VOLUME 84 SUPPLEMENT 1, MAY 2026

EASL CONGRESS

Barcelona Spain
27–30 May 2026

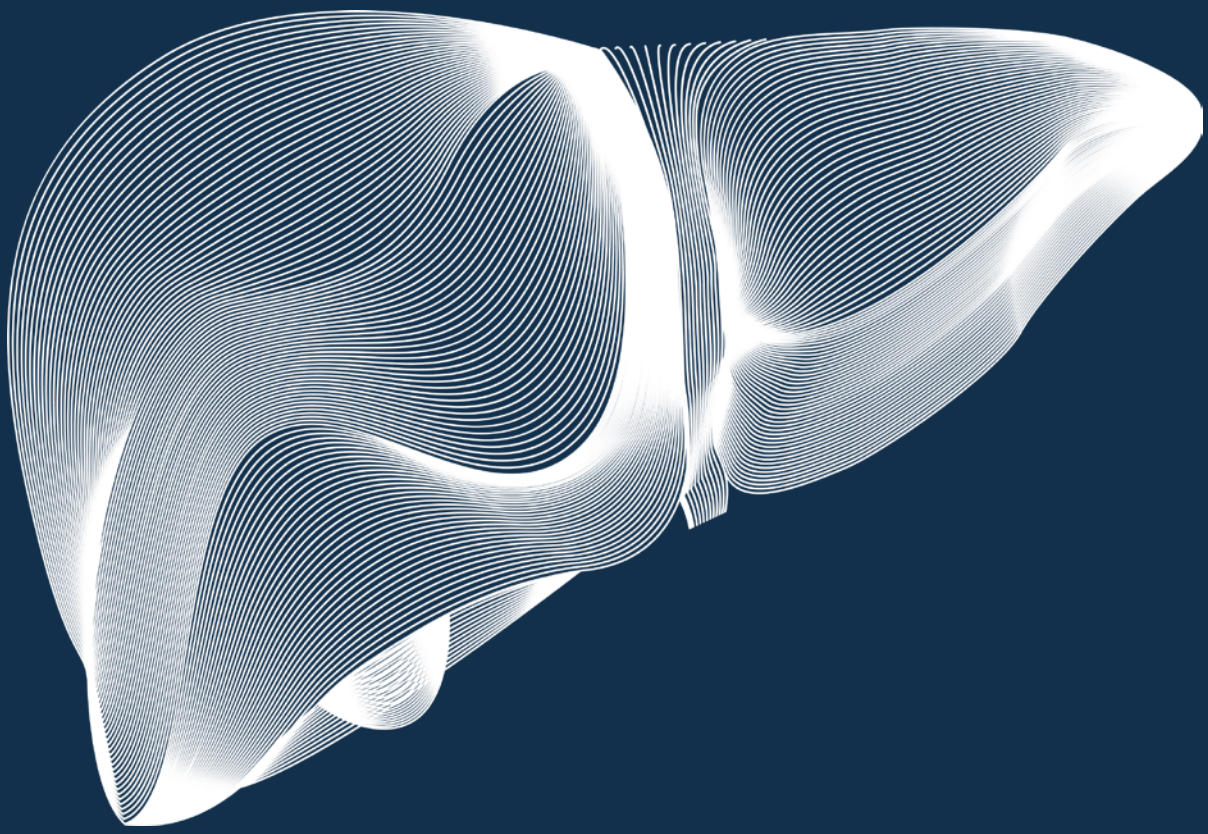

ABSTRACT BOOK

#EASLCongress

easlcongress.eu

JOURNAL OF HEPATOLOGY

The Home of Liver Research

EDITOR IN CHIEF

Vlad Ratziu, France

CO-EDITORS

Annalisa Berzigotti, Switzerland I Tom H. Karlsen, Norway | Phil N. Newsome, UK | Lorenza Rimassa, Italy I Frank Tacke, Germany | Heiner Wedemeyer, Germany

ASSOCIATE EDITORS

Alcohol and Drug-Related Liver Diseases
Guruprasad Aithal, UK
Bin Gao, US
Alexandre Louvet, France

Basic science
Anna Mae Diehl, US
Yasuko Iwakiri, US
Robert Schwabe, US

Cholestasis and Autoimmune Diseases
David Assis, US
Gideon Hirschfield, Canada
Verena Keitel, Germany

Complications of Cirrhosis and Liver Failure
Agustin Albillos, Spain
Alastair O'Brien, UK
Aurelie Plessier, France
Thomas Reiberger, Austria
Puneeta Tandon, Canada
Dominique Thabut, France

Disease Burden and Public Health
Marianne Martinello, Australia

Gut-Liver Axis
Bernd Schnabl, US

Hepatic and Biliary Cancer
Stephen Chan, Hong Kong
Tim Greten, US
Katie Kelly, US
Angela Lamarca, Spain
Tom Luedde, Germany
Jean-Charles Nault, France
Matthias Pinter, Austria

Imaging and Non-Invasive Tests
Maxime Ronot, France

Immunology
Barbara Rehermann, US

Liver Surgery and Transplantation
Andrea Schlegel, US
Nazia Selzner, Canada

MASLD
Quentin Anstee, UK
Jérôme Boursier, France
Amalia Gastaldelli, Italy
George Ioannou, US
Stefano Romeo, Sweden
Vincent Wong, Hong Kong

Paediatric liver diseases
Valerie McLin, Switzerland

Pathology
Dina Tiniakos, UK

Statistics, A.I. and Modelling Outcomes
Julius Chapiro, US
Sylvie Chevret, France
Elise Dumas, Switzerland
Julia Kozlitina, US
Terry Yip, Hong Kong

Viral Hepatitis
Eike Steinmann, Germany
Rachel Wen-Juei Jeng, Taiwan
Sabela Lens, Spain

Specialist consultants
Peter Jepsen (Epidemiology), Denmark
Alexandra Zhernakova (Genomics and big data), Netherlands

Web and social media editor
Rui Castro, Portugal

BREAKTHROUGHS BEYOND THE JOURNAL

Florent Artru, France
Valerie Chew, Singapour
Cornelius Engelmann, Germany
Panu Luukkonen, Finland
Thomas Marjot, UK
David Pinato, UK
Prakash Ramachandran, UK
Lisa Sandmann, Germany
David Trampert, Netherlands

EDITORS EMERITUS

Dame Sheila Sherlock†, Founding Editor, UK (1985-1989)
Jean-Pierre Benhamou†, France (1990-1994)
Gustav Paumgartner†, Germany (1995-1999)
Juan Rodés†, Spain (2000-2004)
Massimo Colombo, Italy (2005-2009)
Didier Samuel, France (2010-2014)
Rajiv Jalan, UK (2015-2019)
Paolo Angeli, Italy (2020-2024)

EDITORIAL BOARD

Manal Abdelmalek, USA
Fredrik Aberg, Finland
Juan Abraldes, Canada
Kosh Agarwal, UK
Alessio Aghemo, Italy
Manon Allaire, France
Emma Andersson, Sweden
Raul Andrade, Spain
Juan Pablo Arab, USA
Marco Arrese, Chile
Tarik Asselah, France
Matias Avila, Spain
Jasmohan Bajaj, USA
Marina Baretti, USA
Thomas Baumert, France
Carmen Berasain, Spain
Marina Berenguer, Spain
Annika Bergquist, Sweden
William Bernal, UK
Christopher Bowlus, USA
Christophe Bureau, France
Patrizia Burra, Italy
Andrés Cárdenas, Spain
Laurent Castera, France
Cyrielle Caussy, France
Landon Chan, Hong Kong
David Cohen, USA
Markus Cornberg, Germany
Helena Cortez-Pinto, Portugal
Leonardo da Fonseca, Brazil
Sarwa Darwish Murad, Netherlands
Laura Dawson, Canada
Claudia de Olivera, Brazil
François Durand, France
Richard Ehman, USA
Manal El-Sayed, Egypt
Jordan Feld, Canada
Claire Francoz, France
Peter Fickert, Austria
Peter Galle, Germany
Jéremie Gautheron, France
Liana Gheorghe, Romania
Olivier Govaere, Belgium
Jordi Gracia-Sancho, Spain
Thierry Gustot, Belgium
Hannes Hagström, Sweden
Yong He, China
Mathias Heikenwälder, Germany
Chiun Hsu, Taiwan
Savneet Kaur, India
Aleksander Krag, Denmark
Andreas Kremer, Switzerland
Karoline Lackner, Austria
Pietro Lampertico, Italy
Nina Le Bert, Singapore
Isabelle Leclercq, Belgium
Maud Lemoine, UK
Hongliang Li, China
Mike Li, USA
Ansgar Lohse, Germany
Anna Lok, USA
Maria Carlota Londoño, Spain
Joachim Lupberger, France
Teresa Macarulla, Spain
Sonya MacParland, Canada
Lungyi Mak, Hong Kong
Mattias Mandorfer, Austria
Jake Mann, UK
Jessica Mellinger, USA
Manuela Merli, Italy
Tim Meyer, UK
Sara Montagnese, Italy
Aldo Montano-Loza, Canada
Laura Nagy, USA
Pierre Nahon, France
Nobuhiro Nakamoto, Japan
Irene Ng, China
Raluca Pais, France
Laura Pallett, UK
Margarita Papatheodoridi, Greece
Valerie Paradis, France
Salvatore Petta, Italy
Salvatore Piano, Italy
Elizabeth Powell, Australia
Xiaolong Qi, China
Pierre-Emmanuel Rautou, France
Nancy Reau, USA
Maru Rinella, USA
Cecilia Rodrigues, Portugal
Manuel Romero-Gómez, Spain
Ian Rowe, UK
Francesco Paolo Russo, Italy
Riad Salem, USA
Shiv K. Sarin, India
Jörn Schattenberg, Germany
Kai Markus Schneider, Germany
Carolin Schneider, Germany
Charlotte Scott, Belgium
Giada Sebastiani, Canada
Christine Sempoux, Switzerland
Yu-Yan Shao, Taiwan
Tracey Simon, USA
Elsa Solà, USA
Mark Sonderup, South Africa
Milan Sonneveld, Netherlands
Silvia Sookoian, Argentina
Mario Strazzabosco, USA
Beicheng Sun, China
Gyongyi Szabo, USA
Parissa Tabrizian, USA
Atsushi Tanaka, Japan
Norah Terrault, USA
Robert Thimme, Germany
Mark Thursz, UK
Natalie Torok, USA
Jonel Trebicka, Germany
Palak Trivedi, UK
Luca Valenti, Italy
Ludovic Vallier, Germany
Schalk van der Merwe, Belgium
Eloi Verrier, France
Silvia Villarinho, USA
Kimberly Watt, USA
Reiner Wiest, Switzerland
Grace Wong, Hong Kong
Mark Yarchoan, USA
Hannele Yki-Jarvinen, Finland
Shira Zelber-Sagi, Israel
Bin Zhou, China

EDITORIAL OFFICE

Head of Publications
Joël Walicki

Editorial Project Manager
Kristina Jajcevic

Editorial Coordinator
Sarita Bhattacharya

Medical Writer
Duncan Anderson

Graphic Arts Project Manager
Pablo Echeverria

EASL GOVERNING BOARD

SECRETARY GENERAL
Debbie Shawcross, UK

VICE SECRETARY
Ana Lleo, Italy

TREASURER
Massimo Pinzani, UK

SCIENTIFIC COMMITTEE
Rui Castro, Portugal
Cyrielle Caussy, France
Emma Culver, UK
Sarwa Darwish Murad, Netherlands
Sabela Lens, Spain
Matthias Pinter, Austria
Bogdan Procopet, Romania

EDUCATIONAL COUNCILLORS
Sven Francque, Belgium

EU POLICY COUNCILLOR
Shira Zelber-Sagi, Israel

EXTERNAL AFFAIRS COUNCILLOR
Francesco Paolo Russo, Italy

INTERNAL AFFAIRS COUNCILLOR
Ahmed Elsharkawy, UK

EASL Office
Journal of Hepatology Editorial Office
7 rue Daubin
1203 Geneva, Switzerland
Tel.: +41 (0) 22 807 0363
E-mail: jhepatology@easloffice.eu

Application for EASL Membership can be done at https://easl.eu/community/join-the-community/

© 2026 European Association for the Study of the Liver. Published by Elsevier B.V. All rights are reserved, including those for text and data mining, AI training, and similar technologies.

This journal and the individual contributions contained in it are protected under copyright, and the following terms and conditions apply to their use in addition to the terms of any Creative Commons or other user license that has been applied by the publisher and the European Association for the Study of the Liver to an individual article:

Photocopying: Single photocopies of single articles may be made for personal use as allowed by national copyright laws. Permission is not required for photocopying of articles published under the CC BY license nor for photocopying for non-commercial purposes in accordance with any other user license applied by the publisher and the European Association for the Study of the Liver. Permission of the publisher and the European Association for the Study of the Liver and payment of a fee is required for all other photocopying, including multiple or systematic copying, copying for advertising or promotional purposes, resale, and all forms of document delivery. Special rates are available for educational institutions that wish to make photocopies for non-profit educational classroom use.

Derivative Works: Users may reproduce tables of contents or prepare lists of articles including abstracts for internal circulation within their institutions or companies. Other than for articles published under the CC BY license, permission of the publisher and the European Association for the Study of the Liver is required for resale or distribution outside the subscribing institution or company. For any subscribed articles or articles published under a CC BY-NC-ND license, permission of the publisher and the European Association for the Study of the Liver is required for all other derivative works, including compilations and translations.

Storage or Usage: Except as outlined above or as set out in the relevant user license, no part of this publication may be reproduced, stored in a retrieval system or transmitted in any form or by any means, electronic, mechanical, photocopying, recording or otherwise, without prior written permission of the publisher and the European Association for the Study of the Liver.

Permissions: For information on how to seek permission visit www.elsevier.com/permissions.

Author rights: Author(s) may have additional rights in their articles as set out in their agreement with the publisher and the European Association for the Study of the Liver (more information at http://www.elsevier.com/authorsrights).

Notice: Books and Journals published by Elsevier comply with applicable product safety requirements. For any product safety concerns or queries, please contact our authorised representative, Elsevier B.V., at productsafety@elsevier.com or Radarweg 29, 1043 NX Amsterdam, Netherlands.

Practitioners and researchers must always rely on their own experience and knowledge in evaluating and using any information, methods, compounds or experiments contained herein. Health care practitioners must exercise their professional judgement and make all treatment-related decisions based solely on the specific conditions of each patient. Because of rapid advances in the medical sciences, independent verification of diagnoses and drug dosages should always be made. The content is provided "as-is" and neither Elsevier nor Society make any representations or warranties, whether express or implied, as to the accuracy, completeness, or adequacy of any content. To the fullest extent permitted by law, neither Elsevier nor Society assume any responsibility for any damages, adverse events, or liability arising from use of information contained herein including for any injury and/or damage to persons or property, whether as a matter of product liability, negligence or otherwise. Inclusion of any advertising material in this publication does not constitute a guarantee or endorsement of the quality or value of such product or service or of any of the representations or claims made by the advertiser.

Publication information: Journal of Hepatology (ISSN 0168-8278). For 2026, volumes 84 and 85 are scheduled for publication. Subscription prices are available upon request from the Publisher or from the Elsevier Customer Service Department nearest you or from this journal's website (http://www.elsevier.com/locate/jhep). Further information is available on this journal and other Elsevier products through Elsevier's website: (http://www.elsevier.com). Subscriptions are accepted on a prepaid basis only and are entered on a calendar year basis. Issues are sent by standard mail (surface within Europe, air delivery outside Europe). Priority rates are available upon request. Claims for missing issues should be made within six months of the date of dispatch.

Orders, claims, and journal inquiries: Please visit our Support Hub page https://service.elsevier.com for assistance.

Advertising information: For advertising and solutions inquiries, please contact Joe Skey, email: joe.skey@formedics.com or Bill Hipple, email: bill.hipple@formedics.com. For reprint queries, please send an email to sales@contentednet.com.

Author enquiries: Visit the Elsevier Support Center (https://service.elsevier.com/app/home/supporthub/publishing) to find the answers you need. Here you will find everything from Frequently Asked Questions to ways to get in touch.
You can also check the status of your submitted article via https://service.elsevier.com/app/answers/detail/a_id/29155/ or find out when your accepted article will be published via https://service.elsevier.com/app/answers/detail/a_id/5981/.

Funding body agreements and policies: Elsevier has established agreements and developed policies to allow authors whose articles appear in journals published by Elsevier, to comply with potential manuscript archiving requirements as specified as conditions of their grant awards. To learn more about existing agreements and policies please visit http://www.elsevier.com/fundingbodies.

Special regulations for authors: Upon acceptance of an article by the journal, the author(s) will be asked to transfer copyright of the article to EASL. Transfer will ensure the widest possible dissemination of information.

Publishing Office: *Journal of Hepatology* (ISSN 0168-8278, USPS 11087) is published monthly by Elsevier B.V., Radarweg 29, Amsterdam, 1043 NX, Netherlands. Airfreight and mailing in the USA by agent named World Container Inc, 150-15, 183rd Street, Jamaica, NY 11413, USA. Periodicals postage paid at Brooklyn, NY 11256.

POSTMASTER: Send address changes to *Journal of Hepatology*, Air Business Ltd, c/o World Container INC 150-15, 183rd St, Jamaica, NY 11413, USA.

Subscription records are maintained at Elsevier B.V. Radarweg 29, 1043 NX Amsterdam, the Netherlands.

Air Business Ltd is acting as our mailing agent.

♾ The paper used in this publication meets the requirements of ANSI/NISO Z39.48-1992 (Permanence of Paper).

Printed by Henry Ling, The Dorset Press, Dorchester, UK

JOURNAL OF HEPATOLOGY

VOLUME **84**, SUPPLEMENT **S1**, PAGES **S1–S1108**

Abstract Book of EASL Congress 2026
27–30 May 2026, Barcelona, Spain

Publication of this Abstract supplement was supported by the European Association for the Study of the Liver (EASL)

ELSEVIER

EASL CONGRESS

London United Kingdom
16–19 June 2027

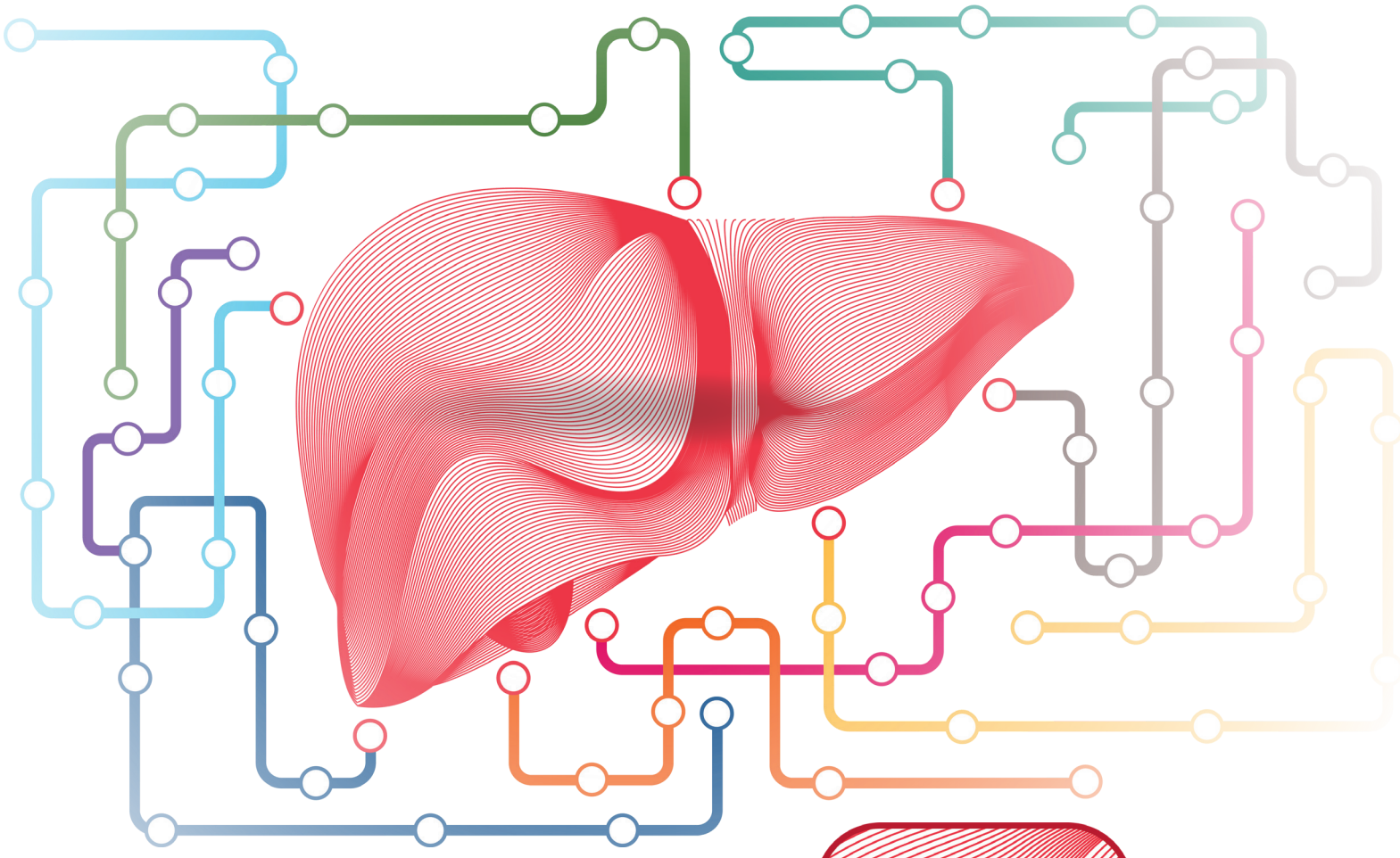

#EASLCongress

easlcongress.eu

SAVE THE DATE!

EASL GUIDELINES 2.0

Your essential app for advanced liver care

Consult EASL Clinical Practice Guidelines anytime, anywhere.

Expand your knowledge with continuously updated resources and tools.

Discover EASL Policy Statements and Policy Dialogues.

GET IT ON Google Play

Download on the App Store

EASL™ The Home of Hepatology

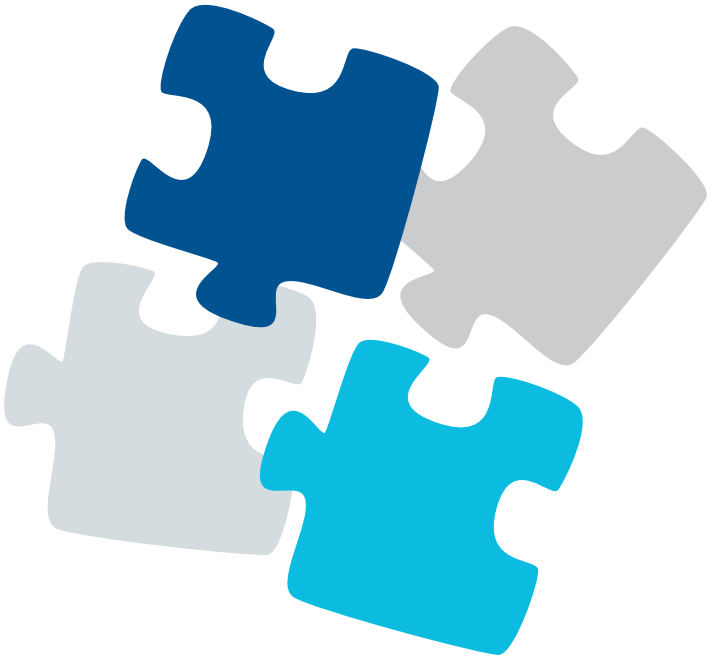

Let’s unite hepatology!

Discover your membership benefits!

Become a member

JOURNAL OF HEPATOLOGY

VOLUME **84**, SUPPLEMENT **1**, PAGES **S1–S1108**

CONTENTS

Oral Presentations S1

GENERAL SESSION I S1

GENERAL SESSION II S4

Late breakers oral session S7

Hepatocyte biology and fibrosis S11

Immune-mediated I S13

Liver tumours – experimental S17

MASLD: Clinical and therapeutical aspects I S19

Interprofessional forum S21

Public health S23

Alcohol S26

Basic Science MASLD S28

Cirrhosis – Clinical and experimental I S30

Cirrhosis – Clinical and experimental II S33

Liver tumours – Clinical S36

Rare liver diseases S39

Regeneration and gut communication S41

Viral hepatitis B/D – Current therapies S43

Viral hepatitis B/D – New therapies S47

Basic viral hepatitis and immunology S49

Cirrhosis – Clinical and experimental III S52

Immune mediated II S55

Liver transplantation S59

MASLD: Clinical and therapeutical aspects II S62

Viral hepatitis – Clinical aspects S65

EASL Clinical Practice Guidelines on management of primary biliary cholangitis and PBC abstracts S67

Poster Presentations S69
Late-breaker Posters S69
Acute liver failure and drug induced liver injury – Clinical S88
Acute liver failure and drug induced liver injury – Experimental and pathophysiology S99
Alcohol-related liver disease and MetALD – Clinical S108
Alcohol-related liver disease and MetALD – Experimental and pathophysiology S129
Cirrhosis and its complications – ACLF and Critical illness S141
Cirrhosis and its complications – Experimental and pathophysiology S162
Cirrhosis and its complications – Other clinical complications except ACLF and critical illness S184
Fibrosis – Stellate cell biology S229
General Hepatology (including non-invasive liver assessment) S246
Gut microbiota and liver disease – Liver-organ crosstalk S260
Hepatocyte biology S270
Immune-mediated and cholestatic – Experimental and pathophysiology S281
Immune-mediated and cholestatic disease – Clinical aspects S294
Liver development and regeneration S357
Liver immunology S362
Liver transplantation and hepatobiliary surgery – Clinical S374
Liver transplantation and hepatobiliary surgery – Experimental and pathophysiology S418
Liver tumours – Clinical aspects except therapy S422
Liver tumours – Experimental and pathophysiology S453
Liver tumours – Therapy S490
MASLD – Clinical aspects except therapy S515
MASLD – Diagnostics and non-invasive assessment S558
MASLD – Experimental and pathophysiology S627
MASLD – Therapy S678
Nurses and Allied Health Professionals – Research project S702
Nurses and Allied Health Professionals – Clinical – service development or improvement project S710
Portal Hypertension (cirrhosis and non-cirrhosis) S719
Public Health – Except Viral Hepatitis S758
Public Health – Viral Hepatitis S797
Rare liver diseases (including paediatric and genetic) – Clinical S827
Rare liver diseases (including paediatric and genetic) – Experimental and pathophysiology S852
Viral hepatitis – Clinical, except HBV, HDV and HCV S864

Viral Hepatitis – Experimental and pathophysiology S868
Viral hepatitis B and D – Clinical aspects S897
Viral hepatitis B and D – Current therapies S934
Viral hepatitis B and D – New therapies, unapproved therapies or strategies S956
Viral hepatitis C – Clinical aspects including follow up after SVR S966
Viral hepatitis C – Therapy and resistance S979
Author Index S982
Disclosures: no commercial relationships S1099
Disclosures: commercial relationships S1104
Reviewers list S1108

Registration of Clinical Trials
The *Journal of Hepatology* endorses the policy of the WHO and the International Committee of Medical Journal Editors (ICMJE) on the registration of clinical trials. Therefore, any trial that starts recruiting on or after July 1, 2005 should be registered in a publicly owned, publicly accessible registry and should satisfy a minimal standard dataset. Trials that started recruiting before that date will be considered for publication if registered before September 13, 2005.
More detailed information regarding clinical trials and registration can be found in New Engl J Med 2004; 351:1250–1251 and New Engl J Med 2005; 352:2437–2438.

Available online at www.sciencedirect.com
ScienceDirect
for online access via your library

A-TANGO

Featuring G-TAK, a novel combinatorial therapy for acute-on-chronic liver failure (ACLF)

Expected Impact

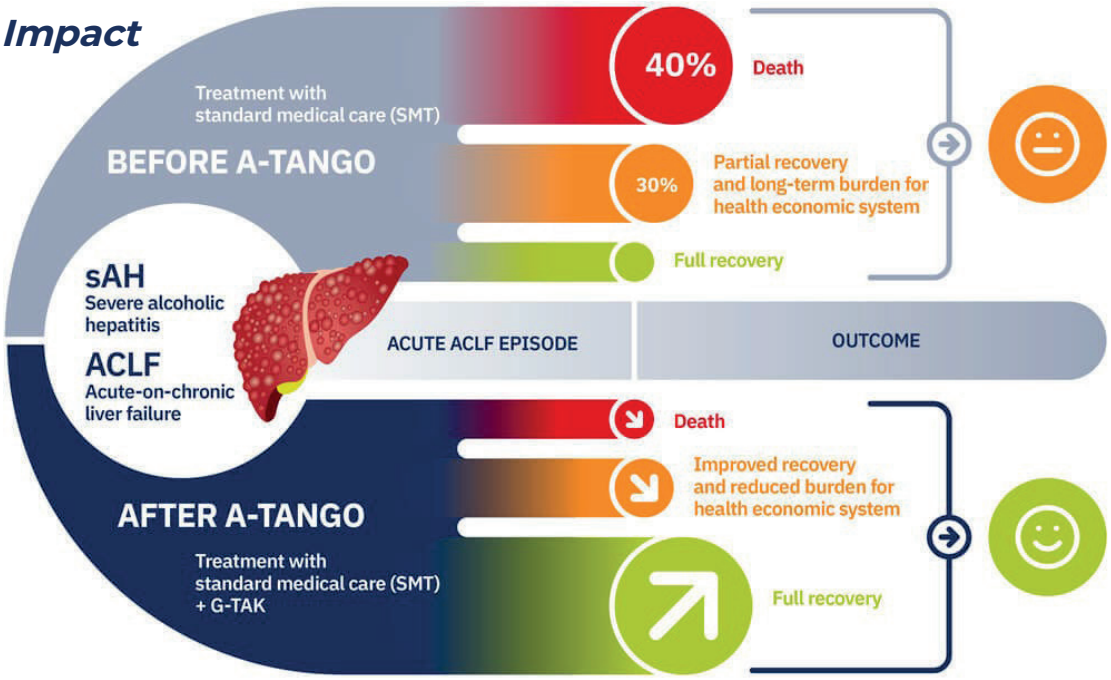

- More than **10 million people** suffer from **decompensated cirrhosis** worldwide.
- Effective treatment of ACLF is an urgent and unmet need.
- A-TANGO performs **Phase II clinical studies of G-TAK,** a novel and innovative therapeutic strategy that aims to **reduce inflammation** and **improve hepatocyte proliferation.**
- A-TANGO also strives to identify **reliable biomarkers** for better patient stratification and increased survival.

13 partners, one goal: Helping cirrhosis patients in Europe and beyond

kick-off
1st March 2021

project duration
5.0 years

grant amount
6.0 million €

a-tango.eu

This project has received funding from the European Union's Horizon 2020 research and innovation programme under grant agreement No 945096.

DECISION

decision-for-liver.eu

DEcompensated CIrrhoSIs: identification of new cOmbiNatorial therapies based on systems approaches

Key facts

- **Project start**: 1st April 2020
- **Duration**: 6.5 years
- **Members**: 21 institutions from 10 European countries
- **EC funding**: € 6 million

AIM 1
Understanding at systems level

- Using **high-throughput technologies** to understand decompensated cirrhosis at systems level
- Re-analyzing standardized biobank samples from **2,200 patients** with decompensated cirrhosis by characterizing
  - **epigenetics »** manuscript in preparation
  - **transcriptomics**
    » Aguilar F et al. J Hepatol (2025)
  - **metabolomics »** manuscript accepted in *Nature Communications*
  - **microRNA »** manuscript in preparation
  - **extracellular vesicles »** presented at EASL2024

AIM 2
New combinatorial therapy

COMBAT-Trial: proof-of-concept, phase II randomized controlled clinical study

- **Goal**: Evaluate safety and tolerability of a novel combinatorial therapy (human albumin and enoxaparin) in patients with decompensated cirrhosis discharged from the hospital; comparison to standard medical treatment

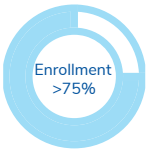

- First patient enrolled in July 2024

PROSPECT study: prospective, multicenter observational cohort study on post-discharge outcomes in patients with cirrhosis and AD

- **Goal**: Test the prognostic accuracy of novel biomarkers identified within DECISION

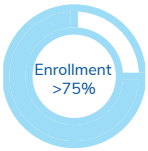

- First patient enrolled in March 2025

AIM 3
Pre-clinical models

- Existing rat models for acute decompensation of cirrhosis leading to ACLF lack full replication of human disease heterogeneity
  » We therefore aim to refine existing animal model-s
- Publications:
  - Development & characterization of **novel rodent ACLF models »** manuscript submitted
  - Acceleration of an advanced **NASH model** by acute and toxic effects of Phenobarbital
    » Kraus N, Uschner FE et al. Cells (2024)

AIM 4
Prognostic and response tests

- Novel and robust **stratification method** identifies three clusters of patients with acute decompensation of cirrhosis (AD)
  » Palomino-Echeverria S et al. J Transl Med (2024)
  » Ortega-Lagerreta A, Palomino-Echeverria S et al. PLOS Comp Bio (2024)
- Potential tool for healthcare providers to enhance patient monitoring or preventative measures using existing electronic health record data and method could guide future clinical trial design
- Further results will be published soon

This project received funding from the European Union's Horizon 2020 research and innovation programme under grant agreement No. 847949.

GENIAL is a pioneering initiative targeting **alcohol-related liver cancer** (**ALD-HCC**). Our primary goal is to identify **genetic** and **environmental** factors contributing to ALD-HCC risk and unravel how their **interactions** drive alcohol-related liver carcinogenesis. By pinpointing individuals at risk, GENIAL will pave the way for innovative **prevention strategies** and potential **chemopreventive targets** to tackle this devastating disease. Moreover, GENIAL is dedicated to **educating** and empowering the entire EU community with vital knowledge for effective disease prevention and **early detection**.

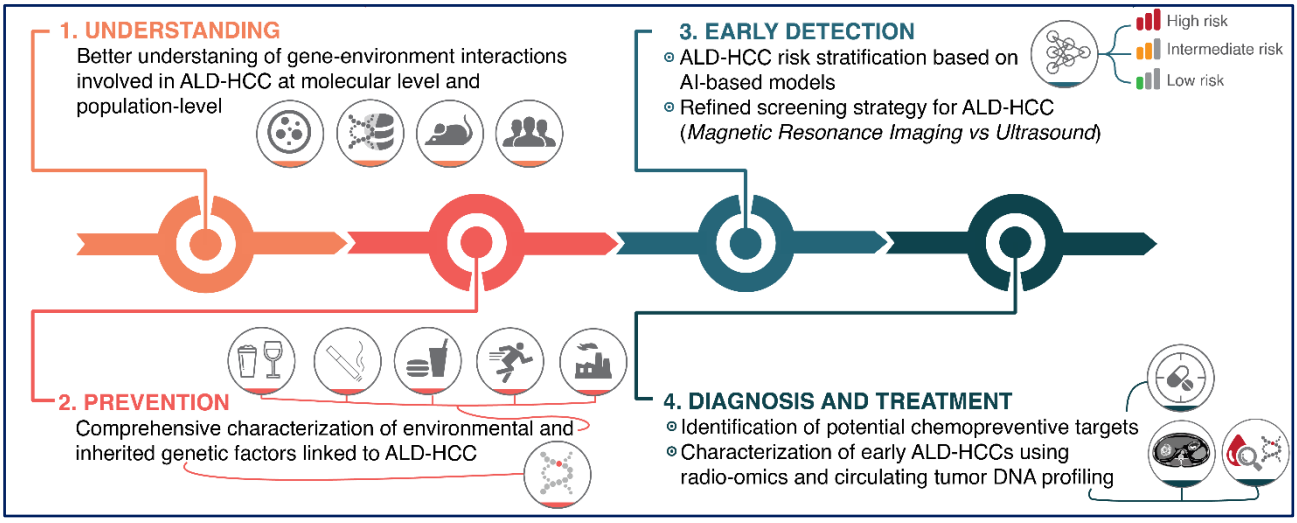

The GENIAL Project is funded by the European Union within the Horizon Europe programme under grant agreement No 101096312.

innovative health initiative · efpia · EuropaBio · MedTech Europe from diagnosis to cure · Vaccines Europe · COCIR Advancing Healthcare

AIM LIVER

A biomarker-based platform for early diagnosis of chronic liver disease to enable personalized therapy

ACADEMIA AND INDUSTRIES ARE CONDUCTING THE LARGEST PROJECT EVER IN THE FIELD OF LIVER DISEASES

AIM:

To design and validate an AI-powered screening platform using biomarkers for the early diagnosis of liver diseases in the general population, and to establish links to care through personalized interventions

Clínic Barcelona · Universitat de Barcelona · Roche · OUH Odense University Hospital Svendborg Hospital · Universitätsmedizin Mainz · Azienda Ospedale Università Padova · IHU ican Foundation for Innovation in Cardiometabolism and Nutrition · Assistance Publique Hôpitaux de Paris · University of Zagreb School of Medicine · Dubrava University Hospital · Università degli Studi di Milano · FNaF F. D. Roosevelt Banská Bystrica · ISGlobal Barcelona Institute for Global Health · Universitat de Barcelona · UAB Universitat Autònoma de Barcelona · ELPA European Liver Patients' Association · Innovation Acta · Siemens Healthineers · Nordic Bioscience · Sysmex Together for a better healthcare journey · echosens · AstraZeneca · Boehringer Ingelheim · novo nordisk · Gilead · UKS Universitätsklinikum des Saarlandes · EASL The Home of Hepatology · Universität Zürich · Mayo Clinic · Newcastle University

Visit our website and follow us on social media

Co-funded by the European Union

This project is supported by the Innovative Health Initiative Joint Undertaking (IHI JU) under grant agreement No 101132901. The JU receives support from the European Union's Horizon Europe research and innovation programme and EFPIA, COCIR, MedTech Europe, Vaccines Europe and EuropaBio.

Funded by the European Union, the private members, and those contributing partners of the IHI JU. Views and opinions expressed are however those of the author(s) only and do not necessarily reflect those of the aforementioned parties. Neither of the aforementioned parties can be held responsible for them.

MICROBiome-based biomarkers to PREDICT decompensation of liver cirrhosis and treatment response

MICROB-PREDICT

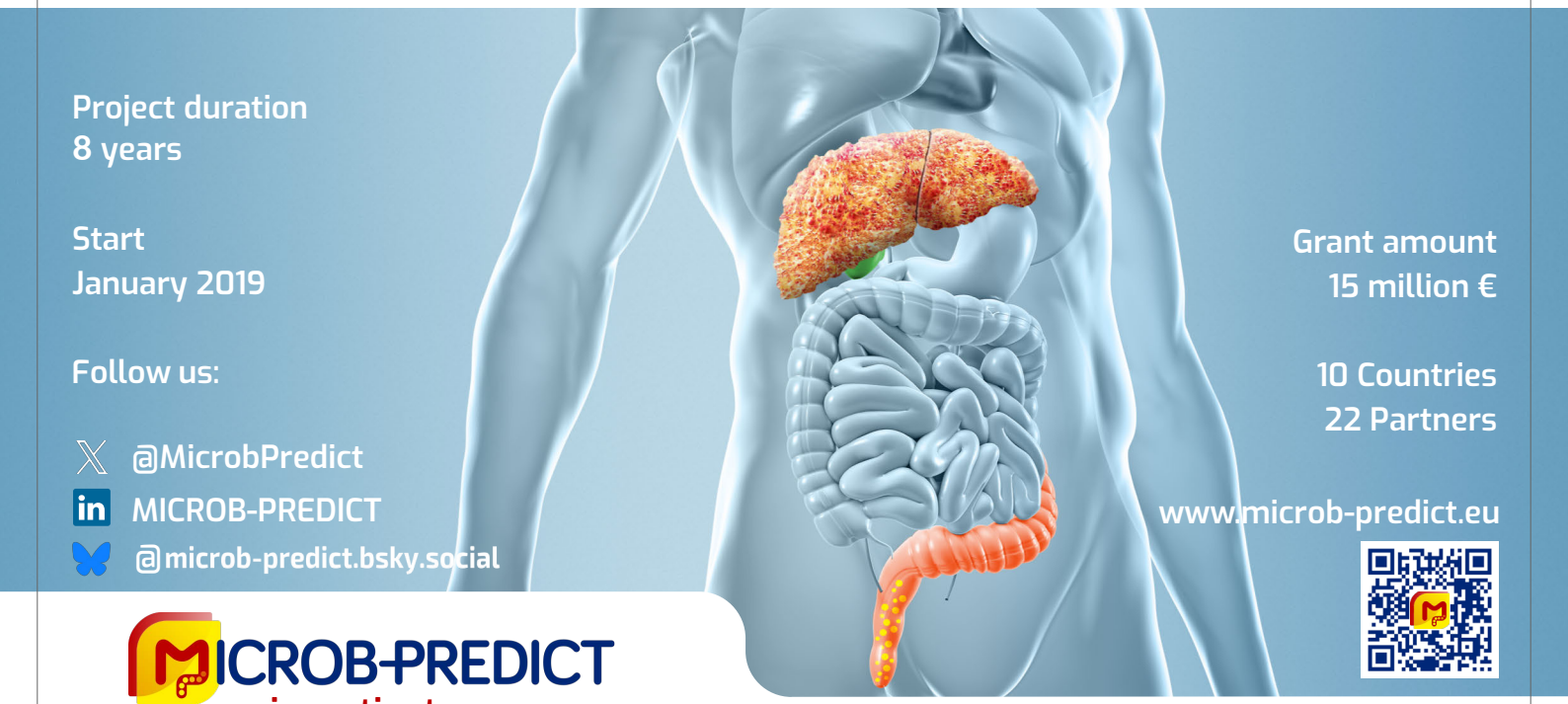

Project duration
8 years

Start
January 2019

Follow us:

@MicrobPredict
MICROB-PREDICT
@microb-predict.bsky.social

Grant amount
15 million €

10 Countries
22 Partners

www.microb-predict.eu

MICROB-PREDICT investigates

the human microbiome to identify predictors and mechanisms associated with the development of decompensation of cirrhosis and progression to acute-on-chronic liver failure (ACLF).

- → New microbiome-based tests for better stratification of cirrhosis patients
- → Personalized prediction and prevention of decompensation and ACLF
- → Clinical trial to predict response to treatment
- → Modern, effective nanobiosensors as clinical tools with improved specificity
- → More personalized treatment
- → Increased survival times
- → Decreased costs for the health systems

EF CLIF EUROPEAN FOUNDATION FOR THE STUDY OF CHRONIC LIVER FAILURE

Universität Münster

UiO : University of Oslo · UCL · University of Copenhagen · VAIOMER Pioneer in Tissue Microbiomes · cea · biobyte solutions · INRA Science & Impact

King's College London · University of Debrecen · IDIBAPS Institut D'Investigacions Biomèdiques August Pi i Sunyer · KU LEUVEN · ICN2 Institut Català de Nanociència i Nanotecnologia · Excelencia Severo Ochoa · OUH Odense University Hospital · LUMC Leids Universitair Medisch Centrum

EASL The Home of Hepatology · ELPA European Liver Patients' Association · concentris research management · Max-Planck-Gesellschaft · EMBL · Universitat de Barcelona

This project has received funding from the European Union's Horizon 2020 research and innovation programme under grant agreement No 825694.

THRIVE

TUMOUR-HOST INTERACTIONS IN LIVER CANCER
OF CHILDHOOD AND ADULTS

THRIVE is a pioneering EU initiative that aims to **enhance** the **outcome of paediatric & adult liver cancer patients** by:

advancing the **understanding** of HCC	identifying **biomarkers** for current therapies	**developing novel treatments** to overcome resistance

THRIVE Consortium

Josep M Llovet - FRCB-IDIBAPS, Spain
Helen Reeves - UNEW, UK
Quentin Anstee - NUTH, UK
Jessica Zucman-Rossi - UPCITE, France
Manel Esteller - IJC-CERCA, Spain
Georg Zeller - LUMC, The Netherlands
Eran Elinav - WEIZMAN, Israel
Carolina Armengol - IGPT-CERCA, Spain
Mathias Heikenwälder - EKUT, Germany
Sven Nahnsen - EKUT, Germany
Manfred Claassen - EKUT, Germany
Jens Puschhof - DKFZ, Germany
Inn-Acta, Italy
ELPA, Belgium
EASL, Switzerland

Funded by the European Union

Funded by the European Union under Grant Agreement Nr. 101136622. Views and opinions expressed are however those of the author(s) only and do not necessarily reflect those of the European Union or the European Health and Digital Executive Agency (HADEA). Neither the European Union nor the granting authority can be held responsible for them.

EASL JOURNAL OF HEPATOLOGY

THURSDAY 28 MAY

GENERAL SESSION I

GS-001

Clinically meaningful rates of functional cure in virologically suppressed patients with chronic hepatitis B infection treated with bepirovirsen: B-Well phase 3 trials

Jinlin Hou[1], Seng Gee Lim[2], Maria Buti[3], Man-Fung Yuen[4], Edward J. Gane[5], Pietro Lampertico[6,7], Norah Terrault[8], Huy Nguyen[9], Hyung Joon Yim[10], Qing Xie[11], Jianmei Lin[12], Yunqing Qiu[13], Rachel Wen-Juei Jeng[14,15], Jeong Heo[16], Cheng-Yuan Peng[17], Chien-Hung Chen[18], Wan-Long Chuang[19], Yao Xie[20], Maria Hlebowicz[21], Nevin Idriz[22], Rajiv Mehta[23], Kosh Agarwal[24], Monica Gomes da Silva[25], Alex Franca[26], Roxana Cernat[27], Apinya Leerapun[28], Carla Coffin[29], Adrian Gadano[30], Pietro Andreone[31,32], Shigetoshi Fujiyama[33], Vasileios Sevastianos[34], Yuichiro Suzuki[35], Vlad Ratziu[36], Ghassan Riachi[37], Hartmut Stocker[38,39], Tien Huey Lim[40], Tarik Asselah[41,42], Yasuhito Tanaka[43], Jacinta Holmes[44], Xieer Liang[1], Jennifer Cremer[45], Tamara Lukic[46], Helene Plein[47], Geoff Quinn[48], Yu Tao[49], Melanie Paff[49], Dickens Theodore[45], Robert Elston[48]. *[1]Nanfang Hospital, Southern Medical University, State Key Laboratory of Multi-organ Injury Prevention and Treatment, Key Laboratory of Infectious Diseases Research in South China, Ministry of Education, Guangzhou, China; [2]National University Health System, Singapore, Singapore; [3]Hospital Universitario Vall D´Hebron, CIBEREHD del Instituto Carlos III, Barcelona, Spain; [4]Department of Medicine, School of Clinical Medicine & State Key Laboratory of Liver Research, Queen Mary Hospital, The University of Hong Kong, Hong Kong, China; [5]Liver Transplant Unit, University of Auckland, Auckland, New Zealand; [6]Foundation IRCCS Ca' Granda Ospedale Maggiore Policlinico, Milan, Italy; [7]CRC "A. M. and A. Migliavacca" Center for Liver Disease, University of Milan, Milan, Italy; [8]University Of Southern California, Los Angeles, United States; [9]San Jose Gastroenterology, San Jose, United States; [10]Korea University Ansan Hospital, Ansan, Korea, Rep. of South; [11]Ruijin Hospital Affiliated to Shanghai Jiao Tong University School of Medicine, Shanghai, China; [12]Sichuan Provincial People's Hospital, Chengdu, China; [13]1st Affiliated Hospital Of Zhejiang University, Hangzhou, China; [14]Chang Gung Memorial Hospital, Linkou, Taiwan; [15]College of Medicine, Chang Gung University, Linkou, Taiwan; [16]College of Medicine, Pusan National University and Biomedical Research Institute, Pusan National University Hospital, Busan, Korea, Rep. of South; [17]China Medical University Hospital, China Medical University, Taichung, Taiwan; [18]Kaohsiung Chang Gung Memorial Hospital, Kaohsiung, Taiwan; [19]Kaohsiung Medical University Hospital, Kaohsiung Medical University, Kaohsiung, Taiwan; [20]Beijing Ditan Hospital, Beijing, China; [21]University of Warmia and Mazury, Olsztyn, Poland; [22]UMHAT Sofiamed, Sofia, Bulgaria; [23]SIDS Hospital and Research Center, Surat, India; [24]Institute of Liver Studies, Kings College Hospital NHS Trust, London, United Kingdom; [25]Department of Public Health, Hospital de Clinicas, Federal University of Paraná, Curitiba, Brazil; [26]Hospital de Cirurgia, NewData Clinical Research, Federal University of Sergipe, Aracaju, Brazil; [27]Clinical Hospital for Infectious Diseases, Ovidius University of Constanta, Constanta, Romania; [28]Chiang Mai University, Chiangmai, Thailand, [29]Snyder Institute, Cumming School of Medicine, University of Calgary, Calgary, Canada; [30]Hospital Italiano de Buenos Aires, Buenos Aires, Argentina; [31]Ospedale Clinicizzato di Baggiovara, AOU di Modena, Modena, Italy; [32]Università di Modena e Reggio Emilia, Modena, Italy; [33]Kumamoto Shinto General Hospital, Kumamoto, Japan; [34]Evangelismos General Hospital, Athens, Greece; [35]University of Yamanashi, Yamanashi, Japan; [36]Hôpital Pitié Salpêtrière, Paris, France; [37]CHU de Rouen, Hôpital Charles Nicolle, Rouen, France; [38]Epimed Gmbh, Berlin, Germany; [39]St. Joseph Hospital, Berlin, Germany; [40]Aotearoa Clinical Trials, Papatoetoe, Auckland, New Zealand; [41]Université de Paris-Cité, INSERM UMR1149, Paris, France; [42]Hôpital Beaujon, Clichy, France; [43]Kumamoto University Hospital, Kumamoto, Japan; [44]St Vincent's Hospital Melbourne, University of Melbourne, Fitzroy, Australia; [45]GSK, Durham, United States; [46]GSK, Dubai, United Arab Emirates; [47]GSK, London, United Kingdom; [48]GSK, Stevenage, United Kingdom; [49]GSK, Collegeville, United States*
Email: jlhousmu@163.com

Background and aims: Functional cure (FC), hepatitis B surface antigen (HBsAg) loss and hepatitis B virus (HBV) DNA < lower limit of quantification (LLOQ) 24 weeks off therapy, is the treatment goal in chronic HBV infection. Bepirovirsen (BPV), an antisense oligonucleotide, is the first anti-HBV therapy in global Phase 3 trials with FC as the primary outcome.
Method: B-Well 1 and 2 are global double-blind Phase 3 trials. Non-cirrhotic adults with nucleos(t)ide analogue (NA)-suppressed chronic HBV infection (HBV DNA <90 IU/mL) and HBsAg > 100–≤ 3000 IU/mL were randomised 2:1 to BPV 300 mg or placebo (PBO) weekly for 24 weeks. Participants (pts) discontinued NAs at Week 48, if eligible. The primary outcome was FC response rate at Week 72 for all pts; defined as HBsAg not detected (qualitative; < 0.05 IU/mL) and HBV DNA < LLOQ (< 20 IU/mL or target not detected) 24 weeks after discontinuing all HBV treatment. Key secondary outcomes included FC response rate for pts with baseline HBsAg ≤ 1000 IU/mL. Safety was assessed via adverse event (AE) and laboratory monitoring.
Results: The full analysis set comprised 650 BPV and 328 PBO pts in B-Well 1 and 570 BPV and 286 PBO pts in B-Well 2. Pts were 71% male, mean age approximately 49 years, 68% Asian, 8% HBeAg positive, and 63% had baseline HBsAg ≤ 1000 IU/mL. No PBO pts achieved FC. Among BPV pts with baseline HBsAg ≤ 3000 IU/mL, 20% and 19% achieved FC in B-Well 1 and B-Well 2, respectively ($p < 0.001$ vs PBO). In BPV pts with baseline HBsAg ≤ 1000 IU/mL, 25% in B-Well 1 and 28% in B-Well 2 achieved FC ($p < 0.001$ vs PBO). Most common AEs with BPV (pooled safety: BPV = 1223, PBO = 611) in Week 1–72 included injection site erythema (31%; PBO 2%), injection site pain (23%; PBO 5%) and alanine aminotransferase (ALT) increase (23%; PBO 4%). ALT increases were transient and generally occurred in Week 5–10; 6% of BPV pts had ALT ≥ 10x upper limit of normal (vs PBO <1%). No cases were adjudicated as meeting drug-induced liver injury criteria. Few AEs were serious (BPV 7%; PBO 4%) or led to permanent treatment discontinuation (BPV 3%; PBO < 1%). Two deaths unrelated to study treatment occurred in the BPV arm.
Conclusion: 24-week BPV treatment induced clinically meaningful and statistically significant FC rates versus PBO in virologically

 © 2026 All rights reserved.

suppressed pts with chronic HBV infection, with an acceptable safety profile, showing the potential for BPV to be a first-in-class finite therapy for FC.
Funding: GSK (202009/NCT05630807; 219288/NCT05630820). [for the B-Well Study Group].

GS-002

The microbe-derived metabolite imidazole propionate promotes the pathogenesis of primary sclerosing cholangitis via p38–mTORC1 signaling

Antonio Molinaro[1,2], Peder Rustøen Braadland[1,3,4], Alba Carreras Palou[2], Guido Carpino[5], Marios Nikolaidis[6], Petra Hanzely[1,3,4], Katharina Beck[2], Ahmad Ali[7,8], Lars Bossen[9,10], Anna Katharina Frank[1,3,4,11], Annika Lundqvist[2], Brian D. Juran[6], Diletta Overi[5], Enya Amundsen-Isaksen[1,3,4], Trine Folseraas[1,3,4,12], Martin Cornillet[13], Holmfridur Helgadottir[1,14], Bryan McCauley[6], Laura Cristoferi[15], Marco Carbone[15], Vincenzo Cardinale[16], Marte Lie Høivik[17,18], Lise Katrine Engesæter[1,3,4,12], Sara Tjønnfjord[1,3,12,17], Adrian McCann[19], Per Ueland[19], Mette Vesterhus[1,14], Tom Hemming Karlsen[1,3,4,12], Henning Grønbæk[9,10], Eugenio Gaudio[5], Konstantinos N. Lazaridis[6], Annika Bergquist[20], Espen Melum[1,3,4,6,12], Fredrik Backhed[2], Johannes R. Hov[1,3,12,17]. *[1]Norwegian PSC Research Center, Department of Transplantation Medicine, Division of Surgery and Specialized Medicine, Oslo University Hospital, Oslo, Norway; [2]The Wallenberg Laboratory, Department of Molecular and Clinical Medicine, Institute of Medicine, Sahlgrenska Academy, University of Gothenburg, Gothenburg, Sweden; [3]Research Institute of Internal Medicine, Division of Surgery and Specialized Medicine, Oslo University Hospital, Oslo, Norway; [4]Institute of Clinical Medicine, Faculty of Medicine, University of Oslo, Oslo, Norway; [5]Department of Anatomical, Histological, Forensic Medicine and Orthopedics Sciences, Sapienza University of Rome, Rome, Italy; [6]Division of Gastroenterology and Hepatology, Mayo Clinic, Rochester, MN, United States; [7]Division of Gastroenterology and Hepatology, School of Medicine, University of Missouri, Columbia, MO, United States; [8]Division of Gastroenterology and Hepatology, University of Missouri School of Medicine, Columbia, United States; [9]Department of Hepatology & Gastroenterology, Aarhus University Hospital, Clinical Institute, Aarhus University, Aarhus, Denmark; [10]Clinical Institute, Aarhus University, Aarhus, Denmark; [11]Hybrid Technology Hub-Centre of Excellence, Institute of Basic Medical Sciences, Faculty of Medicine, University of Oslo, Oslo, Norway; [12]Section of Gastroenterology, Department of Transplantation Medicine, Division of Surgery and Specialized Medicine, Oslo University Hospital Oslo, Oslo University Hospital,, Oslo, Norway; [13]Department of Medicine Huddinge, Center for Infectious Medicine, Karolinska Institutet, Karolinska University Hospital, Stockholm, Sweden; [14]Department of Medicine, Haraldsplass Deaconess Hospital, Bergen, Norway; [15]Department of Medicine and Surgery, University of Milano-Bicocca, Liver Unit, ASST Grande Ospedale Metropolitano (GOM) Niguarda, Milan, Italy; [16]Department of Translational and Precision Medicine, Sapienza University of Rome, Rome, Italy; [17]Institute of Clinical Medicine, Faculty of Medicine, University of Oslo, Department of Gastroenterology, Division of Medicine, Oslo University Hospital,, Oslo, Norway; [18]Department of Gastroenterology, Division of Medicine, Oslo University Hospital, Oslo, Norway; [19]Bevital AS, Bergen, Norway; [20]Unit of Gastroenterology and hepatology, Department of Medicine Huddinge, Karolinska Institutet, Karolinska University Hospital, Stockholm, Sweden*
Email: antonio.molinaro@wlab.gu.se

Background and aims: Although the gut-liver axis is implicated in primary sclerosing cholangitis (PSC), robust clinical and translational evidence of intestinal drivers are scarce. Here, we used an unbiased metabolomic approach to identify microbially produced molecules associated with PSC and its outcomes and experimentally defined their mechanistic role in bile duct inflammation and fibrosis.
Method: We profiled more than 1,100 plasma metabolites in people with PSC (n = 161) before or after liver transplantation (LT) and healthy controls (HC, n = 32) using untargeted LC–MS/MS. Putative microbiota-derived drivers were identified by prioritizing metabolites that (i) were differentially abundant in PSC, (ii) predicted LT-free survival, (iii) remained altered despite LT. Targeted technical and clinical validation were performed in more than 1,600 PSC blood samples from Norway, Sweden and USA, and 560 control samples from inflammatory bowel disease (IBD) without PSC and people with primary biliary cholangitis or metabolic dysfunction-associated steatotic liver disease. Metagenome sequencing was performed in people with PSC (n = 144). Experimental validation was performed by challenging patient-derived cholangiocyte organoids and chow-fed and 3,5-diethoxycarbonyl-1,4-dihydrocollidine (DDC)-fed mice with key disease-associated metabolite.
Results: The histidine metabolite imidazole propionate (ImP) emerged as the most robustly increased metabolite in PSC. ImP was persistently elevated after LT, and consistently predicted reduced LT-free survival in geographically distinct cohorts. PSC-related gut bacteria correlated with ImP concentration in blood and proctocolectomized individuals had reduced ImP levels. People with PSC had higher ImP levels than disease controls, unaffected by IBD status. When challenged with ImP, cholangiocyte organoids secreted pro-inflammatory and pro-fibrogenic factors, and cholangiocyte cell lines displayed mTORC1 activation, which previously has been identified to mediate ImP signaling. In wildtype mice, chronic ImP administration caused biliary fibrosis, portal inflammation and ductular reaction, and ImP exacerbated the biliary injury in DDC-fed mice. The ImP effects were abolished in mice deficient in p38γ/δ MAP kinase isoforms.
Conclusion: We identify gut microbial ImP as a key player in PSC pathophysiology via activation of p38γ/δ-dependent mTORC1 signaling. Targeting ImP production or signaling can represent a therapeutic strategy for PSC.

GS-003

A PNPLA3 antisense oligonucleotide, AZD2693, for the treatment of MASH in I148M homozygous participants: results from the phase 2b FORTUNA study

Rohit Loomba[1], Atsushi Nakajima[2], Marco Arrese[3], Elisabetta Bugianesi[4], Alok Pachori[5], Ola Fjellstrom[6], Janeli Sarv[7], Mathias Liljeblad[8], Kalra Shruti[9], Javier Armisen[10], Lars Hansen[11], Vincent Wai-Sun Wong[12]. *[1]MASLD Research Center, Division of Gastroenterology and Hepatology, University of California at San Diego, La Jolla, United States; [2]Department of Gastroenterology and Hepatology, Yokohama City University Graduate School of Medicine, Yokohama, Japan; [3]Departamento de Gastroenterología, Escuela de Medicina, Pontificia Universidad Católica de Chile, Santiago, Chile; [4]Department of Medical Sciences, University of Turin, Turin, Italy; [5]Late Cardiovascular, Renal and Metabolism, BioPharmaceuticals, R&D, AstraZeneca, Boston, United States; [6]Early Cardiovascular, Renal and Metabolism, BioPharmaceuticals, R&D, AstraZeneca, Gothenburg, Sweden; [7]Biometrics, Late Cardiovascular, Renal and Metabolism, BioPharmaceuticals, R&D, AstraZeneca, Gothenburg, Sweden; [8]Translational Sciences and Clinical Development, Early Cardiovascular, Renal and Metabolism, BioPharmaceuticals, R&D, AstraZeneca, Gothenburg, Sweden; [9]Global Patient Safety, AstraZeneca, Gothenburg, Sweden; [10]Translational Sciences and Clinical Development, Early Cardiovascular, Renal and Metabolism, BioPharmaceuticals, R&D, AstraZeneca, Cambridge, United Kingdom; [11]Late Cardiovascular, Renal and Metabolism, BioPharmaceuticals, R&D, Gaithersburg, United States; [12]Department of Medicine and Therapeutics, The Chinese University of Hong Kong, Hong Kong, Hong Kong*
Email: roloomba@ucsd.edu

Background and aims: The *PNPLA3* I148M genetic variant (rs738409) is the strongest genetic risk factor for MASH and cirrhosis. AZD2693, a *PNPLA3*-targeted, GalNAc-conjugated antisense oligonucleotide, reduced *PNPLA3* mRNA and protein levels in pre-clinical and Phase 1 clinical studies. The Phase 2b FORTUNA study evaluated

the efficacy, safety, and tolerability of AZD2693 versus placebo in homozygous carriers of the *PNPLA3* I148M risk allele with non-cirrhotic MASH and F2–F3 fibrosis.
Method: In this international, multicenter, randomized, double-blind, placebo-controlled trial, 217 participants were randomized across either AZD2693 at 25 and 50 mg or corresponding placebos (pbo) in a 2:2:1:1 ratio and were treated for 52 weeks followed by a 12-week follow up period. Primary endpoint was MASH resolution without worsening of fibrosis based on histology. Secondary endpoint was the proportion of participants with at least one stage of liver fibrosis improvement with no worsening of MASH. Safety and tolerability were assessed.
Results: 87% of randomized participants completed end of treatment biopsy. After 52 weeks of treatment, there was a robust decrease in the PNPLA3 protein as determined by immunostaining. For the primary endpoint, the percentage of responders was 1.4%, 5.5% and 6.8% in the 50 mg, 25 mg, and pbo, respectively. Percent point difference from pbo was −5.2% (95% CI, −15.4% to 5.1%; p = 0.116) and −1.4% (95%CI, −12.0% to 9.2%; p = 0.783) for the 50 mg and 25 mg, respectively. For the secondary endpoint, the percentage of responders was 8.7%, 16.4% and 10.8% in the 50 mg, 25 mg, and pbo, respectively. Percent point difference from pbo was −0.3% (95%CI, −11.9% to11.3%; p = 0.693) and 4.3% (95%CI, −7.2% to15.9%; p = 0.320) for the 50 mg and 25 mg groups, respectively. In a sub-study, there was no significant improvement in liver fat content (mean change from baseline: −1.52 vs −1.65 p = 0.899) and liver stiffness (geometric mean ratio to baseline: 1.17 vs 1.03; p = 0.030, nominal) in the AZD2693 50 mg group vs pbo. AZD2693 was generally well tolerated. Adverse events were similar across groups. Mild, dose-dependent increases in mean alanine aminotransferase levels were observed.
Conclusion: After 52 weeks of treatment, AZD2693 (25 mg or 50 mg) was not better over placebo for either the histological resolution of MASH or the improvement in fibrosis in homozygous carriers of the *PNPLA3* rs738409 risk allele with non-cirrhotic MASH and fibrosis.

GS-004-YI
Hepatocyte-macrophage crosstalk reprograms liver zonation in metabolic dysfunction-associated steatotic liver disease by regulating hepatic HNF4A

Shuai Chen[1], Dabao Shang[2], Xiaogang Xiang[2], Frank Tacke[3], Adrien Guillot[3], Hanyang Liu[3]. [1]*Nanjing Medical University, The Third Affiliated Hospital, Changzhou, China;* [2]*Shanghai Jiao Tong University School of Medicine, Ruijin Hospital, Shanghai, China;* [3]*Berlin, Germany*
Email: brandenliu@live.com

Background and aims: Metabolic dysfunction-associated steatotic liver disease (MASLD) is among the most prevalent chronic liver diseases worldwide and a major contributor to liver-related malignancy. Hepatocytes, organized along the liver lobular axis into periportal (zone 1), mid-lobular (zone 2) and pericentral (zone 3) regions, exert distinct physio-pathological functions, via interactions with microenvironmental factors and non-parenchymal cells. Such zonal heterogeneity is increasingly recognized as a determinant of MASLD initiation and progression, yet its regulatory mechanisms remain under investigation.
Method: Transcriptomic and metabolomic analyses of human MASLD liver samples were performed at single-cell and spatial resolution to define hepatocyte metabolic phenotypes and intercellular interactions. MASLD mouse models were established using a high-fat diet and a choline-deficient, L-amino acid-defined, high-fat diet. Clodronate liposome-mediated macrophage depletion and hepatocyte-specific genetic manipulations were employed to MASLD mouse models. *In situ* multiplex immunofluorescence staining and cultivating primary hepatocytes with macrophages were utilized to study hepatocyte–macrophage crosstalk.
Results: Spatial single-cell analyses demonstrated a progressive dominance of zone 3 metabolic programs over zone 1 with staging steatosis. Zone 2 hepatocytes displayed elevated lipid and carbohydrate metabolic activity, accompanied by increased expression of hepatocyte nuclear factor 4 alpha (HNF4A) during MASLD progression, suggesting a role in maintaining liver functions. In vivo, hepatocyte-specific HNF4A limited hepatic steatosis, whereas zone 2 hepatocytes with reduced HNF4A expression showed enhanced interactions with lipid-associated macrophages (LAMs). Macrophage depletion attenuated liver fibrosis and restored hepatocyte *Hnf4a* expression across the lobular axis. Lipid-associated macrophages modulate metabolic zonation features by regulating hepatocyte HNF4A.
Conclusion: Hepatocyte HNF4A is identified as a key regulator of hepatic metabolic zonation in MASLD, determining a novel metabolic-immune crosstalk mechanism. Targeting hepatocyte-LAM communications may represent a therapeutic strategy to reprogram hepatic metabolism and mitigate disease progression of MASLD.

GS-005
Transjugular intrahepatic portosystemic shunt for refractory hepatic hydrothorax in cirrhosis: a multicenter European study

Marco Tizzani[1], Gian Paolo Caviglia[1], Luis Téllez[2], Sophia Geißelbrecht[3], Francesco Vizzutti[4], Marlene Reincke[5], Chiara Becchetti[6], Luigi Maruzzelli[7], Dario Saltini[8], Marika Rudler[9], Kymentie Ferdinande[10], Enrico Pompili[11], Hélène Larrue[12], Giulia Tosetti[13], Silvia Nardelli[14], Daniela Campion[1], Jesus Donate[2], Anja Tiede[3], Silvia Aspite[4], Michael Schultheiß[5], Marco Solcia[15], Andreina Olavarria[16], Elisabetta Bugianesi[1], Gianluca Svegliati-Baroni[17], Mauro Viganò[18], Salvatore Piano[19], Pierluigi Toniutto[20], Oliviero Riggio[14], Vincenzo La Mura[21], Christophe Bureau[12], Paolo Caraceni[11], Marco Senzolo[10], Dominique Thabut[9,22], Filippo Schepis[8], Roberto Miraglia[7], Aldo Airoldi[6], Dominik Bettinger[5], Fabio Marra[4], Benjamin Maasoumy[3], Agustín Albillos[2], Alfredo Marzano[1], Carlo Alessandria[1]. [1]*Division of Gastroenterology and Hepatology, A.O.U. Città della Salute e della Scienza di Torino, University of Turin, Turin, Italy;* [2]*Gastroenterology and Hepatology Department. Hospital Universitario Ramón y Cajal. IRYCIS. CIBERehd. Universidad de Alcalá. Madrid, Spain, Madrid, Spain;* [3]*Department of Gastroenterology, Hepatology, Infectious Diseases and Endocrinology, Hannover Medical School, Hannover, Germany, German Center for Infection Research (DZIF), Partner-Site Hannover-Braunschweig, Hannover, Germany, Hannover, Germany;* [4]*Department of Experimental and Clinical Medicine, University of Florence, Florence, Italy, Florence, Italy;* [5]*Department of Medicine II, Medical Center University of Freiburg, Faculty of Medicine, University of Freiburg, Germany, Freiburg, Germany;* [6]*Hepatology and Gastroenterology Unit, ASST Grande Ospedale Metropolitano Niguarda, Milan, Italy, Milan, Italy;* [7]*IRCCS ISMETT, Radiology Service, Palermo, Italy and UPMC Italy, Palermo, Italy, Palermo, Italy;* [8]*Severe Liver Diseases Unit (M.E.C.), C.H.I.M.O.M.O. Department, Azienda Ospedaliero-Universitaria di Modena, University of Modena and Reggio Emilia, Modena, Italy, Modena, Italy;* [9]*AP-HP, Sorbonne Université, Liver Intensive Care Unit, Hepatogastroenterology Department, La Pitié-Salpêtrière Hospital and Brain Liver Pitié-Salpêtrière (BLIPS) Study Group, Paris, France, Paris, France;* [10]*Unit of Vascular Liver Diseases and Treatment of Portal Hypertension. Gastroenterology, Department of Surgery, Oncology and Gastroenterology University-Hospital of Padua, Padua, Italy, Padua, Italy;* [11]*Department of Medical and Surgical Sciences, Alma Mater Studiorum University of Bologna, Italy, Unit of Semeiotics, Liver and Alcohol-related Diseases, IRCCS Azienda Ospedaliero-Universitaria di Bologna, Italy, Bologna, Italy;* [12]*Department of Hepatology, University Hospital and Toulouse III - Paul Sabatier University, Toulouse, France, Toulouse, France;* [13]*Division of Gastroenterology and Hepatology, Foundation IRCCS Ca' Granda Ospedale Maggiore Policlinico, Milan, Italy, Milan, Italy;* [14]*Department of Translational and Precision Medicine, Sapienza University of Rome, Italy, Rome, Italy;* [15]*Interventional Radiology Unit, ASST Grande Ospedale Metropolitano Niguarda, Milan, Italy, Milan, Italy;* [16]*Radiology Department. Hospital Universitario*

Ramón y Cajal. Madrid, Spain, Madrid, Spain; [17]Liver Injury and Transplant Unit, Polytechnic University of Marche, Ancona, Italy, Ancona, Italy; [18]Gastroenterology, Hepatology and Transplantation Division, ASST Papa Giovanni XXIII, ASST Papa Giovanni XXIII, Bergamo, Italy, Bergamo, Italy; [19]Unit of Internal Medicine and Hepatology. Department of Medicine – DIMED. University and Hospital of Padova, Italy, Padua, Italy; [20]Hepatology and Liver Transplant Unit, University of Udine, Italy, Udine, Italy; [21]Fondazione IRCCS Ca' Granda Ospedale Maggiore Policlinico, Angelo Bianchi Bonomi Hemophilia and Thrombosis Center, Milan, Italy; Department of Pathophysiology and Transplantation, University of Milan, Milan, Italy, Milan, Italy; [22]AP-HP, Sorbonne Université, Liver Intensive Care Unit, Hepatogastroenterology Department, La Pitié-Salpêtrière Hospital and Brain Liver Pitié-Salpêtrière (BLIPS) Study Group, Paris, France, INSERM UMR_S 938, Centre de recherche Saint-Antoine, Maladies métaboliques, biliaires et fibro-inflammatoire du foie, Institute of Cardiometabolism and Nutrition (ICAN), Paris, France, Paris, France
Email: dottcarloalessandria@gmail.com

Background and aims: refractory hydrothorax (RH) develops in up to 15% of patients with cirrhosis and significantly impairs quality of life and clinical outcome of these patients. Transjugular intrahepatic portosystemic shunt (TIPS) has been suggested as a potential treatment, but data is limited. We aimed to evaluate TIPS clinical efficacy and impact on survival in patients with RH.
Method: retrospective study including all consecutive patients with cirrhosis who underwent TIPS for RH in a 16-year period (2008–2023) across 18 European centers. Endpoints were assessed: after 12 months from TIPS, at the date of liver transplant (LT) or death or of the last available visit during the 12-month follow-up. Clinical response was classified, compared to baseline, as: I - complete (CR) in case of disappearance of symptoms and no further need for thoracenteses; II - partial (PR) as decrease of symptoms and ≥50% reduction of thoracenteses; III - null (NR) as minor or no relief in symptoms and <50% reduction or same/increased number of thoracenteses.
Results: overall, 155 patients were included. Alcohol was the predominant etiology (47%), with moderately impaired liver function (Child-Pugh class B 78%, median MELD-Na 15), prevalent right unilateral hydrothorax (85%) and very common dyspnea (87%). TIPS improved RH in the majority of patients (88% overall), with 61% of CR. At 12 months after TIPS, 76 patients (49%) were alive, 23 (15%) had been transplanted, 36 (23%) had died and 20 (13%) were lost during the follow-up. Mean overall survival was 11.0 ± 0.3 months for CR patients vs 8.4 ± 0.8 months vs 6.9 ± 1.2 months, for PR and NR patients respectively (Log-rank test: $p < 0.001$; Cox regression: HR = 0.22, 0.11–0.43; $p < 0.001$). Significantly improved survival for CR patients was also confirmed when considering CR to TIPS as a time-varying covariate (HR = 0.25, 0.13–0.48; $p < 0.001$). At multivariable analysis, considering LT as competitive event, clinical CR was the only variable independently associated with improved survival (sHR = 0.28,0.15–0.55, $p < 0.001$); conversely, bilateral hydrothorax and higher MELD-Na score were independently associated with poorer survival (sHR = 2.55, 1.34–4.85, p = 0.004 and sHR = 1.10, 95% CI 1.05–1.15, $p < 0.001$, respectively).
Conclusion: our study supports the use of TIPS in patients with cirrhosis and RH, showing that clinical CR is achieved in a relevant proportion of patients and is associated with improved survival.

GS-006

Stereotactic body radiotherapy versus radiofrequency ablation for small (≤3 cm) hepatocellular carcinoma (STEREO): a randomized, non-inferiority, phase 3 trial

Jinhong Jung[1], Jonggi Choi[1], So Yeon Kim[1], So Jung Lee[1], Hyung Jin Won[1], Yong Moon Shin[1], Won-Mook Choi[1], Sung Won Chung[1], Danbi Lee[1], Ju Hyun Shim[1], Kang Mo Kim[1], Young-Suk Lim[1], Han Chu Lee[1]. *[1]Asan Medical Center, Seoul, Korea, Rep. of South*
Email: jkchoi0803@gmail.com

Background and aims: Radiofrequency ablation (RFA) is a well-established curative treatment for hepatocellular carcinoma (HCC) but is limited by tumour location and visibility. While stereotactic body radiotherapy (SBRT) may overcome these technical limitations, prospective randomised evidence comparing SBRT with RFA for HCC measuring ≤3 cm is lacking.
Method: In this phase 3, randomised, non-inferiority trial, adults with unresectable primary or recurrent HCC presenting with one to two lesions measuring 1–3 cm were randomly assigned (1:1) to receive SBRT or RFA. Technical feasibility was assessed prior to treatment, with a predefined crossover allowed if the assigned procedure was not feasible. The per-protocol (PP) population served as the primary analytic cohort. The modified intention-to-treat (mITT) population included all participants who received treatment for the target lesion. The primary endpoint was 2-year local progression-free survival (LPFS), evaluated using a non-inferiority margin of −15%. Secondary endpoints included local control, progression-free survival (PFS), and overall survival (OS) (ClinicalTrials.gov identifier: NCT05433701).
Results: Among 178 randomised participants, 170 comprised the PP population (RFA n = 68; SBRT n = 102). The median follow-up duration for LPFS was 31 months. The 2-year LPFS rates were 92·0% with SBRT and 89·7% with RFA (difference 2·3%; 90% confidence interval [CI] −5·2%–9·9%), meeting the non-inferiority criterion. Local recurrence at two years occurred in 4·4% of RFA-treated patients and 2·0% of SBRT-treated patients. The 2-year PFS rates in the PP population were 55·6% for SBRT and 51·5% for RFA (HR 0·96; 95% CI 0·64–1·44). The 2-year OS rates were 94·0% for SBRT and 94·1% for RFA. Most adverse events were grade 1–2, and no treatment-related deaths occurred.
Conclusion: SBRT was non-inferior to RFA for local tumour control in patients with small, unresectable HCC and represents an effective alternative local therapy.

THURSDAY 28 MAY

GENERAL SESSION II

GS-007

Abbreviated gadoxetic acid–enhanced magnetic resonance imaging versus ultrasonography for hepatocellular carcinoma surveillance in high-risk patients: a randomized controlled trial

Hyo Jung Park[1], Jonggi Choi[1], Dong Wook Kim[1], Sang Hyun Choi[1], Won-Mook Choi[1], Sung Won Chung[1], Danbi Lee[1], Ju Hyun Shim[1], Han Chu Lee[1], Young-Suk Lim[1], Amit Singal[2], So Yeon Kim[1]. *[1]Asan Medical Center, Seoul, Korea, Rep. of South; [2]University of Texas Southwestern Medical Center, Dallas, United States*
Email: sykim.radiology@gmail.com

Background and aims: The AMRIUS trial (Abbreviated Magnetic Resonance imaging using gadoxetic acid versus Ultrasonography for Surveillance of early-stage hepatocellular carcinoma in high-risk patients) aimed to prospectively compare gadoxetic acid-enhanced abbreviated MRI (HBP-AMRI) and ultrasonography (US) for hepatocellular carcinoma (HCC) surveillance in high-risk patients with cirrhosis.
Method: This open-label, randomized controlled trial was conducted at a tertiary referral center in South Korea. Adults (≥20 years) with high-risk cirrhosis (annual HCC incidence > 5%), Eastern Cooperative Oncology Group performance status performance status 0–2, Child–Pugh class A or B, and no prior liver cancer or recent malignancy were enrolled. Participants were randomized 1:1 to biannual HBP-AMRI or US for two surveillance rounds. The primary endpoint was the

detection rate of Barcelona Clinic Liver Cancer (BCLC) stage 0 or A HCC. Secondary endpoints included detection rates of BCLC stage 0 and all-stage HCC, false referral rate, and BCLC stage distribution at initial HCC diagnosis.
Results: Between August 2022 and October 2024, 806 patients were randomized to the HBP-AMRI (n = 403) or US (n = 403) group. A total of 44 participants (5.5%) were diagnosed with HCC (32 in the HBP-AMRI group and 12 in the US group). BCLC stages at diagnosis were stage 0 in 59.1% (26/44), stage A in 31.8% (14/44), stage B in 4.5% (2/44) and stage C in 4.5% (2/44).The median size of detected HCCs was 1.5 cm (range, 1.0–5.0 cm). The detection rate of BCLC stage 0 or A HCC was significantly higher in the HBP-AMRI group (7.7% [29/377]) than in the US group (2.9% [11/382], p = 0.003). HBP-AMRI also showed higher detection rates of BCLC stage 0 HCC than US (6.1% [23/377] vs. 0.8% [3/382], p < 0.001) and all-stage HCC (8.5% [32/377] vs. 3.1% [12/382], p = 0.002). The false referral rate was lower in the HBP-AMRI group (2.1% [15/704]) group than in the US group (4.4% [32/731], p = 0.02). The HBP-AMRI group demonstrated an earlier BCLC stage distribution compared with the US group (p = 0.04).
Conclusion: HBP-AMRI using gadoxetic acid demonstrated superior performance to US for HCC surveillance in high-risk cirrhotic patients, with higher detection rate of early-stage HCC and fewer false referrals (ClinicalTrials.gov, NCT06312826).

GS-008
RNA editing for the treatment of alpha-1 antitrypsin deficiency (AATD)

Pavel Strnad[1], Kenneth Chapman[2], Alice Turner[3], Matthew Conron[4], William J H Griffiths[5], Paul Hernandez[6], John R Hurst[7], Heli Yla-Outinen[8], Varun Goel[9], Joseph Haegele[9], Ken Longo[9], Mark McLaughlin[9], Prashant Monian[9], Michael Monine[9], Padma Narayanan[9], Shushma Patel[9], Abu Siddiqui[9], Andrew Strahs[9], Chikdu Shivalila[9], Lanyie Xie[9], Christopher Wright[9], Cynthia Caracta[9].
[1]University Hospital RWTH Aachen, Aachen, Germany; [2]Department of Medicine, University of Toronto, Toronto, Canada; [3]School of Health Sciences, University of Birmingham, Birmingham, United Kingdom; [4]Department of Respiratory and Sleep Medicine, St Vincent's Hospital Melbourne, Melbourne, Australia; [5]Cambridge Liver Unit, Addenbrooke's Hospital, Cambridge, United Kingdom; [6]Division of Respirology, Department of Medicine, Dalhousie University - QEII Health Sciences Centre, Halifax, Canada; [7]Royal Free London NHS Foundation Trust, London, United Kingdom; [8]Turku University Hospital, Turku, Finland; [9]Wave Life Sciences, Cambridge, United States
Email: pstrnad@ukaachen.de

Background and aims: Severe AATD commonly results from homozygous mutations in the *SERPINA1* gene (Pi*ZZ genotype), where misfolded Z-AAT protein accumulates in hepatocytes, leading to liver injury and disease. Liver retention results in serum and pulmonary deficiency of wild-type M-AAT and increased risk of lung disease. Standard of care aims to address lung disease by augmenting serum protein levels through weekly infusions with human plasma-purified AAT. Liver disease is not addressed by this intervention.
WVE-006, an investigational *N*-Acetylgalactosamine-conjugated RNA editing oligonucleotide, is designed to recruit endogenous ADAR enzymes to edit the *SERPINA1* mRNA in hepatocytes and replace Z-AAT with M-AAT. This approach aims to increase circulating M-AAT protein levels while reducing Z-AAT and address both lung and liver manifestations of severe AATD.
Method: RestorAATion-2 (NCT06405633) is an ongoing phase 1b/2a clinical trial evaluating the safety, tolerability, pharmacodynamics, and pharmacokinetics of single- and multiple-ascending doses of WVE-006 (200, 400, 600 mg; n = 8 all cohorts) in ZZ individuals. Participants receive a single subcutaneous dose of WVE-006 with a 12-week observation period, followed by biweekly (200 mg) or monthly dosing (400, 600 mg) for 12 weeks with a subsequent observation period. M-AAT, Z-AAT and total (M + Z) AAT protein in serum were measured by LC-MS/MS. Functional AAT levels were measured by a neutrophil elastase inhibition assay.
Results: In the 200 mg multidose cohort, mean peak serum M-AAT levels reached 7.2 uM in ZZ individuals. M-AAT levels represented 64.4% of total AAT (11.9 uM) and remained above 50% throughout the observation period. Increases in functional AAT activity were consistent with M-AAT production and were accompanied by a 60.3% reduction in Z-AAT protein. In the 200 and 400 mg single dose cohorts, M-AAT levels increased to 4.8 uM and 5.3 uM, respectively. In the 200 mg cohort, one participant experienced an acute-phase response due to a kidney stone, during which total serum AAT levels reached 20.6 uM (10.6 uM M-AAT). WVE-006 has been generally safe and well tolerated; all adverse events have been mild to moderate, with no serious adverse events.
Conclusion: These data, which show production of M-AAT, lowering of Z-AAT levels, and endogenous upregulation of AAT protein in ZZ individuals during stress provide proof-of-concept for the first RNA editing therapy to enter clinical testing.

GS-009
Safety, feasibility, impact, and proteomic perturbations with growth hormone treatment in alcohol-related hepatitis: a randomized clinical trial

Nipun Verma[1], Parminder Kaur[1], Pratibha Garg[1], Rohit Nadda[1], Arun Valsan[2], Arka De[1], Sunil Taneja[1], Ajay Kumar Duseja[1].
[1]Postgraduate Institute Of Medical Education And Research Chandigarh, Chandigarh, India; [2]Amrita Institute of Medical Sciences and Research Centre, Kanayannur, India
Email: nipun29j@gmail.com

Background and aims: Growth hormone (GH) regulates regeneration, inflammation, and gut barrier function, which are profoundly impaired in alcohol-related hepatitis (AH). This trial evaluated the safety, feasibility, and impact of GH treatment in AH.
Method: Assessor-blinded open-label randomized trial between 2023 and 2025 at a tertiary center (CTRI/2022/12/048572). Patients with AH without malignancy, sepsis, respiratory, circulatory, or renal failure were randomized to standard medical therapy (SMT; n = 34) or GH plus SMT (n = 34). GH was given 2 U/day subcutaneously. Insulin-like growth factor 1 (IGF-1) levels above the population median were recorded. Endpoints included 90-day overall survival (primary endpoint), infection incidence, Model for End-stage Liver Disease (MELD) and Child-Turcotte-Pugh (CTP) scores, day 30 biomarkers, and plasma proteomics (analyzed through a linear mixed-effects model).
Results: Groups were comparable at baseline (median age 41.5 years, all males, 73.5% with acute-on-chronic liver failure). IGF-1 rise was more frequent with GH than SMT (85.3% vs 58.8%; p = 0.031). The GH group had higher 90-day survival (97.1% vs 82.3%; p = 0.044), fewer infections (12.2% vs 57.8%; p < 0.001), and greater improvement in 90-day MELD (beta = –0.24; p = 0.021) and CTP (beta = –0.15; p = 0.005). At day 30, GH treatment was associated with lower cytokeratin 18 (beta = –0.15; p = 0.001), lipopolysaccharide (beta = –0.20; p = 0.004), zonulin (beta = –0.49; p = 0.008), and TNF-alpha (beta = –0.32; p = 0.002), with an increase in IL-10 (beta = 0.40; p = 0.043). Proteomics showed upregulation of pathways related to epithelial barrier integrity (tight junctions, immunoglobulin A-related networks), immune regulation (phagosome function, leukocyte trafficking), cytoskeletal remodeling (Rap1 signaling, actin–myosin organization), regeneration (phosphoinositide 3-kinase-Akt, hypoxia-inducible factor 1 signaling), and modulation of complement-coagulation, ferroptosis, and cell adhesion processes. GH was well tolerated with no treatment-related serious adverse events or discontinuations.
Conclusion: In this initial trial, GH was found to be safe and feasible in AH. It was associated with improved survival, fewer infections, and biomarker and proteomic changes consistent with reduced bacterial translocation, improved intestinal integrity, and regenerative-immune remodeling. Further multicenter studies are needed to test

its efficacy in diverse settings and the mechanisms underlying its action in AH.

GS-010

Circadian disruption drives MASLD by impairing FABP5-dependent incretin secretion via gut microbial TUDCA depletion

Dekai Zheng[1], Zhixin Fang[1], Xuelian Gao[1], Changhao Cheng[1], Xun Wang[1], Ting Zhang[1], Yinghong Zhu[1], Xianhui Qin[2], Kangsen Yang[1], Yuchuan Chen[1], Routing Wang[1], Ziyan Wang[1], Zhixian Lan[1], Jian Sun[1]. *[1]Department of Infectious Diseases, Nanfang Hospital, Southern Medical University, Key Laboratory of Infectious Diseases Research in South China, Ministry of Education, State Key Laboratory of Multi-organ Injury Prevention and Treatment, Guangzhou, China; [2]Division of Nephrology, Nanfang Hospital, Southern Medical University, National Clinical Research Center for Kidney Disease, State Key Laboratory of Multi-organ Injury Prevention and Treatment, Guangzhou, China*
Email: doctorsunjian@qq.com

Background and aims: Circadian rhythm disruption is a potent driver of Metabolic Dysfunction-Associated Steatotic Liver Disease (MASLD), yet the underlying mechanisms remain unclear. We aimed to elucidate the gut-liver signaling pathways linking circadian disruption to MASLD, focusing on the microbiota, metabolites, and enteroendocrine function.
Method: Accelerometer data from 89,695 UK Biobank participants was analyzed to link circadian disruption to MASLD. A chronic jet lag (CJL) mouse model was established to mimic circadian misalignment. Metagenomics, metabolomics, and fecal microbiota transplantation (FMT) were used to identify microbial drivers. Mechanisms were dissected using drug affinity responsive target stability (DARTS), cellular thermal shift assays (CETSA), microscale thermophoresis (MST), and intestinal-specific *Fabp5* knockout mice. Clinical relevance was validated in night-shift workers and acute jet-lagged volunteers.
Results: Epidemiological analysis revealed that blunted circadian amplitude increased MASLD risk independent of genetic susceptibility. In mice, CJL exacerbated diet-induced steatohepatitis. Microbiota depletion and FMT confirmed dysbiosis causality, while metagenomics pinpointed *Lepagella muris* expansion as a key driver. Possessing intrinsic bile salt hydrolase (BSH) activity, its expansion drives enzymatic depletion of tauroursodeoxycholic acid (TUDCA). Mechanistically, we identified Fatty Acid Binding Protein 5 (FABP5) as a direct TUDCA target in enteroendocrine cells. TUDCA competitively displaces fatty acids from FABP5, increasing bioavailability to activate FFAR-mediated GIP and GLP-1 secretion. In CJL, TUDCA depletion allows FABP5 to sequester fatty acids, blunting incretin secretion and promoting metabolic dysfunction. Restoring this axis via BSH inhibitors, TUDCA supplementation, or DPP-4 inhibitors ameliorated CJL-driven MASLD. Crucially, mechanistic signatures including expanded *L. muris*, elevated BSH, TUDCA depletion, and suppressed incretins were mirrored in shift workers and jet-lagged humans. Furthermore, FMT from these donors transferred disease susceptibility to mice.
Conclusion: We identify a novel axis wherein circadian disruption promotes *L. muris*-mediated TUDCA depletion, impairing FABP5-dependent incretin secretion and driving MASLD. Targeting the BSH-TUDCA-FABP5 pathway offers a rationale for precision interventions in circadian-disrupted populations.

GS-011-YI

Underdilated TIPS strategy improves survival and reduces hepatic encephalopathy in refractory ascites: a multicenter international study

Dario Saltini[1], Michael Praktiknjo[2], Marco Senzolo[3], Sarah Lisa Schütte[4], Rakhi Maiwall[5], Marika Rudler[6], Davide Roccarina[7], Christian Jansen[8], Anna Baiges[9], Lukas Hartl[10], Cristian Caporali[11], Markus Kimmann[2], Nancy Farouk[2], Kymentie Ferdinande[3], Charlotte Bouzbib[12], Fabrizio Fanelli[13], Carsten Meyer[8], Fanny Turon[9], Asunción Ojeda[9], Virginia Hernández-Gea[9], Mattias Mandorfer[10], Thomas Reiberger[10], Juan Carlos García-Pagán[9], Johannes Chang[8], Dominique Thabut[6], Benjamin Maasoumy[4], Jonel Trebicka[2], Dominik Bettinger[14], Francesco Vizzutti[7], Filippo Schepis[1]. *[1]Severe Liver Diseases (M.E.C.) Departmental Unit, Department of Medical Specialties, University Hospital of Modena "Policlinico", University of Modena and Reggio Emilia, European Reference Network on Rare Liver Disorders (ERN Rare-Liver), Modena, Italy; [2]Department of Medicine B, University Hospital Muenster., Muenster, Germany; [3]Unit of Vascular Liver Diseases and Treatment of Portal Hypertension, Gastroenterology, Department of Surgical, Oncological and Gastroenterological Sciences, University-Hospital of Padua, Padua, Italy; [4]Department of Gastroenterology, Hepatology, Infectious Diseases and Endocrinology, Hannover Medical School, Hannover, Germany; [5]Department of Molecular and cellular medicine, Institute of Liver and Biliary Sciences, D-1 Vasant Kunj., New Delhi, India; [6]AP-HP, Sorbonne Université, Liver Intensive Care Unit, Hepatogastroenterology Department, La Pitié-Salpêtrière Hospital, 47-83 Boulevard de l'Hôpital, Paris 75013, France; INSERM UMR_S 938, Centre de recherche Saint-Antoine, Maladies métaboliques, biliaires et fibro-inflammatoire du foie, Institute of Cardiometabolism and Nutrition (ICAN), Paris, France; [7]Department of Experimental and Clinical Medicine, University of Florence., Florence, Italy; [8]University Hospital Bonn, Department of Internal Medicine I, Bonn, Germany; [9]Barcelona Hepatic Hemodynamic Laboratory, Liver Unit, Hospital Clínic, Clínic Barcelona; ERN-RareLiver (Health Care Provider of the European Reference Network on Rare Liver Disorders), CSUR (Centro de referencia del Sistema Nacional de Salud en Enfermedad Hepática Vascular Compleja en adultos); FRCB-IDIBAPS (Fundació de Recerca Clínic Barcelona-Institut d'Investigacions Biomèdiques August Pi i Sunyer); CIBEREHD (Centro de Investigación Biomédica en Red Enfermedades Hepáticas y Digestivas); AGAUR SGR202101115; Medicine Department, Faculty of Medicine, and health Science, Universitat de Barcelona, Barcelona, Spain; [10]Division of Gastroenterology and Hepatology, Department of Medicine III, Medical University of Vienna, Vienna, Austria; [11]Division of Interventional Radiology, University Hospital of Modena "Policlinico", Modena, Italy; [12]Liver Intensive Care Unit, Hepatogastroenterology Department, La Pitié-Salpêtrière Hospital, 47-83 Boulevard de l'Hôpital, Paris, France; [13]Department of Radiology, Interventional Radiology Unit, Careggi Hospital., Florence, Italy; [14]Department of Medicine II, Medical Center University of Freiburg, Faculty of Medicine, University of Freiburg, Freiburg, Germany*
Email: fschepis@unimore.it

Background and aims: The optimal dilation strategy for transjugular intrahepatic portosystemic shunt (TIPS) placement in refractory ascites remains debated. Underdilated TIPS (≤7 mm) has been proposed to reduce overt hepatic encephalopathy (OHE), but its survival benefit remains unproven. We compared underdilated versus standard (≥8 mm) TIPS in a multicentric international study.
Method: Data of patients with cirrhosis and refractory ascites undergoing TIPS using ePTFE-covered stents between 2009 and 2025 in 11 centers of 6 countries were retrospectively collected. Primary outcomes were all-cause mortality and OHE, analyzed using Fine–Gray competing-risk models accounting for liver transplantation (mortality) and death or transplantation (OHE). A propensity score-weighted analysis was also performed to account for baseline imbalances. Secondary outcomes included ascites control (need for large-volume paracentesis, LVP) and TIPS dysfunction.
Results: The study included 1,019 patients (mean age 59 ± 10 years; 71% male); 412 (40%) received underdilated TIPS. Baseline MELD score (13.3 vs 13.2; p = 0.687) was comparable between groups. Underdilated TIPS was more frequently performed in patients with alcohol-related cirrhosis (60% vs 52%; p = 0.011) and prior episodes of OHE (23% vs 18%; p = 0.036). Median follow-up was 19 months (IQR 18 months). Underdilated TIPS was associated with a significantly lower cumulative incidence of death compared with standard TIPS

(2-year: 22% vs 27%, p = 0.001; 4-year: 30% vs. 40%; p = 0.001) and a reduced incidence of OHE (1-year: 29% vs 39%, p = 0.003). On multivariable competing-risk analysis adjusted for age, sex, MELD, etiology, PCPG reduction, and prior OHE, underdilation independently reduced the risk of death (sHR 0.74; p = 0.017) and OHE (sHR 0.68; p = 0.001). Results were consistent in propensity score-weighted sensitivity analysis. Ascites control was similar between groups, whether considering all post-TIPS LVPs (39% vs 40%; p = 0.7) or excluding early LVPs (≤30 days post-TIPS; 29% vs 32%; p = 0.3). The incidence of TIPS dysfunction did not differ between underdilated and standard strategies (13% vs 15%; p = 0.2).
Conclusion: In this large international study, underdilation TIPS strategy is associated with improved survival and a lower risk of OHE in patients with cirrhosis and refractory ascites, without impairing ascites control or increasing TIPS dysfunction. These findings support underdilated TIPS as a preferred strategy and may inform future guideline recommendations.

GS-012
Efficacy and safety of tobevibart (VIR-3434) alone or in combination with elebsiran (VIR-2218) in participants with chronic hepatitis delta virus infection: week 96 endpoint results from the phase 2 SOLSTICE trial

Tarik Asselah[1], Anca Streinu-Cercel[2], Alina Jucov[3], Edward J. Gane[4], Heiner Wedemeyer[5], Pietro Lampertico[6,7], Patrick Kennedy[8], Michael A. Chattergoon[9], Bria Bullard[9], Cheng Huang[9], Rima Acosta[9], Cara Pilowa[9], Todd Correll[9], Kosh Agarwal[10]. [1]*Université de Paris Cité, Hôpital Beaujon, Paris, France;* [2]*National Institute for Infectious Diseases Matei Bals, Carol Davila University of Pharmacy and Medicine, Bucharest, Romania;* [3]*Arensia Exploratory Medicine GmbH, Dusseldorf, Germany, Nicolae Testemitanu State University of Medicine and Pharmacy, Chisinau, Moldova;* [4]*University of Auckland, Auckland, New Zealand;* [5]*Department of Gastroenterology, Hepatology, and Endocrinology, Hannover Medical School, Hannover, Germany;* [6]*Division of Gastroenterology and Hepatology, Foundation IRCCS Ca' Granda Ospedale Maggiore Policlinico, Milan, Italy;* [7]*CRC "A. M. and A. Migliavacca" Center for Liver Disease, Department of Pathophysiology and Transplantation, University of Milan, Milan, Italy;* [8]*Centre for Immunobiology and Infection, Blizard Institute, Barts and the London School of Medicine and Dentistry, London, United Kingdom;* [9]*Vir Biotechnology, San Francisco, United States;* [10]*Institute of Liver Studies, King's College Hospital, London, United Kingdom*
Email: tarik.asselah@aphp.fr

Background and aims: Hepatitis delta virus (HDV) infection is the most severe form of viral hepatitis with limited treatment options. The ongoing phase 2 SOLSTICE study is investigating the antiviral activity and safety of the monoclonal antibody tobevibart alone and in combination with the small interfering RNA (siRNA) elebsiran in participants with chronic HDV infection, with or without compensated cirrhosis, on NRTI therapy (NCT05461170).
Method: Safety and efficacy, including trends in HDV and HBV antiviral activity and biochemical markers, were assessed in participants receiving either tobevibart 300 mg plus elebsiran 200 mg subcutaneously (SC) every 4 weeks (tobevibart +elebsiran Q4W) or tobevibart 300 mg SC every 2 weeks (tobevibart Q2W) for 96 weeks.
Results: Data are summarized for all participants at week 72 and ~75% of the cohort at week 96. At week 72, HDV RNA TND (target not detected, no amplification on PCR) was achieved by 77% (24/31) and 53% (17/32) receiving tobevibart+elebsiran Q4W and tobevibart Q2W, respectively. At week 96, HDV RNA TND rates were 88% (21/24) and 46% (11/24) in the tobevibart+elebsiran Q4W and tobevibart Q2W cohorts, respectively. ALT normalized in 55% (17/31) and 69% (22/32) receiving tobevibart+elebsiran Q4W and tobevibart Q2W at week 72, and at week 96, rates were 54% (13/24) and 58% (14/24), respectively. At week 72, 94% of tobevibart+elebsiran Q4W and 19% of tobevibart Q2W participants had HBsAg <10 IU/mL and rates remained similar at week 96. Treatment-emergent adverse events were primarily Grade 1–2, transient, with the most common being influenza-like syndrome occurring with the first dose and generally resolving within 24–48 hrs in both treatment groups. No treatment-related serious adverse events occurred. Seven participants receiving tobevibart +elebsiran Q4W and eight participants receiving tobevibart Q2W have not yet reached the week 96 visits but remain on treatment. Full cohort data through week 96 will be presented.
Conclusion: Participants receiving tobevibart+elebsiran Q4W showed numerically greater rates of HDV RNA TND and HBsAg <10 IU/mL, at weeks 72 and 96 than those receiving tobevibart Q2W. TND rates increased over time with combination therapy, while rates plateaued with monotherapy. Adverse events were generally mild to moderate and transient. These results support further development of tobevibart+elebsiran Q4W, which is now being evaluated in the phase 3 ECLIPSE program for chronic HDV infection.

Late breakers oral session

LBO-001
A phase 2b/3 trial of saroglitazar in primary biliary cholangitis (EPICS III)

Raj Vuppalanchi[1], Alejandra Villamil[2], Yusuf Yilmaz[3], Ramazan Idilman[4], Beatriz Margarita Ameigeiras[5], Farheen Shaikh[6], Meral Akdogan Kayhan[7], Murat Kiyici[8], Kris V. Kowdley[9], Siddharth Aras[10], Chintan Shah[10], Deven Parmar[6], Naga Chalasani[1]. [1]*Indiana University School of Medicine, Indianapolis, United States;* [2]*Hospital Italiano de Buenos Aires, Buenos Aires, Argentina;* [3]*Recep Tayyip Erdoğan University, Rize Merkez, Türkiye;* [4]*Ankara University School of Medicine, Ankara, Türkiye;* [5]*Hospital Ramos Mejía, Buenos Aires, Argentina;* [6]*Zydus Therapeutics Inc, Pennington, New Jersey, United States;* [7]*Health Science University, School of Medicine, Department of Gastroenterology, Bilkent City Hospital, Ankara, Türkiye;* [8]*Bursa Uludağ University School of Medicine, Bursa, Türkiye;* [9]*Velocity Clinical Research, Liver Institute Northwest, Elson S. Floyd College of Medicine, Washington State University, Seattle, Washington, United States;* [10]*Zydus Life Sciences, Ahmedabad, India*
Email: rvuppala@iu.edu

Background and aims: Saroglitazar, a dual PPARα/γ agonist, improved serum alkaline phosphatase (ALP) in patients with primary biliary cholangitis (PBC) in a phase 2a study. We conducted a phase2b/3 study of saroglitazar in patients with PBC who had an inadequate response to or intolerance to ursodeoxycholic acid (UDCA).
Method: EPICS-III is a phase 2b/3 adaptive, double-blind, randomized control trial to evaluate saroglitazar in patients with PBC who had an inadequate response to or intolerance to UDCA. The phase 2b dose-finding portion included 37 participants who received placebo or saroglitazar magnesium 1 mg or 2 mg for 16 weeks. Based on its results, saroglitazar magnesium 1 mg (0.97 mg of saroglitazar) was selected for phase 3, which randomized 148 patients to saroglitazar (n = 97) or placebo (n = 51) for 52 weeks. *The p*rimary endpoint was the biochemical response at week 52, defined as (ALP) <1.67 × ULN, with at least a 15% reduction from baseline, and total bilirubin below ULN. The key secondary endpoint was ALP normalization at week 52.
Results: Baseline characteristics between the two groups in phase 3 were comparable, except for higher baseline ALP and other liver biochemistries in the saroglitazar group. Biochemical response was achieved in 56.7% with saroglitazar compared to 9.8% with placebo (difference, 48.0%; 95% CI, 35.3 to 60.8; p < 0.001). In participants with baseline ALP ≤3 × ULN, biochemical response was 83.1% (49/59) and 14.7% (5/34), respectively. ALP normalization occurred in 8.2% of patients with saroglitazar versus 0% with placebo (difference, 8.5%;

95% CI, 2.9 to 14; p = 0.016), with improvements in ALP levels observed as early as 2 weeks. In participants with moderate-to-severe pruritus, saroglitazar showed greater improvement in pruritus than placebo at week 24 with a treatment difference of −3.2 (95% CI, −5.66 to −0.82; P = 0.009). Adverse events (AE) were reported in 81.1% with saroglitazar versus 90.5% with placebo, and serious adverse events occurred in 6.3% and 11.1%, respectively. Four participants with saroglitazar and 1 participant with placebo reported fractures as AEs. Saroglitazar was not associated with significant weight gain, DILI, renal dysfunction, or increased CPK.
Conclusion: In this Phase2b/3 EPICS III program, saroglitazar significantly improved biochemical response and ALP normalization in individuals with PBC who had an inadequate response to or intolerance to UDCA. Saroglitazar is an effective second line therapy for PBC.

LBO-002

Plasma exchange with albumin 5% significantly increases 90-day overall survival in acute-on-chronic liver failure: topline results of the APACHE trial

Javier Fernández[1,2], Nikolaos Pyrsopoulos[3,4], Jasmohan S. Bajaj[5], Giovanni Perricone[6], Thierry Gustot[7], Thomas Reiberger[8], Thomas Berg[9], Ali Al-Khafaji[10], Alexander Wilmer[11], Mikhael Giabicani[12], Gautam Mehta[13], Agustín Albillos[14], David J. Kramer[15,16], William Bernal[17], Jonel Trebicka[18,19], Mireia Torres[20], Fiona McCarthy[21], Peter Nelson[22], Richard Moreau[1], Miquel Lozano[23], Vicente Arroyo[1], on behalf of APACHE Study Investigators[1,2]. *[1]EF CLIF, EASL-CLIF Consortium and Grifols Chair, Barcelona, Spain; [2]Hospital Clínic, IDIBAPS and CIBERehd, Barcelona, Spain; [3]Division of Gastroenterology and Hepatology, Rutgers-New Jersey Medical School, New Jersey, United States; [4]NYU Grossman School of Medicine, Transplant Institute, New York, United States; [5]Division of Gastroenterology, Hepatology, and Nutrition, Richmond VA Medical Center and Virginia Commonwealth University, Virginia, United States; [6]Hepatology and Gastroenterology Unit, ASST GOM Niguarda, Milan, Italy; [7]Department of Gastroenterology, Hepato-Pancreatology, HUB Erasme Hospital, Université Libre de Bruxelles, Brussels, Belgium; [8]Division of Gastroenterology and Hepatology, Department of Medicine III, Medical University of Vienna, Vienna, Austria; [9]Division of Hepatology, Department of Medicine II, Leipzig University Medical Center, Leipzig, Germany; [10]Department of Critical Care Medicine, University of Pittsburgh Medical Center, Pittsburgh, PA, United States; [11]Medical Intensive Care Unit, Department of General Internal Medicine, University Hospital Leuven, Leuven, Belgium; [12]Department of Anaesthesiology and Critical Care, Beaujon Hospital, DMU Parabol, AP-HP Nord, Clichy, France; [13]Royal Free NHS Foundation Trust Hospital, London, United Kingdom; [14]Gastroenterology and Hepatology Department, Hospital Universitario Ramón y Cajal, IRYCIS, CIBERehd, University of Alcalá, Madrid, Spain; [15]Aurora Critical Care Service, University of Wisconsin School of Medicine and Public Health, Milwaukee, Wisconsin, United States; [16]Wake Forest University, Internal Medicine, Winston-Salem, United States; [17]Liver Intensive Therapy Unit, Institute of Liver Studies, Kings College Hospital, London, United Kingdom; [18]Department of Internal Medicine B, University of Münster, Munster, Germany; [19]Department of Internal Medicine I, Goethe University Frankfurt, University Hospital, Frankfurt, Germany; [20]Clinical Operations, Scientific Innovation Office, Grifols, Barcelona, Spain; [21]Biostatistics, Scientific Innovation Office, Grifols, Dublin, Ireland; [22]Clinical Development, Scientific Innovation Office, Grifols, California, United States; [23]Apheresis & Cellular Therapy Unit, Department of Hemotherapy and Hemostasis, ICAMS, Hospital Clínic de Barcelona, IDIBAPS, University of Barcelona, Barcelona, Spain*
Email: jfdez@clinic.cat

Background and aims: Acute-on-chronic liver failure (ACLF) is characterized by organ failure(s) and high short-term mortality. Liver transplantation (LT) is currently the only life-saving treatment, and therapies to increase survival remain an unmet need. This pivotal trial evaluated the efficacy and safety of high-volume plasma exchange with Albutein 5%® (PE-A5%) in patients with ACLF grade 1b, 2, or 3a (EASL-CLIF criteria).
Method: APACHE was a phase 3, multicenter, randomized, controlled, parallel-group, open-label trial (NCT03702920). Patients were randomized to standard medical treatment (SMT)+PE-A5% or SMT alone. PE-A5% consisted of 2 sessions on consecutive days followed by sessions every other day for a min. of 4 to a max. of 9 sessions depending on clinical response. The primary endpoint was 90-day overall survival (OS) with censoring on LT. Secondary and exploratory endpoints included 90-day transplant-free survival (TFS), 28-day OS, and ACLF grade subgroup analyses. Safety assessments included treatment-emergent adverse events (TEAEs), suspected adverse drug reactions (SADRs) and adverse reactions (ARs).
Results: The study was terminated early for non-clinical reasons at 72% of target patient randomization with 274 patients randomized to SMT+PE-A5% (n = 135) or SMT (n = 139) in 29 centers worldwide. Baseline characteristics were balanced. Median PE sessions in the SMT+PE-A5% group were 4. SMT+PE-A5% significantly increased 90-day OS compared to SMT (Hazard Ratio [HR] [95% CI] = 0.65 [0.45, 0.94]; p = 0.021). 90-day OS HR [95% CI] for ACLF grade 1b, 2, and 3a subgroups were 0.73 [0.27, 2.02], 0.55 [0.34, 0.90], and 0.83 [0.43, 1.59], respectively. For 90-day TFS, 36 LTs and 51 deaths occurred in the SMT+PE-A5% group compared with 20 LTs and 69 deaths in the SMT group with a HR [95% CI] of 0.83 [0.62, 1.12], p = 0.22. 28-day OS HR [95% CI] was 0.67 [0.44, 1.01], p = 0.06. Total TEAEs were more frequent in SMT+PE-A5% group, consistent with known PE side effects; however, TEAEs resulting in death were similar between groups (SMT+PE-A5%: 12 in 9 (7.0%) patients; SMT: 11 in 10 (7.2%) patients). SADRs or ARs to Albutein 5% occurred in <5% of SMT+PE-A5% patients.
Conclusion: SMT+PE-A5% significantly increased 90-day OS compared to SMT in ACLF patients with a numerically greater benefit in ACLF grade 2. TEAEs reflected known safety risks for PE-A5% in ACLF patients. APACHE demonstrates a favorable benefit-risk profile for treatment of ACLF patients with SMT+PE-A5%.

LBO-003

Tune-401: a first-in-class epigenetic silencer of HBV demonstrates deep and durable antiviral activity in the phase 1b/2a proof of concept Tune-401-001 study

Edward J. Gane[1,2], Alina Jucov[3,4], Kendra Congdon[5], Brian Cosgrove[5], Rickey Reinhardt[5], Oluwatobi Olorunyomi[5], Derek Jantz[5], Heidi Zhang[5], John McHutchison[5], Christian Schwabe[6], Kosh Agarwal[7], Man-Fung Yuen[8]. *[1]The University of Auckland, Auckland, New Zealand; [2]New Zealand Liver Transplant Unit, Auckland City Hospital, Auckland, New Zealand; [3]Arensia Exploratory Medicine GmbH, Dusseldorf, Germany; [4]Nicolae Testemitanu State University of Medicine and Pharmacy, Chişinău, Moldova; [5]Tune Therapeutics, Durham, United States; [6]New Zealand Clinical Research, Auckland, New Zealand; [7]Institute of Liver Studies, Kings College Hospital, London, United Kingdom; [8]Queen Mary Hospital, The University of Hong Kong, Hong Kong, China*
Email: edgane@adhb.govt.nz

Background and aims: Tune-401 is a first-in-class epigenetic silencing therapy designed to shut down HBV by directly targeting and silencing both covalently closed circular DNA (cccDNA) and integrated HBV DNA sequences. mRNA encoding an epigenetic silencing protein and guideRNA targeting the HBV genome are delivered intravenously within lipid nanoparticles to hepatocytes. The ongoing Phase 1b/2a Tune-401-001 study is evaluating safety, pharmacokinetics, and pharmacodynamics in patients with chronic hepatitis B (CHB).
Method: Twenty-one CHB patients on nucleos(t)ide therapy (12 HBeAg-negative; 9 HBeAg-positive) have been enrolled. Four single-dose cohorts received either 0.2 mg/kg, 0.45 mg/kg, 0.65 mg/kg, or 0.85 mg/kg (N = 2/6/3/3). An additional multi-dose cohort received three doses of 0.65 mg/kg at approximately 4-week intervals (N = 7).

Primary endpoints are safety and tolerability, with assessment of quantitative serum pgRNA, HBeAg, HBcrAg, and HBsAg. Cohort baseline characteristics for 0.2/0.45/0.65/0.85 mg/kg and multi-dose cohort were: % female 0/50/33/67/14; median age 51/50/51/45/47 years; mean qHBsAg 3.60/3.03/3.11/3.04/3.36 $\log_{10}$ IU/mL.
Results: Tune-401 was generally safe and well tolerated. Most adverse events (AEs) were transient and resolved within two weeks. The most common AEs were infusion-related reactions (Grade 1/2/3, n = 14/6/2). Transient ALT/AST elevations were predominantly mild (Grade 2/3, n = 5/3). Dose-dependent antiviral activity that has been maintained over time has been observed. At 20 weeks post a single dose, mean HBsAg reductions from pre-dose baseline were 29.6% in the 0.45 mg/kg cohort and 54.0% in the 0.65 mg/kg cohort. Multiple patients achieved durable >95% reductions in pgRNA levels and >99% reductions in HBcrAg levels, indicating direct cccDNA silencing. Furthermore, 3/10 patients in the 0.65 mg/kg cohorts achieved pgRNA and HBcrAg biomarker negativity. Two participants (0.85 mg/kg cohort) achieved HBeAg loss with one seroconversion. Preliminary results from the multiple dosing cohort suggest increases in antiviral efficacy from additional doses with no additional safety concerns.
Conclusion: This study provides the first clinical results from targeted epigenetic silencing of HBV with evidence of direct cccDNA repression. The favorable emerging safety profile and deep, durable antiviral activity support continued development of Tune-401 into Ph2 to define the optimal, maximally efficacious dosing regimen to achieve HBV cure.

LBO-004
Safety, pharmacokinetics, and clinical activity of HRX215 after hepatectomy due to colon carcinoma metastases: interim results from pilot cohort of a 1b/2a clinical trial
Patrick Starlinger[1], Rory L. Smoot[1], Susanne Warner[1], Scott Nyberg[1], Lars Zender[2], Hedda Wold[3], Tillmann Taube[3], Wolfgang Albrecht[3], Elias Papatheodorou[3], Linda Greenbaum[3,4]. [1]*Mayo Clinic, Rochester, United States;* [2]*University Hospital, Tuebingen, Tuebingen, Germany;* [3]*HepaRegeniX GmbH, Tuebingen, Germany;* [4]*HepaRegeniX, Tuebingen, Germany*
Email: starlinger.patrick@mayo.edu

Background and aims: Insufficient future liver remnant (FLR) associated risk for post-hepatectomy liver failure (PHLF) represents the major source of morbidity and mortality after liver resection and is the main cause of technical inoperability in patients with colorectal cancer liver metastasis (CRCLM). HRX215 is a potent and selective oral inhibitor of the dual-specific protein kinase mitogen-activated protein kinase kinase 4 (MKK4) and represents the first ever targeted therapy with potential to improve liver regeneration and thereby reduce PHLF risk in patients undergoing hepatectomy. The aim of the study is to assess the safety, pharmacokinetics and efficacy of HRX215 in patients undergoing liver resection for CRCLM.
Method: This phase 1b/2a study consists of two open label (OL) pilot parts (phase 1b) followed by a randomized placebo controlled phase 2a. Safety, pharmacokinetic and liver volume data are available for five participants undergoing minor liver resection for CRCLM who have been enrolled in the first OL pilot part.
Results: Percent liver resection ranged from 2–30%. Four SAEs were reported in study participants, none of which were considered to be causally related to HRX-215. Other reported adverse events (AEs) were mostly mild or moderate (CTCAE severity grade 1–2). No PHLF events were observed. Full recovery of liver volume (measured by MRI) and function as measured by INR and total bilirubin was achieved by postoperative day 7 for all 5 patients. Pharmacokinetic analysis demonstrated HRX215 plasma concentration-time profiles similar to healthy participants. Liver volumes remained at similar levels at the end of the 28 day treatment period and during the ongoing 6 month safety follow up period.
Conclusion: HRX215 was well tolerated in participants undergoing minor liver resection for CRCLM, with safety profile consistent with expected AEs in this patient population and comparable pharmacokinetics to healthy participants. Rapid restoration of liver volume and liver function was observed in all 5 participants. The potential for HRX215 to accelerate liver volume recovery in participants undergoing more extensive liver resections will be investigated in the next phases of the study.

LBO-005-YI
The combination of senolytic drugs, dasatinib plus quercetin, reduces liver fibrosis in metabolic dysfunction–associated steatohepatitis: a phase 2 randomized double-blind placebo controlled study: the TRUTH study
Mijra Koning[1], Artemiy Kovynev[1], Marcos Fondevila[2], Michiel Mommersteeg[3], Bart Verwer[4], Marije Vlug[5], Teaco Kuiper[6], Maarten van den Berg[3], Anne Vrieze[7], Maurice Bizino[8], Annewieke van den Beld[8], Luuk Berk[9], Thomas Boerlage[8], Willem Pieter Brouwer[10], Weena Chen[6], Djuna L. Cahen[6], Robert C. Verdonk[11], Dewkoemar Ramsoekh[1], Michail Doukas[10], Sanne Vermorgen[1], Joanne Verheij[1], R. Bart Takkenberg[1], Jacques Bergman[1], Ulrich Beuers[1], Geert D'Haens[1], Joost P. H. Drenth[1], Tamar Tchkonia[12], Bernd Schnabl[13], James Kirkland[12], Abraham Stijn Meijnikman[1]. [1]*Amsterdam UMC, Amsterdam, Netherlands;* [2]*Department of Medicine, University of California, San Diego, United States;* [3]*Haga Hospital, Den Haag, Netherlands;* [4]*Spaarne Gasthuis, Haarlem, Netherlands;* [5]*Dijklander Hospital, Hoorn, Netherlands;* [6]*Amstelland Hospital, Amstelveen, Netherlands;* [7]*Flevo Hospital, Almere, Netherlands;* [8]*Groene Hart Hospital, Gouda, Netherlands;* [9]*Fransiscus Hosptial, Rotterdam, Netherlands;* [10]*Erasmus Medical Center, Rotterdam, Netherlands;* [11]*St. Antonius Hospital, Nieuwegein, Netherlands;* [12]*Cedars-Sinai Health sciences University, Los Angeles, United States;* [13]*University of California San Diego, San Diego, United States*
Email: mijra.koning@amsterdamumc.nl

Background and aims: Cellular senescence, a stress-induced program characterized by stable nncell-cycle arrest, is a hallmark of aging and a key driver of liver inflammation and fibrosis. Senolytic agents that selectively eliminate senescent cells may modify or reverse key features of metabolic dysfunction–associated steatohepatitis (MASH). Dasatinib plus quercetin (D+Q) is a candidate senolytic therapy for fibrotic MASH. Here, we report a phase 2 double-blind randomized controlled trial evaluating the efficacy and safety of D+Q in patients with fibrotic MASH.
Method: Patients with biopsy-confirmed fibrotic MASH (F2–F3) were randomized (1:1) to receive intermittent D+Q (dasatinib 100 mg/day, quercetin 1000 mg/day) for 3 consecutive days per week for 3 weeks, followed by a 4-week drug-free period, or matching placebo; this 7-week cycle was repeated three times. The primary endpoint was ≥1-stage fibrosis improvement without worsening of MASH, assessed by liver histology using the SAF (Steatosis–Activity–Fibrosis) score on paired biopsies obtained at baseline and end of treatment. All biopsies were centrally scored by three independent pathologists blinded to timepoint and treatment allocation. Efficacy was analysed by intention-to-treat using a chi-squared test. Secondary endpoints included MASH resolution and safety.
Results: A total of 31 patients were randomized (median age 56 years [IQR 47–62.5]; 76% male; Type 2 Diabetes 58%); 17 received D+Q and 14 placebo. There were 4 discontinuations, D+Q (n = 3), placebo (n = 1). Improvement of fibrosis without worsening of MASH was achieved in 8 (47%) patients in the D+Q group vs. 1 (7%) with placebo (p = 0.041). Resolution of MASH occurred in 71% of patients receiving D+Q compared with 15% receiving placebo (p = 0.011). Improvement of the NAFLD Activity Score (NAS) was better with D+Q (−1.43 ± 1.22 vs. −0.39 ± 0.77; p = 0.012). In the D+Q group, 14/17 participants reported adverse events (AE) compared to 6 with placebo. Most reported side effects of D+Q were headache and gastrointestinal complaints. Reported severity of these AEs was mild or moderate and all AEs were resolved without intervention.

Conclusion: Intermittent senolytic treatment with D+Q significantly improved fibrosis and resolved MASH in fibrotic MASH with a favourable safety profile. Our data suggest that senescence drives fibrotic MASH and may be reversible with pharmacological intervention. These findings need confirmation in larger trials with longer follow-up. Clinical trial number NCT05506488.

LBO-006

Efficacy and safety of volixibat, an IBAT inhibitor, in patients with primary sclerosing cholangitis and moderate-to-severe pruritus: results of the VISTAS trial

Cynthia Levy[1], Gideon M. Hirschfield[2], Mitchell Shiffman[3], Muyiwa Awoniyi[4], Deepak Joshi[5], Debra Weinstein[6], Douglas Thorburn[7], Alejandra Villamil[8], Ynto de Boer[9], Parvez Mantry[10], Aldo J. Montano-Loza[11], Münevver Demir[12], Adriaan J. van der Meer[13], Lisa Forman[14], Jessica Dyson[15], Nimer Assy[16], Kidist Yimam[17], Walid Ayoub[18], Thomas Berg[19], Marie-Noëlle Hilleret[20], Christoph P. Berg[21], John Eaton[22], Cláudia Couto[23], Verena Keitel-Anselmino[24], Palak Trivedi[25], Eli Zuckerman[26], Roger McCorry[27], Emily Schonfeld[28], Fernando Cairo[29], Marlyn J. Mayo[30], Julius Wilder[31], Juan F. Gallegos-Orozco[32], Stuart C. Gordon[33], William Gelson[34], Miriam Levy[35], Roman Perri[36], Suresh Venkatachalapathy[37], Gabriel Alejandro Aballay Soteras[38], Marc Deschenes[39], Henry Nguyen[40], Rifaat Safadi[41], Siddharth Sood[42], Emma Culver[43], Alan Bonder[44], Janisha Patel[45], James O'Beirne[46], Nora Cazzagon[47], Mario Álvares-da-Silva[48], Fadi Abu Baker[49], Paulo Bittencourt[50], Pietro Invernizzi[51], Ira Jacobson[52], Gadi Lalazar[53], Avik Majumdar[54], Chirag Patel[55], Magdalena Salcedo Plaza[56], Rodrigo Aires[57], Ehud Zigmond[58], Victor Ankoma-Sey[59], David Bernstein[60], Brian Borg[61], Marco Carbone[62], Géraldine Dahlqvist[63], Tarek Hassanein[64], Paul Hermabessière[65], Pietro Lampertico[66], Kate Lynch[67], Mercedes Martinez[68], Sergio Rodriguez-Tajes[69], Manish Thapar[70], Richard Kalman[70], Frans van der Heide[71], Xavier Verhelst[72], David W. Victor Iii[73], Hallam Gugelmann[74], Tiago Nunes[74], Erik Ness[74], David Sanchez Ramos[74], Jilliann Elliott[74], Tobias Di Marco[74], Jayshree Krishnaswami[74], Clara Kebabian[74], Jolan Terner-Rosenthal[74], Andrew McKibben[74], Raul Aguilar[74], Cory Kostrub[74], Susanna Carou-Keenan[74], Lara Longpre[74], Pamela Vig[74], Joanne Quan[74], Christopher L. Bowlus[75], Kris V. Kowdley[76]. *[1]Schiff Center for Liver Diseases, University of Miami Miller School of Medicine, Miami, Florida, United States; [2]The Autoimmune and Rare Liver Disease Programme, Division of Gastroenterology and Hepatology, Toronto General Hospital, Toronto, Canada; [3]Liver Institute of Virginia, Bon Secours Mercy Health, Richmond, Virginia, United States; [4]Digestive Disease Institute, Department of Gastroenterology, Hepatology and Nutrition, Cleveland Clinic, Cleveland, Ohio, United States; [5]King's College Hospital NHS Foundation Trust, London, United Kingdom; [6]Science 37, Inc., Culver City, California, United States; [7]Sheila Sherlock Liver Centre and UCL Institute for Liver and Digestive Health, Royal Free Hospital, London, United Kingdom; [8]Hospital Italiano de Buenos Aires,, Buenos Aires, Argentina; [9]Amsterdam UMC, Amsterdam, Netherlands; [10]The Liver Institute at Methodist Dallas Medical Center, Dallas, Texas, United States; [11]University of Alberta, Division of Gastroenterology and Liver Unit, Edmonton, Canada; [12]Department of Hepatology and Gastroenterology, Campus Virchow-Klinikum and Campus Charité Mitte, Charité -, Universitätsmedizin Berlin, Berlin, Germany; [13]Erasmus MC, Rotterdam, Netherlands; [14]University of Colorado Anschutz Medical Campus, Aurora, Colorado, United States; [15]Newcastle upon Tyne Hospitals NHS Foundation Trust, Newcastle upon Tyne, United Kingdom; [16]Galilee Medical Center, Nahariya, Israel; [17]California Pacific Medical Center Research Institute, San Francisco, California, United States; [18]Cedars Sinai Medical Center, Los Angeles, California, United States; [19]Division of Hepatology, Department of Medicine II, University of Leipzig Medical Center, Leipzig, Germany; [20]Université Grenoble Alpes, Service hépatogastroenterologie, CHU Grenoble Alpes, Grenoble, France; [21]University Hospital Tubingen Medical Clinic, Tubigen, Germany; [22]Mayo Clinic, Rochester, Minnesota, United States; [23]Hospital das Clinicas da Universidade Federal de Minas Gerais, Belo Horizonte, Brazil; [24]University Hospital Magdeburg, Magdeburg, Germany; [25]University Hospitals Birmingham NHS Foundation Trust, Birmingham, United Kingdom; [26]The Carmel Medical Center, Haifa, Israel; [27]Royal Victoria Hospital Belfast Health and Social Care Trust, Belfast, United Kingdom; [28]Weill Cornell Medical College, New York, New York, United States; [29]Hospital El Cruce, Buenos Aires, Argentina; [30]University of Texas Southwestern Medical Center, Dallas, Texas, United States; [31]Duke School of Medicine, Duke Clinical Research Institute, Durham, North Carolina, United States; [32]University of Utah, Salt Lake City, Utah, United States; [33]Henry Ford Health, Detroit, Michigan, United States; [34]Cambridge Liver Unit, Cambridge, United Kingdom; [35]Liverpool Hospital, Liverpool, Australia; [36]Vanderbilt UMC, Nashville, Tennessee, United States; [37]Nottingham University Hospitals NHS Trust, Nottinghan, United Kingdom; [38]Glenny Corp S.A., Buenos Aires, Argentina; [39]Royal Victoria Hospital McGill University Health Centre, Montreal, Canada; [40]Departments of Medicine and Microbiology, Immunology, and Infectious Diseases (MIID) Snyder Institute for Chronic Disease, Cumming School of Medicine, University of Calgary, Calgary, Canada; [41]1Hadassah Medical Organization, The Liver Institute, Jerusalem, Israel; [42]Northern Health, Melbourne, Australia; [43]John Radcliffe Hospital, Oxford, United Kingdom; [44]Beth Israel Deaconess Medical Center, Boston, Massachusetts, United States; [45]University Hospital Southampton NHS Foundation Trust, Southampton, United Kingdom; [46]UniSc Clinical Trials Birtinya, Queensland, Australia; [47]Department of Surgery, Oncology and Gastroenterology, University Hospital of Padova, ERN RARE-LIVER, Azienda-Ospedale-Università di Padova, Padova, Italy; [48]Hospital de Clínicas de Porto Alegre, Porto Alegre, Brazil; [49]Department of Gastroenterology and Hepatology, Hillel Yaffe Medical Center, Hadera, Israel; [50]Centro de Pesquisa Clínica da Escola Bahiana de Medicina e Saúde Pública, Salvador, Brazil; [51]Fondazione IRCCS San Gerardo dei Tintori, Monza, Italy; [52]NYU Grossman School of Medicine, New York, New York, United States; [53]Shaare Zedek Medical Center, Jerusalem, Israel; [54]Austin Health, Melbourne, Australia; [55]Galen Medical Group, Chattanooga, Tennessee, United States; [56]Hospital General Universitario Gregorio Maranon, Madrid, Spain; [57]Hospital Das Clinicas Da UFG, Goiania, Brazil; [58]The Chaim Sheba Medical Center, Ramat Gan, Israel; [59]Liver Associates of Texas, P.A., Houston, Texas, United States; [60]Northwell Health Center for Liver Diseases, New York, New York, United States; [61]Southern Therapy and Advanced Research LLC., Jackson, Mississippi, United States; [62]University of Milano-Bicocca, ASST GOM Niguarda, Milan, Italy; [63]Cliniques Universitaires Saint-Luc, Brussels, Belgium; [64]Southern California Research Center, Inc., Coronado, California, United States; [65]CMC Magellan, Paris, France; [66]Foundation IRCCS Ca' Granda Ospedale Maggiore Policlinico, Milan, Italy; [67]Royal Adelaide Hospital, Adelaide, Australia; [68]Columbia University Irving Medical Center, New York, New York, United States; [69]Hospital Casa Maternidad, Barcelona, Spain; [70]Einstein Medical Center, Philadelphia, Pennsylvania, United States; [71]University Medical Center Groningen, Groningen, Netherlands; [72]Ghent University Hospital, Ghent, Belgium; [73]Houston Methodist Hospital, Houston, Texas, United States; [74]Mirum Pharmaceuticals, Inc., Foster City, California, United States; [75]University of California, Davis, Davis, California, United States; [76]Liver Institute Northwest, Seattle, Washington, United States*
Email: clevy@med.miami.edu

Background and aims: Primary sclerosing cholangitis (PSC) is a chronic cholangiopathy frequently accompanied by severe cholestatic pruritus and fatigue, leading to substantial impairment in quality of life. No approved pharmacologic treatments are available. Volixibat (VLX) is a minimally absorbed ileal bile acid transporter (IBAT) inhibitor that interrupts the enterohepatic bile acid recirculation, reducing the total bile acid pool, a mechanism implicated in cholestatic pruritus. VISTAS is a 28-week, multicenter, randomized, double-blind, placebo (PBO)-controlled, pivotal study which evaluated the efficacy and safety of VLX for pruritus in PSC. Here we report

an overview of the trial design and baseline characteristics; topline results will be available at the time of presentation.
Method: Following a dose-selection period with a blinded interim analysis, the confirmatory portion of the study evaluated oral VLX 20 mg BID versus PBO in patients with PSC. Eligible participants with moderate-to-severe pruritus (based on a score of ≥4 on a 0–10 numerical rating scale [Adult ItchRO]) were selected for primary endpoint analysis. Primary endpoint was defined as change from baseline (CFB) in worst itch over 28 weeks. Key secondary endpoints included CFB through 28 weeks of: serum bile acid (sBA); PROMIS Fatigue and Sleep Disturbance; proportion of responders with ≥2-point reduction in Adult ItchRO. Safety endpoints included adverse event reporting and laboratory measurements.
Results: In total, 132 participants were eligible for primary endpoint analysis and were randomized to receive either VLX or PBO. At baseline, 47.7% were male, mean (SD) age at enrolment was 43.5 (14.7) years, 90.2% had large-duct, and 9.8% small-duct PSC. 72% had inflammatory bowel disease (IBD); among these, 72.6% had ulcerative colitis, 25.3% Crohn's disease, and 2.1% had unclassified IBD types. Additional baseline characteristics (mean [SD]) included: Adult ItchRO (6.2 [1.5]), sBA (μmol/L; 41.8 [30.0]), ALP (U/L: 357.7 [225.7]), AST (U/L: 68.2 [39.0]), ALT (U/L: 82.1 [55.2]), TB (mg/dL: 10.8 [13.3]) and DB (mg/dL: 5.9 [8.9]). Results for the primary endpoint, key secondary endpoints, and safety will be presented at the congress as the trial was ongoing at the time of abstract submission.
Conclusion: VISTAS is the largest interventional study investigating the efficacy and safety of an IBAT inhibitor in PSC. The results will represent the first controlled evidence of a potential therapy addressing the symptom burden in PSC patients.

THURSDAY 28 MAY

Hepatocyte biology and fibrosis

OS-001-YI
Vascularized liver spheroid-on-chip with liver specific vascular cells

Negar Vahdani[1,2,3], Karin Schmid[1,3], Keely Keller[4], Deborah Stroka[4], Olivier Guenat[1,2]. *[1]Organs-on-Chip Technologies Lab, ARTORG Center, Medical Faculty, University of Bern, Bern, Switzerland; [2]Multidisciplinary Center for Infectious Diseases, Medical Faculty, University of Bern, Bern, Switzerland; [3]Graduate School for Cellular and Biomedical Sciences, Medical Faculty, University of Bern, Bern, Switzerland; [4]Department of Visceral Surgery and Medicine, Inselspital, Bern University Hospital and University of Bern, Bern, Switzerland*
Email: negar.vahdani@unibe.ch

Background and aims: *In vitro* liver models have evolved from 2D monocultures to advanced 3D spheroid and organoid models; however, most existing models lack a functional microvasculature and rely on passive diffusion for oxygen and nutrient delivery. This limitation restricts hepatocyte metabolic activity, functional stability, and long-term culture and does not reflect the highly vascularised nature of the liver. Recent advances in organs-on-chip technology offer a promising strategy for developing perfused, vascularized liver spheroid models. The aim of this study is to develop and characterize a perfused, vascularized liver spheroid-on-chip that enhances hepatocyte functionality.
Method: An open-top microfluidic device was designed with a central chamber to support the formation of a self-assembled microvasculature and the subsequent vascularization of liver spheroids. Liver spheroids were generated by co-culturing primary human hepatocytes (PHH) with human stellate cells (HSCs) and liver sinusoidal endothelial cells (LSECs) and were assessed for albumin secretion, urea production, and CYP3A4 activity. Self-assembled LSECs and HSCs microvasculature were analyzed for vascular morphology, perfusability and permeability. Liver spheroids were transferred onto the microvascular network and fixed for immunostaining after vascularization.
Results: Liver spheroids were generated by co-culturing PHH, HSC, and LSECs cells in 2:1:1 ratio, resulting in spheroids with diameters of 200–250 μm. Compared with PHH monoculture spheroids, co-culture spheroids exhibited increased sphericity and significantly higher albumin secretion and CYP3A4 activity. The self-assembled microvasculature formed connected, perfusable and permeable network. Finally, the spheroids were transferred into a fibrin gel on the microvasculature bed on chip and fixed after 4 days in culture. Immunofluorescent staining showed integration of the vascular network with the spheroids, with vessels extending into the spheroids.
Conclusion: This study successfully developed a vascularized liver-on-chip by integrating co-cultured liver spheroids with a self-assembled microvasculature. The liver spheroids maintained metabolic activity, as evidenced by albumin, urea, and CYP3A4 expression, while the microvasculature exhibited perfusable vessel formation. This model addresses the lack of functioning microvasculature in spheroids and holds promise for advancing translational hepatology research by providing a more physiologically relevant environment.

OS-002-YI
Hepatocyte lipolytic disruption by ATGL-deficiency contributes to MASH-fibrosis via lipotoxic stress in vivo: molecular and single-cell transcriptomic insights

Henriette Horstmeier[1], Tanmoy Chakma[1], Katharina Bonitz[2,3], Thomas Sorz-Nechay[2,3], Katja Sommer[4], Vlad Taru[2], Robert Brettner[1], Hubert Scharnagl[4], Veronica Moreno-Viedma[1], Veronika Mlitz[1], Claudia Fuchs[1], Philipp Schwabl[1,2,4], Thomas Reiberger[2,3], Michael Trauner[1]. *[1]Hans Popper Laboratory of Molecular Hepatology, Medical University of Vienna, Vienna, Austria; [2]Christian Doppler Laboratory for Portal Hypertension and Liver Fibrosis, Medical University of Vienna, Vienna, Austria; [3]CeMM Research Center for Molecular Medicine of the Austrian Academy of Sciences, Vienna, Austria, Vienna, Austria; [4]Medical and Chemical Laboratory Diagnostics, Medical University of Graz, Graz, Austria*
Email: henriette.horstmeier@meduniwien.ac.at

Background and aims: Adipose triglyceride lipase (ATGL/PNPLA2) is the key lipase hydrolysing intracellular triglycerides to glycerol and free fatty acids and thereby regulating hepatic energy balance, and cellular crosstalk. However, the role of ATGL-mediated lipolysis as potential disease modulator via impact on liver fibrosis and portal pressure (PP) remains unclear.
Method: Metabolic dysfunction-associated steatohepatitis (MASH)-fibrosis was induced in hepatocyte-specific ATGL knockout ($Pnpla2^{fl/fl}$Alb-Cre^{+}) mice and controls ($Pnpla2^{fl/fl}$Alb-Cre^{-}) by feeding of a choline-deficient, aminoacid-defined high-fat diet (CDAHFD) or a matched control diet for 12 weeks. PP was measured invasively; fibrosis severity was assessed by serum biochemistry and histology and the liver immunophenotype was profiled by flow cytometry. In a sub-cohort (n = 4/group), hepatocytes (HC), cholangiocytes and non-parenchymal liver cells were isolated before pooling and scRNA-seq using the 10x Chromium Flex platform.
Results: Hepatocyte-specific ATGL knockout (HepATGL-KO) under CDAHFD resulted in hepatocyte lipid loading, reflected by increased liver-to-bodyweight ratio [7.25 ± 0.37 vs. 13.59 ± 0.64%; p < 0.001] and reduced serum FFA levels [0.52 ± 0.04 vs. 0.39 ± 0.03 mmol/L; p = 0.018]. Moreover, HepATGL-KO aggravated fibrosis [collagen proportionate area, CPA: 2.17 ± 0.31 vs. 4.35 ± 0.55%; p = 0.002] and increased PP [6.64 ± 0.24 vs. 7.63 ± 0.30 mmHg; p = 0.028], spleen-to-bodyweight ratio [0.47 ± 0.03 vs. 0.56 ± 0.19%; p = 0.02] and liver

injury [AST: 279 ± 23 vs. 429 ± 35 U/L; $p < 0.001$]. The generated scRNA-seq dataset of 101490 hepatic cells supported by flow cytometry indicated the strongest transcriptomic changes within HC and macrophages. Besides a shift in macrophage identity towards lipid-associated macrophages (LAM), pseudo-bulking analysis of HepATGL-deficient HC subclusters in MASH revealed a lipid-stress response characterized by *Scd1, Lpl* and *Orm3*. Moreover, upregulation of *Col3a1, Col4a3* and *Acta2* supported enhanced profibrotic remodelling in HepATGL-KO.

Conclusion: Our data underlines the crucial role for ATGL as key contributor to MASH-fibrosis, since hepatocyte-loss of ATGL aggravates liver injury, fibrosis and portal hypertension. In our scRNA-seq dataset, ATGL-KO in hepatocytes show disrupted hepatocyte lipid handling and lipotoxic stress which in turn seem to impact HC-LAM crosstalk and cause downstream pro-fibrotic remodelling.

OS-003

A single-cell fixed RNA profiling uncovers key transcriptional and signalling programs in liver fibrosis progression and regression

Le Thi Thanh Thuy[1], Pham Minh Duc[2], Hoang Hai[1], Norifumi Kawada[3]. [1]*Department of Global Education and Medical Sciences, Graduate School of Medicine, Osaka Metropolitan University, Osaka, Japan, Osaka, Japan;* [2]*Department of Hepatology, Graduate School of Medicine, Osaka Metropolitan University, Osaka, Japan, Osaka, Japan;* [3]*Endowsed Departments of Liver Cancer Treatment and Homeostatic Regulation, Graduate School of Medicine, Osaka Metropolitan University, Osaka, Japan, Osaka, Japan*
Email: thuy@omu.ac.jp

Background and aims: Single-cell fixed RNA profiling (FLEX) is a novel technique that captures RNA expression in frozen tissues at a single-cell resolution. We applied FLEX to mouse model of liver fibrosis progression and regression to identify novel anti-fibrotic targets.

Method: Mice were administered intraperitoneal thioacetamide (TAA) for 10 weeks to induce fibrosis, and regression was assessed 2 weeks after cessation. The livers were fixed, dissociated, and analysed using FLEX. Molecular validation included immunoblotting, immunohistochemistry, gene silencing/overexpression, cytokine/phosphokinase arrays, and human liver samples.

Results: Approximately 40,000 liver cells were profiled, integrated, and annotated into 10 major cell types using lineage-specific markers. Pericentral signature restoration in hepatocytes, scar-resolving genes (Mmp14 and Ctsl), fenestrae restoration in liver sinusoidal endothelial cells, anti-inflammatory Kupffer cells, reduced fibrogenic cholangiocytes, and recovery-associated immune cell subsets were observed. During fibrosis, monocyte-derived macrophages secrete semaphorin-4D (SEMA4D), which binds to Plexin B2 on hepatic stellate cells (HSCs). SEMA4D$^+$ cells were upregulated in mouse and human fibrotic livers. Recombinant SEMA4D induces type I collagen in HSCs, whereas humanised monoclonal IgG4 SEMA4D blockade (VX15/2503) attenuates fibrosis *in vivo*. LIM and cysteine-rich domains 1 (LMCD1) was enriched in fibrotic HSCs and suppressed during regression. LMCD1 knockdown reduced the expression of fibrotic protein, while LMCD1 overexpression promoted the expression of fibrotic protein via AKT/mTOR signalling. LMCD1 and SEMA4D are localised in the fibrotic septa and are correlated with the fibrotic stage in humans.

Conclusion: This FLEX-based single-cell atlas revealed critical transcriptional programs and cell-cell interactions, identifying SEMA4D and LMCD1 as promising therapeutic targets for liver fibrosis.

OS-004-YI

Multiomic analysis identifies macrophage oxidised LDL receptor 1 (OLR1) as a novel antifibrotic therapeutic target across multiple aetiologies of human chronic liver disease

Fabio Colella[1], Kexin Kong[1], Eleni Papachristoforou[1], Jacky Tam[1], Juliet Luft[1], Gosia Grzelka[1], Pak Qiu[1], Timothy Kendall[1], Jonathan Fallowfield[1,2], Yingxin Liang[3], Volker Lauschke[3,4,5,6], Prakash Ramachandran[1]. [1]*Centre for Inflammation Research, Institute for Regeneration and Repair, University of Edinburgh, Edinburgh, United Kingdom;* [2]*University of Edinburgh, Institute For Regeneration and Repair, Edinburgh, United Kingdom;* [3]*Department of Physiology and Pharmacology and Center for Molecular Medicine, Karolinska Institutet and University Hospital, Stockholm, Sweden;* [4]*Dr. Margarete Fischer-Bosch Institute of Clinical Pharmacology, Stuttgart, Germany;* [5]*University of Tübingen, Tübingen, Germany;* [6]*Department of Pharmacy, the Second Xiangya Hospital, Central South University, Changsha, China*
Email: fcolell2@ed.ac.uk

Background and aims: Regardless of cause, chronic liver disease (CLD) is characterised by progressive fibrosis which can drive poor clinical outcomes. Monocyte-derived macrophages (MDMs) play a central role in both the progression and resolution of liver fibrosis and represent a promising target for antifibrotic therapies. Recent work has identified TREM2$^+$CD9$^+$ MDMs, termed scar-associated macrophages (SAMac), as the key human MDM population regulating fibrosis. However, it remains unknown how to specifically target SAMac to inhibit their pro-inflammatory pro-fibrotic properties across different causes of CLD.

Method: Human liver single-cell RNA-sequencing (scRNAseq) data from 77 patients (42 healthy, 35 CLD) were analysed. Human liver spatial proteomics was performed using a 34-plex antibody panel on the PhenoCycler-Fusion. Deconvolution of liver bulk RNA-seq data from different CLD aetiologies and stages was carried out using BayesPrism. Mouse CLD was induced by chronic CCl4 or bile duct ligation (BDL). OLR1 modulation was performed on human cells using RNA interference or antibody blockade via MEDI6570.

Results: ScRNAseq identified a distinct CLD-enriched cluster of OLR1$^+$ SAMac with a pro-inflammatory pro-fibrotic gene expression profile. Spatial proteomics confirmed expansion of OLR1$^+$ SAMac in CLD which mapped to areas of fibrosis. Bulk RNA-seq data demonstrated a significant upregulation of OLR1 and expansion of OLR1$^+$ SAMac with histological fibrosis stage across MASLD, ALD, PSC and PBC patients. Expansion of OLR1$^+$ SAMac was further confirmed in the CCl_4 and BDL models of CLD. In primary human MDMs, *OLR1* and *IL1B* expression showed a strong positive correlation across 67 stimulation conditions, suggesting a pro-inflammatory role. Functionally, silencing of OLR1 reduced *IL1B* expression in both THP-1 and primary human MDMs. Co-culture assays demonstrated that OLR1 silencing or blockade in MDMs reduced *COL1A1* and *COL3A1* expression in hepatic stellate cells. Furthermore, OLR1 silencing in multilineage human liver spheroids significantly attenuated fibrillar collagen gene and protein expression.

Conclusion: These data identify OLR1 as a regulator of SAMac phenotype in CLD and highlight the potential of OLR1 blockade as a novel anti-inflammatory antifibrotic therapy. Crucially, OLR1$^+$ SAMacs accumulate across multiple aetiologies of CLD, suggesting that targeting OLR1 could have broad applicability to CLD patients.

OS-005-YI

Plasma cell-free DNA fragmentomics for non-invasive detection of hepatocellular carcinoma (HCC) in chronic liver disease (CLD)

Venkata Ramana Mallela[1], Sultan N. Alharbi[1], Mathew Vithayathil[1], Giulia Manfredi[2], Rosalba Minisini[2], David J. Pinato[3], Rishi Patel[4], Rohini Sharma[1]. [1]*Division of Surgery and Cancer, Imperial College London, Hammersmith Hospital, London, United Kingdom;* [2]*Department of Translational Medicine, University of Eastern Piedmont, Novara, Italy;* [3]*Division of Surgery and Cancer, Imperial College London, Hammersmith Hospital, Department of Translational Medicine, Division of Oncology,*

University of Eastern Piedmont, London, United Kingdom; [4]Eastman Dental School, University College London, London, WC1E 6DE, UK, London, United Kingdom
Email: v.mallela24@imperial.ac.uk

Background and aims: Early detection of hepatocellular carcinoma (HCC) remains difficult in patients with chronic liver disease (CLD undergoing surveillance. Plasma cell-free DNA (cfDNA) fragmentomics, which reflects genome-wide fragmentation patterns influenced by chromatin organisation and nuclease activity, represents a promising non-invasive biomarker. This study aimed to characterise cfDNA fragmentomic differences across healthy controls (HC), CLD, and HCC, and to develop a machine learning model to distinguish these conditions.
Method: A total of 700 participants were included. Plasma cfDNA from 475 individuals (HCC, n = 139; CLD, n = 186; HC, n = 150) in the training cohort underwent shallow whole-genome sequencing. In the training set, CLD etiologies were mainly attributed to alcohol (n = 42), HCV (n = 32), autoimmune liver disease (n = 30), MASLD (n = 24), HBV (n = 19), other causes, n = 3; or unknown etiologies (n = 36), with participants recruited from the United Kingdom and Italy. External validation included 225 participants (HCC, n = 75; CLD, n = 75; HC, n = 75), with CLD predominantly due to viral hepatitis and cirrhosis, including HBV (n = 26) and cirrhosis (n = 49). Fragmentomic features, including genome-wide fragmentation profiles, tumor fraction, fragment size distributions, end-motif frequencies, and mitochondrial cfDNA content, were extracted and integrated using ensemble machine learning models.
Results: HCC exhibited a distinct multidimensional fragmentomic profile compared with CLD and HC. Genome-wide fragmentation scores, tumour fraction, and mitochondrial cfDNA levels were significantly higher in HCC (all $p < 0.0001$). Short cfDNA fragments (<150 bp) were enriched in HCC, minimal in HC, and intermediate in CLD. End-motif analysis demonstrated progressive disease-related changes, with GC- and adenine-rich motifs in HC, thymine-rich motifs in CLD, and tumour-associated GC-rich cleavage patterns in HCC. In external validation, the classifier showed moderate discrimination between HCC and CLD (AUC 0.724) and strong discrimination between CLD and HC (AUC 0.935).
Conclusion: Plasma cfDNA fragmentomics identifies robust biological differences across the liver disease spectrum and enables accurate non-invasive detection of HCC. Integration of multiple fragmentomic features using machine learning supports improved surveillance strategies in at-risk populations and warrants validation in larger prospective cohorts.

Immune-mediated I

OS-006-YI

Development of a multi-biomarker model to predict transplant-free survival in primary sclerosing cholangitis: a multicenter retrospective study

Holmfridur Helgadottir[1,2], Peder Rustøen Braadland[1,3], Ahmad Ali[4], Elizabeth Atkinson[5], Brian D. Juran[6], Bryan McCauley[5], Guri Fossdal[2], Trine Folseraas[1,3,7,8], Sara Tjønnfjord[1,3,7,8], Kirsten Muri Boberg[1,3,7], Morten Karsdal[9], Diana Julie Leeming[9], Andressa de Zawadzki[9], Per Ueland[10,11], Adrian McCann[11], William Rosenberg[12], Martin Cornillet[13], Tom Hemming Karlsen[1,3,7,8], Johannes R. Hov[1,3,7,8], Annika Bergquist[14], Konstantinos N. Lazaridis[6], Mette Vesterhus[1,2,10].
[1]Norwegian PSC Research Center, Department of Transplantation Medicine, Oslo University Hospital, Oslo, Norway; [2]Department of Medicine, Haraldsplass Deaconess Hospital, Bergen, Norway; [3]Research Institute of Internal Medicine, Division of Surgery, Inflammatory Diseases and Transplantation, Oslo University Hospital, Oslo, Norway; [4]Division of Gastroenterology and Hepatology, University of Missouri School of Medicine, Columbia, United States; [5]Division of Clinical Trials and Biostatistics, Mayo Clinic, Rochester, United States; [6]Division of Gastroenterology and Hepatology, Mayo Clinic, Rochester, United States; [7]Institute of Clinical Medicine, University of Oslo, Oslo, Norway; [8]Section of Gastroenterology, Department of Transplantation Medicine, Oslo University Hospital, Oslo, Norway; [9]Nordic Bioscience, Biomarkers & Research, Herlev, Denmark; [10]Department of Clinical Science, University of Bergen, Bergen, Norway; [11]BEVITAL AS, Bergen, Norway; [12]The Institute for Liver and Digestive Health, University College London Division of Medicine, University College London, London, United Kingdom; [13]Center for infectious medicine, Department of Medicine Huddinge, Karolinska Institutet, Stockholm, Sweden; [14]Unit of Gastroenterology and Nutrition, Department of Medicine Huddinge, Karolinska Institutet, Karolinska University Hospital, Stockholm, Sweden
Email: hofihelgad@gmail.com

Background and aims: Predicting liver transplantation or death in primary sclerosing cholangitis (PSC) is challenging due to its heterogeneous course and complex pathogenesis, hindering the design of effective follow-up strategies and clinical trials. We aimed to determine whether a multi-biomarker model, integrating markers of fibrosis, extracellular matrix turnover, inflammation, and microbial metabolism, could improve risk prediction beyond single markers or clinical scores.
Method: We assembled a large cross-sectional PSC cohort from Norway, Sweden and the United States and analyzed biomarkers in frozen serum samples. Prediction models for two and five year liver transplantation-free survival were created using multivariable Cox regression analysis. A full model included eight biomarkers: enhanced liver fibrosis (ELF) test, type III and V collagen formation (PRO-C3, PRO-C5), degradation of type III and IV collagen (C3M, C4M), kynurenine-tryptophan ratio (KTR), neopterin, and pyridoxal 5′-phosphate (PLP). Internal validation and subset-fitting assessed overfitting and generalizability across regions, we compared pragmatic subset models with the full model, and benchmarked all models against the ELF test and established PSC risk scores.
Results: We included 906 PSC patients (64% male, 79% with inflammatory bowel disease, 57% on ursodeoxycholic acid). Median age at sampling was 47 years (IQR 34–60) and half were followed for at least seven years. At two and five years, 12% and 23%, respectively, reached the composite endpoint of liver transplantation or death. On internal validation of the full model, the optimism-corrected C-index was 0.834 (IQR 0.832–0.836) and 0.822 (IQR 0.821–0.822) at two and five years, with corresponding calibration slopes of 0.880 and 0.916. A pragmatic model of ELF, KTR and PLP had a C-index of 0.817 at five years and an improved calibration slope (0.970 vs. 0.917 for the full model). Both models outperformed the ELF-only model (C-index 0.79, calibration slope 0.99) and provided incremental predictive value beyond the Amsterdam-Oxford PSC model and the PSC Risk Estimate Tool.
Conclusion: Our models showed strong discrimination and good calibration. A pragmatic model, capturing fibrosis, inflammation and gut microbial metabolism, achieved predictive performance comparable to the full model. Both models outperformed the ELF test and clinical scores. These findings provide proof-of-principle that integrating markers of distinct disease processes can improve risk prediction in PSC.

OS-007

Norucholic acid leads to biochemical and histologic improvement in primary sclerosing cholangitis: impact of concomitant ursodeoxycholic acid therapy

Michael Trauner[1], Palak J. Trivedi[2], Gerald Denk[3], Martti Färkkilä[4], Peter Schirmacher[5], Stefan G. Hübscher[6], Michael Dill[7], Gerda Elisabeth Villadsen[8], Christoph P. Berg[9], Kristin K. Jørgensen[10,11], Marcel Vetter[12], Münevver Demir[13], Andreas E. Kremer[14], Christoph Schramm[15], Christian Strassburg[16], Heike Bantel[17], Tobias Boettler[18], Ulrich Beuers[19], Alexandre Louvet[20], Emina Halilbasic[1], Sabine Weber[3], Michael Stiess[21], Markus Proels[21], Ralph Müller[21], Peter Fickert[22], Michael Manns[17]. *[1]Division of Gastroenterology and Hepatology, Department of Internal Medicine III, Medical University of Vienna, Vienna, Austria; [2]NIHR Birmingham Biomedical Research Centre, University of Birmingham, Birmingham, United Kingdom; [3]Department of Medicine II, University Hospital LMU, Munich, Germany; [4]Department of Gastroenterology, University of Helsinki and Helsinki University Hospital, Helsinki, Finland; [5]Institute of Pathology, University Hospital Heidelberg, Heidelberg University, Heidelberg, Germany; [6]School of Infection, Inflammation and Immunology, University of Birmingham, Birmingham, United Kingdom; [7]Division of Gastroenterology, University Hospital Heidelberg, Heidelberg, Germany; [8]Department of Hepatology and Gastroenterology, Aarhus University Hospital, Aarhus, Denmark; [9]Department of Gastroenterology, Hepatology and Infectiology, University Hospital Tübingen, Tübingen, Germany; [10]Department of Gastroenterology, Akershus University Hospital, Lørenskog, Norway; [11]Norwegian PSC Research Center, Department of Transplantation Medicine, Clinic of Surgery and Specialized Medicine, Oslo University Hospital Rikshospitalet, Oslo, Norway; [12]Department of Medicine 1, Friedrich-Alexander-University Erlangen-Nürnberg, Erlangen, Germany; [13]Department of Hepatology and Gastroenterology, Charité Universitätsmedizin Berlin, Berlin, Germany; [14]Department of Gastroenterology and Hepatology, University Hospital Zürich, Zürich, Switzerland; [15]Department of Medicine and Martin Zeitz Centre for Rare Diseases, University Medical Centre Hamburg-Eppendorf, Hamburg, Germany; [16]Department of Internal Medicine I, University Hospital Bonn, Bonn, Germany; [17]Department of Gastroenterology, Hepatology, Infectious Diseases and Endocrinology, Hannover Medical School, Hannover, Germany; [18]Department of Medicine II, University Hospital Freiburg, Freiburg, Germany; [19]Department of Gastroenterology and Hepatology, Amsterdam UMC, Locatie AMC, Amsterdam, Netherlands; [20]Services des maladies de l'appareil digestif, CHU de Lille, Lille, France; [21]Dr. Falk Pharma GmbH, Freiburg, Germany; [22]Department of Medicine, Medical University of Graz, Graz, Austria*
Email: michael.trauner@meduniwien.ac.at

Background and aims: Currently no pharmacological therapy is approved for the treatment of primary sclerosing cholangitis (PSC) in most countries. Recently, norucholic acid (NCA) demonstrated superiority over placebo (PBO) in a phase 3 pivotal trial (NUC-5) in PSC that included patients with and without concomitant UDCA as background therapy. The efficacy of NCA in these two cohorts is compared in this subgroup analysis.
Method: NUC-5 was a 192-week double-blind trial investigating 1,500 mg NCA versus PBO once daily in adults with PSC. Inclusion criteria included alkaline phosphatase (ALP) levels ≥1.5-fold upper limit of normal (ULN). Patients on a stable dose of UDCA (≤20 mg/kg body weight/day) for at least 8 weeks prior to baseline could maintain their UDCA regimen throughout the trial. The primary analysis was performed after 96 weeks, with the primary combined endpoint of no worsening in histological disease stage by Ludwig classification plus partial normalization of ALP to <1.5-fold ULN. Secondary endpoints included histological, biochemical, and safety parameters.
Results: Within the full analysis set, 77.1% of NCA and 81.3% of PBO patients took background UDCA, respectively (NCA+UDCA n = 158, PBO+UDCA n = 78, NCA alone n = 47, PBO alone n = 18). Most baseline characteristics were balanced between the subgroups except for ALP levels (NCA+UDCA: 359 U/l, PBO+UDCA: 324 U/l, NCA alone: 373 U/l, PBO alone: 467 U/l). At the primary analysis, 12.7% of NCA patients and 5.1% of PBO patients taking UDCA achieved the primary endpoint ($p = 0.08$) compared with 23.4% and 0% without UDCA ($p < 0.001$), respectively. Improvement in Ludwig histologic disease stage was observed for 23.4% of NCA+UDCA vs. 11.9% of PBO+UDCA patients ($p = 0.18$), compared with 30.3% of patients with NCA alone vs. 6.7% with PBO alone ($p = 0.13$) among patients with paired biopsies. Partial normalization of ALP was more frequent with NCA monotherapy (NCA alone: 25.5%, PBO alone: 5.6%, $p = 0.10$; NCA+UDCA: 18.4%, PBO+UDCA: 15.4%, $p = 0.51$) as was a 40% reduction in ALP from baseline (NCA alone: 31.9%, PBO alone: 0%, $p < 0.001$; NCA+UDCA: 14.6%, PBO+UDCA: 11.5%, $p = 0.50$). Adverse events were generally balanced between NCA patients with and without UDCA.
Conclusion: Treatment with NCA led to improvement in histologic and biochemical outcomes both with and without concomitant UDCA. Co-therapy with NCA plus UDCA was tolerated as well as NCA monotherapy. Higher rates of improvement were observed across all parameters in patients without concomitant UDCA as background therapy.

OS-008

Latest liver stiffness best predicts long-term outcomes in autoimmune hepatitis undergoing serial assessment: a large multicentre cohort study from canal

Yu Jun Wong[1,2], Guan Sen Kew[1,3], Gideon M. Hirschfield[4], Aliya Gulamhusein[4], Madeline Cameron[4], Shagani Thisairajah[1], Hin Hin Ko[5], Nabiha Faisal[6], Kristel Leung[7], Jean-Philippe Wallach[8], Devika Shreekumar[1], Narmeen Umar[1], Karim Qumosani[9], Mina Niazi[10], Julian Hercun[11], Catherine Vincent[11], Angela Cheung[9], Tasha Kulai[12], Tianyan Chen[13], Andrew L. Mason[1], Mark Swain[14], Bettina Hansen[4], Ellina Lytvyak[1], Aldo J Montano-Loza[1]. *[1]Division of Gastroenterology and Hepatology, University of Alberta, Edmonton, Canada, Edmonton, Canada; [2]Department of Gastroenterology & Hepatology, Changi General Hospital, Singapore, Singapore; [3]Woodlands Health Campus, Singapore, Singapore; [4]The Autoimmune and Rare Liver Disease Programme, Division of Gastroenterology and Hepatology, Toronto General Hospital, Toronto, Canada, Toronto, Canada; [5]Division of Gastroenterology, University of British Columbia, Vancouver, Vancouver, Canada; [6]Department of Internal Medicine, Section of Hepatology, University of Manitoba, Manitoba, Canada; [7]Departments of Medicine & Public Health Sciences, Queen's University, Kingston, Ottawa, Canada; [8]Nanaimo Regional Hospital, Nanaimo, Nanaimo, Canada; [9]University of Ottawa's Faculty of Medicine, Ottawa, Canada; [10]Division of Gastroenterology and Hepatology, College of Medicine, University of Saskatchewan Royal University Hospital, Saskatoon, Canada; [11]Liver Unit of the Centre hospitalier de l'Université de Montréal, Montreal, Canada; [12]Department of Medicine, Dalhousie University, Halifax, Nova Scotia, Canada; [13]Gastroenterology, Hepatology and Liver Transplantation, McGill University Health Centre, Royal Victoria Hospital, Montreal, Canada; [14]Division of Gastroenterology and Hepatology, University of Calgary, Calgary, Canada*
Email: wongyujun1985@gmail.com

Background and aims: While liver stiffness measurements (LSM) are widely used for monitoring and prognostication in chronic liver disease, their dynamic prognostic value in autoimmune hepatitis (AIH) remains controversial. We assessed whether dynamic changes in LSM improve the prediction of liver-related events (LRE) in treated AIH.
Method: We analyzed the multicentre Canadian Network for Autoimmune Liver Disease (CaNAL) registry, including AIH patients diagnosed (2010–2025) across 13 Canadian centres, who underwent serial LSMs after diagnosis and treatment. Patients with hepatic decompensation (HD) before LSM, unreliable LSM or LSM<6 months of diagnosis, prior liver transplantation (LT), or follow-up<6 months were excluded. Using a landmark approach, we compare the

prognostic performance of baseline LSM (LSM1, ≥6 months after AIH diagnosis) and the *most recent LSM* (LSMc), to predict the occurrence of HD and LRE (HD, HCC, LT & death) using Cox regression analysis.
Results: Among 523 patients who underwent serial LSMs (median age 46 years, 16% with advanced disease(cACLD) suggested by LSM1≥15 kPa); median LSM decreased from 11.0 kPa (IQR:7–11) to 7.9 kPa (5–9) at LSMc. Over a median follow-up of 150 months, 4.2% developed HD, 1% underwent LT, and 3% demised. Patients who developed HD had higher LSM1 and LSMc, greater absolute and relative LSM changes, lower platelet counts, and IgG levels ($p < 0.05$ for all). In contrast, biochemical responses at 6 months were not associated with subsequent HD or LREs. Despite low event rates reflecting effective contemporary therapy, both LSM1 and LSMc independently predicted HD (HR: 1.07 per kPa for each, $p < 0.001$), with superior discrimination for LSMc (AUROC: 0.812 vs 0.788). Among patients with advanced disease (LSM1≥15 kPa), regression to LSM<15 kPa or ≥20% LSM reduction was associated with a significantly lower risk of LRE ($p < .05$). Importantly, similar risk stratification was observed in patients without advanced disease. An LSMc ≥15 kPa independently predicted LRE, whereas neither complete biochemical response nor LSM change provided incremental prognostic value beyond LSMc in likelihood ratio testing.
Conclusion: In treated AIH, most recent liver stiffness is the strongest predictor of liver-related outcomes, outperforming baseline stiffness and biochemical response. Serial LSM enables dynamic risk stratification and identifies patients at ongoing risk despite apparent biochemical remission, supporting its role in post-treatment surveillance.

OS-009-YI

Mycophenolate mofetil in combination with prednisolone as potential first-line maintenance therapy in treatment-naïve autoimmune hepatitis: 3-year follow-up of the CAMARO-trial

Charlotte Slooter[1], Romée Snijders[2], Anna Stoelinga[3], Katinka Gerrits[4], Tom J.G. Gevers[5], Simon Pape[2], Maaike Biewenga[3], Maarten Tushuizen[3], Robert C. Verdonk[6], Hendrik J.M. de Jonge[7], Jan Maarten Vrolijk[8], Sjoerd Bakker[9], Thomas Vanwolleghem[10], Martine A.M.C. Baven-Pronk[11], Ulrich Beuers[4], Adriaan J. van der Meer[12], Nicole F.M. van Gerven[13], Marijn Sijtsma[14], Brechje van Eijck[15], Manon van Ijzendoorn[16], Manon van Herwaarden[17], Floris van den Brand[4], Kerem Sebib Korkmaz[18], Aad van den Berg[19], Maureen Guichelaar[20], Matthijs Kramer[5], Frank Govaert[21], Sita Jansen[22], Sanne K van der Wiel[22], Leendert H. Oterdoom[23], Ilona Kerkhof[14], Maartje Bartelink[17], Leslie Noach[24], Daphne Hotho[19], Amar Levens[25], Bart van Hoek[3], Ynto de Boer[1], Joost PH Drenth[1]. *[1]Department of Gastroenterology and Hepatology, Amsterdam University Medical Centres, location VU Medical Centre, AGEM Research Institute, Amsterdam, Netherlands; [2]Department of Gastroenterology and Hepatology, Radboud University Medical Centre, European Reference Network RARE-LIVER, Nijmegen, Netherlands; [3]Department of Gastroenterology and Hepatology, Leiden University Medical Centre, Leiden, Netherlands; [4]Department of Gastroenterology and Hepatology, Amsterdam University Medical Centres, location VU Medical Centre, Amsterdam, The Netherlands, Amsterdam, Netherlands; [5]Division of Gastroenterology and Hepatology, Department of Internal Medicine, Maastricht University Medical Centre, European Reference Network RARE-LIVER, Maastricht, Netherlands; [6]Department of Gastroenterology and Hepatology, St. Antonius Hospital, Nieuwegein, Netherlands; [7]Department of Gastroenterology and Hepatology, Jeroen Bosch Hospital's Hertogenbosch, Netherlands; [8]Department of Gastroenterology and Hepatology, Rijnstate Hospital, Arnhem, Netherlands; [9]Department of Gastroenterology and Hepatology, Elisabeth-Tweesteden Hospital, Tilburg, Netherlands; [10]Department of Gastroenterology and Hepatology, Antwerp University Hospital, European Reference Network RARE-LIVER, Edegem, Belgium; [11]Department of Gastroenterology and Hepatology, Groene Hart Hospital, Gouda, Netherlands; [12]Department of Gastroenterology and Hepatology, Erasmus University Medical Centre, Rotterdam, Netherlands; [13]Department of Gastroenterology and Hepatology, Rode Kruis Hospital, Beverwijk, Netherlands; [14]Department of Gastroenterology and Hepatology, St. Jansdal Hospital, Harderwijk, Netherlands; [15]Department of Gastroenterology and Hepatology, Spaarne Gasthuis, Haarlem, Netherlands; [16]Department of Gastroenterology and Hepatology, Hospital Bernhoven, Uden, Netherlands; [17]Department of Gastroenterology and Hepatology, Deventer Hospital, Deventer, Netherlands; [18]Department of Gastroenterology and Hepatology, IJselland Hospital, Capelle aan den Ijssel, Netherlands; [19]Department of Gastroenterology and Hepatology, University Medical Center Groningen, Groningen, Netherlands; [20]Department of Gastroenterology and Hepatology, Medisch Spectrum Twente, Enschede, Netherlands; [21]Department of Gastroenterology and Hepatology, Slingeland Hospital, Doetinchem, Netherlands; [22]Department of Gastroenterology and Hepatology, Reinier de Graaf Gasthuis, Delft, Netherlands; [23]Department of Gastroenterology and Hepatology, Haga Hospital, Den Haag, Netherlands; [24]Department of Gastroenterology and Hepatology, Amstelland Hospital, Amstelveen, Netherlands; [25]Department of Clinical Pharmacy and Toxicology, Leiden University Medical Centre, Leiden, Netherlands*
Email: c.d.slooter@amsterdamumc.nl

Background and aims: The CAMARO trial demonstrated that response rates and tolerability of 24-weeks treatment with mycophenolate mofetil (MMF) plus prednisolone in treatment-naïve autoimmune hepatitis (AIH) resulted in better tolerability and a higher response rate in comparison to azathioprine (AZA) plus prednisolone. We aimed to compare long-term tolerability and maintenance of response in both arms.
Method: We analyzed patients enrolled in the CAMARO trial, a 24-week multicenter randomized controlled trial comparing AZA with MMF, both combined with prednisolone, in treatment-naïve autoimmune hepatitis. Follow-up data were retrospectively collected until October 1, 2025 or the last outpatient visit, allowing up to 3 years of follow-up. The primary endpoint was continued treatment with the randomized study drug with normalization of ALT and/or AST according to local reference ranges.
Results: Three-year follow-up was achieved by 65 patients (93%; 30 AZA, 35 MMF; median follow-up 4.4 years). After 3 years, 53% of patients had continued randomized treatment with normal transaminases in the AZA group compared to 77% in the MMF group ($p = 0.04$). Discontinuation between 24 weeks and 3 years occurred in 21% in both groups (AZA 5/24; MMF 8/38), with intolerance responsible for two discontinuations in each group. Two MMF-treated patients achieved sustained remission and successfully stopped AIH therapy. Among patients without normal transaminases at 24 weeks, on-treatment normalization by 3 years occurred in 6/12 (AZA) and 7/15 (MMF). Median time to biochemical remission was shorter with MMF than with AZA (13 vs 60 weeks; $p < 0.05$). This was confirmed in a sensitivity analysis censoring patients at discontinuation of randomized therapy and in a 4-week landmark analysis to mitigate the influence of prednisolone. No significant differences were observed between AZA and MMF with respect to loss of response (1/12 vs 1/22 of patient with on-treatment normalization at 24 weeks), 3-year steroid-free response rates (54% vs 51%), or median time to prednisolone discontinuation (78 vs 90 weeks) ($p > 0.05$ for all).
Conclusion: MMF was associated with a higher proportion of patients with 3-year on-treatment transaminase normalization and a shorter time to biochemical remission compared to AZA. Among patients who remained on treatment at 24 weeks, with or without response, both AZA and MMF could be safely continued with comparable clinical efficacy. In treatment-naïve AIH, MMF may be considered a first-line maintenance therapy.

OS-010

Management of patients with primary biliary cholangitis in the post-obeticholic era: real-world effectiveness data on elafibranor and seladelpar from the ColHai registry

Alvaro Diaz-Gonzalez[1], Cristina Montón[2], Marina Brosell[2], Agustin Castiella[3], Silvia Torrente[3], Montserrat Garcia-Retortillo[4], Ares Villagrasa[5], Mar Riveiro Barciela[5], Elena Gómez-Domínguez[6], Ana Arencibia Almeida[7], María Del Barrio[1], Helena Hernández Evole[8], Sergio Rodriguez-Tajes[8], Alberto Monescillo[9], Miren Garcia Cortes[10], Juan Pedro Toro Ortiz[10], Jose Manuel Sousa-Martin[11], Javier Ampuero Herrojo[11], Adolfo Gallego Moya[12], Francisca Cuenca Alarcón[13], Marta Casado-Martin[14], Alejandro Rodríguez Mateu[14], Manuel Hernández-Guerra[15], María Pilar Rios[16], Indhira Perez Medrano[17], Raisa Quiñones[18], Laura Alcoba Vega[18], Ismael El Hajra Martínez[19], Vanesa Bernal[20], Eva Fernandez Bonilla[20], Conrado Fernandez-Rodriguez[21], Isabel Conde[22], Raquel Diaz[23], Marina Vidal[23], Berta Lapeña[24], Gema De la Cruz[25], Inmaculada Castello[26], Natalia García Gimeno[27], Magdalena Salcedo Plaza[28], Ainhoa Fernández-Yunquera[28], Margarita Sala Llinás[29], Miguel Fernández-Bermejo[30], Mireia Trias[31], Beatriz Mateos Muñoz[32], María Dolores Antón Conejero[33], Raquel Ríos León[34], Eva Dueñas-Sánchez[35], Janire Prieto[36], Mercedes Vergara[37], María Carlota Londoño[8]. *[1]Gastroenterology and Hepatology Department, Clinical and Translational Research in Digestive Diseases Group, Marqués de Valdecilla University Hospital, Santander, Spain, Research Institute Marques de Valdecilla (IDIVAL), Clinical and Traslational Research in Digestive Pathology Group, Santander, Spain, Santander, Spain; [2]Hospital Clínico Universitario de Valencia, Valencia, Spain; [3]Hospital Universitario de Donostia, San Sebastián, Spain; [4]Sección de Hepatología, Servicio de Digestivo, Hospital del Mar. Institut de Recerca Hospital del Mar, Barcelona, Spain; [5]Liver Unit, Internal Medicine Department, Hospital Universitari Vall d'Hebron, Vall d'Hebron Barcelona Hospital Campus, Barcelona, Spain; Universitat Autònoma de Barcelona, Spain; Centro de Investigación Biomédica en Red de Enfermedades Hepáticas y Digestivas (CIBERehd), Instituto de Salud Carlos III, Madrid, Spain; European Reference Network on Hepatological Diseases (ERN RARE-LIVER), Barcelona, Spain; [6]Servicio de Aparato Digestivo. Hospital Universitario 12 de Octubre. Madrid, España, Madrid, Spain; [7]Sección de Hepatología. Servicio de Aparato Digestivo. Hospital Universitario Nuestra Señora de la Candelaria, Santa Cruz de Tenerife, Spain; [8]Servicio de Hepatologia, Hospital Clinic Barcelona, Fundació Clinic Barcelona, Fundació de Recerca Clínic Barcelona-Institut d'Investigacions Biomèdiques August Pi i Sunyer (FRCB-IDIBAPS), Universitat de Barcelona, Centro de investigación biomédica en red Enfermedades Hepáticas y Digestivas (CIBEREHD), Barcelona, España, Barcelona, Spain; [9]Hospital Universitario Insular de Gran Canaria, Gran Canaria, Spain; [10]Unidad de Gestión Clínica de Aparato Digestivo del Hospital Universitario Virgen de La Victoria de Málaga. IBIMA-plataforma Bionand, Universidad de Málaga. CIBERehd, Málaga, Spain; [11]Hospital Universitario Virgen del Rocío, Sevilla, Spain; [12]Hospital Universitari Sant Pau, Barcelona, Spain; [13]Unidad de Hígado. Servicio de Aparato Digestivo Hospital Clínico San Carlos, Madrid, Spain; [14]Hospital Universitario Torrecárdenas, Almería, Spain; [15]Servicio de Aparato Digestivo. Hospital Universitario de Canarias. La Laguna, España., Santa Cruz de Tenerife, Spain; [16]Hospital Arnau de Vilanova de Valencia, Valencia, Spain; [17]Unidad de Hepatología. Complexo Hospitalario Universitario de Pontevedra. Instituto de Investigación Sanitaria Galicia Sur (IISGS)., Pontevedra, Spain; [18]Complejo Asistencial Universitario de León, León, Spain; [19]Hospital Universitario Puerta de Hierro de Majadahonda, Madrid, Spain; [20]Hospital Universitario Miguel Servet, Zaragoza, Spain; [21]Hospital Universitario Fundación de Alcorcón, Madrid, Spain; [22]Hepatology and Liver Transplantation Unit, Hospital Universitario y Politécnico La Fe, IIS La Fe, Valencia, Spain. Ciberehd, ISCIII, Madrid, Spain, Valencia, Spain; [23]Hospital Universitario Infanta Sofía, Madrid, Spain; [24]Servicio de Aparato Digestivo. Hospital Universitario San Pedro, Logroño, Logroño, Spain; [25]Hospital Universitario de Toledo, Toledo, Spain; [26]Hospital General Universitario de Valencia, Valencia, Spain; [27]Hospital de Manises, Manises, Spain; [28]Hospital General Universitario Gregorio Marañón, Madrid, Spain; [29]Unidad Hepatología. Servicio Digestivo. Hospital Universitario Doctor Josep Trueta. IDIBGI. Girona. CIBEREHD, Girona, Spain; [30]Hospital Universitario de Cáceres, Cáceres, Spain; [31]Hospital Universitari de Mataró, Mataró, Spain; [32]Servicio de Aparato Digestivo. Hospital Universitario Ramón y Cajal, CIBERehd, IRYCIS, Madrid, Madrid, Spain; [33]Hospital Universitario Doctor Peset, Valencia, Spain; [34]Hospital Universitario General de Villalba, Villalba, Spain; [35]Hospital de Viladecans, Viladecans, Spain; [36]Gastroenterología y Hepatología, Hospital de Urduliz Alfredo Espinosa, Vizcaya Departamento de Medicina, Universidad del País Vasco UPV/EHU, Bilbao, Spain; [37]Unidad de Hepatología, Servicio de Digestivo, Parc Taulí Sabadell Hospital Universitari, Institut d'Investigació i Innovació Parc Taulí (I3PT-CERCA), Universitat Autónoma de Barcelona. CIBERehd, Sabadell, Spain*
Email: mlondono@clinic.cat

Background and aims: Obeticholic acid (OCA) withdrawal and approval of new drugs have represented a major shift in the management of patients with PBC. We evaluated the impact of these changes and the early use and effectiveness of elafibranor (ELA) and seladelpar (SEL).

Method: This was a retrospective analysis of 529 patients with PBC across 37 centres from the Spanish ColHai registry. Continuous data are presented as medians and interquartile ranges.

Results: Patients were mostly female (91%) with a median age of 60 years (51.4–67.9), median ALP 1.5 × ULN (1.1–2.1), GGT 1.9 × ULN (0.9–5), AST 1.03 × ULN (0.8–1.4), ALT 0.8 × ULN (0.5–1.3), and bilirubin of 0.6 × ULN (0.4–0.9), 20% had cirrhosis, 20% were on ursodeoxycholic acid (UDCA) monotherapy, 39% on OCA + UDCA, 13% on bezafibrate (BZF) + UDCA, 26% on OCA + UDCA + BZF, and 2% were UDCA intolerant. Follow-up data were available for 317 patients (60%) at month 1, 258 patients (49%) at month 3, and 102 patients (19%) at month 6. Aggregated response data consider the last available follow-up per patient. ELA was administered to 115 patients, with median ALP reduction from baseline of –24% (–38 to –1) at month 1, –24% (–35 to 2) at month 3, and –36% (–42 to –11) at month 6. Response rates by Paris-II and POISE were 42% and 53% in patients on UDCA monotherapy, 70% and 79% in those previously treated with OCA + UDCA, 37% and 47% in those on BZF, and 35% and 58% in those treated with OCA + UDCA + BZF, respectively. SEL was administered to 297 patients, with median ALP reduction of –19% (–34 to 0) at month 1, –26% (40 to –3) at month 3, and –33% (–47 to –2) at month 6. Response rates by Paris-II and POISE were 55% and 65% in patients on UDCA monotherapy, 59% and 69% previously treated with OCA+UDCA, 24% and 31% in those on BZF, and 41% and 56% in those treated with OCA+UDCA+BZF. Among patients previously treated with OCA+UDCA, 18 (10%) and 10 (6%) lost Paris II and POISE responses after OCA discontinuation. Similarly, 27 (23%) and 18 (15%) on OCA+UDCA+BZF lost Paris II and POISE responses after triple therapy discontinuation. Fatigue improved in 16 patients (39%) treated with ELA and 28 (28%) with SEL. Pruritus improved in 14 patients (47%) with ELA and 65 (64%) with SEL.

Conclusion: In this first real-world experience from the ColHai registry, ELA and SEL demonstrated clinically relevant reductions in ALP and early biochemical response in patients with PBC, even in those previously exposed to second-line therapies.

Liver tumours – experimental

OS-011

Germline alterations in the TRAIL apoptotic pathway predispose to hepatocellular adenoma through a benign tumor field effect and convergent somatic evolution

Jessica Zucman-Rossi[1], Louisa Stern[2], Sandrine Imbeaud[2], Shuoshuo Jin[2], Samantha Schaeffer[2], Carolin V. Schneider[3], Sabrine Sidali[2], Eric Trépo[4], Jean-Frédéric Blanc[5], Paulette Bioulac-Sage[5], Julien Calderaro[6], Alexis Laurent[6], Ephrem Salamé[7], Valérie Paradis[8], Catherine Guettier[9], Marianne Ziol[2], Alexandre Louvet[10], Philippe Labrune[11], Olivier Cussenot[12], Emmanuelle Genin[13], Pierre Laurent-Puig[2], Théo Hirsch[2], Jean-Charles Nault[2]. *[1]Université Paris Cité, Paris, France; [2]Centre de Recherche des Cordeliers, PARIS, France; [3]RWTH Aachen University, Aachen, Germany; [4]Université Libre de Bruxelles, Brussel, Belgium; [5]CHU De Bordeaux, Lormont, France; [6]Urgences Hôpital Henri Mondor, Créteil, France; [7]Centre Hosp Régional Universitaire Tours, Loches, France; [8]Beaujon, Clichy, France; [9]Hôpital Bicêtre, Le Kremlin-Bicêtre, France; [10]Hôpital Fourrier- Chu De Lille, Lille, France; [11]Assistance Publique hopitaux de paris, Clamar, France; [12]Assistance publique hopitaux de paris, PARIS, France; [13]inserm, brest, France*
Email: sandrine.imbeaud@inserm.fr

Background and aims: Hepatocellular adenomas (HCA) are rare benign liver tumors whose genetic predisposition remains largely unexplained outside a few monogenic conditions. We aimed to identify inherited genetic factors predisposing to HCA and to determine how germline variation interacts with somatic evolution and environmental risk factors.
Method: We analyzed 669 unrelated HCA patients recruited across multiple European centers using an integrative approach that combined genome-wide association study (GWAS), exome-wide rare-variant burden analyses (ExWAS), and multi-omics profiling. Germline data were compared to large population reference cohorts. Somatic mutations, transcriptomes, and clonal architectures were characterized in 664 tumors from 561 patients using whole-exome sequencing, RNA sequencing, and targeted analyses. Non-tumor liver transcriptomes were analyzed to assess functional consequences of germline variants.
Results: We identified germline alterations in four genes of the TRAIL apoptotic pathway (*TNFSF10*, *TNFRSF10A*, *TNFRSF10B*, and *CASP8*) as the most frequent genetic predisposition to HCA, present in approximately 25% of patients. This architecture combined a common regulatory TNFSF10 risk allele with multiple rare loss-of-function variants, highlighting polygenic and allelic heterogeneity. TRAIL germline variants were strongly associated with the development of multiple adenomas, particularly HNF1A-inactivated HCA, despite shorter exposure to oral contraceptives. Integrated somatic analyses revealed a striking convergent selection of independent HNF1A inactivating mutations across multiple tumors within the same individuals, consistent with a benign tumor field effect. Transcriptomic profiling of non-tumor liver tissue from TRAIL variant carriers showed dysregulation of apoptosis-related pathways, hepatic metabolism, estrogen signaling, and circadian regulators, indicating that germline TRAIL deficiency reprograms the hepatic environment prior to tumor initiation.
Conclusion: Germline impairment of the TRAIL apoptotic pathway represents a major genetic predisposition to HCA and drives benign tumorigenesis through a field effect that biases somatic evolution toward HNF1A inactivation. These findings redefine the role of apoptosis in benign liver tumor development and highlight germline-somatic interplay as a key determinant of tumor multiplicity and subtype selection.

OS-012

In vitro identification of immunogenic tumoral antigens in advanced hepatocellular carcinoma reveals new opportunities for therapeutic applications

Frederik Peeters[1], Orian Bricard[2], Razgar Seyed Rahmani[2], Jieyi Xiong[2], Gino Philips[2], Evy Vanderheyden[2], Thomas Van Brussel[2], Rogier Schepers[2], Sarah Cappuyns[1], Chris Verslype[1,3], Diether Lambrechts[2], Jeroen Dekervel[1]. *[1]Department of Digestive Oncology, UZ Leuven, Leuven, Belgium; [2]Laboratory for Translational Genetics, Center for Cancer Biology, VIB, Leuven, Belgium; [3]KU Leuven, Oncology, Leuven, Belgium*
Email: frederik.peeters@hotmail.com

Background and aims: The antigenic landscape underlying the antitumor immune response remains poorly characterized. Existing methods for antigen identification or prediction are limited in accuracy, often restricted to exonic mutations, and frequently lack experimental validation of immunogenicity. Systematic identification of tumoral antigens is critical for the development of novel immunotherapy strategies in advanced HCC (aHCC). We aimed to map the antigenic repertoire in aHCC using a novel unbiased, transcriptome-wide approach which includes functional validation.
Method: Pre-treatment and on-treatment tumor biopsies were obtained from a patient with aHCC who achieved a complete pathological response following treatment with durvalumab plus tremelimumab. By applying single-cell RNA and T-cell receptor (TCR) sequencing, we identified the TCRs of the 12 most expanded CD8+ T-cell clones in each tissue sample. After excluding duplicate TCRs between timepoints, 19 patient-specific, potentially tumor-antigen directed TCRs were selected. Each TCR was transfected in a T cell line and cocultured with an HLA matched antigen-presenting cell (APC) line expressing the patient-specific tumor transcriptome library. Clusters of APCs with activated T cells were isolated, expanded and the antigenic sequence incorporated in the APC was retrieved by sanger sequencing.
Results: We identified a tumoral antigenic sequence for 10 out of 19 TCRs analyzed. Only 2 of the antigens were based on a mutation, whereas the others represented the reactivation of a novel cancer-testis antigen, overexpressed genes and alternative open reading frames. Expression of several of the detected antigens identified in this patient was also detected in tumors from other HCC patients and across other tumor types within the TCGA dataset, indicating the presence of shared tumor antigens between cancer patients. Remarkably, 4 different TCRs were found to recognize the same antigen. For 9 out of 10 TCRs with an identified tumoral antigen, the corresponding T cell clonotype was detected in the tumor biopsy prior to immune checkpoint inhibition (ICI), indicating an ongoing immune response against these antigens before ICI.
Conclusion: Using a novel antigen detection platform, we confirmed that diverse genomic alterations, ranging from exonic mutations to events in the dark genome, can give rise to immunogenic antigens capable of eliciting T-cell responses. The identification of shared tumoral antigens opens new opportunities for therapeutic applications.

OS-013

Epigenetic control of MASH-driven hepatocarcinogenesisby the histone methyltransferase G9a

Ainara Irigaray-Miramon[1], Amaya Lopez-Pascual[2], Borja Castello[1], Roberto Barbero[3], Elena Adan-Villaescusa[1], Jasmin Elurbide-Tardio[3], Emiliana Valbuena-Goiricelaya[1], Maria U Latasa[1], Iker Uriarte[3], Maialen Lizasoain[1], Miriam Belzunce[1], Pedro Rodrigues[4], Maria Arechederra[5], Bruno Sangro[6], Carmen Berasain[3], Matías A Avila[1], Maite G Fernandez-Barrena[5]. *[1]Hepatology Laboratory, Solid Tumors Program, CIMA, CCUN, University of Navarra, Pamplona, Spain; [2]Hepatology Unit, CCUN, Navarra University Clinic, Instituto de Investigaciones Sanitarias de Navarra IdiSNA, Pamplona, Spain; [3]Hepatology Laboratory, Solid Tumors Program, CIMA, CCUN, University*

of Navarra, CIBERehd, Instituto de Salud Carlos III, Pamplona, Spain; [4]Department of Liver and Gastrointestinal Diseases, Biodonostia Health Research Institute - Donostia University Hospital, University of the Basque Country (UPV/EHU), San Sebastian, Spain; [5]Hepatology Laboratory, Solid Tumors Program, CIMA, CCUN, University of Navarra, CIBERehd, Instituto de Salud Carlos III, Instituto de Investigaciones Sanitarias de Navarra IdiSNA, Pamplona, Spain; [6]Hepatology Unit, CCUN, Navarra University Clinic, CIBERehd, Instituto de Salud Carlos III, Instituto de Investigaciones Sanitarias de Navarra IdiSNA, Pamplona, Spain
Email: magarfer@unav.es

Background and aims: Metabolic dysfunction–associated steatotic liver disease (MASLD) is the most prevalent chronic liver disease worldwide and a growing global health burden. However, the molecular mechanisms driving progression from simple steatosis to steatohepatitis (MASH) and hepatocellular carcinoma (HCC) remain incompletely understood. Epigenetic regulators have emerged as critical mediators of this transition. The histone methyltransferase G9a (EHMT2) has been implicated in hepatocarcinogenesis, but its role in metabolically driven HCC remains unclear. This study aimed to define the hepatocyte-specific contribution of G9a to HCC development in a metabolic inflammatory context.
Method: Wild-type (WT) and hepatocyte-specific G9a knockout (G9aΔhepKO) mice were subjected to a Western diet combined with CCl_4 for 26 weeks, recapitulating key features of MASH-associated HCC. Liver injury, fibrosis, tumor burden, and metabolic alterations were assessed using biochemical, histological, transcriptomic, proteomic, and metabolomic approaches. In parallel, primary hepatocytes from both genotypes were exposed to lipogenic and inflammatory stimuli to model MASH in vitro.
Results: WT mice developed multiple HCC nodules, whereas G9aΔhepKO mice exhibited a marked reduction in tumor incidence and burden. Loss of hepatocytic G9a significantly attenuated fibrosis and induced profound metabolic remodeling, particularly affecting lipid and amino acid metabolism. Multi-omics integration revealed suppression of tumor-promoting, fibrogenic, and mitotic pathways in G9a-deficient livers. Consistently, G9a-deficient hepatocytes failed to sustain the lipogenic and inflammatory programs characteristic of MASH progression in vitro. Notably, Ogdhl, a mitochondrial enzyme with tumor-suppressive properties, was identified as a direct epigenetic target of G9a. Ogdhl was strongly repressed in WT HCC-bearing livers but preserved upon G9a deletion, suggesting that maintenance of OGDHL expression contributes to disrupted tumor metabolic homeostasis.
Conclusion: These findings identify G9a as a central epigenetic driver of MASH-to-HCC progression. Hepatocyte-specific G9a deletion limits fibrosis and hepatocarcinogenesis while restoring metabolic balance, highlighting a critical link between epigenetic regulation and metabolic reprogramming in liver cancer. Targeting G9a may therefore represent a promising therapeutic strategy for metabolically driven HCC.

OS-014-YI

The evolving heterogeneity of intrahepatic cholangiocarcinoma: clonal dynamics, spatial archetypes, and therapeutic opportunities

Claudio Zampato[1], Paula Cantallops Vilà[1], Gemma Garcia Vicién[1], Laura Sererols Viñas[1], Carmen Cárcamo Giráldez[1], Marsela Karemani[2], Daniela Grases[3], Roser Pinyol[4], Daniela Sia[5], Robert F. Schwabe[6], Anna Moles[7], Josep M Llovet[8], Eduard Porta-Pardo[9], Silvia Affo[1]. *[1]Tumor Microenvironment Plasticity and Heterogeneity Research Group, Institut d'Investigacions Biomediques August Pi i Sunyer (IDIBAPS), Barcelona, Spain; [2]Institut de Recerca Biomèdica de Lleida (IRBLleida), Lleida, Spain; [3]Josep Carreras Leukaemia Research Institute, Badalona, Spain; [4]Liver Cancer Translational Research Group, Liver Unit, Institut d'Investigacions Biomèdiques August Pi i Sunyer (IDIBAPS), Hospital Clinic, Universitat de Barcelona, Barcelona, Spain; [5]Mount Sinai Liver Cancer Program, Divisions of Liver Diseases, Department of Medicine, Tisch Cancer Institute, Icahn School of Medicine at Mount Sinai, New York, United States; [6]Columbia University, New York, United States; [7]Institut d'Investigacions Biomèdiques de Barcelona (IIBB-CSIC), Barcelona, Spain; [8]Liver Cancer Translational Research Group, Liver Unit, Institut d'Investigacions Biomèdiques August Pi i Sunyer (IDIBAPS), Hospital Clinic, Universitat de Barcelona, Mount Sinai Liver Cancer Program, Divisions of Liver Diseases, Department of Medicine, Tisch Cancer Institute, Icahn School of Medicine at Mount Sinai, New York, NY, USA; Institució Catalana de Recerca i Estudis Avançats (ICREA), Barcelona, Spain, Barcelona, Spain; [9]Josep Carreras Leukaemia Research Institute (IJC), Barcelona Supercomputing Center (BSC), Barcelona, Spain, Badalona, Spain*
Email: zampato@recerca.clinic.cat

Background and aims: Intrahepatic cholangiocarcinoma (iCCA) is the second most common primary liver cancer, diagnosed at advanced stages and associated with poor prognosis. Its molecular and cellular heterogeneity complicates treatment and contributes to therapy resistance. Here, employing an integrative approach, we investigated structural vulnerabilities to guide innovative therapies for iCCA.
Method: R26R-Confetti mice were injected with AAV8-TBG-Cre for stochastic hepatocyte labelling, followed by iCCA induction via hydrodynamic injection of KRAS G12D/sg-p19 (n = 4) or YAP/AKT plasmids (n = 4). Three Confetti-derived tumor cell lines obtained from each model were used for bulk RNA-seq, CNV profiling, and drug testing. KRAS/p19 tumors (n = 4) and human iCCA (N = 4) underwent Visium CytAssist spatial transcriptomics (ST), integrated with bulk, using non-negative matrix factorization (NMF), and single-cell RNA-seq. CAF depletion was performed in Lrat-Cre iDTR (n = 4 Cre−, 6 Cre+) and aSMA-TK (n = 5 TK−, 8 TK+) mice, followed by spatial transcriptomic profiling using Xenium 5K ST.
Results: Confetti Cre-mediated recombination in hepatocytes enabled in vivo tumor clonal lineage tracing as confirmed by confocal microscopy in 2 iCCA models. Tumor clones showed transcriptomic and genomic heterogeneity and responded differently to Gem, Cis, and Gem/Cis in vitro. To investigate how this heterogeneity is organized and shaped within the TME, we integrated tumor clonal tracing, bulk and single-cell RNA sequencing with ST, unveiling 2 conserved spatial archetypes within each lesion. The core archetype, located in the central tumor area, correlated with tumor and dendritic cells, showed activation of MAPK, Hypoxia response, WNT and EGFR pathways, and was associated with the non-inflamed tumor classical STIM (stromal, tumor, immune microenvironment) class. The edging archetype, located at the tumor periphery, correlated with CAFs, T, B, NK, and macrophages, exhibited activation of TGF-B, PI3K, VEGF and Trail pathways, and was associated with the inflammatory stroma STIM class. Xenium ST revealed that CAF perturbation favored an edging archetype and inflammatory stroma STIM class in iCCA lesions, predicted to enhance immunotherapy response.
Conclusion: Using an integrative approach, we revealed conserved, yet dynamic archetypes shaped by the surrounding stroma, highlighting spatial engineering as a promising therapeutic strategy in iCCA.

OS-015

Personalized RNA-based tumor vaccines targeting neoantigens in hepatocellular carcinoma

Paul Schneider[1], Jenny Schunke[2], Nadja Salomon[2], Akili Özlem[2], Barbara Schroers[2], Mustafa Diken[2], Jörn M. Schattenberg[3], Leonard Kaps[1,3]. *[1]Department of Dermatology, University Medical Center, Mainz, Germany; [2]TRON – Translational Oncology at the University Medical Center of the Johannes Gutenberg University Mainz gGmbH, Mainz, Germany; [3]Department of Medicine II, University Medical Center, Homburg/Saar, Germany*
Email: leonardkaps@googlemail.com

Background and aims: Immune checkpoint inhibitors (ICI) that stimulate the immune system represent an effective therapeutic strategy for hepatocellular carcinoma (HCC). Beyond ICI, mRNA-based tumor vaccines targeting tumor-specific neoantigens (NA) derived from somatic mutations hold promise as a novel personalized immunotherapeutic approach. In this study, mRNA tumor vaccination targeting NA was evaluated in a clinically relevant HCC model.
Method: NA were identified from Dt81Hepa1–6 murine HCC cells via RNA sequencing and prioritized in silico using the VaxRank algorithm. Selected NA were encoded into pentatope mRNA constructs and formulated in lipoplex nanoparticles (LPX). HCC was induced in cirrhotic C57BL/6JrJ mice by CCl_4 gavage (6 weeks), followed by i.s. injection of Dt81Hepa1–6 cells. HCC mice (n = 15 per group) received i.v. vaccinations with NA-mRNA-loaded LPX (LPX:NA-mRNA) or control mRNA (LPX:CTRL) on days 7, 14, and 21 after tumor cell inoculation (TCI). Overall mortality was assessed in vaccinated HCC mice, including cohorts receiving additional murine anti-PD-L1 therapy.
Results: At sacrifice on day 28 after TCI, vaccination with LPX:NA-mRNA elicited a robust cellular immune response. FACS analysis of digested livers revealed a significant increase in total $CD4^+$ and $CD8^+$ T-cell frequencies (both $p < 0.0001$), accompanied by enhanced T-cell proliferation ($CD4^+Ki67^+$ and $CD8^+Ki67^+$, both $p < 0.0001$) and a marked expansion of effector $CD8^+$ T-cells ($CD62L^-CD44^+$, $p < 0.0001$). In parallel, regulatory T-cells ($CD25^+FoxP3^+$) were reduced compared with controls ($p < 0.001$). ELISPOT assays confirmed that splenic T-cells from LPX:NA-mRNA–vaccinated mice mounted strong NA-specific responses to synthetic NA peptides. LPX:NA-mRNA vaccination resulted in a significant reduction in tumor burden, as demonstrated by a decreased number of liver metastases, lower AFP levels, and a reduced tumor area determined by morphometric analysis of H&E-stained liver sections (all $p < 0.05$). During the 56-day follow-up after TCI, mortality was lowest in mice treated with combined LPX:NA-mRNA vaccination and ICI (3/11 deaths), intermediate in LPX:NA-mRNA monotherapy (5/11) and LPX:CTRL plus ICI (6/11), and highest in the LPX:CTRL placebo group (11/12). Treatment was well tolerated without evidence of acute toxicity.
Conclusion: NA-targeted mRNA vaccination was well tolerated and induced a robust tumor-specific T-cell–mediated antitumor response in cirrhotic HCC mice. Combination with ICI further improved overall mortality.

MASLD: Clinical and therapeutical aspects I

OS-016

Week 48 top-line results from the phase 2b, multicenter, randomized, placebo-controlled IMPACT trial of pemvidutide in metabolic dysfunction-associated steatohepatitis

Mazen Noureddin[1], Naim Alkhouri[2], Stephen A. Harrison[2], Rohit Loomba[3], Naga Chalasani[4], Shaheen Tomah[5], Julio Gutierrez[5], John Suschak[5], M. Scot Roberts[5], Rachel Garner[5], Sarah Browne[5], Christophe Arbet-Engels[5], M. Scott Harris[5]. *[1]Houston Methodist Hospital, Houston Research Institute, Pinnacle Clinical Research, Houston, TX, United States; [2]Summit Clinical Research, Clinical Research Institute of Ohio, San Antonio, TX, United States; [3]MASLD Research Center, Division of Gastroenterology and Hepatology, University of California at San Diego, San Diego, CA, United States; [4]Indiana University School of Medicine, Indianapolis, IN, United States; [5]Altimmune, Inc, Gaithersburg, MD, United States*
Email: noureddinmd@pinnacleresearch.com

Background and aims: Pemvidutide is a balanced 1:1 glucagon/GLP-1 dual receptor agonist in development for the treatment of metabolic dysfunction-associated steatohepatitis (MASH). IMPACT was a phase 2b, randomized, placebo-controlled, double-blind trial in patients with biopsy-confirmed MASH and fibrosis stage F2 or F3 (NCT05989711). At 24 weeks, pemvidutide treatment showed statistically significant histologic MASH resolution and high rates of fibrosis improvement. Here we present the 48-week endpoints, including non-invasive tests (NITs), weight loss, and safety.
Method: 212 patients were randomized 1:2:2 to receive once-weekly subcutaneous pemvidutide (1.2 mg or 1.8 mg) administered without dose titration, or placebo. Week 48 read outs included NITs of liver fat content (LFC), hepatic inflammation [corrected T1 (cT1), alanine aminotransferase (ALT)] and fibrosis [ELF, liver stiffness measurement (LSM) by FibroScan®], and weight loss. There was no histological assessment at week 48.
Results: The mean age was 53 years, the mean BMI was 39 kg/m^2, 58% were female, and 43% had type 2 diabetes. At week 48, pemvidutide treatment resulted in LFC changes of −45.2% ($p < 0.0001$), −54.7% ($p < 0.0001$), and −8.2% in the 1.2 mg, 1.8 mg, and placebo groups. Mean changes in cT1 relaxation time in the 1.2 mg, 1.8 mg, and placebo groups were −124 ms ($p < 0.0001$), −140 ms ($p < 0.0001$), and −21 ms. A greater proportion of patients treated with pemvidutide achieved a ≥ 30% reduction in LSM than placebo [1.2 mg (61.1%; $p < 0.0001$), 1.8 mg (63.9%; $p < 0.0001$), placebo (21.2%)]. ELF score changes of −0.49 ($p < 0.0001$), −0.58 ($p < 0.0001$), and +0.16 occurred in the 1.2 mg, 1.8 mg, and placebo groups. A greater proportion of patients receiving pemvidutide achieved concurrent responses in ELF score (≥ 0.5 reduction) and LSM (≥ 30% reduction) compared to placebo [1.2 mg (27.8%; $p = 0.0003$); 1.8 mg (32.4%; $p < 0.0001$); placebo (3.2%)]. The changes in ALT were −37.8 IU/L ($p < 0.0001$), −37.4 IU/L ($p < 0.0001$), and −10.3 IU/L in the 1.2 mg, 1.8 mg, and placebo groups. Mean weight loss in the 1.2 mg, 1.8 mg, and placebo groups was 4.5% ($p < 0.0001$), 7.5% ($p < 0.0001$), and 0.2%. Pemvidutide was well-tolerated with discontinuations due to adverse events of 0%, 1.2%, and 3.5% in the 1.2 mg, 1.8 mg, and placebo groups.
Conclusion: Treatment led to significant, dose-dependent reductions in NITs of MASH inflammation and fibrosis, as well as clinically meaningful weight loss at week 48.

OS-017

CAP-LS-ALT3+ and 4 scores for the prediction of MASLD-related liver related events: a derivation and global validation study

Hye Won Lee[1], Seung Up Kim[1], Terry Cheuk-Fung Yip[2], Vincent Wai-Sun Wong[2]. *[1]Yonsei University College of Medicine, Seoul, Korea, Rep. of South; [2]The Chinese University of Hong Kong, HK, Hong Kong*
Email: ksukorea@yuhs.ac

Background and aims: Fibrosis drives adverse outcomes in metabolic dysfunction–associated steatotic liver disease (MASLD). We developed and validated two open probability scores—CLA3+ (≥F3) and CLA4 (F4)—from controlled attenuation parameter (CAP) and liver stiffness (LS) by vibration-controlled transient elastography (VCTE) and alanine aminotransferase (ALT).
Method: In a multinational cohort of 16 tertiary centers, single-term fractional-polynomial logistic models produced CLA3+/CLA4 probabilities. Prognosis for liver-related events (LREs) was assessed using time-dependent area under receiver operating characteristic curve (AUROC), Brier score, integrated discrimination improvement (IDI), and serial-change analyses. Clinical implementation was evaluated with two-step pathways (FIB-4→CLA3+ for ≥F3; FIB-4→CLA4 for F4).
Results: The derivation cohort included 2,811 patients with liver biopsy. The validation cohort included 11,196 patients with baseline LS, among whom 8,046 had serial LS. Derivation AUROCs were 0.84 (CLA3+) and 0.89 (CLA4). In validation, both achieved the highest integrated AUROC (0.83) with lowest integrated Brier scores (0.0078–0.0081) across comparators for predicting LREs. CLA3+ classified 83.1%/10.8%/6.1% as low/intermediate/high risk (5-year LRE 0.4%/1.5%/11.8%; sensitivity of low-risk cut-off 0.72), and CLA4 92.0%/3.6%/

4.4% (0.5%/4.7%/13.0%; specificity of high-risk cut-off 0.93), achieving the smallest intermediate zone. IDI favored CLA3+ over Agile3+ (+0.013 at 3 years; +0.021 at 5 years), while CLA4 matched Agile4. Serially, categories were stable (86.7% CLA3+; 93.2% CLA4), and ≥10–30% decreases predicted lower subsequent LRE risk. In two-step testing, intermediates were minimized (FIB-4→CLA 3 + 3.9%; FIB-4→CLA4 1.4%) while achieving the highest rule-in enrichment (8.3% 5-year LRE).
Conclusion: CLA3+ and CLA4 generate interpretable, high-performing probabilities from CAP, LS, and ALT, with small indeterminate zones and actionable serial dynamics, and are clinically deployable as second-line tests within FIB-4–based two-step pathways.

OS-018
Hepatic transcriptomic signatures reveal mechanistic insights underlying improved metabolic dysfunction–associated steatohepatitis histology with survodutide, a glucagon/glucagon-like peptide-1 receptor dual agonist, in a phase 2 trial
Raphael Hesse[1], Panagiotis Papavasileiou[2], Ahmad Alhussein[3], Renee Marshall[4], Elena Startseva[3], Ramy Younes[3], Amalia Gastaldelli[5], Arun J. Sanyal[6], Corinna Schoelch[1]. *[1]Boehringer Ingelheim Pharma GmbH & Co. KG, Biberach, Germany; [2]Boehringer Ingelheim Pharma GmbH & Co. KG, Ingelheim, Germany; [3]Boehringer Ingelheim International GmbH, Ingelheim, Germany; [4]Boehringer Ingelheim Pharmaceuticals, Inc., Ridgefield, Connecticut, United States; [5]Cardiometabolic Risk Unit, CNR Institute of Clinical Physiology, Pisa, Italy; [6]Virginia Commonwealth University, School of Medicine, Richmond, Virginia, United States*
Email: raphael.hesse@boehringer-ingelheim.com

Background and aims: Survodutide is a glucagon receptor (GCGR)/glucagon-like peptide-1 receptor (GLP-1R) dual agonist in phase 3 clinical development for the treatment of obesity, and metabolic dysfunction-associated steatohepatitis (MASH). We present data from a prespecified transcriptome analysis from baseline (BL) and W48 liver tissue samples from a phase 2 trial in people with MASH (NCT04771273). The aim was to investigate liver specific on-treatment changes on therapeutic responses to survodutide.
Method: 293 participants received ≥1 dose of survodutide or placebo. Liver biopsy samples were obtained from trial participants at visit 1 and W48. Following ribonucleic acid (RNA) extraction libraries were prepared and sequenced on a NovaSeq sequencer. The sequencing reads were processed with a Boehringer Ingelheim internal pipeline, building upon the implementation of the ENCODE "Long RNA-seq" pipeline followed by differential expression analysis with limma/voom. Pathway analyses were performed using GSEA, ssGSEA and IPA with REACTOME canonical pathways and curated gene sets from the literature.
Results: Biopsy samples that passed QC were available from 48 patients (10 Placebo/38 survodutide). Transcriptomic profiling revealed activation of GCGR signalling in liver tissue following survodutide treatment. Compared with baseline, several genes associated with fibrosis and inflammation, including those involved in TGFB1-, IL4-, and IL13-mediated pathways, were significantly downregulated. Notably, expression of LOXL1, LAMB1, MMP9, PLEC, TGFB1, and multiple collagen genes decreased upon treatment. Gene Set Enrichment Analysis indicated that cellular pathways involved in tissue remodelling, fibrosis, and inflammation were suppressed, while Ingenuity Pathway Analysis suggested that survodutide may mitigate fibrosis progression by limiting hepatic stellate cells migration, preserving hepatocytes, and supporting regeneration. TGFB1 and FOXA2 were identified as potential upstream regulators of these effects.
Conclusion: We present a comprehensive transcriptome analysis by next-generation sequencing from liver biopsies collected in a phase 2 clinical trial with the GCGR/GLP-1R dual agonist survodutide. The observed modulation of liver mRNA expression known to be regulated in fibrotic-and inflammatory processes provide a mechanistic basis for the improvement in fibrosis and supports the biological plausibility that survodutide reduces hepatic inflammation and fibrogenesis.

OS-019
Utility of noninvasive criteria based on vibration controlled transient elastography and enhanced liver fibrosis test in identifying patients with high-risk MASLD
Naim Alkhouri[1], Elizabeth Brombosz[1], Grazina Binkauskiene[1], Winston Dunn[2], Rashmee Patil[1], Rohit Puskoor[1], John Poulos[3], Alma Laura Ladrón de Guevara[4], Vlad Ratziu[5], Marcelo Kugelmas[6], Juan Pablo Arab[7], Meena Bansal[8], Jörn M. Schattenberg[9], Mazen Noureddin[1]. *[1]Summit Clinical Research, San Antonio, United States; [2]University of Kansas, Kansas City, United States; [3]Coastal Research Institute, Fayetteville, NC, United States; [4]CENTRO DE INVESTIGACION Y GASTROENTEROLOGIA, Mexico City, Mexico; [5]Sorbonne University, Paris, France; [6]South Denver Gastroenterology, Denver, United States; [7]Virginia Commonwealth, Richmond, United States; [8]Mount Sinai, New York, United States; [9]Saarland University, Saarbrücken, Germany*
Email: naim.alkhouri@gmail.com

Background and aims: Histologic endpoints in MASH trials have several limitations including the invasive nature of liver biopsy, variability in pathologists' interpretation, and the fact that full regulatory approval still requires improvement in clinical outcomes. Therefore, new criteria based on noninvasive tests (NITs) have been proposed to identify patients with high-risk MASLD that are at the highest risk for progression to cirrhosis and major adverse liver outcomes (MALO). One proposed set of cutoffs for identifying these patients is the combination of LSM 10–20 kPa and ELF 9–10.8. This study aimed to evaluate the efficacy of these criteria in identifying subjects with high-risk MASLD in a multicenter database using fibrosis stage on biopsy as the gold standard.
Method: Patients with LSM, ELF, and available biopsy data were identified from a multicenter database of screening and baseline data from 12 MASH clinical trials. Patients that met LSM 10–20 kPa + ELF 9–10.8 criteria were further analyzed based on fibrosis stage and stratified into F0-F2 vs F3/F4, with F3/F4 individuals at the highest risk of MALO and those with F3 at the highest risk of progression to cirrhosis.
Results: 4,188 patients had liver biopsy, LSM and ELF available (8.0% with F0 on biopsy, 17.3% F1, 25.6.% F2, 23.7% F3, and 25.5% F4). Importantly, the LSM 10–20 kPa + ELF 9–10.8 criteria were met in 18.0% of F0 patients, 23.2% of F1, 33.6% of F2, 41.7% of F3, and 34.7% of F4 patients. Out of 1373 patients that met the LSM and ELF cutoffs and had liver biopsy data available, only 57% (784) had F3/F4, while 43% (589) had F0-F2, including 60 (10%) patients with F0 and 168 (29%) with F1. Patients with F0-F1 that met the LSM and ELF cutoffs were older, more likely to be diabetics, and had higher AST, AST/ALT ratio, HbA1C, and FIB4 index compared to those with F0-F1 that did not meet the criteria.
Conclusion: Using cutoffs of LSM 10–20 kPa and ELF 9–10.8 may overestimate the likelihood of developing cirrhosis and MALO in patients with no evidence of significant fibrosis on liver biopsy. Patients with F0-F1 that met the LSM and ELF criteria were older, more likely to be diabetics, with higher FIB4. More strict criteria are potentially needed in this population to increase the likelihood of identifying high-risk MASLD.

OS-020

Effect of empagliflozin alone or combined with low-dose semaglutide on metabolic dysfunction-associated steatohepatitis and type 2 diabetes – a histology-based randomized, placebo-controlled, double-blind phase 4 trial (COMBAT_T2_NASH)

Sabine Kahl[1], Georgia Xourafa[1], Angela Härtel[2], Berthold Amann[2], Ulrich Dischinger[3], Andreas Geier[3], Katharina Laubner[4], Jochen Seufert[4], Astrid Lerner[5], Ingolf Schiefke[6], Zoltan Kender[7], Stefan Kopf[7], Julia Szendrödi[7], Christian Herder[1], Andrea Tura[8], Birgit Knebel[1], Uta Drebber[9], Andrea Tannapfel[10], Vlad Ratziu[11], Kenneth Cusi[12], Andreas Birkenfeld[13], Martin Hrabe de Angelis[14], Annette Schürmann[15], Michele Solimena[16], Michael Roden[1]. *[1]German Diabetes Center, German Center for Diabetes Research, Duesseldorf, Germany; [2]Franziskuskrankenhaus Berlin, Berlin, Germany; [3]University Hospital Wuerzburg, Wuerzburg, Germany; [4]University Hospital Freiburg, Freiburg, Germany; [5]Eugastro GmbH, Leipzig, Germany; [6]Klinikum St. Georg gGmbH, Leipzig, Germany; [7]University Clinics Heidelberg, Heidelberg, Germany; [8]CNR Institute of Neuroscience, Padua, Italy; [9]Cologne University, Cologne, Germany; [10]Ruhr University Bochum, Bochum, Germany; [11]Sorbonne Université and Hospital Pitié Salpêtrière, Paris, France; [12]University of Florida, Gainesville, United States; [13]University Hospital Tübingen, Tübingen, Germany; [14]Helmholtz Center Munich, Munich, Germany; [15]German Institute of Human Nutrition, Potsdam-Rehbrücke, Germany; [16]University Hospital Dresden, Dresden, Germany*
Email: michael.roden@ddz.de

Background and aims: Whether sodium-glucose co-transporter-2 inhibitors and their combination with glucagon-like peptide-1 receptor agonists improve diabetes-related metabolic dysfunction-associated steatohepatitis (MASH) is currently unknown.
Method: This randomized controlled trial compared effects of empagliflozin (10 mg qd) plus semaglutide (1 mg qw; COMBI) with empagliflozin alone (10 mg qd; EMPA) versus placebo (PLAC) on biopsy-confirmed MASH with F1-F3 fibrosis in 61 people with type 2 diabetes. The primary endpoint was MASH resolution without fibrosis progression at 48 weeks. Secondary endpoints included changes in NAFLD activity score (NAS), activity component (lobular inflammation+ballooning) and steatosis. Statistical analyses included Fisher exact test, ANCOVA and 2-sided t-test as appropriate. Data are given as mean and standard deviation.
Results: Participants (47.5% female, age 56 ± 11 years, BMI 33 ± 5 kg/m^2, HbA1c 7.4 ± 1%) received COMBI (n = 23), EMPA (n = 17) or placebo (n = 21), of whom 54 had paired biopsies available. Body weight decreased with COMBI (-8.6 ± 5.4 kg) but not with EMPA (−0.4 ± 7.4 kg) vs. PLAC (0.1 ± 3.4 kg; p < 0.0001 and 0.82) after 48-week treatment. Also, HbA1c improved with COMBI only (−1.3 ± 0.9%) but not with EMPA (-0.4 ± 0.7%) compared to PLAC (−0.1 ± 0.9%; p = 0.0002 and p = 0.25). The proportion of participants with MASH resolution without progression of fibrosis was nominally higher in COMBI (9.5%) but not in EMPA (0%) vs. PLAC (5.6%; both p = 1.0). NAS improved in COMBI (−1.3 ± 1.0), but not in EMPA (−0.1 ± 0.7) vs. PLAC (−0.1 ± 1.1; p = 0.0002 and p = 0.9221). COMBI showed greater reductions in steatosis (−0.38 ± 0.35) and activity component (-0.90 ± 0.90) than PLAC (0.06 ± 0.38 and – 0.14 ± 0.97; p < 0.0001 and p = 0.0078), whereas EMPA (−0.17 ± 0.36 and 0.07 ± 0.68) lead to non-significant changes vs. PLAC. Likewise, transaminases and cytokeratin-18 fragments M30/M65 decreased only with COMBI (all p < 0.01 vs. PLAC).
Conclusion: In people with moderately-controlled type 2 diabetes, the proportion of participants achieving MASH resolution without progression of fibrosis was nominally higher with combined empagliflozin and low-dose semaglutide as compared to placebo after 48 weeks of treatment. Combined treatment was also superior to placebo for improvements in both MASH-related steatosis and inflammation. These effects were likely mediated by the semaglutide-induced reductions in body mass and glycemia.
Clinicaltrials.gov NCT04639414.

Interprofessional forum

OS-021

A nursing educational intervention positively impacts adherence in a cohort of patients with Wilson disease

Anna Miralpeix[1,2,3], Montserrat Rodríguez[4], Núria Fabrellas[2,3,5], Mercè Torra[2,6], Anna Pocurull Aparicio[1,2], Cristina Collazos[1], Elia Canga[1,2,3], Xavier Forns[1,2,5,7], Zoe Mariño[1,2,5,7,8]. *[1]Liver Unit, Hospital Clínic, Barcelona, Spain; [2]Institut d'Investigacions Biomèdiques August Pi i Sunyer (IDIBAPS), Barcelona, Spain; [3]Facultat d'Infermeria, Escola de Doctorat, Universitat de Barcelona, Barcelona, Spain; [4]Pharmacy Service, Hospital Clínic, Barcelona, Spain; [5]Centro de Investigación Biomédica en Red, Enfermedades hepáticas y digestivas (CIBERehd), Barcelona, Spain; [6]Biochemistry and Molecular Genetics Service, Hospital Clínic, Barcelona, Spain; [7]Facultat de Medicina i Ciències de la Salut, Universitat de Barcelona, Barcelona, Spain; [8]ERN-RARE Liver, Hospital Clínic, Barcelona, Spain*
Email: amiralpeix@recerca.clinic.cat

Background and aims: Wilson Disease (WD) is a rare genetic disorder of copper metabolism requiring lifelong treatment with complex regimens and frequent adverse events. Poor adherence is associated with worse clinical outcomes and healthy habits are key to prevent progression and hepatic comorbidities. A nursing educational program was implemented at Hospital Clínic to empower patients, detect barriers and design individualized plans to improve adherence. Here we present the follow-up results.
Method: This single-center, prospective intervention included two visits (baseline V0 and 6-month follow-up V1) led by the same specialized nurse. Treatment adherence was assessed by: 1) medical chart review, 2) pharmacy refill data (low if <80%), and 3) self-reported by patients with the ARMSe questionnaire (low if score ≥16). Adherence to Mediterranean diet was evaluated with MEDAS-14 questionnaire (adapted for low-copper intake and hepatic disease) and physical activity with IPAQ questionnaire. Variables were compared using McNemar's, Chi-square and Mann–Whitney U tests and presented as median (IQR) or n (%), as appropriate.
Results: 54 WD patients were included and followed-up: 54% female, median age 39 (29–47) years, time since diagnosis 20 (14.5–28) years, 72% hepatic phenotype, 50% on chelators and 50% on zinc, treatment duration of 12 (2–20) years. No drug changes occurred between visits. Low adherence by ARMSe decreased from 39% at V0 to 24% at V1 (p = 0.039); with forgetfulness and multiple daily doses as the main barriers. At V1, non-adherent patients were younger (29 vs 40 years, p = 0.032), with non-significant trends to higher ALT and exchangeable copper. No differences were found by sex, phenotype, treatment, educational level or occupation. Clinical and pharmacy-based adherence did not significantly change, but agreement among the three methods improved from 55% to 69%. Non-significant improvement in physical activity was found, but adherence to the adapted Mediterranean diet significantly increased (54% vs 72%, p = 0.031).
Conclusion: This individualized nursing intervention showed a positive impact on treatment adherence and dietary habits in WD patients, despite the limitations of a small sample size and a single 6-month follow-up visit. Continued educational efforts remain essential, as nearly one-quarter of the patients remained non-adherent to treatment, and special attention should be given to younger patients who are generally less compliant. Long-term follow-up is planned to assess sustained impact.

OS-022-YI

Prolonged fasting during hospitalization is associated with poor prognosis in patients with cirrhosis

Astrid Ruiz Margáin[1], Sidney Lopez Moreno[1], Mariana Barrat Remes[1], Mariana Lopez Caracas[1], Renata Montemayor Salazar[1], Abraham Sanchez Gomez[1], Berenice M. Román-Calleja[1], Nayelli C. Flores-Garcia[1], Ricardo Macias-Rodriguez[1]. [1]*Instituto Nacional de Ciencias Médicas y Nutrición Salvador Zubirán, Ciudad de México, Mexico*
Email: astrid.ruizm@incmnsz.mx

Background and aims: Prolonged fasting is common in hospitalized patients with cirrhosis due to procedures, clinical instability, or complications; however, data on its frequency, duration, and clinical impact remain scarce. Fasting may accelerate muscle loss and worsen malnutrition, contributing to functional decline and increased morbidity and mortality. We aimed to evaluate the frequency of fasting during hospitalization and its association with short-term mortality in patients with cirrhosis.
Method: Retrospective cohort study in hospitalized patients with cirrhosis between 2023 and 2025. Primary outcome was 3-month mortality. Total fasting days were defined as the cumulative number of full fasting days, whether continuous or intermittent. Descriptive statistics, chi-square test, independent and paired t-tests, Kaplan–Meier and Cox proportional hazards regression were used.
Results: 228 patients were included (median age 58 years); MASLD (17.1%), alcohol-related liver disease (16.2%), and HCV (11%) were the most common etiologies. Overall, 81.6% experienced at least one fasting period, with recurrent episodes during hospitalization; up to five fasting periods occurred in 5% of patients. Most fasting periods were related to clinically justified indications; however, fasting duration frequently extended beyond the immediate indication. The main reasons for fasting were pre-procedural (63.6%), high-dose vasopressors (14.1%), post-procedural (8.1%), delayed initiation of nutritional support (5.1%), hepatic encephalopathy (4%), and oral intolerance (2%). Phase angle, a validated marker of sarcopenia, declined significantly during hospitalization in both groups but was more pronounced in patients with fasting ≥6 days (3.8 to 3.0, $p < 0.001$) than in those fasting <6 days (4.0 to 3.8, $p = 0.005$). Baseline phase angle was similar between groups ($p = 0.151$), whereas final values differed significantly ($p < 0.001$). Three-month survival was lower in patients with fasting ≥6 days compared with <6 days (45% vs 70%, $p = 0.002$). In multivariable Cox models, fasting ≥6 days remained independently associated with higher 3-month mortality after adjustment for MELD-Na and length of hospital stay (HR 2.08, 95% CI 1.05–4.13).
Conclusion: Prolonged fasting during hospitalization in patients with cirrhosis is associated with worsening sarcopenia, and increased 3-month mortality, independent of liver disease severity and length of hospital stay, reducing the frequency of fasting periods may represent a potentially modifiable risk factor.

OS-023

Development and content validation of a symptom burden scale for liver cirrhosis

Laurence Seynhaeve[1], Tilde Penninck[2], Charlotte De Vloo[3], Sofie De Meulder[1], Jef Dewyspelaere[1], Luc Harlet[1], Jochen Decaestecker[1], Kymentie Ferdinande[1], Lise-Marie Kinnaer[4]. [1]*Department of Hepatology, AZ Delta Hospital, Roeselare, Belgium, Roeselare, Belgium;* [2]*Department of Hepatology, AZ Maria Middelares Gent, Belgium, Gent, Belgium;* [3]*AZ Delta, Department of Gastroenterology and Hepatology, Rumbeke, Belgium, Roeselare, Belgium;* [4]*Department of Public Health and Primary Care, University Centre for Nursing and Midwifery, Ghent University, Ghent, Belgium, Ghent, Belgium*
Email: laurence.seynhaeve@azdelta.be

Background and aims: Liver cirrhosis is a progressive condition in which healthy liver tissue is replaced by fibrosis, representing a major global health burden and accounting for nearly 2% of deaths in Europe. It results from chronic liver diseases such as alcohol use disorder, viral hepatitis, and MASLD, and may progress from a compensated to decompensated stage with reduced survival. Patients experience a substantial and heterogeneous symptom burden that significantly impairs quality of life. Existing generic and liver disease–specific instruments do not fully capture the multidimensional symptom burden and lived experiences of patients with cirrhosis. Therefore, a validated, patient-centered tool applicable to both clinical practice and research is needed. This study aims to develop a cirrhosis-specific symptom burden instrument and evaluate its content validity.
Method: A rapid review identified the most frequently reported symptoms in liver cirrhosis, grouped into physical, psychological, and social domains. A hepatologist, clinical nurse specialist, and patient education expert ensured clinical relevance. The preliminary instrument included 35 items. Content validity was assessed using a two-round Delphi study with healthcare professionals and patients. Items were rated for relevance, clarity, and feasibility on a 5-point Likert scale. Participants could also give qualitative feedback on clarity and missing elements. The Item-Content Validity Index (I-CVI; cut-off ≥ 0.78) and Scale-Content Validity Index (S-CVI; cut-off ≥ 0.90) were calculated to quantify agreement.
Results: After two Delphi rounds, 24 items met the predefined threshold for content validity I-CVI ≥ 0.78, resulting in a tool structured across four domains: physical, psychological, social and treatment adherence. The final S-CVI was 0.89 for healthcare professionals and 0.85 for patients. Qualitative feedback led to refinements in content, item formulation, response options and the removal of redundant questions.
Conclusion: We developed a symptom burden instrument specifically designed for patients with liver cirrhosis. The tool demonstrates good content validity and has the potential to serve as a patient-centered measure for systematic symptom assessment. Its implementation in clinical practice may improve symptom recognition, guide individualized care and enhance shared decision-making. Further psychometric testing in larger patient populations is warranted to confirm reliability and construct validity.

OS-024

Becoming a different person - Living with hepatic encephalopathy

Rikke Werge[1], Marie Louise Hamberg[2], Susanne Lauridsen[2,3], Thora Thomsen[4,5]. [1]*Copenhagen University Hospital, Amager Hvidovre, Hvidovre, Denmark;* [2]*Copenhagen University Hospital, Herlev Gentofte, Herlev, Denmark;* [3]*WHO-CC Parker Institute, Copenhagen, Copenhagen, Denmark;* [4]*Zealand University Hospital, Koege, Denmark;* [5]*University of Southern Denmark, Odense, Denmark*
Email: rikke.parsberg.werge.02@regionh.dk

Background and aims: People living with liver cirrhosis experience a high symptom burden and low HR-QoL. Hepatic encephalopathy (HE) occurs in up to 75% of those with cirrhosis but is sparsely described from the individual's perspective. Due to recurrent cognitive impairment, a marginalized diagnosis, and a healthcare discourse emphasizing involvement and self-responsibility, these individuals appear vulnerable when navigating a complex healthcare system.
Research reveals a lack of qualitative insight into the lived experiences of HE among people with liver cirrhosis. This study aimed to explore how these people experience living with HE as a recurring condition in everyday life, and how they are met by healthcare professionals (HCPs).
Method: A qualitative explorative study was conducted within the framework of Interpretive Description. Semi-structured interviews were performed with four participants and four HCPs. Data were analyzed thematically using Braun and Clarke's six-step approach and reported according to COREQ guidelines.

Results: The overarching theme *"Becoming a different person"* captured the profound physical, cognitive, and existential transformations related to HE. Three main themes were constructed:
1. Change and loss – Participants described changes in identity, self-understanding, and social relationships, accompanied by loss of control and experiencing isolation.
2. New paths – Participants adopted mental and practical strategies to navigate fluctuating cognitive function in order to maintain daily life.
3. HE in clinical encounters – requires empathy, flexibility, continuity and unconventional approaches from HCPs. Stigma associated with cirrhosis, and it's expected association to alcohol use disorder further intensified vulnerability.
Conclusion: HE is experienced as a transformative and isolating condition, deeply affecting identity, autonomy, and social roles through increased vulnerability of those affected. The clinical encounter is shaped by the cognitive impairment caused by HE, requiring tailored and sensitive care from HCPs. Findings highlight the need for individualized care, early and repeated education of staff, as well as development of HE-specific consultations. Addressing the related stigma and supporting relatives are essential to improving quality of life.

OS-025
Dietary practices and beliefs in individuals with primary sclerosing cholangitis – Associations with symptoms and pleasure in eating

Catarina Lindqvist[1], Adam Schumacher[2], Martine Walmsley[3], Nora Cazzagon[4], Annika Bergquist[5]. *[1]Gastroenterology and Nutrition Unit, Department of Medicine Huddinge, Karolinska Institutet, Section Clinical Nutrition, Karolinska University Hospital, European Reference Network on Hepatological Diseases (ERN RARE-LIVER), Stockholm, Sweden; [2]Gastroenterology and Nutrition Unit, Department of Medicine Huddinge, Karolinska Institutet, Stockholm, Sweden; [3]PSC Support, European Reference Network on Hepatological Diseases (ERN RARE-LIVER), Oxford, United Kingdom; [4]Department of Surgery, Oncology and Gastroenterology, University of Padova, Azienda Ospedale, Università Padova, European Reference Network on Hepatological Diseases (ERN RARE-LIVER), Padova, Italy; [5]Gastroenterology and Nutrition Unit, Department of Medicine Huddinge, Karolinska Institutet, Department of Upper Abdominal Diseases, Karolinska University Hospital, European Reference Network on Hepatological Diseases (ERN RARE-LIVER), Stockholm, Sweden*
Email: catarina.lindqvist.1@ki.se

Background and aims: Primary sclerosing cholangitis (PSC) is a progressive cholestatic liver disease commonly associated with inflammatory bowel disease (IBD) and currently has no cure. Individuals with PSC frequently seek information on diet and its potential influence on disease progression. The aim of this study was to investigate dietary practices and beliefs of individuals with PSC.
Method: A survey was developed by members of the PSC working group within the European Reference Network (ERN) Rare Liver. The survey included multiple-choice and open-ended questions on PSC, IBD, symptoms, dietary beliefs and practices, eating-related symptoms, and sources of dietary advice. The anonymous, open survey was available online on the EU Survey platform in 11 languages from January to June 2025 and was distributed via ERN newsletter and webpage, healthcare centres and patient organisations. Descriptive statistics were performed.
Results: A total of 839 individuals with PSC from 33 countries responded (mean age 48 ± 15 years; 55% female). IBD was reported in 57%, liver cirrhosis in 28%, and previous liver transplantation in 16%. While 88% reported wanting dietary advice, only 38% had received PSC-specific dietary guidance. More than half preferred consultation with a health-care professional. Vitamins or supplements were prescribed in 32%, self-initiated in 24%, and 16% had both prescribed and self-initiated use. Two-thirds reported changing dietary habits after PSC diagnosis. Specific foods were reported to worsen symptoms in 42%, with fatty foods most frequently mentioned, followed by red meat and dairy products. Only 26% reported no eating-related symptoms and 48% reported two or more symptoms. Abdominal pain (43%) was the most common symptom affecting normal eating, followed by diarrhoea (34%) and digestive difficulties (31%). Thirty-two percent stated that PSC reduced their enjoyment of eating, mainly because certain foods caused unwanted symptom. Among respondents with IBD, 44% considered IBD the main condition influencing their diet, 14% considered PSC, and 28% had difficulties determining which disease had the greatest impact.
Conclusion: Many individuals with PSC report dietary changes and symptom-related eating difficulties, yet few receive professional dietary guidance, highlighting an unmet need for structured nutritional support in PSC care.

Public health

OS-026-YI
Understanding long-term hepatobiliary morbidity after intrahepatic cholestasis of pregnancy in the UK, and how this varies by ethnicity

Rebecca Lissmann[1], Fabiola Eto[1], Stamatina Iliodromiti[1], Julia Zollner[2], Caroline Ovadia[3], Catherine Williamson[4], Jennifer Jardine[5]. *[1]Queen Mary University of London, London, United Kingdom; [2]University College London, London, United Kingdom; [3]The University of Edinburgh, Edinburgh, United Kingdom; [4]Imperial College London, London, United Kingdom; [5]University of Cambridge, Cambridge, United Kingdom*
Email: r.lissmann@qmul.ac.uk

Background and aims: Intrahepatic cholestasis of pregnancy (ICP) is associated with impaired bile flow in the liver and adverse pregnancy outcomes. Existing smaller studies in predominantly ethnically homogenous European populations have suggested an association between ICP and long-term hepatobiliary morbidity. We aimed to understand the association between ICP and subsequent hepatobiliary morbidity in England, and to explore how this varied by ethnic group.
Method: Hospital Episode Statistics records of births in 2000–2021 were linked to primary care (CPRD Aurum) and secondary care (Hospital Episode Statistics) data. Women with an ICP diagnosis during the first recorded pregnancy were compared with those without. Incidence of subsequent hepatobiliary morbidity (including composite hepatobiliary disease, gallstone disease, other liver disease, pancreatitis, infectious liver disease, fibrosis and cirrhosis, hepatobiliary malignancy, and end stage liver disease) was established. Cox regression was used to estimate time-related associations. Models incorporated maternal age at birth and ethnicity.
Results: 3,701,995 women were included in the analysis, of whom 31,082 (0.8%) were diagnosed with ICP in their first recorded pregnancy. Median follow-up time was 10.4 years (IQR 5.8–15.0). Incidence of ICP varied by ethnicity: 0.8% in white, 1.3% in South-Asian, 0.5% in Black, 0.7% in Mixed, and 0.9% in Other ethnic groups. Those with a recorded ICP diagnosis were more likely to progress to liver morbidity compared to those without: composite hepatobiliary disease aHR 2.38 (CI 2.29–2.48, $p < 0.001$), pancreatitis aHR 2.43 (95% CI 2.13–2.76, $p < 0.001$), gallstones aHR 2.24 (95% CI 2.14–2.34, $p < 0.001$), hepatobiliary malignancy aHR 4.05 (95% CI 1.91–8.56, $p < 0.001$), fibrosis and cirrhosis aHR 2.92 (95% CI 2.22–3.84, $p < 0.001$), other liver disease aHR 2.52 (2.30–2.75, $p = <0.001$), infectious liver disease aHR 2.10 (95% CI 1.75–2.52, $p < 0.001$)), and end stage liver disease aHR 2.05 (95% CI 1.42–2.98, $p < 0.001$). Compared to White women, Black and South Asian women had an increased risk of subsequent severe hepatobiliary morbidity.

Conclusion: This study provides the strongest evidence to date of an association between ICP and hepatobiliary morbidity. We have explored how this association varies by ethnicity. Postpartum follow-up and inclusion of ICP in hepatobiliary risk stratification appear to be important. Interventions should tackle health inequalities between ethnic groups.

OS-027

A prospective, randomized, double-blind, placebo-controlled, phase III, multicenter study to evaluate the immunogenicity and safety of recombinant hepatitis-e vaccine in healthy adults & adolescents

Premashis Kar[1], Ayush Jasrotia[1], Nikhil Nagre[1], Jata Shankar Kumar[1].
[1]*Max Super Speciality Hospital, Vaishali, W-3, Ashok Marg, near Radisson Blu Hotel, Sector-1, Vaishali, Ghaziabad, Uttar Pradesh 201010, Ghaziabad, Uttar Pradesh 201010, India*
Email: premashishkar@gmail.com

Background and aims: Hepatitis E virus (HEV) remains a major cause of acute viral hepatitis in developing countries, with significant morbidity among young adults and pregnant women. A recombinant HEV vaccine offers a promising preventive approach. This Phase 3 study was conducted to evaluate the immunogenicity and safety of a purified recombinant Hepatitis-E Vaccine (E. coli) in a healthy Indian population.
Method: This was a multicenter, randomized, double-blind, placebo-controlled trial. Healthy Indian adults and adolescents (aged 16–65 years) seronegative for anti-HEV IgG (IgG <0.9) were enrolled and randomized in a 1:1 ratio to receive either the Hepatitis-E vaccine or placebo. The vaccination schedule consisted of three doses administered at Month 0 (Day 1), Month 1 (Day 31 ± 7), and Month 6 (Day 181 ± 14), with final evaluation at Month 7 (Day 211 ± 14). The primary endpoint was seroconversion rate 1 month after the third dose. Secondary endpoints included changes in geometric mean titres (GMT) of anti-HEV antibodies and safety assessments based on adverse events (AEs) and clinical/laboratory monitoring.
Results: Out of 347 screened subjects, 190 were enrolled (96 males, 94 females; median age 34 years). At study completion, seroconversion rates were significantly higher in the vaccine group compared to placebo (ITT: 75% vs 18%, PP: 89% vs 22%; $p < 0.001$). Mean GMT increases were also significantly greater in the vaccine group (ITT: 3.17 vs 0.15; PP: 3.68 vs 0.13; $p < 0.0001$). A total of 29 adverse events were reported among 13 subjects. The most common AEs were headache (n = 7), pyrexia (n = 3), eosinophilia (n = 3), and fatigue (n = 3), all of which were mild and resolved without sequelae. No serious adverse events or deaths occurred. Laboratory, vital, and physical examination parameters remained within normal limits.
Conclusion: The recombinant Hepatitis-E Vaccine (E. coli) demonstrated strong immunogenicity with a statistically significant increase in seroconversion and GMT compared to placebo, and was well tolerated. These results support its use in HEV-endemic regions to reduce the burden of hepatitis E.

OS-028

Early readmission in high-income countries contributes towards lower mortality-results from CLEARED global study

Ashok Kumar Choudhury[1], Florence Wong[2], Jacob George[3], Qing Xie[4], Peter Hayes[5], Ramazan Idilman[6], Mark Topazian[7], Mario Álvares-da-Silva[8], Hailemichael Desalegn[7], Wai-Kay Seto[9], Aldo Torre[10], Patrick S. Kamath[11], Shiv Kumar Sarin[1], Zhujun Cao[4], Anand Kulkarni[12], Abha Nagral[13], Neil Rajoriya[14], Henok Fisseha[7], Chuanwu Zhu[15], Nabil Debzi[16], Alberto Farias[17], Minghua Su[18], Sebastián Marciano[19], Robert Livingstone[20], Yanhang Gao[21], René Malé Velazquez[22], Coskun Ozer Demirtas[23], Yongfang Jiang[24], Jose Antonio Velarde-Ruiz Velasco[25], Hiang Keat Tan[26], Caiyan Zhao[27], Maria Sarai González-Huezo[28], Sumeet Asrani[29], Lei Wang[30], Mingqin Lu[31], Matheus Truccolo Michalczuk[32], Zeki Karasu[33], Jacqueline Cordova-Gallardo[34], Cameron Gofton[35], Michael Gounder[36], Jawaid Shaw[37], Xin Zheng[38], Aloysious Aravinthan[39], Ruveena Bhavani[40], Dinesh Jothimani[41], Kessarin Thanapirom[42], Sevda Aghayeva[43], Dinc Dincer[44], Shalimar Shalimar[45], Minghua Lin[46], Bin Xu[47], Xiaoping Wu[48], Chenghai Liu[49], James Fung[50], Helena Katchman[51], Gustavo Pereira[52], Mohamed El-Kassas[53], Marie Jeanne Lohoues[54], Dominik Bettinger[55], Hanna Aberra[56], Nilang Patel[57], Ashish Kumar[58], Anil Arora[58], Surender Singh[59], Sunil Taneja[60], Arun Valsan[61], Akash Shukla[62], CE Eapen[63], Akash Roy[64], Anil Anand[65], Amey Sonavane[66], Mithun Sharma[12], Mohamed Rela[41], Paul J. Thuluvath[67], K. Rajender Reddy[68], Brian Bush[69], Jasmohan Bajaj[37]. [1]*Institute of Liver and Biliary Sciences, new delhi, India;* [2]*University of Toronto, Toronto, Canada;* [3]*The Westmead Institute for Medical Research, Westmead, Australia;* [4]*Ruijin Hospital, Shanghai Jiao Tong University School of Medicine, Shanghai, China;* [5]*Division of Health Sciences, Deanery of Clinical Sciences, University of Edinburgh, Edinburgh, UK, Edinburgh, United Kingdom;* [6]*Ufuk University-Faculty Of Medicine, Ankara, Türkiye;* [7]*St.paul's Hospital Millennium Medical College, Addis Ababa, Ethiopia;* [8]*Hospital de Clínicas de Porto Alegre, Universidade Federal do Rio Grande do Sul, Porto Alegre, Brazil, Alegre, Brazil;* [9]*The University of Hong Kong, Hong Kong SAR, China, Hong Kong, China;* [10]*Instituto Nacional De Ciencias Médicas Y Nutrición Salvador Zubirán, Ciudad de México, Mexico;* [11]*Mayo Clinic College of Medicine & Science, Rochester, United States;* [12]*Asian Institute Of Gastroenterology, Hyderabad, India;* [13]*Jaslok Hospital, Mumbai, India;* [14]*University Hospital Birmingham Nhs Trust, Birmingham, Northern Ireland;* [15]*The Fifth People's Hospital of Suzhou, Hospital of Suzhou, Suzhou, China;* [16]*Mustapha Bacha University Hospital of Algiers, Algiers, Algeria;* [17]*Hospital das Clínicas da Faculdade de Medicina da Universidade de São Paulo, São Paulo, Brazil;* [18]*The First Affiliated Hospital of Guangxi Medical University, Nanning, China;* [19]*Hospital Italiano de Buenos Aires, Buenos Aires, Argentina;* [20]*Royal Berkshire Hospital, Reading, United Kingdom;* [21]*The First Hospital of Jilin University, Jilin, China;* [22]*Instituto de la Salud Digestiva, Guadalajara, Guadalajara, Mexico;* [23]*Marmara University, Istanbul, Türkiye;* [24]*The Second XiangYa Hospital of Central South University, Changsha, China;* [25]*Hospital Civil de Guadalajara Fray Antonio Alcalde, Guadalajara, Mexico;* [26]*Singapore General Hospital, Singapore, Singapore;* [27]*The Third Affiliated Hospital of Hebei Medical University, Hebei, China;* [28]*Centro Médico ISSEMYM, Mexico City, Mexico;* [29]*Baylor University Medical Center, Dallas, United States;* [30]*Second Hospital of Shandong University, Shandong, China;* [31]*The First Affiliated Hospital of Wenzhou Medical University, Wenzhou, China;* [32]*Hospital de Clínicas de Porto Alegre, Universidade Federal do Rio Grande do Sul, Porto Alegre, Brazil;* [33]*Ege University School of Medicine, Izmir, Türkiye;* [34]*Hospital General Dr. Manuel Gea Gonzalez, Mexico City, Mexico;* [35]*Royal North Shore Hospital, Sydney, Australia;* [36]*The Westmead Institute for Medical Research and Westmead Hospital, University of Sydney, Sydney, Australia;* [37]*Virginia Commonwealth University and Richmond VA Medical Center, Richmond, United States;* [38]*Tongji Medical College, Huazhong University of Science and Technology, Wuhan, China;* [39]*NIHR Nottingham Biomedical Research Centre, Nottingham University Hospitals NHS Trust and University of Nottingham, Nottingham, United Kingdom;* [40]*Universiti of Malaya, Kuala Lumpur, Malaysia;* [41]*Rela Institute, Chennai, India;* [42]*Chulalongkorn University, Bangkok, Thailand;* [43]*University Hospital, Baku, Azerbaijan;* [44]*Akdeniz University School of Medicine, Antalya, Türkiye;* [45]*All India Institute of Medical Sciences, New Delhi, India, New Delhi, India;* [46]*Mengchao Heapatobiliary Hospital of Fujian Medical University, Fuzhou, China;* [47]*Beijing Youan Hospital, Capital Medical University, Beijing, China;* [48]*The First Affiliated Hospital of Nanchang University, Nanchang, China;* [49]*Shuguang Hospital Affiliated to Shanghai University of Traditional Chinese Medicine, Shanghai, China;* [50]*The University of Hong Kong, Hong Kong SAR, China;* [51]*Tel Aviv Sourasky Medical Center, Tel Aviv, Israel;* [52]*Hospital Federal de Bonsucesso, Rio de Janeiro, Brazil;* [53]*Sohag University, Cairo, Egypt;* [54]*CHU Cocody, Abidjan, Abidjan, Côte d'Ivoire;* [55]*University of Freiburg, Freiburg, Germany;* [56]*University Hospital and King Faisal Hospital, Kigali, Rwanda, Rwanda, Central African Republic;*

[57]Ruijin Hospital, Shanghai Jiao Tong University School of Medicine, Shanghai, China, Shanghai, China; [58]Sir Gangaram Hospital and GRIPMER, Delhi, India; [59]SGPGI, LUCKNOW, India; [60]PGIMER, Chandigarh, India; [61]Amrita institute of medical sciences, Kochi, India; [62]Seth GS Medical college and KEM Hospital, mumbai, India; [63]CMC, VELLORE, India; [64]Apollo Multispeciality Hospitals, Kolkata, India; [65]Kims, Bhubaneswar, India; [66]APOLLO Hospital, Mumbai, India; [67]Mercy Medical Center, Baltimore, United States; [68]University of Pennsylvania, Philadelphia, United States; [69]Virginia Commonwealth University and Richmond VA Medical Center, Ruijin Hospital, Shanghai Jiao Tong University School of Medicine, Shanghai, China, Richmond, United States
Email: doctor.ashokchoudhury@gmail.com

Background and aims: Early readmission after hospitalization for decompensated cirrhosis is associated with adverse outcomes, yet its predictors and global disparities poorly characterized. We aimed to identify determinants of 30-day readmission following index non-elective hospitalization and its impact on short-term outcomes.
Method: The CLEARED Consortium prospectively enrolled hospitalized patients with cirrhosis globally. Patients who died, underwent liver transplantation (LT) during index admission, or lost to follow-up were excluded. The primary outcome was 30-day readmission. Centers were categorized as high-income (HIC), upper-middle–income (UMIC), or low/low-middle–income countries (LMICs).
Results: A total of 8,263 hospitalized patients with cirrhosis enrolled in registry, of which 5,692 were analyzed with mean age of 56.16 ± 13.31 years, 64.1% male and predominant etiology being alcohol (41.1%). Within 30 days of discharge, 1,610 patients (28.3%) were readmitted. Readmitted patients had higher rates of prior ascites (70.3% vs. 61.5%), overt hepatic encephalopathy (22.7% vs. 13.4%), hyponatremia (31.2% vs. 24.4%), acute kidney injury (21.6% vs. 13.0%), hospitalization (61.2% vs. 44.0%) and infection (25.3% vs. 15.9%) within the preceding 6 months (all $p < 0.001$). Viral etiologies, particularly hepatitis C (13.9% vs. 10.1%, $p < 0.001$), higher MELD-Na scores (27 vs. 25, $p < 0.001$), and admissions with anasarca or dyselectrolytemia were common among readmitted patients. Thirty-day readmission was associated with higher mortality (10.4% vs. 4.8%) and LT rates (8.9% vs. 3.6%) (both $p < 0.001$). Readmission rates were highest in HICs (37.1%) with a low post-readmission mortality. On multivariable analysis, HCV etiology (OR 1.48), 6-month hospitalization (OR 1.66) or infection (OR 1.22), at admission presence of anasarca (OR 1.39) and higher MELD-Na (OR 1.02 per point) independently predicted readmission (all $p \leq 0.03$). LMIC (OR 0.41) and UMIC (OR 0.62) residence were independently associated with lower odds of readmission than HICs (both $p < 0.001$) but a higher mortality.
Conclusion: Early readmission and recent healthcare utilization occurs in one-quarter of hospitalized patients with cirrhosis and identifies a population with a poor short-term survival and higher need of LT. Higher rate of readmissions, lower mortality and higher transplant rate in high-income countries than the low- and middle-income countries, likely a reflection of barriers to access rather than lower disease burden.

OS-029

Impact of rapid testing and self-administered risk questionnaires on hepatitis C screening rates

María Jesus Vivancos-Gallego[1], Marta Rosas Cancio-Suarez[1], Javier Martinez[1], Beatriz Romero[2], Pilar Perez[3], Marta Lor[4], Pablo López-Cepero Sierra[5], Ma Aranzazu Alonso[3], María Luisa Careaga[6], Ana Isabel Moreno[7], Margarita Herrero[8], Alvaro Ureña[9], Josefa Castro[10], Maria Jesus Perez-Elias[1]. [1]Infectious Diseases, Hospital Universitario Ramón y Cajal, IRYCIS, Madrid, Spain, CIBER de Enfermedades Infecciosas (CIBERINFEC), Instituto de Salud Carlos III, Madrid, Spain, Alcalá de Henares University, Alcalá de Henares, Madrid, Spain, Madrid, Spain; [2]Microbiology, Hospital Universitario Ramón y Cajal, IRYCIS, CIBER de Enfermedades Infecciosas (CIBERINFEC), Instituto de Salud Carlos III, Madrid, Spain, Alcalá de Henares University, Alcalá de Henares, Madrid, Spain, Madrid, Spain; [3]Centro de Salud Garcia Noblejas, Madrid, Spain; [4]Centro de Salud Aquitania, Madrid, Spain; [5]Centro de Salud Canal de Panama, Madrid, Spain; [6]Centro de Salud Cirajas, Madrid, Spain; [7]Centro de Salud Alpes, Madrid, Spain; [8]Centro de Salud Mar Baltico, Madrid, Spain; [9]Centro de Salud Canillejas, Madrid, Spain; [10]Centro de Salud Benita de Avila., Madrid, Spain
Email: mjesus.vivancos@gmail.com

Background and aims: Underdiagnosis remains a major barrier to Hepatitis C (HCV) elimination. The ATENEA study assesses whether the implementation of rapid testing combined with a self-administered risk assessment in Primary Care (PC) settings could enhance HCV detection.
Method: This is a cluster-randomized, stepped-wedge trial (clinicaltrials.gov ID: NCT06528626) conducted across eight PC centers between July 2023 and February 2025. An initial 4-month observation phase (July–October 2022) was implemented in all centers, followed by 4-month intervention periods: Control (standard practice after training on HIV screening) Rapid hepatitis C testing (RT) Combined intervention (RT + self-administered risk questionnaire; RT+Q) Intervention type was modeled as a categorical variable with four levels, using the observation phase as the reference. We calculated HCV screening coverage (HCV tests performed) and total and new HCV diagnoses per 100,000 patients attended. Poisson regression models, adjusted for period and clustering by center, were fitted to estimate incidence rate ratios (IRRs) with 95% confidence intervals.
Results: A total of 40 center-period observations were analyzed. The study population included 237,670 individuals, with 14,975 HCV tests performed, yielding 208 positive results (26 newly diagnosed). Compared with the observation phase (2,120 HCV tests were conducted with 23 positives), HCV Screening rates increased by 124% in the RT+Q phase (IRR = 2.24; 95% CI: 2.00–2.50; $p < 0.001$) and by 96% in the RT phase (IRR = 1.96; 95% CI: 1.34–2.87; $p = 0.001$), while Control phase demonstrated a non-significant increase (IRR = 1.54; $p = 0.131$). The Prevalence of Anti-HCV significantly increased in the RT+Q phase (IRR = 2.83; 95% CI: 1.95–4.13; $p < 0.001$), with non-significant upward trend in RT phase (IRR = 1.75; $p = 0.105$), and Control phase revealed no differences (IRR = 0.84; $p = 0.799$).
Conclusion: The implementation of rapid hepatitis C testing combined with self-administered risk questionnaires in Primary Care significantly enhances screening activity.

OS-030

A multicentre randomised controlled trial of screening for MASLD in patients with type 2 diabetes not known to have liver disease in primary care

Ryan Buchanan[1], Tina Reinson[1], Josh Bilson[1], Scott Harris[1], Chinonso Nwoguh[1], Keith Cooper[1], Mary Onoja[1], Karen Malone[2], Chris D Byrne[1]. [1]University of Southampton, Southampton, United Kingdom; [2]Woolston & Town Hill Primary Care Network, Southampton, United Kingdom
Email: rmb1d14@soton.ac.uk

Background and aims: Current guidance for liver disease assessment in type 2 diabetes mellitus (T2DM) varies, and in the United Kingdom (UK) testing for MASLD fibrosis is largely limited to individuals with ultrasound-confirmed steatosis or abnormal liver enzymes. We evaluated the clinical effectiveness and costs of alternative fibrosis assessment strategies.
Method: REFLEX was an unblinded, individual-level, 1:1 randomised controlled multicentre trial conducted across primary and secondary care in the Wessex region of England (population ~8 million). The protocol was published (BMJ Open 2025) and the study prospectively registered. Adults with Systematised NOmenclature of MEDicine code registered T2DM and no known liver disease or liver testing in the preceding two years were eligible. Participants were randomised

to either a 'FibroScan First' pathway or to Usual Care. The primary outcome was referral for hepatocellular carcinoma (HCC) surveillance within 12 months of randomisation. Secondary analyses modelled two-step strategies using ELF or Fib-4 as initial tests prior to FibroScan. A cost-effectiveness evaluation is ongoing.
Results: 634 participants were randomised (318 'FibroScan First'; 316 Usual Care). At 12 months, only 13 (4%) participants in Usual Care had undergone fibrosis assessment. In contrast, 313 participants in the 'FibroScan First' arm received a scan; 39 met criteria for hepatology referral. Twelve participants (4%) were diagnosed with F4 fibrosis and commenced HCC surveillance, and a further 64 (20.1%) were diagnosed with F2/F3 fibrosis. No cases of F4 or F2/F3 disease were identified in Usual Care. Total pathway costs were £33,518/€38,200 for 'FibroScan First' and £1,105/€1259 for Usual Care. Modelling two-step pathways reduced case detection: F4 disease fell to 6 (2%) cases using ELF and 5 (2%) using Fib-4. Costs were £33,103/€37,735 for ELF +FibroScan and Fib4+FibroScan £7,325/€8,350.
Conclusion: Usual care in this trial identified no cases for HCC surveillance over 12 months. A 'FibroScan First' screening strategy substantially increased detection of clinically significant disease leading to cancer surveillance. Two-step strategies using ELF or Fib-4 missed around half of cases with cirrhosis. Ongoing cost-effectiveness modelling analyses will determine whether early diagnosis offsets increased upfront costs.

FRIDAY 29 MAY

Alcohol

OS-031
Safety and pharmacokinetic results from a Phase 2 safety lead-in in participants with hepatic impairment support continued development of GSK4532990 in alcohol-related liver disease

Young Kul Jung[1], Theresa Fleming[2], Itziar Irurzun[3], Grace Kang[4], Hirotoshi Ebinuma[5], Eric Lawitz[6], Giovanni Perricone[7], William Sanchez[8], Raj Vuppalanchi[9], Patrick Weston[10], Phillip Sundin[4], Brandon Swift[11], Nikhil Vergis[2], Sandhya Nirodi[12], Stuart Kendrick[12], MeeJ Kim[13]. *[1]Korea University College of Medicine, Seoul 02841, Korea, Rep. of South; [2]GSK, London, United Kingdom; [3]GSK, Madrid, Spain; [4]GSK, Collegeville, PA, United States; [5]International University of Health and Welfare Narita Hospital, Chiba, Japan; [6]Texas Liver Institute, University of Texas Health, San Antonio, TX, United States; [7]Hepatology and Gastroenterology Unit, ASSt Grande Ospedale Metropolitano Niguarda, Milan, Italy; [8]Floridian Clinical Research, Miami Lake, FL, United States; [9]Indiana University School of Medicine, Indianapolis, IN, United States; [10]Synergy Healthcare of Tampa, FL, United States; [11]GSK, Durham, NC, United States; [12]GSK, Stevenage, United Kingdom; [13]GSK, Rockville, MD, United States*
Email: 93cool@hanmail.net

Background and aims: Alcohol-related liver disease (ALD) is a leading cause of morbidity, mortality and liver transplantation. Silencing of *hydroxysteroid 17-beta-dehydrogenase-13 (HSD17B13)* is a promising option, as loss-of-function (LOF) is associated with reduced ALD progression. GSK4532990, an N-acetylgalactosamine conjugated siRNA, selectively targets *HSD17B13* in hepatocytes to mimic the LOF mutation. We report safety and pharmacokinetics (PK) from a Phase 2 study safety lead-in of GSK4532990 in participants (pts) with ALD (NCT06613698).
Method: Eligible pts (18–70 yrs) had a history of alcohol consumption consistent with ALD/met-ALD, with either Child-Turcotte-Pugh (CTP) A or CTP-B hepatic impairment. Pts received a subcutaneous dose of GSK4532990 and were evaluated over 8 weeks for safety (vital signs, ECG, laboratory tests, adverse events [AEs]). Intensive PK were collected on Day 1 and analysed non-compartmentally.
Results: In total, 16 pts (n = 8 per CTP cohort) completed the study (no withdrawals). Eleven pts experienced treatment-emergent AEs (TEAEs); 4 had TEAEs related to study treatment. The most common treatment-related AEs were injection site reactions. Eight serious TEAEs were reported in 5 pts; none were related to study treatment. Two CTP-A pts experienced protocol-defined liver events, adjudicated as not causally related to GSK4532990. There were no safety findings regarding laboratory parameters, ECG and vital sign changes from baseline (BL). BL median (min, max) AST (U/L) was 120 (45, 194) for CTP-A, 56 (42, 120) for CTP-B pts; median change from BL (U/L) at Week (W)8 was −44 (−102, 201) for CTP-A, −7 (−67, 9) for CTP-B. Median ALT values at W8 were also reduced, despite similar median PeTH at W8 vs. BL. Median T_{max} was 6.0 hrs post-dose for CTP-A and CTP-B pts. Geometric mean apparent $t_{1/2}$ (coefficient of variation %) was 6.4 (10.4; CTP-A) and 7.2 (19.8; CTP-B) hrs. Geometric mean C_{max} and AUC_{0-24h} were at least 19- and 24-fold lower for both cohorts, compared with corresponding exposures maximum tolerated dose in monkey toxicology studies.
Conclusion: No safety concerns were identified in pts with CTP-A and CTP-B hepatic impairment after a single dose of GSK4532990. Liver biochemistry improved in both cohorts despite ongoing alcohol consumption. PK were comparable between CTP-A and CTP-B pts and demonstrated wide safety multiples relative to nonclinical toxicology. These results supported initiation of the main study and continued development of GSK4532990 in ALD.

OS-032-YI
Burden of MetALD and alcohol-related liver disease in the European general population: insights from the 30,199-patient LiverScreen cohort

Stine Johansen[1,2], Elisa Pose[3,4,5], Maja Thiele[1,2], Laurent Castera[6], Guillem Pera[7], Salvatore Piano[8], Isabel Graupera[3,4,5], Pere Torán[7], Katrine Tholstrup Bech[1,2], Helle Schnefeld[1,2], Marta Tonon[8], Anita Madir[9], Daniel Jan Havaj[10], Jesse Pustjens[11], Mirko Zoncapè[12], Peter R. Galle[13], Peter Andersen[1,2], Judit Pich[14], Johanne Kragh Hansen[1,2], Neil Guha[15], Jörn M. Schattenberg[16], Emmanuel Tsochatzis[12], Willem Pieter Brouwer[11], Juan M. Pericàs[5,17,18], Lubomir Skladany[10], Ivica Grgurevic[9], Llorenç Caballeria[7], Pere Ginès[3,4,5], Aleksander Krag[1,2]. *[1]FLASH - Centre for Liver Research, Department of Gastroenterology and Hepatology, Odense University Hospital, Odense, Denmark; [2]Department of Clinical Research, Faculty of Health Sciences, University of Southern Denmark, Odense, Denmark; [3]Liver Unit, Hospital Clínic of Barcelona, Barcelona, Spain; [4]Fundació de Recerca Clínic Barcelona - Institut d'Investigacions Biomèdiques August Pi i Sunyer (FCRB - IDIBAPS), Barcelona, Spain; [5]Centro de Investigación Biomédica en Red Enfermedades Hepáticas y Digestivas (CIBEREHD), Madrid, Spain; [6]Department of Hepatology, Hôpital Beaujon, Assistance Publique-Hôpitaux de Paris, Clichy, Université de Paris, Paris, France; [7]Unitat de Suport a la Recerca Metropolitana Nord, Fundació Institut Universitari per a la Recerca a l'Atenció Primària de Salut Jordi Gol i Gurina (IDIAPJGol), Barcelona, Spain; [8]Unit of Internal Medicine and Hepatology, Department of Medicine - DIMED, University and Hospital of Padova, Padova, Italy; [9]Department of Gastroenterology, Hepatology and Clinical Nutrition, University Hospital Dubrava, Zagreb, Croatia; [10]Division of Hepatology, Gastroenterology and Liver Transplantation, Department of Internal Medicine II, Slovak Medical University Faculty of Medicine, F. D. Roosevelt University Hospital, Banska Bystrica, Slovakia; [11]Department of Gastroenterology and Hepatology, Erasmus MC-University Medical Centre, Rotterdam, Netherlands; [12]UCL Institute for Liver and Digestive Health, Royal Free Hospital, University College of London (UCL), London, United Kingdom; [13]Department of Internal Medicine I, University Medical Center of the Johannes Gutenberg-University, Mainz, Germany; [14]Clinical Trial Unit, Hospital Clínic, Barcelona, Barcelona, Spain; [15]NIHR Nottingham Biomedical Research*

Centre, Nottingham University Hospitals NHS Trust and the University of Nottingham, Nottingham, United Kingdom; [16]Department of Medicine II, Saarland University Medical Center, Saarland University, Homburg, Germany; [17]Liver Unit, Hospital Universitari Vall d´Hebron, Vall d'Hebron Institut de Recerca (VHIR), Vall d'Hebron Barcelona Hospital Campus, Barcelona, Spain; [18]Universitat Autònoma de Barcelona, Barcelona, Spain
Email: stine.johansen@rsyd.dk

Background and aims: Alcohol-related liver disease (ALD) and metabolic dysfunction and ALD (MetALD) represent an under-recognized part of the steatotic liver disease spectrum, particularly at early, asymptomatic stages. Population-level data on their prevalence and fibrosis severity are limited, and the joint impact of alcohol and cardiometabolic risk factors remains poorly defined. We aimed to estimate the prevalence and severity of ALD and MetALD in the European general population using the LiverScreen cohort.
Method: We conducted a prospective screening study in individuals aged ≥40 years from the general population in nine European countries. We recorded demographic, clinical, and standard laboratory parameters, and assessed liver fibrosis using liver stiffness measurements (LSM). Individuals with LSM ≥ 8 kPa and/or ALT ≥ 1.5 × the upper limit of normal were referred for hepatology consultation including liver biopsy in patients who agreed to the procedure.
Results: We included 30,199 individuals from the general population (mean age 58 ± 10 years; 57% women). Overall, 7.1% reported harmful alcohol use (women/men: ≥14/21 drinks/week) and 70% had at least one cardiometabolic risk factor. At inclusion, 31% had steatotic liver disease (ALD = 0.4%; MetALD = 2%; MASLD = 28%), while 69% had no steatotic liver disease. The prevalence of significant fibrosis was highest in ALD, with 10.9% having LSM ≥ 10 kPa, followed by MetALD (7.5%) and MASLD (4.3%). In patients with MetALD or ALD, only 5.2% had ALT ≥ 1.5 × the upper limit of normal; however, exceeding this threshold was associated with a markedly higher risk of MetALD or ALD (odds ratio 3.4, 95% CI 2.4–4.5; p < 0.001). Among the 2,457 individuals referred for hepatology consultation, 331 underwent liver biopsy. Advanced fibrosis (≥F3) was present in 28% (93/331). Among biopsied patients with ALD or MetALD, 39% had advanced fibrosis, significantly higher than in those with MASLD (27%).
Conclusion: In this large, population-based cohort, ALD and MetALD accounted for a small proportion of patients with steatotic liver disease but were associated with a higher burden of advanced fibrosis. These findings underscore a substantial yet underrecognized burden of ALD and MetALD in the general population, highlighting the need for earlier and more systematic identification.

OS-033
Efficacy and safety of bovine colostrum in the treatment of severe alcohol- associated hepatitis

Sandeep Sidhu[1], Ajay Kumar Duseja[2], Shalimar Shalimar[3], Sandeep Nijhawan[4], Dharmesh Kapoor[5], Omesh Goyal[6], Harsh Kishore[7], Prasanna Samuel Premkumar[8], Saravanaraj Karuppasamy[8]. *[1]Christian Medical College Ludhiana, Ludhiana, India; [2]Postgraduate Institute Of Medical Education And Research Chandigarh, Chandigarh, India; [3]All India Institute of Medical Sciences, Delhi, India, New Delhi, India; [4]Sawai Man Singh Medical College, Jaipur, India; [5]Yashoda Hospitals, Secunderabad, India; [6]Dayanand Medical College and Hospital, Ludhiana, India, Ludhiana, India; [7]Dayanand Medical College and Hospital, Ludhiana, India; [8]Christian Medical College, Vellore, Vellore, India*
Email: sandeepsidhu1963@gmail.com

Background and aims: Severe alcohol-associated hepatitis (sAH) is associated with high short-term mortality. sAH is linked to gut dysbiosis, intestinal barrier dysfunction, bacterial translocation, and heightened liver inflammation. Bovine colostrum is a naturallyoccurring, immunoglobulin G-enriched oral preparation containing lactoferrin and short-chain fatty acids. We evaluated the efficacy and safety of bovine colostrum in patients with sAH.
Method: This phase 3, parallel-group, double-blind, randomised, placebo-controlled trial was conducted at five academic tertiary care centres in India. Between 2017 and 2023, 174 patients with sAH were centrally randomised using the Trans European Network for Clinical Trials Services to receive freeze-dried bovine colostrum (20 g) or placebo (pasteurised bovine milk powder, 20 g) three times daily for 4 weeks. Eighty-nine patients were assigned to the colostrum group and 85 to the placebo group. Patients, investigators, and statisticians were masked to treatment allocation. The primary outcome was 90-day survival, assessed in the intention-to-treat population.
Results: Ninety-day survival was significantly higher in the colostrum group (86.5%; 95% confidence interval 77.2–92.5) than in the placebo group (43.5%; 32.9–54.7) (p < 0.0001), despite similar baseline Model for End-Stage Liver Disease (MELD) scores (median 30.2 vs. 31.5). Restricted mean survival time was 79.6 days (interquartile range 74.1–85.1) in the colostrum arm and 47.2 days (39.3–55.0) in the placebo arm (p < 0.0001). Secondary outcomes showed significant reductions in MELD scores, serum endotoxin and tumor necrosis factor-alpha levels, and thirteen episodes of sepsis in the colostrum group vs. 29 in the placebo arm (p = 0.009) in the first month. Serious adverse events reflected disease severity and were not due to the intervention.
Conclusion: This study demonstrated a significant improvement in 90-day survival with bovine colostrum in patients with sAH. Corticosteroids were not used as a comparator arm because MELD scores were ~30. However, this treatment warrants confirmation in additional populations.

OS-034
Multilevel remodeling of the glucocorticoid receptor axis underlies corticosteroid resistance in severe alcoholic hepatitis

Qun Cai[1], Marco Fidaleo[1], Graziella Privitera[1], Meiqian Hu[1], Changze Hong[1], MohammadMahdi Saeidinejad[1], Fausto Andreola[1], Rajiv Jalan[1]. *[1]University College London, Royal Free Campus, Institute for Liver and Digestive Health, London, United Kingdom, London, United Kingdom*
Email: quncai@zju.edu.cn

Background and aims: Severe alcoholic hepatitis (SAH) causes acute decompensation and high short-term mortality. Corticosteroids benefit only a subset of patients, and mechanisms of non-response are unclear. Because steroid effects depend on the glucocorticoid receptor (GR) and GR isoform balance shaped by alternative splicing, we investigated whether dysregulated GR signaling and splicing regulation in hepatocytes and peripheral monocytes contributes to steroid non-response in SAH.
Method: We prospectively enrolled patients with SAH(n = 25), stable cirrhosis (SC, n = 10) and healthy controls (HC, n = 10). In an independent SAH cohort (n = 50), patients were classified as corticosteroid responders (R, n = 21) or non-responders (NR, n = 29) using the Lille model. Liver biopsies were stained for GRα+β, GRβ and Serine-Rich Splicing Factor 3/5/9. Peripheral blood monocytes from HC, SC and SAH were analyzed for cytoplasmic/nuclear GRα/GRβ and GR transactivation after dexamethasone, with additional experiments using SAH plasma and the TLR4 inhibitor (YAQ005). Underlying mechanistic studies were performed in HHL-5 cells exposed to EtOH, LPS and DEXA.
Results: In SAH cohort, NR had higher mortality (28-day 14.2% vs 0%; 90-day 17.9% vs 4.8%). In liver biopsies, responders showed a GRα-high/GRβ-low pattern with an increased GRα/GRβ ratio, while non-responders exhibited reduced nuclear GRα, enhanced GRβ in ballooned/steatotic hepatocytes and reduced nuclear SRSF3. In monocytes, dexamethasone increased GRα nuclear translocation and GR transactivation in healthy and SC subjects, but not in SAH, which displayed relatively increased GRβ. SAH plasma induced a steroid-resistant phenotype in healthy monocytes, partially reversed

by YAQ005. In HHL-5 cells, dexamethasone increased nuclear GRα and the GRα/GRβ ratio in controls, whereas EtOH+LPS, but not EtOH or LPS alone, reduced nuclear SRSF3, shifted GR isoforms towards GRβ and blunted DEXA-induced GRα nuclear translocation.
Conclusion: SAH is characterised by multilevel disruption of the GRα/GRβ–SRSF3 axis in the liver and circulating monocytes, providing a mechanistic basis for corticosteroid resistance. The data provide potential candidate biomarkers and therapeutic targets focusing on ensuring GR balance, increasing SRSF3 expression and monocyte GR function. The restoration of GR balance following inhibition of TLR4 indicates a potential novel therapy and should be explored further in suitable models.

OS-035
Impact of glucagon-like peptide-1 therapy on alcohol-related outcomes in cirrhosis: real-world evidence from a multi-center United States cohort
Islam Mohamed[1], Basil Jalamneh[1], Mohamad Ibrahim[2], Judy Sheffeh[3], Prasun Jalal[2]. [1]*Cleveland Clinic Foundation, Cleveland, United States;* [2]*Baylor College of Medicine, Houston, United States;* [3]*Henry Ford Warren Hospital, Warren, United States*
Email: jalal@bcm.edu

Background and aims: Alcohol use disorder (AUD) is a major contributor to alcohol-related liver disease (ALD)-related complications, including hepatic decompensation and liver transplant waitlist removal. Sustained abstinence is central to improving outcomes and current pharmacologic strategies for preventing relapse show limited effectiveness. Glucagon-like peptide 1 (GLP-1) receptor agonists may reduce alcohol cravings through central reward modulation and improve metabolic dysfunction, which often coexists with ALD, but real-world evidence evaluating their clinical impact is limited. This study aimed to assess the effects of GLP-1 receptor agonists on alcohol relapse and liver-related complications among individuals with ALD using TriNetX United States Collaborative Network.
Method: We conducted a retrospective cohort study using the TriNetX global network of 111 healthcare organizations to evaluate adults with alcohol-related liver disease exposed to GLP-1 receptor agonists versus unexposed controls. The index date was the first prescription for exposed patients and the corresponding diagnosis date for controls, with outcomes assessed from 30 to 365 days. Propensity score matching balanced clinical and laboratory factors. Primary outcomes included alcohol-related events, liver disease progression, hospitalization, transplant listing, and phosphatidylethanol positivity. Time-to-event analyses used Kaplan–Meier methods with hazard ratios.
Results: After propensity matching, 9,293 patients were included in each cohort. GLP-1 RA exposure was associated with a significantly lower risk of alcohol remission events (HR 0.76, 95% CI 0.69–0.84), alcohol withdrawal (HR 0.43, 95% CI 0.37–0.51), and alcohol intoxication (HR 0.37, 95% CI 0.31–0.45). GLP-1 RA use was also associated with reduced risks of alcohol-associated hepatitis (HR 0.49, 95% CI 0.43–0.57), cirrhosis progression (HR 0.58, 95% CI 0.46–0.72), all-cause hospitalization (HR 0.46, 95% CI 0.39–0.55), and hepatic decompensation (HR 0.58, 95% CI 0.51–0.66). No significant differences were observed in liver transplant listing or PEth positivity.
Conclusion: In this large real-world cohort with alcohol-related liver disease, glucagon-like peptide 1 receptor agonists were associated with reduced alcohol-related events, slower liver disease progression, and fewer hospitalizations. These findings suggest a potential adjunctive role for glucagon-like peptide 1 therapy in mitigating relapse and improving outcomes, warranting further prospective evaluation.

Basic Science MASLD

OS-036-YI
CD74+ macrophage attenuates metabolic dysfunction-associated steatotic liver disease by driving efferocytosis-dependent metabolic reprogramming and phenotype switch
Yang Xiao[1], Tian Lan[1], Yuanshui Long[1], Chengwei Tang[1], Zhiyin Huang[1], Jinhang Gao[1]. [1]*Department of Gastroenterology and Hepatology, West China Hospital, Sichuan University, Chengdu, China*
Email: xiaoyangsg@foxmail.com

Background and aims: Macrophages clear hepatocytes that undergo programmed cell death (PCD) through efferocytosis to promote tissue regeneration. How efferocytic macrophages regulate metabolic dysfunction-associated fatty liver disease (MASLD) and liver fibrosis through metabolic reprogramming remains to be fully deciphered. We aim to investigate the role and mechanism of CD74$^+$ macrophages in efferocytosis and MASLD.
Method: RNA-sequencing and metabolomics were employed to analyze phenotypes of macrophages after efferocytosing apoptotic, pyroptotic, and necroptotic hepatocytes. Macrophage-specific *Cd74* knockdown mice were fed with CDAHFD diet for 12 weeks to induce MASLD. Single-cell RNA sequencing (scRNA-seq), spatial transcriptomics, and multiplex immunofluorescence (mIF) were performed in the liver of CDAHFD diet-fed mice, and fluorescence-activated cell sorting and live cell imaging in cells, to evaluate CD74$^+$ macrophages-mediated efferocytosis.
Results: Depending on the type of PCD, efferocytosis of dying hepatocytes triggered distinct transcriptional and metabolic phenotypes in macrophages, while *Cd74* expression was consistently upregulated. *Cd74* deletion in macrophages inhibited efferocytosis of dying hepatocytes *in vitro*. Mechanistically, Co-immunopercipitation assay showed that CD74 bind to GAS6, a bridging molecule crucial for the detection and engulfment of dying cells. ScRNA-seq and mIF from patients revealed that the number and proportion of CD74$^+$ macrophages and efferocytosis of dying hepatocytes were increased with the progression of liver fibrosis. Spatial transcriptomics revealed that macrophage-specific *Cd74* knockdown inhibited efferocytosis, resulting in an increased number of apoptotic hepatocytes and liver fibrosis and steatosis in MASLD mouse model, confirmed by staining. Metabolomics showed decreased level of S-adenosylmethionine (SAM), the main source of methionie essential for histone methylation, and increased level of nicotinamide in efferocytic macrophages, which further increased SAM consumption. These metabolic changes inhibited histone methylation and downstream transcription of macrophage cathepsin S, a profibrotic factor that induced hepatic stellate cell activation and liver fibrosis.
Conclusion: CD74$^+$ macrophages represent a macrophage subset characterized by high efferocytic capacity. Efferocytosis of dying hepatocytes triggered metabolic reprogramming-mediated histone modification, which reversed the profibrotic phenotype of macrophages and inhibited liver fibrosis.

OS-037
Hepatic STARD1-dependent Oxysterol generation emerges as a novel cardiovascular risk factor in MASH
Sandra Torres Núñez[1], Eduardo Garcia[2], Susana Núñez[1], Vicent Ribas[1], Leire Goicoechea[1], Hala Jaara[1], Ana Garcia[3], Mariana Acevedo[1], Ana Cenarro[4], Emma Muñoz[5], Naira Rico[6], Ana Paula Dantas[7], Francisco Jiménez-Trinidad[3], Eduard Guasch[3,5], Xavier Lopez[5], Montserrat Rigoll[3], Josefina Casas[8], Rocío Munoz-Hernández[9], Manuel Romero-Gómez[9], Vicenta Llorente-Cortes[10], José Fernandez-Checa[1,11], M. Carmen Garcia-Ruiz[1,11]. [1]*Department of Molecular and Cellular Biomedicine, Institute of Biomedical Research of Barcelona (IIBB), CSIC, Barcelona, Spain, CIBEREHD, Madrid, Spain,*

Instituto de Investigaciones Biomédicas August Pi i Sunyer (IDIBAPS), Liver Unit, Hospital Clinic I Provincial de Barcelona, Barcelona, Spain, Barcelona, Spain; [2]Department of Experimental Pathology, Institute of Biomedical Research of Barcelona (IIBB), CSIC, Barcelona, Spain, Barcelona, Spain; [3]Department of Cardiology, Cardiovascular Clinical Institute, Arrythmia Unit, Hospital Clìnic, Universitat de Barcelona, Centro de Investigación Biomédica en Red de Enfermedades Cardiovasculares (CIBERCV), Madrid, Spain, Barcelona, Spain; [4]Instituto Investigación Sanitaria Aragón, Hospital Universitario Miguel Servet, Zaragoza, Spain, Centro de Investigación Biomédica en Red de Enfermedades Cardiovasculares (CIBERCV), Madrid, Spain, Zaragoza, Spain; [5]Instituto de Investigaciones Biomédicas August Pi i Sunyer (IDIBAPS), Barcelona, Spain, Barcelona, Spain; [6]CORE Laboratory, Biochemistry and Molecular Genetics Department, Biomedical Diagnostic Centre, Hospital Clínic, Barcelona, Spain, Barcelona, Spain; [7]Department of Cardiology, Cardiovascular Clinical Institute, Arrythmia Unit, Hospital Clìnic, Universitat de Barcelona, Barcelona, Spain; [8]Research Unit on BioActive Molecules (RUBAM), Departament de Química Orgànica Biològica, Institut D'Investigacions Químiques I Ambientals de Barcelona, Consejo Superior de Investigaciones Científicas (CSIC), Barcelona, Spain, Barcelona, Spain; [9]UCM Digestive Diseases and Ciberehd, Virgen del Rocío University Hospital, CSIC, Institute of Biomedicine of Seville, University of Seville, CIBEREHD, Madrid, Spain, Seville, Spain; [10]Department of Experimental Pathology, Institute of Biomedical Research of Barcelona (IIBB), CSIC, Barcelona, Spain, Centro de Investigación Biomédica en Red de Enfermedades Cardiovasculares (CIBERCV), Madrid, Spain, Barcelona, Spain; [11]Department of Medicine, Keck School of Division of Gastrointestinal and Liver disease, University of Southern California, Los Angeles, CA, United States., Los Angeles, United States
Email: carmen.garcia@iibb.csic.es

Background and aims: Metabolic dysfunction–associated fatty liver disease (MAFLD) is associated with extrahepatic complications, particularly cardiovascular disease (CVD), yet the mechanistic liver–heart connection remains unclear. Cholesterol trafficking to mitochondria via STARD1 promotes MAFLD progression and hepatocellular carcinoma. Mitochondrial cholesterol is converted by CYP27A1 into 27-hydroxycholesterol (27-OHC), the most abundant circulating oxysterol, which is elevated in MAFLD patients and induces atherosclerosis in mice. This study investigated the role of hepatic STARD1 in MAFLD progression and cardiac remodeling, focusing on 27-OHC as a mediator of the liver–heart axis.
Method: Male hepatocyte-specific StARD1 knockout ($StARD1^{\Delta Hep}$) and control ($StARD1^{f/f}$) mice were fed a standard diet or a high-fat, high-cholesterol (HFHC) diet (60% fat, 0.5% cholesterol) for up to 10 months. Liver injury, steatosis, and fibrosis were assessed histologically. Cardiac remodeling was evaluated by fibrosis staining, magnetic resonance imaging (MRI), and lipidomic analyses of cholesterol esters (CE), triglycerides (TG), ceramides, and 27-OHC. Cardiac expression of LRP-1 and cathepsin D (CatD) was analyzed in mouse hearts and in human cardiac myocytes treated with 27-OHC. Circulating 27-OHC was measured in serum from MAFLD patients.
Results: HFHC-fed $StARD1^{\Delta Hep}$ mice showed reduced liver injury, hepatocyte ballooning, steatosis, and fibrosis compared with $StARD1^{f/f}$ controls, confirming STARD1's role in MAFLD progression. Hearts from HFHC-fed $StARD1^{\Delta Hep}$ mice exhibited reduced LRP-1 and CatD expression and preserved cardiac output by MRI. Cardiac CE and TG content increased with HFHC feeding but did not differ between genotypes. Hepatic 27-OHC was nearly undetectable in $StARD1^{\Delta Hep}$ mice, while cardiac 27-OHC was reduced by ~50%, indicating that a substantial fraction of cardiac 27-OHC originates from the liver in a STARD1-dependent manner. Ceramide profiles were unchanged between genotypes.In vitro, 27-OHC reduced viability, increased ROS, and induced LRP-1 and CatD in human cardiac myocytes. Serum from MAFLD patients showed elevated circulating 27-OHC, supporting translational relevance.
Conclusion: Hepatic STARD1 promotes MAFLD progression and generates 27-OHC, contributing to cardiac remodeling and dysfunction. Elevated circulating 27-OHC in MAFLD patients supports a mechanistic liver–heart axis and identifies STARD1–27-OHC as potential therapeutic targets to mitigate liver–heart complications.

OS-038
Environmental chemical exposure as a modifier of disease severity in metabolic dysfunction–associated steatotic liver disease

Tuulia Hyötyläinen[1], Shashank Gupta[2], Andi Alijagic[2], João Barbosa[2], Jade Chaker[2], Maria Grau[3], Daniel Duberg[2], Antonio Vidal-Puig[4], Stefania Carobbio[5], Vlad Ratziu[6], Jörn M. Schattenberg[7], Elisabetta Bugianesi[8], Ann Daly[9], Quentin M. Anstee[9], Matej Orešič[10].
[1]Orebro University, Örebro, Sweden; [2]Örebro universitet, Örebro, Sweden; [3]Cipf Centre d'Investigació Príncep Felip, Valencia, Spain; [4]University of Cambridge, Príncipe Felipe Research Center, Cambridge, United Kingdom; [5]Príncipe Felipe Research Center, Valencia, Spain; [6]Assistance Publique-Hôpitaux de Paris, Paris, France; [7]Saarland University Medical Centre, Hamburg, Germany; [8]University of Turin, Torino, Italy; [9]Newcastle University, Newcastle upon Tyne, Northern Ireland; [10]Örebro universitet, University of Turku, Örebro, Sweden
Email: tuulia.hyotylainen@oru.se

Background and aims: Metabolic dysfunction–associated steatotic liver disease (MASLD) is the most prevalent chronic liver disease worldwide, yet excess adiposity alone does not explain interindividual susceptibility or disease progression. Environmental exposures, particularly endocrine-disrupting chemicals such as per- and polyfluoroalkyl substances (PFAS), may act as disease modifiers by exacerbating metabolic stress and impairing hepatic adaptive capacity. Our aim was to identify associations between real-life chemical exposures and MASLD severity and to study underlying metabolic pathways relevant to liver pathology.
Method: We performed an exposome-wide analysis in 1,521 adults from the European Steatotic Liver Disease (SLD) Registry, covering the spectrum of steatosis, inflammation, and fibrosis. Plasma PFAS and metabolic profiles were analysed using liquid chromatography–mass spectrometry. Associations with liver-related phenotypes were assessed using multivariable and sex-stratified analyses. Findings were combined with PFAS exposure experiments in mice and hepatocyte-like HepaRG cells to support mechanistic interpretation.
Results: PFAS and parabens were associated with MASLD severity, correlating with histologically characterised steatosis, ballooning, and fibrosis, with non-invasive fibrosis measures (fib4 and fibroscan) as well as markers of insulin resistance in sex-specific manner. PFAS exposure was linked to disturbances in bile acid metabolism, lipid metabolism (phosphatidylcholines and sphingolipids), amino acids and gut microbiota–derived metabolites, with stronger associations in males. Upregulation of several bile acids was also associated with fibrosis, especially in males (9 bile acids with adjusted $p < 0.1$, $t > 2.8$), and with lipids in both females and males (182 and 167 lipids in females and males, respcectly, adj. $p < 0.01$). These metabolic signatures were directionally consistent across human, *in vivo*, and *in vitro* models and were most pronounced under steatotic conditions, suggesting synergistic effects.
Conclusion: Integrated human and experimental data indicate that PFAS exposure is associated with more advanced MASLD through disruption of bile acid homeostasis, lipid metabolism, mitochondrial pathways, and the gut–liver axis. Environmental chemical exposure may therefore represent a clinically relevant modifier of MASLD progression, supporting the inclusion of exposome-informed perspectives in risk stratification and preventive strategies in hepatology.

OS-039-YI

DNMT3A establishes an epigenetic macrophage immunometabolic program driving inflammation and fibrosis in MASH

Amaia Navarro-Corcuera[1], Naroa Goikoetxea-Usandizaga[1], Carolina Conter[1], Patricia Peña-Sanfélix[1], Leidy Estefanía Zapata-Pavas[1], Nerea Ferreiro[1], María Luz Martínez-Chantar[1]. [1]*CIC bioGUNE, Basque Research and Technology Alliance, BRTA, building 801A, 48160, Derio, Spain*
Email: anavarro@cicbiogune.es

Background and aims: Metabolic dysfunction–associated steatohepatitis (MASH) is a leading cause of cirrhosis, hepatocellular carcinoma, and liver transplantation, with fibrosis stage representing the strongest predictor of mortality. Current therapies show limited antifibrotic efficacy, underscoring the need to target core fibro-inflammatory mechanisms. Macrophages are central drivers of MASH progression, yet the epigenetic programs locking them into pathogenic states remain undefined. We hypothesized that the de novo DNA methyltransferase DNMT3A acts as a master regulator of macrophage immunometabolic reprogramming that sustains inflammation and fibrosis in MASH.
Method: We used a diet- and toxin-induced FAT-MASH mouse model that recapitulates human steatohepatitis and advanced fibrosis. Macrophage heterogeneity was resolved by single-cell RNA-seq. DNMT3A expression and localization were assessed in murine and human MASH livers by transcriptomic and protein analyses. Causal and translational studies integrated myeloid-specific *Dnmt3a* knockout mice, pharmacological DNMT3A inhibition, epigenomic profiling (EM-seq, ChIP-seq), metabolic assays, and comparison with Resmetirom.
Results: Single-cell RNA-seq analysis in FAT-MASH mouse livers identified Kupffer-like macrophages, monocyte-derived macrophages, and lipid-associated macrophages (LAMs) enriched within inflammatory and fibrotic niches. LAMs expressing Trem2, Cd9, Spp1, and Lgals3 accumulated within fibrotic septa and correlated with histological disease severity. FAT-MASH mice developed extensive macrophage infiltration forming crown-like structures around lipid-laden hepatocytes, accompanied by robust induction of pro-inflammatory cytokines (TNF-alpha, IL-1beta, IL-6), hepatic stellate cell activation, increased collagen deposition, and bridging fibrosis. DNMT3A was strongly upregulated in Trem2^high macrophage subsets in both murine and human MASH livers and spatially localized to fibrotic regions. Functional data supported a DNMT3A-dependent epigenetic program that stabilizes glycolytic, pro-inflammatory, and pro-fibrotic macrophage states in MASH.
Conclusion: DNMT3A defines a previously unrecognized epigenetic checkpoint linking macrophage immunometabolism to persistent inflammation and fibrosis in MASH. Targeting DNMT3A-dependent macrophage programs represents a compelling immune–epigenetic strategy with potential to enhance antifibrotic efficacy beyond current therapies.

OS-040

Sexually dimorphic palmitoylation of UTY of liver sinusoidal endothelial cells drives advanced metabolic dysfunction-associated steatohepatitis (MASH) via PGF2α/SPIN1 axis

Rui-Qi Li[1], Xi-Xuan Wang[1], Jun Guo[2], Hao Ren[1], Tianhao Mao[3], Cai-Yun Zhang[3], Zihao Liang[4], Dawei Yang[5], Yuzheng Zhuge[6], Feng Zhang[6], Wei Chen[4], Changhua Yi[4], Qingfang Xiong[1], Shu-Ling Chen[5], Wei Zhang[6], Yongfeng Yang[1]. [1]*Department of Hepatology, The Second Hospital of Nanjing, Medical School, Southeast University, Nanjing, China;* [2]*Department of Hepatology, The Second Hospital of Nanjing, Medical School, Affiliated to Nanjing University of Chinese Medicine, Nanjing, China;* [3]*Nanjing Key Laboratory of Hepatology, Nanjing University of Chinese Medicine, Nanjing, China;* [4]*Clinical Research Centre, The Second Hospital of Nanjing, Affiliated to Nanjing University of Chinese Medicine, Nanjing, China;* [5]*Department of Pharmacy, The Second Hospital of Nanjing, Affiliated to Nanjing University of Chinese Medicine, Nanjing, China;* [6]*Department of Gastroenterology, Nanjing Drum Tower Hospital, Affiliated Hospital of Medical School, Nanjing University, Nanjing, China*
Email: 627364595@qq.com

Background and aims: The pronounced male predominance in advanced metabolic dysfunction-associated steatohepatitis (MASH) remains mechanistically undefined beyond hormonal influences. Here, we identify a Y chromosome-encoded epigenetic circuit centered on UTY (ubiquitously transcribed tetratricopeptide repeat-containing protein Y-linked) that orchestrates sex-specific MASH through metabolic reprogramming of liver sinusoidal endothelial cells (LSECs).
Method: Utilizing endothelial-specific Uty knockout (Uty EC-CKO) male mice subjected to GAN diets for 20 weeks (MASH), we combined multi-omics profiling, chromatin topology analysis, and intercellular communication assays to delineate the UTY-mediated sexual dimorphism in MASH progression.
Results: Male LSECs exhibited enhanced UTY demethylase activity through Cys379 palmitoylation, driving H3K27me3 erasure at the prostaglandin F synthase (PGFS) promoter. PGFS-derived PGF2α secretion from male LSECs was 2.5- fold higher than females, activating co-cultured hepatic stellate cells (HSCs) via SPIN1 stabilization. PGF2α binding to SPIN1 disrupted its MARCH9-mediated ubiquitination, enabling SPIN1-H3K4me3 complex formation at fibrogenic loci (TGFβ1, Wnt5a). PGF2α exacerbated proinflammatory cytokine release in M1 macrophages. Pharmacological inhibition of UTY palmitoylation (2-BP) or SPIN1-H3K4me3 interaction attenuated collagen deposition by 48–62% in male models, while female fibrogenesis remained unaffected.
Conclusion: Our work unveils a Y chromosome-driven paradigm wherein palmitoylated UTY licenses male-dominant MASH through epigenetic-metabolic coupling in LSECs. The UTY-PGF2α-SPIN1 axis represents a precision therapeutic target for addressing sex disparities in MASH.

Cirrhosis – Clinical and experimental I

OS-041

Development of new criteria for response to plasma volume expansion at 24 hours in patients with cirrhosis and acute kidney injury

Simone Incicco[1], María José Moreta[2], Roberta Gagliardi[1], Selene Iavarone[3], Marta Tonon[1], Elisa Pose[3], Carmine Gambino[1], Jordi Gratacós-Ginès[3], Nicola Zeni[1], Isabel Graupera[3], Valeria Calvino[1], Núria Fabrellas[4], Pere Ginès[5], Paolo Angeli[1], Adrià Juanola[3], Salvatore Piano[1]. [1]*University of Padua, Padua, Italy;* [2]*Liver Unit, Hospital Clínic of Barcelona, Barcelona, Catalunya, Spain, Barcelona, Catalunya, Spain;* [3]*Liver Unit, Hospital Clínic of Barcelona, Barcelona, Catalunya, Spain, Institut d'Investigacions Biomèdiques August Pi i Sunyer (IDIBAPS), Barcelona, Catalunya, Spain, Barcelona, Catalunya, Spain;* [4]*Institut d'Investigacions Biomèdiques August Pi i Sunyer (IDIBAPS), Barcelona, Catalunya, Spain, Faculty of Nursing, University of Barcelona, Barcelona, Catalunya, Spain, Barcelona, Spain;* [5]*Liver Unit, Hospital Clínic of Barcelona, Barcelona, Catalunya, Spain, School of Medicine and Health Sciences, University of Barcelona, Barcelona, Catalunya, Spain, Institut d'Investigacions Biomèdiques August Pi i Sunyer (IDIBAPS), Barcelona, Catalunya, Spain, Barcelona, Catalunya, Spain*
Email: salvatore.piano@unipd.it

Background and aims: Recently, the ADQI/ICA consensus suggested shortening albumin expansion from 48 to 24 hours in patients with cirrhosis and AKI. However, a significant proportion of responses

occurs between 24 and 48 hours. We aimed to develop new criteria to assess response after 24 hours of albumin expansion.
Method: Consecutive inpatients with decompensated cirrhosis and AKI stage≥1b were enrolled at the Hospital of Padova and followed until 90 days, death, or liver transplant. All patients underwent diuretic withdrawal and 48-hour albumin expansion. Serum creatinine (SCr) was assessed at 24 and 48 hours. AKI response was defined as ≥1 stage reduction or resolution. Discrimination ability of 24-hour percentage SCr changes to predict 48-hour response was assessed by the area under the ROC curve, and optimal cut-offs for response and non-response were identified using a likelihood ratio(LR)–based approach (LR+≥6 and LR-≤0.2). External validation was performed in a cohort from Hospital Clínic of Barcelona.
Results: 387 patients with decompensated cirrhosis and AKI were included (mean age 61.6 ± 10.7 years; 72% male). AKI response occurred in 28% of patients at 24 hours and 53% at 48 hours. Among patients classified as non-responders at 24 hours, 35% achieved response at 48 hours (i.e. 48% of all 48-hour responders). 24–hour percentage sCr changes showed high discrimination ability for predicting 48-hour response (AUROC = 0.87, 95%CI = 0.83–0.90, p < 0.001). According to the LR, 24-hour response was classified as full response (≥10% sCr decrease, FR), partial response (0–<10% sCr decrease, PR), or non-response (any increase of sCr, NR). 45%, 25%, and 31% of patients were classified as FR, PR, and NR, with 48-hour response rates of 89%, 36%, and 14%, respectively. The new classification independently predicted AKI resolution during hospitalization /.(FR: OR = 10.19, p < 0.001; PR: OR = 2.09, p = 0.027) and 90-day mortality (FR: sHR = 0.54, p = 0.006; PR: sHR = 0.63, p = 0.031). In the validation cohort (n = 379), discrimination ability of 24-hour percentage sCr changes was confirmed (AUROC 0.85, p < 0.001) as well as the accuracy of the new 24-hour response classification in predicting AKI response at 48 hours, AKI resolution and 90-day mortality.
Conclusion: The ADQI/ICA recommendation to assess albumin response at 24 hours misclassifies many patients as non-responders. The proposed 24-hour response criteria reduce misclassification and may guide decision-making in cirrhosis and AKI.

OS-042

Pulmonary hypertension phenotypes and severity independently predict non–liver-related mortality in compensated cirrhosis: applying the 2022 ESC/ERS criteria

Dario Saltini[1], Antonio Piscopo[2], Tomas Guasconi[1], Marcello Bianchini[1], Andrea Salomè Velasco Mayorga[2], Giustina Lo Cascio[2], Giulia Catania[3], Nicolò Giglioli[4], Filippo Scianò[1], Fabiola Milosa[4], Rosina Maria Critelli[4], Filippo Schepis[1]. [1]*Severe Liver Diseases (M.E.C.) Departmental Unit, Department of Medical Specialties, University Hospital of Modena "Policlinico", University of Modena and Reggio Emilia, European Reference Network on Rare Liver Disorders (ERN Rare-Liver), Modena, Italy;* [2]*Gastroenterology Unit, University Hospital of Modena "Policlinico", University of Modena and Reggio Emilia, Modena, Italy;* [3]*Faculty of Medicine and Surgery; University of Modena And Reggio Emilia, Modena, Italy;* [4]*EpatoGastro Lab – RBA-Labs CHIMOMO Department – University of Modena and Reggio Emilia, Modena, Italy*
Email: fschepis@unimore.it

Background and aims: Pulmonary hypertension (PulH) is increasingly recognized in cirrhosis, yet its prognostic impact in asymptomatic compensated patients remains undefined. The 2022 ESC/ERS guidelines lowered the diagnostic threshold (mPAP >20 mmHg) and introduced a novel "unclassified PulH" phenotype, both untested in hepatology. We investigated whether PulH phenotype and severity independently influence long-term survival beyond liver disease progression.
Method: We retrospectively analyzed consecutive patients undergoing paired hepatic venous pressure gradient and right-heart catheterization between 2016 and 2023. PulH was classified according to 2022 ESC/ERS criteria as pre-capillary (mPAP >20 mmHg, PCWP ≤15 mmHg, PVR ≥2 WU), post-capillary (mPAP >20 mmHg, PCWP >15 mmHg, PVR <2 WU), or unclassified (mPAP >20 mmHg, PCWP ≤15 mmHg, PVR <2 WU). Severity was stratified as mild (mPAP 21–24 mmHg) or overt (mPAP ≥25 mmHg). Patients receiving beta-blockers, diuretics, or cardioactive drugs were excluded. Primary endpoints were 5-year transplant-free survival (5y-TFS) and 5-year non–liver-related mortality (5y-NLRM), censoring at first decompensation, HCC, or ACLF to isolate the extrahepatic impact of PulH.
Results: Of 1,632 screened patients, 325 met inclusion criteria. PulH prevalence was 61%, with unclassified PulH being most common (30%), followed by post-capillary (17%) and pre-capillary (14%). Liver function was preserved (MELD 10.4 ± 3.8; Child-Pugh 5.7 ± 1.2) and clinically significant portal hypertension was present in 83%. Over a mean follow-up of 4.9 ± 2.7 years, 115 patients died (35%) and 49 underwent liver transplantation (15%). Five-year TFS was 67%, 61%, and 53% for no-PulH, unclassified, and pre/post-capillary PulH, respectively (p = 0.01), with corresponding 5y-NLRM rates of 6%, 14%, and 26% (p < 0.001). Direct comparisons across severity categories showed significant differences in TFS and NLRM between no-PulH and both mild and overt PulH. A dose-response relationship emerged, with even mild PulH significantly worsening outcomes. On multivariable analysis, PulH phenotype and severity independently predicted mortality, together with age, Child-Pugh score, and hemoglobin.
Conclusion: In compensated cirrhosis, asymptomatic PulH—even mild or unclassified—independently predicts non–liver-related death, supporting integration of the 2022 ESC/ERS criteria into hepatological risk stratification.

OS-043-YI

Efficacy and safety of low-dose versus standard-dose human albumin in decompensated cirrhosis with acute kidney injury: a randomized controlled trial

Aman Agrawal[1], Deep Patel[1], Ajay Kumar[1], Ujjwal Sonika[1], Siddharth Srivastava[1], Ashok Dalal[1], Sanjeev Sachdeva[1]. [1]*Department of Gastroenterology, Govind Ballabh Pant Institute of Postgraduate Medical Education and Research (GIPMER), New Delhi, India*
Email: amanagrawal.sms96@gmail.com

Background and aims: Acute kidney injury (AKI) complicates 20–50% of decompensated cirrhosis (DC) hospitalizations and significantly increases mortality. Current guidelines recommend 20% human albumin at 1 g/kg/day (maximum 100 g) for 2 days as initial volume resuscitation, based primarily on expert consensus. However, this regimen carries substantial risks of fluid overload and poses significant cost burden, particularly in resource-limited settings. Evidence defining the minimal effective albumin dose remains scarce. This randomized controlled trial aimed to evaluate whether low-dose albumin could achieve comparable efficacy to standard dosing for AKI resolution while offering improved safety.
Method: Hospitalized patients with DC and ICA-defined AKI ≥Stage 1B (serum creatinine ≥1.5 mg/dL) were screened at a tertiary center (April 2024-August 2025). Exclusions included chronic kidney disease, heart failure, albumin allergy, and hemodynamic instability. Patients were randomized 1:1 to receive 20% albumin at either standard dose (1 g/kg/day, maximum 100 g) or low dose (0.5 g/kg/day, maximum 40 g) for 48 hours. Non-responders received vasoconstrictor therapy as per standard protocol. Primary endpoint was complete AKI resolution at 48 hours (serum creatinine within 0.3 mg/dL of baseline). Secondary outcomes included adverse events, hemodynamic response, and mortality.
Results: Sixty patients were enrolled (54 males [90%]; mean age 46.2 ± 8.7 years). Alcohol was the predominant etiology (75%). Baseline characteristics were balanced: mean MELD-Na 28.15 ± 7.33, Child-Pugh C 71.7%, mean creatinine 2.9 ± 1.52 mg/dL. Complete AKI resolution at 48 hours was identical in both groups (11/30 [36.7%]

each; p = 1.0), indicating comparable efficacy. Hemodynamic improvements in mean arterial pressure and IVC diameter were comparable. Fluid overload occurred exclusively in the standard-dose group (6/30 [20%] vs 0/30 [0%]; p = 0.024). In-hospital mortality trended lower with low-dose albumin (6.7% vs 20.0%; p = 0.254), as did 90-day mortality (20.0% vs 46.7%; p = 0.054). Kaplan-Meier analysis confirmed AKI resolution as a strong predictor of 90-day survival (86.4% vs 55.3%, log-rank p = 0.014).
Conclusion: Low-dose albumin (0.5 g/kg/day) achieved comparable efficacy to standard dosing for AKI resolution in decompensated cirrhosis while demonstrating superior safety and reduced costs. These findings align with recent 2024 EASL-ADQI-ICA guidance emphasizing individualized, cautious albumin use and warrant validation in larger multicentre trials.

OS-044
Confocal laser endomicroscopy for assessment of intestinal barrier function in liver cirrhosis: results from a multicenter study using a novel method
Marcel Sorribas Olivera[1], Benedikt Simbrunner[2], Jessica Schaerer[3], Marco Felber[4], Jordi Codinach[5], Mattias Mandorfer[2], Michael Trauner[2], Thomas Reiberger[2], Johann Hammer[6], Reiner Wiest[3]. [1]*Department of Disease Biology, Molecular Cell Biology Group, Almirall, Sant Feliu de Llobregat, Spain, Department of Agri-Food Engineering and Biotechnology, Universitat Politècnica de Catalunya (UPC), Castelldefels, Spain, Sant Feliu de Llobregat, Spain;* [2]*Division of Gastroenterology and Hepatology, Department of Medicine III, Medical University of Vienna, Vienna, Austria, Clinical Research Group MOTION, Medical University of Vienna, Vienna, Austria, Vienna Hepatic Hemodynamic Lab, Division of Gastroenterology and Hepatology, Department of Medicine III, Medical University of Vienna, Vienna, Austria, Vienna, Austria;* [3]*Department of Visceral Surgery and Medicine, Inselspital, Bern University Hospital, University of Bern, Bern, Switzerland, Bern, Switzerland;* [4]*Departement for BioMedical Research, University of Bern, Bern, Switzerland, Department of Visceral Surgery and Medicine, Inselspital, Bern University Hospital, University of Bern, Bern, Switzerland, Bern, Switzerland;* [5]*Department of Bioengineering. School of Engineering. Universitat Ramon Llull - Institut Químic de Sarrià (URL-IQS). 08017 Vía Augusta, 390 (Barcelona), Spain, Barcelona, Spain;* [6]*Division of Gastroenterology and Hepatology, Department of Medicine III, Medical University of Vienna, Vienna, Austria, Vienna, Austria*
Email: marcel.sorribas@gmail.com

Background and aims: Intestinal barrier dysfunction drives complications in advanced chronic liver disease (ACLD). Confocal laser endomicroscopy (CLE) enables real-time, high-resolution visualization of fluorescein leakage across the epithelium during endoscopy. We assessed intestinal permeability by CLE in two independent cohorts and introduced two novel quantitative approaches designed to overcome the limitations of the current scoring systems by providing objective, reproducible measurements; and investigate potential correlations of the CLE with ACLD disease severity and subsequent clinical course.
Method: After intravenous fluorescein administration, CLE of the small intestine was performed in two cohorts: (1) Bern cohort (n = 5 healthy individuals, n = 16 ACLD patients) and (2) Vienna cohort (n = 48 ACLD patients). Image analysis included established Confocal Leak, Gap, and Watson scores, plus two novel quantitative approaches: the 3-layer approach (fluorescence in lumen, epithelium and lamina propria) and the 3-line approach (fluorescence intensity from epithelial base, middle, and apex). These metrics were correlated with ACLD disease severity, liver function, hepatic venous pressure gradient (HVPG) and liver-related events (LREs: decompensation, ACLF, liver-related mortality).
Results: Healthy controls showed no evidence of fluorescein leakage, while ACLD patients frequently exhibited transepithelial fluorescein permeation into the gut lumen. Permeability increased with clinical stage (Vienna cohort: compensated vs. first vs. further decompensation: 24%, 57%, 71%; p = 0.019). Both new quantification methods clearly distinguished healthy, compensated and decompensated states, with negligible interobserver variability. Across cohorts, CLE surrogates of intestinal barrier dysfunction—especially 3-line apex/base ratios and slopes—correlated with HVPG (apex/base ratio: r = 0.575, p < 0.001), liver function (e.g., albumin: r = –0.553, p < 0.001) and higher LRE occurrence during follow-up.
Conclusion: CLE enables direct visualization of intestinal barrier dysfunction in ACLD, that is linked to severity of portal hypertension, liver failure, and to clinical prognosis. The novel 3-line approach provides robust, quantitative assessment of permeability, offering a promising tool for direct endoscopic assessment of intestinal barrier permeability and disease monitoring.

OS-045
Dysregulated Kynurenine metabolism promotes hepatic encephalopathy via neuroinflammation
Michitaka Matsuda[1], Shinji Kondo[1], Taiji Yamazoe[1], Masaaki Mino[1], Eiji Kakazu[1], Tatsuya Kanto[1]. [1]*Japan Institute for Health Security, The Research Center for Hepatitis and Immunology, Chiba, Japan*
Email: matsuda.m@jihs.go.jp

Background and aims: Dysregulated metabolites due to liver diseases are potentially neurotoxic and cause neurologic complications, including hepatic encephalopathy (HE). While hyperammonemia has been used as a biomarker of HE, currently available treatments targeting hyperammonemia are not always effective. The study aims to identify novel metabolites responsible for the development of HE.
Method: Bile duct ligation (BDL) was performed on a C57BL/6 mouse to create the HE model. The open field test evaluated the neurobehavioral changes in the mice. The cellular dynamics of the brain during HE development were evaluated by using bulk/spatial/single-cell transcriptome analyses. The metabolic profiling of the mouse brain, liver, and blood was conducted by an LC-MS-based metabolomics approach. HE-associated metabolites, including Kynurenine, were measured in the serum of patients with liver diseases. Microglia were isolated from the mouse brain and treated with Kynurenine. IDO, an enzyme that metabolizes Tryptophan into Kynurenine, was chemically inhibited by 1-MT in vitro and in vivo.
Results: From 6 days after BDL induction, the mice revealed abnormal behavior and upregulated the neuroinflammation-associated genes in the brain. Immune profiling revealed an increased number of pro-inflammatory macrophage populations in the brain, indicating that microglial activation is involved in the development of HE. Importantly, no hyperammonemia was observed until 14 days after BDL surgery, suggesting non-ammonia factors contributed to neuroinflammation at this early stage. Metabolomic profiling identified kynurenine as an abnormal metabolite increased in the blood, liver, and brain of the model mice. Systemic administration of Kynurenine induced neuroinflammation and abnormal behavior of the wild-type mouse. In vitro, Kynurenine treatment activated microglia isolated from wild-type mice, indicating that elevated Kynurenine induces neuroinflammation via microglial activation. In the liver of HE model mice and cirrhosis patients, IDO, an enzyme that metabolizes tryptophan into Kynurenine, was upregulated. Oral administration of 1-MT, an IDO inhibitor, decreased systemic Kynurenine levels and suppressed neuroinflammation in the HE model mouse.
Conclusion: The transcriptomic and metabolomic profiling of the HE model mice and patients identified kynurenine as a novel immunometabolic factor that is increased early in the development of HE. Kynurenine could be a novel biomarker and therapeutic target of HE.

Cirrhosis – Clinical and experimental II

OS-046

Post-TIPS recompensation is achievable and associated with excellent survival: EUROTIPS-german cirrhosis study group multicenter study

Michael Praktiknjo[1], Wagner Enrique Ramírez[2], Markus Kimmann[1], Anna Baiges[2], Kymentie Ferdinande[3], Lukas Hartl[4], Sheila González-Padilla[5], Dario Saltini[6], Alvaro Giráldez-Gallego[7], Marika Rudler[8], Jesus Donate[9], Wim Laleman[10], Dhiraj Tripathi[11], Laure Elkrief[12], Martin Sebastian McCoy[1], Marlene Reincke[13], Amos Zeller[14], Maike Rebecca Pollmanns[15], Christian Jansen[16], Eirini Claas[17], Julian Pohl[18], Sonia Torres[2], Alberto Zanetto[3], Marlene Hintersteininger[4], Jose Sanchez-Serrano[5], Lukas Sturm[13], Georgios Konstantis[14], Karsten Große[15], Carsten Meyer[19], Tony Bruns[15], Moritz Passenberg[14], Michael Schultheiß[13], Paloma Lluch-García[5], Mattias Mandorfer[4], Giulio Barbiero[20], Andreea Fodor[2], Cornelius Engelmann[18], Tobias Weismüller[17], Johannes Chang[16], Theresa Hildegard Wirtz[15], Jassin Rashidi-Alavijeh[14], Dominik Bettinger[13], Frank Erhard Uschner[1], Luis Téllez[9], Dominique Thabut[8], Filippo Schepis[6], María Pilar Ballester[5], Thomas Reiberger[4], Marco Senzolo[3], Jonel Trebicka[1], Juan Carlos García-Pagán[2], Zeyu Wang[1], Virginia Hernández-Gea[2]. *[1]Department of Medicine B, University Hospital Münster, Münster, Germany; [2]Hepatic Hemodynamic Laboratory, Liver Unit, Hospital Clínic Barcelona, Barcelona, Spain; [3]Unit of Vascular Liver Diseases and Treatment of Portal Hypertension, University-Hospital of Padua, Padua, Italy; [4]Division of Gastroenterology and Hepatology, Department of Medicine III, Medical University of Vienna, Vienna, Austria; [5]Hepatology Unit, Digestive Disease Department, Hospital Clínico Universitario de Valencia, Valencia, Spain; [6]Severe Liver Diseases Unit, University Hospital of Modena, University of Modena and Reggio Emilia, Modena, Italy; [7]Digestive Diseases Department, Hospital Universitario Virgen del Rocío, University of Seville, Seville, Spain; [8]Liver Intensive Care Unit, Hepatogastroenterology Department, La Pitié-Salpêtrière Hospital, Sorbonne Université; INSERM UMR_S 938, Paris, France; [9]Department of Gastroenterology and Hepatology, Hospital Universitario Ramón y Cajal, IRYCIS, Universidad de Alcalá, Madrid, Spain; [10]Department of Gastroenterology and Hepatology, University Hospitals Leuven, KU Leuven, Leuven, Belgium; [11]Liver Unit, University Hospitals Birmingham NHS Foundation Trust, Birmingham, United Kingdom; [12]Faculté de médecine de Tours and Hepato-Gastroenterology Service, CHRU Tours, Université Paris-Cité, Tours, France; [13]Department of Medicine II, Medical Center University of Freiburg, Faculty of Medicine, University of Freiburg, Freiburg, Germany; [14]Department of Gastroenterology, Hepatology and Transplant Medicine, University of Duisburg-Essen, Essen, Germany; [15]Medical Department III, University Hospital RWTH Aachen, Aachen, Germany; [16]Department of Internal Medicine I, University Hospital Bonn, Bonn, Germany; [17]Department of Gastroenterology, Hepatology and Oncology, Vivantes Humboldt-Hospital, Berlin, Germany; [18]Department of Hepatology and Gastroenterology, Charité – Universitätsmedizin Berlin, Campus Virchow Klinikum, Berlin, Germany; [19]Department of Diagnostic and Interventional Radiology, University Hospital Bonn, Bonn, Germany; [20]Unit of Interventional Radiology, University Hospital of Padua, Padua, Italy*
Email: michael.praktiknjo@ukmuenster.de

Background and aims: The Baveno VII definition of recompensation of decompensated cirrhosis excluded patients with TIPS. However, patients achieving etiologic control/cure may still recompensate with/after TIPS, but the incidence of recompensation and its impact on survival is unknown. This study investigates the concept of recompensation in decompensated patients treated with TIPS.

Method: This retrospective multicenter study included prospective TIPS patients from the EuroTIPS consortium (derivation cohort, 8 centers) and retrospective patients from a national real-life cohort (validation cohort, 7 centers). Recompensation was defined according to Baveno VII criteria (except exclusion of TIPS): (i) control of etiology, (ii) resolution of decompensating events off diuretics and laxatives/rifaximin for 12 months, and (iii) improvement of liver function to Child Pugh A. Primary outcome was achievement of recompensation. Secondary outcomes were 1-, 3- and 5-year transplant-free survival.

Results: In total, 1106 patients with controllable etiology (alcohol: n = 819, 74%; viral: n = 121, 11%; autoimmune/PBC: n = 166, 15%) were included. The derivation cohort included 242 patients (82% male), median age of 57 years and MELD of 11. Median follow up was 3.2 years. Etiology was controlled in 202 patients (83.3%) at TIPS implantation. Of those, 27 (13.4%) achieved recompensation status at a median of 1.1 years after TIPS with a 1-, 3-, 5-year survival of 100%, 96%, 77% compared to 77%, 56%, 40% in the non-recompensated patients (p = 0.001). The validation cohort included 864 patients with 551 (63.8%) controlled etiology at baseline. Of those, 88 (15.9%) achieved recompensation at a median of 1.4 years after TIPS, with a 1-, 3-, 5-year survival of 100%, 90%, 87% compared to 82%, 68%, 53% in the non-recompensated patients (p = 0.001). Lower MELD (sHR 0.82, 0.69–0.96) and alcohol etiology (sHR 0.28, 0.11–0.69) were independently associated with recompensation in both cohorts.

Conclusion: Our data support the concept that recompensation after TIPS is indeed achievable. Patients with recompensation after TIPS show excellent transplant-free survival. These findings suggest that the role of post-TIPS recompensation may merit consideration in future refinements of current definitions.

OS-047

A longitudinal multi-modal cfDNA framework for early detection and adaptive monitoring of hepatocellular carcinoma

Rong Fan[1], Liangxu Guo[1], Lei Chen[2], Yunsong Qian[3], Chunying Wang[4], Xiaolong Liu[5], Xiaotang Fan[6], Guoqing Jiang[7], Dan Zheng[8], Pujun Gao[9], Honglian Bai[10], Jie Xia[11], Chuanxin Wang[12], Yanlong Yu[13], Yanhang Gao[14], Jingfeng Liu[15], Jian Sun[1], Hong-Yang Wang[2], Jinlin Hou[1]. *[1]Department of Infectious Diseases, Nanfang Hospital, Southern Medical University, Guangzhou, China; [2]Department of Hepatobiliary Medicine, Shanghai Eastern Hepatobiliary Surgery Hospital, Shanghai, China; [3]Hepatology Department, Ningbo Hwamei Hospital, University of Chinese Academy of Sciences, Ningbo, China; [4]Xuzhou Infectious Disease Hospital, Xuzhou, China; [5]The United Innovation of Mengchao Hepatobiliary Technology Key Laboratory of Fujian Province, Mengchao Hepatobiliary Hospital of Fujian Medical University, Fuzhou, China; [6]Department of Hepatology, First Affiliated Hospital of Xinjiang Medical University, Urumqi, China; [7]Department of Hepatobiliary Surgery, Clinical Medical College, Yangzhou University, Yangzhou, China; [8]Department of Gastroenterology, The Central Hospital of Wuhan, Tongji Medical College, Huazhong University of Science and Technology, Wuhan, China; [9]The First Hospital of Jilin University, Jilin, China; [10]The Department of Infectious Disease, The First People's Hospital of Foshan, Foshan, China; [11]Department of Infectious Diseases, Southwest Hospital, Third Military Medical University (Army Medical University), Chongqing, China; [12]Department of Clinical Laboratory, The Second Hospital, Cheeloo College of Medicine, Shandong University, Jinan, China; [13]Chifeng Clinical Medical School of Inner, Mongolia Medical University, Chifeng, China; [14]First hospital of jilin university, jilin, China; [15]The United Innovation of Mengchao Hepatobiliary Technology Key Laboratory of Fujian Province, Mengchao Hepatobiliary Hospital of Fujian Medical University, Clinical Oncology School of Fujian Medical University, Fujian Cancer Hospital, Department of Hepatopancreatobiliary Surgery, Clinical Oncology School of Fujian Medical University,Fujian Cancer Hospital, Fujian, China*
Email: rongfansmu@163.com

Background and aims: Current guideline-based surveillance for hepatocellular carcinoma (HCC) in patients with cirrhosis remains insufficiently sensitive and lacks flexibility for dynamic risk assessment under irregular monitoring intervals. This study aimed to develop a longitudinal, multimodal cfDNA framework that captures evolving molecular trajectories and enables flexible, adaptive monitoring across variable follow-up schedules.
Method: We conducted a prospective, multicenter cohort study (NCT03588442) enrolling 3444 patients with cirrhosis across 16 hospitals. A total of 6344 serial plasma samples were collected for cfDNA profiling at three predefined follow-up timepoints: T1 (baseline), T2 (6 months), and T3 (12 months). A multi-channel transformer framework, HepaTrack, built with attention-based temporal sequence modeling and incorporating a masking strategy to simulate irregular follow-up scenarios, was developed to integrate copy number, fragmentomic, and sequence-derived cfDNA features, capturing coordinated molecular dynamics for flexible longitudinal modeling of HCC occurence.
Results: During the 12-month follow-up, 109 participants were diagnosed with HCC and 3335 remained free of HCC. By integrating six cfDNA-derived molecular profiles, HepaTrack captured temporal molecular dynamics throughout hepatocarcinogenesis, enabling risk prediction, detection discrimination, and longitudinal monitoring in diverse settings. In the prediction scenario using cfDNA from 6 to 12 months pre-diagnosis, sensitivities were 0.65–0.78 at T1 and 0.74–0.80 at T2, rising to 0.80–0.85 when combining T1 + T2, with overall specificities of 0.93–0.98 across internal and external cohorts. In the detection scenario within 0-6 months pre-diagnosis, sensitivities were 0.82–0.81 at T3, 0.80–0.98 for T1-T3, 0.88–1.00 for T2 + T3, and 0.98–1.00 when all three timepoints (T1 + T2 + T3) were included, with specificities maintained between 0.94 and 0.98. Population-scale simulations showed that applying HepaTrack at single timepoints (T1, T2, T3) detected 1319, 1384, and 1609 HCC cases per 100000 individuals, compared with 619 using alpha-fetoprotein plus ultrasound, representing an approximately a 2.1–2.6-fold increase, with higher sensitivities (0.70, 0.74, 0.86 vs. 0.63) and specificities (0.96, 0.95, 0.97 vs. 0.84).
Conclusion: HepaTrack is a scalable cfDNA framework enabling dynamic HCC surveillance and early detection via multimodal trajectory integration.

OS-048

Efficacy and safety of recombinant human albumin injection in the treatment of hypoalbuminemia in patients with cirrhotic ascites: a phase III randomized, blinded, positive-controlled trial

Xu Li[1], Xinrui Wang[1], Yawen Luo[2], Bin Xu[3], Guoqiang Zhang[4], Shangyuan Cai[5], Jinlin Hou[6], Liang Hong[7], Xiaoping Wu[8], Xing Li[9], Kaizhong Luo[10], Tao Yang[11], Wei Xiang[11], Junqi Niu[1], Yanhang Gao[1].
[1]The First Hospital of Jilin University, China-Singapore Belt and Road Joint Laboratory on Liver Disease Research, Jilin Provincial Key Laboratory of Metabolic Liver Diseases, Changchun, China; [2]The Affiliated Hospital of Zunyi Medical University, Zunyi, China; [3]Beijing Youan Hospital, Capital Medical University, Beijing, China; [4]Luoyang Central Hospital Affiliated to Zhengzhou University, Luoyang, China; [5]The First Affiliated Hospital of Henan University, Kaifeng, China; [6]Nanfang Hospital, Southern Medical University, Guangzhou, China; [7]Rui'an People's Hospital, Ruian, China; [8]The First Affiliated Hospital of Nanchang University, Nanchang, China; [9]Pingxiang People's Hospital, Pingxiang, China; [10]The Second Xiangya Hospital of Central South University, Changsha, China; [11]Tonghua Anrate Biopharmaceutical Co., Ltd, Tonghua, China
Email: yanhang@mail.jlu.edu.cn

Background and aims: Hypoalbuminemia from impaired hepatic synthesis is pivotal in cirrhotic ascites and poor outcomes. Plasma-derived human serum albumin (HSA) is standard but limited by resource scarcity and pathogen risks. Recombinant human albumin (rHA) is a scalable alternative. This phase III trial verified rHA's efficacy equivalence to HSA in serum albumin (ALB) improvement, non-inferiority in ascites reduction, and safety/immunogenicity.
Method: Multicenter randomized double-blinded trial planned to enroll 414 patients aged 18–75 years (BMI ≥18.0 kg/m^2, ALB <30 g/L, cirrhotic ascites Grade 1–2). Patients were randomized 1:1 to rHA (10 g/vial, 20%) or HSA (Alburaas®) 20 g daily IV for 7 days, then with a 12-week follow-up period. Primary endpoint: ALB change from baseline to Day 7 (including early discontinuation for ALB ≥40 g/L with Day 7 assessment). Key secondary endpoint: ascites improvement rate (non-inferiority margin −10%). Analyses used Full Analysis Set (FAS), Per-Protocol Set (PPS), Safety Set (SS), Immunogenicity Analysis Set; primary endpoint via mixed-effects model for repeated measures (MMRM), non-inferiority via stratified Newcombe method.
Results: 416 patients randomized (1:1 rHA:HSA), 414 dosed (rHA 206 vs. HSA 208). Baseline characteristics balanced. Primary endpoint: least squares mean (LSM) ALB change 13.047 (SE = 0.2564) g/L (rHA) vs. 12.302 (SE = 0.2566) g/L (HSA), between-group difference 0.745 (95% CI:0.065–1.425) g/L (within equivalence margin −2 to 2 g/L). Key secondary endpoint: ascites improvement rate 55.3% (rHA) vs. 54.3% (HSA), difference 1.1% (95% CI:-8.47%–10.61%, lower bound > −10%). ALB ≥35 g/L rate (89.8% vs. 88.0%, p = 0.5709), median time to ALB ≥35 g/L (7 days both), plasma colloid osmotic pressure (COP) change (3.69 ± 0.219 vs. 3.75 ± 0.216 mmHg, p = 0.8473), as well as changes in body weight, abdominal circumference, ascites depth, and clinical symptom improvement (dyspnea, shortness of breath, abdominal distension) were comparable. Median time to retreatment: not reached (rHA) vs. 96.0 days (HSA). No rHA-related serious adverse events (SAEs); 1.9% HSA-related SAEs. Immunogenicity: 3/206 (1.46%) patients had transient low-titer anti-drug antibodies (ADA), no efficacy/safety impact.
Conclusion: Recombinant human albumin is efficacy-equivalent to HSA in ALB improvement, non-inferior in ascites reduction, with sustained effects, favorable safety, and low immunogenicity, serving as a reliable HSA alternative for cirrhotic ascites-related hypoalbuminemia.

OS-049

Natural killer cell immune dysfunction characterizes patients with acute-on-chronic liver failure

Rosa Martin-Mateos[1], Leticia Munoz[2], Alejandro Miranda[2], Ferran Aguilar[3], Juanjo Lozano[4], Zhujun Cao[5], Maria Papp[6], Alberto Farias[7], Liliana Mendes[8], Carlo Alessandria[9], Luciana Lofego Goncalves[10], Martin Janicko[11], Victor Vargas Blasco[12], Sebastián Marciano[13], Gustavo Pereira[14], Salvatore Piano[15], Christian Jansen[16], Adelina Lozano Miranda[17], Daniel Mazo[18], Mauricio Castillo[19], Eduardo Morales Sorribas[20], Loreto López Vergara[20], Lorena Paule[21], Raquel Sánchez Martín[21], Wim Laleman[22], Jonel Trebicka[3,23], Vicente Arroyo[3], Joan Clària[24], Richard Moreau[3], Agustín Albillos[1].
[1]Hospital Universitario Ramón y Cajal, IRYCIS, Universidad de Alcalá, CiberEHD, Madrid, Spain; [2]Universidad de Alcalá, CiberEHD, Madrid, Spain; [3]European Foundation for the Study of Chronic Liver Failure (EF CLIF), Barcelona, Spain; [4]CIBERehd, Barcelona, Spain; [5]Department of Infectious Diseases, Ruijin Hospital, School of Medicine, Shanghai Jiao Tong University, Shanghai, China; [6]University of Debrecen, Faculty of Medicine, Institute of Medicine, Department of Gastroenterology, Debrecen, Hungary; [7]Faculdade de Medicina, Universidade Federal de Minas Gerais, Instituto Alfa de Gastroenterologia, Hospital das Clínicas da Universidade Federal de Minas Gerais, Belo Horizonte, Brazil; [8]Hospital de Base do Distrito Federal, Brasilia, Brazil; [9]Division of Gastroenterology and Hepatology, A. O.U. Città della Salute e della Scienza di Torino, University of Turin, Turin, Italy; [10]Gastroenterology and Hepatology Unit, Hospital Universitário Cassiano Antônio Moraes, Universidade Federal do Espírito Santo, Vitòria, Brazil; [11]Pavol Jozef Safarik University in Kosice, Kosice, Slovakia; [12]Hospital Vall d'Hebron, Universitat Autònoma de Barcelona, Barcelona, Spain; [13]Liver Unit and Department of Research, Hospital Italiano de Buenos Aires, Buenos Aires, Argentina; [14]Gastroenterology and

Hepatology Unit, Bonsucesso Federal Hospital (Ministry of Health), Rio de Janeiro, Brazil; [15]University of Padova, Padova, Italy; [16]University of Bonn, Bonn, Germany; [17]Hospital Nacional Guillermo Almenara, Universidad Nacional de San Marcos, Lima, Peru; [18]Universidade Estadual de Campinas, Campinas, Brazil; [19]Servicio de Gastroenterología y Hepatología, Hospital de Especialidades Centro Médico Nacional La Raza IMSS, Ciudad de Mexico, Mexico; [20]Department of Critical Care, Hospital Universitario Ramón y Cajal, Madrid, Spain; [21]University of Alcalá, Madrid, Spain; [22]Department of Gastroenterology and Hepatology, Division of Liver & Biliopancreatic disorders and Liver Transplantation, University Hospitals Leuven, Leuven, Belgium; [23]Department of Internal Medicine B, University of Münster, Münster, Germany; [24]EF CLIF, Hospital Clínic de Barcelona, IDIBAPS, CIBERehd & Universitat de Barcelona, Barcelona, Spain
Email: rosamartinmat@hotmail.com

Background and aims: Cirrhosis-associated immune dysfunction is characterized by progressive systemic inflammation and immunodeficiency. Patients with acute-on-chronic liver failure (ACLF) display the highest grade of both components. The underlying dysfunctional mechanisms across the different immune cell populations and their prognostic relevance remain unclear. This study investigated the transcriptomic profiles and phenotypic alterations of circulating NK cells in ACLF.

Method: RNA sequencing was performed on whole-blood samples from 25 healthy controls and 422 patients included in the seminal ACLARA and PREDICT studies sponsored by the European Foundation CLIF (123 with ACLF and 299 with acute decompensation). Immune cell composition was inferred by cell deconvolution using SingleR and CIBERSORT, and differentially expressed genes were identified (log_2FC >1.5, FDR <0.05; DESeq2). Findings were validated in independent translational cohorts by multiparametric flow cytometry, assessing NK-cell phenotype and effector function both at baseline and after stimulation.

Results: Transcriptomic analysis revealed a marked dysregulation of the lymphoid compartment in ACLF, with a significant reduction in T and NK cells. Flow cytometry confirmed lower circulating NK-cell counts affecting both cytotoxic and immunomodulatory subsets, while a population with a partially deactivated or exhausted phenotype showed a relative increase. Patients who died had significantly fewer circulating NK cells, linking NK-cell loss to poor prognosis. Phenotypic analysis revealed an inhibitory and functionally exhausted NK-cell profile in ACLF, characterized by increased NKG2A (inhibitory) and decreased NKG2D (activating) expression. These changes were associated with reduced cytotoxic (↓CD57) and secretory activity (↓perforin and IFNγ after stimulation), together with changes in maturation, migration (↓CXCR3), proliferation (Ki67), and apoptosis (Annexin V/caspase), suggesting accelerated but ineffective cellular turnover and an overall state of effector hyperresponsiveness.

Conclusion: ACLF induces a profound immune dysregulation, with a major impact on the NK-cell compartment. Circulating NK cells are markedly reduced, and their phenotypic and functional profile reflects an exhausted effector state that may contribute to poor outcomes.

OS-050-YI

A genome-wide association study identifies SUSD1 as a risk locus for renal impairment in decompensated cirrhosis

Lukas Otero Sanchez[1], Joan Clària[2], Clelia Galvanin[1], Ferran Aguilar[3], Layese Richard[4], Matteo Serra[5], Laura Jiménez-Gracia[6], Darko Castven[7], Soňa Fraňková[8], Milan Jirsa[9], David Tornai[10], Anna Curto-Vilalta[3], Alberto Queiroz Farias[11], Maria Papp[10], Patricia Momoyo Zitelli[11], Paolo Caraceni[12], Giacomo Zaccherini[13], Luciana Lofego Goncalves[14], Carlo Alessandria[15], Gustavo Pereira[16], Wim Laleman[17], Adrian Gadano[18], Salvatore Piano[19], Angelo Z. Mattos[20], Desislava Germanova[21], Valerio Lucidi[21], Soret Daphnee[22], Line Carolle Ntandja Wandji[22], Frank Erhard Uschner[23], Aldo Torre[24], Victor Vargas Blasco[25], Liliana Mendes[26], Rajeshwar Prosad Mookerjee[27], Carlos Benitez[28], Mario Álvares-da-Silva[29], Myriam Remmelink[30], Paulo Bittencourt[31], Agustín Albillos[32], Cláudia Couto[33], Rafael Bañares[34], Manuel Mendizabal[35], Delphine Degré[1], Claudio Toledo[36], Martin Janičko[37], Daniel F Mazo[38], Pietro Gatti[39], Mauricio Castillo[40], William Bernal[41], Adelina Lozano Miranda[42], P. Martin Padilla[43], Alexander Zipprich[44], René Malé Velazquez[45], Christophe Moreno[1], Andre Lyra[46], Flair Jose Carrilho[47], Juan C Nieto[6], Javier Fernández[48], Jonel Trebicka[49], Rajiv Jalan[50], Paolo Angeli[19], Horia Ștefănescu[51], Pierre-Emmanuel Rautou[52], Stephan Buch[53], Alexandre Louvet[22], Jens U. Marquardt[7], Thierry Gustot[1], Holger Heyn[6], Vicente Arroyo[3], Nathalie Ganne-Carrié[54], Jan Sperl[8], Richard Moreau[3,52], Philippe Mathurin[22], Pierre Nahon[54], Eric Trépo[1]. *[1]Department of Gastroenterology, Hepatopancreatology and Digestive Oncology, Hôpital Universitaire de Bruxelles, Université Libre de Bruxelles, Brussels, Belgium, Laboratory of Experimental Gastroenterology, Université Libre de Bruxelles, Brussels, Belgium, Department of Hepatogastroenterology, Hôpital Pitié Salpêtrière-Assistance Publique-Hôpitaux de Paris, Paris, France, Bruxelles, Belgium; [2]Hospital Clínic De Barcelona, Barcelona, Spain; [3]European Foundation for the Study of Chronic Liver Failure (EF CLIF) and Grifols Chair, Barcelona, Spain, Barcelona, Spain; [4]Université Paris Est Créteil, INSERM, IMRB, Equipe CEpiA (Clinical Epidemiology and Ageing), Unité de Recherche Clinique (URC Mondor), Service de Santé Publique, Assistance Publique Hôpitaux de Paris (AP-HP), Hôpitaux Universitaires Henri Mondor, F-94000, Créteil, Paris, France; [5]Breast Cancer Translational Research Laboratory J-C Heuson, Université Libre de Bruxelles (ULB), Hôpital Universitaire de Bruxelles (HUB), Institut Jules Bordet, Brussels, Brussels, Belgium; [6]Centro Nacional de Análisis Genómico, C/Baldiri Reixac 4, 08028 Barcelona, Spain, Barcelona, Spain; [7]Department of Medicine I, University Medical Center Schleswig-Holstein, Lübeck 23562, Germany, Lubeck, Germany; [8]Department of Hepatogastroenterology, Institute for Clinical and Experimental Medicine, 14021 Prague, Czech Republic, Prague, Czech Republic; [9]Laboratory of Experimental Hepatology, Center for Experimental Medicine, Institute for Clinical & Experimental Medicine, Prague, Czech Republic, Prague, Czech Republic; [10]Division of Gastroenterology, Department of Internal Medicine, Faculty of Medicine, University of Debrecen, Debrecen, Hungary, Debrecen, Hungary; [11]Department of Gastroenterology, Hospital das Clínicas, University of Sao Paulo School of Medicine, Sao Paulo, Brazil, Sao Paulo, Brazil; [12]Unit of Semeiotics, Liver and Alcohol-related Diseases, IRCCS Azienda Ospedaliera-Universitaria di Bologna, Italy, Department of Medical and Surgical Sciences, University of Bologna, Italy, Bologna, Italy; [13]IRCCS Azienda Ospedaliero-Universitaria di Bologna, Unit of Semeiotics, Liver and Alcohol-related Diseases, Bologna, Italy; [14]Gastroenterology and Hepatology Unit, Hospital Universitário Cassiano Antônio Moraes, Universidade Federal do Espírito Santo, Vitória, Brazil, Vitoria, Brazil; [15]Division of Gastroenterology and Hepatology, A.O.U. Città della Salute e della Scienza di Torino, University of Turin, Turin, Italy, Turin, Italy; [16]Gastroenterology and Hepatology Unit, Bonsucesso Federal Hospital (Ministry of Health), Rio de Janeiro, Brazil, Rio de Janeiro, Brazil; [17]Department of Gastroenterology & Hepatology, Division of Liver and Biliopancreatic disorders, UZ Leuven, KU LEUVEN, LEUVEN, Belgium, Leuven, Belgium; [18]Liver Unit and Department of Research, Hospital Italiano de Buenos Aires, Buenos Aires, Argentina, Buenos aires, Argentina; [19]University of Padova, Padova, Italy, Padova, Italy; [20]Federal University of Health Sciences of Porto Alegre, and Gastroenterology and Hepatology Unit, Irmandade Santa Casa de Misericórdia de Porto Alegre, Porto Alegre, Brazil, Porto Alegre, Brazil; [21]Department of Digestive Surgery and Transplantation, Hôpital Universitaire de Bruxelles, Université Libre de Bruxelles, Belgium, Brussels, Belgium; [22]Université Lille, CHU de Lille, Service des maladies de l'appareil digestif, Hôpital Huriez, INFINITE-U1286, Lille, France, Lille, France; [23]JW Goethe University Hospital, Frankfurt, Germany, Frankfurt, Germany; [24]Departamento de Gastroenterología, Instituto Nacional de Ciencias Médicas y Nutrición 'Salvador Zubirán', Mexico City, Mexico, Mexico City, Mexico; [25]Liver Unit, Hospital Universitario Vall d´Hebron, Facultad*

de Medicina, Universidad Autónoma de Barcelona, Barcelona, Spain, Barcelona, Spain; [26]Hospital de Base do Distrito Federal, Brasilia, Brazil, Brasilia, Brazil; [27]UCL Medical School, Royal Free Hospital, London, United Kingdom, London, United Kingdom; [28]Departamento de Gastroenterología, Facultad de Medicina, Pontificia Universidad Católica de Chile, Santiago, Chile, Santiago, Chile; [29]Gastrointestinal and Liver Unit, Hospital de Clínicas de Porto Alegre, Universidade Federal do Rio Grande do Sul, Brazil, Porto Alegre, Brazil; [30]Department of Pathology, Hôpital Universitaire de Bruxelles, Université Libre de Bruxelles, Brussels, Belgium, Brussels, Belgium; [31]Hospital Português da Bahia, Brazil, Bahia, Brazil; [32]Department of Gastroenterology, Hospital Universitario Ramón y Cajal, IRYCIS, University of Alcalá, CIBEREHD, Madrid, Spain, Madrid, Spain, [33]Faculdade de Medicina, Universidade Federal de Minas Gerais; Instituto Alfa de Gastroenterologia, Hospital das Clínicas da Universidade Federal de Minas Gerais, Belo Horizonte, Brazil; [34]Department of Gastroenterology and Hepatology. Hospital General Universitario Gregorio Marañón. Instituto de Investigación Sanitaria Gregorio Marañón. Facultad de Medicina (Universidad Complutense of Madrid), CIBERehd, Madrid, Spain, Madrid, Spain; [35]Unidad de Hígado y Trasplante Hepático, Hospital Universitario Austral, Pilar, Argentina, Pilar, Argentina; [36]Gastroenterology Unit, Hospital Valdivia, Universidad Austral de Chile, Valdivia, Chile; [37]Pavol Jozef Safarik University in Kosice and Pasteur University hospital, Kosice, Slovakia, Kosice, Slovakia; [38]Division of Gastroenterology, University of Campinas, Campinas, Brazil, Campinas, Brazil; [39]Internal Medicine PO Ostuni, ASL Brindisi, Italy, Brindisi, Italy; [40]Servicio de Gastroenterología y Hepatología, Hospital de Especialidades Centro Médico Nacional La Raza Instituto Mexicano del Seguro Social, Mexico City, Mexico, Mexico City, Mexico; [41]King's College Hospital, London, United Kingdom, London, United Kingdom; [42]Unidad de Hígado, Hospital Nacional Arzobispo Loayza, Lima, Perú, Lima, Peru; [43]Hospital Nacional Guillermo Almenara, Universidad Nacional de San Marcos, Lima, Perú, Lima, Peru; [44]University Hospital Halle-Wittenberg, Halle (Saale), Jena University Hospital, Jena, Germany, Jena, Germany; [45]Instituto de Salud Digestiva y Hepática, Guadalajara, México, Guadalajara, Mexico; [46]Hospital Universtário Professor Edgard Santos, Salvador, Brazil, Salvador, Brazil; [47]Hospital São Rafael, Salvador, Brazil, Salvador, Brazil; [48]Hospital Clínic de Barcelona, IDIBAPS, CIBERehd and Universitat de Barcelona, Barcelona, Spain, Barcelona, Spain; [49]Department of Internal Medicine B, University of Münster, Münster, Germany, Munster, Germany; [50]Liver Failure Group. Institute for Liver and Digestive Health, Division of Medicine, University College London, Royal Free Campus, London, United Kingdom, London, United Kingdom; [51]Liver Unit, Regional Institute of Gastroenterology and Hepatology 'Octavian Fodor,' University of Medicine and Pharmacy 'Iuliu Hatieganu,' Cluj-Napoca, Romania, Cluj-Napoca, Romania; [52]Service d'Hépatologie, Hôpital Beaujon, Centre de Référence des Maladies Vasculaires du Foie, FILFOIE, European Reference Network on Hepatological Diseases, Clichy, France, Clichy, France; [53]Department of Medicine I, Dresden University Hospital, Dresden 01307, Germany, Dresden, Germany; [54]AP-HP, Hôpitaux Universitaires Paris Seine Saint-Denis, APHP, Liver Unit, Bobigny, Université Sorbonne Paris Nord, F-93000 Bobigny, Inserm, UMR-1138 "Functional Genomics of Solid Tumors," Centre de recherche des Cordeliers, Université de Paris, Paris, Paris, France
Email: lukas.otero.sanchez@ulb.be

Background and aims: Renal impairment (RI) is a frequent and life-threatening complication of decompensated cirrhosis, yet genetic susceptibility factors remain unknown. We performed the first genome-wide association study (GWAS) to identify genetic variants associated with RI in this critically ill population and provide insights into pathophysiological mechanisms.
Method: The derivation phase included 3,220 patients across five cohorts (83% European, 17% Admixed American ancestry). The validation phase included 1,728 European ancestry patients across four independent cohorts. Linear regression models adjusted for the first 10 principal components, age and sex assessed genetic associations with serum creatinine (sCr) as a surrogate of RI. Separate analyses were integrated through trans-ancestry and cohort meta-analyses. Single-cell and spatial transcriptomics mapped GWAS signals to cell types in the liver, blood and kidney.
Results: The rs2099161[C > T] variant at the *SUSD1* locus showed genome-wide significant association with sCr (trans-ancestry derivation: beta = 0.16, 95% CI: 0.11–0.21; $p = 4.32 \times 10^{-10}$; independent validation: beta = 0.09, 95% CI: 0.03–0.16; $p = 5.34 \times 10^{-3}$). Combined meta-analysis of all nine cohorts demonstrated homogeneous effect sizes (beta = 0.13, 95% CI: 0.09–0.17; $p = 8.31 \times 10^{-11}$; $I^2 = 0\%$). This association was specific to decompensated cirrhosis, with no effect in compensated cirrhosis (n = 3,139; beta = 0.00, 95% CI: – 0.05 to 0.05; p = 0.99) or the general population (n = 402,683; beta = –0.01, 95% CI: – 0.01 to 0.00; $p = 3.78 \times 10^{-3}$). The rs2099161[C] risk allele was significantly associated with kidney failure at inclusion ($p = 6.34 \times 10^{-4}$), with CC homozygotes showing OR = 1.60 (95% CI: 1.21–2.11) compared to TT homozygotes. Similar associations were observed for terlipressin requirement (p = 0.027; CC vs TT: OR = 2.06, 95% CI: 1.06–3.92). Transcriptomic analyses identified plasmacytoid dendritic cells (pDCs) as the primary *SUSD1*-expressing cell type with elevated expression in patients with RI across compartments. Patients with RI showed increased pDC abundance and type I interferon signaling in liver and kidney tissues.
Conclusion: *SUSD1* is a risk locus for RI specifically in decompensated cirrhosis across diverse ancestries and cohorts. Our results highlight gene-environment interactions and implicate the pDC-interferon axis as a candidate mechanism linking liver dysfunction to kidney injury.

Liver tumours – Clinical

OS-051-YI
Olanzapine improves appetite, weight and quality of life in patients with hepatocellular carcinoma: a multicenter, randomized controlled trial

Sagnik Biswas[1], Vijay Alexander[2], Vignesh Dwarkanathan[3], Sanchita Gupta[1], Arun Valsan[4], Gurasis Boparai[1], Amruthavarshini Nagabhushana[2], Santhosh Kumar[2], Arnav Aggarwal[1], Goldwin Cecil[2], Sarthak Saxena[1], Arathi Venu[4], Monita Gahlot[1], George Puthusseril[4], Shubham Jain[1], Ayush Agarwal[1], Anoop Koshy[4], Shrinkhala Verma[1], Amitabha Mandal[1], Naman Singh[1], Samagra Agarwal[1], Soumyadeep Choudhury[1], Priya Nair[4], S Sudhindran[4], Ashish Singh[2], Ankur Goyal[1], Raju Sharma[1], Shivanand Gamangatti[1], Ashish Goel[2], Shalimar[1]. *[1]All India Institute of Medical Science, New Delhi, India; [2]Christian Medical College, Vellore, India; [3]ESIC Hospital, Chennai, India; [4]Amrita Institute Of Medical Sciences, Kochi, India*
Email: sagnik_biswas@yahoo.co.in

Background and aims: To assess the role of olanzapine (OLN) in improving weight, appetite and quality-of-life (QoL) in patients with intermediate/advanced HCC and cachexia along with its safety in this patient group.
Method: In this multicentre, open-label randomized controlled trial (December 2024-May 2025), 166 adult (18–70 years) patients with intermediate/advanced HCC and cachexia (defined as involuntary loss of ≥5% weight over the prior 6 months) were randomly assigned (1:1) to receive OLN (5 mg/day) with nutritional counselling (OLN +NC) or NC alone. We included patients who were treatment naïve or those who received prior therapy but had progressive disease with ongoing weight loss. Treatment modality for HCC was decided based on stage of disease and suitability for locoregional/systemic therapy. Primary outcome was to compare the proportion of patients reporting improvement in weight (>5% from baseline) over 12 weeks between the two groups (modified intention-to-treat

analysis). Secondary outcomes included change in anorexia (Visual analogue and Functional Assessment of Anorexia/Cachexia Therapy scale), muscle mass (assessed by computerized tomography scan), handgrip strength (dynamometry), exercise tolerance (6-minute walk test), caloric intake and QoL (Functional Assessment of Cancer Therapy-Hepatobiliary questionnaire).
Results: Baseline characteristics were comparable in both groups. A higher proportion of patients in the OLN+NC group (39.7%) reported weight gain (>5%) as compared to 15.3% in the NC alone group (absolute risk difference [ARD]: 24.4% [95% CI: 10.9 to 37.9]; p < 0.001). Weight gain was noted in both treatment-naïve and experienced patients. A higher number of patients in the OLN+NC group reported reduction in anorexia (36.5% vs NC: 15.1%, ARD: 21.4 [95% CI: 5.3–37.7]; p = 0.01) accompanied by improved median daily caloric intake (OLN+NC: +135 [−45 to 312.5] kcal vs NC: −29 [−355 to 210] kcal; p = 0.002). Patients using OLN also reported improved QoL (46.2% vs NC: 28.2%, ARD: 17.9 [95% CI: 3.5 to 32.4]; p = 0.02) with significantly better sense of physical well-being and lower incidence of negative symptoms due to HCC. No significant between-group differences were observed in muscle mass, handgrip strength or exercise tolerance. OLN was not associated with any major drug related adverse events.
Conclusion: A 12-week course of olanzapine improves weight, appetite and QoL in patients with intermediate/advanced HCC with cachexia and is well tolerated in this patient group (CTRI:2024/12/077603).

OS-052
Circulating methylated SEPT9 for detection of hepatocellular carcinoma in patients with cirrhosis: a prospective multicenter phase 3 diagnostic validation study

Abderrahim Oussalah[1], Maël Silva Rodriguez[1], Guillaume Conroy[2], Mouni Bensenane[3], Hélène Rousseau[4], Ahmet Ayav[5], Jean-Louis Guéant[6], Houda Camara[4], Cédric Baumann[4], Valérie Laurent[7], Jean-Pierre Bronowicki[3]. *[1]University Hospital of Nancy, Department of Genomic Medicine, Division of Biochemistry, Molecular Biology, and Nutrition, Faculty of Medicine of Nancy, INSERM UMR_S 1256, Nancy, France; [2]Mercy Hospital, Department of Gastroenterology and Hepatology, Metz, France; [3]University Hospital of Nancy, Department of Gastroenterology and Liver Diseases, Nancy, France; [4]University Hospital of Nancy, Methodology, Data Management and Statistics Unit, Nancy, France; [5]University Hospital of Nancy, Department of Hepato-Pancreato-Biliary Surgery, Nancy, France; [6]Joan Klein Jacobs Center for Precision Nutrition and Health, Cornell University, Ithaca, United States; [7]University Hospital of Nancy, Department of Radiology, Nancy, France*
Email: abderrahim.oussalah@univ-lorraine.fr

Background and aims: Hepatocellular carcinoma (HCC) surveillance in patients with cirrhosis remains suboptimal, with inadequate early-stage detection. Alpha-fetoprotein (AFP) demonstrates insufficient sensitivity. We previously showed promising diagnostic accuracy for methylated *SEPT9* (mSEPT9), a cell-free DNA-based epigenetic biomarker. The primary objective was to evaluate the diagnostic accuracy of plasma mSEPT9 compared with AFP for detecting HCC in patients with cirrhosis undergoing surveillance. Exploratory objectives included evaluation of combination strategies and assessment of the relationship between replicate positivity and circulating methylated DNA load.
Method: In this prospective, multicenter, phase 3 diagnostic validation study (NCT03311152), we enrolled 574 patients with cirrhosis undergoing HCC surveillance at two tertiary centers in France. HCC was diagnosed according to AASLD and EASL criteria by hepatologists unaware of mSEPT9 results. We compared mSEPT9 testing (triple-negative, single-positive, double-positive, or triple-positive based on three biological replicates) with AFP greater than 20 ng/mL. Combination strategies included Tier 1 (either biomarker positive, prioritizing sensitivity) and Tier 2 (both biomarkers positive, prioritizing specificity). The primary endpoint was diagnostic accuracy assessed by AUROC, sensitivity, specificity, predictive values, and likelihood ratios using frequentist and Bayesian approaches.
Results: Among 574 participants (median age 63 years; 72% male; median Child-Pugh score 5), 118 had HCC, with 51 (43.2%) at BCLC stage 0 or A. mSEPT9 achieved an AUROC of 0.79 (95% CI 0.74 to 0.84), compared with 0.71 (95% CI 0.66 to 0.76) for AFP (p = 0.002; Bayes factor 713, extreme evidence). Tier 1a (at least single-positive mSEPT9 or AFP greater than 20 ng/mL) achieved 87.8% sensitivity and 95.0% negative predictive value. Tier 2 (triple-positive mSEPT9 and AFP greater than 20 ng/mL) achieved 99.6% specificity and 95.1% positive predictive value. Tier 1c (triple-positive mSEPT9 or AFP greater than 20 ng/mL) achieved 74.8% sensitivity with 85.9% specificity. For early-stage disease (BCLC 0-A), Tier 1a achieved 74.5% sensitivity versus 23.5% for AFP alone (3.2-fold improvement).
Conclusion: Circulating mSEPT9 combined with AFP substantially improved HCC detection in patients with cirrhosis, particularly for early-stage disease amenable to curative treatment. These findings support integrating mSEPT9 into surveillance algorithms to enhance early detection.

OS-053
Fecal microbiota transplantation combined with atezolizumab plus bevacizumab in hepatocellular carcinoma refractory to atezolizumab plus bevacizumab: final results of the open label, single-arm, FAB-HCC pilot study

Katharina Pomej[1], Adrian Frick[1], Bernhard Scheiner[1], Maximilian Baumgartner[2], Klaus Schmetterer[1], Lorenz Balcar[1], Larissa Pajancic[1], Abelina Kreuter[1], Petra Pjevac[3], Joana Silva[3], Bela Hausmann[3], Thomas Köcher[4], Carlos Reyna-Blanco[1], Katharina Lampichler[1], Nataliya Rohr-Udilova[1], Adrija Chakrabarty[1], Anton Klotz[1], Annika Lampl[1], Kerstin Zinober[1], Katharina Regnat[1], Michael Trauner[1], David Berry[3], Thomas Vogl[1], Dietmar Tamandl[1], Christoph Gasche[1], Matthias Pinter[1]. *[1]Medical University of Vienna, Vienna, Austria; [2]CeMM Research Center for Molecular Medicine of the Austrian Academy of Sciences, Vienna, Austria; [3]University of Vienna, Centre for Microbiology and Environmental Systems Science, Vienna, Austria; [4]Metabolomics Service and Research Facility, Vienna Biocenter Core Facilities, Vienna, Austria*
Email: matthias.pinter@meduniwien.ac.at

Background and aims: Modulation of the gut microbiome (i.e., fecal microbiota transplant (FMT)) may help to overcome resistance to immune checkpoint inhibitors.
Method: In this single-center, single-arm pilot study (ClinicalTrials.gov ID: NCT05750030), we included patients with advanced HCC who progressed on atezolizumab/bevacizumab. Patients received a single FMT via colonoscopy from an anti-PD-1-responding HCC donor or a healthy donor, combined with atezolizumab/bevacizumab q3w. The primary endpoint was safety, measured by incidence and severity of treatment-related adverse events (TRAEs). The main secondary endpoint was best overall response according to mRECIST and RECISTv1.1. For exploratory analyses, blood and stool samples were collected longitudinally. Stool samples were processed for 16S rRNA sequencing and HPLC-MS metabolomics; amplicon-sequencing-variants were analyzed using DESeq2, differential abundance of metabolites and bacterial taxa were assessed using Maaslin2. Peripheral blood mononuclear cells were analyzed on CYTOFlex flow cytometer. Phage-display immunoprecipitation sequencing was performed on plasma samples to profile systemic IgG-epitope repertoires against gut microbiota and environmental antigens using a phage library comprising 357,000 peptides.
Results: Between August 2023 and November 2024, 12 patients were included (male, n = 10; Child-Pugh A, n = 11; BCLC C, n = 10). Grade 3–4 TRAEs included arterial hypertension (n = 5) and proteinuria (n = 3), both related to bevacizumab, and diarrhea (n = 1), related to FMT. No serious TRAEs were observed. Objective response rate according to

mRECIST and RECISTv1.1 was 33% and 25%, respectively. Median progression-free survival was 6.9 (95%CI, 3.0–10.8) months (mRECIST) and 4.3 (95%CI, 0.2–8.5) months (RECISTv1.1). FMT resulted in a significant shift of recipient microbiome towards donor microbiome. Healthy-donor FMT was associated with higher engraftment compared with anti-PD-1-responder-FMT, and increased recipient fecal and plasma concentrations of certain bile acids. Responders had a higher proportion of peripheral naïve CD4+ CD45RA+ T cells at baseline, and we observed trends in certain T cell and monocyte populations after FMT. Responders showed greater shifts in systemic IgG antibody reactivity after FMT, consistent with a more pronounced early remodeling of humoral immune responses.
Conclusion: FMT combined with atezolizumab/bevacizumab was safe and achieved a high response rate in patients with atezolizumab/bevacizumab-refractory HCC.

OS-054

A confidence-aware artificial intelligence pathology model for cholangiocarcinoma diagnosis

Yue Cheng[1,2,3], Nael Azouzi[4], Astrid Laurent Bellue[5], Zhuxian Guo[1,2,3], Taek Chung[6], Qinghe Zeng[7], Arezoo Ghodsifard[1,2,3], Thomas Albrecht[8], Stephanie Roessler[8], Camille Boulagnon-Rombi[9], Mukul Vij[10], Mohamed Rela[10], Reha Akpinar[11,12], Jeremy Augustin[1,2,3,4], Celine Bazille[13], Shaodian Xu[1,2,3], Shenhong Kong[1,2,3], Emmanuele Lechapt-Zalcman[4], Christophe Tournigand[14], Emmanuelle Kempf[14], Brustia Raffaele[1,2,3,15], Jean-Michel Pawlotsky[1,3,16], Chiara Braconi[17], Stefano Caruso[1,2,3], Marianne Ziol[18], Benjamin Goeppert[19], Luca Di Tommaso[11,12], Young Nyun Park[6], Julien Calderaro[1,2,3,4].
[1]Institut Mondor, INSERM, U955, Créteil, France; [2]MINT-Hep, Mondor Integrative Hepatology, Créteil, France; [3]Université Paris-Est, Créteil, France; [4]Department of Pathology, Henri-Mondor Hospital, Assistance Publique-Hôpitaux Paris (AP-HP), Créteil, France; [5]Department of Pathology, Bicêtre Hospital, Assistance Publique-Hôpitaux Paris (AP-HP), Université Paris-Saclay, Le Kremlin-Bicêtre, France; [6]Department of Pathology, Graduate School of Medical Science, Brain Korea 21 Project, Yonsei University College of Medicine, Seoul, Korea, Rep. of South; [7]Else Kroener Fresenius Center for Digital Health, Faculty of Medicine and University Hospital Carl Gustav Carus, TUD Dresden University of Technology, Dresden, Germany; [8]Institute of Pathology, Heidelberg University, Medical Faculty, University Hospital Heidelberg, Liver Cancer Center Heidelberg (LCCH), Heidelberg, Germany; [9]Department of Pathology, Centre Hospitalier Universitaire de Reims, Hôpital Robert-Debré, Reims, France; [10]The Institute of Liver Disease & Transplantation, Dr Rela Institute & Medical Centre, Bharath Institute of Higher Education and Research, Chennai, India; [11]Department of Biomedical Sciences, Humanitas University, Pieve Emanuele, Milan, Italy; [12]Department of Pathology, IRCSS Humanitas Research Hospital, Rozzano, Milan, Italy; [13]Department of Pathology, CHU de Caen, 14000 Caen, ISTCT, GIP CYCERON, CNRS, UNICAEN, Normandie Université, Caen, France; [14]Medical Oncology Department, Henri-Mondor Hospital, Assistance Publique-Hôpitaux Paris (AP-HP), Créteil, France; [15]Department of Digestive and Hepato-pancreatic-biliary Surgery, Henri-Mondor Hospital, Assistance Publique-Hôpitaux Paris (AP-HP), Créteil, France; [16]Department of Virology, Hôpitaux Universitaires Henri Mondor, Assistance Publique-Hôpitaux de Paris, Créteil, France; [17]Beatson West of Scotland Cancer Centre, Gartnavel General Hospital, 1053 Great Western Rd, Glasgow, United Kingdom; [18]AP-HP, Hôpitaux Universitaires Paris Seine Saint-Denis, Pathology Unit; Inserm, UMR-1138 "Functional Genomics of Solid Tumors," Centre de Recherche des Cordeliers, Université de Paris; Biological Resource Center liver biobank GH Paris-Seine-Saint-Denis, Saint-Denis, France; [19]Institute of Pathology, RKH Hospital Ludwigsburg, Ludwigsburg, Germany
Email: yue.cheng.chloe@gmail.com

Background and aims: Intrahepatic cholangiocarcinoma (ICCA) is a highly lethal primary liver cancer. Histologically, ICCA is difficult to diagnose as its morphological and immunohistochemical features significantly overlap with those of metastatic adenocarcinomas. This leads to additional workup and treatment delays. We aimed to develop and prospectively validate a clinically oriented artificial intelligence (AI) model that differentiates ICCA from metastatic cancers on routine liver biopsy whole-slide images (WSIs) and provides case-level confidence estimates.
Method: The retrospective cohort comprised 544 adults with ICCA (n = 281) or liver metastases (n = 263) from five European liver centres, split into training and internal test sets. The model was obtained by applying pathology foundation models and training the slide-level aggregators. To quantify prediction confidence, an out-of-distribution detection module (G-ODIN) was added and case-level confidence scores were derived from predictive entropy (PE). Diagnostic performance was assessed by area under the receiver operating characteristic curve (AUC) and false positive rate (FPR). PE distributions were compared using Mann–Whitney U tests. The model was further prospectively validated in two independent cohorts from France (Avicenne and Reims University Hospitals) and Asia (Rela Institute, India and Yonsei University of Medicine, South Korea).
Results: On the internal test set, the model achieved an AUC of 0.86 and an FPR of 0.19 (best performance using CONCH/TITAN). After addition of the G-ODIN module, we observed that PE was lower in correctly classified cases vs misclassified cases, confirming that it could be used as a confidence metric (p = 0.003). After PE thresholding (threshold of 0.54), AUC reached 0.944 with an FPR of 0. The model was further prospectively validated using the PE threshold. In the French prospective cohort (n = 25), all samples were correctly classified (AUC of 1, 32% of patients could be predicted according to PE thresholding). In the Asian cohort (n = 136), all but one patient were correctly classified (AUC of 0.965, 23.5% of patients could be predicted according to PE thresholding).
Conclusion: We developed and prospectively validated a confidence-based artificial intelligence model to assist the differential diagnosis between ICCA and liver metastases on routine liver biopsies. Our approach may help reduce unnecessary investigations and treatment delays for patients with suspected ICCA.

OS-055

Serum procalcitonin: a new tumor biomarker for the diagnosis and monitoring of fibrolamellar hepatocellular carcinoma

Jean-Charles Nault[1], Claudia Campani[1], Théo Hirsch[2], Ethan Neumann[3], Waqar Arif[3], Sandrine Imbeaud[2], Marina Baretti[3], Marianne Ziol[1], Sabrina Sidali[1], Pauline Roger[2], Manon Allaire[1], Mohamed Bouattour[4], Fabio Marra[5], Brice Fresneau[6], Neus Llarch[7], Jean Marie Peron[8], René Gerolami[9], Eric Nguyen Khac[10], Pierre Nahon[1], Nathalie Ganne[1], Julien Calderaro[1], Aurélie Beaufrère[1], Valérie Paradis[1], Catherine Guettier[1], Angela Sutton[1], Mark Yarchoan[3], Jessica Zucman-Rossi[2]. *[1]APHP, PAris, France; [2]Centre de Recherche Des Cordeliers, Paris, France; [3]John Hopkins Hospital, Baltimore, United States; [4]AP-HP, Hôpital Beaujon, Liver Cancer and Innovative Therapy, CLICHY, France; [5]Department of Experimental and Clinical Medicine, Internal Medicine and Hepatology Unit, University of Firenze, Firenze, Italy; [6]Institut Gustave Roussy, Villejuif, France; [7]Barcelona Clinic Liver Cancer (BCLC) Group, Barcelona, Spain; [8]Department of Hepatogastroenterology, Rangueil University Hospital, 31059 Toulouse, France, Toulouse, France; [9]Unité hépatologie, Hôpital de la Timone, Marseille, France, Assistance Publique-Hôpitaux de Marseille (APHM), Marseille, France; [10]Hepato-Gastroenterology Department, CHU Amiens, Amiens, France*
Email: naultjc@gmail.com

Background and aims: Fibrolamellar carcinoma (FLC) is a rare primary liver cancer that develops in non-cirrhotic livers, typically affecting young patients who usually present with normal levels of known serum tumor biomarkers. The observation of markedly elevated serum procalcitonin (PCT) in one patient led us to investigate the potential role of PCT as a biomarker in a larger cohort of FLC cases.

Method: Serum PCT concentrations were measured in 34 samples from 18 patients with metastatic FLC, as well as in 64 patients with hepatocellular carcinoma (HCC), 24 with cholangiocarcinoma (CCA), and 20 patients with cirrhosis without HCC, from European and U.S. cohorts. Using RNA sequencing, we analyzed the expression of the CALCA gene, which encodes PCT, in 27 FLCs, 331 HCCs, 39 CCAs, 71 hepatoblastomas, 34 hepatocellular adenomas, and 55 non-tumoral liver samples. Spatial transcriptomic analysis was performed on three FLCs, and PCT immunohistochemistry (IHC) was conducted on 13 FLCs and 34 other primary or secondary liver cancers.
Results: The median serum PCT level was significantly elevated in 8 FLC patients (55.2 µg/L) compared with HCC (0.14 µg/L), CCA (0.16 µg/L), and cirrhosis (0.11 µg/L; P = 0.0005) in the European cohort. These findings were independently validated in a U.S. cohort of 10 FLC patients compared with HCC and CCA cases (P = 0.0002). Across cohorts, elevated serum PCT was observed in 83% of FLC cases versus only 3% of HCC and CCA patients (P < 0.0001). In four patients followed longitudinally, PCT levels correlated with radiological response, stability, or progression according to RECIST 1.1 criteria. For example, serum PCT increased from 51 µg/L (102× the upper limit of normal) to 581 µg/L (1,162× ULN) following tumor progression under immunotherapy. RNA sequencing revealed significant CALCA overexpression in FLC compared to other primary liver tumors (P < 0.0001), with an AUC of 0.975 versus CCA, and 0.994 versus HCC, demonstrating excellent diagnostic sensitivity and specificity for this rare liver cancer. Spatial transcriptomics localized CALCA expression specifically to tumor cells harboring the DNAJB1-PRKACA fusion gene. Immunohistochemistry confirmed PCT overexpression in tumor cells in 77% of FLCs, but not in other primary or secondary liver cancers (P < 0.0001).
Conclusion: Procalcitonin is a sensitive and specific biomarker for fibrolamellar hepatocellular carcinoma, both in serum and tumor tissue, with potential clinical utility for diagnosis and monitoring of treatment response.

Rare liver diseases

OS-056

Efficacy and safety of CAM2029 in patients with polycystic liver disease: phase 2b POSITANO study

Marie C. Hogan[1], Frederik Nevens[2], Arun Jesudian[3], K. Rajender Reddy[4], Richard Taubert[5], Jonel Trebicka[6], Peter Almgren[7], Ulrika Axling[7], Peter Jönsson[7], Fredrik Tiberg[7], Joost P.H. Drenth[8]. *[1]Mayo Clinic, Rochester, MN, United States; [2]University Hospitals KU Leuven, Leuven, Belgium; [3]Weill Cornell Medicine, New York, NY, United States; [4]University of Pennsylvania, Philadelphia, PA, United States; [5]Medizinische Hochschule Hannover, Hannover, Germany; [6]Universitätsklinikum Münster, Münster, Germany; [7]Camurus AB, Lund, Sweden; [8]Amsterdam University Medical Center, Amsterdam, Netherlands*
Email: hogan.marie@mayo.edu

Background and aims: Somatostatin analogues (SSAs; eg octreotide and lanreotide) have indicated efficacy in reducing liver volume in investigator-driven clinical trials in polycystic liver disease (PLD) but efficacy has not yet been established in randomised clinical trials. CAM2029 is a novel subcutaneous, extended-release octreotide depot, based on the FluidCrystal® technology, designed for convenient administration by patients using an autoinjector pen. Here we report the 53-week (W) core phase results of the Phase 2b POSITANO (NCT05281328) study evaluating CAM2029 in patients with PLD.
Method: The core phase consisted of a 53W double-blind, randomised, placebo-controlled period enrolling patients with symptomatic PLD and height-adjusted total liver volume (htTLV) ≥ 1800 mL/m. Patients received either CAM2029 10 mg weekly or every 2 weeks, or placebo weekly. Primary endpoint was difference in htTLV change from baseline to W53 between CAM2029 (combined doses) and placebo. Secondary endpoints included change in PLD-related symptoms (per newly developed PLD-Symptoms [PLD-S] score), change in total liver cyst volume and safety.
Results: Seventy-one patients were randomised (CAM2029 combined n = 48; placebo n = 23). Mean age was 54.1 years, 85.9% were female and median htTLV was 3070 mL/m. Treatment was completed by 87.2% for CAM2029 combined and 87.0% for placebo. The primary endpoint was met, with a statistically significant estimated relative treatment difference in htTLV from baseline to W53 of 4.3% (95% confidence interval [CI]: 8.4, 0.1; p = 0.0443) between CAM2029 and placebo. CAM2029 reduced total liver cyst volume growth, with an estimated relative treatment difference from baseline to W53 of 8.7% (95% CI: 15.2, 1.8; p = 0.0159) between CAM2029 and placebo. CAM2029 improved PLD-S score from baseline to W53; however, no significant difference was observed between CAM2029 and placebo (estimated relative treatment difference: 2.7; 95% CI: 10.5, 5.2; p = 0.5041). CAM2029 was well tolerated, with a safety profile consistent with other injectable SSAs. Most adverse events (AEs) were grade 1–2 for both CAM2029 and placebo. The most frequent AEs with CAM2029 were diarrhoea (68.1%), injection site pruritus (42.6%), injection site pain (40.4%) and abdominal pain (36.2%).
Conclusion: CAM2029 reduced total liver and liver cyst volume growth, supporting further evaluation as a potential PLD treatment. The study is ongoing to evaluate long-term CAM2029 treatment in an open-label extension period up to 120 weeks.

OS-057

Tiomolibdate choline stabilizes liver disease and improves neurological symptoms as well as quality-of-life in treatment-experienced Wilson disease patients

Valentina Medici[1], Aftab Ala[2], Karl Heinz Weiss[3], Edward J. Gane[4], Zoe Mariño[5,6,7], Chandler Robinson[8], Andrew Cittadine[8], Declan Tuffy[8], George Boon Bee Goh[9], Marina Berenguer[10], Thomas Sandahl[11], Fred Askari[12]. *[1]University of California Davis Medical Center, Sacramento, United States; [2]King's College Hospital NHS Foundation Trust, London, United Kingdom; [3]Krankenhaus Salem, Heidelberg, Germany; [4]University of Auckland, Grafton, New Zealand; [5]Hospital Clínic De Barcelona, Barcelona, Spain; [6]Liver Unit, Hospital Clinic, IDIBAPS, Barcelona, Spain, Barcelona, Spain; [7]Liver Unit, Hospital Clínic Barcelona, IDIBAPS, CIBERehd, Universitat de Barcelona, Barcelona, Spain, Barcelona, Spain; [8]Monopar Therapeutics, Wilmette, United States; [9]Singapore Health Services, Singapore, Singapore; [10]Hospital Universitario Y Politécnico La Fe, Valencia, Spain; [11]Aarhus University Hospital, Aarhus, Denmark; [12]University of Michigan-Ann Arbor, Ann Arbor, United States*
Email: vmedici@health.ucdavis.edu

Background and aims: Wilson disease (WD) is a rare autosomal recessive disorder characterized by excess copper (Cu) accumulation resulting in hepatic and neurologic damage as well as psychiatric symptoms. Tiomolibdate choline (TMC; ALXN1840), a once-daily oral agent with extremely high affinity for binding Cu, has been shown to improve Cu balance and prevent toxic effects of Cu overload in WD patients. A Phase 2 study was conducted in treatment-experienced WD patients to evaluate the effect of TMC on both liver pathology and clinical symptoms of WD.
Method: This open-label, multicenter Phase 2 trial evaluated the efficacy of TMC monotherapy through 48 weeks in treatment-experienced (≥ 1 year on standard of care) WD patients. Hepatic, neurologic, and quality of life assessments were performed at Baseline and Week 48; patients in the extension period had assessments repeated at Week 96. Liver biopsy was performed at Baseline and Week 48 to assess the impact of TMC on hepatic Cu concentration, stage of fibrosis, and grade of steatosis. Neurologic and clinical outcomes were assessed by the Unified WD Rating Scale

(UWDRS) and Clinical Global Impression (CGI) scale. Quality of life was assessed by the EuroQoL 5-Dimensions (EQ5D) UK Health Index.
Results: 29 WD patients were enrolled with a median [IQR] prior treatment duration of 13.8 years [10.9]; 23 continued in the extension period. At Week 48, the majority of patients showed improvement or stabilization in hepatic pathology, including Non-alcoholic Fatty Liver Disease Activity Score (NAS; 71% improved or stabilized) and Non-alcoholic Steatohepatitis Clinical Research Network (NASH CRN) fibrosis score (67% improved or stabilized). There was a statistically significant improvement in liver stiffness by transient elastography (mean [SD] – 1.19 kPa (2.15); p = 0.0122). Hepatic Cu concentration was not statistically different at Week 48. Statistically significant improvements in UWDRS, CGI, and EQ5D UK Health Index were observed at Week 48 and persisted through Week 96.
Conclusion: TMC treatment for up to 2 years resulted in improvement or stabilization of parameters of liver pathology as well as improvement in neurologic and clinical outcomes in heavily pretreated patients. Stability in hepatic Cu concentration indicates effective Cu control by TMC. Higher doses and/or a longer time period may lead to reductions in liver Cu. These results support TMC's role as a valuable treatment option for WD patients.

OS-058

Assessment of liver injury and genotype among children and adults with lysosomal acid lipase deficiency: analysis of the international LAL D registry

William Balistreri[1], Ali Canbay[2], Thomas Kerr[3], Sophie Kitchen[4], Florian Abel[5], Lorenzo D'Antiga[6]. *[1]UC Department of Pediatrics, Cincinnati Children's Hospital Medical Center, Cincinnati, United States; [2]Department of Internal Medicine, Ruhr-Universitat Bochum, Bochum, Germany; [3]Department of Gastroenterology and Hepatology, UT Southwestern, Dallas, United States; [4]Epidemiology and Real World Science, Alexion, AstraZeneca Rare Disease, Boston, United States; [5]Department of Global Medical Affairs, Alexion, AstraZeneca Rare Disease, Boston, United States; [6]Department of Medicine and Surgery, University of Milano–Bicocca, Milan, Italy*
Email: william.balistreri@cchmc.org

Background and aims: Lysosomal acid lipase deficiency (LAL-D) is a rare inherited lysosomal storage disease characterized by liver injury and dysregulated lipid metabolism. This analysis assessed liver damage and dyslipidemia by genotype among patients with LAL-D.
Method: Children and adults enrolled in the International LAL-D Registry were included regardless of treatment status with sebelipase alfa (LAL enzyme replacement therapy [ERT]). Infants who started ERT at <6 months were excluded. Biochemical and clinical features, including liver biopsy results, and *LIPA* genotype were assessed at baseline (registry enrollment date for untreated patients, last assessment before ERT start for treated patients) in all patients. Transaminases were assessed longitudinally in treated patients.
Results: As of August 2025, 281 patients with LAL-D (163 children: 45% female, 92% White; 118 adults: 54% female, 90% White) were included. Median time from onset of manifestations to diagnostic testing was 1.6 y (children) and 10.0 y (adults). The most common manifestations that raised suspicion of LAL-D were elevated aspartate aminotransferase (AST; 77% of children, 47% of adults), elevated alanine aminotransferase (ALT; 76%, 53%), and hepatomegaly (67%, 50%). Among 142 patients with liver biopsy results at baseline, 60% had macrovesicular and microvesicular steatosis and 44% had lobular inflammation; proportions were similar among children and adults. Among 231 patients with *LIPA* sequencing results, most were homozygous (41%) and compound heterozygous (28%) for c.894G>A. ALT levels were ≥2 times the upper limit of normal in 49% of children and 25% of adults homozygous for c.894G>A; proportions for compound heterozygotes for c.894G>A were 63% and 22%. Among patients with ≥1 c.894G>A variant, fibrosis scores tended to be worse for younger versus older patients. Most patients of any genotype with elevated transaminases co-presented with dyslipidemia. The proportion of ERT-treated patients with elevated ALT decreased from 92% (157/170) at baseline to 53% (89/167) at last follow-up (median 7.4 years); results were similar between children and adults. The proportion of ERT-treated patients with elevated AST also decreased (86% [146/169] to 33% [54/165]).
Conclusion: Across *LIPA* genotypes, liver damage was a common feature of LAL-D among pediatric and adult patients; children typically present with elevated transaminases. ERT was associated with improvements in transaminase levels.

OS-059-YI

Prevalence and novel predictors of recurrent intrahepatic cholestasis of pregnancy using the 2023 EASL guidelines in a cohort of over 250 subsequent pregnancies

Nina Rodriguez[1], Jacqueline Slobin[1], Lauren Alpert[1], Cecilia Katzenstein[1], Keith Sigel[1], Rhoda Sperling[1], Caroline Ovadia[2], Catherine Williamson[3], Tatyana Kushner[4]. *[1]Icahn School of Medicine at Mount Sinai, New York, United States; [2]University of Edinburgh, Edinburgh, Scotland, United Kingdom; [3]Imperial College London, London, United Kingdom; [4]Weill Cornell Medicine, New York, United States*
Email: nina.rodriguez@icahn.mssm.edu

Background and aims: The 2023 EASL guidelines propose a risk stratification framework for suspected intrahepatic cholestasis of pregnancy (ICP), but the predictive validity in subsequent pregnancies is unknown. We assessed whether EASL group classification in an index pregnancy could predict the risk of ICP recurrence and disease severity in later pregnancies.
Method: We conducted a retrospective cohort study at a large U.S. health system (2009–2024). Groups were assigned per the 2023 EASL guidelines for suspected ICP: A (bile acids (BA) < 19 µmol/L, normal ALT/AST), B (BA < 19 µmol/L, elevated ALT/AST), or C (BA ≥ 19 µmol/L). Confirmed ICP was defined as BA ≥10 µmol/L. Recurrent ICP was defined as peak BA ≥10 µmol/L in a subsequent pregnancy among those with confirmed ICP in the index pregnancy. Regression models estimated risk ratios (RRs) for predictors of ICP recurrence and progression between EASL groups.
Results: Among 4,386 patients with suspected ICP in an index pregnancy (median age: 32 years, 45% Hispanic), we identified 265 with a subsequent pregnancy with BAs ordered: 158 in Group A (7% with confirmed ICP), 64 in B (29% with confirmed ICP), and 43 in C. Confirmed ICP recurred in 46% (66/145; 95% CI 37–54%). Recurrent ICP was associated with symptom onset before 28 weeks in the index pregnancy (27% vs 10%), Hispanic ethnicity (62% vs 38%), and gallstones (27% vs 9%), all p < 0.01. Index pregnancy BAs ≥ 40 (n = 44, 30%) or ≥ 100 µmol/L (n = 14, 10%) were not significantly associated with ICP recurrence, whereas index pregnancy EASL group classification significantly stratified recurrence risk (51% in C, 49% in B, 20% in A; p = 0.020). Among those with confirmed ICP in the index pregnancy, both Group B (aRR 2.5, 95% CI 1.1–5.6) and C (aRR, 2.4 95% CI 1.1–5.2) had higher risk of recurrence compared to A. EASL group agreement across pregnancies was fair: 53% remained in the same group, 35% shifted to a lower-risk group, and 12% moved to a higher-risk group. Among suspected ICP patients initially in A or B, peak BAs ≥ 10 µmol/L in the index pregnancy was associated with higher risk of progressing to C (RR 3.9, 95% CI 1.4–11.0). Adverse obstetric outcomes did not differ significantly between those with and without ICP recurrence.
Conclusion: ICP recurs frequently, yet BA levels in the index pregnancy alone were not associated with recurrence. EASL-defined groups meaningfully stratified future risk, highlighting heterogeneity within suspected ICP and the value of this framework for longitudinal risk assessment.

OS-060

Incidence, clinical characteristics and outcomes of checkpoint inhibitor-induced liver injury (ChILI): a multicentre UK-wide retrospective cohort study

Edmond Atallah[1], Thomas Moore[1], Hester Franks[1,2] and The UK National Oncology Trainee Collaboration for Healthcare Research (NOTCH)[3]. [1]*Nottingham University Hospitals NHS Trust, Nottingham, United Kingdom;* [2]*University of Nottingham, Division of Cancer and Stem Cells, BioDiscovery Institute, Nottingham, United Kingdom;* [3]*The UK National Oncology Trainee Collaboration for Healthcare Research (NOTCH), Clatterbridge, United Kingdom*
Email: edmond.atallah@gmail.com

Background and aims: Immune checkpoint inhibitors (CPI) have become the leading cause of drug-induced liver injury (DILI) cases in national registries. Current evidence on the incidence and outcomes of checkpoint inhibitor-induced liver injury (ChILI) is derived from studies with small sample sizes and lacks systematic evaluation. Here, we present a national real-world analysis of the incidence, clinical characteristics, and outcomes of ChILI in all patients who received CPI over 5 years.
Method: Using the prospective electronic prescribing and management system for Systemic Anti-Cancer Therapy (SACT) in the UK, all adult patients who received CPI for melanoma or renal cell carcinoma with or without concurrent targeted therapy between January 2018 and December 2022 at 20 centres were identified. Patients were systematically screened for acute liver injury ≥ Grade 2 by the Common Terminology Criteria for Adverse Events (CTCAE v5). Detailed clinical data, including CPI, investigations, treatment and outcomes, were collected. Causality assessment and formal adjudication were performed centrally. ChILI pattern and severity grading were assessed using the international expert working group criteria and CTCAE.
Results: Out of 8080 patients who received CPI, 724 had acute liver injury and were included (9%). ChILI occurred in 535 patients (7% of all who received CPI). Hepatocellular was the most common pattern of injury occurring in 220 patients (41%). Three-quarters of ChILI patients (404) developed Grade 3/4 liver injury, 82 developed jaundice (15%), and 13 met severe DILI criteria (2%). 10 ChILI patients developed cholangiopathy (2%), and 2 had sinusoidal obstruction syndrome (SOS) (0.4%). None of the patients progressed to acute liver failure (ALF) or died due to ChILI. 46 out of 535 ChILI patients improved without receiving steroids (9%). Among the 489 who received steroids, 143 had over 3 months of treatment (29%), 122 received additional immunosuppression (25%), and 89 had significant steroid-related side effects (18%). Among the 250 patients who were challenged with CPI (47%), ChILI recurred in 68 patients (27%).
Conclusion: In this largest real-world cohort of ChILI to date, no patients developed ALF or died due to ChILI. Distinctive ChILI subtypes, cholangiopathy and SOS, are rare but require clinical suspicion and early investigations. There is significant heterogeneity in ChILI management and prolonged steroid use in >25% of patients; a prospective clinical trial is needed to inform clinical practice.

Regeneration and gut communication

OS-061

Microbial pathways differentiate between patients with cirrhosis who are hospitalized withis 90 days in a multi-national cohort

Jasmohan Bajaj[1], Darja Nikitina[2], Masoumeh Sikaroodi[3], Mario Álvares-da-Silva[4], Aldo Torre[5], Ramazan Idilman[6], Ki Tae Suk[7], Mette Lauridsen[8], Elise Jonasson[8], Matheus Truccolo Michalczuk[4], Hye Won Lee[7], Satya Priya Sharma[7], Jesus Alejandro Ruiz Manríquez[5], Edita Kiudeliene[2], Dilara Turan Gökçe[6], Sai Bojja[3], Juozas Kupcinskas[2], Patrick Gillevet[3]. [1]*Virginia Commonwealth University, Richmond, United States;* [2]*Lithuanian University of Health Sciences, Kaunas, Lithuania;* [3]*George Mason University, Manassas, United States;* [4]*Hospital de Clínicas de Porto Alegre, Porto Alegre, Brazil;* [5]*Instituto Nacional de Ciencias Médicas y Nutrición Salvador Zubirán, San José del Rincón, Mexico;* [6]*Ankara Bilim Üniversitesi, Ankara, Türkiye;* [7]*Hallym University College of Medicine, Chuncheon, Korea, Rep. of South;* [8]*Sdu University Of Southern Denmark, Ejsberg, Denmark*
Email: jasmohan.bajaj@vcuhealth.org

Background and aims: Prediction of hospitalizations is important in cirrhosis to ensure timely prevention. Microbial composition is altered in cirrhosis but functionality, which is the host-bacterial interface, needs further evaluation. Aim: define microbial pathways linked with 90-day hospitalization in a multi-national cirrhosis cohort.
Method: Cirrhosis outpatients were recruited from 7 countries (USA, Türkiye, Korea, Denmark, Lithuania, Brazil & Mexico). Demographics, cirrhosis severity (MELD, complications, medications), diet, were recorded, stool collected & pts followed for 90 days for hospitalizations. Metagenomics & pathway analysis using HUMAnN were performed. PERMANOVA & regression analysis was performed using Maaslin2 for 90-day hospitalizations prediction.
Results: 682 patients with cirrhosis (170 US, 90 Brazil, 99 Korea, 93 each Lithuania & Mexico, 84 Türkiye, & 53 Denmark) were enrolled. 60% were men, MELD 12 ± 5, albumin3.5 ± 0.70, Na 138 ± 7. Most common etiology was alcohol (35%) then viral (31%) & MASLD (17%). 56% were decompensated (35% on lactulose, 19% on rifaximin, 44% prior ascites, 19% prior variceal bleed, 31% on NS βblockers). Diet varied (most with yogurt & coffee). 90-day Hospitalizations: Seen in 169 (25%), most of which 133(79%) were liver-related. Country-wise rate differed with lowest in Brazil & Türkiye & highest in Lithuania & Korea. Bacterial pathway analysis: PERMANOVA adjusted for country showed differences between hospitalized versus not ($p = 0.001$). There were differences in pathway diversity ($p = 0.004$) but not richness. Maaslin2: Pathways ↓ in hospitalized: All had $p < 0.01$, carbohydrate storage and biosynthesis (sucrose synthesis II, glycogen degradation II), amino acid biosynthesis (L-ornithine & L-methionine synthesis), nucleotide & aromatic compound degradation Pathways ↑ in hospitalized fermentation, alternative substrate utilization, *de novo* nucleotide biosynthesis, cell wall recycling, lipid metabolism, and Enterobacteriaceae-associated functions (heterolactic fermentation, ethanolamine utilization, glycerol and hexitol fermentation, pyrimidine biosynthesis, & enterobacterial common antigen biosynthesis).
Conclusion: In a multinational outpatient cirrhosis cohort, gut microbial functional pathways focused on urea cycle and bioenergetics intermediates were lower, while ammoniagenic and Enterobacterial pathways were higher in those who were hospitalized within 90 days. Microbial pathway profiling could improve risk prediction in cirrhosis beyond single center studies.

OS-062

Endothelial IRF1/CD36/TGF-β1 axis drives metabolic reprogramming and impairs liver regeneration in aging

Minjie Zhao[1], Xuesong Xu[2], Riccardo Perriera[3], Weilong Hong[4], Clelia Ferraro[3], Xing Lai[5], Salvatore Gruttadauria[3], Jianping Gong[6], Massimo Pinzani[3], Junhua Gong[2], Giovanni Zito[3]. [1]*Department of Hepatobiliary Surgery, The Second Affiliated Hospital of Chongqing Medical University, Chongqing 400010, China; Centre for Lipid Research & Key Laboratory of Molecular Biology for Infectious Diseases (Ministry of Education), Institute for Viral Hepatitis, Department of Infectious Diseases, the Second Affiliated Hospital, Chongqing Medical University, Chongqing 400016, China; University of Pittsburgh Medical Center-Mediterranean Institute for Transplantation and Highly Specialized Therapies (UPMC-ISMETT), 90127 Palermo, Italy, Palermo, Italy;* [2]*Department of Hepatobiliary Surgery, The Second Affiliated Hospital of Chongqing Medical University, Chongqing 400010, China; Centre for*

Lipid Research & Key Laboratory of Molecular Biology for Infectious Diseases (Ministry of Education), Institute for Viral Hepatitis, Department of Infectious Diseases, the Second Affiliated Hospital, Chongqing Medical University, Chongqing 400016, China; Chongqing, China; [3]ISMETT-Istituto Mediterraneo per i Trapianti Ismett IRCCS, Palermo, Italy; [4]Department of Anesthesiology, The Second Affiliated Hospital of Chongqing Medical University, Chongqing 400010, P.R. China; Mitochondrial Medicine and Critical Illness Organ Protection Research Center, The Second Affiliated Hospital of Chongqing Medical University, Chongqing 400010, P.R. China; Basic Medicine Research and Innovation Center for Novel Target and Therapeutic Intervention, Ministry of Education, the Second Affiliated Hospital of Chongqing Medical University, Chongqing 400010, P.R. China, Chongqing, China; [5]Department of Hepatobiliary Surgery, The People's Hospital of Chongqing Tongnan District, Chongqing 402660, China; Basic Medicine Research and Innovation Center for Novel Target and Therapeutic Intervention, Ministry of Education, the Second Affiliated Hospital of Chongqing Medical University, Chongqing 400010, P.R. China; Chongqing, China; [6]Department of Hepatobiliary Surgery, The Second Affiliated Hospital of Chongqing Medical University, Chongqing 400010, China; Centre for Lipid Research & Key Laboratory of Molecular Biology for Infectious Diseases (Ministry of Education), Institute for Viral Hepatitis, Department of Infectious Diseases, the Second Affiliated Hospital, Chongqing Medical University, Chongqing 400016, China; Basic Medicine Research and Innovation Center for Novel Target and Therapeutic Intervention, Ministry of Education, the Second Affiliated Hospital of Chongqing Medical University, Chongqing 400010, P.R. China; Chongqing, China
Email: mjzhao8818@163.com

Background and aims: The diminished regenerative capacity of the liver in aging individuals represents a major clinical obstacle. Although liver sinusoidal endothelial cells (LSECs) are essential regulators of the hepatic regenerative niche, the molecular basis for their functional decline with age remains largely undefined. This study investigates the mechanistic role of CD36 upregulation in aged LSECs and its contribution to impaired liver regeneration via metabolic and signaling dysregulation.
Method: Partial hepatectomy (PHx) was conducted in young and aged mice, with subsequent single-cell RNA sequencing of the liver. Aged mice with endothelial-specific CD36 knockout (CD36-/-) were generated to evaluate liver regeneration. In vitro, CD36-overexpressing endothelial SK-HEP1 cells were subjected to etoposide-induced senescence, followed by assessment of senescence markers and functional assays. 2D(transwell) and 3D(assembloids) co-culture systems were employed to examine the paracrine effects of endothelial cells on hepatocyte proliferation. Transcriptional regulation of CD36 by IRF1 was validated using chromatin immunoprecipitation (ChIP) and dual-luciferase reporter assays.
Results: Single-cell transcriptomics identified CD36 as markedly upregulated in aged liver endothelial cells, correlating with enhanced lipid metabolism pathways and suppression of cell-cycle expression. Conditional ablation of CD36 in endothelium significantly enhanced hepatocyte proliferation and restored regenerative capacity in aged mice post-PHx. Mechanistically, CD36 overexpression amplified palmitate uptake, driving metabolic reprogramming and activating the TGF-β1 signaling. This led to endothelial dysfunction via induction of endothelial-to-mesenchymal transition, coupled with potent cell-cycle arrest in hepatocytes. Mechanistically, we found that CD36 expression is directly driven by the transcription factor IRF1, whose levels were higher in aged LSECs.
Conclusion: Our findings unveil a previously unrecognized regulatory axis—IRF1/CD36/TGF-β1—in aged LSECs that disrupts liver regeneration through integrated metabolic reprogramming and inhibitory paracrine signaling. This axis represents a key mechanism underlying age-related liver regenerative failure and highlights potential therapeutic targets for improving postoperative recovery in elderly patients.

OS-063
Treatment of liver cirrhosis using hepatocyte-derived liver progenitor-like cells: a prospective, open label, single arm, safety trial

Kang He[1], Xuejing Zhu[2], Yaoping Shi[3], Weijian Huang[4], Weifeng Yu[5], Bo Zhai[3], Hexin Yan[4], Qiang Xia[1]. *[1]Department of Liver Surgery, School of Medicine, Renji Hospital, Shanghai Jiao Tong University, Shanghai, China; [2]Celliver Biotechnology Inc., Shanghai, China; [3]Department of Interventional Oncology, School of Medicine, Renji Hospital, Jiaotong University, Shanghai, China; [4]Department of Anesthesiology and Critical Care Medicine, School of Medicine, Renji Hospital, Shanghai Jiaotong University, Shanghai, China, Celliver Biotechnology Inc., Shanghai, China, Key Laboratory of Anesthesiology (Shanghai Jiao Tong University), Ministry of Education, Shanghai, China; [5]Department of Anesthesiology and Critical Care Medicine, School of Medicine, Renji Hospital, Shanghai Jiaotong University, Shanghai, China, Key Laboratory of Anesthesiology (Shanghai Jiao Tong University), Ministry of Education, Shanghai, China*
Email: hexin.yan@celliver.com

Background and aims: Liver transplantation demand is constrained by donor scarcity and surgical risks, creating an urgent need for novel therapies targeting cirrhosis' core pathophysiology: hepatic stellate cell (HSC) activation, excessive type I collagen (Col1a1) deposition (fibrosis), and hepatocyte apoptosis/impaired regeneration. This study evaluated the safety and therapeutic potential of hepatocyte-derived liver progenitor-like cells (HepLPCs) for cirrhosis, validating its mechanism against these pathophysiological defects.
Method: We developed expandable hepatocyte-derived liver progenitor-like cells (HepLPCs) from primary human hepatocytes, defined their antifibrotic and pro-regenerative mechanisms, also validated efficacy in a TAA-induced rat cirrhosis model. Biodistribution studies tracked the in vivo clearance of xenogeneic HepLPCs, and preclinical safety was evaluated in 36 cynomolgus monkeys. Based on these data, a first-in-human trial was conducted in nine cirrhosis patients, who received HepLPCs via transhepatic arterial infusion without immunosuppression.
Results: HepLPCs secreted high levels of MMP-1/-3 (key antifibrotic MMP subtypes) and HGF. MMP-1/-3 specifically degraded Col1a1 from activated HSCs. HGF bound its receptor c-MET to promote hepatocyte proliferation and inhibit apoptosis. In TAA rats, HepLPCs reduced α-SMA expression and Col1a1 deposition, while increasing Ki67-positive hepatocytes. Biodistribution showed HepLPCs clearance within 1 week; fluorescence tracking + immunohistochemistry confirmed no long-term engraftment in liver or other organs. Preclinical studies in monkeys showed no dose-limiting toxicities. In the clinical trial, no serious adverse events occurred; minor events were cirrhosis-related. Treatment was well-tolerated without transfusion reactions. While Child-Pugh and MELD scores did not change significantly, some patients showed improved liver biochemistry (increased albumin synthesis), coagulation profiles (increased prothrombin activity), and portal hypertension indicators (decreased portal vein pressure) over 6 months.
Conclusion: HepLPCs transplantation exhibits promising safety and potential efficacy in cirrhosis, with mechanisms precisely targeting fibrosis and impaired hepatocyte regeneration. The available evidence supports a predominantly paracrine mechanism underlying these therapeutic effects. These data support further clinical investigation, particularly in decompensated cirrhosis and acute-on-chronic liver failure.

OS-064-YI
Intestinal sirtuin 1 controls liver regeneration by altering hepatocyte priming and promoting metabolic remodelling

Vinicius Dias Nirello[1], Sian Seaman[1], Paula Ruiz[1], Mark Philo[1], Mar Moreno-Gonzalez[1], Patrick Varga-Weisz[2], Naiara Beraza[1]. *[1]Quadram Institute, Norwich, Northern Ireland; [2]University of Essex, Colchester, Northern Ireland*
Email: mark.philo@quadram.ac.uk

Background and aims: The liver rapidly restores its mass after injury, yet how the gut–liver axis contributes to this process remains unclear. Bile acids (BA) and their metabolism are key regulators of liver regeneration. Previous work highlighted the role of both liver- and intestinal-specific FXR in this process. SIRT1 regulates FXR signalling and BA metabolism, but the role of intestinal-specific SIRT1 in modulate the liver regenerative response remains undefined. Here, we aimed to define how intestinal SIRT1 shapes early signalling and metabolic reorganisation after partial hepatectomy (PHx).
Method: Intestinal-specific SIRT1-deficient mice (SIRT1^int-KO) and wildtype littermates underwent PHx. Liver tissue collected at 0, 6 and 24 h was analysed by bulk RNA-seq. STAT3 activation, hepatic BA and progenitor cell expansion was evaluated by immunoblotting, targeted metabolite profiling and immunohistochemistry.
Results: At 6 h post-PHx, both genotypes suppressed metabolic regulators (e.g., *Srebf1*, *Ppard*, *Mlxipl*) and activated a core inflammatory programme. However, SIRT1^int-KO livers displayed a distinct signature marked by (i) reduced STAT-associated genes (*Jak3*, *Osmr*, *Il15*, *Ccl5*), (ii) induction of interferon-stimulated genes (*Ifi*, *Gbp*, Oas families), and (iii) activation of stress pathways including *Atf3* and *Eif2ak3*/PERK. Correspondingly, STAT3 phosphorylation was markedly reduced in SIRT1^int-KO mice despite comparable TNF-α and IL-6 levels, indicating defective hepatocyte priming. By 24 h, transcriptomic divergence intensified. WT livers initiated broad metabolic reprogramming—fatty-acid oxidation, amino-acid metabolism and organic-acid catabolism—whereas SIRT1^int-KO livers failed to engage these pathways and instead sustained chemokine expression (*Ccl2*, *Ccl3*, *Cxcl10*), extracellular-matrix genes (*Col1a1*, *Loxl1*, *Adamts2*) and senescence regulators (*Cdkn1a*/*p21*). These molecular features aligned with pronounced parenchymal injury, hepatic BA accumulation and expansion of liver progenitor cells. Mechanistically, impaired intestinal FXR–FGF15 signalling was strongly associated with these defects, and targeted intestinal FXR agonism with Fexaramine restored liver regeneration in SIRT1^int-KO mice.
Conclusion: Intestinal SIRT1 is required for the transcriptional and metabolic transitions that support liver regeneration, including cell priming and the reactivation of lipid and amino-acid metabolic networks, protecting from a BA–driven inflammatory and senescent state.

OS-065
Evidence for bile acid-mediated ileal barrier function deficits in primary sclerosing cholangitis

Nicholas Ilott[1], Nicholas Provine[1], Matthias Friedrich[1], Claire Pearson[1], Kyla Dooley[1], Amelia Heslington[2], Miriam Tomczak[3], Kate Coldwell[1], Elizete Araujo Batista Neves[1], Anna Hoyle[1], Yukari Kimura[1], Megan Perry[1], Shana-Lee Bownes[1], Kaye Eve-Rowe[1], Calliope Dendrou[1], Charlotte Rich-Griffin[4], Iolanda Vendrell[1], Lisa Gartner[5], Ida Parisi[1], Oyindamola Ajisegiri[1], Amy Cross[1], Joanna Hester[1], Roman Fischer[1], Fadi Issa[1], Fiona Powrie[1], Holm Uhlig[1], Emma Culver[1], Paul Klenerman[1]. *[1]University of Oxford, Oxford, United Kingdom; [2]University of Newcastle, Newcastle, United Kingdom; [3]University Medical Center Hamburg-Eppendorf, Hamburg, Germany; [4]Nonacus, Birmingham, United Kingdom; [5]The Francis Crick Institute, London, United Kingdom*
Email: nicholas.ilott@kennedy.ox.ac.uk

Background and aims: Primary sclerosing cholangitis (PSC) is a rare progressive disease of the bile ducts and liver. Primary causes and factors influencing progression remain unknown although likely involve autoimmune-related damage to cells of the biliary tree and pathologic gut-liver communication. Given a high prevalence of ulcerative colitis in PSC, research into pathological intestinal involvement in liver disease has largely focussed on the large intestine. However, reduced bile flow from the liver has the potential to impact on homeostatic barrier-protective functions of the small intestine, including the main site of bile acid reuptake – the terminal ileum (TI). This could lead to disease progression through pathobiont-induced damage to the liver, as well as dysbiosis-associated right-sided colonic inflammation.
Method: Using a combination of scRNA-seq, spatial transcriptomics and proteomics of TI biopsies from patients with PSC-UC, UC and healthy controls we demonstrate changes across multiple cell types in PSC-UC.
Results: In both CD4 and CD8 memory T cells, we show evidence of decreased expression of genes involved in oxidative phosphorylation (OXPHOS) in the TI of patients with PSC-UC, supporting altered barrier immunity. We also show that mature enterocytes of the TI can be characterised by spatially organised cell states. The phase II detoxification gene, *Glutathione-S-transferase alpha 1* (*GSTA1*) marks one enterocyte state that is enriched at the base of villi and is co-expressed with multiple other detoxification enzymes. Genes within this co-expression module are downregulated in ileal samples from patients with PSC-UC, supporting altered detoxification capacity in ileal enterocytes in patients with PSC. Inverse correlations between GSTA1 protein abundance and alkaline phosphatase (ALP) levels in patients with PSC, and reduced *Gsta1* mRNA expression in a mouse model of cholestatic liver disease, support a direct role for reduced bile flow in downregulating GSTA1 and related detoxification proteins. Results from gnotobiotic mouse models suggests that *Gsta1* expression is tuneable through microbiome manipulation, with evidence that the presence of microbes that can deconjugate conjugated primary bile acids contribute to reduced expression of *Gsta*1.
Conclusion: We have identified new pathways that are disrupted in the small intestine of patients with PSC. These pathways represent potential new targets for treatment that can be tuned by microbiome intervention.

Viral hepatitis B/D – Current therapies

OS-066
Long-term virological and clinical outcomes in patients with hdv-related cirrhosis treated with bulevirtide monotherapy for up to 4 years (save-d study)

Elisabetta Degasperi[1], Maria Paola Anolli[1], Dana Sambarino[1], Marta Borghi[1], Riccardo Perbellini[1], Liana Gheorghe[2], Mirela Chitul[2], Christoph Schramm[3], Hartmut Schmidt[3], Mathias Jachs[4], Thomas Reiberger[4], Ivana Carey[5], Kosh Agarwal[5], Maria Buti[6], Adriana Palom[6], Giampiero D'Offizi[7], Francesco De Maria[7], Caroline Zöllner[8], Frank Tacke[8], Christopher Dietz-Fricke[9], Heiner Wedemeyer[9], Margarita Papatheodoridi[10], George Papatheodoridis[10], Florian van Bömmel[11], Sabela Lens[12], Maurizia Brunetto[13], Alessandro Federico[14], Elena Rosselli Del Turco[15], Magdalena Meszaros[16], Alessia Ciancio[17], Alvaro Giráldez-Gallego[18], Filipe Calinas[19], Fabien Zoulim[20], Soo Aleman[21], Nasser Semmo[22], Sophie Metivier[23], Carla Coffin[24], Sebastien Poulin[25], Alessandra Mangia[26], Marie-Noëlle Hilleret[27], Uta Merle[28], Mariana Cardoso[29], Alexandra Martins[30], Catarina Gouveia[31], Karen Doucette[32], Sergio Borgia[33,34], Alessandro Loglio[35], Teresa Santantonio[36], Nicola Coppola[37], Adriano Pellicelli[38], Juliette Foucher[39], Bruno Roche[40], Xavier Causse[41], Louis Dalteroche[42], Jérôme Dumortier[43], Nathalie Ganne-Carrié[44], Frederic Heluwaert[45], Isabelle Ollivier-Hourmand[46], Dominique Roulot[47], Isabelle Rosa[48], Cristina Fonseca[49], Ana Margarida Vieira[50], Francesca Pileri[51], Monia Maracci[52], Matteo Tonnini[53], Jean-Pierre Arpurt[54], Karl Barange[55], Eric Billaud[56], Lucia Parlati[57], Anne Gervais[58], Anne Minello Franza[59], Massimo Puoti[60], Ana Horta[61], Mariana Machado[62], Dalia Fernandes[63], Joaquim Oliveira[64], Joao Vaz Alves[65], Pietro Lampertico[1,66,67]. *[1]Division of*

Gastroenterology and Hepatology, Foundation IRCCS Ca' Granda Ospedale Maggiore Policlinico, Milan, Italy; [2]Center for Digestive Diseases and Liver Transplantation, Fundeni Clinical Institute, Bucharest, Romania; [3]Department of Gastroenterology, Hepatology and Transplant Medicine, Medical Faculty, University of Duisburg-Essen, Essen, Germany; [4]Division of Gastroenterology and Hepatology, Department of Medicine III, Medical University of Vienna, Vienna, Austria; [5]Institute of Liver Studies, King's College Hospital,, London, United Kingdom; [6]Liver Unit, Internal Medicine Department, Hospital Universitari Vall d'Hebron, Vall d'Hebron Barcelona Hospital Campus, Barcelona, Spain; [7]Division of Infectious Diseases - Hepatology, Department of Transplantation and General Surgery, Istituto Nazionale per le Malattie Infettive "L. Spallanzani" IRCCS, Rome, Italy; [8]Department of Hepatology and Gastroenterology, Charité Universitätsmedizin Berlin, Berlin, Germany; [9]Department of Gastroenterology, Hepatology, Infectious Diseases and Endocrinology at Hannover Medical School, Hannover, Germany; [10]1st Department of Gastroenterology, General Hospital of Athens "Laiko", Medical School of National & Kapodistrian University of Athens, Athens, Greece; [11]Division of Hepatology, Department of Medicine II, Leipzig University Medical Center, Laboratory for Clinical and Experimental Hepatology, Leipzig, Germany; [12]Liver Unit, Hospital Clínic, IDIBAPS, Universitat de Barcelona, Barcelona, Spain; Centro de Investigación Biomédica en Red de Enfermedades Hepáticas y Digestivas (CIBEREHD), Barcelona, Spain; [13]Department of Clinical and Experimental Medicine, University of Pisa and Hepatology Unit, University Hospital of Pisa, Pisa, Italy; [14]Division of Hepatogastroenterology, Department of Precision Medicine, Università della Campania "Luigi Vanvitelli", Naples, Italy; [15]Department of Medical and Surgical Sciences, Unit of Infectious Diseases, "Alma Mater Studiorum" University of Bologna, S. Orsola-Malpighi Hospital, Bologna, Italy; [16]Liver Transplantation and Hepatogastroenterology Unit, CHU Montpellier, CHU Montpellier, Montpellier, France; [17]Department of Medical Sciences, University of Turin, Gastroenterology Division of Città della Salute e della Scienza of Turin, University Hospital, Turin, Italy; [18]Hospital Virgen del Rocío, IBIS, Sevilla, Spain; [19]Serviço de Gastrenterologia, ULS de São José, Lisboa, Portugal; [20]Lyon Hepatology Institute, Université Claude Bernard Lyon 1, Hospices Civils de Lyon, INSERM Unit 1052 - CRCL, Lyon, France; [21]Infectious Disease Clinic, Karolinska University Hospital, Stockholm, Sweden; [22]Department of Visceral Surgery and Medicine, Inselspital, Bern University, Bern, Switzerland; [23]Hepatology Unit, CHU Rangueil, Toulouse, France; [24]Division of Gastroenterology and Hepatology, Department of Medicine, Cumming School of Medicine, University of Calgary, Calgary, Canada; [25]Service de microbiologie-infectiologie, CISSS des Laurentides, Hôpital de St-Jérôme et Clinique I.D, St-Jérôme, St-Jerome, Canada; [26]Liver Unit, Fondazione IRCCS "Casa Sollievo della Sofferenza", San Giovanni Rotondo, Italy; [27]University Grenoble Alpes, Hepatology and Gastroenterology Unit, CHU Grenoble Alpes, 38043 Grenoble, France, Inserm U 1209, CNRS UMR 5309, Team Cell Dynamics, Immunity, Metabolism & Cancer, Institute for Advanced Biosciences, Grenoble, France; [28]Department of Internal Medicine IV, Gastroenterology & Hepatology, Heidelberg University Hospital, Heidelberg, Germany; [29]Gastroenterology Department, ULS de São José, Lisbon, Portugal; [30]Serviço de Gastrenterologia, ULS de Amadora/Sintra, Sintra, Portugal; [31]Serviço de Gastrenterologia, ULS de Loures/ Odivelas, Odivelas, Portugal; [32]Division of Infectious Diseases, Department of Medicine, University of Alberta, Edmonton, Canada; [33]Osler Hepatitis Centre Brampton Civic Hospital, William Osler Health System, and McMaster University, Division of Infectious Diseases, Hamilton, Canada; [34]Osler Hepatitis Centre, Infectious Diseases, William Osler Health System, Brampton, Canada; [35]Gastroenterology, Hepatology and Transplantation Division, ASST Papa Giovanni XXIII, Bergamo, Italy; [36]Department of Medical and Surgical Sciences, Infectious Diseases Unit, University of Foggia, Foggia, Italy; [37]Department of Mental Health and Public Medicine - Infectious Diseases Unit, University of Campania Luigi Vanvitelli, Naples, Italy; [38]Liver Unit, San Camillo Hospital, Department of Transplantation and General Surgery, Rome, Italy; [39]Hepatology Department, Haut-Lévêque Hospital, Bordeaux, France; [40]Hepato-Biliary Center, AP-HP Hôpital Universitaire Paul Brousse, Paris-Saclay University, Research INSERM-Paris Saclay Unit 1193, Villejuif, France; [41]Service d'Hépato-Gastroentérologie CHU d'Orléans, Orleans, France; [42]Service d'Hépato-Gastroentérologie CHU de Tours, Tours, France; [43]Department of Digestive Diseases, Hospices Civils de Lyon, Edouard Herriot hospital, Claude Bernard Lyon 1 University, Lyon, France; [44]AP-HP, Avicenne Hospital, Hepatology Department, Bobigny, France; [45]Centre Hospitalier Annecy Genevois, 74000, Annecy, France; [46]Department of Hepatogastroenterology, CHU de Caen Normandie, Caen, France; [47]Liver Unit, Avicenne hospital, AP-HP, Sorbonne Paris Nord University, Bobigny, France; [48]Service d'hépatogastroentérologie, Centre Hospitalier Intercommunal, Creteil, France; [49]Serviço de Gastrenterologia, ULS de Almada/ Seixal, Almada, Portugal; [50]Serviço de Gastrenterologia, ULS do Algarve, Algarve, Portugal; [51]Division of Internal Medicine and Center for Hemochromatosis, University of Modena and Reggio Emilia, Modena, Italy; [52]Institute of Infectious Diseases and Public Health, Università Politecnica delle Marche, Ancona, Italy; [53]Division of Internal Medicine, Hepatobiliary and Immunoallergic Diseases, IRCCS Azienda Ospedaliero-Universitaria di Bologna, Bologna, Italy; [54]Department of Gastroenterology, CH d'Avignon, Avignon, France; [55]Department of Gastroenterology, Toulouse University Hospital, Toulouse, France; [56]Université de Nantes, INSERM UIC 1413, Department of Infectious Diseases, CHU Hôtel Dieu, Nantes, France; [57]Université Paris Cité, Assistance Publique des Hôpitaux de Paris, Hôpital Cochin, Hepatology/Addictology department, Paris, France; [58]Assistance Publique des Hôpitaux de Paris, Hôpital Bichat Claude Bernard, Service des Maladies Infectieuses et Tropicales, Paris, France; [59]CHU Dijon, Service d'Hépato-gastroentérologie et oncologie digestive, Inserm EPICAD LNC-UMR1231, Université de Bourgogne-Franche Comté, Dijon, France; [60]School of Medicine and Surgery University of Milano Bicocca, Milano, Italy; [61]Serviço de Infecciologia, ULS de Santo António, Portugal, Santo Antonio, Portugal; [62]Serviço de Gastrenterologia, ULS do Estuário do Tejo, Portugal, Lisboa, Portugal; [63]Serviço de Gastrenterologia, ULS de Braga, Portugal, Braga, Portugal; [64]Serviço de Infecciologia, ULS de Coimbra, Portugal, Coimbra, Portugal; [65]Serviço de Infecciologia, ULS de Lisboa Ocidental, Lisboa, Portugal; [66]CRC "A. M. and A. Migliavacca" Center for Liver Disease, Department of Pathophysiology and Transplantation, University of Milan, Milan, Italy; [67]D-SOLVE consortium, an EU Horizon Europe funded project (No 101057917), Milan, Italy
Email: elisabetta.degasperi@policlinico.mi.it

Background and aims: Bulevirtide (BLV) is approved by EMA for treatment of chronic hepatitis Delta (CHD), however data about long-term outcomes in patients with cirrhosis are limited.
Method: CHD patients with cirrhosis treated with BLV 2 mg/day in the SAVE-D study (51 centers) were included. Virological (HDV RNA undetectable or ≥2 Log_{10} decline *vs.* baseline), biochemical (ALT<40 U/L), combined response, viral breakthroughs (VBK: 1 Log_{10} HDV RNA increase *vs.* previous timepoint) and liver-related events (LREs) were assessed. Clinically significant portal hypertension (CSPH) was defined according to Baveno VII criteria.
Results: 424 patients treated with BLV up to 192 weeks (W) were included: age 50 (IQR 40–58) years, 61% men, ALT 78 (51–128) U/L, liver stiffness measurement (LSM) 16.5 (12.6–25.3) kPa, platelets 101 (68–149) x10^9/L, 96% CPT score A, 51% with varices, 9% with previous decompensation, 90% on NUC. Baseline HDV-RNA was 5.4 (4.2–6.3) Log_{10}IU/mL and qHBsAg 3.7 (3.2–4.1) Log_{10}IU/mL. After W144 of BLV, 70%, 67%, 51% and 34% of patients achieved virological, biochemical, combined response, and HDV RNA undetectability, respectively. In 42 patients with available W192 data, the corresponding figures were 76%, 60%, 52% and 33%. Patients with <1 Log_{10} HDV RNA decline *vs.* baseline decreased from 20% (W48) to 14% (W144). VBK occurred in 8% between W48-W96 (75% normal ALT)) and 10% between W96-W144 (70% normal ALT). 26 patients developed a LRE, 9 decompensation and 17 HCC: the 3-year cumulative incidences were 2.7% (95% CI 1–4%) and 5.3% (95% CI 2–7%), respectively. The corresponding figures in patients with *vs.* without baseline CSPH were 5.9% *vs.* 0.5%

for decompensation (p = 0.004) and 8.4% *vs.* 2.5% for HCC (p = 0.01), respectively. Lower baseline albumin independently predicted LREs (HR 0.13, p = 0.0003). The 3-year liver transplantation (LT)/death-free survival was 88.8% (95% CI 85–92%): 29 patients underwent LT (22 HCC, 7 decompensation) and 13 patients died, 8 of LREs. Persistence on-treatment was maintained by 94% of patients, 20 discontinued BLV monotherapy (7 add-on IFN, 2 skin allergy, 2 decompensation, 3 undetectable HDV RNA, 3 non-compliance, 2 non-response, 1 clinical trial entry), 7 were lost to follow-up.
Conclusion: Most CHD patients with cirrhosis treated for up to 4 years with BLV 2 mg/day monotherapy achieved a virological and/or biochemical response. The incidence of LREs remained low and was associated with lower baseline albumin and CSPH.

OS-067
Is undetectability of HDV RNA for 96 weeks on Bulevirtide associated with a sustained virological response off-treatment in the real life? Results from the French ANRS HD EP01 HEPDELTA cohort

Helene Fontaine[1], Marc Bourliere[2], Miroslava Subic-Levrero[3], Caroline Jezequel[4], Sophie Metivier[5], Juliette Foucher[6], Nathalie Ganne-Carrié[7], Jérôme Dumortier[8], Magdalena Meszaros[9], Vlad Ratziu[10], Veronique Loustaud-Ratti[11], Vincent Leroy[12], Louis Dalteroche[13], Lucia Parlati[14], Anne Minello Franza[15], Violaine Ozenne[16], Frederic Heluwaert[17], Jérôme Gournay[18], Armand Abergel[19], Philippe Mathurin[20], Laurent Alric[21], Karine Lacombe[22], Isabelle Rosa[23], Simona Tripon[24], Ghassan Riachi[25], Marie-Noëlle Hilleret[26], Nicolas Robillard[27], Corentin Rouvray[28], Christelle Tual[27], Claire Fougerou-Leurent[27], Fatoumata Coulibaly[29], Eric Rosenthal[29], Segolene Brichler[30,31], Patrizia Carrieri[32], Lawrence Serfaty[33], Dominique Roulot[34], Fabien Zoulim[3]. *[1]Hepatology Unit - Beaujon Hospital - APHP, Clichy, France; [2]Hepato-gastroenterology department, Hôpital Saint Joseph, Marseille, France; [3]Hepato-gastroenterology department, Hôpital de la Croix Rousse, Hospices Civils de Lyon, Lyon, France; [4]Liver Diseases Department, Hôpital Pontchaillou, Rennes, France; [5]Hepato-gastroenterology department, Hôpital Rangueil, Toulouse, France; [6]Hepato-gastroenterology department, Hôpital Haut-Lévêque, Bordeaux, France; [7]Hepatology department, Hôpital Avicenne, Bobigny, France; [8]Hepato-gastroenterology department, Hôpital Herriot, Hospices Civils de Lyon, Lyon, France; [9]Hepato-gastroenterology department, Hôpital Saint-Eloi, Montpellier, France; [10]Hepato-gastroenterology department, Hôpital La Pitié Salpêtrière, AP-HP Assistance Publique - Hôpitaux de Paris, Paris, France; [11]Hepato-gastroenterology department, Hôpital Dupuytren, Limoges, France; [12]Hepato-gastroenterology department, Hôpital Henri Mondor, AP-HP Assistance Publique - Hôpitaux de Paris, Créteil, France; [13]Hepato-gastroenterology department, Hôpital Trousseau, Tours, France; [14]Hepato-gastroenterology department, Hôpital Cochin, AP-HP Assistance Publique - Hôpitaux de Paris, Paris, France; [15]Hepato-gastroenterology department, Hôpital du Bocage, Dijon, France; [16]Hepatology department, Hôpital Saint Antoine, AP-HP Assistance Publique - Hôpitaux de Paris, Paris, France; [17]Hepato-gastroenterology department, CH de la région Annécienne, Annecy, France; [18]Hepatology department, Hôtel Dieu, Nantes, France; [19]Digestive and Hepatobiliary Centre, Hôpital Estaing, Clermont-Ferrand, France; [20]Digestive System Diseases Department, Hôpital Claude Huriez, Lille, France; [21]Internal medicine department, Hôpital Rangueil, Toulouse, France; [22]Infectious and Tropical Diseases Department, Hôpital Saint Antoine, AP-HP Assistance Publique - Hôpitaux de Paris, Paris, France; [23]Hepato-gastroenterology department, CH intercommunal, Créteil, France; [24]Hepato-gastroenterology department, Nouvel hôpital civil, Strasbourg, France; [25]Hepato-gastroenterology department, Hôpital Charles Nicolle, Rouen, France; [26]Hepato-gastroenterology department, Hôpital Michallon, Grenoble, France; [27]Pharmacology Department, Hôpital Pontchaillou, Rennes, Inserm, CIC 1414, Rennes, France; [28]Pharmacology Department, Hôpital Pontchaillou, Rennes, Inserm, CIC 1414, Rennes, France, Rennes, France; [29]ANRS I MIE, Paris, France; [30]CNR Hépatites, Hôpital Avicenne, Bobigny, France; [31]CNR Hépatites, Hôpital Avicenne, Bobigny, France, Bobigny, France; [32]Aix Marseille Univ, Inserm, IRD, SESSTIM, Sciences Economiques & Sociales de la Santé & Traitement de l'Information Médicale, ISSPAM, Marseille, France; [33]Hepato-gastroenterology department, Hôpital de Hautepierre, Strasbourg, France; [34]Hepatology Department, Hôpital Avicenne, Bobigny, France*
Email: helene.fontaine@aphp.fr

Background and aims: In the phase 3 study (Myr301), HDV RNA remained undetectable (Robogene 2.0 assay: LL0D 6 IU/ml) 2 years after discontinuation of Bulevirtide (BLV) 2 or 10 mg/day for 96 to 144 weeks, in 23/148 (15.5%) patients of the total population and in 90% patients with undetectable HDV RNA for 96 weeks on BLV, suggesting a finite duration of treatment in these patients. The aim of this sub-study of HEPDELTA cohort, aiming to study the natural history of HDV infection according different treatment modalities, was to analyse this result in the real life.
Method: 344 patients were treated (161 with BLV 2 mg alone, 154 with BLV + Pegylated Interferon (PegIFN), 29 with BLV for at least six months then BLV + PegIFN): 42.4 ± 11.3 years, 67% males, 41% sub-Saharan origin, 7125% with cirrhosis, HDV RNA 5.9 + 1.4 $\log_{10}$ IU/ml, 83.3% genotype 1 and 12.5% of genotype 5. The HDV RNA undectectability (less sensitive test), during treatment, was 38.5, 59.3 and 53.3% at W96, 38.5, 44 and 50% at W144 and 46.2, 72.7 and 20% of patients at W192, in the 3 groups, respectively.
Results: The virological response was 26.2, 43.2 and 30% at FU 24, 38.5, 29.7 and 22.2% at FU 48, 35.7, 44.0 and 25.0% at FU 96 and 42.9, 70.00 and 0% at FU 144, respectively. Among the 161 patients receiving BLV alone, 79 (49%) discontinued treatment, including 23 with undetectable HDV RNA at the end of treatment (EOT) (mean duration 103.3 ± 56.4 weeks): 9 patients (39.1%) relapsed during follow-up ≥ 48 weeks off-treatment. In 13 with undetectable HDV RNA for ≥96 weeks, 5 discontinued treatment: 1 (20%) relapsed after >48 weeks of follow-up. Among the 154 treated with BLV + PegIFN, 92 (59.7%) discontinued treatment, including 42 with undetectable HDV RNA at EOT (mean BLV and PegIFN duration of 109.4 ± 77.5 and 72.9 ± 52 weeks, respectively): 18 (42.8%) relapsed. In 25 of them, with undetectable HDV RNA for ≥ 96weeks on treatment, 11 discontinued treatments: 4 (36.4%) relapsed within 48 weeks off treatment. Among 29 receiving BLV for > 6 months then BLV + Peg IFN, one patient with undetectable HDV RNA for ≥96 weeks discontinued treatments with HBsAg loss and remained responder after 48 weeks off-treatment.
Conclusion: In the real life HEPDELTA cohort as in MYR 301, the sustained virological response at 48 weeks off treatment remains high in patients with HDV RNA undetectability for > 96 weeks during BLV (80%) or BLV + peg IFN (67%) treatment.

OS-068-YI
The new EASL treatment indications for HBeAg-negative chronic hepatitis B virus infection reduce grey-zone patients and reflect better routine clinical practice

Margarita Papatheodoridi[1], Sofia Paraskevopoulou[1], Panagiota Ioannidou[1], Paraskevi Fytili[1], Alkistis Maria Papatheodoridi[1], Stratigoula Sakellariou[2], Evangelos Cholongitas[1], Ioannis Vlachogiannakos[1], George Papatheodoridis[1]. *[1]1st Academic Department of Gastroenterology, General Hospital of Athens "Laiko", Medical School of National & Kapodistrian University of Athens, Athens, Greece; [2]1st Department of Pathology, Medical School of National & Kapodistrian University of Athens, General Hospital of Athens "Laiko", Athens, Greece*
Email: gepapath@med.uoa.gr

Background and aims: The 2025 EASL HBV clinical practice guidelines (CPGs) expand treatment indications (TxI) for HBeAg-negative chronic HBV (CHBVe-) patients (pts) promoting earlier treatment initiation in grey-zone (GZ) cases, but their real life implementation is unknown. We assessed how the 2025 TxI compared to the 2017 EASL TxI apply in our GZ CHBVe- pts and how they are associated with

treatment initiation in CHBVe- in clinical practice over the recent years (yrs).
Method: All CHBVe- pts with ≥1 visit between 2010 and 2019 were included if they had no TxI by the 2017 CPGs based on baseline ALT/HBV DNA defined as HBV DNA >20,000 IU/ml and ALT >2 × ULN. Pts with coinfection, immunosuppression, decompensation or HCC, alcohol abuse or other liver injury were excluded. Parameters based on a predefined CRF were collected. Among pts without TxI during yr-1, typical HBeAg-negative chronic infection (CIe-) pts were defined those with persistently ALT ≤ULN and HBV DNA <2000 and GZ pts were considered those who did not fulfill the typical CHBVe- definition. Former (2017) TxI were: a) HBV DNA >20,000 and ALT >2 × ULN, b) HBV DNA ≥2000 and Ishak-stage (F) 3–4 or liver stiffness (LS) 9.1–12/12.1–15 kPa in case of ALT ≤/>ULN or c) detectable HBV DNA and F5–6 or LS>12/>15 kPa in case of ALT≤/>ULN. New (2025) TxI were: A) detectable HBVDNA and LS >8 Kpa or F≥4 or B) HBV DNA ≥2000 and ALT >ULN or LS 7.1–8 kPa or F3.
Results: Of 2012 chronic HBV pts, 1501 (75%) (males 60%, mean age 44 ± 15 yrs, BMI 26 ± 4 kg/m^2, follow-up 6.0 ± 4.6 yrs) were included. Using 2017 vs 2025 EASL CPGs, 679 (45%) vs 660 (44%) were CIe-, 577 (38%) vs 297 (20%) were GZ and 245 (16%) vs 544 (36%) were pts with TxI (A: 259, B: 285), respectively. New (2025) TxI during yr-1 were met by 19 (2.8%) former CIe-, 280 (48.5%) former GZ and all 145 pts with 2017 TxI. Of 297 former GZ pts without new TxI, 238 (80%) had HBV DNA ≥2000 but ALT ≤ULN and 59 (20%) had ALT >ULN but HBV DNA <2000 (all LS ≤7 kPa). Therapy during yr-1 was initiated in 366/544 (67%) pts with new TxI, 34/297 (11.4%) new GZ and 9/660 (1.4%) new CIe- pts ($p < 0.001$). The 1-/3-/5-yr treatment initiation rates were 67/77/85% in pts with as well as 4.5/9/16% in pts without new TxI within yr-1 (log-rank, $p < 0.001$).
Conclusion: The EASL 2025 TxI reduce by half the GZ CHBVe- pts and reflect better treatment policies in routine clinical practice over the last 15 years identifying the majority of pts clinicians are already more likely to treat.

OS-069
Efficacy and safety of interferon combined with antiretroviral therapy in people with HIV/HBV co-infection: a prospective observational study

Yaozu He[1], Weiyin Lin[1], Hong Li[1], Fei Gu[1], Peishan Du[1], Shaozhen Chen[1], Xiaoping Tang[2], Linghua Li[1]. [1]*Infectious Disease Center, Guangzhou Eighth People's Hospital, Guangzhou Medical University Guangzhou, Guangzhou, China;* [2]*Institute of Infectious Disease, Guangzhou Eighth People's Hospital, Guangzhou Medical University, Guangzhou, China*
Email: llheliza@126.com

Background and aims: To evaluate the efficacy and safety of interferon combined with antiretroviral therapy (ART) for achieving HBV functional cure (HBsAg seroclearance) in HBV/HIV co-infected individuals.
Method: In this prospective observational study, we enrolled HBV/HIV co-infected adults on stable ART (>1 year) with HBeAg-negative status, HBsAg <1500 IU/mL, HIV RNA <20 copies/mL, and HBV DNA <100 IU/mL. Participants were allocated to two groups according to patient preference and physician recommendation: pegylated interferon α-2b (PEG-IFN α-2b) weekly for 48 weeks added to ongoing ART (n = 30) or continued ART alone (n = 90). All ART regimens contained two drugs with anti-HBV activity (3TC or FTC plus TDF or TAF). Primary endpoint was HBsAg seroclearance (quantitative HBsAg <0.05 IU/mL) at weeks 24 and 48. Secondary endpoints included early interferon response by week 24 (HBsAg decline >1 $\log_{10}$ IU/mL from baseline or seroclearance) and safety.
Results: Of the 2045 screened individuals with HBV/HIV co-infection, 409 met the preliminary criteria. Thirty entered the PEG-IFN α-2b plus ART group, and 90 entered the ART-alone group. Baseline features were balanced, except for a younger age in the PEG-IFN group (mean 41.8 ± 6.9 vs 45.7 ± 7.4 years; P = 0.011). Gender, ART duration, baseline HBsAg levels, and CD4 count were comparable between the groups (all P > 0.05). At week 24, 27 participants in the PEG-IFN group and 87 in the ART-alone group completed follow-up. HBsAg seroclearance was observed in 4/27 (14.8%) of those receiving PEG-IFN α-2b plus ART, versus none in the ART-alone group. Early interferon response occurred in 15/27 (55.6%) of the PEG-IFN group. As the study is still ongoing, only a subset of participants has completed the 48-week follow-up. At 48 weeks, 18 patients in the PEG-IFN α-2b plus ART group completed follow-up, with 7 (38.8%) achieving HBsAg seroclearance. In the ART-alone group, 54 patients completed 48 weeks of follow-up, with only 1 (1.9%) achieving HBsAg seroclearance. The difference in seroclearance rates between the two groups was statistically significant (P < 0.001). Adverse events in the PEG-IFN group were frequent but manageable, with no severe interferon-related adverse events leading to discontinuation.
Conclusion: PEG-IFN α-2b added to ART shows potential for HBsAg seroclearance in selected individuals with HIV/HBV co-infection, with acceptable tolerability.

OS-070-YI
Peg-IFN add-on versus nucleos(t)ide analogue withdrawal in patients with chronic hepatitis B – a pooled analysis of two global cohorts (RETRACT-B and PROSPER studies)

Edo J. Dongelmans[1], Grishma Hirode[2], Florian van Bömmel[3], Rachel Wen-Juei Jeng[4], Rong-Nan Chien[4], Chien-Hung Chen[5], Tung-Hung Su[6], Jia-Horng Kao[6], Wai-Kay Seto[7], Lesley Patmore[1], Lilian Liang[8], Shao-wen Jiang[9], Dag Henrik Reikvam[10], Marte Holmberg[11,12], Seng Gee Lim[13], Fabien Zoulim[14], Arno Furquim d'Almeida[15], Scott K. Fung[2], Margarita Papatheodoridi[16], Benjamin Maasoumy[17], Bettina E. Hansen[1,18], Richard Post[1], Anna Pocurull Aparicio[19], Yuxian Huang[20], Jose A. Carrión[21], Norah Terrault[22], Marc Ghany[23], Fabrice Carrat[24], Nathalie Ganne-Carrié[25,26], Asgeir Johannessen[11,12], Thomas Vanwolleghem[15], Sabela Lens[19], Teresa Broquetas[27], Qiankun Hu[28], Markus Cornberg[29], Man-Fung Yuen[7], Grace Wong[8], George Papatheodoridis[16], Thomas Berg[3], Marc Bourliere[30], Qing Xie[9], Yao-Chun (Holden) Hsu[31], Jordan J. Feld[2], Harry L.A. Janssen[1,2], Milan J. Sonneveld[1]. [1]*Erasmus University Medical Center, Rotterdam, Netherlands;* [2]*Toronto Centre for Liver Disease, Toronto General Hospital, University Health Network, Toronto, Canada;* [3]*Leipzig University Medical Center, Leipzig, Germany;* [4]*Chang Gung Memorial Hospital Linkou Medical Center, Chang Gung University, Taoyuan City, Taiwan;* [5]*Kaohsiung Chang Gung Memorial Hospital, Kaohsiung City, Taiwan;* [6]*National Taiwan University Hospital, Taipei City, Taiwan;* [7]*The University of Hong Kong, Hong Kong SAR, China;* [8]*Medical Data Analytics Centre (MDAC), The Chinese University of Hong Kong, Hong Kong SAR, China;* [9]*Shanghai Ruijin Hospital, Jiao Tong University School of Medicine, Shanghai, China;* [10]*Oslo University Hospital, Institute of Clinical Medicine, University of Oslo, Oslo, Norway;* [11]*Institute of Clinical Medicine, University of Oslo, Oslo, Norway;* [12]*Vestfold Hospital, Tønsberg, Norway;* [13]*National University Health System, Yong Yoo Lin School of Medicine, National University of Singapore, Singapore, Singapore;* [14]*Lyon Hepatology Institute (IHU EVEREST), UMR PaThLiv U1350, INSERM, Université Claude Bernard Lyon 1, Hospices civils de Lyon, Lyon, France;* [15]*Antwerp University Hospital, Viral Hepatitis Research Group, Laboratory of Experimental Medicine and Pediatrics, University of Antwerp, Antwerp, Belgium;* [16]*Medical School of National and Kapodistrian University of Athens, General Hospital of Athens "Laiko," Athens, Greece;* [17]*Hannover Medical School, Hannover, Germany;* [18]*University of Toronto, Toronto, Canada;* [19]*Hospital Clinic Barcelona, IDIBAPS and CIBEREHD, University of Barcelona, Barcelona, Spain;* [20]*National Medical Centre for Infectious Diseases, Huashan Hospital, Fudan University, Shanghai Public Health Clinical Center, Fudan University, Shanghai, China;* [21]*Hospital del Mar, Institut Hospital del Mar D'Investigacions Mèdiques, PSMAR, Universitat Pompeu Fabra, Facultat de Ciències de la Salut i de la Vida, Barcelona, Spain;* [22]*Keck School of Medicine of University of Southern California, Los Angeles, United States;* [23]*National Institutes of Health, Bethesda, United*

States; [24]Sorbonne Université, INSERM, Institut Pierre Louis d'Épidémiologie et de Santé Publique, IPLESP, Paris, France; [25]Service d'Hépatologie, Hôpital Avicenne, Université Sorbonne Paris Nord, UFR SMBH, Bobigny, France; [26]Cordeliers research center, Sorbonne Université, Inserm, Université de Paris, team « Functional Genomics of Solid Tumors », Equipe labellisée Ligue Nationale Contre le Cancer, Labex OncoImmunology, Paris, France; [27]Hospital del Mar, Institut Hospital del Mar D'Investigacions Mèdiques, PSMAR, Barcelona, Spain; [28]Shanghai Public Health Clinical Center, Fudan University, Shanghai, China; [29]Hannover Medical School, Centre for Individualised Infection Medicine (CiiM), A Joint Venture of Helmholtz Centre for Infection Research and Hannover Medical School, Hannover, Germany; [30]Hôpital Saint Joseph, Aix Marseille University, Inserm, IRD, SESSTIM, Sciences Économiques and Sociales de la Santé and Traitement de l'Information Médicale, ISSPAM, Marseille, France; [31]School of Medicine, E-Da Hospital/I-Shou University, Kaohsiung City, Taiwan
Email: e.dongelmans@erasmusmc.nl

Background and aims: Both nucleo(s)tide analogue (NA) withdrawal and pegylated-interferon (peg-IFN) add-on are strategies to increase HBsAg loss rates in chronic hepatitis B patients on long-term NA therapy. It remains unclear which strategy is superior.
Method: We compared HBsAg loss rates in HBeAg negative patients who stopped NA therapy with patients who received peg-IFN add-on using individual participant data from two global cohorts: (1) RETRACT-B, including patients who withdrew NA therapy and, (2) PROSPER, which studied NA-treated patients allocated to 48 weeks of peg-IFN add-on. The primary outcome was the cumulative HBsAg loss rate at 2-years after NA-stop or start of peg-IFN add-on (Kaplan-Meier method). Secondary outcome included ALT-flares (5≥×ULN). Robustness of the findings was subsequently confirmed after IPTW balancing. Analyses were performed in the overall population and stratified by ethnicity.
Results: In total, 2,095 patients were included (NA-stop: n = 1,772; peg-IFN add-on: n = 323). In comparison to NA-stop, peg-IFN treated patients were younger (48 vs. 52 years, p < 0.001), more often male (83 vs. 72%, p < 0.001), non-Asian (38 vs. 19%, p < 0.001), and had higher baseline ALT (26 vs. 23, p = 0.002). Baseline HBsAg (2.8 vs. 2.7 log10 IU/mL, p = 0.30), duration of NA therapy (4.3 vs. 3.1 years, p = 0.97) and patients with cirrhosis (8 vs. 11%, p = 0.10) were similar. The cumulative 2-year HBsAg loss rate was higher for patients treated with peg-IFN add-on vs. NA-stop (16 vs. 5%, p < 0.001; IPTW: 13 vs. 5%, p < 0.001). Importantly, the superiority of peg-IFN add-on was apparent in Asians (20 vs. 3%, p < 0.001; IPTW: 13 vs. 3%, p < 0.001), but not in non-Asians (9 vs. 13%, p = 0.37; IPTW: 8 vs. 12%, p = 0.54). Results were consistent for patients with baseline HBsAg <1,000 IU/mL, with higher HBsAg loss rates observed with peg-IFN add-on vs. NA-stop in Asians (30 vs. 5%, p < 0.001; IPTW: 20 vs. 5%, p < 0.001), but not in non-Asians (19 vs. 33%, p = 0.13; IPTW: 27 vs. 35%, p = 0.68). ALT-flares were more common after NA-stop (24 vs. 6%, p < 0.001; IPTW: 23 vs. 5%, p < 0.001), being consistent in Asian (24 vs. 7%, p < 0.001; IPTW: 24 vs. 5%,p < 0.001) and non-Asian patients (22 vs. 6%, p < 0.001, IPTW: 21 vs. 3%, p = 0.016).
Conclusion: Peg-IFN add-on resulted in higher HBsAg loss rates when compared to NA withdrawal in Asian patients, while responses were similar in non-Asians. These findings pave the way for personalised decision-making on the optimal strategy to increase HBsAg loss rates in patients on NA therapy.

Viral hepatitis B/D – New therapies

OS-071

PD-1 inhibitor plus Peg-IFNα therapy: efficacy and predictors of HBsAg clearance in CHB patients with a suboptimal early response to Interferon

Chenrui Liu[1], Yaping Li[1], Meng Zhang[1], Guoe Gou[1], Miao Hao[1], Muqi Wang[1], Yikai Wang[1], Shuangsuo Dang[1]. *[1]The Second Affiliated Hospital of Xi'an Jiaotong University, Xi'an, China*
Email: dang212@126.com

Background and aims: Despite being a cornerstone HBsAg clearance therapy, interferon often yields poor responses and risks T-cell exhaustion. PD-1 inhibitors offer a potential strategy but are limited as monotherapy. This study followed HBsAg outcomes in CHB patients over 24 weeks of PD-1 inhibitor plus Peg-IFNα treatment and a 24-week off-treatment period to identify characteristics of responders.
Method: This study enrolled interferon-experienced CHB patients (prior interferon ≥24 weeks with HBsAg decline <0.5 $\log_{10}$ IU/mL at week 24, HBsAg <1500 IU/mL, HBeAg-negative, HBV DNA <5 IU/mL) without PD-1 inhibitor contraindications. Patients received 24 weeks of PD-1 inhibitor (1 mg/kg, Q8–12W) plus Peg-IFNα (180 μg/week), followed by 24 weeks off-treatment. HBsAg status at end of follow-up (EOF) defined clearance and non-clearance groups. Baseline predictors were analyzed via univariate and binary logistic regression.
Results: Of 91 enrolled patients (69 male, 22 female), 26 (28.5%; 22M, 4F) achieved HBsAg clearance at EOF, with no unexpected safety signals. Baseline levels differed significantly between clearance and non-clearance groups for globulin (25.2 [23.2–29.0] vs. 27.65 [25.55–30.725] g/L, P = 0.013), albumin-to-globulin ratio (1.73 [1.485–1.9275] vs. 1.565 [1.3825–1.7925], P = 0.04), HBsAg (2.8 [0.6925–5.62] vs. 51.115 [4.025–294.925] IU/mL, P < 0.001), and HBsAb (2.645 [1.575–9.04] vs. 0.88 [0.4275–1.6975] IU/mL, P < 0.001). Based on a week-4 HBsAg decline >0.5 $\log_{10}$ IU/mL, patients were classified as early (n = 33) or poor early responders (n = 58). HBsAg clearance rates were 54.5% (18/33) and 13.7% (8/58), respectively. In binary logistic regression, only baseline HBsAg (OR 0.991, 95% CI 0.984–0.999, P = 0.017) and a week-4 HBsAg decline >0.5 $\log_{10}$ IU/mL (OR 10.233, 95% CI 2.706–38.699, P < 0.001) were independent predictors of week-48 clearance. ROC analysis for week-4 HBsAg decline yielded an AUC of 0.808 (0.700–0.917, P < 0.001), with an optimal cutoff of 0.418 $\log_{10}$ IU/mL (Se = 0.769, Sp = 0.754). Baseline HBsAg had an AUC of 0.790 (0.691–0.889, P < 0.001), with an optimal cutoff of 10.165 IU/mL (Se = 0.677, Sp = 0.846).
Conclusion: PD-1 inhibitor combined with Peg-IFNα achieved an HBsAg clearance rate of approximately 28.5% in interferon-experienced CHB patients with a suboptimal early response, supporting its potential as a viable clinical cure strategy. Baseline HBsAg <10 IU/mL and week-4 HBsAg decline ≥0.418 $\log_{10}$ IU/mL were predictive of HBsAg clearance at week 48.

OS-072

Safety, tolerability, pharmacokinetics, and pharmacodynamics of GSK3965193 in patients with chronic hepatitis B (CHB)

Martin Leivers[1], Stephen Atkinson[2], Sarah Mole[2], Christine Livingston[1], Ahmed Nader[1], B S Pooja[3], Susmita Sanyal[4], Eric Billaud[5,6], Caroline Jezequel[7], Marie-Noëlle Hilleret[8], Pietro Lampertico[9], Young-Suk Lim[10], Jeong Heo[11], Won Young Tak[12], Ashley Brown[13], Daniel Forton[14], Curtis Cooper[15], Carla Coffin[16], Anchalee Avihingsanon[17], Shilpy Joshi[1], Michael Maguire[2], Puneet Dhawan[1], Kiran Gumireddy[1], Anil Kesarwani[1], Nadia Noormohamed[1]. *[1]GSK, Collegeville, United States; [2]GSK,*

Stevenage, United Kingdom; [3]GSK, Bengaluru, India; [4]GSK, Hyderabad, India; [5]Department of Infectious Diseases, CHU Hôtel-Dieu, Nantes, France; [6]CIC UIC 1413 INSERM, CHU Nantes, Nantes, France; [7]CHU Pontchaillou, Rennes, France; [8]Department of Hepatogastroenterology, CHU Grenoble Alpes, Grenoble, France; [9]Foundation IRCCS Ca' Granda Ospedale Maggiore Policlinico, Milan, Italy; [10]Asan Medical Center, University of Ulsan College of Medicine, Seoul, Korea, Rep. of South; [11]College of Medicine, Pusan National University and Biomedical Research Institute, Pusan National University Hospital, Busan, Korea, Rep. of South; [12]Kyungpook National University Hospital, School of Medicine Kyungpook National University, Daegu, Korea, Rep. of South; [13]Imperial College Healthcare NHS Trust, London, United Kingdom; [14]St George's NIHR Clinical Research Facility, St George's University Hospital, London, United Kingdom; [15]University of Ottawa, Ottawa, Canada; [16]Cumming School of Medicine, University of Calgary, Calgary, Canada; [17]HIVNAT, Thai Red Cross AIDS Research Centre and Excellence Centre in Tuberculosis, Faculty of Medicine, Chulalongkorn University, Bangkok, Thailand
Email: martin.r.leivers@gsk.com

Background and aims: GSK3965193 (GSK193) is a novel, orally bioavailable, small molecule inhibitor of the human non-canonical poly(A) polymerases PAPD5/7, designed to reduce the HBV antigen HBsAg through destabilization of HBV RNA. This first-in-patient study aimed to assess the safety, tolerability, pharmacokinetics (PK), and pharmacodynamics (PD) of GSK193 in patients with chronic hepatitis B (CHB).
Method: This was a multicenter, randomized, double-blind, placebo-controlled phase 1 study (ClinicalTrials.gov: NCT05330455). In Part 3 of the study, HBeAg positive and negative patients on nucleoside analogs were randomized to GSK193 (0.5 mg, QD; n = 14) or placebo (QD; n = 4) for 28 days. PK, PD (HBV biomarkers) and safety monitoring, including nerve conduction assessments at baseline, days 15 and 29, were assessed.
Results: GSK193 had an acceptable safety profile and was well tolerated in CHB patients at the tested dose and duration. In part 3, no serious treatment-emergent adverse events (TEAEs) or TEAEs > Grade 2 occurred. The most common TEAEs were dizziness, fatigue, dysgeusia, and headache, all of which occurred more frequently with GSK193 than placebo. No significant changes were observed in nerve conduction assessments. Following administration, GSK193 was rapidly absorbed, with a median T_{max} of 3.0 h and median $t_{1/2}$ of 7.9 h. No accumulation was observed after 28 daily doses. A plasma target concentration corresponding to the protein-binding–adjusted preclinical liver EC90 was exceeded for 24 hours following the 0.5 mg dose, confirming PK model-based predictions. GSK193 treatment resulted in a posterior mean for the maximum HBsAg reduction from baseline of 0.50 log10 IU/mL (95% credible interval [CrI]: 0.3, 0.7) which was higher than in the placebo group (0.08 log10 IU/mL; 95% CrI: 0.05, 0.09). Individually, the highest observed maximum reduction of HBsAg levels with GSK193 was 1.66 log10 IU/mL compared to 0.10 log10 IU/mL with placebo. On average, this maximum reduction was achieved within 24 days with GSK193. Upon cessation of GSK193 administration, HBsAg levels generally rebounded to baseline within 2 weeks.
Conclusion: GSK193 at the tested dose was tolerated, showed favorable safety and pharmacokinetic profile, and demonstrated preliminary evidence of antiviral activity through HBsAg reduction, supporting further clinical development of GSK193 as part of a regimen for treating CHB.
Funding: GSK (study 214760).

OS-073

A single VRON-0200 prime dose, followed by a monthly antiviral combination regimen, resulted in rapid, profound, and durable HBsAg declines in chronically hepatitis B-infected patients

Edward J. Gane[1], Sue Currie, Tien Huey Lim[2], Andrew Luber[3], Marie Bonhomme[4], Grace Wong[5]. *[1]Auckland City Hospital, Auckland, New Zealand; [2]Middlemore Hospital, Auckland, New Zealand; [3]Virion Therapeutics, LLC, Philadelphia, United States; [4]PPD, Part of Thermo Fisher Scientific, Richmond, United States; [5]The Chinese University of Hong Kong, Hong Kong, Hong Kong*
Email: scurrie@viriontx.com

Background and aims: VRON-0200 is an immune-modulator containing a checkpoint modifier targeting HBV core and pol (but not S) antigens, designed to enhance, broaden, and prolong T cell responses. The Phase 1b study demonstrated that VRON-0200 induces anti-HBV immune activation/restoration, with durable HBsAg declines after a single dose. This study report evaluates the safety,immunogenicity,and HBsAg data from chronically-HBV(CHB) infected patients(pts), on NUCs, that received VRON-0200, alone, or in combination with investigational antivirals.
Method: CHB pts, NUC-suppressed with HBsAg <500 IU/mL (Cohorts 1 and 2;C1/2), or <1,000 IU/mL (Cohort 3;C3), were randomized to receive i.m. VRON-0200 prime on D1, w/wo VRON-0200 boost on D91;C3 receive VRON-0200 prime, followed by 6 monthly doses of elebsiran plus tobevibart (E+T) starting on D28, alone, or with a VRON-0200 boost on D196. Safety, virologic, and immunologic assessments were performed. HBsAg (ELISA; LLOD:0.05 IU/mL),and T cell frequencies (IFNɣ ELISpot) were measured.
Results: As of December 19, 2025, 35 pts were included: 28 (80%) male, 30 (86%) Asian, median age:46 yrs, and median BL HBsAg,179 IU/mL(range:10–1169). In 12,073 pt safety days, 38 TRAEs were reported: 4-GR2,34-GR1, with no treatment-related SAEs or D/Cs. In C1/2, all 27 reached EOS(D360); at D360, 359 days post VRON-0200 prime dose, 23/27(85%) had sustained and/or continued HBsAg declines;12/23(52%) had >50% declines, and 4 pts had $\geq 1 \log_{10}$IU/mL reduction from baseline. A boost dose did not enhance responses, and HBsAg declines were independent of BL HBsAg levels. IFNɣ ELISpot responses did not appear to be associated with HBsAg declines. In C3, within 7 days of first E+T dose, rapid and profound HBsAg declines were observed (100% ≤2 IU/mL; 1 below LLOD) and were independent of BL HBsAg levels. At Day 196 (28 days post last E+T dose), 100% were ≤1 IU/mL; 3 of 7 below LLOD. C3 results, at least 3 months post last E+T dose, to be reported.
Conclusion: In this Phase 1b study, VRON-0200 alone, or in combination, had no observed safety concerns, and was well tolerated. VRON-0200-induced anti-HBV activity was enhanced in combination with antivirals and produced rapid and profound HBsAg declines in all patients. This novel approach, where anti-HBV immunity is "sparked" (i.e. primed) with VRON-0200, and then "fanned" (i.e. boosted) by HBV removal, supports the potential of VRON-0200 as a foundational backbone agent for future HBV Functional Cure regimens. A Phase 2b study (SPARK-B) is in planning.

OS-074

Marked sensitivity to an entry inhibitor in Mongolian patients with chronic hepatitis delta: 24-week results from a phase IIb multicentre randomised controlled trial of Hepalatide

Janchiv Oyunbileg[1], Xiaolu Tang[2], Shirnin Tamir[3], Batjargal Azjargal[4], Munkhzaya Chogsom[5], Otgonjargal Nomingerel[3], Batzorig Orgil[3], Xian Gao[2], Fei Cai[2], Wenhui Liu[2], Hanzhi Fang[2], Hongli Liu[2]. *[1]National Center for Public Health, Ulaanbaatar, Mongolia; [2]Shanghai HEP Pharma Co., Ltd., Shanghai, China; [3]SFCS Site Management LLC, Ulaanbaatar, Mongolia; [4]National Center for Communicable Diseases, Ulaanbaatar, Mongolia; [5]National Cancer Center of Mongolia, Ulaanbaatar, Mongolia*
Email: jobileg@gmail.com

Background and aims: HBV/HDV entry inhibitors represent a major advance in the direct antiviral treatment for chronic hepatitis delta (CHD). Bulevirtide is the first approved therapy for CHD in Europe as an orphan drug. In the phase II MYR202 trial, 24 weeks of bulevirtide 2 mg achieved a combined response rate of 21%. However, efficacy and safety data from hyperendemic regions remain limited, where entry inhibitors are urgently needed. Mongolia is among the countries with the highest reported prevalence of CHD worldwide.

This study reports a phase IIb trial of the entry inhibitor hepalatide in Mongolian CHD patients.
Method: This multicentre, randomised, open-label, delayed-treatment–controlled trial enrolled adults aged 18–65 years with compensated CHD and quantifiable HDV RNA in Mongolia (NCT06505928). Participants were randomised 1:1:1 to once-daily subcutaneous hepalatide 2.1 mg, hepalatide 4.2 mg, or delayed treatment for 48 weeks, followed by a 96-week extension with hepalatide 2.1 mg. Virological response was defined as undetectable HDV RNA or a ≥ 2 $\log_{10}$ decline, and biochemical response as alanine aminotransferase normalisation. Combined response and safety were assessed at the 24-week interim analysis.
Results: Ninety subjects (81 Mongolian, 1 Kazakh, and 8 of other ethnicities) were randomised to the 2.1 mg, 4.2 mg, or delayed treatment groups (n = 31, 29, and 30). Eighty-nine participants completed the 24-week period, with one discontinuation in the 2.1 mg group. Hepalatide was generally well tolerated, with no grade ≥ 3 treatment-related adverse events. At week 24, virological response rates were 51.6%, 62.1%, and 0.0%, with mean HDV RNA changes of −1.96, −2.30, and + 0.04 $\log_{10}$ IU/mL. Biochemical response occurred in 77.4%, 65.6%, and 13.3% of patients, while combined response rates were 48.4%, 41.4%, and 0.0%. All virological, biochemical, and combined responses in both hepalatide groups were significantly higher than in the delayed treatment group ($p < 0.001$ for each comparison).
Conclusion: Hepalatide demonstrated significant virological, biochemical, and combined responses with good tolerability in Mongolian patients with CHD. Relative to historical bulevirtide data predominantly from Caucasian cohorts, the high combined response rates observed in the study may indicate heightened sensitivity to entry inhibitors in this highly endemic Mongolian population. These findings may suggest long-term clinical relevance of entry inhibitors in Mongolian CHD patients.

OS-075
Lonafarnib/ritonavir and peg-Interferon alfa drive histological improvement and inflammation resolution in chronic hepatitis D: results of the multicenter phase 3 D-LIVR study
Robert Taylor[1], Ohad Etzion[2], Saeed Sadiq Hamid[3], Tarik Asselah[4,5], George Sebastian Gherlan[6], Maria Buti[7], Pietro Lampertico[8], Adela Turcanu[9], Tsarynna Petrivna[10], Liana Gheorghe[11], George Stancu[11], Natalia Voronkova[12], Natalia Barsukova[13], Soo Aleman[14], Jordan J. Feld[15], Jean-Karl Sirois[16], Armaan Hirani[1], Hebaalla Agha[1], Leen Kawas[1], Nancy S. Reau[17], Christopher Koh[18], Theo Heller[18], Cihan Yurdaydin[19], Xue Hua[1], Jeffrey Glenn[1,20]. *[1]EIT Pharma, Inc., Kirkland, United States; [2]Soroka, University Medical Center, Be'er Sheva, Israel; [3]Aga Khan University, Karachi, Pakistan; [4]Hopital Beaujon, University of Paris, Clichy, France; [5]University of Paris, Paris, France; [6]Carol Davila University of Medicine and Pharmacy, Bucharest, Romania; [7]Hospital Universitari Vall d'Hebron, Barcelona, Spain; [8]Fondazione IRCCS CA' Granda Ospedale Maggiore Policlinico, Milan, Italy; [9]The State University of Medicine and Pharmacy, Chisinau, Moldova; [10]International Institute of Clinical Research, Kyiv, Ukraine; [11]Institutul Clinic Fundeni, Bucharest, Romania; [12]H-Clinic, Moscow, Russian Federation; [13]Center for Targeted Therapy, LLC., Moscow, Russian Federation; [14]Korolinska Universitetssjukheset, Huddinge, Sweden; [15]University Health Network, Toronto, Canada; [16]YBR Analytics, Toronto, Canada; [17]Rush University Medical Center, Chicago, United States; [18]Liver Disease Branch, NIDDK, NIH, Bethesda, United States; [19]Koc University School of Medicine, Istanbul, Türkiye; [20]Stanford University School of Medicine, Palo Alto, United States*
Email: jeffrey.glenn@eitpharma.com

Background and aims: Lonafarnib (LNF) boosted with ritonavir (LNF/RTV) is an oral therapy for chronic hepatitis D (CHD) that may be combined with peg-interferon-alfa (Peg). LNF has a dual mechanism, inhibiting the host farnesyltransferase to disrupt HDV virion assembly, and inducing interferon-stimulated gene expression. Improvement of liver histology in CHD is a key predictor of long-term clinical benefit, and reducing hepatic inflammation is a necessary precursor to hepatic histology improvement. Therefore, we evaluated the impact of LNF/RTV with and without Peg on inflammatory and histological outcomes in D-LIVR, the largest phase 3 randomized placebo-controlled CHD trial to date.
Method: Oral LNF/RTV with or without PEG was evaluated in placebo controlled 407 patients with CHD, largest number of histology biopsies for CHD in a single study. The primary endpoint was a composite score of ≥ 2 log HDV RNA reduction and ALT normalization compared to baseline at week 48 on-treatment, with improvement in liver histology as a secondary endpoint. Histological response was defined as a ≥2-point improvement in modified Ishak Histologic Activity Index (HAI) without worsening of fibrosis. This study examines the relationship between ALT normalization and histological improvement.
Results: Both LNF/RTV monotherapy and LNF/RTV+Peg met the primary composite endpoint with significant improvement over placebo (LNF/RTV: 10%, $p = 0.004$, LNF/RTV+ Peg: 19% $p < 0.0001$). Peg monotherapy had limited composite response rate (9%, $p = 0.09$ vs placebo) at 48 weeks on treatment driven by limited ALT normalization. In contrast, ALT was significantly normalized in both LNF/RTV (25%, $p = 0.0003$ vs placebo) and LNF/RTV+Peg (34%, $p < 0.0001$ vs placebo) arms. Importantly, LNF/RTV+Peg resulted in a statistically significant histological improvement at 48-weeks on-treatment ($p = 0.01$) and LNF/RTV monotherapy directionally improved histological endpoints.
Conclusion: In patients with chronic hepatitis D, reduction of hepatic inflammation is a critical step toward histological improvement and long-term clinical benefit. LNF/RTV, a first-in-class oral CHD therapy, alone and in combination with peg-interferon alfa, significantly reduces HDV viral load and normalizes ALT, and combination treatment translates into meaningful improvements in liver histology after only 48 weeks of treatment. These findings support LNF/RTV-based regimens as disease-modifying therapies for CHD and highlight the added histological benefit of combination therapy.

SATURDAY 30 MAY

Basic viral hepatitis and immunology

OS-076-YI
Long-read sequencing unveils extensive HBV-DNA integration driving massive HBsAg production and sustaining HDV persistence
Stefano D'Anna[1], Lorenzo Piermatteo[1], Ilaria Grossi[1], Giuseppina Brancaccio[2], Luca Carioti[3], Andrea Di Lorenzo[4], Tommaso Poldiallai[1], Lorenza Pasqualini[5], Elisabetta Teti[4], Marco Iannetta[4], Caterina Pasquazzi[6], Miriam Lichtner[6], Umberto Cillo[7], Alessandro Vitale[7], Enrico Gringeri[7], Maria Magrofuoco[7], Leonardo Baiocchi[8], Simona Francioso[8], Ilaria Lenci[8], Apostolos Koffas[9], Maria Lorena Abate[10], Giovanni Battista Gaeta[11], Antonella Olivero[10], Loredana Sarmati[4], Mario Rizzetto[10], Upkar Gill[9], Patrick Kennedy[9], Gian Paolo Caviglia[10], Valentina Svicher[1], Romina Salpini[1]. *[1]University of Rome Tor Vergata, Department of Biology, Rome, Italy; [2]Infectious Diseases, Link Campus University Rome, Department of Life Sciences, Health and Health Professions, Rome, Italy; [3]University of Rome Tor Vergata, Department of Experimental Medicine, Rome, Italy; [4]University Hospital of Rome Tor Vergata, Infectious Diseases Unit, Rome, Italy; [5]Agilent Technologies Italia - Milano, Cernusco sul Naviglio, Italy; [6]Sant'Andrea Hospital, Rome, Italy; [7]University of Padua, Hepatobiliary Surgery and Liver*

Transplantation Unit, Department of Surgery, Oncology and Gastroenterology, Padua, Italy; [8]University Hospital of Rome Tor Vergata, Hepatology Unit, Rome, Italy; [9]Blizard Institute, Barts and The London School of Medicine and Dentistry, Queen Mary University of London, London, United Kingdom; [10]University of Turin, Department of Medical Sciences, Turin, Italy; [11]University L. Vanvitelli, Infectious Disease Unit, Naples, Italy
Email: stefanodanna26@gmail.com

Background and aims: HDV relies on HBsAg for its infectivity. HBsAg transcripts originate from cccDNA via the conventional poly-A signal and from integrated double-stranded linear HBV-DNA via the cryptic poly-A signal. Here, we evaluated intrahepatic HBV/HDV reservoir and the contribution of HBsAg production from linear HBV-DNA integration in sustaining HDV activity and pathogenetic potential.
Method: 70 liver biopsies from eAg- patients (pts) (74% NUC-treated) were included: 35 with chronic hepatitis delta (CHD) and 35 with chronic hepatitis B (CHB). Droplet-digital PCR quantified cccDNA, pgRNA, HDV-RNA and HBsAg transcripts from cccDNA and integrated HBV-DNA. In 19 CHD pts, long-read Nanopore sequencing assessed HBV-DNA integrations including those containing at least the entire ORF-S up to the cryptic poly-A signal (S-integrants). RNA-seq evaluated viral gene expression.
Results: In CHD pts, median (IQR) cccDNA, pgRNA and cccDNA-derived HBsAg transcripts were 1 (0.02–12), 8 (1–147) and 1 (0.2–41) copies/1000cells, all >1 log lower than in CHB pts ($p < 0.001$). HDV-RNA was 787 (1–7596) copies/1000cells. cccDNA strongly correlated with pgRNA and cccDNA-derived HBsAg transcripts ($p < 0.001$) but not with HDV-RNA ($P = 0.60$). Despite limited intrahepatic HBV reservoir, >1 HBV-DNA integrant was detected in 73.7% (14/19) of CHD pts (5 [2–6] number of unique events per pt). Notably, 10/14 (71.4%) CHD pts carried S-integrants. S-integrant carriers had high levels of integrated-derived HBsAg transcripts (32410 [16733–53180] cps/1000cells), which were absent in pts without HBV-DNA integrants, as confirmed by RNA-seq. S-integrant carriers had higher cccDNA and pgRNA ($p < 0.005$ for both), supporting that an active cccDNA fuels HBV-DNA integration, while HDV-RNA was similar regardless of S-integrants ($p = 0.5$). Moreover, S-integrant carriers had higher serum HBsAg (4.3 [4.0–4.4] vs 3.7 [3.5–3.9] logIU/ml, $p = 0.04$). By AUROC, HBsAg >4logIU/ml predicted the occurrence of S-integrants with the best accuracy (75% sensitivity and 75% specificity). Finally, in 7/10 pts, S-integrants localised in 26 human genes regulating cell proliferation, most of which ($N = 21$) are known to dysregulate hepatocytes proliferation.
Conclusion: This study provides the first direct evidence that S-integrants sustain massive HBsAg production, supporting HDV persistence. High serum HBsAg (>4 logIU/ml) may reflect an enrichment of HBV-DNA integration. Localization of integrants in proliferation-related genes suggests a role in paving the way to hepatocarcinogenesis.

OS-077
Clinical efficacy of BRII-179 therapeutic vaccine provided by a mismatched T cell epitope of prehistoric origin

Nina Le Bert[1], Akshay Binayke[1], Shubhankar Ambike[1], Previtha Dawn[1], Ying Tan[2], Anthony Tan[1], Yazhini Avaiarasi[1], Shoukit Hang[3], Yun Ji[4], Qing Zhu[4], Antonio Bertoletti[1]. *[1]Duke-Nus Medical School, Singapore, Singapore; [2]Brii Biosciences Inc, Beijing, China; [3]T Cell Diagnostic Pte Ltd, Singapore, Singapore; [4]Brii Biosciences Inc, Durham, United States*
Email: antonio@duke-nus.edu.sg

Background and aims: Therapeutic vaccines for HBV cure aim to restore dysfunctional HBV-specific T and B cells. BRII-179 is a therapeutic vaccine composed of recombinant HBV envelope proteins. Clinical trials combining siRNA, BRII-179, and PegIFN-alpha demonstrated that BRII-179 modulates HBV-specific immunity and increases rates of HBsAg loss (Wong, G. L.-H. *et al*. Elebsiran and PEG-IFNα for chronic hepatitis B infection: a partially randomized, open-label, phase 2 trial. *Nat. Med.* (2025) doi:10.1038/s41591-025-04049-z).
Method: We studied CHB patients on nucleo(t)side analogue therapy who received BRII-179 plus siRNA ($n = 77$), with a subset subsequently treated with siRNA and PegIFN-alpha ($n = 31$). We performed T cell epitope mapping, functional characterization and longitudinal tracking of vaccine-induced T cells, quantification and phenotyping of HBs-specific B cells, and sequence analysis comparing vaccine and infecting HBV strains.
Results: Anti-HBs titers after BRII-179 treatment correlated not with pre-existing PreS1/PreS2/S-specific T cells, but with expansion of IL-2-producing CD4T cells targeting two adjacent epitopes in the PreS1 N-terminal domain. These epitopes, mismatched with patients' infecting genotypes (B and C), were induced by a PreS1 sequence of a rare genotype G considered a remnant of prehistoric HBV lineages. The vaccine-induced CD4T cells produced predominantly IL-2 and were detected in most vaccinated patients across diverse HLA-class II backgrounds. They remained functionally stable for over two years, and persisted during subsequent PegIFN-alpha/siRNA treatment. Despite lacking cross-reactivity with contemporary HBV genotypes, patients with these epitope-mismatched CD4T cells showed marked progressive maturation of HBs-specific B cells, suggesting intramolecular help between vaccine-specific T cells and HBs-specific B cells.
Conclusion: Enhanced HBsAg loss rates following siRNA and PegIFN-alpha treatment are associated with the expansion of epitope-mismatched vaccine-specific CD4T cells and HBs-specific B cell maturation. These findings underscore the role of HBs-specific B cells in achieving HBsAg loss. The notable immunogenicity of this ancient HBV sequence raises the possibility that viral epitopes lost during evolution may hold the key to eliciting therapeutically effective antiviral immunity.

OS-078
Metabolic dysfunction-associated steatotic liver disease induces hepatocellular ferroptosis and activates intrahepatic macrophages by upregulating lipocalin-2 to accelerate the clearance of Hepatitis B surface antigen

Yan Han[1], Jing Tang[1], ZhiWei Chen[1], Hong Ren[1]. *[1]Department of infectious diseases, The second affiliated hospital of Chongqing Medical University., Chongqing, China*
Email: renhong0531@cqmu.edu.cn

Background and aims: To date, it remains challenging to cure chronic hepatitis B (CHB). Intriguingly, recent cohort studies have revealed that metabolic dysfunction-associated steatotic liver disease (MASLD) can promote the spontaneous clearance of HBsAg in CHB patients. This study aims to uncover the underlying mechanism.
Method: C57BL/6J mice were administered rAAV8-1.3HBV via tail-vein injection to establish chronic HBV infection. Subsequently, either a Methionine-Choline Deficient (MCD) or a Choline-Deficient, L-Amino Acid-defined, High-Fat Diet (CDAHFD) regimen was fed to the mice to induce a CHB concurrent with MASLD model. Bulk RNA-seq of liver tissue and single-cell RNA sequencing (scRNA-seq) of hepatocytes and immune cells were conducted to investigate the mechanism. In vitro, the conditioned medium from lipocalin-2 (Lcn2)-overexpressing or ferroptosis-induced hepatocytes was co-cultured with macrophages to mimic cell-cell crosstalk.
Results: In the MASLD/CHB co-diseased group, both mouse models exhibited markedly reduced serum HBsAg levels compared to baseline. ScRNA-seq of hepatocytes revealed a substantial decrease in HBV mRNA-positive cells in the co-diseased group. Bulk RNA-seq indicated significant upregulation of the hepatic ferroptosis pathway, which was further corroborated by iron overload and elevated malondialdehyde (a lipid peroxidation product). Treatment with Liproxstatin-1, a ferroptosis inhibitor, increased serum HBsAg levels. To assess whether hepatic ferroptosis triggers an immune response, we analyzed intrahepatic immune cells via scRNA-seq and found significant macrophage activation. In vitro studies demonstrated that

this activation was characterized by the upregulation of M1 markers and, importantly, the phosphorylation and nuclear translocation of key proteins in the TLR4/NF-κB/IRF3 axis. Following macrophage depletion with Gacl3, serum HBsAg levels elevated. Notably, Liproxstatin-1 treatment could also attenuate macrophage activation. At Last, we found that Lcn2, a key metabolic gene in MASLD, was markedly upregulated. Inhibition of Lcn2 significantly alleviated hepatic ferroptosis and reduced macrophage infiltration, leading to a significant rebound in the serum HBsAg level.
Conclusion: Our study demonstrated that MASLD can induce hepatocellular ferroptosis and activate intrahepatic macrophages via Lcn2 upregulation, thereby accelerating HBsAg clearance. This finding provides new insights into the MASLD-HBV interplay.

OS-079
SR-1891, a first long-acting capsid assembly modulator, induces safe, profound and durable antiviral suppression after a single subcutaneous dose in mouse models of chronic hepatitis B
Romano Di Fabio[1], Marco Manenti[1], Alessandro Grillo[1], Pietro Di Lucia[1], Elisa Bono[2], Leonardo Giustini[2], Lorena Donnici[3], Katherine Squires[4], Gaston Picchio[2], Raffaele De Francesco[3,5], Matteo Iannacone[1,2], Micol Ravà[1], Luca G. Guidotti[1,2]. *[1]Vita-Salute San Raffaele University, Milan, Italy; [2]IRCCS San Raffaele Scientific Institute, Milan, Italy; [3]INGM, National Institute of Molecular Genetics "Romeo ed Enrica Invernizzi," Milan, Italy; [4]Former Antios Therapeutics, Mendham, NJ, USA, Mendham, NJ, United States; [5]Department of Pharmacological and Biomolecular Sciences, Università degli Studi di Milano, Milan, Italy*
Email: guidotti.luca@hsr.it

Background and aims: Novel suppressive therapies that improve both antiviral potency and adherence over current nucleos(t)ide analogues are likely to be needed to curb the global burden of chronic HBV infection in the foreseeable future. Here, we report the discovery and initial preclinical characterization of SR-1891, a highly potent capsid assembly modulator (CAM) that leverages intrinsic long-acting properties following subcutaneous administration.
Method: SR-1891 was administered as a single subcutaneous dose (150 mg/kg) to HBV-replicating immunocompetent transgenic mice (HBV Tg, baseline viremia 10^7–10^8 copies/mL) or HBV-infected immunodeficient liver-humanized mice (HBV Hu, baseline viremia 8 × 10^8–4 × 10^9 copies/mL). This dose is comparable to those used in the preclinical development of lenacapavir, a long-acting CAM approved for HIV treatment. At abstract submission, HBV Tg and HBV Hu cohorts had been followed through days 14 and 28, respectively. Control animals received continuous oral entecavir (ETV; 0.1 mg/kg/day in drinking water), a regimen commonly used in mouse studies to approximate human clinical exposure. Serum HBV DNA, HBV RNA and ALT were measured at multiple time points before and after dosing. In selected HBV Tg mice, liver injury and hepatocellular capsid distribution were assessed histologically on day 14.
Results: Relative to pre-dose serum HBV DNA, ETV produced progressive multi-log10 declines after 14 days in HBV Tg (−3.4 log10) and HBV Hu (−1.9 log10) mice, and after 28 days in HBV Hu mice (−2.8 log10), without reducing serum HBV RNA. In contrast, SR-1891 achieved ≈10-fold greater decreases in serum HBV DNA than ETV at all assessed time points, reaching −4.3 log10 at day 14 in HBV Tg mice and −3.0 log10 at day 14 in HBV Hu mice, with an ≈8-fold difference still evident at day 28 in HBV Hu mice (−3.7 log10). SR-1891 also induced progressive declines in serum HBV RNA, reaching ≥2 log10 reductions versus baseline and ETV by day 14 (last assessment) in both models. No ALT elevations were detected in HBV Tg mice, and day-14 histology showed no liver injury or aberrant hepatocellular capsid accumulation.
Conclusion: SR-1891 is a first long-acting CAM that, after a single subcutaneous dose, achieves greater and more durable antiviral effects than daily oral ETV. Ongoing studies of serum and hepatic viral markers, including HBeAg, HBsAg and cccDNA before and after days 14–28, as well as ADME profiling and PK/PD analyses, will be reported at the meeting.

OS-080-YI
The spatial single-cell landscape in the hepatitis B virus/hepatitis D virus-coinfected human liver reveals spatially confined immunosuppressive virus-immune niches
Yuan Suo[1], Shirin Nkongolo[2,3,4], Carolin Mogler[5], Ira Godbole[1], Günter Päth[1], Stephan Urban[3], Robert Thimme[1], Bertram Bengsch[1,6,7]. *[1]Clinic for Internal Medicine II, University Medical Center Freiburg, Freiburg, Germany; [2]Internal Medicine IV (Gastroenterology, Hepatology, Infectious Diseases), University Hospital Heidelberg, Heidelberg, Germany; [3]Molecular Virology, Department of Infectious Diseases, University Hospital Heidelberg, Heidelberg, Germany; [4]German Center for Infection Research, partner site Heidelberg, Heidelberg, Germany; [5]Institute of Pathology, School of Medicine & Health, Technical University of Munich, Munich, Germany; [6]Signaling Research Centres BIOSS and CIBSS, Freiburg, Germany; [7]German Cancer Consortium (DKTK), Heidelberg, Germany, Partner Site Freiburg, Freiburg, Germany*
Email: yuan.suo@uniklinik-freiburg.de

Background and aims: Chronic hepatitis B virus (HBV) and hepatitis D virus (HDV) infection can lead to severe viral hepatitis and progression to liver cirrhosis and liver failure. The mechanisms underlying the failure of the immune system to clear HDV remain poorly understood. This study aimed to comprehensively characterize virus-host interactions in the spatial microenvironment in the HDV-infected human liver at single-cell resolution.
Method: Liver samples from 21 chronic HBV/HDV-infected patients were analyzed using MIBI-TOF imaging. The imaging panel comprised 40 markers for liver parenchymal cells and liver architecture, immune lineages and functional markers. Virus-infected cells were identified by hepatitis D antigen (HDAg) and hepatitis B virus core and surface antigens (HBsAg, HBcAg).
Results: We identified 18 different cell types, with hepatocytes accounting for the majority of cells, as expected. 4.3% of hepatocytes stained positive for the viral antigens HDAg, HBsAg, and/or HBcAg. Virus antigen-positive hepatocytes were biased towards either a dominant $HBsAg^+$ or $HDAg^+$ population. $HDAg^+$ hepatocyte density correlated with serum HDV RNA levels ($R^2 = 0.9212$, $P < 0.0001$) and the density of virus marker-positive hepatocytes was associated with immune cell infiltration ($R^2 = 0.2013$, $P = 0.0413$). Macrophages and CD8T cells were the most abundant immune cells (8.95% and 8.59%). Zonation analysis identified hepatic zones 1–3, and predominant stromal regions. Zone 3 exhibited the highest density of virus antigen-positive hepatocytes, whereas immune cells were most densely localized in Zone 1 and the stromal region. Spatial interactions between immune and virus-positive cells were further analyzed by distance analysis. Macrophages were significantly enriched within viral regions ($P = 0.011$), and showed higher immunosuppressive PD-L1 and CD204 expression in close proximity to hepatocytes with viral antigens. Cellular interaction analysis revealed those hepatocytes to interact more with macrophages, which in turn displayed enriched interactions with exhausted and progenitor exhausted CD8T cells.
Conclusion: Intrahepatic analysis of HDV patients identifies distinct spatial virus-immune niches in HBV/HDV infection. Phenotypic gradients around virus marker-positive hepatocytes suggest prominent interactions between HDV-infected hepatocytes and M2-like macrophages, suggesting the establishment of an immunosuppressive niche involved in regulating adaptive immunity.

Cirrhosis – Clinical and experimental III

OS-081

Transjugular intrahepatic portosystemic shunt (TIPS) in patients with porto-sinusoidal vascular disease (PSVD): a retrospective multicenter international study from the vascular liver diseases group (VALDIG)

Laura Turco[1], Virginia Hernández-Gea[2], Dario Saltini[3], Luis Téllez[4], Antonina Antonenko[5], Francesco Vizzutti[6], Rosario La Delfa[6], Mauro Viganò[7], Dhiraj Tripathi[8], Francesca D'Arcangelo[8], Julia Eichholz[9], Chiara Becchetti[10], Stefania Gioia[11], Pierre-Emmanuel Rautou[12], Aurélie Plessier[12], Alberto Zanetto[13], Elisa Pinto[13], Kymentie Ferdinande[13], Chengjian Wu[14], Martina Lucà[15], Oana Nicoara-Farcau[16], Nancy Farouk[17], Marlene Reincke[18], Feng Zhang[19], Madalina Gabriela Indre[1], Lukas Hartl[20], Laure Elkrief[21], Sagnik Biswas[22], Francesco Santopaolo[23], Wim Laleman[24], Nicola Pugliese[25], Margaret Teng[26], Louise China[26], Magdalena Meszaros[27], Michele Bevilacqua[28], Arun Valsan[29], Nicolás Ortiz-López[30], José Ferrusquía-Acosta[31], Alessio Aghemo[25], Mattias Mandorfer[20], Thomas Reiberger[32], Maria Cristina Morelli[33], Dominik Bettinger[18], Michael Praktiknjo[34], Bogdan Procopet[16], Giulia Tosetti[15], Luo Xuefeng[14], Silvia Nardelli[11], Aldo Airoldi[10], Benjamin Maasoumy[9], Stefano Fagiuoli[7], Annalisa Berzigotti[5], Agustín Albillos[4], Filippo Schepis[3], Juan Carlos García-Pagán[2], Marco Senzolo[35].

[1]Internal Medicine Unit for the Treatment of Severe Organ Failure, IRCCS Azienda Ospedaliero-Universitaria di Bologna, Bologna, Italy; [2]Barcelona Hepatic Hemodynamic Laboratory, Liver Unit, Hospital Clínic, Institut de Investigacions Biomèdiques August Pi i Sunyer (IDIBAPS), Barcelona, Spain; [3]Severe Liver Diseases (M.E.C.) Departmental Unit, Department of Medical Specialties, University Hospital of Modena "Policlinico", University of Modena and Reggio Emilia, Modena, Italy; [4]Department of Gastroenterology and Hepatology, Hospital Universitario Ramón y Cajal, Instituto Ramón y Cajal de Investigación Sanitaria (IRYCIS), Universidad de Alcalá, Madrid, Spain; [5]Department of Visceral Surgery and Medicine, Inselspital, Bern University Hospital, University of Bern, Bern, Switzerland; [6]Department of Experimental and Clinical Medicine, University of Florence, Florence, Italy; [7]Gastroenterology Hepatology and Transplantation Unit, ASST Papa Giovanni XXIII, Bergamo, Italy; [8]Liver Unit, University Hospitals Birmingham NHS Foundation Trust, Birmingham Health Partners, Birmingham, United Kingdom; [9]German Center for Infection Research (DZIF), Hannover-Braunschweig, Germany; [10]Hepatology and Gastroenterology, ASST Grande Ospedale Metropolitano Niguarda, Milan, Italy; [11]Department of Translational and Precision Medicine, Sapienza University of Rome, Rome, Italy; [12]AP-HP, Hôpital Beaujon, Service d'Hépatologie, DMU DIGEST, Centre de Référence des Maladies Vasculaires du Foie, FILFOIE, Clichy, France; [13]Gastroenterology and Multivisceral Transplant Unit, Padua University Hospital, Padua, Italy; [14]Department of Gastroenterology and Hepatology, Sichuan University-University of Oxford Huaxi Joint Centre for Gastrointestinal Cancer, West China Hospital, Sichuan University, Chengdu, China; [15]A. M. e A. Migliavacca Center for Liver Disease, Division of Gastroenterology and Hepatology, Fondazione IRCCS Ca' Granda Ospedale Maggiore Policlinico, University of Milan, Milan, Italy; [16]Regional Institute of Gastroenterology and Hepatology "Prof. Dr. Octavian Fodor", Cluj-Napoca, Romania; [17]Department of Medicine I, University Hospital Bonn, Bonn, Germany; [18]Department of Medicine II, Medical Center University of Freiburg, Faculty of Medicine, University of Freiburg, Freiburg, Germany; [19]Department of Gastroenterology, Affiliated Drum Tower Hospital of Nanjing University Medical School, Nanjing, Jiangsu, China; [20]Division of Gastroenterology and Hepatology, Department of Medicine III, Medical University of Vienna, Vienna, Austria; [21]Faculté de Médecine de Tours et CHRU de Tours, Hôpital Trousseau, Service d'Hépatogastroentérologie, Tours, France; [22]Department of Gastroenterology and Human Nutrition Unit, All India Institute of Medical Sciences, New Delhi, India; [23]Liver Unit-CEMAD, Centro Malattie Apparato Digerente, Medicina Interna e Gastroenterologia, Fondazione Policlinico Universitario Gemelli IRCCS, Rome, Italy; [24]Department of Gastroenterology and Hepatology, Division of Liver & Biliopancreatic disorders and Liver Transplantation, University Hospitals Leuven, Leuven, Belgium; [25]Department of Biomedical Sciences, Humanitas University, Pieve Emanuele (MI), Italy; Division of Internal Medicine and Hepatology, Department of Gastroenterology, IRCCS Humanitas Research Hospital, Rozzano, Italy; [26]Department of Hepatology and Liver Transplantation, Royal Free Hospital, London, United Kingdom; [27]Department of Hepatogastroenterology, Hepatology and Liver Transplantation Unit, Saint Eloi Hospital, Montpellier, France; [28]Liver Unit, Department of Medicine, University and Azienda Ospedaliera Universitaria Integrata of Verona, Verona, Italy; [29]Department of Hepatology, Amrita Institute of Medical Sciences, Koci, India; [30]Sección de Gastroenterología, Departamento de Medicina, Hospital Clínico Universidad de Chil, Santiago, Chile; [31]Liver Unit. Parc Taulí Hospital Universitari. Institut d'Investigació i Innovació Parc Taulí (I3PT-CERCA), Universitat Autònoma de Barcelona, Sabadell, Spain; [32]Division of Gastroenterology and Hepatology, Department of Medicine III, Medical University of Vienna, Vienna, Italy; [33]1 Internal Medicine Unit for the Treatment of Severe Organ Failure, IRCCS Azienda Ospedaliero-Universitaria di Bologna, Bologna, Italy; [34]Department of Medicine B, University Hospital Münster, Münster, Germany; [35]Gastroenterology and Multivisceral Transplant Unit, Padua University Hospital, Padua, Unit of Vascular Liver Disease and Treatment of Portal Hypertension, Gastroenterology, University Hospital of Padova, Health Care Provider of the European Reference Network on Rare Liver Disorders (ERN Rare-Liver), Padua, Italy

Email: laurarturco.md@gmail.com

Background and aims: TIPS is well-established for portal hypertension (PH) in cirrhosis, but knowledge in PSVD is limited. This study evaluated TIPS efficacy and outcomes in PSVD.

Method: Retrospective, multicenter study in patients with histologically confirmed PSVD undergoing TIPS across 31 centers. Time-to-event outcomes were analyzed using Cox proportional hazards models and competing-risks event analysis.

Results: The cohort comprised 300 patients, 63% male, with a median age of 51 years (36–62). 51% had associated conditions, predominantly drug exposure (27%), hematological (22%) or immunological disorders (19%). Pre-TIPS portal vein thrombosis (PVT) was present in 45%, occlusive in 12%. 28% patients were on anticoagulation treatment before TIPS. All received covered stents dilated to < 8 (20%), 8–10 (56%), or 10 mm (16%); dilation was not documented in 8% of cases. Median portal pressure gradient (PPG) decreased from 19 (15–23) to 8 mmHg (5–11). The primary indication for TIPS placement was variceal bleeding (66%), followed by recurrent/refractory ascites (19%) and PVT (13%). After TIPS, 91% did not rebleed, ascites was controlled in 62%, and 22% discontinued diuretics. Stent dysfunction occurred in 22% and was independently correlated with the presence of complete PVT before TIPS (HR: 3.15, 95% CI 1.58–6.25; p = 0.0011). Cardiac failure occurred in 6%, liver failure in 2%. Overt hepatic encephalopathy (oHE) occurred in 18% at 1 and 21% at 3 years, with pre-TIPS ascites as an independent risk factor (HR: 3.43, 95% CI 1.70–6.92; p = 0.0006). During follow-up [27 months (12–60)], 6% underwent transplant, 17% died (11 liver-related). Transplant-free survival was 90% at 1 year, 69% at 5 years. Ascites control (HR: 0.32, 95% CI 0.15–0.68; p = 0.0032), immunological disorders (HR: 3.56, 95% CI 1.30–9.76; p = 0.013), bacterial infection after TIPS (HR: 1.93, 95% CI 1.06–3.52; p = 0.031 and oHE (HR: 2.10, 95% CI 1.02–4.29; p = 0.043) predicted transplant/death. For non-liver related deaths, chronic kidney disease (HR: 3.57, 95% CI 1.49–8.58; p = 0.0045), bacterial infection (HR: 2.93, 95% CI 1.61–5.34; p = 0.0004), and hematological disorders (HR: 2.61, 95% CI 1.11–4.85; p = 0.0261) were independent factors.

Conclusion: TIPS effectively manages PH complications in PSVD despite high stent dysfunction. Multidisciplinary evaluation remains essential given the influence of associated conditions on survival.

OS-082

Assessment of the Toulouse algorithm for predicting heart failure after TIPS in the EuroTIPS multicenter cohort

Sarah Shalaby[1], Charlotte Bouzbib[2], Marika Rudler[2], Hélène Larrue[3], Lucie Cavailles[3], Jesus Donate[4], Emma Vanderschueren[5], Lara Biribin[6], Theresa Müllner-Bucsics[7], Lukas Hartl[7], Tomas Guasconi[8], Valentina Adotti[9], Enric Reverter[10], David Toapanta[10], Xavier Borrat[11], Marta Iriarte[12], Barbarba Vidal[12], Asunción Ojeda[1], Sonia Torres[1], Valeria Perez[1], Fanny Turon[1], Marco Pavesi[13], Emma Vidal[13], Marco Senzolo[6], Francesco Vizzutti[9], Filippo Schepis[8], Thomas Reiberger[7], Wim Laleman[5], Luis Téllez[4], Christophe Bureau[3], Dominique Thabut[2], Virginia Hernández-Gea[1], Juan Carlos García-Pagán[1], Anna Baiges[1]. *[1]Barcelona Hepatic Hemodynamic Laboratory, Liver Unit, Hospital Clínic Barcelona, Universitat de Barcelona, FRCB-IDIBAPS, CIBEREHD, CSUR, ERN-RareLiver, Barcelona, Spain, Barcelona, Spain; [2]AP-HP, Sorbonne Université, Liver Intensive Care Unit, Hepatogastroenterology Department, La Pitié-Salpêtrière Hospital, 47-83 Boulevard de l'Hôpital, Paris 75013, France, INSERM UMR_S 938, Centre de recherche Saint-Antoine, Maladies métaboliques, biliaires et fibroinflammatoire du foie, Institute of Cardiometabolism and Nutrition (ICAN), Paris, France, Paris, France; [3]4- Service d'Hépatologie Hôpital Rangueil CHU Toulouse 1 avenue Jean Poulhes 31059 Toulouse France et Université Paul Sabatier Toulouse 3, Toulouse, France, Toulouse, France; [4]Servicio de Gastroenterología y Hepatología. Instituto Ramón y Cajal de Investigación Sanitaria (IRYCIS). Centro de Investigación Biomédica en Red (CIBERehd). Universidad de Alcalá, Madrid, Spain, Madrid, Spain; [5]Department of Gastroenterology and Hepatology, Division of Liver & Biliopancreatic disorders and Liver transplantation, University Hospitals Leuven, KU Leuven, Leuven, Belgium, Leuven, Belgium; [6]Gastroenterology, University-Hospital of Padua, Health Care Provider of the European Reference Network on Rare Liver Disorders (ERN-Rare Liver), Padua, Italy, Padova, Italy; [7]Vienna Hepatic Hemodynamic Lab, Division of Gastroenterolongy and Hepatology, Department of Medicine III, Medical University of Vienna, Vienna, Austria, Vienna, Austria; [8]Severe Liver Diseases (M.E.C.) Departmental Unit, Department of Medical Specialties, Azienda Ospedaliero-Universitaria of Modena, University of Modena and Reggio Emilia, Modena, Italy, Modena, Italy; [9]Department of Experimental and Clinical Medicine, University of Florence, Florence, Italy; | 11- Liver Unit, IDIBAPS, and CIBEREHD, Liver ICU, Hospital Clinic, University of Barcelona, Barcelona, Spain, Florence, Italy; [10]Liver Unit, IDIBAPS, and CIBEREHD, Liver ICU, Hospital Clinic, University of Barcelona, Barcelona, Spain, Barcelona, Spain; [11]Clinical Informatics, Hospital Clinic, Barcelona, 08036, Spain, Barcelona, Spain; [12]Department of Cardiology, Cardiovascular Institute, Hospital Clínic, University of Barcelona, Barcelona, Spain, Barcelona, Spain; [13]Barcelona Clinical Coordinating Center (BCCC) - Fundació Món Clínic, Barcelona, Spain, Barcelona, Spain*
Email: shalaby@recerca.clinic.cat

Background and aims: TIPS is an effective treatment for complications of portal hypertension but carries a relevant risk of heart failure (HF) occurring in 10–20% of cases. The previously published Toulouse algorithm (TA), based on baseline BNP/NT-proBNP levels and simple echocardiographic parameters, suggested a negligible risk of post-TIPS HF in patients with BNP < 40 pg/mL or NT-proBNP <125 pg/mL, and a high risk (> 50%) in those with elevated NT-proBNP and signs of diastolic dysfunction. This algorithm has only been validated in a small cohort of patients with refractory ascites. The aim of the present study was 1) to assess the external validity of the Toulouse algorithm and 2) to further refine prediction strategies.

Method: Retrospective multicenter study within the EuroTIPS registry. Consecutive patients with cirrhosis treated with TIPS were included if baseline BNP or NT-proBNP, echocardiography and 12-month follow-up were available. Patients were included between 2015 and 2024. HF was defined by typical CF symptoms, objective evidence of pulmonary congestion and need for new-onset or intensified diuretic therapy.

Results: A total of 255 patients were included (76% men, median age of 59 years). Most common etiologes were alcohol-related in 45% and MASLD in 30%; TIPS indication was refractory ascites in 50% and secondary prevention of bleeding in 31%. Prior history of ischemic heart disease and valvular disease was present in 6% and 4% of patients, respectively. Post-TIPS HF occurred in 28 patients (11%). Seven of the 117 (6%) patients classified as negligible HF risk by TA developed CF. Conversely, only 12 of 84 patients (14%) classified as high risk by TA developed CF, compared with a previously reported incidence of 51% in this group. The AUC of TA for predicting CF was 0.62, without relevant improvement according to TIPS indication. Subsequently, based on univariable and multivariable analysis, a new predictive model including baseline NT-proBNP, serum sodium and metabolic syndrome was developed. The model was internally validated using bootstrap resampling and showed a concordance statistic of 0.78, with a time-dependent AUC of 0.83 at 1 year. Echocardiographic parameters were not associated with post-TIPS HF.

Conclusion: In this large international cohort, the Toulouse algorithm showed limited accuracy to predict post-TIPS HF. A new model based on NT-proBNP, metabolic syndrome and sodium levels may better identify patients at risk of HF after TIPS.

OS-083-YI

Evidence-based definition of major and minor histological criteria for the diagnosis of porto-sinusoidal vascular disease

Alexandre Sayadi[1], Christine Sempoux[2], Annette Gouw[3], Alberto Quaglia[4], Alba Díaz[5], Dina G. Tiniakos[6], Maria Guido[7], Prodromos Hytiroglou[8], Miguel Albuquerque[9], Camille Pignolet[10], Matthieu Tihy[11], Luiz Antônio Rodrigues de Freitas[12], Kenichi Harada[13], Romil Saxena[14], Prasenjit Das[15], Sanjay Kakar[16], Puja Sakhuja[17], Venancio Alves[18], Maha Guindi[19], David E Kleiner[20], Robert Minnee[21], Michail Doukas[22], Sarwa Darwish Murad[23], Lucile Moga[24], Virginia Hernández-Gea[25], Pierre-Emmanuel Rautou[24], Valérie Paradis[1]. *[1]Université Paris Cité, Centre de recherche sur l'inflammation, INSERM U1149;Service de Pathologie, AP-HP.Nord, Hôpital Beaujon, FHU MOSAIC2, SIRIC InsiTu, Clichy, France; [2]Service of Clinical Pathology, Institute of Pathology, Lausanne University Hospital, University of Lausanne, Lausanne, Switzerland; [3]Department of Pathology and Medical Biology, University Medical Center Groningen, Groningen, Netherlands; [4]Department of Cellular Pathology, UCL Cancer Institute, Royal Free Hospital, London, United Kingdom; [5]Pathology Department,Hospital Clinic, Universitat de Barcelona, FRCB-IDIBAPS (Fundació de Recerca Clínic Barcelona-Institut d'Investigacions Biomèdiques August Pi i Sunyer), CIBEREHD (Centro de Investigación Biomédica en Red Enfermedades Hepáticas y Digestivas), Barcelona, Spain; [6]Department of Pathology, Aretaieion University Hospital, School of Medicine, National and Kapodistrian University of Athens, Athens, Greece, Faculty of Medical Sciences, Translational and Clinical Research Institute, Newcastle University, Newcastle, United Kingdom; [7]Department of Medicine, DIMED, University of Padua, Padua, Italy; [8]Department of Pathology, School of Medicine, Aristotle University, Thessaloniki, Greece; [9]Service de Pathologie, AP-HP.Nord, Hôpital Beaujon, FHU MOSAIC2, SIRIC InsiTu, Clichy, France; [10]Université Paris Cité, Centre de recherche sur l'inflammation, INSERM U1149, Paris, France; [11]Université Paris Cité, Centre de recherche sur l'inflammation, INSERM U1149, Service de Pathologie, AP-HP.Nord, Hôpital Beaujon, FHU MOSAIC2, SIRIC InsiTu, Clichy, France; [12]Faculdade de Medicina da Bahia (UFBA), Brazil, Instituto de Pesquisas Gonçalo Moniz-Fundação Osvaldo Cruz, Salvador-Bahia, Brazil; [13]Department of Human Pathology, Kanazawa University Graduate School of Medicine, Kanazawa, Japan; [14]Department of Pathology and Laboratory Medicine, Emory University School of Medicine, Atlanta, GA, United States; [15]Department of*

Pathology, All India Institute of Medical Sciences, New Delhi, India; [16]University of California San Francisco Pathology Department, San Francisco, CA, United States; [17]Department of GI Surgery& Pathology, GB Pant Institute of Postgraduate Medical Education & Research and Maulana Azad Medical College, Delhi University, JLN Marg, New Delhi, India; [18]Departamento de Patologia - Faculdade de Medicina, Universidade de São Paulo, São Paulo, Brazil; [19]Department of Pathology and Laboratory Medicine, Cedars-Sinai Medical Center, Los Angeles, CA, United States; [20]Laboratory of Pathology, National Cancer Institute, National Institutes of Health, Bethesda, MD, United States; [21]Department of Hepato-Pancreato-Biliary (HPB)/Transplant Surgery, Erasmus MC Transplant Institute, University Medical Center Rotterdam, Rotterdam, Netherlands; [22]Department of Pathology, Erasmus University Medical Center, Rotterdam, Netherlands; [23]Department of Gastroenterology and Hepatology, Erasmus MC Transplant Institute, Erasmus MC, Rotterdam, Netherlands; [24]Université Paris Cité, Centre de recherche sur l'inflammation, INSERM U1149; Service d'Hépatologie, AP-HP, Hôpital Beaujon, DMU DIGEST, Centre de Référence des Maladies Vasculaires du Foie, FILFOIE, Health Care Provider of the European Reference Network on Rare Liver Diseases (ERN-RARE-LIVER), Clichy, France; [25]Barcelona Hepatic Hemodynamic Laboratory, Liver Unit, Hospital Clínic, Clínic Barcelona, FRCB-IDIBAPS (Fundació de Recerca Clínic Barcelona-Institut d'Investigacions Biomèdiques August Pi i Sunyer), CIBEREHD (Centro de Investigación Biomédica en Red Enfermedades Hepáticas y Digestivas), Health Care Provider of the European Reference Network on Rare Liver Diseases (ERN-RareLiver), CSUR (Centro de referencia del Sistema Nacional de Salud en Enfermedad Hepática Compleja), AGAUR SGR2021 01115, Barcelona, Spain
Email: alexandre.sayadi@aphp.fr

Background and aims: Definition of porto-sinusoidal vascular disease (PSVD) currently relies on specific and non-specific histological lesions, based on expert opinion. The aim of this study was to establish evidence-based histological criteria for diagnosing PSVD.
Method: We used a four-step strategy (1) Definition of normal liver vasculature by morphometric analysis of 10 normal surgical liver samples measuring area, axis, and number of vascular structures. (2) Definition of elementary histological lesions of PSVD based on literature data and results of step #1, and their reproducibility between 9 European pathologists. Inter-reader reproducibility was established by analyzing 58 liver biopsies (42 PSVD patients and 16 normal liver biopsies), using intra-class correlation (ICC) and Fleiss' kappa. (3) Identification of histological lesions associated with PSVD diagnosis: review of another cohort of 218 liver biopsies from 88 patients with PSVD and portal hypertension, 89 patients with chronic liver disease without cirrhosis and 41 living liver donors. Patients with venous outflow obstruction were excluded. Major histological criteria were defined as having a specificity > 95% and a sensitivity > 10% for PSVD. Minor histological criteria were defined as having a specificity between 80 and 95% and a sensitivity > 10% for PSVD. (4) External validation of these major and minor criteria was done by 9 independent pathologists from USA, Brazil, India and Japan.
Results: (1) and (2) resulted in an atlas of 15 histological lesions previously associated with PSVD including their precise definition, based on morphometry and expert consensus. Portal venule stenosis (PVS) had the highest ICC across the 9 raters (0.51), while nodular regenerative hyperplasia (NRH) had a Fleiss' kappa at 0.26, with pairwise kappa ranging from 0.12 to 0.67. (3) Three major histological criteria were identified: PVS in ≥ 50% of portal tracts; muscularized portal veins and NRH. Three minor criteria were identified: PVS in 25 to 50% of portal tracts; regenerative changes and abnormal distribution of vascular structures. Presence of these 3 minor features in the same biopsy reached the definition of a major criterion (specificity 98%, sensitivity 17%). (4) Results were validated by the external group of pathologists.
Conclusion: This study, by identifying major and minor histological lesions associated with PSVD, represents a turning point in the revised 2026 definition of this disease.

OS-084

Futility criteria for TIPS placement in patients with refractory acute variceal bleeding: a EuroTIPS study

Charlotte Bouzbib[1], Luc Haudebourg[2], Anna Baiges[3], Louis Dalteroche[4], Laure Elkrief[4], Charlotte Frappreau[4], Hélène Larrue[5], Christophe Bureau[5], Lucie Cavailles[5], Dhiraj Tripathi[6], Faisal Khan[6], David Patch[7], Jonel Trebicka[8], Michael Praktiknjo[9], Markus Kimmann[8], Nils Manegold[8], Josune Cabello Calleja[8], Filippo Schepis[10], Tomas Guasconi[10], Wim Laleman[11], Emma Vanderschueren[11], Thomas Reiberger[12], Mattias Mandorfer[12], Lukas Hartl[12], Marco Senzolo[13], Lara Biribin[13], Johannes Chang[14], Christian Jansen[14], Nina Böhling[14], Jakub Grobelski[14], Fabio Marra[15], Francesco Vizzutti[15], Alexander Zipprich[16], Cristina Ripoll[16], Henrik Karbannek[16], Marlen Hinz[16], Dominik Bettinger[17], Michael Schultheiß[17], Lukas Sturm[17], Pablo Bellot Garcia[18,19], Agustín Albillos[20], Luis Téllez[20], Jesus Donate[20], Rebeca Pintado Garrido[21], Alvaro Giráldez-Gallego[22], María Pilar Ballester[23], R. Bart Takkenberg[24], Raoel Maan[25], Bogdan Procopet[26], Oana Nicoara-Farcau[26], Silvia Nardelli[27], Sarah Raevens[28], Lauren Tang[29], See Teikchoon[29], Navjyot Hansi[29], Andres Conthe[30], Aurélie Walter[31], Isabelle Ollivier-Hourmand[31], Louise Lebedel[31], Jean-Charles Nault[32], Nathalie Ganne-Carrié[32], Olivier Sutter[32], Jean Marie Peron[5], Sonia Torres[3], Virginia Hernández-Gea[3], Manon Allaire[1], Juan Carlos García-Pagán[3], Dominique Thabut[1], Marika Rudler[1]. *[1]Pitié-Salpêtrière Hospital, Paris, France; [2]Neurology ICU, APHP Sorbonne Universite, Pitie-Salpêtrière Hospital, 83 boulevard de l'hôpital, Paris, France; [3]Barcelona Hepatic Hemodynamic Laboratory, Liver Unit, Hospital Clínic, Clínic Barcelona, ERN-RareLiver, CSUR, FRCB-IDIBAPS, Universitat de Barcelona, Barcelona, Spain; [4]Tours University Hospital, Tours, France; [5]Hôpital Rangueil CHU Toulouse, Toulouse, France; [6]Queen Elizabeth Hospital, University Hospitals Birmingham, Birmingham, United Kingdom; [7]Royal Free London NHS Foundation Trust, London, United Kingdom; [8]University Hospital Münster, Münster, Germany; [9]Department of Medicine B, University Hospital Münster, Münster, Germany; [10]Azienda Ospedaliero - Universitaria Policlinico di Modena, Modena, Italy; [11]University Hospitals Leuven, Leuven, Belgium; [12]Medical University of Vienna, Vienna, Austria; [13]University Hospital of Padua, Padua, Italy; [14]University Hospital Bonn, Bonn, Germany; [15]Università degli studi di Firenze, Firenze, Italy; [16]Friedrich Schiller Universität, Jena, Germany; [17]University Medical Center Freiburg, Freiburg, Germany; [18]HGU Alicante, Alicante, Spain; [19]University General Hospital Dr. Balmis, Liver Unit, Alicante; [20]Hospital Universitario Ramon y Cajal, Madrid, Spain; [21]Valladolid, Valladolid, Spain; [22]Digestive Diseases Department, Hospital Universitario Virgen del Rocío, Institute of Biomedicine (HUVR/CSIC/US), University of Seville, Seville, Spain; [23]Clinic University Hospital of Valencia, Valencia, Spain; [24]Amsterdam University Medical Centers, Amsterdam, Netherlands; [25]Erasmus MC, Rotterdam, Netherlands; [26]Octavian Fodor Regional Institute of Gastroenterology and Hepatology, Cluj-Napoca, Romania; [27]Sapienza Università di Roma, Roma, Italy; [28]Ghent University, Gent, Belgium; [29]Cambridge University Hospitals NHS Foundation Trust, Cambridge, United Kingdom; [30]General Universitary Hospital Gregorio Marañón, Madrid, Spain; [31]Caen Hospital, Caen, France; [32]Avicenne Hospital, Bobigny, France*
Email: charlotte.bouzbib@aphp.fr

Background and aims: In patients with cirrhosis and refractory acute variceal bleeding, salvage/rescue transjugular intrahepatic portosystemic shunt (TIPS) placement is associated with a 6-week mortality rate of 30–50%. International guidelines raise the question of placing a TIPS in patients with 6-week mortality > 90%, i.e. in patients with a Child-Pugh score ≥ 14, or in patients with lactate ≥ 12 mM and/or a MELD score ≥ 30, especially if they are not candidate for liver transplantation (LT). The aim of this study was to prospectively validate these futility criteria.
Method: This was an ancillary multicenter study within the EuroTIPS registry, which included all consecutive patients with cirrhosis and treated with salvage/rescue TIPS between 2020 and 2024 in 19

centers in Europe. Patients were followed up at 1, 3, 6, 9 and 12 months, or until death or LT. The primary endpoint was 42-day mortality (LT as a competing event). We also aimed to develop a futility score for TIPS placement, and to validate it in a previously published retrospective multicenter European cohort.
Results: Overall, 177 pts were included (73.4% men, age 54 years, alcohol-related cirrhosis 76%, Child-Pugh score 9, MELD score 16, ACLF 23%, salvage/rescue TIPS 78.5%/21.5%). Forty-two-day mortality was 24.3%, with no significant difference between salvage and rescue TIPS ($p = 0.14$). In multivariate analysis, factors independently associated with 42-day mortality were higher age, ascites, higher bilirubin, INR and creatinine and vasopressors at TIPS placement. Only one patient had a Child-Pugh score ≥ 14, precluding validation of this criterion. Among the 27 patients with a MELD score ≥ 30 and/or lactate ≥ 12 mM, the 42-day transplant-free survival rate was 37%. A futility score was developed using the previously listed factors associated with 42-day mortality: the AUROC for the prediction of 42-day mortality was 0.808 and 42-day mortality was 100% in patients with a score ≥ 90 in our derivation cohort. In the validation cohort of 164 patients, 29 patients (17.7%) had a score ≥ 90, with a 42-day mortality rate of 93.1%.
Conclusion: In this prospective series, rescue/salvage TIPS was associated with a better prognosis than previously reported, possibly due to patient's selection. Previously described futility criteria were not validated. A new score should be used to discuss rescue/salvage TIPS on a case-by-case basis in patients who are not candidate for LT.

OS-085-YI
The natural history of porto-sinusoidal vascular disorder without portal hypertension: a multicenter retrospective VALDIG study
Edeline Kaze[1], Sarah Raevens[2], Géraldine Dahlqvist[3], Margherita Saracco[4], Lucile Moga[5], Nicola Pugliese[6], Elisa Farina[7], Emma Murcia[8], Lorenz Balcar[9], Carina Boros[10], Martina Lucà[11], Lorenzo Argiento[11], Heloïse Giudicelli-Lett[12], Thomas Vanwolleghem[13], Ann Driessen[13], Sarah Shalaby[14], Wagner Enrique Ramírez[14], Djamal Tazibt[15], Odile Goria[16], Laure Elkrief[17], Jean Delwaide[18], Astrid Marot[19], Quentin Schoevaerdts[19], Christophe Moreno[20], Jean Paul Cervoni[15], Virginia Hernández-Gea[14], Juan Carlos García-Pagán[14], Sven Francque[13], Dominique Thabut[12], Carla Cafasso[21], Marianne Ziol[10], Pierre Nahon[10], Georg Semmler[9], Bernhard Scheiner[9], Christophe Bureau[8], Mauro Viganò[7], Alessandro Loglio[7], Alessio Aghemo[6], Aurélie Plessier[5], Pierre-Emmanuel Rautou[5], Pamela Baldin[3], Laurine Verset[20], Anne Hoorens[2], Pierre Deltenre[22]. *[1]Hôpital Érasme-Cliniques Universitaires de Bruxelles, cliniques de l'Europe, Bruxelles, Belgium; [2]Ghent University Hospital, Gent, Belgium; [3]Cliniques Universitaires Saint-Luc, Bruxelles, Belgium; [4]Azienda Ospedaliera Cittàdella Salute e della Scienza di Torino, Torino, Italy; [5]Hôpital Beaujon, Université Paris-Cité, Clichy, France; [6]Humanitas University, Rozzano, Italy; [7]ASST Papa Giovanni XXIII, Bergamo, Italy; [8]Hôpital Rangueil, Toulouse, France; [9]Medizinische Universität Wien, Wien, Austria; [10]Hôpital Avicenne, Bobigny, France; [11]Fondazione Irccs Ca Granda Ospedale Maggiore Policlinico, Milano, Italy; [12]Hôpital Universitaire de la Pitié-Salpêtrière, Paris, France; [13]Antwerp University Hospital, Edegem, Belgium; [14]Hospital Clínic De Barcelona, Barcelona, Spain; [15]Chu Besançon, Besançon, France; [16]Hôpital Charles Nicolle, Rouen, France; [17]Hôpital Trousseau CHU de Tours, Tours, France; [18]Centre Hospitalier Universitaire Sart Tilman, Liege, Belgium; [19]CHU UCL Namur-Site de Godinne, Yvoir, Belgium; [20]Hôpital Érasme-Cliniques Universitaires de Bruxelles, Bruxelles, Belgium; [21]University of Milan, Milano, Italy; [22]Hôpital Érasme-Cliniques Universitaires de Bruxelles, Clinique Saint-Luc Bouge, CHU UCL Namur-Site Godinne, Bruxelles, Belgium*
Email: kazeedeline@gmail.com

Background and aims: Data on the natural history of patients with histological lesions of porto-sinusoidal vascular disorder (PSVD) who do not show signs of portal hypertension (PH) are scarce. We aimed to describe the natural history of these patients and identify risk factors for progression.
Method: A retrospective study was conducted to collect health-related data on patients with a histopathological diagnosis of PSVD and no sign of PH. Patients with any sign of PH were excluded and a liver biopsy of at least 15 mm was required. Associated conditions were defined as the use of any medication or the presence of any disease that could be associated with PSVD. They were considered severe if they were potentially associated with reduced life expectancy. Main endpoints were the development of signs or complications of PH and death.
Results: 227 patients from 18 centers were included (92 men [41%], median age 46 years). Indication for liver biopsy was abnormal liver tests in 186 patients (82%). Histological findings were nodular regenerative hyperplasia, obliterative portal venopathy, incomplete septal cirrhosis, a combination of these histological lesions, or sinusoidal dilatation with or without other signs indicative of PSVD, in 126 (56%), 41 (18%), 2 (1%), 14 (6%) and 44 (19%) patients, respectively. Associated conditions were observed in 100 patients (46%), of which 55 (24%) were considered as severe. During a median follow-up of 37 months (95% CI: 27–46), 3 patients (1.3%) developed PH-related manifestations (ascites in 2 patients, esophageal varices in 1 patient). The cumulative incidence of PH-related manifestations at 10 years was 6% (95% CI: 2–20%). Nineteen patients (8%) died, 17 from non-hepatic causes and 2 from complications related to preexisting cholangiocarcinoma. No patient died from PH-related complications. Independent predictors of death were age (relative risk [RR]: 1.07, 95% CI: 1.03, 1.11, $p < 0.001$) and presence of a severe associated condition (RR: 4.76, 95% CI: 1.55–14.65, $p = 0.006$). The 10-year survival rate was 84% (95% CI: 77–92%): 95% (95% CI: 89–100) in patients without an associated condition, 100% in patients with a non-severe associated condition, and 58% (95% CI: 41–76) in patients with a severe associated condition ($p < 0.001$).
Conclusion: Most patients with PSVD without PH will not develop it. Sixteen percent of patients die within 10 years, mostly from non-hepatic causes, and the risk of death is independently associated with the severity of the associated condition.

Immune mediated II

OS-086
Event-free survival of maralixibat-treated patients with progressive familial intrahepatic cholestasis compared with aligned real-world data of untreated patients from NAPPED
Pedro Miranda Afonso[1], Alise D.E. de Groot[2], Mark Nomden[2], Paola Mian[2], Benjamin Shneider[3], Emmanuel Gonzalès[4], Irena Jankowska[5], Etienne Sokal[6], Richard J. Thompson[7], Andrea Goldstein[8], Douglas B. Mogul[8], Shannon Vandriel[8], Seema Alam[9], Cigdem Arıkan[10], Henrik Arnell[11], Madeleine Aumar[12], Amer Azaz[13], Emna Barkaoui[14], Maria Belen Pallitto[15], Marisa Beretta[16], Jernej Brecelj[17], Pier Luigi Calvo[18], Mara Cananzi[19], Huey-Ling Chen[20,21,22], Guillermo Costaguta[23,24], Elisa de Carvalho[25], Dominique Debray[26], Antal Dezsőfi-Gottl[27], Angelo Di Giorgio[28], Ozlem Durmaz[29], Alexandre Fabre[30], Sandra Ferreira[31], Ryan T. Fischer[32], Björn Fischler[11], Cristina Campos Gonçalves[33,34], Enke Grabhorn[35], Tassos Grammatikopoulos[7], Girish Gupte[36], Winita Hardikar[37], Loreto Hierro Llanillo[38], Giuseppe Indolfi[39], Emmanuel Jacquemin[4], Carolina Jimenez-Rivera[40], Marianne Hørby Jørgensen[41], Agustina Kadaristiana[7], Wikrom Karnsakul[42], Nanda Kerkar[43,44], Kyung Mo Kim[45], Jae Sung Ko[46], Denitza Kofinova[47], Nolwenn Laborde[48], Patryk Lipiński[49], Rohan Malik[50], Saeed Mohammad[51], Yael Mozer-Glassberg[52], Gabriella Nebbia[53], Emanuele Nicastro[54], Felipe Ordoñez[55], Anna Orłowska-Wójcicka[5], Arti Pawaria[56],

Esra Polat[57], Tudor Lucian Pop[58,59], Jesús Quintero Bernabeu[60], Giusy Ranucci[61], Aathira Ravindranath[62], Nathalie Rock[63], Ioannis Roilidis[64], Mathias Ruiz[65], Thomas Sandahl[66], Srinivas Sankaranarayanan[67], Mohammad Shagrani[68,69], Eyal Shteyer[70], Pooja Spector[71], James E. Squires[72], Ekkehard Sturm[73], Cristina Targa[74], Marise Tofoli[75], Bethany Tucker[7], Christos Tzivinikos[76], Wendy L. van der Woerd[77], Georg-Friedrich Vogel[78], Heng Wang[79], Jian-She Wang[80], Sabina Wiecek[81], Aglaia Zellos[82], Andréanne N. Zizzo[83], Henkjan J. Verkade[84], Bettina Hansen[1,85,86]. [1]*Department of Epidemiology and Biostatistics, Erasmus Medical Center, Rotterdam, Netherlands;* [2]*Clinical Pharmacy and Pharmacology, University of Groningen, University Medical Center Groningen, Groningen, Netherlands;* [3]*Division of Pediatric Gastroenterology, Hepatology, and Nutrition, Department of Pediatrics, Baylor College of Medicine, Houston, Texas, United States;* [4]*Pediatric Hepatology and Liver Transplantation Unit, National Reference Centre for Rare Pediatric Liver Diseases, FILFOIE, ERN RARE LIVER, Bicêtre Hospital, AP-HP. Université Paris-Saclay, Le Kremlin-Bicêtre, and Inserm U1193, Hepatinov, University of Par, Orsay, France;* [5]*Children's Memorial Health Institute, Warsaw, Poland;* [6]*Pediatric Gastorenterology and Hepatology, Université Catholique de Louvain, Cliniques St Luc, Brussels, Belgium;* [7]*Paediatric Liver, GI and Nutrition Centre, King's College Hospital, London, England, United Kingdom;* [8]*Mirum Pharmaceuticals, Inc., Foster City, California, United States;* [9]*Pediatric Hepatology, Institute of Liver and Biliary Sciences, New Delhi, India;* [10]*Department of Pediatric Gastroenterology and Organ Transplant, Koc University School of Medicine, Istanbul, Türkiye;* [11]*Pediatric Gastroenterology, Astrid Lindgren Children's Hospital, Karolinska University Hospital and Division of Pediatrics, CLINTEC, Karolinska Institutet, Stockholm, Sweden;* [12]*Department of Pediatric Gastroenterology Hepatology and Nutrition CHU Lille, Univ. Lille, Inserm U1286- INFINITE- Institute for Translational Research in Inflammation, Lille, France;* [13]*Pediatric Gastroenterology, Hepatology and Nutrition, Sheikh Khalifa Medical City, Abu Dhabi, United Arab Emirates;* [14]*Department of Pediatrics, Tunis Children Hospital, Tunis, Tunisia;* [15]*Department of Gastroenterology and Hepatology, Hospital Italiano, CABA, Buenos Aires, Argentina;* [16]*Faculty of Health Sciences, Wits Donald Gordon Medical Centre, University of the Witwatersrand, Johannesburg, South Africa;* [17]*Department of Gastroenterology, Hepatology and Nutrition, University Children's Hospital Ljubljana; Department of Pediatrics, Faculty of Medicine, University of Ljubljana, Ljubljana, Slovenia;* [18]*Regina Margherita Children's Hospital, Azienda Ospedaliera Città Della Salute e Della Scienza University Hospital, Turin, Italy;* [19]*Unit Of Gastroenterology, Digestive Endoscopy, Hepatology and Care of the Child With Liver Transplantation, University Hospital of Padova, Padova, Italy;* [20]*Department of Pediatrics, National Taiwan University Children's Hospital, Taipei, Taiwan;* [21]*Department and Graduate Institute of Medical Education and Bioethics, National Taiwan University College of Medicine, Taipei, Taiwan;* [22]*Hepatitis Research Center, National Taiwan University Hospital, Taipei, Taiwan;* [23]*CHU de Quebec-Université Laval, Quebec City, Canada;* [24]*Sanatorio de Niños de Rosario, Santa Fe, Argentina;* [25]*Pediatric Gastroenterology Department, Hospital de Base do Distrito Federal, Hospital da Criança de Brasília, Centro Universitário de Brasília, Brasília, Distrito Federal, Brazil;* [26]*Gastroenterology-Hepatology-Nutrition Unit, APHP-Necker Enfants Malades University Hospital, Paris, France;* [27]*Pediatric Center, Semmelweis University, Budapest, Hungary;* [28]*Department of Medicine, University of Udine, Udine, Italy;* [29]*Department of Child Health and Diseases, Gastroenterology, Hepatology and Nutrition, Istanbul Faculty of Medicine, Istanbul, Türkiye;* [30]*APHM, Hôpital de la Timone Enfant, Service de Pédiatrie Multidisciplinaire, Marseille, France;* [31]*Maxillofacial Surgery Department, Centro Hospitalar e Universitário de Coimbra, Coimbra, Portugal;* [32]*Section of Hepatology, Department of Gastroenterology, Children's Mercy Kansas City, Kansas City, Kansas, United States;* [33]*European Reference Network on Hepatological Diseases (ERN RARE-LIVER), Hamburg, Germany;* [34]*Pediatric Gastroenterology/ Hepatology Center Lisbon, Lisbon, Portugal;* [35]*Pediatric Hepatology and Liver Transplantation, University Medical Center Hamburg Eppendorf, Hamburg, Germany;* [36]*Liver Unit (Including Small Bowel Transplantation), Birmingham Women's and Children's Hospital, Birmingham, England, United Kingdom;* [37]*Department of Gastroenterology and Clinical Nutrition, Royal Children's Hospital, Melbourne, Australia;* [38]*Service of Pediatric Hepatology and Transplantation, Children's Hospital La Paz, La Paz University Hospital, Madrid, Spain;* [39]*Meyer Children's Hospital, IRCCS, Florence, Italy;* [40]*Department of Pediatrics, Children's Hospital of Eastern Ontario, University of Ottawa, Ottawa, Canada;* [41]*Department of Pediatrics and Adolescent Medicine, Rigshospitalet Copenhagen University Hospital, Copenhagen, Denmark;* [42]*Department of Pediatrics, Johns Hopkins University School of Medicine, Baltimore, Maryland, United States;* [43]*Massachusetts General Brigham for Children, Boston, Massachusetts, United States;* [44]*University of Rochester Medical Center, Rochester, New York, United States;* [45]*Department of Pediatrics, Asan Medical Center Children's Hospital, Seoul, Korea, Rep. of South;* [46]*Department of Pediatrics, Seoul National University College of Medicine, Seoul, Korea, Rep. of South;* [47]*Department of Pediatric Surgery, University Multiprofile Hospital for Active Treatment and Emergency Medicine "N.I. Pirogov", Sofia, Bulgaria;* [48]*Unité de Gastro-entérologie, Hépatologie, Nutrition et Maladies Héréditaires du Métabolisme pédiatriques, Hôpital des Enfants, CHU de Toulouse, Toulouse, France;* [49]*Department of Pediatrics, Medical Center of Postgraduate Education, Warsaw, Poland;* [50]*Department of Pediatrics, All India Institute of Medical Sciences, New Delhi, India;* [51]*Monroe Carell Jr. Children's Hospital & Vanderbilt University School of Medicine, Nashville, Tennessee, United States;* [52]*Institute of Gastroenterology, Nutrition and Liver Diseases, Schneider Children's Medical Center of Israel, Petah Tikva, Israel;* [53]*Fondazione Irccs Ca' Granda Ospedale Maggiore Policlinico, Milano, Italy;* [54]*Pediatric Hepatology, Gastroenterology and Transplantation, Hospital Papa Giovanni XXIII, Bergamo, Italy;* [55]*Section of Pediatric Gastrohepatology, Fundación Cardioinfantil, Bogota, DC, Colombia;* [56]*Department of Pediatric Gastroenterology, Hepatology & Liver Transplantation, Amrita Institute of Medical Sciences, Kochi, India;* [57]*Department of Pediatric Gastroenterology, Hepatology, and Nutrition, Sancaktepe Training and Research Hospital, Istanbul, Türkiye;* [58]*2nd Pediatric Discipline, Department of Mother and Child, Iuliu Hatieganu University of Medicine and Pharmacy, Cluj-Napoca, Romania;* [59]*2nd Pediatric Clinic, Emergency Clinical Hospital for Children, Cluj-Napoca, Romania;* [60]*Hospital Universiatri Vall d'Hebron, Barcelona, Spain;* [61]*Pediatric Department for the Treatment and Study of Abdominal Diseases and Abdominal Transplantation, IRCCS ISMETT (Mediterranean Institute for Transplantation and Advanced Specialized Therapies), University of Pittsburgh Medical Center, Palermo, Italy;* [62]*Department of Pediatric Gastroenterology, Apollo BGS Hospital, Mysuru, Karnataka, India;* [63]*Division of Pediatric Gastroenterology, University Hospital of Geneva, Geneva, Switzerland;* [64]*Third Pediatric Department, Hippokration Hospital, Aristotle University of Thessaloniki, Thessaloniki, Greece;* [65]*Hôpital Femme Mère Enfant, Hospices Civils de Lyon, Bron, France;* [66]*Department of Hepatology and Gastroenterology, Aarhus University Hospital, Aarhus, Denmark;* [67]*Department of Pediatric Gastroenterology and Hepatology, Kanchi Kamakoti Childs Trust Hospital, Chennai, India;* [68]*Liver & SB Transplant & Hepatobiliary-Pancreatic Surgery, King Faisal Specialist Hospital & Research Center, Riyadh, Saudi Arabia;* [69]*Alfaisal University, College of Medicine, Riyadh, Saudi Arabia;* [70]*The Juliet Keiden Institute of Pediatric Gastroenterology and Nutrition, Shaare Zedek Medical Center, Jerusalem, Israel;* [71]*Department of Pediatrics, Columbia University Irving Medical Center, New York, New York, United States;* [72]*Division of Pediatric Gastroenterology and Hepatology, Department of Pediatrics, University of Pittsburgh School of Medicine, Pittsburgh, Pennsylvania, United States;* [73]*Pediatric Gastroenterology and Hepatology, University Children's Hospital Tübingen, Tübingen, Germany;* [74]*Pediatric Gastroenterology Service, Hospital da Criança Santo Antônio, Universidade Federal de Ciências da Saúde de Porto Alegre, Complexo Hospitalar Santa Casa, Porto Alegre, Rio Grande do Sul, Brazil;* [75]*Department of Pediatric Gastroenterology, State Hospital for Children and Adolescents, Goiania, Brazil;* [76]*Department of Pediatric Gastroenterology, Al Jalila Children's Specialty Hospital, Dubai, United*

Arab Emirates; [77]Pediatric Gastroenterology, Hepatology and Nutrition, Wilhelmina Children's Hospital, University Medical Center Utrecht, Utrecht, Netherlands; [78]Department of Paediatrics I, Institute of Cell Biology, Medical University of Innsbruck, Innsbruck, Austria; [79]DDC Clinic for Special Needs Children, Middlefield, Ohio, United States; [80]Department of Gastroenterology, Children's Hospital of Fudan University, Shanghai, China; [81]Department of Pediatrics, Medical University of Silesia, Katowice, Poland; [82]Pediatric Gastroenterologist, Academic Scholar, First Department of Pediatrics, Aghia Sophia Children's Hospital, National and Kapodistrian University of Athens, Athens, Greece; [83]Department of Paediatrics, London Children's Hospital, Western University, London, Ontario, Canada; [84]Pediatric Gastroenterology-Hepatology, University of Groningen, University Medical Center Groningen, Groningen, Netherlands; [85]Toronto Center for Liver Disease, University Health Network, Toronto, Canada; [86]IHPME, University of Toronto, Toronto, Canada
Email: bettina.hansen@utoronto.ca

Background and aims: Progressive Familial Intrahepatic Cholestasis (PFIC) is a group of hepatocellular bile acid transport disorders that lead to pruritus, growth failure, lipid-soluble vitamin deficiency, and liver failure. Maralixibat, an ileal bile acid transporter inhibitor, is approved for PFIC-related cholestatic pruritus in patients ≥12 months of age in the US and treatment of PFIC ≥3 months of age in Europe. We compared event-free survival (EFS), time to surgical biliary diversion (SBD), liver transplant (LT), or death in maralixibat-treated patients from the MARCH, MARCH-ON, and RISE trials with aligned real-world data of untreated patients from the NAPPED study.
Method: We randomly selected NAPPED eligible untreated patients with genetically confirmed biallelic non-truncating bile salt export pump (nt-BSEP) or FIC1 deficiencies. To balance baseline characteristics, inverse probability of treatment weights (IPTW) were applied derived from propensity scores for receiving maralixibat (vs. being in NAPPED) estimated from age, sex, PFIC type, total bilirubin, alanine aminotransferase, and aspartate aminotransferase. EFS and SBD-free were compared using IPTW-adjusted Kaplan-Meier curves and Cox models.
Results: Among patients ≥1 year old, 41 maralixibat-treated patients (nt-BSEP, N = 28; FIC1, N = 13) were compared with 256 untreated NAPPED patients (nt-BSEP, N = 201; FIC1, N = 55). At 3 years, EFS was 0.74 (95%CI, 0.59–0.92) in the maralixibat cohort versus 0.42 (95%CI, 0.35–0.51) in NAPPED; the corresponding SBD-free survival probabilities were 0.98 (95%CI, 0.94–1.00) and 0.67 (95%CI, 0.6–0.76), respectively. EFS was significantly better with maralixibat (hazard ratio [HR], 0.29; 95%CI, 0.16–0.54; $p < 0.0001$). The HR for SBD-free probability was 0.05 (95%CI, 0.01–0.39, $p = 0.0036$). In a sensitivity analysis restricted to patients who remained event-free during the first 6 months, the HRs were 0.46 (95%CI, 0.23–0.91; $p = 0.0252$) for EFS and 0.08 (95%CI, 0.01–0.57, $p = 0.0125$) for SBD-free probability.
Conclusion: Maralixibat treatment was associated with improved event free survival in nt-BSEP and FIC1 patients.

OS-087-YI
Enhanced liver fibrosis test and vibration controlled transient elastography as surrogate endpoints in primary sclerosing cholangitis

Tim Middelburg[1,2], Jutta van Crevel[1,2], Bregje Mol[1,2], Liesbeth de Vries[3], Johannes Bogaards[4], Cyriel Ponsioen[1,2].
[1]Amsterdam UMC, Department of Gastroenterology & Hepatology, Amsterdam, Netherlands; [2]Amsterdam Gastroenterology, Endocrinology & Metabolism, Amsterdam, Netherlands; [3]Hagaziekenhuis Den Haag, Den Haag, Netherlands; [4]Amsterdam UMC, Department of Epidemiology & Data Science, Amsterdam, Netherlands
Email: t.e.middelburg@amsterdamumc.nl

Background and aims: Enhanced Liver Fibrosis (ELF) and Vibration Controlled Transient Elastography (VCTE) have shown promising results for prediction of transplant-free survival in primary sclerosing cholangitis (PSC). However, the individual risk associated with their changes over time and the variability therein are unknown.
Method: This prospective study included annual ELF and VCTE data of PSC patients. Joint models were used to assess overall and risk-group–specific changes over time and the overall association with PSC-related death or liver transplantation, reported as longitudinal hazard ratios (HR). Risk groups at baseline were defined using recommended cut-offs for ELF (<7.7, 7.7–10.6, >10.6) and VCTE (<6.5, 6.5–9.9, >9.9 kilopascal). VCTE was log-transformed to account for right skewness. Linearity of longitudinal trajectories was assessed using likelihood ratio tests, comparing linear and quadratic trendlines. Overall variability was evaluated with random slope effects and residual variance, and expressed as the overall coefficient of variation (CV).
Results: Joint model analysis of ELF included 118 participants (10 events) with 446 measurements over a median follow-up of 5.0 years [Q1-Q3: 3.9–5.5], whereas VCTE analysis included 198 participants (26 events) and 787 measurements over a median 5.8 years [Q1-Q3: 3.8–7.3]. Median baseline ELF was 9.29 [Q1-Q3: 8.55–10.18), with an estimated annual increase of 0.16 (95% CI: 0.12–0.21), associated with a 22% (95% CI: 10–35) higher hazard per year. Median baseline VCTE was 7.1 kPa (Q1-Q3: 5.1–10.1), with an estimated annual increase of 0.04 (95% CI: 0.03–0.06) on the log-scale, associated with a 6% (95% CI: 3–9) higher hazard per year. Risk-group-specific slopes showed no significant differences for both ELF and VCTE. ELF followed a linear trajectory ($p = 0.31$ for non-linearity), whereas VCTE demonstrated a significantly increased slope over time, even on the log-scale ($p = 0.02$ for non-linearity). The overall CV was 13.7% for ELF and 32.3% for VCTE.
Conclusion: Both ELF and VCTE increase over time in PSC patients, which is associated with an increased individual risk for PSC-related death or liver transplantation. However, the longitudinal trajectory for ELF is more stable and predictable than that for VCTE, and annual increases in ELF are associated with a greater increase in hazard compared with the average annual increase in VCTE. These findings support ELF as a candidate surrogate endpoint of transplantation-free survival in PSC.

OS-088
Portal endothelial–biliary epithelial crosstalk shapes early primary sclerosing cholangitis

Laura Liebig[1,2], Nico Will[2], Eric Lindberg[3], Alena Laschtowitz[4], Silja Steinmann[2], Yang Xu[2], Marcial Sebode[2], Nicola Gagliani[2,5], Dorothee Schwinge[2], Norbert Hübner[1,4,6], Christoph Schramm[2,7].
[1]Max Delbrück Center for Molecular Medicine, Berlin, Germany; [2]Uke Hamburg, Hamburg, Germany; [3]University Hospital Ludwig-Maximilians, Munich, Germany; [4]Charité - Universitätsmedizin, Berlin, Germany; [5]Karolinska Institute, Stockholm, Sweden; [6]German Center for Cardiovascular Research (DZHK), Berlin, Germany; [7]Martin Zeitz Centre for Rare Diseases, Hamburg, Germany
Email: lauraanne.liebig@mdc-berlin.de

Background and aims: Primary sclerosing cholangitis (PSC) is a chronic immune-mediated cholestatic liver disease likely driven by dysregulated hepatic cell interactions. Its association with inflammatory bowel disease and reported intestinal and biliary dysbiosis suggest microbial influences on early disease development. Here, we aimed to define stage-specific transcriptional cell states and intercellular signaling pathways in PSC with a focus on early-stage disease.
Method: Single-nucleus RNA sequencing of fresh-frozen human liver samples ($n_{TOTAL} = 63$) included PSC spanning early, intermediate, and advanced disease stages ($n_{PSC} = 20$), as well as autoimmune hepatitis, other chronic liver diseases, and controls; spatial transcriptomics covered PSC across stages and controls ($n_{TOTAL} = 22$). Data were analyzed using unsupervised clustering, differential gene expression, and interactome analysis.

Results: From early PSC onward, biliary epithelial cells (BECs) exhibited prominent disease-associated cell states and transcriptional changes, with reduced progenitor-like BECs and progressive expansion of reactive ductular cells. Early PSC was marked by altered epithelial barrier function, extracellular matrix and basement membrane reorganization, as well as microbial sensing and inflammatory signaling, which intensified with disease progression. Interactome and spatial transcriptomic analyses identified early activation of portal vein–associated endothelial cells with increased IL6 expression and predicted IL6–IL6R signaling toward BECs in the portal tracts, accompanied by sustained downstream IL6 signaling and persistent BEC activation across disease stages. Early immune and stromal involvement included TNF-expressing Kupffer cells, IFNG signaling from $CD8^+$ T cells toward BECs, CCL2-mediated $CD4^+$ T cell–BEC interactions, and expansion of activated fibroblasts engaging with BECs, consistent with early periductal matrix remodeling.
Conclusion: Our data show that early PSC involves disease-specific remodeling of biliary epithelial cell states. A newly described epithelial–vascular interaction may explain the close link between PSC and intestinal inflammation. Disrupted epithelial function and portal endothelial IL-6 signaling, together with immune and fibroblast interactions, place BECs at the center of intestinal and portal inflammatory signaling. Ongoing functional validation will further define the contribution of endothelial activation to PSC pathogenesis.

OS-089

CNP-104, an investigational antigen-specific therapy, demonstrates favorable impact across multiple analyses of liver stiffness measurement in a Phase 2a randomized, placebo-controlled trial in PBC

Christopher L. Bowlus[1], Adam Elhofy[2], Molly Frey[2], Derrick McCarthy[2], Erik Wambre[3], Stephen Caldwell[4], Roberto J Firpi[5], Brett Fortune[6], Michael Galambos[7], Stuart C Gordon[8], Denise Harnois[9], Tarek Hassanein[10], Matthew Robert Kappus[11], Eric Lawitz[12], Scott McHenry[13], Bhaktasharan Patel[14], Raymond Phillips[15], Daniel Pratt[16], Jatinder Pruthi[17], Govarthanan Rajendiran[18], Gautham Reddy[19], Manuel Rodriguez[20], Marina Silveira[21], Bobby Zervos[22], Paul Peloso[2], Eric Gershwin[1].
[1]University of California-Davis, Sacramento, United States; [2]COUR Pharma, Chicago, United States; [3]Icahn School of Medicine at Mount Sinai, New York, United States; [4]University of Virginia, Charlottesville, United States; [5]University of Florida, Gainesville, United States; [6]Montefiore Medical Center, Bronx, United States; [7]Digestive Healthcare of Georgia, Atlanta, United States; [8]Henry Ford Health, Wayne State University School of Medicine, Detroit, United States; [9]Mayo Clinic Florida, Jacksonville, United States; [10]Southern California Research Center, Coronado, United States; [11]Duke University School of Medicine, Durham, United States; [12]Texas Liver Institute, University of Texas Health San Antonio, San Antonio, United States; [13]Washington University School of Medicine in St. Louis, St. Louis, United States; [14]Peak Gastroenterology Associates, Colorado Springs, United States; [15]GI Pros Research, Naples, United States; [16]Massachusetts General Hospital, Harvard Medical School, Boston, United States; [17]Om Research, Lancaster, United States; [18]Sanford Medical Center, Sioux Falls, United States; [19]University of Chicago, Chicago, United States; [20]Florida Research Institute, Lakewood Ranch, United States; [21]Yale School of Medicine, New Haven, United States; [22]Cleveland Clinic Weston Hospital, Weston, United States
Email: mfrey@courpharma.com

Background and aims: Primary biliary cholangitis (PBC) is a progressive autoimmune liver disease with significant unmet needs. Increasing evidence supports using liver stiffness measurement (LSM) by vibration-controlled transient elastography (VCTE) as a predictor of clinical outcomes independent of liver biochemistries. CNP-104 is a novel tolerogenic nanoparticle encapsulating PDC-E2, previously shown to impact the underlying autoimmunity of PBC via antigen-specific decreases in pathogenic Th17T cells and expansion of tolerogenic T cells. Here we present the first-in-human results of CNP-104 on LSM in adults with PBC.
Method: This randomized, double-blind, placebo-controlled trial enrolled 42 patients with PBC with an incomplete biochemical response to ursodeoxycholic acid. Two doses of CNP-104 or placebo were administered IV one week apart, randomized 2:1 (CNP-104: n = 25; placebo: n = 16). The study included safety monitoring, exploratory clinical endpoints including liver stiffness via FibroScan®, and mechanistic immune endpoints including antigen-specific Th17 T cells with a pre-specified analysis through Day 120.
Results: Baseline LSM for CNP-104 and placebo were 9.60 ± 11.35 kPa and 10.45 ± 11.35 kPa, (p = 0.87) respectively. LSM increased in the placebo arm and remained stable in the CNP-104 arm through Day 180 (p = 0.0005). Fewer CNP-104 treated participants had a ≥ 2 kPa increase from baseline compared to placebo at Day 120 (17% vs. 40%, respectively) and Day 180 (25% vs. 47%, respectively). Response rates across increasing percent change thresholds at Day 120 and 180 demonstrated a consistently higher LSM response rate in the CNP-104 arm compared to placebo (decrease ≥ 0% at Day 120: 65% vs. 18%, respectively; p = 0.0026). The separation seen in this analysis suggests a CNP-104 treatment effect across a range of progressor definitions. Among all patients who had a reduction in PDC-E2-specific Th17 cells, LSM decreased significantly compared to those who had an increase in this pathogenic immune population through Day 180 (p = 0.001), suggesting a mechanistic link. CNP-104 had a favorable safety profile.
Conclusion: CNP-104 treatment stabilized LSM compared to placebo across multiple definitions of progression. The correlation between modulation of PDC-E2-specific Th17 cells and lower LSM suggests an effect mediated by restoring antigen-specific immune tolerance. These findings support further investigation of CNP-104 as a novel therapy for PBC.

OS-090

Increased risk of major adverse cardiovascular events in patients with primary biliary cholangitis, a population-based national cohort study in Sweden

Ida Henriksson[1], Carl Eriksson[2], Linnea Widman[3], Axel Wester[3], Nils Nyhlin[1], Hannes Hagström[4]. *[1]Department of Gastroenterology, Faculty of Medicine and Health, Örebro University, Örebro, Sweden; [2]Department of Gastroenterology, Faculty of Medicine and Health, Clinical Epidemiology Division, Department of Medicine Solna, Karolinska Institutet, Stockholm, Örebro, Sweden; [3]Department of Medicine, Huddinge, Karolinska Institutet, Stockholm, Sweden; [4]Department of Medicine, Huddinge, Karolinska Institutet, Division of Hepatology, Department of Upper GI, Karolinska University Hospital, Stockholm, Sweden*
Email: ida.henriksson@regionorebrolan.se

Background and aims: Primary biliary cholangitis (PBC) is an autoimmune liver disease, where previous studies have shown conflicting results regarding cardiovascular morbidity and mortality. The aims of this study are to assess the risk of Major Adverse Cardiovascular Events (MACE) in PBC and to explore the influence of disease severity.
Method: Nationwide register-based study on all patients with PBC diagnosed in Sweden between 2002 and 2022, matched with up to ten controls from the general population on age, sex, year of diagnosis and municipality. The primary outcome was incident MACE, adjusted for cardiovascular risk factors in a Cox regression model. Patients with cirrhosis were analyzed separately.
Results: We identified 3 332 patients and 28 076 matched controls. Of patients with PBC, 743 (22%) experienced MACE, with an incidence rate of 30.5/1000 person-years (PY), compared to 18.9/1000 PY in controls. This corresponds to 12 additional MACE events per 100 persons with PBC over 10 years. The association was strongest for cardiovascular death, (aHR = 2.19, 95%CI = 1.95–2.46) and congestive

heart failure (aHR = 1.73, 95%CI = 1.50–2.00). Among patients with PBC and cirrhosis, the incidence rate of total MACE was 87/1000 PY:s compared to 27/1000 PY:s in those without cirrhosis.
Conclusion: PBC is associated with an increased risk of MACE compared to matched controls. The highest rates are seen in patients with cirrhosis. Efforts to reduce cardiovascular risk is needed in patients with PBC.

Liver transplantation

OS-091
Long-term outcomes of patients with complete immunosuppression withdrawal after liver transplantation: a multicentre, worldwide study

Manuel Rodríguez-Perálvarez[1], Bruno Sensi[2], Giuseppe Tisone[2], Sandy Feng[3], Garrett Roll[3], Jose Ignacio Herrero[4], Eliano Bonaccorsi-Riani[5], Jose Antonio Pons[6], Pablo Ruiz[7], Marina Berenguer[8], Caroline den Hoed[9], George V. Mazariegos[10], Rachel Smith[10], Alessandro Parente[11], Varuna Aluvihare[11], Alberto Sanchez-Fueyo[11], Xiang Xuan Eunice Tan[12], Susana Calretas[13], Jacopo Lanari[14], Marco Spada[15], Aldo J Montano-Loza[16], Vincent E. de Meijer[17], Jacques Pirenne[18], Callum Riley[19], Daljeet Chahal[20], Eleonora De Martin[21], Stefano Di Sandro[22], Damiano Patrono[23], Ignacio Garcia Juarez[24], Alba Cachero[25], Gupse Adali[26], Davide Ghinolfi[27], Stefania Camagni[28], Ana Arias[29], Nuru Bayramov[30], Osama Elbahr[31], Tommaso Maria Manzia[2], Rodney Rogers[3], Tavakhol Mehdi[3], Dana Jakoubek[3], María Pascual Coloma[4], Mercedes Iñarrairaegui[4], Maxime Foguenne[5], Olga Ciccarelli[5], Alberto Baroja[6], Jordi Colmenero[7], Victoria Aguilera Sancho[8], Wojciech Polak[9], Ellina Lytvyak[16], Pablo Ramírez[6], Patrizia Bocagni[14], Ewan Glassey[11], Neil Rajoriya[19], Hans Blokzijl[17], Mark Muthiah[12], Roberta Angelico[2]. *[1]Hospital Universitario Reina Sofía, CORDOBA, Spain; [2]University of Rome Tor Vergata, Rome, Italy; [3]University of California, San Francisco, California, United States; [4]Clinica Universidad de Navarra, Pamplona, Spain; [5]University Hospital Saint-Luc, Brussels, Belgium; [6]Hospital Universitario Virgen Arrixaca, Murcia, Spain; [7]Hospital Clínic, Barcelona, Spain; [8]Hospital Universitario La Fe, Valencia, Spain; [9]Erasmus MC Transplant Institute University Medical Center Rotterdam, Rotterdam, Netherlands; [10]UPMC Children's Hospital of Pittsburgh, Pittsburgh, United States; [11]King's College London, London, United Kingdom; [12]National University Hospital, Singapore, Singapore; [13]Hospitais da Universidade de Coimbra, Coimbra, Portugal; [14]Padua University Hospital, Padua, Italy; [15]Bambino Gesù Children's Hospital IRCCS, Rome, Italy; [16]University of Alberta Hospital, Alberta, Canada; [17]University Medical Center Groningen, Groningen, Netherlands; [18]University Hospitals Leuven, Leuven, Belgium; [19]University Hospitals Birmingham NHS Foundation Trust, Birmingham, United Kingdom; [20]University of British Columbia, Vancouver, Canada; [21]Universite Paris-Saclay, Villejuif, France; [22]University Hospital of Modena "Policlinico", Modena, Italy; [23]Azienda Ospedaliero Universitaria Città della Salute e della Scienza di Torino, Turin, Italy; [24]Instituto Nacional de Ciencias Médicas y Nutrición "Salvador Zubirán", Mexico city, Mexico; [25]Hospital Universitario de Bellvitge, Hospitalet De Llobregat, Spain; [26]University of Health Sciences Istanbul Umraniye Training and Research Hospital, Istambul, Türkiye; [27]Azienda Ospedaliero Universitaria Pisana, Pisa, Italy; [28]ASST Papa Giovanni XXIII, Bergamo, Italy; [29]Hospital Universitario Puerta de Hierro, Madrid, Spain; [30]Azerbaijan Medical University, Baku, Azerbaijan; [31]Menoufia University, Shebin El Kom, Egypt*
Email: ropeml@hotmail.com

Background and aims: Immunosuppression withdrawal after liver transplantation (LT) is feasible in selected individuals but the risk of chronic graft damage is unknown. We aimed to describe the clinical characteristics and long-term outcomes of patients with successful immunosuppression withdrawal after LT.
Method: Retrospective cohort study involving 31 LT centers in 15 countries. Adult and pediatric patients with complete immunosuppression withdrawal for ≥12 months following LT were eligible. Patients receiving multi-organ or re-transplants were excluded. We evaluated long-term outcomes, including evidence of histological graft injury, rejection, and mortality.
Results: A total of 287 patients (223 adults and 64 children) were included, representing 0.46% of the reference LT population. The prevalence of complete immunosuppression withdrawal ranged from 0% to 4.4% in adults and from 0% to 13.3% in children. The median time from LT to immunosuppression withdrawal was 9.4 years, followed by 7.8 years of post-withdrawal follow-up. The most common reasons for immunosuppression withdrawal were participation in a clinical trial (53%), patient decision (25.1%), and immunosuppression-related side effects (16.7%). Immunosuppression withdrawal was associated with a metabolic improvement including reductions in diabetes (34.1% to 19.7%) and hypertension (58.7% to 31.4%). Paired liver biopsies before and after immunosuppression withdrawal were available in 108 patients (37.6%) and among them 43.5% achieved operational tolerance. Worsening fibrosis (≥1 Ishak's stage) and new-onset inflammation occurred in 30.5% and 22.2% of patients, respectively. Five-year overall survival after immunosuppression withdrawal was 93%, and no patient experienced immunologically mediated graft loss. Neither worsening fibrosis nor inflammation had an impact on mortality (HR = 1.77 [95%CI 0.63–4.96] and HR = 1.46 [95%CI 0.39–5.49], respectively).
Conclusion: Immunosuppression withdrawal is seldom attempted after LT and mostly within clinical trials. Although some patients may experience mild histological changes during follow-up, the risk of immunologically mediated graft loss is negligible. Patients showed excellent overall survival rates with fewer metabolic comorbidities. Future studies should focus on safely expanding immunosuppression withdrawal to a broader subset of LT patients.

OS-092-YI
Eurotransplant experience with model for end-stage liver disease standard exceptions for hepatopulmonary syndrome and portopulmonary hypertension

Maïté Verstraeten[1,2], Axel J. T. Jens[3], Gabriela Berlakovich[4], Martina Sterneck[5], Felix Braun[6], Caroline den Hoed[7], Blaž Trotovšek[8,9], Danko Mikulic[10], Tamas Benkoe[11,12], Anja Geerts[1,2], Xavier Verhelst[1,2], Hans Van Vlierberghe[1,2], Sarah Raevens[1,2]. *[1]Hepatology Research Unit, Department of Internal Medicine and Paediatrics, Ghent University, Ghent, Belgium; [2]Department of Gastroenterology and Hepatology, Ghent University Hospital, Ghent, Belgium; [3]Eurotransplant International Foundation, Leiden, Netherlands; [4]Division of Transplantation, Medical University of Vienna, Vienna, Austria; [5]Department of Internal Medicine, University Medical Center Hamburg-Eppendorf, Hamburg, Germany; [6]Sektion für Klinische Transplantationsmedizin, Klinik für Allgemeine, Viszeral-, Thorax-, Transplantations- und Kinderchirurgie, Universitätsklinikum Schleswig-Holstein (UKSH), Campus Kiel, Kiel, Germany; [7]Erasmus MC Transplant Institute, University Medical Center Rotterdam, Department of Gastroenterology and Hepatology, Rotterdam, Netherlands; [8]Department of Abdominal Surgery, University Medical Center Ljubljana, Ljubljana, Slovenia; [9]Medical Faculty Ljubljana, University of Ljubljana, Ljubljana, Slovenia; [10]Center for Solid Organ Transplantation, University Hospital Merkur, Zagreb, Croatia; [11]Department of Surgery, Transplantation and Gastroenterology, Semmelweis University, Budapest, Hungary; [12]Department of General-, Visceral-, Transplantation-, and Thoracic Surgery, University Hospital Frankfurt, Frankfurt, Germany*
Email: maite.verstraeten@ugent.be

Background and aims: Hepatopulmonary syndrome (HPS) and portopulmonary hypertension (PoPH) are severe pulmonary vascular

complications of end-stage liver disease (ESLD) and portal hypertension. Some patients are eligible for Model for End-Stage Liver Disease (MELD) standard exception (SE) liver transplantation (LT) prioritization in Eurotransplant. Data on waitlist and post-transplant outcomes under current SE policies remain limited.

Method: We analysed Eurotransplant registry data (2006–2022) for adult LT candidates with approved SE for HPS (n = 117) or PoPH (n = 25), compared with 710 matched controls (matching based on age, sex, MELD score, and liver disease etiology) without SE. Outcomes included overall survival, waitlist outcomes, and post-LT survival. Survival analyses were performed using Kaplan-Meier, Cox proportional hazards, and Fine and Gray competing risks models.

Results: Overall mortality was similar between HPS and controls (HR 1.23, 95% CI 0.93–1.63, p = 0.16), but higher in PoPH (HR 1.79, 95% CI 1.06–3.00, p = 0.028). Pre-transplant mortality was comparable across groups (for HPS: HR 1.02, 95% CI 0.68–1.53, p = 0.92; for PoPH: HR 1.22, 95% CI 0.55–2.72, p = 0.62). Post-LT survival was similar for HPS and controls (HR 1.11, 95% CI 0.73–1.67, p = 0.63), but significantly poorer for PoPH (HR 2.39, 95% CI 1.17–4.89, p = 0.017). At 6 months, survival rates were 88.1% (95% CI 84.7% - 91.6%) for control patients, 92.3% (95% CI 86.6% - 98.4%) for HPS and 57.1% (95% CI 36.3% - 89.9%) for PoPH; and at 1 year 84.7% (95% CI 81% - 88.7%), 87% (95% CI 79.7% - 94.8%), and 57.1% (95% CI 36.3% - 89.9%) respectively. Infection was the leading cause of post-LT mortality; cardiovascular events were more frequent in PoPH recipients.

Conclusion: LT candidates with SE for severe HPS achieve comparable overall and post-LT survival to non-SE recipients, supporting the appropriateness of current SE policy. Conversely, PoPH patients demonstrate markedly poorer post-LT outcomes, highlighting the need for careful candidate selection, optimized pre-transplant management, and perioperative strategies to improve survival.

OS-093

Cell-free chromatin for identifying T cell-mediated liver rejection

Abed Khakayla[1], Achraf Imam[1], Gavriel Fialkoff[2], Israa Sharkia[2], Ronen Sadeh[2], Omri Or[2], Jenia Gutin[2], Rifaat Safadi[1,3], Yael Milgrom[3], Orit Pappo[4], Severin Jacobi[5], Bastian Engel[6], Richard Taubert[6], Jonathan Frederik Brozat[7], Frank Tacke[7], Cornelius Engelmann[7], Esther Harpenas[8], Nofar Rosenberg[9], Ophir Hay[9], Eithan Galun[9], Nir Friedman[8]. *[1]Hadassah-Hebrew University Medical Center, Department of General surgery and Transplantation Unit, Jerusalem, Israel; [2]Senseera LTD, Jerusalem, Israel; [3]Hadassah-Hebrew University Medical Center, The Liver Unit Institute of Gastroenterology and Liver Diseases, Jerusalem, Israel; [4]Hadassah-Hebrew University Medical Center, Department of Pathology, Jerusalem, Israel; [5]Ludwig-Maximilians-Universität München, Munich, Germany; [6]Hannover Medical School, Department of Gastroenterology, Hepatology, Hannover, Germany; [7]Charité - Universitaetsmedizin Berlin, Department of Hepatology and Gastroenterology, Berlin, Germany; [8]Hebrew University of Jerusalem, Faculty of Medicine, Jerusalem, Israel; [9]Hadassah-Hebrew University Medical Center, The Goldyne Savad Institute for Gene Therapy, Jerusalem, Israel*
Email: nir.friedman@mail.huji.ac.il

Background and aims: T cell-mediated rejection (TCMR) complicates up to 30% of liver transplant recipients, predominantly within the first post-transplant year, and requires timely immunosuppressive intervention. Current diagnosis relies on invasive liver biopsy, which is unsuitable for frequent monitoring and delays the diagnosis. Emerging evidence supports the use of liquid biopsies as minimally invasive tools for real-time assessment of tissue injury and immune activity.

Method: Cell-free chromatin immunoprecipitation followed by sequencing (cfChIP-seq) targeting H3K4me3 - a histone mark associated with active or poised promoters - is a non-invasive method that provides a genome-wide scale readout of transcriptional activity and cell-state in the tissues of origin. A Chromatin Rejection Score (CRS), reflecting TCMR-specific signals, was developed in an exploratory cohort of cfChIP-seq plasma samples (n = 4,988) and evaluated in an independent cohort of liver transplant recipients (Jerusalem) who underwent a for-cause biopsy (TCMR, n = 17; non-TCMR, n = 23). Additional validation was performed on n = 50 samples with biopsy-verified TCMR status from a multicenter German cohort.

Results: CRS robustly discriminated biopsy-confirmed TCMR from other causes of post-transplant liver injury, achieving an area under the receiver operating characteristic curve (AUC) of 0.99 (95% CI 0.98–1), outperforming conventional transaminase markers ALT and AST (AUC 0.76, 0.68, resp.). This performance was reproduced on the external validation cohort. In longitudinal analyses, increases in CRS often preceded histopathological confirmation of TCMR and decreased rapidly following initiation of corticosteroid therapy, preceding the normalization of transaminase levels. Finally, we show that the same results can be obtained using a rapid-turnaround digital PCR method for CRS readout, demonstrating the feasibility of a quick and cost-effective assay at the medical center.

Conclusion: cfChIP-seq is an accurate, reproducible, and reliable biomarker for diagnosing and monitoring TCMR through minimally invasive molecular profiling of liver allograft injury. cfChIP-seq has the potential to enable early diagnosis, reduce the need for liver biopsies and guide effective immunosuppressive management in liver transplant recipients. By incorporating the digital PCR method it can provide real-time indication of rejection onset and rapid assessment of treatment responses.

OS-094

Liver transplantation for hepatocellular carcinoma: prognostic impact of complete pathologic response and influence of treatment modality- a U.S. national database study

Benjamin Tran[1], Rebecca Marino[1], Justine Aziz[2], Joseph DiNorcia[1], Julia Torabi[1], Myron Schwartz[1], Sander Florman[1], Kirema Garcia-Reyes[2], Rahul Patel[2], Edward Kim[2], Parissa Tabrizian[1]. *[1]Liver Transplant and Hepatobiliary Surgery, Recanati/Miller Transplantation Institute, Icahn School of Medicine at Mount Sinai, New York, United States; [2]Department of Diagnostic, Molecular and Interventional Radiology, Icahn School of Medicine at Mount Sinai, New York, United States*
Email: benjamin.tran2@mountsinai.org

Background and aims: Complete pathologic response (cPR) in hepatocellular carcinoma (HCC) is associated with improved post-liver transplant (LT) outcomes. However, national cPR rates, modality-specific differences, and predictors remain undefined. We evaluated the significance of cPR in a large national U.S. cohort.

Method: A retrospective study was performed using the UNOS database of adult LT recipients with HCC (2012–2024). cPR was defined as absence of viable tumor on explant pathology. Predictors of cPR were assessed using logistic regression. Cumulative incidence of cPR was estimated using Fine–Gray competing risk models. Overall (OS) and recurrence-free survival (RFS) were analyzed using Kaplan–Meier estimates.

Results: Among 7,398 LT recipients, 2,167 (29.3%) achieved cPR with poor imaging–pathology concordance (30.5%), with imaging demonstrating fewer lesions than pathology (thus overestimating response) in 42.6% of cases ($\kappa = 0.17$, $p < 0.001$). At listing, patients with cPR had smaller tumors (max size 2.3 vs 2.7 cm), lower total tumor diameter (2.7 vs 3.2 cm), and lower AFP levels (10 vs 11 ng/mL; all $p < 0.001$). These significant differences persisted at LT. Higher cPR rates were associated with patients achieving a longer waitlist period prior to LT (>18 months vs <6 months; OR 1.94, 95% CI 1.57–2.40). cPR rates were higher after Y-90 radioembolization (41.2%) and ablation (36.4%) than TACE (24.0%; p <0.001). On multivariable analysis, cPR likelihood increased with Y-90 (adjusted OR 1.89, 95% CI 1.46–2.05) and ablation (adjusted OR 1.23, 95% CI 1.08–1.39) compared to TACE. Increasing tumor burden (TTB ≥13 vs ≤3: OR 0.33,95% CI 0.13–0.86) and elevated AFP (≥100 ng/mL: OR 0.92, 95% CI 0.86–1.05) were independently associated with reduced cPR. Interaction analyses

showed that Y-90 benefit was greatest when administered within 6 months of waitlisting (OR 2.40, 95% CI 1.59–3.61) and among all-comer patients (OR 1.58, 95% CI 1.17–3.26). Competing risk analyses confirmed that Y-90 achieved the highest cumulative incidence of cPR across transplant eligibility regardless of the extent of disease. Patients with cPR had superior OS (5-year: 86.6% vs.77.4%) and RFS (76.9% vs 63.1%) compared with patients not achieving cPR ($p < 0.001$).

Conclusion: In this cohort, nearly one-third of LT recipients with HCC achieved cPR, associated with greater OS and RFS. Y-90 radioembolization was independently associated with higher cPR rates, with greatest benefit when administered early and among patients with higher tumor burden.

OS-095-YI

Non-vascular, non-cirrhotic portal hypertension following liver transplantation is largely caused by combination of portosinusoidal injury and allograft rejection

Iulia Minciuna[1,2,3], Michail Doukas[4], Valérie Paradis[5], Raoel Maan[6,7], Caroline den Hoed[1,7], Anne Van Eldere[1,7], Sandra Coenen[1,7], Wojciech Polak[7,8], Jeroen de Jonge[7,8], Bogdan Procopet[2,3], Sarwa Darwish Murad[1,7]. *[1]Department of Gastroenterology and Hepatology, Erasmus University Medical Center Rotterdam, Rotterdam, Netherlands; [2]University of Medicine and Pharmacy "Iuliu Hatieganu", Cluj-Napoca, Romania; [3]Regional Institute of Gastroenterology and Hepatology "O. Fodor", Cluj-Napoca, Romania; [4]Department of Pathology, Erasmus University Medical Center, Rotterdam, Netherlands; [5]Department of Pathology, AP-HP Hôpital Beaujon, Clichy, Paris, France; [6]Department of Gastroenterology and Hepatology, Erasmus University Medical Center, Rotterdam, Netherlands; [7]Erasmus MC Transplant Institute, Erasmus University Medical Center, Rotterdam, Netherlands; [8]Department of Surgery, Division of HPB and Transplant Surgery, Erasmus MC Transplant Institute, Erasmus University Medical Center, Rotterdam, Netherlands*
Email: Iuliabreaban@yahoo.com

Background and aims: Portal hypertension (PH) may develop after liver transplantation (LT) due to vascular complications or recurrence of cirrhosis. However, in rare cases, post-transplant PH (PTPH) occurs outside this setting which has been associated to a variety of histological entities, including sinusoidal obstruction syndrome (SOS), nodular regenerative hyperplasia (NRH) and several allograft rejection forms. In this study, we hypothesize that there is a considerable degree of overlap between these entities that contribute PTPH.

Method: From 2007–2022, 1004 adults underwent LT in our institution. Patients with non-cirrhotic, non-vascular PTPH (i.e. new-onset ascites, varices, portal hypertensive bleeding or newly detected portosystemic collaterals), who underwent liver biopsy for this indication were compared to matched LT patients with liver test abnormalities. Two independent pathologists, blinded to the cases, reviewed all biopsies systematically using internationally accepted criteria for acute and chronic T-cell mediated rejection (TCMR), acute and chronic antibody mediated rejection (AMR), portosinusoidal vascular disorder and SOS.

Results: Overall, 19 patients developed PTPH without vascular cause or recurrent liver disease. Upon systematic assessment, all patients (100%) with PTPH met histological criteria for PSVD, 63% for acute and 63% for chronic TCMR, 47% for SOS, 26% for cAMR and 16% for AMR. Global inter-pathologist agreement was 84%. Interestingly, 74% showed both features of rejection and PSVD. However, only 26% had isolated microvascular injury at the portosinusoidal (PSVD only, $n = 2$) and/or centrilobulair (PSVD and SOS, $n = 3$) level. Compared to matched controls, PTPH was significantly more frequently associated with PSVD (100% vs 5%, $p < 0.001$), SOS (47% vs 16%; $p = 0.03$) and chronic TCMR (63% vs 16%, $p = 0.03$). There were no differences in acute TCMR (63% vs 79%), acute AMR (16% vs 16%) and chronic AMR (26% vs 16%). Outcome was dismal in PTPH, with poor response to therapy and significantly lower 10-year patient (26% vs 76%, $p = 0.01$) and graft survival (18% vs 76%, $p = 0.001$).

Conclusion: Non-cirrhotic, non-vascular PTPH is a rare but serious complication, which is most often caused by a combination of allograft rejection and portosinusoidal injury. Increased vigilance and a systematic, unbiased approach by pathologists are needed to identify these overlapping features, since this may guide targeted treatment and enhance response.

OS-108

Home-based exercise and motivational programme before and after liver transplantation (EXALT): a multicentre randomised, controlled trial

Matthew Armstrong[1], Samir Mehta[2], Joan Duda[3], Sally Fenton[3], Chiemelie Ngonadi[1], Alice Freer[1], Ashlea Hargreaves[1], Nigel Cope[4], Dawn Brant[2], Yongzhong Sun[2], Dr. Clare Melikian[4], Dan Martin[5], Felicity Williams[1]. *[1]Liver Unit, Queen Elizabeth University Hospital Birmingham, UK, NIHR Birmingham Biomedical Research Centre, University of Birmingham, UK, Birmingham, United Kingdom; [2]Birmingham Clinical Trials Unit, University of Birmingham, Birmingham, United Kingdom; [3]School of Sports, Exercise and Rehabilitation Sciences, University of Birmingham, Birmingham, United Kingdom; [4]Hepatobiliary and Liver transplant Anaesthesia Department, Royal Free Hospital, London, United Kingdom; [5]Peninsula Medical School, University of Plymouth, Plymouth, United Kingdom*
Email: mattyarm2010@googlemail.com

Background and aims: Physical frailty is associated with mortality and reduced health-related quality of life (HRQoL) after liver transplantation. Exercise interventions may improve transplantation outcomes, but data from clinical trials are limited and adherence strategies are lacking. We evaluated the efficacy of a personalised home-based exercise and motivational programme in patients undergoing liver transplantation.

Method: EXALT trial was a multicentre, randomised-controlled trial in two supra-regional UK transplant centres. Patients awaiting liver transplantation were randomly assigned (1:1) to a remotely monitored, physiotherapist-delivered, home-based exercise and motivational programme (Exercise group) or a patient advice leaflet (Control group) up to 52 weeks pre- and 24 weeks post-transplantation. The primary outcome was the physical component summary (PCS) of the short form-36v2.0 HRQoL questionnaire 24 weeks post-transplantation. We used a repeated-measures, mixed-effects linear regression model (adjusted for age, sex, site, and disease severity) in patients who underwent transplantation within 52 weeks of randomisation.

Results: Between May 2022 and May 2024, 269 patients were enrolled (134 exercise group, 135 control group). 180 (67%) were male and mean age was 51.8 years (SD 12.3). 85 (63%) patients underwent transplantation in each group. At 24 weeks post-transplantation, the improvement in PCS score was greater in the exercise group compared to the control group (least-squares mean difference +4.7, 95% CI 1.7 to 7.8; $p < 0.01$). The exercise group had greater improvements compared to control group in physical frailty (liver frailty index; least-squares mean difference -0.3, 95%CI -0.6 to -0.1; $p < 0.01$), aerobic exercise capacity (duke activity status index; least-squares mean difference +5.6, 95%CI 1.7 to 9.5; $p < 0.01$) and autonomous motivation towards exercise (Behavioural Regulation in Exercise Questionaire-2 least-squares mean difference +0.6, 95%CI 0.1 to 0.9; $p = 0.01$) at 24 weeks post-transplantation. There were similar rates of surgical complications and adverse events between groups. 90-day and 1-year post-transplant survival was 100% and 98% in the exercise group compared to 94% and 92% in the control group.

Conclusion: This personalised home-based exercise and motivational programme significantly improved physical health-related quality of life, frailty and physical fitness after liver transplantation, and enhanced patient's autonomous motivation for long-term engagement in exercise.

MASLD: Clinical and therapeutical aspects II

OS-096

Belapectin reduces varices development in high-risk MASH cirrhosis by modulating fibrogenesis balance as reflected by Pro-C3/CTX-III ratio

Mazen Noureddin[1], Naim Alkhouri[2], Mitchell Shiffman[3], Raj Vuppalanchi[4], Nadege Gunn[5], Khurram Jamil[6], Seth Zuckerman[6], Andrew Volosov[6], Naga Chalasani[4]. [1]*Houston Methodist Hospital, Houston, TX, United States;* [2]*Summit Clinical Research, Clinical Research Institute of Ohio, San Antonio, TX, United States;* [3]*Liver Institute of Virginia, Richmond, VA, United States;* [4]*Indiana university school of medicine, Indianapolis, United States;* [5]*Impact Research Institute, Waco, TX, United States;* [6]*Galectin Therapeutics, Norcross, GA, United States*
Email: khurramjamil@yahoo.com

Background and aims: Belapectin, a galectin-3 inhibitor, reduced new varices development in the per-protocol population of the Phase 2b/3 NAVIGATE trial. As variceal formation reflects fibrosis progression and portal hypertension, we evaluated whether belapectin 2 mg/kg's clinical benefit is linked to attenuation of active fibrogenesis, using the Pro-C3/CTX-III ratio, a marker of collagen formation versus degradation.
Method: NAVIGATE (NCT04365868) randomized patients with compensated MASH cirrhosis, portal hypertension, and no baseline varices to belapectin 2 mg/kg, 4 mg/kg, or placebo every 2 weeks for 18 months, stratified by T2DM. Of 357 randomized (119 per group), 287 completed 18 months with both baseline and end-of-treatment endoscopy, forming the per-protocol population. Baseline characteristics were balanced (mean age 60 years; 65% female; platelets 131 × 10^9/L; LSM 24.8 kPa; 67% T2DM). This study examined new varices and changes in Pro-C3/CTX-III at week 78 in subjects at high risk of progression, including those with baseline ELF >11.3, an ELF increase ≥0.5, or a Pro-C3/CTX-III ratio above median at baseline.
Results: Belapectin consistently lowered varices incidence across all ELF categories, with the largest effect in patients with baseline ELF >11.3 (22.7% vs. 42.9% with placebo). In this subgroup, Pro-C3/CTX-III worsened by 4.3% with placebo but improved by 13.6% with belapectin. Among patients with baseline Pro-C3/CTX-III above the median, placebo worsened by 2.2% versus a 9.3% improvement with belapectin. In all subjects with ELF increases ≥0.5 subjects receiving belapectin experienced markedly less progression in Pro-C3/CTX-III relative to placebo (15.9% vs 40.4%, p = 0.004), reflecting reduced collagen formation and enhanced degradation with belapectin.
Conclusion: In advanced MASH cirrhosis, belapectin 2 mg/kg reduces new varices and attenuates active fibrogenesis, as evidenced by favorable shifts in the Pro-C3/CTX-III ratio in high-risk ELF subgroups. These data suggest that belapectin's anti-fibrotic effects may contribute to reducing the risk of portal hypertension–associated complications.

OS-097

Liver fibrosis is the only predictor of adverse outcomes: time to remove metabolic dysfunction associated steatohepatitis (MASH) resolution as a clinical trial endpoint

Zobair M. Younossi[1], Ming-Lung Yu[1,2], Leyla de Avila[1], Salvatore Petta[1,3], Hannes Hagström[1,4], Seung Up Kim[1,5], Atsushi Nakajima[1,6], Javier Crespo[1,7], Laurent Castera[1,8], Naim Alkhouri[1,9], Ming-Hua Zheng[1,10], Sombat Treeprasertsuk[1,11], Prooksa Ananchuensook[1,11], Shalimar Shalimar[1,12], Emmanuel Tsochatzis[1,13], K T Shenoy[1,14], Leena Mohan[1,15], Jian-Gao Fan[1,16], Stuart Roberts[1,17], Khalid A Alswat[1,18], Vincent Wai-Sun Wong[1,19], Yusuf Yilmaz[1,20], Winston Dunn[21], Sven Francque[1,22], Ahmed Cordie[1,23], Saleh Alqahtani[1,24], Mattias Ekstedt[25], George Boon Bee Goh[1,26], Claudia Pinto Oliveira[1,27], Mário Pessoa[1,28], Wah-Kheong Chan[1,29], Marlen Ivon Castellanos Fernández[1,30], Ajay Kumar Duseja[1,31], Juan Pablo Arab[1,32], George Papatheodoridis[1,33], Giada Sebastiani[1,34], Cristiane A. Villela-Nogueira[1,35], Roberta D'Ambrosio[36], Pietro Lampertico[1,36], Khalid Al Naamani[1,37], A.G. (Onno) Holleboom[1,38], Arun Valsan[1,39], Arathi Venu[39], Mohamed El-Kassas[1,40], Grazia Pennisi[3], Ying Shang[41], Wen-Yue Liu[42], Hye Won Lee[5], Takashi Kobayashi[6], Satoru Kakizaki[1,43], Cyrielle Caussy[1,44], Brian Pearlman[1,45], Paula Iruzubieta[7], Rida Nadeem[46], Felice Cinque[34], Margarita Papatheodoridi[33], Mirko Zoncapè[47], Rui-Xu Yang[16], Sherlot Juan Song[19], Nicholas Dunn[21], Zouhir Gadi[22], Ming-Lun Yeh[48], Kevin Kim Jun Teh[26], Sanjiv Mahadeva[29], Licet Gonzalez Fabian[49], Ahmed Almohsen[50], Nathalie Leite[35], Nicola Pugliese[1,51], Johan Vessby[52], Chencheng Xie[53,54], Narendra S Choudhary[55], Ethan Friend[56], Maria Poca[57], Takumi Kawaguchi[1,58], Francesco Paolo Russo[59], Adrian Gadano[1,60], Luis Antonio Diaz[1,61], Ashwani K. Singal[1,62], Bérénice Ségrestin[1,44], Nadege Gunn[1,56], Didac Mauricio[1,63], Marco Arrese[1,64], Anna Ludovica Fracanzani[1,65], Rosa Lombardi[1,65], Alessio Aghemo[51], Shira Zelber-Sagi[1,66], Brian Lam[1], Andrei Racila[1,67], Maria Stepanova[1,67]. [1]*The Global NASH Council (GNC), Washington, DC, United States;* [2]*Hepatobiliary Division, Department of Internal Medicine, Kaohsiung Medical University Hospital, Kaohsiung Medical University, Kaohsiung, Taiwan;* [3]*Section of Gastroenterology, PROMISE Department, University of Palermo, Palermo, Italy;* [4]*Division of Hepatology, Department of Upper GI Diseases, Karolinska University Hospital, Stockholm, Sweden;* [5]*Department of Internal Medicine, Yonsei University College of Medicine, Seoul, Korea, Rep. of South;* [6]*Department of Gastroenterology and Hepatology, Yokohama City University Graduate School of Medicine, Yokohama, Japan;* [7]*Gastroenterology and Hepatology Department, Clinical and Translational Research in Digestive Diseases, Valdecilla Research Institute (IDIVAL), Marques de Valdecilla University Hospital, Santander, Spain;* [8]*Department of Hepatology, Hospital Beaujon, Assistance Publique-Hôpitaux de Paris, Université Paris-Cité, Paris, France;* [9]*Summit Clinical Research, San Antonio, Texas, United States;* [10]*MAFLD Research Center, Department of Hepatology, The First Affiliated Hospital of Wenzhou Medical University, Wenzhou, China;* [11]*Division of Gastroenterology, Department of Internal Medicine, Chulalongkorn University, Bangkok, Thailand;* [12]*Department of Gastroenterology and Human Nutrition Unit, All India Institute of Medical Sciences, New Delhi, India;* [13]*University College London Institute for Liver and Digestive Health, Royal Free Hospital, London, United Kingdom;* [14]*Department of Gastroenterology, Sree Gokulam Medical College and Research Foundation, Trivandrum, Kerala, India;* [15]*Population Health and Research Institute, Medical College P O, Trivandrum, Kerala, India;* [16]*Department of Gastroenterology, Xinhua Hospital affiliated to Shanghai Jiao Tong University School of Medicine, Shanghai, China;* [17]*Alfred Hospital Gastroenterology Department, Monash University, Melbourne, Australia;* [18]*Liver Disease Research Center, Department of Medicine, College of Medicine, King Saud University, Riyadh, Saudi Arabia;* [19]*Medical Data Analytics Center, Department of Medicine and Therapeutics, The Chinese University of Hong Kong, Hong Kong, China;* [20]*Department of Gastroenterology, School of Medicine, Recep Tayyip Erdogan University, Rize, Türkiye;* [21]*Internal Medicine, Kansas University Medical Center, Kansas City, Kansas, United States;* [22]*Department of Gastroenterology and Hepatology, Antwerp University Hospital, Edegem, Belgium;* [23]*Cairo University Hospitals HIV Clinic, Endemic Medicine Department, Cairo University Hospitals, Cairo, Egypt;* [24]*Liver, Digestive, and Lifestyle Health Research Section, and Organ Transplant Center of Excellence, King Faisal Specialist Hospital and Research Center, Riyadh, Saudi Arabia;* [25]*Department of Gastroenterology and Hepatology, Department of Health, Medicine, and Caring Sciences, Linköping University, Linköping, Sweden;* [26]*Department of Gastroenterology & Hepatology, Singapore General Hospital, Singapore, Singapore;* [27]*Department of Gastroenterology, Faculdade Medicina da Universidade de Sao Paulo, Sao Paulo, Brazil;* [28]*Department of Gastroenterology, Hospital das Clínicas da Faculdade de Medicina da Universidade de São*

Paulo - HCFMUSP, São Paulo, Brazil; [29]Gastroenterology and Hepatology Unit, Department of Medicine, University of Malaya, Kuala Lumpur, Malaysia; [30]Department of Research and Teaching, Institute of Gastroenterology, University of Medical Sciences of Havana, Havana, Cuba; [31]Department of Hepatology, Postgraduate Institute of Medical Education and Research, Chandigarh, India; [32]Stravitz-Sanyal Institute for Liver Disease and Metabolic Health, Division of Gastroenterology, Hepatology, and Nutrition, Department of Internal Medicine, Virginia Commonwealth University School of Medicine, Richmond, Virginia, United States; [33]1st Academic Department of Gastroenterology, Medical School of National and Kapodistrian University of Athens, General Hospital of Athens "Laiko", Athens, Greece; [34]Division of Gastroenterology and Hepatology, Department of Medicine, McGill University Health Centre, Montreal, Canada; [35]School of Medicine, Internal Medicine Department and Hepatology Division, Clementino Fraga Filho University Hospital, Federal University of Rio de Janeiro, Rio de Janeiro, Brazil; [36]Division of Gastroenterology and Hepatology, Foundation IRCCS Ca' Granda Ospedale Maggiore Policlinico, Milan, Italy; [37]Division of Gastroenterology and Hepatology, Department of Medicine, The Medical City for Military and Security Services, Muscat, Oman; [38]Department of Vascular Medicine, Amsterdam University Medical Center, Amsterdam, Netherlands; [39]Centre for Metabolic Liver Disease and Integrated Liver Care Unit, Amrita Institute of Medical Sciences, Kochi, Kerala, India; [40]Endemic Medicine Department, Faculty of Medicine, Capital University, Cairo, Egypt; [41]Department of Medicine, Huddinge, Karolinska Institutet, Stockholm, Sweden; [42]Department of Endocrinology, the First Affiliated Hospital of Wenzhou Medical University, Wenzhou, China; [43]Department of Clinical Research, NHO Takasaki General Medical Center, Takasaki, Japan; [44]Département Endocrinologie, Diabète et Nutrition, Hôpital Lyon Sud, Hospices Civils de Lyon, Pierre-Bénite, Lyon, France; [45]Department of Graduate Medical Education, Hamilton Medical Center, Medical College of Georgia, Dalton, Georgia, United States; [46]Arizona Liver Health, Chandler, Arizona, United States; [47]Liver Unit, Department of Internal Medicine, University and Azienda Ospedaliera Universitaria Integrata of Verona, Verona, Italy; [48]Center of Excellence for Metabolic Associated Fatty Liver Disease, National Sun Yat-sen University, Kaohsiung, Taiwan; [49]Department of Pathological Anatomy, Institute of Gastroenterology, University of Medical Sciences of Havana, Havana, Cuba; [50]Department of Medicine, Schulich School of Medicine, Western University & London Health Sciences Centre, London, Ontario, Canada; [51]Division of Internal Medicine and Hepatology, Department of Gastroenterology, IRCCS, Humanitas Research Hospital, Rozzano, Italy; [52]Department of Medical Sciences, Gastroenterology Research Group, Uppsala University, Uppsala, Sweden; [53]Division of Hepatology, Avera McKennan Hospital & University Health Center, Sioux Falls, South Dakota, United States; [54]Univerity of Iowa, Iowa City, United States; [55]Hepatology, and Institute of Liver Transplantation and Regenerative Medicine, Medanta The Medicity, Gurugram, Haryana, India; [56]Velocity Clinical Research, Waco, Texas, United States; [57]Department of Gastroenterology, CIBEREHD, IR Sant Pau, Hospital de la Santa Creu i Sant Pau, Barcelona, Spain; [58]Division of Gastroenterology, Department of Medicine, Kurume University School of Medicine, Kurume, Japan; [59]Department of Surgery, Oncology and Gastroenterology, University of Padova Gastroenterology Unit, Azienda Ospedaliera - Universita Padova, Padova, Italy; [60]Liver Unit, Hospital Italiano de Buenos Aires, Buenos Aires, Argentina; [61]MASLD Research Center, Division of Gastroenterology and Hepatology, University of California San Diego, San Diego, California, United States; [62]Department of Medicine, Division of Gastroenterology, Hepatology, and Nutrition, University of Louisville, Louisville, Kentucky, United States; [63]Department of Endocrinology & Nutrition, CIBERDEM, IR Sant Pau, Hospital de la Santa Creu i Sant Pau, Barcelona, Spain; [64]Departamento de Gastroenterología, Escuela de Medicina, Pontificia Universidad Católica de Chile, Santiago, Chile; [65]Unit of Metabolic Disease, Fondazione IRCCS Ca' Granda Ospedale Maggiore Policlinico, Milan, Italy; [66]School of Public Health, Faculty of Social Welfare and Health Sciences, University of Haifa, Haifa, Israel; [67]Center for Outcomes Research in Liver Disease, Washington, DC, United States
Email: zobair.younossi@cldq.org

Background and aims: MASH pathologic diagnosis requires steatosis, lobular inflammation, and hepatocyte ballooning with significant inter- and intra-observer variability leading to large screen failures in clinical trials. Nevertheless, "MASH resolution" has been an endpoint in most recent clinical trials. Also, most non-invasive tests (NITs) are being developed as surrogates of fibrosis rather than MASH. We evaluated associations between histological features of MASH, fibrosis stage, and clinical outcomes.
Method: Adults with MASLD from 41 countries (G-MASLD) were included if they had liver biopsy with MASLD Activity Score (steatosis 0–3, inflammation 0–3, ballooning 0–2), fibrosis stage (0–4), and longitudinal follow-up for mortality and clinical events (decompensation, HCC, transplant, death).
Results: 9,712 MASLD patients were included [age 51 ± 13 years; 49% male; 66% obesity; 51% type 2 diabetes (T2D); 54% hypertension (HTN)]. Advanced fibrosis (AF, F3–F4) was present in 42%, and 15% had significant fibrosis (SF, F2). Patients with AF were older, more often female, and had more T2D and HTN (all $p < 0.001$). NAS scores were higher in AF (mean 4.9 ± 1.4 vs. 3.8 ± 1.6), with greater frequency of NAS≥5 (64% vs. 35%), grade 3 lobular inflammation (30% vs. 3%), and grade 2 hepatocyte ballooning (57% vs. 19%) (all $p < 0.0001$). Higher NAS was associated with AF (OR per 1-point increase 1.64, 95% CI 1.58–1.70; NAS ≥5 vs <5: OR 3.32, 3.00–3.68; all $p < 0.0001$). Lobular inflammation (grade 2: OR 2.23; grade 3: OR 8.02) and hepatocyte ballooning (grade 1: OR 3.42; grade 2: OR 7.87) were independently associated with AF (all $p < 0.0001$). However, predicting long-term outcomes using Cox models (adjusted for country, age, sex, obesity, T2D, and HTN) showed that only AF predicted all-cause mortality (aHR 2.10, 1.65–2.68) and clinical events (aHR 3.73, 3.07–4.53; both $p < 0.0001$). After adjustment for AF or AF+SF, neither NAS nor its components (including hepatocyte ballooning) were associated with adverse outcomes (all $p > 0.05$), a pattern unchanged in fibrosis subgroups (no SF/AF, SF, AF) or when adjusting for liver stiffness ≥10 kPa.
Conclusion: MASH features are associated with AF but not with adverse outcomes after adjustment for fibrosis. Although inflammatory pathways remain important therapeutic targets, variability in pathologic assessment of MASH and its inability to predict clinically relevant outcomes make MASH resolution a suboptimal primary endpoint; fibrosis-related NITs should instead be prioritized as the key endpoint.

OS-098-YI

Distinguishing persistent from transient liver stiffness elevation using blood-based non-invasive tests: Longitudinal results from the European LiverScreen consortium

Jesse Pustjens[1], Katrine Tholstrup Bech[2], Laurens A. van Kleef[1], Guillem Pera[3], Helle Schnefeld[2], Katrine Lindvig[2], Robert J. de Knegt[1], Peter Andersen[2], Johanne Kragh Hansen[2], Llorenç Caballeria[3], Carla Chacon[3], Pere Torán[3], Anna Soria[4], Marta Cervera Carbonell[5], Íngrid Arteaga[3], Anita Arslanow[4], Sarwa Darwish Murad[1], Harry L.A. Janssen[1], Aleksander Krag[2], Isabel Graupera[3], Pere Ginès[3], Maja Thiele[2], Willem Pieter Brouwer[1]. *[1]Department of Gastroenterology and Hepatology, Erasmus MC, University Medical Centre, Rotterdam, the Netherlands, Rotterdam, Netherlands; [2]Centre for Liver Research, Department of Gastroenterology and Hepatology, Odense University Hospital, Odense, Denmark, Institute of Clinical Research, University of Southern Denmark, Odense, Denmark, Odense, Denmark; [3]Unitat de Suport a la Recerca Metropolitana Nord, Institut Universitari d'Investigació en Atenció Primària Jordi Gol, Mataró, Barcelona, Spain, Barcelona, Spain; [4]Liver Unit, Hospital Clínic, University of Barcelona, Barcelona, Catalonia, Spain, Institut D'Investigacions Biomèdiques August Pi I Sunyer (IDIBAPS), Barcelona, Spain, Barcelona, Spain;*

[5]*Institut D'Investigacions Biomèdiques August Pi I Sunyer (IDIBAPS), Barcelona, Spain, Centro de Investigación en Red de Enfermedades Hepáticas y Digestivas (CIBEREHD), Barcelona, Spain, Barcelona, Spain*
Email: j.pustjens@erasmusmc.nl

Background and aims: Liver stiffness measurements (LSM) have a well-established role in liver disease screening, but high regression rates among initial elevated values have been reported. Blood-based non-invasive tests (NITs) may help distinguish transient from persistent LSM elevation over long-term follow-up in a general population-based setting.
Method: This prospective, longitudinal study, conducted at three European centres (Barcelona, Rotterdam, Odense), was part of the LiverScreen consortium. We assessed LSM over a four-year interval. Persistent LSM elevation was defined as LSM ≥8 kPa at both baseline and follow-up, and transient elevation as a decrease to <8 kPa at follow-up. First, we stratified the prevalence of follow-up LSM elevation according to baseline LSM and NIT-scores (FIB-4, MAF-5, LiverRisk Score [LRS], and LiverPRO). Next, we evaluated the ability of NITs to detect persistent LSM elevation using area under the curve (AUC) analyses Finally, we analyzed transitions in NIT-score categories over follow-up and subsequent LSM elevation.
Results: Among 4536 participants (median follow-up 4.3 years [IQR 4.1–8.2]; median age 62 years [56–68]; 52% female), 5.5% (n = 251) had baseline LSM ≥8 kPa. Of these, 38% had persistent LSM elevation at follow-up. Among individuals with elevated baseline LSM but low NIT-scores, transient LSM elevation rates were high, ranging from 81% (LiverPRO) to 74% (FIB-4). Conversely, when baseline NIT-scores were high, persistent LSM elevation rates ranged from 43% (LiverPRO) to 47% (MAF-5). A sequential high NIT-score at follow-up further increased persistent elevated LSM prevalence ranging from 45% (LiverPRO) to 54% (FIB-4). Baseline NITs scores demonstrated moderate to excellent ability to predict persistent LSM elevation (AUC: MAF-5: 0.872; LRS: 0.852; LiverPRO: 0.845; FIB-4: 0.700). In individuals with a low baseline LSM and serial low NIT-scores, elevation at follow-up occurred in 1.4% (MAF-5) to 2.2% (FIB-4), compared to 5.3% (FIB-4) and 12.9% (MAF-5) when NIT-scores remained high during follow-up.
Conclusion: During long-term follow-up, transient LSM elevations were more frequent than persistent elevations. MAF-5, LRS, and LiverPRO provide excellent predictive value for long-term persistent LSM elevation. Low baseline NIT-scores can reduce the likelihood of persistent elevation to 19%, while repeated high NIT-scores can increase this likelihood to 54%.

OS-099

AI-powered cell-free DNA methylation profiling for identification of treatment-eligible MASLD patients: a multi-cohort validation study

Jörn M. Schattenberg[1], Soheil Damangir[2], Hamed Amini[2], Leila Bazargan[2], Chong Lu[2], Kitty Yale[3], Reshma Shringarpure[3], Lynn Lips[3], Brent A. Neuschwander-Tetri[4], Rohit Loomba[5], Manal F. Abdelmalek[6], Anna Mae Diehl[7]. [1]*Saarland University Medical Center, Homburg, Germany;* [2]*Hepta Bio, Inc., Foster City, United States;* [3]*Akero Therapeutics, Inc., South San Francisco, United States;* [4]*Saint Louis University, St. Louis, United States;* [5]*University of California, San Diego, La Jolla, United States;* [6]*Mayo Clinic, Rochester, United States;* [7]*Duke University, Durham, United States*
Email: soheil@hepta.bio

Background and aims: With the approval of resmetirom and semaglutide for the treatment of MASH with moderate-to-advanced fibrosis (F2-F3), accurate identification of treatment-eligible patients has become a critical clinical need. Current non-invasive tests (NITs) result in missing almost a third of the treatment-eligible patients as they were predominantly developed for detecting advanced fibrosis (F3-F4). We developed and validated an AI-powered cell-free DNA (cfDNA) methylation platform optimized for detecting MASH with F2-F3 to address this diagnostic gap.
Method: This multi-cohort study includes 553 biopsy-confirmed MASLD patients from 3 independent cohorts across the US and Europe: (1) Duke MASLD Biobank (n = 276), (2) University Medical Center Mainz Biobank (n = 73), and (3) Akero Therapeutics' SYNCHRONY Phase 3 screening population (n = 204). Deep methylation sequencing of plasma cfDNA was performed, generating 112 terabytes of genomic data. A novel transformer architecture (LiquidTransformer 89 million parameters), trained on a 20,000 core cluster, was developed to identify clinically significant fibrosis. Test performance was evaluated for the detection of: (1) significant fibrosis (F2-F3) in non-cirrhotic patients and (2) cirrhosis (F4). Performance was compared head-to-head against Fib4, VCTE and ELF on matched samples. All performance results were measured on the validation set.
Results: For detection of treatment-eligible fibrosis, F2-F3, and cirrhosis detection the test achieved AUC of 0.83 and 0.80 respectively. In direct comparison on matched subsets of samples, cfDNA methylation test outperformed Fib4 (AUC 0.82 vs 0.71) across all datasets with delta AUC 0.07, 0.07 and 0.13 for Duke, Mainz and Akero respectively. On a subset of Akero samples n = 201 where other comparators were available the test (AUC = 0.82) outperformed ELF (AUC = 0.69), VCTE (AUC = 0.67) and Fib4 (AUC = 0.64). Notably, the Akero cohort represents a clinically pre-selected population yet the model maintained robust performance. Performance was consistent across sex and diabetes status.
Conclusion: This AI-powered cfDNA methylation platform accurately identifies MASLD patients eligible for treatment while excluding cirrhosis, directly addressing a diagnostic gap in current guideline-recommended NIT pathways. The technology demonstrates consistent performance across independent international cohorts including a clinical trial screening population, uniquely positioning it to be considered for integration into treatment decision algorithms.

OS-100

Norucholic acid reduces histological and biochemical inflammation in metabolic dysfunction-associated steatohepatitis: results from the phase 2b randomized clinical trial NUT-3

Emina Halilbasic[1], Karel Dvořák[2], Safadi Rifaat[3], Gerlinde Teuber[4], Peter Schirmacher[5], Carolin Lackner[6], Małgorzata Inglot[7], Münevver Demir[8], Frederik Nevens[9], Mark Wright[10], Matthew Armstrong[11], Rudolf Stauber[12], Sandra Noh[5], Michael Stiess[13], Andreas Geier[14], Michael Trauner[1]. [1]*Division of Gastroenterology and Hepatology, Department of Internal Medicine III, Medical University of Vienna, Vienna, Austria;* [2]*Regional Hospital Liberec, Liberec, Czech Republic;* [3]*Liver Institute, Hadassah-Hebrew University Hospital, Jerusalem, Israel;* [4]*Practice PD Dr. med. G. Teuber, Frankfurt am Main, Germany;* [5]*Institute of Pathology, University Hospital Heidelberg, Heidelberg, Germany;* [6]*Institute of Pathology, Medical University of Graz, Graz, Austria;* [7]*Wroclaw Medical University, Wroclaw, Poland;* [8]*Department of Hepatology and Gastroenterology, Charité Universitätsmedizin Berlin, Berlin, Germany;* [9]*Department of Gastroenterology and Hepatology, UZ Leuven, Leuven, Belgium;* [10]*Department of Hepatology, Southampton General Hospital, Southampton, United Kingdom;* [11]*NIHR Birmingham Biomedical Research Centre, University of Birmingham, Birmingham, United Kingdom;* [12]*Division of Gastroenterology and Hepatology, Department of Internal Medicine, Medical University of Graz, Graz, Austria;* [13]*Dr. Falk Pharma GmbH, Freiburg, Germany;* [14]*Division of Hepatology, Department of Medicine II, University Hospital Wuerzburg, Wuerzburg, Germany*
Email: michael.trauner@meduniwien.ac.at

Background and aims: The semi-synthetic bile acid homologue norucholic acid (NCA) was shown in a prior phase 2a trial to improve liver enzymes in metabolic dysfunction-associated steatotic liver disease. Here, we report the results of a phase 2b trial of NCA on liver

histology in metabolic dysfunction-associated steatohepatitis (MASH).
Method: In this placebo-controlled, randomized clinical trial, MASH patients with a NAFLD activity score (NAS) ≥4 and fibrosis stage of F2 or F3 were randomized to treatment with 1,500 mg NCA, 1,000 mg NCA, or placebo once daily for 72 weeks. The primary endpoint was resolution of MASH with no worsening of fibrosis, or improvement of fibrosis with no worsening of MASH, from baseline visit to week 72. Secondary endpoints included components of the primary endpoint as well as change in NAS, change in the histologic Steatosis, Activity, and Fibrosis (SAF) score, changes in liver biochemistry, and safety outcomes.
Results: The trial enrolled 83, 70 and 63 patients in the 1,500 mg NCA, 1,000 mg NCA, and placebo arms, respectively. At week 72, 33.7% of patients in the 1,500 mg NCA arm, 20.0% in the 1,000 mg NCA arm, and 30.2% in the placebo arm achieved the primary endpoint (1,500 mg NCA vs placebo: p = 0.30, 1,000 mg NCA vs placebo: p = 0.92). Resolution of MASH with no worsening of fibrosis was observed in 27.7% of 1,500 mg NCA patients vs. 19.0% of placebo patients (p = 0.18), while improvement of fibrosis with no worsening of MASH was reported for 18.1% of 1,500 mg NCA patients vs. 20.6% of placebo patients. The absolute change in total NAS was −1.7 for 1,500 mg NCA vs. −0.9 for placebo (p = 0.005), with changes of −0.5 vs. − 0.1, respectively, in the inflammation subscore (p = 0.002). Improvement in the SAF inflammation subscore was also significantly greater with 1,500 mg NCA (−0.4 vs. −0.2, p = 0.02). NCA led to significantly higher rates of ALT normalization (1,500 mg NCA: 29.0%, placebo: 10.5%, p = 0.01) and significantly greater reduction in gamma-glutamyltransferase than placebo. The pooled rates of patients with adverse events were 92.8% for NCA and 87.3% with placebo, with serious adverse events reported for 15.7% of NCA patients and 9.5% of placebo patients.
Conclusion: NCA was not superior to placebo in the composite primary endpoint. Statistical superiority was observed in multiple histologic and biochemical parameters of inflammation. The known favorable safety profile of NCA was confirmed.

Viral hepatitis – Clinical aspects

OS-101-YI
Association between end-of-treatment biomarkers and HBV genotype in severe biochemical flares after nucleos(t)ide analogue cessation: results from five prospective studies within the PROSTOP consortium

Fleur Ballet[1,2], Arno Furquim d'Almeida[1,2], Marte Holmberg[3,4], Simon Hume[5,6], Anna Pocurull Aparicio[7], Magnus Lindh[8], Axelle Vanderlinden[1,2], Barbara Testoni[9], Fabien Zoulim[9], Benoit Kabamba[10], Veerle Matheeussen[11], Kumar Visvanathan[5,6], Dag Henrik Reikvam[4,12], Niel Hens[13,14], Sabela Lens[7], Alexander Thompson[5,6], Asgeir Johannessen[3,4,12], Thomas Vanwolleghem[1,2]. *[1]University of Antwerp, Viral Hepatitis Research Group, Laboratory of Experimental Medicine and Pediatrics, Antwerp, Belgium; [2]Antwerp University Hospital, Department of Gastroenterology and Hepatology, Edegem, Belgium; [3]Vestfold Hospital Trust, Department of Infectious Diseases, Tonsberg, Norway; [4]University of Oslo, Institute of Clinical Medicine, Faculty of Medicine, Oslo, Norway; [5]St Vincent's Hospital, Gastroenterology Department, Melbourne, Australia; [6]St Vincent's Hospital, Department of Infectious Disease and Immunology Research Centre, Melbourne, Australia; [7]University of Barcelona, Liver Unit, Hospital Clinic, FCRB-IDIBAPS, Barcelona, Spain; [8]University of Gothenburg, Department of Infectious Diseases, Sahlgrenska Academy, Gothenburg, Sweden; [9]Université Claude Bernard Lyon 1, Lyon Hepatology Institute, UMR Inserm U1350 PaThLiv, Lyon, France; [10]Clinique Universitaires Saint-Luc, Department of Microbiology, Brussels, Belgium; [11]Antwerp University Hospital, Laboratory of Medical Microbiology, Antwerp, Belgium; [12]Oslo University Hospital, Department of Infectious Diseases, Oslo, Norway; [13]University of Antwerp, Centre for Health Economics Research and Modelling of Infectious Diseases (CHERMID), Vaccine & Infectious Disease Institute (VAXINFECTIO), Antwerp, Belgium; [14]University of Hasselt, Data Science Institute, Interuniversity Institute for Biostatistics and statistical Bioinformatics (I-BioStat), Hasselt, Belgium*
Email: fleur.ballet@uantwerpen.be

Background and aims: Hepatitis B core-related antigen (HBcrAg), hepatitis B core IgG antibodies (anti-HBc) and HBV RNA are emerging biomarkers in chronic hepatitis B, and bear potential for predicting severe biochemical flares (SBFs; ALT >10xULN) after nucleos(t)ide analogue (NUC) cessation. Recently, hepatitis B virus (HBV) genotype (gt) A was identified as a protective factor against SBFs. We aimed to investigate the relationship between these biomarkers and HBV genotype to provide more insight into the mechanisms behind this effect and guide future treatment strategies.
Method: Individual patient-level data from five international prospective NUC-stop studies within the PROSTOP consortium were pooled. All patients were HBeAg negative, long-term virologically suppressed, and none had advanced liver fibrosis. Multivariate mixed linear and logistic regression models were used to assess associations between biomarkers and gt, with study included as a random effect. Models were adjusted for age, sex, and log-transformed HBsAg levels. HBcrAg and anti-HBc were analysed as continuous log-transformed variables while HBV RNA was analysed as undetectable versus detectable.
Results: A total of 343 patients with available gt (A: 58 (16.9%), B: 70 (20.4%), C: 59 (17.2%), D: 131 (38.2%), E: 23 (6.7%), F: 2 (0.6%)) were included. HBcrAg, anti-HBc and HBV RNA were available for 320, 338 and 153 patients, respectively. Combined HBcrAg and anti-HBc data were available for 296 patients, and all three biomarkers for 140 patients. Anti-HBc levels were significantly higher in gt A compared to C, D and E (log_{10} units difference 0.52, 0.45 and 0.64 respectively, all p < 0.001). Conversely, HBcrAg levels were significantly lower in gt A compared to B and C (log_{10} units difference −1.09 and −1.07 respectively, all p < 0.001). Compared with gt A, gt D was associated with lower odds of having detectable HBV RNA (OR 0.23, 95% CI 0.06–0.83, p = 0.03).
Conclusion: In this large, pooled analysis of five prospective NUC cessation studies, genotype A was significantly associated with higher anti-HBc and lower HBcrAg levels, both known protective factors for SBFs. This relation could partially explain the low number of post-cessation severe flares observed in patients with HBV gt A and provide mechanistic insight to inform biomarker-guided individualized NUC cessation strategies.

OS-102
Long term survival benefits of DAA in HCV related HCC patients: results from England National HCV registry

Maria Guerra Veloz[1], Rathiga Rudra[2], Simon Hume[3], Daniel Clayton-Chubb[3], Renita George[1], Sarah Selemani[1], Paul Ross[1], Janet Dearden[2], Aileen Marshall[3], Peter Sandwith[2], Matthew Foxton[4], Kosh Agarwal[1], Douglas Macdonald[3]. *[1]King's College Hospital, Institute of Liver Studies, London, United Kingdom; [2]Department of Hepatology, Barts Health NHS Trust, London, United Kingdom; [3]Royal Free Hospital, London, United Kingdom; [4]Chelsea & Westminster NHS Foundation Trust, London, United Kingdom*
Email: maria.guerraveloz@nhs.net

Background and aims: Patients with Hepatitis C virus (HCV) related hepatocellular carcinoma (HCC) have largely been excluded from European HCV National treatment registries and so the survival benefits in this cohort are unclear. Since 2015, NHS England has approved direct acting antiviral (DAA) therapies for all viraemic patients, including those with HCC. The aim of this study is to assess

the HCV care cascade and overall survival (OS) benefits in those with HCC.
Method: Patients with HCV related HCC from the National Hepatitis C registry in Greater London between 2015 and 2025 were included. Patients' data was cross referenced with their local multidisciplinary HCC team records. Two cohorts were compared (DAA therapy initiation vs non initiation).
Results: 343 patients with complete records were included. The majority were male (79%) with compensated cirrhosis (62.7%) and genotype 3 (45.5%). DAA therapies were started in 78.7% (270) and 88.5% (239) had an outcome reported. SVR was achieved in 88.7% (212/239) of patients. In those patients who started DAA therapies, the cancer stage distribution was BCLC 0/A 64.4%, B 16.7%, C 10% and D 4.4%, whereas in those who did not it was 45.7%, 5.7%, 18.6% and 30% respectively ($p < 0.005$). Almost 80% had untreated HCC at the time of DAA therapy initiation. The median OS was longer in patients who received DAA therapies (68 (95% IC 48–87) months)) in comparison with those who did not (15 (95% CI 7–23) months)) (Log Rank $p < 0.001$). Moreover, OS was longer in those with BCLC stage 0/A who achieved SVR (128 months; 95% CI 112–144) in comparison with those BCLC stage 0/A who did not receive DAA therapies (25 (95% CI 12–37) months)). The median OS for those with BCLC stage B/C who achieved SVR was 35 (95% IC 26–44) months in comparison with those who did not receive DAA therapies, which was 9 (95% IC 0–19) months. In the multivariate Cox regression model, [adjusted by sex, age, BCLC stage, liver function (ALBI grade)], non-DAA therapy initiation (HR 7; 95%CI 3.8–13, $p < 0.001$), non-SVR (HR 2.3, $p < 0.001$,) BCLC stage C/D (HR 1.43, $p < 0.001$) and non-curative cancer treatments (HR 1.95) were the risk factors associated with mortality.
Conclusion: In this cohort, more than two thirds of patients with HCV-related HCC initiated DAA therapies leading to a higher rate of SVR. DAA therapies along with SVR are associated with improvement in overall survival independent of BCLC stage and so treatment should be started in eligible patients.

OS-103-YI
Identifying individuals for hepatocellular carcinoma (HCC) surveillance after hepatitis B surface antigen (HBsAg) seroclearance: refining risk thresholds by age, sex, cirrhosis, diabetes and risk scores

Terry Cheuk-Fung Yip[1], Vincent Wai-Sun Wong[2], Mandy Sze-Man Lai[3], Jimmy Che-To Lai[1], Vicki Wing-Ki Hui[3], Lilian Liang[3], Yee-Kit Tse[2], Henry L.Y. Chan[4], Grace Lai-Hung Wong[2]. *[1]Medical Data Analytics Centre (MDAC), Department of Medicine and Therapeutics, The Chinese University of Hong Kong, Hong Kong, Institute of Digestive Disease, The Chinese University of Hong Kong, Hong Kong, Li Ka Shing Institute of Health Sciences, Faculty of Medicine, The Chinese University of Hong Kong, Hong Kong, Hong Kong; [2]Medical Data Analytics Centre (MDAC), Department of Medicine and Therapeutics, The Chinese University of Hong Kong, Hong Kong, Institute of Digestive Disease, The Chinese University of Hong Kong, Hong Kong, Hong Kong, Hong Kong; [3]Medical Data Analytics Centre (MDAC), Department of Medicine and Therapeutics, The Chinese University of Hong Kong, Hong Kong, Hong Kong; [4]Department of Internal Medicine, Union Hospital, Hong Kong, Medical Data Analytics Centre (MDAC), The Chinese University of Hong Kong, Hong Kong, Hong Kong*
Email: tcfyip@cuhk.edu.hk

Background and aims: Current European and American guidelines provide no specific HCC surveillance recommendations for patients with HBsAg loss, despite a lower HCC incidence than patients with chronic hepatitis B (CHB); target groups remain those with cirrhosis, men > 40 years, women > 50 years, and PAGE-B ≥ 10. We evaluated HCC risk after HBsAg loss by age, sex, cirrhosis, and diabetes, and evaluated PAGE-B and modified PAGE-B (mPAGE-B) scores.
Method: Using a territory-wide database in Hong Kong, we included adults with monoinfected CHB who cleared HBsAg from Jan 2000 to Dec 2020, followed until Mar 2025. Exclusions were liver transplantation or HCC before HBsAg loss and follow-up < 6 months. Annual HCC incidence was estimated with death as a competing risk. Subgroups potentially met surveillance threshold if the upper 95% CI of annual incidence was ≥ 0.2%. We calculated the 5-year integrated time-dependent area under the receiver operating characteristic curve (iAUC) for PAGE-B and mPAGE-B. Cirrhosis was defined by diagnosis codes, fibrosis-4 index > 3.25, and/or aspartate aminotransferase to platelet ratio index > 2.
Results: Of 9,733 patients included (mean age 57.4 ± 13.8 years, 40.0% female, 13.1% cirrhosis, 21.4% diabetes), 181 (1.9%) developed HCC at a median (IQR) follow-up of 9.2 (6.5–13.1) years. Annual HCC incidence was 0.47% (0.37%–0.58%) with cirrhosis and 0.11% (95% CI 0.09%–0.14%) without cirrhosis. In men without cirrhosis, the annual HCC incidence was 0.01% (95% CI 0.001%–0.08%) for HBsAg loss ≤ 40 years, 0.08% (0.03%–0.17%) for 41–50 years, and 0.18% (0.14%–0.23%) for > 50 years. In women without cirrhosis, the annual HCC incidence was 0.01% (95% CI 0.001%–0.04%) for HBsAg loss ≤ 50 years, 0.06% (0.02%–0.13%) for 51–60 years, and 0.13% (0.07%–0.23%) for > 60 years. In patients without cirrhosis, the 5-year iAUC was 0.749 (95% CI 0.695–0.801) for PAGE-B and 0.768 (0.716–0.814) for mPAGE-B. Annual HCC incidence was 0.17% (95% CI 0.13%–0.21%) for PAGE-B ≥ 12, and 0.17% (0.14%–0.22%) for mPAGE-B ≥ 11. In the absence of cirrhosis, the annual HCC incidence was 0.17% (95% CI 0.12%–0.25%) with diabetes and 0.09% (0.07%–0.12%) without diabetes.
Conclusion: Patients with HBsAg loss who have cirrhosis warrant HCC surveillance. When cirrhosis is absent, thresholds are met by men > 50 years and women > 60 years at HBsAg loss, and by those with diabetes. PAGE-B and mPAGE-B accurately stratify HCC risk; cut-offs after HBsAg loss should be higher than those used in CHB.

OS-104
Rolling FIB-4 as a dynamic predictor of liver disease progression in HCV patients: insights from the french HEPATHER cohort

Lucia Parlati[1], Clovis Lusivka-Nzinga[2], Marc Bourliere[3], Fabrice Carrat[2], Pierre Nahon[4], Vincent Mallet[1,5]. *[1]Cochin Hospital, Hepatology Departement, Paris, France; [2]Sorbonne Université, Inserm, iPLesp, Paris, France, Paris, France; [3]Hopital Saint Joseph, Marseille, France; [4]Hôpital Avicenne, Bobigny, France; [5]AP-HP, Paris, France*
Email: lucia.parlati@aphp.fr

Background and aims: Single FIB-4 measurements may inadequately capture liver-related risk. Rolling FIB-4, defined as the cumulative area under consecutive FIB-4 measurements anchored to baseline, reflects longitudinal hepatic risk. We assessed its ability to predict 5-year liver disease progression in adults with hepatitis C (HCV).
Method: Patients with HCV enrolled in the prospective French ANRS CO22 HEPATHER cohort (2006–2015) were analyzed. Liver disease progression was defined as hepatocellular carcinoma (HCC) or decompensated cirrhosis, with death or liver transplantation treated as competing events. Fine–Gray competing-risk models estimated 5-year cumulative incidence. The cohort was split into training (2/3) and independent test (1/3) sets. Predictive performance of baseline FIB-4, rolling FIB-4, and their combination was evaluated. Discrimination was assessed using ROC curves at a fixed 5-year horizon, with AUC comparisons by the DeLong test. Calibration was assessed on the test set and corrected using logistic recalibration.
Results: Among 8,436 patients, 52% were men and the median age was 56 years (Q1–Q3: 50–64), 34% had cirrhosis. Overall, 93.6% received direct-acting antivirals, of whom 95.6% achieved SVR. Over a median follow-up of 5.96 years (IQR: 4.20–7.67), 353 patients (4.2%) experienced liver disease progression, 438 (5.2%) experienced a competing event, and 7,645 (90.6%) were censored. Baseline FIB-4 and rolling FIB-4 showed good discrimination for 5-year progression (AUC = 82.3% [79.8–84.8] and 83.7% [81.2–86.2], respectively). In multivariable Fine–Gray models including both indices, rolling FIB-4 remained independently associated with progression ($p < 0.0001$), whereas baseline FIB-4 was no longer significant ($p = 0.44$). Adding

rolling FIB-4 to a clinically adjusted Fine–Gray competing-risk model significantly improved 5-year risk prediction compared with baseline FIB-4 alone (ΔAUC = 0.0378; p = 0.006), achieving excellent predictive performance (AUC ≈ 0.90). Direct comparison of multivariable models confirmed a significant gain with rolling FIB-4 (ΔAUC = 0.0259; p < 0.0001). Recalibration improved agreement between predicted and observed risks without altering discrimination (AUC = 0.902).
Conclusion: Rolling FIB-4 improves 5-year prediction of liver disease progression beyond baseline FIB-4 in HCV patients, providing dominant prognostic information when integrated into clinically adjusted competing-risk models, with robust discrimination and calibration after validation.

OS-105-YI
Acute hepatitis E in ACLF is associated with higher organ-failure burden and delayed recovery, but not independent mortality risk
Hao Xing Lai[1], Sabrina Xin Zi Quek[2], Liang Shen[1], Seng Gee Lim[2], Mark Muthiah[2], Ashok Kumar Choudhury[3], Shahinul Alam[4], Sanjiv Saigal[5], Dong Joon Kim[6], CE Eapen[7], Ashish Goel[7], Qin Ning[8], Harshad Devarbhavi[9], Virendra Singh[10], Akash Shukla[11], Saeed Sadiq Hamid[12], Jinhua Hu[13], Soek-Siam Tan[14], Anil Arora[15], Manoj Kumar Sharma[3], Mohamed Rela[16], Dinesh Jothimani[17], Nagaraja Rao Padaki[18], Anand Kulkarni[18], Hasmik Ghazinyan[19], Zhongping Duan[20], Ajit Sood[21], Omesh Goyal[21], Laurentius A. Lesmana[22], Rinaldi Lesmana[23], Sombat Treeprasertsuk[24], Yuemin Nan[25], Samir Shah[26], Tao Chen[27], V.M. Dayal[28], Shaojie Xin[29], Fazal Karim[30], Zaigham Abbas[31], Jose Sollano[32], Kemal Fariz Kalista[33], Ananta Shrestha[34], Diana Payawal[35], Masao Omata[36], Shiv Kumar Sarin[3], Guan Huei Lee[2].
[1]National University of Singapore Yong Loo Lin School of Medicine, Singapore, Singapore; [2]National University Hospital System, Singapore, Singapore; [3]Institute of Liver and Biliary Sciences, New Delhi, India; [4]Bangabandhu Sheikh Mujib Medical University, Dhaka, Bangladesh; [5]Max Super Specialty Hospital, New Delhi, India; [6]Hallym University College of Medicine, Chuncheon, Korea, Rep. of South; [7]Christian Medical College Vellore, Vellore, India; [8]Tongji Hospital of Tongji Medical College, Huazhong University of Science and Technology, Wuhan, China; [9]St John's Medical College, Bangalore, India; [10]Postgraduate Institute of Medical Education and Research, Chandigarh, India; [11]Seth GS Medical College and KEM Hospital, Mumbai, India; [12]Aga Khan University Hospital, Karachi, Pakistan; [13]302 Military Hospital, Beijing, China; [14]Selayang Hospital, Selayang, Malaysia; [15]Sri Ganga Ram Hospital, New Delhi, India; [16]Dr. Rela Institute and Medical Centre, Chennai, India; [17]Dr. Rela Institute & Medical Centre, Chennai, India; [18]Asian Institute of Gastroenterology Hyderabad, Hyderabad, India; [19]Nork Clinical Hospital of Infectious Disease, Yerevan, Armenia; [20]Beijing Youan Hospital, Capital Medical University, Beijing, China; [21]Dayanand Medical College, Ludhiana, India; [22]Digestive Disease & Oncology Centers, Medistra Hospital, Jakarta, Indonesia; [23]RSCM, Jakarta, Indonesia; [24]Chulalongkorn University, Bangkok, Thailand; [25]Hebei Medical University, Shijiazhuang, China; [26]Global Hospital, Mumbai, India; [27]Tianjin Institute of Hepatobiliary Disease, Tianjin, China; [28]IGIMS, Patna, India; [29]Beijing 302 Hospital, Beijing, China; [30]Sir Salimullah Medical College Mitford Hospital, Dhaka, Bangladesh; [31]Ziauddin University, Karachi, Pakistan; [32]University of Santo Tomas, Manila, Philippines; [33]Cipto Mangunkusumo General Hospital, Jakarta, Indonesia; [34]Alka Hospital, Lalitpur, Nepal; [35]Fatima University Medical Center, Manila, Philippines; [36]University of Tokyo, Tokyo, Japan
Email: mdcleegh@nus.edu.sg

Background and aims: Hepatitis E virus (HEV) is a leading cause of acute viral hepatitis, but its prognostic impact in acute-on-chronic liver failure (ACLF) is unclear. We evaluated organ-failure trajectories and survival in ACLF patients with acute HEV infection within the APASL ACLF Research Consortium (AARC).
Method: We analysed 5,612 prospectively enrolled ACLF admissions from 25 countries (2004–2021). Acute HEV was defined by HEV IgM positivity. Organ failures (day 0/4/7) and survival were compared between HEV and non-HEV; multivariable Cox regression was performed in patients with complete covariate data.
Results: Acute HEV was present in 340/5,612 patients (6.1%). At admission, HEV patients had higher platelet counts, higher bilirubin levels, and lower albumin levels (all p < 0.05). HEV was associated with a higher organ-failure burden at presentation: any organ failure (95.0% vs 91.7%; p = 0.032), ≥3 organ failures (41.2% vs 31.7%; p < 0.001), and renal failure (37.4% vs 29.2%; p = 0.001). Among those with day-4 assessments, persistent organ failure remained higher (87.6% vs 77.7%, p < 0.001), and organ-failure distribution was worse (p < 0.001). By day 7, liver failure (66.0% vs 58.2%, p = 0.028), renal failure (21.4% vs 16.1%, p = 0.046), and ≥3 organ failures (24.3% vs 14.6%, p < 0.001) remained higher. Kaplan–Meier survival was worse (median 12 vs 18 days; log-rank p < 0.001), but HEV was not independently associated with mortality in Cox regression (n = 3,409; HR 1.09, 95% CI 0.93–1.28; p = 0.299). Fewer HEV patients received liver transplantations (2.9% vs. 5.7%), and among those who did, 90 day survival rates were significantly lower compared to non-HEV transplant recipients (0% vs 5.5%, p = 0.003).
Conclusion: Acute HEV-associated ACLF is characterised by greater renal and multi-organ failure and delayed early recovery with poorer unadjusted survival; however, HEV is not an independent mortality determinant after adjustment, suggesting baseline organ-failure burden largely explains the excess risk.

EASL Clinical Practice Guidelines on management of primary biliary cholangitis and PBC abstracts

OS-106
Safety and efficacy of pemafibrate (K-808), a selective peroxisome proliferator-activated receptor alpha modulator, in patients with primary biliary cholangitis: twelve-week data from the randomized, placebo-controlled, PEMA-PBC dose-finding study
Gideon M. Hirschfield[1], Kris V. Kowdley[2], Marco Carbone[3], David E. Jones[4], Albert Parés[5], Cynthia Levy[6], Shinji Shimoda[7], Andrey Belous[8], Ryohei Tanigawa[9], Hideki Suganami[9], Atsushi Tanaka[10]. *[1]The Autoimmune and Rare Liver Disease Programme, Toronto General Hospital, Toronto, Canada; [2]Washington State University, Liver Institute Northwest, Velocity Clinical Research, Seattle, United States; [3]University of Milano-Bicocca, Milan, Italy; [4]Newcastle University, Clinical and Translational Research Institute, Newcastle, United Kingdom; [5]University of Barcelona, Hospital Clinic, Barcelona, Spain; [6]University of Miami, Milan, United States; [7]Kansai Medical University, Osaka, Japan; [8]Kowa Pharma Development, Boston, United States; [9]Kowa Company, Tokyo, Japan; [10]Teikyo University, Tokyo, Japan*
Email: gideon.hirschfield@uhn.ca

Background and aims: Treatment goals for patients living with primary biliary cholangitis (PBC) include improving alkaline phosphatase levels (ALP), with normalization increasingly recognized as the ideal response to therapy. We report 12-week data from the Phase 2, double-blind, randomized, placebo-controlled, multicenter trial of extended-release pemafibrate (K-808), a highly selective peroxisome proliferator-activated receptor (PPAR) alpha modulator, in patients with inadequate response or intolerance to ursodeoxycholic acid (UDCA); NCT06247735.
Method: Eligible non-cirrhotic patients with ALP >1.5× upper limit of normal (ULN, 116 U/L) after at least 1 year of treatment with, or intolerance to, UDCA were randomized to receive either K-808 0.2 mg/day, 0.4 mg/day or placebo for 12 weeks, followed by a 52-week extension. The primary endpoint was percentage change from baseline in ALP. The key secondary endpoint was ALP normalization.

Additional endpoints included achievement of POISE criteria (ALP <1.67× ULN, with a reduction from baseline ≥ 15%, and total bilirubin ≤1× ULN), patient-reported outcomes with PBC-40, 5-D Pruritus Scale, Pruritus and Fatigue Numerical Rating Scale (NRS). Safety endpoints included adverse events (AEs).
Results: In total, 46 patients were randomized, with 15, 15 and 16 receiving K-808 0.2 mg, 0.4 mg and placebo, respectively. Mean (SD) age was 60.0 (12.3) years; 80.4% were female; 52.2% were from North America and 47.8% from Japan; BMI was 26.7 (7.5) kg/m^2. Baseline ALP levels were 216.5 (49.8), 263.8 (124.9) and 271.5 (172.4) U/L, and 1, 3 and 2 patients had ALP >3× ULN in K-808 0.2 mg, 0.4 mg and placebo groups, respectively. At week 12, least-squares mean changes in ALP were −47.7%, −48.5% and −1.3%; ALP normalized in 66.7%, 60.0% and 0% of patients. In the subpopulation with baseline ALP >1.67× ULN (n = 32), ALP normalized in 44.4%, 60.0% and 0%, and POISE criteria were achieved in 88.9%, 70.0% and 0%. There were numerically greater improvements in endpoints of fatigue and pruritus with K-808. No serious AEs or safety concerns were identified during the 12-week treatment period.
Conclusion: In patients with PBC who have insufficient response or intolerance to UDCA, addition of pemafibrate (K-808), a highly selective PPAR alpha modulator, for 12 weeks, led to clinically meaningful, and statistically significant, biochemical improvements in ALP, including normalization in ≥60% of participants. There were no safety concerns.

OS-107

Linafexor in UDCA-inadequate PBC: a phase 2 trial of a pulsatile FXR agonist

Xiao Xiao[1], Hong You[2], Jia Shang[3], Youwen Tan[4], Li Yang[5], Hongliang He[6], Sujun Zheng[7], Kai Wang[8], Junqi Niu[9], Qian Cao[10], Tingbo Liang[11], Shi Ouyang[12], Min Zhang[13], Rong Lin[14], Bingliang Lin[15], Wen Zhang[16], Aiming Yang[16], Min Lian[17], Weituo Zhang[18], Xiangwei Hua[19], Rong Deng[19], Gaihong Wang[19], Hualing Pan[19], Julia Yang[19], Zhenwei Zhang[19], Peter Wang[19], H. Eric Xu[19], Xiong Ma[1]. *[1]Renji Hospital, Shanghai Jiaotong University School of Medicine, Shanghai, China; [2]Beijing Friendship Hospital, Capital Medical University, Beijing, China; [3]Henan Provincial People's Hospital, Henan, China; [4]The Third People's Hospital of Zhenjiang, Zhenjiang, China; [5]West China Hospital, Chengdu, China; [6]Anhui Provincial Hospital, Hefei, China; [7]Beijing Youan Hospital, Beijing, China; [8]Qilu Hospital of Shandong University, Jinan, China; [9]The First Hospital of Jilin University, Jilin, China; [10]Sir Run Run Shaw Hospital, Hang Zhou, China; [11]The First Affiliated Hospital, Hangzhou, China; [12]The Fifth Affiliated Hospital of Guangzhou Medical University, Guangzhou, China; [13]The Second Xiangya Hospital of Central South University, Changsha, China; [14]Union Hospital, Tongji Medical College of Huazhong University of Science and Technology, Wuhan, China; [15]The Third Affiliated Hospital, Sun Yat-Sen University, Guangzhou, China; [16]Peking Union Medical College Hospital, Beijing, China; [17]Renji Hospital, Shanghai Jiao Tong University School of Medicine, Shanghai, China; [18]Clinical Research Institute, Shanghai Jiao Tong University School of Medicine, Shanghai, China; [19]Cascade Pharmaceuticals, Inc, Shanghai, China*
Email: maxiongmd@hotmail.com

Background and aims: Up to 40% of patients with primary biliary cholangitis (PBC) have an inadequate response to ursodeoxycholic acid (UDCA), highlighting an unmet medical need. Linafexor is a novel pulsatile farnesoid X receptor (FXR) agonist with an ultra-short half-life (approximately 1 hour), designed to deliver choleretic and anti-inflammatory effects while minimizing the toxicity associated with continuous FXR occupancy. We evaluated the efficacy and safety of linafexor in patients with PBC and an inadequate response to UDCA.
Method: In this multicenter, double-blind, phase 2 trial, patients with PBC and an inadequate response to UDCA (alkaline phosphatase [ALP] >1.67× upper limit of normal [ULN] after ≥6 months of UDCA) or UDCA intolerance were randomized 1:1:1 to linafexor 2 mg, linafexor 4 mg, or placebo once daily for 12 weeks, followed by a 40-week open-label extension (OLE). The primary endpoint was percent change in ALP from baseline to week 12. Secondary endpoints included composite biochemical response (ALP <1.67×ULN, ≥15% ALP reduction, and normal total bilirubin), changes in other liver biochemistries, and safety.
Results: Among 74 randomized patients, the mean percent change in ALP from baseline to week 12 was −18.1% (95% CI, −28.1 to −8.1) with linafexor 2 mg and −20.6% (95% CI, −30.9 to −10.4) with linafexor 4 mg, compared with +5.6% (95% CI, −3.9 to 15.2) with placebo (P < 0.001 for both comparisons). Composite biochemical response was achieved in 20.8% (2 mg), 33.3% (4 mg), and 3.8% (placebo). Significant reductions were also observed in gamma-glutamyl transferase, aminotransferases, and immunoglobulin M levels. Improvements in biochemical markers were sustained throughout the OLE, and placebo crossover participants exhibited significant improvements upon initiating linafexor. Cumulative composite response rates reached 39.6% (original linafexor) and 30.8% (crossover). During the double-blind phase, pruritus was the most common treatment-related adverse event; nearly all cases were mild to moderate (only one Grade 3 CTCAE event). Throughout the study period, no new safety signals emerged during the OLE, and no cases of drug-induced liver injury (DILI) were reported.
Conclusion: Linafexor, a novel pulsatile FXR agonist, demonstrated significant and durable improvements in biochemical markers with a manageable safety profile in patients with PBC. Based on these phase 2 findings, phase 3 clinical trials are now underway.

EASL | JOURNAL OF HEPATOLOGY

Late-breaker Posters

LBP-001

Primary care liver fibrosis detection pathway in people with type 2 diabetes: results from the PRELUDE1 prospective, pragmatic, electronic health record-embedded, parallel-arm cohort study

Kushala Abeysekera[1], Michael James[2], Stuart Rison[3], Huei-Tyng (Philippe) Huang[2], John Moore[4], Ann Archer[1], Gillian Hood[2], Imogen Salisbury[2], Matthew Hickman[1], James Brindley[2], William Alazawi[2]. *[1]Bristol University, Bristol, United Kingdom; [2]Barts Liver Centre, Blizard Institute, Queen Mary University of London, London, United Kingdom; [3]Wolfson Institute of Population Health, Queen Mary University of London, London, United Kingdom; [4]Charlotte Keel Medical Practice, Bristol, United Kingdom*
Email: w.alazawi@qmul.ac.uk

Background and aims: People with type 2 diabetes mellitus (T2DM) are at increased risk of steatotic liver disease. Guidelines recommend calculated scores (e.g. Fib-4) followed by second-tier (e.g. vibration controlled transient elastography (VCTE)) to risk-stratify patients, inform specialist referral and treatment eligibility. Adoption of these guidelines in primary care practices (PCPs) remains low (~5%). PRELUDE1 was a large, prospective pragmatic, electronic health record (EHR)-embedded parallel-arm cohort study in UK PCPs. We assessed adding Fib-4 to T2DM annual reviews followed by VCTE in community versus hospital settings.
Method: Ten PCPs (in London and Bristol) were included and allocated at start of study to community or hospital scanning arms. Fib-4 was included by requesting a specific T2DM annual review set or adding a Fib-4 order set to routine bloods. People with Fib-4≥1.3 were referred for VCTE (LSM≥8.0 referred to specialist care). Clinical, demographic and laboratory data were extracted from EHR.
Results: Total study population (n = 8705) was balanced across community (n = 4599) and hospital (n = 4106) arms with no clinically-meaningful differences in demographic or metabolic parameters. Mean age was 61 years, 55% male, 41% South Asian ethnicity and 67% in the two most-deprived national quintiles. At baseline, 294 (3.4%) people had Fib-4 scores which increased to 2999 (34.3%) by study-end (community 32.3%; hospital 36.8%) of whom 1115 (37.2%) had Fib-4≥1.3. Significantly more patients attended VCTE in community than hospital settings (78.3% vs 71.7%, p = 0.007), driven by differences in London PCPs: 81.6% in community, 56.9% in hospital (p < 0.001), but not between cities themselves. Of all scans performed, 25.5% (n = 168) had LSM≥8.0 and 15.5% (n = 102) LSM≥10 with no statistically significant differences between settings or cities. Increasing Fib-4 threshold to 2.0 for VCTE referral in people aged >65 would have reduced referrals by 45.5% to n = 608, increased rates of LSM≥8.0 and LSM≥10 to 31.0% and 20.0% respectively but not identified 32.3% (n = 55) of all people with LSM≥8.0 kPa, over half of whom had LSM≥10 kPa.
Conclusion: In this EHR-embedded pragmatic study conducted in socioeconomically diverse populations, adding Fib-4 testing to T2DM annual reviews markedly increased availability of scores from baseline. Patient attrition through second-tier testing was more pronounced in hospital-referring PCPs. Fibrosis testing in T2DM is feasible and should be tailored to local population needs. ISRCTN14585543.

LBP-004-YI

Real-world validation of elafibranor in UDCA non-responders previously treated with OCA or fibrates — results from the ELEVATE-PBC study

Alessandra Bonfichi[1], Elisa Merelli[1], Alessio Gerussi[1], Laura Cristoferi[1], Eugenia Nofit[1], Maria Pia Calabrese[2], Stefano Fagiuoli[3], Andrea Mega[4], Federica Malinverno[1], Daphne D'Amato[1], Sara Labanca[5], Erica Nicola Lynch[6], Armando Curto[6], Fabrizio Bronte[7], Salvatore Fortunato Tantillo[7], Antonino Castellaneta[8], Filomena Morisco[9], Federica Cerini[10], Caparra Francesca[10], Raffaella Viganò[11], Marina Clemente[11], Ester Vanni[12], Maurizio Russello[13], Mariarita Cannavò[13], Caterina Cusumano[14], Clara Agnolon[14], Domenico Alvaro[15], Domenico Montecalvo[15], Vincenzo Cardinale[15], Silvia Nardelli[15], Francesca Terracciani[16], Antonio De Vincentis[16], Pietro Lampertico[17], Valeria Pace Palitti[18], Lucia Napoli[19], Maria Teresa Migliano[19], Alessandro Federico[20], Fiammetta Di Nardo[20], Fabio Marra[21], Marcello Persico[22], Tommaso Sarcina[22], Giovanni Raimondo[23], Saveria Lory Croce'[24], Lisa Fusaro[24], Mariaconsiglia Bragazzi[25], Federico Cotti[25], Grazia Anna Niro[26], Chiara Lillo[26], Chiara Ricci[27], Paolo Poisa[27], Francesco Losito[28], Teresa Zolfino[29], Chiara Scudu[29], Francesco Azzaroli[30], Elton Dajti[30], Maurizia Brunetto[31], Francesca Romana Ponziani[32], Cristina Rigamonti[33], Carla De Benedittis[33], Gabriele Missale[34], Pietro Andreone[35], Luchino Chessa[36], Alessandra Deidda[36], Natalia Terreni[37], Francesco Bellanti[38], Ilaria Cavalli[39], Francesca Toffolon[39], Alessandro Granito[40], Dante Pio Pallotta[40], Alessandra Mangia[41], Mariagrazia Marulli[41], Nora Cazzagon[42], Vincenza Calvaruso[43], Davide Salvioni[44], Marco Marzioni[45], Umberto Vespasiani-Gentilucci[16], Edoardo Giovanni Giannini[5], Mauro Viganò[3], Pietro Invernizzi[1], Ana Lleo[46], Marco Carbone[47]. *[1]Division of Gastroenterology and Center of Autoimmune Liver Diseases, San Gerardo Hospital, University of Milano Bicocca, Monza, Italy; [2]Department of Biomedical Sciences, Division of Internal Medicine and Hepatology, Department of Gastroenterology, Humanitas Clinical and Research Center IRCCS Rozzano, Italy, Milan, Italy; [3]Gastroenterology Hepatology and Transplantation Unit, ASST Papa Giovanni XXIII, Bergamo, Italy; [4]Gastroenterology Unit, Ospedale Generale Regionale di Bolzano, Bolzano, Italy; [5]Gastroenterology Unit, Department of Internal Medicine, University of Genoa, Genoa, Italy; [6]Gastroenterology Research Unit, Department of Experimental and Clinical Biomedical Sciences "Mario Serio," University of Florence, Florence, Italy; [7]Gastroenterology Unit, Department of Medicine, Ospedali Riuniti Villa Sofia-, V. Cervello, Palermo, Italy; [8]Section of Gastroenterology, Department of Precision and Regenerative Medicine and Ionian Area, University of Bari, Bari, Italy; [9]Gastroenterology Unit, Department of Clinical Medicine and Surgery, Federico II University of Naples, Naples, Italy; [10]Hepatology Unit, San Giuseppe Hospital, Milan, Italy; [11]Hepatology and Gastroenterology Unit, ASST GOM Niguarda, Milan, Italy; [12]Gastroenterology Unit, Città della Salute e della Scienza University Hospital, Turin, Italy; [13]Liver Unit of ARNAS Garibaldi-Nesima, Catania, Italy; [14]Department of Gastroenterology, Verona University Hospital, Verona, Italy; [15]Department of Medicine and Medical Specialties, Sapienza University*

 © 2026 All rights reserved.

ELSEVIER

of Rome, Rome, Italy; [16]Department of Hepatology, University Campus Bio-Medico, Rome, Italy; [17]CRC "A. M. and A. Migliavacca" Center for the Study of Liver Disease, Division of Gastroenterology and Hepatology, Fondazione IRCCS Cà Granda Ospedale Maggiore Policlinico, University of Milan, Milan, Italy; [18]Internal Medicine Unit, Santo Spirito Hospital, Pescara, Italy; [19]Department of Internal Medicine, AUSL Romagna, Faenza, Italy; [20]Department of Clinical and Experimental Internal Medicine, University of Campania Luigi Vanvitelli, Naples, Italy; [21]Dipartimento di Medicina Sperimentale e Clinica, University of Florence, Florence, Italy; [22]Department of Medicine and Surgery, "Scuola Medica Salernitana," Internal Medicine and Hepatology Unit, University of Salerno, Salerno, Italy; [23]Department of Human Pathology, University Hospital of Messina, Messina, Italy; [24]Department of Medicine, Surgery and Health Sciences, University of Trieste, Trieste, Italy; [25]Department of Medical and Surgical Sciences and Biotechnologies, Sapienza University, Rome, Italy; [26]Gastroenterology Unit, Fondazione IRCCS "Casa Sollievo Sofferenza," San Giovanni Rotondo, Foggia, Italy; [27]Gastroenterology Unit, Department of Clinical and Experimental Sciences, University of Brescia and Spedali Civili, Brescia, Italy; [28]Gastroenterology Unit, National Institute of Gastroenterology, IRCCS "S de Bellis" Research Hospital, Castellana Grotte, Bari, Italy; [29]Gastroenterology Unit, ARNAS Brotzu, Cagliari, Italy; [30]Department of Medical and Surgical Sciences, University of Bologna, Bologna, Italy; [31]Department of Clinical and Experimental Medicine, University of Pisa, Pisa, Italy; [32]Division of Internal Medicine, Gastroenterology-Hepatology Unit, Fondazione Policlinico Universitario Agostino Gemelli, Rome, Italy; [33]Department of Internal Medicine, Università del Piemonte Orientale, Novara, Italy; [34]Department of Medicine and Surgery, Unit of Infectious Diseases and Hepatology, University of Parma, Parma, Italy; [35]Division of Internal Medicine, Department of Medical and Surgical Sciences, Maternal-Infantile and Adult, University of Modena and Reggio Emilia, Modena, Italy; [36]Department of Medical Sciences and Public Health, University of Cagliari, Cagliari, Italy; [37]Hepatology Unit, Valduce Hospital, Como, Italy; [38]Department of Medical and Surgical Sciences, University of Foggia, Foggia, Italy; [39]Division of Internal Medicine, Cremona Hospital, Cremona, Italy; [40]Department of Medical and Surgical Sciences, University of Bologna, Sant' Orsola-Malpighi Hospital, Bologna, Italy; [41]Liver Unit, Fondazione IRCCS "Casa Sollievo della Sofferenza," San Giovanni Rotondo, Foggia, Italy; [42]Department of Surgery, Oncology and Gastroenterology -, University of Padova, Padova, Italy; [43]Gastroenterology and Hepatology Unit, Department of Health Promotion Sciences Maternal and Infantile Care, Internal Medicine and Medical Specialities, University of Palermo, Palermo, Italy; [44]Amaf (Associazione malattie autoimmuni del fegato), Monza, Italy; [45]Clinic of Gastroenterology and Hepatology, Università Politecnica delle Marche, Ancona, Italy; [46]Department of Biomedical Sciences, Division of Internal Medicine and Hepatology, Department of Gastroenterology, Humanitas Clinical and Research Center IRCCS, Rozzano, Italy; [47]Department of Hepatology and Gastroenterology, ASST Grande Ospedale Metropolitano Niguarda, Milan, Italy
Email: alessandra.bonfichi@gmail.com

Background and aims: Ursodeoxycholic acid (UDCA) represents the first-line therapy in patients with Primary Biliary Cholangitis (PBC), although up to 40% of patients respond inadequately. Elafibranor, a PPAR agonist, is an emerging alternative that reduces ALP with a favourable safety profile. The ELEVATE-PBC study evaluated real-world efficacy and safety of elafibranor in patients with inadequate response or intolerance to prior therapy or naïve to other second-line therapies.
Method: In this multicentre study, we included adult patients from the *Italian PBC Registry* treated with elafibranor since October 2024. Biochemical response (BR) was defined as ALP <1.67×ULN with normal bilirubin; complete BR as normal ALP and bilirubin. Longitudinal data at baseline, 3- and 6-month after elafibranor initiation were analysed descriptively and reported as median and interquartile range (IQR) for continuous variables and proportions for categorical variables.
Results: We included 281 patients, predominantly females (n = 244, 86.8%), with a median age of 61 years (IQR 54–67). The median disease duration was 8.9 years. Cirrhosis was present in 77 patients (27.4%). Autoimmune hepatitis overlap was present in 20 patients (7.1%). Median liver stiffness (LS) was 7.2 kPa. Prior fibrate use was reported in 80 (28.5%) patients, whereas 193 (68.7%) were on obeticholic acid. Median washout intervals from the last obeticholic acid and fibrate courses to elafibranor initiation were 7.5 (3.7–10.3) and 0.11 (0.0–9.5) months, respectively. 71 patients (25.3%) were on statins. Median baseline values of ALP were 1.72×ULN, total bilirubin 0.67 mg/dl and ALT 0.9×ULN. At baseline, 131 patients (47%) presented BR and 24 (8.6%) complete BR. Follow-up data were available for 78 patients at 3-month and 39 patients at 6-month. At 3-month, BR was reached by 64 patients (84.2%) and complete BR by 40 patients (41.0%), while at 6-month these endpoints were achieved by 32 (82.1%) and 16 (41%) patients, respectively. No increase in serum creatinine values or total bilirubin were observed at 6-month. Responses were similar regardless of prior second-line therapies. Treatment was discontinued in 15 patients, mainly due to gastro-intestinal intolerance (7 cases; 46.6%). Longer follow-up data will be available at the time of presentation.
Conclusion: Preliminary real-world data from the ELEVATE-PBC study confirm trial findings — elafibranor is effective and safe in a large cohort of UDCA non-responsive patients previously treated with OCA or fibrates.

LBP-005
Treatment of hepatitis C in pregnancy with Sofosbuvir/Velpatasvir: interim results from the STORC study

Catherine Chappell[1], Jasmin Charles[2], Marcela Smid[2], Kara Rood[3], Tatyana Kushner[4], Mia Biondi[5], Jordan J. Feld[6], Mark Yudin[7], Genevieve Eastabrook[8], Sarah Osmundson[9], Todd Davies[10], John Cafardi[11], Leslie Meyn[1], Stacey Scherbakovsky[12], Kyung Min Kwon[12], Cathleen Letterio[12], Sharon Hillier[1]. *[1]University of Pittsburgh, Pittsburgh, United States; [2]University of Utah Health, Salt Lake City, United States; [3]The Ohio State University, Columbus, United States; [4]Weill Cornell Medical College, New York, United States; [5]York University, Toronto, Canada; [6]University Health Network, Toronto, Canada; [7]Unity Health Toronto, Toronto, Canada; [8]London Health Sciences Centre, London, Canada; [9]Vanderbilt University, Nashville, United States; [10]Marshall University, Huntington, United States; [11]University of Cincinnati, Cincinnati, United States; [12]Gilead Sciences, Foster City, United States*
Email: chappellca@upmc.edu

Background and aims: Pregnancy presents a key opportunity to treat hepatitis C virus (HCV) infection, improving maternal outcomes and reducing perinatal transmission. However, safety data for direct-acting antivirals in pregnancy remain limited. The STORC study is an international, multi-center study evaluating sofosbuvir/velpatasvir (SOF/VEL) in pregnant people with HCV.
Method: In this open-label, single-arm study, pregnant people with HCV infection were enrolled between 20 and 30 weeks' gestation and treated with a 12-week course of SOF/VEL. HCV RNA testing was performed at screening, enrollment, delivery and 12 weeks after SOF/VEL completion (SVR12). The primary outcomes were gestational age at delivery and SVR12. Infants were followed for 12 months.
Results: Between July 2022 and March 2026, 100 pregnant people with HCV were screened and 83 enrolled. Participants had a median age of 33 (range 18–44). 79 (95.2%) participants had FIB-4 scores <1.45; 4 (4.8%) had scores 1.45 to <3.25, including two with elevated AST/ALT and two with low platelets. None of the participants had decompensated cirrhosis. At enrollment, participants had a median HCV RNA of 4.59 (range 2.61, 6.18) log copies/mL. Three participants discontinued treatment after one dose due to vomiting (n = 2) and declining further treatment (n = 1). After initiation of SOF/VEL, 51/52 (98.0%) had an undetectable HCV RNA at time of delivery. To date, 61 participants have completed the SVR12 visit and of those 59 (96.7%)

were cured. Of the two participants with treatment failure, one missed 20 doses and had HCV re-exposure via her sexual partner and the other missed 28 doses and had HCV re-exposure due to return to injection drug use. Among 52 participants with HCV RNA results at delivery, 12 were within the SVR4 window; 11 (91.7%) had concordant SVR12 results, and the discordant case was treatment failure with HCV re-exposure. Of the 73 participants who have delivered, median gestational age was 38+5 weeks (range 30+1, 42+0), 8 (10.9%) had preterm delivery at less than 37 weeks, and none had cholestasis of pregnancy. All adverse events related to SOF/VEL were less than grade 2, except one participant had grade 3 nausea. Of 59 infants tested for HCV RNA, all were undetectable within 2–12 months of age.
Conclusion: Interim STORC data support the safety of SOF/VEL after 20 weeks' gestation, with high HCV cure rates and possible prevention of cholestasis and perinatal HCV transmission.

LBP-007
Comparative study of the efficacy and safety of systemic glucocorticosteroids on liver enzyme activity in patients with autoimmune hepatitis without liver cirrhosis
Volodymyr Cherniavskyi[1], Leonid Pavlovskyi[1], Liudmyla Onyshchuk[1].
[1]*Bogomolets National Medical University, Kyiv, Ukraine*
Email: onishluda@gmail.com

Background and aims: Autoimmune hepatitis (AH) is a chronic progressive disease that leads to the early development of liver fibrosis and cirrhosis. To prevent these complications, timely appointment of effective and safe treatment is necessary. The key drugs in the treatment of AH remain glucocorticosteroids. However, whether they are all equally effective and safe remains a subject of discussion and the interest of this work.
Aim: To compare the effects of methylprednisolone, prednisolone, and budesonide on reducing liver enzyme activity in patients with AH without liver cirrhosis.
Method: We conducted a prospective randomized cohort study of 70 patients with AH. All patients were equally divided into three groups. Patients in the first group received methylprednisolone 24 mg per day. Patients in the second group received prednisolone 30 mg per day. The third group of patients received budesonide 9 mg per day. Assessment of ALT and AST activity, as well as side effects, was carried out at 4, 8 and 12 weeks. All patients were prescribed azathioprine 50 mg per day according to the standard of treatment at the end of the second week with subsequent dose titration to 100 mg per day.
Results: In patients of the three groups at the beginning of treatment, the average values of ALT activity were 95 ± 14.8, 98 ± 15.3, 99 ± 14.8, AST 65 ± 9.1, 59 ± 8.7, 55 ± 8.7 (p = 0.870 for ALT and p = 0.177 for AST). After 4 weeks, ALT activity in patients of the three groups did not differ significantly and was 58 ± 13.1, 62 ± 9.7 and 67.5 ± 8.5 (p = 0.064). After 8 weeks, ALT activity in patients of the three groups was 37 ± 5.8, 39 ± 7.7, 44 ± 6.9 and did not differ significantly (p = 0.0820). At the end of week 12, ALT activity in patients of the three groups was within the reference values (p = 0.065). AST activity in patients of the three groups at 4, 8 and 12 weeks was within normal limits and did not differ significantly (p = 0.269 after 4 weeks, p = 0.652 after 8 weeks, p = 0.139 after 12 weeks). The frequency of side effects after 4, 8 and 12 weeks was the lowest in patients of the first and third groups 20 and 15% respectively (p = 0.001). At the same time, in patients who took prednisolone, the frequency of side effects was observed in 30% of cases.
Conclusion: The administration of methylprednisolone, prednisolone, or budesonide to patients with AH without cirrhosis is equally effective in improving liver enzyme. Methylprednisolone and budesonide are safer than prednisolone in patients with AH without cirrhosis.

LBP-008
Longitudinal multi-omics reveals regenerative programs and predictive plasma signatures in human liver regeneration
Martin Cornillet[1], Dan Sun[1], Ghada Nouairia[2], Emelie Barreby[1], Anna Emilia Kern[3], Kristoffer Huitfeldt Sola[4], Hassan Foroughi[5], Lena Berglin[1], Helene Johansson[4], Ahmed Elewa[6], Ruth Baumgartner[4], Bengt Isaksson[7], Andras Simon[6], Ewa Ellis[4], Torkel Brismar[4], Annika Bergquist[2], Stefan Gilg[4], Claudia Kutter[5], Ernesto Sparrelid[4], Niklas Björkström[1]. [1]*Center for Infectious Medicine, Department of Medicine Huddinge, Karolinska Institutet, Huddinge, Sweden;* [2]*Unit of Gastroenterology and Nutrition, Department of Medicine Huddinge, Karolinska Institutet, Huddinge, Sweden;* [3]*Medical University of Vienna, Department of General Surgery, Division of Visceral Surgery, Vienna, Austria;* [4]*Department of Clinical Science, Intervention and Technology (CLINTEC), Karolinska Institutet and Karolinska University Hospital Huddinge, Huddinge, Sweden;* [5]*Department of Microbiology Tumor and Cell Biology & Science for Life Laboratory, Karolinska Institutet, Solna, Sweden;* [6]*Department of Cell and Molecular Biology, Karolinska Institutet, Solna, Sweden;* [7]*Division of Surgical Departments, Södersjukhuset, Stockholm, Sweden*
Email: martin.cornillet.jeannin@ki.se

Background and aims: Animal models using partial hepatectomy (PH) have established our understanding of how liver regeneration could possibly occur in humans. This has considerable implications for regenerative medicine, such as prediction of post-hepatectomy liver failure (PHLF) upon major resections. As translation to humans has been limited and challenging, we aimed to provide both basic knowledge and proof-of-concept insights for clinical applications in the human setting.
Method: Two-stage hepatectomy combined with longitudinal multi-omics was used as the human model at the Karolinska University Hospital. The study included 21 patients subjected to Associating Liver Partition and Portal Vein Ligation for Staged Hepatectomy (ALPPS). Serial liver biopsies (segments 3 and 5), peripheral blood mononuclear cells, and plasma were collected. Separately, preoperative plasma samples from 120 patients subjected to major hepatectomy from which 60 developed PHLF was analyzed (3 cohorts of 40 patients, ISGLS grade B or C, including metastatic colorectal cancer, hepatocellular carcinoma, klatskin, cholangiocarcinoma and gallbladder cancers).
Results: Analysis of longitudinal matched liver biopsies during the proliferative phase (stage 2) identified transcriptomic and epigenetic modules preferentially mobilized in the regenerating future liver remnant (FLR) rather than the matched deportalized tissue. Integration of these modules revealed the main pathways, transcription factors, cytokines, and oncogenes involved. To study the initiation phase, we performed serum profiling the days prior and following Stage 1 and identified the main pathways active during the metabolic remodeling, including evidence for nucleotide salvage and lipolysis. Finally, using machine learning techniques, we revealed a proteomic signature capturing the regenerative potential of human liver. This plasma signature predicted efficient regeneration or liver failure after major hepatectomy in three independent cohorts, even in patients with sFLR below 20%. Deconvolution of this signature identified HNF4 as master regulator and potential therapeutic target.
Conclusion: Overall, we validate key knowledge from experimental PH models and provide novel insights into human liver regeneration with clinical implication for prediction of PHLF.

LBP-009
Synthetic data generation by artificial intellegence predicts clinical outcomes in untreated and Bulevirtide-treated patients with chronic hepatitis Delta
Saverio D'amico[1], Elisabetta Degasperi[2,3,4], Stella De Nicola[5], Nicola Pugliese[5,6], Maria Paola Anolli[2,3,4], Marta Borghi[2,3,4], Sara Baccino[1], Ferrari Ivan[1], Dominique Roulot[7], Matteo Della Porta[1], Alessio Aghemo[5,6], Pietro Lampertico[2,3,4,8]. [1]*IRCCS Humanitas*

Research Hospital, Rozzano, Italy; [2]Division of Gastroenterology and Hepatology, Foundation IRCCS Ca' Granda Ospedale Maggiore Policlinico, Milan, Italy; [3]European Reference Network on Hepatological Diseases (ERN RARE-LIVER), Milan, Italy; [4]D-SOLVE Consortium, an EU Horizon Europe funded project (No 101057917), Milan, Italy; [5]Division of Internal Medicine and Hepatology, Department of Gastroenterology, IRCCS Humanitas Research Hospital, Rozzano, Italy; [6]Department of Biomedical Sciences, Humanitas University, Pieve Emanuele, Italy; [7]Liver Unit, Avicenne Hospital, AP-HP, Sorbonne Paris Nord University, Bobigny, France; [8]CRC "A. M. and A. Migliavacca" Center for Liver Disease, Department of Pathophysiology and Transplantation, University of Milan, Milan, Italy
Email: pietro.lampertico@unimi.it

Background and aims: Bulevirtide (BLV) monotherapy induces virological and biochemical responses in patients with CHD, but the possibility to evaluate its impact on clinical outcomes is currently limited by unavailability of comparable untreated controls. Synthetic data (SD) mimic real-patient statistical and clinical properties, potentially overcoming these limitations. We aimed to generate and validate high-fidelity SD evaluating disease outcomes in BLV-treated versus untreated CHD patients with cirrhosis.
Method: Clinical data from 344 CHD patients with cirrhosis treated with BLV in the SAVE-D study and two historical BLV-untreated cohorts from Italy and France (n = 298) were used to train models. Two settings were defined: A) 1:1 generation of both cohorts assessing clinical fidelity and privacy standards; B) generation of balanced, augmented cohorts (n = 3000/group), reproducing clinical endpoints and addressing matching challenges. SD were evaluated using SAFE framework (PMID: 41197110) against a real data pool excluded from the training phase. Fidelity and privacy were evaluated by Clinical Synthetic Fidelity (CSF) score (average of statistical metrics) and Nearest Neighbour Distance Ration (NNDR) (optimal 0.65–0.85). Propensity score matching (logistic regression) aligned clinical and demographic covariates (SMD <0.1). Primary endpoint compared three-year incidences of liver-related events (hepatocellular carcinoma [HCC] and decompensation).
Results: In setting A, synthetic cohorts of BLV-treated and untreated patients showed high fidelity and privacy (CSF 90%/94%, NNDR 0.71/0.85). In setting B, propensity score matching identified 624 pairs from 3,000 SD samples per group with consistent SAFE metrics. 3-year cumulative incidences of decompensation and HCC were similar across real *vs.* synthetic BLV-treated and untreated patients: decompensation 2.7% *vs.* 4.2% (BLV-treated) and 11.3% *vs.* 10.0% (untreated), HCC 6.6% *vs.* 8.5% (BLV-treated) and 3.6% *vs.* 4.8% (untreated), respectively. Compared to real patients, the synthetic cohort significantly improved statistical robustness, due to the larger pool of matched individuals with perfectly comparable characteristics (real: p = 0.054 and p = 0.378 *vs.* synthetic: p = 0.039 and p = 0.546).
Conclusion: High-fidelity synthetic patient-level data accurately reproduce clinical outcomes in untreated and BLV-treated CHD patients with cirrhosis. This strategy may overcome some of the challenges in rare diseases.

LBP-010

Safety, tolerability, pharmacokinetics, and pharmacodynamics of DA-1726, an oxyntomodulin analogue, in a higher-dose phase 1 cohort with exploratory noninvasive liver assessment

Chris Fang[1], Yuna Chae[2], Robert Homolka[1], Ji Eun Lee[1], Kyunghyun Lee[1,3], Sung-Jin Kim[1,3], Mi-Kyung Kim[2], Hyung Heon Kim[1]. *[1]MetaVia Inc., Cambridge, United States; [2]Dong-A ST Co., Ltd, Yongin-Si, Korea, Rep. of South; [3]Dong-A ST Co., Ltd, Seoul, Korea, Rep. of South*
Email: ynchae@donga.co.kr

Background and aims: Obesity is associated with metabolic complications, including metabolic dysfunction–associated liver disease. DA-1726 is an oxyntomodulin analogue, acting as a dual glucagon-like peptide-1 and glucagon receptor agonist. In this first-in-human phase 1 study (NCT06252220), a higher-dose cohort further evaluated the safety, tolerability, pharmacokinetics (PK), and pharmacodynamics of DA-1726 in obese but otherwise healthy adults, with exploratory noninvasive assessment of liver-related parameters.
Method: In this 48 mg multiple-ascending dose cohort, nine participants received DA-1726 or placebo in a 6:3 randomization ratio. Participants received once-weekly subcutaneous dosing for four weeks without dose titration; six entered an optional four-week extension phase at the same dose (four DA-1726; two placebo).
Results: In this interim analysis, DA-1726 was generally well tolerated. Gastrointestinal (GI) adverse events (AEs) were mainly transient and mild to moderate, with no treatment-related discontinuations or serious AEs. Participants receiving DA-1726 showed progressive reductions in body weight, with mean percent changes from baseline of −6.1% at Day 26 and −9.1% at Day 54 ($p < 0.05$ vs placebo at Day 26), without evidence of plateau through Week 8. Significant changes were also observed in waist circumference (−5.8 cm at Day 26; −9.8 cm at Day 54; $p < 0.05$ vs placebo). At Day 54, the mean change from baseline in controlled attenuation parameter (CAP) was −20.0 dB/m in the 48 mg group versus +24.0 dB/m in the placebo group. Modest improvement from baseline was also observed in liver stiffness measurement (LSM) by vibration-controlled transient elastography (VCTE; −10.3% vs. +13.8% with placebo), with directional improvement from baseline in FibroScan-aspartate aminotransferase (FAST) score. Cardiovascular parameters, including heart rate and Fridericia-corrected QT interval (QTcF), remained stable with no clinically significant changes observed despite glucagon receptor activation, supporting a favorable safety profile.
Conclusion: DA-1726 was generally well tolerated up to 48 mg, with predominantly mild-to-moderate GI AEs and no new safety signals. Clinically meaningful and statistically significant weight loss was observed. In addition, exploratory FibroScan-based assessments suggest early trends toward improvement in liver-related parameters, supporting further evaluation in longer-term studies.

LBP-011

Pharmacological effects of apixaban and edoxaban in patients with liver cirrhosis

Lucas Gautier[1], Cindy Pereira Portela[1], Debora Bertaggia Calderara[1], Lucas Veuthey[1], Alessandro Aliotta[1], Maxime Zermatten[1], Elise Mdawar-Bailly[2], Sophie Kasmi[2], Darius Moradpour[2], Montserrat Fraga Christinet[2], Lorenzo Alberio[1]. *[1]Division of Haematology and Central Haematology Laboratory, Centre Hospitalier Universitaire Vaudois (CHUV), Lausanne, Switzerland; [2]Division of Hepatology and Gastroenterology, Centre Hospitalier Universitaire Vaudois (CHUV), Lausanne, Switzerland*
Email: lucas.gautier@chuv.ch

Background and aims: While several patients with liver cirrhosis (LC) require long-term anticoagulation because of atrial fibrillation or venous thromboembolism, data on direct oral anticoagulants (DOAC) use remain limited. Here, we evaluated the pharmacological profiles of two DOAC in this population.
Method: This monocentric clinical trial (NCT05869591) enrolled non-anticoagulated patients with Child-Pugh A (n = 38) and B (n = 4) LC, randomised to receive either edoxaban 60 mg OD (n = 21) or apixaban 5 mg BID (n = 21) for 7 days. Pharmacokinetic and pharmacodynamic parameters were measured at day (d) 1, 3, 8, and 9. Preliminary results include DOAC peak and trough concentrations, *ex vivo* thrombin generation (TG) parameters, and *in vivo* markers of coagulation (prothrombin fragments 1+2 [F1+2], thrombin–antithrombin complexes [TAT], D-dimers [DD]).
Results: The cohort included 12 female (29%) and 30 male (71%) patients, all with preserved renal function and a median MELD score of 8 (range 6–18); 50% were thrombocytopenic (median platelet count 147 G/L; range 58–358). DOAC concentrations exhibited

distinct profiles, with median peak and trough levels of 204 and 17 ng/mL for edoxaban and 158 and 92 ng/mL for apixaban, respectively. No patient had trough concentrations above the values observed in patients without LC [1]. As expected, *ex vivo* TG parameters changed in line with DOAC levels. Overall, compared to non-anticoagulated baseline, DOAC significantly reduced *ex vivo* TG ($p < 0.01$) and *in vivo* coagulation markers (F1+2, TAT, DD; $p < 0.01$). At d8, DOAC significantly decreased F1+2 and DD (−24% and −23%, respectively; $p < 0.01$); the reduction in DD was −32% with edoxaban ($p = 0.08$) and −22% with apixaban ($p < 0.05$). Patients with thrombocytopenia exhibited less DD reduction compared to those with platelets ≥150 G/L (−6% versus −37%; $p < 0.05$).

Conclusion: Edoxaban showed higher peak and lower trough levels than apixaban, which displayed greater variability at trough without exceeding the usual range observed in patients without LC. Based on F1+2 and DD, both DOAC appeared effective in patients with LC. Noteworthy, the only factor identified to impact the anticoagulant effect *in vivo* was platelet count, with thrombocytopenia correlating with a significantly lower DD reduction.

Reference

1. de Vries *et al. Thromb Haemost* 2025;125:563–573.

LBP-012

High rate and sustained HBsAg loss achieved with HT-101 plus HT-102 combination therapy in HBeAg-negative, nucleos(t)ide analogue-suppressed patients: ongoing off-treatment results from a multicenter Ib/IIa study

Xieer Liang[1], Chen Liang[2], Jianmei Lin[3], Bei Zhong[3], Huiqing Liang[4], Wen Xie[5], Yujuan Guan[6], Zhihong Liu[1], Xun Qi[2], Dong Wang[7], Zhipeng Zhang[8], Lijuan Ding[8], Zhiping Cui[8], Huaien Song[8], Kun Yue[8], Jinlin Hou[1]. *[1]Department of Infectious Diseases, Nanfang Hospital, Southern Medical University, Guanghzou, China; [2]Liver Disease Department, Shanghai Public Health Clinical Centre, Shanghai, China; [3]Infectious Diseases Department, Qingyuan People's Hospital, Guanghzou, China; [4]Infectious Diseases Department, Xiamen Traditional Chinese Medicine Hospital, Xiamen, China; [5]Liver Disease Department, Beijing Ditan Hospital, Beijing, China; [6]Liver Disease Department, Guangzhou Eighth People's Hospital, Guanzhou, China; [7]Hepa Thera Biopharmaceutical Co.Ltd., Shanghai, China; [8]Hepathera, Shanghai, China*
Email: jlhousmu@163.com

Background and aims: HT-101, a GalNAc-conjugated small interfering RNA targeting the S-region of the hepatitis B virus (HBV) genome, and HT-102, a human monoclonal antibody directed against the antigenic loop of HBsAg, have demonstrated synergistic efficacy for HBsAg clearance in patients with chronic HBV infection. Here we report off-treatment follow-up data from the ongoing China-based study (NCT07183306/CTR20244730).

Method: This multicenter, open-label, partial dose-escalation study enrolled HBeAg-negative patients on stable nucleos(t)ide analogue (NA) therapy, with serum HBsAg levels from 100 to 3,000 IU/mL. Participants were assigned to five treatment groups: A (HT-101 400 mg), B (HT-102 300 mg for 24 weeks, followed by HT-101 400 mg for week 24 to 48], C (HT-101 100 mg + HT-102 300 mg), D (HT-101 200 mg + HT-102 300 mg), and E (HT-101 400 mg + HT-102 300 mg). HT-101 and/or HT-102 were administered subcutaneously every 4 weeks for 24 or 48 weeks, with follow-up for up to 48 weeks post-treatment. The primary endpoint was the incidence of treatment-emergent adverse events (TEAEs). Secondary endpoints included HBsAg kinetics, virological and pharmacodynamic markers, and immunogenicity.

Results: Both Group A and Group B have completed the 48-week visit, while Groups C–E have completed the 32-week visit. At week 24, HBsAg seroclearance was observed in 4/20 (20%) participants in Group A and 3/4 (75%) maintained HBsAg loss from end of treatment (week 24) through week 48. In Group B, 4/8 (50%) achieved HBsAg seroclearance at week 48. At week 32 (8 weeks post-treatment), the HBsAg seroclearance rates were 4/8 (50%) in Group C, 8/10 (80%) in Group D, and 8/10 (80%) in Group E respectively. Among combination therapy recipients (Groups C–E), 20/22 (91%) of those who achieved HBsAg seroclearance at week 24 remained HBsAg negative at week 32 (8 weeks off-treatment). The therapy was well tolerated, with most TEAEs being grade 1–2 in severity (e.g., injection site reactions). No drug-related serious adverse events, grade ≥3 events, or alanine aminotransferase flares were observed.

Conclusion: Combination therapy with HT-101 and HT-102 achieved very high rate of HBsAg loss which was sustained for 8 weeks post-treatment. HT-101 monotherapy demonstrated durable HBsAg loss for up to 24 weeks post-treatment. These results support the continued development of HT-101 and HT-102 as a promising strategy for achieving functional cure in patients with chronic HBV infection.

LBP-013

A phase Ib multiple dose ascending study of HH-006 in treatment-naïve participants with chronic hepatitis B virus infection

Xieer Liang[1], Xihua Fu[2], Yujuan Guan[3], Zhihong Liu[1], Wencong Dai[1], Zuoheng Xu[2], Ying Zhuang[4], Guangyu Li[4], Liangfeng Zou[4], Zhongmin Zhou[4], Yonghe Qi[4], Pan Chen[4], Xiyu Zhang[4], Bin Ye[4], Yin Zhang[4], Bin Chen[4], Jianhua Sui[4], Wenhui Li[5], Jinlin Hou[1]. *[1]Nanfang Hospital, Southern Medical University, Guangzhou, China; [2]The Affiliated Panyu Central Hospital of Guangzhou Medical University, Guangzhou, China; [3]Guangzhou Eight People's Hospital, Guangzhou Medical University, Guangzhou, China; [4]Huahui Health Ltd., Beijing, China; [5]National Institute of Biological Sciences, Beijing, China*
Email: jlhousmu@163.com

Background and aims: HH-006 is a human monoclonal antibody (mAb) targeting the PreS1 domain of HBV large (L) envelope protein, with an engineered Fc region to enhance half-life and Fc function. HH-006 has demonstrated a favorable safety profile and the expected pharmacokinetic (PK) profile in healthy volunteers in a phase Ia study. The objectives of this study were to evaluate the safety, tolerability, PK, and antiviral activity of HH-006 in chronic HBV infection (CHB).

Method: This study is a randomized, double-blind, and placebo-controlled study. A total of 36 treatment-naïve CHB participants were enrolled and randomized (9:3 within each dose cohort). At baseline, the mean ± SD HBsAg level among participants was 1,756.4 ± 1,312.52 IU/mL, the mean ± SD HBV DNA level was 3.6 ± 1.38 $\log_{10}$ IU/mL, and the mean ± SD ALT level was 33.4 ± 22.37 U/L. Participants in each dose group (120 mg, 240 mg and 480 mg) received HH-006 or placebo subcutaneous (S.C.) once a week on Day 1, Day 8, Day 15, Day 22 and Day 29, with 24 weeks of follow-up.

Results: All HH-006 treatment-emergent adverse events (TEAEs) were Grade 1 or 2, with no adverse events of special interest (AESIs), serious adverse events (SAEs), or AEs leading to treatment discontinuation. On-treatment AEs were reported in 92.6% (25/27) of participants in the HH-006 treatment groups and 88.9% (8/9) in the placebo group, while treatment-related AEs occurred in 81.5% and 77.8% of participants, respectively. Systemic exposure of HH-006 was increased in a near dose-proportional manner across the 120–480 mg dose range. Following SC injection, the T_{max} ranged from 1 to 3 days post-dose, the mean elimination half-life ranged from 30.6 to 42.6 days. Decreases of HBV DNA and HBsAg were observed across all dose cohorts. At 4 weeks after the final dose, the mean ± SD HBV DNA reduction from baseline was −0.62 ± 0.61, −0.78 ± 0.37, −0.69 ± 0.57 in the HH-006 groups and −0.34 ± 0.72 $\log_{10}$ IU/mL in the placebo group. The maximal HBsAg decrease in the study period was −0.34, −0.40, −0.46 $\log_{10}$ IU/mL in HH-006 treated groups, compared with −0.13 $\log_{10}$ IU/mL in the placebo group.

Conclusion: HH-006 was safe and well-tolerated and demonstrated antiviral activity, with an approximately dose-proportional PK profile, in treatment-naïve patients with CHB. Further studies are

warranted to explore HH-006's potential as single agent or combination use for functional cure of HBV.

LBP-014

Safety, tolerability, pharmacokinetics and pharmacodynamics of an orally innovative GalNAc-conjugated thyroid hormone receptor-beta agonist (Kylo-0603) in healthy volunteers: a multiple ascending dose study

Xingjiang Hu[1], Youlei Wang[1], Qiao Zhang[1], Caixia Yan[1], Zhuojun Zhou[1], Yumei Gu[2], Qinsheng Zhang[2], Tao Guan[2], Kunyuan Cui[2,3], Qingwei Zhao[1]. *[1]Zhejiang Provincial Key Laboratory for Drug Evaluation and Clinical Research, Department of Clinical Pharmacy, The First Affiliated Hospital, Zhejiang University School of Medicine, Hangzhou, China; [2]Hygieia Pharmaceuticals Co., Ltd., Hangzhou, China; [3]Kylonova (Xiamen) Biopharma Co., Ltd., Xiamen, China*
Email: huxingjiang@zju.edu.cn

Background and aims: Metabolic dysfunction-associated fatty liver disease (MAFLD) affects over one-fourth of the global adult population and is the leading cause of liver disease worldwide. Kylo-0603, a liver-targeted small molecule, is an orally N-acetylgalactosamine-conjugated thyroid hormone receptor-β agonist designed to improve MAFLD by increasing hepatic fat metabolism and reducing lipotoxicity. A single-center, randomized, double-blind, placebo-controlled, phase 1 study aimed to evaluate the safety, tolerability, pharmacokinetics and pharmacodynamics of Kylo-0603 in Chinese healthy volunteers (NCT06365580).
Method: Sixty participants were randomized to receive once-daily Kylo-0603 at doses of 1.2, 2, 4, 8, 12, and 16 mg, or placebo for 14 days. Subjects were followed for an additional 7 days off drug for safety assessment.
Results: Means age of 60 participants was 29.7 years old (SD: 5.45) and 50% was female. The exposure of Kylo-0603 exhibited nonlinear manner. The plasma concentrations of Kylo-0603 at doses of 1.2–16 mg were below the lower limit of quantification within 8 hours after administration on Day 1 or Day 14 (except for one participant in 16 mg cohort), without accumulation after multiple doses. The half-life of Kylo-0603 ranged from 0.5 to 1.5 hours. Kylo-0603 was primarily excreted though feces. Kylo-0603 was safe and well-tolerated in this study. No treatment- or dose-related trends were observed for adverse events (AEs). No serious AEs were reported. The majority of AEs and all treatment-related AEs were Grade 1. No gastrointestinal AEs were reported in Kylo-0603 group. No alanine aminotransferase elevations exceeded 1.5×ULN in 1.2–16 mg cohorts. The mean levels of thyroid hormones including thyrotropin (TSH), free triiodothyronine (T3), total T3, free thyroxine (T4) and total T4 in each dose cohort mostly fluctuated within the normal reference range, without symptoms or signs of thyroid dysfunction. Clinically meaningful placebo-adjusted reductions in serum low-density lipoproteins cholesterol levels were observed at doses of 8 mg, 12 mg and 16 mg ($p < 0.05$) on Day 15, with the maximal reduction up to 28.5% in 12 mg cohort. In addition, significant reductions in total cholesterol, Apolipoprotein B, and triglycerides were observed.
Conclusion: Kylo-0603 was safe and well-tolerated in Chinese healthy volunteers in this two-week study. It has great potential to become an innovative therapy for MAFLD with its beneficial effect on lipid parameters.

LBP-015

Thybetador, a potent and selective THR-β agonist: results from a phase 1 first-in-human study in healthy volunteers and participants with elevated LDL-C

Xiangwei Hua[1], Hualing Pan[1], Rong Deng[1], Jia Sun[1], Gaihong Wang[1], Guanguan Zhao[1], Shengsheng Yang[1], Guozhi Li[1], Yun Liu[2], Julia Yang[1], Zhenwei Zhang[1], Peter Wang[1], H. Eric Xu[1]. *[1]Cascade Pharmaceuticals, Inc, Shanghai, China; [2]Shanghai Xuhui District Central Hospital, Shanghai, China*
Email: eric.xu@cascadepharm.com

Background and aims: Thybetador (CS060380) is a novel thyroid hormone receptor-beta (THR-β) agonist. *In vitro*, Thybetador demonstrated high potency, and exhibited >100-fold selectivity for THR-β over THR-α (relative to T3). This Phase 1 first-in-human study evaluated the safety, tolerability, pharmacokinetics (PK), and pharmacodynamics (PD) of Thybetador in healthy volunteers and participants with elevated low-density lipoprotein cholesterol (LDL-C).
Method: The trial comprised two randomized, double-blind, placebo-controlled parts: a Single Ascending Dose (SAD) study (0.2, 1, 2, 5, and 10 mg) and a Multiple Ascending Dose (MAD) study (0.1–2 mg once daily). The SAD part included a food-effect sub-study to assess the impact of a high-fat meal on PK. Safety, PK parameters, and PD markers (including sex hormone-binding globulin [SHBG] and lipid profiles) were assessed.
Results: Thybetador was well tolerated in both SAD group and MAD group. The most common treatment-emergent adverse events (TEAEs) were transient elevations in ALT or AST and reversible reductions in free T4 or total T4, consistent with the mechanism of action. SAD exposure of Thybetador was linear within the dose range of 0.2–10 mg. Plasma concentrations peaked 2–4.5 hours post-dose, with a geo-mean half-life (t1/2) of 9.1–10.9 hours, supporting once-daily (QD) dosing. Food intake had no significant impact on PK. In the MAD study, steady state was achieved within approximately one week. Tmax and t1/2 were similar in SAD and MAD cohorts. The mean of Rac_AUCtau ranged between 1.166–1.495, indicating no obvious accumulation. SHBG, a key PD marker for THR-β activation, increased dose-dependently (0.25–2 mg), rising >100% at 0.25 mg and >200% at 2 mg. Significant reductions were observed in LDL-C, triglycerides (TG), total cholesterol (TC), apolipoprotein B (Apo-B) and Lp(a) after 14 days of treatment.
Conclusion: In this Phase I trial, Thybetador exhibited a favorable safety profile and PK characteristics in both SAD and MAD studies. Robust PD effects were observed in the MAD study. Based on these findings, Phase II investigations are currently ongoing.

LBP-016

Immunogenetic predictors of hepatitis D virus infection progression in Uzbekistan: implications for a national screening strategy

Malika Khodjaeva[1], Zebiniso Sofiya Ismailova[1], Erkin Musabaev[1], Nargiz Ibadullaeva[1], Aziza Khikmatullaeva[1], Shokhista Bakieva[1]. *[1]Research Institute of Virology, Republican Specialized Scientific and Practical Medical Center of Epidemiology, Microbiology, Infectious and Parasitic Diseases, Tashkent, Uzbekistan*
Email: drmusabaev1956@gmail.com

Background and aims: Hepatitis D virus (HDV) infection is the most severe form of viral hepatitis, characterized by rapid progression to liver cirrhosis and hepatic failure. The high prevalence of HDV in Uzbekistan necessitates early identification of patients at high risk of disease progression. National strategies, in accordance with Presidential Resolution No. PP-243 (May 16, 2022), include expanded HDV screening among patients with hepatitis B. Uzbekistan is currently the only Central Asian country implementing a systematic screening approach. Identification of clinically relevant immunogenetic markers is therefore of particular importance. This study aimed to investigate host immunogenetic factors associated with HDV clinical outcomes and assess their relevance for clinical practice and public health.
Method: Patients with HDV infection were stratified into: benign chronic hepatitis, progressive chronic hepatitis, and HDV-associated cirrhosis (Child-Pugh A-C). Immunogenetic analysis included human leukocyte antigen (HLA)-B Bw4/Bw6, interleukin-10 (IL10)-1082C>T (rs1800896), and interleukin-28B (IL28B) polymorphisms

(rs12979860, rs8099917). Associations between immunogenetic markers and disease severity were analyzed to identify predictors of progression for risk stratification and clinical decision-making.
Results: Patients with cirrhosis more frequently exhibited the HLA-B Bw4/Bw4 genotype and a licensed natural killer (NK) cells phenotype (OR 1.67 and OR 2.22). The IL10-1082 TT genotype was significantly more common in progressive hepatitis and cirrhosis (p = 0.033) and absent in benign cases. IL28B rs12979860 genotype distribution differed significantly (p = 0.001): TT predominated in progressive disease, whereas CC was associated with a benign course. The G allele (TG/GG) of rs8099917 was detected exclusively in progressive hepatitis and cirrhosis (p = 0.03). These findings demonstrate a strong association between host immunogenetic profile and HDV progression.
Conclusion: Immunogenetic markers, particularly within the HLA-B/KIR axis and cytokine pathways, are associated with HDV severity and may serve as predictors of progression. Their integration into clinical practice may enable early risk stratification, improve clinical decision-making, and optimize patient management. At the population level, this approach may reduce progression to cirrhosis and hepatic failure through earlier targeted intervention.

LBP-017

Longitudinal analysis of routine laboratory data prospectively identifies clinically significant hepatic fibrosis from the general population, outperforming standard fibrosis scores: validation from the LiveWell multi-modal screening study

Timothy Jobson[1,2], Catherine Denver[1,2], Christina Owen[1], Neil Stevens[2], Axelle Caudrillier[3], Yasmin Hamadache[3], Heath O'Brien[3], Patrick Short[3], Jamie Webb[3], Katie Barnes[3]. *[1]Somerset NHS Foundation Trust, Taunton, United Kingdom; [2]Predictive Health Intelligence Ltd, Wellington, United Kingdom; [3]Sano Genetics Ltd, London, United Kingdom*
Email: katie@sanogenetics.com

Background and aims: Clinically significant hepatic fibrosis (F2+) defines eligibility for emerging metabolic dysfunction-associated steatotic liver disease (MASLD) therapies, but population-level identification is challenging. hepatoSIGHT is a National Health Service (NHS) adopted tool using the Cumulative Liver Damage Index (CLDI, approximating the integral of alanine aminotransferase over time) derived from routine blood tests. We prospectively validated a two-stage approach: CLDI population enrichment followed by a multi-biomarker model including a polygenic risk score (PRS; PGS002283). Data available March 2026.
Method: The general population was risk-stratified by CLDI; the highest-risk 7% (cases) and age- and sex-matched controls across two age cohorts (25–35 and 45–55 years) were recruited for transient elastography (TE) and saliva-based genetic testing performed by Sano Genetics. Logistic regression models using longitudinal laboratory data in hepatoSIGHT were assessed by Receiver Operating Characteristic Area Under the Curve (ROC-AUC). Mediation analysis examined the PRS-CLDI relationship.
Results: 994 participants were recruited. CLDI significantly predicted F2+ fibrosis (TE greater than or equal to 8 kPa; odds ratio (OR) 3.87, p < 0.001) and F4 cirrhosis (OR 5.02, p < 0.01). The best hepatoSIGHT model (age, sex, CLDI, platelet minimum and mean, HbA1c mean; 45–55 age cohort) achieved ROC-AUC 0.748 (95% confidence interval (CI) 0.584–0.890). A model incorporating body mass index (BMI) and extended to the combined age cohorts (age, sex, BMI, CLDI, platelet mean) improved performance (ROC-AUC 0.884, 95% CI 0.79–0.957). This outperforms the published population-level AUC for Fibrosis-4 index (FIB-4) (0.572; Graupera et al., 2022). The number needed to scan (NNS) using TE to identify one F2+ case was 8. Mediation analysis showed a significant indirect effect of PRS via CLDI (p = 0.026), validating CLDI as capturing cumulative genetic hepatic risk.
Conclusion: hepatoSIGHT operates as a two-stage screen: CLDI enriches the highest-risk 7% from routine data; a multi-biomarker model then stratifies this group precisely. This achieves NNS of 8 for F2+ identification by TE, and outperforms published FIB-4 population benchmarks in discriminative performance. PRS mediation validates the biological coherence of CLDI. hepatoSIGHT offers a deployable, evidence-based pathway to identify patients eligible for emerging MASLD therapies. Validation in a large population is warranted.

LBP-018

Improvements in fatigue in patients with primary biliary cholangitis treated with elafibranor: patient-reported outcome measurement information system fatigue short form 7a (PFSF 7a) data from the phase III ELATIVE® trial

David E. Jones[1], Andreas E. Kremer[2], Cynthia Levy[3,4], Nuno Antunes[5], Darren Asquith[6], Nathan Touati[7], Mark Swain[8]. *[1]Translational and Clinical Research Institute and NIHR Newcastle Biomedical Research Center, Newcastle University, Newcastle Upon Tyne, United Kingdom; [2]Department of Gastroenterology and Hepatology, University Hospital Zurich, University of Zurich, Zurich, Switzerland; [3]Schiff Center for Liver Diseases, University of Miami, Miami, Florida, United States; [4]Division of Digestive Health and Liver Diseases, University of Miami School of Medicine, Miami, Florida, United States; [5]Ipsen, Cambridge, Massachusetts, United States; [6]Ipsen, London, United Kingdom; [7]Ipsen, Paris, France; [8]Liver Unit, Department of Medicine, Cumming School of Medicine, University of Calgary, Calgary, Alberta, Canada*
Email: david.jones@newcastle.ac.uk

Background and aims: Fatigue is the most common and debilitating symptom in primary biliary cholangitis (PBC). In the phase III ELATIVE® trial (NCT04526665), elafibranor (ELA) improved fatigue in patients (pts) with PBC. Here, a breakdown of the Patient-Reported Outcome Measurement Information System Fatigue Short Form 7a (PFSF 7a; a 7-item, 5-point Likert scale tool) was used to further assess the impact of ELA vs placebo (PBO) on fatigue, with changes in total T-score and individual items evaluated.
Method: In ELATIVE®, pts were randomised 2:1 to ELA 80 mg or PBO. Mean (standard error [SE]) change from baseline (BL; CfB) in individual PFSF 7a items raw score (1 = lowest fatigue; 5 = highest fatigue) and total PFSF 7a T-score (lower score represents greater improvements) and achievement of a minimal clinically important difference (MCID; T-score improvement ≥3) were evaluated through Week (Wk) 52 for pts with moderate-to-severe fatigue at BL (T-score ≥60). Statistical testing at Wk 52 was conducted using Student t-test and Fisher exact test for CfB and MCID, respectively.
Results: For pts receiving ELA vs PBO, 46/107 (43.0%) vs 20/52 (38.5%) had moderate-to-severe fatigue at BL. Improvements in PFSF 7a T-score with ELA vs PBO were observed through Wk 52 (mean [SE] CfB: Wk 4: −3.7 [0.9] vs −0.7 [0.9]; Wk 26: −5.6 [1.1] vs −3.9 [1.3]; Wk 52: −6.5 [1.2] vs −2.6 [1.6]; Wk 52: p = 0.076). Greater proportions of pts receiving ELA vs PBO achieved a MCID in PFSF 7a T-score at Wk 4 (24/45 [53.3%] vs 4/20 [20.0%]) and Wk 26 (29/45 [64.4%] vs 6/15 [40.0%]); at Wk 52, statistically significant differences for ELA vs PBO were seen (28/42 [66.7%] vs 5/16 [31.3%]; p = 0.020). Pts receiving ELA vs PBO had greater improvements (mean [SE] CfB) at Wk 52 for the majority of PFSF 7a items, particularly those evaluating mental and physical fatigue: 'extreme exhaustion' (−0.9 [0.2] vs −0.2 [0.3]); 'too tired to think clearly' (−0.7 [0.1] vs −0.2 [0.3]); 'too tired to bath or shower' (−0.7 [0.2] vs −0.1 [0.3]). These items showed greater improvements for ELA vs PBO at all timepoints assessed and had the highest proportions of pts reporting an improvement of ≥1 point/item at Wk 52 (61.9% vs 31.3%; 57.1% vs 31.3%; 54.8% vs 25.0%, respectively).
Conclusion: In these post hoc analyses, a significantly higher proportion of pts receiving ELA vs PBO achieved a MCID in fatigue reduction. Greater improvements with ELA vs PBO were observed through Wk 52 for most PFSF 7a items, suggesting ELA improves multiple aspects of fatigue in PBC.

LBP-019-YI

Data for action: real-world hepatitis c virus and human immunodeficiency virus co-and hepatitis c virus mono-infection epidemiology to inform strategic hepatitis c virus elimination in south africa

Bongani Khanyi[1], Murad Ruf[2], Morubula Manamela[3], Jayendrie Thaver-Kleitmann[3], Ntsakisi Maluleke[4], Lesego Lenabe[5], Sibahle Ngongo[5], Zinhle Makatini[6], Imraan Essa[7], Urvisha Bhoora[5], Nishi Prabdial-Sing[8]. *[1]University of the Witwatersrand-Medical School, Johannesburg, South Africa; [2]Gilead Sciences Europe, Uxbridge, Northern Ireland; [3]National Institute for Communicable Diseases, Johannesburg, South Africa; [4]Gilead Sciences South Africa, Johannesburg, South Africa; [5]University of Pretoria, Tshwane, South Africa; [6]Medical Faculty, Bloemfontein, South Africa; [7]Addington Hospital, Durban, South Africa; [8]National Institute for Communicable Diseases, University of the Witwatersrand, Johannesburg, South Africa*
Email: 2331628@students.wits.ac.za

Background and aims: Real-world data on hepatitis C virus (HCV) burden in South Africa (SA) is scarce. Modelling estimates for active HCV range between 265–920,000. Although, pan-genotypic DAAs are available in the public health sector since 2023, access is only through tertiary hospitals, currently. The 2022 WHO HCV guidelines include, along with harm reduction services, HIV treatment (ART) services as priority settings for integrated service delivery. Whereas SA is committed to elimination goals, funding is a limitation. At present, harm reduction services in SA are mostly reliant on donor funding with only the City of Tshwane providing state services. To inform elimination prioritisation in SA, we aimed to generate HCV epidemiological data in these public health service settings.
Method: We screened adult patients from five public HIV-ART clinics in four cities (2× Johannesburg, Tshwane, Cape Town, and Durban), and unselected People who use drugs (PWUD) clients with known HIV status from two harm reduction sites in Tshwane. HCV-Ab+ were centrally RNA confirmed. We calculated prevalence estimates with 95% confidence intervals overall, by site and sex, with Fisher's exact and Chi-square tests for associations.
Results: With 2,970 of 4,000 (74.3%) HIV-ART patients across five sites were tested, 63.7% were female. Overall HCV-RNA+/HIV coinfection prevalence in ART sites was 0.20% [0.04–0.36], all HCV infections were exclusively in males, 0.56% [CI: 0.11–1.01]. We found no significant prevalence variation across the five sites ($p > 0.05$). We also tested 151/200 (75.5%) PWUD clients, 87% were male, 81% were on Opiate agonist therapy (OAT). There were no significant differences in proportions of client sex or OAT) use between sites. 90% of HCV-Ab tested RNA+, overall RNA prevalence of 35% [CI:27.5–42.7]. More than a third (39%) were HIV coinfected. Testing is ongoing.
Conclusion: As all HCV infections were found in male patients at the adult public HIV ART clinics, once-off HCV screening in adult male HIV-ART patients may be considered. Moreso, we found high rates of active HCV infection with substantial proportions of HCV/HIV coinfection in PWUD clients across both harm reduction sites. To meaningfully advance HCV elimination and prevent accelerated liver disease in HIV coinfected patients, South Africa should embrace both, harm reduction services and public health care facilities at population-level and make DAA accessible through local clinics and community-based service models.

LBP-020

A global Delphi consensus to define chronic liver disease severity: replacing cirrhosis with a stage-based model

Aleksander Krag[1,2], Nikolaj Torp[1,2], Stine Johansen[1,2], Emmanuel Tsochatzis[3], Mary E. Rinella[4], Diana Romero[5], Cristina Ripoll[6], Jaime Bosch[7], Thomas Reiberger[8,9], Annalisa Berzigotti[7], Guadalupe Garcia-Tsao[10,11]. *[1]FLASH -, Centre for Liver Research, Department of Gastroenterology and Hepatology, Odense University Hospital, Odense, Denmark; [2]Department of Clinical Research, Faculty of Health Sciences, University of Southern Denmark, Odense, Denmark; [3]UCL Institute for Liver and Digestive Health, Royal Free Hospital, University College of London (UCL), London, United Kingdom; [4]University of Chicago, Pritzker School of Medicine, Chicago, United States; [5]City University of New York Graduate School of Public Health and Health Policy (CUNY SPH), New York, United States; [6]Internal Medicine IV, Jena University Hospital, Friedrich Schiller University, Jena, Germany; [7]Department of Visceral Surgery and Medicine (Hepatology), Inselspital, Bern University Hospital, University of Bern, Bern, Switzerland; [8]Division of Gastroenterology and Hepatology, Department of Medicine III, Medical University of Vienna, Vienna, Austria; [9]Christian Doppler Lab for Portal Hypertension and Liver Fibrosis, Medical University of Vienna, Vienna, Austria; [10]Digestive Diseases Section, Department of Medicine, Yale University, New Haven, United States; [11]Digestive Diseases Section, Department of Medicine, VA-CT Healthcare System, West Haven, United States*
Email: aleksander.krag@rsyd.dk

Background and aims: The term 'cirrhosis' has historically been used to define the late stage of chronic liver disease (CLD) based on histology. Evolving insights into disease mechanisms, wider availability of non-invasive tests (NITs), evidence for reversibility with effective etiologic therapies, and updated natural history studies suggest that the static concept of 'cirrhosis' no longer reflects current understanding of advanced chronic liver disease (ACLD). This study aimed to evaluate whether a modern stage-based definition of CLD severity is warranted among global stakeholders in hepatology.
Method: A structured, modified Delphi process was conducted to investigate international expert consensus, endorsed by the Baveno Cooperation and guided by an expert methodologist. Following a literature review and input from the Baveno Cooperation leadership, a conceptual framework was developed to inform the Delphi statements. Delphi panellists were identified by Baveno Cooperation nomination and through a literature review. Statements were scored using a 5-point Likert scale with opportunity to provide comments. Statements were revised between the Delphi rounds based on agreement and qualitative feedback to improve consensus. Consensus was predefined as a supermajority (≥67% 'agree' or 'somewhat agree').
Results: A total of 456 panellists from 52 countries across six continents participated (83% response rate; 456 of 547 invited). Round 1 included 24 statements, achieving a mean agreement of 86% and generating 1,458 comments. Round 2 had an 83% response rate (377 of 456), included 30 statements, and reached a mean agreement of 93%, with all statements achieving ≥85% agreement and 875 comments. Panellists agreed that cirrhosis-based terminology is outdated and the traditional reliance on histology is misaligned with current clinical practice given the widespread use of NITs. There was strong consensus that the term 'cirrhosis' does not provide sufficient granularity to identify clinically meaningful distinctions, particularly regarding the degree of portal hypertension. A stage-based framework for CLD severity (CLD stages I–IV) was strongly supported: CLD stage I (non-ACLD), CLD stage II (cACLD without clinically significant portal hypertension [CSPH]), CLD stage III (cACLD with CSPH) and CLD stage IV (decompensated, dACLD).
Conclusion: This global Delphi consensus demonstrates broad expert support for moving beyond cirrhosis-based terminology towards a stage-based definition of chronic liver disease.

LBP-021

24-week safety and efficacy of brelovitug monotherapy for the treatment of chronic hepatitis D: data from phase 2b of AZURE-1

Tatyana Kushner[1], David Yardeni[2], Marta Dobryanska[3], Alina Jucov[4], Douglas T. Dieterich[5], Jordan J. Feld[6], Maia Butsashvili[7], Ekaterine Dolmazashvili[8], Dragomir Gerov[9], Tamar Khuchua[10], Tarek Saadi[11], David Kaplan[12], James Park[13], Dimitar Pavlov[14], Mariana Penkova Radicheva[9], Carla Coffin[15], Edward J. Gane[16], Sébastien Poulin[17], Ira Jacobson[18], Miriam Levy[19], Mark S. Sulkowski[20], Norah Terrault[21], Karen Doucette[22],

Nancy S. Reau[23], Simone Strasser[24], Tomohiro Tanaka[25], Ashley Duzik[26], Susanna Tan[27], Sue Naim[27], Will Garner[27], Craig Pace[27], Hassan Javanbakht[27], Nancy Shulman[27], Saeed Sadiq Hamid[28], Cihan Yurdaydin[29]. *[1]Weill Cornell Medicine, New York, New York, United States; [2]Soroka University Medical Center, Beersheva, Israel; [3]Arensia Exploratory Medicine GmbH, Nicolae Testemitanu State University of Medicine and Pharmacy, Kyiv, Ukraine; [4]Arensia Exploratory Medicine GmbH, Nicolae Testemitanu State University of Medicine and Pharmacy, Chişinău, Moldova; [5]Icahn School Of Medicine At Mount Sinai, New York, New York, United States; [6]Toronto Centre for Liver Disease, University Health Network, Toronto General Hospital, Toronto, Canada; [7]ClinicNeolab, Tbilisi, Georgia; [8]Hepatology Clinic Hepa, Tbilisi, Georgia; [9]University Multiprofile Hospital For Active Treatment, Plovdiv, Bulgaria; [10]Geo Hospitals Tbilisi Multiprofile Medical Center, Tbilisi, Georgia; [11]Rambam Health Care Campus, Haifa, Israel; [12]University Of Pennsylvania Perelman School of Medicine, Philadelphia, Pennsylvania, United States; [13]Northwell Health Center for Liver Disease and Transplantation, New York, New York, United States; [14]Multiprofile Hospital for Active Treatment, Plovdiv, Bulgaria; [15]University of Calgary, Cumming School of Medicine, Calgary, Canada; [16]New Zealand Clinical Research (NZCR), Auckland, New Zealand; [17]CMU du Quartier Latin, Montreal, Canada; [18]NYU Grossman School Of Medicine, New York, New York, United States; [19]Liverpool Hospital, Liverpool, Australia; [20]The Johns Hopkins Hospital, Baltimore, Maryland, United States; [21]Keck School Of Medicine Of The University Of Southern California, Los Angeles, California, United States; [22]University of Alberta, Edmonton, Canada; [23]Rush University System For Health, Chicago, Illinois, United States; [24]Royal Prince Alfred Hospital, Sydney, Australia; [25]University of Iowa, Iowa City, Iowa, United States; [26]Long Beach Research Institute, Long Beach, California, United States; [27]Mirum Pharmaceuticals, Inc., Foster City, California, United States; [28]Aga Khan University, Karachi, Pakistan; [29]Koc University Hospital, Istanbul, Türkiye*
Email: tak4011@med.cornell.edu

Background and aims: Chronic Hepatitis D (CHD) is the most severe form of viral hepatitis and current treatments are limited. Brelovitug (BJT-778) is a fully human anti-hepatitis B surface antigen monoclonal antibody. AZURE-1 is a global, randomized, controlled, seamless Phase 2b/3 trial evaluating brelovitug versus delayed treatment (DT) for the treatment of CHD. Here we report on the efficacy and safety from the Phase 2b portion of AZURE-1.
Method: Participants were randomized 2:2:1 to receive open-label brelovitug 300 mg subcutaneous (SC) weekly (QW) self-administered at home, 900 mg SC every 4 weeks (Q4W) administered in the clinic, or delayed treatment (DT) for 24 weeks followed by brelovitug 300 mg QW. Key inclusion criteria were hepatitis D virus (HDV) RNA >500 IU/mL, ALT >upper limit of normal (ULN), and Child-Pugh Score <7; HIV co-infection and compensated cirrhosis with or without portal hypertension was allowed. There were no exclusion criteria for liver stiffness, bilirubin, albumin, INR or maximum ALT. The primary endpoint was a composite of virologic response (HDV RNA ≥2 $\log_{10}$ IU/mL decrease or undetectable HDV RNA) and ALT normalization at W24.
Results: A total of 53 participants were randomized; 21 to 300 mg QW, 20 to 900 mg Q4W, and 12 to DT. The mean (SD) age overall was 46 (8.2) years, 49 (92%) were White, 37 (70%) were male, and 28 (53%) had cirrhosis. Mean (SD) baseline HDV RNA was 5.5 (0.83) $\log_{10}$ IU/mL and ALT was 124 (95.3) U/L, including 11 (21%) with ALT ≥5×ULN and 8 (15%) with liver stiffness >25 kpa. At W12, virologic response occurred in 80% (16/20) including one out of window response, 50% (10/20), and 0% (0/12) for the 300 mg QW, 900 mg Q4W, and DT groups, respectively. At W12, mean (SD) ALT (U/L) values declined from 116 (91.2) at baseline to 46 (17.3) with 300 mg QW, 132 (105.5) to 51 (25.7) with 900 mg Q4W, and 124 (91.4) to 101 (51.7) in DT. Seven participants reported mild injection site reactions and 1 reported mild flu-like syndrome. There were no treatment-related SAEs, Grade ≥3 AEs, or AEs leading to study discontinuation. Further reductions in HDV RNA and ALT are observed after W12. Results at W24 will be shared at time of presentation as the trial is still ongoing.
Conclusion: In individuals with CHD with and without cirrhosis, brelovitug was associated with early improvements in HDV RNA, ALT and was well-tolerated. Multiple Phase 3 trials are ongoing.

LBP-022-YI

Single-dose of a novel monoclonal anti-HBV antibody (HepB mAb19) demonstrates sustained HBsAg suppression beyond 48 weeks: interim results from first-in-human phase I RUHBV1 and SAMBA trials

Han Ngoc Le[1], Siri Nana Halling Svensgaard[2], Zijun Wang[3], Jesper Damsgaard Gunst[2], Vanessa Igbokwe[1], Sidsel Dahl Winther Andersen[2], Henriette Graversen[2], Andre Moraes Nicola[3], Caroline Zöllner[4], Martin Kluge[4], Rachel Scheck[1], Pinkus Tober-Lau[1], David Hillus[1], Münevver Demir[4], Frank Tacke[4], Leif Erik Sander[1], Florian Kurth[1], Michel C. Nussenzweig[3], Thomas Rasmussen[2], Marina Caskey[3], Christian Gaebler[1], Ole S. Søgaard[2]. *[1]Department of Infectious Diseases and Critical Care Medicine, Charité–Universitätsmedizin Berlin, Berlin, Germany; [2]Department of Infectious Diseases, Aarhus University Hospital, Aarhus, Denmark; [3]Laboratory of Molecular Immunology, The Rockefeller University, New York, United States; [4]Department of Hepatology and Gastroenterology, Campus Virchow-Klinikum (CVK) and Campus Charité Mitte (CCM), Charité—Universitätsmedizin Berlin, Berlin, Germany*
Email: ngoc-han.le@charite.de

Background and aims: Chronic hepatitis B (CHB) remains a significant global health burden with persistently low rates of functional cure. This interim analysis reports on HepB mAb19 (mAb19), a highly potent, broadly neutralizing monoclonal antibody targeting hepatitis B surface antigen (HBsAg) and incorporating a half-life-extending modification at the Fc region. HepB mAb19 is currently being evaluated in HBeAg-negative CHB patients with HBV DNA below lower limit of quantification receiving standard antiviral therapy in the SAMBA trial in Denmark and Germany and the RUHBV1 trial in the United States. Enrollment was completed in Mid-March 2026.
Method: A total of 35 participants were enrolled (71% male, median age 43 years), with a median HBsAg level of 2418 IU/mL and median liver stiffness below 7 kPa. 20 participants received a single intravenous infusion of mAb19 in four ascending dose groups: 1 mg/kg (n = 8), 3 mg/kg (n = 4), 10 mg/kg (n = 4), and 30 mg/kg (n = 4), with one to two placebo recipients per group. Another 15 participants were enrolled in the open-label group with a defined maximum tolerated dosing of 30 mg/kg. Participants are followed for up to 48 weeks with regular assessments of safety, clinical laboratory, pharmacokinetics, and HBV serology parameters.
Results: Rapid declines in serum HBsAg were observed within 24 hours post-infusion across all dose groups, with a mean reduction of 1.14 $\log_{10}$ IU/ml by day 7. While lower doses resulted in transient reductions lasting up to week 24, participants completing follow-up in the highest dose group demonstrated persistent HBsAg reduction beyond 48 weeks, accompanied by high anti-HBs responses, suggesting durable, dose-dependent antiviral effects of mAb19. To date, all participants receiving infusion with 30 mg/kg have maintained reduced HBsAg levels at follow-up, including one case of sustained HBsAg loss at week 24. No serious adverse events (SAEs) or dose-limiting toxicities were observed. All AEs were transient and predominantly mild (grade 1). Six transient infusion reactions presenting with flu-like symptoms were observed that were possibly related to high baseline HBsAg (mean HBsAg 12478 IU/ml).
Conclusion: HepB mAb19 demonstrated a favourable safety profile and induced rapid, dose-dependent reductions in HBsAg. Sustained suppression beyond 48 weeks and a case of HBsAg loss following a single infusion support its potential for functional cure and provide a strong rationale for further clinical development.

LBP-023

Real-world outcomes in patients with primary biliary cholangitis who initiated elafibranor treatment with baseline alkaline phosphatase levels between 1× to 1.67× the upper limit of normal

Cynthia Levy[1,2], Channa Jayasekera[3], Seema T. Meloni[4], Matthew Sobiesk[4], Deborah Nikolla[4], Christelle Pommie[5], Hugo Gomes da Silva[5], Christopher L. Bowlus[6]. [1]*Schiff Center for Liver Diseases, University of Miami, Miami, Florida, United States;* [2]*Division of Digestive Health and Liver Diseases, University of Miami School of Medicine, Miami, Florida, United States;* [3]*Mayo Clinic, Phoenix, Arizona, United States;* [4]*Ipsen, Cambridge, Massachusetts, United States;* [5]*Ipsen, Paris, France;* [6]*Division of Gastroenterology and Hepatology, UC Davis School of Medicine, Sacramento, California, United States*
Email: clevy@med.miami.edu

Background and aims: Elafibranor (ELA), a peroxisome proliferator-activated receptor (PPAR)-alpha/delta agonist approved as a second-line (2L) treatment (Tx) for primary biliary cholangitis (PBC), demonstrated significant efficacy in the phase III ELATIVE® trial (NCT04526665). Patients (pts) with mildly elevated alkaline phosphatase (ALP; <1.67× upper limit of normal [ULN]) were not included in ELATIVE®. However, these pts can have significant disease burden and could be candidates for Tx. To our knowledge, this is the first real-world study to examine outcomes in pts with PBC with ALP >1 to <1.67× ULN treated with a PPAR agonist.
Method: This retrospective, observational study used the US HealthVerity network, which links data from claims, electronic health and laboratory provider records. The study identification period was Jun 2024–Dec 2025. The date of first observed ELA exposure was defined as the index date (baseline [BL]). Adult pts with PBC who received ≥1 dose of ELA during the study identification period were included. BL characteristics were assessed at the most recent visit prior to index date. Biochemical responses (including change from baseline [CfB]) were assessed using laboratory data through month (M)6 post-index for pts that started ELA as monotherapy or with ursodeoxycholic acid, without another 2L Tx; a post hoc analysis examined the excluded cohort of pts with prior 2L Tx that was discontinued by index date.
Results: A total of 321 pts had ≥1 ELA dose and no prior 2 L Tx. Of those, 111 had both pre- and post-index data, 53 with BL ALP between >1 to <1.67× ULN. At BL, mean (SD) age was 57 (11) years and 94.3% were female. Mean (SD) duration of ELA Tx was 187 (119) days. Mean (SD) ALP decreased from 174 (33) U/L at BL to 131 (52) U/L by M6 ($p < 0.001$), with mean (SD) CfB of −42 (60) U/L and percent CfB of −22.1% (37.1). By M6, 84.9% had an ALP reduction and 58.5% achieved ALP normalisation. In a post hoc analysis of pts with prior 2L Tx (n = 15), mean (SD) ALP was 177 (30) U/L at BL and 144 (50) U/L by M6 ($p < 0.03$), with mean (SD) CfB of −34 (45) U/L and percent CfB of −18.9% (24.8). By M6, 80.0% had an ALP reduction and 46.7% achieved ALP normalisation.
Conclusion: This is the first real-world study to show the effectiveness of ELA in pts with PBC with BL ALP between > 1 and < 1.67 × ULN, where clinically and statistically significant ALP reductions were seen and the majority achieved normalisation by M6. These data may help inform decision-making regarding Tx optimisation.

LBP-024

In F0-F1 and F2-F3 MASH, ≥5% weight loss (WL) significantly lowers VCTE and ELF independent of biopsy fibrosis improvement; resmetirom and not placebo reduction of ELF and VCTE are associated with biopsy improvement of fibrosis, independent of WL

Rohit Loomba[1], Quentin M. Anstee[2], Rebecca Taub[3], Dominic Labriola[3], Robin Mogg[3], Suneil Hosmane[3], Jörn M. Schattenberg[4], Vlad Ratziu[5]. [1]*San Diego School of Medicine, San Diego, United States;* [2]*Newcastle, Newcastle, United Kingdom;* [3]*Madrigal Pharmaceuticals, Conshohocken, United States;* [4]*Saarland University Medical Center, Saarbrücken, Germany;* [5]*Inserm, Paris, France*
Email: rebeccataub@yahoo.com

Background and aims: Resmetirom (Res) is approved for the treatment of adults with MASH and liver fibrosis. Changes in liver stiffness (VCTE), and ELF, a test for F3/F4 stage, are proposed as surrogate endpoints for fibrosis response in MASH. Weight loss (WL) reduces liver stiffness and collagen markers in patients (pts) without significant liver fibrosis (F0-F1) who have obesity/metabolic risk in whom serum markers of fibrosis may be elevated. In Res and placebo (Pbo) treated pts, the impact of ≥5% WL on VCTE and ELF and association with biopsy fibrosis improvement (FI) was examined in F0–F1 and F2–F3 MASH from MAESTRO Phase 3 trials.
Method: Baseline (BL) and Week 52 (W52) VCTE, ELF components were determined in MAESTRO-NASH (NCT03900429) (F2–F3), and MAESTRO-NAFLD-1 (NCT04197479) (F0–F1). Logistic regression models were used to explore associations between Res or Pbo mediated changes (absolute difference for ELF, difference of log transformed for VCTE), changes in weight (≥5% vs <5% WL) and biopsy FI.
Results: In F0-F1 ~14% had ≥5% WL at W52. Mean BL VCTE was 7.6 kPA; ELF, 9.2. In F0–F1, Res did not reduce VTCE, ELF (doi: 10.1038/s41591-023-02603-1). VCTE was significantly reduced in F0–F1 with ≥5% WL (−1.7 kPa, −25.0% (80 mg), −1.2 kPa, −24.3% (100 mg), −1.6 kPa 22.4% (Pbo)) versus (v) <5% WL (0.0 kPa, −3.9% (80 mg); −0.3 kPa, −6.1% (100 mg), −0.3 kPa, −8.9% (Pbo)). ELF was reduced in ≥5% WL v <5% WL with P3NP component showing the most significant reduction: ≥5% WL, −8.8% (80 mg), −8.4% (100 mg), −11.0% (Pbo) v <5%WL, 2.5% (80 mg), −1.8% (100 mg), −2.7% (Pbo). In F2–F3, Res reduced VCTE and ELF (DOI: 10.1056/NEJMoa2309000). Mean BL VCTE was 13.3 kPa; ELF, 9.8. A subset had ≥5% WL at W52 (17% (80 mg), 22%(100 mg), 12% Pbo). VCTE was reduced with WL ≥5% (−3.0 kPa, −18.9% (80 mg), −6.1 kPa, −35.6% (100 mg), −3.5 kPa, −27.8%, (Pbo)) v WL<5% (−2.1 kPa, −10.7% (80 mg), −2.4 kPa, −11.4% (100 mg), −0.49, 0.5% (Pbo)). Independent effects of WL and FI, respectively, on VCTE were demonstrated for Res [$p < 0.001$, $p < 0.001$] and not Pbo [$p < 0.001$, $p = 0.13$]. ELF was reduced with WL ≥5% (−0.32 (80 mg), −0.53 (100 mg), −0.19 (Pbo) v WL<5% (−0.07 (80 mg), −0.07 (100 mg), 0.13 (Pbo)). Independent effects of WL and FI, respectively, on ELF were demonstrated for Res [$p < 0.001$, $p < 0.001$] and not Pbo [$p < 0.001$, $p = 0.14$].
Conclusion: Confounding effects of WL on ELF and VCTE that may be independent of FI must be considered in analyzing MASH treatments. With Res treatment, independent correlations of WL and FI with ELF/VCTE reductions were observed.

LBP-025

Once-monthly efimosfermin alfa in participants with metabolic dysfunction-associated steatohepatitis with F2/F3 fibrosis: post hoc results from a 24-week, randomized, double-blind, placebo-controlled, phase 2 trial

Rohit Loomba[1], Kris Kowdley[2], Muhammad Y. Sheikh[3,4], Nomita Kim[5], Anita Kohli[6], Eric Lawitz[7,8], Brenda Jeglinski[9], Kelly Kutch[9], Jose Manuel Trigo[9], Patricia Mendez[10], Margaret Koziel[9], Stuart Kendrick[11], Sumanta Mukherjee[10], Mazen Noureddin[12]. [1]*University of California San Diego, San Diego, United States;* [2]*Liver Institute Northwest, Velocity Clinical Research, Elson S Floyd College of Medicine, Seattle, United States;* [3]*Fresno Clinical Research Center, Fresno, United States;* [4]*California Health Sciences University, Clovis, United States;* [5]*IMA Clinical Research, Austin, United States;* [6]*Arizona Liver Health/Arizona Clinical Trials, Chandler, United States;* [7]*Texas Liver Institute, San Antonio, United States;* [8]*Univerity of Texas Health San Antonio, San Antonio, United States;* [9]*Boston Pharmaceuticals, Waltham, United States;* [10]*GSK, Collegeville, United States;* [11]*GSK, Stevenage,*

United Kingdom; [12]Houston Methodist Hospital, Houston Research Institute, Houston, United States
Email: NoureddinMD@houstonresearchinstitute.com

Background and aims: Efimosfermin alfa, a once-monthly fibroblast growth factor 21 analog, showed histological improvements in fibrosis and metabolic dysfunction-associated steatohepatitis (MASH) activity compared with placebo among participants (pts) with F2/F3 fibrosis after 24 weeks of treatment in a Phase 2 trial (NCT04880031). This *post hoc* analysis assessed changes in non-invasive tests (NITs) liver stiffness measurement (LSM), enhanced liver fibrosis (ELF), and type III collagen pro-peptide (PRO-C3) with efimosfermin in pts with F2/F3 at baseline/biopsy-confirmed MASH from parts B, C, and D.
Method: In this pooled analysis, 120 pts were randomized to receive placebo (n = 40), efimosfermin 225 mg every 4 weeks (Q4W; n = 12), or efimosfermin 300 mg Q4W (n = 68) for 24 weeks. The proportion of patients with a response (defined as ELF reduction ≥0.5, LSM reduction ≥30%, and fibrosis improvement of ≥1 stage without MASH worsening) and PRO-C3 levels were assessed at the closest point to 24 weeks.
Results: Pts receiving placebo, efimosfermin 225 mg, and efimosfermin 300 mg had a mean age of 54.4, 62.3, and 53.8 years and 43%, 75%, and 41% had F3 fibrosis, respectively. By 24 weeks, a higher proportion of pts in the placebo group (33%; 13/40) had no changes in LSM, ELF, or fibrosis improvement than those in the efimosfermin 225 mg (17%; 2/12) or efimosfermin 300 mg (21%; 14/68) groups. A greater proportion of pts in the efimosfermin 225 mg and 300 mg groups achieved a response (8% [1/12] and 7% [5/68], respectively) compared with placebo (3%; 1/40). There was also a greater combined reduction in LSM and ELF in the efimosfermin 225 mg and 300 mg groups (42% [5/12] and 19% [13/68], respectively) than placebo (10%; 4/40). PRO-C3 levels decreased by approximately 20% as early as Week 4 with efimosfermin and remained suppressed through Week 24, while placebo showed smaller, later changes.
Conclusion: Efimosfermin (both doses) produced greater and simultaneous improvements in LSM, ELF, and fibrosis versus placebo; the strong correlation between ELF and LSM improvements supports an early and sustained anti-fibrotic effect. Although there were study limitations with a small sample size of pts receiving efimosfermin 225 mg and the short duration used to assess clinical benefits, these NIT findings complement the histological results and support continued evaluation in F2/F3 MASH for longer durations in the Phase 3 trials.

LBP-026
Hepatic recompensation is associated with sustained transplant-free survival in primary biliary cholangitis decompensated cirrhosis: an international multicenter study from the Global-PBC study group

Adrielly Martins[1], Yu Jun Wong[2], Adriaan J. van der Meer[3], Tiki D. Blom[3], Nikolaos Gatselis[4], George Dalekos[4], María Carlota Londoño[5], Sergio Rodriguez-Tajes[5], Gideon M. Hirschfield[6], Aliya Gulamhusein[6], Guilherme Cançado[7], John Eaton[8], Nick Nguyen[8], Jef Verbeek[9], Cláudia Couto[7], Xavier Verhelst[10], Anja Geerts[10], Atsushi Tanaka[11], Marlyn J. Mayo[12], Mark Pedersen[12], Christos Triantos[13], Konstantinos Papantoniou[13], Conrado Fernandez-Rodriguez[14], Andrew L. Mason[2], Bettina E. Hansen[3], Aldo J. Montano-Loza[2], Cynthia Levy[1]. *[1]University of Miami, Miami, United States; [2]University of Alberta, Changi General Hospital, Alberta, Canada; [3]Erasmus MC, Rotterdam, Netherlands; [4]General University Hospital of Larissa, Larissa, Greece; [5]Universitat de Barcelona, Barcelona, Spain; [6]University of Toronto, Toronto, Canada; [7]Universidade Federal de Minas Gerais, Belo Horizonte, Brazil; [8]Mayo Clinic, Rochester, United States; [9]University Hospitals Leuven, Leuven, Belgium; [10]Ghent University Hospital, Ghent, Belgium; [11]Teikyo University School of Medicine, Tokyo, Japan; [12]University of Texas Southwestern Medical Center, Dallas, United States; [13]University of Patras, Patras, Greece; [14]University Rey Juan Carlos, Madrid, Spain*
Email: axm8717@med.miami.edu

Background and aims: Hepatic recompensation has been described in several forms of chronic liver disease. Whether recompensation occurs in primary biliary cholangitis (PBC) remains understudied. We aimed to determine its rate in decompensated PBC and evaluate its impact on liver transplant-free survival (TFS).
Method: We conducted a retrospective international multicenter cohort study using the Global PBC Study Group database (16 centers; North America, South America, Europe, and Asia). Patients with PBC cirrhosis and a documented index decompensating event (ascites, variceal bleeding, or hepatic encephalopathy [HE]) were included; those with PBC-autoimmune hepatitis overlap or without proper follow-up were excluded. Recompensation was defined as the composite of MELD 3.0 < 10, absence of new decompensating event throughout 12 months after index decompensation (ID), and no ongoing use of diuretics or HE treatments for at least 12 months. All patients were treated with ursodeoxycholic acid for at least 12 months. Among patients event-free at 12 months, Kaplan-Meier and Cox regression assessed predictors of TFS. Sensitivity analysis used imputed MELD 3.0 values.
Results: Of 348 patients with decompensated PBC (86% female, median age at ID 63 years, median MELD 3.0 at ID 14), index events included ascites (73%), variceal bleeding (22%), and HE (14%). At 12 months, 195 patients (56%) were event-free; 12 (6.2%) achieved recompensation. Without the treatment-free criterion, 33 additional patients qualified (45 total, 23.1%). Among these 195 patients (139 events; median follow-up 50.1 months), those with MELD 3.0 < 10 at 12 months had markedly longer TFS than those without (median 97.5 vs 44.0 months; log-rank p < 0.001). Failure to achieve MELD 3.0 < 10 predicted liver transplantation or death on univariate (HR 2.34, 95%CI 1.45–3.78, p < 0.001) and multivariable analysis adjusted for treatment-free status (HR 2.34, 95%CI 1.45–3.78, p < 0.001). Treatment-free status alone was not independently associated with TFS (p = 0.3). Findings were consistent in the imputed sensitivity analysis for missing MELD 3.0 values (HR 1.92, 95%CI 1.27–2.89, p = 0.002).
Conclusion: Hepatic recompensation is not only achievable but clinically meaningful in decompensated PBC. A MELD 3.0 < 10 at 12 months identifies a subgroup with substantially improved TFS.

LBP-027
ARO-INHBE demonstrates clinically meaningful reductions in liver fat as monotherapy and in combination with low-dose tirzepatide in adults with obesity

John Baker[1], Jane Kerr[2], Renate Koops[3], Grigoriy Shekhtman[4], Eric Garcia-Medel[4], Ran Fu[4], James Hamilton[4], Ildiko Lingvay[5], Carel Le Roux[6], Rohit Loomba[7], Arun J. Sanyal[8], Rinki Murphy[9]. *[1]Middlemore Hospital, Te Whatu Ora Counties Manuaku, Middlemore, New Zealand; [2]New Zealand Clinical Research, Christchurch, New Zealand; [3]Aoteoroa Clinical Trials, Auckland, New Zealand; [4]Arrowhead Pharmaceuticals, Pasadena, United States; [5]Division of Endocrinology, University of Texas Southwestern Medical Center, Dallas, United States; [6]University College Dublin, Dublin, Ireland; [7]Division of Gastroenterology and Hepatology, University of California at San Diego, San Diego, United States; [8]Division of Gastroenterology, Hepatology, and Nutrition, Virginia Commonwealth University, Richmond, United States; [9]Department of Medicine, Faculty of Medical and Health Sciences, University of Auckland, Auckland, New Zealand*
Email: r.murphy@auckland.ac.nz

Background and aims: Excess hepatic fat is a key driver of metabolic dysfunction-associated steatohepatitis (MASH). The *INHBE* gene encodes Activin E, a hepatokine thought to promote fat storage in adipocytes. Predicted *INHBE* loss of function variants are associated with a favorable metabolic profile and lower risk of type 2 diabetes (T2DM). ARO-INHBE is an investigational siRNA designed to silence hepatic *INHBE* expression.

Method: Participants with obesity (BMI 30–50 kg/m^2), with T2DM (HbA1c 6.7%–9.5%) and without T2DM (HbA1c <6.5%), were enrolled in a Phase 1/2a, randomized, placebo-controlled study evaluating the safety, tolerability, pharmacokinetics, and pharmacodynamics of ARO-INHBE. Participants received one (D1) or two (D1 and D29) subcutaneous doses of ARO-INHBE, as monotherapy (n = 6 per group, allocated 2:1 to 50, 100, 200, or 400 mg vs placebo[PBO]), or in combination with 5 mg tirzepatide (n = 12 per group; allocated 2:1 to 100, 200, or 400 mg vs PBO), and were followed for up to 169 days. The primary endpoint was incidence of treatment-emergent adverse events (TEAEs). Exploratory endpoints included changes in serum Activin E levels, body composition (MRI), liver fat content (LFC) by MRI proton density fat fraction (MRI-PDFF), and biochemical parameters.
Results: Of 121 participants, 78 (64.5%) were female; mean age was 45.3 years; 20% had T2DM. Baseline mean BMI was 36.9 kg/m^2, mean LFC was 8.9%; 42.1% had LFC ≥8%. ARO-INHBE achieved durable and dose-dependent reductions in serum Activin E, with a mean maximum reduction of 85.3% after a single 400 mg dose. Participants without T2DM with baseline LFC ≥8% receiving ≥200 mg ARO-INHBE monotherapy (n = 10; baseline LFC 14.5 ± 5.1%), had a placebo-adjusted post-dose LFC reduction of 44% ($p < 0.01$). In participants with T2DM (baseline LFC 16.9 ± 9.1%), combination therapy with ARO-INHBE 400 mg and TZP 5 mg led to greater LFC reduction than TZP alone (−59% [n = 7] vs −20% [n = 6], p = 0.01). ARO-INHBE was well-tolerated. Most TEAEs were mild and no TEAEs led to study or study drug discontinuation. No adverse laboratory trends (including HbA1c, ALT, and lipids) were observed.
Conclusion: RNAi-mediated silencing of *INHBE* with ARO-INHBE was well-tolerated and produced clinically meaningful reductions in LFC as monotherapy or combination therapy with low-dose tirzepatide in individuals with obesity with and without T2DM. Targeting Activin E may represent a novel therapeutic strategy for MASH and obesity-related metabolic dysfunction. The AROINHBE-1001 study is ongoing.

LBP-028-YI

Preventing vertical transmission of hepatitis B virus in Democratic Republic of Congo by combining birth-dose vaccine and tenofovir: a randomized double-blind placebo-controlled trial

Patrick Ngimbi[1], Nefer Batsuli[2], Linda James[2], Myriam Bonze[1], Elysée Bayayana[1], Jusline Pani[1], Gaëtan Bondo[1], Bienvenu Tukebana[1], Jeansy Mavinga[1], Martine Tabala[3], Melchior Kashamuka Mwandagalirwa[3], Charles Mbendi[3], Gavin Cloherty[4], Mark Anderson[4], Jonathan B. Parr[2], Lauren Tompkins[2], Julie Dumond[2], Mackenzie Cottrell[2], Feng-Chang Lin[2], Sylvia Becker-Drepps[2], Camille Morgan[2], Alix Boisson-Walsh[5], Marcel Yotebieng[6], Ernest Sumaili[1], Samuel Mampunza[1], Peyton Thompson[2]. *[1]Université Protestante du Congo, Kinshasa, Congo, Dem. Republic of (formally known as Zaire); [2]University of North Carolina at Chapel Hill, Chapel Hill, United States; [3]École de Santé Publique, Université de Kinshasa, Kinshasa, Congo, Dem. Republic of (formally known as Zaire); [4]Abbott Laboratories, Altavista, United States; [5]Rutgers University, New Brunswick, United States; [6]Albert Einstein College of Medicine, New York City, United States*
Email: nnb4@unc.edu

Background and aims: Eliminating vertical transmission of hepatitis B virus (HBV) is possible by combining birth-dose (HepB-BD) vaccine and maternal antiviral prophylaxis; these strategies are not yet available in low-resource settings like Democratic Republic of Congo (DRC). We conducted a randomized double-blind placebo-controlled trial of prophylaxis for all HBV-infected women (regardless of viral load). Our trial is among the first to evaluate this approach and launched prior to updated WHO guidelines recommending prophylaxis-for-all where viral load testing is inaccessible.
Method: We screened pregnant women at three maternity centers in Kinshasa using HBV surface antigen (HBsAg) rapid tests. Eligible participants (age ≥18, HBsAg+, HIV−, normal creatinine <1.3 mg/dL) were randomized at 28–32 weeks' gestation to placebo or tenofovir disoproxil fumarate (TDF), taken once daily from enrollment through 4 weeks postpartum. Infants received HepB-BD, preferably <24 hours of life. Primary outcomes were effectiveness (infant HBsAg status at 6 months), safety (side effects, alanine aminotransferase (ALT) levels, and hepatitis flares [ALT ≥5× the upper limit of normal]) and surveyed acceptability of study activities. Secondary outcomes included medication adherence via survey and dried blood spot (DBS) tenofovir diphosphate (TFVdp) concentrations, and receipt/timeliness of HepB-BD.
Results: 307 of 14,027 (2.2%) pregnancies screened were HBsAg+. 119/164 (73%) enrolled mothers and 115/151 (76%) infants completed follow-up. There was no vertical transmission: 115 infants tested HBsAg-negative at 6 months. No major safety concerns were observed: 34 (41%) TDF and 24 (29%) placebo recipients reported mild-to-moderate side effects, ALT levels were similar between arms, and there were no hepatitis flares. Acceptability was high (93% in placebo and 87% in TDF arm). Adherence was lower by DBS TFVdp concentrations than self-report: 42% on TDF reported taking 2–6 doses/week and 58% took 7 doses/week, but concentrations indicated 84% took <2, 16% 2–6 and 0% 7 doses/week. 85% of infants received HepB-BD; 53% were timely, with lower coverage in the TDF vs placebo arm (81% vs 89% vaccinated; 49% vs 56% timely). Viral load testing is in progress.
Conclusion: No infants were HBV+ in this prophylaxis-for-all plus HepB-BD trial in DRC, despite suboptimal antiviral adherence and untimely birth-dose vaccine. A layered approach was safe and should be considered in DRC and similar low-resource settings to maximize prevention.

LBP-029

Weight loss–independent Glucagon effect led to rapid, clinically significant reductions in MASH severity, including steatosis and liver stiffness, during a 48-week randomized controlled trial of dual agonist DD01

Mazen Noureddin[1,2], Rashmee Patil[3], Dimple Desai[4], Rohit Puskoor[5], Winston Dunn[3,6], Jaehee Shin[7], Dennis To[8], Adam Bell[8], Daniel Lee[8], Yen-Huei Lin[8]. *[1]Houston Methodist Hospital, Department of Medicine, Sherrie and Alan Conover Center for Liver Disease and Transplantation, JC Walter Jr Transplant Center, Houston, United States; [2]Houston Research Institute, Houston, United States; [3]Pinnacle Clinical Research, San Antonio, United States; [4]South Texas Research Institute, Edinburg, United States; [5]Pinnacle Clinical Research, Austin, United States; [6]University of Kansas Medical Center, Kansas City, United States; [7]D&D Pharmatech Co, Seongnam-si, Korea, Rep. of South; [8]Neuraly, Inc., Gaithersberg, United States*
Email: noureddinmd@pinnacleresearch.com

Background and aims: DD01 is a dual GLP-1/glucagon receptor agonist designed to leverage complementary metabolic pathways for the treatment of MASLD/MASH. While GLP-1 receptor agonism improves glycemic control and reduces caloric intake, glucagon receptor activation promotes hepatic lipid oxidation, increases energy expenditure, and may directly reduce liver fat independent of weight loss. DD01 is being investigated for these liver-directed effects in MASH.
Method: DD01-DN-02 is an ongoing phase 2 48-week randomized, double-blind, placebo-controlled trial (NCT06410924), with endpoints at 12 (primary) and 48 (secondary) weeks. Key inclusion criteria for this study are ≥10% liver fat content (LFC) by MRI-PDFF and having 2 metabolic risk factors (MASLD population) OR biopsy showing F1–F3 fibrosis with NAS≥4 (MASH population). Participants were randomized 1:1 to receive 40 mg DD01 (with 2-week dose escalation only) or placebo weekly via subcutaneous injection.
Results: A total of 67 patients were randomized, 33 to the DD01 arm and 34 to the placebo arm. DD01 treatment resulted in substantial and clinically meaningful reductions in hepatic steatosis, with >50%

reduction in LFC in >70% of subjects after 12 weeks ($p < 0.0001$ vs placebo). Rapid reductions in LFC were accompanied by significant reductions in liver stiffness as assessed by MRE and compared to placebo-treated subjects (−19.7 vs −7.2; $p < 0.01$) and a significant relative reduction in ELF score (−2.5 vs 1.5; $p < 0.01$). In DD01-treated patients who lost ≥5% bodyweight at 12 weeks, there was an 81.1% (−85.3, −76.9) reduction in MRI-PDFF from baseline ($p < 0.0001$). Among patients with <5% bodyweight loss, those treated with DD01 achieved a 37.4% reduction in MRI-PDFF (95% CI, −72.9, −1.9), versus an increase of 1.6% (−30.4, 33.6) in placebo subjects. In the same population, there was a 19.2% (−37.5, −0.9) reduction in MRE in the DD01 arm, versus a 7.7% (−24.2, 8.9) reduction in the placebo arm ($p = 0.02$). Histological outcomes, including Week 48 biopsy data, are expected to be available at the time of conference presentation.
Conclusion: DD01 demonstrated significant reductions in liver fat and improvements in markers of MASH severity at 12 weeks, including in patients with minimal weight loss, supporting potential weight-independent hepatic effects. Further data, including histological outcomes at 48 weeks, will help clarify the durability and clinical relevance of these findings.

LBP-030

Rotational thromboelastometry–guided transfusion strategy versus conventional management in difficult-to-treat acute variceal bleeding in ACLF: a randomised controlled trial

Madhumita Premkumar[1], Prerna Sharma[1], Anchal Sandhu[1], Kamal Kajal[1], Harish Bhujade[1], Arka De[1], Sweta Rose[1], Muhammad Ashraf[1], S. Balaraja[1], Naveen Dandia[1], Ajay Kumar Duseja[1], Jasmina Ahluwalia[1], Narender Kumar[1], Deepy Zohmangaihi[1], K. Rajender Reddy[2]. *[1]Postgraduate Institute of Medical Education and Research, Chandigarh, India; [2]Penn Medicine, Philadelphia, United States*
Email: drmadhumitap@gmail.com

Background and aims: Acute variceal bleeding (AVB) in acute-on-chronic liver failure (ACLF) is portal hypertension-driven and managed with vasoactive therapy and endoscopic control. However, a subset may be difficult to treat, requiring substantial transfusion support, predisposing to adverse events (AEs).
Method: In this single-centre, randomised, double-blind trial, patients with difficult-to-treat AVB were assigned (1:1) to a rotational thromboelastometry (ROTEM)-guided or a standard coagulation test (SCT)-guided transfusion strategy. Difficult-to-treat AVB was defined as (i) bleeding from multiple sites in addition to the primary variceal source (esophageal [EV], gastric[GV], or both), including post-EVL ulcer bleeding; and/or (ii) failure to control bleeding despite appropriate pharmacologic and endoscopic therapy, and/or (iii) requirement for escalation to rescue therapies such as balloon tamponade, Danis-Ella self-expanding metal stent(SEMS) placement, or pre-emptive or salvage TIPS. The primary endpoint was the rebleeding rate at 48 hours, Day 5, and Day 42. Secondary endpoints included blood component utilisation, intensive care need, AEs, and survival.
Results: Of 1,341 screened patients, 262 were randomised (ROTEM, n = 132; SCT, n = 130; aged 45.1 ± 11.6 years; MELD-Na 24.2 ± 9.7; 89% men; 64.5% alcohol-associated; 73% had shock). Difficult-to-treat bleeding included multiple bleeding sites (n = 113), active spurting (n = 112), or failure-to-control bleed (n = 37; 17-TIPS and 20-SEMS). Bleeding sources were small esophageal varices (EV, 9.2%), large EV (76.7%) and gastric varices (14.1%). Baseline characteristics were comparable. Rebleeding rates at 48–120 hours (4.6%), 6–42 days (13.4%), and 42–180 days (8.8%) were similar. ROTEM significantly reduced the need for fresh frozen plasma (29.2% vs 7.6%) and platelet units (26.9% vs 9.1%; $p < 0.001$), and transfusion-related AEs (6.8% vs 14.6%; $p = 0.047$), without differences in ICU admission or 180-day mortality (34.7%). Independent predictors of rebleeding were multiple bleeding sites (adjusted hazard ratio[aHR] 1.9;95%CI:1.1–2.5; $p = 0.007$) and CLIF-C ACLF score (aHR 1.04; 95%CI: 1.01–1.07; $p = 0.022$). Rebleeding (subdistribution HR [sHR] 1.4; 95%CI:1.2–3.9; $p = 0.026$), and Grade 2 ACLF grade (sHR 5.0;95%CI:1.5–16.3; $p = 0.007$), and Gr 3 (sHR 18.9;95%CI:5.5–65.6; $p < 0.001$) predicted 180-day mortality.
Conclusion: In ACLF with difficult-to-treat AVB, ROTEM-guided transfusion reduced plasma and platelet exposure and AEs without compromising bleeding control or survival.

LBP-031

AHB-137 monotherapy elicits high functional cure rates and sustained DNA suppression in treatment-naïve chronic hepatitis B participants: results from an ongoing phase II study

Yunqing Qiu[1], Haibing Gao[2], Dazhi Zhang[3], Youwen Tan[4], Meihong Yu[1], Xiaowei Xu[1], Xiangmei Wang[2], Shan Zhong[3], Xingbei Zhou[4], Mingyue Chen[5], Kaili Zhang[5], Chen Yang[5], Yeming Pan[5], Di Zhao[5], Miao Wang[5], Cheng Yong Yang[5,6], Guofeng Cheng[5,6], Hao Wang[5]. *[1]The First Affiliated Hospital, Zhejiang University School of Medicine, Hangzhou, China; [2]Mengchao Hepatobiliary Hospital of Fujian Medical University, Fuzhou, China; [3]The Second Affiliated Hospital of Chongqing Medical University, Chongqing, China; [4]The Third People's Hospital of Zhenjiang, Zhenjiang, China; [5]Ausper Biopharma Co., Ltd., Hangzhou, China; [6]Ausperbio Therapeutics Inc., Foster City, United States*
Email: qiuyq@zju.edu.cn

Background and aims: AHB-137 has demonstrated promising efficacy with a favorable safety profile in nucleos(t)ide analogue (NA) suppressed HBeAg-negative chronic hepatitis B (CHB) patients. The ongoing phase II study (NCT06829329) evaluates AHB-137 in treatment-naïve CHB patients. Here we present the End of Study (EOS) results from Part A.
Method: Part A is a randomized, double-blind, placebo-controlled study in treatment-naïve CHB participants (baseline (BL) HBsAg 100–10,000 IU/mL, HBV DNA 20–2,000 IU/mL). Participants received 16-week AHB-137 (300 mg) or placebo (4:1) weekly as monotherapy (without NA), followed by a 24-week off-treatment follow-up. Primary endpoint was complete response (CR; HBsAg <0.05 IU/mL and HBV DNA <10 IU/mL) at End of Treatment (EOT). Functional cure (FC; sustained CR) was evaluated at EOS (24 weeks off all treatment). Efficacy and safety were evaluated using per-protocol set (PPS) and safety set (SS), respectively.
Results: The PPS included 31 participants (AHB-137, n = 25; placebo, n = 6). AHB-137 monotherapy demonstrated rapid and potent HBV DNA suppression, with 100% of participants achieving HBV DNA <10 IU/mL by week 16 (EOT). Profound HBsAg reduction was also observed: 84% (16/19) of participants with BL HBsAg ≤3,000 IU/mL achieved HBsAg loss by EOT; all 6 participants with BL HBsAg >3,000 IU/mL showed ≥4.5 $\log_{10}$ IU/mL HBsAg reduction, and 3 achieved HBsAg loss. Overall, 68% (17/25) achieved CR at EOT. Safety was consistent with prior studies in NA-suppressed patients, with most treatment related adverse events being Grade 1–2, including reversible ALT/AST elevations associated with rapid HBsAg decline. One treatment-related SAE was reported, characterized by ALT elevation with concomitant bilirubin and HBV DNA increases. No clinical symptoms were reported, and the event resolved completely without sequelae. At EOS, 32% (8/25) achieved FC. Responses were particularly favorable in participants with BL HBsAg ≤1,000 IU/mL, with 70% (7/10) achieving FC. Among those with BL HBsAg >1,000 IU/mL, 33% (5/15) achieved partial cure at EOS, with sustained HBV DNA suppression and HBsAg <10 IU/mL.
Conclusion: In treatment-naive CHB participants, AHB-137 monotherapy demonstrated potent inhibition of HBV DNA replication and profound reduction of HBsAg, resulting in a high FC rate. Overall, AHB-137 was generally well-tolerated, coupled with durable off-treatment HBV DNA suppression. These data support the further development of AHB-137 in a broader CHB population.

LBP-032

Denifanstat and resmetirom combination therapy rapidly decreased atherogenic lipids in healthy adults in Phase 1 open-label trial

Mary E. Rinella[1], Arun J. Sanyal[2], Wen-Wei Tsai[3], Shipra Gupta[3], Cristina Alonso[4], Katharine Grimmer[3], Eduardo Martins[3], Marie O' Farrell[3], Rohit Loomba[5]. *[1]University of Chicago, Chicago, IL, United States; [2]Virginia Commonwealth University School of Medicine, Richmond, VA, United States; [3]Sagimet Biosciences, San Mateo, CA, United States; [4]Rubio Metabolomics, Derio, Bizkaia, Spain; [5]UC San Diego School of Medicine, La Jolla, CA, United States*
Email: wen-wei.tsai@sagimet.com

Background and aims: Increased *de novo* lipogenesis drives development of MASH, with fatty acid synthase (FASN) being the key enzyme. In a Ph2b trial, an oral FASN inhibitor Denifanstat (Deni) improved fibrosis and MASH resolution and prevented progression to cirrhosis. Resmetirom (Res), an FDA-approved thyroid hormone receptor beta agonist for MASH with F2/F3 fibrosis, reduced liver fat by increasing lipid oxidation. Combination of Deni and Res may increase efficacy through complementary mechanisms of liver fat reduction and Deni's direct anti-fibrotic effect, as demonstrated in preclinical MASH models. This Ph1 trial evaluated safety, PD and PK of the combination.
Method: Forty healthy adults (20/cohort) received 50 mg Deni and weight-based Res (80/100 mg). Cohorts 1 and 2 completed 7 days of monotherapy lead-in for Deni or Res respectively followed by 7 days of combination therapy. Blood was analyzed for multi-omic profiling, and Deni and Res PK.
Results: All treatments were generally well tolerated. Total cholesterol was significantly decreased by 23.4 and 16.4 mg/dL at the end of treatment (EOT) in cohorts 1 and 2 ($p < 0.001$), and decreased by 6.6 and 13.2 mg/dL with monotherapy of Deni and Res at day 7. The observed reductions ranged from ~1.1-fold decrease to greater than a 2.4-fold decrease relative to a hypothetical additive reduction, suggesting a potential synergistic lipid lowering effect with combination. LDL-cholesterol also dropped by 16.7 mg/dL (cohort 1) and 13.6 mg/dL (cohort 2) at EOT ($p < 0.001$). Polyunsaturated triglycerides (TG) were specifically increased by 2-week Deni treatment, while Deni and Res decreased saturated TG both alone and in combination. Serum sex hormone binding globulin was increased by 40% with Res monotherapy ($p < 0.001$), but not with Deni, and further increased to 58% with combination therapy at EOT ($p < 0.001$), showing rapid target engagement for Res. At day 7 (monotherapy) and day 14 (combination), plasma $AUC_{0\text{-}tau}$ (ng*h/mL) for Deni was 13110 and 14970; for Res $AUC_{0\text{-}tau}$, it was 7054 and 4580.
Conclusion: These Phase 1 results showed strong target engagement for Deni and Res, alone and in combination. The combination significantly reduced atherogenic lipids, suggesting cardiovascular benefits. Together with prior fibrosis improvement data, the safety, PD/biomarker and PK results support further clinical evaluation of Deni/Res combination for MASH and fibrosis.

LBP-033

Elafibranor treatment results in rapid reductions in biochemical markers and symptom burden in real-world practice: interim results from the prospective, non-interventional ELFINITY phase IV global study in patients with primary biliary cholangitis

Jörn M. Schattenberg[1,2], Peter Fickert[3], Kris V. Kowdley[4,5], Ashis Mukhopadhya[6], Seema Jaitly[7], Christelle Pommie[8], Marwan Sleiman[8], Phil Troke[7], Michael Trauner[9]. *[1]Department of Internal Medicine II, Saarland University Medical Center, Homburg, Germany; [2]Saarland University, Saarbrücken, Germany; [3]Department of Internal Medicine, Division of Gastroenterology and Hepatology, Medical University Graz, Graz, Austria; [4]Liver Institute Northwest, Seattle, United States; [5]Elson S. Floyd College of Medicine, Washington State University, Washington, United States; [6]Department of Gastroenterology, Aberdeen Royal Infirmary, NHS Grampian, Aberdeen, United Kingdom; [7]Ipsen, London, United Kingdom; [8]Ipsen, Paris, France; [9]Department of Internal Medicine III, Division of Gastroenterology and Hepatology, Medical University of Vienna, Vienna, Austria*
Email: joern.schattenberg@uks.eu

Background and aims: Elafibranor (ELA) is a peroxisome proliferator-activated receptor (PPAR)-alpha/delta agonist approved for primary biliary cholangitis (PBC) second-line treatment. We present Month (M)3 data from the ongoing global, prospective, non-interventional phase IV ELFINITY study (NCT06447168) assessing real-world effectiveness and safety of ELA.
Method: ELFINITY will recruit ~424 patients (pts) receiving ELA 80 mg/day in real-world settings, to be followed for up to 5 years. Change from baseline (BL; CfB) in ALP, ALP normalisation and biochemical response (ALP <1.67× upper limit of normal [ULN] with ≥15% reduction from BL, and TB ≤ ULN) were reported at M3. A subgroup analysis was conducted to evaluate obeticholic acid (OCA)-experienced pts in ALP categories (<1, 1–<1.67, 1.67–<3 and ≥3× ULN) at BL and at M3. Moderate-to-severe (mod–sev) fatigue was defined as PBC-40 Fatigue ≥29 or Functional Assessment of Chronic Illness Therapy (FACIT)-Fatigue ≤30 (lower scores indicate higher fatigue), and mod–sev pruritus as PBC-40 Itch ≥7 or 5-D Itch ≥12. Pts with mod–sev symptoms achieving minimum clinically important differences (MCID) were reported (improvements PBC-40 Fatigue ≥5, PBC-40 Itch ≥1.5 and 5-D Itch ≥3). FACIT-Fatigue CfB was reported at M3. Pts receiving ≥1 dose were assessed. Completion of PRO instruments was not mandatory; missing data were not imputed.
Results: As of Oct 25, 55 pts were included in this analysis; 53 received ≥1 dose. Of pts with BL data, 27/51 (53%) had ALP ≥1.67× ULN. Mean (SD) ALP CfB to M3 was –0.7× ULN (0.7). At M3, 28/51 (55%) had biochemical response and 11/49 (22%) with BL ALP > ULN had ALP normalisation; 3 maintained normal BL ALP to M3. Of OCA-experienced pts, 7 improved and 1 worsened by 1 ALP category at M3; 8 maintained the same category. At BL, 25/44 (57%) had mod–sev fatigue by PBC-40 Fatigue and 18/44 (41%) by FACIT-Fatigue. In these pts, 8/14 (57%) improved ≥ MCID in PBC-40 Fatigue and mean (SD) FACIT-Fatigue CfB was 8.2 (13.1; n = 10) at M3. BL mod–sev pruritus was reported in 9/44 (20%) pts by PBC-40 Itch and 14/43 (33%) by 5-D Itch, of whom 3/3 (100%) and 6/8 (75%) improved ≥ MCID at M3. By M3, 6 pts discontinued. 26/53 (49%) had TEAEs, none serious/severe. TEAEs in ≥5 pts included fatigue (n = 6), headache (n = 5), diarrhoea (n = 5) and nausea (n = 5).
Conclusion: In this M3 interim analysis, ELA led to rapid improvements in ALP and both fatigue and pruritus, and was well tolerated, suggesting ELA is effective in real-world practice.

LBP-034-YI

Real-world experience with seladelpar in primary biliary cholangitis: first results from the Italian RESTART-PBC study

Francesca Terracciani[1], Antonio De Vincentis[1], Alessandra Mangia[2], Mauro Viganò[3], Edoardo Giovanni Giannini[4], Cristina Rigamonti[5], Federica Cerini[6], Ilaria Arena[7], Marco Carbone[8], Raffaella Viganò[8], Maurizia Brunetto[9], Nora Cazzagon[10], Francesco Giuseppe Foschi[11], Leonardo De Marco[12], Andrea Galli[13], Francesca Romana Ponziani[14], Eugenia Nofit[15], Laura Cristoferi[15], Alessio Gerussi[15], Ana Lleo[16], Pietro Lampertico[17], Fabrizio Bronte[18], Elisabetta Lorefice[19], Pietro Andreone[20], Grazia Anna Niro[21], Filomena Morisco[22], Valeria Pace Palitti[23], Maurizio Russello[24], Stefano Brillanti[25], Fabio Piscaglia[26], Antonino Castellaneta[27], Luchino Chessa[28], Fabio Marra[29], Marco Marzioni[30], Raffaele Cozzolongo[31], Pier Maria Battezzati[32], Gaetano Bertino[33], Vincenza Calvaruso[34], Valeria Piazzolla[2], Francesca Colapietro[3], Sara Labanca[4], Carla De Benedittis[5], Giulia Francesca Manfredi[5], Caparra Francesca[6], Marco Saracino[7], Marina Clemente[8], Barbara Coco[9], Iris Bocaj[10], Lucia Napoli[11], Erica Nicola Lynch[13], Leonardo Stella[14], Daphne D'Amato[15], Maria Pia Calabrese[16], Elisabetta Degasperi[17], Salvatore Fortunato Tantillo[18], Marta Baldini[19], Filippo Gabrielli[20],

Rosa Cotugno[21], Valentina Cossiga[22], Mariarita Cannavò[24], Giada Alterini[25], Antonella De Feudis[27], Alessandra Deidda[28], Filippo Biagi[29], Luca Maroni[30], Sara Vavassori[32], Alfredo Risicato[33], Maria Cristina Neglia[34], Pietro Invernizzi[15], Umberto Vespasiani-Gentilucci[1]. [1]*University Campus Bio-Medico of Rome, Internal Medicine and Hepatology, University Campus Bio-Medico of Rome, Roma, Italy;* [2]*Liver Unit, IRCCS Casa Sollievo della Sofferenza, S. Giovanni Rotondo, Italy;* [3]*Papa Giovanni XXIII Hospital, Bergamo, Italy;* [4]*University of Genoa, IRCCS Ospedale Policlinico San Martino, Genoa, Italy;* [5]*A.O.U. Maggiore della Carità, Novara, Italy;* [6]*Hepatology Division San Giuseppe Hospital, MultiMedica IRCCS, Università degli Studi di Milano, Milan, Italy;* [7]*Ospedale di RHO, Rho, Italy;* [8]*ASST Grande Ospedale Metropolitano Niguarda, Milan, Italy;* [9]*Hepatology Unit, Reference Center of the Tuscany Region for Chronic Liver Disease and Cancer, University Hospital of Pisa and Department of Clinical and Experimental Medicine, University of Pisa, Pisa, Italy;* [10]*Department of Surgery, Oncology and Gastroenterology, University of Padova, Padua, Italy;* [11]*Presidio Ospedaliero di Faenza, UO Medicina Interna, Faenza, Italy;* [12]*AULSS 1 Dolomiti, Ospedale San Martino di Belluno, Belluno, Italy;* [13]*Azienda Ospedaliera Universitaria Careggi, Gastroenterologia Clinica, Florence, Italy;* [14]*Fondazione Policlinico Universitario Agostino Gemelli IRCCS, Rome, Italy;* [15]*ASST Monza Ospedale San Gerardo, Gastroenterologia, Centro delle Malattie Autoimmuni del Fegato, Monza, Italy;* [16]*Division of Internal Medicine and Hepatology, Department of Gastroenterology, IRCCS Humanitas Research Hospital, Rozzano-Mi, Italy;* [17]*Division of Gastroenterology and Hepatology, Foundation IRCCS Ca' Granda Ospedale Maggiore Policlinico, Milan, Italy;* [18]*University of Palermo, Italy; Ospedali Riuniti Villa Sofia V. Cervello, Palermo, Italy;* [19]*"San Giuseppe" Hospital, Gastroenterology Unit, Empoli, Italy;* [20]*Ospedale Civile di Baggiovara, AOU di Modena, Modena, Italy;* [21]*IRCCS Casa Sollievo della Sofferenza, S. Giovanni Rotondo (Foggia), Italy;* [22]*Ospedale policlinico Federico II di Napoli, Naples, Italy;* [23]*Internal Medicin Unit, Santo Spirito Hospital, Pescara, Italy, Pescara, Italy;* [24]*Azienda Ospedaliera di Rilievo Nazionale e di Alta Specializzazione Garibaldi, UO Epatologia, Catania, Italy;* [25]*Azienda Ospedaliera Universitaria Senese, Siena, Italy;* [26]*IRCCS Azienda Ospedaliero Universitaria di Bologna -, UOC di Medicina Interna, Malattie epatobiliari e immunoallergologiche, Bologna, Italy;* [27]*UO Gastroenterologia, Policlinico di Bari, Bari, Italy;* [28]*Azienda ospedaliero università di Cagliari, Policlinico universitario Monserrato, Cagliari, Italy;* [29]*UO Medicina Interna ed Epatologia, Azienda Ospedaliera Universitaria Careggi, Florence, Italy;* [30]*Azienda Ospedaliero Universitaria delle Marche, Ancona, Italy;* [31]*IRCCS S de Bellis, Castellana Grotte, Italy;* [32]*ASST Santi Paolo e Carlo, Milan, Italy;* [33]*Gastroenterology and Hepatology Unit, University Hospital Policlinico Vittorio Emanuele, Catania, Italy;* [34]*Section of Gastroenterology and Hepatology, University of Palermo, Palermo, Italy*
Email: f.terracciani@unicampus.it

Background and aims: A substantial proportion of patients with PBC do not respond adequately to first-line UDCA therapy. Seladelpar, a selective PPAR-δ agonist, has been recently approved as second-line treatment. The RESTART-PBC study aims to evaluate its effectiveness and safety in a real-world setting.
Method: In this multicenter observational study, adult patients from the Italian PBC Registry treated with seladelpar according to approved criteria were included. Prior seladelpar trial participants were excluded. Biochemical response was evaluated in those with at least one follow-up assessment, and defined as: adequate (ALP <1.67×ULN and normal bilirubin), POISE (adequate plus ≥15% ALP reduction), and complete (normal ALP and bilirubin). Symptoms were assessed using Worst Itch Numeric Rating Scale (WI-NRS), PBC-40, and 5-D Itch. Longitudinal changes were analyzed with linear mixed-effects models and reported as LS-means (95%CI). Kaplan–Meier estimates were used for cumulative response.
Results: Overall, 167 patients were included [median age 55 years; 90% female; median disease duration 6.3 years; 54 (32%) with cirrhosis; 19 (11%) with PBC/autoimmune hepatitis variant]. Prior second-line exposure included fibrates (48 patients, 29%) and/or obeticholic acid (96 patients, 57%), with median washouts of 7 (IQR 0–287) and 189 (IQR 110–249) days, respectively. At baseline, 48% of patients were already in adequate and 9% in complete response. Among the 129 patients with at least one follow-up assessment, median follow-up after seladelpar start was 6 months. Probabilities of maintaining/attaining adequate, POISE, and complete response were 67%, 46%, and 31% at 3 months, and 80%, 62%, and 42% at 6 months, remaining stable at 9 months. Responses were similar regardless of prior second-line therapy or washout duration. Discontinuation occurred in 3 patients (2.4%): 2 for intolerance and 1 for drug interaction. WI-NRS significantly decreased at 3 months (−1.03; −40%) and over time ($p < 0.001$). Among patients with WI-NRS≥4, 58% improved to <4. Improvements were also observed in PBC-40 total score ($p < 0.001$) and fatigue ($p = 0.030$).
Conclusion: These interim real-world data confirm seladelpar effectiveness and safety regardless of prior second-line exposure. Initiation at ALP <1.67×ULN in a substantial subgroup of both switch and naïve patients suggests a shift toward earlier, proactive treatment aiming at ALP normalization, particularly in advanced fibrosis.

LBP-035

Scalable bioreactor production of functional iPSC-derived hepatic microtissues demonstrates unprecedented therapeutic efficacy in a preclinical model of acute liver failure

Dilyana Todorova[1], Elise Warter[1], Kenita Fock-Sing[1], Helene Riesterer[1], Charlene Francois[1], Solenn Guilbert[1], Jens Schroeder[1], Emilie Faggiani[1], Peter Andersen[1,2]. [1]*Treefrog Therapeutics, Bordeaux, France;* [2]*Johns Hopkins School of Medicine, Department of Medicine, Baltimore, United States*
Email: dilyana.todorova@treefrog.fr

Background and aims: Pluripotent stem cell (PSC)–derived cell replacement therapies represent a promising strategy for restoring liver function in patients suffering from multiple types of liver disease including acute or chronic liver failure. Early clinical and preclinical studies have demonstrated the safety and feasibility of PSC-derived approaches, including both single-cell suspensions and 3D tissue formats. However, clinical efficacy remains limited, underscoring the need for improved graft functionality and robust, scalable manufacturing processes to enable clinical translation and commercialization.
Method: iPSC-derived hepatic microtissues were generated using TreeFrog Therapeutics' proprietary high-throughput cell encapsulation technology (C-Stem™) in standard stirred-tank bioreactors, creating a biomimetic 3D microenvironment that supports growth factor-guided differentiation. In vitro functionality was assessed by quantifying albumin, alpha-1-antitrypsin (A1AT), factor VII secretion, urea production, and cytochrome P450 (CYP3A4) activity in comparison with primary human hepatocytes (PHH). Comprehensive characterization of microtissue composition and cellular identity was performed using molecular and histological analysis. In vivo efficacy was evaluated in a carbon tetrachloride (CCl_4)-induced mouse model of acute liver failure following transplantation of microtissues on a biocompatible scaffold.
Results: iPSC-derived hepatic microtissues generated with C-Stem™ displayed expression of key hepatic markers, characteristic morphology and robust functional activity. Levels of albumin, A1AT, factor VII secretion, ureagenesis, and CYP3A4 activity approached or exceeded those observed in PHH. In vivo, transplantation of hepatic microtissues resulted in a 70% increase in survival in CCl_4-treated mice compared to controls, demonstrating significant therapeutic benefit comparable to PHH.
Conclusion: This study demonstrates the superior functional performance and therapeutic efficacy of C-Stem™-produced iPSC-derived hepatic microtissues in a preclinical model of liver failure. The observed survival benefit, combined with a scalable and reproducible manufacturing process, supports the development of a clinically and commercially viable cell therapy product and provides a

strong rationale for progression toward clinical trials following safety validation.

LBP-036

Pemvidutide treatment led to fibrosis regression after 24 weeks in patients with metabolic dysfunction-associated steatohepatitis: quantitative digital pathology analysis from the IMPACT phase 2b, multicenter, randomized, placebo-controlled trial

Naim Alkhouri[1,2], Shaheen Tomah[3], Julio Gutierrez[3,4], John Suschak[3], Yukti Choudhury[5], Elaine Chng[5], Jay Yang[3], M. Scot Roberts[3], Rachel Garner[3], Sarah Browne[3], M. Scott Harris[3], Christophe Arbet-Engels[3], Mazen Noureddin[1,6,7]. [1]*Summit Clinical Research, San Antonio, United States;* [2]*Clinical Research Institute of Ohio, Westlake, United States;* [3]*Altimmune, Gaithersburg, United States;* [4]*Scripps Clinic, La Jolla, United States;* [5]*Histoindex Pte. Ltd, Singapore, Singapore;* [6]*Houston Methodist Hospital, Houston, United States;* [7]*Houston Research Institute, Houston, United States*
Email: nalkhouri@summitclinicalresearch.com

Background and aims: Pemvidutide is a balanced 1:1 glucagon/GLP-1 dual receptor agonist in development for the treatment of metabolic dysfunction-associated steatohepatitis (MASH) where the direct hepatic effects of glucagon may provide greater efficacy over existing therapies. IMPACT was a 48-week, phase 2b, randomized, placebo-controlled, double-blind trial in patients with biopsy-confirmed MASH and fibrosis stage F2 or F3 (NCT05989711). At the week 24 (W24) primary endpoint, pemvidutide treatment showed statistically significant histologic MASH resolution and trends toward fibrosis improvement by conventional pathology reading. Artificial intelligence (AI) and noninvasive tests (NITs)-based analyses showed consistent evidence of anti-fibrotic activity as early as 24 weeks. Here, we evaluated fibrosis regression using second harmonic generation (SHG)/two-photon excited fluorescence (TPEF) microscopy imaging with a quantitative AI-based image analysis algorithm, Histoindex qFibrosis®.
Method: 212 patients were randomized 1:2:2 to receive once-weekly subcutaneous pemvidutide (1.2 mg or 1.8 mg) administered without dose titration, or placebo (PBO). Between January and March 2026, biopsies from 183 patients (1.2 mg [n = 35]; 1.8 mg [n = 77]; PBO [n = 71]) with unstained slides available at baseline (BL) and W24 were imaged by SHG/TPEF and analyzed using qFibrosis®. The qFibrosis® analysis incorporated a correction for the steatotic area of each BL and W24 slide image.
Results: At W24, qFibrosis®-based continuous analyses showed significant improvements in fibrosis in both the 1.2 mg and 1.8 mg pemvidutide doses. Mean changes in continuous qFibrosis® values of −1.25 and −1.08 were observed in the 1.2 mg and 1.8 mg, respectively, compared with −0.15 in PBO ($p < 0.001$ for both). Regression of fibrosis by at least 1-stage occurred in 68.6% ($p < 0.001$ vs. PBO), 54.5% ($p = 0.002$ vs. PBO), and 29.6% of patients in the 1.2 mg, 1.8 mg, and PBO groups, respectively. Overall, 58.9% of patients receiving pemvidutide had a ≥1 qFibrosis® stage regression.
Conclusion: Pemvidutide treatment for 24 weeks resulted in significant fibrosis regression in patients with F2 or F3 MASH as measured by qFibrosis® quantitative digital pathology. These data, together with previous AI- and NIT-based analyses, may support an antifibrotic effect with pemvidutide treatment as early as 24 weeks.

LBP-037

Seladelpar leads to decreases in serum proteins associated with PBC disease severity: proteomic analysis from the pivotal RESPONSE trial

Michael Trauner[1], Yan Liang[2], Peyvand Amini[2], Grant Budas[2], Kyung Min Kwon[2], Barry Crittenden[2], Anna Zagorska[2]. [1]*Division of Gastroenterology and Hepatology, Department of Internal Medicine III, Medical University of Vienna, Vienna, Austria;* [2]*Gilead Sciences Inc., Foster City, United States*
Email: anna.zagorska@gilead.com

Background and aims: Seladelpar (SEL), a first-in-class delpar (selective PPAR-delta agonist), is approved for second-line treatment of PBC and has shown efficacy in improving cholestasis and pruritus in the pivotal Phase 3, placebo (PBO)-controlled RESPONSE study (NCT04620733). Based on these clinical findings, the aim of this analysis is to further evaluate the effects of SEL on longitudinal changes in serum proteins.
Method: In the RESPONSE study, 193 patients with PBC were randomized 2:1 to receive SEL 10 mg or PBO for 12 months. Serum proteomes were profiled from 862 samples from 180 patients at baseline, months 1, 3, 6 and 12 using 11k SomaScan Assay version 5.0, which measured 9852 human proteins. Data normalization, calibration, and quality control processes were performed according to the manufacturer's instructions. Baseline correlations between protein levels and clinical metrics were evaluated using Spearman correlation. Longitudinal changes were analyzed with mixed-effects models, estimating PBO-adjusted changes from baseline at each post-baseline time point.
Results: At month 12, 71 proteins were significantly upregulated and 87 were significantly downregulated from baseline in the SEL arm, compared to the PBO arm (adjusted p-value <0.05). SEL treatment led to a decrease in proteins known to be associated with cholestasis (NT5E, PIGR, STX2), pruritic conditions (FOLH1, IL-22, IL18R1), inflammation (SAA1, MIF, IL1RL1), and fibrosis (WNT5A, FBLN5, THY1). SEL treatment also increased canonical PPAR-delta targets involved in improving lipid metabolism (ACADVL, APOA1, FGF21). Notably, 60 proteins which decreased with SEL showed correlation ($r > 0.3$, adjusted p-value <0.05) with markers of cholestasis (ALP, GGT, total bile acid), pruritus (IL-31, ATX, clinical pruritus scores) and fibrosis (liver stiffness, ELF score) at baseline.
Conclusion: SEL treatment resulted in rapid, sustained and significant changes in serum proteome over time. SEL led to reductions in proteins associated with cholestasis, pruritus, inflammation and fibrosis consistent with the biochemical and clinical symptomatic improvements observed in patients treated. SomaScan analysis identified potential novel biomarkers reflective of PBC disease severity and markers indicative of PPAR-delta pathway engagement that will require further validation.

LBP-038

A novel trientine tetrahydrochloride formulation administered once-a-day for people living with Wilson disease: results from a phase 2 study

Emmanouil Tsochatzis[1], Andrew Holt[2], Elaine Kamara[3], Samuel Shribman[4], Varinder Athwal[5], Katherine Martin[5], David Nicholl[2], Richard Parker[6], Joanna Moore[6], Farah Lawrence-Wilde[3], Nick Manamley[3], C. Omar Kamlin[3], Aftab Ala[7]. [1]*Royal Free Hospital, London, United Kingdom;* [2]*University Hospital Birmingham, Birmingham, United Kingdom;* [3]*Orphalan SA, London, United Kingdom;* [4]*National Hospital for Neurology and Neurosurgery, University of London, London, United Kingdom;* [5]*University of Manchester, Manchester University NHS Foundation Trust Hospitals, Manchester, United Kingdom;* [6]*Leeds University Hospitals NHS Trust, Leeds University, Leeds, United Kingdom;* [7]*Liver Institute, Kings College Hospital, Royal Surrey County Hospital, London, United Kingdom*
Email: emmanouil.tsochatzis@nhs.net

Background and aims: Wilson's disease (WD) is a rare disorder of impaired copper transport requiring lifelong therapy. Adherence is challenging (at least twice daily, separate from food/other medications), thus simplifying treatment may be beneficial. The aim of this study was to assess tolerability, adherence, treatment satisfaction of a novel trientine tetrahydrochloride formulation administered once-a-day (QD TETA-4HCl), compared with standard of care (SoC).
Method: Phase 2 decentralised study (NCT07010575) of adults with WD (Leipzig score ≥4) on maintenance therapy prescribed at least twice daily either a chelator, zinc salts, or combination identified by 6

UK tertiary centres. Following enrolment subjects were switched to receive QD TETA-4HCl (mg-for-mg rounded to nearest full tablet for chelators or 600 mg trientine base [2 tablets] for zinc conversion) for 28-days followed by SoC for 28-days. Adverse events (AEs) and non-ceruloplasmin bound copper (NCC-Sp) was measured. Patient reported outcomes included treatment satisfaction questionnaire for medication (TSQM-9; 3 domains convenience, effectiveness, satisfaction) and Morisky medication adherence score (MMAS-8; less than 6 considered poorly adherent).

Results: Ten (7 male) patients, mean (range) age 35.3 (21–55) years enrolled with hepatic (2), neurologic (3), mixed (3), asymptomatic (2) phenotypes. SoC therapies were trientine (4), zinc (3), DPA (2), combination (1) and switched to either 2 or 3 QD TETA-4HCl tablets. Nine AEs (8 mild, 1 moderate [thrombocytopaenia]) were reported in 7 subjects; no dose changes occurred, all resolved. Mean (90% CI) serum NCC-Sp at baseline, 28d after QD TETA-4HCl and after 28d SoC was unchanged; 46.2 (37.1, 55.3), 48.6 (39.7, 57.4) and 49.3 (40.6, 58.0) mcg/L respectively. TSQM-9 convenience domain showed significant improvements; mean (90% CI) at baseline, 28d after QD TETA-4HCl and 28d after SoC was 43.1 (26.3, 59.9), 85.0 (78.4, 91.6) [p = p = 0.008], and 40.7 (26.9, 54.4), respectively. At the same timepoints, TSQM-9 Effectiveness did not change; 61.1 (54.5, 67.7), 67.3 (54.2, 80.4) and 66.1 (60.0, 72.3) and TSQM-9 Satisfaction improved; 69.9 (61.1, 78.7), 85.7 (75.3, 96.1) [p = 0.057], and 67.3 (58.5, 76.1). At same timepoints, adherence significantly improved; MMAS-8 score was 4.8 (3.7, 5.8), 7.7 (7.4, 8.0) [p = 0.002] and 5.0 (4.0, 5.9).

Conclusion: People living with WD report positive impact on convenience and adherence after 28d of QD TETA-4HCl whilst demonstrating favourable tolerability and biomarker stability.

LBP-039

Survodutide reduces steatosis and fibrosis in a MASH human liver spheroid model through direct glucagon receptor agonism

Philip Vonschallen[1], Radina Kostadinova[1], Agnieszka Pawlowska Pawlowska[1], Joel Zvick[1], Natacha Levy[1], Bonnie Razzaghi[1], Anna Savchenko[1], Francisco Verdeguer[1], Thomas Klein[2]. *[1]Insphero, Schlieren, Switzerland; [2]Boehringer Ingelheim Pharma, GmbH & Co. KG, Biberach, Germany*
Email: philip.vonschallen@insphero.com

Background and aims: Survodutide, a novel glucagon receptor (GCGR)/glucagon-like peptide-1 receptor (GLP1R) dual agonist is currently in Phase 3 clinical trials for obesity and metabolic dysfunction-associated steatohepatitis (MASH). Here we report insights into the mechanism of action of Survodutide in human MASH liver spheroids.

Method: Human liver spheroids phenocopying MASH human livers were investigated to decipher the mechanism of GCGR/GLP1R agonism. Concentration dependent (0.3–10 µM) treatment with Survodutide in liver spheroids was compared with 3 µM long-acting glucagon receptor agonist (LaGCGR) and 3 µM Tirzepatide (GLP1R/GIPR). Spheroids were treated for 10 days followed by the measurement of intracellular triglycerides and glycogen. The fibrotic biomarkers procollagen type I (PNIP) and type III peptide (PIIINP) were detected from the media supernatant at days 7 and 10. Additional spheroids were harvested at day 10 to perform RNAseq.

Results: Triglyceride content in spheroids detected at day 10 was significantly ($p < 0.001$) reduced in all concentrations of Survodutide starting from 0.3 µM (Survodutide = 751 pmol/microtissue (MT), versus DMSO control = 1086 pmol/MT). LaGCGR showed a similar lipid lowering efficacy (757 pmol/MT $p < 0.001$) whereas tirzepatide (1067 pmol/MT) showed no effect. Intracellular glycogen content was significantly reduced with Survodutide treatment at all concentrations, most pronounced at 3 µM (37 ng/MT; p-value <0.05) and with 3 µM LaGCGR (39 ng/MT). However, Tirzepatide (122 ng/MT) failed to elicit any change in glycogen content versus control (88 ng/MT). PIIINP detection in the supernatant as a fibrotic marker showed concentration dependent reduction by Survodutide (EC50 = 0.36 µM), most pronounced at 3 µM (0.08 ng/MT/day, $p < 0.001$) and LaGCGR 3 µM (0.07 ng/MT/day, $p < 0.001$) vs control (0.17 ng/MT/day). Tirzepatide showed no effect (0.17 ng/MT/day). RNAseq analysis demonstrated differences between Survodutide and Tirzepatide in regulation of transcriptional programs known for glucagon receptor activating drugs such as activation of catabolic pathways including glycolysis, fatty acid oxidation and oxidative phosphorylation.

Conclusion: Collectively, the combination of biochemical, biomarkers and transcriptomic analysis in this study suggests a liver-targeted effect of Survodutide to prevent steatosis and fibrosis in MASH patients, which distinguishes from Tirzepatide's mechanism of action.

LBP-040

Functional cure rate in chronic hepatitis B virus infected participants receiving elebsiran and pegylated interferon alfa: final results from the phase 2 ENSURE study

Grace Lai-Hung Wong[1], Man-Fung Yuen[2], Bingliang Lin[3], Mark Douglas[4], Chong Zhu[5], Ke Cao[5], Alex Tian[5], Xiaofei Chen[5], Qing Zhu[6], David Margolis[6], Zhi Hong[6], Jidong Jia[7]. *[1]Department of Medicine and Therapeutics, The Chinese University of Hong Kong, Hong Kong, China; [2]Department of Medicine, School of Clinical Medicine, The University of Hong Kong, Hong Kong, China; [3]The Third Affiliated Hospital, Sun Yat-, Sen University, Guangzhou, China; [4]The Westmead Institute for Medical Research, The University of Sydney and Westmead Hospital, Sydney, Australia; [5]Brii Biosciences (Beijing) Co. Limited, Beijing, China; [6]Brii Biosciences, Inc., Durham, NC, United States; [7]Liver Research Center, Beijing Friendship Hospital, Capital Medical University, Beijing, China*
Email: wonglaihung@mect.cuhk.edu.hk

Background and aims: The ENSURE study is a controlled, partially-randomized evaluation of an HBV targeting siRNA, elebsiran, plus pegylated interferon alfa (PEG-IFN) versus PEG-IFN alone. Published results show a higher hepatitis B surface antigen (HBsAg) loss rate in combination cohorts versus PEG-IFN at 24 weeks (W) post the end of treatment (EOT). Additionally, prior treatment with BRII-179 led to a higher HBsAg loss in those with previous hepatitis B surface antibody (anti-HBs) response. Here, we report the functional cure (FC) result, defined as sustained HBsAg loss with undetectable HBV DNA for at least 24W after stopping all treatment, including nucleos(t)ide analogues (NA).

Method: In Part 1, virologically suppressed participants with chronic HBV infection on NA therapy, with screening HBsAg >100 and ≤3000 IU/mL, were randomized at a ratio of 1:1:1 to one of three cohorts: elebsiran 200 mg or 100 mg + PEG-IFN, or PEG-IFN alone, for 48W. In Part 2, participants who previously received elebsiran and BRII-179 were enrolled to receive elebsiran 100 mg + PEG-IFN for 48W. NA was given daily until stopping criteria were met at 24W post EOT. An additional 24W NA discontinuation monitoring period (NDMP) was conducted to confirm FC in participants who stopped NA.

Results: 55 and 31 participants enrolled in Part 1 and Part 2, respectively. In Part 1, 4/19 (21%) and 5/18 (28%) participants from the elebsiran 200 mg or 100 mg + PEG-IFN cohorts were eligible for stopping NA compared to 1/18 (6%) in PEG-IFN cohort. At the end of NDMP, FC was achieved in 2/19 (11%) and 3/18 (17%) participants from the elebsiran 200 mg or 100 mg + PEG-IFN cohorts, respectively, compared to 1/18 (6%) in the PEG-IFN cohort. In Part 2, 9/31 (29%) participants met NA stopping criteria. At the end of NDMP, 8/31 (26%) participants achieved FC, with 7/19 (37%) in BRII-179 anti-HBs responders compared to 1/12 (8%) in non-responders. In combination treated participants achieving HBsAg loss at EOT, HBsAg rebound rates were 38% and 55% in those with or without BRII-179 exposure, respectively. No participants who had HBsAg rebound had ALT flare. All 12 participants with positive baseline hepatitis B e antigen did not achieve sustained HBsAg loss.

Conclusion: Compared to PEG-IFN, the addition of elebsiran resulted in higher FC rate. Furthermore, BRII-179 experienced participants achieved higher FC rate, especially in anti-HBs responders, suggesting that BRII-179 might play an important role in achieving lasting immunological control of the virus.

LBP-041

HSK31679, a thyroid hormone receptor beta agonist, improves histological outcomes in Asian patients with MASH and F2–F3 fibrosis: a 52-week phase 2b randomized, double-blind, placebo-controlled trial

Feng Xue[1], Jianfeng Liu[2], Jinjun Chen[3], Xing Li[4], Sikui Wang[5], Yawen Luo[6], Bangjie Zhang[7], Jiawei Geng[8], Weihong Wang[9], Rui Zhao[10], Chuanwu Zhu[11], Junjun Bi[12], Xiqing Guo[13], Lungen Lu[14], Guang-Ming Li[15], Hong Peng[16], Li Dong[17], Guohong Ge[18], Danying Cheng[19], Xianfei Zhong[20], Lvfeng Yao[21], Feng Gao[22], Shiyao Chen[23], Jiaojian Lv[24], Liang Xu[25], Guodong Zhang[26], Xiaozhong Wang[27], Gang He[28], Yaocai Li[29], Xiuping Jin[30], Wang Jing[31], Huiying Rao[32], Shuilin Sun[33], Yunzhen Shi[34], Min Meng[35], Jing Zhang[36], Muyessar Maimaitiyiming[37], Chao Wu[37], Cunliang Deng[38], Zong Zhang[39], Yan Bi[40], Xiaohua Li[41], Tingting Wu[42], Weifang Zeng[42], Lai Wei[43]. *[1]Hepatopancreatobiliary Center, Beijing Tsinghua Changgung Hospital, Key Laboratory of Digital Intelligence Hepatology (Ministry of Education), School of Clinical Medicine, Tsinghua Medicine, Tsinghua University, Department of Gastroenterology, Binzhou Medical University Hospital, Beijing, China; [2]Cangzhou People's Hospital, Cangzhou, China; [3]Nanfang Hospital, Guangzhou, China; [4]Pingxiang People's Hospital, Pingxiang, China; [5]Liaocheng People's Hospital, Liaocheng, China; [6]Affiliated Hospital of Zunyi Medical University, Zunyi, China; [7]The Third Affiliated Hospital of Xinxiang Medical University, Xinxiang, China; [8]The First People's Hospital of Yunnan Province, Kunming, China; [9]Huzhou Central Hospital, Huizhou, China; [10]The Sixth People's Hospital of Shenyang, Shenyang, China; [11]The Affiliated Infectious Diseases Hospital of Soochow University, Suzhou, China; [12]People's Hospital of Zezhou County, Jincheng, China; [13]Chongqing University Three Gorges Central Hospital, Chongqing, China; [14]Shanghai General Hospital, Shanghai, China; [15]The Sixth People's Hospital of Zhengzhou, Zhengzhou, China; [16]Guizhou Provincial People's Hospital, Guizhou, China; [17]The First Affiliated Hospital of Nanjing Medical University, Nanjing, China; [18]Changzhou Third People's Hospital, Changzhou, China; [19]Beijing Ditan Hospital, Beijing, China; [20]The People's Hospital of Leshan, Leshan, China; [21]Mengchao Hepatobiliary Hospital of Fujian Medical University, Fuzhou, China; [22]Linyi People's Hospital, Linyi, China; [23]Minhang Hospital, Fudan University, Shanghai, China; [24]Lishui People's Hospital, Lishui, China; [25]Tianjin Second People's Hospital, Tianjin, China; [26]Pingmei Shenma Medical Group General Hospital, Pingdingshan, China; [27]Xinjiang Uygur Autonomous Region Traditional Chinese Medicine Hospital, Urumqi, China; [28]Jiangmen Central Hospital, Jiangmen, China; [29]Maoming People's Hospital, Maoming, China; [30]North China University of Science and Technology, Tangshan, China; [31]Affiliated Traditional Chinese Medicine Hospital of Southwest Medical University, Luzhou, China; [32]Peking University People's Hospital, Beijing, China; [33]The Second Affiliated Hospital of Nanchang University, Nanchang, China; [34]Dongyang People's Hospital, Dongyang, China; [35]Anyang People's Hospital, Anyang, China; [36]Beijing Youan Hospital, Beijing, China; [37]The First People's Hospital of Kashi Prefecture, Kashgar, China; [38]Mianyang 404 Hospital, Mianyang, China; [39]Shandong Public Health Clinical Centre, Jinan, China; [40]The Affiliated Drum Tower Hospital of Nanjing University Medical School, Nanjing, China; [41]Shanghai Seventh People's Hospital, Shanghai, China; [42]Haisco Pharmaceutical Group Co., Ltd., Chengdu, China; [43]Hepatopancreatobiliary Center, Beijing Tsinghua Changgung Hospital, Key Laboratory of Digital Intelligence Hepatology (Ministry of Education), School of Clinical Medicine, Tsinghua Medicine, Tsinghua University, Beijing, China, Beijing, China*
Email: weilai@tsinghua.edu.cn

Background and aims: Resmetirom, a liver-targeted thyroid hormone receptor beta agonist, has been approved in the United States and European Union for noncirrhotic MASH with moderate-to-advanced fibrosis, based largely on data from predominantly White populations. In our phase 2a study, HSK31679 reduced liver fat content (LFC) in Asian patients with metabolic dysfunction-associated steatotic liver disease. This phase 2b trial evaluated the histological efficacy and safety of HSK31679 after 52 weeks in Asian patients with MASH and F2/F3 fibrosis, including a substantial proportion of non-obese patients.
Method: In this multicenter, randomized, double-blind, placebo-controlled phase 2b trial, 186 patients with biopsy-confirmed MASH and F2/F3 fibrosis were randomized 1:1:1 to once-daily oral HSK31679 80 mg, HSK31679 160 mg, or placebo. The primary endpoint was improvement in MASH without worsening of fibrosis at week 52. Secondary endpoints included improvement in MASH with at least one-stage fibrosis improvement, at least 30% relative reduction in LFC by MRI-PDFF, and changes in lipid parameters.
Results: Baseline characteristics were comparable across groups. At week 52, the primary endpoint was met in 37.3% and 30.0% of participants receiving HSK31679 80 mg and 160 mg, respectively, versus 10.0% with placebo (both $p < 0.001$). In the BMI-stratified analyses, both doses showed higher rates of response than placebo in participants with BMI <28 kg/m^2 (nominal $p < 0.05$ for both comparisons). Rates of MASH improvement with at least one-stage fibrosis improvement were 22.0%, 18.3%, and 5.0%, respectively (both $p < 0.05$ vs placebo). More participants receiving HSK31679 achieved ≥30% reduction in MRI-PDFF at week 52 (52.5% and 53.3% vs 25.0%; both $p < 0.01$). HSK31679 also improved multiple lipid parameters, with no significant difference in body weight change between groups. HSK31679 was generally safe and well tolerated; gastrointestinal adverse events were slightly more frequent than with placebo but were mild to moderate, and no drug-related serious adverse events, discontinuations, or deaths occurred.
Conclusion: HSK31679 significantly increased the rate of MASH improvement without worsening of fibrosis at week 52, with reductions in LFC and improvements in multiple lipid parameters, with a favorable safety and tolerability profile. Histological benefit was also observed in non-obese participants despite no significant between-group difference in body-weight change.

LBP-042

Safety, tolerability, sustained hepatitis B surface antigen reduction and HBsAg clearance ratio in chronic hepatitis B patients treated with long-term BW-20507

Man-Fung Yuen[1], Grace Lai-Hung Wong[2], Chitchai Rattananukrom[3], Pisit Tangkijvanich[4], Khuanchai Supparatpinyo[5], Sakkarin Chirapongsathorn[6,7]. *[1]The University of Hong Kong, Queen Mary Hospital, Hong Kong, China; [2]The Chinese University of Hong Kong, Hong Kong, China; [3]Division of Gastroenterology and Hepatology, Department of Medicine, Srinagarind Hospital, Faculty of Medicine, Khon Kaen University, Khon Kaen, Thailand; [4]Center of Excellence in Hepatitis and Liver Cancer, Chulalongkorn University, Bangkok, Thailand; [5]Research Institute for Health Sciences, Chiang Mai University, Chiang Mai, Thailand; [6]Phramongkutklao Hospital and College of Medicine, Bangkok, Thailand; [7]Phramongkutklao Hospital and College of Medicine, Royal Thai Army, Bangkok, Thailand*
Email: mfyuen@hku.hk

Background and aims: BW-20507 is an N-acetylgalactosamine conjugated small interfering RNA (siRNA) designed to target the hepatitis B virus (HBV). Preclinical studies have demonstrated its distinct antiviral activity and promising potential for the treatment of HBV infection. Here, we present preliminary data from an ongoing study evaluating the long-term safety, tolerability, and antiviral activity of BW-20507 in patients with chronic HBV infection (CHB).
Method: This is a long-term treatment phase in subjects who previously received 3 doses of BW-20507 and had been followed for

40 weeks. Subjects enrolled in the study will receive BW-20507 300 mg every 4 weeks for 24 weeks (7 doses), followed by every 8 weeks for 72 weeks (9 doses). Subjects who meet the predefined nucleoside analogs (NUCs) discontinuation criteria may stop NUCs between Weeks 48 and 72 and will be closely monitored, with NUCs re-initiated as needed according to the prespecified retreatment criteria. During the follow-up period (Weeks 96–120), no further BW-20507 will be administered, and subjects will either continue NUCs or be monitored off NUCs, with re-initiation based on the same retreatment criteria.
Results: Twenty-two patients (mean age 46.6 years old; M: F 20:2; HBeAg positive 22.7%) with CHB were enrolled. Up to the cutoff date, all subjects had completed the D197 visit (Week 28 visit). Treatment was well tolerated in all subjects, with a favorable safety profile. No treatment discontinuations occurred and no treatment-related SAE was reported. Mean baseline HBsAg level was 569.0 IU/mL (2.76 $\log_{10}$ IU/mL). 21 (95.5%) and 19 (86.4%) patients had baseline HBsAg <3,000 IU/mL and <1000 IU/mL respectively. On Day 197, the mean maximal reduction of HBsAg was 2.85 $\log_{10}$ IU/mL and all of the subjects achieved HBsAg <3 IU/mL. Ten (45.5%) subjects achieved HBsAg clearance for at least 1 follow-up visit. HBsAg clearance rate was 87.5% (7/8) in subjects with baseline HBsAg ≤50 IU/mL, versus 52.6% (10/19) in those with HBsAg ≤1000 IU/mL.
Conclusion: Long-term treatment with BW-20507 was well tolerated and demonstrated a favorable safety profile in patients with CHB. Continued BW-20507 treatment can lead to higher rates of HBsAg clearance over time.

LBP-043
First evidence of elimination and inactivation of cccDNA in liver biopsies collected from patients with chronic hepatitis B treated with PBGENE-HBV
Man-Fung Yuen[1], Alina Jucov[2,3], Emily Harrison[4], James Harris[5], Keely Dulmage[4], Andrew Van Cott[4], Abhishek Chandiramani[4], Neil Leatherbury[4], Janel Lape[4], Peter Balfe[5], Jeff Smith[4], Cassandra Gorsuch[4], Stanley Frankel[4], Jane McKeating[5], Mark S. Sulkowski[4,6], Edward J. Gane[7]. *[1]Queen Mary Hospital, The University of Hong Kong, Hong Kong, Hong Kong; [2]Arensia Exploratory Medicine GmbH, Düsseldorf, Germany; [3]Nicolae Testemitanu State University of Medicine and Pharmacy, Chişinău, Moldova; [4]Precision BioSciences Inc., Durham, United States; [5]Nuffield Department of Medicine, University of Oxford, Oxford, United Kingdom; [6]Division of Infectious Diseases, Johns Hopkins Bayview Medical Center, Johns Hopkins University & Medicine, Baltimore, United States; [7]New Zealand Clinical Research, Auckland, New Zealand*
Email: mfyuen@hku.hk

Background and aims: PBGENE-HBV is a first-in-class gene editor utilizing ARCUS technology designed to cure hepatitis B by elimination or inactivation of cccDNA, the sole source of new infectious viral particles and HBV replication. The PBGENE-HBV target site is highly conserved in both cccDNA and integrated HBV DNA and is essential in cccDNA for viral polymerase function.
Method: PBGENE-HBV is being evaluated in a Phase 1 trial for safety and efficacy in participants controlled on nucleos(t)ide analogs (Yuen et al. AASLD abstract 5017). Liver biopsies were analyzed from two voluntary participants dosed in Cohort 2 (0.4 mg/kg). In one participant, biopsies were collected pre-treatment and after the second dose administration. In the other participant, a post-treatment biopsy only was collected after the third and final dose. Both short- and long-read sequencing techniques have been utilized to evaluate editing of cccDNA and integrated HBV DNA. In addition, HBV RNA and HBsAg in the blood were evaluated for antiviral activity.
Results: Sequencing confirmed editing of cccDNA and integrated HBV DNA at both the DNA and RNA level with a high degree of concordance. In the first participant, paired biopsies showed a 10-fold (1-log) decrease in the percentage of cccDNA-derived RNA transcripts after two administrations of PBGENE-HBV, supporting cccDNA elimination. In the 0.16% of cccDNA-derived transcripts remaining, edits were present in 23% of sequences, supporting cccDNA inactivation. In a second participant who underwent a post-treatment biopsy only, collected after 3 doses, edits were found in 80% of remaining cccDNA transcripts, suggesting cumulative effect of repeat administrations of PBGENE-HBV. This patient had detectable pgRNA in the blood at baseline which became and remained undetectable after dosing, corresponding with undetectable pgRNA in the biopsy. In all biopsy samples, HBsAg transcripts were expressed predominantly from integrated HBV DNA rather than cccDNA. Durable HBsAg declines in the blood were observed in both participants 9 months after initial dosing.
Conclusion: Biopsy data demonstrate the first evidence of elimination and inactivation of cccDNA in HBV patients through gene editing with PBGENE-HBV. Antiviral activity was evidenced by loss of detectable pgRNA, as well as durable HBsAg declines. These data support continued evaluation of PBGENE-HBV dose and schedule as a curative therapy.

LBP-044
Integrated serum proteomics and N-glycoproteomics for non-invasive biomarkers in primary biliary cholangitis
Dong Zhao[1], Liangjun Zhang[1], Zuzhi Xu[1], Xiaoman Xie[1], Qiong Pan[1], Jin Chai[1]. *[1]the First Affiliated Hospital (Southwest Hospital) of Third Military Medical University (Army Medical University), Cholestatic Liver Diseases Center, the First Affiliated Hospital (Southwest Hospital) of Third Military Medical University (Army Medical University), Metabolic Dysfunction-Associated Steatotic Liver Disease (MASLD) Medical Research Center, the First Affiliated Hospital (Southwest Hospital) of Third Military Medical University (Army Medical University), Chongqing, China*
Email: jin.chai@cldcsw.org

Background and aims: Primary biliary cholangitis (PBC) is an autoimmune disease characterized by small bile duct injury and cholestasis. Diagnosis based on current serological tests and clinical treatment with ursodeoxycholic acid (UDCA) are challenging, particularly with autoimmune hepatitis (AIH) overlap. In this study, we aim to identify non-invasive serum biomarkers for PBC to reduce reliance on liver biopsy.
Method: We performed proteomics and N-glycoproteomics on 737 serum samples from controls, patients with PBC, AIH, and their overlap syndrome (PBC+AIH) across nine centers. The cohort is divided into discovery and validation sets. Machine learning was applied to build biomarker panels with serum omics and clinical variables in the discovery cohort, which were further confirmed in the validation cohort.
Results: A diagnostic panel comprising one protein, one N-glycoprotein, and conventional clinical variables, achieved ROC-AUC >0.9 in distinguishing PBC, greatly improving the diagnostic accuracy over current serological diagnosis. Additionally, two models for staging PBC and UDCA treatment response were developed. A five-protein panel can realize ROC-AUC >0.8 in differentiating early-stage from later stage of PBC. Another panel incorporating one protein, one N-glycoprotein, and clinical variables, exhibited satisfactory performance in predicting UDCA treatment response with ROC-AUC >0.9. SHAP analysis highlighted the important contribution of novel biomarkers to the model, supporting their potential biological relevance in PBC progression.
Conclusion: Our study has identified a few panels of serum biomarkers that effectively differentiate PBC from other autoimmune liver diseases, stage PBC without a liver biopsy, and predict the UDCA treatment response.

WEDNESDAY 27 TO SATURDAY 30 MAY

Acute liver failure and drug induced liver injury – Clinical

TOP-178

Predicting in-hospital mortality in drug-induced liver injury

Jeril Lasington[1], Lawin Steve Mathew Lasington[2]. [1]*New York Medical College, Valhalla, United States;* [2]*Rutgers University-Newark Arch, Newark, United States*
Email: lawinsteve.ls@gmail.com

Background and aims: Drug-induced liver injury (DILI) causes substantial morbidity and is the leading cause of acute liver failure (ALF) in Western countries. Unlike other liver diseases, no validated prognostic scores exist specifically for DILI. We developed an interpretable machine learning (ML) model to predict in-hospital DILI mortality and identify key risk factors across injury patterns and drug classes.
Method: This retrospective cohort study used the National Inpatient Sample (2019–2022) to identify adult DILI hospitalizations (ICD-10: K71.x). Patients were classified by injury pattern (ALF, hepatocellular necrosis, cholestatic, acute hepatitis, chronic) and causative drug class using T-codes. The primary outcome was in-hospital mortality. Four ML algorithms (Logistic Regression, Random Forest, XGBoost, LightGBM) were trained using temporal validation (2019–2021 training, 2022 testing) with 69 clinical features. SMOTE addressed class imbalance. Performance was evaluated using AUC-ROC, sensitivity, and specificity. SHAP analysis identified key predictors.
Results: Among 11,296 DILI hospitalizations, overall mortality was 5.9%. Mortality varied by injury pattern: ALF 16.4%, severe hepatocellular necrosis 9.6%, chronic DILI 5.5%, cholestatic 3.4%, and acute hepatitis 2.9%. By drug class, antineoplastic agents had the highest mortality (7.3%), followed by cardiovascular drugs (7.2%) and acetaminophen (6.5%). Random Forest achieved the best performance (AUC 0.912; sensitivity 84.7%; specificity 86.0%).SHAP analysis showed systemic severity markers dominated prediction: organ failure count (1.32), age (0.86), respiratory failure (0.70), underlying malignancy (0.59), mechanical ventilation (0.46), and metabolic acidosis (0.36). Specific drug class contributed minimally compared to physiologic derangement, suggesting clinical trajectory rather than causative agent determines outcomes.
Conclusion: This ML model accurately predicts DILI mortality using routine clinical data. Key findings: (1) ALF carries 5-fold higher mortality than other DILI phenotypes; (2) antineoplastic agents, not acetaminophen, have the highest mortality; (3) systemic organ failure burden, rather than causative drug, dominates mortality prediction. These findings support developing a DILI-specific prognostic score emphasizing physiologic severity over etiology for early identification of high-risk patients requiring intensive monitoring or transplant evaluation.

TOP-192

Acyl-CoA synthetase long-chain family member 4 as a novel prognostic biomarker for poor outcome in drug-induced liver injury

Yu Wang[1], Pengchong Li[2], Xue Wang[1], Mengmeng Zhang[1], Yan Wang[1], Zikun Ma[1], Yao Meng[1], Tiantian Guo[1], Jiahao Yuan[1], Yubo Zhong[1], Jinxin Gu[1], Cen Zhang[1], Sihan Dong[1], Jun Li[3], Xinyan Zhao[1], Jidong Jia[1]. [1]*Liver Research Center, Beijing Friendship Hospital, Capital Medical University, Beijing, China, State Key Laboratory of Digestive Health, Beijing, China, National Clinical Research Center of Digestive Diseases, Beijing, China, Beijing, China;* [2]*Department of Gastroenterology, Beijing Friendship Hospital, Capital Medical University, Beijing, China, State Key Laboratory of Digestive Health, Beijing, China, National Clinical Research Center of Digestive Diseases, Beijing, China, Beijing, China;* [3]*The First Affiliated Hospital, Zhejiang University School of Medicine, Hangzhou, Zhejiang, China, Hangzhou, China*
Email: wang-yu@mail.ccmu.edu.cn

Background and aims: Early risk stratification in drug-induced liver injury (DILI) remains a major clinical challenge. We aimed to identify a novel biomarker to improve prognostic assessment in DILI and to evaluate whether its prognostic value is specific to DILI compared with autoimmune and virus-related liver disease.
Method: We performed proteomic profiling of human liver tissue from patients with DILI and analyzed publicly available single-nucleus RNA sequencing (snRNA-seq) datasets from DILI-associated acute liver failure (DILI-ALF) and healthy controls. Candidate molecules were validated in in vitro and in vivo DILI models. A multicentre prospective DILI cohort (NCT05060289) was used to evaluate the prognostic performance of serum biomarkers, benchmarked against five established DILI prognosis models. Disease specificity was assessed in independent cohorts of autoimmune hepatitis (AIH) and chronic hepatitis B (CHB).
Results: Liver proteomics revealed marked activation of ferroptosis and identified acyl-CoA synthetase long-chain family member 4 (ACSL4) as a central hub in DILI-ALF. SnRNA-seq analysis showed consistent upregulation of ACSL4 in hepatocytes from DILI-ALF patients compared with healthy controls, which was confirmed by double immunofluorescence staining. In vitro and in vivo DILI models further supported a pathogenic role of ACSL4-mediated ferroptosis, as siRNA-mediated ACSL4 knockdown in vitro and pharmacological ACSL4 inhibition in vivo both attenuated liver injury. In the prospective DILI cohort, serum ACSL4 concentrations were significantly higher in patients with poor outcomes than in those with favourable outcomes (924.98 vs. 471.06 pg/mL, $p < 0.001$). ACSL4 demonstrated excellent prognostic performance (AUROC = 0.953), significantly outperforming Hy's Law, nHy's Law and Robles-Diaz (all $p < 0.001$), and marginally surpassing DrILTox ALF (AUROC = 0.884) and MELD (AUROC = 0.884). Moreover, in a real-world validation cohort, the ACSL4-based model achieved an AUROC of 0.904 (95% CI, 0.750–1.000). In contrast, elevated ACSL4 levels were not observed in AIH or CHB patients with poor outcomes.
Conclusion: ACSL4 is a novel biomarker with high accuracy for predicting poor outcome in DILI. Its prognostic elevation appears specific to DILI relative to AIH and CHB and it performs comparably or better than existing prognostic models. ACSL4 shows strong potential for early risk stratification and may help guide clinical decision-making in patients with suspected DILI.

SAT-056

Active pharmacovigilance and performance of K18, M-CSFR, and GLDH as DILI biomarkers for diagnosis and prognosis in a complex hospitalized population in Brazil

Raquel Boff[1], Vittoria Sampaio[1], Paola Hoff Alves[1], Ana Lazzari[1], Isabela Carvalhal[2], Tiago Onofrio Soares[2], Theo Futuro Telöken[3], Nelson Suarez Uribe[1], Hidayat Ullah Kassim[1], Rui Davila[4], Fernando Hertz Wolff[5], Jeronimo De-Conto-Oliveira[4], Mercedes Robles-Díaz[6], Dvora Joveleviths[1]. [1]*Universidade Federal Do Rio Grande Do Sul, Porto Alegre, Brazil;* [2]*Pontifícia Universidade Católica do Rio Grande do Sul, Porto Alegre, Brazil;* [3]*Universidade Do Vale Do Rio*

Dos Sinos, Porto Alegre, Brazil; [4]Hospital de Clínicas de Porto Alegre, Porto Alegre, Brazil; [5]Hospital Moinhos De Vento, Porto Alegre, Brazil; [6]Universidad De Málaga, Málaga, Spain
Email: raquelboff80@gmail.com

Background and aims: Drug-Induced Liver Injury (DILI) diagnosis is complex, relying on the exclusion of other causes and non-specific liver tests with suboptimal sensitivity. This study evaluated the diagnostic potential of Cytokeratin-18 (K18), Macrophage Colony-Stimulating Factor Receptor (MCSFR), and Glutamate Dehydrogenase (GLDH) in hospitalized patients with DILI, pre-existing liver disease (PLD), and controls, were comorbidities and polypharmacy complicate investigation.
Method: Prospective study with active pharmacovigilance conducted between 2019 and 2025 for biomarker development, analyzing medical history by RedCap under international DILI criteria (alanine aminotransferase (ALT) >5× upper limit of normal (ULN), ALT 3–5× ULN with total bilirubin (TB) >2 mg/dL, and alkaline phosphatase (ALP) >2× ULN). Cases were adjudicated by RUCAM and expert opinion. Biomarkers were quantified via ELISA/Luminex. Diagnostic performance was assessed by ROC curves (AUC) and associations by Spearman's coefficient.
Results: From 2,500 records, 23 cases of DILI, 41 cases of PLD, and 18 controls (similar clinical profiles but normal aminotransferases) were confirmed. Active pharmacovigilance (RUCAM score) detected 20 DILI cases, significantly outperforming traditional methods (Naranjo), which reported only 2. The primary suspected drug classes were antibiotics (39.0%), antifungals (14.1%), and antineoplastics (9.4%). The mean age was 50.24 years (SD 15.59), with a 60.9% female (DILI group). Median DILI latency: 60.15 days (SD 85.4); 45.8% (n = 10) showed a hepatocellular pattern. RUCAM scores were distributed as: 3–5 (n = 6; 26.1%), 6–8 (n = 15; 65.2%), and ≥9 (n = 2; 8.7%). The biomarkers K18, MCSFR, and GLDH did not show significant differences in diagnostic of DILI, AUC values of 0.610, 0.565, and 0.554, respectively. In PLD, K18 (AUC 0.696) outperformed ALT (AUC 0.557) in differential diagnosis. GLDH (AUC 0.806) and MCSFR (AUC 0.707) predicted mortality in DILI and pre-existing liver disease, respectively.
Conclusion: Biomarkers provide critical insight into the progression and severity of DILI, playing a significant prognostic role. ALT's non-specificity reinforces the need for clinical evaluation.

SAT-057

Drug-induced liver injury: a survey among members of the society of liver disease in Africa

Maurizio Bonacini[1], Patricia Jones[2], Wendy Spearman[3], Manal El-Sayed[4], Karin Siebelt[5]. *[1]Mission Gastroenterology, San Francisco, United States; [2]University of Miami, Coral Gables, United States; [3]University of Cape Town, Cape Town, South Africa; [4]Ain-Shams Univ., Cairo, Egypt; [5]Amed Education, Amsterdam, Netherlands*
Email: bonacim08@gmail.com

Background and aims: Drug-induced liver injury (DILI) represents the most common cause of liver failure in Europe, most frequently acetaminophen (APAP), idiosyncratic cases ranking second. The USA DILI network has published detailed descriptions of DILI and provided regulators with surveillance data. There is no known DILI registry in Africa. The aim is to report African practitioners' experiences with DILI.
Method: A survey was co-developed by AASLD/SOLDA, consisting of 28 questions about participant demographics and their experience with DILI. This was sent to 2038 SOLDA members. 337 responses were received from 36 African countries.
Results: 51% of responders were physicians, 7% nurses, 4% pharmacists and 38% other practitioners. Thirty-one percent were Gastrointestinal/Liver, 23% Infectious Diseases, 17% general medicine and 29% other. Two thirds were in academic and/or public positions and 1/3 in private practice. Countries were geographically well represented, the highest response number being from Nigeria (64). When asked about DILI significance, 58.5% answered significant or very significant, 30.5% moderately significant and 11% not very significant. Respondents estimated that 56% of their patients take traditional remedies or herbal or dietary supplements (HDS). 52% percent of practitioners see ≥6 DILI cases/year. The median number of prescription medications DILI seen was 5/year. Most frequently cited culprits: Tuberculosis (TB) medications (47.6%), APAP (24.5%), antibiotics (17%, 40% of which were Amoxycillin/clavulanate), HIV meds (13.6%) and NSAIDS (9%). Median number of DILI due to traditional meds or HDS was 3 cases/year for each category. About 55% of respondents have seen a fatal case of DILI. Of the 80 fatal cases, the most common culprits were HDS (37), TB medications (19), analgesics/APAP (14); HIV drugs (7), antibiotics (2) and Ecstasy (1). Greater than 75% have access to liver and serological tests to exclude competing causes and 46% to liver biopsies. HLA testing is available to 30% of respondents. Fifty-five percent note that a registry is not available in their country; 86% would report cases to a central DILI registry.
Conclusion: Almost 60% of African practitioners view DILI as a significant problem. TB medications are the main culprits but HDS may have more impact on mortality. Most responders have access to basic liver/serology tests and almost 50% to liver biopsies. The vast majority would contribute to a DILI registry. These data support the creation of an African DILI registry.

SAT-058

Our experience of immune-mediated hepatotoxicity: five-year data from a London cancer centre

Annabelle Chung[1], Alberto Fusi[1], Arjuna Singanayagam[1], Styliani Germanou[1]. *[1]St George's Hospital, London, United Kingdom*
Email: annabelle.chung@stgeorges.nhs.uk

Background and aims: Immune-mediated hepatotoxicity (IMH) is a well-known adverse effect of immune checkpoint inhibitors (ICI). Management involves interruption to immunotherapy, steroid treatment, and second line immunosuppression in steroid-refractory cases, usually on the Acute Oncology Care Unit to avoid hospital admissions. Here, we aimed to assess the management and outcomes of IMH in our cancer service over the last 5 years.
Method: Cancer patients who received ICIs and subsequently developed IMH between 2021 and 2025 at St George's Hospital, London, UK, were analysed. Data collected from our electronic records included patient demographics, cancer treatment, IMH management and outcomes. Grading of hepatitis was defined as per published guidelines.
Results: 46 patients were included, the majority with lung (41.3%), skin (28.3%) or renal cell (19.6%) cancer. ICI regimes varied - singlet ICI (34.8%), dual ICI (28.3%) or with chemotherapy (37.0%). 28.2% of patients showed evidence of hepatic steatosis on imaging. The proportion of patients with Grade 3–4 IMH did not differ between those with hepatic steatosis (8/11, 72.7%) and those with a normal ultrasound (19/26, 73.1%). Overall, 72.3% of all cases were Grade 3–4. Average time between ICI treatment and onset of hepatitis was 116.6 days (range 12–412), following an average of 3.3 cycles (range 1–10). Patients treated with dual ICIs (PD-1 with CTLA-4; n = 12) experienced a shorter mean time to IMH (83.6 days) compared to those receiving singlet ICI (142.6 days; n = 34). 93.5% of patients were managed with high dose corticosteroids - 72.7% were steroid-responsive. 25% required an additional agent with mycophenolate mofetil (MMF). Mean length of treatment was 61.5 days, excluding 3 patients (8.8%) who require MMF indefinitely. 7 patients died during treatment, but only one death was toxicity-related. 80.9% of cases resolved. Only 23.9% of patients (n = 11) were rechallenged with singlet ICI following IMH and recurrence did not occur. 93.5% of patients required at least 1 visit to our ambulatory unit (mean 7.6, range 1–23). 17% of patients required inpatient admission, however this has reduced between 2021 (40%) and 2025 (0%).

Conclusion: Our five-year data demonstrates that IMH can be managed effectively on an outpatient basis. Although IMH is treatable, it often leads to cessation of ICIs. Guidance on rechallenging ICI remains dependent on clinician experience and multidisciplinary team input, thus highlighting the ongoing challenges of managing IMH.

SAT-059

Trastuzumab is associated with acute hepatitis and chronic porto-sinusoidal vascular disease in the french-speaking network for the study of the hepatotoxicity of health products (REFHEPS)

Bénédicte Delire[1], Lucy Meunier[2], Magdalena Meszaros[2], José Ursic Bedoya[2], Isabelle Rosa[3], Amel Zahhaf[2], Eleonora De Martin[4], François Duhoux[5], Cédric van Marcke[5], William Jacot[6], Séverine Guiu[6], Yves Horsmans[1], Dominique Larrey[2,7].
[1]Department of Hepato-Gastroenterology, Cliniques Universitaires Saint-Luc et Institut de Recherche Clinique (IREC), Université Catholique de Louvain., Brussels, Belgium; [2]Liver unit, Hopital St Eloi, CHU Montpellier, France, 34, Montpellier, France; [3]Service d'Hépato-Gastroentérologie, CHIC de Créteil, 40 Avenue de Verdun, 94010 Créteil cedex, France, Créteil, France; [4]AP-HP Hôpital Paul Brousse, Centre Hépato-Biliaire, Inserm UMR-S 1193, Université Paris-Saclay, Villejuif, France, Villejuif, France; [5]Department of Medical Oncology, King Albert II Cancer Institute, Cliniques Universitaires Saint-Luc, Brussels, Institut de Recherche Expérimentale et Clinique (IREC), Pole of Medical Imaging, Radiotherapy and Oncology (MIRO), Université Catholique de Louvain (UCLouvain), Brussels, Brussels, Belgium; [6]Department of Medical Oncology, Institut du Cancer de Montpellier, Inserm U1194, Montpellier University, Montpellier, France, Montpellier, France; [7]CHU Montpellier, Liver Unit, Montpellier, France
Email: benedicte.delire@saintluc.uclouvain.be

Background and aims: Trastuzumab (TRA) is a targeted therapy that exists as either a monoclonal antibody or an antibody-drug conjugate:TRA-deruxtecan (T-DXd)/TRA-emtansine (T-DM1). All are used to treat breast cancer (BC) and other solid tumors and are associated with drug-induced liver injury (DILI).
Method: Patients assessed by the French-speaking network for the study of the hepatotoxicity of health products (REFHEPS) between January 2022 and December 2025 were evaluated. Those with TRA/T-DXd/T-DM1-induced liver toxicity were included. Hepatotoxicity was defined as ALT or AST ≥5× ULN, ALP ≥2× ULN, or total bilirubin ≥2× ULN associated with ALT ≥3× ULN or the appearance of signs of portal hypertension (PH).Approval by an ethics committee (IRB number: 198711).
Results: Twenty-three of the 332 cases collected in the REFHEPS involved TRA/T-DXd/T-DM1: 12 T-DM1, 7 T-DXd, 1 T-DM1 and nivolumab, 1 T-DM1 and pertuzumab, 1 TRA, and 1 TRA+pertuzumab+tucatinib. All but one of the patients were female, median age 59 years (33–82). Twenty-one patients were treated for BC, 1 for ovarian tumor and 1 for bladder carcinoma. DILI phenotype was cholestatic in 4 cases, cytolytic in 3 and mixed in 1. Fifteen patients did not meet the biological criteria for DILI but had minimal biological abnormalities and/or signs of PH. When applicable, the median RUCAM score was 7 and DILIN grade for causality assessment was probable. Hepatic damage was symptomatic in 6 cases, three had variceal haemorrhage. Fifteen patients in the cholestatic/ minimal biological abnormalities and PH groups had liver biopsy. Histological analysis was consistent with porto-sinusoidal vascular liver disease (PSVD) in all patients whose evolution was chronic. PSVD was related to T-DM1 in 9 cases, to T-DXd in 7, to T-DM1 and nivolumab in 1, to T-DM1 and pertuzumab in 1, and to TRA in 1. In the cytolytic and mixed group, 2 patients had a biopsy showing an acute lobular hepatitis in one case and a cholestatic hepatitis in the other. Two patients experienced resolution of liver enzymes while another patient only showed improvement in hepatic tests after three months.One patient died due to oncological progression and liver failure. Acute hepatitis was associated with T-DM1 in 2 cases, to T-DXd in 1 and to a combination of TRA-Pertuzumab-Tucatinib in 1.
Conclusion: TRA, T-DXd and T-DM1 are associated with DILI, including acute hepatitis and chronic PSVD. Further data are needed to predict the development of clinical PH in patients treated with these molecules.

SAT-060

Hepatotoxicity patterns associated with antibody-drug conjugates in clinical trials: a systematic review and meta-analysis

Yinuo Dong[1], Yang Zhi[1], Xiao-Yun Li[2], Xiaohong Lei[3], Yimin Mao[1].
[1]Renji Hospital, Shanghai Jiaotong University School of Medicine, Shanghai, China; [2]The First Affiliated Hospital, Fujian Medical University, Fuzhou, China; [3]Shanghai Tenth People's Hospital, Shanghai, China
Email: noradong@sjtu.edu.cn

Background and aims: Antibody-drug conjugates are widely used in cancer therapy, yet hepatotoxicity remains a key safety concern that may interrupt treatment and, in rare cases, cause fatal outcomes. We conducted a systematic review and meta-analysis to characterize the incidence, severity, and patterns of hepatotoxicity associated with contemporary antibody-drug conjugates in clinical trials.
Method: We performed a systematic review and meta-analysis of prospective clinical trials evaluating antibody-drug conjugates in adult patients with solid tumors or hematological malignancies. PubMed, Embase, Web of Science, and the Cochrane Library were searched from inception to September 15, 2025. Hepatotoxicity outcomes were defined by the Common Terminology Criteria for Adverse Events and included any grade and grade ≥3 elevations of alanine aminotransferase (ALT), aspartate aminotransferase (AST), alkaline phosphatase (ALP), gamma-glutamyl transferase (GGT), and total bilirubin (TBIL), as well as veno-occlusive disease (VOD). Pooled incidences were estimated and between study heterogeneity was assessed. Prespecified subgroup analyses were conducted by payload class, antibody target, treatment strategy, cancer type, and linker type.
Results: A total of 164 clinical trials comprising 201 cohorts and 16,584 patients were included. Laboratory defined hepatotoxicity was frequent, with pooled incidences of any grade ALT and AST elevations of 20.7% and 22.07%, while grade ≥3 elevations occurred in 3.61% and 3.43%, respectively. Cholestatic pattern abnormalities were less common, with pooled incidences of any grade ALP, GGT, and TBIL elevations of 10.92%, 8.42%, and 8.45%, and grade ≥3 events of 2.54%, 3.27%, and 2.92%. VOD was infrequent and was confined to calicheamicin-based antibody-drug conjugates, specifically gemtuzumab ozogamicin and inotuzumab ozogamicin. Subgroup analyses indicated that payload class was a key determinant of severe hepatotoxicity, with DNA-damaging payloads showing the highest incidence of grade ≥3 events, whereas topoisomerase I inhibitor based payloads consistently showed the lowest. Compared with monotherapy, combination regimens were associated with higher incidences of hepatocellular injury.
Conclusion: Hepatotoxicity associated with antibody-drug conjugates is common but mostly low grade, with severe events confined to specific platforms. Recognition of payload-, target-, and treatment-related risk differences may help optimize ADC use and hepatic monitoring in clinical practice.

SAT-061-YI

Acute liver failure: a 10-year analysis emphasizing the critical role of multidisciplinary approach

Michela Helga Falzone[1], Rachele Gastaldi[1], Margherita Saracco[1], Gabriella Tomaiuolo[1], Chiara Manuli[1], Silvia Strona[1], Maria Torrani Cerenzia[1], Chiara Stratta[2], Maurizio Berardino[2], Francesco Lupo[3], Renato Romagnoli[3], Silvia Martini[1]. *[1]SSD Insufficienza epatica e trapianto epatico, AOU Città della salute e della scienza di Torino, Turin, Italy; [2]SC Anestesia e Rianimazione 2, AOU Città della salute e della scienza di Torino, Turin, Italy; [3]SC Chirurgia Generale*

2, AOU Città della salute e della scienza di Torino, Turin, Italy
Email: michelahelga.falzone@unito.it

Background and aims: Acute liver failure (ALF) is a life-threatening condition in patients (pts) without prior liver disease. Survival depends on etiology, timely referral, complication management and liver transplant (LT). In Europe 8% of LTs are performed annually for ALF. We reported ALF LT outcomes in Italian high-volume LT Centre over the last 10 years (y).
Method: Emergency ALF LTs (Jan 2016–Sep 2025) were included, with follow-up ending in Oct 2025. Revised King's College criteria were used to determine the need for emergency LT.
Results: Of 1542 total LTs, 32 (2.1%) were performed for ALF. Median (med) age was 49 y [IQR 28–58], 50% male. Etiologies: 44% viral (mainly HBV), 13% autoimmune, 13% Wilson, 9% heat stroke, 6% drug-induced (valproate, disulfiram), 6% A. phalloides, 6% HELLP, 3% indeterminate. Onset was 59% hyperacute, 25% acute and 16% subacute (O'Grady classification). Med transfer time from peripheral centers to our Centre was 1 day (d) [1–3]. At presentation: med bilirubin 13.7 mg/dl [6.5–20.1], INR 4.0 [2.8–5.7], creatinine 1.1 mg/dl [0.6–1.4], MELD 35 [29–38]. Hepatic encephalopathy grade 3–4 affected 19 pts, with med arterial ammonia of 258 mcmol/l [182–395], 79% requiring endotracheal intubation; no one developed intracranial hypertension. Pre-LT complications were acute kidney injury (AKI) (53%), hemodynamic instability needing vasopressors (47%), infections (25%). 17 pts (53%) underwent hemodialysis (HD) — 5 for AKI, 8 for hyperammonemia, 4 for both; 3 pts (9.4%) plasmapheresis. Med transfer-to-listing time was 1 d [0–2] and LT waiting time 1 d [1–2]. Med MELD was 36 [32–41]. One intraoperative death occurred due to cardiac arrest at reperfusion. Med extubation time was 3 d [1–6]; ICU stay 7 d [4–11]; overall hospitalization 26 d [16–54]. Post-LT 11/17 pts (65%) needed HD, 16/31 (52%) had infections and 12/31 (39%) early neurologic complications (delayed consciousness recovery, seizures). We observed 1/31 Yerdel-I portal vein thrombosis (43 d post-LT), 6/31 early acute rejection (med RAI 4/9) and 12/31 biliary complications (1 re-LT 39 d post-LT due to biliary necrosis). After a med follow-up of 4.3 y [1.7–6.3], mortality was 9.7%: 1 septic shock and 1 lymphoma within 3 months, 1 lung cancer after 6 y. 1- and 5- survival rates were 93%, 9-y 80%.
Conclusion: Emergency life-saving LT for ALF is a rare indication. Despite illness severity, high survival rate underscores the value of prompt multidisciplinary care.

SAT-062
Rechallenge after a DILI episode: importance of the pattern and the medication class

María Fernández-Aguilera[1], Maria Calvo-Orteu[2], Anna Pocurull Aparicio[3], Jose A. Carrión[4], Inés Sáenz de Miera[5], Mercedes Vergara[6], Maria Poca[7], Elia Canga[3], Alba Ardevol[8], Xavier Ariza[9], Alberto Amador[10], Joaquín Sáez-Peñataro[2], Xavier Forns[3], Mar Riveiro Barciela[1]. [1]*Liver Unit, Internal Medicine Department, Hospital Universitario Vall d'Hebron, Universitat Autònoma de Barcelona, CIBEREHD, Barcelona, Spain;* [2]*Servei de Farmacologia Clínica, Hospital Clínic, IDIBAPS, Barcelona, Spain;* [3]*Hospital Clínic, IDIBAPS, Universitat de Barcelona, CIBEREHD, Barcelona, Spain;* [4]*Hospital del Mar, IMIM, Universitat Pompeu Fabra, Barcelona, Spain;* [5]*Joan XXIII Universitary Hospital, Tarragona, Spain;* [6]*Unidad de Hepatologia, Servicio de Aparato Digestivo, Hospital Universitario Parc Taulí, Institut d'Investigació i Innovació Parc Taulí (I3PT-CERCA), Universitat Autònoma de Barcelona, CIBEREHD, Sabadell, Spain;* [7]*Hospital de la Santa Creu i Sant Pau, Universitat Autònoma de Barcelona, CIBEREHD, Barcelona, Spain;* [8]*Hospital Germans Trias i Pujol, Badalona, Spain;* [9]*Hospital Moisès Broggi, Universitat de Barcelona, Sant Joan Despí, Spain;* [10]*Hospital Universitario de Bellvitge, IDIBELL, Universitat de Barcelona, Hospitalet de Llobregat, Spain*
Email: mariafdezaguilera@gmail.com

Background and aims: Drug-induced liver injury (DILI) is the most frequent cause of acute liver failure (ALF) in high-income countries. While positive rechallenge has been associated with high mortality and liver transplant rate, data on "negative rechallenge" and the risk factors associated with DILI relapse are scarce. This study aimed to assess the incidence, characteristics, and safety of drug rechallenge in a real-world cohort.
Method: All DILI cases included in the DILI-cat registry were collected. Classical DILI criteria were used (ALT ≥5×ULN; AP ≥2×ULN or ALT ≥3 ULN + bilirubin ≥2×ULN). In patients who were retreated with a drug from the same family, time to retreatment, relapse and its severity were also recorded.
Results: 274 DILI cases were recorded in 10 university hospitals. Roughly, half were women, median age 59 years, 33% with history of dyslipidemia, 15% diabetes, 31% arterial hypertension and 10% chronic liver disease (mainly MASLD). Regarding DILI, most frequent drugs were antibiotics (21%), lipid-lowering (18%), oncohematological drugs (18%) and analgesics (11%). Biochemical pattern: hepatocellular (54%), cholestatic (29%) and mixed (17%). Up to 81% presented a RUCAM >6 points (likely or very likely causality). Forty-eight patients (18%) had exposure to ≥1 potentially hepatotoxic drug. Up to 40% patients were admitted to hospital, 4 (2%) developed ALF, but none died or required liver transplant. Overall, 41 (15%) subjects were retreated within a median time of 5 months (IQR 2–11) from the initial DILI episode. Retreatment was more common among DILI due to lipid-lowering (12/38, 32%) and oncohematological drugs (16/41, 30%), in comparison to antibiotics or antituberculosis agents ($p = 0.021$). Higher rechallenge rate was observed among subjects presenting with cholestatic pattern, in contrast to hepatocellular or mixed (28% vs 15% vs 19%, $p = 0.10$). Positive rechallenge (i.e. DILI relapse) was observed in 3/41 (7%) retreated patients. Two of the 3 cases were reported after exposure to the same drug: Irinotecan/oxaliplatin, latency time 1 month, hepatocellular pattern; co-trimoxazole, latency 6 months, cholestatic. The third occurred after switching within the analgesic class (metamizole to ibuprofen, cholestatic pattern, latency 1 month)). None of the relapses developed severe hepatitis.
Conclusion: Rechallenge after a DILI episode is not infrequent in clinical practice, and the rate of relapse is relatively low, especially among oncohematological and lipid-lowering drugs.

SAT-067
Multicenter evaluation of large language models versus hepatologists for prognostic prediction in drug-induced liver injury

Haoshuang Fu[1], Yanan Du[1], Gangde Zhao[2], Yan Zhuang[3], Tianhui Zhou[1], Rongtao Lai[1], Ruidong Mo[1], Qing Xie[1]. [1]*Department of Infectious Diseases, Ruijin Hospital, Shanghai Jiao Tong University School of Medicine, Shanghai, China;* [2]*Department of Infectious Diseases, Ruijin North Hospital, Shanghai Jiao Tong University School of Medicine, Shanghai, China;* [3]*Department of Infectious Diseases, Wuxi Xinrui Hospital, Shanghai Jiao Tong University School of Medicine, Wuxi, China*
Email: 15670612801@163.com

Background and aims: Drug-induced liver injury (DILI) is the leading cause of acute liver failure in Western countries, and approximately 20% of patients progress to chronicity, potentially resulting in cirrhosis. The large language models (LLMs) provide new opportunities for clinical decision support. However, their prognostic value in DILI remains unclear. This study evaluated the performance of LLMs in predicting DILI outcomes and compared them with human experts.
Method: A total of 943 patients with RUCAM scores >6 were enrolled from three medical centers and classified as recovery, chronicity, or death at 6-month follow-up. Patients were divided into internal and external cohorts by enrolling centers. Three LLMs (GPT-5.1, Gemini-2.5 Pro, and DeepSeek-3.2) were evaluated using zero-shot prompting, and ensemble strategies (voting, OR, and AND rules) were applied to improve predictive stability. Junior, middle, and senior

hepatologists independently estimated the probability of progression to chronicity or death. Model performance was assessed using AUROC, accuracy, sensitivity, specificity, and agreement metrics.
Results: For chronic DILI, the senior hepatologist achieved the highest AUROC (0.61) and accuracy (70%). Among LLMs, GPT-5.1 showed the best performance (AUROC 0.59) with an accuracy of 53%, outperforming junior and middle hepatologists but remaining numerically inferior to senior expertise. DeepSeek demonstrated the highest sensitivity (0.80), whereas the middle hepatologist exhibited the highest specificity (0.86). Gemini-2.5 Pro showed the strongest agreement with the senior hepatologist ($\kappa = 0.43$). For lethal DILI, the senior hepatologist achieved an AUROC of 0.87 with accuracy of 83%, while GPT-5.1 yielded the highest LLM AUROC (0.86) with accuracy of 77%, outperforming junior and middle hepatologists but remaining inferior to senior expertise. Gemini-2.5 Pro demonstrated the highest sensitivity (0.86), whereas the middle hepatologist achieved the highest specificity (0.83). Across overall, internal, and external cohorts, the LLM-AND strategy maintained stable AUROC and accuracy without substantial inter-cohort variation.
Conclusion: LLMs demonstrated clinically relevant prognostic capability for DILI outcomes. The AND ensemble strategie improved robustness across cohorts and achieved performance comparable to senior hepatologists, supporting the potential role of aggregated LLMs as reliable decision-support tools in DILI prognosis.

SAT-068

Long-term outcomes following checkpoint inhibitor-induced liver injury

Kenza Faouzi[1], Alexandre Maria[1], Stéphanie Faure[1], Candice Lesage[1], Cyril Coustal[1], Marie Dupuy[1], Charles Catney[1], Georges-Philippe Pageaux[1], Quentin Thomas[2], Xavier Quantin[2], Lucy Meunier[1], Lina Hountondji[1]. *[1]Regional University Hospital Center of Montpellier, Montpellier, France; [2]Montpellier Cancer Institute, Montpellier, France*
Email: lina.hountondji@outlook.fr

Background and aims: Immune checkpoint inhibitors (ICIs) have become a cornerstone in the treatment of many cancers, significantly improving patient prognosis and survival. However, checkpoint inhibitor-induced liver injury (CHILI) occurs in up to 25% of treated patients and raises major challenges regarding the resumption of anticancer therapy once hepatitis has resolved. ICI rechallenge is associated with a 20–30% risk of hepatitis recurrence, and alternative treatments are often preferred despite limited data This study aimed to evaluate oncological management after CHILI and the risk of liver toxicity recurrence according to subsequent anticancer strategies over a two-year follow-up.
Method: CHILI-Outcomes is a retrospective, observational, multicenter study including adult patients treated with ICIs and discussed at the ImmunoTox multidisciplinary board. Clinical and biological data were collected at diagnosis and during follow-up up to 24 months. Data on cancer characteristics, oncological treatments, treatment rechallenge, hepatitis recurrence, and survival were analyzed. Chronic CHILI was defined as persistent abnormal liver tests at 6 months.
Results: Eighty-three patients were included between December 2018 and August 2023, predominantly men (61.4%), with a median age of 66.5 years. The main cancer types were lung cancer (35%) and melanoma (30.1%), mostly stage IV (66.2%). ICIs were mainly anti-PD(L)1 monotherapy (73.5%), and hepatitis severity was predominantly CTCAE grade III (75.9%). Corticosteroids were used in 74.4% of patients, and 5.1% required second-line immunosuppression. Chronic CHILI developed in 7.2% of patients. After a median follow-up of 25.5 months, 66.3% of patients resumed anticancer therapy, including ICIs (52.4%), tyrosine kinase inhibitors (29.5%), or chemotherapy (17.9%). Hepatitis recurred in 13 patients after ICI rechallenge and was attributed to ICIs alone in 11 cases and to combined ICI plus TKI in 2 cases. A favorable oncological response (complete, partial or stable) was observed in 33.7% of patients at 6 months (n = 28) and in 31.3% at 12 months (n = 26). Overall mortality was 43%, mainly related to cancer progression, while death from liver failure remained rare (8.4%).
Conclusion: In conclusion, most patients resumed anticancer treatment after CHILI, frequently with ICI rechallenge. Although hepatitis recurrence was more common with ICIs, long-term morbidity and mortality were primarily driven by oncological progression, with a low rate of chronic liver injury.

SAT-069

Significant liver fibrosis in patients with steatotic liver disease treated with Tamoxifen or Aromatase inhibitors: a cardiometabolic risk–driven phenomenon

Jae Yoon Jeong[1], Na Ryung Choi[1], Jung Hee Kim[2], Ju-Yeon Cho[3], Won Sohn[4]. *[1]Ewha Womans University Mokdong Hospital, Ewha Womans University College of Medicine, Seoul, Korea, Rep. of South; [2]Hallym University Dongtan Sacred Heart Hospital, Dongtan, Korea, Rep. of South; [3]Saint Louis University School of Medicine, Saint Louis University Hospital, St. Louis, United States; [4]Kangbuk Samsung Hospital, Sungkyunkwan University School of Medicine, Seoul, Korea, Rep. of South*
Email: jyjeong76@hanmail.net

Background and aims: This study aimed to assess the risk of liver fibrosis in patients with steatotic liver disease (SLD) receiving tamoxifen or aromatase inhibitors. In particular, we investigated cardiometabolic factors associated with liver fibrosis in this population and compared the impact of tamoxifen and aromatase inhibitors on liver fibrosis.
Method: We conducted a cross-sectional study using a cohort from a tertiary referral hospital that included patients with SLD and breast cancer treated with tamoxifen or aromatase inhibitors. Liver fibrosis was assessed using transient elastography (TE). Significant fibrosis was defined as a liver stiffness measurement (LSM) ≥8.0 kPa. We evaluated the risk of significant fibrosis and fibrosis-related risk factors, including cardiometabolic factors such as overweight/obesity, prediabetes/diabetes, high blood pressure/hypertension, hypertriglyceridemia, and decreased high-density lipoprotein cholesterol levels.
Results: A total of 413 patients were included: 268 received tamoxifen and 145 received aromatase inhibitors. The mean age was 53 years. The mean LSM was 4.86 ± 2.52 kPa, and the prevalence of significant fibrosis was 6.3% (n = 26). In multivariable analysis, significant fibrosis was independently associated with hypertriglyceridemia (odds ratio [OR] 3.23, 95% confidence interval [CI] 1.08–9.55, p = 0.035) and high blood pressure/hypertension (OR 2.63, 95% CI 1.03–6.77, p = 0.044). However, the use of tamoxifen was not associated with a higher risk of significant fibrosis compared with aromatase inhibitors (OR 1.32, 95% CI 0.56–3.09, p = 0.531). There was no significant difference in the prevalence of significant fibrosis between patients receiving tamoxifen and those receiving aromatase inhibitors. The mean LSM values were 4.88 ± 2.52 kPa in the tamoxifen group and 4.82 ± 2.16 kPa in the aromatase inhibitor group (p = 0.841).
Conclusion: In patients with SLD and breast cancer receiving tamoxifen or aromatase inhibitors, liver fibrosis is more strongly associated with cardiometabolic risk factors than with endocrine therapy itself. These findings suggest that careful management of cardiometabolic risk factors is crucial in patients with SLD undergoing endocrine therapy.

SAT-070

Clinical relevance of albumin binding kinetics in patients undergoing extracorporeal albumin detoxification

Stine Koball[1,2,3], Adrian Dominik[1,3], Sebastian Koball[1], Michael Hinz[1], Jan Stange[1]. [1]*University of Rostock, Rostock, Germany;* [2]*Albutec GmbH, Rostock, Germany;* [3]*ProMedTec Germany GmbH, Rostock, Germany*
Email: stine.koball@gmail.com

Background and aims: Liver failure is associated with toxin accumulation that impairs albumin binding, increases toxin bioavailability, and promotes secondary organ failure with adverse clinical outcomes. Current extracorporeal liver support strategies like Multiple Pass Albumin Dialysis aim to restore albumin detoxification capacity by removing albumin-bound toxins and water-soluble toxins. This study aimed to characterize albumin binding kinetics using a dansylsarcosine-based method, evaluating its clinical relevance in patients with liver failure undergoing extracorporeal albumin detoxification. Functional assessment of albumin may provide essential guidance for timing and selection of detoxification therapies.
Method: Data was analyzed using the OPALESCE trial database, including patients treated with Molecular Adsorbents Recirculating System (MARS) and Open Albumin Dialysis (OPAL) therapy. Albumin binding kinetics at Sudlow site II were assessed by dansylsarcosine titration and ligand binding curve analysis using a modified binding model. The parameters Bmax (maximum number of binding sites) and Kd (binding affinity, defined as the ligand concentration at half saturation) were derived. Kinetic parameters were validated against previously published albumin function markers, including albumin binding capacity and electron spin resonance-based measures and then correlated with clinical scores.
Results: Higher Bmax values and lower Kd values were associated with better clinical status, including improved organ function scores. Correlations were observed with Glasgow Coma Scale, Sepsis-related Organ Failure Assessment score, Hepatic Encephalopathy Grade, Model for End-stage Liver Disease score, and Acute-on-Chronic Liver Failure-related scores. Treatment with extracorporeal albumin detoxification resulted in measurable improvements in albumin binding kinetics, reflected by increasing Bmax and decreasing Kd values, consistent with trends observed in established albumin function markers. These findings indicate partial reversibility of impaired albumin binding through extracorporeal support.
Conclusion: Dansylsarcosine-based kinetic modeling enables functional characterization of albumin binding in liver failure. Albumin binding function impaired by toxin accumulation shows improvement after extracorporeal albumin detoxification. Differentiation between reversible and irreversible albumin dysfunction may support individualized therapeutic decision-making and optimization of liver support strategies.

SAT-071

The dosage effect of polyene phosphatidylcholine injection for treating patients with acute drug-induced liver injury: a cohort trial

Ming Kong[1], Jiaqi Li[1], Yu Chen[1]. [1]*Beijing Youan Hospital, Capital Medical University, Beijing, China*
Email: chybeyond1071@ccmu.edu.cn

Background and aims: Polyene phosphatidylcholine (PPC) injection is widely used for various liver diseases in China. However, the optimal dosage of PPC injection for acute drug-induced liver injury (DILI) remains unclear. This study aims to investigate the dosage effect of polyene phosphatidylcholine in treating DILI.
Method: We conducted a cohort study involving patients with acute drug-induced liver injury who were admitted to Beijing Youan Hospital, Capital Medical University, Beijing, China. The patients were equally divided into two groups: the control group received 930 mg/d of PPC injection combined with other hepatoprotective agents; the study group received 1860 mg/d of PPC injection combined with the same other hepatoprotective agents, with a treatment duration of 7–14 days. The primary endpoint was above 50% reduction in alanine aminotransferase (ALT) after 7days treatment.
Results: A total of 60 patients with acute DILI were enrolled, with 30 patients in each group. There were no significant statistical differences in baseline ALT, aspartate aminotransferase (AST), total bilirubin (TBIL), age, or gender between the two groups. After 7 days treatment, the proportion of above 50% reduction in ALT was significantly higher in study group than control group (86.7% vs. 63.3%, $p = 0.037$). After 14 days treatment, the proportion of above 50% reduction in ALT was higher in study group (96.0% vs. 72.4%, $p = 0.028$), and the reduction proportion in AST was greater in study group (−79.3% [−86.9%, −68.1%] vs. −61.3% [−78.4%, −34.6%], $p = 0.035$). There were no serious adverse reactions in each group.
Conclusion: In this study, the study group showed more significant reductions in ALT and AST, which preliminarily indicates that higher dosage of polyene phosphatidylcholine is more effective in DILI, with well tolerated.

SAT-072

RECAM versus RUCAM for drug-induced liver injury diagnosis: a systematic review and validation study

Weiqian Lou[1], Chengwei Chen[2], Rongtao Lai[1]. [1]*Department of Infectious Diseases, Ruijin Hospital, Shanghai Jiao Tong University School of Medicine, Shanghai, China;* [2]*Liver Disease Research Center, 905th Hospital of PLA Navy, Shanghai, China*
Email: lairongtao1202@163.com

Background and aims: Drug-induced liver injury (DILI) has emerged as the predominant etiology of acute liver injury worldwide. While RUCAM served as the gold standard causality assessment method for three decades, the introduction of the electronic revision RECAM in 2022 generated substantial debate concerning diagnostic superiority and real-world applicability. To compare the diagnostic accuracy of RECAM against RUCAM across heterogeneous patient cohorts and determine the feasibility of RECAM as a replacement tool in routine clinical practice.
Method: A systematic literature search of PubMed, Embase, and Web of Science (January 2020–December 2024) identified validation studies directly comparing RECAM and RUCAM performance. Inclusion criteria required reporting of the area under receiver operating characteristic curve (AUROC), sensitivity, specificity, or inter-rater agreement (weighted kappa). We extracted data stratified by population characteristics, DILI phenotype (conventional pharmaceuticals versus herbal products), and discriminatory metrics.
Results: Two large-scale multicenter validation cohorts met inclusion criteria. Japanese investigators (RECAM-J 2023) evaluated 538 confirmed DILI patients and 128 alternative diagnosis controls, demonstrating an AUROC of 0.88 for probable/highly probable DILI detection after excluding viral hepatitis penalty scores. Chinese multicenter data encompassed 481 DILI cases (301 conventional drugs, 180 herbals) and 100 liver injury mimics spanning five tertiary centers. RECAM outperformed RUCAM across all subgroups: combined cohort AUROC 0.947 versus 0.867 ($P = 0.0016$), conventional agents 0.923 versus 0.819 ($P = 0.0185$), and herbal products 0.972 versus 0.911 ($P = 0.0199$). Principal scoring divergence between instruments derived from latency period interpretation, hepatitis B serology weighting, and prior drug hepatotoxicity classification. RECAM exhibited enhanced inter-observer reproducibility, electronic health record integration potential, and concordance with adjudicated expert consensus diagnoses.
Conclusion: RECAM demonstrates better diagnostic accuracy than RUCAM in diverse populations, particularly for herbal medicine-induced liver injury. Prospective validation among general practitioners and in specialized scenarios (e.g., immune checkpoint inhibitors, chronic DILI, transplant recipients) remains necessary before RUCAM replacement can be recommended.

SAT-073

Extreme hyperferritinemia is associated with high short-term mortality in acute liver failure and acute-on-chronic liver failure

Jonathan Lee[1], Diana Garcia[1], Costica Aloman[2,3], Nancy S. Reau[1]. [1]*Rush University Medical Center, Chicago, United States;* [2]*Westchester Medical Center, Valhalla, United States;* [3]*New York Medical College, Valhalla, United States*
Email: jonoslee@outlook.com

Background and aims: Ferritin has been studied as a prognostic biomarker. Studies have shown a significant correlation between marked ferritinemia and increased all-cause mortality in chronic liver diseases. Past investigations into the causes of extreme hyperferritinemia (EHF) have observed a high prevalence of liver disease, but few studies have focused on the type of liver injury and their associated mortality. This study aims to characterize the most common etiologies of EHF and to explore their associated prognostic outcomes.
Method: We performed a retrospective, single-center study on all adult patients presenting with a serum ferritin level >10,000 μg/L between January 1, 2014 and December 31, 2024. Demographics, laboratory values, etiology of EHF, and survival duration from time of ferritin result to death were collected. Chi-square and unpaired T-tests were used for bivariate analysis, as appropriate. A p-value of <0.05 was deemed statistically significant.
Results: 718 adult patients (mean age 56 years) met inclusion criteria with a median follow-up period of 272 days. Most patients were male (55.6%) and a plurality were Black (42.9%). The mean ferritin level was 23860 μg/L (range 10014–60000 μg/L). 377 (52.5%) patients lived and 341 (47.5%) patients died on follow-up. Mean ferritin levels were significantly higher in non-survivors than survivors (25107 vs 22675 μg/L, $p = 0.004$). Older age was significantly associated with mortality (60.2 vs 53.8 years, $p < 0.001$). EHF was most associated with liver disease (28.3%), infection (25.9%), and malignancy (15.9%). Acute liver failure (ALF) (88.7%) and acute-on-chronic liver failure (ACLF) (9.4%) comprised the majority of liver disease etiologies associated with EHF. The most common ALF etiologies were ischemic hepatitis (68.9%) and drugs/toxins (19.4%), whereas alcohol-associated hepatitis (84.2%) was the most common underlying chronic liver disease state identified in ACLF. ALF was associated with a significantly higher mean ferritin level than ACLF (28947 vs 20654 μg/L, $p = 0.004$). 54.4% of ALF patients died (mean survival 35 days) versus 42.1% of ACLF patients (mean survival 7 days).
Conclusion: There was a high prevalence of ALF and ACLF in EHF. EHF was associated with poor prognosis and significant overall short-term mortality. Our findings underscore the potential value of ferritin as an additional tool for overall mortality risk stratification. Future research should explore the prognostic value of non-EHF in ALF and ACLF.

SAT-074

Antineoplastic drug–associated hepatic steatosis: evidence from the FDA adverse event reporting system

Yanjie Lin[1], Gui-Qiang Wang[2], Hong Zhao[2]. [1]*Department of Infectious Disease, Center for Liver Disease, Peking University First Hospital, Beijing, China;* [2]*Department of Infectious Disease, Center for Liver Disease, Peking University First Hospital, Department of Infectious Diseases, Peking University International Hospital, Beijing, China*
Email: zhaohong_pufh@bjmu.edu.cn

Background and aims: Since drug-induced hepatic steatosis is relatively rare but closely related to adjusting the treatment of the primary disease, preventing liver steatosis and its inflammation. This study investigated the risk factors of drug-induced hepatic steatosis by analyzing a large dataset from the FDA Adverse Event Reporting System (FAERS).
Method: The reporting odds ratios (ROR) and information component (IC) were used to evaluate the reports of hepatic steatosis from the first quarter of 2004 to the third quarter of 2024. Univariate, LASSO and multivariate regression analyses were used to explore the risk factor. Moreover, the time to onset of hepatic steatosis was also assessed.
Results: Overall, 16,767 cases related to fatty liver disease were found in FAERS. In total, 117 drugs were found to be associated with hepatic steatosis, with antineoplastic drugs (28/117), antiviral drugs (18/117), psychotropic drugs (17/117), and immunomodulatory drugs (12/117) being the most common. Age under 41 years old, a heavier weight and 13 different drugs, including 3 antineoplastic drugs of interest, namely Methotrexate, Pegaspargase, and Tamoxifen, were risk factors for hepatic steatosis. The median time to onset was 123.50 days, while the onset of Pegaspargase was faster, with a median time of only 19 days ($p < 0.001$).
Conclusion: With the increasing variety of drugs, it's necessary to focus on hepatic steatosis and steatohepatitis caused by drugs, and adjust the therapeutic drugs in a timely manner to reduce the incidence of liver fibrosis, liver cirrhosis and prevent the interruption of treatment for the primary disease.

SAT-075

Predicting the unpredictable: machine learning outperforms MELD for ICU mortality in acute liver failure

Jeril Lasington[1], Lawin Steve Mathew Lasington[2]. [1]*New York Medical College, Valhalla, United States;* [2]*Rutgers University-Newark Arch, Newark, United States*
Email: jeril.lasington@gmail.com

Background and aims: Acute liver failure (ALF) carries high ICU mortality, yet validated ICU-specific prediction tools remain limited. Traditional scores like MELD were not designed for acute presentations in critically ill patients. We developed and validated machine learning (ML) models to predict hospital mortality in ALF using readily available clinical parameters.
Method: This retrospective cohort study used MIMIC-IV (v3.1) to identify adults with ALF requiring ICU admission (2008–2022). Patients with pre-existing chronic liver disease or cirrhosis were excluded to focus on acute presentations. Predictors from the first 24 hours included demographics, vital signs, laboratory values, and ICU interventions. Four ML algorithms (Logistic Regression, Random Forest, XGBoost, Gradient Boosting) were trained using 80/20 stratified splits with five-fold cross-validation. Performance was evaluated using AUC-ROC, AUPRC, and calibration analysis. SHAP analysis assessed feature importance.
Results: Among 2,024 ALF patients (mean age 60.1 years; 56.2% male), hospital mortality was 40.7%. Vasopressor support was required in 48.4% and mechanical ventilation in 46.1%. Random Forest achieved highest discrimination (AUC 0.804, 95% CI 0.765–0.841), significantly outperforming MELD (AUC 0.609) with 32% relative improvement. Cross-validation demonstrated model stability (AUC 0.79 ± 0.03). At optimal threshold, sensitivity was 59%, specificity 82%, PPV 69%, and NPV 74%. Feature importance revealed markers of shock (lactate, MAP), metabolic derangement (pH), and hepatocyte injury (ALT) as dominant predictors. Top features included maximum lactate (0.078), minimum pH (0.069), age (0.062), minimum MAP (0.055), and shock index (0.052).
Conclusion: ML significantly outperforms traditional MELD for ICU mortality prediction in ALF. The model identified clinically interpretable predictors emphasizing hemodynamic instability and metabolic derangement over liver-specific parameters alone. This tool may assist early risk stratification and resource allocation for critically ill ALF patients.

SAT-076

Impact of liver biopsy on causality assessment in checkpoint inhibitor–induced liver injury

Lucy Meunier[1], Alexandre Maria[1], Benjamin Riviere[1], Bénédicte Delire[2], Yves Horsmans[2], Dominique Larrey[1,3,4], Eleonora De Martin[5], Lucia Parlati[6], Marie Dupuy[1], Stéphanie Faure[1], Lina Hountondji[1]. [1]*Montpellier Hospital, Montpellier, France;* [2]*Saint Luc University, Bruxelles, Belgium;* [3]*CHU Montpellier, 34, Montpellier, France;* [4]*CHU Montpellier, Liver Unit, Montpellier, France;* [5]*Villejuif hospital, Paris, France;* [6]*Cochin Hospital, Paris, France*
Email: lucy-meunier@chu-montpellier.fr

Background and aims: The diagnosis of checkpoint inhibitor–induced liver injury (CHILI) remains challenging due to the lack of specific biomarkers. Consequently, the reliability of the RUCAM score for assessing causality of liver test abnormalities under ICIs, as well as the role of liver biopsy in diagnosing and staging CHILI, remains uncertain. The aim of this study was to evaluate whether liver histology impacts causality assessment in suspected CHILI.
Method: This study included adult patients diagnosed with CHILI who were followed for 6 months after liver biopsy at Montpellier University Hospital. All enrolled patients underwent a standardized causality assessment using the RUCAM score, independently calculated by two senior hepatologists responsible for patient inclusion. Discrepancies were resolved by consensus. RUCAM is a 14-point causality assessment tool categorized as follows: ≤0 (excluded), 1–2 (unlikely), 3–5 (possible), 6–8 (probable), and ≥9 (highly probable).
Results: Among the 50 patients, 58% were male, with a median age of 65 years (range 29.8–83.4). The median time from ICI initiation to hepatitis onset was 81 days (range 10–561). Anti–PD-1 monotherapy was the most frequently implicated regimen (n = 30; 60%). Liver injury patterns were hepatocellular in 42% (n = 21), cholestatic in 34% (n = 17), and mixed in 24% (n = 12). The median RUCAM score prior to liver biopsy was 7 (probable) (range 1–11), and 42 patients (84%) were classified as having probable or highly probable CHILI after biopsy. Interobserver agreement for RUCAM scoring was almost perfect, with an absolute agreement of 90.0% (κ = 0.80; 95% CI [0.63–0.97]). No discordance was observed in histological interpretation between observers. Although liver biopsy findings did not modify the RUCAM score, they contributed to confirming or questioning the diagnosis in 80% of cases (n = 40).
Conclusion: In patients with suspected CHILI, liver biopsy significantly influences causality assessment without modifying the RUCAM score. While RUCAM demonstrates good interobserver reproducibility, its limitations in CHILI underscore the added value of histological evaluation in selected cases. Causality assessment in CHILI is complex, as time to onset may be prolonged and concomitant treatments are frequent. Additional factors, including response to corticosteroids and the presence of other immune-related adverse events, should be integrated into diagnostic evaluation.

SAT-077

Lipopolysaccharide binding protein as a predictive biomarker for the onset of acute kidney injury in cirrhosis

Tadashi Namisaki[1], Masafumi Oyama[1], Tatsuya Nakatani[1], Kosuke Kaji[1], Hitoshi Yoshiji[1]. [1]*The Department of Gastroloenterology, Nara Medical University, Kashihara, Japan*
Email: tadashin@naramed-u.ac.jp

Background and aims: We aimed to identify plasma biomarkers that predict the onset and clinical outcomes of acute kidney injury (AKI) in patients with liver cirrhosis (LC).
Method: This retrospective case–control study included 182 patients with LC: 91 patients who developed AKI (AKI group) and 91 patients who did not develop AKI (non-AKI group) as controls. Plasma levels of lipopolysaccharide-binding protein (LBP), soluble CD163 (sCD163), and soluble mannose receptor (sMR) were measured at the time of AKI diagnosis in the AKI group and at a comparable clinical assessment in the non-AKI group. We investigated independent risk factors for AKI onset using multivariable logistic regression. Within the AKI group, we further examined predictors of 90-day mortality from AKI onset and poor treatment response (lack of AKI improvement) using multivariable models, and compared cumulative survival between groups stratified by biomarker cutoffs.
Results: Compared with the non-AKI group, the AKI group had significantly higher plasma levels of renin, angiotensin II, LBP, sCD163, and sMR. In multivariable analysis, LBP ≥2550 ng/mL was independently associated with AKI onset in patients with LC (odds ratio [OR] 4.30; 95% confidence interval [CI] 1.82–10.2; p < 0.001). Among patients with AKI, sMR levels were significantly higher in those who died within 90 days of AKI onset than in those who survived beyond 90 days. sMR ≥1595 ng/mL was an independent risk factor for 90-day mortality (OR 5.98; 95% CI 1.70–21.1; p = 0.0054), and cumulative survival was significantly lower in the high-sMR group (≥1595 ng/mL) than in the low-sMR group (<1595 ng/mL). In addition, sMR levels were significantly higher in patients with poor treatment response than in those whose AKI improved. sMR ≥1460 ng/mL was identified as a risk factor for poor treatment response (OR 3.52; 95% CI 1.09–11.3; p = 0.035), and treatment response rates were significantly higher in the low-sMR group (<1460 ng/mL) than in the high-sMR group (≥1460 ng/mL).
Conclusion: In patients with LC, elevated LBP may predict AKI onset, whereas elevated sMR may predict short-term survival and treatment response after AKI develops. These biomarkers may reflect endotoxin-related inflammation and macrophage activation and could enable earlier risk stratification and more tailored management of cirrhosis-associated AKI.

SAT-078

Association between biochemical patterns of DILI and histological findings in liver biopsies

Tayna Domingos[1], Vinicius Nunes[1], Luiz Antônio Rodrigues de Freitas[1], Genário Oliveira Santos Júnior[1], Raymundo Parana Ferreira Filho[1], Maria Schinoni[1]. [1]*University Hospital of Bahia, Salvador, Brazil*
Email: tayna.s.domingos@gmail.com

Background and aims: Drug-induced liver injury (DILI) presents a broad clinical and histological spectrum. While the biochemical classification into hepatocellular, cholestatic, and mixed patterns is central to clinical evaluation, its correlation with histology and severity remains limited.This study aimed to identify the histological correlates responsible for the clinical severity associated with different biochemical patterns of DILI.
Method: A cross-sectional study was conducted in individuals with DILI who underwent liver biopsy.Clinical, biochemical, and histopathological variables were evaluated.
Results: A sample of 58 patients was analyzed according to their biochemical pattern: hepatocellular (n = 41), cholestatic (n = 7), and mixed (n = 10). The hepatocellular pattern showed greater clinical severity, with progression to acute liver failure (ALF) in 73.2% of cases, compared to 0% in the cholestatic pattern and 40% in the mixed pattern (p < 0.05). This group presented higher medians of ALT (740 U/L), AST (889 U/L), and INR (2.35), in contrast to the cholestatic (ALT 208 U/L; AST 134 U/L; INR 1.0) and mixed (ALT 281.5 U/L; AST 306 U/L; INR 1.0) patterns. The presence of massive/submassive necrosis (n = 31) was significantly associated with the biochemical profile (p < 0.05). The group with necrosis consisted mainly of hepatocellular (83.9%) and mixed (16.1%) patterns, while the group without necrosis included all cholestatic cases (25.9%), as well as portions of the hepatocellular (55.6%) and mixed (18.5%) patterns. Clinical severity was higher in the group with necrosis, where 93.5% of patients progressed to ALF/transplant, compared to 18.5% in the group without necrosis (p < 0.05). Biochemically, necrosis presented higher values of: AST [median 843 (349–3041) vs. 348 (151–1000) U/L; p < 0.05], ALT [693 (467–1365) vs. 320 (210–935) U/L; p < 0.05], and INR [3.27 (2–5) vs. 1.02 (1–1.38); p < 0.05]. Furthermore, Hy's Law was

present in 83.8% of those with massive/submassive necrosis ($p < 0.05$). In contrast, hepatocellular ballooning was more frequent in the cholestatic pattern (71.4%) compared to the hepatocellular (9.8%) and mixed (20%) patterns ($p < 0.05$),indicating predominant cellular activity without progression to liver failure.
Conclusion: DILI severity is primarily driven by massive/submassive necrosis. While the hepatocellular pattern identifies risk, necrosis extent is the key prognostic determinant, surpassing isolated inflammation.These findings reinforce histological-biochemical integration for risk stratification.

SAT-079

Plasma exchange improves transplant-free survival in acute liver failure: a patient-level meta-analysis

Miguel Sogbe[1], Javier Perez de Rojas[2], Monica Rubio-Ardanaz[1], Paloma Sangro[3], Manuel de la Torre[3], Delia D'Avola[3], Mercedes Iñarrairaegui[1], Josepmaria Argemi[1], Bruno Sangro[1,3], Jose Ignacio Herrero[1]. *[1]Liver Unit, Clinica Universidad de Navarra, Pamplona, Spain, Centro de Investigación Biomédica en Red de Enfermedades Hepáticas y Digestivas (CIBEREHD), Pamplona, Spain, Instituto de Investigación Sanitaria de Navarra (IdiSNA), Pamplona, Spain, Pamplona, Spain; [2]Department of Preventive Medicine Clinica Universidad de Navarra, Universidad de Navarra, Pamplona, Spain; [3]Liver Unit, Clinica Universidad de Navarra, Madrid, Spain, Centro de Investigación Biomédica en Red de Enfermedades Hepáticas y Digestivas (CIBEREHD), Pamplona, Spain, Instituto de Investigación Sanitaria de Navarra (IdiSNA), Pamplona, Spain, Madrid, Spain*
Email: msogbe@unav.es

Background and aims: Acute liver failure (ALF) is associated with high short-term mortality, and liver transplantation (LT) remains the only definitive treatment. However, limited organ availability and strict eligibility criteria restrict its applicability and point to the need for effective alternative therapies. Plasma exchange (PE) has been proposed as a liver support strategy in ALF, but existing evidence is conflicting. We aimed to assess the impact of PE on transplant-free survival in ALF and to evaluate post-transplant outcomes when PE is used as a bridge to LT.
Method: A systematic search of PubMed/MEDLINE and Scopus was conducted to identify eligible studies published up to March 2025. Studies comparing PE with standard medical treatment (SMT), with LT allowed in both groups, were included. Eligible studies were required to report Kaplan-Meier survival curves with log-rank results and/or hazard ratios (HRs). Individual patient data were reconstructed from published Kaplan-Meier curves. The primary endpoint was transplant-free survival. Secondary analyses evaluated post-transplant survival among patients undergoing LT after PE versus SMT. Pooled HRs were estimated using one-stage Cox proportional hazards models with shared frailty, with sensitivity analyses using alternative meta-analytic approaches.
Results: Six studies comprising 447 patients were included. Among patients managed without LT, mortality was 47.6% (77/162) in the PE group compared with 80.8% (160/198) in the SMT group. PE was associated with significantly improved transplant-free survival (HR: 0.39; 95% CI, 0.29–0.52) compared to SMT. This finding was robust across sensitivity analyses, including cluster-robust Cox regression (HR: 0.41; 95% CI, 0.30–0.55) and a two-stage fixed-effects meta-analysis (pooled HR: 0.37; 95% CI, 0.28–0.49), with moderate heterogeneity (Cochran's $Q = 8.45$, $p = 0.13$; $I^2 = 40.8\%$). Among patients undergoing LT, mortality was 14.0% (6/43) in the PE+LT group and 18.1% (8/44) in the SMT+LT group. PE was not associated with improved post-transplant survival (HR: 0.84; 95% CI, 0.29–2.44).
Conclusion: In patients with ALF, PE is associated with a significant improvement in transplant-free survival but does not confer a clear survival benefit as bridge to LT. These findings support the use of PE as an effective supportive therapy for patients with ALF who are not immediate candidates for LT.

SAT-083

Concomitant medications associated with acute liver injury risk following amoxicillin/clavulanate exposure unexplained by other causes: signal detection analyses using electronic health record data

Richard Noriega[1,2], Jimmy Efird[3,4], Timothy Arnold[5,6], Chad Dorn[1,2], Ruth Reeves[1,2], Ayako Suzuki[1,7]. *[1]Health Services Research, Tennessee Valley Healthcare System VA, Nashville, TN, United States; [2]Department of Biomedical Informatics, Vanderbilt University Medical Center, Nashville, TN, United States; [3]VA Cooperative Studies Program Coordinating Center, Boston VA, Boston, MA, United States; [4]School of Medicine, Case Western Reserve University, Cleveland, OH, United States; [5]Human Systems Integration, Office of Clinical Informatics, Office of Health Informatics, Digital Health Office, Veterans Health Administration, Washington, DC, United States; [6]College of Pharmacy, University of Michigan, Ann Arbor, MI, United States; [7]Gastroenterology, Duke University, Durham, United States*
Email: ayako.suzuki@duke.edu

Background and aims: Drug-induced liver injury (DILI) is an increasingly important public health issues. Although several genetic risk factors for DILI have been identified, clinical risk factors remain poorly defined, limiting risk stratification. We developed an electronic health record (EHR)-based framework to identify acute liver injury following amoxicillin/clavulanate exposure unexplained by alternative causes (ALI-AMX/CLAV) as a scalable DILI phenotype (PMID: 36547811). Using this approach, we explored concomitant medications associated with the risk of ALI-AMX/CLAV to identify potential clinical risk determinants.
Method: We analyzed Veterans Health Administration EHR data (1999–2015), comprising 1.4 million AMX/CLAV exposures in a predominately male population. We identified 2,249 ALI-AMX/CLAV cases and 4,427 acute liver injury cases associated with other causes (ALI-OTR). All medications co-administered at the time of AMX/CLAV exposure were extracted. Odds ratios (ORs) with 95% confidence intervals (CIs) were computed for each concomitant medication by comparing ALI-AMX/CLAV and ALI-OTR cases with AMX/CLAV-exposed referents without ALI. Models were adjusted for age, sex, race/ethnicity, care setting (inpatient vs. outpatient), and pre-existing liver conditions. Associations were categorized as specific to ALI-AMX/CLAV, ALI-OTR or shared across ALI phenotypes.
Results: Among AMX/CLAV-exposed individuals, 1582 unique concomitant medications were identified. After adjustment, 32 medications were associated with increased odds of ALI-AMX/CLAV only, 79 with ALI-OTR only, and 341 and 45 medications were associated with increased or decreased odds of both ALI-AMX/CLAV and ALI-OTR, respectively. Of the 32 medications specific to ALI-AMX/CLAV, 3 were anti-cholinergic, 9 had potential immunostimulatory effects, 4 were anti-androgenic, and 4 were antiviral agents, including two anti-HIV medications.
Conclusion: Distinct concomitant medications associated with increased odds of ALI-AMX/CLAV, many with immunostimulatory or anticholinergic properties, were identified. Anti-androgenic agents, potentially counteracting androgen-mediated immunosuppression, also emerged as important risk determinants in this male-dominant population. These findings generate biologically plausible mechanistic hypotheses for modifiers of AMX/CLAV-related liver injury risk and highlight the utility of EHR-based signal detection for future DILI risk assessment strategies.

SAT-084-YI

Development and external validation of the RE-AD score: a clinical-based machine learning tool for acute decompensation prediction in compensated advanced chronic liver disease

Marco Vicardi[1], Lorenz Balcar[2], Leonardo Antonio Natola[1], Filippo Cattaazzo[1], Manuele Bicego[1], Vincenzo Dimaria[1], Michele Bevilacqua[1], Aldo Filice[1], Anna Mantovani[1], Katia Donadello[1], Laura Alaimo[1], Georg Semmler[2], David Poulakos[2], Adrian Wunderbaldinger[2], Jan Embacher[2], Lucie Simonis[2], Andrea Ruzzenente[1], Veronica Paon[1], Donatella Ieluzzi[1], Nicola Zeni[3], Roberta Gagliardi[3], Rosa Lombardi[4], Enrico Polati[1], Luca Dalle Carbonare[1], David Sacerdoti[1], Mattias Mandorfer[2], Salvatore Piano[1], Andrea Dalbeni[1]. [1]*University of Verona and University and Hospital Trust (AOUI) of Verona, Verona, Italy;* [2]*Medical University of Vienna, Wien, Austria;* [3]*University of Padova, Padova, Italy;* [4]*Fondazione IRCCS Ca' Granda Ospedale Maggiore Policlinico, Milano, Italy*
Email: marcovica98@gmail.com

Background and aims: Patients with compensated advanced chronic liver disease (cACLD) remain at risk of acute decompensation (AD), including acute-on-chronic liver failure, which carries high short-term mortality. Most available prognostic tools primarily predict overall hepatic decompensation and include a substantial proportion of non-acute decompensation (NAD) events, which usually follow a more indolent course. Therefore, accurate prediction of short-term AD in cACLD remains challenging. We aimed to develop and externally validate the Risk Estimation of Acute Decompensation (RE-AD) score, using machine learning (ML) to predict AD within 12 months and compare its performance with established scores.
Method: This multicenter retrospective study included consecutive cACLD patients from Verona and Vienna University Hospitals (2017–2024), followed for 12 months or until AD. The development cohort (n = 1,440) was analyzed using regularized ML with Leave-One-Out cross-validation and LASSO feature selection. External validation was performed in an independent cohort from Padua (n = 110). Model performance was assessed in terms of discrimination, calibration, and clinical utility. RE-AD was compared with FIB-4, APRI, ALBI, RESIST-HCV, ANTICIPATE ± NASH, Baveno VII criteria, and SAVE.
Results: Overall, 81 of 1,550 patients (5.2%) developed AD within 12 months. RE-AD incorporates age, number of hospital admissions (elective and non-elective) and infection episodes requiring antibiotics in the previous 12 months, serum albumin, and INR. Internal validation showed good discrimination (AUC 0.818, 95% CI 0.78–0.85), acceptable calibration, and high negative predictive value (99.1%), outperforming most comparators except for ALBI and SAVE. In external validation, RE-AD showed excellent discrimination (AUC 0.910, 95% CI 0.84–0.98), ranking highest among all comparators. High sensitivity (90.0%) and negative predictive value (98.9%) supported its role as a rule-out tool.
Conclusion: RE-AD is a clinically interpretable ML-based score designed to predict short-term acute decompensation in cACLD, addressing a clinical gap not fully covered by existing tools. The score demonstrated preserved discrimination across internal and external cohorts and relies exclusively on routinely available clinical variables, unlike some established scores (e.g. SAVE) requiring less frequently assessed information such as varices. These features support the use of RE-AD for individualized risk stratification and rule-out strategies in cACLD.

SAT-085

Fulminant autoimmune hepatitis: clinical presentation, diagnostic modalities, outcome and prognostic factors

Alejandra Villamil[1], Eduardo Mullen[1], Paola Casciato[1], Maria Acosta[1], Juan Bandi[1]. [1]*Hospital Italiano de Buenos Aires, Ciudad Autonoma de Buenos Aires, Argentina*
Email: alejandra.villamil@hospitalitaliano.org.ar

Background and aims: Fulminant autoimmune hepatitis (AIH) is one of the leading causes of acute liver failure (ALF) in Latin America (18–26%). Early diagnosis and prompt initiation of corticosteroids may be lifesaving and could prevent the need for liver transplantation (LT). However, rapid diagnostic tools and reliable prognostic markers remain limited. Aims: To characterize the clinical presentation, diagnostic modalities, outcomes, and prognostic factors associated with fulminant AIH.
Method: A retrospective analysis was conducted on 307 consecutive patients evaluated for fulminant hepatic failure between 1994 and 2023. Eighty-six patients (28%) fulfilled simplified criteria for fulminant AIH; 7 with cirrhosis were excluded. Patients were analyzed in two periods based on the availability of transjugular liver biopsy (Group 1: 1994–2005, n = 28; Group 2: 2006–2023, n = 51). Autoantibodies, IgG, gammaglobulin, and ceruloplasmin were obtained in all cases; LC1 testing was added in 2009. Meprednisone (1 mg/kg orally or via nasogastric tube) was initiated at diagnosis.
Results: Seventy-nine fulminant AIH patients were evaluated. Encephalopathy was hyperacute in 1 patient, acute in 33 (41.7%), and subacute in 45 (55.9%). Overall, 63/79 (80%) patients died or required LT within a median of 7.8 days (range 1–34). Sixteen (20%) survived, 47 (60%) underwent LT, and 16 (20%) died without LT. Prognosis improved in Group 2 (71% vs 87% LT or death; $p < 0.05$), parallel to shorter time to diagnosis and steroid initiation (2.1 ± 1.7 vs 4.6 ± 2.1 days; $p < 0.05$). Liver biopsy (performed in 46/51 Group 2 patients) defined diagnosis in 29% and revealed massive or hemorrhagic centrilobular necrosis, both associated with poor outcomes. On multivariate analysis, independent predictors of poor prognosis were grade III/IV encephalopathy at treatment initiation (OR 5.11; 95% CI 2.18–10.23; $p = 0.04$) and lack of ≥20% improvement in PT/INR by day 3 of steroids (OR 6.07; 95% CI 1.49–27.45; $p = 0.01$). Early initiation of steroids (<36 hours of admission) was associated with better survival/ liver transplantation.
Conclusion: Early diagnosis—particularly through rapid-access liver biopsy—facilitates timely steroid therapy and improves survival in fulminant AIH. The integration of rapid ELISA-based autoantibody testing warrants further evaluation in high-prevalence settings.

SAT-086

A simple five-variable model integrating GWAS variants predicts chronic outcomes in drug induced liver injury

Weiwei Lou[1], Jingjing Jiang[1], Weiqian Lou[1], Xichen Zhu[1], Rongtao Lai[1], Qing Xie[1]. [1]*Department of Infectious Diseases, Ruijin Hospital, Shanghai Jiao Tong University School of Medicine, Shanghai, China*
Email: lairongtao1202@163.com

Background and aims: In clinical practice, progression to chronic liver injury occurs in 6%-39% of drug induced liver injury (DILI) cases. However, reliable prognostic tools remain lacking. We aimed to investigate whether genetic variants associated with DILI susceptibility may predict chronic outcomes and thus fill the gap between genetic discovery and clinical translation.
Method: Between 2018 and 2023, we prospectively enrolled 338 well characterized DILI patients at Shanghai Ruijin Hospital. Chronic DILI was defined as persistent liver test abnormalities beyond 6 months. It developed in 167 (49.4%) patients. We analyzed the genotype of two significant single nucleotide polymorphisms (rs72631567, rs28531257), which were combined with routinely available laboratory parameters. These lab parameters included peak alanine aminotransferase, low-density lipoprotein cholesterol, and monocyte count. A light gradient boosting machine learning algorithm was trained on 270 patients and validated independently on 68 patients.
Results: Both genetic variants at rs72631567 and rs28531257 showed significant associations with chronic DILI progression. The integrated model achieved an area under the curve (AUC) of 0.92 (95% confidence interval 0.89–0.95) in the training cohort and 0.81 (0.70–0.91) in validation, substantially outperforming clinical variables alone (AUC, 0.57, $P < 0.001$). SHAP analysis revealed that rs72631567 contributed the greatest predictive weight, followed by peak transaminase levels.

Conclusion: The current work demonstrates that susceptibility variants from genome-wide association studies can be prognostic. Our five-variable tool requires only standard blood tests and straightforward genotyping. Early identification of high-risk patients may help determine the intensity of monitoring and therapeutic decisions, thus making precision medicine practical for DILI management.

SAT-087

Individualised treatment benefit of double plasma molecular adsorption system in patients with liver failure

Cai Gao[1], Beiling Li[2], Jian Zu[1], Rajiv Jalan[3], Jinjun Chen[2,4], Yee Hui Yeo[5]. *[1]School of Mathematics and Statistics, Xi'an Jiaotong University, Xi'an, China; [2]Hepatology Unit, Department of Infectious Diseases, Nanfang Hospital, Southern Medical University, Guangzhou, China; [3]Institute for Liver and Digestive Health, University College Hospital, Royal Free Campus, London, United Kingdom; [4]Department of Infectious Diseases, Key Laboratory of Molecular Biology for Infectious Diseases (Ministry of Education), Institute for Viral Hepatitis, the Second Affiliated Hospital, Chongqing Medical University, Chongqing, China; [5]Cedars-Sinai Medical Center, West Hollywood, United States*
Email: yeehui.yeo@cshs.org

Background and aims: Despite increasing use of the double plasma molecular adsorption system (DPMAS) in patients with liver failure, reported short-term survival benefits remain inconsistent, suggesting substantial heterogeneity in treatment response. Simple comparisons between DPMAS and standard medical treatment (SMT) may therefore be clinically insufficient. We aimed to estimate individualised treatment benefit and identify patients most likely to benefit from DPMAS.
Method: We conducted a prospective, multicentre cohort study of adults with liver failure (total bilirubin ≥12 mg/dL and international normalised ratio ≥1.5) treated with DPMAS or SMT across 50 hospitals. The primary endpoint was 28-day transplant-free mortality. Individualised treatment effects were estimated using a machine learning–based causal framework, predicting 28-day mortality under SMT and DPMAS for each patient. Absolute risk reduction was calculated as the difference between predicted risks, and patients were categorised into high-, indeterminate-, and low-benefit groups. Model interpretability was assessed to identify key variables associated with treatment benefit. Baseline characteristics across benefit strata were compared to identify distinct phenotypes.
Results: A total of 1,210 patients with liver failure were included, of whom 625 received DPMAS and 585 received SMT. Crude 28-day transplant-free mortality was 14.9% in the DPMAS group and 20.9% in the SMT group. Among the tested models, a CatBoost classifier within a doubly robust machine learning framework demonstrated the best performance. Predicted individualised treatment effects showed marked heterogeneity. Patients in the high-benefit tertile experienced an estimated absolute risk reduction of up to 13.7%, with a 22.06% difference in 28-day survival benefit between the high- and low-benefit groups. Key variables differentiating benefit strata were identified. The low-benefit group comprised two predominant phenotypes: patients with low baseline risk and mild disease, and patients with advanced, refractory multi-organ failure.
Conclusion: In this large multicentre cohort, the survival benefit of DPMAS was highly heterogeneous. Individualised treatment effect modelling identified clinically distinct subgroups with substantial differences in benefit, supporting a targeted-use strategy for DPMAS to improve patient selection and inform future clinical trials.

SAT-088

HLA-B*35:01 as a potent genetic risk factor for drug-induced liver injury in chinese patients: a prospective multicenter study

Mengmeng Zhang[1], You Deng[1], Yun Zhu[2], Liwei Liu[3], Liuyi Chang[4], Zhengsheng Zou[2], Liang Wang[5], Zikun Ma[1], Yao Meng[1], Tiantian Guo[1], Mengyu Zhao[1], Meng He[1], Xinyan Zhao[1]. *[1]Liver Research Center, Beijing Friendship Hospital,Capital Medical University, Beijing, China; [2]The Fifth Medical Center of PLA General Hospital, Beijing, China; [3]Beijing You'an Hospital, Capital Medical University, Beijing, China; [4]Yuncheng Central Hospital, Shanxi Medical University, Shanxi, China; [5]The Second Hospital & Clinical Medical School, Lanzhou University, Lanzhou, China*
Email: zhangmengmeng707@163.com

Background and aims: Idiosyncratic drug-induced liver injury (DILI), distinct from intrinsic type, is unpredictable and can lead to severe outcomes, including liver transplantation or death in 5–10% of cases. However, the genetic architecture of DILI in Chinese patients remains poorly defined. This study aimed to identify HLA susceptibility loci in a well-defined Chinese DILI cohort to facilitate the identification of high-risk individuals.
Method: Between June 2022 and December 2025, we prospectively enrolled patients from eleven centers across China. Patients with unclear drug exposure or confounding liver diseases (e.g., alcoholic liver disease, autoimmune hepatitis) were excluded. DILI diagnosis and culprit drug identification were adjudicated by a panel of three independent clinical experts for each case. To account for multiple comparisons across HLA alleles, the false discovery rate (FDR) was controlled using the Benjamini-Hochberg procedure, with reported q-values <0.05 considered significant. All analyses were performed using R software (version 4.4.1).
Results: A total of 547 patients were enrolled including 350 (64%) female and median age 55 years (IQR 45–64). Herb-induced liver injury was the predominant cause (299/547, 54.7%), with *Polygonum multiflorum* (90/547, 16.5%), *Scutellaria baicalensis* (65/547, 11.9%), and *Psoralea corylifolia* (35/547, 6.4%) identified as the most common agents. Hepatocellular injury was the major clinical phenotype. Among them, 374 patients had complete high-resolution HLA genotyping data. In this genetically characterized cohort, HLA-B*35:01 was carried by 136 patients (36.4%), including 6 homozygotes. The allele frequency was significantly elevated compared to population controls (0.225 vs. 0.001; $p = 3.30 \times 10^{-43}$), yielding an odds ratio (OR) of 54.4 (95% CI 18.24–256.37). This association remained significant after rigorous multiple testing correction ($q = 1.37 \times 10^{-41}$). Notably, the frequency of HLA-B*35:01 did not differ significantly between DILI cases attributed to *Polygonum multiflorum* or *Scutellaria baicalensis* and those caused by other herbs.
Conclusion: This study identifies HLA-B*35:01 as a key genetic risk factor for DILI in Chinese patients. Its association across multiple herbs suggests a shared pathogenic mechanism, supporting the potential for genetic risk assessment.

SAT-089-YI

Clinical characteristics, risk factors, and outcomes of immunotherapy-related hepatotoxicity: experience from a large retrospective cohort

Yang Zhi[1], Yinuo Dong[1], Jieting Tang[1], Yimin Mao[1]. *[1]Division of Gastroenterology and Hepatology, Renji Hospital, Shanghai Jiao Tong University School of Medicine, NHC Key Laboratory of Digestive Disease, Shanghai, China*
Email: maoym11968@163.com

Background and aims: Immunotherapy-related hepatotoxicity (IRH) is an increasingly recognized adverse event of immune checkpoint inhibitors (ICIs) that may compromise treatment continuity and outcomes. This study aimed to define the clinical characteristics, risk factors, and outcomes of IRH in a large real-world cohort of patients treated with ICIs.
Method: We conducted a retrospective, multicenter, electronic medical record-based study. Patients with malignancies who received ICI therapy at five tertiary centers in China from November 2018 to November 2024 with available liver biochemistry data both before and after ICI initiation were screened for eligibility. Patients with normal baseline liver biochemistry who developed abnormalities, as well as those with abnormal baseline who experienced a marked worsening following ICI therapy, were initially identified and

underwent causality assessment through an expert opinion process. Patients with confirmed IRH were classified into the IRH group, whereas those with non-IRH constituted the control group. The severity of liver injury was assessed using both the Common Terminology Criteria for Adverse Events (CTCAE) and the international expert working group (EWG) criteria for drug-induced liver injury (DILI).

Results: Of 15,835 patients screened, 4,641 (29.3%) were adjudicated as having IRH, while 10,043 served as non-IRH controls. Based on CTCAE criteria, 3,736 patients (80.5%) experienced grade 1 liver injury and 444 (9.6%) developed high-grade IRH (≥ grade 3). In contrast, by EWG criteria, 4,148 patients (89.4%) did not meet the diagnostic threshold for DILI, and only 9 (0.2%) were classified as having ≥ grade 3 liver injury. Although biochemical normalization was observed in most patients, 50 (1.1%) died or required liver transplantation within 21 days of the first IRH episode. Multivariable analysis demonstrated that younger age and anti-cancer regimen were independently associated with all-grade IRH. Hepatocellular carcinoma and higher baseline aminotransferase levels were additionally associated with an increased risk of high-grade IRH. Among patients with high-grade IRH, 184 (41.4%) were rechallenged with ICI, of whom 86 (46.7%) developed recurrent IRH, including 29 (33.7%) with high-grade IRH.

Conclusion: Marked discrepancies were observed between CTCAE and EWG grading of IRH severity. Younger age and anti-cancer regimen were consistently associated with increased risk of IRH, and rechallenge appeared feasible even in patients with prior high-grade IRH.

Acute liver failure and drug induced liver injury – Experimental and pathophysiology

TOP-193-YI

Serum glycomics at admission predict liver transplantation-free survival in patients with acetaminophen-induced acute liver failure

Lorenz Grossar[1], Nicky Somers[1], Emma Butaye[1], Nicolas Debusschere[1], Thomas Vanwolleghem[2], Géraldine Dahlqvist[3], Jean Delwaide[4], Jef Verbeek[5], Lindsey Devisscher[6], Sander Lefere[1], Leander Meuris[7], Nico Callewaert[7], Sarah Raevens[8], Anja Geerts[8], Hans Van Vlierberghe[8], Xavier Verhelst[8]. *[1]Ghent University, Department of Internal Medicine and Paediatrics, Liver Research Centre Ghent, Ghent, Belgium; [2]Antwerp University Hospital, Department of Gastroenterology and Hepatology, Antwerp, Belgium; [3]Hepatogastroenterology and Liver Transplantation, Cliniques Universitaires Saint-Luc, Brussels, Belgium; [4]Department of Gastroenterology and Hepatology, CHULiege, Liège, Belgium; [5]Department of Gastroenterology and Hepatology, University Hospitals Leuven, Leuven, Belgium; [6]Liver Research Centre Ghent, Ghent University, Gut-Liver Immunopharmacology Unit, Ghent, Belgium; [7]VIB Center for Medical Biotechnology, VIB, Department of Biochemistry and Microbiology, Ghent University, Ghent, Belgium; [8]Ghent University Hospital, Department of Gastroenterology and Hepatology, Liver Research Centre Ghent, Ghent, Belgium*
Email: lorenz.grossar@ugent.be

Background and aims: Acute liver failure (ALF) is a rare but potentially life-threatening clinical syndrome characterized by hepatocellular damage and impaired liver function. In the Western world, the majority of cases are caused by acetaminophen (APAP) overdose. In subjects not responding to medical therapy, emergency liver transplantation (ELT) is required to avoid fatal outcome. The decision to list a subject for ELT is based on imperfect prediction rules with strong specificity, but limited sensitivity, thereby providing good ruling-in capacity but unacceptably poor ruling-out performance. We investigated the potential to derive a serum glycomics biomarker able to predict transplant-free survival.

Method: We performed a prospective, multicenter study in five referral centers for ELT in Belgium, between 2014 and 2024. In 91 patients with APAP-related ALF, serum samples were collected within 24 hours of admission for analysis of the total serum N-glycome. Relative glycan abundancies underwent central log-ratio transformation before comparison between outcome groups to enable robust comparison of compositional data. Elastic net regression was used to derive a glycan score predictive of ELT. The optimal cut-off for classification was defined by the Youden index.

Results: Seven out of 91 (7.7%) subjects underwent ELT, with two deaths occurring after liver transplantation. Another five (5.5%) subjects died without undergoing prior ELT. In subjects in need of ELT, we observed an increase of the agalacto, core-fucosylated glycan NGA2F, and of the agalacto, core-fucosylated, bisecting glycan NGA2FB (independent t-test, p-values 0.0356 and 0.0239, respectively). After elastic net regression, a glycan score predictive of liver transplantation was derived, mainly characterized by a relative increase of undergalactosylation and fucosylation, and decreased branching of glycans. At the optimal cut-off of 0.0815, this biomarker predicted ELT with a sensitivity of 85.7%, specificity of 73.8%, and a negative predictive value of 98.4%. The area under the receiver operating curve was 0.833 (95% confidence interval: 0.711–0.955).

Conclusion: A distinct glycomic signature can be determined on serum admission samples of APAP-ALF patients, reliably ruling-out subjects not requiring ELT. Application of this serum biomarker could avoid unnecessary harm in subjects who would otherwise undergo ELT, and thus avoid significant morbidity and healthcare costs.

TOP-194

A novel mechanism by which the FABP4/CD36 axis exacerbates cholestasis via antagonizing FXR signaling

Yuelin Xiao[1], Tianhui Zhou[1], Haoshuang Fu[1], Shuying Song[1], Ziqiang Li[1], Qing Xie[1]. *[1]Department of Infectious Diseases, Ruijin Hospital, Shanghai Jiao Tong University School of Medicine, Shanghai, China*
Email: cherlynxiao@163.com

Background and aims: Cholestatic liver injury involves multi-cell crosstalk, with liver macrophage activation key to amplifying injury. However, specific mediators directly disrupting bile acid (BA) homeostasis remain unclear. Farnesoid X receptor (FXR), a master regulator of BA metabolism (synthesis, transport, detoxification), is a common cholestasis driver due to impaired function. Our prior clinical data showed fatty acid-binding protein 4 (FABP4)—a macrophage-enriched lipid chaperone—is significantly elevated in cholestatic liver disease serum. Given its role in metabolic inflammation, we proposed that FABP4 drives liver injury not only through classical pro-inflammatory effects but, more importantly, by directly interfering with the hepatoprotective FXR signaling axis, thereby dominating the dysregulation of BA homeostasis.

Method: We used a multidisciplinary approach (genetic: Fxr-deficient mice; pharmacological: FABP4 inhibitor BMS309403) to induce cholestasis with alpha-naphthylisothiocyanate (ANIT). Liver injury was assessed via histology, serum biochemistry (ALT/AST, ALP, etc), and inflammatory markers. Molecular mechanisms were explored using immunohistochemistry, Western blotting, qRT-PCR, and in vitro experiments.

Results: In vivo results showed that inhibition of FABP4 by BMS309403 significantly protected WT mice against ANIT-induced liver injury, inflammation, and cholestasis. However, this protection was lost in *Fxr*$^{-/-}$ mice. Regardless of whether they received BMS309403 treatment, *Fxr*$^{-/-}$ mice exhibited comparable levels of necrosis, inflammation, elevated serum ALT/AST levels, and cholestasis, suggesting that the regulatory effect of the BMS inhibitor on key downstream targets (i.e, the BA synthetic enzymes CYP7A1 and

CYP8B1) is entirely dependent on FXR. In vitro experimental analysis also confirmed this hierarchical relationship: when FXR was silenced, the ability of BMS309403 or FABP4 knockdown to regulate gene networks was weakened. Furthermore, inhibiting FABP4 or its partner CD36 directly modulated FXR, CYP7A1, and CYP8B1 in primary hepatocytes, placing the FABP4/CD36 complex upstream of FXR signaling.
Conclusion: This study confirms macrophage-derived FABP4 is a key upstream FXR signaling suppressor in cholestatic liver disease. It drives cholestatic injury by blocking this core hepatoprotective pathway, causing uncontrolled BA toxicity. We reveal a novel immune-metabolic circuit (FABP4/CD36 to FXR) and validate FABP4 as a potential target for restoring BA homeostasis in cholestasis.

TOP-207
Serpine1 as a potential therapeutic target in pyrrolidine alkaloids-induced hepatic sinusoidal obstruction syndrome
Yifan Ma[1], Hong Gao[1]. [1]*Zhongshan Hospital, Fudan University, Evidence-based Medicine Center, Fudan University, Shanghai, China*
Email: gao.hong@zs-hospital.sh.cn

Background and aims: Hepatic sinusoidal obstruction syndrome (HSOS) induced by pyrrolidine alkaloids (PAs) is a life-threatening liver injury lacking standardized models that reflect its chronic progression in humans. This study aimed to establish a clinically relevant chronic PA-HSOS murine model and identify therapeutic targets by dissecting molecular mechanisms underlying endothelial injury.
Method: A 28-day murine PA-HSOS model was developed using key alkaloids (including seneciphylline, senecionine, and their N-oxide derivatives) from Gynura segetum, mirroring human exposure. Disease progression was evaluated via hematological profiling, CT imaging, histopathology, and transcriptomic analysis. A hepatocyte-liver sinusoidal endothelial cell (LSECs) co-culture system validated molecular pathways, while TM5441, a Serpine1 inhibitor, was tested for therapeutic efficacy.
Results: The murine model recapitulated human PA-HSOS features, including elevated liver enzymes (ALT and AST), coagulation dysfunction (prolonged PT/APTT and increased D-dimer), hepatomegaly, sinusoidal fibrosis, and loss of function of LSECs. RNA sequencing identified Serpine1 as the top upregulated gene, linked to p53 signaling. Co-culture experiments confirmed Serpine1-driven activation of the p53 pathway, promoting endothelial senescence. TM5441 treatment reduced the Serpine1-p53 axis activity, improved liver function, normalized coagulation, and restored LSECs integrity, with attenuated inflammation and fibrosis.
Conclusion: This study establishes the first chronic PA-HSOS model that faithfully mimics human disease and identifies Serpine1 as a pivotal therapeutic target. Targeting the Serpine1-p53 pathway with TM5441 represents a promising strategy for mitigating endothelial injury.

THU-056
Isoniazid exposure triggers hepatocyte exosome driven Rac 1 mediated engulfment of non-viable hepatocytes and activation of hepatic stellate cells
Suman Santra[1], Debasree Bishnu[2], Shyamalendu Medda[3], Payal Mirza[1], Swagata Purkait[2], Sreosi Chakraborty[1], Gopal Dhali[1], Abhijit Chowdhury[4]. [1]*Centre for Liver Research, School of Digestive and Liver Diseases, Institute of Post Graduate Medical Education and Research, Kolkata, India;* [2]*John C. Martin Centre for Liver Research and Innovations, Kolkata, India;* [3]*Department of Anatomy, Institute of Post Graduate Medical Education and Research, Kolkata, India;* [4]*Indian Institute of Liver and Digestive Sciences, John C. Martin Centre for Liver Research and Innovations, Kolkata, India*
Email: sumansantra22@yahoo.in

Background and aims: Drug-induced liver injury (DILI) is a major global health concern. Anti-tubercular drugs account for the majority of DILI cases in India. Isoniazid (INH) is frequently associated with hepatotoxicity and can progress to chronic liver injury. The mechanisms linking INH-induced hepatocyte injury to hepatic stellate cell (HSC) activation and fibrosis remain incompletely understood. Exosomes are increasingly recognized as mediators of hepatocyte–non-parenchymal cell communication. This study aimed to evaluate whether exosomal microRNAs (miRNAs) released from INH-treated hepatocytes promote efferocytosis of HSCs and drive HSCs activation in chronic DILI.
Method: Exosomes were isolated from conditioned media of E47 cell line with or without INH treatment and were characterized using NTA, electron microscopy and Western blotting. Small RNA sequencing was performed to compare miRNA profiles between the 2 groups. Differentially expressed miRNAs were analyzed for functional relevance to phagocytosis and efferocytosis pathways. Selected miRNAs were validated using miRNA mimic transfection. Efferocytosis of HSCs and their activation were assessed by confocal microscopy, collagen type I (Col1a1) expression, and collagen secretion.
Results: Exosomal profiling demonstrated distinct miRNA cargo between with or without INH-treated hepatocytes. RNA sequencing identified multiple differentially expressed miRNAs. Top 10 down-regulated miRNAs in INH-treated exosomes were related to phagocytosis and cytoskeletal regulation. Among these, hsa-miR-145-5p was identified as a key regulator targeting RAC1, a mediator of cellular engulfment. Functional restoration of miR-145-5p using a miRNA mimic altered RAC1 expression and modulated HSC behavior. HSCs exposed to exosomes from INH-treated hepatocytes had increased engulfment of dead hepatocytes and phenotypic activation as evidenced by increased Col1a1 expression and total collagen secretion.
Conclusion: Exosomal miRNAs released from INH-treated hepatocytes contribute to HSC activation by promoting engulfment of dead hepatocytes. Down regulation of hsa-miR-145-5p and subsequent RAC1-dependent signalling appear to play a central role in this process. These findings highlight a novel exosome-mediated mechanism linking hepatocyte injury to fibrogenic HSC activation in INH-induced chronic DILI and suggest that targeting exosomal miRNA signalling may represent a potential therapeutic strategy to limit fibrosis in DILI.

THU-057-YI
Targeting impaired efferocytosis in acute-on-chronic liver failure: human mechanistic insights and murine macrophage therapeutic efficacy
Sunidhi Diwakar[1], Deepanshu Maheshwari[1], Nidhi Nautiyal[1], Sandeep Kumar[1], Manisha Manisha[1], Anupam Kumar[1]. [1]*Institute of Liver & Biliary Sciences, New Delhi, India*
Email: dr.anupamkumar.ilbs@gmail.com

Background and aims: Impaired efferocytosis contributes to inflammation and defective repair in cirrhosis and ACLF, but its role in ACLF remains unclear. We assessed efferocytosis in ACLF vs healthy and compensated (Comp.) cirrhosis patients and tested whether healthy bone marrow–derived Mϕ restore efferocytosis and promote liver repair in an ACLF mouse model.
Method: Blood samples were collected from healthy (n = 10), comp. cirrhosis (n = 20), and ACLF (n = 50) patients. $CD14^+$ monocytes were differentiated into Mϕ using Mϕ Colony-Stimulating Factor over 7 days. Efferocytosis and MER Tyrosine Kinase (MERTK)/T-cell Immunoglobulin and Mucin domain-containing protein 4 (TIM4) expression were analysed via flow cytometry and confocal imaging. Mϕ proteomics was performed and Energy metabolism assessed with Seahorse bioanalyzer. Mitochondrial (Mt) respiration's impact on efferocytosis in healthy assessed with rotenone, complex I inhibitor. In a murine ACLF model, Green Fluorescent Protein (GFP^+) Mϕ or saline were injected post-injury, followed by imaging, histology, and functional analysis.

Results: Mϕ single efferocytosis showed marked decline from healthy to cirrhosis to ACLF ($p < 0.0001$). Continuous efferocytosis was similarly low in ACLF and cirrhosis, but lower than in healthy ($p < 0.0001$). MERTK ($p < 0.001$) and TIM4 ($p < 0.001$) were higher in ACLF vs healthy and cirrhotic Mϕ. Global protein profiling of Mϕ showed early Mt biogenesis, fatty acid oxidation defects in cirrhosis, worsening in ACLF. Mϕ Mt energy metabolism declined from cirrhosis ($p < 0.001$) to ACLF ($p < 0.001$) compared to healthy. Healthy Mϕ showed ($p < 0.01$) reduction in efferocytosis with rotenone-induced Mt respiration defects. These data show Mt defects impair Mϕ efferocytosis in ACLF, despite increased efferocytosis receptors. Healthy mice Mϕ therapy in ACLF mouse model improved liver histology, reducing ballooning, necrosis, Inflammation. It decreased fibrosis ($p < 0.001$), High mobility group box 1($p < 0.0001$), Apoptotic$^+$ cells ($p < 0.001$), while enhancing hepatocyte proliferation ($p < 0.0001$) in treated group vs controls. therapy increased liver F4/80$^+$ ($p < 0.001$), efferocytosis ($p < 0.001$), phagocytosis ($p < 0.001$) vs controls, increased in-vitro BM cell maturation to Mϕ ($p < 0.0001$), efferocytosis function ($p < 0.0001$).
Conclusion: Impaired Mt metabolism reduces Mϕ efferocytosis in ACLF despite increased MERTK and TIM4. Healthy Mϕ transfer restores efferocytosis, reduces liver injury and inflammation, promotes regeneration, supporting Mϕ therapy in ACLF.

THU-058

Sex-dependent modulation of acetaminophen-induced liver injury in diet-induced metabolic steatohepatitis

José Fernandez-Checa[1], Laura Fábrega[1], Paula Segales[2], Susana Nuñez[1], Manuel Romero-Gómez[3], M. Carmen Garcia-Ruiz[1].
[1]Institute of Biomedical Research of Barcelona, IIBB-CSIC, CIBEREHD, Barcelona, Spain; [2]Institute of Biomedical Research of Barcelona, IIBB-CSIC, Barcelona, Spain; [3]Unit of Digestive Diseases, Hospital Universitario Virgen del Rocio, CIBEREHD, Sevilla, Spain
Email: checa229@yahoo.com

Background and aims: Metabolic Dysfunction–Associated Steatohepatitis (MASH) alters hepatic lipid metabolism, inflammatory signaling and stress responses, potentially modifying susceptibility to drug-induced liver injury (DILI). Acetaminophen (APAP) overdose is the leading cause of acute DILI worldwide, yet the impact of diet-induced MASH on APAP hepatotoxicity, particularly in a sex-dependent context, remains poorly defined. This study aimed to determine whether MASH differentially sensitizes male and female livers to APAP-induced injury and to identify the underlying metabolic and stress-related mechanisms.
Method: Male and female C57BL/6J mice were fed a standard chow or a high-fat, high-cholesterol diet (HFHC; 60% kcal fat, 0.5% cholesterol) for 12 weeks to induce MASH features. Mice then received a single dose of APAP (300 mg/kg) and were sacrificed 4 hours post-administration. Hepatic injury and key metabolic, inflammatory, and stress-related pathways were assessed using biochemical, histological, and molecular approaches.
Results: HFHC feeding induced hepatic steatosis and metabolic dysfunction in both sexes but resulted in more severe macrosteatosis in males. This was associated with a stronger suppression of fatty acid oxidation pathways and enhanced lipogenic signaling in male livers. APAP administration exacerbated liver injury in HFHC-fed mice, with males displaying higher transaminase levels and impaired autophagic flux.
Inflammatory analyses revealed a pronounced pro-inflammatory response in males, characterized by macrophage and neutrophil infiltration and increased expression of pro-inflammatory mediators, whereas females exhibited a comparatively attenuated inflammatory profile with upregulation of anti-inflammatory and reparative markers. Combined HFHC feeding and APAP exposure amplified mitochondrial and ER stress signaling by STARD1–SAB axis activation, predominantly in males. Sex-specific differences were also observed in cholesterol metabolism, suggesting distinct adaptive capacities to metabolic and xenobiotic stress.
Conclusion: Diet-induced MASH enhances susceptibility to APAP hepatotoxicity in a sex-dependent manner. Although APAP sensitizes both sexes, male mice exhibit greater metabolic disruption, stress signalling activation, inflammation, and liver injury, while females show relative protection. These findings highlight biological sex as a critical modifier of DILI risk in MASH and support the need for sex-informed approaches in drug safety and liver disease management.

THU-059-YI

Estrogen deficiency-induced hepatic steatosis confers protection against drug-induced liver injury via NRF2 activation: implications for postmenopausal liver health

José García Consuegra[1,2,3], Naroa Goikoetxea-Usandizaga[4,5], Ana Sagrera Aparisi[1,2,3], Ariadna Gil Martín[2], Irene González-Recio[4], Amaia Navarro-Corcuera[4], Raul J. Andrade[5,6], Maria Isabel Lucena[5,7], Paolo Grumati[8], James W. Dear[9], María Luz Martínez-Chantar[4,5], Sara Cogliati[1,2,3].
[1]Autonomous University of Madrid (UAM), Madrid, Spain; [2]Centro de Biología Molecular Severo Ochoa (CBM UAM-CSIC), Madrid, Spain; [3]Instituto Universitario de Biología Molecular (IUBM UAM), Madrid, Spain; [4]Liver Disease Lab, CIC bioGUNE, Basque Research and Technology Alliance (BRTA), Derio, Spain; [5]Center for the Study of Liver and Gastrointestinal Diseases (CIBERehd), Carlos III National Institute of Health, Madrid, Spain; [6]Unidad de Gestión Clínica de Enfermedades Digestivas, Instituto de Investigación Biomédica de Málaga-IBIMA, Hospital Universitario Virgen de la Victoria, Universidad de Málaga, Málaga, Spain; [7]Servicio de Farmacología Clínica, Instituto de Investigación Biomédica de Málaga-IBIMA, Hospital Universitario Virgen de la Victoria, UICEC SCReN, Universidad de Málaga, Málaga, Spain; [8]Telethon Institute of Genetics and Medicine (TIGEM), Pozzuoli, Italy; [9]Pharmacology, Toxicology and Therapeutics, Centre for Cardiovascular Science, University of Edinburgh, Edinburgh, United Kingdom
Email: jgconsuegra@cbm.csic.es

Background and aims: Estrogens exert a significant influence on liver physiology, with clear sex-based differences and metabolic alterations following menopause or ovariectomy (OVX). While their protective role against chronic liver diseases has been widely proposed, their involvement in drug-induced liver injury (DILI) remains poorly understood. Given the increasing prevalence of polypharmacy and acetaminophen (APAP) use in postmenopausal women, our study aims to explore how long-term oestrogen deprivation, mimicking the postmenopausal state, modulates susceptibility to APAP-induced liver injury. Understanding this relationship may provide key insights for improving clinical management and risk assessment in postmenopausal patients.
Method: 12-week-old female mice were either ovariectomized (OVX) or sham-operated. After 5 months they were treated with an APAP overdose (600 mg/Kg) and sacrificed after 6 hours.
Results: The TUNEL assay, revealed that OVX mice have less necrotic tissue than control, that correlated with less levels of GPT and GOT. Our results also showed that OVX animals exhibited an improved oxidized-to-reduced glutathione ratio and, overall, higher glutathione levels, an indicator of enhanced cellular well-being. These results were consistent with increased transcript levels of protective genes against cellular oxidative stress, such as HO-1, GCLC, GSR and GSTA, targets of the transcription factor NRF2.
Previous research had highlighted that NRF2 is activated by lipids that accumulates within the cells and prime the cells to protection against oxidative stress. As oestrogen deprivation induces hepatic lipid accumulation, we hypothesized a lipid-mediated protective mechanism. We demonstrated that after OVX there is an accumulation of fatty acids and less fatty acid oxidation (FAO), further validated by liver bulk RNA-seq analysis. Our data in mouse were corroborated by gene expression data from a cohort of human liver biopsies where we found higher levels of NRF2 and HO-1 expression in old women

(more than 50 years) than in younger women and men suggesting similar mechanisms activated in humans.
Conclusion: Estrogen deprivation leads to lipid accumulation within the liver, that further activates the oxidative stress response elements via NRF2 that might be exhibiting a protecting phenotype against APAP induced injury. These results are promising and open the door to diet-derived treatments against drug-induced liver injuries.

THU-060
Neutrophil calcium dynamics and recruitment in acetaminophen induced liver injury
Barbara Fidelix Santana[1], Guilherme Gomes[1], Isadora Feng[1], Sandhra Carvalho[1], Maria Eduarda Favalessa[1], Yuri Capato[1], Marcelo Souza[1], Maria Fernanda Amorim[1], Alfredo Goes[1], André Oliveira[1], Maria de Fátima Leite[1]. [1]*UFMG, ICB UFMG, Belo Horizonte, Brazil*
Email: bfidelixs@gmail.com

Background and aims: Acetaminophen (APAP) overdose is a major cause of drug-induced liver injury (DILI), in which neutrophils play a key role by responding to hepatocyte-derived danger signals and coordinating tissue repair. This study investigated how intracellular and extracellular calcium regulate neutrophil migration toward APAP-injured liver spheroids.
Method: Human neutrophils isolated from healthy donors were co-cultured with HepG2 liver spheroids pre-treated with APAP. Neutrophil migration and intracellular calcium dynamics were analyzed using confocal microscopy and automated cell tracking. Intracellular and extracellular calcium were selectively inhibited using BAPTA/AM and EGTA, respectively.
Results: Neutrophils exposed to APAP-treated spheroids exhibited enhanced recruitment compared with control spheroids, migrating longer distances (138.0 ± 96.8 micrometers vs. 75.9 ± 32.7 micrometers, $p < 0.001$) and accumulating preferentially near injured tissue (83.5 ± 10.3 percent vs. 66.2 ± 2.4 percent, $p = 0.034$). APAP injury did not alter the peak amplitude of intracellular calcium signals in neutrophils compared with controls ($p = 0.21$), indicating that increased recruitment was not driven by calcium signal magnitude. Chelation of extracellular calcium markedly impaired neutrophil motility, reducing migration distance and abolishing directional movement (all $p \leq 0.003$). Under these conditions, APAP treatment failed to promote neutrophil recruitment, demonstrating that calcium influx is essential for injury-directed migration. In contrast, inhibition of intracellular calcium mobilization did not suppress motility but significantly reduced directionality ($p = 0.01$), indicating loss of guided migration. Combined inhibition of extracellular calcium entry and intracellular calcium mobilization resulted in reduced neutrophil motility and directionality, with no differences between APAP-treated and control spheroids.
Conclusion: Collectively, our data demonstrate that although mobilization of calcium from intracellular stores is required for neutrophil directionality toward APAP-injured cells, it is not sufficient to sustain neutrophil migration. Instead, calcium entry emerges as the rate-limiting step for effective neutrophil motility. Given the critical role of neutrophils in liver repair during DILI, elucidating the mechanisms governing their recruitment to sites of injury may provide novel opportunities to improve the clinical management of patients with DILI.

THU-061
Cell-microcapsule-mediated oral delivery of nanoenzymes alleviates drug-induced liver injury via the gut-liver axis
Xiaoyu Huang[1 2,2], Fengmei Wang[1]. [1]*Tianjin First Central Hospital, Nankai University, Tianjin, China;* [2]*Nankai University, Tianjin, China*
Email: wangfengmeitj@126.com

Background and aims: Drug-induced liver injury (DILI) represents a major clinical challenge characterized by mitochondrial dysfunction, excessive reactive oxygen species (ROS) production, and inflammation. This study aims to investigate a novel liver-targeted oral delivery system utilizing cell-encapsulated nano-antioxidants to alleviate DILI and elucidate its mechanisms involving redox homeostasis and gut microbiota modulation.
Method: We designed a liver-targeted oral delivery system encapsulating nanoenzymes within cell vesicles to generate biocompatible anti-inflammatory nanoparticles. These nanoparticles are designed to resist gastric acid degradation and facilitate absorption via intestinal M cells for translocation to the liver. To validate safety and efficacy, a mouse model of DILI induced by APAP was employed. The therapeutic agents were administered orally one day prior to and concurrently with APAP injection. Mice were euthanized 24 hours later. Liver tissues were collected for histopathological examination, measurement of inflammatory cytokines, and molecular analyses including Western blotting.
Results: The cell microcapsules loaded with nanoenzymes demonstrated excellent ROS scavenging capacity, high stability within the intestinal environment, and favorable biocompatibility. In vivo tracking confirmed that the microcapsules effectively targeted macrophages in the liver. In the APAP-induced DILI mouse model, the nanoenzyme-loaded yeast cell microcapsules significantly alleviated body weight loss, hepatic fibrosis, and hepatocyte necrosis compared to the control group. Treatment also resulted in a marked reduction of inflammatory cytokines. Mechanistically, the intervention remodeled the gut microbiota, characterized by an increase in short-chain fatty acid levels through the suppression of harmful bacteria and the enhancement of beneficial bacterial populations.
Conclusion: This natural product-targeted oral delivery system offers a novel therapeutic approach for drug-induced liver injury through synergistic anti-inflammatory, antioxidant, and gut microbiota-modulating effects. The study elucidates the precise mechanism by which these nano-antioxidant agents protect against liver injury, laying the groundwork for the future development of nano-therapeutic materials for DILI management.

THU-062
A preclinical model of acute alcoholic hepatitis (AAH) in humanized liver mice
Eleanna Kaffe[1], Negin Farzad[2], Ruiqi Li[2], Yuval Kluger[2], Rong Fan[2], Wajahat Mehal[2], Richard Flavell[2]. [1]*Univ of Penn, Philadelphia, United States;* [2]*Yale University, New Haven, United States*
Email: eleana.kaffe@pennmedicine.upenn.edu

Background and aims: Acute Alcoholic hepatitis (AAH) is characterized by hepatocyte dysfunction, cholestasis, immune dysregulation, and high mortality[1–5]. A major limitation in the field is lack of preclinical models that reproduce all the above features. We evaluated whether a mouse with a humanized liver and immune system (HL-HIS) recapitulates key features of AAH.
Method: HL-HIS mice, containing human hepatocytes, human non-parenchymal cells (NPCs), and human immune system, were exposed to short-term alcohol feeding. Hepatocyte function, immune composition, and transcriptomic changes were analyzed and compared with human AAH datasets.
Results: Alcohol exposure induced severe steatosis, human-specific hepatocyte injury, cholestasis, impaired cholesterol-to–bile acid conversion, immune profile as in AAH and transcriptomic changes resembling the immune and hepatocyte dysfunction seen in AAH. Hepatocyte dysfunction included impaired antioxidant defense and bile acid synthesis as well as loss of HNF4α signaling. Immune profiling revealed reduced circulating T cells, increased hepatic cytotoxic T cells, and reduced liver-resident NK and Kupffer cells with impaired antimicrobial/antiviral programs. Hepatocyte steatosis and dysfunction were strongly dependent on signals from human NPCs.
Conclusion: HL-HIS mice faithfully model cholestasis, immune dysregulation, and hepatocyte dysfunction in AAH, providing a translational platform to dissect disease mechanisms. This model

reveals for the first time that hepatocyte steatosis and dysfunction are regulated in a paracrine manner and are not a direct effect of alcohol.

References

1. Yamazaki T. & Schnabl B. Acute alcohol-associated hepatitis: Latest findings in non-invasive biomarkers and treatment. *Liver Int* 45, e15608 (2025). PMC10646153
2. Gao C. *et al.* Single-cell Profiling of Intrahepatic Immune Cells Reveals an Expansion of Tissue-resident Cytotoxic CD4(+) T Lymphocyte Subset Associated With Pathogenesis of Alcoholic-associated Liver Diseases. *Cell Mol Gastroent Hepatol* 19, 101411 (2025). PMC11719870
3. Zhao X. *et al.* Single-cell landscape of the intrahepatic ecosystem in alcohol-related liver disease. *Clin Transl Med* 15, e70198 (2025). PMC11746962
4. Argemi J. *et al.* Defective HNF4alpha-dependent gene expression as a driver of hepatocellular failure in alcoholic hepatitis. *Nat Comm* 10, 3126 (2019). PMC6635373
5. Kim A. *et al.* Diminished function of cytotoxic T- and NK- cells in severe alcohol-associated hepatitis. *Metab Target Organ Damage* 2 (2022). PMC11326509

THU-067

PLPP2 drives liver repair and regeneration via remodeling phosphatidylethanolamine metabolism after acute liver injury

Fan Li[1], Yiming Wang[2], Hao Wang[1], Ling Lu[1], Ming Ni[1]. [1]*The First Affiliated Hospital of Nanjing Medical University, Nanjing, China;* [2]*Peking Union Medical College Hospital, Chinese Academy of Medical Sciences and Peking Union Medical College, Beijing, China*
Email: drlifan1999@163.com

Background and aims: Acute liver injury is commonly caused by overdose-drug, toxins, or ischemia. The liver possesses a remarkable regenerative capacity, wherein metabolic remodeling plays a crucial role. However, the specific metabolic shift that initiates hepatocyte regeneration remains unclear. We aimed to identify the key metabolic process driving the transition from liver injury to regeneration.
Method: We employed multi-time-point proteomic and metabonomic profiling to identify the key metabolic pathway and associated regulatory genes. We analysed liver samples from DILI patients and employed gene-modified mice. Transcriptomic and metabolomic were applied to validate the underlying mechanism.
Results: Multi-time-point multi-omics analyses demonstrated that phosphatidylethanolamine undergoes a dynamic metabolic reprogramming, with PLPP2 exhibiting synchronous changes among the enzymes regulating PE metabolism. Liver biopsy samples from patients with drug-induced liver injury corroborated the PLPP2 alterations. In murine models, hepatocyte-specific deletion of PLPP2 demonstrated its protective effect against ALI. Mechanistically, the resolution of ER stress was accompanied by a robust upregulation of PLPP2 during the regenerative phase. This shift promotes liver repair and regeneration by initiating the PE biosynthesis. PE, upon binding to PEBP1, modulated its affinity and strengthened its interaction with GLI1, thereby disrupting the association between ITCH and GLI1 and preventing the ubiquitination and degradation of GLI1. Additionally, PE promotes autophagy by facilitating the lipidation of LC3B. The increase of in ER-localized PE mediated by PLPP2 also contributed to alleviation of ER stress, thus establishing a positive feedback loop. Pharmacologic activation of PLPP2 may represent a promising therapeutic strategy for ALI.
Conclusion: The transition from reduction to elevation of PE maps to the pathological shift of liver from injury to regeneration following ALI, wherein PLPP2 serves as a switch initiating PE biosynthesis. Thus, targeting PLPP2 may represent a promising therapeutic strategy for ALI.

THU-068

Alarmin interleukin-33 protects against liver injury and promotes hepatocyte proliferation in acute liver failure

Mengqi Li[1], Hongshan Wei[2], Fan Xiao[3]. [1]*Capital Medical University, Beijing, China;* [2]*Department of Gastroenterology, Beijing Ditan Hospital, Capital Medical University, Beijing, China;* [3]*National Center for Infectious Diseases, Beijing Ditan Hospital, Capital Medical University, Beijing Key Laboratory of Viral Infectious Diseases, Institute of Infectious Diseases, Beijing Institute of Infectious Diseases, Beijing, China*
Email: lmq000330@163.com

Background and aims: Interleukin-33 (IL-33), a member of the interleukin-1 (IL-1) family, regulates immunity and tissue repair, but its role in acute liver failure (ALF) remains unclear. This study evaluated the effects and mechanisms of IL-33 in concanavalin A (Con A)-induced murine ALF.
Method: Female C57BL/6J mice received concanavalin A (Con A, 10 mg/kg) with or without recombinant interleukin-33 (1 microgram per mouse, 2 h prior). Hepatic injury was assessed by serum transaminase levels and histological analysis. Interleukin-33 and inflammatory cytokines were quantified by enzyme-linked immunosorbent assay, quantitative real-time polymerase chain reaction, and Luminex. Flow cytometry was performed to analyze hepatic regulatory T cells and ST2-positive regulatory T cells, while hepatocyte proliferation (Ki-67) was evaluated by immunohistochemistry. Survival following lethal Con A challenge (25 mg/kg) was also assessed.
Results: Interleukin-33 was markedly upregulated during concanavalin A-induced liver injury ($p < 0.001$). Pretreatment with interleukin-33 was associated with reduced alanine aminotransferase ($p < 0.001$) and aspartate aminotransferase ($p < 0.001$) levels, as well as attenuated histological damage in concanavalin A (10 mg/kg)-treated mice ($p < 0.05$); however, increased mortality was observed under lethal challenge. Interleukin-33 treatment was associated with elevated serum interleukin-1 beta ($p < 0.001$), monocyte chemoattractant protein 1 ($p < 0.01$), and tumor necrosis factor alpha ($p < 0.05$) levels, together with increased hepatic interleukin-1 beta ($p < 0.05$) and monocyte chemoattractant protein 1 ($p < 0.05$), while hepatic tumor necrosis factor alpha expression was reduced ($p < 0.001$). In addition, interleukin-33 was associated with increased hepatic regulatory T cell proliferation ($p < 0.05$) and programmed cell death protein 1 expression ($p < 0.05$), particularly in ST2-positive regulatory T cells, as well as enhanced hepatocyte Ki-67 expression ($p < 0.001$).
Conclusion: Interleukin-33 appears to exert dual effects in acute liver failure, being associated with attenuated hepatic injury, enhanced immunoregulatory responses, and increased hepatocyte proliferation, while also increasing mortality under conditions of excessive immune activation. These findings suggest that interleukin-33 may represent a potential therapeutic target for acute liver failure; however, optimized combination strategies may be required to balance therapeutic efficacy and safety.

THU-069

Hepatocyte-specific activation of Mad2l1 protects against acute liver injury by preserving mitochondrial stress responses and restraining inflammatory amplification

Qiuhong Liu[1], Qingqing Hu[1]. [1]*The First Affiliated Hospital, College of Medicine, Zhejiang University, Hangzhou, China*
Email: liuqh@zju.edu.cn

Background and aims: Acute liver injury (ALI) and liver failure syndromes are characterized by severe hepatocyte damage and rapid deterioration of liver function occurring within a short period of time. Mad2l1 is a key protein in the spindle-assembly checkpoint (SAC) that can significantly affect the cell cycle and effectively induce apoptosis. However, the role of Mad2l1 in ALI has not yet been examined.

Method: Intrahepatic Mad2l1 expression was determined in both human and mouse ALI models. *Mad2l1*+/-, Alb^{cre} *Mad2l1*$^{f/f}$, and wild-type mice were were challenged by two independent ALI models, induced by acetaminophen (APAP) and lipopolysaccharide/D-galactosamine (LPS/D-GalN). Liver samples were collected for proteomics and post-translational modification proteomics (PTM) analysis. Histological, biochemical, and molecular studies were performed to evaluate liver injury in mice. Primary hepatocytes and hepatic cell lines were exposed to APAP or LPS/TNF-α for in vitro analysis.
Results: Intrahepatic Mad2l1 expression was significantly upregulated in human and mouse ALI models. Mice with systemic, liver-specific, or hepatocyte-specific Mad2l1 deficiency were vulnerable to ALI. Consistently, immunoblotting revealed increased expression of inflammatory, mitochondrial stress, and cell-death markers in Mad2l1-deficient livers, whereas hepatocyte-targeted Mad2l1 overexpression conferred protection. Integrated proteomics and PTM profiling revealed revealed injury-type–dependent programs: LPS/D-GalN injury featured suppression of mitochondrial oxidative phosphorylation/respirasome and RNA processing/translation (including reduced YTHDF2), alongside enrichment of complement–coagulation/platelet activation and leukocyte trafficking/phagocytosis pathways with prominent acylation remodeling; APAP injury preferentially showed peroxisome-centered metabolic rewiring with limited early PTM changes. Mad2l1 perturbation was further associated with altered ferroptosis-related proteins and mitochondrial oxidative stress markers in both cells and liver tissues.
Conclusion: Hepatocyte-targeted Mad2l1 deficiency worsens APAP- and LPS/D-GalN–induced liver injury by disrupting mitochondrial stress programs and amplifying inflammation, whereas Mad2l1 overexpression is protective. Hepatocyte-specific Mad2l1 might be a novel therapeutic target for ALI.

THU-070

Construction of engineered biliary trees with P-glycoprotein efflux function and enhanced resistance to drug-induced injury

Jun Li[1], Shiwen Ma[1], Jiaxian Chen[1], Meiqian Hu[1], Jiaojiao Xin[1], Dongyan Shi[1], Jing Jiang[1]. [1]*State Key Laboratory for Diagnosis and Treatment of Infectious Diseases, The First Affiliated Hospital, Zhejiang University School of Medicine, Hangzhou, China*
Email: lijun2009@zju.edu.cn

Background and aims: The reconstruction of functional biliary trees (FBT) is crucial in the development of bioengineered liver. Decellularized liver scaffolds (DLS), a common platform for FBT, suffer from mechanical instability, resulting in luminal collapse and consequent hypoxic stress that severely impairs FBT function. Additionally, current engineered biliary constructs lack the necessary injury resistance to endure the pathological microenvironment associated with end-stage liver disease. This work aimed to construct macro-scale FBT with enhanced injury resistance using rat DLS optimized by genipin and mouse primary cholangiocytes.
Method: The newly developed FBTs were systematically evaluated through functional assays, transcriptomic analysis, and hepatotoxic drug-induced injury testing to validate their structural stability and injury resistance.
Results: The FBT exhibited an optimized microenvironment with enhanced structural stability and fluid mechanical properties, which facilitated cholangiocyte adhesion and alleviated hypoxic stress, as evidenced by downregulation of the HIF pathway. Morphological evaluation revealed that the bioengineered FBT recapitulated the hierarchical branching architecture of native biliary networks, with well-organized luminal structures and proper apical-basal polarity. Scanning electron microscopy identified elongated, upright primary cilia projecting from the luminal cholangiocytes, while JC-1 staining confirmed preserved mitochondrial membrane potential—indicative of cellular health. Functionally, the FBT exhibited enhanced bile acid transport, marked by the upregulation of *Slc51a/Slc51b* (encoding OST-α/OST-β) and *Abcc3* (encoding MRP3), along with enhanced retinoic acid synthesis capacity. Compared to 2D monolayers, the FBT exhibited a superior polarity barrier and enhanced efflux capacity for toxic substances, supported by the upregulation of Abcb1a, which encodes the key efflux transporter P-glycoprotein (P-gp). Notably, such FBT maintained homeostasis and exhibited unique resistance to hepatotoxic injury. This toxic resistance was linked to P-gp-mediated efflux function in FBT, as demonstrated by the impairment of this protection following verapamil-mediated activity inhibition of P-gp.
Conclusion: The efflux transporter P-gp plays a critical role in the injury resistance of FBT. Our macro-scale FBT, with enhanced toxic efflux function and injury resistance, provides a promising strategy for bioengineered liver construction and clinical translation.

THU-071-YI

Bacteroides intestinalis AM1 remodels liver microbiome and toxic metabolites, highlighting a novel therapeutic strategy in acute liver failure

Sushmita Pandey[1,2], Neha Sharma[1], Nupur Sharma[1], Sadam H. Bhat[1], Vipul Sharma[1], Yash Magar[1], Abhishak Gupta[3], Babu Mathew[1], Gaurav Tripathi[1], Vasundhra Bindal[1], Sanju Yadav[1], Manisha Yadav[1], Rakhi Maiwall[1], Anju Katyal[2], Shiv Kumar Sarin[1], Jaswinder Maras[1]. [1]*Institute of Liver & Biliary Sciences, New Delhi, India;* [2]*Dr. B R Ambedkar Center for Biomedical Research, University of Delhi, New Delhi, India;* [3]*Artemis Hospital Gurgaon, Gurugram, India*
Email: jassi2param@gmail.com

Background and aims: Acute liver failure (ALF), clinical syndrome of rapid hepatocellular injury with metabolic and linked microbial derangements. We investigated metabolic and microbial markers associated to predisposition to early mortality in ALF patients. We use Bacteroides intestinalis-AM1 to improve ALF outcomes.
Method: A plasma metabolomic and metaproteomic signature predicting non-survival in ALF was identified in 40 patients and 5 healthy controls and validated in 270 ALF patients using high-resolution mass spectrometry and machine-learning approaches. The therapeutic efficacy of *Bacteroides intestinalis* AM-1 was further confirmed in a preclinical acetaminophen-induced ALF mouse model.
Results: ALF non survivors (ALF-NS) exhibited elevated levels of primary bile acids and tryptophan metabolites, associated with inflammation, cell death, and mitochondrial dysfunction ($p < 0.01$, FDR<0.01, FC>1.5). Elevated chenodeoxycholic acid (CDCA; logFC >10) was associated with an increased risk of early mortality in ALF patients (hazard ratio >1.7; $p < 0.05$), which was independently validated in preclinical ALF mouse model. Additionally, ALF-NS exhibited an increased prevalence of pathogenic bacterial species Firmuctes, actinobacteria and others (FC.1.5; $p < 0.05$) and significant impairment of key microbial modulators involved in bile acid and other toxic metabolite regulation like chenodeoxycholic acid and cholic acid ($p < 0.05$). Oral *Bacteroides intestinalis* AM-1 (10^9 CFU/mL) supplementation in APAP-treated mice reduced muricholic acid and CDCA levels by restoring beneficial commensals like bacteriodes, lactobacillus and others ($p < 0.05$). *Bacteroides intestinalis* AM-1 enhanced glutathione-mediated NAPQI detoxification via upregulation of L-histidine amino-ligase and glutathione synthetase enzymes (FC>1.5; $p < 0.05$), while suppressing IL-1β/TLR4 signaling, oxidative stress, mitochondrial dysfunction, and caspase-3-mediated necroptosis in the liver of preclinical ALF model ($p < 0.05$).
Conclusion: Elevated plasma chenodeoxycholic acid (CDCA) is associated with poor prognosis in acute liver failure. Increase in pathogenic microbiome and loss of detoxifying commensals increase early mortality risk. *Bacteroides intestinalis* AM-1 restores microbiome balance, enhances glutathione synthesis, and reduces toxic metabolites, inflammation, mitochondrial dysfunction, and necro-apoptosis in a preclinical ALF model, thereby showing clear therapeutic benefits in a preclinical ALF model.

THU-072

Uncovering immune related mechanisms in drug-induced liver toxicity of sitaxsentan using human ex vivo precision-cut liver slices

Kevin Schmidt[1], Dana Oldenkott[1], Angelika Stucki-Koch[1], Josef Fangmann[2], Heiko Aselmann[2], Katherina Sewald[1], Jan Fiedler[1], Susann Dehmel[1]. [1]*Fraunhofer Institute for Toxicology and Experimental Medicine, Hannover, Germany;* [2]*Krh Hospital Siloah, Hannover, Germany*
Email: kevin.schmidt@item.fraunhofer.de

Background and aims: Hepatotoxicity is a major reason for failure in clinical development and post-marketing withdrawal of therapeutics. Overcoming limitations of other pre-clinical liver models, human precision-cut liver slices (hPCLiS) retain the 3D complexity of the hepatic microenvironment, which is necessary to understand immune-related mechanisms in drug induced liver injury (irDILI). Here, we aim to uncover irDILI of endothelin receptor antagonist (ERA) sitaxsentan, withdrawn from the market due to hepatotoxicity.
Method: hPCLiS were prepared from tumor-distant liver resections using a Krumdieck slicer and cultivated under carbogen atmosphere. Immune cell abundance in hPCLiS was analyzed via flow cytometry. Immune responsiveness was shown by stimulation of hPCLiS with LPS, poly I:C, and anti-CD3/28 beads. HPCLiS were treated with sitaxsentan, ambrisentan, or acetaminophen (APAP) for 48 h. Release of lactate dehydrogenase into culture supernatant and cellular metabolic activity measurement by WST-1 turnover were used as indicators for general cytotoxicity. Cytokine protein levels as well as mRNA expression of inflammatory and hepatocyte markers were assessed using multiplex MSD platform and qPCR, respectively.
Results: Flow cytometry analysis revealed comprehensive immune cell presence (20–40%) including high T cell content (66%) with more abundant $CD8^+$ than $CD4^+$ cells (ratio 2.5) and 17% NKT cells. Of note, distinct cytokine secretion profiles of hPCLiS exposed to LPS, poly I:C, and anti-CD3/28 beads confirmed immune reactivity of the tissue. While no changes in general cytotoxicity were visible for both investigated ERAs, sitaxsentan preferentially induced secretion of IL-12p70, IL-13 and IL-2 hinting at Kupffer cell and NKT cell activation. In contrast, ambrisentan exposure did not induce such distinct cytokine pattern, which aligns with the less toxic clinical profile of the drug. Expectedly, toxicity of APAP in escalated doses was reflected by decreased metabolic activity and IFN-γ induction.
Conclusion: In summary, our data suggest early activation of Kupffer cells after sitaxsentan treatment, which could trigger further immune cell activation leading to hepatotoxicty. Shedding light on the yet unknown irDILI effects of sitaxsentan, the herein presented results advocate for hPCLiS as an invaluable pre-clinical model to assess safety of novel therapies, particularly addressing concerns about immune-mediated liver toxicity.

THU-073-YI

Plasma bacteriophage diversity correlates with microbiome diversity and contributes todiseases severity and poor outcome in acute liver failure

Neha Sharma[1], Sushmita Pandey[1], Manisha Yadav[1], Vasundhra Bindal[1], Sanju Yadav[1], Nupur Sharma[1], Babu Mathew[1], Gaurav Tripathi[1], Vipul Sharma[1], Rakhi Maiwall[1], Shvetank Sharma[1], Shiv Kumar Sarin[1], Jaswinder Maras[1]. [1]*Institute of Liver and Biliary Sciences, New Delhi, India*
Email: jassi2param@gmail.com

Background and aims: Acute liver failure (ALF) causes rapid liver injury and high infection-related mortality, but despite links to gut–liver axis disruption and microbial dysbiosis, the role of altered bacteriophage diversity in disease severity is still unclear.
Method: A total of 40 ALF patients and 5 Healthy controls(HC) were enrolled. Baseline Samples were collected before antibiotics. Plasma Peptide based bacteriophage diversity, metaproteome, and circulating indicator of gut barrier injury and microbial translocation (FABP2, LBP, and CD14) was analysed on ALF Non-Survivors(ALF-NS); n = 32, ALF-survivors(ALF-S); n = 8 and HC; n = 5.
Results: ALF-NS exhibited increased intestinal permeability and microbial translocation, with elevated FABP2 (1.62-fold), LBP (3.03-fold), and CD14 (8.01-fold), alongside marked gut microbiome dysbiosis identified bacterial peptides >15 phylum and >25 genera and showed higher Alpha/Beta diversity with increase in Firmicutes, Actinobacteria and others, functionally associated to energy, amino acids, xenobiotic metabolism compared to ALF-S and HC($p < 0.05$). ALF showed predominance of lytic phages (59.0%) with reduced temperate phages (27.6%) compared to HC. ALF-NS exhibited phageome restructuring with reduced Myoviridae (15.27% vs S 19.63%) and Inoviridae (0.83% vs S 1.46%), alongside enrichment of Corticoviridae (0.19% vs S 0.07%) and Siphoviridae (27.87% vs S 24.51%), and increased pathogenic phages including *Enterobacteria phage K11*, *Vibrio phage KVP40* ($p < 0.05$). Also, Shannon index viral diversity correlates with Shannon Diversity of bacterial ($R^2>0.9$, $p < 0.05$). Cross-correlation analysis revealed that increased *Lactococcus phage rt1*(11.8-fold) in ALF-NS was inversely associated with reduced abundance of beneficial commensal *Lactococcus* ($R^2>0.7$, $p < 0.05$). In ALF-NS, enrichment of pathobionts *Enterobacter* and *Pseudomonas* was inversely associated with marked depletion of their bacteriophages *Pseudomonas* phage D3 (0.065-fold) and *Enterobacteria* phage N4 (0.36-fold) ($p < 0.05$). This phage loss demonstrated strong prognostic performance (AUROC > 0.9) and was associated with increased mortality risk (hazard ratio 1.4; 95% CI 1.12–1.83; log-rank $p < 0.05$) showing that phage diversity in ALF regulates bacterial abundance and disease severity.
Conclusion: ALF-NS exhibit a pronounced loss of pathobiont-targeting bacteriophages, driving microbial dysbiosis, heightened disease severity, underscoring bacteriophage diversity as a critical regulator of microbial balance and ALF progression.

THU-074

Biomolecular mapping of circulating extracellular vesicles to develop AI driven prognostic panels for stratifying acute liver failure patients at risk of early mortality

Neha Sharma[1], Sushmita Pandey[2], Vasundhra Bindal[2], Manisha Yadav[2], Sanju Yadav[2], Nupur Sharma[2], Babu Mathew[2,3], Gaurav Tripathi[2], Vipul Sharma[2], Rakhi Maiwall[2], Shvetank Sharma[2], Jaswinder Maras[2]. [1]*Institute of Liver and Biliary Sciences, New Delhi, India;* [2]*Institute of Liver and Biliary Sciences, New Delhi, India;* [3]*Institute of Liver and Biliary Sciences (ILBS), New Delhi, India*
Email: jassi2param@gmail.com

Background and aims: Acute liver failure (ALF) is a severe condition with high mortality, marked by microbial and metabolic factors in the blood. Plasma-derived exosomes, reflecting inflammation, offer a non-invasive tool to identify ALF patients at high risk of early mortality.
Method: Plasma samples from 50 ALF (25 non-survivors(ALF-NS), 25 survivors(ALF-S) patients and 20 controls were processed for extracellular vesicle isolation using protein organic solvent precipitation (PRoSPR) and characterized by transmission electron microscopy, dynamic light scattering, nanoparticle tracking analysis, and proteomic analysis, followed by meta-proteomic and metabolomic profiling. An identified diagnostic metabolite panel was validated in a separate cohort (220 ALF; 153 ALF-NS, 67 ALF-S) using HRMS and machine learning.
Results: Plasma-derived exosomes (120–200 nm) were characterised with a concentration of $3.25 \times 10^{11} \pm 0.55$ particles/mL, zeta potential of -30.67 ± 3.6 mV, and >20 EV-specific proteins (Vesiclepedia) ($p < 0.01$). Exosomal metabolomics identified over 1,000 metabolites, with more than 800 significantly altered in ALF. ALF-NS showed pronounced enrichment of long-chain fatty acid β-oxidation, and bile acid pathways, linking metabolic dysregulation to inflammation and disease severity. Bacterial-peptide identified >15 phyla and >25 genera based alpha/beta diversity was higher in ALF-NS

corresponding to increase in Bacteroidota, Actinomycetota functionally linked to energy and xenobiotic metabolism ($p < 0.05$). Higher EV levels of *Enterococcus ceocorum* and Klebsiella pneumoniae in non-survivors correlated with metabolites, Clinical parameters and severity ($r^2 > 0.8$, $p < 0.05$). A panel of five extracellular vesicle–derived metabolites showed strong prognostic potential in acute liver failure, achieving (AUC = 0.98) and a high hazard ratio (17.58). Deoxycholic acid-3-glucuronide(8.8 fold) showed highest normalized importance and predicted early-mortality with >95% accuracy/sensitivity/specificity using ANN and ML. Interestingly, Upregulation of β-glucuronidase (>2-fold) and reduced ABCC3 (MRP3) impaired bile acid efflux, driving intracellular bile acid accumulation and exacerbating hyperinflammation and oxidative stress in acute liver failure non-survivors.

Conclusion: Plasma-derived exosome metabolite cargo panel indicates hyper-inflammation and advanced glycation specific to non-survivors, potentially identifying ALF patients at risk of early mortality.

THU-075

Assessing drug-mediated inhibition of liver transporter function with functional MRI: proof of concept

Sam Jenkins[1], Oliver Spear[1], Elliot Checkley[1], Marta Tibiletti[2], Thazin Min[3], Paul Hockings[4], Aleksandra Galetin[5], Gerry Kenna[2], Geoff Parker[2,6], Gunnar Schuetz[7], Daniel Scotcher[5], John Waterton[2,8], Ian Rowe[3,9], Steven Sourbron[10], Benjamin Rea[3,10]. [1]*Sheffield Teaching Hospitals NHS Trust, Sheffield, United Kingdom;* [2]*Bioxydyn Ltd, Manchester, United Kingdom;* [3]*Leeds Teaching Hospitals NHS Trust, Leeds, United Kingdom;* [4]*Antaros Medical, Chalmers University of Technology, Gothenburg, Sweden;* [5]*Centre for Applied Pharmacokinetic Research, The University of Manchester, Manchester, United Kingdom;* [6]*UCL Hawkes Institute, Department of Medical Physics and Biomedical Engineering, University College London, London, United Kingdom;* [7]*Bayer AG, Berlin, Germany;* [8]*Centre for Imaging Sciences, Faculty of Biology Medicine & Health, The University of Manchester, Manchester, United Kingdom;* [9]*Leeds Institute for Medical Research, University of Leeds, Leeds, United Kingdom;* [10]*University of Sheffield, Sheffield, United Kingdom*
Email: s.sourbron@sheffield.ac.uk

Background and aims: Assessing the risk of drug-mediated liver injury (DILI) and liver-mediated drug-drug interactions (DDI) for new drugs requires biomarkers that respond to drug effects on hepatic transporters. Unfortunately, predictions of changes in liver exposure are currently difficult to verify clinically. A potential solution is provided by dynamic MRI with the contrast agent gadoxetate, a known substrate of OATP1B1, OATP1B3, NTCP, MRP2 and MRP3. A recent study in rats with six test drugs has demonstrated that this method can detect different levels of transporter inhibition. The aim of this study was to test whether these results translate to humans, using two strong inhibitors (rifampicin and ciclosporin) and one drug that is not expected to inhibit gadoxetate transport (metformin).

Method: This prospective study included 20 healthy volunteers, split between rifampicin (n = 8), ciclosporin (n = 6) and metformin (n = 6) groups. Each participant underwent two visits separated by 1–4 weeks. At the second visit, a clinical dose of rifampicin (600 mg), metformin (1000 mg) or ciclosporin (100 mg) was administered orally prior to imaging. MRI data were analysed to measure the uptake rate k(he) of gadoxetate from extracellular space (e) into hepatocytes (h), and the excretion rate k(bh) from hepatocytes (h) to bile (b). Two MRI scans were performed on each visit, the first to measure acute drug effects, and the second to assesses functional recovery after acute inhibition. One quarter of a clinical dose of gadoxetate was administered for each scan.

Results: Rifampicin reduced k(he) with −93 ± 1.6% ($p < 0.001$) and k(bh) with −55 ± 29% ($p = 0.015$). Ciclosporin reduced k(he) with −79 ± 6.4% ($p = 0.002$) and k(bh) with −70 ± 20% ($p < 0.001$). Metformin did not have a measurable effect on k(he) (13 ± 53%, $p = 0.99$) or on k(bh) (−2.0 ± 45%, $p = 0.37$). In the ±4 hours after peak drug concentration, k(he) increased with 215 ± 88% for ciclosporin ($p = 0.005$) and 29 ± 12%, for metformin ($p = 0.005$), but did not change significantly for rifampicin (44 ± 45%, $p = 0.1$). k(bh) did not show systematic changes in the same time frame for any of the drugs.

Conclusion: Results demonstrate that gadoxetate MRI can characterise drug-mediated inhibition of hepatocellular uptake and biliary excretion in humans. The method may be useful for assessment of DILI and DDI during drug development, and potentially in patient management.

Disclosure: Transporter assessment for DILI or DDI is an off-label use of gadoxetate.

THU-076

Variation of CD39-positive tregs in idiosyncratic drug-induced liver injury

Maria Vargas[1], Stuart Astbury[1], Jane I. Grove[1], Guruprasad Aithal[1]. [1]*University of Nottingham, NIHR Nottingham Biomedical Research Centre, Nottingham, United Kingdom*
Email: guru.aithal@nottingham.ac.uk

Background and aims: The pathogenesis of idiosyncratic drug-induced liver injury (DILI) involves a loss of immune tolerance, primarily characterised by a $CD8^+$ cytotoxic T cell response. The liver is considered an immunologically tolerant organ; a key inhibitory mechanism of this tolerance is mediated by regulatory T cells (Tregs), which not only inhibit antigen-presenting cells but also secrete anti-inflammatory cytokines such as interleukin-10 (IL-10) and transforming growth factor-beta (TGF-β). CD39 is an ectonucleotidase expressed on Tregs. It converts adenosine triphosphate into adenosine monophosphate, which is then converted into anti-inflammatory adenosine (by CD73), conferring immune-suppressive activity. $CD39^+$ Tregs are reduced in other autoimmune inflammatory diseases. We aimed to evaluate the Treg response in DILI.

Method: We evaluated CD39 expression in Treg cells ($CD4^+CD25^{hi}CD127^{low}FOXP3^+$), using peripheral blood samples from 11 DILI cases and 11 controls (5 healthy and 6 autoimmune hepatitis [AIH]). Cell subtype results are shown as proportions, while marker expression is shown by geometric mean fluorescence intensity (gMFI). Statistical analysis was performed using the Kruskal-Wallis test, with a significance threshold of $p < 0.05$. Outliers were identified using the ROUT method with Q1%.

Results: We observed decreased counts of total T cells ($CD3^+$), $CD4^+$, and $CD8^+$ T cells in DILI samples. Treg levels in DILI were 4.3% (0.3–14.1) of the $CD4^+$ subset, compared to 2.8% (0.8–5.7) in healthy controls and 2.8% (0.7–5.7) in AIH controls, showing no significant differences between the groups. In DILI, $CD39^+$ Tregs decreased significantly compared with healthy controls (56.6% of Tregs [6.4–96.8] vs. 90.5% [69.7–95.2], $p = 0.0158$), whereas $CD39^{low}$ Tregs increased in DILI relative to healthy controls (42.9% [3.2–93.4] vs. 4.7% [0.9–29.7], $p = 0.046$). $TGFβ^+$Tregs were significantly higher in DILI samples (3.4% of Tregs, range 1–31.6; $p = 0.0306$) compared to healthy controls (0.9%, range 0.75–2.9). No significant correlation was observed between CD39 and TGFβ expression (Spearman r = −0.3 in healthy controls; AIH r = 0.7; and DILI r = 0.52, p = ns). Therefore, the downregulation of $CD39^+$ Tregs in DILI does not correlate with TGFβ secretion.

Conclusion: Tregs in DILI are present in normal numbers and express elevated TGFβ. However, they exhibit functional deficits, particularly a decrease in the $CD39^+$ Treg subset, potentially contributing to the pathogenesis of DILI.

THU-077

Systematic drug screening in a patient-derived bile duct organoid biobank deciphers context-dependent bile duct injury mechanisms

Ziye Chen[1], Tianzi Luo[2], Mingming Ren[2], Yadi Geng[2], Yakun Liu[2], Meidai Liang[2], Zixuan Wang[3], Hui Bai[2], Yunfang Wang[1]. [1]*Beijing Tsinghua Changgung Hospital, School of Clinical Medicine, Tsinghua Medicine, Tsinghua University,, Beijing, China;* [2]*Clinical Translational Science Center, Beijing Tsinghua Changgung Hospital, Beijing, China;* [3]*Liver Research Center, Beijing Tsinghua Changgung Hospital, Beijing, China*
Email: medical_chan@163.com

Background and aims: Drug-induced liver injury (DILI) is a major cause of clinical trial attrition. The mechanisms of its cholangiopathic subtype (DIBDI) are poorly understood, and crucially, how pre-existing biliary disease affects injury and repair remains unknown. Current bile duct organoid (BDO) models, limited in pathological scope, cannot address this. We therefore constructed a comprehensive BDO biobank to systematically investigate how disease background dictates susceptibility to and recovery from DIBDI.
Method: We established a biobank of patient-derived BDOs representing key pathological states (normal, dilation, cholangitis, choledocholithiasis), which were validated for morphological, phenotypic, and functional fidelity. To systematically investigate drug-induced injury, we screened six pharmacologically diverse agents known to cause bile duct damage (including glibenclamide, omeprazole, amitriptyline, chlorpromazine, moxifloxacin, azithromycin) using this platform. A refined injury model was then established, enabling the functional assessment of damage and repair dynamics. Finally, we employed integrated label-free imaging and Drug-seq to decipher the state-specific metabolic phenotypes and molecular mechanisms.
Results: Validation confirmed the high fidelity of our BDO biobank to patient tissues. Utilizing this platform for multi-drug screening, we discovered that drug-induced injury susceptibility is highly context-dependent, varying with both the specific agent and the underlying pathology. Drug-seq analysis provided high-resolution, dynamic transcriptomic landscapes for each drug-state combination. This approach identified both shared and state-specific signaturesof injury. A set of pathways—most prominently involving p53 signaling, cytoskeletal remodeling, and mitochondrial clearance—was consistently modulated across multiple drugs. The expression dynamics of genes within these pathways (e.g., *TESC*, *MUC1*, *GDF15*) defined distinct molecular trajectories that predicted and explained the functional sensitivity outcomes, mapping molecular perturbations directly to phenotypic responses.
Conclusion: Collectively, we have established a unique and pathologically diverse BDO biobank and we have enabled the first systematic exploration of how pre-existing disease dictates DIBDI outcomes. This work directly addresses a long-standing gap in mechanistic models and provides essential insights for stratifying hepatotoxicity risk and guiding targeted therapeutic interventions.

THU-078

Characterisation and applicability of a 3D coculture spheroid model for drug-induced liver injury

Neele Wewer[1], Lisa Rogalski[1], Julia Böhme[1], Maxi Paul[1], Dajana Lichtenstein[1]. [1]*German Federal Institute for Risk Assessment, Berlin, Germany*
Email: neele.wewer@bfr.bund.de

Background and aims: Conventional 2D monoculture lack the complex network of cell–cell and cell–matrix interactions that are crucial for maintaining physiological functionality. Many toxicological responses in hepatic tissue are dependent on the interplay between different liver cell types, which cannot be fully replicated in monocultures. To improve the predictability of human toxicity, we developed a 3D liver model by coculturing four different cell types as a spheroid, providing a more accurate *in vitro* representation of human liver physiology.
Method: For determination of optimal culture conditions, various cell lines, different cell numbers per spheroid, and suitable coculture media were evaluated. The final model comprises hepatocytes (HepaRG), macrophages (THP-1), endothelial cells (HMEC-1) and hepatic stellate cells (HHSteC), with 4,000 cells per spheroid in total. The spheroids were maintained for six days with cell-type ratios resembling those found *in vivo* in human liver tissue. The model was functionally characterized by morphological assessment, fluorescence imaging of cell-specific markers, mRNA expression analysis, and quantification of liver-specific secretion markers, specific CYP enzymes and transporters. To demonstrate the model's applicability, both mono- and coculture spheroids were exposed to reference compounds known to target liver-related endpoints.
Results: The presence of all four cell types as well as their typical morphological phenotypes could be provided by fluorescence imaging. To investigate the effects of a more physiological environment on hepatic function, mRNA and protein quantification data of the 3D coculture model were compared with those from a 3D monoculture of HepaRG cells after three and six days. Data exhibited similar protein expression of liver-specific CYP enzymes and transporters in mono- and coculture spheroids despite the differences in HepaRG cell numbers. Treatment with reference compounds displayed endpoint-specific responses, causing drug-induced liver injury such as phospholipidosis, inflammation, and impaired xenobiotic metabolism.
Conclusion: In conclusion, this 3D liver model is a promising *in vitro* system displaying relevant human liver physiology and enables the investigation of drug-induced liver injury mechanisms.

THU-079

Macrophage GPR65 sensing of lactate triggers pro-inflammatory polarization and aggravates APAP-induced liver injury

Miaomiao Wu[1]. [1]*Anhui Medical University, Hefei, China*
Email: wumiaomiao@ahmu.edu.cn

Background and aims: Acetaminophen-induced liver injury (AILI) is the leading cause of acute liver failure (ALF), yet the mechanisms driving excessive inflammation and disease progression remain poorly defined. Elevated serum lactate is a strong predictor of poor prognosis in APAP-related ALF, but the mechanistic basis for this association is unclear.
Method: Mouse models of AILI were combined with genetic and pharmacologic inhibition of lactate-GPR65 signaling, bone marrow transplantation, and macrophage-targeted AAV-F4/80-mediated modulation to determine functional of Macrophage GPR65. Bulk and single-cell RNA sequencing, macrophage functional assays, and analyses of blood samples from patients were performed to elucidate the underlying immunometabolic mechanisms and clinical relevance.
Results: We demonstrate that lactate functions not as a passive metabolic by-product but as an active immunometabolic driver in AILI. Excessive glycolysis caused marked lactate accumulation, which activated the macrophage GPR65 to induce pro-inflammatory polarization and promote inflammatory mediator release. Genetic deletion or pharmacologic blockade of lactate production or GPR65 signaling markedly attenuated AILI. GPR65 was selectively enriched in macrophages within the APAP-damaged liver and was also elevated in circulating monocytes of patients, correlating with inflammatory cytokines and disease severity. Single-cell analyses revealed that GPR65 promotes sustained differentiation of monocytes into CD68+ inflammatory macrophages, whereas Gpr65 deficiency favored the emergence of HMOX1+ macrophages with tissue-repair features, thereby reshaping the hepatic immune microenvironment toward reduced inflammation.
Conclusion: This study identifies lactate–GPR65 signaling as a key immunometabolic pathway that governs macrophage pro-

inflammatory polarization and amplifies hepatic inflammation during AILI, establishing GPR65 as a potential therapeutic target in drug-induced and inflammatory liver injury.

THU-083

IPA ameliorates acute-on-chronic liver failure by suppressing neutrophil extracellular trap formation

Hang You[1], Jing Xiao[1], Zongyi Liu[1], Yong Sun[1], Yu Zhang[1], Li Wei[1], Ning Ling[1], Hong Ren[1], Peng Hu[1], Shiying Li[1], Mingli Peng[1].
[1]*Department of Infectious Diseases, Key Laboratory of Molecular Biology for Infectious Diseases (Ministry of Education), Institute for Viral Hepatitis, the Second Affiliated Hospital, Chongqing Medical University, Chongqing, China, Chongqing, China*
Email: 1336438976@qq.com

Background and aims: Acute-on-chronic liver failure (ACLF) is characterized by numerical alterations and impaired function of neutrophils. Accumulating evidence suggests that gut microbiota and their metabolites play a pivotal role in the pathogenesis of HBV-related ACLF. This study aimed to investigate the potential role of the tryptophan metabolite indole-3-propionic acid (IPA) in HBV-ACLF.
Method: Using an integrated multi-omics approach combining metagenomic sequencing, targeted metabolomics, and bioinformatics, we profiled the gut microbiota–metabolite associations in ACLF and compared them with those in patients with decompensated cirrhosis (DC), compensated cirrhosis (CC), and chronic hepatitis B (CHB). The protective effects of IPA on ACLF mice were examined through in vivo and in vitro experiments, and the mechanism underlying IPA-mediated inhibition of neutrophil extracellular trap (NET) formation was further validated by immunoprecipitation, immunofluorescence, and related methods.
Results: Analysis of the CHB–CC–DC–ACLF disease progression revealed that, based on metagenomics, both α- and β-diversity of the gut microbiota were significantly lower in the ACLF stage than in the DC, CC, and CHB stages. Gene enrichment analysis indicated significant alterations in tryptophan metabolism, with marked downregulation of key enzymes involved in IPA metabolism (FLDB, ACDA). Further analysis showed a significant reduction in IPA-producing microbial taxa (Firmicutes, Ruminococcus and Faecalimonas). Targeted metabolomics demonstrated that IPA levels in plasma, feces, and liver tissue were markedly decreased in ACLF and closely correlated with AST, ALT, TBil, and INR. IPA supplementation improved survival in ACLF mice, ameliorated liver and kidney function, and suppressed the expression of inflammatory cytokines (TNF-α, IL-6). Mechanistically, IPA reduced the proportion of pro-inflammatory neutrophils and inhibited NET formation. Furthermore, IPA attenuated hepatocyte apoptosis by targeting the MAPK/p38 signaling pathway.
Conclusion: Our findings underscore the potential of the microbial metabolite IPA in ameliorating ACLF. As a gut-derived metabolite, IPA represents a promising therapeutic candidate with translational potential.

THU-084

Defective antigen-presenting cell interleukin 23 support limits interleukin 22 production by mucosal-associated invariant T cell and tissue repair in chronic drug-induced liver injury

Cailun Zou[1], Zherui Liu[2], Zhuoya Deng[3], Zhengsheng Zou[2,4].
[1]*Department of Gastroenterology, China-Japan Friendship Hospital, Beijing, China;* [2]*Peking University 302 Clinical Medical School, Beijing, China;* [3]*Beijing Youan Hospital, Capital Medical University, Beijing, China;* [4]*Senior Department of Hepatology, Chinese PLA General Hospital, Beijing, China*
Email: zoucl302@163.com

Background and aims: Chronic drug-induced liver injury (DILI) is characterised by persistent hepatic inflammation and impaired tissue repair, yet the immunological mechanisms driving chronicity remain poorly defined. Mucosal-associated invariant T (MAIT) cells are highly enriched in the liver and implicated in tissue repair through interleukin 22, but their role in chronic DILI and the upstream signals regulating MAIT-cell repair functions are unclear. We aimed to define MAIT-cell involvement in chronic DILI and identify upstream molecular pathways governing MAIT-cell-mediated hepatic repair as potential therapeutic targets.
Method: We analysed MAIT cells in healthy controls (HC, n = 30), acute DILI (n = 43) and chronic DILI (n = 50) by flow cytometry. Plasma IL-23 was measured in HC (n = 26), acute DILI (n = 27) and chronic DILI (n = 27). Data-independent acquisition plasma proteomics was performed in HC (n = 8), acute DILI (n = 10) and chronic DILI (n = 10). Phorbol 12-myristate 13-acetate (PMA)-differentiated THP-1 macrophages were conditioned with pooled patient serum and analysed for IRAK4 and phosphorylated p65. Healthy-donor MAIT cells were stimulated with recombinant IL-23 or co-cultured with serum-conditioned macrophages to quantify IL-22 expression in MAIT cells.
Results: MAIT-cell proportions were reduced in both acute and chronic DILI versus HC, but chronic DILI showed higher HLA-DR expression, indicating persistent activation. Cytotoxic markers did not increase in chronic versus acute DILI. IL-22-positive MAIT cells were lower in chronic than acute DILI and inversely correlated with alanine and aspartate aminotransferase within chronic DILI. Chronic DILI serum reduced MAIT IL-22 ex vivo despite inducing HLA-DR. Proteomics highlighted suppressed toll-like receptor signalling, including reduced IRAK4 and nuclear factor kappa B 1, and THP-1 macrophages exposed to chronic DILI serum showed reduced IRAK4 and p65 phosphorylation. Plasma IL-23 correlated positively with IL-22-positive MAIT cells in chronic DILI ($r = 0.411$; $p = 0.033$). Recombinant IL-23 increased MAIT IL-22 dose-dependently, whereas chronic DILI-conditioned macrophages supported weaker MAIT IL-22 responses than acute DILI-conditioned macrophages.
Conclusion: Chronic DILI is characterised by persistently activated MAIT cells with selective IL-22 deficiency driven by impaired APC innate signalling and reduced IL-23 support. Targeting the APC-IL-23-MAIT-IL-22 axis may provide a mechanism-based therapeutic strategy for chronic DILI.

Alcohol-related liver disease and MetALD – Clinical

TOP-208-YI

Fecal microbiota transplant for alcohol use disorder in patients with cirrhosis: a randomized controlled trial

Srajit Singh[1], Vinod Arora[1], Mohit Varshney[1], Vikas Khillan[1], Sukriti Baweja[1], Pramod Gautam[1], Rajan Vijayaraghavan[1], Harshvardhan Tevethia[1], Manisha Yadav[1], Shiv Kumar Sarin[1].
[1]*Institute of Liver & Biliary Sciences, New Delhi, India*
Email: vinod_ucms@yahoo.com

Background and aims: Alcohol use disorder (AUD) worsens outcomes in alcohol related liver disease (ALD), with limited approved pharmacological therapies and a high relapse rate. Gut dysbiosis is increasingly recognised to influence alcohol craving, relapse, and disease progression. Preliminary studies suggest that fecal microbiota transplantation (FMT) may reduce alcohol craving; however, data in patients with ALD, particularly from Asia, remain limited. We evaluated the safety and efficacy of FMT as an adjunctive therapy for AUD in patients with ALD.
Method: In this single centre, randomised controlled trial, 54 patients with ALD and AUD were randomised in 1:1 ratio to receive either a single session of FMT delivered via upper gastrointestinal endoscopy plus standard medical therapy (SMT, comprising baclofen and structured AUD counselling) or SMT alone. The primary endpoint was the proportion of patients achieving and maintaining alcohol

abstinence at one month. Secondary endpoints included alcohol abstinence at 3 and 6 months; lapse and relapse severity; alcohol craving Obsessive Compulsive Drinking Scale (OCDS) and the Alcohol Use Disorders Identification Test (AUDIT) score; adverse events; disease severity scores like MELD and MELD Na and gut microbiota changes analysed before and after FMT using stool metagenomic analysis.
Results: Baseline characteristics including age (43.3 vs 45.6); CTP (6.8 vs 7.4); MELD (11.9 vs 12.7); OCDS (22.2 vs 21.6) and AUDIT (20.5 vs 19.3) scores were comparable between both arms. At 1 month, complete abstinence showed a favourable trend in FMT arm (52% vs 33.3%) and reached significance at 3 months, compared to SMT (22% vs 0%, $p < 0.023$), with sustained benefits at 6 months (11% vs 0). Relapse rates were significantly lower in the FMT arm at 3 and 6 months (36% vs 79.2%, $p = 0.04$; 45.5% vs 100%, $p < 0.01$). OCDS and AUDIT scores declined earlier and significantly more in FMT group ($p < 0.05$) at 1, 3 and 6 months. FMT resulted in improvement in MELD and MELD Na scores. Stool metagenomic analysis revealed that abstinent FMT patients had reduced alpha diversity along with increased ruminococcaceae, bifidobacteriaceae and decreased prevotellaceae and clostridiaceae, whereas relapse was associated with expansion of clostridiaceae and bacteroidaceae species.
Conclusion: FMT administration reduced relapse episodes and improves liver severity scores in ALD patients with AUD, with concordant gut microbiome changes supporting a mechanistic link.

TOP-209-YI

GLP-1 RA use reduces the incidence of alcohol-associated hepatitis and risk of death in type 2 diabetes mellitus and alcohol use disorder in a routine clinical care stetting

Neha Shah[1], Vinay Jahagirdar[1], Kavin Parmar[1], Arun J. Sanyal[1].
[1]*Virginia Commonwealth University School of Medicine, Richmond, United States*
Email: shahn24@vcu.edu

Background and aims: Alcohol-associated hepatitis (AH) is an important complication of alcohol use disorder (AUD). GLP-1 receptor analogs (GLP-1 RA) have recently been shown to reduce alcohol craving and are being evaluated for AUD. It is not known if GLP-1 RA reduces the risk of AH in those with AUD. The aim of this study was to determine if GLP-1 RA use reduced (1) the risk of developing AH and (2) other liver and cardio-renal-metabolic (CRM) outcomes and (3) improve mortality in those with T2DM and AUD.
Method: A retrospective analysis of adults with T2DM and AUD from 2020–2025 was performed using the TriNetX collaborative research database, which includes patient level anonymized data from over 100 million individuals across multiple health systems in USA and Europe. GLP-1 RA use was established from prescriptions and outcomes assessed during period of active prescription use. Key outcomes were mortality, AH, ascites, encephalopathy, atrial fibrillation, heart failure and MACE. Those who received GLP-1 RA were compared to propensity score match (PSM) controls who did not. PSM was done for age, gender, race, BMI, nicotine dependence, hypertension, laboratory parameters (bilirubin, AST, ALT, creatinine, INR, A1C) and statin use. The absolute and relative risks from time-dependent proportional hazards models were computed. Time to event analyses with Kaplan-Meier curves and across-group comparisons with logrank test were done.
Results: A total of 131900 individuals with T2DM with AUD were identified with 15300 who received a GLP-1 RA for at least 1 year. Following PSM, GLP-1 RA decreased the incidence of AH (HR: 0.20–0.27, $p < 0.0001$ for all) with greatest decrease in those > 60 yrs. Within 6 mo-3 yrs, absolute risk of AH decreased to 0.2% to 0.8% with GLP-1 RA, compared to 1.3% to 2.0% without GLP-1 RA (HR 0.2–0.4 $p <$ 0.0001 for all). GLP-1 RA improved other liver related events: new diagnosis cirrhosis (HR 0.21–0.57), ascites (0.21–0.32), encephalopathy (HR: 0.24–0.54) $p < 0.01$ for all. It also decreased atrial fibrillation (HR: 0.31–0.44), heart failure (HR: 0.33–0.44) and 5-point MACE (HR: 0.26–0.75) $p < 0.001$ for all. It further decreased sepsis (HR: 0.24–0.31). Overall GLP-1 RA reduced all-cause mortality (HR: 0.29–0.42, $p < 0.0001$ for all).
Conclusion: GLP-1 RA use reduced development of AH in those with AUD and T2DM. These data provide a strong rationale to study this in a prospective randomized trial inclusive of diabetic and non-diabetic individuals.

TOP-210

The impact of prior bariatric surgery on patients with compensated and decompensated alcohol-related liver disease: results of an observational multicenter study

Astrid Marot[1,2], Jackie Bitton[3], Sofia Belhoussine Drissi[3], Laura Weichselbaum[3], Delphine Degré[3], Thierry Gustot[3], Eric Trepo[3], Olivier Borgniet[1], Hassane Njimi[3], Marc Van Hoof[4], Pierre Deltenre[4], Christophe Moreno[3]. [1]*CHU UCL Namur, Yvoir, Belgium;* [2]*CHU UCL Namur, Yvoir;* [3]*HUB Erasme, Brussels, Belgium;* [4]*St Luc Bouge, Namur, Belgium*
Email: astridmarot@gmail.com

Background and aims: Recent data suggest an increased risk of alcohol-related liver disease (ARLD) in patients with prior bariatric surgery (BS). The aims were to evaluate the impact of prior BS on mortality in patients with ARLD at different stages of severity (i.e. compensated ARLD, decompensated ARLD, and alcohol-associated hepatitis [AAH]) and to assess the risk of hepatic decompensation in those with compensated ARLD both with and without prior BS in a large multicenter retrospective study.
Method: We included 794 patients with ARLD in 3 Belgian centers between January 4th 2010 and 31st December 2024. The median follow-up was 2.6(IQR 0.4–6.8) yrs. Cumulative incidence functions were applied in patients with AAH and those with compensated and decompensated ARLD separately. Competing-risks regression procedures were performed.
Results: Almost 15% of patients (115/794) with ARLD had a prior BS. At inclusion, 377 patients had a compensated ARLD, 189 had a decompensated ARLD, and 228 had an AAH. Compared to the non-BS group, patients with a prior BS were predominantly female (50.4%vs 27.5% $p < 0.001$), younger (51 vs 56 yrs $p < 0.001$) with a higher proportion of Child-Pugh C (47.4% vs 27.4% $p < 0.001$). They were also younger at transplantation (48 vs 58 yrs, $p < 0.001$) and at death (50 vs 59 yrs $p < 0.001$). In patients with AAH, cumulative incidence of death at 6 months was not different between both groups (33.9%vs 47.4% $p = 0.1$). In multivariate analyses, age (SHR1.03 $p = 0.001$) and MELD score (SHR1.08 $p < 0.001$) were independently associated with mortality but not prior BS. In patients with compensated and decompensated ARLD, cumulative incidence of death at 3 yrs was not different between both group (23.1%vs 21.5% $p = 0.77$). In multivariable analyses, MELD score (SHR1.19 $p < 0.001$) abstinence (SHR0.31 $p = 0.01$) and prior BS (SHR5.98 $p = 0.03$) were independently associated with mortality. In compensated ARLD, hepatic decompensation was more frequent in the BS group compared to the non-BS group. In multivariable analyses, MELD score (SHR1.12 $p <$ 0.001) and prior BS (SHR2.24 $p = 0.02$) were independently associated with hepatic decompensation.
Conclusion: Despite being younger at inclusion, liver transplantation and death, ARLD patients with a prior BS have more severe liver disease than those with no prior BS. Prior BS is associated with higher mortality in patients with compensated and decompensated ARLD, but not in patients with AAH. In compensated ARLD, prior BS is also associated with a higher risk of first hepatic decompensation.

TOP-222

Alcohol-related liver disease with latent fibrosis: an indolent phenotype in abstinent patients

David Heitmann[1], Lucía Ramón[2], Lorenzo Ciocca[1], Queralt Herms[1], Martina Perez-Guasch[1,2,3], Ruth Nadal[3], Marta Cervera Carbonell[3], Nicole Casanova[3], Cautar El Maimouni[1,3], María José Moreta[1,3], Anna Soria[1,3], Adrià Juanola[1,2,3], Isabel Graupera[1,2,3], Núria Fabrellas[2,3], Jordi Gratacós-Ginès[1,3], Pere Ginès[1,2,3], Elisa Pose[1,2,3]. *[1]Hospital Clínic De Barcelona, Barcelona, Spain; [2]Universitat de Barcelona - Facultat de Medicina i Ciències de la Salut, Barcelona, Spain; [3]Institut d'Investigacions Biomèdiques August Pi i Sunyer, Barcelona, Spain*
Email: heitmann@clinic.cat

Background and aims: Liver fibrosis, together with alcohol abstinence, is the main prognostic factor in alcohol-related liver disease (ArLD). Liver stiffness measurement (LSM) by transient elastography, which correlates with the degree of fibrosis, has also prognostic value. Some patients show advanced fibrosis on liver biopsy but discordantly low LSM, suggesting a distinct clinical phenotype. The aim was to characterize these patients and assess their prognosis.
Method: We prospectively includedconsecutive patients with ALD who underwent liver biopsy at Hospital Clínic of Barcelona from 2013 to 2025 (LiverModel cohort). Patients with non-advanced fibrosis (METAVIR <F3), clinical decompensation at baseline, and lacking baseline LSM were excluded. Two groups were defined according to LSM: <10 kPa and ≥10 kPa. Liver-related events (LRE) included portal hypertension–related decompensation, hepatocellular carcinoma, liver transplantation, or liver-related death. Prognosis was assessed by an Andersen–Gill Cox regression model (allowing recurrent events), adjusted for age and sex. A subanalysis was performed in patients with sustained abstinence throughout follow-up, assessed by self-report and family interview, or by urinary ethyl glucuronide when available.
Results: A total of 115 patients were included: 23 (20%) with LSM < 10 kPa and 92 (80%) with LSM ≥10 kPa. The proportion of females (26% vs. 23%) and mean age (64 vs. 60 years) were similar (p > 0.05). No differences were observed in the prevalence of metabolic risk factors. Patients with LSM <10 kPa had lower MELD scores (9 vs. 11, p = 0.01). Abstinence at inclusion (48% vs. 43%) and its duration (4 vs. 5 months) did not differ (p > 0.05). Over a median follow-up of 3.6 years, 7 LRE occurred in 2 patients with LSM <10 kPa, while 43 LRE occurred in 23 patients with LSM≥ 10 kPa. In the overall cohort, LSM≥ 10 kPa showed a trend toward a higher risk of LRE (HR 2.14; 95% CI 0.59–7.71; p = 0.25). In patients with sustained abstinence (n = 71), no patient with LSM <10 kPa experienced a LRE, whereas 17 patients with LSM≥ 10 kPa accumulated 29 LRE. Predictive models could not estimate a finite HR due to complete separation between groups, indicating a near-zero risk in LSM <10 kPa. Patients whose LSM decreased from ≥10 kPa at baseline to <10 kPa during follow-up (n = 35) did not develop any LRE.
Conclusion: Abstinent patients with advanced fibrosis but LSM < 10 kPa have a very low risk of LRE, suggesting the existance of latent fibrosis with a favorable prognosis.

FRI-041-YI

Increasing phosphatidylethanol correlates with increasing liver stiffness – a prospective longitudinal analysis of 1397 individuals at risk of steatotic liver disease

Katrine Tholstrup Bech[1], Nikolaj Torp[1], Helle Schnefeld[1], Stine Johansen[1], Camilla Dalby Hansen[1], Katrine Thorhauge[1], Johanne Kragh Hansen[1], Mette Lehmann Andersen[2], Ida Villesen[1], Anine Andersen[1], Charlotte Mary Gjøl[1], Gunilla Calov[1], Markus Maagaard[1], Ea Kyed[1], Ellen Lyngbeck Jensen[1], Maria Fogt[1], Kathrine Sejer Sørensen[1], Peter Andersen[1], Marianne Bergmann[3], Aleksander Krag[1], Maja Thiele[1], Mads Israelsen[1]. *[1]FLASH - Centre for Liver Research, Department of Gastroenterology and Hepatology, Odense University Hospital, Department of Clinical Research, University of Southern Denmark, Odense, Denmark; [2]Department of Gastroenterology and Hepatology, Herlev Hospital, Herlev, Denmark; [3]Department of Biochemistry and Immunology, Sygehus Lillebælt, University Hospital of Southern Denmark, Vejle, Denmark*
Email: katrine.tholstrup.bech@rsyd.dk

Background and aims: The role of phosphatidylethanol (PEth) for subclassification within SLD is emerging, but the use of repeated assessment remains unstudied. We examined how longitudinal changes in alcohol intake assessed by PEth and self-report correlated with changes in liver stiffness in SLD.
Method: Prospective, single-centre study of adults with type 2 diabetes, BMI ≥30 kg/m^2, or current/prior excessive alcohol consumption. We measured PEth, self-reported alcohol intake, and liver stiffness using vibration-controlled transient elastography (VCTE) at two visits with two years apart. We defined changes in alcohol intake as moderate if PEth changed ≥20 ng/mL, and substantially if ≥80 ng/mL. Similarly, moderate if self-reported intake changed ≥10 g/day and substantially if ≥20/30 g/day (F/M). A relative change in VCTE ≥30% was considered significant. We used logistic regression analyses to investigate the correlation between changes in alcohol measures versus VCTE.
Results: We included 1397 participants with a mean time of 2.3 years (±0.6) between visits. Baseline age was 57 years (±9), 62% were male, and 18% had VCTE ≥8 kPa. At follow-up, changes in alcohol intake were more frequently detected by PEth than by self-report, both for increases (moderate: 24% vs. 10%; substantial: 14% vs. 3%) and decreases (moderate: 29% vs. 20%; substantial: 16% vs. 8%). For VCTE, 11% increased and 25% decreased. In univariable analyses, increased VCTE correlated with increased PEth (moderate: OR 1.59, 95% CI 1.11–2.28, p = 0.012; substantial: OR 1.96, 95% CI 1.30–2.98, p = 0.001), but was not correlated with self-reported alcohol intake (moderate: OR 1.04, 95% CI 0.60–1.80, p = 0.90; substantial: OR 0.75, 95% CI 0.27–2.12, p = 0.59). Neither decrease in PEth nor self-reported alcohol intake correlated with VCTE decrease. In multivariable analyses, PEth increases were the only predictors of VCTE increase (moderate: OR 1.61, 95% CI 1.11–2.34, p = 0.012 vs. substantial: OR 1.99, 95% CI 1.30–3.06, p = 0.002), while type 2 diabetes, BMI ≥30 kg/m^2, age, sex, and follow-up time were not.
Conclusion: Increasing phosphatidylethanol levels rather than self-reported alcohol consumption predicts worsening of liver stiffness in low-prevalence populations. Consequently, alcohol biomarkers may be the best suited tool for monitoring alcohol intake in patients with steatotic liver disease.

FRI-042

Current management of acute alcoholic hepatitis in France: results from a prospective cohort of 466 patients

Jean-François Cadranel[1], Thierry Thévenot[2], Armand Abergel[3], José Ursic Bedoya[4], Sarah Mouri[5], Jerome Boursier[6], Noemi Reboux[7], Nicolas Carbonell[8], Marco Vano[9], Moana Gelu-Simeon[10], Marika Rudler[5], Francois Durand[9], Honore Zougmore[1], Philippe Pulwermacher[1]. *[1]Ghpso Creil, Creil, France; [2]Chu Besançon, Besançon, France; [3]Chu Clermont-Ferrand, Cournon-d'Auvergne, France; [4]Chu Montpellier, Montpellier, France; [5]CHU Pitié Salpêtrière, Paris, France; [6]Chu Angers, Angers, France; [7]Internat La Cavale Blanche, Brest, France; [8]CHU Saint-Antoine Paris, Paris, France; [9]CHU Beaujon, Clichy, France; [10]CHU Pointe à Pitre, Pointe à Pitre Guadeloupe, France*
Email: jeanfrancois.cadranel@ghpso.fr

Background and aims: The objectives of this prospective multicentre study conducted in general hospitals, university hospitals were to collect the results of a prospective cohort of patients (pts) with acute alcoholic hepatitis (AAH), focusing, in cases of severe AAH, on the role of transjugular liver biopsy (TLB), treatment with N-acetylcysteine (NAC), prolonged corticosteroid (C) therapy in cases with an

intermediate Lille score on day 7, and transfer to a liver transplant centre (LTC).
Method: From October 2022 to March 2024, a pre-established anonymous Google questionnaire to be completed for each patient with AAH was sent to participating departments. Patients with severe AAH are the subject of this analysis. The results were expressed as mean ± standard deviation; a multivariate analysis was performed. The study focused on liver biopsy requierment, and use of N Acetylcystein and criteria for transfer to liver transplant center.
Results: 358 patients with severe AHF were included in this analysis. 266 (64.3%) were from a university hospital. Mean age 54 years (10). H 246 (74.2%). Mean TP 37% (12.3). The Maddrey score was 68.5 (45.4). 86.4% of patients were in Pugh stage C. Average MELD score 25.4 (6.34). 82.1% underwent TLB (215). TLB was performed much more often in university hospitals than in general hospitals (215 (82.1) vs 56 (51), p < 0.01). There was no difference in the use of NAC between university hospitals and general hospitals. Sixty-nine patients (19.2%) received NAC-C treatment. The PT of these patients was lower, 33.4 (11.6) vs. 37.5 (12), p = 0.01. 87 patients (24.3%) were transferred to a TC. Transfer to a TC was much more common in patients followed at a CHU: 78 (30%) vs. 9 (10%), p < 0.001; in cases of high MELD score (1.01 [1 to 1.01, p = 0.0013], Child-Pugh score C (3.75 [1.45–13.1, p = 0.001]. Transfer to TC was also more common in cases where C was discontinued in the event of an intermediate score on day 7: 4.70 [2.27–10.6, p < 0.01]; whereas patients who received NAC were transferred less often (9.52%, 23%) [0.36–0.15, 0.75, p < 0.02]. In multivariate analysis, transfer to TC was less common in cases treated with NAC-C (0.14 [0.04–0.5, p = 0.003]) and more common in cases where C was discontinued on day 7 in cases with an intermediate score (3.58 [1.27–10, p = 0.015]).
Conclusion: Potential benefits of routine LB, combination of NAC/C and prolongation in cases of intermediate Lille score to reduce transfers to liver transplant centers should be evaluated.

FRI-043
Sequential day-4 and day-7 Lille model to minimize unnecessary corticosteroid exposure in non-responders with severe alcohol-related hepatitis
Nicolas Conquet[1], Laura Weichselbaum[2], Nicolas Goossens[1], Marie Ongaro[1], Eric Trépo[2], Massimo Leo[1], Laurent Spahr[1], Christophe Moreno[2], Clemence Canivet[1]. [1]*Division of Gastroenterology, Hepatology and Nutrition, HUG, Geneva, Switzerland;* [2]*Department of Gastroenterology, Hepatopancreatology, and Digestive Oncology, Hôpital Universitaire de Bruxelles, Université Libre de Bruxelles, Brussels, Belgium*
Email: clemence.canivet@hug.ch

Background and aims: Early evaluation of corticosteroid response using the day-4 Lille Model (LM4) has been proposed as an alternative to the conventional day-7 assessment (LM7) in severe alcohol-related hepatitis (AH). However, a subset of patients classified as responders at LM4 subsequently become non-responders at LM7, a group associated with poorer prognosis. We aimed to assess, in a multicenter European cohort, the performance of a sequential LM4–LM7 strategy to predict 3-month mortality and reduce unnecessary corticosteroid exposure.
Method: We included biopsy-proven severe AH (Maddrey ≥32) from Geneva (12/2016–08/2024) and Brussels (07/2006–07/2015). Response was defined as LM <0.45. The primary endpoint was 3-month mortality (death or liver transplantation). A 2-step algorithm was developed in Geneva and validated in Brussels: (1) discontinuation of corticosteroids in LM4 non-responders; (2) among LM4 responders, discontinuation in LM7 non-responders. Data are expressed as median (IQR).
Results: *Derivation cohort (n = 64):* age of 54 (49–59) years, 67% male; baseline bilirubin 211 (108–309) µmol/L, INR 1.8 (1.6–1.9). *Validation cohort (n = 166):* age of 53 (46–58) years, 62% male; bilirubin 256 (142–410) µmol/L, INR 1.8 (1.6–2.2). Three-month mortality was 33% and 37%, respectively. In the derivation cohort: 42 (66%) and 38 (59%) patients were considered as responders at LM4 and LM7, respectively. Median LM4 and LM7 values were similar (0.36 vs 0.35; p = 0.87), with concordant responder/non-responder classification in 58/ 64 patients. In the validation cohort: 97 and 105 patients were considered LM4 and LM7 responders, respectively, with agreement in 152/166 patients. Median LM4 was 0.32 (0.16–0.64) and LM7 0.26 (0.09–0.62, p = 0.87). *Two-step algorithm*: LM4 allowed early corticosteroid discontinuation in 22 patients in the derivation cohort. LM7 reclassified 12% of LM4 responders (5/42) as non-responders, with 60% mortality. Overall, mortality was 16% in responders versus 56% in non-responders. In the validation cohort, 69 patients discontinued corticosteroids at day 4, and LM7 reclassified only 3 additional patients (66% mortality). Mortality remained markedly higher in non-responders than responders (61% vs 29%).
Conclusion: A sequential LM4–LM7 strategy enables earlier withdrawal of ineffective corticosteroid therapy without risk of undertreatment, while maintaining prognostic accuracy. Prospective studies are warranted to confirm its clinical utility.

FRI-044
Hot & cold fibrosis biomarkers as prognostic tools for assessment of cardiovascular and liver-related events in patients with alcohol-related liver disease
Andressa de Zawadzki[1], Maja Thiele[2], Stine Johansen[2], Ida Villesen[2], Peter Andersen[2], Ida Ziegler Spedtsberg[2], Morten Karsdal[1], Diana Julie Leeming[1], Aleksander Krag[2]. [1]*Nordic Bioscience Clinical Studies A, Herlev, Denmark;* [2]*Centre for Liver Research, Department of Gastroenterology and Hepatology, Odense University Hospital, Odense, Denmark, Department of Clinical Research, Faculty of Health Sciences, University of Southern Denmark, Odense, Denmark, Odense, Denmark*
Email: anza@nordicbio.com

Background and aims: Alcohol overuse increases the risk of alcohol-related liver disease (ALD) and cardiovascular disease (CVD). Patients with advanced ALD face higher risks of liver-related complications, CVD and infections. Non-invasive tests have been widely used to assess risk of liver-related outcomes, however, biomarkers to identify ALD patients at risk of CVD remain an unmet clinical need. This study evaluates the prognostic value of PRO-C6 (endotrophin), a fibroblast activity biomarker linking wound healing and fibrogenesis, combined with C4G (T cell activity biomarker, reflecting hot & cold fibrosis endotypes) for predicting cardiovascular and liver-related events in patients with ALD.
Method: Serum levels of nordicPRO-C6 (type VI collagen formation) and nordicC4G (type IV collagen fragment degraded by granzyme-B, a T cell specific protease) were assessed in the GALAXY EU funded cross-sectional cohort of 450 patients with biopsy-proven ALD including 5 years of follow up. The prognostic utility of baseline levels of PRO-C6 and C4G for CVD and decompensation was evaluated using Aalen–Johansen cumulative incidence curves with death as a competing risk. Fine–Gray models estimated hazard ratios across biomarker tertiles to define risk stratification cut-offs.
Results: In 450 patients with ALD, elevated levels of the fibroblast activity biomarker PRO-C6 were associated with an increased risk of CVD ($PRO\text{-}C6_{cutoff}$ = 8.0 ng/mL, HR_{CVD} = 2.35, p < 0.01) and decompensating events ($PRO\text{-}C6_{cutoff}$ = 11.2 ng/mL, $HR_{decompensation}$ = 4.87, p < 0.001). Increased C4G levels stratified ALD at higher risk of decompensation ($C4G_{cutoff}$ = 33.0 ng/mL, $HR_{decompensation}$ = 3.40, p < 0.01), without prognostic utility for CVD events. The ratio PRO-C6/C4G differed significantly between patients with and without CVD events (p < 0.001). Combined PRO-C6 and C4G cut-offs improved risk stratification, with lower C4G levels correlating to a poor CVD prognosis and higher C4G levels linked to higher risk of liver-related events.
Conclusion: Increased fibroblast activity is linked to higher risk of liver-related and cardiovascular events in patients with ALD. Furthermore, a distinct immune cell T-cell activity endotype

enables to stratify ALD patients at risk of specific clinical outcomes. Patients with decreased immune cell activity (cold fibrosis endotype) have a poorer prognosis for CVD outcomes, whereas those with increased immune cell activity (hot fibrosis endotype) have a higher risk of liver-related events.

FRI-050

Dynamics of steatotic liver disease subtype classification and predictors of significant fibrosis in Latin America: the STELLA study

Luis Antonio Diaz[1], Francisco Idalsoaga[2], Mário Pessoa[3], Claudia Pinto Oliveira[3], Patricia Momoyo Zitelli[3], Scherezada Mejia[4], Ezequiel Ridruejo[5], Mirta Peralta[6], Cesar Castro[7], Jorge Luis Garavito Rentería[7], Rommel Zambrano Huailla[7], Gustavo Ayares[2], Nancy Solis[2], Francisco Barrera[2], María Paz Orellana[2], Sebastián Marciano[8], Adrian Gadano[8], Jorge Martinez[8], María José Acosta[8], Martin Tagle[9], Hugo Cedrón[9], Ismael de Jesus Yepes Barreto[10,11], Dalis Pérez[10], Maria Saavedra[12], Samuel Perez[12], Estefanía Liza[13], Javier Diaz-Ferrer[13], Lorena Castro[14], Loreto Aguilar[14], Roberto Pérez Ravier[15], María Belen Martínez[15], Natalie Vilcinskas Y Botteron[15], Manuel Mendizabal[16], Daniela Simian[17], Juan Pablo Roblero[17], Pamela Gil[17], Arun J. Sanyal[18], Juan Pablo Arab[18], Marco Arrese[2]. *[1]University of California San Diego, La Jolla, United States; [2]Pontificia Universidad Católica de Chile, Santiago, Chile; [3]Hospital das Clínicas da Faculdade de Medicina da U S P, São Paulo, Brazil; [4]Hospital Juárez De México, Ciudad de México, Mexico; [5]Centro de Educación Médica e Investigaciones Clíni, Buenos Aires, Argentina; [6]Hospital De Infecciosas Francisco Muñiz, Buenos Aires, Argentina; [7]Hospital Nacional Arzobispo Loayza, Lima, Peru; [8]Hospital Italiano de Buenos Aires, Buenos Aires, Argentina; [9]Clínica Anglo Americana, San Isidro, Lima, Peru; [10]Centro Médico Gastropack, Cartagena, Colombia; [11]UNIVERSIDAD DE CARTAGENA, Cartagena, Colombia; [12]Clínica Ces, Medellín, Colombia; [13]Hospital Edgardo Rebagliati Martins, Lima, Peru; [14]Clínica Universidad de Los Andes, Santiago, Chile; [15]Hospital Central de Mendoza, Mendoza, Argentina; [16]Hospital Universitario Austral, Pilar, Argentina; [17]Hospital Clínico Universidad de Chile, Santiago, Chile; [18]Virginia Commonwealth University, Richmond, United States*
Email: luisdiazpiga@gmail.com

Background and aims: Latin America is underrepresented in prospective steatotic liver disease (SLD) studies despite a high metabolic burden. This multinational study aims to identify the main predictors of significant fibrosis among adults with SLD in Latin America.

Method: Cross-sectional analysis of prospectively enrolled adults with SLD (2023 criteria) at 14 tertiary centers in six countries (Argentina, Brazil, Chile, Colombia, Mexico, and Peru). We recorded self-reported alcohol intake and the Chilean Mediterranean Dietary Index (MDI, adapted for regional use). Fibrosis was assessed by liver biopsy and/or vibration-controlled transient elastography (VCTE). Significant fibrosis was defined as ≥F2 on biopsy or VCTE ≥8 kPa (if biopsy unavailable). Predictors of significant fibrosis were examined using binary logistic regression, including age, sex, ethnicity, body mass index (BMI), type 2 diabetes mellitus (T2DM), MDI, family history of advanced fibrosis, and SLD subtype.

Results: We included 634 participants (median age 63 [54–70] years; 59.8% women; 42.2% self-reported Hispanic/Latino ethnicity; 22.0% had a first-degree relative with advanced fibrosis). The median BMI was 30.3 [26.9–33.9] kg/m^2, and the T2DM prevalence was 46.9%. The median alcohol intake was 0 [0–28] g/week. Based on prior clinician-assigned SLD subtype, 85.3% were MASLD, 5.7% MetALD, and 9.0% ALD. At enrollment, 62.8% with prior MetALD reported alcohol intake within the MASLD alcohol range, while 52.6% and 43.9% with prior ALD were within the MASLD and MetALD alcohol ranges, respectively. Significant fibrosis prevalence was 49.7%. In the adjusted model, age (OR 1.03, 95% CI 1.00–1.06; p = 0.023), Hispanic/Latino ethnicity (OR 3.61, 95% CI 1.67–7.78; p = 0.001), T2DM (OR 4.41, 95% CI 2.31–8.42; p < 0.0001), ALD (reference MASLD; OR 21.85, 95% CI 4.18–114.18; p < 0.0001), and family history of advanced fibrosis (OR 2.30, 95% CI 1.11–4.76; p = 0.025) were independently associated with higher odds of significant fibrosis, whereas higher MDI adherence was associated with lower odds (OR 0.77, 95% CI 0.65–0.92; p = 0.004).

Conclusion: In this multicenter study, significant fibrosis was mainly associated with ALD, T2DM, older age, and family history, while higher Mediterranean diet adherence was protective. Lower self-reported alcohol intake at enrollment than implied by prior diagnoses highlights the need for longitudinal ascertainment of prior alcohol exposure to improve SLD subtype classification and clinical decision-making (FONDECYT 1241450).

FRI-051

Medications for alcohol use disorder after liver transplantation in the US: patterns, timing, and survival

Wei Zhang[1], Luis Antonio Diaz[2], Cassy Sun[3], Kelly Hsu[4], Stephanie Mrowczynski[5], Heidi Yeh[6], Ana Ivkovic[7], Peng-Sheng Ting[5], Emily Bethea[7], Giuseppe Morelli[5]. *[1], Newton, United States; [2]University of California San Diego, Pontificia Universidad Católica de Chile, La Jolla, United States; [3]Harvard T.H. Chan School of Public Health, Boston, United States; [4]Tuft University School of Medicine, Boston, United States; [5]Tulane School of Medicine, New Orleans, United States; [6]Division of transplant surgery, Massachusetts General Hospital, Boston, United States; [7]Massachusetts General Hospital, Boston, United States*
Email: wzhang50@mgh.harvard.edu

Background and aims: Alcohol-associated liver disease (ALD) is now the leading indication for liver transplantation (LT). Up to 20% of LT recipients resume alcohol use within 1 year and 30–40% within 5 years, worsening graft outcomes and long-term prognosis. Despite this high risk, post-transplant use of medications for alcohol use disorder (MAUD) has not been systematically evaluated. We aimed to characterize real-world MAUD prescribing after LT and examine its association with post-transplant mortality.

Method: We conducted a retrospective cohort analysis of adults transplanted for ALD at two liver transplant centers in the United States. We fit a Cox proportional hazards model with time since LT (days) as the analysis time. Covariates were age at LT, sex, race, Model for End-Stage Liver Disease (MELD) score at LT, any documented post-LT alcohol relapse, and MAUD use. The endpoint was time to death after LT.

Results: We included 274 recipients; the median age at LT was 55.2 years (IQR 44.9–61.7), 29.2% were women, and 91.2% were White or Caucasian. The median follow-up was 4.4 years (IQR 2.6–6.5). Post-LT MAUD was prescribed in 21.2% of patients. Among patients who received MAUD, the most common therapies after LT were naltrexone (72.4%), acamprosate (27.6%), gabapentin (20.7%), and topiramate (5.2%). Some patients received more than one MAUD. Among MAUD initiators, 34.8% started treatment before relapse and 65.2% after relapse. In the adjusted model, alcohol relapse was independently associated with a higher hazard of mortality (HR 4.00; 95% CI 1.15–13.92; p = 0.029). Age, sex, race, and MELD at LT were not significant predictors. MAUD use showed a non-significant trend toward lower mortality (HR 0.31; 95% CI 0.06–1.57; p = 0.159).

Conclusion: In this cohort study, the use of MAUD after LT in ALD remains low and was commonly initiated reactively after alcohol relapse. Alcohol relapse after LT strongly predicted adverse outcomes, whereas receipt of MAUD was associated with a favorable but non-significant association with survival. These findings support the systematic integration of MAUD into routine post-LT care and support multicenter evaluation of this approach.

FRI-052

The impact of early alcohol abstinence on further decompensation in alcohol-associated liver disease

Diego Drumond Westgeest e Sousa[1], Yigit Yazarkan[1], Alberto Calleri[1], Blake Kassmeyer[2], Kamalpreet S. Hara[1], Tiffany Wu[1], Puru Rattan[1], Vijay Shah[1], Patrick S. Kamath[1], Douglas Simonetto[1]. [1]*Mayo Clinic, Division of Gastroenterology and Hepatology, Rochester, Minnesota, United States;* [2]*Mayo Clinic, Division of Clinical Trials and Biostatistics, Rochester, Minnesota, United States*
Email: diegowestgeest@gmail.com

Background and aims: Further decompensation is common in patients with cirrhosis and is associated with worse clinical outcomes. However, the impact of early alcohol abstinence and alcohol-associated hepatitis (AH) on subsequent decompensation in alcohol-associated liver disease (ALD) remains poorly defined. We aimed to assess the impact of early alcohol abstinence and AH on further decompensation in ALD.
Method: Consecutive adult patients hospitalized for decompensated ALD (2020–2024) were identified via the Rochester Epidemiology Project using validated ICD-9/10 codes with manual confirmation. AH was defined according to NIAAA criteria. Cumulative incidence of further decompensation was estimated using competing-risk methods, with death, liver transplantation, and TIPS treated as competing events. The effect of further decompensation on mortality was assessed using time-dependent Cox models. Landmark analyses at 3 months evaluated the impact of alcohol abstinence on further decompensation using adjusted cause-specific Cox models.
Results: A total of 121 patients were included; 90 (74.4%) were male, with a median age of 58 years (IQR, 46.1–66.0). Ascites was the most common initial decompensation, followed by encephalopathy and variceal bleeding, and 24 (19.8%) patients presented with multiple events at first hospitalization. Median follow-up was 23.8 months (IQR, 5.0–47.0), during which further decompensation occurred in 87 (71.9%) patients after a median of 3.7 months (IQR, 1.3–8.6). The cumulative incidence of further decompensation did not differ between patients presenting with single versus multiple initial decompensation events (Gray's test $p = 0.39$). In time-dependent Cox models, further decompensation was associated with a significantly higher risk of all-cause mortality (HR 5.39, 95% CI 2.46–11.81; $p < 0.001$). In adjusted cause-specific Cox models, alcohol abstinence within 3 months was independently associated with a reduced hazard of further decompensation (HR 0.40, 95% CI 0.20–0.81; $p = 0.01$), while older age and the presence of AH were associated with increased risk (HR 1.04, 95% CI 1.02–1.07; $p < 0.001$ and HR 2.50, 95% CI 1.31–4.80; $p = 0.006$, respectively).
Conclusion: Further decompensation strongly predicts mortality in ALD. Early alcohol abstinence within 3 months is associated with a reduced risk of subsequent decompensation, whereas the presence of alcohol-associated hepatitis identifies patients at higher risk, underscoring the need for closer follow-up and targeted interventions.

FRI-053

Alcohol-related hepatitis modifies the prognostic value of laboratory dynamics after abstinence in decompensated alcohol-related cirrhosis

Jan Embacher[1,2,3], Georg Semmler[1,2], Lorenz Balcar[1,2], Georg Kramer[1,2], Christian Sebesta[1,2], Paul Thöne[1,2], Marlene Hintersteininger[1,2], Lukas Hartl[1,2], Mathias Jachs[1,2], Benedikt Simbrunner[1,2,3], Daniel König[4,5], Michael Trauner[1,2], Mattias Mandorfer[1,2], Thomas Reiberger[1,2,3], Benedikt Hofer[1,2,3]. [1]*Division of Gastroenterology and Hepatology, Department of Medicine III, Medical University of Vienna, Vienna, Austria;* [2]*Clinical Research Group MOTION, Medical University of Vienna, Vienna, Austria;* [3]*Christian Doppler Lab for Portal Hypertension and Liver Fibrosis, Medical University of Vienna, Vienna, Austria;* [4]*Department of Psychiatry and Psychotherapy, Medical University of Vienna, Vienna, Austria;* [5]*Comprehensive Center for Clinical Neurosciences and Mental Health, Medical University of Vienna, Vienna, Austria*
Email: jan.embacher@meduniwien.ac.at

Background and aims: Alcohol abstinence improves outcome and facilitates hepatic recompensation in alcohol-related cirrhosis (ALD). Although disease severity determines recompensation, lab-based surrogates of hepatic function may be unreliable in severe-acute conditions such as alcohol-related hepatitis (AH). We therefore evaluated the context-dependent prognostic value of MELD and albumin at abstinence and 90 days (D90) for predicting recompensation (Baveno VII) and liver-related death (LRD).
Method: Patients with decompensated ALD who achieved abstinence and had paired laboratory assessments at baseline (time of abstinence) and after 90 (±30) days of abstinence were included. Alcohol relapse and liver transplantation were treated as competing events.
Results: Among 100 patients (72% male, median age 54 years), 56 presented with AH at baseline. Patients with AH were younger (52 vs. 58 years) and showed higher baseline levels of bilirubin, AST, and INR. At D90, a 20% decrease in MELD was more common in patients with AH (70% vs. 39%), whereas a 20% increase in albumin occurred at a similar rate (43% vs. 50%). Over a median follow-up of 43 months, 24% of patients recompensated, and 16% experienced LRD. In patients without baseline AH, neither baseline MELD or albumin were associated with recompensation, while both D90-MELD and D90-albumin showed a trend (SHR 0.89, $p = 0.063$; SHR 1.08, $p = 0.092$) in a competing-risks regression analysis and D90-MELD predicted LRD (SHR 1.16, $p < 0.001$). In contrast, a 20% MELD decrease strongly predicted recompensation (SHR 4.60, $p = 0.020$). This effect was further amplified by concomitant 20% albumin increase (SHR 8.31, $p < 0.001$), while 20% albumin increase alone only showed a trend (SHR 2.99, $p = 0.095$). No LRD occurred among patients without AH achieving combined MELD/albumin improvement. In AH patients, neither baseline nor D90 values predicted recompensation, yet D90-albumin (SHR 0.84, $p = 0.005$) and D90 MELD (SHR 1.18, $p = 0.003$) predicted LRD. Further, while a 20% MELD decrease was numerically linked to recompensation (SHR 2.98, $p = 0.147$), and LRD (SHR 0.27, $p = 0.065$), there was no association for albumin dynamics.
Conclusion: While the prognostic value of lab-based surrogates of hepatic function in patients with decompensated ALD at the time of abstinence is limited by concomitant AH, re-assessment after 90 days of abstinence and evaluation of early biochemical improvements substantially improve prognostic accuracy.

FRI-054

Community-based alcohol-related liver disease early recognition and assessment (CALDERA): effect on drinking behaviour, markers of liver injury and emergency hospital attendance

Callum Higgins[1], Peter Strathern[1], Cherry Fung[1], Kirsty McCaughey[1], Aileen Billsdon-McGrane[2], Claire Kerr[2], Derek Scollon[2], Ewan H Forrest[1,3]. [1]*University of Glasgow, Glasgow, United Kingdom;* [2]*Department of Gastroenterology, Glasgow Royal Infirmary, Glasgow, United Kingdom;* [3]*Glasgow Royal Infirmary, Glasgow, United Kingdom*
Email: ewan.forrest@ggc.scot.nhs.uk

Background and aims: Early detection of alcohol-related liver disease (ALD) is vital to prevent progressive liver damage. This study assessed the effects of liver assessment including vibration controlled transient elastography (VCTE) in patients with alcohol use disorder (AUD) attending the community Glasgow Alcohol and Drug Recovery Service (GADRS).
Method: Liver assessment was available for patients attending the North East (NE) GADRS for AUD. This included VCTE by FibroScan to measure liver stiffness (LSM). Two patient cohorts were studied. Cohort 1 consisted of patients who attended community GADRS between July and October 2024 and compared those who had a liver assessment with those who had not. Any cause hospital Emergency

Department (ED) attendance in the year prior to and after initial ADRS review was recorded. Cohort 2 consisted of patients who attended NE GADRS between 2019 and January 2025 who had more than one liver assessment. Estimated alcohol use (UK units) in the week prior to each assessment was noted and changes in LSM were annualised. Again, ED attendance in the year prior to and after the index assessment was recorded. Results are expressed with 95% Confidence Intervals.
Results: In Cohort 1, 98 patients had a liver assessment group and 119 did not. In the year after assessment there was an absolute reduction in ED attendances by 37 (20%) in those who had a liver assessment compared with a fall of 5 (2%) ED attendances in those who didn't ($p < 0.001$). In Cohort 2, 112 patients had had follow-up VCTE with a median interval of 0.91 (0.73, 1.10) years. The median baseline LSM was 6.2 (5.4, 7.4): 41 (36%) had a LSM >8 kPa and 15 (13%) >12 kPa. On comparison between those with high LSM (>8 kPa) and those with low LSM (<8kPa) at index assessment, there was a reduction in follow-up LSM (-1.39 *vs* 0.22 kPa; $p = 0.012$) and alcohol use (−70 *vs* 0.0 units; $p = 0.003$) amongst high LSM patients. High LSM patients had a reduction in ED attendances by 10 (14%) compared with a rise of 16 (11%) ED attendances in low LSM patients ($p < 0.001$).
Conclusion: Detection of advanced ALD is feasible in the community using VCTE. After liver assessment, emergency hospital attendance fell compared with those who did not have a liver assessment. In those who had repeat liver assessments, the fall in ED attendance was most obvious in those with a high baseline LSM. Those with high initial LSM were also more likely to reduce their alcohol consumption and improve their LSM reading on follow-up.

FRI-055
Alcohol-metabolite associations differ by liver steatosis status: a metabolomics study in finnish men
Konsta Hakkarainen[1,2], Fredrik Åberg[3], Lilian Fernandes Silva[2], Anniina Oravilahti[2], Taru Tukiainen[2], Markku Laakso[2], Ville Männistö[1,2]. *[1]Department of Medicine, Kuopio University Hospital, Kuopio, Finland; [2]Faculty of Health Sciences, School of Medicine, Institute of Clinical Medicine, University of Eastern Finland, Kuopio, Finland; [3]Transplantation and Liver Surgery, Helsinki University Hospital and University of Helsinki, Helsinki, Finland*
Email: konsta.hakkarainen@gmail.com

Background and aims: Recent studies have shown that alcohol-induced liver injury is amplified in the presence of steatotic liver disease, but the underlying metabolic alterations remain poorly characterized. We examined whether liver steatosis modifies the associations between alcohol consumption and circulating plasma metabolites in a large population-based cohort of men.
Method: A total of 10188 middle-aged men (mean age 57.5 ± 7.1 yrs, mean BMI 27.9 ± 4.8 kg/m2, mean alcohol use 105.8 ± 141.7 g/wk) from the METabolic Syndrome In Men (METSIM) study were classified as having non-steatotic or steatotic liver using Fatty Liver Index (FLI, <30 vs. >60), with validation using Hepatic Steatosis Index (HSI, <30 vs. ≥36). Plasma metabolites were quantified using the Metabolon Global Discovery panel. Alcohol-metabolite associations were assessed by regression models with multiple confounder adjustment. Overlap weighting was performed to consider differences in alcohol use distributions between liver steatosis groups. The Benjamini-Hochberg Procedure was used for multiple testing correction.
Results: Of 1259 metabolites, a total of 222 showed statistically significant differences in the alcohol–metabolite interaction between steatosis groups, consistently identified using both FLI and HSI (Benjamini-Hochberg-corrected p-values from 0.048 to 2.4×10^{-42}). Of these metabolites, 57% were lipids, 21% xenobiotics, and 13% amino acids, with the remaining metabolites distributed across smaller pathway categories. Several metabolites considered to have protective effects against oxidative stress (such N-acetylglycine and N-acetylmethionine), showed a weaker alcohol-associated increase in individuals with liver steatosis, suggesting a possible reduced hepatic capacity to counteract oxidative stress in steatosis. Interestingly alcohol interaction with theanine, previously reported to have protective effects against alcohol-induced liver injury, was similarly lower. In contrast, several lipids demonstrated stronger alcohol-associated increases in liver steatosis.
Conclusion: Differences in alcohol-metabolite associations between those with and without liver steatosis suggest increased susceptibility to alcohol-related toxicity in individuals with steatosis. These findings support the concept that steatosis alters systemic metabolic responses to alcohol, potentially contributing to elevated liver injury risk.

FRI-056
The evaluation of a novel multidisciplinary hepatology clinic
Gideon Hanibal[1], Heather Lewis[1]. *[1]Department of Hepatology, St Mary's Hospital, Imperial College Healthcare NHS Trust, London, United Kingdom, London, United Kingdom*
Email: gideon.hanibal21@imperial.ac.uk

Background and aims: Alcohol-related liver disease (ALD) is a leading cause of liver morbidity and mortality, intrinsically linked with alcohol use disorder (AUD). Multidisciplinary care models integrating hepatology and addiction services may improve patient outcomes, but direct comparisons to standard hepatology care are limited. This retrospective study evaluated the effectiveness of a multidisciplinary alcohol hepatology clinic versus a general hepatology clinic in reducing alcohol consumption and improving clinical-related outcomes in ALD patients.
Method: Data from 142 patients (71 per cohort) attending a multidisciplinary alcohol clinic or a general hepatology clinic at St Mary's Hospital were analysed. Demographics, alcohol consumption, abstinence rates, Fibroscan Liver Stiffness Measurement (LSM) and Fibroscan Controlled Attenuation Parameter (CAP) scores were collected pre- and post-clinic intervention. Use of pharmacological treatment for AUD was also recorded. Statistical significance was set at $p < 0.05$.
Results: Both clinics showed significant reductions in weekly alcohol consumption (multidisciplinary: mean 65.2 to 35.8 units/week, $p < 0.01$; general hepatology: 65.2 to 54.4 units/week, $p = 0.03$). When comparing clinics, the multidisciplinary clinic achieved a significantly greater median reduction in consumption (30 vs 14 units/week, $p = 0.03$) and higher abstinence rates (41.7% vs 19.1%, $p = 0.02$). Pharmacological treatment use was also significantly higher in the multidisciplinary clinic (50.7% vs 4.41%, $p < 0.01$). Fibroscan LSM improved significantly in the multidisciplinary cohort (median 14.3 to 10.1 kPa, $p = 0.01$), but not in the general hepatology clinic. No significant changes were observed in Fibroscan CAP scores.
Conclusion: The multidisciplinary clinic demonstrated superior improvements in alcohol reduction, abstinence, pharmacotherapy use and liver fibrosis. However, its retrospective design and baseline cohort differences limit comparability and generalisability, warranting future prospective, multi-centre research. This pilot study supports multidisciplinary clinics as an effective model for improving alcohol and clinical-related outcomes in ALD patients. Larger, prospective studies are necessary to support broader clinical implementation.

FRI-057
Postbiotic-driven enhancement of the gut barrier reduces systemic inflammation in patients with alcohol-related liver disease
Johanne Kragh Hansen[1,2], Mads Israelsen[1,2], Evelina Stankevic[3], Suguru Nishijima[4], Sara Stinson[3], Peter Andersen[1,2], Stine Johansen[1,2], Camilla Dalby Hansen[1,2], Ida Villesen[1,2], Katrine Thorhauge[1,2], Nikolaj Torp[1,2], Marisa Isabell Keller[3], Gitte Hedegaard Jensen[5], Sönke Detlefsen[2,5], Diana Julie Leeming[6], Andressa de Zawadzki[6], Michael Kuhn[4], Morten Karsdal[6],

Jonel Trebicka[7,8], Hans Israelsen[9], Cristina Legido-Quigley[10,11], Peer Bork[4,12,13], Manimozhiyan Arumugam[2,3], Torben Hansen[3], Maja Thiele[1,2], Aleksander Krag[1,2]. *[1]Department of Gastroenterology and Hepatology, Centre for Liver Research, Odense University Hospital, Odense, Denmark; [2]Department of Clinical Research, Faculty of Health Sciences, University of Southern Denmark, Odense, Denmark; [3]Novo Nordisk Foundation Center for Basic Metabolic Research, Faculty of Health and Medical Sciences, University of Copenhagen, Copenhagen, Denmark; [4]Molecular Systems Biology Unit, European Molecular Biology Laboratory, Heidelberg, Germany; [5]Department of Pathology, Odense University Hospital, Odense, Denmark; [6]Nordic Bioscience A/S, Biomarkers & Research, Herlev, Denmark; [7]Department of Internal Medicine B, University of Münster, Münster, Germany; [8]European Foundation for the Study of Chronic Liver Failure, Barcelona, Germany; [9]Nordic Rebalance A/S, Hillerød, Denmark; [10]Steno Diabetes Center Copenhagen, Herlev, Denmark; [11]Institute of Pharmaceutical Science, King's College London, London, United Kingdom; [12]Max Delbrück Centre for Molecular Medicine, Berlin, Denmark; [13]Department of Bioinformatics, Biocenter, University of Würzburg, Würzburg, Germany*
Email: johanne.kragh.hansen@rsyd.dk

Background and aims: Gut barrier impairment is a driver of hepatic inflammation in alcohol-related liver disease (ALD) due to translocation of microbial products. However, microbial translocation may also cause systemic low-grade chronic inflammation. ReFerm®, an oat-based postbiotic fermented with *Lactobacillus plantarum* 299v, improves gut barrier integrity, but its impact on systemic inflammation is unclear. This post-hoc analysis of the GALA-POSTBIO trial examined associations between ReFerm®-induced barrier improvements and systemic inflammation in patients with ALD.
Method: In the randomized GALA-POSTBIO trial, 56 patients with advanced ALD were allocated 1:1 to ReFerm® or the control product Fresubin® (medical protein supplement) for 24 weeks. Systemic inflammation was assessed by plasma C-reactive protein (CRP). Intestinal barrier integrity was evaluated via plasma intestinal fatty acid–binding protein (I-FABP). Patients were classified as responders or non-responders based on a reduction in I-FABP relative to baseline.
Results: Median age was 63 years (IQR 57–67), 83% were male, and most had cirrhosis (F2/F3/F4: 4/15/33). Alcohol intake was similar between groups. Forty-one patients completed the study per protocol, with I-FABP results for 36. Baseline CRP was comparable (ReFerm® 1.8 mg/L (IQR 0.7–4.3) vs. Fresubin® 1.9 mg/L (IQR 1.1–3.6)). At 24 weeks, CRP decreased in the ReFerm® group (1.2 mg/L (IQR 0.6–2.2)) but increased in the Fresubin® group (2.5 mg/L (IQR 1.2–3.1)), with the between-group difference approaching significance ($p = 0.053$). Reduction in I-FABP, indicating improved gut barrier, was more frequent with ReFerm® (OR 5.2, 95% CI 1.25–21.57; $p = 0.044$). Among ReFerm® patients with decreased I-FABP, CRP was lower than in those with increased I-FABP (1.2 vs. 4.0 mg/L, $p = 0.06$), a pattern not seen in the Fresubin® group.
Conclusion: Postbiotic supplementation improved gut barrier integrity, which was associated with lower systemic inflammation in advanced ALD. These findings support further research in whether this effect is direct or mediated by improved liver inflammation.

FRI-058-YI

Prevalence and timing of comorbidities among patients with alcohol-related liver cirrhosis: a nationwide study of 11,989 patients with cirrhosis

Gustav Jakobsson[1,2], Ying Shang[2], Linnea Widman[2], Hannes Hagström[2,3]. *[1]Capio Sankt Görans Sjukhus, Stockholms Stad, Sweden; [2]Department of Medicine, Huddinge, Karolinska Institute, Huddinge, Sweden; [3]Division of Hepatology, Department of Upper GI, Karolinska University Hospital, Stockholm, Sweden*
Email: gustav.jakobsson@ki.se

Background and aims: Alcohol-related liver cirrhosis (ARLC) is the most severe and end-stage form of alcohol-related liver disease caused by long-term heavy alcohol consumption. ARLC seldom causes any symptoms before hepatic decompensation, leading to diagnosis at a late stage when the prognosis is dismal. Patients with ARLC may have a different set of comorbidities than the general population, thus identifying these comorbidities could allow for screening of pre-cirrhotic disease in specific patient groups. Our aim was to compare the prevalence of comorbidities among patients with ARLC and the general population and to assess the timing of comorbidity diagnoses relative to ARLC diagnosis.
Method: We used Swedish national registers to identify all new cases of ARLC (ICD-10 code: K70.3) from 2006 to 2020 (n = 11,989) with up to 10 controls (n = 113,657), matched on age, sex, and place of residence. Comorbidities were identified from 1998 to 2020 using ICD-codes from all in- and outpatient contacts with specialized care. To capture conditions primarily treated in primary care, we additionally used data on drug dispensation from the National Prescribed Drug register.
Results: At the time of ARLC diagnosis, the most prevalent comorbidities among cases were alcohol use disorder (51.3% vs 3.3% in the general population), hypertension (51.8% vs 37.7%), anemia (46.5% vs 15%), fractures (32.2% vs 14.7%) and depressive disorders (31.2% vs 16.1%). All differences were significant (p-value< 0.001). The median time to diagnosis of comorbidities before ARLC was 55.6 months for alcohol use disorder (IQR 17.3–108.9), 23.0 months for anemia (IQR 9.3–72.0), 78.5 months for hypertension (IQR 39.0–122.5), 71.7 months for fractures (IQR 30.3–124.7) and 67.0 months for depressive disorders (IQR 28.9–113.1).
Conclusion: Our study shows that the prevalence of comorbidities differs between patients with ARLC and the general population. Several of these comorbidities were diagnosed years before ARLC, suggesting that it is possible to identify high-risk groups where targeted screening for liver disease or targeted interventions could be possible and thereby modify disease progression. For instance, more than 50% of patients who later develop ARLC have a prior diagnosis of AUD, diagnosed at a median of 4 years before ARLC diagnosis. Our findings suggest a window of opportunity in which high-risk groups for future liver disease may be identified well before cirrhosis develops.

FRI-059

Limited overlap between high phosphatidylethanol, alcohol use disorder, and liver fibrosis in 6,231 individuals screened for steatotic liver disease

Stine Johansen[1,2], Katrine Tholstrup Bech[1,2], Helle Schnefeld[1,2], Johanne Kragh Hansen[1,2], Camilla Dalby Hansen[1,2], Ellen Lyngbeck Jensen[1,2], Ea Kyed[1,2], Markus Maagaard[1,2], Gunilla Calov[1,2], Mette Lehmann Andersen[1,2,3], Maria Fogt[1,2], Anine Andersen[1,2], Charlotte Mary Gjøl[1,2], Katrine Thorhauge[1,2], Peter Andersen[1,2], Ida Villesen[1,2], Nikolaj Torp[1,2], Maja Thiele[1,2], Aleksander Krag[1,2], Mads Israelsen[1,2]. *[1]FLASH - Centre for Liver Research, Department of Gastroenterology and Hepatology, Odense University Hospital, Odense, Denmark; [2]Department of Clinical Research, Faculty of Health Sciences, University of Southern Denmark, Odense, Denmark; [3]Department of Gastroenterology and Hepatology, Herlev Hospital, Herlev, Denmark*
Email: stine.johansen@rsyd.dk

Background and aims: Excessive alcohol intake is common, yet only a minority of individuals develop significant liver fibrosis. Conversely, many patients with alcohol-related liver disease (ALD) do not meet criteria for alcohol use disorder (AUD). Understanding of the co-existence is limited and based on self-reported alcohol intake, which is prone to underreporting. Phosphatidylethanol (PEth), a direct alcohol biomarker, allows for more accurate quantification of recent alcohol intake. We aimed to investigate how PEth implementation influences understanding of the relationship between liver fibrosis severity, AUD and alcohol intake.
Method: We conducted a prospective screening study including individuals from the general population or at risk of steatotic liver

disease due to excessive alcohol intake or metabolic dysfunction. Assessment included liver stiffness measurement (LSM), PEth, and risk of AUD using the Alcohol Use Disorders Identification Test (AUDIT). We estimated the prevalence and overlap of recent alcohol intake corresponding to MetALD (PEth 20–199 ng/mL) and high alcohol intake corresponding to ALD (PEth ≥200 ng/mL), high risk of AUD (AUDIT ≥16), and significant fibrosis (LSM ≥10 kPa).
Results: We investigated 6,231 individuals for steatotic liver disease. Median age was 57 (52–62) years, 52% were women and 28% reported excessive drinking for >5 years. At inclusion, 3.4% had LSM ≥10 kPa; 8.3% had AUDIT ≥16, 42% had PEth 20–199 ng/mL, and 17% PEth ≥200 ng/mL. In patients with significant fibrosis, high risk of AUD was found in 10% with MetALD and 49% with ALD. Conversely, among patients with high risk of AUD and high alcohol intake (AUDIT ≥16, PEth ≥200), 12% had significant fibrosis. Overlap between all three markers increased was limited: fewer than 3% (38 of 1,363) had AUDIT ≥16, LSM ≥10 kPa, and PEth ≥200 ng/mL concurrently. Both AUDIT ≥16 and PEth ≥200 ng/mL were associated with an increased risk of significant fibrosis ($OR_{AUDIT\ \geq 16}$: 1.37 (95%CI 1.04–1.70), p < 0.001) & $OR_{PEth\ \geq 200}$: 1.10 (95%CI 0.81–1.39), p < 0.001).
Conclusion: High PEth, high AUDIT scores, and increased LSM display limited overlap, indicating that self-reported high risk of alcohol use disorder, objective high alcohol intake, and liver fibrosis identify largely distinct patient groups. Only 1 in 10 with high PEth and high risk of AUD have significant liver fibrosis. In contrast, 10 to 50% of those with elevated PEth and significant fibrosis are at high risk of AUD.

FRI-060
Cardiometabolic risk factors are not associated with lower lifetime alcohol consumption in newly diagnosed patients with alcohol-related liver disease: a clinical cohort study
Linnea Juhl Vestergaard[1], Gro Askgaard[1], Lone Galmstrup Madsen[1], Peter Jepsen[2], Anna Emilie Kann[1], Jonas Hedelund Rønn[1]. *[1]Zeland University Hospital, Naestved, Denmark; [2]Aarhus University Hospital, Aarhus, Denmark*
Email: linve@regionsjaelland.dk

Background and aims: It is thought that cardiometabolic risk factors (CMRFs) act synergistically with alcohol consumption in the development of cirrhosis. Therefore, patients with CMRFs might develop alcohol-related liver disease at a lower level of alcohol consumption.
We aimed to assess whether a lower lifetime alcohol consumption was associated with CMRFs in newly diagnosed patients with alcohol-related liver disease (ALD).
Method: We included patients with newly diagnosed ALD at Zealand University Hospital, Denmark, 2021–2025. All patients underwent a standardized clinical assessment, including anthropometrics, biochemical tests (including Phosphatidyl ethanol [PEth]), and transient elastography. Lifetime alcohol consumption was assessed by the Lifetime Drinking History interview. CMRFs included obesity (BMI ≥30), hypertension, diabetes, and dyslipidemia (treated or measured). One standard drink equaled 12 g of pure ethanol. We used logistic regression to estimate odds ratios (OR) for CMRFs according to lifetime alcohol consumption, adjusted for sex, age and Child-Pugh class.
Results: Among 109 patients with ALD, 76% were men, mean age was 62 years, and 74.7% had cirrhosis. Patients reported a median lifetime alcohol consumption of 53,952 drinks (IQR: 31,968; 84,984) over a median of 41 drinking years, corresponding to a median weekly consumption of 25 drinks (IQR: 14; 41) during drinking periods. Median PEth was 0.22 micromole/L (IQR: 0.01; 1.21). Number of CMRFs was 0 or 1 in 46% of patients, 2 in 32%, and 3 or 4 CMRFs in 23% of patients. The median number of CMRFs was 1 for patients with a lifetime alcohol consumption of < 45,000 drinks and 2 for patients with a lifetime alcohol consumption of 45,000–70,000 drinks and ≥ 70,000 drinks. Lifetime alcohol consumption was not associated with CMRFs with adjusted ORs of 1.41 (95% CI: 0.48–4.08) for obesity, 2.23 (0.80–6.19) for diabetes, 1.18 (0.49–2.86) for hypertension, and 1.56 (0.66–3.70) for dyslipidemia when a lifetime alcohol consumption of ≥ 45,000 drinks was compared to < 45,000 drinks. Patients with 3–4 CMRFs vs 0–2 CMRFs tended to have a higher lifetime alcohol consumption of ≥ 45,000 vs. < 45,000 (OR of 3.18 [0.99–10.2], p = 0.051).
Conclusion: Cardiometabolic risk factors were not associated with lower lifetime alcohol consumption in newly diagnosed ALD patients. On the contrary, having multiple cardiometabolic risk factors tended to be associated with higher lifetime alcohol consumption.

FRI-061
Hazardous alcohol use amongst persons with compensated cirrhosis from different etiologies: a liver cirrhosis network study
Mandana Khalili[1], Miranda Gurra[2], Douglas Simonetto[3], Norah Terrault[4], Lauren Bonner[2], David Goldberg[5], Jasmohan Bajaj[6], Arun J. Sanyal[6], Nicole Welch[7], Bilal Hameed[1], Neehar D. Parikh[8], Elliot Tapper[8], Rohit Loomba[9], Monica Tincopa[9], Patricia Jones[5], Elizabeth Verna[10], Robert S. Brown, Jr.[11], Cynthia Moylan[12], Patrick S. Kamath[3], Matthew Robert Kappus[12], Srinivasan Dasarathy[7]. *[1]University of California San Francisco, San Francisco, United States; [2]Northwestern University, Chicago, United States; [3]Mayo Clinic, Rochester, United States; [4]University of Southern California, Los Angeles, United States; [5]University of Miami, Miami, United States; [6]Virginia Commonwealth University, Richmond, United States; [7]Cleveland Clinic, Cleveland, United States; [8]University of Michigan, Ann Arbor, United States; [9]University of California San Diego, La Jolla, United States; [10]Columbia University, New York, United States; [11]Cornell University, New York, United States; [12]Duke University, Durham, United States*
Email: mandana.khalili@ucsf.edu

Background and aims: Alcohol-associated liver disease (ALD) is the most common etiology of cirrhosis in the United States. We aim to describe alcohol use among a large prospectively assembled cohort of patients living with cirrhosis and different etiologies of liver disease.
Method: Baseline demographics, clinical characteristics, and alcohol use in adults (≥18 years) with compensated cirrhosis enrolled in 10 U. S. centers within Liver Cirrhosis Network (LCN) Cohort Study were assessed. Etiology of liver disease was investigator assigned and categorized as ALD, metabolic-dysfunction associated liver disease (MASLD), viral hepatitis, ALD + another etiology (combo-ALD), and other. Alcohol Use Disorders Identification Test -Consumption (AUDIT-C) evaluated alcohol use in past 12 months. In those with positive AUDIT-C score (3+ in women, 4+ in men), full AUDIT was performed.
Results: Among 1205 participants, characteristics were: median age 62 (IQR 52, 69) years, 50% male, 75% White, 27% Hispanic, 30% with high school or less education, and 44% employed. Overall, 8.7% had positive AUDIT-C score and 277 (23%) had an ALD or combo-ALD etiology. Eight patients with MASLD had alcohol use levels that met MetALD criteria. A significant proportion of ALD (26%) or combo-ALD (22%) had positive AUDIT-C score vs. MASLD (3.4%), viral hepatitis (5.9%), and other etiology (4.3%). Among those with positive AUDIT-C and ALD or combo-ALD, 61% and 28%, respectively, had high-risk or greater drinking (AUDIT score 16+). Among the ALD subgroups, a higher proportion had a history of prior cirrhosis decompensation compared to non-ALD (22% vs. 4%). On vibration-controlled transient elastography, the mean CAP score in ALD and combo-ALD was lower compared to MASLD (median [IQR] = 249 [211, 281] and 260 [229, 298] vs. 282 [246, 316], respectively), and 43% and 37% had no steatosis (vs. 20% in MASLD). Similarly, among 514 with MR elastography, the proton density fat fraction was lower in ALD and combo-ALD vs MASLD (median = 2.8% and 3.6% vs. 5.5%) despite similar mean liver stiffness measures (median = 5.1 and 4.6 vs. 5.1 kPA).
Conclusion: At LCN entry, overall, 8.7% of participants with compensated cirrhosis and 23% of ALD groups had a positive

AUDIT-C score, with nearly two-thirds of ALD group reporting high-risk drinking. This highlights the importance of screening for alcohol use among those with cirrhosis in order to provide interventions to reduce alcohol intake in this at-risk population.

FRI-062

Impact of on-demand nalmefene–mediated alcohol reduction on liver function and noninvasive fibrosis and steatosis measures in patients with alcohol use disorder and metabolic dysfunction–associated alcohol-related liver disease

Yohei Koizumi[1,2], Masashi Hirooka[2], Yoichi Hiasa[2]. [1]*Koizumi Clinic, Yawatahama, Ehime, Japan;* [2]*Department of Gastroenterology and Metabology, Ehime University Graduate School of Medicine, Toon, Ehime, Japan*
Email: shachiyo2@yahoo.co.jp

Background and aims: Patients with metabolic dysfunction–associated alcohol-related liver disease (MetALD) are at risk of progressive hepatic steatosis and fibrosis due to the combined effects of metabolic dysfunction and ongoing alcohol consumption. Early-stage, patient-centered alcohol reduction strategies and reliable tools for short-term treatment monitoring are needed in this emerging disease entity. This study aimed to evaluate the impact of on-demand nalmefene–mediated alcohol reduction on alcohol consumption and its effects on liver function and noninvasive elastography-based measures of hepatic fibrosis and steatosis in patients with alcohol use disorder (AUD) and MetALD.
Method: This pilot study included 48 patients with MetALD and 55 patients with metabolic dysfunction–associated steatotic liver disease (MASLD) as a control group. Patients with MetALD received on-demand nalmefene (18 mg), self-administered on days perceived to carry a high risk of alcohol consumption, over a 24-week period, while MASLD patients underwent standard lifestyle intervention. Liver function tests, liver stiffness assessed by shear wave elastography, and hepatic fat quantification using attenuation imaging were evaluated at baseline and at 12 and 24 weeks.
Results: All patients in the MetALD group received at least one dose of nalmefene, and 42 completed the 24-week follow-up. Monthly heavy drinking days decreased by a mean of 15.5 days, and mean daily alcohol consumption was reduced by 48.7 g/day. At week 24, the nalmefene-treated MetALD group showed significantly greater reductions in serum transaminases ($P = 0.037$) and gamma-glutamyl transferase ($P = 0.041$) compared with the MASLD group. Liver stiffness decreased by 22% and hepatic fat content by 19%, showing trends toward improvement, although these changes did not reach statistical significance. Nalmefene was generally well tolerated, with mostly mild adverse events, including dizziness and nausea.
Conclusion: On-demand nalmefene was associated with clinically meaningful reductions in alcohol consumption and biochemical markers of liver injury in patients with alcohol use disorder and MetALD. Favorable short-term trends in noninvasive elastography-based measures support their potential role as sensitive tools for treatment monitoring in early-stage MetALD. A patient-driven pharmacological alcohol reduction strategy combined with metabolic risk management may represent a feasible early intervention and monitoring pathway for this population.

FRI-067

Recompensation in alcohol related liver disease is infrequent and should not delay transplantation assessment

Arushi Kumar[1], Ian Rowe[1,2], Richard Parker[1,2]. [1]*Leeds Teaching Hospital NHS Trust, Leeds, United Kingdom;* [2]*Leeds Institute for Medical Research, University of Leeds, Leeds, United Kingdom*
Email: arushi.kumar2@nhs.net

Background and aims: Alcohol-related liver disease (ArLD) is the most prevalent cause of liver-related mortality. Liver transplantation remains an effective solution in selected patients with decompensated disease. Recent studies have outlined definitions of recompensation and shown an associated survival benefit; however, translating this to clinical practice remains undetermined. We aim to quantify the rates of recompensation in decompensated ArLD and compared the risk of death at specific timepoints to inform decisions regarding the timing of liver transplantation.
Method: The ALLHEAL study is a prospective database study of patients with ArLD. We examined outcomes in people with decompensated alcohol-related cirrhosis (d-AC) or alcohol-related hepatitis (AH) at the time of entry to the study. Multi-state modelling and landmark modelling was used to describe outcomes over time in those who remained decompensated at three months, six months, one year and two years after baseline. Rates of recovery compared to baseline were explored and recompensation was based on Baveno, excluding the requirement for removal of the aetiologica agent i.e alcohol to explore the role of abstinence.
Results: 143 patients were included: the median age was 52 years (IQR 44–58), 52% were male and 30 (21%) had AH. Over a median follow-up of 79 months (IQR 20–101), 70 (49%) patients died and 13 (9.1%) underwent liver transplantation. Recompensation occurred in 30 (21%) patients with a cumulative incidence of 11% (6.7–17%) at one year and 15% (10–22%) at two years from baseline. The cumulative incidence of recompensation was consistently lower than the risk of death or transplantation which was 30% (23–38%) and 41% (32–49%) at one year and two years from baseline respectively. This was also noted in the 64 patients who were abstinent during follow-up, although rates of transplantation were higher. In multivariable analysis, abstinence during follow-up (SDH 2.62, 1.10–2.67, $p = 0.030$), first presentation of liver disease (SHD 3.39, 1.45–7.96, $p = 0.005$) and the presence of AH at baseline (SDH 3.61, 1.37–9.55, $p = 0.010$) were associated with a greater likelihood of recompensation.
Conclusion: In decompensated ALD, recompensation is uncommon and outweighed by the risk of death or transplantation. Delaying transplantation in the hope of recompensation may lead to worse outcomes in most patients. Proactive consideration of liver transplantation at the same time as alcohol rehabilitation could offer better outcomes in ArLD.

FRI-068

Beyond maddrey and MELD: machine learning transforms mortality prediction in critically ill alcohol-associated hepatitis

Jeril Lasington[1], Lawin Steve Mathew Lasington[2]. [1]*New York Medical College, Valhalla, United States;* [2]*Rutgers University-Newark Arch, Newark, United States*
Email: jeril.lasington@gmail.com

Background and aims: Alcohol-associated hepatitis (AAH) carries substantial short-term mortality, particularly among ICU patients. Traditional prognostic scores including MELD and Maddrey's Discriminant Function (DF) were developed for transplant prioritization and corticosteroid eligibility rather than ICU mortality prediction. We developed machine learning (ML) models for predicting ICU mortality in AAH and compared performance against established clinical scores.
Method: This retrospective cohort study used MIMIC-IV (v3.1) to identify adults with AAH requiring ICU admission (2008–2022). Predictors from the first 24 hours included demographics, liver function tests, renal parameters, metabolic markers, hemodynamics, cirrhosis complications, and ICU interventions. Four ML algorithms (Logistic Regression, Random Forest, XGBoost, Gradient Boosting) were trained using 80/20 stratified splits with five-fold cross-validation. Performance was compared against MELD, MELD-Na, Maddrey DF, and SOFA using bootstrap DeLong testing ($n = 2000$).
Results: Among 1,084 AAH patients (mean age 49.2 years; 62.1% male; 45.2% with concurrent cirrhosis), hospital mortality was 27.8%. Random Forest achieved highest discrimination (AUC 0.872, 95% CI 0.819–0.918), significantly outperforming MELD (0.769, +13%, $p = 0.0007$), MELD-Na (0.757, +15%, $p = 0.0002$), Maddrey DF (0.806, +8%, $p = 0.029$), and SOFA (0.820, $p = 0.031$). Feature importance revealed

bilirubin as the dominant predictor, followed by sepsis, creatinine, INR, and pH, reflecting the multiorgan nature of severe AAH. Notably, sepsis emerged as the second most important predictor, highlighting infection's critical role in AAH mortality.
Conclusion: ML significantly outperforms all traditional scoring systems for ICU mortality prediction in AAH. The integration of hepatic dysfunction (bilirubin, INR), systemic illness (sepsis, lactate), and renal impairment explains this superior performance. These findings support developing AAH-specific ICU prognostic tools beyond liver-centric scores, with particular attention to early sepsis identification and aggressive infection management in this vulnerable population.

FRI-069
Mortality prediction in alcohol-associated hepatitis
Jeril Lasington[1], Lawin Steve Mathew Lasington[2]. [1]*New York Medical College, Valhalla, United States;* [2]*Rutgers University-Newark Arch, Newark, United States*
Email: jeril.lasington@gmail.com

Background and aims: Alcohol-associated hepatitis (AAH) hospitalizations and mortality increased during the COVID-19 pandemic. Traditional prognostic scores (MELD, Maddrey DF, Lille) were developed in earlier cohorts and require laboratory values often missing from administrative databases. We developed an interpretable machine learning (ML) model to predict in-hospital AAH mortality using admission-level variables and examined pandemic-era trends.
Method: This retrospective cohort study used the National Inpatient Sample (2019–2022) to identify adult AAH hospitalizations (ICD-10: K70.10, K70.11). Patients were categorized by severity: AAH without ascites, AAH with ascites, hepatorenal syndrome (HRS), and hepatic failure. The primary outcome was in-hospital mortality. Four ML algorithms (Logistic Regression, Random Forest, XGBoost, LightGBM) were trained using temporal validation (2019–2021 training, 2022 testing) with 55 clinical features including demographics, MELD proxies, hepatic decompensation, infections, and alcohol-related complications. Procedural variables were excluded to avoid data leakage. SHAP analysis enabled model interpretation.
Results: Among 109,005 AAH hospitalizations, overall mortality was 4.3%. Mortality rose significantly: 3.8% (2019) to 4.7% (2022), a 25% relative increase ($p < 0.001$). Hospitalizations grew 19% from 2019–2021 before declining in 2022. Mean age was 47.3 years; 65.5% were male. Mortality by severity: HRS 24.2%, hepatic failure 15.8%, AAH with ascites 4.9%, AAH without ascites 1.7%. LightGBM achieved excellent performance (AUC 0.916; sensitivity 83.3%; specificity 86.0%). Top SHAP predictors were acute kidney injury (1.17), sepsis (0.69), age (0.40), renal dysfunction (0.39), and metabolic acidosis (0.35). Liver-specific predictors included HRS (0.28) and coagulopathy (0.25).
Conclusion: This ML model accurately predicts AAH mortality using admission-level data. Key findings are that AAH hospitalizations and mortality rose substantially during the pandemic; HRS carries 14-fold higher mortality than AAH without ascites; AKI and sepsis are dominant predictors, supporting early fluid resuscitation and infection monitoring. This tool can identify high-risk patients at admission for early goals-of-care discussions, ICU triage, and transplant evaluation.

FRI-070
Metabolic comorbidities are associated with lower in-hospital mortality in alcoholic liver disease hospitalizations: a nationwide analysis (NIS 2019–2022)
Jeril Lasington[1], Lawin Steve Mathew Lasington[2]. [1]*New York Medical College, Valhalla, United States;* [2]*Rutgers University-Newark Arch, Newark, United States*
Email: jeril.lasington@gmail.com

Background and aims: The overlap between metabolic dysfunction and alcohol-related liver disease (MetALD) is increasingly recognized, but its impact on acute outcomes remains unclear. We investigated the association between metabolic comorbidities (obesity, type 2 diabetes, hypertension, dyslipidemia) and in-hospital mortality among patients hospitalized with alcoholic liver disease (ALD).
Method: Using the National Inpatient Sample (2019–2022), we identified adult ALD hospitalizations (weighted N = 2,008,684). Metabolic comorbidity was defined as ≥1 condition present. Multivariable logistic regression assessed associations with in-hospital mortality, adjusting for age, sex, decompensation, cirrhosis, alcohol use disorder, and critical illness markers (sepsis, acute kidney injury, mechanical ventilation). Subgroup and dose-response analyses by metabolic burden score (0–4) were performed.
Results: Overall mortality was 5.8%. Patients with metabolic comorbidities (64.8%) had lower crude mortality than those without (5.4% vs. 6.6%; $p < 0.001$). After full adjustment, metabolic comorbidity was associated with reduced mortality (aOR 0.684; 95% CI 0.673–0.695). A dose-response relationship emerged: aOR 0.801 per 1-unit increase in burden score (p-trend <0.001), with mortality declining from 6.6% (burden 0) to 3.9% (burden 4). Protection was consistent across most subgroups and strongest in older patients (aOR 0.55 for ≥70 years), but absent in females (aOR 1.02). Patients without metabolic comorbidities were younger yet had higher rates of acute decompensation and alcohol-related severity markers, largely explaining this inverse association.
Conclusion: Metabolic comorbidities were paradoxically associated with lower in-hospital mortality in ALD, showing a clear dose-response effect. This likely reflects phenotypic differences: pure ALD patients experience more severe acute alcohol injury, while those with metabolic overlap follow more chronic courses with fewer precipitating events. These findings underscore heterogeneity within ALD/MetALD populations and have implications for acute risk stratification.

FRI-071
Restoration of ethanol-induced Bifidobacterium bifidum depletion ameliorates alcohol-related liver disease
Yating Li[1], Xiaowei Xu[1], Lanjuan Li[1]. [1]*State Key Laboratory for Diagnosis and Treatment of Infectious Diseases, National Clinical Research Center for Infectious Diseases, National Medical Center for Infectious Diseases, Collaborative Innovation Center for Diagnosis and Treatment of Infectious Diseases, Infectious Diseases Department, The First Affiliated Hospital, Zhejiang University School of Medicine, Hangzhou, China*
Email: liyating1991@126.com

Background and aims: Alcohol-related liver disease (ALD) is characterized by intestinal barrier dysfunction and gut microbiota dysbiosis. Analysis of our clinical cohort documented a marked depletion of the *Bifidobacterium* genus in patients with ALD and the functional screening has identified *Bifidobacterium bifidum (B. bifidum)* as a particularly depleted species with protective properties. Based on this, the present study aims to investigate the therapeutic potential of *B. bifidum* against ALD and elucidate its underlying mechanisms.
Method: The study enrolled 140 participants, including 40 healthy controls, 55 ALD patients, and 45 patients with non-metabolic liver disease. An ALD mouse model was established using a Lieber-DeCarli ethanol diet for 8 weeks. Based on human cohort findings, *B. bifidum* isolated and cultured from healthy human donor feces, was administered via oral gavage daily during the 8-week modeling period. An integrated approach combining bacterial 16S rRNA gene sequencing, targeted/untargeted metabolomic profiling, liquid chip technology, and validation of critical regulatory factors at transcriptional and translational levels was employed.
Results: Cohort analysis revealed a marked depletion of *Bifidobacterium* genus in ALD. Functional screening identified *B. bifidum* as a protective candidate. In murine models, pretreatment

with *B. bifidum* significantly ameliorated liver weight and the liver-to-body weight ratio, hepatic steatosis, and lowered serum aminotransferase levels. The intervention restored gut barrier integrity, reducing LPS-binding protein and increasing tight junction proteins. Furthermore, *B. bifidum* administration mitigated gut microbial dysbiosis, characterized by a reduction in the abundance of pathogenic taxa (*Klebsiella*, *Proteus* and *Escherichia-Shigella*) and an enrichment of beneficial genera (*Actinobacteria* and *Bifidobacterium*). These microbiome alterations were functionally correlated with shifts in lipid metabolism. Mechanistically, *B. bifidum*-derived metabolites, particularly short-chain fatty acids suppressed the hepatic expression of *de novo* lipogenesis genes (*Accα*, *Fasn*, *Srebp-1c*). *B. bifidum* modulated the hepatic TLR expression profile, specifically downregulating TLR2/TLR4 while upregulating TLR12, which consequently attenuated the production of pro-inflammatory cytokines (*Il1b*, *Il6*, *Tnfa*).

Conclusion: Our findings suggest that *B. bifidum* has potential as a probiotic for preventing and treating ALD, offering novel insights into liver disease management.

FRI-072

Physical activity reduces the risk of alcohol-attributable liver fibrosis and liver-related events

Chuan Liu[1], Shanghao Liu[1], Bicheng Ye[1], Chiwei Zhang[1], Mengxian Zheng[1], Xiaolin Wang[1], Yuping Chen[1], Yinqiu Zhang[1], Jiawei Zhang[1], Ling Yang[1], Huapeng Lin[2], Caihong Gu[3], Shuo Yan[4], Lili Ye[5], Yong-Fen Zhu[6], Lan Ma[7], Liping Wang[7], Wenjuan Wang[8], Nayi Zhang[9], Jing Li[9], Yuanhang Liao[10], Chaoliang Xiong[10], Hui Shi[11], Haisong Xin[12], JianSong Ji[13], Jianxiang Song[14], Zhenyu Dai[15], Xiao Liang[16], Guo Zhang[8], Yijun Tang[17], Xiaolong Qi[1]. *[1]Liver Disease Center of Integrated Traditional Chinese and Western Medicine, Department of Radiology, Zhongda Hospital, Medical School, Southeast University, Nanjing, China; [2]Department of Gastroenterology and Hepatology, Shanghai Ninth People's Hospital, Shanghai Jiao Tong University School of Medicine, Shanghai, China, Shanghai, China; [3]Department of Critical Care Medicine,The First Affiliated Hospital of Kangda College of Nanjing Medical University, Lianyungang, China; [4]Department of Ultrasound, People's Hospital of Huanghua, Cangzhou, China; [5]Department of Oncology Center, The Fifth Affiliated Hospital of Wenzhou Medical University, Lishui, China; [6]Zhejiang Key Laboratory of Multi-omics Precision Diagnosis and Treatment of Liver Diseases, Department of Liver and Infectious Diseases, Sir Run Run Shaw Hospital, Zhejiang University School of Medicine, Hangzhou, China; [7]Department of Infectious Diseases, Bozhou People's Hospital, Bozhou, China; [8]Department of Gastroenterology, Guangxi Hospital Division of The First Affiliated Hospital, Sun Yat-sen University, Nanning, China; [9]Department of Internal medicine, Qingdao Public Health Clinical Center, Qingdao, China; [10]The Department of Gastroenterology, Yichun People's Hospital, Yichun, China; [11]Department of Neurosurgery, The First Affiliated Hospital of Kangda College of Nanjing Medical University, Lianyungang, China; [12]Department of Orthopedics, People's Hospital of Huanghua, Huanghua, China; [13]Zhejiang Key Laboratory of Imaging and Interventional Medicine, Zhejiang Engineering Research Center of Interventional Medicine Engineering and Biotechnology, Department of Radiology, Lishui Central Hospital, The Fifth Affiliated Hospital of Wenzhou Medical University, Lishui, China; [14]Department of Cardiothoracic Surgery, Affiliated Yancheng Hospital, School of Medicine, Southeast University, Yancheng Third People's Hospital, Yancheng, China; [15]Department of Radiology, Affiliated Yancheng Hospital, School of Medicine, Southeast University, Yancheng Third People's Hospital, Yancheng, China; [16]Department of General Surgery, Sir Run-Run Shaw Hospital, Zhejiang University School of Medicine, Hangzhou, China; [17]Department of Respiratory and Critical Care Medicine, Taihe Hospital, Hubei University of Medicine, Shiyan, China*
Email: liuchuan101z@163.com

Background and aims: The impact of physical activity on alcohol-attributable liver fibrosis and liver-related events (LREs) is under-researched. Our study aims to investigate the influence of physical activity on liver fibrosis and LREs in individuals who consume alcohol at least once per month.

Method: This prospective study included a total of 261,927 participants and comprised cross-sectional and longitudinal components. The cross-sectional component analyzed data from the Chinese LiverHealth cohort (N = 6,867) and the UK Biobank cT1 cohort (N = 19,919), with liver fibrosis (defined as liver stiffness ≥ 8 kPa measured by FibroScan or cT1 ≥ 800 ms by magnetic resonance imaging) as the outcome. The longitudinal component enrolled 255,060 participants from the UK Biobank, including a wearable device subcohort (N = 56,484), with LREs (specifically hepatocellular carcinoma, cirrhosis, and its complications) as the outcome. Physical activity was assessed via questionnaire or wearable device. In the wearable device cohort, moderate-to-vigorous physical activity (MV-PA) bouts were derived using a two-level Random Forest classifier and categorized as short (<3 in), medium (3 to <5 min; 5 to <10 min), and long (>10 min).

Results: Compared with inactive participants (reported no MV-PA), the multivariable-adjusted odds ratio (OR) for liver fibrosis was significantly lower among those with physical activity (OR, 0.776 [0.616–0.977], p = 0.031 in the LiverHealth cohort; OR, 0.979 [0.970–0.988], p < 0.001 in the UK Biobank cT1 cohort). In the longitudinal UK Biobank cohort, physical activity was independently associated with a lower risk of LREs in multivariable Cox regression analyses (hazard ratio [HR], 0.774 [0.699–0.856], p < 0.001). Furthermore, in the wearable device cohort, compared with bouts of less than 3 minutes, the risk of LREs was lower for bouts of 3 to <5 minutes (HR, 0.499 [0.250–0.998], p = 0.049), 5 to <10 minutes (HR, 0.459 [0.256–0.822], p = 0.009), and >10 minutes (HR, 0.328 [0.186–0.581], p < 0.001). Additionally, a near-linear dose-response relationship was observed between the daily duration of MV-PA and LRE risk in longitudinal UK biobank cohort and wearable device subcohort.

Conclusion: Physical activity is significantly associated with a reduced risk of alcohol-attributable liver fibrosis and liver-related events.

FRI-073

Digital pathology and multi-omic profiling in abstinent patients with alcohol-related decompensated cirrhosis shows significant degrees of fibrosis regression associated to clinical improvement

Lisa Longato[1], Luc Francis[1], Gareth Muirhead[1], Tu Vinh Luong[2,3], Jennifer Watkins[2,3], Nafia Guljar[1], Athiva Shankar[1], Cristina Albert[1], Massimo Pinzani[3,4], Gautam Mehta[3], Anne E. Wyman[5], Kevin Moore[3], Camila Gabriela De Brito[2], Vandana Gupta[5], Paresh Thakker[5], Mathieu Petitjean[6], Morten Karsdal[7], Bevan Emma Huang[1], Chris Stevenson[1], Haakan Wennbo[5], Giuseppe Mazza[1]. *[1]Engitix Therapeutics, London, United Kingdom; [2]Department of Cellular Pathology, Royal Free London NHS Foundation Trust, London, United Kingdom; [3]Institute for Liver and Digestive Health, University College London, London, United Kingdom; [4]Irccs Ismett-Upmc, Palermo, Italy; [5]Early Clinical Development GI Therapeutic area unit Takeda Pharmaceuticals, Boston, United States; [6]PharmaNest Inc., Princeton, United States; [7]Nordic Bioscience A/S, Herlev, Denmark*
Email: Lisa.Longato@engitix.com

Background and aims: Sustained alcohol abstinence is known to improve the prognosis of patients with alcohol-related liver disease (ALD) at every stage of the disease. This study was aimed at the in-depth histological and molecular characterization of fibrosis regression in a cohort of abstinent ALD patients.

Method: Extent of fibrosis regression in explants from a cross-sectional cohort of 42 patients with decompensated ALD cirrhosis who underwent liver transplant was assessed by conventional and digital pathology. Serum biomarkers were assessed by ELISA and livers were profiled by scRNAseq and spatial transcriptomics.

Results: Pathologist-led assessment of histological features according to a modified Beijing classification categorized 70% of the cohort with

features of fibrosis regression, either moderate (n = 24) or advanced (n = 5). The remaining non-regressive samples were shown to display either features of progressive disease (n = 3) or an indeterminate pattern of fibrosis regression (n = 10). AI-assisted digital pathology analysis confirmed the histologic features, showing a significant decrease in the phenotypic fibrosis composite score in the regressive vs non-regressive groups (mean ± SEM: 3.2 ± 0.2 vs 5.2 ± 0.2; P < 0.05). Patients showing regression had been abstinent for longer (25.8 ± 3.5 vs 9.2 ± 0.9 months) and displayed selectively improved indices of hepatic function such as reduced bilirubin (40.4 ± 5.2 vs 155.3 ± 25.9 µM/L), INR (1.38 ± 0.06 vs 1.63 ± 0.11) and MELD-Na (13.4 ± 0.9 vs 20.2 ± 1.2) compared to non-regressive patients, respectively (all P < 0.05). The same patients displayed significantly (P < 0.05) reduced ELF scores (11.9 ± 0.2 vs 13.4 ± 0.4) and ProC3 levels (31.8 ± 2.4 vs 58.3 ± 9.0). scRNAseq analysis revealed shifts in the composition of liver cells in regressive samples, specifically increased hepatocytes and mononuclear phagocytes, and reduced cholangiocytes and connective tissue cells. The increase in macrophages was largely driven by the selective expansion of 2 subpopulations in regressive samples. Spatial profiling showed nodule expansion in regression with upregulation of metabolic pathways in nodules relative to septal areas.

Conclusion: Histological fibrosis regression can be achieved in patients with decompensated ALD cirrhosis who maintain abstinence. Patients with fibrosis regression display improved measures of organ function, reduced serum biomarkers of fibrosis, and a molecular/cellular signature indicative of reduced damage, parenchymal regeneration, and ongoing tissue repair.

FRI-074

Bio-molecular landscape of hyper-oxidized and cysteinylated albumin signature linked to immune activation and hyperinflammation in severe alcohol-related hepatitis

Babu Mathew[1], Sushmita Pandey[1], Gaurav Tripathi[1], Vasundhra Bindal[1], Vipul Sharma[1], Nupur Sharma[1], Yash Magar[1], Manisha Yadav[1], Neha Sharma[1], Sanju Yadav[1], Shvetank Sharma[1], Shiv Kumar Sarin[1], Jaswinder Maras[1]. [1]*Institute of Liver & Biliary Sciences, New Delhi, India*
Email: jassi2param@gmail.com

Background and aims: Severe alcohol-associated hepatitis (SAH) is characterized by oxidative stress and systemic inflammation. In SAH, reduced human mercaptalbumin (HMA) shifts toward oxidized isoforms, HNA1 (cysteinylated) and HNA2 (hyper-oxidized), which are pro-inflammatory. The macromolecular cargo bound to these isoforms may influence disease severity and outcomes.

Method: We enrolled 125 adults: 60 with SAH (30 survivors, 30 non-survivors), 50 with decompensated cirrhosis, and 15 healthy controls. HNA1 and HNA2 were purified by anion exchange chromatography and analyzed using UHPLC-HRMS–based multi-omics. Albumin-bound macromolecules were quantified and correlated with functional status, severity scores, and survival using multivariate statistical analysis.

Results: Albumin redox fractionation revealed distinct macromolecular signatures linked to severity, mortality, and therapeutic relevance. In SAH non-survivors, HMA was enriched with inflammatory and oxidative cargo including L-cystathionine (FC = 5.7), N,N-Dimethylhistidine (FC = 3.3), ceramide Cer(t18:1(6OH)/24:0(2OH)) (FC = 3.4), and PRMT1 (FC = 11), along with bacterial peptides from *Ehrlichia chaffeensis* (FC = 10.9). Pathways involved mitochondrial immune responses and IL-23 signaling. HNA1 displayed a pathogenic profile with elevated Elaidic carnitine (FC = 5.9), Heptanoylcarnitine (FC = 4.3), histidine (FC = 3.8), leukotriene C4 (FC = 3.1), TG(17:2/20:5/20:5) (FC = 7.9), and tetranor-PGE1 (FC = 6.5). Proteins including MAP4K1 (FC = 8) and Interferon-α1 (FC = 6.6), and peptides from *Listeria monocytogenes* and *Klebsiella pneumoniae* indicated microbial translocation. Pathways included necroptosis, interferon, and prostaglandin signaling. HNA2 carried hyper-inflammatory and hypoxia-related cargo: Eicosadienoic acid (FC = 5.3), PE(P-16:0/15:1) (FC = 5.4), PPIA (FC = 5), and peptides from *Campylobacter concisus*. Pathways involved TNFR1, HIF-1, and kynurenine signaling. HNA1/HNA2-bound molecules correlated strongly with MELD-Na, DF, ALBI, and PALBI. PPIA (HR = 1.68) and Eicosadienoic acid (HR = 1.30) emerged as predictors and candidate drug targets. HNA2 was most strongly associated with sustained inflammation, hypoxia, and metabolic exhaustion.

Conclusion: In SAH patients who died within 30 days, HNA2 binds hyper-inflammatory, hypoxia-responsive, and microbial molecules, amplifying systemic inflammation and metabolic failure, establishing HNA2 as a potential therapeutic target.

FRI-075

Association of protein-calorie malnutrition with in-hospital complications in patients hospitalized with alcohol-associated cirrhosis

Jazmin Mexia Cabrales[1], Fatima Shafiq[1], Hassan Sinan[1], Madonna Johnson[1], Frances Lee[2]. [1]*Department of Medicine, NYC Health + Hospitals/Elmhurst, Icahn School of Medicine at Mount Sinai, New York City, United States;* [2]*Icahn School of Medicine at Mount Sinai, New York, United States*
Email: jazmin.mexia@gmail.com

Background and aims: Malnutrition is highly prevalent among patients with cirrhosis and is particularly common in alcohol-associated liver disease. Despite EASL guidelines recommendations for early nutritional assessment, malnutrition is frequently under-recognized during hospitalization. Data evaluating the association between malnutrition and clinical outcomes among hospitalized patients with alcohol-associated cirrhosis remains limited.

Method: We conducted a single-center retrospective cohort study using the Mount Sinai TriNetX electronic health record (EHR) network. Adults ≥18 years hospitalized with alcohol-associated cirrhosis were identified and categorized into two cohorts based on the presence or absence of a documented diagnosis of malnutrition. Propensity score matching (1:1 nearest neighbor), was performed using age, sex, comorbidities and baseline markers of cirrhosis severity, including ascites, portal hypertension, esophageal varices, chronic kidney disease, diabetes, and heart failure. Outcomes were assessed 1–90 days after the index event and included: short-term all-cause mortality, acute kidney failure, spontaneous bacterial peritonitis, acute hepatic failure and 90-day readmission. Risk ratios (RRs) with 95% confidence intervals (CIs) were calculated with statistical significance set at p < 0.05.

Results: After propensity score matching, 1,550 patients with alcohol-associated cirrhosis and documented malnutrition were compared with 1,550 patients without malnutrition. Patients with malnutrition experienced a significantly higher incidence of acute kidney injury compared with those without malnutrition (21.2% vs 10.5%; risk ratio [RR] 2.03, 95% CI 1.66–2.47; p < 0.0001). Malnutrition was also associated with a higher risk of spontaneous bacterial peritonitis (6.8% vs 3.3%; RR 2.04, 95% CI 1.47–2.84; p < 0.0001). Acute hepatic failure, ninety-day readmission rates and all-cause mortality did not differ significantly between groups.

Conclusion: Among hospitalized patients with alcoholic cirrhosis, protein-calorie malnutrition was independently associated with a markedly increased risk of acute kidney injury and spontaneous bacterial peritonitis, but not with short-term mortality, readmission or acute hepatic failure. These findings suggest that malnutrition in alcohol-associated cirrhosis is a strong marker of vulnerability to in-hospital complications and highlight the importance of early nutritional recognition and intervention during hospitalization.

FRI-076-YI

Alcohol-associated amino acid signature linked to zonal glutamine synthetase serves as a biomarker of metabolic adaptation in steatotic liver disease

Masaaki Mino[1], Eiji Kakazu[1], Taiji Yamazoe[1], Michitaka Matsuda[1], Tatsuya Kanto[1]. [1]*Japan Institute for Health Security, The Research Center for Hepatitis and Immunology, Ichikawa, Japan*
Email: kakazu.e@jihs.go.jp

Background and aims: The impact of alcohol on free amino acids (FAAs) and intrahepatic metabolism within the spectrum of steatotic liver disease remains poorly understood. We aimed to identify an alcohol-specific FAA signature using a large-scale biobank and elucidate its pathological and metabolic basis through human tissue and murine models.
Method: We analyzed a Japanese population biobank (n = 23,036). Subjects were classified into MASLD (n = 3,504), MetALD (n = 519), and alcohol-related liver disease (ALD) (n = 899) based on alcohol intake and steatotic liver indices (FLI≥60, HSI>36, and questionnaire data). Plasma concentrations of 20 FAAs were quantified using LC–MS/MS. In a clinical cohort of chronic liver disease (n = 1,326), we examined the glutamate/glutamine (Glu/Gln) ratio across modified ALBI (mALBI) grades. Zone 3 glutamine synthetase (GS) expression was evaluated in an ALD human tissue microarray (n = 53; fibrosis stages F0–F4). Mechanistically, C57BL/6J mice were subjected to the national institute on alcohol abuse and alcoholism (NIAAA) ethanol-binge protocol (n = 5), and livers were analyzed 9 h post-binge by metabolomics and RNA-seq.
Results: In the biobank, steatotic liver was associated with broad FAA remodeling (16 increased and 4 decreased vs controls). A characteristic "High-Glu/Low-Gln" signature was progressively enhanced from MASLD to MetALD to ALD. In the clinical cohort, the Glu/Gln ratio differed by etiology; in MASLD, the ratio declined with worsening liver function, whereas in MetALD and ALD, it increased up to mALBI grade 2b and dropped sharply at grade 3. In human tissue samples, GS expression in zone 3 increased with fibrosis progression (F0–F3), suggesting compensatory upregulation, but was lost in cirrhosis (F4). Murine models corroborated this mechanism, showing hepatic Glu accumulation, induction of zone 3-enriched genes (*Cyp2e1, Cyp1a2*), and glutathione depletion, consistent with alcohol-driven pericentral oxidative stress. These findings suggest that zone 3 GS is upregulated in earlier stages but becomes lost in advanced fibrosis stages.
Conclusion: The alcohol-induced Glu/Gln signature reflects biphasic zone 3 glutamine synthetase dynamics and may serve as a mechanistic biomarker capturing the transition from metabolic adaptation to failure in MetALD/ALD.

FRI-077

Quantifying biological and clinical modifiers of phosphatidylethanol in treatment-seeking alcohol use disorder

Andrew Palmer[1,2], Jason Connor[1,2], Gerald Holtmann[1,2], John Saunders[1], Paul Clark[1,2]. [1]*The University of Queensland Herston, Herston, Australia;* [2]*Princess Alexandra Hospital, Woolloongabba, Australia*
Email: andrew.palmer@uq.edu.au

Background and aims: Hazardous alcohol consumption and alcohol use disorder (AUD) are leading causes of preventable morbidity and mortality. However, alcohol exposure remains largely quantified by self-report, which is vulnerable to recall bias, social desirability bias, and underreporting. Phosphatidylethanol (PEth) is a sensitive and specific biomarker of recent alcohol intake, yet interpretive thresholds vary across studies and between individuals at comparable intake levels. We aimed to estimate (i) the variance in PEth explained by self-reported intake; (ii) the diagnostic performance of conventional indirect biomarkers at established PEth thresholds; and (iii) the contribution of biological and clinical covariates to PEth variability in a treatment-seeking AUD cohort.
Method: We conducted a prospective cross-sectional study of treatment-seeking adults with moderate to severe AUD recruited between April 2023 and January 2025 from a quaternary hospital alcohol and drug service in Brisbane, Australia. Alcohol intake was assessed using the 30-day Timeline Follow-Back (TLFB; standard drink = 10 g ethanol). The primary outcome was blood PEth 16:0/18:1 measured by LC–MS/MS. Predictors included clinically plausible cohort-derived laboratory variables screened in bivariate analyses (AST, ALT, GGT, ferritin, time since last drink) and a priori variables previously reported to influence PEth (BMI, haemoglobin, advanced fibrosis, age, sex, socioeconomic status).
Results: Seventy-three participants were included; 75% were male, with a mean age of 49 years (IQR 39–56). PEth was strongly correlated with mean daily alcohol intake ($r = 0.82$, $p < 0.001$). Each additional standard drink per day was associated with a 69.6 ng/mL increase in PEth (95% CI 56.4–82.8, $p < 0.001$). A core multivariable model including intake, AST, and ALT explained 79.6% of PEth variance (adjusted $R^2 = 0.780$). Addition of a priori predictors did not significantly improve model performance ($\Delta R^2 = 0.029$, $p = 0.142$). At a PEth threshold >210 ng/mL, ALT demonstrated the strongest discrimination for significant alcohol exposure (AUC = 0.74), followed by AST (AUC = 0.68) and GGT (AUC = 0.67).
Conclusion: In treatment-seeking adults with moderate to severe AUD, PEth closely reflects recent self-reported alcohol intake assessed by TLFB, with liver function tests providing additional biological context.

FRI-078

Long-term mortality under the new steatotic liver disease classification

Parucha Paruchakul[1], Moongmun Anuntasainont[1], Mingkwan Ratanapipop[1], Sakkarin Chirapongsathorn[2]. [1]*Department of Medicine, Phramongkutklao Hospital and College of Medicine, Bangkok, Thailand;* [2]*Division of Gastroenterology and Hepatology, Department of Medicine, Phramongkutklao Hospital and College of Medicine, Bangkok, Thailand*
Email: toop.parucha@gmail.com

Background and aims: The 2023 reclassification of steatotic liver disease (SLD) distinguishes metabolic dysfunction–associated SLD (MASLD), MASLD with increased alcohol intake (MetALD), and alcohol-associated liver disease (ALD). However, the long-term mortality implications of this framework, particularly in Asian populations, remain unclear.
Method: We conducted a retrospective longitudinal cohort study of adults diagnosed with SLD by ultrasonography in 2014, reclassified using the 2023 SLD criteria and followed for up to 11 years. All-cause and cause-specific mortality were assessed using Kaplan–Meier analysis and multivariable Cox models, with cancer- and cardiovascular (CVD)-specific mortality evaluated after excluding patients with pre-existing cancer or CVD.
Results: Among 1,279 patients (median age 57 years; 57% male), 88% had MASLD, 3% MetALD, and 3% ALD. During a median follow-up of 10.8 years, 67 deaths occurred. ALD had the highest mortality incidence (58.6 per 1,000 person-years) and the lowest 10-year survival (58.9%). After adjustment, ALD was independently associated with increased all-cause mortality compared with MASLD (adjusted hazard ratio [aHR] 4.0; 95% CI 1.1–14.2), whereas MetALD showed no excess risk. Older age, diabetes, chronic kidney disease, and advanced fibrosis were independent predictors of mortality. Liver- and cancer-related deaths predominated in ALD, while CVD-specific mortality was similar across SLD subtypes. After excluding patients with pre-existing cancer, ALD remained strongly associated with increased overall mortality (64.6 per 1,000 person-years; aHR 7.6; 95% CI 1.9–29.6), the lowest 10-year survival (55.5%), and a median survival of 10.7 years. Significant differences in all-cause, liver-related, hepatocellular carcinoma–related, and cancer-related mortality were observed across SLD subtypes (log-rank $p < 0.001$). Among patients

without pre-existing CVD, ALD was also associated with increased overall mortality (aHR 4.5; 95% CI 1.2–16.3), while CVD-specific mortality did not differ significantly.
Conclusion: In this long-term Asian cohort, the 2023 SLD reclassification provided meaningful prognostic stratification. ALD was associated with markedly higher all-cause, liver-related, and cancer-related mortality and poorer survival than MASLD, whereas MetALD did not increase mortality risk. Cardiovascular mortality was similar across SLD subtypes, supporting the clinical utility of the updated SLD reclassification.

FRI-079-YI
Higher socioeconomic status is associated with alcohol under-reporting: a PEth-based analysis of 6,000 individuals screened for SLD
Helle Schnefeld[1,2], Johanne Kragh Hansen[1,2], Mads Israelsen[1,2], Katrine Tholstrup Bech[1,2], Camilla Dalby Hansen[1,2], Katrine Thorhauge[1,2], Maria Fogt[1], Ea Kyed[1,2], Kathrine Sejer Sørensen[1], Anine Andersen[1,2], Stine Johansen[1,2], Nikolaj Torp[1,2], Ida Villesen[1,2], Peter Andersen[1], Sönke Detlefsen[3], Maja Thiele[1,2], Aleksander Krag[1,2]. *[1]FLASH - Centre for Liver Research, Odense, Denmark; [2]SDU - University of Southern Denmark, Odense, Denmark; [3]Department of Pathology, Odense, Denmark*
Email: helle.schnefeld@rsyd.dk

Background and aims: Steatotic liver disease (SLD) subgrouping relies on current, self-reported alcohol intake and is prone to misclassification due to recall bias. People with low socioeconomic status (SES) have higher alcohol-related morbidity and mortality; however, how SES influences the accuracy of self-reported alcohol intake is less well understood. Phosphatidylethanol (PEth) is a direct biomarker reflecting alcohol consumption over the prior 1–4 weeks. We investigated the association between SES and discordance between self-reported alcohol intake and PEth.
Method: Single-centre, cross-sectional liver fibrosis screening study in the general Danish population and individuals at risk of SLD. SES was assessed by income, education, employment, and living situation. Alcohol use was self-reported (past week and past 3 months) and categorised according to SLD nomenclature. PEth was classified into three categories (<20 ng/mL, 20–199 ng/mL, ≥200 ng/mL). Under-reporting was defined as self-reported intake below the PEth-indicated category. SES trends were evaluated using Cuzick's test and ordinal logistic regression.
Results: We screened 6,364 participants, median age 57 years, 52% female. Alcohol intake was low in 77%, moderate in 16% and high in 7%, while PEth was low in 42%, moderate in 41% and high in 17%. Among 6,082 participants with complete data, 45% under-reported and 4% over-reported their alcohol intake relative to PEth, while 51% showed concordance. Under-reporting increased with higher SES, most notably by income (36% lowest vs 58% highest income; $p < 0.001$), and remained significant after adjustment for age, sex, and education. Full-time employment had the highest adjusted probability of under-reporting (46%) whereas those outside the labour market reported less (36–39%; $p < 0.001$). Individuals living alone under-reported less than those cohabiting (40% vs 46%; $p < 0.001$). Education was not associated with under-reporting.
A cumulative binary SES score (0–4, higher scores indicating higher SES), showed a dose–response relationship based on income, education, labour market attachment, and living alone/other showed a dose–response. Under-reporting decreased from 52% at SES = 0 to 32% at SES = 4 ($p < 0.001$).
Conclusion: SES was strongly associated with discrepancies between self-reported alcohol intake and PEth. Higher-SES individuals substantially under-reported their intake, leading to systematic misclassification. SES-related bias should be explicitly considered when alcohol intake informs SLD assessment.

FRI-083
Type 2 diabetes mellitus and alcohol use disorder amplify both cardio-renal-metabolic and liver related outcomes and mortality risk compared to either disorder alone
Neha Shah[1], Vinay Jahagirdar[1], Kavin Parmar[1], Arun J. Sanyal[1]. *[1]Virginia Commonwealth University School of Medicine, Richmond, United States*
Email: shahn24@vcu.edu

Background and aims: Alcohol use disorder (AUD) and type 2 diabetes mellitus (T2DM) are both highly prevalent and often co-exist in the same person. The impact of T2DM on AUD-related liver outcomes and the impact of AUD on cardio-renal-metabolic (CRM) outcomes is not established in routine clinical practice settings. The aim of this study was the quantify the impact of concomitant T2DM and AUD on CRM and liver outcomes relative to either disorder alone in a large real-world practice setting.
Method: We evaluated mortality, CRM and liver outcomes in those with T2DM + AUD vs propensity score matched (PSM) controls with T2DM (analysis 1) or AUD alone (analysis 2). PSM was done for demographics, BMI, laboratory (bilirubin, AST, ALT, INR, creatinine, A1C), nicotine dependence and statin use. Those on a GLP-1 RA were excluded. Independent analyses by age decile strata from 30 yrs. onwards was performed. The key outcome measures were death, new diagnosis of cirrhosis, ascites, hepatic encephalopathy, alcohol associated hepatitis, 5-point MACE, atrial fibrillation and obesity-related cancers. Absolute risk (AR %) and Hazard ratios (HR) were computed using time-dependent proportional hazards model. Kaplan-Meir analyses were done to assess time to event with cross-group comparisons with logrank test (significance $p < 0.05$).
Results: 131900, 639437 and 2420891 cases of T2DM+AUD, AUD alone and T2DM alone were eligible for analysis prior to PSM. *T2DM +AUD vs T2DM*: In T2DM, coexistent AUD increased mortality (AR 2.2–6.1, HR 1.3–1.6), ascites (HR 2.7–3.3), encephalopathy (HR 6.9–7.9), MACE (HR 1.4–2.0), and atrial fibrillation (HR 1.4–1.8) and sepsis (HR 1.7–2.0) ($p < 0.001$ for all) across all age deciles studied. Cancer risk (HR 1.3, 95% CI 1.2–1.4) was increased in those with age > 60 yrs. *T2DM+AUD vs AUD*: T2DM increased the risk of death (HR 1.4–1.6), new diagnosis of cirrhosis (HR 1.5–1.8) and heart failure (HR 2–3) ($p < 001$ for all) in all age deciles studied. Importantly, the risk of alcohol associated hepatitis was increased in ages 30–59 yrs (HR: 1.1–1.5) ($p < 0.05$ for all).
Conclusion: T2DM +AUD increased mortality and CRM outcomes compared to either one alone. T2DM increases liver-related outcomes including development of alcohol associated hepatitis in those with AUD. AUD increases cardiometabolic outcomes in those with T2DM.

FRI-084
Triangulated alcohol assessment substantially increases identification of MetALD and ALD in a population-based study of steatotic liver disease
Juho Siltanen[1,2], Lara Lehtoranta[3], Annamari Lundqvist[3], Anniina Ojanen[3], Linda Mustelin[3], Lotta Joutsi-Korhonen[4,5], Tuukka Helin[5], Ville Männistö[2], Fredrik Åberg[3,4,6]. *[1]Kuopion yliopisto, Kuopio, Finland; [2]Kuopion yliopistollinen sairaala, Kuopio, Finland; [3]Terveyden Ja Hyvinvoinnin Laitos, Oulu, Finland; [4]University of Helsinki, Helsinki, Finland; [5]Department of Clinical Chemistry, Diagnostic Center, Helsinki University Hospital, Helsinki, Finland; [6]Transplantation and Liver Surgery, Helsinki University Hospital, Helsinki, Finland*
Email: siltanen.juho@gmail.com

Background and aims: Steatotic liver disease (SLD) subclassification is currently based on self-reported average alcohol intake. A triangulated assessment combining self-reports, AUDIT-C and phosphatidylethanol (PEth) was recently proposed to improve subclassification accuracy. In a general population survey, we evaluated how applying triangulated alcohol assessment alters the prevalence and proportion of SLD subclasses.

Method: Of participants in the Finnish Healthy Finland 2023 survey, 1576 adults residing in Uusimaa were invited to a liver substudy. 1090 (69%) participated. SLD was defined as ultrasound-derived fat fraction (UDFF ≥) 5%. Alcohol use was assessed using self-reported 7-day consumption, AUDIT-C, and PEth. Subclassification into MASLD, MetALD and ALD by triangulation was done as previously described (Torp et al. Lancet Gastroenterol Hepatol 2025;10:975). The given method balances allocation to higher risk groups if conflict exists between indicators, emphasizing self-reported consumption. Participants with any missing alcohol consumption data were excluded, leaving 717 individuals for analysis.
Results: Among 717 individuals (mean age 52 years, 45% men, mean BMI 27.3 kg/m2, diabetes 6.5%), 419 (58.4%) had SLD. Mean alcohol use was 56 ± 99.3 g/wk, mean AUDIT-C 3.8 ± 2.1 points, and mean PEth 0.04 ± 0.08 µmol/L. Using mean alcohol use alone, 390 were classified as MASLD (population prevalence 54.4%, proportion of SLD 93.1%), 14 as MetALD (2.0%, 3.3%), 6 as ALD (0.8%, 1.4%) and 9 as other (1.3%, 2.1%), which were omitted from further analysis. Using the triangulated assessment, 160 were classified as MASLD (population prevalence (22.3%, proportion of SLD 38.2%), 236 as MetALD (32.9%, 56.3%), and 14 as ALD (2.0%, 3.3%). Applying a pragmatic "maximum-of-three" indicator subclassified SLD cases into 160 with MASLD (population prevalence 22.3%, proportion of SLD 38.2%), 211 with MetALD (29.4%, 50.4%), and 40 with ALD (5.6%, 9.5%).
Conclusion: Triangulating alcohol assessment substantially alters SLD subclassification in the general population, with major implications for SLD epidemiology and clinical care. Reliance on alcohol self-reports alone likely underestimates, especially MetALD. Accurate evaluation of alcohol consumption should therefore integrate multiple complementary indicators.

FRI-085
Biological impact of anemia on phosphatidylethanol concentrations in advanced liver disease: analysis of the RH7 cohort

Lubomir Skladany[1], Svetlana Adamcova Selcanova[2], Daniela Žilinčanová[2], Jana Čiefová[2], Daniel Jan Havaj[2], Karolina Sulejova[2], Martin Janičko[3], Lukas Laffers[4], Luis Antonio Diaz[5], Juan Pablo Arab[6]. *[1]HEGITO - Department of Hepatology, Gastroenterology and Liver Transplantation of F. D. Roosevelt University Hospital, Banska Bystrica, Slovakia; 2nd Department of Internal Medicine, Medical school of PJ Safarik University and L. Pasteur University hospital in Kosice, Slovakia, Banska Bystrica, Slovakia; [2]HEGITO - Department of Hepatology, Gastroenterology and Liver Transplantation of F. D. Roosevelt University Hospital, Banska Bystrica, Slovakia, Banska Bystrica, Slovakia; [3]2nd Department of Internal Medicine, Medical school of PJ Safarik University and L. Pasteur University hospital in Kosice, Slovakia, Kosice, Slovakia; [4]Department of Mathematics, Faculty of Natural Sciences, Matej Bel University, Banska Bystrica; Slovakia, Department of Economics, Faculty of Economics and Administration, Masaryk University. Brno, Czech Republic, Banska Bystrica, Slovakia; [5]Departamento de Gastroenterologia, Escuela de Medicina, Pontificia Universidad Catolica de Chile, Santiago, Chile, Santiago, Chile; [6]Stravitz-Sanyal Institute of Liver Disease and Metabolic Health, Division of Gastroenterology, Hepatology, and Nutrition, Department of Internal Medicine, Virginia Commonwealth University School of Medicine, USA, Departamento de Gastroenterologia, Escuela de Medicina, Pontificia Universidad Catolica de Chile, Santiago, Chile, Virginia, United States*
Email: lubomir.skladany@gmail.com

Background and aims: Phosphatidylethanol (PEth) is an established erythrocyte-bound biomarker of alcohol exposure. However, its reliability may be influenced by biological factors affecting red blood cell mass and turnover. Anemia is common in patients with advanced chronic liver disease (ACLD) and may alter PEth concentrations independently of alcohol intake. We aimed to evaluate the impact of anemia severity on PEth levels and to identify hemoglobin thresholds associated with systematically reduced PEth concentrations.
Method: In a large cohort of patients with ACLD, PEth concentrations were analyzed across anemia severity categories (none, mild, moderate, severe). Group comparisons were performed, and a data-driven regression tree model was applied to identify hemoglobin (Hb) thresholds associated with altered PEth levels. Clinical severity markers, including MELD score and liver frailty index (LFI), were assessed across anemia strata.
Results: Mean PEth concentrations declined stepwise with increasing anemia severity, with a statistically significant difference across groups (p = 0.028). The most pronounced reduction occurred between non-anemic patients and those with moderate-to-severe anemia. Increasing anemia severity was concurrently associated with worsening clinical status, reflected by higher MELD and LFI values, consistent with advanced disease and malnutrition. Regression tree analysis identified Hb <14 g/dL as the primary threshold associated with markedly reduced PEth concentrations, independent of liver disease etiology. This threshold aligned with the observed stepwise decline across anemia categories.
Conclusion: Anemia is an independent biological modifier of PEth concentrations in patients with ACLD. Reduced erythrocyte mass and shortened red blood cell lifespan likely lead to systematic underestimation of alcohol exposure by PEth in anemic patients. These findings have important implications for the clinical interpretation of PEth and highlight the need to consider hemoglobin levels when using PEth in advanced liver disease.

FRI-086
Impact of cardiometabolic risk factors on the prognosis of alcohol-related hepatitis: a study in the era of the new steatotic liver disease nomenclature

Pablo Solis-Munoz[1,2,3], María De la Flor-Robledo[3,4], Jorge Rivas-Izquierdo[5], Miguel Fernández-Bermejo[1,2], Daniel Martín Holgado[1], Sergio Casiano-Manzano[1], Zulianni Jiménez-Colmenarez[1], Joaquín Domínguez-Humanes[1], Carmelo García-Monzón[6,7], José Antonio Solís-Herruzo[8,9]. *[1]Department of Gastroenterology. Hepatology Unit. Hospital Universitario de Cáceres., Cáceres, Spain; [2]Instituto Universitario de Biomarcadores de Patologías Moleculares (IBPM). Universidad de Extremadura., Cáceres, Spain; [3]Faculty of health sciences. Universidad Alfonso X El Sabio. Villanueva de la Cañada, Madrid. Spain, Villanueva de la Cañada, Madrid, Spain; [4]Department of Anaesthesiology. Hospital Universitario Severo Ochoa, Leganés, Madrid, Spain; [5]Gastroenterology and Hepatology Unit. Unidad Médica Angloamericana, Madrid, Spain; [6]Liver Research Unit, Hospital Universitario Santa Cristina, Instituto de Investigación Sanitaria del Hospital Universitario de La Princesa, Madrid, Spain; [7]Centro de Investigación Biomédica en Red de Enfermedades Hepáticas y Digestivas (CIBEREHD), Instituto de Salud Carlos III, Madrid, Spain; [8]Gastroenterology and Hepatology Laboratory, Research Institute, Hospital Universitario 12 de Octubre, Madrid, Spain; [9]Department of Medicine. Medical School, Universidad Complutense de Madrid, Madrid, Spain*
Email: pablo.a.solis@hotmail.com

Background and aims: Cardiometabolic risk factors (CMRF) have traditionally been overlooked in alcohol-related liver disease (ALD), and their impact on alcohol-relaated hepatitis (AH) remains unexplored. We aimed to assess the influence of CMRF, including number and control, on complications and mortality in patients with AH using the newly proposed steatotic liver disease (SLD) nomenclature and diagnostic criteria.
Method: In this prospective cohort study, we analyzed 100 patients with biopsy-proven AH. Clinical and laboratory data, including obesity, hypertension, diabetes, triglycerides, and HDL cholesterol levels, were collected upon admission, according to the new SLD framework. Patients were followed up for complications during admission and for one year to assess mortality.

Results: Patients with AH and CMRF had higher mortality (46% vs. 25%, p = 0.049) and more complications, notably acute kidney injury (52% vs. 29%, p = 0.030) and infection (31% vs. 9.6%, p = 0.014) than those without CMRF. Logistic regression showed that only patients with ≥3 CMRF had more complications, and mortality, both all-cause (82% vs. 25%, p < 0.001) and liver-related (53% vs. 22%, p = 0.019), while those with 1–2 CMRF had outcomes similar to those of patients without CMRF. These patients also had higher MELD (30 vs. 24, p = 0.010) and Maddrey's mDF (52 vs. 46, p = 0.011) scores than those with 2 or less CMRF. In the multivariable analysis, the MELD score, infections, and diabetes were independently associated with 1-year mortality. Furthermore, patients with poorly controlled CMRF had a higher mortality risk than those with well-controlled CMRF (OR 4.7 [1.4–18]; p = 0.016). A new, intuitive cardiometabolic control (CMC) score integrating the number and degree of CMRF control was also associated with short- and long-term mortality.
Conclusion: The presence, burden, and degree of control of cardiometabolic risk factors significantly influenced outcomes of AH in our cohort. Patients with clustered (≥3) or poorly controlled CMRF had higher risks of complications and mortality, highlighting the potential value of metabolic assessment and management in ALD, particularly in those who later develop AH.

FRI-087-YI
Episodic heavy drinking and implications for steatotic liver disease nomenclature: a national USA study
Yinan Su[1], Jennifer Dodge[2,3], Brian Lee[2]. [1]*Keck School of Medicine, University of Southern California, Los Angeles, United States;* [2]*Division of Gastroenterology and Liver Diseases, University of Southern California, Keck School of Medicine, Los Angeles, United States;* [3]*Department of Population and Public Health Sciences, University of Southern California Keck School of Medicine, Los Angeles, United States*
Email: yinansu@usc.edu

Background and aims: International agencies define heavy drinking by average increased alcohol consumption OR episodic heavy consumption, which do not always coexist. However, SLD nomenclature only captures average alcohol consumption to define subgroups. We assessed prevalence of episodic heavy drinking among SLD subgroups, and differences in liver fibrosis among MASLD with (vs. without) episodic heavy drinking, compared to MetALD and ALD.
Method: We performed a cross-sectional analysis using the nationally-representative US National Health and Nutrition Examination Survey (NHANES) 2017–2023, including adults with vibration-controlled transient elastography (VCTE) data. Episodic heavy drinking was ≥4 drinks (women) and ≥5 (men) on any day, at least once per month. SLD was defined as controlled attenuation parameter ≥248 dB/m and/or liver stiffness measurement (LSM) ≥8 kPA by VCTE. Significant and advanced liver fibrosis were LSM ≥8 and ≥12 kPA by VCTE. Multivariable logistic regression evaluated the association of episodic heavy drinking with liver fibrosis, adjusting for age, gender, and average alcohol consumption. SLD subgroup prevalence was compared using consensus nomenclature vs. if episodic heavy drinking was considered as increased alcohol use under nomenclature.
Results: Among 8,006 adults, 4,571 had SLD: 3,969 had MASLD, 373 had MetALD, and 144 had ALD per consensus nomenclature. Among MASLD, 632 (15.9%) had episodic heavy drinking, which was associated with higher likelihood of significant (aOR 1.69 [95%CI 1.11–2.58]) and advanced (aOR 2.76 [1.58–4.80]) liver fibrosis vs. without episodic heavy drinking. The adjusted weighted-prevalence of significant liver fibrosis among MASLD with episodic heavy drinking (23.6% [17.6–29.6%]) was higher than MASLD without episodic heavy drinking (15.6% [13.5–17.6%]). Reclassifying those with SLD and episodic heavy drinking as MetALD or ALD decreased weighted-prevalence of MASLD (48.0% [46.0–50.0%] to 40.4% [38.5–42.4%]), and increased MetALD (5.3% [5.6–6.1%] to 12.9% [11.9–13.9%]), while ALD was similar (1.9% [1.5–2.3%] to 2.1% [1.7–2.5%]).
Conclusion: Episodic heavy drinking is prevalent in MASLD and associated with 3-fold higher odds of advanced liver fibrosis. Reclassifying these patients to MetALD would more than double the estimated prevalence of MetALD, and highlights the importance of alcohol patterns in clinical risk stratification.

FRI-088
Triglycerides identify a lower-risk phenotype and predict mortality in clinically suspected alcohol-associated hepatitis
Ana Suárez-Saro Fernández[1], Mónica Barreales Valbuena[1], Alvaro Hidalgo[1], Elena Gómez-Domínguez[1], Berta De las Heras[1], Maria Amo[1], Carolina Muñoz Codoceo[1], Irina Calvo[1], Maria Luisa Manzano Alonso[1], Raquel Muñoz Gómez[1], Ana Martin Algibez[1], Maria Inmaculada Fernández Vázquez[1].
[1]*Hospital universitario 12 de octubre, Madrid, Spain*
Email: anasaro1996@gmail.com

Background and aims: Phenotypic heterogeneity is increasingly recognised in alcohol-associated hepatitis (AH). Higher triglyceride (TG) levels may indicate a low-risk phenotype with relatively preserved hepatic function, but this remains insufficiently characterised. We aimed to assess whether admission TG levels predict short and mid-term mortality in clinically suspected AH.
Method: We retrospectively included consecutive patients admitted with clinically suspected AH. TG were analysed categorically (<150, 150–224, ≥225 mg/dL) and as a log-transformed continuous variable. Baseline characteristics, liver severity scores and 28-, 90- and 180-day mortality were compared across TG groups. Associations with mortality were evaluated using logistic regression, Cox models and Kaplan–Meier analysis, adjusting for age, sex, prior cirrhosis and MELD.
Results: TG measurements were available in 185 of 209 patients with suspected AH. Higher TG levels were associated with a milder biochemical profile (lower INR, transaminases, bilirubin, urea, MDF, GAHS and MELD; p < 0.05). Mortality was consistently higher in the low-TG group (<150 mg/dL) compared with patients with TG≥225 mg/dL at 28 days (13.5% vs 2.9%, p = 0.050), 90 days (22.5% vs 4.5%, p = 0.003) and 180 days (28.1% vs 7.3%, p = 0.002). In univariable logistic regression, TG≥225 mg/dL was associated with substantially reduced mortality at all time points (OR: 0.19–0.22). Log-transformed TG showed a similarly protective association (OR: 0.17–0.23). In multivariable models, logTG remained independently associated with reduced 180-day mortality (OR: 0.28; 95% CI 0.10–0.80). Cox regression confirmed these findings, with logTG showing an adjusted HR of 0.34 (95% CI 0.15–0.77). Kaplan–Meier curves demonstrated higher survival in patients with elevated TG (p = 0.002).
Conclusion: Among patients with clinically suspected AH, higher admission TG levels may identify an alcohol foamy degeneration-like phenotype associated with lower biochemical severity and reduced mortality. TG could serve as an inexpensive and accessible biomarker to refine risk stratification and guide clinical decision-making in AH, a finding that warrants prospective validation.

FRI-089
Use of biopsy to diagnose alcoholic hepatitis in a setting a high prevalence of alcohol consumption
Vanessa Trentzsch[1], Cristina Ripoll[1], Andreas Stallmach[1], Alexander Zipprich[1]. [1]*Jena University Hospital, Department of Internal Medicine IV (Gastroenterology, Hepatology, Infectious Diseases and Central Endoscopy), Jena, Germany*
Email: alexander.zipprich@med.uni-jena.de

Background and aims: Criteria for diagnosis of alcoholic hepatitis (AH) have been proposed, however validation in routine clinical practice is scarce. Furthermore, lack of response to corticosteroids leads to doubts regarding the diagnosis if histological confirmation

was not undertaken. The aim of this study was to evaluate the usefulness of biopsy for the diagnosis of AH.
Method: Between 2019 und 2023, 186 patients underwent transjugular liver biopsy, 74 patients because of the clinical suspicion of AH. NIAAA Alcoholic Hepatitis Consortia Criteria were applied to all patients: (1) jaundice < 8 weeks, 2) recent harmful alcohol consumption, 3) AST < 50 IU/ml, 4) AST/ALT 1.5, 5) both AST and ALT < 400 IU/ml, 6) Bilirubin > 3 mg/dL). Comparison of the number of positive criteria, including probable AH (all criteria) and possible AH (not all criteria fulfilled) and histological diagnosis was done. Usefulness of biopsy was evaluated as the proportion of patients who had alternative diagnoses or were non-responders to prednisolone out of the total population who were biopsied with the clinical suspicion of AH. Results are reported as median (IQR) and n (%) as appropriate.
Results: A total of 74 patients underwent liver biopsy with the clinical suspicion of AH (age 54 years (43–64 years) male 45 (61%), MELD 25 (22–30)). These patients fulfilled 4 (n = 6), 5 (n = 21) or 6 (n = 47) of the NIAAA criteria. From these patients, 60 had histological evidence of AH (81%). Among patients with possible AH (n = 27), 37% [n = 3 (50%) with 4 and n = 7 (33%) with 5 criteria] had other diagnoses while among patients with probable AH (n = 47), 9% (n = 4) had an alternative diagnosis. A total of 42 patients received treatment with corticosteroids (10 with possible and 32 with probable AH). Of these, all but one patient had histological confirmation. Among those who were treated, 12 were non-responders at 7 days according to Lille score (including 1 patient without histological confirmation). Taking into account the number of patients in whom the biopsy excluded an AH (n = 14) and in those in whom it was confirmed (despite lack of response to corticosteroids n = 11), the biopsy provided fundamental support for clinical decision-making in 25 (34%) of patients.
Conclusion: Use of biopsy in the diagnosis of AH is useful in all patients since even in patients who fulfil all diagnostic criteria, 9% had no AH. In one third of patients, biopsy provided essential information in clinical decision making against and after non-response to therapy.

FRI-090-YI
AI-based quantitative histologic comparison of disease architecture across steatotic liver disease subclassifications
Ida Villesen[1,2], Laura Pikkupeura[3], Bilal El-Masri[4], Maria Jimenez-Ramos[5], Peter Andersen[1], Anine Andersen[1], Helle Schnefeld[1,2], Johanne Kragh Hansen[1,2], Kathrine Sejer Sørensen[1], Katrine Tholstrup Bech[1,2], Ea Kyed[1,2], Stephen Atkinson[5], Robert Henderson[5], Dmytro Dvornikov[5], Christina Jayson[6], Darren Fahy[6], Mads Israelsen[1,2], Aleksander Krag[1,2], Torben Hansen[3], Sönke Detlefsen[4], Marc Goldfinger[5], Maja Thiele[1,2].
[1]FLASH - Centre for Liver Research, Odense, Denmark; [2]SDU - University of Southern Denmark, Odense, Denmark; [3]Novo Nordisk Foundation Center for Basic Metabolic Research, Faculty of Health and Medical Sciences, University of Copenhagen, Copenhagen, Denmark; [4]Department of Pathology, Odense University Hospital, Odense, Denmark; [5]GSK Stevenage, Gunnels Wood Road, Stevenage, Hertfordshire, United Kingdom; [6]PathAI Inc., Boston MA, United States
Email: ida.falk.villesen@rsyd.dk

Background and aims: The steatotic liver disease (SLD) nomenclature incorporates both alcohol consumption and metabolic risk factors. Yet, histological differences across the SLD spectrum remain unexplored by novel techniques. We aimed to investigate whether fibrosis distribution, inflammation and cellular composition differed between patients with MASLD, MetALD and ALD when deploying a quantitative histological AI tool.
Method: Single-centre study in Odense, Denmark. Patients were biopsied at first visit. All patients had confirmed MASLD, MetALD or ALD based on metabolic dysfunction and self-reported alcohol intake and phosphatidylethanol measurements. Patients were matched for age and fibrosis stage. A clinical pathologist at Odense performed initial assessment. LiverExplore (PathAI, Boston, Research Use Only; not for use in diagnostic procedures) extracted quantitative histology features from digital H&E whole slide images. The AI-based pathology tool quantitatively differentiated cell subtypes, including distribution and density of immune cells, ballooned and steatotic hepatocytes and fibroblasts. Further, LiverExplore identified different fibrosis subtypes and amount per tissue. We compared the density of cell types and fibrosis distributions using Kruskal-Wallis with p-value correction for multiple testing.
Results: We included 80 patients: 38 MASLD, 20 MetALD, and 22 ALD. Fibrosis stages were distributed as follows (n): F0/1, F1/18, F2/24, F3/27, and F4/10. Mean age was 59 ± 9 years, 72% male. Patients with ALD had substantially more perisinusoidal fibrosis than MASLD and MetALD patients, across both F0–2 and F3–4. Additionally, patients with ALD showed more overall fibrosis, already from earlier stages (F0–2). However, when comparing the densities of injured or healthy hepatocytes and immune cells we found no statistically significant difference between the SLD subgroups. PCA analysis revealed no stratification by fibrosis or SLD subtyping. However, distinct patient clusters emerged according to ballooning, steatosis and lobular inflammation (scored by pathologists) agnostic to SLD subtyping.
Conclusion: Patients with ALD exhibit a greater fibrosis burden than MASLD, particularly within the perisinusoidal compartment, compared across similar fibrosis stages. These architectural differences do not appear to be driven by increased immune cell infiltration or greater hepatocyte injury. PCA analysis suggests distinct histopathological subtypes that are not a function of the driving risk factors of disease.

FRI-091
The gender equity model for liver allocation accurately predicts 90-day mortality and acute kidney injury in alcohol-associated hepatitis
Lankai Xu[1], James Vu[1], Lindsey Immers[1], Jordan Holliday[1], Robert Pecha[1], Lydia Aye[1], Vikrant Rachakonda[1]. *[1]University of California Davis Medical Center, Sacramento, United States*
Email: lcxu@health.ucdavis.edu

Background and aims: The Model for End-Stage Liver Disease (MELD) is commonly used to determine mortality risk in alcohol-associated hepatitis (AH). MELD includes serum creatinine (Cr), which is related to muscle mass, and hence MELD may underestimate disease severity in women due to gender differences in body composition. MELD 3.0 and the Gender Equity Model for Liver Allocation (GEMA) have been developed to address gender disparities in liver disease assessment. The aim of the study was to compare liver disease models for outcome prediction in AH.
Method: This was a retrospective study of 582 patients hospitalized with probable or definite AH from July 2017 to September 2024. Clinical, demographic and laboratory data were obtained at admission. AUROC analysis of logistic regression models was used to compare performance of MELD, MELD-Na, MELD 3.0, GEMA and GEMA-Na for predicting 90-day mortality.
Results: 250 (41.2%) women and 342 (58.8%) men were included. Median age was 45 years, and 267 (45.9%) were Caucasian. 28-day mortality was 19.8%, and 90-day mortality was 32.6%. Compared to men, women exhibited lower BMI [27.0 (IQR 23.4–31.3) kg/m2 vs. 28.0 (IQR 24.2–32.9) kg/m2, $p < 0.035$] with higher serum bilirubin [8.5 (IQR 5.6–17.0) mg/dl vs. 7.6 (IQR 4.6–14.1) mg/dl, $p = 0.023$] and lower serum Cr [0.77 (IQR 0.59–1.15) mg/dl vs. 0.95 (IQR 0.69–1.47) mg/dl, $p < 0.001$]. There were no significant gender differences in MELD, MELD-Na, MELD 3.0, GEMA, and GEMA-Na. GEMA exhibited highest accuracy for predicting 90-day mortality [AUROC: 0.808 (95% CI 0.765–0.851)] with sensitivity of 0.78 and specificity of 0.68 at an optimal cutoff of 23. GEMA exhibited superior performance for 90-day mortality compared to MELD [AUROC: 0.782 (95% CI 0.737–0.827), $p = 0.003$ vs GEMA], MELD-Na [AUROC: 0.776 (95% CI 0.729–0.823)), $p = 0.002$ vs GEMA], MELD 3.0 [AUROC 0.788 (95% CI 0.743–0.833)), $p = 0.028$ vs GEMA] and GEMA-Na [AUROC

0.790 (95% CI 0.744–0.837), $p = 0.013$ vs GEMA]. Acute kidney injury (AKI) developed in 166 patients (28.5%), and GEMA [AUROC:0.858 (95% CI 0.824–0.892)] was superior to MELD [AUROC: 0.797 (95% CI 0.756–0.837), $p < 0.001$], MELD-Na [AUROC: 0.786 (95% CI 0.744–0.828), $p < 0.001$ vs. GEMA], MELD 3.0 [AUROC: 0.800 (95% CI 0.758–0.842), $p < 0.001$], and GEMA-Na [AUROC: 0.844 (95% CI 0.807–0.880), $p = 0.024$].
Conclusion: GEMA demonstrates superior performance for predicting 90-day mortality and acute kidney injury in AH. Prospective studies are planned to assess GEMA to model disease severity in AH.

FRI-092-YI
Integration of polygenic risk score with metabolomics (MetPRS) identifies a protective sphingolipid signature that predicts survival in alcohol-related liver disease
Vaishali Yadav[1], S Muralikrishna Shasthry[1], Mohit Varshney[1], Kanica Kaushal[1], Rishabh Sharma[1], Nirupma Trehanpati[1], Sukriti Baweja[1], Shiv Kumar Sarin[1], Gayatri Ramakrishna[1]. [1]*Institute of Liver & Biliary Sciences, New Delhi, India*
Email: rgayatri@ilbs.in

Background and aims: Alcoholic liver disease (ALD) exhibits marked inter-individual variability in disease severity and survival, suggesting an important role for genetic susceptibility and downstream metabolic alterations. We aimed to understand how genetic risk interacts with metabolic pathways to identify patients at higher risk of adverse outcomes.
Method: ALD Patients (n = 84) were genotyped for four gene variants (PNPLA3 rs738409, MBOAT7 rs641738, TM6SF2 rs58542926, and HSD17B13 rs72613567), and a cumulative genetic risk score (CGRS, 1–7) was derived. Untargeted LC–MS based plasma metabolomics was performed. Associations between genetic risk, metabolite profiles, and survival were assessed using correlation and regression-based models to predict mortality.
Results: ALD patients were stratified into low genetic risk (LGR) (score 1–2; $n = 61$) and high genetic risk (HGR) (score 5–7; $n = 23$) groups. The CGRS alone showed moderate predictive ability for one-year survival (AUC = 0.64, p = 0.02). Out of 164 metabolites only five (sphingosine-1-phosphate (S1P), sphinganine-1-phosphate (DHS-1P), 20-oxopregn-5-en-3-yl hydrogen sulfate, hydroxytryptophol (5-HTOL), and dopamine showed strong prognostic performance for survival (combined AUC = 0.89, $p < 0.001$). Among these, S1P was log2 fold higher in survivors and showed the highest predictive value (AUC = 0.79). Genetic risk integration with S1P further improved discrimination between survivors and non-survivors in the low genetic risk (AUC = 0.93). Correlation analysis revealed that in the low-risk group, S1P (r = 0.50, $p = 0.039$), DHS-1P (r = 0.57, $p = 0.018$), and 20-oxopregn-5-en-3-yl hydrogen sulfate (r = 0.66, $p = 0.004$) were positively associated with survival, whereas these associations were attenuated in the high-risk group ($p < 0.001$). In contrast, 5-HTOL and dopamine showed consistent negative associations with survival in both LGR (r ≈–0.50, $p = 0.039$; r = –0.35, $p = 0.017$) and HGR individuals (r ≈–0.36, $p = 0.002$; r = –0.29, $p = 0.015$), indicating poorer outcomes with higher levels.
Conclusion: Integrated genetic–metabolic(Met PRS) profiling significantly outperforms individual markers in predicting ALD survival. We identified a distinct prognostic divergence: LGR individuals exhibit a protective metabolic endotype, characterized by sphingolipids and steroid sulfates while HGR individuals lack this signature. Contrary, the HGR individuals are characterized by decrease of protective lipid metabolites and shifts towards detrimental neuroamines.

FRI-093
Recompensation criteria and clinical outcomes in decompensated alcohol-associated liver disease: a population-based study in Olmsted county
Yigit Yazarkan[1], Diego Drumond Westgeest e Sousa[1], Alberto Calleri[1], Blake Kassmeyer[2], Kamalpreet S. Hara[1], Puru Rattan[1], Tiffany Wu[1], Patrick S. Kamath[1], Vijay Shah[1], Douglas Simonetto[1]. [1]*Division of Gastroenterology and Hepatology, Mayo Clinic, Rochester, United States;* [2]*Division of Clinical Trials and Biostatistics, Mayo Clinic, Rochester, United States*
Email: yyazarkan99@gmail.com

Background and aims: The prevalence of alcohol-associated liver disease (ALD) is increasing, together with increased mortality and need for liver transplantation (LT). Alcohol abstinence may lead to hepatic recompensation; however, reported recompensation rates remain variable and are largely derived from European cohorts, with estimates of 7–18% using the Baveno VII criteria. We aimed to evaluate the impact of broader criteria on recompensation rates and survival in patients with ALD.
Method: Adult residents of Olmsted County, Minnesota (USA), with decompensated ALD diagnosed between 2020–2024 were identified through the Rochester Epidemiology Project using ICD codes and confirmed by chart review. Recompensation required sustained alcohol abstinence, >12 months without decompensation with improved liver function, and was defined using 3 criteria: Baveno VII (no therapy), expanded Baveno (low-dose therapy: spironolactone ≤200 mg/day; furosemide ≤20 mg/day; lactulose/rifaximin), and extended Baveno (medium-dose therapy: furosemide ≤60 mg/day). Recompensation incidence and its association with mortality were assessed using competing-risk models, treating LT, TIPS, and death as competing events.
Results: Among 121 patients with decompensated ALD, 56 (46%) achieved sustained alcohol abstinence (66% biomarker-confirmed). Median age was 55 years (IQR 44–62), 79% were male, and obesity, hypertension, and diabetes were present in 55%, 77%, and 46%, respectively. Ascites was the most common decompensating event (75%). At alcohol cessation, median MELD 3.0 was 19 (15–23). Cumulative incidence of recompensation at 1 and 3 years was 3.7% and 23% (Baveno VII), 3.7% and 42% (expanded Baveno), and 7.4% and 57% (extended Baveno) (Gray's test, p < 0.001). Five-year mortality after the 12-month landmark analysis was 63% in non-recompensated patients and significantly lower in patients meeting Baveno VII (33%), expanded Baveno (28%), or extended Baveno criteria (32%) (Gray's test, p = 0.049). In subdistribution hazard models, expanded and extended Baveno recompensation were associated with reduced mortality (sHR 0.24,95% CI 0.06–1.04; p = 0.057 and 0.23, 95% CI 0.07–0.76; p = 0.016).
Conclusion: In a contemporary US County population with decompensated ALD, broader recompensation definitions captured higher rates of recompensation and were consistently associated with improved survival. These findings support the adoption of expanded recompensation criteria for outcome assessment and highlight the need for confirmation in future studies.

FRI-094
Trends in transplant outcomes for alcohol-related cirrhosis and alcohol-related hepatitis in the United States over 15 years
Maria Stepanova[1], Giacomo Germani[1,2], Robert Wong[1,3], Fatema Nader[1], Rohit Satoskar[1,4], Saleh A. Alqahtani[1], Linda Henry[1], Patrizia Burra[1,2], Ashwani K. Singal[1,5], Zobair M. Younossi[1]. [1]*The global NASH/MASH council, Washington DC, United States;* [2]*Department of Surgery, Oncology and Gastroenterology, University of Padova, Italy, Padova, Italy;* [3]*Division of Gastroenterology and Hepatology, Stanford University School of Medicine, Palo Alto, CA, United States, Palo Alto, United States;* [4]*Georgetown University Medical Center, Washington DC,*

Washington DC, United States; [5]University of Louisville School of Medicine and Avera Transplant Institute, Louisville, United States
Email: zobair.younossi@cldq.org

Background and aims: Alcohol-related liver disease (ALD) is the leading indication for liver transplantation (LT) in the US and Europe. Within the ALD spectrum, severe alcohol-related hepatitis (AH) has high short-term mortality. We compared characteristics and outcomes of LT patients with ALD cirrhosis (AC) versus AH.
Method: Adult LT candidates and recipients with a primary listing diagnosis of AC or AH were identified from the U.S. Scientific Registry of Transplant Recipients (SRTR), 2006–2022. Demographic and clinical characteristics, waitlist and post-transplant outcomes were compared between two groups.
Results: We included 182,468 adult LT candidates (25% for AC and 0.9% for AH). Over time, LT listing for AC increased from 17% (2006) to 41% (2022). The number of listings with AH were <100 cases per year until 2018 (1.2%) with a subsequent increase to 3.6% (2022). In comparison to candidates with AC, those with AH were younger (44 ± 10 vs. 53 ± 10 years), less commonly male (67% vs. 71%), more commonly covered by a private insurance (63% vs. 53%), with higher MELD scores (32 ± 10 vs. 23 ± 10) (all $p < 0.01$). Of those with ALD, 79% of AH vs. 64% of AC eventually received a LT (77% vs. 47% within 3 months, $p < 0.0001$), 5% vs. 6% died on the list, 3% vs. 5% were removed due to deterioration, and 4% vs. 5% due to improvement. Post-transplant mortality in AH vs. AC was as follows: 1-year 5% vs. 6%, 3-year 10% vs. 13%, 5-year 15% vs. 20% (all $p > 0.01$). In multivariate analysis, being on life support was the only predictor of post-transplant mortality in AH: aHR (95% CI) = 1.77 (1.15–2.73), $p = 0.01$. In patients with AC, post-transplant mortality was higher in those with type 2 diabetes (T2D): 1-year 8% vs. 6%, 3-year 16% vs. 12%, 5-year 24% vs. 19%, 10-year 45% vs. 36%, all $p < 0.0001$. In AC, independent predictors of post-transplant mortality included earlier calendar year (aHR (95% CI) = 0.957 (0.950–0.964) per year), older age (1.027 (1.023–1.030) per year), black race (1.27 (1.11–1.46)), non-Hispanic ethnicity (0.81 (0.75–0.88)), lack of college education (0.88 (0.82–0.94)), Medicaid coverage (1.19 (1.10–1.29)), T2D (1.29 (1.21–1.39)), lower functional status (0.995 (0.993–0.996) per 1 point), the presence of HCC (1.20 (1.08–1.33)), being on life support (1.23 (1.11–1.36)), having received TIPSS (1.20 (1.10–1.31)), and re-transplantation (1.63 (1.34–2.00)).
Conclusion: The share of liver transplantation for both AC and AH is growing, with 5-year survival of >80% in both groups.

FRI-095

Clinician and patient perspectives on stigma, knowledge, and care gaps in alcohol-related liver disease (ALD)

Zobair M. Younossi[1], Phunchai Charatcharoenwitthaya[1,2], Maja Thiele[1], Shira Zelber-Sagi[1,3], Ashwani K. Singal[1], Aleksander Krag[1,4], Hirokazu Takahashi[1], Yuichiro Eguchi[1], Ajeet Bhadoria[1,5], Ajay Kumar Duseja[1,6], KT Shenoy[1,7], Khalid Al Naamani[1,8], Aung Bwa[1,9], Giacomo Germani[1,10], Nicola Pugliese[1,11], Ming-Hua Zheng[1,12], Jian-Gao Fan[1,13], Yusuf Yilmaz[1,14], George Papatheodoridis[1,15], Mohamed El-Kassas[1,16], Mario Guimarães Pessoa[1,17], Claudia Pinto Oliveira[1,17], Cristiane Villela Nogueira[1,18], Ming-Lung Yu[1,19], Frank Tacke[1,20], Neeraj Bhala[1,21], Wah-Kheong Chan[1,22], Marco Arrese[1,23], Wendy Spearman[1,24], Javier Crespo[1,25], Munkhbat Batmunkh[1,26], Hasmik Ghazinyan[1,27], Robert Wong[1,28], Vincent Wai-Sun Wong[1,29], Lamia Haque[1,30], Juan Pablo Arab[1,31], Luis Antonio Diaz[1,32], Ali A Weinstein[1,33], Jenn Jones[1,34], Michael Betel[1,35], Jane Ranagan[36], Markos Kalligeros[1,37], Fatema Nader[1,38], Linda Henry[1,38], Maria Stepanova[1,38]. *[1]The global NASH/MASH council, Washington DC, United States; [2]Division of Gastroenterology, Department of Medicine, Faculty of Medicine Siriraj Hospital, Mahidol University, Bangkok, Thailand, Bangkok, Thailand; [3]School of Public Health, Faculty of Social Welfare and Health Sciences, University of Haifa, Haifa, Israel; [4]Centre for Liver Research, Department of Gastroenterology and Hepatology, Odense University Hospital and University of Southern Denmark, Odense, Denmark, Odense, Denmark; [5]All India Institute of Medical Sciences (AIIMS), Rishikesh, India; [6]Department of Hepatology, Post Graduate Institute of Medical Education and Research, Chandigarh, India; [7]Department of Gastroenterology, Sree Gokulam Medical College and Research Foundation, Kerala, India, Kerala, India; [8]Division of Gastroenterology and Hepatology, Department of Medicine, The Medical City for Military and Security Services, Muscat, Oman, Muscat, Oman; [9]Yangon GI and Liver Centre, Yangon, Myanmar, Yangon, Myanmar; [10]Department of Surgery, Oncology and Gastroenterology, Padua University Hospital, Padua Italy, Padua, Italy; [11]Division of Internal Medicine and Hepatology, Department of Gastroenterology, Humanitas Research Hospital, Rozzano, Milan, Italy, Milan, Italy; [12]MAFLD Research Center, Department of Hepatology, the First Affiliated Hospital of Wenzhou Medical University, Wenzhou, China, Wenzhou, China; [13]Department of Gastroenterology, Xinhua Hospital, Shanghai Jiao Tong University School of Medicine, Shanghai, China, Shanghai, China; [14]Department of Gastroenterology, School of Medicine, Recep Tayyip Erdoğan University, Rize, Türkiye, Rize, Türkiye; [15]1st Academic Department of Gastroenterology, Medical School of National and Kapodistrian University of Athens, General Hospital of Athens "Laiko", Athens, Greece, Athens, Greece; [16]Endemic Medicine Department, Faculty of Medicine, Capital University, Cairo, Egypt, Cairo, Egypt; [17]Departamento de Gastroenterologia, Hospital das Clínicas (LIM 07) da Faculdade de Medicina daUniversidade de São Paulo, São Paulo, Brasil, Sao Paulo, Brazil; [18]School of Medicine, Hepatology Division, Universidade Federal do Rio de Janeiro,Brazil, Rio de Janeiro, Brazil; [19]22. Kaohsiung Medical University Hospital, Kaohsiung Medical University, Kaohsiung, Taiwan and Center of Excellence for Metabolic Associated Fatty Liver Disease, National Sun Yat-sen University, Kaohsiung, Taiwan, Kaoshiung, Taiwan; [20]Department of Hepatology and Gastroenterology, Charité - Universitätsmedizin Berlin, Berlin, Germany, Berlin, Germany; [21]Melbourne Digestive Diseases Centre (MDDC), Royal Melbourne Hospital and University of Melbourne Medical School, Parkville Victoria, Australia, Victoria, Australia; [22]Gastroenterology and Hepatology Unit, Department of Medicine, University of Malaya, Kuala Lumpur, Malaysia, Kuala Lumpur, Malaysia; [23]Departamento de Gastroenterología, Escuela de Medicina, Pontificia Universidad Católica de Chile, Santiago, Chile, Santiago, Chile; [24]Division of Hepatology, Department of Medicine, Faculty of Health Sciences, University of Cape Town, Cape Town, South Africa, Cape Town, South Africa; [25]Gastroenterology and Hepatology Department, Clinical and Translational Research in Digestive Diseases, Valdecilla Research Institute (IDIVAL), Marqués de Valdecilla University Hospital, Spain, Santander, Spain; [26]Graduate School, Mongolian National University of Medical Sciences, Ulaanbaatar, Mongolia, Ulaanbaatar, Mongolia; [27]Hepatology Department, NORK Clinical Hospital of Infectious Diseases, Yerevan, Armenia, Yerevan, Armenia; [28]Division of Gastroenterology and Hepatology, Stanford University School of Medicine, Palo Alto, United States; [29]Medical Data Analytics Center, Department of Medicine and Therapeutics, The Chinese University of Hong Kong, Hong Kong, Hong Kong; [30]Digestive Diseases, Yale Medicine, New Haven, CT, USA, New Haven, United States; [31]Division of Gastroenterology, Hepatology, and Nutrition of Virginia Commonwealth University School of Medicine, Richmond, VA, USA, Richmond, United States; [32]Division of Gastroenterology & Hepatology, UC San Diego, La Jolla CA, USA, La Jolla, United States; [33]Department of Global and Community Health, George Mason University, Fairfax, VA, USA, Fairfax, United States; [34]Sober Livers, Aurora, CO, United States, Aurora, United States; [35]Fatty Liver Alliance, Toronto, Canada; [36]Chronic Liver Disease Foundation, Clark, New Jersey, United State, Clark, United States; [37]Division of Gastroenterology and Hepatology, Beth Israel Deaconess Medical Center, Harvard Medical School, Boston, MA, USA, Boston, United States; [38]Center for Outcomes Research in Liver Diseases, Washington DC, USA, Washington DC, United States*
Email: zobair.younossi@cldq.org

Background and aims: Alcohol-associated stigma, gaps in clinician knowledge about ALD and alcohol use disorder (AUD), and

suboptimal practice patterns may adversely affect ALD management. We evaluated stigma and ALD management from both clinician and patient perspectives.

Method: Two global, web-based anonymous surveys were conducted. Clinicians reported ALD-related knowledge, perceptions (discomfort, empathy, perceived patient responsibility, alcohol underreporting, frustration with care), and practice patterns (alcohol screening, fibrosis assessment, and AUD management). Patients with ALD reported alcohol-related behaviors, and stigma, including self-stigma (cognitive, affective, behavioral domains) and perceived stigma (stereotypes, discrimination, shame, social isolation).

Results: A total of 440 clinicians (290 gastroenterology/hepatology [GI/Hep], 150 non-GI/Hep) and 305 ALD patients completed surveys. GI/Hep clinicians were more often based at tertiary or transplant centers and cared for more ALD patients than non-GI/Hep clinicians (all $p < 0.05$). Despite recognizing the importance of ALD, non-GI/Hep clinicians reported greater discomfort taking care of ALD patients and more frequently attributed responsibility, lack of motivation, and poor self-control to patients (all $p < 0.05$). Overall, 86% of clinicians believed patients underreported alcohol use. Noninvasive fibrosis assessment was commonly recommended (85%). Barriers to care included stigma, limited resources, time constraints, and insufficient addiction medicine training. AUD pharmacotherapy was underutilized, particularly in decompensated cirrhosis. Among patients, 54% reported cirrhosis and 56% had ≥1 chronic condition. Current alcohol use was reported by 36% and 51% had prior AUD treatment (mainly outpatient). Perceived stigma was reported by 92%, including shame (82%), stereotyping (72%), and social isolation (61%). Mean self-stigma score was 27 ± 9 (range 9–45), highest in the cognition domain. Alcohol underreporting due to shame, guilt, or fear was reported by 47%. Among suggested terms, alcohol-related liver disease was considered least stigmatizing by both clinicians (40%) and patients (51%).

Conclusion: ALD-related stigma is prevalent among both clinicians and patients and is associated with clinician discomfort in providing care, reduced disclosure of alcohol use, and suboptimal management of AUD. Findings from this international survey support prioritizing multifaceted stigma-reduction strategies.

FRI-099

Development and validation of a disease-specific health-related quality of life questionnaire (HRQL) for alcohol-related liver disease (CLDQ-ALD)

Zobair M. Younossi[1], Maria Stepanova[1], Leyla de Avila[1], Issah Younossi[1], Andrei Racila[1]. [1]*Center for Outcomes Research in Liver Diseases, Washington DC, USA, Washington DC, United States*
Email: zobair.younossi@cldq.org

Background and aims: Alcohol-related liver disease (ALD) is a leading cause of advanced liver disease and a major indication for liver transplantation. Despite its substantial clinical, humanistic, and societal burden, ALD-specific HRQL instruments are lacking. Accurate HRQL assessment is essential in clinical research and therapeutic trials in ALD. Accordingly, this study aimed to develop and validate an ALD-specific HRQL instrument using a standard protocol for disease-specific HRQL instrument development.

Method: A comprehensive list of HRQL items was generated based on ALD patients' individual interviews and focus groups, existing HRQL instruments, and input from expert healthcare providers. Items were reduced through administration to patients with ALD, calculation of item impact scores, assessment of face validity, exploratory factor analysis, and evaluation of within-domain consistency and redundancy. The final CLDQ-ALD instrument then underwent initial steps for psychometric validation.

Results: The initial questionnaire comprised 90 items. Across two rounds of item reduction, it was completed by 91 patients with ALD (round 1: n = 19 [26% <45 years, 47% male, 5% with type 2 diabetes (T2D), 68% with cirrhosis, 26% current alcohol use]; round 2: n = 72 [32% <45 years, 69% male, 18% with T2D, 39% with cirrhosis, 40% current alcohol use]) and reduced to 40 final items. Exploratory factor analysis identified nine factors explaining >95% of the total variance. Based on factor loadings, items were assigned to nine domains (Fatigue, Alcohol, Function, Physical, Abdominal Symptoms, Itching, Sleep, Emotional, and Worry). Face and construct validity were assessed, along with concordance with the validated CLDQ instrument (CLDQ-MASH). The final CLDQ-ALD demonstrated good to excellent psychometric performance, with high internal consistency (Cronbach's α >0.85 across all domains and >0.90 in 5 of 9 domains). Item-domain correlations exceeded 0.60 for 39 of 40 items and were <0.90 for all items, with each item correlating most strongly with its assigned domain. No substantial floor or ceiling effects were observed. Known-groups validity demonstrated mean score differences >0.5 in relevant domains by sex, presence of T2D, current alcohol use, depression, clinically overt fatigue, and cirrhosis. Additional psychometric analyses are ongoing.

Conclusion: The CLDQ-ALD is a disease-specific HRQL instrument for use in clinical research and therapeutic trials involving patients with ALD.

FRI-100

Cell-free DNA as a biomarker of liver fibrosis in alcohol-related liver disease

Paola Zuluaga Blanco[1], Daniel Fuster[1], Berta Martín[2], Marvin Bueno-Vélez[3], Mireia Torres[3], Mar Muñoz[2], Miguel Angel Peinado[2], Robert Muga[1]. [1]*Hospital Germans Trias I Pujol, Universidad Autónoma de Barcelona-Campus de Bellaterra, Badalona, Spain;* [2]*Igtp Institut Germans Trias I Pujol, Badalona, Spain;* [3]*Hospital Germans Trias I Pujol, Badalona, Spain*
Email: ypzuluaga.germanstrias@gencat.cat

Background and aims: The study of cell-free DNA (cfDNA) methylation in alcohol-related liver disease (ALD) is limited, but there is an emerging interest on it, especially in hepatocellular carcinoma. Most studies have focused on tissue DNA methylation, showing that ALD is associated with aberrant methylation patterns, which may contribute to disease progression. We aimed to describe the global characteristics of cfDNA methylation according to the degree of liver fibrosis (LF) in Alcohol Use Disorder (AUD) patients referred to treatment.

Method: Pilot study of cfDNA methylation microarrays (ILLUMINA) in a cohort of patients with Alcohol Use Disorder (AUD) admitted to detoxification program. We excluded patients with alcohol-related cirrhosis or/and other liver diseases. We quantified cfDNA by fluorometry, we inferred the putative contribution of different tissue to the origin of the cfDNA using cell-type methylation atlas and validated deconvolution standalone program. We also performed an analysis to determine the pace of biological aging using DunedinPACE. We used the Shear Wave Elastography (SWE) to stratify the stage of LF according to the median of ten determinations of kPa value. We stratified in F0-F1 (kPa < 7.0), F2 (kPa 7.1–8) and F3 (kPa > 8). We correlated the results with liver parameters.

Results: We included 47 patients (78% men) with mean age of 49.7 ± 7.6 years and mean alcohol consumption of 173 ± 78 gr/day. The mean biological age was 57 ± 10.8 years with differences from the real age of 7.3 ± 6.29 years ($p < 0.01$). The amount of cfDNA was higher in patients with more advanced stages of LF; 50.41 ± 10.83 ng/µL in F0–F1 (n = 29), 56.39 ± 13.01 ng/µL in F2 (n = 8) and 99.18 ± 100.42 ng/µL in F3 (n = 10); $p = 0.02$. The contribution of liver tissue of the cfDNA was greater in patients with more advanced stages of LF; 2.40 ± 5.06% in F0–F1; 6.17 ± 8.19% in F2 and 4.37 ± 4.70% in F3; $p = 0.04$. The percentage of liver tissue origin was directly correlated with AST ($r = +0.35$, $p < 0.01$) and ALT ($r = +0.20$, $p < 0.01$) and inversely correlated with serum bilirubin ($r = -0.12$, $p = 0.01$) and Lactato Dehydrogenase enzyme ($r = -0.11$, $p = 0.02$).

Conclusion: Cell aging by epigenetic footprint show accelerated ageing in patients with AUD. Cellular aging, the amount of cfDNA, and the contribution of liver tissue to cfDNA were higher in advanced stages of liver fibrosis. CfDNA may have utility in non-invasive diagnosis and staging of liver fibrosis in patients with ALD.

Alcohol-related liver disease and MetALD – Experimental and pathophysiology

TOP-223

MLCK platelet ignites neutrophil via mitochondrial transfer to trigger liver injury

Juan Wang[1], Xianda Wang[1], Haiyuan Shen[1], Sainan Tang[2], Shuang Wu[3], Yaqun Li[2], Jiayi Zhu[1], Miaomiao Wu[1], Jerrold R. Turner[4], Zi Zuo[2], Hua Wang[1]. *[1]Department of Oncology, the First Affiliated Hospital of Anhui Medical University, Hefei, China, Innovation and Entrepreneurship Laboratory for College Students, Laboratory of Molecular Biology, Department of Biochemistry, Anhui Medical University, Hefei, China, Hefei, China; [2]Innovation and Entrepreneurship Laboratory for College Students, Laboratory of Molecular Biology, Department of Biochemistry, Anhui Medical University, Hefei, China, Hefei, China; [3]School of Pharmacy, Anhui Medical University, Hefei, China, Hefei, China; [4]Department of Pathology, Brigham and Women's Hospital and Harvard Medical School, Boston, Massachusetts, USA, Hefei, China*
Email: wangjuan5102020@163.com

Background and aims: Neutrophil-induced inflammation underlies a wide spectrum of liver pathologies, including alcohol-associated hepatitis (AH), but the triggers of neutrophil activation remain unclear. Platelets are known to contribute to inflammation beyond their roles in hemostasis and thrombosis. This study aims to elucidate the mechanisms of platelet-neutrophil crosstalk in driving NET formation and liver injury, and to explore novel therapeutic targets.
Method: Using single-cell RNA sequencing (scRNA-seq), transmission electron microscopy (TEM), intravital microscopy (IVM), stimulated emission depletion (STED) microscopy, structured illumination microscopy (SIM) and genetic knockout models, we investigated platelet activation, tunneling nanotube (TNT) formation, mitochondrial transfer, and neutrophil extracellular trap (NET) formation in human patients and mouse models of AH, drug-induced liver injury (DILI), and sepsis. In vitro co-culture systems, mitochondrial tracking, pharmacological inhibition, and platelet transfusion experiments were employed to validate mechanistic insights.
Results: We identified a distinct $MLCK^+$ platelet subpopulation that forms TNTs in a Piezo1/Ca^{2+}-dependent manner. These platelets transfer functional mitochondria to CXCR2-high neutrophils via TNTs, fueling oxidative phosphorylation, enhancing glycolytic capacity, and igniting sustained NET formation, which exacerbates liver injury. Genetic ablation of MLCK or pharmacological disruption of the CXCL7-CXCR2 axis abrogated TNT formation, mitochondrial transfer, NET release, and liver injury across multiple models (AH, APAP, GaIN/LPS). Platelet transfusion with *Mylk*-deficient platelets, CXCR2 antagonism (SB225002) or small-molecule inhibitor (T4S1820) attenuated inflammation without increasing bleeding risk.
Conclusion: Our findings establish MLCK-dependent mitochondrial transfer via TNTs as a novel mechanism of platelet-neutrophil crosstalk that drives NET formation and liver injury. Targeting MLCK or the platelet-neutrophil interaction axis offers a promising and safer therapeutic strategy for inflammatory liver diseases by mitigating inflammation without compromising hemostasis.

TOP-224-YI

Inhibition of protein kinase C-η as a strategy to overcome steroid resistance in severe alcohol-related hepatitis

Manisha Yadav[1], Sanju Yadav[1], Neha Sharma[1], Gaurav Tripathi[1], Yash Magar[1], Vasundhra Bindal[1], Jayesh Kumar Sevak[1], Babu Mathew[1], Sushmita Pandey[1], Nupur Sharma[1], Anupama Kumari[1], Shiv Kumar Sarin[1], Jaswinder Maras[1]. *[1]Institute of Liver & Biliary Sciences, New Delhi, India*
Email: jassi2param@gmail.com

Background and aims: Severe alcohol-related hepatitis (SAH) is a life-threatening condition in which corticosteroids benefit only ~60% of patients, and the molecular mechanisms underlying steroid non-response remain poorly defined. This study identified host signaling pathways and bacterial signatures associated with steroid resistance in SAH.
Method: A total of 71 SAH patients who had undergone transjugular liver biopsy were enrolled. Liver biopsies from 19 prednisolone treated patients (10-responders (R), 9-non-responders (NR)) were analysed via phosphoproteomics and metaproteomics to identify key kinase and microbial signatures associated with steroid non-response. Findings were validated in 20 patients (cohort-2) via immunohistochemistry and in another 32 patients (cohort-3) using RNA-seq. Pathway and kinase associated with steroid resistance were identified. A key glucocorticoid-modulating kinase was functionally validated *in vitro* and *in vivo* using NIAAA animal model.
Results: Metaproteomic identified 257 bacterial species. NR had significantly reduced alpha diversity ($p < 0.01$) with enrichment of *S. pneumoniae, Staphylococcus aureus,* and *Pseudomonas aeruginosa* ($p < 0.05$). Phosphoproteomics identified 372 kinases ($p < 0.05$). NR exhibited significant up-regulation of pathways associated with steroid resistance such as Th17 signalling, CREB phosphorylation, JAK-STAT signalling, and glucocorticoid receptor (GR) inhibitors ($p < 0.05$), and down-regulation of pathways necessary for steroid response such as HSP90 activity, DUSP3, ERK inhibition, and ECM maintenance ($p < 0.05$). Kinome analysis showed increased activity of GR antagonist kinases such as PRKCH (Protein kinase c-eta), MINK1, AURKA in NR with reduced activity of DUSP3 ($p < 0.01$). PRKCH correlated with *P. aeruginosa* abundance (r^2 >0.7) and plasma pyocyanin levels (>2FC, $p < 0.05$) which induces PRKCH. PRKCH partial inhibition using staurosporine significantly restored prednisolone sensitivity in vitro ($p < 0.01$). In NIAAA binge model, staurosporine plus prednisolone therapy significantly reduced inflammatory markers and pathways compared to prednisolone alone documenting benefit of combination therapy ($p < 0.01$).
Conclusion: Bacterial metabolite pyocyanin, drives PRKCH activation and contributes to steroid resistance in SAH. Targeting PRKCH restores steroid sensitivity and enhances anti-inflammatory activity offering a new potential therapeutic strategy for overcoming steroid resistance.

FRI-101

Identification of a $LYVE1^+$ macrophage population associated with vascular remodelling enriched at early stages of alcohol-related liver disease

Laia Aguilar-Corominas[1], Alicia Martínez-Álvarez[2], Javier Vicente-Mora[1], Jordi Gratacós-Ginès[3], Isabel Graupera[3], Pere Ginès[4], Elisa Pose[3], Mar Coll[1]. *[1]University of Barcelona (UB), Institut d'Investigacions Biomèdiques August Pi i Sunyer (IDIBAPS), Barcelona, Spain; [2]Institut d'Investigacions Biomèdiques August Pi i Sunyer (IDIBAPS), Barcelona, Spain; [3]Hospital Clinic of Barcelona, Institut d'Investigacions Biomèdiques August Pi i Sunyer (IDIBAPS), Barcelona, Spain; [4]University of Barcelona (UB), Institut d'Investigacions Biomèdiques August Pi i Sunyer (IDIBAPS), Hospital Clinic of Barcelona, Barcelona, Spain*
Email: laguilco22@alumnes.ub.edu

Background and aims: Liver sinusoidal loss and capillarisation, associated with vascular remodelling, increase during the

progression of alcohol-related liver disease (ALD). However, the contribution of immune cells, particularly macrophages, to these processes remains poorly understood. This study aimed to characterize a macrophage population associated with sinusoidal and vascular remodelling during ALD progression.
Method: scRNA-seq analysis was performed on liver biopsies from healthy controls (n = 3) and patients with ALD at early (n = 3) and advanced stages (n = 8). Identified myeloid populations were characterized in silico using signalling pathway databases. Spatial proteomic analysis (CD163, collagen, LYVE1, CD34, PDPN, hepatocyte, actin, CK7, VEGF) was performed using the MACSima™ platform on liver biopsies from healthy controls (n = 6) and patients with ALD without fibrosis (n = 4) or with fibrosis (early F0–F1, n = 6; advanced F3–F4, n = 8). In addition, liver clearing of cirrhotic tissue was performed (CD68, LYVE1). Vascular remodelling signatures were validated by gene set enrichment analysis (GSEA) using bulk transcriptomic data from patients with ALD (healthy controls n = 6; early fibrosis n = 5; advanced fibrosis n = 20).
Results: scRNA-seq identified a distinct LYVE1$^+$ macrophage population enriched at early stages of ALD. In silico functional analysis revealed that LYVE1$^+$ macrophages expressed pathways related to sinusoidal and vascular remodelling. Cell-cell interaction analysis indicated predominant interactions with sinusoidal endothelial cells through CDH5. Spatial proteomic analysis confirmed the presence of this macrophage subpopulation and demonstrated its enrichment in ALD patients with early fibrosis. Analysis of sinusoidal (LYVE1) and classical (CD34) endothelial markers showed increased LYVE1$^+$ sinusoidal structures at early disease stages, followed by a reduction at advanced stages, concomitant with an increase in CD34$^+$ vessels. GSEA revealed increased vascular endothelial proliferation and migration signatures at advanced stages. Liver clearing of cirrhotic tissue demonstrated that LYVE1$^+$ macrophages are in close spatial contact with liver sinusoidal endothelial cells. Importantly, sinusoidal density positively correlated with the abundance of LYVE1$^+$ macrophages along disease progression.
Conclusion: A LYVE1$^+$ macrophage population emerges at early stages of ALD and is associated with sinusoidal and vascular remodelling, suggesting a potential role for LYVE1$^+$ macrophages in sinusoidal integrity.

FRI-102-YI
Hepatic stellate cell-derived Follistatin-like 3 ameliorates alcohol-induced liver injury via inhibition of Activin type II receptor signaling pathway
Gloria Alvarez Sola[1], Sabrina Kogan[2], Russell Goodman[3]. [1]*Liver Center, Division of Gastroenterology. Massachusetts General Hospital, Boston, United States;* [2]*Cornell University, Ithaca, United States;* [3]*Liver Center, Division of Gastroenterology, Massachusetts General Hospital, Endocrine Unit, Massachusetts General Hospital, Boston, United States*
Email: galvarezsola@mgh.harvard.edu

Background and aims: Alcohol-associated liver disease (ALD), characterized by progressive fibrogenesis and loss of hepatic function, has no effective treatments. Activin A, a key profibrogenic factor upregulated in ALD, activates canonical SMAD2/3 signalling in hepatocytes, inducing p21-mediated cell-cycle arrest and senescence. We found that follistatin-like 3 (FSTL3), a secreted antagonist of Activin A, is upregulated in the liver and plasma of ALD patients. We aimed to investigate the role and hepatic cellular origin of FSTL3 in ALD, assess its impact on metabolic function, and evaluate the therapeutic potential of bimagrumab, an anti-Activin type II receptor human monoclonal antibody.
Method: Bioinformatic analyses of human and mouse ALD liver datasets, including single-cell RNA-seq data, were performed to assess FSTL3 expression and its cellular origin. FSTL3 regulation was evaluated in ethanol-treated human liver organoids. The functional role of FSTL3 was investigated in ALD mouse models using AAV-mediated Fstl3 overexpression, global Fstl3 knockout (KO), and treatment with bimagrumab.
Results: FSTL3 was significantly upregulated in human liver biopsies and mouse models of ALD, was induced and secreted in ethanol-treated human liver organoids and was identified as secreted via activated hepatic stellate cells. *In vivo*, Fstl3 overexpression and bimagrumab treatment consistently reduced hepatic fat accumulation, inflammatory markers, and p21 expression in mouse models of ALD. These effects were reversed in ethanol-fed Fstl3-KO mice, which exhibited significantly higher levels of hepatic fat, p21 expression and inflammatory markers compared with wild type. Gene Set Enrichment Analysis revealed repression of hepatic Smad2/3 target gene activation in ethanol-fed mice overexpressing Fstl3. *In vitro*, FSTL3 rescued Activin A-induced loss of Huh7 viability.
Conclusion: Hepatic stellate cell-derived FSTL3 may act as an intrinsic protective factor in ALD by antagonizing Activin A-mediated SMAD2/3 signaling pathway. Enhancing FSTL3 activity or blocking the hepatic Activin type II receptor using antagonists such as bimagrumab may offer a therapeutic approach to limit liver injury and influence early disease mechanisms in ALD.

FRI-103
Impact of fecal microbiota transplant from select human donors on alcohol intake in an immunocompetent alcohol use disorder model is sex-selective
Lauren May[1], Jennifer Wolstenholme[1], Alexander Khoruts[2], Jasmohan Bajaj[1]. [1]*Virginia Commonwealth University, Richmond, United States;* [2]*University of Minnesota, Minneapolis, United States*
Email: jasmohan.bajaj@vcuhealth.org

Background and aims: Alcohol-related liver disease (ALD) and continuing alcohol use disorder (AUD) needs a concerted effort beyond current therapies to address addiction & liver disease. Altered gut microbiome in ALD is a target. Fecal microbiota transplant (FMT) in human trials with germ-free (GF) translation were successful but focused only on males. GF mice are not immunocompetent. Moreover, the impact of different human FMT donors into immunocompetent recipients is unclear. Aim: In immunocompetent mice determine the impact of sex and FMT donor on alcohol consumption.
Method: Conventional male and female C57BL/6 mice received three courses of oral antibiotics (Abx) using validated techniques to enhance human FMT engraftment while remaining immunocompetent. Male & female groups were (1) no-Abx (2) Abx only (3) Abx with FMT from human donors (1, 2 & 3). Stools from 3 healthy human donors from an accredited stool bank were administered using gavage to the assigned mouse groups. Then voluntary alcohol intake and preference in an intermittent two-bottle choice paradigm were assessed for five weeks. We also performed behavioral tests for anxiety-like & locomotor function (open field & Rotarod) during the same timeframe.
Results: We included 10 mice per subgroup and all survived the testing. Alcohol intake: found notable sex differences in response to cross-species FMT and alcohol intake. Two of the three human FMT donors significantly reduced ethanol intake and preference in female mice, while no significant reductions were found in ethanol intake or preference in male mice. Donor 1 reduced ethanol preference by 30.4% and was significantly different from the no-Abx group ($p = 0.0001$, two-way ANOVA), and donor 2 reduced ethanol preference by 21.3% and was also significantly different from the no-Abx group ($p = 0.008$, two-way ANOVA). Other behavioral tests: Anxiety-like and locomotor behavior in the open field did not differ between groups or by sex following FMT or ethanol drinking ($p > 0.05$, one-way ANOVA).
Conclusion: In a model of immunocompetent mice with antibiotic pre-treatment, female mice were affected by FMT donors, which resulted in reduced alcohol intake. The same donors had no significant impact on male mice. The impact of microbial transfer is unique to alcohol behavior because anxiety &locomotion tests were unaffected. This model provides a foundation for further mechanistic

studies and donor selection via FMT to influence drinking in clinical trials & experimental studies.

FRI-104

Thermoneutral housing alters ethanol metabolism and exacerbates hepatic steatosis in a mouse model of alcohol-associated liver disease

José Fernandez-Checa[1], Monica Barrios[2], Laura Fábrega[2], Denise Pinheiro[3], Susana Nuñez[2], M. Carmen Garcia-Ruiz[2]. [1]*Institute of Biomedical Research of Barcelona, IIBB-CSIC, CIBEREHD, Keck School of Medicine, University of Southern California, Los Angeles, CA, USA, Barcelona, Spain;* [2]*Institute of Biomedical Research of Barcelona, IIBB-CSIC, CIBEREHD, Barcelona, Spain;* [3]*Institute of Biomedical Research of Barcelona, IIBB-CSIC, Barcelona, Spain*
Email: checa229@yahoo.com

Background and aims: Alcohol-associated liver disease (ALD) is a major cause of morbidity and mortality. Current models are typically housed at 22°C, the comfort temperature for humans that induce cold stress in rodents, leading to potentially confounding outcomes of relevance for human ALD studies. This study investigates the impact of thermoneutral housing (30°C) on ALD development, hypothesizing that it elicits distinct metabolic and pathological responses compared to standard housing, influencing disease progression.
Method: Male C57BL/6J mice were housed at 22°C or 30°C and subjected to the National Institute on Alcohol Abuse and Alcoholism (NIAAA) acute-on-chronic ethanol feeding model. Hepatic tissue was analyzed for steatosis, inflammation, fibrosis, and ethanol metabolism enzymes. Specifically, we assessed protein expression and activity of cytochrome P450 2E1 (CYP2E1), alcohol dehydrogenase (ADH), and aldehyde dehydrogenase (ALDH), along with blood ethanol and acetaldehyde levels.
Results: Mice housed at 30°C and fed the ethanol diet showed diminished weight gain but exacerbated hepatomegaly and higher quantitative lipid accumulation compared to ethanol-fed mice housed at 22°C. While blood ethanol levels decreased at 30°C, liver acetaldehyde levels significantly increased. Regarding metabolism, 30°C housing resulted in lower CYP2E1 protein expression but significantly higher enzymatic activity, coupled with increased ADH expression and similar ALDH levels, suggesting altered flux through ethanol metabolic pathways. Histopathological analysis further revealed that thermoneutrality significantly exacerbated tissue disorganization and total inflammatory cell infiltration compared to the 22°C group. Notably, specific macrophage infiltration (F4/80) remained comparable between both housing conditions, but thermoneutrality induced increased presence of infiltrating neutrophils. Fibrosis, however, was similar in both housing temperatures.
Conclusion: These data show that thermoneutrality elicits distinct metabolic and inflammatory changes to ethanol response compared to standard housing. This model improves ALD complexity study, offering a more nuanced understanding of environmental factors influence on disease progression.

FRI-105-YI

Exhaled breath condensate bile acid profile correlates with plasma bile acid profile in alcohol related liver diseases

Vasundhra Bindal[1], Gaurav Tripathi[1], Sushmita Pandey[1], Manisha Yadav[1], Neha Sharma[1], Babu Mathew[1], Nupur Sharma[1], Vipul Sharma[1], Yash Magar[1], Sanju Yadav[1], Rakhi Maiwall[1], Shvetank Sharma[1], Jaswinder Maras[1], Shiv Kumar Sarin[1]. [1]*Institute of Liver & Biliary Sciences, New Delhi, India*
Email: shivsarin@gmail.com

Background and aims: Plasma bile acid levels are closely associated with alcohol-related liver disease (ARLD) and reflect hepatic dysfunction. Exhaled breath condensate (EBC) represents a novel, non-invasive matrix for metabolite assessment. We evaluated EBC for assessing identifying different bile acid farctions and compared with plasma bile acids in ARLD patients.
Method: This study enrolled 360 healthy individuals to establish baseline breath bile acid profiles in EBC, assessing postprandial, age, sex, and weight-related variations. Breath and paired plasma bile acids were then analyzed in 120 patients with alcohol-related cirrhosis (ARC) and 120 with severe alcohol-associated hepatitis (SAH) using high-resolution mass spectrometry.
Results: Altogether, 19 bile acids were identified in plasma of which 16 were identified in the breath samples. The most abundant bile acids in both plasma and breath were glycine- and taurine-modified bile acids. Cholic acid and deoxycholic acid were the most affected bile acids, and correlated with changes in gender, age, weight or diet respectively (FC >1.5, $p < 0.05$). Glycochenodeoxycholic acid (FC >6.5, $p < 0.001$), Glycoursodeoxycholic acid (FC >11, $p < 0.001$), and Glycodeoxycholic acid (FC >9.3, $p < 0.001$) were significantly increased in the EBC samples of SAH patients as compared to ARC or controls. Glycochenodeoxycholic acid, glycoursodeoxycholic acid, and glycodeoxycholic acid exhibited strong diagnostic performance in EBC (AUC >0.85) and plasma (AUC ≈0.82), demonstrating high concordance between breath and plasma bile acid profiles.
Conclusion: Glycochenodeoxycholic acid, Glycoursodeoxycholic acid, Glycodeoxycholic acid levels are significantly elevated in breath and plasma of SAH patients compared with alcohol cirrhosis patients, with a diagnostic efficiency of 85%. Exhaled breath condensate is a novel, non-invasive method for detailed bile acid assessment and early prognostication of poor outcome in ARLD patients.

FRI-106

The glucagon/glucagon-like peptide-1 receptor dual agonist survodutide strongly reduces alcohol intake in the lean golden syrian hamster, a preclinical model with spontaneous alcohol preference

Francois Briand[1], Mohsin Hassan[2], Thomas Klein[2]. [1]*Physiogenex, Escalquens, France;* [2]*Boehringer Ingelheim, Biberach, Germany*
Email: f.briand@physiogenex.com

Background and aims: The glucagon/glucagon-like peptide-1 receptor dual agonist survodutide has demonstrated significant benefits in patients with obesity and metabolic dysfunction-associated steatohepatitis. Since excessive alcohol consumption exacerbates outcomes in these patients, we investigated whether survodutide could provide additional benefits by lowering alcohol intake in the golden Syrian hamster, a preclinical model showing a spontaneous preference for alcohol.
Method: Lean (no overweight), 11-week-old, male golden Syrian hamsters were housed with a free access to either normal tap water or 15% alcohol-supplemented water for 7 weeks. Following a 4-week induction period, hamsters were treated s.c. QD with vehicle, semaglutide 15 nmol/kg (used as a positive control) or survodutide 15 nmol/kg for 3 weeks.
Results: During the 4-week induction period, with free access to water or alcohol, hamsters rapidly halved their water intake while progressively increasing their alcohol consumption by 2-fold. Compared with vehicle, both semaglutide and survodutide treatment induced a significant reduction in food intake for 2 weeks, after which food intake returned to vehicle levels. Compared to vehicle, both semaglutide and survodutide treatments resulted in a strong and sustained reduction in alcohol consumption (−55% in cumulative intake for both), while normal tap water intake gradually increased throughout the treatment period (>2-fold cumulative intake with both drugs). Expressed as total water volume consumed during treatment, alcohol intake decreased from 78% to 29% with semaglutide, and from 82% to 20% with survodutide, at the end of the treatment (both $p < 0.0001$ vs. vehicle). Conversely, normal tap water intake increased from 22% to 71% with semaglutide, and from 18% to 80% with survodutide, as a proportion of total water volume consumed t (both $p < 0.0001$). Since lean hamsters were normolipidemic, no major effect on liver fat content and plasma lipid levels

were observed, however, survodutide slightly reduced plasma triglycerides as well as free fatty acids (p = 0.053 vs. vehicle).
Conclusion: The present study demonstrates that survodutide strongly reduces alcohol intake in a hamster model with spontaneous preference for alcohol. These preclinical findings highlight the potential benefits of the glucagon/glucagon like peptide-1 receptor agonist survodutide for the treatment of patients with significant alcohol consumption.

FRI-107
Gut-derived immunoglobulin A activates hepatic macrophages and exacerbates inflammation in alcohol-related liver disease
Min gu Kim[1,2], Min Su Cha[1,2], Deok Hwa Seo[1,2], Gil Won Lee[1,2], Min Seo Park[1,2], Kwon Yong Tak[1,3], Pil Soo Sung[1,2,3]. *[1]The Catholic University of Korea, College of Medicine, Liver Research Center, Seoul, Korea, Rep. of South; [2]Postech-catholic Biomedical Engineering Institute, Department of Biomedicine & Health Sciences, The Catholic University of Korea College of Medicine, Seoul, Korea, Rep. of South; [3]Seoul St. Mary's Hospital, the Catholic University of Korea, Department of Internal Medicine, Division of Gastroenterology and Hepatology, Seoul, Korea, Rep. of South*
Email: pssung@catholic.ac.kr

Background and aims: Mucosal immunoglobulin A (IgA) protects against gut microbes, but its role in alcohol-related liver disease (ALD) is unclear. We tested whether gut-derived IgA accumulates in the liver, binds hepatic macrophages, and amplifies inflammation.
Method: Patients with ALD and controls (ALD n = 222; control n = 20) were assessed for serum IgA, bilirubin and albumin. Liver sections were immunostained for IgA and immune markers; dissociated liver cells were analyzed by flow cytometry to quantify IgA-bound macrophages; hepatic cytokine transcripts were measured by quantitative PCR (qPCR). Mice underwent chronic-plus-binge ethanol feeding with or without fingolimod (FTY720, 1 mg/kg/day) to block gut-to-liver trafficking; serum aspartate/alanine aminotransferase (AST/ALT), IgA, liver immune profiles (single-cell RNA sequencing and flow cytometry), and gut lymphoid IgA-positive cells were evaluated. In vitro, human CD14-positive monocytes were stimulated with plate-coated secretory IgA (sIgA) with or without lipopolysaccharide (LPS); cytokines were quantified by ELISA and conditioned medium was applied to hepatocytes to assess cell death. Statistics: t-test or Mann-Whitney U test as appropriate; correlations: Spearman; two-sided $p < 0.05$.
Results: Serum IgA was higher in ALD than controls and associated with lower albumin and higher bilirubin. High-IgA patients showed increased hepatic IgA deposition and immune infiltration, higher proportions of IgA-bound macrophages, and increased hepatic inflammatory cytokine transcripts. In mice, ethanol increased interleukin-1 beta-high macrophages and expanded IgA-transcript-high plasma cells. Blocking gut-to-liver trafficking (FTY720) reduced serum IgA and AST/ALT and improved histologic liver injury, with lower hepatic Il1b (qPCR). It also decreased IgA binding to macrophages and hepatic IgA and CD138 staining, while IgA and plasma cells accumulated in Peyer's patches. In vitro, sIgA enhanced LPS-induced cytokine secretion by CD14-positive monocytes, and sIgA plus LPS conditioned medium increased hepatocyte death versus LPS alone.
Conclusion: Gut-derived IgA reaches the liver and engages macrophages, exacerbating ALD. Blocking gut-to-liver trafficking reduced systemic/hepatic IgA and IgA-macrophage interactions and improved liver injury readouts, with decreased AST/ALT, attenuated histologic injury, and decreased hepatic Il1b transcripts. These findings support the IgA–macrophage axis as a therapeutic target.

FRI-108-YI
Methyl group donor supplementation modulates gut microbiota and methylome in a metabolic and alcohol-related liver disease murine model
Carolina Díaz-Canul[1], Ángel Vázquez-Esqueda[1], Rebeca Escutia-Gutiérrez[1], Rebeca Rosas-Campos[1], Mónica Ibarra-Hernández[1], Julio Alonso-Vázquez[1], Marina Galicia-Moreno[1], Juan Armendariz-Borunda[1], Ana Soledad Sandoval-Rodriguez[1]. *[1]Universidad de Guadalajara, Centro Universitario de Ciencias de la Salud, Institute for Molecular Biology in Medicine and Gene Therapy, Guadalajara, Mexico*
Email: anasol44@hotmail.com

Background and aims: Metabolic and alcohol-related liver disease (MetALD) is the combined effects of metabolic dysfunction and alcohol consumption, leading to hepatic inflammation and steatosis. Alterations in intestinal barrier function, dysbiosis, bacterial translocation, and dysregulation of DNA methylation contribute to disease progression. The aim was to evaluate the effects of methyl group donor supplementation as a potential therapeutic strategy for metabolic, intestinal, and epigenetic alterations in a MetALD murine model.
Method: Male C57BL/6J mice (10 wks old, 25 g) were randomly assigned to three experimental groups (n = 8): control group (ND); MetALD (20% ethanol in water +45% fat diet); and MetALD + MetMix (MetALD diet + daily gavage of methionine, betaine, zinc sulfate, choline, B9, B6, and B12), maintained for 20 wks. Weekly body weights were measured. Liver and epididymal weights and biochemical analyses (liver enzymes, lipid profile, and hormones) were determined. Histological evaluation was performed on the liver, adipose tissue, and colon. Liver proinflammatory gene expression was measured using qPCR. Gut microbiota was assessed using 16S rRNA gene sequencing, and barrier function was examined using immunohistochemistry of occludin, claudin-1, and E-cadherin expression. Alcian Blue staining was used to quantify the number of goblet cells. DNA methylation was analyzed using the Infinium Mouse Methylation BeadChip. ANOVA with post hoc tests was used for the statistical analysis, with $p < 0.05$ considered significant.
Results: Methyl group donor significantly reduced body weight, epididymal fat mass, serum cholesterol, and high- and low-density lipoprotein levels compared with the MetALD group ($p < 0.05$). A consistent trend toward reduced AST, ALT, triglyceride, very low-density lipoprotein, adipokine, and hepatic Il6 and Tnfa expression was observed. Histological analyses revealed improvements in steatosis, adipocyte hypertrophy, goblet cell number, and occludin, claudin-1, and E-cadherin expression, supporting improved intestinal barrier integrity. Gut microbiota analysis showed differentiation in beta diversity, whereas alpha diversity and the Firmicutes-to-Bacteroidetes ratio displayed an increasing trend. In addition, MetMix supplementation altered the DNA methylation profile.
Conclusion: Methyl group donor treatment improved metabolic and histological parameters, supported intestinal barrier integrity, tended to enhance gut microbiota diversity, and modulated the DNA methylation profile.

FRI-109
Lifestyle and microbiome modification for the management of MetALD in the preclinical DUAL model
Olga Estévez-Vázquez[1,2,3,4], Alisson Quezada Cuadrado[1], Raquel Benedé-Ubieto[1,3], Hector Leal-Lassalle[1,4], Javier Vaquero[2,3,5], Rafael Bañares[2,3,5], Francisco Javier Cubero[1,2,3,4], Yulia Nevzorova[1,2,3,4]. *[1]Departamento de Inmunología, Oftalmología y Otorrinolaringología, Facultad de Medicina, Universidad Complutense de Madrid, Madrid, Spain; [2]Instituto de Investigaciones Sanitarias Gregorio Marañón (IiSGM), 28009, Madrid, Spain; [3]Centro de Investigación Biomédica en Red de Enfermedades Hepáticas y Digestivas (CIBEREHD), Instituto de Salud Carlos III, Madrid, Spain; [4]Instituto universitario de investigación en neuroquímica, Facultad de Medicina,*

Universidad Complutense de Madrid, Madrid, Spain; [5]Servicio de Aparato Digestivo, Hospital General Universitario Gregorio Marañón, 28007, Madrid, Spain
Email: olgaeste@ucm.es

Background and aims: MetALD is term that describes patients with MASLD and simultaneous moderate alcohol consumption. Harmful interaction of alcohol and metabolic risk factors increases the development of steatohepatitis, fibrosis and intestinal dysbiosis. As dietary modifications and physical exercise are the most non-pharmacological recommended therapeutic interventions for MetALD management, in this study we emphasise the beneficial effects of gut microbiota modulation plus lifestyle modifications as an attractive therapeutic strategy to improve the clinical outcome of MetALD.
Method: C57BL/6J male mice received 10% alcohol in sweetened drinking water together with a Western diet (DUAL model) for short (10 weeks) and long (23 weeks) periods. Therapeutic modulations of the microbiome were performed by a) application of probiotic mixture containing 8 strains of *Lactobacillus*, or by b) FMT from healthy donor mice during the last 4 weeks of the short- and long-term feeding period. DUAL diet withdrawal (WTD) was performed by c) the replacement with a chow diet and normal water for 21 days alone or d) in combination of WTD with treadmill sessions (WTD+EX).
Results: The use of probiotics in short-term DUAL feeding did not exert any remarkable benefit in terms of hepatic steatosis, inflammation, or liver fibrosis. FMT from a healthy donor induced mild improvement in liver histology and led to the partial reduction of liver injury, steatosis, hepatic inflammation and fibrosis; however, only in short-term DUAL feeding. DUAL diet withdrawal was the best therapeutic option for early MetALD induced by short-term feeding. Nevertheless, after the long-term DUAL feeding, diet replacement resulted in only a slight improvement of steatohepatitis and fibrosis in the liver. Unless the combination of WTD+EXER led to significant reductions in hepatic steatosis, decreased hepatomegaly, liver damage, hepatic inflammation and attenuated activation of HSC in the advanced stage of MetALD.
Conclusion: Overall, for early-stage MetALD, the efficacy of each therapy ranked as follows: diet withdrawal > FMT > probiotics. Microbiome modulation failed to improve advanced liver phenotypes induced by long-term DUAL feeding. Only the combination of WTD +EXERCISE was the best therapeutic option for advanced MetALD. Our data emphasizes the necessity of prompt dietary and lifestyle intervention in MetALD and suggests that microbiota-targeted therapies may aid recovery if introduced before irreversible hepatic changes occur.
PID2023-150260OB-I00

FRI-110

Aldehyde dehydrogenase 2 deficiency promotes alcohol-associated liver fibrosis via AMPK/DRP1-dependent oxidized mtDNA

Feiyu Zhang[1], Ying Shi[1], Yanhang Gao[1]. [1]*The First Hospital of Jilin University, Changchun, China*
Email: zhangfeiyu00@163.com

Background and aims: Alcohol-associated liver fibrosis is a critical stage in the development of liver cirrhosis, and the current therapeutic approaches have limited efficacy in its intervention. Therefore, clarifying the mechanism of alcoholic liver fibrosis is of great significance for the development of novel therapeutic strategies. The deficiency of aldehyde dehydrogenase 2 (ALDH2) is closely related to the susceptibility to alcoholic liver fibrosis, but its specific mechanism remains unclear.
Results: This study first found that the liver stiffness of patients with alcoholic liver disease carrying the ALDH2 rs671 mutation was significantly higher than that of ALDH2 wild-type carriers, and the level of oxidized mtDNA (ox-mtDNA) in extracellular vesicles in serum was significantly increased; this result was further verified in an alcoholic liver fibrosis mouse model. Mechanistic studies showed that ALDH2 deficiency could inhibit the phosphorylation of AMPK at Thr172 and enhance the phosphorylation of DRP1 at Ser616, thereby inducing mitochondrial fragmentation and promoting the release of extracellular vesicles rich in ox-mtDNA; these vesicles could activate the cGAS-STING signaling pathway in macrophages, drive the activation of hepatic stellate cells, and further exacerbate the process of liver fibrosis. In addition, inhibiting DRP1 activity in ALDH2 knockout mice could partially reverse mitochondrial fragmentation, reduce the level of ox-mtDNA, and delay the progression of fibrosis.
Conclusion: This study revealed a new mechanism by which ALDH2 deficiency promotes alcohol-associated liver fibrosis through the AMPK/DRP1/ox-mtDNA extracellular vesicle axis, providing a theoretical basis for intervention strategies targeting mitochondrial homeostasis.

FRI-111

Therapeutic potential of mesenchymal stem cells in severe alcoholic hepatitis: integrative analysis of transcriptomic signatures and in vivo validation

Seul Ki Han[1,2], Mi Ra Lee[1,2], HyunJung Chung[1,2], Soon Koo Baik[1,2], Jin Suk Lee[2], Moon Young Kim[1,2]. [1]*Department of Internal Medicine, Wonju Severance Christian Hospital, Wonju, Korea, Rep. of South;* [2]*Regeneration Medicine Research Center, Yonsei University Wonju College of Medicine, Wonju, Korea, Rep. of South*
Email: drkimmy@yonsei.ac.kr

Background and aims: Severe alcoholic hepatitis (SAH) has a high mortality rate, yet effective therapies beyond corticosteroids remain limited. Mesenchymal stem cells (MSCs) are emerging as a potential treatment due to their immunomodulatory properties. This study aimed to identify conserved molecular targets in SAH through meta-analysis of public transcriptomes and to evaluate the therapeutic efficacy and mechanisms of human bone marrow-derived MSCs (hBM-MSCs) in a murine SAH model.
Method: We conducted a meta-analysis of 10 publicly available datasets (8 gene expression and 2 prognostic) to identify robust differentially expressed genes (DEGs) and mortality-related signatures. For validation, an SAH model was established in C57BL/6 mice via 4-week ethanol feeding and thioacetamide (TAA) injection. Mice were treated with vehicle, low-dose (5×10^5), or high-dose (1×10^6) hBM-MSCs. Efficacy was assessed by serum biochemistry and histology. The candidate genes from the meta-analysis were validated using qPCR and Western blotting.
Results: The meta-analysis identified 17 downregulated and 7 upregulated genes consistently associated with SAH. In the mouse model, MSC transplantation significantly ameliorated liver injury, evidenced by reduced ALT, AST, and bilirubin levels, alongside attenuated fibrosis and inflammation. Notably, high-dose MSCs showed superior efficacy. Validation revealed that genes predicted to be upregulated—LYN, TLR2, HDAC9, and MAPK3—were confirmed to be overexpressed in the SAH model at both mRNA and protein levels. Importantly, MSC treatment significantly suppressed the protein expression of these targets, correlating with histological recovery. While some predicted downregulated genes showed discordance between mRNA and protein levels, the suppression of LYN, TLR2, HDAC9, and MAPK3 was consistent and dose-dependent.
Conclusion: This study demonstrates that hBM-MSCs effectively mitigate liver injury, inflammation, and fibrosis in a severe alcoholic hepatitis model, with dose-dependent efficacy. The integration of transcriptomic meta-analysis with in vivo protein-level validation successfully identified LYN, TLR2, HDAC9, and MAPK3 as key pathogenic targets modulated by MSC therapy. These findings suggest that MSCs represent a viable therapeutic strategy for SAH, and the identified gene signatures may serve as potential biomarkers for treatment response.

FRI-115

Ethanol reprograms hepatic lymphatic endothelial cells to promote proinflammatory immune trafficking in alcohol-associated hepatitis

Young-Ri Shim[1], Guqing Luo[1], Yilin Yang[1], Jain Jeong[1], Naotaka Kugiyama[1], Teruo Utsumi[1], Matthew J. McConnell[1], Yasuko Iwakiri[1]. [1]*New Haven, United States*
Email: yasuko.iwakiri@yale.edu

Background and aims: Alcohol intake delays wound healing and exacerbates alcohol-associated hepatitis(AH), yet mechanisms remain incompletely understood. The lymphatic system regulates inflammation through immune trafficking. We hypothesized that ethanol alters lymphatic endothelial cell (LyEC) phenotype, leading to dysregulated immune behavior and worsens AH.
Method: A mouse AH model (NIAAA model) was used to isolate hepatic LyECs for RNA-sequencing and immune profiling. Primary human liver LyECs were used for ethanol exposure and co-culture with human peripheral blood mononuclear cells (PBMCs). Immune phenotypes were analyzed by fow cytometry. Human relevance was assessed using liver scRNA-seq from controls and alcohol-associated cirrhosis (GSE136103).
Results: RNA-seq of LyECs from ethanol-fed mice showed strong induction of stress/detoxification genes (Mt1, Mt2, Aldh1a1; padj $<1 \times 10^{9}$) and inflammatory mediators (Il6, Ccl2, Cxcl1, Cxcl10; padj <0.05), indicating pro-inflammatory reprogramming. In parallel, Ccl21b, which regulates CCR7-dependent immune trafficking, was markedly reduced($>2^{3}$ $\log_2$-fold; padj <0.01), suggesting impaired lymphatic guidance. Ethanol also downregulated junctional/mechanosensory genes (Gja4, Pecam1; padj <0.05), while inducing flow-responsive transcription factors(Klf2, Klf4; 2.4-fold; padj <0.02). In vitro, ethanol (100 mM)-treated human LyECs increased CXCL10 (3.7-fold) and CCL2 (2.4-fold; $p < 0.05$). Ethanol-treated LyECs enhanced PBMC migration, with recruited cells expressing higher CXCR3 (1.42-fold, $p < 0.01$; receptor for CXCL10) and CXCR2 (1.9-fold, $p < 0.0001$; chemokine receptor mediating CCL2-driven chemotaxis). CXCL10 knockdown reduced CD4+ T-cell migration($p = 0.06$). Recruited cells were mainly CD4+ T cells and monocytes, not neutrophils or B cells. Attracted CD4+ T cells showed higher CXCR3 ($p < 0.05$). Human liver scRNA-seq confirmed increased CXCR3 in CD4+ T cells from alcohol-associated cirrhosis. Finally, ethanol-fed mice showed enhanced LyEC - CD3+ T cell interactions, with a 1.43-fold increase in hepatic T-cell accumulation ($p < 0.05$) correlating with lymphatic vessel density ($r^2 = 0.61$, $p < 0.0001$), and increased hepatic CXCR3+CD4+ T cells, including IL-17+ subsets ($p < 0.01$).
Conclusion: Ethanol reprograms LyEC toward a dysfunctional, pro-inflammatory states with impaired immune guidance and selective recruitment of CXCR3+ pathogenic CD4+ T cells. LyEC dysfunction defines a new pathogenic mechanism contributing to impaired tissue repair and AH progression.

FRI-116

Performance of MAF-5 versus FIB-4 for predicting liver fibrosis across alcohol intake levels: NHANES 2017–2023

Nikhil Kalita[1], Luis Antonio Diaz[1], Kaleb Tesfai[1], Rohit Loomba[1]. [1]*University of California San Diego, La Jolla, United States*
Email: nikhil.kalita@gmail.com

Background and aims: The Metabolic-Associated Fatty Liver Disease-5 (MAF-5) score is a recently proposed fibrosis risk index designed to overcome limitations of the Fibrosis-4 (FIB-4) index, particularly in individuals with metabolic dysfunction-associated steatotic liver disease (MASLD). However, its performance across levels of alcohol consumption has not been evaluated. This study aimed to validate the performance of MAF-5 in individuals with increased alcohol intake.
Method: The sample included participants from NHANES 2017–2020 and 2021–2023, aged ≥21 years with vibration-controlled transient elastography data. Participants with chronic liver disease, other than SLD, were excluded. Alcohol intake was quantified in grams per week and categorized into weighted tertiles with equivalent sample sizes. Alcohol intake tertiles were defined as low (0.420–6.44 g/week), moderate (6.78–50.76 g/week), and high ($51.02–4.9 \times 10^{3}$ g/week). Survey weights were applied for all analyses. The risk for significant fibrosis (>8 kPa) was assessed using the numeric MAF-5 and FIB-4 indexes. Associations were evaluated using logistic regression overall and by alcohol intake tertile. Discriminatory performance was assessed using AUROC estimation.
Results: The study population consisted of 11,917 participants and was 49.80% male. Overall, 9.59% of participants had significant fibrosis. Both MAF-5 and FIB-4 scores were associated with significant fibrosis across all logistic regression models in the overall sample and within each alcohol intake tertile ($p < 0.05$). MAF-5 demonstrated consistently higher discriminatory performance than FIB-4 across all alcohol intake strata. Overall AUROCs were 0.78 for MAF-5 and 0.63 for FIB-4 ($p < 0.001$). When comparing MAF-5 versus FIB-4, all AUCs were significantly different ($p < 0.001$): in low intake (0.81 vs 0.57), moderate intake (0.77 vs 0.59) and high intake (0.77 vs 0.65) groups, respectively. MAF-5 had better rule-out performance compared with FIB-4 (NPV 98.26% vs 92.22%, respectively).
Conclusion: In a nationally representative U.S. population, MAF-5 demonstrated superior discrimination for significant liver fibrosis compared with FIB-4, even in individuals with increased alcohol intake. These findings suggest that MAF-5 remains a robust tool for assessing fibrosis risk, irrespective of alcohol consumption, and may offer improved clinical utility for fibrosis screening and referral decisions across heterogeneous exposure profiles.

FRI-117

Increased serum concentration and hepatic expression of Fibroblast growth factor 19 suggests it is a potential diagnostic biomarker for alcohol-related hepatitis

Patrycja Kiczynska[1], Alastair M. Kilpatrick[2,3], Laura Martinez-Gili[2], Daniel Rodrigo-Torres[3], Stuart J. Forbes[3], Benjamin H. Mullish[2,4], Julian Walters[5], Mark R. Thursz[2,6], Luke D. Tyson[2,6]. [1]*Imperial College London School of Medicine, London, United Kingdom;* [2]*Department of Metabolism, Digestion and Reproduction, Division of Digestive Diseases, Imperial College London, 10th Floor QEQM Wing, St Mary's Hospital, London W2 1NY, United Kingdom, London, United Kingdom;* [3]*Centre for Regenerative Medicine, Institute for Regeneration and Repair, The University of Edinburgh, Edinburgh BioQuarter, 5 Little France Drive, Edinburgh EH16 4UU, United Kingdom, Edinburgh, United Kingdom;* [4]*Department of Hepatology, St Mary's Hospital, Imperial College Healthcare NHS Trust, London, UK, London, United Kingdom;* [5]*Department of Gastroenterology, Imperial College Healthcare NHS Trust and Division of Digestive Diseases, Imperial College London, Hammersmith Hospital, London W12 0NN, UK, London, United Kingdom;* [6]*Imperial College Healthcare NHS Trust, London, United Kingdom*
Email: patrycja.kiczynska21@imperial.ac.uk

Background and aims: Alcohol-related hepatitis (AH) is a severe form of alcohol-related liver disease, with high mortality. However, it is hard to distinguish from decompensated alcohol-related cirrhosis without AH (DC). Liver biopsy is the gold standard but is invasive and not always available. Serum bile acids (BAs) are elevated in AH, but faecal BAs are reduced. Fibroblast growth factor 19 (FGF19) is usually produced by ileal enterocytes in response to farnesoid X receptor (FXR) activation by BAs. FGF19 acts on hepatocytes to reduce bile acid synthesis. FGF19 may be elevated in AH, despite cholestasis. We evaluated FGF19 as a diagnostic biomarker of AH.
Method: Baseline (D0) serum FGF19 was measured by enzyme-linked immunosorbent assay (ELISA) in 240 clinically-diagnosed AH patients and 189 DC patients from the MICAH cohort. Serum FGF19 was determined in 46 biopsy-proven AH patients from the ISAIAH clinical trial of canakinumab, at D0 and 28 days after treatment (D28).

Paired D0 and D28 RNA-seq data was available for these patients. Serum FGF19 concentrations were compared by Mann-Whitney U, correlation with hepatic FGF19 expression assessed by Spearman's rank, associations by binary logistic regression, and biomarker performance by area under the receiver operating characteristic curve (AUROC) analysis. Significance tests with Benjamini-Hochberg adjusted p values<0.05 were deemed significant.
Results: Serum FGF19 was higher in AH than DC at D0 (median 1270 [IQR 447–9078] vs 335 [201–919] pg/mL, p < 0.001). In AH, serum FGF19 decreased D0 to D28 (3140 vs 351 pg/mL, p < 0.001). D0 FGF19 distinguished AH from DC (AUROC 0.748, p < 0.001). D0 FGF19 correlated with MELD score (rho = 0.27, p < 0.001), but did not associate with 90-day mortality. Serum FGF19 correlated strongly with hepatic FGF19 expression at D0 (rho = 0.87, p < 0.001), and moderately at D28 (rho = 0.48, p < 0.010). Hepatic FGF19 expression did not correlate significantly with hepatic FXR expression (rho = -0.26, p = 0.051) but correlated with vitamin D receptor (VDR, rho = 0.55, p < 0.001) and retinoic acid receptor alpha (RARA) expression (rho = 0.26, p = 0.045).
Conclusion: Serum FGF19 was significantly higher in AH than DC, and performed moderately as a diagnostic biomarker. In AH, hepatic FGF19 production may compensate for reduced ileal production due to cholestasis. Hepatic FGF19 production may be driven by VDR and RARA activation, known to increase FGF19 transcription in enterocytes. This mechanism warrants further exploration.

FRI-118
Efferocytosis-related biomarkers enable non-invasive identification of at-risk metabolic dysfunction-associated steatohepatitis

Jingjing Jiang[1], Weiwei Lou[2], Weiqian Lou[1], Qing Xie[1], Rongtao Lai[1]. *[1]Department of Infectious Diseases, Ruijin Hospital, Shanghai Jiao Tong University School of Medicine, Shanghai, China; [2]Department of Infectious Diseases, Ruijin Hospital, Shanghai Jiao Tong University School of Medicine, Shanghai, China*
Email: xieqingrjh@163.com

Background and aims: Metabolic dysfunction-associated steatotic liver disease (MASLD) is the leading cause of chronic liver disease worldwide, and patients with Efferocytosis is increasingly recognized as a critical process linking hepatocellular injury, inflammation, and fibrogenesis. However, efferocytosis-related molecular signatures in at-risk MASH have not been systematically explored.
Method: Bulk RNA-sequencing data from patients with MASLD (GSE135251: n = 110 training) were analyzed to identify efferocytosis-related genes (ERGs) associated with at-risk MASH, defined histologically by a NAFLD activity score (NAS) ≥4 and fibrosis stage ≥2. Differential expression analysis was applied to screen for genes linked to at-risk MASH, which were intersected with ERGs to obtain risk-associated ERGs, followed by functional enrichment analyses. Three machine learning approaches—stepwise regression, least absolute shrinkage and selection operator (LASSO), and support vector machine–recursive feature elimination (SVM-RFE)—were applied to identify robust hub genes. A predictive nomogram was constructed and externally validated in an independent cohort (GSE174478: n = 50 validation). In addition, the translational potential of these biomarkers was evaluated using a circulating serum proteomics dataset.
Results: Seventeen ERGs were identified as being significantly associated with at-risk MASH, from which five hub genes (CD24, CHI3L1, TREM2, PTGS2, and LGR6) were selected. A hub gene–based predictive model demonstrated strong discriminative performance in the training cohort (AUC = 0.866, 95% CI: 0.817–0.915) and remained robust in the external validation cohort (AUC = 0.805, 95% CI: 0.714–0.897). A simplified serum-based model incorporating TREM2 and CHI3L1 achieved acceptable discriminatory ability (AUC = 0.736, 95% CI: 0.664–0.808).
Conclusion: This study identifies an efferocytosis-related molecular signature associated with at-risk MASH and explore its potential utility for non-invasive risk stratification. These findings highlight efferocytosis as a biologically relevant pathway in MASH progression and provide a foundation for future mechanism-oriented and translational studies.

FRI-119
C-X-C chemokine receptor type 4 and C-X-C motif chemokine 12 mediate liver injury by cytotoxic CD8 T-cells in alcohol-associated liver disease

Gil Won Lee[1], Min Seo Park[1], Kwon Yong Tak[2], Hee Sun Cho[2], Ji Won Han[1,2], Pil Soo Sung[1,2]. *[1]Department of Medical Sciences, Graduate School of The Catholic University of Korea, Seoul, Korea, Rep. of South; [2]Division of Gastroenterology and Hepatology, Department of Internal Medicine, College of Medicine, Seoul St. Mary's Hospital, The Catholic University of Korea, Seoul, Korea, Rep. of South*
Email: pssung@catholic.ac.kr

Background and aims: Alcohol-associated liver disease (ALD) involves chronic immune dysregulation. We hypothesised that CXC chemokine receptor 4 (CXCR4) and its ligand CXC motif chemokine 12 (CXCL12) promote pathogenic CD8 T-cell activation and tissue-directed migration in ALD.
Method: Peripheral blood mononuclear cells (PBMCs) from ALD patients and controls (n = ALD 3, control 3) were analysed by single-cell transcriptomics and flow cytometry to define CXCR4-positive CD8 T-cell states and effector markers. Public transcriptomic datasets were interrogated with gene set enrichment analysis to compare T-cell receptor signalling with cytokine-driven programs (including interleukin 15 and type I interferon). Functional relevance was tested using CXCL12-driven migration assays and hepatocyte co-culture injury assays. Statistics: [tests], two-sided p < 0.05; enrichment was significant at false discovery rate <0.05.
Results: CXCR4-positive CD8 T cells were expanded in ALD and displayed enhanced activation and cytotoxicity, including higher granzyme B and perforin expression than CXCR4-negative cells. Transcriptomic analyses showed preferential enrichment of cytokine-mediated programs (interleukin 15, type I interferon and natural killer-like cytotoxic signatures) with comparatively reduced canonical T-cell receptor signalling, consistent with inflammation-driven activation. CXCL12 selectively promoted migration and enrichment of CXCR4-high CD8 T cells. In hepatocyte co-culture, CXCR4-high CD8 T cells induced greater hepatocyte injury than CXCR4-low/negative cells.
Conclusion: CXCR4-high CD8 T cells represent an activated, cytotoxic population in ALD. The CXCR4-CXCL12 axis couples cytokine-driven activation with directed migration and effector function, supporting this pathway as a potential therapeutic and biomarker target.

FRI-120
Unraveling the progressive remodeling and functional exhaustion of peripheral NK cells in alcohol-related liver disease progression

Young-Sun Lee[1], Ji Hoon Kim[1], Eunho Choi[1], Jong Eun Yeon[1]. *[1]Korea University Guro Hospital, Seoul, Korea, Rep. of South*
Email: lys810@korea.ac.kr

Background and aims: Alcohol-relateded liver disease (ALD) remains a global leading cause of liver-related mortality, yet the immunological drivers of its progression from steatosis to cirrhosis are poorly understood. While Natural Killer (NK) cells are essential for anti-fibrotic surveillance, their functional impairment is a hallmark of chronic liver injury. We sought to elucidate the high-resolution transcriptomic and functional landscape of CD56dim NK cells—the primary cytotoxic subset—across the clinical spectrum of ALD.
Method: We integrated single-cell RNA sequencing (scRNA-seq) and flow cytometry to analyze peripheral blood mononuclear cells (PBMCs) from healthy controls (n = 4), patients with alcoholic fatty liver (AFL, n = 6), and those with alcoholic cirrhosis (n = 3). A

specialized computational pipeline was employed to dissect the CD56dim NK cell compartment, focusing on subset heterogeneity, functional states, and molecular programming.
Results: Analysis of 7,354 high-quality CD56dim NK cells identified four transcriptionally distinct subsets, including a terminally exhausted population. Disease progression was characterized by a profound remodeling of this ecosystem, marked by a massive expansion of exhausted NK cells in cirrhotic patients. These cells exhibited a unique biphasic functional trajectory: a transient hyperactivated state during the AFL stage, followed by a collapse into terminal dysfunction in cirrhosis. Mechanistically, exhausted cells in cirrhosis established a fixed molecular program, upregulating canonical checkpoints (TIGIT, LAG3) alongside novel regulators, specifically the post-transcriptional repressor *ZFP36* and the GPCR-desensitizing protein *ARRB2*.
Conclusion: ALD progression is driven by the systematic expansion and molecular "lockdown" of an exhausted peripheral CD56dim NK cell population. This failure of anti-fibrotic surveillance, defined by a distinct biphasic trajectory, identifies *ZFP36* and *ARRB2* as potential therapeutic targets and offers a robust blood-based molecular signature for disease staging.

FRI-121
Alcohol-induced oxidative stress triggers mitochondrial calcium release through permeability transition pore opening in alcohol-associated steatohepatitis
Kwangwoo Lee[1], Kyurae Kim[1], Jihyo Byun[1], Won-il Jeong[1]. [1]*Korea Advanced Institute of Science and Technology (KAIST), Daejeon, Korea, Rep. of South*
Email: wijeong@kaist.ac.kr

Background and aims: Chronic alcohol consumption leads to mitochondrial calcium (Ca^{2+}) accumulation in hepatocytes. The subsequent mitochondrial Ca^{2+} efflux into the cytosol triggers a cascade of glutamate release, and immune activation, ultimately driving the progression of alcohol-associated steatohepatitis (ASH). However, the mechanism underlying mitochondrial Ca^{2+} release remains unclear. One potential mediator is the mitochondrial permeability transition pore (mPTP), a channel known for its activation in response to mitochondrial reactive oxygen species (ROS). Thus, we investigated the relationship between alcohol-induced mitochondrial ROS production and mPTP-mediated Ca^{2+} efflux in ASH.
Method: For ASH induction, mice were fed ethanol (EtOH) for 2 weeks plus a single binge. Mitochondrial ROS and Ca^{2+} levels were measured *in vivo* and *in vitro* by flow cytometry and fluorescence imaging, using MitoSOX, Calcein AM, and Rhod-2 AM. Mito-TEMPO and Cyclosporine A were applied to inhibit ROS generation and mPTP opening, respectively. Mouse hepatocytes and human HCC cells were subjected to EtOH treatment. Bulk RNA sequencing, quantitative RT-PCR, and Western blotting were conducted for additional analyses.
Results: Bulk RNA-sequencing and qRT-PCR analyses revealed the upregulation of mPTP-related genes in EtOH-fed mouse livers and hepatocytes. *In vitro,* low-dose ethanol (20 mM) treatment for 24 hours increased mPTP- and glutamate-related gene expression, primed by the upregulation of *Aldh2*, a key gene for alcohol–mediated mitochondrial ROS production. In mouse hepatocytes, 20 mM EtOH increased mitochondrial ROS and Ca^{2+} accumulation, as measured by MitoSOX and Rhod-2 AM, respectively. Subsequent 100 mM treatment triggered mPTP opening, confirmed by Calcein AM release, which led to mitochondrial Ca^{2+} efflux and enhanced glutamate secretion from hepatocytes. Consistently, intravital live imaging showed that EtOH feeding elevated Rhod-2 AM intensity, which rapidly declined after binge exposure. Notably, treatments of mitochondrial ROS scavenger (Mito-TEMPO) and mPTP inhibitor (Cyclosporine A) blocked mitochondrial Ca^{2+} efflux in hepatocytes, reducing hepatic glutamate release both *in vivo* and *in vitro*. Coincidently, these findings were reproduced in human SNU475 cells.
Conclusion: Our findings reveal the mechanism of mitochondrial Ca^{2+} efflux in ASH development and suggest that targeting mitochondrial Ca^{2+} signaling may provide a therapeutic strategy for ASH.

FRI-122
A Novel murine model of metabolic dysfunction-associated alcoholic liver disease (MetALD) for therapeutic drug evaluation
Hui Li[1], Jiliang Zhang[1], Sitong Zhang[1]. [1]*WuXi AppTec, Shanghai, China*
Email: li_hui0122@wuxiapptec.com

Background and aims: Metabolic dysfunction-associated alcoholic liver disease (MetALD) is a distinct category that represents a large proportion of metabolic dysfunction-associated steatohepatitis (MASH) patients. With the redefinition of "NASH" to "MASH," MetALD, characterized by the presence of metabolic dysfunction coupled with significant alcohol consumption, has garnered increasing attention in clinical practice. The GAN diet-induced MASH model is a widely recognized MASH model, as it effectively simulates both liver pathology and metabolic dysfunction in MASH. However, like other MASH models, it deliberately excludes the influence of alcohol consumption, failing to replicate the alcohol use in MetALD patients. This study aims to develop a MetALD model for preclinical drug evaluation based on the GAN diet and alcohol consumption, incorporating liver pathology, metabolic features, and the factor of alcohol consumption.
Method: Male C57BL/6 mice were assigned to five groups based on diet, ethanol exposure, and treatment regimen: Healthy + Vehicle, MASH + Vehicle, EtOH + Vehicle, MetALD + Vehicle, and MetALD + Semaglutide. The mice were fed either a chow or GAN diet. Additionally, the EtOH and MetALD groups received ethanol in drinking water and via oral gavage. Semaglutide was administered for six weeks, during which body weight and body composition were monitored. After treatment, liver samples were collected for histological analysis, transcriptomics, and clustering analysis with clinical data.
Results: The MetALD model successfully replicated key features of human pathology, including increased liver damage, steatosis, inflammation, and fibrosis, with the NAS score increasing from 1 to 5 and the liver fibrosis score (LFS) increasing from 0 to 2. Semaglutide administration in MetALD mice reduced the NAS score and LFS score to 3 and 1a/b, respectively, demonstrating the model's ability to simulate phenotypes and verify key drugs for MetALD. Moreover, clustering results indicate a high overlap of key liver genes between MetALD model mice and MetALD patients, suggesting reliable simulation of the model at the mechanistic level.
Conclusion: This novel murine model effectively mimics both pathophysiological and mechanistic characteristics of human MetALD in the context of obesity and alcohol consumption. It potentially serves as an essential tool for understanding the molecular mechanisms underlying MetALD pathogenesis and evaluating potential therapeutic strategies.

FRI-123
Hepatocyte SIRT7 regulates PMN-MDSC differentiation via the FXR–bile acid axis in alcohol-related liver disease
Gaoshuang Liang[1], Yicheng Teng[1], Jing Zhang[1], Jinying Peng[1], Zhuan Li[1]. [1]*Hunan Normal University, ChangSha, China*
Email: zhuanli@hunnu.edu.cn

Background and aims: Polymorphonuclear myeloid-derived suppressor cells (PMN-MDSCs), a pathologically activated subset of neutrophils, have been increasingly implicated in the progression of alcohol-related liver disease (ALD). However, the mechanisms by which injured hepatocytes shape the hepatic immune microenvironment and influence PMN-MDSC differentiation remain poorly understood.
Method: Hepatocyte-specific SIRT7-deficient mice (Alb-Cre SIRT7 −/−) and wild-type littermates were subjected to a Lieber–DeCarli ethanol diet to model ALD. Hepatic immune cell populations were

characterized using flow cytometry and single-cell transcriptomic analysis. The potential interaction between SIRT7 and FXR was examined using co-immunoprecipitation and chromatin immunoprecipitation assays. Targeted metabolomic analyses were performed to assess alterations in bile acid composition. In vitro differentiation assays were used to evaluate the effects of selected bile acids on bone marrow–derived PMN-MDSC differentiation.

Results: Analysis of clinical samples and experimental ALD models indicated an enrichment of CD300ld^{+} PMN-MDSCs in the diseased liver. Hepatocyte-specific deletion of SIRT7 was associated with attenuated alcohol-induced liver injury and a reduction in hepatic PMN-MDSC accumulation. Mechanistic investigations suggested that SIRT7 may interact with FXR and modulate its acetylation status, thereby influencing FXR transcriptional activity on genes involved in bile acid synthesis and transport, including Cyp7a1 and Cyp27a1. Loss of hepatocyte SIRT7 was accompanied by altered bile acid profiles, characterized by a decrease in deoxycholic acid (DCA) levels. Furthermore, in vitro studies supported a potential role for DCA as a metabolic signal capable of enhancing the differentiation of progenitor cells toward a PMN-MDSC-like phenotype.

Conclusion: These data suggested that hepatocyte SIRT7 is closely associated with the regulation of FXR activity and bile acid homeostasis during ALD. Altered bile acid profiles, particularly changes in deoxycholic acid (DCA) levels, may represent an important metabolic link between hepatocyte injury and PMN-MDSC differentiation. Elucidating SIRT7–FXR–bile acid axis may provide a mechanistic basis for understanding hepatocyte–immune cell communication and identify potential targets for therapeutic intervention for ALD.

FRI-124

CREB1-regulated SLC39A1 attenuates alcoholic liver disease by orchestrating autophagy and mitophagy

Xianwei Liu[1], Rui Li[1], Yijin Wang[1]. [1]*Southern University of Science and Technology, Shenzhen, China*
Email: wangyj3@sustech.edu.cn

Background and aims: Alcoholic liver disease (ALD) represents a major global health burden with incompletely understood molecular underpinnings. Zinc transporter SLC39A1 has been implicated in cellular ion homeostasis, yet its functional role in ALD remains elusive. This study aims to decipher a hitherto unrecognized SLC39A1-dependent pathway that confers protection against ALD.

Method: Liver samples from ALD patients were analyzed by immunofluorescence. Hepatocyte-specific Slc39a1 knockout (CKO) mice were subjected to Lieber DeCarli ethanol feeding. Primary hepatocytes were exposed to ethanol in vitro. Liver injury, steatosis, autophagy, and mitophagy were assessed. ChIP and luciferase reporter assays were employed to evaluate CREB1-dependent transcriptional regulation of SLC39A1. Mechanistic insight into SLC39A1-DRP1 interaction was explored using genetic and pharmacological approaches.

Results: Analysis of human samples and GEO datasets revealed upregulated SLC39A1 in ALD patients. Intriguingly, elevated hepatic SLC39A1 correlated with milder liver injury, including reduced steatosis, inflammation, and fibrosis. Ethanol-fed mice exhibited elevated SLC39A1 and associated with improved survival. Conversely, Slc39a1 CKO mice displayed exacerbated liver injury and steatosis. Mechanistically, SLC39A1 deficiency potentiated autophagy flux, evidenced by increased LC3IIB, Atg5, an effect reversed by chloroquine (CQ). Importantly, CQ administration ameliorated liver pathology and improved survival in CKO mice, underscoring the detriment of excessive autophagy. CREB1 was identified as a direct transcriptional activator of SLC39A1, with enhanced promoter binding upon ethanol exposure. Immunofluorescent staining showed a substantial co-localization of SLC39A1 and CREB1 in ALD patients compared to healthy individuals. Furthermore, SLC39A1 physically interacted with DRP1, promoting mitochondrial fission and Fundc1-mediated mitophagy. Disruption of DRP1 genetically or pharmacologically ablated SLC39A1-driven mitophagy, whereas DRP1 overexpression rescued mitophagy and attenuated apoptosis in SLC39A1- deficient hepatocytes.

Conclusion: We reveal a cytoprotective axis where CREB1-driven SLC39A1 curbs alcohol-induced liver injury via dual regulation of autophagy and DRP1-dependent mitophagy. This delineates a novel ALD pathway, nominating SLC39A1 as a therapeutic target.

FRI-125

Spatial transcriptomics reveals metabolic, immune and regenerative reprogramming during disease resolution in severe alcohol-related hepatitis

Ane Otaegui-Chivite[1], Hiromi Kudo[1], Alastair M. Kilpatrick[2], Daniel Rodrigo-Torres[2], Stuart J. Forbes[2], Luke D. Tyson[1], Nikhil Vergis[1], Robert D. Goldin[1], Stephen R. Atkinson[1], Mark R. Thursz[1], Laura Martinez-Gili[1]. [1]*Imperial College London, London, United Kingdom;* [2]*The University of Edinburgh, Edinburgh, United Kingdom*
Email: l.martinez-gili@imperial.ac.uk

Background and aims: Severe alcohol-related hepatitis (sAH) is associated with high mortality. Clinical trials of assets targeting inflammation have shown limited improved outcomes, necessitating identification of alternate therapeutic pathways. We assessed liver spatial transcriptomics changes between baseline and the resolution phase of sAH.

Method: Paired liver biopsies (day 0 and 28) from five sAH patients recruited to the ISAIAH clinical trial (EudraCT: 2017-003724-79; 80% males; 100% treatment arm) were analysed with CosMx human universal 1000-plex RNA panel. Differential gene expression was determined with linear mixed effects models with subject as random intercept. Benjamini-Hochberg-adjusted p values below 0.1 were considered significant. Spatial metrics were computed with Squidpy.

Results: Activated Kupffer cells, myofibroblasts and ductular reaction cholangiocytes were detected at both timepoints. Kupffer cells were the most abundant at day 0 (d0; 22%), followed by hepatocytes (20%), while a higher hepatocyte proportion trend was observed at d28 (29%; $p = 0.11$). Spatial analysis revealed prominent clustering of B cells, myofibroblasts and stellate cells at d0, while hepatocytes were the most spatially clustered at d28. T cells co-localised with Kupffer cells at d0, and with myofibroblasts and cholangiocytes at d28. Expression of liver X receptor beta (NR1H2), apolipoprotein C1 (APOC1) and selenoprotein P (SELENOP) increased at d28 across multiple cell types. Hepatocytes suppressed stress genes (serum amyloid A 1/2 [SAA1/2], alpha-1 antitrypsin [SERPINA1]), and increased growth factors (insulin-like growth factor 1 [IGF1])). Cholangiocytes increased regenerative genes (WNT7B, notch-related genes, frizzled receptors [FZD]). Endothelial and stellate cells downregulated contractile and fibrogenic programs (transgrelin [TAGLN], collagen type I alpha 2 chain [COL1A2], tissue inhibitor of metalloproteinase 1 [TIMP1]). Kupffer cells downregulated activation genes (CD14, toll-like receptor 2 [TLR2]). T cells upregulated immunomodulatory galectin-9 (LGALS9) and chemokines XCL1/2, and B cells cysteine-rich intestinal protein 1 (CRIP1) and CD81.

Conclusion: Resolution of sAH is associated with spatial and functional remodelling of inflammatory and stromal niches, including changes in lymphocytes spatial organisation that may be relevant to tissue repair. Our findings support immune regulation and metabolic resilience as targets for early combination therapies.

FRI-126

Binge alcohol exposure induces neutrophil extracellular trap associated injury in the proximal small intestine

Scott Minchenberg[1,2], Marti Ortega-Ribera[1,2], Alejandro Hionides-Gutierrez[1,2], Siddharth Ghosh Roy[1], Aditi Datta[1], Viliam Brezani[1], Bruna Santos[1], Subhash Kulkarni[1,2], Prashanth Thevkar Nagesh[1,2], Gyongyi Szabo[1,2,3]. [1]*Beth Israel*

Deaconess Medical Center, Boston, United States; [2]Harvard Medical School, Boston, United States; [3]Broad Institute of Mit & Harvard, Cambridge, United States
Email: sminchen@bidmc.harvard.edu

Background and aims: Acute alcohol binges impair intestinal barrier integrity and promote gut-derived inflammatory signaling implicated in alcohol-related liver disease. The proximal small intestine (PSI) is exposed to the highest luminal alcohol concentrations, yet early site-specific inflammatory mechanisms remain poorly defined. We aimed to characterize the inflammatory response to binge alcohol exposure and to assess the roles of oxidative stress and neutrophil extracellular traps (NETs) in intestinal injury.
Method: Eight- to 12-week-old female C57BL/6J mice received daily oral ethanol gavage (3.5 g/kg) for three days. PSI, distal small intestine (DSI), and colon were collected 3 and 24 hours after the final binge. Intestinal injury was assessed by villus height:crypt depth ratios and neutrophil infiltration by Ly6G immunostaining. Neutrophil activation and NET formation were assessed by measuring neutrophil elastase, lipocalin-2, and citrullinated histone H3. Serum endotoxin was quantified by limulus amebocyte lysate assay. To assess oxidative stress, mice received 500 mg/kg N-acetylcysteine (NAC) with ethanol, and to evaluate NET involvement, mice were pretreated with 5 mg/kg DNase I (intraperitoneal) 1 hour prior to each binge. PSI neutrophil chemotactic factors were also assessed.
Results: Three alcohol binges induced a PSI enteropathy with reduced villus height–crypt depth at 3 hours that persisted at 24 hours, while DSI and colon histology remained unchanged. PSI injury was associated with transient neutrophil recruitment and activation peaking at 3 hours, followed by sustained NET formation. Although tissue neutrophil abundance normalized by 24 hours, NET markers, including citrullinated histone H3, remained elevated. Alcohol increased serum endotoxin at 3 hours, consistent with barrier dysfunction. While alcohol increased PSI reactive oxygen species, antioxidant treatment reduced oxidative stress but failed to prevent PSI injury, neutrophil activation, or endotoxemia. In contrast, DNase I pretreatment reduced PSI neutrophil recruitment, activation, NETosis markers, PSI villus blunting, and decreased serum endotoxin.
Conclusion: DNase I pretreatment protects against alcohol-induced PSI enteropathy and gut-derived inflammatory signaling by suppressing neutrophil activation and NET formation. These findings identify extracellular DNA–driven NETosis as a key upstream mechanism of binge alcohol–induced intestinal injury and a potential therapeutic target in alcohol-related liver disease.

FRI-127
Urinary markers of complement and chronic kidney disease are associated with occurrence of acute kidney injury in patients with severe alcohol-associated hepatitis

Luan Prado[1], Megan McMullen[1], Ryan Musich[1], for The AlcHepNet Investigators[1], Laura Nagy[1]. *[1]Department of Inflammation and Immunity, Cleveland Clinic, Cleveland, United States*
Email: pradol2@ccf.org

Background and aims: Patients with severe alcohol-associated hepatitis (sAH) are at risk of developing acute kidney injury (AKI); however, our understanding of the clinical factors and mechanisms for AKI in patients with sAH is an unmet clinical need. Patients with chronic kidney disease (CKD), associated with renal fibrosis, are at increased risk of AKI. Complement, a critical component of innate immunity, is increased in kidneys, urine and plasma of patients with CKD. Further, complement is perturbed in both plasma and urine from patients with sAH. Here we investigated whether urinary biomarkers of complement, fibrosis and CKD are predictive of AKI in patients with sAH and whether kidney injury and fibrosis develop in murine models of heavy alcohol consumption.
Method: Urine collected from 52 patients with sAH at enrollment in the AlcHepNet Observational study (NCT 3850899) was used for global quantitative proteomics. Patients were stratified by estimated glomerular filtration rate (eGFR <60 or >60) and physician diagnosis of AKI during 24 wk follow-up. Male C57BL/6 mice were exposed to the Lieber-DeCarli ethanol diet for 1–2 d at 6% (v/v) ethanol or 5% (v/v) ethanol for 4 w or pair-fed control diets.
Results: Classical urinary biomarkers of AKI, including urinary lipocalin-2 (LCN2), IL-18, and liver fatty acid-binding protein (L-FABP) were detected in the proteomics analysis but did not distinguish patients who developed AKI from those who did not. Further, biomarkers of renal fibrosis and CKD (DKK3) and complement Factor D (CFD), were detected in patients with sAH and were higher in patients with eGFR<60 + AKI. In murine models, expression of tubular injury markers, as well as complement and inflammatory genes were increased in response to 1–2d of 6% ethanol exposure. Kidney injury was further increased after 4 wk/5% ethanol exposure with mice increased expression of mRNA for fibrogenic genes and DKK3 as well as collagen deposition and mild tubular injury.
Conclusion: Biomarkers of complement activation, fibrosis and CKD were increased in the urine of patients with sAH with lower eGFR and a diagnosis of AKI compared to those without AKI, suggesting that CFD and DKK3 are potential prognostic biomarkers for AKI in patients with sAH and low eGFR. Both short term and chronic heavy ethanol exposure in mice resulted in early stages of kidney injury, providing an important pre-clinical murine model to investigate the relation between alcohol, complement and kidney disease.

FRI-132
Disruption of TCA-glutamine metabolism: α-Ketoglutaric acid as a prognostic marker in alcohol-associated liver disease

Sushmita Pandey[1,2], Khan Shahrukh Khan[1], Shreya Sharma[1], Yash Magar[2], Nupur Sharma[2], Babu Mathew[2], Sanju Yadav[2], Manisha Yadav[2], Gaurav Tripathi[2], Vasundhra Bindal[2], Vipul Sharma[2], Jaswinder Maras[2], Anju Katyal[1]. *[1]Dr. B R Ambedkar Center for Biomedical Research, University of Delhi, New Delhi, India; [2]Institute of Liver & Biliary Sciences, New Delhi, India*
Email: anju_katyal@yahoo.com

Background and aims: Alcohol combined with high-fat consumption drives profound metabolic dysregulation in liver disease. This study aimed to characterize time-dependent metabolic alterations using a Wistar rat alcohol-fat model and validate key findings in patients.
Method: Male Wistar rats were subjected to chronic dietary interventions comprising ethanol, high-fat diet, or their combination, alongside a standard control diet, for a total duration of 10 weeks to induce alcohol-associated liver disease. Animals were euthanized at predefined time points (weeks 6, 8, and 10) to capture temporal metabolic alterations during disease progression. Serum samples were collected and subjected to comprehensive untargeted metabolomic profiling using high-resolution mass spectrometry. Key metabolic signatures were subsequently validated in an independent cohort of patients (SAH; n = 350) with alcohol-associated liver disease to establish translational relevance.
Results: Serum and hepatic metabolomic profiling demonstrated a profound, compartment-specific disruption of glutamine and TCA cycle coupling during alcohol-fat-induced liver injury (FC >1.5; $P < 0.05$). Progressive accumulation of circulating α-ketoglutaric acid and 2-ketoglutaramic acid (FC >1.5; $p < 0.05$), alongside depletion of serum glutamate and glutamine ($p < 0.05$), reflects impaired mitochondrial TCA flux and defective nitrogen handling with advancing disease severity. In contrast, intrahepatic enrichment of α-ketoglutaric acid, glutamate, and glutamine indicates metabolic trapping within the injured liver, consistent with mitochondrial dysfunction and altered anaplerosis. Clinically, elevated serum α-ketoglutaric acid showed a robust and reproducible association with disease severity and adverse outcomes, including in patients with alcohol-associated liver disease (AUROC>0.89; $p < 0.05$, FC >2.0), underscoring its potential utility as a translational biomarker for metabolic decompensation and prognostic stratification in alcohol and fat driven liver injury.

Conclusion: Alcohol and fat induced liver disease is characterized by progressive α-ketoglutaric acid accumulation, reflecting mitochondrial and nitrogen metabolic dysfunction, with translational relevance as a prognostic biomarker in patients.

FRI-133

Morphological differences in mitochondria of patients with and without alcohol related liver disease

Meliz Sahuri Arisoylu[1], Sophie Maliakal[1], Sergio Bozzano[1], Una Rastovic[1], Moyosoreoluwa Feyide[1], Bhavanaa Arunakumar[1], Ane Zamalloa[1], Nigel Heaton[1], Elena Palma[1]. *[1]Roger Williams Institute of Liver Studies, School of Immunology & Microbial Sciences, Faculty of Life Sciences and Medicine, King's College London, Foundation for Liver Research and King's College Hospital, London, United Kingdom*
Email: m.arisoylu@researchinliver.org.uk

Background and aims: Changes in hepatocyte mitochondrial morphology and size occur in response to metabolic stressors, including alcohol, in both patients and experimental models. Disproportionate mitochondrial enlargement (megamitochondria) has been described as a maladaptive response but has also been associated with improved clinical outcomes in alcohol-related hepatitis, a form of end-stage alcohol-related liver disease (ALD). However, systematic characterisation of mitochondrial morphology in human liver tissue across health and disease remains limited, partly due to technical constraints and a lack of physiologically relevant models. This study aimed to characterise hepatocyte mitochondrial morphology in patients with different disease backgrounds and to compare these findings with cellular and tissue models to assess their relevance for studying mitochondrial morphology.
Method: For ex vivo analysis, liver samples were obtained from patients with or without ALD. Human precision-cut liver slices (PCLS) were generated from both groups and exposed to acute ethanol at varying concentrations and durations. For in vitro experiments, primary human hepatocytes (PHH) were treated with 100 or 250 mM ethanol for 24 hours. Samples were fixed, mitochondria were visualised by immunofluorescence, and imaging was performed using super-resolution microscopy. Quantitative analyses were restricted to viable hepatocytes, and relative mitochondrial size distributions were compared.
Results: Mitochondrial size distributions varied between patients within each group. Enlarged mitochondria were observed in both groups but were more frequent and larger in ALD patients. In the PCLS model, ethanol exposure increased the frequency of larger mitochondria. Similarly, in the cellular model, enlarged mitochondria were detected in all groups, with both their number and size increasing in a dose-dependent manner following ethanol treatment.
Conclusion: Mitochondrial morphology in human liver tissue is strongly influenced by ethanol exposure and underlying liver health. These findings highlight the need for further research to uncover mechanisms of mitochondrial resilience or vulnerability to alcohol-induced injury. The development of comparable 2D and 3D models to study mitochondrial morphology would not only improve our understanding of the role of this organelle in liver health but also provide a platform for targeting mitochondria in the treatment of liver disease.

FRI-134

Selective farnesoid X receptor agonist INT-787 inhibits ethanol-induced liver injury in mice

David Schöler[1], Sainan Chen[1,2], Marcos Fondevila[1], Aenne Harberts[1], Yanhan Wang[1], Yixin Bai[3,4], Qinghai Liu[3,4], Qihong Yang[3,4], Luciano Adorini[5], Mary Erickson[5], Sanjay Kansra[5], Hidekazu Tsukamoto[3,4,6], Bernd Schnabl[1,7]. *[1]University of California San Diego, La Jolla, United States; [2]Zhujiang Hospital,Southern Medical University, Intensive Care Unit, Guangzhou, China; [3]University of Southern California, Los Angeles, United States; [4]Southern California Research Center for ALPD and Cirrhosis, Los Angeles, United States; [5]Intercept Pharmaceuticals, Inc, Morristown, United States; [6]Department of Veterans Affairs Greater Los Angeles Healthcare System, Los Angeles, United States; [7]VA San Diego Healthcare System, San Diego, United States*
Email: beschnabl@health.ucsd.edu

Background and aims: Farnesoid X receptor (FXR) agonists improve bile acid homeostasis and metabolic function, but their role in ethanol-induced liver injury remains unclear. INT-787 is a novel FXR agonist structurally related to obeticholic acid (OCA). We investigated whether INT-787 protects against ethanol-induced liver injury and whether this involves modulation of the gut-liver axis.
Method: INT-787 and OCA were evaluated in 2 mouse models of ethanol-induced liver disease, the oral Lieber-DeCarli chronic-plus-binge ethanol feeding model for 8 weeks and an intragastric hybrid high-cholesterol/high-fat diet plus ethanol plus binge feeding model (intragastric hybrid ethanol feeding model) for 7 weeks. Hepatic injury was assessed by serum/plasma alanine aminotransferase (ALT) levels, while hepatic steatosis was evaluated by hepatic triglyceride content and histological analysis. Bile acid metabolism was assessed by circulating bile acid levels and hepatic CYP7A1 protein expression, and intestinal permeability was evaluated by circulating lipopolysaccharide (LPS) levels. To assess direct intestinal effects of INT-787 and OCA, differentiated Caco-2 monolayers were exposed to LPS, and transepithelial electrical resistance (TER), tight junction protein expression, and cell viability were analyzed.
Results: Across both *in vivo* models, INT-787 reduced ethanol-induced liver injury, as reflected by lower ALT levels, and attenuated hepatic steatosis, as determined by reduced hepatic triglycerides and histological lipid accumulation. These effects were accompanied by suppression of hepatic CYP7A1 protein expression and reduced circulating bile acid levels, consistent with hepatic FXR activation. In the intragastric hybrid ethanol feeding model, INT-787 additionally reduced intestinal permeability and lowered circulating LPS levels, indicating improved gut barrier function. *In vitro*, INT-787 dose-dependently preserved TER and maintained expression of the tight junction protein 1 (TJP1, also known as ZO-1) in LPS-challenged Caco-2 monolayers without inducing cytotoxicity. This barrier-protective effect exceeded that observed with OCA.
Conclusion: INT-787 inhibits ethanol-induced liver injury and steatosis more effectively than OCA in 2 mouse models through modulation of bile acid metabolism and preservation of intestinal epithelial integrity. These findings support INT-787 as a next-generation FXR agonist with therapeutic potential for alcohol-associated liver disease.

FRI-135-YI

Leucine-rich alpha-2-glycoprotein 1 turnover indicates impaired regenerative signaling in alcohol-associated hepatitis

Nupur Sharma[1], Vipul Sharma[1], Sadam Bhat[1], Sushmita Pandey[1], Sanju Yadav[1], Mothe Shravya[2], Yash Magar[1], Babu Mathew[1], Vasundhra Bindal[1], Gaurav Tripathi[1], Manisha Yadav[1], Rimsha Rimsha[1], Neha Sharma[1], Ranjan Nanda[2], Chhagan Bihari[1], Archana Rastogi[1], Shvetank Sharma[1], Viniyendra Pamecha[1], Shiv Kumar Sarin[1], Jaswinder Maras[1]. *[1]Institute of Liver and Biliary Sciences, New Delhi, India; [2]International Centre for Genetic Engineering and Biotechnology, New Delhi, India*
Email: jassi2param@gmail.com

Background and aims: Severe alcoholic hepatitis (SAH) features inflammation, liver dysfunction, and poor regeneration. We assessed protein turnover as a marker of liver injury and repair in SAH patients, and murine ALD and abstinent models.
Method: SAH patients (n = 10), healthy controls (n = 5), and liver donors (n = 5) received 70% D_2O, with plasma collected at baseline and Days 1, 3, 5, and 7. LC-MS/MS quantified turnover of injury- and regeneration-related proteins linked to disease severity. Key

regenerative markers were validated in platelets from SAH patients, controls, and donors (n = 10 each), and in animal models.
Results: SAH patients showed higher plasma protein turnover than controls (0.38/day vs 0.23/day, $p < 0.05$), reflecting accelerated but dysregulated protein dynamics. Specifically, 37 proteins involved in inflammatory, complement, platelet activation, and ECM remodeling pathways had increased while14 proteins associated with HDL assembly and BCR regulation had reduced turnover (FC >1.5, $p < 0.05$). Functional clustering revealed that turnover of ECM and fibrosis-related proteins strongly correlated with histological severity in SAH ($r^2 = 0.98$, $p < 0.05$). When liver donors were analysed, they exhibited increased turnover of 50 proteins linked to platelet degranulation, complement activation, and HDL remodeling, indicating preserved regenerative signaling. Notably, Leucine-rich alpha-2-glycoprotein 1 (LRG1) emerged as a key regenerative marker. Its turnover and regenerative potential were both significantly reduced in SAH patients (35%) compared to liver donors (100%, $p < 0.05$). Supporting this, a preclinical ALD model demonstrated that alcohol abstinence restored hepatic LRG1 expression, its receptors (IL6R, IL4R, TGFβR2, EGFR), and downstream pro-survival and proliferative signaling pathways (FC >1.5, $p < 0.05$). Platelet degranulation, a source of LRG1, was impaired in SAH, contributing to compromised LRG1-mediated signaling and regeneration.
Conclusion: LRG1 turnover supports liver regeneration and may serve as a novel indicator of liver repair and regenerative capacity in alcohol-associated liver disease.

FRI-136
A high-salt diet aggravates alcohol-associated liver diseases by disrupting the functional homeostasis of liver sinusoidal endothelial cells
Haiyuan Shen[1,2,3], Miaomiao Wu[2,4], Juan Wang[1,2], Li Zuo[2,4], Hua Wang[1]. [1]*Department of Oncology, the First Affiliated Hospital of Anhui Medical University, Hefei, China;* [2]*Innovation and Entrepreneurship Laboratory for college students, Anhui Medical University, Hefei, China;* [3]*School of Pharmaceutical Sciences, Anhui Medical University, Hefei, China;* [4]*Department of Biochemistry, Anhui Medical University, Hefei, China*
Email: shenhayyuan@163.com

Background and aims: Alcohol-associated liver disease (ALD), primarily caused by chronic excessive alcohol consumption, is a leading cause of liver-related mortality worldwide. The global burden of ALD remains a significant concern, particularly when compounded by other prevalent lifestyle risk factors such as high-salt diets. This study aims to investigate the impact of high-salt diet on ALD progression and to identify the key cell types and molecular mechanisms involved, thereby elucidating novel pathogenic pathways and potential therapeutic targets.
Method: C57BL/6 mice were subjected to the Gao-binge model of ALD and fed either a high-salt diet or a normal-salt diet. The extent of alcohol-induced liver injury, steatosis, and inflammation was evaluated across groups. Single-cell RNA sequencing was employed to identify liver cell populations significantly affected by high-salt intake. To elucidate the underlying mechanisms, a comprehensive analysis was conducted using 16S rRNA sequencing, metabolomics, proteomics, and genetic engineering approaches.
Results: High-salt diet reshaped the intrahepatic immune microenvironment. Mechanistically, it upregulates salt-inducible kinase 1 (Sik1) in liver sinusoidal endothelial cells (LSECs), leading to increased release of selectins and intercellular adhesion molecule-1 (ICAM-1), which promotes neutrophil infiltration and exacerbates alcohol-induced liver injury in mice. Furthermore, high-salt intake reduced the abundance of beneficial gut bacteria, such as *Akkermansia muciniphila* and *Lactobacillus reuteri*, while promoting the expansion of harmful bacteria, including *Enterococcus faecalis*. Impaired LSEC function facilitated bacterial translocation to the liver, where colonizing bacteria further induced hepatic inflammation and hepatocyte damage.
Conclusion: High-salt intake exacerbates the progression of ALD by impairing LSEC barrier and inflammatory functions. It promotes the expression of selectins and ICAM-1 on LSECs in a Sik1-dependent manner, leading to neutrophil recruitment and increased bacterial invasion into the liver, thereby triggering inflammation and tissue injury. These findings reveal a novel molecular mechanism in alcohol-induced liver injury and suggest that dietary modification and interventions targeting LSECs may offer potential therapeutic strategies for ALD.

FRI-137
Intestinal GPR119 activation improves alcohol-related liver disease via gut-liver axis and mediates the protective effect of its ligand palmitoleic acid
Mengyao Wang[1], Chang Yuan[1], Zhou Zhao[1], Jian Sun[1]. [1]*Department of Infectious Diseases, Nanfang Hospital, Southern Medical University, Guangzhou, China, State Key Laboratory of Multi-organ Injury Prevention and Treatment, Key Laboratory of Infectious Diseases Research in South China, Ministry of Education, Guangdong Provincial Key Laboratory for Prevention and Control of Major Liver Diseases, Guangdong Provincial Clinical Research Center for Viral Hepatitis, Guangdong Institute of Hepatology, Guangdong Provincial Research Center for Liver Fibrosis Engineering and Technology, Guangzhou, China*
Email: sunjianteam@163.com

Background and aims: Alcohol-related liver disease (ALD) is increasingly seen as a systemic metabolic disorder shaped by the gut liver axis. Re analysis of public serum metabolome data indicates that metabolite set enrichment highlights G-protein-coupled receptors (GPCRs), particularly fatty acid activated GPCRs, within the affected pathways. Among these, the specific role and mechanistic contribution of G protein coupled receptor 119 (GPR119) in ALD remain insufficiently explored.
Method: Enrichment analysis was performed on publicly available serum untargeted metabolomics data derived from a published ALD cohort, comprising 32 healthy controls and 100 ALD patients. ALD mouse models were established using the NIAAA protocol, with mice subjected to chronic-plus-binge ethanol feeding regimen. Intestinal epithelium-specific GPR119 overexpression was achieved in wild-type mice via adeno-associated virus (AAV) vector-mediated gene delivery (Vil1-Gpr119Tg). GPR119 was pharmacologically activated with APD688 (10 mg/kg/day, oral gavage) and with palmitoleic acid (50 and 200 mg/kg/day, oral gavage). Caco-2 cell lines were used for in vitro experiments.
Results: In the ALD cohort, serum metabolites differentially enriched versus healthy controls clustered explicitly within GPCR-signalling pathways. Ethanol-fed mice exhibited a selective post-transcriptional loss of intestinal GPR119, as protein levels declined while Gpr119 mRNA remained signifiantly unchanged. Mechanistically, ethanol enhanced ubiquitination of GPR119 and accelerated its proteasomal degradation. Pharmacological activation with APD688, transgenic over-expression of Vil1-Gpr119Tg, or oral supplementation with the endogenous ligand palmitoleic acid all reinstated the GPR119-cAMP-PKA-CREB cascade in the small intestine. This was accompanied by markedly elevated tight-junction proteins Zonula Occludens-1 and occludin, restoration of mucosal barrier integrity, and simultaneous attenuation of ethanol-driven liver injury.
Conclusion: Alcohol impairs intestinal GPR119 through ubiquitin-mediated degradation, whereas Pharmacological activation or intestinal specific overexpression of GPR119 re-programs the gut-liver metabolite axis and ameliorates experimental ALD. Palmitoleic acid functions as an endogenous GPR119 agonist, offering a readily translatable strategy for ALD therapy. These findings establish GPR119 as a guardian of the gut–liver axis and an attractive, druggable target for ALD intervention.

Cirrhosis and its complications – ACLF and Critical illness

TOP-423

Therapeutic plasma exchange improves short-term survival in acute on chronic liver failure: a randomised controlled trial

Sagnik Biswas[1], Shekhar Swaroop[1], Arnav Aggarwal[1], Ayush Agarwal[1], Poonam Coshic[1], Samagra Agarwal[1], Hem Chandra Pandey[1], Gopal Patidar[1], Rahul Chaurasia[1], Pragyan Acharya[1], Baibaswata Nayak[1], Deepak Gunjan[1], Viren Sardana[2], Ashwani Mishra[1], Shivanand Gamangatti[1], Shalimar[1]. [1]*All India Institute of Medical Science, New Delhi, India;* [2]*Institute of Genomic and Integrative Biology, New Delhi, India*
Email: sagnik_biswas@yahoo.co.in

Background and aims: Therapeutic plasma exchange (TPE) is a promising modality for the management of acute-on-chronic liver failure (ACLF), however, its impact on patient survival is unclear. This randomized controlled trial (RCT) evaluated the efficacy and safety of TPE compared to standard medical therapy (SMT) in ACLF.
Method: In this single-center, open-label RCT (February 2022-March 2025), we randomly (1:1) assigned 194 adult patients (aged 18–60 years) with ACLF (European Association for the Study of the Liver-Chronic Liver Failure Consortium [EASL CLIF-C] Grades 1–3b) to receive SMT plus 5 sessions of TPE (97 patients) or SMT alone (97 patients). The primary outcome was all-cause mortality at 28 days. Secondary outcomes included 90-day mortality, changes in prognostic scores and resolution of organ failures, infections and adverse events.
Results: Baseline characteristics were comparable between the two groups. Alcohol use was the most common cause of underlying liver disease (67.5%) and most patients presented with ACLF Grade 2 (64.5%). Seventy-two (74.2%) patients completed 3 sessions of TPE while 56 (57.7%) received all 5 sessions. Hemodynamic instability was the leading cause for discontinuation of TPE (18/41 patients, 43.9%). The 28-day mortality was significantly lower with TPE (43 patients, 44.3%; 95%CI: 34.2%–54.8%) than SMT (62 patients, 63.9%; 95%CI: 53.5%–73.4%), $p = 0.006$; absolute risk reduction: 19.6% (95% CI: 5.8% to 33.3%), although the 90-day mortality rates between both groups were similar (TPE:66% [55.6–75.3] versus SMT:69.1% [58.9–78]; p = 0.64). Subgroup analysis did not reveal significant heterogeneity across ACLF grade or etiology. TPE resulted in greater reductions in serum bilirubin, international normalized ratio, ammonia, and higher rates of resolution of hepatic and coagulation failure by day 7 as compared to SMT. Infections were more frequent with TPE [20/92 (21.7%) vs 12/102 (11.8%), p = 0.062]. Dyselectrolytemia and shivering were the most common complications after TPE.
Conclusion: TPE significantly improves 28-day survival and organ failure resolution in patients with ACLF, but does not reduce 90-day mortality. Fluid and electrolyte imbalances affect tolerability of TPE in this patient group [CTRI/2022/01/039094].

TOP-424-YI

Continuous terlipressin infusion plus norepinephrine versus norepinephrine alone in acute kidney injury associated with acute-on-chronic liver failure and septic shock: a randomized controlled trial

Jitendra Kumar Singh[1], Rakhi Maiwall[1], Ankit Bhardwaj[1], Harshvardhan Tevethia[1], Rajan Vijayaraghavan[1], Arun Kumar Sood[1], Manoj Kumar[1], Shiv Kumar Sarin[1]. [1]*Institute of Liver & Biliary Sciences, New Delhi, India*
Email: jitendra2602kc@gmail.com

Background and aims: Acute kidney injury (AKI) in acute-on-chronic liver failure (ACLF) with septic shock is driven by severe systemic vasodilatation and splanchnic pooling, often limiting the efficacy of norepinephrine (NE) alone. Terlipressin, a vasopressin analogue, may provide complementary splanchnic vasoconstriction and improve renal perfusion. We evaluated whether continuous low-dose terlipressin infusion combined with NE improves renal and hemodynamic outcomes compared with NE alone.
Method: Single-center open-label RCT of 126 ACLF patients with less-severe septic shock (NE <0.05 µg/kg/min) and AKI randomized to NE alone (n = 63) or terlipressin infusion (1 mg/day, escalated to 4 mg/day by Day 4) plus NE (n = 63). MAP ≥70 mmHg targeted; 20% albumin given. Primary endpoint: Day-4 shock reversal with ≥1-stage AKI improvement; secondary endpoints: Day-7 AKI outcomes, NEE, albumin dose, RRT, 28-day mortality, and adverse events.
Results: Baseline characteristics were comparable: age (46.36 ± 10.09 vs 44.21 ± 12.57 years), AARC score (10.53 ± 1.52 vs 10.46 ± 1.17), eGFR (49.92 ± 20.53 vs 51.03 ± 19.49 mL/min/1.73 m^2), MAP (63.47 ± 2.29 vs 62.56 ± 2.22 mmHg; p = 0.085), lactate (2.35 ± 0.62 vs 2.26 ± 0.55 mmol/L; p = 0.502). Pneumonia was the commonest sepsis source (47.2% vs 43.6%), followed by SBP (19.4% vs 33.3%) in NE vs NE+TERLI. Renal biomarkers were similar: urine NGAL (307.3 ± 237.4 vs 246.6 ± 200.1 ng/mL; p = 0.20) and cystatin-C (2.19 ± 1.15 vs 1.90 ± 0.59 mg/L; p = 0.14). Day-4 shock reversal (92.3% vs 52.8%; p < 0.001) and ≥1-stage AKI improvement (74.4% vs 44.4%; p = 0.008) were higher with NE+TERLI. Day-7 AKI resolution was higher (71.8% vs 44.4%; p = 0.004) with lower progression (12.8% vs 16.7%; p = 0.610). Day-4 NEE was lower (0.01 ± 0.03 vs 0.06 ± 0.08; p = 0.001). Albumin dose (100.6 ± 60.7 vs 96.9 ± 62.2 g; p = 0.78), RRT (15.8% vs 20.6%; p = 0.63) and 28-day mortality (22.2% vs 28.2%; p = 0.55) were comparable. AARC score (adjusted HR 3.01, CI 1.76–5.15; p < 0.001) and baseline lactate (adjusted HR 14.39, CI 2.75–75.32; p = 0.002) independently predicted mortality. Adverse events were higher with NE+TERLI (13.3% vs 4.3%; p = 0.2). Baseline eGFR (OR 1.06, CI 1.02–1.11; p = 0.002) and NE+TERLI (OR 3.60, CI 1.04–12.47; p = 0.043) independently predicted Day-7 AKI recovery.
Conclusion: In patients with ACLF, septic shock, and AKI, continuous low-dose terlipressin combined with norepinephrine is safe and significantly improves early shock reversal and renal recovery while reducing catecholamine requirements.

TOP-437

Immune dysfunction assessed by neutrophil-to-lymphocyte ratio predicts mortality and infection in acute-on-chronic liver failure

Rosa Martin-Mateos[1], Eva Uson[2], Juan Manuel Diaz[2], Alberto Queiroz Farias[3], Maria Papp[4], Paolo Caraceni[5], Aldo Torre[6,7], Salvatore Piano[8], Gustavo Pereira[9], Thierry Gustot[10], Carlo Alessandria[11], Wim Laleman[12], Christian Jansen[13], Manuel Mendizabal[14], Luciana Goncalves[15], Sebastián Marciano[16], Liliana Mendes[17], José Luis Pérez-Hernández[18], Paulo Bittencourt[19], Padilla Machaca Martín[20], Marco Arrese[21], Victor Vargas Blasco[22], Angelo Mattos[23], Claudio Toledo[24], Daniel Mazo[25], Mauricio Castillo[26], Marcelo Silva[14], Martin Janicko[27], Vishal C. Patel[28], Cláudia Couto[29], Cristina Sanchez-Garrido[2], Jonel Trebicka[2,30], Vicente Arroyo[2], Joan Clària[31], Agustín Albillos[1], Richard Moreau[2]. [1]*Hospital Universitario Ramón y Cajal, IRYCIS, Universidad de Alcalá, CiberEHD, Madrid, Spain;* [2]*European Foundation for the Study of Chronic Liver Failure (EF CLIF), Barcelona, Spain;* [3]*Department of Gastroenterology, Hospital das Clínicas, University of Sao Paulo School of Medicine, Sao Paulo, Brazil;* [4]*University of Debrecen, Faculty of Medicine, Institute of Medicine, Department of Gastroenterology, Debrecen, Hungary;* [5]*Department of Medical and Surgical Sciences, University of Bologna, Bologna, Italy;* [6]*Departamento de Gastroenterología, Instituto Nacional de Ciencias Médicas y Nutrición "Salvador Zubirán", Mexico City, Mexico;* [7]*Instituto Nacional de Ciencias Médicas y Nutrición Salvador Zubirán, Mexico City, Mexico;* [8]*University of Padova, Padova, Italy;* [9]*Gastroenterology and Hepatology Unit, Bonsucesso Federal Hospital (Ministry of Health), Rio de Janeiro, Brazil;* [10]*C.U.B. Erasme, Bruxelles, Belgium;* [11]*Division of Gastroenterology and*

Hepatology, A.O.U. Città della Salute e della Scienza di Torino, University of Turin, Turin, Italy; [12]Department of Gastroenterology and Hepatology, Division of Liver & Biliopancreatic disorders and Liver Transplantation, University Hospitals Leuven, Leuven, Belgium; [13]University of Bonn, Bonn, Germany; [14]Unidad de Hígado y Trasplante Hepático, Hospital Universitario Austral, Pilar, Argentina; [15]Gastroenterology and Hepatology Unit, Hospital Universitário Cassiano Antônio Moraes, Universidade Federal do Espírito Santo, Vitòria, Brazil; [16]Liver Unit and Department of Research, Hospital Italiano de Buenos Aires, Buenos Aires, Argentina; [17]Hospital de Base do Distrito Federal, Brasilia, Brazil; [18]Servicio de Gastroenterología y Hepatología, Hospital General de México "Dr. Eduardo Liceaga", Ciudad de Mexico, Mexico; [19]Hospital Português da Bahia, Salvador, Brazil; [20]Hospital Nacional Guillermo Almenara, Universidad Nacional de San Marcos, Lima, Peru; [21]Departamento de Gastroenterología, Facultad de Medicina, Pontificia Universidad Católica de Chile, Santiago, Chile; [22]Hospital Vall d'Hebron, Universitat Autònoma de Barcelona, Barcelona, Spain; [23]Federal University of Health Sciences of Porto Alegre, and Gastroenterology and Hepatology Unit, Irmandade Santa Casa de Misericórdia de Porto Alegre, Porto Alegre, Brazil; [24]Gastroenterology Unit, Hospital Valdivia, Universidad Austral de Chile, Valdivia, Chile; [25]Universidade Estadual de Campinas, Campinas, Brazil; [26]Servicio de Gastroenterología y Hepatología, Hospital de Especialidades Centro Médico Nacional La Raza IMSS, Ciudad de Mexico, Mexico; [27]Pavol Jozef Safarik University in Kosice, Kosice, Slovakia; [28]Roger Williams Institute of Liver Studies, School of Immunology & Microbial Sciences, Faculty of Life Sciences and Medicine, King's College London, Foundation for Liver Research and King's College Hospital, London, United Kingdom; [29]Faculdade de Medicina, Universidade Federal de Minas Gerais; Instituto Alfa de Gastroenterologia, Hospital das Clínicas da Universidade Federal de Minas Gerais, Belo Horizonte, Brazil; [30]Department of Internal Medicine B, University of Münster, Münster, Germany; [31]EF CLIF, Hospital Clínic de Barcelona, IDIBAPS, CIBERehd & Universitat de Barcelona, Barcelona, Spain
Email: rosamartinmat@hotmail.com

Background and aims: Cirrhosis-associated immune dysfunction plays a central role in the pathogenesis of acute-on-chronic liver failure (ACLF), contributing to organ failure, infection, and death. However, current prognostic models do not incorporate direct measures of immune function. The neutrophil-to-lymphocyte ratio (NLR) reflects both systemic inflammation and immune exhaustion and may serve as a simple, readily available biomarker in clinical practice. We aimed to evaluate the prognostic value of NLR for predicting mortality and infection in patients with ACLF.
Method: We analyzed data from 914 patients with ACLF enrolled in two prospective, multicenter EF-CLIF cohorts: 420 from the PREDICT study and 494 from the ACLARA study. Demographic, clinical, and laboratory data were extracted from the databases. Univariate and multivariate logistic regression models identified independent predictors of mortality and bacterial infection. Kaplan–Meier and Cox regression analyses evaluated survival according to NLR cutoffs. The additive prognostic value of an NLR-defined "immune dysfunction" subscore to standard organ-failure models was also assessed.
Results: Mean age was 57.9 ± 12.2 years, 65.4% were male, and main etiologies included alcohol-related liver disease (57.8%) and MASLD (18.8%). Overall 28-day and 90-day mortality rates were 35.1% and 53.6%, respectively. NLR at ACLF onset was significantly higher in non-survivors than in survivors (median 9 [5–17] vs. 5 [3–9], $p < 0.0001$). In multivariate analysis, NLR independently predicted 28-day mortality (OR 1.02, 95% CI 1.00–1.03, $p = 0.024$) and overall mortality (OR 1.03, 95% CI 1.01–1.05, $p = 0.005$), together with age, MELD score, albumin, acute alcohol-associated hepatitis, and bacterial infection. In Cox regression, NLR remained an independent predictor of death (HR 1.01, 95% CI 1.01–1.02, $p < 0.001$). Incorporating an NLR-defined immune dysfunction marker into standard organ-failure models improved prognostic accuracy (AUC 0.68 vs. 0.65; $p = 0.017$). At ACLF development, 58% of patients presented with bacterial infection, and higher NLR values were consistently associated with infection ($p < 0.01$). In multivariable analysis, only NLR and C-reactive protein independently predicted early infection, highlighting their value in identifying high-risk patients.
Conclusion: Elevated NLR independently predicts mortality and infection risk, and may serve as a simple and widely available biomarker to refine risk stratification in clinical practice.

SAT-448
Machine learning identifies soluble VAP-1 as a promising biomarker to discriminate hepatic and extrahepatic precipitants of decompensation in cirrhosis

Majda El Hassani[1], Johanna Reißing[1], Oluwatomi Ibidapo-Obe[1], Mick Frissen[1], Haedge Frederic[1], Karsten Große[1], Mohamad Murad[1], Andreas Stallmach[2], Philipp Reuken[2], Theresa Hildegard Wirtz[1], Tony Bruns[1]. *[1]University Hospital RWTH Aachen-Department of Internal Medicine III, Aachen, Germany; [2]University Hospital Jena-Department of Internal Medicine IV, Jena, Germany*
Email: melhassani@ukaachen.de

Background and aims: Systemic inflammation drives complications in decompensated cirrhosis. Differentiating sterile inflammatory triggers like alcohol-associated hepatitis (AH) from bacterial infections such as spontaneous bacterial peritonitis (SBP) remains a clinical challenge. We used a machine-learning approach to identify discriminating biomarkers.
Method: In this retrospective case-control study, serum samples and routine laboratory parameters from 70 patients with decompensated alcohol-related cirrhosis (35 AH, 35 SBP) were analyzed. 43 serum biomarkers reflecting inflammation and matrix turnover were quantified by bead-based immunoassay. A Random Forest model was trained to discriminate AH from SBP.
Results: Random Forest models identified Soluble Vascular Adhesion protein-1 (sVAP-1) as a top-ranking feature for discriminating AH from SBP, both in combination with and independent of routine laboratory parameters. Circulating sVAP-1 levels were substantially higher in AH than in SBP (median 759 vs 401 ng/mL, $p < 0.0001$), largely reflecting shedding from hepatic sinusoids. sVAP-1 positively correlated with Soluble Interleukin-1 Receptor type 1 (sIL-1R1) ($r_s = 0.384$, $p = 0.03$) an indicator of intense IL-1 pathway activation in AH but surprisingly not with markers of hepatocyte damage. Patients with AH and highest sVAP-1 concentrations showed a trend towards worse 28-day transplant-free survival compared to those with lower levels in univariate Cox regression (HR = 2.75; 95% CI 0.88–8.62; $p = 0.08$), which was significant after adjustment of Model for End-Stage Liver Disease (MELD) in multivariable analysis (aHR = 5.18; 95% CI 1.19–22.64; $p = 0.03$).
Conclusion: The endothelial-derived amine-oxidase sVAP-1 is a promising serum biomarker for discriminating sterile inflammation in AH from extrahepatic infectious precipitants in cirrhosis. Its independence from traditional markers of hepatocyte injury and its prognostic relevance warrant validation in larger studies.

SAT-449
Alterations in primary hemostasis in patients with liver cirrhosis and bacterial infection

Florentia Athanasaki[1], Larisa Vasilieva[2], Efrosyni Nomikou[3], Efthimia Pavlou[3], Stavros Formozis[3], Krystalia Dimitriou[1], Dimitra Krystallaki[1], Nikolaos-Nektarios Karamanolis[1], Iliana Mani[1], Flora Kontopidou[1], Emilia Hadziyannis[1], Alexandra Alexopoulou[1]. *[1]2nd Department of Internal Medicine and Research Laboratory, Medical School, Hippokration General Hospital, National & Kapodistrian University of Athens, Athens, Greece; [2]Department of Gastroenterology, Alexandra General Hospital, 11528 Athens, Athens, Greece; [3]Blood Bank and Haemophilia Unit, Hippokration General Hospital of Athens, Athens, Greece*
Email: florathan91@gmail.com

Background and aims: Reduced platelet (PLT) aggregation has been reported in liver cirrhosis (LC) in comparison with healthy controls. The aim was to assess the alterations and the prognostic role of PLT aggregation and von Willebrand factor (vWF)-related parameters in bacterial infection (BI) superimposed on LC.
Method: The alterations of PLT aggregation by thromboelastography (TEG) 6S PLT mapping assay as well as vWF antigen (WF:Ag), vWF activity (vWF Ristocetin cofactor-vWF:RCo) and FVIII levels were studied in patients with decompensated cirrhosis and BI (DC+BI), stable cirrhosis (SC) and those with infection without LC (Control group). The prognostic value of PLT aggregation was explored in the DC+BI group.
Results: 71 patients were enrolled in DC+BI, 42 in SC and 20 in the Control group. Patients in DC+BI had significantly reduced PLT aggregation in response to Adenosine Diphosphate (ADP) compared to those in SC ($p = 0.029$). Significant elevated levels of wWF:Ag%, wWF:RCo% and FVIII counterbalanced the reduced levels of PLT aggregation ($p < 0.001$, $p < 0.001$ and $p = 0.017$, respectively). Patients in DC+BI and SC (cirrhosis groups) had significantly reduced PLT aggregative response to Arachidonic Acid (AA) compared to Control group ($p = 0.003$ and 0.005, respectively). Within the DC+BI group, those with organ failures [sepsis, Acute Kidney Injury (AKI) or acute-on-chronic liver failure (ACLF)] showed lower values of PLT aggregation (ADP) rate ($p = 0.001$, $p < 0.001$, $p < 0.001$, respectively) vs those without. Moreover, wWF:Ag and wWF:RCo levels were higher in patients with AKI than in those without ($p = 0.009$, $p = 0.004$, respectively), while the same parameters along with FVIII were higher in patients with ACLF than in those with acute decompensation (AD) ($p = 0.003$, $p = 0.017$ and $p = 0.031$, respectively). In the survival analysis of the DC+BI group, non-survivors demonstrated reduced PLT aggregation (ADP), which showed high accuracy in predicting mortality (AUROC = 0.851). PLT aggregation (ADP) less than 70.9% *was* independently associated with mortality [HR 6.536 (95%CI 1.296–32.962), $p = 0.023$] after adjustment for cofactors.
Conclusion: ADP-induced PLT aggregation is reduced in liver cirrhosis with infection in a stepwise manner according to the severity of infection. It also plays a prognostic role as it is associated with 30-day mortality. wWF:Ag and wWF:RCo values are elevated compensating PLT hypo-responsiveness. AA-induced PLT aggregation reduction is identified in cirrhosis groups.

SAT-450

Incidence and associated factors of severe chronic kidney disease after liver transplantation in patients with acute-on-chronic liver failure

Anea Augé[1], Hélène Barraud[1], Pauline Houssel-Debry[2], Valentin Coirier[2], Isaure Breteau[1], Eric Levesque[1], Edouard Bardou-Jacquet[2], Adrian Camino[1], Cyprien Gayat[1], Louis Dalteroche[1], Coralie Fleurent[1], Sébastien L'Hermite[2], Philippe Gatault[1], Florent Artru[2], Laure Elkrief[1]. [1]*Hospital Center of Tours, Tours, France;* [2]*Hospital Center of Rennes, Rennes, France*
Email: aneauge@laposte.net

Background and aims: Liver transplantation (LT) is increasingly performed in patients with severe acute-on-chronic liver failure (ACLF), with adequate short- and long-term survival. However, post-LT renal dysfunction is a major concern, particularly in ACLF patients with severe renal impairment at LT. Post-LT renal outcomes in this population remain poorly characterized. We aimed to assess the incidence, determinants and prognostic impact of severe chronic kidney disease after LT in patients with severe ACLF.
Method: We conducted a retrospective cohort study including all patients with severe ACLF (grade 2 or 3) who underwent LT between 2011 and 2021 in two French tertiary centers. The primary endpoint was the incidence of severe chronic kidney disease (CKD) beyond 6 months after transplantation, defined by an estimated glomerular filtration rate <30 mL/min/1.73 m^2, need for renal replacement therapy (RRT) or kidney transplantation. Cumulative incidence was estimated using competing-risk methods with death as a competing event. Factors associated with severe post-transplant CKD were assessed using Fine and Gray subdistribution hazard (sHR) models.
Results: We included 222 patients (median age 57 years, 72% men, median MELD score 36), of whom 20% had diabetes and 14% required RRT at LT. Among the 196 patients (88%) alive at 6 months, 25 (13%) developed severe CKD and 22 (11%) died without reaching the primary endpoint during a median follow-up of 60 months. The cumulative incidence of severe CKD was 6% at 1 year, 9% at 3 years and 13% at 5 years, with no difference between ACLF grade 2 and 3. Diabetes (sHR 2.7, $p = 0.006$) and RRT at LT (sHR 2.8, $p = 0.042$) were independently associated with severe CKD, whereas basiliximab induction ($n = 95$) was protective (sHR 0.33, $p = 0.02$). Severe CKD was associated with increased risks of subsequent mortality (HR 2.3, $p = 0.04$), infections (HR 2.2, $p = 0.006$) and major adverse cardiovascular events (MACE) (HR 7.7, $p < 0.001$).
Conclusion: In this large two-center cohort of patients transplanted for severe ACLF, severe CKD remained relatively infrequent at 5 years, but was associated with a marked increase in long-term mortality, infectious complications and MACE. These findings underscore the central role of post-transplant renal dysfunction in long-term outcomes and support early identification of high-risk patients and implementation of targeted nephroprotective strategies, including basiliximab-based induction therapy.

SAT-451

Validation of consensus liver failure cut offs to predict 30-day mortality in a nationwide inpatient cirrhosis cohort

Scott Silvey[1], Ohm Patel[2], Nilang Patel[1], Jasmohan Bajaj[1]. [1]*Virginia Commonwealth University, Richmond, United States;* [2]*Richmond Va Medical Center, Richmond, United States*
Email: jasmohan.bajaj@vcuhealth.org

Background and aims: Acute-on-chronic liver failure (ACLF) harmonization is difficult & varying liver failure (LF) cutpoints are proposed. A recent study based on the CLEARED consortium that was put into a multi-stakeholder consensus proposed serum bilirubin >7.5 mg/dL, INR >1.5 with creatinine >1.5 mg/dl, infections & hepatic encephalopathy (HE). Aim: Validate consensus liver failure (LF) definitions in a national cirrhosis cohort.
Method: Cirrhosis inpatients in TriNetX US database from 2009–25 were included. Labs, cirrhosis details & inpatient course were recorded. The primary outcome was 30-day mortality. Prior cut-offs in consensus & CLEARED data (Bilirubin>7.5 mg/dl, creatinine>1.5 mg/dl, INR>1.5 individually or MELD>27 or MELD3.0 > 28 ± HE grade≥2 & infections) were predictive of mortality. Predictive metrics of these thresholds [sensitivity, specificity, positive (PPV) & negative predictive values (NPV)] were calculated. Finally, decision tree models were fit using threshold combinations (1. Bilirubin+INR+Creatinine 2.Bilirubin +INR+Creatinine+HE+Infection, 3.MELD3.0+HE+Infection, 4.MELD3.0 +HE+Infection) to determine relative importance of each component & model AUCs using XGBoost.
Results: 239,482 cirrhosis inpatients were included (60 yrs, 61% men); 9% died at 30-days. Those who died were older, with higher MELD/MELD 3.0 scores & HE/infections. LF thresholds: Individual: Bilirubin>7.5 (sensitivity:30%,specificity:86%, PPV:18%, NPV:92%), INR>1.5 (sensitivity:62%,specificity:66%, PPV:16%, & NPV:94%, Creatinine>1.5 (sensitivity:53%,specificity:74%, PPV:18%, & NPV:94.9%). MELD>27 (sensitivity:37%,specificity:89%,PPV:25%, & NPV:93.1%) & MELD3.0 > 28 had similar metrics (sensitivity:42%, specificity:87%,PPV:25%, & NPV:94%). Finally, 3 individual labs together had sensitivity of 16.2%, specificity of 96.6%, PPV of 33.4%, & NPV of 91.8%. Decision tree analysis: Best-performing model was the three labs+HE/infection (AUC: 0.72 [0.72–0.73]), where creatinine had the highest relative importance (45.0%), then INR (40.3%), bilirubin (9.6%), infection (4.3%), and HE (<1.0%). This was better

than AUCs of individual labs (0.70), MELD+HE/infection (0.68) & MELD3.0+HE/infection(0.69).
Conclusion: Using a threshold of INR>1.5, Bilirubin>7.5 mg/dl & creatinine>1.5 mg/dl at baseline was associated with high inpatient mortality combined with HE and infection in a national cohort of inpatients with cirrhosis. These national data validate prior consensus documents and cohorts, and pave the way for harmonization of ACLF definitions.

SAT-452

Immune failure in ACLF: validation of consensus definitions in two large cohorts of inpatients with cirrhosis

Jasmohan Bajaj[1], Scott Silvey[1], Florence Wong[2], Jacob George[3], Qing Xie[4], Ramazan Idilman[5], Peter Hayes[6], Mario Álvares-da-Silva[7], Aldo Torre[8], Hailemichael Desalegn[9], Mark Topazian[9], Wai-Kay Seto[10], Shiv Kumar Sarin[11], Zhujun Cao[12], Neil Rajoriya[13], Abha Nagral[14], Henok Fisseha[9], Anand Kulkarni[15], Chuanwu Zhu[16], Nabil Debzi[17], Alberto Farias[18], Minghua Su[19], Ashish Goel[20], Sebastián Marciano[21], Robert Livingstone[22], Radha Krishan Dhiman[23], Yanhang Gao[24], René Malé Velazquez[25], Coskun Ozer Demirtas[26], Yongfang Jiang[27], Jose Antonio Velarde-Ruiz Velasco[28], Hiang Keat Tan[29], Caiyan Zhao[30], Maria Sarai González-Huezo[31], Sumeet Asrani[32], Lei Wang[33], Mingqin Lu[34], Matheus Truccolo Michalczuk[35], Zeki Karasu[36], Jacqueline Cordova-Gallardo[37], Cameron Gofton[38], Michael Gounder[39], Jawaid Shaw[1], Xin Zheng[40], Aloysious Aravinthan[41], Ruveena Bhavani[42], Kessarin Thanapirom[43], Dinesh Jothimani[44], Sevda Aghayeva[45], Dinc Dincer[46], Shalimar Shalimar[47], Bin Xu[48], Minghua Lin[49], Xiaoping Wu[50], Chenghai Liu[51], Yan Yue James Fung[52], Helena Katchman[53], Gustavo Pereira[54], Mohamed El Kassas[55], Marie Jeanne Lohoues[56], Dominik Bettinger[57], Hanna Aberra[58], Paul J. Thuluvath[59], Dibya Lochan Praharaj[60], Ajay Kumar Duseja[61], Nilang Patel[1], K. Rajender Reddy[62], Brian Bush[1], Patrick S. Kamath[63], Ashok Kumar Choudhury[11]. *[1]Virginia Commonwealth University and Richmond VA Medical Center, Ruijin Hospital, Shanghai Jiao Tong University School of Medicine, Shanghai, China, Richmond, United States; [2]University of Toronto, Toronto, Canada; [3]The Westmead Institute for Medical Research, Westmead, Australia; [4]Ruijin Hospital, Shanghai Jiao Tong University School of Medicine, Shanghai, China; [5]Ufuk University-Faculty of Medicine, Ankara, Türkiye; [6]University of Edinburgh, Edinburgh, United Kingdom; [7]Hospital de Clínicas de Porto Alegre, Porto Alegre, Brazil; [8]Instituto Nacional De Ciencias Médicas Y Nutrición Salvador Zubirán, Ciudad de México, Mexico; [9]St. Paul's Hospital Millennium Medical College, Addis Ababa, Ethiopia; [10]The University of Hong Kong Li Ka Shing Faculty of Medicine, Pok Fu Lam, Hong Kong; [11]Institute of Liver and Biliary Sciences, New Delhi, India; [12]Chinese University of Hong Kong School of Chinese Medicine Teaching Clinic for C, Shanghai, China; [13]Queen Elizabeth Hospital Birmingham Charity, Birmingham, United Kingdom; [14]Apollo Hospitals Hospital, Navi Mumbai, India; [15]Asian Institute of Gastroenterology, Hyderabad, India; [16]Department of Infectious Diseases, Suzhoa, China; [17]Hôpital Mustapha Pacha, Algiers, Algeria; [18]Hospital das Clínicas da Faculdade de Medicina da U S P, São Paulo, Brazil; [19]Department of Infectious Diseases, Nanning, China; [20]Christian Medical College, Vellore, India; [21]Hospital Italiano de Buenos Aires, Buenos Aires, Argentina; [22]Royal Berkshire Hospital, Reading, United Kingdom; [23]Sanjay Gandhi Postgraduate Institute of Medical Science, Lucknow, India; [24]The First Hospital of Jilin University, Jilin, China; [25]Instituto de la Salud Digestiva, Guadalajara, Mexico; [26]Marmara University Faculty Of Economics Building İbrahim Üzümcü, İstanbul, Türkiye; [27]The Second XiangYa Hospital of Central South University, Changsha, China; [28]Hospital Civil de Guadalajara Fray Antonio Alcalde, Guadalajara, Mexico; [29]Singapore General Hospital, Singapore, Singapore; [30]The Third Affiliated Hospital of Hebei Medical University, Hebei, China; [31]Centro Médico ISSEMYM, Mexico, Mexico; [32]Baylor Dallas (Baylor University Medical Center), Dallas, United States; [33]Second Hospital of Shandong University, Shandong, China; [34]The First Affiliated Hospital of Wenzhou Medical University, Wenzhou, China; [35]Hospital de Clínicas de Porto Alegre, Universidade Federal do Rio Grande do Sul, Porto Alegre, Brazil, Porto Alegre, Brazil; [36]Ege University School of Foreign Languages, Bornova, Türkiye; [37]Hospital General Doctor Manuel Gea González, Ciudad de México, Mexico; [38]Royal North Shore Hospital, Sydney, Australia; [39]Westmead Hospital, Sydney, Australia; [40]Department of Infectious Disease, Union Hospital, Tongji Medical College, Huazhong University of Science and Technology, Wuhan, China; [41]NIHR Nottingham Biomedical Research Centre, Nottingham, Nottingham, United Kingdom; [42]University of Malaya, Kuala, Malaysia; [43]Kimg Chulalongkorn Memorial Hospital, Krung Thep Maha Nakhon, Thailand; [44]Dr. Rela Institute and Medical Centre, Chennai, India; [45]Baku Medical Plaza Hospital, Baku, Azerbaijan; [46]Akdeniz University Faculty of Architecture, Konyaaltı, Türkiye; [47]AIIMS Hospital, New Delhi, India; [48]Beijing Youan Hospital, Capital Medical University, Beijing, China; [49]Mengchao Hepatobiliary Hospital of Fujian Medical University, Fuzhou, China; [50]The First Affiliated Hospital of Nanchang University, Nanchang, China; [51]Shuguang Hospital Affiliated to Shanghai University of Traditional Chinese Medicine, Shanghai, China; [52]The University of Hong Kong, Hong Kong SAR, China, Hong Kong, China; [53]Tel-Aviv Sourasky Medical Center, Tel Aviv, Israel; [54]Hospital Geral de Bonsucesso, Rio de Janeiro, Brazil; [55]Helwan University, Helwan, Egypt; [56]CHU de Cocody, Abidjan, Cote dIvoire, Abidjan, Central African Republic; [57]University Medical Center Freiburg, Freiburg, Germany; [58]University Hospital and King Faisal Hospital, Kigali, Rwanda; [59]Mercy Medical Center, Baltimore, United States; [60]Kims, Bhubaneswar, India; [61]Post Graduation of Medical Education and Research, Chandigarh, India; [62]University of Pennsylvania, Philadelphia, United States; [63]Mayo Clinic School of Medicine, Rochester, United States*
Email: jasmohan.bajaj@vcuhealth.org

Background and aims: A recent global consensus on cirrhosis organ failures proposed "immune failure" (IF: SBP, bacteremia, Vibrio, fungal infections and sepsis) and recommended prospective validation. Aim: Validate the impact of IF on 30-day mortality.
Method: We used CLEARED Consortium and Veterans Corporate Data Warehouse (VA-CDW). CLEARED includes cirrhosis inpatients recruited globally where cirrhosis details, country income (high/upper-mid/low income HIC/UMIC/LIC), inpatient course, and infections were recorded. Concurrent VA-CDW data from 2020–24 with data from all Veteran cirrhosis inpatients using validated ICD10 codes was utilized. Patients were divided into IF, non-IF-infections and neither. Logistic regression for 30-day mortality was performed across both cohorts.
Results: CLEARED: 6505 patients (56 years, 64% men) of whom 17% had IF, 17% no-IF infection and 66% neither were included. Highest mortality rate was in IF (38%) versus no-IF-infection (23%) and neither (13%, $p < 0.001$). IF patients had worse cirrhosis severity, comorbidities, and were highest in LICs. Multi-variable regression: IF linked with higher mortality vs neither (OR 2.21:1.83–2.66) and non-IF-infection (OR 2.04:1.06–2.58;both $p < 0.001$) with not being in HIC (LIC: OR-2.34/UMIC:1.7,$p < 0.001$), older age, cirrhosis complications, higher MELD-Na and WBC count. LT listing was protective. VA-CDW: 28,760 patients (68 yrs, 96% men) of whom 13% had IF, 13% and 74% neither. Highest mortality rate was in IF (30%) then no-IF-infections (12%) and neither (8%, $p < 0.001$). Multi-variable regression: IF still showed higher mortality vs neither (OR-2.37:2.13–2.62), and no-IF-infection (OR-2.25:1.96–2.58) both $p < 0.001$; other variables linked with mortality were age, cirrhosis complications, MELD-Na and higher WBC.
Conclusion: Immune failure defined in a recent consensus as presence of SBP, bacteremia, fungal infections and sepsis were linked with high 30-day mortality as compared to other infections in two large independent inpatient cirrhosis cohorts.

SAT-453

Right ventricle- pulmonary artery uncoupling in critically ill decompensated chronic liver disease patients: an exploratory observational stud

Aniruddha Banerjee[1], Deepak Tempe[1], Rakhi Maiwall[2]. [1]*Department of Anaesthesia and Critical Care, Institute of Liver and Biliary Sciences, Delhi, India;* [2]*Department of Hepatology, Institute of Liver and Biliary Sciences, Delhi, India*
Email: banerjeeaniruddha194@gmail.com

Background and aims: Right ventricle-pulmonary artery (RV-PA) uncoupling, a state of right ventricular (RV) dysfunction relative to its afterload, is a known predictor of mortality in various critical illnesses. However, its prevalence and prognostic significance in critically ill patients with decompensated chronic liver disease (CLD) are unknown. This study aimed to determine the prevalence of RV-PA uncoupling in this population and evaluate its association with disease severity and clinical outcomes.
Method: This prospective observational study was conducted in the intensive care unit (ICU) of a tertiary liver institute. We enrolled 250 adult patients with decompensated CLD requiring ICU care. A comprehensive transthoracic echocardiogram was performed within 48 hours of admission. RV-PA uncoupling was defined by a tricuspid annular plane systolic excursion to pulmonary artery systolic pressure (TAPSE/PASP) ratio of ≤0.33 mm/mmHg. Clinical, hemodynamic, and laboratory data were collected, and patients were followed for 28-days in the ICU.
Results: The prevalence of RV-PA uncoupling was 26.8% (67 out of 250 patients). Patients with uncoupling had significantly higher liver disease severity scores on admission (mean model for end-stage liver disease – sodium score: 36.0 ± 8.3 vs 31.0 ± 9.0, $p < 0.01$). The uncoupling group demonstrated greater hemodynamic instability, requiring significantly higher vasopressor support ($p < 0.01$), and had more severe respiratory failure, evidenced by a lower arterial oxygen tension to fraction of inspired oxygen ratio (PF ratio) ($p \leq 0.02$). Persistently elevated serum lactate levels were also significantly associated with uncoupling ($p < 0.01$). Kaplan-Meier survival analysis revealed significanty ($p < 0.01$) shorter survival span in uncoupling group (8.19 vs 17.05 days).
Conclusion: RV-PA uncoupling is common in critically ill patients with decompensated CLD and is a powerful, independent predictor of early mortality. It serves as an integrated marker of advanced liver disease severity and systemic circulatory collapse. The non-invasive bedside assessment of the TAPSE/PASP ratio is a valuable tool for risk stratification, and the identification of uncoupling should prompt aggressive, RV-protective management strategies in this high-risk population.

SAT-457

Beta-blockers for prevention of further decompensation and associated renal outcomes

Brendan Brew[1], Angus Jeffrey[1,2,3], Adam Testro[1], Marie Sinclair[1,4], Penelope Hey[1], Karl Vaz[1], Avik Majumdar[1,4]. [1]*Austin Hospital, Heidelberg, Australia;* [2]*Sir Charles Gairdner Hospital, Nedlands, Australia;* [3]*The University of Western Australia, Crawley, Australia;* [4]*The University of Melbourne, Parkville, Australia*
Email: brewy4@gmail.com

Background and aims: Non-selective beta blockers (NSBBs) are indicated for prevention of decompensation in cirrhosis. This study evaluated the impact of NSBBs initiated after a first decompensating event (ascites, hepatic encephalopathy [HE], or variceal bleeding) on further decompensation, renal outcomes, and mortality.
Method: This retrospective cohort study included adults with cirrhosis admitted with a first decompensation at a single tertiary liver transplant centre in Australia between January 2015 and March 2025. Patients were followed until further decompensation requiring hospitalisation, death, or liver transplant (LT). The primary outcome was further decompensation. Secondary outcomes were liver-related death (LRD) and LT, and acute kidney injury (AKI). Competing risks analysis was performed.
Results: A total of 310 patients were followed for a median of 21.3 months (IQR 6.4–45.5) of which 112 (36.1%) received NSBB therapy (87.5% carvedilol, 12.5% propranolol), of whom 66 (58.9%) achieved target dose. Median age was 61 years (49–69), median MELD 16 (12–20), and a majority 55.4% had alcohol-related liver disease. Median time from first decompensation to NSBB initiation was 2.5 months (IQR –0.04–34.2); three patients were on NSBBs prior to admission. In those who received NSBB therapy compared to not, the cumulative incidence of further decompensation after 5 years was lower in patients who had first decompensation with ascites (53% vs 74%, $p = 0.023$) and variceal bleeding (52% vs 81%, $p = 0.013$). There was no difference seen in HE (67% vs 73%, $p = 0.602$). Cumulative incidence of LRD and LT was also reduced after ascites-related first decompensation (27% vs 49%, $p = 0.007$), but not after variceal bleeding (23% vs 48%, $p = 0.102$) or HE (28% vs 58%, $p = 0.058$). Median creatinine before NSBB initiation was 69 µmol/L (57–86.5) versus 71 µmol/L (59.5–95.5) at follow-up ($p = 0.96$), measured after a median of 31.5 days (IQR 15–116). Only nine AKI events (8%) occurred.
Conclusion: NSBB therapy following a first decompensation with ascites or variceal bleeding was associated with reduced further decompensation and improved clinical outcomes, without adverse renal effects. These findings demonstrate the safety and effectiveness of NSBBs in patients with decompensated cirrhosis, supporting their use in this group.

SAT-458-YI

Beneficial impact of consequent non-selective beta-blocker intake on patient outcomes in all stages of chronic liver disease

Josune Cabello Calleja[1], Christophe Junot[2], Florence Castelli[2], Celine Chollet[2], Wenyi Gu[1,3,4], David Tornai[5], Michael Kuhn[6], Robert Schierwagen[1], Sabine Klein[1], Michael Praktiknjo[1], Manimozhiyan Arumugam[7], Minneke Coenraad[8], Maria Papp[5], Aleksander Krag[9], Jonel Trebicka[1,9,10]. [1]*Department of Internal Medicine B, University Hospital Muenster, Muenster, Germany;* [2]*Centre de Recherche sur l'Inflammation, INSERM, Université Paris Cité, Paris, France;* [3]*Department of Gastroenterology, Ren Ji Hospital, School of Medicine, Shanghai Jiao Tong University, Shanghai, China, Shanghai Institute of Digestive Disease, NHC Key Laboratory of Digestive Diseases, Shanghai, China;* [4]*Department of Internal Medicine I, University Hospital Frankfurt, Goethe University Frankfurt, Frankfurt, Germany;* [5]*Division of Gastroenterology, Department of Internal Medicine, University of Debrecen, Debrecen, Hungary;* [6]*European Molecular Biology Laboratory (EMBL), Heidelberg, Germany;* [7]*Faculty of Health and Medical Sciences, University of Copenhagen, Copenhagen, Denmark;* [8]*Department of Gastroenterology and Hepatology, Leiden University Medical Center, Leiden, Netherlands;* [9]*Department of Gastroenterology and Hepatology, Odense University Hospital, Odense, Denmark;* [10]*European Foundation for Study of Chronic Liver Failure (E-CLIF), Barcelona, Spain*
Email: josune.cabello@ukmuenster.de

Background and aims: Non-selective beta-blockers (NSBB) are commonly used in in patients with chronic liver disease as primary or secondary prophylaxis of variceal bleeding. However, their role on the overall survival of CLD at different disease stages is still under discussion.
Method: This study analyzed 3,622 patients from six multicentre cohorts to evaluate the impact of non-selective beta-blocker (NSBB) use during hospital admissions on short- and long-term survival across CLD stages: non-cirrhotic CLD, stable decompensated cirrhosis (SDC), unstable decompensated cirrhosis (UDC), pre–acute-on-chronic liver failure (pre-ACLF), and ACLF. To account for confounding and healthy survivor bias, propensity score matching 1:1 was applied. Overall mortality was analysed using Fine & Gray competing risk regression with liver transplantation as a competing event. In a subgroup from MICROBPREDICT cohort, a metabolomic analysis was

performed, including manual integration and peak quality assessments.
Results: NSBB use (n = 741; 35.8%) consistently reduced mortality in all CLD stages. ACLF patients profited notably from NSBB with a lower 28-day mortality (19.8% vs. 35.2%, p = 0.02). Pre-ACLF patients also showed reduced short- and long-term mortality (28-day: 19.8% vs. 21.7%, p < 0.05; 1-year: 57.4% vs. 71.4%, p = 0.04). Additionally, NSBB use was independently related to lower overall mortality in all patients (OR: 0.76, 95% CI: 0.60–0.97, p = 0.025), and in pre-ACLF patients when adjusted by other confounders. After propensity score matching, cumulative incidence curves confirmed a significant reduction in mortality for overall cohort, ACLF and pre-ACLF (Gray test p < 0.05). In a metabolomic subgroup analysis, propranolol and carvedilol metabolites were detected in various biosamples, with strongest signals in urine. Metabolites were not detected in all patients with NSBB treatment in the medical history. Patients in which NSBB metabolites were detected showed slightly lower mortality compared to those without detected metabolites, but the difference was not statistically significant.
Conclusion: Patients who received NSBB treatment showed improved survival outcomes, even in the most severe stages, like pre-ACLF or ACLF. However, our metabolomic analysis raises some doubts regarding patient adherence to NSBB therapy. Inadequate compliance may reduce the effectiveness of NSBBs.

SAT-459
Impact of cirrhosis on short- and mid-term outcomes of critically ill patients requiring invasive mechanical ventilation
Gemma Cerezal-Gómez[1,2], Alfonso Muriel[3,4], Mariano Gómez-Rubio[1,5], Fernando Frutos-Vivar[1,6], Óscar Peñuelas[1,5,6]. [1]*Hospital Universitario de Getafe, Getafe, Spain;* [2]*Universidad de Valladolid- Faculty of Medicine, Valladolid, Spain;* [3]*Centro de Investigación en Red de Epidemiología y Salud Pública, Madrid, Spain;* [4]*Universidad de Alcalá de Henares, Madrid, Spain;* [5]*Universidad Europea de Madrid- Faculty of Biomedical and Health Sciences, Villaviciosa de Odón, Spain;* [6]*Centro de Investigación en Red de Enfermedades Respiratorias, CIBERES, Madrid, Spain*
Email: gemmacerezal@gmail.com

Background and aims: Cirrhosis is a significant cause of morbidity and mortality worldwide, with up to 10% of patients requiring admission to an intensive care unit (ICU). Although invasive mechanical ventilation (IMV) has traditionally been associated with a very poor prognosis in this population, contemporary data suggest improving outcomes. The aim of this study was to evaluate clinical practice and outcomes in critically ill patients with cirrhosis requiring IMV.
Method: We performed a subgroup analysis of patients with pre-existing cirrhosis included in a prospective, multicenter, international cohort study enrolling consecutive adult patients admitted to 457 ICUs in 42 countries between October 2022 and June 2024 who required IMV for more than 12 hours (Global Burden of Mechanical Ventilation, GEMINI study). Demographic and clinical variables were collected at baseline, daily during the first ICU week, and until ICU discharge. Outcomes included ICU, in-hospital, and 6-month mortality. Multivariable logistic regression model was applied to evaluate the effect of cirrhosis on mortality and is expressed as odds ratio (OR) with 95% confidence interval (CI).
Results: Of 7,239 patients, 363 (5%) had cirrhosis. Compared with non-cirrhotic patients, those with cirrhosis were younger (59 ± 12 vs. 61 ± 18 years, p = 0.01) and predominantly male (75% vs. 62%, p < 0.001). At ICU admission, they presented greater disease severity, including a higher incidence of sepsis (25.6% vs. 16.5%, p < 0.001) and organ failure. No differences were observed in ICU or hospital length of stay. Mortality was significantly higher in patients with cirrhosis: ICU mortality 42.2% vs. 31.7%, in-hospital mortality 49.5% vs. 37.1%, and 6-month mortality 63.9% vs. 40.3% (all p < 0.001). After adjustment, cirrhosis was independently associated with increased ICU mortality (OR 1.64; 95% CI 1.35–2.08; p < 0.001) and in-hospital mortality (OR 1.67; 95% CI 1.32–2.11; p < 0.001), but not with 6-month mortality (OR 1.25; 95% CI 0.91–1.72; p = 0.164).
Conclusion: In this large cohort of mechanically ventilated ICU patients, cirrhosis was independently associated with increased ICU and in-hospital mortality, while no independent association with 6-month mortality was observed. These findings highlight the sustained prognostic impact of chronic liver disease beyond ICU discharge and support the need for integrated hepatology–ICU management and post-ICU follow-up.

SAT-460
Clinical benefit of artificial liver support system on 90-day survival in patients with acute-on-chronic liver failure
Xiao Che[1], Jingran Jiao[2], Shuang Li[3], Rui Zhao[1], Manman Xu[1], Yu Chen[1]. [1]*Fourth Department of Liver Disease (Difficult & Complicated Liver Diseases and Artificial Liver Center), Beijing You'an Hospital, Capital Medical University, Beijing Key Laboratory of Liver Regeneration and Artificial Liver Transformation Research, Beijing You'an Hospital, Capital Medical University, Beijing, China;* [2]*Beijing Key Laboratory of Liver Regeneration and Artificial Liver Transformation Research, Beijing You'an Hospital, Capital Medical University, Beijing, China;* [3]*Blood Purification Center, Beijing Youan Hospital, Capital Medical University, Beijing, China*
Email: chechexx@163.com

Background and aims: Acute-on-chronic liver failure (ACLF) is a clinical syndrome with high mortality. This study evaluated the effect of artificial liver support systems (ALSS; dual plasma molecular adsorption system combined with plasma exchange, DPMAS + PE) on 90-day transplant-free survival in patients with ACLF.
Method: Consecutive hospitalized patients with ACLF who received ALSS or standard medical therapy (SMT) were prospectively enrolled at Beijing You'an Hospital, Capital Medical University, between January 2022 and June 2025. ALSS and SMT patients were compared using 1:1 propensity score matching (PSM) based on key baseline covariates. Survival outcomes were assessed using Kaplan-Meier analysis and multivariable Cox regression.
Results: A total of 624 patients were included (ALSS group, n = 235; SMT group, n = 390). After PSM, 235 pairs were analyzed. The 90-day survival was higher in the ALSS group than in the SMT group (58.3% vs. 43.4%, $P < 0.05$). Survival benefit was observed in patients with ACLF 0–1 (64.5% vs. 47.6%, $P < 0.05$) and in those with MELD-Na ≥25 (53.3% vs. 28.6%, $P < 0.05$), but not in ACLF grade 2–3 or MELD-Na < 25 (In patients with 15 ≤ MELD-Na <25, survival curves intersected). In interaction analysis, patients with ACLF 0–1 and 15 ≤ MELD-Na <25, showed improved 90-day survival with ALSS (59.8% vs. 43.0%, $P < 0.05$) and independently reduced 90-day mortality (HR 0.56, 95% CI 0.37–0.89; $P < 0.05$). Older age (HR 1.02 per year; $P < 0.05$) and decompensated cirrhosis (HR 1.97, $P < 0.05$) were associated with increased mortality.
Conclusion: ALSS conferred a survival benefit in patients with EASL-CLIF ACLF 0–1 and intermediate MELD-Na scores.

SAT-461
Dynamic innate immune trajectories assessed by SeptiLoop identify immunoparalysis associated with nosocomial infection in decompensated cirrhosis
Juan Manuel Diaz[1,2,3], José Alcaraz[4], Richie Alexander Inge-Cox[1,2,3], Natalia Jimenez-Esquivel[1], Sandra Blaya[1], Ignacio Retta[1], Loredana Cosmina Sabau[4], Juliana Zapatero[1], Enrique Hernández Jiménez[5], Eduard Guerrero[5], Queralt Caus-Capdevila[5], Vanessa Roman[5], Joan Clària[3,6], Javier Fernández[1,3]. [1]*Liver ICU, Liver Unit, Hospital Clínic de Barcelona, Barcelona, Spain;* [2]*Fundació de Recerca Biomedica Clinic – Institut D'investigació Biomédic August Pi i Sunyer (FRCB-IDIBAPS), Barcelona, Spain;* [3]*European Foundation for the Study of Chronic Liver Failure (EF CLIF), Barcelona, Spain;* [4]*CORE Laboratory, Department of Biochemistry*

and Molecular Genetics, Hospital Clínic, Barcelona, Spain; [5]Loop Dx, StartUB! - University of Barcelona, Barcelona, Spain; [6]Biochemistry and Molecular Genetics Service, Hospital Clínic, IDIBAPS, University of Barcelona and CIBERehd, Barcelona, Spain
Email: juanmanuel.diaz@efclif.com

Background and aims: Patients with decompensated cirrhosis and acute-on-chronic liver failure (ACLF) develop immune dysfunction that increases susceptibility to nosocomial infections. Immunoparalysis, a key driver of infection risk in this setting, cannot currently be monitored dynamically at the bedside. SeptiLoop, a rapid in vitro assay of stimulated tumor necrosis factor (TNF) alpha production, may allow assessment of innate immune competence. We aimed to characterize longitudinal SeptiLoop trajectories in acute decompensation (AD) and ACLF and to evaluate whether early changes are associated with nosocomial infection.
Method: Prospective observational study including consecutive patients nonelectively hospitalized for AD of cirrhosis and admitted to the intensive care unit or regular ward at Hospital Clínic of Barcelona (September 2024–November 2025). Patients were classified as AD or ACLF at baseline according to EASL-CLIF criteria. SeptiLoop was measured at baseline and on days 1, 3, 7, 15 and 28 (404 tests in 91 patients). Delta SeptiLoop 0–7 was defined as the change from day 0 to day 7. Longitudinal trajectories were analyzed using mixed-effects models. Fine–Gray competing-risk analyses evaluated the association between delta SeptiLoop 0–7 and nosocomial infection, adjusted for ACLF and MELD-Na.
Results: Baseline SeptiLoop measurements showed no association with disease severity, infection or mortality. In contrast, trajectories differed markedly: AD showed an upward pattern consistent with immune recovery, whereas ACLF showed persistently low values and a progressive decline (days 3 to 7; $p < 0.001$). Patients who developed nosocomial infection had a downward SeptiLoop trajectory, whereas those without infection showed an increase (group by time $p < 0.01$). An early decline in delta SeptiLoop 0–7 was associated with a higher risk of nosocomial infection (sHR 0.45, 95% CI 0.23–0.92; $p = 0.028$). SeptiLoop did not independently predict 28-day mortality, which was driven by ACLF.
Conclusion: Baseline SeptiLoop measurements have limited prognostic value, but dynamic trajectories identify a clinically relevant immune phenotype. An early decline reflects functional immunoparalysis and is associated with an increased risk of nosocomial infection, supporting the use of SeptiLoop for immune monitoring in AD and ACLF.

SAT-464

Bilirubin trajectory phenotypes in patients with cirrhosis admitted to intensive care: an externally validated joint latent class mixed model with implications for future definitions of acute-on-chronic liver failure

Thomas Dixon[1], Tasneem Pirani[1], William Bernal[1], Mark Mcphail[1].
[1]*Liver Intensive Therapy Unit, King's College Hospital NHS Foundation Trust, London, United Kingdom*
Email: thomasdixon@nhs.net

Background and aims: Patients with cirrhosis admitted to the Intensive Care Unit (ICU) show heterogeneous organ failure trajectories. In acute-on-chronic liver failure (ACLF), bilirubin is variably expressed, and high bilirubin trajectories may capture distinct phenotypes with different survival. We aimed to identify early, reproducible, outcome-relevant bilirubin trajectory phenotypes during the first week of ICU admission using latent class mixed modelling.
Method: We analysed ICU patients with cirrhosis at our institution who had ≥2 bilirubin results during the first 7 days of ICU admission (n = 870). To identify latent trajectories in bilirubin levels while accounting for informative dropout, we fitted a joint latent class mixed model. We evaluated 2–5 class solutions, prioritising model fit, clinical interpretability, and bootstrap stability for model selection. The three-class model was selected and applied to an external MIMIC-IV cohort.
Results: The derivation cohort comprised 870 patients (61.0% male, 37.9% in-hospital mortality). A three-class solution was optimal, yielding three bilirubin trajectories: low-stable, high-improving, and high-worsening. Assignment certainty was high (mean posterior probability ≥0.87). In-hospital mortality was 32.5% (233/717) for low-stable, 51.1% (24/47) for high-improving, and 68.9% (73/106) for high-worsening. At ICU admission, higher bilirubin trajectories were associated with greater organ failure burden: the mean number of organ failures (SOFA subscore ≥3 per organ component) was higher in the high-worsening (2.3) and high-improving (2.2) classes compared with the low-stable class (1.6).
In external validation (n = 3,264), in-hospital mortality was 18.3% (545/2,971) for low-stable, 35.7% (10/28) for high-improving, and 57.7% (153/265) for high-worsening; the preserved mortality gradient and high assignment certainty (mean posterior probability ≥0.89) support reproducibility of these trajectory phenotypes across cohorts.
Conclusion: Longitudinal bilirubin phenotyping yields reproducible, survival-linked subgroups and is associated with organ failure burden. This supports trajectory-informed interpretation of routine bilirubin measurements for risk stratification in critically ill patients with cirrhosis. These findings suggest that significant hyperbilirubinaemia and/or early bilirubin dynamics warrant consideration as potential eligibility criteria in future iterations of ACLF definitions.

SAT-465

Assessing the effectiveness of an educational intervention to improve BASL bundle compliance and optimise care in the first 24 hours for patients with acute decompensation of cirrhosis in a district general hospital

Osama Elshabasy[1], Emily Hebden[1], Yousuf Ismail[1], Patrick Robinson[1].
[1]*Yeovil District Hospital, Yeovil, United Kingdom*
Email: Osama.elshabasy@gmail.com

Background and aims: Morbidity and mortality from chronic liver disease in the UK have risen markedly over the past 50 years. The National Confidential Enquiry into Patient Outcome and Death (NCEPOD) reported that fewer than 50% of patients admitted with alcohol-related liver disease received good-quality inpatient care (1). To address this, the British Association for the Study of the Liver (BASL) developed a care bundle to standardise management within the first 24 hours for patients with decompensated cirrhosis (2). However, uptake remains low, with bundle use reported in only 11.4% of admissions (2). This study aimed to assess baseline BASL bundle compliance and evaluate the impact of a targeted educational intervention in a district general hospital.
Method: An audit of patients admitted with DC was undertaken to evaluate adherence to key elements of the BASL care bundle, including early diagnostic ascitic tap and timely recognition and management of sepsis. Baseline compliance was assessed retrospectively over four months, during which no patients had a complete bundle performed.The educational intervention was targeted at resident doctors most frequently responsible for clerking patients with DC. Post-intervention compliance was subsequently reassessed over a two month period.
Results: Following the educational intervention, overall compliance improved, with 45% of patients admitted with decompensated cirrhosis receiving the full BASL care bundle. Improvements were noted in timely diagnostic ascitic tap on admission. Some areas which included requesting cultures and CXR continued to show poor adherence.
Conclusion: Baseline compliance with the BASL care bundle was poor, consistent with findings from national audits. A focused, low-cost educational intervention targeting resident doctors led to a clinically meaningful improvement in bundle compliance. This demonstrates that teaching resident doctors can effectively improve

early care for cirrhotic patients. Ongoing educational initiatives and further streamlining of bundle implementation is required to sustain and improve compliance.

SAT-466-YI

Global ROTEM-derived haemostatic profiles predict major non-portal hypertensive bleeding in acute-on-chronic liver failure

Kymentie Ferdinande[1], Elisa Pinto[2], Jochen Decaestecker[3], Charlotte De Vloo[3], Cristiana Bulato[4], Elena Campello[5], Alberto Ferrarese[2], Martina Gambato[6], Giacomo Germani[2], Francesco Paolo Russo[2], Patrizia Burra[2], Paolo Simioni[5], Hans Van Vlierberghe[7], Katrien MJ Devreese[8], Alberto Zanetto[2], Marco Senzolo[6]. *[1]Department of Surgery, Oncology, and Gastroenterology, University of Padova, Padova, Italy; Department of Gastroenterology and Hepatology, University Hospital of Ghent, Ghent, Belgium, Department of Gastroenterology and Hepatology, AZ Delta Hospital Rumbeke, Rumbeke, Belgium, Padova, Italy; [2]Department of Surgery, Oncology, and Gastroenterology, University of Padova, Padova, Italy, Gastroenterology/Multivisceral Transplant Unit, Padua University Hospital, Padova, Italy, Padova, Italy; [3]Department of Gastroenterology and Hepatology, AZ Delta Hospital, Rumbeke, Belgium, Rumbeke, Belgium; [4]Thrombotic and Hemorrhagic Diseases Unit, General Internal Medicine, Padova University Hospital, Padova, Italy, Padova, Italy; [5]Department of Medicine, University of Padova, Padova, Italy, First Chair of Internal Medicine, Padua University Hospital, Padova, Italy, Padova, Italy; [6]Gastroenterology/Multivisceral Transplant Unit, Padua University Hospital, Padova, Italy, Padova, Italy; [7]Department of Gastroenterology and Hepatology, Ghent University Hospital, Ghent, Belgium, Ghent, Belgium; [8]Coagulation Laboratory, Department of Laboratory Medicine. Ghent University Hospital, Ghent, Belgium, Department of Diagnostic Sciences, Ghent University, Ghent, Belgium, Ghent, Belgium*
Email: kymentie.ferdinande@studenti.unipd.it

Background and aims: Patients with acute-on-chronic liver failure (ACLF) are at high risk of non-portal hypertensive (NPH) bleeding. Although rotational thromboelastometry (ROTEM) assesses whole-blood haemostasis, interpretation is limited by isolated parameters. The area under the ROTEM curve (AUC), integrating clot kinetics and strength, is no longer routinely reported. We aimed to develop a reproducible method to estimate AUC INTEM/EXTEM and to evaluate its predictive value for major NPH bleeding in ACLF.
Method: In a prospectively followed multicentre ACLF cohort (n = 95), INTEM and EXTEM AUCs were estimated using AUC = 176.47–0.579×(time to MCF)-0.346 × CT+0.802 × CFT+ 100.12 × MCF. Agreement with device-reported AUCs was assessed using Lin's concordance correlation coefficient (CCC). NPH bleeding was defined as acute spontaneous or post-procedural bleeding, excluding PH–related bleeding. Discrimination was assessed by ROC analysis with Youden-derived cut-offs. Independent predictors were identified using MELD-adjusted LASSO-penalised logistic regression including bacterial infection, acute kidney injury, platelet count and fibrinogen.
Results: Patients were predominantly male (62%), with alcohol-related liver disease as the main aetiology (61%) and a median MELD of 25. 30/95 patients (31.6%) developed major NPH bleeding after a median of 13 days, most commonly mucosal, procedure-related, soft-tissue or intracranial bleeding. Estimated AUCs showed excellent agreement with device-reported values (INTEM CCC 0.952; EXTEM CCC 0.955; $p < 0.001$). AUC INTEM/EXTEM and a combined score integrating AUC INTEM/EXTEM and MCF FIBTEM decreased stepwise with increasing ACLF severity, with significant differences between ACLF grade I and III. Discrimination for NPH bleeding was good for AUC INTEM (AUROC 0.803; cut-off 3597; sensitivity 0.70, specificity 0.82; $p < 0.001$), AUC EXTEM (AUROC 0.787; $p < 0.001$), MCF FIBTEM (AUROC 0.763; $p < 0.001$), and the combined score (AUROC 0.802; cut-off 7239; sensitivity 0.70, specificity 0.83; $p < 0.001$). In MELD-adjusted models, AUC INTEM below the cut-off independently predicted bleeding (λ.min OR 4.82, 95% CI 1.67–13.17; λ.1se OR 1.95, 95% CI 1.03–4.81), as did the combined AUC score (λ.min OR 5.38, 95% CI 1.91–15.24; λ.1se OR 2.16, 95% CI 1.04–5.33).
Conclusion: An extrapolation-based method accurately estimates ROTEM-derived AUCs in ACLF; low AUC INTEM and the composite score independently predict major NPH bleeding. Prospective validation is needed to define actionable thresholds.

SAT-467-YI

Geographical variation in rifaximin use, gut microbiota composition, and outcomes in european patients with decompensated cirrhosis

Susan Fischer[1], Josune Cabello Calleja[2], Felix Salim[3], Wenyi Gu[2], Wieneke Michels[1], Annarein Kerbert[1], Marisa Isabell Keller[3], Pere Ginès[4], Wim Laleman[5], Maria Papp[6], Joan Claria[4], Richard Moreau[7], Vicente Arroyo[7], Debbie L. Shawcross[8], Rajiv Jalan[9], Peer Bork[3], Aleksander Krag[10], Christophe Junot[11], Matthias Mann[12], Sabine Klein[2], Itziar de Lecuana[13], Anton Jan van Zonneveld[1], Manimozhiyan Arumugam[14], Michael Kuhn[3], Jonel Trebicka[2], Minneke Coenraad[1]. *[1]Leiden University Medical Center, Leiden, Netherlands; [2]Universitätsklinikum Münster, Münster, Germany; [3]European Molecular Biology Laboratory, Heidelberg, Germany; [4]Hospital Clinic of Barcelona, Barcelona, Spain; [5]UZ Leuven, Leuven, Belgium; [6]University of Debrecen, Debrecen, Hungary; [7]European Foundation for the Study of Chronic Liver Failure, Barcelona, Spain; [8]The Institute of Liver Studies King's College, London, United Kingdom; [9]University College London, London, United Kingdom; [10]Odense Universitetshospital, Odense C, Denmark; [11]INRAE, Paris, France; [12]Max Planck Institute of biochemistry, Munich, Germany; [13]Faculty of Medicine and Health Sciences, University of Barcelona, Barcelona, Spain; [14]Center for Basic Metabolic Research, University of Copenhagen, Copenhagen, Denmark*
Email: s.e.fischer@lumc.nl

Background and aims: Cirrhosis causes substantial morbidity and mortality, with outcomes potentially varying across European regions due to differences in healthcare systems, demographics, and treatment strategies. This study investigated the association between geographical region and the clinical phenotype among hospitalized European patients with acutely decompensated cirrhosis (AD). As a secondary objective, regional variation in gut microbiota composition and its association with mortality was investigated.
Method: Clinical data on disease phenotype and mortality from 2,377 hospitalized patients with AD enrolled in three European prospective cohorts (CANONIC, PREDICT, FCRB) across 16 countries were collected. Patients were grouped into Northern/Western (n = 962, N/W), Eastern (n = 181, E), and Southern Europe (n = 1234, S). Disease phenotypes were classified as acute-on-chronic liver failure (ACLF, at admission and pre-ACLF combined), unstable decompensated cirrhosis (UDC), and stable decompensated cirrhosis (SDC). In a subcohort of patients with stool samples available (n = 248), gut microbiota composition was assessed by shotgun metagenomic sequencing with taxonomic profiling and multivariable microbiome analyses adjusting for antibiotic (AB) exposure and clinical variables.
Results: Disease phenotype distribution differed between regions, with lower UDC and higher SDC in Eastern Europe ($p < 0.001$). The prevalence of ACLF/pre-ACLF at admission was similar across regions (N/W 30%, E 34%, S 29%; $p = 0.339$). 28- and 90-day mortality did not differ, while 1-year mortality was higher in Eastern Europe (40% vs. 33% N/W and 30% S; $p = 0.035$). Baseline gut microbiota composition differed significantly by region and was strongly influenced by AB exposure. Rifaximin use was highest in Southern Europe (35% vs. 26% N/W and 10% E; $p < 0.001$). Overall microbiota structure was dominated by *Bacteroides*, while Southern Europe showed a distinct shift toward an *Enterococcus*-enriched microbiota. Bacterial infections were more common in Eastern Europe (44% vs. 27% N/W and 28% S; $p = 0.029$). These regional microbiota differences persisted after adjustment for AB use, but were not associated with disease phenotype or mortality.

Conclusion: ACLF prevalence and mortality were largely comparable across European regions in patients with decompensated cirrhosis. Regional variation in gut microbiota composition does not independently determine survival outcomes.

SAT-468

Clinical impact of bacterial infections in acutely decompensated cirrhosis: insights from 4.97 million admissions

Javier Fernández[1,2], Yacine Hajji[3], Jonel Trebicka[2,4], Thierry Artzner[2,5], William Bernal[2,6], Joan Clària[2,7], Lise Lotte Gluud[2,8], Jennifer Lai[9], Jacqueline O'Leary[10], Pierre-Emmanuel Rautou[2,11,12], Debbie L. Shawcross[13,14], Bart Staels[15], Florence Wong[16], Cristina Sanchez-Garrido[2], Eva Uson[2], Athéna Crespin[3], Berenice Alard[3], Jennifer Jara Vargas[3], Maxime Anné[3], Stephanie Ferreira[3], Dean Hum[3], Jeremy Magnanensi[3], Pejvack Motlagh[3], Sakina Sayah Jeanne[3], Pierbruno Ricci[3], Katharina Staufer[3], Arun J. Sanyal[17,18], Richard Moreau[2,11,19], Jasmohan Bajaj[20], Paolo Angeli[2,21]. *[1]Liver ICU, Liver Unit, Hospital Clinic, IDIBAPS and CIBEREHD, Barcelona, Spain, Barcelona, Spain; [2]European Foundation for the Study of Chronic Liver Failure (EF CLIF), Barcelona, Spain, Barcelona, Spain; [3]Genfit S.A., Loos, France; [4]Department of Internal Medicine B, University Hospital Münster, Münster, Germany, Münster, Germany; [5]Liver Transplant Unit, Hôpitaux Universitaires de Strasbourg, France, Strasbourg, France; [6]Liver Intensive Therapy Unit, Kings College Hospital, London, United Kingdom, London, United Kingdom; [7]Hospital Clínic-IDIBAPS, CIBERehd, University of Barcelona, Barcelona, Spain; Barcelona, Spain; [8]Gastrounit Medical Division, Hvidovre Hospital, Hvidovre, Denmark, Hvidovre, Denmark; [9]Department of Medicine, University of California, San Francisco, California, San Francisco, California, United States; [10]University of Texas, Southwestern, Dallas, United States, Dallas, United States; [11]Université Paris-Cité, Inserm, Centre de recherche sur l'inflammation, UMR 1149, Paris, France, Paris, France; [12]AP-HP, Hôpital Beaujon, Service d'Hépatologie, DMU DIGEST, Centre de Référence des Maladies Vasculaires du Foie, FILFOIE, ERN RARE-LIVER, Clichy, France, Clichy, France; [13]Institute of Liver Studies, Kings College London, London, UK, London, United Kingdom; [14]Roger Williams Institute of Liver Studies, Faculty of Life Sciences and Medicine, King's College London, London, United Kingdom, London, United Kingdom; [15]Université de Lille, Inserm, CHU Lille, Institut Pasteur de Lille, U1011-EGID, Lille, France, Lille, France; [16]Department of Medicine, University of Toronto, Toronto General Hospital, Toronto, ON, Canada, Toronto, Canada; [17]Department of Medicine, Virginia Commonwealth University of Medicine, Richmond, Virginia, USA, Richmond, Virginia, United States; [18]Stravitz-Sanyal Institute for Liver Disease and Metabolic Health, Virginia Commonwealth University School of Medicine, Richmond, VA, USA, Richmond, Virginia, United States; [19]Hôpital Beaujon, Service d'Hépatologie, Clichy, France, Clichy, France; [20]Division of Gastroenterology, Hepatology, and Nutrition, Department of Internal Medicine, Virginia Commonwealth University School of Medicine, Richmond, VA, USA, Richmond, Virginia, United States; [21]University of Padova, Italy, Padova, Italy*
Email: yacine.hajji@genfit.com

Background and aims: Acute decompensation (AD) of cirrhosis is defined by an acute development or worsening of ascites, hepatic encephalopathy (HE), and/or variceal bleeding (VB). It is unclear whether bacterial infections (BI) should be considered as an AD event "per se" or a precipitating/aggravating decompensation factor. Using real-world data, we evaluated the impact of BI on patient outcomes either alone or combined with other AD events.

Method: All hospitalizations (hosp) of patients with cirrhosis recorded between April-2016 and February-2025 in Komodo's Healthcare Map US real-world database and associated with at least one AD or BI event were included. Hosp were categorized by types of AD events (ascites, HE, VB) reported regardless of initial or subsequent AD event. BI were considered community-acquired if they were reported within 48 h after admission, and nosocomial if they occurred thereafter. Length of hosp stay (LOS), AD re-hospitalization rates, and mortality within 28/90/180d were compared between hosp with or without BI using fold changes (FC).

Results: A total of 4,974,364 hosp from 1,620,164 patients were extracted (male: 58%, mean age at admission: 63 ± 13 years, median LOS: 6 days [IQR: 4, 10]). Presence of ascites was reported in 46% of hosp, HE in 24%, and VB in 11%. A total of 40% of hosp reported community-acquired infections (CAI) without AD, 40% had AD without CAI, and 20% had both CAI and AD. Among hosp with ascites, HE, or VB, CAI was observed in 36%, 37%, and 24% of cases, respectively. VB and CAI alone showed the lowest 28/90/180d mortality (2/5/8% and 4/8/11%, respectively) while HE and ascites alone had higher mortality rates (4/10/15% and 5/13/19%, respectively). The 28-d mortality in hosp with VB, HE, or ascites increased when CAI was present (7, 10, 12% respectively). In hosp with at least 1 AD event, the median LOS (4–7 d) and 28-d mortality (2–8%) consistently increased with bacterial infection, either community-acquired or nosocomial (FC ranging 1.4–1.9 and 2.8–3.1 for LOS; 2.3–3.5 and 2.4–4.5 for mortality). Re-hospitalization rates at 28-d (15–35%) were modestly affected by CAI and nosocomial infections with FC ranging 0.9–1.3 and 1.0–1.5 across groups.

Conclusion: While BI alone was associated with low mortality and re-hospitalization rates, infections precipitating or complicating any AD event consistently increased mortality and prolonged LOS. These findings support the view that BI acts mainly as an aggravating factor in decompensated cirrhosis.

SAT-473

Examining the newly proposed consensus organ failure thresholds for acute on chronic liver failure

Jonas Ho[1], Sakktivel Elangovan[1], Jeanette Ng[1], Yan Ling Ong[1], Jessica Tan[1], Eugene Wong[1], Hiang Keat Tan[2], Chanda Ho[2], Marianne De Roza[3], Jason Pik Eu Chang[2], Prema Raj[2], Rahul Kumar[1]. *[1]Changi General Hospital, Singapore, Singapore; [2]Singapore General Hospital, Sinagapore, Singapore; [3]Sengkang General Hospital, Singapore, Singapore*
Email: rahul.kumar@singhealth.com.sg

Background and aims: Recently, efforts have been made to harmonize the heterogeneous definitions of acute-on-chronic liver failure (ACLF). New organ-specific thresholds have been proposed for defining organ failure (OF)[1,2]. These individual cut-offs and their implications for mortality require further exploration. The study aims to examine the specific OF cut-off and its impact on 28- and 90-day mortality.

Method: This prospective study was conducted as part of the multicentre SoLiDaRity collaborative, designed to predict decompensation, ACLF, and mortality in cirrhosis. A total of 396 consecutive hospital admissions for acute decompensation were included in the analysis. OFs, encompassing liver (LF), kidney (KF), circulatory (CF), respiratory (RF), immune (IF), and acute encephalopathy (AE), were defined as per the new criteria[2]. Standard statistical tests, along with Cox regression, were used to assess the risk of death associated with the proposed OF cut-offs.

Results: Majority were male (67.2%), and the mean age was 64.4 ± 11.5 years. Alcohol (43%) and MASLD (30%) were predominant aetiologies. The mortality was 11.1% and 25% at 28 and 90 days. Individually, LF was present in 14.1%, KF in 5.6%, AE in 14.6%, CF in 9.6%, RF in 5.8% and IF in 9.3%. On Cox regression, LF (HR:2.11; 95%CI: 1.07–4.17), KF (HR:5.39; 95%CI: 2.59–11.23), CF (HR:5.87;95%CI:3.13–10.92), and RF (HR: 4.90; 95%CI: 2.35–10.21) were individual predictors of 28-day mortality, but IF (HR: 0.983; 95%CI:0.35–2.74) and AE (HR: 1.29; 95%CI:0.63–2.79) were not. Furthermore, in the multivariable Cox regression (MVA), while KF, CF, and RF were independent predictors of 28-day mortality, LF was not. Similar results were observed for 90-day mortality, except that LF was also an independent predictor in MVA. Although IF did not predict 28- or 90-day mortality, a neutrophil-to-lymphocyte ratio of ≥9 was a predictor

at both time points. Kaplan-Meier analysis showed that the pooled mortality of patients with any OF by the new definition was 19.7% at 28 days and 33.7% at 90 days, compared with 5.6% and 18.7%, respectively, in those without any OF.
Conclusion: The new organ-specific cut-offs stratify mortality, with kidney, circulatory, and respiratory failures as the strongest independent predictors. Immune failure and encephalopathy require further refinement, supporting the prognostic relevance of objective inflammatory markers such as the neutrophil-to-lymphocyte ratio.

References

PMID: 39961976
PMID: 40499736

SAT-474

Exploring rhabdomyolysis in critically ill decompensated cirrhotic patients – a retrospective analysis of a german transplant centre

Lukas Hofmann[1], Romy Winkler[1], Janett Fischer[1], Florian van Bömmel[1], Sirak Petros[2], Lorenz Weidhase[2], Thomas Berg[1], Jonas Schumacher[1]. *[1]Division of Hepatology, Department of Medicine II, Leipzig University Medical Center, Leipzig, Germany, Leipzig, Germany; [2]Medical ICU, University Hospital Leipzig, Leipzig, Germany, Leipzig, Germany*
Email: jonas.schumacher@medizin.uni-leipzig.de

Background and aims: Rhabdomyolysis, characterized by excessive skeletal muscle breakdown and elevated serum myoglobin levels, is a potentially life-threatening condition frequently complicated by acute kidney injury (AKI). In patients with decompensated liver cirrhosis (dLC), AKI commonly results from hypovolemia or hepatorenal syndrome. Yet the contribution of rhabdomyolysis to renal dysfunction and mortality remains poorly defined.
We aimed to determine the real-world incidence, etiology, and clinical impact of rhabdomyolysis in critically ill patients with dLC.
Method: dLC-patients admitted to the intensive care unit (ICU) between June 2024–May 2025 were included and screened for signs of rhabdomyolysis defined by myoglobin serum levels ≥1000 ng/ml. Clinical and laboratory data were obtained at admission and from rhabdomyolysis-diagnosis for 10 consecutive days. Patients were followed for 90 days.
Results: Among 117 dLC-patients 25 (21.4%) presented with rhabdomyolysis. 28- and 90-Day transplant-free survival rates differed significantly between patients with and without rhabdomyolysis (8/25 (32%) vs 55/92 (59.8%), $p = 0.014$; and 4/25 (16%) vs. 44/92 (47.8%), $p = 0.005$). Outcomes in Statin-associated rhabdomyolysis (SAR) were even worse with transplant-free survival rates of 22.2% and 11.1%, respectively. SAR was the leading cause of rhabdomyolysis (9/25, 36%). Plasma myoglobin levels were significantly higher in SAR compared to non-SAR ($p < 0.001$). Nearly all affected patients 24/25 (96%) presented with acute-on-chronic liver failure, and 22/25 (88%) developed concomitant AKI.
Conclusion: Rhabdomyolysis and specifically SAR might represent an underestimated contributor to AKI and mortality in patients with dLC. Elevated myoglobin levels may serve as a prognostic marker of poor outcome and warrant systematic evaluation in future studies.

SAT-475

Serological responses COVID-19 vaccination: a potential biomarker to predict liver-related complications in patients with compensated advanced liver disease (cACLD)

Changze Hong[1,2], María Pilar Ballester[3], Giovanni Perricone[4], Manuela Merli[5], Maria Buti[6], José Luis Calleja Panero[7], German Soriano[8], Pierluigi Toniutto[9], Javier Ampuero[10], Francesco Paolo Russo[11], David Sacerdoti[12], Minneke Coenraad[13], Marina Berenguer[14], Salvatore Piano[11], Angelo Sangiovanni[15], Agustín Albillos[16], Amir Gander[17], Vishal C. Patel[18], Paolo Caraceni[19], Gavin Wright[20], Paula Iruzubieta[21], Raul J. Andrade[22], Francisco Javier Garcia-Samaniego[23], Xavier Verhelst[24], Eva Uson[25], Cristina Sanchez-Garrido[25], Gautam Mehta[1,17], Rajiv Jalan[1,17] on behalf of the COBALT Consortium[26]. *[1]Institute for Liver and Digestive Heath, University College London, London, United Kingdom; [2]Hepatology Unit, Department of Infectious Diseases, Nanfang Hospital, Southern Medical University, Guangzhou, China; [3]Department of Gastroenterology and Hepatology, Hospital Clínico Universitario de Valencia, Valencia, Spain; [4]ASST Grande Ospedale Metropolitano Niguarda, Hepatology and Gastroenterology Unit, Milano, Italy; [5]Department of Translational and Precision Medicine, University of Rome Sapienza, Roma, Italy; [6]Liver Unit, Hospital Universitario Valle de Hebron, Barcelona, Spain; [7]Department of Gastroenterology and Hepatology, Hospital Universitario Puerta de Hierro Majadahonda, IDIPHIM, Madrid, Spain; [8]Hospital de la Santa Creu i Sant Pau, Barcelona, Spain; [9]Hepatology and Liver Transplantation Unit, Azienda Sanitaria Universitaria Integrata, University of Udine, Udine, Italy; [10]Hospital Universitario Virgen del Rocio, Sevilla. Instituto de Biomedicina de Sevilla, Universidad de Sevilla, Sevilla, Spain; [11]Department of Medicine - DIMED, Unit of Internal Medicine and Hepatology (UIMH), University of Padova, Padova, Italy; [12]Azienda Ospedaiera Universitaria Integrata Verona, Verona, Italy; [13]Department of Gastroenterology and Hepatology, Leiden University Medical Center, RC Leiden, Netherlands; [14]Hepatology, HBP Surgery and Transplantation, Hepatology & Liver Transplant Unit, La Fe University Hospital, Valencia, Spain; [15]Foundation IRCCS Ca' Granda Ospedale Maggiore Policlinico, Division of Gastroenterology and Hepatology, Milan, Italy; [16]Servicio de Gastroenterología, Hospital Universitario Ramón y Cajal, Centro de Investigación Biomédica en Red de Enfermedades Hepáticas y Digestivas (CIBEREHD), Instituto Ramón y Cajal de Investigación Sanitaria (IRYCIS), Madrid, Spain; [17]Royal Free London NHS Foundation Trust, London, United Kingdom; [18]Faculty of Life Sciences and Medicine, King's College London, London, United Kingdom; [19]Department of Medical and Surgical Sciences, University of Bologna, Bologna, Italy; [20]Mid & South Essex NHS Foundation Trust, Basildon, United Kingdom; [21]Gastroenterology and Hepatology Department, Marqués de Valdecilla University Hospital, Santander, Spain; [22]Servicio de Aparato Digestivo, Hospital Universitario Virgen de la Victoria, Universidad de Málaga, Málag, Spain; [23]Liver Unit, Hospital Universitario La Paz, CIBERehd, IdiPAZ, Universidad Autónoma de Madrid, Madrid, Spain; [24]Department of Gastroenterology and Hepatology, Ghent University Hospital, Grent, Belgium; [25]European Foundation for the Study of Chronic Liver Failure (EF CLIF), EASL-CLIF Consortium and Grifols Chair, Barcelona, Spain; [26]the COBALT Consortium, London, United Kingdom*
Email: r.jalan@ucl.ac.uk

Background and aims: Patients with compensated advanced chronic liver disease (cACLD) have dysregulated innate and adaptive immunity, worsening with the stage of the disease. This is referred to as cirrhosis-associated immune dysfunction (CAID) and is characterized by a variety of abnormalities in immune profiles. However, there are no specific biomarkers of CAID that have been validated to be associated with future complications of cACLD. As immune response to vaccines provides a composite perspective on immune function, we hypothesized that serological response to COVID-19 vaccine may serve as a biomarker to identify cACLD patients at risk of developing liver-related complications.
Method: cACLD patients were included from the COBALT study, a prospective, observational cohort study. Participants with liver transplantation (LT) before study inclusion or those without serological or follow-up data were excluded. Serum concentrations of IgG directed against COVID-19 Spike and IgM against COVID-19 S1 receptor binding domain (RBD) were measured at week-7 following vaccination. Participants were followed up after the second vaccination dose for 1-year or until the third vaccine dose. The liver-related complications were evaluated using competing risk analysis, in which LT was treated as a competing event.
Results: A total of 95 cACLD patients were included in this study. The median age was 62 (IQR: 56–69) years, and 67.4% patients were male. Alcohol-associated liver disease (40%) was predominant. Over a

median follow-up time of 151 (IQR: 107–289) days, 16 patients developed liver-related complications, 13 patients received LT, and 8 patients had non-liver-related complications (including 5 COVID-19 infections). The levels of anti-S1-RBD IgM and anti-spike IgG were both comparable between different clinical outcome groups (both p > 0.05). We then used tertiles of vaccine response among the healthy population (n = 41) as the cut-off points of the cACLD populations. cACLD patients with a lower level of anti-S1-RBD IgM developed significantly greater liver-related complications compared to those with medium or high levels (sHR: 0.37, 95%CI: 0.14–0.98, p = 0.042).
Conclusion: Impaired serological response after COVID-19 vaccination was associated with the development of liver-related complications suggesting that serological responses to vaccination could serve as a composite biomarker of immune function to predict future liver-related complications in cACLD patients.

SAT-476

ATANGO organ failure (OF) score performs better than EASL-CLIF, NACSELD and APASL scores for the diagnosis of acute-on-chronic liver failure (ACLF) in the independent COSSH cohort

Meiqian Hu[1], Jinjin Luo[2], Nipun Verma[3], Sina Jameie-Oskooei[1], Xi Liang[2], Jiaqi Li[4], Tianzhou Wu[5], Jiang Li[6], Peng Li[7], Qian Zhou[2], Jiaojiao Xin[2], Dongyan Shi[2], Jing Jiang[2], Xin Chen[8], Bing Zhu[9], Tingting Feng[10], Jian-Ming Zheng[11], Yuxian Huang[11], Feng Ye[12], Bingqi Li[13], Yan Huang[14], Shaoli You[15], Cornelius Engelmann[16], Yu Chen[17], Jun Li[2], Rajiv Jalan[1]. *[1]University College London, Royal Free Campus, Institute for Liver and Digestive Health, London, United Kingdom; [2]State Key Laboratory for Diagnosis and Treatment of Infectious Diseases, National Clinical Research Center for Infectious Diseases, National Medical Center for Infectious Diseases, The First Affiliated Hospital, Zhejiang University School of Medicine, Hangzhou, China; [3]Department of Hepatology, Postgraduate Institute of Medical Education and Research, Chandigarh, India; [4]Department of Gastroenterology, Zhejiang Provincial People's Hospital, People's Hospital Affiliated of Hangzhou Medical College, Hangzhou, China; [5]International Health Care Community, Pacific Care Home, Hangzhou, China; [6]Department of Infectious Disease, The First Affiliated Hospital of Anhui Medical University, Hefei, China; [7]Department of Gastroenterology, The First Affiliated Hospital, Zhejiang University School of Medicine, Hangzhou, China; [8]Zhejiang Provincial Key Laboratory of Pancreatic Disease, The First Affiliated Hospital, Zhejiang University School of Medicine, Hangzhou, Zhejiang, China, Institute of Pharmaceutical Biotechnology, Zhejiang University School of Medicine, Hangzhou, China; [9]Department of Hepatology, Liver Vascular Disease Diagnosis And Treatment Center, The Fifth Medical Center of PLA General Hospital, Beijing, China; [10]Department of Infectious Diseases, The First Affiliated Hospital of Suzhou University, Suzhou, China; [11]Department of Infectious Diseases, Huashan Hospital, Fudan University, Shanghai, China; [12]Department of Infectious Disease, The First Affiliated Hospital of Xi'an Jiaotong University, Xi'an, China; [13]Department of Infectious Diseases, The Third Affiliated Hospital of Sun Yat-sen University, Guangzhou, China; [14]Department of Infectious Diseases, Xiangya Hospital, Central South University, Changsha, China; [15]Senior Department of Hepatology, The Fifth Medical Center of Chinese PLA General Hospital, Beijing, China; [16]Charité-Universitaetsmedizin Berlin, Clinic for Hepatology and Gastroenterology, Berlin, Germany; [17]Beijing Municipal Key Laboratory of Liver Failure and Artificial Liver Treatment Research, Fourth Department of Liver Disease, Beijing Youan Hospital, Capital Medical University, Beijing, China*
Email: humeiqian@zju.edu.cn

Background and aims: ACLF is a complex syndrome associated with high short-term mortality, with no agreement between continents on its diagnostic criteria. In order to try and harmonize the definitions, the ATANGO score was developed and validated in over 8000 patients from Europe, Latin America, India and China. In order to determine the comparative value of the ATANGO score, the performance of all models for the diagnosis and prognosis of ACLF was tested in an independent cohort–the Chinese (COSSH) cohort, developed in Hepatitis B patients.
Method: Data from 3,370 hospitalized cirrhosis patients with acute decompensation in the COSSH cohort were analyzed. Five ACLF diagnostic models were compared, including A-TANGO, EASL-CLIF (European), COSSH-ACLF (Chinese), the APASL (Asia), and NACSELD (USA). Prognostic performance was assessed using net reclassification improvement (NRI), C-indices, and integrated discrimination improvement (IDI).
Results: Among 3,370 patients, the A-TANGO and COSSH-ACLF models identified the largest numbers of ACLF patients (1,134 and 1,155), compared with the EASL-CLIF (706), APASL-ACLF (437), and NACSELD-ACLF (93) models. The 28-/90-day mortality rates were 32.5%/49.0% for A-TANGO model and 31.6%/48.6% for COSSH-ACLF framework, whereas NACSELD-ACLF framework identified the fewest patients but with the highest mortality (62.9%/67.9%). Only 39-patients met criteria for diagnosis of ACLF in all five models and these patients had extremely high mortality (87.5%/93.3%). The A-TANGO model showed the best reclassification using NRI compared with EASL-CLIF, COSSH-ACLF, APASL-ACLF, and NACSELD-ACLF models (11.81%, 7.71%, 37.4%, and 45.9%). Using the CLIF-organ failure (OF) score as the reference, the COSSH-ACLF II, COSSH-ACLF, and A-TANGO OF scores demonstrated improved discrimination (IDI: 4.09%, 0.62%, and 0.81%). C-index analyses further confirmed that COSSH-ACLF II, COSSH-ACLF, and A-TANGO OF scores provided the best discrimination for 28-day mortality (0.857, 0.848, and 0.832).
Conclusion: The A-TANGO models performs as well as the COSSH model in the COSSH cohort for the diagnosis of ACLF and for prediction of short-term mortality. The other 3-models underestimate the diagnosis of ACLF markedly. As further attempts are made to harmonize definitions for the diagnosis and prognosis of ACLF, the data from this study would support the use of ATANGO score for non-HBV patients whilst COSSH score be used for HBV patients.

SAT-477

Prognostic value of minimal hepatic encephalopathy assessment in patients with acute and chronic liver disease

Nicholas Zeuzem[1], Yu Ri Im[1], Samuel Scholl[1], Alina Bauschen[1], Timo Lehr[1], Katharina Merk[1], Julian Allgeier[1], Christian M. Lange[1], Christiana Graf[1]. *[1]LMU University Hospital, München, Germany*
Email: christiana.graf@med.uni-muenchen.de

Background and aims: Minimal hepatic encephalopathy (mHE) may predict overt hepatic encephalopathy (oHE). However, the prognostic value of different mHE assessment tools across various stages of liver disease remains unclear. The aim of this study was to evaluate the predictive value of mHE testing for clinical outcomes.
Method: Patients with liver cirrhosis or severe acute liver injury without overt HE at inclusion were prospectively enrolled. mHE was assessed using the Psychometric Hepatic Encephalopathy Score (PHES), Critical Flicker Frequency (CFF), Animal Naming Test (ANT), and EncephalApp Stroop test. mHE was defined as ≥2 of 3 tests abnormal using age- and education-adjusted norms. Serial mHE assessment was performed in a subgroup. Primary endpoints were the development of oHE and liver transplantation-free survival.
Results: A total of 121 patients were included: 46% male, median age 56 years, median MELD was 17. Disease stages comprised compensated cirrhosis (20%), stable decompensated cirrhosis (13%), unstable decompensated cirrhosis (17%), pre-ACLF (18%), ACLF (13%), and severe acute liver injury (19%). Main etiologies were alcohol-related (40%) and autoimmune/cholestatic liver diseases (29%). At baseline, mHE was present in 14% (17/121). During median follow-up of 9 months, 24 patients (20%) developed oHE, 25 (21%) underwent liver transplantation, and 11 (9%) died. CFF as continuous variable was significantly associated with oHE (HR 0.91 per Hz, 95% CI 0.84–0.98, p = 0.011), remaining significant after MELD adjustment (aHR 0.91, p = 0.015). Serial assessment was available in 58 patients. Unfavorable mHE trajectory (new onset or persistently abnormal) was associated

with higher oHE rates (60% vs 16%, p < 0.001). In MELD-adjusted regression, unfavorable trajectory strongly predicted oHE (aHR 5.62, 95% CI 2.06–15.39, p < 0.001). Sensitivity analysis restricted to patients with cirrhosis (n = 98) confirmed these findings.
Conclusion: CFF as continuous variable predicts oHE development in patients with acute and chronic liver disease. Serial mHE assessment identifies high-risk patients independent of MELD score, supporting integration of mHE testing into clinical practice.

SAT-478

Use and effectiveness of lactulose and rifaximin in patients with cirrhosis and hepatic encephalopathy highlight need for new treatments: insights from real-world data

Jacqueline O'Leary[1], Jonel Trebicka[2,3], Jennifer Jara Vargas[4], Jeremy Magnanensi[4], Javier Fernández[3,5], Thierry Artzner[6,7], William Bernal[7,8], Joan Clària[7,9], Lise Lotte Gluud[3,10], Jennifer Lai[11], Richard Moreau[7,12], Pierre-Emmanuel Rautou[7,12,13], Christopher F. Rose[14], Debbie L. Shawcross[15,16], Bart Staels[17], Florence Wong[18], Cristina Sanchez-Garrido[7], Eva Uson[7], Berenice Alard[4], Maxime Anné[4], Athéna Crespin[4], Stephanie Ferreira[4], Yacine Hajji[4], Dean Hum[4], Pejvack Motlagh[4], Pierbruno Ricci[4], Sakina Sayah Jeanne[4], Katharina Staufer[4,19], Paolo Angeli[7,20], Arun J. Sanyal[21,22], Dominique Thabut[23,24], Jasmohan Bajaj[25]. [1]*University of Texas, Southwestern, Dallas, United States;* [2]*Department of Internal Medicine B, University Hospital Münster, Münster, Germany;* [3]*European Foundation for the Study of Chronic Liver Failure, Barcelona, Spain;* [4]*Genfit S.A., Loos, France;* [5]*Liver ICU, Liver Unit, Hospital Clinic, IDIBAPS and CIBEREHD, Barcelona, Spain;* [6]*Liver Transplant Unit, Hôpitaux Universitaires de Strasbourg, Strasbourg, France;* [7]*European Foundation for the Study of Chronic Liver Failure (EF CLIF), Barcelona, Spain;* [8]*Liver Intensive Therapy Unit, Kings College Hospital, London, United Kingdom;* [9]*Hospital Clínic-IDIBAPS, CIBERehd, University of Barcelona, Barcelona, Spain;* [10]*Gastrounit Medical Division, Hvidovre Hospital, Hvidovre, Denmark;* [11]*Department of Medicine, University of California, San Francisco, California, United States;* [12]*Université Paris-Cité, Inserm, Centre de recherche sur l'inflammation, Paris, France;* [13]*Hôpital Beaujon, Service d'Hépatologie, Paris, France;* [14]*Hepato-Neuro Laboratory, CRCHUM, Université de Montréal, Montreal, Canada;* [15]*Institute of Liver Studies, Kings College London, London, United Kingdom;* [16]*Roger Williams Institute of Liver Studies, Faculty of Life Sciences and Medicine, King's College London, London, United Kingdom;* [17]*Université de Lille, Inserm, CHU Lille, Institut Pasteur de Lille, U1011-EGID, Lille, France;* [18]*Department of Medicine, University of Toronto, Toronto General Hospital, Toronto, Canada;* [19]*Division of Gastroenterology and Hepatology, Department of Medicine III, Medical University of Vienna, Vienna, Austria;* [20]*University of Padova, Padua, Italy;* [21]*Department of Medicine, Virginia Commonwealth University of Medicine, Richmond, Virginia, United States;* [22]*Stravitz-Sanyal Institute for Liver Disease and Metabolic Health, Virginia Commonwealth University School of Medicine, Richmond, Virginia, United States;* [23]*Department of Hepatogastroenterology, Hôpital Pitié Salpêtrière-Assistance Publique-Hôpitaux de Paris, Liver Intensive Care Unit, Paris, France;* [24]*Centre de recherche Saint-Antoine, Inserm, Sorbonne Université, Paris, France;* [25]*Division of Gastroenterology, Hepatology, and Nutrition, Department of Internal Medicine, Virginia Commonwealth University School of Medicine, Richmond, Virginia, United States*
Email: jennifer.jaravargas@genfit.com

Background and aims: Overt hepatic encephalopathy (HE) carries high risk of hospitalization (hosp), recurrence and mortality. While lactulose (L) remains the cornerstone of HE management, evidence suggests adding rifaximin (R) enhances clinical outcomes. This study aims to characterize treatment patterns of L and/or R and assess their impact on clinical outcomes in hospitalized patients (pts) with HE.
Method: All hosp from 04/2016–02/2025 of pts with cirrhosis and HE defined by ICD codes, treated with L and/or R were extracted from the Komodo's Healthcare Map U.S. real-world database. Three treatment options during hospitalization were evaluated: L monotherapy (L_m), R monotherapy (R_m), L and R dual therapy (LR_d). Further sub-categorization was based on L and/or R prescription the month prior to hosp to describe pharmaceutical patterns. Evaluated clinical outcomes were 28d mortality and length of stay (LOS).
Results: The study cohort included 211,171 pts with 414,305 hosp. Mean age at admission was 61y, 56% were male. Only 44% had one hosp, 23% had two and 33% had three or more. Treatment during hosp was L_m in 50% of cases, R_m in 19%, and LR_d in 31%. Pharmaceutical patterns varied across hosp: the most common being L_m with prior L (27%), LR_d with prior LR (21%) and L_m without prior L/R (19%). Hosp with L_m without prior L/R were predominantly first admissions (72%), showing an overall 28d mortality rate of 4.1% and a median LOS of 7d. Hosp with LR_d without prior L/R were also mainly first hosp (64%), and were associated with a slightly higher 28d mortality (5%), the longest median LOS (11d) and the highest proportion of cases with bacterial infection and/or other type of acute decompensation reported on top of HE (76%). Hosp with L_m or LR_d and prior L were typically second or later hosp (>64%), with higher 28d mortality for L_m (9.3%) vs LR_d (6%) [$p < 0.001$]. Prior treatment with LR was predominantly associated with third hosp onwards (>60%), with lower 28d mortality for LR_d (7.3%) compared with L_m (8.1%) [$p < 0.001$] and R_m (9.1%) [$p < 0.001$].
Conclusion: In this large US-based cohort, treatment patterns for hospitalized pts with HE reveals substantial heterogeneity. L monotherapy still predominates, indicating potential to possibly reduce LOS and mortality with earlier dual therapy. Over half of pts were readmitted with high readmission rates persisting even under dual therapy, highlighting the need for optimized strategies and novel therapies to improve outcomes.

SAT-480

Beyond MELD: machine learning mortality prediction in cirrhotic patients with sepsis

Jeril Lasington[1], Lawin Steve Mathew Lasington[2]. [1]*New York Medical College, Valhalla, United States;* [2]*Rutgers University-Newark Arch, Newark, United States*
Email: lawinsteve.ls@gmail.com

Background and aims: Sepsis remains a leading cause of mortality in cirrhotic patients, with ICU mortality rates exceeding 40–50%. Traditional prognostic scores (MELD, MELD-Na, SOFA, CLIF-SOFA) were developed for different clinical contexts and may not optimally capture the unique pathophysiology of sepsis superimposed on chronic liver disease. We developed and validated machine learning (ML) models for predicting ICU mortality in cirrhotic patients with sepsis and compared their performance against established clinical scores.
Method: This retrospective cohort study used the MIMIC-IV (v3.1) database to identify adult patients (≥18 years) with cirrhosis and concurrent sepsis requiring ICU admission (2008–2022). Cirrhosis and sepsis were identified using ICD-9/10 codes. Predictors included demographics, liver function tests, renal parameters, sepsis markers, hemodynamics, neurological status, cirrhosis complications, and ICU interventions collected within 24 hours of admission. Four ML algorithms (Logistic Regression, Random Forest, XGBoost, Gradient Boosting) were trained using 80/20 train-test splits with stratified sampling. Performance was evaluated using AUC-ROC, AUPRC, and Brier score with five-fold cross-validation. ML models were compared against MELD, MELD-Na, SOFA, and CLIF-SOFA scores using bootstrap resampling (n = 1000) for confidence intervals.
Results: Among 1,612 patients (mean age 60.1 years; 56.2% male), hospital mortality was 45.7%. Random Forest and Logistic Regression achieved the highest discrimination (AUC 0.787, 95% CI 0.740–0.834), significantly outperforming CLIF-SOFA (0.710), SOFA (0.710), MELD (0.708), and MELD-Na (0.708). Random Forest achieved sensitivity 65.3%, specificity 77.8%, PPV 71.1%, and NPV 72.9%. Top predictors integrated sepsis severity markers (lactate, pH, temperature) and

liver-specific dysfunction (bilirubin, INR, creatinine), reflecting the intersection of both disease processes.
Conclusion: ML models significantly outperform traditional scoring systems for predicting ICU mortality in cirrhotic patients with sepsis, achieving an 11% relative improvement in AUC. Key predictors capture both sepsis severity and hepatic dysfunction, supporting development of cirrhosis-specific sepsis prognostic tools.

SAT-481
Machine learning model for non-sodium predictors of ICU mortality drivers in cirrhotic hyponatremia
Jeril Lasington[1], Lawin Steve Mathew Lasington[2]. [1]*New York Medical College, Valhalla, United States;* [2]*Rutgers University-Newark Arch, Newark, United States*
Email: lawinsteve.ls@gmail.com

Background and aims: Hyponatremia is common in cirrhosis and incorporated into MELD-Na to improve mortality prediction. However, in patients with established hyponatremia, the prognostic value of sodium level itself remains unclear. We hypothesized that once hyponatremia develops, factors beyond sodium drive ICU mortality. We aimed to identify key mortality predictors using machine learning (ML) and evaluate whether MELD-Na provides incremental value over MELD in this pre-selected population.
Method: This retrospective cohort study used MIMIC-IV (v3.1) to identify adults with cirrhosis and hyponatremia requiring ICU admission (2008–2022). Predictors from the first 24 hours included liver function, renal parameters, metabolic markers, hemodynamics, sodium values, and cirrhosis complications. Four ML algorithms (Logistic Regression, Random Forest, XGBoost, Gradient Boosting) were trained using 80/20 splits with five-fold cross-validation. Performance was compared against MELD, MELD-Na, SOFA, and sodium alone using bootstrap DeLong testing (n = 2000).
Results: Among 1,437 patients (mean age 58.4 years; 61.2% male; mean sodium 128.3 mEq/L), hospital mortality was 26.7%. Random Forest achieved superior discrimination (AUC 0.784, 95% CI 0.721–0.841), significantly outperforming MELD (0.672, $p < 0.001$) and MELD-Na (0.665, $p < 0.001$) which is 18% relative improvement. Critically, MELD-Na provided no advantage over standard MELD (p = NS), and sodium alone showed no prognostic value (AUC 0.503, equivalent to random chance). Feature importance analysis revealed non-sodium factors dominated prediction: bilirubin, INR, anion gap, lactate, and hemodynamic parameters ranked highest, while all sodium parameters fell outside the top 20 predictors.
Conclusion: In cirrhotic patients with established hyponatremia, ML significantly outperforms traditional scores while revealing that sodium loses prognostic value once hyponatremia is present. Liver synthetic function (bilirubin, INR) and metabolic-hemodynamic status and not sodium level were found to be the drivers of mortality risk. These findings suggest clinicians should focus prognostic assessment on hepatic and metabolic parameters rather than sodium correction in this population.

SAT-482
Single-nucleus RNA sequencing identifies a GATA4+ liver sinusoidal endothelial cell subpopulation in acute-on-chronic liver failure
Xiayao Li[1], Xiaohan Qian[1], Wenxin Zhoudi[1], Yangfan Shen[1], Xiaowei Xu[1]. [1]*The First Affiliated Hospital, Zhejiang University School of Medicine, Hangzhou, China*
Email: lixiayao2001@163.com

Background and aims: Liver sinusoidal endothelial cell (LSEC) dysfunction is a persistent feature of liver diseases, yet its phenotypic regulation in acute-on-chronic liver failure (ACLF) remains poorly understood. This study aimed to delineate the heterogeneity and functional characteristics of LSECs in ACLF using single-nucleus RNA sequencing, and to identify key molecules and signaling pathways involved in liver inflammation and repair.
Method: We performed snRNA-seq on explanted liver tissues from five HBV-ACLF patients underwent liver transplantation. Public snRNA-seq datasets of healthy human livers were integrated as controls using Harmony. Following quality control and normalization, LSECs were extracted and re-clustered. Pathway enrichment was assessed using AddModuleScore, developmental trajectories were inferred by Monocle, intercellular communication was analyzed by CellChat and gene regulatory network was analyzed by pySCENIC.
Results: After analyzing 5,247 LSECs which were re-clustered into 7 subpopulations, we identified a distinct GATA4$^+$ LSEC subpopulation that was expanded in the liver of patients with HBV-ACLF. These GATA4$^+$ LSECs present in all ACLF samples, characterized by high expression of GATA4, ENG, IL33 but low expression of STAB2, LYVE1, suggesting the dysfunction and remodeling of LSECs in ACLF. Pathways related to cell migration, morphogenesis, and cytoskeletal organization were enriched in this subpopulation, reflecting a liver pro-repair signature. In a trajectory analysis, GATA4$^+$ LSECs located at the branch after healthy LSECs, indicating the endothelial phenotypic transition in ACLF. Cell-cell interaction analysis revealed enhanced interactions between GATA4$^+$ LSECs and hepatocytes, cholangiocytes and hepatic stellate cells via the BMP-SMAD axis. Notably, GATA4, a transcription factor, is the master regulator of LSEC differentiation, which may drive endothelial dysfunction by regulating the expression of its target gene ENG.
Conclusion: GATA4$^+$ LSECs constitute a distinct subset enriched in ACLF livers and exert LSEC dysfunction and liver pro-repair effects, suggesting potential therapeutic targets targeting LSECs for ACLF.

SAT-483
The GCS paradox: machine learning shows glasgow coma scale has no prognostic value in hepatic encephalopathy
Jeril Lasington[1], Lawin Steve Mathew Lasington[2]. [1]*New York Medical College, Valhalla, United States;* [2]*Rutgers University-Newark Arch, Newark, United States*
Email: jeril.lasington@gmail.com

Background and aims: Hepatic encephalopathy (HE) is a major cirrhosis complication requiring ICU admission, with mortality rates of 30–50%. Traditional prognostic tools including MELD, SOFA, and Glasgow Coma Scale (GCS) are commonly used, but their performance in HE remains unclear. Importantly, GCS interpretation is confounded by the potentially reversible nature of HE-related mental status changes. We developed machine learning (ML) models to predict ICU mortality in HE and evaluated whether GCS provides independent prognostic value.
Method: This retrospective cohort study used MIMIC-IV (v3.1) to identify adults with HE requiring ICU admission (2008–2022). Predictors from the first 24 hours included demographics, liver function, renal parameters, GCS components, HE precipitants (sepsis, AKI, GI bleeding, hyponatremia), and cirrhosis complications. Four ML algorithms (Logistic Regression, Random Forest, XGBoost, Gradient Boosting) were trained using 80/20 splits with five-fold cross-validation. Performance was compared against MELD, MELD-Na, SOFA, and GCS using bootstrap DeLong testing (n = 2000).
Results: Among 1,314 HE patients (mean age 57.2 years; 64.8% male), hospital mortality was 32.3%. Logistic Regression achieved highest discrimination (AUC 0.801, 95% CI 0.740–0.856), significantly outperforming MELD (0.669, +20%, p = 0.0001), MELD-Na (0.647, +24%, $p < 0.0001$), and SOFA (0.645, +24%, $p < 0.0001$). Strikingly, GCS alone showed no prognostic value (AUC 0.531), performing no better than random chance. Feature importance revealed sepsis as the dominant predictor, followed by lactate, creatinine, sodium, and INR. The underlying precipitant, rather than HE severity or GCS, determined outcomes.
Conclusion: ML significantly outperforms traditional scores for HE mortality prediction. Critically, GCS alone has no prognostic value in HE, reflecting the reversible nature of HE-related encephalopathy. Clinicians should not use GCS for prognostication in HE; instead,

focus should be on identifying precipitants, particularly sepsis and AKI which drive mortality risk. These findings support precipitant-focused risk stratification rather than reliance on neurological assessment alone.

SAT-484

Incidence and risk factors for acute-on-chronic liver failure in outpatients with cirrhosis–a prospective multicenter cohort study

Isadora Bombassaro[1], Angelo Mattos[2], Luciana Goncalves[3], Gustavo Pereira[4], Mario Álvares-da-Silva[5], Carlos Antonio Rodrigues Terra Filho[6], Liliana Mendes[7], Patrícia Goncalves[8], Juliana Maya[4], Gabriel Guerreiro[5], Daniel Meohas[6], Angelo Z. Mattos[1]. *[1]Federal University of Health Sciences of Porto Alegre, Irmandade Santa Casa de Misericórdia de Porto Alegre, Porto Alegre, Brazil; [2]Ufcspa- Fund Univ Federal De Ciências Da Saúde De Porto Alegre, Porto Alegre, Brazil; [3]Universidade Federal do Espírito Santo, Vitória, Brazil; [4]Hospital Geral de Bonsucesso, Rio de Janeiro, Brazil; [5]Hospital de Clínicas de Porto Alegre, Porto Alegre, Brazil; [6]Universidade Do Estado Do Rio De Janeiro, Hospital da Lagoa, Rio de Janeiro, Brazil; [7]Hospital de Base, Brasília, Brazil; [8]Hospital Universitário Cassiano Antônio Moraes, Vitória, Brazil*
Email: angmattos@hotmail.com

Background and aims: Acute-on-chronic liver failure (ACLF) has been extensively studied in hospitalized patients, but its incidence and risk factors in outpatients remain poorly defined. This study evaluated the incidence and independent risk factors for ACLF in an outpatient cohort of individuals with cirrhosis.
Method: This is a prospective multicenter cohort study, in which baseline data were collected at the first outpatient visit of individuals with cirrhosis, who were then followed until the development of ACLF or the competing outcomes (liver transplant and death). ACLF was defined according to the Chronic Liver Failure Consortium criteria. Cumulative incidence functions for ACLF were calculated, and multivariable analyses were performed using the Fine–Gray competing risk model, in which subdistribution hazard ratios (HRs) and their 95% confidence intervals (CIs) were estimated.
Results: A total of 881 patients were included (78.1% - Child-Pugh A, 19.9% - Child-Pugh B, 2% - Child-Pugh C). The cumulative incidence of ACLF was 4.7% (n = 36) in 12 months and 5.9% (n = 45) in 36 months. Independent risk factors for ACLF at 12 months included lower levels of hemoglobin (HR = 0.80; 95% CI = 0.69–0.93, p = 0.003) and albumin (HR = 0.45; 95% CI = 0.26–0.76, p = 0.003), higher levels of creatinine (HR = 1.44; 95% CI = 1.08–1.91, p = 0.013), and the presence of ascites (HR = 2.12; 95% CI = 1.03–4.33, p = 0.040) at the baseline.
Conclusion: ACLF incidence was relatively low, consistent with the predominance of compensated cirrhosis at the beginning of the follow-up. Anemia and baseline markers of impaired liver and kidney function were independently associated with the development of ACLF.

SAT-489

Body composition is a predictor of treatment response and survival in hepatorenal syndrome (HRS-AKI)

Sina Oesinghaus[1], Julian Pohl[1], Dominik Geisel[2], Nick-Lasse Beetz[2], Frank Tacke[1], Cornelius Engelmann[1]. *[1]Charité Campus Virchow, Department of Gastroenterology and Hepatology, Berlin, Germany; [2]Charité Campus Virchow, Department of Radiology, Berlin, Germany*
Email: sina.oesinghaus@charite.de

Background and aims: Advanced liver cirrhosis is characterized by systemic complications, including hepatorenal syndrome (HRS-AKI) and sarcopenia. Despite their co-occurrence, the interplay between body composition, pharmacotherapy response and survival remains poorly defined. While terlipressin plus albumin is the standard of care, 30–40% of patients do not respond. AI based CT body composition analysis (BCA) offers a novel approach to identify risk factors in these vulnerable patients. This study investigated BCA-derived predictive markers for terlipressin response and 90-day transplant-free survival.
Method: 106 HRS-AKI patients receiving terlipressin at Charité Centers (2018–2022) were retrospectively included in this study. Treatment response after 7 days was defined based on the reduction of peak serum creatinine by ≥25%. Using BCA, the tissue area at the L3 level was measured and standardized by height [cm^2/m^2] to calculate skeletal muscle index (SMI), subcutaneous fat index (SFI) and visceral fat index (VFI). A Sarcopenic Visceral Obesity Index was defined as SVI = SMI × SFI/VFI. Regression and competing risk analyses identified independent predictors of treatment response and 90-day mortality.
Results: Out of 106 patients 77% were male and 33% female with a median age of 63 years. Overall, 39.6% presented with ACLF grade I, 20.8% with grade II, 4.7% with grade III and 34.9% without ACLF at diagnosis of AKI. The median MELD score was 25. Mean SMI was 40.2 ± 8.7 cm^2/m^2 in men and 35.8 ± 5.8 cm^2/m^2 in women. At 90 days, 57.5% of patients had died and 2.8% had undergone liver transplantation. The overall terlipressin response rate was 25.5%. In a multivariate competing risk model, day 7 treatment response was a significant protective factor for 90-day mortality (sHR 0.42; 95% CI 0.20–0.90; p = 0.026). While SMI, SFI, and VFI alone showed no association with transplant-free survival, a lower SVI was associated with a higher 90-day mortality (sHR 0.64; 95% CI 0.41–1.00; p = 0.050). Multivariate Cox models identified low SMI (HR 1.52; 95% CI 1.06–2.19; p = 0.03) and low SVI (HR 1.40; 95% CI 1.071.82; p = 0.01) as robust independent predictors of terlipressin non-response.
Conclusion: Reduced muscle mass (SMI) and altered muscle-to-fat distribution (SVI) are independent predictors of terlipressin non-response which is a critical determinant of 90-day transplant free survival. BCA-based stratification may help guide early treatment strategies in HRS-AKI.

SAT-490

Acute kidney injury in decompensated cirrhosis without underlying chronic kidney disease represents a distinct high-risk phenotype compared to acute-on-chronic kidney disease

Rahul Thakkar[1], Kavish Patidar[2], Olivia Walker[1], Gerald Ogola[1], Patrick S. Kamath[3], Sumeet Asrani[1]. *[1]Baylor Scott & White Health, Dallas, United States; [2]Houston Methodist, Houston, United States; [3]Mayo Clinic, Rochester, United States*
Email: rahul.thakkar@bswhealth.org

Background and aims: Acute kidney injury (AKI) is a critical prognostic factor in decompensated cirrhosis and acute-on-chronic liver failure (ACLF). The 2025 Consensus on Organ Failures in Cirrhosis has formalized the definition of acute-on-chronic kidney disease (AoCKD), but data characterizing the prognostic divergence between AoCKD and *de novo* AKI remain limited. This study evaluated the mortality impact of acute serum creatinine (sCr) change across baseline renal function and chronic kidney disease status.
Method: We conducted a retrospective cohort study of adult patients with decompensated cirrhosis admitted to intensive care units across 54 hospitals in a large integrated healthcare system (2019–2022). The primary outcome was 30-day all-cause mortality. Patients were stratified based on admission sCr (admit sCr), maximum absolute change in sCr during their stay (delta sCr), and presence or absence of chronic kidney disease (CKD). Mortality trajectories were analyzed as a function of Delta sCr across distinct admission baselines, stratified by CKD status.
Results: Mortality increased with larger delta sCr in all patients across admission sCr values, but the steepness of this increase differed between non-CKD and CKD cohorts. For most admit sCr/delta sCr combinations, non-CKD patients exhibited higher mortality rates than their CKD counterparts. The maximum absolute mortality difference between non-CKD and CKD patients followed a bell-shaped pattern across admission sCr values, peaking at an admit sCr of 2.5 mg/dL (22% difference) and narrowing at the extremes (10–11% at admit sCr of 1.0 and 4.0 mg/dL). At an admission sCr of 2.5 mg/dL,

patients without pre-existing CKD exceeded 60% mortality with a delta sCr of 1.0 mg/dL, whereas patients with CKD required a delta sCr of 3.0 mg/dL to reach comparable mortality.
Conclusion: Acute rises in serum creatinine were associated with a greater increase in 30-day mortality among patients without pre-existing CKD compared to those with CKD in decompensated cirrhosis, supporting *de novo* AKI as a distinct high-risk phenotype from acute-on-chronic kidney disease. These findings suggest that prognostic frameworks and renal endpoints in ACLF intervention trials should account for baseline kidney status, as equivalent creatinine changes may not confer equivalent mortality risk.

SAT-491

Long-term efficacy of double plasma molecular adsorption system with sequential low-volume plasma exchange for intermediate-stage HBV-ACLF: a randomized controlled trial

Chan Xie[1], Jia Chen[1], Wenxiong Xu[1], Liang Peng[1]. [1]*Third Affiliated Hospital of Sun Yat-sen University, Guangzhou, China*
Email: xchan@mail.sysu.edu.cn

Background and aims: The mortality rate of hepatitis B virus (HBV)-related acute-on-chronic liver failure (ACLF) remains high despite standard care. Artificial liver support systems are widely used, but long-term data remains limited. This study aimed to investigate the safety and long-term efficacy (up to 2 years) of the double plasma molecular adsorption system combined with sequential low-volume plasma exchange (DPMAS+LPE) specifically in patients with intermediate-stage HBV-ACLF.
Method: In this randomized controlled trial, patients diagnosed with intermediate-stage HBV-ACLF were enrolled and randomly assigned (1:1) to either a trial group or a control group. Both groups received standard medical treatment (SMT), including antiviral therapy and comprehensive supportive care. Patients in the trial group additionally received three sessions of DPMAS+LPE, administered once every two days. The primary endpoint was 2-year transplantation-free survival (TFS), the second endpoints included treatment safety, 2-year cumulative overall survival (OS).
Results: A total of 56 patients (28 per group) completed the 2-year follow-up, with no severe treatment-related adverse events recorded in the trial group. The trial group achieved significantly superior short-term outcomes compared to the control group, evidenced by higher cumulative TFS (53.6% vs. 25.0%, $p = 0.029$) and OS (64.3% vs. 35.7%, $p = 0.033$) at 3 months. Notably, this survival advantage was sustained over the long term; the trial group maintained numerically higher survival rates at 2 years (OS: 50.0% vs. 28.6%; TFS: 35.7% vs. 21.4%) compared to the control group, although the difference did not reach statistical significance in this cohort ($p > 0.05$).
Conclusion: DPMAS+LPE is a safe intervention that significantly improves short-term survival in intermediate-stage HBV-ACLF. Importantly, this early therapeutic efficacy translates into a clinically meaningful trend toward better long-term prognosis, with survival benefits persisting up to 2 years. Therefore, DPMAS+LPE is recommended as an effective strategy for management in this population.

SAT-492

Individualised nutrition support improves outcomes in hepatitis B virus-related acute-on-chronic liver failure patients at nutritional risk: a randomised controlled trial

ZhiPeng Li[1,2], Yeqiong Zhang[1], Qiumin Luo[1], Chan Xie[1], Liang Peng[1]. [1]*Department of Infectious Diseases Third Affiliated Hospital of Sun Yat-sen University, Guangzhou, China;* [2]*Third Affiliated Hospital of Sun Yat-sen University, Guangzhou, China*
Email: lizhp28@mail.sysu.edu.cn

Background and aims: Patients with acute-on-chronic liver failure (ACLF) are at high nutritional risk, which adversely affects prognosis, yet robust evidence for nutritional interventions is scarce. This study evaluated the safety and efficacy of individualised nutritional support for hepatitis B virus-related ACLF (HBV-ACLF).
Method: In this single-centre, investigator-initiated, open-label randomised controlled trial, HBV-ACLF patients meeting COSSH criteria with NRS-2002 ≥3 were randomised 1:1 to individualised nutritional support (energy target 1.2 × REE; protein 1.2 g/kg/day) or control (standard dietary advice). Assessments were performed at baseline, day 30, and day 90. Primary endpoints were 30- and 90-day transplant-free mortality. Secondary endpoints included safety, the incidence of adverse clinical outcomes, liver severity scores (MELD, COSSH-ACLF IIs), anthropometry (mid-arm circumference), muscle function (handgrip strength, gait speed, SPPB), and quality of life (EQ-5D).
Results: Between December 2023 and March 2025, 572 patients with HBV-ACLF were screened, 80 were randomised, and 78 (39 in the control group and 39 in the intervention group) were analysed in the modified intention-to-treat population. Individualised nutrition significantly reduced transplant-free mortality at day 30 (2.6% vs. 20.5%, $p = 0.033$) and day 90 (17.9% vs. 38.5%, $p = 0.044$) compared to controls. Adverse clinical outcome rates were also lower (day 30: 25.6% vs 56.4%, $p = 0.006$; day 90: 33.3% vs 74.4%, $p < 0.001$), with no excess in serious events, gastrointestinal reactions, complications, or hyperglycemia. The intervention group achieved greater improvements in MELD and COSSH-ACLF II scores, anthropometric indices, muscle function, adverse clinical outcomes and EQ-5D scores (all $p < 0.05$).
Conclusion: In HBV-ACLF patients at nutritional risk, individualised target-driven nutritional support is safe, lowers 30- and 90-day transplant-free mortality, reduces adverse clinical outcomes, and improves hepatic function, muscle performance, and quality of life. These findings provide prospective, randomised evidence supporting early, goal-driven, and function-oriented nutrition treatments with dynamic assessments as a practical strategy in ACLF care.

SAT-493

A phase I clinical trial evaluating the safety and efficacy of the QH-1A combination bio-artificial liver support system incorporating ex-vivo mesenchymal stem cells for the treatment of acute-on-chronic liver failure patients

Liang Peng[1], Chan Xie[1], Wenxiong Xu[1], Jia Chen[1], Xiyao Chen[1]. [1]*Third Affiliated Hospital of Sun Yat-sen University, Guangzhou, China*
Email: pliang@mail.sysu.edu.cn

Background and aims: Acute-on-chronic liver failure (ACLF) has high mortality, and artificial liver support is a key therapeutic approach. Compared with mechanical artificial liver systems, bio-artificial liver support better mimics native hepatic function. This study evaluated the safety and preliminary efficacy of the QH-1A bio-artificial liver support system incorporating ex vivo mesenchymal stem cells (MSCs) in ACLF patients.
Method: This single-center, open-label Phase I clinical trial (approved by NMPA China) assessed QH-1A's safety and preliminary efficacy. All patients received standard medical treatment, including antiviral therapy and comprehensive supportive care. Patient plasma was separated with a plasma separator and perfused through an MSC-seeded hollow-fiber cartridge, allowing MSC-derived extracellular vesicles (including exosomes) and other bioactive factors to return to the patient. Participants were sequentially enrolled into 4-hour (n = 3), 6-hour (n = 3), and 8-hour (n = 3) cohorts with escalating durations. Follow-ups were conducted post-treatment, on Days 3, 7, and 28. Escalation decisions were made by an independent Safety Evaluation Committee based on 28-day safety data.
Results: Nine patients were enrolled from May to October 2025. The 28-day liver transplantation-free survival rate was 88.89% (one patient underwent liver transplantation on Day 26 due to unimproved condition). For safety, 25 related adverse events occurred; only 1 patient had a serious adverse event, with no treatment discontinuation. At Day 28, clinical parameters improved across all cohorts. TBIL decreased from baseline levels of 324.40 (248.10, 361.90), 424.00 (393.20, 462.00), and 265.60 (224.20, 333.10) μmol/L

to 83.20 (63.20, 192.30), 313.60 (151.70, 531.80), and 51.10 (43.20, 116.50) μmol/L in the 4-, 6-, and 8-hour groups, respectively. INR improved significantly in the 4- and 8-hour groups, dropping from 1.89 (1.53, 2.10) and 2.23 (1.65, 2.31) to 1.44 (1.18, 1.68) and 1.23 (1.20, 1.59), respectively. Correspondingly, their COSSH-ACLF II scores decreased from 6.40 (6.00, 6.80) and 7.40 (6.90, 7.40) to 5.40 (4.50, 5.50) and 5.50 (4.90, 6.50), respectively.
Conclusion: The QH-1A bio-artificial liver support system exhibited good safety and tolerability in ACLF patients, improving liver function, coagulation parameters, and clinical severity scores. It may be a promising ACLF treatment, with further studies needed to validate its safety and efficacy.

SAT-494
Elevated plasma aldosterone predicts liver-related mortality in decompensated cirrhosis
Clemens Renhardt[1,2,3], Benedikt Simbrunner[1,2,3,4], Mathias Jachs[1,2,3], Benedikt Hofer[1,2,3,4], Georg Kramer[1,2,3], Christian Sebesta[1,2,3], Marlene Hintersteininger[1,2,3], Paul Thöne[1,2,3], Paula Hoefinger[1,2], Lorenz Balcar[1,2,3], Georg Semmler[1,2,3], Rodrig Marculescu-Ferrari[5], Michael Trauner[1,3], Mattias Mandorfer[1,2,3], Thomas Reiberger[1,2,3,4], Lukas Hartl[1,2,3]. *[1]Division of Gastroenterology and Hepatology, Department of Medicine III, Medical University of Vienna, Vienna, Austria; [2]Vienna Hepatic Hemodynamic Lab, Division of Gastroenterology and Hepatology, Department of Medicine III, Medical University of Vienna, Vienna, Austria; [3]Clinical Research Group MOTION, Division of Gastroenterology and Hepatology, Department of Medicine III, Medical University of Vienna, Vienna, Austria; [4]Christian Doppler Lab for Portal Hypertension and Liver Fibrosis, Medical University of Vienna, Vienna, Austria; [5]Department of Laboratory Medicine, Medical University of Vienna, Vienna, Austria*
Email: n12028120@students.meduniwien.ac.at

Background and aims: Portal hypertension (PH) - as the main driver of hepatic decompensation - is associated with circulatory dysfunction that triggers the compensatory activation of the renin-angiotensin aldosterone system. However, the prognostic value of plasma aldosterone concentration (ALDO) in contemporary patients with compensated (cACLD) and decompensated (dACLD) advanced chronic liver disease remains unknown.
Method: Patients with ACLD undergoing hepatic venous pressure gradient (HVPG) measurement between 05/2018 and 08/2024 within the prospective VICIS study (NCT03267615) and available ALDO were included. Patients were followed up for 2 years; the event of interest was decompensation in cACLD and liver-related death in dACLD patients.
Results: Overall, 595 patients (cACLD: n = 210; dACLD: n = 385; median age: 58 years; 69.6% male; median MELD: 14 points; median HVPG: 17 mmHg) were included. While only 18 cACLD patients (8.6%) were treated with mineralocorticoid receptor antagonists (MRA), 302 dACLD patients (78.4%), were treated with MRA. ALDO (was significantly increased in dACLD (246 vs. cACLD: 76 pg/mL; p < 0.001). In dACLD patients, HVPG (per mmHg; B: 0.032; 95%CI: 0.012–0.053; p = 0.002), MELD (per point; B: 0.045; 95%CI: 0.021–0.070; p < 0.001) and sodium (per mmol/L; B: –0.133; 95%CI: –0.155 ––0.111; p < 0.001) were strongly linked to ALDO (log-transformed) in univariate analysis of linear regression, however, only sodium (per mmol/L; B: –0.131, 95%CI: –0.155 ––0.107; p < 0.001) remained independently linked to ALDO on multivariate analysis. In cACLD patients (median follow-up 18.3 months), ALDO was not associated with first decompensation in competing risk regression analysis. In dACLD (median follow-up 23.2 months), ALDO predicted liver-related mortality (aSHR: 1.062, [97.5%CI: 1.001–1.125]; p = 0.044) independently of sex, age, MELD-Na and albumin.
Conclusion: ALDO levels substantially increase in dACLD and are strongly linked to low plasma sodium levels. ALDO is an independent risk factor for liver-related death in dACLD.

SAT-495
Predictors of reversibility of acute-on-chronic liver failure at 6 months: a prospective study
Shreyas Sarvesh[1], Rajan Vijayaraghavan[1], Ashok Kumar Choudhury[1], Rakhi Maiwall[1], Chitranshu Vashitshtha[1], Ankur Jindal[1], S. Muralikrishna Shasthry[1], Vinod Arora[1], Harshvardhan Tevethia[1], Satender Pal Singh[1], Guresh Kumar[1], Ankit Bhardwaj[1], Vikram Bhatia[1], Manoj Kumar[1], Shiv Kumar Sarin[1]. *[1]Institute of Liver & Biliary Sciences, New Delhi, India*
Email: rajanvf40@gmail.com

Background and aims: Acute-on-chronic liver failure (ACLF) is a rapidly progressive condition and carries a high short-term mortality. Although a proportion of patients achieve reversal of key elements that define ACLF, only a few have been analysed prospectively under defined timelines. We aimed to determine baseline factors that could predict reversal of ACLF within 180 days.
Method: ACLF patients, admitted either in the ward or in the ICU, were prospectively enrolled and followed for 365 days. Reversal of ACLF was defined as: bilirubin <5 mg/dL and INR <1.5, with no hepatic encephalopathy, and either resolution of ascites or no ascites. The objective was to determine the proportion of patients achieving reversibility by 180-days and 'early reversal' by 90-days, and baseline factors predicting reversibility at 6-months.
Results: A total of 475 patients were enrolled, of whom 44.6% required ICU admission. Alcohol was the predominant acute insult (75.6%), followed by drug-induced liver injury (12%) and hepatitis B (7.16%). Overall, ACLF reversal at 180 days was achieved in 52.4% (n = 249) patients, while early reversal at 90 days occurred in 33.5% (n = 183). Among patients surviving beyond 28 days, reversal rates increased to 62.9% at 90 days and 69.8% at 180 days.Patients achieving reversal had significantly lower baseline BMI, Child–Turcotte–Pugh score, MELD-Na score, and AARC score (all p < 0.001). On multivariable analysis, higher serum albumin (HR 1.74, 95% CI 1.11–2.74, p = 0.016), HDL cholesterol (HR 1.03, 95% CI 1.00–1.06, p = 0.025), and platelet count (HR 1.92, 95% CI 1.16–3.19, p = 0.011) were independently associated with increased likelihood of reversibility. Alcohol as the acute insult was associated with a nearly threefold higher probability of reversal compared with other etiologies (HR 2.83, 95% CI 1.60–5.01, p < 0.001). Conversely, higher ferritin levels (HR 0.60, 95% CI 0.45–0.79, p < 0.001), shock (HR 0.53, p = 0.008), SBP(HR 0.46, p = 0.002), HE, and need for RRT were associated with poorer reversibility. Prolonged rifaximin or norfloxacin was independently associated with improved reversal (HR 2.27, p < 0.001).
Conclusion: More than half of patients with ACLF achieve reversal by 6 months, whereas early reversal within 90 days is uncommon. Baseline inflammatory burden, organ failures, and metabolic reserve strongly influence reversibility. Extending the assessment window to 180 days may better define meaningful recovery and therapeutic endpoints in ACLF.
Clinical trial registration: NCT-06387160.

SAT-496
Statin use in liver cirrhosis is associated with a reduced risk of hepatic decompensation and mortality
N. Apoorva Sasikumar[1], Cheng Han Ng[2,3,4], Saori Hieda[5], Vincent Chen[6], Jimmy Che-To Lai[7], Karn Wijarnpreecha[8], Rahul Kumar[9], Apichat Kaewdech[10], Masayuki Ueno[11], Anand Kulkarni[12], Ming-Hua Zheng[13], Akash Roy[14], Ken Liu[15,16], Chitchai Rattananukrom[17], Mazen Noureddin[18], Mohammad Shadab Siddiqui[19], Mark Muthiah[1,2,20], Hirokazu Takahashi[21]. *[1]Alexandra Hospital, Singapore, Singapore; [2]National University Hospital, Singapore, Singapore; [3]Kurume University School of Medicine, Kurume, Japan; [4]Graduate School of Medicine, Yokohama City University, Kanagawa, Japan; [5]Saitama Medical University, Saitama, Japan; [6]University of Michigan Medical School, Michigan, United States; [7]The Chinese University of Hong Kong, Hong Kong, Hong Kong; [8]University of Arizona College of Medicine*

Phoenix, Arizona, United States; [9]Changi General Hospital, Singapore, Singapore; [10]Prince of Songkla University, Songkhla, Thailand; [11]Kurashiki Central Hospital, Kurashiki, Japan; [12]Asian Institute of Gastroenterology, Hyderabad, India; [13]First Affiliated Hospital of Wenzhou Medical University, Wenzhou, China; [14]Apollo Multispeciality Hospital, Kolkata, India; [15]Royal Prince Alfred Hospital, Sydney, Australia; [16]University of Sydney, Sydney, Australia; [17]Srinagarind Hospital, Khon Kaen University, Khon Kaen, Thailand; [18]Houston Methodist Hospital and Houston Research Institute, Texas, United States; [19]University of Virginia School of Medicine, Virginia, United States; [20]National University Centre for Organ Transplantation, National University Health System, Singapore, Singapore; [21]Saga University, Saga, Japan
Email: e1354047@u.nus.edu

Background and aims: Statins possess pleiotropic effects beyond lipid lowering that may beneficially modify the course of liver cirrhosis. However, their use in compensated cirrhosis remains limited due to safety concerns and the paucity of large-scale data. We evaluated the association between statin use and the risks of hepatic decompensation and all-cause mortality in patients with compensated liver cirrhosis.
Method: We performed a retrospective, multinational, longitudinal cohort study within the Cirrhosis Outcome and Research Endeavour (CORE) consortium, including consecutive adults with compensated cirrhosis across 13 tertiary centers in eight countries. Compensated cirrhosis was defined by liver stiffness measurement ≥10 kPa and absence of prior decompensation. Statin exposure was defined at baseline. Outcomes were hepatic decompensation and all-cause mortality, analyzed using Fine–Gray competing-risk regression. Multivariable models adjusted for demographic, metabolic, and liver disease–related covariates. Inverse probability of treatment weighting (IPTW) was used to support causal inference.
Results: Among 2,564 patients (median follow-up 3.09 years), 901 (35.1%) were statin users. Statin use was associated with a significantly lower risk of hepatic decompensation in multivariable analyses (adjusted subdistribution hazard ratio [SHR] 0.70, 95% CI 0.57–0.86). Findings were consistent across moderate- and high-risk cirrhosis strata. Statin use was associated with lower all-cause mortality in partially adjusted models, though this association was attenuated after full adjustment. In IPTW-weighted analyses, statin use was associated with reduced risks of hepatic decompensation (SHR 0.55, 95% CI 0.37–0.80) and all-cause mortality (SHR 0.65, 95% CI 0.46–0.91).
Conclusion: In this large multinational cohort, statin use was associated with reduced hepatic decompensation and improved survival in compensated cirrhosis, supporting a potential disease-modifying role warranting prospective evaluation.

SAT-497

Optimizing linezolid therapy in acute-on-chronic liver failure through interprofessional therapeutic drug monitoring in the ICU

Georgios Athanasoulas[1], Alexander Kratzer[1], Sophia Rusch[1], Sophie Schlosser-Hupf[1], Patricia Mester-Pavel[1], Vlad Pavel[1], Martina Müller-Schilling[1], Stephan Schmid[1]. [1]*Universitätsklinikum Regensburg, Regensburg, Germany*
Email: stephan.schmid@ukr.de

Background and aims: Acute-on-chronic liver failure (ACLF) is a rapidly progressive syndrome associated with severe infections and high mortality. Linezolid is a key reserve antibiotic for the treatment of multidrug-resistant infections but is characterized by a narrow therapeutic window and high pharmacokinetic variability, particularly in critically ill patients with liver dysfunction. Therapeutic drug monitoring (TDM) may optimize efficacy while reducing toxicity. This study aimed to evaluate the clinical impact of an interprofessional TDM-based approach for individualized linezolid therapy in ICU patients with and without ACLF.
Method: This prospective study was conducted on a medical intensive care unit with hepatology specialization. Fifty-one critically ill patients receiving linezolid therapy, with and without ACLF, were included. Linezolid was administered as a continuous infusion following an initial loading dose. Weekly TDM was performed using high-performance liquid chromatography (HPLC). Serum concentrations, implementation of interprofessional recommendations, linezolid consumption, and clinical course were analyzed. Outcomes were compared between ACLF and non-ACLF patients.
Results: Initial TDM revealed marked variability in linezolid exposure: 29% of patients were within the therapeutic target range (2–10 mg/L), 21% were below target (<2 mg/L), and 50% exceeded the upper limit (>10 mg/L), including extreme concentrations >20 mg/L. Therapy adjustments were recommended in 20 cases, with full adherence by the treating teams. Subsequent measurements demonstrated improved target attainment. Notably, more than 80% of patients with supratherapeutic concentrations (>10 mg/L) had ACLF. No hematological or other relevant adverse events were observed under TDM-guided therapy. The structured involvement of medical students supported interprofessional learning and reinforced antibiotic stewardship principles in the ICU.
Conclusion: An interprofessional TDM-based strategy enables safe and individualized linezolid therapy in critically ill patients with ACLF. High rates of supratherapeutic exposure in ACLF patients underscore the need for systematic TDM in this population. This approach enhances patient safety, promotes rational use of reserve antibiotics, and represents an effective model for integrating precision medicine and interprofessional education in intensive care.

SAT-498

Machine learning based prediction of early organ failure in acute-on-chronic liver failure

Garima Singhal[1], Ashok Kumar Choudhury[1], Vinod Arora[1], Shiv Kumar Sarin[1] AARC APASL ACLF Research Consortium[1]. [1]*Institute of Liver and Biliary Sciences, New Delhi, India*
Email: doctor.ashokchoudhury@gmail.com

Background and aims: Acute-on-chronic liver failure (ACLF) is a dynamic syndrome characterized by rapid progression to multiorgan failure and high short-term mortality. However, predictive models to identify patients at risk of developing organ failure (OF) after presentation—particularly among those without OF at baseline—remain limited. We aimed to develop and validate machine-learning models to predict early development of organ failure.
Method: We analysed data from the AARC registry, including detailed clinical, laboratory, and organ failure assessments. After data preprocessing, the cohort was randomly divided into derivation (70%) and validation (30%) datasets. Multiple machine-learning models—XGBoost, Random Forest, Decision Tree, and Logistic Regression—were used. Model performance was assessed using area under the receiver operating characteristic curve (AUROC), accuracy, sensitivity, specificity, positive predictive value (PPV), and negative predictive value (NPV) to predict development of new-onset organ failure by day 4.
Results: A total of 8,683 patients were included (mean age 44.6 ± 11.6 years; 87% male), with alcohol as the predominant etiology (56.8%). At presentation, 92.85% had at least one organ failure, while 621 patients (7.15%) had no organ failure. Among these, 16.4% developed new-onset organ failure by day 4, which was associated with significantly increased 90-day mortality (HR 1.37; 95% CI 1.32–1.43; p = 0.001). After feature selection, 25 variables were retained for model development. The Random Forest model demonstrated the best performance (accuracy 0.92, AUROC 0.87, sensitivity 0.70, specificity 0.96, PPV 0.77, and NPV 0.94). The most influential predictors were baseline serum albumin, PT-INR, serum lactate, hepatic encephalopathy, and new-onset sepsis by day 4. Decision tree analysis accurately stratified patients into high-risk (lactate >1.62 mmol/L and albumin <2.2 g/dL), intermediate-risk (lactate

<1.62 mmol/L and albumin >2.2 g/dL or lactate >1.62 mmol/L with INR >2.0), and low-risk (INR <2.0 and lactate <1.62 mmol/L) categories, with corresponding risks of early organ failure of 58.4%, 15.3%, and 8.1%, respectively.
Conclusion: Among ACLF patients without organ failure at baseline, nearly one-sixth develop new-onset organ failure within 4 days, conferring a higher mortality risk. A simple combination of serum lactate, albumin, and PT-INR provides effective early risk stratification and may aid prognostication, intensive monitoring, and transplant decision-making in ACLF.

SAT-499
Presence of sarcopenia or chronic kidney disease does not influence the level of venous ammonia in outpatients with stable cirrhosis
Rajit Soni[1], Pooi Ling Loi[1], Hiang Keat Tan[2], Marianne De Roza[3], Chanda Ho[2], Jason Pik Eu Chang[2], Prema Raj S/O Jeyaraj[4], Rahul Kumar[1]. [1]*Changi General Hospital, Singapore, Singapore;* [2]*Singapore General Hospital, Singapore, Singapore;* [3]*Sengkang General Hospital, Singapore, Singapore;* [4]*Duke-Nus Medical School, Singapore, Singapore*
Email: rajit.soni94@gmail.com

Background and aims: Hyperammonaemia in cirrhosis is multifactorial. Although skeletal muscle and kidneys are thought to play a key role in extrahepatic ammonia clearance, the influence of sarcopenia and chronic kidney disease (CKD) on circulating ammonia levels in stable outpatients with cirrhosis has not been systematically evaluated. We aimed to determine whether sarcopenia or CKD affects venous ammonia concentrations in this population.
Method: This prospective study was conducted as part of the multicentre SoLiDaRity collaborative, designed to predict decompensation, acute-on-chronic liver failure, and mortality in cirrhosis. Consecutive outpatients with cirrhosis attending hepatology clinics were enrolled. Sarcopenia was assessed using the right psoas muscle index (PMI), calculated from available computed tomography scans at the level of the third lumbar vertebra. CKD was defined by an estimated glomerular filtration rate (eGFR) <60 mL/min/1.73 m^2 for ≥3 months, together with loss of corticomedullary differentiation on renal ultrasonography, and further staged. Venous ammonia and routine biochemical parameters were measured at enrolment. Standard statistical methods were used to compare ammonia levels across groups. The study was approved by the institutional review boards of participating centres and conducted in accordance with the Declaration of Helsinki.
Results: A total of 280 patients were included. The median venous ammonia level at enrolment was 25.5 µmol/L (Interquartile range [IQR] 18–43.5). Median ammonia levels were 29 µmol/L (IQR 19–52) in patients without sarcopenia and 24.5 µmol/L (IQR 15–39) in those with sarcopenia ($p = 0.054$). Across CKD stages, median ammonia levels were 30 µmol/L (IQR 19–53) in stage 0, 24 µmol/L (IQR 17–39) in stages 1–2, 26 µmol/L (IQR 15–51) in stage 3, and 34 µmol/L (IQR 18.5–68) in stages 4–5, with no significant difference observed ($p = 0.068$). In contrast, ammonia levels increased significantly with worsening liver disease severity: 21 µmol/L (IQR 16–29) in Child–Turcotte–Pugh (CTP) class A, 46 µmol/L (IQR 27–69) in class B, and 57 µmol/L (IQR 42–77) in class C ($p < 0.001$).
Conclusion: In stable outpatients with cirrhosis, venous ammonia levels are primarily driven by the severity of hepatic dysfunction and are not independently influenced by sarcopenia or chronic kidney disease. These findings highlight liver disease severity, rather than extrahepatic ammonia clearance, as the dominant determinant of circulating ammonia in stable cirrhosis.

SAT-500
Fairness-aware machine learning predicts 30-day mortality in vietnamese patients with decompensated cirrhosis
Hien Tran[1]. [1]*School of Biomedical Engineering - Vietnam National University HCMC International University, Ho Chi Minh, Vietnam*
Email: doctor.tranhuuhien@gmail.com

Background and aims: Decompensated cirrhosis carries high short-term mortality and existing scores (Child-Pugh, MELD) may underperform in Asian populations. We aimed to build fairness-aware machine learning (ML) models to predict 30-day mortality in a Vietnamese cohort and to compare them with established scores.
Method: We prospectively enrolled 100 adults hospitalized for decompensation at a tertiary center. After standard preprocessing, hybrid feature selection and synthetic oversampling addressed class imbalance. The primary model was a regularized logistic regression within a stacked ensemble; performance was evaluated on a held-out test set using area under the receiver operating characteristic curve (AUROC) and decision curve analysis (DCA). Benchmarks included Child-Pugh, MELD, MELD-Na, MELD 3.0, ALBI and PALBI. Interpretability used Shapley additive explanations (SHAP).
Results: Median age was 53 years (IQR 46–63); 21.4% were female. Major etiologies were alcohol-related (53.0%) and viral hepatitis (42.3%). Logistic regression achieved the highest test AUROC of 0.990 with accuracy 94.1%, outperforming all prognostic scores (AUROC 0.751–0.912; $p < 0.05$ for pairwise comparisons). DCA showed greater net benefit across clinically relevant thresholds (e.g., net benefit 0.441 at 50% risk vs 0.324 for MELD 3.0). SHAP ranked international normalized ratio and total bilirubin as the most influential predictors.
Conclusion: A fairness-aware ML framework, particularly logistic regression, improved discrimination and clinical utility for 30-day mortality prediction in decompensated cirrhosis. External validation in independent populations is warranted for generalizability.

SAT-501
Myeloid cell 5-lipoxygenase activation and its metabolite product 5-HETE promote systemic inflammation and hepatocyte ferroptosis in acute-on-chronic liver failure
Huilan Tu[1], Xinyi Xu[1], Ruoqi Zhou[1], Xia Yu[1], Xianbin Xu[1], Jiyang Chen[1], Xiuding Zhang[1], Xinxin Liu[1], Ying Hu[1], Jifang Sheng[1], Yu Shi[1]. [1]*The First Affiliated Hospital, Zhejiang University School of Medicine, Hangzhou, China*
Email: 12318425@zju.edu.cn

Background and aims: Acute-on-chronic liver failure (ACLF) is characterized by profound systemic inflammation, yet upstream inflammatory circuits remain incompletely defined. We investigated whether myeloid 5-lipoxygenase (5-LOX) activation and its oxylipins (5-HETE, leukotrienes) drive inflammation in ACLF and associate with hepatocyte ferroptosis.
Method: We enrolled 145 participants (26 healthy controls, 31 chronic liver disease, 33 decompensated cirrhosis, 55 ACLF). We performed bulk RNA-seq (whole-blood leukocytes, neutrophils, liver) and liver scRNA-seq, quantified plasma 5-LOX products by targeted oxylipin metabolomics, and calculated a 5-LOX pathway score in deconvoluted leukocyte subsets. Intrahepatic 5-LOX^+ myeloid cells were assessed by multiplex immunofluorescence. Oral zileuton was tested in LPS/D-GalN and ConA murine liver failure. Iron and ferroptosis markers were assessed in patients and mice, including a high-iron diet model. 5-HETE effects were tested in THP-1–derived macrophages and THLE-2 hepatocytes.
Results: 5-LOX/leukotriene pathway transcripts increased stepwise across disease stages and peaked in ACLF, which were enriched in neutrophils and monocytes/macrophages, and correlated with inflammatory activation and ACLF severity. Plasma 5-HETE and leukotrienes were markedly elevated in ACLF and associated with liver injury and systemic inflammation. Liver omics and tissue validation showed heightened hepatic 5-LOX activation with increased 5-LOX^+ macrophages and neutrophils. In both murine

models, hepatic 5-HETE increased; zileuton reduced 5-HETE and liver injury. In vitro, 5-HETE robustly activated the ATF4/CHOP integrated stress response and the NR4A/KLF2/4-driven immunometabolic program in THP-1–derived macrophages, accompanied by increased glycolysis and lipid peroxidation. Patients with ACLF and murine liver failure exhibited increased serum and hepatic iron and ferroptosis-associated changes, which were mitigated by 5-LOX inhibition. A high-iron diet model supported an association between hepatic ferroptosis and 5-LOX pathway activation. In THLE-2 cells, 5-HETE exposure induced ferroptosis-related alterations.
Conclusion: Myeloid 5-LOX activation is tightly linked to systemic inflammation and severity in ACLF, and 5-HETE associates with hepatocyte ferroptosis, supporting 5-LOX as a therapeutic target.

SAT-505

Development and outcome of ACLF in patients with autoimmune hepatitis, primary biliary cholangitis and primary sclerosing cholangitis compared to patients with non-autoimmune chronic liver disease: analysis of a multicentric international cohort

Xavier Verhelst[1], Cristina Sanchez-Garrido[2], Ferran Aguilar[2], Hans Van Vlierberghe[1], Sarah Raevens[1], Anja Geerts[1], Sebastián Marciano[3], Manuel Mandizabal[4], Aldo Torre[5], Vishal C. Patel[6], Flair Jose Carrilho[7], Berta Romero-Grimaldo[2], Alberto Queiroz Farias[8], Jonel Trebicka[9], Wim Laleman[10], Salvatore Piano[11], Joan Clària[2], Paolo Angeli[11], Thierry Gustot[12], Richard Moreau[2]. *[1]Department of Gastroenterology and Hepatology, Ghent University Hospital, Ghent, Belgium; [2]EF CLIF, Barcelona, Spain; [3]Hospital Italiano de Buenos Aires, Buenos Aires, Argentina; [4]Austral University Hospital, Buenos Aires, Argentina; [5]Departamento de Gastroenterología, Instituto Nacional de Ciencias Médicas y Nutrición "Salvador Zubirán," Mexico City, Mexico; [6]Roger Williams Institute of Liver Studies, School of Immunology & Microbial Sciences, Faculty of Life Sciences and Medicine, King's College London, Foundation for Liver Research and King's College Hospital, London, United Kingdom; [7]Hospital das Clínicas, University of São Paulo School of Medicine, Sao Paulo, Brazil; [8]University of Sao Paulo, Sao Paulo, Brazil; [9]Department of Internal Medicine B, University of Muenster, Muenster, Germany; [10]Department of Gastroenterology & Hepatology, Section of Liver- & Biliopancreatic Disorders and Liver Transplantation, University Hospitals Leuven, Leuven, Belgium; [11]Department of Medicine, University of Padova, Padova, Italy; [12]HUB Hopital Erasma, Brussels, Belgium*
Email: xavier.verhelst@uzgent.be

Background and aims: Acute on chronic liver failure (ACLF) is a clinical syndrome of acute decompensation observed in patients with cirrhosis characterized by very high morbidity and mortality. The aim of this project was to describe the clinical characteristics and outcomes of patients with autoimmune hepatitis (AIH), primary biliary cholangitis (PBC) and primary sclerosing cholangitis (PSC) compared to non-autoimmune related liver disease.
Method: Patient data collected by the EF CLIF consortium in 3 prospective studies (CANONIC, PREDICT and ACLARA) were used to study patient characteristics, the development of ACLF (within 28 days of admission) and patient outcome (28- and 90-day mortality) in patients with AIH, PBC and PSC, compared to patients with non-autoimmune related liver disease.
Results: Patients with AIH (n = 122), PBC (n = 114), PSC(n = 56) and 3179 controls were included (Alcohol: n = 2271; MAFLD: n = 541; HepC: n = 711; and HepB: n = 182). AIH and PSC patients were younger compared to the controls (46.8 and 48.1 vs. 58.2; $p < 0.01$). Immunosuppressants were significantly more used in AIH, PBC and PSC versus controls (resp. 63%, 21%, 21% vs. 1%; $p < 0.01$). As a precipitating factor more bacterial infections were observed (AIH 53%, PBC 38%, PSC 58% versus 32%; $p < 0.01$, $p = 0.28$, $p < 0.01$). AIH patients showed a higher prevalence of ACLF at admission (OR 1.71; 34% vs 23%; $p = 0.01$). In PBC and PSC a trend was observed towards a higher prevalence of ACLF at admission (31% and 33% versus 23%, $p = 0.07$ and $p = 0.12$). There was no difference in the severity of ACLF at presentation. PSC patients tended to have a higher incidence of ACLF development (OR 2.22; 28.1% vs 15%, $p = 0.07$). At admission higher values of bilirubin were present in AIH, PSC and PBC ($p < 0.01$), a higher INR in AIH and PSC ($p < 0.01$), higher CRP (28.8 and 54.2 versus 20.8; $p < 0.01$) and serum TNF-alpha levels (44.54 and 40.49 vs. 27.05; $p < 0.01$) in AIH and PSC patients. Levels of IL-8 were decreased in AIH (4.21 vs. 7.06; $p < 0.01$). There was however no significant difference in 28-day and 90-day mortality between patients with AIH, PBC or PSC and controls.
Conclusion: Patients with AIH hospitalised for an acute decompensation of cirrhosis have a higher incidence of ACLF at admission compared to other aetiologies. PSC patients tended to develop more ACLF after admission, without significant impact on mortality. Clinical, biochemical and immunological characteristics of AIH, PBC and PSC patients with ACLF require further research.

SAT-506-YI

Elevated serum concentrations of Angiopoietin-2 link endothelial dysfunction, vascular destabilization, and poor outcomes across stages of cirrhosis

Lea von Ehren[1], Johanna Reißing[1,2,3], Mohamed Ramadan Mohamed[1], Haedge Frederic[1], Mick Frissen[1], Oluwatomi Ibidapo-Obe[1], Majda El Hassani[1], Andreas Stallmach[4], Philipp Reuken[4], Theresa Hildegard Wirtz[1], Tony Bruns[1]. *[1]University Hospital RWTH Aachen, Department of Internal Medicine III, Aachen, Germany; [2]Aachen, Aachen, Germany; [3]University Hospital RWTH Aachen, Department for Internal Medicine III, Aachen; [4]Friedrich Schiller University Jena, Jena University Hospital, Department of Internal Medicine IV, Jena, Germany*
Email: lvonehren@rwth-aachen.de

Background and aims: Endothelial dysfunction is a hallmark of advanced cirrhosis, driving portal hypertension and potentially aggravating organ failure. We aimed to characterize the relationship between Angiopoietin-2 (ANGPT2), a key regulator of vascular stability, and a comprehensive network of inflammatory, endothelial, and angiogenic mediators across the spectrum of liver disease severity.
Method: Serum concentrations of ANGPT2 and a panel of 20 related biomarkers were quantified by multiplex immunoassay in cohorts of healthy controls (n = 20), patients with compensated cirrhosis (n = 20), decompensated cirrhosis without acute-on-chronic liver failure (n = 20) and with acute-on-chronic liver failure (ACLF, n = 40). Angiopoietin-2 mRNA was analyzed in gut and liver from two murine models of fibrosis (CCl4 and bile duct ligation) and in cultured human endothelial cells.
Results: Angpt2 was upregulated in liver, colon and small intestine in both animal models of cirrhosis with comparable expression of ANGPT2 between human liver sinusoidal and macrovascular endothelial cells. In patients, circulating ANGPT2 levels increased progressively with the severity of liver disease, being highest in ACLF. Serum ANGPT2 correlated with upstream inflammatory drivers and cell death pathways (IL-6, sCD163, FasR, progranulin) and was tightly associated with downstream markers of endothelial activation and injury (ICAM-1, Thrombomodulin). Higher ANGPT2 serum concentrations indicated poor transplant-free survival, particularly in patients with decompensated cirrhosis ($p < 0.0001$, log-rank test).
Conclusion: Circulating ANGPT2 levels are an indicator of systemic inflammation and endothelial dysfunction in cirrhosis. ANGPT2 may provide a mechanistic link that translates the inflammatory insult into vascular destabilization and poor outcomes associated with clinical decompensation and ACLF.

SAT-507

Definition of renal failure with stage ≥2 acute kidney injury and final serum creatinine ≥2 mg/dL has the best prognostication for mortality in a global cirrhosis cohort

Florence Wong[1], K. Rajender Reddy[2], Patrick S. Kamath[3], Peter Hayes[4], Jacob George[5], Ashok Kumar Choudhury[6,7], Ramazan Idilman[8], Wai-Kay Seto[9], Qing Xie[10], Aldo Torre[11], Mario Álvares-da-Silva[12], Danielle Adebayo[13,14], Adam Doyle[15], Zhujun Cao[16], Hiang Keat Tan[17], Adrian Gadano[18], Mark Topazian[19], Abha Nagral[20], Alberto Farias[21], Minghua Su[22], Nabil Debzi[23], Neil Rajoriya[24], Cameron Gofton[25], Chuanwu Zhu[26], Coskun Ozer Demirtas[27], Katina Zheng[1], Henok Fisseha[19], Ashish Goel[28], Sebastián Marciano[18], Nafisa Salih[13], Radha Krishan Dhiman[29], Yanhang Gao[30], Anand Kulkarni[31], René Malé Velazquez[32], Yongfang Jiang[33], Jose Antonio Velarde-Ruiz Velasco[34], Caiyan Zhao[35], Maria Sarai González-Huezo[36], Sumeet Asrani[37], Lei Wang[38], Mingqin Lu[39], Matheus Truccolo Michalczuk[12], Sezgin Barutcu[40], Jacqueline Cordova-Gallardo[41], Michael Gounder[5], Jawaid Shaw[42], Xin Zheng[43], Aloysious Aravinthan[44], Dinesh Jothimani[45], Kessarin Thanapirom[46], Carlos Benitez[47], Dinc Dincer[48], Anoop Saraya[49], Bin Xu[50], Minghua Lin[51], Shiv Kumar Sarin[6], Xiaoping Wu[52], Chenghai Liu[53], Richard Goodheart[15], Nazokat Otajonova[37], Yingling Wang[26], Sevda Aghayeva[2], Yu Sung Kim[25], Haydar Adanir[48], Patricia Momoyo Zitelli[54], Somaya Albhaisi[55], Marco Arrese[47], Abdullah Emre Yıldırım[40], Man Su[22], Tongluk Teerasarntipan[46], Xinrui Wang[30], Busra Haktaniyan[56], Liou Wei Lun[17], Hak-Keith Leung[57], Yanyun Zhang[53], Hasan Basri Yapıcı[27], Francisco Félix Tellez[32], Feng Peng[33], Belimi Hibat Allah[23], Suresh Vasan Venkatachalapathy[44], WeI Wang[35], CE Eapen[28], Araceli Bravo Cabrera[36], Qunfang Rao[52], Ajay Jhaveri[20], Rosemary Faulkes[24], Yijing Cai[39], Lilian Torres Made[32], Jing Liu[43], Amey Sonavane[58], Linlin Wei[50], Mithun Sharma[31], Sanjiv Mahadeva[57], Haibing Gao[51], Shalimar Shalimar[49], Dedong Yin[38], Brian Bush[55], Scott Silvey[55], Jasmohan Bajaj[55].

[1]University of Toronto, Toronto General Hospital, Toronto, Canada; [2]University of Pennsylvania, Philadelphia, United States; [3]Mayo Clinic, Rochester, United States; [4]University of Edinburgh, Edinburgh, United Kingdom; [5]Westmead Hospital, University of Sydney, Westmead, Australia; [6]Institute of Liver & Biliary Sciences, New Delhi, India; [7]Institute of Liver and Biliary Sciences, Hepatology, Delhi, India; [8]Gazi University Faculty Of Medicine, Ankara, Türkiye; [9]The University of Hong Kong, Pok Fu Lam, Hong Kong; [10]Jiao Tong University, Ruijin Hospital, Shanghai, China; [11]Instituto Nacional de Ciencias Médicas y Nutrición Salvador Zubirán, Mexico City, Mexico; [12]Hospital de Clínicas de Porto Alegre, Universidade Federal do Rio Grande do Sul, Porto Alegre, Brazil; [13]Royal Berkshire NHS Foundation Trust, Reading, United Kingdom; [14]Royal Berkshire Hospital NHS Trust, Gastroenterology, Reading, United Kingdom; [15]Royal Perth Hospital, Perth, Australia; [16]Jiao Tong University of Shanghai, Ruijin Hospital, Shanghai, China; [17]Singapore General Hospital, Singapore, Singapore; [18]Hospital Italiano de Buenos Aires, Buenos Aires, Argentina; [19]St Paul's Hospital, Addis Ababa, Mayo Clinic, Rochester, Addis Ababa, Ethiopia; [20]Jaslok Hospital, Mumbai, India; [21]University of Sao Paolo, Sao Paolo, Brazil; [22]The First Affiliated Hospital of Guangxi Medical University, Nanning, China; [23]Mustapha Bacha University Hospital, Algiers, Algeria; [24]Queen Elizabeth University Hospitals, Birmingham, United Kingdom; [25]Royal North Shore Hospital, Sydney, Australia; [26]The Fifth People's Hospital of Suzhou, Suzhou, China; [27]Marmara University School of Medicine, Istanbul, Türkiye; [28]Christian Medical College, Vellore, India; [29]Sanjay Gandhi Postgraduate Institute of Medical Research, Lucknow, India; [30]The First Hospital of Jilin University, Jilin, China; [31]Asian Institute of Gastroenterology, Hyderabad, India; [32]Instituto de la Salud Digestiva, Guadalajara, Mexico; [33]The Second XiangYa Hospital of Central South University, Changsha, China; [34]Hospital Civil de Guadalajara Fray Antonio Alcalde, Guadalajara, Mexico; [35]The Third Affiliated Hospital of Hebei Medical University, Hebei, China; [36]Centro Médico ISSEMYM, Mexico City, Mexico; [37]Baylor University Medical Center, Dallas, United States; [38]Second Hospital of Shandong University, Shandong, China; [39]The First Affiliated Hospital of Wenzhou Medical University, Wenzhou, China; [40]Gaziantep University School of Medicine, Gaziantep, Türkiye; [41]Hospital General Dr. Manuel Gea Gonzlez, Mexico City, Mexico; [42]Richmond VA Medical Center, Richmond, United States; [43]Union Hospital, Tongji Medical College, Huazhong University of Science and Technology, Wuhan, China; [44]University of Nottingham, Nottingham, UK and NIHR Nottingham Biomedical Research Centre, Nottingham University Hospitals NHS Trust, Nottingham, United Kingdom; [45]Dr. Rela Institute and Medical Centre, Chennai, India; [46]Chulalongkorn University and King Chulalongkorn Memorial Hospital, Bangkok, Thailand; [47]Pontificia Catholic University of Chile, Santigo, Chile; [48]Akdeniz University School of Medicine, Antalya, Türkiye; [49]All India Institute of Medical Sciences, New Delhi, India; [50]Beijing Youan Hospital, Capital Medical University, Beijing, China; [51]Mengchao Hepatobiliary Hospital of Fujian Medical University, Fuzhou, China; [52]The First Affiliated Hospital of Nanchang University, Nanchang, China; [53]Shuguang Hospital Affiliated to Shanghai University of Traditional Chinese Medicine, Shanghai, China; [54]Hospital das Clínicas da Faculdade de Medicina da Universidade de São Paulo, San Paolo, Brazil; [55]Virginia Commonwealth University, Richmond, United States; [56]Ankara University, School of Medicine, Ankara, Türkiye; [57]University of Malaysia, Kuala Lumpur, Malaysia; [58]Apollo Hospital, Mumbai, India

Email: florence.wong@utoronto.ca

Background and aims: Acute kidney failure (AKF) in cirrhosis has variably been defined as serum creatinine (sCr) ≥2.5 mg/dL (International Ascites Club), or sCr ≥2 mg/dL (EASL-CLIF), or stage ≥2 AKI ± RRT (Consensus paper 2025). It is unclear which provides the best prognostic value. Aim: To identify an AKF definition that provides the strongest prediction of 30-day mortality in patients with cirrhosis & AKF.

Method: The global CLEARED Consortium enrolled non-electively admitted patients with cirrhosis from 127 sites in 37 countries. Patients with AKI with sCr of >0.3 mg/dL were allotted into one of 3 definitions of AKF: A) stage ≥2 AKI & final sCr <2 mg/dL (modified Consensus) (n = 219), B) AKI with sCr ≥2 mg/dL but no doubling (modified EASL-CLIF) (n = 430), C) stage ≥2 AKI & final sCr ≥2 mg/dL (overlap Gp) (n = 740) and compared with D) all other AKI cases (No AKF) (n = 816). Demographics, cirrhosis details, inpatient course and 30-day mortality were collected. Multivariable logistic regression model was fitted to identify factors independently associated with the strongest AKF definition.

Results: 2205 (age = 57 yrs, 65% men) of 8143 enrolled patients had AKI and sCr and outcome data for analysis. At enrolment, Group (Gp) B had high prevalence of diabetes (44%) or hypertension (38%) ($p < 0.05$ vs. other 3 Gps), and most cirrhosis complications with ascites (79%), prior AKI/HRS (55%), hypoNa (32%), and 68% admitted in past 6 Ms ($p < 0.05$ vs. other 3 Gps). However, Gp C had the highest median admission MELD-Na of 30 ($p < 0.001$ vs. other 3 Gps) and became the sickest with their AKI, triggered commonly by infection (35.3%) ($p < 0.001$ vs. other 3 Gps). More Gp C patients developed encephalopathy (44.5%) and electrolytes imbalance (38.5%) with their AKI ($p < 0.001$ vs. other 3 Gps for both). Median peak sCr were 1.53 mg/dL, 2.85 mg/dL and 3.84 mg/dL for Gps A, B, & C respectively ($p < 0.001$). 33% of Gp C received terlipressin ($p = 0.023$ vs. Gps A & B) and 89% received albumin ($p < 0.001$ vs. Gps A & B). AKI was unresolved in 44% in Gp C vs. Gp B = 34%, and Gp A = 21% ($p < 0.001$). In-hospital and 30-day mortality were 45% & 55% for Gp C, vs. 25% & 35% for Gp B, vs. 18% & 25% for Gp A ($p < 0.001$ for both). SBP as the AKI trigger, electrolyte imbalance, high WBC or high MELD-Na at admission were factors associated with AKF as defined in Gp C ($p < 0.05$ for all).

Conclusion: In a global cirrhosis cohort, stage ≥2 AKI with final sCr ≥2 mg/dL links with the worst 30-day mortality after AKI, especially when triggered by SBP.

SAT-508

Exploratory study of early diagnostic markers for hepatitis B-related acute-on-chronic liver failure based on plasma cell-free deoxyribonucleic acid methylation sequencing

Wenxin Zhoudi[1], Yangfan Shen[1], Xiayao Li[1], Zhangya Pu[1], Xiaowei Xu[1]. [1]*State Key Laboratory for Diagnosis and Treatment of Infectious Diseases, National Clinical Research Center for Infectious Diseases, Collaborative Innovation Center for Diagnosis and Treatment of Infectious Diseases, College of Medicine, The First Affiliated Hospital, Zhejiang University, Hangzhou, China, Hangzhou, China*
Email: di.zhou@zju.edu.cn

Background and aims: Acute-on-Chronic Liver Failure (HBV-ACLF), characterized by acute hepatic decompensation in chronic liver disease patients, is predominantly triggered by hepatitis B virus (HBV) reactivation in China and carries high short-term mortality. Circulating cell-free DNA (cfDNA) has emerged as a prognostic non-invasive biomarker in HBV-ACLF. To address the need for early detection, this study profiles cfDNA methylation in HBV-ACLF and validates findings in ACLF animal model to identify potential early diagnostic markers.
Method: This study enrolled 110 HBV-ACLF patients, 25 patients with HBV-related liver cirrhosis, 25 patients with chronic HBV infection, and 107 healthy controls. Plasma cfDNA methylation was profiled by Reduced Representation Bisulfite Sequencing RRBS, and bioinformatics identified pathways and differentially methylated genes (DMGs) relevant to early ACLF diagnosis. Selected DMGs were validated in an ACLF mouse model, assessing promoter methylation and its effect on gene expression.
Results: Elevated plasma cfDNA levels in HBV-ACLF patients correlated with disease severity and survival, declining during recovery. Methylation analysis highlighted immune pathway involvement, including LYVE1-associated regulation of macrophages, neutrophil responses, and $CD8^+$ T cell differentiation, with survival-linked differences in NOD2 and TGF-β/IL-6 signaling. Disease progression showed increasing promoter methylation of RAB8A and MGLL, and decreasing methylation of DUSP22, MPG, MIB2, FKBP5, and PSENEN. In ACLF mouse model, reduced MPG and FKBP5 promoter methylation correlated with elevated gene and protein expression, supporting their methylation-dependent role in pathogenesis.
Conclusion: This study characterized the methylation landscape of HBV-ACLF across disease stages (CHB, cirrhosis, ACLF), severity, outcome, and recovery. Seven genes (DUSP22, MGLL, MPG, RAB8A, MIB2, FKBP5, PSENEN) were identified as potential early diagnostic markers. Mouse model validation implicated MPG and FKBP5 in ACLF pathogenesis via promoter methylation regulation, providing a basis for further mechanistic investigation.

SAT-509

Timing of diagnostic paracentesis from first physician contact and in-hospital outcomes in cirrhosis with ascites

Alexander Zhu[1], Meghan Cloutier[1], Ikjot Singh[1], Edward Tamale[1], Inioluwa Dada[1], Anthony Martinez[1,2]. [1]*Department of Internal Medicine, University at Buffalo, Buffalo, United States;* [2]*Department of Gastroenterology and Hepatology, University at Buffalo, Buffalo, United States*
Email: alexander.b.zhu@gmail.com

Background and aims: Timely diagnostic paracentesis is recommended for hospitalized patients with cirrhosis and ascites, and earlier performance has been associated with improved outcomes. Prior studies predominantly define timing relative to hospital admission, which may not accurately reflect delays from initial clinical evaluation. We aimed to examine associations between timing of diagnostic paracentesis, measured from the first physician contact, and in-hospital outcomes among patients with cirrhosis and ascites.
Method: We conducted a retrospective cohort study of adults with cirrhosis and ascites hospitalized at a tertiary care safety-net hospital between 2023 and 2024 who underwent diagnostic paracentesis. Time to diagnostic paracentesis was measured from the first physician contact, defined using the timestamp of the initial physician evaluation. Early diagnostic paracentesis was defined as occurring within 24 hours of first physician contact. Outcomes included in-hospital mortality, acute kidney injury (AKI), hepatic encephalopathy (HE), and length of stay (LOS). Associations between the timing of diagnostic paracentesis and in-hospital outcomes were examined using multivariable regression models adjusted for MELD-Na and age.
Results: Among 192 hospitalizations, 89 (46.4%) received early paracentesis, and 103 (53.6%) received delayed paracentesis. AKI occurred less frequently in the early paracentesis group compared with the delayed group (31.5% vs 53.4%; $p = 0.002$), as did HE (20.2% vs 37.9%; $p = 0.008$). After adjustment for MELD-Na and age, early paracentesis remained associated with lower odds of AKI (adjusted OR 0.31, 95% CI 0.15–0.62; $p = 0.001$) and HE (adjusted OR 0.43, 95% CI 0.22–0.83; $p = 0.012$). Median LOS was shorter in the early paracentesis group (7 days [IQR 3–12]) compared with the delayed group (13 days [IQR 7–21.5], $p < 0.0001$). In-hospital mortality was numerically lower among patients who received early paracentesis (13.5% vs 21.4%), although this difference did not reach statistical significance ($p = 0.154$).
Conclusion: Diagnostic paracentesis performed within 24 hours of the first physician contact was associated with lower rates of acute kidney injury and hepatic encephalopathy, and with shorter length of stay, among hospitalized patients with cirrhosis and ascites. Measuring paracentesis timing from first physician contact may provide a more clinically meaningful quality metric than admission-based timing and better identify modifiable delays in care.

SAT-510-YI

Reduced thrombin generation capacity in decompensated cirrhosis and acute-on-chronic liver failure is associated with short-term mortality

Alexander Zubko[1], Jonathan Frederik Brozat[2], Rana Ismail[2], Julian Pohl[2], Hannah Schwarz[2], Philipp Enghard[3], Jan Kruse[3], Frank Tacke[2], Christoph Sucker[4], Cornelius Engelmann[2]. [1]*Charité - Universitätsmedizin Berlin, Department of Hepatology and Gastroenterology, CCM and CVK, Augustenburger Platz 1, 13353 Berlin, Berlin, Germany;* [2]*Charité - Universitätsmedizin Berlin, Department of Hepatology and Gastroenterology, CCM and CVK, Augustenburger Platz 1, 13353 Berlin, Berlin, Germany;* [3]*Department of Nephrology and Medical Intensive Care, Charité-Universitätsmedizin, 13353 Berlin, Berlin, Germany, Berlin, Germany;* [4]*Medical Care Center (Medizinisches Versorgungszentrum), COAGUMED Gerinnungszentrum, Berlin, Germany*
Email: Alexander.Zubko@charite.de

Background and aims: In liver cirrhosis, haemostasis is rebalanced through concomitant alterations of pro- and anticoagulant pathways, limiting the clinical interpretability of conventional coagulation tests such as INR and platelet count. We evaluated thrombin generation assay (TGA) profiles in acute decompensation (AD), acute-on-chronic liver failure (ACLF) compared with healthy controls and explored associations with organ failure and short-term outcome.
Method: In 136 participants (AD n = 74; ACLF grade I–III n = 49; controls n = 13), TGA was performed at baseline from platelet-poor plasma and quantified by tLag, tPeak, peak thrombin (Peak), velocity index (VI) and area under the curve (AUC). Cox proportional hazards models were used to estimate hazard ratios (HR) for 90-day mortality. Elastic-net regression (lambda.min) was applied to derive a composite TGA score based on Peak, VI and AUC.
Results: Compared with AD, ACLF patients showed more pronounced laboratory abnormalities (INR, bilirubin and creatinine, all $p < 0.01$) and had higher disease severity scores (MELD 25 vs. 14; CLIF-C OF 9

vs. 5; p < 0.001). Onset of thrombin generation was delayed in ACLF (median tLag 5.0) compared with AD (3.85) and controls (3.6) (p = 0.007), while time to peak remained comparable (p = 0.148). Quantitative thrombin capacity (AUC) was preserved in AD and controls (p = 0.784) but substantially reduced in ACLF (all p < 0.001 vs. AD/controls). Higher INR and bilirubin correlated with lower Peak, VI and AUC (all p < 0.001). Across AD and ACLF, reduced thrombin capacity (Peak, VI and AUC) correlated with 28-day and 90-day mortality (all p < 0.05). In univariable Cox models, higher Peak, VI and AUC were each associated with a lower risk of 90-day mortality. The elastic-net-derived composite TGA score showed robust prognostic performance (HR 0.546, 95% CI 0.403–0.739; p = 0.001) and remained independently associated with mortality after adjustment for either platelet count, INR, age, sex category or aetiology (platelets HR 0.539 [0.398–0.732], p = 0.001; INR HR 0.645 [0.451–0.921], p = 0.016, respectively).

Conclusion: While the concept of rebalanced haemostasis applies in AD, the development of ACLF represents a turning point characterized by profound alterations in quantitative thrombin generation. The predictive performance of single and composite TGA parameters support TGA as a global coagulation marker for risk stratification in acutely ill patients with cirrhosis.

Cirrhosis and its complications – Experimental and pathophysiology

TOP-438

Targeting the sEH–EET axis with DPP-4 inhibitor and ARNI ameliorates portal hypertension in experimental cirrhosis

Masafumi Oyama[1], Kosuke Kaji[1], Hitoshi Yoshiji[1]. [1]*Department of Gastroenterology, Nara Medical University Hospital, kashihara, Japan*
Email: k184066@naramed-u.ac.jp

Background and aims: Portal hypertension (PH) is a major complication of cirrhosis, and non-selective beta-blockers (NSBBs) are recommended as the standard therapy; however, in some cases, their use may be limited due to systemic hypotension and renal dysfunction. Epoxyeicosatrienoic acids (EETs) improve hepatic microcirculation but are rapidly inactivated by soluble epoxide hydrolase (sEH), whose expression is increased in cirrhotic livers. Inhibition of sEH increases EET levels and has been reported to reduce portal pressure and fibrosis. Dipeptidyl peptidase-4 inhibitors (DPP-i) and angiotensin receptor–neprilysin inhibitors (ARNI) are suggested to maintain EETs through sEH suppression, but their combined effects remain unclear. This study aimed to evaluate the effects of DPP-i and ARNI on portal pressure and liver fibrosis in experimental models of cirrhosis.

Method: F344 rats were fed a choline-deficient, L-amino acid-defined, high-fat diet (CDAHFD) for six weeks to induce cirrhosis. Thereafter, rats received oral administration of vehicle, vildagliptin (10 mg per kg), sacubitril/valsartan (30 mg per kg), combined vildagliptin and sacubitril/valsartan, or carvedilol (10 mg per kg) for an additional six weeks. Portal pressure and systemic hemodynamics were measured, and hepatic sEH activity, EET levels, endothelial function, vascular remodeling, and liver fibrosis were assessed by enzyme-linked immunosorbent assay, quantitative polymerase chain reaction, Western blotting, and immunohistochemistry.

Results: In CDAHFD rats, portal pressure elevation was significantly attenuated by DPP-i or ARNI, and combination therapy showed a reduction comparable to NSBB. Unlike NSBB, DPP-i and ARNI did not alter mean arterial pressure, heart rate, or cardiac output. Both drugs increased vasodilatory markers (Gch, Ddah1), enhanced eNOS phosphorylation, and reduced moesin phosphorylation. Sinusoidal capillarization (CD34), pathological angiogenesis (Vegfa, Ptgs2, Pigf, Vwf), Hedgehog pathway activation, and profibrotic gene expression (Acta2, Col1a1, Tgfb1, Ctgf) were suppressed. sEH expression and activity were elevated in CDAHFD rats and were reduced by both agents, with concomitant increases in hepatic EETs.

Conclusion: DPP-i and ARNI improved portal hypertension and liver fibrosis and demonstrated additive benefits when combined. This therapeutic strategy may represent a novel treatment option for cirrhosis-associated portal hypertension.

TOP-439

Oxidized mitochondrial DNA released from injured hepatocytes drives macrophage STING activation in acute-on-chronic liver failure

Qiankun Hu[1], Xueyun Zhang[2], Yuxian Huang[1,2]. [1]*Shanghai Public Health Clinical Center, Fudan University, Shanghai, China;* [2]*Huashan Hospital, Fudan University, Shanghai, China*
Email: yxhuang@fudan.edu.cn

Background and aims: Acute-on-chronic liver failure (ACLF) is characterized by a systemic inflammatory response leading to multi-organ failure and high short-term mortality. Although mitochondrial injury is a prominent feature of ACLF, whether mitochondria-derived danger signals initiate innate immune activation remains poorly defined. We aimed to determine whether oxidized mitochondrial DNA (ox-mtDNA) released from injured hepatocytes acts as a pathogenic trigger of macrophage-driven inflammation in ACLF.

Method: Clinical samples, murine ACLF models, and hepatocyte-macrophage systems were integrated to characterize mtDNA release, oxidative modification, and activation of cytosolic DNA-sensing pathways. Transcriptomic, histological, and molecular analyses were performed to delineate activated innate immune pathways and cell-specific immune responses. The role of cGAS-STING signaling was evaluated using myeloid-specific STING-deficient mice ($STING^{fl/fl}$-$LyzM^{cre}$) and pharmacologic inhibition of cGAS or STING.

Results: In both patients with ACLF and experimental murine models, hepatocellular mitochondrial damage was accompanied by a marked increase in circulating mtDNA copy numbers, with ox-mtDNA representing the dominant form. The accumulation of ox-mtDNA preceded maximal cytokine induction and coincided with early activation of innate immune pathways in the liver. Among cytosolic DNA sensors, cGAS-STING signaling was robustly activated in hepatic macrophages in both murine and human ACLF. In vitro, ox-mtDNA exhibited enhanced immunostimulatory capacity compared with non-oxidized mtDNA, potently activating macrophage cGAS-STING signaling and downstream TBK1-IRF3 and NF-κB pathways. In vivo, intraperitoneal administration of ox-mtDNA in combination with D-galactosamine induced acute liver injury and inflammatory cell infiltration, recapitulating key pathological features of ACLF. Importantly, myeloid-specific deletion of STING or pharmacologic inhibition of cGAS or STING markedly attenuated macrophage activation, reduced hepatic necroinflammation, and improved survival in ACLF mice.

Conclusion: Ox-mtDNA released from injured hepatocytes functions as an upstream pathogenic driver of ACLF by activating macrophage cGAS-STING signaling. Targeting oxidized mtDNA-driven innate immune activation represents a promising therapeutic strategy for attenuating inflammation-driven liver failure.

TOP-440

L-Homoarginine as a novel prognostic biomarker and therapeutic target in cirrhotic dilutional hyponatremia: an integrated study from clinical cohort to mechanistic exploration

Xue Mei[1], Hai Li[2], Guohong Deng[3], Xian-Bo Wang[4], Xin Zheng[5], Yan Huang[6], Jinjun Chen[7], Zhong-Ji Meng[8], Yanhang Gao[9], Feng Liu[10], Yu Shi[11], liujuan Ji[1], Yuyi Zhang[1], Wei Yuan[1], Zhi-Ping Qian[1]. [1]*Shanghai Public Health Clinical Center, Fudan University, Shanghai, China;* [2]*Ren Ji Hospital, School of Medicine, Shanghai Jiao Tong University, Shanghai,*

China; [3]Department of Infectious Diseases, Southwest Hospital, Third Military Medical University, Chongqing, China; [4]Center of Integrative Medicine, Beijing Ditan Hospital, Capital Medical University, Beijing, China; [5]Department of Infectious Diseases, Institute of Infection and Immunology, Union Hospital, Tongji Medical College, Huazhong University of Science and Technology, Wuhan, China; [6]Department of Infectious Diseases, Hunan Key Laboratory of Viral Hepatitis, Xiangya Hospital, Central South University, Changsha, China; [7]Hepatology Unit, Department of Infectious Diseases, Nanfang Hospital, Southern Medical University, Guangzhou, China; [8]Department of Infectious Diseases, Hubei Clinical Research Center for Precise Diagnosis and Treatment of Liver Cancer, Taihe Hospital, Hubei University of Medicine, Shiyan 442000, Hubei, China; [9]Department of Hepatology, The First Hospital of Jilin University, Changchun, China; [10]Department of Infectious Diseases and Hepatology, The Second Hospital of Shandong University, Jinan, Jinan, China; [11]The State Key Laboratory for Diagnosis and Treatment of Infectious Diseases, The First Affiliated Hospital of School of Medicine, Zhejiang University, Hangzhou, China
Email: meiw258@163.com

Background and aims: Dilutional hyponatremia (DH) is a life-threatening complication of cirrhosis with no effective therapy, driven by arginine vasopressin-mediated renal aquaporin-2 (AQP2) upregulation. We aimed to identify key pathogenic metabolites through metabolomics and validate their mechanistic role in AQP2 dysregulation.
Method: We analyzed data and plasma from a multicenter prospective cohort (CATCH-LIFE) of cirrhotic patients (n = 1013; 253 with hyponatremia). Untargeted metabolomics was performed to screen differential metabolites. Key findings were validated by targeted metabolomics, in a bile duct ligation (BDL) rat model of cirrhotic DH, and in human renal tubular epithelial (HK-2) cells under hypotonic stress.
Results: Clinical Cohort: Serum sodium was an independent predictor for 90-day adverse outcomes (per 1 mmol/L increase: OR 0.95, 95% CI 0.93–0.97, $p < 0.001$). Patients with uncorrected hyponatremia at day 7 had a 46% increased risk (HR 1.46, 95% CI 1.05–2.02, $p < 0.001$) compared to those corrected, and exhibited higher rates of cirrhosis complications ($p < 0.05$). Metabolomics Discovery: Among 514 significantly altered plasma metabolites in hyponatremic patients, the arginine biosynthesis pathway was most enriched. L-homoarginine (L-hArg) was the most significantly depleted metabolite in the refractory hyponatremia subgroup and demonstrated superior predictive value for 28-day outcomes (AUC = 0.702, 95% CI 0.61–0.79, $p < 0.0001$) compared to other candidates. In Vivo Validation: In BDL-induced cirrhotic rats with DH, L-hArg supplementation significantly downregulated both renal AQP2 mRNA and protein expression ($p < 0.05$) compared to saline-treated controls, paralleling a trend toward higher serum sodium levels. Notably, L-hArg treatment restored AQP2 expression to levels comparable to non-hyponatremic controls. In Vitro Mechanistic Insight: In HK-2 cells, L-hArg potently inhibited the upregulation of AQP2 protein on the cell membrane induced by hypotonic stress ($p < 0.05$). Furthermore, L-hArg treatment enhanced cellular antioxidant capacity, evidenced by increased levels of nitric oxide (NO), superoxide dismutase (SOD), and glutathione (GSH) ($p < 0.05$), without affecting cell proliferation.
Conclusion: L-hArg depletion as a novel hallmark of refractory cirrhotic DH. L-hArg effectively suppresses renal AQP2 expression *in vivo* and *in vitro*, positioning it as a potent dual-purpose biomarker for prognosis and a promising therapeutic candidate for this high-mortality condition.

FRI-382

Neurofilament light chain proteins are a sensitive biomarker of neuronal damage in hepatic encephalopathy

Clelia Asero[1], Francesca Polito[2], Maria Stella Franzè[1], Antonio Battaglia[3], Claudia Ligresti[3], Teresa Maltese[2], M'hommed Aguenoz[1], Vincenzo Macaione[1], Irene Cacciola[4].
[1]Università Degli Studi Di Messina, Department of Clinical and Experimental Medicine, University of Messina, Messina, Italy, Division of Medicine and Hepatology, University Hospital of Messina, Messina, Italy, Messina, Italy; [2]Università Degli Studi Di Messina, Messina, Italy; [3]Università Degli Studi Di Palermo, Division of Medicine and Hepatology, University Hospital of Messina, Messina, Italy, Palermo, Italy; [4]Università Degli Studi Di Messina, Division of Medicine and Hepatology, University Hospital of Messina, Messina, Italy, Department of Clinical and Experimental Medicine, Messina, Italy
Email: clelia.asero@gmail.com

Background and aims: Hepatic encephalopathy (HE) is a severe complication of liver cirrhosis. Although traditionally considered reversible, growing evidence suggests that HE episodes may lead to persistent neuronal damage. This study aimed to evaluate the potential role of neurofilament light chain proteins (NfL) as biomarkers for detecting neuronal injury associated with HE.
Method: Between May 1st, 2024, and April 30th, 2025, 133 patients were consecutively enrolled at the Liver Unit of the University Hospital of Messina. Exclusion criteria included active alcohol use and/or illicit drug consumption, and the presence of neurological disorders. For each patient serum NfL concentrations were measured using Single Molecular Array Technology. The study design included two phases: 1) evaluation of NfL concentration differences across the study population, 2) analysis of correlations between NfL levels and clinical/biochemical parameters routinely used for HE diagnosis [West Haven criteria, ammonia levels, Animal Naming Test (ANT)], as well as anthropometric and nutritional indicators [body mass index (BMI), handgrip strength, calf circumference].
Results: The study population (56.4% males; median age 69 years) included 28 non-cirrhotic (21.1%) and 105 cirrhotic patients (78.9%), 34 of them (32.3%) with a diagnosis of HE. Statistical analysis revealed significant differences in NfL levels across the three groups ($p = 0.001$), with a progressive increase in NfL levels from non-cirrhotic patients (mean rank = 43.13) to cirrhotic patients with HE (mean rank = 78.94). ROC curve analysis demonstrated good discriminative ability of NfL for HE detection with an AUC of 0.753 (95% C.I. 0.630–0.876, $p = 0.001$). Significant negative correlations were observed between NfL levels and ANT scores (Rho = –0.320, $p = 0.001$), suggesting that higher neurofilaments levels were related to poorer cognitive performance, while positive associations were detected for West Haven grades (Rho = 0.168, $p = 0.05$) and ammonia levels (Rho = 0.222, $p = 0.021$), indicating that higher NfL concentrations corresponded to more severe HE grades. Also, higher NfL levels were associated with lower BMI ($p = 0.009$), reduced handgrip strength ($p = 0.008$) and calf circumference < 31 cm ($p = 0.043$), reflecting the impact of sarcopenia on HE development.
Conclusion: NfL is a promising biomarker for HE. Its use in clinical practice may improve early detection and stratification of HE severity in cirrhotic patients.

FRI-383

Effect of nitazoxanide on organ failures in disease models of alcohol-mediated acute-on-chronic liver failure (ACLF)

Sabine Klein[1], Marie Bobowski-Gerard[2], Frank Erhard Uschner[1], Camille Vanbésien[2], Philippe Delataille[2], Simon Debaecker[2], Dean Hum[2], Bart Staels[3], Jonel Trebicka[1], Sakina Sayah Jeanne[2].
[1]Hospital of the Goethe University Frankfurt, University Hospital Münster, Germany, Munster, Germany; [2]GENFIT SA, Loos, France; [3]Univ. Lille, Institut Pasteur de Lille, CHU Lille, Inserm U1011, Lille, France
Email: marie.gerard@genfit.com

Background and aims: Acute-on-chronic liver failure (ACLF) in patients with cirrhosis is characterized by multiple organ failures and is associated with high short-term mortality. Acute alcohol hepatitis is a common ACLF precipitant, triggering immune dysfunction and cell death. We previously demonstrated the beneficial effect of nitazoxanide (NTZ) on systemic inflammation as well as liver and kidney function in lipopolysaccharide-induced ACLF models. The aim of this study was to assess the efficacy of NTZ on cell death and multiple organ failure in alcohol-induced disease models.
Method: To assess the effect of NTZ on organ failure, Sprague-Dawley rats were administered with CCl_4 (1 mg/kg, i.p.) combined with 0.06 g/L phenobarbital and 4 to 16% ethanol in drinking water for up to 16 weeks. When rats reached the decompensated stage (i.e., appearance of ascites), a binge of ethanol at 6 g/kg was given orally to precipitate ACLF. NTZ (150 mg/kg, p.o.) was administered one hour after ethanol binge, then twice daily for 3 days. Markers for organ failure were assessed using blood analysis, pulse oximetry and animal behaviour testing. To assess the *in vitro* effect of NTZ on alcohol-mediated cell death, immortalized human hepatocytes were stimulated with 0.6 mM ethanol and treated with tizoxanide (TZ), NTZ's circulating active metabolite. Cell death was evaluated through measurement of caspase 3 activation and cleavage.
Results: In ACLF rats, NTZ administered post-alcohol binge significantly improved brain dysfunction as shown by a reduction of neurological behaviour scoring: 2.7 vs 1 in the NTZ vs the vehicle group ($p = 0.02$). Peripheral blood oxygenation also improved upon NTZ treatment as shown by an increase of oxygen saturation rate (88% vs. 60% in the vehicle group, $p < 0.001$). NTZ also reduced serum levels of blood urea nitrogen (−29%, $p = 0.05$) and AST (−43%, $p = 0.008$) relative to vehicle in ACLF rats, indicating improvement of liver and kidney function. In human hepatocytes, TZ blunted ethanol-induced apoptosis in a dose-dependent manner as shown by a reduction of caspase 3/7 activity and caspase 3 cleavage ($IC_{50} = 1.9$ µM).
Conclusion: NTZ protects from multiple organ failure (brain, respiratory, liver and kidney) in alcohol-induced ACLF models, which could be explained in part by a direct anti-cell death effect. These findings further support the development of NTZ (investigational drug G1090N) as a new therapeutic approach for ACLF.

FRI-384
Differential activity of nitazoxanide vs rifaximin in lipopolysaccharide-induced disease models

Marie Bobowski-Gerard[1], Philippe Delataille[1], Simon Debaecker[1], Camille Vanbésien[1], Athéna Crespin[1], Bart Staels[2], Jonel Trebicka[3], Sakina Sayah Jeanne[1]. [1]*GENFIT SA, Loos, France;* [2]*Univ. Lille, Institut Pasteur de Lille, CHU Lille, Inserm U1011, Lille, France;* [3]*Hospital of the Goethe University Frankfurt, University Hospital Münster, Germany, Munster, Germany*
Email: marie.gerard@genfit.com

Background and aims: Nitazoxanide (NTZ), an antimicrobial compound with large spectrum activity, has shown promising effects on HE in 3 clinical studies. Moreover, we demonstrated anti-inflammatory and organ protective activities of NTZ in disease models of acute-on-chronic liver failure, a severe complication of chronic liver disease associated with multi-organ failure. Rifaximin is a poorly absorbed antibiotic, indicated for the prevention of hepatic encephalopathy (HE) recurrence in cirrhotic patients. The primary mechanism of rifaximin is thought to occur through is effects on the gut microbiome, although other potential beneficial activities, such as anti-inflammatory effects, have been reported. To better understand the mechanisms of action of NTZ vs rifaximin, we compared their activities on lipopolysaccharide (LPS)-induced inflammatory response *in vivo* and *in vitro*.
Method: Endotoxemia was induced in healthy rats by intraperitoneal (i.p.) injection of LPS (1 mg/kg). A single oral dose of NTZ (300 mg/kg) or rifaximin (50 mg/kg) was administered 15 min after LPS. Serum was collected at 3 and 5 hours post-LPS stimulation and cytokine levels and hepatic function parameters analyzed. TZ, the active metabolite of NTZ, or rifaximin (0.3 to 30 µM) were applied *in vitro* for 6 hours to human PBMCs concomitant with LPS stimulation. Cytokine secretion in the supernatant was measured using a Luminex.
Results: In rats with endotoxemia, NTZ lowered LPS-induced serum cytokine release by 26% for IL-6 ($p = 0.03$), 45% for IL-10 ($p = 0.04$), and 43% for TNF-alpha ($p = 0.14$), in comparison with the vehicle group. LPS-induced levels of hepatic markers were also reduced upon NTZ administration: total bile acids by 100% ($p < 0.001$) and AST by 70% ($p = 0.06$). Finally, NTZ restored albumin levels by 50% ($p = 0.007$). In contrast, rifaximin had no effect on LPS-induced serum levels of inflammatory cytokines and hepatic markers (AST, ALT, albumin, total bile acids), in comparison with the vehicle group. In LPS-stimulated PBMC, TZ dose-dependently inhibited cytokine secretion IL-6 ($IC_{50} = 6.9$ µM; Emax = −88%) and TNF-alpha ($IC_{50} = 0.7$ µM; Emax = −39%), whereas rifaximin showed no effect.
Conclusion: Although both NTZ and rifaximin exhibit broad-spectrum antibiotic activity, these findings highlight NTZ's superior ability to rapidly mitigate systemic inflammation and liver injury/function in LPS-induced disease models.

FRI-385-YI
Serum-conditioned nanoplastics trigger hepatocyte injury and inflammation in human liver tissue

Paula Boeira[1], Valentin Tastet[1], Kieran Smith[1,2], Eleanor Walker[1,2], Namrata Pandey[1], Glenn Harper[3], Nathaniel Clark[4], Michael Wilde[5], Matthew Bowles[2], Charlotte Hitchins[2], Christopher Briggs[2], David Stell[2], Aditya Kanwar[2], David Sheridan[2], Richard Thompson[6], Matthew Cramp[1,2], Ashwin Dhanda[1,2], Somaiah Aroori[1,2], Jemimah Denson[7], Shilpa Chokshi[1,8]. [1]*Centre of Environmental Hepatology, Faculty of Health, University of Plymouth, Plymouth, United Kingdom;* [2]*South West Liver Unit, University Hospitals Plymouth NHS Trust, Plymouth, United Kingdom;* [3]*Plymouth Electron Microscopy Centre, University of Plymouth, Plymouth, United Kingdom;* [4]*School of Health Professions, Faculty of Health, University of Plymouth, Plymouth, United Kingdom;* [5]*School of Geography, Earth and Environmental Sciences, Faculty of Science and Engineering, University of Plymouth, Plymouth, United Kingdom;* [6]*Marine Institute, School of Biological and Marine Sciences, University of Plymouth, Plymouth, United Kingdom;* [7]*Cellular and Anatomical Pathology Department, University Hospitals Plymouth NHS Trust, Plymouth, United Kingdom;* [8]*The Roger Williams Institute of Liver Studies, Faculty of Life Sciences and Medicine, King's College London, Plymouth, United Kingdom*
Email: paula.boeira@plymouth.ac.uk

Background and aims: Hepatic accumulation of micro- and nanoplastics (MNPs) has increased over the past decade in parallel with the surge in global plastic pollution and has been reported in patients with cirrhosis. While animal studies demonstrate MNP induced hepatotoxicity, inflammation, and fibrogenesis, mechanistic human data is lacking, identifying a poorly understood risk factor.
Method: Human precision-cut liver slices (hPCLS) preserving native architecture, multicellularity, and immunocompetence from macroscopically normal liver tissue adjacent to resected metastases ($n = 10$) were cultured for 48 h with fluorescent 54 nm polypropylene nanoplastics (PP-NP; 2–25 µg/mL), directly or following pre-incubation with autologous human serum (untreated/heat-inactivated). Hepatotoxicity was assessed by histology (evaluation by histopathologist), cytotoxicity assays, biochemistry, apoptosis/necrosis, confocal microscopy, transmission electron microscopy and flow cytometry. RNA analysis was used to define transcriptional pathways of injury. Immortalized human hepatocytes (IHH) were used to validate key findings.
Results: Subcellular and endosomal accumulation of PP-NPs was observed in >85% of hepatocytes, accompanied by marked hepatotoxicity ($n = 10$; LDH/ALT/AST rise $p < 0.01$) and histological/transcriptional evidence of cellular damage resembling drug-induced liver injury. Serum pre-conditioning significantly exacerbated

toxicity (n = 10; LDH, ALT, AST rise p < 0.001), whereas heat-inactivated serum abolished this effect. IHH recapitulated responses observed in hPCLS. High levels of necrosis were observed and subjects with a significant alcohol history exhibited increased susceptibility to plastic-induced liver injury, suggesting that pre-existing hepatic stress may amplify MNP toxicity.
Conclusion: This study provides mechanistic evidence of plastic-induced liver injury in human tissue. Serum-conditioned nanoplastics, but not heat-inactivated controls, triggered injury at real-world exposure levels, demonstrating that heat-labile serum proteins are mediators of MNP toxicity. Integrated transcriptomic and histological analyses revealed inflammatory and cell-death pathways, establishing a causal mechanism for hepatotoxicity. The heightened susceptibility in patients with alcohol history supports a second-hit model in which nanoplastics exacerbate pre-existing liver stress. These data position MNPs as a clinically relevant environmental risk factor with implications for liver disease progression and exposure regulation.

FRI-386
Monocyte distribution width predicts infection and mortality in acutely decompensated cirrhosis

Robert G Brenig[1,2], Lukas Jutzi[1], Anne Geng[1], Kelly Da Silva[2], Patrizia Künzler-Heule[3], Beatrice Frauchiger[4], Laura Infanti[4,5], Mark J W McPhail[6], Julia Wendon[6], David Semela[3], Christine Bernsmeier[1,2,6]. *[1]Department of Biomedicine, University of Basel, Basel, Switzerland; [2]University Centre for Gastrointestinal and Liver Disease Basel, University Hospital Basel, Basel, Switzerland; [3]Department of Gastroenterology and Hepatology, HOCH Health Ostschweiz – Cantonal Hospital St.Gallen, St. Gallen, Switzerland; [4]Regional Blood Transfusion Center Swiss Red Cross Northwestern Switzerland, Basel, Switzerland; [5]Division of Haematology, University Hospital Basel, Basel, Switzerland; [6]Institute of Liver Studies, King's College Hospital, King's College London, London, United Kingdom*
Email: robert.brenig@unibas.ch

Background and aims: Innate immune dysfunction is a hallmark of advanced cirrhosis and is associated with susceptibility to infection, acute decompensation (AD) and adverse prognosis. Monocyte distribution width (MDW), a measure of monocyte size heterogeneity reflecting cellular activation, has shown diagnostic value in sepsis but remains poorly characterised in cirrhosis. We aimed to evaluate MDW as a biomarker of preserved innate immune activity and to assess its association with disease severity, susceptibility to infection, and short-term prognosis from compensated to acutely decompensated cirrhosis.
Method: Patients with compensated or AD cirrhosis were recruited at two Swiss tertiary centres, along with healthy controls (HC) (Cantonal Hospital St.Gallen [SG]: HC/ Child A/B/C, n = 13/33/25/12; University Hospital Basel [BS]: n = 23/40/29/4). An independent cohort of patients with AD (n = 25) was included from King's College London (KCL). Peripheral blood monocytes were identified by flow cytometry using a CD14/CD16/HLA-DR gating strategy. MDW was analysed retrospectively defined as the standard deviation of forward scatter width.
Results: In the SG cohort, MDW correlated with diverse cirrhosis severity scores (Child: r = 0.24, p = 0.03; MELD: r = 0.24, p = 0.03; ALBI: r = 0.27, p = 0.02), albumin (r = –0.24, p = 0.04), portal hypertension (HVPG: r = 0.41, p = 0.01), and immune markers (CD16: r = 0.23, p = 0.04; HLA-DR: r = -0.25, p = 0.03). Associations with severity scores were confirmed in the BS cohort (Child: r = 0.23, p = 0.05; MELD: r = 0.26, p = 0.04), here MDW also correlated with CRP (r = 0.32, p = 0.01) and INR (r = 0.30, p = 0.02). In AD patients from the BS cohort, MDW increased significantly within 24 hours of AD onset (d0-d1 = 1277, p = 0.01). MDW at AD onset predicted primary infection (AUROC 0.90, p = 0.03), secondary infection within 14 days (AUROC 0.88, p = 0.04), and 1-month mortality (AUROC 0.91, p = 0.02). In AD patients from the BS and KCL cohorts, failure of the MDW to increase within the first 1–3 days after AD onset (d0-d1–3 = –1389) was a strong predictor of transplantation or death within 28 days (AUROC 0.93, p = 0.02).
Conclusion: MDW was associated with cirrhosis severity, infection risk and short-term mortality. Notably, early dynamic changes in MDW within 1–3 days after AD onset predicted 28-day transplant-free survival. Despite small cohorts, these findings support MDW as a simple, inexpensive biomarker for risk stratification and immune monitoring in AD.

FRI-387-YI
Apical sodium-dependent bile acid transporter (ASBT) inhibition improves hepatic and extrahepatic manifestations in a mouse model of cirrhosis

Francisco Javier Caballero-Camino[1,2], Noelia Pastor de los Toyos[1], Mireia Tena-Garitaonaindia[1], Santiago Iturbe-Rey[1], Beatriz Val[1], Maider Huici-Izagirre[1], Laura Izquierdo-Sánchez[1,2], Maria Jesus Perugorria[1,2], Pedro Rodrigues[1,2,3], Luis Bujanda[1,2,4], Peter Åkerblad[5], Erik Lindstrom[5], Jesus M Banales[1,2,3,6]. *[1]Department of Liver and Gastrointestinal Diseases, Biogipuzkoa Health Research Institute - Donostia University Hospital - University of the Basque Country (UPV/EHU), San Sebastian, Spain; [2]National Institute for the Study of Liver and Gastrointestinal Diseases (CIBERehd, "Instituto de Salud Carlos III"), Madrid, Spain; [3]IKERBASQUE, Basque Foundation for Science, Bilbao, Spain; [4]Department of Medicine, Faculty of Medicine and Nursing, University of the Basque Country (UPV/EHU), San Sebastian, Spain; [5]Ipsen, Gothenburg, Sweden; [6]Department of Biochemistry and Genetics, School of Sciences, University of Navarra, Pamplona, Spain*
Email: fcojavier.caballerocamino@bio-gipuzkoa.eus

Background and aims: Liver cirrhosis is estimated to cause about one million deaths worldwide each year. In addition to the pathological changes within the liver, extrahepatic complications including, portal hypertension and persistent systemic inflammation, are major drivers of disease progression and clinical outcomes. Disrupted bile acid (BA) homeostasis, particularly increased BA concentrations, is a hallmark of cirrhosis; however, its pathological contribution remains poorly understood. Here, we evaluated the role of the sodium-dependent bile acid transporter (ASBT) in a mouse model of cirrhosis, using either a gut-restricted ASBT inhibitor (elobixibat) or a systemic ASBT inhibitor (ritivixibat).
Method: A mouse model of advanced fibrosis with cirrhotic features was established through chronic (12-week) administration of carbon tetrachloride (CCl_4). Starting from the 3rd week of CCl_4 administration, elobixibat or ritivixibat were provided in chow at doses of 2.5 and 12 mg/kg/day respectively. Liver histology was assessed blindly by an expert pathologist. Serum BA species were quantified using UHPLC-MS.
Results: Mice exposed to chronic CCl_4 administration developed advanced liver fibrosis, inflammation, steatohepatitis and splenomegaly, along with increased serum transaminases, bilirubin, and iron levels compared with healthy controls. Consistent with previous findings in cirrhotic patients (Sauerbruch T, *et al*. Front. Physiol. 2021), total serum bile acid (TBA) levels were elevated in CCl_4-challenged mice, accompanied by a higher proportion of primary and conjugated BAs. Chronic treatment with either ritivixibat or elobixibat reduced serum TBA levels and restored the balance of primary/secondary and conjugated/unconjugated BAs in CCl_4-exposed mice. These improvements were accompanied by significant reductions in liver fibrosis, steatohepatitis and transaminases, as well as normalization of splenomegaly, serum iron levels, and perivenous hepatic iron deposition. Importantly, serum TBA concentrations—as well as the proportions of primary and conjugated BAs—positively correlated with the histopathological liver phenotype, biochemical serum markers of hepatic injury (transaminases and bilirubin), and spleen size across all study groups.
Conclusion: ASBT inhibition restores bile acid homeostasis and significantly improves hepatic and extrahepatic features of advanced

fibrosis, supporting its potential as a therapeutic strategy for advanced liver disease.

FRI-388-YI

Maladaptive emergency myelopoiesis (EM) is already activated in patients with the less severe forms of acutely decompensated cirrhosis (ADC), and its amplification drives progression towards severity

Zhujun Cao[1,2], Ferran Aguilar[1], Beatriz García-Torre[1], Juanjo Lozano[3], Rosa María Martín Mateos[4], Maria Papp[5], Alberto Farias[6], Liliana Mendes[7], Carlo Alessandria[8], Luciana Lofego Goncalves[9], Martin Janicko[10], Victor Vargas Blasco[11], Sebastián Marciano[12], Gustavo Pereira[13], Salvatore Piano[14], Christian Jansen[15], Adelina Lozano Miranda[16], Daniel Mazo[17], Mauricio Castillo[18], Wim Laleman[19], Agustín Albillos[20], Jonel Trebicka[21], Joan Clària[22], Richard Moreau[1]. *[1]European Foundation for the Study of Chronic Liver Failure (EF CLIF), Barcelona, Spain; [2]Department of Infectious Diseases, Ruijin Hospital, Shanghai Jiao Tong University School of Medicine, Shanghai, China; [3]CIBERehd, Barcelona, Spain; [4]Department of Gastroenterology and Hepatology, Hospital Universitario Ramón y Cajal, Instituto Ramón y Cajal de Investigación Sanitaria (IRYCIS), Madrid, Spain; [5]University of Debrecen, Faculty of Medicine, Institute of Medicine, Department of Gastroenterology, Debrecen, Hungary; [6]Department of Gastroenterology, Hospital das Clínicas, University of Sao Paulo School of Medicine, Sao Paulo, Brazil; [7]Hospital de Base do Distrito Federal, Brasilia, Brazil; [8]A.O.U. Città della Salute e della Scienza Torino, Torino, Italy; [9]Gastroenterology and Hepatology Unit, Hospital Universitário Cassiano Antônio Moraes, Universidade Federal do Espírito Santo, Vitória, Brazil; [10]Pavol Jozef Safarik University in Kosice, Kosice, Slovakia; [11]Hospital Universitari Vall d´Hebron, Barcelona, Spain; [12]Liver Unit and Department of Research, Hospital Italiano de Buenos Aires, Buenos Aires, Argentina; [13]Gastroenterology and Hepatology Unit, Bonsucesso Federal Hospital (Ministry of Health), Rio de Janeiro, Brazil; [14]University of Padova, Padova, Italy; [15]University of Bonn, Bonn, Germany; [16]Unidad de Hígado, Hospital Nacional Arzobispo Loayza, Lima, Peru; [17]Division of Gastroenterology (Gastrocentro), University of Campinas (Unicamp), Campinas, Brazil; [18]Servicio de Gastroenterología y Hepatología, Hospital de Especialidades Centro Médico Nacional La Raza IMSS, Ciudad de México, Mexico; [19]Department of Gastroenterology and Hepatology, Division of Liver & Biliopancreatic disorders and Liver Transplantation, University Hospitals Leuven, KU Leuven, Leuven, Belgium; [20]Department of Gastroenterology, Hospital Universitario Ramón y Cajal, IRYCIS, University of Alcalá, CIBEREHD, Madrid, Spain; [21]Department of Internal Medicine B, University of Münster, Münster, Germany; [22]EF CLIF, Hospital Clínic de Barcelona, IDIBAPS, CIBERehd & Universitat de Barcelona, Barcelona, Spain.*
Email: richard.moreau@efclif.com

Background and aims: Whether maladaptive EM (i.e., amplified myelopoiesis with immunosuppressive features), which is associated with acute-on-chronic liver failure (ACLF) and pre-ACLF, is also seen in less severe forms of ADC is unknown. The dynamicity of maladaptive EM with disease progression is also unknown. We addressed these questions here.

Method: We analyzed whole-blood RNA-seq data obtained in 25 healthy subjects (HS) and on admission from 501 patients who were classified as AD (ADC without ACLF by day-28, n = 299), pre-ACLF (ADC developing ACLF by day-28, n = 79), and ACLF (n = 123). In addition, we performed multivariable ordinal regression with the adjacent categories logit model to analyze the association between transcriptional changes and the progression of disease from HS to ACLF through AD and pre-ACLF.

Results: Compared to the group of HS, each patient's group presented with features of activated EM, including neutrophilia, monocytosis, upregulation of the *STAT3* gene and its target *CEBPB* (which encodes a master transcription factor driving EM), together with upregulation of genes related to immature and mature neutrophils and monocyte subsets. Each patients group also had upregulation of genes related to low-density neutrophils and myeloid suppressor cells (known to suppress lymphocyte functions), features indicating that EM was maladaptive. Flow cytometry analysis confirmed the presence of maladaptive EM in AD. Using weighted gene co-expression network analysis, we identified 24 gene programs, of which one was representative of maladaptive EM (member genes included, e.g., transcription factor *CEBPA*, granule genes [*RETN, NAPRT, NEU1, RNASE2, CTSC*], and immunosuppressive genes [*IL10, CD163, C1QA/B, MERTK, MARCO, HMOX1*]). Multivariable ordinal regression with the adjacent categories' logit model revealed that amplifying the maladaptive EM gene program was associated with a higher risk of disease progression to the next most severe stage (common odds ratio [cOR], 1.83; 95% CI, 1.59–2.11), after adjustments for differences in age, sex, BMI, and clinical precipitants.

Conclusion: Maladaptive EM is already activated among patients who present with the less severe forms of ADC. Moreover, amplification of the maladaptive EM gene program per se may drive progression to severe forms of ADC, findings suggesting that this program should be a target for future therapies aiming to prevent disease progression.

FRI-393

Germline variants influence cirrhosis and HCC through distinct pathways

Marijana Vujkovic[1], David Kaplan[1], Jonas Ghouse[2], Baoli Chang[3], Joseph Brancale[4], Adam Lewis[5], David Zhang[3], Michael Levin[3], Olivea Veatch[6], Josephine Johnson[1], Carolin V. Schneider[7], Anurag Verma[1], Kirk Wangensteen[8], Eleonora Scorletti[3], Dipender Gill[9], Chigoziri Konkwo[4], Alexis Garofalo[3], Lindsay Guare[3], Tae-Hwi Linus Schwantes-An[10,10], Marco Abreu[10], Helene Gellert-Kristensen[11], Ole B Pedersen[12], Christian Erikstrup[13], Johan S Bundgaard[11], Erik Soerensen[11], Sisse Rye Ostrowski[14], Henning Bundsgaard[14], Kyung-Min Lee[15], Abraham Shaked[3], Kim Olthoff[3], Maarouf Hoteit[16], Elizabeth Speliotes[17], Yanhua Chen[17], Antonino Oliveri[17], Lishi Yin[17], Luca Valenti[18,18], Francesco Malvestiti[19], Daniele Marchelli[19], Lorenzo Miano[19], Quentin M. Anstee[20], Ann K Daly[20], Heather Cordell[20], Rebecca Darlay[20,20], Niek Verweij[21], George Hindy[21], Adam Locke[21], Kentaro Matsuura[22], Sumeet Asrani[23], Giuliano Testa[23], Luca Lotta[21], Marcus Jones[21], Daniel Dochtermann[24], Trina Norden-Krichmar[25], Craig Teerlink[26], Poornima Devineni[24], Saiju Pyarajan[24], Daniel Rader[3], Yasuhito Tanaka[27], Benjamin Voight[1], Silvia Vilarinho[4], Lisa Bastarache[5], Stefan Stender[28], Philip Tsao[29], Timothy Morgan[25], Julie Lynch[26], Kyong-Mi Chang[1]. *[1]Philadelphia VA Medical Center & University of Pennsylvania, Philadelphia, United States; [2]University of Copenhagen and Aarhus University Hospital, Copenhagen and Aarhus, Denmark; [3]University of Pennsylvania, Philadelphia, United States; [4]Yale School of Medicine, New Haven, United States; [5]Vanderbilt University Medical Center, Nashville, United States; [6]University of Kansas Medical Center, Kansas City, United States; [7]University Hospital RWTH Aachen & German Cancer Research Center (DKFZ), Aachen & Dresden, Germany; [8]Mayo Clinic, Rochester, United States; [9]Imperial College London, London, United Kingdom; [10]VA Long Beach Healthcare System & Indiana University School of Medicine, Long Beach & Indianapolis, United States; [11]Copenhagen University Hospital, Copenhagen, Denmark; [12]Zealand University Hospital & University of Copenhagen, Koge & Copenhagen, Denmark; [13]Aarhus University Hospital and Aarhus University, Aarhus, Denmark; [14]Copenhagen University Hospital & University of Copenhagen, Copenhagen, Denmark; [15]VA Salt Lake City, Salt Lake City, United States; [16]Hospital of University of Pennsylvania, Philadelphia, United States; [17]University of Michigan, Ann Arbor, United States; [18]Università degli Studi di Milano & Fondazione IRCCS Ca' Granda Ospedale Maggiore Policlinico Milano, Milan, Italy; [19]Università degli Studi di Milano, Milan, Italy; [20]Newcastle University, New Castle, United Kingdom; [21]Regeneron Genetics Center, Tarrytown, United States; [22]Nagoya City University, Nagoya, Japan; [23]Baylor Scott & White Health, Dallas, United States; [24]VA Boston Healthcare System, Boston, United States; [25]VA Long Beach and UC Irvine, Long Beach and Irvine, United*

States; [26]VA Salt Lake City and University of Utah, Salt Lake City, United States; [27]Kumamoto University, Kumamoto, Japan; [28]Copenhagen University Hospital & University of Copenhagen, Copenhagen, United States; [29]VA Palo Alto, Palo Alto, United States
Email: kmchang@upenn.edu

Background and aims: Cirrhosis and hepatocellular carcinoma (HCC) are long-term complications of chronic liver disease (CLD). We aimed to study the genetic basis of cirrhosis and HCC relative to CLD risk factors and clinical risk prediction.
Method: Multi-ancestry genome-wide association studies (GWAS) for cirrhosis and HCC included cohorts from North America, Europe and Asia with: 1) 35,481 all-cause cirrhosis cases vs 2.36M population controls; 2) replication cohort of 8,806 cirrhosis cases vs 328,061 population controls; 3) 35,481 all-cause cirrhosis cases vs 191,491 CLD controls; 4) 6,680 HCC cases vs 1.76M population controls; 5) 4,995 HCC cases vs 706,432 population controls; 6) 6,680 HCC cases vs 191,491 CLD controls. Genome-wide significance (GWS) was defined by p-value < 5×10^{-8}. We also conducted coding variant, gene burden, immunogenetic, causal mediation, multi-state survival, risk prediction, drug target discovery and treatment response analyses in a subset of the cohorts.
Results: All-cause cirrhosis GWAS with population controls identified 27 GWS cirrhosis-associated loci, including 10 novel loci of which three (*FGF21*, *RPTOR*, and *IFNL3/4)* were replicated in independent cirrhosis cohorts. Cirrhosis GWAS using CLD controls showed 6 GWS loci (*PNPLA3, SERPINA1, HLA, TM6SF2, HKDC1*), of which *CD81* was novel. HCC GWAS with population controls identified 11 GWS HCC-associated loci of which three were novel (*EPHA2, CD81, TENM4*), without GWS loci for HCC GWAS with cirrhosis controls. In causal mediation analyses, 15 cirrhosis loci showed differential effects on cirrhosis risk via underlying etiologies (e.g. alcohol, metabolic, viral) and 6 HCC loci influenced HCC risk through cirrhosis. In a gene-burden analysis of rare variants from whole-genome sequencing data in the VA Million Veteran Program (n = 102,677), we identified *GSTA5* as a novel cirrhosis-associated gene, while *APOB* and *ATP9B* were associated with and replicated for HCC. Furthermore, a high genetic risk score for cirrhosis was associated with a nearly doubled risk of CLD progression to cirrhosis (HR = 1.94, $P = 2 \times 10^{-68}$) and cirrhosis progression to HCC (HR = 1.65, $P = 7 \times 10^{-8}$). Finally, among individuals with chronic hepatitis C, cirrhosis risk following therapy was modified by *PNPLA3*, *IFNL3/4*, and *CD81* variants for PEG-IFN, and by *APOE* lead variant for DAA.
Conclusion: These findings define genetic basis of HCC and cirrhosis, with distinct interplays with underlying CLD causes and potential prognostic implications.

FRI-394-YI
Reduced cardiorespiratory fitness and its physiological determinants in patients with cirrhosis: evidence of cirrhosis-induced myopathy

Alexis Couret[1], Fabrice Rannou[2], Bruno Pereira[2], Camille Marcantei[1], François Le Calvez[1], Valérie Julian[2], Martine Duclos[2], Fréderic Costes[2], Leon Muti[3], Benjamin Buchard[3], Sarah Arbogast[3], James King[4], Delphine Weil-Verhoeven[5], Armand Abergel[3], Gael Ennequin[1].
[1]Clermont Auvergne University, Clermont-Ferrand, France; [2]CHU Gabriel-Montpied, Clermont-Ferrand, France; [3]CHU Estaing, Clermont-Ferrand, France; [4]Loughborough University, Loughborough, United Kingdom; [5]Chu Besançon, Besançon, France
Email: Alexis.couret@uca.fr

Background and aims: Cirrhosis induces multi-organ dysfunction, yet the specific physiological determinants underlying reduced cardiorespiratory fitness (CRF) remain poorly defined. This study aims to compare patients with cirrhosis to healthy controls to assess and identify the main contributors to CRF.
Method: Forty-five patients with cirrhosis and 45 age- and sex-matched controls underwent incremental cardiopulmonary exercise testing (CPET) on a cycle ergometer. The pulmonary, cardiac, vascular, and muscular components of CRF were measured, including peak oxygen uptake (VO_{2Peak}), ventilatory efficiency (VE/VCO_2), oxygen uptake efficiency slope (OUES) and chronotropic response. Non-invasive hemodynamic monitoring (Physioflow®) was used to estimate cardiac output and arteriovenous oxygen difference (a-vO_2). In pre-transplantation settings, a sub-group of twenty-five patients with cirrhosis did plethysmography and diffusing capacity evaluation.
Results: Patients with cirrhosis exhibited markedly reduced CRF compared with controls (VO_{2Peak}: 15.4 ± 5.5 vs 29.3 ± 7.5 $ml.min^{-1}.kg^{-1}$, $p < 0.001$) and the decline correlated to Child-Pugh score. Kinetic parameters (OUES: 1467 ± 544 vs 2216 ± 584, Lowest VE/VCO_2: 35.3 ± 9.3 vs 27.6 ± 4.5, Wilkoff index: 0.50 ± 0.28 vs 0.95 ± 0.19; $p < 0.001$) were also significantly impaired and chronotropic incompetence was highly prevalent (89%). Cardiac output during exercise was preserved but a-vO_2 was decreased (10.7 ± 3.0 vs 14.1 ± 1.1 $mlO_2.dl^{-1}$, $p = 0.002$), indicating a defective peripheral oxygen extraction in patients with cirrhosis. Multivariate regression analysis ($r^2 = 0.79$) identified maximal heart rate and muscle performance (5-sit to stand) as independent predictors of $VO_{2Peak.}$
Conclusion: Reduced CRF in cirrhosis appears to result mainly from impaired skeletal muscle oxygen utilisation, compounded by chronotropic incompetence. Muscle function has shown to be the most important determinant of CRF impairment with evidence of cirrhosis-induced myopathy. These findings emphasize the value of integrative functional evaluation in cirrhosis management.

FRI-395-YI
Recapitulating cirrhosis in vitro using a primary liver microphysiological system and patient plasma profiling

Laura de Jong[1], Luuk de Haan[2,3], Vincent van Duinen[2], Iris Schilt[2], Tomás Coimbra[2], Sander de Ruiter[2], Lenie van den Broek[2], Minneke Coenraad[1]. *[1]Leiden University Medical Center, Leiden, Netherlands; [2]MIMETAS BV, Oegstgeest, Netherlands; [3]Leiden Academic Centre for Drug Research, Leiden, Netherlands*
Email: l.m.de_jong@lumc.nl

Background and aims: Liver cirrhosis is the end stage of chronic liver disease and a major cause of liver-related mortality. Progress in understanding its pathophysiology and developing therapies is hampered by the lack of preclinical models that mimic the multicellular architecture and complexity of the cirrhotic liver. This study aims to develop a human liver microphysiological system (MPS) that mimics key features of cirrhosis and to investigate how patient plasma from different stages of cirrhosis affects liver phenotype in the MPS.
Method: Plasma from patients with compensated cirrhosis, decompensated cirrhosis, and acute-on-chronic liver failure (ACLF) was profiled using targeted lipidomics and Olink Reveal proteomics. In parallel, we developed a primary human liver model using OrganoPlate Graft technology by embedding primary hepatocytes, liver-derived endothelial cells, stellate cells, and Kupffer cells in hydrogel under unidirectional flow. Cirrhosis-like features were induced through combined LPS/TGF-β exposure with controlled lipid loading.
Results: Lipidomics on plasma showed widespread lipid suppression with selective accumulation of free fatty acids, lactosylceramides, and phosphatidic acids in decompensated and ACLF patients, but not in compensated disease. Proteomic profiling revealed stage-specific remodeling, with clear separation by principal component analysis (PC1 30%, PC2 15%) and 519, 717, and 758 proteins altered in compensated, decompensated, and ACLF patients, respectively. IL-6, HAVCR, CA9 and MUC13 were among the most consistently altered hits. To evaluate the impact of disease-stage specific plasma on liver phenotype, we developed a human liver MPS containing four cell types, which maintained core hepatic functions, including stable albumin production (>5 µg/mL/day) and CYP activity for 19 days. The model was immunocompetent, with a 4-fold IL-6 increase after LPS

stimulation, and showed a perfusable vascular network. The 10-day cirrhosis trigger induced lipid accumulation and inflammatory and pro-fibrotic mediator release, recapitulating steatosis and fibrosis. Plasma exposure experiments on the MPS model are ongoing.
Conclusion: Plasma profiling revealed disease stage-specific lipid and proteomic alterations. To explore the functional impact of these changes, we developed a human liver MPS that maintained hepatic function and recapitulated cirrhosis-like steatosis and fibrosis, establishing a platform with the potential to link patient plasma profiles to liver phenotype.

FRI-396
Dyslipidemia is associated with impaired fibrinolysis in patients with cirrhosis
Fynn Elvers[1], Jelle Adelmeijer[1], Marilena Stamouli[2], William Bernal[3], Vishal C Patel[2], Ton Lisman[1]. *[1]Surgical Research Laboratory and Section of Hepatobiliary Surgery and Liver Transplantation, Department of Surgery, University of Groningen, University Medical Center Groningen, Groningen, Netherlands; [2]Roger Williams Institute of Liver Studies, School of Immunology & Microbial Sciences, Faculty of Life Sciences and Medicine, King's College London, Foundation for Liver Research and King's College Hospital, London, United Kingdom; [3]Liver Intensive Therapy Unit, Institute of Liver Studies, Kings College Hospital, London, United Kingdom*
Email: fynn.l.elvers@gmail.com

Background and aims: Patients with cirrhosis frequently show abnormalities in lipid profiles and circulating proteins of clot breakdown (fibrinolysis). Recent studies suggest that fibrinolytic proteins regulate lipid metabolism and that dyslipidemia is associated with fibrinolytic abnormalities. However, these mechanisms have not yet been studied in experimental models of liver disease or patients with cirrhosis. We aimed to study the relationships between fibrinolytic parameters and lipid profiles across stages of cirrhosis.
Method: Plasma and serum samples were collected from patients admitted to King's College Hospital, United Kingdom. We studied 33 patients with stable cirrhosis (SC), 42 with decompensated cirrhosis (DC), 43 with acute-on-chronic liver failure (ACLF) and 29 with sepsis without liver disease (as a reference for systemic inflammation), and compared them to reference values from 38 healthy controls. We quantified fibrinolysis by clot lysis time (CLT), plasminogen (PLG), plasminogen activator inhibitor 1 (PAI-1), and tissue-plasminogen activator (tPA), and assessed serum lipids through apolipoprotein-A1 (ApoA1), very low-density lipoprotein (VLDL), LDL, high-density lipoprotein, lipoprotein (a) (Lp(a)), triglycerides and total cholesterol.
Results: CLT was shortened in SC and DC, and prolonged in ACLF and sepsis. PLG decreased, while PAI-1 and tPA increased progressively with cirrhosis severity and in sepsis. Triglycerides were similar to controls in cirrhosis but high in sepsis. All other lipids decreased progressively with cirrhosis severity and in sepsis. In multiple-testing adjusted correlation analysis for cirrhosis, we found statistically significant ($p < 0.05$) associations for ApoA1 with CLT ($r = -0.24$), PAI-1 ($r = -0.29$), tPA ($r = -0.22$) and PLG ($r = 0.39$, $p < 0.001$), for triglycerides with CLT ($r = 0.32$), and for LDL ($r = 0.29$) and Lp(a) ($r = 0.28$) with PLG. In sepsis, LDL ($r = 0.53$), VLDL ($r = 0.44$), Lp(a) ($r = 0.48$), total cholesterol ($r = 0.52$) and triglycerides ($r = 0.44$) correlated with PLG.
Conclusion: Progressive cirrhosis was characterized by a shift toward impaired fibrinolysis and declining lipid levels. ApoA1 showed inverse, and triglycerides, LDL, and Lp(a) positive, associations with fibrinolytic parameters, consistent with prior experimental and non-cirrhotic human studies. Our findings suggest that dyslipidemia is linked to impaired fibrinolysis in cirrhosis which may contribute to thrombosis risk, warranting further mechanistic studies.

FRI-397-YI
Increased ceftriaxone exposure in hospitalised patients with decompensated cirrhosis compared to patients without cirrhosis revealed by population pharmacokinetic modelling (TACTILE study)
Solaiman Ezzafzafi[1], Reinier van Hest[1], Ron Mathôt[1], Midas B. Mulder[2], Brenda De Winter[3], Joost PH Drenth[1], Raoel Maan[3], Marten Lantinga[1]. *[1]Amsterdam UMC, Amsterdam, Netherlands; [2]Haaglanden MC, Den Haag, Netherlands; [3]Erasmus MC, Rotterdam, Netherlands*
Email: s.ezzafzafi@amsterdamumc.nl

Background and aims: Bacterial infections are a leading cause of decompensation and mortality in patients with cirrhosis. Guidelines recommend adequate antibiotic treatment, but pathophysiological changes in decompensated cirrhosis alter drug pharmacokinetics (PK), potentially resulting in unpredictable and complex drug behaviour. Ceftriaxone (CFX) is widely used in decompensated cirrhosis, however liver-related alterations may affect the PK despite predominant renal clearance. There is limited PK data to inform proper dosing in liver cirrhosis. This study investigated whether CFX exposure was changed in patients with cirrhosis compared to hospitalised patients without cirrhosis. Funding: Gastrostart (24-2023).
Method: The TACTILE study is a multicentre observational study in hospitalised patients with decompensated cirrhosis and ascites treated with intravenous CFX 2 g/day. Waste material blood samples were collected to measure unbound (pharmacologically active) CFX plasma concentrations (CFX_u). A published population PK (popPK) model developed in non-cirrhosis patients was used to predict CFX_u in patients with cirrhosis. Measured CFX_u were compared with model-predicted CFX_u, and bias (mean prediction error, MPE) and precision (normalised root mean squared error, NRMSE) were assessed as measures of predictive performance. In case of significant bias and/or imprecision, the popPK model would be refitted with the obtained CFX_u to assess differences in PK.
Results: The analysis included 75 CFX_u measurements from 19 patients with cirrhosis (median age 62 years [IQR 50–71], eGFR 84 mL/min/1.73 m^2 [IQR 51–106], MELD-Na score 18 [IQR 16–25], n = 7 Child-Pugh B and n = 12 Child-Pugh C). Measured CFX_u in patients with cirrhosis (range 1–76 mg/L) were significantly underestimated by the popPK model in non-cirrhosis patients, with a MPE of −25% [95% CI −38 to −11] and substantial imprecision of 79% (NRMSE; 95% CI 68–89). Refitting the popPK model revealed CFX_u clearance in patients with cirrhosis to be 4.2 L/h (95% CI 3.5–5) compared to 7.2 (95% CI 6.3–8.2) L/h in the population of non-cirrhosis patients that served as a basis for development of the original popPK model.
Conclusion: CFX exposure is higher in hospitalised patients with decompensated cirrhosis when compared to patients without cirrhosis. This finding reveals that renally cleared drugs warrant cirrhosis-specific dosing recommendations and challenges the assumption that drugs independent of liver metabolism are unaffected by advanced chronic liver disease.

FRI-398
Comparing the intrahepatic effects of carvedilol and simvastatin in experimental liver cirrhosis
Yeldos Nulan[1,2,3], Eric Felli[2,3], Cong Wang[2,2], Sonia-Emilia Selicean[2,3], Manuel Prampolini[1,2,3], Annalisa Berzigotti[2,3], Jordi Gracia-Sancho[2,3,4], Jaime Bosch[2,3]. *[1]Graduate School for Cellular and Biomedical Sciences (GCB), University of Bern, Bern, Switzerland; [2]Department of Visceral Surgery and Medicine, Inselspital, Bern University Hospital, University of Bern, Bern, Switzerland; [3]Department for BioMedical Research, Hepatology, University of Bern, Bern, Switzerland; [4]Liver Vascular Biology Research Group, CIBEREHD, IDIBAPS Research Institute, Barcelona, Spain*
Email: nulan.yeliduosi@unibe.ch

Background and aims: Portal hypertension (PH) arises primarily due to increased intrahepatic vascular resistance (IHVR) driven by structural alterations, such as architectural remodeling due to hepatic stellate cells (HSCs) activation, and elevated hepatic vascular tone resulting from liver sinusoidal endothelial cells (LSECs) dysfunction. Non-selective-beta-blockers (NSBBs) lower PH through extrahepatic actions. Recently, in experimental cirrhosis, we found that carvedilol, a newer generation NSBB with additional anti-alpha1-adrenergic activity, achieves a superior reduction in portal pressure (PP) compared to traditional NSBBs by decreasing IHVR. Simvastatin, a type of HMG-CoA reductase inhibitor, is well established in reducing IHVR by 1) improving LSECs phenotype and increasing NO release, and 2) deactivating HSCs, both through the Krüppel-like factor 2 (KLF2) transcription pathway. This study aims to evaluate the potential synergistic effects of carvedilol and simvastatin in reducing HSCs and LSECs activation and dysfunction both in vitro and in vivo in a rat model of cirrhosis.
Method: *In vitro*: LSECs and HSCs were isolated from cirrhotic rats (i.p. thioacetamide 12 weeks) and then cultured with carvedilol (C)/simvastatin (S)/carvedilol plus simvastatin (C+S) for 24 hours. Endothelial function was assayed by NO bioavailability. Cell contraction assays were performed in cirrhotic HSCs. (n = 3–5). *In vivo*: hepatic hemodynamics were assessed in cirrhotic rats treated with carvedilol (10 mg/kg/day) or simvastatin (25 mg/kg/day) or carvedilol plus simvastatin for 2 weeks (n = 6–9). Hepatic remodeling was evaluated by measuring the collagen proportionate area (CPA), and HSCs activation were assessed via immunofluorescence detection of alpha-smooth muscle actin (α-SMA) in liver sections.
Results: In vitro: NO release was increased in all experimental groups vs vehicle, by 2.2, 2.3 and 2.2 fold-change respectively. HSCs cell contraction was reduced by 49% in C,78% in S, and 84% in C+S. In vivo: All treatments reduced PP by 29.7% (C), 16.9% (S), and 29.5% (C+S). CPA-positive area in liver tissue slides was reduced by 35.1%, 35.0% and 26.4% respectively. αSMA-positive area was reduced by 33.5%, 32.7%, and 32.5% respectively (all $p < 0.05$).
Conclusion: These results indicate that combined carvedilol and simvastatin treatment is comparable to their individual effects, ameliorating endothelial function and reducing hepatic stellate cell activation and support further characterization of their synergistic effects.

FRI-399

Neutrophil-derived miR-223 suppresses inflammasome activation and ameliorates pyroptotic cell death in peritoneal macrophages during spontaneous bacterial peritonitis

Mick Frissen[1], Majda El Hassani[1], Karsten Große[1], Philipp Reuken[2], Stefanie Quickert[2], Johanna Reißing[1], Oluwatomi Ibidapo-Obe[1], Tony Bruns[1]. *[1]University Hospital RWTH Aachen - Department of Internal Medicine III, Aachen, Germany; [2]University Hospital Jena - Department of Internal Medicine IV, Jena, Germany*
Email: mfrissen@ukaachen.de

Background and aims: Spontaneous bacterial peritonitis (SBP) is a frequent complication of decompensated cirrhosis often precipitating acute-on-chronic liver failure. While the peritoneal influx of neutrophils is a hallmark of peritonitis, the regulatory signaling between infiltrating cells and resident peritoneal macrophages (PMφ) remains poorly defined. We hypothesized that microRNAs (miRNAs) serve as local mediators in this peritoneal immune crosstalk.
Method: We performed multiplex microRNA profiling on paired serum and ascitic fluid samples from patients with decompensated cirrhosis before and during SBP, and candidate miRNAs were validated using qRT-PCR. To dissect cellular origin and functional impact, we utilized primary human neutrophil and PMφ *ex vivo* models as well as mechanistic studies using miRNA mimic technology.
Results: miRNA profiling revealed a distinct peritoneal miRNA landscape during SBP, characterized by a significant enrichment of miR-223 in ascites but not in serum. We identified infiltrating neutrophils as the primary source of extracellular miR-223. *In vitro*, isolated PMφ exposed to conditioned medium from circulating neutrophils of patients with SBP exhibited robust inflammatory gene expression and inflammasome activation, which was ameliorated by a synthetic miR-223 mimic, which suppressed *NLRP3* expression and abrogated Caspase-1-mediated pyroptosis.
Conclusion: Our findings define an intercellular resolution circuit in SBP, wherein infiltrating neutrophils release miR-223 to act as a molecular brake on resident macrophages. By dampening NLRP3 inflammasome activation and preventing pyroptosis, this paracrine transfer limits excessive peritoneal inflammation.

FRI-400

IGF1r receptor is involved in the Th17-mediated response in chronic liver disease

Ani Gasparyan[1,2,3], Oriol Juanola[1,2], Paula Boix[1,2], Isabel Gómez-Hurtado[1,2], Manuel Sánchez[1], Albina Espana[1], Esther Caparrós[1,2], Rubén Francés[1,2]. *[1]Laboratorio de Inmunobiología Hepática e Intestinal, Departamento de Medicina Clínica, UMH, San Juan, Spain; [2]ISABIAL Investigación en Inmunobiología Hepática e Intestinal, Alicante, Spain; [3]Departamento de Farmacología, UMH, San Juan, Spain*
Email: rfrances@umh.es

Background and aims: The immune system plays a key role in the development of chronic liver disease (CLD) orchestrating the transition from compensated to decompensated disease. One of the main factors involved in the regulation of Th17-Treg balance is the insulin-like growth factor (IGF) system. However, the exact role of the IGF1-IGF1r pathway in CLD remains unclear. Therefore, the main goal of this study was to further explore the role of the IGF1-IGF1r duo in regulating the functionality and maintenance of Th1y cells, as well as the interaction with other liver damage-associated ligands in a model of experimental cirrhosis.
Method: Two experimental approaches were used. Firstly, an animal model of experimental cirrhosis by CCL4 administration was carried out in a total 20 C57BL/6J male mice (6–8 weeks of age). And, secondly, an in vitro model was used to stimulate naïve T cells differentiation into Th17 cells simulating the pro-inflammatory microenvironment in the liver. These cells were used to co-culture with hepatocyte and to evaluate Th17-mediated response under different experimental conditions. Flow cytometry, relative RNA gene expression, western blotting and ELISA were used.
Results: Flow cytometry studies revealed higher expression of IGF1r receptors in Th17 cells from spleens of cirrhotic mice vs controls (12.7 ± 1.4 vs. 1.4 ± 0.7 units, $p < 0.0001$) and a higher percentage of IGF1r+ cells ((24.9 ± 0.2 vs. 16.1 ± 0.7%, $p = 0.0009$). An increase in the gene expression of Igf1r (6.1 ± 3.9 vs. 1.1 ± 0.5 units, $p = 0.0003$) and Igf1 (2.2 ± 0.7 vs. 1.1 ± 0.3 units, $p = 0.0001$) were observed in co-cultured lymphocytes and hepatocytes, respectively. In addition, higher IGF1 ligand levels were observed in the co-culture supernatant (0.32 ± 0.01 vs. 0.27 ± 0.02 units, $p = 0.0001$). Ligand-exposure studies revealed a synergistic action between IGF1r and TLR4 in Th17, as IGF1 ligand increased IL-17 expression but even higher IL-17 was observed with the combination of IGF1 and HMGB1 ligands (19.7 ± 0.9 vs. 14.65 ± 1.0 units, $p = 0.0003$). The use of IGF1r antagonist reduced IL-17 expression compared to controls (5.17 ± 1.64 vs. 16.8 ± 5.0 units, $p = 0.012$).
Conclusion: Blocking IGF1r reduces the activity of primary differentiated Th17 lymphocytes. Given the synergistic activity of IGFr1 with other innate receptors, its modulation may constitute a new tool for reducing Th17 expansion present during advanced CLD.

FRI-401-YI

Whole blood, microglial and astrocytic, transcriptomics and metabolomics reveals the association of type I interferon-associated immune-metabolic reprogramming in overt hepatic encephalopathy

Meiqian Hu[1], María Pilar Ballester[2], Anindro Bhattacharya[3], Ferran Aguilar[4], Francois Fenaille[5], Cristina Sanchez-Garrido[4], Richard Moreau[4], Vicente Arroyo[4], Victor Vargas Blasco[6], Wim Laleman[7], Joan Claria[4], Jonel Trebicka[4], Juan Antonio Carbonell-Asins[8], Christopher F. Rose[9], Rajiv Jalan[1].
[1]University College London; Royal Free Campus, Institute for Liver and Digestive Health, London, United Kingdom; [2]Digestive Disease Department, Hospital Clínico Universitario de Valencia, Valencia, Spain; [3]University of Pennsylvania, Department of Bioengineering, Philadelphia, United States; [4]European Foundation for the Study of Chronic Liver Failure (EF CLIF), Barcelona, Spain; [5]Université Paris-Saclay, CEA, INRAE, Département Médicaments et Technologies pour la Santé, MetaboHUB, Gif-sur-Yvette, France; [6]Facultad de Medicina, Unidad docente Vall d'Hebron, Universidad Autónoma de Barcelona, Barcelona, United Kingdom; [7]Department of Gastroenterology & Hepatology, Division of Liver & Biliopancreatic disorders and Liver Transplantation, University Hospitals Leuven, KU LEUVEN, Leuven, Belgium; [8]INCLIVA Biomedical Research Institute, Valencia, Spain; [9]Hepato-Neuro Laboratory, CRCHUM, Université de Montréal, Montreal, Canada
Email: humeiqian@zju.edu.cn

Background and aims: Overt hepatic encephalopathy (OHE) is a severe neuropsychiatric complication of decompensated cirrhosis. Beyond hyperammonemia, increasing evidence suggests that systemic immune dysregulation and metabolic alterations contribute to its pathogenesis. We aimed to characterize the immune-metabolic landscape associated with OHE using integrative multi-omics analyses.
Method: Transcriptomic profiling was performed in 78-patients with decompensated cirrhosis from the PREDICT cohort, comparing patients with OHE and age- and sex-matched non-OHE controls (1:2). Differential expression, pathway enrichment (GO and KEGG), and gene set enrichment analyses were conducted. In a subset of 37-patients with paired transcriptomic and metabolomic data, integrative analyses were used to explore immune-metabolic interactions. Transcriptomic data from microglia and astrocytes isolated from bile duct ligation (BDL) and sham-operated mice were analyzed for supportive validation.
Results: Whole blood transcriptomics revealed that OHE was characterized by robust activation of type I interferon signaling and innate antiviral responses, including upregulation of interferon-stimulated genes, RIG-I-like receptor signaling components, and chemokines involved in immune cell recruitment. Genes related to tryptophan metabolism (IDO1, IL4I1) were significantly upregulated. Gene set enrichment analysis further confirmed enhanced innate immune and interferon responses, accompanied by downregulation of pathways related to glial and astrocyte differentiation. Metabolomic profiling identified distinct metabolic alterations in OHE, with prominent enrichment of pathways related to carnitine synthesis, ammonia recycling, amino-acid and purine metabolism. Integrative correlation analysis demonstrated significant associations between interferon-related genes and metabolites involved in carnitine metabolism and the tryptophan-kynurenine pathway. In keeping with the systemic data, interferon-stimulated genes, including Mx1, were markedly upregulated in microglia and astrocytes from BDL mice.
Conclusion: OHE is associated with a systemic type I interferon-driven immune activation coupled with metabolic reprogramming. These alterations may contribute to impaired glial homeostasis and neuroinflammation, providing important mechanistic insights into the pathogenesis of OHE and potential therapeutic targets related to type 1 interferon and tryptophan metabolism pathways.

FRI-402

A peritoneal macrophage-Th1/Th17 axis drives inflammation in spontaneous bacterial peritonitis

Oluwatomi Ibidapo-Obe[1], Majda El Hassani[1], Johanna Reißing[1], Mick Frissen[1], Haedge Frederic[1], Mohamad Murad[1], Karsten Grosse[1], Tony Bruns[1]. *[1]Department of Internal Medicine III, University Hospital RWTH, Aachen, Germany*
Email: oibidapo@ukaachen.de

Background and aims: Bacterial infections like spontaneous bacterial peritonitis (SBP) are a major cause of morbidity and mortality in cirrhosis. We investigated the phenotype and function of peritoneal T helper cells in ascitic fluid (AF) and their interaction with peritoneal macrophages during SBP.
Method: We profiled blood and AF T helper cells from cirrhosis patients with and without SBP using unsupervised mass cytometry (CyTOF) and flow cytometry. Cytokines and chemokines were quantified in plasma and AF by Luminex and ELISA. Sorted AF T helper cell subsets were analysed by sequencing. To mimic peritoneal infection, we co-cultured AF CCR6$^+$ CD4$^+$ T cells with autologous macrophages and heat-killed *E. coli*.
Results: Peritoneal, resident-like CD69$^+$ T helper cells were abundant in AF compared to blood and showed heterogeneous CD127 expression. Unlike their CD127lo counterparts, CD4$^+$ CD69$^+$ CD127$^+$ cells displayed an activated effector phenotype, co-expressing CCR6 with CD161, CD49a, and CXCR3. Upon stimulation, these cells produced both IL-17 and IFN-γ, and gene profiling confirmed a pathogenic Th1/Th17 signature distinct from circulating T cells. During SBP, these Th1/Th17 cells (CD4$^+$ CXCR3$^+$ CCR6$^+$) were enriched in AF but not blood. Peritoneal levels of the CCR6 ligand CCL20 correlated with the severity of local and systemic inflammation. In vitro, *E. coli*-exposed macrophages produced CCL20 and pro-inflammatory cytokines, which enhanced IFN-γ and IL-17 production by co-cultured CCR6$^+$ T cells.
Conclusion: Our findings reveal a macrophage-Th1/Th17 inflammatory circuit in SBP, driven by CCL20-mediated recruitment and sustained by macrophage-derived cytokines. Peritoneal CCR6$^+$ T helper cells represent a key driver of peritoneal inflammation and a potential target for modulating immunity in cirrhosis-associated infections.

FRI-403

Ascites bactericidal capacity in patients with decompensated cirrhosis

Isanka Ratnasekera[1], Min-Duy Phan[2,3], Nhu Nguyen[2,3], Eline Jessen[1], Sahar Keshvari[1], Yvette Ong[4], Timothy Kidd[5], Steven Hancock[2,3], David Hume[1], Elizabeth Powell[6], Matthew Sweet[2,3], Mark Schembri[2,3], Katharine Irvine[1,3]. *[1]Mater Research - The University of Queensland, Brisbane, Australia; [2]Institute for Molecular Bioscience, The University of Queensland, Brisbane, Australia; [3]Australian Infectious Diseases Research Centre, The University of Queensland, Brisbane, Australia; [4]School of Biomedical Sciences, Queensland University of Technology, Brisbane, Australia; [5]School of Chemistry and Molecular Biosciences, The University of Queensland, Brisbane, Australia; [6]QIMR-Berghofer Medical Research Institute, Brisbane, Australia*
Email: katharine.irvine@uq.edu.au

Background and aims: Patients with decompensated cirrhosis are at high risk of developing bacterial infections. The most common infection is spontaneous bacterial peritonitis (SBP) in ascites fluid, caused by gut bacterial translocation. We aimed to investigate the bactericidal activity of cell-free ascites fluid and ascites macrophages.
Method: We performed bacterial killing assays using cell-free ascites fluid or ascites macrophages from patients with decompensated cirrhosis without active infection. We performed a genetic screen for EXPEC and K. pneumoniae genes that confer resistance to ascites fluid killing and validated novel targets in patient samples and in vivo in a mouse model.

Results: Non-pathogenic *Escherichia coli* K12 was rapidly killed in cell-free ascites fluid, associated with complement deposition, but ExPEC and *K. pneumoniae* strains were completely resistant to killing. A transposon-based genome-wide screen identified a requirement for genes involved in O-antigen biosynthesis for survival of both organisms in cell-free ascites fluid, including the transcription factor RfaH, which controls expression of surface polysaccharides. Although ExPEC were resistant to fluid-mediated killing, ascites macrophages, especially VSIG4^{Hi} cells, phagocytosed and killed ExPEC and non-pathogenic *E. coli* with similar efficacy. Mice with toxin-induced cirrhosis had higher bacterial burdens in the liver than control mice when infected with ExPEC, but rapidly cleared an *rfaH* mutant attenuated for capsule and O-antigen biosynthesis.
Conclusion: Together, these data identify critical roles for capsule and O-antigen in host evasion by SBP-associated pathogens. While pathobionts may cause infections in some patients with decompensated cirrhosis, especially those with impaired cellular immunity, many patients may be able to effectively defend against translocating intestinal commensal bacteria. Targeting bacterial virulence factors and/or host macrophage functions may reduce the risk of SBP in cirrhosis.

FRI-404

Lymphatic vessel dilatation with Rspo3-Wnt dysregulation drives impaired intestinal regeneration in cirrhosis-associated portal hypertensive duodenopathy

Deepika Jakhar[1], Pinky Juneja[1], Aarti Sharma[1], Simran Sharma[1], Ahona Roy[1], Phool Chand[1], Archana Rastogi[1], Vikram Bhatia[1], Savneet Kaur[1]. [1]*Institute of Liver & Biliary Sciences, New Delhi, India*
Email: savykaur@gmail.com

Background and aims: Portal hypertensive duodenopathy (PHD), a common complication of portal hypertension and cirrhosis, involves mucosal and vascular alterations, with largely undefined pathogenic mechanisms. Emerging evidence has identified intestinal lymphatic vessels (LVs) as critical regenerative niche; however, their role in PHD remains ambiguous. This study aimed to investigate the association between duodenal LVs and intestinal regeneration in patients with cirrhosis and PHD.
Method: A total of 30 patients with liver cirrhosis and 15 control subjects (dyspepsia) were recruited. All subjects underwent upper gastrointestinal endoscopy and were assessed for PHD. Intestinal stem cells marker (Lgr5), LV density and diameter (podoplanin score-sum of intensity and density of pdpn+ vessels), along with gene expression of regeneration factors were analyzed in biopsies from the second part of duodenum (D2) by IHC and RT-PCRs.
Results: Controls had normal endoscopic findings and among cirrhosis patients, 50% showed ulcers, red and/or white spots, erythema, and mucosal edema. Cirrhosis patients had higher dilated pdpn+ LV histological score versus controls (5.9 ± 1.1 vs 2.1 ± 0.5. p = 0.04). As compared to controls, cirrhotics showed thickened mucosa and decreased villi:crypt ratio (2.4 + 0.24 vs 0.8 ± 0.2, p = 0.02). Endoscopically, most patients (but not all) with higher pdpn score showed D2-lymphangiectasia spots. We did not observe any other correlation between pdpn score and endoscopy findings in patients. Expression of the intestinal stem marker, Lgr5 was decreased in patients with cirrhosis as compared to controls (3 fold, p = 0.05). Gene expression of intestinal repair and injury factors secreted by Paneth cells, Notch-2 (18 fold, p = 0.02), BMP-2(20 fold, p = 0.01), EGF(2 fold, p = 0.05) were increased in cirrhotics vs controls. However, expression of lymphangiogenic factors, Rspo3 (6 fold, p = 0.02) and Wnt2b (6 fold, p = 0.02) was decreased in patients as compared to controls.
Conclusion: A high duodenal LV density is a common feature in patients with cirrhosis, irrespective of the endoscopic findings. Despite activation of Notch signaling, impaired lymphangiocrine Rspo3–Wnt signaling likely drives mucosal injury and defective intestinal stem cell–mediated regeneration leading to PHD in some of these patients.

FRI-409-YI

Insulin-like growth factor 1 suppression worsens with cirrhosis severity and mortality, and therapeutic restoration improves outcomes in decompensated cirrhosis: a clinical-experimental study

Parminder Kaur[1], Wenting Tan[2], Pratibha Garg[1], Abeba Habtesion[2], Pinaki Dutta[1], Cornelius Engelmann[2], Gaurav Sharma[1], Alexandra Phillips[2], Naveen Kalra[1], Rui Zhang[3], Takayuki Kondo[2], Guohong Deng[3], Yunjie Dan[3], Sunil Taneja[1], Fausto Andreola[2], Ajay Kumar Duseja[1], Rajeshwar Prosad Mookerjee[2], Virendra Singh[1], Rajiv Jalan[2], Nipun Verma[1]. [1]*Post Graduate Institute of Medical Education and Research, Chandigarh, India;* [2]*Institute for Liver and Digestive Health, University College London, Royal Free Campus, London, United Kingdom, London, United Kingdom;* [3]*Department of Infectious Diseases, Southwest Hospital, Third Military Medical University, Chongqing, Chongqing, China*
Email: r.jalan@ucl.ac.uk

Background and aims: Insulin-like growth factor 1 (IGF-1) is reduced in advanced cirrhosis but its role in mediating hepatic inflammation, senescence and liver regeneration is unknown. This clinic-experimental study explores the role of IGF-1 in disease progression and evaluated outcomes of restoring IGF-1 axis.
Method: This study has 4 study parts. 1. Circulating IGF-1 was measured in 2-patient cohorts - (China; n = 221) (India; n = 257) and related to disease severity and mortality. 2. 2-models of cirrhosis (bile-duct ligation and CCL4) and lipopolysaccharide (LPS)-induced acute-on-chronic liver failure (ACLF) were used to test TLR4 (YAQ005) and RIPK1 inhibition (necrostatin-1) and impact on IGF-1 axis. 3. Effect of rhIGF-1 restoration on liver function, fibrosis, survival, liver and muscle transcriptomics was assessed. 4. Decompensated cirrhosis patients were randomized to standard medical therapy (SMT) or adjunct growth hormone (GH) 2 IU/day, titrated to normal IGF-1; primary endpoint: complication-free survival (CFS).
Results: 1. In both cohorts, IGF-1 levels declined stepwise from chronic hepatitis to stable cirrhosis to acute decompensation (AD) (all p < 0.05), and lower IGF-1 independently predicted 28-, 90-, 180-, and 365-day mortality.
2. In animal-models, hepatic IGF-1 expression decreased in ACLF (3.4-fold and 2.3-fold; p < 0.05); TLR4 or RIPK1 inhibition reduced mortality significantly and restored hepatic IGF-1.
3. rhIGF-1 improved reduced fibrosis (p < 0.05), lowered ammonia (p = 0.045), and improved coma-free survival (85.7% vs 33.3%; p = 0.048). Hepatic transcriptomics confirmed downregulation of injury, senescence and inflammatory pathways; muscle transcriptomics identified pathways related to cellular stress responses, inflammatory signalling, and muscle development.
4. At 12-months, CFS improved with GH vs SMT (HR 0.57; 0.34 to 0.96; p = 0.035). Patients who normalized IGF-1 on GH (responders; n = 22) had higher CFS vs SMT (77.0% vs 22.2%; HR 0.19; p = 0.001). GH prevented AD or ACLF occurrence (sHR 0.47; p = 0.010) with highest benefit in IGF-1 responders (sHR 0.04; p = 0.002). GH also improved the skeletal muscle index, liver frailty, myostatin, cell death, and neutrophil phagocytic capacity with maximal effects in IGF-1 responders. Fewer serious adverse events were noted in GH vs SMT group (23.9% vs 50.0%; p = 0.018).
Conclusion: Downregulation of IGF-1 axis is a pathophysiologically relevant feature of decompensated cirrhosis and data supports later phase clinical trials of IGF-1 in this condition.

FRI-410-YI

Circulating bile-acid profiles delineate disease severity and identify a metabolic fingerprint of ACLF

Georgios Konstantis[1], Moritz Passenberg[1], Maiju Myllys[2], Zaynab Hobloss[2], Jörg Reinders[2], Ahmed Ghallab[2,3], Andreas Schütte[1], Nargiz Nuruzade[1], Clara Guntlisbergen[1], Björn Jung[1], Benedikt Hild[1], Jan Best[1], Katharina Willuweit[1], Hartmut Schmidt[1], Jan G. Hengstler[2], Jassin Rashidi-Alavijeh[1]. [1]*Department of Gastroenterology, Hepatology and Transplant Medicine, Medical Faculty, University of Duisburg-Essen, Duisburg, Germany, Essen, Germany;* [2]*Department of Toxicology, Leibniz Research Centre for Working Environment and Human Factors, Technical University Dortmund, Dortmund, Germany, Dortmund, Germany;* [3]*Forensic Medicine and Toxicology Department, Faculty of Veterinary Medicine, Qena University, Qena, Egypt, Qena, Egypt*
Email: georgios.konstantis@uk-essen.de

Background and aims: Bile-acid (BA) synthesis, conjugation and microbiome-dependent transformation are tightly linked to liver function and become progressively disrupted with advancing chronic liver disease. However, comprehensive data on circulating BA patterns across the full spectrum of cirrhosis remain limited. We aimed to characterize BA profiles across compensated and decompensated stages and to determine whether they delineate disease severity and define an ACLF-specific metabolic signature.
Method: Circulating BA were quantified across compensated cirrhosis (194), non-acute decompensation (111), acute decompensation (AD, 48), and acute-on-chronic liver failure (ACLF, 41). Between-group differences were assessed with false discovery rate (FDR) control. Global metabolic structure was explored using unsupervised dimensionality reduction and clustering. Supervised models were applied to derive phenotype-specific BA signatures and to evaluate discrimination of ACLF and ACLF grades using ROC analyses. Pathway enrichment was assessed using established metabolomics tools.
Results: Multiple BA differed significantly across disease stages after FDR correction, indicating progressive BA remodeling with worsening cirrhosis. The dominant signal was a marked depletion of secondary BA with progression to decompensation, reaching lowest levels in ACLF (e.g. DCA, LCA, GDCA, GLCA). In parallel, conjugated primary BA were relatively enriched in ACLF, most notably TCDCA and TCA. Unsupervised analysis revealed a strong structure (PC1–2 ~ 54% of variance) and identified two metabolically distinct clusters associated with clinical stage (Cramér's V = 0.39), separating compensated from decompensated disease. Supervised modeling yielded the strongest discrimination for ACLF (AUROC 0.79), defining an interpretable ACLF-specific fingerprint combining increased conjugated primary BA and reduced secondary BA. Discriminatory performance increased with ACLF grade for key BA (e.g. TCDCA AUROC 0.63 for ACLF-1 vs AD and 0.88 for ACLF-3 vs AD). Infection status did not modify the ACLF-associated BA pattern. Pathway analysis identified primary BA biosynthesis as the only significantly enriched pathway.
Conclusion: Circulating BA profiles exhibit a strong, severity-aligned pattern across the cirrhosis spectrum. ACLF is characterized by a distinct metabolic fingerprint marked by loss of secondary and enrichment of conjugated primary BA, reflecting ACLF disease biology and severity.

FRI-411

Systemic markers of fibroblast- and immune cell activity in post-TIPS endotyping within patients with severe clinical evolution

Alejandro Mayorca Guiliani[1], Christian Labenz[2], Eva Maria Schleicher[2], Paul Schneider[2], Jasmin Soehngen[2], Michael Bernhard Pitton[3], Julia Weinmann-Menke[2], Peter R. Galle[2], Simon Johannes Gairing[2], Myriam Meineck[2], Diana Julie Leeming[1], Morten Karsdal[1]. [1]*Nordic Bioscience A/S, Herlev, Denmark;* [2]*Department of Internal Medicine I, University Medical Center of the Johannes Gutenberg-University Mainz, Mainz, Germany, Mainz, Germany;* [3]*Department of Radiology, University Medical Center of the Johannes Gutenberg-University Main, Mainz, Germany, Mainz, Germany*
Email: christian.labenz@unimedizin-mainz.de

Background and aims: Transjugular intrahepatic portosystemic shunt (TIPS) is an established treatment for cirrhosis complications, such as ascites or variceal bleeding. Circulating extracellular matrix (ECM) biomarkers may aid in identifying patients with poor post-TIPS prognosis by endotyping patients according to ECM remodeling activity.
Method: 89 patients living with cirrhosis undergoing TIPS at the University Hospital Mainz were enrolled and followed for further decompensation, hepatic encephalopathy (HE), ascites, variceal bleeding and death/liver transplantation. Serum collected at TIPS placement and outpatient visits was analyzed for white blood cell count, IL-6, IL-8, C-reactive protein, ammonia, bilirubin, creatinine, fibroblast activity (nordicPRO-C3, nordicPRO-C6), neutrophil activity (CPa9-HNE), macrophage activity (VICM), and ECM degradation biomarkers of type III and IV collagen (nordicC3M, nordicC4M, nordicCTX-III). Unsupervised k-means clustering was applied to baseline variables to define patient clusters, subsequently assessed for associations with post-TIPS outcomes using Kaplan–Meier survival analysis and multivariable Cox proportional hazards models
Results: Median age was 62 (52–67 yo), predominant etiology was alcohol related liver disease (ALD) (56%) and predominant indication was ascites (88%). We identified 3 clusters (1 = 29, 2 = 35, 3 = 25). Cluster 1, (*fibrogenic*), was characterized by high PRO-C3, C3M and PRO-C6, suggesting high fibroblastic activity. Cluster 2 (*quiescent*) had lower ECM biomarkers but high ammonia, albumin and bilirubin. Cluster 3 (*fibrolytic*) had a high ECM degradation and immune activation profile. Kaplan–Meier analysis showed a significantly lower and delayed HE incidence in the fibrolytic cluster compared with the other two (log-rank p = 0.013); in contrast, Cox regression identified the fibrogenic cluster as having a significantly higher risk of further decompensation (p = 0.016). In Cox regression analysis adjusted for MELD score and age, the quiescent cluster was not significantly associated with post-TIPS hepatic encephalopathy (HR 0.50, 95% CI 0.17–1.41; p = 0.20)
Conclusion: ECM biomarkers identified three endotypes, fibrogenic, quiescent, and fibrolytic. Patients in the fibrogenic cluster demonstrated an elevated risk of further decompensation and post-TIPS HE. The fibrolytic cluster was protective for developing HE. These findings suggest that ECM remodeling reflects post-TIPS disease activity and pathophysiology.

FRI-412

Balancing immune dysfunction in ACLF: ASK1 inhibitor SRT-015 mitigates inflammatory responses while enhancing immune antibacterial defenses

Vanessa Legry[1], Ophélie Hanot[1], Berta Romero-Grimaldo[2], Cristina López-Vicario[2], Bryan J. Contreras[2], María Belén Sánchez-Rodríguez[2], Carlos Rojano-Alfonso[2], Ines Vanhille-Campos[2], Richard Moreau[3], Jean-Marie Brusq[1], Bart Staels[4], Sakina Sayah Jeanne[1], Joan Clària[2]. [1]*GENFIT SA, LOOS, France;* [2]*Hospital Clinic-IDIBAPS, Universitat de Barcelona, European Foundation for the Study of Chronic Liver Failure (EF CLIF), Barcelona, Spain;* [3]*European Foundation for the Study of Chronic Liver Failure (EF CLIF), Barcelona, Spain;* [4]*Université de Lille, Institut Pasteur de Lille, INSERM U1011, CHU Lille, Lille, France*
Email: vanessa.legry@genfit.com

Background and aims: Patients with cirrhosis develop significant immune dysfunction, characterized by the simultaneous presence of systemic inflammation, which correlates with disease progression, and immune paralysis, which increases the susceptibility to bacterial infections leading to complications such as acute-on-chronic liver failure (ACLF). Currently, there are limited therapeutic options addressing the underlying pathogenic mechanisms of ACLF. Given that systemic inflammation contributes to tissue damage in ACLF,

anti-inflammatory agents should halt disease progression, without exacerbating immune paralysis. SRT-015, an investigational Apoptosis Signal-Regulating Kinase 1 (ASK1) inhibitor, has demonstrated efficacy in reducing systemic inflammation and liver injury in preclinical models of liver failure and ACLF. This study aimed to further characterize the effect of SRT-015 on the functions of innate and adaptive immune cells using healthy donor blood cells as a proof-of-concept.

Method: The effects of SRT-015 (2–10 μM) on cytokine production and B cell and monocyte immunophenotype were assessed in peripheral blood mononuclear cells (PBMCs), while its actions on bacterial phagocytosis, degranulation and migration were tested in polymorphonuclear leukocytes (PMNs). The effects of SRT-015 on cytokine secretion and polarization were evaluated in monocyte-derived macrophages (MDM).

Results: In PBMCs, SRT-015 significantly reduced LPS-induced production of pro-inflammatory cytokines (IL-6, IL-1β, CXCL10, and TNFα), while shifting B-cell composition toward a memory phenotype, increasing memory B cells by 60% and decreasing naïve B cells by 34%. No changes in the composition of classical, intermediate or non-classical monocytes were observed. In PMNs, SRT-015 increased *E. coli* phagocytosis (+52%, p = 0.02) without negatively affecting complementary antibacterial effector functions, including degranulation and cell migration. In MDMs, SRT-015 significantly attenuated LPS-induced production of pro-inflammatory cytokines (IL-6, IL-1β, MIP-1α), while preserving IL-4 -driven macrophage M2 polarization.

Conclusion: This proof-of-concept study demonstrates the potential of the investigational drug SRT-015 to reduce systemic inflammation while enhancing antibacterial activity and preserving immune cell function, supporting its further development for advanced liver disease and ACLF.

FRI-413

Modulation of the gut microbiome by Yaq-001 ameliorates fecal microbiome transplant (FMT) induced liver injury from cirrhotic specific pathogen-free mice to germ-free mice

Jinxia Liu[1], Jose G Guevara[2], Haifeng Wu[3], Qin Jin[4], Huoyan Ji[5], Saeed Shoaie[2], Rajiv Jalan[6]. *[1]UCL Institute for Liver and Digestive Health, Upper third floor, Royal Free Campus, Rowland Hill Street, Hampstead, London, NW3 2PF, Nantong, China; [2]Centre for Host-Microbiome Interactions, Faculty of Dentistry, Oral & Craniofacial Sciences, King's College London, SE1 9RT, UK, London, United Kingdom; [3]Department of Gastroenterology, Affiliated Hospital of Nantong University, Nantong, 226001, China, Nantong, China; [4]Department of Pathology, Affiliated Hospital of Nantong University, Nantong, 226001, China, Nantong, United Kingdom; [5]Department of Laboratory Medicine, Affiliated Hospital of Nantong University, Nantong, 226001, China, Nantong, China; [6]UCL Institute for Liver and Digestive Health, Upper third floor, Royal Free Campus, Rowland Hill Street, Hampstead, London, NW3 2PF, London, United Kingdom*
Email: r.jalan@ucl.ac.uk

Background and aims: The gut microbiome is critically involved in the pathogenesis of liver diseases. Yaq-001, a non-absorbable, gut-restricted microbiome therapeutic, has demonstrated potential in restoring microbiome balance, mitigating endotoxemia, systemic inflammation, hepatic fibrosis, and liver cell death in specific pathogen-free (SPF) mice with liver cirrhosis. This study aims to investigate the mechanisms through which Yaq-001 modulates the liver-gut axis using FMT from SPF to germ-free (GF) mice.

Method: Two mouse models of cirrhosis were utilized: (a) SPF mice: carbon tetrachloride (CCl4)-induced cirrhosis for 6-weeks in SPF mice; *4 groups: control (n = 6), control-Yaq-001 (n = 6), CCl4 (n = 12), and CCl4-Yaq-001 (n = 12)*, and (b) GF mice: Fecal samples from SPF mice were used for FMT in GF mice for 9-weeks, combined with CCl4 administration for 3 weeks; *4 groups: FMT from SPF control (n = 6), FMT from SPF control-Yaq-001 (n = 6), FMT from SPF CCl4 (n = 10), and FMT from SPF CCl4-Yaq-001 (n = 10)*. Yaq-001 (0.4 g/100 g body weight per day) was administered to SPF mice for 6-weeks. Blood and tissue samples were collected for subsequent analysis of biochemistry, colonic and liver bulk RNA sequencing, and fecal samples for I6S RNA microbiome analysis.

Results: GF mice that received FMT from Yaq-001-pretreated, CCl4-exposed SPF mice donors exhibited markedly attenuated liver damage, as evidenced by significantly reduced serum ALT, hepatic fibrosis (CPA), apoptosis (TUNEL), and endotoxemia, compared to those receiving microbiota from untreated SPF-CCl4 donors. Microbiome analysis confirmed that Yaq-001 pretreatment reshaped microbial communities, enriching for beneficial taxa negatively correlated with injury biomarkers and depleting harmful taxa positively correlated with damage. Transcriptomic profiling revealed that Yaq-001's effects extended to host gene expression, modulating pathways involved in metabolism and stress response in both the liver and intestine. A key finding was the upregulation of intestinal Cyp2e1 following Yaq-001, which correlated negatively with injury markers.

Conclusion: The core mechanisms underlying the protective effect of Yaq-001 on inflammation and liver injury involves restructuring the gut microbiome, which in turn regulates host gene expression programs both locally and also in distant organs such as the liver. The data support its future development as a microbiome therapeutic for diverse diseases associated with dysbiosis.

FRI-414

Dual molecular targeting of Pttg1 and NO delivery restores hemodynamics, halts fibrogenesis and decreases liver steatosis in advanced liver disease

Manuel Macías-Herranz[1], Rocío García-Pérez[2], Andrea Díaz-Tendero[3], María Calvo[4], Gregori Casals[5], Cristina Fornaguera[6], Salvador Borrós[3], Wladimiro Jiménez[1], Guillermo Fernández-Varo[7]. *[1]Biochemistry and Molecular Genetics Service, Hospital Clínic of Barcelona, Institut d'Investigacions Biomèdiques August Pi i Sunyer (IDIBAPS), Barcelona, CIBEREHD, ISCIII, Madrid, Spain, Department of Biomedicine, University of Barcelona, Barcelona, Spain; [2]Hepatopancreatobiliary Surgery & Transplantation, General & Digestive Surgery Service, Digestive & Metabolic Disease Institute (ICMDM), Hospital Clínic of Barcelona, Barcelona, Spain; [3]Grup d'Enginyeria de Materials (Gemat), Institut Químic de Sarrià (IQS), Universitat Ramon Llull (URL), Barcelona, Spain; [4]Advanced Optical Microscopy-Clinic Campus, Scientific and Technological Center, University of Barcelona, Barcelona, Spain; [5]Biochemistry and Molecular Genetics Service, Hospital Clínic of Barcelona, Institut d'Investigacions Biomèdiques August Pi i Sunyer (IDIBAPS), Barcelona, CIBEREHD, ISCIII, Madrid, Spain, Department of Fundamental and Clinical Nursing, Faculty of Nursing, University of Barcelona, L'Hospitalet de Llobregat, Barcelona, Spain; [6]Grup d'Enginyeria de Materials (Gemat), Institut Químic de Sarrià (IQS), Universitat Ramon Llull (URL), Barcelona, Spain, Institució Catalana de Recerca i Estudis Avançats (ICREA), Barcelona, Spain; [7]Biochemistry and Molecular Genetics Service, Hospital Clínic of Barcelona, Institut d'Investigacions Biomèdiques August Pi i Sunyer (IDIBAPS), Barcelona, CIBEREHD, ISCIII, Madrid, Spain*
Email: gfvaro@recerca.clinic.cat

Background and aims: Advanced liver fibrosis is a critical stage in chronic liver disease progression, characterized by severe hemodynamic impairment, extracellular matrix accumulation, and increased risk of cirrhosis and hepatocellular carcinoma. Pituitary tumor transforming gene 1 (*Pttg1*) regulates fibrogenic and oncogenic pathways, while nitric oxide (NO) modulates vascular tone and cellular activation. We investigated the therapeutic potential of combining *Pttg1* silencing with NO delivery using poly(β-amino ester) nanoparticles functionalized with retinol (ret-pBAE NPs) for specific liver targeting in a rat model of advanced fibrosis.

Method: Twenty-three Wistar rats with CCl_4-induced fibrosis (plus phenobarbital for 17 weeks) were randomized to receive either *Pttg1* siRNA + NO donor-loaded ret-pBAE NPs (n = 12) or vehicle (n = 11).

Hemodynamic parameters (mean arterial pressure [MAP], portal pressure [PP]), serum liver function markers, hepatic collagen and steatosis, and expression of profibrogenic genes were assessed.
Results: Combined therapy significantly improved MAP (110 vs. 115 mmHg, $p < 0.001$) and reduced PP (10 vs. 7 mmHg, $p < 0.001$). ALT, AST and total bilirubin levels decreased markedly (225 vs. 85 U/L, $p < 0.01$; 445 vs. 199 U/L, $p < 0.01$; and 0.45 vs. 0.10 mg/dl, $p < 0.05$, respectively), indicating improved hepatic function. Hepatic collagen content and steatosis were reduced by 47% and 48%, respectively ($p < 0.001$). Molecular analysis revealed strong downregulation of *Pttg1* and key profibrogenic genes (*Col1alpha2, alpha-SMA, Dlk1, Pdgfrb, Timp1*). It is important to emphasize that the combined therapy elicited a significant upregulation of *Mmp2* and *Mmp9* expression, accompanied by a concomitant downregulation of *Timp1*. This modulation resulted in a substantial increase in the *Mmp2/Timp1* gene expression ratio, and an even more pronounced elevation in the *Mmp9/Timp1* ratio. Collectively, these findings indicate a perturbation in the transcriptional equilibrium governing extracellular matrix (ECM) turnover, thereby facilitating its accelerated degradation.
Conclusion: Dual targeting of *Pttg1* and NO delivery via ret-pBAE NPs exerts robust antifibrotic and hepatoprotective effects in advanced liver fibrosis. These findings support the translational potential of combined RNA interference and NO modulation strategies as innovative therapies for chronic liver disease.

FRI-415-YI

Bone marrow mitochondrial dysfunction drives pathogenic myelopoiesis and monocyte–macrophage dysfunction in cirrhosis

Manisha Manisha[1], Deepanshu Maheshwari[1], Nidhi Nautiyal[1], Sandeep Kumar[1], Sunidhi Diwakar[1], Rajni yadav[1], Vaibhav Tiwari[1], Anupama Kumari[1], Dinesh Mani Tripathi[1], Shiv Kumar Sarin[1], Anupam Kumar[1]. [1]*Institute of Liver and Biliary Sciences, New Delhi, India*
Email: dr.anupamkumar.ilbs@gmail.com

Background and aims: Cirrhosis is characterized by sustained recruitment of dysfunctional monocytes/macrophages that drive chronic inflammation, fibrosis progression, and failure of hepatic repair. Although demand-driven myelopoiesis is required to meet increased immune needs in chronic liver injury, the mechanisms by which this process becomes pathogenic at the level of the bone marrow(BM) remain unclear. We investigated whether dysfunction of BM hematopoietic stem and progenitor cells (HSPCs) underlies the generation of pathogenic monocyte–macrophages in cirrhosis, and whether correcting this dysfunction can reprogram pathogenic myelopoiesis toward a reparative phenotype.
Method: Proteomic and metabolomic profiling of cirrhotic HSPCs were performed to identify bioenergetic defects. Mitochondrial integrity and ultrastructure were characterized via flow cytometry and electron microscopy. Bone marrow derived Macrophages (BMDMs) functionality was evaluated using phagocytosis and efferocytosis assays. Therapeutic potential of Mesenchymal Stem Cells (MSCs) was investigated using in vitro and in vivo cirrhotic models. Efficacy was determined by assessing HSC expansion, macrophage functional restoration, and histological quantification of liver fibrosis and regeneration.
Results: Proteomic and metabolic profiling reveals significant bioenergetic defect in cirrhotic HSCs, characterized by the down-regulation of ETC,TCA enzymes and the coactivators PGC-1α and TFAM($p < 0.01$). Cirrhotic HSPCs exhibit elevated ROS levels, reduced mitochondrial mass and membrane potential($p < 0.01$).Electron microscopy revealed mitochondrial fragmentation in cirrhotic HSPCs. BMDMs from cirrhotic HSPCs exhibited dysfunctional phenotype with significantly impaired phagocytosis and efferocytosis($p < 0.05$). In vitro co-culture of MSCs and HSCs improves HSPCs bioenergetics through mitochondria transfer. In-Vivo, MSC infusion significantly expanded the HSC pool($p < 0.05$). BMDMs derived from rescued HSPCs showed increased phagocytosis($p < 0.001$) and efferocytosis ($p < 0.001$). Finally, Restoring BMDMs function via reprogramming of HSPCs led to a significant reduction in liver fibrosis ($p < 0.001$) and promotes hepatic regeneration ($p < 0.001$).
Conclusion: Bone marrow mitochondrial dysfunction drives pathogenic myelopoiesis and impaired monocyte–macrophage responses in cirrhosis. MSC-mediated restoration of hematopoietic mitochondrial health reprograms myelopoiesis toward a reparative state, reducing liver fibrosis and promotes hepatic regeneration.

FRI-416-YI

Treg metabolic dysfunction precedes cirrhosis-associated immune dysfunction: implications for therapeutic intervention

Diana Marin-Correa[1], Celio Xavier Da Costa Dos Santos[2], Ravi Kumar[2], Yoana Arroyo[3], Ada Sera Kurt[1], Jorge Torres[1], Alison Taylor[1], Mzamo Mbelle[1], Roberto Savoldelli[1], Evangelos Triantafyllou[4], Timothy Tree[3], Ajay Shah[2], Alberto Sanchez-Fueyo[1], Niloufar Safinia[1]. [1]*Roger Williams Institute of Liver Studies, Faculty of Life Science and Medicine, King's College London, London, United Kingdom;* [2]*Department of Cardiovascular Sciences, King's College London, London, United Kingdom;* [3]*Faculty of Life Science and Medicine King's College London, School of Immunology & Microbial Sciences, London, United Kingdom;* [4]*Faculty of Medicine Imperial College London, London, United Kingdom*
Email: diana.marin_correa@kcl.ac.uk

Background and aims: Chronic liver injury drives fibrosis through inflammation and oxidative stress, leading to cirrhosis. Advanced cirrhosis features cirrhosis-associated immune dysfunction (CAID), marked by systemic inflammation, innate immune paralysis, multi-organ failure, and increased mortality. We have shown that cirrhotic Tregs are functionally impaired due to dysregulated nuclear factor erythroid 2-related factor 2 (NRF2) signaling, a master regulator of antioxidant and metabolic responses. We hypothesize that NRF2 dysfunction in cirrhosis impairs Treg metabolic plasticity, preventing maintenance of immunosuppressive capacity within the pro-oxidant, metabolically dysregulated systemic milieu of CAID.
Method: Peripheral blood was obtained from healthy volunteers and patients stratified by Baveno VIII criteria: fibrosis (F3–4), compensated and decompensated advanced chronic liver disease (cACLD and dACLD). Acute-on-chronic liver failure (ACLF) samples served as positive CAID controls. After PBMC isolation, we measured: 1) monocyte phenotypic and functional profiling by flow cytometry; 2) Treg suppressive capacity by micro-suppression assays; 3) bulk RNA sequencing; 4) targeted metabolomics of cellular lysates and serum by LC-MS; and 5) metabolic profiling by SCENITH.
Results: ACLF monocytes displayed the classic CAID phenotype: upregulated inhibitory receptors (PD1, PDL1, MERTK), downregulated HLA-DR and CD86, and impaired phagocytosis and cytokine production. In contrast, cACLD monocytes were phenotypically and functionally equivalent to controls, confirming intact innate immunity. Despite preserved monocyte function, cACLD Tregs showed significantly reduced suppression, identifying an early Treg-intrinsic defect preceding innate dysfunction. Transcriptomic analysis revealed reprogrammed gene networks regulating suppressive function, stability, and metabolism. SCENITH showed diminished glycolytic capacity with compensatory increases in fatty acid oxidation and amino acid catabolism, consistent with metabolic stress adaptation in a chronic inflammatory milieu.
Conclusion: Treg dysfunction constitutes an early event in disease progression. Transcriptional and metabolic Treg reprogramming occurs during compensated disease when innate immunity remains otherwise intact, establishing Treg metabolic dysregulation as a early driver of CAID. These findings position metabolic intervention as a rational strategy to restore Treg function and limit immune-mediated hepatic injury in early-stage cirrhosis.

FRI-418

Inflammation and viscoelastic haemostasis assessment in a wistar rat model of cirrhosis and peritonitis

Iuliana Nenu[1], Andra Tichindeleanu[1], Ioan Topor[1], Serban Trella[1], Rares Craciun[2], Horia Ștefănescu[3], Bogdan Procopet[2], Zeno Sparchez[2]. [1]"Iuliu Hatieganu" University of Medicine and Pharmacy, Physiology Department, Cluj-Napoca, Romania; [2]"Iuliu Hatieganu" University of Medicine and Pharmacy, 3rd Medical Clinic, Department 4 - Internal Medicine; "Prof. Dr. O. Fodor" Regional Institute of Gastroenterology and Hepatology, Cluj-Napoca, Romania; [3]"Prof. Dr. O. Fodor" Regional Institute for Gastroenterology and Hepatology, Cluj-Napoca, Romania
Email: iuliana.nenu@gmail.com

Background and aims: In cirrhosis with spontaneous bacterial peritonitis, inflammation and coagulation are tightly linked. Fresh frozen plasma (FFP) is often administered for coagulopathy, but may not reduce inflammatory burden and could promote hypercoagulability. We compared FFP support with adjuvant simvastatin in Wistar rats.
Method: Cirrhosis was induced in Wistar rats by bile duct ligation and allowed to develop for 16 weeks. Abdominal ultrasound was used to confirm advanced liver disease. Peritonitis was induced by intraperitoneal Escherichia coli inoculation (1.0 × 10^8 colony-forming units, CFU). Infected rats received 14-day antibiotics: ceftriaxone 100 mg/kg/day or meropenem 25 mg/kg/day, subcutaneously once daily. Simvastatin was given by oral gavage (25 mg/kg/day) for 14 days. Plasma support consisted of FFP transfusion every 2 days for 14 days from healthy donor rats. Tissue tumor necrosis factor alpha (TNF-a), interleukin 6 (IL-6) and interleukin 1 beta (IL-1b) were quantified. Coagulation was assessed by ClotPro EX-test and IN-test measuring clotting time (CT), clot formation time (CFT) and maximum clot firmness (MCF). Group comparisons for inflammation tests was made with one-way ANOVA test.
Results: In peritonitis treated with meropenem, simvastatin was associated with lower inflammatory cytokines versus FFP: TNF-a: 8.864 versus 13.241 pg/g protein, IL-6: 4.864 versus 8.307 pg/g protein, and IL-1b: 20.629 versus 42.938 pg/g protein. No statistically significant differences were observed between groups ($p > 0.05$). Across the other groups (ceftriaxone-treated peritonitis and non-infected cirrhosis groups with or without simvastatin), cytokine levels varied by group without a consistent reduction associated with FFP. Across infected cohorts receiving FFP (with either antibiotic), ClotPro showed faster clot build-up and higher firmness consistent with a hypercoagulable profile (EX-test CFT about 22 s with MCF 66.5 to 69.3 mm; IN-test CT 93 to 109.7 s with MCF 69 to 71.3 mm). Simvastatin-treated infected cohorts tended to show closer-to-reference viscoelastic profiles.
Conclusion: In Wistar rats with cirrhosis and peritonitis, repeated FFP transfusion showed no anti-inflammatory signal and was associated with a consistent hypercoagulable viscoelastic pattern, suggesting lack of benefit and potential prothrombotic imbalance. Adjuvant simvastatin showed lower inflammation and comparatively more balanced coagulation profiles.

FRI-419

Beyond status markers: profound disruption of vitamin d metabolism in decompensated cirrhosis and its clinical implications

Anika Nier[1], Julia Kühn[1], Stefanie Quickert[2], Christian Weißenborn[2], Philipp Reuken[2], Tony Bruns[3], Alexander Zipprich[2], Alexander Kluttig[4], Rafael Mikolajczyk[4], Marko Damm[5], Gabriele Stangl[1]. [1]Martin Luther University Halle-Wittenberg, Halle (Saale), Germany; [2]Jena University Hospital, Jena, Germany; [3]University Hospital RWTH Aachen, Aachen, Germany; [4]Institute of Agricultural and Nutritional Sciences, Halle (Saale), Germany; [5]University Clinic Halle (Saale), Halle (Saale), Germany
Email: Anika.Nier@landw.uni-halle.de

Background and aims: Vitamin D (VD) deficiency is common in chronic liver disease (CLD), but the clinical relevance of disturbed VD metabolism remains unclear. In advanced disease, routine 25-hydroxyvitamin D (25(OH)D) assessment may underestimate clinically relevant metabolic failure. Thus, we performed a comprehensive, pathway-wide analysis of VD metabolism across CLD stages and assessed clinical associations.
Method: Patients with decompensated cirrhosis and ascites from University Hospital Jena (n = 39) and German National Cohort (NAKO) participants with (n = 57) or without (n = 48) steatosis were included, matched for age, sex and sampling season; vitamin D supplementation was present in a subset. Plasma and ascitic vitamin D_3 (VD_3), 25$(OH)D_3$, 24,25-dihydroxyvitamin D_3 [24,25$(OH)_2D_3$, catabolism], precursor sterol 7-dehydrocholesterol (7-DHC), 1,25-dihydroxyvitamin D [1,25$(OH)_2D$, active hormone], vitamin D binding protein (DBP) and fibroblast growth factor 23 (FGF23, 1,25$(OH)_2D$ suppressor) were quantified by HPLC–MS/MS or ELISA. Free metabolites were calculated. 90-day survival was analysed by MELD-adjusted Cox regression stratified by median DBP or 25$(OH)D_3$ and predefined 1,25$(OH)_2D$ cut-offs; spontaneous bacterial peritonitis (SBP) in the preceding 3 months was analysed as binary.
Results: VD metabolism was preserved in NAKO groups but globally disrupted in decompensated cirrhosis, independent of VD supplementation (plasma total 25$(OH)D_3$ – 70%, total 1,25$(OH)_2D$ – 60% $p < 0.0001$; free 25$(OH)D_3$ – 35%, free 1,25$(OH)_2D$ – 28%, $p = 0.002$). Plasma VD_3 was detectable in <50% and 24,25$(OH)_2D_3$ in <20% of patients. Plasma 7-DHC (−45%) and DBP (−54%) were reduced, while FGF23 was elevated (+60%, all $p < 0.0001$). Seasonal variation of plasma 25$(OH)D_3$ and 1,25$(OH)_2D$ was lost in cirrhosis. Plasma and ascitic metabolites correlated (25$(OH)D_3$ $r = 0.5$, $p < 0.006$; 1,25$(OH)_2D$ $r = 0.8$, $p < 0.0001$). While plasma 25$(OH)D_3$ was not outcome-associated, low plasma 1,25$(OH)_2D$ showed a trend toward impaired survival (HR 5.1, 95%CI 0.7–39.3; adjusted HR 5.6, 95%CI 0.7–43.4). Low plasma DBP independently predicted 90-day mortality (HR 4.9, 95%CI 1.3–17.9; adjusted HR 4.8, 95%CI 0.9–20.2) and SBP (OR 7.0, 95%CI 1.3–38.4; adjusted OR 8.9, 95%CI 1.3–59.7).
Conclusion: Steatosis does not substantially impair VD metabolism, while decompensated cirrhosis shows profound, supplementation-resistant disruption. DBP emerges as a MELD–independent biomarker for mortality and SBP, extending its role beyond VD transport and underscoring limits of current supplementation.

FRI-420

Acute-on-chronic liver failure is associated with impaired function of mitochondria in the liver

Lena Oeckl[1], Mona-May Langer[1], Helena Stadler[1], Severin Jacobi[2], Dionysios Koliogiannis[2], Markus Guba[2], Hans Zischka[3], Christian M. Lange[1]. [1]Department of Internal Medicine II, LMU University Hospital, Munich, Germany; [2]Department of Visceral Surgery, LMU University Hospital, Munich, Germany; [3]Institute of Molecular Toxicology and Pharmacology, Helmholtz, Institute of Toxicology and Environmental Hygiene, Technical University, Munich, Germany
Email: lena.oeckl@med.uni-muenchen.de

Background and aims: In patients suffering from advanced liver cirrhosis, the development of Acute-on-chronic liver failure (ACLF) is a very frequent syndrome with a high short-term mortality. It is characterized by an intense systemic inflammation associated with different combinations of organ failure. Mitochondrial dysfunction is known to play a crucial role in ACLF, contributing to the development of organ failure and immune dysfunction. This study aims to further characterize mitochondrial dysfunction with progression of liver cirrhosis in the context of a severe inflammatory environment and identify pathophysiological pathways.
Method: Liver tissue was collected from patients undergoing liver transplantation and further processed for Oroboros high resolution respirometry. Mitochondrial morphology was assessed by performing electron microscopy and immunofluorescence staining using

mitochondrial markers. Serum from healthy specimens (= control group) and patients suffering from ACLF was collected for stimulation of HepG2-cells prior to Oroboros analysis as well as cell viability and ATP-assays.
Results: Morphological impairments such as mitochondrial swelling, cristae rarefication and membrane rupture were clearly visible in EM of ACLF patients. Intensity of TOM20 staining was decreased in advanced cirrhosis, indicating loss of mitochondrial mass. The respirometry analysis performed with liver tissue showed a clearly higher mitochondrial membrane instability in ACLF and a significant downregulation of the glycerophosphat pathway ($p = 0.03$), correlating negatively with increasing MELD score. Malat-stimulated complex I respiration, however was higher in ACLF ($p = 0.01$), correlating positively with the MELD score. Non-mitochondrial respiration by oxidative side-reactions was significantly upregulated in patients suffering from ACLF ($p = 0.03$). HepG2s stimulated with ACLF-serum for 3 h showed a significantly higher respiration than the control ($p = 0.02$). Especially, serum from patients with high cytokine levels and inflammatory markers led to an increased mitochondrial respiration, however with a lower viability and less ATP-production compared to the control group.
Conclusion: We suggest that the pro-inflammatory environment in ACLF leads to a significant overstimulation of mitochondria which is not only ineffective regarding energy supply, but may also harm the cells, ultimately causing cell death.

FRI-421
GLP-1 agonist lowers portal pressure by modulating hepatic vascular tone in a toxin-induced cirrhotic rat model
Maria Andres-Rozas[1], Peio Aristu[1], Tomas Jelenik[2], Jenny Egecioglu Norlin[3], Morten Fog-Tonnesen[4], Jordi Gracia-Sancho[5], Anouk Oldenburger[6]. *[1]Barcelona Liver Bioservices, Barcelona, Spain; [2]Diabetes Pharmacology Novo Nordisk A/S, Bagsværd, Denmark; [3]Late translational Medicine Novo Nordisk A/S, Bagsværd, Denmark; [4]CC TA Early project Novo Nordisk A/S, Bagsværd, Denmark; [5]IDIBAPS - Hospital Clínic Barcelona - CIBEREHD, Barcelona, Spain; [6]Early Translational Medicine Novo Nordisk A/S, Bagsværd, Denmark*
Email: auog@novonordisk.com

Background and aims: Metabolic dysfunction-associated steatohepatitis (MASH) promotes fibrosis and vascular dysfunction that increases intrahepatic resistance, leading to portal hypertension and cirrhosis complications. GLP-1 agonists improves MASH in clinical trials and preclinical models, but data on their effects on hemodynamic parameters in advanced or late-stage cirrhosis is limited. We evaluated portal haemodynamics and liver endpoints in a thioacetamide (TAA) rat cirrhosis model and tested the effects of a GLP-1 agonist.
Method: Male Sprague–Dawley rats received TAA (250 mg/kg, i.p., twice weekly) for 10 weeks to induce cirrhosis and portal hypertension, followed by a 3-week TAA-free period during which animals were administered vehicle or a GLP-1 agonist (15 nmol/kg/day, s.c.). End-point measurements included haemodynamic parameters like portal pressure, portal blood flow and intrahepatic vascular resistance (IHVR), organ weights, and histological analyses.
Results: TAA caused portal hypertension due to increased IHVR, and splenomegaly. A 3-week TAA-free interval partially restored haemodynamics but the key pathological features remained impaired: portal pressure and IHVR were increased by 38% and 40%, respectively, compared to healthy controls. Liver fibrosis and spleen weight were increased after TAA treatment and remained unchanged after its removal. Thus, a 3-week washout preserves a cirrhotic model suitable for haemodynamic intervention studies. The GLP-1 agonist significantly lowered portal pressure (10%), which was accompanied by trend to an increased portal flow (23%) and reduced IHVR (22%). These effects are independent of modest body-weight loss (6%). The GLP-1 agonist lowered mean arterial pressure and modestly raised heart rate; fibrosis was unchanged.
Conclusion: The TAA model recapitulates key features of compensated cirrhosis and portal hypertension and is well suited for translational haemodynamic studies. The GLP-1 agonist rapidly lowered portal pressure by reducing IHVR, an effect independent of fibrosis and of weight loss. Fibrosis is in this model not affected by the GLP-1 agonist probably due to the short treatment period. Overall, the GLP-1 agonist appears to reduce portal hypertension through mechanisms that are distinct from effects on body weight or fibrosis. However, human haemodynamic data remain limited, and translational confirmation is required. Future studies should define the vascular-tone pathways that mediate the observed decreases in portal pressure.

FRI-425
Changing epidemiology and clinical presentation of hepatic cirrhosis: data from the Sorpresa study
Tommaso Sarcina[1], Mario Masarone[1], Emanuele Errigo[2], Paolo Angeli[3], Simone Incicco[3], Francesca Ponziana[4], Leonardo Stella[4], Giovan Giuseppe Di Costanzo[5], Debora Angrisani[5], Alessandro Federico[6], Marcello Dallio[6], Andrea Pasta[7], Enrico Pompili[8,9], Pietro Torre[1], Filomena Morisco[10], Luisa Ranieri[10], Nicola Coppola[11], Maria Stanzione[11], Alessio Aghemo[12], Stella De Nicola[12], Edoardo Giannini[7], Vito Di Marco[2], Marcello Persico[1]. *[1]Department of Medicine, Surgery and Dentistry "Scuola Medica Salernitana", University of Salerno, Salerno, Italy, Salerno, Italy; [2]Department of Health Promotion, Mother & Child Care, Internal Medicine & Medical Specialties (PROMISE), Gastroenterology Unit, University of Palermo, Palermo, Italy, Palermo, Italy; [3]Department of Surgery, Oncology and Gastroenterology, Gastroenterology Unit, University of Padua, Padua, Italy, Padova, Italy; [4]Liver Unit, CEMAD – Centro Malattie dell'Apparato Digerente, Internal Medicine and Gastroenterology, Università Cattolica del Sacro Cuore, Fondazione Policlinico Universitario Gemelli IRCCS, Rome, Italy, Roma, Italy; [5]Liver Unit, Antonio Cardarelli Hospital, 80131 Naples, Italy, Napoli, Italy; [6]Hepatogastroenterology Unit, Department of Precision Medicine, University of Campania Luigi Vanvitelli, Naples, Italy, Napoli, Italy; [7]Gastroenterology Unit, Department of Internal Medicine, University of Genoa, Genoa, Italy, Genova, Italy; [8]Department of Medical and Surgical Sciences, University of Bologna, Bologna, Italy; [9]Unit of Semeiotics, Liver and Alcohol-Related Diseases, IRCCS Azienda Ospedaliero-Universitaria di Bologna, Bologna, Italy; [10]Department of Clinical Medicine and Surgery, Diseases of the Liver and Biliary System Unit, University of Naples, Naples, Italy, Napoli, Italy; [11]Department of Mental Health and Public Medicine, Section of Infectious Diseases, Second University of Naples, 80131 Naples, Italy, Napoli, Italy; [12]Division of Internal Medicine and Hepatology, IRCCS Humanitas Research Hospital, Rozzano, Italy, Rozzano, Italy*
Email: tsarcina@unisa.it

Background and aims: Hepatic cirrhosis represents the final stage of most chronic liver diseases and is commonly driven by viral, alcoholic, metabolic or mixed etiologies. In recent years, both the epidemiology and clinical presentation of cirrhosis have been rapidly evolving; however, contemporary national data characterizing this scenario are lacking. To describe the current epidemiological profile and initial clinical presentation of hepatic cirrhosis in Italy during 2024.
Method: In this prospective, multicenter study, 1195 patients with cirrhosis were consecutively enrolled from 11 tertiary hepatology centers across Italy. Eligible participants included individuals with a new diagnosis of cirrhosis or those presenting for the first time to participating centers in 2024. Demographic, socioeconomic, etiological, clinical and laboratory data were collected at baseline. The

relative contribution of individual risk factors was assessed using Pareto chart analysis.
Results: Among 1195 enrolled patients, MASLD was the most prevalent etiology (28.8%), following by viral etiology (20.5%), Alcohol Liver Disease (ALD) (19.4%) and other causes (10.2%), but 251 patients (21%) had a mixed etiology (Met-ALD, Met- virus, ALD-virus, Met-ALD-virus). In the Pareto analysis of individual risk factors, arterial hypertension ranked first, followed by type 2 diabetes mellitus, alcohol abuse, obesity, HCV infection, HBV infection. Despite the growing metabolic burden, viral hepatitis remains a major contributor, representing 41.2% (202 patients of 490) of etiology, among patients at their access to the centers, but with cirrhosis already known, confirming its persistent epidemiological impact despite antiviral therapies and vaccination programs.
Conclusion: This study highlights the evolving epidemiology of cirrhosis, characterized by an increasing contribution of MASLD and a predominance of early-stage, compensated disease (Child-Pugh A) at diagnosis. The comorbidity profile associated with cirrhosis is also emphasized: arterial hypertension was the most prevalent risk factor, although diabetes and obesity appear to exert a more direct pathogenetic impact on liver injury. Viral hepatitis continues to impose a substantial clinical burden, underscoring the need to strengthen vaccination, screening and linkage-to-care strategies. Overall, the frequent overlap of hepatic risk factors, observed in approximately one-fifth of patients, reflects the increasing complexity of cirrhosis management and contributes to a higher disease burden.

FRI-426

Inhibition of VCP alleviates inflammatory injury in acute-on-chronic liver failure through STING-dependent enhancement of macrophage efferocytosis

Zhangya Pu[1], Wenxin Zhoudi[2], Yangfan Shen[3], Qingqing Hu[4], Xiaohan Qian[1], Lingxiao Zhu[1], Zhongyang Xie[5], Xiaoxin Wu[1], Shangci Chen[1], Xiayao Li[1], Xiaowei Xu[1]. *[1]State Key Laboratory for Diagnosis and Treatment of Infectious Diseases, National Clinical Research Center for Infectious Diseases, National Medical Center for Infectious Diseases, Collaborative Innovation Center for Diagnosis and Treatment of Infectious Diseases, The First Affiliated Hospital, Zhejiang University School of Medicine, Hangzhou, China; [2]State Key Laboratory for Diagnosis and Treatment of Infectious Diseases, National Clinical Research Center for Infectious Diseases, National Medical Center for Infectious Diseases, Collaborative Innovation Center for Diagnosis and Treatment of Infectious Diseases, The First Affiliated Hospital, Zhejiang University School of Medicine, H, China; [3]State Key Laboratory for Diagnosis and Treatment of Infectious Diseases, National Clinical Research Center for Infectious Diseases, National Medical Center for Infectious Diseases, Collaborative Innovation Center for Diagnosis and Treatment of Infectious Diseases, The First Affiliated Hospital, Zhejiang University School of Medicine, Han, China; [4]State Key Laboratory for Diagnosis and Treatment of Infectious Diseases, National Clinical Research Center for Infectious Diseases, National Medical Center for Infectious Diseases, Collaborative Innovation Center for Diagnosis and Treatment of Infectious Diseases, The First Affiliated Hospital, Zhejiang University School of Medicine, Hangz, China; [5]State Key Laboratory for Diagnosis and Treatment of Infectious Diseases, National Clinical Research Center for Infectious Diseases, National Medical Center for Infectious Diseases, Collaborative Innovation Center for Diagnosis and Treatment of Infectious Diseases, The First Affiliated Hospital, Zhejiang University School of Medicinev, Hangzhou, China*
Email: Fleur.puzhangya@outlook.com

Background and aims: Acute-on-chronic liver failure (ACLF) is a severe clinical syndrome characterized by systemic inflammation and immune dysregulation, which leads to high short-term mortality. The valosin-containing protein (VCP), a member of the AAA-ATP family, participates in multiple cellular functions and has been implicated in the progression of various diseases. This study aimed to elucidate the role and underlying mechanisms of VCP in the progression of ACLF, with the goal of identifying potential therapeutic targets for future intervention.
Method: To assess VCP expression, liver samples from patients and mice model of ACLF were analyzed. The functional role of macrophage-specific VCP and its underlying molecular mechanisms in ACLF were investigated in mice model using the VCP small-molecule inhibitor and adeno-associated virus (AAV). Additionally, validation of these mechanisms was performed in an in-vitro macrophage cell model.
Results: We found that VCP expression is markedly upregulated in the liver tissues of both patients and mice model of ACLF. In the CCl4/LPS-induced mice ACLF model, inhibition of VCP significantly attenuated liver injury, as evidenced by reduced serum levels of liver enzymes, decreased hepatic inflammation, and improved histopathological outcomes. Mechanistically, VCP inhibition exerted its protective effects through a dual regulatory mechanism: it suppressed the activation of the STING signaling pathway while concurrently enhancing macrophage efferocytosis. Importantly, the administration of a STING agonist effectively reversed these protective effects in vivo, which was further validated in an in-vitro macrophage cell model.
Conclusion: The findings demonstrate that inhibition of VCP expression in ACLF protects against liver injury by enhancing macrophage-mediated efferocytosis of damaged cells. Overall, these results suggest that VCP may represent a potential therapeutic target for the treatment of ACLF.

FRI-427

SIRT5 rs12216101 T > G variant is associated with hepatic encephalopathy and impaired ammonia metabolism in patients with cirrhosis

Federico Salomone[1], Antonio Gil-Gómez[2], Federica Barreca[3,4], Miriam Longo[5], German Soriano[6], Rubén Francés[7], Rocío Gallego-Durán[2], Javier Ampuero Herrojo[2], Marco Tafani[3], Paola Dongiovanni[5], Manuel Romero-Gómez[2]. *[1]Azienda Sanitaria Provinciale di Catania, Catania, Italy; [2]Instituto de Biomedicina de Sevilla, IBiS/Hospital Universitario Virgen del Rocío/CSIC/Universidad de Sevilla, Sevilla, Spain; [3]Dipartimento di Medicina Sperimentale, Università di Roma "La Sapienza", Roma, Italy; [4]La Sapienza University of Rome, Medicina Sperimentale, Roma, Italy; [5]Medicine and Metabolic Diseases, Fondazione IRCCS Ca' Granda Ospedale Maggiore Policlinico, Milan, Italy; [6]Department of Gastroenterology, Hospital de la Santa Creu y Sant Pau, Barcelona, Spain; [7]Department of Clinical Medicine, Miguel Hernandez University, Alicante, Spain*
Email: federicosalomone@rocketmail.com

Background and aims: Hepatic encephalopathy (HE) arises from impairment of ammonia homeostasis. Genetic factors conferring susceptibility to HE are poorly understood. SIRT5 regulates the activity of key enzymes involved in ammonia metabolism by desuccinylating lysine residues. In this study, we aimed to examine the impact of SIRT5 rs12216101 T > G variant on HE and ammonia homeostasis in patients with cirrhosis.
Method: The rs12216101 was genotyped in a retrospective cohort of 598 outpatients followed at four liver units in Spain. Multivariate regression analysis, Kaplan-Meyer curves and Cox regression analysis were performed to assess the predictive value of rs12116101 for HE and decompensating events. Immunoprecipation on liver samples was performed to assess the impact of rs12216101 T > G on succinylation levels of target proteins. To evaluate the role of SIRT5 in intestinal and liver ammonia metabolism, CaCo2 and HepG2 were treated with 50 μM of the SIRT5 activator MC3138 for 24 and 48 h under glucose deprivation.
Results: Patients were followed-up for 30.1 ± 23.1 months. At multivariate regression analysis, adjusted for age, sex and MELD score, rs12216101 T > G variant was associated with the development of decompensation during the follow-up [aHR 1.374

(1.118–1.688); p = 0.002]. At Cox regression analsys, the presence of the G allele was independently associated with the development of hepatic encephalopathy [HR 1.533 (1.153–2.036); p = 0.003]. In a subcohort of patients (n = 219), G-allele carriers displayed an impaired response to the glutamine overload test having a higher ammonia increase at 60 min (58.3 ± 52.6 vs 41.6 ± 35.5 umol/L; p = 0.005). Liver samples from subjects with the GG genotype displayed higher levels of succinyl lysines, indicating reduced SIRT5 activity. Treatment of CaCo2 and HepG2 with MC3138 led to a reduction of ammonia in the medium due respectively to higher desuccinnylation of Glutaminase C (inhibition) and of Carbamoyl-Phosphate Synthase 1 (activation).
Conclusion: SIRT5 rs12216101 T > G variant confers susceptibility to HE in cirrhosis by disrupting intestinal glutaminolysis and urea cycle in the liver.

FRI-428-YI
Endothelial forkhead box O1 (FoxO1) signalling in acute decompensation and acute-on-chronic liver failure: evidence from in vivo models and in vitro exposure to patient plasma
Fabian Schachteli[1], Sabine Klein[1,2], Maximilian Joseph Brol[1,2], Robert Schierwagen[1,2], Pia Lembeck[1], Sara Zarei[1], Sara Noemi Reinartz Groba[1], Wenyi Gu[1,2], Christoph Welsch[2], Jonel Trebicka[1,2,3], Frank Erhard Uschner[1,2]. [1]*Department of Internal Medicine B, University Hospital Münster, Münster, Germany;* [2]*Hospital of the Goethe University Frankfurt, Frankfurt am Main, Germany;* [3]*European Foundation for the Study of Chronic Liver Failure, Barcelona, Spain*
Email: fabian.schachteli@ukmuenster.de

Background and aims: Endothelial dysfunction is a hallmark of acute decompensation (AD) and acute-on-chronic liver failure (ACLF). Forkhead box O1 (FoxO1) regulates endothelial metabolic and growth programmes and could link inflammatory triggers to impaired endothelial repair. We investigated the role of FoxO1 signalling in AD/ACLF *in vivo* and *in vitro*.
Method: In rats, AD was induced by bile duct ligation (BDL) or carbon tetrachloride (CCl4) injections, with or without Western diet or ethanol. ACLF was triggered by lipopolysaccharide injections, alcohol binge or transnasal stool inoculation. For *in vivo* FoxO1 inhibition, the FoxO1 inhibitor AS1842856 was administered intravenously to AD rats. Hepatic FoxO1 pathway activity was assessed in liver tissue by complementary RNA (cRNA) microarray, Western blot and quantitative PCR (qPCR). Human umbilical vein endothelial cells (HUVECs) were incubated with the FoxO1 inhibitor AS1842856 or with plasma from healthy controls and patients with AD/ACLF. Endothelial function was assessed *in vitro* (angiogenesis, proliferation, viability, apoptosis, autophagy, senescence) using tube formation, scratch and MTT assays.
Results: Compared with AD and healthy controls, ACLF induction reduced hepatic FoxO1 signalling *in vivo*. In AD rats, FoxO1 inhibition increased mean arterial pressure (MAP) and decreased the international normalised ratio (INR), while increasing the neurological severity score (NSS). *In vitro*, only ACLF plasma (but not AD plasma or control plasma) significantly downregulated FoxO1. Both AS1842856 and ACLF plasma significantly reduced angiogenesis and proliferation, without increasing autophagy, senescence or apoptosis.
Conclusion: In ACLF, FoxO1 signalling seems to be inhibited in humans and in experimental models and thereby to impair angiogenesis and proliferation, inducing endothelial dysfunction in ACLF.

FRI-429-YI
Multi-etiology liver proteomic profiling of advanced chronic liver disease stages
Sonia-Emilia Selicean[1], Christian Mueller[2], Pfister Stefan[3], Maria Schwerk[4], Aenne Harberts[1], Felix Piecha[1], Lutz Fischer[5], Martina Sterneck[1], Julian Schulze zur Wiesch[1], Samuel Huber[1], Ansgar W. Lohse[1], Victor Puelles[4], Pietro Scatturo[3], Peter Huebener[1]. [1]*I. Department of Medicine, University Medical Center Hamburg-Eppendorf, Hamburg, Germany;* [2]*Bioinformatics Core, University Medical Center Hamburg-Eppendorf, Hamburg, Germany;* [3]*Leibniz Institute of Virology, Hamburg, Germany;* [4]*III. Department of Medicine, University Medical Center Hamburg-Eppendorf, Hamburg, Germany;* [5]*Department of Visceral Transplant Surgery, University Medical Center Hamburg-Eppendorf, Hamburg, Germany*
Email: Soniaselicean@gmail.com

Background and aims: Liver cirrhosis follows complex and heterogeneous trajectories that may shift between distinct clinical states of compensation (CC), decompensation (DC) and acute-on chronic liver failure (ACLF). Deciphering intrahepatic signalling pathways associated with distinct disease stages may identify therapeutic targets to modulate disease progression.
Method: A total of 100 human liver samples from non-cirrhotic (NC) controls (marginal tissue obtained during liver surgery) and liver explants from patients with CC, DC, or ACLF due to alcohol-related liver disease (ARLD), primary sclerosing cholangitis (PSC), or hepatitis C virus (HCV) were subjected to quantitative bulk Liquid Chromatography-Tandem Mass Spectrometry (LC-MS/MS) analysis.
Results: Out of over 4,500 proteins profiled across all conditions, between 5–12% were differentially expressed between NC and CC, 0–0,8% between CC and DC, and 0,3–4% between DC and ACLF livers across all etiologies. Principal component analysis revealed robust stage-dependent clustering in ARLD and HCV, but much less in PSC livers, possibly related to cholestasis-associated hyperbilirubinemia in this condition. NC-to-CC transition was expectedly marked by a high abundance of fibrogenic and extracellular matrix proteins, and a downregulation of proteins related to detoxification and metabolism in CC. DC-to-ACLF transition was dominated by perturbations of metabolic homeostasis and inflammatory responses, characterized by downregulation of PPAR signalling, glycolysis–gluconeogenesis, fatty acid metabolism, detoxification and expression of CYP450 family members. Inflammation-related proteins (e.g. resistin, neutrophil elastase, myeloperoxidase) were amongst the most abundantly expressed proteins in ACLF livers. Regulator activity analysis inferred signatures compatible with SMAD3 overactivation during NC-to-CC transition, whereas DC-to-ACLF progression was compatible with inhibition of HNF4α and PPAR-α/γ activity.
Conclusion: Chronic liver disease progression is associated with distinct, stage-dependent hepatic proteomic signatures. While fibrosis-related proteins predominate across cirrhosis stages, an overabundance of inflammatory proteins and metabolic decline characterize DC–ACLF progression. The contribution of stage-specific hepatic cellular composition remains to be clarified. Modulation of dysregulated protein networks may carry therapeutic potential in advanced chronic liver disease.

FRI-430
Nintedanib improves cardiac rhythm stability and contractility in bile duct ligated-induced cirrhotic cardiomyopathy in cirrhotic rats
Hira Shafique[1], Qamar Niaz[1], Muhammad Adil Rasheed[1], Khalid Abdul Majeed[2], Nasir Ali[3], Ghulam Mustafa[4], Aneela Zameer Durrani[5], Sania Mehreen[6], Muhammad Shafique[1]. [1]*Department of Pharmacology and Toxicology, Faculty of Bio-Sciences, University of Veterinary and Animal Sciences, Lahore, Pakistan;* [2]*Department of Physiology, Faculty of Bio-Sciences, University of Veterinary and Animal Sciences, Lahore, Pakistan;* [3]*Department of Cardiac Surgery, Army Cardiac Hospital, Lahore, Pakistan;* [4]*Department of Pathology, Faculty of Veterinary Sciences, University of Veterinary and Animal Sciences, Lahore, Pakistan;* [5]*Department of Veterinary Medicine, Faculty of Veterinary Sciences, University of Veterinary and Animal Sciences, Lahore, Pakistan;* [6]*Department of Zoology, Faculty of Fisheries*

and Wildlife, University of Veterinary and Animal Sciences, Lahore, Pakistan
Email: qamar.niaz@uvas.edu.pk

Background and aims: Cirrhotic cardiomyopathy (CCM) is a myocardial dysfunction in advanced liver disease with chronotropic dysfunction. Vasodilator agents and diuretics are not recommended in CCM due to decreased vascular resistance and electrolyte imbalance. Nintedanib (Nin), "a tyrosine Kinase inhibitor," is used to treat idiopathic pulmonary fibrosis. Thus, we evaluated Nin against liver inflammation and fibrosis to alleviate the chronotropic dysfunction in CCM in bile duct ligation (BDL)-induced cirrhotic rats.
Method: A total of 64 rats of body weight 250–280 g were selected and grouped as Sham-Saline, Sham-Nin 30, Sham-Nin 60, Sham-Lac (lactulose) 1.5, and BDL-Saline, BDL-Nin 30, BDL-Nin 60, and BDL-Lac 1.5. Sham (control) and BDL surgery (experimental) wa performed to induce liver cirrhosis for 28 days. The Nin 30 and 60 mg/kg and Lac 1.5 g/kg were used to treat the liver cirrhosis for 14 days. Post-treatment, liver and heart histopathology, in vivo chronotropic study, QTc interval, liver function tests (AST, ALT, ALP, albumin, and bilirubin), heart IL-6, TNF α, BNP, and MDA, and serum troponin-I (trop-I) were evaluated.
Results: The average heart rate was decreased with higher doses of adrenaline and noted irregular in the BDL-Saline group, and was increased in BDL-Nin 30 (regular-irregular) and BDL-Nin 60 (regular) groups. The QTc interval was increased in the BDL-Saline group, and was decreased equally in the BDL (Nin 30 and 60) groups. The liver histopathology showed severe inflammation and fibrosis in the BDL-Saline group and moderate and mild in BDL (Nin 30 and 60) groups. The heart showed coagulative and degenerative necrosis in all BDL groups. The BNP, MDA, TNF-α, and IL-6 in heart tissue were increased in the BDL-Saline group and decreased BNP in BDL (Nin 30 and 60) groups, MDA and IL-6 in BDL-Nin 60 group, TNF-α in BDL [Nin 30 (less) and 60 (more)] groups. The serum ALT, AST, ALP, bilirubin, and trop-I increased and albumin reduced in the BDL-Saline group, and decreased AST, ALP, and trop-I more in the BDL-Nin 60 group relative to the BDL-Nin 30, decreased bilirubin with no difference in the BDL (Nin 30 and 60) groups, increased albumin evenly in the BDL (Nin 30 and 60) groups, and increased ALT only in the BDL-Nin 60 group.
Conclusion: Nin 60 mg/kg is more effective in alleviating the chronotropic dysfunction in CCM by improving the liver inflammation and fibrosis, liver function tests (AST, ALP, and bilirubin), myocardial injury (trop-I), and cardiac stress (MDA and BNP) in BDL rats.

FRI-431-YI

LSECtin attenuation in cirrhosis correlates with disease severity and inflammation and can be experimentally recovered by IL-10/IL-13 administration

Benedikt Simbrunner[1,2,3,4,5], Oriol Juanola[6,7,8], Enrique Ángel-Gomis[6,7], Isabel Gómez-Hurtado[7,8], Katharina Bonitz[1,4,5], Thomas Sorz-Nechay[1,2,4,5], Vlad Taru[1,4,5], Katja Sommer[1,2,4,5], Benedikt Hofer[1,2,3,4,5], Kerstin Zinober[1,3,4], Katharina Regnat[1,3,4], Francisco Navarrete Rueda[7,9], Albina Espana[6], Mattias Mandorfer[1,2,3], Michael Trauner[1,2], Philipp Schwabl[1,2,3,4,5], Thomas Reiberger[1,2,3,4,5], Esther Caparrós[6,7,8], Rubén Francés[6,7,8].
[1]Medizinische Universität Wien, Division of Gastroenterology and Hepatology, Wien, Austria; [2]Clinical Research Group MOTION, Medical University of Vienna, Vienna, Austria; [3]Vienna Hepatic Hemodynamic Lab, Division of Gastroenterology and Hepatology, Department of Medicine III, Medical University of Vienna, Vienna, Austria; [4]Christian Doppler Laboratory for Portal Hypertension and Liver Fibrosis, Medical University of Vienna, Vienna, Austria; [5]CeMM Research Center for Molecular Medicine of the Austrian Academy of Sciences, Vienna, Austria; [6]Universidad Miguel Hernández-Campus de San Juan de Alicante, Sant Joan d'Alacant, Spain; [7]Instituto ISABIAL, Hospital General Universitario Dr. Balmis, Alicante, Alicante, Spain; [8]CIBERehd, Instituto de Salud Carlos III, Madrid, Spain; [9]Instituto de Neurociencias, Universidad Miguel Hernández-CSIC, San Juan de Alicante, Alicante, Spain
Email: benedikt.simbrunner@meduniwien.ac.at

Background and aims: Liver sinusoidal endothelial cell (LSEC) C-type lectin (LSECtin) is a key regulator of hepatic immune homeostasis and reduced in cirrhosis. Experimental studies showed that LSECtin overexpression restores LSEC immunoregulatory function, mediated by anti-inflammatory cytokines IL10 and IL13. This study investigated the relationship between LSECtin and portal hypertension and disease severity in patients with cirrhosis and explored the cytokine-driven regulation of LSECtin expression in experimental cirrhosis.
Method: This translational project combined human data from patients with cirrhosis and experimental mouse studies from two centers. In the human cohort (n = 86), hepatic LSECtin mRNA expression was quantified in liver biopsies and correlated with clinical stage, biomarker profiles, and hepatic IL10 and IL13 expression. In CCl_4 and CDAHFD mouse models of cirrhosis (induction period 12 weeks, respectively), hepatic single-cell RNA sequencing (scRNA-Seq) assessed LSECtin regulation in LSECs at peak fibrosis and during regression (3, 7, 14 days after cessation of injury). Interventional studies in the CCl_4 model examined whether exogenous IL-10 or IL-13 administration induces LSECtin expression.
Results: In patients with cirrhosis, hepatic LSECtin mRNA decreased across disease stages (log-fold median vs compensated cirrhosis [CC]: first decompensation −0.88 [−2.25;−0.05]; further decompensation −2.86 [−3.31;−1.45]; $p < 0.001$), similar to hepatic IL10 mRNA expression (−0.31 [0.77] and −0.67 [0.98] vs CC; $p = 0.045$). LSECtin mRNA expression correlated negatively with HVPG (Spearman's r = −0.553), MELD (r = −0.634), and biomarkers ELF (r = −0.718), VWF (r = −0.388), and IL-6 (r = −0.534); and correlated positively with hepatic IL10 mRNA (r = 0.352) and IL13 mRNA (r = 0.351, $p < 0.05$ for all analyses). In hepatic scRNA-Seq analyses, LSECtin expression in LSECs was downregulated at peak fibrosis, followed by upregulation during fibrosis regression in both CCl_4 and CDAHFD models. In the CCl_4 model, IL-10 and IL-13 injections increased the proportion of LSECtin-positive LSECs (CIR-VEH: 25.6%; CIR-IL10: 45.5%; CIR-IL13: 48.5%; $p = 0.035$) indicating partial restoration of LSECtin expression.
Conclusion: Downregulation of LSECtin expression in patients with cirrhosis correlates with clinical disease stage, portal hypertension, and inflammation. In murine models, LSECtin is recovered during fibrosis regression and cytokine administration,supporting IL10/IL13–dependent pathways as regulators of LSECtin in cirrhosis.

FRI-432

Characterization of the toll-like receptor ligandome across the clinical spectrum of alcohol-related cirrhosis

Benedikt Simbrunner[1,2,3,4,4], Raphaela Staltner[5], Benedikt Hofer[1,2,3,4,6], Lorenz Balcar[1,2,3], Vlad Taru[1,3,4,6], Lukas Hartl[1,2,3], Georg Kramer[1,2,3], Georg Semmler[1,2,3], Kerstin Zinober[1,3,4], Katharina Regnat[1,3,4], Michael Trauner[1,2], Mattias Mandorfer[1,2,3], Ina Bergheim[5], Thomas Reiberger[1,2,3,4,6].
[1]Medizinische Universität Wien, Division of Gastroenterology and Hepatology, Wien, Austria; [2]Clinical Research Group MOTION, Medical University of Vienna, Vienna, Austria; [3]Vienna Hepatic Hemodynamic Lab, Division of Gastroenterology and Hepatology, Department of Medicine III, Medical University of Vienna, Vienna, Austria; [4]Christian Doppler Laboratory for Portal Hypertension and Liver Fibrosis, Medical University of Vienna, Vienna, Austria; [5]Department of Nutritional Sciences, Molecular Nutritional Science, University of Vienna, Vienna, Austria; [6]CeMM Research Center for Molecular Medicine of the Austrian Academy of Sciences, Vienna, Austria
Email: benedikt.simbrunner@meduniwien.ac.at

Background and aims: Disruption of the intestinal barrier in alcohol-related (ALD) cirrhosis facilitates translocation of microbial products, most commonly exemplified in literature by

lipopolysaccharide (LPS). Recent evidence indicates that a broader spectrum of pathogen-associated molecular patterns (PAMPs) reaches the circulation in cirrhosis that may trigger inflammation through different Toll-like receptors (TLR). This study aimed to characterize the circulating "TLR ligandome" across the disease severity spectrum of ALD cirrhosis.

Method: Concentrations of TLR1–9 ligands in serum samples were estimated using an assay employing HEK-293 cells stably transfected with the respective human TLRs. Cells were stimulated with 20 μL serum from patients with compensated (CC, n = 20), stable decompensated cirrhosis (SDC, n = 17), or acute decompensation with and without acute-on-chronic liver failure (AD ± ACLF, n = 20), and healthy controls (n = 12). Secreted Embryonic Alkaline Phosphatase (SEAP) reporter activity was quantified on a microplate reader. Each assay included positive and negative controls.

Results: Disease severity as reflected by MELD (CC 11.5 [9.0–14.0], SDC 12.0 [10.0–16.0], AD-ACLF 19.0 [18.0–24.5]; $p < 0.001$) and IL-6 levels (5.85 [4.12;9.40], 12.9 [6.84–22.7], and 27.6 [24.1–41.8]; $p < 0.001$) increased across cirrhosis stages. All TLR assays showed significantly increased activity in cirrhosis stages compared to healthy controls, with modest activation in CC and SDC; but a pronounced activation peak in AD-ACLF. SEAP reporter activity reflecting TLR ligand concentration correlated strongly among all TLRs, indicating either shared TLR recognition or simultaneous presence of various circulating ligands (Spearman's rho >0.500 for all). Positive correlations with inflammatory biomarkers (IL-6, C-reactive protein: CRP) were observed for TLR2, TLR4, TLR7, TLR8, and TLR9. Notably, TLR4 ligand concentration additionally correlated with LPS-binding protein (LBP) levels.

Conclusion: Cell-based TLR reporter assays detect a broad repertoire of circulating TLR ligands in patients with ALD cirrhosis, extending beyond canonical TLR4 activation. The marked activation spike in AD-ACLF and correlations with systemic inflammation support the concept of various circulating PAMPs in cirrhosis peaking in AD-ACLF. The findings highlight the importance of further studies on TLR-activating ligands that shape inflammatory trajectories in cirrhosis.

FRI-433

Integrated metaproteomics reveals parasitic protein signatures associated with inflammation, oxidative stress, regeneration, and mortality in acutely decompensated cirrhosis

Shreya Singh[1], Rohit Nadda[1], Pratibha Garg[1], Sunil Taneja[1], Ajay Kumar Duseja[1], Sumeeta Khurana[1], Trayambak Basak[2], Nipun Verma[1]. *[1]Postgraduate Institute of Medical Education and research, Chandigarh, India; [2]Indian Institute of Technology, Mandi, Himachal Pradesh, Mandi, India*
Email: drnipun29j@gmail.com

Background and aims: The role of circulating parasite-derived proteins in modulating host biological pathways and clinical outcomes in acutely decompensated cirrhosis remains poorly defined. We investigated parasite protein signatures in acute decompensation (AD) and evaluated their associations with host pathway activity and mortality.

Method: In a prospective cohort of 100 patients with AD and 10 healthy controls, plasma proteomic profiling was performed using LC-MS/MS. Parasite-derived peptides were assigned using Unipept version 3.0.1, and diversity metrics were assessed. Differentially expressed parasite proteins (DEPs) between survivors and non-survivors, were identified through inferential statistics, discriminant analysis and machine learning. Associations with inflammatory markers, clinical outcomes, and host pathway enrichment scores (ssGSEA) were evaluated.

Results: Parasite diversity was higher in AD vs. healthy controls, and in non-survivors vs. survivors, reflected by increased alpha diversity and beta diversity ($p < 0.05$). Ten mortality-associated DEPs were identified. *Plasmodium falciparum* reticulocyte-binding homolog 1 (PfRH1) emerged as the strongest predictor of mortality (VIP > 2.2) and correlated with systemic inflammation (NLR, $r = 0.36$, $p = 0.004$). Helminth-derived proteins, *Necator americanus* histone-H4 (NECAME_16786), was enriched in survivors and associated with lymphocyte predominance and total protein levels. PfRH1 showed positive correlations with host Toll-like receptor signalling, MAPK signalling, and inflammatory response pathway, all enriched in non-survivors, and negative correlation with regulatory TGF-beta signalling. Conversely, NECAME_16786 was positively associated with p53 signalling which was enriched in survivors and negatively associated with reactive oxygen species (ROS) pathway which was enriched in non-survivors. Helminth, *Fasciola gigantica* DUB-like protein, FGIG_02690 had negative correlations with ROS pathway.

Conclusion: Circulating parasite proteins are detectable in AD cirrhosis and are systematically associated with host inflammatory, stress, and regulatory pathways, with prognostic relevance. PfRH1 is linked to heightened systemic inflammation and mortality, whereas helminth-derived proteins are associated with a more regulatory host response. These findings raise the possibility of unrecognised low-density parasite exposure in hepatic and immune dysfunction and suggests that helminth-derived immune modulators warrant further therapeutic investigation.

FRI-434

Targeting disrupted immunometabolism-induced mitochondrial bioenergetic failure using YAQ006 and YAQ005 reduces mortality in ACLF

Supachaya Sriphoosanaphan[1,2,3], Annarein Kerbert[1], Tingting Qi[1], Abeba Habtesion[1], Fausto Andreola[1], Jan-Willem Taanman[4], Francesco De Chiara[5], Rajiv Jalan[1]. *[1]Liver Failure Group, Institute for Liver and Digestive Health, University College London, London, United Kingdom; [2]Division of Gastroenterology, Department of Medicine, Faculty of Medicine, Chulalongkorn University, Bangkok, Thailand; [3]Centre of Excellence in Liver Diseases, King Chulalongkorn Memorial Hospital, Thai Red Cross Society, Bangkok, Thailand; [4]Department of Clinical and Movement Neurosciences, Queen Square Institute of Neurology, University College London, London, United Kingdom; [5]Institute for Bioengineering of Catalonia, Barcelona, Spain*
Email: r.jalan@ucl.ac.uk

Background and aims: Hyperammonemia contributes to morbidity and mortality in advanced liver disease and has significant impact on immune function and metabolism, particularly in patients with ACLF. Integrated multiomic profiling demonstrated that ammonia triggers hepatic mitochondrial bioenergetic collapse through a specific, Toll-like receptor 4 (TLR4)-dependent immunometabolic axis[1]. Although ammonia lowering using ornithine phenylacetate (YAQ006) successfully reverses hepatic encephalopathy, it does not improve survival in ACLF. Given the underlying mechanism of ammonia-induced organ injury in ACLF, we aimed to evaluate whether YAQ006 is synergistic with YAQ005 (a TLR4 antagonist) in reducing mortality in ACLF.

Method: We studied two distinct rodent models: 1) A rat model of ACLF induced by bile duct ligation (4 weeks) followed by lipopolysaccharide (LPS) challenge (0.025 mg/kg, i.p.); and 2) A mouse model of ornithine transcarbamylase deficiency ($Otc^{spf\text{-}ash}$) fed a high-protein diet for 7 days acting as hyperammonemic controls. In the ACLF model, YAQ005 (10 mg/kg, i.p.) was administered 3 hours before LPS, and YAQ006 (0.3 g/kg, oral gavage) was given twice daily for 5 days. In the $Otc^{spf\text{-}ash}$ model, YAQ005 and YAQ006 were administered during the final 4 days. Endpoints included ammonia levels, ALT and 6-hour coma-free survival.

Results: In the ACLF model, BDL-LPS rats developed severe hyperammonemia (280.5 ± 38.7 μmol/L) and all animals died. Monotherapy with either YAQ006 or YAQ005 reduced plasma ammonia to 130–145 μmol/L ($p < 0.001$ vs. BDL-LPS). Combination therapy provided synergistic benefit, further reducing ammonia to 73.4 ± 11.5 μmol/L ($p < 0.001$ vs. monotherapies) and reducing liver

injury (ALT 115.1 vs. 321.0 U/L, $p < 0.001$). Notably, the combination achieved 100% coma-free survival, significantly higher than YAQ006 (62.5%) or YAQ005 (75.0%) alone (both $p < 0.01$). In contrast, in the $Otc^{spf\text{-}ash}$ mice, while YAQ006 and YAQ005 significantly reduced ammonia and ALT (both $p < 0.001$), the combination provided no additive benefit, suggesting that the synergy is specific to the inflammatory context.
Conclusion: Combined ammonia scavenging with YAQ006 and TLR4 inhibition with YAQ005 provides synergistic survival benefit in ACLF. The therapeutic synergy observed in inflammatory models of hyperammonemia but not in congenital urea-cycle deficiency highlights disease-context specificity and suggests a novel therapeutic framework for ACLF.
Reference: 1. Sriphoosanaphan S et al. EASL Congress 2025

FRI-435
Ammonia-induced mitochondrial bioenergetic failure is driven through a TLR4-dependent mechanism that specifically targets Complex IV
Supachaya Sriphoosanaphan[1,2,3], Francesco De Chiara[4], Fausto Andreola[1], Harry Horsley[5], Nicola Mordan[6], Jan-Willem Taanman[7], Rajiv Jalan[1]. *[1]Liver Failure Group, Institute for Liver and Digestive Health, University College London, London, United Kingdom; [2]Division of Gastroenterology, Department of Medicine, Faculty of Medicine, Chulalongkorn University, Bangkok, Thailand; [3]Centre of Excellence in Liver Diseases, King Chulalongkorn Memorial Hospital, Thai Red Cross Society, Bangkok, Thailand; [4]Institute for Bioengineering of Catalonia, Barcelona, Spain; [5]Centre for Kidney and Bladder Health, University College London, London, United Kingdom; [6]Eastman Dental Institute, University College London, London, United Kingdom; [7]Department of Clinical and Movement Neurosciences, Queen Square Institute of Neurology, University College London, London, United Kingdom*
Email: r.jalan@ucl.ac.uk

Background and aims: The pathogenesis of ammonia-induced hepatotoxicity remains incompletely understood. While hyperammonemia causes mitochondrial dysfunction, the molecular events linking ammonia to organelle failure are undefined. We previously identified Toll-like receptor 4 (TLR4) as a critical mediator of ammonia-induced liver injury *in vivo* and showed that YAQ005, a TLR4 inhibitor, could significantly reduce ammonia[1,2]. Here, we aimed to explore the mechanisms and define the role of TLR4 in this pathway.
Method: In AML12 murine hepatocytes, we assessed gene expression (qPCR), mitochondrial respiration (Seahorse XF) and oxidative phosphorylation (OXPHOS) enzyme activities (spectrophotometry and Blue Native PAGE). Mitochondrial reactive oxygen species (ROS) and membrane potential were quantified by live-cell confocal imaging. TLR4-mitochondrial co-localisation was assessed by immunofluorescence. Ultrastructural changes were examined by transmission electron microscopy (TEM).
Results: Ammonia (NH_4Cl) exposure induced profound mitochondrial dysfunction, characterised by suppressed basal and maximal respiration ($p < 0.001$) and a specific inhibition of Cytochrome c oxidase (OXPHOS Complex IV). This bioenergetic collapse was accompanied by a mitochondrial ROS surge and membrane depolarisation. Mechanistically, ammonia significantly upregulated *Tlr4* mRNA expression ($p = 0.002$), an effect mitigated by treatment with YAQ005 ($p = 0.001$). Inhibition of TLR4 with YAQ005 also prevented the functional defects, restoring OXPHOS Complex IV activity and respiratory capacity without altering extracellular ammonia levels, confirming a direct protective effect. Notably, ammonia increased TLR4 protein abundance and its spatial association with the mitochondrial network (Pearson's r 0.76; $p = 0.046$). This recruitment was associated with mitochondrial stress and structural remodelling, including cristae effacement and mitophagy, which were attenuated by TLR4 blockade.
Conclusion: These findings identify TLR4 as a direct, cell-autonomous mediator of ammonia-induced mitochondrial dysfunction. We propose a novel mechanism whereby ammonia triggers the transcriptional upregulation and mitochondrial recruitment of TLR4, leading to specific Complex IV inhibition and bioenergetic failure. This provides a mechanistic rationale for the use of TLR4 inhibitor (YAQ005) to protect hepatocyte mitochondrial function in hyperammonemia.
Reference: 1. Kerbert A et al. Sci Adv. 2025;11(10):eado1648
2. Sriphoosanaphan S et al. EASL Congress 2025

FRI-436
Peritoneal remodeling in patients with liver cirrhosis and ascites: a possible pathogenic link to impaired fluid homeostasis and altered peritoneal immunity
Helena Stadler[1], Mona-May Langer[1], Quan Yin[1], Lena Oeckl[1], Marc Weiß[1], Alina Bauschen[1], Severin Jacobi[2], Christian M. Lange[1]. *[1]Department of Medicine II, University Hospital LMU, Munich, Germany; [2]Department of General- Visceral- and Transplant-Surgery, University Hospital LMU, Munich, Germany*
Email: helena.stadler@med.uni-muenchen.de

Background and aims: In homeostasis, the peritoneum plays a central role in maintaining fluid homeostasis and local immune surveillance within the abdominal cavity. Previous studies have shown structural remodeling in the peritoneum of patients with liver cirrhosis, including fibrosis, dilated lymphatics and increased vascularization. Despite the potential impact of peritoneal remodeling on permeability and immune responses, the underlying mechanisms and consequences in the context of liver cirrhosis and ascites remain poorly understood. Therefore, this study aims to characterize the structural and cellular remodeling in the peritoneum of patients with liver cirrhosis.
Method: Specimens of parietal peritoneum were obtained in non-cirrhosis-related elective abdominal interventions and during liver transplantations. H&E and Masson's trichrome staining were performed for histological evaluation, while real-time PCR, spatial transcriptomics and immunofluorescence was used to assess molecular and cellular remodeling. Single-cell sequencing was performed on ascites samples collected during routine paracentesis.
Results: The collagen-positive area in the peritoneum was found to be greater in patients with liver cirrhosis than in controls, with significantly higher collagen content in patients with massive versus moderate ascites ($p = 0.02$). In line with that, spatial transcriptomic analysis revealed an increased abundance of fibroblasts ($p = 0.01$) and myofibroblast ($p = 0.045$) in peritoneum of patients with decompensated liver cirrhosis compared to controls. Additionally, peritoneal mesothelial cells, as well as detached mesothelial-like cells in ascites showed signs of mesothelial-to-mesenchymal transition. This fibrotic and remodeling environment in the peritoneum of patients with decompensated liver cirrhosis was further characterized by a predominance of anti-inflammatory M2 macrophages in the peritoneum. Moreover, lymphatic and vascular endothelium showed an upregulation of activation and inflammatory markers, which may contribute to altered fluid homeostasis and lymphatic drainage.
Conclusion: We suggest that the pro-inflammatory environment in the peritoneal cavity of patients with liver cirrhosis promotes fibrotic remodeling of the peritoneum. The altered peritoneal microenvironment may contribute to development and persistence of ascites and abdominal infections by affecting fluid homeostasis and immune cell polarization and trafficking.

FRI-441-YI
Targeting glycolytic rewiring rescues liver sinusoidal endothelial cell mitochondrial bioenergetics and vascular barrier integrity mitigates endotoxin mediated portal hypertension in cirrhosis
Vaibhav Tiwari[1], Rajni yadav[1], Mamta Kumari[2], Manisha Manisha[1], Aishwarya Bhatnagar[1], Himanshi Himanshi[1], Bitan Guchhait[1],

Mahesh Vijay Patil[1], Savneet Kaur[1], Subhadeep Roy[3], Anupam Kumar[1], Shiv Kumar Sarin[1], Dinesh Mani Tripathi[1]. [1]*Institute of Liver & Biliary Sciences, New Delhi, India;* [2]*National Institute Of Pharmaceutical Education & Research Kolkata, Kolkata, India;* [3]*Birla Institute Of Technology, Mesra, India*
Email: dineshmanitripathi@gmail.com

Background and aims: Endotoxemia aggravates portal hypertension (PHT) in cirrhosis, fundamentally driven by dysfunctional LSECs. In cirrhosis, metabolic reprogramming of LSECs under influence of endotoxemia remains unexplored. We hypothesized that metabolic shift toward 6-phosphofructo-2-kinase/fructose-2,6-biphosphatase 3 (PFKFB3) driven glycolysis disrupts LSEC mitochondrial function, vascular integrity, leading to coagulation, thrombosis and contributing to PHT. We aimed to investigate the role of PFKFB3 and its pharmacological modulation in restoring LSEC bioenergetics and mitigating PHT during sepsis in cirrhosis.
Method: Sepsis was induced in non-cirrhotic (Caecum ligation puncture) and with LPS(1 mg/kg) in CCL_4 cirrhotic rats treated with PFKFB3-inhibitor 3PO (50 mg/kg, i.p). Hemodynamics, LSECs functionality and remodeling were assessed. Metabolomics and bioenergetics of LSECs were analysed. Endothelial integrity was quantified using Trans-endothelial electrical resistance (TEER), vascular permeability (Lucifer yellow, Dextran 40 kDa), tube formation and leukocyte adhesion assays. Molecular validation [gene/protein profiling of PFKFB3, HMGB1 endothelial junctional markers (VE-cadherin/Claudin-5)] was performed and survival was studied.
Results: PFKFB3 inhibition significantly attenuated portal pressure and hyperdynamic circulation in both cirrhotic and non-cirrhotic groups. Treatment reversed the glycolytic shift, evidenced by reduced ECAR($p < 0.001$) and restored mitochondrial respiration (OCR) ($p < 0.01$). LSECs treated with 3PO showed significant improvement in mitochondrial biomass (MTG), potential (MTR) and oxidative stress. Electron microscopy revealed marked increase in diameter and number of LSEC fenestrae. TEER and permeability assays demonstrated restored endothelial barrier integrity ($p < 0.01$) upon treatment. PFKFB3 blockade in LSECs markedly reduced monocyte/neutrophil adhesion, and promotes tube formation ($p = 0.01$). Mechanistically, Glycolytic (PFKFB3, HK1, LDHA) and inflammatory mediators (IL-1β, HMGB1, ICAM-1) were reduced significantly in both cells and tissue. Improved endothelial junction proteins (VE-cadherin/Claudin-5) expression conferred improved barrier integrity upon treatment. Consequently, cellular inhibition of PFKFB3 improved liver injury markers and overall survival (28%).
Conclusion: Targeting PFKFB3 reverses glycolytic reprogramming and rescues LSEC mitochondrial function, thereby ameliorating vascular dysfunction and portal hypertension during sepsis in cirrhosis.

FRI-442
Stage-dependent central and peripheral dysregulation of platelet biogenesis in experimental cirrhosis

Carolina Franco[1,2], Iris Asensio[1,2], Marta Puerto[1,2,3], Elena Vázquez-Ogando[1,2], Johanna Sierra[1,2], Christian Ruiz-Martin[1,2], David Blanco[1,2], Jose Fortea[1,2,3], Cristina Ripoll[1,2,3], Ignacio Benedicto[4,5], Francisco Javier Cubero[1,3,6,7], Jean Campbell[8], Rafael Bañares[1,2,3,9], Javier Vaquero[1,2,3]. [1]*Instituto de Investigación Sanitaria Gregorio Marañón (IiSGM), Madrid, Spain;* [2]*Hospital General Universitario Gregorio Marañón, Madrid, Spain;* [3]*CIBEREHD, Madrid, Spain;* [4]*Centro de Investigaciones Biológicas Margarita Salas (CIB), Consejo Superior de Investigaciones Científicas (CSIC), Madrid, Spain;* [5]*Centro Nacional de Investigaciones Cardiovasculares (CNIC), Madrid, Spain;* [6]*Department of Immunology, Ophthalmology and ENT, Facultad de Medicina, Univ. Complutense, Madrid, Spain;* [7]*Instituto Universitario de Neuroquímica (IUIN), Facultad de Medicina, Univ. Complutense, Madrid, Spain;* [8]*Northwestern University, Seattle, United States;* [9]*Facultad de Medicina, Universidad Complutense, Madrid, Spain*
Email: j.vaquero@iisgm.com

Background and aims: Thrombocytopenia is a hallmark of chronic liver disease (CLD), largely due to hypersplenism and reduced thrombopoietin (TPO) production. Here, we investigated peripheral and bone marrow (BM) determinants of platelet production across stages of experimental cirrhosis.
Method: Male SD rats receiving oral carbon tetrachloride (CCl4) for 2–12 weeks were classified into early, intermediate, and advanced stages based on liver-to-body weight (L/BW) ratio. We examined systemic, hepatic, and hematologic parameters, including TPO across vascular beds, hepatic and BM Tpo/Mpl mRNA, portal pressure, and BM megakaryocyte (MGK) counts (H&E). Liver (n = 27) and BM (n = 31) RNA-seq were analyzed with LIMMA or DESeq2, and GSEA. Separate rat cohorts received the TPO-receptor agonist romiplostim to assess BM responsiveness.
Results: CCl4 induced progressive fibrosis, portal hypertension, and hepatic dysfunction. Platelet counts varied widely but correlated with L/BW ratio, not with plasma TPO, portal pressure, or hepatic function. The normal association of transhepatic venous TPO gradient with platelet count was lost in cirrhosis. In cirrhotic rats, BM Tpo and Mpl mRNA expression decreased, and MGK numbers rose early but failed to increase at advanced stages despite thrombocytopenia. BM RNA-seq showed limited differential expression (64 genes) in rats treated with CCl4, with enrichment of inflammation-related and suppression of metabolic pathways. Of note, stage-resolved analyses revealed distinct programs: early stage had proliferative/stress and ribosome-biogenesis signatures with reduced differentiation and energy metabolism; intermediate stage had persistent metabolic stress with increased immune/antimicrobial pathways and reduced proliferation; advanced stage had exacerbated inflammatory activation with dysregulated ribosome biogenesis and suppression of stress-response and differentiation pathways. GSEA focused on platelet/MGK-related gene sets showed a shift from enrichment to suppression at advanced stage. Romiplostim increased platelet counts in controls ($p < 0.001$) and in cirrhotic rats ($p < 0.05$), without worsening liver injury or portal hypertension. BM transcriptomic responses to romiplostim were preserved in cirrhosis.
Conclusion: Liver disease induces complex, dynamic, and stage-dependent changes in both peripheral and central regulators of platelet production. The preserved response to romiplostim supports that BM progenitors remain functional despite disease-related transcriptional reprogramming.

FRI-443
Whole blood ex vivo targeted lipidomic profiling as an immunometabolic target screening tool in decompensated liver disease

Joseph D Wilson[1,2], Roosey Sheth[1,2], Francesca Trovato[1,2], Mark J W McPhail[1,2]. [1]*Roger Williams Institute of Liver Studies, King's College London, London, United Kingdom;* [2]*King's College Hospital NHS Foundation Trust, London, United Kingdom*
Email: joseph.wilson10@nhs.net

Background and aims: Lipidomic analysis of patients with decompensated cirrhosis and acute-on-chronic liver failure (AD/ACLF) has revealed targets of potential therapeutic and/or biomarker potential. The AD/ACLF lipidome has significant immune dysfunction implications. Currently, lipidomic analysis is performed on plasma or serum, thus negating the impact of metabolically active cells on the observed lipidome. We devised a whole blood, scalable, *ex vivo* platform for targeted lipidomic profiling and assessing therapeutic modulation. We assessed the lipidomic response to autotaxin (ATX) inhibition given the immunomodulatory importance of the lysophosphatidylcholine-autotaxin-lysophosphatidic acid (LPC-ATX-LPA) axis.
Method: Whole blood from AD/ACLF patients (n = 8) and healthy controls (HCs) (n = 4) was cultured *ex vivo* in a RPMI media and foetal bovine serum mixture for 18–24 h with or without the ATX inhibitor HA130 at 100 nM. Supernatants, generated from whole blood centrifugation, were subject to flow injection analysis-tandem mass

spectrometry (FIA-MS/MS) on the Biocrates LxQuant platform. A total of three hundred and twenty-five lipid species were measured. Lipid concentrations were normalised to the median, log-transformed, and pareto-scaled, prior to multivariate analysis by principal components analysis (PCA) and orthogonal least squares discrimant analysis (OPSL-DA).
Results: PCA and OPSL-DA demonstrated distinct whole blood lipidomic profiles of HC and AD/ACLF ($R^2Y = 0.920$; $Q^2 = 0.807$), indicative of good model fit, and predictive performance verified using permutation testing (n = 1000). Sixteen lipid species had a variable importance of projection (VIP) value >2, the majority of which were phosphatidylcholines (38%), acyl carnitines (25%), and cholesteryl esters (19%). They were dominated by phosphatidylcholine O-38:1, phosphatidylcholine 32:1, phosphatidylcholine 32:0, cholesteryl ester 20:5, and hexadecenoylcarnitine. ATX inhibition reduced phosphoenalomine concentrations in both HCs and AD/ACLF.
Conclusion: We demonstrate that our whole blood *ex vivo* lipidomic profiling successfully discriminates between AD/ACLF and HCs, with phosphatidylcholines being highly discriminatory in OPLS-DA analysis. A previously unknown off target effect of ATX inhibition was identified with potentially important immunomodulatory and therapeutic relevance. This model should be further explored to expand this platform and investigate promising drug targets prior to human experimental medicine studies.

FRI-444-YI
Data-driven biomarker phenotypes refine risk stratification in advanced chronic liver disease
Adrian Wunderbaldinger[1], Benedikt Simbrunner[1], Lorenz Balcar[1], Lukas Hartl[1], Benedikt Hofer[1], Mathias Jachs[1], Georg Kramer[1], Paul Thöne[1], Christian Sebesta[1], Bernhard Scheiner[1], Philipp Schwabl[1], Albert Friedrich Stättermayer[2], Michael Trauner[1], Mattias Mandorfer[1], Thomas Reiberger[1], Georg Semmler[1]. *[1]Division of Gastroenterology and Hepatology, Department of Medicine III, Medical University of Vienna, Vienna Hepatic Hemodynamic Lab, Division of Gastroenterology and Hepatology, Department of Medicine III, Medical University of Vienna, Clinical Research Group MOTION, Medical University of Vienna, Vienna, Austria; [2]Division of Gastroenterology and Hepatology, Department of Medicine III, Medical University of Vienna, Clinical Research Group MOTION, Medical University of Vienna, Vienna, Austria*
Email: adrian.wunderbaldinger@meduniwien.ac.at

Background and aims: Traditionally, patients with advanced chronic liver disease (ACLD) are categorized based on their clinical appearance, but their outcomes within specific disease stages like compensated cirrhosis, decompensated cirrhosis and further decompensation are highly heterogeneous. Here, data-driven clustering based on pathophysiological biomarker profiles may unravel prognostically relevant phenotypes.
Method: We prospectively analyzed ACLD patients at the time of first hemodynamic characterization (baseline) at a tertiary care center between 2017 and 2021. We assessed the subsequent clinical course including first and further decompensation and liver-related death (LRD). Unsupervised clustering was performed using partitioning around medoids on a biomarker panel capturing portal hypertension (hepatic venous pressure gradient [HVPG]), endothelial dysfunction (von Willebrand Factor [VWF] antigen), fibrosis (enhanced liver fibrosis [ELF] test), liver function (MELD, albumin, bile acids), systemic inflammation (C-reactive protein [CRP], interleukin-6 [IL-6], procalcitonin [PCT]), and circulatory dysfunction (N-terminal pro-brain-type natriuretic peptide [NT-proBNP], copeptin).
Results: A total of 451 patients (72% male, alcohol-related liver disease as main aetiology [36%]) were included. Distribution of disease stages were as follows: 168 (37%) patients had compensated, 166 (37%) patients had decompensated cirrhosis, and 117 (26%) patients were further decompensated. Within the ACLD spectrum (i.e., not considering clinical stages), we identified two clusters with the following key variable contribution in descending order: Albumin > HVPG > VWF > ELF > others. In total 29% of cACLD, 72% of decompensated cirrhosis and 86% of further decompensation were allocated to the more advanced disease cluster. This cluster identified compensated patients at significantly higher risk of first decompensation (HR: 4.57 [95%CI: 2.31–9.076], p < 0.001), even when adjusted for presence of clinically significant portal hypertension (aHR: 3.75 [95% CI: 1.86–7.57], p < 0.001). In decompensated cirrhosis, this cluster was associated with further decompensation (HR: 1.86 [1.02–3.38], p = 0.042) and LRD (HR: 2.84 [1.09–7.39], p = 0.032).
Conclusion: Patient clustering based on key biomarker profiles reduces the complexity and pathophysiological heterogeneity of ACLD, identifies patients at risk for further disease progression and may serve as an enrichment strategy for clinical trials.

FRI-445
Updated natural history of contemporary compensated advanced chronic liver disease patients
Adrian Wunderbaldinger[1], Lorenz Balcar[1], Lucie Simonis[1], Jan Embacher[1], Georg Kramer[1], Benedikt Simbrunner[1], Mathias Jachs[1], Lukas Hartl[1], Bernhard Scheiner[1], Michael Trauner[1], Thomas Reiberger[1], Mattias Mandorfer[1], Georg Semmler[1]. *[1]Division of Gastroenterology and Hepatology, Department of Medicine III, Medical University of Vienna, Vienna Hepatic Hemodynamic Lab, Division of Gastroenterology and Hepatology, Department of Medicine III, Medical University of Vienna, Clinical Research Group MOTION, Medical University of Vienna, Vienna, Austria*
Email: adrian.wunderbaldinger@meduniwien.ac.at

Background and aims: Due to significant improvements in non-invasive diagnosis and clinical management, the natural history of contemporary patients with compensated advanced chronic liver disease (cACLD) is unclear, especially regarding the multistate disease course of cACLD. Similarly, data on prognostic factors for specific clinical transitions remain limited.
Method: We studied 1140 consecutive cACLD patients presenting at a hepatology outpatient clinic from 2015 (i.e., following the introduction of interferon-free therapies) to 2022. The occurrence of first and further decompensation, acute-on-chronic liver failure (ACLF), and death were recorded. Baseline profiles were obtained at baseline and longitudinally (32,789 individual time points for laboratory values, 1,617 LSMs) and incorporated in a multistate modelling framework.
Results: 61% were male, median age was 55 years, 42% had steatotic liver disease, and 37% viral hepatitis. Median LSM at baseline was 16.0 kPa, median MELD 7, median albumin 43.1 g/dL. The median follow-up was 3.9 years. The probability to remain compensated was 94% at 1 year, 89% at 2 years, and 74% at 5 years, and the probability of having experienced (only) first decompensation was low with 2.6% at 1, 3.8% at 2, and 3.5% at 5 years. At the same time, 0.3% experienced further decompensation at 1, 2.1% at 2, and 3.1% at 5 years while 3.1% had died at 1, 6.6% at 2 and 20% at 5 years, respectively. Within 5 years, patients starting in compensated state were estimated to spend 51.9 months in compensated compared to only 2.7 months in decompensated and further decompensated state. Baseline information on LSM, albumin, MELD and platelet count was associated with first decompensation and further decompensation (LSM, platelet count, MELD), but not any subsequent endpoints (adjusted for age, sex and aetiological cure). Using updated biomarker profiles significantly enhanced the associations of MELD (associated with all subsequent stage transitions) and C-reactive protein (non-liver-related death from cACLD and liver-related death from first decompensation).
Conclusion: The prognosis of cACLD patients in the era of aetiological therapies is improved as compared to historic data and should inform trial design. However, the disease course gets accelerated as soon as first hepatic decompensation has occurred. Baseline biomarkers provide little information for subsequent events other than first decompensation. In contrast, updated biomarkers provide incremental stage-specific information.

FRI-452-YI

Intrahepatic low shear–induced mitochondrial redox dysfunction in liver sinusoidal endothelial cells drives microvascular dysfunction and contributes to acute portal hypertension

Rajni Yadav[1], Vaibhav Tiwari[1], Himanshi Himanshi[1], Aishwarya Bhatnagar[1], Manisha Manisha[1], Savneet Kaur[1], Anupam Kumar[1], Shiv Kumar Sarin[1], Dinesh Mani Tripathi[1]. [1]*Institute of Liver & Biliary Sciences, New Delhi, India*
Email: dineshmanitripathi@gmail.com

Background and aims: Physiological shear regulates LSEC mediated hepatic vascular homeostasis, whereas disturbed shear promotes microvascular dysfunction. However, the consequences of acute reduction in intrahepatic shear below physiological level remain less explored. We investigated how low shear remodels the sinusoidal microenvironment and initiates early vascular complications.
Method: Intrahepatic low shear model was developed by 50–60% portal vein ligation. Intrahepatic blood Flow was assessed by hemodynamics, intra-vital imaging in sham, D1, D2 post PPVL. Liver tissue and isolated LSECs at D2 metabolomics and proteomics was performed. Bioenergetics of LSECs was analysed using Seahorse Extracellular Flux Assay and mitochondrial biomass and potential was measured using MitoTracker dye. Electron microscopy was performed.
Results: Marked reduction in PBF (−42%, −48% at D1, D2 respectively) post PPVL indicate intrahepatic low shear, further confirmed by intravital imaging of portal-vein. Rise in PP (+110%, +135% at D1, D2 respectively) indicating intrahepatic flow resistance. Mechanistically, early alterations dominated by mitochondrial remodelling in LSECs revealed enhanced glycolytic flux- pyruvate levels (log2FC +1.7), reduced mitochondrial fatty-acid β-oxidation, accumulation of L-palmitoylcarnitine (Log2FC- 1.53) indicating carnitine shuttle dysfunction, decrease maximal respiration indicating impaired oxidative phosphorylation. Increased NAD^+ levels (log2FC 2.1) indicate disrupted mitochondrial redox balance. Reduced mitochondrial mass, membrane potential, increased ROS (Sham- 12% vs D2-76% at D2) confirm mitochondrial injury. This altogether disrupts redox sensitive actin protein cdc42 (FC+3), actin-related protein-2 (FC +4.3) and gelsolin (FC −3.5) indicating increased actin polymerisation. Consequently, lead to defenestration (porosity- 18% sham vs 7.9% at D2), while TEM revealed elongated LSECs with increased cytoplasmic-to-nuclear ratio (≥2.1:1 at D2 vs sham = 1:1.5). These endothelial alterations coincided activation of immune and complement-coagulation cascade, establishing a thrombo-inflammatory microenvironment, as evidenced by increased S100A8/A9 expression, elevated serum vWF, reduced ADAMTS13. Together these processes aggravate sinusoidal microvascular dysfunction culminating in acute portal hypertension.
Conclusion: Low shear induces glycolytic uncoupling and mitochondrial redox dysfunction in LSECs, driving cytoskeletal remodelling, thrombo-inflammation, and acute portal hypertension.

FRI-453-YI

Investigating the impact of carboxylated polystyrene nanoplastics in liver using hepatic cell lines and human precision-cut liver slices

Namrata Pandey[1], Paula Boeira[1], Nathaniel Clark[2,3], Eleanor Walker[1], Somaiah Aroori[1,4], Jemimah Denson[4], Richard Thompson[5], Matthew Cramp[1,4], Shilpa Chokshi[1,6], Ashwin Dhanda[1,4]. [1]*Centre of Environmental hepatology, Faculty of Health, University of Plymouth, Plymouth, United Kingdom;* [2]*School of Health Professions, Faculty of Health, University of Plymouth, Plymouth, United Kingdom;* [3]*School of Biomedical Sciences, Faculty of Health, University of Plymouth, Plymouth, United Kingdom;* [4]*South West Liver Unit, University Hospitals Plymouth NHS Trust, Plymouth, United Kingdom;* [5]*School of Biological and Marine Sciences, Faculty of Science and Engineering, University of Plymouth, Plymouth, United Kingdom;* [6]*Roger Williams Institute of Liver Studies, Faculty of Medicine, King's College London, London, United Kingdom*
Email: namrata.pandey@plymouth.ac.uk

Background and aims: Large plastic products degrade during use and after disposal into small particles described as microplastics (<5 mm, MP) and nanoplastics (<1 µm, NP). These MP/NPs accumulate in the environment and can enter the human body via ingestion and inhalation. Several studies have reported MP/NP in human tissue, raising concerns about potential adverse health outcomes. Existing research on NP toxicity is variable and lacks sufficient understanding of the liver-associated pathophysiology. To understand the impact of NP on the liver, we determined the uptake and effects of commercially available carboxylate-modified 20 nm polystyrene nanoparticles (PS NPs) in three hepatic models: human carcinoma hepatocytes (HepG2), immortalised human hepatocytes (IHH), and human precision-cut liver slices (hPCLS).
Method: We visualised and quantified PS NPs uptake in all three hepatic models using confocal microscopy and flow cytometry. We analysed post-exposure cytotoxicity by assessing cell viability, and measuring hepatic injury markers. We also examined the subtle physiological effects of PS NPs in the HepG2 cells by estimating relative reactive oxygen species (ROS) production using the DCFHDA assay and by comparing mitochondrial respiration in cells using the Agilent Seahorse XFe96 analyser.
Results: Exposure experiments show a model and dose-dependent uptake of PS NPs after 24 and 48 hours of exposure in all three hepatic models. 63.0 ± 31.5% IHH cells showed uptake at a concentration of 0.1 µg/mL, which is considerably lower than the measured plastic concentration in human blood (1.8–4.7 µg/mL). Cell viability of IHH cells decreased from 95.2 ± 2% in the control group to 9.7 ± 7.1% at 100 µg/mL after 48 hours of exposure. Early signs of cell injury were observed with high levels of AST enzyme in the media of IHH and hPCLS at high PS NPs concentrations. HepG2 cells showed no changes in cell viability, redox state, or mitochondrial respiratory parameters after exposure to PS NPs.
Conclusion: The study demonstrates that PS NPs can readily accumulate in hepatocytes, even at a concentration as low as 0.1 µg/mL in IHH cells, and cause cell damage and reduce cell viability at high doses. The effect of PS NPs is model-dependent, highlighting the need for physiologically relevant toxicity models to study the underlying mechanisms of NP cytotoxicity. These findings emphasise the urgent need to investigate the health effects of NP pollution on human liver health using humanised toxicity models.

Cirrhosis and its complications – Other clinical complications except ACLF and critical illness

TOP-454-YI

Impact of apixaban on hepatic decompensation in cirrhosis (ApiHep): a randomized controlled trial

Ayush Agarwal[1], Samagra Agarwal[1], Sagnik Biswas[1], Arnav Aggarwal[1], Sarthak Saxena[1], Hem Singh[1], Shivani Pandey[1], Jasmita Dass[1], Sonu Kumar[1], Shubham Jain[1], Shekhar Swaroop[1], Vishal Chauhan[1], Ankit Agarwal[1], Mukul Aggarwal[1], Ashwani Mishra[1], Ankur Goyal[1], Shivanand Gamangatti[1], Raju Sharma[1], Deepak Gunjan[1], Baibaswat Nayak[1], Shalimar Shalimar[1]. [1]*All India Institute of Medical Sciences, New Delhi, New Delhi, India*
E-mail: drshalimar@gmail.com

Background and aims: Evolving data suggest that anticoagulation is safe in patients with cirrhosis and may improve decompensation-free survival in selected patients with hepatic dysfunction. This study aimed to assess the efficacy and safety of the direct oral anticoagulant apixaban in patients with cirrhosis.

Method: In this single-center, parallel-group, open-label randomized controlled trial, patients aged 18–60 years with cirrhosis (Child–Pugh B7–C10) without splenoportal axis thrombosis were randomized (1:1) to receive apixaban (5 mg daily) and standard of care (SOC) or SOC alone for 12 months. The primary outcome was proportion of patients with new-onset or further hepatic decompensation (as defined by Baveno VII) at 1 year. Secondary outcomes included frequency of liver-related events, overall and liver-related mortality, and adverse events. Analyses were performed using modified intention-to-treat and per-protocol approaches.
Results: 134 patients were randomized (67 apixaban; 67 control). Baseline characteristics were comparable between the groups (mean age 43.4 ± 9.5 years; 91.0% males; 51.5% alcohol-related cirrhosis, 30.6% viral and 10.5% MASLD related; CTP 8 [7–9]; MELD-Na 17.1 ± 4.4). Over a median follow up of 12 months, apixaban significantly reduced new-onset or further decompensation compared to control (32.8% vs. 52.2%; absolute risk difference −19.4 [−35.8 to −3.0]; p = 0.036), confirmed in per-protocol analysis (31.2% vs 53.3%, p = 0.01). Secondary outcomes showed trends toward reduced ascites (6.0% vs. 16.4%; p = 0.06), hepatic encephalopathy (20.9% vs. 34.3%; p = 0.08) and variceal bleeding (7.5% vs 13.4%; p = 0.3) with apixaban. Overall and liver-related mortality at 1 year were similar between the groups. Adverse events (55.2 vs 53.7%: p = 0.86), any bleeding (41.8 vs 46.3%; p = 0.6) and major bleeding (9.0% vs. 11.9%; p = 0.57) did not differ between the two groups.
Conclusion: In patients with Child-Pugh B/C cirrhosis without portal venous thrombosis, apixaban significantly reduced new-onset or further hepatic decompensation without increasing hemorrhagic events.
(CTRI/2023/09/058018).

TOP-455-YI

Pre-treatment serum albumin concentration predicts clinical outcomes in patients with cirrhosis receiving long-term albumin

Enrico Pompili[1,2], Giacomo Zaccherini[3], Silvia Nardelli[4], Salvatore Piano[5], Carlo Alessandria[6], Sergio Neri[7], Francesco Giuseppe Foschi[8], Fabio Levantesi[9], Aldo Airoldi[10], Loredana Simone[11], Gianluca Svegiati-Baroni[12], Stefano Fagiuoli[13], Fabio Marra[14], Raffaele Cozzolongo[15], Giulia Iannone[1,2], Maurizio Biselli[1,2], Oliviero Riggio[4], Paolo Angeli[5], Mauro Bernardi[1], Maurizio Baldassarre[2], Paolo Caraceni[1,2]. *[1]Department of Medical and Surgical Sciences, Alma Mater Studiorum University of Bologna, Bologna, Italy; [2]Unit of Semeiotics, Liver and Alcohol-related diseases, IRCCS Azienda Ospedaliero-Universitaria di Bologna, Bologna, Italy; [3]IRCCS Azienda Ospedaliero-Universitaria di Bologna, Unit of Semeiotics, Liver and Alcohol-related Diseases, Bologna, Italy; [4]Department of Translational and Precision Medicine, Sapienza University of Rome, Roma, Italy; [5]Unit of Internal Medicine and Hepatology, Department of Medicine - DIMED, University and Hospital of Padova, Padova, Italy; [6]Division of Gastroenterology and Hepatology, Città della Salute e della Scienza Hospital, University of Turin, Torino, Italy; [7]Department of Clinical and Experimental Medicine, University of Catania, Catania, Italy; [8]Internal Medicine, Hospital of Faenza, Azienda Unità Sanitaria Locale of Romagna, Faenza, Italy; [9]Internal Medicine, Hospital of Bentivoglio, AUSL of Bologna, Bologna, Italy; [10]Liver Unit, Department of Hepatology and Gastroenterology, Niguarda Hospital, Milano, Italy; [11]Gastroenterology Unit, University Hospital Ferrara, Ferrara, Italy; [12]Department of Gastroenterology, Polytechnic University of Marche, Ancona, Italy; [13]Gastroenterology and Transplant Hepatology, Papa Giovanni XXIII Hospital, Bergamo, Italy; [14]Department of Experimental and Clinical Medicine, University of Florence, Firenze, Italy; [15]Division of Gastroenterology, National Institute of Gastroenterology S De Bellis, Castellana Grotte (Bari), Italy*
E-mail: enrico.pompili2@studio.unibo.it

Background and aims: Long-term albumin (LTA) therapy has been shown to improve survival and reduce cirrhosis-related complications in patients with cirrhosis and uncomplicated ascites. To identify the patients deriving the greatest benefit from LTA, this study aimed to evaluate whether baseline serum albumin (SA) levels can predict clinical response to treatment.
Method: This is a post-hoc analysis of the ANSWER trial including 431 patients with cirrhosis and uncomplicated grade 2 or 3 ascites randomized to Standard Medical Treatment (SMT) alone or SMT + LTA up to 18 months. To identify the most discriminatory baseline SA threshold, cut-offs between 2.5 and 4.2 g/dL (0.1 g/dL increments) were tested. For each value, 18-month survival was compared between treatment arms using the log-rank test, and the cut-off with the lowest p-value was selected. The threshold was internally validated using a bootstrap resampling technique with 1000 replicates. The primary endpoint was 18-month survival; secondary endpoints included the incidence rates (IR) of cirrhosis-related complications. Each endpoint was compared between the two subgroups stratified by baseline SA concentration.
Results: Patients did not differ in baseline SA concentration (SMT 3.1 ± 0.5 vs SMT+LTA 3.1 ± 0.6 g/dL, p = 0.86). The baseline SA cut-off associated with the greatest survival benefit was 3.2 g/dL, which was confirmed by the internal validation via bootstrap analysis. Overall, 275 patients (64%) had baseline SA ≤ 3.2 g/dL (132 SMT, 143 SMT+LTA). The 18-month survival was significantly higher in SMT +LTA than SMT in patients with baseline SA ≤ 3.2 g/dL (HR 0.47, 95%CI 0.29–0.77, p = 0.002), while it was similar in patients with SA > 3.2 g/dL (HR 1.04, 95%CI 0.41–2.63, p = 0.93), who show a low mortality rate in both treatment groups. Conversely, the cumulative incidence of paracentesis was significantly lower in the SMT+LTA group compared to SMT, both in patients with SA ≤ 3.2 g/dL (HR 0.45, 95% CI 0.31–0.65, p < 0.001) and in those with SA > 3.2 g/dL (HR 0.52, 95% CI 0.32–0.87, p = 0.010). Similarly, both subgroups showed a significant reduction in complications (i.e., spontaneous bacterial peritonitis [SBP], non-SBP infections, grade III/IV hepatic encephalopathy).
Conclusion: LTA provides survival and morbidity benefits in patients with at least mild-to-moderate hypoalbuminemia, whereas in those with normal SA levels, its advantages are confined to reducing morbidity. Baseline SA may therefore help for prioritizing LTA therapy when resources are constrained.

TOP-456-YI

Prognostic impact and predictive factors of cardiac decompensation following TIPS implantation in cirrhosis– data from the multicenter CARTIPS study

Tammo Lambert Tergast[1], Carolin Zimpel[2], Sarah Lisa Schütte[1], Leander Lorenz[2], Lukas Sturm[3], Dominik Bettinger[3], Michael Schultheiß[3], Tony Bruns[4], Karsten Große[4], Johannes Chang[5], Kim Uekermann[5], Christian Labenz[6], Simon Johannes Gairing[6], Felix Piecha[7], Golda Staub[7], Jassin Rashidi-Alavijeh[8], Marko Damm[9], Stefanie Quickert[10], Michael Praktiknjo[11], Sophie Schlosser-Hupf[12], Cornelius Engelmann[13], Leonard Kaps[14], Julia M. Grottenthaler[15], Jens U. Marquardt[2], Benjamin Maasoumy[1]. *[1]Medizinische Hochschule Hannover, Department of Gastroenterology, Hepatology, Infectious Diseases and Endocrinology, Hannover, Germany; [2]Department of Medicine I, University Medical Center Schleswig Holstein Campus Lübeck, Lübeck, Germany; [3]Department of Medicine II, Medical Center University of Freiburg, Faculty of Medicine, University of Freiburg, Freiburg, Germany; [4]University Hospital RWTH Aachen, Clinic for Gastroenterology, Metabolic Diseases and Internal Intensive Care Medicine (Medical Clinic III), Aachen, Germany; [5]University Hospital Bonn, Department of Internal Medicine I, Bonn, Germany; [6]University Medicine Mainz, Medical Clinic and Polyclinic, Mainz, Germany; [7]University Medical Centre Hamburg-Eppendorf, I. Medical Clinic and Polyclinic, Hamburg, Germany; [8]University Hospital Essen, Clinic for Gastroenterology, Hepatology and Transplantation Medicine, Essen, Germany; [9]Internal Medicine I, University Hospital Halle, Halle, Germany; [10]Department of Internal Medicine IV/Jena University Hospital, Jena, Germany; [11]University Hospital Münster, Medical Clinic B, Münster, Germany; [12]Department of Internal Medicine I, University Hospital Regensburg, Regensburg, Germany; [13]University Medicine*

Charite Berlin, Division of Hepatology and Gastroenterology, Berlin, Germany; [14]Department for Medicine II, University Medical Center Saarland, Homburg, Germany; [15]Department of Gastroenterology, Gastrointestinal Oncology, Hepatology, Infectiology, and Geriatrics, University Hospital Tuebingen, Tuebingen, Germany
E-mail: tergast.tammo@mh-hannover.de

Background and aims: Cardiac decompensation (CD) after implantation of transjugular intrahepatic portosystemic shunts (TIPS) for treatment of portal hypertension related complications is a frequent complication. Thus far, only few studies evaluated prognostic relevance of CD, as well as its potential risk factors. Recently, the Toulouse algorithm or pathological E/A have been proposed to predict post-TIPS CD. However, validation in large independent cohorts are lacking. Here, we aimed to investigate the impact and predictors of post-TIPS CD in a large multicenter cohort.
Method: All patients that received TIPS between 2009 and 2025 for portal hypertension derived complications were retrospectively included in this study across 15 tertiary care centers. All included patients received qualified transthoracic echocardiography (TTE) before TIPS implantation. Primary outcome of this study was development of CD within 365 days post-TIPS implantation as defined by current guidelines of the European Society of Cardiology. Fine and Gray competing risk analyses were used to determine association between risk factors and endpoints, treating death and liver transplantation as competing events.
Results: Overall, 1410 patients were included. Median age was 59 years, ascites was the leading factor for TIPS implantation (76%), most patients were male (65%) and alcohol-related liver disease was the main underlying cause of the liver disease (61%). Cardiac decompensation was documented in 14% of all patients and was associated with significantly increased mortality (HR: 1.90, 95%CI 1.23–7.74; P <0.001). Pathological elevated BNP/proBNP and moderate/severe aortic stenosis were significantly linked to CD (HR 3.08, 95%CI 1.23–7.74, P = 0.02 and HR: 2.79, 95%CI 1.02–7.69, P = 0.04). Patients stratified as "high risk" according to the Toulouse algorithm had significantly higher risk for CD (incidence: 11% vs. 21%; HR: 1.91; 95% CI 1.048–3.49; P = 0.04), while pathological E/A, i.e. <0.8 or >2, was numerically associated with CD (HR: 1.43, 95%CI 0.97–2.10, P = 0.07). CD was rare in patients with normal E/A and BNP/proBNP levels (incidence 3% vs. 17%, HR: 5.29 95% CI 1.28–21.96, P = 0.02).
Conclusion: CD is associated with mortality after TIPS implantation. The Toulouse algorithm predicts CD, however some patients are missed. Basic TTE values in combination with BNP/proBNP indicate those with a low risk of post-TIPS CD.

TOP-469-YI

Remote patient monitoring reduces liver-related hospital readmissions in patients with acutely decompensated cirrhosis

Alberto Calleri[1], Yihong Deng[2], Gabriel Prusch Fernandes[1], Kamalpreet S. Hara[1], Mindy Mickelson[2], Katherine Williams[3], Sara Kloft-Nelson[3], Angela Leuenberger[3], Lindsey Sangaralingham[2], Patrick S. Kamath[1], Vijay Shah[1], Daniel Penrice[1], Douglas Simonetto[1]. *[1]Division of Gastroenterology and Hepatology, Mayo Clinic, Rochester, United States; [2]Robert D and Patricia E Kern Center for the Science of Health Care Delivery, Mayo Clinic, Rochester, United States; [3]Center for Digital Health, Mayo Clinic, Rochester, United States*
E-mail: alberto.calleri.md@gmail.com

Background and aims: Patients with decompensated cirrhosis experience frequent, costly, and often preventable hospitalizations. Despite benefits of remote patient monitoring (RPM) in several chronic diseases, evidence in advanced liver disease remains limited. This study assessed the impact of a cirrhosis-specific RPM program (CiRPM) on post-hospitalization outcomes for patients with acutely decompensated (AD) cirrhosis.
Method: A three-cohort observational study was conducted including adults hospitalized for AD cirrhosis. Patients enrolled in CiRPM (2021–2024) were compared with contemporary controls (C-control) and historical controls (H-control, 2018–2019). CiRPM consisted of 90 days of home monitoring of vitals, body weight, and symptom questionnaires with virtual nurse assessment and hepatologist consultation. This analysis focused on the cumulative incidence of 90-day liver-related hospitalization (LRH). Subgroup analyses evaluated effects by cause of decompensation, liver disease etiology, and disease severity (CLIF-C AD). Confounding was addressed using IPTW with multiple imputation; time-to-event analyses used Cox regression.
Results: Of 430 patients (156 CiRPM, 152 H-control, 122 C-control), the mean age was 59 years, with 41% female, 65% alcohol-associated liver disease (ALD) etiology and mean CLIF-C AD of 56. The 90-day cumulative incidence of LRH was lower in the CiRPM group (39%, 95% CI 29–48) compared to H-control (52%, CI 41–61) and C-control (58%, CI 46–67). CiRPM was associated with a lower risk of LRH relative to C-control (HR 0.57, CI 0.37–0.87; p = 0.01) and H-control (HR 0.67, CI 0.43–1.03; p = 0.07), with a number needed to treat of 5–8 patients. In patients with ALD, CiRPM significantly reduced hospitalizations due to fluid imbalance compared to H-control (OR 0.40, CI 0.25–0.63; p < 0.001) and C-control (OR 0.37, CI 0.24–0.58; p < 0.001). Among patients with non-ALD etiologies, CiRPM was associated with fewer encephalopathy-related hospitalizations compared to H-control (OR 0.29, CI 0.13–0.67; p = 0.004) and C-control (OR 0.36, CI 0.15–0.85; p = 0.02). Patients with CLIF-C AD ≥ 60 experienced the greatest reduction in 90-day LRH (HR 0.43, CI 0.24–0.77; p = 0.005 vs H-control and HR 0.51, CI 0.29–0.91; p = 0.02 vs C-control).
Conclusion: CiRPM significantly reduced liver-related hospitalization, particularly among patients with ALD, fluid imbalance, and advanced disease severity (CLIF-C AD ≥ 60), supporting targeted remote monitoring as scalable post-discharge strategy for this high-risk population.

TOP-470-YI

Longitudinal trajectories of IL-6 and vWF predict clinical outcomes in advanced chronic liver disease independent of liver function

Georg Kramer[1,2,3,4], Dalila Costa[2,5], Benedikt Hofer[1,2,3], Benedikt Simbrunner[1,2,3], Ana Frias[5], Ricardo Silvestre[5], Joana Camões Neves[5], João Belmiro[5], Kerstin Zinober[1,4], Vlad Taru[1,4], Christian Sebesta[1,2,3], Paul Thöne[1,2,3], Marlene Hintersteininger[1,2,3], Lorenz Balcar[1,2,3], Lukas Hartl[1,2,3], Mathias Jachs[1,2,3], Georg Semmler[1,2,3], Michael Trauner[1,3], Mattias Mandorfer[1,2,3], Thomas Reiberger[1,2,3,4]. *[1]Division of Gastroenterology and Hepatology, Department of Medicine III, Medical University of Vienna, Vienna, Austria, Vienna, Austria; [2]Vienna Hepatic Hemodynamic Laboratory, Division of Gastroenterology and Hepatology, Department of Medicine III, Medical University of Vienna, Vienna, Austria, Vienna, Austria; [3]Clinical Research Group MOTION, Medical University of Vienna, Vienna, Austria, Vienna, Austria; [4]Christian-Doppler Laboratory for Portal Hypertension and Liver Fibrosis, Medical University of Vienna, Vienna, Austria, Vienna, Austria; [5]Life and Health Sciences Research Institute (ICVS), University of Minho; Gastroenterology Department, Braga Hospital, Portugal, Braga, Portugal*
E-mail: georg.kramer@meduniwien.ac.at

Background and aims: Systemic inflammation (SI) and portal hypertension (PH) drive cirrhosis progression. We longitudinally analyzed stage-specific trajectories of Interleukin-6 (IL-6) – a surrogate for SI – and von Willebrand Factor Antigen (vWF) – a marker of PH – in patients with compensated (cACLD), decompensated (dACLD) and recompensated advanced chronic liver disease to determine their impact on clinical transitions.
Method: This prospective two-center study (Vienna/Braga, 2017–2024) included ACLD patients at first combined measurement of vWF and IL-6, with consecutively ≥2 measurements of IL-6, vWF and MELD ≥ 6 months between the first and last measurement. We applied a 5-state multi-state model (cACLD, first and further decompensation, clinical recompensation [CR], liver-related death

[LRD]) and a Bayesian joint modeling framework to link longitudinal biomarker trajectories (linear mixed-effects models) with state transition hazards (Cox regression), adjusted for MELD as a time-dependent covariate (last-observation-carried-forward).
Results: 472 patients (273 cACLD, 199 dACLD) were included (mean age 53.5 ± 12.8 years; 67.1% steatotic liver-disease; median MELD 11 [IQR: 8–15]), contributing 3954 vWF and 2918 IL-6 values. During a median follow-up of 35.5 (25.5–96.6) months, 138 transitions to first decompensation, 124 to further decompensation, 56 to CR and 35 to LRD occurred. Rising IL-6 trajectories predicted the transition to first decompensation (per 20% increase [+20%], adjusted hazard ratio [aHR]: 1.21, p < 0.001), further decompensation (per +20%, aHR: 1.17, p < 0.001) and LRD (per +20%, aHR: 1.15, p < 0.001), independent of MELD. Conversely, falling IL-6 was associated with CR (per 20% decrease, aHR: 1.17, p = 0.007 from first decompensation, aHR: 1.18, p < 0.001 from further decompensation). Rising vWF independently predicted first (per +20%, aHR: 1.39, p < 0.001) and further decompensation (per +20%, aHR: 1.19, p < 0.001), but not CR or death.
Conclusion: Longitudinal modeling reveals that rising trajectories of SI (IL-6) and PH (vWF) drive liver disease progression independently of hepatic dysfunction (MELD). While rising vWF predicts progression – particularly to first decompensation, IL-6 trajectories predict courses from first to further decompensation and mortality (rising levels), but also towards recompensation (falling levels). These data highlight the dynamic and stage-dependent prognostic relevance of PH and SI in ACLD, with cessation of SI being a key facilitator of cirrhosis recompensation.

TOP-471-YI
The modified hepatic encephalopathy staging tool has significantly greater diagnostic consistency, prognostic performance and clinical impact compared with the West Haven criteria

Annarein Kerbert[1], Caterina Chesta[2], Pooja Balachandran[2], Aaryan Panchal[2], Jing Xia[2], Darren Rubin[3], Rajeshwar Prosad Mookerjee[2], Tarek Hassanein[4], Rajiv Jalan[2]. *[1]Leiden University Medical Center, Leiden, Netherlands; [2]University College London, London, United Kingdom; [3]Yaqrit Discovery Limited, London, United Kingdom; [4]Southern California Liver Centers, San Diego, United States*
E-mail: j.c.kerbert@lumc.nl

Background and aims: Hepatic encephalopathy (HE) is a serious complication of advanced liver cirrhosis, necessitating accurate and consistent diagnosis and staging in clinical practice and research. The widely used West Haven criteria (WHC) suffer from significant inter-observer variability. This study aimed to develop the modified Hepatic Encephalopathy Staging Tool (mHEST) as a more objective and reproducible method for HE assessment in regulated clinical trials. Its diagnostic consistency, prognostic performance and clinical impact were compared with the WHC.
Method: The study comprised 2 parts. *Part 1* involved revising the original HEST score, based on feedback from an expert panel. Key changes included removing asterixis and adding standardized questions. A two-round online validation survey was conducted: 49 healthcare professionals from 6 countries evaluated 6 video vignettes of actors portraying various HE stages. After viewing an mHEST training video, participants assessed the vignettes twice (5–10 days apart) using mHEST. Inter- and intra-rater agreement were analyzed. In *Part 2*, a prospective, single-center study enrolled 128 hospitalized patients with acutely decompensated cirrhosis. Trained professionals independently assessed HE, using both WHC and mHEST. Ammonia levels were measured at baseline and clinical outcomes were assessed upto one year. Diagnostic consistency, prognostic performance, and impact on existing scoring systems were compared.
Results: In *Part 1*, inter-rater concordance across vignettes ranged from 83.3–100%, and intra-rater agreement from 81.0–100%. In *Part 2*, inter-rater reliability was profoundly higher with mHEST than with WHC (kappa = 0.934 vs. 0.367). mHEST improved the performance of scoring systems incorporating HE assessment, including Child-Pugh and CLIF-C Organ Failure scores. Plasma ammonia levels significantly increased stepwise with rising mHEST grades, but not with WHC grades. In particular, significantly higher ammonia levels were detected in patients with mHEST grade 2 compared to those with grade 0/1 (p < 0.0001), which was not seen with WHC. Unlike WHC, mHEST grade 0/1 was independently associated with a better 1-year survival (HR = 0.515, 95% CI = 0.270–0.982, p = 0.044) in multivariate Cox regression models.
Conclusion: mHEST is a user-friendly tool for HE-assessment outperforming the WHC in diagnostic accuracy, prognostic performance and clinical impact. It has been accepted by the U.S. Food and Drug Administration as an endpoint for HE clinical trials.

TOP-472
Real-world effectiveness of Tolvaptan for hyponatremia in cirrhosis across global regions: a target trial emulation

Kazuya Okushin[1], Ryosuke Tateishi[1], Mitsuhiro Fujishiro[1], Takeya Tsutsumi[1], Kazuhiko Koike[1], Tomohiro Tanaka[2]. *[1]The University of Tokyo, Tokyo, Japan; [2]University of Iowa, Iowa City, United States*
E-mail: tomohiro-tanaka@uiowa.edu

Background and aims: Tolvaptan, an oral vasopressin V2-receptor antagonist, promotes electrolyte-free water excretion, and is widely used in Asian countries, including Japan for the treatment of ascites. However, its role in Western countries is largely limited to the management of hyponatremia due to regulatory restrictions and concerns over hepatotoxicity.
Method: We conducted a retrospective cohort study using the TriNetX Research Network, which aggregates electronic health records from healthcare organizations across global regions, emulating a target trial of cirrhotic patients with hyponatremia. Eligible adults were assigned to tolvaptan plus sodium supplementation (tolvaptan group) or sodium supplementation alone (control). Patients with autosomal dominant polycystic kidney disease were excluded. The primary outcome was 30-day all-cause mortality; secondary outcomes included correction of hyponatremia, changes in liver and renal function parameters, and initiation of hemodialysis. Survival was analyzed using Kaplan-Meier curves with the log-rank test and Cox proportional hazards models. Propensity score matching was applied to balance baseline covariates.
Results: Among 188,707 eligible patients, 2130 received tolvaptan. After 1:1 matching, 1983 patients were analyzed in each group. Baseline demographics and comorbidities were well balanced, although serum sodium remained slightly lower in the tolvaptan group (standardized mean difference, 0.522). Thirty-day mortality was lower in the tolvaptan group compared with controls (14.4% vs. 16.1%; log-rank test p = 0.09, with hazard ratio [HR] 0.87, 95% confidence interval [CI] 0.74–1.02). By the end of the follow-up, serum sodium levels were significantly lower in the tolvaptan group compared with the control group (131.7 ± 133.1 mmol/L, p < 0.001). Hemodialysis initiation did not differ significantly (3.6% vs. 3.7%; log-rank p = 0.76, HR 0.95, 95% CI 0.68–1.33). Renal and liver function parameters were generally comparable, with no evidence of excess hepatotoxicity.
Conclusion: In this large real-world target trial emulation across global regions with ethnic diversity, tolvaptan use was not significantly associated with short-term mortality in cirrhotic patients with hyponatremia, although point estimates consistently favored the tolvaptan group. Further evaluation of the safety and effectiveness of tolvaptan in diverse clinical settings is warranted.

WED-415
Clostridioides difficile mortality in cirrhotic patients matches other bacterial infections in the antimicrobial resistance era

Dimitra Krystallaki[1], Florentia Athanasaki[1], Eleni Geladari[2], Krystalia Dimitriou[1], Nikolaos-Nektarios Karamanolis[1], Iliana Mani[1],

Vasileios Sevastianos[2], Anna Xanthaki[3], Alexandra Alexopoulou[1].
[1]*Second Department of Internal Medicine and Research Laboratory, Hippokration General Hospital, Medical School, National & Kapodistrian University of Athens, Greece, Athens, Greece;* [2]*Third Department of Internal Medicine and Liver Outpatient Clinic, Evangelismos General Hospital, Athens, Greece;* [3]*Microbiology Department, Hippokration General Hospital, Athens, Greece*
E-mail: dimikryst@gmail.com

Background and aims: Bacterial infections (BI) are common in advanced liver cirrhosis and the type of infection may affect prognosis. *Clostridioides difficile* infection (CDI) has been associated with increased short-term mortality but comparative data with other type of BI in the era of increasing antimicrobial resistance are limited. This study aimed to compare outcomes between cirrhotic patients with CDI and those with other BI, and to identify independent predictors of mortality.
Method: We retrospectively analyzed consecutively admitted patients with liver cirrhosis in two tertiary hospitals: with CDI (January 2022–June 2025) and other BI (June 2024–January 2025). CDI was diagnosed based on symptoms of colitis and positive stool antigen and toxin A/B by enzyme immunoassay. Other BI diagnosis was based on the World Health Organization criteria (Aware Antibiotic Book). For all cases, second BI (distinct site and pathogen) and multidrug-resistant organisms (MDRO) were recorded. Patients with advanced hepatocellular carcinoma, recurrent CDI, or fungal infections were excluded.
Results: A total of 101 patients were included (36 CDI, 65 non-CDI), most with decompensated cirrhosis (92.1%). Patients with CDI, compared to those with other BI, were older (median age 73 vs 63 years, p = 0.024), had more comorbidities (Charlson Comorbidity Index 7 vs 6, p = 0.004), more frequent prior exposure to antibiotics (80.6% vs 58.5%, p = 0.024), proton pump inhibitors (66.7% vs 41.5%, p = 0.016), rifaximin (58.3% vs 35.4%, p = 0.026), hospitalizations (80.6% vs 58.5%, p = 0.005), and previous CDI (27.8% vs 3.1%, p < 0.001). Second BI were more prevalent in the CDI group (44.4% vs 21.5%, p = 0.016), while MDRO prevalence was similar between groups (22.2% vs 33.8%, p = 0.261). Thirty- and 90-day mortality did not differ significantly between groups (log-rank p = 0.691 and p = 0.564, respectively). In the overall cohort, Cox regression multivariate model identified Child–Pugh score (HR 1.44, 95% CI 1.13–1.83, p = 0.003) and MDRO (HR 3.07, 95% CI 1.06–8.87, p = 0.039) as independent predictors of 30-day mortality. Among CDI patients, second BI by MDRO independently predicted 30-day mortality (HR 6.04, 95% CI 1.01–36.2, p = 0.049).
Conclusion: In hospitalized cirrhotic patients with infection, short-term mortality appears to be primarily determined by liver disease severity and MDRO, rather than the presence of CDI. In CDI, MDRO-related second infections are the main determinant of 30-day prognosis.

WED-416
Reevaluating hypercoagulability in the portal vein and the impact of TIPS on platelet activation in cirrhosis

Viktoria Moeller[1], Anselm Kunstein[1], Christian Weigel[1], Alexander Killer[1], Eric Tietz[1], Kai Jannusch[1], Mihael Vucur[1], Tom Luedde[1], Peter Minko[1], Johannes Bode[1], Carolin Angendohr[1].
[1]*Universitätsklinikum Düsseldorf, Düsseldorf, Germany*
E-mail: carolohr@gmx.de

Background and aims: In liver cirrhosis, dysregulated hemostasis predisposes patients to hemorrhage and thrombotic complications. The portal vein represents a frequent site of thrombosis, but the underlying mechanisms remain unclear. Previous studies suggested that the portal vein represents a hypercoagulable environment, promoting platelet activation and subsequent thrombogenesis.
Method: We enrolled 34 patients with liver cirrhosis undergoing transjugular intrahepatic portosystemic shunt (TIPS) implantation. Platelet count, activation, and reactivity were assessed by flow cytometry before and after TIPS, as well as across multiple vascular compartments including the portal vein, superior mesenteric vein, hepatic vein, and peripheral vein. In addition, we measured key coagulation factors involved in secondary hemostasis in the indicated vessels.
Results: Platelet counts declined with advancing liver disease, but no changes in platelet activity or reactivity were observed. Despite elevated platelet counts in the portal vein, we found no evidence of increased platelet activation or reactivity. Moreover, no differences in secondary hemostasis were detected across the different vascular compartments. TIPS implantation did not lead to a short-term increase in platelet activation.
Conclusion: Contrary to prior reports, the portal vein does not appear to constitute a hypercoagulable environment. TIPS implantation does not trigger acute platelet activation. These findings suggest that relief of portal hypertension, and the resulting reduction in venous stasis, may exert a greater influence on thrombosis risk than interventions targeting hemostasis.

WED-417
Is 100 the new 250? Ascites fluid PMN >100 has the highest predictive value and odds for 30-day mortality in a national cirrhosis cohort undergoing paracentesis

Scott Silvey[1], Nilang Patel[1], Jasmohan Bajaj[1]. [1]*Virginia Commonwealth University, Richmond, United States*
E-mail: jasmohan.bajaj@vcuhealth.org

Background and aims: An ascites PMN count ≥ 250/ml is considered a corollary for Spontaneous Bacterial Peritonitis (SBP) in the absence of cultures. With changing bacteriology & cirrhosisdemographics, this threshold may need re-evaluation. Aim: Determine impact of differing PMN thresholds on 30-day mortality in a national cirrhosis cohort.
Method: Using the Veterans Affairs Corporate Data Warehouse (VA-CDW), we collected data from Veterans admitted between 2009 and 2024 for cirrhosis & ascites and who received paracentesis ≤ 24 hours into admission. Only patients with valid PMN counts were included. The outcome was 30-day death post-paracentesis. Baseline admission data were compared between groups who died/did not at 30-days. We analyzed PMN thresholds ranging from 50 to 500 with the goal of identifying the cutoff value that optimized positive predictive value (PPV) & odds ratio (OR) of death. We tested this range of PMN values & used smooth splines to fit curves to this data, visually selecting the point where PPV/OR did not increase substantially. Other metrics (sensitivity, specificity, NPV) were also calculated.
Results: 4111 Veterans with cirrhosis & ascites + paracentesis ≤ 24hrs into admission were included (median age 66, 96.3% male, 31.1% alcohol), of which 16.9% died at 30-days. The median PMN count was 19 [IQR: 6–68], which was significantly higher between those who did/did not die (33 vs. 18, $p < 0.001$). Patients who died had higher comorbidities (6 vs 5, p < 0.001), WBC count (8.8 vs 6.8, p < 0.001) & cirrhosis severity (MELD-Na 22 vs 18, albumin 2.8 vs 2.7, both p < 0.001) and. PMN threshold analysis: PMN count ≥ 100 (prevalence: 20.3%) optimized both PPV & OR of death (PPV 25.3%, Sensitivity 30.4%, Specificity 81.8%, NPV 85.2%), and the OR of death vs. those below this threshold was 1.96 (95% CI: [1.63–2.35], $p < 0.001$). Specifically, these metrics increased rapidly until a value of 100 was reached, at which point diminishing returns became evident. Using the defined cutoff for SBP (PMN > 250), the PPV (26.4%) and ORs (1.97 [1.59–2.42]) increased only marginally. Between 100–250 PMNs, an increase in PMN count of 50 corresponded to 11% further increased odds of death, but this increase was not statistically significant ($p = 0.53$).
Conclusion: An ascites fluid PMN ≥ 100/ml is associated with the highest odds ratio for 30-day death in a national cohort of inpatients with cirrhosis. This was comparable to higher values including ≥250/ml used for SBP. A lower PMN count could be considered for optimal prognostication.

WED-418

Dynamic assessment of the AMMON model can guide preventative therapies of patients at risk of liver-related events

Paloma Poyatos-García[1], Jose Sanchez-Serrano[1], Anabel Fernández-Iglesias[2], Rocío Gallego-Durán[3], Carmen Vinaixa[4], Paloma Lluch-García[1], Juan Antonio Carbonell-Asins[5], Rajiv Jalan[6], María Pilar Ballester[1]. [1]*Hospital Clinico Universitario de Valencia, Valencia, Spain;* [2]*Fundació de Recerca Clinic Barcelona-IDIBAPS, Barcelona, Spain;* [3]*Instituto de Biomedicina de Sevilla, Sevilla, Spain;* [4]*Hospital Universitario y Politécnico La Fe, Valencia, Spain;* [5]*Instituto de Investigación Sanitaria INCLIVA, Valencia, Spain;* [6]*University College London, London, United Kingdom*
E-mail: mapibafe@gmail.com

Background and aims: Hyperammonaemia is an independent predictor of hospitalization with liver-related events (LRE) in patients with cirrhosis. The AMMON model, which integrates ammonia with other clinical variables through a machine learning approach, has demonstrated superior performance than traditional severity scores to predict all LRE and death. However, its dynamic role in guiding personalized preventative therapies for patients at risk is unclear. The primary aim of the study was evaluate the dynamic role of the AMMON-OHE model to predict LRE. Exploratory aims were to study the relationship between the model and pathophysiological factors associated with LRE.
Method: A prospective, longitudinal study of consecutive outpatients with cirrhosis followed at two liver units in Valencia between November 2022 and November 2024 was conducted. Clinical, laboratory, and inflammatory, vascular and fibrogenic markers data were collected at baseline, 3, and 6 months. Patients were followed until LRE, liver transplantation, death or study closure in November 2025. Patients were stratified into risk groups (high, medium and low), and dynamic AMMON-OHE categories (stable, progression, regression or remission -low risk-) were defined based on the model changes.
Results: A total of 177 patients were included (75% male; median age 63 years; 63% alcohol-related cirrhosis) exhibited median (IQR) Child-Pugh and MELD-Na of 5 (5–7), and 9 (7–11), respectively. Median plasma ammonia was 36 μg/dL (0.4 × ULN). The cumulative incidence of 1-year LRE differed significantly across dynamic AMMON categories ($p = 0.006$): 44% (remained high risk), 40% (progression), 29% (regression), 20% (remained medium risk), and 10% (remained low risk). Dynamic assessment of the model accurately stratified the risk of hospitalization with LRE both at 3 and 6-months, with the best cut-off to minimize the risk of OHE being remission. AMMON-OHE categories correlated with inflammatory markers (CRP, IL-6), vascular factors (angiopoietin 2, ICAM1, vWF) and PDGFRβ.
Conclusion: Repeated assessment of the AMMON model provides robust dynamic stratification for hospitalization with LRE in outpatients with cirrhosis. These findings support its potential utility in guiding personalized preventative therapeutic strategies in clinical practice and reveal associations with underlying vascular and fibrogenic pathophysiological mechanisms.

WED-419

Culture-independent nanopore metagenomics for pathogen detection in the ascitic fluid for spontaneous bacterial peritonitis in liver cirrhosis patients

Chhagan Bihari[1], Rosmy Babu[2], Vikas Khillan[1], Pratibha Kale[1], Ramesh Prasad[1], Rakhi Maiwall[1], Omkar Rudra[1], Shiv Kumar Sarin[1]. [1]*Institute of Liver and Biliary Sciences New Delhi, Delhi, India;* [2]*ILBS, DELHI, India*
E-mail: drcbsharma@gmail.com

Background and aims: Spontaneous bacterial peritonitis (SBP) is a life-threatening complication of decompensated cirrhosis with high short-term mortality. Conventional ascitic fluid culture has limited sensitivity, leading to frequent culture-negative SBP. We evaluated whole-genome nanopore metagenomics to characterize microbial profiles, mortality-associated taxa, and concordance with culture across SBP groups.
Method: Adults (18–65 years) with decompensated cirrhosis and suspected SBP were enrolled, and ascitic fluid was collected before antibiotics administration. Interim assessment of 48 culture-positive SBP samples and 72 each of culture-negative SBP and non-neutrocytic ascites were sequenced using Oxford Nanopore P2 Solo after low-biomass DNA extraction, followed by stringent filtering.
Results: 91.7% (44/48) of culture-positive SBP, 40.2% (29/72) of culture-negative SBP, and 16.7% (12/72) of non-neutrocytic ascites samples had high-confidence bacterial DNA ($p < 0.001$). Alpha diversity was lowest in culture-positive SBP ($p = 0.0005$) whereas Bray-Curtis dissimilarity varied significantly between groups ($p = 0.00016$). Pseudomonas aeruginosa, Escherichia coli, Klebsiella pneumoniae, Enterococcus faecium, and Stenotrophomonas maltophilia were the most common results of conventional culture in culture-positive SBP which matched metagenomic profiles that were dominated by E. coli, K. pneumoniae, Salmonella enterica, Acinetobacter baumannii, S. maltophilia, and P. aeruginosa, with a shorter turnaround time of 9 hours vs. 5 days. Salmonella enterica, P. aeruginosa, E. coli, and Staphylococcus aureus were found in all culture-negative SBP while Bacillus, Streptomyces, and Staphylococcus species predominated in non-neutrocytic ascites. However, species-specific read counts 4.8 times lesser than culture-positive SBP. Non-neutrocytic ascites demonstrated an even lower burden; 6.8 times lower than culture-positive SBP. Within 30 days 9.1% (4/44) of culture-positive SBP and 6.9% (2/29) of culture-negative SBP died from septic shock. fatal cases were enriched for S. maltophilia with an average of 53477 read counts per sample and S. aureus (4885 reads) and E. coli (1581 reads), respectively.
Conclusion: Metagenomics aligns with conventional culture in culture-positive SBP, however with a reduced turnaround time, while significantly enhancing pathogen detection in culture-negative cases.

WED-420

Extreme heat exposure is associated with an increased risk of all-cause hospitalization in patients with cirrhosis

Therese Bittermann[1,2], Douglas Schaubel[1], Qufei Wu[1], Charles Leonard[1], David Kaplan[1]. [1]*University of Pennsylvania, Philadelphia, United States;* [2]*Queensland Institute of Medical Research Berghofer, Brisbane, Australia*
E-mail: tess.bittermann@health.qld.gov.au

Background and aims: Extreme heat exposure is associated with increased morbidity and mortality in patients with chronic diseases, but the impact on patients with cirrhosis is unknown. This study evaluated the impact of extreme heat exposure on all-cause hospitalization in a validated retrospective cohort of U.S. veterans with incident cirrhosis.
Method: We combined data from the U.S. Veterans Health Administration and publicly available daily maximum temperature (Tmax) data at 3414 weather stations between 2008 and 2021. Extreme heat events were defined as any day (± 3 days) with Tmax >95th percentile for that calendar day/weather station during the study period. Multivariable proportional rates models evaluated the association of extreme heat events on all-cause hospitalization, adjusted for demographics, severity of liver disease, comorbidities, Socioeconomic Deprivation Index (SDI) and climate type. Subgroup analyses were pursued to investigate differences in the impact of heat on outcomes.
Results: The study cohort included 131,793 U.S. veterans with incident cirrhosis between 2008 and 2021. Median follow-up was 1178 days (IQR: 389–2275). The cohort was 96.9% male with median age 63 years (IQR: 58–69). Liver disease etiology included 36.4% with hepatitis C virus, 38.0% with metabolic dysfunction associated steatotic liver disease and 23.9% alcohol. Overall, 60.6% were Child-

Turcotte-Pugh (CTP) class A, 33.8% CTP B and 5.6% CTP C at baseline. High socioeconomic deprivation (SDI 80–100) was present in 24.7%. The most common climate types were mixed-humid (31.9%), cold (29.4%) and hot-humid (20.2%). Extreme heat was significantly associated with an increase in all-cause hospitalization: adjusted rate ratio (RR) 1.79 (95% CI: 1.77–1.80). The excess hospitalization risk was not altered by CTP class (RR 1.80 for class A, RR 1.77 for class B/C) or socioeconomic deprivation (RR 1.79 for SDI <80, HR 1.82 for SDI 80–100). Minimal differences were also observed by climate type, with the HR for hospitalization ranging from 1.76 in hot-humid to RR 1.88 in marine and mixed-dry climates.

Conclusion: Extreme heat is greatly associated with increased all-cause hospitalization in patients with cirrhosis. The magnitude of this risk is unaffected by baseline severity of liver disease, socioeconomic deprivation or climate type. Understanding the impact of climate-related stress, such as extreme heat, on patients with cirrhosis is critical to developing adaptations in care and public health interventions that improve outcomes.

WED-421

Food insecurity, frailty, and oral health are key drivers of impaired quality of life in a large US multicenter cohort of adults with compensated cirrhosis

Adam Buckholz[1], Ani Kardashian[2], David Goldberg[3], Neehar D. Parikh[4], Mandana Khalili[5], Manal F. Abdelmalek[6], Bilal Hameed[5], Matthew Robert Kappus[7], Monica Tincopa[8], Nicole Welch[9], Arun J. Sanyal[10], Patricia Jones[3], Vijay Shah[6], Russell Rosenblatt[1], Rohit Loomba[8], Amreen Dinani[7], Srinivasan Dasarathy[9], Norah Terrault[2], Ann Kan[11], Abigail Smith[11], Elliot Tapper[4], Jasmohan Bajaj[10]. *[1]NewYork-Presbyterian/Weill Cornell Medical Center, New York, United States; [2]University of Southern California, Los Angeles, United States; [3]University of Miami, Miami, United States; [4]University of Michigan, Ann Arbor, United States; [5]University of California San Francisco, San Francisco, United States; [6]Mayo Clinic Health System, Rochester, United States; [7]Duke University, Durham, United States; [8]University of California San Diego, La Jolla, United States; [9]Cleveland Clinic, Twinsburg, United States; [10]Virginia Commonwealth University, Richmond, United States; [11]Northwestern University, Chicago, United States*
E-mail: apb9012@med.cornell.edu

Background and aims: Cirrhosis is associated with impaired quality of life (QoL). Most studies have assessed QoL in decompensated cirrhosis, but data in compensated patients are limited. We examined factors associated with QoL in a large prospective, multicenter cohort of adults with compensated cirrhosis.

Method: The Liver Cirrhosis Network Cohort study prospectively enrolled adults from 10 representative sites across the US with compensated cirrhosis based on liver biopsy within 5 years or a combination of imaging, liver stiffness, and/or blood-based biomarkers and no decompensation within 1 year. Baseline data collection included sociodemographics, medical history, and surveys, including the Patient Reported Outcomes Measurement Information System (PROMIS)-29 Profile v2.1 to calculate an overall preference score (PROPr) ranging from 0 (worst) to 1 (ideal) and 7 domain-level T-scores. Multivariable linear and logistic regression models were fitted for PROPr and probability of T-scores >1 standard deviation (SD) away from the population mean for subdomains where >20% of participants demonstrated impairment. LASSO was used to guide variable selection among sociodemographic/clinical covariates.

Results: Of 1156 participants, median age was 62 years, 76% were white, 44% employed, 13% were food insecure, 34% had fair/poor oral health, and median MELD was 8. Median PROPr T-score was 0.44, and 27%, 23%, and 22% had impaired pain interference (PI), physical functioning (PF), and fatigue scores, respectively. Median PROPr did not vary by etiology of liver cirrhosis. In multivariable analysis, food insecurity (b = –0.14), frailty measured by the Liver Frailty Index (LFI; b = –0.07) and poor oral health (b = –0.05) were associated with worse PROPr (all $p < 0.001$). Food insecurity and higher LFI (more frailty) were also associated with higher odds of impaired T-scores for PF (odds ratio [OR] = 2.61 and 2.64, respectively), PI (OR = 3.07 and 1.77, respectively), and fatigue (OR = 2.54 and 1.49, respectively), all $p < 0.001$. Worse oral health was associated with higher odds of impaired PF and PI (OR = 1.30 and 1.25, $p = 0.002$ and 0.007, respectively), but not with impaired fatigue.

Conclusion: QoL impairment is substantial even in compensated cirrhosis and is associated with food insecurity, frailty, and poor oral health in cross-sectional analysis of a prospective multi-center cohort. Proactive screening for social determinants of health could lead to measures that improve QoL and outcomes in this population.

WED-425

Clinical presentation and determinants of disease progression in cirrhosis: data from the SORPRESA study cohort

Vincenza Calvaruso[1], Gabriele Di Maria[1], Paolo Angeli[2], Simone Incicco[2], Francesca Romana Ponziani[3], Antonio Liguori[3], Giovan Giuseppe Di Costanzo[4], Debora Angrisani[4], Alessandro Federico[5], Mario Romeo[5], Andrea Pasta[6], Paolo Caraceni[7,8], Sara Bighini[9], Mario Masarone[10], Filomena Morisco[11], Maria Guarino[11], Nicola Coppola[12], Gianfranca Stornaiuolo[12], Alessio Aghemo[13], Stella De Nicola[13], Calogero Cammà[1], Marcello Persico[10], Edoardo Giannini[6], Vito Di Marco[1]. *[1]University of Palermo, PROMISE Department. Gastroenterology and Hepatology Section, Gastroenterology Unit, AOUP Paolo Giaccone, Palermo, Palermo, Italy; [2]2Department of Surgery, Oncology and Gastroenterology, Gastroenterology Unit, University of Padua, Padua, Italy, Padua, Italy; [3]3Liver Unit, CEMAD – Centro Malattie dell'Apparato Digerente, Internal Medicine and Gastroenterology, Università Cattolica del Sacro Cuore, Fondazione Policlinico Universitario Gemelli IRCCS, Rome, Italy, Rome, Italy; [4]Liver Unit, Antonio Cardarelli Hospital, 80131 Naples, Italy, Naples, Italy; [5]Department of Clinical and Experimental Medicine, Second University of Naples, 80131 Naples, Italy, Napled, Italy; [6]Gastroenterology Unit, Department of Internal Medicine, University of Genoa, Genoa, Italy, Gastroenterology Unit, IRCCS Ospedale Policlinico San Martino, Genoa, Italy, Genoa, Italy; [7]Unit of Semeiotics, Liver and Alcohol-related diseases, IRCCS Azienda Ospedaliero-Universitaria di Bologna, Bologna, Italy; [8]Department of Medical and Surgical Sciences, University of Bologna, Bologna, Italy; [9]Division of Internal Medicine, Hepatobiliary Diseases and Immunoallergology, IRCCS Azienda Ospedaliero-Universitaria di Bologna, Bologna, Italy, Department of Medical and Surgical Sciences, University of Bologna, Bologna, Italy, Bologna, Italy; [10]Department of Medicine, Surgery and Dentistry "Scuola Medica Salernitana," University of Salerno, Salerno, Italy, Salerno, Italy; [11]Department of Clinical Medicine and Surgery, Diseases of the Liver and Biliary System Unit, University of Naples "Federico II", Naples, Italy, Naples, Italy; [12]Department of Mental Health and Public Medicine, Section of Infectious Diseases, Second University of Naples, 80131 Naples, Italy, Naples, Italy; [13]Division of Internal Medicine and Hepatology, IRCCS Humanitas Research Hospital, Rozzano, Italy, Rozzano, Italy*
E-mail: vincenza.calvaruso@unipa.it

Background and aims: Understanding the aetiology, disease stage at diagnosis, and patterns of decompensation of cirrhosis is essential to define prognosis and optimize management. This study aimed to describe the contemporary clinical presentation of cirrhosis in Italy, characterize disease stages, and identify factors associated with hepatic decompensation.

Method: SORPRESA is a prospective, multicentre cohort study conducted in 11 tertiary hepatology centres in Italy during 2024. Consecutive patients with newly diagnosed cirrhosis or first clinical presentation were enrolled. Demographic, socioeconomic, etiological, clinical, and laboratory data were collected at baseline. Disease progression across three stages (compensated, first decompensation, multiple decompensations) was analysed using cumulative ordinal logistic regression. Covariates included aetiology (ALD,

MASLD, MetALD, HCV, HBV, autoimmune and other causes), age, sex, obesity (BMI ≥ 30 kg/m^2), diabetes, education, employment, family status, and housing conditions. A multinomial logistic regression model was applied to evaluate predictors of first decompensation, classified as acute (AD) or non-acute (NAD), versus compensated disease.

Results: A total of 1195 patients were included (mean age 64 ± 11.6 years; 73% male): 232 had ALD, 345 MASLD, 80 MetALD, 246 HCV, 159 HBV, 72 autoimmune, and 63 other aetiologies. Overall, 609 patients had compensated and 586 decompensated cirrhosis; among the latter, 416 experienced a first decompensation (232 AD, 184 NAD) and 170 multiple events. Aetiology emerged as the strongest predictor of progression: compared with ALD/MetALD, MASLD (OR = 0.67, 95% CI 0.48–0.96, p = 0.027) and viral/other causes (OR = 0.58, 95% CI 0.43–0.79, p < 0.001) were associated with lower risk of worsening. Obesity was protective only in the first transition (OR = 0.57, p < 0.001), suggesting an "obesity paradox." Living alone due to widowhood/divorce ("forced solitude") showed a borderline risk effect (OR = 1.39, p = 0.051). In the multinomial model, ALD significantly increased the relative risk ratio of both AD (RRR = 1.85, p = 0.001) and NAD (RRR = 2.08, p < 0.001) at first decompensation compared to compensated disease.

Conclusion: Alcohol-related and metabolic-associated liver diseases, together with social isolation, are associated with worse clinical outcomes in cirrhosis. These findings highlight the need for integrated medical and social interventions to improve prognosis.

WED-426

Glucagon-like peptide-1 receptor agonists reduce the risk of decompensation in patients with type 2 diabetes across different stages of liver disease

Montserrat Camps Fajol[1,2], Anna Brujats[1,2], Maria Poca[1,2], Càndid Villanueva[1,2], Ramon Bataller[3], Victor Gomariz[1], Andreu Ferrero[1], Edilmar Alvarado-Tapias[2,4,5]. *[1]Department of Gastroenterology and Hepatology, Hospital de la Santa Creu i Sant Pau, Institut de Recerca Sant Pau (IR Sant Pau), Barcelona, Spain; [2]Department of medicine, Universitat Autònoma de Barcelona, Barcelona, Spain; [3]Hospital de la Santa Creu i Sant Pau, Barcelona, Spain; [4]Department of Gastroenterology and Hepatology, Hospital de la Santa Creu i Sant Pau, Institut de Recerca Sant Pau (IR Sant Pau), Department of Medicine, Universitat Autònoma de Barcelona, Barcelona, Spain; [5]Centro de Investigación Biomédica en Red de Enfermedades Hepáticas y Digestivas (CIBEREHD), Instituto de Salud Carlos III, Madrid, Spain*
E-mail: mcampsf@santpau.cat

Background and aims: Advanced chronic liver disease (ACLD) is associated with high morbidity and mortality, particularly after progression to decompensation. Obesity, type 2 diabetes mellitus and alcohol intake, accelerate disease progression. Glucagon-like peptide-1 receptor agonists (GLP-1 RA) improve metabolic and inflammatory parameters; however, their association with hepatic decompensation across different stages of liver disease remains unclear. This study aimed to evaluate the association between GLP-1 RA use and the risk of first and further hepatic decompensation in patients with type 2 diabetes and compensated ACLD (cACLD), decompensated ACLD (dACLD) and alcohol-related liver disease (ArLD).

Method: A systematic review of studies published between 2022 and 2025 was conducted using MEDLINE, Embase and CENTRAL. Observational studies comparing GLP-1 RA users with non-users or standard type 2 diabetes treatments were eligible. Included populations comprised adults with type 2 diabetes, with or without liver disease, including steatotic liver disease, cACLD, dACLD and ArLD. Two reviewers screened studies, extracted data and assessed risk of bias. A random-effects meta-analysis with restricted maximum likelihood estimation and meta-regression analyses was performed. Outcomes were reported as hazard ratios (HR) with 95% confidence intervals (CI).

Results: Thirteen observational studies comprising 2.121.028 patients were identified. Moderate heterogeneity was observed (I^2 = 39.2%), mainly driven by differences in study populations. Meta-regression showed no significant moderating effect of sex, treatment duration or follow-up (global p = 0.13). GLP-1 RA were associated with a reduced risk of hepatic decompensation in the pooled population (HR = 0.76, 95% CI 0.72–0.81; p < 0.001). In patients with cACLD (seven studies), GLP-1 RA were associated with a lower risk of first decompensation (HR = 0.73, 95% CI 0.65–0.83; p < 0.001). Among patients with dACLD (five studies), GLP-1 RA use was associated with a reduced risk of further decompensation (HR = 0.74, 95% CI 0.67–0.81; p < 0.001). Although based on limited evidence (two studies), GLP-1 RA were also associated with a reduced risk of decompensation in ArLD (HR = 0.63, 95% CI 0.50–0.79; p < 0.001).

Conclusion: GLP-1 RA use was associated with a reduced risk of hepatic decompensation across different stages of liver disease. Randomized controlled trials are needed to confirm these findings and identify patient subgroups most likely to benefit.

WED-427-YI

Predictive model of postoperative mortality in patients with cirrhosis. Surgical risk score for patients with cirrhosis (S-RISC)

Lidia Canillas[1], Natalia Jimenez-Esquivel[2], Alberto Amador[3], Anna Brujats[4,5], Jordi Sánchez[5,6], Amalia Pelegrina[7], Carlos Pardo[2], Sergi Homdedeu Montaña[3], Montserrat Camps Fajol[4], Carla de Sárraga[6], Juan Álvarez[8], Xavier Duran[9], Fernando Burdio[7], Enric Reverter[2], Jose A. Carrión[1]. *[1]Department of Medicine and Life Sciences, Universitat Pompeu Fabra, Liver Unit, Gastroenterology Department, Hospital del Mar, IMIM (Hospital del Mar Medical Research Institute), Barcelona, Spain; [2]Liver Unit, Hospital Clinic, Institut d'Investigacions Biomèdiques August Pi i Sunyer (IDIBAPS), Barcelona, Spain; [3]Liver Unit, Gastroenterology Department, Hospital Universitari de Bellvitge, Hepatobiliary and Pancreatic Diseases Research Group, IDIBELL, Universitat de Barcelona, Hospitalet de Llobregat, Spain; [4]Department of Gastroenterology and Hepatology, Hospital de la Santa Creu y Sant Pau, Sant Pau Research Institute (IR Sant Pau), Universitat Autònoma de Barcelona, Barcelona, Spain; [5]Network Biomedical Research Center for Liver and Digestive Diseases (CIBERehd), Carlos III Health Institute, Madrid, Spain; [6]Hepatology Unit, Gastroenterology Department, Hospital Parc Taulí, Parc Taulí Research and Innovation Institute (I3PT), Universitat Autònoma de Barcelona, Sabadell, Spain; [7]Department of Medicine and Life Sciences, Universitat Pompeu Fabra, IMIM (Hospital del Mar Medical Research Institute), Department of General Surgery, Hospital del Mar, Barcelona, Spain; [8]Department of Medicine and Life Sciences, Universitat Pompeu Fabra, IMIM (Hospital del Mar Medical Research Institute), Anesthesiology Department, Hospital del Mar, Barcelona, Spain; [9]Biostatistics Unit, Hospital del Mar Research Institute, Barcelona, Spain*
E-mail: lcanillas@psmar.cat

Background and aims: The current reference model for predicting postoperative mortality in cirrhosis is the VOCAL-Penn score. However, its predictive performance may decline in cohorts from our clinical setting. The aims of this study were: (1) to develop and validate a new model, and (2) to compare its performance with the VOCAL-Penn score.

Method: We conducted a multicenter, retrospective study in patients with cirrhosis undergoing major extrahepatic surgery. Two cohorts were included: non-transplant centers (A–training) and transplant centers (B–validation). Variables related to comorbidity, liver disease severity, and surgical urgency and complexity (minimal–low/moderate/high/extreme) were collected. Univariate analyses were performed using χ^2 and Mann–Whitney U tests. The predictive model was developed using binary logistic regression. Model discrimination (AUROC) was assessed in cohorts A and B and compared with the VOCAL-Penn score.

Results: A total of 2045 patients were included: cohort A (n = 1046) and cohort B (n = 999). Median age was 65 years, 68% were male, and

cirrhosis was alcohol-related in 49.6% and viral in 31.6%. Median platelet count was 127×10^9/L (IQR 86–178×10^9/L). Ascites was present in 36.5%, and esophageal varices in 69% of endoscopies (n = 1669). Surgery was urgent in 38.1% of cases. Surgical complexity was minimal–low (18.7%), moderate (54.8%), high (16.4%), and extreme (10.2%). Ninety-day postoperative mortality was 10.9% in cohort A (n = 114) and 10.1% in cohort B (n = 101). In cohort A, mortality was associated with age, ASA class, bilirubin, albumin, INR, creatinine, sodium, hemoglobin, platelet count, ascites, emergency surgery, and surgical complexity. Independent predictors of mortality [adjusted OR (IQR); p] were: age [1.08 (1.06–1.11); p < 0.001], bilirubin [1.38 (1.20–1.60); p < 0.001], INR [2.16 (1.30–3.58); p = 0.003], sodium [0.93 (0.89–0.98); p = 0.006], platelets [0.99 (0.99–0.99); p = 0.034], ascites [2.32 (1.27–4.24); p = 0.006], emergency surgery [2.01 (1.23–3.26); p = 0.005], and moderate [2.51 (1.11–5.70); p = 0.027], high [6.79 (2.74–16.81); p < 0.001], and extreme [11.96 (4.67–30.60); p < 0.001] surgical complexity. The AUROC for S-RISC versus VOCAL-Penn were 0.856 vs. 0.792 in cohort A (p = 0.002), and 0.872 vs. 0.826 in cohort B (p = 0.042).

Conclusion: The S-RISC model demonstrates excellent discrimination for predicting postoperative mortality in patients with cirrhosis in different hospital settings. In our clinical setting, S-RISC outperforms the VOCAL-Penn score.

WED-428

Transient hepatic elastography as a composite marker of advanced chronic liver disease severity

Aloma Campeche-Leão[1], Lais Garcez[2], Rosângela de Jesus[2], Helma Pinchemel Cotrim[3], Lourianne Cavalcante[2]. [1]*Hepatology and Gastroenterology, General Hospital Roberto Santos, Salvador, Brazil;* [2]*Federal University of Bahia, Hepatology and Gastroenterology, Salvador, Brazil;* [3]*School of Medicine, PPGMS, Federal University of Bahia, Salvador, Brazil*
E-mail: Lourianne@gmail.com

Background and aims: Advanced chronic liver disease (ACLD) with portal hypertension is associated with progressive hepatic dysfunction and adverse outcomes. Transient elastography (TE, FibroScan®) is widely used to assess liver stiffness, but its role as a composite marker integrating clinical severity, nutritional status, and muscle function remains unclear. We aimed to investigate whether TE reflects a multidimensional burden of disease in ACLD.

Method: We conducted a cross-sectional study (March 2024–July 2025) at a tertiary hepatology center in Brazil. Adults (>18 years) with ACLD and portal hypertension were included. Exclusion criteria: ascites, hepatocellular carcinoma, major decompensated comorbidities, inability to consent. Variables: liver stiffness (kPa, TE; categorized <15, 15–24.9, ≥25), age, sex, Child-Pugh, MELD-Na, nutritional status (GLIM), sarcopenia (EWGSOP), arm muscle circumference, and handgrip strength (HGS). Statistical analysis: linear regression and categorical comparisons (Jamovi v2.7.6).

Results: 132 patients were included. Higher TE values were associated with older age, higher MELD-Na, and worse Child-Pugh class (p < 0.05). Sarcopenia prevalence increased across TE strata (p < 0.001). Regression analysis showed each year of age (+0.15–0.20 kPa) and each MELD-Na point (+0.80–1.10 kPa) independently predicted higher stiffness. Malnutrition (GLIM) was more frequent in patients with ≥25 kPa (36.6%). HGS declined with increasing TE, particularly below EWGSOP cut-offs.

Conclusion: Liver stiffness by TE correlates not only with hepatic severity scores but also with nutritional and muscular impairment. TE may serve as a composite marker of systemic disease burden in ACLD, supporting integrated assessment strategies that combine elastography with functional and nutritional evaluation to improve risk stratification and patient care.

WED-429-YI

Artificial intelligence-based models enabling accurate diagnosis of spontaneous bacterial peritonitis using laboratory tests in China: a multicentre, retrospective cohort study

Zhiji Chen[1], Zhihang Zhou[1], Song He[1]. [1]*Second Affiliated Hospital of Chongqing Medical University, Chongqing, China*
E-mail: 894137655@qq.com

Background and aims: Spontaneous bacterial peritonitis (SBP) is the most common infection among patients with cirrhosis. Due to the widespread use of antibiotics and weakened immune systems, timely diagnosis of SBP is challenging. Laboratory tests are widely used in clinical practice, and some have demonstrated diagnostic and prognostic value for SBP. Our goal is to systematically evaluate the value of routine laboratory tests in predicting SBP and to develop a robust and generalizable integrated artificial intelligence (AI) model to assist in the identification of SBP patients.

Method: In this multicenter retrospective cohort study, we collected laboratory findings and clinical characteristics of patients with cirrhotic ascites (including those with confirmed and undiagnosed SBP) who visited 10 hospitals in China between January 1, 2014, and December 1, 2025. We employed a multi-criteria decision-based classification fusion (MCF) risk prediction framework to construct a comprehensive prediction tool integrating the prediction results of 10 artificial intelligence classification models for the diagnosis of SBP. This tool was evaluated on an internal validation set (5235 participants) and an external validation set (1879 participants). The primary endpoint was the predictive accuracy of the model in identifying SBP.

Results: We included 5235 participants in the internal validation set and 1879 participants in the external validation set. The MCF model achieved an area under the receiver operating characteristic (AUC) of 0.929 (95% CI 0.918–0.950) on the internal validation set and an AUC of 0.884 (0.882–0.887) on the external validation set. Compared to polymorphonuclear neutrophils (PMN) count, the model demonstrated higher AUC and sensitivity in identifying SBP. Even after excluding polymorphonuclear neutrophils (PMN) count, the MCF model still achieved acceptable predictive accuracy and outperformed state-of-the-art models in SBP prediction. MCF is packaged as an SBP prediction tool and made publicly available to provide estimated probabilities of SBP based on input laboratory test values.

Conclusion: When using laboratory test results from 10 hospitals, the MCF model consistently performed satisfactorily in the diagnosis of SBP. This model provides a low-cost, readily available, and accurate diagnostic tool for SBP.

WED-430

Computed tomography-defined sarcopenic obesity: an emerging risk factor for cardiovascular and cerebrovascular mortality in cirrhosis

Yanhua Chen[1], Cuncao Wu[2], Zixing Wang[3], Rui Huang[3]. [1]*Peking University Hepatology Institute, Peking University People's Hospital, School of Basic Medical Sciences, Peking University Health Science Center, Beijing, China;* [2]*Department of Cardiology, Peking University People's Hospital, Beijing, China;* [3]*Peking University Hepatology Institute, Peking University People's Hospital, Beijing, China*
E-mail: cyaoh66@163.com

Background and aims: Sarcopenic obesity (Sa-O) and cardiovascular and cerebrovascular (CCV) disease share multiple overlapping risk factors and adversely affect prognosis in cirrhosis. But direct evidences linking Sa-O to CCV mortality in this population remain scarce. This study was thus designed to explore whether Sa-O can serve as an effective predictor of CCV mortality in cirrhosis.

Method: Body composition was obtained from L3 CT scans in this retrospective cirrhotic cohort. Sa-O (co-existence of sarcopenia and obesity) was assessed via three criteria: skeleton muscle index (SMI) < 38 cm^2/m^2 (female), <42 cm^2/m^2 (male) for sarcopenia; obesity was respectively defined by: (a) visceral adipose tissue area (VATA) ≥

80 cm^2; (b) visceral-to-subcutaneous adipose ratio > 1.47 for men and >1.29 for women; (c) body mass index ≥ 25 kg/m^2. The primary outcome was CCV mortality which was evaluated utilizing Fine-Gray models across three definitions in univariable, multivariable and subgroup analyses.

Results: Of 983 cirrhotic patients (male: 595 [60.5%]; age [standard deviation]: 58.4 [12.2] years; CCV deaths: 46 [4.7%]; follow-up duration [interquartile range]:4.56 [1.81–7.28] years), 181 (18.4%), 79 (8.0%), and 41 (4.2%) met criterion A, B and C for Sa-O, with 17 (9.4%), 7 (8.9%), and 5 (12.2%) CCV deaths occurring respectively. The three criteria delineated distinct phenotypes: criterion A (predominantly viral etiology) captured an intermediate profile; criterion B (predominantly alcohol-related with a male predominance) exhibited the greatest frailty and inflammation; and criterion C (predominantly non-viral, non-alcoholic, with a female predominance) had the most severe liver dysfunction. In competing risk analyses, only criteria A and C independently predicted CCV death. Notably, multivariable adjustment attenuated the hazard ratio (HR) for criterion A from 2.88 (95% Confidence Interval [CI]: 1.58–5.22, p = 0.0005) to 2.42 (95% CI: 1.22–4.79, p = 0.0115), whereas amplified that of criterion C from 2.92 (95% CI: 1.12–7.59, p = 0.0282) to 3.16 (95% CI: 1.26–7.92, p = 0.0143). Distinct adjustment effects may reflect underlying phenotypes heterogeneity, given that the intermediate profile of criterion A was less affected by extremes and severity of liver disease. Results were robust across the subgroup and sensitivity analyses.

Conclusion: The study confirms the use of VATA-defined Sa-O as an effective tool for CCV mortality risk stratification in cirrhotic patients.

WED-431-YI

Physical frailty is the most important predictor of early mortality in hospitalized patients with decompensated cirrhosis

Francesca D'Arcangelo[1], Laura Vivian[1], Alberto Ferrarese[1], Martina Gambato[1], Giacomo Germani[1], Marco Senzolo[1], Francesco Paolo Russo[1], Patrizia Burra[1], Alberto Zanetto[1].
[1]Gastroenterology/Multivisceral Transplant Unit, Padua University Hospital, Italy, Department of Surgery, Oncology and Gastroenterology, University of Padova, Padua, Italy, Padua, Italy
E-mail: francesca.darcangelo02@gmail.com

Background and aims: Patients with cirrhosis are at high risk of malnutrition, sarcopenia and frailty. However, most available evidence derives from North American outpatient cohorts. This study prospectively examined the impact of frailty and sarcopenia on short-term clinical outcomes in hospitalized individuals with cirrhosis.

Method: All consecutive patients with cirrhosis admitted to our unit between October 2021 and March 2023 were screened. Exclusion criteria were: age <18 or >70 years, pre-existing musculoskeletal disorders, and prior liver transplantation. At admission, the Liver Frailty Index (LFI) was assessed and patients were classified as robust (<3.2), pre-frail (3.2–4.5), or frail (>4.5). Skeletal muscle mass was measured through CT scan when performed during hospitalization; sarcopenia was defined as SMI <50 cm^2/m^2 in males and <39 cm^2/m^2 in females. Cox regression analysis was used to identify predictors of primary outcome.

Results: A total of 127 patients were included (median age 59 years; 68.5% male). Median MELD was 22 (IQR 17–27); 70% Child-Pugh class C cirrhosis. Alcohol was the leading aetiology (62%). Frailty was present in 48.8% of the cohort. CT-based muscle assessment was available for 94 patients, revealing sarcopenia in 60%. Patients with both frailty and sarcopenia showed an increased need for ICU care compared with robust and non-sarcopenic individuals. Frailty—but not sarcopenia—was associated with prolonged hospitalization (15 [9–27] vs. 6.5 [4–15] days in robust patients; p = 0.001). No significant differences in rehospitalization rates were observed based on frailty (p = 0.589) or sarcopenia (p = 0.065). Over a median follow-up of 96 days (37–384), 39.4% of patients died. Both frailty and sarcopenia were linked to higher mortality (60% vs. 20% and 58% vs. 38%, respectively; p < 0.001 and p = 0.009). In multivariate analysis, frailty (HR 3.377; 95% CI 1.729–6.597; p < 0.001) and ACLF (HR 2.354; 95% CI 1.124–4.929; p = 0.023) were the only independent predictors of mortality. The association between frailty and mortality persisted in post-hoc analyses stratified by ACLF status.

Conclusion: Frailty and sarcopenia are highly prevalent among hospitalized patients with cirrhosis and are associated with greater healthcare resource use. Frailty emerges as the strongest determinant of early mortality after hospitalization. Thus, the assessment of frailty should be considered in all patients with cirrhosis hospitalized due to acute decompensation.

WED-432

A clinical prediction model for severe hepatic encephalopathy and mortality post-transjugular intrahepatic portosystemic shunt in patients with cirrhosis

Stijn de Reus[1], Wenjing Wang[2], Michelle Spaan[1,3], Ellen Werner[1], Diederik Bijdevaate[4], Kay Pieterman[4], Harry L.A. Janssen[1,5], Adriaan J. van der Meer[1], Bettina E. Hansen[2,6], Raoel Maan[1].
[1]Department of Gastroenterology and Hepatology, Erasmus MC, Rotterdam, Netherlands; [2]Department of epidemiology, Erasmus MC, Rotterdam, Netherlands; [3]Department of Gastroenterology and Hepatology, Amsterdam UMC, Amsterdam, Netherlands; [4]Department of Radiology and Nuclear Medicine, Erasmus MC, Rotterdam, Netherlands; [5]Toronto Centre for Liver Disease, Toronto General Hospital, University Health Network, Toronto, Canada; [6]IHPME, University of Toronto & Toronto Centre for Liver Disease, University Health Network, Toronto, Canada
E-mail: s.dereus.1@erasmusmc.nl

Background and aims: Transjugular intrahepatic portosystemic shunt (TIPS) indications are expanding in patients with portal hypertension. However, hepatic encephalopathy (HE) affects up to 50% of patients, which may present substantial clinical challenges, if severe. Prediction models identifying patients at high risk of severe HE or death can guide patient selection for TIPS.

Method: We retrospectively included consecutive cirrhotic patients receiving TIPS between January 2007 and December 2023 in a tertiary center. Patients with prior liver transplant (LT) were excluded. TIPS-indications were defined according to EASL guidelines and ascites as absent, controlled or refractory.

The primary composite endpoint was severe HE (leading to hospitalization) or all-cause mortality within three months, with LT as the competing event. Predictor selection was performed using Least Absolute Shrinkage and Selection Operator, and modeling was done using a Fine-Gray regression. Model validation was performed by 10-fold cross-validation and calibration.

Results: In total, 358 patients were included; 241 (67%) were male and the median age was 57 years (IQR 50–64). Alcohol-associated cirrhosis was the most common etiology in 191 patients (54%), followed by metabolic steatohepatitis in 44 (12%) and viral hepatitis in 39 (11%). TIPS indication was refractory ascites in 152 patients (42%). Of 175 patients receiving TIPS for variceal bleeding (49%), secondary prophylactic TIPS was the most frequent in 76 (43%). At three months, 124 patients had experienced composite endpoint (35%) and 10 had undergone LT (3%). Cumulative incidence of severe HE/death was 40.9% (95%CI 35.7–46.2). Age, diabetes, indication, etiology, ascites severity and MELD were included in the model. The model reached an AUC of 0.76 (95% CI 0.70–0.82) vs. an AUC of 0.69 for MELD and 0.66 for Child-Pugh score (CPS). Internal validation confirmed model performance (AUC 0.73). Calibration showed 124 observed vs. 127 predicted events at 90 days (36.4% vs 37.5%). Risk stratification into tertiles identified low-, intermediate-, and high-

risk groups, with three-month cumulative incidences of 15.0% (95% CI 8.2–21.8), 31.2% (22.5–40.0), and 62.7% (53.5–71.8).
Conclusion: We developed a competing-risk-based prediction model identifying patients at lower and higher risk for early adverse outcomes, which outperformed CPS/MELD. This model could support pre-procedural risk assessment using clinical parameters.

WED-433

Prevalence and associated factors of non-variceal upper gastrointestinal bleeding among cirrhosis patients on follow-up at a tertiary hospital in Ethiopia

Mahlet Desalegn[1], Henok Fisseha[1], Makida Girma[1], Kaleb Berhane[2], Wasihun Zewde[1]. [1]*St. Paul's Hospital Millennium Medical College, Addis Ababa, Ethiopia;* [2]*Adera Medical Centre, Addis Ababa, Ethiopia*
E-mail: malidmitik@yahoo.com

Background and aims: Liver cirrhosis is a major cause of morbidity and mortality worldwide. Upper gastrointestinal bleeding can be variceal or non-variceal. Non-variceal upper gastrointestinal bleeding accounts for 24–42% of bleeding episodes in cirrhotic patients with a mortality rate of 15–30%. Understanding its prevalence and associated factors is critical for prevention and improved outcomes. This study assessed the prevalence and predictors of NVUGIB among cirrhotic patients at a tertiary hospital in Addis Ababa, Ethiopia.
Method: A hospital-based cross-sectional study was conducted from December 2020 to December 2023 with a total of 234 patients in the study. The collected data were analyzed using Statistical Package for Social Sciences version 26.0. Bivariable and multivariable logistic regression were used to assess association between dependent and independent variables. Adjusted odds ratio with a 95% confidence interval was used to estimate the strength of association, and level of statistical significance was declared at p value <0.05.
Results: The prevalence of non-variceal upper gastrointestinal bleeding was 31.6% (95% CI: 26.0–37.8). with a mean (±SD) age of 39 ± 14 years. Independent predictors of non-variceal upper gastrointestinal bleeding included longer duration of cirrhosis (AOR = 1.01, 95% CI: 1.001–1.019, p = 0.03) and Human Immunodeficiency virus Infection (HIV) (AOR = 51.72, 95% CI: 5.65–471.8, p < 0.001). Lower odds of non-variceal upper gastrointestinal bleeding were observed in older patients (AOR = 0.96, 95% CI: 0.93–0.99, p = 0.007), those with hepatitis C virus (AOR = 0.12, 95% CI: 0.05–0.66, p = 0.009) or schistosomiasis (AOR = 0.03, 95% CI: 0.006–0.19, p < 0.001) as the cause of cirrhosis, prior beta-blocker use (AOR = 0.32, 95% CI: 0.14–0.70, p = 0.005), and higher international normalized ratio (AOR = 0.57, 95% CI: 0.36–0.89, p = 0.014). Non-variceal upper gastrointestinal bleeding patients also had lower systolic blood pressure at presentation (AOR = 0.97, 95% CI: 0.95–0.99, p = 0.010) but required fewer blood product transfusions (AOR = 0.25, 95% CI: 0.08–0.71, p = 0.009).
Conclusion: Non-variceal upper gastrointestinal bleeding (NVUGIB) accounted for nearly one-third of bleeding cases among patients with cirrhosis. It was significantly associated with longer duration of cirrhosis, younger age, and the presence of comorbidities. Implementing screening strategies to identify high-risk patients and adopting preventive measures are recommended to reduce the burden of NVUGIB.

WED-435

Sex-stratified prognostic associations of body fat composition and sarcopenia-related parameters in liver cirrhosis

Kei Endo[1], Hidekatsu Kuroda[1], Keisuke Kakisaka[1], Takayuki Matsumoto[1]. [1]*Iwate Medical University School of Medicine, Yahaba, Japan*
E-mail: keiendo@iwate-med.ac.jp

Background and aims: It remains unclear whether fat- and sarcopenia-related parameters show different prognostic associations between sexes. We aimed to evaluate sex-stratified associations of body fat composition and sarcopenia-related parameters with mortality in patients with liver cirrhosis.
Method: We retrospectively analyzed 535 patients with liver cirrhosis without hepatocellular carcinoma between January 2016 and October 202. Skeletal muscle index (SMI), subcutaneous adipose tissue index (SATI), and visceral adipose tissue index (VATI) were quantified using computed tomography at the third lumbar vertebra, and handgrip strength (HGS) was measured. Prognostic analyses were performed using Cox proportional hazards models adjusted for age, albumin–bilirubin score, and etiology (base model), separately for men and women. Associations with mortality were assessed using restricted cubic spline functions. Model discrimination was evaluated using Harrell's C-index with internal bootstrap validation (1000 resamples).
Results: During a median follow-up of 4.8 years, 134 patients died. Among 535 patients, 294 were men, the median age was 68 years, and 225 had virus-related cirrhosis. In men, restricted cubic spline analyses showed significant associations of SMI (P total < 0.01) and HGS (P total < 0.01) with mortality, with lower values conferring higher risk. SATI demonstrated a non-linear association with mortality (P total = 0.03, P non-linearity = 0.02), with increased risk at both low and high values, whereas VATI was not significantly associated (P total = 0.07). In women, SATI showed a significant linear association with mortality (P total = 0.03), while SMI (P total = 0.55), HGS (P total = 0.12), and VATI (P total = 0.09) were not significantly associated. In men, the optimism-corrected C-index of the base model was 0.698, which improved with the addition of HGS (0.746) and SMI (0.736), whereas SATI (0.699) and VATI (0.717) provided limited improvement. In women, the base model C-index was 0.790, and discrimination improved with fat-related parameters (SATI 0.800, VATI 0.805), while muscle-related parameters provided minimal improvement (SMI 0.795, HGS 0.796).
Conclusion: In sex-stratified analyses, muscle mass and strength were associated with prognosis in men, whereas subcutaneous adiposity showed a significant association in women. These findings suggest that the prognostic relevance of sarcopenia- and fat-related metrics may vary by sex, supporting the potential value of sex-stratified risk assessment in cirrhosis.

WED-436

The efficacy of Rifaximin in preventing liver cirrhosis complications, including spontaneous bacterial peritonitis, encephalopathy, variceal bleeding, and all-cause mortality in adult patients with liver cirrhosis : a meta-analysis

Camille Feliciano[1]. [1]*Skyline Hospital and Medical Center, San Jose Del Monte, Bulacan, Philippines*
E-mail: camillefelicianomd@gmail.com

Background and aims: Spontaneous bacterial peritonitis (SBP), hepatic encephalopathy, and variceal bleeding are serious complications of liver cirrhosis associated with a high recurrence rate and increased mortality. Norfloxacin, which is the most commonly used drug for the secondary prophylaxis of SBP, has been linked to the emergence of quinolone-resistant and Gram-positive SBP due to prolonged use. Rifaximin's broader antibacterial spectrum and non-absorbable nature make it a compelling alternative to Norfloxacin. This study aimed to evaluate the efficacy of Rifaximin in the prevention of liver cirrhosis complications including spontaneous bacterial peritonitis, encephalopathy, variceal bleeding, as well its effects on all-cause mortality.
Method: PubMed and Cochrane Library database were searched for articles published until August 24, 2023. Outcomes noted were occurrence of SBP, development of hepatic encephalopathy and variceal bleeding, adverse events, and mortality rate. Meta-analysis assessed the pooled Odds Ratios (ORs) with a 95% Confidence Interval by using Review Manager 5.3. A total of two hundred patients with liver cirrhosis Child-Pugh B and C were assigned to the Rifaximin group with dosages ranging from 800 mg to 1200 mg daily, while a

total of two hundred and seven patients with liver cirrhosis Child Pugh B and C were assigned to the Norfloxacin group with dosages of 400 mg to 800 mg daily, with a treatment duration of 6 months to 1 year. Study endpoints were: occurrence of SBP, hepatic encephalopathy, variceal bleeding, and all cause mortality.
Results: In this study, Rifaximin demonstrated significant efficacy in preventing SBP (Odds Ratio 0.19; $p < 0.0001$) and reducing all-cause mortality (Odds Ratio 0.55; $p = 0.02$), suggesting a strong clinical benefit over Norfloxacin. With an OR of 0.33 (95% CI: 0.17 to 0.64; $p = 0.001$), Rifaximin also shows significant efficacy in preventing hepatic encephalopathy. However, the effect on variceal bleeding was not statistically significant (Odds Ratio 0.76; $p = 0.74$).
Conclusion: Rifaximin demonstrates superior efficacy in preventing liver cirrhosis complications, including spontaneous bacterial peritonitis and hepatic encephalopathy, compared to the current standard of care, Norfloxacin. Additionally, Rifaximin exhibits a more favorable adverse effect profile and a reduced risk of antibiotic resistance.

WED-441
Uncontrolled ammonia is associated with increased healthcare resource utilization in hepatic encephalopathy
Jonathan Fischer[1], Christian Roy[1], Elliot Tapper[2]. [1]*Korro Bio, Cambridge, United States;* [2]*University of Michigan, Ann Arbor, United States*
E-mail: jfischer@korrobio.com

Background and aims: Ammonia is a key driver of hepatic encephalopathy (HE), and achieving ammonia control is essential for preventing morbidity and mortality. However, real-world ammonia control in HE remains poorly understood. We aimed to identify the proportion of patients with HE receiving standard therapies with uncontrolled ammonia and the impact of elevated ammonia on clinical outcomes.
Method: Patients with cirrhosis, HE treated with lactulose and/or rifaximin, ammonia ≥ 52.5 µM, and Model for End-Stage Liver Disease (MELD) ≤ 20 were identified in the All of Us database in 2022. Rifaximin-treated patients with uncontrolled ammonia and MELD ≤ 20 were chosen to identify a stable population with unmet needs that may be suitable for future outpatient clinical trials. Treatment patterns and inpatient healthcare utilization were analyzed, and ammonia findings compared to a urea cycle disorder (UCD) population with pathogenic or likely pathogenic single nucleotide polymorphisms in urea cycle genes.
Results: Of 3524 identified cirrhosis patients, 582 (16.5%) received HE pharmacotherapy, including 219 (38% of treated patients) treated with rifaximin. Among rifaximin-treated patients with ammonia measures, median ammonia was 69 µM, and 76% exhibited levels ≥ 1.5x upper limit of normal. Ammonia levels were higher in rifaximin-treated patients than in a UCD cohort (16 patients, median 56 µM). 75% of the rifaximin-treated patients with elevated ammonia had MELD ≤ 20. These patients with elevated ammonia and stable MELD demonstrated a significant increase in healthcare burden: mean HE-related hospitalizations were 2.33 versus 1.10 in all rifaximin-treated patients (incidence rate ratio (IRR) = 2.13, $p < 0.001$), and all-cause hospitalizations were 3.71 versus 1.96 (IRR = 1.89, $p < 0.01$).
Conclusion: Ammonia control remains a significant challenge that leads to a substantial healthcare burden in HE. Rifaximin-treated patients with uncontrolled ammonia and MELD ≤ 20 had significantly increased healthcare resource utilization compared to all rifaximin-treated HE patients, underscoring both the clinical severity and economic burden of inadequately controlled ammonia. Higher ammonia levels in HE patients compared to those in UCD highlight that current gut-targeted approaches may be insufficient for achieving adequate ammonia control in HE. These findings support the critical unmet need for novel therapies that directly target ammonia metabolism to reduce HE recurrence, improve patient outcomes, and decrease healthcare burden.

WED-442-YI
Distinct disease trajectories and prognosis of further decompensation of cirrhosis
Roberta Gagliardi[1], Rakhi Maiwall[2], Francesco Vizzutti[3], Laura Buttler[4], Lucie Simonis[5], Enrico Pompili[6], Charlotte Bouzbib[7], Marlene Reincke[8], Hélène Larrue[9], Marta Tonon[1], Adrian Wunderbaldinger[5], Marika Rudler[7], Alessio Mastro[3], Ana Coedo[10], Fabio Marra[3], Dominik Bettinger[8], Paolo Caraceni[6], Agustín Albillos[10], Lorenz Balcar[5], Benjamin Maasoumy[4], Dominique Thabut[7], Salvatore Piano[1]. [1]*Department of Medicine, University of Padova, Padova, Italy;* [2]*Institute of Liver and Biliary Sciences, New Delhi, India;* [3]*Department of Experimental and Clinical Medicine, University of Florence, Florence, Italy;* [4]*Department of Gastroenterology, Hepatology, Infectious Diseases and Endocrinology, Hannover Medical School, Hannover, Germany;* [5]*Division of Gastroenterolongy and Hepatology, Department of Medicine III, Medical University of Vienna, Vienna, Austria;* [6]*Department of Medical and Surgical Science, University of Bologna; IRCCS Azienda Ospedaliera-Universitaria di Bologna, Bologna, Italy;* [7]*AP-HP, Sorbonne Université, Liver Intensive Care Unit, Hepatogastroenterology Department, La Pitié-Salpêtrière Hospital, 47- 83 Boulevard de l'Hôpital, Paris, France;* [8]*Department of Medicine II, Medical Center University of Freiburg, Faculty of Medicine, University of Freiburg, Freiburg, Germany;* [9]*University Hospital of Toulouse, Toulouse, France;* [10]*Gastroenterology and Hepatology Department. Hospital Universitario Ramón y Cajal. IRYCIS. CIBERehd. Universidad de Alcalá., Madrid, Spain*
E-mail: salvatore.piano@unipd.it

Background and aims: Further decompensation (FD) in cirrhosis, defined as the development of a second distinct portal hypertension-driven decompensating event, jaundice or recurrence of variceal bleeding, ascites or hepatic encephalopathy (HE), represents a critical prognostic stage associated with markedly increased mortality compared with first decompensation. However, the prognostic impact of different types of FD and the clinical trajectories after FD are not well characterized. The primary aim of this study was to characterize disease trajectories and mortality risk in patients with cirrhosis experiencing FD.
Method: We conducted a multicentre, retrospective, observational study including patients with cirrhosis followed at 10 centers in 6 countries who developed at least one episode of FD (according to Baveno VII criteria). Demographic, clinical, laboratory, endoscopic and treatment data were collected at first FD episode. All subsequent FD episodes were recorded until death, liver transplant or last follow-up (median time 371 days). Analysis of mortality was adjusted for age, sex, etiology, MELD-Na, ACLF and albumin at first FD.
Results: We enrolled 1523 patients (32% female, mean age 57.6 years, alcohol-related cirrhosis 59.2%). The most frequent first FD events were refractory ascites (23.1%), HE (14.5%), recurrent ascites (13.3%) and bleeding (10.7%), whereas recurrent bleeding (7.9%), SBP (6.9%), jaundice (6.8%), hepatorenal syndrome (HRS) (6.3%), ascites (6.2%) and recurrent HE (4.3%) were less common. Subsequent decompensation patterns differed significantly according to the type of first FD. The two-year cumulative incidence of mortality was 37.4%. In multivariable competing risk analysis (using recurrent bleeding as a reference group), ascites (sHR = 2.50; $p < 0.001$), refractory ascites (sHR = 2.01; $p = 0.002$), bleeding (sHR = 2.38; $p < 0.001$), HE (sHR = 1.77; $p = 0.018$) and HRS (sHR = 3.35; $p < 0.001$) as type of FD had a higher risk of mortality, whereas jaundice, SBP, recurrent ascites or recurrent HE did not. Age, MELD-Na, ACLF and albumin at FD were independently associated with mortality as well.
Conclusion: Distinct phenotypes of FD are associated with distinct clinical trajectories and prognosis. Patients developing a second distinct portal hypertension-driven decompensating event, as well as those with refractory ascites and hepatorenal syndrome have the worst prognosis. These findings have important implications for risk stratification and potential phenotype-driven therapeutic management.

WED-443

Rectus femoris cross sectional area predicts further decompensation and mortality in patients surviving hospitalization for acute decompensation of cirrhosis

Roberta Gagliardi[1], Simone Incicco[1], Valeria Calvino[1], Marta Tonon[1], Carmine Gambino[1], Nicola Zeni[1], Sara Montagnese[1], Salvatore Piano[1]. [1]*Unit of Internal Medicine and Hepatology, Department of Medicine, University and Hospital of Padova, Padova, Italy*
E-mail: salvatore.piano@unipd.it

Background and aims: Sarcopenia is common in patients with cirrhosis and is associated with poor clinical outcomes. Further decompensation (FD) represents a critical prognostic stage with higher mortality than first decompensation, yet its association with sarcopenia remains poorly defined. Ultrasound measurement of rectus femoris cross-sectional area (RF-CSA) is a simple bedside tool to assess sarcopenia. This study evaluated the association between RF-CSA and the risk of FD and mortality in patients with cirrhosis surviving a hospitalization for acute decompensation (AD).
Method: Patients with cirrhosis discharged after a hospitalization for AD between 2019 and 2025 were prospectively enrolled. Clinical, demographic and laboratory data were collected during admission and on discharge. RF-CSA was measured at two-thirds of the distance from the anterior superior iliac spine to the superior patellar border. Previously identified RF-CSA thresholds (4.87 cm^2 in males; 2.42 cm^2 in females) were used to diagnose sarcopenia. Follow-up continued until death, liver transplantation or 180 days. Episodes of FD, defined as the development of a second portal hypertension–driven decompensating event and/or jaundice, recurrent variceal bleeding, recurrent/refractory ascites, recurrent hepatic encephalopathy (HE), spontaneous bacterial peritonitis and/or hepatorenal syndrome, were recorded.
Results: A total of 183 patients were included (mean age 65 ± 11 years; median MELD 16). Most had alcohol-related cirrhosis (61%) and ascites (70%). During the follow-up, 68 patients (37%) developed FD. These patients were older (66 ± 11 vs. 62 ± 10 years; p = 0.006), had a higher prevalence of HE (54% vs. 21%; p < 0.001), and showed lower RF-CSA values (2.87 [IQR 2.15–3.64] vs. 3.53 [IQR 2.65–4.82] cm^2; p = 0.003). Patients with sarcopenia according to RF-CSA thresholds had a higher risk of FD (42% vs. 22%; p = 0.012) and mortality (28% vs. 14.3%; p = 0.003). In multivariable analysis (adjusted for age, gender, MELD, and HE), RF-CSA was an independent predictor of both FD (sHR = 0.81; p = 0.035) and mortality (sHR = 0.67; p = 0.009).
Conclusion: In cirrhotic patients surviving a hospitalization for AD, sarcopenia assessed by RF-CSA is independently associated with FD and mortality at 180 days. Interventions aimed at preserving or increasing muscle mass may help reduce the risk of FD and improve patient outcomes.

WED-444

Comparative assessment and external validation of ultrasound-derived quadriceps indices against bioelectrical impedance analysis for sarcopenia screening in chronic liver disease

Paolo Gallo[1], Valentina Flagiello[1], Daniela Lemme[1], Antonio De Vincentis[2], Simone Di Cola[3], Andrea Falcomatà[1], Francesca Terracciani[1], Antonio Picardi[1], Umberto Vespasiani-Gentilucci[1]. [1]*Clinical Medicine and Hepatology Unit, Fondazione Policlinico Universitario Campus Bio-Medico, Via Alvaro del Portillo, 21, Roma, Italy;* [2]*Internal Medicine Unit, Fondazione Policlinico Universitario Campus Bio-Medico, Via Alvaro del Portillo, 21, Roma, Italy;* [3]*Department of Translational and Precision Medicine, Sapienza University of Rome, Roma, Italy*
E-mail: paolo.gallo@policlinicocampus.it

Background and aims: Sarcopenia is a common complication in chronic liver disease (CLD). Muscle ultrasound (US)-measurements are increasingly investigated as feasible bedside tools despite limited standardization. We aimed to evaluate whether US-derived quadriceps indices can serve as surrogates of appendicular skeletal muscle mass (ASMM) measured by bioelectrical impedance analysis (BIA) in patients with compensated cirrhosis.
Method: A prospective, two-phase study was conducted. In phase 1, we evaluated the correlation and agreement between US-based quadriceps measurements (average compression index-ACI- and average feather index -AFI-) and ASMM assessed by BIA in patients with compensated cirrhosis and a history (active disease or under surveillance) of hepatocellular carcinoma (HCC). Phase 2 externally validated these findings in an independent cohort of patients with compensated cirrhosis, regardless of HCC history.
Results: Phase 1 included 88 patients (mean age 73 years [SD7], 78% male). ACI and AFI showed significant correlations with ASMM/height^2 [r = 0.35 (95%CI 0.15–0.52), p = 0.001; r = 0.45 (95%CI 0.27–0.60), p < 0.001, respectively]. In sex-adjusted models, linear regression analysis confirmed AFI [β = 0.64 (95%CI 0.37–0.92)] and ACI [β = 0.50 (95%CI 0.21–0.78)] as significantly associated with ASMM/height^2 (p < 0.001 for both associations). In addition, Bland–Altman analysis showed a good level of agreement for these indices [bias and LoA of 0.007 (−0.239;0.253) and 0.021 (−0.205;0.247) for ACI and AFI, respectively]. Inter-rater reliability was high (ICC 0.94–0.96). Phase 2 included 47 patients (mean age 70 years [SD10], 66% male). In this external cohort, both indices confirmed good correlations [ACI r = 0.49 (95%CI 0.23–0.68), p < 0.001; AFI r = 0.50 [95%CI 0.25–0.69], p < 0.001]. In age- and sex-adjusted models, ACI [β = 0.89 (95%CI 0.44–1.33), p < 0.001] and AFI [β = 0.79 (95%CI 0.34–1.24), p < 0.001] remained independently associated. Finally Bland–Altman analysis confirmed excellent agreement in this population.
Conclusion: US-derived quadriceps measurements provide reproducible and non-invasive surrogates of skeletal muscle mass defined by BIA in patients with compensated cirrhosis, and retain good performance in external validation, supporting their use as a feasible and cost-effective tool for the assessment of sarcopenia in patients with CLD.

WED-445

Predictors of clinical course in patients surviving acute decompensation of cirrhosis

Carmine Gambino[1], Antonio Accetta[1], Enrico Pompili[2,3], Roberto Filomia[4], Chiara Passalacqua[5], Giulia Iannone[2], Concetta Pitrone[4], Gianluca Fusco[5], Clelia Asero[4], Giulia La Manna[5], Giacomo Zaccherini[2,6], Irene Cacciola[4], Giovanni Squadrito[5], Paolo Caraceni[2], Paolo Angeli[1], Salvatore Piano[1]. [1]*University of Padova, Unit of Internal Medicine and Hepatology, Department of Medicine, Padua, Italy;* [2]*IRCCS Azienda Ospedaliero-Universitaria di Bologna, Unit of Semeiotics, Liver and Alcohol-related Diseases, Bologna, Italy;* [3]*Department of Medical and Surgical Sciences, University of Bologna, Bologna, Italy;* [4]*University Hospital of Messina, Medicine and Hepatology Unit, Messina, Italy;* [5]*University Hospital of Messina, Internal Medicine Unit, Messina, Italy;* [6]*University of Bologna, Department of Medical and Surgical Sciences, Bologna, Italy*
E-mail: carmine.gabriele.gambino@gmail.com

Background and aims: Three different clinical trajectories have been described in PREDICT study in patients surviving acute decompensation (AD) of cirrhosis, namely stable decompensated cirrhosis (SDC), unstable decompensated cirrhosis (UDC) and pre-ACLF, yet their prediction at the time of discharge remains challenging. The aim of this study is to investigate predictors of clinical courses at discharge after AD and 1-year mortality.
Method: We included 646 patients (age 63 [54–73] years; male 414 (64.1%); alcohol 297 [46%]; MELD 14 [11–18]) surviving AD of cirrhosis at the three tertiary care centers (University of Bologna, Messina and Padova), from 2011 to 2020. Patients were followed up until liver transplantation (LT), death or 1 year. Clinical and laboratory data at admission, during hospitalization and at discharge were collected.

Results: At 90-day after discharge, 369 (57.1%) patients were identified as SDC, 226 (35%) as UDC and 51 (7.9%) as pre-ACLF. Twenty-two (3.4%) patients underwent LT. At discharge, SDC patients showed, if compared to both UDC and pre-ACLF patients, lower WBC count (4.31 vs 4.83 vs 4.77 × 10^9/L; p = 0.039), creatinine (0.80 vs 0.87 vs 0.87 mg/dL; p = 0.011), bilirubin (1.70 vs 2.11 vs 3.08 mg/dL; p < 0.001), INR (1.32 vs 1.36 vs 1.57; p < 0.001) and MELD (12 vs 14 vs 17; p < 0.001); moreover, they showed higher haemoglobin (104 vs 103 vs 99 g/L; p = 0.01) and platelet count (97 vs 79 vs 73 × 10^9/L; p = 0.047). In a multivariable multinomial logistic regression model (adjusted for age, gender, aetiology, haemoglobin, CRP, albumin, and MELD – all at discharge) with SDC as reference, age (p < 0.01) and MELD (p < 0.001) were independently associated with clinical course, being each 1-point increase in MELD associated with 7.7% higher odds of UDC (OR 1.077, p < 0.001) and 24.6% higher odds of pre-ACLF (OR 1.246, p < 0.001). At 1-year after discharge, mortality rate was higher in pre-ACLF if compared to UDC and SDC (14.8% vs 35% vs 50.6%; p < 0.0001), and 66 (10.2%) patients underwent LT. In a multivariable model (adjusted for age, gender, aetiology, clinical trajectory, creatinine, bilirubin, INR and CRP at discharge), older age (sHR = 1.047; p < 0.001), higher CRP (sHR = 1.01; p < 0.0001), UDC (sHR = 3.10; p < 0.001) and pre-ACLF (sHR = 5.71; p < 0.001) were independent predictors of 1-year mortality.
Conclusion: We confirmed three distinct clinical trajectories after AD of cirrhosis with significantly different mortality. Older age and higher MELD at discharge independently predicted UDC and pre-ACLF trajectories.

WED-446

Neutrophil gelatinase-associated Lipocalin as an early biomarker of outcome after TIPS

Sophia Geißelbrecht[1,2], Christian Niehaus[1,3,4], Anja Tiede[1,2], Hannah Schneider[1], Jim Benjamin Mauz[1], Birgit Bremer[1], Jennifer Witt[1], Martin Kabelitz[1], Christian Labenz[5], Simon Johannes Gairing[5], Eva Maria Schleicher[5], Markus Cornberg[1,2,3,4,6], Anke R.M. Kraft[1,2,3,4,6], Bernhard Meyer[7], Christine Falk[6,8], Heiner Wedemeyer[1,2,3,6], Benjamin Maasoumy[1,2,6].
[1]Department of Gastroenterology, Hepatology, Infectious Diseases and Endocrinology, Hannover Medical School, Hannover, Germany; [2]German Center for Infection Research (DZIF), Partner-site Hannover-Braunschweig, Hannover, Germany; [3]Centre for Individualised Infection Medicine (CiiM), a joint venture between the Helmholtz Centre for Infection Research (HZI) and Hannover Medical School (MHH), Hannover, Germany; [4]Twincore, Centre for Experimental and Clinical Infection Research, a joint venture between the Helmholtz Centre for Infection Research (HZI) and the Hannover Medical School (MHH), Hannover, Germany; [5]Department of Internal Medicine, University Medical Center of the Johannes Gutenberg-University Mainz, Mainz, Germany; [6]Cluster of Excellence RESIST (EXC2155), Hannover Medical School, Hannover, Germany; [7]Department of Diagnostic and Interventional Radiology, Hannover Medical School, Hannover, Germany; [8]Institute of Transplant Immunology, Hannover Medical School, Cluster of Excellence RESIST (EXC2155), Hannover Medical School, Hannover, Germany
E-mail: Geisselbrecht.Sophia@mh-hannover.de

Background and aims: Renal function is an important predictor in end-stage liver disease. However, serum Creatinine (sCr) is influenced by other cirrhosis-related factors such as sarcopenia and malnutrition. This study evaluated the potential of neutrophil gelatinase-associated lipocalin (NGAL) as a novel biomarker for predicting outcomes after transjugular intrahepatic portosystemic shunt (TIPS).
Method: Consecutive patients with decompensated cirrhosis undergoing TIPS insertion between 08/2019 and 04/2025 at centers in Hannover and Mainz were prospectively enrolled. SCr and plasma NGAL levels were measured before TIPS and at 1, 6, 12 and 24 months. Fine-Gray competing risk models were used to analyze survival (competing event: liver transplantation (LT)) and acute kidney injury (AKI) (competing events: death and LT) within three months and two years after TIPS, estimating subdistribution hazard ratios (sHRs) and absolute standardized hazard ratios (aSHRs). Multivariable models were adjusted for age, albumin, bilirubin, and sCr, while univariable models were conducted without adjustment.
Results: A total of 246 patients (median age 60 years, median MELD 3.0 score 15, 53% alcohol-related cirrhosis) were analyzed. Overall, patients showed improved sCr (p < 0.001) and NGAL (p = 0.048) over the course of 12 months, with the greatest benefit observed in patients with impaired renal function (sCr ≥ 1.5 mg/dL and high NGAL ≥ 187 ng/mL). At baseline, NGAL was significantly associated with IL-6 levels (β = 0.51, 95% CI 0.27–0.74; p < 0.001), corresponding to an ~42% increase in IL-6 per NGAL doubling. In univariate competing risk models, higher baseline NGAL was associated with increased two-year mortality (sHR: 1.001; p = 0.047) and AKI (sHR: 1.001; p = 0.04). Baseline NGAL was independently associated with three-month mortality in a multivariable competing risk model (asHR: 1.003; p < 0.001). In contrast, baseline NGAL was not associated with two-year mortality (asHR: 1.001; p = 0.34) or AKI (three-month asHR: 1.00; p = 0.8; two-year asHR: 1.00; p = 0.62) in multivariable competing risk models. However, NGAL levels at one month after TIPS insertion were associated with two-year mortality (asHR: 1.002; p = 0.04) and AKI (asHR: 1.003; p = 0.001).
Conclusion: Baseline NGAL levels were strong predictors of early mortality after TIPS, while NGAL levels at one month post-TIPS were associated with long-term mortality and the development of AKI, supporting NGAL as an early risk stratification biomarker after TIPS.

WED-447

Baseline characteristics of a prospective, multi-center study on the natural history of compensated cirrhosis: the liver cirrhosis network

Kara Wegermann[1], Abigail Smith[2], Srinivasan Dasarathy[3], Nicole Welch[3], Elizabeth Verna[4], Robert S. Brown, Jr.[5], Cynthia Moylan[1,6], Patrick S. Kamath[7], Vijay Shah[7], Patricia Jones[8], Elliot Tapper[9], Rohit Loomba[10], Claude Sirlin[10], Bilal Hameed[11], Andrew Stolz[12], Arun J. Sanyal[13], Jasmohan Bajaj[13], Daniela Ladner[2], Mandana Khalili[11], Norah Terrault[12], Neehar D. Parikh[9], David Goldberg[8].
[1]Duke University, Durham, United States; [2]Northwestern University, Evanston, United States; [3]Cleveland Clinic Foundation, Cleveland, United States; [4]New York-Presbyterian/Columbia University Irving Medical Center, New York, United States; [5]Weill Cornell Medical College of Cornell University, New York, United States; [6]Veterans Affairs Medical Center Durham Qmi, Durham, United States; [7]Mayo Clinic, Rochester, United States; [8]University Miami Miller School-Medical, Miami, United States; [9]University of Michigan Health, Ann Arbor, United States; [10]University of California San Diego, La Jolla, United States; [11]University of California San Francisco, San Francisco, United States; [12]Keck School of Medicine of USC, Los Angeles, United States; [13]Virginia Commonwealth University School of Medicine, Richmond, United States
E-mail: kara.wegermann@duke.edu

Background and aims: Factors driving decompensation among patients with compensated cirrhosis are incompletely understood. The multi-center NIH-sponsored Liver Cirrhosis Network (LCN) Cohort Study aims to elucidate natural history of compensated cirrhosis and develop risk stratification tools. The LCN also includes patients with recompensated cirrhosis, an emerging population with poorly described characteristics and natural history. Here, we describe baseline characteristics of the study population compared to other large US cohorts of patients with cirrhosis, and we compare characteristics of participants with always compensated versus recompensated cirrhosis.
Method: The LCN Cohort Study is a prospective, 3-year observational study at 10 US sites. Adults with compensated cirrhosis were enrolled based on: a) liver biopsy within 5 years or b) 2 of the following: liver biopsy >5 years ago, VCTE ≥ 12.5 kPa, MRE ≥ 5 kPa, imaging with

nodular liver and splenomegaly within 1 year, esophageal varices within 3 years, FIB-4 > 2.67 or platelets < 150,000 within 6 months. We performed a subgroup analysis of participants with recompensation, defined as prior ascites, variceal bleeding, or hepatic encephalopathy without treatment of decompensation ≥ 1 year. We compared demographic and clinical characteristics of our cohort to CDC death and OPTN transplant registry data.

Results: We enrolled 1221 participants from 2022 to 2025. Compared to the contemporary OPTN transplant waitlist registry, LCN participants were older (median age 62 vs 57 years), more often female (50% vs 39%), and more likely to have MASH (56% vs 19%), while a smaller proportion had alcohol-associated liver disease (ALD, 18% vs 44%). The age, race, ethnicity, and sex distribution mirrored the US population dying from cirrhosis in the CDC data from 2022 to 2023. Among 1221 LCN participants, 100 (8.0%) had a history of decompensation followed by recompensation. Recompensated participants had a lower BMI (median 28.7 vs 31.3 kg/m^2, p < 0.001), were less likely to have diabetes (30% vs 47%, p < 0.001) and were more likely to have ALD (55% vs 15%, p < 0.001).

Conclusion: LCN Cohort Study participants have similar demographics to the broader cirrhosis population in the US. The overall cohort had a lower prevalence of ALD compared to a liver transplant waitlist population, but those with recompensated cirrhosis were more likely to have ALD.

WED-448-YI

Development of a composite biomarker to predict risk of AKI and mortality following an acute decompensation of cirrhosis

Olivia Greenham[1], Kohilan Gananandan[1], Peter Holland-Fischer[2], Konstantin Kazankov[3], Rohit Sawhney[4], Naina Shah[1], Carolyn Hyde[5], Pragyan Acharya[6], Rajiv Jalan[1], Karen Louise Thomsen[1,3], Rajeshwar Prosad Mookerjee[1,3]. *[1]Liver Failure Group University College London, London, United Kingdom; [2]Aalborg University Hospital, Aalborg, Denmark; [3]Aarhus University Hospital, Aarhus, Denmark; [4]Eastern Health, Monash University, Melbourne, Australia; [5]Bio-Analysis Centre, London, United Kingdom; [6]All India Institute Of Medical Science, Delhi, India*
E-mail: olivia.greenham@nhs.net

Background and aims: Development of acute kidney injury (AKI) in cirrhosis patients is associated with worse outcomes. The current AKI diagnostic standard, serum creatinine, lacks sensitivity and specificity. Neutrophil gelatinase associated lipocalin (NGAL), reflecting renal tubular injury and dimethylarginines (ADMA and SDMA) related to endothelial dysfunction, are both processes involved in new AKI following acute decompensation (AD). The study aimed to assess the ability for plasma (p) pNGAL, pADMA, pSDMA and urine (u) uNGAL to predict outcomes in patients with AD.

Method: Stored plasma/urine samples were analysed from 122 patients at UCL recruited to DASIMAR, a prospective, observational study in AD patients. Simple plex assays for uNGAL and pNGAL, and mass spectrometry for pADMA and pSDMA were performed on paired urine and plasma samples taken at baseline (T1) and a second time point within 7 days (T2). Using a logistic regression model, increases in a composite of standardised variables (z scores), expressed as 1-standard-deviation (1SD), were used to predict outcomes.

Results: Of 122 patients (66% male, 51 years age, 71% ArLD), 21% had AKI with similar demographics to those with no AKI. 16% withh AKI and 9% with no AKI died within 3 months. Median uNGAL and pNGAL were significantly higher in the AKI group [uNGAL 106 vs 62 ng/ml p = 0.01, pNGAL 132 vs 71 ng/ml p < 0.001].

Univariate analysis showed higher pSDMA and uNGAL values at T1 and T2 were associated with an increased risk of new AKI. A 1SD increase in composite pSDMA and uNGAL at T1 and T2 was associated with a 1.7 and 1.9 fold respective increased risk for new AKI [OR 1.7 (CI1.3–2.6) p = 0.002] [OR 1.9 (CI1.3–3.2) p = 0.004]. Higher values of all 4 biomarkers at T2 were associated with increased 3 month mortality on univariate analysis. A 1SD increase in both composites pADMA and pNGAL, and pSDMA and uNGAL, at T2, resulted in a 1.9 fold and 1.5 fold respective increase in 3 month mortality risk [OR 1.9 (CI1.3–3.2) p = 0.009] [OR 1.5 (CI 1.1–3.1) p = 0.03].

Conclusion: Our data shows higher composite scores of uNGAL and pSDMA are associated with a greater risk of developing new AKI events during AD admissions, which may represent both renal tubular injury and endothelial dysfunction. Higher pSDMA, pADMA, and NGAL levels within 7 days of admission are also associated with an increased 3 month mortality, suggesting repeat measures of these novel markers may inform prognosis and guide early intervention, though this requires further validation.

WED-449

Real-world management of cirrhotic patients following the HALO program: a retrospective observational study

Tarek Hassanein[1], Fatma Barakat[2], Cristina Coll Ortega[3], Thomas Ardiles[4], Christopher Blanchette[5]. *[1]Southern California Liver Centers, Coronado, United States; [2]SCTI Research Foundation, Coronado, United States; [3]Grifols, Sant Cugat del Valles, Spain; [4]Grifols, Shared Services North America, Durham, United States; [5]Rutgers University, Center for Health Outcomes, Policy, and Economics, Ernest Mario School of Pharmacy, Piscataway, United States*
E-mail: thassanein@livercenters.com

Background and aims: Advanced stages of liver cirrhosis are associated with high rates of complications that pose a major burden to patients (pts) and healthcare systems. The Health and Liver Optimization (HALO) program was uniquely developed and implemented across 8 integrated clinics in Southern California for over a decade. This novel program includes tailored monitoring and close follow up and management of cirrhotic pts including monitoring of liver function, lifestyle modification, and supplemental use of human albumin. The aims of this analysis is to describe demographics, clinical characteristics and healthcare resource use of cirrhotic pts following the HALO program.

Method: This is a retrospective observational study of adult pts with seen at one of the clinics following the HALO program between January 2014 and December 2018 and had a confirmed diagnosis of cirrhosis (as documented by imaging or liver biopsy) during that time frame (index date). Pts previously transplanted, diagnosed with liver cancer, or those who did not have at least one follow-up visit before December 2019 were excluded. Follow-up was until December 2022, unless pt was transplanted, diagnosed with HCC, died, or was lost to follow-up.

Results: A total of 889 patients met the inclusion criteria. 52.4% were male. Mean age was 59.5 ± 10.2 years. 51.4% Hispanic or Latino and 91.1% were White or Caucasian. 37.9% had a history of HCV, 22.4% alcohol-related liver disease, 20.7% MASLD/MASH. The median follow-up duration was 34.4 months (1–119 months) with a median number of visits per pt during follow up of 14 (2–117). 24.5% received at least one albumin infusion. 16.6% underwent at least one paracentesis during follow-up. Only 10.9% had received TIPS. 52.3% were hospitalized at least once, largely not liver-related. 10.8% developed Hepatocellular Carcinoma. Most pts were alive at the end of follow-up (85.3%). 96.1% (854) of pts were not listed for transplant, primarily (in 772 pts) because their MELD score did not exceed 15 throughout their follow-up.

Conclusion: Implementing the Health and Liver Optimization (HALO) program in patients with Cirrhosis and End-Stage Liver Disease with the goal of pt stablization resulted in 1) low mortality, 2) lower hospitalization rate and duration, 3) decreased need for paracentesis or TIPS, and 4) significant improvement in early detection of liver cancer. These findings highlight the need for optimized and tailored strategies in advanced liver disease care.

WED-450

Predictive factors for explantation or mortality after tunneled peritoneal catheters in patients with cirrhosis and refractory ascites

Jérémy Hassoun[1], Natasha Ollier[2], Julien Vionnet[2], Montserrat Fraga Christinet[2], Joana Sofia Vieira Barbosa[2], Clemence Canivet[1], Giulia Magini[1], Laurent Spahr[1], Nicolas Goossens[1]. [1]*Hôpitaux Universitaires de Genève, Genève, Switzerland;* [2]*CHUV-Centre Hospitalier Universitaire Vaudois, Lausanne, Switzerland*
E-mail: nicolas.goossens@hug.ch

Background and aims: Tunneled peritoneal catheters (PeCa) implantation represents a therapeutic option in patients with cirrhosis and refractory ascites who are not candidates for transjugular intrahepatic portosystemic shunt (TIPS). Early outcomes and complications remain poorly described. In patients undergoing PeCa implantation for refractory ascites, we aimed to study predictive factors for early catheter explantation or mortality.
Method: We retrospectively analysed 74 cirrhotic patients with contraindication to TIPS who underwent a PeCa implantation in two tertiary centers in Switzerland between 2014 and 2023. The primary outcome was catheter explantation or mortality within 90 days (90-d) after implantation. Predictive factors were evaluated using logistic regression analyses. Continuous values were described as median (IQR) and categorical as n (%).
Results: 74 patients (15% female) were included with a median age of 68 years (60–76); BMI of 23.2 kg/m^2 (21–27), MELD-score of 14 (11–18), and Child-Pugh score of 9 (8–10). Previous spontaneous bacterial peritonitis (SBP) was present in 31% (23/74) of patients prior to PeCa implantation. Within 90-d, the primary endpoint occurred in 52% (39/74) of the patients, including 28% (11/39) PeCa explantation and 72% (28/39) liver transplantation (LT) or death. Causes for explantation were SBP (73%), bleeding (9%), PeCa dysfunction (9%) or cellulitis (9%). Factors associated with the 90-d primary endpoint in univariable analyses included: MELD-score ($p = 0.04$), ECOG performance status (ECOG-PS) ≥ 2 ($p < 0.01$), female sex ($p = 0.01$), and previous hepatocellular carcinoma (HCC) history ($p = 0.01$). SBP prior to implantation was not associated with the outcome (odds ratio [OR] 0.6, $p = 0.32$). In multivariable analysis, ECOG-PS ≥ 2 (OR 1.9, $p < 0.01$), female sex (OR 2.7, $p = 0.02$) and history of HCC (OR 1.4, $p = 0.02$) were independently associated with 90-day outcome. After PeCa implantation, SBP was documented in 23% (17/74) within 90-d, occurring at a median of 20 days (11–56) after implantation and PeCa could be maintained in 47% (8/17) at 90-d follow-up.
Conclusion: PeCa placement is a feasible option for the management of refractory ascites in patients with cirrhosis who are not eligible for TIPS. Higher ECOG-PS, female sex and a history of HCC were associated with PeCa explantation or death during the study period. Previous SBP was not associated with 90-d primary outcome.

WED-451-YI

Post-TIPS decline in von Willebrand factor levels is independently associated with improved survival

Marlene Hintersteininger[1,2,3], Simon Johannes Gairing[4], Katrin Kirsch[4], Theresa Müllner-Bucsics[1], Susanna Riegler[1], Lukas Reider[5], Lorenz Balcar[1,2,3], Eva Maria Schleicher[4], Jasmin Soehngen[4], Lukas Müller[6], Michael Bernhard Pitton[6], Julia Weinmann-Menke[4], Peter R. Galle[4], Michael Trauner[1,3], Mattias Mandorfer[1,2,3], Thomas Reiberger[1,2,3,7], Christian Labenz[4], Lukas Hartl[1,2,3]. [1]*Division of Gastroenterology and Hepatology, Department of Medicine III, Medical University of Vienna, Vienna, Austria;* [2]*Vienna Hepatic Hemodynamic Lab, Division of Gastroenterology and Hepatology, Department of Medicine III, Medical University of Vienna, Vienna, Austria;* [3]*Clinical Research Group MOTION, Medical University of Vienna, Vienna, Austria;* [4]*Department of Internal Medicine 1, University Medical Center of the Johannes Gutenberg-University, Mainz, Germany;* [5]*Division of Cardiovascular and Interventional Radiology, Department of Biomedical Imaging and Image-guided Therapy, Vienna, Austria;* [6]*Department of Radiology, University Medical Center of the Johannes Gutenberg-University, Mainz, Austria;* [7]*Christian Doppler Lab for Portal Hypertension and Liver Fibrosis, Medical University of Vienna, Vienna, Austria*
E-mail: marli.hintersteininger@gmail.com

Background and aims: Transjugular intrahepatic portosystemic shunt (TIPS) placement is an established option for patients with portal hypertension (PH)-related complications. Von Willebrand factor antigen (VWF) is a dynamic non-invasive marker for prognostication in patients with cirrhosis and PH. This study set out to investigate the prognostic relevance of VWF dynamics after TIPS in a bicentric cohort.
Method: All patients with liver cirrhosis who underwent TIPS placement at the University Medical Center Mainz between 2022 and 2025 (Mainz cohort) and the Medical University of Vienna between 2008 and 2025 (Vienna cohort) with available longitudinal VWF measurements at baseline (BL) and at 3 months (M3) of follow-up (FU) were included. Relative VWF change (ΔVWF) was calculated as the ratio of VWF at M3 to VWF at BL. Liver transplantation was considered as a competing event.
Results: A total of 142 patients (Mainz cohort: n = 49; Vienna cohort: n = 93) receiving TIPS (76.1% ascites; 43.9% bleeding) with a median age of 58 years, male predominance (69.7%) and a median MELD of 12 were included. Median BL VWF levels were 322.0% and significantly decreased to a median of 275.5% at M3 ($p < 0.001$) with 57.7% of patients displaying a decline of VWF at M3. Median relative ΔVWF was 0.97. A similar percentage of patients exhibited a VWF decline at M3 in the Vienna (60.2%) and in the Mainz cohort (53.1%; $p = 0.412$). Interestingly, patients with a decline at M3 had significantly higher BL VWF levels compared to those without (359.5% vs. 250.0%; $p < 0.001$), while MELD (12 vs. 12; $p = 0.841$) and liver disease etiology (ALD: 58.5% vs. 53.3%; $p = 0.753$) were comparable. The median FU duration was 14 months. Patients without VWF decline at M3 demonstrated a higher cumulative incidence of death at one year of FU compared to those with VWF decline (16.1% vs. 6.9%; $p = 0.030$). In multivariable competing risk regression analysis adjusted for age and MELD at M3, ΔVWF was an independent risk factor for death (adjusted subdistribution hazard ratio [asHR]: 3.10; 95%CI: 1.24–7.72; $p = 0.015$).
Conclusion: VWF levels decrease in more than half of the patients after TIPS placement. ΔVWF at M3 is an independent risk factor for death, underscoring the prognostic value of VWF dynamics after TIPS.

WED-452

Combined presence of cirrhosis-related hypogonadism and sarcopenia is common and independently linked to impaired survival

Marlene Hintersteininger[1,2,3], Sophia Wirth[4], Tim Zalewski[4], Lorenz Balcar[1,2,3], Mathias Jachs[1,2,3], Benedikt Hofer[1,2,3,5], Georg Kramer[1,2,3], Christian Sebesta[1,2,3], Paul Thöne[1,2,3], Paula Hoefinger[1,2], Ulrika Asenbaum[4], Martina Scharitzer[3,4], Albert Friedrich Stättermayer[1,2], Rodrig Marculescu[6], Michael Trauner[1,3], Mattias Mandorfer[1,2,3], Thomas Reiberger[1,2,3,5], Lukas Hartl[1,2,3], Katharina Lampichler[3,4]. [1]*Division of Gastroenterology and Hepatology, Department of Medicine III, Medical University of Vienna, Vienna, Austria;* [2]*Vienna Hepatic Hemodynamic Lab, Division of Gastroenterology and Hepatology, Department of Medicine III, Medical University of Vienna, Vienna, Austria;* [3]*Clinical Research Group MOTION, Medical University of Vienna, Vienna, Austria;* [4]*Division of General and Paediatric Radiology, Department of Biomedical Imaging and Image-guided Therapy, Medical University of Vienna, Vienna, Austria;* [5]*Christian Doppler Lab for Portal Hypertension and Liver Fibrosis, Medical University of Vienna, Vienna, Austria;* [6]*Department of Laboratory Medicine, Medical University of Vienna, Vienna, Austria*
E-mail: marli.hintersteininger@gmail.com

Background and aims: Hypogonadism and sarcopenia are highly prevalent in male patients with liver cirrhosis (LC). Low testosterone levels have been linked to sarcopenia through disruption of the hypothalamic-pituitary-gonadal axis and impaired muscle protein synthesis, yet their overlap and combined prognostic impact in male patients with LC remains unknown.
Method: Male patients undergoing cross-sectional imaging (CT or MRI) within 180 days of the measurement of total testosterone (TT) and hepatic venous pressure gradient (HVPG) were included. Total psoas muscle thickness at the level of L3 (TPMT-L3) was independently measured by two radiologists, and the mean value was used for analysis. Hypogonadism was defined as TT levels <12 nmol/L. Sarcopenia was defined as a TPMT-L3 <12 mm/m (normalized to body height). Liver transplantation and death were considered as competing events.
Results: A total of 225 patients (median age: 59 years, alcohol-related etiology: 49.6%; decompensated LC: 68.4%, median MELD: 14) with median TT of 9.9 nmol/L (median bioavailable testosterone: 2.9 nmol/L) and median TPMT-L3 of 12.8 mm/m were included. Interreader agreement for TPMT-L3 measurements was good, with an intraclass correlation coefficient of 0.88 (95%CI: 0.84–0.91). Sarcopenia was present in 98 patients and hypogonadism in 129 patients, while combined sarcopenia-hypogonadism was found in 64 patients. Patients with sarcopenia had significantly lower TT levels compared to those without (7.7 vs. 11.9 nmol/L; $p = 0.006$). TT levels correlated positively with TPMT-L3 ($\rho = 0.26$) and albumin ($\rho = 0.42$) and inversely with MELD ($\rho = -0.53$; all $p < 0.001$). During a median follow-up of 24 months, patients with concomitant sarcopenia-hypogonadism had a significantly higher risk of all-cause mortality (asHR:1.82; 95%CI:1.04–3.19; $p = 0.036$) and liver-related death (asHR:2.57; 95%CI:1.39–4.75; $p = 0.003$) after adjustment for age, MELD, albumin and HVPG. Consistently, these patients exhibited a markedly higher 1-year cumulative incidence of death (41.3% vs. 13.6%; $p < 0.001$) and liver-related death (39.7% vs. 6.9%; $p < 0.001$) compared to patients without sarcopenia-hypogonadism.
Conclusion: About two third of male LC patients with sarcopenia show hypogonadism. The concomitant presence of sarcopenia-hypogonadism identifies a subgroup at particularly high risk of short-term mortality. The effectiveness of testosterone substitution to improve sarcopenia and outcomes in patients with LC needs further investigation.

WED-453

Elevated growth differentiation factor 15 reflects disease-driving mechanisms in cirrhosis and predicts liver disease progression and mortality

Benedikt Hofer[1,2,3,4], Thomas Perkmann[5], Ksenia Brusilovskaya[1,3,6], Lorenz Balcar[1,2,4], Marlene Hintersteininger[1,2,4], Georg Kramer[1,2,4], Benedikt Simbrunner[1,2,3,4,6], Esther Caparrós[7,8,9], Rubén Francés[7,8,9,10], Beate Eichelberger[11], Silvia Lee[12], Kerstin Zinober[1,2,3], Benjamin Bödendorfer[5], Borka Radovanovic-Petrova[5], Paul Thöne[1,2,4], Christian Sebesta[1,2,4], Mathias Jachs[1,2,4], Lukas Hartl[1,2,4], Philipp Schwabl[1,2,3,4,6], Mattias Mandorfer[1,2,4], Simon Panzer[11], Thomas Reiberger[1,2,3,4,6], Thomas Gremmel[12,13,14,15]. *[1]Division of Gastroenterology and Hepatology, Department of Medicine III, Medical University of Vienna, Vienna, Austria; [2]Vienna Hepatic Hemodynamic Laboratory, Division of Gastroenterology and Hepatology, Department of Medicine III, Medical University of Vienna, Vienna, Austria; [3]Christian Doppler Lab for Portal Hypertension and Liver Fibrosis, Medical University of Vienna, Vienna, Austria; [4]Clinical Research Group (CRG) MOTION, Medical University of Vienna, Vienna, Austria; [5]Department of Laboratory Medicine, Medical University of Vienna, Vienna, Austria; [6]Center for Molecular Medicine (CeMM) of the Austrian Academy of Sciences, Vienna, Austria; [7]CIBEREHD, Instituto de Salud Carlos III, Madrid, Spain; [8]Hepatic and Intestinal Immunobiology Group, Department of Clinical Medicine, Miguel Hernández University, San Juan de Alicante, Elche, Spain; [9]Instituto IDIBE, Miguel Hernández University, Elche, Spain; [10]Instituto ISABIAL, Hospital General Universitario de Alicante, Alicante, Spain; [11]Department of Blood Group Serology and Transfusion Medicine, Medical University of Vienna, Vienna, Austria; [12]Department of Internal Medicine II, Medical University of Vienna, Vienna, Austria; [13]Institute of Cardiovascular Pharmacotherapy and Interventional Cardiology, Karl Landsteiner Society, St. Pölten, Austria; [14]Department of Internal Medicine I, Cardiology and Intensive Care Medicine, Landesklinikum Mistelbach-Gänserndorf, Mistelbach, Austria; [15]Karl Landsteiner University of Health Sciences, Krems, Austria*
E-mail: benedikt.s.hofer@meduniwien.ac.at

Background and aims: Growth differentiation factor 15 (GDF-15), a cytokine of the transforming growth factor-beta superfamily, modulates inflammation and cellular stress response. It has been implicated in the pathogenesis of various chronic diseases and may inhibit platelet function. We aimed to investigate the role of GDF-15 in cirrhosis by examining its link to disease-driving mechanisms, platelet activation, hepatic decompensation, and mortality.
Method: We prospectively recruited patients with cirrhosis undergoing hepatic venous pressure gradient (HVPG) and platelet activation measurements. Platelet activation was assessed by flow cytometry, including platelet surface P-selectin and glycoprotein IIb/IIIa (GPIIb/IIIa) expression after agonist stimulation. Serum GDF-15 levels were measured using an electrochemiluminescence immunoassay.
Results: A total of 106 patients (70.8% male, median age 55.1 years) were followed for a median of 51.5 (26.0–58.2) months. At baseline, 39.6% were compensated, median MELD was 11, median HVPG 18 mmHg, and median GDF-15 2880 (1850–4770) pg/mL. Higher GDF-15 levels were linked to more pronounced hepatic synthetic dysfunction (MELD Spearman's ρ: 0.50; albumin ρ: –0.57), portal hypertension (HVPG ρ: 0.47), systemic inflammation (C-reactive protein ρ: 0.45; interleukin 6 [IL-6] ρ: 0.55; procalcitonin ρ: 0.58) and fibrosis/fibrogenesis (liver stiffness ρ: 0.67; enhanced liver fibrosis test ρ: 0.64) (all $p < 0.001$). GDF-15 was higher in patients with detectable bacterial DNA in blood (3520 vs. 2250 pg/mL; $p < 0.001$) and correlated with lipopolysaccharide (ρ: 0.34; $p = 0.010$) and lipoteichoic acid (ρ: 0.37; $p = 0.004$). GDF-15 was not significantly linked to platelet activation after adjusting for liver disease severity, except for higher levels in patients with undetectable GPIIb/IIIa after stimulation. During follow-up, 38 patients decompensated and 21 died (61.9% liver-related). GDF-15 predicted decompensation in a multivariable model adjusted for HVPG, MELD, albumin and IL-6 (aHR per 100 pg/mL: 1.015; 95%CI: 1.004–1.026; $p = 0.007$). Similarly, there was a significant link between GDF-15 and a higher risk of liver-related (HR: 1.019; 95%CI: 1.007–1.032; $p = 0.002$) and all-cause mortality (HR: 1.019; 95%CI: 1.009–1.029; $p < 0.001$).
Conclusion: In patients with cirrhosis, GDF-15 reflects disease-driving mechanisms and facilitates risk stratification for hepatic decompensation, liver-related and all-cause mortality.

WED-457

MRI-derived splenic indices as novel predictors of liver decompensation

Kim Hogenberg[1], Jasper van Leengoed[1], Laura Boer[1], Job van der Palen[1], Donald Bouman[1], Maureen Guichelaar[1]. *[1]Medisch Spectrum Twente, Enschede, Netherlands*
E-mail: maureenguichelaar@yahoo.com

Background and aims: Liver decompensation places a major burden on healthcare systems. Early identification using MRI-derived markers, including sarcopenia and splenic characteristics, may enable preventive intervention. This study evaluated their prognostic value for predicting decompensation in cirrhosis.
Method: A retrospective analysis was performed on a large cohort of patients liver cirrhosis who underwent annual MRI scanning for HCC surveillance (2010–2024). Patients were excluded if they had <3 follow-up MRI scans or in case they had liver decompensation before

their first MRI scan. The MRI-derived variables included sarcopenic indices (transversal psoas muscle thickness (TPMT)/height, psoas muscle circumference (PMC) and splenic indices (splenic volume and splenic diffusion-weighted imaging derived parameters including, b-value ratios and apparent diffusion coefficient (ADC)). A mean of values at 4 regions of interest in the spleen was registered. Sarcopenia was diagnosed if TPMT of <17.3 mm/m for men and <10.4 mm/m for women.
Results: A total of 132 patients (62.9% men, mean age 68.1 ± 11.6 years) were included in the study of which 53 patients (40%) had sarcopenia. Mean follow-up was 29.8 ± 9.8 months during which 38 patients (29%) developed liver decompensation. A greater decrease in PMC and TPMT/height over time was observed in patients who developed liver decompensation (resp. $p = 0.07$; $p = 0.023$), indicating progressive muscle loss. Patients who developed liver decompensation had significantly larger splenic volumes and higher ADC and b-value ratios ($p < 0.001$), which increased over three years ($p < 0.01$). Logistic regression models of independent risk factors (splenic volume, b-value ratios and ADC at 1 and 3 years prior to liver decompensation) showed AUC's of resp. 0.79 and 0.75.
Conclusion: MRI-derived quantitative splenic indices demonstrated significant potential for predicting liver decompensation, outperforming sarcopenic indices. Validation in larger cohorts is warranted to confirm these findings and refine predictive models for clinical applicability.

WED-458
Machine learning prediction of covert hepatic encephalopathy in patients with liver cirrhosis based on clinical characteristics
Tiantian Hu[1,2,3], Baoyue Sheng[1], Qingqing Lei[1], Haoxiang Zhu[1,2], Yun-Hui Yang[1], Richeng Mao[1], Jie Tong[1], Xiaoting Zhao[1], Changrong Yuan[3], Zheng Zhu[3], Jinyu Wang[1,2], Jiming Zhang[1,2,4].
[1]Department of Infectious Diseases, Shanghai Key Laboratory of Infectious Diseases and Biosafety Emergency Response, National Medical Center for Infectious Diseases, Huashan Hospital, Fudan University, Shanghai, China; [2]Shanghai Institute of Infectious Diseases and Biosecurity, Key Laboratory of Medical Molecular Virology (MOE/MOH), Shanghai Medical College, Fudan University, Shanghai, China; [3]Fudan University School of Nursing, Fudan University, Shanghai, China; [4]Department of Infectious Diseases, Jing'An Branch of Huashan Hospital, Fudan University, Shanghai, China
E-mail: 23111170004@m.fudan.edu.cn

Background and aims: Covert hepatic encephalopathy (CHE) is a common but frequently underdiagnosed complication of liver cirrhosis, associated with impaired quality of life and adverse clinical outcomes. Early identification of patients at high risk for CHE remains challenging in routine clinical practice. This study aimed to develop and externally validate machine learning–based predictive models for CHE in patients with liver cirrhosis using readily available clinical characteristics.
Method: A longitudinal cohort study was conducted among patients with liver cirrhosis at Huashan Hospital, Fudan University, from September 2023 to November 2025. Patients without overt hepatic encephalopathy at baseline were enrolled, and covert hepatic encephalopathy (CHE) was diagnosed using the Psychometric Hepatic Encephalopathy Score (PHES). The retrospective cohort (Study population 1, n = 309) was randomly divided into training and test sets (8:2), while an independent prospective cohort (Study population 2, n = 68) served as external validation. Missing data were addressed using multiple imputation. Feature selection was conducted in the training set using multicollinearity control, LASSO regression, and stability assessment. Six machine learning models were developed and optimized, with performance evaluated by discrimination, calibration, decision curve analysis, and SHAP-based interpretability.
Results: Among 377 included patients, 251 (66.6%) were diagnosed with CHE. Six predictors were selected for model development. The Random Forest model demonstrated the most stable performance across datasets, with AUCs of 0.9253 in the training set, 0.9118 in the test set, and 0.9189 in the external validation set. High sensitivity and favorable F1 scores were consistently observed. The model showed good calibration and superior clinical net benefit in decision curve analysis. SHAP analysis identified hepatitis B virus infection status, serum albumin level, and blood ammonia concentration as the most influential predictors. To support clinical application, a web-based risk prediction tool was developed and made publicly available.
Conclusion: A machine learning–based Random Forest model using routine clinical parameters demonstrated strong discrimination, calibration, and clinical utility for predicting covert hepatic encephalopathy in patients with liver cirrhosis. This model may facilitate early risk stratification and support clinical decision-making in real-world practice.

WED-459
The advanced liver disease MDT: a new model improving palliative care provision for patients with decompensated advanced chronic liver disease
Katharine Hutchison[1,2], Cristina Gatti[2], Amelia Stockley[2], Benjamin Hudson[2]. *[1]University of Exeter, Exeter, United Kingdom; [2]Exeter, United Kingdom*
E-mail: katharine.hutchison@nhs.net

Background and aims: Despite a high burden of physical and psychological symptoms, patients with decompensated advanced chronic liver disease (dACLD) seldom receive palliative care. Prognostic uncertainty, challenges with patient selection, and a lack of evidence-based frameworks are key barriers to timely referral. We describe outcomes from a novel model of care in which patients with dACLD are managed through an Advanced Liver Disease MDT (ALMDT) from onset of decompensation. Input from Allied Health Professionals (AHPs e.g. physiotherapy, dietetics) and palliative care (PC) specialists is obtained, and palliative interventions including advance care planning are considered, in parallel with disease modifying therapies (e.g. transplantation). Outcomes over a 3-year period are compared with patients managed without ALMDT input.
Method: All patients discussed at the ALMDT between July 2021-June 2024 were reviewed. Hospital records identified patients dying from dACLD without ALMDT discussion, including those with multiple decompensations or death on index admission. Data collected included demographics, PC and AHP input, ACP completion, transplant referral, mortality, and healthcare utilisation in the last year of life (LYOL).
Results: 248 patients were included in analysis. Of these, 171 were managed via the ALMDT, with a 12-month survival of 61.4%. 27 patients died after multiple decompensations without ALMDT input, and 50 died on index presentation. Non-ALMDT patients were more often female, from more deprived areas, and had higher rates of alcohol-related liver disease. PC referral occurred in 58.5% of ALMDT patients vs 7.4% of non-ALMDT patients. ALMDT patients had higher referral rates to physiotherapy/OT (56% vs 18.5%) and dietetics (57% vs 37%); ACP completion was 74% vs 0%. 28 patients died >12 months after ALMDT discussion (discussed early) and 66 died <12 months (discussed late). Early discussion was associated with higher day-case paracentesis rates (80.5% vs 52% late vs 16% never discussed), fewer Emergency Department attendances in LYOL (mean of 2.7 vs 3.7 if discussed late vs 4.4 if never discussed), and fewer inpatient days in LYOL (mean of 23.2 vs 35.4 if discussed late vs 32.3 if never discussed). 54% of patients discussed early died at home, vs 32% of those discussed late.
Conclusion: Managing dACLD through an ALMDT facilitates timely PC and AHP support without precluding curative options. Early discussion is associated with lower healthcare costs in the LYOL and improved end of life care.

WED-460-YI

Glucagon-like peptide- 1 receptor agonists improve survival and reduce healthcare utilization in decompensated hepatitis C cirrhosis

Jeeva Jaganathan[1], Marina Takawy[2], Hazem Abosheaishaa[1], Ghada Mohamed[3], Madhavi Reddy[1]. [1]*The Brooklyn Hospital Center, Brooklyn, United States;* [2]*Rochester Regional Health Unity Hospital, Rochester, United States;* [3]*Lahey Hospital and Medical Center, Burlington, United States*
E-mail: stanjeeva@gmail.com

Background and aims: Hepatitis C virus (HCV) infection remains a major cause of cirrhosis and liver-related mortality worldwide despite effective direct-acting antiviral (DAA) therapies. HCV causes hepatic steatosis by interfering with lipid metabolism and activating fatty acid synthesis pathways, accelerating disease progression. Glucagon-like peptide- 1 receptor agonists (GLP-1 RAs) have been shown to reduce lipogenesis and inflammation resulting in reduced hepatic decompensation risk in Metabolic Dysfunction-Associated Steatotic Liver Disease (MASLD) and cirrhosis patients with type 2 diabetes. However, the impact of GLP-1 RAs on outcomes in HCV cirrhosis patients remains unstudied. To assess the effect of GLP-1 receptor agonists on clinical outcomes in decompensated HCV cirrhosis.
Method: Patients with HCV-related cirrhosis and decompensation (ascites, hepatic encephalopathy or variceal bleeding) were identified using the TriNetX US Collaborative Network. The index event was GLP-1 RA initiation (GLP-1 RA users) who were compared with matched non-users in a 1:1 ratio. Outcomes were assessed over one year including all-cause mortality, liver-related decompensation events, critical care utilization, inpatient admissions and transplant-related outcomes. Propensity score matching balanced demographics and comorbidities including diabetes, obesity, hypertension, and malnutrition between cohorts. Kaplan-Meier survival analysis and Cox proportional hazards regression were used.
Results: Overall, 4798 patients (GLP-1 RA users) and equal matched non-users were identified. GLP-1 RA users had substantially lower all-cause mortality compared to non-users (3.1% vs 13.7%; hazard ratio [HR] 0.21, 95% CI 0.18–0.26; $p < 0.001$). GLP-1 RA users demonstrated reduced liver-related decompensation events (HR 0.38, 95% CI 0.31–0.46; $p < 0.001$). Inpatient hospitalization (8.8% vs 17.3%, relative risk [RR] 0.51, 95% CI 0.42–0.62) and critical care utilization (4% vs 9.7%, RR 0.41, 95% CI 0.34–0.50) were significantly lower in GLP-1 RA users. Additionally, trends towards reduced transplant waitlist placement (0.7% vs 2.0%) and liver transplantation (0.4% vs 1.5%) were observed.
Conclusion: In this nationwide propensity-matched cohort study of decompensated HCV-related cirrhosis patients, GLP-1 RA use was associated with significantly improved survival, reduced complications, and reduced healthcare utilization. Prospective studies are warranted to confirm beneficial effects and safety profile of GLP-1 RAs in this population.

WED-461-YI

Neurofilament light chain in serum predicts overt hepatic encephalopathy in liver cirrhosis

Elise Jonasson[1], Birgitte Jacobsen[1], Lea Ladegaard Grønkjær[1], Mette Lauridsen[1]. [1]*Esbjerg Hospital, University Hospital of Southern Denmark, Esbjerg, Denmark*
E-mail: elise.jonasson.nielsen@rsyd.dk

Background and aims: Overt hepatic encephalopathy (OHE) remains a frequent and severe complication in patients with cirrhosis, however there is a lack of predictive biomarkers. Neurofilament light chain (NfL) is a marker of early central nervous system injury and have been explored in serum as a diagnostic biomarker of minimal hepatic encephalopathy and OHE. We aimed to investigate the prognostic potential of NfL in serum for predicting OHE.
Method: This prospective cohort study included 112 patients. Serum NfL was measured at study inclusion and patients were divided into two groups based on NfL levels (low NfL < 47.6 pg/mL and high NfL ≥ 47.6 pg/mL). During follow up, OHE, liver transplantation and death was registered. Cumulative incidence functions were estimated, and Gray's test was used for unadjusted comparisons. Adjusted absolute risk differences at 6 months, 1 year, and 2 years were estimated using pseudo-observations and generalized linear models, adjusting for prior OHE.
Results: Median follow-up time was 371 days (IQR 291–520), 18 patients developed OHE and 16 patients died or underwent liver transplantation. Cumulative incidence functions showed a higher incidence of OHE in patients with high NfL ($p = 0.007$, Gray's test). At 6 months, 1 year, and 2 years, the cumulative incidence of OHE was consistently lower in patients with low NfL (3.5%, 7.8%, and 13%, respectively) compared with patients with high NfL (16%, 28% and 35%, respectively). In analyses adjusted for prior OHE, high NfL was associated with an increased absolute risk of OHE at all evaluated time points. Patients with high NfL had progressively higher absolute risk of OHE, with adjusted risk difference of 13 percentage points at 6 months ($p = 0.030$), 22 percentage points at 1 year ($p = 0.010$), and 25 percentage points at 2 years ($p = 0.035$), compared with patients with lower NfL. A history of OHE was independently associated with a markedly higher absolute risk of OHE at all time points (all $p < 0.01$).
Conclusion: High NfL ≥ 47.6 pg/mL identifies patients at increased risk of developing OHE. The consistently large absolute risk differences observed across all time points suggest that NfL captures underlying vulnerability to future OHE beyond prior OHE status alone. Serum NfL may therefore represent a useful biomarker for early risk stratification and identification of patients who could benefit from closer monitoring or preventive strategies, either alone or as add on to psychometric tests.

WED-462

Neurofilament light chain in cerebrospinal fluid and serum identifies minimal and overt hepatic encephalopathy

Elise Jonasson[1], Lea Ladegaard Grønkjær[1], Birgitte Jacobsen[1], Mette Lauridsen[1]. [1]*Esbjerg Hospital, University Hospital of Southern Denmark, Esbjerg, Denmark*
E-mail: elise.jonasson.nielsen@rsyd.dk

Background and aims: Minimal hepatic encephalopathy (MHE) is common in patients with liver cirrhosis but remains underdiagnosed due to limitations of psychometric testing. Neurofilament light chain (NfL) and glial fibrillary acidic protein (GFAP) have been proposed as markers of early central nervous system injury and have been explored in serum as biomarkers of hepatic encephalopathy (HE). Both remain unexplored in cerebrospinal fluid (CSF), even though CSF is pathophysiological closer to the site of end-organ damage. We aimed to investigate NfL and GFAP in CSF and serum across the spectrum of HE and to assess their diagnostic utility for HE.
Method: In this cross-sectional study, patients with liver cirrhosis and age- and sex-matched healthy controls (HC) underwent lumbar puncture, blood sampling, and psychometric testing. Patients were divided into three groups based on Psychometric Hepatic Encephalopathy Score: i) unimpaired, ii) MHE and iii) OHE (West Haven Criteria ≥ grade 1). NfL and GFAP were measured in CSF and serum by Simoa HD-X Analyzer (Quanterix, Billerica, MA, USA). Associations between CSF and serum concentrations were assessed using Spearman correlation, and receiver operating characteristic (ROC) analyses evaluated diagnostic performance for HE.
Results: Thirty-five patients (57% unimpaired, 26% MHE, 17% OHE) and 14 HC were included. CSF and serum NfL were higher in MHE and OHE compared to unimpaired patients and healthy controls. There was no difference between unimpaired patients and HC. CSF GFAP was modestly elevated in MHE and OHE versus healthy controls, whereas serum GFAP did not differ between groups. CSF and serum concentrations were strongly correlated for NfL (rho = 0.89, p <

0.0001) and moderately for GFAP (rho = 0.50, p = 0.0004). ROC analyses showed good diagnostic performance of NfL for identifying MHE and OHE, with AUCs of 0.88–0.90 in CSF and 0.93–0.95 in serum. A CSF NfL cut-off of 1144 pg/mL yielded 93% sensitivity and 75% specificity. GFAP showed lower and inconsistent discriminatory ability, particularly in serum.
Conclusion: NfL in CSF and serum reflect neuroaxonal injury in MHE and OHE and shows strong diagnostic performance, outperforming GFAP. Serum NfL therefore emerges as a promising biomarker for early detection of hepatic encephalopathy, either alone or to enhance the specificity of psychometric testing.

WED-463

Treatment with albumin improves circulatory function in patients with cirrhosis and hypovolemic hyponatremia: insights from a randomized controlled trial, the ALBUCAT study

Adrià Juanola[1], María José Moreta[1], Cristina Solé[2], Martina Perez-Guasch[1], Jordi Gratacós-Ginès[1], Anna Soria[1], Berta Cuyàs[3], Marta Martín-Llahí[4], Ann Ma[1], Enrico Pompili[1], Irene Fernández[5], Maria Amorós[6], Anna Cruceta[7], Sonia Diestro[8], Gemma Domenech[1], Jose Rios[8], Jordi Sánchez[2], Núria Fabrellas[9], Isabel Graupera[1], Elisa Pose[1], Pere Ginès[1]. *[1]Liver Unit, Hospital Clínic of Barcelona, Barcelona, Catalonia, Spain, Institut d'Investigacions Biomèdiques August Pi i Sunyer (IDIBAPS), Barcelona, Catalonia, Spain, Centro de Investigación Biomédica en Red de Enfermedades Hepáticas y Digestivas (CIBERehd), Barcelona, Spain; [2]Departament of Gastroenterology and Hepatology. Parc Tauli Hospital Universitari. Institut d'Investigació i Innovació Parc Taulí (I3PT-CERCA). Universitat Autònoma de Barcelona, Sabadell, Spain, Centro de Investigación Biomédica en Red de Enfermedades Hepáticas y Digestivas (CIBERehd), Sabadell, Spain; [3]Department of Gastroenterology, Hospital de la Santa Creu i Sant Pau, Universitat Autònoma de Barcelona, Barcelona, Spain, Centro de Investigación Biomédica en Red de Enfermedades Hepáticas y Digestivas (CIBERehd), Barcelona, Spain; [4]Hospital de Sant Joan Despí Moisès Broggi, Sant Joan Despí, Spain; [5]Liver Unit, Hospital Clínic of Barcelona, Barcelona, Catalonia, Spain, Barcelona, Spain; [6]Institut d'Investigacions Biomèdiques August Pi i Sunyer (IDIBAPS), Barcelona, Catalonia, Spain, Clinical Trial Unit, Hospital Clínic of Barcelona, Barcelona, Spain, Barcelona, Spain; [7]Clinical Trial Unit, Hospital Clínic of Barcelona, Barcelona, Spain, Barcelona, Spain; [8]Biostatistics and Data Management Core Facility, Institut d'Investigacions Biomédiques August Pi i Sunyer (IDIBAPS), Hospital Clínic of Barcelona, Barcelona, Spain, Barcelona, Spain; [9]Faculty of Nursing, University of Barcelona, Barcelona, Catalonia, Spain, Institut d'Investigacions Biomèdiques August Pi i Sunyer (IDIBAPS), Barcelona, Catalonia, Spain, Centro de Investigación Biomédica en Red de Enfermedades Hepáticas y Digestivas (CIBERehd), Barcelona, Spain*
E-mail: pgines@clinic.cat

Background and aims: The ALBUCAT trial demonstrated that intravenous human albumin (HA) administration increases serum sodium levels and reduces 28-day mortality in patients with decompensated cirrhosis and hypervolemic hyponatremia. However, the pathogenic mechanisms underlying these beneficial effects remain incompletely understood. We therefore evaluated circulatory biomarkers involved in sodium and water homeostasis to elucidate the pathophysiological effects of albumin in these patients.
Method: Plasma samples from participants in the multicenter, open-label, randomized ALBUCAT trial were analyzed. Patients with serum sodium ≤ 133 mEq/L were randomized 1:1 to receive intravenous HA for up to 10 days (1 g/kg on day 1 followed by 40 g/day) plus standard of care (SoC; fluid restriction and diuretic withdrawal) or SoC alone. Renin, aldosterone, noradrenaline, copeptin and prostaglandin E2 (PGE2) were measured at baseline, day 5 and day 10 or end of treatment.
Results: Plasma samples were available in 48 of 52 patients (92%): 26 in the SoC group and 22 in the HA group. Baseline biomarker levels did not differ between groups. Under SoC, plasma renin showed no significant changes over time (1491 µUI/mL at baseline and 2000 µUI/mL at day 10; p = 0.052). In contrast, HA administration was associated with a marked and sustained reduction in renin concentrations, from 1763 µUI/mL at baseline to 785 µUI/mL at day 5 and 881 µUI/mL at day 10 (both p = 0.002), resulting in significantly lower levels compared with SoC at day 10 (p = 0.040). Aldosterone followed a similar pattern, remaining stable under SoC while decreasing significantly after HA administration (global treatment-by-time interaction p = 0.002). Copeptin showed a directionally concordant but non-significant trend toward lower levels after HA, with an early decrease at day 5, whereas noradrenaline and PGE2 were unaffected. Notably, reductions in renin and aldosterone concentrations were most pronounced in patients treated with HA who ultimately achieved hyponatremia resolution, whereas non-responders—particularly under SoC—showed no consistent changes over time.
Conclusion: HA administration was associated with a selective reduction in renin and aldosterone levels, predominantly among patients who achieved hyponatremia resolution. These findings suggest that effective improvement in circulatory function with suppression of the renin–angiotensin–aldosterone system underlies the clinical benefits of HA in hypervolemic hyponatremia.

WED-464

Comparative prognostic performance of MELD-based and GEMA scores: a real-world cohort study

Furkan Kabukcu[1], Burcu Gürbüz[2], Hakan Oral[3], İbrahim Nahit Şendur[2], Bengi Ozturk[2], Taylan Kav[2], Onur Keskin[2]. *[1]Hacettepe University Faculty of Medicine, Department of Internal Medicine, Ankara, Türkiye; [2]Hacettepe University Faculty of Medicine, Department of Gastroenterology and Hepatology, Ankara, Türkiye; [3]Hacettepe University Faculty of Medicine, Department of Haematology, Ankara, Türkiye*
E-mail: furkankabukcu@gmail.com

Background and aims: Accurate prognostic stratification in cirrhosis is essential for clinical decision-making and liver transplantation prioritization. We aimed to compare the prognostic performance of MELD, MELD-Na, MELD 3.0, GEMA, and GEMA-Na scores for predicting liver-related outcomes and transplant-free survival.
Method: We retrospectively included cirrhotic patients followed between January 2020 and December 2025. A total of 178 patients were analyzed. MELD, MELD-Na, MELD 3.0, GEMA, and GEMA-Na scores were calculated. The primary outcome was a composite endpoint of all-cause mortality or liver transplantation, with transplant-free survival evaluated in secondary analyses. Survival analyses were performed using Kaplan–Meier method. Discriminative performance was assessed using ROC curves, with pairwise comparisons performed using the DeLong test. Cox proportional hazards models and Harrell's C statistics were used to assess independent prognostic values.
Results: The median age was 57 years (range 18–89), and 90/178 patients (50.6%) were male. During follow-up, 68/178 (38.2%) patients died and 20/178 (11.2%) underwent liver transplantation. Median follow-up duration was 35.4 months (0.5–70.6). Median MELD was 10 (6–31), MELD-Na was 11 (6–32), MELD 3.0 was 12 (6–32), GEMA was 11 (6–28), GEMA-Na was 13 (8–35). Patients with scores above predefined cut-off values for all models had significantly shorter survival (all p < 0.001). MELD 3.0 demonstrated the highest discriminative ability for prediction of the primary outcome (AUC = 0.759), followed by GEMA-Na (AUC = 0.724) and MELD-Na (AUC = 0.715). Pairwise ROC comparisons showed significantly superior performance of MELD 3.0 compared with MELD and GEMA scores (all p < 0.05). Kaplan–Meier analyses using predefined cut-off values demonstrated significant separation of survival curves across all scoring systems (log-rank p < 0.001). In Cox regression analyses, MELD 3.0 and GEMA-Na were significant predictors, with MELD 3.0 showing the highest time-dependent discriminative performance

(Harrell's C = 0.747). For transplant-free survival, MELD 3.0 and GEMA-Na remained the strongest predictors. Harrell's C statistic for transplant-free mortality was highest for MELD 3.0 (C = 0.780).
Conclusion: MELD 3.0 and GEMA-Na demonstrated superior prognostic performance compared with traditional MELD and MELD-Na models for predicting liver-related outcomes and transplant-free survival. Overall, MELD 3.0 showed the strongest prognostic performance among the scoring systems.

WED-465
Low health literacy in patients with steatotic liver disease and depressive symptoms
Leonard Kaps[1], Christian Labenz[2], Alexander Barton[1], Jörn M. Schattenberg[1], Maurice Michel[1]. [1]*Department of Medicine II, University Medical Center, Homburg/Saar, Germany;* [2]*Department of Internal Medicine I, University Medical Center of the Johannes Gutenberg-University, Mainz, Germany*
E-mail: leonardkaps@googlemail.com

Background and aims: Health literacy (HL) describes patients' ability to access, understand, and use health information to manage their health and navigate the healthcare system. While HL is known to influence outcomes in chronic diseases, data in chronic liver disease - particularly steatotic liver disease (SLD) - are limited, and the potential impact of comorbid depression on HL remains largely unexplored. This study aimed to investigate whether depressive symptoms are associated with impaired health literacy in patients with SLD.
Method: In this bicentric study, 198 patients with SLD (173 in Homburg and 25 in Mainz, Germany) were enrolled from 2019 to 2025 at tertiary medical centers. Health literacy was assessed using the German validated Health Literacy Questionnaire (HLQ), comprising nine subscales. SLD and compensated advanced chronic liver disease (cACLD) were diagnosed using liver stiffness measurement (LSM; FibroScan). Steatosis was defined by a controlled attenuation parameter (CAP) ≥ 275 dB/m; cACLD was indicated by LSM ≥ 15 kPa, while values ≤ 10 kPa ruled out cACLD. Depressive symptoms were assessed using the Hamilton Depression Rating Scale (HDRS) and the Patient Health Questionnaire (PHQ-9).
Results: Forty-nine patients (33%) exhibited depressive symptoms. There were no differences between patients with and without depressive symptoms regarding gender, ≥10 years of schooling, LSM, or body mass index (BMI). Patients with depressive symptoms had significantly lower HLQ scores in subscale 3 ("Actively managing my health," $p < 0.05$), subscale 6 ("Ability to actively engage with healthcare providers," $p < 0.0001$), subscale 7 ("Navigating the healthcare system" $p < 0.001$), and subscale 9 ("Understanding health information well enough to know what to do", $p < 0.05$). Overall, subscale 3 showed the lowest scores, whereas subscales 6 and 9 showed the highest. Patients with cACLD scored lower only in subscale 9 compared with those without cACLD. In multivariable regression analyses, associations between depressive symptoms and lower HLQ scores remained significant for subscales 6 and 7 after adjustment for gender, age, BMI, years of schooling, and cACLD.
Conclusion: Depressive symptoms are common in patients with SLD and are associated with impaired health literacy, particularly regarding engagement with healthcare providers and navigation of the healthcare system.

WED-466
Burden and outcomes of multidrug-resistant spontaneous bacterial peritonitis: experience from a resource-constrained setting
Chitta Ranjan Khatua[1], Lelin Kumar Jena[1], Partha Sarathi Behera[1], Aniket Ranjan[1], Prajna Anirvan[2], Manas Kumar Panigrahi[3], Shivaram Prasad Singh[2]. [1]*MKCG Medical College, Brahmapur, India;* [2]*Kalinga Gastroenterology Foundation, Cuttack, India;* [3]*AIIMS Bhubaneswar, Bhubaneswar, India*
E-mail: gudduchhotu3@gmail.com

Background and aims: Spontaneous bacterial peritonitis (SBP) is a common and life-threatening condition, and multidrug-resistant (MDR) bacterial infections further adversely affect patient outcomes. We performed a prospective study to evaluate the impact of MDR infections on outcomes in SBP.
Method: From October 2016 to August 2025, all cirrhosis patients with SBP were included and on hospitalization, all relevant clinical parameters were recorded. Outcomes were compared between patients with and without MDR bacterial infections, with a three-month follow-up to assess both short- and long-term impacts of MDR infections.
Results: Out of 1667 cirrhosis patients, 10.9% (n = 182) had SBP. MDR infection was prevalent in 22.5% (n = 41). Enterococcus (46.4%) and E. coli (36.6%) were common isolated bacteria, followed by Klebsiella (7.3%), Staphylococcus aureus (4.9%), Pseudomonas aeruginosa (2.4%), and Acinetobacter (2.4%). Patients with MDR infections had higher Model for End-Stage Liver Disease (MELD) scores ($p < 0.001$), MELD-Na scores ($p < 0.001$), Child-Turcotte-Pugh (CTP) scores ($p < 0.001$), a higher incidence of acute-on-chronic liver failure (ACLF) (83.8% vs. 47.9%; $p < 0.001$), and acute kidney injury (AKI) (86.5% vs. 51.4%; $p < 0.001$). MDR infection was also associated with decreased ascitic protein levels (1.20 g/dL vs 1.60 g/dL; P = 0.015). Furthermore, patients with MDR infection demonstrated increased frequency of multiple site infections (61% vs. 19.1%; $p < 0.001$), and had decreased in-hospital survival (HR = 0.227; 95% CI = 0.132–0.391; $p < 0.001$), also at 28 days (HR = 0.325; 95% CI = 0.204–0.517; $p < 0.001$), and 90 days (HR = 0.336; 95% CI = 0.226–0.500; $p < 0.001$).
Conclusion: One tenth of decompensated cirrhosis patients had SBP, with more than one fifth having MDR infection. Enterococcus and E. coli were commonly isolated MDR bacteria. MDR infections were associated with lower ascitic fluid protein levels, a higher frequency of infections at multiple sites, and an increased prevalence of ACLF and AKI. SBP with MDR bacteria was associated with a lack of clinical response to antibiotic treatment and increased short-term and long-term mortality.

WED-467
Impact of long-term albumin administration on mortality and cirrhosis-related complications: are these data sufficient to change practice?
W. Ray Kim[1], Cristina Coll Ortega[2], Cristina Fuster[2], Thomas Ardiles[3], Shrikar Reddy Badikol[4], Rahul Rajkumar[4], Elisabet Viayna[2]. [1]*Mayo Clinic College of Medicine & Science-Arizona, Division of Gastroenterology and Hepatology, Phoenix, United States;* [2]*Grifols, Sant Cugat del Vallès, Spain;* [3]*Grifols, Research Triangle Park, United States;* [4]*Boston Strategic Partners, Inc., Boston, United States*
E-mail: cristina.coll@grifols.com

Background and aims: Long-term albumin (LTA) administration has been evaluated in several clinical trials as a disease-modifying therapy to reduce mortality and prevent cirrhosis-related complications in patients with decompensated cirrhosis and ascites, with conflicting results. In light of recently published clinical trial data, we conducted a systematic literature review (SLR) and meta-analysis (MA) of all available clinical trials to assess the impact of LTA on long-term mortality and cirrhosis-related complications.
Method: Included studies were clinical trials identified through PubMed (1995–present) and conference abstracts (2022–2025) in adults with cirrhosis and ascites comparing at least 4 weeks of LTA therapy with standard of care or placebo and reporting at least 12-month mortality. The primary endpoint was 12- to 36-month mortality; secondary endpoints included ascites, refractory ascites (RA), hepatic encephalopathy (HE), renal dysfunction, spontaneous bacterial peritonitis (SBP), hyponatremia, and gastrointestinal (GI) bleeding, each assessed at ≥12 months follow-up when available. A

random-effects model was used to estimate odds ratios (ORs) and 95% confidence intervals (CIs). Heterogeneity was assessed using Chi-squared and I-squared statistics.
Results: Of 22 studies screened, 7 met the eligibility criteria, including 1431 subjects altogether. Fifteen studies were excluded: 13 lacked a comparator, 1 was not a clinical trial, and 1 did not involve adult patients. LTA was associated with a significant reduction in 12- to 36-month mortality (OR: 0.66 [95% CI: 0.47–0.93], p = 0.02). The odds of developing ascites (OR: 0.30 [95% CI: 0.16–0.54], p < 0.0001), RA (OR: 0.52 [95% CI: 0.33–0.81], p < 0.01), HE (OR: 0.62 [95% CI: 0.41–0.95], p = 0.03), renal dysfunction (OR: 0.45 [95% CI: 0.21–0.97], p = 0.04) and SBP (OR: 0.30 [95% CI: 0.16–0.54], p < 0.0001) were significantly lower in the LTA group. No significant differences were observed for hyponatremia (OR: 0.62 [95% CI: 0.36–1.06], p = 0.08) or GI bleeding (OR: 1.15 [95% CI: 0.60–2.23], p = 0.67).
Conclusion: These data indicate that LTA is associated with a significant reduction in mortality and key cirrhosis-related complications, supporting its potential role as a disease-modifying intervention in patients with decompensated cirrhosis and ascites. Future research is needed to define the patient population most likely to benefit and to optimize treatment protocols, including individualized therapeutic strategies.

WED-468
Lack of social network and support are predictors of mortality in cirrhosis. Results from an incidence cohort with long-term follow-up

Thit Mynster Kronborg[1], Malene Barfod O'Connell[1], Frederikke Agerbo[2], Søren Møller[3,4], Nina Kimer[1,3]. *[1]Gastro Unit, Medical Division, University Hospital Hvidovre, Denmark, Department of Clinical Medicine, Copenhagen University, Copenhagen, Denmark; [2]Biostatistics Sanos, Søborg, Denmark; [3]Department of clinical medicine, Copenhagen University, Diagnostic Unit, Department of clinical physiology and nuclear medicine, Hvidovre University Hospital, Copenhagen, Denmark; [4]Diagnostic Unit, Department of Clinical Physiology and Nuclear Medicine, Hvidovre University Hospital, Hvidovre, Denmark*
E-mail: nina.kimer@regionh.dk

Background and aims: Liver cirrhosis is a severe disease with high mortality and increased risk of admissions. Recently, frailty, as both a physical and social concept, has been suggested as a reliable predictor.
The study aimed to investigate different facets of frailty in cirrhosis and examine its potential to predict mortality and admissions.
Method: Data from a prospective cohort study of patients with newly diagnosed cirrhosis were analysed. Physical tests (Short Physical Performance Battery and Hand grip strength) were performed, along with questionnaires regarding quality of life, sociodemographic factors, loneliness, regarding both structural and functional social dimensions. Follow-up of admissions and mortality was registered for at least three years.
Results: A total of 208 patients were included. We found a significant reduction in mortality for patients with handgrip > 30 kg (Hazard ratio 0.50 [0.27, 0.94]), Short physical performance battery > 8 points (0.39 [0.23, 0.66]) and not receiving home care (0.48 [0.27;0.85]). We found a significantly increased risk of death in patients with no psychological support (2.02 [1.12, 3.62]) and when the closest contact was other than family (2.15 [1.42, 3.25]) Being married (0.68 [0.47, 0.97]), not receiving home care (0.58 [0.37, 0.92]), higher scores on physical performance (>8 (0.55 [0.36, 0.83]), and quality of life (>5 (0.50 [0.33, 0.76]) was associated with a reduced risk of admission to hospital.
Conclusion: Lack of close family contact and no psychological support from relatives predict mortality in patients with liver cirrhosis. Physical frailty has a major impact on survival.

WED-473
Beyond age and disease severity: the pivotal role of intestinal and systemic inflammation as drivers of physical frailty in advanced chronic liver disease

Tomáš Koller[1], Daniel Jan Havaj[2], Dana Knutova[1], Daniela Žilinčanová[2], Petra Vrbova[1], Svetlana Adamcova Selcanova[2], Lubomir Skladany[2]. *[1]Lekárska fakulta Univerzity Komenského a Univerzitná nemonica Bratislava, 5. interná klinika, Odd. gastroenterológie a hepatológie, Bratislava, Slovakia; [2]Fakultná nemocnica FD Roosevelta, Odd. hepatológie, gastroenterológie a transplantácie (HEGITO), 2. interná klinika Slovenskej zdravotníckej univerzity, Banská Bystrica, Slovakia*
E-mail: koller.tomas@gmail.com

Background and aims: In hospitalized patients with advanced chronic liver disease (ACLD), physical frailty is a potent, independent predictor of adverse outcomes. While driven by multifactorial causes—including age, protein catabolism, and inflammation—identifying reversible factors is essential for developing targeted therapeutic interventions.
Method: Data were analyzed from the two-center, prospective RH7 cirrhosis registry. We included patients with complete records for anthropometrics, etiology, and frailty status as measured by the Liver Frailty Index (LFI). Assessments included disease severity (MELD-Na, MELD3, CLIF-C AD), protein metabolism (serum albumin), systemic inflammation (WBC, lymphocyte %, CRP), intestinal inflammation (fecal calprotectin), and active alcohol use (phosphatidylethanol >0.3μmol/l or history of heavy drinking).
Results: The cohort included 697 patients (median age: 57; 62.4% male). Alcohol-related cirrhosis was the primary etiology (64.4%), with 18.6% active heavy drinkers. Median MELD-Na was 18.3; 23.8% had refractory ascites. The median LFI was 4.28 (IQR 3.7–5.0); frailty was defined as LFI ≥ 5.25 (80th percentile). Multivariate analysis identified six independent predictors of frailty (Model AUROC = 0.818; 95% CI: 0.786–0.846):
• Age (OR 1.07; 95% CI 1.05–1.09)
• Alcohol-related cirrhosis (OR 1.78; 1.05–2.92)
• Serum albumin (OR 0.94; 0.90–0.98)
• Serum CRP (OR 1.01; 1.0–1.02)
• MELD-Na (OR 1.11; 1.07–1.15)
• Fecal calprotectin (OR 1.07; 1.04–1.10)
Notably, refractory ascites, active heavy drinking, and WBC count were not independently associated with frailty status.
Conclusion: Physical frailty in hospitalized ACLD patients is driven by age, hepatic dysfunction, and a distinct inflammatory profile characterized by both systemic (CRP) and intestinal (fecal calprotectin) markers. These data suggest that intestinal inflammation and protein metabolism are more closely linked to frailty than heavy drinking or mechanical complications like ascites, highlighting new potential therapeutic targets for intervention.

WED-474
Circulating fibronectin reflects disease severity and predicts variceal bleeding in advanced chronic liver disease

Georg Kramer[1,2,3,4], Irina Andreea Lie-Undurean[1,2,3], Benedikt Simbrunner[1,2,3,4], Mathias Jachs[1,2,3], Lorenz Balcar[1,2,3], Benedikt Hofer[1,2,3,4], Lukas Hartl[1,2,3], Georg Semmler[1,2,3], Christian Sebesta[1,2,3], Paul Thöne[1,2,3], Marlene Hintersteininger[1,2,3], Philipp Schwabl[1,2,3,4], Michael Trauner[1,3], Mattias Mandorfer[1,2,3], Thomas Reiberger[1,2,3,4]. *[1]Division of Gastroenterology and Hepatology, Department of Medicine III, Medical University of Vienna, Vienna, Austria, Vienna, Austria; [2]Vienna Hepatic Hemodynamic Laboratory, Division of Gastroenterology and Hepatology, Department of Medicine III, Medical University of Vienna, Vienna, Austria, Vienna, Austria; [3]Clinical Research Group MOTION, Medical University of Vienna, Vienna, Austria, Vienna, Austria; [4]Christian-Doppler Laboratory for Portal*

Hypertension and Liver Fibrosis, Medical University of Vienna, Vienna, Austria, Vienna, Austria
E-mail: georg.kramer@meduniwien.ac.at

Background and aims: Fibronectin is a multifunctional extracellular matrix glycoprotein involved in coagulation, tissue remodeling and immune regulation. We investigated the role of fibronectin in advanced chronic liver disease (ACLD), focusing on its association with key disease-related pathways and clinical outcomes.
Method: Patients with ACLD undergoing hepatic venous pressure gradient (HVPG) measurement and laboratory phenotyping were prospectively recruited. Baseline serum fibronectin was related to markers of liver function, fibrosis, inflammation and coagulation. First and further decompensating events were analyzed using Fine-Gray competing-risk regression, with hepatocellular carcinoma, non-liver-related death and liver transplantation as competing events.
Results: At baseline, 108 (36.2%) had compensated and 190 (63.8%) decompensated ACLD. Median MELD score was 12 (IQR 9–16), median HVPG 17 (IQR 12–21) mmHg and median fibronectin level were 32.95 (IQR 25.50–41.68) mg/dL. Fibronectin levels were significantly lower in decompensated than compensated ACLD (30.25 vs. 38.75 mg/dL; $p < 0.001$). Lower fibronectin levels were associated with impaired hepatic synthetic function (albumin $\rho = 0.43$; INR $\rho = -0.54$; MELD $\rho = -0.47$), more pronounced portal hypertension (HVPG $\rho = -0.22$), systemic inflammation (IL-6 $\rho = -0.38$; CRP $\rho = -0.17$) and extracelluar matrix remodeling assessed by the enhanced liver fibrosis (ELF) test ($\rho = -0.20$; all $p < 0.01$). Fibronectin correlated positively with key coagulation parameters, including fibrinogen ($\rho = 0.55$), antithrombin III activity ($\rho = 0.51$) and protein C activity ($\rho = 0.50$; all $p < 0.001$). During a median follow-up of 29.5 months, 20 patients (6.7%) experienced first decompensation and 75 (25.2%) further decompensation, of whom 15 patients (5.0%) developed first variceal bleeding. 47 (15.8%) patients died from liver-related causes. Interestingly, higher fibronectin levels were independently associated with an increased risk of first variceal bleeding (aSHR 6.41; $p = 0.020$) after adjustment for HVPG and MELD 3.0. In contrast, fibronectin was not significantly associated with non-bleeding decompensating events.
Conclusion: In patients with ACLD, fibronectin correlates to biomarkers representing distinct disease-related pathomechanisms. While lower levels generally reflect advanced liver dysfunction, higher fibronectin levels independently identify patients at increased risk for variceal bleeding.

WED-475

Hypoleptinemia in cirrhosis is associated with increased one-year-mortality in women undergoing transjugular intrahepatic portosystemic shunt

Frederike Krus[1], Shreeya Sharma[1], Paulina Bauer[1], Robert Schierwagen[1], Jannik Sonnenberg[1], Simone Anna Keimburg[1], Philipp Wöhler[1], Sabine Klein[1], Maximilian Joseph Brol[1], Frank Erhard Uschner[1], Kai-Henrik Peiffer[1], Sara Noemi Reinartz Groba[1], Martin Sebastian McCoy[1], Michael Praktiknjo[1], Jonel Trebicka[1,2], Julia Fischer[1]. [1]*University of Münster, Faculty of Medicine and University Hospital of Münster, Department of Internal Medicine B, Münster, Germany;* [2]*European Foundation for the Study of Chronic Liver Failure - EFClif, Barcelona, Spain*
E-mail: frederike.krus@ukmuenster.de

Background and aims: Leptin, a metabolic hormone predominantly secreted by white adipose tissue, regulates systemic metabolism and modulates immune responses to bacterial infection (BI). In chronic liver disease, leptin exerts pro-inflammatory and pro-fibrogenic effects, contributing to hepatic fibrosis. Circulating leptin levels are known to differ substantially between sexes, with higher levels observed in women. However, the clinical relevance of these sex-specific differences for leptin in patients with cirrhosis remains unclear. This study aimed to investigate the role of circulating leptin with a particular focus on sex-specific outcomes in cirrhosis.
Method: In this study, leptin levels were analyzed in a cohort of patients with liver cirrhosis ($n = 157$) who underwent Transjugular intrahepatic portosystemic shunt (TIPS) placement. Leptin levels were measured in plasma samples taken from the right atrium, hepatic vein, portal vein, and cubital vein at the time of TIPS implantation using enzyme-linked immunosorbent assay (ELISA).
Results: In our cohort, circulating leptin levels correlated positively with body mass index (BMI, $p < 0.0001$), which was identified as an independent determinant of leptin concentrations. Based on BMI-adjusted leptin levels, 24% of patients were classified as hypoleptinemic. Unexpectedly, hypoleptinemic patients were predominantly of female sex and obese. Hypoleptinemia was associated to a significantly increased one-year mortality ($p = 0.0462$), an effect predominantly observed in female patients ($p = 0.0145$) compared to those of male sex ($p = 0.8270$). Paired portal and hepatic vein measurements revealed significantly higher leptin concentrations in the portal vein compared to the hepatic vein ($p < 0.0001$), indicating hepatic leptin clearance. Notably, in advanced disease stages (CHILD C cirrhosis and MELD score > 15), this portal–hepatic venous gradient was no longer detectable ($p = 0.2413$ and $p = 0.2101$).
Conclusion: Women with liver cirrhosis may develop a relative leptin deficiency, despite higher physiological leptin levels identifying leptin as a sex-specific prognostic factor in advanced liver cirrhosis. Hepatic leptin clearance decreases with cirrhosis progression, potentially worsening outcome. These findings highlight leptin metabolism as a promising target for further mechanistic and therapeutic studies in liver cirrhosis.

WED-476

Prevalence, risk factors, and clinical outcomes of micronutrient deficiencies in patients with cirrhosis: a prospective cohort study

Narisorn Lakananurak[1], Warasinee Hathayamat[1], Phatcharaporn Chanwidoon[1]. [1]*Department of Medicine Faculty of Medicine Chulalongkorn University, Bangkok, Thailand*
E-mail: narisorn.l@chula.ac.th

Background and aims: Patients with cirrhosis are highly vulnerable to malnutrition and micronutrient deficiencies. Current guidelines recommend empiric supplementation, yet inappropriate use may cause toxicities and liver injury, particularly with fat-soluble vitamins and certain trace elements. Data on prevalence, risk factors, and clinical impact of micronutrient abnormalities in cirrhosis remain scarce. This study aimed to evaluate prevalence, risk determinants, and outcomes of micronutrient deficiencies in cirrhotic patients.
Method: This is a prospective cohort study. A total of 110 patients with cirrhosis were enrolled at outpatient clinics. Serum vitamin A, vitamin D, vitamin E, zinc, copper, and high-sensitivity C-reactive protein (hs-CRP) were measured. Demographics, cirrhosis severity, and complications were recorded. Patients were followed for 6 months to assess clinical outcomes including infection, mortality, hepatic encephalopathy, ascites, and readmission.
Results: Hepatitis B infection was the leading cause of cirrhosis (25.5%), followed by alcohol-related cirrhosis (18.2%) and cirrhosis related to metabolic dysfunction-associated steatohepatitis (MASH) (16.4%). Regarding disease severity, 61.8% of patients were classified as Child-Pugh A, 24.5% as Child-Pugh B, and 13.6% as Child-Pugh C. Micronutrient deficiencies were frequent: vitamin A (51.2%), vitamin D (34.9%), vitamin E (4.8%), zinc (60%), and copper (12.7%). Half of the patients (50%) had multi-micronutrient deficiencies (≥2 deficiencies). Mean ± standard deviation (SD) hs-CRP levels were 3.6 ± 4.7 mg/dL, which did not influence micronutrient status (<20 mg/dL). Independent risk factors for multi-micronutrient deficiencies were Child-Pugh class B/C (odds ratio (OR) 7.8; 95% confidence interval (CI) 1.9–31.5; $p = 0.004$) and Model for End-Stage Liver Disease (MELD) score > 11 (OR 5.2; 95% CI 1.5–18.4; $p = 0.010$). After adjustment for cirrhosis severity, multi-micronutrient deficiencies

were significantly associated with infectious complications (hazard ratio (HR) 4.7; 95% CI 1.2–18.8; p = 0.031).
Conclusion: Micronutrient deficiencies are highly prevalent in cirrhosis, with zinc, vitamin A, and vitamin D most commonly affected. Multi-micronutrient deficiencies are frequent and linked to adverse outcomes, particularly infection, independent of cirrhotic severity. Child-Pugh B/C and MELD >11 identify high-risk patients who may benefit from targeted micronutrient evaluation and supplementation.

WED-477
Prognosis after TIPS in patients aged ≥70 years: a multicentre french cohort study
Hélène Larrue[1], Julie Tainturier[2], Olivia Pietri[3], Laurent Milot[4], Charlotte Bouzbib[5], Baptiste Giguet[6], Sophie Metivier[1], Marie-Noëlle Hilleret[7], Jean Paul Cervoni[8], Fanny Lebosse[9], Louis Dalteroche[2], Lena Dube[6], Angelo Della Corte[9], Zakaria Maghlaoua[7], Dominique Thabut[5], Marc Bourliere[3], Florent Artru[6], Marika Rudler[5], Floriane Sellier[3], Laure Elkrief[2], Christophe Bureau[1], Jérôme Dumortier[4]. *[1]Toulouse University Hospital, Toulouse, France; [2]CHU de Tours, Tours, France; [3]Hôpital Saint-Joseph, Marseille, France; [4]Hôpital Edouard Herriot, Lyon, France; [5]AP-HP Sorbonne Université, Hôpital Universitaire Pitié-Salpêtrière, Paris, France; [6]University hospital centre Pontchaillou, Rennes, France; [7]CHU de Grenoble, Grenoble, France; [8]CHU de Besançon, Besançon, France; [9]Hôpital de la Croix Rousse, Lyon, France*
E-mail: larruehelene@gmail.com

Background and aims: Transjugular intrahepatic portosystemic shunt (TIPS) is an effective treatment for complications of clinically significant portal hypertension; however, its use in elderly patients remains controversial. Data regarding outcomes and prognostic stratification after TIPS in patients aged ≥70 years are limited. We aimed to assess survival, further decompensation, and prognostic determinants after TIPS in this population.
Method: We conducted a retrospective multicentre cohort study including consecutive patients aged ≥70 years who underwent TIPS between 2010 and 2024 in nine tertiary hepatology centres in France. Overall survival and further decompensation-free survival were evaluated up to 24 months. Prognostic factors were analysed using univariable and multivariable Cox models. In patients undergoing TIPS for refractory ascites (RA), a machine-learning model (XGBoost) was additionally developed to explore individualized prognostic stratification.
Results: A total of 402 patients were included (66.7% men; mean age 73.9 ± 3.5 years). TIPS was performed electively in 76.4% of cases, most frequently for RA (51.7%). During a median follow-up of 338 days, 210 patients died, corresponding to an estimated 2-year overall survival of 47.8%. Overall survival did not differ according to the period of TIPS placement (before vs after 2017). Survival varied according to indication, with lower 2-year survival in patients treated for RA (42.2%) and rescue TIPS (39.9%). Nearly half of the cohort (49.8%) experienced at least one episode of further decompensation, with decompensation-free survival rates of 49.0% at 1 year and 41.8% at 2 years; hepatic encephalopathy occurred in 43.8% of patients. No patient underwent liver transplantation. In the overall cohort, age, male sex, serum bilirubin, INR, and ascites were independently associated with mortality. An XGBoost model integrating multiple prognostic variables was created and improved individualized risk prediction.
Conclusion: Outcomes after TIPS in patients aged ≥70 years remain heterogeneous and strongly depend on indication. Patients treated for refractory ascites showed poor long-term survival, even in this large and contemporary multicentre cohort from expert centres, highlighting the need for careful patient selection in this setting. Advanced age and markers of liver failure identify patients at higher risk. Machine-learning approaches may help refine prognostic stratification beyond conventional scores in this growing population.

WED-478
Shear wave elastography combined with ALBI score enhances prediction of hepatic decompensation in advanced chronic liver disease
Jaejun Lee[1], Jung Hyun Kwon[1], Soon Kyu Lee[1]. *[1]Catholic University of Korea, Seoul, Korea, Rep. of South*
E-mail: pwln0516@gmail.com

Background and aims: Hepatic decompensation (HD) is a key determinant of prognosis in advanced chronic liver disease (ACLD). Shear wave elastography (SWE) is widely used to assess fibrosis, but its prognostic value for HD remains uncertain. We evaluated SWE alone and combined with ALBI for risk prediction.
Method: 2759 patients with ACLD who underwent SWE between 2019 and 2025 were analyzed. The endpoint was time to first HD event. Predictive performance of SWE, alone and with ALBI, was evaluated in training (n = 1839) and test (n = 920) sets.
Results: SWE alone showed good performance for predicting HD (C-index 0.760) and OS. A 10-kPa threshold effectively stratified risk, with high-risk patients having higher hazards of HD and death ($P < 0.001$). SWE and ALBI showed no statistical interaction, supporting their potential for complementary synergistic effects when combined. Integrating SWE with ALBI grade created a simple three-tier classification that further improved stratification, with high-risk patients (SWE >10 kPa and ALBI grade 2/3) having a 16.6-fold risk of HD and a 21.4-fold risk of death compared with low-risk patients ($P < 0.001$). A Cox model in the training set generated a weighted linear formula (SWE + 20 × ALBI), termed the SALBI score, achieving the highest accuracy (C-index: training 0.802, test 0.820), outperforming SWE, ALBI, FIB-4, and MELD. The SALBI score stratified high- versus low-risk groups with 13.0-fold and 15.0-fold risks in train and test sets ($P < 0.001$).
Conclusion: SWE is a robust prognostic marker for HD. A linear score combining SWE with ALBI further improves prediction and provides a practical tool for stratification.

WED-479
Prevalence of alcohol use among patients with cirrhosis in the United States: a prospective cohort study
Ria Loomba[1], Kaleb Tesfai[2], Ricki Bettencourt[2], Nikhil Kalita[2], Chinar Sheth[2], Egbert Madamba[2], Veeral Ajmera[2], Luis Antonio Diaz[2]. *[1]Georgetown University, Washington, United States; [2]University of California San Diego, MASLD Research Center, La Jolla, United States*
E-mail: luisdiazpiga@gmail.com

Background and aims: Alcohol use is a leading risk factor for hepatic decompensation and hepatocellular carcinoma among patients with cirrhosis. AASLD and EASL practice guidelines universally recommend complete abstinence from alcohol use in patients with cirrhosis. However, many patients with cirrhosis continue to consume alcohol despite these recommendations. Therefore, we aimed to determine the prevalence of alcohol use using validated questionnaire as well as phosphatidyl ethanol (PEth), a quantitative and objective biomarker of alcohol use, in a prospective cohort of patients with cirrhosis in the United States.
Method: This prospective study included adults with cirrhosis residing in Southern California. Cirrhosis was diagnosed based on AASLD criteria, either on liver biopsy, imaging, and/or laboratory and clinical evidence. We performed a standardized interview, physical exam, laboratory testing (including PEth), vibration-controlled transient elastography (VCTE) and magnetic resonance imaging (MRI). Alcohol consumption was quantified using the Lifetime Drinking History and Alcohol Use Disorders Identification Test (AUDIT). Current alcohol use was defined as either a positive test on PEth or confirmed alcohol use based upon self-report on AUDIT.
Results: The cohort comprised of 183 adults with cirrhosis. The mean (±SD) age in years and body mass index (BMI) was 59.1 ± 11.6 and 29.8 (±6.2) kg/m 2, respectively. 56% were female and 48% were of Hispanic ethnicity. The mean (±SD) LSM was 24.1 kPa (±17.1). 88

(48.1%) had MASLD cirrhosis, 52 (28.4%) had alcohol-associated cirrhosis, and 21 (11.5%) had viral hepatitis related cirrhosis. The prevalence of current alcohol use was 31%. Among those with continued alcohol use, 79% provided self-reports of alcohol consumption, but PEth testing revealed occult alcohol use in 21% (N = 12) who denied alcohol consumption on validated questionnaire. We then compared MELD, FIB-4, platelets, HDL, MCV, ANI, LSM by VCTE, LSM by MRE among those with alcohol use versus those without alcohol use. Alcohol use among cirrhosis patients was associated with higher MRI-PDFF (p-value < 0.01).
Conclusion: Alcohol use is present in 31% of patients with cirrhosis, and PEth testing in cirrhosis can uncover occult alcohol use. Future guidelines may consider PEth testing to detect occult alcohol in cirrhosis to improve the outcomes of patients with cirrhosis.

WED-480
Breaking the habit: evaluating the routine use of spontaneous bacterial peritonitis prophylaxis
Shauna Madigan[1,2], Eugene Phan[3], Keshani Alagiyage[4], Kathleen Davy[4], Kirsty Campbell[5], Jeyamani Ramachandran[4], Mohamed Asif Ali Chinnaratha Mohamedashrafali[3]. *[1]Leeds Teaching Hospitals NHS Trust, Leeds, United Kingdom; [2]Lyell McEwin Hospital, Gastroenterology, Elizabeth Vale, Australia; [3]Lyell McEwin Hospital, Adelaide, Australia; [4]Flinders Medical Centre, Adelaide, Australia; [5]Royal Darwin Hospital, Darwin, Australia*
E-mail: shaunamadigan@gmail.com

Background and aims: Spontaneous bacterial peritonitis (SBP) is the most common bacterial infection in patients with decompensated cirrhosis and is associated with high mortality and morbidity. Despite advances in medical care, 1-year mortality after the first episode of SBP ranges from 31% to 93%. SBP prophylaxis is given to patients either as primary prophylaxis (PP) to prevent the initial episode or secondary prophylaxis (SP) to prevent recurrence. The evidence for this practice is based on outdated data published more than two decades ago. With the emergence of multidrug-resistant organisms (MDRO), routine SBP prophylaxis practices need to be re-evaluated. We aimed to investigate the impact of PP and SP on survival and the development of MDRO.
Method: Data was collected retrospectively for patients admitted with cirrhosis-related ascites from three tertiary centres in Australia between January 2022 and December 2023, with follow-up until death or December 2024.
Results: A total of 379 patients were included, 61% being male, a median (IQR) age of 62 (19) years, MELD-Na score of 21 (9) and follow-up of 1.2 (1.9) years. Alcohol was the predominant aetiology (59%) for cirrhosis, and 73 (19.2%) had MDRO at baseline. On index admission, 13 (3.4%) patients were already on SP, 21 (5.5%) were on PP, and 51 (13.5%) patients were diagnosed with SBP. Post index admission, 32 (8.4%) and 48 (21%) patients were commenced on PP and SP, respectively. During the follow-up, 52 (13.7%) patients had an episode of SBP. The mean SBP-free survival was similar between those on PP and those meeting criteria but not commenced on PP [2.9 v 2.7 years, c2 = 3.7, p = 0.2], and with or without SP [2.2 v 2.0 years, c2 = 1.1, p = 0.3]. Overall survival was similar between those not on SP [median (95%CI): 1.7 (1.2–2.1) years] and those on SP [median (95%CI):1.8 (1.5–2.2) years], c2 = 0.5, p = 0.5. Overall, the risk of developing MDRO culture-positive SBP during follow-up was significantly higher for those on either PP or SP [27.5% v 9.4%, c2 = 18.1, p < 0.001]. The risk was only higher for those who had MDRO positive status at baseline [64.7% v 5.4%, c2 = 29.6, p < 0.001] but not for those with MDRO –ve status at baseline [17.5% v 10.3%, c2 = 2.5, p = 0.1].
Conclusion: This study shows that in a real-world setting, the use of PP and SP for SBP does not have a survival benefit. In fact, those who have MDRO at baseline have worse survival outcomes if started on prophylaxis. Future randomised controlled trials are required to justify PP and SP for SBP.

WED-481
Dynamic network collapse in decompensated hepatic cirrhosis
Yanpei Mai[1], Suzhen Jiang[1], Shuo Yang[2], Zixing Wang[1]. *[1]Peking University Hepatology Institute, Beijing, China; [2]Peking University People's Hospital Radiology Department, Beijng, China*
E-mail: wangzixing@pkuph.edu.cn

Background and aims: Alterations in intrahepatic communication networks – driven by fibrotic bridging, vascular shunting, and metabolic dysfunction – serve as latent biomarkers for impending cirrhotic decompensation. However, the dynamic hepatic connectomes and its role in signaling decompensation remain unexplored.
Method: We enrolled hepatic cirrhotic patients (2022–2025) undergoing gadoxetic acid-enhanced upper abdominal MRI with ≥5 imaging phases (non-contrast, arterial early, arterial late, portal venous, equilibrium). Dynamic contrast-enhanced T1-weighted MRI using a GE Discovery 750 3.0 T or Siemens Prisma 3.0 T scanner with standardized axial acquisition. Liver partitioned into 8 segments (I-VIII). Representative slices. Circular ROIs placed centrally in Segments I–VIII, avoiding vessels and lesions. 837 radiomic features per segment were extracted via PyRadiomics. Sliding window (window size = 3 phases) was applied to build topological networks. Intersegmental connectivity quantified by Pearson correlation, with sparsity controlled at 0.2. Small-worldness, modularity, hub distribution, nodal centrality were analyzed.
Results: Significant network reorganization was observed in decompensated compared to compensated livers within the arterial-portal venous-equilibrium window. This included an increase in modularity (indicating functional fragmentation: 0.066 vs. 0.038), sigma (reflecting heightened randomness: 1.514 vs. 1.434), and a decrease in average path length (suggesting impaired information transfer efficiency: 0.786 vs. 0.818); all P < 0.05. Segment V dominated the liver network in compensation (20% hub prevalence, consistent with its anatomical centrality). Decompensation triggered hub redistribution: Peripheral Segments II–V & VII–VIII: 12–15%; Marginal Segments I & VI: 8–10%. This indicate collapse of compensatory network. The betweenness centrality of Segment I (measure of its information-bridging role) predicted decompensation risk: 18.2%, 54.2%, and 83.3% in low, medium and high risk stratus, respectively. High-risk groups showed significantly elevated HRs for onset of ascites, hepatic encephalopathy and variceal bleeding; all P < 0.05.
Conclusion: This study pioneers a network paradigm for cirrhosis prognostication, shifting from isolated segmental biomarkers to system-level monitoring. The arterial-portal-equilibrium phase offers a critical window for detecting connectome-driven decompensation signals, with Segment I centrality emerging as a clinically important predictor.

WED-482
Association between occupational exposure and hepatocellular carcinoma risk in Egypt: a preliminary case–control analysis
Mohamed Mahmoud Marey[1], Malak A. Hassan[1], Nada Mohamed Faragallah[1], Mariam H. Ghallab[1], Rana Saleh Sharaf[1], Mohamed Mohamed Belal[1], Ahmed Kamal Hussein. *[1]Faculty of Medicine-Alexandria University, Alexandria, Egypt*
E-mail: mohamed.mahmoud2101@alexmed.edu.eg

Background and aims: Occupational exposures have been explored for various cancers, but the association has not been as well-established in hepatocellular carcinoma (HCC). This case-control study aims to explore the role of occupational risk factors in the development of HCC among cirrhotic patients in Egypt.
Method: This case-control study was conducted at Alexandria Main University Hospital, Egypt. Data collection took place between February 2025 and December 2025 by trained personnel using predesigned questionnaires. The control group included cirrhotic patients who achieved negative viremia (HCV or HBV) after treatment for at least 2 years. The cases group included patients with HCC on top of cirrhosis who have achieved negative viremia (HCV or HBV) after

treatment for at least 2 years. Preliminary analysis was conducted using Jamovi software.
Results: The mean age of HCC cases was higher than cirrhotic controls (64.5 ± 10.0 vs 60.8 ± 10.9 years). Males predominated among HCC cases (61.3%), whereas controls showed a slight female predominance (53.5%). Hepatitis C was the predominant cause of cirrhosis among HCC cases (93.5%), while controls had more heterogeneous etiologies, including HCV (40.2%) and MASLD (33.3%). Agriculture was the most common occupation in both groups, accounting for 38.7% of HCC cases and 35.6% of controls.
In this preliminary case–control analysis, rural residence showed an increase in the odds of HCC compared with cirrhotic controls (OR: 1.12; 95% CI: 0.49–2.53). Farming as a primary occupation was associated with HCC risk (OR: 1.02; 95% CI: 0.45–2.35). Exposure to pesticides or fertilizers was not associated with an increase in HCC odds (OR: 0.62; 95% CI: 0.13–2.99), as was employment in an industrial setting (OR: 0.61; 95% CI: 0.21–1.77).
Conclusion: While limited by sample size and preliminary power, these findings suggest that traditional occupational and socio-economic risk factors may play a role in HCC development among cirrhotic patients after sustained viral clearance. Importantly, the study design using cirrhotic patients without HCC as controls rather than general population comparators intentionally minimized the dominant carcinogenic effects of active HCV or HBV infection and cirrhosis-related disease progression, allowing a more isolated evaluation of non-viral, occupational, and socioeconomic exposures. Larger studies are warranted to refine HCC risk stratification in the Egypt's post HCV elimination era.

WED-483
Viscoelastic haemostatic assessment in cirrhosis using ClotPro®: clinical interpretation of manufacturer-derived viscoelastic reference ranges

Buzias Maria[1], Cristiana Grapa[1], Marta Besleaga[1], George Cioclu[1], Mohammad Al Khalili[1], Cristian Tefas[2], Zeno Sparchez[2], Bogdan Procopet[2], Rares Craciun[2]. *[1]"Iuliu Haţieganu" University of Medicine and Pharmacy, Cluj-Napoca, Romania; [2]Gastroenterolgy Department, "Prof. Dr. O. Fodor" Regional Institute of Gastroenterology and Hepatology, Department of Internal Medicine, "Iuliu Haţieganu" University of Medicine and Pharmacy, Cluj-Napoca, Romania, Cluj-Napoca, Romania*
E-mail: rarescraciun@ymail.com

Background and aims: Patients with cirrhosis frequently exhibit abnormal conventional coagulation tests (CCTs), including prolonged INR, thrombocytopenia and hypofibrinogenemia. Viscoelastic testing (VET) enables functional assessment of clot initiation and firmness. ClotPro® (enicor GmbH, Munich, Germany) is a cartridge-based VET device with limited validation in advanced liver disease. We aimed to evaluate haemostatic profiles in cirrhosis using ClotPro® and the clinical relevance of manufacturer-derived reference ranges and exploratory viscoelastic thresholds.
Method: We performed a cross-sectional analysis of consecutive adult patients with cirrhosis and abnormal CCTs undergoing ClotPro® testing. EX- and IN-tests were analyzed. Clot initiation was assessed by clotting time (CT), reflecting coagulation factor activity, and clot firmness by maximum clot firmness (MCF), reflecting platelet and fibrinogen contribution. Parameters were interpreted using manufacturer-provided adult reference ranges.
Results: 120 patients were included (Child A/B n = 59, Child C n = 61). Using manufacturer-derived reference ranges, clot firmness was frequently classified as reduced: EX-MCF was below range in 94/120 (78.3%) and IN-MCF in 88/120 (73.3%) patients, with no difference between Child classes ($p = 0.93$). Clot initiation deteriorated with disease severity. EX-CT was longer in Child C (69 [57–83] vs 55 [49–66] s, $p = 0.002$), and EX-CT above the upper reference limit was more frequent in Child C (35/61, 57.4% vs. 15/59, 25.4%; $p = 0.001$). Despite abnormal CCTs and frequent classification as hypocoagulable, only 24/120 (20.0%) patients reached an exploratory viscoelastic threshold commonly considered clinically actionable in ROTEM-guided bleeding algorithms (EX-CT >80 s), including 18/65 (27.7%) patients with INR >2. Among patients with fibrinogen <1.5 g/L, a composite viscoelastic abnormality was present in 29/36 (80.6%), while in patients with platelet count $<50 \times 10^3$/µL, it occurred in 49/52 (94.2%) patients.
Conclusion: In cirrhosis with abnormal standard coagulation tests, application of manufacturer-derived ClotPro® reference ranges classifies most patients as hypocoagulable. However, only a minority demonstrate viscoelastic abnormalities reaching exploratory thresholds that would support correction of coagulation factor, fibrinogen or platelet deficits. These findings highlight the importance of functional viscoelastic interpretation and the need for disease-specific ClotPro® thresholds in cirrhosis.

WED-484
The kidney-liver axis decoded: machine learning redefines mortality prediction in cirrhotic patients with acute kidney injury

Jeril Lasington[1], Lawin Steve Mathew Lasington[2]. *[1]New York Medical College, Valhalla, United States; [2]Rutgers University-Newark Arch, Newark, United States*
E-mail: jeril.lasington@gmail.com

Background and aims: Acute kidney injury (AKI) occurs in 20–50% of hospitalized cirrhotic patients and is a major mortality driver. Traditional scores including MELD and SOFA incorporate renal parameters but were not designed for the unique pathophysiology of AKI in cirrhosis, which includes hepatorenal syndrome (HRS), prerenal azotemia, and acute tubular necrosis. We developed machine learning (ML) models for predicting ICU mortality in cirrhotic patients with AKI and compared performance against established scores.
Method: This retrospective cohort study used MIMIC-IV (v3.1) to identify adults with cirrhosis and concurrent AKI or HRS requiring ICU admission (2008–2022). Predictors from the first 24 hours included renal parameters, liver function, metabolic markers, hemodynamics, AKI subtype, cirrhosis complications, and ICU interventions. Four ML algorithms (Logistic Regression, Random Forest, XGBoost, Gradient Boosting) were trained using 80/20 stratified splits with five-fold cross-validation. Performance was compared against MELD, MELD-Na, and SOFA using bootstrap DeLong testing (n = 2000).
Results: Among 2720 patients (mean age 59.8 years; 64.1% male; 22.1% HRS), hospital mortality was 34.3%. Logistic Regression achieved highest discrimination (AUC 0.841, 95% CI 0.805–0.872), significantly outperforming MELD (0.729, +15%, $p < 0.0001$), MELD-Na (0.726, $p < 0.0001$), and SOFA (0.728, $p < 0.0001$). Creatinine trajectory (both maximum and minimum values) emerged as the strongest predictor, followed by lactate, age, sepsis, and hepatic dysfunction markers. Subgroup analysis revealed superior performance in non-HRS AKI (AUC 0.855) compared to HRS (AUC 0.744), suggesting HRS may require distinct prognostic approaches.
Conclusion: ML significantly outperforms traditional scores for ICU mortality prediction in cirrhotic patients with AKI. The dominance of creatinine trajectory suggests dynamic AKI course impacts prognosis more than single-timepoint measurements. These findings support developing AKI-specific prognostic tools integrating renal trajectory, hepatic function, and systemic illness severity. External validation is warranted.

WED-485
Refining non-acute decompensation to improve risk stratification in advanced chronic liver disease

Martin Sebastian McCoy[1], Marta Tonon[2], Jan Hähner[1], Hannah Guembel[1], Stine Johansen[3], Frank Erhard Uschner[1], Maximilian Joseph Brol[1], Lena Wolters[1], Thies Wedemeyer[1], Ronja Hartmann[1], Mareike Schroeder[1], Marvin Petrikowski[1],

Julia Fischer[1], Florian Rennebaum[1], Jörn Arne Meier[1], Josune Cabello Calleja[1], Eduardo Cervantes-Alvarez[1], Philip Ferstl[4], Richard Moreau[5], Christoph Welsch[4], Stefan Zeuzem[4], Kai-Henrik Peiffer[1], Aleksander Krag[3], Salvatore Piano[2], Paolo Angeli[2], Michael Praktiknjo[1], Jonel Trebicka[1,3,4,5]. *[1]Department of Internal Medicine B, University of Münster, Münster, Germany, Münster, Germany; [2]Unit of Internal Medicine and Hepatology (UIMH), Department of Medicine (DIMED), Padova, Italy; [3]Centre for Liver Research, Department of Gastroenterology and Hepatology, Odense University Hospital, Odense, Denmark, Odense, Denmark; [4]Department of Internal Medicine I, Goethe University, Frankfurt, Germany, Frankfurt, Germany; [5]European Foundation for Study of Chronic Liver Failure, EF-Clif, Barcelona, Spain, Barcelona, Spain*
E-mail: martinsebastian.mccoy@ukmuenster.de

Background and aims: Non-acute decompensation (NAD) has been proposed to bridge the gap between compensated cirrhosis (CC) and acute decompensation (AD). However, its application for risk stratification is limited by inconsistent definitions. We compared NAD definitions with different ascites severities to compare prognostic performance and risk stratification.
Method: In this multicenter observational study, an outpatient derivation cohort (n = 565) was validated in an independent outpatient cohort (n = 632) and contextualized using a hospitalized AD cohort (n = 1512). Ascites severity and sustained diuretic therapy were evaluated at the lower boundary between CC and NAD. Three NAD frameworks were compared: STRICT criteria (HE grade ½ or ascites grade 2), EXTENDED (incl. ascites grade 1) and INCLUSIVE (incl. diuretic-controlled ascites). Primary endpoints were mortality and progression to AD.
Results: Across outpatient cohorts, patients with ascites grade 1 or diuretic-controlled ascites showed worse outcomes than ascites/diuretic-free individuals. A stepwise risk gradient was observed across ascites phenotypes, with increasing mortality, disease progression, and systemic inflammation. In the derivation cohort, 3-year mortality remained low among ascites/diuretic-free patients (6.4%) but converged at 17% in patients with diuretic-controlled and grade 1 ascites ($p < 0.01$). In the validation cohort, this gradient was reproduced without convergence (3-year mortality: 2.7%, 10.1%, and 24.4%, respectively; $p < 0.001$). Applying these risk patterns to INCLUSIVE NAD criteria increased prevalence from 11% to 62%. While STRICT criteria identified patients at highest risk, they misclassified early decompensation: over 75% of patients progressing to AD within 1 year were classified as non-NAD/compensated, compared with 14% under the INCLUSIVE definition. Consequently, mortality among non-NAD/compensated patients declined stepwise with framework expansion, indicating improved risk separation. In a merged cohort of 2077 patients, INCLUSIVE NAD represented a distinct intermediate-risk phenotype between CC and AD.
Conclusion: Diuretic-controlled ascites is a functional marker of decompensation, aligning with the BAVENO-based concept of recompensation. STRICT NAD criteria identify high-risk patients but lack sensitivity for early decompensation. INCLUSIVE NAD definitions improve identification of at-risk individuals, strengthen long-term risk stratification and facilitate clinical adoption.

WED-489-YI
Frailty in patients with advanced chronic liver disease is reduced using BCAA supplementation (Amino L40) combined with community-based structured exercise programme

Matthew McKenna-Barry[1,2], Reza Saeidi[1,2], Ciara O'Connor[1,2], Noel McCaffrey[3], John Ryan[1,2], Karen Boland[1,2]. *[1]Royal College of Surgeons in Ireland, Dublin, Ireland; [2]Beaumont Hospital, Dublin, Ireland; [3]ExWell Medical, Irish Wheelchair Association, Dublin, Ireland*
E-mail: matthewmckennab24@rcsi.com

Background and aims: Frailty, the reduced physiological reserve to health stressors, increases the risk of death, decompensation and hospitalisation for patients with advanced chronic liver disease (ACLD). Effective therapies are required to mitigate this syndrome.
Method: Patients with ACLD were recruited from a single centre. The intervention consisted of 12 weeks once daily 30 g Amino L40 (Ajinomoto Inc) (7 g protein, 23 g carbohydrate, 2.72 g leucine, 0.76 g isoleucine and 0.8 g valine) and a community based structured exercise programme combining aerobic and resistance exercises twice weekly. This pilot cohort were recruited sequentially and compared to patients in an ongoing randomised controlled trial of two wings; standard of care with dietician evaluation (control) or once daily 30 g Amino L40 alone. Liver Frailty Index (LFI) was measured at induction, 3 weeks and 12 weeks. Mann-Whitney U testing was performed to analyse continuous outcomes.
Results: 122 patients were recruited, 26 were assigned to combination, 48 to control and 48 to Amino L40 alone. There were no statistically significant differences of gender, age, aetiology or MELD between groups. Interim analysis was performed for 17 combination patients, 35 Amino L40 alone patients and 33 control patients at week 3 while recruitment is ongoing. Interim analysis was performed for 10 combination patients, 37 Amino L40 alone patients and 40 control patients at week 12 while recruitment is ongoing.
Combination patients completed median 15.5 (IQR 11–21.75) exercise classes at week 12. Adherance with Amino L40 was median 99% (IQR 90–100%) for combination and 85% (67–100%) for Amino L40 alone. Change in LFI from induction to week 3 for the combination group was median −0.42 (IQR −0.5–−0.28), −0.23 (−0.45–−0.10), $p = 0.036$ in comparison to combination, for Amino L40 alone and −0.17 (−0.32–0.11), $p = 0.002$ in comparison to combination, for control. Change in LFI from induction to week 12 for the combination group was median −0.59 (IQR −0.77–−0.36), −0.35 (−0.5–−0.11), $p = 0.029$ in comparison to combination, for Amino L40 alone, and −0.11 (−0.40–0.2), $p = 0.003$ in comparison to combination, for control. Statistically significant differences in thigh muscle thickness by ultrasound or phase angle were not seen between groups.
Conclusion: The provisional results of this study show that combination structured exercise and Amino l40 resulted in a significant reduction in LFI for patients with ACLD in comparison to Amino l40 alone or control treatment.

WED-490
A comparison of thromboelastometry-guided versus standard of care blood product transfusion strategies in patients with liver cirrhosis undergoing dental extractions

Irina Girleanu[1], Cristina-Maria Muzica[1], Laura Huiban[1], Sebastian Zenovia[1], Raluca Avram[1], Iulian Buzincu[1], Anca Trifan[1]. *[1]Universitatea de Medicină și Farmacie 'Grigore T. Popa' Iași, Iași, Romania*
E-mail: gilda_iri25@yahoo.com

Background and aims: Dental extractions are frequently needed in patients with liver cirrhosis, especially before liver transplantation. The aim of this study was to evaluate the efficacy and safety of a ROTEM-based algorithm in managing the administration of prophylactic blood components to cirrhotic patients undergoing dental extractions.
Method: All cirrhotic patients who were consecutively admitted to a tertiary university hospital from November 2024 to May 2025 and underwent dental extractions were included in the study. The patients were randomly assigned to two groups, with each subjected to a protocol to guide blood product transfusion [fresh frozen plasma (FFP), platelets and/or cryoprecipitate] prior to dental extraction: the standard-of-care (SOC) group -a transfusion protocol based on standard coagulation tests and thromboelastometry group-a transfusion protocol based on rotational thromboelastometry.
Results: Overall, 52 cirrhotic patients were included, with 26 in each group. There were no clinically significant differences regarding the baseline characteristics between the study groups. Postoperative bleeding occurred after two procedures in the SOC group. Patients

from the ROTEM group received less FFP transfusions than the SOC group (3.8% vs. 30.8%, p = 0.010). Blood products transfusion was needed less in patients evaluated using ROTEM compared to the SOC group (30.8% vs. 80.8%, p = 0.0001). There were no differences regarding the length of the hospital stay (p = 0.829) and 30-days survival (p = 0.298) between the two study groups.
Conclusion: Using ROTEM-guided blood product transfusion before dental extraction can prevent excessive blood products transfusion in patients with liver cirrhosis and should be used instead SOC tests.

WED-491
Physician perspectives on palliative care referral and integration in liver cirrhosis: a mixed-methods study
Chung Yau Nah[1], Raphael Lee[1], Xuan Yong Lee[1], Choon Pooh Heng[1], Wan Fen Yip[2]. [1]*Woodlands Health Campus, Singapore, Singapore;* [2]*National Healthcare Group, Singapore, Singapore*
E-mail: brandon.nah@gmail.com

Background and aims: Early integration of palliative care (PC) improves symptom control, advance care planning (ACP) and quality of life in patients with liver cirrhosis, yet referrals remain inconsistent and delayed. This study aimed to explore inter-specialty perspectives on PC integration and referral barriers.
Method: This preliminary analysis is part of a single-centre mixed-methods study surveying physicians from Internal Medicine (IM), Gastroenterology and Hepatology (GH) and Palliative Medicine (PM) at a tertiary hospital in Singapore. A cross-sectional questionnaire assessed perceptions of referral timing, ACP, symptom management, receptiveness and barriers using a 5-point Likert-scale (1 = strongly disagree; 5 = strongly agree), with non-parametric group comparisons and correlation analyses.
Results: 22 physicians participated, representing majority of physicians across departments (GH 9/10; IM 7/9; PM 6/9; 64% consultants; 50% female). While early PC was considered appropriate for decompensated cirrhosis (DC) (GH/IM mean 4.19; PM 4.00), referrals and goals-of-care (GOC) discussions were often delayed (GH/IM 4.25; PM 4.17). Primary physicians were viewed as mainly responsible for disease education, prognostic discussions and GOC conversations. PM physicians perceived lower patient (PM 2.50; GH/IM 3.31, p = 0.024) and family (PM 2.67; GH/IM 3.38, p = 0.027) receptiveness to PC than GH/IM physicians, with higher receptiveness associated with greater willingness to refer. Perceptions of psychosocial care responsibility differed, with each specialty attributing greater responsibility to the other (GH/IM 2.81 vs PM 4.00, p = 0.018; PM 2.33 vs GH/IM 3.50, p = 0.036). Key barriers differed; PM physicians reported greater concern about PC's perceived impact on primary physician–patient relationship (4.17 vs 2.38, p = 0.001), discomfort initiating PC discussions (4.59 vs 2.50, p = 0.001) and limited institutional support (3.83 vs 2.50, p = 0.003). All agreed that clear referral criteria, training primary physicians in prognostic discussions and increased awareness of PC among patients and medical colleagues facilitated referral.
Conclusion: Despite broad recognition of PC's role in DC, specialty-specific differences and barriers persist. Addressing clinician discomfort, clear referral criteria and clarifying the complementary roles of primary and specialist PC may facilitate earlier and more consistent integration. Findings will inform focus group discussions to develop context-specific strategies for timely PC referral.

WED-492
Phase angle as a predictor of mortality in patients with liver cirrhosis
Lenka Nosáková[1], Diana Vážanová[1], Jakub Hoferica[1], Eva Baranovičová[2], Katarína Dirnbachová[2], Peter Banovcin[1]. [1]*Department of Internal Medicine – Gastroenterology, University Hospital Martin, Jessenius Faculty of Medicine in Martin, Comenius University in Bratislava, Martin, Slovakia;* [2]*Martin Biomedical Centre – BioMed, Jessenius Faculty of Medicine in Martin, Comenius University in Bratislava, Martin, Slovakia*
E-mail: lenka.bubernakova@gmail.com

Background and aims: Conventional scoring systems used to assess survival in patients with liver cirrhosis are believed to have several limitations. The aim of our study was to assess the relationship between phase angle, the MELD-Na and CPT scoring systems, and mortality in patients with liver cirrhosis.
Method: From October 2022 to January 2024, we conducted a prospective observational study on patients with liver cirrhosis. The study's primary goal was to evaluate the relationship between body composition and patient survival. Body composition was measured using bioelectrical impedance analysis with the TANITA MC-780MA device, which provided us with phase angle (Pha) values. Patients were dichotomized into sarcopenic and non-sarcopenic groups based on Pha values. This cutoff point was determined using the "maximizing log-rank statistic" method. Patient survival was analyzed using the Cox regression model. Differences between variables were expressed as mean differences (MD). Correlations between variables were assessed using Spearman's correlation coefficient.
Results: We enrolled 41 patients with liver cirrhosis, 14 women (34.1%). The average age of patients with sarcopenia was 59.9 ± 8.38 years, while in the non-sarcopenic group it was 56.7 ± 10.5 years. Sarcopenic patients had an average phase angle that was 2.2 lower compared to non-sarcopenic patients (MD: 2.2; 95% CI: 0.679–3.37; p = 0.007). The average BMI was significantly lower in sarcopenic patients compared to non-sarcopenic patients (26.5 ± 4.36 vs. 29.8 ± 5.21 kg/m^2; p < 0.05). The average MELD-Na score was 14.88 ± 5.25 in the sarcopenic group and 14.75 ± 7.96 in the non-sarcopenic group, which was not a statistically significant difference. In our study, we observed a relationship between mortality and Pha value, where a 1-degree decrease in Pha was associated with a 10% increase in mortality during the follow-up period (HR 1.10; 95% CI: 0.95–1.26; p = 0.196). A significant difference in Pha values was observed between patients with CPT stage A and B cirrhosis. However, we did not observe a correlation between Pha and disease prognosis as expressed by MELD-Na score (rho = –0.054; p = 0.743).
Conclusion: Our results suggest a higher tendency toward mortality in liver cirrhosis patients with lower phase angle values. No association was observed between Pha and MELD-Na score. Further studies with larger patient samples are needed to confirm our findings.

WED-493
The safety of anticoagulant treatment in cirrhotic patients with portal vein thrombosis and severe thrombocytopenia
Irina Girleanu[1], Georgeta Oancea[1], Ioana Coruga[1], Cristina-Maria Muzîcă[1], Laura Huiban[1], Cojocariu Salloum[1], Ana-Maria Singeap[1], Sebastian Zenovia[1], Remus Stafie[1], Stefan Chiriac[1], Adrian Rotaru[1], Simona Juncu[1], Carol Stanciu[1], Anca Trifan[1]. [1]*Universitatea de Medicină și Farmacie 'Grigore T. Popa' Iași, Iași, Romania*
E-mail: gilda_iri25@yahoo.com

Background and aims: Portal vein thrombosis (PVT) is a frequent complication of liver cirrhosis. Although anticoagulation is recommended in selected patients, severe thrombocytopenia represents a relative contraindication. We aimed to assess the safety of anticoagulant treatment in cirrhotic patients with PVT and severe thrombocytopenia.
Method: We performed a prospective observational study including 121 cirrhotic patients treated with anticoagulation for non-malignant PVT. After the anticoagulant initiation, the patients were follow-up for 1 year. Severe thrombocytopenia was defined as a platelet count $<50 \times 10^9$/L.
Results: Severe thrombocytopenia was present in 25 patients (20.7%). Patients with severe thrombocytopenia had higher MELD-Na scores compared with those with platelet counts $\geq 50 \times 10^9$/L (median 19 vs.

15, p = 0.03). Most of the patients were diagnosed with partial PVT (70.3%). The majority of the patients received apixaban or rivaroxaban (81 patients, 66.9%), 33 patients (29.7%) were treated with enoxaparin, and only 4 patients (3.4%) received acenocoumarol. There were no differences regarding the type of anticoagulant treatment between the study groups. Hemorrhagic complications occurred in 28.0% of patients with severe thrombocytopenia and in 18.8% of those without (p = 0.40). Major bleeding events were uncommon and did not differ between groups (4.0% vs. 6.3%, p = 1.00). There was no difference in the mortality rates between the two study groups (8.0% vs. 18.8%, p = 0.24).
Conclusion: Anticoagulant therapy in cirrhotic patients with PVT appears safe even in the presence of severe thrombocytopenia, with low rates of major bleeding and no increase in mortality. These findings warrant confirmation in prospective studies.

WED-494-YI
Socioeconomic deprivation and clinical characteristics of patients with newly-diagnosed cirrhosis in Italy: evidence from the SORPRESA cohort

Andrea Pasta[1], Sara Cariati[1], Antonino Lombardo[2], Paolo Angeli[3], Simone Incicco[3], Francesca Romana Ponziani[4], Leonardo Stella[4], Giovanni Di Costanzo[5], Debora Angrisani[5], Alessandro Federico[6], Marcello Dallio[6], Giulia Pilara[7], Giacomo Zaccherini[7,8], Mario Masarone[9], Filomena Morisco[10], Mario Capasso[10], Nicola Coppola[11], Maria Stanzione[11], Alessio Aghemo[12], Stella De Nicola[12], Marcello Persico[9], Vito Di Marco[2], Edoardo Giovanni Giannini[1]. *[1]Gastroenterology Unit, Department of Internal Medicine, University of Genoa, Genoa, Italy, Gastroenterology Unit, IRCCS Ospedale Policlinico San Martino, Genoa, Italy, Genoa, Italy; [2]Department of Health Promotion, Mother & Child Care, Internal Medicine & Medical Specialties (PROMISE), Gastroenterology Unit, University of Palermo, Palermo, Italy, Palermo, Italy; [3]Department of Surgery, Oncology and Gastroenterology, Gastroenterology Unit, University of Padua, Padua, Italy, Padua, Italy; [4]Liver Unit, CEMAD – Centro Malattie dell'Apparato Digerente, Internal Medicine and Gastroenterology, Università Cattolica del Sacro Cuore, Fondazione Policlinico Universitario Gemelli IRCCS, Rome, Italy, Rome, Italy; [5]Liver Unit, Antonio Cardarelli Hospital, 80131 Naples, Italy, Naples, Italy; [6]Hepatogastroenterology Unit, Department of Precision Medicine, University of Campania Luigi Vanvitelli, Naples, Italy, Naples, Italy; [7]Department of Medical and Surgical Sciences, Alma Mater Studiorum University of Bologna, Italy, Unit of Semeiotics, Liver and Alcohol-related Diseases, IRCCS Azienda Ospedaliero-Universitaria di Bologna, Italy, Bologna, Italy; [8]Unit of Semeiotics, Liver and Alcohol-related Diseases, IRCCS Azienda Ospedaliero-Universitaria di Bologna, Italy, Bologna, Italy; [9]Department of Medicine, Surgery and Dentistry "Scuola Medica Salernitana", University of Salerno, Salerno, Italy, Salerno, Italy; [10]Department of Clinical Medicine and Surgery, Diseases of the Liver and Biliary System Unit, University of Naples "Federico II", Naples, Italy, Naples, Italy; [11]Department of Mental Health and Public Medicine, Section of Infectious Diseases, Second University of Naples, 80131 Naples, Italy, Naples, Italy; [12]Division of Internal Medicine and Hepatology, IRCCS Humanitas Research Hospital, Rozzano, Italy, Milan, Italy*
E-mail: andrea.pasta@edu.unige.it

Background and aims: Socioeconomic determinants may influence the trajectory of cirrhosis beyond traditional clinical scores. This study aimed to evaluate the association between degrees of material deprivation (MD) and the demographic, etiological, and clinical characteristics of patients with newly diagnosed cirrhosis.
Method: In this prospective, multicenter study, patients with newly diagnosed cirrhosis were consecutively enrolled from 11 tertiary hepatology centers across Italy in 2024. MD was quantified across multiple domains and summarized as standardized z-scores. Demographic, etiological, and comorbidity profiles were compared between patients in the highest and lowest MD tertiles.
Results: A total of 1195 patients were included (mean age 64 ± 11.6 years; 73% male): 232 had ALD, 345 MASLD, 80 MetALD, 246 HCV infection, 159 HBV infection, 72 autoimmune liver disease, and 63 other etiologies. Patients with the highest MD were younger (60 ± 13 vs. 62 ± 10 years, p < 0.001) and more frequently female (25.4% vs. 17.9%, p < 0.001). Harmful alcohol consumption (40.8% vs. 20.6%, p < 0.001) and drug addiction (13.5% vs. 4.1%, p < 0.001) were more common among those with greater deprivation. Conversely, patients with the lowest MD exhibited more metabolic features, including higher BMI (28.4 vs. 26.5 kg/m^2, p = 0.033), arterial hypertension (51.8% vs. 41.5%, p = 0.009), and diabetes (44.1% vs. 33.1%, p = 0.162). ALD prevalence was higher among the most deprived (47.3% vs. 24.8%, p < 0.001), while MASLD was more frequent among the least deprived (53.8% vs. 33.1%, p < 0.001). No significant differences were observed for viral hepatitis (p = 0.590) or autoimmune liver disease (p = 0.762). Cluster analysis identified three distinct constellations: social disadvantage, metabolic dysfunction, and autoimmune/viral profiles.
Conclusion: This nationwide cohort delineates three phenotypic patterns of cirrhosis at diagnosis. Material deprivation is strongly linked to alcohol-related and behavioral risk factors, while metabolic and autoimmune/viral forms prevail in more advantaged contexts. Integrating social risk assessment into clinical stratification may improve targeted prevention and management strategies in cirrhosis.

WED-495-YI
Efficacy and safety of low-dose albumin infusion in patients of decompensated cirrhosis with acute kidney injury

Deep Patel[1], Aman Aggrawal[1], Ajay Kumar[1], Ashok Dalal[1], Siddharth Srivastava[1], Ujjwal Sonika[1], Sanjeev Sachdeva[1]. *[1]Govind Ballabh Pant Institute of Postgraduate Medical Education and Research, New Delhi, India*
E-mail: ajaykumar.aiims@gmail.com

Background and aims: Acute kidney injury (AKI) in patients with decompensated cirrhosis (DC), is managed with 20% Human Albumin infusion for initial 48 hours, however studies evaluating albumin infusion dose are limited. Also, human albumin infusion is associated with risk of volume overload, allergic reactions and is costly. This study evaluates the efficacy and safety of low-dose albumin (0.25–0.3 g/kg/d for 48 hours) in patients with DC and AKI stage IB or above.
Method: Patients with decompensated cirrhosis with AKI admitted in tertiary care centre from September 2022 to August 2025 screened and enrolled after excluding patients with Chronic kidney disease, Hepatocellular Carcinoma, respiratory or circulatory failure and on maintenance albumin therapy. The patients received intravenous 20% Human Albumin (100 ml) for 2 consecutive day, the response to albumin was defined as reduction of serum creatinine to within 0.3 mg/dl of the baseline value. The baseline demographic, clinical, biochemical data with response to albumin at 48 hours, adverse effects and mortality were noted.
Results: A total of 252 patients (n = 215 [83%] males, mean age 46.5 ± 11.3 years) were enrolled. Alcohol was the most common aetiology (62.6%), followed by hepatitis C (12.3%). The median MELD-Na was 28.46, and 182 patients (72.2%) were in Child–Pugh C. AKI resolution was noted in 116 (44.7%) patients, 59 patients (23.4%) after 24 hours and additional 57 patients (22.6%) after 48 hours of albumin infusion. Significant volume overload was seen in 2 patients (0.7%), mean duration of hospital stay was 7.98 ± 4.63 days. In hospital mortality was observed in 25.7% (n = 65).
Conclusion: The Low-dose albumin (0.25–0.3 g/kg/d for 48 hours) is safe and effective for volume repletion in decompensated cirrhosis patients with AKI.

WED-496

Myosteatosis is associated with a higher postoperative incidence of ACLF and mortality in patients with liver cirrhosis, independent of Child-Pugh and VOCAL-Penn scores

Felix Piecha[1], Mattis Kreutzer[2], Alexandra Linke[1], Nina Böhling[2], Alexander Isaak[2], Christoph Riedel[1], Maike Theis[2], Jörg C. Kalff[2], Torid Jacob[3], Juliana Goediker[3], Jonel Trebicka[3], Johannes Kluwe[1], Peter Huebener[1], Jürgen Rockstroh[2], Samuel Huber[1], Ansgar W. Lohse[1], Peter Bannas[1], Christian Strassburg[2], Alois Martin Sprinkart[2], Luetkens Julian[2], Michael Praktiknjo[3], Johannes Chang[2]. [1]*University Medical Center Hamburg-Eppendorf, Hamburg, Germany;* [2]*University Hospital Bonn, Bonn, Germany;* [3]*University Hospital Münster, Münster, Germany*
E-mail: f.piecha@uke.de

Background and aims: Patients with liver cirrhosis are at an increased risk for postoperative morbidity and mortality. Surgical outcomes are determined by the severity of liver disease and the type of surgery. Sarcopenia, defined as the quantitative and qualitative loss of skeletal muscle mass, strength, and function, is common in cirrhosis patients and an independent risk factor for adverse outcomes. This study aimed to assess the impact of myosteatosis as a marker of qualitative muscle impairment on the development of postoperative acute-on-chronic liver failure (ACLF) and overall transplant-free survival in cirrhotic patients undergoing surgery.
Method: In this retrospective, bicentric analysis, consecutive patients undergoing elective procedures between 2010 and 2022 without ACLF at the time of surgery were included. A contrast-enhanced CT in the portal venous phase within three months prior was required. Myosteatosis was defined according to current guideline recommendations (<41 HU for BMI <25 kg/m^2; <33 HU for BMI ≥ 25 kg/m^2). Subpopulation analyses included stratification by Child-Pugh score and risk assessment according to the Veterans Outcomes and Costs Associated with Liver Disease (VOCAL) Penn score. The primary endpoint was ACLF development within 28 days after surgery, the secondary endpoint overall one-year transplant-free survival.
Results: A total of 223 patients were included. The majority was male (157/223, 70%) and had alcohol-related liver cirrhosis (103/223, 46%). At the time of surgery, most patients were classified as Child-Pugh B (106/223, 48%), with a median MELD score of 10 (IQR 8–13). The most common surgical procedures according to VOCAL-Penn categories were open abdominal procedures (122/223, 55%). Myosteatosis was present in 157/223 patients (70%). Postoperatively, 60/223 patients (27%) developed ACLF within 28 days, and 67/223 patients (30%) died within one year. Patients with myosteatosis had a higher incidence of postoperative ACLF (31% vs. 16%, p = 0.02) and one-year mortality (35% vs. 16%, p = 0.003). These associations remained significant across Child-Pugh stages and VOCAL-Penn risk strata.
Conclusion: Myosteatosis, as a marker of muscle impairment, is independently associated with an increased risk of postoperative ACLF development and increased one-year mortality — independently of the Child-Pugh stage and VOCAL-Penn risk assessment. These findings support the inclusion of myosteatosis in preoperative risk assessment for patients with liver cirrhosis.

WED-497

Periprocedural bleeding in patients with cirrhosis: a prospective study

Adonis Protopapas[1], Erofili Papathanasiou[1], Vaia Kyritsi[1], Alexandra Tsankof[1], Christos Savopoulos[1], Andreas Protopapas[1]. [1]*First Propaedeutic Department of Internal Medicine, Aristotle University of Thessaloniki, AHEPA University Hospital, Thessalloniki, Greece*
E-mail: adoprot@hotmail.com

Background and aims: Patients with cirrhosis are often considered to have a high risk of periprocedural bleeding, even in low-risk procedures. The aim of this study was to prospectively assess bleeding episodes in patients with cirrhosis undergoing non-surgical procedures.
Method: All non-surgical procedures performed in patients with cirrhosis in our department between May and October 2025 were prospectively documented, along with patient characteristics. The procedures were categorized as low-, indeterminate-, or high-risk according to a recent international consensus.
Results: Seventy-four patients undergoing a total of 204 procedures were included. Of these procedures, 49.0% were performed in patients with hepatocellular carcinoma, and 83.8% in patients with decompensated cirrhosis. The patients had a median MELD-Na score of 17.5 [6–37.7] and a median Child-Pugh score of 8 [5–13]. Furthermore, median platelet and INR values were 122 [23–391] and 1.23 [0.89–4.4], respectively. The most frequently performed procedures were therapeutic paracentesis (36.3%), diagnostic paracentesis (20.6%), esophagogastroduodenoscopy (14.2%), endoscopic variceal ligation (6.9%), central venous catheter insertion (5.4%), and transjugular intrahepatic portosystemic shunt placement (4.4%). The majority of procedures were classified as low risk (79.8%), with only 2% being high risk. 20.3% of patients were under anticoagulation during the procedure. Minor bleeding occurred in 4.4% of procedures, with no cases of major bleeding. There was a correlation of minor bleeding cases with anticoagulation use (p = 0.018).
Conclusion: In this prospective cohort, periprocedural bleeding in patients with cirrhosis was infrequent and limited to minor events, supporting the safety of most non-surgical procedures in this population.

WED-498

Prevalence and prognostic impact of hyperferritinemia in advanced chronic liver disease

Clemens Renhardt[1,2,3], Georg Kramer[1,2,3], Christian Sebesta[1,2,3], Marlene Hintersteininger[1,2,3], Paul Thöne[1,2,3], Benedikt Hofer[1,2,3,4], Benedikt Simbrunner[1,2,3,4], Mathias Jachs[1,2,3], Lukas Hartl[1,2,3], Paula Hoefinger[1,2], Lorenz Balcar[1,2,3], Georg Semmler[1,2,3], Albert Friedrich Stättermayer[1,2], Michael Trauner[1,3], Mattias Mandorfer[1,2,3], Thomas Reiberger[1,2,3,4]. [1]*Division of Gastroenterology and Hepatology, Department of Medicine III, Medical University of Vienna, Vienna, Austria;* [2]*Vienna Hepatic Hemodynamic Lab, Division of Gastroenterology and Hepatology, Department of Medicine III, Medical University of Vienna, Vienna, Austria;* [3]*Clinical Research Group MOTION, Division of Gastroenterology and Hepatology, Department of Medicine III, Medical University of Vienna, Vienna, Austria;* [4]*Christian Doppler Lab for Portal Hypertension and Liver Fibrosis, Medical University of Vienna, Vienna, Austria*
E-mail: n12028120@students.meduniwien.ac.at

Background and aims: Hyperferritinemia is commonly associated with Metabolic dysfunction–associated steatotic liver disease (MASLD) and linked to hepatic inflammation and fibrosis. We assessed serum ferritin levels in well-characterized patients with advanced chronic liver disease (ACLD) and investigated the prognostic value of hyperferritinemia.
Method: Our study included ACLD patients of the VICIS study (NCT03267615), undergoing hepatic venous pressure gradient (HVPG) measurement from 01/2017 to 08/2025. We assessed serum ferritin levels and laboratory values reflecting iron homeostasis, inflammation and metabolic dysfunction. Patients were followed until death or liver transplantation.
Results: 1181 ACLD patients were included: ALD: 53.1%; decompensated (dACLD): 64.5%; median values for age: 57 years; MELD-Na: 14 points; HVPG: 17 mmHg, and ferritin: 126 µg/L. Hyperferritinemia (≥400 µg/L) was present in n = 232 (19.6%) including n = 89 (38.4%) with extensively elevated Transferrin saturation (> 60%; p < 0.001) and n = 3 (0.3%) with genetic HFE variants. Ferritin levels did not significantly differ between compensated (cACLD) and dACLD (median 132 vs. 121 µg/L; p = 0.210). ALD patients (median: 171 µg/L; IQR: 345 µg/L) had higher Ferritin levels than MASLD patients (median: 71.2 µg/L; IQR 164 µg/L; p < 0.001) and other etiologies (median: 104 µg/L; IQR: 210 µg/L; p < 0.001).

Hyperferritinemia was associated with higher total (≥200 mg/dL; p = 0.005) and higher LDL (≥100 mg/dL; p < 0.001) cholesterol, and higher uric acid levels (≥7 mg/dL; p = 0.018). As expected for acute phase proteins, ferritin levels correlated with CRP (Spearman = 0.28; p < 0.001) and IL-6 (Spearman = 0.26; p < 0.001). Follow-up data was available in 841 patients (median follow-up: 26.7 months). Hyperferritinemia was associated with liver-related mortality (log-rank p = 0.002). In multivariate Cox proportionate hazard analysis, hyperferritinemia was not an independent predictor of liver-related death (aHR: 0.978, 95% CI: 0.656–1.456; p = 0.911) while age (aHR: 1.027, 95% CI: 1.012–1.041; p < 0.001), MELD-Na (aHR: 1.096, 95% CI: 1.061–1.133; p < 0.001), and HVPG (aHR: 1.043, 95% CI: 1.019–1.067; p < 0.001) remained as independent risk factors for mortality.
Conclusion: Hyperferritinemia is common in cirrhosis and mainly linked to dysmetabolism and inflammation. Hyperferritinemia was not an independent risk factor for liver-related mortality.

WED-499
Closing the coding gap: International classification of diseases (ICD)-10 code K76.82 for hepatic encephalopathy achieves rapid uptake in U.S. real-world practice

Dominique Thabut[1,2], Pierbruno Ricci[3], Berenice Alard[3], Maxime Anné[3], Athéna Crespin[3], Stephanie Ferreira[3], Yacine Hajji[3], Dean Hum[3], Jennifer Jara Vargas[3], Jeremy Magnanensi[3], Pejvack Motlagh[3], Katharina Staufer[3], Jasmohan Bajaj[4], Jennifer Lai[5], Florence Wong[6], Jacqueline O'Leary[7]. [1]*Department of Hepatogastroenterology, Hôpital Pitié Salpêtrière-Assistance Publique-Hôpitaux de Paris, Liver Intensive Care Unit, Paris, France;* [2]*Centre de recherche Saint-Antoine, Inserm, Sorbonne Université, Paris, France;* [3]*Genfit S.A., Loos, France;* [4]*Virginia Commonwealth University School of Medicine, Richmond, United States;* [5]*Department of Medicine, University of California, San Francisco, United States;* [6]*University of Toronto, Toronto, Canada;* [7]*University of Texas, Southwestern, Dallas, Dallas, United States*
E-mail: pierbruno.ricci@genfit.com

Background and aims: Hepatic encephalopathy (HE) is a frequent and major complication of cirrhosis. Its epidemiologic assessment in administrative databases has been limited by coding constraints. Before October 2022, ICD-10 lacked a specific HE code, requiring reliance on generic codes or medication proxies (lactulose, rifaximin). Evidence on the diagnostic performance and real-world uptake of the new HE-specific code K76.82 is scarce and limited to hospital cohorts. We aimed to evaluate K76.82 adoption in U.S. clinical practice using a large dataset and assess its impact on coding specificity, critical for reimbursement tracking, and evaluation of HE care pathways.
Method: We analyzed Komodo's Healthcare Map, a U.S. claims database, including adults with cirrhosis hospitalized for acute decompensation (ascites, variceal bleeding, HE) and/or bacterial infection between January 2021 and December 2024 (N = 2,121,419). Annual use of K76.82 ICD code was compared with K72.90, K72.91, R27.8, R40.2, and K72.90 plus lactulose or rifaximin. In total, 2,845,899 codes occurrences were considered and normalized to 100% per year. Yearly proportions reflect each strategy's share of HE-coded events among all combined strategies. A Cochran–Armitage trend test was applied to evaluate the statistical significance of changes in the proportion of HE-coded events across years.
Results: K76.82 adoption rose rapidly: 17.81% in 2022, 64.99% in 2023, and 66.49% in 2024. Conversely, K72.90 declined from 70.07% in 2022 to 28.59% in 2023, remaining stable in 2024 at 28.34%. Codes K72.91 and K72.90 with lactulose/rifaximin dropped sharply between 2022 and 2024 (from 4.62% to 0.75% and from 3.11% to 0.68%, respectively), while R27.8 and R40.2 remained stable at about 2% each. A Cochran–Armitage test confirmed a significant upward trend in K76.82 adoption (p < 0.0001).
Conclusion: Within two years of introduction, K76.82 achieved substantial adoption in HE coding-related U.S. practice, progressively replacing nonspecific codes used for HE in the past and medication-based proxies, thereby enhancing specificity for HE identification in administrative datasets. This improvement supports more accurate evaluation of care pathways and reimbursement monitoring. To our knowledge, this is the first large-scale analysis (> 2 million patients) demonstrating real-world utilization; similar assessments in European cohorts are warranted to confirm coding harmonization.

WED-500
Post trans-jugular intrahepatic portosystemic shunt development of hepatic encephalopathy is not changed by early prophylactic treatment and does not increase mortality

Anna Rozenfeld Hemed[1], Niv Zmora[1], Oren Shibolet[1], Liane Rabinowich[1]. [1]*Tel-Aviv Medical Center, Tel Aviv and Gray Faculty of Medicine, Tel Aviv University, Tel Aviv, Israel*
E-mail: annaroz7@gmail.com

Background and aims: Background: Hepatic encephalopathy (HE) after transjugular intrahepatic portosystemic shunt (TIPS) affects 35–50% of patients. Use of prophylactic agents (Lactulose and Rifaximin) to prevent post-TIPS HE remains controversial and currently not recommended by professional guidelines. Aim: To assess real world practice and identify potential predictors for post-TIPS HE and benefit from post-TIPS prophylaxis.
Method: Retrospective cohort study of patients undergoing TIPS at the Tel-Aviv Medical Center (2016–2024). The primary outcome was HE, with secondary outcomes of liver transplantation (LT) and mortality.
Results: Seventy-one patients underwent TIPS, the median age was 64.5 years and 53% were male. Primary liver disease was metabolic-dysfunction-associated-steatohepatitis in 34%, viral (20%), and alcohol (22%). Indications for TIPS were variceal bleeding (53.5%) and refractory ascites (35%). Prior to the procedure 22% had has at least one episode of HE and 24% were treated with Lactulose and/or Rifaximin. At the time of the procedure, Child-Pugh class was A/B/C in 25%/62%/6%, with a median MELD-Na of 10. Following TIPS, 55% received prophylactic treatment (Lactulose, rifaximin, or both). HE developed in 62% (14% in-hospital, 55% within one year). Development of HE was not predicted by pre-or post-TIPS MELD-Na or Child-Pugh score, TIPS diameter and post-TIPS gradient, or post-procedure ammonia levels. Rates of HE also did not differ according to initial prophylaxis treatment (56% with treatment, 69% without, p = 0.28), however in both groups INR was related to risk for post-TIPS-HE (p = 0.01). Statin therapy was documented in 18% of patients. Post-TIPS HE occurred in 21% of statin-treated patients compared to 17% of those not receiving statins (p = 0.71), with no association between statin use and HE development. Overall mortality was 26% vrsus 19% among patients developing HE. Four patients underwent LT.
Conclusion: Early post-TIPS prophylactic was predominantly administered to patients previously treated for HE and did not reduce post-TIPS HE rates. Development of HE was not associated with increased mortality.

WED-501-YI
Comparison of the safety and efficacy of tailored versus fixed-dose albumin in cirrhosis with sepsis-associated acute kidney injury: a randomised controlled trial

Shreyas Sarvesh[1], Rakhi Maiwall[1], Ankit Bhardwaj[1], Satender Pal Singh[1], Rajan Vijayaraghavan[1], Chitranshu Vashitshtha[1], Ankur Jindal[1], Shalini Thapar[1], Dr. Prashant Mohan Agarwal[1], Mradul Daga[1], Deepak Tempe[1], Manoj Kumar[1], Shiv Kumar Sarin[1]. [1]*Institute of Liver & Biliary Sciences, New Delhi, India*
E-mail: rakhi_2011@yahoo.co.in

Background and aims: Sepsis-associated acute kidney injury (SA-AKI) in cirrhosis is marked by circulatory dysfunction and frequent cardiopulmonary complications. Fixed-dose albumin may cause more pulmonary complications. We compared a point-of-care

ultrasound (POCUS)–guided tailored albumin strategy with fixed-dose albumin in cirrhotic patients with SA-AKI.
Method: In this single-centre, open-label randomised controlled trial, adults with cirrhosis and SA-AKI with proven or suspected sepsis were randomised 1:1 to POCUS-guided tailored 25% albumin or fixed-dose albumin (1 g/kg/day). The primary outcome was AKI resolution at 48 hours without cardiopulmonary complications.
Results: A total of 100 patients were analysed (tailored, n = 50; fixed, n = 50). Baseline characteristics were comparable, including age, MELD-Na, SOFA score, lactate, and proven sepsis (86% vs 84%; p = 0.98). The majority had spontaneous bacterial peritonitis (58% vs 52%; p = 0.64), and nosocomial acquisition was seen in (30% vs 28%; p = 0.89). AKI resolution (complete/partial) at 48 hours without cardiopulmonary complications was significantly higher with tailored dosing (42% vs 14%; p = 0.03). By day 7, AKI recovery remained superior in the tailored group (78.0% vs 52%; p = 0.02). Cumulative albumin dose was significantly lower in the tailored arm at 48 hours (107.1 ± 35.5 g vs 147.0 ± 24.8 g; p < 0.001) and at day 7 (162.1 ± 77.5 g vs 228.4 ± 80.8 g; p < 0.001). Cardiopulmonary complications were markedly reduced with tailored dosing (22% vs 78%; p < 0.001). On multivariate analysis, POCUS-guided tailored strategy (OR = 4.81,0.94–24.62) lower SOFA score (OR = 0.53,0.30–0.95), andNT-proBNP (OR = 0.997,0.995–1.000, and lower urea (OR = 0.94,0.90–0.98), and Δchange in inferior vena cava diameter (OR = 0.34,0.16–0.73,) independently predicted AKI resolution. The patients who required oxygen support were lower in the tailored-dose group versus the fixed-dose group (22% vs 80%; p < 0.001). The time to initiation of vasopressor therapy was delayed in the tailored-dose group [80 h (78–86) vs 42 h (29–50); p < 0.001].
Conclusion: POCUS-guided tailored albumin therapy leads to early AKI resolution with a significantly lower incidence of cardiopulmonary complications, the need for dialysis, and a reduced cumulative albumin dose in cirrhosis with SA-AKI. Lower SOFA score and NT-proBNP, the delta change in vena cava diameter and lower urea independently predict AKI resolution in SA-AKI.
Clinical trial.gov - CTRI registration CTRI/2025/02/079902

WED-505
RAAS inhibitors reduces mortality in a real-world multicentre study of liver cirrhosis
N Apoorva Sasikumar[1], Margaret Teng[1,2], Cheng Han Ng[2,3,4], Vincent Chen[5], Jimmy Che-To Lai[6], Karn Wijarnpreecha[7], Rahul Kumar[8], Apichat Kaewdech[9], Masayuki Ueno[10], Anand Kulkarni[11], Ming-Hua Zheng[12], Akash Roy[13], Ken Liu[14,15], Chitchai Rattananukrom[16], Mazen Noureddin[17], Mohammad Shadab Siddiqui[18], Mark Muthiah[1,2,19], Hirokazu Takahashi[20]. *[1]Alexandra Hospital, Singapore, Singapore; [2]National University Hospital, Singapore, Singapore; [3]Kurume University School of Medicine, Kurume, Japan; [4]Graduate School of Medicine, Yokohama City University, Kanagawa, Japan; [5]University of Michigan Medical School, Michigan, United States; [6]The Chinese University of Hong Kong, Hong Kong, Hong Kong; [7]University of Arizona College of Medicine Phoenix, Arizona, United States; [8]Changi General Hospital, Singapore, Singapore; [9]Prince of Songkla University, Songkhla, Thailand; [10]Kurashiki Central Hospital, Kurashiki, Japan; [11]Asian Institute of Gastroenterology, Hyderabad, India; [12]First Affiliated Hospital of Wenzhou Medical University, Wenzhou, China; [13]Apollo Multispeciality Hospital, Kolkata, India; [14]Royal Prince Alfred Hospital, Sydney, Australia; [15]University of Sydney, Sydney, Australia; [16]Srinagarind Hospital, Khon Kaen University, Khon Kaen, Thailand; [17]Houston Methodist Hospital and Houston Research Institute, Texas, United States; [18]University of Virginia School of Medicine, Virginia, United States; [19]National University Centre for Organ Transplantation, National University Health System, Singapore, Singapore; [20]Saga University, Saga, Japan*
E-mail: tenglpm@gmail.com

Background and aims: Renin–angiotensin–aldosterone system inhibitors (RAASi), including angiotensin-converting enzyme inhibitors and angiotensin receptor blockers, are frequently prescribed in patients with cirrhosis for cardiometabolic comorbidities, yet their impact on liver-related outcomes remains uncertain. This study evaluated the association between RAASi use and risks of hepatic decompensation and all-cause mortality in a real-world multicentre cohort of patients with liver cirrhosis.
Method: We conducted an observational study of 1063 patients with cirrhosis, including 501 RAASi users and 562 non-users. RAASi users were older and had a higher burden of metabolic comorbidities and chronic kidney disease. Inverse probability of treatment weighting (IPTW) was applied to balance baseline characteristics. Subdistribution hazard ratios (SHRs) were estimated for hepatic decompensation and all-cause mortality, with stratified analyses by cirrhosis risk category and exploratory analyses by decompensation and mortality subtypes.
Results: After IPTW, covariate balance was achieved with minimal residual imbalance. RAASi use was not associated with a reduced risk of hepatic decompensation in the overall cohort (SHR 0.87, 95% CI 0.63–1.21) or across individual decompensation phenotypes, including ascites, variceal bleeding, hepatic encephalopathy, and spontaneous bacterial peritonitis. In contrast, RAASi use was associated with a significantly lower risk of all-cause mortality (SHR 0.54, 95% CI 0.34–0.88). This mortality benefit was most pronounced in patients with moderate-risk cirrhosis (SHR 0.43, 95% CI 0.21–0.90) and was not statistically significant in high-risk cirrhosis. No differential associations were observed for hepatic versus non-hepatic causes of death.
Conclusion: In this multicentre real-world cohort, RAAS inhibitor use was associated with reduced all-cause mortality without an increase in hepatic decompensation. These findings support the safety of RAASi in selected patients with cirrhosis and suggest a potential survival benefit, particularly at moderate disease severity.

WED-506
Influence of albumin treatment duration on outcome of terlipressin therapy in patients with hepatorenal syndrome – acute kidney injury
Eva Maria Schleicher[1], Christian Labenz[1], Frank Erhard Uschner[2], Julian Pohl[3], Moritz Passenberg[4], Michael Praktiknjo[2], Christoph Welsch[5], Henrik Karbannek[6], Nina Böhling[7], Karsten Große[8], Marlene Reincke[9], Benjamin Maasoumy[10], Paul Jamme[11], Julian Cardinal von Widdern[12], Marcus Mücke[5], Jonel Trebicka[2], Cornelius Engelmann[3], Jassin Rashidi-Alavijeh[4], Cristina Ripoll[6], Dominik Bettinger[9]. *[1]University Medical Center of the Johannes Gutenberg-University, Mainz, Germany; [2]Department of Internal Medicine B, University Hospital Münster, Münster, Germany; [3]Department of Hepatology and Gastroenterology, Charité-Universitätsmedizin Berlin, Berlin, Germany; [4]Department of Gastroenterology, Hepatology and Transplant Medicine, University of Duisburg-Essen, Essen, Germany; [5]Medical Clinic 1, University Hospital, Goethe-University Frankfurt, Frankfurt am Main, Germany; [6]Department of Internal Medicine IV, Jena University Hospital, Jena, Germany; [7]Department of Internal Medicine I, Bonn University Hospital, Bonn, Germany; [8]Department of Internal Medicine III, University Hospital RWTH Aachen, Aachen, Germany; [9]Department of Medicine II, Medical Center University of Freiburg, Freiburg, Germany; [10]Department of Gastroenterology, Hepatology, Infectious Diseases and Endocrinology, Hannover Medical School, Hannover, Germany; [11]Department of Internal Medicine II, LMU University Hospital Munich, München, Germany; [12]Department of Internal Medicine I, University Hospital Halle, Martin-Luther-University Halle-Wittenberg, Halle, Germany*
E-mail: eva.schleicher@unimedizin-mainz.de

Background and aims: Volume expansion with albumin is recommended to establish a diagnosis of hepatorenal syndrome–acute kidney injury (HRS-AKI). Determining the optimal duration of albumin administration involves a careful balance between

minimizing the risk of overtreatment and ensuring timely diagnosis and therapy, while acknowledging the potential, but uncertain, impact on prognosis. Therefore, this study aimed to compare the effects of different albumin treatment durations on terlipressin response and the prognosis of patients with HRS-AKI treated with terlipressin and albumin.

Method: This multicenter retrospective study recruited 490 patients with HRS-AKI treated with terlipressin at 12 German centers. 145 patients were available for further analysis. The cohort was dichotomized into patients treated with albumin before initiation of terlipressin for <24 hours and for 24–60 hours. Patients were followed for treatment response to terlipressin, death, hemodialysis (HD), or liver transplantation (LTX).

Results: Median MELD score of the cohort was 25 [IQR 21; 31]. Most patients were classified as Child-Pugh class C (55%) or B (45%). Chronic kidney disease (CKD) was reported in 32%. Acute-on-chronic liver failure (ACLF) was present in 67% of patients, and 26% had a history of HRS-AKI. At the time of AKI diagnosis, stage 1 AKI was observed in 41% of patients, stage 2 in 28%, and stage 3 in 31%. During follow-up, 59 patients (40.7%) reached a complete response to treatment with terlipressin, and 96 patients (66.2%) died or received a LTX. In a multivariable Fine and Gray analysis of predictors of any response to terlipressin therapy, albumin duration was not associated with a complete response to terlipressin (sHR 0.94; 95% CI 0.65–1.34; $p = 0.70$). In further multivariable models the influence of albumin treatment duration on the likelihood of achieving any response did not change (HR 1.01; 95% CI 0.69–1.47; $p = 0.95$). Of note, albumin treatment duration did not affect HD-/LTX-free survival, neither in univariable nor multivariable analyses.

Conclusion: This study provides real-world evidence to inform current clinical practice by demonstrating that albumin treatment duration (24 or 48 hours) had no significant impact on terlipressin treatment response. These results suggest that ensuring a sufficient duration of albumin therapy (48 hours) can prevent unnecessary terlipressin overtreatment and help optimize management protocols for HRS-AKI by aligning timely diagnosis with optimal treatment effectiveness.

WED-507

Dynamic spleen stiffness measurement as a prognostic tool in critically Ill patients with cirrhosis and ACLF

Elena von Maldeghem[1], Philipp Kalus[1], Sophia Rusch[1], Patricia Mester-Pavel[1], Vlad Pavel[1], Martina Müller-Schilling[1], Stephan Schmid[1]. [1]*Universitätsklinikum Regensburg, Regensburg, Germany*
E-mail: stephan.schmid@ukr.de

Background and aims: Non-invasive elastography techniques are well established for the assessment of liver fibrosis and portal hypertension. While liver stiffness measurement is routinely applied, spleen stiffness has emerged as a promising surrogate marker of portal hypertension. However, data on its feasibility and clinical relevance in the intensive care unit (ICU), particularly in patients with cirrhosis and acute-on-chronic liver failure (ACLF), remain scarce. This prospective study aimed to evaluate the feasibility of serial spleen stiffness measurements using acoustic radiation force impulse (ARFI) elastography in critically ill patients and to assess their association with clinical course and outcomes.

Method: A total of 44 ICU patients with chronic liver disease, with and without ACLF, were prospectively enrolled. Spleen stiffness was measured every 2–4 days using ARFI elastography. Clinical parameters including liver and renal function, ventilation settings, use of organ support therapies, and outcome data were recorded and analyzed.

Results: ARFI-based spleen stiffness measurement was feasible in all patients. Higher spleen stiffness values were significantly associated with the need for renal replacement therapy ($p < 0.001$) and invasive mechanical ventilation ($p < 0.001$). An inverse correlation was observed between ventilation pressures and spleen stiffness ($p = 0.017$), suggesting a potential mechanical influence on measurements. No significant associations were found with age, body mass index, or vasopressor requirement. Serial measurements revealed dynamic changes in spleen stiffness that paralleled the clinical course and evolution of organ dysfunction.

Conclusion: Serial ARFI-based spleen stiffness measurement is feasible and reliable in critically ill patients with cirrhosis in the ICU setting. Beyond reflecting portal hypertension, spleen stiffness values were associated with extrahepatic organ dysfunction and markers of organ failure. Spleen stiffness may therefore represent a non-invasive, bedside-available biomarker for dynamic risk stratification and clinical monitoring in patients with cirrhosis and ACLF.

WED-508

Systemic inflammation identifies patients with decompensated cirrhosis at high risk for further decompensating events

Christian Sebesta[1,2,3], Benedikt Simbrunner[1,2,3,4], Georg Kramer[1,2,3,4], Paul Thöne[1,2,3], Marlene Hintersteininger[1,2,3], Jan Embacher[1,3], Lucie Simonis[1,3], Lorenz Balcar[1,2,3], Benedikt Hofer[1,2,3,4], Lukas Hartl[1,2,3], Mathias Jachs[1,2,3], Georg Semmler[1,2,3], Philipp Schwabl[1,2,3,4], Bernhard Scheiner[1,2,3], Dalila Costa[1,5,6], Albert Friedrich Stättermayer[1,2], Michael Trauner[1,3], Mattias Mandorfer[1,2,3], Thomas Reiberger[1,2,3,4]. [1]*Division of Gastroenterology and Hepatology, Department of Medicine III, Medical University of Vienna, Vienna, Austria, Vienna, Austria;* [2]*Vienna Hepatic Hemodynamic Lab, Division of Gastroenterology and Hepatology, Department of Medicine III, Medical University of Vienna, Vienna, Austria, Vienna, Austria;* [3]*Clinical Research Group MOTION, Medical University of Vienna, Vienna, Austria, Vienna, Austria;* [4]*Christian-Doppler Laboratory for Portal Hypertension and Liver Fibrosis, Medical University of Vienna, Vienna, Austria, Vienna, Austria;* [5]*Gastroenterology Department, Braga Hospital, Braga, Portugal, Braga, Portugal;* [6]*Life and Health Sciences Research Institute (ICVS), School of Medicine, University of Minho, Braga, Portugal, Braga, Portugal*
E-mail: christian.a.sebesta@meduniwien.ac.at

Background and aims: In decompensated cirrhosis (DC), hepatic dysfunction, portal hypertension (PH) and systemic inflammation (SI) may represent differential drivers of further decompensation (FD) and liver-related death (LRD). This study aimed to (i) validate our recently proposed SI biomarker C-reactive protein (CRP, ≥0.5 mg/dL) and interleukin-6 (IL-6, ≥14 pg/mL) cutoffs (Costa/Simbrunner et al; JHepatol 2021) in a temporal validation cohort and (ii) evaluate their prognostic significance beyond MELD and PH severity.

Method: Patients with DC had SI biomarkers, MELD and hepatic venous pressure gradient (HVPG) measured and were followed for FD events and LRD as key outcomes. Multivariable regression models were adjusted for MELD, HVPG and SI biomarkers. Stratifications for MELD ≥ 15 (liver transplant cut-off) and HVPG ≥ 16 mmHg (severe PH) were applied.

Results: 278 patients (median age: 56 years; 64% male, alcohol: 66%) with DC (ascites: 92%, encephalopathy: 29%; bleeding: 8%) and median MELD: 13 and median HVPG: 19 mmHg were included. The incidence of FD and LRD after 1 year (Y1) was 27.7% and 13.7%, while 6.5% underwent transplantation. In multivariable Cox models adjusted for MELD and HVPG, both CRP and IL-6 were independently associated with 90-day FD (aHR logCRP: 2.48, $p < 0.001$; aHR logIL-6: 1.48, $p = 0.004$) and Y1 FD (aHR logCRP: 2.30, $p < 0.001$; aHR logIL-6: 1.37, $p = 0.007$). In models for LRD additionally adjusted for age, CRP predicted 90-day LRD (aHR logCRP: 2.50, $p = 0.035$), whereas logIL-6 showed only a trend (aHR logIL-6: 1.63, $p = 0.054$). Neither biomarker was associated with Y1 LRD. In competing-risk analyses (competing events: transplantation and non–LRD), CRP ≥ 0.5 mg/dL and IL-6 ≥ 14 pg/mL were both associated with a higher cumulative incidence of FD ($p < 0.05$). DC patient stratification by CRP ≥ 0.5 mg/dL and IL-6 ≥ 14 pg/mL, consistently identified patients at particularly high risk of

FD across MELD (≥15 vs. <15) and HVPG (≥16 vs <16 mmHg) risk groups.
Conclusion: In patients with DC, the SI biomarkers CRP and IL-6 predict the risk of FD events independently of hepatic dysfunction (MELD) and PH severity (HVPG). SI biomarkers may therefore be valuable for clinical risk stratification and for enriching DC trials with patients at high short-term risk for decompensating events.

WED-509-YI
Impact of jaundice on outcomes in patients with cirrhosis and ascites and implications for the definition of further decompensation
Lorenz Balcar[1,2], Markus Maagaard[3,4], Enrico Pompili[5,6], Valeria Santori[7], Lucie Simonis[1,2], Roberta Gagliardi[7], Jan Embacher[1,2], Mads Israelsen[3,4], Adrian Wunderbaldinger[1,2], Antonio Accetta[7], Christian Sebesta[1,2], Mattias Mandorfer[1,2], Michael Trauner[1], Paolo Angeli[7], Aleksander Krag[3,4], Thomas Reiberger[1,2], Paolo Caraceni[5,6], Salvatore Piano[7], Georg Semmler[1,2,3,4], Marta Tonon[7], Nikolaj Torp[3,4]. *[1]Division of Gastroenterology and Hepatology, Department of Medicine III, Medical University of Vienna, Vienna, Austria; [2]Vienna Hepatic Hemodynamic Lab, Division of Gastroenterology and Hepatology, Department of Medicine III, Medical University of Vienna, Vienna, Austria; [3]Centre for Liver Research (FLASH), Department of Gastroenterology and Hepatology, Odense University Hospital, Odense, Denmark; [4]Department of Clinical Research, Faculty of Health Sciences, University of Southern Denmark, Odense, Denmark; [5]Department of Medical and Surgical Sciences, University of Bologna, Bologna, Italy; [6]Unit of Semeiotics, Liver and Alcohol-Related Diseases, IRCCS Azienda Ospedaliero-Universitaria di Bologna, Bologna, Italy; [7]Unit of Internal Medicine and Hepatology (UIMH), Department of Medicine (DIMED), University of Padova, Padova, Italy*
E-mail: georg.semmler@meduniwien.ac.at

Background and aims: The role of jaundice in the natural history of cirrhosis is controversially discussed. Hence, the aim of this study was to evaluate the prognostic information derived from jaundice in patients with cirrhosis and ascites as single first decompensation.
Method: Retrospective cohort study including 875 patients with cirrhosis and ascites from four European tertiary centres followed from first hepatic decompensation with ascites (baseline). Time-dependent analyses were performed to evaluate the role of jaundice according to different bilirubin cut-offs (≥3/6/12 mg/dL) for liver-related mortality next to further decompensation as defined by Baveno VII.
Results: The median age was 57 years, the primary aetiology was alcohol-related liver disease (55%), 51% had grade 3 ascites and median MELD score was 14 at first hepatic decompensation. Bilirubin ≥ 3 mg/dL was present in 35% and ≥6 mg/dL in 10%, respectively. Patients were followed for a median of 3.9 years. The cumulative incidence of jaundicedefined by bilirubin ≥ 3 mg/dL at 1 year was 47%, 20% of ≥6 mg/dL, and 6.1% of ≥12 mg/dL, with ≥3 mg/dL yielding the best discrimination regarding liver-related mortality and being further investigated. Jaundice was an independent predictor of liver-related mortality in univariable and multivariable Cox regression analyses adjusting for age, sex, ascites grade, MELD, albumin and aetiological cure, but its consideration as further decompensation event worsened discrimination as compared to further decompensation without jaundice alone (C-statistics: 0.814 vs. 0.767, $p < 0.001$). Specifically, Simon-Makuch estimates for liver-related mortality were 23% vs. 6.6% in those with and without jaundice at 1 year, 43% vs. 4.0% in those with and without further decompensation, and 23% vs. 2.7% in those with the combined endpoint further decompensation and/or jaundice.
Conclusion: Jaundice is frequently co-occurring with ascites as first hepatic decompensation, and is associated with liver-related mortality. However, implementation of jaundice into the definition of further decompensation did not improve prognostication. This suggests that these two events should rather be handled separately than lumped together.

WED-510
Differentiation of minimal and grade 1 hepatic encephalopathy using neurophysiological, neuropsychological, magnetic resonance spectroscopic, and systemic inflammatory parameters
Barjesh Sharma[1,2,2], Lalit Kummetha[1], Shrey Bhatt[1], Venkatesh Sudharsan[1], Siddharth Srivastava[1], Kalpana Bansal[1], Bhawna Mahajan[1], Neera Chaudhry[1], Monica Tandon[1], Sanjeev Sachdeva[1], Ajay Kumar[1], Ashok Dalal[1], Ujjwal Sonika[1]. *[1]Govind Ballabh Pant Institute of Postgraduate Medical Education and Research (G.I.P.M.E.R), Gastroenterology, New Delhi, India; [2]Govind Ballabh Pant Hospital, Gastroenterology, New Delhi, India*
E-mail: barjeshchandersharma@gmail.com

Background and aims: Hepatic encephalopathy (HE) is traditionally classified into overt and minimal HE (MHE). The International Society for Hepatic Encephalopathy and Nitrogen Metabolism clubbed MHE and grade 1 HE in "covert" HE. However, these appear as distinct entities. This study aimed to compare inflammatory markers, magnetic resonance spectroscopy (MRS), Bispectral Index (BIS), spectral electroencephalography (EEG) parameters, and the natural history of MHE and grade 1 HE.
Method: In this prospective study, 150 cirrhotics were categorised into three groups: no HE (n = 50), MHE (n = 50), and grade 1 HE (n = 50). Patients were assessed using West Haven criteria grading, the psychometric hepatic encephalopathy score (PHES), critical flicker frequency (CFF), MRS, analysis of inflammatory markers (cytokines, endotoxin), Bispectral index (BIS), and spectral EEG. All patients were followed for HE progression, complications, hospitalisations, and mortality over 12 months.
Results: Patients with grade 1 HE showed significantly higher levels of ammonia (164.08 ± 30.12 vs 123.42 ± 19.97), endotoxins (0.60 ± 0.05 vs 0.47 ± 0.04) and cytokines compared to MHE. MRS revealed reduced myoinositol/choline ratios and elevated glutamine in HE groups. BIS and EEG metrics effectively distinguished MHE from grade 1 HE with high diagnostic accuracy. Model for End-Stage Liver Disease (MELD), IL-12, BIS, and EEG changes were independent predictors of survival.
Conclusion: MHE and grade 1 HE exhibit distinct inflammatory, neuropsychological, and neurophysiological profiles, as well as differences in survival. Incorporating multimodal biomarkers (CFF, MRS, BIS, EEG, and cytokines) facilitates early differentiation and risk stratification between MHE and grade 1 HE. These findings show that MHE and grade 1 HE are distinct entities.

WED-511
Burden and predictors of fatigue among patients with chronic liver disease
Ankita Singh[1], Akash Shukla[1], Gaurav Lodha[1]. *[1]Seth G S Medical College, Mumbai, India*
E-mail: drakashshukla@yahoo.com

Background and aims: Fatigue impairs health-related quality of life in chronic liver disease and is driven by both central and peripheral components, which should be evaluated in combination to enable a more accurate assessment of its overall burden. In this study, we aim to study the prevalence of fatigue in different etiologies and their predictors.
Method: Single-centre, cross-sectional study of patients with compensated advanced chronic liver disease (CACLD) and decompensated cirrhosis. FACIT-F (functional assessment of chronic illness therapy – fatigue scale), CES-D (centre for epidemiologic studies depression scale) and LFI (Liver frailty index) were used for comprehensive assessment of fatigue in the study population. Fatigue severity based on FACIT-F scores was categorized as mild (30–39), moderate (20–29), and severe (<20). CES-D scores >16 was considered to be associated with depressive features.

Results: A total of 100 patients were included in the study. The median age was 48 years (IQR 39–55), and 73 were men. Alcohol-related liver disease was the most common etiology (31%), followed by metabolic dysfunction–associated steatotic liver disease (MASLD) (19%) and hepatitis B (13%). 17 patients had cACLD, 69 were CTP-B and 14 were CTP C cirrhosis. The median FACIT-F score was 36 (IQR 25–42). Mean handgrip strength was 21 ± 6 kg, and mean LFI score was 4.3 ± 0.43. Overall, 62 patients reported fatigue, categorized as mild, moderate, and severe in 27 (43.5%), 22 (35.5%), and 13 (21%) of patients, respectively. Median CES-D score was 11 (IQR 4–23) and depressive features were observed in 42% of patients. Prevalence of fatigue was comparable between patients with CACLD and decompensated cirrhosis (64.7% vs 61.4%, p = 0.801). The presence of fatigue correlated with higher CES-D (p = 0.009) & LFI scores (p < 0.001); and with etiology [MASLD (15/19, 78.9%) and HCV (4/5, 80%) vs alcohol (54.8%), HBV (38.46%) and other etiologies].
Conclusion: Fatigue affects approximately two-thirds of patients with advanced chronic liver disease, and correlates with depressive features and etiology (MASLD and HCV) rather than decompensation.

WED-512-YI
Safety and outcomes of glp-1 receptor agonists in patients with cirrhosis: a meld-matched real-world cohort study
Abdullah Sohail[1], Zhexiang He[1], Sara Naimimohasses[1], Antonio Sanchez[1]. [1]*The University of Iowa, Iowa City, United States*
E-mail: antonio-sanchez@uiowa.edu

Background and aims: The safety of glucagon-like peptide-1 receptor agonists (GLP-1 RA) in cirrhosis is uncertain because these agents may alter gastrointestinal motility, biliary physiology, and metabolic parameters relevant to hepatic function. Prior studies have been limited by small sample sizes and inadequate adjustment for liver disease severity. Using a large, multicenter, real-world dataset, we evaluated the safety of GLP-1 RAs in patients with cirrhosis.
Method: Adults with cirrhosis were identified in the TriNetX Research Network and stratified into GLP-1 RA users and non-users. Patients with a history of liver transplantation, hepatocellular carcinoma, or pregnancy were excluded. Propensity score matching (1:1) generated two balanced cohorts of 28,091 patients each, matched on demographics, comorbidities, and MELD-related laboratory parameters (bilirubin, INR, creatinine, and sodium), yielding equivalent baseline liver disease severity. Outcomes at 90, 180, and 365 days included all-cause mortality, ascites, hepatic encephalopathy, spontaneous bacterial peritonitis (SBP), esophageal variceal bleeding, sepsis, pancreatitis, gastroparesis, and gallbladder disease.
Results: At 90 days, mortality was significantly lower in GLP-1 RA users (4.0%) than in non-users (8.4%) (risk difference −4.4%, 95% CI −4.8 to −4.0; p < 0.001). At 180 days, SBP occurred in 0.7% of GLP-1 RA users versus 1.6% of non-users (risk difference −0.9%, 95% CI −1.1 to −0.8; p < 0.001), while variceal bleeding rates were similar (1.5% vs 1.6%; p = 0.515). At 1 year, mortality remained significantly lower among GLP-1 RA users (7.3%) than non-users (13.7%) (risk difference −6.4%, 95% CI −6.9 to −5.9; p < 0.001), with corresponding survival probabilities of 91.6% and 83.6%. Across all time points, GLP-1 RA use was not associated with increased risk of hepatic decompensation, infectious complications, pancreatitis, gastroparesis, or gallbladder disease; hazard ratios consistently favored GLP-1 RA users, including an HR of 0.39 for SBP at 180 days (95% CI 0.33–0.46).
Conclusion: In this large matched real-world cohort of patients with cirrhosis with MELD-aligned baseline liver disease severity, GLP-1 RA exposure was not associated with excess hepatic or gastrointestinal complications. It was associated with significantly lower short- and intermediate-term mortality and reduced SBP incidence. These data support the safety of GLP-1 RAs in appropriately selected patients with cirrhosis and highlight the need for prospective validation.

WED-513
Outpatient albumin infusions reduce paracentesis without increasing costs in cirrhosis: a national real-world cost-comparison study
Siddharth Sood[1,2], Michael Mil[2], Nicholas Hannah[1,2,3], Catherine Yu[1], Natalie Ngu[4,5], Thang Dao[6], Jeremy Tse[5], James Williams[7], Lauren Tang[8], Callista Vania Raharjo[9], Benjamin Mead[10], Anna Ham[10], Samuel Wong[8], Ethan Tang[11], Dmitrii Shek[12], Daniel Clayton Chubb[4,13], Diana Lewis[1], Ammar Majeed[4,13], Jacob George[10,14,15], Kate Lynch[11,16], Golo Ahlenstiel[12,17], Rohit Sawhney[4,7], Jason Behary[9,18], Avik Majumdar[2,8], Jacinta Holmes[2,6], Sally Bell[4,5], Stuart Roberts[4,13]. [1]*Northern Health, Epping, Australia;* [2]*The University of Melbourne, Parkville, Australia;* [3]*The Royal Melbourne Hospital, Parkville, Australia;* [4]*Monash University, Clayton, Australia;* [5]*Monash Health, Clayton, Australia;* [6]*Saint Vincent's Hospital Melbourne, Fitzroy, Australia;* [7]*Eastern Health, Box Hill, Australia;* [8]*Austin Hospital, Heidelberg, Australia;* [9]*Saint George Hospital, Kogarah, Australia;* [10]*Westmead Hospital, Westmead, Australia;* [11]*Royal Adelaide Hospital, Adelaide Central Business District, Australia;* [12]*Blacktown Hospital, Blacktown, Australia;* [13]*Alfred Hospital, Melbourne CBD, Australia;* [14]*University of Sydney, Camperdown, Australia;* [15]*Storr Liver Centre, The Westmead Institute for Medical Research, Westmead, Australia;* [16]*The University of Adelaide, Adelaide Central Business District, Australia;* [17]*Western Sydney University, Blacktown, Australia;* [18]*University of New South Wales, Kensington, Australia*
E-mail: siddharth.sood1@nh.org.au

Background and aims: Refractory ascites reduces quality of life and drives high healthcare costs. Long-term human albumin therapy (HA) shows benefits in select groups, but real-world effectiveness remains unclear, limiting widespread adoption beyond a few countries. We evaluated healthcare utilisation and costs of HA compared to a historical cohort in Australia - the largest real-world analysis of HA outside Italy.
Method: A retrospective real-world healthcare cost-comparison study was conducted across 11 Australian centres through the Gastroenterology Society of Australia Liver Faculty Clinical Research Network comparing patients starting HA with a historical cohort. Exclusions: TIPPS, transplant, or PVT. Costs were based on predetermined estimates: A$357.55 for a medical day unit infusion, A $68.50 per 20 g albumin, A$1230 for outpatient abdominal or pleural paracentesis, and A$2195/night for inpatient admissions or ED presentation. Patients were censored at transplant, death, or 6 months follow-up. Appropriate statistical tests were applied to compare groups.
Results: We analysed 134 HA patients and 140 controls. Both groups were matched for age (p = 0.61), gender (p = 0.15), and MELD-Na (median 19.0 HA v 17.8 controls, p = 0.07). HA patients received 2298 infusions (avg 40 g/session). Ascites severity improved in more patients receiving HA (57.1%) than controls (26.7%) (RR 2.14, p < 0.0001) with a correlating reduction in paracentesis: 405 paracentesis in HA (median 0 per 100 patient days (100ptd) [IQR 0–1.7] vs 763 paracentesis in controls (2.7/100ptd [IQR 1.1–4.4]) p < 0.0001. Over 6 months there was no differences between groups with relation to admissions (188 vs 223, p = 0.27) nor length of stay (2.19 vs 2.72 days/100ptd, p = 0.15). Mortality did not differ (22/134 (16.4%) v 33/140 (23.6%)), although Kaplan-Meier curves appeared to diverge at 6 months (p = 0.67). More liver transplants occurred in the HA group (8, 5.97%) compared to controls (2, 1.43%), p = 0.045. Total healthcare costs for the HA group were A$4,643,788, compared to A $5,761,856 over 6 months. The median cost per patient/100ptd was A $12,627 (IQR 7459–28,369) for HA group and A$12,966 (IQR 5127–33,389) for controls, p = 0.72.
Conclusion: In a real-world Australian setting, HA did not increase healthcare costs. Importantly, patients receiving HA required significantly fewer paracentesis. Depending on local healthcare systems, HA

appears to offer a cost-neutral approach to improving care for patients with cirrhosis.

WED-514

Half-dose albumin for the prevention of post-paracentesis circulatory dysfunction (PPCD) in cirrhotic patients with acute decompensation undergoing paracentesis <5 liters: a randomized controlled trial

Pongnarin Nawalerspunya[1], Witchayaporn Praguylertluk[1], Suppana Chuensakul[2], Thanaput Kunlayawutipong[3], Suraphon Assawasuwannakit[4], Siwanon Nawalerspanya[5], Apichat Kaewdech[1], Naichaya Chamroonkul[1], Phunchai Charatcharoenwitthaya[6], Pimsiri Sripongpun[1]. *[1]Prince of Songkla University, Division of Internal Medicine, Faculty of Medicine, Hat Yai, Thailand; [2]Naresuan University Hospital, Amphoe Mueang Phitsanulok, Thailand; [3]Chiang Mai University, Amphoe Mueang Chiang Mai, Thailand; [4]Panyananthaphikkhu Chonprathan Medical Center Srinakharinwirot University, Amphoe Pak Kret, Thailand; [5]Paholpolpayuhasena Hospital, Amphoe Mueang Kanchanaburi, Thailand; [6]Siriraj Hospital Mahidol University, Bangkok, Thailand*
E-mail: pim072@hotmail.com

Background and aims: Albumin replacement (8 g/L) is suggested for large-volume paracentesis (>5 L) to prevent post-paracentesis circulatory dysfunction (PPCD), but not for modest-volume paracentesis (MVP; <5 L) in ambulatory settings, according to standard clinical guidelines. Nonetheless, patients with acute decompensation (AD) are more hemodynamically vulnerable. A prior study suggested that without albumin, patients with acute-on-chronic liver failure undergoing MVP experience PPCD rates of up to 70%, a risk significantly lowered by standard-dose albumin administration (8 g/L). Data regarding PPCD in AD settings are limited. Given the substantial cost of standard therapy and pilot data suggesting the non-inferiority of half-dose (4 g/L) in ambulatory settings, we aimed to determine whether half-dose albumin is effective in preventing PPCD in patients with AD undergoing MVP.
Method: This is a preliminery analysis of a multicenter, randomized, open-label, controlled trial. We included hospitalized patients with AD undergoing MVP. Patients with BCLC-D hepatocellular carcinoma, disseminated intravascular coagulation, and serum creatinine >1.5 mg/dL were key exclusion criteria. Eligible patients were randomized to receive either albumin replacement 4 g/L of ascites removed (ALB group) or no albumin replacement (Control group). The primary endpoint was PPCD, defined as a >50% increase in plasma renin activity on day 6 above baseline. Secondary outcomes included PPCD-related complications, in-hospital mortality, and 28-day mortality.
Results: Of 89 screened patients from 5 centers, 22 were eligible for analysis (ALB group: n = 9; Control group: n = 15). The cohort was 81.8% male with a mean age of 60.4 ± 11 years, baseline BMI of 25.2 ± 5.5 kg/m^2, and baseline serum albumin level of 2.7 ± 0.6 g/dL. The predominant etiology of cirrhosis was alcohol-related (50%). PPCD incidence was 44.4% in the ALB group vs 58.3% in the control group (p = 0.67). Acute kidney injury (AKI) within 6 days occurred in 11.1% vs 7.7% (p = 1.0), in-hospital mortality was 11.1% vs 15.4% (p = 1.0) in the ALB and control groups, respectively, and 28-day mortality was not significantly different between the two groups.
Conclusion: MVP increases the risk of PPCD in cirrhotic patients with AD. In this preliminary study, half-dose albumin replacement did not reduce the incidence of PPCD, AKI, in-hospital mortality, or 28-day mortality. The lower albumin dose may explain the difference in findings compared to earlier study.

WED-515

Early mortality prediction in cirrhotic patients presenting to the emergency department: the CIRR-SOS score

Leonardo Stella[1,2], Giuseppe Marrone[1], Luca Miele[1,3], Marco Biolato[1], Antonio Liguori[1,3], Antonio Gasbarrini[1,3], Francesco Franceschi[1,3], Francesca Romana Ponziani[1,3], Marcello Covino[1,3]. *[1]IRCCS Fondazione Policlinico A. Gemelli, Rome, Italy; [2]Link Campus University, Rome, Italy; [3]Università Cattolica del Sacro Cuore, Roma, Rome, Italy*
E-mail: leonardo.dr.stella@gmail.com

Background and aims: Patients with cirrhosis frequently present to the emergency department (ED) and are at high risk of early death. Existing prognostic scores are unreliable. We developed a pragmatic early-mortality score (the CIRRhotic patients Rapid Short-term Outcome Score, CIRR-SOS) for adults with cirrhosis presenting to the ED, and compared its performance with established prognostic systems.
Method: We performed a retrospective cohort study of consecutive adults with known cirrhosis presenting to the ED of a tertiary referral center between 2015 and 2024. 4.401 patients were included (28-day mortality 7.3%, 320 deaths). Candidate predictors were derived from vital signs, laboratory tests, and comorbidity burden (Charlson Comorbidity Index, CCI). Stepwise AUC-maximizing logistic regression with collinearity control was used to derive CIRR-SOS. Internal validation used five-fold stratified cross-validation under classic refit and fixed-score schemes, bootstrap resampling, and assessment of discrimination (AUC), calibration (Brier score, calibration plots), reclassification (continuous NRI), and clinical utility (decision curve analysis). CIRR-SOS was compared with other prognostic scores. Survival and risk trajectories were evaluated across CIRR-SOS tertiles using Kaplan–Meier and cumulative incidence analyses, and phenotypic clusters were explored via multidomain radar and chord plots.
Results: The ten independent predictors included in the CIRR-SOS were bilirubin, INR, creatinine, white blood cell count, hemoglobin, oxygen saturation, arterial pressure range, respiratory rate, and comorbidity burden. The apparent AUC for 28-day mortality was 0.701 (95% CI 0.676–0.723), with a Brier score of 0.072 and good calibration. Both probability-based and point-based CIRR-SOS models achieved AUC 0.701, outperforming MELD, MELD-Na, CLIF-C AD, mSOFA, qSOFA, and CCI (all DeLong p < 0.02), and showed uniformly positive continuous NRI (Net Reclassification Improvement) versus all comparators. Cross-validation and bootstrap analyses confirmed stable performance (mean AUC ~ 0.70) with consistent retention of core predictors. CIRR-SOS tertiles defined low-, intermediate-, and high-risk groups with 28-day mortalities of 9.1%, 18.8%, and 28.6%, respectively, with early separation of the high-risk group and later divergence between intermediate and low risk.
Conclusion: CIRR-SOS can be a simple, ED-focused, and clinically interpretable tool for early mortality risk stratification in adults with cirrhosis.

WED-516

A combination of normal inflammation parameters does not rule out infection in patients with acute decompensation

Marija Stojiljkovic[1], Stefanie Quickert[2], Vanessa Trentzsch[2], Philipp Reuken[2], Andreas Stallmach[2], Alexander Zipprich[2], Cristina Ripoll[2]. *[1]Jena University Hospital, Department of Internal Medicine IV (Gastroenterology, Hepatology, Infectious Diseases and Central Endoscopy), Jena, Germany; [2]Jena University Hospital, Jena, Germany*
E-mail: vanessa.trentzsch@med.uni-jena.de

Background and aims: Acute decompensation (AD) in cirrhosis is frequently precipitated by infections. Work-up to rule out infections may be resource and time consuming. C reactive protein alone is not useful to rule out infection, since this may be normal in cirrhosis despite infection. Nevertheless, in clinical practice decisions are based on a combination of parameters including both clinical signs and several lab tests. The aim of this study was to evaluate whether

the combination of biochemical inflammatory parameters can be used to rule out infection in patients with AD.
Method: Retrospective monocentric study including all patients with cirrhosis and AD and confirmed infections were included. Patients with increase in 1, 2 or 3 inflammatory parameters [CRP (c-reactive protein), leucocytes and PCT (procalcitonin)]. Variables are reported as n (percent), or median (IQR) according to distribution.
Results: A total of 123 patients (Child Pugh A 16 (13%), B 49 (39.8%), C 58 (47.2%), MELD 19 (14–25), median age 63 (52–71) years, male 77 (63%) with mainly alcohol related liver disease 74 (61%) were included. Infections included pneumonia in 23, UTI (urinary tract infections) in 42, bacteremia in 22, cholangitis in 1, SBP (spontaneous bacterial peritonitis) 12, combination in 23. Only 25/122 (21%) had fever (≥37.8°C). Median CRP, PCT and leucocytes was (41.8 (20.9–67.4) mg/dL, 0.58 (0.22–1.18) ng/ml, 8.8 (6.2–14) 10^3/mL, respectively. Notably, 8 patients (6,5%) had completely normal inflammatory parameters. None of these patients had fever, one patient had left shifting (84%) and one patient had leucopenia. From the other patients 29.3, 34.1 and 30.1% of patients had 1, 2 or 3 high serum inflammatory parameters. Isolated CRP was the only inflammatory parameter in all patients who had only one inflammatory parameter, albeit in 3 patients this increase was only mild (≤10 mg/dL). If slight abnormal levels CRP (<10 mg/dL) and leucocytes (<15.000) are disregarded, than up to 11% (n = 13) of infections would be overseen.
Conclusion: Bacterial infections occur in 6.5% of patients despite normal inflammatory markers, and must thoroughly excluded even when laboratory values are unremarkable.

WED-517
Prognostic value of morphological imaging features in liver cirrhosis: a cohort study
Signe Swerkersson[1,2,3], Wolf Bartholomä[1,2,4], Olof Dahlqvist Leinhard[1,2,5], Mikael Forsgren[1,2,5], Henrik Stjernman[6], Daniel Sjögren[1,7], Patrik Nasr[1,2,8], Markus Holmberg[1], Peter Lundberg[1,2,4], Martin Rejler[6,9], Nils Dahlström[1,2,4], Stergios Kechagias[1], Mattias Ekstedt[1,2]. *[1]Department of health, medicine and caring sciences, Linköping university, Linköping, Sweden; [2]Center for medical image science and visualization (CMIV), Linköping university, Linköping, Sweden; [3]Clinical department of radiology, Capio St Göran hospital, Stockholm, Sweden; [4]Clinical department of radiology in Linköping, Region Östergötland, Linköping, Sweden; [5]AMRA Medical AB, Linköping, Sweden; [6]Department of internal medicine, Ryhov hospital, Region Jönköping County Council, Jönköping, Sweden; [7]Department of medicine, Eksjö Hospital, Region Jönköping County Council, Eksjö, Sweden; [8]Wallenberg center for molecular medicine (WCMM), Linköping university, Linköping, Sweden; [9]The Jönköping academy for improvement of health and welfare, Hälsohögskolan, Jönköping university, Jönköping, Sweden*
E-mail: signe.swerkersson@liu.se

Background and aims: Current guidelines prioritize liver stiffness measurement for diagnosing and monitoring cirrhosis, while imaging is considered supportive. Nevertheless, Magnetic Resonance Imaging (MRI), Computed Tomography (CT), and ultrasound remain widely used. Certain MRI features—such as surface nodularity and portosystemic collaterals—may indicate disease progression and risk of decompensation, yet their prognostic value and reproducibility are poorly defined. We aimed to determine whether morphological MRI features predict decompensation and to measure interreader agreement of the assessments.
Method: In a prospective, multicenter cohort study 150 patients with liver cirrhosis underwent hepatocellular carcinoma surveillance with abbreviated MRI. Baseline T1-weighted dynamic contrast MRIs were independently scored by two radiologists using a 5-point cirrhosis impression score based on anatomical features of chronic liver disease and portal hypertension (1 = none, 2 = subtle, 3 = moderate, 4 = evident, and 5 = severe changes). Patients were categorized into two groups: none–moderate changes versus evident–severe changes. Interreader agreement was evaluated with Cohen's kappa. Decompensation events during 2-year follow-up were compared between groups using Fisher's exact test ($p < 0.05$ considered significant).
Results: Of 131 evaluated patients (mean age 64 ± 11 years; 43% women), 31% had prior decompensation, but 90% were Child-Pugh A at baseline. Steatotic liver disease was predominant (72%), with 43% alcohol-related liver disease. Imaging grades were none (7%), subtle (16%), moderate (27%), evident (36%), and severe (13%). Nine patients (7%) developed decompensation (ascites, encephalopathy, and/or variceal bleeding) within a median of 220 days. All events occurred in the evident–severe group (9/60; 15%), none in the none–moderate group (0/71; $p < 0.001$). Sensitivity and negative predictive value were 100%, whereas specificity was 58% and positive predictive value 15%. Interreader agreement was moderate-substantial (kappa = 0.59).
Conclusion: Morphological MRI features are strongly associated with the risk of decompensation in cirrhosis and demonstrate good reproducibility between readers. These findings validate the clinical relevance of imaging-based stratification and suggest that morphological assessment may complement current monitoring strategies.

WED-521
Oral anticoagulant use and clinical outcomes in patients with cirrhosis: a United States national cohort study
Tomohiro Tanaka[1], Andrea Holcombe[2], Gosia Clore[2], Mingyue Sun[3], Alexandra Bixby[4], Jennifer Lai[5], David Axelrod[4]. *[1]University of Iowa Carver College of Medicine, Iowa City, United States; [2]Center for Access & Delivery Research and Evaluation (CADRE), Iowa City VA Health Care System, Iowa City, United States; [3]University of Iowa Health Care, Iowa City, United States; [4]University Hospitals - Cleveland Medical Center, Cleveland, United States; [5]University of California San Francisco, San Francisco, United States*
E-mail: tomohiro-tanaka@uiowa.edu

Background and aims: While the long term oral anticoagulation (OAC) in patients with cirrhosis has shifted from coumadin to direct oral anticoagulants (DOACs) based on ease of use and patient preference, the impact of this shift on patient mortality and access to liver transplantation (LT) has not been well characterized in a contemporary data set.
Method: We used Epic Cosmos, a vendor-facilitated patient-level electronic health record aggregation that includes longitudinal diagnoses, procesures, laboratory results, and prescription-dispensation records across participating health systems in the United States. We assessed the rate of morality and gastrointestinal bleeding (GIB) in adults with cirrhosis who were initiated DOACs with with patients placed on warfarin between January 2019 to November 2024. Four distinct propensity score (PS) matched cohorts were developed based on indication for OAC: all-indications, Atrial fibrillation (AF), venous thromboembolism (DVT/PE), and portal vein thrombosis (PVT). Mortality risk was calculated using Fine-Gray models with LT as a competing risk, and gastrointestinal bleeding (GIB) risk was assessed with death and LT as competing risks.
Results: Among 93,663 OAC initiators in the cohort, DOAC use increased from 74% in 2019 to more than 95% in 2024 (P <0.001). Among all patients, DOACs use was associated with higher risk of mortality (Subdistribution hazard ratio [sHR] 1.14, 95% CI 1.06–1.20) and GIB (sHR 1.16, 95% CI 1.04–1.28). In contrast, among patients with AF, DOACs did not increase either mortality or GIB (sHR 0.99, 95% CI 0.87–1.11 and sHR 1.19, 0.93–1.52, respectively). In the DVT/PE and PVT cohorts, DOACs were associated with a higher risk of mortality (sHR 1.22, 95% CI 1.10–1.33 and sHR 1.45, 95% CI 1.25–1.67, respectively), but not with GIB; DOAC users were less likely to undergo liver transplantation than warfarin users (Gray's test, p <0.001). Findings were consistent between the primary Fine-Gray models and supplemental Cox proportional hazard models, as well as across per-protocol marginal structural models and sensitivity analyses.

Conclusion: Among patients with cirrhosis who require oral anticoagulants for PE/DVT or PVT, DOAC use was associated with higher mortality and a lower likelihood of LT than warfarin. No differences were noted in the cohort with AF. This mortality differential highlights the need to better understand underlying mechanisms and support individualized, indication- and context-specific OAC for patients with cirrhosis.

WED-522

Rifaximin improves myosteatosis in decompensated cirrhosis - randomized trial

Sunil Taneja[1], Abhik Halder[1], Madhurima Sharma[1], Harish Bhujade[1], Yaswant Kumar[1], Amol Patil[1], Arka De[1], Nipun Verma[1], Madhumita Premkumar[1], Ajay Kumar Duseja[1]. *[1]Postgraduate Institute Of Medical Education And Research, Chandigarh, India*
E-mail: drsuniltaneja@hotmail.com

Background and aims: Myosteatosis has emerged as a distinct phenotype associated with muscle dysfunction, poor transplant outcomes and overall mortality in patients with decompensated cirrhosis. This study aimed to evaluate the efficacy of rifaximin in ameliorating myosteatosis in patients with decompensated cirrhosis.
Method: Out of 137 screened patients with decompensated cirrhosis, 95 (69.3%) had CT-defined myosteatosis. Eighty eligible patients were randomly assigned 1:1 to receive rifaximin plus standard medical therapy (rSMT, n = 40) and standard medical therapy alone (SMT, n = 40). The primary outcome was improvement in myosteatosis at six months. Secondary outcome measures included impact on frailty, body fat composition, muscle mass, prognostic scores, hospitalisation and survival.
Results: The cohort had a male predominance (68.8%, n = 55), with a mean age of 54 ± 9.0 years. The leading cause of cirrhosis was MASLD (52.5%, n = 42), followed by MetALD (22.5%, n = 18) and alcohol related cirrhosis (17.5%, n = 14). The rSMT group showed significant improvement in mean muscle attenuation (HU) from 16.97 ± 12.24 to 23.25 ± 9.92 ($p < 0.00$), compared to the SMT group ($p = 0.01$) at 6 months. The delta change in HU was significantly greater with rSMT (6.28 ± 5.94 vs. 4.48 ± 13.83; $p < 0.00$), with 88.9% showing HU improvement. Logistic regression identified rSMT as an independent predictor of ≥5% HU gain (OR = 0.33, $p = 0.04$). LFI improved modestly in both groups with no between-group difference. In the rSMT group, fat mass decreased from 21.15 (16.62–25.02) at baseline to 20.60 (17.62–24.20) at 6 months ($p = 0.03$). In the SMT group, fat mass decreased from 21.60 (15.05–29.38) to 21.05 (15.25–29.68) ($p = 0.34$). rSMT led to a significant increase in muscle mass ($p < 0.00$), while SMT showed a decline ($p = 0.00$); delta change favoured rSMT ($p < 0.00$). The phase angle improved in both groups, although the difference was non-significant. Prognostic scores improved significantly in the rSMT group, with greater reductions in MELD Na (−3.39 ± 5.36 vs. −1.10 ± 5.00; $p < 0.05$). Ascites control was superior in rSMT (75% vs. 42.1%; $p = 0.01$). Hospitalisation rates were lower (2.8% vs. 23.7%) and survival was higher (97.5% vs. 92.5%) in rSMT, though not statistically significant.
Conclusion: Rifaximin therapy in decompensated cirrhosis has a significant impact on improving myosteatosis, muscle mass, and disease severity, with better ascites control, a reduction in hospitalisation rate, and a trend toward improved survival.

WED-523

A multicentre multistate modelling on the natural history of liver decompensation: longitudinal analysis of 1450 patients

Nicole Shu Ying Tang[1], Eunice Xiang Xuan Tan[1,2,3], Nicholas Syn[1], Daniel Huang[1,2,3], Anand Kulkarni[4], Ming-Hua Zheng[5,6], Vincent Chen[7], Chitchai Rattananukrom[8], Jimmy Che-To Lai[9], Karn Wijarnpreecha[10], Rahul Kumar[11], Apichat Kaewdech[12], Masayuki Ueno[13,14], Akash Roy[15], Ken Liu[16,17], Mazen Noureddin[18,19], Mohammad Shadab Siddiqui[20], Hirokazu Takahashi[21,22], Cheng Han Ng[2,23,24], Mark Muthiah[1,2,3]. *[1]Yong Loo Lin School of Medicine, Singapore, Singapore; [2]Division of Gastroenterology and Hepatology, Department of Medicine, National University Hospital, Singapore, Singapore; [3]National University Centre for Organ Transplantation, National University Health System, Singapore, Singapore; [4]Department of Hepatology and Liver Transplant, Asian Institute of Gastroenterology, Hyderabad, India; [5]MAFLD Research Center, Department of Hepatology, First Affiliated Hospital of Wenzhou Medical University, Wenzhou, China; [6]Key Laboratory of Diagnosis and Treatment for the Development of Chronic Liver Disease, Zhejiang, Wenzhou, China; [7]Division of Gastroenterology and Hepatology, Department of Internal Medicine, University of Michigan, Ann Arbor, MI, United States; [8]Division of Gastroenterology and Hepatology, Department of Medicine, Faculty of Medicine, Srinagarind Hospital, Khon Kaen University, Khon Kaen 40002, Thailand; [9]Medical Data Analytics Centre, Department of Medicine and Therapeutics, The Chinese University of Hong Kong, Hong Kong, Hong Kong; [10]Division of Gastroenterology and Hepatology, Department of Medicine, University of Arizona College of Medicine, Phoenix, Arizona, United States; [11]Department of Gastroenterology, Changi General Hospital, Singapore, Singapore; [12]Gastroenterology and Hepatology Unit, Division of Internal Medicine, Faculty of Medicine, Prince of Songkla University, Songkhla, Thailand; [13]Department of Gastroenterology and Hepatology, Kurashiki Central Hospital, Kurashiki, Japan; [14]Department of Gastroenterology and Hepatology, Graduate School of Medicine, Kyoto University, Kyoto, Japan; [15]Institute of Gastrosciences and Liver Transplantation, Apollo Multi-speciality Hospitals, Kolkatta 700054, India; [16]A.W. Morrow Gastroenterology and Liver Centre, Australian Liver Transplant Unit, Royal Prince Alfred Hospital, Sydney, New South Wales, Australia; [17]Sydney Medical School, University of Sydney, Sydney, New South Wales, Australia; [18]Department of Medicine, Sherrie and Alan Conover Center for Liver Disease & Transplantation, Houston Methodist Hospital, Houston, TX, United States; [19]Houston Research Institute, Houston, TX, United States; [20]Division of Gastroenterology & Hepatology, School of Medicine, University of Virginia, Charlottesville, VA, United States; [21]Liver Center, Saga University Hospital, Saga, Japan; [22]Division of Metabolism and Endocrinology, Department of Medicine, Faculty of Medicine, Saga University, Saga, Japan; [23]Division of Gastroenterology, Department of Medicine, Kurume University School of Medicine, Kurume, Kurume, Japan; [24]Department of Gastroenterology and Hepatology, Yokohama City University School of Medicine, Kanazawa-ku, Yokohama, Japan*
E-mail: nicole.sytang@outlook.com

Background and aims: Cirrhosis often remains silent until decompensation, after which survival deteriorates sharply. Contemporary, transition-aware estimates are limited, especially in Asian-predominant cohorts. We analysed trajectories from compensated advanced chronic liver disease (cACLD) through sequential decompensations to death.
Method: In this multicentre study, we analyzed retrospective data from an adult cohort with liver stiffness ≥ 15 kPa from vibration-controlled transient elastography across 13 institutions internationally. Decompensation included ascites, hepatic encephalopathy, spontaneous bacterial peritonitis, or variceal bleeding. Multistate models were constructed to characterize patient trajectories across four main clinically meaningful states: baseline cACLD, first decompensation, a subsequent second decompensation, and death. Etiology-specific subgroup analyses were conducted, and effects of univariable predictors on transitions were also examined.
Results: Among 1450 patients, 162 (11.2%) developed a first decompensation over median follow-up of 4.27 years. From baseline cACLD, first decompensation occurred at 2.49 per 100 person-years with a median time of 1.57 years (IQR: 0.75–3.54), while death occurred at a rate of 1.01 per 100 person-years with a median time of 4.05 years (IQR: 2.55–6.30). The rate of a second decompensation was higher following the first decompensation, at 43.73 per 100 person-years at a median time of 0.44 (IQR: 0.19–1.07) years. Patients with alcohol-associated liver disease had the highest rate of progression

from baseline to first decompensation, whereas patients with metabolic dysfunction-associated steatotic liver disease had the highest progression rate into a second decompensation following a first decompensating event.
Conclusion: Most patients with cACLD remain compensated, but once decompensation occurs, trajectories accelerate and worsens survival. Transition-aware, etiology-stratified estimates enable individualized prognostication and earlier risk-guided intervention, including timely transplant referral.

WED-524
Active smoking is linked to persisting systemic inflammation and higher mortality after TIPS
Tammo Lambert Tergast[1], Marlene Hintersteininger[2], Ida Edler[1], Anja Tiede[1], Sarah Lisa Schütte[1], Jim Benjamin Mauz[1], Theresa Müllner-Bucsics[2], Paul Hemetsberger[2], Patrik Attalla[2], Lorenz Balcar[2], Benedikt Hofer[2], Michael Trauner[2], Mattias Mandorfer[2], Heiner Wedemeyer[1], Benjamin Maasoumy[1], Thomas Reiberger[2], Lukas Hartl[2]. *[1]Medizinische Hochschule Hannover, Department of Gastroenterology, Hepatology, Infectious Diseases and Endocrinology, Hannover, Germany; [2]Division of Gastroenterology and Hepatology, Department of Medicine III, Medical University of Vienna, Vienna, Austria*
E-mail: tergast.tammo@mh-hannover.de

Background and aims: Insertion of a transjugular intrahepatic portosystemic shunt (TIPS) is an effective therapy for patients with cirrhosis and portal hypertension-related complications. Smoking is common in patients with cirrhosis, however data on its effect on clinical outcomes after TIPS implantation are scarce. This study investigates the impact of smoking or history of smoking on the clinical course after TIPS implantation.
Method: All consecutive patients with cirrhosis undergoing covered TIPS implantation at the Vienna General Hospital (2005–2022) or Hannover Medical School (2009–2021) with available information on smoking status were included in this study. Furthermore, information regarding systemic inflammation using C-reactive protein (CRP) as a surrogate were collected at baseline (BL), 3 (M3) and 6 months (M6) after TIPS placement. To determine the clinical impact of smoking on clinical outcomes, competing risk regression (CRR) was performed.
Results: Overall, 616 patients were included (66% male, median MELD: 12; alcohol-related liver disease was the main etiology: 65.6%). Regarding smoking status, 106 (17.2%) individuals were former and 230 (37.3%) were active smokers. The median number of packyears among former and active smokers was 30.0 and 11.6% were diagnosed with chronic obstructive pulmonary disease. Severity of systemic inflammation decreased significantly after TIPS placement in never smokers (CRP at BL: 0.93 mg/dL vs. M3: 0.73 mg/dL vs. M6: 0.70 mg/dL; $p = 0.026$) and former smokers (CRT at BL: 0.87 mg/dL vs. M3: 0.43 mg/dL vs. M6: 0.46 mg/dL; $p < 0.001$), but not in active smokers (CRP at BL: 0.75 mg/dL vs. M3: 0.49 mg/dL vs. M6: 0.77 mg/dL; $p = 0.859$). On adjusted CRR analysis, both never smokers (asHR: 0.60, 95%CI: 0.36–0.82; $p = 0.004$) and former smokers (asHR: 0.54, 95%CI: 0.37–0.97; $p = 0.037$) showed a significantly lower risk of death compared to active smokers.
Conclusion: Ongoing smoking is associated with persisting inflammation after TIPS implantation and is independently linked to higher mortality.

WED-525
Incidence and predictors of overt hepatic encephalopathy after elective TIPS in cirrhosis: data from a prospective multicenter randomized controlled trial
Apolline Leproux[1], Luc Haudebourg[2], Hélène Larrue[3], Nicolas Weiss[2], Caroline Jezequel[4], Isabelle Mabile-Archambeaud[5], Louis Dalteroche[6], Sébastien Dharancy[7], Patrick Borentain[8], Frédéric Oberti[9], Aurélie Plessier[10], Nathalie Ganne-Carrié[11], Nicolas Carbonell[12], Marika Rudler[1], Christophe Bureau[3], Dominique Thabut[1]. *[1]Hepato-gastro-enterology Unit, APHP Sorbonne Universite, Pitie-Salpêtrière Hospital, 83 boulevard de l'hôpital, Paris, France; [2]Neurology ICU, APHP Sorbonne Universite, Pitie-Salpêtrière Hospital, 83 boulevard de l'hôpital, Paris, France; [3]Hepatology Unit, University Hospital of Toulouse and Toulouse III Paul Sabatier University, 1 avenue Jean Poulhes, Toulouse, France; [4]Hepatology Unit, University Hospital of Rennes Pontchaillou, 2, rue Henri Le Guilloux, Rennes, France; [5]Hepato-gastro-enterology and Digestive Oncology Unit, University Hospital Hôtel Dieu, 1 place Alexis Ricordeau, Nantes, France; [6]Hepatology Unit, Hôpital Trousseau, Tours University, Tours, France; [7]Hepato-gastro-enterology Unit, Huriez Hospital, Lille, France; [8]Hepato-gastro-enterology Unit, AP-HM, Timone University Hospital, 264, rue Saint-Pierre, Marseille, France; [9]Hepato-gastro-enterology Unit, University Hospital, HIFIH Laboratory, Angers, France; [10]Hepatology Unit, Beaujon University Hospital, 100 boulevard du general Leclerc, Clichy, France; [11]Hepatology Unit, Avicenne Hospital, APHP, Sorbonne Paris Nord University, INSERM UMR S-1138, FunGeST team, Centre de Recherche des Cordeliers, Sorbonne Universite, Paris, France; [12]Hepatology Unit, Saint Antoine University Hospital, 184 rue du Faubourg Saint Antoine, Paris, France*
E-mail: dthabut@gmail.com

Background and aims: Elective transjugular intra hepatic portosystemic shunt (TIPS) placement increases liver-transplant free survival (LTFS) and reduces further decompensation in cirrhosis with recurrent/refractory ascites or recurrent variceal bleeding. Although post-TIPS overt hepatic encephalopathy (OHE) remains frequent, predictive factors are difficult to establish due to heterogeneous retrospective studies, and its impact on mortality is debated. This study aimed to identify predictors of OHE and severe OHE (SOHE) after TIPS and to assess their prognostic value in a homogeneous population issued from a randomized controlled trial.
Method: This is an ancillary study of a multicenter, randomized, double-blind, placebo-controlled trial assessing the efficacy of rifaximin versus placebo in preventing OHE (grade ≥ 2) after elective TIPS in patients with cirrhosis. The primary endpoint was the incidence of OHE and SOHE (grade ≥ 3) at 3 months. Secondary endpoints included the incidence of OHE and SOHE (grade ≥ 3) at one-year, predictive factors for OHE and SOHE and liver-transplant free survival (LTFS), analyzed using Fine and Gray competing risk models and Cox regression, including time-dependent and landmark analyses.
Results: Among 186 patients who underwent TIPS, OHE occurred in 36.0% at 3 months and 46.2% at one year, and SOHE in 11.8% and 18.2%, respectively. Older age (HR 1.05, 95% CI 1.01–1.08, $p = 0.004$) and diabetes (HR 2.24, 95% CI 1.38–3.63, $p = 0.001$) were independently associated with OHE occurrence at both timepoints, while rifaximin was protective. MELD score independently predicted early SOHE ($p = 0.046$). MELD score ($p < 0.001$) and baseline B-type Natriuretic Peptide (BNP) ($p = 0.005$) were independently associated with reduced one-year LTFS. OHE, whether early or late, did not impact LTFS, but SOHE occurrence was significantly associated with reduced one-year LTFS ($p < 0.001$).
Conclusion: In patients who underwent elective TIPS, age and diabetes are independent predictors of post-TIPS OHE. Only severe OHE occurrence significantly impacted liver-transplant free survival.

WED-526-YI
Intestinal abundance of Enterococcus is linked to a higher risk of infection post transjugular intrahepatic portosystemic shunt (TIPS-) insertion: first results from the TIPINF study
Anja Tiede[1,2], Jenny Fiebig[3], Laura Buttler[1], Annika Zietz[1], Jim Benjamin Mauz[1], Jennifer Witt[1], Lea Wagner[1], Liv Grete Ahl[1], Matti Peperhove[4], Tammo Lambert Tergast[1], Sabrina Woltemate[3], Heiner Wedemeyer[1,2], Marius Vital[2,3], Benjamin Maasoumy[1,2]. *[1]Hannover Medical School, Department of Gastroenterology, Hepatology, Infectious Diseases and Endocrinology, Hannover, Germany; [2]German*

Center for Infection Research (DZIF), Hannover-Braunschweig, Germany; [3]Hannover Medical School, Institute for Medical Microbiology and Hospital Epidemiology, Hannover, Germany; [4]Hannover Medical School, Department of Diagnostic and Interventional Radiology, Hannover, Germany
E-mail: tiede.anja@mh-hannover.de

Background and aims: Intestinal dysbiosis has been linked to portal hypertension and disease progression in patients with cirrhosis. Moreover, distinct clusters of intestinal dysbiosis correlated with specific clinical complications such as hepatic encephalopathy (HE) and infections in decompensated cirrhosis. Transjugular intrahepatic portosystemic shunt (TIPS-) insertion is a relevant treatment option for portal hypertension. However, the impact of gut dysbiosis on the clinical course post TIPS-insertion remains largely unexplored.
Method: A number of 106 consecutive patients with decompensated liver cirrhosis undergoing TIPS-insertion between 09/2022 and 03/2025 were prospectively included in the TIPINF study. Patients were followed-up for occurrence of infection, HE, and death for one year post-TIPS. Of 47 patients, baseline stool samples (prior to TIPS) were available for the current analysis. Microbiome composition was assessed by metagenomic shotgun sequencing. Microbial clustering was based on Bray-Curtis dissimilarity and relative bacterial abundances.
Results: Patients were predominantly male (57%) with a median age of 60 years and MELD of 10. Most TIPS were implanted for treatment of refractory ascites (70%), with alcohol-related liver disease (47%) being the most common cirrhosis etiology. We identified three distinct microbiota patterns in our cohort: An Enterococcus-dominated (C1), a Bifidobacteria-dominant (C2), and a diverse microbiome clustering most similar to those of healthy individuals (C3). Of note, Enterococcus-dominance was linked to an intestinal abundance of fungi species e.g. Candida. During follow-up, 15 patients (32%) developed a bacterial infection. Enterococcus-abundance was linked to a significantly higher risk of bacterial infection (C1 vs C2+C3: HR 2.75, p = 0.04) in a competing risk analysis, which remained significant in the multivariable model after adjusting for baseline-MELD (C1 vs C2+C3: HR 4.24, p = 0.002). Moreover, patients with Enterococcus-dominance had a numerically higher incidence of overt HE (50% vs 31%). However, neither competing risk analysis for HE-development during follow-up nor Cox regression analysis for 1-year-mortality were statistically significant (C1 vs C2+C3: HR 1.95, p = 0.19; HR 2.24, p = 0.17).
Conclusion: Intestinal dysbiosis is associated with adverse clinical outcomes after TIPS-implantation. An Enterococcus-dominated microbiome is independently associated with an increased risk of post-TIPS bacterial infections.

WED-527
Effect of PPI exposure and discontinuation on infection outcomes in cirrhosis

Arianna Toscano[1], Maria Stella Franzè[1], Clelia Asero[1], Gaia Caccamo[1], Roberto Filomia[1], Concetta Pitrone[1], Carlo Saitta[1], Irene Cacciola[1].
[1]Unit of Medicine and Hepatology, University Hospital of Messina, Unit of Medicine and Hepatology, Department of Clinical and Experimental Medicine, University of Messina, Messina, Italy
E-mail: arianna.toscano13@gmail.com

Background and aims: Proton pump inhibitors (PPIs) are frequently prescribed, often without appropriate indications. Concerns are rising about inappropriate PPI use, as increasing evidence suggests a potential association between PPI exposure and several complications, including bacterial infections (BIs). This study aimed to evaluate the impact of PPI use on infections features, antibiotic failure, and survival in cirrhotic patients hospitalized for BIs.
Method: We retrospectively analysed 232 cirrhotic patients [137 males, median age 67 years] accounting for 255 infectious episodes, consecutively hospitalized from January 2009 to December 2016. Clinical, laboratory and microbiological data were collected. Data on PPI use, indication, type, and treatment discontinuation at discharge in case of improper prescription were collected. Follow-up was continued until the last available contact.
Results: One-hundred seventy-seven out of 232 patients (76.3%) were PPI users. Compared with non-users, PPI users presented higher rates of decompensation at admission (p = 0.010), higher procalcitonin levels (p = 0.014), a greater prevalence of spontaneous bacterial peritonitis (p = 0.031), as well as significantly higher rate of second antibiotic failure (p = 0.015). No significant differences were observed in mortality at 1 and 3 months or in readmission rates. In the univariate regression analysis, PPI use was associated with increased risk of jaundice (HR 1.85, 95% CI 1.29–2.66; p < 0.001), ascites (HR 3.14, 95% CI 1.99–5.00; p <0.001), and hepatic encephalopathy (HR 1.83, 95% CI 1.27–2.62; p = 0.001). PPI discontinuation was associated with a significantly reduced risk of death at both univariate (HR 0.31, 95% CI 0.15–0.64; p = 0.001) and multivariable ((HR 0.41, 95% CI 0.20–0.85, p = 0.017) regression analyses. Kaplan–Meier analysis confirmed significantly improved survival in patients who discontinued PPIs after infection resolution (p < 0.001).
Conclusion: Our findings suggest that ongoing PPI exposure may contribute to the development of major liver-related complications, whereas withdrawal of unnecessary PPI therapy was associated with a significant survival benefit. These findings support the importance of critically reassessing PPI indications in cirrhotic patients.

WED-528
UCH-L1 and GFAP as novel biomarkers for early detection of hepatic encephalopathy

Pere Vaquer-Grimalt[1], Apol·lonia Moll[2], María del Carmen Gassent[2], Ana Belén Martínez[3], Maria Inés Barceló[3], Lucía Bonet-Vidal[1], Juana Maria Ferrer[4], Ana Escarda Gelabert[1], Margalida Vanrell Garau[1], Daniel Morell[5], Lydia Sastre[1]. *[1]Department of Hepatology, Hospital Universitario Son Espases, Palma, Spain; [2]Department of Radiology, Hospital Universitario Son Espases, Palma, Spain; [3]Department of Neurology, Hospital Universitario Son Espases, Palma, Spain; [4]Department of Immunology, Hospital Universitario Son Espases, Palma, Spain; [5]Department of Laboratory Medicine, Hospital Universitario Son Espases, Palma, Spain*
E-mail: perevaquergrimalt@hotmail.com

Background and aims: Hepatic encephalopathy (HE) is a major decompensation in cirrhosis and a leading cause of hospitalization, with substantial clinical, psychosocial, and economic consequences. Diagnostic strategies have remained inadequate, particularly for covert HE, which relies on the Psychometric Hepatic Encephalopathy Score (PHES), a tool infrequently used and insufficiently sensitive. As a result, many patients remain undiagnosed despite their increased risk of progression. We evaluated brain-injury biomarkers as objective and accessible tools for detecting minimal HE (MHE) and overt HE (OHE).
Method: Single-center, cross-sectional study including healthy controls, cirrhotic outpatients (non-HE and MHE), and hospitalized patients with OHE. Exclusion criteria were prior OHE, neurological or psychiatric disease, hepatocellular carcinoma, recent major surgery, chronic heart disease, long-standing type 2 diabetes, or HIV. All outpatients and controls underwent PHES, StroopApp®, EEG, and brain MRI; MHE was defined by ≥2 abnormal tests. UCH-L1, GFAP, ammonia, IL-6, S100β, and enolase were measured using commercial immunoassays. ROC analysis assessed diagnostic performance.
Results: Sixty-seven participants were included (controls, n = 15; non-HE, n = 14; MHE, n = 27; OHE, n = 11). Biomarker levels increased stepwise across HE stages. UCH-L1 was significantly higher in MHE vs non-HE (143.2 ± 37.7 vs 88.2 ± 15.1 pg/mL; p = 0.003), and GFAP showed a similar pattern (27.9 ± 12.2 vs 17.2 ± 5.2 pg/mL, p = 0.008). Ammonia, S100β, and IL-6 were markedly elevated only in OHE (p < 0.0001). Enolase showed no discriminatory value. UCH-L1 discriminated HE vs non-HE with an AUC of 0.89, while GFAP showed

moderate discrimination (AUC = 0.75). ROC 95% CI and optimal sensitivity/specificity values are being calculated.
Conclusion: UCH-L1 and GFAP emerge as promising biomarkers for the objective detection of MHE, a stage frequently missed by current diagnostic strategies. In contrast, ammonia, S100β, and IL-6 were associated exclusively with OHE, supporting distinct biological pathways across HE severity. These findings suggest that brain-injury biomarkers may improve early diagnosis and risk stratification in cirrhosis, warranting prospective validation.

WED-529
Severity at diagnosis and progression in chronic liver disease by aetiology: a nationwide cohort study of 146,654 individuals in Sweden, 2002–2022
Juan Vaz[1], Ulf Strömberg[1], Ying Shang[2], Axel Wester[2], Andrea Lindfors[2], Hannes Hagström[2]. [1]*School of Public Health and Community Medicine, Institute of Medicine, Sahlgrenska Academy, University of Gothenburg, Gothenburg, Sweden;* [2]*Department of Medicine, Huddinge, Karolinska Institutet, Stockholm, Sweden*
E-mail: juan.vaz@gu.se

Background and aims: Many individuals with chronic liver disease (CLD) are diagnosed at an advanced stage, but population-level evidence comparing severity at presentation and subsequent progression across CLD aetiologies remains limited. We aimed to assess the burden of major adverse liver outcomes (MALOs) at diagnosis across aetiologies, identify factors associated with MALOs at presentation, and estimate the cumulative incidence of MALOs among individuals presenting with non-cirrhotic CLD.
Method: Using nationwide Swedish register data, we identified all adults (≥18 years) diagnosed with CLD between 2002 and 2022. CLD was classified by single or combined aetiologies. MALOs at presentation were defined as decompensated cirrhosis, liver failure, hepatocellular carcinoma, liver transplantation, or liver-related death within prespecified time windows. Multinomial logistic regression was used to examine factors associated with MALOs at the first presentation. Among individuals presenting with non-cirrhotic CLD, cumulative incidence functions accounting for competing risks were used to estimate progression to MALOs.
Results: We identified 146,654 adults with CLD. The most common aetiologies were hepatitis C (20%), alcohol-related liver disease (ALD; 18%), metabolic dysfunction-associated steatotic liver disease (MASLD; 13%), and hepatitis B (12%). At diagnosis, 13.4% of individuals presented with MALOs, with ascites being the most common (8% of overall, accounting for 61% of all MALOs). MALOs were most common among individuals with ALD (41%) and cryptogenic cirrhosis (38%). ALD was associated with markedly increased odds of MALOs at presentation (adjusted odds ratio [aOR] 40.8, 95% confidence interval [CI] 37.3–44.7). Among 102,923 individuals presenting with non-cirrhotic CLD, ALD –alone or in combination with other aetiologies– was associated with the highest 10-year cumulative incidence of progression to MALOs.
Conclusion: More than one in eight individuals with CLD in Sweden were diagnosed only after a MALO has occurred. Severity at presentation and subsequent progression vary substantially by underlying disease patterns, with ALD conferring particularly high risk.

WED-530
Machine learning and generative artificial intelligence models outperform established prognostic scoring systems in predicting acute decompensation in patients with chronic liver disease
Mathew Vithayathil[1], James Bell[1], Alexander Cole[1], Claudia Moore-Gillon[1], David Kockerling[1], Rooshi Nathwani[1], Lucia Possamai[1], Heather Lewis[1], Nowlan Selvapatt[1], Maud Lemoine[1], Ameet Dhar[1]. [1]*Imperial College London, London, United Kingdom*
E-mail: mathew.vithayathil@doctors.org.uk

Background and aims: Patients with cirrhosis are at risk of acute decompensation but robust predictors are lacking. This study developed and validated a machine learning model to predict risk of liver decompensation necessitating admission in patients being managed in a dedicated cirrhosis service.
Method: Cirrhosis patients from a tertiary hepatology centre were retrospectively included. Patients were randomly divided into training and validation cohorts. Baseline clinical variables relating to demographics, disease aetiology, biochemistry, liver complications (ascites, encephalopathy, varices) and liver-related pharmacotherapy (beta-blockers, diuretics, rifaximin) were collected. Models using baseline variables to predict 6-month episodes of liver decompensation resulting in admission were developed using 8 supervised learning algorithms, including the TabPFN generative foundation model, and 13 feature selection techniques. The top 3 performing machine learning/feature selection combinations were combined using ensemble learning. Model performance was benchmarked against established liver prognostic scores. K-means clustering stratified patients for acute decompensation risk.
Results: 403 patients were included in training (n = 270) and validation (n = 133) cohorts. The ensemble model consisting of logistic regression, ridge regression and neural network algorithms was predictive of 6-month decompensation in training (AUC 0.75, 95% CI 0.68–0.82) and validation (AUC 0.84, 95% CI 0.72–0.94). Feature selection identified bilirubin, albumin, INR, ascites and diuretic use as the key predictor variables. The model significantly outperformed CP grade (AUC 0.78, $p < 0.001$), MELD (AUC 0.77, $p = 0.03$ and UKELD (AUC 0.72, $p < 0.001$) in predicting 6-month risk of decompensation admission during validation. Unsupervised machine learning identified 3 distinct risk groups, with significant differences in median time-to-decompensation in training and validation (high-risk: 3.0 months, 95% CI 0.5–6.0 vs. moderate-risk: 25.7 months, 95% CI 8.8–36.7 vs. low-risk: median not reached, 95% CI 47.2-upper limit not reached; $p < 0.001$) cohorts.
Conclusion: Machine learning based algorithms using routine clinical variables outperform established prognostic liver scores in predicting risk of admission due to decompensation in patients managed in a dedicated cirrhosis service. Ensemble models can stratify risk of admission, allowing for personalised care strategies including follow-up intervals and ambulatory monitoring in higher risk groups.

WED-531
Optimal glycaemic targets to prevent major adverse cardiovascular events and risk of hypoglycaemia in patients with type 2 diabetes and cirrhosis
Mary Yue Wang[1], Sherlot Juan Song[1], Nana Peng[1], Grace Lai-Hung Wong[1], Vincent Wai-Sun Wong[1], Jimmy Che-To Lai[1], Terry Cheuk-Fung Yip[1]. [1]*The Chinese University of Hong Kong, Sha Tin, Hong Kong*
E-mail: maryyo@link.cuhk.edu.hk

Background and aims: Glycaemic management in patients with T2DM and cirrhosis is challenging due to limited options of anti-diabetic agents and risk of hypoglycaemia. We aimed to determine the association between glycaemic control and clinical outcomes and compare optimal glycaemic targets in individuals with T2DM, with and without cirrhosis.
Method: This retrospective study included adult individuals with T2DM, with or without cirrhosis, after excluding individuals with missing demographic data, type 1 diabetes, missing haemoglobin A_{1c} (HbA_{1c}) records within 1 year, and major adverse cardiovascular events (MACE) before T2DM diagnosis or within 1 year. The primary outcome was MACE. All-cause mortality and hypoglycaemia were secondary outcomes. Restricted cubic spline analysis was used to assess potential non-linear relationship between time-weighted average (TWA) HbA_{1c} and the outcomes. Cause-specific hazard

ratios (CSHR) and 95% confidence interval (CI) were estimated, treating non-MACE-related death as competing risks.
Results: Of 695,549 patients with T2DM, 16,007 (2.3%) had compensated cirrhosis (mean age 68.8 years, 58.5% men) and 3331 (0.5%) had decompensated cirrhosis (mean age 67.9 years, 59.3% men). TWA HbA_{1c} level had a linear relationship with risk of MACE in compensated cirrhosis group (CSHR of per 1% HbA_{1c} increase [95% CI]: 1.09 [1.06–1.12], p <0.001), decompensated cirrhosis group (CSHR of HbA_{1c} [95% CI]: 1.11 [1.06–1.17], p <0.001) and non-cirrhosis group (CSHR of HbA_{1c} [95% CI]: 1.09 [1.08–1.09], p <0. A HbA_{1c} level of 6–7% had the lowest mortality incidence in all T2DM patients with or without cirrhosis. Patients with decompensated cirrhosis had the highest 10-year incidence of hypoglycaemia compared to the compensated cirrhosis and non-cirrhosis groups (15.91 vs 9.05 vs 3.92 per 100 person-years, respectively). Hypoglycaemia was associated with an increased risk of all-cause mortality in all groups (adjusted HR [95% CI]: non-cirrhosis group: 4.18 [4.08–4.28], compensated cirrhosis group: 2.80 [2.52–3.12], decompensated cirrhosis group: 2.70 [2.34–3.11], all p < 0.001).
Conclusion: HbA_{1c} <7% works equally well for T2DM patients with or without cirrhosis as it is associated with a lower risk of MACE and all-cause mortality. However, excessively low HbA_{1c} levels should be managed with caution in cirrhotic patients, given the potential impact of extrahepatic complications and higher risk of mortality and hypoglycaemia.

WED-532
Exploratory analysis of neurofilament light chain across steatotic liver disease suggests utility in hepatic encephalopathy but not in obesity-related cognitive dysfunction

Elise Jonasson[1], Lea Ladegaard Grønkjær[1], Birgitte Jacobsen[1], Mette Lauridsen[1], Charlotte Wernberg[1]. [1]*Liver Research Group, Department of Gastroenterology and Hepatology, University Hospital of South Denmark, Esbjerg, Denmark*
E-mail: elise.jonasson.nielsen@rsyd.dk

Background and aims: Overt hepatic encephalopathy (OHE) remains a severe complication of cirrhosis, while obesity is associated with cognitive dysfunction. There is an unmet need for markers of minimal hepatic encephalopathy (mHE), OHE, and cognitive dysfunction. Neurofilament light chain (NfL) is a marker of neuroaxonal injury and has been proposed as a biomarker of OHE. We aimed to explore NfL across the spectrum of steatotic liver disease (SLD) in patients undergoing cognitive testing.
Method: We analysed two prospective cohorts, with data on cognitive testing using the Continuous Reaction Time (CRT), Portosystemic Encephalopathy Syndrome (PSE), and Repeatable Battery for the Assessment of Neuropsychological Status (RBANS). Patients with cirrhosis were classified as no mHE, mHE, or OHE (n = 38/31/16) based on PSE results or admission with OHE. The second cohort included patients with obesity undergoing liver biopsy, classified as no-MASLD + normal cognition, MASLD + normal cognition, or MASLD + cognitive impairment (n = 17/42/20), defined as ≥2 abnormal tests or RBANS sum score <79. NfL was measured in biobank samples collected at the time of testing, including in 19 healthy controls.
Results: We included 187 patients. The cirrhosis and obesity cohorts differed markedly in sex (69% vs. 32% men), age (63 ± 15 vs. 49 ± 23 years), BMI (28 [6] vs. 42 [8] kg/m^2), and median Nfl levels (23.1 [20] vs. 8.6 [4] pg/ml). The biopsy-confirmed MASLD in the obesity cohort was predominantly mild–moderate, with steatohepatitis in 23/42 vs. 6/20 patients, and fibrosis stages F1/F2/F3 in 10/23/9 and 12/7/1, respectively. In the cirrhosis cohort, NfL increased stepwise across severity: no mHE 14.6 (13), mHE 27.7 (24), and OHE 36.9 (51) pg/ml (p < 0.001). NfL was significantly higher in mHE and OHE compared with healthy controls and cirrhosis without mHE (p < 0.001), with no difference between mHE and OHE (p = 0.3). In contrast, NfL levels were low, had a slight trend, but overlapped across cognitive subgroups in the obesity cohort (p = 0.1). Healthy controls had a median NfL of 12.1 (6.8) pg/ml.
Conclusion: Nfl levels increase with worsening HE in cirrhosis, supporting its role as a biomarker of neuroaxonal injury in HE. In obesity-related MASLD, NfL levels were lower and not associated with cognitive impairment, potentially reflecting BMI-related suppression and limited statistical power. Larger, adequately powered studies are needed to clarify the utility of NfL across the SLD spectrum.

WED-533
Rifaximin improves hyperammonemia through alteration in duodenal microbiota in patients with liver cirrhosis

Shunhei Yamashina[1], Akira Uchiyama[1], Masahiro Tada[1], Kei Ishizuka[1], Maki Morinaga[1], Hiroo Fukada[1], Reiko Yaginuma[1], Kyoko Fukuhara[1], Kazuyoshi Kon[1], Kenichi Ikejima[1]. [1]*Department of Gastroenterology, Juntendo University School of Medicine, Tokyo, Japan*
E-mail: syamashi@juntendo.ac.jp

Background and aims: Hepatic encephalopathy in cirrhosis is associated with gut dysbiosis; however, the small-intestinal microbiota remains incompletely understood compared with stool-based assessments. Proton pump inhibitor treatment has been reported to be associated with a higher risk of small intestinal bacterial overgrowth. Small intestinal bacterial overgrowth has also been linked to hepatic encephalopathy in cirrhosis. Here, we investigated the effects of rifaximin on duodenal microbiota and hyperammonemia in patients with cirrhosis and examined whether these effects differed according to concomitant acid-suppressive therapy.
Method: Twelve adults with cirrhosis and esophageal varices received rifaximin (1200 mg/day) for 12 weeks. Duodenal aspirates were obtained by upper endoscopy before and after treatment with rifaximin, and serum ammonia was measured at both time points. Acid-suppressive therapy was defined as proton pump inhibitor or potassium-competitive acid blocker use. 16S rRNA sequencing was processed with QIIME 2/DADA2. Alpha diversity and weighted UniFrac-based beta diversity (principal coordinate analysis; PERMANOVA) were assessed, and Differentially abundant taxa were identified using LEfSe.
Results: Serum ammonia and aspartate aminotransferase (AST) decreased significantly after rifaximin, whereas platelets, alanine aminotransferase, albumin, bilirubin and gamma-glutamyl transpeptidase were unchanged. The reductions in ammonia and AST were significant mainly in the acid-suppressive group. In the duodenal microbiota, rifaximin decreased Faith phylogenetic diversity, the Shannon index, and observed amplicon sequence variants, while Pielou evenness was preserved. Weighted UniFrac distances showed separation of microbial communities between before and after treatment. LEfSe identified reduced relative abundance of *Peptostreptococcales Tissierellales* and *Parvimonas micra* after rifaximin; in the acid-suppressive subgroup, *Selenomonas* was also reduced.
Conclusion: Rifaximin improved hyperammonemia accompanied by changes in the duodenal microbiota in patients with cirrhosis. These effects appeared more pronounced in patients receiving acid-suppressive therapy, suggesting that small-intestinal dysbiosis may influence treatment response.

WED-537
Targeted albumin therapy for recompensation in decompensated HBV-related cirrhosis: baseline characteristics of a multicenter randomized trial

Wanting Yang[1], Qi Wang[1], Hong Zhao[1], Ligai Liu[1], Ruyu Liu[2], Jinhua Hu[3], Huiling Xiang[4], Shenghao Li[5], Haiyan Kang[6], Jia Li[7], Guanlin Zhou[8], Liang Xu[9], Yu Wang[10], Bing Qiao[11], Guang-Ming Xiao[12], Fenghua Liu[13], Ying Guo[14], Jianru Jia[15], Yuemin Nan[16], Jianxiang Liu[17], Xiaoyuan Xu[17], Wen Xie[1]. [1]*Center of*

Liver Diseases, Beijing Ditan Hospital, Capital Medical University, Beijing, China, Beijing, China; [2]Department of Hepatology Division 3, Beijing Ditan Hospital, Xuzhou Hospital, Capital Medical University, Xuzhou, China Department of Hepatology Division 3, Xuzhou Infectious Diseases Hospital, Xuzhou, China, Department of Hepatology Division 2, Beijing Ditan Hospital, Capital Medical University, Beijing, China, Xuzhou, China; [3]Senior Department of Hepatology, the Fifth Medical Center of PLA General Hospital, Beijing 100039, China, Beijing, China; [4]Department of Gastroenterology and Hepatology, Tianjin University Central Hospital (The third Central Hospital of Tianjin), Tianjin, China; [5]Department of Hepatology 1, The Third People's Hospital of Kunming/ Yunnan Clinical Center for Infectious Diseases, Kunming, China; [6]The Fifth Hospital of Shijiazhuang, Shijiazhuang, China; [7]Department of Gastroenterology and Hepatology, Tianjin Second People's Hospital, Tianjin, China, Tianjin, China; [8]The Fifth People's Hospital of Ganzhou, Ganzhou, Jiangxi, China, Ganzhou, China; [9]The Second People's Hospital Affiliated to Tianjin Medical University, Tianjin, China, Tianjin Institute of Hepatology, Tianjin Second People's Hospital, Tianjin, China, Tianjin, China; [10]Beijing Friendship Hospital, Capital Medical University, Beijing, China; [11]Department of Integrated Traditional Chinese and Western Medicine, Qingdao Public Health Clinical Center, Qingdao, 266033, Shandong, China, Qingdao, China; [12]Department of Hepatology, Guangzhou Eighth People's Hospital, Guangzhou, Guangdong, China, Guangzhou, China; [13]Infection Department of Liaocheng People's Hospital, Liaocheng, China; [14]Department of Hepatology, The Third People's Hospital of Taiyuan, Taiyuan, Taiyuan, China; [15]Baoding People's Hospital., Baoding, China; [16]Hebei Medical University Third Hospital, Shijiazhuang, China; [17]Peking University First Hospital, Beijing, China
E-mail: wantingyang1999@163.com

Background and aims: China bears a high burden of hepatitis B, and effective management of hepatitis B–related cirrhosis remains a major clinical challenge. Although "cirrhosis recompensation" has recently been recognized as a distinct disease stage and carries substantial theoretical and societal value, practical treatment guidelines are lacking. We established a prospective cohort study with the proportion of patients achieving recompensation at week 72 as the primary endpoint to evaluate an optimized human albumin–based treatment strategy.
Method: Patients with decompensated HBV-related cirrhosis were recruited from 17 centers across China and centrally randomized to an intensive or standard treatment group. Based on validated Baveno VII recompensation criteria in entecavir-treated patients, an albumin target of 34 g/L was set for the intensive group. Albumin was infused at baseline, with levels rechecked after 3–5 days and discontinued once ≥34 g/L was achieved. Albumin levels were reassessed at weeks 8, 16, and 24, and additional infusions were given if targets were not met. In the standard group, the albumin target was 30 g/L, with other interventions identical to the intensive group.
Results: From December 2023 to July 2025, 148 patients with decompensated HBV-related cirrhosis were enrolled and randomized into the standard (n = 74) and intensive (n = 74) treatment groups. The total albumin infusion volume (intensive group, 100 g (IQR: 70 g–150 g) vs. standard group, 70 g (IQR: 50 g-100 g), p = 0.0005) and post-infusion albumin concentrations (intensive group, 35.4 g/L (IQR: 34.0 g/L–37.4 g/L) vs. standard group, 33.2 g/L (IQR: 30.9 g/L–36.2 g/L), p = 0.0029) differed significantly, confirming differences in treatment intensity. Baseline characteristics were well-matched between groups, including age (p = 0.3851), sex (p = 0.4869), Child-Pugh score (p = 0.3913), mean serum albumin levels (p = 0.5022), and diuretic use at enrollment (p = 0.1725). All patients continue active follow-up for the primary endpoint (rate of recompensation), with final analyses planned upon trial completion.
Conclusion: The baseline characteristics in our study were evenly distributed, and the protocol successfully achieved a significant difference in albumin infusion volume between the standard and intensive treatment groups. Upon completion of this trial, the assessment of recompensation rates in both groups is expected to provide key evidence to optimize albumin therapy regimens for patients with decompensated hepatitis B-related cirrhosis.

WED-538
Prefrailty and frailty predict hospitalisation in patients with cirrhosis

Ismael de Jesus Yepes Barreto[1], Dagoberto Duarte[1], Luis Molina[1], Jorge Yepes[1], Maria Valera[1], Fernando Garcia[1]. *[1]Universidad de Cartagena, Asociacion Colombiana de Hepatologia, Cartagena de Indias, Colombia*
E-mail: ismayep@yahoo.com

Background and aims: The Liver Frailty Index (LFI) has emerged as a clinically relevant predictor of hospitalisation and adverse outcomes in cirrhosis, reflecting reduced functional reserve and impaired response to stressors. However, the LFI was primarily developed and validated in North American and European populations, with limited representation of Latin American patients. Given regional differences in muscle mass and strength, its prognostic performance may vary across populations. We aimed to evaluate the prognostic value of the LFI for hospitalisation in patients with cirrhosis in Colombia.
Method: We conducted a prospective observational cohort study including consecutive adult patients with cirrhosis attending an outpatient hepatology centre in Cartagena, Colombia, between November 2024 and June 2025. Cirrhosis was diagnosed using clinical, biochemical, imaging, elastographic, and/or histological criteria. Frailty was assessed at baseline using the LFI, based on handgrip strength, chair stands, and balance tests, and categorised as robust (<3.2), prefrail (3.2–4.5), or frail (>4.5). Patients were followed every 60 days to assess hospitalisation. Associations between frailty status and hospitalisation were analysed using chi-square tests.
Results: A total of 121 patients were included; 61.2% were female, and most had compensated disease (80.8% Child–Pugh A, 19.2% Child–Pugh B). According to the LFI, 23.1% were robust, 57.0% prefrail, and 19.8% frail. During a median follow-up of 11.1 months, 26.4% experienced at least one hospitalisation. Hospitalisation rates increased progressively across frailty categories: prefrail vs robust (29.0% vs 10.7%, p = 0.05) and frail vs robust (37.5% vs 10.7%, p = 0.02). Patients classified as Child–Pugh B had higher hospitalisation rates than those with Child–Pugh A (65.2% vs 16.5%, p < 0.001). Additional factors associated with hospitalisation included prior hospitalisation, first episode of hepatic decompensation, older age, lower body mass index, and lower serum albumin levels.
Conclusion: Liver Frailty Index was strongly associated with hospitalisation risk not only among frail patients but also in those classified as prefrail. These findings indicate that prefragility represents an early and clinically relevant stage of vulnerability rather than a benign condition.

WED-539
Health literacy is independently associated with frailty in cirrhosis

Ismael de Jesus Yepes Barreto[1], Nicole Chamorro[1], Guillermo Donado[1]. *[1]Universidad de Cartagena, Asociacion Colombiana de Hepatologia, Cartagena de Indias, Colombia*
E-mail: ismayep@yahoo.com

Background and aims: Health literacy (HL) is the ability to obtain, process, and understand health information to make appropriate health decisions. In cirrhosis, limited HL and frailty are independently associated with adverse outcomes, higher healthcare utilisation, and mortality. Frailty can be assessed using the Hepatic Frailty Index (HFI). The association between HL and frailty in cirrhosis has not been previously evaluated The aim of this study was to assess the association between health literacy and frailty in patients with cirrhosis.
Method: We conducted a cross-sectional, observational, and analytical study including patients with a confirmed diagnosis of cirrhosis

who attended outpatient care between September and December 2025. All participants completed the Spanish version of the Short Assessment of Health Literacy (SAHL-S), a validated instrument to assess health literacy. Frailty was evaluated using the Hepatic Frailty Index. Frailty was defined as an HFI score ≥ 4.5. Continuous and categorical variables were described as means (standard deviation) and percentages, respectively. Univariate and multivariable logistic regression analyses were performed to identify factors associated with frailty.

Results: A total of 98 patients with cirrhosis were included. According to the hepatic frailty classification, 16.5% were classified as robust, 63.7% as prefrail, and 19.8% as frail. The majority of patients were female (56.1%), and most had compensated disease; 87.4% were classified as Child–Pugh A, 11.6% as Child–Pugh B, and 1.1% as Child–Pugh C. Mean age was 64.6 ± 12.8 years. Adequate health literacy was observed in 82.1% of patients. In univariate analysis, adequate health literacy was associated with a lower risk of frailty, while increasing age was associated with a higher risk. No significant association was observed between Child–Pugh class and frailty. In multivariable logistic regression analysis, adequate health literacy remained independently associated with a lower likelihood of frailty (OR 0.26, 95% CI 0.07–0.89, p = 0.032), after adjustment for age. Older age was also independently associated with frailty (OR 1.07 per year, 95% CI 1.01–1.13, p = 0.025).

Conclusion: In patients with cirrhosis, health literacy was independently associated with frailty, beyond age and liver disease severity. These findings suggest that health literacy is a modifiable determinant of frailty and support incorporating health literacy assessment into routine cirrhosis care.

WED-540-YI

Ammonia is an inconsistent marker of clinical outcomes in people with cirrhosis and hepatic encephalopathy: evidence from ten pooled systematic reviews and meta-analyses

Harry Zacharias[1], Lise Lotte Gluud[2], Marsha Morgan[1]. [1]*UCL Institute for Liver & Digestive Health, Division of Medicine, Royal Free Campus, Rowland Hill Street, London, United Kingdom;* [2]*Gastrounit, Medical Division, Copenhagen University Hospital Hvidovre, Hvidovre, Denmark*
E-mail: h.zacharias@ucl.ac.uk

Background and aims: Ammonia plays a central role in the pathophysiology of hepatic encephalopathy (HE). However, the clinical utility of blood ammonia measurements in patients with cirrhosis is debated. Cochrane systematic reviews are conducted using rigorous standards for data identification, extraction, analysis, and interpretation. The treatment of HE has been subject to a series of Cochrane reviews in which data on blood ammonia were collected as a secondary outcome. This study aimed to further explore the clinical utility of ammonia in patients with cirrhosis, using data from these Cochrane reviews.

Method: Ten Cochrane systematic reviews evaluating, in turn, L-acetyl-carnitine, non-absorbable disaccharides, branched-chain amino acids, flumazenil, L-ornithine-L-aspartate, ammonia-lowering agents, probiotics, rifaximin, other antibiotics, and dopaminergic agents were included. Data were extracted from studies comparing these active agents with placebo/no treatment on timing of ammonia sampling, HE classification, mortality, and HE outcomes. Associations between ammonia (as standardised mean differences) and outcomes (as log risk ratios) were examined using random-effects meta-regressions.

Results: Data were available from 125 randomised clinical trials, involving 8342 people (4376 cases, 3966 controls). Information on ammonia was available in 68 (54%) trials, HE outcome data in 90 (72%); and mortality data in 96 (77%) trials. There were no significant correlations between ammonia and HE or mortality outcomes when all trial data were pooled, nor when stratified by treatment type or by type of HE (minimal, acute episodic, persistent/recurrent). However, when stratified by timing of sampling (baseline, end of treatment, change from baseline), baseline ammonia showed a significant inverse association with HE outcomes (slope = –0.50 [95% CI –0.86 to –0.14], p = 0.007, 41 RCTs, n = 2735).

Conclusion: Associations between ammonia and clinical outcomes were inconsistent across all trials, which likely represents between-study methodological heterogeneity. A higher ammonia at baseline was associated with a larger relative treatment effect on HE outcomes, but this likely reflects baseline risk and trial context rather than a useful biomarker of responsiveness to treatment. Hence, the clinical utility of blood ammonia measurement remains unclear. Its role in specifically defined contexts must be identified and tested with rigorous, concordant methodologies in order to define its utility as a clinical biomarker.

WED-541-YI

Clinical application of extensively drug-resistant organism (XDRO) colonization screening in patients with acute decompensation of cirrhosis (AD) in low and high prevalence countries

Nicola Zeni[1], Juan Bañares[2], Parminder Kaur[3], Marzia La Franca[4], Archana Angrup[5], Simone Incicco[4], Roberta Gagliardi[4], Valeria Calvino[4], Marta Tonon[4], Sunil Taneja[6], Ajay Kumar Duseja[3], Paolo Angeli[4], Nipun Verma[3], Salvatore Piano[4]. [1]*University of Padua, Padua, Italy;* [2]*Liver Unit, Digestive Diseases Division, Hospital Universitari Vall d'Hebron, Vall d'Hebron Institut de Recerca (VHIR), Vall d'Hebron Barcelona Hospital Campus, Barcelona, Spain;* [3]*Department of Hepatology, PGIMER, Chandigarh, India;* [4]*Unit of Internal Medicine and Hepatology, Department of Medicine, University and Hospital of Padua, Padua, Italy;* [5]*Department of Medical Microbiology, PGIMER, Chandigarh, India;* [6]*Department of Hepatology, PGIMER, Chandigarh, Italy*
E-mail: nicola.zeni.1@gmail.com

Background and aims: Bacterial infection often precipitates AD and the increasing prevalence of XDRO infection complicates empirical antibiotic therapy and worsens clinical outcomes. Data on XDRO colonization in cirrhotic patients admitted to regular wards are scarce. Our study aimed to evaluate the prevalence of rectal XDRO colonization and its clinical impact in hospitalized patients with AD.

Method: A retrospective observational study was conducted with 232 patients in Padua Hospital, Italy and a validation cohort of 176 patients from PGIMER Chandigarh, India, all admitted for AD, undergoing XDRO surveillance with rectal swab within 48 hours of admission. Patients were followed-up until death, liver transplant or 90-days, to assess the development of XDRO-related infections as well as acute-on-chronic liver failure (ACLF), ICU transfer and 28-day and 90-day mortality according to rectal swab results.

Results: In Italian study cohort (61 ± 12 years old; 64% male, median MELD score 18), 39 (16.8%) tested positive for colonization by XDRO (CR *enterobacteriaceae* accounted for 60% of cases). Patients colonized by XDRO had higher incidence of XDRO infections (33% vs 4.4%; p = 0.017) and rectal swab guided antibiotic treatment would have covered 90% of pathogens. In multivariable analysis (adjusted by age, sex and MELD score), XDRO colonization was associated with higher risk of developing XDRO infections [HR = 3.93; p = 0.006]; moreover it was associated with an increased risk of developing ACLF (OR = 3.18, p = 0.002), being transferred to the ICU (OR = 3.40; p = 0.004), and mortality at 28-days (sHR = 4.39; p < 0.001) and 90-days (sHR = 4.50; p < 0.001). In Indian cohort a higher proportion of patients tested positive for XDRO colonization than Italian cohort (54.4% vs. 16.8%, p < 0.001). A higher prevalence of XDRO infection development in XDRO colonized patients (45% vs 19% p < 0.001) was confirmed and in multivariate analysis colonization was associated to XDRO infection development (sHR = 3.01, p < 0.001). The same XDRO was found in 77% of patients with culture-proven infections. XDRO colonization was not associated to an increased mortality risk, ACLF development or ICU transfer.

Conclusion: Irrespective of XDRO prevalence, colonization by XDRO is associated with an increased risk of developing XDRO infections, but not mortality, ACLF development and ICU transfer risk. Rectal swab could be a valuable screening tool for guiding empirical antibiotic treatment strategy in these patients.

WED-542

Portosystemic ammonia gradient (PAG) predicts risk of overt hepatic encephalopathy occurrence in patients after TIPS

Chuanfu Ding[1], Feng Zhang[1], YuZheng Zhuge[1]. [1]*Department of Gastroenterology, Nanjing Drum Tower Hospital, Affiliated Hospital of Medical School, Nanjing University, Nanjing, Jiangsu, China, Nanjing, China*
E-mail: fzdndx@126.com

Background and aims: Overt hepatic encephalopathy (OHE) is a major complication after transjugular intrahepatic portosystemic shunt (TIPS) placement. However, reliable prediction of post-TIPS OHE remains challenging. We propose a novel index - the portosystemic ammonia gradient (PAG). This study aims to evaluate the effect of PAG in predicting OHE after TIPS.
Method: In this prospective pilot study, 38 cirrhotic patients undergoing elective TIPS were enrolled. PAG was defined as the difference between portal vein ammonia (PVA) and inferior vena cava ammonia (IVCA), measured simultaneously with portosystemic pressure gradient (PPG) before and after TIPS. Clinical outcomes, including OHE, were recorded, and the predictive performance of pre- and post-TIPS PAG and PPG was compared using ROC analysis.
Results: The mean PAG decreased from 42.9 ± 24.2 μmol/L pre-TIPS to 17.5 ± 8.9 μmol/L post-TIPS ($P < 0.001$). During 6-month follow-up, 13 patients (34.2%) developed OHE. Pre-TIPS PAG was lower in patients with OHE than in those without (29.3 ± 19.7 vs. 49.9 ± 23.6 μmol/L, $P < 0.001$). Logistic regression showed post-TIPS PPG (OR = 0.76, 95% CI: 0.57–0.97, $P = 0.04$) and pre-TIPS PAG (OR = 0.96, 95% CI: 0.92–0.99, $P = 0.02$) as independent OHE predictors. Pre-TIPS PAG had the highest predictive accuracy (AUC = 0.748), outperforming post-TIPS PPG, CTP, and MELD (AUC = 0.649, 0.605, 0.560). Patients with lower pre-TIPS PAG (<25.95 μmol/L) had higher cumulative OHE incidence (HR = 0.19, 95% CI: 0.06–0.60; $P = 0.004$).
Conclusion: PAG reflects residual hepatic ammonia metabolism and is a promising prognostic index for post-TIPS OHE, guiding individualized risk stratification and preventive strategies.

WED-543

Assessing synthetic and cholestatic function for decompensation and mortality in compensated cirrhosis: a multi-centre cohort study

David Zhang[1], Margaret Teng[2,3], Nicole Shu Ying Tang[1], Vincent Chen[4], Jimmy Che-To Lai[5,6], Karn Wijarnpreecha[7], Rahul Kumar[8], Apichat Kaewdech[9], Thanawin Pramotedham[10], Anand Kulkarni[11], Ming-Hua Zheng[12,13], Akash Roy[14], Ken Liu[15,16], Chitchai Rattananukrom[17], Mazen Noureddin[18], Mohammad Shadab Siddiqui[19], Mark Muthiah[1,2], Cheng Han Ng[2,20,21], Hirokazu Takahashi[22]. [1]*Alexandra Hospital, Singapore, Singapore;* [2]*Division of Gastroenterology and Hepatology, Department of Medicine, National University Hospital, Division of Gastroenterology, Department of Medicine, Alexandra Hospital, Singapore, Singapore, Singapore;* [3]*Division of Gastroenterology, Department of Medicine, Alexandra Hospital, Singapore, Singapore, Singapore;* [4]*University of Michigan Medical School, Ann Arbor, Ann Arbor, United States;* [5]*Department of Medicine and Therapeutics, The Chinese University of Hong Kong, Shatin, Hong Kong;* [6]*Li Ka Shing Institute of Health Sciences and State Key Laboratory of Digestive Disease, The Chinese University of Hong Kong, Shatin, Hong Kong;* [7]*Division of Gastroenterology and Hepatology, University of Arizona College of Medicine, Phoenix, United States;* [8]*Department of Gastroenterology and Hepatology, Changi General Hospital, Singapore, Singapore;* [9]*Gastroenterology and Hepatology Unit, Division of Internal Medicine, Faculty of Medicine, Prince of Songkla University, Hat Yai, Thailand;* [10]*Division of Gastroenterology and Hepatology, Department of Medicine, National University Hospital, Singapore, Singapore;* [11]*Department of Hepatology and Liver Transplantation, Asian Institute of Gastroenterology, Hyderabad, India;* [12]*MAFLD Research Center, Department of Hepatology, the First Affiliated Hospital of Wenzhou Medical University, Wenzhou, China;* [13]*Key Laboratory of Diagnosis and Treatment for The Development of Chronic Liver Disease in Zhejiang Province, Wenzhou, China;* [14]*Department of Gastrosciences and Liver Transplantation, Apollo Multispeciality Hospital, Kolkata, West Bengal, India;* [15]*Department of Gastroenterology, Royal Prince Alfred Hospital, Sydney, Australia;* [16]*University of Sydney, Sydney, Australia;* [17]*Division of Gastroenterology and Hepatology, Department of Medicine, Faculty of Medicine, Srinagarind Hospital, Khon Kaen University, Khon Kaen, Thailand;* [18]*Houston Methodist Hospital and Houston Research Institute, Houston, United States;* [19]*University of Virginia School of Medicine, Charlottesvile, United States;* [20]*Division of Gastroenterology, Department of Medicine, Kurume University School of Medicine, Kurume, Japan;* [21]*Graduate School of Medicine, Yokohama City University, Kanagawa, Japan;* [22]*Division of Metabolism and Endocrinology, Faculty of Medicine, Saga University, Saga, Japan*
E-mail: chenhanng@gmail.com

Background and aims: Liver cirrhosis remains a major global health burden, yet accurate prognostication of hepatic decompensation remains a clinical challenge. Conventional biochemical indices: albumin, bilirubin, and INR form the cornerstone of clinical assessment but primarily reflect static hepatic function. This study characterised the relationship between these biochemical parameters and outcomes of decompensation and mortality.
Method: We conducted a retrospective multicentre cohort study using the Cirrhosis Outcomes and Research Endeavour (CORE) consortium, comprising 4090 adults with compensated advanced chronic liver disease across 12 centres in North America, Asia, and Australia. Associations between albumin, bilirubin, and INR levels and outcomes were evaluated using Cox proportional hazards and Fine-Gray competing risk models. Optimal thresholds were identified using maximally selected log-rank statistics and examined across subgroups stratified by liver stiffness measurement (LSM).
Results: Derangements in albumin, bilirubin, and INR were independently associated with higher risks of mortality and hepatic decompensation (all $p < 0.05$). However, differences between groups, though statistically significant, were of limited clinical significance, with biomarker values concentrated within narrow physiological ranges. Optimal prognostic thresholds were ≤39.7 g/L for albumin, ≥1.0 for INR, and ≥16.1 μmol/L for bilirubin in predicting mortality, with similar cut-offs for decompensation (38.0 g/L, 1.1, 22.2 μmol/L).
Conclusion: Standard biochemical indices remain essential for baseline assessment and provides foundational information on disease status. However, they exhibit limited dynamic predictive value for identifying individuals at risk of decompensation. Further refinement of existing prognostic models, particularly through the integration of dynamic clinical trajectories or molecular biomarkers, may offer substantially improved risk stratification and prognostication in compensated cirrhosis.

WED-544

Metabolic dysfunction exacerbates residual liver risks in virologically suppressed HBV cirrhosis

Ling Zhou[1], Jiankang Song[1], Mingchen Wang[1], Qiaoping Wu[1], Peishuang Xu, Jinjun Chen[2], HaiYu Wang[1]. [1]*Department of Infectious Diseases, Nanfang Hospital, Southern Medical University, Guangzhou, China, State Key Laboratory of Multi-organ Injury Prevention and Treatment, Key Laboratory of Infectious Diseases Research in South China (Southern Medical University), Ministry of Education, Guangzhou, China;* [2]*Department of Infectious Diseases, Key Laboratory of Molecular Biology for Infectious Diseases (Ministry of Education), Institute for Viral Hepatitis, the Second Affiliated Hospital, Chongqing Medical University,*

Chongqing, China, Department of Infectious Diseases, Nanfang Hospital, Southern Medical University, Guangzhou, China, Chongqing, China
E-mail: 375612668@qq.com

Background and aims: The independent prognostic role of metabolic dysfunction (MD) in virologically suppressed HBV-related cirrhosis remains unclear. This study aimed to evaluate the prognostic value of MD and its components, by combining them with the Baveno VI-SSM model for risk stratification of LREs (hepatic decompensation and hepatocellular carcinoma).
Method: We enrolled 855 patients with HBV-related compensated cirrhosis who had achieved sustained virological suppression (undetectable HBV DNA for ≥6 months) on antiviral therapy. Patients were recruited from April 2019 to April 2022 at Nanfang Hospital, China. Participants were categorized by MD status (present [≥1 cardiometabolic risk factor] vs. absent) and glycemic status (normal, prediabetes, diabetes). Cumulative incidence of LREs was analyzed using Kaplan–Meier curves and multivariable Cox regression. Risk stratification further combined MD with the Baveno VI-SSM criteria (liver stiffness measurement [LSM] <20 kPa and platelet count >150 × 10^9/L, or spleen stiffness measurement [SSM] ≤ 40 kPa).
Results: MD was present in 75.8% (648/855) of patients (mean age 48.6 [SD 9.46] years; 83.3% male; 13.9% diabetes; median LSM 10.4 [IQR 7.4–17.0] kPa; median SSM 42.0 [27.3–65.2] kPa). During median follow-up of 31.0 months (IQR 26.5–43.5), MD patients had higher cumulative LRE incidence than non-MD (7.1% vs. 1.4%; log-rank P = 0.0026). Decompensation occurred exclusively in MD (P = 0.035), with higher HCC incidence (P = 0.023). Multivariable analysis showed MD independently raised LRE risk (aHR 3.48, 95% CI 1.07–11.33), adjusted for age, sex, BMI, baseline LSM, ALT, and FIB-4. Risk escalated dose-dependently by glycemic status (normal < prediabetes < diabetes; [HR for prediabetes: 2.46, 95% CI 2.17–5.17; p = 0.007]; [HR for diabetes: 4.01, 95% CI 1.63–9.89; p < 0.001]). By 48 months, cumulative LRE incidence diverged markedly within the MD subgroup: 13.9% in the unfavorable Baveno VI-SSM category versus 2.4% in the favorable (log-rank P < 0.001; HR 6.24, 95% CI 3.46–11.26). Decompensation rates were 4.5% versus 0% and HCC rates 9.4% versus 2.4% (HR 4.13, 95% CI 2.08–8.20; P < 0.001).
Conclusion: Metabolic dysfunction, especially dysglycemia, independently predicts liver disease progression in virologically suppressed hepatitis B virus-related compensated cirrhosis. Integrating metabolic assessment with the Baveno VI-SSM model enhances risk stratification, facilitating targeted surveillance and intervention for high-risk subgroups.

WED-545
Perioperative mortality, morbidity and sex-specific outcomes in cirrhotic patients undergoing non-hepatic surgeries: a multi-centered cohort study propensity score analysis
Julie Zhu[1], Victoria Straub[2], Patrick Gallagher[1], Ian Epstein[1], Magnus McLeod[3], Kara Matheson[4], Boris Gala-Lopez[5]. [1]*Digestive Care and Endoscopy, Dalhousie University, Halifax, Canada;* [2]*Faculty of Medicine, Dalhousie University, Halifax, Canada;* [3]*PEI Health, Charlottetown, Canada;* [4]*Research Methods Unit, NSHA, Halifax, Canada;* [5]*Department of Surgery, Dalhousie University, Halifax, Canada*
Email: julie.zhu@nshealth.ca

Background and aims: Patients living with cirrhosis may experience higher mortality and morbidity after non-liver related surgeries. We aim to evaluate the impact of cirrhosis and sex on 90-day outcomes after five non-hepatic surgeries.
Method: This is a population cohort study using provincial administrative health data. Data pull and dataset linkage were performed on those underwent partial/total colectomies, abdominal hernia repairs, hip/knee arthroplasties, bariatric surgeries or cholecystectomies in 10 centers from 2010 to 2022. Three primary outcomes were all cause-mortality, LOS, and readmission within 90 days of discharge (if survived). Propensity score analysis was based on inverse probability of treatment weighting, adjusting for baseline characteristics. Conditional logistic regression models were used to estimate odds ratio (OR) for all-cause mortality and marginal Cox frailty models to estimate hazard ratio (HR) for LOS and readmission. Multivariable analyses and sensitivity analysis were performed.
Results: Among a total of 158749 de-identified pts, 42228 with hospital admissions formed the analysis cohort. Outcomes of 1630 with cirrhosis were compared with 40,598 without cirrhosis. 51.7% (21845) were female. In adjusted analysis, the odds of 90-day all-cause mortality was higher for cirrhosis (OR 3.52 (95% CI 2.86, 4.34) p < 0.0001) compared to those without. Surgery type (global p < 0.0001) was also an independent risk factor in mortality. The association between surgery type and mortality varied by cirrhosis (interaction p-value < 0.0001). There was no statistically significant difference in mortality between sexes (OR 0.94 (95% CI 0.83, 1.05) p 0.2709). Cirrhosis (HR 0.43 (95% CI 0.40, 0.45) p < 0.0001), female sex (HR 0.93, 95% CI (0.91, 0.95) p < 0.0001) and surgery type (global p <0.001) were strong predictors of prolonged LOS in adjusted analysis. Readmission post discharge was independently associated with cirrhosis (HR 1.93 95% (CI 1.73, 2.15) p < 00001) and surgery type (p < 0.0001). Major orthopedic surgeries had the highest readmissions after index surgery (HR 1.91 95% CI (1.76, 2.07) p < 0.0001) compared to cholecystectomy.
Conclusion: Cirrhotic patients had higher post-op mortality, and various complications. The study also highlighted sex in determining post-op LOS, surgical type such as major orthopedic, non-elective surgeries in determining post-op outcomes. The results have major implications on resource allocation and perioperative care in patients with cirrhosis.

Fibrosis – Stellate cell biology

TOP-342-YI
Hepatic B cells interact with invariant natural killer T cells via CD40 to stimulate hepatic stellate cells
Jihyo Byun[1], Kyurae Kim[1], Kwangwoo Lee[1], Won-il Jeong[1]. [1]*Korea Advanced Institute of Science and Technology (KAIST), Daejeon 34051, Korea, Rep. of South*
Email: wijeong@kaist.ac.kr

Background and aims: Hepatic B cells contribute to liver fibrosis by secreting cytokines that activate hepatic stellate cells (HSCs), yet the mechanisms remain unclear. In the fibrotic microenvironment, damaged hepatocytes release damage-associated molecular patterns (DAMPs), including lipid-related molecules. In addition, B cells can present lipid antigens to invariant natural killer T (iNKT) cells via CD1d–T cell receptor (TCR) engagement, together with CD40–CD40L co-stimulatory signaling. Thus, this study examined the potential role of B-iNKT cell interactions in liver fibrosis.
Method: Wild-type (WT) and B cell-specific CD40-deficient mice were treated with carbon tetrachloride (CCl_4). Then, blood chemistry, histological staining, immunofluorescence, and qRT-PCR were performed. Primary hepatic cells were analyzed by bulk RNA sequencing, single-cell RNA sequencing (scRNA-seq), and flow cytometry. *In vitro* migration assays and co-culture experiments were conducted using hepatocytes, B cells, iNKT cells, and HSCs.
Results: Bulk RNA-seq revealed significant upregulation of B cell activation markers, including *Cd40, Cd86*, and *Cxcr4* in the fibrotic livers of WT mice compared to controls. Consistently, flow cytometry and immunostaining demonstrated marked accumulation of B cells and their interaction with activated HSCs (aHSCs) within fibrotic septa. Moreover, scRNA-seq and qRT-PCR analyses revealed aHSCs as the principal source of the B cell-recruiting chemokine ligand, CXCL12. In line with this, *in vitro* chemotaxis assays showed enhanced

B cell migration toward aHSCs, confirming their interaction, whereas aHSCs expressed neither TCR nor CD40L to stimulate B cells. Instead, we observed upregulated CD1d and CD40 in B cells isolated from CCl_4-treated mice or co-cultured with conditioned media from damaged hepatocytes, suggesting that B-iNKT cell interactions in fibrotic areas contribute to HSC stimulation. Both *in vivo* and *in vitro*, CD40 deficiency in B cells reduced CD1d and B-iNKT interactions, thereby attenuating HSC activation and liver fibrosis through decreased expression of *Tnfa* and *Tgfb*1.

Conclusion: Our findings indicate that aHSCs recruit B cells to the fibrotic niche through the CXCL12-CXCR4 axis, where hepatocyte-derived lipid-related DAMPs may initiate B-iNKT cell interactions. These interactions promote the production of fibrotic mediators by B cells via CD1d/TCR and CD40/CD40L signaling. Collectively, this mechanism highlights a potential therapeutic strategy for treating liver fibrosis.

TOP-343-YI

LSECtin delivered to hAPCs by functionalized nanoparticles ameliorates chronic liver damage in experimental cirrhosis

Oriol Juanola[1], Vicente Candela[2], Esther Caparrós[1], Isabel Gómez-Hurtado[1], Paula Boix[3], Ani Gasparyan[3,4], Albina Espana[3], Hong Liang[3], Ana Blas-García[5], Ramón Martínez-Máñez[6], Rubén Francés[1]. *[1]Grupo de Inmunobiología Hepática e Intestinal, Dpto, Medicina Clínica, Universidad Miguel Hernández, San Juan, Alicante, España; IIS ISABIAL, Hospital General Universitario Dr. Balmis, Alicante, España; CIBERehd, Instituto de Salud Carlos III, Madrid, España; San Juan de Alicante, Spain; [2]Instituto Interuniversitario de Investigación de Reconocimiento Molecular y Desarrollo Tecnológico (IDM), Universitat Politècnica de València, Universitat de Valencia, Spain; Unidad Mixta UPV-CIPF de Investigación en Mecanismos de Enfermedades y Nanomedicina, Valencia, Universitat Politècnica de València, Centro de Investigación Príncipe Felipe, València, Spain; CIBER de Bioingeniería, Biomateriales y Nanomedicina (CIBER-BBN), Madrid, Spain, Valencia, Spain; [3]Grupo de Inmunobiología Hepática e Intestinal, Dpto. Medicina Clínica, Universidad Miguel Hernández, San Juan, Alicante, España; IIS ISABIAL, Hospital General Universitario Dr. Balmis, Alicante, España; San Juan de Alicante, Spain; [4]Universidad Miguel Hernández de Elche, Pharmacology, San Juan, Spain; [5]CIBERehd, Instituto de Salud Carlos III, Madrid, España; Fundación para el Fomento de la Investigación Sanitaria y Biomédica en la Comunidad Valenciana (FISABIO)., Departamento de Fisiología, Universitat de València, Valencia, Spain, Valencia, Spain; [6]Instituto Interuniversitario de Investigación de Reconocimiento Molecular y Desarrollo Tecnológico (IDM), Universitat Politècnica de València, Universitat de Valencia, Spain, CIBER de Bioingeniería, Biomateriales y Nanomedicina (CIBER-BBN), Madrid, Spain; Departamento de Química, Universitat Politècnica de València, Spain, Valencia, Spain*
Email: rfrances@umh.es

Background and aims: We have described a loss of expression of LSECtin in hepatic antigen-presenting cells in human cirrhotic liver biopsies that correlates with an expansion of a proinflammatory hepatic Th17 immune response.

Method: This project aims at delivering genetic cargo into the hepatic antigen presenting cells to restore the LSECtin expression for reducing the T-cell mediated inflammation. We used immortalized Kuppfer cells (imKCs) and liver sinusoidal endothelial cells (imLSECs), primary hepatic cells, and organs obtained from control and cirrhotic mice treated or untreated with functionalized nanoparticles. 10w-old male mice were subjected to a chronic liver injury protocol with 2 weekly oral doses of weight-controlled CCl_4 for 3 months. Control mice received vehicle (olive oil). A subgroup of mice received functionalized nanoparticles intraperitoneally twice per week in the last two weeks of liver injury protocol.

Results: Functionalized nanoparticles reached mainly the liver and its content was expressed by the endothelial cells found in the hepatic sinusoids. Administration of functionalized nanoparticles retrieved the gene and protein expression of LSECtin in the liver of mice with cirrhosis; and this effect is observed mainly in isolated hepatic LSECs, but not in isolated hepatic macrophages. The recovery of LSECtin expression in the cirrhotic liver is associated with lower infiltration of T lymphocytes (CD3) which suffer an immune reprogramming towards an antiinflammatory Treg phenotype. As consequence of reduced liver inflammation, we observe lower deposition of extracellular matrix proteins in the liver of mice with cirrhosis treated with functionalized nanoparticles, and improved liver function due to reduced circulating levels of ALT/AST and restored levels of albumin when compared to untreated cirrhosis mice. Mice with cirrhosis treated with functionalized nanoparticles showed reduced neuroinflammation due to reduced infiltration of myeloid cells in the brain and reduced protein expression of granzyme B in brain tissue homogenates.

Conclusion: LSECtin delivery by funcionalized nanoparticles increased the hepatic expression of LSECtin in experimental cirrhosis, leading to a reduction of T-cell mediated inflammation and fibrosis progression.

TOP-344

SIRT4 enhances NK cell cytotoxicity against hepatic stellate cells and reverses liver fibrosis via the AMPKα/p53/NKG2DL axis

Huan Chen[1], Feng Zhang[1], Yuzheng Zhuge[1]. *[1]Nanjing Drum Tower Hospital, Affiliated Hospital of Medical School, Nanjing University, Nanjing, China*
Email: ch960361753@163.com

Background and aims: Natural killer (NK) cells possess potent antifibrotic activity in liver fibrosis (LF) by directly targeting and suppressing activated hepatic stellate cells (HSCs). SIRT4, a key mitochondrial regulatory protein, is known to bridge cellular energy metabolism and viability. Nevertheless, its specific role in regulating NK cell-mediated cytotoxicity against HSCs has remained undefined.

Method: Liver fibrosis models were established in SPF C57BL/6 mice via CCl_4 injection or DDC diet. Human liver tissues were from fibrotic patients and healthy donors. Mouse HSCs were isolated by collagenase perfusion and density gradient centrifugation, activated by culture; human HSCs (LX-2) were cultured routinely. Splenic NK cells were isolated and cultured with IL-2. SIRT4 overexpression (pcDNA3.1-SIRT4) and knockdown (si-SIRT4) were performed in HSCs. Therapeutically, AAV8-pGAFP-SIRT4 mediated HSC-specific SIRT4 overexpression, with NK cell depletion to verify effect dependency. Functional and molecular assays detected NK cell cytotoxicity, AMPKα-p53 signaling, and ULBP1/2 expression.

Results: We observed a significant downregulation of SIRT4 in activated HSCs, in mouse models of LF (induced by CCl_4 or DDC), and in liver tissues from patients with fibrosis. Functional studies revealed that SIRT4 overexpression in HSCs enhanced their susceptibility to NK cell-mediated killing, whereas SIRT4 knockdown impaired it. Mechanistically, SIRT4 activates AMPKα, leading to enhanced phosphorylation and nuclear translocation of p53. Activated p53 directly binds to the promoters of ULBP1 and ULBP2, key ligands for the NKG2D receptor, and transactivates their expression. This SIRT4-AMPKα-p53 signaling axis thereby upregulates NKG2D ligands on HSCs, promoting NK cell recognition and cytotoxicity. Therapeutically, HSC-specific overexpression of SIRT4 via an adeno-associated virus vector (AAV8-pGAFP-SIRT4) activated hepatic NK cells, enhanced the clearance of activated HSCs, and effectively attenuated liver injury and fibrosis in mice. This antifibrotic effect was abolished upon NK cell depletion.

Conclusion: Our findings establish SIRT4 as a critical regulator of NK cell cytotoxicity against HSCs, operating through the novel AMPKα-p53-ULBP1/2 pathway. HSC-targeted SIRT4 gene therapy represents a promising and novel therapeutic strategy for the treatment of liver fibrosis.

FRI-304

Evaluation of clinically approved drugs in a Sprague-Dawley rat model of liver fibrosis induced by choline-deficient, L-amino acid defined (CDAA) diet

Jianing Zhou[1], Yanhao Qiu[1], Laia Vilà[1,2], Emma Barroso[1,2], Juan Carlos Laguna[1,2,3], Marta Alegret[1,2,3], Núria Roglans[1,2,3]. [1]*School of pharmacy and food sciences, Universitat de Barcelona, Barcelona, Spain;* [2]*IBUB, Barcelona, Spain;* [3]*CIBERObn, Barcelona, Spain*
Email: roglans@ub.edu

Background and aims: We have previously demostrated that pemafibrate, telmisartan and bempedoic acid administration prevents hepatic steatosis development in an experimental model of simple metabolic-associated steatotic liver disease (MASL) in Sprague-Dawley (SD) rats. In the current study, we aim to evaluate the effectiveness of these drugs for the treatment of liver fibrosis in a male rat model supplemented with a high-sucrose, high-fat, choline-deficient, L-amino acid-defined (CDAA) diet during three months.
Method: 42 Male (M) SD rats were randomly distributed into 5 groups: (1) control (CT; n = 6), which were fed standard chow, (2) CDAA (n = 8), (3) Pemafibrate (PEM; n = 8), (4) Telmisartan (TEL; n = 10) and (5) Bempedoic acid (BEMA; n = 10), which were fed the CDAA diet. All groups were maintained on their respective diet for three months. In the treatment groups, their respective compound was incorporated in the CDAA chow during the last month of feeding. At the end of the treatment period, blood samples were collected for serum isolation and liver tissue for RNA and protein extraction. Inflammatory and fibrotic processes were determined throw gene expression and serum analytes.
Results: After 3 months, CDAA diet increased significantly serum levels of hepatic injury markers, including alanine aminotransferase (ALT) (2.6X) and aspartate aminotransferase (AST) (1.75X). Among the tested compounds, bempedoic acid was the only one to significantly reduce transaminase levels, whereas telmisartan and pemafibrate each lowered one of them. Furthermore, all drug treatments reverted mRNA expression of several genes associated with MASH development compared with the CDAA group including genes related to fibrogenesis (*Acta2, Col1a1, Col1a2*), profibrotic mediators (*Tgf-ß, Pai-1*), extracellular matrix remodelling regulators (*Timp-1*), pro-inflammatory cytokines (*Tnf-α, Il1b*) and macrophage marker (*F4.80*). These findings are consistent with the ACTA2 and Col1A1 protein expression results, obtained by western blot analysis.
Conclusion: Our preliminary results suggest that the MASH induced by high-sucrose, high-fat, choline-deficient, L-amino acid defined diet (CDAA) in rats can be reversed through treatment with pemafibrate, telmisartan, and bempedoic acid. Nonetheless, these conclusions remain preliminary and additional experiments are needed to validate these results.
Grants: PID2023-146140OB-I00, funded by funded by MICIU/AEI/10.13039/501100011033 and FEDER-UE and 2021SGR-00345.

FRI-305

The YAP/TAZ-regulated long non-coding RNA SNHG16 promotes hepatic stellate cell activation

Amira Abdelhamid[1], Aya Osama[2], Hannah Rashwan[2], Ibrahim Fayed[1], Diana Hanna[3], Esther Menze[3], Sameh Magdeldin[2,4], Carsten Sticht[5], Ebtehal El-Demerdash[3,6], Kai Breuhahn[7], Nada El-Ekiaby[1], Ahmed Abdelaziz[1]. [1]*School of medicine, Newgiza university (NGU), Cairo, Egypt;* [2]*Proteomics and metabolomics unit, Basic research department, Children's cancer hospital (CCHE-57357), Cairo, Egypt;* [3]*Department of pharmacology & toxicology, Faculty of pharmacy, Ain Shams university, Cairo, Egypt;* [4]*Department of physiology, Faculty of veterinary medicine, Suez Canal university, Ismailia, Egypt;* [5]*Core facility next generation sequencing, Medical faculty Mannheim, Heidelberg university, Mannheim, Germany;* [6]*Preclinical and translational research center, Faculty of pharmacy, Ain Shams university, Cairo, Egypt;* [7]*Institute of pathology, University hospital Heidelberg, Heidelberg, Germany*
Email: amira.abdelhamid@ngu.edu.eg

Background and aims: Hippo pathway effectors, yes-associated protein (YAP) and transcriptional coactivator with PDZ-binding motif (TAZ), are key regulators of hepatic stellate cell (HSC) activation in liver fibrosis. Long non-coding RNAs (lncRNAs) are recognized as upstream modulators of YAP/TAZ and central contributors to HSC activation. However, their roles as downstream targets of YAP/TAZ in liver fibrosis remain unclear. Building on our prior identification of a YAP/TAZ-regulated lncRNA signature in hepatocellular carcinoma (HCC), this study aimed to characterize lncRNAs downstream of YAP/TAZ in HSCs and determine their contribution to HSC activation.
Method: To identify YAP/TAZ-regulated lncRNAs, YAP/TAZ knockdown (KD) was performed in LX-2 cells followed by RNA sequencing. Differentially expressed (DE) lncRNAs were shortlisted, and SNHG16 was selected for validation. SNHG16 levels were quantified by qRT-PCR after YAP/TAZ overexpression to evaluate its YAP/TAZ-mediated regulation, and after TGF-beta stimulation to assess its response to fibrogenic signaling. The functional impact of SNHG16 KD was assessed by quantifying HSC activation markers (alpha-SMA, COL1A1, TIMP2, TGF-beta, and MMP2) via qRT-PCR, with alpha-SMA protein levels validated by western blot (WB) and immunofluorescence (IF). Whole-proteome analysis was carried out in LX-2 cells after SNHG16 KD. DE proteins were identified, and enrichment analyses were used to characterize the biological processes and pathways impacted.
Results: YAP/TAZ KD resulted in 145 DE lncRNAs. Among these, SNHG16 was downregulated and selected for validation. Overexpression of YAP or TAZ elevated SNHG16 expression ($p < 0.0001$ and $p = 0.0266$, respectively). TGF-beta stimulation also induced SNHG16 ($p = 0.004$), implicating its role in fibrogenesis. Functionally, SNHG16 KD reduced mRNA levels of alpha-SMA ($p < 0.0001$), COL1A1 ($p < 0.0001$), TGFB1 ($p = 0.002$), and TIMP2 ($p = 0.0015$), and increased MMP2 ($p = 0.039$). alpha-SMA protein levels were decreased as indicated by WB ($p = 0.0161$) and IF ($p = 0.0435$). SNHG16 KD suppressed HSC proliferation ($p < 0.0001$), transwell migration ($p < 0.0001$), and colony formation ($p = 0.0005$). Whole proteome analysis showed SNHG16 KD dysregulated 328 proteins, enriched in cell cycle control, metabolic processes, and stress-response reprogramming in HSCs.
Conclusion: SNHG16 may act as a YAP/TAZ-dependent lncRNA that regulates various aspects of HSC biology. Its silencing could therefore be a potential therapeutic target in liver fibrosis.

FRI-306-YI

Anticoagulation attenuates liver fibrosis via targeting neutrophil extracellular traps and proteasome

Yingjie Ai[1,2], Detlef Schuppan[2], Shiyao Chen[1]. [1]*Zhongshan Hospital, Fudan University, Shanghai, China;* [2]*University Medical Center, Johannes Gutenberg University, Institute of Translational Immunology and Research Center for Immunotherapy, Mainz, Germany*
Email: 23111210016@m.fudan.edu.cn

Background and aims: Neutrophil extracellular traps (NETs) contribute to liver fibrosis by sustaining inflammation and activating hepatic stellate cells. Given that anticoagulants demonstrate antifibrotic potential in preclinical models and they modulate neutrophil activation and NETs formation, anticoagulation may suppress NETs release and thereby attenuate fibrogenesis. The 20S proteasome, the catalytic core of the ubiquitin–proteasome system, regulates immune responses and oxidative stress. This study aimed to investigate whether anticoagulation mitigates liver fibrosis through modulation of NETs and 20S proteasome activity.
Method: Advanced liver fibrosis was induced in mice via intraperitoneal injection of thioacetamide (TAA, 150 mg/kg), three times per week for 12 weeks. Mice were randomly divided into a treatment group (the factor X antagonist Edoxaban, Edo) and a control group

(Ctr) (each n = 6). Edo was given as a suspension by gavage (30 mg/kg in 0.2 ml) daily for 3 weeks, while controls received the same volume of saline, from week 10. Liver fibrosis, NETs formation and 20S proteasome subunit genes were assessed via RNA sequencing, WB and IHC.
Results: Masson's trichrome and Sirius Red staining revealed significantly reduced hepatic collagen deposition in the Edo group. RT-qPCR and WB demonstrated marked downregulation of fibrosis-related genes, including Col1a1, Fn, and Acta2 in the Edo group. Differential gene expression analysis also revealed enrichment in the NETs formation pathway. HE staining of the Edo group showed a significantly reduced neutrophil infiltration while IHC revealed reduced expression of NETs markers, including Myeloperoxidase and Neutrophil elastase. WB confirmed lower levels of citrullinated histone H3, another hallmark of NETs. Further correlation analysis across 68 NETs-associated genes identified multiple 20S proteasome subunit genes (Psmb7, Psma5, Psma6, Psmb1, Psmd8, Psmc2, Psmc5, Psmd6 etc.) as positively correlated with NETs markers and significantly downregulated in the Edo group. These transcriptomic alteration was validated by reduced protein expression detected via WB and IHC. Moreover, 20S proteasome activity assay demonstrated a significant decline in enzymatic activity upon anticoagulation.
Conclusion: Our findings suggest that anticoagulant therapy alleviates liver fibrosis by suppressing NETs formation and modulating proteasome activity. These results reveal a potential interplay between coagulation, innate immunity, and proteostasis in fibrogenesis.

FRI-307
ALR deficiency promotes HSCs activation and deteriorates liver fibrosis by perturbation of MCU-mediated calcium homeostasis
Ye Li[1], Yan-bo Wei[1], Ming-qiang Liu[1], Ling-Yue Dong[1], Wei An[1].
[1]*Capital medical university, Beijing, China*
Email: anwei@ccmu.edu.cn

Background and aims: Hepatic stellate cells (HSCs) activation is a pivotal pathogenesis for liver fibrosis (LF). Mitochondrial calcium (mCa^{2+}) dyshomeostasis is reportedly to contribute HSCs activation. We previously demonstrated that ALR overexpression could inhibit HSCs activation potentially through regulating mitochondrial calcium uniporter (MCU). However, the precious mechanisms dealt with ALR interaction with MCU remains unexplored. This study is aiming to unveil whether ALR inhibition on LF progression is associated to maintenance of mCa^{2+} homeostasis through interplay with MUC.
Method: *Alr* liver-knockout (ALR^{-CKO}) mice were established and LF were prepared either by fed choline-deficient high-fat diet (CD-HFD) or bile-duct ligation (BDL).
Results: We demonstrated that ALR expression was continuously downregulated in fibrotic livers of patients (F0-F4). Similarly, HSCs activation and LF lesion were deteriorated following CD-HFD or BDL treatment. The in-vitro study showed that *Alr*-deletion promoted mCa^{2+} influx by disrupting the dimerization of mitochondrial calcium uptake 1/2 (MICU1/2), the core regulatory components of MCU complex, which was coincided with HSCs activation. We confirmed that MICU1/2 dimerization was remarkably reduced both in human and mouse fibrotic liver tissues, which was positively correlated with decreasing ALR expression. Intriguingly, as confirmed by Co-IP assay, ALR appeared to interact mildly with MICU1 or MICU2, implying that ALR-offering modulation on MICU1/2 dimerization might probably be mediated by an alternative molecule. It is known that CHCHD4 is central to the functions of the mitochondrial disulfide relay system (DRS). To identify if ALR, as a member of DRS, could putatively modulate MICU1/2 dimerization via affecting CHCHD4 redox capacity, we then unveil on interaction between ALR and CHCHD4. Molecular analysis demonstrated that ALR could strengthen CHCHD4 activity via redox modification, enhance MICU1/2 dimerization, restrain mCa^{2+} overflow and ultimately HSCs activation. Further bioinformatic analysis and experiment results showed three cysteine residues at C4, C53, and C55 in CHCHD4 were apparently crucial to assist in MICU1/2 dimerzation since mutations of these cysteines resulted in significant loss of ALR interacting with CHCHD4, impairing ALR ability to restrict HSCs activation.
Conclusion: In all, current study elucidates novel mechanism for ALR alleviation of LF by promoting MICU1/2 topology and inhibiting mCa^{2+} dyshomeostasis in HSCs.

FRI-308
Lysyl oxidase inhibition disrupts angiogenin directed hepatic stellate cell activation influence by hepatoma cells
Basundhara Das[1], Bornika Roy[1], Prachi Sharma[1], Maryam Shaikh[2], Sampa Ghose[3], Subhrajit Biswas[1]. [1]*Amity Centre for Liver Research (ACLR), Amity Institute of Molecular Medicine & Stem Cell Research (AIMMSCR), Amity University Uttar Pradesh, Sector 125, Noida, India;* [2]*Heersink School of Medicine, University of Alabama at Birmingham, Birmingham, United States;* [3]*Department of Medical Oncology, All India Institute of Medical Sciences, New Delhi, India*
Email: dhara4713@outlook.com

Background and aims: Liver cancer progression relies on hepatoma cells fostering a supportive tumour microenvironment, often by activating hepatic stellate cells (HSCs). Lysyl oxidase, a matrix-modulating enzyme secreted abundantly by activated HSCs, plays a crucial role as collagen crosslinker in creating this microenvironment. Angiogenin (ANG) is known to play a key role in Hepatocellular Carcinoma (HCC)-mediated HSC activation. In previous studies, although individual inhibition of ANG and LOX has shown in reducing HCC influenced HSC activation and HCC progression respectively, their mechanistic interaction is unexplored. This study investigates targeting the enzymatic activity of LOX to abrogate HCC-mediated HSC activation via angiogenin and thereby reduce ECM remodeling during HCC progression.
Method: HCC stimulated LX2 (HSCs) cells were treated with a pan-LOX inhibitor (βAPN) or a specific LOXL2 inhibitor (LOXL2IN) *in vitro*. Angiogenin expression and nuclear localization were assessed via western blotting and immunofluorescence. CCl_4 was used to generate fibrotic/ cirrhotic background in orthotopic tumours by directly injecting Hepa1-6 cells in BL/6 mice to study the effect of βAPN (100 mg/kg) or LOXL2IN (10 mg/kg) *in vivo*. Liver sections were analyzed for fibrosis/cirrhosis, tumor size, histological staining as well as immunohistochemistry of Angiogenin, αSMA and ECM components (collagen, elastin).
Results: HepG2 secretes angiogenin as an inducer of LX2 cells' activation by altering various ECM proteins. We have stimulated LX2 cells by HepG2-conditioned media, where the expressions of LOX, LOXL2, αSMA were upregulated along with both angiogenin expression and its nuclear translocation. LOX inhibition significantly reduced αSMA and angiogenin expression in protein lysates and prevented nuclear translocation of angiogenin, rather retaining it peripherally/cytoplasmically or secreted, thereby mitigating HCC-mediated LX2 activation. *In vivo*, LOX inhibition reduced tumor size with less Ki67 expression and altered angiogenin localization in αSMA^{+} cells, aborogated ECM components.
Conclusion: Targeting LOX enzymatic activity effectively disrupts the self-sustaining cycle of hepatoma cells via HSCs by indirectly hindering the angiogenin axis, specifically its nuclear translocation and further transcriptional stimulation of lysyl oxidase gene family, suggesting a promising therapeutic strategy in HCC.

FRI-313
Resmetirom ameliorates fibrogenesis in hepatic stellate cells via thyroid hormone receptor alpha-fatty-acid-amide hydrolase 1 signalling pathway
Alba Cabaleiro[1], Eva Novoa[1], Borja López-Picallo[1], Natalia Lima[1], Cristina Roibello[1], Carmen Pena[2], Jose Iglesias-Moure[1], Ana Senra[1], María Luz Martínez-Chantar[3], Anabel Fernández-Iglesias[4],

Jordi Gracia-Sancho[4], Susana Bravo[2], Carlos Dieguez[1], Marta Varela-Rey[1], Vincent Prevot[5], Markus Schwaninger[6], Miguel Lopez[1], Ruben Nogueiras[1]. [1]*Universidad de Santiago de Compostela-Campus Vida, Santiago de Compostela, Spain;* [2]*Department of Biochemistry and Molecular Biology, CIMUS, IDIS, Universidade de Santiago de Compostela, Santiago de Compostela, Spain;* [3]*Liver Disease Lab, BRTA CIC bioGUNE, Centro de Investigación Biomédica en Red de Enfermedades Hepáticas y Digestivas, Bizkaia, Spain;* [4]*Hospital Clínic De Barcelona, Barcelona, Spain;* [5]*Univ. Lille, Inserm, CHU Lille, Laboratory of Development and Plasticity of the Neuroendocrine Brain, Lille, France;* [6]*Universität Zu Lübeck, Lübeck, Germany*
Email: albalopez.cabaleiro@usc.es

Background and aims: Resmetirom is a liver-directed, thyroid hormone receptor beta (THRb)- selective agonist approved for treating metabolic-associated steatohepatitis (MASH) with moderate to advanced fibrosis. While Resmetirom hepatocyte-specific effects are well-established, its impact on other hepatic cells, particularly hepatic stellate cells (HSCs), the main fibrogenic cells, remains unknown. Accordingly, the aim of this study is to elucidate a potential direct role of Resmetirom in HSCs activation and fibrogenesis onset.
Method: Animal models, immortalized cell lines, and primary murine and human HSCs were used in combination with pharmacological treatments and genetic manipulation of thyroid hormone receptor-α (THRa) and fatty acid amide hydrolase (FAAH) to evaluate the effects of Resmetirom on the fibrogenic process.
Results: Resmetirom ameliorates MASH in mice through actions in both hepatocytes and HSCs. Resmetirom attenuates transforming growth factor beta-1(TGF-B1)-induced HSC activation via THRa and increased FAAH expression and activity. In contrast, their inhibition prevents Resmetirom from reducing fibrotic marker expression and the elevated glycolytic activity typical of activated HSCs.
Conclusion: These results uncover an unrecognized mechanism of action for Resmetirom, demonstrating that its antifibrotic efficacy extends beyond hepatocytes to include direct effects on HSCs via THRa and FAAH. Furthermore, these results may support future patient stratification, as individuals harboring THRa mutations could exhibit reduced responsiveness to treatment.

FRI-314

Targeting TRIM54: a potential protective strategy against liver injury in cirrhosis

Fan-E Cheng[1], Yaxi Zhang[1], Shihao Zheng[1], Wenying Qi[1], Size Li[1], Qiuyue Wang[1], Xinyu Zhao[1], Chunfeng Mei[1], Xiaobin Zao[2], Yong'an Ye[3]. [1]*Dongzhimen Hospital, Beijing University of Chinese Medicine, Beijing, China;* [2]*Key Laboratory of Chinese Internal Medicine of Ministry of Education and Beijing, Dongzhimen Hospital, Beijing University of Chinese Medicine, Beijing, China;* [3]*Institute of Liver Diseases, Dongzhimen Hospital, Beijing University of Chinese Medicine, Beijing, China*
Email: 18801020531@163.com

Background and aims: Cirrhosis represents the terminal stage of various chronic liver diseases, hallmarked by progressive fibrosis, architectural distortion, and eventual functional failure. TRIM54, a key member of the TRIM family, has been implicated as a central regulator in multiple hepatic pathological processes. However, its precise function and underlying mechanisms in the initiation and progression of cirrhosis remain elusive. This study aims to systematically elucidate the biological role of TRIM54 and delineate its molecular regulatory network during cirrhotic progression, thereby providing novel theoretical insights and identifying potential therapeutic targets for this disease.
Method: To investigate the role of TRIM54 in cirrhosis, we established two complementary rodent models: a DEN-induced rat model and a CCl_4-induced mouse model of liver cirrhosis. Phenotypic and mechanistic validation was performed using an AAV8-mediated liver-specific knockdown of TRIM54. This intervention was assessed through a combination of serum biochemical analysis, histopathological staining, Western blotting, and quantitative real-time PCR (qRT-PCR). Furthermore, an integrated multi-omics analysis was conducted by combining transcriptomic and proteomic sequencing data.
Results: TRIM54 expression was significantly upregulated in cirrhotic tissues, and its expression level was positively correlated with fibrosis markers (α-SMA and Col1a1). Concurrently, knockdown of TRIM54 led to marked improvements in liver function, accompanied by a reduction in fibrosis and inflammation, as well as suppression of Wnt/β-catenin signaling pathway activation. Integrated multi-omics analysis revealed significant co-enrichment of the Wnt signaling pathway, ubiquitin-mediated proteolysis, and PPAR signaling pathway at both the gene and protein levels, further validating that TRIM54 knockdown exerts its regulatory effects through these pathways. Mechanistically, TRIM54 was shown to promote the ubiquitination and subsequent degradation of AXIN1, thereby modulating the activation status of the Wnt/β-catenin signaling pathway.
Conclusion: The mechanism by which TRIM54 drives cirrhosis involves the ubiquitination-mediated degradation of AXIN1, leading to constitutive activation of the Wnt/β-catenin pathway. Notably, knockdown of TRIM54 reverses this activation and ameliorates disease progression, supporting its therapeutic potential.

FRI-315

Effects of combined Atorvastatin and Ambrisentan treatment on hemodynamic alterations and liver fibrosis in a translational rat model of advanced MASLD

M Serra Cusidó[1,2], Imma Raurell[1,2,3,4], María Martínez-Gómez[1,2,4], Eduard Mas[1,3], Juan M. Pericàs[1,2,3,4], Joan Genesca[1,2,3,4]. [1]*Liver Disease Group, Vall d'Hebron Research Institute, Barcelona, Spain, Barcelona, Spain;* [2]*Universitat Autònoma de Barcelona, Barcelona, Spain, Barcelona, Spain;* [3]*Liver Unit, Area of Digestive Diseases, Hospital Universitari Vall d'Hebron, Barcelona, Spain, Barcelona, Spain;* [4]*Spanish Network of Biomedical Research Centers, Liver and Digestive Diseases (CIBERehd), Spain, Barcelona, Spain*
Email: maria.cusido@vhir.org

Background and aims: Metabolic dysfunction-associated steatotic liver disease (MASLD) is characterized by hepatic steatosis, which can progress to inflammation, fibrosis, and portal hypertension (PH). Despite its increasing clinical burden, therapeutic options remain limited due to the lack of translational animal models. Previous work from our group developed a non-fibrotic NASH model, which, when treated with Atorvastatin (Ato) and Ambrisentan (Amb) reduced steatohepatitis and PH. Considering those results, in this study we evaluate the combined effect of Ato and Amb on liver fibrosis, endothelial dysfunction, and hemodynamic alterations in a recently developed translational model of MASLD with advanced fibrosis.
Method: Male Sprague-Dawley rats were fed for 20 weeks with control diet (CD) or high-fat high-cholesterol diet supplemented with cholic acid and a glucose/fructose beverage (HFD). During the last 4 weeks, HFD rats received 10 mg/kg Ato, 2 mg/kg Amb, or both. At endpoint, liver hemodynamic was assessed, hepatic stellate cells (HSC) were isolated and liver samples were collected.
Results: MASLD rats exhibited increased AST/ALT, PH, insulin resistance, steatohepatitis and advanced fibrosis, corresponding to our known model features. Neither Ato nor Amb alone or combined reduced body weight or insulin resistance. Endothelial dysfunction was reversed by AtoAmb as P-Enos and KLF2 were restored. Markedly, AtoAmb led to fibrosis regression, evidenced by (1) decreased histological fibrosis stage, (2) reduced collagen deposition, (3) downregulation of Col1a1 and alpha-SMA to near-control levels, and (4) lower levels of metalloprotease inhibitor TIMP1. Moreover, AtoAmb HSC prevented collagen gel from contracting, indicating reduced cellular contractility. However, severe steatosis and PH remained unaffected. Linear modelling of portal pressure showed a poor association with fibrosis but a stronger correlation with steatosis

severity, both assessed histologically and quantitative, suggesting steatosis as the main driver to sinusoidal compression and so PH.
Conclusion: The combination of AtoAmb demonstrated a synergistic antifibrotic effect in a translational rat model of MASLD but failed to reduce PH, likely due to persistent severe steatosis and sinusoidal compression. These findings highlight the dissociation between fibrosis and portal pressure in advanced MASLD and emphasize the need for multi-targeted strategies addressing both lipid accumulation and fibrosis for effective PH management.

FRI-316
MicroRNA-based predictive staging of liver fibrosis severity in chronic liver disease
Alejandro del Castillo-Cruz[1,2,3], Victoria Cairoli[4,5,6], Júlia Cacho-Pujol[1,2,3], Lucía Calderón-Robles[1], Núria Benítez-Paredes[1], María Victoria Preciado[4,5,6], Pamela Valva[4,5,6], Anna Moles[1,2,7]. *[1]Instituto de Investigaciones Biomédicas de Barcelona (IIBB-CSIC), Barcelona, Spain; [2]IDIBAPS, Barcelona, Spain; [3]Universitat de Barcelona, Barcelona, Spain; [4]Instituto Multidisciplinario de Investigaciones en Patologías Pediátricas (IMIPP), Buenos Aires, Argentina; [5]CONICET-GCBA, Buenos Aires, Argentina; [6]Hospital de Niños Ricardo Gutiérrez, Buenos Aires, Argentina; [7]CiberEHD, Madrid, Spain*
Email: alejandro.cc.lab@gmail.com

Background and aims: Chronic liver diseases (CLD) are an increasingly common cause of global morbidity and mortality, characterized by persistent inflammation, activation of hepatic stellate cells, and extracellular matrix accumulation. In the absence of specific antifibrotic therapies and validated biomarkers, microRNAs (miRNAs) have emerged as key epigenetic regulators of fibrogenesis and liver regeneration. This study aims to characterize their expression profile in murine models and human CLD samples to evaluate their diagnostic, functional, and therapeutic potential.
Method: Levels of miR-92a-3p, miR-122-5p, miR-194-5p, miR-320a-3p, and miR-423-3p were quantified by RT-qPCR in livers of C57BL6/J mice subjected to different progressive experimental liver fibrosis models: CCl_4 (4 and 8 weeks, and reversal), BDL (7 and 14 days), MASH (6 months WD+CCl_4 and 2 months CDAHFD). The degree of fibrosis was confirmed by Sirius Red staining, RT-qPCR for Col1A1, TGFβ and hydroxyproline (HP) levels in liver tissue. Results from experimental models were validated in liver tissue and serum extracellular vesicles from patients with chronic hepatitis C (CHC), stratified according to fibrosis stage (METAVIR) $F < 2$ ($n = 16$) vs $F \geq 2$ ($n = 13$).
Results: Murine models showed a progression of liver fibrosis associated with classical markers (SR, Col1A1, TGFβ and HP), allowing differentiation between early and advanced stages. miRNA analysis revealed differential expression according to fibrosis severity: miR-92a-3p, miR-122-5p, miR-194-5p, miR-320a-3p, and miR-423-3p decreased in early stages in the CCl_4 and MASH models, whereas in BDL only miR-122-5p, miR-194-5p, and miR-423-3p decreased. While miR-122-5p, miR-194-5p and miR-423-3p showed a positive correlation with the degree of fibrosis in CCl_4 and MASH, in BDL only miR-122-5p did. These findings were validated in liver tissue and serum extracellular vesicles from CHC patients, where a similar modulation of miRNAs was observed according to fibrosis severity.
Conclusion: Hepatic expression of miR-122-5p, miR-194-5p and miR-423-3p is associated with the degree of fibrosis across different murine models of progressive liver disease and in patients, indicating their potential as biomarkers and therapeutic targets to stage fibrosis progression in chronic liver disease.

FRI-317
Modulation of collagen-binding integrins as a therapeutic strategy to inhibit liver fibrosis
Fatemeh Derakhshandeh[1], Stefan Hamelmann[1], Inaam Nakchbandi[1]. *[1]Heidelberg University Hospital, Heidelberg, Germany*
Email: fatemeh.derakhshandeh@uni-heidelberg.de

Background and aims: Aberrant tissue repair results in extracellular matrix (ECM) accumulation and fibrosis in almost all organs. Integrins are heterodimeric receptors that integrate signals from the matrix. Activation and downstream signaling of integrins leads to changes in the composition of ECM components like collagen. Previous studies highlighted the effects of integrins in various signaling pathways that regulate the onset and progression of fibrosis. Our aim was to study how integrins affect fibrosis and try to pharmacologically modulate these integrins.
Method: In vitro and in vivo studies, fluorescence polarization, proteomic analysis.
Results: siRNA-mediated depletion and genetic deletion of alpha11 and beta1 integrin subunits increased TGF-beta mRNA expression in hepatocytes. Subsequently, several polypeptides were tested for their ability to reduce TGF-beta, and the most effective was the pentapeptide Glycine-Leucine-Glutamine-Glycine-Glutamic (GLQGE) (International patent, PCT/EP2020/071319). GLQGE reduced TGF-beta expression by more than half ($p < 0.001$) in hepatocytes and lowered alpha-smooth muscle actin (alpha-SMA) expression (as a measure of activation) and collagen type I production in primary hepatic stellate cells and in NIH3T3 cells (by 30-50 percent, $p < 0.05$). Fluorescence polarization and in vitro assays, including integrin-specific knockdown controls (in NIH3T3 cells), confirmed that GLQGE binds to both alpha10beta1 and alpha11beta1 integrins. Daily administration of GLQGE in mice for 10 days at the end of a 6-week CCl_4 fibrosis model reduced TGF-beta protein to a third, and decreased alpha-SMA by 40 percent and collagen I by 20 percent ($p < 0.05$ for all). The reduction in alpha-SMA protein suggested that GLQGE directly suppressed the activation of hepatic fibroblasts. Proteomic analysis confirmed modulation of integrin signalling.
Conclusion: By acting on integrins, GLQGE inhibits hepatic stellate cell activation directly through integrin alpha10beta1 and alpha11-beta1, and indirectly via TGF-beta suppression in hepatocytes. This dual mechanism significantly reduces collagen production and alpha-SMA expression in vitro and in a liver fibrosis mouse model, providing clear experimental evidence that GLQGE effectively mitigates liver fibrosis.

FRI-318
Potential protective cooperation of interleukin-6-induced miRNA-9 during acute liver injury may underlie reparative and anti-fibrotic responses
Dana Eidelshtein[1], S. Nahum Goldberg[2], Eithan Galun[1], Jonathan Axelrod[1]. *[1]Hadassah University Hospital-Ein Karem, Goldyne Savad Institute of Gene Therapy, Jerusalem, Israel; [2]Hadassah University Hospital-Ein Karem, Department of Radiology, Goldyne Savad Institute of Gene Therapy, Jerusalem, Israel*
Email: dana.eidelshtein@mail.huji.ac.il

Background and aims: The role of interleukin-6 (IL-6) as a central cytokine involved in suppressing liver injury and fibrosis while promoting regeneration, has been known for several decades, yet its downstream mechanisms remain incompletely defined. MicroRNA-9 has been reported to exert anti-fibrotic effects in chronic liver disease, but its regulation during acute inflammatory liver injury is poorly understood. We aimed to define the relationship between interleukin-6 signaling and miR-9 and to assess whether this axis represents an endogenous mechanism that limits injury and fibrotic progression following acute liver injury.
Method: Single-cell RNA sequencing (scRNA-seq) analysis was used to identify cytokine-driven transcriptional programs following radiofrequency ablation (RFA) induced injury in mice- a clinically relevant

model of acute liver injury. In vitro, hepatocyte-derived cell lines were stimulated with IL-6 followed by quantitative PCR to analyze miR-9 host gene expression and intracellular and secreted mature miR-9 levels.
Results: ScRNA-seq and bioinformatics analysis of mouse liver on days 1 and 7 post-RFA indicated that early activation of interleukin-6 and STAT3 signaling was accompanied by increased miR-9-3HG expression in hepatocytes. Elevated IL-6 mRNA and miR-9 levels post-RFA were confirmed by qPCR analysis of total liver RNA. Incubation of hepatocyte-derived cell lines, HUH-7 and Hepa 1-6, with IL-6 or an IL-6/sIL-6 receptor fusion protein (HIL-6) induced MIR9 gene and mature miR-9 expression in a dose-dependent manner, but not in either HepG2 cells or human stellate cell-derived LX-2 cells.
Conclusion: These findings identify a novel IL-6–miR-9 axis linking inflammatory signaling and the regulation of protective regenerative and anti-fibrogenic responses following acute liver injury. Understanding how IL-6–driven miR-9 induction shapes hepatic cell interactions in the liver parenchyma may provide valuable insight into the mechanisms modulating fibrosis and repair post-injury.

FRI-319
Naringenin attenuates thioacetamide-induced liver fibrosis though epigenomic and transcriptomic reprogramming
Roberto Flores Peña[1], Fernando Caloca Camarena[1], Scarlet Arceo-Orozco[2], Jorge Alejandro Salto-Sevilla[2], Rebeca Rosas-Campos[3], Marina Galicia Moreno[2], Hugo Christian Monroy-Ramirez[2], Juan Armendariz-Borunda[4].
[1]Programa de doctorado en farmacología, Departamento de fisiología, Centro universitario de ciencias de la salud. Universidad de Guadalajara, Instituto de biología molecular en medicina y terapia génica, Centro universitario de ciencias de la salud, Universidad de Guadalajara, Guadalajara, Mexico; [2]Instituto de biología molecular en medicina y terapia génica, Centro universitario de ciencias de la salud, Universidad de Guadalajara, Guadalajara, Mexico; [3]Tecnológico de Monterrey, EMCS, Guadalajara, Mexico; [4]Instituto de biología molecular en medicina y terapia génica, Centro universitario de ciencias de la salud, Universidad de Guadalajara, Tecnológico de Monterrey, EMCS, Guadalajara, Mexico
Email: floresp_roberto@hotmail.com

Background and aims: Hepatic fibrosis (HF) arises from the trans differentiation of quiescent hepatic stellate cells (HSC) into a myofibroblast-like phenotype, leading to an imbalance in extracellular matrix (ECM), collagen accumulation, and progressive liver injury. Epigenetic mechanisms may contribute to the persistence of HSC activation and disease progression. Naringenin (NAR), a flavonoid with anti-inflammatory and antifibrotic properties, may counteract these processes. We aimed to evaluate the antifibrotic and epigenetic effects of NAR in a thioacetamide (TAA)-induced HF model.
Method: Male Wistar rats (~200 g) were randomly allocated to five groups (n = 5): untreated (UT); NAR control (100 mg/kg/day, oral) for 4 weeks (NAR 4W); TAA (200 mg/kg, i.p., three times/week) for 4 weeks (TAA 4W); TAA for 8 weeks (TAA 8W); and TAA for 4 weeks followed by NAR for 4 weeks (TAA 4W + NAR 4W). Liver injury and fibrosis were assessed by histology (hematoxylin and eosin, Masson's trichrome, picrosirius red) and Smooth muscle alpha actin (alpha-SMA) immunohistochemistry. Transcriptomic changes were analyzed by ribonucleic acid (RNA) sequencing. Global deoxyribonucleic acid (DNA) methylation (5-methylcytosine, 5mC) was evaluated by dot blot, while DNMT isoforms and histone H3 acetylation were analyzed by western blot. Statistical analysis was performed using one-way ANOVA with Tukey's post hoc test ($p \leq 0.05$).
Results: TAA induced a different fibrosis-associated transcriptomic profile compared with UT. NAR attenuated these alterations, shifting gene expression towards a non-fibrogenic state. Consistently, NAR reduced histopathological injury, collagen I/III deposition, and alpha-SMA immunoreactivity. Fibrosis was associated with increased nuclear DNMT1 and DNMT3A expression and elevated global 5mC levels, whereas NAR reversed these epigenetic changes and restored histone H3 acetylation marks (H3K9ac and H3K14ac).
Conclusion: NAR mitigates HF and reverses epigenetic alterations associated with fibrosis, thus expanding its mechanisms of action as an epigenetic modulator and making it a potential candidate for the treatment of this disease. Further studies are required to clarify additional mechanisms and establish long-term safety before clinical application.

FRI-320
Identification of Sfrp1 in portal fibroblast and biliary fibrosis development
Wenrui Gao[1], Siham Benyahia[1], Haquima El Mourabit[1], Thierry Jaffredo[2], Sara Lemoinne[1], Chantal Housset[1], Nicolas Chignard[1], Axelle Cadoret[1]. *[1]Sorbonne Université, Inserm, Centre de Recherche Saint-Antoine (CRSA), Team Metabolic and biliary diseases of the liver, Paris, France; [2]Sorbonne Université, CNRS, INSERM, Institut de Biologie Paris Seine (IBPS), Laboratoire de Biologie du Développement, Paris, France*
Email: wenrui.gao@inserm.fr

Background and aims: Liver fibrosis results from the accumulation of extracellular matrix produced by myofibroblasts (MFs). In biliary disease, fibrosis arises in the portal area from MFs originating either from portal fibroblasts (PFs) or hepatic stellate cells (HSCs). The aim of our work is to identify the specific role of MFs derived from PFs or HSCs in biliary fibrosis.
Method: Mesenchymal cells were obtained from the bilio-vascular tree of the Abcb4 KO mouse model of biliary fibrosis and the CCl4 model of non-biliary fibrosis after enrichment by FACS by depleting cells expressing EpCAM, CD31, CD45 and CD11b. Mesenchymal cells underwent scRNAseq and resulting data were analyzed with Seurat v5. Fibrogenic cells (HSCs and PFs) were annotated as quiescent or myofibroblastic based on known markers in homeostatic and fibrotic settings. A differential gene expression analysis was performed to identify genes that could discriminate PFs from HSCs.
Results: Portal mesenchymal cells were isolated from Abcb4 KO mice and of CCl4-injected mice with an equivalent amount of liver fibrosis, as ascertained by Sirius red staining and Col1a1 gene expression. Within the scRNAseq data, we first identified fibrogenic cell populations from biliary and non-biliary fibrosis, respectively, and then merged and further annotated them as 8 clusters of MFs and 12 clusters of qPFs and/or qHSCs. Uniform Manifold Approximation and Projection (UMAP) visualization showed distinct projections between fibrogenic cell populations from biliary and non-biliary fibrosis, indicating specific cellular processes involvement. Gene expression analysis identified 12,294 differentially expressed genes (DEGs) between the PF and HSC lineages. Among DEGs, four genes were evidenced that were expressed in PF cells (pct.PF > 50%) and which expression was significantly higher ($p < 0.01$, logFC > 1.8) than in HSCs. Among these four genes, Sfrp1 showed an increased gene expression proportional to fibrotic tissue accumulation in Abcb4 KO and DDC-fed mice, as ascertained on whole liver by RT-qPCR.
Conclusion: By combining cell isolation and scRNAseq analysis, we show a specific involvement of PFs in the portal space during biliary fibrosis, while HSCs are solicited in non-biliary fibrosis. Furthermore, we identified Sfrp1 as a specific marker of the PF lineage that will allow us to better understand the specific involvement of these cells in liver fibrosis.

FRI-321
UBC13 prevents hepatic stellate cell activation by K63 ubiquitination of HMGB1
Sui Guoyan[1], Yoon-Seok Roh[1]. *[1]Department of Pharmacy, Chungbuk National University College of Pharmacy, Cheong-Ju, Korea, Rep. of South*
Email: ysroh@cbnu.ac.kr

Background and aims: Ubiquitination is a critical post-translational modification that regulates hepatic stellate cell (HSC) activation, a key event in the progression of liver fibrosis. Although K48-linked ubiquitination has been extensively characterized, the biological functions of global K63-linked ubiquitination in HSCs remain poorly understood. UBC13, an E2 ubiquitin-conjugating enzyme, specifically catalyzes K63-linked ubiquitination. In current study, we investigated the mechanisms underlying Ubc13-mediated global K63-linked ubiquitination in HSCs and its role in fibrotic progression.
Method: HSC-specific *Ubc13*-deletion mice were generated by crossing *Ubc13*$^{fl/fl}$ mice with Lrat^{Cre} or Pdgfrb^{CreERT2} mice. Liver fibrosis was induced by intraperitoneal injection of 20% carbon tetrachloride or by feeding 3,5-diethoxycarbonyl-1,4-dihydrocollidine diet. Ubiquitin-proteomics analyses were conducted using EV-LX2 and UBC13-overexpressing LX2 cells. Immunoprecipitation–mass spectrometry analyses (IP-MS) were performed in HEK293 T cells transfected with UBC13+K63 or HMGB1+K63 plasmids. RNA-sequencing was performed using EV-LX2 and HMGB1-overexpressing LX2 cells under TGF-β stimulation. UBC13 and α-SMA expression were also analyzed in cirrhotic patient liver samples to evaluate clinical relevance.
Results: During HSC activation, global K63-linked ubiquitination was markedly reduced, while K48-linked ubiquitination remained unchanged. UBC13 expression was significantly downregulated in activated HSCs from both human and murine fibrotic livers. In mice, HSC-specific deletion of *Ubc13* enhanced glycolysis-driven HSC activation and exacerbated liver fibrosis. Mechanistic analyses using ubiquitin proteomics and IP–MS revealed that UBC13 promotes the interaction between TRIM28 and HMGB1, thereby facilitating K63-linked ubiquitination of HMGB1 at Lys147 and its subsequent lysosomal degradation. This degradation restrains glycolysis-driven HSC activation, an effect recapitulated by UBC13 overexpression. Notably, UBC13 expression inversely correlated with α-SMA levels in livers of cirrhosis patients, supporting the translational relevance of the findings.
Conclusion: Hepatic stellate cell UBC13 restrains liver fibrosis through regulation of K63-linked ubiquitination-mediated HMGB1.

FRI-322
IGFBPs, MMPs, and cytokines as predictors of liver fibrosis: comparative analysis of biomarkers

Gabriela Gutierrez Reyes[1], Abigail Hernandez-Barragan[1], Marisela Hernandez-Santillan[1], Moises Martinez-Castillo[1], Ángel Daniel Santana Vargas[2], Paula Cordero-Pérez[3], José Luis Pérez-Hernández[2]. *[1]Universidad Nacional Autónoma de México, UNAM, School of Medicine, UIME, HIPAM Lab, Hospital General de México Dr. Eduardo Liceaga, Mexico City, Mexico; [2]Hospital General de México Dr. Eduardo Liceaga, Gastroenterology and Hepatology Department, Clinic of dream, Mexico City, Mexico; [3]Universidad Autónoma de Nuevo León, University Hospital Dr. José Eleuterio González, School of Medicine, Liver Unit, Monterrey, Mexico*
Email: gabgurey@yahoo.com.mx

Background and aims: Backgroung: Identifying serum biomarkers capable of effectively distinguishing fibrosis stages is critical for early diagnosis and therapeutic monitoring in chronic liver disease. AIM: To evaluate the diagnostic performance of insuline growth factor binding proteins (IGFBPs), cytokines, and matrix metalloproteinases (MMPs) across different fibrosis stages.
Method: A prospective, cross-sectional, multicenter study was conducted. Untreated patients with chronic hepatitis C (cHC) were recruited and classified using FibroScan® and/or FibroTest®. Receiver operating characteristic (ROC) curves were analyzed to compare serum levels of IGFBP 1-7 (ng/ml), cytokines in pg/ml (IL-1a, IL-2, IL-10. IL-12p70), and MMPs (2, 7 and 9; ng/ml) between F0, F1F2, and F3F4 fibrosis groups. Statistical significance was set at $p < 0.05$, and area under the curve (AUC), sensitivity (Se), and specificity (Sp) were reported.
Results: A total of 461 cHC patients met inclusion criteria and were classified into F0 (n = 130), F1–F2 (n = 55), and F3–F4 (n = 216). The IGFBPs: **4** (AUC = 0.754, $p < 0.001$; cut-off: 8.43 ng/mL; sensitivity = 70.9%, specificity = 88.6%); **5** (AUC = 0.722, $p = 0.002$; cut-off: 7.52 ng/mL); **2** (AUC = 0.711, $p = 0.003$; cut-off: 47.56 ng/mL); **7** (AUC = 0.714, $p = 0.002$; cut-off: 3.66 ng/mL); **3**(AUC = 0.660, $p = 0.023$; cut-off: 25.89 ng/mL): IL-10 (AUC = 0.679, $p = 0.009$; cut-off: 5.55 pg/mL; sensitivity = 61.9%, specificity = 84.6%) For advanced fibrosis (F3F4 vs F2), IGFBP-4 had the highest performance, followed by IGFBP-5, IGFBP-2, and IGFBP-7, the latter with the highest specificity (91.4%). IGFBP-3 also reached significance. Among cytokines and MMPs, IL-10 and MMP-7 discriminated F1F2 vs F3F4.
Conclusion: IGFBP-4, IGFBP-5, IGFBP-7, and IL-10 showed significant accuracy in distinguishing fibrosis stages, particularly in identifying mild fibrosis. Their high specificity and robust AUC values support their role as non-invasive biomarkers that may complement diagnostic of fibrosis and also can be used in other liver diseases that MASLD or MetALD.

FRI-323
Matricellular serum biomarkers predict fibrosis severity and clinical outcomes in autoimmune hepatitis and primary biliary cholangitis

Ludwig Horst[1], Rambabu Surabattula[2], Alexander Fierenz[1], Füssel Katja[1], Ansgar W. Lohse[1], Marcial Sebode[1], Sudha Rani Myneni[2], Detlef Schuppan[2,3,4], Christoph Schramm[1,5,6]. *[1]University Medical Center Hamburg-Eppendorf, Hamburg, Germany; [2]University Medical Center of the Johannes Gutenberg University Mainz, Mainz, Germany; [3]Beth Israel Deaconess Medical Center, Boston, United States; [4]European Union Innovative Medicines Initiative 2 (IMI2) Joint Undertaking under grant agreement 777377: LITMUS (Liver Investigation: Testing Biomarker Utility in Steatohepatitis), Mainz, Germany; [5]Martin-Zeitz Center for Rare Diseases, Hamburg, Germany; [6]Hamburg Center for Translational Immunology (HCTI), Hamburg, Germany*
Email: l.horst@uke.de

Background and aims: Autoimmune hepatitis (AIH) and primary biliary cholangitis (PBC) are major autoimmune liver diseases for which reliable biomarkers of fibrosis progression and prognosis remain limited. Thrombospondin-2 and -4 (TSP2/-4), insulin-like growth factor-binding protein 7 (IGFBP7), and cluster of differentiation 163 (CD163) have recently demonstrated predictive potential as biomarkers in people with metabolic dysfunction-associated steatohepatitis. We therefore hypothesised that these markers may serve as predictors of fibrosis and outcome in AIH and PBC.
Method: Serum levels of TSP2, TSP4, IGFBP7, and CD163 were quantified by validated ELISA in 166 individuals with AIH and 117 with PBC treated at the University Medical Center Hamburg-Eppendorf. Biomarkers were evaluated in relation to liver stiffness measured by transient elastography, disease activity, and patient outcomes, including liver-related endpoint-free survival.
Results: In multivariable regression analyses, TSP2, IGFBP7, CD163, and TSP4 were independently and positively associated with liver stiffness in both AIH and PBC ($p < 0.001$–0.007). ROC analyses showed that TSP2 and IGFBP7 effectively discriminated between patients with and without advanced fibrosis (≥F3; AUC 0.83–0.88). In AIH, elevated baseline serum levels of TSP2 and IGFBP7, indicative of advanced fibrosis, were significantly associated with reduced liver-related endpoint-free survival (liver-related death, liver transplantation, and complications of cirrhosis; Log-Rank $p < 0.001$–0.032).
Conclusion: Circulating TSP2, IGFBP7, CD163, and TSP4 were strongly associated with advanced fibrosis in individuals with AIH and PBC. Moreover, especially TSP2 was linked to liver-related endpoint-free survival in AIH, highlighting its promise as a prognostic biomarker.

FRI-324

Lipometabolic reprogramming via ATGL inhibition improves liver fibrosis and promotes hepatic activated CD8+ tissue-resident memory T cells (TRM) in vivo

Henriette Horstmeier[1], Tanmoy Chakma[1], Katharina Bonitz[2,3], Thomas Sorz-Nechay[2,3], Katja Sommer[3], Vlad Taru[2], Veronica Moreno-Viedma[1], Thierry Claudel[1], Robert Brettner[1], Hubert Scharnagl[4], Claudia Fuchs[1], Philipp Schwabl[1,2,3], Thomas Reiberger[2,3], Michael Trauner[1]. [1]*Hans Popper Laboratory of Molecular Hepatology, Medical University of Vienna, Vienna, Austria;* [2]*Christian Doppler Laboratory for Portal Hypertension and Liver Fibrosis, Medical University of Vienna, Vienna, Austria;* [3]*CeMM Research Center for Molecular Medicine of the Austrian Academy of Sciences, Vienna, Austria, Vienna, Austria;* [4]*Medical and Chemical Laboratory Diagnostics, Medical University of Graz, Graz, Austria*
Email: henriette.horstmeier@meduniwien.ac.at

Background and aims: Lipid immunometabolism is a key regulator of immune function and hepatic necroinflammation, thereby potentially impacting liver fibrosis. Controlled by the activity of adipose triglyceride lipase (ATGL), the lipolytic cleavage of triacyl glycerides to free fatty acids and glycerol shapes energy homeostasis, tissue biosynthesis and cell signaling. Given the lack of antifibrotic treatment options, we investigated the therapeutic potential of ATGL-inhibition in fibrosis in a time-resolved manner *in vivo*.
Method: Fibrosis was induced in C57BL/6 mice by carbon tetrachloride (CCl_4; 3x/week, 2 ml/kg, oral gavage) for 1, 2, 4 and 8 weeks in parallel to treatment with the ATGL-inhibitor Atglistatin (ATGLi) (2x/day; 200µmol/kg, oral gavage and via diet 2 mmol/kg chow), while the control groups received olive oil as vehicle control. Liver injury was assessed biochemically, while hepatic collagen proportionate area (CPA) and lipid accumulation were assessed by histology and portal pressure was measured invasively. Further analysis was conducted using multi-organ flow cytometry, bulkRNA sequencing and untargeted metabolomics.
Results: ATGL-Inhibition was confirmed by elevated liver-to-body-weight ratio [5.73 ± 0.11 vs. 4.6 ± 0.14%, $p < 0.0001$] and histologic hepatocellular lipid accumulation. Starting from week 2, ATGLi strongly reduced liver injury [AST: 1163 ± 872 vs. 4532 ± 2427 U/L, $p = 0.0001$], fibrosis [CPA: 5.72 ± 1.00 vs. 2.71 ± 1.20%, $p < 0.0001$] and portal hypertension [PP: 5.57 ± 0.55 vs. 7.76 ± 1.09 mmHg, $p < 0.0001$]. Flow cytometry revealed the expansion of hepatic, lymph nodal and splenic $CD8^+$T cells upon ATGL-inhibition, further identified as effector $CD44^{hi}CD62^{Lo}$ T-cells (T_{eff}) [49.96 ± 5.70 vs. 23.44 ± 10.06%, $p < 0.0001$, rel. to $CD8^+$] and $CD69^+$ tissue-resident memory T cells ($CD8^+$TRM) [34.67 ± 4.69 vs. 14.52 ± 5.96%, $p < 0.0001$, rel. to $CD8^+$]. Metabolomic profiling uncovered the increased biosynthesis of nucleotides, amino acids and redox equivalents.
Conclusion: Our data suggests improved liver fibrosis and portal hypertension upon ATGLi treatment in fibrosis. Mechanistically, ATGL inhibition promoted anti-oxidative and proliferative tissue metabolic activity. In kinetic synchrony, we observed the expansion of hepatic $CD8^+T_{eff}$ and $CD8^+$TRM, potentially maintaining their activation state and target profibrotic agents due to the optimized metabolic niche. Collectively, this points towards a novel antifibrotic mechanism via immunometabolic reprogramming.

FRI-329

Constitutive MAS1 G protein-coupled receptor participates in the pathogenesis of liver fibrosis

Philipp Althaus[1], Fernando Magdaleno[2,2], Robert Schierwagen[1], Frank Erhard Uschner[1], Maximilian Joseph Brol[1], Thomas Walther[3], Jonel Trebicka[1], Sabine Klein[1]. [1]*Münster University Hospital, Münster, Germany;* [2]*Epistem Limited, Manchester, United Kingdom;* [3]*University College Cork, Department of Pharmacology and Therapeutics, Cork, Ireland*
Email: sabine.klein@ukmuenster.de

Background and aims: The activation of the renin-angiotensin system (RAS) in experimental and human liver cirrhosis, leads to increased levels of angiotensin-II (Ang-II) and angiotensin type 1 receptor (AT1R) stimulation, thus contributing to liver fibrosis and portal hypertension (PTH) by activating HSCs. Mas-related G protein-coupled receptor (MAS1) is increased in the cirrhotic liver, representing an alternate mechanism that opposes the effects of the Ang-II/AT1R axis. Thus, we investigated the protective role of MAS1 as a potential antifibrotic receptor constitutively activated in liver fibrosis.
Method: Human blood samples were measured for Angiotensin levels. Gene and protein expressions were investigated in human donors and recipients. Wildtype (wt) and Mas-receptor knock out mice ($Mas1^{-/-}$) received CCl_4, MCD, WD or a bile-duct ligation (BDL) to induce liver fibrosis. BDL mice were treated with Ang(1-7) or AVE0991. To assess PHT, the portal pressure (PP) was measured. Murine livers were histologically analyzed and gene and protein expressions were measured. Hepatic stellate cells (HSC) were isolated from mice and cell lines were transfected with Mas1 plasmid.
Results: MAS1 deficiency stimulates Ang-II/AT1R signaling and thereby aggravates fibrosis and PTH in BDL and CCl_4-mice. *In vivo* studies showed that Ang-(1-7) and AVE0991 lowered portal pressure (PP) in MAS1 deficient mice after BDL, suggesting another receptor different than MAS1 involved in vasoconstriction. *In vitro*, Ang-(1-7) did not attenuate expression of fibrotic markers and contraction in MAS1 transfected HSC cells, suggesting that constitute activation of MAS1 is sufficient to relax HSC.
Conclusion: Constitutive activation of MAS1 in HSC reduces liver fibrosis and PTH.

FRI-330

Platelet derived growth factor receptor beta as a pan-fibrotic drug delivery target

Sylvia Klomp[1], Diederick van Doorn[2], Joanne Verheij[3], Harm Jan Bogaard[4], Guus van Dongen[5], Bart Nijmeijer[6], Rychon van Dasselaar[6], Joey Muns[6], Kevin Adamzek[6], Arthur Eibergen[6], Ronald Boellaard[7], Ben Zwezerijnen[7], Daniëlle Vugts[7], Anton Vonk[1], Cyriel Ponsioen[2], R. Bart Takkenberg[2]. [1]*Amsterdam University Medical Center, Department of Pulmonary Medicine, Amsterdam, Netherlands;* [2]*Amsterdam University Medical Center, Department of Gastroenterology and Hepatology, Amsterdam, Netherlands;* [3]*Amsterdam University Medical Center, Department of Pathology, Department of Pathology, Antwerp University Hospital/University of Antwerp, Belgium, Amsterdam, Netherlands;* [4]*Amsterdam University Medical Center, Department of Pulmonary Medicine, LinXis Biopharmaceuticals, Amsterdam, Netherlands;* [5]*LinXis Biopharmaceuticals, Amsterdam University Medical Center, Department of Radiology and Nuclear Medicine, Amsterdam, Netherlands;* [6]*LinXis Biopharmaceuticals, Amsterdam, Netherlands;* [7]*Amsterdam University Medical Center, Department of Radiology and Nuclear Medicine, Amsterdam, Netherlands*
Email: s.d.klomp@amsterdamumc.nl

Background and aims: Hepatic fibrosis is a dynamic process characterized by excessive extracellular matrix deposition following chronic liver injury. Regardless of type or etiology, liver fibrosis is driven by activated, collagen-producing myofibroblasts. Activated myofibroblasts overexpress platelet-derived growth factor receptor (PDGFR)-beta. This surface receptor may therefore be useful for diagnosis and disease monitoring, as well as for fibrosis-selective drug delivery. SP02SP26-ABD (Fibrobody®), a high-affinity, species-cross-reactive PDGFR-beta–binding construct, was developed as a pan-fibrosis vector for non-invasive imaging of, and selective intracellular targeted drug delivery to, activated myofibroblasts. This study aimed to evaluate the potential of the Fibrobody in targeting fibrotic tissue and its ability to discriminate fibrosis stages across different disease etiologies, using metabolic dysfunction–

associated steatotic liver disease (MASLD) and primary sclerosing cholangitis (PSC) as two distinctly different types of liver fibrosis.
Method: Mouse models of MASLD (choline-deficient, L-amino acid-defined high-fat diet) and PSC (chronic 3,5-diethoxycarbonyl-1,4-dihydrocollidine feeding) were utilized. Liver fibrogenesis was assessed by (immuno)histochemistry. Biodistribution and (intra-) hepatic uptake of ^{89}Zr-labelled Fibrobody were evaluated by PET-CT, *ex vivo* tissue distribution and autoradiography. Human liver specimens from patients with MASLD (n = 37) and PSC (n = 18) were analyzed using Sirius Red and alpha-smooth muscle actin (SMA) staining for fibrosis staging. PDGFR-beta expression was correlated with these fibrosis markers.
Results: In the mouse models, PDGFR-beta overexpression was selectively localized to the fibrotic liver tissue and corresponded with specific and high hepatic accumulation of ^{89}Zr-Fibrobody. In human MASLD and PSC liver samples, PDGFR-beta expression co-localized with collagen (in Sirius Red) and alpha-SMA. PDGFR-beta expression increased with fibrosis severity, enabling discrimination between stages in both MASLD and PSC.
Conclusion: Preclinical data confirm that PDGFR-beta is a robust marker of fibrotic remodeling in liver fibrosis. Furthermore, the data confirm that the Fibrobody is a selective and efficient PDGFR-beta-targeting vector. These results warrant further exploration into the diagnostic and therapeutic potential of the Fibrobody which will be further elucidated in planned and ongoing (pre-) clinical studies.

FRI-331
Targeting DNA stress response as a synthetic lethal strategy for activated hepatic stellate cells
Eui Jin Lee[1], Ja Hyun Koo[1]. [1]*Seoul National University, Seoul, Korea, Rep. of South*
Email: euijin1204@snu.ac.kr

Background and aims: Hepatic stellate cells (HSCs) drive liver fibrosis through myofibroblastic transdifferentiation, a process closely linked to rapid cell proliferation and YAP/TAZ activation. This hyper-proliferative state inherently leads to the accumulation of constitutive DNA damage. To maintain genomic instability, rapidly diving cells, such as cancer cells or stem cells, express high levels of DNA damage response proteins. However, the key element that let the activated HSCs survive in rapidly proliferating state remains unexplored. Therefore, the aim of this study is to identify critical survival regulator that enable activated HSCs to undergo hyper-proliferative state.
Method: To investigate synthetic lethality as a strategy to selectively target activated HSCs, we performed a kinase inhibitor library screening for seeking target kinase that inhibits YAP/TAZ activation. We validated the hit candidates using primary mouse HSCs and the human HSC line LX-2 and evaluated DNA damage accumulation to verify the specificity and mechanism of action. We utilized CCl_4-induced mouse liver fibrosis model to assess the therapeutic efficacy of the compound.
Results: Our screening identified Checkpoint kinase 1 (CHK1) as a critical survivor regulator for activated HSCs to maintain genomic instability. We showed that activated HSCs and fibrotic livers have elevated levels of constitutive DNA damage markers. Pharmacological inhibition of CHK1 effectively suppressed the activation and proliferation of HSCs, and it amplified DNA damage in activated HSCs, while quiescent HSCs remained unaffected. The administration of CHK1 inhibitors in CCl_4-induced mouse liver fibrosis model showed markedly attenuated liver fibrosis and improved liver function.
Conclusion: Our data showed that activated HSCs heavily rely on CHK1 to maintain their genomic instability in rapidly proliferating state. Therefore, targeting CHK1 represents a promising and selective therapeutic strategy for liver fibrosis.

FRI-332
Pathological role of argininosuccinate synthase 1 in metabolic dysfunction-associated steatotic liver disease-related liver fibrosis
Yen-Tung Chen[1], Lawrence Wirawan[2], Ming-Lung Yu[3], Ji-Min Li[4]. [1]*Institute of Precision Medicine, College of Medicine, National Sun Yat-sen University, Center of Excellence for Metabolic Associated Fatty Liver Disease (CEMAFLD), National Sun Yat-sen University, Kaohsiung, Taiwan;* [2]*School of Life Sciences, Indonesia International Institute for Life Sciences, Jakarta Timur, Indonesia;* [3]*Center of Excellence for Metabolic Associated Fatty Liver Disease (CEMAFLD), National Sun Yat-sen University, Department of Internal Medicine, Kaohsiung Medical University Hospital, Kaohsiung Medical University, Kaohsiung, Taiwan;* [4]*National Sun Yat-sen University, Kaohsiung, Taiwan*
Email: jmili@g-mail.nsysu.edu.tw

Background and aims: Metabolic dysfunction-associated steatotic liver disease (MASLD) is the most prevalent chronic liver disease worldwide, with liver fibrosis representing a critical stage in disease progression and limited therapeutic options. Emerging evidence indicates that metabolic reprogramming plays a key role in fibrotic diseases. Argininosuccinate synthase 1 (ASS1), a key enzyme in arginine biosynthesis, has been shown by our group to be down-regulated in pulmonary fibrosis, where its loss leads to disease progression. However, the role of ASS1 in MASLD-associated liver fibrosis remains largely unexplored. This study aimed to investigate the contribution of the metabolic enzyme ASS1 to liver fibrosis in MASLD.
Method: Normal and MASLD mouse models were established by feeding a normal diet (ND) or a Western diet (WD) with 5% fructose in drinking water for 48 weeks. ASS1 expression in liver tissues was assessed by immunohistochemistry (IHC) and immunofluorescence (IF) staining. The role of ASS1 in hepatic stellate cell (HSC) activation was evaluated using wound-healing and Transwell invasion assays, while downstream signaling pathways were analyzed by RNA sequencing (RNA-seq) and confirmed by immunoblotting.
Results: Analysis of published RNA-seq datasets revealed significantly reduced *ASS1* expression in liver tissues from patients with NAFL and NASH, which was inversely correlated with *FAP* expression. A decline in *ASS1* mRNA levels was also observed in activated HSCs. In WD-fed mice, IHC staining of liver tissues with strong alpha-SMA expression revealed markedly diminished ASS1 levels, particularly in HSCs, which was further confirmed by IF staining showing reduced ASS1 expression in alpha-SMA-positive cells. Consistently, whole-liver homogenates from WD mice exhibited decreased ASS1 expression accompanied by increased alpha-SMA levels. *In vitro*, TGF-beta1 treatment of LX-2 cells significantly suppressed ASS1 expression. Moreover, ASS1 silencing enhanced LX-2 cell migration and invasion and notably increased fibrotic markers, including alpha-SMA, fibronectin, and COL1A1. Mechanistically, RNA-seq analysis identified enrichment of PI3K-Akt and mTOR signaling pathways in ASS1-deficient LX-2 cells.
Conclusion: Taken together, these findings suggest that down-regulated ASS1 expression is a hallmark of activated HSCs and drives the progression of liver fibrosis, supporting ASS1 as a potential therapeutic target for MASLD-related liver fibrosis.

FRI-333-YI
Decellularized liver matrix hydrogels suppress hepatic stellate cell activation via ROS-independent NRF2 activation
Jia Li[1], Qi Zhou[1], Junyu Wang[1], Yakun Li[1], Manon Buist-Homan[1], Vincent E. de Meijer[1], Martin Harmsen[1], Klaas Nico Faber[1], Han Moshage[1]. [1]*Umcg, Groningen, Netherlands*
Email: j.li03@umcg.nl

Background and aims: Hepatic stellate cells (HSCs) are the primary source of extracellular matrix (ECM) in liver fibrosis. Decellularized ECM (dECM)-derived hydrogels show therapeutic potential due to superior biocompatibility, yet the molecular mechanisms underlying their anti-fibrotic effects remain unclear. This study investigates

cellular pathways mediating dECM hydrogel-induced HSC deactivation.
Method: Soft (healthy liver stiffness) and stiff (fibrotic liver stiffness) hydrogels were fabricated from porcine liver dECM (LdECM), with stiffness modulated by ruthenium (Ru) crosslinking. Primary rat activated HSCs (aHSCs) cultured on tissue culture polystyrene (TCPS), soft or stiff hydrogels for 48 hours produced conditioned medium (CM). Fresh aHSCs on TCPS were treated with CM for 72 hours. A transwell co-culture system was then used to distinguish the effects of matrix-derived soluble factors from cellular paracrine signaling. Proteomic analysis, qPCR, and western blotting were used to assess HSC activation markers and identify key regulatory pathways. The role of reactive oxygen species (ROS) was investigated using the antioxidant N-acetylcysteine (NAC).
Results: Both CM treatment and co-culture with acellular LdECM hydrogels, regardless of stiffness, significantly suppressed proliferation and activation markers including collagen type 1 and alpha-smooth muscle actin in aHSCs. This demonstrated that soluble factors released from the hydrogel matrix are the dominant drivers of HSC deactivation, independent of direct cellular crosstalk. Proteomic profiling of treated aHSCs revealed a significant upregulation of the antioxidant defense system. This was validated by increased expression of key antioxidant enzymes. Mechanistically, LdECM hydrogels induced the nuclear translocation of nuclear factor erythroid 2-related factor 2 (NRF2). Crucially, this NRF2 activation was ROS-independent, as co-treatment with NAC failed to block NRF2 nuclear entry despite further reducing intracellular ROS levels.
Conclusion: LdECM hydrogels attenuate HSC activation by promoting a potent antioxidant program driven by the ROS-independent activation of NRF2. This finding reveals a novel mechanism where biomaterials can directly reprogram the cellular redox state to regulate HSC fate, offering a new therapeutic rationale for liver fibrosis.

FRI-334
Geniposidic acid suppresses hepatic stellate cell activation by regulating protein kinase B and glycogen synthase kinase 3-beta signaling

Yakun Li[1], Jia Li[1], Manon Buist-Homan[1], Han Moshage[1]. [1]*Umcg, Groningen, Netherlands*
Email: yakunli96@gmail.com

Background and aims: Activation of hepatic stellate cells (HSCs) is a central event in the progression of liver fibrosis and is characterized by excessive deposition of extracellular matrix. Geniposidic acid (GPA), a natural iridoid glycoside derived from *Gardenia jasminoides*, has been reported to exert hepatoprotective effects in conditions such as Metabolic dysfunction-Associated Steatotic Liver Disease (MASLD). However, its direct role in regulating HSC activation remains unclear. This study aimed to investigate the effects of GPA on activated HSCs *in vitro* and to elucidate the underlying molecular mechanisms.
Method: Primary HSCs were isolated from male Wistar rats and fully activated by culturing on uncoated plastic for 7 days. Activated HSCs were treated with GPA (100 or 200 μM) for 72 h. Gene expression was analyzed by quantitative PCR, while protein levels were assessed by Western blotting and immunofluorescence. Real-time cell proliferation was monitored using the xCELLigence system. The Glycogen Synthase Kinase 3-beta (GSK-3 beta) inhibitor SB216763 was employed to verify pathway involvement.
Results: GPA significantly inhibited the proliferation of activated HSCs, reduced transcription of *Acta2* (alpha-smooth muscle actin), and decreased both mRNA and protein expression of collagen type I. In addition, GPA downregulated arginase 1 expression, indicating suppression of the arginine metabolic program associated with HSC activation. Mechanistically, the antifibrotic effects of GPA were associated with reduced protein kinase B (AKT) phosphorylation and concomitant activation of GSK-3-beta. Pharmacological inhibition of GSK-3 beta by SB216763 abolished the antifibrotic effects of GPA.
Conclusion: GPA attenuates HSC activation by modulating the AKT/GSK-3 beta signaling pathway. As a naturally occurring dietary and medicinal compound, GPA represents a promising candidate for antifibrotic intervention.

FRI-335
Anti-hepatic fibrosis effects and mechanistic investigation of small-molecule inhibitors targeting collagen β(1-O) galactosyltransferase

Jing Luo[1], Hongshan Wei[1]. [1]*Beijing ditan hospital, Beijing, China*
Email: 2211110783@pku.edu.cn

Background and aims: To screen small-molecule inhibitors targeting GLT25D1 to block collagen fibril synthesis/secretion with anti-fibrotic potential and elucidate their mechanism.
Method: The human GLT25D1 structure (AlphaFold2-predicted) was used with MOE software to screen >220,000 compounds. Anti-fibrotic efficacy of the lead compound (Tub B) was validated in three hepatic fibrosis mouse models. Effects on collagen synthesis, secretion, ER stress, and apoptosis in TGF-β1-activated LX-2 cells were assessed via WB, qRT-PCR, immunofluorescence, flow cytometry, and TEM.
Results: GLT25D1 deficiency (in mice and LX-2 cells) reduced fibrosis and collagen synthesis. Screening identified 23 GLT25D1 inhibitors. Tub B significantly inhibited collagen secretion in LX-2 cells in vitro and demonstrated hepatoprotection in vivo, reducing ALT/AST and fibrosis pathology in all three models. SPR confirmed Tub B binding to GLT25D1. Tub B treatment caused ER accumulation of COL1A1, induced ER ultrastructural damage, increased apoptosis markers, and activated the PERK-eIF2α-ATF4 UPR pathway.
Conclusion: Tub B, an inhibitor of collagen β(1-O) galactosylation, promotes collagen ER retention in HSCs, triggering PERK-eIF2α-ATF4-mediated ER stress and apoptosis, thereby attenuating hepatic fibrosis progression.

FRI-336
PTTG1 silencing via siRNA, effectively downregulates profibrogenic genes in LX2 cells and human precision cut liver slices

Manuel Macías-Herranz[1], Rocío García-Pérez[2], Andrea Díaz-Tendero[3], Guillermo Fernández-Varo[4], Cristina Fornaguera[5], Salvador Borrós[3], Wladimiro Jiménez[1]. [1]*Biochemistry and Molecular Genetics Service, Hospital Clínic of Barcelona, Institut d'Investigacions Biomèdiques August Pi i Sunyer (IDIBAPS), Barcelona, CIBEREHD, ISCIII, Madrid, Spain, Department of Biomedicine, University of Barcelona, Barcelona, Spain;* [2]*Hepatopancreatobiliary Surgery & Transplantation, General & Digestive Surgery Service, Digestive & Metabolic Disease Institute (ICMDM), Hospital Clínic of Barcelona, Barcelona, Spain;* [3]*Grup d'Enginyeria de Materials (Gemat), Institut Químic de Sarrià (IQS), Universitat Ramon Llull (URL), Barcelona, Spain;* [4]*Biochemistry and Molecular Genetics Service, Hospital Clínic of Barcelona, Institut d'Investigacions Biomèdiques August Pi i Sunyer (IDIBAPS), Barcelona, CIBEREHD, ISCIII, Madrid, Spain;* [5]*Grup d'Enginyeria de Materials (Gemat), Institut Químic de Sarrià (IQS), Universitat Ramon Llull (URL), Barcelona, Spain, Institució Catalana de Recerca i Estudis Avançats (ICREA), Barcelona, Spain*
Email: wjimenez@clinic.cat

Background and aims: Liver fibrosis is driven by activation of hepatic stellate cells (HSCs) and overexpression of profibrogenic genes such as *COL1alpha1* and *alpha-SMA*. Pituitary tumor-transforming gene 1 (*PTTG1*) has emerged as a key regulator of cell proliferation and extracellular matrix remodeling, making its inhibition a promising antifibrotic target. This study aimed to evaluate the impact of *PTTG1* silencing via siRNA on the expression of profibrogenic genes in human liver tissue *in vitro* and *ex vivo*.

Method: Two complementary human experimental models were used: LX2 cells (a human hepatic stellate cell line) and Human Precision Cut Liver Slices (hPCLS). LX2 cells were treated with retinol-functionalized poly(β-amino ester) nanoparticles (ret-pBAE NPs) delivering *PTTG1*-targeted siRNA. In the *ex vivo* model, we obteined hPCLS from liver explants of cirrotic patients undergoing liver transplantation with Alcoholic liver disease (ALD) or Metabolic dysfunction–Associated Alcohol-related Liver Disease (MetALD) etiologies. hPCLS were incubated with Vivofectamine® Liver lipoplexes loaded with the same *PTTG1* siRNA. We tested the viabilitry of hPCLS after incubation through ATP assay. Gene expression of *PTTG1, COL1alpha1*, and *alpha-SMA* was quantified by RT-qPCR.
Results: In LX2 cells, *PTTG1* siRNA induced a significant reduction in *PTTG1* (−62%), *COL1alpha1* (−63%), and *alpha-SMA* (−72%) compared to controls. In hPCLS, the ATP assay indicates that the metabolic activity of hPCLS was within the normal limits at 72 hours in culture under both experimental conditions. *PTTG1* silencing decreased *PTTG1* (−21%), *COL1alpha1* (−88%), and *alpha-SMA* (−75%) in comparison to non treatrd hPCLS. These findings demonstrate the antifibrotic effect of *PTTG1* inhibition in a human derived cell line and in a multicellular, three-dimensional human liver model that closely mimics *in vivo* conditions.
Conclusion: *PTTG1* silencing via siRNA markedly downregulates key profibrogenic genes in both human hepatic stellate cells and hPCLs. These results highlight the potential of *PTTG1* interference as an innovative therapeutic strategy to mitigate the progression of human liver fibrosis.

FRI-337-YI

Transforming growth factor-β1 disrupts hepatic zonation and induces fibrotic endothelial remodeling in vivo

Lukas Neckermann[1], Pia Erdösi[1], Alaa Hammad[1], Eleusa Karavasili[1], Juri Paulischkis[1], Matthias Ebert[2], Steven Dooley[1], Anne Dropmann[1], Seddik Hammad[1]. *[1]Molecular Hepatology Section, Department of Medicine II, Medical Faculty Mannheim, Heidelberg University, Mannheim, Germany; [2]II. Medical Clinic, Medical Faculty Mannheim, University of Heidelberg, Mannheim, Germany*
Email: lukas.neckermann@medma.uni-heidelberg.de

Background and aims: Transforming growth factor-β1 (TGF-β1) is a key driver of hepatic fibrosis; however, its role in disrupting hepatic metabolic zonation and the liver sinusoidal endothelial cell (LSEC) niche remains incompletely understood. We sought to define the molecular and spatial consequences of chronic TGF-β1 signaling using a novel AAV8-based in vivo model integrated with spatial transcriptomic profiling.
Method: C57BL/6 mice received AAV8-TGF-β1 (low/high dose) or AAV8-YFP (control). Following expression, biochemical profiling and histological analyses were performed. GeoMX Digital Spatial Profiling (DSP) was employed to resolve zonal transcriptomic alterations. Complementary in vitro experiments were performed in hepatocytes and hepatic endothelial cells.
Results: AAV8-mediated TGF-β1 overexpression resulted in dose-dependent hepatocellular injury with elevated ALT, AST, and GLDH. Mechanistically, TGF-β1 induced SMAD2/3 phosphorylation and nuclear translocation, assembling transcriptional complexes with SMAD4 that repressed HNF4α, a master regulator of hepatocyte identity and metabolic zonation. Immunohistochemical analysis demonstrated loss of pericentral glutamine synthetase expression and periportal expansion of LYVE1- and E-cadherin-positive zones, reflecting disruption of metabolic zonation. TGF-β1 triggered LSEC capillarization evidenced by diminished LYVE1 and elevated CD34 expression with laminin deposition, accompanied by perisinusoidal α-SMA accumulation and basement membrane formation, confirming stellate cell activation. Spatial transcriptomic analysis via GeoMX revealed downregulation of WNT2/RSPO3 signaling pathways, consistent with erosion of pericentral WNT-driven hepatocyte identity and a shift toward periportal transcriptional programs.
Conclusion: Sustained hepatic TGF-β1 expression drives hepatocellular injury, loss of zonation, endothelial capillarization, and stellate cell activation, collectively establishing a profibrogenic hepatic microenvironment. This AAV8-TGF-β1 model provides a platform for mechanistic dissection of spatially defined TGF-β1-driven liver injury and remodeling.

FRI-338

Fibrosis-staging proteome biomarkers from human cohort evaluated as treatment response biomarkers in rat model

Diana Samodova-Sommer[1], Jeanette de Wett Brodersen[2], Christian Toft Madsen[1], Henning Hvid[3], Annabelle Hoegl[4], Gianluca Mazzoni[5], Lea Mørch Harder[5], Mads Grønborg[6], Marie Louise Therkelsen[1], Morten Fog-Tonnesen[7], Lise Lotte Gluud[8], Trine Pagh Ludvigsen[9], Elisabeth Galsgaard[10], Anouk Oldenburger[10]. *[1]Discovery ADME Novo Nordisk A/S, Bagsværd, Denmark; [2]Lead Pharmacology Novo Nordisk A/S, Bagsværd, Denmark; [3]Pathology & Imaging, Novo Nordisk A/S, Bagsværd, Denmark; [4]Biomarker Assay Development 1 Novo Nordisk A/S, Bagsværd, Denmark; [5]Cohort & Disease Informatics Novo Nordisk A/S, Bagsværd, Denmark; [6]Centre for Bioanalysis & ADME Novo Nordisk A/S, Bagsværd, Denmark; [7]CC TA Early project Novo Nordisk A/S, Bagsværd, Denmark; [8]Copenhagen University Hospital Hvidovre, University of Copenhagen, Copenhagen, Denmark; [9]Late Translational Medicine Novo Nordisk R&D US, Lexington, MA, United States; [10]Early Translational Medicine Novo Nordisk A/S, Bagsværd, Denmark*
Email: auog@novonordisk.com

Background and aims: Metabolic dysfunction-associated steatohepatitis (MASH) lacks reliable circulating biomarkers reflecting progressive liver pathology, and which are translatable between preclinical models and patients. We aimed to correlate plasma biomarkers in a rat diet-induced MASH model (choline-deficient high-fat diet; CDHFD) to hepatic disease progression markers detectable in human MASH patients. We focused on C7 (complement component 7), ADAMTSL2 (ADAMTS-like protein 2), IGFBP7 (Insulin-like growth factor binding protein 7) and TIMP1 (tissue inhibitor of metalloproteinases 1) based on their link to fibrosis stage in human MASH patients.
Method: Rats were fed CDHFD to induce MASH. The 12-week study included biweekly blood sampling and staggered termination at 4, 8, and 12 weeks for liver histology and proteomics. Intervention initiation after 4 weeks: continued CDHFD plus oral ALK5 inhibitor (3 mg/kg q.d.) for 8 weeks or return to chow. Rat plasma and liver were analyzed by LC-MS/MS-based proteomics on an Evosep One LC with Astral MS (100SPD, DIA). To correlate, human plasma from the Fatty Liver Disease in Nordic Countries (FLINC) study was used (NCT04340817), depleted of abundant proteins and analyzed by DIA LC-MS (Q-Exactive HF-X).
Results: After 12 weeks, spleen weight and fibrosis (10-fold rise in Picrosirius Red staining) were increased as expected, consistent with late-stage MASH. At 8 weeks, fibrosis fell 54% with ALK5 inhibitor and 73% with chow reversal. In rat plasma and liver, C7, ADAMTSL2 and IGFBP7 rose progressively and correlated with fibrosis severity. After 8 weeks, ALK5 inhibition and chow reversal reduced C7 in plasma and liver; hepatic IGFBP7 declined with both interventions; ADAMTSL2 decreased in plasma and liver after ALK5 inhibition. These biomarker changes mirror histological antifibrotic effects. The circulating biomarker signatures seen in rats translated to humans with MASH and correlated with disease status in a patient cohort.
Conclusion: In a rat CDHFD model, longitudinal biomarker analysis correlated with fibrosis severity and showed consistent hepatic and plasma changes. Plasma elevations of the same biomarkers were observed in a human MASH cohort and correlated with fibrosis severity, supporting their translational relevance. Pharmacological intervention with ALK5 inhibitor modulated these biomarkers in the rat, but additional analysis with multiple compounds is needed to

understand the complete translational relevance of these biomarkers.

FRI-339

Acetyl-CoA carboxylase 2 inhibition in hepatic stellate cells drives their activation and enhances liver fibrosis

Tamara Parracho[1], Valentina Dorta[1], Marcos Fondevila[1,2], Jose Iglesias-Moure[1], Cristina Roibello[3], Sara Martínez-Martínez[1], Eva Novoa[1,4], Lucía Ramos-Lage[3], Maria J Gonzalez Rellan[1,5], Begoña Porteiro[1], Ana Senra[1], Alba Cabaleiro[1], Jose Maria Lanza-Arnaiz[6], Xabier Buque[7], Miguel Lopez[1,4], María Luz Martínez-Chantar[8,9], Francisco Javier Cubero[9,10], Robert F. Schwabe[11], Carlos Dieguez[1,4], Miguel Fidalgo[1], Diana Guallar[3], Vincent Prevot[12], Markus Schwaninger[13], Javier Crespo[14], Patricia Aspichueta[9,15], Marta Varela-Rey[3], Paula Iruzubieta[14], Ruben Nogueiras[1,4,16]. *[1]Department of Physiology, CIMUS, University of Santiago de Compostela, Santiago de Compostela, Spain; [2]Department of Medicine, University of California San Diego, La Jolla, CA, United States; [3]Department of Biochemistry and Molecular Biology, CIMUS, IDIS, Universidade de Santiago de Compostela, Santiago de Compostela, Spain; [4]CIBER Fisiopatologia de la Obesidad y Nutrición (CIBERobn), Madrid, Spain; [5]Lunenfeld-Tanenbaum Research Institute, Mount Sinai Hospital, Toronto, Ontario, Canada; [6]Departamento de Biología Molecular, Centro de Biología Molecular Severo Ochoa (CBMSO, UAM-CSIC), Universidad Autónoma de Madrid (UAM), Madrid, Spain; [7]Department of Physiology, Faculty of Medicine and Nursing, University of Basque Country UPV/EHU, Vizcaya, Spain; [8]Liver Disease Lab, Center for Cooperative Research in Biosciences (CIC bioGUNE), Basque Research and Technology Alliance (BRTA), Vizcaya, Spain; [9]CIBER Enfermedades Hepáticas y Digestivas (CIBEREHD), Instituto de Salud Carlos III, Madrid, Spain; [10]Department of Immunology, Ophthalmology & ENT, Complutense University School of Medicine, Institute for Research in Neurochemistry (IUIN), Complutense University of Madrid, Health Research Institute Gregorio Marañón (IiSGM), Madrid, Spain; [11]Department of Medicine, Columbia University, New York, United States; [12]Univ. Lille, Inserm, CHU Lille, Laboratory of Development and Plasticity of the Neuroendocrine Brain, Lille Neuroscience & Cognition, European Genomic Institute for Diabetes (EGID), Lille, France; [13]University of Lübeck, Institute for Experimental and Clinical Pharmacology and Toxicology, Lübeck, Germany; [14]Gastroenterology and Hepatology Department, Marqués de Valdecilla University Hospital. Clinical and Translational Digestive Research Group, IDIVAL, Santander, Spain; [15]IIS Biobizkaia Health Institute, Barakaldo, Spain; [16]Galicia Agency of Innovation (GAIN), Xunta de Galicia, Santiago de Compostela, Spain*
Email: tamara.parracho.martinez@usc.es

Background and aims: Acetyl-CoA carboxylase 2 (ACC2) is an enzyme localized to the outer mitochondrial membrane that inhibits fatty acid β-oxidation. Although its role in hepatocytes is well established, its function in hepatic stellate cells (HSCs) remains undefined.
Method: ACC2 expression was assessed in HSCs isolated from patients and mice with liver fibrosis. Genetic modulation of ACC2 was performed in cultured HSCs, and mice with HSC-specific deletion of ACC2 were subjected to different fibrosis-inducing diets.
Results: ACC2 expression was markedly reduced in activated human HSCs, displaying a negative correlation with fibrosis severity. Similar reductions were observed in rodent models of liver fibrosis, as well as in primary human HSCs and LX-2 cells activated by transforming growth factor-β1 (TGFβ1), fetal bovine serum (FBS), or saturated fatty acids. Ectopic ACC2 expression attenuated TGFβ1-, FBS-, and fatty acid–induced HSC activation by decreasing carnitine palmitoyltransferase-1 levels and mitochondrial respiration. Conversely, genetic silencing of ACC2 was sufficient to activate HSCs. Consistently, mice with HSC-specific ACC2 deficiency exhibited accelerated liver fibrosis when fed fibrosis-inducing diets, including a choline-deficient high-fat diet and a Western diet.
Conclusion: These findings demonstrate that loss or inhibition of ACC2 in HSCs promotes their activation and accelerates liver fibrosis, likely through enhanced fatty acid oxidation.

FRI-340

Impact of PNPLA3 p.I148M variant on qFibrosis-based collagen morphology in MASLD: analysis from Milan biobank cohort

Giulia Periti[1], Kutbuddin Akbary[2], Francesco Malvestiti[1,3], Serena Pelusi[1], Marco Maggioni[1], Luisa Ronzoni[1], Sara Margarita[1], Alessandro Cherubini[1], Jessica Rondena[3], Roberta D'Ambrosio[1], Daniele Dondossola[1], Daniele Prati[1], Dean Tai[2], Luca Valenti[1,3]. *[1]Fondazione Irccs Ca Granda Ospedale Maggiore Policlinico, Milano, Italy; [2]HistoIndex pte Ltd, Singapore, Singapore; [3]Università Degli Studi Di Milano, Milano, Italy*
Email: giulia.periti@gmail.com

Background and aims: PNPLA3 p.I148M variant is a major genetic determinant of metabolic dysfunction-associated steatotic liver disease (MASLD) evolution, promoting hepatic fat accumulation and fibrosis through altered hepatocyte lipid metabolism and hepatic stellate cell activation. Its effects on fibrosis morphology and spatial collagen organization are not adequately captured by conventional semi-quantitative histological staging. We aimed to evaluate associations between PNPLA3 p.I148M variant and collagen morphometric features in MASLD using artificial intelligence (AI)-based digital pathology analysis of liver biopsies.
Method: Fifty liver biopsies from MASLD patients in the Milan Biobank were analyzed using qFibrosis (qF), a stain-free Second Harmonic Generation/Two-Photon Excitation (SHG/TPE) microscopy platform with quantitative AI-based collagen morphometry. Associations between PNPLA3 genotype and collagen features were assessed using generalized linear models under an allelic genetic model, normalized for %SHG collagen and tissue area.
Results: Mean age was 55.8 ± 11.1 years, BMI 29.8 ± 4.4 kg/m^2; 90% were male and 40% had advanced fibrosis. PNPLA3 genotypes were I/I (28%), I/M (44%), and M/M (28%). Pathologist-based fibrosis staging correlated strongly with qF staging ($R^2 = 0.84$, $p < 0.0001$). PNPLA3 variant was associated with higher qF stage ($\beta = 0.66 \pm 0.20$, $p = 0.0014$), mortality risk score ($p = 0.016$), and multiple periportal collagen morphometric features, including increased thin and elongated collagen strings ($p < 0.05$). In advanced fibrosis, additional associations were observed in zone 2 and centrivenular regions ($p < 0.05$). Unsupervised analyses identified integrated periportal-perivascular steatosis-fibrosis patterns linked to PNPLA3, enabling development of a collagen-based score predicting PNPLA3 homozygosity (qPNPLA3).
Conclusion: PNPLA3 p.I148M variant is associated with distinct, region-specific collagen architectural patterns not captured by conventional histology. qFibrosis-based collagen morphometry reveals genotype-specific fibrosis patterns correlated with staging and allows development of prognostic indices. These findings support use of quantitative digital pathology to improve patient stratification, risk assessment, evaluation of antifibrotic response in genetically driven MASLD, warranting validation in larger, independent cohorts.

FRI-341

Male rats exhibit exacerbated hepatic and metabolic alterations than females in response to a high fat high fructose high cholesterol diet

Yanhao Qiu[1], Jianing Zhou[1], Núria Roglans[1,2,3], Emma Barroso[1,2], Marta Alegret[1,2,3], Juan Carlos Laguna[1,2,3], Laia Vilà[1,2]. *[1]School of pharmacy and food sciences, Universitat de Barcelona, Barcelona, Spain; [2]Barcelona, Spain; [3]CIBERObn, Barcelona, Spain*
Email: yqiuqiux231@alumnes.ub.edu

Background and aims: Currently, there are no approved pharmacological treatments for metabolic dysfunction-associated steatohepatitis (MASH). The aim of this study is to establish and characterize a

physiological model of MASH to enable the subsequent evaluation of candidate drugs.
Method: Male and female Sprague-Dawley rats were randomly distributed into 2 groups and fed a control (CT) or HFHFrHc diet for 6 months. At the end of the study, the animals were sacrificed and serum, liver and adipose tissues were obtained. Zoometric, liver histology, serum and liver triglyceride (TG) and cholesterol (C) concentrations, serum analytes and liver hydroxyproline (LHP) content were determined. Liver tissue was properly stored for RNA and protein extraction.
Results: After 6 months on a HFHFrHc diet, both male and female rats exhibited a comparable increase in body weight to that observed in CT rats. However, in both sexes, the HFHFrHc diet induced an increase in the liver weight relative to body weight compared with CT rats. Accordingly, HFHFrHc diet induced hepatic steatosis, characterized by elevated TG and C content in liver tissue. Serum TG levels were also significantly augmented in both sexes. Glucose and insulin levels only raised in HFHFrHc-fed male rats, leading to a reduced ISI index indicative of impaired insulin sensitivity in this group. LHP content was increased in both male and female rats fed the HFHFrHc diet, although the magnitude of this increase was greater in males (65% vs. 25% in females). Furthermore, serum ALT and AST levels were elevated exclusively in HFHFrHc male rats. Col1a1 protein levels also increased in both male and female rats fed the HFHFrHc diet; however, the extent of the increase was greater in males (3.2-fold) than in females (1.9-fold). Notably, females exhibited sex-specific differences in baseline antioxidant defenses, as evidenced by higher expression levels of Sod2 and Gpx1 regardless of dietary condition.
Conclusion: These preliminary findings demonstrate a sexual dimorphism in the response of SD rats to a HFHFrHc diet, with males developing a more severe phenotype characterized by impaired glucose metabolism and signs of hepatic injury and suggests a potential role for antioxidant activity in protecting females from fibrosis development. Grants: PID2023-146140OB-I00, funded by funded by MICIU/AEI/10.13039/501100011033 and FEDER-UE and 2021SGR-00345.

FRI-345-YI
Fibrosis stage-specific human hepatic stellate cell cultures exhibit distinct metabolic and matrix remodelling phenotypes in response to fibrogenic factors
Lai Wei[1], Una Rastovic[1], Sara Campinoti[1], Kavitha Kirubendran[1], Maya Medic[1], Bruna Almeida[1], Fabio Grundland Freile[1], Albert Hughes[1], Yunxi (Daisy) Gao[1], Tanya Shaw[2], Elena Palma[1], Shilpa Chokshi[1,3], Luca Urbani[1]. *[1]Roger Williams Institute of Liver Studies, School of Immunology and Microbial Sciences, Faculty of Life Sciences and Medicine, King's College London, Foundation for Liver Research and King's College Hospital, London, United Kingdom; [2]Centre for Inflammation Biology and Cancer Immunology, School of Immunology and Microbial Sciences, King's College London, London, United Kingdom; [3]Centre of Environmental Hepatology, Faulty of Health, University of Plymouth, University of Plymouth, Plymouth, United Kingdom*
Email: luca.urbani@researchinliver.org.uk

Background and aims: Liver fibrosis involves dysfunctional extracellular matrix (ECM) remodelling by activated hepatic stellate cells (HSCs), resulting in excess matrix deposition, disrupted tissue architecture, and impaired liver function. Recent omics studies identified distinct HSC populations and showed ECM dynamics vary by fibrosis stage and aetiology, but current models lack stage-specific ECM complexity and HSC functional profiling. We investigated ECM remodelling and metabolic and functional patterns *in vitro* using primary human HSCs from livers across different fibrosis stages.
Method: Primary human HSCs (n = 12) were isolated from livers with early to advanced fibrosis, classified as fibrosis grade (FG) 0 (no fibrosis), 1 (mild-moderate) and 2 (established-advanced). Cells were stimulated with TGF-β and assessed for phenotype and metabolism using RNAseq, immunofluorescence and Seahorse analysis. Cell-derived matrices (CDMs) were generated, decellularised, and characterised by proteomics, immunofluorescence, and computational analysis of matrisome composition and fibre architecture. Inhibitors of identified ECM-remodelling enzymes were tested for model validation.
Results: Human HSCs exhibited fibrosis stage-dependent phenotypic, metabolic, and transcriptomic profiles. FG1 HSCs showed the highest activation and collagen expression in response to TGF-β, while FG2 HSCs displayed increased senescence markers. FG1 cells were also more metabolically active. Transcriptomics revealed ECM deposition and remodelling genes consistently modulated by TGF-β, with higher expression in FG1 and FG2 cells for core and matrix-associated proteins and inflammatory markers. CDM analysis showed FG1 HSCs produced more ECM with greater fibre alignment, features linked to fibrosis progression and stiffening. FG1 cells were also most responsive to inhibition of ECM regulator TGM2 with ZDON, showing reduced collagen deposition and altered high-density fibre alignment.
Conclusion: Patient-derived HSCs and CDM models revealed fibrosis stage-specific metabolic and ECM remodelling patterns and differential antifibrotic responses, highlighting the need for stage-tailored therapeutic strategies.

FRI-346
Transcriptomic profiling and label-free collagen imaging of hepatic stellate cells cultured as 3D magnetic levitation spheroids
Nataliya Rohr-Udilova[1], Sandra Tüchler[1], Maximillian Lahsnig[2], Katharina Regnat[1], Karin Pfisterer[1], Matthias Pinter[1], Michael Trauner[1]. *[1]Medical University of Vienna, Vienna, Austria; [2]University of Vienna, Vienna, Austria*
Email: nataliya.rohr-udilova@meduniwien.ac.at

Background and aims: Hepatic stellate cells (HSCs) produce extracellular matrix (ECM) in the liver. Increased activation of these cells represents a hallmark of liver fibrosis. Conventional adherent growth on plastic flasks induces HSC activation, which can be mitigated by magnetic levitation–based culture systems.
We aim to characterize pathways and processes in HSCs cultured as 3D magnetic levitation spheroids compared to standard 2D flask cultures.
Method: We used LX-2 immortalized human hepatic stellate cells as the model system. Cultures were performed in two formats: traditional 2D adherent culture and 3D magnetic levitation culture. Bulk mRNA sequencing was conducted in four independent biological replicates to analyze differential gene expression and perform gene ontology (GO) pathway enrichment analysis. Standard normalization and multiple-testing correction were applied. Additionally, 3D visualization of the extracellular matrix collagen was carried out using Second Harmonic Generation (SHG) microscopy which enables label-free 3D visualization.
Results: HSCs were cultured for two weeks using an optimized magnetic levitation protocol, followed by bulk mRNA sequencing. Bulk RNA-seq comparing 2D adherent and 3D magnetic levitation cultures revealed more than 6% differentially expressed genes (FDR-controlled). Representative changes include upregulation of HGF, LUM, PDGFRA, MMP1, COL7A1 and downregulation of COL1A1, LOX, SMAD3, SOX9, COL5A. Gene enrichment analysis performed with ClusterProfiler identified three major clusters with pronounced enrichment in 3D versus 2D cultures: (1) receptor signalling activation and regulation, (2) collagen extracellular matrix and cell-cell junctions, and (3) immune cell migration. SHG imaging revealed radial collagen structures within the 3D magnetic levitation spheroids.
Conclusion: Compared to traditional 2D culture, 3D magnetic levitation suggests a transcriptional shift toward reduced HSC activation markers, with altered immune and extracellular matrix pathways. Functional validation of activation status will be addressed

in future work including primary human HSC. Magnetic levitation culture may provide a valuable approach to study HSC biology and fibrosis.

FRI-347

The non-transcriptional activity of IRF3 induces profibrotic cytoplasmic stress granules

Jared Travers[1], Yingting Zhang[1], Emily Huang[1], Megan McMullen[1], Laura Nagy[1]. [1]*Cleveland Clinic Research, Cleveland, United States*
Email: nagyl3@ccf.org

Background and aims: Nucleic acid-induced activation of the antiviral transcription factor interferon regulatory factor 3 (IRF3) mediates hepatic fibrogenesis in murine models of fibrosis. IRF3 executes multiple transcriptional and non-transcriptional functions which contribute to the development of metabolic liver diseases. In this study, we aimed to delineate the relative contributions of the transcriptional and non-transcriptional activities of IRF3 to hepatic fibrosis.
Method: Wild-type (WT), *Irf3*-deficient ($Irf3^{-/-}$), and mice only expressing non-transcriptional IRF3 activity ($Irf3^{S1/S1}$) were subjected to the chronic carbon tetrachloride (CCl_4) model of liver fibrosis. Molecular mechanisms were investigated using primary murine HSCs and LX2 immortalized human HSCs.
Results: Expression of fibrogenic genes and hepatic fibrosis were decreased in primary HSC cultures and CCl_4-exposed liver tissue, respectively, obtained from $Irf3^{-/-}$ mice as compared to WT and $Irf3^{S1/S1}$ mice. Differentiation of primary murine HSCs in culture or stimulation of LX2 cells with transforming growth factor-beta (TGFβ) induced accumulation of endogenous double-stranded RNA (dsRNA), which triggered the assembly of pro-fibrotic IRF3-containing cytoplasmic stress granules. Finally, TGFβ-induced stress granule assembly was reduced upon short interfering RNA (siRNA)-mediated *IRF3* gene silencing in LX2 cells or in primary HSCs cultured from $Irf3^{-/-}$, but not $Irf3^{S1/S1}$, mice.
Conclusion: The non-transcriptional activity of IRF3 in HSCs mediates a novel profibrotic TGFβ-dsRNA-stress granule axis. These results suggest that cytoplasmic stress granules are important regulators of fibrosis and underscore the importance of antiviral pathways to sterile fibrotic responses.

FRI-348

Interleukin-33 and Serotonin drive hepatic fibrosis in alveolar echinococcosis via the gut-liver axis

Aliya Tulading[1], Guzinayi Abudukadi[1], Hai-Zhang Ma[2], Jing Wu[1], Yilizhati Azhati[1], Alimujiang Mamuti[1], Maiwulanjiang Maimaiti[1], Chun-Hui Lv[1], Rong-Dong He[1], Ming-Juan Wang[1], Repikaiti Yasheng[1], Mirizhati Nuermaimaiti[1], Guliziran Keranmu[1], Hui-cheng Zeng[1], Tao Li[1], Tuerganaili Aji[1], Yingmei Shao[1], Hao Wen[1], Tuerhongjiang Tuxun[1]. [1]*First Affiliated Hospital of Xinjiang Medical University, Urumqi, China;* [2]*Qilu Hospital, Shandong University, Jinan, China*
Email: 13276605069@163.com

Background and aims: Hepatic alveolar echinococcosis is characterized by progressive periparasitic fibrosis. Although both interleukin-33 and serotonin (5-hydroxytryptamine, 5-HT) are elevated in HAE patients, their functional interaction and underlying mechanisms in fibrosis remain unclear. This study aimed to elucidate the role and mechanism of the IL-33/5-HT axis in HAE-induced liver fibrosis.
Method: Clinical samples from patients with HAE, hepatic hemangioma, and hepatocellular carcinoma were analyzed using ELISA, quantitative PCR, western blotting, and immunohistochemistry. *Echinococcus multilocularis*-inoculated wild-type and IL-33 knockout mice were used to assess the fibrotic response. *In vitro* functional experiments were performed on hepatic stellate cells (HSCs) using agonist/antagonist treatments targeting the 5-HT receptor 2B (5-HTR2B).
Results: Serum levels of IL-33 and 5-HT were significantly elevated and correlated in HAE patients. Spatial localization of IL-33 and 5-HTR2B was observed within the fibrotic area. Infected IL-33 knockout mice exhibited attenuated fibrosis and disrupted 5-HTR2B signaling. Mechanistically, 5-HT promoted the activation, proliferation, migration, and extracellular matrix production of HSCs in a 5-HTR2B-dependent manner via ERK and AKT phosphorylation—all of which were effectively inhibited by the antagonist sarpogrelate.
Conclusion: Our findings reveal a pathogenic gut-liver axis pathway: IL-33 stimulates the gut to release 5-HT, which subsequently activates HSCs via the 5-HTR2B and downstream ERK/AKT signaling, thereby driving the fibrotic process in HAE. Targeting 5-HTR2B represents a potential therapeutic strategy for HAE-induced fibrosis.

FRI-349

The dual integrin inhibitor Bexotegrast, indicated for idiopathic pulmonary fibrosis, shows a anti-fibrotic phenotype in human MASH liver spheroids

Francisco Verdeguer[1], Radina Kostadinova[1], Philip Vonschallen[1], Jesus Glaus[1], Joel Zvick[1], Natacha Levy[1], Mathieu Petitjean[2], Adi Lightstone[2], Li Chen[2]. [1]*Insphero, Schlieren, Switzerland;* [2]*PharmaNest, Princeton, United States*
Email: francisco.verdeguer@insphero.com

Background and aims: Metabolic dysfunction-associated steatohepatitis (MASH) is a progressive, severe disease characterized by hepatic lipid accumulation, inflammation, and fibrosis. Despite some recent drug approvals, challenges remain in identifying novel anti-fibrotic compounds. Human preclinical models, including organoids/spheroids, provide powerful and translational approaches for drug discovery. This study tested anti-fibrotic compounds targeting TGF-beta signalling, indicated for idiopathic pulmonary fibrosis (IPF), in human liver spheroids.
Method: A human-derived 3D spheroid model containing primary human hepatocytes, Kupffer cells, liver endothelial cells, and stellate cells from healthy donors was used to induce a MASH phenotype for 10 days. Bexotegrast (PLN-74809) and PLN-1474, were first tested in an initial screening setup (screening A) across a 6-concentration range in triplicates, measuring Pro-Collagen 1(PC-1) at day 10 post-treatment. Bexotegrast was then selected for additional phenotypic characterization of the fibrotic biomarkers PC-1, Pro-collagen III (PIIINP), and Tissue Inhibitor of Metalloproteinases 1 (TIMP1) at days 5, 7, and 10 after MASH induction and drug treatment. Spheroids collected on day 10 underwent histology and Sirius Red staining, quantified with FibroNest digital pathology.
Results: Both PLN-1474 and Bexotegrast produced dose-dependent reductions in PC-1 in the initial screening A. Follow-up experiments with Bexotegrast showed statistically significant reductions in PC-1 and PIIINP at days 5, 7, and 10, and in TIMP1 at days 5 and 7. Bexotegrast also demonstrated a strong reduction in Sirius Red staining.
Conclusion: Human-derived 3D spheroid models serve as cost-effective and predictive tools for identifying successful anti-fibrotic drug candidates. Bexotegrast (PLN-74809) and PLN-1474, repurposed from ongoing idiopathic pulmonary fibrosis (IPF) trials, demonstrated promising anti-fibrotic effects in human MASH liver spheroids.

FRI-350

ESOR1 links liver fibrosis to hepatocellular carcinoma progression via endothelial EGFR signaling

Jin Wang[1,2]. [1]*Capital Medical University, Beijing, China;* [2]*Beijing Ditan Hospital, Beijing, China*
Email: 591073988@qq.com

Background and aims: Progressive liver fibrosis and hepatocellular carcinoma are pathologically interconnected, yet the molecular mechanisms linking fibrotic remodeling to tumor-promoting microenvironments remain incompletely understood. Liver sinusoidal

endothelial cells are central regulators of hepatic homeostasis and extracellular matrix (ECM) dynamics. C6orf120 is a previously uncharacterized ECM-associated protein with no defined role in chronic liver disease. Here, we report the first functional characterization of C6orf120 and propose its designation as EGFR Spatial Organizer 1 (ESOR1), based on its role in endothelial EGFR regulation across distinct fibrotic contexts.

Method: Wild-type and ESOR1-deficient mice were subjected to bile duct ligation (BDL) or carbon tetrachloride (CCl_4) administration to induce cholestatic and toxic liver fibrosis. Liver fibrosis and tissue mechanics were assessed by histology, second harmonic generation imaging, and ultrasound-based elastography. Single-cell RNA sequencing of pooled liver samples was performed to characterize endothelial cell states, followed by subclustering and gene program analyses. Endothelial EGFR signaling was examined using biochemical and imaging-based approaches. The impact of ESOR1 on tumor progression was evaluated in subcutaneous hepatocellular carcinoma models.

Results: Genetic ablation of ESOR1 consistently attenuated liver fibrosis induced by both BDL and CCl_4, accompanied by reduced collagen deposition and tissue stiffness. Single-cell transcriptomic analyses revealed that fibrotic injury induced profound LSEC dysfunction, characterized by loss of canonical LSEC identity and acquisition of capillarized endothelial features, whereas ESOR1 deficiency partially restored LSEC differentiation programs. Mechanistically, ESOR1 promoted endothelial EGFR activation and downstream transcriptional responses associated with receptor organization and ECM remodeling, which were blunted in ESOR1-deficient mice. Consistent with its role in shaping the fibrotic microenvironment, loss of ESOR1 significantly suppressed hepatocellular carcinoma growth and ECM accumulation in vivo.

Conclusion: We identify ESOR1 (formerly C6orf120) as a previously unrecognized extracellular matrix protein that regulates endothelial EGFR signaling to coordinate LSEC dysfunction, fibrotic remodeling, and hepatocellular carcinoma progression across distinct fibrotic etiologies, highlighting ESOR1 as a potential therapeutic target in chronic liver disease and HCC.

FRI-351
Hepatocyte ATF4 drives liver fibrosis via the YAP-SOX9-Osteopontin axis

Hao Wang[1], Wang Yiming[1], Ming Ni[1]. [1]*The First Affiliated Hospital, Nanjing Medical University, Nanjing, China*
Email: wyknyd@163.com

Background and aims: Liver fibrosis represents a pathological response to chronic injury, characterized by extracellular matrix accumulation and architectural disruption. While damaged hepatocytes are known to initiate fibrogenic signaling, the intracellular transcriptional machinery orchestrating their cross-talk with the hepatic microenvironment remains obscure. This study investigates the role of hepatocyte Activating Transcription Factor 4 (ATF4) in driving fibrosis progression via the regulation of the YAP/SOX9/Osteopontin (OPN) axis.

Method: We employed hepatocyte-specific ATF4 knockout mice $ATF4^{HKO}$ and subjected them to bile duct ligation (BDL) or methionine-choline deficient (MCD) diets to simulate cholestatic and metabolic fibrosis, respectively. Mechanistic investigations, including chromatin immunoprecipitation (ChIP), luciferase reporter assays, and RNA sequencing, were performed on primary hepatocytes. Furthermore, primary hepatocyte organoids were established and treated with ISRIB, a specific inhibitor of the integrated stress response, to evaluate the therapeutic potential of pharmacologically targeting ATF4 translation.

Results: Our results identify ATF4 as a critical driver of liver fibrosis across different etiologies. Hepatocytes with elevated ATF4 expression displayed a pro-fibrotic phenotype mediated by the upregulation of Yes-associated protein (YAP). Mechanistically, ATF4 promotes YAP expression, which subsequently functions as a transcriptional co-activator to directly induce SOX9 transcription. This upregulation of SOX9 triggers the secretion of OPN, a potent paracrine factor that activates hepatic stellate cells. Genetic ablation of ATF4 significantly attenuated fibrosis in vivo. Consistently, pharmacological blockade of ATF4 synthesis using ISRIB in hepatocyte organoids effectively suppressed the YAP-SOX9-OPN cascade and mitigated the fibrotic phenotype.

Conclusion: This study establishes hepatocyte ATF4 as a master regulator of fibrogenesis by orchestrating the YAP-SOX9-OPN signaling cascade. These findings suggest that disrupting this transcriptional axis—either genetically or pharmacologically—offers a promising therapeutic strategy to interrupt hepatocyte-stellate cell communication and halt the progression of liver fibrosis.

FRI-352
Umbilical cord mesenchymal stem cell-derived extracellular vesicles attenuate hepatic stellate cell activation via mitochondrial modulation

Junyu Wang[1,2], Qi Zhou[2], Jia Li[2], Manon Buist-Homan[2], Peter Olinga[1,2], Klaas Nico Faber[2], Martin Harmsen[2], Han Moshage[2]. [1]*University of Groningen, Groningen, Netherlands;* [2]*University Medical Center Groningen, Groningen, Netherlands*
Email: j.wang03@umcg.nl

Background and aims: Liver fibrosis is a major driver of chronic liver disease progression and remains without effective antifibrotic therapy. Mesenchymal stem cell (MSC)-derived secretome has shown promise in alleviating liver fibrosis; however, the molecular mediators and mechanisms underlying these effects remain incompletely defined. This study aimed to elucidate the antifibrotic mechanism of umbilical cord-derived MSC (UC-MSC) secretome, focusing on the contribution of extracellular vesicles (EVs) and their modulation of mitochondrial function in activated hepatic stellate cells (aHSCs).

Method: Human UC-MSCs were isolated and characterized by morphology and expression of specific surface markers. Serum-free conditioned medium from UC-MSCs (CM^{UC-MSC}) was collected after 48 hours of culture. EVs were isolated from CM^{UC-MSC} using ultracentrifugation and characterized by nanoparticle tracking analysis, cryogenic electron microscopy, and surface marker expression. Primary hepatic stellate cells (HSCs) were treated with complete CM^{UC-MSC}, the soluble factor fraction (SF^{UC-MSC}), or the EV fraction (EV^{UC-MSC}) of the UC-MSC secretome. Fibrosis-related gene and protein expression were determined using qPCR, immunofluorescence, and Western blotting.

Results: Both CM^{UC-MSC} and EV^{UC-MSC} reduced the *Acta2*/αSMA and cell proliferation, with EV^{UC-MSC} also reduced *Col1a1*/collagen type I expression in aHSCs. Depletion of EVs (SF^{UC-MSC}) attenuated these effects in aHSCs. The UC-MSC-derived secretome did not induce apoptosis or senescence and did not alter mitochondrial fusion or fission. Notably, it enhanced mitochondrial respiration without affecting glycolytic flux in aHSCs.

Conclusion: UC-MSC-derived secretome, particularly its EV fraction, attenuates HSC activation by enhancing mitochondrial respiration, thereby offering a promising therapeutic approach for liver fibrosis. These findings underscore the potential of MSC-derived EVs as effective and safer alternatives for fibrotic liver disease treatment and highlight the need for further studies to delineate their molecular interactions with key fibrotic signaling pathways.

FRI-353
The stiffness of liver-derived extracellular matrix hydrogels regulates hepatic stellate cell activation

Qi Zhou[1], Junyu Wang[1], Jia Li[1], Janette Heegsma[1], Vincent E. de Meijer[1], Pingnan Sun[2], Han Moshage[1], Klaas Nico Faber[1], Martin Harmsen[1]. [1]*University Medical Center Groningen, Groningen, Netherlands;* [2]*Shantou University Medical College, Shantou, China*
Email: j.wang03@umcg.nl

Background and aims: Hepatic stellate cell (HSC) activation is a central driver of liver fibrosis and is associated with excessive extracellular matrix (ECM) deposition, remodeling, and increased tissue stiffness. However, the specific contribution of ECM mechanical properties to HSC activation remains incompletely understood. This study aimed to develop a three-dimensional (3D) liver-derived ECM (L-ECM) hydrogel model with tunable stiffness to investigate the role of ECM mechanics in regulating HSC activation.
Method: Porcine L-ECM hydrogels with stiffnesses ranging from healthy to cirrhotic liver were generated using ruthenium-based photocrosslinking. Primary rat HSCs and the human HSC cell line LX-2 were embedded in the hydrogels and cultured for 2 or 4 days. HSC viability, morphology, collagen fibril organization, and expression of fibrosis-related genes and proteins were assessed. Additionally, L-ECM hydrogels derived from healthy and cirrhotic human liver tissues were compared to evaluate the relative contributions of ECM composition and mechanics to HSC activation.
Results: Porcine L-ECM hydrogels suppressed activation of primary HSCs and LX-2 cells in a stiffness-dependent manner, with lower stiffness strongly inhibiting activation and higher stiffness partially attenuating this effect. Human L-ECM hydrogels similarly suppressed HSC activation. Notably, when stiffness was comparable, no differences in HSC activation were observed between healthy and cirrhotic human L-ECM hydrogels.
Conclusion: ECM mechanical properties exert a dominant influence on HSC activation compared with ECM composition alone. These findings highlight mechanosignaling in HSCs as a critical therapeutic target, complementing biochemical strategies to prevent or reverse liver fibrosis.

FRI-354

Dynamic changes in type III collagen formation and degradation are associated with fibrotic activity following hepatic injury in rats

Thomas Wiggers[1], Mark Kuipers-Skarsfeldt[1], Ydalina Maria Moreno[1], Guillermo Fernández-Varo[2], Wladimiro Jiménez Povedano[2,3], Morten Karsdal[1], Diana Julie Leeming[1]. *[1]Nordic Bioscience A/S, Herlev, Denmark; [2]Biochemistry and Molecular Genetics Service, Hospital Clínic of Barcelona, Institut d'Investigacions Biomèdiques August Pi i Sunyer (IDIBAPS), Barcelona, CIBEREHD, ISCIII, Madrid, Spain, Barcelona, Spain; [3]Department of Biomedicine, University of Barcelona, Barcelona, Spain, Barcelona, Spain*
Email: twm@nordicbio.com

Background and aims: Non-invasive markers of collagen turnover enable assessment of drug effects on the extracellular matrix. Type III collagen formation (fibrogenesis) and degradation (fibrolysis) can be assessed with nordicPRO-C3™ and nordicCTX-III™, respectively. A shift toward fibrolysis has recently been associated with hepatic fibrosis improvement in patients with metabolic dysfunction-associated steatohepatitis (MASH), making PRO-C3 and CTX-III relevant targets for translational studies of hepatic fibrosis. We developed rodent versions of CTX-III (rCTX-III) and PRO-C3 (rPRO-C3) and applied them in two preclinical models of hepatic fibrosis.
Method: A chemiluminescent sandwich immunoassay for nordic rCTX-III and a competitive enzyme-linked immunosorbent assay for nordic rPRO-C3 were developed for rodent blood samples using monoclonal antibodies. rCTX-III detects a protease-generated neo-epitope in a cross-linked dimeric analyte, while rPRO-C3 targets a pro-peptide neo-epitope. rCTX-III and rPRO-C3 were measured in serum of two rat models: 83 rats with CCl_4-induced fibrosis by inhalation (1 L/min) twice weekly for 8, 12, 16, or 20 weeks (wks) and given water containing phenobarbital (0.3 g/L), including regression groups with 15 or 20 wks of CCl_4 followed by 6 wks of washout compared with healthy controls (n = 7 per group); and a bile-duct ligation model for 1 (n = 7), 2 (n = 7), or 3 wks (n = 8), plus 3-week sham surgery (n = 8) and baseline (n = 13).
Results: Within the CCl_4 model, control rats showed stable nnserum rPRO-C3 and rCTX-III levels. rPRO-C3 was increased at 12 wks ($p = 0.067$) and 20 wks ($p < 0.05$) of CCl_4 treatment, and at 15 wks of CCl_4 treatment followed by 6 wks of CCl_4 washout ($p < 0.05$) compared to controls. rCTX-III increased at 8 wks ($p < 0.05$), 12 wks ($p = 0.066$), 16 wks ($p < 0.01$) and 20 wks ($p = 0.062$) of CCl_4 treatment, but showed no difference compared to controls after 15 or 20 wks of CCl_4 followed by 6 wks of washout. In the bile-duct ligation model, rPRO-C3 levels were increased by 3 wks post-surgery ($p < 0.001$), while rCTX-III levels were increased at 1 week ($p < 0.001$), 2 wks ($p < 0.01$) and 3 wks ($p < 0.01$) compared to baseline.
Conclusion: We developed robust assays for the rodent fibrolysis marker rCTX-III and fibrogenesis marker rPRO-C3 and applied them in two hepatic fibrosis models, showing increased type III collagen turnover after injury. rCTX-III and rPRO-C3 may serve as translational biomarkers in antifibrotic drug development.

FRI-355

SOX9 drives hepatic stellate cell activation via a PFKFB3-mediated glycolysis-histone lactylation positive feedback loop

Guanglin Xiao[1], Zhiling Deng[1], Ke Qiu[1], Hong Ren[1]. *[1]Department of Infectious Diseases, Key Laboratory of Molecular Biology for Infectious Diseases, Ministry of Education, Institute for Viral Hepatitis, The Second Affiliated Hospital, Chongqing Medical University, Chongqing, China*
Email: renhong0531@cqmu.edu.cn

Background and aims: The molecular drivers initiating and sustaining aerobic glycolysis reprogramming in activated hepatic stellate cells (HSCs) are unclear. This study aimed to identify HSC-specific targets that facilitate this metabolic shift and elucidated their molecular mechanisms.
Method: We identified the core gene that drives hepatic fibrosis by promoting glycolysis, using six machine learning algorithms applied to a candidate gene set derived from the intersection of glycolysis-related genes, differentially expressed genes (GEO datasets), and key WGCNA modules. The expression of the core gene in HSCs was confirmed by immunofluorescence (IF) staining. The mechanism by which the core gene regulates glycolysis in HSCs was determined using chromatin immunoprecipitation (ChIP) assays.
Results: Integrated transcriptomic and single-cell RNA sequencing analysis of human liver fibrosis identified the glycolytic regulator SOX9 as a key pro-fibrotic molecule. SOX9 was upregulated in human fibrotic livers and mouse fibrosis models (induced by CCl_4 or TAA). Co-localization studies using markers for HSCs (alpha-SMA) demonstrated that SOX9 expression was predominantly enriched in activated HSCs during fibrogenesis. To establish a causal role, we constructed an AAV6 vector (AAV6-postn-shSox9) for HSC-specific knockdown of Sox9 in mice. Central carbon-targeted metabolomics of liver tissues revealed that Sox9 knockdown reduced glycolytic flux while enhancing TCA cycle activity compared to the control vector group. Similarly, modulating SOX9 in LX-2 cells regulated glycolysis and activation. Mechanistically, SOX9 directly transactivated the glycolytic enzyme gene PFKFB3, whose inhibition reversed SOX9-driven phenotypes. Elevated lactate from increased glycolysis triggered histone lactylation, which we identified as an upstream regulator of SOX9. Screening of eight histone lactylation sites in LX-2 cells under multiple conditions pinpointed H4K5la as the specific modification linked to SOX9 upregulation.
Conclusion: This study identifies SOX9 as an upstream regulator of glycolysis in HSCs and demonstrates the existence of a "glycolysis-lactate-histone lactylation" positive feedback loop centered on SOX9 during HSC activation.

FRI-356

Proinsulin connecting peptide attenuates transforming growth factor β1-induced profibrogenic responses in immortalized human hepatic stellate cells

Reiko Yaginuma[1], Kazuyoshi Kon[1], Kyoko Fukuhara[1], Shunsuke Ikejima[1], Masahiro Tada[1], Kei Ishizuka[1], Maki Morinaga[1], Hiroo Fukada[1], Akira Uchiyama[1], Shunhei Yamashina[1], Kenichi Ikejima[1]. [1]*Department of Gastroenterology, Juntendo University Graduate School of Meicine, Tokyo, Japan*
Email: yagirei@juntendo.ac.jp

Background and aims: Insulin resistance is one of the hallmarks of metabolic dysfunction in steatotic liver disease including MASLD and MetALD. Besides hyperinsulinemia, serum proinsulin connecting peptide (C-peptide) levels are elevated simultaneously; however, the biological roles of C-peptide in the pathogenesis of steatohepatitis have not been elucidated yet. Therefore, here we investigated the direct effect of C-peptide on profibrogenic responses in hepatic stellate cells (HSCs) utilizing immortal human HSC line LX-2.
Method: LX-2 cells were incubated with C-peptide (10 nM) in the presence of TGFβ1 (2.5 ng/mL) for 20 hr, and mRNA expression levels of type I collagen (COL1A1), α-smooth muscle actin (ACTA2), TGFβ1/3, SMAD4, MMP-1/-13, and TIMP-1 were quantified by RT-qPCR. Hydroxyproline contents in culture were determined colorimetrically.
Results: In LX-2 cells, incubation with TGFβ1 for 20 hr increased COL1A1 mRNA nearly 4.8-fold over basal levels; however, co-incubation with 10 nM C-peptide blunted this induction almost 26% ($p < 0.0001$). Indeed, TGFβ1-induced increases in cellular hydroxyproline contents were drastically prevented by simultaneous incubation with C-peptide for 72 hr. Further, TGFβ1-induction in ACTA2 mRNA, a hallmark of HSC transactivation, were also prevented nearly 26% by co-incubation with C-peptide ($p < 0.05$). Furthermore, TGFβ1-inductions in MMP-13 and TIMP-1 mRNA levels in LX-2 cells were also blunted by co-incubation with C-peptide significantly. Moreover, mRNA levels of SMAD4 were significantly decreased when LX-2 cells were incubated with C-peptide both in the absence or presence of TGFβ1, the levels being 17% and 22% lower than basal levels, respectively. Interestingly, C-peptide significantly decreased expression levels of TGFβ3 mRNA, but not TGFβ1 mRNA, in LX-2 cells both in the absence and presence of TGFβ1, the levels being 22% and 26% lower than controls, respectively. In addition, C-peptide decreased MMP-1 mRNA levels in LX-2 cells about 12% in the absence of TGFβ1 ($p < 0.05$).
Conclusion: These findings clearly demonstrated that C-peptide attenuates TGFβ1-induced collagen production and matrix-related gene expressions in LX-2 cells, indicating that C-peptide exerts proper biological effects in HSCs rather than a remnant peptide during insulin production. It is therefore hypothesized that C-peptide most likely plays a modulatory role in the progression of hepatic fibrosis in MASLD/MetALD.

General Hepatology (including non-invasive liver assessment)

TOP-550

Coagulopathy and lactate dehydrogenase predict fetal loss in liver dysfunction during pregnancy

Reshma Reshma[1], Premashis Kar[2], Jagdeep Kaur[3], Ayush Jasrotia[2]. [1]*Government Medical College, Amritsar, Max Superspeciality Hospital, Vaishali, Ghaziabad, India;* [2]*Max Superspeciality Hospital Vaishali, Ghaziabad, India;* [3]*Government Medical College, Amritsar, India*
Email: reshma.mallick92@gmail.com

Background and aims: Liver dysfunction during pregnancy is a major contributor to maternal and perinatal morbidity. We aimed to describe the clinical spectrum and identify laboratory predictors of adverse fetal outcomes in a tertiary cohort of pregnancy-related liver dysfunction.
Method: In this prospective observational cohort, pregnant women with liver dysfunction were enrolled and followed from admission until 6 weeks postpartum. Primary fetal outcomes were stillbirth and intrauterine growth restriction. Routine laboratory parameters, including international normalised ratio and lactate dehydrogenase, were assessed. Multivariable logistic regression was performed to identify independent predictors of intrauterine fetal death and growth restriction.
Results: Among 245 pregnancies, diagnoses included intrahepatic cholestasis of pregnancy (U2, 37.5%), preeclampsia (SU, 28.2%), eclampsia (50, 20.4%), HELLP syndrome (8, 3.3%), acute viral hepatitis (S, 2.4%), hyperemesis-related hepatic injury (S, 2.4%), chronic hepatitis (11, 4.5%), and acute fatty liver of pregnancy (3, 1.2%). Preterm delivery occurred in 131 (53.5%); stillbirth in 34 (13.U%); intrauterine growth restriction in U1 (37.1%); and maternal death in 15 (S.1%). In patient-level modelling for intrauterine fetal death events (n = 32), international normalised ratio (adjusted odds ratio 18.U7 per 1-unit increase; U5% confidence interval 1.1U–303.41) and lactate dehydrogenase (adjusted odds ratio 1.24 per 100 U/L increase; U5% confidence interval 1.04–1.47) were independent predictors. For intrauterine growth restriction, international normalised ratio was independently associated (adjusted odds ratio 1S.S3; U5% confidence interval 2.34–118.31), while serum albumin was protective (adjusted odds ratio 0.55 per 1 g/dL increase; U5% confidence interval 0.34–0.8 U).
Conclusion: In pregnancy complicated by liver dysfunction, coagulopathy and elevated lactate dehydrogenase independently predict fetal loss, and hypoalbuminaemia identifies risk of growth restriction. Simple laboratory-based risk stratification may support earlier escalation, multidisciplinary management, and closer fetal surveillance.

TOP-552

Alcohol use at the time of transient elastography does not affect liver stiffness measurement

Jordi Gratacós-Ginès[1,2,3], Lorenzo Ciocca[4], Nikolaj Torp[5,6], Queralt Herms[1], Aleksander Krag[5,6], Pere Ginès[1,2,3,7], Maja Thiele[5,6], Elisa Pose[1,2,3,7]. [1]*Liver Unit, Hospital Clínic de Barcelona, Barcelona, Spain;* [2]*Institut d'Investigacions Biomèdiques August Pi i Sunyer, IDIBAPS, Barcelona, Spain;* [3]*Centro de Investigación Biomédica en Red en Enfermedades Hepáticas y Digestivas, CIBERehd, Madrid, Spain;* [4]*Università Vita-Salute San Raffaele, Milano, Italy;* [5]*Odense University Hospital, Odense, Denmark;* [6]*University of Southern Denmark, Odense, Denmark;* [7]*Universitat de Barcelona, Barcelona, Spain*
Email: EPOSE@clinic.cat

Background and aims: It is unclear whether alcohol use at the time of transient elastography (TE) affects liver stiffness measurement (LSM) independently from the presence of steatohepatitis.
Method: Cross-sectional analysis of two prospective screening cohorts for liver disease with TE: 1) DECIDE (Denmark, 2017–2022): General population with metabolic risk factors and/or harmful alcohol consumption; and 2) ALCOFIB (Spain, 2019–2024): Participants attending an addiction unit due to harmful alcohol consumption. Alcohol consumption was assessed by the measurement of urinary ethylglucoronide (uETG) or phosphatidylethanol (PEth), and groups were defined as follows: a) No/low consumption: uETG <200 ng/mL or PEth <20 ng/mL; b) Intermediate: uETG 200–2000 ng/mL or PEth 20–200 ng/mL; c) High: uETG >2000 ng/mL and PEth >200 ng/mL. AST was selected as the indirect marker of steatohepatitis. Controlled attenuation parameter (CAP) was used to assess steatosis. Steatotic liver disease (SLD) subtypes were defined based on the latest international consensus nomenclature.

Results: A total of 3519 participants were included in the study. Both sexes were represented in similar proportions (52% males) and the median age was 57 years. Intermediate and high alcohol consumption were observed in 991 (30%) and 826 (25%) individuals, respectively. Four hundred fifty-four (13%) individuals had elevated AST levels. Median LSM was 4.8 kPa, and 345 (10%) participants had LSM ≥8 kPa. In multivariable linear regression analysis adjusted for covariables, alcohol use was not associated with LSM (B coefficients for intermediate and high consumption: −0.330 [−1.107–0.448] and −0.359 [−1.891–1.172], respectively). Conversely, AST (B = 0.065 [0.050–0.080]) and CAP (B = 0.007 [0.004–0.010]) were independently associated with LSM. Moreover, distribution of LSM was similar among alcohol consumption groups. In a secondary analysis using logistic regression, only AST and CAP, but not ongoing alcohol, were associated with LSM ≥8 kPa. Other notable factors associated with LSM were body mass index, blood glucose, GGT and platelet levels. Overall, similar results were observed in the different SLD subtypes.
Conclusion: Ongoing alcohol use at the time of TE does not affect LSM. Repeated LSM after alcohol abstinence should only be considered in patients with elevated liver enzymes.

SAT-512

Potential of reflex testing with the CORE model triggered by liver enzyme abnormalities to improve risk prediction in the general population

Fredrik Åberg[1], Lotta Hallamaa[1], Rickard Strandberg[2,3], Hannes Hagström[2,4]. [1]*Helsinki University Hospital and University of Helsinki, Helsingfors, Finland;* [2]*Department of Medicine Huddinge, Karolinska Institutet, Stockholm, Sweden;* [3]*Red Door Analytics, Stockholm, Sweden;* [4]*Division of Hepatology, Department of Upper GI Diseases, Karolinska University Hospital, Stockholm, Sweden*
Email: fredrik.aberg@helsinki.fi

Background and aims: The Cirrhosis Outcome Risk Estimator (CORE) risk-prediction model combines routine liver blood tests (ALT, AST, GGT) to estimate individual risk of liver-related events in the general population. We hypothesized that a reflex strategy—calculating CORE whenever any enzyme exceeds the upper limit of normal—would efficiently capture individuals at elevated CORE-predicted risk.
Method: In four Finnish health examination studies (FINRISK 2002, 2007, and 2012, and Health 2000) representative of the general population, we analyzed 24,000 participants (mean age 50 years, 46% men) with ALT, AST, and GGT measurements. To evaluate the suitability of a reflex-testing strategy, we calculated the proportion of individuals with CORE-predicted 10-year risk >1%, >3%, >5%, >7%, and >10% who would be identified by elevated liver enzymes, defined using IFCC-recommended sex-specific upper limits of normal (men/women: ALT 42/30 U/L; AST 35/33 U/L; GGT 68/40 U/L).
Results: Elevated GGT was the most sensitive marker, identifying 87% of those with CORE ≥1%, 99% with CORE ≥3%, and 100% with CORE ≥5%. Elevated AST detected 83%, 100%, and 100%, respectively, while elevated ALT detected 71%, 92%, and 95%. A dual-enzyme reflex strategy, where CORE was calculated if either ALT or GGT was elevated, detected 98% of individuals with CORE >1% and 100% of those with CORE >3%. A similar increase in detection was achieved by lowering the abnormality thresholds for ALT, AST, or GGT by only 5 U/L. Using elevated GGT alone as the reflex trigger, 87% of CORE tests could be avoided compared to testing the entire population.
Conclusion: A laboratory-integrated reflex-testing strategy, where CORE is automatically calculated whenever ALT, AST, or GGT is elevated, could provide an efficient and low-cost approach to identify individuals at high risk of future major adverse liver outcomes in clinical practice. As GGT was the most sensitive trigger, the reflex strategy could even be restricted to GGT alone.

SAT-513

High fibrosis-4 index is linked to hepatic decompensation and liver cancer in a nationwide matched cohort

Fadi Abu Baker[1], Rawi Hazzan[2], Tarek Saadi[3], Ariel Israel[4]. [1]*Hillel Yaffe Medical Center, Hadera, Israel;* [2]*Clalit Healthcare North District, Afula, Israel;* [3]*Rambam Healthcare Campus, Haifa, Israel;* [4]*Leumit Healthcare Services, Tel Aviv, Israel*
Email: Fa_fd@hotmail.com

Background and aims: The Fibrosis-4 (FIB-4) index is widely used to estimate hepatic fibrosis non-invasively, yet its real-world performance for identifying patients at risk for clinically relevant hepatic outcomes remains incompletely defined. We evaluated liver disease etiologies, advanced hepatic complications, and longitudinal hepatic outcomes in adults with high versus low FIB-4.
Method: In a nationwide real-world matched cohort study, adults aged 40 to 80 years with available laboratory values were included. Individuals with FIB-4 >= 2.67 (n = 21,540) were matched 1 to 1 to controls with FIB-4 <1.45 (n = 21,540) by age, sex, ethnicity, and socioeconomic status. Cross-sectional analyses assessed liver disease etiologies and complications, and longitudinal analyses evaluated incident cirrhosis and hepatic decompensation over a median follow-up of 6.2 years.
Results: At baseline, high FIB-4 was associated with higher prevalence of metabolic dysfunction-associated steatotic liver disease (MASLD) (10.5% vs 6.0%). Viral hepatitis was more common, including hepatitis B virus (HBV) infection (2.1% vs 0.6%; odds ratio (OR) 3.55, 95% confidence interval (CI) 2.91 to 4.34) and hepatitis C virus (HCV) infection (3.5% vs 0.3%; OR 11.98, 95% CI 9.29 to 15.44). Baseline cirrhosis was present in 7.10% versus 0.12% (OR 62.32, 95% CI 39.23 to 87.99). Advanced complications were markedly more frequent, including ascites (4.51% vs 0.35%; OR 13.53, 95% CI 10.69 to 17.12), encephalopathy (0.85% vs 0.06%; OR 15.46, 95% CI 8.62 to 27.73), and esophageal varices (1.81% vs 0.005%). Hepatobiliary malignancies were more prevalent, including hepatocellular carcinoma (0.55% vs 0.04%; OR 14.83, 95% CI 7.28 to 35.18) and cholangiocarcinoma (0.30% vs 0.03%; OR 9.31, 95% CI 4.27 to 24.07). During follow-up, incident cirrhosis occurred in 2.82% versus 0.03% (OR 104.06, 95% CI 47.53 to 284.29), and new-onset hepatic decompensation occurred in 4.39% versus 0.07% (OR 29.28, 95% CI 13.88 to 44.53).
Conclusion: In a large nationwide matched cohort, FIB-4 >= 2.67 identified individuals with substantially higher prevalence of MASLD and viral hepatitis, a markedly greater baseline burden of cirrhosis and advanced complications, and a pronounced long-term risk of incident cirrhosis and hepatic decompensation, alongside increased hepatobiliary malignancy. These findings support FIB-4 as a pragmatic tool to prioritize hepatology evaluation and risk-stratified surveillance pathways.

SAT-514

Diagnostic utility of the splenic-to-liver stiffness ratio in porto-sinusoidal vascular disease (PSVD): a multicentric study

Ayush Agarwal[1], Arun Valsan[2], Shubham Jain[1], Arathi Venu[2], Shiv Verma[1], Dhruv Advani[1], Sinchana Lakshmi[1], Pavit Singh[1], Arnav Aggarwal[1], Vishal Chauhan[1], Sarthak Saxena[1], Sagnik Biswas[1], Prasenjit Das[1], Shalimar Shalimar[1]. [1]*All India Institute of Medical Sciences, New Delhi, New Delhi, India;* [2]*Amrita Institute of Medical Sciences, Kochi, Kochi, India*
Email: ayushgrm@gmail.com

Background and aims: Differentiating porto-sinusoidal vascular disease (PSVD) from cirrhosis remains a significant clinical challenge due to overlapping features of portal hypertension. Liver stiffness measurement (LSM) has limited accuracy, particularly in the intermediate grey-zone range. As PSVD is characterized by elevated portal pressure without advanced hepatic fibrosis, splenic stiffness measurement (SSM) and the splenic-to-liver stiffness ratio (SSM/LSM) may better identify these patients. This study aimed to evaluate

the diagnostic performance of LSM and the SSM/LSM ratio in differentiating PSVD from cirrhosis.
Method: In this multicentric case–control study, biopsy-proven PSVD and cirrhosis patients with valid transient elastography were included. LSM and SSM were assessed with dedicated probes using the FibroScan Expert 630. Centre 1 (AIIMS, New Delhi) served as the derivation cohort, while Centre 2 (Amrita Institute, Kochi) was used for external validation. Diagnostic performance of LSM and SSM/LSM ratio was assessed using area under the receiver operating characteristic curve (AUROC). Optimal cutoffs derived in Centre 1 were applied unchanged to Centre 2, and sensitivity and specificity were compared. Subgroup analysis was performed in the LSM grey zone (10–20 kPa). Histological features associated with high LSM in PSVD were identified.
Results: A total of 183 patients were included (93 PSVD, 90 cirrhosis). Median LSM was significantly lower and SSM/LSM ratio significantly higher in PSVD across both centres ($p < 0.001$). In Centre 1 ($n = 109$), SSM/LSM ratio demonstrated excellent diagnostic accuracy comparable to LSM (AUROC 0.90 vs 0.87, $p = 0.39$), with an optimal cutoff of >2.8. On external validation (Centre 2, $n = 74$), the SSM/LSM ratio demonstrated superior specificity (61.5% vs 25.6%, $p < 0.001$) with comparable sensitivity (97.1% vs 100%) compared to LSM. In the grey-zone LSM subgroup, SSM/LSM ratio showed significantly higher diagnostic accuracy than LSM (AUROC 0.83 vs 0.65, $p = 0.02$). Among PSVD patients, elevated LSM was significantly associated with histological sinusoidal dilatation ($p = 0.001$), perisinusoidal fibrosis ($p = 0.008$), and portal tract vascular abnormalities ($p = 0.02$).
Conclusion: The splenic-to-liver stiffness ratio outperforms LSM alone in differentiating PSVD from cirrhosis in the LSM grey zone, and maintains diagnostic robustness on external validation.

SAT-515
Mortality prediction using non-invasive fibrosis scores independent of chronic liver disease in patients with COVID-19
Maximilian Joseph Brol[1], Elena Rosenquist[1], Julia Fischer[1], Richard Vollenberg[1], Frank Erhard Uschner[1], Frank Tacke[2], Münevver Demir[2], Jonel Trebicka[1,3], Phil Robin Tepasse[1]. *[1]Münster University Hospital, Department of Internal Medicine B, Münster, Germany; [2]Charité - Universitätsmedizin Berlin, Department of Hepatology and Gastroenterology, Campus Virchow-Klinikum (CVK) and Campus Charité Mitte (CCM), Berlin, Germany; [3]European Foundation for the Study of Chronic Liver Failure-EF Clif, Barcelona, Spain*
Email: maximilian.brol@ukmuenster.de

Background and aims: Liver is an important organ in immunological responses. Chronic liver disease may influence outcomes in coronavirus disease 2019 (COVID-19), although this association may be driven by comorbidities rather than liver disease itself. Non-invasive scores based on routine lab tests (NIT) are commonly used to estimate liver fibrosis, despite being potentially confounded by non-hepatic systemic illness. This study aimed to evaluate the impact of chronic liver disease and the prognostic value of non-invasive fibrosis scores in COVID-19.
Method: This retrospective cohort study of prospectively collected data analyzed two cohorts of the German National Pandemic Cohort Network: (i) a university-hospital based high-resolution cohort (HRC) included hospitalized patients with detailed data ($n = 373$) and (ii) a cross-sectoral cohort (CSC) including patients with routine clinical data ($n = 2033$) across all levels of care. Outcomes were compared between patients with and without chronic liver disease. NITs, including FIB-4, APRI and NFS, were analyzed in all patients regardless of known liver disease at diagnosis. Survival analyses, multivariable Cox proportional hazards models, and ROC analyses were performed.
Results: Chronic liver disease was more frequently diagnosed in the HRC than in the CSC (11.2% vs. 6.0%). In the CSC, patients with chronic liver disease had higher unadjusted mortality than those without liver disease (17.4% vs 9.8%, $p = 0.028$), but this association was not significant after adjustment for comorbidities (HR 1.544, $p = 0.061$). In contrast, all NITs were significantly higher in non survivors across both cohorts at diagnosis of COVID, independent of pre-existing liver disease. High risk categories of FIB-4 (>2.67), APRI (>1.5), and NFS (>0.675) were independently associated with increased mortality. In multivariable Cox regression analysis, high risk categories of FIB-4 and APRI (HRC HR 7.057, $p < 0.001$; CSC HR 2.584, $p < 0.001$) were independently associated with increased mortality. Prognostic discrimination for mortality was above 0.7 for each NIT in both cohorts, with best performance for NFS in the HRC (AUROC: 0.832).
Conclusion: NITs, applied irrespective of known liver disease, were strong and independent predictors of mortality, indicating that these scores may capture systemic disease severity beyond liver specific pathology. These findings support the use of NITs for risk stratification in COVID-19 patients regardless of underlying liver disease status.

SAT-516
The impact of CFTR genotype on liver impairment in patients with cystic fibrosis
Valentina Cossiga[1], Mario Capasso[1], Emanuela Pellegrino[1], Paola Iacotucci[2], Simona Albano[1], Lorenza Ferrillo[3], Filippo Vetrone[1], Jolanda Somma[3], Luisa Ranieri[1], Maria Guarino[1], Vincenzo Carnovale[3], Filomena Morisco[1]. *[1]Department of Clinical Medicine and Surgery, Departmental Program "Diseases of the liver and biliary system", University of Naples Federico II, Naples, Italy; [2]Departement of Advanced Biomedical Sciences - University of Naples "Federico II", Naples, Italy; [3]Departement of Translational Medical Sciences - University of Naples "Federico II", Naples, Italy*
Email: valentina.cossiga@gmail.com

Background and aims: Cystic fibrosis-associated liver disease (CFLD) is a significant cause of morbidity and the third cause of death in this genetic disease. However, evidence of CFLD is usually subclinical until the disease is advanced, so CFLD is underdiagnosed. The aim of this study is to evaluate the impact of CFTR (Cystic Fibrosis Transmembrane conductance Regulator) genotype (F508del allele mutation) on liver impairment in patients with cystic fibrosis.
Method: A retrospective monocentric study was conducted at University of Naples Federico II enrolling all consecutive patients with cystic fibrosis with liver involvement (clinical, biochemical or instrumental abnormalities) referred to hepatological evaluation. Non-invasive evaluation of liver fibrosis with transient elastography was performed in all patients, together with the collection of clinical and biochemical data.
Results: Thirty-eight patients (65.7% male, mean age 35.1 ± 10.7 yrs) were enrolled. The cohort was divided into 3 groups according to CFTR genotype: group A homozygotes patients with F508del mutation (7 patients, 18.4%), group B heterozygous F508del mutation patients (13 patients, 34.2%) and group C including other mutations (18 patients, 47.3%). Group A showed a significant more severe CFLD compared to groups B and C as demonstrated by higher liver stiffness (27.8 ± 21.9kPa vs 8.7 ± 5.3 kPa vs 7.2 ± 4.0kPa; group A vs group B $p = 0.006$ and group A vs group C $p = 0.001$), higher FIB-4 score (2.7 ± 2.5 vs 0.9 ± 0.4 vs 0.8 ± 0.5; group A vs groups B and C $p = 0.01$), higher spleen diameter (171 ± 37 mm vs 126 ± 17 mm vs 117 ± 27.8 mm; group A vs group B $p = 0.0007$ and group A vs group C $p = 0.001$) and lower platelets count (155714 ± 135294/mm^3 vs 218692 ± 155628/mm^3 vs 287166 ± 131486/mm^3; group A vs groups B and C $p < 0.05$).
Conclusion: Homozygotes F508del allele mutation patients have severe CFLD with advanced liver fibrosis and significant portal hypertension. Our findings suggest that these patients should be promptly evaluated by hepatologists since diagnosis. Further studies with larger sample size are required to confirm this data.

SAT-517

Impact of adult population screening for liver cirrhosis using routine blood tests on rate of transient elastography referrals from primary care: a prospective intervention study

Joan Flores[1], Christina Trambas[2], Natasha Jovanovic[2], Bree James[2], Alexander Thompson[3], Jessica Howell[3]. *[1]Canberra Hospital, University of Melbourne, St Vincent's Hospital Melbourne, Canberra, Australia; [2]St Vincent's Pathology, Fitzroy, Australia; [3]St Vincent's Hospital Melbourne, University of Melbourne, Fitzroy, Australia*
Email: ericka@flores.com.au

Background and aims: Cirrhosis is often diagnosed late due to a lack of population screening programs. This study evaluated the effect of reflex reporting of Aspartate to Platelet Index (APRI) for routine blood test events on referral rate for vibration controlled transient elastography (VCTE).
Method: This prospective intervention study was conducted between 19 May 2024 to 18 May 2025 at a single tertiary hospital and statewide pathology service. Reflex calculation and reporting of APRI on routine blood test events in adults >18 years who had elevated ALT (laboratory upper limit 30 IU/mL females, 35 IU/mL males) commenced on November 19, 2024. Reports included APRI explanation, recommendation that VCTE be ordered for APRI >1.0 with link to VCTE referral. Pathology, demographic, appointment and VCTE data were collected from pathology service and hospital records. Monthly rate of VCTE referrals and proportion from primary care in the 6 months post intervention were compared to 6 months pre-intervention via regression modelling and Chi square test respectively.
Results: 23,764 blood test events in 12,031 individuals with elevated ALT had APRI reported. Of these, 8,339 were individuals with blood tests ordered in the community. 686 (8%) had APRI>1 and 175 (2%) had APRI>2. Median age of those with APRI>1 was 58 years (IQR 43, 71 years) and most were male (62% vs 38%, $p < 0.001$). Mean rate of individuals with APRI>1 who would require VCTE referral was 114 per month. There were 1192 VCTE referrals during the study period, of which 73 (6.1%) were from non-hepatology specialists including general practitioners (GPs). Mean weekly number of VCTE referrals increased from 0.09 per week pre-intervention to 0.53 per week post-intervention (post-estimation linear trend $p = 0.014$). The proportion of referrals from non-hepatology specialists and GPs increased from 3.0% (20/ 664) pre-intervention to 10.0% (53/ 528) post intervention (X^2 $p < 0.001$); referrals from GPs increased from 2.1% (14/664) pre-intervention to 4.2% (22/528, X^2 $p = 0.04$) post intervention. Post intervention, 17% (9/ 53) of people referred by non-hepatology specialists had F3 or 4 stage fibrosis on VCTE, compared to 5% (1/20) of those referred pre-intervention.
Conclusion: Reflex reporting of APRI on routine blood tests increased the proportion of VCTE referrals from non-liver specialists, without overwhelming VCTE service capacity. Reflex reporting of APRI by pathology services may be an effective, low-cost intervention to increase early diagnosis of cirrhosis.

SAT-521

Feasibility of adult population screening for liver cirrhosis using routine blood tests in Australia: a prospective cohort study

Joan Flores[1,2,3], Christina Trambas[1,4], Natasha Jovanovic[4], Bree James[4], Thai Hong[1], Zina Valaydon[5], Alexander Thompson[1,3], Jessica Howell[1,3]. *[1]Saint Vincent's Hospital Melbourne, Fitzroy, Australia; [2]Canberra Hospital, Garran, Australia; [3]University of Melbourne, Parkville, Australia; [4]Saint Vincent's Pathology, Fitzroy, Australia; [5]Western Health, Footscray, Australia*
Email: ericka@flores.com.au

Background and aims: Blood biomarker algorithms APRI and FIB-4 are recommended in guidelines for cirrhosis screening in people with liver disease. However, awareness and use in primary care are low. We evaluated the feasibility of reflex reporting of APRI and FIB-4 scores by a pathology service on routine blood tests to identify people at risk of cirrhosis.
Method: In this prospective cohort study, anonymised blood test results and demographic data were extracted for all St Vincent's Pathology statewide blood test events ordered in primary care between 8 August 2022 and 31 January 2023. APRI and FIB-4 were calculated for blood test events where FBE and LFTs were ordered together, restricted to adults aged 18 to 80 years with elevated ALT above the laboratory upper limit of normal (30 IU/mL females, 35 IU/mL males).
Results: 15,637 of 38,190 (41%) of individuals tested had elevated ALT. Of these, 6% (N = 478) had APRI >1.0 and 1% (N = 119) had APRI >2.0. Elevated APRI was more common in males (4% vs 3%, $p < 0.001$) but did not vary with age. 27% (N = 4694) had FIB-4 >1.3 and 3% (N = 519) had FIB-4 >2.67. FIB-4 >2.67 was more common in males (4 vs 2%, $p < 0.001$). Odds of FIB-4 >1.3 increased exponentially with age >45 years ($p < 0.001$). Kappa agreement between APRI >1 and FIB-4 >2.67 was 98% (SE 0.005). Median monthly rate of test events which would trigger transient elastography referral was 93 per month for APRI >1.0 and 87 per month for FIB-4 >2.67.
Conclusion: Reflex calculation and reporting of APRI >1.0 and FIB-4 >2.67 by pathology services on routine blood tests in primary care is a potentially feasible approach for population-level cirrhosis screening. Further studies are needed to determine the impact on cirrhosis case identification and referral to specialist care.

SAT-522

Diagnostic performance of the ELF score for liver fibrosis staging in chronic liver disease: a comparative study with FibroScan, serum markers, and liver biopsy

Tatsuya Fujino[1], Shingo Namino[1], Kazumi Yamasaki[1], Tomoyuki Suehiro[1], Yuki Kugiyama[1], Tomohito Kojima[1], Yasuhide Motoyoshi[1], Akira Saeki[1], Shinya Nagaoka[1], Atsumasa Komori[1], Hiroshi Yatsuhashi[1,2]. *[1]NHO Nagasaki Medical Center, Omura, Japan; [2]Clinical Research Center, National Hospital Organization Nagasaki Medical Center, Nagasaki, Japan*
Email: Yatsuhashihiroshi@gmail.com

Background and aims: This study aimed to validate the correlation between the Enhaned Liver Fibrosis(ELF) score and fibrosis stages based on FibroScan (liver stiffness measurement; LSM), and to compare its diagnostic performance with the FIB-4 index, APRI, and M2BPGi. Furthermore, we evaluated the association between the ELF score and histological fibrosis stages in patients who underwent liver biopsy.
Method: Two cohorts were analyzed: Cohort A: 373 patients with chronic liver disease (HBV, n = 105; HCV, n = 250; MASLD, n = 18) who underwent FibroScan and blood tests on the same day. Based on LSM values, they were classified into F1 (≤7.0 kPa, n = 213), F2 (7.1–9.9 kPa, n = 50), F3 (10.0–12.9 kPa, n = 34), and F4 (≥13.0 kPa, n = 76). Cohort B: 277 patients (126 males, 151 females; mean age 59.5 ± 14.4 years) with liver biopsy and ELF measurements. Etiologies included HBV (n = 71), HCV (n = 148), and MASLD (n = 58). Histological stages were F1 (n = 134), F2 (n = 68), F3 (n = 38), and F4 (n = 37). Statistical analyses included correlation analysis, group comparisons, and receiver operating characteristic (ROC) analysis.
Results: In Cohort A, the ELF score showed significant positive correlations with M2BPGi (r = 0.757), FIB-4 (r = 0.699), and APRI (r = 0.654) (all $p < 0.001$). Median ELF scores increased progressively with LSM-based stages (F1: 9.25, F2: 10.14, F3: 10.50, F4: 11.92; $p < 0.001$). For the diagnosis of stage ≥ F2, the ROC for ELF was 0.837, outperforming FIB-4 (0.806) and APRI (0.824). For ≥ F3, ELF demonstrated the highest specificity (0.928). For ≥ F4, ELF achieved the highest AUROC (0.874) among the three markers. In Cohort B (biopsy-proven), median ELF scores also rose significantly across all histological stages (F1: 9.81, F2: 10.53, F3: 11.39, F4: 12.07). The AUROCs for the diagnosis ≥ F2, ≥ F3, ≥ F4 were 0.778, 0.811, and 0.836, respectively, showing improved diagnostic performance with advancing fibrosis.

Conclusion: The ELF score effectively reflects fibrosis progression in chronic liver diseases (HBV, HCV, and MASLD) and demonstrates superior or comparable diagnostic performance to FIB-4, APRI, and M2BPGi. The strong correlation with M2BPGi suggests these markers may serve as complementary non-invasive tools. Furthermore, the clear stepwise increase in ELF scores according to histological stages underscores its clinical utility for identifying advanced fibrosis. Further studies focusing on etiology-specific analysis and longitudinal changes are warranted.

SAT-523

Genetic determinants of clinical phenotypes in pediatric liver transplant recipients with inherited liver diseases

Eyad Gadour[1], Ibrahim Hassan[1], Razan Bader[1], Hadi Kuriry[1], Ahmed Zidan[1], Mohammed Alqahtani[1]. *[1]King Fahad Specialist Hospital, Multiorgan Transplant Centre of Excellence, Pediatric Liver Transplantation, Dammam, Saudi Arabia*
Email: eyadgadour@doctors.org.uk

Background and aims: Inherited liver diseases (ILDs) in children present significant clinical heterogeneity, complicating diagnosis, prognosis, and management. Although genetic diagnosis is now routine, detailed genotype-phenotype correlations remain underexplored, particularly in familial cohorts. This study aimed to elucidate precise genotype-phenotype relationships in pediatric ILDs by analyzing clinical, histopathological, and genetic data from sibling pairs undergoing liver transplantation.
Method: We performed a retrospective cohort study at a tertiary liver transplant center in France, including 26 pediatric patients (13 sibling pairs) with genetically confirmed ILDs who underwent liver transplantation.Statistical analyses using Fisher's exact test and one-way ANOVA (IBM SPSS v28) assessed associations between genotypes and clinical/histological features. Significance was set at $p < 0.05$.
Results: The cohort predominantly comprised infants diagnosed before 1 year of age (76.9%, n = 20). Seven genes were implicated: ABCB11, ABCB4, AGXT, UGT1A1, GBE1, BCKDHA, and DCDC2. PFIC II (ABCB11 mutations) was the most prevalent diagnosis (30.8%, n = 8). Ascites was present in 23.1% (6/26) of patients and showed a trend toward association with genotype, although this did not reach statistical significance ($p = 0.053$). Histopathological analysis revealed cirrhosis as the predominant biopsy finding, occurring in 57.7% (15/26) of cases, and was uniformly associated with ABCB4, specific ABCB11 variants (c.2453A>T, homozygous c.2944G>A), GBE1, and DCDC2 mutations. Eight patients (30.8%) exhibited normal liver histology, which was restricted to carriers of AGXT, UGT1A1, and the ABCB11 c.2296G>A mutation. Mean PELD scores varied by genotype, ranging from 16.5 in patients homozygous for ABCB4 c.3838T>C to 38.5 in another homozygous ABCB4 c.3838T>C pair; however, these differences did not reach statistical significance ($p = 0$).
Conclusion: This study delineates robust genotype-phenotype correlations in pediatric ILDs within a familial cohort. The AGXT mutation defines a unique non-icteric renal phenotype, while specific ABCB11 and DCDC2 variants confer high risk for early coagulopathy and severe hepatocellular dysfunction. The lack of significant correlation between genotype and PELD scores highlights the multifactorial nature of disease severity. These findings emphasize the importance of comprehensive genetic testing for prognostic stratification and personalized clinical management in pediatric ILDs.

SAT-524

Percutaneous liver biopsy in Spain: current clinical practice and safety in the era of non-invasive tests

Mariano Gómez-Rubio[1], Rodrigo Nájera-Muñoz[1], Miguel Fernández-Bermejo[2], Valle Cadahía-Rodrigo[3], Rocio Calvo Hernandez[4], Diego Rojo[5], Luis Cortés García[6], Laura Paola Barreto-Anchury[7], Pablo Flores-Diez[3], Sergio Perez-Rodriguez[4], Laura Pages[8], María Galochino[6], Gemma Carrion Alonso[9], Cristina Martínez Cuevas[10], Sara María Monsalve Alonso[11], María Ojeda Remizova[12], Luis Eduardo Durán Durán[13], Esther Badia-Aranda[14], Ana Guiberteau[15], Leticia González-Moreno[16], María Rodríguez-Peláez[3], Benjamin Polo Lorduy[4], María Teresa Salcedo[17], Adela Navarro[6], Isabel Serra[7], Sonia Martín-Chavarri[9], Alicia SanJosé Crespo[10], Pablo Cavanagh Pérez-Nievas[11], Manuel Crespo Sánchez[12], Antonio Diaz[18], Maria Luisa Gutiérrez[19], Gadea Hontoria-Bautista[14], Cristina Corchado-Berjano[15], María Caldas-Álvarez[16], Carla Lucio-Fernández[20], Silvia Montoliu[21]. *[1]Department of Digestive Diseases. Hospital Universitario de Getafe, Universidad Europea de Madrid. Faculty of Biomedical and Health Sciences, Getafe, Madrid, Spain; [2]Department of Digestive Diseases. Hospital Universitario de Cáceres, Cáceres, Spain; [3]Department of Digestive Diseases. Hospital Universitario Central de Asturias, Oviedo, Spain; [4]Department of Digestive Diseases. Fundación Jiménez Díaz, Madrid, Spain; [5]Liver Unit, Division of Digestive Diseases. Hospital Universitario Vall D'Hebron, Barcelona, Spain; [6]Department of Digestive Diseases. Hospital Universitario Lozano Blesa, Zaragoza, Spain; [7]Department of Hepatology, Hospital Universitario Doctor Josep Trueta, Girona, Spain; [8]Liver Unit, Dvision of Digestive Diseases, Hospital Universitario Vall d'Hebron, Barcelona, Spain; [9]Department of Digestive Diseases, Hospital Universitario Infanta Leonor, San Sebastián de los Reyes, Madrid, Spain; [10]Department of Digestive Diseases, Hospital Universitario Rio Hortega, Valladolid, Spain; [11]Department of Digestive Diseases, Hospital Universitario Infanta Sofía, San Sebastián de los Reyes, Madrid, Spain; [12]Department of Digestive Diseases, Hospital Universitario San Agustín, Avilés, Asturias, Spain; [13]Department of Digestive Diseases, Hospital Universitario Fundación de Alcorcón, Alcorcón, Spain; [14]Department of Digestive Diseases, Hospital Universitario de Burgos, Burgos, Spain; [15]Department of Digestive Diseases, Hospital Universitario de Badajoz, Badajoz, Spain; [16]Department of Digestive Diseases, Hospital Universitario de La Princesa, Madrid, Spain; [17]Pathology Department, Hospital Universitario Vall D'Hebron, Barcelona, Spain; [18]Department of Digestive Diseases, Hospital del Sureste, Arganda del Rey, Madrid, Spain; [19]Department of Digestive Diseases, Hospital Universitario Fundación de Alcorcón, Alcorcón, Madrid, Spain; [20]Department of Digestive Diseases, Hospital Universitario Severo Ochoa, Leganés, Madrid, Spain; [21]Department of Digestive Diseases, Hospital Universitario Joan XXIII, Tarragona, Spain*
Email: mgomezrubio@salud.madrid.org

Background and aims: In the era of non-invasive tests, the role of percutaneous liver biopsy (PLB) in routine clinical practice is evolving. However, contemporary real-world data on its use, safety and clinical impact in Spain are lacking. This study aimed to describe current PLB practice and outcomes in a nationwide setting.
Method: We conducted a multicentre, retrospective observational study including 18 Digestive and Hepatology units in Spain. PLBs performed in 2012 and 2022 were analysed, covering a reference population of 10,227,640 inhabitants. Data were collected through the national PBHPE REDCap® registry (AEED, Spanish Association of Digestive Ultrasound). Utilisation rates, clinical indications, procedural characteristics, diagnostic yield and complications were assessed.
Results: A total of 1,126 PLBs were included, with an annual rate of 11.0 biopsies per 100,000 inhabitants. Mean age was 53.8 years and 51.2% were women; 64.5% of procedures were performed in outpatients. The main indications were abnormal liver tests (45.3%), autoimmune hepatitis (15.5%), hepatitis C (14.2%) and steatotic liver disease (12.0%). Pre-procedural coagulation assessment was performed in 83.3% of cases. Most biopsies (63.7%) were performed by experienced physicians (>100 procedures), predominantly gastroenterologists/hepatologists (87.9%). Ultrasound guidance was used in 95.4% of cases, either with pre-procedural skin marking (51%) or real-time guidance (49%). Automatic needles were employed in 69.6% of procedures, most commonly 16G (66.9%). Adequate liver tissue for

diagnosis was obtained in 91.0%, with a mean specimen length of 19.6 mm. Fibrosis stages were F0 (46.1%), F1 (23.1%), F2 (13.6%), F3 (9.8%) and F4 (7.4%). Pain was absent or mild in 95.8% of patients. No complications occurred in 93.9%. Severe complications were uncommon (1.1%), including liver haematoma (0.8%) and hemoperitoneum (0.3%). One procedure-related death (0.09%) was reported.
Conclusion: Despite the widespread use of non-invasive techniques, PLB remains an important diagnostic tool in clinical practice, particularly in cases of diagnostic uncertainty and immune-mediated liver diseases. When performed by experienced specialists with ultrasound guidance, PLB is safe, well tolerated and provides a high diagnostic yield. Optimising patient selection is essential to maximise clinical impact while maintaining a low risk profile.

SAT-525
Do large language models think like hepatologists? A multi-dimensional real-world study
Nada Abedin[1], Amaryllis Görz[1], Maximilian Freiherr von Beust[2], Anita Pathil-Warth[1], Ulrike Mihm[1], Stefan Zeuzem[1], Georg Dultz[1]. *[1]Medical Clinic 1, University Hospital Frankfurt, Frankfurt am Main, Germany; [2]Independent Researcher, Frankfurt, Germany*
Email: abedin@med.uni-frankfurt.de

Background and aims: Large language models (LLMs) are increasingly evaluated for clinical diagnosis, yet most studies focus exclusively on accuracy. Few studies have examined LLM performance across multiple dimensions in specialized domains such as hepatology and with real-life cases. We aimed to evaluate LLM performance using a multi-dimensional framework encompassing accuracy, guideline adherence, treatment quality, safety, and comparison to actual practice in a real-life cohort.
Method: We performed a retrospective study of 304 hepatology cases from a single-center outpatient clinic at University Hospital Frankfurt with a 1-year follow-up. Each case was evaluated using a LLM (Claude Sonnet 4.5) augmented with retrieval-augmented generation with access to hepatology guidelines (DGVS, EASL). The LLM received first-appointment data only, while ground truth diagnoses were established by specialists with longitudinal follow-up (mean 3.4 visits). Five dimensions were assessed: (1) diagnostic accuracy (exact and category-level), (2) guideline adherence, (3) treatment quality, (4) critical misses, and (5) comparison to actual management. Performance was stratified by disease category, complexity, and confidence level using Wilson confidence intervals and chi-square analysis.
Results: Diagnostic accuracy was 68.5% (95% CI 62.6%–73.8%) for exact diagnosis and 76% (95% CI 70.9%–80.4%) for category, achieved with first-appointment data only. The LLM demonstrated excellent guideline adherence (96.7%, 294/304) with correct guideline selection (92.4%, 281/304) and appropriate treatment recommendations (96.1%, 292/304). Recommendations were superior to actual management in 14.8% (45/304) and equal in 79.6% (242/304). Critical misses occurred in 7.9% (24/304), predominantly affecting rare diseases. Viral hepatitis showed highest accuracy (82.5% exact, 91.3% top-3). Confidence calibration was significant (high 60.5% vs moderate 35.8%, $p = 0.0006$).
Conclusion: LLMs demonstrate moderate accuracy but excellent clinical reasoning and guideline adherence. Despite single-timepoint limitations, LLMs showed appropriate reasoning in 96% of cases and outperformed actual recommendations in 15%. LLMs are appropriate for clinical decision support with mandatory human oversight and can enhance guideline compliance and time-to-treatment significantly. Multi-dimensional evaluation frameworks are essential for assessing medical AI beyond traditional accuracy metrics.

SAT-527
Reevaluating liver enzyme reference ranges in chronic kidney disease: a population-based study
Karem Awad[1], Benaya Rozen Zvi[2], Fadi Abu Baker[3], Mifleh Tatour[4], Abdellatif Zhalka Zhalka[5], Rawi Hazzan[6]. *[1]Department of Nephrology and Hypertension, Emek Medical Center, Afula, Israel, Rappaport Faculty of Medicine, Technion - Institute of Technology, Haifa, Israel, Afula, Israel; [2]Department of Nephrology and Hypertension, Rabin Medical Center, Petah Tikva, Israel, Gray Faculty of Medical & Health Sciences, Tel-Aviv University, Tel-Aviv, Israel, Petah Tiqva, Israel; [3]Department of Gastroenterology and Hepatology, Hillel Yaffe Medical Center, Hadera 38100, Israel, Rappaport Faculty of Medicine, Technion - Institute of Technology, Haifa, Israel, Hadera, Israel; [4]Clalit Health Services, Northern Region, Israel, Azrieli Faculty of Medicine, Bar-Ilan University, Safed, Israel, Nof hagalil, Israel; [5]Department of Internal Medicine B, Emek Medical Center, Afula, Israel, Afula, Israel; [6]Clalit Health Service, Barilan University, Nazareth, Israel*
Email: rawihazzan1@gmail.com

Background and aims: Alanine aminotransferase (ALT) and aspartate aminotransferase (AST) are essential liver biomarkers, but consistently low values complicate their interpretation in chronic kidney disease (CKD). Current reference ranges may contribute to the underdiagnosis of hepatic disorders in this population.
Method: We conducted a retrospective, population-based cohort study using the Clalit Health Services database, which included 820,707 adult patients with a normal body mass index (BMI) and valid AST/ALT results. Patients were stratified by CKD stage and gender. The relationship between enzyme levels and estimated glomerular filtration rate (eGFR) was assessed using descriptive statistics and regression analysis.
Results: ALT and AST levels were significantly lower in CKD patients compared to the general population, with a progressive decline across CKD stages. In males, the mean ALT decreased from 24.4 U/L in Stage I to 13.5 U/L in Stage V; in females, ALT declined from 16.0 U/L to 12.8 U/L. AST values also reduced from 23.6 U/L to 15.6 U/L in males and from 19.5 U/L to 16.5 U/L in females. A strong positive correlation. was observed between ALT and eGFR, particularly in males. Enzyme variability was most significant in early CKD and narrowed in advanced stages. Non-parametric Regression models further confirmed that the association between aminotransferase levels and eGFR is modified by both age and gender, with younger patients exhibiting steeper declines in eGFR.
Conclusion: Our study highlights the urgent need for Kidney Disease-Specific thresholds for liver enzymes. We found that ALT and AST levels decline progressively with increasing severity of CKD, independent of overt liver disease, and this trend is consistent across genders. The narrowing variability and lower enzyme concentrations in advanced CKD highlights the risk of underdiagnosing liver disease when using standard Reference ranges. Implementing CKD-specific thresholds could significantly improve the detection and management of hepatic disorders in this population.

SAT-528
CT-derived spleen volume combined with routine labs accurately differentiates PSVD from cirrhosis across global cohorts
Subin Heo[1], Maxime Ronot[2], Pierre-Emmanuel Rautou[2], Pomohaci Mihai[3], In Hye Song[1], Hyo Jeong Kang[1], Youngeun Yoo[1], Lucile Moga[2], Shantha Valainathan[2], Sung-Cheol Yun[1], Won-Mook Choi[1], Seung Soo Lee[1]. *[1]Asan Medical Center, Seoul, Korea, Rep. of South; [2]Hôpital Beaujon, Clichy, France; [3]University of Medicine and Pharmacy "Carol Davila," Bucharest, Romania*
Email: dr.choi85@gmail.com

Background and aims: Porto-sinusoidal vascular disorder (PSVD) is an often overlooked etiology of portal hypertension and is commonly mistaken for cirrhosis. This study aims to evaluate differences in CT-based volumetric and laboratory characteristics between PSVD and

cirrhosis and to build and externally validate a noninvasive diagnostic model.
Method: We retrospectively analyzed 101 patients with PSVD and 202 with cirrhosis from Korea (Eastern cohort) and 45 patients with PSVD and 100 with cirrhosis from France (Western cohort), all presenting with portal hypertension and matched for its severity. Liver and spleen volumes were automatically measured on contrast-enhanced CT and normalized to individualized reference volumes. After feature comparison, a conditional logistic regression model (PSVD-VL) incorporating standardized spleen volume, aspartate aminotransferase, platelet count, and international normalized ratio was developed in the Eastern cohort and validated in the Western cohort. Rule-in and rule-out thresholds were predefined to aim for 90% specificity and sensitivity.
Results: Standardized spleen volume was markedly higher in PSVD than in cirrhosis in both cohorts (Eastern: 5.14 vs 3.59, $p < 0.001$; Western: 5.20 vs 3.46, $p < 0.001$), whereas markers of hepatic synthetic function and hepatocellular injury were comparatively preserved in PSVD. The PSVD-VL model achieved an area under the receiver operating characteristic curve of 0.86 (95% CI, 0.81–0.91) in the Eastern cohort and 0.79 (95% CI, 0.71–0.87) in the Western cohort for diagnosing PSVD. Applying the rule-in and rule-out thresholds enabled classification of 69% and 67% of patients in the Eastern and Western cohorts, respectively, with correct assignment rates of 86% and 83%.
Conclusion: Compared with cirrhosis of equivalent portal hypertension severity, PSVD is characterized by disproportionate splenomegaly and relatively preserved liver function. A model integrating CT-derived spleen volume with routine laboratory tests demonstrated consistent performance across geographically distinct cohorts and may facilitate more accurate identification of PSVD in clinical practice.

SAT-529
Malnutrition beyond BMI in chronic liver disease: a prospective study of nutritional risk, sarcopenia, and food insecurity

Benjamin Kaschube[1], Monika Rau[1], Andreas Geier[1], Hans Benno Leicht[1], Gerd Sauter[1], Florian P. Reiter[1], Lisa Duemmler[1].
[1]University Hospital Würzburg, Department of Internal Medicine II, Division of Hepatology, Würzburg, Germany
Email: kaschube_b@ukw.de

Background and aims: Malnutrition and sarcopenia are common in chronic liver disease and are associated with impaired quality of life and adverse outcomes. Food insecurity has recently been linked to MASLD, advanced fibrosis, and mortality, but data for patients with chronic liver disease in Germany are lacking. Despite their clinical relevance, systematic screening is not routinely performed. This study aimed to determine the prevalence of malnutrition, sarcopenia, and food insecurity in a large real-world cohort and to identify associated risk factors.
Method: In this prospective study, 981 outpatients with chronic liver disease attending a tertiary care center were screened for malnutrition, sarcopenia, and food insecurity between 11/22–04/24 using validated tools (LDUST, SARC-F, and FIES). Routine clinical characteristics and laboratory parameters were recorded. Descriptive analyses were performed to determine prevalence rates and to assess associations between nutritional status and patient characteristics.
Results: The cohort compromised 981 outpatients (53% female; mean age 55 years). MASLD was the most common etiology (20.5%), followed by viral hepatitis (19.0%) and cholestatic liver disease (16.6%); 18.9% had cirrhosis and 7.6% HCC. Using LDUST, 47.3% of patients were identified as being at risk of malnutrition, with highest prevalence in those with liver cirrhosis (LC), HCC, or prior liver transplantation. Malnutrition risk was not limited to low BMI, as among LDUST-positive patients, obesity (BMI >30 kg/m^2) was more frequent than BMI <25 kg/m^2 (34.1% vs. 31.5%). SARC-F screening was positive in 10.1%, predominantly in patients with ALD and LC, and was associated with older age and cardiometabolic comorbidities. Notably, 96% of patients with a positive SARC-F screening were also at risk of malnutrition. FIES screening was positive in 6.5% (n = 64) of patients, most frequently in viral hepatitis, and was associated with younger age but not with BMI, liver stiffness or cardiometabolic comorbidities. In addition, 9.7% of patients reported a worsened diet due to rising food costs since 2022.
Conclusion: Nearly half of liver outpatients were at risk of malnutrition, including many with overweight or obesity, confirming that malnutrition extends beyond low BMI. Screening for malnutrition, sarcopenia, and food insecurity identifies complementary risk profiles, while rising food costs since 2022 underscore the need to integrate nutritional and socioeconomic assessment into routine hepatology care.

SAT-530
A machine learning approach to non-invasively predict hepatic decompensation in compensated advanced chronic liver disease: the CIRI model

Georg Kramer[1,2,3], Anders Hildeman[4], Caterina Tozzi[5], Roza Maghsood[4], Vinusha Kalatharan[6], Kinga Jastrzebska[4], Hyewonnina Koo[4], Nils Svangård[4], Claire Donoghue[4], Benedikt Simbrunner[1,2,3], Benedikt Hofer[1,2,3], Mattias Mandorfer[1,2,3], Thomas Reiberger[1,2,3], Jan Oscarsson[4], Philip Ambery[4]. *[1]Division of Gastroenterology and Hepatology, Department of Medicine III, Medical University of Vienna, Vienna, Austria, Vienna, Austria; [2]Vienna Hepatic Hemodynamic Laboratory, Division of Gastroenterology and Hepatology, Department of Medicine III, Medical University of Vienna, Vienna, Austria, Vienna, Austria; [3]Clinical Research Group MOTION, Medical University of Vienna, Vienna, Austria, Vienna, Austria; [4]Data Sciences and Artificial Intelligence, BioPharmaceuticals R&D, Astra Zeneca, Gothenburg, Sweden, Gothenburg, Sweden; [5]Data Sciences and Artificial Intelligence, BioPharmaceuticals R&D, Astra Zeneca, Barcelona, Spain, Barcelona, Spain; [6]Data Sciences and Artificial Intelligence, BioPharmaceuticals R&D, Astra Zeneca, Mississauga, Canada, Mississauga, Canada*
Email: georg.kramer@meduniwien.ac.at

Background and aims: Clinically significant portal hypertension (CSPH), defined as a hepatic venous pressure gradient (HVPG) ≥10 mmHg, identifies patients with compensated advanced chronic liver disease (cACLD) at risk of hepatic decompensation. As invasive HVPG measurement is not widely available, reliable non-invasive alternatives are needed. We developed and validated the Cirrhosis Risk Identifier (CIRI), a machine-learning model based solely on 11 routine demographic and laboratory variables, trained to predict first hepatic decompensation and benchmarked it against established blood-based scores (MELD, FIB-4), HVPG and liver stiffness measurement (LSM).
Method: CIRI was trained in cACLD patients from the U.S. Optum's de-identified Clinformatics Data Mart Database (Optum) (training n = 112,618; tuning n = 18,765) and validated in an independent Optum validation cohort (n = 18,852) and a prospective European cohort from Vienna, Austria (n = 210) with paired HVPG and LSM. The endpoint was first hepatic decompensation (ascites, overt encephalopathy, variceal bleeding), with hepatocellular carcinoma and death as competing events.
Results: In the Optum validation cohort (median MELD 8 [IQR 6–12]), 3887 patients (20.6%) decompensated over 18.5 months median follow-up; in Europe (median MELD 9 [IQR 8–12]), 37 patients (17.1%) decompensated over 27.5 months. Steatotic liver disease was the predominant etiology (Optum 54.2%; Europe 44.0%). CIRI showed strong discrimination for first decompensation with time-dependent AUROCs at 1 and 2 years of 0.816 and 0.815 in Optum, and 0.836 and 0.769 in Europe, outperforming MELD and FIB-4 in both cohorts (all $p < 0.05$). In Europe, CIRI performed comparably to HVPG (all $p > 0.9$) and better than LSM (all $p < 0.01$). In Fine-Gray models, CIRI independently predicted decompensation after adjustment for non-selective beta-blockers in Optum (adjusted subdistribution hazard

ratio [aSHR]: 1.67; p < 0.001) and after adjustment for HVPG, non-selective beta-blockers, INR and etiological cure in Europe (aSHR 1.66; p = 0.017). Model performance was robust across etiologies and in sensitivity analyses including FIB-4 ≥1.3 subgroups.
Conclusion: The machine-learning-based CIRI model demonstrated robust prognostic performance and effective risk stratification in cACLD. Its predictive accuracy was validated in large U.S. and European cohorts, with discrimination of decompensation risk comparable to HVPG, supporting its potential as a non-invasive tool to identify "at-risk" cACLD patients.

SAT-531
Association between small intestinal bacterial overgrowth and chronic liver disease in patients with functional gastrointestinal disorders: a cross-sectional study in southern Vietnam
Ngan Le[1]. [1]*Tam Anh general Hospital, Gastroenterology, Ho Chi Minh, Viet Nam*
Email: bsquynhngan@gmail.com

Background and aims: Small intestinal bacterial overgrowth (SIBO) is increasingly recognized as an important factor in the gut–liver axis and may contribute to chronic liver disease (CLD). In Vietnam, and more broadly in Southeast Asia, clinical data on the association between SIBO and chronic liver disease are particularly lacking. Therefore, we conducted the first clinical study in Southern Vietnam to investigate the association between SIBO and chronic liver disease in a real-world cohort of patients with functional gastrointestinal disorders. **Aim:** To evaluate the association between SIBO and chronic liver disease in patients presenting with functional gastrointestinal symptoms.
Method: A cross-sectional study was conducted on 188 patients undergoing breath testing for SIBO. Clinical features, endoscopic findings, metabolic comorbidities, liver enzymes, and abdominal ultrasound results were analyzed. Inclusion Criteria: Completion of glucose breath test, availability of endoscopy, ultrasound, and laboratory data, No antibiotic use within 4 weeks Exclusion Criteria: Prior intestinal resection, Active malignancy, Severe systemic illness interfering with breath testing.
Results: A total of 188 patients were included in the analysis. The mean age was 47.84 ± 14.8 years (range 14–80 years), with a male predominance (107 men and 81 women). Functional gastrointestinal disorders were common in the cohort, including gastroesophageal reflux disease (16.5%), functional dyspepsia (45.7%), and irritable bowel syndrome (60.6%). SIBO was identified in 66 of 188 patients (35.1%). Chronic liver disease was diagnosed in 16 patients (8.5%). The prevalence of chronic liver disease was significantly higher among patients with small intestinal bacterial overgrowth compared with those without SIBO (55.2% vs. 44.8%, p = 0.01).
Conclusion: Small intestinal bacterial overgrowth is highly prevalent among patients with functional gastrointestinal disorders, particularly in those with functional gastrointestinal symptoms accompanied by chronic liver disease. The significant association observed between intestinal bacterial overgrowth and chronic liver disease highlights the potential role of gut dysbiosis in the gut–liver axis and in the progression of chronic liver conditions. These findings underscore the importance of considering the evaluation and management of small intestinal bacterial overgrowth in patients with functional gastrointestinal disorders, especially when chronic liver disease is present.

SAT-532
Direct prothrombin concentration as replacement for INR improves accuracy of MELD in 90-day mortality prediction in patients with acute decompensation of cirrhosis
Markus Maagaard[1,2], Nikolaj Torp[1,2], Mads Israelsen[1,2], Alastair O'Brien[3], Aleksander Krag[1,2]. [1]*Centre for Liver Research, Department of Gastroenterology and Hepatology, Odense University Hospital, Odense, Denmark;* [2]*Institute of Health Sciences, University of Southern Denmark, Odense, Denmark;* [3]*Institute for Liver and Digestive Health, University College London, London, United Kingdom*
Email: markus.maagaard@rsyd.dk

Background and aims: The international normalized ratio (INR) is a core component of the Model for End-Stage Liver Disease (MELD) score. However, INR is influenced by heparins and direct oral anticoagulants (DOACs), thereby compromising its validity as a marker of hepatic synthetic function in an inpatient setting. In contrast, prothrombin concentration (CPT) is not affected by anticoagulants and may more directly reflect liver synthetic capacity. We investigated whether replacing INR with CPT improves the prognostic discrimination of MELD for 90-day mortality in patients with cirrhosis hospitalized with acute decompensation.
Method: We analysed samples from 313 patients admitted to hospital with acute onset or worsening of complications of cirrhosis. CPT was quantified from Li-Hep plasma stored at −80°C until analysis. Measurements were performed in a single 5-minute reaction step by an aptamer-based electrochemical biosensor (Solsten, DK). The primary endpoint was difference in prediction of 90-day survival between CPT and INR. We further investigated if prognostic discrimination of the MELD score, as assessed by Harrell's C, was improved by substituting INR with CPT ($MELD_{CPT}$).
Results: When comparing MELD and $MELD_{CPT}$, Harrell's C was 0.61 for the original MELD, and 0.69 for $MELD_{CPT}$ (p = 0.037). Mean cohort age was 54 years (±11), 28% were female, the dominant cirrhosis etiology was alcohol-related (90%), and 90-day mortality was 26%. The median MELD was 18 (IQR: 15–23), with median bilirubin of 5.6 mg/dL (IQR: 2.6–10.5), median creatinine of 0.78 mg/dL (IQR: 0.59–1.01) and median INR of 1.6 (IQR: 1.4–2.0). Median $MELD_{CPT}$ was 21 (IQR: 19–25), with median CPT of 843 nmol/L (IQR: 610–903). In univariable analyses both CPT (HR = 1.08, 95% CI: 1.03–1.15, p = 0.004) and INR (HR = 1.03, 95% CI: 1.02–1.05, p < 0.001) were associated with 90-day mortality. Training and validation sets were sampled as a 7:3 distribution of patients stratified only on occurrence of events. Multivariable Cox regression - replacing INR with CPT and keeping bilirubin and creatinine weighting as in the original MELD score - made an optimal prediction model expressed as: $-1.74 \times CPT + 9.57 \times \log(\text{Creatinine}) + 3.78 \times \log(\text{Bilirubin}) + 16$.
Conclusion: Using only direct measurements of CPT showed prognostic performance like established liver biomarkers. When CPT replaced INR in the MELD score, the $MELD_{CPT}$ showed greater prognostic discrimination. These findings suggest CPT as a potential prognostic biomarker in patients with decompensated cirrhosis.

SAT-533
Serum bile acids profile analysis predicts severity and progression of liver disease
Yanpei Mai[1], Qinshuo Wang[1], Suzhen Jiang[1], Linlin Cao[2], Xin Wen[1], Tianyi Xue[1], Yuxi Shi[1], Yanhui Yang[1], Huiying Rao[1], Zixing Wang[1]. [1]*Peking University Hepatology Institute, Beijing, China;* [2]*Peking University People's Hospital Laboratory Department, Beijng, China*
Email: wangzixing@pkuph.edu.cn

Background and aims: Bile acids profoundly influence the onset and progression of liver disease through signaling regulation, inflammatory responses, and interactions within the gut-liver axis. During the progression from hepatitis to cirrhosis and ultimately hepatocellular carcinoma, the bile acid profile undergoes dynamic changes. However, the association between specific bile acids and distinct stages of liver disease progression remains unclear. Identifying bile acids with stage-specific signatures holds significant value for elucidating the mechanisms of liver disease progression and establishing early warning systems.
Method: We enrolled 889 patients with liver disease from Peking University Hepatology Institute, categorized as whether of severe conditions (with irreversible liver fibrosis and cirrhosis that is related

to fundamental changes in monitoring frequency, complication risks, treatment regimens, and prognosis) and whether of advanced stages (liver function failure or malignant transformation). Predictive capability of different bile acids was initially assessed by regression model and then confirmed by random forest algorithm for outcome classification. Ten machine learning algorithms were employed to construct liver disease discriminative models. The training-to-validation ratio for each model was 7:3, with 5-fold cross-validation applied to calculate predictive performance.

Results: Among all patients, 185 (20.8%) had severe liver diseases, and 117 (13.2%) were in the advanced stage. Among the 15 bile acids, TCDCA, TCA, GCDCA, GCA, and TUDCA demonstrated the strongest predictive ability for liver disease outcomes. Variable importance derived from the random forest algorithm further validated the robust predictive efficacy of these five bile acids. Naive Bayes demonstrated the highest predictive capability for both classification outcomes, effectively distinguishing patients with severe liver disease and those with advanced liver disease with validation set AUC values of 0.873 (0.821–0.925) and 0.901 (0.854–0.948), respectively.

Conclusion: This study found that the serum bile acid profile composed of specific bile acids can effectively distinguish the severity and advanced stage of liver disease. Abnormal changes are closely associated with key pathological processes such as hepatitis, cirrhosis, and the development of hepatocellular carcinoma. Mechanistic and clinical research targeting these bile acids holds promise as a novel strategy for the assessment and treatment of liver disease.

SAT-537

Nurse-led clinics improve hepatocellular carcinoma surveillance rates and survival in patients with cirrhosis

Mohammad Malik[1], Liezel Robinson[1], Shivam Ghosh[1], George Macfaul[1], Ali Azzam[1], Palak Trivedi[2], Prakash Gupta[1]. *[1]Milton Keynes University Hospital, Milton Keynes, United Kingdom; [2]National Institute for Health and Care Research Birmingham Biomedical Research Centre, Birmingham, United Kingdom*
Email: mmalik458@gmail.com

Background and aims: It is well established that patients with cirrhosis have an increased risk of developing life-threatening complications such as hepatocellular carcinoma (HCC), decompensation, spontaneous bacterial peritonitis and variceal haemorrhage. Current international guidelines recommend the regular monitoring of patients with cirrhosis by way of biannual ultrasound scans, blood tests and screening endoscopy to enable earlier treatment and reduce mortality. However, in practice HCC surveillance remains underutilised, often due to limited hepatologist availability and thus novel strategies are required to successfully manage the increasing burden of liver cirrhosis worldwide. This study evaluated the impact of a dedicated, nurse-led hepatology surveillance service on clinical outcomes in patients with cirrhosis.

Method: We conducted a single-centre retrospective cohort study including patients diagnosed with cirrhosis between January 2020 and June 2025 (n = 409). Clinical outcomes were compared before and after implementation of a nurse-led hepatology surveillance clinic which began in June 2023, with patients receiving conventional hepatologist-led follow up or the novel nurse-led service. Outcomes of interest included adherence to 6-monthly HCC ultrasound surveillance, HCC diagnoses, variceal bleeds, liver transplant clinic referrals and overall survival times.

Results: In our study, 57.0% of patients were male, mean age was 62.3 years and mean follow-up was 25.0 months. Overall adherence to 6-monthly HCC ultrasound surveillance significantly increased following implementation of the nurse-led clinic (7.3% pre-implementation versus 54.9% post-implementation; $p < 0.001$). Survival analysis demonstrated significantly longer survival times among patients on the nurse-led surveillance pathway compared to conventional follow-up (61.6 versus 48.0 months; $p < 0.001$).

Conclusion: Implementation of our novel nurse-led surveillance pathway was associated with significantly increased HCC surveillance rates and longer survival times in patients with cirrhosis compared with conventional follow up. This study has important implications for the management of patients with Child-Pugh A cirrhosis, particularly when medical facilities have limited hepatologist capacity to maintain adequate surveillance.

SAT-538

Quantification of hepatic steatosis: a prospective multicenter head-to-head comparison of histopathology, digital pathology and MRI-PDFF

David Marti-Aguado[1], Clara Alfaro-Cervello[1], Matias Fernández-Patón[2], Gustavo Rojas-Echarry[3], Judith Pérez[3], Amadeo Ten-Esteve[3], María José Gastaldo[3], Cristina Garcia[4], Irene Navarrete-Pérez[5], Leonor Cerda-Alberich[2], Victor Merino[1], Alexandre Perez Girbes[5], Cristina Montón[1], Victor Puglia[4], Antonio Ferrández[1], Mercedes De La Torre Sanchez[6], Victoria Aguilera Sancho[5], Desamparados Escudero-García[1], Salvador Benlloch[4], Jose Miguel Carot[7], Luis Marti-Bonmati[5]. *[1]Incliva - Instituto De Investigación Sanitaria, Valencia, Spain; [2]Instituto De Investigación Sanitaria La Fe, Valencia, Spain; [3]Hospital Universitario Y Politécnico La Fe, Valencia, Spain; [4]Hospital Arnau De Vilanova, Valencia, Spain; [5]Hospital Universitari I Politècnic La Fe, València, Spain; [6]Hospital General Universitario De Valencia, Valencia, Spain; [7]Universidad Politécnica de Valencia, Valencia, Spain*
Email: davidmmaa@gmail.com

Background and aims: Accurate quantification of hepatic lipid content is essential for grading steatosis and monitoring therapeutic response. Hepatic steatosis can be assessed by liver biopsy—using conventional histopathology (invasive gold standard) or digital image analysis (DIA)—and by magnetic resonance–proton density fat fraction (MRI-PDFF), considered the non-invasive gold standard. This study critically evaluated the correlation and agreement between these diagnostic methods for hepatic steatosis quantification.

Method: This prospective, multicenter diagnostic accuracy study included patients with chronic liver disease who underwent paired liver biopsy and MRI between 2017 and 2025. Histological samples were quantitatively assessed by conventional histopathology (percentage of macrovesicular steatosis) and digitized for DIA (proportional area of lipid vacuoles). MRI-PDFF quantified liver fat content across the entire liver volume (~1000 cm^3), compared with a biopsy sample representing approximately 0.05 cm^3. Digital pathology was considered the reference standard ("ground truth").

Results: A total of 384 patients with paired biopsy and MRI were included (59% women; 62% MASLD; 32% obesity; 26% diabetes). Mean hepatic lipid content was 20.4% by conventional histopathology, 9.0% by DIA, and 8.5% by MRI-PDFF. Significant correlations were observed between all methods ($p < 0.001$): $r = 0.87$ for histopathology vs DIA, $r = 0.88$ for histopathology vs MRI-PDFF, and $r = 0.91$ for MRI-PDFF vs DIA. Linear regression analysis demonstrated a systematic overestimation of steatosis by conventional histopathology across the entire range compared with digital pathology and MRI-PDFF, which display nearly identical quantitative behaviour. Using standard histopathology cut-offs for steatosis grading (S1: 5%, S2: 33%, S3: 66%), the corresponding thresholds were non-equivalent and substantially lower when applied to quantitative reference methods: S1: 5.8% (DIA) and 4.8% (MRI-PDFF).
S2: 12.0% (DIA) and 11.2% (MRI-PDFF).
S3: 19.6% (DIA) and 18.8% (MRI-PDFF).

Conclusion: Despite evaluating vastly different liver volumes, MRI-PDFF mirrors DIA showing a linear equivalence for hepatic steatosis assessment. Conventional histopathology systematically distorts steatosis severity. These findings support MRI-PDFF as the most

accurate and reproducible reference standard for hepatic steatosis quantification, with implications in clinical practice and treatment trials.

SAT-539

The presence of mild degree steatosis does not impact the clinical course of portosinusoidal vascular disorder

Iulia Minciuna[1], Ana Maria Fit[2], Ioana Rusu[2], Oana Nicoara-Farcau[1], Corina Radu[3], Cristian Moldovan[4], Cristina Adela Iuga[4], Andreea Fodor[1], Tudor Cosma[1], Buzias Maria[1], Horia Ștefănescu[3], Bogdan Procopet[1]. *[1]Regional Institute of Gastroenterology and Hepatology "O. Fodor," University of Medicine and Pharmacy "Iuliu Hatieganu," Cluj-Napoca, Cluj-Napoca, Romania; [2]Department of Pathology, Regional Institute of Gastroenterology and Hepatology "O. Fodor," Cluj-Napoca, Romania; [3]Regional Institute of Gastroenterology and Hepatology "O. Fodor," Cluj-Napoca, Romania; [4]Department of Personalized Medicine and Rare Diseases, MEDFUTURE-Institute for Biomedical Research, University of Medicine and Pharmacy "Iuliu Hatieganu," Cluj-Napoca, Cluj-Napoca, Romania*
Email: Iuliabreaban@yahoo.com

Background and aims: An association between portosinusoidal vascular disorder (PSVD) and steatotic liver disease has been suggested based on shared genetic variants (i.e. PNPLA3) and disease severity (similar metabolomic profiles observed in cirrhosis vs PSVD with steatosis). However, the impact of steatosis on the clinical and histological features of PSVD remains unclear. We aimed to assess the prevalence of steatosis in PSVD and to characterize patients with both conditions.
Method: In this retrospective study, all adult patients with PSVD who underwent liver biopsy between 2015 and 2024 were included. Biopsies were blindly re-evaluated for fibrosis stage, steatohepatitis activity, and PSVD-related microvascular lesions. In 14 biopsies, NET area was assessed by confocal immunofluorescence.
Results: A total of 45 PSVD patients were included, among which 29 (64.4%) had steatosis on liver biopsy. In patients with PSVD and steatosis, 93.1% had mild steatosis, 96.5% incipient (F0-F1) fibrosis, 17.2% lobular inflammation and 27.6% portal inflammation. However, none had metabolic associated steatohepatitis. We could not find any statistically significant differences between patients with pure PSVD vs those with PSVD and steatosis in terms of clinical features: either non-specific (81.3% vs 86.2%) or specific (56.3% vs 55.2%) signs of portal hypertension, the presence of metabolic comorbidities (18.8% vs 27.6%), the median liver stiffness value (8.2 kPa (2.4–24.8) vs 6 kPa (3.6–12)), the median HVPG value (5.5 mmHg (1–15) vs 5 (2–23)); in terms of histological features either specific- obliterative venopathy (68.8% vs 72.4%), nodular regenerative hyperplasia (18.8% vs 20.7%) or non-specific- portal tract abnormalities (87.5% vs 82.8%), sinusoidal dilatation (62.5% vs 51.7%), mild perisinusoidal fibrosis (43.8 vs 58.6%); $p < 0.05$. Moreover, there was no difference in NETS area between patients with pure PSVD vs those with additional steatosis. However, patients with architectural disturbances had a higher NETS area than those without (19808 vs 10562 μm^2, $p = 0.02$).
Conclusion: The coexistence of mild degree liver steatosis with PSVD histological features was not associated with increased portal pressure gradients or a higher prevalence of clinical signs of portal hypertension, or with the development of a certain specific/non-specific histological features. The presence of NETs in PSVD patients could be linked to the development of architectural disturbances.

SAT-540

Review of palliative care involvement in advanced liver disease

David O. Sullivan[1], Lenin Ekpotu[1], Dee Noone[1], Laura Stobie[1], Monica Blount[1], Pauline Dillon[1], Matthew McKenna Barry[1], John Ryan[1]. *[1]Hepatology Unit, Beaumont Hospital, Dublin, Ireland*
Email: davidosullivan805@gmail.com

Background and aims: Advanced or decompensated liver disease carries a high symptom burden and poorer prognosis than many advanced malignancies. Despite this, many patients are not referred to palliative care until very late in the course of their disease, often until their terminal admission. We aimed to review palliative care referrals in advanced liver disease, and the duration from referral to death.
Method: A retrospective audit was performed on patients with a history of decompensated cirrhosis or hepatocellular carcinoma (HCC) attending the Liver Support Clinic (LSC) in Beaumont Hospital between 2020 and 2024. Data collected included the patient's name, date of birth, medical record number, the aetiology of their liver disease, their HCC status, their date of death, their location of death (either inpatient or out of hospital), their cause of death, whether or not a palliative care referral had been sent, and the time from referral to death.
Results: Of 513 patients attending the LSC, 57 patients died during the time period. 24 (42%) were referred to palliative care, with 18 (75%) referred during their terminal admission. The median time from referral to death was 4 days, and 62% died within one week from the referral. For those referred prior to their terminal admission, median time from referral to death was 43 days, and 2 days for those referred on terminal admission. 44% of patients with HCC were referred, compared with 42% of those without cancer; 50% of HCC patients were referred prior to their terminal admission, compared with only 17% of non-HCC patients. 52.6% died as an inpatient in an acute hospital bed; of the 23 that died out of hospital, most of these died suddenly and unexpectedly.
Conclusion: The palliative care service is under-utilised in those with cirrhosis. The majority of referrals to palliative care occur only days from death, when death is imminent. We believe this late timing severely limits the potential benefits of palliative care input. Those who were diagnosed with HCC were more likely to be referred to palliative care earlier, which is likely due to the more established role for the palliative care service in the management of advanced cancers. Overall, the findings of this audit demonstrate that referrals to palliative care in those with advanced liver disease occurs late and is usually prompted by an acute terminal event. Earlier involvement of palliative care could be used to address symptom burden, facilitate advance care planning, and improve end of life outcomes.

SAT-541

External validation of the VOCAL-Penn score for extrahepatic surgical risk assessment in cirrhosis in asian and european populations

Ana Ostojic[1], Prachiti Gokhe[2], Sai Sarada V[2], Guduru Venkat Rao[2], Petra Dinjar Kujundžić[3], Lucija Maleta[1], Ivica Grgurević[3,4], K. Rajender Reddy[5], Anand Kulkarni[2]. *[1]University Hospital Center Zagreb, Zagreb, Croatia; [2]Asian Institute of Gastroenterology, Hyderabad, India; [3]University Hospital Dubrava, Zagreb, Croatia; [4]University of Zagreb School of Medicine, Zagreb, Croatia; [5]University of Pennsylvania, Philadelphia, United States*
Email: anandvk90@gmail.com

Background and aims: Individuals with cirrhosis have higher perioperative morbidity and mortality than the general population, regardless of the type or extent of surgery. Multiple risk scores are used to support perioperative decision-making, including MELD, MELD-Na, Mayo risk score, and VOCAL-Penn score, each with distinct strengths and limitations. The VOCAL-Penn score is the more recent recommended surgical risk stratification in patients with cirrhosis as per the recent EASL clinical practice guideline. The aim of this study was to validate the performance of the VOCAL-Penn score in patients undergoing extrahepatic surgery in Asian and European tertiary hospital centers.
Method: A retrospective analysis of 182 patients with cirrhosis undergoing non-liver surgery in three tertiary hospitals (1 in India, and 2 in Croatia). For all patients, VOCAL-Penn scores were calculated. The discriminative performance of the VOCAL-Penn score in predicting 30-day and 90-day mortality was evaluated using the area under

the receiver operating characteristic (ROC) curve (C-statistics), Brier scores, and the Index of Prediction Accuracy (IPA).
Results: Most patients were male (n = 142 (77.2%)). The most common etiology of cirrhosis was MASH in India (n = 75 (64.7%)), while the leading cause in Croatia was alcohol-associated liver disease (n = 46 (69.7%)). Arterial hypertension (n = 73 (40.1%)) and diabetes (n = 68 (37.4%)) were the most frequent comorbidities. Across all three centers, most surgeries were performed electively (83.5%). The most common procedure type was open abdominal surgery (64.3%), followed by abdominal wall surgery (19.2%). Three (1.65%) patients died within 30 days and 20 (11.17%) died within 90 days after surgery. For 30-day mortality, VOCAL-Penn demonstrated good discrimination, with a C-statistic of 0.798 (95% CI: 0.512–1.000). For 90-day mortality, discrimination was strong, with a C-statistic of 0.889 (95% CI: 0.817–0.961). Brier scores were low at both time points (0.016–0.072), indicating good model calibration. The Index of Prediction Accuracy (IPA) was −1.0% at 30 days and 27.1% at 90 days.
Conclusion: In this multinational cohort, VOCAL-Penn score showed strong discrimination for 90-day mortality, while reducing the prediction error by 27% compared with a model assuming an average-risk patient. Lower discrimination for 30-day mortality might be due to few events. Model calibration remained good at both time points.

SAT-542

Evaluating artificial intelligence for the diagnosis of drug-induced liver injury in clinical practice

Anna Pocurull Aparicio[1], Martin Gómez-Loira[2], Miren Garcia Cortes[3], Marina Silveira-Balloni[1], Ernest Saenz[2], Jose Pinazo Bandera[3], Elia Canga[1], Raul J. Andrade[3], Juan Turnes[4], Xavier Forns[1]. *[1]Hospital Clinic, University of Barcelona, IDIBAPS, CIBEREHD, Barcelona, Spain; [2]Galicia Sur Health Research Institute, Pontevedra, Spain; [3]Hospital Universitario Virgen de la Victoria, University Of Málaga, IBIMA-BIONAND, CIBEREHD, Málaga, Spain; [4]University Hospital Complex of Pontevedra, Galicia Sur Health Research Institute, Pontevedra, Spain*
Email: xforns@clinic.cat

Background and aims: Drug-induced liver injury (DILI) remains a challenging diagnosis due to the absence of specific biomarkers and the need to exclude alternative causes of liver disease. This study aimed to evaluate the performance of large language models (LLM) in the causality assessment of DILI and to compare their assessments with structured expert opinion process.
Method: We evaluated eight state-of-the-art LLM (GPT-5.2 Pro, Claude Opus 4.5, Gemini 3 Pro, Gemma 3–27B, DeepSeek V3.2, Qwen3-30B, Kimi K2-Thinking, and Mixtral 8 × 22B) on 34 real-world cases. Expert opinion adjudication served as ground truth. Models received blinded clinical vignettes, comprehensive case presentations, and were required to predict both DILI diagnosis (yes/no/indeterminate) and the specific causative drug. We tested two conditions: (1) baseline assessment using only clinical vignettes task-oriented prompts, and (2) context-augmented assessment, where models received LiverTox drug hepatotoxicity entries and EASL/AASLD DILI guidelines as reference material.
Results: Based on expert opinion, 3 cases were considered non-DILI and 31 DILI. The drugs most commonly implicated were anticancer (13), antibiotics (8), analgesics (5) and lipid-lowering drugs (5); the median RUCAM score was 7 (IQR 6–8). The predominant pattern of liver injury was hepatocellular (62%), followed by cholestatic (24%). Most cases were considered of high complexity, with frequent concomitant medication: median of 6 drugs (IQR: 4–8). Experts assigned one single culprit drug in 21 cases, 2 potential drugs in 9 cases, and 3 drugs in one case. Discrepancies among experts occurred in 7 (22%) of the 31 DILI cases. Performance of the 8 language models with context-augmented assessment (measured by Matthews Correlation Coefficient, MCC) ranged from –0,04 to 1,0. Kimi-K2 achieved the highest performance (MCC = 1,0), with concordance with expert opinion in 30 cases (88%). Augmentation with external knowledge (LiverTox hepatotoxicity profiles and EASL/AASLD guidelines) substantially improved performance in 6/8 models, with a mean MCC improvement of 122%.
Conclusion: This proof-of-concept study suggests that knowledge-augmented LLM systems can effectively synthesize clinical presentations, polypharmacy patterns, and hepatotoxicity databases to support DILI causality assessment. This could simplify and standardize DILI diagnosis, especially in centers with limited expert consultation and in high complexity cases.

SAT-543

The use of non-invasive tests to detect and direct management of cirrhosis does not reduce the incidence or delay the onset of first severe decompensation events or improve survival: first report of the ELUCIDATE trial

William Rosenberg[1], Sudeep Tanwar[1], Myka Ransom[2], Annah Muli[2], Deborah Stocken[2], Paul Richardson[3], Rebecca Jones[4], Sulleman Moreea[5], Chin Lye Ch'ng[6], James Neuberger[7], Peter Selby[2]. *[1]University College London, Institute for Liver and Digestive Health, Division of Medicine, London, United Kingdom; [2]University Of Leeds, Leeds, United Kingdom; [3]Royal Liverpool University Hospital, Liverpool, United Kingdom; [4]Leeds Teaching Hospitals N H S Trust, Leeds, United Kingdom; [5]Bradford Royal Infirmary, Bradford, United Kingdom; [6]Singleton Hospital, Swansea, United Kingdom; [7]Queen Elizabeth Hospital, Birmingham, United Kingdom*
Email: w.rosenberg@ucl.ac.uk

Background and aims: Cirrhosis is often diagnosed late, limiting opportunities for surveillance and treatment of portal hypertension (PHTN) or hepatocellular cancer (HCC). ELUCIDATE, a multicentre, two arm, parallel group randomised controlled trial investigated use of the Enhanced Liver Fibrosis (ELF) test to facilitate earlier detection of cirrhosis and treatment of PHTN or HCC, to improve survival compared to standard best care (SC) in people with chronic liver disease (CLD).
Method: Thirty-seven UK centres screened 1303 CLD patients. Those eligible (ELF>8.4) were randomised to ELF guided management (cirrhosis screening if ELF>9.5) (438), or SC (440). All participants were reviewed every 6 months for 30 months with investigations for PHTN and HCC started if cirrhosis was suspected, and complications treated according to best practice. Long-term follow-up (LFU) was performed at 10 years by interrogating routine national data sources. Time from randomisation to first severe complication of cirrhosis (FSCC) due to PHTN, HCC or liver death is reported; deaths from other causes were treated as competing events. The equality of cumulative incidence functions between trial arms was investigated with Gray's test.
Results: FSCC was recorded for 122 patients (63% bacterial peritonitis), with 99 additional non-liver deaths. Median time from randomisation to FSCC was 5.1 years (IQR 1.8, 7.1) ELF v. 2.3 years (IQR 0.4, 2.9) SC, with no statistically significant difference between arms (HR_{adj} = 0.91, 95% CI: 0.63, 1.30, p = 0.60). After diagnosis of cirrhosis FSCC was recorded for 49/279 (17.6%) ELF arm and 9/18 (50%) SC patients. Baseline ELF test score predicted FSCC (HR = 1.32 [95% CI 1.2, 1.5] p < 0.001). There were 152 deaths from any cause (77 ELF, 75 SC). Median survival was 7.8 years (IQR 4.6, 9.8) with no statistically significant difference between arms (HR_{adj} = 0.89, 95% CI: 0.64, 1.24, p = 0.49). Death or incurable HCC was less frequently FSCC in the ELF arm (4/62 v 12/60); (HR = 0.28 [0.10, 0.74] p = 0.017).
Conclusion: ELF facilitated early detection of cirrhosis and risk, creating opportunities for interventions. Compared to standard care, 30 months ELF-directed cirrhosis surveillance and management was not associated with reductions in mortality, or the incidence and timing of the first severe complication of cirrhosis, even though this was less likely death or incurable HCC. Any benefits associated with early diagnosis of cirrhosis are likely to be few and modest at the cost of more invasive testing.

SAT-544

Point-of-care quadriceps ultrasound combining thickness and elastography improves detection of cross-sectional imaging-defined sarcopenia in cirrhosis

Satyam Mishra[1], Somali Ghosh[1], Akash Roy[1], Srijita Ghosh Sen[1], Surabhi Jajodia[1], Usha Goenka[1]. [1]*Apollo Multispeciality Hospitals, Kolkata, India*
Email: satyammishra1998@gmail.com

Background and aims: Sarcopenia is common in cirrhosis, but computed tomography (CT) and magnetic resonance imaging (MRI) based cross-sectional muscle assessment is has limited bedside use, is costly, and is unsuitable for serial monitoring. We evaluated quadriceps ultrasound thickness and two-dimensional shear wave elastography (SWE) stiffness against CT/MRI-derived psoas muscle index (PMI), and tested whether combining morphometric measures and elastography improves detection of CT-defined sarcopenia.
Method: In this prospective cross-sectional study, 110 individuals with underwent clinically indicated CT or MRI and bedside quadriceps assessment within one month. Rectus femoris and vastus lateralis muscle thickness were measured at standardized mid-thigh landmarks, with three measurements obtained and averaged for each muscle. Muscle stiffness of the rectus femoris (RF_ and vastus lateralis (VL) was evaluated using two-dimensional shear wave elastography (2D SWE), with three to five valid acquisitions. Sarcopenia was defined using CT/MRI-derived PMI with sex-specific cut-offs. Associations with PMI were examined using Spearman's correlation, and diagnostic performance was evaluated using receiver operating characteristic analysis and multivariable logistic regression, with area under the curve (AUC) comparisons performed using the DeLong test.
Results: CT-PMI defined sarcopenia was present in 24.5%. RF thickness correlated best with PMI ($\rho = 0.572$, $p < 0.001$), followed by VL thickness ($\rho = 0.425$, $p < 0.001$); stiffness correlations were weaker (RF $\rho = 0.22$, $p = 0.016$; VL $\rho = 0.21$, $p = 0.028$). RF thickness was lower in sarcopenic patients (median 13.5 vs 18.8 mm, $p < 0.001$) and VL thickness was also reduced ($p = 0.006$). RF thickness showed good discrimination [AUC, 0.793) with an optimal cutoff of 16.9 mm (sensitivity 85.2%, specificity 71.1%). A combined model using RF/VL thickness and stiffness improved AUC to 0.854 and significantly outperformed RF thickness alone (AUC difference 0.06, 95% $p = 0.034$). At the optimal probability cutoff of 0.183, sensitivity was 92.6%, specificity 73.5% and negative predictive value 96.8%.
Conclusion: Standardised quadriceps ultrasound, particularly RF thickness, can identify PMI defined sarcopenia in cirrhosis at the bedside. Although SWE stiffness is a weak standalone surrogate of muscle mass, its integration with morphometry improves diagnostic performance and supports a pragmatic screening strategy where cross-sectional imaging is not feasible.

SAT-545-YI

Lifetime survival and penetrance in HFE p.C282Y/p.H63D compound heterozygous and p.H63D homozygous individuals – a liver clinic cohort study

Wolfgang Straka[1], Lorenz Pammer[1], Martina Saretto[1], Bernhard Pfeifer[2,3], Sabrina Neururer[2,3], Rosa Schmidl[1], Maria Rosina Troppmair[1], Marlene Panzer[1], Sonja Wagner[1,4], Elke Pertler[1,4], Florian Kronenberg[5], Claudia Lamina[5], Herbert Tilg[1], Heinz Zoller[1,4], Benedikt Schaefer[1]. [1]*Medical University of Innsbruck, Department of Medicine I, Gastroenterology, Hepatology and Endocrinology, Innsbruck, Austria;* [2]*Division for Digital Medicine and Telehealth, UMIT TIROL - Private University for Health Sciences and Health Technology, Hall, Austria;* [3]*Tyrolean Federal Institute for Integrated Care, Tirol Kliniken Gmbh, Anichstrasse 35, Innsbruck, Austria;* [4]*Christian Doppler Laboratory for Iron and Phosphate Biology, Medical University of Innsbruck, Innsbruck, Austria;* [5]*Institute of Genetic Epidemiology, Medical University of Innsbruck, Innsbruck, Austria*
Email: wolfgang.straka@i-med.ac.at

Background and aims: Hemochromatosis is a common genetic disorder in individuals of European ancestry. In addition to the genetic cause, severity of iron overload is affected by risk factors. Penetrance and survival vary across screening and clinical cohorts. Relevance of p.C282Y/H63D compound heterozygotes and H63D homozygotes remains controversial. EASL hemochromatosis guidelines emphasize management based on phenotypic presentation and risk factors. This population-based cohort study of HFE-genotyped individuals aims to assess life expectancy, age- and sex- specific risks of disease penetrance and survival.
Method: The presented study includes individuals from Tyrol, Austria, who were referred to the liver clinic and genotyped for both the p.H63D and p.C282Y variant in HFE between 1997 and 2021. Clinical data and laboratory parameters, including risk factors and comorbidities were retrospectively assessed from the electronic health records. The long-term follow-up enabled an assessment of the life expectancy and cancer incidence. Further comparisons were made using *HFE* p.C282Y homozygotes, *HFE*-wildtype (wt) individuals and a matched propensity score, population-based control group.
Results: Inclusion criteria were met by 507 p.C282Y/p.H63D compound-heterozygotes and 301 p.H63D homozygotes which were compared with 602 *HFE*-wt and 542 p.C282Y/p.C282Y homozygous individuals as well as the matched controls. Cumulative lifetime risk for the development of provisional iron overload was significantly lower in p.C282Y/p.H63D compound heterozygotes (1.17%) and p.H63D homozygotes (0.45%) as compared to 18% in p.C282Y homozygous patients. The lowest life expectancy was found in *HFE*-wt individuals, with a median estimated survival of 81.70 years, followed by p.H63D homozygotes (82.59), p.C282Y homozygotes (86.23) and p.C282Y/p.H63D compound heterozygotes (87.35). The multivariate regression analysis showed that the genotype itself was not a statistically significant predicator for survival. Worse survival was associated with a higher rate of comorbidities.
Conclusion: Lifetime penetrance for provisional iron overload is 20 times lower in p.C282Y/p.H63D compound heterozygosity and 50 times lower among p.H63D homozygotes compared to p.C282Y homozygosity. *HFE* genotype is not an independent predicator for survival and the observed increase in mortality in p.H63D homozygous individuals is primarily driven by comorbidities.

SAT-546

Glutamate dehydrogenase outperforms transaminases and bilirubin in stratifying choledocholithiasis

Jan Sutter[1], Soleman Almadok[1], Giulia Heide[1], Julian Schulze zur Wiesch[1], Samuel Huber[1], Ansgar Lohse[1].
[1]*I. Department of Medicine, University Medical Center Hamburg-Eppendorf, Hamburg, Germany*
Email: j.sutter@uke.de

Background and aims: Choledocholithiasis (CDL) is a common condition that can lead to serious complications, requiring effective risk stratification for timely intervention. While current guidelines use clinical predictors, imaging, and laboratory markers for risk assessment, the role of glutamate dehydrogenase (GLDH) in CDL remains poorly understood. This study aims to evaluate its potential as a clinical biomarker for identifying patients with CDL.
Method: This single-center cohort study identified 23,103 patients who presented to the emergency department of the University Medical Center Hamburg-Eppendorf and underwent routine abdominal laboratory testing between May 2021 and December 2023. Patients were classified into CDL and other diagnoses. To assess the predictive value of age, sex and laboratory markers for CDL, we developed a random forest machine learning model, conducted a backward stepwise logistic regression and performed receiver operating characteristic (ROC) analysis.

Results: 152 patients were diagnosed with CDL and 22,951 with other diagnoses. In the random forest machine learning model, GLDH emerged as the most significant feature for predicting CDL. ROC analysis revealed that GLDH had the highest area under the curve of 0.93 among laboratory markers. At the upper limit of normal, GLDH demonstrated the best sensitivity (92%) compared to aspartate aminotransferase (AST), alanine aminotransferase (ALT) and bilirubin. High GLDH levels exceeding 150 U/L demonstrate the highest specificity (99%) for CDL, outperforming AST, ALT and bilirubin.
Conclusion: GLDH outperforms AST, ALT and bilirubin as a screening and predictive marker for CDL, supporting its inclusion in clinical guidelines for risk stratification.

SAT-547

Linkage of effective cirrhosis management may be critical for the realization of any benefits associated with early detection of cirrhosis: explanatory analyses from the ELUCIDATE randomised trial

Sudeep Tanwar[1], Myka Ransom[2], Annah Muli[2], Deborah Stocken[2], Paul Richardson[3], Sulleman Moreea[4], Rebecca Jones[5], Chin Lye Ch'ng[6], James Neuberger[7], Peter Selby[2], William Rosenberg[1]. *[1]University College London, Institute for Liver and Digestive Health, Division of Medicine, London, United Kingdom; [2]University Of Leeds, Leeds, United Kingdom; [3]Royal Liverpool University Hospital, Liverpool, United Kingdom; [4]Bradford Royal Infirmary, Bradford, United Kingdom; [5]Leeds Teaching Hospitals N H S Trust, Leeds, United Kingdom; [6]Singleton Hospital, Swansea, United Kingdom; [7]Queen Elizabeth Hospital, Birmingham, United Kingdom*
Email: w.rosenberg@ucl.ac.uk

Background and aims: The ELUCIDATE trial found no statistically significant reduction in mortality, incidence or timing of first severe cirrhosis complications (FSCC) with Enhanced Liver Fibrosis test (ELF) guided cirrhosis detection and management, compared to standard care (SC). EASL cirrhosis surveillance guidance highlights that early treatment of varices and hepatocellular carcinoma (HCC) reduces morbidity and mortality. We hypothesised that the lack of improvement in clinical outcomes may be attributable to poor adherence to protocol-defined surveillance and interventions. We examined between-arm adherence and the association between baseline ELF score and clinical events.
Method: Case report-form review determined adherence to protocol-defined care, by arm, over 30 months from randomisation, including 6 monthly scheduled follow-up before and after diagnosis of cirrhosis; HCC surveillance (alpha-fetoprotein [AFP] testing and imaging) and interventions; endoscopic screening for varices, and prophylaxis. Association between baseline ELF score and the primary endpoint of FSCC was assessed 10 years post randomisation using routine healthcare data. Exploratory analyses examined the prognostic performance of the protocol defined ELF threshold (9.5).
Results: Baseline ELF score was a strong independent predictor of FSCC (positive predictive value of ELF>9.5 for FSCC = 26%). Each unit increase in ELF (centred at 9.5) was associated with a greater risk of FSCC (HR = 1.32, [95% CI 1.16–1.50]; p < 0.001). Adherence to protocol-defined surveillance was poor in both arms. Pre-cirrhotic and post-cirrhotic visit compliance was low but higher in the ELF arm than SC (29.8% vs 19.7% and 16.2% vs 21.1% respectively). After cirrhosis detection, compliance with timing of AFP and imaging for ELF and SC arms were 12.6% vs 11.8% and 29.5% vs 14.3% respectively. Endoscopic surveillance adherence was suboptimal with only 54.4% of ELF arm cirrhotic patients having at least one OGD compared to 60% in the SC arm. Only 56% of ELF and 43% of SC patients with varices received treatment.
Conclusion: While ELF effectively predicted risk of FSCC, poor adherence to cirrhosis surveillance and management protocols may have prevented early detection of cirrhosis translating into clinical benefit. If confirmed in the final analysis of ELUCIDATE this highlights the need to link the implementation of effective care pathways to strategies designed to improve early detection of cirrhosis.

SAT-548

Development and validation of a non-invasive model for predicting advanced liver fibrosis in patients with metabolic dysfunction-associated steatotic liver disease and dysglycemia

Zhang Xuejie[1], Feixiang Xiong[1], Chen Dandan[1], Jialiang Chen[1], Zhou Yang[1], Wu Tong[1], Ji Xiaomin[1], Yuyong Jiang[1], Yixin Hou[1]. *[1]Beijing Ditan Hospitall, Capital Medical University, Beijing, China*
Email: zhangxuejie027668@163.com

Background and aims: The confluence of metabolic dysfunction-associated steatotic liver disease (MASLD) and dysglycemia delineates a high-risk subgroup characterized by a substantially increased likelihood of progressive liver fibrosis. This study aimed to develop and validate a novel, parsimonious non-invasive model for the accurate prediction of advanced fibrosis (stage F3–F4) in this at-risk population.
Method: A retrospective analysis was conducted in 606 consecutive adults with biopsy-proven MASLD and dysglycemia from Beijing Ditan Hospital (2010–2025). The cohort was randomly split into training (n = 424) and validation (n = 182) cohorts. Multivariable logistic regression analysis identified BMI, ALT, and WBC as independent predictors for constructing a non-invasive model to assess advanced liver fibrosis in patients with MASLD and concomitant dysglycemia. The performance of the proposed model was evaluated by the area under the receiver operating characteristic curve (AUROC), sensitivity, specificity, positive predictive value (PPV), and negative predictive value (NPV), and compared with two validated non-invasive serum indices: the Aspartate-to-Platelet Ratio Index (APRI) and the Fibrosis-4 (FIB-4) index.
Results: Three variables were identified as independent predictors of advanced fibrosis: BMI (adjusted odds ratio [aOR] 1.40 per 1 kg/m^2 increase, 95% CI: 1.30–1.51; $P < 0.001$), ALT (aOR 1.01 per 1 U/L increase, 95% CI: 1.01–1.01; $P < 0.001$), and WBC (aOR 1.15 per 1×10^9/L increase, 95% CI: 1.01–1.31; $P = 0.035$). The model demonstrated excellent discriminative performance, with the training cohort showing an AUC of 0.865 (95% CI: 0.826–0.905), specificity of 67.8%, sensitivity of 89.9%, PPV of 84.2%, and NPV of 78%. The validation cohort exhibited an AUC of 0.900 (95% CI: 0.855–0.946), specificity of 71.4%, sensitivity of 91.6%, PPV of 85.8%, and NPV of 81.8%. It significantly outperformed both FIB-4 and APRI across all performance metrics, exhibited excellent calibration, and provided superior net clinical benefit across a wide range of risk thresholds.
Conclusion: We developed a highly accurate and validated non-invasive model based on BMI, ALT, and WBC for predicting advanced fibrosis in patients with MASLD and dysglycemia. Its simplicity and reliance on readily available parameters render it ideally suited for deployment in primary care and diabetology settings, where it could refine risk stratification and guide specialist referrals.

SAT-549

Prognostic value of handgrip strength in 1,294 japanese patients with liver cirrhosis: a large-scale multicenter cohort study from the NHO network

Hiroshi Yatsuhashi[1], Kazumi Yamasaki[1], Hayato Yamana[2], Shinobu Imai[3], Atsushi Naganuma[4], Rie Sugimoto[5], Motoyuki Kohjima[6], Tsutomu Yamashita[7], Satoru Iwamoto[8], Keisuke Ario[9], Masaaki Shimada[10], Shintaro Takaki[11], Takeaki Satoh[12], Kiyoshi Furuta[13], Ryotaro Sakamori[14]. *[1]NHO Nagasaki Medical Center, Omura, Japan; [2]Jichi Medical University, Shimotsuke, Japan; [3]Showa University Graduate School of Pharmacy, Tokyo, Japan; [4]NHO Takasaki Genral Medical Center, Takasaki, Japan; [5]NHO Kyushu Cancer Center, Fukuoka, Japan; [6]NHO Kyushu Medical Center, Fukuoka, Japan; [7]NHO Oita Medical Center, Oita, Japan; [8]NHO Kyoto Medical Center, Kyoto,*

Japan; [9]NHO Ureshino Medical Center, Ureshino, Japan; [10]NHO Nagoya Medical Center, Nagoya, Japan; [11]NHO Kure Medical Center, Kure, Japan; [12]NHO Ku, Kokura, Japan; [13]NHO Matsumoto Medical Center, Matsumoto, Japan; [14]NHO Osaka National Hospital, Osaka, Japan
Email: Yatsuhashihiroshi@gmail.com

Background and aims: Handgrip strength (HGS) has recently emerged as a critical prognostic marker in Western patients with chronic liver disease. While HGS reflects systemic muscle strength and serves as a primary indicator of sarcopenia, large-scale clinical evidence in the Japanese cirrhotic population remains limited. We aimed to investigate the impact of HGS on long-term survival in a large multicenter cohort.
Method: This study prospectively enrolled 1294 patients with liver cirrhosis (694 males, 600 females; mean age 70.7 ± 10.5 years) who visited 36 National Hospital Organization (NHO) hospitals across Japan during 2017. Baseline HGS was measured, and patients were followed for survival outcomes. Clinical characteristics included Child-Pugh class (A/B/C: 950/266/78), etiologies (HCV/HBV/ALD/MASLD/Others: 606/208/241/92/147), and HCC stages (None/I-II/III-IV: 736/405/153). Patients were stratified into sex-specific HGS tertiles: for males, High (≥34.6 kg), Intermediate (27.5–34.4 kg), and Low (≤27.4 kg); for females, High (≥20.0 kg), Intermediate (16.2–19.9 kg), and Low (≤16.1 kg).Survival analysis was performed using the Kaplan-Meier method and Cox proportional hazards models.
Results: The 5-year survival rates significantly declined as HGS decreased (P < 0.0001). • Males: High (78.0%), Intermediate (65.7%), and Low (43.5%). • Females: High (83.1%), Intermediate (72.2%), and Low (64.1%). Multivariate analysis demonstrated that 1) Age, 2) Child-Pugh classification, 3) HCC stage/progression, and 4) HGS tertiles were independent prognostic factors for survival. HGS also showed significant correlations with age, sex, and Child-Pugh score.
Conclusion: HGS is a simple, non-invasive, yet powerful independent predictor of survival in Japanese patients with liver cirrhosis. While conventional scores such as Child-Pugh and MELD provide a "static" assessment of hepatic reserve, HGS captures the "dynamic" physical vitality and systemic resilience of the patient. Integrating HGS with traditional liver-specific markers will allow for more precise risk stratification and the advancement of personalized medicine. Our findings suggest that HGS should be recognized as an essential clinical parameter for monitoring disease progression and the efficacy of therapeutic interventions.

SAT-553

A blood based diagnostic for the identification and risk stratification of fibrosis and cirrhosis based on adverse outcomes

William Young-Greenwald[1], Sam Asgarian[1], Amar Das[1], Angela Watkins[1], Craig Eagle[1], AmirAli Talasaz[1]. *[1]Guardant Health, Palo Alto, United States*
Email: byounggreenwald@guardanthealth.com

Background and aims: Liver Fibrosis/Cirrhosis affects ~4.5 million individuals in the US and can lead to adverse outcomes including death. While current blood-based diagnostics are used to identify individuals with Fibrosis/Cirrhosis, they do not adequately risk stratify those who are likely to advance in disease or have adverse health outcomes, creating an unmet medical need. Here, we present a novel blood-based diagnostic test that identifies individuals with Fibrosis/Cirrhosis at levels better/equal to commercially available tests for screening liver fibrosis. This test also provides a severity index enabling providers to identify patients at the highest risk and monitor and/or treat them before severe health events occur.
Method: A deidentified database of >50,000 individuals who underwent blood-based diagnostic testing was queried for individuals with Fibrosis/Cirrhosis diagnosed within 5 years prior to a negative Guardant Shield test. A machine learning model was trained on Guardant Shield and Infinity DNA methylation data to develop a quantitative risk score of Fibrosis/Cirrhosis disease severity and to classify individuals into disease/healthy. Classification was evaluated in 10-fold cross-validation, and risk stratification was evaluated on a separate holdout set of patients which was divided into four categories: (1) those with a clinical diagnosis of any-stage Fibrosis/Cirrhosis; (2) those not in category (1) but with fatty liver disease; (3) those in categories (1) or (2) and have had an adverse outcome (as defined by Cirrhosis, portal hypertension, HCC, Acute Myocardial or Cerebral Infarction, or Heart Failure within 12 months post-blood test); and (4) all other individuals. Risk stratification was examined by comparing the relative model AUCs of sample groups 1–3 vs group 4.
Results: Our model identified those with Fibrosis (F1–3) or Cirrhosis (F4) with an AUC of 0.79 (Kocak 2025) and 0.84 (Tamaki 2024), respectively, compared to 0.66 with the FIB4 index or 0.85 with the ELF score. Individuals who had adverse outcomes had a higher risk score from our model with AUC improvements of 0.2 and 0.08 for category 3 or 2 vs 1, respectively.
Conclusion: Here, we present a novel DNA methylation-based model for Fibrosis/Cirrhosis identification and risk stratification built on the Guardant Shield platform performing at levels equal to or better than current methods. The results warrant further study to bring more precision to this area of medicine.

SAT-554

Associations of liver steatosis and fibrosis with staging and mortality risk of cardiovascular-kidney-metabolic syndrome: evidence from two community-based studies

Yilin Zhang[1], Shanghao Liu[1], Qiong Liu[2], Haisong Xin[3], Hui Shi[4], Jianxiang Song[5], Lan Ma[6], Puqiang Liu[7], Yuxia Qi[8], Yijun Tang[9], Yang Bo[10], JianSong Ji[11], Yingxia Yang[12], Xiao Liang[13], Huizhen Fan[14], Ruyu Liu[15], Deqiang Luo[16], Qing He[17], Hui Yang[18], Xin Huang[19], Zhaowei Tong[20], Xiongwei He[21], Xingguo Xiao[22], Wen Kang[23], Xixing Ma[1], Jianhai Wei[24], Rong Hu[25], Zhenyu Dai[5], Liping Wang[6], Jianping Zhang[7], Lina Han[8], Zhong-ji Meng[9], Guo Zhang[12], Kejun Liu[10], Lili Ye[26], Yong-Fen Zhu[27], Jianwen Sheng[14], Xiangkun Jiao[28], Xiufeng Zhang[29], Fenghe Chang[16], Wenjia Yang[16], Fengjuan Chen[17], LinQing He[18], Siyi Feng[30], Qi Wang[20], Jiangwen Liu[21], Yanhong Liu[22], Jing Huang[23], Gao-Jun Teng[1], Jianan Wang[2], Xiaolong Qi[1]. *[1]Zhongda Hospital, Nanjing, China; [2]The Second Affiliated Hospital of Zhejiang University School of Medicine, Hangzhou, China; [3]People's Hospital of Huanghua, Huanghua, China; [4]The First Affiliated Hospital of Kangda College of Nanjing Medical University, Lianyungang, China; [5]Affiliated Yancheng Hospital, Yancheng, China; [6]Bozhou People's Hospital, Bozhou, China; [7]Pu County People's Hospital, Linfen City, China; [8]Qingdao Public Health Clinical Center, Qingdao, China; [9]Taihe Hospital, Shiyan, China; [10]General Hospital of Ningxia Medical University, Yinchuan, China; [11]Lishui Central Hospital, Lishui, China; [12]Guangxi Hospital Division of The First Affiliated Hospital, Nanning, China; [13]Sir Run-Run Shaw Hospital, Hangzhou, China; [14]Yichun People's Hospital, Yichun, China; [15]Xuzhou Infectious Diseases Hospital, Xuzhou, China; [16]Baiyin Central Hospital, Baiyin, China; [17]Shenzhen third People's Hospital, Shenzhen, China; [18]The Second Affiliated Hospital of Guangzhou Medical University, Guangzhou, China; [19]Mengchao Hepatobiliary Hospital of Fujian Medical University, Fuzhou, China; [20]Huzhou Central Hospital, Huzhou, China; [21]Medical Department of Shihezi City People's Hospital, Shihezi, China; [22]Zhengzhou Central Hospital Affiliated to Zhengzhou University, Zhengzhou, China; [23]Tangdu Hospital, Xi'an, China; [24]People's Hospital of Huanghua, Cangzhou, China; [25]The First Affiliated Hospital of Kangda College of Nanjing Medical University, Lianyungang, China; [26]The Fifth Affiliated Hospital of Wenzhou Medical University, Lishui, China; [27]Sir Run Run Shaw Hospital, Hangzhou, China; [28]Beijing Ditan Hospital Xuzhou Hospital, Xuzhou, China; [29]Central Hospital of Baiyin City, Baiyin City, China; [30]Mengchao Hepatobiliary Hospital, Fuzhou, China*
Email: qixiaolong@vip.163.com

Background and aims: Cardiovascular-kidney-metabolic (CKM) syndrome integrates cardiovascular, renal, and metabolic dysfunction, elevating risks of cardiovascular disease (CVD) and premature mortality. Liver steatosis and fibrosis contribute to endothelial

dysfunction, atherosclerosis, and renal injury, but remain poorly defined within the CKM framework. We aimed to investigate the associations of liver steatosis and liver fibrosis with staging and mortality risk of CKM syndrome.
Method: We analyzed two community-based studies from LiverHealth project, which enrolled adults from ten provinces across China, and the U.S. National Health and Nutrition Examination Survey (NHANES) 1999–2018. Liver steatosis and fibrosis were assessed using vibration-controlled transient elastography in LiverHealth project and the U.S. Fatty Liver Index and Fibrosis-4 index in NHANES. CKM stages were defined according to American Heart Association guidelines. Multinomial logistic regression and Cox proportional hazards models were used to assess associations with CKM staging and mortality risk, respectively.
Results: A total of 20,591 Chinese and 19,867 U.S. participants were included. In the Chinese cohort, the prevalences of steatosis stages S1–S3 were 13.0%, 6.3%, and 24.8%, respectively; fibrosis stages F1 and ≥F2 accounted for 14.8% and 4.3%, and 7.7% of participants had advanced CKM (stages 3–4). Increasing grades of liver steatosis and fibrosis were both associated with progressively higher odds of advanced CKM (P for trend <0.001). In the U.S. cohort, liver steatosis was present in 33.6% of participants, fibrosis risk was classified as low, intermediate, and high in 81.6%, 15.5%, and 2.9%, respectively, and 15.7% had advanced CKM. Both liver steatosis (OR 1.51, 95% CI 1.36–1.67) and high-risk fibrosis (OR 1.68, 95% CI 1.33–2.12) were independently associated with advanced CKM. Over a median follow-up of 10.5 years, 1,693 all-cause deaths and 497 CVD deaths occurred among participants with CKM stages 0–3. After adjustment for CKM stage, liver steatosis was not significantly associated with mortality, whereas fibrosis was associated with increased risks of all-cause (HR 1.94, 95% CI 1.64–2.31) and CVD mortality (HR 1.69, 95% CI 1.23–2.33).
Conclusion: Liver steatosis and fibrosis were associated with advanced CKM stages. Liver fibrosis but not steatosis was independently related to increased all-cause and CVD mortality in individuals with CKM stages 0–3.

SAT-555
Diagnostic value of MR elastography and MRI-proton density fat fraction in cirrhosis based on explant liver histology
Eun-Ki Min[1], Seung-Seob Kim[2], Seung Up Kim[3], Jae Geun Lee[1], Deok-Gie Kim[1]. *[1]Department of Surgery, The Research Institute for Transplantation, Yonsei University College of Medicine, Seoul, Korea, Rep. of South; [2]Department of Radiology and Research Institute of Radiological Science, Yonsei University College of Medicine, Seoul, Korea, Rep. of South; [3]Department of Internal Medicine, Yonsei University College of Medicine, Seoul, Korea, Rep. of South*
Email: mek1012@yuhs.ac

Background and aims: Accurate assessment of advanced fibrosis and steatosis is essential for prognostication in chronic liver disease. This study aimed to evaluate the diagnostic performance of MRI in assessing liver fibrosis and steatosis in patients undergoing liver transplantation (LT).
Method: Patients who underwent LT between January 2019 and December 2023 with pretransplant MR elastography (MRE) and MRI-based proton density fat fraction (MRI-PDFF) examinations were included. Explanted livers were assessed for fibrosis and steatosis, with cirrhosis subclassified using the Laennec system. Diagnostic performance was evaluated using area under the receiver operating characteristic curve (AUC) analysis.
Results: Among 187 patients (median age, 57 years), 72.2% were male. Hepatitis B virus (55%) and alcoholic liver disease (21.4%) were the most common etiologies. The median Model for End-Stage Liver Disease (MELD) score was 11. MRE detected cirrhosis (F4) with an AUC of 0.92 (95% confidence interval [CI], 0.87–0.97) and severe cirrhosis (F4c) with an AUC of 0.85 (95% CI, 0.79–0.91), at threshold values of 4.76 and 6.43 kPa, respectively. MRI-PDFF identified steatosis with an AUC of 0.83 (95% CI, 0.76–0.89) at a threshold of 2.80%. Comparisons of patients stratified by the threshold values for cirrhosis and severe cirrhosis revealed significant differences in MELD scores, history of portal hypertension-related complications, liver function parameters, and intraoperative transfusion requirements (all $p < 0.05$).
Conclusion: MRI demonstrated high diagnostic accuracy for detecting cirrhosis and steatosis in patients with advanced fibrosis undergoing LT. MRE further stratified cirrhosis severity, supporting its role in non-invasive risk assessment and prognostication.

Gut microbiota and liver disease – Liver-organ crosstalk

TOP-357
Targeting gut microbial nitrogen recycling and intestinal uptake of ammonium attenuates progression of chronic liver disease
Yinghong Zhu[1], Routing Wang[1], Ziyan Wang[1], Zhengjiang Li[1], Sile Liu[2], Jian Qu[3], Dekai Zheng[1], Puling Lai[1], Ziqi Liu[1], Yuxin Liu[1], Jingqiong Xun[4], Yue Ning[5], Jian Sun[1]. *[1]Department of Infectious Diseases, Nanfang Hospital, Southern Medical University, Guangzhou, China, State Key Laboratory of Multi-organ Injury Prevention and Treatment, Key Laboratory of Infectious Diseases Research in South China, Ministry of Education, Guangdong Provincial Key Laboratory for Prevention and Control of Major Liver Diseases, Guangdong Provincial Clinical Research Center for Viral Hepatitis, Guangdong Institute of Hepatology, Guangdong Provincial Research Center for Liver Fibrosis Engineering and Technology, Guangzhou, China; [2]Hunan Provincial People's Hospital and The First-Affiliated Hospital of Hunan Normal University, Changsha, China; [3]Huaihua Hospital of Traditional Chinese Medicine, Huaihua, China; [4]The People's Hospital of Guizhou Province, Guiyang, China; [5]The Quzhou Affiliated Hospital of Wenzhou Medical University, Quzhou, China*
Email: sunjian@smu.edu.cn

Background and aims: Although gut dysbiosis is linked to chronic liver disease (CLD), common microbial drivers across etiologies are poorly defined. To address this, we analyzed clinical and public cohorts encompassing metabolic dysfunction-associated steatotic liver disease (MASLD), alcohol-associated liver disease (ALD), and chronic hepatitis B (CHB) to identify shared pathogenic microbiota and their mechanisms.
Method: Fecal (n = 149) and serum (n = 397) samples from healthy donors and patients (MASLD, ALD, CHB) were collected across 4 centers. Gut microbiome profiling was conducted via shotgun metagenomic sequencing, and public single-cell datasets were analyzed to identify cell types involved in NH_4^+ transport. The role of nitrogen-recycling bacteria (NRB) and NH_4^+ in chronic liver disease was investigated using multiple mouse models (diet-induced, alcohol-induced, CCl_4-induced, HBV) and validated in intestine-specific *Slc12a2* knockout mice. *In vitro* studies employed THLE-2 hepatocytes, HIEC-6 intestinal epithelial cells (IECs), and small intestinal organoids. Analytical methods for mechanisms included serum biochemistry, histopathology, multiplex immunohistochemistry, transmission electron microscopy, Western blot, and co-immunoprecipitation.
Results: We observed a significant enrichment of NRB in CLD patients and found that the levels of their metaboliteNH_4^+ were positively correlated with the progression of CLD in both fecal and serum samples. Subsequently, we discovered NH_4^+ impaired the small intestinal barrier function and passed into the IECs via SLC12A2. In IECs, NH_4^+ was metabolized into glutamine, consuming ATP and elevating acetyl-CoA. The increased acetyl-CoA drove acetylation of the DEFA1, which reduced its ubiquitination and enhanced its

stability and secretion. Secreted DEFA1 bound to TFR1 on hepatocytes, stabilizing TFR1 and enhancing iron uptake. Increasing iron levels subsequently upregulated STEAP3 and NCOA4 and thus promoted the Fenton reaction, resulting in the ROS production and ferroptosis. Besides, we found furosemide sodium (Fus) inhibited the SLC12A2 expression of NH_4^+ surppressing the DEFA1/TFR1/ferroptosis and ultimately inhibiting CLD progression.
Conclusion: We first identify NRB and NH_4^+ as key modulators of CLD progression, unveil NH_4^+/SLC12A2/DEFA1/TFR1/ferroptosis axis for underlying disease progression in CLD patients, and reveal Fus as a potential agent for the treatment of CLD progression.

TOP-358

Exploring biomarkers for immunotherapy benefit in unresectable hepatocellular carcinoma based on microbiome-immunomics

Ningning Zhang[1], Kaipeng Liu[1], Shuwen Zhang[1], Wenwen Zhu[1], Xuanchen Liu[1], Hao Yu[1], Tian Liu[1], Jihui Hao[1]. [1]*Tianjin Medical University Cancer Institute and Hospital, Tianjin, China*
Email: haojihui@tjmuch.com

Background and aims: The immune-checkpoint inhibitors (ICIs) had significantly improved the prognosis of patients with unresectable hepatocellular carcinoma (HCC). However, only approximately 30% of patients achieve objective response from targeted therapy combined with immunotherapy. There is an urgent need to develop effective predictive biomarkers for immunotherapy efficacy.
Method: This study prospectively enrolled 137 patients with unresectable HCC who received ICI combined with targeted therapy as first-line treatment. Integrating peripheral blood flow cytometry, fecal metagenomics, and targeted metabolomics of short-chain fatty acids (SCFAs), we explored the predictive value of peripheral blood PD-1$^+$CD8$^+$T cells and the potential regulatory mechanism of the gut microbiota-SCFAs-peripheral blood PD-1$^+$CD8$^+$T cell axis.
Results: Peripheral blood PD-1$^+$CD8$^+$T cells were independent predictive factors for durable clinical benefit and overall survival (OS) in patients with unresectable HCC. Stratification of patients using a cutoff value of 5.0% showed that the sensitivity, specificity, and accuracy of predicting DCB were 82.0%, 76.1%, and 79.5%, respectively. Patients in the PD-1$^+$CD8$^+$T cells-High group had a higher rate of sustained benefit, as well as longer progression-free survival and OS, compared with those in the PD-1$^+$CD8$^+$T cells-Low group. The gut microbiota of patients in the PD-1$^+$CD8$^+$T cells-High group exhibited higher alpha-diversity and beta-diversity, along with increased abundance of SCFA-producing bacteria such as *Segatella copri*, *Faecalibacterium prausnitzii*, and *Eubacterium* sp., compared with the PD-1$^+$CD8$^+$T cells-Low group. Significant differences in fecal metabolites were observed between the two groups, with butyrate and valeric acid upregulated in the PD-1$^+$CD8$^+$T cells-High group. Multivariate correlation analysis and mediation analysis indicated that changes in the abundance of *Faecalibacterium prausnitzii* may indirectly affect the proportion of peripheral blood PD-1$^+$CD8$^+$T cells by regulating butyrate levels, with the mediating effect accounting for 17.0% of the total effect.
Conclusion: Peripheral blood PD-1$^+$CD8$^+$T cells are expected to serve as a novel peripheral blood biomarker for predicting the efficacy of immunotherapy in patients with unresectable HCC. Additionally, this study initially constructed a potential regulatory axis of "*Faecalibacterium prausnitzii* - butyrate - peripheral blood PD-1$^+$CD8$^+$T cells".

SAT-329-YI

ACLF metabolic markers can identity or exclude bacterial infections in acutely decompensated cirrhosis

Frederik Holz[1], Sania Arif[2], Wenyi Gu[2], Michael Praktiknjo[2], Frank Erhard Uschner[2], Maximilian Joseph Brol[2], Maria Papp[3], Camila Alvarez-Silva[4], Michael Kuhn[5], Marisa Isabell Keller[5], Wim Laleman[2,6], Minneke Coenraad[7], Debbie L. Shawcross[8], Joan Clària[9], Richard Moreau[10], Peer Bork[5], Manimozhiyan Arumugam[4], Christophe Junot[11], Dusko Ehrlich[12], Benjamin Lelouvier[13], Jonel Trebicka[2,6,14], Olaf Tyc[1,15], Robert Schierwagen[2]. [1]*Goethe University Frankfurt, University Hospital, Medical Clinic 1, Biomedical Research Laboratory, 60596, Frankfurt, Germany;* [2]*Medical Clinic B, University of Muenster, 48149, Münster, Germany;* [3]*Department of Internal Medicine, Division of Gastroenterology, Faculty of Medicine, University of Debrecen, Debrecen, Hungary;* [4]*Novo Nordisk Foundation Center for Basic Metabolic Research, University of Copenhagen, Copenhagen, Denmark;* [5]*Molecular Systems Biology Unit, European Molecular Biology Laboratory, Heidelberg, Germany;* [6]*Division of Liver and Biliopanreatic Disorders, KU Leuven, University of Leuven, Leuven, Belgium;* [7]*Department of Gastroenterology and Hepatology, Leiden University Medical Center,, Leiden, Netherlands;* [8]*Roger Williams Institute of Liver Studies, School of Immunology and Microbial Sciences, Faculty of Life Sciences and Medicine, King's College London, Foundation for Liver Research and King's College Hospital NHS Foundation Trust, London, United Kingdom;* [9]*Department of Biochemistry/Molecular Genetics, Hospital Clinic/ University of Barcelona, Barcelona, Spain;* [10]*INSERM, Université Paris Cité, Centre de Recherche sur l'Inflammation (CRI), Paris, France;* [11]*CEA, INRAE, Département Médicaments et Technologies pour la Santé (DMTS), SPI, MetaboHUB-IDF, Université Paris-Saclay, 91191, Gif-sur-Yvette, France;* [12]*University Paris-Saclay, INRAE, MetaGenoPolis, 78350, Jouy-en-Joas, France;* [13]*Vaiomer, 31670, Labège, France;* [14]*Department of Gastroenterology and Hepatology, Leiden University Medical Center, Leiden, Netherlands;* [15]*Goethe University Frankfurt, University Hospital Frankfurt, Medical Clinic 2, Department of Infectious diseases, Frankfurt*
Email: sania.arif@ukmuenster.de

Background and aims: Bacterial infections (BI) often precipitate acute decompensation (AD) and may progress to acute-on-chronic liver failure (ACLF). However, routinely used clinical markers such as leukocyte count and C-reactive protein (CRP) do not reliably indicate the presence of BI, as they may reflect systemic inflammation rather than infection. Early detection of BI and/or its exclusion is critical to improve clinical outcomes, highlighting the need for reliable, non-invasive biomarkers. This study aimed to identify metabolomic biomarkers associated with BI in patients with AD.
Method: We investigated metabolomic and microbiome profiles in AD patients undergoing transjugular intrahepatic portosystemic shunt (TIPS) placement, with or without bacterial infection. Pairwise statistical analyses and differential metabolite expression were performed on ACLF- and sepsis-related metabolites across portal, hepatic, and cubital venous compartments. Metabolites identified as BI-associated were further evaluated in cubital vein samples by assessing concentration differences and correlations with clinical parameters. Diagnostic performance was assessed using receiver operating characteristic (ROC) curve analysis. Model performance of selected metabolites was evaluated by ROC–AUC, repeated cross-validation, and permutation testing to assess robustness and avoid overfitting.
Results: Differential analysis across circulatory compartments identified 8 metabolites as potential BI-associated metabolites. Given the clinical relevance of cubital blood sampling, these metabolites were further examined in this compartment. Two of those metabolites emerged as robust individual biomarkers for BI, demonstrating strong discriminatory power (AUC = 0.816 and 0.787, respectively). Importantly, a combined predictive model incorporating both metabolites significantly improved diagnostic performance (AUC = 0.92).
Conclusion: Two specific metabolites represent promising non-invasive biomarkers for the detection of bacterial infection in patients with acute decompensated cirrhosis and may facilitate treatment of BI, potentially improving clinical outcomes in this high-risk population.

SAT-330

Systemic inflammation aggravated by translocating environmental bacteria Aquitalea Magnusonii DNA in patients with chronic liver disease

Olaf Tyc[1,2], Frank Erhard Uschner[1,3], Sania Arif[3], Nathalie Jung[4], Wenyi Gu[3], Cristina Ortiz[1], Sabine Klein[3], Sandra Torres[1,5], Nico Kraus[1], Kristian Pedersen[6], Chun Kew[7], Wenbo Chen[7,8], Michael Rooney[9], Hira Arif[10], Nicolas Pons[11], Maike Winderbergs[4], Tony Bruns[12], Martin von Bergen[6], Paolina Garbeva[13], Hans Zweer[13], Ivan Dikic[7], Dusko Ehrlich[11], Christophe Junot[14], Benjamin Lelouvier[15], Jonel Trebicka[1,3,16], Robert Schierwagen[1,3]. *[1]Goethe University Frankfurt, University Hospital, Medical Clinic 1, Biomedical Research Laboratory, 60596, Frankfurt, Germany; [2]Goethe University Frankfurt, Hospital, Medical Clinic 2, Department of Infectious diseases, Frankfurt; [3]Medical Clinic B, University of Muenster, 48149, Münster, Germany; [4]Goethe University Frankfurt, Institute of Pharmaceutical Technology, 60438, Frankfurt, Germany; [5]Depart Department of Molecular and Cellular Biomedicine, Institute of Biomedical Research of Barcelona (IIBB), CSIC, 08036, Barcelona, Spain; [6]Department of Molecular Systems Biology, Helmholtz-Centre for Environmental Research—UFZ GmbH, 04318, Leipzig, Germany; [7]Goethe University Frankfurt, Buchmann Institute for Molecular Life Sciences, 60629, Frankfurt, Germany; [8]Goethe University Frankfurt, Institute of Biochemistry II, Faculty of Medicine, 60629, Frankfurt, Germany; [9]Department of Internal Medicine IV, Jena University Hospital and Integrated Research and Treatment Center, Center for Sepsis Control and Care, Jena University Hospital, 07747, Jena, Germany; [10]Department of Biomedical Science and Engineering, Gwangju Institute of Science and Technology, 61005, Gwangju, Korea, Rep. of South; [11]University Paris-Saclay, INRAE, MetaGenoPolis, 78350, Jouy-en-Joas, France; [12]Department of Internal Medicine III, University Hospital RWTH Aachen, 52074, Aachan, Germany; [13]Netherlands Institute of Ecology (NIOO-KNAW), Department of Microbial Ecology, 6708, Wageningen, Netherlands; [14]CEA, INRAE, Département Médicaments et Technologies pour la Santé (DMTS), SPI, MetaboHUB-IDF, Université Paris-Saclay, 91191, Gif-sur-Yvette, France; [15]Vaiomer, 31670, Labège, France; [16]European Foundation for the Study of Chronic Liver Failure, 08021 Barcelona, Spain, Barcelona, Spain*
Email: sania.arif@ukmuenster.de

Background and aims: Disruption of the intestinal barrier ("leaky gut") enables gut microbial components to translocate into the bloodstream and potentially also liver, potentially worsening thereby chronic liver disease. We examined the potential pathogenic role of an aquatic environmental organism *Aquitalea magnusonii* in cirrhosis which has not previously been linked to liver disease progression.
Method: We assessed *A. magnusonii* translocation across human intestinal epithelial layers (Caco-2 and HT29-MTX) *in vitro* and evaluated its dissemination across organs using alcoholic and metabolic steatohepatitis mouse models. Untargeted metabolomics identified ACLF-associated metabolites produced by the bacterium. Proteomic profiling of outer membrane vesicles (OMVs) characterized virulence-related proteins. Hepatic stellate (LX-2) cell line, myeloid and human peripheral blood mononuclear cells were with bacterial supernatants and purified pathogen-associated molecular patterns (PAMPs). Environmental water samples were screened for *Aquitalea* DNA to evaluate potential reservoir sources.
Results: *A. magnusonii* effectively invaded intestinal epithelial monolayers and disseminated to extraintestinal organs in mouse liver disease models. The bacterium produced metabolites enriched in acute-on-chronic liver failure. OMV proteomics revealed elevated levels of virulence factors, including components of flagellar machinery, type IV pili, and ABC transporters. Bacterial supernatants and PAMPs activated TLR2/TLR4-dependent signaling, inducing TNFα, IL-1β and profibrotic markers (COL1A1, TGFβ) in immune and hepatic cells. *Aquitalea* DNA detected in patient samples and tap-water sources suggests the presence of environmental reservoirs, and were associated with higher morbidity.
Conclusion: *A. magnusonii* is an environmental bacterium capable of exacerbating systemic inflammation in liver disease mouse and rat models. Its pathogenic effects involve epithelial barrier translocation, OMV- and PAMP-mediated immune activation, cytokine induction, and secretion of disease-related metabolites. These results highlight the need to consider non-commensal environmental bacteria in the pathogenesis of chronic liver disorders.

SAT-331

Characterization of the intrahepatic microbiome in patients with HBV-related end-stage liver disease

Jiyang Chen[1], Tianzhu Liang[2], Xianbin Xu[1], Xia Yu[1], Zhiwei Li[1], Sisi Yang[1], Ziqing Deng[2], Na Pei[2], Yu Shi[1], Yida Yang[1]. *[1]The First Affiliated Hospital, Zhejiang University School of Medicine, Hangzhou, China; [2]BGI Research, Beijing, China*
Email: yidayang65@zju.edu.cn

Background and aims: Dysregulated microbiota is a hallmark of end-stage liver disease (ESLD). This study aimed to elucidate the composition, functional potential, and host transcriptomic correlations of the intrahepatic microbiome across various stages of hepatitis B virus (HBV)-related ESLD.
Method: We collected liver tissue samples from patients undergoing liver transplantation due to decompensated cirrhosis (DC) (n = 20) or acute-on-chronic liver failure (ACLF) (n = 24), as well as samples from donors (n = 18) who served as controls. Metatranscriptomic sequencing was performed on liver tissues to profile the intrahepatic microbiome, encompassing species composition and functional gene expression, as well as liver transcriptome. An integrated analyse was employed to investigate the correlation between microbial species and host gene expression.
Results: 2208 bacterial species were detected across 13 phyla and 165 genera. Metatranscriptomic profiling revealed that *Proteobacteria* and *Actinobacteria* dominated the intrahepatic microbiome, with *Escherichia coli* and *Pseudomonas* most prevalent across groups. Principal coordinate analysis showed distinct microbial community structures among donors, DC, and ACLF patients. Compared with donors, both groups exhibited increased abundance of *Bacteroides heparinolyticus*, *Moraxella osloensis*, and *Gardnerella vaginalis*, while ACLF patients were further enriched with *Alcaligenes faecalis* and *Burkholderia insecticola*, and DC patients had higher *B. heparinolyticus*. Most taxa originated from the gut, with additional oral- and respiratory-derived species. Despite similar abundance between groups, *E. coli* in ESLD displayed marked functional activation, including nutrient acquisition systems and virulence factors linked to adhesion, invasion, and toxin production. Integrated host–microbiome analysis revealed taxa-specific associations with impaired hepatic metabolic, immune, and structural integrity.
Conclusion: This study delineates the compositional and functional reprogramming of the intrahepatic microbiome in patients with ESLD and its coupling with liver metabolic, immune, and structural pathways. These findings suggest the intrahepatic microbiome as a promising therapeutic target for ESLD.

SAT-332

Antibiotic therapy, not disease severity, shapes the intestinal and oral microbiomes in acutely decompensated cirrhosis

Søren Damsholt[1,2,3], Lotte Lindgreen Eriksen[1,2], Johanne Sloth Lauszus[1,2], Aleksander Krag[4], Nikolaj Torp[4], Stine Johansen[4], Henriette Ytting[5], Peter Holland-Fischer[6], Stine Hansen[6], Mette Lauridsen[7], Elise Jonasson[7], Anne Grosen[8], Christian Erikstrup[8], Susan Mikkelsen[8], Astrid Hvidt[2,3], Louise Thingholm[3], Christian Hvas[1,2], Hendrik Vilstrup[2], Sidsel Støy[1,2,8], Karen Louise Thomsen[1,2]. *[1]Department of Hepatology and Gastroenterology, Aarhus University Hospital, Aarhus, Denmark; [2]Department of Clinical Medicine, Aarhus Unversity, Aarhus, Denmark; [3]Department of Molecular Medicine, Aarhus University Hospital, Aarhus, Denmark; [4]Department of Gastroenterology and Hepatology,*

Odense University Hospital, Odense, Denmark; [5]Gastrounit, Copenhagen University Hospital Hvidovre, Hvidovre, Denmark; [6]Department of Hepatology and Gastroenterology, Aalborg University Hospital, Aalborg, Denmark; [7]Department of Gastroenterology and Hepatology, University of South Denmark, Esbjerg, Denmark; [8]Department of Clinical Immunology, Aarhus University Hospital, Aarhus, Denmark
Email: soerdm@rm.dk

Background and aims: Intestinal microbial disturbances are associated with advancing stages of cirrhosis, but the impact of commonly prescribed medications and disease severity in patients with decompensated cirrhosis remains unknown.
Method: We performed shotgun metagenomic sequencing on faecal and saliva samples from 100 patients with acutely decompensated cirrhosis and on faecal samples from 112 healthy faeces donors as comparators. Group differences in alpha diversity (Shannon) were tested using the Wilcoxon test and associations with disease severity and medication usage were tested using linear regressions. Differences in Bray-Curtis beta diversity were tested with PERMANOVA.
Results: The patients' mean age was 58 (±10) years, 75% were men and the median MELD score was 14.5 [11.2–17.9]. Alcohol was the dominant etiology of cirrhosis (75%) and 55% received antibiotic treatment prior to sample collection. Compared with healthy donors, patients had a 55% lower faeces alpha diversity (2.6 [2.0–3.5] vs. 4.6 [4.1–4.5], $p < 0.001$), and a significant beta diversity dissimilarity ($R^2 = 0.15$, $p < 0.001$). Correspondingly, the oral microbiome diversity was low in patient samples (2.8 [2.0–3.3]). Importantly, 26% of patients exhibited prominent single-species dominance in their faecal sample, where a single species on average accounted for 43 (±22) % of species present. These were most frequently *Enterococcus faecium* (n = 8) and *Bifidobacterium longum* (n = 6). Disease severity had no relation to microbiome diversity, whereas antibiotic treatment was associated with reduced alpha diversities in both faeces (−3.0, $p < 0.001$) and saliva (−0.6, $p < 0.001$), and also with marked beta diversity dissimilarity in both faeces ($R^2 = 0.03$, $p < 0.001$) and saliva ($R^2 = 0.02$, $p = 0.02$). Other medications (proton pump inhibitors, beta-blockers and lactulose), and type of decompensation was not associated with microbiome diversity measures when adjusted for antibiotic treatment ($p > 0.05$).
Conclusion: Patients with acutely decompensated cirrhosis exhibit a markedly reduced intestinal and oral microbial diversity, with frequent prominent single-species dominance. Antibiotic treatment, but not disease severity or type of decompensation, is associated with decreased microbial diversity in this group of patients and contribute to single-species dominance. Our findings do not support causal relation between cirrhosis stage and disturbed microbiome, which is rather ascribable to antibiotic treatment.

SAT-333

An integrated multiomics signature and network analysis differentiating metabolic dysfunction-associated steatotic liver disease and metabolic associated steatohepatitis: a pilot study

Shereen El Sobky[1], Nada El-Ekiaby[1], Injie Fawzy[1], Amira Abdelhamid[1], Heba Attia[2], Ibrahim Fayed[1], Yasser Badr[1], Mohammed Emadeldeen[3], Ahmed Nagy[4], Mohamed Negm[5], Mohamed Negm[6], Ahmed Moustafa[7], Mohamed El-Kassas[8], Mohamed Farag[9], Ramy Aziz[2], Ahmed Abdelaziz[1]. *[1]School of Medicine, Newgiza University (NGU), Giza, Egypt; [2]Department of Microbiology and Immunology, Faculty of Pharmacy, Cairo University, Center for Genome and Microbiome Research, Faculty of Pharmacy, Cairo University, Cairo, Egypt; [3]Hepatology and Gastroenterology department, National Hepatology and Tropical Medicine Research Institute, Cairo, Egypt; [4]School of Medicine, Newgiza University (NGU), Kasr Al-Ainy Viral Hepatitis Center (KAVHC), Kasr Al-Ainy University Hospital, Cairo University, Giza, Egypt; [5]Clinical and research center for intestinal disorders, Cairo University, School of Medicine, Newgiza University (NGU), Cairo, Egypt; [6]Department of Pathology, Faculty of Medicine, Cairo University, Cairo, Egypt; [7]Department of Biology & Biotechnology Graduate Program, American University in New Cairo, Cairo, Egypt; [8]Faculty of Medicine, Helwan University, Cairo, Egypt; [9]Department of Pharmacognosy, Faculty of Pharmacy, Cairo University, Healthcare faculty, Saxony Egypt University (SEU), Badr City, Cairo, Egypt*
Email: shereen.el.sobky@gmail.com

Background and aims: Liver biopsy is the gold standard and the most reliable method, to date, to differentiate between metabolic dysfunction-associated steatotic liver disease (MASLD) and metabolic associated steatohepatitis (MASH) using NAS score. A NAS score ≥5 indicates MASH, while <5 indicates MASLD. Accordingly, there were several attempts to discover new diagnostic biomarkers that can outweigh invasive diagnostic procedures. Growing evidence has shown a causal role for gut-microbiome in MASLD onset. One way for gut-microbiome to affect MASLD is through altering intestinal lumen metabolites. Additionally, bioinformatics analysis predicted potential link between the gut-microbiome, its metabolites, and 38 host proteins in MASLD, suggesting PPARG and FXR to be among the affected host proteins. Accordingly, we aimed at performing an integrative multiomics analysis between patients with MASLD and patients with MASH to investigate potential signature that can distinguish them and determine new players that might affect their pathogenesis.
Method: Serum, stool, formalin fixed paraffin embedded (FFPE) tissue biopsies and clinical data were collected for 21 patients with MASLD and MASH. 16S NGS was performed to determine gut-microbial profile. Gas chromatography/ mass spectrometry (GC/MS) was performed for fecal and serum metabolome analysis. Immunohistochemistry was performed for the detection and quantification of subcellular localization of PPARs, FXR and their upstream regulator SIRT1. Integrative multiomics analysis was performed using mixOmics package v6.28.0 on Rstudio v2023.12.1.402.
Results: Our model identified a signature of 20 gut-bacterial genera, 10 fecal and 30 serum metabolites, and 3 host proteins to potentially discriminate between MASLD and MASH. Moreover, network and in silico analysis suggested myristic, lauric, octanoic and nonanoic acids to putatively affect PPARA and FXR, and *Coprobacter* as an important contributor in MASLD/MASH status. The same three fecal metabolites (myristic, lauric, and octanoic acids) had almost identical interaction networks with four bacterial genera (*Victivallis*, *Eisenbergiella*, *Flavonifractor*, and *Coprobacter*), serum nonaoic acid and PPARA as well as NAS and S scores.
Conclusion: Our pilot study identified potential signature that could differentiate between MASLD and MASH, and unraveled new potential players that might affect MASLD/MASH status.

SAT-334

Rifaximin ameliorates liver fibrosis and hepatocarcinogenesis in experimental MASH by inhibiting the gut–liver axis and Epiregulin–IL-8–driven angiogenesis

Kosuke Kaji[1], Norihisa Nishimura[1], Masafumi Oyama[1], Tatsuya Nakatani[1], Tadashi Namisaki[1], Hitoshi Yoshiji[1]. *[1]Department of Gastroenterology, Nara Medical University, Kashihara, Japan*
Email: kajik@naramed-u.ac.jp

Background and aims: Gut–liver axis plays a key role in metabolic dysfunction–associated steatohepatitis (MASH) progression, whereby gut-derived lipopolysaccharide (LPS) promotes hepatic inflammation, fibrogenesis, and angiogenesis through toll-like receptor 4 (TLR4) signaling. Rifaximin, a non-absorbable gut-selective antibiotic, has been shown to improve intestinal barrier function and reduce endotoxemia. This study aimed to investigate the effect of rifaximin on liver fibrosis and early hepatocarcinogenesis in MASH, with focus on the LPS–epiregulin–IL-8–angiogenesis pathway.
Method: MASH was induced in male Fischer 344 rats by feeding a choline-deficient, L-amino acid-defined high-fat diet (CDAHFD) for 12 weeks. Rifaximin (30 mg/kg/day) or vehicle was orally administered throughout the experimental period. Liver histology including

fibrosis and early hepatocarcinogenesis, portal LPS levels, Kupffer cell activation, and hepatic LPS/TLR4 signaling were analyzed. Angiogenesis-related markers, including epiregulin, IL-8, CD34-positive neovascularization, and proangiogenic gene expression, were examined. Intestinal barrier integrity was evaluated by histology, tight junction protein expression, intestinal LPS levels, and FITC-dextran permeability assays.
Results: Rifaximin significantly attenuated hepatic inflammation and fibrosis in CDAHFD-fed rats, reducing hepatic hydroxyproline content and profibrogenic gene expression. The glutathione S-transferase placental form (GST-P)-positive preneoplastic lesions were markedly decreased, accompanied by suppression of cell proliferation–related genes. Rifaximin lowered portal LPS levels and inhibited Kupffer cell activation, with downregulation of Lbp, Cd14, Tlr4, and proinflammatory cytokines. Notably, hepatic epiregulin and IL-8 expression were significantly reduced, correlating with decreased CD34-positive neovascularization and suppression of angiogenesis-related genes. These effects were associated with restoration of intestinal barrier function, including improved villus architecture, increased tight junction protein expression, and decreased gut permeability.
Conclusion: Rifaximin attenuates liver fibrosis and early hepatocarcinogenesis in murine MASH by restoring intestinal barrier integrity, limiting gut-derived LPS translocation, and suppressing the LPS–TLR4–epiregulin–IL-8–associated angiogenic pathway. These findings identify rifaximin as a potential chemopreventive strategy targeting the gut–liver axis in MASH-related hepatocarcinogenesis.

SAT-335
Acute hypobaric hypoxia remodels the intestinal metaproteome, disrupting barrier function and promoting inflammation-driven dysbiosis
Rupinder Kalra[1], Sanju Yadav[2,3], Jaswinder Maras[2], Ved Dwivedi[4], Nasir Salam[3], Narendra Sharma[1]. *[1]Banasthali Vidyapith, Newai, India; [2]Institute of Liver and Biliary Sciences, New Delhi, India; [3]Jamia Millia Islamia, New Delhi, India; [4]ICGEB, New Delhi, India*
Email: drnarendraks@gmail.com

Background and aims: Hypoxia disrupts intestinal homeostasis and compromising barrier integrity, promoting inflammation and expansion of pathogenic microbes. These changes drive dysbiosis, increase intestinal permeability, and contributing to systemic inflammation and gut–liver axis dysfunction; however, the underlying mechanisms remain obscure.
Method: Male SD rats (n = 6/group) were exposed to simulated hypobaric hypoxia (25,000 ft) for 1, 3, or 7 days. Intestinal tissues were analyzed by metaproteomics, proteomics and metabolomics to identify differentially expressed bacterial peptides, define time-dependent taxonomic and functional signatures, and correlate microbial alterations with intestinal metabolome, intestinal barrier dysfunction and inflammation.
Results: Hypobaric hypoxia induced profound intestinal metaproteomic remodeling, with 216 differentially expressed bacterial peptides across exposure durations, of which 93 were consistently increased (FC>1.5, $p < 0.05$). These changes were associated with enrichment of 15 pathogenic taxa, including Clostridia, Salmonella, and others (FC>2.5), and Mycoplasmoides gallisepticum (FC>2.5), linked to inflammation, metabolic dysregulation, and epithelial barrier disruption. In contrast, seven commensal-associated metaproteins (e.g., Bacteroidales, Nostocaceae) were downregulated, indicating loss of colonization resistance. Intestinal metabolomics revealed marked, time-dependent metabolic reprogramming, with significant enrichment of arginine proline (FC>3.5), tryptophan metabolism (FC>3.5), pyrimidine, lysine, and purine metabolism (R^2>0.7, $p < 0.05$). Functional pathway analysis highlighted perturbations in peptidoglycan and fatty acid biosynthesis, histidine, biotin, glutathione metabolism, and prodigiosin biosynthesis, reflecting oxidative stress and enhanced microbial virulence. Concomitantly, the host intestinal proteome showed significant reduction of tight junction proteins (ZO-1, ZO-2, ZO-3; FC>3.5), adherens junction proteins (E-cadherin), and mucosal defense factors (MUC2, defensins, REG3γ; FC >1.5, $p < 0.05$) there by driving intestinal barrier failure.
Conclusion: Intestinal metaproteomics shows that hypobaric hypoxia induces time-dependent gut dysbiosis with pathogenic enrichment and commensal loss, driving metabolic rewiring, barrier dysfunction, increased permeability, microbial translocation, and gut–liver axis impairment, highlighting the microbiome as a key mediator and therapeutic target.

SAT-336
Hypobaric hypoxia induces sustained pathogenic alterations in gut microbiota and contributes to injury in a preclinical model of hypoxia
Rupinder Kalra[1], Sanju Yadav[2,3], Jaswinder Maras[2], Ved Dwivedi[4], Nasir Salam[3], Narendra Sharma[1]. *[1]Banasthali Vidyapith, Newai, India; [2]Institute of Liver and Biliary Sciences, New Delhi, India; [3]Jamia Millia Islamia, New Delhi, India; [4]ICGEB, New Delhi, India*
Email: drnarendraks@gmail.com

Background and aims: Hypobaric hypoxia modulates liver function and remodels the gut microbiome. Stool metaproteomics reveals functional microbial shifts and metabolic pathway alterations that contribute to hypoxia-induced liver injury and inflammation.
Method: Male SD rats were exposed to simulated hypobaric hypoxia equivalent to 25,000 ft altitude for 1, 3, and 7 days in a hypoxia chamber. Stool samples were subjected to metaproteomic and metabolomic analyses. Differential protein expression profiling, followed by taxonomic and functional annotation, was performed to identify time-dependent microbial signatures and their association with liver inflammation.
Results: Hypobaric hypoxia in rats caused liver inflammation, elevated AST and ALT levels, reduced body weight, and increased liver-to-body weight ratio ($p < 0.05$). Stool metaproteomics revealed distinct α/β diversity changes and 211 differentially expressed bacterial peptides across hypoxia exposure. Hypoxia induced > 180 bacterial peptides while >10 were downregulated at all day of exposure (FC>1.5, $p < 0.05$). Comparative analysis identified 172 bacterial taxa, including 49 taxa; *Streptococcus* and *Klebsiella* associated with gut and liver inflammation and enriched in nicotinate nicotinamide and sphingolipid metabolism. These findings link hypoxia to gut dysbiosis, barrier dysfunction and increased susceptibility to secondary infections. Stool metabolome analysis validated significant dysregulation of tryptophan metabolism and carnitine dysregulation all associate to pathogenic metabolic transformation (R2>0.7, $p < 0.05$). Interestingly, increase in streptococcus correlates >0.7 with spermidine and spermine accumulation. Suggesting that hypoxia increased Streptococcus acts as a metabolic amplifier and increases accumulation of Spermidine, S-Adenosyl-L-methionine (SAM), Spermine, Putrescine >1.5 FC, $p < 0.05$ creates a pathogenic loop that contributes to inflammation and liver injury.
Conclusion: Our study shows that hypobaric hypoxia induces pronounced, time-dependent functional remodelling of the gut microbiome. Sustained enrichment of pathogenic bacteria and depletion of protective taxa may contribute to hypoxia associated gastrointestinal dysfunction and systemic inflammation, highlighting potential microbial targets for therapeutic intervention in hypoxia linked liver diseases.

SAT-337
Odoribacter splanchnicus attenuates western diet–induced MASLD by restoring hepatic lipid metabolism
Soon Sun Kim[1], Moon Gyeong Yoon[1], Se Ha Jang[2], Geum Ok Baek[1], Hyun Sun Jung[2], Jae Youn Cheong[1], Jung Woo Eun[1]. *[1]Ajou University School of Medicine, Suwon, Korea, Rep. of South; [2]Ajou University School of Medicine, Ajou University Graduate School of Medicine, Suwon, Korea, Rep. of South*
Email: jetaimebin@gmail.com

Background and aims: Metabolic dysfunction–associated steatotic liver disease (MASLD) affects both obese and non-obese individuals, and emerging evidence highlights a pivotal role of the gut microbiome in its pathogenesis. This study aimed to identify a gut microbial strain associated with MASLD prevention or treatment and to validate its hepatoprotective effects using *in vitro* and *in vivo* models.
Method: Gut microbiome profiling was performed using 16S rRNA sequencing of fecal samples obtained from healthy controls and patients with MASLD, including both obese and non-obese individuals. *Odoribacter splanchnicus* was identified as a candidate strain significantly reduced in MASLD patients. *In vitro*, the anti-steatotic effects of *O. splanchnicus*–conditioned media were evaluated in free fatty acid–treated HepG2 and Hepa1–6 cells. *In vivo* efficacy was assessed using a 13-week Western diet–induced MASLD mouse model, followed by biochemical, histological, and hepatic gene expression analyses.
Results: *O. splanchnicus*–conditioned media dose-dependently reduced lipid accumulation in hepatocyte cell lines, indicating a direct anti-steatotic effect. In Western diet–fed mice, supplementation with *O. splanchnicus* significantly improved liver enzyme levels (AST, ALT, and GGT), attenuated hepatic steatosis, inflammation, and fibrosis, and reduced macrophage infiltration. Mechanistically, *O. splanchnicus* restored the expression of key regulators of fatty acid oxidation (Ppar-α, Acox1, and Cpt1a) and bile acid signaling (Fxr), while suppressing inflammatory gene expression (Tnf-α and Tlr-4).
Conclusion: These findings demonstrate that *Odoribacter splanchnicus* exerts hepatoprotective and anti-steatotic effects by improving hepatic lipid metabolism and inflammatory responses. This strain represents a promising microbiome-based therapeutic candidate for MASLD across obese and non-obese populations.

SAT-338

The biliary metagenome in malignant cholestasis: analysis of samples obtained during EUS-guided biliary drainage

Łukasz Krupa[1], Georges Schmarz[2], Robert Staroń[1], Hartmut Schmidt[3], Jacqueline Rehner[4], Soeren Becker[4], Marcin Krawczyk[3]. *[1]Medical Department, University of Rzeszów, Rzeszów, Poland; [2]Chair for Clinical Bioinformatics, Saarland University, Saarbrücken, Germany; [3]Essen University Hospital, Department of Gastroenterology, Hepatology and Transplant Medicine, Medical Faculty, University of Duisburg-Essen, Essen, Germany; [4]Institute of Medical Microbiology and Hygiene, Saarland University, Homburg, Germany*
Email: marcinjan.krawczyk@uk-essen.de

Background and aims: Biliary obstruction is a common complication of pancreatic and hepatobiliary malignancies. In the recent years, the role of microbiota in hepatobiliary tumors has gained increasing attention. Endoscopic retrograde cholangiopancreatography (ERCP) is the standard method for biliary drainage in malignant cholestasis. However, when ERCP fails, endosonography-guided biliary drainage (EUS-BD) represents an effective alternative. This study aims to characterise biliary microbial composition in patients with end-stage malignant cholestasis undergoing EUS-BD.
Method: We prospectively enrolled 43 patients (22 women, age 33–89 years) with malignant cholestasis, predominantly due to pancreatic cancer (n = 23) and cholangiocarcinoma (n = 11). Bile samples were collected during EUS-BD (26 hepaticogastrostomies and 17 choledochoduodenostomies) following unsuccessful ERCPs. Metagenomic profiling of bile was performed using next generation sequencing (NGS).
Results: Microbial analysis was successfully performed in all samples. Four samples exhibited minimal microbial diversity with a Shannon diversity index below 0.5: two samples contained Enterococcus faecalis and Klebsiella pneumoniae and the other two samples contained Streptococcus epidermidis and Streptococcus mitis. Differential abundance analyses revealed distinct microbial signatures associated with tumor types. Patients with pancreatic cancer showed an overrepresentation of Streptococcus intermedius (q-val. = 0.032), whereas Cryptobacterium curtum was more abundant in cholangiocarcinoma (q-val. = 0.013). In patients with other malignancies, Actinomyces bouchesdurhonensis was significantly overrepresented (q-val. = <0.001). No significant association between microbial composition of bile and patients survival was observed.
Conclusion: EUS-BD allows collection of bile samples suitable for metagenomic analyses. We detected a differential abundance of species in different end-stage heapatobiliary malignancies. Larger cohorts are needed to further explore the relationship between biliary microbiota, confounding factors, tumor type and its progression.

SAT-341

Bacteroides intestinalis AM-1 reshapes the gut microbiome and preserves intestinal barrier function to mitigate acetaminophen-induced liver injury

Sushmita Pandey[1,2], Neha Sharma[1], Nupur Sharma[1], Vipul Sharma[1], Yash Magar[1], Babu Mathew[1,3], Gaurav Tripathi[1], Vasundhra Bindal[1], Sanju Yadav[1], Manisha Yadav[1], Anju Katyal[4], Shiv Kumar Sarin[1], Jaswinder Maras[1]. *[1]Institute of Liver & Biliary Sciences, New Delhi, India; [2]Dr. B R Ambedkar Center for Biomedical Research, University of Delhi, New Delhi, India; [3]Institute of Liver and Biliary Sciences (ILBS), New Delhi, India; [4]Dr. B R Ambedkar Center for Biomedical Research, University of Delhi, New Delhi, India*
Email: jassi2param@gmail.com

Background and aims: Intestinal dysbiosis exacerbates liver injury, and expansion of pathogenic gut microbiota not only increases the risk of liver failure but also drives gut dysregulation, making the intestinal microbiome a key, targetable risk factor in acute liver failure (ALF). We investigate the role of intestinal and plasma metaproteomic alterations in acute liver failure (ALF) and evaluate microbiome-targeted therapeutic correction in preclinical model of ALF.
Method: Intestinal and plasma meta-proteomes were analyzed in patients with drug induced liver failure ALF (n = 116) and in an acetaminophen (APAP)-induced preclinical model. Key meta-protein alterations were identified and correlated with disease severity and clinical outcomes. Finally, the therapeutic potential of Bacteroides intestinalis AM-1 (Bi) in restoring dysregulated microbiome signatures, improving intestinal homeostasis and ALF-associated pathophysiology was evaluated in detail.
Results: Intestinal and plasma meta-proteomic analyses revealed a significant enrichment of pathogenic bacterial peptides, including Firmicutes and Enterobacteriaceae (FC >1.5; $p < 0.05$), in both ALF patients and APAP-induced preclinical models. This was accompanied by a marked reduction in beneficial commensals such as *Bacteroides* and *Lactobacillus* ($p < 0.05$), correlating with severe disruption of intestinal homeostasis. Oral Bi supplementation effectively restored microbial balance, increasing beneficial taxa while reducing pathogenic bacterial peptides, including Enterobacteriaceae and Clostridiaceae ($p < 0.05$). Bi treatment significantly improved intestinal barrier integrity through upregulation of mucosal and tight-junction proteins, including occludin, MUC2, and MUC1 (FC >2.5; $p < 0.05$). These gut-protective effects translated into marked hepatic benefits, with up to 70% reduction in hepatic necrosis and significantly lower serum AST and ALT levels ($p < 0.05$). Mechanistically, Bi activated intestinal FXR–FGF15 signaling (FC >1.5; $p < 0.05$), correcting FXR dysregulation associated with drug-induced injury and preserving intestinal mitochondrial fitness and redox homeostasis in acute liver failure.
Conclusion: Bacteroides intestinalis AM-1 restores microbiome fitness, re-established intestinal homeostasis, and attenuated experimental APAP-induced liver injury. These findings suggest Bi as a potential probiotic therapy for drug-induced hepatotoxicity.

SAT-345

Machine learning uncovers functional microbial signatures in cirrhosis patients with type 2 diabetes mellitus

In Gyu Park[1], Sang Joon Yoon[1], Sung-Min Won[1], Ki Kwang Oh[1], Un Joo Lee[2], Younglim Ham[3], Ki Tae Suk[1]. *[1]Hallym university, Institute for Liver and Digestive Diseases, Chuncheon-si, Korea, Rep. of South; [2]Hallym University, Department of Electronic Engineering, Chuncheon-si, Korea, Rep. of South; [3]Daewon University College, Department of Nursing, Jaecheon, Korea, Rep. of South*
Email: ktsuk@hallym.ac.kr

Background and aims: Patients with comorbid liver cirrhosis and type 2 diabetes mellitus (T2DM) termed Cirrhotic Diabetes Mellitus (CDM) have worse clinical outcomes than those with either condition alone. Current taxonomic profiling approaches inadequately capture CDM-specific functional microbial interactions. We developed an interpretable machine learning framework to identify functional biomarkers that distinguish this complex comorbid phenotype.
Method: We enrolled 149 participants stratified into four groups: normal controls (NC, n = 59), T2DM (n = 46), cirrhosis (n = 30), and CDM (n = 14). Shotgun metagenomic sequencing was performed to extract both microbial taxonomic profiles and functional genes (KEGG Orthology [KO]). To address the non-linear interactions inherent in high-dimensional metagenomic data, we constructed an interpretable ML framework using XGBoost. This was coupled with Boruta feature selection and SHAP (SHapley Additive exPlanations) analysis to robustly identify key biomarkers and visualize their contribution to disease stratification.
Results: The model demonstrated robust diagnostic performance. Differentiating cirrhosis from NC, it achieved an Area Under the Receiver Operating Characteristic (AUROC) of 0.92 (discovery) and 0.79 (validation), with SHAP confirming *Dorea longicatena* and *Collinsella aerofaciens* as top predictors. Strikingly, for the challenging stratification of CDM from cirrhosis alone, the framework showed robust generalization with a validation AUROC of 0.94. Explainable AI revealed that in CDM, microbial KOs contributed significantly more than taxa. Specifically, the uracil permease gene *uraA* (K02824) was the top predictor, highlighting that functional alterations are more critical than taxonomic shifts in defining this high-risk phenotype.
Conclusion: This study establishes an integrative ML framework that successfully stratifies the complex multimorbidity of cirrhosis and diabetes. By utilizing XGBoost to capture non-linear functional interactions, we identified distinct microbial signatures associated with the CDM phenotype. These findings underscore the potential of function-based microbiome markers for precision risk stratification in advanced liver disease.

SAT-346

The interplay of serum and stool metabolomic profiles in non-progressive and progressive alcohol-related liver disease

Eemeli Puhakka[1], Krista Ahola[1], Hany Ahmed[2], Retu Haikonen[1], Sophie Leclercq[3], Kati Hanhineva[4], Luca Maccioni[3,5], Camille Amadieu[6], Marko Lehtonen[1], Ville Männistö[1], Jaana Rysä[1], Peter Stärkel[3], Olli Kärkkäinen[1]. *[1]University of Eastern Finland, Kuopio University Hospital, Kuopio, Finland; [2]University of Turku, Turku, Finland; [3]Uclouvain, Ottignies-Louvain-la-Neuve, Belgium; [4]University of Turku-Main building, Turku, Finland; [5]National Institutes of Health, Bethesda, United States; [6]University of Bordeaux, Pessac, France*
Email: epuhakka@uef.fi

Background and aims: Liver diseases are on the rise worldwide, in part due to the increase in alcohol-related liver disease (ALD) and metabolic dysfunction-associated steatotic liver disease. ALD is a progressive disease, which has large variation in the rate of progression between individuals with the same alcohol intake. The interplay between gut microbiota, intestinal permeability and liver function has been hypothesized to contribute to the metabolic processes causing ALD progression. In the present study, the aim was to examine metabolomic profiles in stool samples of non-progressive ALD and progressive ALD patients.
Method: The study was composed of 2 study groups, a non-progressive ALD group (N = 31) and an early stage progressive ALD group (N = 36). The stratification between the patient groups was done with elastography and liver function tests (aspartate aminotransferase and alanine aminotransferase). Patients with elevated liver function test results and high elastography scores were assigned to the progressive ALD group. Patient groups took part in a voluntary alcohol rehabilitation program in Brussels, Belgium between 2017 and 2019. Patients had their blood drawn and stool samples collected on the day of the admission. Both the serum and stool samples were analyzed with non-targeted liquid chromatography mass spectrometry metabolomics.
Results: In the metabolomics analysis of the stool samples, 86 identified metabolites had a p-value <0.05 and 11 identified metabolites had a p-value below the corrected alpha level (0.0009). Primary finding was that stool dopamine (Cohen's d = –0.92), phenylalanine (d = –0.92), phenylephrine (d = –0.92), tyrosine (d = –0.84) and 3-dehydroshikimate (d = –1.03) had their levels significantly lower in the progressive ALD group when compared to the non-progressive ALD group. Furthermore, stool levels of phenylalanine, dopamine, tyrosine and phenylephrine all had a moderate reverse correlation (|r|>0.4) with serum glutamate and glycine bound bile acid levels.
Conclusion: The low levels of dopamine and tyrosine in stool of the progressive-ALD point towards a shift in the bacterial species of the gut. Decreased phenylephrine levels could be linked to alterations in gut lining and permeability. The strong reverse correlation with glycine bound bile acids and glutamate indicates an interplay in disease progression. In conclusion, the metabolomic changes indicate a thorough alteration in the functional characteristics of gut lining.

SAT-347-YI

Incomplete microbial and metabolic recovery during the regression phase of carbon tetrachloride-induced liver fibrosis

Katja Sommer[1,2,3], Katharina Bonitz[1,3,4], Thomas Sorz-Nechay[1,2,3,4], Henriette Horstmeier[1], Vlad Taru[1,4], Kerstin Zinober[1], Katharina Regnat[1], Hubert Scharnagl[5], Michael Trauner[1], Philipp Schwabl[1,2,3,4], Thomas Reiberger[1,2,3,4], Benedikt Simbrunner[1,2,3,4]. *[1]Division of Gastroenterology and Hepatology, Department of Internal Medicine III, Medical University of Vienna, Vienna, Austria; [2]Clinical Research Group MOTION, Medical University of Vienna, Vienna, Austria; [3]CeMM Research Center for Molecular Medicine of the Austrian Academy of Sciences, Vienna, Austria; [4]Christian Doppler Laboratory for Portal Hypertension and Liver Fibrosis, Medical University of Vienna, Vienna, Austria; [5]Medical and Chemical Laboratory Diagnostics, Medical University of Graz, Graz, Austria*
Email: katja.sommer@meduniwien.ac.at

Background and aims: Disruption of the intestinal barrier and subsequent microbial translocation contribute to inflammation and portal hypertension in chronic liver disease. We aimed to characterize gut-liver axis changes at carbon tetrachloride (CCl_4)–induced liver injury and after natural disease regression in mice, which may uncover therapeutic targets for strengthening gut barrier function and attenuating inflammatory cascades in liver disease.
Method: Liver fibrosis was induced in male C57BL/6J mice via bodyweight–adapted CCl_4 gavage (2 mL/kg, 3×/week as 20% olive oil solution) for 12 weeks (n = 12). Additionally, a regression group was examined after two-week CCl_4 cessation (n = 12). Control mice received only olive oil (n = 12). Portal pressure (PP) was measured and ileal and hepatic samples collected for transcriptomic profiling, histology and immune-cell phenotyping by flow cytometry. Serum samples were collected for metabolomics and ileum stool for 16S ribosomal RNA sequencing.

Results: Regression significantly reduced PP (7.15 vs. 6.10 mmHg; p = 0.010) and collagen proportionate area (7.14 vs. 4.90%, p = 0.030) compared to peak disease. Ileal immune cell profiling showed decreased $CD45^+$ intraepithelial lymphocyte proportions (−15.75%, p = 0.020) and increased $CD45^+$ lamina propria cells (+34.13%, p = 0.030) in regression. Microbial communities differed significantly between groups (PERMANOVA: p = 0.001). Peak fibrosis showed loss of *Dubosiella* and Muribaculaceae, with expansion of *Ileibacterium*, *Akkermansia*, and *Turicibacter* (in total 30% abundance) compared to controls. Microbial profiles did not normalize in regression; *Ileibacterium* remained elevated (~30% relative abundance; >2 log2-fold increase vs. peak and control), indicating persisting dysbiosis in the anaerobic niche. Serum metabolomics revealed marked alterations, with glutamic acid (log2 fold change [log2FC] = 1.00, p = 0.006) and tauro-muricholate (log2FC = 2.22, p = 0.006) elevated in peak disease compared to controls. Purine-degradation metabolites were enriched in regression compared to peak disease, including hypoxanthine (log2FC = 3.42, p = 0.127) and xanthine (log2FC = 3.34, p = 0.006) as major drivers of group separation.
Conclusion: CCl_4-induced liver fibrosis was linked to microbial, metabolic and immune disturbances, while regression was marked by persistent *Ileibacterium* overabundance and sustained metabolic stress despite partial hepatic structural recovery.

SAT-348
Diet and exercise mitigate MASLD and exert beneficial effects on skeletal muscle via organ crosstalk in diet-induced obese mice
Henrique Souza-Tavares[1], Laura Ramos-da-Silva[1], Nathan Dantas-Miranda[1], Gustavo Silva-Pereira[1], Maria Amancio-Lisboa[1,2], Gabriela Medeiros[1], Flavia Silva-Veiga[1], Vanessa Souza-Mello[1]. [1]*Rio de Janeiro State University, Rio de Janeiro, Brazil;* [2]*Instituto Federal do Rio de Janeiro-Reitoria, Rio de Janeiro State University, Rio de Janeiro, Brazil*
Email: souzatavareshenriqueuerj@gmail.com

Background and aims: Ultra-processed food intake and a sedentary lifestyle, associated with metabolic dysfunction-associated liver disease (MASLD) and sarcopenia, contribute to obesity onset. Hence, the effects of lifestyle change therapy on the muscle-liver axis merit further investigation. This study aimed to evaluate the impact of dietary intervention and physical exercise, alone or in combination, on the modulation of the muscle-liver axis in mice fed excess saturated fat and sucrose.
Method: Adult male C57BL/6J mice were fed a control diet (C) or a diet rich in saturated fat and sucrose (HFS) for ten weeks. The HFS group was then subdivided into four groups (n = 15 each), for a six-week treatment: C (control group), HFS (HFS diet group), HFS-C (C diet, mimicking a dietary treatment), HFS-Ex (HFS diet + exercise), and HFS-CEx (C diet + exercise). High-intensity interval training (HIIT) was performed on a treadmill for mice on alternate days, with each session lasting 15 minutes. At sacrifice, blood samples, triceps surae (gastrocnemius and soleus), and the liver were harvested and evaluated by biochemical, stereological, and molecular biology analyses. The differences were tested using Brown-Forsythe and Welch ANOVA with Dunnett T3 post hoc test (P < 0.05).
Results: The HFS group showed overweight, oral glucose intolerance, a proinflammatory adipokine profile, reduced lean mass, and increased hepatic steatosis volume density. All treatments (diet, exercise, or combination) led to reduced body and fat masses, increased lean mass, and improved adipokine profile. However, only the exercised groups showed increased irisin concentrations, resulting in the most pronounced MASLD reductions through AMP-activated protein kinase (AMPK)/Sirtuin-1 (SIRT1)/Peroxisome proliferator-activated receptor gamma coactivator 1-alpha (PGC1a) activation, improved mitochondrial dynamics, and increased oxidative capacity. All treatments increased muscle fibroblast growth factor 21 (*Fgf21*) expression, a hepatokine linked to the preserved muscle mass and improved mitochondrial dynamics markers.
Conclusion: Lifestyle change therapy (diet, exercise, or combination) improved the body composition and adipokine profile of HFS-fed mice. Enhanced skeletal muscle *Fgf21* and hepatic irisin reinforce crosstalk between these organs, preserving muscle mass and alleviating MASLD. The diet-and-exercise combination was the most effective therapy, leading to complete rescue of body composition, oral glucose tolerance, and hepatic cytoarchitecture.

SAT-349
Pharmabiotics, phocaeicola dorei, ameliorates liver fibrosis by alleviating macrophage efferocytosis of neutrophils
Ki Tae Suk[1], Jung A. Eom[1], In Gyu Park[1], Goo Hyun Kwon[1], Younglim Ham[2], Dong Joon Kim[1]. [1]*Hallym University, Institute for Liver and Digestive Diseases, Chuncheon, Korea, Rep. of South;* [2]*Daewon University, Department of Nursing, Jecheon, Korea, Rep. of South*
Email: ktsuk@hallym.ac.kr

Background and aims: Liver fibrosis results from chronic inflammation, dysregulated immune responses, and persistent activation of hepatic stellate cells (HSCs). Increasing evidence shows that gut microbiota influence hepatic immunity and fibrogenesis. *Phocaeicola dorei* has been reported to ameliorate metabolic diseases. Its role in liver fibrosis remains unclear. We hypothesized that *P. dorei* attenuates liver fibrosis by suppressing neutrophil activation and limiting macrophage-mediated efferocytosis of apoptotic neutrophils, thereby reducing downstream HSC activation.
Method: Fecal samples were collected from healthy controls and patients (n = 285) to assess the clinical relevance of *P. dorei*. In mice models (3,5-diethoxycarbonyl-1.4-dihydrocollidine [DDC] diet and TAA [thioacetamide] injection), *P. dorei* (10^9 CFU/g twice/week) was orally administered. Fibrosis severity, collagen deposition, immune-cell infiltration, and chemokine expression were assessed by histology, Sirius Red staining, immunofluorescence, and qPCR. HSCs were isolated for RNA sequencing to identify pathway changes modulated by *P. dorei*. Primary HSCs, LX-2, THP-1, and HL-60 cell lines were used for mechanical validation.
Results: The relative abundance of *P. dorei* increased progressively with worsing liver disease in human cohort. *P. dorei* administration significantly reduced fibrosis, neutrophil degranulation and efferocytosis pathways, as indicated by decreased *Ly6g* and *F4/80* expression. In parallel, the dysregulated expression of neutrophil-associated chemokines, including *Cx3cl1*, and *Cx3cr1* was restored by *P. dorei* treatment. In vitro, *P. dorei* culture supernatant markedly inhibited macrophage-mediated efferocytosis.
Conclusion: Collectively, *P. dorei* attenuates liver fibrosis by suppressing neutrophil and macrophage infiltration and disrupting efferocytosis through interference with interactions between apoptotic bodies and macrophages. Our results identify *P. dorei* as a potential microbiome-based therapeutic candidate for liver fibrosis.

SAT-350
Liver atrophy drives transcriptomic reprogramming of extrahepatic organs in experimental cirrhosis
Javier Vaquero[1,2,3], Iris Asensio[1,2], Marta Puerto[1,2,3], Carolina Franco[1,2], Elena Vázquez-Ogando[1,2], Raquel Herrero[4,5], Laura Moreno[1,5,6], Johanna Sierra[1,2], Christian Ruiz-Martin[1,2], Diego Rincón Rodriguez[1,2,3,7], Mario Romero[1,2], Jordi Gracia-Sancho[3,8,9], Ignacio Benedicto[10,11], Jean Campbell[12], Francisco Javier Cubero[1,3,13,14], Rafael Bañares[1,2,3,7]. [1]*Instituto de Investigación Sanitaria Gregorio Marañón (IiSGM), Madrid, Spain;* [2]*Hospital General Universitario Gregorio Marañón, Madrid, Spain;* [3]*CIBEREHD, Madrid, Spain;* [4]*Serv. Medicina Intensiva, Hospital Universitario de Getafe, Madrid, Spain;* [5]*Galapagar, Spain;* [6]*Departamento de Farmacología, Facultad de Medicina, Universidad Complutense, Madrid, Spain;* [7]*Facultad de Medicina, Universidad Complutense, Madrid, Spain;* [8]*Liver Vascular Biology Research Group, Hospital Clínic de Barcelona, IDIBAPS, Barcelona, Spain;* [9]*Bern University Hospital, University of Bern, Bern, Switzerland;* [10]*Centro de*

Investigaciones Biológicas Margarita Salas (CIB), Consejo Superior de Investigaciones Científicas (CSIC), Madrid, Spain; [11]Centro Nacional de Investigaciones Cardiovasculares (CNIC), Madrid, Spain; [12]Northwestern University, Seattle, United States; [13]Department of Immunology, Ophthalmology and ENT, Facultad de Medicina, Univ. Complutense, Madrid, Spain; [14]Instituto Universitario de Neuroquímica (IUIN), Facultad de Medicina, Univ. Complutense, Madrid, Spain
Email: j.vaquero@iisgm.com

Background and aims: Advanced chronic liver disease (CLD) is a systemic and inflammatory condition, but how molecular programs evolve across organs remains incompletely defined. Here, we examined transcriptomic changes in the liver and distant organs in experimental CLD, with a focus on the impact of liver atrophy.
Method: Male SD rats received oral carbon tetrachloride (CCl4) or vehicle for 2–12 weeks. Liver atrophy was defined as liver-to-body weight ratio < mean–1 SD of controls. Bulk RNA-seq from liver, mesentery, lung, ileum, kidney, and heart was analyzed in CLD rats without or with atrophy, and compared with controls. Differential expression and GO Biological Process GSEA were used to identify organ-specific and shared pathways.
Results: Animals with liver atrophy formed a distinct transcriptomic cluster by unsupervised PCA across all organs. In the liver, both stages of CLD showed activation of extracellular matrix programs, chemokine signaling, antimicrobial humoral responses, neutrophil recruitment, and TGF-β signatures. Concomitantly, mitochondrial/metabolic programs were repressed, including oxidative phosphorylation, electron transport chain, fatty acid β-oxidation, acetyl-CoA metabolism, and mitochondrial translation. These changes intensified with liver atrophy, which further suppressed xenobiotic/retinoid–terpenoid catabolism and NADPH-regenerating processes. Transcriptomic responses in extrahepatic organs were stage-dependent. Rats without liver atrophy showed mainly organ-restricted changes (xenobiotic/retinoid/terpenoid metabolic induction in lung, proliferative pathways in heart, no major shifts in kidney). After liver atrophy developed, multiple organs converged on innate immune activation, coupled with mitochondrial metabolic dysfunction: a) The mesentery and lung showed prominent leukocyte chemotaxis/trafficking, myeloid/neutrophil activation, and humoral immune responses, with reciprocal depletion of developmental/neurogenic programs, b) The heart and kidneys exhibited granulocyte/complement activation, phagocytosis and leukocyte–endothelial adhesion with marked repression of oxidative phosphorylation and fatty-acid β-oxidation (strongest in heart), c) The ileum preferentially upregulated extracellular matrix programs while suppressing oxidative phosphorylation/electron transport pathways.
Conclusion: Liver atrophy drives a systemic transcriptional transition in experimental CLD, from early organ-specific adaptations to late multi-organ immune activation and bioenergetic failure.

SAT-351
Integrated multi-omics analysis identifies gut microbiota – lipid - metabolite signatures associated with metabolic dysfunction – associated steatotic liver disease in overweight adults

Miloš Vratarić[1], Sofija Ignjatović[1], Bojana Mićić[1], Uroš Gašić[1], Ivana Božić -Antić[2], João Barbosa[3], Daniel Duberg[3], Anh Nguyen[4], Mark Davids[5], Amir H. Alizadeh Bahmani[5], Tuulia Hyötyläinen[3], Matej Orešič[4], Max Nieuwdorp[5], Danijela Vojnović-Milutinović[1], Ana Djordjevic[1], Nataša Veličković[1]. *[1]Institute for Biological Research "Siniša Stanković"- National Institute of Republic of Serbia, Belgrade, Serbia; [2]Euromedik Healthcare System, Belgrade, Serbia; [3]School of Science and Technology, Örebro University, Örebro, Sweden; [4]School of Medical Sciences, Örebro University, Örebro, Sweden, [5]AmsterdamUMC, University of Amsterdam, Amsterdam, Netherlands*
Email: milos.vratarić@ibiss.bg.ac.rs

Background and aims: Metabolic dysfunction–associated steatotic liver disease (MASLD) is characterized by complex interactions between the gut microbiota and host lipid metabolism, mediated by bacterial metabolites. Single-omics approach provides limited insight into these interactions, and integrated multi-omics analysis is needed for a better understanding of the gut-liver axis. This study aims to investigate differences in gut microbiota composition, and lipid and metabolite profiles characteristic of overweight adults with and without MASLD, using an integrated multi-omics approach.
Method: We conducted a cross-sectional observational study and performed fecal metagenomics analysis, as well as untargeted metabolomics and lipidomics analysis of plasma samples from overweight male and female patients with ultrasound-confirmed MASLD (n = 71) and without MASLD (n = 49). DIABLO framework was used to identify multi-omics biomarker panels of bacterial taxa, metabolites, and lipids that can distinguish overweight participants with and without MASLD.
Results: The MASLD group showed a less favorable metabolic profile, characterized by higher body mass index and waist circumference, elevated hepatic enzymes, fasting glucose and triglycerides. Single-omics block analyses provided moderate discrimination between groups, with areas under the curve (AUCs) ranging from 0.657 to 0.734. Integration of all three omics layers using the DIABLO framework improved discrimination, yielding an AUC of 0.811. Lipidomic block in Non-MASLD was dominated by lysophosphatidylcholines (LPCs), including LPC O-22:4, LPC O-20:1, LPC O-22:2, while metabolomics block featured mainly Non-MASLD- dominant contributors. In the microbiota block, Non-MASLD group showed higher abundance of *Romboutsia*, *Gemmiger formicilis*, and *Roseburia*, whereas MASLD showed higher *Acutalibacter*, *Blautia caecimuris*, the *Ruminococcus gnavus* group. Cross-layer correlation analysis identified *B. caecimuris* as the strongest cross-omics correlate, showing positive correlations with proinflammatory genera *Holdemania*, *Bilophila* and *Schaalia*, and negative correlations with beneficial *Parasutterella excrementihominis* and *Turicibacter sanguinis* in MASLD group.
Conclusion: Using a multi-omics integration approach, our study reveals microbial consortia associated with the MASLD phenotype in overweight patients. The next step will be to identify small synergistic bacterial consortia as potential therapeutic candidates for MASLD.

SAT-352-YI
Loss of crypt-adjacent barrier-supportive macrophages promotes gut barrier failure and organ injury in alcohol-related hepatitis

Joscha Vonderlin[1], Manqiang Lin[1], Juan Wang[1], Pavitra Kumar[1], Paul Horn[1], Michael Sigal[1], Frank Tacke[1], Felix Heymann[1], Moritz Peiseler[1], Cornelius Engelmann[1]. *[1]Department of Hepatology and Gastroenterology, Charité-Universitätsmedizin Berlin, Campus Virchow-Klinikum and Campus Charité Mitte, Berlin, Germany*
Email: joscha.vonderlin@charite.de

Background and aims: Patients with alcohol-related hepatitis (AH) are at high risk for progression to acute-on-chronic liver failure (ACLF). Intestinal dysbiosis and gut barrier dysfunction contribute to organ injury and inflammation, yet the underlying mechanisms remain poorly understood. We investigated gut barrier dysfunction and the role of intestinal macrophages in organ injury during acute-on-chronic metabolic injury.
Method: *CX3CR1-GFP* reporter mice were fed a Western diet with 10% ethanol for four weeks followed by ethanol binge 24 h before sacrifice. Liver injury was assessed by TUNEL staining, gut barrier dysfunction by multiplex IHC and multiphoton intravital microscopy (IVM). Immune cells were characterized by spectral flow cytometry, dysbiosis by 16 s rRNA seq. Single-cell RNA seq and 10× Xenium spatial platform was used for (spatial) transcriptional profiling. Macrophage-epithelial crosstalk was functionally tested in intestinal assembloid co-cultures. Human validation was performed with 10× Xenium spatial transcriptomics of colon biopsies from ACLF patients.
Results: Liver injury was most pronounced under acute-on-chronic stress. Whereas acute ethanol binge affected the small intestine, chronic and acute-on-chronic injury predominantly targeted the colon, resulting in impaired gut integrity, loss of barrier function,

Ly6Chi monocyte accumulation, reduced GFP$^+$ macrophage size by IVM and dysbiosis. Whilst macrophages after acute ethanol binge promoted proliferation in intestinal assembloids, this effect was abrogated in chronic and acute-on-chronic condition. Single-cell RNA sequencing revealed profound remodeling of colon macrophage compartments under chronic and acute-on-chronic stress, characterized by marked shifts in tissue-resident and monocyte-derived macrophage composition. Loss of crypt-adjacent *Retnla*$^+$*Lpl*$^+$ macrophages led to loss of barrier-supportive factors (Wnt11, PGE2), impaired epithelial regeneration, and extensive inflammatory and stress-related transcriptional reprogramming under acute-on-chronic condition.
Conclusion: The colon is a central driver of organ injury in metabolic and alcohol-related liver disease. Loss of gut function and altered colonic macrophage composition emerge as key contributors, highlighting potential targets to prevent progression to ACLF. We identify a crypt-adjacent, barrier-supportive macrophage population whose loss under chronic metabolic stress is associated with increased gut permeability and susceptibility to secondary insults in gut and liver.

SAT-353
Gut microbiota metabolite butyrate ameliorated acute-on-chronic liver failure by regulating macrophage polarization
Jing Xiao[1], Hang You[1], Zongyi Liu[1], Yong Sun[1], Yu Zhang[1], Li Wei[1], Hong Ren[1], Shiying Li[1], Peng Hu[1], Mingli Peng[1]. [1]*Department of Infectious Diseases, Key Laboratory of Molecular Biology for Infectious Diseases (Ministry of Education), Institute for Viral Hepatitis, the Second Affiliated Hospital, Chongqing Medical University, Chongqing, China*
Email: xiaojingabu@163.com

Background and aims: Gut microbiota dysbiosis and its metabolites disorders drive the progression of Acute-on-chronic liver failure (ACLF) through the gut-liver axis, but the specific mechanisms and intervention targets remain unclear. This study reveals the core protective role and mechanism of the microbially derived metabolite butyrate in ACLF.
Method: Blood and stool samples were collected from 50 patients with liver disease at different stages and subjected to metagenomic, metabolomic, and transcriptomic sequencing to elucidate the microbiota-metabolism-immune characteristics of ACLF. We evaluated changes in gut microbiota composition, short-chain fatty acids, intestinal barrier integrity, liver injury, and immune cell function following fecal microbiota transplantation (FMT) and butyrate supplementation, and explored specific regulatory mechanisms in ACLF mouse models and RAW264.7 cells.
Results: ACLF patients exhibited a significant reduction in gut microbial diversity, characterized by depletion of butyrate-producing bacteria (*Eubacterium, Clostridium, Ruminococcus, Blautia and Odoribacter*) and enrichment of opportunistic pathogens (*Klebsiella*, *Escherichia* and *Enterococcus*). Concurrent with decreased fecal butyrate levels, ACLF patients exhibited elevated levels of intestinal barrier markers D-lactic acid and lipopolysaccharide (LPS), and peripheral monocyte/macrophage infiltration and enhanced M1 polarization. FMT experiments confirmed that microbiota from ACLF patients could induce butyrate metabolic deficiency, barrier impairment, and exacerbated hepatic inflammation in recipient mice. Mechanistically, butyrate supplementation effectively reversed these pathological alterations. It remodeled the gut microbiota, promoting the colonization of beneficial bacteria *Odoribacter*, repaired intestinal tight junction protein expression, reduced plasm LPS levels, and significantly suppressed M1 macrophage polarization both in the liver and peripheral blood. Further investigation revealed that butyrate inhibited the phosphorylation of the mitogen-activated protein kinase signaling pathway within macrophages, thereby suppressing their polarization towards the pro-inflammatory M1 phenotype.
Conclusion: This study reveals a dysfunctional microbiota-metabolism-immune axis centered on butyrate depletion in ACLF, modulating butyrate represented a potential therapeutic strategy for ACLF.

SAT-354-YI
Bile mycobiome diversity classifies fungal peptide signature for early prediction of gallbladder carcinoma
Sanju Yadav[1], Nupur Sharma[1], Manisha Yadav[1], Neha Sharma[1], Gaurav Tripathi[1], Sushmita Pandey[1], Babu Mathew[1], Vasundhra Bindal[1], Vipul Sharma[1], Viniyendra Pamecha[1], Jaswinder Maras[1]. [1]*Institute of Liver and Biliary Sciences, New Delhi, India*
Email: jassi2param@gmail.com

Background and aims: Carcinoma of Gallbladder (CAGB) has poor prognosis. While the bile microbiome and lipidome are associated with CAGB development, the contribution of fungal mycobiome is unexplored. Our study aims to investigate the fungal Mycobiome diversity and correlate it with the incidence of CAGB with classification of top fungal peptides to potentially stratify CAGB patients.
Method: Bile samples were collected from patients undergoing cholecystectomy for Gallstone (GS) disease (n = 30), patients undergoing surgery for CAGB (n = 30), and healthy liver donors (n = 20) were subjected to fungal peptide-based diversity analysis and metabolomics. Results were cross-validated in 80 patients on the plasma samples, correlated with clinical parameters, and subjected to machine learning analysis.
Results: Fungal peptide-based diversity analysis identified 6-Phyla and 24-Fungal species differentially regulated in the bile samples of the study cohort. Fungal diversity (alpha and beta diversity) was significantly higher in CAGB as compared to GS or HC ($p < 0.05$). 93 fungal peptides were upregulated and 63 were downregulated in CAGB ($p < 0.05$, FC>1.5). Linear discriminant analysis significantly segregated CAGB patients with marked increase in Aspergillus wentii (log2FC-12.21), Nosema bombycis (log2FC-11.25), Saccharomyces (log2FC-10.89), Saccharomyces cerevisiae (log2FC-10.68), and Schizosaccharomyces pombe (log2FC-10.38; $p < 0.05$) in the bile samples. Fungal-metabolite correlation analysis (r2>5, $p < 0.05$) identified Aspergillus wentii, Nosema bombycis, and others directly associated with lysine biosynthesis, taurine, and hypotaurine metabolism, fatty acid, and other in bile, and cysteine and methionine metabolism, ascorbate metabolism, purine metabolism, and others in plasma. Probability of detection (POD) calculated using fungal peptides showed a diagnostic efficiency of 96% for segregation of CAGB patients. The identified top 5 fungal peptides were validated using Single Reaction Monitoring analysis that predicted early mortality>90% accuracy/sensitivity, and specificity in a Machine Learning model.
Conclusion: CAGB patients showcase a distinct fungal diversity and identifies fungal peptide panel capable of segregation and early diagnosis of CAGB patients.

SAT-355
Microbial Streptococcal collagen like-1 protein activates fibrosis via transforming growth factor beta receptor 1 kinase in alcohol-associated liver disease
Manisha Yadav[1], Gaurav Tripathi[1], Jayesh Kumar Sevak[1], Vasundhra Bindal[1], Neha Sharma[1], Sanju Yadav[1], Nupur Sharma[1], Babu Mathew[1], Yash Magar[1], Sushmita Pandey[1], Rimsha Rimsha[1], Abhishak Gupta[2], Anupama Kumari[1], Shvetank Sharma[1], Shiv Kumar Sarin[1], Jaswinder Maras[1]. [1]*Institute of Liver & Biliary Sciences, New Delhi, India;* [2]*Artemis Hospital Gurgaon, Gurugram, India*
Email: jassi2param@gmail.com

Background and aims: Alcohol alters gut microbiota, leading to immune dysregulation and liver injury. We investigated how alcohol-related gut microbiota (AGM) reprogram hepatic kinase signaling to drive inflammation and fibrosis in alcohol related liver disease (ALD), and whether these effects can be reversed by fecal microbiota transplantation (FMT).
Method: Liver kinome and stool metaproteome changes were studied in rats (n = 6/group) colonized with severe alcohol-related

hepatitis patients stool (Group I) or ALD rats colonised with healthy human-donors stool (Group II). AGM-linked liver kinome changes were correlated with bacterial genera. Microbial protein; Streptococcal collagen-like protein 1 (Scl1) showed affinity for TGFβR1 and was screened in stool (n = 24), liver (n = 19) of SAH patients and ALD rats. The diagnostic utility of Scl1 for predicting outcome in SAH was validated in 88 patients, and FMT was employed to reduce streptococcal and Scl1 levels.

Results: Stool metaproteomics showed significant increase in *Streptococcus, Staphylococcus,* and *Clostridium* genera both in group I and group II stool (FC>1.5, $p < 0.05$) along with 34kinases associated with inflammation (Mapk14, Map3k10), fibrosis (Tgfbr1, Igf1r), lipid metabolism and regeneration (Met, Bmpr1a) in liver. FMT from healthy donors to ALD rats reversed the expression of *Streptococcus* (10-fold), *Staphylococcus* (3-fold), and *Clostridium* (5-fold), along with 18 kinases associated with inflammation (Btk, Camk4, Nuak1) and fibrosis (Tgfbr1, Col4a1, Fgfr2). Streptococcus showed strong correlation with TGFbR1 kinase. Scl1 (mimics human-collagen structurally) showed strong affinity for TGFβR1 and was significantly elevated in SAH and ALD-rat stool and liver samples (FC>2, $p < 0.05$). Expression of Scl1 was highest amongst all the known ligands for TGFβR1 such as cola1, cola2, tgfb1, and tgfb2 as its abundance was highest suggesting Scl1 as a major contributor for TGFβR1-activation Following FMT, Scl1-levels in plasma and *Streptococcus*-levels in stool significantly reduced by 2.1-folds and 1.9-folds respectively in SAH-patients and Scl1 also predicted poor response and 30-day mortality with high accuracy 0.92-AUC.

Conclusion: Alcohol-induced gut dysbiosis promotes accumulation of Streptococcal Scl1 protein in human gut which mimics human collagen thus has affinity for binding and activating TGFβR1 kinase. Scl1 also predicts poor response in SAH. FMT from healthy donors restores microbial balance and mitigates harmful host-microbe interactions.

SAT-356

Bifidobacterium pseudolongum-derived inosine mitigates polystyrene nanoplastics-induced hepatic injury by inhibiting the polarization of M1 macrophages

Kaikai Zhang[1], Yuchuan Chen[1], Jiayuan Wan[1], Jianzheng Yang[2], Lijian Chen[2], Anding Zhou[2], Qingyuan Li[2], Nian Zhou[2], Jiuyang Ding[2], Qi Wang[2], Jian Sun[1]. *[1]Department of Infectious Diseases, Nanfang Hospital, Southern Medical University, Guangzhou, China, State Key Laboratory of Multi-organ Injury Prevention and Treatment, Key Laboratory of Infectious Diseases Research in South China, Ministry of Education, Guangdong Provincial Key Laboratory for Prevention and Control of Major Liver Diseases, Guangdong Provincial Clinical Research Center for Viral Hepatitis, Guangdong Institute of Hepatology, Guangdong Provincial Research Center for Liver Fibrosis Engineering and Technology, Guangzhou, China; [2]Guangzhou Key Laboratory of Forensic Multi-Omics for Precision Identification, School of Forensic Medicine, Southern Medical University, Guangzhou, China*
Email: sunjian@smu.edu.cn

Background and aims: Nanoplastics (NPs) are ubiquitous pollutants that disturb gut microbiota and cause hepatic injury. Gut microbiota is considered a contributing factor to multiple hepatic injuries. However, its role in NPs-induced hepatic injury remains unclear. Here, we aims to reveal the microbial mechanisms underlying NPs-induced hepatic injury and explore possible strategies targeted at gut microbiota.

Method: 7-week-old male C57BL/6J mice were orally administered with NPs for 28 days to induce hepatic injury. Gut microbiota from NPs-adminstered mice was transplanted into recipients by fecal microbiota transplantation to investigate the role of gut microbiota. *Bifidobacterium pseudolongum* (*B.p*) colonization and its metabolite inosine supplementation were performed to explore their protection on NPs-induced hepatic injury.

Results: Exposure to NPs significantly reduced gut probiotic *Bifidobacterium pseudolongum* (*B.p*) and its metabolite inosine. Gut microbiota from NPs-adminitered mice partially reproduced NPs-related impairment of gut homeostasis and hepatic injury in recipient mice. Moreover, *B.p* colonization improved NPs-induced impairment of gut homeostasis and hepatic injury, and its protective effects were reproduced by supplementation with inosine. Mechanically, *B.p* colonization ameliorated NPs-induced decrease of hepatic inosine and subsequently normalized the expression of its target adenosine receptor A2a (A2AR). Meanwhile, increased inosine inhibited the miR155/SOCS1/NF-κB pathway and repressed NPs-induced hepatic M1 macrophage polarization. Additionally, miR155 knockout alleviated NPs-induced hepatic injury by inhibiting M1 macrophage polarization, but did not influence the suppression of NPs on A2AR. *In vitro*, CGS21680 (an agonist of A2AR) repressed lipopolysaccharide (LPS)-induced polarization of M1 macrophages by inhibiting the miR155/SOCS1/NF-κB pathway.

Conclusion: Gut microbiota partly mediates NPs-induced hepatic injury. *B.p*-derived inosine represses NPs-induced M1 macrophages polarization by inhibiting the miR155/SOCS1/NF-κB pathway via targeting A2AR. Our findings further clarifies the role of gut microbiota in NPs-induced hepatic injury and provides a potential microbial therapeutic strategy.

Hepatocyte biology

TOP-328

Single-cell and spatial transcriptomic profiling of cross-species livers: evaluating genetically engineered pig livers for clinical xenotransplantation

Siming Kong[1], Mingshuo Wang[1], Rongyan Yao[1], Yakun Liu[1], Congwen Bian[2], Bin Wang[1], Tianzi Luo[1], Hui Bai[1], Yunfang Wang[1], Zhong Zeng[2], Jiahong Dong[3]. *[1]Center for Clinical and Translational Science, Beijing Tsinghua Changgung Hospital, Tsinghua University, Beijing, China, Beijing, China; [2]Department of Organ Transplantation, The First Affiliated Hospital of Kunming Medical University, Kunming, China, Kunming, China; [3]Beijing Tsinghua Changgung Hospital, School of Clinical Medicine, Tsinghua University, Beijing, China, Beijing, China*
Email: ksm09410@163.com

Background and aims: Liver xenotransplantation from genetically engineered pigs holds great clinical potential to address the donor organ shortage. However, the molecular and cellular compatibility of pig livers with human physiology remains incompletely understood, particularly regarding lobular zonation and cell-type-specific gene expression. This study aims to perform an integrated single-cell and spatial transcriptomic comparison of human, macaque, wild-type, and gene-edited pig livers, in order to identify transcriptional features that may inform graft selection and immune modulation in clinical xenotransplantation.

Method: Liver tissues from healthy human donors, macaques, wild-type pigs, and multi-gene-edited pigs (8- and 10-gene edits targeting xenoantigens and immunoregulation) were analyzed. Single-cell RNA sequencing (10× Genomics) and spatial transcriptomics (Visium and Stereo-seq) were performed. Cross-species integration, cell type annotation, and zonation analysis were conducted using Seurat, Harmony, and spatial mapping tools. Comparative analyses assessed evolutionary conservation across species and transcriptional alterations in gene-edited pigs relative to wild-type and human reference livers in major hepatic cell types.

Results: Integrated single-cell and spatial transcriptomic analysis revealed a conserved architecture of major hepatic cell types across human, macaque, and wild-type pig livers. We identified distinct transcriptional gradients from periportal to pericentral zones in

metabolic and immune-related pathways common to all species, including—importantly—the first spatial characterization of zonation patterns in pig liver. Compared to wild-type pigs, livers from both 8- and 10-gene-edited pigs showed downregulation of key xenoantigen-related genes in endothelial and Kupffer cells. Spatial analysis indicated preserved lobular organization in edited livers, with intact zonation gradients and transcriptional changes in periportal regions associated with immune regulation.
Conclusion: This study establishes a cross-species transcriptional and spatial resource for liver xenotransplantation research, highlighting the potential of gene-edited pig livers to approximate human hepatic molecular and structural features. Our findings underscore the value of zonation-aware profiling in evaluating donor livers and support further preclinical validation of multi-gene-edited pigs for clinical translation.

THU-303

Dimorphic response between the classical and alternative pathways of liver bile acid synthesis after feeding a high in sucrose and fat, choline-deficient, L-amino acid defined diet to Sprague-Dawley rats

Jianing Zhou [1], Yanhao Qiu[1], Laia Vilà[1,2], Emma Barroso[1,3], Marta Alegret[1,3,4], Núria Roglans[1,3,4], Juan Carlos Laguna[1,3,4]. *[1]School of Pharmacy and Food Sciences, Universitat de Barcelona, Barcelona, Spain; [2]Barcelona, Spain; [3]IBUB, Barcelona, Spain; [4]CIBERObn, Barcelona, Spain*
Email: jclagunae@ub.edu

Background and aims: We have previously shown a clear sexual dimorphism in the fibrotic response of SD rats to a CDAA diet, with only males developing MASH (*J Hepatol* 2025 82 (Suppl 1) FRI-344). In the present work we demonstrate that the CDAA diet also modifies the liver biosynthesis of bile acids (BA) in a dimorphic way.
Method: Male (M) and female (F) SD rats were randomly distributed into 2 groups each: (1) control (CT; standard rodent chow, n = 4), and (2) CDAA (n = 8) and were fed the CT and CDAA diets for three months. At the end of the treatment, rats fasted for 2 h were sacrificed and liver tissue and faecal content were collected and properly stored. The concentrations of 10 BA (cholic acid, chenodeoxycholic acid (CDCA), deoxycholic acid (DCA), lithocholic acid (LCA), ursodeoxycholic acid (UDCA), α-muricholic acid (MCA), β-MCA, hyocholic acid (HCA), hyodeoxycholic acid (HDCA), and murideoxycholic acid (MDCA)) in rat faeces were determined by ultra-high-performance liquid chromatography coupled to tandem mass spectrometry (UHPLC-MS/MS), as described previously (Biomed&Pharmacother 177 (2024) 117067). Liver expression of pertinent genes related to primary BA synthesis was determined.
Results: Control-fed M and F SD rats showed almost no differences in their faecal BA concentrations, except in the case of DCA (×0.59 F *vs* M, p = 0.029). CDAA-fed M and F rats showed marked increases in primary, and total faecal BA concentrations with respect to CT values. However, only CDAA-fed F SD rats showed significant increases in CDCA, UDCA, DCA, LCA, HCA, HDCA, MDCA and MDCA and secondary BA. Furthermore, the total concentration of 12-OH BA (CA, DCA and MDCA) was decreased in CDAA-fed F (×0.78 F *vs* M, p = 0.012), while the total concentration of non-OH BA (CDCA, alpha and beta MCA, HCA, UDCA and LC) was increased (×2.09 F *vs* M, p = 0.0001), pointing to a shift from the classical to the alternative pathway of BA synthesis. Changes in the expression of key enzymes of BA synthesis, such as cytochrome (CYP) 7A1, CYP7B1 and CYP8B1 were in accordance with this shift in the predominant biosynthetic pathway.
Conclusion: There is a clear sexual dimorphism in liver bile acid synthesis induced by feeding a CDAA diet to SD, characterized by an increased activity of the alternative pathway of BA synthesis and an increased production of secondary BA only in F rats.
Funded by PID2023-146140OB-I00 (MICIU/AEI/10.13039/501100011033) and FEDER-UE and 2021SGR-00345.

THU-313

Expandable non-tumorigenic primary-like human hepatocytes from humanized mouse livers retain hepatic function, enable in vivo engraftment, and support robust HBV infection assays

Lennard Anders[1], Lisa Staffeldt[2,3], Lisa Groß[1], Luise Herling[1], Natalie Herzog[1], Anika Volmar[3], Götz Rövenstrunk[3], Tassilo Volz[2,4], Jan-Heiner Küpper[1], Maura Dandri[2,4], Stefan Lüth[3,5], Janine Kah[2,3,5], Sarah Kammerer[1]. *[1]Institute of Biotechnology, BTU Cottbus-Senftenberg, Brandenburg, Germany; [2]Department of Internal Medicine, University Medical Center Hamburg-Eppendorf, Hamburg, Germany; [3]Faculty of Health Sciences Brandenburg, Brandenburg Medical School Theodor Fontane, Brandenburg, Germany; [4]German Center for Infection Research, Hamburg-Lübeck-Borstel Partner Site, Hamburg, Germany; [5]Department of Gastroenterology, Center for Translational Medicine, University Hospital Brandenburg, Brandenburg Medical School Theodor Fontane, Brandenburg, Germany*
Email: lennard-anders@b-tu.de

Background and aims: Freshly isolated primary human hepatocytes (PHH) are the gold standard for liver metabolism and hepatitis B virus (HBV) studies, but limited availability and rapid loss of function limit routine use. We aimed to establish expandable primary-like human hepatocytes (PLHH) from humanized mouse livers and to evaluate their drug metabolism capacity, *in vivo* behavior, and HBV permissiveness.
Method: Single donor PHH were isolated from urokinase-type plasminogen activator/severe combined immunodeficiency (uPA/SCID) mice after successful liver engraftment. Upcyte technology was used to induce proliferation, followed by clonal selection and characterization by quantitative polymerase chain reaction (qPCR) and immunofluorescence. Cytochrome P450 (CYP) activities were quantified by high-performance liquid chromatography with and without induction. Liver repopulation was tested by intrasplenic transplantation into uPA/SCID mice. Carcinogenic properties were evaluated by orthotopic transplantation of luciferase-labeled cells into NOD SCID gamma (NSG) mice. For HBV infection, cultivated cells were inoculated and extracellular HBV DNA was quantified after sequential medium washes; intracellular HBV DNA was quantified by qPCR.
Results: Selected clones proliferated with a population doubling time of 41.0 ± 1.7 h while retaining hepatocyte-like morphology and marker expression. Clones showed donor-dependent CYP expression/activity and were CYP-inducible. Human marker-positive clusters were detected in recipient uPA/SCID livers after transplantation. In NSG mice, bioluminescence signals from transplanted cells were absent or declined over time, indicating no tumour formation. In contrast, HuH7 (positive control) transplantation led to increased liver size and weight. After HBV inoculation, initial supernatant HBV DNA reached 1.4×10^9 IU/mL in Upcyte clones versus 2.7×10^8 IU/mL in HepaRG and decreased with washes to 4.96×10^6 IU/mL (Upcyte clone HU5221), 1.42×10^6 IU/mL (HepaRG) and 1.5×10^5 IU/mL (clone HU1721). Intracellular HBV DNA was up to 80 times higher in Upcyte clones than in HepaRG.
Conclusion: Expandable PLHH isolated and generated from humanized mouse livers combine proliferative capacity with maintaining CYP-dependent drug metabolism, *in vivo* liver repopulation without tumorigenicity, and are suitable for robust HBV studies. This platform can complement PHH for scalable studies on xenobiotic metabolism, HBV biology and many more.

THU-314

Hepatocyte succinate dehydrogenase/complex II loss drives metabolic rewiring critical for liver homeostasis

David Carneros[1], María Ángeles Rodríguez-Hernández[1], Maria Jesus Perugorria[2], Patricia Altea-Manzano[3], Victor Ramos-Herrero[1], Jose Antonio Gonzalez-Reyes[4], Jose López-Barneo[5], Guillermo López-Lluch[6], Matilde Bustos[1]. *[1]Area of Liver, Digestive and Inflammatory Diseases, Institute of Biomedicine of*

Seville (IBiS), Virgen del Rocio University Hospital (HUVR), Spanish National Research Council (CSIC), University of Seville (US), Seville, Spain; [2]Department of Liver and Gastrointestinal Diseases, Biodonostia Research Institute, Donostia University Hospital, University of the Basque Country (UPV-EHU), Donostia-San Sebastian, Spain, CIBERehd, Instituto de Salud Carlos III (ISCIII), Madrid, Spain, Department of Medicine, Faculty of Medicine and Nursing, University of the Basque Country, UPV/EHU, Leioa, Spain, Donostia, Spain; [3]Andalusian Molecular Biology and Regenerative Medicine Centre-CSIC, Seville, Spain; [4]Departamento de Biología Celular, Fisiología e Inmunología, Universidad de Córdoba, Campus de Excelencia Internacional Agroalimentario, ceiA3, Cordoba, Spain; [5]Instituto de Biomedicina de Sevilla (IBiS) Hospital Universitario Virgen del Rocío/CSIC/Universidad de Sevilla, Seville, Spain, Sevilla, Spain; [6]Department of Physiology, Anatomy and Cell Biology, Andalusian Centre for Developmental Biology, CABD-CSIC, Pablo de Olavide University, Seville, Spain
Email: mbustos-ibis@us.es

Background and aims: Cell-type reprogramming in the liver contributes to the changes accompanying liver disease by regulating nutrient availability and producing metabolites that influence disease progression, resolution, or cancer cell growth. Mitochondria integrate cellular metabolism with cell fate decisions and play a central role in liver disease progression. Succinate dehydrogenase (SDH) functions in both the TCA cycle and the electron transport chain and is essential for tissue homeostasis and cell proliferation. This study aimed to investigate how metabolic alterations resulting from SDH deregulation influence hepatocyte plasticity, potentially revealing novel therapeutic strategies targeting metabolic vulnerabilities.
Method: Hepatocarcinoma (HCC) and control tissues (surrounding or normal liver) from two independent patient cohorts were used to investigate gene expression. A hepatocyte-specific SDH knockout mouse model (LSDH) was generated using the Cre-LoxP system. Biochemical and morphological analyses, including optical and ultrastructural studies, were performed. Mitochondrial metabolism was assessed by measuring OXPHOS protein levels and activity, Seahorse assays, and genomic and targeted quantitative liquid chromatography–mass spectrometry (LC-MS) analyses.
Results: *SDHD* mRNA expression and SDH enzymatic activity were significantly reduced in human HCC samples compared with non-tumor and healthy liver tissues. Hepatocyte-specific loss of SDH demonstrated its critical role in maintaining metabolic homeostasis. LSDH mouse livers exhibited liver damage and altered cellular bioenergetics, characterized by a metabolic shift toward increased glycolysis, glycolytic capacity, and glycolytic reserve. SDH ablation promoted pyruvate consumption to sustain maximal glycolytic flux, associated with increased pyruvate carboxylase expression and reduced pyruvate dehydrogenase activity. Metabolic remodeling induced by SDH loss activated the mammalian target of rapamycin (mTOR) pathway, enhanced lipid synthesis, enriched integrated stress response (ISR) gene expression, and impaired mitochondrial complexes I and IV. Notably, the deleterious effects of SDH inhibition were partially mitigated by a specialized diet.
Conclusion: These findings reveal hepatocyte plasticity under SDH deficiency and define a therapeutically exploitable metabolic vulnerability, enabling intervention strategies aimed at restoring metabolic homeostasis or inducing cell death, depending on the therapeutic objective.

THU-315-YI
Hepatic CNNM1 mediates metabolic and epigenetic adaptation to inverted feeding in night-shift worker models

Carolina Conter[1], Giselle Abruzzese[1], Naroa Goikoetxea-Usandizaga[1,2], Irene González-Recio[1], Eleonora Davoli[1], Davide Pietrafesa[3], Emily Perbellini[1], Amaia Navarro-Corcuera[1], José García Consuegra[4], Nerea Ferreiro[1], Claudia M. Rejano-Gordillo[1], Patricia Peña-Sanfélix[1], Leidy Estefanía Zapata-Pavas[1], Jon Ander Barrenechea-Barrenechea[1], Jessica Nurcis[5], Giada Mordenti[1], Mikel Azkargorta[1], Felix Elortza[1], Atish Mukherji[6], Frank Jühling[6], Virginia López[7,8,9,10], Marta Moreno-Torres[2,11,12], Ramiro Jover[2,11,12], Thomas Baumert[6,13,14,15], Matías A. Avila[2,16,17], Ruben Nogueiras[18,19], Mario Fernández[7,8,9,10], Olga Barca-Mayo[20], Luis Alfonso Martinez-Cruz[1], María Luz Martínez-Chantar[1,2]. *[1]Center for Cooperative Research in Biosciences (CIC bioGUNE), Basque Research and Technology Alliance (BRTA), Bizkaia Technology Park, Building 801A, Derio, Spain; [2]Centro de Investigación Biomédica en Red de Enfermedades Hepáticas y Digestivas (CIBERehd), Instituto de Salud Carlos III, Madrid, Spain; [3]Department of Biology, University of Rome Tor Vergata, Rome, Italy; [4]Departamento de Biología Molecular, Centro de Biología Molecular Severo Ochoa, Consejo Superior de Investigaciones Científicas-Universidad Autónoma de Madrid (CSIC-UAM), Madrid, Spain; [5]Dipartimento di Scienze Cliniche e Biologiche, Universitá di Torino, Torino, Italy; [6]University of Strasbourg, Institute of Translational Medicine and Liver Diseases (ITM), Inserm UMR_S1110, Strasbourg, France; [7]Cancer Epigenetics and Nanomedicine Laboratory, Centro de Investigación en Nanomateriales y Nanotecnología-Consejo Superior de Investigaciones Científicas (CINN-CSIC), Universidad de Oviedo, Oviedo, Spain; [8]Instituto de Investigación Sanitaria del Principado de Asturias (ISPA-FINBA), Universidad de Oviedo, Oviedo, Spain; [9]Instituto Universitario de Oncología del Principado de Asturias (IUOPA), Universidad de Oviedo, Oviedo, Spain; [10]Centro de Investigación Biomédica en Red de Enfermedades Raras (CIBERER), Instituto de Salud Carlos III (ISCIII), Madrid, Spain; [11]Department of Biochemistry and Molecular Biology, University of Valencia, Valencia, Spain; [12]Joint Research Unit in Experimental Hepatology, Health Research Institute La Fe (IIS La Fe), Valencia, Spain; [13]Gastroenterology and Hepatology Service, Strasbourg University Hospitals, Strasbourg, France; [14]Institut Universitaire de France, Paris, France; [15]IHU, Strasbourg, France; [16]Instituto de Investigaciones Sanitarias de Navarra (IdiSNA), Pamplona, Spain; [17]Hepatology Laboratory, Solid Tumors Program, CIMA, CCUN, University of Navarra, Pamplona, Spain; [18]Department of Physiology, CiMUS, University of Santiago de Compostela, Santiago de Compostela, Spain; [19]CIBER Fisiopatología de la Obesidad y Nutrición (CIBEROBN), Instituto de Salud Carlos III, Córdoba, Spain; [20]Circadian and Glial Biology Lab, Physiology Department, Molecular Medicine and Chronic Diseases Research Centre (CiMUS), University of Santiago de Compostela, Santiago de Compostela, Spain*
Email: cconter@cicbiogune.es

Background and aims: Circadian misalignment, as occurs during night-shift work, challenges the liver to adjust its metabolic and transcriptional pathways in response to altered feeding times. Analysis of publicly available liver transcriptomic datasets revealed oscillatory expression of the Cyclin M1 magnesium transporter (CNNM1), a protein normally expressed at low levels in the liver, suggesting a potential role in hepatic adaptation to feeding-time shifts. Here, we investigated whether CNNM1 is required for the liver to respond to inverted feeding.
Method: Male Alb-Cre mice were assigned to three groups: ad libitum control, inverted feeding, or inverted feeding with hepatic *Cnnm1* silencing via a Cre-dependent AAV8. Inverted feeding was implemented using smart-cage feeders (8am–8pm) to simulate night-shift conditions for 3 weeks, with identical diet composition and caloric intake across groups. Liver samples were analyzed using metabolic, proteomic, and epigenetic approaches.
Results: Hepatic *Cnnm1* silencing considerably disrupted the liver's adaptive response to inverted feeding. In response to inverted feeding, livers underwent robust transcriptional and proteomic remodeling, reflecting metabolic adaptation to the shifted feeding schedule. By contrast, livers with hepatic *Cnnm1* silencing largely failed to respond to inverted feeding and instead maintained transcriptional and proteomic profiles similar to ad-libitum controls, indicating a loss of feeding-time–dependent metabolic flexibility. In particular, lipid biosynthesis, that were strongly activated in inverted-

feeding mice,remained largely unchanged in *Cnnm1*-silenced livers at both transcriptional and protein levels. Epigenetically, proteomic analysis identified KDM5A, a histone demethylase, as a downstream effector associated with CNNM1 silencing, while Western blot confirmed modulation of WDR5, a key chromatin regulator. These changes were accompanied by alterations in associated histone marks, demonstrating that CNNM1 is required for adaptive chromatin remodeling during inverted feeding.
Conclusion: CNNM1, although typically expressed at low levels in the liver, is essential for both metabolic and epigenetic reprogramming in response to circadian feeding disruption. Its absence locks the liver in a control-like state, preventing adaptation to inverted feeding and highlighting that even a decreased expressed magnesium transporter can exert a profound effect on hepatic metabolic flexibility in mice mimicking night-shift work conditions.

THU-316
When the clock breaks: H2S as a link between night shift work and metabolic health
Carolina Conter[1], Naroa Goikoetxea-Usandizaga[1,2], Rui Zhou[1,3], Giselle Abruzzese[1], Irene González-Recio[1], Nerea Ferreiro[1], Eleonora Davoli[1], Patricia Peña-Sanfélix[1], Leidy Estefanía Zapata-Pavas[1], Mikel Azkargorta[1], Felix Elortza[1], Marta Moreno-Torres[2,4,5], Ramiro Jover[2,4,5], Alba Tomás-Alvarado[6], Olga Barca-Mayo[7], Manuel Tena-Sempere[8,9,10], Raul M. Luque[8,9,10], Francisco J. Ortega[10,11], José Luis Cantero[12,13], Juan Pedro Bolaños[6,14,15], Montserrat Romero[16,17,18,19], Antonio Zorzano[16,17,18], Luis Alfonso Martinez-Cruz[1], María Luz Martínez-Chantar[1,2]. *[1]Center for Cooperative Research in Biosciences (CIC bioGUNE), Basque Research and Technology Alliance (BRTA), Bizkaia Technology Park, Building 801A, Derio, Spain; [2]Centro de Investigación Biomédica en Red de Enfermedades Hepáticas y Digestivas (CIBERehd), Instituto de Salud Carlos III, Madrid, Spain; [3]Animal Nutrition Institute, Sichuan Agricultural University, Chengdu, China; [4]Department of Biochemistry and Molecular Biology, University of Valencia, Valencia, Spain; [5]Joint Research Unit in Experimental Hepatology, Health Research Institute La Fe (IIS La Fe), Valencia, Spain; [6]Institute of Functional Biology and Genomics, University of Salamanca, Salamanca, Spain; [7]Circadian and Glial Biology Lab, Physiology Department, Molecular Medicine and Chronic Diseases Research Centre (CiMUS), University of Santiago de Compostela, Santiago de Compostela, Spain; [8]Department of Cell Biology, Physiology, and Immunology, University of Córdoba, Córdoba, Spain; [9]Instituto Maimónides de Investigación Biomédica de Córdoba (IMIBIC), Córdoba, Spain; [10]CIBER Fisiopatología de la Obesidad y Nutrición (CIBEROBN), Instituto de Salud Carlos III, Córdoba, Spain; [11]Service of Diabetes, Endocrinology and Nutrition (UDEN), Institut d'Investigació Biomèdica de Girona (IDIBGI), Girona, Spain; [12]Laboratory of Functional Neuroscience, Pablo de Olavide University, Seville, Spain; [13]CIBER de Enfermedades Neurodegenerativas (CIBERNED), Instituto de Salud Carlos III, Madrid, Spain; [14]Centro de Investigación Biomédica en Red sobre Fragilidad y Envejecimiento Saludable (CIBERFES), Instituto de Salud Carlos III, Madrid, Spain; [15]Institute of Biomedical Research of Salamanca, University Hospital of Salamanca, University of Salamanca, Salamanca, Spain; [16]Institute for Research in Biomedicine (IRB Barcelona), The Barcelona Institute of Science and Technology, Barcelona, Spain; [17]Departament de Bioquímica i Biomedicina Molecular, Facultat de Biologia, Universitat de Barcelona, Barcelona, Spain; [18]CIBER de Diabetes y Enfermedades Metabólicas Asociadas (CIBERDEM), Instituto de Salud Carlos III, Madrid, Spain; [19]Institut de Biomedicina de la Universitat de Barcelona (IBUB), Universitat de Barcelona (UB), Barcelona, Spain*
Email: cconter@cicbiogune.es

Background and aims: Night-shift work disrupts circadian rhythms, increasing the risk of metabolic and liver dysfunction. Feeding schedules are emerging as key regulators of hydrogen sulfide (H_2S) metabolism, redox balance, and one-carbon pathways. We aimed to determine how circadian feeding disruption affects peripheral metabolism, particularly hepatic transsulfuration and related pathways, and whether a targeted plant-based diet can restore metabolic homeostasis and induce metabolic rewiring.
Method: Male C57BL/6 mice were assigned to three groups: ad libitum control feeding with chow diet, inverted feeding with chow diet, or inverted feeding with a plant-based diet composed of chickpea, pea, and lentil flours for three weeks. Inverted feeding was implemented using smart-cage feeders (8am–8pm) to simulate night-shift conditions. Hepatic and systemic H_2S production, oxidative stress, and metabolites in the transsulfuration, methionine, folate and polyamines pathways were measured. Transcript levels of the H_2S-producing enzymes cystathionine beta-synthase (CBS), cystathionine gamma-lyase (CSE), and mercaptopyruvate sulfurtransferase (MPST) were quantified.
Results: Inverted feeding increased mice body weight, fasting glucose, and insulin resistance. At the hepatic level, it reduced H_2S production, induced oxidative stress, and disrupted methionine, transsulfuration, folate, and polyamine metabolism, accompanied by significant downregulation of CBS expression. Inverted feeding with the plant-based diet restored hepatic H_2S levels, improved redox balance, and induced profound metabolic rewiring, normalizing folate- and betaine-dependent fluxes across interconnected pathways. Hepatic phosphoserine aminotransferase expression increased 185-fold, reflecting extensive adaptive remodeling of liver metabolism.
Conclusion: Our murine model of night shift work disrupts H_2S-dependent transsulfuration and alters one-carbon metabolism, leading to oxidative stress and metabolic imbalance in the liver. A legume-based plant diet effectively reverses these changes, promotes metabolic rewiring, increases H_2S availability, and restores methionine, transsulfuration, folate, and polyamine metabolism. These results highlight how night shift work may influence liver metabolism and suggest that targeted dietary interventions could help mitigate the metabolic consequences associated with night shift schedules.

THU-317
Peptide-decorated DNA nanostructures enable programmable lysosomal interference in liver cells
Petra Elblová[1], Minghui Liu[2], Alicia Calé[1], Hana Andělová[3], Mariia Lunova[4], Milan Jirsa[4], Nicholas Stephanopoulos[2], Oleg Lunov[3]. *[1]Department of Optical and Biophysical Systems, Institute of Physics of the Czech Academy of Sciences, Prague, 18221, Czech Republic, Faculty of Mathematics and Physics, Charles University, Prague, 12116, Czech Republic, Prague, Czech Republic; [2]School of Molecular Sciences, Arizona State University, Tempe, Arizona 85287, United States, Biodesign Center for Molecular Design and Biomimetics, Arizona State University, Tempe, United States, Tempe, United States; [3]Department of Optical and Biophysical Systems, Institute of Physics of the Czech Academy of Sciences, Prague, 18221, Czech Republic, Prague, Czech Republic; [4]Institute for Clinical & Experimental Medicine (IKEM), Prague, 14021, Czech Republic, Prague, Czech Republic*
Email: elblova@fzu.cz

Background and aims: DNA nanostructures provide programmability at the molecular level and geometric control. Although lysosomes are an essential focus within cells for liver cell metabolism, immune response signaling, and cell death pathways, there have been no rational approaches toward manipulating lysosomal functionality. We set out with the objective of developing a simple biodegradable DNA nanostructure platform with controlled lysosomal interference within liver cell models and understanding the influences of surface chemistry and cell mechanics.
Method: A six-helix bundle DNA structure was created and electrostatically coated with either a decalysine peptide or a bioplex peptide composed of an aurein 1.2 sequence. The cell models were based on human liver cell lines, including HepG2 and Huh7, as well as an Alexander cell line. Uptake experiments were conducted under

specific geometric constraints. The effects on lysosomal localization, pH, structure, metabolism, immune response, and cytotoxicity were measured. Techniques included high-resolution confocal microscopy and Förster resonance energy transfer.
Results: Uptake of DNA nanostructures was highly dependent on actin cytoskeletal rearrangement due to geometric constraints, thus underlining the importance of cellular mechanics as a determinant for nanostructure internalization. After internalization, the nanostructures localized within lysosomes, and these lysosomes displayed responses based on surface peptide conjugation. At low doses, conjugation with decalysine-coated nanostructures caused lysosomal acidification and changes in cellular metabolism without inducing cytotoxic effects. Conversely, aurein-based peptide-coated nanostructures triggered an increase in lysosomal pH and innate immune signaling. Higher doses caused permeabilization of lysosomal membranes and mitochondrial dysfunction and death. Notably, these responses could be controlled based on concentration using the same DNA scaffold.
Conclusion: DNA nanostructures with minimal peptide decoration offer a rational and flexible platform for targeted interference in lysosomes within hepatocytes. By combining nanostructure research with cellular biomechanics, it becomes possible to have controlled modulation of lysosomal function and activity, as well as immune and cell viability responses. These research works have set fundamental guidelines for the generation of organelle-directed nanomaterials.

THU-318
Bile pressure-dependent metabolic collapse and cytoskeletal remodeling in hepatocytes in experimental model of biliary hypertension
Himanshi Himanshi[1], Rajni Yadav[1], Vaibhav Tiwari[1], Aishwarya Bhatnagar[1], Kapish Gupta[2], Amar Mukund[1], Shridhar Sasturkar[1], Savneet Kaur[1], Shiv Kumar Sarin[1], Dinesh Mani Tripathi[1]. [1]*Institute of Liver & Biliary Sciences, New Delhi, India;* [2]*Indian Institute of Technology, Guwahati, India*
Email: dineshmanitripathi@gmail.com

Background and aims: Cholestasis can cause severe hepatotoxicity and increased biliary pressure leading to biliary hypertension. Dynamic changes occurring in hepatocytes in biliary pressure dependent manner remains unexplored. We aimed to investigate bile canalicular metabolic dynamics and adaptation in response to bile fluid stasis and underlying mechanisms.
Method: Primary hepatocyte isolated from bile duct ligation model (BDL) after 2 h, 4 h, 24 h, 7 d, molecular analysis, unbiased proteomics, metabolomic studies were done. Bile fluid dynamics, Biochemical, histological, imaging, SEM/TEM carried out.
Results: Increased hepatocyte CD13 expression and SEM confirmed progressive bile canalicular dilation. Multiomic profiling of primary hepatocyte post BDL reveals cellular reprogramming. At 24 h proteomics revealed early cytoskeletal destabilization (KRT6A −4, KRT14 −1.6, MACF1 −3.4, DSTN −2, ACTB −1.8 and cofilin −1.6). Suppression of junctional proteins (Connexin32 −2.3, Connexin26 −1.9, IntegrinB1 −2.1 and Claudin −1.8) indicating loss of hepatocyte polarity and canalicular integrity supported by depletion of spisulosine and sphinganine. Nuclear-deformation aligned with transmission of mechanical stress to nucleus, consistent with TEM. Metabolically, early BDL(2–4 h) induced rapid metabolic suppression, redox adaptation (GSTA1 −2.2, GLUL −3.3 and CYP2C11 −3.3), alongside metabolomic enrichment of carnitine (+3.1) and sulfur-containing metabolites. By 24 h, suppression of glycolysis (GCK −2.1, PFKFB1 −1.6) and lipid b-oxidation (CROT −2.5, ACSF2 −1.9, HSD17B12 −3.2), together with mitochondrial dysfunction (NDUFA3 +2.1, NDUFC2 +1.9, COQ3 −1.9, TIMM22 +2, GFM1 +1.5), depletion of spermine (−2.5) and PGE2 (-3.09) reflected metabolic collapse. By 7 d, hepatocytes exhibited inflammatory activation (haptoglobin +2.54, complement C3 +2.1), while persistent suppression of detoxification and failure of metabolic recovery. These alterations paralleled rising biliary pressure (12.2 mmHg immediate; 16 mmHg at 2–4 h, 14.2 mmHg at 24 h, 20 mmHg at 7d), similar to patients (12.6 mmHg), defining a pressure-driven cascade causing hepatocyte structural and metabolic failure.
Conclusion: Biliary hypertension disrupts bile canalicular membrane, drives cytoskeletal and nuclear changes and induces cellular stress with metabolic dysfunction in hepatocytes. This pressure-driven remodeling underlies cholestatic injury, and targeting early adaptive responses may limit disease progression.

THU-319
Molecular dynamics simulations reveal how hepatitis B virus preS1 haplotypes modulate the protective efficacy of the host sodium taurocholate cotransporting polypeptide S267F variant
Po-Hsien Hsu[1,2], Hsiang-Hsuan Chuang[2,3], Ding-Lian Wang[2,4], Chih-Jen Huang[2], Mei-Hung Pan[2], Hwai-I Yang[2]. [1]*Graduate Institute of Life Sciences, College of Biomedical Sciences, National Defense Medical University, Taipei, Taiwan;* [2]*Genomics Research Center, Academia Sinica, Taipei, Taiwan;* [3]*School of Medicine, Chung Shan Medical University, Taichung, Taiwan;* [4]*Graduate Institute of Life Science, National Defense Medical University, Taipei, Taiwan*
Email: ericchu102001@gmail.com

Background and aims: Chronic hepatitis B virus (HBV) infection is a global driver of hepatocellular carcinoma (HCC). Viral entry into hepatocytes relies on the interaction between the myristoylated preS1 domain and the host receptor sodium taurocholate cotransporting polypeptide (NTCP). The East Asian-predominant NTCP S267F variant confers protection against HBV infection and HCC; however, its protective efficacy shows marked inter-individual heterogeneity. While S267F impairs viral binding *in vitro*, the structural basis for how specific preS1 variants bypass this restriction to cause clinical heterogeneity remains unclear. We investigated these mechanisms using all-atom molecular dynamics simulations (MDS).
Method: Building on our prior deep sequencing analysis of the REVEAL-HBV cohort (n = 377), which identified NTCP S267F-dependent differences in preS1 haplotype distribution defined by residues 10, 17, and 35 (QSG vs. KAR), these haplotypes were selected as representative variants for structural simulation. Simulations of myristoylated preS1–NTCP complexes in phospholipid bilayer systems were prepared using CHARMM-GUI and performed using GROMACS with the CHARMM36 m force field. Four combinations (NTCP WT/S267F and preS1 QSG/KAR) were simulated with 1-μs production runs. Binding free energies and interfacial contact frequency were used to characterize binding stability and conformational dynamics.
Results: In alignment with our previous clinical findings that NTCP S267F confers protection against QSG-associated HCC risk, MDS demonstrated that the NTCP S267F substitution introduces steric hindrance, impairing binding stability for the QSG haplotype. In contrast, the KAR preS1 haplotype exhibited conformational compatibility with both NTCP variants, maintaining embedding and interfacial interactions across receptor backgrounds. Quantitative MDS metrics suggested that the KAR variant partially compensates for the structural constraints imposed by S267F, thereby preserving effective receptor engagement sufficient to avoid complete entry disruption.
Conclusion: Our results demonstrate that preS1 haplotypes defined by residues 10, 17, and 35 are critical determinants of the protective efficacy of the host NTCP S267F variant. The ability of the KAR haplotype to maintain receptor binding in the presence of S267F provides molecular-level evidence of host-driven viral adaptation and offers a mechanistic explanation for the observed heterogeneity in HCC risk reduction among carriers of this protective host genotype.

THU-320

Plectin-dependent hepatocyte mechanics modulate liver fibrogenesis

Markéta Jiroušková[1], Srikant Ojha[1], Katerina Korelova[1], Lenka Sarnová[1], Herbert Schiller[2], Daniel Kytyr[3], Eva Sticova[4], Martin Gregor[1]. [1]*Institute of Molecular Genetics of the Czech Academy of Sciences, Prague, Czech Republic;* [2]*Helmholtz Munich, Research Unit Precision Regenerative Medicine, Comprehensive Pneumology Center, Munich, Germany;* [3]*Institute of Theoretical and Applied Mechanics of the Czech Academy of Sciences, Prague, Czech Republic;* [4]*Institute for Clinical and Experimental Medicine, Prague, Czech Republic*
Email: marketa.jirouskova@img.cas.cz

Background and aims: The development of chronic liver disease on the background of fibrosis is associated with profound alterations in liver mechanical properties, which predispose the liver to malignant transformation. Using hepatocyte-specific deletion of the major cytolinker protein plectin as a model of altered hepatocyte cytoarchitecture, we investigated how modulation of the hepatic mechanical environment affects fibrosis development.
Method: Liver-specific plectin knockout ($Ple^{\Delta alb}$) mice and their wild-type counterparts were subjected to hepatotoxic fibrosis induced by carbon tetrachloride. Primary hepatocytes were used to characterize the consequences of plectin loss on hepatocyte mechanical properties, cytoskeletal organization and function *in vitro*.
Results: Exploratory analysis of human chronic liver disease datasets from the Gene Expression Omnibus revealed significant upregulation and dynamic regulation of plectin gene expression across fibrotic stages. Hepatocyte-specific plectin deficiency resulted in alterations of liver mechanical properties and was associated with significantly attenuated fibrosis development *in vivo*. Analysis of hepatic stellate cells demonstrated their delayed activation in the $Ple^{\Delta alb}$ hepatocyte environment both *in vitro* and *in vivo*, attributable to reduced parenchymal stiffening following hepatotoxic injury, as determined by atomic force microscopy. Furthermore, plectin loss enhanced hepatocyte keratin expression in response to injury, leading to activation of the pro-survival Akt pathway. *In vitro* analyses revealed that actin cytoskeleton dysregulation in plectin-deficient hepatocytes increased actomyosin contractility, contributing to protection against hepatotoxic injury. Consequently, portal vein-associated hepatocytes in $Ple^{\Delta alb}$ livers exhibited increased nuclear YAP localization, resulting in reduced apoptosis mediated in part by upregulated EGFR expression. Additionally, actin cytoskeleton dysregulation led to an expanded subpopulation of Annexin A2-positive migratory hepatocytes, which contributed to accelerated tissue repair following liver injury.
Conclusion: Together, our findings findings uncover a previously unrecognized role of plectin-dependent cytoskeletal organization in liver fibrogenesis and identify cytoskeleton-dependent mechanotransduction as a promising therapeutic target for limiting fibrosis progression.

THU-321

Precursor of chemically expanded hepatocytes (pre-cHep) with 1-million-fold expansion potential and liver repopulation capacity

Keisuke Kaji[1], Mylinh Huynh[1], Jakob Jeriha[1], Rebecca Granskog[1], Cherie Law[2], Yuichiro Higuchi[3], Stephen Tsui[2], Hiroshi Suemizu[3]. [1]*University of Edinburgh, Edinburgh, United Kingdom;* [2]*Chinese University of Hong Kong, Hong Kong, China;* [3]*Central Institute for Experimental Medicine and Life Science, Kawasaki, Japan*
Email: keisuke.kaji@ed.ac.uk

Background and aims: Cryopreserved primary human hepatocytes (PHH) are indispensable for toxicology testing, drug screening, and disease modelling, but their limited lot sizes and variable quality hinder standardisation. Alternative cell sources, including pluripotent stem cell-derived hepatocyte-like cells, induced hepatocytes generated by fibroblast reprogramming, and immortalised hepatocyte lines, generally lack mature hepatocyte functions. Reprogramming mature hepatocytes into a proliferative state and organoid culture have recently emerged as promising strategies to expand fully functional hepatocytes; however, these cells have not maintained robust liver repopulation capacity beyond approximately 10^4-fold expansion. Therefore, we aimed to optimise hepatocyte expansion culture conditions to generate large quantities of fully functional hepatocytes for research and therapeutic applications.
Method: Previous studies have reported culture conditions that convert mature human hepatocytes into bipotent liver progenitors with high proliferative potential. In our hands combining these conditions resulted in loss of re-differentiation capacity to hepatocytes within one month. We therefore hypothesised that supplementing the culture medium with factors that promote hepatocyte maturation would keep the cells closer to mature hepatocytes and prolong their ability to re-differentiate.
Results: Consistent with this hypothesis, supplementation with forskolin, dibutyryl-cAMP, and IL-6 enabled reprogramming of mature human hepatocytes into precursor cells. These precursors of chemically expanded hepatocytes (pre-cHep) proliferated for over 30 days and achieved up to a 10^6-fold expansion, theoretically yielding 10^{12} cells from an initial 1×10^6, hepatocytes. Throughout this period, pre-cHep retained liver repopulation capacity comparable to cryopreserved PHH in immunocompromised mice. Moreover, pre-cHep efficiently differentiated into chemically expanded hepatocytes (cHep) in 7 days under 3D culture conditions, and these cHep exhibited global gene expression profiles closely resembling those of 3D-cultured adult PHH.
Conclusion: We successfully established pre-cHep lines from 9 of 10 donors (0–10 years old), underscoring the robustness and reproducibility of this culture system. Pre-cHep/cHep therefore represent a bona fide alternative to primary hepatocytes for diverse in vitro applications and constitute a potential cell source for future hepatocyte-based therapeutic strategies.

THU-322-YI

Liver-ETFDH deletion leads to cholestasis and glucose homeostasis disruption

Jose Maria Lanza-Arnaiz[1,2], Beñat Salegi Ansa[1,2], Tzoline Topdjian Panosian[1], Pablo Sánchez-Aguilera[1], Laura Formentini[1,2,3]. [1]*Centro de Biología Molecular Severo Ochoa (CBM), Universidad Autónoma de Madrid (UAM), Madrid, Spain;* [2]*Instituto de Investigación Hospital 12 de Octubre, i+12, Madrid, Spain;* [3]*Instituto de Biología Molecular (IUBM), Universidad Autónoma de Madrid (UAM), Madrid, Spain*
Email: jmlanza@cbm.csic.es

Background and aims: Electron transfer flavoprotein dehydrogenase (ETFDH) is a mitochondrial coenzyme Q reductase that acts as a central metabolic hub, coupling fatty acid oxidation (FAO) and amino acid catabolism to oxidative phosphorylation. Despite its fundamental role in cellular energy homeostasis and mitochondrial function, the pathophysiological relevance of ETFDH in liver biology remains largely unexplored. Therefore, our aim was to generate and characterize the first liver-specific ETFDH knockout mouse model, enabling the dissection of ETFDH-dependent metabolic and signalling pathways in hepatic pathophysiology.
Method: An albumin-Cre–driven ETFDH knockout (ETFDH–/–) mouse model was generated. Hepatic structure and function were assessed using serum biochemistry, histological analyses, transmission electron microscopy, and integrated proteomic and lipidomic profiling. Glucose and lipid metabolism were evaluated under both fed and fasting conditions using complementary in vivo and ex vivo metabolic approaches, including indirect calorimetry in metabolic cages, glucose and insulin tolerance tests, ex vivo liver slice metabolism, and blood hormone measurements.
Results: Hepatocyte-specific deletion of ETFDH caused a severe disruption of hepatic homeostasis. ETFDH–/– livers displayed

pronounced fibrosis and elevated serum alanine aminotransferase levels. Ultrastructural analysis revealed onion-like aberrant structures in bile canaliculi, indicative of intrahepatic cholestasis, further supported by elevated serum bile acid levels. Metabolic analyses revealed profound alterations in hepatic glucose and lipid metabolism, including impaired ketogenesis and FAO, leading to hypoglycaemia. Excess glycogen accumulation was observed under both fed and fasting conditions, indicating defective glycogenolysis. In vivo testing demonstrated glucose intolerance with preserved insulin sensitivity. Consistently, ETFDH−/− mice failed to secrete insulin in response to a glucose challenge, ultimately resulting in a systemic energy crisis and premature death due to severe hypoglycaemia during juvenile development.
Conclusion: Liver-specific deletion of ETFDH results in major disruptions of hepatic energy metabolism, affecting both fatty acid and glucose homeostasis. These alterations are associated with impaired cellular energy balance and secondary dysregulation of pancreatic endocrine function. Collectively, these findings identify ETFDH as a critical regulator of liver homeostasis and systemic metabolic balance.

THU-323
Integrated proteomic and glycoproteomic landscape of human and pig liver: a cross-species comparative analysis
Yakun Liu[1], Rongyan Yao[1], Siming Kong[1], Mingshuo Wang[1], Congwen Bian[2], Bin Wang[1], Tianzi Luo[1], Hui Bai[1], Yunfang Wang[1], Zhong Zeng[2], Jiahong Dong[3]. *[1]Center for Clinical and Translational Science, Beijing Tsinghua Changgung Hospital, Tsinghua University, Beijing, China; [2]Department of Organ Transplantation, The First Affiliated Hospital of Kunming Medical University, Kunming, China; [3]Beijing Tsinghua Changgung Hospital, School of Clinical Medicine, Tsinghua University, Beijing, China*
Email: mikeliuair@gmail.com

Background and aims: Liver xenotransplantation using pigs is limited by short graft survival. Although genetic editing has successfully eliminated major xenoantigens, profound molecular differences between pig and human livers persist. These residual incompatibilities have not been systematically interpreted from an integrated proteomic and glycoproteomic perspective. Here, we conducted the first human–pig liver proteome and glycoproteome comparative analysis to elucidate species- and gene-editing-dependent molecular incompatibilities and to assess whether unresolved protein and glycoform differences underlie limited xenograft survival.
Method: Perfused liver samples from two human donors (healthy human liver, HHL; brain-dead human liver, BDHL) and six pigs (wild-type pig liver, WTPL; 8 gene-edited pig liver, 8GEPL; 10 gene-edited pig liver, 10GEPL) were analyzed using label-free quantitative proteomics and glycoproteomics. Data-independent acquisition mass spectrometry was performed with searches against an in-house spectral library and the UniProt database.
Results: Proteomic analysis showed that HHL and WTPL share conserved core metabolic functions, whereas BDHL differs markedly. Compared with WTPL, 10GEPL upregulated defense and complement pathways while suppressing metabolism, whereas 8GEPL displayed attenuated though more variable changes. Notably, glycoproteomic profiling revealed increased fucosylation and sialofucosylation in gene-edited pig livers and aberrant glycosylation pattern in BDHL. After inspecting site-specific glycosylation differences across species, thirteen immune, metabolic, complement, and coagulation-related glycoproteins (e.g. Haptoglobin, C4A, THY1) were identified and may relate to limited xenograft survival. Specifically, elevated CD5L, a macrophage activation marker, indicated sustained immune activation in gene-edited pig livers, suggesting unintended immunogenic effects of genetic engineering.
Conclusion: This study conducted the first comparative analysis of human and pig liver proteome and glycoproteome, and revealed recipient-context differences and non-linear molecular effects of gene editing, including novel site-specific glycoform changes on key immune and hemostatic glycoproteins. Together, these findings extended the molecular definition of xenograft incompatibility beyond protein abundance and established a quantitative molecular framework for understanding xenograft incompatibility and guiding translational liver xenotransplantation.

THU-324-YI
Hyperoxidized albumin triggers proteasomal and lysosomal dysfunction compromising albumin endocytosis, degradation and recycling in alcohol-associated liver disease
Babu Mathew[1], Nupur Sharma[1], Deepanshu Sharma[2], Sushmita Pandey[1], Sadam H. Bhat[1], Vipul Sharma[1], Gaurav Tripathi[1], Vasundhra Bindal[1], Manisha Yadav[1], Neha Sharma[1], Sanju Yadav[1], Shvetank Sharma[1], Shiv Kumar Sarin[1], Jaswinder Maras[1]. *[1]Institute of Liver & Biliary Sciences, New Delhi, India; [2]National Institute of Immunology, New Delhi, India*
Email: jassi2param@gmail.com

Background and aims: Human serum albumin (HSA) circulates mainly as functional human mercaptalbumin (HMA), while oxidized human Nonmercaptalbumin 1 (HNA1) and human Nonmercaptalbumin 2 (HNA2) comprise about 25% and 5% respectively. In alcohol-associated liver disease (ALD), HNA1 and HNA2 are markedly increased. Although known as severity biomarkers, their intrahepatic effects on proteasomal and lysosomal activity and albumin recycling remain poorly defined.
Method: We examined the pathogenic impact of oxidized albumin isoforms using three approaches: (i) administration of HMA, HNA1, or HNA2 to healthy rats (n = 6/group) followed by proteomic, metabolomic, and albumin isoform functionality analyses in liver and plasma; (ii) repetition of these treatments in ethanol-fed ALD rats (n = 6/group); and (iii) validation in human liver biopsy and plasma from individuals with alcohol-associated cirrhosis (AAC, n = 10) and severe alcohol-associated hepatitis (SAH, n = 12) using RNA sequencing and proteomics.
Results: Exogenous HNA1 and HNA2 induced acute liver dysfunction, with HNA2 producing the greatest increases in injury markers and inflammatory mediators (FC>1.5, $p < 0.05$). HNA1 at SAH-relevant concentration (2.5 g/kg) increased lipogenesis and fibrogenic signaling (TGF-β, IL-17A), whereas HNA2 preferentially activated IL-6, MAPK, and NF-κB pathways (FC>1.5, $p < 0.05$) compared with HMA in healthy rats. Proteins mediating albumin endocytosis (Fcgrt, Cubn, Lrp2, Amn), endosomal docking (Vamp4, Stx2, Stx6), proteasomal degradation (Ecpas, Psma3, Psmb3), lysosomal function, and vesicular trafficking were reduced after HNA1 exposure and further decreased after HNA2 ($p < 0.05$), indicating impaired protein recycling and potential accumulation of pathogenic albumin. Hepatic proteasome expression reduced with increased IL-6 and TNF-α ($p < 0.05$). In ALD rats, HNA2 caused death within 2hours and suppressed proteins involved in albumin endocytosis, trafficking, and exocytosis ($p < 0.05$). These effects were confirmed in SAH plasma and biopsy, showing reduced HMA, accumulation of HNA1/HNA2, and downregulation of genes involved in albumin recycling (FC>1.5, $p < 0.05$).
Conclusion: Hyper-oxidized albumin disrupts hepatic endocytosis, endosomal docking, lysosomal function, exocytosis, and proteasome activity, leading to defective albumin recycling and degradation, thereby driving proteostasis failure, liver injury, and worsening clinical outcomes in ALD.

THU-329
Regulation of hepatic physiology and metabolism by the mitochondrial NAD+ transporter, SLC25A51
Sarmistha Mukherjee[1], Ricardo Velázquez Aponte[1], Gabriel Adzika[1], Nicole Bye[1], Hannah Vanblarcom[1], Teresa Xiao[1], Adarsh Ramamurthy[1], Joseph Baur[1]. *[1]University of Penn-Medical, Philadelphia, United States*
Email: Sarmuk@pennmedicine.upenn.edu

Background and aims: A development in the field has been the identification of SLC25A51 as a mammalian mitochondrial NAD^+ carrier by our group and others. We have recently employed modulation of SLC25A51 to alter the mitochondrial NAD^+ pool in hepatocytes and to establish that it is limiting during liver regeneration. Overexpression of SLC25A51 is sufficient to recapitulate the enhancement of liver regeneration seen with systemic NAD^+ supplementation. Studies on compartmentalization of NAD^+ within the cell will be critical to understand how it can be selectively therapeutic targeted in various metabolic disorders.
Method: We engineered tissue specific floxed mouse lines for inducible knockout of SLC25A51 to extend our studies in young adult mice as whole-body homozygous loss is embryonic lethal. Adeno-associated viral vectors expressing either Cre recombinase or enhanced green fluorescent protein (control) under the control of thyroxine-binding globulin promoter were used to generate mice with liver-specific knockout of *Slc25a51* (LKO).
Results: LKO mice trended towards hypoglycemia at baseline and had significantly lower blood glucose levels in glucose tolerance test. These mice also maintained significantly lower blood glucose when gluconeogenic substrates like pyruvate and glycerol were used. During 16 h fast and 4 h re-fed states, LKO animals showed remarkable decrease in plasma triglycerides, insulin, and cholesterol. Despite maintaining a comparable body weight, LKO mice had significantly enlarged livers and dramatic depletion of liver glycogen. Livers isolated from LKO mice showed decreased hepatic NAD^+, NADH and ATP levels. As expected, mitochondrial NAD^+ and NADH levels were significantly lower, and complex I–dependent respiration was impaired. During an exhaustive treadmill protocol, LKO mice failed to run and had lower VO_2 max. Subsequently, SLC25A51 deletion markedly compromised liver regeneration and blocked the ability of nicotinamide riboside supplementation to promote hepatocyte proliferation.
Conclusion: Our data suggest that SLC25A51 regulates hepatocyte mitochondrial energetics and hepatic redox state and is crucial for liver regeneration. We are using multi-omics approaches and stable isotope tracing experiments to determine the changes in major metabolic pathways following SLC25A51 manipulation. Overall, this study offers mechanistic insight into the role of SLC25A51 in liver physiology and provides evidence for specific functions of discrete subcellular NAD^+ pools in hepatocytes *in vivo*.

THU-330-YI
Hepatocyte desmosterol modulation influences the development of colorectal liver metastasis

Ane Nieva-Zuluaga[1], Ane Ortiz-Palma[1], Beatriz Arteta[2], Maider Apodaka-Biguri[1], Idoia Fernández-Puertas[1], Unai Garzon-Basterra[1], Paul Gómez-Jauregui[1], Natalia Sainz-Ramirez[1], Kendall Alfaro-Jiménez[1], Beatriz Gómez Santos[1], Mikel Gastaca[3], Javier Bustamante[4], Jesus M. Banales[5], Anastasios Giannou[6], Samuel Huber[6], Luis Bujanda[5], Xabier Buque[1], Patricia Aspichueta[7]. [1]*Department of Physiology University of the Basque Country UPV/EHU, Faculty of Medicine and Nursing, Leioa, Spain;* [2]*Department of Cellular Biology and Histology, University of the Basque Country UPV/EHU, Faculty of Medicine and Nursing, Leioa, Spain;* [3]*Hepatobiliary Surgery and Liver Transplantation Unit, Biocruces Bizkaia Health Research Institute, Cruces University Hospital, University of the Basque Country, BioBizkaia Research Health Institute, Barakaldo, Bizkaia, Spain, Bilbao, Spain;* [4]*Hepatology and Liver Transplantation Unit, Cruces University Hospital, BioBizkaia Research Health Institute, Barakaldo, Bizkaia, Spain, Bilbao, Spain;* [5]*Department of Liver and Gastrointestinal Diseases, Biogipuzkoa Health Research Institute, Donostia University Hospital, University of the Basque Country UPV-EHU, Ikerbasque, National Institute for the Study of Liver and Gastrointestinal Diseases (CIBERehd, Carlos III Health Institute), Madrid, Spain, San Sebastian, Spain;* [6]*Section of Molecular Immunology und Gastroenterology, I. Department of Medicine, University Medical Center Hamburg-Eppendorf, Hamburg Center for Translational Immunology (HCTI), University Medical Center Hamburg-Eppendorf, 20246 Hamburg, Germany, Hamburg, Germany;* [7]*Department of Physiology University of the Basque Country UPV/EHU, Faculty of Medicine and Nursing, Leioa, Spain, BioBizkaia Research Health Institute, Barakaldo, Bizkaia, Spain, National Institute for the Study of Liver and Gastrointestinal Diseases (CIBERehd, Carlos III Health Institute), Madrid, Spain, Bilbao, Spain*
Email: ane.nieva@ehu.eus

Background and aims: Colorectal liver metastasis (CRLM) is the second leading cause of cancer-related mortality. Alterations in cholesterol (CL) metabolism are a hallmark of CRLM, where tumor cells shift between increased synthesis and uptake depending on their genetic background. Desmosterol, a CL synthesis intermediate, is elevated in several cancers, while inhibition of Δ(24)-sterol reductase (DHCR24), the enzyme regulating the balance between desmosterol and CL, is beneficial in hepatocellular carcinoma. The aims of the study were: (1) to investigate the remodeling of desmosterol and CL synthesis in human CRLM and (2) to determine if desmosterol accumulation by *Dhcr24* inhibition in hepatocytes affects CRLM proliferation.
Method: Serum, liver tumor (T) and surrounding tissue (ST) from CRLM patients (n = 20) were analyzed. CRLM was induced *in vivo* in mice fed either a chow diet or a Western diet. *Pcsk9* overexpression and *Dhcr24* inhibition in hepatocytes were achieved using ApoE-hAAT1-AAV8 and GalNAc-conjugated antisense oligonucleotides (ASO), respectively. Lipid content and protein levels were quantified. *In vitro* proliferation assays were performed using conditioned media from isolated hepatocytes.
Results: Human CRLM tumors exhibited downregulation of all enzymes involved in CL synthesis, including DHCR24, compared with ST. This proteomic remodeling was associated with increased levels of desmosterol and CL in tumors, suggesting enhanced CL uptake from circulation and accumulation of intermediates not used for *de novo* synthesis. In concordance, reduced serum LDL-CL and increased hepatic LDLR levels in both human samples and preclinical CRLM models were found. In mice, hepatocyte-specific *Pcsk9* overexpression reduced liver metastasis by inhibiting LDL-CL uptake, thereby promoting *de novo* cholesterol synthesis and reducing desmosterol accumulation in ST. Conversely, hepatocyte-specific *Dhcr24* inhibition increased desmosterol levels and promoted CRLM progression, accompanied by elevated LDL-CL. Conditioned media from *Pcsk9*-overexpressing hepatocytes, characterized by reduced desmosterol, decreased CRC cell proliferation *in vitro*. In contrast, direct treatment of CRC cells with desmosterol enhanced proliferation.
Conclusion: Dysregulation of CL synthesis and uptake in CRLM alters desmosterol levels in both hepatocytes and tumor cells. Targeting desmosterol metabolism specifically in hepatocytes may represent a promising strategy to reduce CRLM progression.

THU-331
Defining hepatocyte size–mechanotransduction set point that preserves human hepatocyte identity in vitro and in vivo

Masashi Okawa[1], Yein Woo[1], Garnik Arustamyan[1], Daniel Pinski[1], Meng Li[1], Takeshi Saito[1]. [1]*University of Southern California, Los Angeles, United States*
Email: mo_224@usc.edu

Background and aims: Cell identity maintenance is highly dependent on preserving cell size, morphology, and polarity, which are supported by the extracellular matrix (ECM). Isolation of primary human hepatocytes (HHs) involves dislodgement from the native ECM; thus, in vitro culture of HHs lacks structural support, predisposing cells to aberrant mechanotransduction and subsequent identity loss. However, the mechanisms that initiate these maladaptive responses, their kinetics, and their relationship to morphological changes leading to loss of hepatocyte identity remain elusive. This study aims to define the hepatocyte size "set point" that protects

against maladaptive mechanotransduction and preserves cellular identity.
Method: HHs were seeded at different densities as 2D monolayers to tune cell geometry, from laterally spread cells at low density to spatially confined cells at high density. Cells were also cultured on plates with varying stiffness to modulate cell–matrix tension, and then subjected to serial cellular force measurements and quantitative assessment of morphological architecture. They were compared with transcriptomic profiles generated by scRNA-seq to quantify the expression of hepatocyte identity markers and mechanotransduction pathway targets, including YAP/TAZ-associated pathways, to define the hepatocyte identity–preserving size and mechanical force set point. These readouts were benchmarked against human cirrhotic liver tissue samples.
Results: Reduction in seeding density and plate stiffness led to the emergence of distinct HH subpopulations with heterogeneous cell sizes, including compact cells within the size range observed in normal liver tissue and spread cells to variable extents. This morphological heterogeneity was correlated with the magnitude of forces from adjacent cells and was accompanied by maladaptive mechanotransduction signaling, resulting in transcriptomic heterogeneity into distinct subpopulations, including progenitor- and transdifferentiated-like cells. Genes upregulated in identity-lost cells were similarly upregulated in hepatocytes of cirrhosis individuals.
Conclusion: This study defines hepatocyte size–force set points required to preserve hepatocyte identity and provides a mechanistic framework for understanding hepatocyte dysfunction in cirrhosis. These findings are exploitable to refine HH culture strategies, thereby enhancing the quality of in vitro liver biology and disease modeling and supporting the development of regenerative medicine for liver diseases.

THU-332
Signaling through the insulin receptor induces growth via cell cycle re-entry in hepatocyte spheroids engrafted in the anterior chamber of the eye
Nuria Oliva-Vilarnau[1], Barbara Leibiger[1], Ingo Leibiger[1], Per-Olof Berggren[1], Noah Moruzzi[1]. [1]*The Rolf Luft Research Center for Diabetes and Endocrinology, Karolinska Institutet, Karolinska University Hospital, Stockholm, Sweden*
Email: noah.moruzzi@ki.se

Background and aims: Monitoring of functional changes in hepatocytes, the endocrine pancreas and their crosstalk during metabolic disease development is pivotal to identify early mechanisms. The anterior chamber of the eye (ACE) is a suitable transplantation site that serves as an optical window to longitudinally monitor pancreatic islets and hepatocyte spheroids non-invasively at cellular resolution. Our aim is to implement such *in vivo* platforms to study crosstalk between endocrine pancreas and liver in metabolic disease.
Method: Murine hepatocyte spheroids and pancreatic islets are transplanted singularly or together in close proximity into the ACE of recipient mice and imaged by confocal microscopy. Recipient mice are fed an obesogenic diet to identify changes in signaling factors during disease development. Intravenously administered fluorescent probes are imaged *in vivo* to identify vascularization and FUCCI reporter hepatocytes are employed to assess cell cycle activity and number of cells in real time. The role of signaling via the insulin receptor in the crosstalk is evaluated via liver insulin receptor knockout (LIRKO) hepatocyte spheroids.
Results: Co-transplantation of murine hepatocyte spheroids and pancreatic islets in close proximity results in remarkable growth compared to spheroids transplanted without islets in the contralateral eye. Hepatocyte spheroids transplanted singularly also enlarge upon high-fat-high-fructose diet administration in recipient mice. In both cases, growth is explained by cell cycle re-entry of hepatocytes, as evidenced by FUCCI reporter hepatocytes. Hepatocytes lacking the insulin receptor show dramatically impaired growth in the experimental conditions described above, indicating insulin as the main factor at play.
Conclusion: We established a platform for longitudinal imaging of crosstalk between hepatocyte spheroids and islets *in vivo*, which enables identification of key interplay factors. Our data indicates the potent mitogenic role of insulin on hepatocytes *in vivo*, either as an endocrine or as a paracrine factor.

THU-333-YI
Role of CNNM1 in magnesium homeostasis and hepatocellular dysfunction during aging
Patricia Peña-Sanfélix[1], Leidy Estefanía Zapata-Pavas[1], Irene González-Recio[1], Naroa Goikoetxea-Usandizaga[1,2], María Luz Martínez-Chantar[1,2], Luis Alfonso Martinez-Cruz[1], Raul M. Luque[3], Ignacio Gil-Duque[3]. [1]*Liver Disease Lab, CIC bioGUNE, Basque Research and Technology Alliance (BRTA), Derio, Spain;* [2]*Centro de Investigación Biomédica en Red de Enfermedades Hepáticas y Digestivas (CIBERehd), Carlos III National Institute of Health, Madrid, Spain;* [3]*Maimónides Institute of Biomedical Research of Córdoba (IMIBIC), Department of Cell Biology, Physiology and Immunology of University of Córdoba, Reina Sofia University Hospital, CIBER Pathophysiology of Obesity and Nutrition (CIBERobn), Cordoba, Spain*
Email: ppena@cicbiogune.es

Background and aims: Aging is associated with progressive metabolic and inflammatory dysfunction in the liver. Magnesium is essential for cellular energy metabolism and organelle function, and its deficiency has been linked to age-related diseases. CNNM1, a member of the cyclin and CBS domain divalent metal cation transporter family, has been identified as an age-regulated magnesium transporter in experimental models, while showing minimal basal expression under physiological conditions. Its upregulation with ageing suggests a pathogenic role in hepatocyte dysfunction. We investigated the impact of CNNM1 and magnesium on hepatic metabolism during ageing.
Method: Hepatic CNNM1 expression was modulated *in vivo* using AAV vectors for hepatocyte-targeted overexpression or silencing in young and aged mice. Primary mouse hepatocytes were used for mechanistic studies. Mitochondrial function, oxidative stress and metabolic flux were assessed using established assays. Systemic metabolic function was evaluated by glucose, pyruvate and insulin tolerance tests. Gene and protein expression were analysed by qPCR and immunoblotting, and tissue and cellular alterations were examined by histological and immunostaining approaches. Immune cell populations were characterised by flow cytometry.
Results: Aging was associated with increased hepatic Cnnm1 expression and a redistribution of magnesium in hepatocytes, with reduced cytosolic and increased mitochondrial magnesium levels. CNNM1 overexpression in young hepatocytes recapitulated key features of liver ageing, including impaired mitochondrial respiration, endoplasmic reticulum stress and altered magnesium compartmentalisation. CNNM1 silencing in aged hepatocytes restored magnesium balance and mitochondrial function. Systemically, overexpression impaired glucose tolerance, whereas silencing improved glucose, pyruvate, and insulin tolerance. At the cellular level, CNNM1 overexpression disrupted iron homeostasis and increased hepatic iron, while silencing attenuated iron dysregulation and lipid peroxidation. In parallel, CNNM1 knockdown reduced pro-inflammatory cytokine expression, and reshaped hepatic immune cell composition.
Conclusion: CNNM1 could be acting as a key hepatocyte-intrinsic regulator by altering magnesium and iron balance, mitochondrial function, and inflammation during liver aging. Targeting CNNM1-dependent pathways may represent a promising strategy to restore hepatocellular homeostasis in liver aging.

THU-334-YI

A human induced pluripotent stem cells-based liver assembloid platform for investigating ischemia/reperfusion injury

Riccardo Perriera[1], Clelia Ferraro[1], Minjie Zhao[1,2], Martina Morsicato[1], Salvatore Gruttadauria[3], Valentina Agnese[1], Massimo Pinzani[1], Giovanni Zito[1]. [1]*Research Department, Istituto Mediterraneo per i Trapianti e Terapie ad alta specializzazione (IRCCS-ISMETT), Palermo, Italy;* [2]*Department of Hepatobiliary Surgery, Second Hospital Affiliated to Chongqing Medical University, Chongqing, China;* [3]*Abdominal Surgery and Organ Transplant Unit, Department for the Treatment and Study of Abdominal Diseases and Abdominal Transplantation, Istituto Mediterraneo per i Trapianti e Terapie ad alta specializzazione (IRCCS-ISMETT), Palermo, Italy*
Email: rperriera@ismett.edu

Background and aims: Ischemia reperfusion injury (IRI) is one of the leading causes of liver graft failure. Although machine perfusion improves the quality of marginal donor livers, damage to the vasculature and parenchyma often leads to irreversible injury, compromising graft function. To investigate the complex interactions between endothelial cells and hepatocytes under IRI, we developed an assembloid model by combining human induced pluripotent stem cell (hiPSC)-derived liver organoids (LOs) with human umbilical vein endothelial cells (HUVECs). To identify novel IRI-associated markers, assembloids were subjected to an in vitro IRI assay, followed by transcriptomic analysis using RNA sequencing.
Method: hiPSC-LOs were generated using an established differentiation protocol in a matrix-free system combining two commercially available kits. Organoid maturation was enhanced by molecular inhibition of GSK-3 during differentiation. The maturation of hiPSC-LOs and hiPSC-derived assembloids (hiPSC-Assemb) was assessed by RNA sequencing, and compared with tissue-derived liver organoids (TLOs) and their corresponding endothelial assembloids (T-Assemb). The IRI assay was subsequently applied to both hiPSC-based and tissue-derived models to identify novel IRI-associated markers through comparative transcriptomic analysis.
Results: GSK-3 inhibition significantly increased the expression of hepatocyte markers and promoted the maturation of specific cells within hiPSC-LOs, indicating improved hepatic differentiation. In hiPSC-Assemb, interactions between hiPSC-LOs and HUVECs further enhanced hepatocyte marker expression and functional activity. RNA sequencing revealed dynamic crosstalk between parenchymal and endothelial cells within the assembloid models. Moreover, the transcriptional profile following the IRI assay identified the regulation of unrecognized genes implicated in injury and stress response pathways.
Conclusion: hiPSC-Assemb represent a versatile and powerful platform for studying liver biology and complex liver pathologies. The ability to differentiate and integrate multiple cell types within a single assembloid constitutes a key advantage of this model, enabling the investigation of multifactorial liver injuries such as IRI. Transcriptomic analysis of liver assembloids reveals liver-specific gene expression patterns and the identification of novel targets during IRI, providing a valuable framework for further mechanistic and translational studies.
Ministero della Salute-Ricerca Corrente.

THU-335

Hepatic molecular pathways associated with pemafibrate treatment in a rat model of metabolic-associated steatotic liver disease

Yanhao Qiu[1], Jianing Zhou[1], Núria Roglans[1,2,3], Emma Barroso[1,2], Marta Alegret[1,2,3], Juan Carlos Laguna[1,2,3], Laia Vilà[1,2]. [1]*School of Pharmacy and Food Sciences, Universitat de Barcelona, Barcelona, Spain;* [2]*Barcelona, Spain;* [3]*CIBERObn, Barcelona, Spain*
Email: yqiuqiux231@alumnes.ub.edu

Background and aims: We have previously shown that pemafibrate (Pema) administration prevents steatosis development in an experimental model of simple metabolic-associated steatotic liver disease (MASL) in Sprague-Dawley (SD) (*Biomed Pharmacother* 2024 177:117067). Here, we investigated previously undescribed pathways that may contribute to the beneficial effects of Pema treatment in MASLD.
Method: Female SD rats were randomly assigned to three groups (n = 8 per group): (1) control, receiving standard diet; (2) high-fat diet with 10% (w/v) fructose in drinking water (HFHFr); and (3) HFHFr plus Pema at 0.5 mg/kg/day. Rats were fed the HFHFr diet for three months, while treated animals received the diet supplemented with Pema during the last month. At the end of the treatment, liver tissue was properly stored for RNA and protein extraction.
Results: Pema increased the expression of several genes involved in mitochondrial function, including Tfam, Nrf2, Sirt3, Ppargc1a, as well as mitochondrial complex IV subunits (Mt-co1, Mt-co2, and Mt-co3); PPARGC1α protein levels were also elevated. Given the link between mitochondrial function and antioxidant defences, metallothioneins Mt1 and Mt2 were evaluated, revealing increased *Mt2* expression along with higher catalase levels. As MT2 has been associated with autophagy regulation, autophagic markers were analyzed. Pema-treated rats exhibited increased phosphorylated ULK levels, reduced LC3-II/I ratio, and decreased lysosomal acid lipase expression, indicating autophagy inhibition. Finally, we assessed the expression of the vitamin D receptor (VDR), as it has been reported to modulate the expression of several genes altered in our study. Both Vdr gene and protein expression were increased in Pema-treated rats, together with enhanced expression of direct VDR target genes such as Angptl8 and Pparγ2. Further, VDR expression positively correlated with Tfam, Nrf2, Mt-co1, Mt2, and catalase expression, suggesting that VDR may contribute to some of the effects induced by Pema treatment in our MASL model.
Conclusion: Overall, our findings suggest the involvement of additional molecular pathways underlying the beneficial effects of Pema in MASL, with VDR signaling identified as a potential mediator of its hepatic actions. Nevertheless, further research is required to comprehensively clarify the underlying mechanisms. Grants: PID2023-146140OB-I00, funded by funded by MICIU/AEI/10.13039/501100011033 and FEDER-UE and 2021SGR-00345.

THU-336

Remodeling of the bile acid connectome across the hepatitis-cirrhosis-hcc axis: network analysis reveals stage-specific hubs and potential therapeutic targets

Qinshuo Wang[1], Zixing Wang[2], Huiying Rao[3], Xin Wen[4], Tianyi Xue[4], Yanpei Mai[2], Suzhen Jiang[2], Shuo Yang[2], Yuxi Shi[4], Yanhui Yang[2], Linlin Cao[3]. [1]*Peking University Hepatology Institute, Peking University Health Science Center, Peking University People's Hospital Laboratory Department, Beijing, China;* [2]*Peking University Hepatology Institute, Beijing, China;* [3]*Peking University People's Hospital Laboratory Department, Beijing, China;* [4]*Peking University Hepatology Institute, Peking University Health Science Center, Beijing, China*
Email: caoll@bjmu.edu.cn

Background and aims: While bile acids are established players in liver disease progression and are components of predictive models, the dynamics of BA networks across disease stages remain unexplored. We hypothesize that the transition from hepatitis to cirrhosis and hepatocellular carcinoma (HCC) is driven not just by changes in individual BA concentrations, but by a fundamental rewiring of BA interaction networks. This study aims to systematically map and quantify the BA network topology across this disease spectrum to identify hub BAs that may coordinate metabolic dysregulation.
Method: We prospectively enrolled 889 patients from Peking University Hepatology Institute in 2025, categorized into six groups: Hepatitis B, MAFLD, HBV-MAFLD, compensated cirrhosis, decompensated cirrhosis, and HCC. Serum levels of individual BAs were quantified using LC-MS. For each group, a BA co-abundance network G = (V,E) was constructed, where nodes (V) represent BAs

and edges (E) represent strong correlations (|Spearman's r| >0.65, capturing both synergistic and inhibitory relationships. Network topology was analyzed using density, clustering coefficient, and modularity. Cross-group comparisons of BA profiles and core identities pinpointed hub BAs whose relative changes are linked to global network restructuring.
Results: We found significant differences in network structure across the Hepatitis-Cirrhosis-HCC Axis. Specifically, network density-reflecting the frequency of interactions between bile acids- increased from 0.09–0.14 (MAFLD, HBV and overlap), 0.15–0.17 (CC and DC), to 0.22 (HCC); clustering coefficient-reflecting the degree of collaboration among BAs within functional modules-rose from 0.58 to 0.74 accordingly. Analysis of network hubs revealed that UDCA as a core BA in MAFLD, where as glycine-conjugated BAs dominated the other groups. That is, GDCA composed 6.4%–8.1% of the BA pool for HBV, and was identified as a driver for progression to CC. GCDCA becomes the hub when further progressing to DC, whereas GCA acts as a consistent hub within the networks throughout the full disease spectrum.
Conclusion: This work moves beyond individual BA quantification to define the "BA connectome" in liver disease. Identifying the dynamic hub BAs provides novel insights into the critical control points of metabolic dysregulation at each stage. These hubs represent potential biomarkers for disease monitoring and novel therapeutic targets for interrupting progression.

THU-337
Integrating proteomics and metabolomics analysis identifies molecular links associated to liver injury in preclinical model of acute hypoxia stress

Sanju Yadav[1,2], Rupinder Kalra[3], Manisha Yadav[1], Gaurav Tripathi[1], Neha Sharma[1], Nupur Sharma[1], Sushmita Pandey[1], Vipul Sharma[1], Babu Mathew[1], Vasundhra Bindal[1], Narendra Sharma[3], Ved Dwivedi[4], Jaswinder Maras[1], Nasir Salam[2]. *[1]Institute of Liver and Biliary Sciences, New Delhi, India; [2]Jamia Millia Islamia, New Delhi, India; [3]Banasthali Vidyapith, Newai, India; [4]ICGEB, New Delhi, India*
Email: nsalam@jmi.ac.in

Background and aims: Acute hypobaric hypoxia induces metabolic stress, disrupting redox homeostasis and promoting liver injury; however, the molecular mechanisms linking hypoxia to hepatic dysfunction remain poorly defined. This study aimed to characterize time-dependent liver-specific proteomic and metabolomic alterations during acute hypoxic exposure.
Method: Male SD rats (n = 16/group) were exposed to simulated hypobaric hypoxia (25,000 ft) for 1, 3, or 7 days. Liver tissues were subjected to untargeted proteomic and metabolomic analyses to define temporal molecular perturbations associated with hepatic stress.
Results: Hypoxia induced significant liver injury, evidenced by elevated serum bilirubin, AST, and ALT levels and a reduced liver-to-body weight ratio ($p < 0.05$). Liver metabolomics showed a time-dependent remodelling, of 341-up, 20-down at day-1, 316 up, 22-down at day-3, and 356 up, 10 down at day-7 (FC>1.5, $p < 0.05$). These changes predominantly involved activation of inflammatory and mitochondrial redox pathways, including tryptophan (C00099, C00025), amino sugar metabolism (C00140), folate metabolism (C00576), and the TCA cycle(C00025), alongside suppression of nitrogen metabolism (C00262, C00086), indicating impaired detoxification (>2FC, $p < 0.05$). Proteomic analysis showed extensive dysregulation of (1091-up, 586-down) proteins at day-1, 1104-up and 821 down at day-3, and 453-up and 606 down at day-7 (FC>1.5, $p < 0.05$). Proteins associated with stress and lipid metabolism (FADS1, ACOX2, ACOT8), fatty acid metabolism (ACADVL, CPT1B), and calcium signalling (PTGS1) were enriched (>2FC, $p < 0.05$). Integrated multi-omics showed strong correlations between increased TCA cycle activity and inflammatory signaling pathways ($R^2>0.7$, $p < 0.05$). Network-level analysis further linked apoptotic (BAX, APAF1, CDH1, PRKCD), platelet activation (ATP2B3, PPP2R1B) and Eph–ephrin signalling (EPHA7, MYH9, LYN, EPHA3), angiotensinogen (ACE, CMA1) with altered nucleotide, amino acid, and antioxidant metabolism, identifying Eph–ephrin signalling as a key contributor to hypoxia-induced liver inflammation.
Conclusion: Acute hypobaric hypoxia induces early liver injury marked by redox imbalance, metabolic rewiring, and inflammatory activation, with coordinated proteomic–metabolomic disruptions highlighting Eph–ephrin signalling as a key driver of hypoxia-induced hepatic inflammation and a potential therapeutic target.

THU-338-YI
Type I interferon-mediated liver injury and hepatocarcinogenesis upon hepatic autophagy inhibition

Lea Aylin Yücel[1], Farina Schneider[2], Callum Hall[3], George Kassiotis[3], Marcus Krüger[4], Reinhard Büttner[2,5], Manolis Pasparakis[4,5,6], Tom Luedde[1,7], Vangelis Kondylis[1,2,5,8]. *[1]Clinic for Gastroenterology, Hepatology and Infectious Diseases, University Hospital Düsseldorf, Düsseldorf, Germany; [2]Institute for Pathology, University Hospital Cologne, Cologne, Germany; [3]The Francis Crick Institute London, London, United Kingdom; [4]Institute for Genetics, University of Cologne, Cologne, Germany; [5]Center for Molecular Medicine (CMMC), Medical Faculty and University Hospital Cologne, University of Cologne, Cologne, Germany; [6]Cologne Excellence Cluster for Aging and Aging Associated Diseases (CECAD), University of Cologne, Cologne, Germany; [7]Center for Integrated Oncology Aachen Bonn Cologne Düsseldorf (CIO ABCD), Düsseldorf, Germany; [8]University Hospital Düsseldorf, Department of Gastroenterology Hepatology and Infectious diseases, Medical Faculty at Heinrich-Heine-University Düsseldorf, Düsseldorf, Germany*
Email: LeaAylin.Yuecel@med.uni-duesseldorf.de

Background and aims: Liver injury drives chronic liver disease (CLD), progressively inducing inflammation, fibrosis and cirrhosis, thereby increasing the risk of hepatic malignancy. Autophagy is a catabolic process that maintains cytoplasmic quality via degradation of cellular material, and its dysregulation promotes CLD progression, such as alcoholic steatohepatitis (ASH) and metabolic dysfunction-associated steatohepatitis (MASH). In this project, we aimed to identify pathways involved in liver injury and hepatocarcinogenesis in mice with liver parenchymal cell-specific ATG16L1 ablation (LPC-KO), which develop spontaneous liver injury, progressing with age to steatohepatitis, fibrosis and tumor formation.
Method: Quantitative proteomics were used to identify early differences between ATG16L1-deficient and control livers. Transgenic mouse lines were generated to assess the role of the autophagy receptor Sequestosome-1/p62 and different mediators of type I interferon (IFN) signalling in vivo together with biochemical and (immuno)histochemical analyses. Immunoprecipitation (IP) with J2 antibody followed by RNA sequencing (RNAseq) was used to look for potential dsRNA sources activating type I IFN signalling.
Results: p62 ablation ameliorated liver injury, hepatomegaly, and delayed hepatocarcinogenesis in ATG16L1 LPC-KO mice. Proteomic analysis revealed an increased type I IFN signature, which was not normalized upon p62 deficiency. LPC-specific deletion of *Ifnar1* decreased liver injury and tumorigenesis, highlighting the involvement of type I IFN signalling in hepatocyte death. *Mavs*, but not *Sting*, deletion phenocopied the effect of Ifnar1 deficiency, indicating that aberrant accumulation of dsRNAs leads to Mavs-dependent IFN production that mediates the observed liver damage in ATG16L1 LPC-KO mice. J2 IP followed by RNAseq identified significantly altered expression in specific families of endogenous transposable elements (TEs) in livers of these mice as the potential stimuli of type I IFN signalling activation. The involvement of IFN-inducible molecules that regulate cell death, such as Zbp1, are currently being examined.
Conclusion: Our findings suggest that autophagy safeguards hepatocytes from the build-up of endogenous TEs in the context of non-viral liver disease, thus preventing the induction of type I IFN signalling that sensitizes hepatocytes to death. Possible upregulation of endogenous TEs in ASH and MASH patients needs to be elucidated.

Immune-mediated and cholestatic – Experimental and pathophysiology

TOP-295-YI

Centrally-imprinted innate immune tolerance following colitis attenuates cholestatic liver disease: implications for gut-liver axis driven PSC-IBD pathogenesis

Rania Matthys[1,2], Lander Heyerick[1], Zenzi De Vos[1], Lara Morren[1], Hans Van Vlierberghe[3], Anja Geerts[3], Sarah Raevens[3], Sander Lefere[2], Xavier Verhelst[3], Frederik Berrevoet[4], Lindsey Devisscher[1].
[1]Department of Basic & Applied Medical Sciences, Gut-Liver Immunopharmacology Unit, Ghent, Belgium; [2]Liver Research Center Ghent, Ghent University, Ghent University Hospital, Ghent, Belgium; [3]Department of Gastroenterology and Hepatology, Ghent University Hospital, Ghent, Belgium; [4]Department of General, Hepatobiliary Surgery and Liver Transplantation, Ghent University Hospital, Ghent, Belgium
Email: rania.matthys@ugent.be

Background and aims: Primary sclerosing cholangitis (PSC) is a chronic cholestatic liver disease frequently associated with inflammatory bowel disease (IBD). While the role of IBD in PSC remains unclear, evidence suggests a protective effect of PSC-IBD. Monocytes and macrophages are key drivers of PSC, and innate immune cells can develop long-lasting functional memory after inflammatory insults. We aim to determine how colitis shapes innate immune responses in the bone marrow and how these centrally imprinted responses translate to cholestatic liver disease severity in vivo.
Method: Acute colitis was induced in mice using 2% dextran sulphate sodium (DSS) for 5 days. Bone marrow was collected at defined timepoints post-colitis and differentiated ex vivo into bone marrow–derived macrophages (BMDMs), which were subjected to secondary stimulation and analyzed by RT-qPCR. To assess in vivo consequences, acute cholestatic liver disease was induced by common bile duct ligation (CBDL) 8 weeks after DSS exposure, with and without bone marrow transplantation (BMTx). BM of mice that underwent acute colitis was used to confirm our results.
Results: Acute colitis induced sustained elevation of pro-inflammatory cytokines (Il1b, Il6, Il12, TNFalpha) in BMDMs for up to 6 weeks, returning to baseline by 8 weeks post-colitis. Ex vivo restimulation of these BMDMs at 8 weeks post-colitis revealed reduced expression of glycolysis-related genes (mTOR, Hif1alpha, Mct1), indicating an innate immune memory state consistent with immune tolerance. In vivo, cholestatic liver injury induced 8 weeks after colitis showed a trend toward reduced hepatic inflammatory markers (Ccr2, TNFalpha, Nlrp3). Similarly, CBDL mice that received bone marrow from colitis-exposed donors displayed reduced hepatic expression of Ccr2, TNFalpha, Nlrp3, and Ccr5, along with lower hepatic mTOR and Hif1alpha levels, supporting centrally programmed immune tolerance.
Conclusion: A single episode of colitis induces innate immune memory in bone marrow derived macrophages that persists for at least 8 weeks. This memory is characterized by a tolerant phenotype, reflected by reduced inflammatory and metabolic gene expression upon restimulation. Bone marrow transplantation experiments indicate that this tolerant state is encoded at the level of hematopoietic progenitors, highlighting a central BM-driven mechanism that may contribute to innate immune dysregulation relevant to PSC-IBD.

TOP-296-YI

Liver-specific CNNM4 silencing alleviates fibrosis by restoring bile acids homeostasis in cholestatic preclinical models and human liver slices

Naroa Goikoetxea-Usandizaga[1,2], Maitane Asensio[2,3], Irene González-Recio[1], Jorge Simon[1], Marina Serrano-Maciá[1], Marta Romero[3], Beatriz Sanchez de Blas[3], Maria Andres-Rozas[4], Ana Martínez-Alcocer[4], Ute Schaeper[5], Małgorzata Milkiewicz[6], Piotr Milkiewicz[6,7], Ruben Nogueiras[8,9], Jelena Mann[10,11], Jordi Gracia-Sancho[2,4], Jose Marin[2,3], María Luz Martínez-Chantar[1,2].
[1]Liver Disease Lab, CIC bioGUNE, Derio, Spain; [2]CIBEREHD, Madrid, Spain; [3]Experimental Hepatology and Drug Targeting (HEVEFARM), IBSAL, University of Salamanca, Salamanca, Spain; [4]Liver Vascular Biology Research Group, Barcelona Hepatic Hemodynamic Laboratory, IDIBAPS, Barcelona, Spain; [5]Silence Therapeutics GmbH, Berlin, Germany; [6]Department of Medical Biology, Pomeranian Medical University, Szczecin, Poland; [7]Translational Medcine Group, Pomeranian Medical University, Szczecin, Poland; [8]Department of Physiology, Research Centre of Molecular Medicine and Chronic Diseases, University of Santiado De Compostela, Santiago de Compostela, Spain; [9]CIBERobn, Santiago de Compostela, Spain; [10]Newcastle Fibrosis Research Group, Bioscience Institute, Faculty of Medical Sciences, Newcastle University, Newcastle, United Kingdom; [11]FibroFind, Newcastle, United Kingdom
Email: mlmartinez@cicbiogune.es

Background and aims: Primary biliary cholangitis (PBC) and primary sclerosing cholangitis (PSC) are progressive cholestatic liver diseases leading to cirrhosis, liver failure, and transplantation. Existing therapies are only partially effective, leaving an urgent need for novel interventions. Magnesium (Mg^{2+}) is an essential regulator of cellular metabolism, mitochondrial function, and endoplasmic reticulum homeostasis. Dysregulated Mg^{2+} has been observed in liver injury, but its role in cholestasis remains unknown. We investigated hepatic Mg^{2+} homeostasis as a driver of cholestatic liver injury and assessed CNNM4, a Mg^{2+} exporter, as a targetable mechanism.
Method: Mg^{2+} transporters were analyzed in liver biopsies from PBC and PSC patients and in murine cholestasis models (bile duct ligation and Mdr2−/− mice). CNNM4 was silenced using GalNAc-conjugated siRNA. Liver injury, inflammation, fibrosis, and bile acid (BA) metabolism were assessed in vivo, with proteomic profiling. Translational relevance was directly tested in precision-cut human liver slices (PCLS) from patients.
Results: CNNM4 expression was consistently upregulated in human cholestatic livers and murine models. GalNAc-siCnnm4 restored hepatic Mg^{2+}, reduced inflammation and fibrosis. Mechanistically, NIRBAD confirmed that GalNAc-siRNA therapy reduces liver BA emptying time by one-third in Mdr2-/- mice, similar to wild-type mice. Proteomics revealed an antifibrotic and anti-inflammatory signature linked to Mg^{2+} restoration. Critically, in PCLS from patients, CNNM4 silencing robustly decreased fibrotic and inflammatory markers, demonstrating translational efficacy in human tissue.
Conclusion: Altered Mg^{2+} homeostasis drives cholestatic liver injury. CNNM4 inhibition restores Mg^{2+} balance, reverses hallmark features of cholestasis, and reduces fibrosis in both preclinical models and human liver slices. These findings provide compelling preclinical and human evidence supporting CNNM4-targeted therapy as a novel, liver-directed strategy for PBC and PSC.

FRI-260

RTY-406 is a dual-acting ABCB4/MDR3 and ABCB11/BSEP positive functional modulator that demonstrates efficacy in a model of primary sclerosing cholangitis

Eric Bell[1], Nathan Fuller[1], Youhwa Jo[1], Jennifer Truong[1], John Miller[1], Robert Hughes[1]. *[1]Rectify Pharmaceuticals, Boston, United States*
Email: ebell@rectifypharma.com

Background and aims: ATP binding cassette subfamily B member 4 (ABCB4/MDR3) and 11 (ABCB11/BSEP) facilitate the translocation of phosphatidylcholine (PL) and the efflux of bile acids (BA) from hepatocytes to the canalicular space, respectively. Mutations in these transporters cause monogenic cholestatic diseases (PFIC3 [MDR3 deficiency]/PFIC2 [BSEP deficiency]) and are associated with the hepatobiliary diseases intrahepatic cholestasis of pregnancy (ICP) and low phospholipid-associated cholelithiasis (LPAC), highlighting their critical role in maintaining hepatobiliary health. We have

discovered RTY-406, a novel, potent, dual-acting ABCB4/BSEP positive functional modulator (PFM) that significantly reduces cholestasis and cholangitis in an animal model of PSC.
Method: RTY-406 was evaluated with twice daily oral dosing for 6 weeks in *Abcb4* heterozygous animals fed a lithogenic diet, a model that recapitulates multiple hallmarks of PSC[1,2]. Peripheral markers of cholestasis, serum BA and alkaline phosphatase (ALP), were monitored, as well as bile components and the incidence of cholesterol crystal formation in the gallbladder. Gene expression, chemokine measurements, and histology were evaluated on liver tissue for markers of ductular reaction, cholangitis, and fibrosis.
Results: RTY-406 increased biliary levels of PL, demonstrating Abcb4 target engagement, and reduced the incidence of gallbladder crystal formation. Serum levels of BA, ALP and the levels of liver taurocholic acid (TCA) were reduced by RTY-406, indicating Bsep target engagement and efficacy on cholestatic markers. Analysis of liver tissue demonstrated RTY-406 reduced pro-inflammatory chemokines, markers of ductular reaction, monocyte/neutrophil infiltration of bile ducts, and biliary fibrosis.
Conclusion: RTY-406, a first-in-class, orally active dual PFM for ABCB4/BSEP, was characterized in a mixed genetic/diet induced model of PSC. By enhancing the function of Abcb4 and Bsep, RTY-406 conferred a beneficial impact on relevant markers of cholestasis and biliary health. These data demonstrate the potential of our dual BSEP/ABCB4 PFM to provide a benefit for hepatobiliary diseases such as PSC.

FRI-261
RTY-406, a candidate drug for primary sclerosing cholangitis (PSC), a dual-acting ABCB4/MDR3 and ABCB11/BSEP positive functional modulator, demonstrates target modulation in non-human primates
Eric Bell[1], Nathan Fuller[1], John Miller[1], Pol Boudes[1], Robert Hughes[1].
[1]*Rectify Pharmaceuticals, Boston, United States*
Email: ebell@rectifypharma.com

Background and aims: ATP binding cassette subfamily B member 4 (ABCB4/MDR3) and 11 (ABCB11/BSEP) translocate phosphatidylcholine (PL) and bile acids (BA) from hepatocytes to bile ducts, respectively. While RTY-406, a novel dual-acting ABCB4/BSEP positive functional modulator (PFM), has demonstrated efficacy in rodent models of cholestasis, validating target modulation and safety in a higher species de-risks clinical translation. We used non-human primates to assess and validate mechanism of action and hepatobiliary health serum biomarkers to support early clinical development.
Method: RTY-406 was evaluated in two independent repeat-dose studies in Cynomolgus monkeys with durations of 14 days and 28 days. Animals receiving daily oral dosing were assessed for sustained pharmacodynamic effects on peripheral markers suitable for clinical monitoring. Markers of bile acid metabolism, including total cholesterol (CHO) were used to monitor mechanism of action, while Alkaline Phosphatase (ALP), gamma-glutamyl transferase (GGT), Alanine Aminotransferase (ALT) and Aspartate Aminotransferase (AST), were used to monitor hepatobiliary health.
Results: In both the 14-day and 28-day studies, RTY-406 demonstrated a favorable profile with no adverse signals in liver function tests. ALT and AST levels confirmed the absence of hepatocellular injury. CHO, ALP, and GGT levels were all dose-dependently reduced, indicating appropriate target modulation consistent with the anticipated mechanism of action of RTY-406.
Conclusion: These 14- and 28-day studies in Cynomolgus monkeys establish a translatable biomarker profile for RTY-406. Use of bile acid synthesis markers combined with ALP, GGT, ALT, and AST provides a robust panel for parallel monitoring of target modulation and hepatobiliary health. These data de-risk translation to human studies, offering a specific set of serum biomarkers that further support clinical development of RTY-406 for PSC.

FRI-262-YI
Pathogenic MUC1$^+$ cholangiocytes drive fibrogenic crosstalk via the EFNA5–EPHA2 axis in cholestatic liver injury
Dinesh Mani Tripathi[1], Aishwarya Bhatnagar[1], Rajni Yadav[1], Himanshi Himanshi[1], Vaibhav Tiwari[1], Savneet Kaur[1], Chhagan Bihari[1], Nidhi Jalan Sakrikar[2], Shridhar Sasturkar[1], Shiv Kumar Sarin[1]. [1]*Institute of Liver and Biliary Sciences, New Delhi, India;* [2]*Mayo Clinic, Rochester, Minnesota, United States*
Email: dineshmanitripathi@gmail.com

Background and aims: Liver injury is characterized by a ductular reaction marked by expansion of biliary epithelial cells (BECs), which contribute to both regeneration and disease progression. Pathogenicity arises from heterogeneous BEC subpopulations that remain poorly understood. We aim to define the role of MUC1$^+$ BECs in driving fibrogenesis through paracrine signaling and to identify the underlying pathways.
Method: Cholestatic injury was induced by bile duct ligation (BDL; day 2, 4, 7) and DDC diet (2 and 4 weeks). Biliary markers were analyzed by qPCR. MUC1 expression was assessed by immunohistochemistry (IHC) in murine and human liver tissue, followed by sorting of EpCAM$^+$MUC1± and EFNA5 gene expression was validated. MUC1$^+$ organoids were generated and characterized by immunofluorescence. Conditioned media (CM)–based co-culture, collagen gel contraction, and tube formation assays were performed. STRING network and protein docking analyses were conducted.
Results: Both models showed increased ductular stress and progenitor markers OPN (BDL 9-fold; DDC 5-fold), SSTR (5-fold), and ciliary remodeling by IFT27 (3-fold). IHC showed progressive expansion of MUC1$^+$ ductules from 4% - 2D, 7% - 4D, 9%- 7D, 15% - 28D. In DDC, the MUC1$^+$ increased 7% -2W; 4%- 4W. Gene analysis revealed a 12-fold increase in intrahepatic MUC1 compared with the extrahepatic compartment, and a transient increase in BCL2. At the cellular level, MUC1 increased 7-fold. MUC1$^+$ organoids increased in number (25–30 per 50,000 cells) and size (10-fold) with CK19$^+$MUC1$^+$ duct-like structures. CM showed progressive endothelin-1 elevation (23, 91, 383 pg/ml) and induced stellate cell activation (a-SMA 3-fold; COL1A1 2-fold), collagen contraction, angiogenic marker expression (TIE2, eNOS, VCAM ~2-fold), and enhanced tube formation. Direct co-culture showed an increased a-SMA population (15%). Based on prior ligand–receptor interaction studies, EFNA5 gene expression was enriched in EpCAM$^+$MUC1$^+$ BECs. EPHA2 receptor is present in activated stellate cells, supported by docking analysis. STRING analysis revealed a key fibrogenic hub linked to the PDGF and collagen pathways.
Conclusion: Cholestatic injury drives expansion of pathogenic MUC1$^+$ biliary epithelial cells that promote fibrosis through paracrine mechanisms. EFNA5 expression was detected in MUC1$^+$ cells, while its cognate receptor EPHA2, expressed on hepatic stellate cells, shows strong links to PDGFR and collagen pathways, supporting a cholangiocyte–stromal axis in fibrosis progression.

FRI-263
Mosaic X chromosome loss is more frequent in primary biliary cholangitis but does not influence transplant-free survival
Chiara Caime[1], Emil Hiitola[2], Rosanna Asselta[3], Tatiana Cajuso[4], Davide Bernasconi[5], Pietro Invernizzi[6], Andrea Ganna[7], FinnGen FinnGen[4], Mikko Myllymäki[2], Alessio Gerussi[6]. [1]*Division of Gastroenterology, Center for Autoimmune Liver Diseases, European Reference Network on Hepatological Diseases (ERN RARE-LIVER), Fondazione IRCCS San Gerardo dei Tintori, Monza, Italy; Department of Medicine and Surgery, University of Milano-Bicocca, Monza, Italy; Institute for Molecular Medicine Finland, University of Helsinki, Helsinki,*

Finland, Monza, Italy; [2]Hematology Research Unit Helsinki, University of Helsinki and Helsinki University Hospital Comprehensive Cancer Center, Helsinki, Finland; Translational Immunology Research program, University of Helsinki, Helsinki, Finland; iCAN Digital Precision Cancer Medicine Flagship, Helsinki, Finland, Helsinki, Finland; [3]Department of Biomedical Sciences, Humanitas University, Milan, Italy; IRCCS Humanitas Research Hospital, Rozzano, Milan, Italy, Milan, Italy; [4]Institute for Molecular Medicine Finland, University of Helsinki, Helsinki, Finland, Helsinki, Finland; [5]Bicocca Bioinformatics Biostatistics and Bioimaging Centre, School of Medicine and Surgery, University of Milan-Bicocca, Milan, Italy; Department of Clinical Research and Innovation, ASST Grande Ospedale Metropolitano Niguarda, Milan, Italy, Milan, Italy; [6]Division of Gastroenterology, Center for Autoimmune Liver Diseases, European Reference Network on Hepatological Diseases (ERN RARE-LIVER), Fondazione IRCCS San Gerardo dei Tintori, Monza, Italy; Department of Medicine and Surgery, University of Milano-Bicocca, Monza, Italy, Monza, Italy; [7]Institute for Molecular Medicine Finland, University of Helsinki, Helsinki, Finland; Analytic and Translational Genetics Unit, Massachusetts General Hospital, Boston, MA, USA; Program in Medical and Population Genetics, Broad Institute of MIT and Harvard, Cambridge, MA, USA, Helsinki, Finland
Email: alessio.gerussi@unimib.it

Background and aims: Primary Biliary Cholangitis (PBC) is a chronic autoimmune liver disease with strong female predominance. Variants on the X chromosome contribute to genetic susceptibility to PBC. Mosaic chromosomal alterations (mCAs), including age-related clonal hematopoiesis and loss of the X chromosome (mLOX), have been implicated in autoimmune diseases, but their prevalence and clinical relevance in PBC remain poorly defined.
Method: We detected mCAs using MOsaic CHromosomal Alterations (MoChA) caller across FinnGen (N = 520,210) and UK Biobank (UKBB; N = 482,789) to assess population-level prevalence. We identified 791 PBC patients from FinnGen and 453 from UKBB. In the FinnGen cohort, after excluding 141 males and 70 females with incomplete X chromosome data, we evaluated mLOX prevalence and clinical outcomes in 580 female PBC patients (mLOX: N = 208; no mLOX: N = 372). Age-adjusted Cox proportional hazards models assessed the impact of mLOX on death or liver transplantation in FinnGen, analyzed separately for all-cause and liver-related outcomes. UKBB data were used for prevalence validation only.
Results: Overall mCA prevalence was 28.9% in FinnGen and 12.7% in UKBB, increasing with age; the most frequent events were mLOX in females (11.9% and 5.1%) and loss of the Y chromosome (mLOY) in males (14.7% and 16.1%). Among the 580 female PBC patients analyzed, mLOX was significantly elevated compared to FinnGen participants with PBC (OR = 1.58; CI: 1.19–2.11; p = 0.0018), validated via meta-analysis with UKBB (OR = 1.60; CI: 1.22–2.08; p = 0.0006). In FinnGen, despite an increased prevalence, mLOX was not associated with increased risk of death or liver transplantation (HR = 0.80; 95% CI: 0.49–1.32; p = 0.391), nor with liver-related death or transplantation (HR = 1.23; 95% CI: 0.66–2.43; p = 0.475).
Conclusion: Female PBC patients show 60% higher rates of mLOX than population-matched controls, but mLOX does not associate with transplant-free survival. These findings suggest mLOX may contribute to PBC pathogenesis without affecting disease prognosis.

FRI-264
Endoplasmic reticulum stress-mediated PPARα-DDX3X interaction modulates Con A-induced liver injury in mice

Zihao Fan[1], 玲 徐[1], Feng Ren[1]. *[1]Beijing Institute of Hepatology/Beijing Youan Hospital, Capital Medical University, Beijing, China*
Email: fzh_925@163.com

Background and aims: Dysfunction of endoplasmic reticulum (ER) stress is involved in the pathogenesis of immune-mediated liver injury, but its molecular mechanism has not been fully elucidated. Previous studies have shown that PPARα and DDX3X play important roles in ER stress-related dysfunction. This study further explored how PPARα and DDX3X interact to regulate ER stress-related dysfunction in immune-mediated liver injury.
Method: Liver injury was induced in C57BL/6J mice via concanavalin A (Con A). DDX3X hepatocyte-specific knockout ($DDX3X^{\Delta Hep}$) mice and control ($DDX3X^{fl/fl}$) mice were utilized to investigate the role of DDX3X in liver injury. 4-PBA was used to inhibit ER stress, while siRNA, AAV-shRNA, and LV were used to regulate PPARα expression. Tunicamycin (TM) was used to induce ER stress in primary hepatocytes, and autoimmune hepatitis (AIH) patients were included for validation.
Results: Inhibition of ER stress alleviates ConA-induced liver injury by increasing PPARα expression and reducing both DDX3X levels and phosphorylation in the liver. PPARα activation attenuates liver injury and suppresses the phosphorylation of DDX3X, which is regulated by ER stress. A phospho-deficient DDX3X mutant (p.T323A) significantly reduces ConA-induced liver injury in mice. Mechanistically, phosphorylation of DDX3X promotes its cytoplasmic–nuclear translocation and hepatocyte apoptosis during ER stress. Moreover, PPARα interacts with the DDX3X helicase domain in the cytoplasm, masking the phosphorylation site (p.323), to inhibit the nuclear translocation of DDX3X and decrease the downregulation of CHOP expression. Additionally, colocalization of PPARα and DDX3X is observed in the livers of AIH patients, elevated serum DDX3X levels were linked to AIH-associated liver failure, and sustained reduction of DDX3X was correlated with a better prognosis.
Conclusion: This study highlights the role of the PPARα-DDX3X interaction in regulating DDX3X phosphorylation during ER stress and promoting DDX3X nuclear translocation and hepatocyte apoptosis. Therefore, targeting the ER stress-PPARα-DDX3X pathway represents a novel therapeutic approach for immune-mediated liver injury.

FRI-265-YI
Acetylcholine-producing B cells regulate regulatory T-cell function within the bile duct ligation–induced fibrotic liver microenvironment

Nastaran Fazel Modares[1]. *[1]University Health Network, Toronto, Canada*
Email: nastaran.fazel@gmail.com

Background and aims: Chronic cholestatic liver injury leads to progressive fibrosis driven by sustained inflammation and dysregulated immune responses. While cytokine-mediated immune regulation in fibrosis is well characterized, the contribution of neuroimmune signaling pathways remains poorly understood. Acetylcholine (ACh), traditionally viewed as a neurotransmitter, can be produced by immune cells and exerts immunomodulatory effects. Whether immune-derived ACh regulates immune homeostasis and fibrogenic pathways during chronic cholestatic liver injury is unknown.
Method: Cholestatic liver fibrosis was induced by bile duct ligation (BDL) in young mice. Acetylcholine-producing lymphocytes were identified using ChAT-GFP reporter mice, and B cell–specific cholinergic deficiency was studied using conditional ChAT knockout models. Immune cell composition and activation were assessed by flow cytometry and histological analyses, alongside evaluation of inflammatory and fibrogenic pathways.
Results: BDL-induced fibrosis was associated with a progressive decline in hepatic $ChAT^{+}$ B cells, accompanied by altered immune composition within the liver. Loss of cholinergic B-cell function correlated with reduced regulatory T-cell abundance and increased expression of profibrotic and inflammatory markers, including a-sma–associated pathways. This suggests that disruption of cholinergic immune regulation may exacerbate disease progression. Histological analyses demonstrated increased fibrotic remodeling in the absence of immune-derived acetylcholine, indicating impaired immune restraint of fibrogenic responses.
Conclusion: These findings identify immune-derived acetylcholine as an important regulator of immune balance during cholestatic liver injury. Disruption of cholinergic immune signaling contributes to

altered Treg homeostasis and enhanced fibrogenic signaling. Neuroimmune pathways may therefore represent previously unrecognized modulators of liver fibrosis and potential targets for limiting disease progression in chronic liver injury.

FRI-266

Identification of molecular targets from the interactome of primary sclerosing cholangitis and their therapeutic modulation

Claudia Fuchs[1], Oleksandr Petrenko[1,2,3], Carolina Mangana[2], Thomas Sorz-Nechay[1,2,3], Kerstin Zinober[1,3], Benedikt Hofer[1,2,3], Benedikt Simbrunner[1,2,3], Frank Assen[4], Wolfgang Weninger[4], Klaus Kaczirek[5], Georg Gyoeri[6], Gabriela Berlakovich[6], Barbara Maier[2], Espen Melum[7], Anna Katharina Frank[7], Philipp Schwabl[1,2,3], Michael Trauner[1], Thomas Reiberger[1,2,3].
[1]Division of Gastroenterology and Hepatology, Department of Internal Medicine III, Medical University of ViennaMedical University of Vienna, Vienna, Austria; [2]CeMM Research Center for Molecular Medicine of the Austrian Academy of Sciences, Vienna, Austria; [3]Christian Doppler Laboratory for Portal Hypertension and Liver Fibrosis, Medical University of Vienna, Vienna, Austria; [4]Department of Dermatology, Medical University Vienna, Vienna, Austria; [5]Department of General Surgery, Medical University of Vienna, Vienna, Austria; [6]Department of Transplant Surgery, Medical University of Vienna, Vienna, Austria; [7]Norwegian PSC Research Center, Division of Surgery and Specialized Medicine, Oslo University Hospital, Oslo, Norway
Email: claudia.fuchs@meduniwien.ac.at

Background and aims: Primary sclerosing cholangitis (PSC) is a rare cholestatic liver disease characterized by chronic bile duct inflammation and fibrosis, progressing to advanced liver disease. Since the cellular and molecular drivers of PSC progression remain poorly defined, we designed a prospective-translational study to profile the PSC liver interactome at single-cell resolution to identify disease-specific molecular targets, supported by multiomics evidence, and demonstrate their therapeutic modulation via predicted small molecule ligands.
Method: We recruited three patients diagnosed with PSC cirrhosis scheduled for liver transplantation. Non-parenchymal cells (NPCs) were isolated from explanted livers and subjected to scRNA-seq and paired snRNA-seq and data were integrated with healthy and non-PSC cirrhotic controls using scVI. Differential interactions were identified using MultiNicheNet. Top ligand-receptor pairs were validated via imaging mass cytometry (IMC) and whole-tissue proteomics (with/without scaffold enrichment), cross-referencing significant transcriptomic changes in *Mdr2*$^{-/-}$ mice. Selected molecular targets underwent ligand screening with AutoDock Vina, followed by *in vitro* validations of the predicted small molecules on PSC patient-derived cholangiocyte organoids.
Results: We obtained 35501 single-cell transcriptomes from PSC livers, identifying distinct cell types (e.g., *ITGAX*/*CD1C+* dendritic cells, DC; *KRT19*/*CFTR+* cholangiocytes). PSC-specific interactions included *THBS1-CD36* between hepatic stellate cells (HSCs) and sinusoidal cells as well as HSCs and DCs. IMC confirmed increased numbers of THBS1+ HSCs and DC in fibrotic areas, as well as numbers of SLIT2+ PSC ductuli. PSC proteomics and *Mdr2*$^{-/-}$ transcriptomics further showed significant upregulation of *Thbs1*, *Nrp1*, and Slit2. bulkRNA sequencing of PSC organoids showed that treatment with ligandsTHBS1, NRP1, and SLIT2 downregulates NF-kB signature expression. GW-493838 combined with BMS270394 notably downregulated both TGF-beta and Notch signatures.
Conclusion: In advanced human PSC we discovered a range of molecular targets - by multi-molecular approaches, a reduced number of potential targets – selected by *Mdr2*$^{-/-}$ animal model validation and *in silico* drug screening. Finally, disease-modulating effects of of these predicted small molecules were investigated using PSC patient-derived cholangiocyte organoids suggesting NRP1 and THBS1 as relevant therapeutic targets.
OP and CF share first authorship; MT and TR share senior authorship.

FRI-267

Modelling the reactive cholangiocyte phenotype in cholangiopathies using human biliary organoids for evaluation of novel therapeutic compounds

Fabian Heinreichsberger[1], David Pereyra[2], Claudia Fuchs[1], Michael Trauner[1]. *[1]Hans Popper Laboratory of Molecular Hepatology, Division of Gastroenterology and Hepatology, Department of Internal Medicine III, Medical University of Vienna, Vienna, Austria; [2]Department of General Surgery, Division of Visceral Surgery, Medical University of Vienna, Department of Vascular Biology and Thrombosis Research, Centre of Physiology and Pharmacology, Medical University of Vienna, Vienna, Austria*
Email: fabian.heinreichsberger@meduniwien.ac.at

Background and aims: Cholangiocytes actively contribute to inflammation during cholestatic disorders by acquiring a "reactive cholangiocyte phenotype." Multifactorial pathways involving bacterial metabolites, accumulating bile acids (BAs) or proinflammatory cytokines play significant roles in cholangiocyte activation. This study aims to (i) characterize the molecular pathways underlying cholangiocyte reactivity and (ii) explore the therapeutic effects of the hydrophilic BAs norucholic acid (NCA) and tetrahydroxylated BAs (THBA) on activated cholangiocytes.
Method: Human extrahepatic cholangiocyte organoids (ECOs) were challenged either with 10 ng/ml LPS & 100 U/L IFNγ or 50 ng/ml IL-17A & 2 ng/ml TNFa. Hydrophilic BAs (250 μM NCA or 0,1–100 μM THBA) were added to explore their therapeutic potential in preventing cholangiocyte activation. Gene expression profiles of inflammatory mediators were analyzed by qPCR.
Results: mRNA-expression profiling demonstrated that the combination of IL-17A and TNFα exerted synergistic effects, elevating Ccl20 128-fold, significantly above separated treatments (7-fold IL-17a; 21,1-fold TNFa, P < 0,0001). Co-treatment with 0.1 μM THBA significantly attenuated the IL-17A/TNFα-mediated inflammatory response, reducing Ccl2 (by 23%, P = 0,013), Cxcl2 (by 60%, P = 0,015) Il-8 (by 53%, P = 0,039) and Ccl20 (by 40%, P = 0,027) expression. NCA decreased Ccl2 (by 22%, P = 0,015), and Cxcl2 (by 45%, P = 0,05). LPS/IFNγ stimulation induced pro-inflammatory chemokine expression in ECOs 5-fold Cxcl2 (P = 0,005), 12,3-fold Ccl2 (P = 0,003), 764,9-fold Cxcl10 (P = 0,0008)). Co-treatment with THBA demonstrated dose-dependent anti-inflammatory effects, reducing Ccl2 (P = 0,0019) and Cxcl2 (P = 0,0198) back to near-baseline levels and Cxcl10 by about 50% (P = 0,001) at 0.1 μM.
Conclusion: THBA & NCA attenuate the reactive cholangiocyte phenotype arguing for their therapeutic potential in cholangiopathies.

FRI-268-YI

T helper cells influence the fate decision of facultative liver stem cells

Ben Higgins[1], Gareth Hardisty[1], Pei-Chi Huang[1], Man Chun Wong[1], Matamoana Muller[1], Hei-Ip Hong[1], Naruhiro Kimura[2], Tim Kendall[1], David Withers[3], Philip Newsome[3], Prakash Ramachandran[1], Wei-Yu Lu[1]. *[1]University of Edinburgh, Centre for Inflammation Research, Edinburgh, United Kingdom; [2]Division of Gastroenterology and Hepatology, Niigata University, Niigata, Japan; [3]Department of Immunology and Immunotherapy, University of Birmingham, Birmingham, United Kingdom*
Email: s2263267@ed.ac.uk

Background and aims: During liver disease, a compensatory biliary regenerative mechanism, termed ductular reaction (DR), occurs. A hallmark of DR is the acquisition of a facultative stem cell phenotype by the cholangiocytes, accompanied by infiltration and proliferation of CD4$^+$ T helper cells. However, the role of these T helper cells during DR is unclear. Thus, we aimed to (1) characterise the immune composition and immune-cholangiocyte spatial organisation of the biliary niche during DR, and (2) define the influence of T helper subsets on cholangiocyte function and fate.

Method: 30-plex imaging utilising the Akoya PhenoCycler was performed on human cholestatic and steatotic explant livers to resolve the spatial immune-cholangiocyte organisation. An *Mdm2*$^{fl/fl}$ transgenic mouse model of liver injury in conjunction with antibody-based CD4 depletion was used to assess T helper cell function during DR *in vivo*. Immune- and cholangiocyte-enriched scRNA sequencing was conducted to investigate immune interactions and characterise cellular heterogeneity. The functional role of defined T helper subsets was validated using co-culture with intrahepatic cholangiocyte organoids (ICOs).
Results: T helper cells were enriched within the biliary niche, particularly in cholestatic liver diseases. Single-cell transcriptomic analysis identified distinct cholangiocyte subpopulations, including a subset marked by a stem-like transcriptional signature. T helper cell depletion disrupted this population, leading to transcriptional downregulation of key pathways involved in liver regeneration, including EGFR and Notch signalling. Co-culture experiments resulted in cholangiocytes with divergent transcriptomic profiles and phenotypes, demonstrating subset-specific regulation of cholangiocyte cell fate. Notably, Th17 cells and IL-17A promoted a stem-like cholangiocyte phenotype and induced pro-inflammatory chemokines associated with DR. Consistently, disease progression is associated with an increased Th17 to Treg ratio and enrichment of key IL-17A signalling pathways.
Conclusion: T helper cell subsets regulate the plasticity of cholangiocytes during DR. Th17-derived IL-17A programs a stem-like cholangiocyte state through modulation of regenerative and inflammatory pathways, revealing immune control of biliary regeneration.

FRI-269
Reactive biliary epithelial cells distinctly respond to toxic bile acids and favor pro-inflammatory macrophage polarization through GAS6-AXL signaling pathway in cholestatic liver
Tian Lan[1,2], Guo Yin[1], Hanyang Liu[1], Natalia Martagón Calderón[3], Franco-Leonardi Bianca[4], Yuanshui Long[2], Pavitra Kumar[1], Hilmar Berger[1], Milad Rezvani[3], Frank Schaap[5,6], Frank Tacke[1], Adrien Guillot[1]. [1]*Department of Hepatology & Gastroenterology, Charité Universitätsmedizin Berlin, Campus Virchow-Klinikum and Campus Charité Mitte, Berlin, Germany;* [2]*Department of Gastroenterology and Hepatology, West China Hospital, Sichuan University, Chengdu, China;* [3]*Department of Pediatric Gastroenterology, Nephrology and Metabolic Medicine, Charité Universitätsmedizin Berlin, Berlin, Germany;* [4]*Department of Physiology and Biophysics, Institute of Biomedical Sciences, University of Sao Paulo, Sao Paulo, Brazil;* [5]*Department of Surgery, NUTRIM Institute of Nutrition and Translational Research in Metabolism, Maastricht University, Maastricht, Netherlands;* [6]*Department of General, Visceral and Transplantation Surgery, RWTH Aachen University, Aachen, Germany*
Email: tian.lan@charite.de

Background and aims: Cholestatic liver diseases are characterized by toxic bile acid (BA) accumulation, biliary epithelial cell (BEC) activation, and macrophage accumulation. However, how the interaction between reactive BEC and toxic BA impacts macrophages remains to be fully elucidated. Growth-arrest specific protein 6 (GAS6) is a secreted protein with complex and sometimes contradictory effects on liver repair and immune response by binding to its receptor AXL. Current data shows that BECs represent a major source of GAS6. However, the role of BEC-derived GAS6 in chronic liver disease remains to be fully deciphered.
Method: Mouse intrahepatic cholangiocyte organoids (mICO) were generated from wild-type and *Mdr2*-deficient (KO) mice. Bulk RNA sequencing, seahorse assay, and multiplex immunofluorescence (mIF) were used to characterize the mICO phenotypes. BEC-specific *Gas6* knockdown mice were generated by AAV-delivered siRNA. Dissociated WT and KO mICO were seeded into the multicellular biliary-niche-on-a-chip system (BoC), together with mouse primary hepatic stellate cells, endothelial cells, and macrophages. The BoC was perfused with fresh blood circulating immune cells.
Results: KO mICO showed increased proliferation and expression of pro-inflammatory and pro-fibrotic factors when compared to WT mICO, mimicking the phenotype of reactive BECs *in vivo*. When stimulated with toxic BA, KO mICO showed higher viability and distinct transcriptomic profiles compared with WT mICO. Seahorse assays revealed that KO mICO were more metabolically active and adapted better to stress inducers. Public dataset mining and cellchat analysis revealed that BEC interacts with macrophages through GAS6-AXL signaling in cholestatic liver disease. Mouse primary macrophages treated with conditioned medium from WT and KO mICO showed pro-inflammatory polarization. This effect was partly reversed by inhibiting GAS6-AXL pathway in cell culture and in the BoC system. BEC-specific *Gas6* knockdown prevented DDC diet-induced liver injury and fibrosis, and upregulated liver cell proliferation in mice. In line, intraperitoneal injection of GAS6 protein inhibited liver cell proliferation, exaggerated liver injury and inflammation in mice fed with a CDE diet.
Conclusion: Reactive cholangiocytes have distinct transcriptomic and metabolic profiles and respond differently to toxic BA stimulation, favoring pro-inflammatory macrophage polarization and impairing liver regeneration through GAS6-AXL signaling in cholestatic liver disease.

FRI-270
Gut microbiota-bile acid axis drives pathogenic gamma delta T differentiation in autoimmune hepatitis
Junxing Li[1], Han Wang[2], Dong Xu[1]. [1]*Department of Infectious Diseases, Tongji Hospital, Tongji Medical College, Huazhong University of Science and Technology, Hubei, Wuhan, China;* [2]*Department of Gastroenterology, Tongji Hospital, Tongji Medical College, Huazhong University of Science and Technology, Hubei, Wuhan, China*
Email: 1141539455@qq.com

Background and aims: Autoimmune hepatitis (AIH) is a chronic immune mediated liver disease driven by dysregulated hepatic immunity. Gamma delta T cells (γδT) are an important component of liver resident immune populations, yet their role in AIH and the mechanisms governing their differentiation remain unclear. This study aimed to investigate the contribution of hepatic γδT cells to AIH and to determine whether the gut microbiota bile acid axis influences their differentiation and pathogenic function.
Method: AIH was induced in mice by transfection of human autoantigen cytochrome P450 2D6 (CYP2D6). Hepatic γδT cells were characterized using single cell RNA sequencing. Human AIH liver samples were analyzed to validate findings from the mouse model. The functional role of γδT cells was assessed using γδT cell deficient mice. Transcriptional profiles of hepatic γδT cells were analyzed to identify regulatory and pro inflammatory gene programs. Liver metabolomics and 16S rRNA sequencing were performed to assess bile acid metabolism and gut microbiota composition. Antibiotic treatment was used to modulate gut microbiota and evaluate effects on bile acid metabolism, γδT differentiation and AIH severity.
Results: Single cell analysis revealed a marked accumulation of hepatic γδT cells in AIH mice, dominated by the γδT1 subset. Consistently, human AIH liver samples showed increased γδT cell infiltration with a γδT1 biased phenotype. In AIH livers, regulatory associated genes in γδT, including Nfatc1, Dusp2, Klf4, Vegfb and Bach2it1, were significantly downregulated, while pro inflammatory genes such as Bag3, Usp18 and Tab3 were upregulated. Genetic deletion of γδT cells markedly alleviated liver inflammation and fibrosis. Mechanistically, γδT1 cells were essential for effective dendritic cell antigen presentation. Metabolomic analysis indicated that γδT1 differentiation was associated with altered bile acid metabolism, which was driven by gut microbiota dysbiosis characterized by increased Allobaculum and Desulfovibrio. Antibiotic

treatment restored bile acid homeostasis, reduced hepatic γδT1 cells and ameliorated AIH severity.
Conclusion: γδT1 cells accumulate in AIH and promote liver inflammation by enhancing dendritic cell mediated antigen presentation. Their pro inflammatory differentiation is driven by bile acid metabolic dysregulation secondary to gut microbiota imbalance. Targeting the gut microbiota-bile acid-γδT1 axis may represent a novel therapeutic strategy for AIH.

FRI-271
Long-term effects of antibiotics in promoting liver fibrosis during cholestatic liver disease
Jack Hales[1], Cristina Lumbreras-Perales[1], Mar Moreno-Gonzalez[1], Raymond Kiu[1,2], Pablo Elizalde-Garcia[1], Shikha Saha[1], Mark Philo[1], Lindsay Hall[1,2], Naiara Beraza[1]. *[1]Quadram Institute, Norwich, United Kingdom; [2]University of Birmingham, Birmingham, United Kingdom*
Email: jack.hales14@gmail.com

Background and aims: Cholestatic liver disease is defined as an autoimmune disease with a strong genetic component, while its increased incidence point towards environmental triggers. The role of the gut microbiota during liver disease is increasingly accepted, while the mechanisms mediating its contribution to disease progression remain largely undefined. Antibiotics disrupt gut microbial communities and the potential long-term effects on liver disease susceptibility remain poorly understood. This study aimed to investigate the potential long-term effects of antibiotic-induced gut microbiome disruption on the progression of cholestatic liver disease.
Method: Mice (C57Bl/6, 8–12 weeks) received broad-spectrum antibiotics (ABx) for 7 days, with a 3-week wash-out ("recovery") period before bile duct ligation (BDL). 7 days after BDL, liver, and serum samples were collected and analysed using immunological, histological, and immunohistochemical (IHC) techniques. Shotgun sequencing and LC-MS approaches were used in faecal samples obtained from the same animals; before and after ABx, after recovery and after BDL.
Results: In ABx-treated mice, gut microbiota biomass was restored at 3 weeks post-treatment (recovery), as measured by 16 s rRNA qPCR in faecal samples. Still, shotgun sequencing revealed persistent alterations in microbiome composition, including non-recovery of commensal such as Bacteroides thetaiotaomicron (Bt), with distinct bile acids and short-chain fatty acid profiles. 7 days after BDL, ABx +recovery mice showed exacerbated liver fibrosis, assessed by Sirius Red staining, compared to mice not receiving ABx. Flow cytometry and further F4/80 IHC revealed reduced macrophage recruitment in the livers of ABx-treated mice versus untreated mice at 7 days post-BDL, accompanied by impaired phagocytic capacity and reduced expression of MMP2, indicating an altered macrophage response.
Conclusion: Antibiotics cause lasting gut microbiome alterations, including loss of key commensal bacteria that exacerbate liver fibrosis in cholestatic liver disease, despite microbiota biomass recovery. Pointing to Bt as a potential strategy to attenuate ABx-mediated aggravation in cholestatic liver disease.

FRI-272
Methyldopa reduces plasma bile acid concentrations in a murine model of estrogen-induced cholestasis
Dina Manna[1], Hana Lastuvkova[1], Jolana Schreiberova[1], Lenka Jandova[1], Milos Hroch[1], Martin Ambroz[2], Mária Krutáková[2], Martin Lenicek[3], Hirsova Petra[4], Marian Kacerovsky[5], Petr Pavek[2], Stanislav Micuda[1]. *[1]Univerzita Karlova-Lékařská Fakulta v Hradci Králové, Hradec Králové, Czech Republic; [2]Univerzita Karlova-Farmaceutická Fakulta v Hradci Králové, Hradec Králové, Czech Republic; [3]General University Hospital in Prague and First Faculty of Medicine, Charles University, Prague, Czech Republic; [4]Mayo Clinic, Rochester, United States; [5]University Hospital Olomouc, Olomouc, Czech Republic*
Email: manad@lfhk.cuni.cz

Background and aims: Intrahepatic cholestasis of pregnancy (ICP) is the most common gestational liver disorder and is characterized by elevated serum bile acid (BA) concentrations. This results in increased placental barrier penetration and adverse pregnancy outcomes, such as preterm birth and meconium-stained amniotic fluid. Epidemiological studies indicate that ICP is associated with an increased risk of preeclampsia, often requiring treatment with antihypertensive medications such as methyldopa; however, the impact of methyldopa on BA homeostasis remains unclear.
Method: We examined methyldopa in a murine model of estrogen-induced cholestasis. Female C57BL/6J mice received ethinylestradiol (10 mg/kg, s.c.) with or without methyldopa (250 mg/kg, p.o.) for 7 days. BA profiles were quantified by LC–MS across plasma, bile, liver, urine, intestine, and feces. Hepatic, ileal, and renal expression of BA-related enzymes/transporters was assessed by RT-qPCR and Western blotting.
Results: In estrogen-induced cholestatic mice, methyldopa decreased total BA concentrations in plasma and liver without increasing fecal or urinary BA excretion. This reduction was associated with upregulation of phase I/II enzymes (Cyp2b10, Ugt1a1, Sult2a1) and transporters (Abcb11, Slc10a1, Abcc3/4), consistent with transcriptional changes indicative of indirect constitutive androstane receptor (CAR) activation via p-ERK downregulation. Methyldopa also lowered hepatic free cholesterol in cholestatic mice, accompanied by downregulation of Hmgcr and upregulation of Acat2, suggesting altered cholesterol handling that limits substrate availability for BA synthesis.
Conclusion: Methyldopa lowered plasma BA concentrations under estrogen-induced stress by reducing BA synthesis and enhancing detoxification. In the context of pregnancy-related BA dysregulation, these findings suggest that methyldopa, when used to treat hypertensive disorders of pregnancy, may attenuate BA accumulation and potentially delay the onset of cholestatic phenotypes—an observation that generates hypotheses warranting clinical validation.

FRI-273
Increased miR-27b expression in early primary biliary cholangitis impairs mitophagy via prohibitin-2 suppression
Joanna Abramczyk[1], Jesus M Banales[2], Piotr Milkiewicz[3], Malgorzata Milkiewicz[1]. *[1]Department of Medical Biology, Pomeranian Medical University, 70-111 Szczecin, Poland, Szczecin, Poland; [2]Donostia University Hospital, University of the Basque Country UPV/EHU, CIBERehd, Ikerbasque, 20014 Donostia, San Sebastian, Spain; Department of Biochemistry and Genetics, School of Sciences, University of Navarra, 31008 Pamplona, Spain, San-Sebastian, Spain; [3]Department of Translational Medicine, Pomeranian Medical University, Liver and Internal Medicine Unit, Department of General, Transplant and Liver Surgery of the Medical University of Warsaw, Warsaw, Poland, Szczecin, Poland*
Email: joanna.abramczyk@pum.edu.pl

Background and aims: Impaired mitophagy, a form of autophagy responsible for the degradation of damaged mitochondria, has been implicated in the pathogenesis of primary biliary cholangitis (PBC) and may contribute to the generation of disease-specific anti-mitochondrial antibodies. miR-27b is a microRNA involved in the regulation of mitophagy through modulation of the PINK1/Parkin pathway and suppression of prohibitin-2 (PHB2), a key mediator of Parkin-mediated mitophagy leading to defective clearance of damaged mitochondria. This study aimed to investigate the role of miR-27b in the pathogenesis of PBC.
Method: Expression of miR-27b and protein levels of PHB2 were analyzed in liver tissue at different stages of PBC, including early-stage PBC with fibrosis stages F0–F2 (esPBC, n = 17), advanced PBC with fibrosis stage F4 (n = 10), PSC (n = 10), and controls (n = 15). miR-27b expression was also evaluated in normal human cholangiocytes (NHC) and in H69 human cholangiocytes in culture with or without experimentally overexpression of miR-506 (H69 miR-506; a PBC cholangiocyte model). NHC were exposed to glycochenodeoxycholic

acid (GCDCA), lithocholic acid (LCA), and lipopolysaccharide (LPS). miR-27b overexpression was experimentally overexpressed by transfection with mirVana® miRNA Mimics. The role of miR-27b in autophagy was quantified by flow cytometry using the Muse® Autophagy LC3 Kit. MicroRNA, mRNA, and protein levels were assessed by qPCR and Western blot, respectively.
Results: Increased expression of miR-27b was observed only in the early stages liver tissue of esPBC (9-fold increase vs. advanced PBC, PSC, and controls), accompanied by a 30% reduction in PHB2 protein levels. Under baseline conditions, miR-506 cholangiocytes were characterized by 4-fold higher levels of miR-27b compared with controls. Incubation of NHC with GCDCA (150 µM) or LCA (100 µM), but not LPS, increased miR-27b expression (3-fold and 5.5-fold vs. control, respectively). Enhanced miR-27b expression in NHC cells led to an increased proportion of autophagic cells (1.8-fold vs. control) and an 80% reduction in PHB2 protein levels.
Conclusion: This study demonstrates that enhanced miR-27b expression at early stages of PBC and the consequent inhibition of PHB2 accumulation on damaged mitochondria may contribute to defective mitophagy, representing a potential therapeutic target in PBC.

FRI-274
Myeloid deletion of SIRT1 exacerbates cholestasis-induced liver disease by promoting inflammation and fibrosis in mice
Mar Moreno-Gonzalez[1], Anna Isaacs-Ten[1], Pablo Luri Martin[1], Ane Álava[1], Naiara Beraza[1]. [1]*Quadram Institute, Food Microbes and Health Institute Strategic Programme, Norwich, United Kingdom*
Email: mar.moreno-gonzalez@quadram.ac.uk

Background and aims: Sirtuin1 (SIRT1) has been described as a key macrophage regulator during inflammation. We previously described that myeloid-specific SIRT1 overexpression contributes to cholestatic disease progression, promoting liver damage and fibrosis. Here, we investigate whether the modulation of SIRT1 in macrophages could ameliorate liver injury and fibrosis by rewiring macrophage metabolism and autophagy, regulating inflammation.
Method: Cholestasis was induced in myeloid-specific SIRT1 knockout mice (SIRT1 Mye−/−) and wild-type (WT) littermates via bile duct ligation (BDL) or 3,5-diethoxycarbonyl-1,4-dihydrocollidine (DDC) feeding. After 7 days, serum transaminases were measured and liver tissues were analysed by quantitative PCR (qPCR), immunohistochemistry (IHC) and immunofluorescence (IF). To evaluate autophagy, Bone Marrow-Derived Macrophages (BMDMs) from SIRT1 Mye −/− and WT mice were stimulated with labelled apoptotic bodies, and LC3B puncta were quantified.
Results: 7 days after BDL, SIRT1 Mye−/− showed increased serum Aspartate Aminotransferase (AST) and Alanine Aminotransferase (ALT) levels compared to WT. In line with this, SIRT1 Mye−/− mice had increased macrophage infiltration in the liver. IHC analysis of cytokeratin-19 (CK-19) evidenced increased biliary epithelial expansion in SIRT1 Mye−/− supporting ductular reaction. Additionally, Sirius red and αSMA staining and quantification showed increased fibrosis in SIRT1 Mye−/− 7 days after BDL compared to controls. Similarly, after 1 week of DDC feeding, SIRT1 Mye−/− mice had elevated levels of inflammatory cytokines (Il-1b, CCL2, TNFα) in the liver compared to WT controls. IHC analysis revealed increased CK-19-positive areas and increased liver fibrosis in SIRT1 Mye−/− compared to controls, as determined by Sirius red staining and αSMA IF. *In vitro*, we found decreased LC3B puncta in SIRT1-deficient macrophages after stimulation with apoptotic bodies compared to WT, indicating impaired autophagy activity.
Conclusion: SIRT1 deletion in myeloid cells contributes to the aggravation of cholestasis-mediated liver disease by promoting inflammation, ductular reaction and fibrosis. Mechanistically, SIRT1 deletion reduces autophagy in macrophages. These findings suggest that fine-tuning of SIRT1, rather than elimination, in macrophages may represent a novel therapeutic strategy for this condition.

FRI-275
Disease-specific microbiome signatures distinguish primary sclerosing cholangitis from inflammatory bowel disease
Burcin Özdirik[1,2], Daniel Fasulo[3], Peter Lee[3], Frank Tacke[2], Mark Driscoll[3], Bernd Schnabl[1]. [1]*University California San Diego, Charité - Universitätsmedizin Berlin, La Jolla, United States;* [2]*Charité-Universitätsmedizin Berlin, Berlin, Germany;* [3]*Intus - Biosciences, Farmington, United States*
Email: bozdirik@health.ucsd.edu

Background and aims: Primary sclerosing cholangitis (PSC) is an immune-related cholangiopathy lacking treatment options outside of liver transplantation. The gut-liver axis, particularly the contribution of gut microbiota, has emerged as a key pathway in PSC pathogenesis. Although PSC is frequently associated with inflammatory bowel disease (IBD), robust microbiome markers that reliably distinguish PSC from IBD alone remain elusive. In a novel approach, we employ PCR amplification of the bacterial rRNA operon to identify microbiome signatures that distinguish PSC from IBD alone and healthy controls.
Method: Microbiome profiling was performed across 96 patients with PSC (PSC-only n = 30, PSC-IBD only n = 66), 87 patients with IBD (Crohn's disease n = 42; Ulcerative Colitis n = 45), and healthy controls from two different cohorts (n = 55; n = 82). A ~2,500-base amplicon spanning the 16S and 23S rRNA genes was generated and mapped to a custom 16S–23S rRNA reference database. Marker discovery was conducted in defined training subsets, followed by classification using logistic regression and random forest models with cross-validation and independent evaluation sets.
Results: We developed a PSC-specific marker set comprising Enterobacteriaceae, Lachnospiraceae, and Oscillospiraceae that distinguishes PSC from IBD and healthy controls with 91–94% accuracy (AUC = 0.98). Further, in comparisons of PSC-IBD versus IBD-only, 27 microbial markers covering 10 taxonomic categories achieved 84% accuracy under cross validation by Random Forest. Key species included *Enterococcus faecalis*, *Klebsiella pneumoniae*, *Streptococcus thermophilus*, and *Fusobacterium ulcerans*. Incorporation of additional IBD markers improved sensitivity and subgroup performance, particularly in PSC-IBD with ulcerative colitis.
Conclusion: Distinct microbiome signatures differentiate PSC from healthy controls and from IBD alone, supporting a PSC-specific microbial phenotype with diagnostic potential.

FRI-276-YI
Modelling biliary epithelial responses to microbial signals using a bile duct on a chip platform
Sarah Peisl[1,2,3,4], Henry Hoyle[1,2,5], Enya Amundsen-Isaksen[1,2,6], Jeremy Yeoh[1,2,5,6], Stefan Krauss[5], Deborah Stroka[3,4], Espen Melum[1,2,5,6,7]. [1]*Norwegian PSC Research Center, Department of Transplantation Medicine, Division of Surgery and Specialized Medicine, Oslo University Hospital Rikshospitalet, Oslo, Norway;* [2]*Research Institute of Internal Medicine, Division of Surgery and Specialized Medicine, Oslo University Hospital Rikshospitalet, Oslo, Norway;* [3]*Department of Visceral Surgery and Medicine, Bern University Hospital, University of Bern, Bern, Switzerland;* [4]*Graduate School for Cellular and Biomedical Sciences, University of Bern, Bern, Switzerland;* [5]*Hybrid Technology Hub, Institute of Basic Medical Science, University of Oslo, Oslo, Norway;* [6]*Institute of Clinical Medicine, Faculty of Medicine, University of Oslo, Oslo, Norway;* [7]*Section of Gastroenterology, Department of Transplantation Medicine, Division of Surgery and Specialized Medicine, Oslo University Hospital Rikshospitalet, Oslo, Norway*
Email: sarah.peisl@unibe.ch

Background and aims: Cholangiopathies such as primary sclerosing cholangitis are characterized by chronic biliary inflammation, with increasing evidence implicating microbial products in disease pathogenesis. Cholangiocytes are exposed to microbes and microbial signals in bile and express receptors capable of sensing microbe-

associated molecular patterns (MAMP) that may engage in pro-inflammatory signalling. Mechanistic insights on how distinct microbial signals affect cholangiocyte function remain limited. We therefore aimed to integrate MAMPs with an *in vitro* bile-duct-on-a-chip model to study microbial–epithelial interactions relevant to cholangiopathies.

Method: A 3D-printed bile duct-on-a-chip with a collagen-embedded tubular channel lined by a confluent, polarized cholangiocyte layer was used. As cell source cholangiocyte organoids generated from bile duct brushings collected during ERCP were used. Lipopolysaccharide (LPS), lipoteichoic acid (LTA), and flagellin were applied apically in the chip for 24 hours at increasing concentrations with continuous flow within the channel. Epithelial responses were assessed by permeability to dextran, basal cytokine secretion (IL-8, CCL-20) by ELISA, and gene expression by qPCR, including tight junction (Claudin-2, Claudin-3) and functional markers (ASBT, CFTR).

Results: LPS, LTA and flagellin induced stimulus- and dose-dependent cholangiocyte responses. Low-dose LPS (0.1 µg/mL) was associated with an adaptive epithelial response, with unchanged permeability, upregulation of tight junction (Claudin-2 1.4-fold, Claudin-3 1.4-fold), functional markers (ASBT 5.0-fold, CFTR 2.2-fold), and suppressed IL-8 secretion (Δ –67 pg/mL). LPS 10 µg/mL was associated with increased 10 kDa dextran permeability (59% vs 15%, p = 0.007), reduced ASBT expression (0.6-fold), and IL-8 secretion (Δ +254 pg/mL). Compared with LPS, LTA and flagellin were associated with stronger inflammatory responses at low doses, with marked IL-8 induction (LTA 0.5 µg/mL: Δ +694 pg/mL; flagellin 1 ng/mL: Δ +1287 pg/mL) and CCL-20 release (LTA 5 µg/mL: Δ +251 pg/mL; flagellin 10 ng/mL: Δ +2436 pg/mL), not observed with LPS.

Conclusion: The bile duct on a chip model enables investigation of cholangiocyte responses to distinct microbial signals in a more physiological manner than previously reported. Using this platform, we identified stimulus- and dose-dependent differences in cholangiocyte sensitivity to apical MAMP, establishing the chip as relevant system to study microbial–epithelial interactions.

FRI-282

Molecular classification of Indian gallbladder cancer reveals TP53-driven and oncogene-addicted subgroups

Gayatri Ramakrishna[1], Vipin Yadav[1], Archana Rastogi[1], Vaishali Yadav[1], Varun Suroliya[2], Anupama Bhattacharya[2], Ashily Koshy[1], Abhilasha Yadav[1], Rishabh Sharma[1], Ragini Kilambi[1], Nihar Mohapatra[1], Nirupma Trehanpati[1], Viniyendra Pamecha[1], Shiv Kumar Sarin[1]. [1]*Institute of Liver & Biliary Sciences, New Delhi, India;* [2]*Artemis Hospital Gurgaon, Gurugram, India*
Email: gayatriramakrishna@gmail.com

Background and aims: Gallbladder cancer (GBC) is an aggressive biliary malignancy with high incidence in northern India. Despite known associations with gallstones and genetic predisposition, its molecular heterogeneity remains poorly defined. This study integrated genomic and immunohistochemical markers to define molecular subsets of GBC and compare tumors arising with or without gallstones.

Method: DNA from 32 gallbladder specimens was analysed using targeted next-generation sequencing using a 42-gene somatic mutation panel. Variant analysis and genetic clustering were performed using an R-based pipeline. Immunohistochemistry (IHC) was conducted for prognostic markers, including AQP1, S100P, MUC5AC, CRP, and Podoplanin.

Results: Both genders were equally represented, with gallstones present in 50% and underlying fatty liver in 59.4% cases. Histopathology revealed adenocarcinoma as the predominant subtype (78%), followed by adenosquamous carcinoma (12%). The mutation profile revealed C > T transitions as the most frequent base substitution, amongst the pathogenic variants. *TP53* was the most frequently mutated gene (56%), followed by *EGFR* (25%), *BRAF* (22%), *RB1* (19%), and *KRAS* and *PIK3CA* (12% each). Novel *RET* and *IDH1/2* variants were detected in 12% of cases. Clinically actionable targets (*IDH, ERB2, BRAF, KRAS*) were identified in 28% of tumors. Integration of mutation profiles with clinical and IHC-based prognostic markers identified three molecular subgroups of gallbladder cancer: (1) GBC1 (*TP53*-mutant): predominantly female, adverse clinicopathological features, median survival 23 months, weak podoplanin and intense AQP1 expression; (2) GBC2 (*TP53*-wild type with *RET*/*IDH* mutation): favourable prognosis, median survival 27 months, moderate AQP1 and podoplanin; (3) GBC3 (*TP53*-wild type with *EGFR*/*BRAF* mutation): predominantly male, poorest survival (13 months), intense stromal podoplanin expression. Gallstone-associated GBC exclusively harboured *IDH1* variants (19% vs 0%, p = 0.06), whereas non–stone GBC showed a higher frequency of *BRAF*/*MAP2K2* (12% vs 31%, p = 0.2) alterations.

Conclusion: In Indian patients with GBC, *TP53* inactivation defines a major subclass with moderate to good prognosis, whereas *TP53*–wild-type tumors follow an alternative oncogene-addicted pathway with poor prognosis linked to stromal podoplanin. While BRAF enrichment in non–stone tumors indicates dominance of the RAS-MAPK pathway, the IDH1 variants, which were exclusive to gallstone-associated GBC, suggest metabolic adaptation.

FRI-283

Retrieval-augmented pc-deployable small language models achieve comparable performance to frontier systems for autoimmune liver disease guideline-based decision support

Ernest Saenz[1], Martin Gómez-Loira[2], Juan Turnes[2], Indhira Pérez-Medrano[2], Ezequiel Ridruejo[3], Jimmy Daza[1], Lucia Coli[1], Timo Itzel[1], Andreas Teufel[1]. [1]*Department of Medicine II, Division of Hepatology, Medical Faculty Mannheim, Heidelberg University, Mannheim, Germany;* [2]*University Hospital Complex Of Pontevedra, Pontevedra, Spain;* [3]*Hepatology Section, Department of Medicine, Centro de Educación Médica e Investigaciones Clínicas Norberto Quirno "CEMIC", Buenos Aires, Argentina*
Email: ernest.phd@gmail.com

Background and aims: Autoimmune liver diseases expertise remains concentrated in academic centers, creating barriers to guideline concordant care in community settings. Large language models (LLMs) show promise for clinical decision support but raise concerns regarding cost sustainability, privacy and data governance. We evaluated whether smaller, locally deployable on consumer hardware models with retrieval-augmented generation (RAG) could match frontier commercial systems for autoimmune hepatitis (AIH), primary biliary cholangitis (PBC), and primary sclerosing cholangitis (PSC) clinical questions.

Method: Clinicians averaging 15 years of hepatology practice constructed a 117 question corpus addressing AIH (29.9%), PBC (35.9%), and PSC (34.2%) across diagnostic criteria, treatment algorithms, and risk stratification. Reference guidelines included EASL, AASLD, BSG, UK-PBC, APASL, DGVS, and Japanese society recommendations. Fifteen LLMs spanning 3B-1T+ parameters completed 5,265 baseline inferences. Three architecturally-diverse models (dense transformer, mixture-of-experts, hybrid state-space model (SSM); 12B-1T parameters) were subsequently evaluated with top-5 guideline passage retrieval. Outcomes included accuracy with 95% confidence intervals, inference latency, answer stability, and per-query cost and we used pairwise McNemar's tests and model per disease interaction effects.

Results: Without RAG, performance varied significantly: GPT-5.1 achieved 93.0% accuracy (95% CI: 90.2–95.3%), best local models 84.0–86.3%. With RAG, architecturally-diverse models converged: GPT-5.1 95.4%, Kimi K2 (1T MoE) 94.6%, Magistral-24B (local) 94.8%, Nemotron-12B (local) 95.0% (overlapping CIs, no significant pairwise differences). Disease-specific RAG performance: AIH 97–100%, PSC 100%, PBC 85–87% across all models. Additionally, 67/105 (63.8%) pairwise comparisons showed significant differences without RAG

versus 0/6 (0%) with RAG ($p < 0.001$ for interaction effect elimination).
Conclusion: For guideline-based autoimmune liver disease questions, small locally-deployable models with guideline retrieval demonstrated non-inferior accuracy to frontier expensive commercial systems. This approach may enable equitable access to LLM-assisted decision support while maintaining institutional data control on hospital-grade computers. Prospective clinical validation and assessment of non-guideline scenarios remain necessary before implementation.

FRI-284
A novel therapeutic strategy for cholemic nephropathy: mineralocorticoid receptor antagonists attenuate bile acid–induced renal injury in vivo and in vitro via the rac1–mineralocorticoid receptor pathway
Sigrid Schulte[1], Susanne Zweerink[1], Diran Herebian[2], Jochen Fries[3], Dirk Nierhoff[1], Christoph Neumann-Haefelin[1], Hans-Michael Steffen[1], Ulrich Töx[1]. *[1]University Hospital Cologne, Department of Gastroenterology and Hepatology, Cologne, Germany; [2]University Hospital Duesseldorf, Department of Paediatrics Neonatology and Paediatric Cardiology Metabolism laboratory, Duesseldorf, Germany; [3]University Hospital Cologne, Institute for Pathology, Cologne, Germany*
Email: sigrid.schulte@uk-koeln.de

Background and aims: Cholemic nephropathy (CN) represents an important cause of renal dysfunction in patients with cholestasis and advanced liver disease. While activation of the mineralocorticoid receptor (MR) has been implicated in renal injury, the interaction between the small GTPase RAS-related C3 botulinum toxin substrate 1 (Rac1) and MR signaling, and its contribution to CN progression, remain poorly understood. This study investigated the effects of MR antagonism on histopathological renal alterations in a bile duct ligation (BDL) rat model and examined bile acid–induced cytotoxicity in human proximal tubular epithelial cells, with a particular focus on the Rac1–MR signaling pathway.
Method: Sixty male Wistar rats were randomly assigned to three groups: sham operation, BDL without treatment, and BDL with spironolactone treatment (100 mg/kg body weight/day) for 28 days. Renal tissue was harvested for histological and immunohistochemical analysis. In parallel, the bile acid profile of a cholestatic patient with histological evidence of CN (serum bilirubin 9.3 mg/dL, creatinine 4.5 mg/L) was determined. HK-2 cells were exposed to a bile acid cocktail reflecting this patient-specific profile, with or without potassium canrenoate and/or the Rac1 inhibitor NSC23766. Cytotoxicity was assessed using the CytoTox-Glo® assay.
Results: In vivo, BDL induced characteristic histopathological features of cholemic nephropathy in untreated animals, whereas these changes were markedly attenuated in spironolactone-treated rats. Immunohistochemical analysis demonstrated reduced renal Rac1 expression in the treatment group. In vitro, exposure of HK-2 cells to the bile acid cocktail resulted in pronounced cytotoxicity after 24 hours. Co-treatment with potassium canrenoate (10 µM) and NSC23766 (100 µM) significantly reduced cytotoxicity ($p = 0.001$). Both agents alone also conferred partial protection.
Conclusion: These findings demonstrate a significant protective effect of mineralocorticoid receptor antagonists in experimental cholemic nephropathy, both in vivo and in vitro. Beyond the classical aldosterone–MR axis, activation of the Rac1–MR signaling pathway appears to play a critical role in bile acid–induced renal injury. Further studies are warranted to elucidate the therapeutic potential of targeting this pathway in cholestasis-associated kidney disease.

FRI-285
Thioredoxin reductase 1 regulates the nucleotide binding oligomerization domain containing 2-receptor interacting serine/threonine kinase 2 signaling pathway during cholestatic liver injury
Colin Shearn[1], Aimee Anderson[1], Michael Devereaux[1], Edward Schmidt[2], Ronald Sokol[3]. *[1]The University of Colorado Anschutz Medical Campus, Aurora, United States; [2]Montana State University, Hungarian Veterinary Medical University, Bozeman, United States; [3]The University of Colorado Anschutz Medical Campus, Children's Hospital Colorado, Aurora, CO, United States*
Email: Colin.Shearn@CUAnschutz.edu

Background and aims: The cholestatic liver disease primary sclerosing cholangitis (PSC), is characterized by periportal inflammation with progression to hepatic fibrosis and ultimately cirrhosis. Bacterial PAMPs have been shown to activate the Nucleotide Binding Oligomerization Domain Containing 2- Receptor Interacting Serine/Threonine Kinase 2 (Nod2-Ripk2) intracellular inflammatory signaling pathway in the intestine. Approximately 80% of PSC patients have an additional diagnosis of Crohn's disease, increasing the susceptibility of the liver to exposure of bacterial Pathogen-Associated Molecular Patterns (PAMPs) originating from the intestine. We have recently shown that Thioredoxin Reductase (TrxR1) signaling plays an important role in regulation of inflammation during cholestasis. The objective of this study was to determine if Nod2-Ripk2 signaling is upregulated in PSC and to examine the impact of pharmacological and genetic targeting of thioredoxin reductase 1 on Nod2-Ripk2 signaling in cell culture and a murine model of cholestatic liver injury.
Method: Protein and mRNA expression of the Nod2-Ripk2 signaling pathway was examined in liver tissue isolated from WT and murine models of cholestasis as well as in patients diagnosed with end stage PSC. In addition, the effect of inhibition or genetic ablation of TrxR1 signaling on Nod2-Ripk2 signaling was analyzed in cultured macrophages, cholangiocytes as well as in the bile duct ligation (BDL) model of cholestatic injury.
Results: Increased protein and mRNA expression of the Nod2-Ripk2 signaling pathway was present in human PSC as well as in liver isolated from mice following 3 day BDL as well as after feeding 3,5-Diethoxycarbonyl-1,4-Dihydrocollidine (DDC) for 3 days. Immunohistochemical analysis of livers from human cholestatic patients as well as 3 day DDC fed and 3 day BDL mice and revealed increased hepatic Nod2 and Ripk2 staining. Pharmacological targeting of TrxRd1 inhibited Flagellin-LPS mediated Nod2-Ripk2 activation in RAW264.7 macrophages and H69 cholangiocytes. Finally, hepatospecific deletion as well as pharmacological targeting of TrxR1 inhibited BDL-dependent induction of hepatic Nod2-Ripk2 signaling.
Conclusion: These data demonstrate that the Nod2-Ripk2 inflammatory pathway is activated in murine cholestasis as well as in human PSC and implicate TrxR1-signaling as an important regulator of Nod2-Ripk2 activation.

FRI-286
cfChIP-seq liquid biopsy distinguishes autoimmune hepatitis from other liver diseases
Gavriel Fialkoff[1], Ami Ben Ya'akov[2], Issra Sharkia[1], Ronen Sadhe[1], Jenia Gutin[1], Abed Khakayla[3], Achraf Imam[3], Rifaat Safadi[4], Ophir Hay[4], Nofar Rosenberg[5], Yael Milgrom[4], Nir Friedman[1], Eithan Galun[5], Eyal Shteyer[2]. *[1]The Rachel and Selim Benin School of Computer Science and Engineering, Hadassah-Hebrew University Medical Center, Jerusalem, Israel; [2]The Juliet Keidan Institute of Pediatric Gastroenterology, Shaare Zedek Hospital, Jerusalem, Israel; [3]Department of General Surgery and Transplantation Unit, Hadassah-Hebrew University Medical Center, Jerusalem, Israel; [4]Hadassah-Hebrew University Medical Center The Liver Unit Institute of Gastroenterology and Liver Diseases, Hadassah-Hebrew University Medical Center, Jerusalem, Israel; [5]The Goldyne Savad Institute for Gene Therapy,*

Hadassah-Hebrew University Medical Center, Jerusalem, Israel
Email: eithang@hadassah.org.il

Background and aims: Autoimmune hepatitis (AIH) is a chronic immune-mediated liver disease associated with substantial morbidity and mortality. Diagnosis and monitoring typically rely on liver biopsy, despite its invasiveness and limitations. Liquid biopsies show promise as noninvasive alternatives, but their utility in AIH remains underexplored. Here, we show that plasma-based chromatin immunoprecipitation followed by sequencing (cfChIP-seq) can detect hepatocyte-specific transcriptional activity in AIH and serve as a diagnostic and monitoring biomarker.
Method: We profiled circulating cell-free nucleosomes marked by H3K4me3—an active histone modification—in plasma samples from children and adults that underwent liver biopsy in two medical centers. Clinical data, lab results and histological results were recorded and correlated to the cfChip results. Diagnosis of AIH was based on the International Autoimmune Hepatitis Group scoring index. cfChIP-seq results were compared with liver RNA-seq from matched biopsies. A machine learning classifier was trained to distinguish AIH cfChIP-seq profiles from those of other liver diseases.
Results: In total, 345 patients participated in the study and were classified into distinct groups: AIH patients confirmed by biopsy (42 children and 49 adults), healthy controls (six pediatric and eight adult), and individuals with other liver conditions (35 children and 211 adults).cfChIP-seq revealed immune-related transcriptional signatures in hepatocyte-derived nucleosomes unique to AIH patients, corroborated by matched liver RNA-seq data. When tested on individuals with elevated transaminase levels, a cfChIP-seq-based classifier discriminated AIH from other liver conditions, including MASH and DILI, with high accuracy (AUC = 0.94. 79% sensitivity at 90% specificity). The cfChIP-seq signal reflected ongoing intrahepatic transcriptional activity and distinguished AIH from non-autoimmune liver injuries.
Conclusion: Plasma cfChIP-seq captures hepatocyte-specific gene activity and offers a non-invasive, accurate method for diagnosing and monitoring AIH. This approach could reduce reliance on liver biopsy, improve diagnostic precision, enable continuous monitoring of treatment response, and provide novel insights into AIH pathogenesis.

FRI-287

Renal apical sodium-dependent bile acid transporter (ASBT) inhibition increases whole-body bile acid clearance in healthy pigs by enabling renal elimination as quantified by 11C-CSar PET/CT

Michael Soerensen[1], Frederik Teicher Kirk[2], Maja Kanstrup Jørgensen[2], Mie Ringgaard Dollerup[2], Aage Kristian Olsen Alstrup[2], Dirk Bender[2], Erik Lindstrom[3], Thomas Sandahl[2]. *[1]Viborg Regional Hospital, Aarhus University Hospital, Viborg, Denmark; [2]Aarhus University Hospital, Aarhus, Denmark; [3]Ipsen, Gothenburg, Sweden*
Email: michsoer@rm.dk

Background and aims: Cholestasis, defined as decreased bile flow, can lead to systemic accumulation of bile acids (BAs). Ileal BA transporter (IBAT) inhibitors prevent reabsorption of BAs in the gut, thereby increasing fecal BA excretion and reducing systemic BA accumulation. IBAT is also expressed in proximal renal tubules, then referred to as ASBT (apical sodium-dependent bile acid transporter). Accordingly, ASBT inhibitors increase urinary excretion of BAs in bile duct ligated mice but have not been tested in larger animal models. The aim of this preclinical study was to quantify the acute effects of systemic ASBT inhibition on urinary BA excretion, whole-body BA clearance, and changes in hepatic transport kinetics in a porcine model using functional, positron emission tomography (PET) with the synthetic conjugated BA tracer ^{11}C-CSar.
Method: Eight anesthetized female pigs (Danish Landrace × Yorkshire crossbred; mean weight 42 kg) underwent two successive 60-min ^{11}C-Csar PET recordings: A baseline PET with vehicle administered as an IV bolus + infusion followed by a PET with vehicle + the ASBT inhibitor elobixibat. Arterial blood was collected successively for measurements of ^{11}C-CSar and elobixibat concentrations. Time courses of radioactivity concentrations (kBq/mL vs time in minutes) in liver and ureters were obtained. Whole-body clearance was calculated as AUC of blood ^{11}C-CSar divided by injected dose of ^{11}C-CSar. Relative change in urinary excretion was calculated as $AUC_{ureters}/AUC_{blood}$ after treatment relative to $AUC_{ureters}/AUC_{blood}$ before treatment.
Results: Arterial plasma concentrations of elobixibat ranged from 320 to 1078 (mean 673) ng/mL. Visually, pre-treatment with elobixibat clearly increased activity of ^{11}C-CSar in ureters compared to an almost non-visible excretion in vehicle-treated controls. Quantitatively, elobixibat increased urinary excretion of ^{11}C-CSar by a median of 8.2-fold ($P < 0.01$), leading to an increase in whole body clearance from mean 20.4 to 23.8 mL blood/min ($P < 0.01$). Elobixibat did not affect hepatic kinetics of ^{11}C-CSar (all parameters $P > 0.15$).
Conclusion: Intravenous administration of elobixibat increased whole-body clearance of BA in healthy pigs by enabling renal elimination. These findings provide a translational rationale for systemic ASBT inhibition as a strategy to reduce systemic bile acid exposure in patients with severe cholestasis, including patients at risk of cholaemic nephropathy.

FRI-289

Indoles are colon-dependent circulating microbial metabolites associated with prognosis in primary sclerosing cholangitis

Sara Tjønnfjord[1,2,3], Martin Cornillet[4], Ahmad Ali[5], Harry Sokol[6], Holmfridur Helgadottir[7], Brian D. Juran[8], Trine Folseraas[9], Cyriel Ponsioen[10], Marios Nikolaidis[8], Arild Nesbakken[11], Ragnhild Lothe[11], Bryan McCauley[8], Antonio Molinaro[12], Emma Nilsson[13], Stergios Kechagias[14], Fredrik Rorsman[15], Per Ueland[16], Adrian McCann[16], Marte Lie Høivik[17], Tom Hemming Karlsen[9], William Rosenberg[18], Mette Vesterhus[7], Konstantinos N. Lazaridis[8], Annika Bergquist[19], Johannes R. Hov[9], Peder Rustøen Braadland[20]. *[1]Research Institute of Internal Medicine, Division of Surgery, Inflammatory Diseases and Transplantation, Oslo University Hospital, Oslo, Norway; [2]Institute of Clinical Medicine, University of Oslo, Oslo, Norway; [3]Norwegian PSC Research Center, Department of Transplantation Medicine, Oslo University Hospital, Oslo, Norway; [4]Center for Infectious Medicine, Department of Medicine Huddinge, Karolinska Institutet, Karolinska University Hospital, Stockholm, Sweden; [5]Division of Gastroenterology and Hepatology, School of Medicine, University of Missouri, Columbia, Missouri, United States; [6]Sorbonne Université, INSERM, Centre de Recherche Saint-Antoine, CRSA, AP-HP, Saint-Antoine Hospital, Gastroenterology Department, Paris, France; [7] Oslo, Norway; [8]Division of Gastroenterology and Hepatology, Mayo Clinic, Rochester, Minnesota, United States; [9]Norwegian PSC Research Center, Department of Transplantation Medicine, Oslo University Hospital, Institute of Clinical Medicine, University of Oslo, Research Institute for Internal Medicine, Division of Surgery, Inflammatory Diseases and Transplantation, Oslo University Hospital, Oslo, Norway; [10]Department of Gastroenterology and Hepatology, Amsterdam University Medical Center, Amsterdam, Netherlands; [11]Institute of Clinical Medicine, University of Oslo, Department of Molecular Oncology, Institute for Cancer Research, Oslo University Hospital, Oslo, Norway; [12]Department of Molecular and Clinical Medicine/Wallenberg Laboratory, Institute of Medicine, University of Gothenburg and Sahlgrenska University Hospital, Gothenburg, Sweden; [13]Department of Surgery and Gastroenterology, Skåne University Hospital, Skåne, Sweden; [14]Department of Health, Medicine and Caring Science, Linköping University, Linköping, Sweden; [15]Department of Medical Sciences, Gastroenterology and Hepatology, Uppsala University Hospital, Uppsala, Sweden; [16]BEVITAL AS, Bergen,*

Norway; [17]Institute of Clinical Medicine, University of Oslo, Department of Gastroenterology, Oslo University Hospital, Ullevål, Oslo, Norway; [18]The Institute for Liver and Digestive Health, University College London Division of Medicine, University College London, London, United Kingdom; [19]Unit of Gastroenterology and Nutrition, Department of Medicine Huddinge, Karolinska Institutet, Karolinska University Hospital, Stockholm, Sweden; [20]Norwegian PSC Research Center, Department of Transplantation Medicine, Oslo University Hospital, Research Institute for Internal Medicine, Division of Surgery, Inflammatory Diseases and Transplantation, Oslo University Hospital, Oslo, Norway
Email: sara.tjonnfjord@gmail.com

Background and aims: Gut microbiota-derived indoles exert anti-inflammatory effects by activating the aryl hydrocarbon receptor in inflammatory bowel disease (IBD). Primary sclerosing cholangitis (PSC) typically co-occurs with IBD, and many patients undergo colectomy, which was recently associated with improved PSC survival. Here, we aimed to estimate the extent to which indole levels are altered by IBD or colectomy, and whether indoles are associated with PSC outcomes.
Method: Serum levels of indoles and the microbial metabolite trimethylamine-N-oxide (TMAO) were analysed by LC-MS/MS in a cross-sectional Norwegian PSC cohort (n = 315, median follow up 12 years). Colectomy status and IBD activity were evaluated retrospectively. Serum levels of indoles and TMAO were also assessed in a U.S. PSC cohort (n = 509, median follow up 5 years), a cross-sectional Swedish PSC cohort (n = 101), a Norwegian colorectal cancer cohort without PSC (n = 68) and healthy controls (HC, n = 100).
Results: Multiple indoles including indole-3-propionic acid (IPA) were consistently reduced in PSC compared with HC, particularly in those who had undergone colectomy. TMAO was only reduced in colectomized participants. Among people with colorectal cancer without PSC, increasingly extensive colonic resections were associated with progressively greater reductions in IPA and TMAO. Considering colon status in PSC, IPA and TMAO were almost abolished in people with proctocolectomy with ileostomy, while the impact of other types of colectomies including ileoanal pouch was weaker. In PSC with intact colon, higher concentrations of IPA were associated with better liver transplantation-free survival, while the impact of TMAO on survival was limited. There was an apparent survival benefit of high circulating IPA levels also when adjusting for the Amsterdam-Oxford model score (HR per SD increase = 0.69 (0.49–0.98) and 0.28 (0.13–0.63) in the Norwegian and U.S. cohort, respectively). Neither the indoles nor TMAO appeared to differ according to IBD status or activity.
Conclusion: IPA was reduced in people with PSC, and in those with inctact colon, the lowest levels were associated with the poorest outcome. Colectomy, and particularly proctocolectomy, was associated with depletion of key microbial metabolites, both potential disease drivers and protective factors. However, the putative benefit of gut-derived, anti-inflammatory indoles seems to be outweighed by the suggested protective role of proctocolectomy in PSC.

FRI-290-YI
Multi-omics analysis reveals zone-specific hepatocyte antigen presentation and pathogenic CD8+ T cells in autoimmune hepatitis

Han Wang[1], Shuhui Wang[1], Dean Tian[1], Mei Liu[1]. *[1]Department of Gastroenterology, Tongji Hospital, Tongji Medical College, Huazhong University of Science and Technology, Wuhan, China*
Email: hanwang@tjh.tjmu.edu.cn

Background and aims: Autoimmune hepatitis (AIH) is a chronic immune-mediated liver disease with increasing global prevalence. Progress in mechanistic and translational research has been limited by the lack of robust animal models and comprehensive characterization of the hepatic immune microenvironment. Here, we established a stable AIH mouse model and performed integrated multi-omics analyses, combining single-cell and spatial transcriptomics in both mice and human AIH samples, to provide a panoramic view of immune cell dynamics and hepatocyte-immune interactions.
Method: AIH was induced by liver-specific overexpression of the human autoantigen CYP2D6. Liver inflammation and fibrosis were assessed by H&E and Sirius Red staining, and serum autoantibodies by ELISA. Hepatic immune populations were profiled using 10× Genomics single-cell RNA sequencing and spatial transcriptomics. Human AIH liver samples were analyzed by spatial transcriptomics for cross-species validation. Stage-specific roles of $CD4^+$ and $CD8^+$ T cells were evaluated by in vivo depletion, and hepatocyte–immune cell interactions were analyzed across hepatic zones.
Results: By day 14 post-injection, periportal inflammation was evident, with serum autoantibodies detected by day 28. Peak disease at day 35 showed hallmark AIH features, including interface hepatitis, rosette formation, and fibrosis, closely resembling human AIH. Multi-omics analysis revealed dynamic remodeling of hepatic immune populations, including $CD4^+$ T cells, $CD8^+$ T cells, NK cells, and activated Tregs, with prominent immune cell interactions. Effector and tissue-resident memory $CD8^+$ T cells predominated, while $CD4^+$ T cells mainly contributed to disease initiation. Spatial transcriptomics identified zone-specific hepatocyte antigen presentation, with Zone 3 hepatocytes as the primary antigen-presenting cells, a finding validated in human AIH samples. Functional studies demonstrated that $CD8^+$ T cells are the principal pathogenic population, whereas $CD4^+$ T cells play a limited role during acute inflammation.
Conclusion: This AIH mouse model recapitulates key features of human disease and, through integrated multi-omics analyses, provides the first panoramic view of hepatic immune dynamics and zone-specific hepatocyte-immune interactions. The study clarifies stage-specific roles of $CD4^+$ and $CD8^+$ T cells, validates findings in human samples, and establishes a robust platform for mechanistic studies and therapeutic target discovery in AIH.

FRI-291-YI
Cholangiocyte-derived interleukin-15 contributes to the interaction with auto-aggressive CD8+ T cells in primary sclerosing cholangitis

Nico Will[1], Laura Liebig[2], Christian Casar[1], Sabrina Pilz[1], Silja Steinmann[1], Victor Haas[1], Franziska Mangler[1], Tobias Poch[1], Jenny Krause[1], Ulf Panzer[1], Michael Dudek[3], Percy A. Knolle[3], Norbert Hübner[2], Samuel Huber[1], Ansgar W. Lohse[1], Dorothee Schwinge[1], Christoph Schramm[1]. *[1]University Of Hamburg Medical Center Eppendorf Helipad, Hamburg, Germany; [2]Max Delbrück Center For Molecular Medicine, Berlin, Germany; [3]Institut für Molekulare Immunologie, München, Germany*
Email: c.schramm@uke.de

Background and aims: Primary sclerosing cholangitis (PSC) is a progressive autoimmune liver disease with limited treatment options and a presumed pathogenetic contribution of the adaptive immune response. We have previously described that $CD8^+$ T cells are in close interaction with cholangiocytes. We here hypothesized that Interleukin-15 (IL-15), recently described to drive tissue-resident cytotoxic and auto-aggressive responses, may act on hepatic $CD8^+$ T cells to shape their interaction with cholangiocytes.
Method: We analyzed intrahepatic $CD8^+$ T cells using our previously generated CITE-Seq from people with PSC. Peripheral $CD8^+$ T cells from people with PSC (n = 25), PBC (n = 14), and healthy controls (n = 18) were assessed via full-spectrum flow cytometry. IL15 and IL15RA expression were profiled using single-nucleus RNA-seq (sNucSeq) from liver biopsies ($n_{total} = 52$, $n_{PSC} = 25$) and validated in human cholangiocyte organoids on protein level. Portal immune cell composition and cytokine expression were assessed by spatial transcriptomics across PSC stages and controls (n = 22).
Results: CITE-Seq-analysis of intrahepatic $CD8^+$ T cells from people with PSC showed high HLA class II, NKG2D, interferon γ and

granzyme expression, consistent with IL-15–induced auto-aggression. The upregulation of IL-15–associated phenotypic markers was confirmed in peripheral CD8$^+$ T cells from people with PSC using flow cytometry. sNucSeq analysis of liver biopsies revealed significantly increased IL15 and IL15RA-expression in cholangiocytes of PSC livers. IL-15 and IL-15Rα expression was confirmed at the transcriptional and protein levels in human-derived cholangiocyte 3D organoids and was significantly (~10-fold) upregulated upon interferon-γ stimulation. Spatial transcriptomics revealed accumulation of CD8$^+$ T cells with auto-aggressive transcriptomic profiles within portal tracts of PSC livers in proximity of cholangiocytes. Notably, cholangiocytes exhibited the highest expression of IL15 and IL15RA among all cell types of the portal tract. Blocking experiments to functionally validate those findings in mouse models are ongoing.
Conclusion: Our data support a role for IL-15 in driving auto-aggressive CD8$^+$ T cell activation in PSC. Cholangiocytes appear to serve as both source and presenter of IL-15, suggesting an antigen-independent mechanism of cholangiocyte-mediated activation of auto-aggressive CD8$^+$ T cells. The IL-15 axis may therefore represent a novel therapeutic target in PSC.

FRI-298
Integrated multi-omics approaches reveal IL-33 as a central pathogenic factor and potential therapeutic target in autoimmune hepatitis
Long Xu[1], Wanwan Shi[1], Xinghuan Fu[1], Wen-Jing Wang[1], Lin-Hui Hu[1], Xue-Ying Li[1], Yan Wang[1], Gui-Qiang Wang[1]. *[1]Department of Infectious Disease, Center for Liver Disease, Peking University First Hospital, Beijing 100034, China, Beijing, China*
Email: twinkleclinic@163.com

Background and aims: The precise source and causality of Interleukin-33 (IL-33) in autoimmune hepatitis (AIH) remain unclear. This study aims to identify the specific IL-33-producing cell subset, establish its genetic causality, and demonstrate the therapeutic efficacy of targeting IL-33 in AIH.
Method: Two-sample Mendelian randomization (MR) analysis was performed to evaluate the causal relationship between IL-33 and susceptibility to AIH. Serum IL-33 levels were measured in both AIH patients and healthy controls to investigate correlations with specific disease activity markers. To identify the cellular source of IL-33 within the liver, single-cell RNA sequencing (scRNA-seq) combined with multiplex immunofluorescence was used. Additionally, the therapeutic efficacy of an anti-IL-33 monoclonal antibody (Torudokimab) was assessed in an S100-induced AIH murine model by measuring liver injury biomarkers and immunoglobulin levels.
Results: Two-sample MR analysis revealed a causal relationship between IL-33 and susceptibility to AIH, with genetically predicted higher IL-33 levels significantly increasing AIH risk (OR = 1.457, 95% CI: 1.096–1.936, P = 0.010). Clinically, serum IL-33 levels were significantly elevated in AIH patients compared to healthy controls (P < 0.0001). Correlation analysis showed significant positive associations between IL-33 and key disease severity markers, particularly with IgG (R = 0.52, P = 0.00022) and AST (R = 0.50, P = 0.00045), followed by ALT (R = 0.44, P = 0.0023) and IgM (R = 0.40, P = 0.0077). scRNA-seq and immunofluorescence identified a specific subset of liver sinusoidal endothelial cells (LSECs), characterized by NRG3 expression, as the primary source of intrahepatic IL-33. In the S100-induced AIH murine model, treatment with Torudokimab demonstrated strong therapeutic efficacy. Compared to vehicle-treated controls, Torudokimab significantly reduced serum ALT and AST levels (P < 0.0001), effectively normalizing liver enzyme levels, and significantly alleviated the autoimmune response, as evidenced by reduced serum IgG levels (P = 0.0002).
Conclusion: This study establishes the causal role of IL-33 in the pathogenesis of AIH and identifies a specific subset of NRG3$^+$ LSECs as its primary source. Importantly, in vivo data show that targeting IL-33 effectively reverses liver injury and attenuates excessive immunoglobulin production, highlighting its potential as a novel therapeutic strategy for AIH treatment.

FRI-299
Radiocarbon dating and multi-omics of gallstones reveal prolonged residence time accompanied with microbial dysbiosis and bacterial oncometabolites linked to gallbladder cancer
Vipin Yadav[1], Rajveer Sharma[2], Vaishali Yadav[1], Ashi Mittal[1], Garima Bhatia[1], Rishabh Sharma[1], Ragini Kilambi[1], Deepti Sharma[1], Nihar Mohapatra[1], Pratibha Ramchandra Kale[1], Sherin Thomas[1], Archana Rastogi[1], Nirupma Trehanpati[1], Viniyendra Pamecha[1], Shvetank Sharma[1], Shiv Kumar Sarin[1], Gayatri Ramakrishna[1]. *[1]Institute of Liver & Biliary Sciences, New Delhi, India; [2]Inter University Accelerator Centre, New Delhi, India*
Email: rgayatri@ilbs.in

Background and aims: Gallbladder cancer (GBC) is a highly aggressive malignancy with poor outcomes and marked geographic variation, notably in northern India and Chile. Most GBCs arise in the presence of gallstones, yet the biological link between persistence of stone, composition, and malignant transformation remains unclear. This study integrated radiocarbon dating with multi-omics profiling of gallstone cores to elucidate chronological, microbial, and metabolic drivers of carcinogenesis.
Method: Thirty gallstones from patients with gallstone disease (GSD), preneoplastic lesions (PNP), and GBC were analyzed. Radiocarbon (^{14}C) dating estimated gallstone age, while LC-MS–based metabolomics and 16S rRNA sequencing identified metabolic and microbial signatures.
Results: Radiocarbon data revealed extended intracholecystic residence in GBC (median 17.5 years, range 10–55) compared with PNP (13 years) and GSD (11 years) (p < 0.03). Logistic regression confirmed increased cancer risk with longer persistence (AUC = 0.86). Metabolomics demonstrated distinct clustering by disease state. GBC stones exhibited >3-fold higher lysophosphatidylcholines, 4.2-fold elevated sulfoglycolithocholate, 6-fold enrichment of the oncometabolite trimethylamine N-oxide (TMAO), and increased leukotriene B4 and dityrosine, reflecting an inflammatory microenvironment. Conversely, protective lipids such as phosphatidylethanolamines and short-chain fatty acids (e.g., butyrate) were depleted. Metagenomic profiling identified enrichment of *Klebsiella* (FC = 2.46) and *Enterococcus* (FC = 2.20) in GBC cores, correlating strongly (r ≥ 0.7–0.9) with pro-inflammatory and lipid metabolites. Integrated analysis revealed disease-stage–specific microbial-metabolite–metabolite networks. *Klebsiella* and *Enterobacter* were positively associated with bile acids, lysophospholipids, amino-acid conjugates, and TMAO, whereas *Escherichia–Shigella* correlated with cholesterol and ceramide-rich metabolites in non-malignant stones. Butyrate showed inverse associations with pathogenic taxa.
Conclusion: Prolonged gallstone retention (>17 years) drives microbial dysbiosis and metabolic reprogramming toward pro-inflammatory, carcinogenic pathways. The gallstone core reflects the evolving gallbladder microenvironment, where altered LysoPC: PC ratios, TMAO accumulation, and enrichment of inflammatory lipids and secondary bile acids link pathogenic microbes to carcinogenic transformation.

FRI-300-YI
Developing advanced 3D models of cholangiocyte-immune crosstalk
Jeremy Yeoh[1,2,3,4], Henry Hoyle[1,2,3,4], Enya Amundsen-Isaksen[1,2,3,4], Anna Katharina Frank[1,2,4], Aleksandra Aizenshtadt[3], Stefan Krauss[3], Espen Melum[1,2,3,4,5]. *[1]Norwegian PSC Research Center, Department of Transplantation Medicine, Division of Surgery and Specialized Medicine, Oslo University Hospital Rikshospitalet, Oslo, Norway; [2]Research Institute of Internal Medicine, Division of Surgery and Specialized Medicine, Oslo University Hospital Rikshospitalet, Oslo, Norway; [3]Hybrid*

Technology Hub, Institute of Basic Medical Science, University of Oslo, Oslo, Norway; [4]Institute of Clinical Medicine, Faculty of Medicine, University of Oslo, Oslo, Norway; [5]Section of Gastroenterology, Department of Transplantation Medicine, Division of Surgery and Specialized Medicine, Oslo University Hospital Rikshospitalet, Oslo, Norway
Email: w.j.yeoh@medisin.uio.no

Background and aims: Cholangiopathies, such as primary sclerosing cholangitis (PSC), are driven by ongoing inflammation, where immune-cholangiocyte interactions contribute to bile duct dysfunction and liver damage. Currently, relevant human models that recapitulate biliary-immune crosstalk and cell migration are lacking, limiting studies of these mechanisms. Herein, we aimed to radically improve current methods with modified cholangiocyte organoid (CO)-immune co-cultures, as well as develop an immunocompetent organ-on-a-chip (VDUCT) incorporating perfusable primary human bile ducts and vascular channels. These systems will allow for studies of immune-related processes, such as ligand-receptor interactions and immune recruitment, in the context of bile duct physiology.
Method: Primary human cholangiocyte organoids were propagated from endoscopic retrograde cholangiopancreatography (ERCP) brushings, with human umbilical vein endothelial cells (HUVECs) and peripheral blood mononuclear cells sourced either commercially or in-house. Cholangiocytes were seeded on top of Matrigel for 14 days. The VDUCT chip consisted of two parallel hollow channels cast in hydrogel in a 3D printed chip, seeded with cholangiocytes and/or HUVECs. Fluorescent PBMCs were perfused through the vascular channel. Cell populations were visualized using brightfield and/or confocal microscopy.
Results: Surface-seeded CO-immune cell co-culture showed proximity of immune cells to cholangiocyte organoids unlike conventional embedded culture. After 24 h, surface-seeded COs exhibited loss of organoid morphology, while embedded COs largely remained intact. In the VDUCT, cholangiocytes and endothelial cells formed confluent biliary epithelia and vascular endothelia respectively after 10 days in culture, evident by actin, CK19 and CD31 staining. Perfused PBMCs adhered to the endothelium, with approximately 30% extravasated and migrated along a CXCL12 chemotactic gradient. However, no extravasation or migration of immune cells toward the biliary epithelia was observed after 48 h of co-culture, regardless of LPS stimulation.
Conclusion: In sum, our new approach to cholangiocyte-immune co-culture and the VDUCT chip will allow for a new generation of *in-vitro* studies on biliary-immune interactions with direct human and disease relevance. Furthermore, our scalable multi-cellular bile-duct on a chip will allow for parallel regulation of key parameters relevant to bile duct function and immune processes, such as flow rate and shear stress.

FRI-301
Setting-up a biliary niche-on-a-chip for the study of human liver disease-associated ductular reaction

Guo Yin[1], Marlene Kohlhepp[1], Bianca Leonardi, Tian Lan[2], Hanyang Liu[1], Hilmar Berger[1], Milad Rezvani[3], Philip Bufler[3], Frank Tacke[1], Adrien Guillot[1]. *[1]Charité-Universitätsmedizin Berlin, Department of Hepatology & Gastroenterology, Campus Virchow-Klinikum and Campus Charité Mitte, Berlin, Germany, Berlin, Germany; [2]Department of Gastroenterology, West China Hospital, Sichuan University, Chengdu, China; Charité-Universitätsmedizin Berlin, Department of Hepatology & Gastroenterology, Campus Virchow-Klinikum and Campus Charité Mitte, Berlin, Germany, Chengdu, China; [3]Charité - Universitätsmedizin Berlin, Department of Pediatric Gastroenterology, Nephrology and Metabolic Medicine, Berlin 13353, Germany, Berlin, Germany*
Email: guo.yin@charite.de

Background and aims: Ductular reaction (DR), characterized by cholangiocyte proliferation associated with inflammation and liver fibrosis, is a common hallmark of virtually all chronic liver diseases, e. g., metabolic dysfunction-associated steatotic liver disease (MASLD), and primary sclerosing cholangitis (PSC). Yet, DR implications in disease progression remain poorly understood, likely due to the lack of appropriate models. Diverse cells are involved in DR and, therefore, we aimed at developing a versatile in vitro system for cellular crosstalk investigation. We previously reported on a microfluidics-based, multicellular and primary cell-based liver-on-a-chip model mimicking the liver sinusoid and the biliary niche microenvironments. This project aims at refining the model, exploring its physiological relevance for DR studies, and setting up a human cell-based system.
Method: Intrahepatic cholangiocytes were isolated from wild-type (WT) and *Mdr2*-deficient (KO) mice by positive selection and expanded to generate 3-dimensional organoids. Total RNA sequencing and immunostaining confirmed cell identity and evidenced differences associated with DR between the two lines. Mouse or human primary hepatocytes, cholangiocytes, hepatic stellate cells, macrophages and endothelial cells were isolated from the liver and seeded to generate a biliary niche-on-a-chip (BoC). Freshly isolated blood circulating immune cells were perfused. Protein and gene expression were assessed by multiplex immunofluorescence and RT-qPCR, and immune cells were characterized by multispectral flow cytometry. Gene interference was used to knock-down genes associated with distinct pathogenic pathways.
Results: Mouse primary liver and blood cells were successfully isolated and seeded into the BoC. Inflammation and fibrogenesis increased in the BoC seeded with reactive mouse intrahepatic cholangiocyte organoids (mICOs) isolated from *Mdr2*-deficient. Transient gene expression in mICOs or macrophages modulated the BoC inflammatory response. Early results show that human primary liver cells were successfully isolated and characterized by immunofluorescence staining prior seeding in a humanized BoC.
Conclusion: The multicellular BoC is a first-of-its-kind, versatile primary cell-based model that may be used to study DR, allowing to dissect the relevance of cell-type specific molecular pathways for liver biology and pathogenesis ex vivo. Preliminary data support the feasibility of a primary, human cell-based liver-on-a-chip.

FRI-302-YI
Inhibiting cuproptosis mitigates cholangiocyte inflammation in primary biliary cholangitis

Yu-Jie Zhou[1], Nana Cui[1], Qiwei Qian[1], Bingyuan Huang[1], Tianyu Mao[1], Haoyu Wen[1], Yu Chen[1], Qiaoyan Liu[1], Leigh MacConell[2], Meng Yu[2], Liping Liu[2], Ming-Hua Zheng[3], Min Lian[1], Xiao Xiao[1], Zhengrui You[1], Ruqi Tang[1], Merrill E Gershwin[4], Xiong Ma[1]. *[1]Renji Hospital, School of Medicine, Shanghai Jiao Tong University, Shanghai, China; [2]HighTide Therapeutics, Inc., Shenzhen, China; [3]The First Affiliated Hospital of Wenzhou Medical University, Wenzhou, China; [4]University of California at Davis, Davis, United States*
Email: maxiongmd@hotmail.com

Background and aims: Cuproptosis, a newly identified mechanism of cell death features DLAT ($PDC\text{-}E_2$) aggregation, the immunodominant mitochondrial autoantigen of primary biliary cholangitis (PBC). Hitherto therapeutic venues designed to modulate cuproptosis are lacking.
Method: We employed a multi-prong approach, using in-vitro models, and a phase II clinical study to define cuproptosis in PBC. We firstly compared susceptibility to cuproptosis among using a panel of cells. We also investigated the correlation between serum copper levels and pathology in chronic liver diseases. Similarly we investigated the relationships of $PDC\text{-}E_2$ oligomerization and cuproptosis. Then high-throughput screening of cuproptosis inhibitor was performed in cholangiocytes and the mechanism of the

inhibitory effect of berberine on cuproptosis was explored. Finally we explored the therapeutic value of berberine in patients with PBC.
Results: Cholangiocytes are more susceptible to cuproptosis than hepatocytes due to lower expression of metallothionein. Unlike in chronic hepatitis B, MASLD, and autoimmune hepatitis, serum copper was positively correlated with fibrosis stages in PBC. We observed copper overload-triggered aggregation of the DLAT (aka PDC-E_2) autoantigen in cholangiocyte mitochondria. Intriguingly, large EVs released by cuproptotic cells contained intact aggregated PDC-E_2. Co-culture of these EVs with liver-infiltrating immune cells from PBC patients potently expanded and activated PDC-E_2-specific T cells. A widely prescribed medication, berberine, was identified to inhibit cuproptosis. Mechanistically, berberine suppresses cuproptosis through promoting PDC-E_2 degradation and inhibiting pyruvate uptake to mitochondria to bypass PDC-E_2. In PBC mouse models, induction of cuproptosis exacerbated cholangitis, accompanied by increased hepatic infiltration of PDC-E_2-specific T cells, while berberine intervention mitigated cholangiocyte inflammation. Finally, in the phase 2 clinical trial in PBC patients with inadequate response to standard therapy, berberine ursodeoxycholate demonstrated reduced ALP levels at week-12 (-9.82%; 95%CI: −19.5 ~ −0.11; P = 0.048).
Conclusion: We report herein an association between cuproptosis and PBC progression. Berberine treatment represents a promising therapeutic strategy for modulating cuproptosis in associated pathologies.

Immune-mediated and cholestatic disease – Clinical aspects

TOP-277-YI
Real-world effectiveness and safety of seladelpar in primary biliary cholangitis: a nationwide electronic health record-based study

Adrielly Martins[1], Cynthia Levy[1]. [1]*University of Miami, Miami, United States*
Email: axm8717@med.miami.edu

Background and aims: Seladelpar, a selective peroxisome proliferator-activated receptor delta agonist, received United States Food and Drug Administration conditional approval in August 2024 as second-line therapy for primary biliary cholangitis (PBC). However, efficacy and safety data are lacking for patients with autoimmune hepatitis (AIH) overlap syndrome and metabolic dysfunction-associated steatotic liver disease (MASLD)—populations underrepresented in clinical trials. We evaluated the real-world effectiveness and safety of seladelpar across PBC subgroups.
Method: This retrospective cohort study used Epic Cosmos, a federated electronic health record platform. Adults with PBC prescribed seladelpar after approval were included. Patients were classified into mutually exclusive subgroups: PBC alone, PBC-AIH overlap, and PBC-MASLD. The primary outcome was biochemical response at 6 months per POISE criteria (alkaline phosphatase [ALP] less than 1.67 times upper limit of normal [ULN], 15% or greater ALP reduction, and normal bilirubin). Secondary outcomes included ALP normalization and hepatotoxicity (alanine aminotransferase [ALT] greater than 3 or 5 times ULN [xULN]).
Results: Among 666 patients with baseline ALP, 209 (31.4%) had PBC alone, 76 (11.4%) had PBC-AIH overlap, and 381 (57.2%) had PBC-MASLD. Mean age was 63.9 years and 89.8% were female. Cirrhosis was present in 35.6% overall, higher in PBC-AIH (52.6%) and PBC-MASLD (45.4%) than PBC alone (11.5%; $p < 0.001$). At 6 months (n = 248), POISE response rates were 68.8% for PBC alone, 64.2% for PBC-MASLD, and 48.5% for PBC-AIH ($p = 0.13$). Cirrhotic patients had lower 6-month POISE response than non-cirrhotic (55.6% vs 68.5%; $p = 0.04$). ALP normalization rates were 48.4%, 38.4%, and 27.3%, respectively ($p = 0.11$). ALT elevations greater than 3 xULN decreased from baseline (3.5%) to 6 months (1.1%), with no ALT greater than 5 xULN at 6 months. Mean ALT was lower at 6 months across all subgroups. No new drug-induced liver injury cases were observed. Among patients with available eGFR (14%) and creatine kinase (4%) data, no renal or muscle safety concerns were observed.
Conclusion: In this real-world study, biochemical response rates were consistent with phase 3 trial results. MASLD did not attenuate treatment response. Patients with AIH overlap showed numerically lower response rates, warranting further investigation. Seladelpar demonstrated a favorable hepatic safety profile across diverse PBC populations.

TOP-278
Factors associated with the development of primary biliary cholangitis in individuals with antimitochondrial antibodies: a spanish multicenter study

Alvaro Diaz-Gonzalez[1], Helena Hernández Evole[2], Lucía Jiménez[3], Manuel Rodríguez-Perálvarez[3], Jesús M. González[4], Sofía Criado[5], Emily Larrea[5], Antonio Olveira[5], Indhira Perez Medrano[6], Ares Villagrasa[7], Ignacio VazRomero[7], Mar Riveiro Barciela[7], Margarita Sala Llinás[8], María Del Barrio[1], Sergio Rodriguez-Tajes[2], María Carlota Londoño[2], Judith Gómez-Camarero[9], Ismael El Hajra Martínez[10], Beatriz Mateos Muñoz[11], Angela Martínez Herreros[12], Francisca Cuenca Alarcón[13], Sonia Blanco-Sampascual[14], Ana Arencibia Almeida[15], Marta Alonso-Peña[1,16]. [1]*Gastroenterology and Hepatology Department, Clinical and Translational Research in Digestive Diseases Group, Marqués de Valdecilla University Hospital, Santander, Spain; Research Institute Marques de Valdecilla (IDIVAL), Clinical and Traslational Research in Digestive Pathology Group, Santander, Spain, Santander, Spain;* [2]*Servicio de Hepatologia, Hospital Clinic Barcelona, Fundació Clinic Barcelona, Fundació de Recerca Clínic Barcelona-Institut d'Investigacions Biomèdiques August Pi i Sunyer (FRCB-IDIBAPS), Universitat de Barcelona, Centro de investigación biomédica en red Enfermedades Hepáticas y Digestivas (CIBEREHD), Barcelona, España, Barcelona, Spain;* [3]*Unidad de Hepatología y Trasplante Hepático, Hospital Universitario Reina Sofía, IMIBIC, CIBERehd, Córdoba, España, Córdoba, Spain;* [4]*Digestive Diseases Department, Complejo Asistencial Universitario de Salamanca, Laboratorio de Hepatología Experimental y Vectorización de Fármacos (HEVEPHARM), CIBERehd, IBSAL, Spain, Salamanca, Spain;* [5]*Servicio de Aparato Digestivo, Hospital Universitario la Paz, Madrid, España, Madrid, Spain;* [6]*Unidad de Hepatología. Complexo Hospitalario Universitario de Pontevedra. Instituto de Investigación Sanitaria Galicia Sur (IISGS), Pontevedra, Spain;* [7]*Liver Unit, Internal Medicine Department, Hospital Universitari Vall d'Hebron, Vall d'Hebron Barcelona Hospital Campus, Barcelona, Spain; Universitat Autònoma de Barcelona, Spain; Centro de Investigación Biomédica en Red de Enfermedades Hepáticas y Digestivas (CIBERehd), Instituto de Salud Carlos III, Madrid, Spain; European Reference Network on Hepatological Diseases (ERN RARE-LIVER), Barcelona, Spain;* [8]*Unidad Hepatología, Servicio Digestivo, Hospital Universitario Doctor Josep Trueta, IDIBGI, Girona, CIBEREHD, Girona, Spain;* [9]*Servicio de Aparato Digestivo, Hospital Universitario de Burgos, Burgos, Burgos, Spain;* [10]*Hospital Universitario Puerta de Hierro de Majadahonda, Madrid, Spain;* [11]*Servicio de Aparato Digestivo, Hospital Universitario Ramón y Cajal, CIBERehd, IRYCIS, Madrid, Madrid, Spain;* [12]*Servicio de Aparato Digestivo, Hospital Universitario San Pedro, Logroño, Logroño, Spain;* [13]*Unidad de Hígado, Servicio de Aparato Digestivo Hospital Clínico San Carlos, Madrid, Spain;* [14]*Sección de Hepatología. Hospital Universitario Basurto, OSI Bilbao Basurto, Bilbao, Spain;* [15]*Sección de Hepatología, Servicio de Aparato Digestivo, Hospital Universitario Nuestra Señora de la Candelaria, Santa Cruz de Tenerife, Spain;* [16]*Departamento de Anatomía y Biología Celular, Universidad de Cantabria, Santander, Santander, Spain*
Email: diazg.alvaro@gmail.com

Background and aims: Individuals with AMA positivity are at risk of developing Primary Biliary Cholangitis (PBC), although only a minority progress to overt disease. There is limited information on their characteristics and factors associated with PBC development.
Method: Multicenter, retrospective study in 16 Spanish centers. We included individuals with AMA and/or PBC-specific antibodies who did not meet diagnostic criteria for PBC at antibody detection and who were under active follow-up.
Results: 846 individuals were included, predominantly women (82.8%). 770 (91%) were AMA+, 254 (30%) had anti-M2 antibodies, 58 (6.8%) anti-sp100, and 16 (1.9%) anti-gp210. Overall, 306 patients (36.2%) had other autoimmune diseases and 6 (0.7%) had a family history of PBC. 54 individuals (7.3%) reported at least one symptom, the most frequent being fatigue (n = 33, 3.9%) followed by pruritus (n = 11, 1.3%). All patients had alkaline phosphatase (ALP) levels below the upper limit of normal (ULN). Median values of other parameters (xULN; IQR) were AST 0.7 (0.5–0.9), ALT 0.6 (0.4–0.8), GGT 0.4 (0.4–1.6), total bilirubin 0.4 (0.3–0.6), and IgM 0.5 (0.3–0.8). Baseline elastography was available in 113 patients, with a median of 4.7 kPa (IQR 3.7–6.1). Follow-up data were available for 417 individuals. 41 patients (9.8%) developed PBC after a median of 3.2 years (IQR 1.3–6.4), yielding an incidence rate of 1.96 per 100 person-years. At baseline, those who developed PBC had significantly higher ALP (0.79 vs 0.63 × ULN, $p < 0.001$) and GGT levels (1.02 vs 0.63 × ULN, $p < 0.001$). No differences were observed in AST, ALT, bilirubin, IgM, or other parameters. In addition, patients who progressed to PBC had a higher prevalence of AMA titers >1:320 (81.6% vs 60.7%; $p = 0.011$). Baseline fatigue was significantly more frequent among those who developed PBC (14.7% vs 5%; $p = 0.014$). In univariate analysis, baseline ALP, GGT, AMA titers and fatigue were significantly associated with the risk of developing PBC. The optimal ALP × ULN cutoff was 0.73 × ULN (sensitivity 0.71; specificity 0.69). ALP ≥0.73 × ULN (HR 4.9; 95% CI 2.4–10.2), GGT >ULN (HR 2.8; 95%CI 1.4–5.6), AMA titers >1:320 (HR 3.9; 95% CI 1.7–9.3), and baseline fatigue (HR 3.7; 95% CI 1.5–9.2) were independently associated with the development of PBC in the multivariate analysis.
Conclusion: Approximately 10% of AMA-positive individuals developed PBC over a median follow-up of 3.2 years. Baseline fatigue, ALP, GGT and AMA titers were independently associated with the risk of developing PBC.

TOP-279

Male patients with autoimmune hepatitis have lower rates of treatment response and higher risk of liver-related events: a multicenter nationwide longitudinal study of 2000 patients

Ellina Lytvyak[1,2], Gideon M. Hirschfield[3], Yu Jun Wong[1], Shagani Thisairajah[1], Hin Hin Ko[4], Julian Hercun[5], Mina Niazi[6], Catherine Vincent[5], Karim Qumosani[7], Tianyan Chen[8], Angela Cheung[9], Kristel Leung[10], Jean-Philippe Wallach[11], Nabiha Faisal[12], Devika Shreekumar[1], Narmeen Umar[1], Aliya Gulamhusein[3], Andrew L. Mason[1], Mark Swain[13], Bettina E. Hansen[3], Aldo J Montano-Loza[1]. *[1]Division of Gastroenterology and Liver Unit, University of Alberta, Edmonton, Canada; [2]Division of Preventive Medicine, University of Alberta, Edmonton, Canada; [3]The Autoimmune and Rare Liver Disease Programme, Division of Gastroenterology and Hepatology, Toronto General Hospital, Toronto, Canada; [4]Division of Gastroenterology, University of British Columbia, Vancouver, Canada; [5]Liver Unit, Department of Medicine, Centre Hospitalier De l'Université De Montréal, Montreal, Canada; [6]Division of Gastroenterology and Hepatology, College of Medicine, University of Saskatchewan, Royal University Hospital, Saskatoon, Canada; [7]Department of Medicine, Western University, London, Canada; [8]Department of Medicine, McGill University Health Centre, Montreal, Canada; [9]Department of Medicine, University of Ottawa, Ottawa, Canada; [10]Departments of Medicine & Public Health Sciences, Queen's University, Kingston, Canada; [11]Nanaimo Regional Hospital, Nanaimo, Canada; [12]Department of Internal Medicine, Section of Hepatology, University of Manitoba, Winnipeg, Canada; [13]Liver Unit, Division of Gastroenterology and Hepatology, University of Calgary, Calgary, Canada*
Email: montanol@ualberta.ca

Background and aims: Sex is an established determinant of prognosis in liver diseases, yet its influence on outcomes in autoimmune hepatitis (AIH) is unclear. We analyzed a large, representative multicenter Canadian cohort to determine and quantify the influence of sex on clinical course, treatment response, and outcomes in AIH.
Method: We analyzed data of 2000 AIH patients from the Canadian Network for Autoimmune Liver Diseases (CaNAL). Complete biochemical response (CBR) was defined by normalization of ALT and IgG. Poor clinical outcomes were defined as progression to cirrhosis, liver decompensation, hepatocellular carcinoma (HCC), liver transplantation (LT), or death.
Results: Our cohort, encompassing 21,204 person-years of follow-up, was predominantly female (75.0%), Caucasian (69.1%), median age 60.4 [IQR 44.6–71.0] and disease duration 8.5 [3.5–15.6] years. At diagnosis, males were younger than females (43.3 [IQR 26.2–59.1] vs. 51.1 y.o. [34.2–61.8], $p < 0.001$), presented with more severe disease (ALT 8.8 × ULN [3.1–24.1] vs. 7.6 × ULN [2.2–20.5], $p = 0.033$), and higher frequency of cirrhosis (31.3% vs. 26.4%; $p = 0.038$). Males had higher risk of not achieving CBR at 6- and 12-month (OR 1.82 [95% CI 1.34–2.46], $p < 0.001$, and OR 1.48 [1.11–1.97], $p = 0.008$, respectively), translating into lower treatment response rates (26.6% vs. 39.7%, $p < 0.001$, and 37.5% vs. 47.0%, $p = 0.008$, respectively) compared to females. Moreover, males had 1.5 times higher risk of progression to cirrhosis compared to females if they did not achieve 6-month CBR (HR 3.61 [1.27–10.24], $p = 0.016$, vs. HR 2.34 [1.45–3.78], $p < 0.001$), adjusted for age at diagnosis. Males also had a 3-fold females' risk of developing hepatic decompensation if 6-month CBR was not achieved (HR 7.97 [1.07–59.2], $p = 0.042$, vs. HR 2.72 [1.33–5.56], $p = 0.006$), adjusted for cirrhosis at diagnosis and type 2 diabetes. Male sex was associated with a higher risk of LT (HR 1.49 [1.05–2.12], $p = 0.027$), while risk of HCC, liver-related mortality, and event-free survival did not differ.
Conclusion: Males with AIH have greater disease severity, frequency of cirrhosis at diagnosis, and a lower likelihood of achieving CBR than females. Not achieving CBR places males at 1.5-fold higher risk of progression to cirrhosis and 3-fold higher risk of developing decompensation than females. This shows the importance of sex-specific risk stratification and developing targeted strategies to enhance treatment response in males with AIH.

TOP-280

Long-term safety, tolerability and maintenance of efficacy of linerixibat for the treatment of cholestatic pruritus in primary biliary cholangitis

Christopher L. Bowlus[1], Stuart C Gordon[2], David E. Jones[3], Andreas E. Kremer[4], Kris V. Kowdley[5], Cynthia Levy[6], Marlyn J. Mayo[7], Atsushi Tanaka[8], Pietro Andreone[9], Jidong Jia[10], qinglong Jin[11], Keiji Tsuji[12], Linda Casillas[13], Alexander Cobitz[13], Andrea Ribeiro[14], Jing Wang[13], Jennifer B. Shannon[15], Sadia Halim[16], Ivana Lazic[16], Brooke M. Currie[13], Kaitlin Hagan[13], Brandon Swift[15], Ciara Gorey[16], Megan McLaughlin[13], Gideon M. Hirschfield[17]. *[1]University of California Davis School of Medicine, Sacramento, United States; [2]Henry Ford Health, Michigan State University, Detroit, United States; [3]Institute of Translational and Clinical Research and NIHR Newcastle Biomedical Research Center, Newcastle University, Newcastle Upon Tyne, United Kingdom; [4]Department of Gastroenterology and Hepatology, University Hospital Zurich, Zurich, Switzerland; [5]Liver Institute Northwest, Seattle, United States; [6]Division of Digestive Health and Liver Diseases and Schiff Center for Liver Diseases, University of Miami Miller School of Medicine, Miami, United States; [7]University of Texas Southwestern Medical School,*

Dallas, United States; [8]Teikyo University School of Medicine, Tokyo, Japan; [9]Medicina Interna Metabolica, Baggiovara Hospital, Azienda Ospedaliero-Universitaria di Modena and Università di Modena e Reggio Emilia, Modena, Italy; [10]Liver Research Centre, Beijing Friendship Hospital, Capital Medical University, Beijing, China; [11]The First Hospital of Jilin University, Changchun, China; [12]Hiroshima Red Cross Hospital and Atomic-Bomb Survivors Hospital, Hiroshima, Japan; [13]GSK, Collegeville, United States; [14]GSK, Madrid, Spain; [15]GSK, Durham, United States; [16]GSK, London, United Kingdom; [17]The Autoimmune and Rare Liver Disease Programme, Division of Gastroenterology and Hepatology, University Health Network, Toronto General Hospital, Toronto, Canada
Email: clbowlus@health.ucdavis.edu

Background and aims: Cholestatic pruritus is common in primary biliary cholangitis (PBC) and negatively impacts sleep and quality of life, yet effective treatments are lacking. In the Phase 3 GLISTEN study (NCT04950127), linerixibat, an ileal bile acid transporter inhibitor, significantly improved pruritus and pruritus-related sleep interference vs placebo over 24 weeks (wks). This analysis reports interim data from the Linerixibat Long-term Safety and Tolerability (LLSAT [NCT04167358]) Study evaluating linerixibat's long-term safety, tolerability and maintenance of itch improvement.
Method: Patients (pts) with PBC and moderate–severe pruritus when previously enrolled in Phase 3/Phase 2b linerixibat trials were eligible to enrol in this ongoing, open-label, global extension study, in which pts receive oral linerixibat 40 mg twice daily. The primary endpoint is frequency and severity of adverse events (AEs). Key secondary endpoints include: change in laboratory values; assessment of maintenance of efficacy (MOE; percent of pts who achieved an itch response [≥ 3-point reduction from baseline on 0–10 worst itch numerical rating scale (WI-NRS)] at wk 24 also achieving this threshold at wk 52). Stable concomitant PBC/itch therapy is permitted for those assessed for MOE. Analyses are descriptive.
Results: Of 241 pts enrolled up to 4 years, 222 (92%) were receiving ursodeoxycholic acid, 21 (9%) cholestyramine and 88 (37%) fibrates, seladelpar or elafibranor. AEs were reported in 88% of pts; serious AEs in 14%. The most common AE was diarrhoea (44%; led to treatment discontinuation in 7%). Among pts with an AE, 7% experienced hepatobiliary disorders, 6% alanine aminotransferase increase and 3% aspartate aminotransferase increase. Of 41 responders eligible for interim MOE assessment at wk 24 (who reached wk 52 or withdrew early), 30 (73% [95% CI: 58.07–84.31]) maintained itch efficacy at wk 52. Pts who received linerixibat for 52 continuous wks (n = 38; in GLISTEN then LLSAT) had a mean (SD) WI-NRS change from baseline of −4.87 (2.3). For those randomised to 24 wks of linerixibat then 8 wks of placebo in GLISTEN, itch returned then improved to previous levels once linerixibat restarted in LLSAT.
Conclusion: Interim analysis demonstrates that linerixibat treatment up to 4 years is generally well-tolerated with an acceptable safety profile. In addition, when assessed in a portion of pts with WI-NRS data at wks 24 and 52, linerixibat response on itch is maintained.
Funding:GSK (212358).
[for the LLSAT Study Group].

TOP-281

Real world outcomes of primary biliary cholangitis in Latin America

Claudia Couto[1], Guilherme Cançado[1], Jhon Prieto[2], Graciela Castro-Narro[3], Maria Lucia Ferraz[4], Débora Terrabuio[5], Lorena Castro[6], Luciana Faria[1], Alejandra Villamil[7], Esteban Gonzalez Ballerga[8], Cristiane A. Villela-Nogueira[9], Viridiana Guevara[10], Ezequiel Ridruejo[11], Harlim Rodriguez[12], Maria Sarai González-Huezo[13], Fernando Cairo[14], Jonathan Aguirre[15], Elze Maria Gomes Oliveira[16], Adelina Lozano Miranda[17], Nicolás Ortiz-López[18], Janaina Schiavon[19], Paulo Bittencourt[20], Fernando Bessone[21], Maria Margarita Anders[22], Roberto Rafael Perez[23], Manuel Mendizabal[24], Rodrigo Zapata[25,26], Daniela Perez[27], Alma Kuljacha[28], Mario Guimarães Pessoa[5], Hugo Cheinquer[29], Liliana Mendes[30], Cristiane Tovo[31], Pablo Coste[32], Stefanny Cornejo-Hernández[33], Adriana Varon[34], Maria Chiara Chindamo[9], Daniela Simian[18], Raul Lazarte[35], Melisa Dirchwolf[36], Miguel Escobedo[37], Juan Córdoba[2], Ivan López-Mendez[38], Ana Cristina Amaral[4], Sarah Rufino[4], Franco Weisser[39], Andreina Fragenas[7], Ilse Pardo Ivirico[8], Vivian Rotman[9], Carlos Coronel-Castillo[10], Mirta Peralta[11], Danay Guerrero[12], Luis Alejandro Rosales Renteria[13], Manuel Barbero[14], Paula Daniela Chiodi Lopez[40], Ana Sofia Castro[15], Lucas Carvalho[16], Alvaro Urzúa[18], Leonardo Schiavon[19], Daniela Moreno[2], Sebastián Gil[2,41], Diana Carolina Alfonso Vergel[2], Diego Puentes[42], Nalu Navarro-Alvarez[3], Raimundo Araujo Gama[4], Fernanda Gelape[1], Mateus Nardelli[1], Bernardo Moraes[1], Rodrigo Sanchez[6], Matías Bori[8], Rodrigo Toledo-Galván[10], Marlen Ivon Castellanos Fernández[12], Marcela Ibarra[13], Nicolas Dominguez[14], Angelo Mattos[31], Eduardo Cancado[5], Nélia Hernandez[40]. *[1]Federal University of Minas Gerais, Hospital das Clinicas, Instituto Alfa de Gastroenterologia, Belo Horizonte, Brazil; [2]Centro de Enfermedades Hepáticas y Digestivas, Bogotá, Colombia; [3]Departamento de Gastroenterologia, Servicio de Hepatologia y Transplante Hepático, Instituto Nacional de Ciencias Medicas y Nutrición "Salvador Zubirán", Ciudad de México, Mexico; [4]Hospital São Paulo, Ambulatório de Hepatologia, Universidade Federal de São Paulo, São Paulo, Brazil; [5]Hospital das Clínicas da Universidade de São Paulo, São Paulo, Brazil; [6]Clínica Universidad de los Andes, Santiago, Chile; [7]Hospital Italiano de Buenos Aires, Buenos Aires, Argentina; [8]Hospital de Clínicas José de San Martín, Buenos Aires, Argentina; [9]Universidade Federal do Rio de Janeiro, Rio de Janeiro, Brazil; [10]Hospital General de México, Ciudad de México, Mexico; [11]Centro de Educación Médica e Investigaciones Clínicas Norberto Quirno (CEMIC), Buenos Aires, Argentina; [12]Instituto de Gastroenterología de Cuba, La Habana, Cuba; [13]Centro Médico ISSEMyM, Toluca, Mexico; [14]Hospital El Cruce, Buenos Aires, Argentina; [15]Hospital Ángeles Pedregal, Ciudad de México, Mexico; [16]Centro Universitário Lusíada (UNILUS), Santos, Brazil; [17]Clínica Ricardo Palma, Lima, Peru; [18]Hospital Clínico Universidad de Chile, Santiago, Chile; [19]Universidade Federal de Santa Catarina, Florianópolis, Brazil; [20]Hospital Português, Salvador, Brazil; [21]Hospital Provincial del Centenario, Rosario, Argentina; [22]Hospital Alemán, Buenos Aires, Argentina; [23]Hospital Central de Mendoza, Mendonza, Argentina; [24]Hospital Universitario Austral, Pilar, Argentina; [25]Clínica Alemana de Santiago, Santiago, Chile; [26]Facultad de Medicina, Universidad del Desarrollo, Santiago, Chile; [27]Hospital Ángel C. Padilla, Tucumán, Argentina; [28]Hospital Ángeles Valle Oriente, Monterrey, Mexico; [29]Hospital de Clínicas de Porto Alegre, Porto Alegre, Brazil; [30]Hospital de Base do Distrito Federal, Brasília, Brazil; [31]Santa Casa de Misericórdia de Porto Alegre, Porto Alegre, Brazil; [32]Hospital R.A. Calderón Guardia, San José, Costa Rica; [33]Hospital Central Militar, Ciudad de México, Mexico; [34]Hospital Cardio Infantil, Bogotá, Colombia; [35]Clinica Santa María, Santiago, Chile; [36]Hospital Privado de Rosario, Rosario, Argentina; [37]Hospital Universitario "Dr. José Eleuterio González," Monterrey, Mexico; [38]Unidad de Hepatologia y Transplantes, Hospital Médica Sur, Ciudad de México, Mexico; [39]Medicina Interna Clínica Dávila, Santiago, Chile; [40]Unidad Académica de Gastroenterología, Hospital de Clínicas, Montevideo, Uruguay; [41]Hospital Universitario San Ignacio, Bogotá, Colombia; [42]Grupo de Equidad en Salud, Facultad de Medicina, Universidad Nacional de Colombia, Bogotá, Colombia*
Email: cacouto@uol.com.br

Background and aims: Primary biliary cholangitis (PBC) outcomes are mainly reported in Caucasians, lacking data from Latin America. This study aimed to evaluate the biochemical response to ursodeoxycholic acid (UDCA) and second-line therapies using established criteria, and to assess long-term survival and prognosis for PBC in Latin America.
Method: The ALLATIN cohort is a retrospective international multicentre study that enrolled PBC patients from several Latin American countries. Biochemical response was assessed at 6 and 12 months of treatment. Deep response was defined as alkaline phosphatase (ALP)

normalization and bilirubin < 0,6 times the upper limit of normal (ULN).
Results: 2,182 PBC patients (93.3% female) were included –. At diagnosis, median age was 53 years (15–91), 18% were asymptomatic and 27% had advanced liver disease. Baseline mean ALP was 3.63 ± 3.30 × ULN and antimitochondrial antibody positivity was 73.5%. Autoimmune hepatitis and metabolic dysfunction-associated liver disease overlap were reported in 19.8% and 6.3%, respectively. UDCA was prescribed to 96.9%, with 3.6% discontinuation. UDCA response rates after 12 months were: Toronto (57.3%), Paris-2 (39.1%), POISE (38.8%) and deep-response (14.7%). Second-line therapy included fibrates in 27.8% and obeticholic acid in 0.3%. After 12 months of fibrates, response rates were Toronto (58.6%), Paris-2 (36.4%), POISE (42.1%) and deep-response (18.9%). During a mean follow-up of 7.4 ± 5.9 years, 28% developed advanced liver disease, 1.5% had hepatocellular carcinoma and 6.1% underwent liver transplantation. Five- and 10-years survival were 90.2 ± 0.9% and 81.7 ± 1.4%, respectively. Multivariate analysis showed ALP ≥5 .84 × ULN at diagnosis predicted death/transplantation (HR 1.80; 95%CI 1.37–2.34; p < 0.001), and ALP ≥1.46 × ULN at 12 months on UDCA predicted lower transplant-free survival (HR 2.20; 95%CI 1.66–2.94; p < 0.001).
Conclusion: This is the largest Latin American PBC cohort. Low rates of biochemical response to UDCA and modest indication of second-line therapy may be associated with the significant burden of advanced liver disease observed. ALP at baseline and 12-month of UDCA are independent prognostic factors for transplant-free survival. These findings support early risk stratification and timely escalation of therapy in PBC patients from Latin America.

TOP-292-YI
Statin use is associated with reduced cholangiocarcinoma risk in primary sclerosing cholangitis: a national EHR cohort study
Adrielly Martins[1,2], Miki Scaravaglio[3,4], Cynthia Levy[1]. *[1]University of Miami, Miami, United States; [2]Schiff Center for Liver Diseases - University of Miami, Miami, United States; [3]Università Milano-Bicocca, Milano, Italy; [4]University of Cambridge, Cambridge, Northern Ireland*
Email: axm8717@med.miami.edu

Background and aims: Patients with primary sclerosing cholangitis (PSC) face a 10–15% lifetime risk of cholangiocarcinoma (CCA). Statins have demonstrated anti-inflammatory and antineoplastic properties in hepatobiliary cancers, but their association with CCA risk in PSC remains unclear. We evaluated the association between statin use and CCA development in a large PSC cohort.
Method: Using the Epic Cosmos database, we conducted a retrospective cohort study of PSC patients diagnosed between 2005–2025. Relevant statin exposure was defined as ≥2 prescriptions, first prescription ≥90 days after PSC diagnosis, and ≥90 days before CCA diagnosis (for CCA cases). Hazard ratios (HR) were estimated by Cox proportional hazards regression adjusting for age, sex, inflammatory bowel disease (IBD), and cirrhosis. Time-stratified analysis was performed when proportional hazards assumption was violated. Sensitivity analyses examined subgroups by IBD status, cirrhosis, and age.
Results: Of 35,453 PSC patients (mean age 52 years, 51% male, 50% IBD, 58% cirrhosis), 4,485 (13%) met statin exposure criteria and 2,041 (5.8%) developed CCA. CCA incidence was significantly lower in statin users than non-users (3.3% vs 6.1%, p < 0.001). In adjusted analysis, statin use was associated with 69% reduction in CCA risk (HR 0.31, 95% CI 0.26–0.37, p < 0.001). Time-stratified analysis revealed protection was strongest in the first 2 years (HR 0.06, 94% risk reduction), diminished over time (years 2–5: HR 0.38; years 5–10: HR 0.54), and was no longer significant beyond 10 years. In sensitivity analysis excluding CCA diagnosed within 1 year of PSC (likely prevalent disease, n = 904, 44% of cases), statin use remained significantly protective (HR 0.47, 95% CI 0.39–0.56, p < 0.001). Protection was consistent across subgroups: PSC-IBD (HR 0.33) and PSC without IBD (HR 0.28), with cirrhosis (HR 0.34) and without cirrhosis (HR 0.24), and across all age groups (p < 0.001). A dose-response relationship was observed with significant risk reduction across all prescription categories (73% reduction with 2–5 orders; trend p < 0.001).
Conclusion: In a large retrospective cohort of PSC patients, statin use was associated with a substantial reduction in CCA risk across different clinical subgroups. The protective effect was greatest in the early years after diagnosis and increased with greater exposure. These findings support further prospective evaluation of statins in PSC.

TOP-293
Liver biopsy facilitates efficient and high-quality diagnosis and evaluation of treatment outcomes in primary sclerosing cholangitis: results from the phase 3 NUC-5/PSC trial
Sandra Noh[1], Stefan G. Hübscher[2], Thomas Longerich[1], Geoffrey Chase[3], Michael Stiess[3], Peter Fickert[4], Michael Manns[5], Michael Trauner[6], Peter Schirmacher[1]. *[1]Institute of Pathology, University Hospital Heidelberg, Heidelberg, Germany; [2]School of Infection, Inflammation and Immunology, University of Birmingham, Birmingham, United Kingdom; [3]Dr. Falk Pharma GmbH, Freiburg, Germany; [4]Department of Medicine, Medical University of Graz, Graz, Austria; [5]Department of Gastroenterology, Hepatology, Infectious Diseases and Endocrinology, Hannover Medical School, Hannover, Germany; [6]Division of Gastroenterology and Hepatology, Department of Internal Medicine III, Medical University of Vienna, Vienna, Austria*
Email: peter.schirmacher@med.uni-heidelberg.de

Background and aims: NUC-5/PSC was a randomized, controlled, phase 3 trial investigating norucholic acid (NCA) in primary sclerosing cholangitis (PSC) at 74 sites in 16 European countries. A significant benefit of NCA was demonstrated based on the primary and several secondary endpoints comprising structured histopathological evaluation of liver biopsies. Here, we assess the suitability of liver biopsies for clinical investigations and routine diagnosis in PSC based on histological analyses in the trial.
Method: Patients with PSC were treated with NCA or placebo for 192 weeks, with biopsies collected at screening, week 96, and week 192. Eligibility criteria for the trial included confirmation of disease by cholangiography as well as hallmark signs of PSC by liver biopsy within 2 months of baseline. Biopsies were collected according to local procedures. Histological evaluation was performed centrally, with an initial examination of biopsies to confirm diagnosis, and evaluation of efficacy parameters in all biopsies after database lock. These included Ludwig, Ishak, modified Nakanuma score and PSC histoscore staging as well as digital pathology assessment of collagen proportionate area.
Results: A total of 610 biopsies from 335 patients were available at database lock for the primary analysis, with screening biopsies from 334 patients. Mean biopsy length was 21 mm (5.7% <10 mm; 21.3% 10–15 mm; 73.0% >15 mm) with 1.6% containing <6 portal tracts, 34.1% with 6–10 portal tracts, and 64.3% with >10 portal tracts. Expert histological scoring was possible for 98.5% of biopsies, while digital fibrosis assessment was possible for 98.9%. Among the 610 biopsies, 9 were not evaluable due to technical ineligibility. Furthermore, histological evaluation suggested a diagnosis other than PSC (e.g. sarcoidosis, fibropolycystic disease, primary biliary cholangitis) for 3.3% of patients, and a significant comorbid parenchymal disease (e.g. metabolic or toxic etiology) for 3.0%. Biopsy-related adverse events (AEs) were reported for 4.1% of biopsy examinations across all time points, with serious AEs reported for 1.1% and AEs for 0.7% of biopsies, and no discontinuations.
Conclusion: In this international pivotal trial in PSC, the use of locally-collected liver biopsies facilitated high diagnostic sensitivity and efficient analyses with few adverse events. Histopathology of liver biopsy is safe and informative, confirming diagnostic accuracy and therapeutic efficacy in clinical trials and for routine diagnosis of PSC.

TOP-294-YI

The number needed to treat with bezafibrate as second-line therapy to prevent liver transplantation or death in people with primary biliary cholangitis

Ellen Werner[1], Maria A. van de Vrie[1], Maria C. van Hooff[1], Adriaan J. van der Meer[1]. [1]*Erasmus University Medical Center, Rotterdam, Netherlands*
Email: e.werner@erasmusmc.nl

Background and aims: The clinical benefit of bezafibrate (BZF) in primary biliary cholangitis (PBC) has not been extensively reported in absolute measures. We aimed to assess the number needed to treat (NNT) with bezafibrate (BZF) to prevent liver transplantation (LT) or death among people with PBC.
Method: The NNT was calculated based on the LT-free survival probability among ursodeoxycholic acid (UDCA)-treated individuals with PBC included in the Dutch PBC Cohort Study and the reported adjusted HR of BZF on LT or death (aHR 0.33, 95%CI 0.19–0.55) in the Japanese Cohort Study (Tanaka et al. J Hepatol 2021). In addition, the NNT was plotted over the range of the GLOBE score (as a prognostic tool), to allow the estimation of the NNT to prevent one LT or death for the individual with BZF. The NNT to prevent one death or LT within 5 years (NNT5y) or 10 years (NNT10y) is presented.
Results: In total, 2271(63.7%) Dutch people with PBC had an ALP above the upper limit of normal (ULN) after one year of UDCA. Their median age was 57.1 years (IQR 50.1–67.0), 2003 (88.2%) were female and 187 (8.2%) had cirrhosis. During a median follow-up of 7.5 years (IQR 3.5–13.2), 76 patients underwent LT and 411 patients died without LT. Overall, the cumulative 5y and 10y LT-free survival was 90.0% (95% 88.6–91.4) and 79.4% (95% CI 77.2–81.5), respectively. This corresponded to an estimated NNT5y of 15 (95%CI 11–26) and a NNT10y of 7 (95%CI 6–13) to prevent one LT or death. According to the ALP category (1.0–1.67 × ULN, 1.67–3.0 × ULN, and ≥3.0 × ULN) at one year of UDCA, the NNT5y was 20 (95%CI 14–38), 13 (95%CI 9–26), and 7 (95%CI 5–15), and the NNT10y was 8 (95%CI 6–15), 8 (95%CI 6–16), 6 (95%CI 5–11), and 4 (95%CI 3–8), respectively. The NNT5y and NNT10y dropped below 20 from a GLOBE score above 0.19 and –0.81 (corresponding to an estimated cumulative LT-free survival of 92.3% for either 5 or 10 years), which was the case for 768/1741 (44.1%) and 1494/1741 (85.8%) people in the analyses.
Conclusion: The overall projected efficacy of continued BZF therapy in terms of the NNT to prevent LT or death was strong (NNT < 20), also in case people had a relatively favorable ALP level (1.0–1.67 × ULN) after one year of UDCA. These results highlight the potential clinical benefit of off-label BZF therapy in those without ALP normalization with UDCA therapy alone.

SAT-245

High prevalence of low muscle strength and low muscle mass in primary biliary cholangitis: a multimodal assessment including muscle ultrasound

Luise Aamann[1,2,3,4], Kasper Yde Jensen[5], Lene Terslev[3,6], Bente Appel Esbensen[3,6], Louise Diederichsen[6,7], Charlotte Suetta[3,8], Søren Møller[9,10], Henriette Ytting[1,2,3,4]. [1]*The Gastro Unit, Copenhagen University Hospital Hvidovre, Copenhagen, Denmark;* [2]*Department of Digestive Diseases, Transplantation and General Surgery, Section for Liver Diseases, Rigshospitalet, University of Copenhagen, Copenhagen, Denmark;* [3]*Institute of Clinical Medicine, Faculty of Health and Sciences, University of Copenhagen, Copenhagen, Denmark;* [4]*European Reference Network on Hepatological Diseases (ERN RARE-LIVER), Hamburg, Germany;* [5]*Copenhagen Center for Arthritis Research (COPECARE), Center for Rheumatology and Spine Diseases, Copenhagen, Denmark;* [6]*Copenhagen Center for Arthritis Research (COPECARE), Center for Rheumatology and Spine Diseases, Copenhagen University Hospital Rigshospitalet, Copenhagen, Denmark;* [7]*Institute of Clinical Medicine, Faculty of Health and Sciences, University of Copenhagen, Copenhagen, Denmark;* [8]*Geriatric Research Unit, Copenhagen University Hospital, Bispebjerg and Frederiksberg Hospital, Copenhagen, Copenhagen, Denmark;* [9]*Department of Clinical Physiology and Nuclear Medicine, Copenhagen University Hospital Hvidovre, Copenhagen, Denmark;* [10]*Institute of Clinical Medicine, Faculty of Health and Sciences, Copenhagen, Denmark*
Email: luise.aamann@gmail.com

Background and aims: Primary biliary cholangitis (PBC) is a chronic autoimmune cholestatic liver disease associated with fatigue, muscle weakness, and impaired physical performance. Sarcopenia is a known complication of chronic inflammatory diseases, but its prevalence and clinical relevance in PBC are insufficiently described. This study aimed to assess sarcopenia-related features in patients with PBC using a multimodal approach and to evaluate the feasibility of ultrasound for muscle mass assessment.
Method: Adult patients with primary biliary cholangitis were included in a cross-sectional study conducted at the outpatient clinic, Gastro Unit, Copenhagen University Hospital Hvidovre. Sarcopenia was defined according to European Working Group on Sarcopenia in Older People 2 (EWGSOP2) criteria. Muscle strength was assessed using handgrip dynamometry. Muscle mass was evaluated by appendicular skeletal muscle index (ASMI) measured by dual-energy X-ray absorptiometry (DXA), skeletal muscle mass index (SSMI) assessed by bioelectrical impedance analysis (BIA), and right-sided ultrasound measurements of the biceps brachii and rectus femoris without probe compression. Liver stiffness was assessed by transient elastography. Group comparisons were performed using independent t-tests.
Results: Forty-four patients (100% women) with a median (IQR) age of 59 (54–65) years and disease duration of 5.4 (3.0–9.4) years were included; 9% had advanced liver disease (liver stiffness > 15 kPa). Low muscle strength (< 16 kg) was present in 19%, while low muscle mass was found in 19% by DXA (ASMI < 5.5 kg/m^2) and 21% by BIA (SSMI < 6.1 kg/m^2). Disease duration and liver stiffness did not differ between patients with low versus normal muscle strength. Ultrasound measured biceps brachii muscle thickness correlated moderately with ASM ($r = 0.44$, $p = 0.004$) and SSM (0.48, $p = 0.002$) and rectus femoris muscle thickness correlated moderately with ASM ($r = 0.37$, $p = 0.02$) and SSM ($r = 0.44$, $p = 0.005$).
Conclusion: Despite a low prevalence of advanced liver disease, patients with PBC demonstrated a high prevalence of low muscle strength and muscle mass than European reference populations. These findings suggest that sarcopenia-related features occur earlier and more frequently in women with PBC and may contribute to fatigue. Muscle ultrasound appears to be a feasible and clinically useful adjunct for muscle mass assessment and may support easily accessible systematic screening.

SAT-246

High burden of depression, sleep disturbance, and anhedonia in primary biliary cholangitis independent of fibrosis stage and prognostic scores

Gupse Adali[1], Mehmet Ali Saruhan[2], Berkay Dertsiz[2]. [1]*University of Health Sciences Istanbul Umraniye Training and Research Hospital, Istanbul, Türkiye;* [2]*University Of Health Sciences, Istanbul, Türkiye*
Email: gupseadali@gmail.com

Background and aims: Primary biliary cholangitis (PBC) is a chronic immune-mediated cholestatic liver disease associated with a substantial symptom burden. Fatigue, pruritus, sleep disturbances, and psychological symptoms are highly prevalent and may markedly impair health-related quality of life. Data simultaneously evaluating depression, sleep quality, and anhedonia in PBC, particularly in comparison with healthy individuals, are limited. This study aimed to compare depressive symptoms, sleep quality, and anhedonia between patients with primary biliary cholangitis and healthy controls using validated psychometric tests and to explore whether these tests are associated with disease severity.
Method: This cross-sectional study included 88 patients with PBC followed at a tertiary referral center and 50 healthy controls (HC)

without known liver or systemic disease. All participants underwent a standardized psychological assessment using validated self-report instruments: the Beck Depression Inventory for depressive symptom severity, the Pittsburgh Sleep Quality Index for sleep quality, and the Snaith–Hamilton Anhedonia Scale for anhedonia. Moderate-to-severe depression, poor sleep quality, and the presence of anhedonia were defined using established cutoff values.
Results: Patients with PBC had a significantly higher prevalence of moderate-to-severe depression (51.1% vs. 20.0%, $p = 0.001$), poor sleep quality (70.5% vs. 44.0%, $p = 0.004$), and anhedonia (38.6% vs. 18.0%, $p = 0.020$) than controls. Associations between PBC and psychological outcomes remained significant after adjusting for sex. Within the PBC cohort, cirrhosis was present in 9.1%, significant fibrosis in 33.0%, and advanced fibrosis in 15.9% of patients. One-third of patients were non-responders according to the Paris II criteria, 23.9% had concomitant MASLD, and 15.9% were classified as high-risk according to the GLOBE score. No significant associations were observed between quality of life measures and disease severity, including liver stiffness. Similarly, quality of life scores were not associated with the presence of MASLD, Paris II response status, or GLOBE risk category.
Conclusion: Patients with PBC exhibit a substantially higher burden of depression, sleep disturbance, and anhedonia than healthy controls. Importantly, these impairments appear to be independent of biochemical response, fibrosis severity, and prognostic risk scores, underscoring the need for systematic psychological assessment alongside routine disease monitoring in PBC.

SAT-247

Treatment adherence predicts lower risk of disease progression among patients with primary biliary cholangitis in the United States

Robert G. Gish[1], Michel Mendler[2], Edward Mena[2], Chong Kim[3], Yi Pan[4], Mihail Samnaliev[4], Diane Ito[4], Maria Agapova[3]. [1]*Robert G. Gish Consultants LLC, San Diego, United States;* [2]*California Liver Research Institute, Pasadena, United States;* [3]*Gilead Sciences, Foster City, United States;* [4]*Stratevi, Santa Monica, United States*
Email: rgish@robertgish.com

Background and aims: Primary biliary cholangitis (PBC) is an autoimmune liver disease that can progress to cirrhosis, hepatocellular carcinoma, and liver failure. Real-world evidence evaluating the association between PBC treatment adherence and progression to these clinical outcomes is limited. This study aimed to evaluate the association between PBC treatment adherence with PBC disease progression.
Method: This retrospective cohort study utilized Komodo's Healthcare Map insurance claims (01/01/2016–12/19/2024). Adults aged ≥18 years diagnosed with PBC, with continuous insurance coverage, initiating ursodeoxycholic acid (UDCA), obeticholic acid (OCA) or off-label fibrates after 01/01/2017 were eligible. Proportion of days covered (PDC) with continuous treatment with UDCA, OCA and/or off-label fibrates was estimated, with ≥80% considered adherent. Discrete time-to-event models using annual and quarterly intervals as the analytic units estimated associations between adherence and the first occurrence in the data of cirrhosis, decompensated cirrhosis (DC), hepatocellular carcinoma (HC), liver transplant (LT), and all-cause mortality controlling for demographics, baseline comorbidities, and PBC treatment.
Results: The cohort included 54,034 patients with mean/median follow-up of 1,443/1,365 days (SD: 867). Patients were mostly female (84.9%), primarily Medicare-covered (51.0%), and had a mean age of 62 years. The majority (96.7%) initiated UDCA. Over 1, 3, and 5 years, 50%, 29%, and 21% were adherent, respectively. Adherence was associated with lower risk of cirrhosis (Hazard ratio [HR]: 0.88; 95% CI: 0.83–0.93), DC (HR: 0.69; CI: 0.63–0.76), LT (HR: 0.69; 95% CI: 0.58–0.81) and death (HR: 0.82; 95% CI: 0.76–0.88) (all p < .001) and was not a significant predictor of HC (HR: 0.98; 95% CI: 0.82–1.17; p = .819). When quarterly intervals were used, adherence remained associated with lower risk of cirrhosis, DC, LT and death (all p < .001).
Conclusion: In PBC, only about half of patients met the commonly accepted minimum adherence ≥80% threshold after 1 year, dropping to 1 in 5 by five years. As adherence predicts disease progression, therapy selection based on long-term tolerability and patient suitability may improve outcomes in PBC.

SAT-248

Recompensation and further decompensation after index decompensation in patients with autoimmune hepatitis: a real-world study

Arnav Aggarwal[1], Sagnik Biswas[1], Sarthak Saxena[1], Ayush Agarwal[1], Shekhar Swaroop[1], Vishal Chauhan[1], Shubham Jain[1], Samagra Agarwal[1], Shalimar Shalimar[1]. [1]*All India Institute of Medical Sciences, New Delhi, India*
Email: arnav272@gmail.com

Background and aims: Immunosuppression controls inflammation and can reverse fibrosis in autoimmune hepatitis (AIH), but data on hepatic recompensation in AIH-related decompensated cirrhosis are limited. We evaluated incidence and predictors of recompensation and further decompensation, and assessed the impact of recompensation on long-term survival in these patients.
Method: In this retrospective analysis of a prospectively maintained database, patients with decompensated AIH-related cirrhosis (ascites, variceal bleed or hepatic encephalopathy [HE]) treated with immunosuppression were followed from the time of biopsy-confirmed AIH. The primary outcome was cumulative incidence of recompensation, defined as per Baveno VII consensus, estimated using Fine and Gray competing-risk regression with further decompensation and death as competing risks. Secondary outcomes were all-cause mortality and further decompensation, and the effect of recompensation on mortality was assessed using a time-dependent Cox proportional hazard model.
Results: Of 112 patients (71% females; mean age 41 ± 13 years), 75% had ascites, 26% variceal bleeding and 13% HE. The median MELD-Na and CTP scores were 15.7 (11.5–22.7) and 7 (6–10) respectively. Prednisolone, azathioprine and mycophenolate mofetil were used in 89%, 62% and 21% of patients respectively. Over a median follow up of 29 months, 60 (54%) patients achieved recompensation. Younger age, lower CTP score and biochemical response at 6 months independently predicted recompensation, with biochemical response being the strongest predictor (sHR 1.76, 95% CI 1.18–3.13). After recompensation, 9 (15%) patients developed further decompensation (1- and 2-year cumulative incidence 3.4% and 8.5%), whereas among 52 non-recompensated patients, 36 (69%) developed further decompensation and 16 (31%) remained in a stable decompensated state. Recompensation was associated with reduced mortality (HR 0.26, 95% CI 0.07–0.91) compared with non-recompensated patients. Younger age, lower CTP score and biochemical response also independently predicted lower mortality.
Conclusion: More than half of treated AIH-related decompensated cirrhosis treated with immunosuppression can achieve recompensation, which is associated with reduced mortality compared with non-recompensated patients. Younger age, lower baseline CTP score, and biochemical response are key determinants of recompensation and survival.

SAT-249

Plasma C4 as a potential biomarker of cholangiocarcinoma in primary sclerosing cholangitis

Ina Andersen[1], Peder Braadland[2,3], Antonio Molinaro[4], Marcus Henricsson[4], Tom Hemming Karlsen[1,2,3,5], Mette Vesterhus[2,6,7], Johannes R. Hov[1,3,8,9], Trine Folseraas[8,9,10]. [1]*Section of Gastroenterology, Department of Transplantation Medicine, Clinic of Surgery and Specialized Medicine, Oslo University Hospital, Rikshospitalet, Norwegian Center of PSC Research, Clinic of Surgery and*

Specialized Medicine, Oslo University Hospital, Rikshospitalet, Institute of Clinical Medicine, University of Oslo, Norway, Oslo, Norway; [2]Norwegian Center of PSC Research, Clinic of Surgery and Specialized Medicine, Oslo University Hospital, Rikshospitalet, Research Institute of Internal Medicine, Clinic of Surgery and Specialized Medicine, Oslo University Hospital, Rikshospitalet., Oslo, Norway; [3]Research Institute of Internal Medicine, Clinic of Surgery and Specialized Medicine, Oslo University Hospital, Rikshospitalet, Oslo, Norway; [4]Department of Molecular and Clinical Medicine/Wallenberg Laboratories, Sahlgrenska Academy, University of Gothenburg, Sweden; Institute of Medicine, Section of Gastroenterology and Hepatology, Sahlgrenska University Hospital, Gothenburg, Sweden, Gothenburg, Sweden; [5]Institute of Clinical Medicine, University of Oslo, Norway; Research Institute of Internal Medicine, Clinic of Surgery and Specialized Medicine, Oslo University Hospital, Rikshospitalet, Oslo, Norway; [6]Department of Medicine, Haraldsplass Diaconal Hospital, Bergen, Norway, Bergen, Norway; [7]Clinical Institute 2, University of Bergen, Norway, Bergen, Norway; [8]Norwegian Center of PSC Research, Clinic of Surgery and Specialized Medicine, Oslo University Hospital, Rikshospitalet, Oslo, Norway; [9]Institute of Clinical Medicine, University of Oslo, Norway, Oslo, Norway; [10]Section of Gastroenterology, Department of Transplantation Medicine, Clinic of Surgery and Specialized Medicine, Oslo University Hospital, Rikshospitalet, Oslo, Norway
Email: inaand@ous-hf.no

Background and aims: People with primary sclerosing cholangitis (PSC) have an increased risk of cholangiocarcinoma (CCA), a cancer with poor prognosis, highlighting the urgent need for improved biomarkers to predict CCA in PSC. We have previously shown that reduced bile acid synthesis, measured by blood 7-hydroxy-4-cholesten-3-one (C4), is associated with worse outcomes in PSC. Here, we investigated whether plasma C4 could serve as a non-invasive marker of CCA risk in PSC.
Method: C4 and bile acids in plasma profiles were analyzed by ultraperformance liquid chromatography-tandem mass spectrometry in 187 Norwegian individuals with PSC (79% male), categorized as either i) PSC with untreated CCA at sampling (PSC-CCA), ii) PSC developing CCA within two years of sampling (PSC-TO-CCA), and iii) PSC without CCA within two years of sampling (PSC-ONLY). Values are given as median (interquartile range, IQR). Group differences were calculated using Mann-Whitney-U test, and statistical analyses were performed in Stata (v18.0).
Results: In total, n = 168 were categorized as PSC-ONLY, ten as PSC-CCA and nine as PSC-TO-CCA. The distributions of sex and concurrent inflammatory bowel disease were similar in the groups. Median age at sampling was 41.2 years, median time since PSC diagnosis was 2.7 years. The median age in the PSC-ONLY group was lower than in the PSC-CCA and PSC-TO-CCA groups (39 vs. 54.7 and 55.5 years), while time since diagnosis was similar between the groups. The C4 levels were higher in the PSC-ONLY group (11.3 nmol/L, IQR 4–32.2) compared with PSC-CCA (1.8 nmol/L, IQR 1.4–2.6, $p < 0.001$) and were borderline significantly higher than in the PSC-TO-CCA group (2.8 nmol/L, IQR 1.3–8.4, $p = 0.051$). Total bile acids concentration was lower in PSC-ONLY (14.0 µmol/L, IQR 4.4–48.1) compared with PSC-CCA (78.0 µmol/L, IQR 68.0–99.3, $p < 0.001$). The total bile acids in PSC-ONLY were also numerically, but not statistically, lower than in PSC-TO-CCA (37.5 µmol/L, IQR 8.1–39.4, $p = 0.64$) and higher in PSC-CCA than in PSC-TO-CCA ($p = 0.04$). Overall, users of UDCA had lower C4 levels than non-UDCA-users (7.7 nmol/L, IQR 2.1–21.8 vs 22.5 nmol/L, IQR 8.5–45.6, $p < 0.001$). We observed no differences in C4 levels depending on use of UDCA in either group.
Conclusion: Plasma C4 was lower and total bile acids levels were higher in individuals with PSC who had established or were close to CCA development. These findings support C4 as a potential non-invasive biomarker for CCA development of PSC and warrant further investigation.

SAT-250

Long-term biochemical response is associated with a lower risk of decompensation in autoimmune hepatitis, irrespective of non-selective beta-blocker use

Pinelopi Arvaniti[1,2,3,4], Marlene Padilla[1], Ignasi Olivas[1,3], Helena Hernández Evole[1,3], Sergio Rodriguez-Tajes[1,2,3], Alessio Gerussi[5,6], Roberta Lasco[6], Alessandra Bonfichi[6], Alejandra Villamil[7], Sofia Tejado Rico[7], Yu Jun Wong[8,9], Jarell Jie-Rae Tan[8,10], Judith Gómez-Camarero[11], Vincenza Calvaruso[12], Giuliano Genova[12], Mirjam Kolev[3,13], Juan Pedro Toro Ortiz[14], Miren Garcia Cortes[14], Bastian Engel[3,15], Lisa Sandmann[15], Richard Taubert[3,15], Marco Carbone[16], Raffaella Viganò[16], Marina Clemente[16], Sara Lorente[17], Indhira Perez Medrano[18], Montserrat Garcia-Retortillo[19], Konstantinos Papantoniou[20], Christos Triantos[20], Joao Madaleno[3,21], Ellina Lytvyak[22], Aldo J Montano-Loza[22], Laura Harrison[23], Ana Arencibia Almeida[24], Mar Riveiro Barciela[2,3,25], Adrielly Martins[26], Cynthia Levy[26], Marcial Sebode[3,27], Christoph Schramm[3,27,28], Ansgar W. Lohse[3,27], Isabel Conde[29], Raquel Ríos León[30], Natalia García Gimeno[31], Rosa Rota[32], Carmen Álvarez-Navascués[33], Esther Maderuelo[34], Ismael El Hajra[34], George Giannoulis[35], Kalliopi Zachou[35], George Dalekos[35], Ignacio Garcia Juarez[36], Orfanel Pineda-Arzate[36], Virginia Hernández-Gea[1,2,3,37], María Carlota Londoño[1,2,3]. *[1]Liver Unit, Hospital Clínic Barcelona, Fundació de Recerca Clínic Barcelona-Institut d'Investigacions Biomèdiques August Pi i Sunyer (FRCB-IDIBAPS), Universitat de Barcelona, Barcelona, Spain, Barcelona, Spain; [2]Centro de Investigación Biomédica en Red en Enfermedades Hepáticas y Digestivas (CIBEREHD), Spain, Barcelona, Spain; [3]European Reference Network on Hepatological Diseases (ERN RARE-LIVER), Barcelona, Spain; [4]Department of Internal Medicine, General Hospital of Granollers, Barcelona, Spain, Granollers, Spain; [5]Division of Gastroenterology, Center for Autoimmune Liver Diseases, European Reference Network on Hepatological Diseases (ERN RARE-LIVER), Fondazione IRCCS San Gerardo dei Tintori, Monza, Italy, Monza, Italy; [6]Department of Medicine and Surgery, University of Milano-Bicocca, Monza, Italy, Monza, Italy; [7]Unidad de Autoinmunidad Hepática Sección de Hepatología y Trasplante Hepático, Hospital Italiano de Buenos Aires, Argentina., Buenos Aires, Argentina; [8]Department of Gastroenterology & Hepatology, Changi General Hospital Singapore, Singapore, Singapore, Singapore; [9]Duke-NUS Medical School, Singapore, Singapore, Singapore; [10]Yong Loo Lin School of Medicine, National University of Singapore, Singapore, Singapore, Singapore; [11]Servicio de Aparato Digestivo, Hospital Universitario de Burgos, Burgos, España, Burgos, Spain; [12]Gastroenterology and Hepatology Unit, Department of Health Promotion Sciences Maternal and Infantile Care, Internal Medicine and Medical Specialities, PROMISE, University of Palermo, Palermo, Italy; [13]Department of Visceral Surgery and Medicine, Inselspital, Bern University Hospital, University of Bern, Switzerland, Bern, Switzerland; [14]Unidad de Gestión Clínica (UGC) de Aparato Digestivo del Hospital Universitario Virgen de La Victoria de Málaga, IBIMA-plataforma Bionand, Universidad de Málaga, CIBERehd, European Reference Network on Hepatological Diseases (ERN RARE-LIVER), Malaga, Spain; [15]Department of Gastroenterology, Hepatology, Infectious Diseases and Endocrinology, Hannover Medical School, Hannover, Germany, Hannover, Germany; [16]Centre for Autoimmune Liver Diseases, School of Medicine and Surgery, University of Milano-Bicocca, Milano, Italy; Epatologia e Gastroenterologia, ASST Grande Ospedale Metropolitano Niguarda, Milano, Italia, Milano, Italy; [17]Servicio de Hepatología, Hospital Clínico Lozano Blesa, Universidad de Zaragoza, Zaragoza, España, Zaragosa, Spain; [18]Complexo Hospitalario Universitario de Pontevedra, Instituto de Investigación Sanitaria Galicia Sur (IISGS), Pontevedra, España, Pontevedra, Spain; [19]Servicio de Aparato Digestivo, Hospital del Mar-Parc de Salut Mar, Barcelona, España, Barcelona, Spain; [20]Division of Gastroenterology, Department of Internal Medicine, University of Patras, 26504, Patras, Greece, Patras, Greece; [21]Liver Disease Unit - Department of Internal Medicine, Adult Liver Transplant Unit,*

Unidade Local de Saúde de Coimbra - Hospitais da Universidade de Coimbra, Coimbra, Portugal, Coimbra, Portugal; [22]Division of Gastroenterology and Liver Unit, University of Alberta, Edmonton, Alberta, Canada, Alberta, Canada; [23]Liver Unit, Northern General Hospital, Sheffield Teaching Hospitals NHS Foundation Trust, Herries Road, Sheffield, S5 7AU, United Kingdom, Sheffield, United Kingdom; [24]Servicio de Aparato Digestivo, Hospital Universitario Nuestra Señora de la Candelaria, Santa Cruz de Tenerife, España, Tenerife, Spain; [25]Liver Unit, Department of Internal Medicine, University Hospital Vall de Hebron, Barcelona, Spain, Barcelona, Spain; [26]Schiff Center for Liver Diseases, University of Miami Miller School of Medicine, Miami, FL, USA, Miami, United States; [27]Department of Medicine, University Medical Center Hamburg-Eppendorf, Hamburg, Germany, Hamburg, Germany; [28]Martin Zeitz Center for Rare Diseases, University Medical Center Hamburg-Eppendorf, Hamburg, Germany, Hamburg, Germany; [29]Hepatology and Liver Transplantation Unit, Hospital Universitario y Politécnico La Fe, Health Research Institute La Fe, Valencia, Spain; Ciberehd, Instituto de Salud Carlos III (o ISCIII), Madrid, Spain, Valencia, Spain; [30]Aparato Digestivo, Hospital Universitario General Villalba, Madrid, España, Madrid, Spain; [31]Aparato Digestivo, Hospital de Manises, Valencia, España, Valencia, Spain; [32]Aparato Digestivo, Hospital Universitario de Belvitge, Barcelona, España, Barcelona, Spain; [33]Servicio de Aparato Digestivo, Hospital Universitario Central de Asturias, Oviedo, España, Oviedo, Spain; [34]Department of Gastroenterology and Hepatology, Hospital Universitario Puerta de Hierro de Majadahonda, Spain, Majadahonda, Spain; [35]Department of Medicine and Research Laboratory of Internal Medicine National Expertise Center of Greece in Autoimmune Liver Diseases European Reference Network on Hepatological Diseases (ERN RARE-LIVER) General University Hospital of Larissa, Greece, Larissa, Greece; [36]Department of Gastroenterology, Instituto Nacional de Ciencias Médicas y Nutrición Salvador Zubirán, Mexico City, Mexico, Mexico, Mexico; [37]CSUR Centro de referencia del Sistema Nacional de Salud en Enfermedad Hepática Vascular Compleja en adultos, Barcelona, Spain
Email: peni.arvaniti@gmail.com

Background and aims: Baveno VII recommends non-selective beta blockers (NSBB) to prevent decompensation in compensated cirrhosis with clinically significant portal hypertension (CSPH). However, evidence supporting this strategy in autoimmune hepatitis (AIH) is lacking and it remains unclear whether NSBB provides additional benefits beyond those conferred by a long-term biochemical response (BR). We aimed to evaluate the potential of NSBB for preventing decompensation in AIH-related CSPH compared to BR.
Method: Multicentre retrospective study of 266 patients with AIH-related compensated cirrhosis and CSPH with follow-up ≥12 months. CSPH was defined by esophageal varices (EV), HVPG ≥10 mmHg, portosystemic collaterals, liver stiffness ≥25 kPa or spleen stiffness ≥50 kPa. BR was defined as sustained normalization of transaminases during follow-up. Inverse probability of treatment weighting (IPTW) was used to balance baseline covariates (age, sex, body mass index, Child-Pugh score, platelets and EV size) between patients with and without NSBB, considering death and liver transplantation (LT) as competing events.
Results: Most patients were female (66%), with a median age of 58 years (IQR 45–66) and median follow-up of 6 years (IQR 2–11). Overall, 67% (n = 177) received NSBB (propranolol = 70, carvedilol = 107), 53% as primary prophylaxis for high-risk EV. Decompensation occurred in 32% (n = 85), most commonly ascites (66%). At CSPH diagnosis, NSBB treated patients more frequently had high-risk EV (62% vs. 32%, p = 0.001) and lower platelets (108×10^9 vs. 134×10^9, p = 0.003). In IPTW-adjusted analyses, the use of NSBB did not reduce the risk of decompensation (SHR 1.10; 95%CI 0.69–1.78; p = 0.665). In contrast, BR was associated with a significantly lower risk of decompensation (SHR 0.44; 95%CI 0.28–0.72; p = 0.001), an effect that remained consistent in time-dependent analysis, after adjustment for NSBB use and for a composite endpoint of decompensation, death or LT. In stratified analyses, NSBB use was not associated with the risk of decompensation in patients with BR (HR 1.79; 95%CI 0.94–3.43, p = 0.078), whereas it was associated with a significantly lower risk in those without BR (HR 0.40; 95%CI 0.20–0.79; p = 0.009).
Conclusion: In compensated AIH-related cirrhosis, achieving long-term BR was consistently associated with lower risk of decompensation, regardless of NSBB use. This suggests that controlling the inflammatory activity of the disease plays a key role in the prognosis of AIH, even in the presence of CSPH.

SAT-251-YI

S-adenosyl-L-methionine improves health-related quality of life in patients with primary sclerosing cholangitis and inflammatory bowel disease: a subanalysis of a randomized, placebo-controlled trial

Emil Bik[1], Beata Kruk[2], Karolina Wronka[1], Jocelyn Trottier[3], Pawel Piluch[1], Olga Ciepiela[4], Joanna Raszeja-Wyszomirska[1], Olivier Barbier[3], Piotr Milkiewicz[1,5]. *[1]Department of Hepatology, Transplantology and Internal Medicine, Medical University of Warsaw, Warsaw, Poland; [2]Laboratory of Metabolic Liver Diseases, Department of General, Transplant and Liver Surgery, Medical University of Warsaw, Warsaw, Poland; [3]Laboratory of Molecular Pharmacology, CHU-de-Québec & Faculty of Pharmacy, Laval University, Québec, Canada; [4]Department of Laboratory Medicine, Medical University of Warsaw, Warsaw, Poland; [5]Translational Medicine Group, Pomeranian Medical University, Szczecin, Poland*
Email: emilbbik@gmail.com

Background and aims: Patients with primary sclerosing cholangitis (PSC) frequently experience fatigue, anxiety, and impaired health-related quality of life (HRQoL). Despite the relevant impact on daily functioning, currently no therapy has been proven to effectively improve HRQoL in PSC. S-adenosyl-L-methionine (SAMe) is a key methyl donor involved in hepatocellular and neurochemical pathways and may improve well-being. This randomized, double-blind, placebo-controlled trial evaluated the effect of SAMe on HRQoL in PSC patients receiving ursodeoxycholic acid (UDCA).
Method: Sixty-eight PSC patients were randomized 1:1 to receive SAMe or placebo for six months in addition to UDCA. Five patients in the SAMe group and two in the placebo group discontinued the study, leaving 61 participants (29 SAMe, 32 placebo) included in the final analysis. HRQoL was assessed at baseline and after treatment using the State-Trait Anxiety Inventory (STAI-X1/X2), Generalized Anxiety Disorder Scale (GAD-7), Patient Health Questionnaire (PHQ-9), Modified Fatigue Impact Scale (MFIS), and the disease-specific PBC-40 questionnaire. This subanalysis focused on the subgroup of patients with concomitant inflammatory bowel disease (IBD). Changes between baseline and post-treatment values were analyzed using the Mann–Whitney U test.
Results: Among 37 patients with concomitant IBD (19 SAMe, 18 placebo), baseline HRQoL scores were comparable between treatment arms. No significant between-group differences were observed in liver biochemistry during the study period. Compared with placebo, treatment with SAMe resulted in significantly greater improvement in multiple health-related quality of life domains. Median (IQR) reductions in anxiety-related scales were −7 [−12; −3] vs−1 [−5; 3] for STAI-X1 and −7 [−10; −3] vs 0 [−4; 4] for STAI-X2 (SAMe vs placebo, respectively). General anxiety and depressive symptoms also improved (GAD-7: −3 [−4; −2] vs 0 [−2; 2]; PHQ-9: −2 [−3; −1] vs 0 [−1; 2]). Fatigue decreased more markedly in the SAMe group (MFIS: −10 [−15; −6] vs −3 [−8; 2]), and disease-specific quality of life measured by the PBC-40 improved accordingly (−9 [−13; −5] vs −3 [−9; 3]). All between-group differences reached statistical significance (p < .05).
Conclusion: In the subgroup of patients with PSC and concomitant IBD, SAMe supplementation improves anxiety, mood, fatigue, and disease-specific HRQoL.

SAT-252

Baseline anti-mitochondrial antibody titre in addition to gamma-glutamyltranspeptidase and alanine-aminotransferase serum levels anticipate future primary biliary cholangitis development

Davide Bitetto[1], Carlo Fabris[1], Fornasiere Ezio[1], Elisa Fumolo[1], Elena Garlatti Costa[1], Pierluigi Toniutto[1]. [1]*Hepatology and Liver Transplantation Unit, UDINE, Italy*
Email: davide_bitetto@yahoo.it

Background and aims: Antimitochondrial antibodies (AMA) serum positivity represents a major criterion for diagnosing primary biliary cholangitis (PBC). However, AMA positivity may be found in the presence of normal liver enzymes, suggesting that it could predispose to the development of PBC over time. This study aimed to evaluate the incidence and risk factors for PBC development in a cohort of AMA positive patients.
Method: This retrospective-longitudinal study, conducted from January 2014 to December 2023, enrolled all patients tested AMA positive in the central laboratory of the academic hospital in Udine (Italy), that serves a population of 537.943 inhabitants.
Results: 392 patients tested positive for AMA and 133(33.9%) of them fulfilled the diagnostic criteria for PBC. The annual incidence of AMA positivity and PBC was 5.31/100000 and 2.09/100000 inhabitants, respectively. At the time of the first AMA detection, 93/133(69.9%) patients had an established PBC. In the remaining 40 patients, PBC developed during the follow-up with a declining annual rate, ranging from 4.7% to 1%, with a cumulative 5- and 10-years incidences of 11.7% and 13.4% respectively. At the univariate and multivariate time-to-event analysis PBC occurrence was associated with baseline AMA titre>225 UI/L(O.R. 2.01, 95% C.I. 1.39–2.91, $p < 0.001$), levels of gamma-glutamyltranspeptidase (GGT) > 40 UI/L(O.R. 4.25, 95% C.I. 2.76–6.54, $p < 0.001$) and alanine-aminotransferase (AST) > 30 UI/L (O.R 1.69, 95% C.I. 1.16–2.45, $p = 0.005$).
Conclusion: In AMA positive patients, baseline AMA titre, GGT and AST serum levels anticipate the PBC development.

SAT-253

Changes in the clinical presentation of primary biliary cholangitis over the years in a university center in Argentina

Matías Bori[1], Juan Antonio Sorda[1], Ilse Pardo Ivirico[1], Andrea Curia[1], Lina Palma Cerón[1], Natalia Vera[1], Esteban Gonzalez Ballerga[1].
[1]*Hospital de Clínicas "José de San Martín" Universidad de Buenos Aires, Buenos Aires, Argentina*
Email: borimatias@gmail.com

Background and aims: The clinical presentation of primary biliary cholangitis (PBC) has changed globally over time. However, these changes have not been sufficiently analyzed in our local setting. The aim of this study was to evaluate changes in the clinical presentation of PBC over the last 40 years in a university center in Argentina.
Method: A retrospective study including 596 patients with PBC, divided into four groups according to year of diagnosis: <1990 (n = 113), 1990–1999 (n = 206), 2000–2009 (n = 151), and >2009 (n = 106). Variables analyzed included age at diagnosis, disease stage, clinical presentation (asymptomatic or symptomatic), biochemical stage (according to the Rotterdam criteria), and histological stage.
Results: The female-to-male ratio was 24:1 and remained stable over time. There was an increase in the mean age at diagnosis, from 54.3 years (±11.6) before 1990 to 57.2 years (±12.2) after 2009 ($p = 0.0185$). The symptomatic clinical variant decreased from 73.7% to 50.0% ($p < 0.001$), while early biochemical stage diagnosis increased from 18.0% to 77.4% ($p < 0.001$) over the same period. Advanced histological stages (III-IV) decreased from 60.2% before 1990 to 20.8% after 2009 ($p < 0.001$). The proportion of UDCA responders according to Paris-I, Toronto, Paris-II, Rotterdam, and GLOBE score criteria increased over the investigated decades ($p < 0.001$).
Conclusion: Over time, patients with PBC have shown a change in their clinical presentation, characterized by an older age at diagnosis, earlier biochemical and histological stages, and a predominance of asymptomatic clinical forms. These findings are consistent with global reports and may be attributable to better knowledge of the disease, greater availability and access to diagnostic tests, and possibly changes in environmental triggers over time.

SAT-254

Seladelpar effect on lipids and muscle safety with concomitant statin use in patients with primary biliary cholangitis: interim results from the open-label ASSURE study with up to 4 years of treatment

Christopher L. Bowlus[1,2], Yusuf Yilmaz[3], Ehud Zigmond[4], Victor Vargas Blasco[5], Christophe Corpechot[6], Álvaro Díaz-González[7], Sarah Proehl[8], Johnny Chew[8], Kyung Min Kwon[8], Xiangyu Liu[8], Robert Kustra[8], John M. Vierling[9]. [1]*Division of Gastroenterology and Hepatology, University of California Davis School of Medicine, Sacramento, United States;* [2]*Division of Gastroenterology and Hepatology, UC Davis School of Medicine, Sacramento, California, United States;* [3]*Department of Gastroenterology, School of Medicine, Recep Tayyip Erdoğan University, Rize, Türkiye;* [4]*Liver Health Center, Cheba Medical Center, Ramat-Gan, Israel;* [5]*Universitat Autònoma Barcelona, Barcelona, Spain;* [6]*Reference Center for Inflammatory Biliary Diseases and Autoimmune Hepatitis, French Network for Rare Liver Disease in Children and Adults (FILFOIE), European Reference Network RARE-LIVER, Saint-Antoine Hospital and Research Center, Assistance Publique-Hôpitaux de Paris, Sorbonne University, Paris, France;* [7]*Hospital Universitario Marqués de Valdecilla, Instituto de Investigación Valdecilla (IDIVAL), Santander, Spain;* [8]*Gilead Sciences, Inc., Foster City, United States;* [9]*Baylor College of Medicine, Houston, United States*
Email: vierling@bcm.edu

Background and aims: Seladelpar (SEL) is a first-in-class delpar (selective PPAR-delta agonist) indicated for the treatment of primary biliary cholangitis (PBC) in combination with ursodeoxycholic acid (UDCA) in patients (pts) with an inadequate response to UDCA or as monotherapy in pts unable to tolerate UDCA. Dyslipidaemia and use of statins are common in PBC. In the pivotal RESPONSE study (NCT04620733), SEL was associated with reductions in triglycerides (TG), total cholesterol (TC), and low-density lipoprotein cholesterol (LDL-C) at Month (M) 12 vs placebo, independent of statin use. Here, we present an interim analysis of long-term changes in lipids and muscle-related safety in pts treated with SEL from the ongoing open-label Phase 3 ASSURE study (NCT03301506).
Method: Pts from RESPONSE and legacy SEL studies enrolled in ASSURE and received open-label SEL 10 mg once daily. In this analysis, all pts in ASSURE were pooled. Baseline (BL) was defined as SEL initiation in RESPONSE or ASSURE. Post hoc, mean percent change from BL in TG, TC, and LDL-C were analysed through M36. Safety was assessed for the overall population and two subgroups (with or without BL statin use) up to M48. Muscle-related adverse events (AEs) were identified via a predefined search strategy. Data cutoff: 31 Jan 2025.
Results: Among 337 pts in ASSURE, mean BL TG was 116 mg/dL, TC 230 mg/dL, and LDL-C 130 mg/dL. In 122 pts evaluable at M36 of treatment, mean percent change from BL was −15.4% for TG, −12.0% for TC, and −18.6% for LDL-C. There were no meaningful changes in high-density lipoprotein cholesterol. At BL, 87/337 (26%) pts were on a statin. Incidences of AEs and serious AEs (SAEs) were similar in pts on a statin at BL compared with those not on a statin (AEs: 90% vs 91%; SAEs: 20% vs 18%). Muscle-related AE incidence was similar among pts on a statin (9%) vs not (9%). Creatinine kinase (CK) elevations > 3 × the upper limit of normal occurred infrequently both in pts on a statin (1%) and not on a statin (1%). Among 31 pts with muscle-related AEs, only 1 pt (not on a statin) discontinued treatment permanently due to myalgia without a CK elevation.
Conclusion: SEL treatment of pts with PBC resulted in clinically meaningful improvements in lipid profiles that were sustained through M36. Overall, SEL appeared safe regardless of statin use

and without concerns for muscle toxicity with up to 4 years of treatment.

SAT-255

Seasonal variation in intrahepatic cholestasis of pregnancy and its association with adverse pregnancy outcomes: a large retrospective cohort study

Jianghui Cai[1], Mi Tang[1], Xiao Yang[1]. [1]*Chengdu Women's and Children's Central Hospital, Chengdu, China*
Email: caijianghui@126.com

Background and aims: Intrahepatic cholestasis of pregnancy (ICP) is a liver disorder characterized by pruritus and elevated serum bile acids, which is associated with an increased risk of adverse pregnancy outcomes. Evidence suggests that seasonal variation in the onset of ICP exists worldwide. However, the influence of environmental factors, such as the season at diagnosis, on disease severity and perinatal outcomes remains underexplored in ICP. Thus, the present study aims to investigate whether the season of ICP diagnosis is associated with the risk of adverse pregnancy outcomes.
Method: This retrospective cohort study included all patients diagnosed with ICP at Chengdu Women's and Children's Central Hospital from 2015 to 2023. Patients were stratified into four groups based on the season of diagnosis: Spring (March-May), Summer (June-August), Autumn (September-November), and Winter (December-February). Primary outcomes included preterm birth, meconium-stained amniotic fluid (MSAF), asphyxia, and perinatal death. Secondary outcomes included low Apgar scores, NICU admission, peak total bile acid (TBA) levels, and length of maternal hospital stay. Statistical analyses included Chi-square, ANOVA, and multivariate logistic regression adjusting for potential confounders.
Results: Among 1216 ICP patients identified, the distribution of diagnoses across seasons was 20.23% (Spring), 16.28% (Summer), 24.1% (Autumn), and 39.39% (Winter). The incidence of preterm birth was significantly higher in patients diagnosed during winter compared to other seasons (aOR, 1.27; 95% CI, 1.06–1.51, $p < 0.05$). Similarly, rates of MSAF (aOR, 1.21; 95% CI, 1.09–1.37) and the low Apgar scores (aOR, 1.16; 95% CI, 1.07–1.25) were significantly higher in the Winter group. Peak TBA levels were also highest among patients diagnosed in Winter (129 μmol/L, $p < 0.05$). No significant independent seasonal associations were found for other perinatal outcomes, including asphyxia, perinatal death, NICU admission, or length of hospital stay.
Conclusion: The season of ICP diagnosis was significantly associated with the risk of adverse pregnancy outcomes, particularly preterm birth and MSAF. Diagnosis during winter was linked to more severe biochemical profiles and worse clinical outcomes. These findings suggest a potential role of seasonal environmental factors in modulating ICP severity. Further research is warranted to elucidate the underlying mechanisms and explore potential implications for management strategies.

SAT-256-YI

Biochemical changes and clinical outcomes after obeticholic acid withdrawal in patients with primary biliary cholangitis

Beatriz Carrillo Cubero[1], Alba Carmona Frías[1], Paloma Elma Alañón-Martínez[1,2], Jose Luis Montero[1,2,3], Pilar Barrera Baena[1,2,3], Antonio Poyato González[1,2,3], Marta Guerrero-Misas[1,2,3], Manuel De La Mata Garcia[1,2,3], Manuel Rodríguez-Perálvarez[1,2,3]. [1]*Hepatology and Liver Transplant Unit, Reina Sofía University Hospital, Córdoba, Spain;* [2]*Hepatology and Liver Transplant Unit of the Reina Sofía University Hospital, Córdoba, Spain;* [3]*Biomedical Research Center Network for Liver and Digestive Diseases (CIBERehd), Madrid, Spain*
Email: b.carrillocubero@gmail.com

Background and aims: In august 2024, the European Medical Agency revoked marketing authorization of Obeticholic acid (OA) for primary biliary cholangitis (PBC) in the European Union due to uncertainties on risks and benefits. We evaluated the evolution of liver biochemical tests and clinical outcomes in patients who withdrew OA without receiving alternative second line therapies.
Method: Observational retrospective study including adult patients with PBC who withdrew OA following regulatory authorities' recommendation. We excluded patients with decompensated cirrhosis. Patients underwent clinical visits at 6 and 12 months after OA withdrawal including liver biochemical tests. Clinical outcomes of interest were hepatic decompensation, liver transplantation, and death. Patients starting another second line therapy, including fibrates, seladelpar, or elafibranor, were excluded from that time onwards.
Results: 47 patients exposed to OA for 27 months (IQR 17–58) were recruited (97.9% women, aged 59 +/- 9.9 years old), including 29 patients (61.7%) with compensated cirrhosis. At OA withdrawal, 14 patients (29.8%) were taking 10 mg/day and 33 patients (70.2%) were receiving 5 mg/day. Six months and 12 months after OA withdrawal, 72.3% ($n = 34$) and 42.6% ($n = 20$) of patients had not received an alternative second line therapy, respectively, and were included in the liver biochemical analysis. At 6 months, median alkaline phosphatase (AP) and total bilirubin were unchanged but gamma-glutamyl transferase (GGT) raised from 59 UI/L (IQR 26–140) to 95 UI/L (IQR 49–238) ($p = 0.001$), and aspartate aminotransferase (AST) raised from 34 UI/L (IQR 23–49) to 42 UI/L (IQR 27–54) ($p = 0.043$). At 12 months, the only biochemical parameter which continued increasing was GGT at 148 UI/L (IQR 64–249) ($p = 0.002$ compared to baseline). In the whole cohort, 4 patients (8.5%) had hepatic decompensations after OA withdrawal including encephalopathy (3 episodes), ascites (2 episodes) and variceal bleeding (1 episode). Three patients required liver transplantation and one patient died due to infection during hepatic decompensation.
Conclusion: OA withdrawal was associated with a mild elevation of transaminases and a more pronounced and sustained elevation of GGT. The risk of severe hepatic decompensation within the first 12 months is not negligible and claims for caution when considering withdrawal of a second line therapy in patients with PBC, particularly in presence of advanced liver fibrosis.

SAT-257-YI

Serum metabolomic signatures for cirrhosis detection and prediction in primary sclerosing cholangitis

Elisa Catanzaro[1,2,3], Ainhoa Lapitz[1,4,5], Piotr Milkiewicz[6,7], Beata Kruk[6], Mohamad Elgozair[8], Ahmed Fowsiyo[8], Johannes R. Hov[9,10,11], Trine Folseraas[9,10,11], Ina Andersen[9,10,11], Marco Carbone[12,13], Rocio Macias[4,14], Christoph Schramm[15,16], Ludwig Horst[15,16], Cristina Alonso[17], Małgorzata Milkiewicz[7], Laura Izquierdo-Sánchez[1,4], Adelaida La Casta[1], Raul Jimenez-Aguero[1], Maria Jesus Perugorria[1,4,5], Laura Cristoferi[18], Gonzalo Crespo[4,19], Marco Arrese[20], Javier Chahuan[20], Javier Bustamante[21], Angela Lamarca[22], Michael Dill[23,24,25], Domingo Balderramo[26], Luis Bujanda[1,4,5], Lewis Roberts[8], Tom Hemming Karlsen[9,10,11], Luca Fabris[27,28], Nora Cazzagon[2,3], Pedro Rodrigues[1,4,29], Jesus M Banales[1,4,29,30]. [1]*Biogipuzkoa Health Research Institute, San Sebastian, Spain;* [2]*Department of Surgery, Oncology and Gastroenterology, University of Padova, Padova, Italy;* [3]*Gastroenterology Unit, University Hospital of Padova, Padova, Italy;* [4]*CIBERehd, Instituto de Salud Carlos III (ISCIII), Madrid, Spain;* [5]*University of the Basque Country, UPV/EHU, Leioa, Spain;* [6]*Transplant and Liver Surgery of the Medical University of Warsaw, Warsaw, Poland;* [7]*Pomeranian Medical University, Szczecin, Poland;* [8]*Mayo Clinic, Rochester, Minnesota, United States;* [9]*Norwegian PSC Research Center, Oslo, Norway;* [10]*University of Oslo, Oslo, Norway;* [11]*Oslo University Hospital, Oslo, Norway;* [12]*Department of Medicine and Surgery, University of Milano-Bicocca, Milan, Italy;* [13]*Hepatology and Gastroenterology Unit, ASST Grande Ospedale Metropolitano Niguarda, Milan, Italy;* [14]*University of Salamanca, Biomedical Research Institute of Salamanca (IBSAL), Salamanca, Spain;* [15]*Martin Zeitz Center for Rare*

Diseases, University Medical Centre Hamburg-Eppendorf, Hamburg, Germany; [16]Department of Medicine, University Medical Center Hamburg-Eppendorf, Hamburg, Germany; [17]Rubio Metabolomics (OWL Metabolomics), Derio, Spain; [18]Division of Gastroenterology, Center for Autoimmune Liver Diseases, Fondazione IRCCS San Gerardo dei Tintori, Monza, Italy; [19]Hospital Clinic Barcelona, IDIBAPS, Barcelona, Spain; [20]Pontificia Universidad Católica de Chile, Santiago, Chile; [21]Hepatobiliary Surgery and Liver Transplantation Unit, Cruces University Hospital, Bilbao, Spain; [22]Fundación Jiménez Díaz University Hospital, Madrid, Spain; [23]Heidelberg University Hospital, Heidelberg, Germany; [24]German Cancer Research Center (DKFZ) Heidelberg, Heidelberg, Germany; [25]National Center for Tumor Diseases (NCT), NCT Heidelberg, Heidelberg, Germany; [26]Instituto Universitario de Ciencias Biomédicas de Córdoba, Córdoba, Argentina; [27]Department of Molecular Medicine, University of Padua, Padova, Italy; [28]Digestive Disease Section, Yale University, New Heaven, Connecticut, United States; [29]Ikerbasque, Basque Foundation for Science, Bilbao, Spain; [30]University of Navarra, Pamplona, Spain
Email: elisa.catanzaro95@gmail.com

Background and aims: Primary sclerosing cholangitis (PSC) is characterized by marked heterogeneity in disease progression, with variable advancement to cirrhosis, contributing to poor prognosis and challenges in accurate staging. Integrating metabolic information may improve the assessment of disease severity. This proof-of-concept study aimed to identify a serum metabolomic signature for cirrhosis detection in PSC and to evaluate its ability to predict cirrhosis development within five years.
Method: In this international multicenter study, serum samples were obtained from 216 PSC patients enrolled at nine centers across seven countries. Patients were randomly allocated (70:30) to a discovery cohort (n = 154; 22% cirrhosis) and a validation cohort (n = 62; 29% cirrhosis). Metabolomic profiling was performed using ultra-high-performance liquid chromatography–mass spectrometry (UHPLC-MS). Multivariate logistic regression adjusted for age, sex, inflammatory bowel disease, alkaline phosphatase, and bilirubin was used to identify metabolites independently associated with cirrhosis. Candidate metabolites were prioritized using bootstrap-based Elastic Net regression with cross-validation and combined into predictive models. The best-performing model was validated in the independent cohort. Stable metabolites were subsequently used to construct a model for 5-year cirrhosis prediction.
Results: Among 484 detected metabolites, 121 were significantly associated with cirrhosis, of which 27 (16 increased, 11 decreased) remained independently associated after adjustment. A seven-metabolite model differentiated cirrhotic from non-cirrhotic patients in the discovery cohort (AUC = 0.86). In the validation cohort, the model achieved an AUROC of 0.78. Among non-cirrhotic patients (n = 56), 8 (14%) developed cirrhosis during five-year follow-up, despite no baseline differences in FIB-4 scores (p = 0.15). A six-metabolite model derived from the original signature predicted 5-year cirrhosis development with high accuracy (AUROC 0.88), and demonstrated superior discrimination compared with existing prognostic scores Amsterdam-Oxford Score (0.66; p = 0.04) and revised Mayo Risk Score (0.47; p < 0.01).
Conclusion: Serum metabolomic profiles differ according to PSC disease stage, supporting metabolomics as a promising complementary tool for cirrhosis detection. Exploratory analyses indicate potential utility for predicting cirrhosis, supporting further validation in larger independent cohorts and integration into patient stratification models.

SAT-258

Distinct disease phenotypes in primary biliary cholangitis according to extrahepatic comorbidities: results from the Italian national PBC registry

Nora Cazzagon[1], Antonio De Vincentis[2], Martina Benatti[1], Eugenia Nofit[3], Francesca Terracciani[2], Elisa Catanzaro[1], Emanuela Bonaiuto[1], Teresa Zappitelli[1], Giovanni Figorilli[1], Ludovico Abenavoli[4], Giuliano Alagna[5], Domenico Alvaro[6], Pietro Andreone[7], Francesco Azzaroli[8], Leonardo Baiocchi[9], Francesco Bellanti[10], Mariaconsiglia Bragazzi[11], Fabrizio Bronte[12], Andrea Affronti[12], Barbara Coco[13], Vincenza Calvaruso[14], Francesca Capelli[15], Antonino Castellaneta[16], Ilaria Cavalli[17], Luchino Chessa[18], Roberto Chiavaroli[19], Federica Cerini[20], Saveria Lory Croce'[21], Caterina Cusumano[22], Simona Di Cesare[23], Alessandro Granito[24], Fabio Piscaglia[24], Nadia Dal Bo'[25,26], Luca Fabris[27], Mauro Viganò[28], Alessandro Federico[29], Edoardo Giannini[30], Grazia Anna Niro[31], Erica Nicola Lynch[32], Pietro Lampertico[33], Pierenrico Lecis[34], Ana Lleo[35], Alessandra Mangia[36], Fabio Marra[37], Marco Marzioni[38], Andrea Mega[39], Luca Miele[40], Gabriele Missale[41], Filomena Morisco[42], Gerardo Nardone[43], Valeria Pace Palitti[44], Marcello Persico[45], Carlo Saitta[46], Chiara Ricci[47], Cristina Rigamonti[48], Maurizio Russello[49], Susanna Schianchi[50], Cinzia Simoni[51], Francesco Losito[52], Ester Vanni[53], Giovanni Vettori[54], Lorenzo Surace[55], Raffaella Viganò[56], Giovanni Vitale[57], Teresa Zolfino[58], Alessio Gerussi[3], Laura Cristoferi[3], Marco Carbone[56], Pietro Invernizzi[3], Umberto Vespasiani-Gentilucci[2]. *[1]Dipartimento di Scienze Chirurgiche, Oncologiche e Gastroenterologiche, Università di Padova; Gastroenterologia, Azienda Ospedale- Università Padova, Padova, Padova, Italy; [2]Policlinico Universitario Campus Bio-Medico, Roma, Italy; [3]IRCCS San Gerardo dei Tintori, Monza, Italy; [4]Azienda Ospedaliera Universitaria Renato Dulbecco, Catanzaro, Italy; [5]Azienda Ospedale Universitaria di Sassari, Sassari, Italy; [6]Policlinico Umberto I, Roma, Italy; [7]Ospedale Civile di Baggiovara di Modena, Modena, Italy; [8]IRCCS Azienda Ospedaliero Universitaria di Bologna - Policlinico Sant'Orsola, Bologna, Italy; [9]Universita' di Roma Tor Vergata, Roma, Italy; [10]Policlinico Riuniti di Foggia, Foggia, Italy; [11]Ospedale Santa Maria Goretti di Latina, Università "La Sapienza" Polo Pontino, Latina, Italy; [12]Azienda Ospedaliera Ospedali Riuniti Villa Sofia, Palermo, Italy; [13]Dipartimento di Medicina Clinica e Sperimentale -Università di Pisa; UO Epatologia - Azienda Ospedaliero Universitaria Pisana, Pisa, Italy; [14]A.O.U. Policlinico "Paolo Giaccone", Palermo, Italy; [15]Azienda Socio-Sanitaria Ovest Milanese, Milano, Italy; [16]A.O.U. Consorziale - Policlinico Bari, Bari, Italy; [17]Azienda Socio Sanitaria Territoriale (ASST) di Cremona, Cremona, Italy; [18]A.O.U. di Cagliari - Presidio Ospedaliero Duilio Casula Monserrato, Cagliari, Italy; [19]Fondazione Ospedaliera Poliambulanza Brescia- B, Brescia, Italy; [20]Ospedale San Giuseppe - IRCCS Multimedica, Milano, Italy; [21]Azienda Sanitaria Universitaria Giuliano Isontina, Trieste, Italy; [22]Azienda Ospedaliera Universitaria Integrata Verona – A, Verona, Italy; [23]Azienda USL della Romagna, Ospedale "Morgagni Pierantoni", Forlì, Italy; [24]IRCCS A.O.U. Policlinico Sant'Orsola di Bologna, Bologna, Italy; [25]Ospedale regionale Ca' Foncello di Treviso, Treviso, Italy; [26]Ospedale Ca' Foncello, Gastroenterology, Treviso, Italy; [27]Azienda Ospedale- Università Padova, Padova, Italy; [28]ASST Papa Giovanni XXIII, Bergamo, Italy; [29]Azienda Ospedaliera Universitaria Luigi Vanvitelli, Napoli, Italy; [30]IRCCS Ospedale Policlinico San Martino, Genova, Italy; [31]Ospedale Casa Sollievo della Sofferenza- San Giovanni Rotondo, San Giovanni Rotondo, Italy; [32]Gastroenterologia, A.O.U. Careggi, Firenze, Italy; [33]Fondazione IRCCS Ca' Granda Ospedale Maggiore Policlinico, Milano, Italy; [34]Ospedale San Bassiano, Bassano del Grappa, Italy; [35]Division of Internal Medicine and Hepatology, Department of Gastroenterology, IRCCS Humanitas Research Hospital, Rozzano, Milan, Italy; Department of Biomedical Sciences, Humanitas University, Pieve Emanuele, Italy; [36]Epatologia, IRCCS "Casa Sollievo della Sofferenza", San Giovanni Rotondo, Italy; [37]Medicina Interna ed Epatologia, A.O.U. Careggi, Firenze, Italy; [38]Ospedali Riuniti - University Hospital, Ancona, Italy; [39]SABES, Bolzano, Italy; [40]Fondazione Policlinico Universitario Agostino Gemelli IRCCS, Roma, Italy; [41]Azienda Ospedaliero-Universitaria di Parma, Parma, Italy; [42]Programma Dipartimentale Malattie del fegato e delle vie biliari, AOU Federico II, Napoli, Italy; [43]A.O.U. "Federico II," UOC Gastroenterologia ed Epatologia, Napoli, Italy; [44]Azienda USL di Pescara, Pescara, Italy; [45]Medicina interna ed*

Epatologia Università di Salerno, Salerno, Italy; [46]A.O.U. Policlinico Gaetano Martino, Messina, Italy; [47]ASST Spedali Civili Presidio di Brescia, Brescia, Italy; [48]A.O.U. Maggiore della Carità, Novara, Italy; [49]Azienda Ospedaliera di Rilievo Nazionale e di Alta Specializzazione Garibaldi, Catania, Italy; [50]Azienda USL - IRCCS di Reggio Emilia, Reggio Emilia, Italy; [51]ASST Valle Olona - Presidio di Gallarate, Gallarate, Italy; [52]Ospedale S de Bellis - IRCCS, Castellana Grotte, Italy; [53]A.O.U. Città della Salute e della Scienza di Torino, Torino, Italy; [54]Azienda Provinciale per i Servizi Sanitari, Trento, Italy; [55]ASP Catanzaro Presidio Ospedaliero "Giovanni Paolo II", Catanzaro, Italy; [56]ASST Grande Ospedale Metropolitano Niguarda, Milano, Italy; [57]IRCCS Azienda Ospedaliero-Universitaria di Bologna, Bologna, Italy; [58]Presidio Ospedaliero San Michele, ARNAS G. Brotzu di Cagliari, Cagliari, Italy
Email: nora.cazzagon@unipd.it

Background and aims: Primary biliary cholangitis (PBC) commonly occurs alongside extrahepatic autoimmune diseases (EADs) and cardiometabolic conditions (CMCs), yet their clinical relevance remains incompletely defined. We investigated the distribution of these comorbidities and examined whether they identify distinct phenotypic patterns of PBC.
Method: We conduct a retrospective analysis of patients enrolled in the Italian National PBC Registry (PBC322) across 57 centers. Demographics, baseline biochemical data, liver stiffness measurement (LSM), and the presence of a PBC-autoimmune hepatitis (AIH) variant were collected. The occurrence and timing of EADs, CMCs (overweight/obesity, dyslipidemia, hypertension, glucose metabolism disorders), and cardiovascular diseases (CVD: coronary artery disease, cerebrovascular disease, peripheral artery disease) were recorded. Patients with diabetes and/or metabolic syndrome were grouped as D/MS.
Results: Among 3,142 registered patients, 2,340 fulfilled inclusion criteria. The cohort was predominantly female (89%), with a mean age of 54.9 ± 4.3 years and a median disease duration of 4.9 years (IQR 1.5–10.7); mean BMI was 24.9 ± 4.3. At baseline, 23% had cirrhosis and 7% a PBC-AIH variant. EADs were present in 27% of patients, most frequently autoimmune thyroid diseases (11%), Sjogren's syndrome (7%), systemic sclerosis (4%), rheumatoid arthritis (2%), systemic lupus erythematosus (1%), vitiligo (1%) and other EADs (3%). CMCs were highly prevalent, including dyslipidemia (43%), hypertension (37%), diabetes (9%), and obesity (10%). Cirrhosis and CVD were significantly more prevalent in patients with D/MS and EADs+D/MS (cirrhosis 30% and 25%; CVD 7% and 9%) compared with those without comorbidities (23% and 3%) or with EADs alone (19% and 4%) ($p = 0.021$ and $p < 0.001$). Consistently, LSM values were higher in D/MS and EADs+D/MS (7.1 kPa [4.8–11.1] and 6.4 kPa [4.9–9.1]) than in patients with isolated EADs or no comorbidities (5.9 kPa [4.4–8] and 5.8 [4.5–8.4]) ($p = 0.005$). The PBC-AIH variant was more frequently observed in patients with EADs and EAD+D/MS (12% and 15%) than in those with D/MS alone or without comorbidities (4% and 5%; $p < 0.001$).
Conclusion: In a large national PBC cohort, CMCs and EADs delineate distinct disease phenotypes. Diabetes and metabolic syndrome identify patients with more advanced liver involvement and increased cardiovascular burden, whereas EADs are associated with a higher prevalence of the PBC–AIH variant.

SAT-259
Survival and prognostic factors in patients with autoimmune hepatitis-related cirrhosis
Yu Chen[1], Xiao Xiao[1], Xiong Ma[1]. *[1]Renji Hospital, School of Medicine, Shanghai Jiao Tong University, Shanghai, China*
Email: xxiao_sh@163.com

Background and aims: Long-term outcomes and prognostic factors in autoimmune hepatitis (AIH)-related cirrhosis remain poorly characterized. This study aimed to evaluate survival and identify prognostic predictors in patients with AIH-related cirrhosis.
Method: This retrospective cohort study included patients with AIH-related cirrhosis treated with immunosuppressive therapy. Transplant-free survival was analyzed using Kaplan-Meier methods and Cox proportional hazards regression. Multivariable analyses were performed separately for compensated and decompensated stages.
Results: Of the 544 patients, 379 had compensated cirrhosis and 165 had decompensated cirrhosis. During a median follow-up of 62 months (interquartile range [IQR] 38–83), decompensated group showed significantly worse survival than compensated group (60-month survival 85.9% vs. 97.3%, $p < 0.001$), with an adjusted hazard ratio (HR) of 6.26 (95% confidence interval [CI] 3.13–12.55). In the compensated group, older age (HR 1.07 per year, $p = 0.037$) and higher total bilirubin (HR 1.99, $p = 0.028$) were independent predictors of mortality. In the decompensated group, higher platelet count was associated with improved survival (HR 0.39, $p = 0.024$). Second-line immunosuppression was more frequently used among survivors in both groups.
Conclusion: Survival in AIH-related cirrhosis is strongly stage-dependent, with decompensation significantly increasing mortality risk. Age and bilirubin are key predictors in compensated disease, while platelet count is prognostic in decompensated disease. These findings support stage-adapted clinical management and risk-stratified follow-up strategies.

SAT-260-YI
True seronegative autoimmune hepatitis in adults is rare and overestimated
Francesca Colapietro[1], Charlotte Slooter[2], Kalliopi Zachou[3], Daniel E. Di Zeo-Sánchez[4], Mercedes Robles-Díaz[4], Miren Garcia Cortes[4], Sara Santopietro[5], Vincenzo Ronca[6], Maria Pia Calabrese[6], Alessio Gerussi[5], Pietro Invernizzi[5], Raul J. Andrade[4], George Dalekos[3], Joost PH Drenth[2], Ynto de Boer[2], Ana Lleo[6]. *[1]ASST Papa Giovanni XXIII, Bergamo, Italy; [2]Amsterdam UMC, AGEM Institute, Vrije Universitet, Amsterdam, Netherlands; [3]General University Hospital of Larissa, Larissa, Greece; [4]Instituto de Investigación Biomédica de Málaga-IBIMA, Hospital Universitario Virgen de la Victoria, Universidad de Málaga, Malaga, Spain; [5]Università Milano-Bicocca, Milano, Italy; [6]Università Humanitas, IRCCS Humanitas Research Hospital, Pieve Emanuele, Italy*
Email: f.colapietro2@gmail.com

Background and aims: Seronegative autoimmune hepatitis (SnAIH) lacks detectable conventional autoantibodies (ANA, ASMA, anti-LKM, and anti-SLA/LP), posing diagnostic challenges. Increasing evidence suggests SnAIH in adults reflects limitations in autoantibody detection rather than a distinct variant. We systematically re-evaluated all biopsy-proven SnAIH cases in a large international multicenter AIH cohort using standardized testing.
Method: Adult patients with confirmed AIH from the International AIH Group Retrospective Registry were included. Variant syndromes were excluded. Demographic, clinical, histological and serological data were analyzed. Response to treatment at 6 and 12 months, and onset with acute severe AIH (AS-AIH) ($1.5 < INR < 2$, jaundice without encephalopathy) were recorded.
Results: We included 760 adults from five centers with available baseline liver biopsy; after excluding seropositive AIH ($n = 702$), pediatric ($n = 2$) and PBC variant ($n = 4$) cases, 52 SnAIH patients (6.8%) were identified. Of these, 25 completely lacked autoantibody testing, with only one retested (48.1%). Eighteen had partial testing, 94% without anti SLA/LP; six underwent retesting: three patients became positive, and only one remained seronegative. Overall, nine confirmed SnAIH patients (1.2%) were identified, with only one fully retested within 12 months. Median age was 56 years (20–67), 88.9% were females. Median ALT was 16.1 × ULN (6.3–46), IgG were elevated in four cases. All cases presented acutely, including one with AS-AIH. Four (44.4%) had biopsy features suggestive of autoimmune-like drug-induced liver injury (DILI-AIH); one relapsed after

corticosteroid withdrawal. Three out of seven patients (42.9%) failed to normalize ALT at six months. One patient developed cirrhosis.
Conclusion: In this large cohort, true SnAIH is rare (~1%), and less than 20% of cases underwent guideline-recommended retesting. Serological assessment was often incomplete, and nearly half had DILI-AIH-like histology. These results suggest that true SnAIH may be overestimated due to partial testing and assay variability. Strict adherence to the guidelines with standardized, comprehensive, autoantibody assays and systematic retesting in specialized laboratories are needed to clarify whether SnAIH is a distinct clinical entity in adults with AIH.

SAT-261

Postpartum alkaline phosphatase trajectory predicts magnetic resonance cholangiopancreatography based disease progression in women with primary sclerosing cholangitis

Katherine Cooper[1], Daniel Pratt[1]. [1]*Massachusetts General Hospital, Boston, United States*
Email: kcooper5@mgh.harvard.edu

Background and aims: Autoimmune diseases often flare in the postpartum period. In primary sclerosing cholangitis (PSC), identifying biochemical flares is challenged by increases in placental alkaline phosphatase (ALP). We evaluated static and dynamic ALP trajectories after pregnancy and their relation to PSC disease progression.
Method: This is a single center analysis of pregnant women enrolled in a longitudinal PSC registry. The primary outcome was PSC disease progression, defined as change in cholangiogram on magnetic resonance cholangiopancreatography (MRCP) comparing pre and-post pregnancy imaging. Pre-ALP and post-ALP were calcualted for each patient as the mean ALP in the year before pregnancy and after delivery, respectively; ΔALP was calculated as the relative change between pre- and post-ALP. Pre-ALP, post-ALP, and ΔALP were evaluated using receiver operating curves (ROC) and compared with area under the curve (AUC). They were also compared to a prior PSC flare definition, >25% increase in ALP level. To quantify cumulative cholestasis, we defined ALP-time burden as the area under the normalized ALP (ALP/pre-ALP)–time curve using trapezoidal integration.
Results: Among 23 pregnancies (median age 33, 83% IBD, 83% large duct PSC), 14 (61%) met criteria for biochemical flare and 7 (30%) demonstrated MRCP progression. More progressors had a biochemical flare (43% v 11%, p = 0.15) and fewer returned to pre-ALP baseline (0% v 44%, p = 0.05). Pre-ALP (AUC 0.54) and post-ALP (AUC 0.63) poorly discriminated progression whereas Δ ALP showed excellent discrimination at 6 months (AUC 0.94) and 12 months (AUC 0.88). The optimal ΔALP was 58%; a pragmatic threshold of Δ ALP ≥ 50% retained screening standards (sensitivity 100%, specificity 69%) and outperformed the previously used flare definition of ≥25% (AUC 0.85 v. 0.75, Delong p = 0.05). Importantly, cumulative cholestasis was higher in progressors compared to non-progressors (median ALP-time burden 745 vs 488 normalized-ALP-days, p = 0.004).
Conclusion: Our findings suggest that a majority of pregnant women with PSC meet criteria for biochemical flare after delivery. However, rather than distinct flares, the relative change in ALP levels after delivery compared to pre-pregnancy baseline seemingly best correlated with disease progression. Postpartum elevations of ALP in women with PSC warrants careful follow-up, especially when not resolved by 6 months. Larger studies are needed to validate ΔALP as a biomarker of postpartum PSC disease progression.

SAT-262

Geographic heterogeneity in primary biliary cholangitis across Latin America: results from ALLATIN cohort

Claudia Couto[1], Guilherme Cançado[1], Jhon Prieto[2], Graciela Castro-Narro[3], Maria Lucia Ferraz[4], Débora Terrabuio[5], Lorena Castro[6], Luciana Faria[1], Alejandra Villamil[7], Esteban Gonzalez Ballerga[8], Cristiane A. Villela-Nogueira[9], Viridiana Guevara[10], Ezequiel Ridruejo[11], Harlim Rodriguez[12], Maria Sarai González-Huezo[13], Fernando Cairo[14], Jonathan Aguirre[15], Elze Maria Gomes Oliveira[16], Adelina Lozano Miranda[17], Nicolás Ortiz-López[18], Janaina Schiavon[19], Paulo Bittencourt[20], Fernando Bessone[21], Maria Margarita Anders[22], Roberto Rafael Perez[23], Manuel Mendizabal[24], Rodrigo Zapata[25,26], Daniela Perez[27], Alma Kuljacha[28], Mario Guimarães Pessoa[5], Hugo Cheinquer[29], Liliana Mendes[30], Cristiane Tovo[31], Pablo Coste[32], Stefanny Cornejo- Hernández[33], Adriana Varon[34], Maria Chiara Chindamo[9], Daniela Simian[18], Raul Lazarte[35], Melisa Dirchwolf[36], Miguel Escobedo[37], Juan Córdoba[2], Ivan López-Mendez[38], Ana Cristina Amaral[4], Sarah Rufino[4], Franco Weisser[39], Andreina Fragenas[7], Ilse Pardo Ivirico[8], Vivian Rotman[9], Carlos Coronel-Castillo[10], Mirta Peralta[11], Danay Guerrero[12], Luis Alejandro Rosales Renteria[13], Manuel Barbero[14], Paula Daniela Chiodi Lopez[40], Ana Sofia Castro[15], Lucas Carvalho[16], Alvaro Urzúa[18], Leonardo Schiavon[19], Daniela Moreno[2], Sebastián Gil[2,41], Diana Carolina Alfonso Vergel[2], Diego Puentes[42], Nalu Navarro-Alvarez[43], Raimundo Araujo Gama[4], Fernanda Gelape[1], Mateus Nardelli[1], Bernardo Moraes[1], Rodrigo Sanchez[6], Matías Bori[8], Rodrigo Toledo-Galván[10], Marlen Ivon Castellanos Fernández[12], Marcela Ibarra[13], Nicolas Dominguez[14], Angelo Mattos[31], Eduardo Cancado[5], Nélia Hernandez[40]. [1]*Federal University of Minas Gerais, Hospital das Clinicas, Instituto Alfa de Gastroenterologia, Belo Horizonte, Brazil;* [2]*Centro de Enfermedades Hepáticas y Digestivas, Bogotá, Colombia;* [3]*Hospital Médica Sur, Ciudad de México, Mexico;* [4]*Hospital São Paulo, Ambulatório de Hepatologia, Universidade Federal de São Paulo, São Paulo, Brazil;* [5]*Hospital das Clínicas da Universidade de São Paulo, São Paulo, Brazil;* [6]*Clínica Universidad de los Andes, Santiago, Chile;* [7]*Hospital Italiano de Buenos Aires, Buenos Aires, Argentina;* [8]*Hospital de Clínicas José de San Martín, Buenos Aires, Argentina;* [9]*Universidade Federal do Rio de Janeiro, Rio de Janeiro, Brazil;* [10]*Hospital General de México, Ciudad de México, Mexico;* [11]*Centro de Educación Médica e Investigaciones Clínicas Norberto Quirno (CEMIC), Buenos Aires, Argentina;* [12]*Instituto de Gastroenterología de Cuba, La Habana, Cuba;* [13]*Centro Médico ISSEMyM, Toluca, Mexico;* [14]*Hospital El Cruce, Buenos Aires, Argentina;* [15]*Hospital Ángeles Pedregal, Ciudad de México, Mexico;* [16]*Centro Universitário Lusíada (UNILUS), Santos, Brazil;* [17]*Clínica Ricardo Palma, Lima, Peru;* [18]*Hospital Clínico Universidad de Chile, Santiago, Chile;* [19]*Universidade Federal de Santa Catarina, Florianópolis, Brazil;* [20]*Hospital Português, Salvador, Brazil;* [21]*Hospital Provincial del Centenario, Rosario, Argentina;* [22]*Hospital Alemán, Buenos Aires, Argentina;* [23]*Hospital Central de Mendoza, Mendonza, Argentina;* [24]*Hospital Universitario Austral, Pilar, Argentina;* [25]*Clínica Alemana de Santiago, Santiago, Chile;* [26]*Facultad de Medicina, Universidad del Desarrollo, Santiago, Chile;* [27]*Hospital Ángel C. Padilla, Tucumán, Argentina;* [28]*Hospital Ángeles Valle Oriente, Monterrey, Mexico;* [29]*Hospital de Clínicas de Porto Alegre, Porto Alegre, Brazil;* [30]*Hospital de Base do Distrito Federal, Brasília, Brazil;* [31]*Santa Casa de Misericórdia de Porto Alegre, Porto Alegre, Brazil;* [32]*Hospital R.A. Calderón Guardia, San José, Costa Rica;* [33]*Hospital Central Militar, Ciudad de México, Mexico;* [34]*Hospital Cardio Infantil, Bogotá, Colombia;* [35]*Clinica Santa María, Santiago, Chile;* [36]*Hospital Privado de Rosario, Rosario, Argentina;* [37]*Hospital Universitario "Dr. José Eleuterio González," Monterrey, Mexico;* [38]*Unidad de Hepatologia y Transplantes, Hospital Médica Sur, Ciudad de México, Mexico;* [39]*Medicina Interna Clínica Dávila, Santiago, Chile;* [40]*Unidad Académica de Gastroenterología, Hospital de Clínicas, Montevideo, Uruguay;* [41]*Hospital Universitario San Ignacio, Bogotá, Colombia;* [42]*Grupo de Equidad en Salud, Facultad de Medicina, Universidad Nacional de Colombia, Bogotá, Colombia;* [43]*Departamento de Gastroenterologia, Servicio de Hepatologia y Transplante Hepático, Instituto Nacional de Ciencias Medicas y Nutrición "Salvador Zubirán", Ciudad de México, Mexico*
Email: cacouto@uol.com.br

Background and aims: Primary biliary cholangitis (PBC) shows geographical variations in presentation and prognosis. Data from

Latin America is scarce, particularly for cross-country comparisons. This study aimed to describe clinical characteristics, treatment response, and outcomes of PBC across Latin American countries.
Method: The ALLATIN cohort is a retrospective international multicentre study that enrolled 2,182 PBC patients from 13 Latin American countries. For this analysis, participants from the five largest contributing countries were selected (n = 1,980) after excluding those with concomitant liver diseases (n = 564). These were Brazil (40%), Argentina (25.1%), Mexico (17.6%), Chile (9.9%) and Colombia (7.4%), totaling 1,416 participants.
Results: Cohort was predominantly female (93.8%, lower in Argentina, 90%, p = 0.023) with a median age at diagnosis of 53 years (15–90) – subjects from Chile were slightly older (55 [28–80], p < 0.001). Antimitochondrial antibody positivity was 76.3% overall, but notably lower in Colombia (53.3%, p < 0.001). Liver biopsy was performed in 742 participants (52.4%). Hashimoto thyroiditis (14% overall) was more common in Argentina/Chile (20–21%) and less in Mexico/Colombia (8%), p < 0.001. Sjögren syndrome was observed in 9.2%, without difference across countries (p = 0.178). Asymptomatic presentation was reported in 19.3% at diagnosis, highest in Argentina (25.5%, p = 0.003). Response rates to ursodeoxycholic acid (UDCA) after 12 months varied: Toronto (59%), Paris-2 (40.1%), POISE trial (38.7%) and deep-response (14.5%) criteria. Argentina showed higher response rates by Paris-2, POISE and deep-response criteria (p ≤ 0.008). Fibrates were used as second-line therapy in 30.2%, with higher use in Mexico (37.1%) and lower in Colombia (8.6%, p < 0.001). Transplant-free survival differed significantly across countries (log-rank p < 0.001); the risk of death or liver transplantation was higher in Mexico than in Chile (HR 4.36, 95% CI 2.1–10.9, p < 0.001).
Conclusion: In the largest Latin American PBC cohort reported, there was significant heterogeneity in presentation, response to UDCA and long-term prognosis across countries. These findings highlight that even when selecting clear-cut PBC subjects, specific genetic, economic, social and cultural country-related factors influence the disease course. Regional strategies for optimal risk stratification and management should be taken into consideration.

SAT-263

Fibrates outperform obeticholic acid in biochemical response at the cost of higher early discontinuation: insights from the Italian PBC registry

Laura Cristoferi[1], Eugenia Nofit[1], Alessandra Nardi[2], Nora Cazzagon[3,4], Emanuela Bonaiuto[3,4], Pietro Lampertico[5], Elisabetta Degasperi[5], Vincenza Calvaruso[6], Maria Cristina Neglia[6], Umberto Vespasiani-Gentilucci[7], Francesca Terracciani[7], Ana Lleo[8], Francesca Colapietro[8], Ester Vanni[9], Alessandra Risso[9], Federica Malinverno[1], Stefano Fagiuoli[10], Francesco Azzaroli[11], Elton Dajti[11], Francesco Losito[12], Raffaele Cozzolongo[12], Raffaella Viganò[13], Marina Clemente[13], Filomena Morisco[14], Valentina Cossiga[14], Maurizio Russello[15], Mariarita Cannavò[15], Antonino Castellaneta[16], Antonella De Feudis[16], Maurizia Brunetto[17], Barbara Coco[17], Marco Marzioni[18], Luca Maroni[18], Edoardo Giannini[19,20], Sara Labanca[20], Federica Cerini[21], Francesco Pavan[21], Pietro Andreone[22], Filippo Gabrielli[22], Valeria Pace Palitti[23], Cristina Rigamonti[24], Giulia Francesca Manfredi[24], Giovanni Vitale[11], Maria Cristina Morelli[11], Grazia Anna Niro[25], Rosa Cotugno[25], Lucia Napoli[26], Francesco Giuseppe Foschi[26], Marcello Persico[27], Tommaso Sarcina[27], Alessio Gerussi[1,28], Gabriele Missale[29], Daphne D'Amato[28], Alessandra Orlandini[29], Giuliano Alagna[30], Alessandro Granito[31], Fabio Piscaglia[31], Giovanni Raimondo[32], Carlo Saitta[32], Domenico Alvaro[33], Silvia Nardelli[33], Francesco Bellanti[34], Stefano Quiete[34], Giovanni Vettori[35], Luisa Moser[35], Monica Zoeschg[36], Andrea Mega[36], Alessandro Federico[37], Fiammetta Di Nardo[37], Francesca Romana Ponziani[38], Francesca Fianchi[38], Ilaria Cavalli[39], Angela Gobbi[39], Caterina Cusumano[40], Clara Agnolon[40], Francesca Capelli[41], Lavinia Pitotti[41], Leonardo Baiocchi[2], Paola Carnì[2], Teresa Zolfino[42], Chiara Scudu[42], Chiara Ricci[43], Paolo Poisa[43], Luca Fabris[3,4], Alberto Lasagni[4], Pierenrico Lecis[44], Anna Meneghetti[44], Luchino Chessa[45], Francesco Pes[45], Fabrizio Bronte[46], Andrea Affronti[46], Pietro Invernizzi[1], Marco Carbone[13,28], Mauro Viganò[10]. *[1]Division of Gastroenterology, Center for Autoimmune Liver Diseases, European Reference Network on Hepatological Diseases (ERN RARE-LIVER), Fondazione IRCCS San Gerardo dei Tintori, Monza, Italy; [2]Università Tor Vergata, Roma, Italy; [3]Department of Surgery, Oncology and Gastroenterology, University of Padova, Padova, Italy; [4]Azienda Ospedale Università Padova, Padova, Italy; [5]Fondazione Irccs Ca Granda Ospedale Maggiore Policlinico, Milano, Italy; [6]A.O.U. Policlinico "Paolo Giaccone", Palermo, Italy; [7]Research Unit of Hepatology, Department of Medicine and Surgery, Università Campus Bio-Medico of Rome, Clinical Medicine and Hepatology Unit, Fondazione Policlinico Universitario Campus Bio-Medico, Rome, Italy; [8]Department of Biomedical Sciences, Humanitas University, PieveEmanuele; Division of Internal Medicine and Hepatology, Department of Gastroenterology, IRCCS Humanitas Research Hospital, Milan, Italy; [9]A.O.U. Città della Salute e della Scienza di Torino, Turin, Italy; [10]Gastroenterology Hepatology and Transplantation Unit Department of Medicine Azienda Socio Sanitaria Territoriale (ASST) Papa Giovanni XXIII, Bergamo, Italy; [11]Policlinico Sant'Orsola Malpighi, Bologna, Italy; [12]Istituto Nazionale di Gastroenterologia -IRCCS "Saverio de Bellis," Castellana Grotte, Italy; [13]ASST Grande Ospedale Metropolitano Niguarda, Milano, Italy; [14]Programma su "Malattie del Fegato e Vie Biliari" Azienda Ospedaliera Universitaria Federico II, Università Di Napoli Federico II, Napoli, Italy; [15]ARNAS Garibaldi Catania, Catania, Italy; [16]Policlinico di Bari, Bari, Italy; [17]Azienda Ospedaliera Università Pisana, Dipartimenti di medicina Clinica e Sperimentale dell'Università di Pisa, Cisanello, Italy; [18]Azienda Ospedaliera Università Ospedali Riuniti, Ancona, Italy; [19]Dipartimento di Medicina Interna, Università degli Studi di Genova, Genova, Italy; [20]Ospedale Policlinico San Martino, Genova, Italy; [21]Dipartimento di Scienze Cliniche e di Comunità, Università degli Studi di Milano, U.O. Epatologia Ospedale San Giuseppe-Multimedica, Milan, Italy; [22]Ospedale Civile di Baggiovara, Modena, Italy; [23]Azienda USL di Pescara, Pescara, Italy; [24]Department of Translational Medicine, Università del Piemonte Orientale, Novara, Italy; [25]Unità di Gastroenterologia, Fondazione Casa Sollievo della sofferenza, IRCCS, San Giovanni Rotondo, Italy; [26]Presidio Ospedaliero di Faenza, Faenza, Italy; [27]A.O.U. San Giovanni di Dio e Ruggi d'Aragona, Salerno, Italy; [28]Department of Medicine and Surgery, University of Milano-Bicocca, Monza, Italy; [29]A.O. U di Parma, Parma, Italy; [30]Azienda Ospedaliera Universitaria di Sassari, Sassari, Italy; [31]Division of Internal Medicine, Hepatobiliary and Immunoallergic Diseases, IRCCS AUO di Bologna, Bologna, Italy; [32]A.O.U. Policlinico Gaetano Martino, Messina, Italy; [33]AOU Policlinico Umberto I, Università La Sapienza, Roma, Italy; [34]Azienda Ospedaliera Universitaria Policlinico Riuniti Foggia, Foggia, Italy; [35]ASUIT (Azienda Sanitaria Universitaria Integrata del Trentino), Trento, Italy; [36]Azienda Sanitaria dell'Alto Adige, Bolzano, Italy; [37]Università della Campania Luigi Vanvitelli di Napoli, Napoli, Italy; [38]Fondazione Policlinico Universitario A. Gemelli IRCCS, Roma, Italy; [39]ASST Cremona, Cremona, Italy; [40]Azienda Ospedaliera Universitaria Integrata Verona, Verona, Italy; [41]ASST Ovest milanese - Ospedale di Legnano, Legnano, Italy; [42]Presidio Ospedaliero San Michele, ARNAS G. Brotzu di Cagliari, Cagliari, Italy; [43]ASST - Spedali Civili di Brescia, Università di Brescia, Brescia, Italy; [44]Ospedale San Bassiano, Bassano del Grappa, Italy; [45]SS Malattie del Fegato, AOU Cagliari o Liver Unit, University Hospital of Cagliari, Cagliari, Italy; [46]Azienda Ospedaliera Ospedali Riuniti Villa Sofia - V. Cervello, Palermo, Italy*
Email: l.cristoferi@campus.unimib.it

Background and aims: Fibrates (FB) are used off-label as second-line (SL) therapy in primary biliary cholangitis (PBC) with inadequate response/intolerance to ursodeoxycholic acid (UDCA) and for pruritus. We evaluated the effectiveness and safety of FB versus obeticholic acid (OCA) under real-world conditions within the *Italian PBC Registry*.

Method: Patients initiating SL therapy with OCA or FB (fenofibrate/bezafibrate) have been included. Primary endpoints were ALP relative change (×ULN) and ALP < ULN at 1st biochemical assessment (12months +/- 6) after starting SL. Early discontinuation (<6 months) and toxicity were recorded. Patients who received both drugs were included in the analysis only if the 1st assessment was available before changing therapy. Factors associated with ALP < ULN were analysed trough a multivariable logistic regression.
Results: Overall, 737 patients initiated SL therapy (346 OCA, 243 FB, 148 sequential combination). Early discontinuation occurred in 39/243 (16.0%) on FB and 19/346 (5.5%) on OCA, mainly due to intolerance/toxicity ($p < 0.05$). After exclusions for missing follow-up/early therapy switch, 455 patients were included in the analysis (246 OCA, 133 FB, 76 combination therapy cases of whom 64 and 12 started with OCA and FB, respectively); 71(15.6%) had cirrhosis. Baseline ALP levels with OCA and FB were 1.92 × ULN (IQR 1.62–2.64) and 1.68 × ULN (IQR 1.23–2.54), respectively. Median time from baseline assessment to SL initiation was -29 days (IQR −9/−89), and to 1st biochemical assessment 309 days (IQR 233–372) with OCA and 300 days (IQR 224–369) with FB. Median ALP relative changes were −25% (IQR −40% to −8%) for OCA and −46% (IQR −61% to −22%) for FB ($p < 0.0001$). At baseline, 9(2.9%) and 20(13.8%) had normal ALP levels for OCA and FB groups; at first assessment ALP normalization was observed in 41(13.2%) and 88(60.7%), respectively. After adjustment for age, cirrhosis and baseline ALP level, FB therapy was associated with a higher likelihood of ALP normalization compared to OCA (OR 10.3, CI 5.8–18.1, $p < 0.0001$).
Conclusion: In this nationwide real-world cohort study including secondary and tertiary centres, FB achieved greater biochemical improvement than OCA as SL therapy for PBC, at the cost of higher early discontinuation rates. These findings reinforce FB as a potent off-label SL option while underscoring the need for vigilant long-term safety monitoring and continued real-world assessment of emerging therapeutic strategies.

SAT-264

Metabolic dysfunction–associated steatotic liver disease drives a high-risk phenotype in autoimmune hepatitis. Results from the COLHAI registry

Laura Cudero Quintana[1], Yolanda Rodríguez Gil[2], Ignasi Olivas[3], María Carlota Londoño[3], Pinelopi Arvaniti[3], Miren Garcia Cortes[4], Judith Gómez-Camarero[5], Santiago Montull[6], Adrián Lopez Ocaña[4], Manuel Romero-Gómez[7], Álvaro Díaz González[8], Eva Fernandez Bonilla[9], Margarita Sala Llinás[10], María Aragüés Floristán[1], Marta Nabal Mirat[1], Monica Barreales Valbuena[1], Maria Amo[1], Berta De las Heras[1], Maria Luisa Manzano Alonso[1], Ana Martín Algibez[1], Maria Inmaculada Fernández Vázquez[1], Elena Gómez-Domínguez[1]. *[1]Hepatology Unit, Gastroenterology and Hepatology Department, Hospital Universitario 12 de Octubre, Madrid, Spain; [2]Pathology Department, Hospital Universitario 12 de Octubre, Madrid, Spain; [3]Hepatology Unit, Hospital Clínic De Barcelona, Instituto de Investigaciones Biomédicas August Pi i Sunyer (IDIBAPS), Centro de Investigación Biomédica en Red de Enfermedades Hepáticas y Digestivas (CIBEREHD), Department of Internal Medicine, General Hospital of Granollers, Barcelona, Spain, Barcelona, Spain; [4]Gastroenterology and Hepatology Department, Hospital Universitario Virgen De La Victoria, Málaga, Spain; [5]Digestive Department, Hospital Universitario De Burgos, Burgos, Spain; [6]Department of Internal Medicine, General Hospital of Granollers, Barcelona, Spain, Barcelona, Spain; [7]UGC Aparato Digestivo, Hospital Universitario Virgen del Rocío, Sevilla, España; Centro de Investigación Biomédica en Red de Enfermedades Hepáticas y Digestivas (CIBEREHD), Madrid, España; Instituto de Biomedicina de Sevilla (HUVR/CSIC/US), Asociación Española para el Estudio del Hígado, España, Sevilla, Spain; [8]Gastroenterology and Hepatology Department, Clinical and Translational Research in Digestive Diseases Group, Valdecilla Research Institute (IDIVAL), Hospital Universitario Marqués De Valdecilla, Santander, Spain; [9]Gastroenterology and Hepatology Department, Hospital Universitario Miguel Servet, Zaragoza, Spain; [10]Hepatology Unit. Hospital Universitario Doctor Josep Trueta de Gerona, Girona, Spain*
Email: laura.cudero@gmail.com

Background and aims: The coexistence of autoimmune hepatitis (AIH) and metabolic dysfunction–associated liver disease (MASLD) may enhance inflammation, accelerate progression and worsen long-term outcomes. The aim of the study is to assess the prevalence of simple steatosis or metabolic dysfunction- associated steatohepatitis (MASH) in AIH and evaluate its impact on fibrosis, clinical course and prognosis at 3, 5 and 10 years.
Method: Multicenter retrospective study including biopsy-proven AIH (2000–2023). Patients were classified as AIH–MASH, AIH–steatosis or isolated AIH. Kruskal–Wallis, Mann–Whitney and Fisher tests were applied (p < 0.05).
Results: A total of 335 patients were included: 16.7% AIH–MASH, 14.9% AIH–steatosis and 68.4% isolated AIH. Age and sex were similar (>60% women). AIH–MASH and AIH–steatosis showed higher BMI (30.5 and 29.7 vs. 25.7 kg/m^2; $p < 0.05$) and more dyslipidemia (75% and 64% vs. 34.2%; $p < 0.05$) and diabetes (46.4% and 22% vs. 8.4%; $p < 0.05$). Significant fibrosis was more frequent in AIH–MASH (35.7% vs. 16% and 25.2%; $p = 0.01$) with higher liver stiffness (10.4 vs. 5.8 and 7.3 kPa; $p = 0.09$). Portal hypertension features were more common in AIH–MASH at diagnosis (ascites 12.5%, varices 8.9%) and follow-up (ascites 7.7–11.1%; varices 3.9–11.1%). AIH- MASH also showed higher transaminases, IgG and ultrasound signs of chronic liver disease (54.2%, 55% and 44.4% at 3, 5 and 10 years; $p < 0.05$). Hepatocellular carcinoma incidence was higher in AIH MASH (3.9%, 9.5% and 9.1%; $p < 0.05$). Overall mortality increased in AIH–MASH (9.3% vs. 2.1% and 4.8%; $p = 0.3$), with more liver-related deaths; transplant rates were similar (<10%; $p = 0.7$).
Conclusion: MASLD–AIH is associated with more advanced fibrosis, faster progression and worse long-term outcomes, including higher HCC incidence. Intensive metabolic management and surveillance are essential.

SAT-265

Primary biliary cholangitis with concurrent metabolic dysfunction-associated steatotic liver disease demonstrates comparable biochemical response to ursodeoxycholic acid: results from the ELLA-PBC cohort

Paul Yoon[1], Adriana Shen[1], Matthew Chen[1], Tara Foroohar[1], Isai Martinez Rios[1], Sade Brown[1], Jennifer Dodge[1], Brian Lee[2], Kali Zhou[1], Jeffrey Kahn[1], Saro Khemichian[1], Lily Dara[1]. *[1]Keck Hospital of University of Southern California, Los Angeles, United States; [2]Hoag Memorial Hospital, Newport Beach, United States*
Email: psyoon@usc.edu

Background and aims: Metabolic dysfunction-associated steatotic liver disease (MASLD) commonly coexists with primary biliary cholangitis (PBC), but its impact on disease severity, treatment response, and prognosis remains uncertain, particularly in Hispanic patients who are disproportionately affected yet underrepresented in prior studies.
Method: The East Los Angeles Latinx PBC (ELLA-PBC) cohort includes predominantly Hispanic adults (≥18 years) with PBC treated at the University of Southern California Medical Centers (2006–2022). Patients initiating ursodeoxycholic acid (UDCA) with 1-year follow-up were included. MASLD was defined by hepatic steatosis plus ≥1 cardiometabolic risk factor (CMRF) with limited alcohol use. Patients were classified as PBC alone or PBC+MASLD. Predictors of 1-year alkaline phosphatase (ALP) normalization were evaluated using multivariable logistic regression. Transplant-free survival (TFS) was estimated using Kaplan-Meier methods.
Results: Of 157 UDCA-treated patients, 46 (29.3%) had PBC+MASLD. Compared with PBC alone, PBC+MASLD patients were younger (52.5 vs. 58.0 years, $p = 0.045$), more often Hispanic (80.4% vs. 61.3%, $p = 0.048$), and more often underinsured (67.4% vs. 49.6%, $p = 0.04$). BMI

was higher in PBC+MASLD (28.5 vs. 25.5 kg/m2, p = 0.009), while other CMRF were similar. PBC+MASLD patients had less advanced liver disease, with lower rates of cirrhosis, ascites, and hepatic encephalopathy and more favorable albumin, platelet, FIB-4, and APRI values (all p < 0.05). One-year biochemical response did not differ between PBC alone and PBC+MASLD (Paris II: 32.1% vs. 31.1%, p = 0.90; POISE: 39.5% vs. 42.2%, p = 0.75; ALP normalization: 18.2% vs. 13.3%, p = 0.46). MASLD was not associated with ALP normalization in the unadjusted (p = 0.47) or adjusted analyses (aOR 0.94, 95% CI 0.32–2.73, p = 0.91). GLOBE predicted more favorable survival in PBC +MASLD (5-year: 91% vs. 87%, p = 0.03), while UK-PBC risk was similar (p = 0.22). Over median 3.4 years (IQR 2.0–5.1), 25 patients experienced transplant or death. PBC+MASLD patients demonstrated numerically higher 5-year TFS (93.4% vs. 75.8%) with borderline log-rank significance (p = 0.058) and significant Wilcoxon testing (p = 0.018).

Conclusion: Concurrent MASLD was not associated with impaired biochemical response or worse early clinical outcomes in PBC. Instead, patients with PBC+MASLD presented with less advanced disease and demonstrated comparable, and potentially more favorable, prognosis. Larger longitudinal studies are needed to clarify long-term impact.

SAT-266

Cirrhosis progression in primary biliary cholangitis is higher among hispanic patients: results from the ELLA-PBC cohort

Paul Yoon[1], Adriana Shen[1], Matthew Chen[1], Tara Foroohar[1], Isai Martinez Rios[1], Sade Brown[1], Jennifer Dodge[1], Brian Lee[2], Kali Zhou[1], Jeffrey Kahn[1], Saro Khemichian[1], Lily Dara[1]. *[1]Keck Hospital of University of Southern California, Los Angeles, United States; [2]Hoag Memorial Hospital, Newport Beach, United States*
Email: psyoon@usc.edu

Background and aims: Primary biliary cholangitis (PBC) follows a progressive fibrotic course. Although ursodeoxycholic acid slows disease progression, many patients continue to advance. Hispanic patients have lower biochemical response rates in PBC and disproportionately higher mortality across chronic liver diseases, but racial/ethnic differences in cirrhosis progression for PBC remains understudied.

Method: The East Los Angeles Latinx PBC (ELLA-PBC) cohort includes predominantly Hispanic patients (≥18 years) with PBC treated at the University of Southern California Medical Centers (2006–2022). Patients with prior liver transplant or cirrhosis at presentation were excluded. The primary outcome was incident cirrhosis. Five-year cumulative incidence of cirrhosis was estimated from initial presentation using Kaplan-Meier methods and compared by race/ethnicity with the log-rank test. Cox proportional hazards models estimated hazard ratios (HR) for cirrhosis, with multivariable adjustment for covariates with univariable p < 0.10.

Results: Among 180 patients without cirrhosis at presentation, 123 (68.3%) were Hispanic, 35 (19.4%) were non-Hispanic White (NHW), and 22 (12.2%) were other non-White groups. Hispanic patients had higher rates of underinsurance (73.2% vs. 22.9% in NHW; p < 0.001) and higher baseline alkaline phosphatase (307 U/L [IQR 186–557] vs. 228 U/L [IQR 106–418] in NHW; p = 0.03), while other markers of liver disease severity (AST, ALT, bilirubin, APRI, FIB-4) were comparable across groups. Over a median 3.8 years, 34 patients developed cirrhosis. Five-year cumulative incidence was higher among Hispanic vs. NHW patients (28.6% [95% CI 20.1–39.5] vs. 6.5% [95% CI 1.7–23.9]; p = 0.02), while non-White patients had incidence similar to NHW patients (10.1% [95% CI 2.6–34.7]; p = 0.62). In univariable Cox models, Hispanic ethnicity was associated with a 4.5-fold higher risk of cirrhosis vs. NHW patients (HR 4.49 [95% CI 1.07–18.80]; p = 0.04), with no difference in non-White vs. NHW patients (HR 1.62 [95% CI 0.23–11.48]; p = 0.63). This association persisted after adjusting for baseline APRI and BMI (HR 4.17 [95% CI 0.98–17.65]; p = 0.05).

Conclusion: Hispanic patients with PBC had significantly higher 5-year cumulative incidence of cirrhosis, with elevated risk persisting even after adjustment for baseline fibrosis and BMI. These findings identify Hispanic patients as a high-risk group for cirrhosis development in PBC and support earlier therapeutic optimization and closer surveillance in this population.

SAT-267

Hepatic hilar lymphadenopathy identifies advanced fibrosis in primary biliary cholangitis

Youness Dendane[1], Rihab El Kihel[1], Ouiam Elmqaddem[1], Hajar Koulali[1], Abdelkrim Zazour[1], Ghizlane Kharrasse[1], Zahi Ismaili[1]. *[1]Department of Hepato-Gastroenterology, Mohammed VI University Hospital, Oujda, Morocco; Digestive Diseases Research Laboratory (LARMAD), Faculty of Medicine and Pharmacy, Mohammed First University, Oujda, Morocco*
Email: dendane.youness@gmail.com

Background and aims: Hepatic hilar lymphadenopathy is frequently reported on ultrasound in patients with primary biliary cholangitis, but its clinical significance remains unclear. Although often considered benign, its association with liver fibrosis has not been clearly established. This study aimed to assess the relationship between hepatic hilar lymphadenopathy, liver fibrosis severity, and systemic inflammation in primary biliary cholangitis.

Method: We conducted a retrospective study including 62 patients with primary biliary cholangitis treated with ursodeoxycholic acid (13–15 mg/kg/day) and followed for at least 24 months. Patients were classified according to the presence or absence of hepatic hilar lymphadenopathy on baseline ultrasound, defined as lymph nodes larger than 10 mm or explicitly reported by the radiologist. Liver fibrosis was assessed using transient elastography (liver stiffness ≥9 kPa) and FIB-4 score. Systemic inflammation was evaluated by C-reactive protein. Comparisons were performed using appropriate statistical tests, with significance set at p < 0.05.

Results: The mean age was 56 ± 12 years, with a female predominance (79 percent). Hepatic hilar lymphadenopathy was identified in 8 patients (13 percent). Patients with lymphadenopathy did not differ from those without regarding age or sex distribution. In contrast, advanced liver fibrosis assessed by transient elastography was nearly sixfold more frequent in patients with lymphadenopathy compared with those without (62.5 percent vs 11.1 percent; p = 0.018). A FIB-4 score ≥ 3.25 was also more common in the lymphadenopathy group (37.5 percent vs 7.4 percent; p = 0.041). No significant differences were observed in C-reactive protein levels. No cases of hepatic decompensation occurred during follow-up.

Conclusion: Hepatic hilar lymphadenopathy was associated with advanced liver fibrosis independently of systemic inflammation in patients with primary biliary cholangitis. This overlooked ultrasound finding may represent a simple warning sign for advanced fibrosis and should not be considered incidental. Prospective studies are needed to confirm its prognostic value.

SAT-268

Reassessing the utility of the Ferritin-IgG score in predicting complete biochemical response in patients with autoimmune hepatitis from the ColHai registry: is it truly useful?

Alvaro Diaz-Gonzalez[1], Bastian Engel[2], Manuel Hernández-Guerra[3], Indhira Perez Medrano[4], Beatriz Mateos Muñoz[5], Rosa M Morillas[6], Elena Gómez-Domínguez[7], Diana Horta[8], Isabel Conde[9], María Del Barrio[1], Ignasi Olivas[10], Ismael El Hajra Martínez[11], Mar Riveiro Barciela[12], Ana Barreira[12], Carmen López Núñez[13], Carmen Álvarez-Navascués[14], Manuel Rodríguez-Perálvarez[15], Elmar Jaeckel[16], Richard Taubert[2], María Carlota Londoño[10]. *[1]Gastroenterology and Hepatology Department, Clinical and Translational Research in Digestive Diseases Group, Marqués de Valdecilla University Hospital, Santander, Spain; Research Institute Marques de Valdecilla (IDIVAL), Clinical and Traslational Research in*

Digestive Pathology Group, Santander, Spain, Santander, Spain; [2]Department of Gastroenterology, Hepatology, Infectious Diseases and Endocrinology, Hannover Medical School, Hannover, Germany; European Reference Network on Hepatological Diseases (ERN RARE-LIVER), Hamburg, Germany, Hannover, Germany; [3]Servicio de Aparato Digestivo, Hospital Universitario de Canarias, La Laguna, España, Santa Cruz de Tenerife, Spain; [4]Unidad de Hepatología, Complexo Hospitalario Universitario de Pontevedra, Instituto de Investigación Sanitaria Galicia Sur (IISGS), Pontevedra, Spain; [5]Servicio de Aparato Digestivo, Hospital Universitario Ramón y Cajal, CIBERehd, IRYCIS, Madrid, Madrid, Spain; [6]Hepatology Department, Hospital Germans Trias i Pujol and Germans Trias i Pujol Research Institute, IGTP, Badalona; Departament of Medicine, Universitat Autònoma de Barcelona; Centro de investigación biomédica en Red de Enfermedades Hepáticas y Digestivas, CIBERehd, Badalona, Spain; [7]Servicio de Aparato Digestivo, Hospital Universitario 12 de Octubre, Madrid, España, Madrid, Spain; [8]Servicio de Aparato Digestivo, Hospital Universitari Mutua de Terrassa, Terrassa, España, Terrassa, Spain; [9]Hepatology and Liver Transplantation Unit, Hospital Universitario y Politécnico La Fe, IIS La Fe, Valencia, Spain; Ciberehd, ISCIII, Madrid, Spain, Valencia, Spain; [10]Servicio de Hepatologia, Hospital Clinic Barcelona, Fundació Clinic Barcelona, Fundació de Recerca Clínic Barcelona-Institut d'Investigacions Biomèdiques August Pi i Sunyer (FRCB-IDIBAPS), Universitat de Barcelona, Centro de investigación biomédica en red Enfermedades Hepáticas y Digestivas (CIBEREHD), Barcelona, España, Barcelona, Spain; [11]Hospital Universitario Puerta de Hierro de Majadahonda, Madrid, Spain; [12]Liver Unit, Internal Medicine Department, Hospital Universitari Vall d'Hebron, Vall d'Hebron Barcelona Hospital Campus, Barcelona, Spain; Universitat Autònoma de Barcelona, Spain; Centro de Investigación Biomédica en Red de Enfermedades Hepáticas y Digestivas (CIBERehd), Instituto de Salud Carlos III, Madrid, Spain; European Reference Network on Hepatological Diseases (ERN RARE-LIVER), Barcelona, Spain; [13]Unidad Hepatología, Servicio Digestivo, Hospital Universitario Doctor Josep Trueta, IDIBGI, Girona, CIBEREHD, Girona, Spain; [14]Servicio de Aparato Digestivo, Hospital Universitario Central de Asturias, Oviedo, España, Oviedo, Spain; [15]Unidad de Hepatología y Trasplante Hepático, Hospital Universitario Reina Sofía, IMIBIC, CIBERehd, Córdoba, Spain, Córdoba, Spain; [16]Ajmera Transplant Center, Toronto General Hospital, United Health Network, University of Toronto, Toronto, Canada, Toronto, Canada
Email: mlondono@clinic.cat

Background and aims: No predictive tools for Complete Biochemical Response (CBR) in AIH are currently available. A German study proposed a score based on ferritin + IgG as a predictive marker of CBR, and its utility has been included in the AASLD guidelines. We aimed to evaluate the usefulness of this score in an international cohort of patients with AIH.
Method: International multicenter study including 430 patients from Hannover and the ColHai registry. The score (0–2) was calculated by assigning 1 point for ferritin <2.09 × ULN and another for IgG >1.89 × ULN.
Results: At baseline, patients from Hannover were younger ($p = 0.013$) and had higher transaminases, bilirubin ($p < 0.001$), ferritin ($p = 0.007$), and IgG ($p = 0.003$). In the overall cohort (ColHai + Hannover), 78% achieved CBR; however, CBR rates were higher in ColHai at 6 months (50% vs 38%; $p = 0.036$) and 12 months (67% vs 55%; $p = 0.031$). The score was associated with CBR in the Hannover cohort but showed no predictive ability in ColHai (c-statistic at 6 months: 0.51 [95% CI 0.45–0.56]; 12 months: 0.51 [95% CI 0.45–0.57]; during follow-up: 0.54 [95% CI 0.47–0.61]). We found no association with CBR at 6 months (HR 1.01; 95% CI 0.79–1.30), 12 months (HR 0.97; 95% CI 0.78–1.20), or during follow-up (HR 0.93; 95% CI 0.77–1.15). Considering baseline differences, the score was re-evaluated after IPTW-propensity score adjustment, again showing no association with CBR (HR 0.88; 95% CI 0.71–1.10). When analyzing the score components separately, the ferritin cut-off showed no predictive ability in ColHai at 6 months (HR 1.34; 95% CI 0.96–1.88), 12 months (HR 1.16; 95% CI 0.88–1.53), or during follow-up (HR 1.09; 95% CI 0.84–1.41). However, the IgG cut-off of 1.89 × ULN demonstrated predictive ability in the Hannover cohort (HR 0.42; 95% CI 0.24–0.75), in ColHai (HR 0.72; 95% CI 0.51–0.99), and in the combined cohort (HR 0.61; 95% CI 0.46–0.81).
Conclusion: We were unable to validate the usefulness of the score in the ColHai cohort. However, the proposed IgG cut-off was confirmed as a predictor of CBR.

SAT-269

Second-line treatment with novel PPAR agonists in patients with primary biliary cholangitis: real-world experience from a european tertiary care center

Miriam M. Düll[1,2], Jonas Schmid[1,2], Marcel Vetter[1,2], Markus F. Neurath[1,2], Andreas E. Kremer[3], Peter Dietrich[1,2,4].
[1]Department of Medicine 1, University Hospital and Friedrich-Alexander-University Erlangen-Nürnberg, Erlangen, Germany; [2]Deutsches Zentrum Immuntherapie DZI, Erlangen, Erlangen, Germany; [3]Department of Gastroenterology and Hepatology, University Hospital Zürich, University of Zürich, Zürich, Switzerland; [4]Institute of Biochemistry, Emil-Fischer-Zentrum, Friedrich-Alexander-University Erlangen-Nürnberg, Erlangen, Germany
Email: miriam.duell@uk-erlangen.de

Background and aims: A relevant proportion of patients with primary biliary cholangitis (PBC) require second-line therapy due to insufficient response or intolerance to ursodeoxycholic acid (UDCA). After withdrawal of conditional approval for obeticholic acid (OCA) in the EU, alternative treatment strategies became necessary. Elafibranor (ELA), a dual PPAR-α/δ agonist, and seladelpar (SELA), a selective PPAR-δ agonist, were recently introduced for PBC treatment. Real-world data remain limited. We aimed to assess biochemical response, patient-reported outcomes, and safety of ELA and SELA in routine clinical practice.
Method: We prospectively analyzed consecutive PBC patients treated with ELA (80 mg once daily) or SELA (10 mg once daily) at a tertiary referral center between October 2024 and December 2025. Liver biochemistry, treatment history, patient-reported outcomes (PROMIS Fatigue SF-7a and PBC-40 fatigue and pruritus domains), and safety were assessed at baseline and at 3–6-month intervals.
Results: Thirty-one PBC patients (89% female, median age 58.5 years; 29% with advanced fibrosis or cirrhosis) received ELA (n = 22) or SELA (n = 9). Among 27 patients previously treated with OCA, 17 (63%), including four on triple therapy (UDCA+OCA+bezafibrate), were switched to PPAR agonists (ELA n = 13, SELA n = 4), while one-third initiated second-line therapy de novo. All but one patient (UDCA intolerance) remained on UDCA (mean dose 14.9 mg/kg). Median treatment duration was 309 days (IQR 207–355) for ELA and 189 days (IQR 172–201) for SELA. Follow-up data were available for 20, 16, and 3 patients at 3, 6, and 12 months, respectively. At first follow-up, alkaline phosphatase (ALP) decreased in all but two patients, with a median reduction of 28%. POISE response criteria were achieved in 60%, Paris II criteria newly reached in 35%, and 26% newly showed ALP normalization. All patients with available 12-month follow-up achieved ALP normalization (baseline mean ALP 2.1 × ULN). Patients with cirrhosis showed stable or improved MELD and Child-Pugh scores. Three patients discontinued ELA due to mild intolerance; no serious adverse events occurred. Patient-reported fatigue and pruritus scores remained stable throughout treatment.
Conclusion: In this real-world cohort, elafibranor and seladelpar were associated with rapid biochemical improvement and good tolerability. Transition from OCA to PPAR agonists was feasible, including in patients with advanced liver disease, supporting their role as effective second-line options in PBC.

SAT-270

Interleukin-17 blockade in primary sclerosing cholangitis: results from a single-arm, open-label pilot study

Amera Elzubeir[1,2], Juliet High[2], Matthew Hammond[2], Lee Shepstone[2], Martine Walmsley[3], Palak Trivedi[4], Emma Culver[5], Guruprasad Aithal[6], Leo Alexandre[1,2], Simon Rushbrook[1,2]. *[1]Norfolk & Norwich University Hospital, Gastroenterology Department, Norwich, United Kingdom; [2]Norwich Medical School, Faculty of Medicine and Health Sciences, Norwich, United Kingdom; [3]PSC Support, Manchester, United Kingdom; [4]National Institute for Health and Care Research (NIHR) Birmingham Biomedical Research Centre (BRC); Centre for Liver and Gastrointestinal Research, Institute of Immunology and Immunotherapy, University of Birmingham, Liver Unit, University Hospital Birmingham National Health Service Foundation Trust Queen Elizabeth, Birmingham, United Kingdom; [5]Translational Gastroenterology Unit, Oxford University Hospital NHS Foundation Trust; University of Oxford, Oxford, United Kingdom; [6]NIHR Nottingham Biomedical Research Centre, Nottingham University Hospitals NHS Trust and University of Nottingham, Nottingham, United Kingdom*
Email: amera.elzubeir@doctors.net.uk

Background and aims: Primary sclerosing cholangitis (PSC) has no licensed pharmacological therapy. Basic science and translational studies implicate T-helper 17 (Th17) cells and interleukin 17 (IL-17) signalling in PSC pathogenesis. We conducted a pilot study to assess the safety and feasibility of brodalumab, an IL-17 receptor A monoclonal antibody, in PSC (ISRCTN15271834).

Method: SABR-PSC was a phase 2a, single-arm, open-label, multicentre study. Adults (18–75 years) with large-duct PSC received eight brodalumab injections (210 mg) subcutaneously over 13 weeks. Primary outcomes were safety (hepatic and colonic, including post-treatment colonoscopy and histology) and feasibility (adherence, tolerability, recruitment and retention). Exploratory efficacy outcomes included change from baseline to week 16 in alkaline phosphatase (ALP), other liver biochemical analytes, liver stiffness measurements (LSM), enhanced liver fibrosis (ELF) score, 5D-Itch and health-related quality of life (HRQoL).

Results: Six participants were enrolled, and all completed the study (median age: 37.5 years; 83% male; 50% with concomitant inflammatory bowel disease [quiescent]). At baseline, the median ALP was 141 U/L (range: 63–249) and all participants had an ELF score ≥ 7.7 (range: 7.8–9.9). Treatment adherence was excellent (100%). All participants reported ≥ 1 adverse event (AE); the majority were mild. The most common AEs were fatigue, pharyngitis and abdominal pain. No serious AEs and no ALP-defined AEs occurred. At week 16, two participants (33.3%) achieved > 20% reduction in ALP, with accompanying reductions in gamma glutamyl-transferase, LSM and/or ELF; one of whom achieved a > 45% reduction in ALP and subsequent normalisation. Exploratory sub-group analysis suggested larger ALP reductions occurred among those with a baseline ELF score ≥ 9.6. No new diagnoses or exacerbations of inflammatory bowel disease were observed as assessed by faecal calprotectin, partial Mayo score, colonoscopic and histological assessment. 5D-Itch and HRQoL metrics remained stable over the treatment duration.

Conclusion: In this first-in-disease pilot study, brodalumab was safe, well-tolerated and feasible in PSC, with excellent treatment adherence and no emergent adverse gastrointestinal safety signals. Numerical improvement in exploratory efficacy outcomes (ALP, GGT, LSM/ELF) were observed in a subset of patients. A larger-scale randomised controlled trial to further evaluate brodalumab's safety, tolerability and efficacy in PSC is warranted.

SAT-271

Efficacy and tolerance of second line treatments for autoimmmune hepatitis: a multicentric french real life FILFOIE study

Ahmad Kattan[1], Marie-Noëlle Hilleret[2], Teresa Antonini[1], Kerstin Hartig[1], Yasmina Chouik[1], Christine Chambon-Augoyard[3], Sylvie Radenne[1], Francois Bailly[1], Charlotte Costentin[2], Olivier Guillaud[3], Francois Villeret[1], Fanny Lebosse[1], Mathias Ruiz[4], Vincent Leroy[2], Jérôme Dumortier[3], Domitille Erard[1]. *[1]Hepatology, Hospices Civils de Lyon, Lyon, France; [2]Service d'hépato Gastro Entérologie, CHU de Grenoble, Grenoble, France; [3]Federations des Spécialites Digestives, HCL, Lyon, France; [4]Service d'hépato Gastro Entérologie Pédiatrique, Hopital Mère Enfant, Hospices Civils de Lyon, Lyon, France*
Email: domitille.erard@chu-lyon.fr

Background and aims: Autoimmune hepatitis (AIH) is a rare, chronic inflammatory liver disease. First-line treatment is well established, combining steroids and azathioprine to maintain remission. However, 20% of patients do not respond or do not tolerate first-line treatment. The objectives of this study were to describe second-line treatments for AIH, their efficacy and tolerance, in a large French cohort of adult and pediatric patients.

Method: Between 2000 and 2025 in two expert centers, patients followed for AIH who received second-line treatments due to intolerance or ineffectiveness of first-line therapy were retrospectively included.

A complete biochemical response was defined as normalization of transaminases and IgG at 6 months of treatment.

Results: A total of 142 patients were included, with a median age at diagnosis of 42 years and a majority of women (70.4%). A quarter of patients (26.1%) had an associated overlap syndrome. At diagnosis the median cytolysis level was 10.7 ULN (IQR: 4.2–22.4) for AST and 10.0 ULN (IQR: 4.0–20.4) for ALT. A liver biopsy was performed in 124 (87.3%) patients, with cirrhosis in 36 patients (25.4%); 14.7% of patients had severe acute hepatitis (INR > 1.5). First-line treatment was steroids (100%) combined with azathioprine (89.4%). Azathioprine treatment was discontinued in 115 patients (90.6%), mainly due to intolerance (56.5%) and ineffectiveness (34.8%). Mycophenolate mofetil was used as second-line treatment in 90 patients (63.4%), mainly due for intolerance (67.8%). At 6 months, 42.2% of patients had a complete biochemical response (CBR) and 33.3% had discontinued treatment. Tacrolimus was used in 82 patients (57.7%), mainly due to first-line therapy failure (79.3%). At 6 months, 39% of patients had a CBR and 28.0% had discontinued treatment. Among other treatments, 12 patients (8.5%) were treated with cyclosporine, 8 (5.6%) with mTOR inhibitors, 6 (4.2%) with rituximab, and 3 with plasma exchange. During follow-up, a majority of patients (65.5%) received two second-line treatments, and 26.8% received three treatments. At the last follow-up (median duration of 6 years), 70 patients (49.3%) had a complete biochemical response, 101 (71.1%) had cytolysis <1.5 ULN, and 112 (78.9%) had cytolysis <2 ULN. Thirteen patients (9.2%) underwent transplantation, and 4 (2.8%) died.

Conclusion: Second-line treatment of AIH is based on MMF and tacrolimus with good efficacy and few severe clinical events observed during follow up.

SAT-272-YI

Spleen stiffness predicts clinical event-free survival in primary biliary cholangitis: a prospective cohort study

Ilkay Ergenc[1], Hasan Basri Yapıcı[2], Caglayan Keklikkiran[3], Coskun Ozer Demirtas[4], Haluk Kani[4], Michael Heneghan[1,5], Yusuf Yilmaz[3]. *[1]The Roger Williams Institute of Liver Studies, King's College Hospital, London, United Kingdom; [2]Department of Internal Medicine, School of Medicine, Marmara University, Istanbul, Türkiye; [3]Department of Gastroenterology, School of Medicine, Recep Tayyip Erdoğan University, Rize, Türkiye; [4]Department of Gastroenterology, School of Medicine, Marmara University, Istanbul, Türkiye; [5]School of Immunology and Microbial Sciences, Faculty of Life Sciences and Medicine, King's College London, London, United Kingdom*
Email: ergencilkay@gmail.com

Background and aims: Spleen stiffness measurement (SSM) using 100-Hz transient elastography is a promising non-invasive tool to

predict clinically significant portal hypertension (PHT). In Primary Biliary Cholangitis (PBC), PHT can develop before cirrhosis in the early stages due to granulomatous inflammation and cholestasis. PHT is associated with poor prognosis. The aim of this study was to evaluate SSM as a predictor of clinical event-free survival in patients with PBC.
Method: Consecutive PBC patients meeting EASL criteria were invited to participate. Consenting patients with reliable SSM were followed every six months with clinical assessment and liver function tests, and annually with abdominal ultrasound. SSM was performed with FibroScan® Expert 630 by same experienced hepatologist. Elevated SSM was defined as >26.5 kPa, based on published thresholds for probable CSPH. Event-free survival was defined as absence of ascites, variceal bleeding, encephalopathy, spontaneous bacterial peritonitis, hepatorenal syndrome, hepatocellular carcinoma, transplantation, or death.
Results: Of 108 enrolled patients, 98 had reliable SSM and were followed for a median of 51 months (8–57). All had at least one positive diagnostic marker; 52 (48%) had previous liver biopsy. Most were female (94.4%); mean age was 50.4 ± 11 years; median disease duration was 4.6 years (1.7–7.5). Twenty-eight (26.2%) were non-responders by Paris II, and 15 (14%) had cirrhosis. Elevated SSM (>26.5 kPa) was present in 37 (35.7%). SSM correlated weakly with liver stiffness ($r = 0.494$, $p < 0.01$). The prevalence of cirrhosis, biochemical remission, metabolic syndrome, and steatosis was similar between elevated and normal SSM groups. Ten clinical events occurred: 2 (3.2%) in the normal SSM group and 8 (22.9%) in the elevated SSM group ($p = 0.06$), including variceal bleeding ($n = 5$), hepatorenal syndrome ($n = 1$), and ascites ($n = 1$). Six patients died: two due to variceal bleeding, two due to sepsis, one due to ovarian cancer, and one sudden death of unknown cause. Median event-free survival was longer with normal versus elevated SSM (53.1 vs 48.1 months; log-rank $\chi^2 = 9.976$, $p = 0.02$).
Conclusion: Elevated SSM identified patients at higher risk of clinical events and mortality with shorter event-free survival. SSM may improve risk stratification and guide monitoring in PBC.

SAT-273

Clinical outcomes of mycophenolate mofetil as first-line therapy in autoimmune hepatitis: a real-world cohort study

Rut Fernández[1], Eunate Muga[1], Ander García[1], Alex Bausela[1], Maria Senosiáin[1], Patricia Salvador[1], Javier Bustamante[1], José Ramón Fernández[1]. [1]*Hospital Universitario Cruces, Barakaldo, Spain*
Email: fernandezbezanillarut@gmail.com

Background and aims: Standard first-line therapy for autoimmune hepatitis (AIH) consists of corticosteroids (CS) with azathioprine, although intolerance, delayed response and steroid-related toxicity remain major limitations. Mycophenolate mofetil (MMF) has recently emerged as an effective and well-tolerated alternative, supported by the randomized controlled CAMARO trial, but real-world evidence remains limited. We aimed to evaluate the effectiveness and safety of MMF as first-line treatment for AIH in routine clinical practice.
Method: We conducted a retrospective observational study including consecutive immunosuppression-naïve adult patients with newly diagnosed AIH treated with MMF plus CS as first-line therapy at a tertiary referral center between October 2016 and October 2024. Baseline demographic, clinical, biochemical and histological data were collected. Complete biochemical remission (CBR) was defined as normalization of alanine aminotransferase (ALT) and immunoglobulin G (IgG) levels. Outcomes included CBR at 6 and 12 months, time to CBR, CS tapering, relapses, treatment changes and adverse events.
Results: Thirty-two patients were included (mean age 60 years; 69% female). At presentation, 75% had acute hepatitis without severity criteria, 16% acute severe hepatitis and 9% acute decompensation of advanced chronic liver disease. At baseline, median ALT was 991 U/L, median IgG was 1865 mg/dL and median MELD score was 15. CBR was achieved in 90.6% (95% CI 80–100%) at 6 months and 96.9% (95% CI 91–100%) at 12 months, with a median time to remission of 43 days (IQR 21.5–135.3). At 6 months, 22% of patients were receiving CS doses ≤2.5 mg/day, increasing to 65.6% at 12 months. One relapse (3.1%) occurred during follow-up. MMF was discontinued in three patients (9.4%), none due to lack of efficacy. Adverse events occurred in 28.1% (9/32), mainly mild gastrointestinal symptoms; only one patient required permanent MMF withdrawal. No patient required liver transplantation and no deaths were recorded during follow-up.
Conclusion: CBR rates and the safety profile of MMF in this real-world cohort were at least comparable to those reported in randomized trials and large prospective cohorts, including the CAMARO trial and published Greek series. The use of MMF in AIH enables rapid and sustained remission with low CS requirements, limited toxicity and minimal relapse rates, supporting its use as a first-line option for AIH in routine clinical practice.

SAT-274-YI

Long term prognostic impact of persisting histological activity despite biochemical remission in autoimmune hepatitis (AIH)

Sarah Flatley[1], Asha Dube[1], Barbara Hoeroldt[1], Laura Harrison[1], Elaine Wadland[1], Dermot Gleeson[1]. [1]*Sheffield Teaching Hospitals, Sheffield, United Kingdom*
Email: s.flatley@nhs.net

Background and aims: We previously reported that persistent histological activity despite biochemical remission (BR) was found in 45% of AIH patients and was associated with reduced long-term survival. Whether this remains true in more contemporary cohorts and in patients achieving complete biochemical remission (CBR) is unclear. We aimed to reassess the long-term prognostic significance of persistent histological activity despite BR in AIH.
Method: Single-centre cohort study of 496 patients (79% female, age 57 [2–87] years, follow-up 9 [0–36] years) with AIH (1999 IAIHG criteria) presenting 1987–2023 and followed until death/liver transplantation. 445 patients had a diagnostic liver biopsy; 260 underwent follow-up biopsy after a median of 29 months. All biopsies were examined by a single histopathologist (AKD) according to a pre-designed proforma. BR was defined as normal ALT, AST and globulin; CBR additionally required normal IgG. Histological remission was defined as Ishak histological activity index (HAI) ≤3 .
Results: At follow-up biopsy, 205/260 (79%) patients were in BR, and 95/130 (73%) with available IgG data were in CBR. Persistent histological activity (HAI ≥4) was present in 99/205 (48%) patients in BR and 51/95 (54%) patients in CBR. Histological remission was more frequent in patients achieving BR (52% vs 15%, $p < 0.001$) and CBR (46% vs 10%, $p < 0.001$). Serum IgG was not independently associated with histological remission after accounting for BR.
Overall, 20-year death/transplantation rates were 54 ± 3% (all-cause) and 20 ± 3% (liver-related). In the overall cohort, achievement of BR within 12 months was associated with reduced all-cause death/transplantation (HR 0.25, 95% CI: 0.06–0.98, $p = 0.045$), adjusting for other known prognostic variables. CBR showed a similar but non-significant association (HR 0.71, 95% CI: 0.20–1.36, $p = 0.079$).
Among patients achieving BR, mortality did not differ by IgG normalisation (HR 0.71, 95% CI: 0.09–5.34, $p = 0.747$) and persistent histological activity was not associated with all-cause (HR 1.07, 95% CI: 0.59–1.94, $p = 0.837$) or liver-related (HR 1.83, 95% CI: 0.62–9.40, $p = 0.391$) death/transplantation.
Conclusion: 1. BR was significantly associated with improved outcomes, but additional serum IgG normalisation was not of further prognostic value.
2. Persistent histological activity was common despite BR and CBR but was not independently associated with inferior long-term survival. In patients achieving BR or CBR, routine repeat liver biopsy solely for prognostication may not be needed.

SAT-275

Long-term extrahepatic mortality in autoimmune hepatitis: a cohort study

Sarah Flatley[1], Asha Dube[1], Barbara Hoeroldt[1], Laura Harrison[1], Elaine Wadland[1], Dermot Gleeson[1]. [1]*Sheffield Teaching Hospitals, Sheffield, United Kingdom*
Email: s.flatley@nhs.net

Background and aims: Autoimmune hepatitis (AIH) is associated with excess long-term mortality, historically attributed to liver disease. The contribution and causes of extrahepatic deaths remain incompletely defined. We aimed to quantify extrahepatic mortality in AIH compared with the general population and to describe its major causes.
Method: Single-centre retrospective/prospective cohort study of 496 patients (79% female, age 57 [2–87] years, follow-up 9 [0–36] years) with AIH (1999 IAIHG criteria) presenting 1987–2023 and followed until death/liver transplantation or 31/12/23. Causes of death were determined from clinical records and death certificates. Standardised mortality ratios (SMR) for extrahepatic death were calculated using age- and sex-matched regional population data, adjusted for calendar year and to exclude background liver-related mortality.
Results: During follow-up, 168 patients died and 11 underwent liver transplantation. Of 168 deaths, 121 (72%) were extrahepatic. Extrahepatic mortality exceeded that of the general population (SMR 1.31; 95% CI: 1.08–1.75). Extrahepatic deaths were due to cancer (31%; SMR 1.38 [95% CI 0.94–1.83]), infection (24%; SMR 7.77 [4.88–10.66]), vascular disease (21%; SMR 1.44 [0.86–2.02]), frailty or dementia (11%), renal failure (3%), other causes (10%), and unknown causes (2%). On multivariate analysis, older age at diagnosis, diabetes mellitus, and failure to normalise ALT within 12 months, but not the presence of cirrhosis, were independently associated with extrahepatic mortality. Excess infection-related mortality persisted in patients without cirrhosis (n = 324; SMR 7.39 [3.62–11.08]). Causes included pneumonia (n = 19), Covid-19 (n = 3), urosepsis (n = 3), and infective endocarditis, listeria meningitis, and invasive aspergillosis (n = 1 each). At infection onset, 22/26 informative patients (85%) were receiving immunosuppressive therapy, including prednisolone, budesonide, azathioprine and mycophenolate, with no exposure to biologic agents.
Conclusion: In this long-term AIH cohort, most deaths were due to extrahepatic causes and overall extrahepatic mortality exceeded that of the background population. Non-liver deaths were predominantly related to malignancy, vascular disease and infection, emphasising the importance of long-term management of AIH beyond control of liver inflammation alone.

SAT-276

Risk of cancer in patients with autoimmune liver disease treated with acetylsalicylic acid

Paulina Flis[1,2], Hannes Hagström[1,3], Staffan Rosenborg[2,4], Annika Bergquist[1,3], Axel Wester[1,2]. [1]*Gastroenterology and Nutrition Unit, Karolinska Institute, Stockholm, Sweden;* [2]*Division of Clinical Pharmacology, Karolinska University Hospital, Stockholm, Sweden;* [3]*Division of Hepatology, Department of Upper Gastrointestinal Diseases, Karolinska University Hospital, Stockholm, Sweden;* [4]*Department of Laboratory Medicine, Karolinska Institute, Stockholm, Sweden*
Email: paulina.flis@ki.se

Background and aims: Primary biliary cirrhosis (PBC), primary sclerosing cholangitis (PSC), and autoimmune hepatitis (AIH) are the major autoimmune liver diseases (AILD) and are associated with an increased risk of cancer. Epidemiological studies suggest that acetylsalicylic acid (ASA) may have protective effects against several cancers. We therefore investigated the potential cancer-protective effect of ASA in patients with AILD.
Method: Using the population-based DELIVER cohort, Swedish national registers were used to identify all patients with a hospital-based AILD diagnosis between 2006 and 2021. Patients were classified as ASA-exposed (≥180 days of ASA dispensed within 365 days after diagnosis of AILD, based on defined daily doses) or non-exposed. Follow-up started 365 days after AILD diagnosis. Propensity score matching was done to balance potential confounders, including sex, age, education, comorbidities and co-medications. Cox regression was used to estimate hazard ratios (HRs) and 95% confidence intervals (CI) for any cancer. The cumulative incidence of cancer was calculated while accounting for the competing risk of non-cancer death.
Results: We included a total of 698 AILD-patients with a median age of 72 (IQR 63–79) of whom 542 (78%) were female and 106 (15%) had cirrhosis at baseline. 322 (46%) had PBC, 267 (38%) had AIH and 109 (16%) had PSC. During a median follow-up of 3.7 years (IQR 1.5–7.8), any cancer occurred in 37/182 (20%) of ASA-exposed patients and 100/516 (19%) of unexposed patients. Cancer incidence rates per 1000 person-years were similar between ASA-exposed patients (42.7) and comparators (39.2) (HR 1.1, 95% CI 0.7–1.6). The 10-year cumulative incidence of any cancer was 25% (95% CI 18–34%) in ASA-exposed patients and 24% (95% CI 20–29%) in unexposed patients. The incidence of major bleeding did not differ between groups (HR 1.0, 95% CI 0.7–1.5), with 10-year cumulative incidences of 27% (95% CI 19–35%) in ASA-exposed and 24% (95% CI 19–28%) in unexposed patients.
Conclusion: ASA use was not associated with a reduced risk of cancer in patients with AILD, and no increased risk of major bleeding was observed among ASA-exposed patients.

SAT-282

CNP-104, an investigational antigen-specific therapy, demonstrates evidence of improved hepatic function and prognostic risk in a phase 2a randomized, placebo-controlled trial in PBC

Christopher L. Bowlus[1], Adam Elhofy[2], Molly Frey[2], Derrick McCarthy[2], Erik Wambre[3], Stephen Caldwell[4], Roberto J Firpi[5], Brett Fortune[6], Michael Galambos[7], Stuart C Gordon[8], Denise Harnois[9], Tarek Hassanein[10], Matthew Robert Kappus[11], Eric Lawitz[12], Scott McHenry[13], Bhaktasharan Patel[14], Raymond Phillips[15], Daniel Pratt[16], Jatinder Pruthi[17], Govarthanan Rajendiran[18], Gautham Reddy[19], Manuel Rodriguez[20], Marina Silveira[21], Bobby Zervos[22], Paul Peloso[2], Eric Gershwin[1]. [1]*University of California-Davis, Sacramento, United States;* [2]*COUR Pharma, Chicago, United States;* [3]*Icahn School of Medicine at Mount Sinai, New York, United States;* [4]*University of Virginia, Charlottesville, United States;* [5]*University of Florida, Gainesville, United States;* [6]*Montefiore Medical Center, Bronx, United States;* [7]*Digestive Healthcare of Georgia, Atlanta, United States;* [8]*Henry Ford Health, Wayne State University School of Medicine, Detroit, United States;* [9]*Mayo Clinic Florida, Jacksonville, United States;* [10]*Southern California Research Center, Coronado, United States;* [11]*Duke University School of Medicine, Durham, United States;* [12]*Texas Liver Institute, University of Texas Health San Antonio, San Antonio, United States;* [13]*Washington University School of Medicine in St. Louis, St. Louis, United States;* [14]*Peak Gastroenterology Associates, Colorado Springs, United States;* [15]*GI Pros Research, Naples, United States;* [16]*Massachusetts General Hospital, Harvard Medical School, Boston, United States;* [17]*Om Research, Lancaster, United States;* [18]*Sanford Medical Center, Sioux Falls, United States;* [19]*University of Chicago, Chicago, United States;* [20]*Florida Research Institute, Lakewood Ranch, United States;* [21]*Yale School of Medicine, New Haven, United States;* [22]*Cleveland Clinic Weston Hospital, Weston, United States*
Email: mfrey@courpharma.com

Background and aims: Primary biliary cholangitis (PBC) is a progressive autoimmune liver disease with significant unmet needs. Current therapies target bile acid regulation without addressing the underlying autoreactive T-cell mediated pathology. CNP-104 is a first-in-class tolerogenic nanoparticle encapsulating the PBC autoantigen PDC-E2, designed to restore antigen-specific immune

tolerance. Here we report exploratory prognostic risk scores from a Phase 2a study of CNP-104 in PBC.
Method: This randomized, double-blind, placebo-controlled trial enrolled 42 patients with PBC with an incomplete response to ursodeoxycholic acid. Patients were randomized 2:1 to receive two IV doses of CNP-104 (4 or 8 mg/kg) or placebo, one week apart. Exploratory analyses included prognostic risk scores (UK-PBC, GLOBE, and ALBI) and their components. Presented are the pooled CNP-104 (n = 25) and go-forward 4 mg/kg CNP-104 (n = 11) cohorts versus placebo (n = 16).
Results: UK-PBC and ALBI scores worsened in the placebo group but stabilized in both the pooled CNP-104 group (p = 0.014 and p = 0.001, respectively) and the 4 mg/kg group (p = 0.010 and p < 0.0001, respectively) through Day 270. This stabilization indicates a reduced risk of poor clinical outcomes. GLOBE scores increased similarly in the placebo and pooled CNP-104 arms (p > 0.05), but stabilized in the 4 mg/kg group compared to placebo (p = 0.0125). These results reflect the differential impact of CNP-104 on the unique components/weights used in each model (UK-PBC: ALP, bilirubin, ALT, albumin, platelets; ALBI: albumin, bilirubin; GLOBE: age, ALP, bilirubin albumin, platelets). Albumin levels were maintained in pooled CNP-104 and 4 mg/kg cohorts compared to a decrease in placebo at Day 180 (p = 0.040 and p = 0.014, respectively), suggesting albumin as a driver of improvements in prognostic scores. ALP and platelet levels were stable over the course of this analysis. Together, this data suggests that CNP-104 initially has a larger impact on hepatic function than on cholestasis early in the treatment course.
Conclusion: The significant improvement in key prognostic scores with CNP-104 demonstrates early evidence of disease-modifying activity and provides insight into the unique impact of CNP-104 on hepatic function compared to other PBC treatments. These findings support CNP-104 for development as a mechanistically distinct treatment for PBC in larger randomized trials.

SAT-283
Unmet needs of patients with primary biliary cholangitis in Greece: results from the preliminary analysis of the Hellenic autoimmune liver diseases study group
Nikolaos Gatselis[1], Vasiliki Lygoura[1], Stefania Pitsava[1], Martha Orfanidou[1], Konstantinos Papantoniou[2], Maria Loukia Koutsompina[3], Basil Sakellariou[4], Georgios Psarakis[5], Alexandra Alexopoulou[6], Evangelos Cholongitas[7], Christos Triantos[2], Theodoros Androutsakos[3], Emmanouil Manesis[4], Dimitrios N. Samonakis[5], Stella Gabeta[1], Dafni Sveroni[1], Anna Samakidou[1], Kalliopi Zachou[1], Eirini Rigopoulou[1], Dina Tiniakos[8], George Dalekos[1]. *[1]Department of Medicine and Research Laboratory of Internal Medicine, Expertise Center of Greece in Autoimmune Liver Diseases, European Reference Network on Hepatological Diseases (ERN RARE-LIVER), General University Hospital of Larissa, Larissa, Greece; [2]Division of Gastroenterology, Department of Internal Medicine, University of Patras, 26504, Patras, Greece, Patras, Greece; [3]Department of Pathophysiology, Medical School, National and Kapodistrian University of Athens, Athens, Greece; [4]Hepatology Unit, Euroclinic, Athens, Greece; [5]Department of Gastroenterology, University Hospital of Heraklion, Crete, Heraklion, Greece; [6]2nd Department of Internal Medicine, School of Medicine, "Hippokration" General Hospital of Athens, Medical School, National and Kapodistrian University of Athens, Athens, Greece; [7]1st Department of Internal Medicine, "Laiko" General Hospital of Athens, School of Medicine, National and Kapodistrian University of Athens, Athens, Greece; [8]Department of Pathology, Aretaieion Hospital, Medical School, National and Kapodistrian University of Athens, Athens, Greece*
Email: gatselis@me.com

Background and aims: Primary biliary cholangitis (PBC) is the most common autoimmune liver disease, with significant impact on quality of life and survival. We aimed to analyze Greek PBC patients, assess to treatment response during the first year, and explore correlation with outcomes.
Method: Prospectively-collected data were retrospectively analyzed. Response to ursodeoxycholic acid (UDCA) at first year was classified according to alkaline phosphatase (ALP): complete response (ALP ≤ 1 × ULN), partial response (1.67 × ULN ≥ ALP > 1 × ULN), and non-response (ALP > 1.67 × ULN).
Results: Overall, 1385 patients were included (85.6% female; median age 56.4 years). Median delay in diagnosis was 19 months. At baseline, 719/1385 (51.9%) were asymptomatic, 171/1385 (12.3%) had cirrhosis, including decompensation [70/171 (40.9%)]. Fatigue and pruritus at diagnosis were present at 176/1385 (12.7%) and 281/1385 (20.3%), respectively. At month 12 of treatment, 62.2% showed complete response, 27.5% partial, and 10.3% non-response. During follow-up [median (interquartile range): 7 (11) years], 93/1214 patients (7.7%) developed cirrhosis, and 71/194 (37.2%) decompensation. Baseline symptoms were not associated with outcome (decompensation, liver-related-death or liver transplantation). Both non-responders (HR:10.0;95%CI:4.8–20.9; p < 0.001) and partial responders (HR:2.7;95%CI:1.3–5.7; p = 0.007) had increased risk of decompensation. Liver-related-death or liver transplantation occurred in 93/1385 patients (6.7%). Non-response (HR:6.8;95% CI:3.6–12.7; p < 0.001) and partial response (HR:2.2;95%CI:1.2–4.2; p = 0.011) were associated with liver-related mortality.
Conclusion: Cirrhosis at diagnosis is relatively uncommon in PBC, yet it remains a significant concern. Approximately 40% of patients do not achieve ALP normalization after one of UDCA, which is associated with poor prognosis. Therefore, early identification and prompt initiation of second-line therapies seem essential. [on behalf of the Hellenic Autoimmune Liver Diseases Study Group]

SAT-284
Outcomes of cirrhotic patients at the presentation of autoimmune hepatitis and the role of biochemical response as a predictor of survival
Elze Maria Gomes Oliveira[1], Maria Lucia Gomes Ferraz[2], Ana Cristina Amaral[2], Antonio Eduardo Benedito da Silva[2], Patrícia Marinho C Oliveira[3], Lucas Carvalho[4], Luiza Lacks[5], Felipe Oliveira Carvalho[6], Maria Chiara Chindamo[7]. *[1]Centro Universitario Lusiada UNILUS, Santos, Brazil; [2]Universidade Federal de Sao Paulo, Sao Paulo, Brazil; [3]Fleury Medicina e Saude, Sao Paulo, Brazil; [4]Endosoni, Centro Universitario Lusiada, Santos, Brazil; [5]Hospital Beneficência Portuguesa, Santos, Brazil; [6]Hospital Ana Costa, Santos, Brazil; [7]Federal University of Rio de Janeiro, Rio de Janeiro, Brazil*
Email: elzeoliveira@terra.com.br

Background and aims: Autoimmune hepatitis (AIH) generally responds well to immunosuppressive therapy and is associated with a favorable prognosis. Treatment aims to delay fibrosis progression, prevent liver transplantation, and improve survival. Cirrhosis is present at diagnosis in approximately 30% of patients and has been associated with poorer treatment response and worse outcomes. Failure to achieve biochemical remission has been linked to increased rates of liver transplantation and liver-related mortality. This study aimed to evaluate the frequency of cirrhosis at AIH presentation and to assess the impact of biochemical response and liver function at diagnosis on patient survival.
Method: A total of 114 patients with AIH diagnosed according to International Autoimmune Hepatitis Group criteria were included. Cirrhosis was defined by histology or by clinical signs of liver failure and/or portal hypertension. All patients were treated with prednisone combined with azathioprine. Loss of liver function was defined as prothrombin activity <70% and albumin <3.5 g/dL. Biochemical response was defined as normalization of ALT, AST, gammaglobulin, and bilirubin levels.
Results: Among the 114 patients evaluated, 60 (53%) had cirrhosis at diagnosis. Ninety-five percent were female, with a mean age of 28 ± 17 years. Among cirrhotic patients, 57% achieved a biochemical

response. Data from 51 of the 60 cirrhotic patients were available for analysis regarding the presence or absence of biochemical response, disease course with or without decompensation, and survival over a mean follow-up period of 8 ± 4.5 years. Among cirrhotic patients with biochemical response, 29 of 30 (97%) remained free of decompensation, compared with 12 of 21 (57%) cirrhotic patients without biochemical response (p = 0.001). Mean survival time was 14 years in patients with biochemical response and 9 years in those without response (p = 0.03). In patients who achieved biochemical response, comparative analysis according to disease presentation (cirrhosis with or without liver function impairment) showed no significant impact of liver function at diagnosis on survival (10.6 ± 1.1 vs. 10.2 ± 1.2 years; p = 0.86).
Conclusion: The achievement of biochemical response is a strong predictor of decompensation-free survival and improved overall survival in patients with cirrhosis at the time of AIH diagnosis. This favorable prognosis appears to be independent of liver function status at presentation.

SAT-285

Isolated IgG elevation in patients with persistently normal transaminases does not affect the outcome of autoimmune hepatitis: or just a little bit?

Lorenz Grossar[1], Sarah Raevens[2], Christophe Van Steenkiste[3], Isabelle Colle[4], Charlotte De Vloo[5], Hans Orlent[6], Jeoffrey Schouten[7], Marie Gallant[8], Annelien Van Driessche[9], Sander Lefere[1], Lindsey Devisscher[10], Anja Geerts[2], Hans Van Vlierberghe[2], Xavier Verhelst[2]. [1]*Ghent University, Department of Internal Medicine and Paediatrics, Liver Research Centre Ghent, Ghent, Belgium;* [2]*Ghent University Hospital, Department of Gastroenterology and Hepatology, Liver Research Centre Ghent, Ghent, Belgium;* [3]*Maria Middelaresziekenhuis, University of Antwerp, Ghent, Belgium;* [4]*AZorg, Aalst, Belgium;* [5]*AZ Delta, Roeselare, Belgium;* [6]*AZ Sint-Jan, Bruges, Belgium;* [7]*VITAZ, University of Antwerp, Sint-Niklaas, Belgium;* [8]*Jan Ypermanziekenhuis, Ieper, Belgium;* [9]*AZ Glorieux, Ronse, Belgium;* [10]*Liver Research Centre Ghent, Ghent University, Gut-Liver Immunopharmacology Unit, Ghent, Belgium*
Email: lorenz.grossar@ugent.be

Background and aims: Follow-up of disease activity in subjects with autoimmune hepatitis (AIH) mainly relies on normalization of transaminases (TA) and immunoglobulin G (IgG). Complete biochemical response is defined by the international autoimmune hepatitis group consensus criteria as normalization of TA and IgG within six months after induction treatment, and correlates with superior liver-related survival. The association of IgG with survival outcomes is more contested than TA normalization. In a recent retrospective, multicenter cohort, no significant difference in cirrhosis development was observed between subjects with AIH after persistent TA normalization, according to their IgG evolution. We aimed to replicate these findings in our own cohort.
Method: We performed a subset-analysis from our own real-world, multicenter, retrospective cohort of subjects with AIH and identified those with persistently normal TA, and without cirrhosis at initial diagnosis. All available IgG levels were recorded allowing classification of subjects with either persistently normal IgG (IgGn), fluctuating IgG (IgGf), and persistently elevated IgG (IgGe). Development of cirrhosis was assessed by suggestive clinical, laboratory and imaging findings, and/or follow-up biopsy.
Results: From an initial cohort of 213 subjects with AIH, 95 without cirrhosis and with persistently normal TA could be identified. According to IgG evolution, 76 (80.0%) had persistently normal IgG, whereas 17 (17.9%) and 2 (2.1%) were classified as IgGf and IgGe, respectively. During a median follow-up of 8.1 years (interquartile range: 1.2–15.1 years), seven (7.4%) subjects developed cirrhosis. When comparing proportions according to IgG evolution, the proportion of subjects with persistently normal IgG who developed cirrhosis was significantly lower than in those with either persistently elevated or fluctuating IgG: 3/76 (4.0%) versus 1/2 (50%) and 3/17 (17.6%), respectively. Fisher's exact test p-value for differences in proportions between IgGn, IgGf, and IgGe = 0.01635.
Conclusion: In our subset-analysis, development of cirrhosis occurred significantly less in subjects with persistently normal TA and IgG, compared to those with abnormal IgG in follow-up. Our findings are in contrast with a recent publication suggesting no role of IgG in cirrhosis development, emphasizing the importance of large datasets with long-term follow-up when outcome incidence is low.

SAT-286

Burden of recurrent primary sclerosing cholangitis (PSC), re-transplantation, and explant malignancy in a globally representative cohort of patients of >1500 PSC patients undergoing liver transplant

Aliya Gulamhusein[1], Aisha Alawi[2], Leila Amiri[1], Sarah Al-Shakhshir[3], Bilal Bobat[4], Lisa Campbell[4], Hannah Giles[5], Aditya Sheth[5], Sergio Rodriguez-Tajes[6], Helena Hernández Evole[6], Claudia Couto[7], Mateus Nardelli[7], Piotr Milkiewicz[8], Emil Bik[9], Ken Liu[10], Xavier Verhelst[11], Anja Geerts[11], Alejandra Villamil[12], Mark Swain[13], Matthew Sadler[14], Marco Carbone[15], Raffaella Viganò[15], Jessica Dyson[16], Danielle Rayner[16], Christopher L. Bowlus[17], Kidist Yimam[18], Clara Dibenedetto[19], Pietro Lampertico[19], Eunice Tan[20], Brysen Keith[21], Gideon M. Hirschfield[1], Ellina Lytvyak[22], Andrew L. Mason[22], Kym Watt[23], Johannes R. Hov[24], Cynthia Levy[25], Aldo J Montano-Loza[22], John Eaton[26], Palak J. Trivedi[27], Bettina E. Hansen[28]. [1]*Toronto General Hospital, Autoimmune and Rare Liver Diseases Program, Toronto Centre for Liver Diseases, Toronto General Hospital, University Health Network, Toronto, Canada;* [2]*Autoimmune and Rare Liver Diseases Program, Toronto Centre for Liver Diseases, Toronto General Hospital, University Health Network, Toronto, Canada;* [3]*Queen Elizabeth Hospital - Department of Hepatology and Liver transplantation, Birmingham, United Kingdom;* [4]*Charlotte Maxeke Johannesburg Academic Hospital, Johannesburg, South Africa;* [5]*New Zealand Liver Transplant Unit, Auckland, New Zealand;* [6]*Liver Unit, Hospital Clínic, Fundació de Recerca Clínic Barcelona, Barcelona, Spain;* [7]*Departamento de Clínica Médica Instituto Alfa de Gastroenterologia/ Hospital das Clínicas - UFMG, Belo Horizonte, Brazil;* [8]*Department of Hepatology, Transplantology and Internal Medicine, Medical University of Warsaw, Warszawa; Translational Medicine Group, Pomeranian Medical University, Szczecin, Poland, Warsaw, Poland;* [9]*Department of Hepatology, Transplantology and Internal Medicine, Medical University of Warsaw, Warszawa, Warsaw, Poland;* [10]*AW Morrow Gastroenterology and Liver Centre Royal Prince Alfred Hospital, Sydney, Australia;* [11]*Ghent University, Ghent Hepatology Research Unit, Department of Gastroenterology and Hepatology, Ghent University Hospital, Ghent, Belgium;* [12]*Médica Hepatóloga Sección de Hepatología y Trasplante Hepático Hospital Italiano de Buenos Aires, Buenos Aires, Argentina;* [13]*Calgary Liver Unit, University of Calgary, Calgary, Canada;* [14]*Transplant Clinic, Foothills Medical Center, Calgary, Calgary, Canada;* [15]*Centre for Autoimmune Liver Diseases, School of Medicine and Surgery, University of Milano-Bicocca, Milano, Milan, Italy;* [16]*Newcastle upon Tyne Hospitals NHS Foundation Trust, Newcastle, United Kingdom;* [17]*Division of Gastroenterology and Hepatology at the University of California Davis, Davis, United States;* [18]*Autoimmune Liver Disease Program Division of Hepatology and Liver Transplantation California Pacific Medical Center, San Francisco, United States;* [19]*Gastroenterology and Hepatology Division, Foundation IRCCS Ca' Granda Ospedale Maggiore Policlinico, Milan, Italy, Milan, Italy;* [20]*National University Hospital, Singapore, Singapore, Singapore;* [21]*Department of Medicine, University of Miami Miller School of Medicine, Miami, FL, USA, Miami, United States;* [22]*University of Alberta, Edmonton, Canada;* [23]*Division of Gastroenterology and Hepatology, Mayo Clinic, Rochester, Minnesota, USA, Rochester, United States;* [24]*Norwegian PSC Research Center, Oslo, Norway;* [25]*Division of Digestive Health and Liver Diseases, University of Miami School of Medicine, Miami, Florida, Miami, United States;* [26]*Mayo Clinic - Division of Gastroenterology and Hepatology, Rochester, United States;* [27]*University of Birmingham, National Institute for Health*

Research Birmingham Biomedical Research Centre, Centre for Liver and Gastrointestinal Research, Institute of Immunology and Immunotherapy, University of Birmingham, Birmingham, United Kingdom; Liver Unit, University Hospitals Birmingham, Birmingham, United Kingdom; Institute of Translational Medicine, Birmingham, United Kingdom; [28]Department of Epidemiology & Biostatistics, Erasmus MC, Rotterdam, the Netherlands, Erasmus, Netherlands
Email: aliya.gulamhusein@uhn.ca

Background and aims: Primary sclerosing cholangitis (PSC) is an enigmatic chronic cholestatic disease that results in a disproportionate burden of transplant activity across the globe. Herein, we characterize a globally representative cohort of patients (pts) with PSC who underwent liver transplantation (LT) and report burden of recurrent PSC (rPSC), re-transplantation, and malignancy on explant.
Method: Descriptive statistics were used to describe baseline characteristics. Summary statistics were reported as proportions and medians with interquartile ranges. Kaplan-Meier analyses were used to evaluate time dependent regional differences in risk of rPSC.
Results: In total, 1546 pts were included in the analysis from Africa (n = 114), Northern Europe (NE) (n = 405), Mediterranean Europe (n = 61), Oceania (n = 117), North America (NA) (n = 791) and South America (SA) (n = 58). The mean age of PSC diagnosis was 36 (25–48) years (yrs), 65% were male, 55% Caucasian, 76% had IBD, and 10% labelled with an autoimmune hepatitis variant. Mean age at LT was 44 yrs (32–57) and median MELD 14 (8–21). Surgically, 61% had a donation after brain death graft, 9% had a donation after cardiac death graft, 16% had a living donor graft, and 55% had a Roux-en-Y anastomosis. UDCA was used in 39% of pts pre-LT and 22% in the first year post LT. Tacrolimus (83%) and mycophenolate mofetil (52%) were the most common immunosuppressive agents used post LT. Malignancy was detected in 6.2% of all explants (n = 96), with cholangiocarcinoma in 3.2% (n = 50), gallbladder cancer in 1.2% (n = 18) and hepatocellular cancer in 2% (n = 28). Excluding pts referred for LT with indication of neoplasia (n = 60), 4.5% (n = 67) of the cohort had incidental malignancy on explant. The cumulative incidence of rPSC was 2.1% at 1 year, 13.7% at 5 yrs and 26.8% at 10 yrs. There was a lower risk of rPSC in Africa compared to the other regions ($p < 0.05$) but no significant difference in rPSC across Mediterranean or NE, NA, SA, and Oceania. Re-LT occurred in 14.1% (n = 219) a median of 2.3 (0.2–8.6) yrs after first LT, and a third LT was performed in 1.9% (n = 30) pts after a median of 2.6 (0.8–11.5) yrs from second LT. A fourth LT was performed in 3 pts, all from NE at a median of 6.9 (4.8–7.5) yrs from 3rd LT.
Conclusion: PSC pts undergoing LT are at high risk of malignancy on explant, rPSC, and re-transplantation. Understanding predictors of such impactful outcomes remains an important priority.

SAT-287

Efficacy and safety of seladelpar in patients with primary biliary cholangitis and cirrhosis, including those with clinical signs of portal hypertension: interim results from the open-label ASSURE study with up to 4 years of treatment

Aliya Gulamhusein[1], Pietro Invernizzi[2,3], Andrea Galli[4], Francesca Carubbi[5], Sarah Proehl[6], Robert Kustra[6], Jie Liu[6], Kyung min Kwon[6], Daria B. Crittenden[6], Palak J. Trivedi[7,8], Stuart C Gordon[9,10]. *[1]Division of Gastroenterology and Hepatology, Toronto Centre for Liver Disease, University of Toronto, Toronto, Canada; [2]Centre for Autoimmune Liver Diseases and Division of Gastroenterology, European Reference Network (ERN) RARE-LIVER, Fondazione IRCCS San Gerardo dei Tintori, Monza, Italy; [3]Department of Medicine and Surgery, University of Milano-Bicocca, Monza, Italy; [4]Azienda Ospedaliero Universitaria Careggi Gastroenterologia Clinica, Firenze, Italy; [5]Metabolic Medicine Unit, Azienda Ospedaliero Universitaria di Modena, University of Modena and Reggio Emilia, Modena, Italy; [6]Gilead Sciences, Inc., Foster City, United States; [7]National Institute for Health Research Birmingham Biomedical Research Centre, Centre for Liver and Gastrointestinal Research, College of Medical and Dental Sciences, University of Birmingham, Birmingham, United Kingdom; [8]Liver Unit, University Hospitals Birmingham Queen Elizabeth, Birmingham, United Kingdom; [9]Division of Hepatology, Henry Ford Hospital, Wayne State University School of Medicine, Detroit, United States; [10]Michigan State University College of Medicine, East Lansing, United States*
Email: sgordon3@hfhs.org

Background and aims: Seladelpar (SEL) is a first-in-class delpar (selective PPAR-delta agonist) indicated for the treatment of primary biliary cholangitis (PBC) in combination with ursodeoxycholic acid (UDCA) in patients (pts) with an inadequate response to UDCA or as monotherapy in pts unable to tolerate UDCA. In the pivotal RESPONSE study (NCT04620733), SEL had similar efficacy in pts with or without compensated cirrhosis and safety generally similar to placebo. Here, we present an interim analysis of the efficacy and safety of SEL in pts with compensated cirrhosis in the ongoing open-label Phase 3 ASSURE study (NCT03301506).
Method: Pts from RESPONSE and legacy SEL studies enroled in ASSURE and received SEL 10 mg once daily. Pts with cirrhosis per protocol at baseline (BL) were pooled. BL was defined as SEL initiation in RESPONSE or ASSURE. Post hoc, cirrhosis pts were identified as having features of portal hypertension (PHT) if they met ≥ 1 criterion at baseline (BL): platelets < 140×10^3/uL, low albumin, elevated total bilirubin (TB), ascites, or medical history of varices or PHT. Efficacy endpoints through month (M) 36 included composite biochemical response (CBR; alkaline phosphatase [ALP] < 1.67 × the upper limit of normal [ULN], ≥ 15% decrease in ALP, and TB ≤ 1.0 × ULN), ALP normalisation, and other laboratory changes. Safety was also assessed. Data cutoff: 31 Jan 2025.
Results: 53/337 (16%) pts had cirrhosis at BL; most were Child-Pugh (CP)-A, with 4 (8%) CP-B. At BL, mean ALP was 267.5 U/L, TB 0.98 mg/dL, and liver stiffness 20.6 kPa. 29/53 (55%) pts with cirrhosis had features of PHT. Among evaluable pts, 25/51 (49%) achieved CBR at M12, with a similar proportion meeting this endpoint at M36 (9/19 [47%]). Mean percent change from BL in ALP was −35% at M12 and −28% at M36. 15/51 (29%) pts achieved ALP normalisation at M12, and 3/19 (16%) with available data had normal ALP at M36. Adverse events were reported in 50/53 (94%) pts. Four pts experienced events meeting the criteria for a PBC clinical outcome; no events were assessed as related to SEL. No pts with abnormal aspartate aminotransferase (AST) or alanine aminotransferase (ALT) at BL experienced an AST or ALT ≥ 2 × BL.
Conclusion: SEL continues to demonstrate sustained biochemical efficacy and a favourable safety profile in cirrhosis pts with PBC, including pts with features of PHT, with up to 4 years of treatment.

SAT-288

Increased risk of non-Hodgkin lymphoma in autoimmune hepatitis: a large retrospective cohort study

Mifleh Tatour[1], Fadi Abu Baker[2], Tarek Saadi[3], Rawi Hazzan[4]. *[1]Clalit Health Service, Faculty of Medicine, Bar Ilan, Safed, Tel aviv, Israel; [2]Department of Gastroenterology and Hepatology, Hadera, Israel; [3]Rambam Health Care Campus, Haifa, Israel; [4]Clalit Health Service, Azrieli Faculty of Medicine, Bar-Ilan University, Tel aviv, Israel*
Email: rawihazzan1@gmail.com

Background and aims: Autoimmune hepatitis (AIH) is a chronic immune-mediated liver disease that usually requires long-term immunosuppressive therapy. Thiopurines and mycophenolate mofetil (MMF), commonly used in AIH, have been associated with an increased risk of lymphoma in other autoimmune diseases. However, data regarding the risk of non-Hodgkin lymphoma (NHL) in AIH patients are limited. This study aimed to evaluate the incidence of NHL in AIH patients treated with immunosuppressive agents compared with the general population.
Method: We conducted a retrospective population-based cohort study using Clalit Health Services data from 2000–2020. Adult AIH patients treated with azathioprine, 6-mercaptopurine (6-MP), or MMF were included. Patients with inflammatory bowel disease, other

autoimmune diseases, prior lymphoma, or additional chronic liver diseases were excluded. Incident NHL cases were identified through linkage with the Israeli National Cancer Registry. Standardized incidence ratios (SIRs) were calculated by age and sex to compare observed versus expected NHL cases.
Results: A total of 685 AIH patients were included (83.5% female; mean age 53.1 years), with a mean follow-up of 7.5 years. Nine patients developed NHL, all aged ≥45 years at diagnosis. The overall SIR for NHL was 36.5, indicating a markedly increased risk compared with the general population. Six cases occurred in patients treated with azathioprine and two in those treated with MMF; no cases were observed in patients treated exclusively with 6-MP. No statistically significant association was found between specific immunosuppressive agents and NHL risk.
Conclusion: AIH patients treated with standard immunosuppressive regimens exhibit a substantially increased risk of NHL compared with the general population, independent of the specific agent used. These findings highlight the need for heightened clinical awareness and possibly tailored surveillance strategies for lymphoma in AIH. The elevated risk likely reflects a combination of chronic immune dysregulation inherent to AIH and prolonged immunosuppressive therapy, underscoring the importance of balancing long-term treatment benefits against potential malignancy risks. Further large-scale and mechanistic studies are warranted to elucidate causal factors and guide optimal management approaches.

SAT-289

Long-term risk of inflammatory bowel disease in autoimmune hepatitis: over a 20-year population-based study

Mifleh Tatour[1,2], Fadi Abu Baker[3], Tarek Saadi[4], Rawi Hazzan[2,5]. *[1]Clalit Health Service, Faculty of Medicine, Bar Ilan, Safed, Tel aviv, Israel; [2]Bar Ilan University, Safed, Israel; [3]Department of Gastroenterology and Hepatology, Hadera, Israel; [4]Rambam Health Care Campus, Haifa, Israel; [5]Clalit Health Service, Azrieli Faculty of Medicine, Bar-Ilan University, Tel aviv, Israel*
Email: rawihazzan1@gmail.com

Background and aims: Autoimmune hepatitis (AIH) is a chronic immune-mediated liver disease frequently associated with other autoimmune conditions, including inflammatory bowel disease (IBD). Although coexistence of AIH and IBD has been described, the long-term incidence of IBD after AIH diagnosis and its impact on liver outcomes remain insufficiently defined. This study aimed to evaluate the long-term risk of IBD among AIH patients and to assess its influence on cirrhosis and liver-related complications.
Method: We conducted a retrospective, population-based cohort study using Clalit Health Services data, including adult patients diagnosed with AIH between 2000 and 2024. Patients with pre-existing IBD, other chronic liver diseases, or cirrhosis before AIH diagnosis were excluded. Incident IBD cases were identified during follow-up. Demographic, clinical, and treatment variables were analyzed. Kaplan–Meier analysis was used to estimate cumulative IBD incidence, and multivariable logistic regression identified predictors of IBD development. Liver-related outcomes were compared between patients with and without IBD.
Results: Among 1284 AIH patients (80.5% female; median age 51.5 years), 126 (9.8%) developed IBD during a mean follow-up of 4.8 years, most commonly Crohn's disease. The cumulative probability of remaining IBD-free declined progressively to 79.7% at 20 years. Smoking was independently associated with increased IBD risk (adjusted OR 1.76, 95% CI 1.10–2.83). Cirrhosis was significantly more prevalent in AIH patients with IBD compared with those without IBD (73.9% vs 26.3%, $p < 0.0001$). However, rates of major liver-related complications, including ascites, variceal bleeding, hepatic encephalopathy, and hepatocellular carcinoma, did not differ between groups.
Conclusion: IBD develops in a substantial proportion of AIH patients over long-term follow-up, with risk increasing over time. Smoking is a modifiable independent risk factor for IBD development. Although AIH–IBD overlap is associated with a higher prevalence of cirrhosis, it does not appear to increase the risk of advanced liver-related complications. These findings support long-term vigilance for IBD in AIH patients and emphasize the importance of smoking cessation.

SAT-290-YI

Timing matters: prognostic impact of biochemical response assessment in autoimmune hepatitis (AIH)

Helena Hernández-Évole[1], Ana Pascual-Dapena[2], Marta Sánchez-Ric[1], María Fernández-Aguilera[3], Empar Moreno-Penades[3], Nuria Florensa[2], David Heitmann[2], Diogo Simas[2], Fernando Diaz[4], Sara Lermo[4], María Del Barrio[5], Pinelopi Arvaniti[1], Ignasi Olivas[2], Álvaro Díaz-González[6], Magdalena Salcedo Plaza[7], Mar Riveiro Barciela[8], Sergio Rodriguez-Tajes[1], María Carlota Londoño[1]. *[1]Hospital Clínic De Barcelona, Centro de Investigación Biomédica en Red Enfermedades Hepáticas y Digestivas CIBEREHD), Madrid, Spain; IDIBAPS, Barcelona, Spain; [2]Hospital Clínic De Barcelona, Barcelona, Spain; [3]Vall d'Hebron, Barcelona, Spain; [4]Gregorio Marañón, Madrid, Spain; [5]Hospital Valdecilla, Santander, Spain; [6]Hospital Valdecilla, Clinical and Translational Research in Digestive Diseases Group, Valdecilla Research Institute (IDIVAL), Santander, Spain, Santander, Spain; [7]Gregorio Marañón, Gregorio Marañón Health Research Institute (IiSGM), Madrid, Spain; CIBERehd, Madrid, Spain; [8]Vall d'Hebron, CIBERehd, Barcelona, Spain*
Email: hernandez.ievole@gmail.com

Background and aims: Current AIH guidelines define complete biochemical response (CBR) as normalization of transaminases and IgG at 6 months, although the optimal timing for response assessment remains uncertain. We aimed to evaluate whether the timing of CBR or biochemical response (BR; transaminase normalization) assessment influences its prognostic value for future liver-related events (LRE) in patients with AIH.
Method: Retrospective cohort of 423 biopsy-confirmed AIH patients treated with first-line therapy at four Spanish hospitals. Patients with cirrhosis at diagnosis, prior decompensation, variant forms, or fulminant presentation were excluded. LRE was defined as cirrhosis development, decompensation, hepatocellular carcinoma, liver transplantation, or liver-related death. Landmark analyses at 3, 6, 9, and 12 months were performed using Cox proportional hazards assessed the association between CBR and BR with LRE at 3, 6, 9 and 12 months, adjusting for age and sex.
Results: Most patients were women (64.3%) with median age of 55 years (IQR 42–65) and median follow-up (FU) of 6.3 (IQR 3.1–9.7). CBR was achieved in 83% of patients after a median time of 6.5 months (IQR 2.9–14.4) from treatment initiation. CBR rates at 3, 6, 9, and 12 months were 20%, 37%, 50%, and 57%, respectively. During the FU 36 patients developed LRE, none occurred before 9 months and only one by 12 months of treatment. Landmark Cox regression showed that achieving CBR at 6 months was linked to a reduced risk of LRE (HR 0.37, 95% CI 0.14–0.98, $p = 0.044$), with the strongest prognostic value at 9 months (HR 0.35, 95% CI 0.15–0.81, $p = 0.014$). CBR at 3 and 12 months were not significantly related to outcomes.BR was achieved in 87% of patients after a median time of 5.7 months (IQR 2.3–11.8). BR rates at 3, 6, 9 and 12 months were 25%, 43%, 57%, and 65%, respectively. The strongest association between BR and reduced LRE risk was at 9 months (HR 0.45, 95% CI 0.21–0.96, $p = 0.038$).
When compared to BR, CBR resulted in a slight, non-significant improvement in Harell's C statistics at 6 (0.77 vs. 0.76, $p = 0.625$) and 9 months (0.75 vs. 0.77, $p = 0.464$).
Conclusion: In non-cirrhotic patients with AIH, assessing treatment response at 9 months identifies late responders without increasing early clinical risk and provides optimal prognostic discrimination for LRE. BR based on transaminase normalization performs similarly to CBR, suggesting limited added prognostic value of IgG normalization.

SAT-291

Reduced symptom prevalence but significant quality of life impact in patients with primary biliary cholangitis in Spain

Helena Hernández-Évole[1], Ignasi Olivas[2], Diogo Simas[3], Ismael El Hajra Martínez[4], Esther Maderuelo[4], Margarita Sala Llinás[5], Beatriz Mateos Muñoz[6], Ana Arencibia Almeida[7], Raquel Ríos León[8], Cristina Montón[9], Vanesa Bernal[10], Judith Gómez- Camarero[11], Luís Neves da Silva[12], Pinelopi Arvaniti[13], José Presa[14], María Carlota Londoño[1], Sergio Rodriguez-Tajes[1]. *[1]Hospital Clínic, Centro de Investigación Biomédica en Red Enfermedades Hepáticas y Digestivas, IDIBAPS, Barcelona, Spain; [2]Hospital Clínic De Barcelona, Centro de Investigación Biomédica en Red Enfermedades Hepáticas y Digestivas CIBEREHD), Madrid, Spain; IDIBAPS, Barcelona, Spain; [3]Hospital Clínic De Barcelona, Barcelona, Spain; [4]Hospital Universitario Puerta De Hierro Majadahonda, Majadahonda, Spain; [5]Hospital Universitari De Girona Doctor Josep Trueta, Girona, Spain; [6]Hospital Ramón y Cajal, Madrid, Spain; [7]Hospital Universitario Nuestra Señora de la Candelaria, Tenerife, Spain; [8]Hospital General De Villalba, Collado Villalba, Spain; [9]Hospital Clínico Universitario, Valencia, Spain; [10]Hospital Universitario Miguel Servet, Zaragoza, Spain; [11]Hospital Universitario De Burgos, Burgos, Spain; [12]Unidade Local de Saúde de Braga, E.P.E. Sete Fontes - São Victor, Braga, Portugal; [13]Hospital Clínic De Barcelona, 2.Centro de Investigación Biomédica en Red Enfermedades Hepáticas y Digestivas CIBEREHD), Madrid, Spain; IDIBAPS, Barcelona, Spain; [14]Centro Hospitalar De Trás-Os-Montes E Alto Douro, Vila Real, Portugal*
Email: hernandez.ievole@gmail.com

Background and aims: Fatigue and pruritus are common symptoms of primary biliary cholangitis (PBC) and can occur at any disease stage. Previous studies report prevalence rates of pruritus, fatigue, and cognitive impairment in PBC at 80%, 60%, and 35%, respectively. This study aimed to evaluate symptom severity and associated clinical factors in Spanish PBC patients.
Method: A multicenter cross-sectional study at 11 sites used electronic questionnaires (PBC-40, 5D-Itch, EQ-5D-5L) to measure symptoms and quality of life (QoL). Moderate-to-severe (M-S) symptoms were defined as fatigue ≥29, cognitive impairment ≥16, and pruritus ≥9. Clinical and epidemiological data were then collected.
Results: 191 patients were included: 91% women, median age 60 years (IQR 52–66), 88% AMA positive, and 7% with cirrhosis. Most (88%) received UDCA alone; 30.9% had second-line therapy. Based on PBC-40, 30% of patients had pruritus; with 12% experiencing M-S symptoms. Of these, 33% were untreated and 25% denied pruritus upon questioning. The 5D-itch scale identified pruritus in 49%, although 40% denied it. The correlation between 5D-itch and PBC-40 was moderate ($r = 0.648$, $p < 0.001$). Pruritus was linked to higher liver stiffness (OR 1.22, IQR 1.1–1.4) and younger age (OR 0.94, IQR 0.89–0.99). Those who reported no pruritus but were detected by PBC-40 had lower QoL than those without pruritus (0.92 vs 1.00; $p = 0.002$). M-S fatigue was reported by 41% of patients and cognitive impairment by 30%, with neither associated with clinical or biochemical features. M-S fatigue was associated with pruritus (OR 3.5, IQR 1.02–11.86). Patients with cognitive impairment received more psychotropic medications without higher rates of depression or anxiety. Pruritus significantly reduced quality of life (QoL) ($p < 0.0001$), even when mild, and M-S fatigue had a similar impact ($p < 0.0001$). When both symptoms coexisted, QoL was lowest (0.790 vs 0.923, $p < 0.05$). Increased fatigue scores were linked to higher chances of work leave or disability pension (OR 1.08, 95% CI: 1.02–1.14, $p = 0.011$), regardless of average income per consumption unit.
Conclusion: Fatigue, although less common in our Spanish cohort than previously reported, was the primary symptom of PBC and the key factor contributing to reduced QoL and socioeconomic burden. Its strong association with pruritus underscores the importance of using validated scales to detect underreported symptoms. PBC-40 detects early mild pruritus impacting QoL, identifying patients who may benefit from treatment.

SAT-298

Diagnosis, treatment and outcomes of primary biliary cholangitis – insight from 801 patients enrolled for 20 years in the Polish registry of two tertiary centres

Maciej Janik[1], Beata Kruk[1], Ewa Wunsch[2], Karolina Wronka[1], Magdalena Jaroszek[1], Jacek Tomczuk[1], Sebastian Jędruszek[2], Kaja Kozłowska[2], Joanna Raszeja-Wyszomirska[1], Piotr Milkiewicz[1,2]. *[1]Medical University of Warsaw, Warszawa; [2]Pomeranian Medical University, Szczecin, Poland*
Email: mjanik24@gmail.com

Background and aims: Primary biliary cholangitis (PBC) is a rare cholestatic liver disease with limited but expanding treatment options. Data on PBC from Central/Eastern Europe remain scarce. Here, we evaluated diagnosis, treatment and outcomes from a 20-year Polish registry of patients with PBC.
Method: We analysed a cohort of 801 patients with PBC prospectively recruited between 2005 and 2025 at two tertiary centres (Warsaw and Szczecin) collaborating within ERN RARE-LIVER. The registry comprised clinical and patient-reported data at the time of diagnosis, at inclusion, and during follow-up.
Results: The cohort included 719 women (90%), with a median age at diagnosis of 53 years (range: 22–88), and no differences in age compared to males. AMA and ANA antibodies (including, but not limited to, anti-sp100 and anti-gp210) were present in 79% and 68%, respectively. At diagnosis, median (range) ALP and bilirubin levels were 270 (37–2700) IU/mL and 0.9 (0.1–40.5) mg/dL, respectively. Liver biopsy (LB) was performed in 49% of patients (with younger age and/or with worse liver injury markers (ALT, AST, ALP, all $p < 0.01$)), due to suspicion of autoimmune hepatitis (AIH) variant and/or advanced fibrosis. Liver cirrhosis (assessed by LB, liver stiffness or clinical signs) and PBC/AIH variant were diagnosed in 31% and 8% of patients, respectively. More than half of patients (56%) reported any pruritus at diagnosis. These subjects had higher ALP ($p < 0.001$), but no differences in liver cirrhosis status ($p = 0.08$). At the registry inclusion (median 2 (0–27) years after diagnosis), significant fatigue (>33) and itch (>6) were evaluated by PBC-40 in 40% and 39% patients, respectively. Drug regimens comprised of UDCA (98%) and fibrates (43%). Indications for fibrates were: insufficient UDCA response (63%), pruritus (17%), hypertriglyceridemia (11%) or multi-indication. After a median of 6 (0.5–32) years from the diagnosis, 55% had normalised ALP, 35% had ALP 1.0–1.67, and 10% had ALP > 1.67, the upper limit of normal. During the follow-up, 27% patients underwent liver transplantation (LT), and 12% died. Patients who received LT were diagnosed at a younger age, in a non-tertiary centre (82%, both $p < 0.001$), with higher ALP and ALT (both $p < 0.05$), but not bilirubin.
Conclusion: This large Polish PBC cohort provides comprehensive real-world data on diagnosis, symptom burden, treatment patterns and long-term outcomes. Despite widespread UDCA use, many patients required second-line or symptom-relief therapy.

SAT-299

The majority of fatigued primary biliary cholangitis patients do not have clinically significant itch

David E. Jones[1], Jessica Leighton[1], Aaron Wetten[2], Magnus Doverskog[3], Jessica Dyson[2]. *[1]Newcastle University, Newcastle upon Tyne, United Kingdom; [2]Newcastle Upon Tyne Hospitals Nhs Foundation Trust, Newcastle upon Tyne, United Kingdom; [3]Umecrine Cognition, Solna, Sweden*
Email: david.jones@newcastle.ac.uk

Background and aims: Quality of life (QoL) impairment in primary biliary cholangitis (PBC) is significant with the symptoms of itch and fatigue (with and without cognitive symptoms) predominating. Recent advances in itch treatment through the development of the iBAT inhibitors and appreciation of the beneficial effects of the

fibrates and PPAR agonists has, together with the intuitive view that night-time itch that disturbs sleep must contribute to fatigue, led to a view that targeting itch is the key route to symptom improvement in PBC. This study aimed to address the question of whether fatigue in PBC is, indeed, simply a downstream consequence of itch, with the implication that effective itch treatment will address the problem of fatigue at a population level.

Method: The PBC-40 questionnaire was completed by 1964 well-characterised patients in the UK-PBC national cohort. Established cut-offs for moderate/severe symptom severity (ie clinically significant symptoms) vs mild/none (non-clinically significant) were used for each symptom domain (itch, fatigue and cognitive symptoms).

Results: 644 (33%) participants had significant itch. Of these, 520 (81%) also had significant fatigue. 336 (52%) had significant cognitive symptoms and 333 (52%) had fatigue with cognitive symptoms (the form of fatigue with the greatest impact on QoL). Of the 1320 participants with no/mild itch, 608 (46%) had fatigue and 363 (28%) had cognitive symptoms. Overall, 1128 (57%) of the cohort had fatigue, but of those 54% did not have itch. Likewise, of the 699 (36%) of the population with significant cognitive symptoms 52% did not have itch.

Conclusion: Fatigue and cognitive symptoms are common in PBC patients with clinically significant itch. It is therefore logical to target itch treatment as a priority in this group. However, the majority of PBC patients with fatigue and/or cognitive symptoms do not have itch, so we can't expect improvement in their fatigue through itch reduction. Hence, to support a more individualized treatment approach, there is a clear need to develop specific fatigue-targeting therapies to address the quality-of-life issues in this group of patients.

SAT-300

Long-term treatment with elafibranor improves markers of immune response and inflammation in primary biliary cholangitis

David E. Jones[1], Cynthia Levy[2,3], Kris V. Kowdley[4,5], Christopher L. Bowlus[6], Darren Asquith[7], Nuno Antunes[8], Nathan Touati[9], Jörn M. Schattenberg[10]. *[1]Translational and Clinical Research Institute and NIHR Newcastle Biomedical Research Center, Newcastle University, Newcastle Upon Tyne, United Kingdom; [2]Schiff Center for Liver Diseases, University of Miami, Miami, United States; [3]Division of Digestive Health and Liver Diseases, University of Miami School of Medicine, Miami, United States; [4]Liver Institute Northwest, Seattle, Washington, United States; [5]Elson S. Floyd College of Medicine, Washington State University, Washington, United States; [6]Division of Gastroenterology and Hepatology, UC Davis School of Medicine, Sacramento, United States; [7]Ipsen, London, United Kingdom; [8]Ipsen, Cambridge, Massachusetts, United States; [9]Ipsen, Paris, France; [10]Department of Internal Medicine II, Saarland University Medical Center, Homburg, Germany*
Email: david.jones@newcastle.ac.uk

Background and aims: Primary biliary cholangitis (PBC) is a rare autoimmune disease characterised by progressive destruction of small intrahepatic bile ducts. Chronic inflammation results in liver injury, fibrosis and cirrhosis. Markers of immune response (immunoglobulin [Ig]-G and IgM) and inflammation (haptoglobin and C-reactive protein [CRP]) are associated with disease activity. Elafibranor (ELA), a PPARα/δ agonist, significantly improved markers of cholestasis in the phase III ELATIVE® trial (NCT04526665). Here, markers of immune response/inflammation from the trial and ongoing open-label extension (OLE) are presented.

Method: 161 patients (pts) were randomised 2:1 to receive ELA 80 mg or placebo (PBO) daily in the double-blind period (DBP). Pts who completed the DBP could enter the OLE and receive ELA 80 mg. Change from baseline (CfB) in IgG, IgM, haptoglobin and CRP were assessed using a mixed model for repeated measures (adjusted for baseline/stratification factors) at Week (W) 26 and 52 of the DBP and were presented descriptively from OLE start to W156. OLE data are reported for pts who continued ELA (continuous pts [W156 ELA exposure]; baseline at DBP start) and pts who switched from PBO to ELA (crossover pts [W104 ELA exposure]; baseline at OLE start).

Results: 108 pts received ELA and 53 received PBO in the DBP. 138 pts entered the OLE (continuous pts: n = 93; crossover pts: n = 45); 113 remained at W156. In the DBP, significant reductions in IgG, IgM and haptoglobin were observed with ELA vs PBO at W26 and sustained to W52 (W52 IgG least squares [LS] mean CfB: –0.365 g/L [n = 95] vs 0.333 g/L [n = 46, p = 0.009]; IgM LS mean CfB: –0.558 g/L [n = 95] vs 0.025 g/L [n = 46, p < 0.001]; haptoglobin LS mean CfB: –0.166 g/L [n = 93] vs –0.001 g/L [n = 47, p = 0.008]). CRP increases were smaller with ELA vs PBO (W52 LS mean CfB: 0.81 mg/L [n = 93] vs 1.02 mg/L [n = 47, p = 0.051]). In the OLE, reductions in IgG, IgM and haptoglobin were sustained in continuous pts to W156 (W156 mean CfB IgG: –0.556 g/L [n = 72]; IgM: –0.676 g/L [n = 72]; haptoglobin: –0.204 g/L [n = 73]). Reductions in all markers were reproduced in crossover pts (W156 mean CfB IgG: –1.361 g/L; IgM: –0.663 g/L; haptoglobin: –0.231 g/L; CRP: –0.71 mg/L [n = 33 for all]).

Conclusion: Long-term ELA treatment leads to sustained and reproducible reductions in levels of markers of immune response/inflammation, providing a potential role for ELA in influencing mechanistic changes to autoimmune processes in PBC and slowing disease progression.

SAT-301

Investigating the burden of illness in primary sclerosing cholangitis (PSC): a multinational study

Deepak Joshi[1], Guy Lacey[2], Jolan Terner-Rosenthal[2], Lucia Quadrado[2], Robin Howard[2], Jane Moorhouse[3], Oliver Webb[3], Sarah Smart[3], Donna Rowen[4], Philip A. Powell[4], Brian Thorsen[5], Ingo Van Thiel[6], Martine Walmsley[7], Angela Leburgue[8], Francesca Scarpa[9], Marlyn J. Mayo[10]. *[1]King's College Hospital, RW-ILS, London, United Kingdom; [2]Mirum Pharmaceuticals, Inc., Foster City, California, United States; [3]Initiate Consultancy, Ltd., Northampton, United Kingdom; [4]Sheffield Centre for Health and Related Research, University of Sheffield, Sheffield, United Kingdom; [5]PSC Partners Seeking a Cure, Denver, Colorado, United States; [6]Deutsche Leberhilfe, eV, Cologne, Germany; [7]PSC Support, Manchester, United Kingdom; [8]ALBI France, Versailles, France; [9]AMAF Italia (Associazione Malattie Autoimmuni Del Fegato), Muggio, Italy; [10]UT Southwestern Medical Center, Dallas, Texas, United States*
Email: d.joshi@nhs.net

Background and aims: Primary sclerosing cholangitis (PSC) is a rare, chronic liver disease associated with progressive damage to hepatic bile ducts and cholestasis-related symptoms such as pruritus and fatigue, which can impair health-related quality of life (HRQoL). This study aims to better characterize the burden of illness in symptomatic PSC patients.

Method: A survey of patients with PSC matched to a general population sample was initiated in the US, UK, France, Germany and Italy. The web-based survey sent through patient advocacy groups with links to questionnaires contained both quantitative and qualitative elements, including validated outcome measures (e.g., PROMIS Fatigue, SF-36). Pruritus severity was measured by the Adult ItchRO (0–10 scale; 0 = no itch; 10 = worst itch). T-statistics and linear regression analyses were performed to examine the relationship between pruritus severity and HRQoL. Only survey data from the US, UK, and France were available at the time of submission.

Results: 242 individuals (38% male; mean [SD] age 42.3 [12.3] years) were included of which 121 were patients with PSC currently experiencing pruritus (US: n = 50, UK: n = 50, France: n = 21) and 121 from an age- and sex- matched general population cohort (US: n = 50; UK: n = 50; France: n = 21). The median (SD) ItchRO in patients with PSC was 5 (2.30) indicating moderate severity, with 62% of patients reported having to make lifestyle adjustments due to fatigue. Pruritus severity (ItchRO) and fatigue (PROMIS fatigue) were significantly correlated (r = 0.243, p = 0.007) and this relationship remained

significant when controlled for country, age, and sex. Overall, patients with PSC had significantly ($p < 0.05$) lower HRQoL scores across the majority of SF-36 domains vs. the general population. Furthermore, an increase in pruritus severity was associated with worsening HRQoL across the physical component summary, role-physical, bodily pain and social functioning SF-36 domains. PSC symptoms negatively impacted patients' ability to work in half of the population.
Conclusion: Initial findings demonstrate that PSC is associated with debiliating physical, emotional, and social burden, with pruritus severity linked to fatigue and reduced physical function. These symptoms continue to be present and inadequately managed despite multiple medications used, underscoring an unmet need in the treatment of PSC.

SAT-302

The mean corpuscular volume (MCV) is a surrogate for therapeutic azathioprine metabolites in patients with autoimmune hepatitis

Guan Sen Kew[1,2], Yu Jun Wong[2], Shagani Thisairajah[2], Ellina Lytvyak[2], Aldo J Montano-Loza[2]. *[1]Woodlands Health Campus, Singapore, Singapore; [2]University of Alberta Hospital, Edmonton, Canada*
Email: kewguansen@gmail.com

Background and aims: Azathioprine (AZA), combined with prednisone, is still considered the first-line treatment for autoimmune hepatitis (AIH). Recent guidelines suggest testing 6-thioguanine nucleotides (6-TGN) in patients with incomplete biochemical response, intolerance, or non-adherence to therapy, proposing a therapeutic level of >223 pmol/8 × 10^8erythrocytes. However, access to 6-TGN testing can be costly and limited in many countries, leading to the consideration of surrogate blood indices such as mean corpuscular volume (MCV) and white blood cell (WBC) count. This study aims to evaluate the clinical utility of these blood indices in predicting therapeutic 6-TGN levels.
Method: We included 111 patients with AIH who were tested for 6-TG and 6-MMP (6-Methylmercaptopurine) levels because of incomplete biochemical response between 2004 and 2025. Data collected included baseline demographics, hematological and biochemical indices, azathioprine dosage, and corresponding 6-TGN levels, which were analyzed.
Results: 68.5% were female, and 29.7% had cirrhosis. A total of 211 6-TGN samples were collected, with a median value of 278 pmol/8 × 10 8 erythrocytes (IQR 182–490). The median azathioprine dose was 1.31 mg/kg (IQR 0.99–1.67), and 59.7% of samples were collected while patients were also on prednisone. Patients with MCV higher than 94.5 fL (OR = 2.93, $p = 0.004$) and an increase in MCV from baseline (OR = 2.71, $p = 0.004$) are more likely to have therapeutic 6-TGN levels. In contrast, WBC was not a significant predictor (OR = 0.96, $p = 0.516$) of therapeutic 6-TGN levels. Higher azathioprine doses (mg/kg) did not predict higher 6-TGN levels (B = 13.6, $p = 0.718$), but were significantly associated with higher 6-MMP levels (B = 3103.05, $p < 0.001$). The optimal MCV and change in MCV from baseline for predicting therapeutic 6-TGN levels were 94.5 fL, with a sensitivity of 69.4% and specificity of 63.6% (Youden index = 0.33), and +4.5 fL, with a sensitivity of 59.2% and specificity of 79.7% (Youden index = 0.39), respectively.
Conclusion: MCV higher than 94.5 fL and an increase in MCV from baseline were the strongest indicators of therapeutic 6-TGN levels in our cohort of AIH patients. Our findings suggest MCV might be useful in clinical practice as surrogate indicators to assess therapeutic 6-TGN levels, especially in regions where access to 6-TGN testing is limited.

SAT-303

Healthcare resource utilisation and costs associated with alkaline phosphatase normalisation and composite biochemical response among adults prescribed ursodeoxycholic acid for primary biliary cholangitis

Robert G. Gish[1,2], Robert Wong[3], Yi Pan[4], Mihail Samnaliev[4], Diane Ito[4], Chong Kim[5]. *[1]Robert G. Gish Consultants, LLC, San Diego, United States; [2]Hepatitis B Foundation, Doylestown, United States; [3]Division of Gastroenterology and Hepatology, Department of Medicine, Stanford University, Stanford, United States; [4]Stratevi, Santa Monica, United States; [5]Gilead Sciences, Inc., Foster City, United States*
Email: chong.kim9@gilead.com

Background and aims: Patients (pts) with primary biliary cholangitis (PBC) experience a substantial clinical and economic burden. Response to first-line ursodeoxycholic acid (UDCA) in clinical trials varies, and evidence linking biochemical response to economic outcomes is unclear. We aimed to evaluate the association between biochemical response and healthcare utilisation (HCRU) and costs in pts with PBC receiving UDCA.
Method: This observational, retrospective cohort study used Komodo Health data to identify pts with PBC from 1/9/2018 to 30/3/2023. Inclusion criteria: ≥ 1 UDCA prescription (excluding pts receiving obeticholic acid), continuous insurance enrolment for 12 months pre- and post-index, and baseline alkaline phosphatase (ALP) ≥ 1.67 × upper limit of normal (ULN). Post-index ALP normalisation was defined as ALP ≤ 1 × ULN; composite biochemical response (CBR) was defined as ALP < 1.67 × ULN, ALP decrease ≥ 15%, and total bilirubin ≤ 1 × ULN. Regression-adjusted models compared the association on HCRU and costs for pts achieving ALP normalisation or CBR.
Results: At baseline, 4013 pts had ALP ≥ 1.67 × ULN. Two cohorts of 1015 pts and 935 pts were analysed for post-index ALP normalisation and CBR, respectively. Pts achieving ALP normalisation (173/1015 [17%]) or CBR (600/935 [64%]) were older and more likely to be of White race or non-Hispanic ethnicity. In regression-adjusted sensitivity analyses (n = 941), ALP normalisation was associated with significantly fewer inpatient (IP) admissions (rate ratio [RR], 0.26; 95% CI, 0.11–0.64; $p = .003$) and outpatient (OP) visits (RR, 0.85; 95% CI, 0.73–0.99; $p = .036$). Differences in emergency room (ER) visits and prescription use were not significant. Achieving CBR (n = 865) was associated with significantly fewer IP visits (RR, 0.35; 95% CI, 0.20–0.59; $p < .001$), while OP visits, ER visits, and prescription use showed no significant differences. Each 10% reduction in ALP levels was associated with 21% lower IP, 6% lower OP, and 13% lower ER visit rates (all $p < .001$). Costs were significantly lower both for pts with ALP normalisation (–$8250; $p < .001$) and with CBR (–$5691; $p < .001$).
Conclusion: In pts with PBC receiving UDCA, achieving ALP normalisation or CBR was associated with substantial reductions in HCRU and costs. These findings underscore the importance of monitoring biochemical response and considering timely treatment escalation for non-responders to improve clinical outcomes and reduce the economic burden on pts and the healthcare system.

SAT-304

Sustained alkaline phosphatase normalisation and biochemical response are associated with reduced disease progression and clinical outcomes among adults prescribed ursodeoxycholic acid for primary biliary cholangitis

Robert G. Gish[1,2], Robert Wong[3], Yi Pan[4], Mihail Samnaliev[4], Diane Ito[4], Chong Kim[5]. *[1]Robert G. Gish Consultants, LLC, San Diego, United States; [2]Hepatitis B Foundation, Doylestown, United States; [3]Division of Gastroenterology and Hepatology, Department of Medicine, Stanford University, Stanford, United States; [4]Stratevi, Santa Monica, United States; [5]Gilead Sciences, Inc., Foster City, United States*
Email: chong.kim9@gilead.com

Background and aims: Primary biliary cholangitis (PBC) is a chronic, autoimmune liver disease associated with long-term liver injury,

fibrosis, and clinical outcomes including cirrhosis and liver transplantation. Up to 40% of patients (pts) with PBC have inadequate treatment response to first-line ursodeoxycholic acid (UDCA), and incomplete treatment response (eg, alkaline phosphatase [ALP] > the upper limit of normal [ULN]) is associated with worse outcomes. This study evaluated the association of disease progression with sustained biochemical response in pts with PBC treated with UDCA in real-world settings.

Method: This observational, retrospective study used Komodo Health data to identify adults with PBC from 1/9/2018 to 30/3/2023. Key inclusion criteria were ≥ 1 UDCA prescription, 12 months (M) of continuous pre-index insurance coverage, and baseline (BL) ALP ≥ 1.67 × ULN. Pts were assessed for ALP normalisation (ALP ≤ 1 × ULN) and composite biochemical response ([CBR]; ALP < 1.67 × ULN, ≥15% ALP decrease from BL, and total bilirubin ≤ 1 × ULN) at 12 M (± 6 M) following UDCA initiation; pts who achieved either biochemical response but failed to maintain it through the end of follow-up (up to 30 M) were excluded. Cox Proportional-hazard (PH) regression models assessed clinical outcomes following biochemical response, including a composite endpoint of death or liver transplantation.

Results: At BL, 4013 pts had ALP ≥ 1.67 × ULN; 1015 and 935 pts were evaluated for ALP normalisation and CBR at 12 M (± 6 months), respectively. Pts achieving sustained ALP normalisation (173/1015 [17%]) or CBR (600/935 [64%]) were older and less likely to be of African American race or Hispanic ethnicity and more likely to have Medicare coverage. BL cirrhosis was lower for pts who achieved CBR vs those who did not (17% vs 39%; p < .001). In adjusted Cox PH models, CBR was associated with reduced risk of cirrhosis (hazard ratio [HR], 0.52; 95% CI, 0.33–0.83; p = .006), decompensated cirrhosis (HR, 0.20; 95% CI, 0.06–0.63; p = .006), ascites (HR, 0.12; 95% CI, 0.04–0.36; p < .001) and mortality (HR, 0.28; 95% CI, 0.13–0.57; p < .001).

Conclusion: Pts with PBC treated with UDCA who achieve sustained ALP normalisation or CBR had reduced risk of disease progression and fewer clinical outcomes. Incorporating ALP normalisation and CBR into PBC treatment decisions (eg, escalation to second-line options to enhance biochemical response) may help mitigate complications.

SAT-305

Metabolic syndrome drives small dense low-density lipoproteins in primary biliary cholangitis: a lipoprint-based analysis

Tomáš Koky[1], Sylvia Dražilová[1], Martin Janicko[1], Slavomíra Komárová[1], Beáta Hubková[2], Ivana Tóthová[2], Mária Mareková[2], Peter Jarčuška[1]. *[1]2nd Dept of Internal Medicine, PJ Safarik University, Faculty of Medicine and L Pasteur University Hospital, Košice, Slovakia; [2]Dept of Medical and Clinical Biochemistry, PJ Safarik University, Faculty of Medicine, Košice, Slovakia*
Email: tomaskoky1@gmail.com

Background and aims: Primary biliary cholangitis (PBC) is associated with cholestasis-related dyslipidaemia considered largely non-atherogenic. However, concomitant metabolic syndrome may promote atherogenic lipoprotein alterations not captured by conventional lipid parameters. Small dense LDL (sdLDL) is a key atherogenic LDL subfraction, but its determinants in PBC remain unclear. We investigated associations between metabolic syndrome, liver disease characteristics and Lipoprint-derived sdLDL in PBC.

Method: In this cross-sectional single-centre study, patients with PBC underwent Lipoprint-based LDL subfraction analysis. sdLDL was defined as LDL-3–7. Metabolic syndrome and metabolic dysfunction–associated steatotic liver disease (MASLD) were defined by standard criteria, and liver fibrosis as non-advanced (F0–2) or advanced (F3–4) measured by transient elastography (VCTE). Due to skewed distribution, sdLDL was ln-transformed. Associations were assessed using univariable analyses, multivariable linear regression adjusted for relevant metabolic and clinical confounders and logistic regression for detectable sdLDL.

Results: Among 148 patients with PBC, metabolic syndrome was present in 39%. Ln-transformed sdLDL levels were higher in patients with metabolic syndrome than in those without (−2.87 ± 1.53 vs −3.58 ± 1.19; p = 0.004; Cohen's d = 0.53), while no association was observed with MASLD (p = 0.324) or advanced fibrosis (p = 0.155). In multivariable linear regression, metabolic syndrome remained independently associated with higher ln-transformed sdLDL levels (standardized β = 0.26, p = 0.005), with consistent results after adjustment for statin and fibrate therapy (standardized β = 0.27, p = 0.003) and in sensitivity analyses using waist circumference (p = 0.010). In logistic regression, metabolic syndrome was independently associated with detectable sdLDL. Although sdLDL levels were higher in patients with complete biochemical response (CBR), stratified nonparametric analysis showed that in the CBR+ subgroup ln(sdLDL) was higher in patients with metabolic syndrome (Mann–Whitney U = 544.5, p = 0.012), with a similar trend in the CBR− subgroup indicating no effect modification by biochemical response.

Conclusion: In PBC, small dense LDL is driven by metabolic syndrome rather than MASLD, liver fibrosis, or biochemical response to therapy. Lipoprint-based sdLDL profiling may improve cardiovascular risk stratification in this population.

SAT-306

Demographic and clinical characteristics of United States real-world patients with primary biliary cholangitis and alkaline phosphatase between 1 and 1.67 vs ≥ 1.67 × upper limit of normal despite ursodeoxycholic acid treatment

Rachel H. Mackey[1,2], Steve Gao[1], Charlotte Carroll[1], Fang Xia[1], Nirali Kotowsky[1], Lisa Albert[1], Grace M. Chee[1], Susheela Carroll[1], Daria B. Crittenden[1]. *[1]Gilead Sciences, Inc., Foster City, United States; [2]University of Pittsburgh School of Public Health, Pittsburgh, United States*
Email: nirali.kotowsky@gilead.com

Background and aims: For ursodeoxycholic acid (UDCA)-treated patients (pts) with primary biliary cholangitis (PBC), alkaline phosphatase (ALP) ≥ 1.67 × upper limit of normal (ULN) is a recognised threshold warranting second-line (2L) treatment initiation. However, given increasing evidence that any ALP > ULN increases risk of adverse clinical outcomes, we characterised real-world pts with PBC and ALP between 1 and 1.67 × ULN.

Method: Adult pts with PBC were identified in a United States laboratory-linked claims database (HealthVerity Marketplace) from 1/1/2015 to 5/15/2025 at earliest of 2+ PBC diagnosis (dx) codes or an anti-mitochondrial antibody-positive result with either 1+ PBC dx code or any ALP ≥ 1.5 × ULN. ALP index date was the first ALP > ULN on/after PBC dx date directly preceded by ≥ 6 months of UDCA (and no 2L) treatment. Pts with liver cancer, failure or transplant, decompensated cirrhosis, or lack of 12 months continuous medical enrolment on/before ALP index date were excluded. Pts were categorised based on first ALP between 1 and 1.67 × ULN vs pts at first ALP ≥ 1.67 × ULN. Due to overlap between the two groups, no statistical testing was performed.

Results: Characteristics for pts with ALP between 1 and 1.67 × ULN (n = 796) vs ALP ≥ 1.67 × ULN (n = 341) were: male 10% vs 13%, mean age of 58 vs 55 years, prior UDCA duration of 2.5 vs 2.3 years, proportion with portal hypertension 5% vs 7%, diabetes 23% vs 19%, chronic kidney disease 10% vs 11%, osteoporosis 14% vs 11%, fatigue 22% vs 20%, sleep disorders 11% vs 11%, hypertension 49% vs 40%, hyperlipidaemia 56% vs 49%, statin use 32% vs 26%, obesity 23% vs 16%, depression or anxiety 33% vs 27%, and pruritus 7% vs 13%. In pts with ALP between 1 and 1.67 × ULN vs pts with ALP ≥ 1.67 × ULN, 68% and 89%, respectively, had ≥ 1 characteristic associated with worse outcomes, including compensated cirrhosis (23% vs 30%), albumin < lower limit of normal (7% vs 16%), total bilirubin > 0.6 × ULN (25% vs 44%), increased alanine or aspartate aminotransferases (ALT > ULN [37% vs 67%] or AST > ULN [26% vs 66%]), APRI ≥ 1.5 (2% vs 10%), FIB-

4 ≥ 3.25 (9% vs 13%), advanced PBC (Rotterdam criteria: 2% vs 8%), or GLOBE > 0.3 (24% vs 39%).
Conclusion: UDCA-treated pts with PBC with elevated ALP between 1 and 1.67 × ULN have a substantial burden of comorbidities, symptoms, and abnormal liver biochemical and clinical risk factors for disease progression, similarly seen in pts with ALP ≥ 1.67 × ULN. This supports considering 2L therapy in pts with any ALP elevation.

SAT-307
Factors associated with second-line treatment initiation among real-world, second-line–eligible patients with primary biliary cholangitis in the United States
Nirali Kotowsky[1], Oluwadamilola Onasanya[1], Rongjun Shen[1], Steve Gao[1]. [1]*Gilead Sciences, Inc., Foster City, United States*
Email: nirali.kotowsky@gilead.com

Background and aims: Evidence is limited on the frequency of second-line (2L) treatment initiation among United States (US) adults with primary biliary cholangitis (PBC) who are 2L eligible. Clinical characteristics that drive 2L initiation within these groups in the real world are poorly understood.
Method: This was a retrospective cohort study of adults with PBC in the US HealthVerity Marketplace database, with 2L eligibility based on alkaline phosphatase (ALP) ≥ 1.67 × upper limit of normal (ULN) or ALP > 1 to < 1.67 × ULN after completing 12 months (M) of ursodeoxycholic acid (UDCA) from 1/1/15 to 1/5/25. Eligible patients (pts) had continuous insurance enrolment ≥ 12 M before and ≥ 6 M after ALP test date (index), ≥ 80% UDCA adherence over the first 12 M of treatment, and no 2L treatment at baseline (BL). BL characteristics were assessed at index date. Follow-up continued until disenrollment, outcome (2L initiation), mortality, or end of study period. A Cox model was used to estimate the adjusted hazard ratio (HR) and 95% confidence intervals (95% CIs) of 2L initiation among pts with ALP > 1 to < 1.67 × ULN, relative to pts with ALP ≥ 1.67 × ULN.
Results: Among 1031 pts with PBC identified, 315 (30.6%) and 716 (69.4%) had ALP ≥ 1.67 × ULN, or ALP > 1 to < 1.67 × ULN at index, respectively. Overall, 22.9% of the cohort initiated 2L treatment during follow-up; 37.5% and 16.5% had ALP ≥ 1.67 × ULN, or ALP > 1 to < 1.67 × ULN, respectively. Most (79.2%) 2L initiators added a 2L treatment to UDCA, while the remainder switched from UDCA to 2L. Median time from index date to 2L add-on was shorter for the ALP ≥ 1.67 × ULN vs ALP > 1 to < 1.67 × ULN group (280 vs 865 days, p < .01). Across both groups, those who initiated 2L treatment were more likely to be younger (40–64 years). In the ALP ≥ 1.67 × ULN group, comorbid chronic kidney disease was a negative risk factor for 2L initiation (2.5% vs 8.1%, p < .01). In the ALP > 1 to < 1.67 × ULN group, comorbid hypertension was a negative risk factor for 2L initiation (27.1% vs 39.5%, p < .01); Cox regression showed a 0.3 × lower hazard of 2L initiation with ALP > 1 to < 1.67 × ULN vs ALP ≥ 1.67 × ULN (HR [95% CI] = 0.3 [0.2–0.4]).
Conclusion: Despite available 2L treatments for PBC, about 63% of pts with ALP ≥ 1.67 × ULN and 84% of pts with ALP > 1 but < 1.67 × ULN do not receive 2L. Given emerging evidence that any elevated ALP increases the risk for liver transplant or death, these data raise concerns about undertreatment of PBC among US patients.

SAT-308
Characteristics and treatment patterns of primary biliary cholangitis: real-world insights from a linked claims–electronic medical records database
Nirali Kotowsky[1], Oluwadamilola Onasanya[1], Rongjun Shen[1], Steve Gao[1]. [1]*Gilead Sciences, Inc., Foster City, United States*
Email: nirali.kotowsky@gilead.com

Background and aims: With the approval of 2 new therapies for primary biliary cholangitis (PBC), understanding real-world treatment patterns is increasingly important. This retrospective study aims to characterise patient characteristics by the treatment option initiated after diagnosis among patients (pts) with PBC in the US.
Method: This retrospective cohort study used the US HealthVerity Marketplace database to identify adults (at index) from 1/1/2016 to 30/11/2024. The index date was the first PBC case-defining event: a positive anti-mitochondrial antibody (AMA) test, positive antinuclear antibody test preceded by a negative AMA test, PBC diagnosis code, the first of 2 elevated alkaline phosphatase (ALP) test results ≥ 6 months (M) apart, or first-line (1L) ursodeoxycholic acid (UDCA) or second-line (2L; fibrates, obeticholic acid, elafibranor, or seladelpar) treatment for PBC. Eligible pts with PBC were required to have continuous insurance enrolment for M12 before and M6 after index and were classified into 3 groups at baseline (BL; untreated, UDCA only, and 2L treated) defined by their treatment post-index.
Results: Among 12,230 pts with PBC, 19% untreated, 70% UDCA only, and 11% 2L-treated pts were identified. Mean (SD) age in the untreated, UDCA-only, and 2L-treated groups was 55 (15), 57 (13), and 53 (11) years, respectively, with a greater proportion of pts ≥ 65 years in the untreated (27%) vs the 2L-treated group (12%; p < .01). Medical and mental health comorbidities (hypertension, 52%; diabetes, 24%; major depressive disorder, 27%; anxiety disorder, 33%) were significantly more prevalent in the untreated vs the UDCA-only (37%, 16%, 16%, 20%, respectively) and 2L-treated (32%, 15%, 17%, 21%, respectively) groups (p < .01). There was no significant difference in the proportion of comorbid metabolic dysfunction-associated steatohepatitis, autoimmune hepatitis, or alcoholic liver disease between the 3 groups. About 17% of the 2L-treated vs 14% and 13% of the UDCA-only and untreated groups had BL concomitant use of adjunctive anti-itch medications (p < .01). Of the 2L-treated group, ~ 18% had a BL ALP ≥ 1.67 × upper limit of normal (ULN) vs 9% and 7% of the UDCA-only and untreated groups.
Conclusion: Pts untreated for PBC had similar rates of comorbid liver conditions but more cardiovascular and mental health conditions than treated pts with PBC. Despite BL ALP ≥ 1.67 × ULN, ~ 1 in 10 pts with PBC were not receiving PBC treatment nor escalating to 2L treatment.

SAT-313
Topographical phenotyping of pruritus in chronic liver diseases using standardized body mapping
Miriam M. Düll[1,2], Vanessa Karlen[1,2], Jonas Schmid[1,2], Peter Dietrich[1,2,3], Markus F. Neurath[1,2], Sonja Ständer[4], Martin Schmelz[5], Martin Metz[6,7], Tomasz Hawro[8], Andreas E. Kremer[1,2,9]. [1]*Department of Medicine 1, University Hospital and Friedrich-Alexander-University Erlangen-Nürnberg, Erlangen, Germany;* [2]*Deutsches Zentrum Immuntherapie DZI, Erlangen, Erlangen, Germany;* [3]*Institute of Biochemistry, Emil-Fischer-Zentrum, Friedrich-Alexander-University Erlangen-Nürnberg, Erlangen, Germany;* [4]*Department of Dermatology and Center for Chronic Pruritus, University Hospital Münster, Münster, Germany;* [5]*Department of Experimental Pain Research Mannheim, University of Heidelberg, Mannheim, Germany;* [6]*Institute of Allergology, Charité - Universitätsmedizin Berlin, Corporate Member of Freie Universität Berlin and Humboldt-Universität zu Berlin, Berlin, Germany;* [7]*Fraunhofer Institute for Translational Medicine and Pharmacology ITMP, Immunology and Allergology, Berlin, Germany;* [8]*Department of Dermatology, Allergy and Venereology, Center of Excellence for Inflammatory Medicine, University Medical Center Schleswig-Holstein, Lübeck, Germany;* [9]*Department of Gastroenterology and Hepatology, University Hospital Zürich, University of Zürich, Zürich, Switzerland*
Email: miriam.duell@uk-erlangen.de

Background and aims: Pruritus is a frequent and burdensome symptom in chronic liver diseases, significantly impairing quality of life; however, its anatomical distribution across etiologies remains poorly characterized. Standardized body mapping provides a patient-friendly, language-independent approach to systematically capture itch patterns and may help identify disease- or patient-specific phenotypes. We aimed to characterize the anatomical distribution of

pruritus in patients with chronic liver diseases and explore differences across etiological subgroups.
Method: In a cross-sectional study at a tertiary hepatology center, pruritic patients completed front- and back-view body maps indicating current and habitual itch sites. Demographic, clinical, and etiological data were collected. Patients were categorized into immune-mediated and cholestatic liver diseases (ICLD), steatotic liver diseases including MASLD, MetALD, ALD (SLD), and viral liver diseases (VLD). Itch intensity and impact were assessed using mean and worst itch NRS and the 5-D Itch scale. Body maps were digitized and analyzed using automated, observer-independent quantitative image analysis.
Results: Among 656 participants, 173 (26.4%) reported pruritus; complete body maps were available for 150 patients (67.7% female). ICLD represented the largest subgroup (n = 71; 40.7%). Mean itch was 3.8 ± 2.7, worst itch 4.4 ± 2.9, and median 5-D Itch score 11 (IQR 8.5–15). Pruritus predominantly affected the extremities, particularly volar forearms and anterior lower legs, followed by the back. In contrast to previous literature, involvement of the palms and soles was rare. Current and habitual itch patterns were highly concordant. Patients with cirrhosis reported less frequent upper-body involvement than non-cirrhotic patients. Female patients reported itch across more regions than males. No disease-specific exclusive patterns were identified, but extremity-dominant distribution was consistent across all subgroups.
Conclusion: Standardized body mapping reveals a reproducible, extremity-predominant pattern of pruritus in chronic liver diseases, largely independent of etiology. ICLD patients demonstrated the most extensive distribution. These findings support shared pathophysiological mechanisms in hepatobiliary pruritus and underscore body mapping as a robust, complementary approach for itch phenotyping, offering spatial insights beyond conventional intensity-based assessments and potentially greater ease of use for patients.

SAT-314
Genetic predisposition increases the gallstone risk in patients with PSC: single center, prospective analysis

Beata Kruk[1,2], Susanne Weber[3], Frank Lammert[4], Piotr Milkiewicz[5], Marcin Krawczyk[6]. *[1]Laboratory of Metabolic Liver Diseases, Department of General, Transplant and Liver Surgery, Centre for Preclinical Research, Medical University of Warsaw, Warsaw, Poland; [2]Laboratory of Metabolic Liver Diseases, Department of General, Transplant and Liver Surgery, Medical University of Warsaw, Warsaw, Poland; [3]Department of Medicine II, University Hospital Saarland, Homburg, Germany; [4]Center for Health Research Economics Hannover (CHERH), Hannover Medical School (MHH), Hannover, Germany; [5]Liver and Internal Medicine Unit, Department of General, Transplant and Liver Surgery, Medical University of Warsaw, Division of Gastroenterology, Department of Translational Medicine, Pomeranian Medical University in Szczecin, Warsaw, Poland; [6]Department of Gastroenterology, Hepatology and Transplant Medicine, Medical Faculty, University of Duisburg-Essen, Essen, Germany*
Email: beata.kruk@wum.edu.pl

Background and aims: Gallstone disease (GD) is common in primary sclerosing cholangitis (PSC), affecting up to 25% of patients (*Said et al. J Hepatol 2008*). Its development is linked to disturbances in bile acid homeostasis, chronic cholestasis, and impaired gallbladder motility, all frequent in PSC (*Cazzagon et al. J Hep. Rep. 2022*). Here, we investigate the prevalence of GD in a large PSC cohort and assess both clinical and genetic risk factors, including the common polymorphism in the hepatobiliary sterol transporter ABCG8.
Method: A total of 663 adults with PSC (218 women, age 18–74 years, BMI 15.6–39.5 kg/m^2) were prospectively recruited. Data on GD, cholecystectomy and gallbladder cancer were extracted from clinical records, abdominal sonography, and/or MRI. The *ABCG8* p.D19H (rs11887534) polymorphism was genotyped using TaqMan assays.
Results: Among 663 patients, a total of 93 (14%) had history of GD: sixty-six had gallstones and gallbladder *in situ*, whereas 27 had been cholecystectomised before inclusion. Six patients had diagnosis of gallbladder cancer (three before inclusion and three during follow-up). The minor allele frequency *ABCG8* p.D19H was higher in those with GD than in those without (8.6% vs. 4.5%). The variant was associated an approximately twofold increased risk of GD (OR = 2.06; 95% CI, 1.13–3.75; P = 0.018). Among non-genetic risk factors, GD was associated with age (P < 0.001), but not with BMI, sex, or ulcerative colitis (all P > 0.05). In multivariate analysis, both the *ABCG8* p.D19H polymorphism (P = 0.015) and age (P < 0.001) remained independently associated with GD. One of six patients with gallbladder cancer was heterozygous for the transporter variant.
Conclusion: GD-PSC is a multifactorial condition, more common in older patients and those with genetic predisposition. These results further underscore the use of ursodexycholic acid in PSC to mitigate the risk of developing gallstones and their complications in predisposed patients.

SAT-315
Blood extracellular vesicle proteins predict ursodeoxycholic acid response in primary biliary cholangitis

Ainhoa Lapitz[1,2,3], Elisa Catanzaro[1,4,5], Pedro Rodrigues[1,2,6], Stella Gabeta[7], Clara Mancuso[8,9], Nikolaos Gatselis[7], Vasiliki Lygoura[7], Laura Cristoferi[10], Miki Scaravaglio[9,11], Laura Izquierdo-Sánchez[1,2], Maria Jesus Perugorria[1,2,3], Pietro Invernizzi[9,10], Luis Bujanda[1,2,3], George Dalekos[7], Marco Carbone[8,9], Jesus M Banales[1,2,6,12].
[1]Biogipuzkoa Health Research Institute, Donostia-San Sebastian, Spain; [2]National Institute for the Study of Liver and Gastrointestinal Diseases (CIBERehd, "Instituto de Salud Carlos III"), Madrid, Spain; [3]University of the Basque Country (EHU), Leioa, Spain; [4]University of Padova, Padova, Italy; [5]Azienda Ospedale-Università Padova, Padova, Italy; [6]Ikerbasque, Basque Foundation for Science, Bilbao, Spain; [7]General University Hospital of Larissa, Larissa, Greece; [8]ASST Grande Ospedale Metropolitano Niguarda, Milan, Italy; [9]University of Milano-Bicocca, Monza, Italy; [10]Center for Autoimmune Liver Diseases, Fondazione IRCCS San Gerardo dei Tintori, Monza, Italy; [11]Cambridge Stem Cell Institute, Cambridge, United Kingdom; [12]University of Navarra, Pamplona, Spain
Email: ainhoa.lapitz@biodonostia.org

Background and aims: Ursodeoxycholic acid (UDCA) is the standard first-line therapy for primary biliary cholangitis (PBC), improving liver biochemistry and long-term outcomes. However, approximately one-third of patients exhibit incomplete response and require alternative therapies. While clinical criteria may aid to assess response after treatment initiation, reliable pre-treatment biomarkers to predict UDCA efficacy are lacking. This proof-of-concept study aimed to explore baseline proteomic differences in serum extracellular vesicles (EVs) between UDCA non-responders and responders to non-invasively predict treatment response.
Method: 24 serum samples from patients with PBC with elevated alkaline phosphatase (ALP > 1.5× upper limit of normal, ULN) prior to UDCA initiation were included. Treatment response after one year was defined as ALP < 1.5 × ULN, classifying patients as responders (n = 9) or non-responders (n = 15). Serum EVs were isolated by differential ultracentrifugation and analyzed using mass spectrometry–based proteomics. Associations between EV protein abundance and UDCA response were assessed, and candidate biomarkers were integrated into a predictive model using Elastic Net-penalized logistic regression.
Results: Pre-treatment clinical characteristics revealed that non-responders were younger compared to responders, with no significant differences in cirrhosis or biochemical parameters. Proteomic analysis of serum EVs identified 23 proteins with altered abundance in non-responders at baseline. These proteins were functionally related to polyclonal B-cell activation, immune trafficking, and early fibrotic remodeling, reflecting a pre-existing more aggressive immune-driven and fibrogenic disease phenotype in non-responder patients that is not primarily bile acid–dependent. A machine learning six-protein predictive model (HV333, KV230, IGE, LV214,

KVD13 and KV228) distinguished responders from non-responders with an AUC of 0.985 (95% CI 0.947–1.000, p < 0.001), 93.3% sensitivity, and 100% specificity. Patients exhibiting this signature were approximately 184-fold more likely to be non-responders to UDCA.
Conclusion: Serum EV proteins are promising pre-treatment biomarkers to predict UDCA response in PBC. After further validation in larger cohorts, they may enable a personalized medicine approach, identifying patients at high risk of non-response at baseline and guiding tailored treatment strategies, including early consideration of second-line therapies.

SAT-316

Efficacy and safety of seladelpar in patients with primary biliary cholangitis and alkaline phosphatase levels between 1 and 1.67 × upper limit of normal: interim results from the open-label ASSURE study

Cynthia Levy[1,2], Jeong Heo[3], Michael Galambos[4], Xin Qi[5], Justin Smith[5], Susheela Carroll[5], Kyung Min Kwon[5], Sarah Proehl[5], John M. Vierling[6]. *[1]Division of Digestive Health and Liver Diseases, Miller School of Medicine, University of Miami, Miami, United States; [2]Schiff Center for Liver Disease, Miller School of Medicine, University of Miami, Miami, United States; [3]Department of Internal Medicine, Pusan National University and Biomedical Research Institute, Busan, Korea, Rep. of South; [4]Digestive Healthcare of Georgia, Atlanta, United States; [5]Gilead Sciences, Inc., Foster City, United States; [6]Baylor College of Medicine, Houston, United States*
Email: vierling@bcm.edu

Background and aims: Seladelpar (SEL) is a first-in-class delpar (selective PPAR-delta agonist) indicated for the treatment of primary biliary cholangitis (PBC) in combination with ursodeoxycholic acid (UDCA) in patients (pts) with an inadequate response to UDCA or as monotherapy in pts unable to tolerate UDCA. The pivotal RESPONSE (NCT04620733) study evaluated SEL in pts with alkaline phosphatase (ALP) ≥ 1.67 × the upper limit of normal (ULN). Here, we report data from an interim analysis of pts with lower baseline (BL) ALP levels between 1 and 1.67 × ULN in the ongoing Phase 3 ASSURE study (NCT03301506).
Method: Pts from RESPONSE and legacy SEL studies enroled in ASSURE and received open-label SEL 10 mg once daily. Data for this post hoc analysis included pts from legacy studies with ALP levels between 1 and 1.67 × ULN at BL in ASSURE. BL was defined as SEL initiation in ASSURE. Endpoints for this analysis included composite ALP normalisation response (ALP ≤ 1 × ULN and ≥ 15% ALP reduction) and change from BL in laboratory parameters through month (M) 24. Safety was also assessed. Data cutoff: 31 Jan 2025.
Results: A total of 50 pts from legacy SEL studies enroled in ASSURE with ALP levels between 1 and 1.67 × ULN, and 47 reached M24 of treatment as of the data cutoff. At BL, 24% had cirrhosis, and 44% were aged < 50 years at PBC diagnosis. BL means were ALP 156 U/L, gamma-glutamyl transferase (GGT) 117 U/L, total bilirubin (TB) 0.64 mg/dL, and alanine aminotransferase (ALT) 28 U/L. Composite ALP normalisation was achieved by 83% (40/48) and 74% (35/47) of pts at M12 and M24. SEL treatment reduced mean ALP by −40% at 12 M and −35% at M24. GGT and ALT also declined (mean change, respectively: −40% and −23% at M12; −39% and −24% at M24), while TB remained stable overall. No pts had adverse events (AEs) leading to treatment discontinuation; 2 pts (4%) had serious AEs, which were unrelated to treatment.
Conclusion: In pts with PBC enroled in ASSURE with ALP levels between 1 and 1.67 × ULN, treatment with seladelpar up to 24 M led to sustained reductions in markers of cholestasis and high rates of ALP normalisation, which is increasingly recognised as an optimal treatment goal for PBC. SEL appeared overall safe and well tolerated in this population.

SAT-317

A novel machine learning-based diagnostic tool for distinguishing between primary sclerosing cholangitis and IgG4-related cholangitis: an international asian study in China and Japan

Chenyi Jiang[1], Min Lian[2], Atsushi Tanaka[3], Xiong Ma[1]. *[1]Division of gastroenterology and hepatology, Renji Hospital, School of Medicine, Shanghai Jiao Tong University, Institute of aging & tissue regeneration, Renji Hospital, Shanghai Jiao Tong University School of Medicine, Shanghai, China; [2]Division of gastroenterology and hepatology, Renji Hospital, School of Medicine, Shanghai Jiao Tong University, Shanghai, China; [3]Teikyo University School of Medicine, Tokyo, Japan*
Email: ceciliacy2021@126.com

Background and aims: Primary sclerosing cholangitis (PSC) and IgG4-related cholangitis (IRC) are two distinct autoimmune cholangitis that share similar biochemical and imaging features. Distinguishing between them remains a significant clinical challenge. We aimed to develop and validate a machine learning-based diagnostic tool to improve the diagnostic accuracy for PSC and IRC in Asian populations.
Method: This international study includes data from China and Japan. The Chinese data were derived from a multicenter observational cohort study of PSC and IRC (NCT05463445), which enrolled adult patients with imaging-evidence of sclerosing cholangitis from 13 hospitals. Patients with secondary sclerosing cholangitis were excluded. Data from the leading center (n = 382) were used for model development. A separate prospective cohort from the same center (n = 94) was used for temporal validation, and data from the other 12 hospitals (n = 337) were used for external validation. The Japanese data were obtained from nationwide epidemiological studies, comprising 881 patients (524 IRC, 357 PSC) with complete diagnostic data for external validation. The eXtreme Gradient Boosting (XGB) algorithm was used to construct the final model based on four routinely available clinical variables: serum IgG4, age at diagnosis, ALT, and ALP. Model performance was evaluated by the area under the receiver operating characteristic curve (AUROC), sensitivity, specificity, and decision curve analysis.
Results: A total of 1694 patients (813 Chinese, 881 Japanese) were included. The XGB model achieved an AUROC of 0.98 (95% CI 0.96–0.99) in the Chinese development cohort, 0.98 (95% CI 0.95–1.00) in the Chinese temporal validation cohort, 0.96 (95% CI 0.94–0.98) in the Chinese external validation cohort, and 0.91 (95% CI 0.89–0.93) in the Japanese nationwide validation cohort. The model showed good sensitivity (0.78–0.94) and high specificity (0.91–0.97) across all validation cohorts. Decision curve analysis demonstrated a consistent net benefit across a wide range of threshold probabilities in all cohorts, supporting the model's clinical utility.
Conclusion: We developed and validated a simple, four-variable XGB-based diagnostic tool that accurately distinguishes IRC from PSC in Asian populations. The tool will be made publicly available as a web-based calculator, which can assist clinicians in making accurate diagnoses and guide appropriate management decisions.

SAT-318

18F FAPI PET/CT as a non-invasive assessment in autoimmune liver diseases: a prospective pilot study

Zhuwan Lyu[1], Shuxian An[1], Tianyu Mao[1], Xiting Pu[1], Bo Li[1], Jun Zhang[1], Jianjun Liu[1], Xiong Ma[1], Min Lian[1]. *[1]Shanghai Jiaotong University School of Medicine Affiliated Renji Hospital, Shanghai, China*
Email: sophialian24@163.com

Background and aims: Autoimmune liver diseases (AILD), characterized by chronic inflammation and progressive fibrosis, still rely on the invasive liver biopsy as diagnostic method in practice. Our study aims to evaluate the feasibility of fibroblast activation protein inhibitor positron emission tomography/computed tomography (FAPI PET/CT) in quantifying inflammation and fibrosis in AILD patients as a non-invasive method for assessing disease activity.

Method: This prospective pilot study enrolled 15 AILD patients and 3 metabolic dysfunction-associated steatotic liver disease (MASLD) patients. All participants underwent FAPI PET/CT imaging. Hepatic FAPI uptake was quantified using maximum standardized uptake value (SUVmax) and liver-to-background uptake ratio (LBR). All the liver sections were assessed using the Scheuer scoring system. FIB-4 and APRI score were calculated for comparing the predictive accuracy with SUVmax or LBR. Immunohistochemistry and multiplex immunofluorescence characterized FAP expression patterns and spatial relationships with immune cells.
Results: We found that FAPI expression was significantly upregulated in AILD patients compared to that in control groups. The FAPI uptake showed strong correlations with fibrosis stage and inflammatory grade. Clinically, FAPI uptake is related to liver stiffness as well as several serological markers (including platelet number and international normalized ratio) but not autoantibodies (such as antinuclear antibody). FAPI PET/CT demonstrated superior diagnostic performance for detecting significant fibrosis ($S \geq 2$) with an AUROC of 0.992, outperforming transient elastography, FIB-4, and APRI. Histological analysis revealed disease-specific spatial patterns that fibroblast activation protein expression was accumulated in periportal/lobular regions in autoimmune hepatitis (AIH) while in peribiliary areas in primary biliary cholangitis (PBC). Spatial analysis showed closer proximity between FAP+ fibroblasts and T cells or macrophages in AIH compared to PBC.
Conclusion: Our study reveals that FAPI PET/CT directly visualizes active fibroblasts in AILD, demonstrating superior diagnostic performance compared to established tools, suggesting its potential for early intervention and non-invasive monitoring in AILD.

SAT-319

Point-of-care liver stiffness measurement predicts liver-related events in autoimmune hepatitis: results from a large nationwide multicenter longitudinal CaNAL study

Ellina Lytvyak[1,2], Gideon M. Hirschfield[3], Yu Jun Wong[1], Shagani Thisairajah[1], Hin Hin Ko[4], Julian Hercun[5], Mina Niazi[6], Catherine Vincent[5], Karim Qumosani[7], Tianyan Chen[8], Angela Cheung[9], Jennifer Flemming[10], Kristel Leung[10], Jean-Philippe Wallach[11], Nabiha Faisal[12], Devika Shreekumar[1], Narmeen Umar[1], Aliya Gulamhusein[3], Andrew L. Mason[1], Mark Swain[13], Bettina E. Hansen[3], Aldo J Montano-Loza[1]. *[1]Division of Gastroenterology and Liver Unit, University of Alberta, Edmonton, Canada; [2]Division of Preventive Medicine, University of Alberta, Edmonton, Canada; [3]The Autoimmune and Rare Liver Disease Programme, Division of Gastroenterology and Hepatology, Toronto General Hospital, Toronto, Canada; [4]Division of Gastroenterology, University of British Columbia, Vancouver, Canada; [5]Liver Unit, Department of Medicine, Centre Hospitalier De l'Université De Montréal, Montreal, Canada; [6]Division of Gastroenterology and Hepatology, College of Medicine, University of Saskatchewan, Royal University Hospital, Saskatoon, Canada; [7]Department of Medicine, Western University, London, Canada; [8]Department of Medicine, McGill University Health Centre, Montreal, Canada; [9]Department of Medicine, University of Ottawa, Ottawa, Canada; [10]Departments of Medicine & Public Health Sciences, Queen's University, Kingston, Canada; [11]Nanaimo Regional Hospital, Nanaimo, Canada; [12]Department of Internal Medicine, Section of Hepatology, University of Manitoba, Winnipeg, Canada; [13]Liver Unit, Division of Gastroenterology and Hepatology, University of Calgary, Calgary, Canada*
Email: montanol@ualberta.ca

Background and aims: Liver stiffness measurement (LSM) represents a valuable noninvasive tool for the prediction of outcomes in patients with chronic liver disease; however, evidence in autoimmune hepatitis is still scarce. Our study aimed to explore the prognostic potential of LSM in predicting clinical outcomes in autoimmune hepatitis (AIH), accounting for demographic, clinical, and lifestyle factors.
Method: From the nationwide Canadian Network for Autoimmune Liver Diseases registry, we analyzed data of 1148 AIH patients with ≥ 1 reliable LSM at/after diagnosis but before occurrence of any events. We performed landmark analysis using the first LSM and follow-up until the outcome. The primary composite outcome was time to the first onset of liver-related events (LRE), defined as hepatic decompensation, liver transplantation, hepatocellular carcinoma (HCC), or death. LSM cut-offs were established using the highest Youden's index. Complete biochemical response (CBR) was defined as normalization of both ALT and IgG. Predictive performance of models was evaluated using Harrell's C-index, with comparison conducted via a non-parametric bootstrap approach with 1000 replicates.
Results: The majority were females (74.3%) and Caucasians (72.4%). Median age was 59.7 (IQR 42.6–70.9) years, time from diagnosis to first LSM 2.9 years (range 0–43.7), LSM value 8.1 kPa (IQR 5.5–14.2) and CBR at 6 months was present in 58.4%. LSM was associated with reaching the composite endpoint (HR 1.03 [1.01–1.05], $p = 0.007$), after adjusting for cirrhosis at diagnosis (HR 7.01 [2.78–17.66], $p < 0.001$), type 2 diabetes (HR 2.75 [1.19–6.31], $p = 0.017$), age at diagnosis, and lack of CBR at 6-month and at the time of LSM. Addition of LSM increased Harrell's C-index by 0.02 [0.001–0.06] to 0.88 (SE 0.06). Patients with LSM ≥ 11.0 kPa (best cutoff) had 3 times higher risk of reaching composite endpoint [HR 3.23 [1.03–10.1], $p = 0.045$], adjusted for cirrhosis at diagnosis (HR 6.89 [2.78–17.08], $p < 0.001$), type 2 diabetes (HR 2.63 [1.15–6.05], $p = 0.023$), age at diagnosis, and lack of CBR at 6-month and at the time of LSM.
Conclusion: LSM improves the prediction of clinical outcomes in AIH beyond treatment response and other factors. LSM ≥ 11.0 kPa carries a 3-fold higher risk of development of decompensation, HCC, LT, or liver-related death. The incorporation of LSM into routine assessment has the potential to improve risk stratification and to guide individualized treatment and surveillance strategies in AIH.

SAT-320

Impact of metabolic dysfunction-associated steatotic liver disease on treatment response, clinical outcomes and prognosis in primary biliary cholangitis: findings from a large multicenter longitudinal GLOBAL PBC registry

Ellina Lytvyak[1,2], Yu Jun Wong[1,3,4], Bettina E. Hansen[5,6], Laurent Lam[7], Pierre-Antoine Soret[8], Sara Lemoinne[8], Gideon M. Hirschfield[5], Aliya Gulamhusein[5], Albert Pares[9], Ignasi Olivas[9], María Carlota Londoño[9], Sergio Rodriguez-Tajes[9], John Eaton[10], Karim T Osman[10], Christoph Schramm[11,12], Marcial Sebode[11], Ansgar Lohse[11], George Dalekos[13], Nikolaos Gatselis[13], Frederik Nevens[14], Nora Cazzagon[15], Alessandra Zago[16], Francesco Paolo Russo[15], Annarosa Floreani[15,17], Nadir Abbas[18,19], Palak Trivedi[18,19], Douglas Thorburn[20], Francesca Saffioti[20,21], Jade King[20], Davide Roccarina[20], Vincenza Calvaruso[22], Luigi Capodicasa[22], Adele Delamarre[23], Natalia Sobenko[24], Alejandra Villamil[24], Shagani Thisairajah[1], Devika Shreekumar[1], Esli Medina-Morales[25], Alan Bonder[25], Vilas Patwardhan[25], Cristina Rigamonti[26], Marco Carbone[27,28], Pietro Invernizzi[27,29], Laura Cristoferi[29], Adriaan J. van der Meer[30], Rozanne C. de Veer[30], Ehud Zigmond[31], Eyal Yehezkel[31], Andreas E. Kremer[32], Ansgar Deibel[32], Tony Bruns[33], Karsten Große[33], Aaron Wetten[34], Jessica Dyson[34,35], David E. Jones[34], Cynthia Levy[36], Atsushi Tanaka[37], Jérôme Dumortier[38], Georges-Philippe Pageaux[39], Armando Curto[40], Erica Nicola Lynch[40], Andrea Galli[40], Victor De Ledinghen[23], Fabrice Carrat[7], Olivier Chazouillères[8], Aldo J Montano-Loza[1], Christophe Corpechot[8]. *[1]Division of Gastroenterology and Liver Unit, University of Alberta, Edmonton, Canada; [2]Division of Preventive Medicine, University of Alberta, Edmonton, Canada; [3]Duke-NUS Medical School, Singapore, Singapore; [4]Department of Gastroenterology & Hepatology, Changi General Hospital, Simei, Singapore; [5]The Autoimmune and Rare Liver Disease Programme, Division of Gastroenterology and Hepatology, Toronto General Hospital, Toronto, Canada; [6]Department of Epidemiology & Biostatistics, Erasmus MC,*

Rotterdam, Netherlands; [7]Pierre Louis Institute of Epidemiology and Public Health, Sorbonne University, Inserm, France; [8]APHP, Saint-Antoine Hospital, Department of Hepatology, Reference Center for Inflammatory Biliary Diseases and Autoimmune Hepatitis, CRMR MIVB-H, European Reference Network on Hepatological Diseases, ERN Rare-Liver, F-75012 Paris, France; Sorbonne Université, Inserm, Centre de Recherche Saint-Antoine, CRSA, F-75012 Paris, France; Fédération Hospitalo-Universitaire Gut, Liver & Microbiome Research, FHU GLIMMER, Paris, France; [9]Liver Unit, Hospital Clínic, Fundació de Recerca Clínic Barcelona–Institut d'Investigacions Biomèdiques August Pi i Sunyer (FRCB-IDIBAPS), University of Barcelona, Centro de Investigación Biomédica en Red de Enfermedades Hepáticas y Digestivas (CIBEREHD), European Reference Network on Hepatological Diseases (ERN Rare-Liver), Barcelona, Spain; [10]Division of Gastroenterology and Hepatology, Mayo Clinic, Rochester, United States; [11]Department of Medicine I, European Reference Network on Hepatological Diseases (ERN Rare-Liver), University Medical Center Hamburg–Eppendorf, Hamburg, Germany; [12]Martin Zeitz Center for Rare Diseases, University Medical Center Hamburg-Eppendorf, Hamburg, Germany; [13]Department of Medicine and Research Laboratory of Internal Medicine, National Expertise Center of Greece in Autoimmune Liver Diseases, European Reference Network on Hepatological Diseases (ERN Rare-Liver), General University Hospital, Larissa, Greece; [14]Division of Hepatology and Liver Transplantation, European Reference Network on Hepatological Diseases (ERN Rare-Liver), University Hospitals KU, Leuven, Belgium; [15]Department of Surgery, Oncology and Gastroenterology, European Reference Network on Hepatological Diseases (ERN Rare-Liver), University of Padova, Padova, Italy; [16]Public Health and Cancer Prevention Service, Henri Becquerel Comprehensive Cancer Centre, Rouen, France; [17]IRCCS Sacro Cuore Don Calabria Hospital, Negrar Di Valpolicella, Verona, Italy; [18]Liver Unit, University Hospitals Birmingham National Health Service Foundation Trust Queen Elizabeth, Birmingham, United Kingdom; [19]National Institute for Health and Care Research (NIHR) Birmingham Biomedical Research Centre (BRC), Institute of Immunology and Immunotherapy, Centre for Liver and Gastrointestinal Research, University of Birmingham, Birmingham, United Kingdom; [20]University College London Institute for Liver and Digestive Health, Royal Free Hospital, London, United Kingdom; [21]Oxford Liver Unit, Department of Gastroenterology and Hepatology, Oxford University Hospitals NHS Foundation Trust, Oxford, United Kingdom; [22]Section of Gastroenterology and Hepatology, PROMISE, University of Palermo, Palermo, Italy; [23]Department of Hepatology, University Hospitals of Bordeaux, Pessac, France; [24]Autoimmune Liver Diseases Unit, Hospital Italiano de Buenos Aires, Buenos Aires, Argentina; [25]Department of Medicine, Division of Gastroenterology, Beth Israel Deaconess Medical Center, Boston, United States; [26]Department of Translational Medicine, Università del Piemonte Orientale, Novara, Italy; [27]Department of Medicine and Surgery, University of Milano-Bicocca, Monza, Italy; [28]Liver Unit, ASST Grande Ospedale Metropolitano Niguarda, Milano, Italy; [29]Division of Gastroenterology, Center for Autoimmune Liver Diseases, European Reference Network on Hepatological Diseases (ERN RARE-LIVER), IRCCS Fondazione San Gerardo dei Tintori, Monza, Italy; [30]Department of Gastroenterology and Hepatology, Erasmus University Medical Center, Rotterdam, Netherlands; [31]The Research Center for Digestive Tract and Liver Diseases, Tel Aviv Sourasky Medical Center, Tel Aviv, Israel; [32]Department of Gastroenterology and Hepatology, University Hospital Zürich, University of Zürich, Zürich, Switzerland; [33]Department of Medicine III, University Hospital RWTH Aachen, European Reference Network on Hepatological Diseases (ERN Rare-Liver), Aachen, Germany; [34]Department of Hepatology and Liver Transplantation, Newcastle upon Tyne Hospitals NHS Foundation Trust and Newcastle University, Newcastle upon Tyne, United Kingdom; [35]Translational and Clinical Research Institute, Newcastle NIHR Biomedical Research Centre, Newcastle upon Tyne, United Kingdom; [36]Division of Digestive Health and Liver Diseases, Schiff Center for Liver Diseases, University of Miami, Miami, United States; [37]Department of Medicine, Teikyo University, Tokyo, Japan; [38]Department of Gastroenterology and Hepatology, Edouard Herriot Hospital, Hospices Civils de Lyon, Claude Bernard University, Lyon, France; [39]Department of Hepatology and Liver Transplantation, University Hospital, Montpellier, France; [40]Department of Experimental and Clinical Biomedical Sciences "Mario Serio"; Azienda Ospedaliero-Universitaria Careggi; University of Florence, Florence, Italy
Email: montanol@ualberta.ca

Background and aims: Metabolic dysfunction-associated steatotic liver disease (MASLD) is increasingly common, but data on its concomitance with primary biliary cholangitis (PBC) are limited. We aimed to evaluate the impact of MASLD on treatment response, clinical outcomes, and their prediction in people with PBC.
Method: We analyzed 1209 PBC patients across 21 centers in North America, Europe, and Asia, who had ≥ 1 reliable controlled attenuation parameter (CAP) by vibration-controlled transient elastography (VCTE), measured before occurrence of any events, and ≥ 6 months of follow-up. MASLD was defined as CAP ≥ 270 dB/m or histologically confirmed steatosis, plus ≥ 1 cardiometabolic risk factor and no history of heavy alcohol use. Treatment response was measured by conventional criteria. Clinical outcomes included liver decompensation, hepatocellular carcinoma, liver transplantation (LT), or death.
Results: 90.7% were females, with mean age 62.9 ± 11.7 years, and MASLD was diagnosed in 26.6%. Proportion of females (29.1% vs. 26.4%), age at diagnosis (53.3 ± 11.9 vs. 52.4 ± 12.2 y.o.), and time from VCTE to follow-up (2.6 ± 1.6 vs. 2.7 ± 1.7) did not differ between PBC-MASLD and PBC. Liver stiffness measurement (LSM) was higher among PBC-MASLD (10.9 ± 11.3 vs. 9.1 ± 8.3 kPa; p = 0.014), as well as prevalence of diabetes (52.5% vs. 23.9%; p < 0.001) and obesity (54.5% vs. 19.8%; p < 0.001). Treatment response achievement was more frequent in PBC-MASLD, as per Paris-2 (30.7% vs. 20.7%, p = 0.007), Toronto criteria (31.4% vs. 19.7%, p = 0.002), ALP normalization (34.8% vs. 22.2%, p = 0.001), and deep biochemical response (38.7% vs. 21.9%, p < 0.001), with a similar trend for GLOBE score (28.5% vs. 20.0%, p = 0.075). MASLD was not associated with poorer outcomes overall (HR 0.68, p = 0.192) or in the high-risk group (LSM ≥ 15.0 kPa, HR 0.89, p = 0.747). Adjustment for MASLD did not alter the predictive value of LSM, GLOBE, UK-PBC, APRI, or FIB-4 (HR 1.05, p < 0.001; HR 3.15, p < 0.001; HR 2.27, p < 0.001; HR 1.68, p < 0.001; and HR 1.38, p < 0.001), respectively. Probability of LT and liver-related death was similar between PBC-MASLD and PBC (5-year: 2.5 ± 4.7% vs. 3.1 ± 5.6%, p = 0.280; 10-year: 7.4 ± 11.7% vs. 9.1 ± 12.7%, p = 0.213; 15-year: 12.3 ± 16.3% vs. 14.8 ± 17.4%, p = 0.150).
Conclusion: In people with PBC, MASLD is associated with higher treatment response rates and does not negatively affect clinical outcomes or the predictive value of LSM and established prognostic scores.

SAT-321

Development and temporal validation of a perioperative prediction model for secondary sclerosing cholangitis in critically ill cardiac surgery patients

Samy Mady[1], Michael Schoerghuber[1], Lukas Gulden[1], Theresa Lind[1], Florian Rainer[1], Matthias Egger[1], Michael Kolland[1], Peter Fickert[1], Vanessa Stadlbauer[1,2], Nikolaus Schreiber[1]. *[1]Medizinische Universität Graz, Graz, Austria; [2]Center of Biomarker Research CBmed GmbH, Graz, Austria*
Email: vanessa.stadlbauer@medunigraz.at

Background and aims: Secondary sclerosing cholangitis in critically ill patients (SSC-CIP) is a rare but devastating complication after cardiac surgery with very high mortality. The aim was to develop and validate a parsimonious perioperative laboratory-based prediction model to enable early risk stratification of SSC-CIP.
Method: A retrospective observational study included adult patients undergoing cardiac surgery between 2020 and 2024. Case status was

assigned by independent chart review of two clinical experts, classifying patients as definitive SSC-CIP (endoscopic retrograde cholangiography or magnetic resonance cholangiography) or very likely SSC-CIP (prolonged intensive care stay with invasive ventilation, prolonged inotropic support or extracorporeal membrane oxygenation and a typical rise in gamma-glutamyl transferase and alkaline phosphatase after exclusion of other causes). Standard laboratory parameters obtained at postoperative ICU admission were evaluated as candidate predictors. Patients operated between 2020–2022 formed the development cohort, and those operated between 2023–2024 formed an independent validation cohort. Predictor selection and model tuning were conducted in the development cohort using stability selection with L1-penalized logistic regression on bootstrap samples, followed by optimization of model complexity with L2-regularized logistic regression. Model performance was assessed using the area under the receiver operating characteristic curve (AUROC) and the Brier score with uncertainty quantified by non-parametric bootstrapping (2000 resamples).

Results: Among 1769 patients, 976 (15 SSC-CIP) were in the development cohort and 793 (14 SSC-CIP) in the validation cohort. The final model comprised six postoperative laboratory predictors selected via stability-based feature selection: potassium, gamma-glutamyl transferase, platelet count, arterial oxygen partial pressure, procalcitonin and serum osmolality. In the validation cohort, bootstrap resampling yielded a median AUROC of 0.77 (95% confidence interval 0.61–0.92) and a Brier score of 0.22, indicating acceptable discrimination and moderate calibration.

Conclusion: The model based on routine perioperative laboratory parameters showed acceptable discriminative performance for SSC-CIP, but estimates were constrained by the small number of events inherent to this rare condition. Multicenter collaboration and centralized registries are needed to refine predictive accuracy and support clinically actionable risk stratification.

SAT-322

Patient navigation and patient-reported outcomes assessment in primary biliary cholangitis and primary sclerosing cholangitis reveal quality-of-life differences and early indicators of adverse clinical outcomes: a multi-year registry analysis

Ana Marenco-Flores[1,2], Victoria Abadi-Ron[2], Natalia Rojas-Amaris[2], Ava Tsapatsaris[1], Esteban Garita[3], Romelia Barba[4], Leandro Sierra[5], Behnam Saberi[2], Vilas Patwardhan[2], Alan Bonder[2]. *[1]Harvard Medical School, Beth Israel Deaconess Medical Center, Boston, United States; [2]Beth Israel Deaconess Medical Center, Harvard Medical School, Boston, United States; [3]Albert Einstein College of Medicine, Montefiore Medical Center, Bronx, United States; [4]Texas Tech University, Lubbock, United States; [5]Cleveland Clinic, Twinsburg, United States*
Email: ana_marenco@hms.harvard.edu

Background and aims: Patient-reported outcomes (PROs) offer insight into the burden of chronic liver disease. The Chronic Liver Disease Questionnaire (CLDQ) measures quality of life (QoL) across fatigue, activity, emotional function, abdominal, and systemic symptoms. We examined patient navigation data, CLDQ domain trends, and their association with hepatic decompensation in primary biliary cholangitis (PBC) and primary sclerosing cholangitis (PSC) to determine whether PRO patterns and navigation data help identify early indicators of adverse outcomes.

Method: We conducted a retrospective study using a long-standing registry at a tertiary hepatology center (2018–2025). Patients with PBC or PSC completed the CLDQ at baseline and follow-up. We assessed domain scores, completion rates, and changes over time by disease type and compared retained patients with those who dropped out due to death, liver transplantation, or hepatic decompensation. Domain scores required ≥ 50% item completion. Biochemical–QoL associations were examined using Spearman's correlation, and yearly domain scores with SD were plotted to assess longitudinal patterns. Analyses were performed in Stata and Python.

Results: Among 311 patients (183 PBC, 128 PSC) with 1223 visits, retention was 78.1%, with 21.9% dropout from hepatic decompensation (10.9%), liver transplantation (9.0%), or death (1.9%). PSC patients reported higher QoL across most domains, including fatigue (5.48 vs 5.05, $p < 0.001$), systemic (5.41 vs 5.05, $p = 0.008$), activity (5.71 vs 5.44, $p = 0.03$), and abdominal symptoms (5.95 vs 5.69, $p = 0.02$), with similar emotional function ($p = 0.12$). Overall CLDQ scores were higher in PSC (5.68 vs 5.38, $p < 0.001$). Longitudinal plots showed improvement in PSC (+12.5%) and stable scores in PBC. Dropout patients had lower QoL than retained patients (5.29 vs 5.54, $p = 0.02$), with deficits in fatigue ($p = 0.04$) and systemic symptoms ($p = 0.01$). Higher alkaline phosphatase correlated with lower QoL ($r = -0.22$), strongest for fatigue ($r = -0.25$), and declines in activity often preceded hepatic decompensation ($r = -0.34$).

Conclusion: This registry showed strong retention and higher QoL in PSC than in PBC. Hepatic decompensation primarily caused dropouts, with lower fatigue and systemic symptom scores distinguishing non-continued participants. The ALP–QoL relationship supports the use of the CLDQ, and longitudinal domain tracking may help identify patients needing earlier intervention.

SAT-323

Impact of imaging surveillance on outcomes after cholangiocarcinoma diagnosis in primary sclerosing cholangitis

Adrielly Martins[1], Miki Scaravaglio[2], David Goldberg[1], Cynthia Levy[1]. *[1]University of Miami, Miami, United States; [2]University of Cambridge, Cambridge, Northern Ireland*
Email: axm8717@med.miami.edu

Background and aims: Patients with primary sclerosing cholangitis (PSC) carry a lifetime cholangiocarcinoma (CCA) risk of 10–15%, prompting recommendations for systematic surveillance. However, evidence supporting survival benefit from surveillance is limited. We aimed to determine if imaging surveillance improved the overall survival of patients with PSC-CCA.

Method: Using the Epic Cosmos database, we conducted a retrospective cohort study of PSC patients with CCA diagnosed between 2005 and 2025, at least one year after PSC diagnosis. Patients with colorectal cancer were excluded. Surveillance was defined as two or more abdominal imaging studies (magnetic resonance imaging, computed tomography, or ultrasound) performed 6–36 months before CCA diagnosis to distinguish surveillance from diagnostic workup. The primary outcome was all-cause mortality after CCA diagnosis. Cox proportional hazards regression was used, adjusting for age at PSC diagnosis, sex, ulcerative colitis, cirrhosis, and colectomy status. Sensitivity analyses addressed informative censoring by excluding patients lost to follow-up >2 years and by assuming these patients died.

Results: A total of 1031 PSC-CCA patients were included (mean age at CCA 57 years, 61% male, 70% with inflammatory bowel disease, 78% with cirrhosis). Among them, 536 (52%) received surveillance and 495 (48%) did not. Patients in the surveillance group had higher rates of cirrhosis (86% vs 70%, $p < 0.001$) and prior colectomy (50% vs 24%, $p < 0.001$). During a median follow-up of 1.43 years (IQR 0.48–3.64), 352 patients (34%) died and 72 (7%) underwent LT. LT rates were higher in the surveillance group (9.0% vs 4.8%, $p = 0.011$). In the main adjusted analysis, surveillance appeared associated with higher mortality (hazard ratio 1.32, 95% confidence interval [CI] 1.06–1.65, $p = 0.014$). However, this association attenuated and became non-significant in sensitivity analyses excluding patients lost to follow-up (hazard ratio 1.23, 95% CI 0.98–1.53) and assuming lost patients died (hazard ratio 1.12, 95% CI 0.92–1.36).

Conclusion: In this large retrospective cohort of patients with PSC-CCA, imaging surveillance was not associated with improved survival after CCA diagnosis. However, surveillance was associated with

higher LT rates, possibly reflecting earlier detection at transplant-eligible stages, warranting further investigation.

SAT-324

Latent class analysis identifies three distinct patient phenotypes in primary sclerosing cholangitis: implications for clinical trial access and mental health screening

Adrielly Martins[1], Patricia Moreno[1], Joshua Korsenik[2], Christopher L. Bowlus[3], Cynthia Levy[1]. [1]*University of Miami, Miami, United States;* [2]*Harvard University, Cambridge, United States;* [3]*University of California - Davis, Davis, United States*
Email: axm8717@med.miami.edu

Background and aims: Primary sclerosing cholangitis (PSC) patients experience variable symptom burden and psychological distress, yet care approaches often do not account for this heterogeneity. We used latent class analysis (LCA) to identify distinct patient phenotypes and examine associations with quality of care measures.
Method: We analyzed data from 238 PSC patients who completed an online survey (response rate 75%). LCA was performed using 8 indicators: 5 physical symptoms (fatigue, itch, abdominal pain, brain fog, nausea), PROMIS Depression and Anxiety scores (categorized as low/moderate/high), and care confidence. Models with 2–5 classes were compared using Bayesian Information Criterion (BIC). Multinomial logistic regression examined predictors of class membership. Chi-square tests compared quality of care outcomes across classes.
Results: Three phenotypes were identified (N = 220, mean posterior probability = 0.96): [1] Low Symptom Burden (34%): minimal physical symptoms, moderate psychological burden, high care confidence; [2] Physical Burden (26%): high fatigue (89%), moderate other symptoms, high anxiety (73%) but low depression, high care confidence; [3] Physical & Psychological Burden (41%): high fatigue (92%), elevated symptoms across all domains, with 95% moderate/high depression and 100% moderate/high anxiety. IBD prevalence did not differ significantly across phenotypes ($p = 0.78$). There was a trend toward association of cirrhosis with both higher burden phenotypes (OR 2.34–2.44, $p = 0.06$–0.07); and female sex trended toward association with the high-burden group ($p = 0.09$). Patients in the Physical & Psychological Burden group were less likely to report being offered clinical trial participation ($p = 0.024$), and this disparity persisted after adjusting for cirrhosis, female sex, and IBD ($p = 0.046$). Mental health screening was uniformly low across all phenotypes: only 26–31% were asked about depression and 26–28% about anxiety, despite near-universal psychological burden in the highest-risk group.
Conclusion: Over 40% of PSC patients experience major physical and psychological burden. These patients were less likely to report being offered clinical trials, though further investigation is needed to determine whether this reflects eligibility criteria, access barriers, or other factors. Mental health screening rates are low across all phenotypes. Phenotype-based approaches may help identify patient-sin need of psychological support and could inform strategies to optimize clinical trial recruitment.

SAT-361

Bridging the gap in primary sclerosing cholangitis care: results from a patient survey

Adrielly Martins[1], Patricia Moreno[1], Joshua Korsenik[2], Christopher L. Bowlus[3], Cynthia Levy[1]. [1]*University of Miami, Miami, United States;* [2]*Harvard University, Cambridge, United States;* [3]*University of California - Davis, Davis, United States*
Email: axm8717@med.miami.edu

Background and aims: Primary sclerosing cholangitis (PSC) is a rare, chronic liver disease often associated with inflammatory bowel disease (IBD), for which effective treatments are lacking. Prior research suggests significant variability in care delivery, but the patient perspective remains underexplored. This study aimed to assess patients' perceptions of PSC care, including symptom burden, psychological well-being, and alignment between clinical practice and guideline-based recommendations.
Method: An anonymous online questionnaire was distributed through the PSC Partners registry (March–June 2025). Adults with PSC were invited to complete a 52-question survey capturing symptom burden, access to care, adherence to surveillance, and perceptions of care. Validated PROMIS forms assessed anxiety and depression. Analyses examined associations between social deprivation index (SDI), clinical factors, and outcomes.
Results: A total of 238 patients completed the survey (median age 54 years; 52% female; 75% US residents); 67% had concomitant IBD—ulcerative colitis (73%) – and 24% had cirrhosis. Most were followed by a hepatologist (79%) at a university-affiliated center (65%). Fatigue (60%) was the most commonly reported symptom, followed by brain fog (37%), abdominal pain (37%), and pruritus (34%). While physicians frequently asked about physical symptoms (fatigue 70%, pruritus 76%, abdominal pain 78%), inquiries about anxiety (28%) and depression (28%) were less common. PROMIS T-scores indicated mild depression and anxiety. Higher SDI was associated with increased depression ($p = 0.01$) and anxiety ($p = 0.01$), as was cirrhosis with depression ($p < 0.01$). Among patients with IBD, 68% reported annual colonoscopy; and 99% of all respondents reported having undergone at least one colonoscopy. Annual imaging was reported by 89%, and lifetime testing included bone densitometry (74%) and fibrosis assessment through vibration-controlled transient elastography (70%). Scheduling challenges (31%) were the most commonly reported barrier to imaging. Fifty-five percent had been invited to participate in clinical trials and 77% rated their overall care as good or excellent.
Conclusion: Findings from this survey highlight high adherence to recommended surveillance practices but reveal gaps in mental health assessment. SDI and cirrhosis were associated with worse psychological outcomes. These findings emphasize the need for structured mental health screening and attention to social determinants of health in PSC care.

SAT-362

Efficacy and safety of seladelpar vs placebo in patients with primary biliary cholangitis and metabolic syndrome in the pivotal phase 3 response study

Marlyn J. Mayo[1], Eric Lawitz[2], Alejandra Villamil[3], Ewa Janczewska[4], Pietro Andreone[5], María Carlota Londoño[6], Ares Villagrasa[7,8,9], Sarah Proehl[10], Lulu Wang[10], Daria B. Crittenden[10], Christopher L. Bowlus[11]. [1]*Division of Digestive and Liver Diseases, University of Texas Southwestern, Dallas, United States;* [2]*Texas Liver Institute, University of Texas Health San Antonio, San Antonio, United States;* [3]*The Liver Autoimmunity Unit, Hospital Italiano de Buenos Aires, Buenos Aires, Argentina;* [4]*Department of Basic Medical Sciences, Faculty of Public Health in Bytom, Medical University of Silesia, Bytom, Poland;* [5]*Division of Internal Medicine, University of Modena and Reggio Emilia, Baggiovara Hospital, Modena, Italy;* [6]*Liver Unit, Hospital Clínic Barcelona, Instituto de Investigaciones Biomédicas August Pi i Sunyer (IDIBAPS), Centro de Investigación Biomédica en Red de Enfermedades Hepáticas y Digestivas (CIBEREHD), Barcelona, Spain;* [7]*Department of Medicine, Universitat Autònoma de Barcelona, Barcelona, Spain;* [8]*Liver Unit, Hospital Universitario Vall de Hebron, Barcelona, Spain;* [9]*European Reference Network on Rare Liver Disorders (ERN-Liver), Barcelona, Spain;* [10]*Gilead Sciences, Inc., Foster City, United States;* [11]*Division of Gastroenterology and Hepatology, University of California Davis School of Medicine, Sacramento, United States*
Email: clbowlus@health.ucdavis.edu

Background and aims: Seladelpar (SEL) is a first-in-class delpar (selective PPAR-delta agonist) indicated for the treatment of primary biliary cholangitis (PBC) in combination with ursodeoxycholic acid (UDCA) in patients (pts) with an inadequate response to UDCA or as monotherapy in pts intolerant to UDCA. The pivotal Phase 3 RESPONSE (NCT04620733) study excluded pts with metabolic-

associated steatohepatitis. Pts with steatotic liver disease (MASLD) were allowed without formally collecting hepatic steatosis data. We describe the efficacy and safety of SEL in pts with PBC and evidence of concurrent metabolic syndrome (MetS) as a proxy for MASLD in the RESPONSE trial.

Method: Pts with PBC were randomised 2:1 to SEL 10 mg or placebo (PBO) for 12 months (M). In this post hoc subgroup analysis, pts were classified as having MetS if they met ≥ 3 of the following criteria at entry: body mass index (BMI) > 27.6 kg/m^2, elevated triglycerides, low high-density lipoprotein, current treatment for hypertension or diabetes, or elevated blood pressure or fasting glucose. Efficacy endpoints included composite biochemical response (CBR; alkaline phosphatase [ALP] < 1.67 × upper limit of normal [ULN], total bilirubin ≤ ULN, ALP reduction ≥ 15% from baseline [BL]), ALP normalisation, and changes in ALP and other laboratory parameters at M12. Safety was also assessed.

Results: Of 193 pts enrolled, 22% had evidence of MetS at BL (SEL: 24 [19%]; PBO: 18 [28%]). At BL, pts with MetS vs pts without had higher mean BMI (30.4 vs 26.2 kg/m^2), ALP (324.5 U/L vs 311.5 U/L), and liver stiffness (11.5 kPa vs 8.9 kPa), and were more likely to have cirrhosis (24% vs 11%). The percentage of pts achieving a CBR (95% CI) at M12 in the SEL arm was similar in pts with and without MetS (MetS: 42% [22–63]; no MetS: 66% [56–75]) compared with PBO (MetS: 17% [4–41]; no MetS: 21% [11–36]), as was ALP normalisation (SEL: MetS, 17% [5–37] vs no MetS, 27% [19–37]; PBO: MetS, 0% [0–19] vs no MetS, 0% [0–8]). ALP reduction with SEL at M12 was similar regardless of MetS status (mean percent change from BL for SEL vs PBO: MetS, −41% vs 2%; no MetS, −44% vs −9%). Incidence of adverse events (AEs), including cardiovascular AEs, was similar between the SEL and PBO arms irrespective of MetS presence.

Conclusion: MetS was a frequently observed comorbidity in pts with PBC enrolled in RESPONSE. The efficacy and safety profile of SEL was similar in pts with and without MetS. Further studies are needed to better understand the impact of MASLD on PBC management.

SAT-363

Efficacy and safety of seladelpar in patients with primary biliary cholangitis and risk factors for progression including younger age at diagnosis or higher liver stiffness in the pivotal response study

Marlyn J. Mayo[1], Gideon M. Hirschfield[2], Michael Galambos[3], Ira Jacobson[4], Richard Aspinall[5], Christopher L. Bowlus[6], Mitchell Shiffman[7], George Dalekos[8], Kyung min Kwon[9], Lulu Wang[9], Sarah Proehl[9], Daria B. Crittenden[9]. [1]*Division of Digestive and Liver Diseases, University of Texas Southwestern, Dallas, United States;* [2]*The Autoimmune and Rare Liver Disease Programme, Division of Gastroenterology and Hepatology, Toronto General Hospital, Toronto, Canada;* [3]*Digestive Healthcare of Georgia, Atlanta, United States;* [4]*New York University Grossman School of Medicine New York, New York, United States;* [5]*Department of Gastroenterology and Hepatology, Portsmouth Hospitals University NHS Trust, Queen Alexandra Hospital, Portsmouth, United Kingdom;* [6]*Division of Gastroenterology and Hepatology, University of California Davis School of Medicine, Sacramento, United States;* [7]*Liver Institute of Virginia, Bon Secours Mercy Health, Richmond, United States;* [8]*Department of Medicine and Research Laboratory of Internal Medicine, National Expertise Center of Greece in Autoimmune Liver Diseases, General University Hospital of Larissa, Larissa, Greece;* [9]*Gilead Sciences, Inc., Foster City, United States*
Email: marlyn.mayo@utsouthwestern.edu

Background and aims: Seladelpar (SEL) is a first-in-class delpar (selective PPAR-delta agonist) indicated for the treatment of primary biliary cholangitis (PBC). In the Phase 3 RESPONSE trial (NCT04620733), SEL significantly improved cholestasis biomarkers and pruritus vs placebo (PBO) in patients (pts) with PBC. Younger age at diagnosis and higher liver stiffness measurements (LSM) are risk factors for PBC progression. Here, we report data on the high-risk subgroups of pts in RESPONSE.

Method: Pts with PBC were randomised 2:1 to SEL 10 mg or PBO for 12 months (M). Two high-risk subgroups were defined post-hoc: age < 45 years (yrs) vs ≥ 45 yrs at PBC diagnosis, and LSM ≥ 10 kPa vs < 10 kPa at baseline (BL). Efficacy endpoints at M12 included composite biochemical response (CBR; alkaline phosphatase [ALP] < 1.67 × upper limit of normal [ULN], ALP decrease ≥ 15%, and total bilirubin ≤ ULN) and mean percent change in ALP. Safety was also assessed.

Results: Among 193 pts enrolled, 65 pts were age < 45 yrs at diagnosis (SEL, 40; PBO, 25) and 52 pts had a BL LSM ≥ 10 kPa (SEL, 36; PBO, 16). Pts aged < 45 yrs vs ≥ 45 yrs at diagnosis had a mean age at entry of 48 vs 61 yrs; cirrhosis was present in 17% vs 13% of pts per group, respectively, with similar ALP (mean 316 vs 313 U/L). Pts in the younger diagnosis subgroup treated with SEL had a CBR of 45% vs 12% with PBO; in the older diagnosis group, CBR was 69% vs 25% with SEL vs PBO. Mean ALP percent change from BL in the younger group was −35% vs 2% for SEL vs PBO, while in the older age group it was −47% vs −11%. Pts with BL LSM ≥ 10 kPa had a higher prevalence of cirrhosis vs the < 10 kPa group (44% vs 2%) and higher ALP (mean 350 vs 300 U/L). Pts with a higher LSM treated with SEL had a CBR of 47% vs 13% with PBO, with this endpoint observed in 67% vs 24% in the lower LSM group. Mean percent change from BL in ALP was similar in both groups: higher LSM, SEL −40% vs PBO −15%; lower LSM, −43% vs −3%. No treatment-related serious adverse events (AEs) were reported in any pts; liver-, muscle-, and renal-related AEs were similar in both high-risk groups.

Conclusion: SEL improved cholestatic markers in two subgroups of pts with PBC and risk factors for progression based on younger age at diagnosis and elevated liver stiffness. Safety was similar for pts with or without high-risk characteristics. Overall, these results suggest SEL may benefit pts with PBC across clinical risk levels.

SAT-364

Long-term improvements in lipid profiles with elafibranor treatment, and favourable safety with concomitant statin use, in patients with primary biliary cholangitis during the open-label extension of the phase III ELATIVE® trial

Marlyn J. Mayo[1], Christopher L. Bowlus[2], Kris V. Kowdley[3,4], Mark Pedersen[1], Nuno Antunes[5], Darren Asquith[6], Nathan Touati[7], Cynthia Levy[8,9]. [1]*Division of Digestive and Liver Diseases, University of Texas Southwestern Medical Center, Dallas, Texas, United States;* [2]*Division of Gastroenterology and Hepatology, UC Davis School of Medicine, Sacramento, California, United States;* [3]*Liver Institute Northwest, Seattle, Washington, United States;* [4]*Elson S. Floyd College of Medicine, Washington State University, Washington, United States;* [5]*Ipsen, Cambridge, Massachusetts, United States;* [6]*Ipsen, London, United Kingdom;* [7]*Ipsen, Paris, France;* [8]*Schiff Center for Liver Diseases, University of Miami, Miami, Florida, United States;* [9]*Division of Digestive Health and Liver Diseases, University of Miami School of Medicine, Miami, Florida, United States*
Email: marlyn.mayo@utsouthwestern.edu

Background and aims: Patients (pts) with primary biliary cholangitis (PBC) may have increased risk of cardiovascular (CV) disease and dyslipidaemia which may require lipid-modifying therapies. In ELATIVE® (NCT04526665), elafibranor (ELA) led to significantly improved biomarkers of cholestasis in PBC and was associated with atherogenic lipid improvements through 52 weeks (wks). Here, long-term lipid data from the ongoing open-label extension (OLE) are evaluated.

Method: Pts who completed the ELATIVE® double-blind period (DBP) could enter the OLE and receive ELA 80 mg daily. Data are reported for pts who continued ELA treatment (continuous pts) and pts who switched from placebo to ELA (crossover pts). For continuous pts, baseline (BL) was DBP start; for crossover pts, BL was last measurement at/before first ELA dose. Mean change from BL (CfB) in total cholesterol, low-, very low-, high-density lipoprotein cholesterol (LDL-c, VLDL-c, HDL-c) and triglycerides, and CV risk score, are reported through 208 and 104 wks of ELA treatment in continuous and crossover pts, respectively. New muscle-related

adverse events (AE) occurring in the OLE are reported for both groups, and for pts receiving statins.
Results: Overall, 138 pts entered the OLE (93 continuous pts; 45 crossover pts). In continuous pts, improvements in lipids observed at Wk 52 were maintained through Wks 156 (n = 73) and 208 (n = 15), with mean CfB (mg/dL) of: total cholesterol (Wk 156: −25.4; Wk 208: −37.1), LDL-c (Wk 156: −18.8 [n = 72]; Wk 208: −23.2 [n = 14]), VLDL-c (Wk 156: −5.1 [n = 72]; Wk 208: −8.5 [n = 14]) and triglycerides (Wk 156: −28.1; Wk 208: −55.3). In crossover pts, early improvements were sustained through 104 wks of ELA treatment (mean CfB [mg/dL]; n = 33): total cholesterol (−29.3), LDL-c (−18.1), VLDL-c (−4.6) and triglycerides (−23.3). HDL-c mean CfB (mg/dL) remained stable in both continuous (Wk 156: −1.0; Wk 208: −0.3) and crossover (Wk 104: −6.5) pt groups. BL mean CV risk score was low and remained stable in both pt groups. To data cut-off, 4 muscle-related AEs occurred in the OLE (2 continuous ELA; 2 crossover ELA), none treatment-related. In pts receiving statins (continuous ELA: 19 [20.4%]; crossover ELA: 10 [22.2%]), no new muscle-related safety signals were detected.
Conclusion: Long-term ELA treatment in pts with PBC, including crossover pts, was associated with sustained improvements in atherogenic lipids. CV risk remained stable. There were no new treatment-related muscle-related AEs, including in pts receiving statins.

SAT-365
Real-world survey assessing pruritus in PSC in France, Germany, Italy and the United States: results from a matched patient and their treating physician cohort
Marlyn J. Mayo[1], Marco Carbone[2], Will Johnson[3], Lena Amari[3], Guy Lacey[4], Jolan Terner-Rosenthal[4], Lucia Quadrado[4], Robin Howard[4], Verena Keitel-Anselmino[5]. *[1]UT Southwestern Medical Center, Dallas, Texas, United States; [2]University of Milano-Bicocca, Milan, Italy; [3]Adelphi Real World, Bollington, United Kingdom; [4]Mirum Pharmaceuticals, Inc., Foster City, California, United States; [5]University Hospital Magdeburg, Magdeburg, Germany*
Email: marlyn.mayo@utsouthwestern.edu

Background and aims: Primary sclerosing cholangitis (PSC) is a chronic, progressive liver disease characterized by damage to intra- and extrahepatic bile ducts. While studies indicate that almost 90% of patients with PSC experience pruritus at some point in their lives, a recent physicians survey reported that 42% of their patients with PSC had pruritus and almost all physicians (90%) believe that pruritus has a profound impact on a patient's quality of life (QoL). The purpose of the current study is to describe the reported frequency and assessment of pruritus in a matched cohort of patients with PSC to their treating physicians to determine if there are alignment or differences between what physicians and patients report.
Method: Data were extracted from the Adelphi Real World PSC Disease Specific Programme™, a cross-sectional survey with retrospective data collection of physicians and their adult patients (≥18 years old) with PSC in France, Germany, Italy, and the United States from November 2024 to April 2025. The current presentation is focused on physicians' and patients' perceptions and attitudes around their management of PSC. Analyses of the matched cohorts used symmetry significance testing.
Results: Results from physicians (n = 157) and patients with PSC (n = 151) were included in this analysis. There was agreement between physicians and their patients regarding the most common current symptoms (pruritus [68% vs. 68%; p = 1.00]; sleep disturbance due to pruritus [15% vs. 19%; p = 0.2008]), although physicians reported fatigue signficantly less than patients (68% vs. 75%; p = 0.0499). There was also agreement between physicians and patients regarding the most bothersome PSC symptoms (fatigue [77% vs. 74%; p = 0.4497], pruritus [76% vs. 77%; p = 0.8348], sleep disturbance due to pruritus [13% vs. 17%; p = 0.2253]). Physicians were less likely to think their patients' pruritus was mild vs. patients (58% vs 72%; p = 0.0104). Physicians were less likely to believe that current PSC treatments could relieve pruritus (27% vs. 48%). However, both physicians and patients reported that improving pruritus was still a key goal for treatment (72% vs. 69%; p = 0.2482).
Conclusion: While there was agreement on the prevalence of pruritus between physicians and patients, perspectives on the burden of symptoms appeared to differ. These initial data highlight the importance of more explicit assessment of pruritus during clinical encounters and improved physician/patient communication to bridge perceptual differences.

SAT-366
Use of maralixibat for the treatment of cholestatic pruritus in late-onset PFIC
David Bernstein[1], Maly Tiev[1], Jeffrey Crippin[2], Fabian Rodas[3], Adebowale Adeyemi[4], Natasha Chandok[5], Marlyn J. Mayo[6]. *[1]Gastroenterology and Hepatology Ambulatory Network, NYU Grossman School of Medicine, NYU Langone Health, New York, New York, United States; [2]Department of Medicine, Washington University School of Medicine, St. Louis, Missouri, United States; [3]University of Texas Health Science Center San Antonio-UTHSCSA, The Texas Liver Institute, San Antonio, Texas, United States; [4]Division of Gastroenterology, Department of Pediatrics, Nemours Children's Hospital, Wilmington, Delaware, United States; [5]Department of Medicine, McMaster University, Hamilton, Ontario, Canada; [6]UT Southwestern Medical Center, Dallas, Texas, United States*
Email: marlyn.mayo@utsouthwestern.edu

Background and aims: Progressive Familial Intrahepatic Cholestasis (PFIC) has traditionally been characterized as a pediatric cholestatic condition. More recently, it has been recognized that PFIC can be diagnosed at any age. Maralixibat (MRX), an ileal bile acid transporter inhibitor (IBATi), is indicated for the treatment of cholestatic pruritus in patients with PFIC ≥1 year in the US, and for the treatment of PFIC in patients ≥3 months in the EU. However, its use in late-onset PFIC has not been widely reported. Here we describe the efficacy, tolerability, and safety of MRX in late-onset PFIC.
Method: Clinicians treating patients (≥18 years) with a diagnosis of PFIC completed an electronic case report form including clinical and biochemical data. Pruritus was assessed with the Clinician Scratch Scale (CSS), a 0–4 scale where 0 = no evidence of pruritus and 4 = cutaneous mutilation, bleeding or scarring; ≥1-point reduction is considered clinically meaningful. Data are presented using medians and min/max, and categorical variables are as counts and percentages.
Results: Data on 6 patients (2 males) from 6 centers were included: 1 (17%) *ATP8B1*, 2 (33%) *ABCB11*, 2 (33%) *ABCB4*, and 1 (17%) multi-gene deletion at 17q12. Median age at initiation of treatment was 26 (range 10–60) years and duration of treatment was 9 (range 2–129) months. One was being assessed for liver transplant (LT) and 1 was waitlisted. Before treatment, 3 (50%) had CSS of 4, 1 (17%) had a CSS of 3, and 2 (33%) had CSS of 2. Following treatment, all had a clinically meaningful reduction in CSS, with 3 (50%) achieving complete resolution (CSS = 0). Pre- and post-treatment sBA levels were available for 4, 3 (75%) with a substantial reduction in sBA levels (212 to 14, 352 to 16, and 81 to 60 μmol/L). Bilirubin and liver enzymes remained stable or decreased in the majority. Notably, the 2 being evaluated or waitlisted for LT were delisted following clinical improvement. AEs were reported in 3 including diarrhea (n = 3; 50%), transaminase increase that normalized by last clinical follow-up (n = 2; 33%), increase in bilirubin (n = 1; 17%), and abdominal pain (n = 1; 17%). There were no discontinuations or severe liver events (e.g., decompensation).
Conclusion: MRX led to significant improvements in pruritus and sBA in patients with late-onset PFIC, suggesting IBATi may offer benefit in this group. Additional studies evaluating longer follow-up in a larger cohort would allow for better characterization of the benefits of IBATi in late-onset PFIC.

SAT-367

Comparative clinical and immunological features of drug-induced autoimmune-like hepatitis, drug-induced liver injury, and autoimmune hepatitis

Yao Meng[1], Zikun Ma[1], Yuhong Suo[1], Lina Wu[1], Tiantian Guo[1], Mengmeng Zhang[1], Xu Fan[1], Xinyan Zhao[1]. [1]*Beijing Friendship Hospital, Capital Medical University, Beijing, China*
Email: mengyao2954@163.com

Background and aims: Distinguishing drug-induced autoimmune-like hepatitis (DIALH) from drug-induced liver injury (DILI) and autoimmune hepatitis (AIH) is challenging due to overlapping clinical features. We aimed to identify discriminative characteristics through a comparative analysis of clinical indicators and peripheral T-cell subsets.
Method: Clinical and immunological characteristics were compared across three groups: DIALH, DILI, and AIH. Peripheral blood T-cell subsets were analysed by flow cytometry. Group differences were assessed using the Kruskal–Wallis test, followed by pairwise Wilcoxon tests, with $p < 0.05$ considered statistically significant.
Results: A total of 6 cases of DIALH, 38 cases of DILI and 42 cases of AIH were included in the study. The DIALH group exhibited markedly higher peak levels of alanine aminotransferase (ALT) and aspartate aminotransferase (AST) compared to the AIH group [ALT: 588.5 (330.3–789.0) vs. 87.0 (51.0–120.0) U/L, $p < 0.001$; AST: 459.7 (287.8–512.6) vs. 93.0 (56.9–186.8) U/L, $p < 0.001$]. The DILI group showed significantly higher bilirubin levels (TBIL, DBIL) compared to DIALH [TBIL: DILI 72.2 (32.3–146.0) vs. DIALH 18.8 (10.1–27.8) μmol/L, p = 0.007; vs. AIH 23.9 (15.2–65.2) μmol/L, $p < 0.001$]. Serum immunoglobulin G (IgG) levels were significantly higher in both the DIALH and AIH groups compared to the DILI group [DIALH: 1815.0 (1477.5–1912.5), AIH: 1760.0 (1580.0–2070.0), vs. DILI: 1110.0 (971.0–1310.0) mg/dL; DIALH vs. DILI p = 0.009, AIH vs. DILI $p < 0.001$], while levels between DIALH and AIH were comparable ($p = 0.762$). Flow cytometry analysis identified differences in several T-cell subsets. Th2-like Tregs and CCR4+ Memory-Tregs were significantly reduced in DIALH compared to DILI and AIH [both $p < 0.05$].
Conclusion: DIALH shares a predominantly hepatocellular injury pattern with DILI and elevated IgG levels with AIH, but is distinguished by a reduced proportion of Th2-like and CCR4+ memory Tregs, suggesting a specific peripheral immune signature that may aid in its differentiation.

SAT-368-YI

ALNE 2.0: a histopathology-based deep learning model accurately discriminates autoimmune hepatitis and primary biliary cholangitis and helps identify the dominant phenotype in variant cases

Elisa Merelli[1,2], Laura Žigutytė[3], Giorgio Cazzaniga[4], Jessica Dyson[5,6], Abhishek Gairola[5], Ye Htun Oo[7,8,9], George Mells[5,6,10], Michael Heneghan[11], Rebecca Jones[12], Emma Culver[13,14], Douglas Thorburn[15], Kenneth J. Simpson[16], Dermot Gleeson[17,18], Uk-Aih Consortium[19], Marco Carbone[1,20], Laura Cristoferi[2], Roberta Lasco[2], Fabio Pagni[4], Xiong Ma[21,22], Qi Miao[21], Yongfeng Yang[23], Hongli Liu[23], Du-Xian Liu[24], Xing Liu[23], Bastian Engel[25], Richard Taubert[25], Björn Hartleben[26], Ana Lleo[27,28], Francesca Colapietro[27,28], Luca Di Tommaso[27,29], Reha Akpinar[27,29], Andreas Cerny[30], Benedetta Terziroli Beretta-Piccoli[31,32,33], Lorenzo Magenta[30], Claudia Di Bartolomeo[34], Maurizia Bissig[34], Adriaan J. van der Meer[35], Ellen Werner[35], Tiki D. Blom[35], Michail Doukas[36], Joao Madaleno[37,38], Bernardo Canhão[37,38], Maria Agusta Cipriano[38,39], Joana Madeira[38,39], Elisabetta Degasperi[40], Sonia Stella[40], Marco Maggioni[41], Alessia Belotti[41], Vincenza Calvaruso[42], Daniela Cabibi[42], Alberto Quattrocchi[42], Mauro Viganò[43], Alessandro Loglio[43], Andrea Gianatti[44], Lisa Licini[44], María Carlota Londoño[45], Marlene Padilla[45], Alba Díaz[46,47,48], Carla Fuster[46,47,48], Piotr Milkiewicz[49], Maciej Janik[49], Jacek Tomczuk[49], Jakub Grzybowski[50], Alan Bonder[51], Ana Marenco-Flores[51], Imad Nasser[51], Vilas Patwardhan[51], Atsushi Tanaka[52], Kazumichi Abe[53], Kenichi Harada[54], Kaori Yoshimura[54], Conrado Fernandez-Rodriguez[55,56], Marta Quiñones[55], Fernando Pinedo-Moraleda[57], Elena Garcìa-Garcìa[57], Tom J. G. Gevers[38,58,59], Ozgur Koc[38,59], Iryna Samarska[60], Matthias van Haele[60], Jef Verbeek[61], Tania Roskams[62], Umberto Vespasiani-Gentilucci[63,64], Francesca Terracciani[63,64], Simone Carotti[65,66], Chiara Taffon[67,68], David N. Assis[69], Dhanpat Jain[70], Wenyi Luo[70], George Dalekos[71], Cristina Rigamonti[72,73], Alejandra Villamil[74], Aldo J Montano-Loza[75], Nora Cazzagon[76], Joanne Verheij[77], Ángela Remesal-Doblado[78], Zunamys Itzel Carrero[3], Pietro Invernizzi[1,2], Jakob Nikolas Kather[3,79,80,81], Alessio Gerussi[1,2]. [1]*Department of Medicine and Surgery, Università degli Studi di Milano-Bicocca, Monza, Italy;* [2]*Centre for Autoimmune Liver Diseases and Division of Gastroenterology, European Reference Network (ERN) RARE-LIVER, Fondazione IRCCS San Gerardo dei Tintori, Monza, Italy;* [3]*Else Kroener Fresenius Center for Digital Health, Faculty of Medicine, TUD Dresden University of Technology, Dresden, Germany;* [4]*Department of Medicine and Surgery, Pathology, IRCCS Fondazione San Gerardo dei Tintori, University of Milano-Bicocca, Monza, Italy;* [5]*Newcastle upon Tyne Hospitals NHS Foundation Trust, Newcastle, United Kingdom;* [6]*Translational and Clinical Research Institute, Newcastle NIHR Biomedical Research Centre, Newcastle University, Newcastle, United Kingdom;* [7]*College of Medicine and Health, University of Birmingham, Birmingham, United Kingdom;* [8]*Centre for Liver Research, University of Birmingham and University Hospital Birmingham NHS Foundation Trust, Birmingham, United Kingdom;* [9]*Centre for Rare Diseases, European Reference Network on Hepatological Diseases (ERN-RARE-LIVER) Centre, Birmingham, United Kingdom;* [10]*Academic Department of Medical Genetics, University of Cambridge, Cambridge, United Kingdom;* [11]*Institute of Liver Studies, King's College Hospital NHS Foundation Trust, Denmark Hill, London, United Kingdom;* [12]*Leeds Liver Unit, St James's University Hospital, Leeds, United Kingdom;* [13]*John Radcliffe Hospital, Oxford, United Kingdom;* [14]*University of Oxford, Oxford, United Kingdom;* [15]*Liver Unit, Royal Free Hospital, London, United Kingdom;* [16]*Department of Hepatology and Scottish Liver Transplant Unit, Royal Infirmary of Edinburgh, Edinburgh, United Kingdom;* [17]*Liver Unit, Sheffield Teaching Hospitals NHS Foundation Trust, Sheffield, United Kingdom;* [18]*Division of Clinical Medicine, School of Medicine and Population Health, University of Sheffield, University of Sheffield Medical School, Sheffield, United Kingdom;* [19]*Newcastle University, Newcastle upon Tyne, Newcastle, United Kingdom;* [20]*Liver Unit, ASST Grande Ospedale Metropolitano (GOM) Niguarda, Milan, United Kingdom;* [21]*NHC Key Laboratory of Digestive Diseases (Renji Hospital, Shanghai Jiaotong University School of Medicine), Division of Gastroenterology and Hepatology, State Key Laboratory for Oncogenes and Related Genes, Renji Hospital, School of Medicine, Shanghai JiaoTong University; Shanghai Institute of Digestive Disease, Shanghai, China;* [22]*Institute of Aging & Tissue Regeneration, Renji Hospital, School of Medicine, Shanghai JiaoTong University, Shanghai, China;* [23]*Department of Infectious Disease and Liver Disease, Nanjing Key Laboratory of Hepatology, The Second Hospital of Nanjing, Affiliated to Nanjing University of Chinese Medicine, Nanjing, China;* [24]*Department of Pathology, The Second Hospital of Nanjing, Affiliated to Nanjing University of Chinese Medicine, Nanjing, China;* [25]*Department of Gastroenterology, Hepatology, Infectious Diseases and Endocrinology, Hannover Medical School, Hannover, Germany;* [26]*Institute for Pathology, Hannover Medical School, Hannover, Germany;* [27]*Department of Biomedical Sciences, Humanitas University, Pieve Emanuele (Milan), Italy;* [28]*Division of Internal Medicine and Hepatology, Department of Gastroenterology, IRCCS Humanitas Research Hospital, Rozzano (Milan), Italy;* [29]*Department of Pathology, IRCCS Humanitas Research Hospital, Rozzano (Milan), Italy;* [30]*Epatocentro Ticino SA, Lugano, Switzerland;* [31]*Servizio di Gastroenterologia Ed Epatologia, Ente Ospedaliero*

Cantonale, Ospedale Civico, Lugano, Switzerland; [32]Faculty of Medical Biosciences, Università della Svizzera Italiana, Lugano, Switzerland; [33]MowatLabs, Faculty of Life Sciences & Medicine, King's College London, King's College Hospital, London, United Kingdom; [34]Fondazione Epatocentro Ticino SA, Lugano, Switzerland; [35]Department of Gastroenterology and Hepatology, Erasmus University Medical Center, Rotterdam, Netherlands; [36]Department of Pathology, Erasmus MC Cancer Institute, Rotterdam, Netherlands; [37]Liver Disease Unit, Department of Internal Medicine, Unidade Local de Saúde de Coimbra - Hospitais da Universidade de Coimbra, Coimbra, Portugal; [38]European Reference Network on Hepatological Diseases (ERN RARE-LIVER), European Union; [39]Pathology Department, Unidade Local de Saúde de Coimbra - Hospitais da Universidade de Coimbra, Coimbra, Portugal; [40]Division of Gastroenterology and Hepatology, Foundation IRCCS Ca' Granda Ospedale Maggiore Policlinico, Milan, Italy; [41]Department of Pathology, Foundation IRCCS Ca' Granda Ospedale Maggiore Policlinico, Milan, Italy; [42]Department of Health Promotion, Mother and Child Care, Internal Medicine and Medical Specialties (PROMISE), University of Palermo, Palermo, Italy; [43]Gastroenterologia 1 - Epatologia e Trapiantologia ASST Papa Giovanni XXIII, Bergamo, Italy; [44]Anatomia Patologica ASST Papa Giovanni XXIII, Bergamo, Italy; [45]Liver Unit, Hospital Clínic Barcelona, Universitat de Barcelona, Fundació de Recerca Clínic Barcelona-Institut d'Investigacions Biomèdiques August Pi i Sunyer (FRCB-IDIBAPS), Centro de Investigación Biomédica en Red de Enfermedades Hepáticas y Digestivas (CiberEHD), Barcelona, Spain; [46]Pathology Department, CDB, Hospital Clínic Barcelona, Barcelona; Institut d'Investigacions Biomèdiques August Pi i Sunyer (IDIBAPS), Barcelona, Spain; [47]University of Barcelona, Barcelona, Spain; [48]Centro de Investigación Biomédica en Red en Enfermedades Hepáticas y Digestivas (CIBEREHD), Barcelona, Spain; [49]Department of Hepatology, Transplantology and Internal Medicine, Medical University of Warsaw, Warsaw, Poland; [50]Department of Pathology, Medical University of Warsaw, Warsaw, Poland; [51]Division of Gastroenterology, Hepatology, and Nutrition, Beth Israel Deaconess Medical Center, Harvard Medical School, Boston, United States; [52]Department of Medicine, Teikyo University School of Medicine, Tokyo, Japan; [53]Department of Gastroenterology, Fukushima Medical University, Fukushima, Japan; [54]Department of Human Pathology, Kanazawa University Graduate School of Medicine, Kanazawa, Japan; [55]Service of Gastroenterology, Hospital Universitario Fundación Alcorcón, Madrid, Spain; [56]Dept Medical Specialties and Public Health, Universidad Rey Juan Carlos, Madrid, Spain; [57]Servicio de Anatomía Patológica, Hospital Universitario Fundación Alcorcón, Madrid, Spain; [58]Nutrim School for Nutrition and Translational Research in Metabolism, Maastricht University, Maastricht, Netherlands; [59]Department of Gastroenterology and Hepatology, MUMC +, Maastricht, Netherlands; [60]Department of Pathology, GROW - Research Institute for Oncology & Reproduction, Maastricht University Medical Center, Maastricht, Netherlands; [61]Department of Gastroenterology and Hepatology, University Hospitals Leuven, Leuven, Belgium; [62]Department of Imaging and Pathology, KU Leuven and University Hospitals Leuven, Leuven, Belgium; [63]Research Unit of Hepatology, Department of Medicine and Surgery, Università Campus Bio-Medico of Rome, Rome, Italy; [64]Clinical Medicine and Hepatology Unit, Fondazione Policlinico Universitario Campus Bio-Medico, Rome, Italy; [65]Microscopic and Ultrastructural Anatomy Research Unit, Department of Medicine and Surgery, Università Campus Bio-Medico of Rome, Rome, Italy; [66]Predictive Molecular Diagnostics, Fondazione Policlinico Universitario Campus Bio-Medico, Rome, Italy; [67]Operative Research Unit of Anatomical Pathology, Fondazione Policlinico Universitario Campus Bio-Medico of Rome, Rome, Italy; [68]Research Unit of Anatomical Pathology, Department of Medicine and Surgery, Università Campus Bio-Medico of Rome, Rome, Italy; [69]Department of Medicine, Section of Digestive Diseases and Yale Liver Center, Yale School of Medicine, New Haven, United States; [70]Department of Pathology, Yale School of Medicine, New Haven, United States; [71]Department of Medicine and Research Laboratory of Internal Medicine, National Expertise Center of Greece in Autoimmune Liver Diseases, European Reference Network on Hepatological Diseases (ERN RARE-LIVER), General University Hospital of Larissa, Larissa, Greece; [72]Department of Translational Medicine, Università del Piemonte Orientale, Vercelli, Italy; [73]Division of Internal Medicine, AOU Maggiore della Carità, Novara, Italy; [74]Department of Hepatology & Liver Transplantation, Italian Hospital of Buenos Aires, Buenos Aires, Argentina; [75]Division of Gastroenterology and Liver Unit, University of Alberta, Edmonton, Canada; [76]Department of Surgery, Oncology and Gastroenterology, University of Padova, Padua, Italy; [77]Pathology, Amsterdam UMC, Amsterdam, Netherlands; [78]UGC Aparato Digestivo y Farmacología Clínica, Hospital Universitario Virgen de la Victoria, Instituto de Investigación Biomédica de Málaga y Plataforma en Nanomedicina - IBIMA Plataforma BIONAND, Universidad de Málaga, Málaga, Spain; [79]Department of Medicine I, Faculty of Medicine, TUD Dresden University of Technology, Dresden, Germany; [80]Medical Oncology, National Center for Tumor Diseases (NCT), University Hospital Heidelberg, Heidelberg, Germany; [81]Pathology & Data Analytics, Leeds Institute of Medical Research at St James's, University of Leeds, Leeds, United Kingdom
Email: alessio.gerussi@unimib.it

Background and aims: Differentiating autoimmune hepatitis (AIH), from primary biliary cholangitis (PBC), and their variant syndrome (VS) is challenging due to overlapping histological and clinical features. The ALNE deep learning (DL) model has shown promise in AIH–PBC discrimination but has not been validated in large cohorts or applied to VS. We aimed to develop and externally validate a histopathology-based DL model for discriminating AIH, PBC, and characterizing VS using a large, ethnically diverse, multicenter cohort.

Method: We conducted a multicenter study including a training cohort of 1216 patients with AIH (n = 900, mean age at diagnosis 53 ± 16 years, 66% female) and PBC (n = 316, mean age at diagnosis 52 ± 11 years, 73% female). Digitized liver biopsy slides and clinical data were collected from 21 international centers across Europe, Asia, North and South America and processed using the UNI2 foundation model to extract histopathological features. ALNE 2.0, a binary classification model (AIH vs. PBC), was developed using 5-fold cross-validation and externally validated on 207 patients (AIH n = 162, mean age at diagnosis 53 ± 17 years, 67% female; PBC n = 45, 52 ± 9 years, 91% female) from two additional centers. The model was then applied to 198 VS cases from 17 countries (mean age at diagnosis 51 ± 14 years, 53% female), generating a probability score. Logistic and linear regression analyses examined clinical variables associated with AIH vs PBC classification probabilities.

Results: In 5-fold cross-validation (training cohort: AIH n = 900, PBC n = 316), ALNE 2.0 achieved a mean AUROC of 0.92 (95% CI 0.88–0.96), with average precision of 0.97 (95% CI 0.96–0.99) for AIH and 0.79 (95% CI 0.68–0.91) for PBC. In independent external validation (AIH n = 162, PBC n = 45), performance remained high: AUROC of 0.94, average precision of 0.98 for AIH and 0.83 for PBC. In VS cases (n = 198), predictions were evenly distributed (AIH 46.5%, PBC 53.5%), with probabilities polarizing toward AIH or PBC phenotypes rather than intermediate values. Cases classified as AIH had significantly higher alanine aminotransferase levels (OR 1.18, 95% CI 1.02–1.38, p = 0.031) at presentation, while those classified as PBC more frequently exhibited GP210 antibody positivity (coeff. −0.154, 95% CI −0.305 to −0.004, p = 0.045).

Conclusion: ALNE 2.0 accurately discriminates AIH and PBC in a large, ethnically diverse multicenter cohort and provides quantitative assessment of the dominant disease phenotype in VS cases.

SAT-369

Unsupervised machine learning reveals distinct quality-of-life clusters across autoimmune liver diseases

Elisa Merelli[1,2], Damiano Verda[3], Alessandro Piazza[3], Natalie Uhlenbusch[4], Romée Snijders[5,6], Bernd Löwe[4,5], Ansgar W. Lohse[5,7], Maciej Janik[5,8], Piotr Milkiewicz[5,8,9], Patricia Kovats[5,10,11], Maria Papp[5,10], Boglarka Balogh[10],

Francesca Bolis[1], Laura Cristoferi[2], Marco Carbone[1,12], Pietro Invernizzi[1,2], Luise Aamann[5,13,14], Henriette Ytting[5,13,14], Joao Madaleno[5,15,16,17], Bernardo Canhão[15,18], E. T. T. L. Tjwa[6], Joost P. H. Drenth[5,6], Lisbet Grønbæk[5,19,20], Henning Grønbæk[5,19], Vincenzo Ronca[21,22], Kathryn Olsen[5,23], Ye Htun Oo[5,23], Adriaan J. van der Meer[5,24], Bastian Engel[5,25], Alejandro Campos-Murguia[5,25], Richard Taubert[5,25], Ozgur Koc[5,26], Matthijs Kramer[5,26,27], Tom J. G. Gevers[5,18,26], Christoph Schramm[5,7,28], Alessio Gerussi[1,2]. *[1]Department of Medicine and Surgery, Università degli Studi di Milano-Bicocca, Monza, Italy; [2]Centre for Autoimmune Liver Diseases and Division of Gastroenterology, European Reference Network (ERN) RARE-LIVER, Fondazione IRCCS San Gerardo dei Tintori, Monza, Italy; [3]Rulex Innovation Labs, Genova, Italy; [4]Department of Psychosomatic Medicine and Psychotherapy, University Medical Centre Hamburg-Eppendorf, Hamburg, Germany; [5]European Reference Network on Hepatological Diseases (ERN RARE-LIVER), European Union; [6]Department of Gastroenterology and Hepatology, Radboud University Medical Centre, Nijmegen, Netherlands; [7]I. Department of Medicine, University Medical Centre Hamburg-Eppendorf, Hamburg, Germany; [8]Department of Hepatology, Transplantology and Internal Medicine, Medical University of Warsaw, Warsaw, Poland; [9]Translational Medicine Group, Pomeranian Medical University, Szczecin, Poland; [10]Department of Internal Medicine, Division of Gastroenterology, Faculty of Medicine, University of Debrecen, Debrecen, Hungary; [11]Kálmán Laki Doctoral School, Faculty of Medicine, University of Debrecen, Debrecen, Hungary; [12]Liver Unit, ASST Grande Ospedale Metropolitano (GOM) Niguarda, Milano, Italy; [13]Department of Digestive Diseases, Transplantation and General Surgery, Section for Liver Disease, Rigshospitalet, University of Copenhagen, Copenhagen, Denmark; [14]Department of Clinical Medicine, Faculty of Health Sciences, University of Copenhagen, Copenhagen, Denmark; [15]Liver Disease Unit, Internal Medicine Department, Centro Hospitalar e Universitário de Coimbra, Coimbra, Portugal; [16]Liver Transplant Unit, Centro Hospitalar e Universitário de Coimbra, Coimbra, Portugal; [17]Faculty of Medicine, University of Coimbra, Coimbra, Portugal; [18]Nutrim School for Nutrition and Translational Research in Metabolism, Maastricht University, Maastricht, Netherlands; [19]Department of Hepatology & Gastroenterology, Aarhus University Hospital, Aarhus, Denmark; [20]Department of Medicine, Regional Hospital Horsens, Horsens, Denmark; [21]Department of Biomedical Sciences, Humanitas University, Pieve Emanuele (Milan), Italy; [22]Department of Gastroenterology, Division of Internal Medicine and Hepatology, IRCCS Humanitas Research Hospital, Rozzano (Milan), Italy; [23]Liver Transplant and Hepatobiliary Unit, Queen Elizabeth Hospital, University Hospital of Birmingham NHS Foundation Trust & Centre for Liver and Gastro Research, NIHR Biomedical Research Centre, Institute of Immunology and Immunotherapy, University of Birmingham, Birmingham, United Kingdom; [24]Department of Gastroenterology and Hepatology, Erasmus University Medical Centre, Rotterdam, Netherlands; [25]Department of Gastroenterology, Hepatology, Infectious Diseases and Endocrinology, Hannover Medical School, Hannover, Germany; [26]Department of Gastroenterology and Hepatology, MUMC+, Maastricht, Netherlands; [27]GROW—School for Oncology & Reproduction, Maastricht University, Maastricht, Netherlands; [28]Martin Zeitz Centre for Rare Diseases, University Medical Centre Hamburg-Eppendorf, Hamburg, Germany*
Email: alessio.gerussi@unimib.it

Background and aims: Autoimmune liver diseases (AILDs) have a significant impact on health-related quality of life (HRQoL). Using artificial intelligence (AI), we explored HRQoL and related constructs to identify patient phenotypes that transcend traditional diagnostic categories.
Method: A total of 1388 patients with autoimmune hepatitis (AIH), primary biliary cholangitis (PBC), primary sclerosing cholangitis (PSC), or variant syndromes were recruited from 12 European centers (mean age 52 ± 16 years; 71% female). Data included nine validated HRQoL questionnaires assessing physical functioning, fatigue, emotional distress, somatic symptom burden, and illness-related cognitions, along with sociodemographic and clinical variables. Unsupervised K-means clustering was applied to identify homogeneous subgroups based solely on HRQoL profiles, with cluster stability confirmed through internal validation (617 patients, mean age 51.5 ± 16.6 years, 72.0% female). Feature ranking determined the variables most responsible for cluster differentiation.
Results: Clustering identified five distinct HRQoL-based patient clusters transcending diagnostic categories. Cluster A included older, comorbid patients with cirrhosis, moderately impaired physical health but preserved psychological health. Cluster B (predominantly female) showed the lowest HRQoL, marked by fatigue, physical limitations, poor health perception and somatic preoccupation. Cluster C represented clinically stable patients with balanced HRQoL. Cluster D showed moderate disease severity but high emotional burden and strong medication beliefs. Cluster E included younger, mainly male patients with minimal comorbidities and the highest HRQoL. Self-rated health, fatigue and somatic preoccupation were the strongest discriminators. A rule achieving 90% coverage in Cluster B was defined by the following criteria: European Quality-of-life 5-Dimension (EQ-5D) "usual activities" > 1, EQ-5D "health today" ≤ 52, 8-item Somatic Symptom Scale (SSS-8) tiredness/low energy > 0, and Somatic Symptom Disorder-B Criteria Scale (SSD-12) behavioural subscale > 2.
Conclusion: This AI-based, multidimensional analysis identified five HRQoL phenotypes across AILDs, independent of diagnosis. The identification of a severely affected subgroup, identifiable through a simple four-item rule, highlights opportunities for targeted, transdiagnostic interventions.

SAT-370

Symptom experience in patients with primary biliary cholangitis: pilot survey results

Robert Mitchell-Thain[1], Mo Christie[1], Rebecca West[1], William Lobb[2], Nekshan Dalal[3], Alexa Ashton[2], Magnus Doverskog[4], David E. Jones[5]. *[1]PBC Foundation, Dunfermline, United Kingdom; [2]Indegene, Princeton, United States; [3]Indegene, London, United Kingdom; [4]Umecrine Cognition, Solna, Sweden; [5]Newcastle University Hospital, Newcastle Upon Tyne, United Kingdom*
Email: robert@pbcfoundation.org.uk

Background and aims: Primary biliary cholangitis (PBC) is a chronic cholestatic liver disease with significant impact on quality of life. This study aimed to capture symptom burden in PBC, and gain patient perspective on the need for new therapeutic options.
Method: 103 adults with PBC were surveyed using an online instrument on the PBC Foundation app. Respondents were predominantly female (98%) with majority aged 51–70 years (70%). 39% were employed full-time/part-time by choice, 18% were employed part-time or retired due to illness and 9% were unable to work due to illness. 96% of patients were on UDCA with 49% being responders, 6% non-responders, and 44% unsure/not told if they were responders. Only 9% of patients were told they had cirrhosis.
Results: Majority of patients reported experiencing central fatigue (84%) followed by dry eyes/dry mouth (72%), bone/joint pain (71%), peripheral fatigue (69%) and itching/pruritis (45%) in the last 4 weeks. 60% of patients reported experiencing both central and peripheral fatigue. 84% of patients reported moderate to severe fatigue on the PBC-40 questionnaire (48% moderate- score of 29 to 39 and 37% severe- score of ≥40). Central fatigue was patients' most burdensome/severe symptom (51%), followed by peripheral fatigue (41%) and bone ache (37%). Nearly half (49%) of patients reported experiencing their worst days due to central fatigue almost daily. Only 60% patients experiencing central fatigue and 45% experiencing peripheral fatigue discussed it with their clinicians believing fatigue to be "normal" (23%) and that clinicians cannot help (17%). When asked to choose only one symptom to treat, central fatigue overwhelmingly

dominated patient priorities (58%), followed by peripheral fatigue: 15%, all other symptoms combined: 27%.
Conclusion: Fatigue is commonly reported as one of the most prevalent symptoms of PBC. This survey highlights the importance of central (characterized by a lack of self-motivation) and peripheral fatigue (muscle weakness and dysfunction) constructs and the dominance of central fatigue as the most burdensome symptoms for which patients seek treatment. These findings underscore an urgent need for targeted interventions and a patient-focused approach to fatigue management to improve quality of life in PBC.

SAT-371
Nebokitug modulates gut–liver inflammatory and tissue-remodeling signatures in PSC patients with coexisting IBD
Revital Aricha[1], Tom Snir[1], John Lawler[1], Chris Cirillo[1], Dave Weiner[1], Adi Mor[1]. [1]*Chemomab Therapeutics Ltd., Tel Aviv, Israel*
Email: revital.aricha@chemomab.com

Background and aims: Primary sclerosing cholangitis (PSC) co-occurs with inflammatory bowel disease (IBD) in over 60% of affected individuals, reflecting intertwined gut–liver immune pathways. In the Phase 2 SPRING trial of nebokitug, a monoclonal antibody targeting the chemokine CCL24, 62% of enrolled PSC patients had concomitant ulcerative colitis (UC) or Crohn's disease (CD). We evaluated whether CCL24 inhibition modulates inflammatory and tissue-remodeling signatures relevant to PSC-IBD pathogenesis.
Method: SPRING study enrolled adults with PSC, with or without concomitant IBD. UC patients) were required to have emission or mild disease (Partial Mayo ≤2–3; no item >1), and and CD patients had to be in remission (CDAI <150). Concomitant IBD therapies were required to be stable for ≥12 weeks. Patients were treated with nebokitug (10 or 20 mg/kg) vs placebo once every three weeks for 15 weeks. Serum proteins were quantified using the Olink proteomic platform at baseline and Week 15. Biomarker analyses focused on inflammatory cytokines, chemokines, monocyte/macrophage markers, epithelial injury markers, and tissue-remodeling proteins previously associated with UC and CD activity.
Results: Nebokitug treatment led to modulation of inflammatory pathways shared between PSC and IBD. Significant reductions were observed in TNFRII, CXCL9/10/11, IL-6, CD14, IL-18, and IL-17, cytokines known to be strongly linked to IBD activation, mucosal immune recruitment and epithelial injury. Nebokitug also decreased multiple proteins associated with stromal and epithelial remodeling in IBD progression, including S100A12 (UC severity correlate), YKL-40 (IBD activity marker), resistin (predictor of Crohn's disease inflammation), CD38 (UC mucosal inflammation), and VEGF (angiogenesis in CD). Nebokitug demonstrated a significant elevation in MST-1, a negative regulator of inflammation that has been linked to genetic susceptibility and disease modulation in IBD, highlighting potential relevance to intestinal inflammatory pathways.
Conclusion: Treatment with nebokitug for up to 15 weeks resulted in improvements across inflammatory and tissue-remodeling pathways relevant to PSC with coexisting intestinal inflammation. These findings suggest that CCL24 inhibition may beneficially impact shared gut–liver inflammatory circuits.

SAT-372
Nebokitug down-regulates core fibrotic and immune pathways defined by single-cell liver profiling
Revital Aricha[1], Tom Snir[1], John Lawler[1], Chris Cirillo[1], Dave Weiner[1], Adi Mor[1]. [1]*Chemomab Therapeutics Ltd., Tel Aviv, Israel*
Email: revital.aricha@chemomab.com

Background and aims: Primary sclerosing cholangitis (PSC) is an immune-mediated biliary disease with no approved treatments. Recent single-cell analyses of human liver tissue identified four PSC-specific gene expression programs (GEPs), including extracellular matrix (ECM) remodeling, macrophage activation, fibrosis/myofibrosis, and immune-activation pathways. These GEPs are upregulated in livers from patients with PSC compared with those with metabolic dysfunction–associated steatohepatitis (MASH) and healthy controls. We assessed the effects of nebokitug, a CCL24-blocking monoclonal antibody in clinical development for PSC, on these GEPs by examining corresponding protein changes in serum from the SPRING Phase 2 trial.
Method: Serum proteins were quantified using the Olink proximity extension assay (PEA) in patients with PSC enrolled in the SPRING study who were treated with nebokitug 10 mg/kg (n = 21), nebokitug 20 mg/kg (n = 27), or placebo (n = 18). We analyzed the association between the four GEPs and disease severity (defined by elastography >8.7 kPa) and evaluated the effects of nebokitug vs placebo on these protein related GEPs.
Results: Proteins corresponding to all four PSC-related GEPs, reflecting fibrosis-related collagens, fibrotic macrophage activity, myofibroblast pathways, and immune-activation signaling, were significantly elevated in patients with moderate to advanced disease compared with those with mild PSC. Treatment with nebokitug led to dose-dependent reductions in serum proteins associated with these GEPs, with the greatest effects observed in patients with moderate to advanced disease.
Conclusion: Nebokitug treatment was associated with dose-dependent reductions in serum protein signatures linked to key fibrotic and immune pathways implicated in PSC. These findings support CCL24 blockade as a mechanism-based therapeutic approach targeting core molecular drivers of PSC pathogenesis.

SAT-377
AI-driven proteomic profiling differentiates composite improvement following treatment with nebokitug in PSC
Tom Snir[1], Revital Aricha[1], John Lawler[1], Chris Cirillo[1], Dave Weiner[1], Adi Mor[1]. [1]*Chemomab Therapeutics Ltd., Tel Aviv, Israel*
Email: tom.snir@chemomab.com

Background and aims: Primary sclerosing cholangitis (PSC) is a chronic liver disease, characterized by persistent and progressive inflammation and fibrosis. The phase 2 SPRING study of nebokitug, an anti-CCL24-monoclonal antibody, showed anti-inflammatory, anti-fibrotic, and anti-cholestatic activity in PSC patients. We present a machine-learning model trained on treatment-associated proteomic changes to characterize nebokitug's impact on the liver. In addition, integration with a liver-specific atlas proteome allows evaluation of coordinated liver-derived protein changes following treatment.
Method: Serum protein levels in patients with PSC were quantified by Olink explore HT, before and after 15 weeks treatment with nebokitug (10 mg/kg; n = 21, 20 mg/kg; n = 27). All measured proteins were used to model a composite improvement outcome requiring reductions in ELF score, transient elastography, and PRO-C3, using penalized logistic regression (Elastic Net). Feature importance was aggregated from 500 iterations of repeated 5-fold cross-validation. Consensus was defined by features selected in ≥50% of iterations. Model performance was evaluated via AUROC and validated using permutation testing. Pathway and network analyses were performed on contributing proteins. PCA was performed on sub-groups of proteins shown to be liver specific.
Results: The model accurately differentiated patients who met the composite improvement criterion from those who did not, achieving a mean AUROC of 0.92 in repeated cross-validation. Permutation testing confirmed the model's validity, outperforming random noise models (mean null AUROC 0.59; $p < 0.05$). Stability analysis resulted in a protein signature consistently selected across iterations. Pathway analysis showed metabolic, catabolic and extracellular matrix related pathways, predominantly expressed in the liver. Analysis of baseline-to-week 15 changes using a liver-specific atlas proteome allowed clear discrimination between the groups, as shown by PCA.
Conclusion: AI work based on proteomics was successful in distinguishing a composite efficacy improvement outcome to treatment with nebokitug in patients with PSC. Patients who meet

the criteria showed differential expressions of liver proteins, with functional liver related proteins as the main drivers of this change. This analysis highlights treatment-associated improvement following nebokitug therapy, as well as the importance of CCL24 blockade in liver diseases and PSC pathology.

SAT-378-YI

The italian primary biliary cholangitis registry: insights from a nationwide cohort study

Eugenia Nofit[1,2], Laura Cristoferi[1], Alessio Gerussi[1,2], Daphne D'Amato[2], Marco Mario Giacomo Festa[1], Emanuela Bonaiuto[3], Vito Di Marco[4], Francesco Azzaroli[5], Elton Dajti[5], Francesca Colapietro[6], Pietro Lampertico[7], Elisabetta Degasperi[7], Stefano Fagiuoli[2,8], Mauro Viganò[8], Antonino Castellaneta[9], Antonella De Feudis[9], Edoardo Giannini[10], Sara Labanca[10], Francesca Terracciani[11], Giovanni Raimondo[12], Carlo Saitta[12], Maurizio Russello[13,14], Mariarita Cannavò[13], Ester Vanni[15], Alessandra Risso[15], Filomena Morisco[16], Valentina Cossiga[16], Cristina Rigamonti[17], Giulia Francesca Manfredi[17], Gabriele Missale[18], Alessandra Orlandini[18], Raffaele Cozzolongo[19], Francesco Losito[19], Armando Curto[20], Andrea Galli[20], Luca Maroni[21], Maurizia Brunetto[22], Barbara Coco[22], Federica Cerini[23,24], Francesco Pavan[23], Francesco Bellanti[25], Stefano Quiete[25], Lucia Napoli[26], Francesco Giuseppe Foschi[26], Andrea Mega[27], Monica Zoeschg[27], Alessandro Granito[28], Fabio Piscaglia[28], Giovanni Vitale[29], Maria Cristina Morelli[29], Valeria Pace Palitti[30], Marcello Persico[31], Tommaso Sarcina[31], Lorenzo Surace[32], Elisabetta Falbo[32], Raffaella Viganò[33], Federico D'Amico[33], Silvia Nardelli[34], Domenico Montecalvo[34], Gerardo Nardone[16], Alba Rocco[16], Giovanni Vettori[35], Luisa Moser[35], Chiara Ricci[36], Paolo Poisa[36], Fabrizio Bronte[37], Andrea Affronti[37], Alessandro Federico[38], Fiammetta Di Nardo[38], Clara Agnolon[39], Giuliano Alagna[40], Mariaconsiglia Bragazzi[41], Ilaria Cavalli[42], Alessandra Mangia[43], Francesca Fianchi[44], Filippo Gabrielli[45], Teresa Zolfino[46], Grazia Anna Niro[47], Luca Fabris[48], Saveria Lory Croce'[49], Luchino Chessa[50], Anna Meneghetti[51], Luigi Muratori[52], Leonardo Baiocchi[53], Eleonora Grassi[54], Francesca Capelli[55], Ludovico Abenavoli[56], Anna Maria Baragiotta[57], Fabio Marra[58], Nadia Dal Bo'[59], Susanna Schianchi[60], Roberto Chiavaroli[61], Nora Cazzagon[3], Vincenza Calvaruso[4], Ana Lleo[6], Umberto Vespasiani-Gentilucci[11], Marco Marzioni[21], Marco Carbone[2,33], Pietro Invernizzi[1]. *[1]Fondazione Irccs San Gerardo dei Tintori di Monza, Università degli Studi di Milano-Bicocca, Monza, Italy; [2]Università degli Studi di Milano-Bicocca, Milano, Italy; [3]Azienda Ospedale Università Padova, University of Padova, Padova, Italy; [4]Azienda Ospedaliera Universitaria Policlinico Paolo Giaccone, University of Palermo, Palermo, Italy; [5]IRCCS Azienda Ospedaliero-Universitaria di Bologna Policlinico Sant'Orsola, Bologna, Italy; [6]Istituto Clinico Humanitas, Rozzano, Italy; [7]Fondazione Irccs Ca Granda Ospedale Maggiore Policlinico, Milano, Italy; [8]ASST Papa Giovanni XXIII, Bergamo, Italy; [9]Azienda Ospedaliero Universitaria Consorziale Policlinico, Bari, Italy; [10]Ospedale San Martino, Genova, Italy; [11]Fondazione Policlinico Universitario Campus Bio-Medico, Roma, Italy; [12]Azienda Ospedaliera Universitaria di Messina Gaetano Martino, Messina, Italy; [13]Azienda Ospedaliera di Rilievo Nazionale e di Alta Specializzazione Garibaldi, Catania, Italy; [14]LIVER UNIT, ARNAS GARIBALDI-NESIMA, CATANIA; [15]Azienda Ospedaliera Città della Salute e della Scienza, Turin, Italy; [16]Azienda Ospedaliera Universitaria Federico II, Napoli, Italy; [17]Azienda Ospedaliero Universitaria Maggiore della Carità, Novara, Italy; [18]Azienda Ospedaliero-Universitaria di Parma, Parma, Italy; [19]IRCCS S. De Bellis, Castellana Grotte, Italy; [20]Azienda Ospedaliero Universitaria Careggi, Gastroenterologia, Firenze, Italy; [21]Azienda Ospedaliero Universitaria delle Marche, Ancona, Italy; [22]Azienda Ospedaliera-Universitaria Pisana, Pisa, Italy; [23]Ospedale San Giuseppe, Milano, Italy; [24]Dipartimento di Scienze Cliniche e di Comunità Università degli Studi di Milano, Milano, Italy; [25]Azienda Ospedaliera Universitaria Ospedali Riuniti, Foggia, Italy; [26]AUSL Romagna Ospedale "degli Infermi" di Faenza, Faenza, Italy; [27]Azienda Sanitaria dell'Alto Adige, Bolzano, Italy; [28]S. Orsola-Malpighi Hospital, Department of Medical and Surgical Sciences, Bologna, Italy; [29]IRCCS Azienda ospedaliero-universitaria di Bologna - Policlinico Sant'Orsola, Bologna, Italy; [30]Ospedale "Santo Spirito", Pescara, Italy; [31]Azienda Ospedaliera Ospedali Riuniti San Giovanni di Dio e Ruggi d'Aragona, Salerno, Italy; [32]Presidio Ospedaliero Giovanni Paolo II, Lamezia Terme, Italy; [33]ASST Grande Ospedale Metropolitano Niguarda, Milano, Italy; [34]Policlinico Umberto I, Roma, Italy; [35]Presidio Ospedaliero Santa Chiara, Trento, Italy; [36]ASST Spedali Civili, Brescia, Italy; [37]Azienda Ospedaliera Ospedali Riuniti Villa Sofia-Cervello, Palermo, Italy; [38]Azienda Ospedaliera Universitaria Luigi Vanvitelli, Napoli, Italy; [39]Azienda Ospedaliera Universitaria Integrata di Verona, Borgo Trento Hospital, Verona, Italy; [40]Azienda Ospedaliero Universitaria Di Sassari, Sassari, Italy; [41]Ospedale Santa Maria Goretti, Latina, Italy; [42]Azienda Socio-Sanitaria Territoriale di Cremona, Cremona, Italy; [43]IRCCS Casa Sollievo della Sofferenza, San Giovanni Rotondo, Italy; [44]Fondazione Policlinico Universitario Agostino Gemelli IRCCS, Roma, Italy; [45]Ospedale Civile di Baggiovara, Modena, Italy; [46]Presidio Ospedaliero San Michele, ARNAS G. Brotzu, Cagliari, Italy; [47]Fondazione IRCCS Casa Sollievo della Sofferenza, Gastroenterology Unit, San Giovanni Rotondo, Italy; [48]Azienda Ospedale-Università Padova, Padova, Italy; [49]Azienda Sanitaria Universitaria Integrata Di Trieste, Trieste, Italy; [50]Presidio Ospedaliero Duilio Casula, A.O.U. di Cagliari, Monserrato, Italy; [51]Ospedale San Bassiano, Bassano del Grappa, Italy; [52]IRCCS Azienda Ospedaliero Universitaria, Policlinico Sant'Orsola, Medicina Interna e Malattie Immunoreumatologiche, Bologna, Italy; [53]Policlinico Tor Vergata, Roma, Italy; [54]Ospedale di Circolo e Fondazione Macchi, Varese, Italy; [55]Azienda Socio Sanitaria Territoriale Ovest Milanese, Legnano, Italy; [56]Azienda Ospedaliero-Universitaria Renato Dulbecco, Catanzaro, Italy; [57]Azienda Ospedaliera Santa Maria degli Angeli, Pordenone, Italy; [58]A.O.U. Careggi, Internal Medicine and Hepatology, Firenze, Italy; [59]Ospedale Ca' Foncello, Gastroenterology, Treviso, Italy; [60]Azienda Unità Sanitaria Locale IRCCS, Reggio Emilia, Italy; [61]Fondazione Poliambulanza Istituto Ospedaliero, Brescia, Italy*

Email: eugenia.nofit@irccs-sangerardo.it

Background and aims: Primary biliary cholangitis (PBC) is a rare autoimmune liver disease. Epidemiological data in Italy are limited. To address this the Italian PBC Registry was established in 2019 to collect retrospective and prospective data. This study provides an overview of the Registry and its collected data.

Method: The Registry includes demographic, biochemical, staging, and treatment data. Tests at diagnosis are those performed 3 months before to 30 days after diagnosis; tests at 1 year after UDCA were performed 11–15 months after treatment initiation. Categorical variables are reported as frequencies (%), continuous variables are reported as mean ± SD or median and interquartile range. ALP, AST, ALT, GGT are expressed as ratios of their ULN, bilirubin as mg/dL.

Results: From 2019 to 2025 enrolment increased from 128 to 3310 (37 ± 22 patients/month). 3199 were analyzed (111 excluded for missing data). The Registry involves 69 active centers, 61 entering data across Italy (40 North, 9 Center, 20 South/Islands). 2836 (89%) were female with mean age 55.3 ± 12 years, BMI 24.96 ± 4.64, 3067 (96.7%) were Caucasian. Median follow-up was 6.9 years [3.1,12.6]. 2018 (80.3%) reported no alcohol consumption, 456 (18.1%) consumed <10/20 g/day (women/men) and 40 (1.6%) consumed >10/20 g/day (women/men). Never-smokers were 1724 (70%), former 423 (17.2%), current 315 (12.8%). At diagnosis, among 1840 patients (57.5%) with available tests, the mean values were: ALP 1.59 [1.07,2.67], AST 1.25 [0.83,2.10], ALT 1.32 [0.80,2.18], GGT 3.90 [1.89,7.49], bilirubin 0.65 [0.50, 0.92] mg/dL. Liver biopsy was performed in 666 (20.8%) patients and transient elastography in 653 (20.4%) with a median liver stiffness of 6.6 kPa [5.0,9.1]. After one year of UDCA 809 (25.3%) patients had: ALP 1.11 [0.78,1.64], AST 0.78

[0.59,1.06], ALT 0.70 [0.48,1.10], GGT 1.26 [0.70,2.78], bilirubin 0.60 [0.44,0.83] mg/dL. Elevated ALP (>1.67) was observed in 185 (22.9%). However, considering the entire cohort, 923 (28.8%) patients initiated second-line therapy: 429 (46.5%) with Obeticholic Acid (OCA), 277 (30%) with fibrates, 163 (17.7%) with combination therapy (OCA and fibrate). Regarding the new PPAR-targeted therapies, 125 (13.5%) patients initiated Elafibranor and 52 (5.6%) initiated Seladelpar.
Conclusion: The Italian PBC Registry provides a national picture of PBC, supporting disease monitoring and management. Continued commitment from participating centers will enhance data completeness and strengthen the reliability of future analyses.

SAT-379

Alkaline phosphatase and bilirubin levels at one year of fibrate therapy predict long-term outcomes in patients with primary biliary cholangitis receiving second-line treatment

Satoko Ohfuji[1], Kyoko Kondo[2], Keiji Tsuji[3], Mayumi Yamaguchi[4], Yuki Yamashita[5], Hironao Okubo[6], Kazufumi Dohmen[7], Hideyuki Tamai[8], Masaya Tamano[4], Masanori Abe[9], Atsumasa Komori[10], Atsushi Tanaka[11]. *[1]Department of Public Health, Graduate School of Medicine, Osaka Metropolitan University, Osaka, Japan; [2]OMU Core Facilities Life Sciences Section, Osaka Metropolitan University, Osaka, Japan; [3]Department of Gastroenterology, Hiroshima Red Cross Hospital and Atomic-bomb Survivors Hospital, Hiroshima, Japan; [4]Department of Gastroenterology, Dokkyo Medical University Saitama Medical Center, Koshigaya, Japan; [5]Department of Medicine, Division of Gastroenterology, Shinshu University School of Medicine, Matsumoto, Japan; [6]Department of Gastroenterology, Juntendo University Nerima Hospital, Tokyo, Japan; [7]Gastrointestinal and Hepato-Biliary-Pancreatic Center, Chihaya Hospital, Fukuoka, Japan; [8]Department of Hepatology, Wakayama Rosai Hospital, Wakayama, Japan; [9]Department of Community and General Medicine, Ehime University Graduate School of Medicine, Ehime, Japan; [10]NHO Nagasaki Medical Center, Nagasaki, Japan; [11]Department of Medicine, Teikyo University School of Medicine, Tokyo, Japan*
Email: satoko@omu.ac.jp

Background and aims: In patients with primary biliary cholangitis (PBC) treated with ursodeoxycholic acid (UDCA) monotherapy, alkaline phosphatase (ALP) and total bilirubin (T-Bil) levels are well-established predictors of prognosis. However, their prognostic utility in patients receiving combination therapy with UDCA and fibrates remains unclear. This nationwide Japanese retrospective cohort study aimed to validate biochemical response criteria at one year of fibrate therapy as a predictor of transplant-free survival in patients with PBC receiving fibrates as second-line therapy.
Method: Patients with PBC who received bezafibrate (BZF) or pemafibrate (PMF) as second-line treatment due to an incomplete response or intolerance to UDCA between 2001 and 2024 were included. By using laboratory data at one year after starting fibrate treatment, the proportions achieving 1) ALP < 1.67×the upper limit of normal (ULN) and ≥ 15% ALP reduction and T-Bil normalization, 2) both ALP and T-Bil normalization, 3) ALP normalization and T-Bil < 0.6 × ULN were assessed. Then, the association between each biochemical response criteria and transplant-free survival was analyzed by using Kaplan-Meier and Cox proportional hazard models.
Results: A total of 558 patients (BZF: 344, PMF: 214) were included. The median age was 60 years (IQR: 50–68 years), and 460 (82%) were female. At 1 year of fibrate treatment, the median ALP level (×ULN) was 0.81 (IQR: 0.57–1.60), and the median T-Bil level (×ULN) was 0.50 (IQR: 0.40–0.67). 315 (57.3%) achieved 1) ALP < 1.67 × ULN and ≥ 15% ALP reduction and T-Bil normalization, 326 (59.3%) achieved 2) both ALP and T-Bil normalization, and 261 (47.5%) achieved 3) ALP normalization and T-Bil < 0.6 × ULN. During a median follow-up of 4.9 years, 27 (4.8%) patients underwent death or liver transplantation. In the univariate analysis, all three criteria were significantly associated with outcomes. After adjustment of potential confounders, achieving 1) ALP < 1.67 × ULN and ≥ 15% ALP reduction and T-Bil normalization was only a significant predictor, which showing a 69% reduction in hazard (HR = 0.31, 95%CI: 0.11–0.83).
Conclusion: This nationwide Japanese cohort study demonstrates that the ALP and T-Bil levels at one year after initiation of fibrate therapy are valuable predictors for transplant-free survival in patients with PBC receiving fibrates as second-line treatment.

SAT-380

Clinical utility of thiopurine methyltransferase (TPMT) genotype and azathioprine (AZA) metabolites in the management of autoimmune hepatitis (AIH)

Ignasi Olivas[1,2], Judit Julian[3], Ana Maria Lizana[3], Pinelopi Arvaniti[1,2,4], Helena Hernández Evole[1,2,4], Sergio Rodriguez-Tajes[1,2,4], Jaime Sainz[3], Mercè Brunet[3,5], María Carlota Londoño[1,2,4,6]. *[1]Liver Unit, Hosptial Clínic Barcelona, Institut d`Investigació Biomedica August Pi y Sunyer (IDIBAPS), Barcelona, Spain; [2]Fundació de Recerca Clínic Barcelona-Institut d'Investigacions Biomèdiques August Pi Sunyer (FRCB-IDIBAPS), Barcelona, Spain; [3]Department of Biochemistry and Molecular Genetics, Section of Pharmacology and Toxicology, Hospital Clínic Barcelona, Barcelona, Spain; [4]Centro de Investigación Biomédica en Red Enfermedades Hepáticas y Digestivas (CIBEREHD), Barcelona, Spain; [5]Universitat de Barcelona, Barcelona, Spain; [6]Universitat de Barcelona, Centro de Investigación Biomédica en Red Enfermedades Hepáticas y Digestivas (CIBEREHD), Institut d`Investigació Biomedica August Pi y Sunyer (IDIBAPS), Barcelona, Spain*
Email: ignasiolivasalberch@gmail.com

Background and aims: Current AIH guidelines recommend monitoring AZA metabolites, 6-thioguanine (6-TG) and 6-methylmercaptopurine (6-MMP), to optimize therapy. Evidence for their clinical utility is limited, and the relationship between TPMT genotype and AZA metabolites remains unclear. This study evaluated the impact of TPMT genotyping and 6-TG/6-MMP monitoring on the management of AIH.
Method: This prospective study included 112 AIH patients treated with AZA and prednisone. TPMT polymorphisms (*3A, *3B, and *3C) were assessed by qPCR. Erythrocyte 6-TG and 6-MMP concentrations were measured using ultra-high-performance liquid chromatography–mass spectrometry. Therapeutic ranges were defined as 6-TG 235–450 pmol/8 × 10^8 erythrocytes and 6-MMP <5700 pmol/8 × 10^8 erythrocytes. Continuous data are expressed as median (IQR).
Results: Most patients were women (67%), Caucasian (89%), age 55 years (38.9–64.8). Time from AZA initiation to first metabolite measurement was 3.3 years (0.98–6.53) and AZA dose was 100 mg/d (75–125). Testing was performed for insufficient response (IR) in 50 patients (45%) and for AZA dose adjustment in 62 patients (55%) with complete biochemical response (CBR). Among 96 patients with TPMT genotyping, seven (7%) were heterozygous for *3A and the remainder were wild type (WT). Median 6-TG and 6-MMP levels were 386 pmol/8 × 10^8 erythrocytes (IQR 259–566) and 1541 pmol/8 × 10^8 erythrocytes (IQR 0–3976). No differences in 6-TG levels were found between WT and heterozygous patients, while 6-MMP levels were significantly lower in heterozygous patients ($p < 0.001$). AZA dose correlated positively with 6-TG levels in WT ($\rho = 0.34$; 95% CI 0.15–0.52; $p < 0.001$) and heterozygous patients ($\rho = 0.89$; 95% CI 0.40–1.00; $p = 0.012$). 6-TG levels were not associated with CBR, anaemia, or leukopenia ($p > 0.05$). Metabolite-guided management led to treatment changes in 34 patients: in 19 with CBR and 6-TG or 6-MMP above range, AZA was reduced; in 9 with IR and 6-TG below range, AZA was increased; in 6 with IR and 6-TG above range, AZA was switched to MMF. Four patients with IR and undetectable 6-TG were identified as non-adherent.
Conclusion: TPMT genotyping and AZA metabolite monitoring showed interindividual variability and adherence issues, prompting therapeutic adjustments in a substantial proportion of patients with AIH. The lack of association between 6-TG levels and CBR or toxicity

suggests metabolite monitoring may be mainly useful in patients with IR.

SAT-381

Impact of metabolic syndrome on clinical outcomes in primary biliary cholangitis: a retrospective cohort study

Jade Pace[1], Michael Attanasi[1], Brittany Kwait[1], Christopher Dorizas[1], Bryana Belin[2], Maham Ghani[1], Sanjaya Satapathy[1]. *[1]Northwell Health, Manhasset, United States; [2]Donald & Barbara Zucker School of Medicine at Hofstra, Hempstead, United States*
Email: jpace1@northwell.edu

Background and aims: Metabolic syndrome is an increasing area of interest among patients with chronic liver disease and has been associated with adverse outcomes in several conditions. However, its impact on clinical outcomes in primary biliary cholangitis (PBC) remains unclear. We investigated the association between metabolic syndrome and hepatic decompensation and mortality in a retrospective cohort of patients with PBC followed at a tertiary care center. We hypothesized that the comorbidity of metabolic syndrome confers a worse prognosis.
Method: Inclusion criteria consisted of patients at least 18 years of age with an ICD-10 code diagnosis of PBC and positive anti-mitochondrial antibody titer ≥ 1:40 that were admitted over the past 10 years. Metabolic syndrome was defined using established clinical criteria at index admission. Body mass index ≥ 30 kg/m^2 and A1c ≥ 5.6% were used as surrogates for elevated waist circumference and fasting glucose. The primary outcomes were time to first hepatic decompensation (ascites, bilirubin > 3.0, encephalopathy, or esophageal gastrointestinal bleed) and all-cause mortality. Survival was assessed using Kaplan-Meier methods, and Cox proportional hazards models were used to evaluate associations after adjustment for age, sex, and Model for End-Stage Liver Disease (MELD) score where available.
Results: A total of 401 adults with PBC were included. Among this cohort, 137 patients (34%) met criteria for metabolic syndrome. Liver disease severity markers such as bilirubin levels and MELD score were similar between groups. During follow-up, 140 patients (35%) developed hepatic decompensation and 68 patients (17%) died. In multivariable models adjusted for age and sex, metabolic syndrome was not independently associated with hepatic decompensation (hazard ratio [HR] 0.83; 95% confidence interval [CI] 0.63–1.10) or mortality (HR 1.18; 95% CI 0.64–1.82). In MELD-adjusted mortality models (n = 310), metabolic syndrome remained unassociated with mortality (HR 1.08; 95% CI 0.64–1.82). Older age, male sex, and higher MELD score were independently associated with increased mortality.
Conclusion: In this large cohort of patients with PBC, metabolic syndrome was not independently associated with hepatic decompensation or mortality after adjustment for established disease severity markers. These findings suggest that traditional indicators of liver disease severity, rather than metabolic comorbidity burden, primarily drive adverse outcomes in PBC.

SAT-382

Utility of spleen stiffness measurement for the detection of esophageal varices in primary biliary cholangitis (PBC)

Marlene Padilla-Lopez[1,2], Ignacio Vaz-Romero[3], Adriana Ahumada[4], Javier Merino[5], Ivica Grgurević[2,6], Anita Madir[7], Frane Pastrovic[2,8], Filomena Morisco[2,9], Elisabetta Degasperi[2,10], Limas Kupčinskas[2,11], Ruta Vindzgalskyte[2,11], Esther Maderuelo[12], Neus Garcia Ferris[12], Elba Llop Herrera[2,12], Elton Dajti[2,13], Francesco Azzaroli[2,13], Javier Fajardo[14], Anna Brujats[14], Edilmar Alvarado-Tapias[14], Joao Madaleno[2,15], Xavier Verhelst[2,16], Maria Papp[2,17], Boglarka Bozso[2,17], Daniela De la Viña[18], Alejandra Villamil[2,18], Juan Carlos Bandi[18], Pinelopi Arvaniti[1,2,19], Ignasi Olivas[1,2,19], Helena Hernández Evole[1,2,19], Magdalena Salcedo Plaza[20], Mar Riveiro Barciela[2,3,19], María Carlota Londoño[1,2,19], Sergio Rodriguez-Tajes[1,2,19]. *[1]Liver Unit, Hospital Clínic Barcelona, Fundació de Recerca Clínic Barcelona–Institut d'Investigacions Biomèdiques August Pi i Sunyer (FRCB-IDIBAPS), University of Barcelona, Barcelona, Spain; [2]European Reference Network on Rare Liver Diseases (ERN RARE-LIVER), Europa; [3]Liver Unit, Department of Internal Medicine, Vall d'Hebron University Hospital, Barcelona, Spain; [4]Hospital General Universitario Gregorio Marañón, Centro de Investigación Biomédica en Red de Enfermedades Hepáticas y Digestivas (CIBEREHD), Madrid, Spain; [5]Hospital General Universitario Gregorio Marañón, Madrid, Spain; [6]Klinička Bolnica Dubrava, European Reference Network on Rare Liver Diseases (ERN RARE-LIVER), Zagreb, Croatia; [7]Klinička Bolnica Dubrava, Zagreb, Croatia; [8]University Hospital Dubrava, Zagreb, Croatia; [9]Azienda Ospedaliera Universitaria Federico II, Naples, Italy; [10]Division of Gastroenterology and Hepatology, Foundation IRCCS Ca' Granda Ospedale Maggiore Policlinico, Milan, Italy; [11]Lithuanian University of Health Sciences, Kaunas, Lithuania; [12]Hospital Universitario Puerta De Hierro, Madrid, Spain; [13]Gastroenterology Unit, IIRCCS Azienda Ospedaliero-Universitaria di Bologna, Bologna, Italy; [14]Hepatology and Gastroenterology Department, Hospital de la Santa Creu i Sant Pau, Barcelona, IR Sant Pau, Universitat Autonoma de Barcelona, Barcelona, Spain; [15]Hospitais da Universidade de Coimbra, Coimbra, Portugal; [16]Department of Gastroenterology and Hepatology, Ghent University Hospital, Gent, Belgium; [17]University of Debrecen, Clinical Center, Nagyerdei Campus, Debrecen, Hungary; [18]Hospital Italiano de Bueno Aires, Bueno Aires, Argentina; [19]Centro de Investigación Biomédica en Red de Enfermedades Hepáticas y Digestivas (CIBEREHD), Spain, Spain; [20]Hospital General Universitario Gregorio Marañón, Centro de Investigación Biomédica en Red de Enfermedades Hepáticas y Digestivas (CIBEREHD), Barcelona, Spain*
Email: marlenepadillamd@gmail.com

Background and aims: In primary biliary cholangitis (PBC), clinically significant portal hypertension (CSPH) may develop even in precirrhotic stages due to a presinusoidal component, potentially limiting the accuracy of Baveno VII (BVII) criteria for predicting esophageal varices (EV). We aimed to evaluate the utility of spleen stiffness measurement (SSM) in predicting EV and varices needing treatment (VNT) in patients with PBC.
Method: This multicenter cross-sectional study included patients from 14 centers with PBC fulfilling at least one of the following criteria: Liver stiffness measurement (LSM) ≥8 kPa, splenomegaly, platelet count ≤150 × 10^9/L, or ultrasonographic signs of cirrhosis or portal hypertension. LSM and SSM were assessed using transient elastography. Laboratory tests, ultrasound (±6 months from the SSM), and upper endoscopy (±12 m) were collected.
Results: We included 126 patients, 87% women, with a median age of 64 years (IQR 58–71). Overall, 82% had a LSM ≥8 kPa, 48% thrombocytopenia, 49% splenomegaly, and 65% cirrhosis. Median LSM and SSM values were 13.6 kPa (IQR 9.1–21.3) and 36.6 kPa (IQR 25.2–48.6), respectively. EV were present in 39% of patients, of whom 28% had VNT. The prevalence of VNT was significantly higher in patients with LSM >15 kPa (24%) compared with those with LSM 8–15 kPa (4%) or <8 kPa (0%; p = 0.002). For EV prediction, BVII criteria (LSM ≤ 15 kPa and platelet count ≥150 × 10^9/L) showed moderate diagnostic accuracy (AUC 0.71), with a sensitivity (Se) of 85%, specificity (Sp) of 55%, and negative predictive value (NPV) of 85%. LSM alone demonstrated comparable performance (AUC 0.74, Se of 94%, Sp 48% and NPV of 93%) at a cut-off of 9.8 kPa. Platelet count also showed moderate accuracy (AUC 0.70, Se 55%, Sp 82%, NPV 74%) using a cut-off of 127.5 × 10^9/L. SSM achieved the highest diagnostic accuracy for EV detection (AUC 0.79, Se 78%, Sp 74%, NPV 84%) at a cut-off of 37 kPa. Combining SSM ≥37 kPa with a platelet count <127.5 × 10^9/L further improved diagnostic performance (AUC 0.81, Se 45%, Sp 88%, NPV 72%). For VNT prediction, SSM was the strongest predictor (AUC 0.85, Se 93%; Sp 65%; NPV 99%), at a cut-off of 39 kPa, outperforming BVII criteria, LSM, and platelet count (AUC 0.68, 0.74, and 0.77, respectively).
Conclusion: SSM showed superior diagnostic accuracy for predicting esophageal varices and varices needing treatment in patients with

PBC, improving BVII criteria. Its use may enable more accurate risk stratification, including in precirrhotic stages.

SAT-383

Beyond fibrosis: clinical relevance of histological inflammatory patterns in autoimmune hepatitis

Ana Pascual-Dapena[1], Marta Sánchez-Ric[1], Helena Hernández Evole[1], Diogo Simas[1], Nuria Florensa[1], David Heitmann[1], Ignasi Olivas[1], Pinelopi Arvaniti[1], Sergio Rodriguez-Tajes[1], María Carlota Londoño[1]. *[1]Liver Unit, Hospital Clinic Barcelona, Fundació de Recerca Clínic Barcelona-Institut d'Investigacions Biomèdiques August Pi i Sunyer (FRCB-IDIBAPS), Ciberehd, Barcelona, Spain*
Email: mlondono@clinic.cat

Background and aims: Autoimmune hepatitis (AIH) exhibits diverse histological features. Beyond fibrosis, the implications of these patterns in terms of disease presentation, progression, and outcomes remain inadequately defined. We aimed to assess the clinical and prognostic implications of different histological inflammatory patterns in patients with AIH.
Method: We retrospectively evaluated 349 diagnostic liver biopsies from patients with AIH. Histology was classified into four inflammatory patterns: predominant portal inflammation (PI), predominant lobular inflammation (LI), mild portal and lobular inflammation (mPLI), and moderate-to-severe portal and lobular inflammation (m-sPLI). The presence of ductular reaction (DR) was also assessed. Liver-related events (LRE) were defined as cirrhosis development, decompensation, hepatocellular carcinoma, liver transplantation, and liver-related death. Complete biochemical response (CBR) was assessed during follow-up.
Results: Most patients were women (71%), with a median age of 53 years (IQR 42–63) and a median follow-up of 8 years (IQR 5–12). At diagnosis, 33 patients had PI, 34 LI, 84 mPLI, and 112 m-sPLI. DR was present in 41 patients. Patients with predominant LI and m-sPLI showed higher median AST (873 and 710 vs. 217 and 382 U/L), ALT (1015 and 834 vs. 274 and 430 U/L), and bilirubin levels (7 and 5.4 vs. 1.0 and 1.7 mg/dL) compared with PI and mPLI phenotypes (all $p < 0.05$), and more frequently presented with acute AIH (67% and 58% vs. 35% and 43%, respectively; $p = 0.013$). Patients with DR had higher GGT (193 vs. 135 U/L, $p < 0.001$), alkaline phosphatase (236 vs. 155 U/L, $p = 0.004$), and bilirubin levels (7.0 vs. 2.6 mg/dL, $p = 0.021$). CBR rates were 47% at 6 months, 57% at 12 months, and 78% at last follow-up, with no significant differences across histological phenotypes. After excluding patients with cirrhosis at diagnosis ($n = 37$), 66 patients developed LRE during follow-up. Predominant LI was associated with a lower risk of LRE compared with other histological phenotypes (6% vs. 23%; OR 0.21, 95% CI 0.05–0.89; $p = 0.035$), and this association persisted after adjustment for baseline fibrosis (OR 0.22, 95% CI 0.05–0.97; $p = 0.048$).
Conclusion: Distinct histological inflammatory patterns in AIH are associated with different clinical presentations and long-term outcomes. Predominant lobular inflammation identifies a subgroup of patients with a more favourable disease course. Recognition of histological patterns at diagnosis may improve risk stratification in AIH.

SAT-384

Statins are underutilized for cardiovascular disease in patients with PBC

Mark Pedersen[1], Gemma H. X. Weijsters[2], Adriaan J. van der Meer[2], Ellina Lytvyak[3], Allison Mella[3], Sergio Rodriguez-Tajes[4], Helena Hernández Evole[4], Cláudia Couto[5], Henriette Ytting[6], Xavier Verhelst[7], Agnes Paradissis[7], Cynthia Levy[8], Adrielly Martins[8], Marco Carbone[9], Eugenia Nofit[9], Álvaro Díaz-González[10], Konstantinos Papantoniou[11], Christos Triantos[11], Conrado Fernandez-Rodriguez[12], Gideon M. Hirschfield[13], Shani Nagler[13], Chloe Nguyen[13], Bettina E. Hansen[2], Marlyn J. Mayo[1]. *[1]University of Texas Southwestern Medical Center at Dallas, Dallas, United States; [2]Erasmus MC, Rotterdam, Netherlands; [3]University of Alberta, Edmonton, Canada; [4]Hospital Clínic De Barcelona, Barcelona, Spain; [5]Universidade Federal De Minas Gerais, Belo Horizonte, Brazil; [6]Hvidovre Hospital, Hvidovre, Denmark; [7]UZ Gent, Gent, Belgium; [8]University of Miami Miller School of Medicine, Miami, United States; [9]Università degli Studi di Milano-Bicocca, Milano, Italy; [10]Hospital Universitario Marqués De Valdecilla, Santander, Spain; [11]Division of Gastroenterology, Department of Internal Medicine, University of Patras, 26504, Patras, Greece, Patras, Greece; [12]Universidad Rey Juan Carlos, Madrid, Spain; [13]UHN - Toronto General Hospital - Elizabeth St Garage, Toronto, Canada*
Email: mrpeders@gmail.com

Background and aims: Primary biliary cholangitis (PBC) is a chronic, cholestatic liver disease that is associated with dyslipidemia. Retrospective studies have suggested that dyslipidemia in PBC is not associated with increased risk of major adverse cardiovascular events (MACE), or is associated only in the presence of another cardiovascular risk factor. We use data from the multinational Global PBC Study group to examine the treatment patterns of dyslipidemia in PBC.
Method: Retrospective chart review was performed at 13 separate clinical sites in the Global PBC Study group. Data were collected on prior diagnoses of dyslipidemia, hypertriglyceridemia, hypertension, chronic kidney disease (CKD), pharmacotherapy of dyslipidemia, revascularizations (cardiac, cerebral, or peripheral) and MACE (defined as ST-elevation myocardial infarction [STEMI], non-ST-elevation myocardial infarction [NSTEMI], unstable angina, cerebrovascular accident, and transient ischemic attack).
Results: Data were collected on 1926 patients from 9 countries. 799 (24.6%) of these patients carried a diagnosis of dyslipidemia, 652 (20.1%) hypertension, and 136 (7.1%) chronic kidney disease. There were 81 MACE events (5.3%), with 45 of these being cardiac (STEMI, NSTEMI, or unstable angina). Only 40.5% of patients with dyslipidemia and hypertension were on a statin as primary prophylaxis of MACE. Of the 106 patients who had either a MACE or revascularization event for non-MACE reasons (e.g. high-risk coronary lesions), only 58.4% patients ever received a statin.
Conclusion: In this large, multinational population, only 40.5% of patients with two identified risk factors for MACE were prescribed a statin as primary prophylaxis, as is suggested by current AASLD and EASL guidelines. Further, only half the patients with a strong indication for statin use (history of MACE or revascularization procedure) were prescribed a statin. Though further work is needed to define which patients with PBC are at increased risk for MACE, the present data suggest that statins are underutilized in patients with PBC.

SAT-385

Identifying primary biliary cholangitis in the general population: a laboratory based look back exercise

Isobel Phillips[1], Molly Thorpe[1], Abdullah Alhouri[1], Grace Hutchinson[1], Angharad Clements[1], Joanna Gould[1], Molly Flint[1], Eleanor Godward[1], Andrew Yeoman[1]. *[1]Aneurin Bevan University Health Board, Newport, United Kingdom*
Email: andrew.yeoman@wales.nhs.uk

Background and aims: PBC is typically diagnosed via the combination of a positive anti-mitochondrial antibody (AMA) and raised alkaline phsophatase (ALP) levels. The true prevalence is probably underestimated due to a lack of awareness of the disease in non specialist settings. We set out to evaluate whether there are a significant number of patients within our region of Gwent, Wales, that possess the laboratory features that are highly suggestive of PBC but who are currently undiagnosed.
Method: A retrospective search was undertaken within the clinical laboratory system within the Aneurin Bevan University Health Board utilsing data from 1st April 2104 to 30th March 2024. We identified all

pateints with a positive AMA and corrleated this with whether the ALP was elevated, either at the same time as AMA postitivity or at any time point during future follow up. Patients with an existing diagnosis of PBC were also identified via notes review.
Results: A total of 974 unique individuals had a raised AMA, 378 of which have a confirmed diagnosis of PBC given a population prevalence of 69/100,000. Of the remaining 596 individuals without a diagnosis of PBC, 132 (22%) had an eleavted ALP synchronous to the AMA positivity. Of these individuals 65% were referred and assessed by Hepatology and PBC had been excluded. In addition, 464 had a normal ALP of whom 109 (23%) had been referred and seen for specialty assessment. Of the 464 with a normal ALP at time of AMA positivity, 225 (48%) subsequently had at least 1 elevation in the ALP and in 163 (35%) this was persistent. Specilaist clinical review occurred in 60/163 (37%) of this cohort. Overall, there were 149 individuals whose AMA and ALP would be suggestive of PBC prompting specialist assessment but who have not been referred for such.
Conclusion: Despite a high PBC prevalence, around 2/3rds of positive AMAs in our region over a decade are not asscoiated with a confirmed diagnosis of PBC. Furthermore 149 of these individuals (25%) have not been formally reviewed by Hepatology to confirm a diagnosis. Work is now currently underway to identify how many of these individuals have PBC.

SAT-386

Prevalence and clinical impact of metabolic dysfunction-associated steatotic liver disease in primary biliary cholangitis: a tertiary-center experience

Riccardo Plebani[1], Maria Pia Calabrese[1,2], Antonella Ruiu[1,2], Pietro Meschisi[1,2], Stella De Nicola[1,2], Nicola Pugliese[1,2], Vincenzo Ronca[1,2], Alessio Aghemo[1,2], Ana Lleo[1,2]. *[1]Department of Biomedical Sciences, Humanitas University, Department of Gastroenterology, Division of Internal Medicine and Hepatology, IRCCS Humanitas Research Hospital, Rozzano, Milan, Italy; [2]Department of Gastroenterology, Division of Internal Medicine and Hepatology, IRCCS Humanitas Research Hospital, Rozzano, Italy*
Email: ric.plebani@gmail.com

Background and aims: Metabolic dysfunction-associated steatotic liver disease (MASLD) is frequent among general population, as such might coexist with other chronic liver condition such as primary biliary cholangitis (PBC). However, its clinical relevance remains uncertain. While current management effectively targets cholestasis, it is unclear whether patients with concomitant MASLD differ in disease progression. We aimed to assess MASLD prevalence in a tertiary-care PBC cohort, assessing their treatment response and disease course compared with PBC alone.
Method: We conducted a single-centre, retrospective, observational study of consecutive patients with PBC. MASLD was defined by evidence of hepatic steatosis on imaging in the presence of cardiometabolic risk factors. Fibrosis stage was assessed by liver biopsy or liver stiffness measurement. Metabolic dysfunction–associated steatohepatitis (MASH) was defined histologically. Clinical outcomes were assessed at the last available follow-up.
Results: Among 160 patients with PBC, 50 (31%) had concomitant MASLD. Baseline alkaline phosphatase levels were comparable between patients with and without MASLD (median 220, IQR 145–321 vs median 211, IQR 151–381 respectively, $p = 0.80$), while gamma-glutamyltransferase levels were higher in MASLD patients without being statically significant (median 224, IQR 123–438 vs median 274, IQR 167–538, respectively, $p = 0.30$). Liver stiffness measurements were similar between groups, whereas CAP values were significantly higher in patients with MASLD (median 201, IQR 181–233 vs median 255, IQR 227–293, $p < 0.05$). Response to UDCA did not differ between groups. Cirrhosis was less frequent among patients with MASLD compared with those without MASLD (14% vs 32%, $p = 0.029$). Hepatic decompensation occurred in 4% of patients with MASLD and 12% of those without MASLD, without a statistically significant difference between groups. Among patients with MASLD, 8 (18.6%) had fibrosis stage F2–F3; histological MASH was identified in 3 patients.
Conclusion: MASLD was a common overlapping condition in patients with PBC, yet its presence was not associated with clear differences in cholestatic treatment response or short-term clinical outcomes in this cohort. These findings raise the hypothesis that MASLD may have a limited impact on the clinical course of established PBC, although longer follow-up and larger prospective studies are needed.

SAT-387

Meaningful within-patient change on the 5-D itch scale in patients with primary biliary cholangitis experiencing pruritus

David E. Jones[1], Andreas E. Kremer[2], Milena Anatchkova[3], Mary Kate Ladd[3], Anne Skalicky[3], Shubhram Pandey[4], Marvin Rock[5], Susheela Carroll[5], Caroline Burk[5]. *[1]Newcastle University, Newcastle, United Kingdom; [2]University Hospital Zürich, University of Zürich, Zürich, Switzerland; [3]Thermo Fisher Scientific, Waltham, MA, United States; [4]Pharmacoevidence, Mohali, India; [5]Gilead Sciences, Foster City, CA, United States*
Email: david.jones@newcastle.ac.uk

Background and aims: Pruritus is a prominent symptom in primary biliary cholangitis (PBC). In the phase 3 RESPONSE trial (NCT04620733), seladelpar (SEL) vs placebo (PBO) significantly and meaningfully reduced pruritus in patients with PBC as measured using the pruritus numerical rating scale (NRS), the established regulatory standard for pruritus assessment in PBC studies. Findings were supported by consistent results from the 5-D Itch scale, a validated patient-reported measure of pruritus severity and impact. However, a meaningful within-patient change (MWPC) threshold on the 5-D Itch was not established. Here, RESPONSE patient data were analyzed to establish an MWPC threshold on the 5-D Itch.
Method: RESPONSE was a 12-month, double-blind, placebo-controlled trial. The 5-D Itch was completed bi-weekly from run-in to Month (M) 6 and monthly to M12. Anchor-based analyses of the intent-to-treat population (ITT) at M6 and M12 examined the 5-D Itch total score's sensitivity to change and identified an MWPC threshold; all ITT patients with data were evaluated. Patient Global Impression of Severity (PGI-S) and Change (PGI-C) scales (completed at baseline, M6, M12) served as anchors. Spearman's correlation coefficients between 5-D Itch total and PGI-S/PGI-C change scores verified anchor suitability. A distribution-based estimate (0.5 × SD at baseline) supported anchor-based findings. Proportions of 5-point responders for the 5-D Itch were evaluated in the ITT and the subgroup with moderate to severe pruritus (MSPN; baseline Pruritus NRS ≥ 4).
Results: RESPONSE enrolled 193 patients (128 SEL; 65 PBO). PGI-S and PGI-C were deemed suitable anchors ($|\text{Spearman's } \rho| > 0.30$). In patients with a 1-point PGI-S improvement, mean (SD) change in 5-D Itch total was –4.21 (3.64) at M6 and –3.70 (3.47) at M12 (median –5 for both). In patients reporting "moderately better" on the PGI-C, mean (SD) change was –3.49 (4.38) at M6 and –2.38 (3.94) at M12 (median: –2.5 at M6; –3.5 at M12). The distribution-based estimate was 2.39. At M6, 24% on SEL vs 14% on PBO were 5-point responders in the ITT, and 45% on SEL vs 26% on PBO were 5-point responders in the MSPN. At M12, 23% on SEL vs 9% on PBO were 5-point responders in the ITT, and 43% on SEL vs 17% on PBO were 5-point responders in the MSPN.
Conclusion: An MWPC threshold range of –3 to –5.5 points on the 5-D Itch in patients with PBC in RESPONSE was established. Higher proportions of patients on SEL than PBO were 5-point responders at M6 and at M12.

SAT-388

Primary biliary cholangitis education significantly improves competence in recognising which patients would most likely benefit from second line therapy

S Christy Rohani-Montez[1], Marinella Calle[1], Margaux Le Berre[1], Marlyn J. Mayo[2], Mark Swain[3], María Carlota Londoño[4]. [1]*Medscape Education Global, London, United Kingdom;* [2]*UT Southwestern Medical Center, Dallas, TX, United States;* [3]*University of Calgary, Calgary AB, Canada;* [4]*Hospital Clinic Barcelona, Barcelona, Spain*
Email: srohani@medscape.net

Background and aims: Best practices in the management of primary biliary cholangitis (PBC) are evolving with the recent availability of peroxisome proliferator-activated receptor (PPAR) agonists. We sought to improve physician competence according to the Moore's Outcomes Framework, in recognizing who would potentially benefit from these second-line therapies, and to improve knowledge regarding PPAR agonist clinical trial data by providing expert-led accredited education.
Method: Physicians participated in a 55-minute, video-based online CME activity divided into 4 main discussions with different speakers and synchronized slides (available at www.medscape.org/viewarticle/1002582). Education effects were assessed using a 3-question, repeated pairs, pre-/post-assessment study design. One question assessed confidence. Pre- to post-assessment differences were evaluated using the McNemar's test. $P \leq 05$ was considered significant. The activity launched in June 2025, and data collected through October 2025.
Results: Overall significant improvements were seen after participation for gastroenterologists/hepatologists (gastro/heps) with a correct response rate of 44% at pre-assessment vs 62% post-assessment ($p < .001$, Cohen's $d = 0.68$, $N = 272$), and for primary care physicians (PCPs) with a correct response rate of 44% at pre-assessment vs 57% at post-assessment ($p < .001$, Cohen's $d = 0.51$, $N = 457$). Case-based questions assessing when to consider second-line therapy showed significant improvements. The largest gap in knowledge was regarding the therapeutic expectations of PPAR agonists based on current clinical data, specifically how quickly ALP reductions should be expected, but this also significantly improved post-education. After participating, 32% of gastro/heps and 35% of PCPs had measurable improvements in confidence in deciding when to start second-line PBC therapy. When asked what challenges are most often encountered when assessing the need for second-line PPAR agonists amongst inadequate UDCA responders, 30% of gastro/heps and 42% of PCPs said lack of knowledge on PPAR agonist clinical data and 44% of gastro/heps and 43% of PCPs said lack of or limited access to these therapies. Only 8% of gastro/heps and 5% of PCPs said they were not convinced that PPAR agonists would benefit these patients.
Conclusion: This study demonstrates the success of online video-based education in improving competence and confidence in implementing second line PPAR agonists for patients with PBC.

SAT-393

From real patients to digital twins: synthetic cohorts for evidence generation in UDCA-treated primary biliary cholangitis

Vincenzo Ronca[1], Sara Baccino[2], Ferrari Ivan[2], Eugenia Nofit[3], Alessio Gerussi[4], Laura Cristoferi[3], Saverio D'amico[2], Matteo Della Porta[1,2], Pietro Invernizzi[3,4], Marco Carbone[4,5], Ana Lleo[1,2]. [1]*Department of Biomedical Sciences, Humanitas University, Department of Gastroenterology, Division of Internal Medicina and Hepatology, IRCCS Humanitas Research Hospital, Milan, Italy;* [2]*IRCCS Humanitas Research Hospital, Milan, Italy;* [3]*Fondazione IRCCS San Gerardo dei Tintori di Monza, Monza, Italy;* [4]*Department of Medicine and Surgery, University of Milano-Bicocca, Division of Gastroenterology, Center for Autoimmune Liver Diseases, European Reference Network on Hepatological Diseases (ERN RARE-LIVER), Monza, Italy;* [5]*Hepatology and Gastroenterology Unit, Grande Ospedale Metropolitano Niguarda, Milan, Italy*
Email: Vincenzo.ronca@hunimed.eu

Background and aims: Second-line therapies expanded treatment options for primary biliary cholangitis (PBC) patients who are non-responders to ursodeoxycholic acid (UDCA) and at risk of disease progression; however, regulatory approval has relied on biochemical surrogate endpoints rather than hard clinical outcomes. Outcome-based trials remain challenging due to slow disease progression and constraints on placebo use in the presence of approved therapies, highlighting the need for alternative evidence-generation frameworks. We aimed to generate and validate high-fidelity synthetic cohort of UDCA-treated PBC patients.
Method: A total of 1016 UDCA-treated PBC patients were derived from the Italian PBC retrospective registry. Demographics, laboratory test, comorbidities, and clinical outcomes were collected. A patented AI-based generative model was trained on baseline and follow-up variables to generate a synthetic cohort at a 1:1 ratio. Fidelity was assessed by comparing summary statistics, standardised mean differences (SMD), principal component analysis, distance- and correlation-based metrics, and a composite Clinical Synthetic Fidelity (CSF) score. Privacy protection was evaluated by the 5th percentile distance to closest record (DCR) and nearest neighbour distance ratio (NNDR). Biochemical trajectories were compared. Transplant-free survival according to UDCA response, defined by POISE criteria, was analysed in real and synthetic cohorts.
Results: The synthetic cohort closely reproduced baseline demographics and clinical features. Median age was 57 years (IQR 50–66) in both cohorts, with comparable sex distribution and laboratory values. Transplant-free survival curves and hazard separation between synthetic and real cohorts in UDCA responders and non-responders were preserved. All SMDs were <0.05, indicating good balance. Fidelity metrics were high (CSF 0.896; correlation score 0.945; numerical and categorical distance scores 0.878 and 0.886; PCA score 0.877). Privacy analyses showed similar 5th percentile DCR values for real–synthetic (6.02) and real–real (5.58) comparisons, with NNDR values of 0.896 and 0.857. Longitudinal biochemical trajectories overlapped over five years.
Conclusion: High-fidelity synthetic patient-level data accurately reproduce demographic, longitudinal biochemical, and outcome patterns in UDCA-treated PBC. Synthetic cohorts offer a scalable complement to traditional evidence generation, enabling external control arms and exploratory regulatory analyses in slow-progressing diseases.

SAT-394

Frequency of PFIC-associated genetic variants across different adult cholestatic phenotypes

Vivian Rotman[1], Andreia Evangelista[1], Aline Moura Ferraz Pereira[1], Cibele Franz[2], Luciana Agoglia[3], Renata Perez[1], Maria Chiara Chindamo[1]. [1]*Federal University of Rio de Janeiro, Rio de Janeiro, Brazil;* [2]*UNIRIO, Rio de Janeiro, Brazil;* [3]*Federal Fluminense University, Rio de Janeiro, Brazil*
Email: vrotman@gmail.com

Background and aims: Progressive familial intrahepatic cholestasis (PFIC) comprises a group of autosomal recessive disorders caused by pathogenic variants in genes encoding bile acid transport proteins and may progress to advanced liver disease. In adults, PFIC-associated variants are often linked to milder phenotypes and are frequently identified in the heterozygous state, challenging the traditional view of strict recessive inheritance. Data on the prevalence and clinical impact of PFIC-related variants in Brazilian adults remain limited. This study aimed to describe the frequency of PFIC-associated genetic variants and the clinical and demographic characteristics of adults with cholestatic phenotypes.
Method: Adult patients evaluated for cholestatic liver disease underwent genetic analysis of 18 cholestasis-related genes using

next-generation sequencing (Illumina HiSeq 2500/4000) on buccal swab samples. Variants were classified according to ACMG criteria and HGVS nomenclature as pathogenic (P), likely pathogenic (LP), or variants of uncertain significance (VUS). Clinical, laboratory, and demographic data were retrospectively collected from medical records.
Results: Fifty-five patients were included: 64% female with mean age at symptom onset of 36.1 ± 14.5 years. Chronic cholestasis was the predominant clinical phenotype (87.3%), and cirrhosis at diagnosis was observed in 14.5% of patients. PFIC-associated variants were identified in 31 patients (56.4%), predominantly involving the *ABCB4* gene (93.5%). Among these, 22 variants occurred in simple heterozygosity (14 variants were classified as pathogenic, 3 as LP, and 5 as VUS) and 7 in compound heterozygosity (one patient carried VUS in both alleles, while six patients carried a VUS in one allele combined with another variant). *ABCB11* variants were identified in one patient (3.2%) in compound heterozygosity, and *CFTR* variants were also detected in only one patient (3.2%). Typical cholestatic symptoms were frequently observed among individuals carrying VUS.
Conclusion: *ABCB4* variants were highly prevalent among Brazilian adults with cholestatic liver disease. The predominance of simple heterozygosity supports the possibility of alternative inheritance mechanisms or the presence of undetected variants. The association between VUS and classical cholestatic manifestations suggests a potential for future reclassification of some of these variants as pathogenic.

SAT-395
Tacrolimus as second-line therapy in pediatric autoimmune hepatitis: remission and response outcomes in a single-center cohort
Saurabh Saurabh[1]. [1]*Ilbs Pharmacy, New Delhi, India*
Email: saurabh394@gmail.com

Background and aims: A subset of children with autoimmune hepatitis (AIH) remain refractory or intolerant to standard therapy with corticosteroids and azathioprine, constituting a difficult-to-treat phenotype. Evidence for calcineurin inhibitors in this population is limited. We evaluated the efficacy and safety of tacrolimus as second-line immunosuppression in pediatric AIH.
Method: A retrospective cohort of 16 children (age 3–18 years) with AIH (type 1/ 2 or seronegative) treated with tacrolimus were analyzed. Indications included incomplete biochemical response, azathioprine intolerance, or persistent disease activity despite optimized therapy. Tacrolimus dosing targeted trough levels of 4–8 ng/mL. Outcomes assessed were (i) biochemical remission (normal ALT and IgG), (ii) biochemical response (>50% improvement), time to remission, and (iii) adverse events. Median follow-up was 8 months.
Results: Of 16 children receiving tacrolimus, 7 (43.7%) achieved complete biochemical remission, with a median time to remission of 5 months. An additional 5 children (31.2%) demonstrated partial biochemical response. Overall, 12/16 (75%) showed meaningful biochemical improvement. Four children had minimal/no response. Among responders, corticosteroid tapering was feasible in the majority, with several achieving steroid minimization. Tacrolimus was generally well tolerated. Reported adverse events included mild tremors (n = 2), transient hypertension (n = 1), and reversible nephrotoxicity (n = 1).
Conclusion: Tacrolimus is an effective and safe second-line immunosuppressive option in pediatric AIH, achieving remission or substantial biochemical improvement in three-quarters of treated children. These findings support consideration of tacrolimus in difficult-to-treat pediatric AIH and highlight the need for multicenter prospective studies to standardize dosing and long-term surveillance.

SAT-396
Bone mineral density is stable in patients with primary biliary cholangitis receiving up to 3.5 years of elafibranor treatment
Jörn M. Schattenberg[1], Pietro Andreone[2], Michael Heneghan[3], Cynthia Levy[4,5], Nuno Antunes[6], Darren Asquith[7], Seema Jaitly[7], Nathan Touati[8], Marlyn J. Mayo[9]. [1]*Department of Internal Medicine II, Saarland University Medical Center, Homburg, Germany;* [2]*Medicina Interna Metabolica, Baggiovara Hospital, Azienda Ospedaliero-Universitaria di Modena and Università di Modena e Reggio Emilia, Modena, Italy;* [3]*Institute of Liver Studies, King's College Hospital NHS Foundation Trust, London, United Kingdom;* [4]*Schiff Center for Liver Diseases, University of Miami, Miami, Florida, United States;* [5]*Division of Digestive Health and Liver Diseases, University of Miami School of Medicine, Miami, Florida, United States;* [6]*Ipsen, Cambridge, Massachusetts, United States;* [7]*Ipsen, London, United Kingdom;* [8]*Ipsen, Paris, France;* [9]*Division of Digestive and Liver Diseases, University of Texas Southwestern Medical Center, Dallas, Texas, United States*
Email: joern.schattenberg@uks.eu

Background and aims: Patients (pts) with primary biliary cholangitis (PBC) have a higher risk of osteoporosis and fractures. Elafibranor (ELA) demonstrated no negative impact on bone health through 52 weeks (wks) of the phase III ELATIVE® trial (NCT04526665). Here, data from the ongoing open-label extension (OLE) are presented.
Method: Data are reported for pts who completed the double-blind period (DBP) and continued daily ELA 80 mg into the OLE; baseline (BL) was defined as DBP start. Dual energy X-ray absorptiometry (DEXA), the gold standard for assessing bone mineral density (BMD), was used to measure the femoral neck, lumbar spine and total hip regions. Mean (standard deviation [SD]) change from BL (CfB) in BMD absolute values and T-scores are reported through Wk 182. Due to staggered OLE entry, data were pooled for Wk 104 and 130 (Wk 104|130) and Wk 156 and 182 (Wk 156|182). Bone fractures are reported from OLE start to data cut-off (DCO; May 2025).
Results: 93/108 (86.1%) pts continued ELA into the OLE; at BL, 87/93 (93.5%) were female, 34/93 (36.6%) had osteoporosis or osteopenia and mean (SD) age was 56.7 (8.3) years. At BL, mean (SD) femoral neck BMD absolute value was 0.79 g/cm^2 (0.15) which remained stable at Wk 52 (CfB: 0.00 g/cm^2 [0.05]), 104|130 (CfB: 0.00 g/cm^2 [0.03]) and 156|182 (CfB: −0.03 g/cm^2 [0.05]). Mean (SD) lumbar spine BMD absolute value at BL was 0.99 g/cm^2 (0.18); this was stable at Wk 52 (CfB: 0.00 g/cm^2 [0.04]), 104|130 (CfB: 0.00 g/cm^2 [0.05]) and 156|182 (CfB: −0.01 g/cm^2 [0.07]). Mean (SD) total hip BMD absolute value was 0.84 g/cm^2 (0.14) at BL and remained stable at Wk 52 (CfB: 0.00 g/cm^2 [0.04]), 104|130 (CfB: +0.01 g/cm^2 [0.03]) and 156|182 (CfB: +0.04 g/cm^2 [0.18]). Mean (SD) BMD T-scores at BL for femoral neck, lumbar spine and total hip regions were −1.36 (1.1), −1.24 (1.45) and −1.14 (1.16), respectively; these remained stable at Wk 52 (CfB: −0.04 [0.40]; −0.03 [0.49]; +0.03 [0.51]), 104|130 (CfB: −0.01 [0.29]; −0.11 [0.44]; +0.05 [0.36]) and 156|182 (CfB: −0.16 [0.70]; −0.06 [0.77]; +0.00 [0.64]). From OLE start to DCO, 9 fractures occurred in 8/93 (8.6%) pts; most fractures were associated with a fall (7/9 [77.8%]) or trauma (1/9 [11.1%]) and 7/8 (87.5%) pts had confounding factors.
Conclusion: After up to 3.5 years of ELA treatment, BMD remained stable in pts with PBC. Few pts experienced fractures, and most had confounding factors; the observed proportion was consistent with the expected rate in a PBC population, suggesting ELA has no negative impact on bone health.

SAT-397
Histological and morphometric analyses demonstrate antifibrotic activity of norucholic acid in primary sclerosing cholangitis
Hendrik Wiethoff[1], Stefan G. Hübscher[2], Sandra Noh[1], Thomas Longerich[1], Geoffrey Chase[3], Markus Proels[3], Michael Stiess[3], Peter Fickert[4], Hans Heinrich Wedemeyer[5], Michael Trauner[6], Peter Schirmacher[1]. [1]*Institute of Pathology, University Hospital*

Heidelberg, Heidelberg, Germany; [2]School of Infection, Inflammation and Immunology, University of Birmingham, Birmingham, United Kingdom; [3]Dr. Falk Pharma GmbH, Freiburg, Germany; [4]Department of Medicine, Medical University of Graz, Graz, Austria; [5]Department of Gastroenterology, Hepatology, Infectious Diseases and Endocrinology, Hannover Medical School, Hannover, Germany; [6]Division of Gastroenterology and Hepatology, Department of Internal Medicine III, Medical University of Vienna, Vienna, Austria
Email: peter.schirmacher@med.uni-heidelberg.de

Background and aims: Norucholic acid (NCA) was recently shown to confer a significant benefit for patients with primary sclerosing cholangitis (PSC) in the NUC-5/PSC trial. This benefit was demonstrated using endpoints incorporating paired liver biopsies. Here, we present detailed results of histopathological evaluations conducted in the trial.
Method: The NUC-5/PSC trial compared 1500 mg NCA versus placebo (PBO) in patients with PSC over a 192-week double-blind phase, with the primary analysis performed at week 96. Biopsies were collected at screening as well as weeks 96 and 192 according to local procedures. Histological analyses were carried out at the primary analysis, with 201 patients having at least one screening and one post-baseline biopsy (NCA: 144, PBO: 57). Histological evaluation was performed centrally by hematoxylin and eosin and Sirius red staining as well as cytokeratin 7 immunohistochemistry. All biopsies were assessed centrally for multiple histological scores by two expert liver pathologists blinded to treatment allocation and biopsy sequence. Collagen proportionate area (CPA) was evaluated by semiquantitative digital pathology.
Results: Significantly more patients exhibited no worsening in histological disease stage with NCA than PBO as assessed by Ludwig staging (risk difference [RD] 20.7, $p < 0.001$), modified Nakanuma score (RD 16.8, $p = 0.006$), PSC histoscore (RD 16.7, $p = 0.006$), and Ishak staging (RD 18.9, $p = 0.002$). The treatment effect by no worsening in Ludwig stage was consistent across disease severity at baseline, as defined by baseline ALP levels (<2.5x ULN: RD 26.7; ≥2.5x ULN: RD 12.4), liver stiffness by Fibroscan (F0: RD 31.1; F4: 22.0), or Ludwig stage (stages 1+2: RD 22.1; stages 3+4: RD 20.1). Fibrosis as assessed by CPA increased with Ludwig stage: mean (±SD) CPA at baseline was 3.7% (±2.1%) in all patients with Ludwig stage 1, 5.7% (±2.8%) for Ludwig stage 2, 10.0% (±4.2%) for Ludwig stage 3, and 25.4% (±11.6%) for Ludwig stage 4. Mean CPA changed from 8.9% (±6.3%) at baseline to 8.0% (±6.8%) at week 96 among NCA patients compared with 7.8% (±6.7%) to 9.3% (±8.7%) among placebo patients with evaluable biopsies at both time points.
Conclusion: Detailed histological analyses revealed significant antifibrotic treatment effects of NCA in PSC, which were consistent across all different staging systems and degrees of baseline disease severity. In line with staging results, CPA analysis by digital pathology confirmed positive effects of NCA on liver fibrosis.

SAT-398

The burden of fatigue in primary sclerosing cholangitis: results from the WIND-PSC prospective cohort

Christoph Schramm[1], Gideon M. Hirschfield[2], Christopher L. Bowlus[3], Brian Thorsen[4], Bettina E. Hansen[5], Mary Vyas[6], Kidist Yimam[7], Daniel Pratt[8], Craig Lammert[9], Sayed Obaidullah Aseem[10], Aldo J Montano-Loza[11], Michael Li[12], Zuha Jeddy[4], Sammantha Fuller[13], Julia Van Dyke[13], Stephen Rossi[4], Cynthia Levy[14].
[1]UKE - University Medical Center Hamburg-Eppendorf, Department of Medicine, Hamburg, Germany; [2]University of Toronto - UHN, Autoimmune and Rare Liver Disease Programme, Toronto, Canada; [3]University of California at Davis, Department of Medicine, Sacramento, United States; [4]PSC Partners Seeking a Cure, Greenwood Village, United States; [5]Erasmus University Medical Center, Erasmus, Netherlands; [6]PSC Partners Seeking A Cure - Canada, Toronto, Canada; [7]California Pacific Medical Center, Division of General and Transplant Hepatology, San Francisco, United States; [8]Massachusetts General Hospital, Autoimmune and Cholestatic Liver Center, Boston, United States; [9]Indiana University, Department of Medicine, Indianapolis, United States; [10]Virginia Commonwealth University, Department of Medicine, Richmond, United States; [11]University of Alberta, Department of Medicine, Edmonton, Canada; [12]University of California at San Francisco, Department of Medicine, San Francisco, United States; [13]Arbor Research Collaborative For Health, Ann Arbor, United States; [14]University of Miami, Department of Medicine, Miami, United States
Email: clevy@med.miami.edu

Background and aims: Fatigue is a burdensome but poorly understood symptom of primary sclerosing cholangitis (PSC) that significantly impacts quality of life. Data on its persistence and relationship to other symptoms is lacking. WIND-PSC is a global prospective observational study evaluating clinical outcomes, biomarkers and symptom burden in adults with PSC. We report an interim analysis on the incidence, severity, and persistence of fatigue and its correlation to other symptoms.
Method: Adult patients with large duct PSC were prospectively enrolled at 9 sites in North America and Europe. A patient-reported categorical symptom screening tool assessing the frequency, severity and persistence of abdominal pain, anxiety, brain fog, fatigue, insomnia, liver pain, nausea, and pruritus is administered at baseline and every 12 weeks. Evaluation criteria required baseline and a Week 12 and/or 24 assessment.
Results: A total of 261 patients met symptom screening criteria with patient demographics and disease characteristics consistent with other PSC cohorts. Cirrhosis was present in 12% of patients based on a liver stiffness measurement (LSM) >15 kPa and clinical data. Fatigue was the most prevalent symptom at baseline (75%) with severe and frequent/constant symptoms in 18% and 29%, respectively. Other less frequent symptoms were insomnia (62%), anxiety (58%), brain fog (46%), abdominal pain (46%), pruritus (44%), liver pain (36%), and nausea (27%). Most patients had ≥ 2 symptoms at baseline (69%) and only 12% reporting no symptoms. Presence and severity of fatigue at baseline was most strongly correlated (r_S) with insomnia (0.58) followed by brain fog (0.52) and abdominal pain (0.50). Fatigue was not associated with LSM, IBD status, duration of PSC, or any patient demographics. At Week 24, fatigue persisted for 31%, worsened for 13%, newly emerged for 12%, remained absent for 13%, improved for 14%, and resolved for 11% of patients. Change in fatigue at Week 24 was moderately associated with directional change or persistence in brain fog ($p < 0.001$), anxiety ($p < 0.05$), insomnia ($p < 0.05$), and abdominal pain ($p < 0.05$), and aligned with the associations at baseline.
Conclusion: Fatigue is a frequent but poorly understood symptom in people with PSC, independent of disease stage or demographics and linked to the presence and persistence of other symptoms. These data support further studies to understand the factors leading to the occurrence and persistence of fatigue and its impact on health-related quality of life.

SAT-399

Anti-HK1 and Anti-KLHL12 antibodies in primary biliary cholangitis: diagnostic relevance but no prognostic impact

Mirjam Kolev[1], Basil Ummel[1], Henning Nilius[2], Florian Kollert[3], Michael Mahler[4], Gary Norman[5], Chelsea Bentow[4], Michael Horn[2], Michael Nagler[2], Nasser Semmo[1]. *[1]Department of Visceral Surgery and Medicine, Inselspital, Bern University Hospital, University of Bern, Switzerland, Bern, Switzerland; [2]Department of Clinical Chemistry, Inselspital, Bern University Hospital, University of Bern, Switzerland, Bern, Switzerland; [3]Department of Rheumatology and Immunology, Bern University Hospital, University of Bern, Switzerland, Bern, Switzerland; [4]Research and Development, Autoimmunity, Werfen, San Diego, CA, USA, San Diego, United States; [5]Research and Development, Autoimmunity, Werfen, San Diego, CA, San Diego, United States*
Email: mirjam.kolev@insel.ch

Background and aims: Novel antibodies against hexokinase 1 (HK1) and kelch-like 12 (KLHL12) have been proposed as highly specific diagnostic markers for primary biliary cholangitis (PBC) and as potential prognostic indicators. We aimed to assess their diagnostic and prognostic value in a contemporary PBC cohort.
Method: In this retrospective single-center cohort study, 96 PBC patients and 269 non-PBC controls underwent extended serological profiling, including anti-MIT3 (M2), anti-gp210, anti-sp100, anti-HK1, and anti-KLHL12. Diagnostic performance was evaluated using receiver operating characteristic (ROC) curves and area under the curve (AUC) analysis. Transplant-free survival was analyzed with Kaplan–Meier estimates and Cox regression.
Results: Among the 96 PBC patients, 84% were female, with a median age of 56 years (IQR 45.5–65). Median follow-up was 8.3 years (IQR 4.3–12.3). Anti-HK1 and anti-KLHL12 antibodies were detected in 50.0% and 21.9% of patients, respectively. Established markers were positive in 86.5% (anti-MIT3), 19.5% (anti-gp210), and 24% (anti-sp100). Anti-MIT3 alone showed a sensitivity of 86.5% (95% CI, 78.0–92.6%) and specificity of 94.3% (95% CI, 88.1–97.9%). Considering all antibodies together, sensitivity increased to 91.7% (95% CI, 84.2–96.3%) with a modest decrease in specificity to 90.6% (95% CI, 83.3–95.4%). Fifteen patients either died from liver-related events or underwent transplantation. No statistically significant differences in transplant-free survival were observed for anti-HK1, anti-KLHL12, anti-gp210, or anti-sp100 positivity (all $p > 0.05$).
Conclusion: Anti-HK1 and anti-KLHL12 antibodies are common in PBC and provide complementary diagnostic information when added to established serological markers, modestly improving overall sensitivity. However, they were not associated with transplant-free survival, indicating their primary utility is diagnostic rather than prognostic in contemporary PBC patients.

SAT-400
Baseline predictors of treatment failure in autoimmune hepatitis: a multicenter study with external validation
Anna Sessa[1], Edouard Bardou-Jacquet[2], Maud Lemoine[3], Caterina Porciani[4], Lucia Possamai[5], Antonio Saviano[6], Lorraine Blaise[7], Filippo Biagi[8], Marianne Ziol[7], Belinda Smith[5], Fabio Marra[9], Nathalie Ganne-Carrié[7], Eduardo Miraval[10], José Echeveste[10], Maria Anson[10], Josepmaria Argemi[10], Stefano Caruso[11], Sara Lemoinne[4], Robert D. Goldin[3], Pierre Allaume[2], Julien Calderaro[1], Vincent Leroy[1]. *[1]Hôpitaux Universitaires Henri Mondor, Paris-Est Créteil University, Medicine, Créteil, France, Inserm, U955, Team 18, Créteil, France, Créteil, France; [2]Chu Pontchaillou Rennes, Rennes, France; [3]Imperial College of Science Technology & Medicine, St Mary's Hospital, London, United Kingdom; [4]Hôpital Saint-Antoine Ap-Hp Par Chartier Dalix, University of Pisa, Paris, France; [5]Saint Mary's Hospital, London, United Kingdom; [6]Hôpital Civil, Strasbourg, France; [7]Hôpital Avicenne, Bobigny, France; [8]Azienda Ospedaliera Careggi, Firenze, Italy; [9]Azienda Ospedaliero Universitaria Careggi, Firenze, Italy; [10]Clinica Universidad de Navarra, Pamplona, Spain; [11]Faculté de Santé-Upec, Créteil, France*
Email: asessa1990@gmail.com

Background and aims: Lack of treatment response and cirrhosis are associated with hepatic events in autoimmune hepatitis (AIH), yet predictors of treatment failure available at diagnosis remain poorly defined. We aimed to identify baseline predictors of treatment failure in a large multicenter AIH cohort and to externally validate a simple risk stratification.
Method: This retrospective longitudinal study included a training cohort of 351 consecutive patients with AIH and liver biopsy at diagnosis with at least 1 year of follow up treated in 4 French, 1 Italian, and 1 Spanish tertiary centers (2010–2023). An external validation cohort comprised 65 UK patients (2012–2024). Complete biochemical response (CRB) was defined according to EASL guidelines. Candidate predictors were restricted to baseline variables and selected using LASSO. A simple clinical risk score was derived in the training cohort and applied to the validation cohort.
Results: Training and validation cohorts were comparable for age (54 years in both), gender (68% and 78% female), prevalence of cirrhosis (28% and 31%) and treatment regimens (azathioprine + corticoids 88 vs 79%). Compared with the training cohort, UK patients had significantly lower ALT levels (232 vs 495.5 IU/L, $p = 0.001$) and higher IgG levels (25 vs 20 g/L, $p = 0.008$). CBR within one year was achieved in 76% and 81% of patients, while refractory disease occurred in 10% and 9%, respectively. IgG levels and cirrhosis emerged as the main predictors of treatment failure, defining three baseline risk groups: low (IgG <25.9 g/L), intermediate (IgG ≥ 25.9 g/L without cirrhosis), and high risk (IgG ≥25.9 g/L with cirrhosis). In the validation cohort, response rates decreased stepwise across risk groups (88%, 81%, and 64%), mirroring the pattern observed in the training cohort (85%, 63%, and 47%). High-risk patients had reduced odds of response (OR 0.26, 95% CI 0.05–1.17) and increased odds of refractory disease (OR 3.54, 95% CI 0.59–21.21). When used to identify treatment failure, the score demonstrated a specificity of 78% in the validation cohort (89% in the training cohort), a sensitivity of 50% (vs 35%), and a high negative predictive value (94% vs 92%). Incorporating early ALT response status into the baseline score did not improve discrimination.
Conclusion: A simple baseline IgG–cirrhosis score provides reproducible stratification of treatment failure risk in AIH and may have clinical utility for individualized therapeutic strategies.

SAT-401-YI
Early real-world experiences of Elafibranor in primary biliary cholangitis (PBC)
Charlotte Sewell[1,2], Nadir Abbas[2], Diane Lloyd Madden[2], Ahmed M Elsharkawy[2], Amanda Smith[2], James Ferguson[2], Palak Trivedi[1,2]. *[1]University of Birmingham, Birmingham, United Kingdom; [2]Liver Unit, University Hospitals Birmingham NHS Foundation Trust, Birmingham, United Kingdom*
Email: charlottesewell@nhs.net

Background and aims: Elafibranor (Ela), a next-generation peroxisome proliferator-activated receptor (PPAR) alpha/delta agonist, was approved for the treatment of PBC in 2024. Herein, we evaluate early real-world experiences in using Ela as a second-, third-, or fourth-line treatment for PBC.
Method: The effectiveness, safety and tolerability of Ela was evaluated in patients (pts) initiating therapy in combination with ursodeoxycholic acid (UDCA), obeticholic acid (OCA), and amongst those switching from bezafibrate (BZF).
Results: From Dec 2024 to Nov 2025, 54 pts initiated Ela (49 women, median age 57y, median transient elastography score 11.5 kPa). 18 pts had cirrhosis, 47 continued UDCA, 16 combined Ela with OCA and 29 switched from BZF to Ela. To date, n = 45, 33 and 17 have completed 1-, 3- and 6-months follow-up, respectively. 8, 4, and 2 pts discontinued Ela at the same timepoints, principally for gastrointestinal side effects (n = 7). However, 5 pts were able to restart later. In pts continuing Ela, median alkaline phosphatase (ALP) decreased from 2.47x upper limit of normal (ULN) at baseline, to 1.64x, 1.49x and 1.36x ULN at 1, 3 and 6 months respectively ($p < 0.0001$), with 2, 4 and 3 pts attaining normal ALP at the same points. Alanine aminotransferase (ALT) decreased from 0.99x ULN at baseline, to 0.87x, 0.80x and 0.84x ULN at 1,3 and 6 months ($p < 0.03$). Bilirubin was 0.62x ULN at baseline and remained stable at 1, 3 and 6 months. Pts on Ela without OCA showed similar reductions in ALP (from 2.94x ULN at baseline to 1.65x, 1.50x, and 1.32x ULN at 1, 3, and 6 months; $p < 0.001$) to the Ela + OCA group (ALP lowered from 1.88x ULN to 1.44x ULN at 1 month and 1.2x ULN at 3 months; $p < 0.02$). In pts who switched to Ela from BZF, ALP decreased from 2.68x ULN to 1.68x, 1.21x and 1.94x ULN at 1, 3 and 6 months ($p < 0.008$). ALP reductions were similar to those with no prior BZF exposure (2.26x ULN at baseline to 1.65x, 1.50x and 1.15x ULN at 1, 3 and 6 months; $p < 0.008$). No significant reductions in ALT

were observed in the sub-group of pts on Ela+OCA combination therapy, nor in those with prior BZF exposure. In all, n = 21/40 pts with pruritus at baseline reported improvement, 11 no change, and 4 worsening of itch. 24 pts who switched from BZF reported pruritus at baseline, and 12 reported improvement on Ela.
Conclusion: Treatment with Ela in real-world PBC settings is associated with early biochemical and symptomatic improvement, including in pts previously treated with BZF, and in combination with OCA.

SAT-402

MSC-mediated modulation of the IL-4/CD39 Axis in treg cells restores immune tolerance and improves treatment outcomes in steroid-resistant autoimmune hepatitis

Wanwan Shi[1]. [1]*Peking University First Hospital, Beijing, China*
Email: wanwanshi198@163.com

Background and aims: Autoimmune hepatitis (AIH) is an immune-mediated liver disease that poses significant challenges in treatment, particularly for patients who are steroid-resistant. Recent studies have highlighted that reduced CD39 expression on Treg cells, leading to impaired immunosuppressive function, is one of the key pathogenic mechanisms in AIH. Mesenchymal stem cells (MSCs) has demonstrated promising results in treating immune-related diseases. This study aims to explore the role of MSCs in restoring Treg cell function by modulating the IL-4/CD39 axis, providing a novel therapeutic strategy for steroid-resistant AIH patients.
Method: We assessed the expression of IL-4 in peripheral blood mononuclear cells from steroid-resistant AIH patients using flow cytometry, and investigated the correlation between IL-4 expression and CD39 in Treg cells. Additionally, immunofluorescence staining was performed to examine the distribution of CD39 and IL-4 in liver tissue from these patients. To investigate the causal relationship between IL-4 and AIH susceptibility, we conducted a two-sample Mendelian randomization (MR) analysis. Furthermore, we evaluated the therapeutic effects of MSCs in a ConA-induced AIH mouse model by measuring liver injury biomarkers, immunoglobulin levels, and Treg cell subtypes and function, with a focus on the regulation of the IL-4/CD39 axis.
Results: In PBMCs from steroid-resistant AIH patients, we observed significantly elevated IL-4 levels ($P < 0.01$), which correlated negatively with CD39 expression on Treg cells ($R = -0.42$, $P = 0.02$). MR analysis confirmed a significant causal relationship between IL-4 and AIH susceptibility. The analysis using the Inverse Variance Weighted method showed statistical significance (OR = 1.459027, 95% CI: 1.006–2.115, $P = 0.046$) suggesting that IL-4 may increase the risk of AIH. These findings demonstrate a critical link between IL-4, CD39 deficiency, and impaired immune suppression in Treg cells. In AIH mouse models, MSC treatment significantly reduced ALT, AST, and IgG levels ($P < 0.0001$), indicating effective immunoregulation. MSC treatment also significantly increased the proportion of Treg cells, restored CD39 expression and decreased IL-4 expression, suggesting that MSCs restore Tregs function by modulating the IL-4/CD39 axis.
Conclusion: Our findings demonstrate that MSCs can modulate the IL-4/CD39 axis in Treg cells to restore immune tolerance for AIH. This approach represents a novel strategy for treating autoimmune liver diseases.

SAT-403

Analysis of structured and unstructured data from a large electronic health record system identifies frequent pruritus and fatigue in patients with PSC

Anthony Perez[1], Ashley Jaksa[1], Sarah Sidhu[2], Douglas B. Mogul[2], Shannon Vandriel[2], April LaRow[2], Michael Fried[1]. [1]*Target RWE, Durham, North Carolina, United States;* [2]*Mirum Pharmaceuticals, Inc., Foster City, California, United States*
Email: sarah.sidhu@mirumpharma.com

Background and aims: Primary sclerosing cholangitis (PSC) is a progressive cholestatic liver disease featuring bile duct strictures that lead to hepatic injury, cirrhosis, and liver failure. Pruritus and fatigue may occur, but reported prevalence varies widely across studies. We used large electronic health record (EHR) databases, TARGET-LD and TARGET-GASTRO, with over 800,000 patients with liver and gastrointestinal disease that contain both structured and unstructured data to assess dataset robustness and frequency of patient-reported pruritus and fatigue in PSC patients.
Method: PSC patients were identified in TARGET-LD/GASTRO using ICD-10 K83.0. Baseline characteristics, amount of liver enzyme results [alanine aminotransferase (ALT); aspartate aminotransferase (AST); alkaline phosphatase (ALP)], MRCP testing, and diagnoses of pruritus and fatigue were described. For a subset of patients who had unstructured data available (i.e., provider notes), we evaluated the EHR text for positive mentions of pruritus, fatigue, and MRCP testing, using a purpose-built natural language processing (NLP) system to improve prevalence estimates relative to traditional code-based enumeration alone.
Results: We identified a cohort of 3958 PSC patients. Patients had mean age of 54 years at first PSC ICD-10 code and 53% were male. In both the inpatient and outpatient setting, more than 2600 patients (>66%) had at least one lab result for each major liver enzyme (ALT, AST and ALP). Over a third of patients had >4 outpatient lab values for ALT (33.5%, n = 1326), AST (33.7%, n = 1332), and ALP (38.5%, n = 1523). A subgroup of 1427 patients had additional available unstructured data. In this subgroup, structured data identified MRCP in less than half of patients (41%, n = 594), while inclusion of unstructured data revealed twice as many (82%, n = 1080). Structured data rarely identified pruritus (17%, n = 235) and fatigue (20%, n = 216), though frequency was greater with the addition of unstructured data for both pruritus (53%, n = 758) and fatigue (66%, n = 944).
Conclusion: We identified one of the largest reported US EHR datasets of PSC patients with robust data on laboratory values and imaging. While pruritus and fatigue were infrequently coded, additional analysis of unstructured data markedly increased their identification and indicate these are important, prevalent symptoms in PSC. Use of both structured and unstructured elements may provide a new opportunity to understand the natural history of this rare disease.

SAT-404

Concomitant metabolic-dysfunction associated steatotic liver disease in primary biliary cholangitis: no adverse liver outcomes but increased cardiovascular risk in a large real-world cohort

Jarell Jie-Rae Tan[1], Ellina Lytvyak[2], Shao Wei Sean Lam[3], Aldo J Montano-Loza[2], Yu Jun Wong[1,3]. [1]*Department of Gastroenterology & Hepatology, Changi General Hospital, Singapore, Singapore;* [2]*Division of Gastroenterology and Hepatology, University of Alberta, Edmonton, Canada, Edmonton, Canada;* [3]*Duke-NUS Medical School, Singapore, Singapore, Singapore*
Email: wongyujun1985@gmail.com

Background and aims: Metabolic dysfunction-associated steatotic liver disease (MASLD) is increasingly prevalent among patients with primary biliary cholangitis (PBC), but it's impact on long-term clinical outcomes remains unclear. We evaluated whether concomitant MASLD modifies clinical outcomes in PBC.
Method: We performed a retrospective nationwide cohort study using TriNetX (deidentified, patient-level, electronic health records from >110 US healthcare organizations). MASLD was defined as hepatic steatosis plus ≥1 cardiometabolic risk factor. Patients with other chronic liver diseases were excluded. Adults with PBC were classified as PBC-MASLD or PBC alone, and propensity-matched (1:1) on demographics, cirrhosis, ALP, and metabolic comorbidities. Secondary analysis evaluated MASLD patients with new onset of PBC. Outcomes were assessed using time-to-event analyses. Biochemical response was defined as ALP normalization at 1-year.

Primary outcome was hepatic decompensation (HD); secondary outcomes included major adverse cardiovascular events (MACE), liver transplantation (LT), HCC, and all-cause mortality.
Results: Among 3711 PBC patients (86.3% female; mean age 60.6 ± 15 years), 1327 (35.8%) had concomitant MASLD. After matching, 1216 PBC patients were included per group with good balance across matched variables (SMD < 0.10). Over an average follow-up of 4.1 years, PBC-MASLD was not associated with increased risk of HD (HR 1.02, 95%CI: 0.77–1.36), LT, and HCC. Results were consistent in landmark analyses excluding early events. In contrast, PBC-MASLD had a significantly higher risk of MACE than PBC alone (HR 1.31, 95% CI: 1.05–1.63, p = 0.018). ALP normalization at 1-year was more common in PBC-MASLD than PBC alone (55.8% vs 43.8%, p < 0.01). All-cause mortality was higher in PBC/MASLD despite comparable liver-specific outcomes (HR 1.64, 95%CI 1.31–2.05). These findings were consistent in sensitivity analyses that excluded patients without cardiometabolic risk factors and those with a high cardiometabolic burden. In MASLD patients with new-onset PBC, risks of HD and MACE were similar to those of MASLD alone.
Conclusion: Concomitant MASLD did not worsen liver-related outcomes in PBC but was associated with higher cardiovascular risk and poorer survival, challenging the assumption that PBC-MASLD is clinically benign. This suggests excess risk in PBC-MASLD is driven by cardiometabolic disease rather than liver progression, highlighting the need for integrated cardiovascular risk assessment and management.

SAT-409-YI
The burden of cholangiocarcinoma in primary sclerosing cholangitis: a high-volume north american transplant and hepatobiliary surgical center perspective
Natassia Tan[1,2], Robert Grant[3], Jennifer Knox[3], Chaya Shwaartz[4,5], Arndt Vogel[2,3], Ian Mcgilvray[4,5], Laura Dawson[6], Trevor Reichman[4,5], Gonzalo Sapisochin[7], Aruz Mesci[6], Nazia Selzner[5], Gideon M. Hirschfield[1,2], Aliya Gulamhusein[1,2]. *[1]The Autoimmune and Rare Liver Disease Programme, Toronto General Hospital, University Health Network, Toronto, Canada; [2]Toronto Centre for Liver Disease, Toronto, Canada; [3]Princess Margaret Cancer Centre, Toronto, Canada; [4]Division of General Surgery, Toronto General Hospital, Toronto, Canada; [5]Ajmera Transplant Center, University Health Network, Toronto, Canada; [6]Department of Radiation Oncology, Princess Margaret Cancer Centre, University Health Network, Toronto, Canada; [7]Department of General and Abdominal Surgery, Vall d'Hebron University Hospital, Barcelona, Spain*
Email: natassiapinpintan@gmail.com

Background and aims: Primary sclerosing cholangitis (PSC) is associated with a high burden of cholangiocarcinoma (CCA). Optimal management of PSC-CCA is challenging due to strict eligibility criteria of protocols for liver transplant (LT) and risks associated with extensive surgery and/or immunochemotherapy in patients (pts) with significant hepatobiliary (HB) disease. Herein, we describe the management of PSC-CCA in a high-volume PSC, HB, and LT center.
Method: We conducted a single-center retrospective study of all pts with PSC-CCA followed at the University Health Network between January 1st, 2000, to December 31st, 2024.
Results: Of 881 pts with PSC, 54 cases (6%) of PSC-CCA were identified, the majority male (n = 35, 64.8%). Median age of diagnosis of PSC was 38 (IQR 30–47) years (yrs) and 48 (IQR 39–59) yrs for CCA. Perihilar CCA (pCCA) was most common (n = 20, 37%), followed by intrahepatic CCA (iCCA) (n = 17, 31.4%), and distal CCA (dCCA) (n = 8, 14.8%). 40% (8/20) pts were enrolled in the Mayo protocol for LT-pCCA, 50% dropped out due to progressive disease and 50% had LT, one with subsequent Whipple for positive margins. 25% (5/20) of pts with pCCA ineligible for LT had primary resection with adjuvant capecitabine (80%) – with 75% 3-yr overall survival (OS). 50% (10/20) were ineligible for surgery and managed with palliative chemotherapy (CT) (60%) or supportively (40%) with 54% 1-yr and 27% 3-yr OS. Of those with PSC-iCCA, 17.6% (3/17) were managed with LT, 1 with mixed CCA-hepatocellular carcinoma as standard of care, 1 with iCCA <2 cm pre-LT, and 1 with multifocal CCA stable on neoadjuvant CT. 41% (7/17) pts with iCCA had a primary resection with neoadjuvant and/or adjuvant CT with 100% 1-yr OS and 50% 2-yr OS. 35.2% (6/17) pts with iCCA were ineligible for surgical intervention and managed with palliative CT (50%) or supportively (50%) with 55% 1-yr OS. Of the 7 pts with CCA that had LT, median follow up was 1.7 yrs (IQR 1–2.4), with 42% 5-year OS. All pts with dCCA had a Whipple procedure and adjuvant CT, with 75% 1-yr and 37.5% 5-yr OS. In the entire cohort, 29 (53.7%) pts died with 31.1% 5-yr OS after CCA diagnosis.
Conclusion: PSC-CCA carries a dismal prognosis yet selected pts may benefit from aggressive surgical intervention, though management remains heterogeneous even in high volume centers. Optimizing outcomes relies on early diagnosis, incorporation of molecular profiling, and expanding oncologic indications for LT, all on a backbone of multidisciplinary management of these complex pts.

SAT-410
PRO-C3 shows prognostic and trial-endpoint potential in primary sclerosing cholangitis
Usha Tharmathas[1,2,3], Andressa de Zawadzki[4], Diana Julie Leeming[4], Sara Kristina Tjønnfjord[2,3,5], Holmfridur Helgadottir[3,6], Peder Rustøen Braadland[7,8], Gideon M. Hirschfield[9], Trine Folseraas[2,3,5], Lei Ling[10], Johannes R. Hov[2,3,5,8], Morten Karsdal[4], Tom Hemming Karlsen[2,3,5,8], Mette Vesterhus[3,6,11], Kristin Kaasen Jørgensen[1,2,3]. *[1]Dept. of Gastroenterology, Akershus University Hospital, Lørenskog, Norway; [2]Institute of Clinical Medicine, University of Oslo, Oslo, Norway; [3]Norwegian PSC Research Center, Department of Transplantation Medicine, Oslo University Hospital, Oslo, Norway; [4]Nordic Bioscience AS, Herlev, Denmark; [5]Section of Gastroenterology, Department of Transplantation Medicine, Oslo University Hospital, Oslo, Norway; [6]Dept. of Medicine, Haraldsplass Deaconess Hospital, Bergen, Norway; [7]Norwegian PSC Research Center, Department of Transplantation Medicine, Oslo, Norway; [8]Research Institute of Internal Medicine, Division og Surgery and Specialized Medicine, Oslo University Hospital, Oslo, Norway; [9]The Autoimmune and Rare Liver Disease Programme, Division of Gastroenterology and Hepatology, Toronto General Hospital, Toronto, Canada; [10]NGM Biopharmaceuticals, South San Francisco, United States; [11]Department of Clinical Science, Haraldsplass Deaconess Hospital, University of Bergen, Bergen, Norway*
Email: ushanaresh@gmail.com

Background and aims: Primary sclerosing cholangitis (PSC) lacks dynamic biomarkers suitable for short-term evaluation of disease activity. Procollagen type III N-terminal (PRO-C3) reflects active fibrogenesis. This study aimed to estimate the biological variability of PRO-C3 in PSC and its association with relevant clinical outcomes.
Method: The biological variability of PRO-C3 in PSC was assessed in the placebo group (n = 20) of a phase II clinical trial with 7 repeated measurements obtained over 16 weeks[1]. The associations between PRO-C3 and hepatic decompensation and liver transplantation-free survival were evaluated in an observational, cross-sectional PSC cohort (n = 235). Competing risk regression and Cox proportional hazard models with a linear spline were used to identify a threshold of PRO-C3 and to estimate the linear association with clinical outcomes. Absolute risk predictions were estimated for 1-, 2- and 4-year horizons.
Results: The intraindividual coefficient of variation of PRO-C3 was 13.8%, with an intraclass correlation of 0.88. In the observational PSC cohort, the median (IQR) follow-up time was 5 (2–12) years, and baseline alkaline phosphatase and PRO-C3 were 221 (126–364) U/L and 55.2 (40.5–79.6) ng/mL, respectively. Patients in the highest PRO-C3 tertile (>69.7 ng/mL, (n = 78)) had increased subdistribution hazard of hepatic decompensation (sHR 4.11 95% CI 1.33–11.4) and

hazard of liver transplantation or death (HR 2.71, 95% CI 1.69–4.36) compared with the lowest tertile (<45.4 ng/mL, (n = 78)). Above an identified threshold value of 42 ng/mL, each doubling of PRO-C3 was associated with a two-fold increase in the hazard of liver transplantation or death (HR 2.07 95% CI 1.62–2.65). SIMEX correction confirmed the robustness of the threshold and the effect estimate. A two-fold increase in PRO-C3 above 42 ng/mL was associated with a 1.92-, 1.88-, and 1.78-fold risk of liver transplantation or death at 1-, 2, and 4- years, respectively. Model discrimination was moderate across all time horizons (AUROC 0.70–0.71).
Conclusion: PRO-C3 has low biological variability over time in people with PSC. Higher PRO-C3 levels is associated with increased risk of hepatic decompensation and liver transplantation or death, with a linear relationship with the latter endpoint among individuals with PRO-C3 > 42 ng/mL. PRO-C3 may serve as a candidate prognostic biomarker and therapeutic trial endpoint in PSC.

Reference

Hirschfield *et al.*, *J Hepatol*. 2019. 70(3):483–93

SAT-411-YI

Long-term outcome of autoimmune hepatitis: complications, cancer risk and survival in a large nationwide swedish cohort

Richard Thörn[1], Mårten Werner[1], Jonas Wixner[1]. [1]*Umeå University, Department of Public Health and Clinical Medicine, Norrland University Hospital, Umeå, Sweden*
Email: richard.thorn@regionvasterbotten.se

Background and aims: Autoimmune hepatitis (AIH) is a chronic inflammatory liver disease that can lead to end-stage liver disease if untreated. Long-term data on prognosis and risk of AIH-related complications such as hepatic and extrahepatic cancer remain limited. This study aimed to investigate long-term outcome of AIH, focusing on survival, cause of death and cancer risk.
Method: A nationwide cohort of AIH patients linked to all Swedish university hospitals has been established by the national hepatologist collaboration SweHep. Data from this cohort was used in our study and supplemented with data from the Swedish Cause of Death and the National Cancer Registers. Outcomes were compared to a matched Swedish reference population and relative survival (RS) and standardised incidence ratios (SIR) were calculated.
Results: The cohort comprised 1086 patients (24.4% male) with a follow-up time of 18,091 patient-years. Cirrhosis was found in 21.7% at diagnosis and in 35.5% overall by the end of follow-up. The most common causes of death were cancer (29.8%), liver disease (24.4%) and cardiovascular disease (15.4%). Liver disease was a significantly less common cause of death among patients without cirrhosis (8.2%, $p < 0.001$). A slight, yet significant, reduction in RS was observed after 5 years of disease duration. After 12 years, a steeper decline in RS emerged, reaching 50% after 36 years. The SIR for any cancer was 2.60 (95% CI 2.34–2.88), significantly higher in men. Thirty-three patients (3.0%) developed HCC, the vast majority having cirrhosis. The SIR for hepatobiliary cancer among cirrhotic patients was 24.39 (95% CI 16.44–34.57). The annual incidence of HCC in patients with cirrhosis was 0.56%. Among patients who progressed to cirrhosis during follow-up, 12.1% eventually developed HCC (SIR 93.98; 95% CI 57.8–142.79), compared with 5.1% of patients with cirrhosis at AIH diagnosis ($p = 0.013$).
Conclusion: Patients with AIH showed reduced survival, which became more evident after the first decade of disease. Cancer was the most common cause of death and there was an increased overall risk of malignancy, especially in men. The risk of HCC was increased compared to the general population, particularly in patients with cirrhosis, but the risk was notably lower than in other chronic liver diseases. Thus, HCC surveillance might not be cost effective in all patients with AIH cirrhosis, but rather in those with disease progression despite immunosuppressive treatment.

SAT-412

Acute cholangitis in primary sclerosing cholangitis: profile classification of patient-reported symptom burdens predicts recovery from cholangitis episodes

Brian Thorsen[1], Martine Walmsley[2], Mary Vyas[3], Mark Chatterley[2], Stephen Rossi[1]. [1]*PSC Partners Seeking a Cure, Greenwood Village, CO, United States;* [2]*PSC Support, Manchester, United Kingdom;* [3]*PSC Partners Seeking a Cure Canada, Toronto, Canada*
Email: brian@pscpartners.org

Background and aims: Acute cholangitis (AC) is a significant complication in patients living with primary sclerosing cholangitis (PSC). Previous data showed a significant and highly variable symptom burden during AC. We aim to identify patterns in symptom presentation which may link to patient characteristics and post-AC recovery.
Method: A de-identified survey was distributed to adults with PSC and ≥1 AC episode by PSC Partners Patient Registry and PSC Support. Patient characteristics, AC symptom frequency, severity, and change during the latest AC episode, and medical interventions were collected. Symptom profile classes (SPCs) were developed by latent class analysis (LCA) based on severity of AC symptoms, such as liver pain, fatigue, pruritus, fever, nausea, jaundice, anxiety, and depression. SPCs were analyzed for categorical associations with clinical and demographic variables, interventions, and patient-reported recovery after AC.
Results: A total of 564 responses met screening criteria. Clinical characteristics are consistent with other cohorts, except for 45% male. All AC symptoms had >50% prevalence except jaundice (43%) and vomiting (40%), with highest prevalence of fatigue (90%) and liver pain (84%). Three SPCs were identified by LCA and interpretability, labeled as Low, Medium, and High, each containing 25%, 45%, and 30% of patients. Most symptoms had increasing incidence and severity across SPC. The High SPC had the greatest incidence and severity in all symptoms: 100% with moderate/severe fatigue and >75% with moderate/severe liver pain, fever, nausea, anorexia, and insomnia. The Low SPC had mostly lower incidence, including 12% with brain fog vs. 66% and 92% in Medium and High. However, the Low SPC had higher rates of severe liver pain, fever, nausea, and vomiting than the Medium SPC (all $p < 0.05$). Full recovery to baseline health after AC was strongly associated with SPC (Low: 90%, Medium: 76%, High: 52%, $p < 0.001$). Longer recoveries were associated with higher SPC ($p < 0.001$). Antibiotic use was weakly associated with SPC ($p = 0.03$). Women were more likely to be in the High SPC vs. the Low SPC ($p = 0.002$). No other demographics were associated with SPC. The SPC model shows fever and nausea alone during AC indicate a milder or treatable case of AC and a likely full recovery.
Conclusion: There is an overall gradient of symptom burden in AC, and higher burdens have worse recovery. Fatigue, liver pain, fever, nausea, and brain fog are key symptoms to understand the symptom burden of AC.

SAT-413

Natural history of primary biliary cholangitis in Alberta: province-wide registry data on treatment uptake, biochemical response, liver transplantation, and survival

Bryce Tkachuk[1], Aldo J Montano-Loza[2], Abdel-Aziz Shaheen[1]. [1]*University of Calgary, Calgary, Canada;* [2]*University of Alberta, Edmonton, Canada*
Email: az.shaheen@ucalgary.ca

Background and aims: Population-based audits have described primary biliary cholangitis (PBC) management and outcomes, but registry-wide Canadian data are limited. We characterized incident PBC in Alberta, including ursodeoxycholic acid (UDCA) use, biochemical response across published criteria, liver transplantation, and survival.
Method: A validated case-finding algorithm identified 3250 adults with a PBC diagnostic code; charts were reviewed to confirm PBC.

Incident cases from 2005 to 2022 were linked to provincial laboratory and administrative datasets. The reference date was the index date. Baseline and 12-month laboratory results (ALP, bilirubin, AST, GGT, albumin, platelets), AMA status, biopsy results, UDCA prescriptions, and biochemical response (Rochester, Barcelona, Paris I/II, Rotterdam, Toronto, Ehime) were extracted. age-sex adjusted Cox models were used to assess survival.

Results: Patients were predominantly women (1291/1470; 88%) with median age 58 years (IQR 50–67). UDCA was prescribed in 1397 (95%), 61 (4.1%) had liver transplantation, and 278 (18.9%) died during follow-up. Median baseline ALP was 202 U/L (IQR 139–330), bilirubin 10 µmol/L (7–16), AST 49 U/L (32–78), and GGT 209 U/L (99–456). AMA was positive in 87.8%, negative in 8.9%, and unavailable in 3.3%. Biopsy was performed in 559 (38%); among AMA-negative biopsied cases, 86/90 (96%) showed histologic findings of PBC. Biochemical response rates after at least one year of UDCA treatment were Rochester 82%, Barcelona 62%, Paris I 91%, Rotterdam 84%, Toronto 75%, Paris II 81%, and Ehime 54%. At 12 months, ALP decreased to 138 U/L (102–201), and bilirubin remained low at 9 µmol/L (7–14). Using the POISE composite score (12-month ALP < 1.67 ×ULN, normal bilirubin, and ≥ 15% ALP reduction), 37% met response criteria. In age-sex adjusted models, Paris I response best predicted liver transplant-free survival in Alberta (aHR 0.19; 95% CI 0.11–0.34), followed by Rotterdam (aHR 0.23; 95% CI 0.15–0.36) and Rochester criteria (aHR 0.33; 95% CI 0.22–0.50).

Conclusion: In this population-based cohort, PBC primarily affected middle-aged women with a high UDCA prescription rate and predominantly with normal bilirubin. Biochemical response differed substantially by criterion; Toronto and Paris I classified most patients as responders. The low POISE response rate underscores unmet need for second-line therapy in PBC. Variation in the criteria used resulted in changes in responder classification, with potential implications on clinical care.

SAT-414-YI

Secretory immunoglobulin A (sIgA): a new prognostic marker for primary sclerosing cholangitis (PSC)

David Tornai[1], Anita Szabo[1], Laura Hanisch[1], Istvan Tornai[1], Tamas Tornai[2], Péter Antal-Szalmás[3], Maria Papp[1]. *[1]University of Debrecen, Faculty of Medicine, Division of Gastroenterology, Department of Internal Medicine, Debrecen, Hungary; [2]Semmelweis University, Institute of Pancreatic Diseases, Budapest, Hungary; [3]University of Debrecen, Faculty of Medicine, Department of Laboratory Medicine, Debrecen, Hungary*
Email: tornai.david@med.unideb.hu

Background and aims: Primary sclerosing cholangitis (PSC) is a progressive inflammatory disease of the bile ducts, frequently associated with inflammatory bowel disease (IBD). The gut-liver axis is considered a pivotal factor in PSC pathogenesis. In a previous study, we demonstrated that elevated serum levels of secretory (s)IgA —which is produced in the gut and secreted into the lumen—serve as a marker of gut-barrier damage and a strong predictor of short-term mortality in patients with acute-on-chronic liver failure. In this study, we aimed to evaluate the association of serum sIgA with disease severity, clinical characteristics, and outcomes in PSC.

Method: We conducted a cohort study of PSC patients analyzing data collected during annual follow-up visits. Serum sIgA concentrations were measured from baseline samples. We investigated the association between sIgA and clinical parameters and assessed sIgA's prognostic value for a composite endpoint defined as liver transplantation (LTx) or liver-related mortality over a 10-year period.

Results: The cohort included 135 patients (51.9% male; median age: 36.4 years [IQR: 25.5–48.9]). Co-existing IBD was present in 54.1% of patients, autoimmune hepatitis (AIH) variant syndrome in 19.3%, and established liver cirrhosis in 22.2%. sIgA levels were not associated with the presence of IBD or AIH variant syndrome but were significantly higher in patients with cirrhosis (40.8 [14.0–58.4] vs. 10.7 [5.1–27.8] g/mL; $p < 0.001$). sIgA showed significant positive correlations with disease severity scores (Revised Mayo Risk Score, Amsterdam-Oxford Model, UK-PSC), macrophage activation markers (sCD14, sCD163), liver enzymes (AST, ALT, GGT, ALP), liver function tests (total bilirubin, albumin) (all $p < 0.001$), and CRP ($p = 0.007$). Furthermore, sIgA was a significant predictor of the composite endpoint (AUROC: 0.697; 95% CI: 0.612–0.773). Using an optimal cut-off of > 20.1 µg/mL, elevated sIgA was associated with a nearly 5-fold increased risk of adverse outcomes (HR: 4.975; 95% CI: 2.117–11.695; $p < 0.001$).

Conclusion: Serum sIgA levels correlate with disease severity and predict 10-year transplant-free survival in PSC. Notably, sIgA levels were independent of the presence of co-existing IBD, supporting the hypothesis that gut-barrier dysfunction occurs in PSC even in the absence of manifest intestinal inflammation. The correlation with macrophage activation markers further suggests a link with bacterial translocation.

SAT-415

Prognostic utility of circulating macrophage activation markers in primary sclerosing cholangitis: gadget or magic?

David Tornai[1], Peter Ven[2], Istvan Tornai[1], Tamas Tornai[3], Péter Antal-Szalmás[4], Maria Papp[1]. *[1]University of Debrecen, Faculty of Medicine, Division of Gastroenterology, Department of Internal Medicine, Debrecen, Hungary; [2]University of Pécs, Division of Gastroenterology, First Department of Medicine, Pécs, Hungary; [3]Semmelweis University, Institute of Pancreatic Diseases, Budapest, Hungary; [4]University of Debrecen, Faculty of Medicine, Department of Laboratory Medicine, Debrecen, Hungary*
Email: tornai.david@med.unideb.hu

Background and aims: Primary sclerosing cholangitis (PSC) is a progressive cholestatic liver disease with a highly variable clinical course. The reliability of current biomarkers in predicting disease activity and progression remains limited. As dysregulated macrophage activity is increasingly recognized as a pivotal driver of PSC pathophysiology, we aimed to evaluate circulating macrophage activation markers as prognostic tools.

Method: We analyzed serum levels of soluble macrophage activation markers (sCD14, sCD163, sCD206/sMR, and suPAR) in a cohort of 93 Hungarian PSC patients. We assessed associations with disease severity (Revised Mayo Risk Score, UK-PSC, and Amsterdam-Oxford Model [AOM]), gut-barrier function (sIgA), a composite endpoint defined as liver transplantation (LTx) or liver-related mortality over a 10-year period.

Results: The cohort (median age 36 years; 57% male) included 46.2% with co-existing IBD and 21.5% with baseline cirrhosis. During follow-up, 24 patients (25.9%) reached the composite endpoint (14 LTx, 10 liver-related deaths). All four markers were significantly elevated in patients with cirrhosis ($p < 0.01$ for all) and those reaching the composite endpoint (AUROC: sCD206: 0.674; sCD163: 0.789; sCD14: 0.736; suPAR: 0.794; $p < 0.01$ for all). sCD163, sCD14, and suPAR correlated positively with clinical risk scores and all markers correlated with sIgA. In univariate Cox regression, log-transformed sCD14, sCD163, and suPAR predicted the composite outcome. notably, sCD14 demonstrated the highest predictive value (HR: 10.43 CI: 3.81–28.8). After adjusting for clinical risk scores, sCD14 remained an independent predictor across all models, whereas suPAR lost significance when adjusted for AOM, and sCD163 lost significance across all scores. A novel composite score combining optimal cut-offs of these three macrophage markers provided superior risk stratification: patients with 0, 1–2, or 3 positive markers had a 0%, 40.7%, and 81.7% event rate, respectively.

Conclusion: Serum level of macrophage activation markers are increased by PSC severity in and predict long-term outcomes. sCD14 bares additional information to clinical scores and the combination of markers representing different aspects of macrophage activation offers robust risk stratification. The correlation with sIgA highlights

the role of the gut-liver axis in macrophage-mediated disease progression.

SAT-416

Metabolic syndrome as a determinant of inadequate biochemical response to ursodeoxycholic acid in primary biliary cholangitis

Christos Triantos[1], Konstantinos Papantoniou[1], Efthymios Tsounis[2,3], Ioanna Aggeletopoulou[2], Maria Bali[2], Nikitas Kimiskidis[2], Odysseas Ampazis[2], Georgia Diamantopoulou[2], Konstantinos Thomopoulos[2]. *[1]Division of Gastroenterology, Department of Internal Medicine, University of Patras, 26504, Patras, Greece, Patras, Greece; [2]Division of Gastroenterology, Department of Internal Medicine, University of Patras, Patras, Greece; [3]Division of Gastroenterology, Department of Internal Medicine, 251 Hellenic Airforce Hospital, Athens, Greece*
Email: chtriantos@hotmail.com

Background and aims: Ursodeoxycholic acid (UDCA) is the first-line therapy for primary biliary cholangitis (PBC), yet many patients fail to achieve an adequate biochemical response. Metabolic syndrome (MetS) may modify treatment response in PBC, beyond the contribution of individual metabolic risk factors. The aim of the current study was to evaluate the association between MetS and biochemical response to UDCA in patients with PBC.
Method: Data from patients with PBC treated with UDCA at a tertiary referral center in Western Greece were collected retrospectively, with prospective follow-up for outcome assessment. Biochemical response at 12 months was defined as alkaline phosphatase (ALP) $\leq 1.67 \times$ ULN and normalization of total bilirubin. MetS was defined as the presence of three or more established metabolic abnormalities at baseline, including obesity defined by body mass index (BMI), dyslipidaemia, hypertension, and impaired glucose regulation. Comparisons were performed using the Mann–Whitney U and Pearson's chi-square tests, while binary logistic regression was used to identify independent predictors of biochemical response.
Results: A total of 95 PBC patients were included (median age 62 years; 91.6% female; 81.1% AMA positive; 47.4% ANA positive; 13.7% baseline cirrhosis; 15.8% current smokers; 7.4% PBC–autoimmune hepatitis overlap). MetS was significantly more frequent among non-responders than responders (42.1% vs 19.3%; $p = 0.021$). Non-responders were older and had higher baseline ALP, higher ALP at 6 months, and higher baseline bilirubin compared with responders ($p = 0.048$, $p = 0.004$, $p < 0.001$, and $p = 0.035$, respectively). In multivariable analysis adjusted for age, baseline bilirubin, and baseline ALP, MetS independently predicted lack of biochemical response (OR = 3.95, 95% CI : 1.06–14.76; $p = 0.041$). When ALP at 6 months was included instead of baseline ALP, lower ALP at 6 months emerged as an independent predictor of response ($p = 0.016$), while the association with MetS was attenuated (OR = 5.81, 95% CI : 0.85–39.84; $p = 0.073$).
Conclusion: MetS is associated with an increased likelihood of inadequate biochemical response to UDCA in patients with PBC. Early biochemical response, as reflected by ALP at 6 months, seems to be a strong determinant of treatment outcome and may partially mediate the effect of metabolic dysfunction. These findings highlight the potential clinical relevance of metabolic risk assessment in PBC.

SAT-417

Presence of myopathy in patients with primary biliary cholangitis

Yiğit Şahin[1], Yasemin Balaban[1], Mete Üçdal[1], Şaziye Apraş Bilgen[2], Gözde Kart Bayram[1], Beyza Atay[1]. *[1]Hacettepe University Faculty of Medicine Hospital, Altındağ, Türkiye; [2]Hacettepe University Faculty of Medicine Hospital, Ankara, Türkiye*
Email: yb.sahin7@gmail.com

Background and aims: Primary biliary cholangitis (PBC) is a chronic autoimmune cholestatic liver disease frequently associated with extrahepatic manifestations. Although muscle involvement has been described in isolated reports, myopathy remains an under-recognized complication in PBC. This study aimed to systematically evaluate the presence and characteristics of myopathy in patients with PBC.
Method: In this prospective study, 56 adult patients fulfilling EASL diagnostic criteria for PBC were evaluated between December 2024 and December 2025. Clinical symptoms, muscle strength (Medical Research Council, MRC), biochemical markers of muscle injury (creatine kinase [CK], CK-MB, myoglobin, troponin), inflammatory parameters, autoantibodies, and quality-of-life scores (PBC-40 fatigue domain, HAQ) were recorded. Patients with neurological, endocrinopathic, oncological or rheumatologic disorders explaining myopathy were excluded. Patients with elevated muscle enzymes or reduced muscle strength underwent further radiological evaluation. Comparisons were performed using Independent Samples t-test and Mann–Whitney U test.
Results: The cohort was predominantly female (92.9%) with a mean age of 53.7 ± 8.6 years. Muscle-related symptoms were common, including myalgia (39.3%) and muscle weakness (26.8%), despite preserved muscle strength (mean MRC score 4.9 ± 0.3). Two patients (3.6%) exhibited marked CK elevation (>300 U/L). Compared with patients with normal CK levels, those with elevated CK demonstrated significantly higher CK-MB, myoglobin, and troponin levels as expected. Whole-body imaging revealed myositis-like changes or sarcopenia in selected cases.
Conclusion: Myopathy may represent an under-recognized extra-hepatic manifestation of PBC, even in patients without overt muscle weakness. Systematic screening using biochemical markers may facilitate earlier detection of muscle involvement and guide multi-disciplinary evaluation in this population.

SAT-418-YI

Enhanced liver fibrosis test significantly improves the predictive value of the Amsterdam-Oxford model in primary sclerosing cholangitis

Jutta van Crevel[1,2], Tim Middelburg[1,2], Bregje Mol[1,2], Johannes Bogaards[3], Cyriel Ponsioen[1,2]. *[1]Department of Gastroenterology & Hepatology, Amsterdam University Medical Center, Amsterdam, Netherlands; [2]Amsterdam Gastroenterology, Endocrinology & Metabolism, Amsterdam, Netherlands; [3]Department of Epidemiology & Data Science, Amsterdam University Medical Center, Amsterdam, Netherlands*
Email: j.n.vancrevel@amsterdamumc.nl

Background and aims: Reliable individual prognostication in primary sclerosing cholangitis (PSC) remains challenging. The Amsterdam Oxford Model (AOM) predicts transplant-free survival with moderate discrimination (C-statistic 0.67–0.75). The Enhanced Liver Fibrosis (ELF) test has shown promising prognostic value in PSC. This study evaluated whether the predictive value of AOM can be improved by incorporating ELF.
Method: In a prospective Dutch PSC cohort, first available ELF measurements were linked to clinical and laboratory data. Transplant-free survival was defined as time from ELF measurement to PSC-related death or liver transplantation. Cox models assessed AOM, ELF, and their combination, with incremental value evaluated via Wald tests and C-statistics. Next, we applied exploratory LASSO-penalized regression with bootstrap validation on AOM candidate predictors plus ELF. Calibration was assessed by comparing predicted survival with Kaplan-Meier estimates based on risk quartiles.
Results: We included 292 PSC patients (64% male, median age at PSC diagnosis 35 years, 72% inflammatory bowel disease (IBD), 7% features of autoimmune hepatitis (AIH)). Median time from PSC diagnosis to ELF measurement was 5.1 years (IQR 2.6–11.0), with a median follow-up from ELF measurement of 5.6 years (IQR 3.0–13.2). During follow-up, 79 events occurred. AOM and ELF were moderately correlated (Pearson's $r = 0.60$). Prediction by AOM at the time of ELF measurement showed a C-statistic of 0.75 (HR 2.91, 95% CI 2.14–3.96), while prediction by ELF alone showed a C-statistic of 0.78 (HR 2.07,

95% CI 1.77–2.43). Combining AOM and ELF improved the C-statistic to 0.80 (AOM HR: 1.60, 95% CI 1.07–2.38; ELF HR: 1.81, 95% CI 1.50–2.19). Wald tests confirmed that incorporating ELF improved the prediction by AOM ($p < 0.0001$). The LASSO-derived model achieved an optimism-corrected C-statistic of 0.84, and consistently selected ELF (HR 1.55, 95% CI 1.25–1.93) along with PSC subtype, bilirubin, albumin, gamma GT, IBD, sex, AIH and time since PSC diagnosis. Calibration was satisfactory, with good agreement between predicted and observed survival across risk groups.

Conclusion: ELF provided significant incremental prognostic value in addition to AOM alone and was consistently selected in LASSO-penalized modeling. The optimized model demonstrated robust and excellent discriminative performance and good calibration in internal validation, showing promising utility for prognostic assessment in PSC.

SAT-419

Recurrence rate and clinical outcomes for recurrent primary sclerosing cholangitis after liver transplantation: a systematic review with meta-analysis

Lisa van Lierop[1], Qiming Tan[1], Raymond Odsen[1], Janice Kung[1], Aldo J Montano-Loza[1], Abdel Aziz Shaheen[2], Juan Abraldes[1], Frank Hoentjen[1]. *[1]University of Alberta, Edmonton, Canada; [2]University of Calgary, Calgary, Canada*
Email: lvanlier@ualberta.ca

Background and aims: Liver transplant (LT) is a dreaded outcome of end-stage primary sclerosing cholangitis (PSC). PSC recurrence (rPSC) after LT impacts graft survival and patient outcomes, but recurrence rate and clinical outcomes remain unclear. This systematic review with meta-analysis aims to quantify pooled rates of rPSC after LT and to evaluate post-transplant clinical outcomes, including graft and patient survival.

Method: A systematic search of multiple databases was conducted from inception to June 27, 2025, to identify cohort studies reporting rPSC after LT in adults. The primary outcome was the rPSC rate (pooled proportion); secondary outcomes included time to rPSC, rPSC in patients with PSC-IBD or post-colectomy, graft and patient survival, re-transplantation, and all-cause mortality. Pooled rates were estimated via random-effects (DerSimonian and Laird) and generalized linear mixed models (GLMM). Heterogeneity was evaluated using I^2 statistics, and robustness was assessed through leave-one-out sensitivity analyses. Risk of publication bias was assessed using contour-enhanced funnel plots, Egger's test, and trim-and-fill.

Results: Fifty-six articles contributed 59 independent study estimates (7946 LT recipients). The pooled rate of rPSC was 20.4% (95% CI 18.2–22.9%) using a DerSimonian-Laird random-effects model, with a similar estimate obtained using a GLMM approach (19.1%; 95% CI 16.4–22.1%). Heterogeneity was substantial ($I^2 \approx 80\%$), and the 95% prediction interval ranged from 9.5% to 38.6%. Assessment for publication bias demonstrated no significant small-study effects (Egger's $p = 0.38$). The median time to rPSC was 4.1 years. Recurrence occurred in 25.6% of patients with PSC-IBD and 18.8% post-colectomy, with histologic recurrence in 12.0%, re-transplantation in 12.6%, and re-transplantation for rPSC in 30.9%. One-, five-, and ten-year graft survival rates were 80.7%, 70.0%, and 56.4%, respectively; overall patient survival rates were 90.7%, 81.9%, and 73.7%, with a pooled mortality rate of 22.5%.

Conclusion: This meta-analysis provides the most comprehensive estimate to date, demonstrating that rPSC is frequent after LT (about 20%) and carries clinically relevant risks of graft failure, re-transplantation, and death. These findings have important implications for long-term surveillance, patient counseling, and future research objectives.

SAT-420

Serum glycomics are novel biomakers that increase the prognostic value of the GLOBE score in patients with primary biliary cholangitis

Xavier Verhelst[1], Nicky Somers[1], Nikolaos Gatselis[2], Emma Butaye[3], Lorenz Grossar[3], Nicolas Debusschere[3], Anja Geerts[1], Sarah Raevens[1], Hans Van Vlierberghe[1], Gideon M. Hirschfield[4], Christophe Corpechot[5], Atsushi Tanaka[6], Marco Carbone[7], Cynthia Levy[8], Palak J. Trivedi[9], Alejandra Villamil[10], Leander Meuris[11], Nico Callewaert[11], Vasiliki Lygoura[2], Maria C. van Hooff[12], Adriaan J. van der Meer[12], George Dalekos[2], Bettina E. Hansen[12]. *[1]Department of Gastroenterology and Hepatology, Ghent University Hospital, Ghent, Belgium; [2]Department of Medicine and Research Laboratory of Internal Medicine, National Expertise Center of Greece in Autoimmune Liver Diseases, General University Hospital, Larissa, Greece; [3]Liver Research Center Ghent, Ghent University, Ghent, Belgium; [4]Toronto Centre for Liver Disease, University Health Network, University of Toronto, Toronto, Canada; [5]Pierre Louis Institute of Epidemiology and Public Health, Sorbonne University, Inserm, Paris, France; Public Health Unit, Saint-Antoine Hospital, Assistance Publique - Hôpitaux de Paris, Paris, France; [6]Department of Medicine, Teikyo University, Tokyo, Japan; [7]Department of Medicine and Surgery, University of Milano-Bicocca, Monza, Italy; [8]Division of Digestive Health and Liver Diseases, Schiff Center for Liver Diseases, Miami University, Miama, United States; [9]National Institute for Health Research (NIHR) Birmingham Biomedical Research Centre (BRC), Institute of Immunology and Immunotherapy, Centre for Liver and Gastrointestinal Research, University of Birmingham, Birmingham, United Kingdom; [10]Hospital Italiano de Buenos Aires, Buenos Aeres, Argentina; [11]Center for medical Biotechnology, VIB, Ghent, Belgium; [12]Department of Gastroenterology and Hepatology, Erasmus University Medical Center, Rotterdam, Netherlands*
Email: xavier.verhelst@uzgent.be

Background and aims: Primary Biliary Cholangitis (PBC) is a rare progressive chronic liver disease. Prognostic scores are useful for decision making in patients with PBC, but the role of biomarkers is unclear. We studied the association of serum glycomics with disease progression and liver transplant free survival (TFS) in patients with PBC.

Method: In this multicentric international study stored serum samples of 858 PBC patients from 3 European PBC expert centers of the GLOBAL PBC Study Group were included. Serum N-glycomic analysis was performed using DNA sequencer assisted-Fluorophore Assisted Carbohydrate Electrophoresis. A glycomics-based biomarker was developed using uni-and multivariate Cox regression analyses on one time point.

Results: Patients had a mean follow-up of 6.43 years, with an 5- and 10-year (TFS) of 91.6% and 83.1. Poor TFS was associated with an increase of fucosylated glycans (NA2FB, NA3Fbc, NA4Fb) and a decrease of bi-, and tri-antennary glycans (NA2F, NA3), from which the GlycoPBCScore was derived with an area under the curve of 0.82 (95% CI [0.78–0.86], $p < 0.001$). According to a derived cut-off, patients in the 'high risk' group developed more cirrhosis (15.5% vs 6.3%, $p < 0.001$), hepatic decompensation (41.4% vs 15.9%, $p < 0.001$), hepatocellular carcinoma (3.2% vs 0.6%, $p = 0.003$) and had a higher mortality rate (37.4% vs 6.6%, $p < 0.001$), when compared to the 'low risk' group. Hazard ratio (HR) for adverse outcome was 3.36 (95% CI [2.82–4.01], $p < 0.001$) according to this biomarker. In a multivariable Cox proportional hazards model, the association of the GlycoPBCScore with poor TFS was confirmed (HR 2.05, 95% CI [1.66–2.53], $p < 0.001$). Moreover, combining this new glycomics based biomarker with the PBC GLOBE Score increased the prognostic value, leading to a more accurate classification of patients in need of liver transplantation and patients with an uneventful disease course. In particular, a high negative predictive value of 97.3% was observed

using the combination of GLOBE score and GlycoPBCscore, compared to 90% when there was a discordance between the GLOBE score and the biomarker.
Conclusion: The GlycoPBCScore is a new prognostic serum biomarker for liver-transplant free survival in patients with PBC, that provides additional prognostic information if combined with the currently used PBC GLOBE Score. Patients with an uneventful disease course can more accurately be identified.

SAT-421

Real-world experience with Elafibranor in patients with primary biliary cholangitis previously treated with Obeticholic acid: an italian multicenter observational study

Mauro Viganò[1], Domenico Montecalvo[2], Sara Labanca[3], Francesca Romana Ponziani[4], Erica Nicola Lynch[5], Marco Distefano[6], Francesca Terracciani[7], Maria Rita Cannavò[8], Vincenzo Ronca[9], Laura Cristoferi[10], Alessio Gerussi[10], Carla De Benedittis[11], Valeria Pace Palitti[12], Lucia Napoli[13], Teresa Zolfino[14], Giuliano Alagna[15], Vincenza Calvaruso[16], Alessandra Moretti[17], Giulia Rizzo[18], Marco Marzioni[19], Nora Cazzagon[20], Elisabetta Lorefice[21], Davide Roccarina[5], Raffaele Cozzolongo[22], Laura Scribano[23], Giovanni Vitale[24], Barbara Coco[25], Adriano Pellicelli[26], Federica Cerini[27], Antonino Castellaneta[28], Angela Fabbri[29], Alida Andrealli[30], Alessandra Garribba[31], Luca Fabris[20], Eugenia Pesatori[1], Alessandro Loglio[1], Leonardo Stella[4], Maurizio Russello[8], Ana Lleo[9], Cristina Rigamonti[11], Andrea Galli[5], Umberto Vespasiani-Gentilucci[7], Vincenzo Cardinale[2], Silvia Nardelli[2], Domenico Alvaro[2], Eugenia Nofit[10], Stefano Fagiuoli[1], Marco Carbone[32], Pietro Invernizzi[10], Edoardo Giovanni Giannini[3,33].
[1]Gastroenterology, Hepatology and Transplantation Division, ASST Papa Giovanni XXIII, Bergamo, Italy; [2]Policlinico Umberto I, Rome, Italy; [3]IRCCS Ospedale Policlinico San Martino, Genova, Italy; [4]CEMAD Fondazione Policlinico Universitario Agostino Gemelli IRCCS, Università Cattolica del Sacro Cuore, Rome, Italy; [5]AOU Careggi, Firenze, Italy; [6]UOSD Hepatology Unit, ASP Siracusa, Siracusa, Italy; [7]Policlinico Universitario Campus Bio-Medico, Rome, Italy; [8]ARNAS Garibaldi, Catania, Italy; [9]IRCCS Humanitas Research Hospital, Milan, Italy; [10]IRCCS San Gerardo dei Tintori, Monza, Italy; [11]AOU Maggiore della Carità, Novara, Italy; [12]Azienda USL di Pescara, Pescara, Italy; [13]Ospedale degli Infermi, Faenza, Italy; [14]AO Brotzu, Cagliari, Italy; [15]AOU di Sassari, Sassari, Italy; [16]Ospedale Giaccone, Palermo, Italy; [17]San Filippo Neri, Rome, Italy; [18]ASL2 Abruzzo Lanciano Vasto Chieti, Chieti, Italy; [19]AOU delle Marche, Ancona, Italy; [20]AOU Padova, Padova, Italy; [21]Azienda USL Toscana Centro, Empoli, Italy; [22]IRCCS De Bellis, Castellana Grotte, Italy; [23]Ospedale Sant'Antonio, Padova, Italy; [24]IRCCS Azienda Ospedaliero-Universitaria di Bologna, Bologna, Italy; [25]AOUP, Pisa, Italy; [26]Ospedale San Camillo, Rome, Italy; [27]Dipartimento di Scienze Cliniche e di Comunità, Università degli Studi di Milano, Milano, Italy; [28]Policlinico di Bari, Bari, Italy; [29]AUSL della Romagna, Rimini, Italy; [30]Ospedale Valduce, Como, Italy; [31]Ospedale Santa Maria delle Croci, Ravenna, Italy; [32]ASST Grande Ospedale Metropolitano Niguarda, Milan, Italy; [33]Università degli Studi di Genova, Genova, Italy
Email: mvigano@asst-pg23.it

Background and aims: Elafibranor, a dual peroxisome proliferator-activated receptor agonist, has recently been conditionally approved as second-line treatment for patients with Primary Biliary Cholangitis (PBC) and a suboptimal response to ursodeoxycholic acid (UDCA). In this study, we aimed to evaluate the efficacy and safety of elafibranor 80 mg/day in patients with PBC consecutively enrolled in the Italian Elafibranor Early Access Program and who had discontinued Obeticholic acid (OCA) treatment due to revocation of its marketing authorization.
Method: Patients were recruited into the Italian PBC Registry, a multicentre, observational cohort study that includes more than 60 secondary/tertiary centres managing patients with following PBC across Italy. The primary endpoint was the median change in alkaline phosphatase (ALP) levels from the beginning of elafibranor treatment until most recent follow up, and the secondary endpoints were: rate of patients with ALP <1,67 the upper limit of normal (ULN), rate of normalization of ALP (≤1 × ULN), change in pruritus intensity from baseline as measured on the Worst Itch Numeric Rating Scale (WI-NRS) in those with baseline severe-to-moderate pruritus (WI-NRS ≥4) and the occurrence of Adverse Events (AEs).
Results: We included 80 patients whose median age was 60 years, 87% were female, 16% with cirrhosis, 59% with ALP <1.67 ULN and 17% with ALP ≤1 × ULN. Median duration of OCA before initiation of elafibranor was 17 (4–93) months; median time between last OCA use and elafibranor initiation 3 (0–6) months. During a median treatment duration with elafibranor of 6 months (3–9) median ALP significantly decreased from 170 to 119 U/L (p = 0.013), and 77% and 46% of patients had ALP <1.67 × ULN and 46% ALP ≤1 × ULN, respectively. Among 11 patients who had moderate-to-severe pruritus, 10 improved (91%, median improvement: −4 points). Five patients (6%) prematurely discontinued elafibranor because of gastrointestinal AEs.
Conclusion: This real-world experience on the largest cohort reported to date of patients with PBC previously exposed to OCA and treated with elafibranor, suggests that elafibranor is an effective and safe alternative for such patients as a second-line therapy. Given the relatively short treatment duration of treatment with elafibranor, further evaluation with extended follow-up is warranted.

SAT-425

Faecalibacterium prausnitzii regulates biliary repair via the SCFAs–H3K27ac–ELF3 axis in primary biliary cholangitis

Qi Wang[1], Xi Wang[1], Ronghua Jin[1], Minghui Li[1]. *[1]Beijing Ditan Hospital, Capital Medical University, National Center for Infectious Diseases, Beijing, China*
Email: 18263829683@163.com

Background and aims: Primary biliary cholangitis (PBC) is a chronic cholestatic liver disease that primarily affects middle-aged women. Studies suggest that alterations in the gut microbiome are closely associated with the pathogenesis and treatment of PBC, but the underlying mechanisms remain unclear.
Method: This study first conducted gut microbiota analysis of fecal samples from PBC patients and healthy controls using metagenomic sequencing, with LEfSe and other methods employed to identify differential microbial taxa. Subsequently, a bile duct ligation (BDL) mouse model was established and treated with *F. prausnitzii* (1 × 10^9 CFU/day), while ductular reaction and liver fibrosis were evaluated through histopathological staining. For in vitro experiments, a GCDC-induced injury model using human primary biliary epithelial cells (HiBECs) was developed, followed by treatment with varying concentrations of short-chain fatty acids (SCFAs). Furthermore, ChIP assays were performed to detect H3K27ac modification levels, elucidating the specific mechanism by which SCFAs exert their effects through epigenetic regulation of the ELF3/PI3K-Akt pathway. All data were statistically analyzed using two-tailed t-tests/ANOVA with FDR correction ($P < 0.05$ considered statistically significant).
Results: We found that *F. prausnitzii* was significantly reduced in the gut microbiota of PBC patients. Supplementation with *F.prausnitzii* markedly improved BDL-induced biliary injury, including cholangitis, bile duct hyperplasia, and liver fibrosis, while also restoring gut microbial balance and intestinal barrier function. These beneficial effects were linked to SCFAs produced by *F. prausnitzii*. Mechanistic studies revealed that *F. prausnitzii*-derived SCFAs enhanced histone H3K27 acetylation, upregulating the transcription factor ELF3 and subsequently activating the PI3K-Akt signaling pathway to promote bile duct cell repair.
Conclusion: This study demonstrates that *F. prausnitzii* exerts protective effects in PBC. Its depletion in PBC patients and its therapeutic potential in alleviating cholangitis and liver fibrosis,

along with restoring gut function, highlight its promising clinical application for PBC treatment.

SAT-426-YI

Decline in aspartate- and alanine aminotransferase in relation to clinical outcome in people with primary biliary cholangitis after start of ursodeoxycholic acid

Gemma H. X. Weijsters[1], Ellen Werner[1], Tiki D. Blom[1], Maria C. van Hooff[1], Rozanne C. de Veer[1], Ulrich Beuers[2], Joost PH Drenth[2], Frans J. C. Cuperus[3], Remco van Dijk[4], Bart J. Veldt[5], Michael Klemt-Kropp[6], Suzanne van Meer[7], Robert C. Verdonk[8], Hajo J. Flink[9], Jan Maarten Vrolijk[10], Cyriel Y. Ponsioen[11], Ulrike de Wit[12], Johan P. H. Kuyvenhoven[13], Jerome Sint Nicolaas[14], Philip W. Friederich[15], Merel M. Tielemans[16], Marleen De Vree[17], Huseyin Aktas[18], Sunje Abraham[19], Mariëlle J. F. Meijnen[20], Janne van Rooij[21], Nicole S. Erler[22], Harry L. A. Janssen[1], Bettina E. Hansen[23], Adriaan J. van der Meer[1]. *[1]Erasmus University Medical Center, Rotterdam, Netherlands; [2]Amsterdam University Medical Center, Amsterdam, Netherlands; [3]University Medical Center Groningen, Groningen, Netherlands; [4]Leiden University Medical Center, Leiden, Netherlands; [5]Reinier de Graaf Gasthuis, Rotterdam, Netherlands; [6]Noordwest Ziekenhuisgroep, Alkmaar, Netherlands; [7]University Medical Center Utrecht, Utrecht, Netherlands; [8]St. Antonius Hospital, Nieuwegein, Netherlands; [9]Catharina Hospital, Eindhoven, Netherlands; [10]Rijnstate, Arnhem, Netherlands; [11]Maastricht University Medical Center, Maastricht, Netherlands; [12]Elisabeth – Tweesteden Hospital (ETZ), Tilburg, Netherlands; [13]Spaarne Gasthuis Hospital, Haarlem, Netherlands; [14]Amphia Hospital, Breda, Netherlands; [15]Meander Medical Center, Amersfoort, Netherlands; [16]Bravis Hospital, Roosendaal/Bergen op Zoom, Netherlands; [17]Treant Hospital, Emmen/Hoogeveen, Netherlands; [18]Hospital Group Twente (ZGT), Hengelo, Netherlands; [19]Alrijne Hospital, Leiden/Leiderdorp/Alphen aan den Rijn, Netherlands; [20]St Jansdal Hospital, Harderwijk, Netherlands; [21]Tjongerschans Hospital, Heerenveen, Netherlands; [22]Julius Center for Health Sciences and Primary Care, University Medical Center Utrecht, Utrecht, Netherlands; [23]Toronto Centre for Liver Disease, Toronto, Canada*
Email: g.weijsters@erasmusmc.nl

Background and aims: While aspartate aminotransferase (AST) and alanine aminotransferase (ALT) levels during ursodeoxycholic acid (UDCA) are associated with liver-transplant (LT)-free survival and liver-related events in people with primary biliary cholangitis (PBC), this is unclear for the decline in both parameters. The aim of this study was to assess how the percentage reduction of ALT and AST after 1 year UDCA relate to clinical outcome in PBC.

Method: The retrospective Dutch PBC Cohort Study includes every identifiable patient with PBC from 1990 up to last data collection (2019–2023) from all 71 hospitals in the Netherlands. Patients were included if >1 year follow-up after start of UDCA and without autoimmune hepatitis or second-line therapy/immunosuppressants. Where feasible, laboratory values were imputed using joint model multiple imputation. Cox survival analyses were used to study how ΔAST and ΔALT (per 10%) were related to LT-free survival and liver-related events (decompensation, LT, or liver-related death). Continuous variables were fitted as natural cubic spline where needed.

Results: In total, 3139 patients were included. At start of UDCA, median age was 58.0 years (IQR 49.7–67.2), 2745 (87.4%) were female and 203 (6.5%) had cirrhosis. During a median follow-up of 8.0 years (IQR 3.8–13.3), 295 patients developed decompensated cirrhosis, 78 patients underwent LT, and 584 patients died (152 [26%] liver-related; 115 [20%] of unknown cause). Median ΔAST after 1 year was −40% (−59; −15) and median ΔALT was −51% (−69; −25). In multivariable models (including baseline biochemistry), ΔAST (aHR 0.89, 95% CI 0.84–0.93) and ΔALT (aHR 0.94, 95% CI 0.90–0.99) were associated with LT-free survival (both $p < 0.05$). For liver-related events the aHR for ΔAST was 0.90 (95%CI 0.86–0.95) and for ΔALT 0.95 (95%CI 0.91–0.99) (both $p < 0.05$). When combining both ΔAST and ΔALT in one model, ΔAST remained significantly associated with LT-free survival and liver-related events (aHR 0.90, 95%CI 0.86–0.96, $p < 0.001$ and aHR 0.92, 95%CI 0.87–0.98, $p = 0.016$), while ΔALT lost significance. The ΔAST and ΔALT were not related to both outcomes after adjustment for their absolute value at 1 year (aHR~1, $p > 0.4$ for both).

Conclusion: Among people with PBC, the decline in AST during the first year appears to better reflect the clinical benefit of UDCA therapy than the decline in ALT. Yet, to assess prognosis, the decline in the transaminases do not add prognostic value over absolute values of AST and ALT at 1 year.

SAT-427

Early thiopurine metabolite monitoring in autoimmune hepatitis improves biochemical response at 6 months and enables early steroid withdrawal in a prospectively managed cohort

Jan Philipp Weltzsch[1], Moritz Waldmann[2], David Lübbering[1], Ludwig Horst[1], Silja Steinmann[1], Britta Zecher[1], Louisa Lund[1], Stephanie Schulze[1], Thomas Renne[2], Marcial Sebode[1], Christoph Schramm[1], Ansgar W. Lohse[1], Johannes Hartl[1]. *[1]I. Dept. of Medicine, University Medical Centre Hamburg Eppendorf (UKE), Hamburg, Germany; [2]Institute of Clinical Chemistry and Laboratory Medicine, University Medical Centre Hamburg-Eppendorf (UKE), Hamburg, Germany*
Email: j.weltzsch@uke.de

Background and aims: In autoimmune hepatitis (AIH), only 25–55% of patients achieve transaminase normalization after 6 months of standard therapy with azathioprine or mycophenolate mofetil, highlighting the need for improved strategies. We previously showed that, due to poor correlation between weight-adjusted thiopurine doses and metabolite levels of 6-thioguanine/6-methylmercaptopurine (6TGN/6MMP), therapeutic drug monitoring (TDM) improves response rates. Here, we prospectively evaluated whether a dose-adjustment algorithm incorporating early thiopurine metabolite measurements improves treatment responses.

Method: From 06/2022–06/2025, patients with a new diagnosis of AIH treated with thiopurines were prospectively managed according to a published treatment algorithm with early TDM at a median of 2 months and compared with a prospective cohort treated before TDM implementation (02/2017–03/2022). The primary endpoint was biochemical remission (BR), defined as normalization of ALT and AST at 6 months. Secondary endpoints included complete BR (CBR; normalization of ALT, AST and IgG) and steroid-free BR. Multivariable logistic regression assessed associations between TDM and outcomes, adjusting for age, sex, baseline ALT, AST, IgG, bilirubin, INR and fibrosis stage.

Results: A total of 216 patients with AIH were included: 75 were managed using TDM and 141 served as controls. Baseline characteristics (age, sex, ALT/AST levels, IgG, mHAI, INR), were similar between groups, advanced fibrosis tended to be more frequent in controls (23% vs. 12%). In patients with low 6TGN levels lacking BR (34/75, 45%), TDM-guided dose adjustments resulted in improved metabolite profiles (median 6TGN +28% at 6 months vs. baseline measurement; $p < 0.001$). Eight patients (11%) were switched to combination therapy with allopurinol due to shunting toward 6MMP, defined by a 6MMP:6TGN ratio >5. In these patients, the 6MMP:6TGN ratio decreased from 13.3 at baseline to 0.7 at 6 months ($p = 0.016$). Dose escalation based on early TDM achieved BR in 72%, and combination with allopurinol in 63% at month 6. Accordingly, early TDM was overall independently associated with higher rates of BR (72% vs. 52%; OR 2.24; $p = 0.022$), steroid-free BR (41% vs. 17%; OR 3.11; $p = 0.003$), and CBR (71% vs. 46%; OR 2.51; $p = 0.019$) at month 6 compared to controls.

Conclusion: Dose adjustments based on early TDM significantly improved 6-month biochemical response and facilitated early steroid withdrawal, supporting individualized thiopurine dose optimization.

SAT-428-YI

Differentiating acute-onset autoimmune hepatitis from drug-induced autoimmune-like hepatitis: a multicenter study and score development

Haoyu Wen[1,2], Yu Chen[1], Yu-Jie Zhou[1], Tianyu Mao[1], Qi Miao[1], Qiuxiang Lin[3], Zuxiong Huang[3], Yongfeng Yang[4], Xiong Ma[1], Xiao Xiao[1]. [1]*Division of Gastroenterology and Hepatology, Key Laboratory of Gastroenterology and Hepatology, Ministry of Health, State Key Laboratory for Oncogenes and Related Genes, Renji Hospital, School of Medicine, Shanghai Jiao Tong University; Shanghai Institute of Digestive Disease, Shanghai, China;* [2]*Department of Gastroenterology and Hepatology, Guangzhou Key Laboratory of Digestive Diseases, Guangzhou Digestive Disease Center, Guangzhou First People's Hospital, School of Medicine, South China University of Technology, Guangzhou, China;* [3]*Department of Hepatology, Mengchao Hepatobiliary Hospital of Fujian Medical University, Fuzhou, China;* [4]*Department of Infectious Disease and Liver Disease, The Second Hospital of Nanjing, Affiliated to Nanjing University of Chinese Medicine, Nanjing, China*
Email: xxiao_sh@163.com

Background and aims: The incidence of acute-onset autoimmune hepatitis (A-AIH) is rising, but its diagnosis remains challenging, particularly in patients with a history of hepatotoxic drug exposure. The clinical presentations of A-AIH and drug-induced autoimmune-like hepatitis (DI-ALH) at onset are often indistinguishable, complicating their timely diagnosis.
Method: We conducted a three-center retrospective study in China, screening patients with acute liver injury, hepatotoxic drug exposure, and autoimmune features. Patients were definitively classified as DI-ALH if they achieved sustained remission after culprit drug cessation, or as A-AIH if they relapsed. We compared the two groups across baseline demographics, laboratory indices, immunological profiles, and liver histology. After evaluating the performance of established AIH diagnostic criteria, we developed and independently validated a novel multivariable logistic regression model to improve discrimination between A-AIH and DI-ALH.
Results: Of 458 patients screened, 238 met the inclusion criteria and constituted the final cohort: 94 with A-AIH and 144 with DI-ALH. Compared to DI-ALH, A-AIH patients had significantly higher IgG levels, lower platelet counts, and higher autoantibody titers. Histologically, A-AIH exhibited more severe portal inflammation, interface hepatitis, fibrosis, and rosette formation. The discriminatory capacity of both the 2022 and 2008 histological criteria was limited and comparable (AUC 0.62 vs. 0.59, p = 0.616). The novel Dx-AID score —incorporating platelet count, IgG, autoantibodies, and histological features—achieved high diagnostic accuracy in both the derivation cohort (AUC 0.84, 95% CI: 0.77–0.91) and the independent validation cohort (AUC 0.83, 95% CI: 0.72–0.94).
Conclusion: A-AIH and DI-ALH share many clinical similarities, but they differ in immunological and histological profiles. The Dx-AID score effectively integrates these key differences, providing a clinically actionable tool for early differentiation and guiding personalized treatment decisions.

SAT-429

Biochemical criteria in relation to clinical outcome in people with primary biliary cholangitis using ursodeoxycholic acid

Ellen Werner[1], Gemma H. X. Weijsters[1], Tiki D. Blom[1], Maria C. van Hooff[1], Rozanne C. de Veer[1], Ulrich Beuers[2], Joost P. H. Drenth[2], Frans J. C. Cuperus[3], Remco van Dijk[4], Bart J. Veldt[5], Michael Klemt-Kropp[6], Suzanne van Meer[7], Robert C. Verdonk[8], Hajo J. Flink[9], Jan Maarten Vrolijk[10], Cyriel Ponsioen[2], Matthijs Kramer[11], Pieter C. J. ter Borg[12], Robert Roomer[13], Edith M. M. Kuiper[14], Stephan Schmittgens[15], Yasser A. Alderslieste[16], Koen R. Beukema[17], Leendert H. Oterdoom[18], Martine A. M. C. Baven-Pronk[19], Anne Vrieze[20], Ingrid C. A. W. Konings[21], Nicole S. Erler[22], Harry L. A. Janssen[1,23], Bettina E. Hansen[1,24,25], Adriaan J. van der Meer[1]. [1]*Erasmus University Medical Center, Rotterdam, Netherlands;* [2]*Amsterdam University Medical Center, Amsterdam, Netherlands;* [3]*University Medical Center Groningen, Groningen, Netherlands;* [4]*Leiden University Medical Center, Leiden, Netherlands;* [5]*Reinier de Graaf Gasthuis, Delft, Netherlands;* [6]*Noordwest Ziekenhuisgroep, Alkmaar, Netherlands;* [7]*University Medical Center Utrecht, Utrecht, Netherlands;* [8]*St.Antonius Hospital, Nieuwegein, Netherlands;* [9]*Catharina Hospital, Eindhoven, Netherlands;* [10]*Rijnstate, Arnhem, Netherlands;* [11]*Maastricht University Medical Center, Maastricht, Netherlands;* [12]*Ikazia, Rotterdam, Netherlands;* [13]*Franciscus Gasthuis & Vlietland, Rotterdam, Netherlands;* [14]*Maasstad Hospital, Rotterdam, Netherlands;* [15]*Nij Smellinghe Hospital, Drachten, Netherlands;* [16]*Beatrix Hospital, Gorinchem, Netherlands;* [17]*Medisch Spectrum Twente, Twente, Netherlands;* [18]*Haga Hospital, Den Haag, Netherlands;* [19]*Groene Hart Hospital, Gouda, Netherlands;* [20]*Flevo Hospital, Almere, Netherlands;* [21]*Admiraal de Ruyter Hospital, Goes/Vlissingen/Zierikzee, Netherlands;* [22]*Julius Center for Health Sciences and Primary Care, University Medical Center Utrecht, Utrecht, Netherlands;* [23]*Toronto Centre for Liver Disease, University of Toronto, Toronto, Canada;* [24]*IHPME, University of Toronto, Toronto, Canada;* [25]*Toronto Center for Liver Disease & TGHRI, University Health Network, Toronto, Canada*
Email: e.werner@erasmusmc.nl

Background and aims: Various biochemical criteria have been proposed to evaluate prognosis with ursodeoxycholic acid (UDCA) in people with Primary Biliary Cholangitis (PBC). Most results, however, are derived from tertiary cohorts. We aimed to assess the relation between the various criteria and clinical outcome in a nationwide cohort of people with PBC.
Method: The retrospective Dutch PBC Cohort Study (DPCS) includes in-depth clinical data of every identifiable individual with PBC in the Netherlands from 1990 up to last data collection (2019–2023) in all 71 Dutch hospitals. Clinical data were obtained through medical chart review. Where feasible, imputation was performed using joint model multiple imputation. People were included in case of at least one year of follow-up (FU) after initiating UDCA. Survival analyses were used to evaluate the various biochemical criteria in relation to liver transplantation (LT) or death.
Results: In total, 3566 patients were included with a median age of 57.6y (IQR 49.5–66.9) of whom 3131 (87.8%) were female, 294 (7.2%) had cirrhosis and 3376 (83.0%) were treated in non-academic hospitals. At one year of UDCA, 79.9% met Paris I (ALP $\leq 3 \times$ ULN, AST $\leq 2 \times$ ULN, and Total Bilirubin [TB] $\leq$ ULN), 75.0%, the Rotterdam criteria (normal TB and albumin), 74.5% Toronto (ALP $\leq 1.67 \times$ ULN), 65.2% Barcelona (normal ALP or 40% ALP decrease), 57.4% PARIS II (ALP and AST $\leq 1.5 \times$ ULN with TB $\leq$ ULN), 53.0% POISE (ALP$<1.67 \times$ ULN, ALP decrease $\geq$15% from baseline, and TB $\leq$ ULN), and 25.6% the Global Deep Response (normal ALP and TB $\leq 0.6 \times$ ULN. Median FU was 8.0 years (IQR 3.9–13.3) during which 622 patients died and 95 patients underwent LT. Irrespective of the criteria, those who met these had a favorable LT-free survival as compared to those with did not ($p < 0.001$ for all). Over the various criteria, the cumulative 10-year survival ranged between 85.5% (95%CI 83.9–87.2, Toronto) and 89.2% (95%CI 86.3–92.2, Global Deep Response) among those with a biochemical response. However, among those with an incomplete response, the cumulative 10-year survival ranged between 54.7% (95%CI 49.3–60.7, Rotterdam) and 81.8% (95%CI 79.9–63.7, Global Deep Response).
Conclusion: This large, recent, representative nationwide PBC cohort study, supports that all previously suggested biochemical criteria at one year of UDCA therapy are associated with the LT-free survival. The prognosis was similar between the responders to the various criteria, but varied substantially depending on which of the criteria was not met after one year of UDCA.

SAT-432

Validation of the GLOBE score in a nationwide cohort of people with primary biliary cholangitis

Ellen Werner[1], Gemma H. X. Weijsters[1], Tiki D. Blom[1], Lina Assadrati[1], Maria C. van Hooff[1], Rozanne C. de Veer[1], Ulrich Beuers[2], Joost P. H. Drenth[2], Frans J. C. Cuperus[3], Remco van Dijk[4], Bart J. Veldt[5], Michael Klemt-Kropp[6], Suzanne van Meer[7], Robert C. Verdonk[8], Hajo J. Flink[9], Jan Maarten Vrolijk[10], Cyriel Ponsioen[2], Matthijs Kramer[11], Martijn J. ter Borg[12], Khalida Soufidi[13], Djuna L. Cahen[14], Lauren A. van der Waaij[15], Hans H. K. Thio[16], Roberta M. Manzat-Saplacan[17], Lisette J. H. van Dam[18], Ludger S. M. Epping[19], Matthias C. Jurgens[20], Marcel Cazemier[21], Nicole S. Erler[22], Harry L. A. Janssen[1,23], Bettina E. Hansen[1,24,25], Adriaan J. van der Meer[1]. *[1]Erasmus University Medical Center, Rotterdam, Netherlands; [2]Amsterdam University Medical Center, Amsterdam, Netherlands; [3]University Medical Center Groningen, Groningen, Netherlands; [4]Leiden University Medical Center, Leiden, Netherlands; [5]Reinier de Graaf Gasthuis, Delft, Netherlands; [6]Noordwest Ziekenhuisgroep, Alkmaar, Netherlands; [7]University Medical Center Utrecht, Utrecht, Netherlands; [8]St.Antonius Hospital, Nieuwegein, Netherlands; [9]Catharina Hospital, Eindhoven, Netherlands; [10]Rijnstate, Arnhem, Netherlands; [11]Maastricht University Medical Center, Maastricht, Netherlands; [12]Maxima Medical Center, Eindhoven, Netherlands; [13]Zuyderland Medical Center, Heerlen, Netherlands; [14]Hospital Amstelland, Amstelveen, Netherlands; [15]Martini Hospital, Groningen, Netherlands; [16]Saxenburgh Medical Center, Hardenberg, Netherlands; [17]Wilhelmina Hospital Assen, Assen, Netherlands; [18]Ommelander Hospital, Scheemda, Netherlands; [19]Maasziekenhuis Pantein, Boxmeer, Netherlands; [20]St. Jans Gasthuis Weert, Weert, Netherlands; [21]BovenIj Hospital, Amsterdam, Netherlands; [22]Julius Center for Health Sciences and Primary Care, University Medical Center Utrecht, Utrecht, Netherlands; [23]Toronto Centre for Liver Disease, University of Toronto, Toronto, Canada; [24]IHPME, University of Toronto, Toronto, Canada; [25]Toronto Center for Liver Disease & TGHRI, University Health Network, Toronto, Canada*
Email: e.werner@erasmusmc.nl

Background and aims: Prognostic tools in Primary Biliary Cholangitis (PBC) are mostly derived from tertiary cohorts. The GLOBE score is commonly used to predict the liver transplantation-free survival (LTFS). We aimed to evaluate the prognostic performance of the GLOBE score in a nationwide cohort of people with PBC.
Method: The Dutch PBC Cohort Study is a retrospective study which includes in-depth clinical data from every identifiable individual with PBC in the Netherlands from 1990 up to last data collection (2019–2023) in all 71 Dutch hospitals. Where feasible, imputation was performed using joint model multiple imputation. Inclusion criteria were ursodeoxycholic acid (UDCA) initiation and availability of the GLOBE score parameters alkaline phosphatase (ALP), total bilirubin (TB), platelets and albumin at one year after start of UDCA. Survival analyses were performed to assess the relation between the GLOBE score and LT or death. Discriminative ability of the GLOBE score was assessed with the c-statistic and the accuracy of the predicted probabilities were assessed through calibration plots. The Integrate Brier Score (IBS) summarized prediction error over time.
Results: In total, 2637 patients were included of whom 2056 (78.0%) were treated in non-academic hospitals. At baseline, median age was 57.2 years (IQR 49.3–66.9), 2319 (87.9%) were female and 203 (7.7%) had cirrhosis. At one year of UDCA, ALP was 1.2 × ULN (IQR 0.9–1.7) and TB was 0.5 × ULN (IQR 0.4–0.7). Overall, the median GLOBE score was −0.1 (IQR −0.7–0.6). During a median follow-up (FU) of 7.9 years (IQR 3.9–13.3) years, 74 underwent LT and 491patients died. The GLOBE-score was independently associated with LT or death (adjusted HR 3.05, 95%CI 2.68–3.47, p < .001). The c-statistic was 0.79 (95%CI 0.77–0.82). Calibration showed an IBS of 0.05 over a 10y follow-up. In the 25% of people with highest GLOBE scores (>0.56) the observed 10y LT-free survival probability was 60.3% (95%CI 55.7–65.2) vs a predicted 10y LT-free survival of 59.2%. These were 97.5% (95%CI 96.0–99.0) vs 94.1% for people with a GLOBE score of <−0.66 (lowest 25%) and 90.1% (95%CI 88.0–92.2) vs 85.3% for people with a GLOBE score −0.66 to 0.56 (middle 50%).
Conclusion: In this nationwide cohort of people with PBC, a higher GLOBE score was associated with risk of LT or death with an accurate discriminative ability. Especially for people with PBC at greater risk of LT or death, the GLOBE's projected prognosis was very accurate.

SAT-433

Alkaline phosphatase in relation to clinical outcome according to subgroups of people with primary biliary cholangitis

Ellen Werner[1], Gemma H. X. Weijsters[1], Tiki D. Blom[1], Maria C. van Hooff[1], Rozanne C. de Veer[1], Ulrich Beuers[2], Joost P. H. Drenth[2], Frans J. C. Cuperus[3], Remco van Dijk[4], Bart J. Veldt[5], Michael Klemt-Kropp[6], Suzanne van Meer[7], Robert C. Verdonk[8], Hajo J. Flink[9], Jan Maarten Vrolijk[10], Cyriel Ponsioen[2], Matthijs Kramer[11], Johannes Schmidt[12], Frank C. Bekkering[13], Stephan H. C. van Stiphout[14], Nicole F. M. van Gerven[15], Sven J. van den Hazel[16], Paul J. Bus[17], A. van der Beek[18], Sigrid Vandebosch[19], Maaike J. Denters[20], Paul G. van Putten[21], Nicole S. Erler[22], Harry L. A. Janssen[1,23], Bettina E. Hansen[1,24,25], Adriaan J. van der Meer[1]. *[1]Erasmus University Medical Center, Rotterdam, Netherlands; [2]Amsterdam University Medical Center, Amsterdam, Netherlands; [3]University Medical Center Groningen, Groningen, Netherlands; [4]Leiden University Medical Center, Leiden, Netherlands; [5]Reinier de Graaf Gasthuis, Delft, Netherlands; [6]Noordwest Ziekenhuisgroep, Alkmaar, Netherlands; [7]University Medical Center Utrecht, Utrecht, Netherlands; [8]St.Antonius Hospital, Nieuwegein, Netherlands; [9]Catharina Hospital, Eindhoven, Netherlands; [10]Rijnstate, Arnhem, Netherlands; [11]Maastricht University Medical Center, Maastricht, Netherlands; [12]Dijklander Hospital, Hoorn, Netherlands; [13]Ijsselland Hospital, Capella a/de Ijssel, Netherlands; [14]Elkerliek Hospital, Helmond, Netherlands; [15]Rode Kruis Hospital, Beverwijk, Netherlands; [16]Slingeland Hospital, Doetinchem, Netherlands; [17]Laurentius Hospital, Roermond, Netherlands; [18]Hospital Rivierenland, Tiel, Netherlands; [19]ZorgSaam Hospital, Oostburg/Terneuzen/Hulst, Netherlands; [20]Zaans Medical Center, Zaandam, Netherlands; [21]Antonius Zorggroep, Sneek, Netherlands; [22]Julius Center for Health Sciences and Primary Care, University Medical Center Utrecht, Utrecht, Netherlands; [23]Toronto Centre for Liver Disease, University of Toronto, Toronto, Canada; [24]IHPME, University of Toronto, Toronto, Canada; [25]Toronto Center for Liver Disease & TGHRI, University Health Network, Toronto, Canada*
Email: e.werner@erasmusmc.nl

Background and aims: Alkaline phosphatase (ALP) has been associated with prognosis in people with primary biliary cholangitis (PBC). The strength of this association is likely influenced by specific patient and disease characteristics. We aimed to assess the relation between ALP at one year of ursodeoxycholic acid (UDCA) and clinical outcome in subgroups of people with PBC.
Method: The retrospective Dutch PBC Cohort Study (DPCS) includes every identifiable patient with PBC in the Netherlands from 1990 up to last data collection (2019–2023) in all 71 Dutch hospitals. Clinical data were obtained through medical chart review. Where feasible, imputation was performed using joint model multiple imputation. Patients were included in case of ≥1 year of follow-up after initiating UDCA. Laboratory values are presented as upper limits of normal (ULN). The association between ALP and liver transplant (LT) or death was evaluated using Cox survival analyses. Depending on the subgroup, analyses were adjusted for sex, age, cirrhosis at baseline, total bilirubin (TB), use of immunosuppressives and calendar year.
Results: In total, 3566 patients were included (median age 57.6 years (IQR 49.5–66.9), 3131 (87.8%) were female). At baseline, 2433/3422 (71.1%) had early disease stage (normal TB and albumin) and 989/3422 (28.9%) moderately advanced (abnormal TB or albumin). The median follow-up was 8.0 years (IQR 3.9–13.3) during which 95 patients underwent LT and 622 patients died. At one year after start of

UDCA, median ALP was 1.2 (IQR 0.9–1.6) and median TB was 0.5 (IQR 0.4–0.7). Overall, the aHR of ALP was 1.40 (95%CI 1.28–1.52, p < .001). The aHR of ALP was significant in the assessed subgroups (all p < .05); 1.27 (95%CI 1.10–1.46) in those with an early stage vs 1.31 (95%CI 1.18–1.44) in those with a moderately advanced stage, 1.41 (95%CI 1.07–1.86) in males vs 1.19 (95%CI 1.03–1.38) in females, 1.26 (95%CI 1.06–1.50) in people aged <45y up to 1.30 (95%CI 1.12–1.50) in people >65y and 1.24 (95%CI 1.10–1.39) when UDCA was initiated <2010 vs 1.40 (95%CI 1.22–1.60) ≥2010. The aHR of ALP at one year was 1.58(95%CI 1.16–2.15) in those with a baseline ALP <2 and 1.21 (95%CI 1.05–1.40) in those with a baseline ALP >4. Baseline TB ≤ 0.6 resulted in an aHR for ALP of 1.18 (95%CI 1.01–1.38) vs 1.24 (95%CI 1.01–1.40) for TB > 0.6.
Conclusion: This large nationwide cohort supports that ALP at one year after start of UDCA is a consistent prognostic marker for the population with PBC, across all clinically relevant subgroups.

SAT-434

Utilization of maralixibat, an ileal bile acid transporter inhibitor, for the treatment of intrahepatic cholestasis of pregnancy: a case series

Lizemarie Wium[1], Caroline Ovadia[2], Kate Wiles[3], Jenny Chambers[4,5], Alice Mitchell[4], Jemma Johns[1,6], Salma Jabak[1], Sarah-Louise Sinclair-Bell[1], Bansri Bharania[1], Rebecca Allen[3], Janet Dearden[3], Arron Jones[3], Naomi Primrose[7], Muna Noori[7], Douglas B. Mogul[8], Jolan Terner-Rosenthal[8], Pamela Vig[8], Catherine Williamson[4]. *[1]King's College Hospital NHS Trust, London, England, United Kingdom; [2]University of Edinburgh, Edinburgh, Scotland, United Kingdom; [3]Barts Health NHS Trust, London, England, United Kingdom; [4]Institute of Reproductive and Developmental Biology, Imperial College London, London, England, United Kingdom; [5]ICP Support, Poole, England, United Kingdom; [6]King's College London, London, England, United Kingdom; [7]Imperial College Healthcare NHS Trust, London, England, United Kingdom; [8]Mirum Pharmaceuticals, Inc., Foster City, California, United States*
Email: catherine.williamson@imperial.ac.uk

Background and aims: Intrahepatic cholestasis of pregnancy (ICP) is characterized by elevated maternal total serum bile acids (TBA) and liver transaminases. Maralixibat (MRX) is an ileal bile acid transporter (IBAT) inhibitor that effectively reduces pruritus and total serum bile acid (TBA) levels in non-gestational cholestasis. This case series reviewed the effectiveness and tolerability of MRX on hypercholanemia and pruritus in recurrent, severe ICP.
Method: Retrospective analysis of four cases of recurrent, severe ICP with marked hypercholanemia and pruritus with insufficient ursodeoxycholic acid response treated with MRX through a compassionate use program was conducted. Key clinical, biochemical, and safety data were collected.
Results: Case 1 was a 37 year old White woman (heterozygous p.[V444A] *ABCB11*), previous stillbirth and miscarriage. She had elevated TBA (118 µmol/L) but no recorded pruritus. She began MRX treatment (70 µg/kg/d, uptitrated to 175 µg/kg/d) at 28 + 0 weeks' gestation. MRX reduced TBA (<40 µmol/L) and the patient delivered a live baby at 35 + 5 gestational weeks. Case 2 was a 36 year old Black woman (homozygous p.[V444A] *ABCB11*), previous live birth at 37 weeks' gestation. She developed pruritus at 17 weeks and elevated TBA (219 µmol/L) at 22 + 4 weeks' gestation. She began MRX treatment (70 µg/kg/d, uptitrated to 210 µg/kg/d) at 28 + 5 weeks' gestation and pruritus and TBA improved (<40 µmol/L). Due to a sudden unexplained increase in TBA, the clinical team induced instead of increasing the MRX dose. A healthy baby was delivered at 34 + 5 weeks of gestation. Case 3 was a 42 year old South Indian woman (ICP-associated genetic variants not detected), previous stillbirth and fetal loss after placental abruption. TBA was elevated (237 µmol/L) and she began MRX treatment (300 µg/kg BID) and saw an improvement in TBA (<40 µmol/L). A healthy baby was delivered at 34 weeks' gestation. Case 4 was a 38 year old White woman (heterozygous, p.[V444A] *ABCB11*) two previous stillbirths. TBA was elevated (148 µmol/L) since nine weeks' gestation. She began MRX treatment (70 µg/kg/d, uptitrated to 300 µg/kg/d) at 18 weeks' gestation. TBA was reduced (52–93 µmol/L), then rose (125 µmol/L) at 31 weeks when a decision was made to expedite delivery. She delivered a live baby at 31 + 2 weeks' gestation. Mild GI events occurred in three patients during MRX treatment but were manageable.
Conclusion: These findings suggest that maralixibat may effectively manage ICP by lowering TBA and improving pruritus.

SAT-435

Early liver stiffness measurement improves the prediction of liver-related events beyond biochemical remission in newly diagnosed autoimmune hepatitis

Yu Jun Wong[1,2], Guan Sen Kew[1,3], Gideon M. Hirschfield[4], Aliya Gulamhusein[4], Madeline Cameron[4], Shagani Thisairajah[1], Hin Hin Ko[5], Nabiha Faisal[6], Kristel Leung[7], Jean-Philippe Wallach[8], Devika Shreekumar[1], Narmeen Umar[1], Karim Qumosani[9], Mina Niazi[10], Julian Hercun[11], Catherine Vincent[11], Angela Cheung[12], Tianyan Chen[13], Tasha Kulai[14], Andrew L. Mason[1], Mark Swain[15], Bettina Hansen[4], Ellina Lytvyak[1], Aldo J Montano-Loza[1]. *[1]Division of Gastroenterology and Hepatology, University of Alberta, Edmonton, Canada, Edmonton, Canada; [2]Department of Gastroenterology & Hepatology, Changi General Hospital, Singapore, Singapore; [3]Woodlands Health Campus, Singapore, Singapore; [4]The Autoimmune and Rare Liver Disease Programme, Division of Gastroenterology and Hepatology, Toronto General Hospital, Toronto, Canada, Toronto, Canada; [5]Division of Gastroenterology, University of British Columbia, Vancouver, Vancouver, Canada; [6]Department of Internal Medicine, Section of Hepatology, University of Manitoba, Manitoba, Canada; [7]Departments of Medicine & Public Health Sciences, Queen's University, Kingston, Ottawa, Canada; [8]Nanaimo Regional Hospital, Nanaimo, Nanaimo, Canada; [9]Department of Medicine, Western University, London, Ontario, Canada; [10]Division of Gastroenterology and Hepatology, College of Medicine, University of Saskatchewan Royal University Hospital, Saskatoon, Canada; [11]Liver Unit of the Centre hospitalier de l'Université de Montréal, Montreal, Canada; [12]University of Ottawa's Faculty of Medicine, Ottawa, Canada; [13]McGill University Health Centre, Royal Victoria Hospital, Montreal, Canada; [14]Department of Medicine, Dalhousie University, Halifax, Nova Scotia, Canada; [15]Division of Gastroenterology and Hepatology, University of Calgary, Calgary, Canada*
Email: wongyujun1985@gmail.com

Background and aims: Biochemical remission (BR) is the primary treatment target in autoimmune hepatitis (AIH), yet it may not fully capture residual fibrosis or long-term risk. The prognostic role of liver stiffness measurement (LSM) in AIH, particularly when performed early after diagnosis and treatment initiation, remains unclear. We evaluate whether *early LSM* provides independent prognostic value for liver-related events (LRE) beyond BR in AIH.
Method: From the Canadian Network for Autoimmune Liver Disease registry, we identified AIH patients (diagnosed 2010–2025) across 13 centres who underwent *early LSM* (<12 months after AIH diagnosis and treatment initiation). A landmark analysis was performed using the first *early* LSM. The primary composite outcome was time to first LRE, defined as hepatic decompensation, liver transplantation, hepatocellular carcinoma, or death. BR was defined as ALT normalization, with sensitivity analysis using complete BR (ALT and IgG normalization) at 6 months.
Results: Among 305 AIH patients (median age: 55 years, 32.1% cirrhosis at diagnosis), median time to *early* LSM was 2.1 months (IQR: 0.5–5.6), and median LSM was 12.6 kPa (IQR:7.5–23.1). ALT normalization was achieved in 57.6% and 72.6% at 6 and 12 months, respectively. Over a median follow-up of 58 months, 29 patients developed LRE, most commonly hepatic decompensation. Despite low absolute event rate typical of treated AIH cohorts, patients with LREs had significantly higher LSM and lower platelet counts at diagnosis (all p < 0.05). LSM ≥15 kPa independently predicted LREs

(HR 4.6, 95%CI: 1.9–11.2, p < 0.0001). Importantly, 52% of patients with LSM ≥15 had already achieved BR at 6 months. The association between LSM ≥15 kPa and LREs remained robust after adjustment for BR status, diabetes, MELD score, and prior decompensation. Cox-adjusted survival analysis demonstrated significantly reduced LRE-free survival in patients with LSM ≥ 15 kPa (aHR: 3.95, 95%CI: 1.44–10.89). Among patients with repeated LSM <6 months, no LRE occurred in patients achieving ≥20% LSM reduction or LSM regression to <15 kPa, whereas all LRE occurred in patients without LSM improvement.
Conclusion: Biochemical remission does *not* fully eliminate long-term risk in AIH. *Early* LSM ≥15 kPa identifies a clinically important high-risk subgroup despite apparent biochemical control. Incorporating early LSM into post-treatment assessment may enable more precise risk stratification and guide surveillance intensity in AIH.

SAT-436
Challenging the paradigm: IBD status does not independently predict hepatic outcomes in a large, long-term PSC cohort
Yu Jun Wong[1,2], Guan Sen Kew[1,3], Ellina Lytvyak[1], Devika Shreekumar[1], Shagani Thisairajah[1], Andrew L. Mason[1], Aldo J Montano-Loza[1]. *[1]Division of Gastroenterology and Hepatology, University of Alberta, Edmonton, Canada, Edmonton, Canada; [2]Department of Gastroenterology & Hepatology, Changi General Hospital, Singapore, Singapore; [3]Woodlands Health Campus, Singapore, Singapore*
Email: wongyujun1985@gmail.com

Background and aims: Inflammatory bowel disease (IBD) is integral for risk stratification, surveillance strategies, and clinical trial design in primary sclerosing cholangitis (PSC). However, whether IBD independently predicts hepatic outcomes beyond established markers of disease severity remains uncertain. We aim to evaluate whether IBD status, subtype, and diagnostic timing independently predict the first occurrence of hepatic decompensation (HD) or hepatobiliary malignancy in PSC.
Method: We analysed 611 patients with PSC (EASL criteria) from a tertiary Canadian cohort (1974–2024). The primary outcome was first HD. Fine–Gray model (competing risks: liver transplantation (LT), death, cholangiocarcinoma, hepatocellular carcinoma, gallbladder adenocarcinoma, and colorectal cancer) evaluated the association of IBD with HD risk in PSC patients. Multivariable Cox and Poisson regression provided complementary analyses, adjusting for established risk factors including *cirrhosis*. Prespecified sensitivity analyses assessed IBD subtype (Ulcerative colitis *vs.* Crohn's disease) and IBD diagnosis timing (before and after PSC diagnosis).
Results: Among 611 PSC patients (mean age 34 ± 16 years, 64% male), 72% had concomitant IBD (71% ulcerative colitis, 29% Crohn's disease), with 26% diagnosed after PSC. PSC patients with IBD were younger, more frequently male, more likely to have small-duct PSC, and had higher platelet counts (all p < 0.05). Over a mean follow-up of 9.4 (±7.7) years, 30% experienced HD, 37.2% underwent LT, and 5% developed hepatobiliary malignancy. In competing risk analysis, IBD was *not* associated with HD (Fine-Gray sHR: 0.83, 95%CI: 0.51–1.27; Poisson adjusted IRR 0.70, 95%CI: 0.46–1.04). Null associations persisted for LT-free survival and hepatobiliary malignancy in Cox-models, and across IBD subtype and diagnostic timings. Instead, *cirrhosis* at diagnosis was the strongest independent predictor of HD across all adjusted models (Fine-Gray sHR: 2.85, p = 0.008; Poisson adjusted IRR: 2.84, p = 0.002).
Conclusion: In this large, long-term PSC cohort, concomitant IBD, regardless of subtype or diagnostic timing, was *not* independently associated with HD, transplant-free survival, or hepatobiliary malignancy in PSC, across competing-risks, Cox, and Poisson regression. Conversely, cirrhosis was an independent predictor of HD. Hepatic risk stratification should prioritize disease severity markers like *cirrhosis* over IBD status, advocating a shift towards risk-based surveillance and trial design.

SAT-441
One in four adults have already developed cirrhosis at the time of primary biliary cholangitis diagnosis among a national cohort of veterans in the United States
Robert Wong[1], Zeyuan Yang[2], Ramsey C. Cheung[1]. *[1]Stanford University School of Medicine, VA Palo Alto Health Care System, Palo Alto, United States; [2]VA Palo Alto Health Care System, Palo Alto, United States*
Email: rwong123@stanford.edu

Background and aims: Primary biliary cholangitis (PBC) is a progressive cholestatic liver disease associated with significant morbidity and mortality. Delays in timely diagnosis and linkage to treatment contributes to continued liver injury and progression to cirrhosis and liver-related mortality. We aim to evaluate the prevalence of cirrhosis at time of PBC diagnosis among a national cohort of U.S. Veterans, which reflects delays in timely diagnosis and linkage to care.
Method: Adults with PBC were identified using National Veterans Affairs data from January 1, 2010 to April 30, 2025. PBC was diagnosed based on established definitions and incorporated the presence of ≥1 inpatient or ≥2 outpatient ICD-9/10 diagnosis codes for PBC. The proportion of patients with cirrhosis at time of PBC diagnosis was identified using validated algorithms based on ICD-9/10 diagnosis codes. Comparisons of cirrhosis proportions at time of PBC diagnosis was stratified by sex, age, and race/ethnicity and compared between groups utilized chi-square methods.
Results: Overall prevalence of PBC was 51.6 per 100,000 persons. Among 2147 adults with PBC (mean age 64.6 years, 79.5% men, 78.4% non-Hispanic white, 11.7% African American, 7.1% Hispanic, 2.2% Asian), 24.9% had concurrent diabetes mellitus, 48.9% dyslipidemia, 59.5% hypertension, and median alkaline phosphatase was 157 U/L (IQR 103–256). Overall, 25.3% (95% CI 23.6–27.0) had evidence of cirrhosis at time of PBC diagnosis, which was similar in men (25.3%, 95% CI 23.4–27.2) and women (25.4%, 95% 21.8–29.0). Proportion with cirrhosis at PBC diagnosis was significantly higher in younger patients age 18–39y (40.0% vs. 28.9% in age 40–59y, p < 0.05). Compared to non-Hispanic whites, proportion with cirrhosis was similar among Asians and Hispanics, but African Americans had significantly lower proportion with cirrhosis at diagnosis (20.5% vs. 26.3%, p = 0.02). When stratified by sex and race/ethnicity, the proportion of patients with cirrhosis at diagnosis was lowest among Asian women (14.3%) and highest among Asian men (28.6%).
Conclusion: Among a national cohort of U.S. Veterans with PBC, more than one in four already had developed cirrhosis at time of PBC diagnosis. This was particularly observed for non-Hispanic whites and Asian men. Greater awareness and vigilance are needed to improve timely diagnosis and treatment of patients with PBC to prevent liver-related morbidity and mortality.

SAT-442
Real-world efficacy and safety of fibrates in patients with primary biliary cholangitis
Ewa Wunsch[1], Karolina Wronka[2], Maciej Janik[2], Beata Kruk[3], Sebastian Jędruszek[1], Kaja Kozłowska[1], Magdalena Jaroszek[2], Jacek Tomczuk[2], Joanna Raszeja-Wyszomirska[2], Piotr Milkiewicz[1,2]. *[1]Division of Gastroenterology, Department of Translational Medicine, Pomeranian Medical University in Szczecin, Szczecin, Poland; [2]Department of Hepatology, Transplantology and Internal Medicine, Medical Universty of Warsaw, Warsaw, Poland; [3]Laboratory of Metabolic Liver Diseases, Department of General, Transplant and Liver Surgery, Medical University of Warsaw, Warsaw, Poland*
Email: ewa.wunsch@pum.edu.pl

Background and aims: Fibric acid derivatives are used off-label as second-line therapy in patients with primary biliary cholangitis (PBC) with an inadequate response to ursodeoxycholic acid (UDCA) and are

recommended by EASL for the treatment of cholestatic pruritus. However, real-world data on their effectiveness and safety remain limited. We aimed to assess the real-world clinical use, efficacy and tolerability of fibrates in patients with PBC.
Method: This study included all consecutive patients with PBC treated since 2019 in two Polish tertiary university centers. Patients with decompensated liver cirrhosis, after liver transplantation or lost to follow-up were excluded. Clinical, laboratory and drug regimens data were extracted from medical records and analyzed retrospectively.
Results: Among 396 patients with PBC (361 females, mean age 52 ± 12 years), 145 (37%; 132 females, mean age 56 ± 12 years) received fibrates as add-on therapy to UDCA. The main indications were inadequate biochemical response to UDCA according to Barcelona criteria (68%), cholestatic pruritus (21%) and dyslipidaemia (16%). Fenofibrate was the initial agent in 143 (97%) of cases, while bezafibrate - in two remaining patients. Fibrate therapy was associated with a significant improvement in liver biochemistry (reduction in ALP from 248 ± 12 to 160 ± 8 IU/L, $p < 0.001$; GGT from 185 ± 14 to 120 ± 11 IU/L, $p < 0.001$; and ALT from 57 ± 3 to 47 ± 2 IU/L, $p = 0.002$). No differences were observed in albumin, INR, platelets and creatinine levels. Adverse events were reported in 30 (20%) of patients, most frequently myopathy, gastrointestinal intolerance, renal function deterioration and hypertransaminasemia. Due to lack of efficacy or tolerability, fenofibrate treatment was switched to bezafibrate in 10 patients, with recurrent intolerance observed in half of them. Overall, fibrate therapy was discontinued in 22 patients (15%). Owing to insufficient response, elafibranor was initiated recently in two patients, while linerixibat was introduced in two patients with refractory pruritus.
Conclusion: In real-world clinical practice, more than one-third of patients with PBC require second-line therapy. Fibrates provide significant biochemical improvement in vast majority of these patients; however, adverse events occur in a substantial proportion, leading to the discontinuation of therapy. This finding highlights the need for novel therapeutic alternatives with better tolerability, reinforcing the importance of expanding the treatment landscape in PBC.

SAT-443

Liver transplantation for cholestatic liver diseases: trends in primary biliary cholangitis and primary sclerosing cholangitis in the US and Europe over two decades

Zobair M. Younossi[1], Giacomo Germani[1,2], Robert Wong[1,3], Maria Stepanova[1], Fatema Nader[1], Vincent Karam[1,4], René Adam[1,5], Saleh Alqahtani[1,6], Rohit S. Satoskar[1,7], Linda Henry[1], Patrizia Burra[1,2]. *[1]The Global NASH/MASH Council, Washington DC, United States; [2]Department of Surgery, Oncology and Gastroenterology, University of Padova, Padova, Italy; [3]Division of Gastroenterology and Hepatology, Stanford University School of Medicine, Palo Alto, United States; [4]The European Society for Organ Transplantation, Paris, France; [5]Hopital Paul Brousse, Villejuif, France; [6]Liver, Digestive, and Lifestyle Research Section, and Organ Transplant Center of Excellence, King Faisal Specialist Hospital and Research Center, Riyadh, Saudi Arabia; [7]Georgetown Medical Center, Washington DC, United States*
Email: zobair.younossi@cldq.org

Background and aims: Cholestatic liver diseases [primary biliary cholangitis (PBC) and primary sclerosing cholangitis (PSC)] are indications for liver transplantation (LT). We assessed demographics, clinical features, and outcomes of LT recipients with PBC and PSC in the US and Europe.
Method: Adult LT recipients with PBC or PSC were identified from the European Liver Transplant Registry (ELTR) and U.S. Scientific Registry of Transplant Recipients (SRTR) (2000–2022).
Results: A total of 22,034 LT recipients were included (PBC n = 8774; PSC n = 13,260). PBC recipients were older (56 ± 10 vs. 46 ± 13 years) and predominantly female (85% vs. 31%) (both $p < 0.0001$). HCC was present in 5.4% of PBC, and cholangiocarcinoma in 2.4% of PSC patients. PBC patients had more ascites (66% vs. 50%) and hepatic encephalopathy (46% vs. 32%) (all $p < 0.0001$), and higher MELD scores (20 ± 9 vs. 19 ± 9, $p < 0.0001$). In the entire dataset, PBC as a proportion of all LTs declined from 6.2% (2000) to 2.9% (2022) ($p < 0.0001$), while PSC remained stable (5.9% to 5.7%, $p > 0.05$). Although the declines in PBC-LTs were observed in both SRTR and ELTR, PSC showed a recent increase in ELTR: 4.9% to 7.3% ($p < 0.05$). Post-transplant survival for PBC: 1-year 90%, 3-year 85%, 5-year 81%, 10-year 68%; for PSC: 1-year 92%, 3-year 86%, 5-year 81%, 10-year 69%. In multivariable survival analyses, post-transplant mortality in PBC was independently associated with earlier calendar year (aHR = (95% CI) = 0.980 (0.970–0.991) per year), older age (1.029 (1.023–1.035) per year), male sex (1.31 (1.16–1.48)), moderate (1.15 (1.02–1.29)) and severe hepatic encephalopathy (1.70 (1.40–2.06)), presence of HCC (1.31 (1.08–1.60)), and higher donor age (1.008 (1.005–1.010) per year) (all $p < 0.05$). In PSC, post-transplant mortality was also associated with earlier calendar year (0.975 (0.967–0.984) per year), older age (1.024 (1.021–1.028) per year), male sex (1.15 (1.05–1.26)), higher MELD score (1.017 (1.012–1.022) per 1 point), presence of cholangiocarcinoma (2.14 (1.74–2.64)), receiving a transplantation in a small transplant center (<15/year, aHR = 1.51 (1.09–2.09)), and older donor's age (1.007 (1.005–1.010) per year) (all $p < 0.05$).
Conclusion: Liver transplantations for PBC have declined, likely reflecting improved medical therapy, while PSC have remained stable, with recent increases in Europe. Three-year post-transplant survival exceeds 85% for both groups and continues to improve.

SAT-444

Fecal microbiota transplantation as an adjunctive therapy for refractory cholestatic liver disease: a prospective single-center exploratory study

Yu Zhang[1], Qi Wang[1], Minghui Li[1], Huichun Xing[1], Yifan Xu[1]. *[1]Beijing ditan hospital, Beijing, China*
Email: rainybaby_2527@126.com

Background and aims: Treatment options for refractory cholestatic liver disease are limited. This study evaluated the efficacy and safety of fecal microbiota transplantation (FMT) in patients with an inadequate response to standard therapy.
Method: Seventy patients with cholestatic liver disease, including those with primary biliary cholangitis and primary sclerosing cholangitis, who exhibited an insufficient biochemical response to at least 12 months of standard therapy (e.g., ursodeoxycholic acid) were enrolled. All patients received three weekly administrations of FMT via colonoscopy-guided enema while continuing their existing treatment regimen. The primary efficacy endpoint was the alkaline phosphatase (ALP) response rate at week 12, defined as a reduction of >40% from baseline or normalization of ALP levels. Secondary endpoints included changes in other liver biochemical parameters (serum total bile acids, γ-glutamyltransferase, total bilirubin), the Visual Analogue Scale for pruritus, the Chronic Liver Disease Questionnaire for quality of life, and the incidence of adverse events.
Results: At week 12, the intention-to-treat analysis yielded an overall ALP response rate of 68.6% (48/70). In the primary biliary cholangitis subgroup (n = 15), the response rate was 53.3% (8/15). Compared to baseline, significant reductions were observed in median levels of serum total bile acids, γ-glutamyltransferase, and total bilirubin (all $P < 0.001$). Pruritus scores and quality of life measures also showed significant improvement ($P < 0.01$). Regarding safety, only two patients (2.9%) experienced mild, transient adverse events (one with self-limiting low-grade fever and one with mild diarrhea). No serious adverse events or procedure-related infections were reported.
Conclusion: This preliminary study suggests that adjunctive FMT may improve biochemical response and alleviate clinical symptoms in patients with cholestatic liver disease refractory to standard therapy, demonstrating a favorable safety and tolerability profile. The

therapeutic effect is potentially mediated through the restoration of gut microbial ecology and subsequent modulation of the entero-hepatic bile acid circulation. These findings support the rationale for conducting larger-scale randomized controlled trials.

SAT-445

Clinical characteristics and predictors of poor biochemical response in patients with primary biliary cholangitis: a single-centre study from Xinjiang, China

Caihua Chang[1], Yilihamu Abulitifu[2], Yongping Zhang[2]. [1]*Xinjiang Uygur Autonomous Region People's Hospital, Uruqmi, China;* [2]*Xinjiang Uygur Autonomous Region People's Hospital, Urumqi, China*
Email: 2468005130@qq.com

Background and aims: The incidence of PBC has increased globally and in China in recent years. A comprehensive understanding of clinical characteristics and predictors of poor biochemical response to ursodeoxycholic acid (UDCA) is essential for early identification and optimized management. Data on PBC patients from Xinjiang are limited. This study aimed to analyze the clinical features and factors associated with poor biochemical response in PBC patients in Xinjiang.
Method: We retrospectively enrolled PBC patients diagnosed between November 2020 and November 2025 who received UDCA-based therapy for ≥12 months. Demographic data, clinical manifestations, laboratory parameters, treatment, and outcomes were collected. According to the Barcelona criteria, patients were classified as biochemical responders or non-responders. Multivariable logistic regression was used to identify predictors of poor response.
Results: A total of 190 PBC patients were included, predominantly female (female-to-male ratio ≈9:1), with a mean age of 55.46 ± 12.71 years. Clinically significant portal hypertension(CSPH) was present in 62 patients(32.63%), cirrhosis in 58(30.53%), and decompensated cirrhosis in 21(11.05%). Pruritus and fatigue were reported in 28.42% and 33.16% of patients, respectively, while jaundice occurred in 23.16%. Concomitant metabolic-associated fatty liver disease and autoimmune hepatitis were each observed in 13.68% of patients. Median APRI and FIB-4 scores were 0.74(0.34–1.88) and 2.13(1.19–4.50), respectively. Median alkaline phosphatase was 132.50 U/L, γ-glutamyl transferase 117.00 U/L, alanine aminotransferase 35.45 U/L, aspartate aminotransferase 47.00 U/L, total bilirubin 13.90 μmol/L, and direct bilirubin 5.18 μmol/L. Antimitochondrial antibody positivity was detected in 63.69% of patients and gp210 antibodies in 18.95%. Most patients(88.42%) received UDCA monotherapy, with a biochemical response rate of 61.75%. Multivariable logistic regression identified baseline CSPH(OR = 9.20, 95% CI 1.34–63.17), IgM positivity (OR = 9.62, 95% CI 3.99–23.18), anti-gp210 positivity(OR = 6.77, 95% CI 1.86–24.65) and CHE(OR = 0.79, 95% CI 0.65–0.96) as independent predictors of poor biochemical response to UDCA ($P < 0.05$).
Conclusion: PBC patients in Xinjiang often present with advanced disease. UDCA monotherapy remains insufficient for a substantial proportion of patients. Baseline CSPH, CHE, IgM and anti-gp210 positivity may facilitate early risk stratification and support timely initiation of combination or second-line therapy.

Liver development and regeneration

TOP-327-YI

A 3D atlas of liver tissue microarchitecture during regeneration reveals how hepatocyte division preserves bile canalicular integrity

Dilan Martinez Torres[1,2], Valeria Candia-Campano[1,2], Cristian Perez Gallardo[1,2], Hernán Morales-Navarrete[3], Fabián Segovia-Miranda[1,2]. [1]*Department of Cell Biology, Faculty of Biological-Sciences, Universidad de Concepción, Concepcion, Chile;* [2]*Grupo de Procesos en Biología del Desarrollo (GDeP), Faculty of Biological Sciences, Universidad de Concepción, Concepcion, Chile;* [3]*Bio-Cheminformatics Research Group, Universidad de Las Américas, Quito, Ecuador*
Email: dilanm954@gmail.com

Background and aims: The liver exhibits a remarkable regenerative capacity, restoring its mass within approximately seven days after 70% partial hepatectomy in mice. Successful regeneration, however, requires more than hepatocyte proliferation, demanding the coordinated reconstruction of a highly organized three-dimensional tissue architecture that supports bile and blood flow. This architecture arises from hepatocyte multipolar polarity, aligning apical membranes to form bile canaliculi while maintaining basal sinusoidal interfaces. During regeneration, hepatocytes divide in a crowded environment while preserving bile canalicular integrity, a critical barrier preventing toxic bile acid leakage. How these architectural and functional constraints are maintained remains poorly understood. Here, we generated a time-resolved 3D atlas of liver tissue architecture and used it to investigate how dividing hepatocytes preserve bile canalicular integrity.
Method: Eight- to ten-week-old C57BL/6J mice were subjected to a 70% partial hepatectomy. Fixation was performed by transcardial perfusion at daily intervals (days 1–7) post hepatectomy, followed by the collection of 200 μm vibratome liver sections. Sections were stained for cell borders (phalloidin), bile canaliculi (CD13), sinusoids (FLK-1), and nuclei (DAPI), and subsequently cleared using the SeeDB protocol. Images were acquired using a multiphoton microscope and were processed, reconstructed in 3D, and analyzed using Fiji and MotionTracking software powered by neural networks.
Results: The 3D atlas provides a comprehensive overview of liver tissue organization throughout regeneration. Analysis of hepatocyte division across metaphase, anaphase, and cytokinesis revealed that the spatial organization of apical membranes preserves bile canalicular continuity and consistently positions apical domains between sister cells to generate a new bile canalicular segment. Apical, basal, and lateral membrane domains were symmetrically inherited by daughter cells.
Conclusion: This 3D atlas provides a quantitative, tissue-scale framework to study liver regeneration. By linking hepatocyte division to the preservation of bile canalicular integrity, our work highlights how functional tissue architecture is maintained during regeneration. Moreover, this dataset establishes a foundation for computational and biophysical modeling of tissue growth, polarity maintenance, and network remodeling.

THU-339

Graphene oxide nanoparticles mitigate ethanol-induced liver injury by modulating miR21, miR-122 and miR-214–associated autophagy pathways

Hiral Aghara[1], Palash Mandal[1]. [1]*Charotar University of Science and Technology Gate, Petlad, India*
Email: hiralaghara@gmail.com

Background and aims: Alcohol-associated liver disease (ALD) is characterized by hepatic lipid accumulation, inflammation, and impaired autophagy, leading to progressive liver injury. Dysregulation of microRNAs (miRNAs), including miR-21, miR-122, and miR-214, plays a key role in regulating lipid metabolism and inflammatory responses during ethanol-induced liver damage. Graphene oxide nanoparticles (GNPs) have emerged as biologically active nanomaterials with the potential to modulate cellular stress responses. This study aimed to evaluate whether GNPs mitigate ethanol-induced liver injury by restoring autophagy through miRNA modulation.
Method: In vitro studies were performed using HepG2 hepatocyte cells exposed to ethanol, followed by GNP treatment. The protective effects of GNPs were assessed using Oil Red O staining and analysis of

autophagy and inflammation-associated mRNA expression. To assess in vivo relevance, male Wistar rats were fed a liquid diet containing 5% ethanol for 28 days. During the ethanol-feeding period, rats received oral administration of GNPs (10 mg/kg), at 5-day intervals. Hepatic injury was evaluated using serum biochemical parameters, histopathological assessment, and lipid staining. Hepatic mRNA expression of autophagy- and inflammation-related genes, along with miRNA expression profiling (miR-21, miR-122, and miR-214), was performed at the end of the study.
Results: Ethanol exposure induced significant lipid accumulation and suppression of autophagy associated mRNA expression in HepG2 cells, accompanied by increased inflammatory gene expression. GNP treatment markedly reduced intracellular lipid accumulation and restored autophagy-related mRNA expression. In vivo, chronic ethanol feeding resulted in hepatic steatosis, elevated serum biochemical markers of liver injury, and histological evidence of liver damage. GNP administration significantly attenuated these effects, reducing hepatic lipid accumulation and improving liver histology. Ethanol-induced dysregulation of hepatic miRNAs, characterized by decreased miR-122 and increased miR-21 and miR-214 expression, was normalized following GNP treatment. These changes were associated with restoration of autophagy-related mRNA expression and attenuation of inflammatory signalling.
Conclusion: GNPs mitigate ethanol-induced liver injury by modulating miR-21, miR-122, and miR-214–associated autophagy pathways. These findings support GNPs as a protective nanoplatform for limiting disease progression in alcohol-associated liver disease.

THU-340-YI
Engineered extracellular vesicles derived from mesenchymal stem cells enriched with insulin-like growth factor I restore impaired liver regeneration after partial hepatectomy in fibrotic livers
Mailín Casadei[1,2,2], María José Cantero[1], Bárbara Bueloni[1], Fátima Huamán Ormeño[1], Lucía Perez[1], Lucía Lameroli[1], Brian Martinez Ruiz[1], Catalina Atorrasagasti[1], Juan Bayo Fina[1], Esteban Fiore[1], Guillermo Mazzolini[1]. [1]*Instituto de Investigaciones en Medicina Traslacional CONICET-Universidad Austral, Pilar, Argentina;* [2]*Instituto de Investigaciones en Medicina Traslacional CONICET-Austral, Pilar, Argentina*
Email: mcasadei@austral.edu.ar

Background and aims: The liver exhibits a remarkable regenerative capacity, however, this ability is progressively impaired during chronic liver injury. In this context, mesenchymal stem cell–derived extracellular vesicles (MSC-EV) represent a promising cell-free therapeutic strategy due to their immunomodulatory and pro-regenerative properties. Moreover, EV can be genetically engineered to deliver therapeutic molecules such as insulin-like growth factor I (IGF-I), a well-established hepatoprotective and pro-regenerative factor. The aim of this study is to evaluate whether IGF-I–loaded EV can restore liver regeneration in fibrotic mouse livers using a partial hepatectomy (PHx) model.
Method: EV were isolated from umbilical cord–derived MSC transduced with adenoviruses encoding green fluorescent protein (GFP-EV) or IGF-I (IGF-I-EV). Fibrosis was induced in adult male C57BL/6 mice by intraperitoneal administration of thioacetamide (0.2 mg/g body weight, 3 times/week) for 8 weeks, followed by 66% PHx. One hour later, mice received a single intravenous dose of vehicle, GFP-EV or IGF-EV (0.05 mg/mouse) and were euthanized 3 days later for liver sample collection (n = 6/group). Liver regeneration was assessed by liver index (liver/body weight) and regeneration rate (% of recovered liver mass), PCNA immunohistochemistry and qPCR analysis of Pcna, Hgf and Igf-I genes. Liver injury was evaluated by serum alanine and aspartate aminotransferase and lactate dehydrogenase levels.Fibrosis was analyzed by Sirius Red staining and gene expression of Col1A2 and Acta2, while inflammation was assessed by expression of Tnf-alpha, Il1-beta, iNOS, Il10 and Arg1.
Results: IGF-I-EV enhanced liver regeneration in fibrotic mice after PHx, restoring liver index and liver regeneration rate to levels comparable to non-fibrotic PHx controls. This was associated with increased PCNA-positive hepatocytes and upregulation of regeneration-related genes. This effect was associated with reduced liver injury, as evidenced by lower serum aspartate aminotransferase and lactate dehydrogenase levels. Importantly, IGF-I-EV attenuated fibrosis after resection, as shown by reduced collagen deposition and downregulation of Col1A2 and Acta2. This was accompanied by a dampened inflammatory response, with decreased expression of pro-inflammatory genes such as Tnf-alpha, Il1-beta and iNOS.
Conclusion: Our data support IGF-I–EV as a potential strategy to restore impaired liver regeneration in the context of partial hepatectomy in fibrotic livers.

THU-341
Macrophages drive spatially specific liver regeneration via arginine metabolism reprogramming: the translational potential of arginine supplementation
Jinwei Chen[1], Min Tang[1], Xiaorong Xu[2]. [1]*Tongji University, Tongji University Affiliated Tongji Hospital, Shanghai Tenth People's Hospital, Shanghai, China;* [2]*Tongji University, Shanghai Tenth People's Hospital, Shanghai, China*
Email: 2411217@tongji.edu.cn

Background and aims: Liver regeneration follows a strict spatiotemporal pattern, typically initiated by periportal hepatocytes. The mechanisms underlying this zonation-specific initiation, particularly how immune cells set the spatiotemporal program by modulating metabolic reprogramming, remain unclear. This study aimed to reveal how myeloid S100A4^{+} macrophage deficiency reshapes the regenerative landscape and elucidates its role in driving arginine metabolic reprogramming via IL-6 signaling to activate the proliferative program in specific hepatocyte zones.
Method: Myeloid-specific S100A4 knockout (S100A4 cKO) mice and a 70% partial hepatectomy model were used. Zonation-specific transcriptional programs in regenerating hepatocytes were analyzed by single-cell RNA sequencing (scRNA-seq) and spatial transcriptomics. High-resolution multiplex immunofluorescence, flow cytometry, metabolomics, and in vivo functional experiments were employed for validation.
Results: In S100A4 cKO mice, the core regenerative region shifted from the periportal zone (zone 1) to the mid-lobular zone (zone 2), with enhanced liver weight restoration and proliferation. Single-cell and spatial analyses showed coordinated activation of IL-6 signaling and arginine anabolic pathways in zone 2 hepatocytes. cKO elevated hepatic IL-6 levels and upregulated hepatocyte IL-6 receptor expression, driving sustained JAK-STAT3 activation. STAT3 directly promoted expression of arginine synthesis enzymes ASS1 and OTC, increasing de novo arginine synthesis. Arginine accumulation activated mTORC1 to drive the cell cycle while its metabolites suppressed ferroptosis, specifically unlocking zone 2 hepatocyte proliferation. Exogenous arginine supplementation effectively recapitulated this spatially specific regeneration enhancement, demonstrating translational potential.
Conclusion: This study identifies myeloid S100A4 as a key regulator of liver regeneration spatial programming. Its deficiency activates the IL-6-arginine metabolic axis, triggering zonation-specific metabolic reprogramming that determines regeneration location and intensity. Arginine supplementation may therefore support liver regeneration, benefiting patients awaiting transplants or recovering from resection.

THU-345-YI

Cell type-specific role of CD44 in liver regeneration

Tanja Derowski[1], Sophia Bernatik[1], Kohnke-Ertel Birgit[1], Fabian Delugré[1], Franziska Ihli[1], Magdalena Kolmstetter[1], Fabian Geisler[1], Carolin Mogler[2], Roland M. Schmid[1], Ursula Ehmer[1]. *[1]Department for Internal Medicine II, TUM School of Medicine and Health, Technical University of Munich, TUM University Hospital, Munich, Germany; [2]Institute of Pathology, School of Medicine, Technical University of Munich, Comparative Experimental Pathology, School of Medicine, Technical University of Munich, Munich, Germany*
Email: tanja.derowski@gmail.com

Background and aims: CD44 is barely detectable in healthy adult livers but is strongly upregulated during chronic liver injury. Previous data suggest that CD44 promotes proliferation in hepatocytes and cells of the ductular reaction (DR) via injury- and cell type-specific pathways. Here, we aimed to uncover the cell-type dependent molecular mechanisms downstream of CD44.
Method: Hepatocyte injury was induced in *Cd44*$^{-/-}$ and age-matched C57BL/6J control mice by a choline-deficient, ethionine-supplemented diet (CDE). As a model of chronic cholestatic liver injury, *Mdr2*$^{-/-}$; *Cd44*$^{-/-}$ mice and age-matched *Mdr2*$^{-/-}$ control mice were used. Formalin-fixed, paraffin-embedded livers were analyzed by single-nucleus RNA sequencing.
Results: Compared to the healthy liver, *Mdr2*$^{-/-}$ and CDE liver injury models both showed expansion of hepatic stellate cells (HSCs), immune cells, and cells of the DR. CD44 expression was mainly found in DR cells, cholangiocytes, and immune cells. In both models, *Cd44*$^{-/-}$ mice displayed a marked reduction of DR cells, while effects on overall immune cells and HSCs were largely negligible. Pathway analysis indicated differential regulation of several pathways such as MAPK, mTOR, Myc, and Wnt signaling – in part in a cell-type dependent manner.
Conclusion: Our data support the role of CD44 as a key driver of the ductular reaction and proliferation in liver injury with cell-type specific activation of several pro-proliferative downstream pathways as potential targets in the treatment of chronic liver injury.

THU-346

Engineering a fibrotic organoid chip revealing ductular reaction driven by matrix-derived forces

Mengqi Zhu[1,2,3], Yu Du[1,2], Mian Long[1,2]. *[1]Insitute of Mechanics, Chinese Academy of Sciences, Beijing, China; [2]School of Engineering Science, University of Chinese Academy of Sciences, Beijing, China; [3]School of Materials Science and Engineering, East China University of Science and Technology, Shanghai, China*
Email: zmq17i@126.com

Background and aims: Ductular reaction (DR) is a hallmark of chronic liver diseases, characterized by compensatory proliferation of biliary epithelial cells (BECs). Temporal delay between extracellular matrix (ECM) deposition and BEC expansion suggests a critical role of fibrotic niche in DR progression. During fibrosis, ECM undergoes profound biomechanical remodeling, becoming stiffer and generating altered mechanical stresses. However, the mechanism by which these matrix-derived mechanical cues drive DR remains poorly understood, largely due to the absence of in vitro models that recapitulate the dynamic 3D mechanical microenvironment of fibrotic liver. Here, we developed a novel bioengineered fibrotic organoid chip (FOC) that incorporates *in vivo* matrix composition, multicellular architecture, and measurable mechanical cues, dissecting the mechanotransductive pathways of DR.
Method: The FOC was created by seeding BECs and fibroblasts within a collagen/Matrigel matrix into microfabricated arrays of microwells with microcantilevers. Self-organized 3D microtissues were cultured for 6 days. Matrix remodeling was assessed via second harmonic generation (SHG) imaging, tissue stiffness by nanoindentation, and contractile forces in real time through cantilever deflection. Mechanical stresses on organoids were quantified using embedded elastic round microgels (ERMGs), together with numerical simulations.
Results: The FOC supported the well-defined co-culture of biliary organoids and fibroblasts, both maintaining phenotypic markers. The FOC formed fibrotic briding band with aligned collagen fibers, increased stiffness, and progressive contraction over time. Organoids within fibrotic niches showed enhanced growth and morphological deformation under contraction. ERMG-based force mapping revealed a shift from tensile to compressive stress on organoids in fibrotic tissues. Pharmacological inhibition of ROCK or myosin II reduced both tissue contraction and organoid growth. Redistribution of α2 integrin under fibrotic cues and reduced BECs growth under inhibition further indicated mechanosensitive regulation of proliferation.
Conclusion: This study established a biomimetic FOC recapitulating key structural and mechanical features of DR, and demonstrated that matrix-derived contractile forces and stiffness actively promote BEC expansion and deformation through mechanotransductive pathways involving ROCK/myosin and α2 integrin, highlighting the role of biomechanical cues in chronic liver disease progression.

THU-347-YI

Generation of sinusoidal-like endothelial cells from human induced pluripotent stem cells (hiPSCs) for 3D liver models

Clelia Ferraro[1], Riccardo Perriera[1], Minjie Zhao[2], Martina Morsicato[1], Salvatore Gruttadauria[1], Valentina Agnese[1], Massimo Pinzani[1], Giovanni Zito[1]. *[1]ISMETT - Istituto Mediterraneo per i Trapianti Ismett IRCCS, Palermo, Italy; [2]Department of Hepatobiliary Surgery, Chongqing, China*
Email: cleliaferr93@gmail.com

Background and aims: The liver is a highly complex vascularized organ in which liver sinusoidal endothelial cells (LSECs) play a central role in tissue architecture, metabolic exchange, and paracrine signaling. Advanced three-dimensional (3D) in vitro models are required to recapitulate this complexity. Human induced pluripotent stem cells (hiPSCs) provide a valuable platform to generate defined components of the hepatic microenvironment. This study aimed to generate endothelial cells with sinusoidal potential from hiPSCs and to assess whether a 3D microenvironment promotes maturation toward a sinusoidal phenotype.
Method: hiPSCs were differentiated into endothelial-like cells using four protocols (A–D) applied at defined time points. Cell populations were characterized by morphology and transcriptional analysis of endothelial markers. Selected endothelial cells were then integrated into 3D liver models.
Results: Protocols A and C induced expression of CD36 and STAB2, suggesting metabolic and scavenger activity, but showed weak and variable PECAM, CDH5, and ERG expression, with only transient LYVE1 detection. Protocol B did not promote endothelial commitment. In contrast, Protocol D generated cells with a stable endothelial identity, consistent STAB2 and CD36 expression, and low but reproducible LYVE1 levels, compatible with an immature sinusoidal phenotype. These cells were suitable for incorporation into 3D assembloids, where further maturation is expected.
Conclusion: We identify an optimized strategy to generate LSEC-like cells from hiPSCs, providing a robust platform for 3D liver models to study endothelial maturation and cell–cell interactions in a physiologically relevant microenvironment.
This work was supported by project PNRR-MCNT2-2023-12378263 CUP I73C24000390007, Funded by the European Union - Next Generation EU - NRRP M6C2 - Investment 2.1 Enhancement and strengthening of biomedical research in the NHS.

THU-350

Interleukin-17a induces hepatocyte conversion into hepatic progenitor-like cells with stem cell characteristics

Pei-Chi Huang[1], Ben Higgins[1], Man Chun Wong[1], Gareth Hardisty[1], Jonathan Fallowfield[1,2,2], Wei-Yu Lu[1]. [1]*University of Edinburgh, Institute For Regeneration and Repair, Edinburgh, United Kingdom;* [2]*Centre for Inflammation Research, Institute for Regeneration and Repair, University of Edinburgh, Edinburgh, United Kingdom*
Email: p.huang-15@sms.ed.ac.uk

Background and aims: Liver transplantation is the only treatment for end-stage disease, while the lack of available donor organs makes alternative therapies warranted. Low proliferation of hepatocytes *in vitro* is the main challenge in using hepatocytes for cellular therapy. Proinflammatory signals play important roles in mediating tissue repair, cell proliferation and plasticity. We aim to investigate if proinflammatory cytokines could promote hepatocyte cellular plasticity and expansion *in vitro*, ultimately improving the repopulation capacity of expanded hepatocytes.
Method: RFP+ hepatocytes were isolated from tdTomato^{LSL} transgenic mice. Isolated hepatocytes were cultured with either Tissue Necrosis Factor (TNF)-alpha or Interleukin (IL)-17a *in vitro* on collagen-coated plates. Expanded cells were characterised and transplanted into the mouse with p21 overexpressed hepatocytes.
Results: Expanded Primary Hepatocytes (ExPHs) cultured with either TNF-alpha or IL-17a were reprogrammed towards a progenitor phenotype with the upregulation of *Krt19*, *Sox9,* and *Epcam* and downregulation of hepatic markers (*Hnf4a, Hnf1a* and *Asgr1)*. Both TNF-alpha and IL-17a activated the NFkB pathway and promoted ExPHs proliferation. Interestingly, IL-17a ExPHs had the highest expression of biliary and hepatic genes and maintained a higher epithelial phenotype and hepatocyte functions compared to the TNF-alpha expanded group. Bulk RNA sequencing identified the upregulation of stem cell markers (*Prom1* and *Tnfrsf12a)*, on IL-17a ExPHs. Epithelial-Mesenchymal Transition (EMT) genes were upregulated on TNF-alpha ExPHs with the downregulation of cell adhesion and epithelial markers, revealing the instability of TNF-alpha ExPHs. Functionally, IL-17a ExPHs can be differentiated into cells with hepatocyte or biliary function. On the contrary, TNF-alpha ExPHs failed to secrete albumin and store glycogen. We successfully transplanted IL-17a ExPHs into injured mouse livers, and these RFP+ IL-17a ExPHs engrafted the injured liver, and improved mouse survivability compared to the sham transplanted group.
Conclusion: Pro-inflammatory cytokines improve hepatocyte expandability and promote cellular plasticity *in vitro*, while IL-17a treatment stabilised hepatocytes during long-term culture with epithelial properties and hepatocyte functions. The long-term function and stability of ExPHs *in vivo* remains to be tested.

THU-351

Hepatic-lobule-mimetic spheroids composed of chemically derived hepatic progenitors and endothelial cells enhance liver regeneration via spatial patterning

Hee Ju Kim[1], Elsy Soraya Salas Silva[1], Minji Park[2], Ji Hyun Shin[1], Songwan Jin[2], Dongho Choi[1]. [1]*Department of Surgery, Hanyang University College of Medicine, 222, Wangsimni-ro, Seongdong-gu, Seoul, Korea, Rep. of South;* [2]*Research Institute, T&R Biofab. Co. Ltd., Siheung-si, Gyeonggi-do, Korea, Rep. of South*
Email: crane87@hanyang.ac.kr

Background and aims: Conventional 3D hepatic models often fail to recapitulate the hierarchical vascular architecture and functional maturation of native liver tissue. To address this, we established hepatic-lobule-mimetic spheroids composed of mouse chemically derived hepatic progenitors (mCdHs) and endothelial cells (SVEC4-10). This study aimed to systematically evaluate how spatial patterning influences hepatic development and identify the optimal architecture for liver regeneration.
Method: We utilized a preset extrusion-based microfluidic bioprinting strategy to fabricate three defined architectures: non-structured, core-shell, and segmented. This approach enabled precise control over cellular arrangement. Spheroids were evaluated for morphological stability, hepatic differentiation, and angiogenic potential in vitro. Furthermore, orthotopic transplantation into fumarylacetoacetate hydrolase-deficient (*Fah-/-*) mice was performed to assess in vivo engraftment, biocompatibility, and structural integrity.
Results: Among the three architectures, segmented spheroids maintained a stable tripartite geometry for four days and displayed markedly enhanced hepatic differentiation. By Day 10, the segmented group showed a 1.5–1.8-fold increase in albumin and urea secretion relative to other groups. Immunohistochemical analysis revealed spatially confined SOX9+ progenitors within the central region, indicative of zonal maturation, while Matrigel assays demonstrated organized CD31+ angiogenic sprouting specific to structured architectures. In vivo transplantation confirmed that segmented spheroids achieved superior engraftment and structural retention compared to counterparts, leading to significant functional recovery *in Fah-/-* mice.
Conclusion: Collectively, these findings demonstrate that precise spatial control within spheroids significantly improves hepatic maturation and vascularization. The segmented architecture, confirmed as the most effective model in both in vitro and in vivo settings, offers a scalable and translationally relevant platform for regenerative medicine and liver disease modeling.
This research was supported by a grant of Korean ARPA-H Project through the Korea Health Industry Development Institute (KHIDI), funded by the Ministry of Health & Welfare, Republic of Korea (RS-2024-00512447), This research was supported by a grant of the Korea-US Collaborative Research Fund(KUCRF), funded by the Ministry of Science and ICT and Ministry of Health & Welfare, Republic of Korea (RS-2025-16063805).

THU-352

Surface-modified MSC exosomes with PEGylation and SE-1 antibody conjugation for enhanced circulation and LSEC-targeted therapy in liver fibrosis

Mi Ra Lee[1,2], Jin Suk Lee[2], HyunJung Chung[1,2], Seul Ki Han[1,2], Soon Koo Baik[1,2], Moon Young Kim[1,2]. [1]*Department of Internal Medicine, Wonju Severance Christian Hospital, Wonju, Korea, Rep. of South;* [2]*Regeneration Medicine Research Center, Yonsei University Wonju College of Medicine, Wonju, Korea, Rep. of South*
Email: drkimmy@yonsei.ac.kr

Background and aims: Liver fibrosis involves the defenestration of liver sinusoidal endothelial cells (LSECs), which disrupts physiological exchange between blood and hepatocytes. While mesenchymal stem cell (MSC)-derived exosomes show anti-fibrotic potential, their clinical use is limited by a lack of liver-targeting specificity. We aimed to develop a targeted delivery system by engineering exosomes to display antibodies against the SE-1 receptor, a specific marker on LSECs, to enhance hepatic accumulation and therapeutic efficacy.
Method: High-purity exosomes were isolated from the conditioned media of human MSCs using a Tangential Flow Filtration (TFF) system. To improve systemic stability and targeting capability, the exosomal surface was modified with polyethylene glycol (PEG) and conjugated with anti-SE-1 antibodies (Exo+SE-1). The physicochemical characteristics of the engineered exosomes were analyzed via nanoparticle tracking analysis (NTA), and cytotoxicity was evaluated using the Cell Counting Kit-8 (CCK-8) assay. Targeting specificity was assessed *in vitro* using primary LSECs. Furthermore, *in vivo* biodistribution and tissue accumulation were examined in a murine model following intravenous administration to verify the liver-homing ability of Exo+SE-1.
Results: The engineered Exo+SE-1 exhibited a uniform size distribution and high stability in physiological buffers due to PEGylation. *In*

vitro binding assays demonstrated that Exo+SE-1 bound significantly and specifically to SE-1-expressing LSECs compared to non-targeted control exosomes. In *in vivo* studies, the surface modification effectively reduced reticuloendothelial system (RES) clearance, resulting in a prolonged circulation half-life. Notably, biodistribution analysis revealed that Exo+SE-1 showed significantly enhanced accumulation in the liver tissue compared to unmodified exosomes, confirming effective active targeting to the hepatic endothelium.
Conclusion: This study establishes that SE-1 antibody-conjugated MSC exosomes can effectively target LSECs, overcoming the biodistribution limitations of native exosomes. By restoring LSEC function and delivering therapeutic cargo directly to the injury site, Exo+SE-1 represents a promising, clinically viable nanotherapeutic platform for the precision treatment of liver fibrosis and regeneration.

THU-353
Spatio-temporal omics identifies ZEB1-BMP4 in hepatic stellate cells as a key axis for liver regeneration after acute injury
Jun Li[1], Bingqi Li[1], Heng Yao[1], Jing Jiang[1], Jiaojiao Xin[1], Xi Liang[1], Dongyan Shi[1]. [1]*State Key Laboratory for Diagnosis and Treatment of Infectious Diseases, National Clinical Research Center for Infectious Diseases, National Medical Center for Infectious Diseases, Collaborative Innovation Center for Diagnosis and Treatment of Infectious Diseases. The First Affiliated Hospital, Zhejiang University School of Medicine, Hangzhou, China*
Email: lijun2009@zju.edu.cn

Background and aims: The liver rapidly restores its structure and function after acute liver injury (ALI). Hepatic stellates cells (HSCs) are promptly activated upon ALI; however, the mechanisms through which HSCs contribute to liver repair remain unclear. This study aims to elucidate how HSCs orchestrate Mlxipl$^+$ hepatocytes to promote liver regeneration.
Method: The ALI mouse model was established via intraperitoneal injection of the anti-CD95 antibody JO2. Liver tissues and blood samples were collected at days 0, 1, 3 and 7 post-injury. Single-cell RNA sequencing (scRNA-seq) and spatial transcriptomics (ST) were performed on liver tissues to explore the mechanism driving self-repair. Transcription factors (TF) and ligand-receptor analysis were conducted between HSCs and Mlxipl$^+$ hepatocytes to identify key signaling pathways involved in liver repair, and then were validated experimentally through functional interventions. Clinical relevance was evaluated using plasma, peripheral blood mononuclear cells and liver tissues derived from patients with acute and acute-on-chronic liver failure.
Results: The ALI mouse model was successfully established, characterized with regional necrosis of liver tissue and elevated liver function makers. A spatiotemporal atlas of liver injury and repair was constructed by integrating scRNA-seq and ST data. Dynamic cell-cell interactions were observed among hepatocytes, endothelial cells and mesenchymal cells. Notably, similarity in cellular communication patterns at days 3 and 7 indicated that the process of liver repair stabilized by day 3. Sub-clustering analysis further revealed strong interactions between HSCs and both classical and Mlxipl$^+$ hepatocytes, mediated through extracellular matrix regulation. TF analysis and ChIP-qPCR confirmed that ZEB1 in HSCs binds to and transcriptionally regulates the BMP4 promoter. The overexpression and knockdown of ZEB1 correspondingly altered BMP4 expression ($p < 0.0001$). Plasma BMP4 levels were significantly higher in liver failure patients than in healthy controls ($p < 0.01$). Exogenous BMP4 supplementation also alleviated injury in primary hepatocytes in vitro.
Conclusion: This study maps the spatiotemporal dynamics of liver repair, highlighting the decline and rebound of HSCs and hepatocytes during injury and recovery. We identify the ZEB1-BMP4 axis in HSCs as a key mechanism promoting Mlxipl$^+$ hepatocyte proliferation and tissue regeneration, offering a novel therapeutic target for ALI.

THU-354
Liver protein turnover map classifies a mitochondrial regenerative protein panel essential for liver recovery
Nupur Sharma[1], Sadam H Bhat[1], Anupama Kumari[1], Himanshi Himanshi[1], Prachi Sinha[1], Sushmita Pandey[1], Sanju Yadav[1], Babu Mathew[1], Vasundhra Bindal[1], Gaurav Tripathi[1], Manisha Yadav[1], Neha Sharma[1], Vipul Sharma[1], Mothe Shravya[2], Ranjan Nanda[2], Sukriti Baweja[1], Dinesh Mani Tripathi[1], Shiv Kumar Sarin[1], Jaswinder Maras[1]. [1]*Institute of Liver and Biliary Sciences, New Delhi, India;* [2]*International Centre for Genetic Engineering and Biotechnology, New Delhi, India*
Email: jassi2param@gmail.com

Background and aims: Partial hepatectomy (PHx) is a well-established model for studying acute liver regeneration; yet, molecular distinctions between successful regeneration and recovery from chronic liver injury remain unclear. Alcohol-related liver disease (ALD) exhibits impaired regeneration and progressive hepatic dysfunction. We investigated protein turnover dynamics during liver regeneration and identified key regenerative proteins disrupted in ALD and the effect of alcohol abstinence.
Method: A deuterium oxide (D_2O) labeling approach was used to measure protein turnover in rats with PHx, ALD, and alcohol abstinence. Animals received a priming intraperitoneal dose of 99.9% D_2O (0.35 mL/g) on Day 0, followed by 8% D_2O in drinking water for 7 days. Liver samples were collected on Days 1, 3, 5, and 7. Turnover and pathway analyses identified key regenerative proteins, which were validated by siRNA knockdown in HepG2 cells.
Results: PHx-induced regeneration showed liver-to-body weight ratio and ALT/AST normalized by Day-7. D_2O-analysis revealed 358 proteins with increased turnover post-PHx, particularly in mitochondrial metabolism, protein synthesis, and oxidative phosphorylation (FC>1.5, $p < 0.05$). ALD showed suppressed turnover of 27 PHx-associated proteins, reflecting impaired regenerative capacity. Abstinence partially restored regenerative responses, with 30 proteins commonly elevated in PHx and Abstinence. Among these, GOT2, ETFA, ETFB, HADH, and RPS19 were top-ranked regenerative markers. Their siRNA-mediated knockdown in HepG2 cells reduced expression by 70–90% ($p < 0.001$), decreased BrdU incorporation (50–60%, $p < 0.001$), reduced PCNA expression (~2-fold, $p < 0.01$), and delayed wound closure ($p < 0.01$), confirming their roles in hepatocyte proliferation. Proteomics revealed that GOT2 and RPS19, which are most compromised regenerative proteins linked to the cell cycle (FC > 1.5, $p < 0.05$), were affected post-knockdown.
Conclusion: Using PHx, we identified core regenerative proteins with increased turnover, indicating active liver regeneration. In ALD, these proteins showed suppressed turnover, reflecting impaired regeneration, while alcohol abstinence partially restored their turnover, suggesting recovery of regenerative programs. Overall, shared mitochondrial and biosynthetic turnover pathways were highlighted as essential for liver repair and as potential therapeutic targets.

THU-355-YI
Lymphangiocrine signal, Wnt7a is a key driver of cholangiocyte proliferation during liver regeneration
Aarti Sharma[1], Pinky Juneja[1], Deepika Jakhar[1], Jayesh Kumar Sevak[1], Ashwini Vasudevan[1], Simran Sharma[1], Impreet Kaur[1], Viniyendra Pamecha[1], Dinesh Mani Tripathi[1], Archana Rastogi[1], Shiv Kumar Sarin[1], Sumeet Singh[2], Savneet Kaur[1]. [1]*Institute of Liver & Biliary Sciences, New Delhi, India;* [2]*Laboratory of Regeneration and Stress Biology, Institut de Recherche Interdisciplinaire en Biologie Humaine et Moléculaire (IRIBHM-Jacques E. Dumont), Université libre de Bruxelles, Belgium, Department of Life Sciences, School of Natural Sciences, Shiv Nadar Institution of Eminence, India, Bruxelles, Belgium*
Email: savykaur@gmail.com

Background and aims: Liver lymphatic vessels (LVs) and lymphatic endothelial cells (LyECs) were characterized after 70% partial

hepatectomy (PHx) to delineate their unexplored contribution to liver regeneration.
Method: We developed 70% PHx rat models and studied LVs and other hepatic cells at different time points. LC-MS/MS of LyECs was performed to identify specific protein signatures. Wnt7a, an identified secreted protein, was further investigated by *in-vivo* studies using lymphangiogenesis inhibitor in rat PHx models and in Wnt7a-knockout zebrafish. Effects of Wnt7a were evaluated on both primary rodent and human cholangiocyte (chol)-organoids. Serum Wnt7a levels were measured in live donor liver transplant (LDLT) and liver biopsies of post-transplant liver failure (PTLF) and post-hepatectomy liver failure (PHLF) patients.
Results: As compared to sham, increased number of dilated PDPN+ LVs were observed in portal areas at day (D) 2 post-PHx (2.56-fold, $p < 0.0001$). Proteomics of LyECs at D2 post-PHx revealed significant upregulation of a secreted protein, Wnt7a compared to sham. *In-vitro* studies of primary rat liver cells with Wnt7a established it as a potent stimulator of hepatocyte and cholangiocyte proliferation. *In-vivo* lymphangiogenesis inhibition by vegfr3 inhibitor in PHx models and *in-vivo* loss-of-function of Wnt7a in zebrafish resulted in reduction of bile ducts by 30 ± 2.7% and 45 ± 5.2% respectively. Mechanistically, Wnt7a activated downstream frizzled 7 (FZD7) receptor in cholangiocytes, driving their proliferation via planar cell polarity /FZD7-AKT-JAK-STAT pathway. In presence of Wnt7a, human chol-organoid proliferation was significantly increased as compared to untreated controls (1.8-fold, $p = 0.006$). In comparison to pre-operative baseline levels, elevated Wnt7a levels were seen in LDLT donors at D2 post-operatively (2.75-fold, $p = 0.04$). Patients with PTLF and PHLF showed weak expression of PDPN+Wnt7a+ LVs along with severe ductopenia.
Conclusion: Portal lymphangiogenesis constitutes a critical component of the regenerative response following 70% PHx. Specifically, Wnt7a secreted by LVs interacts with its cognate receptor, FZD7, on the cholangiocyte membrane and this novel lymphangiocrine signaling axis serves as a primary driver of biliary cell proliferation in the regenerating liver.

THU-356
SLC1A5-dependent glutamine transport regulates macrophage senescence and efferocytosis during liver regeneration
Hao Wang[1], Haoran Hu[1], Jian Xu[1], Yuechen Wang[1], Yue Yu[1], Feng Cheng[1], Haoming Zhou[1]. *[1]The First Affiliated Hospital with Nanjing Medical University, Nanjing, China*
Email: hmzhou@njmu.edu.cn

Background and aims: Liver regeneration is an extraordinary process vital for the maintenance of homeostasis, governed by complex metabolic and immune interactions, particularly concerning the function of macrophages. Prior research underscores the significant role of these immune cells in the repair of tissue; nevertheless, the precise mechanisms that govern macrophage phenotypes and their functions throughout liver regeneration are not well understood. This study aims to investigate the role of SLC1A5, a neutral amino acid transporter responsible for glutamine transport, in macrophage senescence and efferocytosis during liver regeneration.
Method: We employed myeloid-specific SLC1A5 knockout mice ($SLC1A5^{fl/fl}Lyz2^{cre}$) in conjunction with a partial hepatectomy model to examine the effects of macrophage SLC1A5 deficiency on liver regeneration. Bone marrow-derived macrophages (BMDMs) were extracted and subjected to RNA sequencing and a range of functional assays to assess macrophage senescence, efferocytosis, and cytokine production levels.
Results: The results indicate that SLC1A5 is essential for thwarting macrophage senescence and maintaining efferocytosis during liver regeneration. Macrophages lacking SLC1A5 showed elevated senescence markers and transitioned towards a pro-inflammatory phenotype, marked by increased levels of TNF-α and IL-6. Significantly, efferocytosis was compromised due to the reduced expression of Gas6, a critical ligand for macrophage efferocytosis. Treatment with L-glutamine and recombinant Gas6 effectively restored macrophage functions and enhanced liver regeneration in vivo.
Conclusion: This investigation demonstrates that SLC1A5 is integral in modulating macrophage functions via glutamine transport during liver regeneration. The enhancement of glutamine availability may offer a new therapeutic strategy to alleviate macrophage senescence and promote liver recovery following injury.

Liver immunology

TOP-325-YI
Time-resolved single-cell profiling of liver fibrosis regression identifies monocyte-derived Kupffer cells as central mediators of resolution
Katharina Bonitz[1,2], Thomas Sorz-Nechay[1,2], Henriette Horstmeier[1], Katja Sommer[1,2], Vlad Taru[1], Oleksandr Petrenko[1,2], Benedikt Hofer[1], Benedikt Simbrunner[1], Kerstin Zinober[1], Katharina Regnat[1], Hubert Scharnagl[3], Raphael Bednarsky[1,2], Christoph Bock[1,2], Michael Trauner[1], Stefan Günther Kauschke[4], Peng Sun[4], Eric Simon[4], Philipp Schwabl[1], Thomas Reiberger[1,2]. *[1]Medical University of Vienna, Vienna, Austria; [2]CeMM Research Center for Molecular Medicine of the Austrian Academy of Sciences, Vienna, Austria; [3]University Hospital Graz, Graz, Austria; [4]Boehringer Ingelheim Pharma GmbH & Co.KG, Biberach an der Riss, Germany*
Email: katharina.bonitz@meduniwien.ac.at

Background and aims: After cessation of liver injury fibrosis can spontaneously regress. However, the underlying molecular mechanisms of liver fibrosis regression remain poorly understood. Hepatic macrophages are key drivers of fibrosis progression, and understanding their transcriptomic changes in liver disease regression may uncover therapeutic targets.
Method: Liver fibrosis was induced in two murine models by administration of carbon tetrachloride (CCl_4) or by Choline-Deficient L-Amino Acid-Defined High Fat Diet (MASH) for 12 weeks. Healthy controls received olive oil or CHOW diet for 12 weeks. After disease induction spontaneous regression was allowed for 3, 7 and 14 days in the CCl_4 model, and for 7, 14 and 28 days in the MASH model. Animals were sacrificed at peak of disease and at the indicated timepoints of regression. At each study endpoint we assessed disease severity including collagen proportionate area, portal pressure and transaminases, and performed hepatic scRNA-Seq.
Results: Disease induction led to pronounced fibrosis, portal hypertension and liver injury compared to healthy controls – followed by significant improvements over the course of regression. We generated a single-cell fibrosis regression atlas with 183.000 cells across both models and all timepoints. Transcriptional state changed most in hepatic macrophages with seven distinct macrophage subpopulations. They contained monocyte-derived populations, such as scar-associated macrophages (Trem2+, Cd9+) and Kupffer cell (KC) signatures. While embryonically derived KCs (EmKCs: Clec4f+, Timd4+, Vsig4+) were exclusive to healthy controls, monocyte-derived KCs (MoKC: Clec4f+, Timd4-, Clec1b+) expanded in fibrosis regression in both disease models. Expansion of Clec1b+ MoKCs in regression was confirmed by flow cytometry. Differential gene expression analysis between MoKCs and EmKCs revealed an upregulation of genes encoding Matrix metalloproteinases (MMPs), most notably *Mmp12*, indicating a prominent role of MoKCs in extracellular matrix degradation facilitating liver disease regression.
Conclusion: We show that in two murine models of regressive liver disease, the strongest transcriptomic changes of all cell types occurred in hepatic macrophage populations. We identified an expanding

MoKC cluster, that replenishes the niche depleted EmKCs after liver disease. MoKCs demonstrated high *Mmp* expression – suggesting a key role in resolving liver fibrosis.

TOP-326

Prognostic immuneclassification in intrahepatic biliary tract cancer

Ira Godbole[1], Jannis Heyer[2], Konrad Kurowski[2], Philipp Holzner[3], Robert Thimme[1], Peter Bronsert[2], Bertram Bengsch[1]. [1]*Clinic for Internal Medicine II (Gastroenterology, Hepatology, Endocrinology and Infectious Diseases, Freiburg University Medical Center), Faculty of Medicine, University of Freiburg, Freiburg, Germany;* [2]*Institute of Pathology, Faculty of Medicine, University Hospital Freiburg, Freiburg, Germany;* [3]*Department of General and Visceral Surgery (Center for Surgery, Freiburg University Medical Center), Freiburg, Germany*
Email: ira.godbole@uniklinik-freiburg.de

Background and aims: Intrahepatic cholangiocarcinoma (iCCC), a major subtype of biliary tract cancer (BTC), is a highly aggressive malignancy with poor prognosis. Although immune checkpoint inhibitors are increasingly used in BTC, the spatial organization of the tumor immune microenvironment (TiME) and its relationship to outcome remain incompletely understood. Using spatial immune analysis within this project, we investigated how CD8 T cell infiltration and localization relative to tumor stroma and parenchyma define immunotypes with prognostic relevance, independent of treatment.
Method: Resectable iCCC tissue microarrays from a monocentric cohort of 98 patients, predominantly with grade 2 and grade 3 tumors, were analyzed using immunohistochemistry (IHC; n = 95) and 42-plex imaging mass cytometry (IMC; n = 27). The IMC panel covered tumor, immune, extracellular matrix, and architectural markers, enabling single-cell phenotyping with detailed CD8 T cell characterization. Tumor and stromal masks enabled regional CD8 T cell density quantification. Cut-offs were defined using cutoffR and validated in the IHC cohort using matched CD8 and collagen staining. Immune subclasses were spatially clustered to identify immune neighbourhoods and cell–cell interactions. Overall survival was assessed using Kaplan–Meier analysis of clinically annotated data.
Results: Spatial analysis identified three immune neighbourhoods with distinct compositions: IN1 enriched for cytotoxic and dysfunctional CD8 states, IN2 dominated by myeloid and macrophage populations, and IN3 showing higher frequencies of B cells and CD4 T cell subsets ($p < 0.001$). Based on CD8 T cell density and spatial localization, tumors were classified as depleted (<180 CD8 cells/mm^2; 59/95, 62.1%; mean OS 22.47 months), compartmentalized (tumor-to-stroma CD8 ratio <0.45; 6/95, 6.3%; mean OS 40.33 months), or enriched (ratio >0.45; 30/95, 31.5%; mean OS 60.9 months). Kaplan–Meier analysis showed significantly different survival, with enriched tumors outperforming depleted tumors ($p = 0.00696$) and compartmentalized tumors showing intermediate outcomes. Enriched tumors displayed increased CD8$^+$CD45RO$^+$ memory T cells, whereas depleted tumors showed higher FoxP3$^+$ regulatory T cells and myeloid-dominated neighbourhoods ($p = 0.0001$).
Conclusion: We establish a spatial CD8-based immune classification for iCCC that correlates with survival in immunotherapy-naïve patients and reflects intrinsic TiME biology, providing a robust framework for prognostic stratification.

WED-321-YI

Regulatory T cells polarise to TregTh1 in autoimmune cholangitis, yet cells remain functional, enabling GMP Treg therapy

Ayma Asif[1], Naomi Richardson[1], Grace Wootton[1], Kayani Kayani[1], Ye Htun Oo[1], Amber Bozward[1]. [1]*University of Birmingham, Birmingham, United Kingdom*
Email: a.g.bozward@bham.ac.uk

Background and aims: Primary biliary cholangitis (PBC) is an autoimmune cholestatic liver disease characterised by effector T cell–mediated biliary injury. Regulatory T cells (Tregs) are critical for restoring hepatic immune tolerance, yet their phenotype, functional stability and suitability for cell therapy in PBC remain incompletely defined. FoxP3 mutation in mice present with PBC like pathology in the liver. We investigated the frequency, phenotype, immunometabolic profile, lineage stability and suppressive function of Tregs in PBC, and assessed the feasibility of generating clinical-grade good manufacturing practice (GMP) Tregs for therapeutic application.
Method: Peripheral blood mononuclear cells and liver tissue were obtained from patients with PBC, other liver diseases and controls. Tregs were identified as CD4$^+$CD25$^+$CD127^{low} cells and analysed by flow cytometry for phenotypic, functional and metabolic markers. Suppression and lineage-stability assays were performed under Th1 and Th17 polarising conditions. Cytokines were quantified in serum and liver supernatant using LEGENDplex. GMP-grade Tregs were isolated, expanded and phenotyped under GMP conditions.
Results: The frequency of circulating Tregs was comparable between PBC (n = 13) and controls (n = 21). PBC Tregs expressed functional markers CD39, CTLA-4, and FoxP3, with the CD39^{high} subset exhibiting the highest CTLA-4 and FoxP3 expression ($p < 0.0001$). Naïve Tregs (CD45RA$^+$CCR7$^+$) were significantly reduced in PBC compared with AIH, ALD, and healthy donors ($p = 0.0350$, $p = 0.0132$, and $p = 0.0405$), with a reciprocal increase in effector memory Tregs versus ALD and HFE ($p < 0.0001$ and $p = 0.0045$). PBC Tregs remained metabolically competent, with no differences in mitochondrial mass or membrane potential. Under Th1-polarising conditions, PBC Tregs showed reduced FoxP3 stability compared with HFE ($p < 0.05$) without increased IFN-γ or TNF-α production, and suppressive function was preserved. PBC livers were enriched for IL-6 and IFN-γ compared with donor and MASH/ALD samples (all $p < 0.005$). Clinically relevant numbers of GMP-grade Tregs were successfully expanded from PBC patients while retaining phenotype and suppressive capacity.
Conclusion: Tregs in PBC retain suppressive capacity and metabolic competence despite phenotypic plasticity within an inflamed cytokine rich milieu. GMP-grade Treg therapy in PBC is feasible, applying CD39^{high} Tregs and preconditioning strategies targeting IL-12/Th1 pathways may enhance lineage stability and therapeutic efficacy.

WED-322

In silico prediction of microrna-t cell receptor constant region interactions: novel insights into autoimmune liver disease pathogenesis

Kiandokht Bashiri[1]. [1]*Georgetwon University/MedStar Washington Hospital Center, Washington DC, United States*
Email: kiandokht.bsh@gmail.com

Background and aims: Autoimmune liver diseases (ALDs), including autoimmune hepatitis (AIH), primary biliary cholangitis (PBC), and primary sclerosing cholangitis (PSC), are marked by dysregulated T cell responses causing hepatic inflammation. T cell receptor (TCR) constant regions (TRAC for alpha; TRBC1/TRBC2 for beta) ensure TCR stability and signaling. MicroRNAs (miRNAs) regulate immune genes post-transcriptionally, with altered profiles in ALD. This novel in silico study predicted miRNA targeting of TCR constants, cross-referenced with ALD miRNAs, and performed functional enrichment to uncover pathogenic roles.
Method: Human mRNA sequences (TRAC: 4631 nt, ENSG00000277734; TRBC1: 1448 nt; TRBC2: 1489 nt) were analyzed via miRDB (scores ≥ 50), cross-validated with TargetScan. Predictions overlapped with ALD-associated miRNAs from PubMed and GEO datasets. Functional enrichment used miEAA for pathways (KEGG) and tissue specificity.
Results: MiRDB predicted 158 miRNAs for TRAC, 44 for TRBC1, and 39 for TRBC2. Twelve miRNAs were shared between TRBC1 and TRBC2, including hsa-miR-4455. A key disease-associated candidate, hsa-miR-4725-3p, targeted both TRAC (score 64) and TRBC2 (score 84)

and is reported to be upregulated in untreated AIH (fold change >2; $p < 0.05$). Enrichment analysis revealed strong over-representation of T-cell receptor signaling among TRAC-targeting miRNAs ($p = 3.60 \times 10^{-10}$), along with significant enrichment in RIG-I–like receptor signaling ($p = 3.60 \times 10^{-10}$), indicating alpha-chain–specific immune regulation. TRBC1-associated miRNAs were enriched in ECM–receptor interaction pathways ($p = 2.61 \times 10^{-5}$), while TRBC2-associated miRNAs were enriched in blood-specific tissues ($p = 2.57 \times 10^{-4}$) and platelet activation ($p = 1.51 \times 10^{-4}$), suggesting hematopoietic context–dependent modulation.
Conclusion: This in silico analysis identifies multiple high-confidence miRNAs targeting TCR constant regions, with TRAC exhibiting the strongest immunologic pathway enrichment, suggesting α-chain–specific vulnerability to miRNA-mediated dysregulation in ALD. hsa-miR-4725-3p emerges as a compelling dual-target regulator associated with AIH activity, providing a mechanistic link between altered miRNA profiles and T-cell hyperactivation. These findings highlight miRNA–TCR interactions as a previously unrecognized layer of immune dysregulation in ALD. In vitro validation is warranted.

WED-323
Myeloid progenitor cells are enriched and adopt a pro-inflammatory profile in liver fibrosis

Katharina Bonitz[1,2], Emanuel Pietschmann[1], Sarah Dobner[2], Fanni Toth[2], Thomas Sorz-Nechay[1,2], Henriette Horstmeier[1], Katja Sommer[1,2], Benedikt Hofer[1], Benedikt Simbrunner[1], Vlad Taru[1], Jan Embacher[1], Kerstin Zinober[1], Katharina Regnat[1], Michael Trauner[1], Philipp Schwabl[1], Laura de Rooij[2], Thomas Reiberger[1,2]. [1]*Medical University of Vienna, Vienna, Austria;* [2]*CeMM Research Center for Molecular Medicine of the Austrian Academy of Sciences, Vienna, Austria*
Email: katharina.bonitz@meduniwien.ac.at

Background and aims: Liver cirrhosis is associated with an increase in myeloid-derived cells both in the liver and the systemic circulation. However, the role of haemopoietic progenitor cells (HPCs) in cirrhosis remains poorly investigated.
Method: Peripheral blood mononuclear cells were isolated from patients with liver cirrhosis (LC) and healthy controls (HC) by gradient centrifugation. Samples were either used for flow cytometry (HC n = 10, LC n = 25) or scRNA-Seq (HC n = 3, LC n = 6). For flow cytometry cells were stained with an 8-color panel to distinguish HPC populations. For scRNA-Seq with ParseBio, samples were sorted for $CD45^{dim}$, excluding mature immune cells. The scRNA-Seq analysis was performed with Seurat, yielding 10265 cells after quality control.
Results: In LC patients the HPC compartment shifted compared to HC. We found a decrease in CD34+CD38+ progenitor cells (LC: 3.37% vs. HC: 7.25%; $p = 0.005$). However, within the progenitor population LC patients had an increase in CD34+CD38+CD45RA-CD123+ common myeloid progenitor cells (CMPs: LC 0.66% vs. HC 0.07%; $p = 0.003$). ScRNA-Seq analysis confirmed a trend towards higher relative abundance of CMPs in LC (28.79% vs HC: 11.00%; $p = 0.282$). To understand if CMPs are functionally different in LC vs HC conditions, we performed differential gene expression analysis and found *CD36*, *LILRB1* and *KCNG2* as the three top upregulated and *WDR49*, *ABTB3*and *CDS1* as the three major downregulated genes in CMPs of LC patients compared to HC. Gene set enrichment analysis revealed that CMPs in LC had a pro-inflammatory phenotype and showed an upregulation of metabolic pathways and oxidative phosphorylation. Monocyte-primed progenitors, which expressed more mature markers, than CMPs, retained a similar enrichment of inflammatory and metabolic pathways in LC, suggesting early shifts in myeloid progenitors persist during differentiation.
Conclusion: LC patients present an increase in CMPs within their hematopoietic progenitor compartment. This CMP population exhibits a pro-inflammatory phenotype that is retained during differentiation – suggesting an early priming towards a potentially disease-driving myeloid lineage.

WED-324-YI
Human liver spatial transcriptomics reveals macrophage-driven antiviral responses distinguishing seronegative fulminant hepatitis from autoimmune hepatitis

Amber Bozward[1], Mahboobeh Behruznia[1], John Cole[2], Scott Davies[1], Kylie Savoye[1], Chiranjit Das[1], Matthew Pugh[1], Grace Wootton[1], Fabian Spill[1], Owen Cain[3], Alan McNally[1], Ye Htun Oo[1]. [1]*University of Birmingham, Birmingham, United Kingdom;* [2]*University of Glagow, Glasgow, United Kingdom;* [3]*University Hospitals Birmingham, Birmingham, United Kingdom*
Email: a.g.bozward@bham.ac.uk

Background and aims: Autoimmune hepatitis (AIH) and seronegative fulminant hepatitis (SNH) share overlapping clinical and histological features, yet their causative factors and underlying immune mechanisms remain poorly understood resulting in liver transplantation. Spatial transcriptomics offers an opportunity to resolve cell-type-specific and tissue-contextual differences across both diseases to explore discovery pathways for diagnostic and translational therapeutic avenues.
Method: We profiled explant human liver from AIH (n = 3), SNH (n = 3), and donor (n = 3) controls using CosMx™ high-plex spatial transcriptomics, complemented by Visium transcriptome-wide spatial profiling (AIH (n = 5), SN (n = 6)), immunohistochemistry, confocal microscopy and metatranscriptomics. The same patient samples were analysed across all platforms. Cell types were annotated using Seurat, SingleR, and spatial context validation. Cell–cell communication was assessed with CellChat.
Results: SNH exhibited a macrophage-dominated antiviral transcriptional signature, characterised by enrichment of interferon-stimulated genes (e.g., MX1, ISG15), consistent with a heightened antiviral response. Metatranscriptomics analysis confirmed viral sequences in SNH samples. Spatial mapping identified CD63 as a significantly upregulated marker in SNH patients, confirmed with immunohistochemistry, implicating vesicle trafficking and exosome-associated pathways in antiviral immunity and highlighting CD63 as a potential diagnostic marker. In contrast, AIH samples demonstrated increased B cell–T cell proximity with reduced TNFSF14 (LIGHT)-HVEM pathway activity, indicating disrupted costimulatory signalling.
Conclusion: Our study provides the first multi-platform spatial transcriptomic analysis of AIH and SNH, revealing macrophage-driven antiviral immunity as a key immunopathological feature of SNH, distinct from the adaptive immune-dominant profile in AIH. The identification of CD63 as an upregulated marker in SNH and reduced LIGHT pathways activity in AIH could be future diagnostic markers for these diseases, demonstrating the power of spatially resolved multi-platform analysis to uncover disease-specific immune architectures, informing future diagnostic strategies and targeted therapeutic approaches for patients.

WED-329-YI
Development of ex vivo models to study the response to immunotherapy in hepatocellular carcinoma

Carla Castro Alejos[1], Diana Llopiz[1], Andrea Moreno Ardila[1], Maria Ruiz[1], Leyre Silva[1], Uxua Mancheño[1], Eduardo Miraval[2], José Echeveste[2], Sandra Hervás-Stubbs[1], Miguel Sogbe[2], Josepmaria Argemi[2], Bruno Sangro[2], Pablo Sarobe[1]. [1]*Centro de Investigación Médica Aplicada-UNAV, Pamplona, Spain;* [2]*Clinica Universidad de Navarra, Pamplona, Spain*
Email: psarobe@unav.es

Background and aims: Immunotherapy based on immune checkpoint inhibitors (ICI) has become first-line treatment for patients with advanced hepatocellular carcinoma (HCC). However, only 25–35% of treated patients respond to these therapies. Recently, ex vivo culture systems of tumor fragments have been used to study the response of tumor-infiltrating lymphocytes to different immunotherapies and potentially predict treatment outcomes. Our aim was to

establish an ex vivo culture system for HCC to analyze the characteristics of tumors showing responses to ICIs approved for HCC.
Method: One mm^3 fragments were generated from tumors obtained from mice or patients with early HCC, frozen and kept for future experiments. Thawed fragments were cultured in a collagen/Matrigel matrix with different ICI combinations (Roelofsen LM, et al. STAR Protoc. 2023) and IFN-gamma released to the supernatants was measured by ELISA. Tumor lymphocytic infiltrate was characterized by flow cytometry.
Results: In vivo, subcutaneous tumors generated with the HCC cell line PM299L showed partial responses when treated with the ICIs approved for HCC based on PD-L1+CTLA-4 or PD-L1+VEGFR blockade ($p < 0.05$). Ex vivo, treatment with anti-PD-L1 + anti-CTLA-4 antibodies of fragments generated from these tumors showed IFN-gamma production with a remarkable inter- and intra-tumoral heterogeneity. IFN-gamma production was associated with different signals of immune infiltration: responding tumors had higher proportions of leukocytes ($CD45^+$ cells) ($p = 0.007$), T lymphocytes ($p = 0.03$) and CD8 T cells ($p = 0.009$). Overall, tumors that showed positive responses induced by PD-L1+CTLA-4 blockade also responded to PD-L1+VEGFR. No responses to ICI were detected when using fragments of the immune-desert NM53 HCC tumor. Interestingly, cultures of orthotopic tumors with lymphocyte levels equivalent to those found in subcutaneous responding tumors did not show any response, suggesting the presence of additional control mechanisms. Preliminary results using tumor fragments from a cohort of 13 patients with early HCC showed that ex vivo treatment with durvalumab + tremelimumab or atezolizumab + bevacizumab combination immunotherapies induced responses in some patients: according to the response definition criteria, responses ranged from 8 to 24% for PD-L1+CTLA-4 blockade and reached a 38% for PD-L1 +VEGF.
Conclusion: These results suggest that this system could be useful to identify responding patients and to characterize mechanisms associated with response to ICI.

WED-330-YI
Liver associated invariant T cells are enriched in PSC patients, secrete IFN-γ in response to IL-12 and IL-18, and can potentially contribute to Treg plasticity

Scott Davies[1], Annabelle Schofield[1], Grace Wootton[1], Ye Htun Oo[1,2].
[1]*Centre for Liver and Gastrointestinal, Institute of Biomedical Research, Department of Immunology and Immunotherapy, School of Infection, Inflammation and Immunology, College of Medicine and Health, Birmingham, United Kingdom;* [2]*University Hospital Birmingham Nhs Trust, Birmingham, United Kingdom*
Email: s.p.davies.1@bham.ac.uk

Background and aims: Primary Sclerosing Cholangitis (PSC) is an immune-mediated biliary disease that occurs in close associate with inflammatory bowel disease (IBD). Recently, T cells which are MHC-II restricted, innate-like, commensal-reactive (T_{MIC}) and cytokine-responsive with polyfunctional effector properties were reported in IBD patients and associated mouse model. T_{MIC} cells had a reported phenotype of $CD161^{hi}$, $Va7.2^{negative}$ $PLZF^+$. We aimed to assess their presence and function in the blood and liver of PSC patients.
Method: The abundance and phenotype of T_{MIC} cells were assessed in PSC patients by flow cytometry staining of peripheral blood mononuclear cells (PBMCs) and multiplex immunofluorescence staining of FFPE liver tissue. T_{MIC} function was tested by overnight treatment of liver-infiltrating mononuclear cells (LIMCs) with cytokine cocktails. TCR Va7.2 staining was used to exclude MAIT cells. Stability and suppression capacity of PSC-derived Tregs was assessed in presence of Th1/Th17 polarising cytokine conditions or bile acids. Treg phenotype in blood and liver of PSC and control donors was assessed by flow cytometry.
Results: Immunofluorescence staining of liver tissues showed the presence of T_{MIC}-like cells in PSC with a higher frequency in PSC patients compared to donors (66% vs 25%). These cells were observed in proximity to bile ducts and $FoxP3^+$ $CD4^+$ cells in PSC livers. Flow cytometry phenotyping of PSC PBMCs demonstrated T_{MIC} frequency of (46% ± 7%; n = 7), 36% higher than non-diseased controls (10% ± 5%; n = 4). T_{MIC}-like cells expressed IL-18R (46% ± 8%), IL-7R (CD127;85% ± 2%), and IL-12R (6% ± 1%). Treatment of LIMCs with IL-18 and IL-12 caused increased IFN-γ expression by T_{MIC} (20% ± 7% vs 4% ± 2%, n = 4. PSC liver-derived Tregs maintained functional markers CTLA-4 (72% ± 10%) and FoxP3 (96% ± 2; n = 12). IFN-γ and IL-12 treatment of PSC-derived Tregs resulted in lineage plasticity towards Treg-Th1 phenotype (Tbet; 14% ± 8%, IFN-γ; 56% ± 18%; n = 3) and reduced capacity to suppress proliferation of effector T cells by 24% compared to control suppression (40% ± 8% vs.16% ± 2%). Lithocholic acid treatment of Treg reduced CD25 expression (37% ± 19%).
Conclusion: Liver associated invariant T cells (LAIT), which share the T_{MIC} phenotype, are present in PSC patients. LAIT cells respond to IL-12 and IL-18 and secrete IFN-γ. IFN-γ and IL-12, as well as lithocholic acid, reduced Treg suppressive capacity. These factors may perpetuate chronic cholangiopathy in PSC.

WED-331-YI
Impact of alcohol consumption on the immune architecture in hepatocellular carcinoma

Margaux Delaporte[1,2], Marine Roux[3], Maëlle Guillout[4], Nicolas Gallez[1], Julien Chaigneau[3], Anthony Sébillot[4], Jerome Boursier[3], Michel Samson[1], Céline Raguénès-Nicol[1].
[1]*Université de Rennes, INSERM, Irset - UMR_S 1085, Rennes, France;* [2]*Irset | Institut de recherche en santé, environnement et travail, Rennes, France;* [3]*Hepato-Gastroenterology and Digestive Oncology Department, Angers University Hospital, HIFIH Laboratory UPRES EA3859, SFR 4208, Angers, France;* [4]*University Rennes, CNRS, Inserm, Biosit UAR 3480 US_S 018, France-BioImaging (ANR-24-INBS-0005 FBI BIOGEN), Core Facility H2P2, Rennes, France*
Email: margaux.delaporte.1@univ-rennes.fr

Background and aims: Hepatocellular carcinoma (HCC) remains a major cause of cancer-related mortality and personalized-medicine such as immunotherapy has highly variable efficacy so far. This is partly due to heterogeneity in the tumor immune microenvironment, classified as "hot" or "cold" based on immune cell infiltration. Although chronic alcohol consumption is known to induce oxidative stress and sustain a pro-inflammatory state, the combined effects of metabolic dysfunction-associated liver disease (MASLD) and alcohol misuse, on the HCC immune microenvironment remain poorly understood. We aimed to determine whether alcohol consumption shapes the HCC immune architecture and modulates its "hot" or "cold" status, clues to understanding immunotherapy responsiveness.
Method: We developed a 24-marker multiplex Immunofluorescence panel to characterize immune cell populations in HCC biopsies stratified by alcohol consumption. Biopsies of tumors and non-tumors from 53 patients were processed to identify and localize 20 populations of cells in lymphoid, myeloid and stromal subsets. Cellular quantification, spatial analysis, and unsupervised clustering allow us to describe the heterogeneity among patients. Alcohol weekly consumption was also incorporated as a key stratification variable to determine its influence on the immune landscape.
Results: Tumors with a higher number of infiltrating immune cells were particularly enriched in specific subsets of lymphocytes as well as dendritic cells and neutrophils, consistent with an inflamed and immunologically active microenvironment. Using principal component analysis, we identified a cellular profile captured by PC2 that discriminates immune-high from immune-low tumor phenotypes ($p = 0.022$), and this profile was significantly associated with alcohol consumption ($p < 0.001$). Spatial analyses further revealed denser CTL and T-helper cell clusters within hot tumors, indicating a higher degree of local immune organization and coordinated immune activity.

Conclusion: These findings demonstrate that alcohol consumption is significantly associated with a specific immune microenvironment of HCC, with immune-high phenotype. This immune signature may partly explain immunotherapy responsiveness and support improved patient stratification and tailored therapeutic strategies that integrate alcohol-related immune alterations.

WED-332-YI

Hepatitis B virus specific T cell immunity to guide discontinuation of nucleoside analogue therapy in hepatitis B e antigen negative chronic hepatitis B

Raquel Encijo Heredia[1,2], Julia Peña Asensio[1], Rocío López[1,3], Joaquín Míquel[1,4], Marta Vila[5], Maria Francesca Cortese[5,6], Ariadna Rando-Segura[5,6], Miguel Torralba[1,2,7], Juan Ramón Larrubia[1,2,4], Henar Calvo Sánchez[1,2,4]. *[1]Translational Research Group on Cellular Immunology (GITIC), Instituto de Investigación Sanitaria de Castilla La Mancha (IDISCAM), Guadalajara, Spain; [2]Department of Medicine and Medical Specialties, University of Alcalá, Alcalá de Henares, Spain; [3]Service of Immunology, University Hospital of Guadalajara, Guadalajara, Spain; [4]Service of Gastroenterology, University Hospital of Guadalajara, Guadalajara, Spain; [5]Department of Microbiology, Liver Unit, Vall d'Hebron Institut de Recerca (VHIR), Vall d'Hebron Barcelona Hospital Campus, Barcelona, Spain; [6]Carlos III Health Institute, Network Center For Biomedical Research in Hepatic and Digestive Diseases (CIBERehd), Madrid, Spain; [7]Service of Internal Medicine, University Hospital of Guadalajara, Guadalajara, Spain*
Email: raquelencijo45@gmail.com

Background and aims: Criteria for safely discontinuing nucleoside analogue (NUC) therapy in hepatitis B e antigen negative chronic hepatitis B (CHBe(-)) remain poorly defined. Although treatment withdrawal can lead to functional cure in a subset of patients, reliable immunological predictors of durable viral control are lacking. We aimed to prospectively evaluate whether quantitative and functional hepatitis B virus specific T cell responses can predict relapse-free survival after treatment discontinuation.
Method: Twenty-eight CHBe(-) patients who elected to discontinue long-term NUC therapy were prospectively followed for a median of 5 years. Patients were classified as functional cure, inactive carrier, grey zone, late relapser or early relapser according to virological and biochemical outcomes. Baseline hepatitis B surface antigen (HBsAg) and hepatitis B core related antigen (HBcrAg) levels were quantified. Hepatitis B virus specific T cell immunity was assessed after ten-day antigen specific expansion using interferon gamma enzyme linked immunospot assays with multiple viral peptide pools and multi-parametric flow cytometry to quantify functional CD8 T cell degranulation and cytokine production. Relapse-free survival was analysed using Kaplan–Meier methods according to T cell functionality.
Results: Patients achieving functional cure showed very low antigen burden, defined as HBsAg below 100 IU/mL and HBcrAg below 2 log, together with low interferon gamma spot forming cell responses. In contrast, inactive carriers displayed the strongest multispecific T cell responses, followed by grey zone, late relapsers and early relapsers. Late relapsers exhibited high cytokine intensity, consistent with transient hyperactivation of functionally impaired T cells, whereas early relapsers showed minimal enzyme linked immunospot and CD8 T cell activity. Importantly, patients with two or more functional enzyme linked immunospot responses had no relapse during follow-up, while more than 60% of patients with one or no responses experienced relapse. Relapse-free survival differed significantly between these groups.
Conclusion: Very low antigen levels identify patients who can safely discontinue NUC therapy. Among patients with higher antigen burden, multispecific hepatitis B virus specific T cell responses strongly predict durable viral control, whereas weak responses identify individuals at high risk of relapse. Immune profiling may enable personalised, immune guided treatment discontinuation in CHBe(-).

WED-333-YI

Understanding the impact of the liver microenvironment on the fate of regulatory T cells

Maegen Fleming[1], Elena Perpinan[1], Ada Sera Kurt[1], Elisavet Kodela[1], Marwa Elgosbi[1], Roberto Savoldelli[1], Leonard Bellersheim[1], Nicolas Sompairac[2], Alberto Sanchez-Fueyo[1], Niloufar Safinia[1]. *[1]Roger William's Institute of Liver Studies, School of Immunology and Microbial Sciences, King's College London, SE5 9NU, London, United Kingdom; [2]School of Cancer & Pharmaceutical Sciences, Comprehensive Cancer Centre, King's College London, SE1 1UL, London, United Kingdom*
Email: maegen.fleming@kcl.ac.uk

Background and aims: Regulatory T cell therapies (Tregs) possess considerable therapeutic potential for autoimmune liver disease and liver transplantation. However, fundamental questions remain regarding how Tregs interact with the hepatic microenvironment, potentially limiting their therapeutic efficacy. In previous work we have shown that Tregs exist at a lower frequency in healthy liver tissue, compared to other non-lymphoid organs, and enrich in the tumour tissue of hepatocellular carcinoma (HCC). Additionally, intrahepatic Tregs are more apoptotic than circulating and intratumoral Tregs. This suggests the liver poses a hostile environment to these essential immunosuppressive cells. To generate effective liver-specific Treg-based therapeutics, capable of both trafficking to and surviving within the liver tissue, an understanding of the factors controlling Treg stability and function is crucial.
Method: We obtained surgically resected liver tissue specimens and performed single-cell RNA sequencing (scRNAseq) on purified Tregs and conventional CD4+ T cells from histologically intact liver tissue, matched peripheral blood, alongside paired non-tumoral/tumour tissue from HCC patients. To study the effects of distinct hepatic microenvironments on Tregs, healthy blood-derived Tregs were treated in vitro with secretomes derived from both liver and tumoral tissues.
Results: Transcriptomic analysis displayed marked differences in Tregs isolated from intrahepatic tissue compared to their circulatory and tumoral counterparts. Gene set enrichment analysis (GSEA) revealed augmentation of inflammatory-associated and apoptotic pathways in intrahepatic Tregs relative to circulatory Tregs. Enhanced cytokine signalling, mTOR pathway activation, and metabolic reprogramming was shown in intrahepatic Tregs compared to intratumoral Tregs. Following in-vitro secretome co-cultures, Tregs treated with healthy liver secretomes were shown to be reduced in number and more apoptotic than those cultured in tumour secretomes.
Conclusion: Tregs adapt by transcriptomic, signalling, and metabolic changes in response to environmental exposure. In vitro co-culture experiments, with liver-derived secretomes, mirrored the reduced frequency and viability of Tregs observed in patient samples. These results indicate that tissue factors play critical roles in determining the survival and efficacy of Tregs. Identifying afflicted pathways will crucially inform the development of future strategies for liver-targeted immunotherapies.

WED-334

Proteomics-driven immune landscape profiling in acute decompensation identifies suppressive monocytes as key determinants of disease progression and mortality

Pratibha Garg[1], Nipun Verma[1], Parminder Kaur[1], Sunil Taneja[1], Ajay Kumar Duseja[1]. *[1]Department of Hepatology, Postgraduate Institute of Medical education and Research, Chandigarh, India*
Email: pgargbhawan@gmail.com

Background and aims: Acute decompensation (AD) in cirrhosis is a paradoxical immune state of systemic inflammation coupled immunoparalysis. Although dysregulated myeloid responses are known,

the relative contribution of distinct immunoregulatory cell phenotypes in shaping disease progression and mortality remains poorly defined.

Method: We performed untargeted LC-MS/MS plasma proteomics in 100 patients with AD (21 AD no-ACLF, 79 ACLF) at admission. Identified proteins were annotated to immune cell–specific signatures using CellMarker2.0, and immune cell enrichment was quantified using single-sample gene set enrichment analysis (ssGSEA). Enrichment profiles were compared across disease state (AD vs ACLF), baseline severity (grade 0–1 vs 2–3), disease course over 30 days (non-severe vs severe trajectory), and 30-day mortality. Predictive performance of immune phenotypes was evaluated using ROC analysis.

Results: At presentation, ACLF was distinguished from AD by early amplification of myeloid immune subsets, predominantly suppressive monocytes (SMs), which were 3.36-fold higher in ACLF ($p = 0.004$), alongside attenuated $CD8^+$ T-cytotoxic immunity (fold change 0.42, $p = 0.013$). Patients presenting with severe disease at baseline (grade 2–3) demonstrated similar enrichment of SMs ($p = 0.023$) alongside early contraction of naïve and cytotoxic T-cell pools. Baseline immune landscape guided disease trajectory. Patients following severe disease course over 30 days exhibited 6.26-fold enrichment of SMs ($p < 0.001$), alongside enrichment of DCs, non-classical monocytes, and M2 macrophages, and progressive depletion of $CD8^+$ cytotoxic and naïve T cells; mortality reflected persistence of this immune state with 7.4 folds-higher SMs and further reduction of CD8+ T-cells (FC: 0.38, $p = 0.018$). SMs, annotated as MO-MDSC like cells ($CD33^{++}CD11b^{++}CD11c^{+}CD14^{+}CD16^{-/+}$HLA-DR-$CD15^{-}CD66b^{-}CD123^{-}$), emerged as the most discriminative phenotype demonstrating robust prediction of severe disease course and 30-day mortality (AUC 0.87–0.89), with performance improving to AUC to 0.906 when combined with baseline CLIF-C OF score.

Conclusion: Untargeted immune landscape mapping in AD identifies MO-MDSC-like suppressive monocytes as central drivers of disease severity, and mortality, supporting disease progression is governed by immunoregulatory myeloid reprogramming, rather than hyperinflammation alone, and highlighting them as clinically informative biomarkers and potential targets for immune-modulatory strategies.

WED-336

Dual TIGIT and PD-1 blockade reverses CD8+ T cell dysfunction in acute-on-chronic liver failure

Yidi Jia[1], Yao Zhang[1], Xueyun Zhang[1], Yan Wang[2], Yuqi Liu[1], Xiaoting Zhao[1], Mengqi Zhu[1], Yuxian Huang[1], Jiming Zhang[1].
[1]Department of Infectious Diseases, Shanghai Key Laboratory of Infectious Diseases and Biosafety Emergency Response, National Medical Center for Infectious Diseases, Huashan Hospital, Fudan University, Shanghai, China, Shanghai, China; [2]Department of Geriatrics, Huashan Hospital, Fudan University, Shanghai 200040, China, Shanghai, China
Email: seven_jyd@163.com

Background and aims: Acute-on-chronic liver failure (ACLF) is characterized by the rapid hepatic decompensation and multiorgan failure, with a 90-day mortality rate approaching 60%. Overwhelming bacterial infections, driven by anti-bacterial immunity deficiency, are a leading precipitating factor triggering 35% of ACLF cases. Although dual blockade of immune checkpoints TIGIT/PD-1 has demonstrated activity in oncology, its potential to promote anti-bacterial immunity in ACLF remains unexplored. The aim of this study was to evaluate whether TIGIT and PD-1 are co-upregulated on T cells in ACLF and whether dual checkpoint blockade could improve their function.

Method: Patients with ACLF ($n = 77$) were enrolled within 24 hours of hospitalization, alongside healthy controls (HC, $n = 38$) and patients with cirrhosis patients (LC, $n = 52$). $CD8^+$T cells were isolated from peripheral blood mononuclear cells (PBMCs) for flow cytometric phenotyping and functional assays. T cell responses were assessed following CD3/CD28 stimulation, with or without ex vivo blockade using anti-TIGIT and/or anti-PD-1 antibodies.

Results: TIGIT expression was significantly increased on $CD8^+$ T cells from patients with ACLF (median 35.0%, IQR 28.7–47.3%) compared to HCs (median 15.7%, IQR 9.8–21.2%) and LC patients (median 29.4%, IQR 20.9–40.2%), with upregulation of PD-1 co-expression ($PD\text{-}1^+$ $TIGIT^+$ $CD8^+$T cells: median 60.2%, IQR 36.9–68.5%; $PD\text{-}1^+$ $TIGIT^-$ $CD8^+$T cells: median 29.5%, IQR 15.7–42.1%; $p < 0.0001$). Increased frequencies of $TIGIT^+$ $CD8^+$T cells correlated with ACLF severity (EASL CLIF grade 1: median 23.3%, IQR 16.2–32.5%; grade 2: median 34.5%, IQR 30.1–40.7%; grade 3: median 41.25%, IQR 29.7%-56.8%; $p < 0.05$, respectively) and evidence of bacterial translocation (without bacterial infection: median 33.85%, IQR 23.8–41.1%; with bacterial infection: median 34.7%, IQR 28.5–56.0%; $p = 0.0363$). Ex vivo TIGIT blockade alone restored the proliferative capacity (CD25, CD69) and cytokine production (IFN-gamma, IL-2, TNF-alpha) of $CD8^+$ T cells from ACLF patients. Notably, combined TIGIT and PD-1 blockade resulted in significantly greater enhancement of proliferation and cytokine release compared to single-agent TIGIT inhibition.
Conclusion: Dual TIGIT/PD-1 blockade potently enhances the ex vivo functionality of $CD8^+$ T cells in ACLF. These findings support further investigation into co-blockade of TIGIT and PD-1 as a promising immunotherapeutic strategy for ACLF.

WED-337-YI
Retinoids reprogram TREM2$^+$ monocyte-derived macrophages toward a restorative phenotype via redox control to attenuate liver fibrosis

Kyurae Kim[1], Jang Su Jeon[2], Sung Eun Choi[1], Jihyo Byun[1], Kwangwoo Lee[1], Sang Kyum Kim[2], Won-il Jeong[1]. [1]*Korea Advanced Institute of Science and Technology (KAIST), Daejeon, Korea, Rep. of South;* [2]*Chungnam National University, Daejeon, Korea, Rep. of South*
Email: wijeong@kaist.ac.kr

Background and aims: Hepatic macrophages regulate the progression and regression of liver fibrosis by interacting with hepatic stellate cells (HSCs). Among the heterogeneous macrophages, $TREM2^+$ monocyte-derived macrophages (MDMs) emerge in injured livers. Recent studies highlight restorative roles of these cells, the regulation of which remains poorly understood. Here, we aimed to investigate how HSC-derived retinoids program MDMs toward a restorative phenotype during liver fibrosis.
Method: Liver fibrosis was induced in mice by CCl_4 injection. Hepatic macrophages were isolated and analyzed by single-cell RNA sequencing (scRNA-Seq) using the 10X Genomics platform. Macrophage frequency, cellular ROS, and nitric oxide levels were assessed by flow cytometry. HSC-mediated regulation of MDMs was evaluated by *in vitro* co-culturing and retinoid supplementation.
Results: scRNA-Seq identified $TREM2^+$ MDMs, which differentiate from infiltrating monocytes in fibrotic liver, and revealed a restorative subset expressing anti-inflammatory and tissue-remodeling genes. In this subset, KEGG pathway analysis of differentially expressed genes found retinoid metabolism to be highly enriched, along with selective expression of retinoid-responsive genes such as transcription factors, receptors, and metabolizing enzymes. Immunofluorescence staining of fibrotic liver tissue showed that MDMs were localized within fibrotic septa, where activated HSCs release retinoids. *In vitro*, inducible MDMs co-cultured with HSCs or treated with retinoids showed upregulated retinoid-responsive genes (*Rara*, *Stra6l*, *Rbp4*) and anti-inflammatory macrophage markers (*Arg1*, *Il10*), while reducing inflammatory cytokine expression. In addition, retinoids increased NRF2 levels, a master regulator of antioxidant responses, and lowered cellular ROS levels. Interestingly, retinoids induced robust ARG1 expression, driving a metabolic switch in arginine metabolism from nitric oxide production toward polyamine synthesis, thereby conferring restorative macrophage properties. Importantly, retinoid supplementation in mice attenuated liver fibrosis by reprogramming phenotypes of hepatic MDMs toward a restorative state.
Conclusion: This study demonstrates that HSC-derived retinoids act as key regulators, endowing $TREM2^+$ MDMs with restorative functions through redox control mediated by NRF2 upregulation and reprogramming of arginine metabolism in liver fibrosis. Taken together, we propose that modulating MDM properties could be a target for antifibrotic strategies.

WED-338
A TNF-producing neutrophil subset drives age-dependent hepatotoxicity

Jin Lee[1], Gen-Sheng Feng[1]. [1]*University of California San Diego, La Jolla, United States*
Email: jil327@ucsd.edu

Background and aims: Cancer therapy in the elderly is particularly challenging due to heightened treatment-associated detrimental effects, which often lead to treatment discontinuation and increased mortality. The mechanisms by which aging contributes to the detrimental effect of cancer therapy remain poorly understood.
Method: To identify age-associated pathogenic factors in an unbiased manner, we performed single-cell RNA sequencing (scRNA-seq) and bulk RNA sequencing on non-parenchymal cells (NPCs) isolated from young (5-month-old) and aged (20-month-old) livers. Immune cell profiling and functional analyses were conducted using flow cytometry, multiplexed antibodies staining, and Luminex cytokine/chemokine assays. Fundamental biochemical assays, as well as gene deletion and cell depletion models were performed *in vivo* and *ex vivo* to investigate underlying mechanisms.
Results: We recently found that a synthetic double-stranded RNA (dsRNA), poly-inosinic:cytidylic acid (polyIC) that induces interferons (IFNs) and inflammatory response, effectively suppressed liver cancer in multiple murine models when administered to young mice, especially in combination with anti-PD-L1 antibody. Given that the majority of liver cancer patients are over 60 years of age, we evaluated the anti-tumor effect of polyIC in aged mice. Surprisingly, old mice, with or without liver tumors, died suddenly with massive liver necrosis following polyIC administration at doses well tolerated by young mice. We found no evidence implicating IFNs in mediating this toxic effect. However, single-cell and functional analyses unearthed a $CD14^+$ neutrophil subset featured by robust TNFα induction by polyIC exclusively in the aged liver. Impaired NR3C1 expression and elevated NF-κB and AP-1 signaling drive a skewing toward Tnf^+over $Saa1^+$ neutrophils in the aged liver. TNF neutralization rescued polyIC-induced mortality, while also enhancing its antitumor effect in aged mice. Bioinformatic analysis revealed significant association of a Tnf^+Saa1^- neutrophil gene signature with reduced survival in liver cancer patients over 60.
Conclusion: This study uncovers a previously unknown detrimental mechanism in the aged liver, which is undetectable under basal conditions. We provide a new strategy to improve therapeutic outcomes in elderly patients by mitigating treatment-associated toxicity.

WED-339
Lactate triggers HBV-Specific CD8+ T cell exhaustion through mitophagy suppression-mediated mitochondrial dysfunction

Zhipeng Liu[1], Yuhao Wang[1], Xiaoyi Liu[1], Libo Tang[1], Yongyin Li[1]. [1]*Department of Infectious Diseases, Nanfang Hospital, Southern Medical University, Key Laboratory of Infectious Diseases Research in South China (Southern Medical University), State Key Laboratory of Multi-organ Injury Prevention and Treatment, GuangZhou, China*
Email: yongyinli@foxmail.com

Background and aims: Hepatitis B virus (HBV) -specific T cells exhibit an exhausted phenotype associated with glycolytic metabolic disruption and perturbation of mitochondrial homeostasis. However, their relationship and underlying mechanisms remain elusive. Since lactate, a key glycolytic metabolite that can modulate immune

response, we investigated its role in HBV-specific T cell dysfunction during chronic HBV infection.
Method: We recruited 242 patients with chronic HBV infection and 78 health controls. The metabolic characteristics of peripheral blood mononuclear cells (PBMC) were comprehensively analyzed using RNA-seq, metabonomics and scRNA-seq. Additionally, we systematically evaluated the glucose uptake, mitochondrial function, autophagy flux, and mitophagy activity of HBV-specific $CD8^+$ T cells using flow cytometry from both PBMC and liver mononuclear cells (LMC). To investigate lactate-mediated T cell exhaustion, we performed exogenous stimulations with Bay-876, lactate, Oligomycin, and Midivi-1, and assessed through multiparametric cytokine profiling and functional assays.
Results: The glucose metabolic status in PBMC was significantly activated during HBV infection, accompanied by the accumulation of lactate. Specifically, HBV-specific $CD8^+$ T cells exhibited more dramatically increased Glut1 expression and 2-NBDG uptake than global T cells, especially in intrahepatic HBV-specific $CD8^+$ T cells. Restraining glucose uptake via Bay-876 improved HBV-specific T cell function, while lactate accelerated their dysfunction. Mechanistically, lactate elicited aberrant mtROS production and mitochondrial membrane potential via suppressing mitophagy dysfunction. Meanwhile, reversing mitochondrial dysfunction by MitoQ and MitoTempo restored the HBV-specific T cells function. However, aggravating mitophagy impairment by Midivi-1blunted the production of IFN-γ and TNF-α in HBV-specific T cell. Concurrently, dysfunctional autophagy also significantly contributed to HBV-specific T cells dysfunction, but this effect was independent of the lactate-mediated exhaustion pathway.
Conclusion: Lactate drives HBV-specific T cell exhaustion by disrupting mitochondrial function via restraining mitophagy. These results highlight lactate metabolism as a potential therapeutic target for chronic HBV infection.

WED-340-YI
Hepatocyte senescence controls RORγt+ cell populations in the liver and is sensitive to metabolic zonation

Yuxin Li[1], Jake Sherrick[1], Soumyajit Saha[2], Kevin Yiyu Fan[1], Hanan Almakhayitah[1], Nadiya Boyar[1], Kulvinder Gill[1], Daniel Kearns[1], Aekkachai Tuekprakhon[1], Zania Stamataki[1]. *[1]Centre for Liver and Gastrointestinal Research, School of Infection and Immunology, University of Birmingham, Birmingham, United Kingdom, National Institute for Health and Care Research (NIHR), Birmingham Biomedical Research Centre (BRC), BIRMINGHAM, United Kingdom; [2]London School of Hygiene and Tropical Medicine, Keppel Street, London, United Kingdom, Norwich Medical School, University of East Anglia, Norwich, United Kingdom, London, United Kingdom*
Email: yxl1800@student.bham.ac.uk

Background and aims: Hepatocyte senescence is a hallmark of chronic liver disease and ageing, contributing to inflammation, fibrosis and impaired regeneration through alterations of the hepatic microenvironment. Senescence-associated secretory phenotypes (SASPs), including IL-1β, IL-6 and TGF-β, promote differentiation of $ROR\gamma t^+$ T cells which drive liver inflammation, fibrosis and tissue repair. We recently discovered that live $ROR\gamma t^+$ cells were engulfed by enclysis in human livers. We hypothesised that senescence-associated inflammatory mediators enhance enclysis to control pathogenic $ROR\gamma t^+$ cell populations in liver disease, and explored the role of hepatic lipids.
Method: Hepatocyte senescence was induced in Huh-7 cells using doxorubicin, with cell cycle arrest confirmed by p21 immunofluorescence. Enclysis was quantified by high-content imaging (n = 6). Intracellular lipid and cholesterol accumulation were assessed by BODIPY and filipin staining. The effects of SASP cytokines (IL-1β, IL-6, IL-8 and TGF-β) and cholesterol on enclysis were tested in vitro. Cholesterol synthesis was inhibited using atorvastatin. Enclysis of $ROR\gamma t^+$ cells was analysed in non-cirrhotic and cirrhotic human liver tissues (n = 60) using digital histopathology and spatial QuPath algorithms to define metabolically distinct liver zones.
Results: Senescent $p21^+$ hepatocytes showed increased enclysis and secreted factors that also influenced neighbouring $p21^-$ cells. SASPs IL1-β and IL-8 increased enclysis, but IL-6 and TGF-β did not. Senescent hepatocytes accumulated intracellular lipids and cholesterol, as demonstrated by increased BODIPY and filipin staining. Cholesterol loading enhanced enclysis, while atorvastatin reversed the senescence-associated, cholesterol-dependent increase in enclysis and reduced T-cell engulfment. Enclysis of $ROR\gamma t^+$ cells was increased in autoimmune, viral and metabolic liver disease compared with healthy liver, and was spatially enriched in the mid-lobular zone associated with regeneration.
Conclusion: Hepatocyte senescence drives enclysis through IL-1β/IL-8 signalling and cholesterol accumulation, linking metabolic rewiring to immune regulation in the diseased liver. Spatially enriched enclysis within the mid-lobular zone limits $ROR\gamma t^+$ cell expansion and may restrain inflammation while preserving regenerative capacity. These findings highlight cholesterol-dependent enclysis as a novel therapeutic axis for senotherapeutic and lipid-targeting strategies in chronic liver disease.

WED-341
Decoupling of monocyte subset expansion and immune competence in hepatitis B–related acute-on-chronic liver failure

Xiaoqin Liu[1], Jingmao Yang[2], Yunyun Wang[1], Ruicong Chen[1], Mingqin Lu[1]. *[1]Department of Infectious Diseases, The First Affiliated Hospital of Wenzhou Medical University, Wenzhou, China; [2]Department of Gastroenterology, The First Affiliated Hospital of Wenzhou Medical University, Wenzhou, China*
Email: lizwondering@sina.com

Background and aims: Hepatitis B–related acute-on-chronic liver failure (HBV-ACLF) is characterized by intense systemic inflammation and high susceptibility to bacterial infection, suggesting profound immune dysfunction. Monocytes are central to antigen presentation and innate pathogen sensing, yet how monocyte subset remodeling relates to immune competence in HBV-ACLF remains unclear. We aimed to characterize global and subset-specific monocyte functional alterations and to determine whether changes in monocyte composition are coupled or decoupled from immune function.
Method: Peripheral blood monocytes from patients with HBV-ACLF (n = 67), chronic hepatitis B, and healthy controls were analyzed by multiparameter flow cytometry. Monocyte subsets were defined by CD14 and CD16 expression. Antigen presentation and pathogen sensing were assessed using human leukocyte antigen–DR (HLA-DR) and Toll-like receptor 4 (TLR4) as primary markers, together with additional immunoregulatory markers including triggering receptor expressed on myeloid cells 2 (TREM2). Analyses were performed according to bacterial infection status and longitudinal disease trajectories based on the Model for End-Stage Liver Disease (MELD) score changes.
Results: HBV-ACLF was associated with marked monocyte functional remodeling. Expression of HLA-DR and TLR4 was progressively reduced from controls to chronic hepatitis B and further to HBV-ACLF, indicating impaired antigen presentation and pathogen sensing (all $p < 0.0001$). In contrast, immunoregulatory markers, including TREM2, were significantly increased ($p < 0.0001$). Intermediate monocytes were markedly expanded in HBV-ACLF ($p < 0.0001$). Regulatory and repair-associated markers tracked with subset expansion, whereas host-defense functions showed an inverse relationship. Despite numerical expansion, HLA-DR and TLR4 expression remained markedly reduced in specific subsets ($p < 0.01$), demonstrating a decoupling between monocyte composition and immune competence. Bacterial infection and disease deterioration further amplified this decoupling, while partial recovery was observed in patients with improving disease course.

Conclusion: HBV-ACLF is characterized by structured and dynamic monocyte immune remodeling, in which subset expansion selectively reinforces immunoregulatory programs while essential host-defense functions are functionally exhausted. This composition–function decoupling provides a mechanistic framework for immune imbalance and susceptibility to infection in HBV-ACLF.

WED-345

PD-1+ follicular helper T cells as the key discriminator: a combined model with plasmablasts for distinguishing autoimmune hepatitis from drug-induced liver injury

Zikun Ma[1], Yuhong Suo[1], Yao Meng[1], Yubo Zhong[1], Tiantian Guo[1], Mengmeng Zhang[1], Min Li[1], Xu Fan[1], Xinyan Zhao[1]. [1]*Liver Research Center, Beijing Friendship Hospital, Capital Medical University, State Key Laboratory of Digestive Health, National Clinical Research Center of Digestive Disease, Beijing, China*
Email: mazikun0114@163.com

Background and aims: Non-invasive differentiation of autoimmune hepatitis (AIH) from drug-induced liver injury (DILI) remains clinically challenging. We aimed to identify specific circulating T/B-cell subsets for distinguishing AIH from DILI.
Method: This prospective case-control study (Beijing Friendship Hospital, 2024–2025) focused on treatment-naive AIH and DILI patients. Diagnostic gold standard was based on clinicopathological data, and treatment response. Fresh peripheral blood was collected for flow cytometric analysis of T/B lymphocyte subsets. Least absolute shrinkage and selection operator (LASSO) and multivariate logistic regression selected predictors for final models. Diagnostic performance was assessed via area under the curve (AUC), calibration curves, decision curves, bootstrapping, and DeLong's test. SHapley Additive exPlanations (SHAP) values quantified each predictors' contribution.
Results: A total of 158 patients (86 with AIH and 72 with DILI), as well as 41 healthy controls (HC), were included, matched for age and sex. Most patients were women (121, 77%), median age 52 (42–61) years. AIH and DILI differed significantly (all $P < 0.001$) in serum transaminases, bilirubin, and immunological G levels. Circulating programmed death (PD)-1^+ follicular helper T (Tfh) cells [7% (5–8) vs. 3% (3–3) vs. 4% (4–4)] and plasmablasts [14% (5–29) vs. 2% (1–4) vs. 2% (1–4)] were significantly elevated in AIH vs. DILI and HC (all $P <$ 0.001). LASSO and multivariate logistic regression selected PD-1^+Tfh cells [odds ratio (OR) 7×10^{42}, *95%* confidence interval (CI) 2×10^{16}–3×10^{69}, $P = 0.002$] and plasmablasts (OR 1×10^{8}, *95%* CI 2–9×10^{15}, $P = 0.044$) for the final model. This combined model, distinguishing AIH from DILI, achieved an AUC of 0.957 (*95%* CI: 0.929–0.985) with internal validation at 0.956 (*95%* CI: 0.949–0.958), showing good calibration and net benefit. It significantly outperforming PD-1^+ Tfh cells or plasmablasts alone (AUCs 0.957 vs. 0.921vs. 0.859, DeLong's $P < 0.05$). SHAP analysis identified PD-1^+Tfh cells (SHAP: 0.273) as the most influential contributor, outweighing plasmablasts (SHAP: 0.150).
Conclusion: Combining the PD-1^+ Tfh cells with plasmablasts in a logistic regression model provides an accurate, clinically applicable, minimally invasive tool to distinguish AIH from DILI. SHAP values highlighted the importance of PD-1^+ Tfh cells as the strongest positive discriminator for AIH vs. DILI.

WED-346

Single-cell profiling reveals altered natural killer cell composition and transcriptional programs in MASLD-related HCC

Barbara Oliviero[1], Emma Busarello[2], Alessia La Gaipa[1], Marcello Maestri[1], Salvatore Corallo[3], HCC Multidisciplinary Team[1], Toma Tebaldi[2], Mario Umberto Mondelli[1], Stefania Mantovani[1]. [1]*Fondazione IRCCS Policlinico San Matteo, Pavia, Italy;* [2]*University of Trento, Trento, Italy;* [3]*Fondazione IRCCS Policlinico San Matteo, University of Pavia, Pavia, Italy*
Email: s.mantovani@smatteo.pv.it

Background and aims: Liver cancer is a leading cause of cancer death, and its incidence is expected to rise over the next 20 years. Hepatocellular carcinoma (HCC), comprising 85–90% of primary liver cancers, has a poor prognosis. While viral-associated HCC is declining, metabolic dysfunction-associated steatotic liver disease (MASLD)-related HCC is increasing, and the role of NK cells in this context remains poorly understood.
Method: Surgically resected non-MASLD-HCC (n = 7) and MASLD-HCC (n = 6) and matched non-tumor liver tissues were collected from treatment-naïve patients. CD45$^+$ cells were profiled by single-cell RNA sequencing using BD Rhapsody™, and 46,979 high-quality cells were analyzed for differential expression, pathway enrichment, and cell–cell communication.
Results: Unsupervised clustering and marker gene expression analysis revealed 24 distinct immune cell populations, including three NK cell subsets: one circulating (cC4) and two tissue-resident (trC2, trC14). Total NK cells were reduced in tumors compared to liver-infiltrating cells, with the greatest decrease observed in trC2 cells, independent of HCC etiology. Tumor-infiltrating NK-cell subset transcriptional profiles differed between MASLD- and non–MASLD-HCC. In MASLD-HCC, cC4 cells displayed altered immune regulatory pathways and upregulation of lipid-related metabolic pathways, suggesting adaptation to a lipid-rich microenvironment. In the same context, TrC2 and trC14 cells showed downregulation of pathways related to NK activation, cytotoxicity, neutrophil activation, and T cell signaling, alongside enrichment of inflammatory and metabolic pathways. CellChat analysis revealed altered cell–cell interactions in MASLD-HCC, with cC4 showing the strongest reduction in incoming and outgoing signaling, while trC2 displayed high communication activity. TrC2 displayed increased interactions with macrophages, CD8$^+$ T cells, and proliferating cells, reduced interactions with MAIT and mast cells, and enhanced signaling through FASLG, CADM, ICAM, and TRAIL pathways.
Conclusion: All tumor NK cell subsets derived from MASLD-HCC upregulated lipid-related pathways, whereas only tissue-resident NK cells downregulated pathways associated with neutrophil activation and NK cell cytotoxicity. These findings indicate that all three NK cell subsets in MASLD-HCC exhibit metabolic and functional alterations, though the specific changes differ among the clusters, collectively contributing to a less cytotoxic phenotype and potentially impaired anti-tumor immunity.

WED-347

Lessons from single-cell transcriptomics in chronic hepatitis B: refinement without redefinition

Akhilesh Mulay[1], James Cai[1], Jantarika Arora[1], Gerard Hernandez-Mir[1], Patrick Kennedy[1,2], Upkar Gill[1,2]. [1]*Centre for Immunobiology & Infection, The Blizard Institute, Barts and The London Faculty of Medicine & Dentistry, Queen Mary University of London, London, United Kingdom;* [2]*Department of Hepatology, Barts Health NHS Trust, London, United Kingdom*
Email: u.gill@qmul.ac.uk

Background and aims: Single-cell RNA sequencing (scRNA-seq) is increasingly applied to chronic hepatitis B (CHB) cohorts to characterise immune dysfunction and identify pathways relevant to hepatitis B virus (HBV) cure. Although many core aspects of HBV immunopathology were recognised before scRNA-seq, it has enabled higher-resolution characterisation of intrahepatic immune states and interactions; but its incremental translational contribution to cure-directed advances in CHB warrants critical evaluation.
Method: MEDLINE was searched via PubMed using a predefined strategy identifying human studies applying scRNA-seq to CHB. Of 221 records identified, 42 underwent full-text review, with 26 included. Data were extracted using a structured proforma, including sequencing platform, tissue source, immune populations analysed, disease phase, treatment status, and links to HBV cure.

Results: Twenty-six studies applied scRNA-seq to CHB, predominantly using microfluidic droplet-based platforms, with sampling from blood and intrahepatic tissue. Capture of neutrophils and liver parenchymal cells were limited due to dissociation protocols and cell fragility. Although innate populations were studied less frequently than adaptive cells, scRNA-seq verified innate dysfunction contributes to impaired adaptive immunity. Specific macrophage and NK cell subsets, including FCGR3A+ macrophages, were implicated in immunoregulatory and inflammatory pathways, while functional cure was associated with enrichment of immune-active innate populations, including neutrophils, Kupffer cells, and liver-resident NK cells with enhanced effector activity. Adaptive immune findings reinforced existing paradigms of dysfunctional, largely non-HBV-specific liver-resident CD8 T cells, Treg expansion and impaired B-cell maturation. Recovery-associated populations, including IL-2 linked cytotoxic CD4 T cells and attenuated HBV polymerase-specific CD8 T cells, provided mechanistic context for the limited efficacy of checkpoint-based strategies in CHB. Across studies, small sample sizes, heterogeneous cohorts, limited HBV-specific profiling, and infrequent functional validation constrained generalisability.
Conclusion: In CHB, scRNA-seq refines rather than transforms concepts of immune dysfunction, defining liver-resident immune states and cure-associated innate-adaptive networks, enabling dataset reuse. Progress toward functional cure requires strategic, sustainable application of scRNA-seq with longitudinal sampling and validation to aid HBV cure.

WED-348

Impaired vaccine-induced adaptive immunity cross-reactive to emerging influenza viruses in chronic liver diseases

Lisa-Marie Müller[1,2], Wasihun Hailemichael[1,2], David Reeg[1,3], Kevin Ciminski[4], Peter Reuther[4], Martin Schwemmle[4], Robert Thimme[1], Maike Hofmann[1], Hendrik Luxenburger[1].
[1]University Medical Center Freiburg, Department of internal medicine II, Freiburg im Breisgau, Germany; [2]University Freiburg, Faculty of biology, Freiburg im Breisgau, Germany; [3]University Freiburg, Faculty of medicine, Freiburg im Breisgau, Germany; [4]University Medical Center Freiburg, Institute of Virology, Freiburg im Breisgau, Germany
Email: lisa-marie.noll@uniklinik-freiburg.de

Background and aims: Patients with chronic liver disease frequently exhibit immune dysregulation and increased susceptibility to infections, including influenza virus. Vaccination is a key preventive strategy, particularly for influenza A virus due to its seasonal circulation and pandemic potential. The emergence of highly pathogenic avian influenza (HPAI) viruses has raised concerns regarding protection in vulnerable populations. An open question is whether seasonal influenza vaccination induces cross-reactive immunity against emerging strains. This study aimed to assess adaptive cross-reactive immune responses to avian influenza following seasonal influenza vaccination in patients with chronic liver disease compared with healthy individuals.
Method: Patients with liver cirrhosis (n = 6), liver transplant recipients (LTR, n = 13), and healthy controls (< 60 years, n = 10; > 60 years, n = 6) were vaccinated with a seasonal influenza vaccine lacking H5. Peripheral blood mononuclear cells (PBMC) and serum were collected 120–180 days post-vaccination. PBMCs were stimulated with overlapping peptide (OLP) pools spanning the H5 protein of A/Astrakhan/3212/2020. H5-specific $CD4^+$ and $CD8^+$ T cell responses were analyzed by intracellular cytokine staining. Neutralizing antibodies were measured by plaque reduction neutralization test.
Results: H5-specific $CD8^+$ T cell responses were rare and of low magnitude in all cohorts. H5-reactive $CD4^+$ T cell responses were detectable in LTR and cirrhotic patients, but epitope breadth was significantly reduced in LTR compared with age-matched healthy controls ($p = 0.004$). The breadth of polyfunctional IL-2^+TNF$^+$ $CD4^+$ T cell responses was reduced in LTR ($p < 0.001$) and cirrhotic patients ($p = 0.0011$), with reduced magnitude and functionality in selected OLP pools. Neutralizing antibody titers against seasonal H1 and avian H5 were comparable across cohorts, with high H1- and low H5-specific titers.
Conclusion: Seasonal influenza vaccination induces only limited cross-reactive adaptive immunity to avian influenza in patients with chronic liver disease. Although humoral responses were comparable to healthy individuals, low H5-specific antibody titers indicate that cross-reactivity is mainly mediated by $CD4^+$ T cells. However, in LTR and cirrhotic patients, these responses show reduced breadth and functional strength, suggesting limited protection against emerging high-risk influenza strains and emphasizing the need for targeted pandemic preparedness strategies in this vulnerable group.

WED-349

Retinoic acid signaling in hepatic stellate cells orchestrates plasmacytoid dendritic cell recruitment and immune tolerance: implications for cholestatic liver injury

Nobuhiro Nakamoto[1], Yuzo Koda[1], Akihisa Ueno[2], Kentaro Miyamoto[1], Toshiaki Teratani[1], Ryosuke Kasuga[1], Yukie Nakadai[1], Haruka Okada[1], Nobuhito Taniki[1], Keisuke Ojiro[1], Takanori Kanai[1]. *[1]Division of Gastroenterology and Hepatology, Keio University School of Medicine, Tokyo, Japan; [2]Department of Pathology, Keio University School of Medicine, Tokyo, Japan*
Email: nobuhiro.z2@keio.jp

Background and aims: Plasmacytoid dendritic cells (pDCs) are enriched in the steady-state liver and exert immunosuppressive functions beyond their antiviral roles. However, the mechanisms regulating hepatic pDC accumulation remain unclear. Hepatic stellate cells (HSCs) store vitamin A and regulate retinoic acid (RA) metabolism, but upon activation they lose vitamin A–containing lipid droplets and exhibit impaired RA responsiveness. This study aimed to investigate the role of RA signaling in HSCs in hepatic pDC recruitment and liver disease pathogenesis.
Method: pDC dynamics were analyzed in murine models under physiological and pathological conditions. Single-cell RNA sequencing, and immunohistochemistry were used to identify chemokine sources and spatial relationships. Cell-specific CXCL12 knockout mice were generated to define the contribution of HSC-derived CXCL12. Functional relevance was examined using the 3,5-diethoxycarbonyl-1,4-dihydrocollidine (DDC) cholestatic liver injury model. Clinical relevance was assessed by serum vitamin A levels and intrahepatic pDCs in patients with primary sclerosing cholangitis (PSC).
Results: RA signaling was essential for hepatic pDC maintenance; vitamin A deficiency (VAD) or RA receptor inhibition reduced hepatic pDCs, whereas RA administration increased pDC abundance in the liver. Single-cell transcriptomic analyses identified HSCs as the dominant source of CXCL12, which was further enhanced by RA. RA treatment promoted spatial co-localization of Desmin-positive HSCs and pDCs in vivo, and HSC-derived CXCL12 promoted pDC migration via the CXCL12–CXCR4 axis, as confirmed by in vitro chemotaxis assays. HSC-specific CXCL12 depletion abolished both basal and RA-induced pDC accumulation, whereas hepatocyte-specific depletion had a lesser effect. In the DDC model, HSC activation was accompanied by reduced CXCL12 expression and decreased hepatic pDC abundance. RA supplementation partially restored pDCs and ameliorated liver injury, whereas pDC depletion exacerbated disease with reduced regulatory T cells and increased pro-inflammatory immune populations. In human PSC, advanced disease was associated with reduced serum vitamin A levels and loss of portal BDCA-2–positive pDCs.
Conclusion: RA signaling in HSCs induces CXCL12, orchestrating hepatic pDC recruitment and immune tolerance. Disruption of this pathway contributes to cholestatic liver injury, while restoring RA signaling or HSC-derived CXCL12 may offer a therapeutic strategy for chronic cholestatic liver diseases.

WED-350

Soluble liver antigen (SLA)-specific CD4+ T cells phenotypes in the blood of patients with autoimmune hepatitis (AIH) correlate with the clinical situation

Carina Saggau[1], Philipp Hofmann[2], Yang Xu[3], Nicola Gagliani[3], Johannes Herkel[3], Petra Bacher[2], Johannes Hartl[3], Rainer Günther[4], Alexander Scheffold[1]. [1]*Institute of Biotechnology, Technical University Berlin, Berlin, Germany;* [2]*Institute of Medical Immunology, University Hospital Schleswig-Holstein & Christian-Albrechts University Kiel, Kiel, Germany;* [3]*University Medical Center Hamburg-Eppendorf, Hamburg, Germany;* [4]*Division of Hepatology/Transplant Hepatology, UKSH, Campus Kiel, Kiel, Germany*
Email: Carina.Saggau@uksh.de

Background and aims: Anti-SLA autoantibodies represent the only disease-specific autoantibodies in AIH and are associated with reduced overall survival. However, the autoreactive SLA-specific $CD4^+$ T helper (Th) cells that orchestrate autoantibody production and drive the pathogenic immune response remain difficult to detect. Consequently, their functional and molecular characteristics, and their precise role in disease pathogenesis, remain poorly defined.
Method: To address this, we used activation-based antigen-reactive T cell enrichment (ARTE) to characterize *ex vivo* SLA-specific CD4+ Th cells isolated from the blood of patients and healthy controls. We performed multiparameter cytometric characterization, single cell RNA-sequencing and re-expression of autoreactive T cell receptors (TCRs) to confirm specificity and identify peptide/HLA class II recognition. Furthermore, we performed single cell RNA-sequencing of SLA-reactive T cells from the blood and the entire CD4+ T cell compartment from paired liver biopsies enabling tracking of autoantigen-specific T cells in the tissue.
Results: Compared to healthy donors, autoreactive memory Th cells were highly increased in the blood of SLA-antibody-positive AIH patients. These cells exhibited a phenotypically altered, yet heterogenous T cell profile. Exhaustion-associated co-inhibitory receptors were significantly elevated and were co-expressed with variable amounts of FOXP3. The cytokine profile (e.g. expression of IL-21, IFN-g) of SLA-reactive T cells in the blood of AIH patients indicated a TpH phenotype. Thus, T cell responses in AIH patients could be clearly distinguished phenotypically from those of healthy donors, and the heterogeneity within the AIH patient cohort correlated with the individual clinical status (e.g. active disease vs remission, mild disease vs severe course). Paired patient samples were used to track SLA-specific TCRs from the blood and identified by ARTE in scRNA & TCRSeq data from liver tissue-derived memory CD4 T cells. The autoreactive T cells were enriched 10- to 100-fold in tissue versus blood reflecting the respective phenotype of SLA-specific T cells in the blood.
Conclusion: Our data suggest that SLA-specific T cells play a central role in AIH pathogenesis, including the generation of SLA-specific antibodies, and that it is possible to clinically stratify patients based on autoreactive T cell phenotyping. This may help to improve monitoring of treatment response and may define novel autoantigen-specific therapeutic strategies.

WED-351

Using immunohistochemistry to determine the enclysis of T cells in cholestatic and viral liver diseases

Soumyajit Saha[1,2], Yuxin Li[3,4], Kevin Yiyu Fan[3,4], Hanan Almakhayitah[3,4], Aekkachai Tuekprakhon[3,4], Zania Stamataki[3,4]. [1]*London School of Hygiene and Tropical Medicine, London, United Kingdom;* [2]*University of East Anglia, Norwich, United Kingdom;* [3]*Centre for Liver and Gastrointestinal Research, School of Infection and Immunology, University of Birmingham, Birmingham, United Kingdom, Birmingham, United Kingdom;* [4]*National Institute for Health and Care Research (NIHR), Birmingham Biomedical Research Centre (BRC), Birmingham, United Kingdom*
Email: soumyajit2349s@gmail.com

Background and aims: Hepatocytes engulf live $CD4^+$ cells in a process called enclysis. The $CD4^+$ cells can be seen inside hepatocytes. Enclysis has been reported for $Foxp3^+$ cells which are killed inside the hepatocyte and $Tbet^+$ cells which are not killed, but enclysis in $ROR\gamma t^+$ cells has not been investigated, despite their association with pathology. Here, $ROR\gamma t^+$ cells found inside hepatocytes were investigated in primary biliary and primary sclerosing cholangitis, and hepatitis C and B infection. This can improve our understanding of liver disease and may lead to development of better prognostic and therapeutic methods.
Method: RORγt was detected in liver sections by immunohistochemistry. Using QuPath software, the liver tissue was divided into anatomic regions — periportal, midlobular and perifibrous. QuPath's cell detection system was used to distinguish hepatocytes and non-hepatocytes. RORγt was expected to be seen in the latter. Whether a cell was $ROR\gamma t^+$ was determined using the mean optical density of the stain. The number of $ROR\gamma t^+$ cells which were inside and outside hepatocytes was quantified. The proportion of $ROR\gamma t^+$ cells which were inside was compared between anatomic regions of the liver, between disease aetiologies, and between the same anatomic region in different disease aetiologies.
Results: Viral diseases ($n = 22$) had higher proportions of $ROR\gamma t^+$ cells inside hepatocytes than cholestatic diseases ($n = 19$) with the differences being starkest in the midlobular region ($p < 0.01$). Hepatitis B virus infected livers had the highest proportions of $ROR\gamma t^+$ cells inside hepatocytes while primary sclerosing cholangitis livers had the lowest ($p < 0.05$). The midlobular region also had the highest proportion of engulfed $ROR\gamma t^+$ in all diseases ($p < 0.0001$).
Conclusion: The $ROR\gamma t^+$ cells inside hepatocytes were likely enclysed. Previous research showed no difference between $Foxp3^+$ cell enclysis in immune-mediated conditions compared to viral infection. We found greater $ROR\gamma t^+$ cell engulfment in viral infection than cholestatic diseases. There were large differences in $ROR\gamma t^+$ cell enclysis between anatomic regions of the liver and between diseases. This shows that enclysis is sensitive to anatomic regions and disease aetiology and should be studied separately for different T cell subsets. Combining this with existing data on anatomic differences in inflammation in these diseases suggests that the level of enclysis in the midlobular region reduces inflammation, pointing to potential prognostic and therapeutic avenues.

WED-352

Collectin-11 of the lectin pathway mediates complement-dependent hepatic ischemia-reperfusion injury in mice

Tatsuro Sugaya[1,2], Manabu Hayashi[2], Yumi Ishida[1], Takeshi Machida[1], Masayuki Sekimata[3], Hiromasa Ohira[2], Hideharu Sekine[1].
[1]*Department of Immunology, Fukushima Medical University School of Medicine, Fukushima, Japan;* [2]*Department of Gastroenterology, Fukushima Medical University School of Medicine, Fukushima, Japan;* [3]*Radioisotope Research Center, Fukushima Medical University, Fukushima, Japan*
Email: tsugaya@fmu.ac.jp

Background and aims: Hepatic ischemia-reperfusion injury (IRI) is associated with post-liver transplant complications, and its pathogenic mechanism needs to be elucidated. The complement system is an innate immune system that maintains biological homeostasis through the recognition and elimination of foreign pathogens and apoptotic cells, and has been reported to be involved in hepatic IRI. Collectin-11 (CL-11) is a pattern recognition molecule that recognizes terminal L-fucose of glycans on targets and initiates activation of the complement lectin pathway (LP). However, contribution of CL-11 in hepatic IRI is unknown. In this study, we aimed to clarify whether CL-11 is involved in hepatic IRI.
Method: CL-11-deficient ($CL\text{-}11^{-/-}$) mice were generated by CRISPR/Cas9 system. IRI in the liver was induced by 60 minutes segmental hepatic ischemia and 6 hours of reperfusion. Liver injury was assessed by measurement of serum transaminase levels and

histological scoring using Suzuki scoring system. Deposition of complement component 3 (C3) in the liver was evaluated by immunohistochemical (IHC) staining. *In vitro* inhibitory effects of adding various sugars, including L-fucose, added to mouse sera on LP activity were evaluated by a C4 deposition assay measuring C4 deposition levels on mannan-coated plates. *In vivo* inhibitory effect of intraperitoneally administered L-fucose on liver injury in a hepatic IRI-induced model was evaluated by measuring serum transaminase levels and liver histological scores.
Results: In the hepatic IRI-induced model, *CL-11*$^{-/-}$ mice showed significantly lower levels of liver injury compared with wild-type (WT) mice, as assessed by serum transaminase levels and histological scores. IHC staining revealed marked C3 deposition in the liver of WT mice, but almost no deposition was observed in the liver of *CL-11*$^{-/-}$ mice underwent hepatic IRI. A significant reduction of C4 deposition on mannan-coated plate was observed only when L-fucose was added in the serum mixture. In a hepatic IRI-induced model, mice administered with L-fucose had significantly reduced serum transaminase levels and histological severity compared with control mice.
Conclusion: Our results showed that CL-11 is involved in hepatic IRI most likely via activation of the LP in mice, and administration of L-fucose can be a promising therapeutic approach for hepatic IRI.

WED-353-YI
Oxysterol-binding protein-related protein 2 drives sterol accumulation and neutrophil dysfunction in sepsis associated with alcohol related cirrhosis

Gaurav Tripathi[1], Vasundhra Bindal[1], Sushmita Pandey[1], Neha Sharma[1], Manisha Yadav[1], Vipul Sharma[1], Nupur Sharma[1], Babu Mathew[1], Sanju Yadav[1], Yash Magar[1], Meenu Bajpai[1], Shvetank Sharma[1], Rakhi Maiwall[1], Shiv Kumar Sarin[1], Jaswinder Maras[1]. [1]*Institute of Liver & Biliary Sciences, New Delhi, India*
Email: jassi2param@gmail.com

Background and aims: Neutrophil dysfunctionality is a hallmark of sepsis in alcohol related cirrhosis (ARC), characterised by impaired pathogen clearance, yet its underlying mechanisms remain poorly understood.
Method: Untargeted multimomics profiling was performed on neutrophils from healthy controls, non-septic ARC, and septic/septic shock ARC patients. A total of 185 patients were randomized into discovery (n = 150) and validation (n = 35) cohorts. Results were validated using omics, ELISA, neutrophil functionalities, and flow cytometry.
Results: Among 9,115 proteins and 1,414 metabolites identified, 6,488 proteins (FC > 1.5, p < 0.05) and 729 metabolites (FC > 1.5, p < 0.05) were significantly altered in septic ARC patients. Lipid and sterol homeostasis emerged as key dysregulated pathways. Further analysis identified OSBPL2 (FC > 3892, AUC = 0.93) and LDLR (FC > 4.47, AUC = 0.92) as important regulators of neutrophil dysfunction in sepsis. Elevated OSBPL2 expression causes sterol overload with elevated cholesterol (FC > 6), 25-hydroxycholesterol (FC > 500), in sepsis and shock patients, causing them to become foamy in nature. Sterol accumulation induces mitochondrial stress (THEM4 FC > 5, HIF1A FC > 7) with impaired oxidative phosphorylation, ROS elevation, and ER stress (HSPA1A FC > 3, AMFR FC > 189) with disrupted protein folding specifically in sepsis. These neutrophils showed membrane rigidity, impaired vesicular trafficking, leading to defective degranulation via dysregulated KLC1 (FC > 59), STX4 (FC > 15), and ITGB2 (FC > 11, p < 0.05). Increase in oxidative stress and ROS further promoted NETosis, upregulating ALOX5 (FC > 24), PRKCD (FC > 44), and FPR2 (FC > 5). Sterol accumulation also increases expression of anti-apoptotic proteins like BIRC (FC > 15.9, p < 0.01) and decreases expression of proapoptotic proteins like TP53 (FC < –10.3, p < 0.05), thereby increasing the lifespan of these bulky foamy neutrophils. The expression of OSBPL2 was further validated as a predictor of sepsis and foamy neutrophils in an independent cohort, with an AUC > 0.95. Benchamarking against clinical scores such as SOFA, MELD, and others. Validation was conducted using flow cytometry, mass spectrometry, and ELISA.
Conclusion: OSBPL2-positive neutrophils act as lipid reservoirs, causing lipid accumulation and activation of anti-apoptotic signaling, along with increased mitochondrial and ER stress, resulting in a aged foamy neutrophil phenotype in sepsis. This makes OSBPL2 a crucial predictive marker for sepsis and immune exhaustion in neutrophils.

WED-354
Ugonin J suppresses hepatocyte inflammation via GPX2-mediated redox regulation

Li-Yun Wang[1], Chih-Chuang Liaw[2], Yu-Hsuan Tseng[1], Ming-Lun Yeh[3], Ming-Lung Yu[1]. [1]*The Center of Excellence for Metabolic Associated Fatty Liver, National Sun Yat-sen University, Kaohsiung, Taiwan;* [2]*Department of Marine Biotechnology and Resources, National Sun Yat-sen University, Kaohsiung, Taiwan;* [3]*The Center of Excellence for Metabolic Associated Fatty Liver, National Sun Yat-sen University, Kaohsiung Medical University, Kaohsiung, Taiwan*
Email: sindy.wly@gmail.com

Background and aims: Hepatocyte-derived oxidative stress plays a pivotal role in regulating inflammatory signaling and immune crosstalk during metabolic and inflammatory liver diseases. Ugonin J, a bioactive flavonoid, has been reported to exhibit antioxidant properties; however, its role in hepatocyte redox–immune regulation remains unclear. This study aimed to investigate whether Ugonin J modulates hepatocyte inflammatory responses through a GPX2–reactive oxygen species (ROS)–dependent mechanism.
Method: Mouse AML12 hepatocytes and human HepG2 cells were treated with Ugonin J for 24 hours. Cytokine and chemokine profiles were analyzed in conditioned media (AML12) or cell lysates (HepG2) using multiplex immune panels. GPX2 expression and intracellular ROS levels were assessed by qPCR, immunoblotting, and fluorescent ROS assays.
Results: In AML12 hepatocytes, Ugonin J markedly suppressed the secretion of pro-inflammatory cytokines and chemokines, including CCL3, GM-CSF, IL-1β, IL-6, IL-12p40, and TNF-α, indicating a robust anti-inflammatory effect. This was accompanied by induction of GPX2 expression and significant attenuation of intracellular ROS levels. In contrast, HepG2 cell lysates showed increased intracellular levels of several immune-related cytokines following Ugonin J treatment, while the ROS- and NF-κB-dependent chemokine IL-8 was consistently reduced. These findings suggest differential regulation of intracellular immune signaling versus paracrine inflammatory output between normal and transformed hepatocytes.
Conclusion: Ugonin J exerts hepatocyte-protective anti-inflammatory effects by enhancing GPX2-mediated antioxidant capacity and suppressing ROS-driven inflammatory signaling. The distinct responses observed between normal and cancerous hepatocytes highlight a context-dependent redox–immune crosstalk, supporting the therapeutic potential of Ugonin J in inflammation-driven liver diseases.

WED-355
Targeting the STING pathway as a strategy to suppress hepatitis B virus replication

Mingyuan Zhang[1], Xiaomei Wang[1], Hongqin Xu[1], Yanhang Gao[2], Junqi Niu[1]. [1]*Department of Hepatology, Center of Infectious Diseases and Pathogen Biology, The First Hospital of Jilin University, Changchun 130021, China, Jilin Provincial Key Laboratory of Metabolic Liver Diseases, The First Hospital of Jilin University, Jilin University, Changchun 130021, China, China-Singapore Belt and Road Joint Laboratory on Liver Disease Research, The First Hospital of Jilin University, Jilin University, Changchun 130021, China Conflict of Interest, Changchun, China;* [2]*Department of Hepatology, Center of Infectious Diseases and Pathogen Biology, The First Hospital of Jilin University, Changchun 130021, China, Jilin Provincial Key Laboratory of Metabolic Liver Diseases, The First Hospital of Jilin University, Jilin University, Changchun 130021, China,*

China-Singapore Belt and Road Joint Laboratory on Liver Disease Research, The First Hospital of Jilin University, Jilin University, Changchun 130021, China, Changchun, China
Email: junqiniu@jlu.edu.cn

Background and aims: Activation of the host immune system is a promising strategy for treating hepatitis B (HBV). The stimulator of interferon genes (STING) signaling pathway acts as an innate immune sensor for viral DNA. We aimed to determine whether STING activation can inhibit HBV replication in the liver.
Method: We evaluated STING expression in peripheral blood mononuclear cells (PBMCs) and liver biopsy specimens from patients with chronic hepatitis B (CHB). We examined the effect of the STING agonist 5,6-dimethylxanthone-4-acetic acid (DMXAA) on HBV replication and the immune response in a mouse model of HBV infection (rAAV8-HBV1.3). Additionally, we depleted macrophages in vivo to assess their role in DMXAA's antiviral effects.
Results: STING expression in CHB patients was higher in the immune-active phase than in the inactive phase or uninfected healthy controls, suggesting an association between elevated STING expression and immune activation. In a mouse model with persistent HBV replication, repeated DMXAA administration produced dose-dependent reductions in serum HBV DNA, HBsAg, and HBeAg levels, accompanied by an enhanced hepatic immune response. DMXAA treatment significantly enhanced macrophage secretion of interferon-beta (IFN-beta) and interleukin-6 (IL-6) in a dose-dependent manner, highlighting a correlation between STING agonist concentration and the production of these immune mediators. Transcriptome sequencing of liver tissues revealed 856 differentially expressed genes (DEGs) involved in immune-related signaling pathways. In Kupffer cell-deficient mice, DMXAA's ability to inhibit HBV replication was significantly attenuated.
Conclusion: STING pathway activation enhances the immune response against HBV by upregulating the expression of immune-related genes. Hepatic Kupffer cells play an important role in STING-mediated inhibition of HBV replication. Targeting the STING pathway in macrophages represents a promising strategy for inhibiting HBV replication and warrants investigation in future studies.

WED-356
VISTA deficiency exacerbates the development of acute-on-chronic liver failure by promoting Tc1 differentiation
Yao Zhang[1], Xueyun Zhang[1], Yidi Jia[1], Jiajia Han[1], Yuxian Huang[1], Richeng Mao[1], Jiming Zhang[1]. *[1]Shanghai Key Laboratory of Infectious Diseases and Biosafety Emergency Response, National Medical Center for Infectious Diseases, Huashan Hospital, Fudan University, SHANGHAI, China*
Email: youxiang08707@163.com

Background and aims: Acute-on-chronic liver failure (ACLF) has a high early mortality, and there is abundant evidence that persistent inflammatory response and immune activation are the core pathogenesis of ACLF. However, the mechanism of immune disorder has not been fully clarified. Previous studies have shown that deficiency of V-type immunoglobulin domain-containing suppressor of T-cell activation (VISTA) exacerbates the progression of inflammatory diseases. Moreover, the immune response mediated by $CD8^+$T cells can directly cause liver damage and is closely related to the dysregulation of inflammatory response in ACLF patients. Our study was designed to investigate the role of VISTA expression on $CD8^+$T cells in the pathogenesis of ACLF.
Method: We assessed the expression and function of VISTA on $CD8^+$ T cells in blood samples from healthy controls, patients with stable cirrhosis, and ACLF patients. Transcriptome sequencing was performed to determine the relevant pathways, which was then verified by Western blot. Inhibitors of relevant signaling pathways were added to the $CD8^+$ T cells to explore the key signal mechanism.
Results: In ACLF patients, the expression of VISTA was significantly reduced in the $CD8^+$ T cells compared with healthy subjects and stable cirrhosis patients, especially in the effector memory and terminally differentiated effector memory cells with high CD45RA expression subsets. The expression of VISTA on $CD8^+$ T cells was associated with disease severity and prognosis. VISTA downregulation contributed to the activation and proliferation of $CD8^+$ T cells, and enhanced the differentiation of type 1 cytotoxic T cells (Tc1), as well as heightened inflammatory cytokine secretion. This effect was mediated through the activation of the extracellular signal-regulated kinase 1 and 2 (Erk1/2) signaling pathway.
Conclusion: Our study reveals that VISTA downregulation drives ACLF progression by amplifying Tc1-mediated inflammation. This insight not only advances the mechanistic understanding of ACLF pathogenesis but also nominates VISTA as a potential candidate for therapeutic intervention.

Liver transplantation and hepatobiliary surgery – Clinical

TOP-503
Medication adherence and liver transplantation survival: a nationwide cohort study
Ilias Kounis[1], Cyrille Feray[1], Bruno Roche[1], Thomas Breard[1], Antoine Martin[2], Isabelle Boytchev[2], Eric Vibert[1], Audrey Coilly[1], Antoine Meyer[2]. *[1]AP-HP Hôpital Paul-Brousse, Centre Hépato-Biliaire, Villejuif, France; [2]Service de Gastroentérologie, University Hospital of Bicêtre, Assistance Publique-Hôpitaux de Paris, Kremlin Bicêtre, France*
Email: ilias.kounis@aphp.fr

Background and aims: Although the impact of non-adherence to immunosuppressants is well established after kidney transplantation, national-scale data on liver transplantation (LT) remain limited. We aimed to quantify medication adherence after LT and evaluate its association with graft survival.
Method: Using the French National Health Data System (SNDS), we conducted a nationwide cohort study of first-time LT recipients aged >15 years (2010–2022). Adherence was estimated monthly using a time-dependent medication possession ratio (MPR) over a rolling 12-month period. The primary endpoint was graft survival (death/retransplantation), which was analysed using a time-dependent Cox model adjusted for social deprivation, organic and psychiatric comorbidities, liver disease aetiology, and severity indicators.
Results: Among 10,191 LT recipients (median age 55 years, 73.3% male), the mean MPR remained high (85–90%) up to 13 years post-LT. Over a median 6.8-year follow-up, the incidence of death/retransplantation was 4.6 per 100 personyears, rising from 4.2 (MPR≥90%) to 6.5 (MPR<70%). Compared with MPR ≥90%, the adjusted hazard ratios (aHR) for death/retransplantation were 1.14 (MPR 80–90%), 1.39 (70–80%), and 1.64 (<70%) (p-trend<0.001), demonstrating a clear dose–response relationship. Low adherence (<70%) was strongly associated with death (aHR 1.60), retransplantation (aHR 2.26), and biopsy-proven rejection (aHR 3.71) but not with serious infection or severe chronic kidney disease. The excess risk was most pronounced in recipients ≤40 years (aHR 3.47) and those with a low comorbidity burden.
Conclusion: In this nationwide cohort, adherence to maintenance immunosuppression was a major modifiable determinant of long-term graft and patient survival after LT, with no signal for increased infection or nephrotoxicity at higher adherence levels. Systematic adherence monitoring and targeted interventions, particularly for younger and otherwise healthy recipients, should be integrated into routine post-transplant care.

TOP-518

Waitlist outcomes are better and post-transplant outcomes are similar in alcohol associated hepatitis vs. alcohol associated cirrhosis: a UNOS analysis

Mangesh Pagadala[1], Ashwani K. Singal[2], Winston Dunn[3], Robert Wong[4], Patrizia Burra[5], Yong-Fang Kuo[6], Umang Arora[7], Anil Arora[8], Saleh Alqahtani[9]. *[1]Liver Institute Methodist Dallas, Irving, United States; [2]University of Louisville, Louisville, United States; [3]University of Kansas Medical Center, Westwood, United States; [4]Stanford University, Stanford, United States; [5]University of Padua, Padova, Italy; [6]University of texas medical branch galveston, Galveston, United States; [7]Mayo Clinic, Rochester, United States; [8]Sir Ganga Ram Hospital, New Delhi, India; [9]Weill Cornell Medicine, New York, United States*

Email: mangeshpagadala@mhd.com

Background and aims: Alcohol liver disease, including alcohol cirrhosis (AC) and alcohol hepatitis (AH), is the leading indication for liver transplantation (LT). In our previous study (UNOS database), post-LT outcomes in AH were like LT recipients for AC However, data are limited on long-term post-transplant and on waitlist outcomes comparing AH and AC.

Method: Adult LT listings for ALD in the UNOS database (01/2004–03/2025) were stratified to AH and AC indications using UNOS codes. Living donor LT was excluded. Analyses compared AH vs. AC on a) trends on listings and LT; b) 90-day cumulative waitlist (WL) mortality and receipt of LT using competing risk analysis; and c) 10-yr. post-LT graft and patient survival. Propensity score matching (PSM) was performed to balance baseline demographic, clinical, and disease severity variables at listing. Sub-hazard ratios (SHR) and 95% confidence intervals (95% CI) reported for WL outcomes using Fine and Gray models and HR (95% CI) reported outcomes using cox proportional models.

Results: Of 63,025 listings [4168 (6.6%) AH], listings for AH increased from 3.1% in 2004 to 16.1% in 2025. AH vs. AC candidates were younger (45 vs. 53 yrs.) and females (35 vs. 29%), P < 0.001. AH candidates were likely to be obese, on life support and have better functional status despite higher MELD score. Unadjusted cumulative 90-day WLM was lower in AH (13.9 vs. 24.5%) with HR (95% CI) of 0.88 (0.78–0.98), P = 0.019. The 90-d LT probability was higher in AH (76.9% vs 60.3%), 2.53 (2.43–2.63), P < 0.001. In the PSM cohort after matching for demographics and MELD score, 90-d WL mortality was similar comparing AH vs. AC, 0.916 (0.801–1.046), P = 0.195. However, AH candidates had slightly higher probability of 90-d LT, 1.050 (1.003–1.100), P = 0.037. Other predictors for WLM were age, MELD score, hepatic encephalopathy and being on life support at listing. Of 40,902 LT [3233 (7.9%) AH], LT for AH increased from 2.3% to 16.1% between 2004 and 2025. In the PSM cohort, 10-yr. post-LT outcomes were similar in AH compared to AC on graft [88 vs. 82%, Log Rank P = 0.329, 1.09 (0.96–124), P = 0.177] and patient survival [90 vs. 84%, P = 0.988, 1.01 (0.88–1.16), P = 0.873].

Conclusion: Our study shows candidates with AH compared to AC have lower WL mortality, higher probability of LT, and similar long-term post-LT outcomes. These findings support the ongoing LT for AH, while highlighting a need to evaluate equity in organ access for the broader spectrum of patients with alcohol associated liver disease.

TOP-519

Liver transplantation for portal vein tumor thrombus in the immunotherapy era: outcomes and risk stratification in a multi-institutional study

Rebecca Marino[1], Laura Kulik[2], Albert CY Chan[3], CL Chiang[4], Neehar D. Parikh[5], Matthew DeMaio[5], Christian Toso[6], Massimo Leo[7], Fanpu Ji[8], Manon Allaire[9], Eric Vibert[10,11], Ju Dong Yang[12], Mohammad Saeid Rezaee-Zavareh[13], Oliver Scatton[14], Fernando Rotellar[15], Anjana Pillai[16], Elizabeth Aby[17], Jun Li[18], Sander Florman[1], Neil Mehta[19], Parissa Tabrizian[1]. *[1]Liver Transplant and Hepatobiliary Surgery, Recanati/Miller Transplantation Institute, Icahn School of Medicine at Mount Sinai, New York, United States; [2]Division of Gastroenterology and Hepatology, Department of Medicine, Northwestern University, Chicago, United States; [3]Liver Transplant Center, Queen Mary Hospital, Department of Surgery, The University of Hong Kong, Hong Kong, Hong Kong; [4]Department of Clinical Oncology, The University of Hong Kong, Hong Kong, Hong Kong; [5]Division of Gastroenterology and Hepatology, University of Michigan, Ann Arbor, United States; [6]Hôpitaux universitaires de Genève (HUG), Division of Digestive Surgery, Genève, Switzerland; [7]Hôpitaux universitaires de Genève, Service de gastroentérologie et hépatologie, Genève, Switzerland; [8]Department of Hepatology, Xi'an Jiaotong University Second Affiliated Hospital, Xi'an, China; [9]Service d'Hépato-gastroentérologie, AP-HP Sorbonne Université, Hôpital Universitaire Pitié-Salpêtrière, Paris, France; [10]Centre Hépato-Biliaire, Hôpital Paul Brousse, Paris, France; [11]AP-HP, Centre Hépato-Biliaire, VILLEJUIF, France; [12]Division of Digestive and Liver Diseases, Cedars-Sinai Medical Center, Los Angeles, United States; [13]Middle East Liver Diseases Center, Tehran, Iran; [14]Service de Chirurgie Hépato-biliaire et Transplantation Hépatique, Hôpital Pitié-Salpêtrière, Paris, France; [15]HPB and Liver Transplant Unit, University of Navarra, Pamplona, Spain; [16]Department of Medicine, University of Chicago, Chicago, United States; [17]Division of Gastroenterology, Hepatology, and Nutrition, University of Minnesota, Minneapolis, United States; [18]Shanghai Jiahui International Hospital, Shanghai, China; [19]Division of Gastroenterology and Hepatology, University of California San Francisco, San Francisco, United States*

Email: parissa.tabrizian@mountsinai.org

Background and aims: Downstaging selected patients with HCC and PVTT can achieve acceptable post-transplant survival, challenging prior dogma. The impact of immune checkpoint inhibitors (ICI) on transplant outcomes in PVTT remains unclear. This study aims to evaluate post-transplant outcomes in the immunotherapy era, define risk stratification, and guide liver transplant selection in PVTT.

Method: We retrospectively analyzed 57 patients with HCC and PVTT listed for transplantation across 13 international centers. Patients were grouped into ICI + LT (n = 22), LT without prior ICI (n = 23), and ICI without LT (n = 12, including 7 waitlist dropouts). Multivariable Cox regression identified independent predictors of 1- and 3-year survival, which were used for risk stratification. OS and DFS were evaluated using Kaplan–Meier analyses across cohorts and risk-based subgroups.

Results: Compared with LT alone, ICI + LT was associated with higher radiographic response rates (CR/PR: 90.9% vs 69.5%, p = 0.022) and longer waitlist time (7.5 vs 1.5 months, p = 0.005). At transplant, the ICI cohort had more favorable tumor features, including lower total tumor diameter (2.0 vs 3.5 cm, p = 0.01), reduced PVTT burden (Vp3–Vp4: 4.5% vs 39.1%, p = 0.02), and lower AFP (AFP<20 ng/mL: 63.6% vs 30.4%, p = 0.035). Three-year OS was comparable between ICI + LT and LT-alone groups (75.6% vs 65.9%, p = 0.302). On multivariable analysis, combined LRT + ICI (HR 0.42,CI 0.26–0.54, p < 0.001), radiographic response (HR 0.22,CI 0.14–0.55, p < 0.001), AFP reduction ≥ 50% (HR 0.62,CI 0.40–0.85, p = 0.016), and meeting Milan criteria at LT (HR 0.19,CI 0.13–0.58, p < 0.001) improved OS, whereas waitlist time ≤ 3 months and Vp3–Vp4 were associated with worse survival (p < 0.001). High-risk patients (no combined therapy, no radiographic or AFP response, no downstaging, waitlist time ≤ 3 months, Vp3–Vp4) derived benefit from ICI + LT versus LT alone (2-year OS: 58.3% vs 38.1%, p = 0.045; DFS: 60.0% vs 33.3%, p = 0.021). Among ICI-treated recipients, LRT conferred additional benefit (2-year OS: ICI alone 55.6% vs ICI + LRT 85.7%, p = 0.043). Mild rejection occurred in 2/22 patients (9.1%) receiving ICI.

Conclusion: In the largest multi-institutional study, selected patients with HCC and PVTT achieved excellent post-transplant survival. In high-risk PVTT, ICI-based therapy—particularly combined LRT + ICI—significantly improved oncologic outcomes, highlighting tumor biology as a key determinant for candidate selection and immunotherapy use in PVTT transplant pathways.

TOP-520-YI

Rejection-associated transcripts distinguish between different types of rejection after liver transplantation

Alejandro Campos-Murguia[1], Richard Taubert[1], Bastian Engel[1], Sophia Heinrich[1], Björn Hartleben[1], Friederike Dellbrügge[1], Fabian Dranicki[1], Luise Gatzweiler[1], Milad Ghahraman[1], Sinan Yilmaz[1], Heiner Wedemeyer[1]. [1]*Hannover Medical School, Hannover, Germany*
Email: taubert.richard@mh-hannover.de

Background and aims: Long-term outcomes after liver transplantation (LT) are largely determined by the chronic side effects of immunosuppression. Accurate assessment of the graft alloimmune status may enable more individualized immunosuppressive management. Rejection-associated transcripts offer the potential to improve the identification and classification of rejection phenotypes. The relevance of antibody-mediated rejection (AMR) after LT has recently been confirmed by reports on liver cirrhosis progression in 40–50% of AMR cases, despite not relevant liver enzyme elevation and independent from the presence of donor-specific antibodies (DSA). The identification of a unique molecular signature using bulk RNA sequencing confirmed involvement of similar pathways after LT. The aim of this study was to validate a selected gene set using high-throughput quantitative PCR (qPCR) as a targeted and clinically applicable approach to distinguish AMR from other forms of graft injury.
Method: Expression of a 91-gene panel, selected based on previously reported genes uniquely associated with TCMR and AMR, was quantified using high-throughput quantitative PCR. Univariate and multivariate analyses, as well as least absolute shrinkage and selection operator (LASSO) regression, were performed to identify genes discriminating between different types of rejection.
Results: A total of 226 liver biopsies obtained after LT between 2018 and 2022 were included, comprising both surveillance and indication biopsies. Of these, 17 showed clinical TCMR, 31 subclinical TCMR, 21 AMR histology without detectable DSA, and 6 AMR with positive DSA. Additionally, 41 biopsies showed no type of inflammation, and 110 biopsies had other diagnoses not included in the aforementioned categories, 71 of the 91 genes demonstrated statistically significant differential expression across groups. Distinct gene expression signatures discriminating TCMR from AMR were identified in both univariate and multivariate analyses adjusted for age, sex, and time after LT. AMR cases with and without DSA exhibited similar molecular patterns. LASSO analysis identified a subset of 31 genes with high discriminatory power for different rejection phenotypes.
Conclusion: This study validates the presence of a distinct molecular signature characterizing AMR as a separate rejection entity after LT even in the absence of DSA. The prognostic value of these high throughput qPCR transcript set is currently under investigation.

FRI-447

Fenofibrate is associated with improvement in chronic cholangiopathy after liver transplantation: a single-center experience

Fredrik Åberg[1], Johanna Savikko[1], Eija Tukiainen[1], Ville Sallinen[1], Aki Uutela[1], Ines Beilmann-Lehtonen[1], Marko Vannas[1], Tea Kontio[1], Arno Nordin[1]. [1]*Helsinki University Hospital and University of Helsinki, Helsingfors, Finland*
Email: fredrik.aberg@helsinki.fi

Background and aims: Non-anastomotic biliary stricturing (NAS; cholangiopathy) after liver transplantation (LT) is a major complication with limited treatment options. Fenofibrate has shown benefit in early-onset ischemic cholangiopathy related to donation after circulatory death LT. We report our single-center experience using fenofibrate for refractory, long-standing NAS following donation after brain death LT.
Method: In 2023–2025, 18 LT recipients (mean age 53 years, 61% men, 50% PSC, 28% re-LT) with progressive symptomatic NAS despite ERC, UDCA ± antibiotic prophylaxis were started on fenofibrate 145 mg OD (dose reduced in renal dysfunction). This was a retrospective within-subject pre–post study with repeated measures and up to 12-month post-fibrate follow-up. Biochemical response was defined as alkaline phosphatase (ALP) normalization or ≥40% reduction. Clinical response was defined as improvement in patient-reported symptoms (chills, fever attacks, nausea, pruritus, abdominal pain) or reduced cholangitis frequency.
Results: Mean time from LT to NAS onset was 31 months, and mean time from NAS diagnosis to fibrate initiation was 33 months. After fenofibrate initiation, cholestasis improved in all patients, with a median on-treatment ALP reduction of 35% (IQR 22–51) by 1 month, maintained up to the end of the 12-month follow-up. A biochemical response was achieved by 72% of patients and a clinical response by 63%. Among 15 patients treated >90 days, response rates were 80% and 71%, respectively. Overall agreement between biochemical and clinical response criteria was 81%. In a linear mixed-effects model adjusting for time and patient-level variability, ALP levels decreased on average by 163 IU/L (95% CI −233 to −92) during active fenofibrate treatment compared with non-treatment periods ($p < 0.001$). The absence of a significant time trend ($p = 0.23$) suggests the reduction was attributable to fenofibrate rather than natural fluctuation or recovery. Fibrate response rates did not differ significantly by age, sex, pre-treatment ALP, LT indication (PSC vs other), or NAS duration pre-fibrate (all $p > 0.1$). Creatinine increased on average 27% from baseline by 1 month and thereafter remained stable. Five of 18 patients discontinued fenofibrate due to side effects and/or incomplete response. In patients who stopped fenofibrate, ALP increased.
Conclusion: These observed benefits of fibrates in long-standing post-LT NAS warrant further evaluation in prospective trials.

FRI-448

Donor and recipient pharmacogenetic variation at the POR locus is associated with acute rejection and biliary strictures after liver transplantation

Fredrik Åberg[1], Maria Semenova[2], Ville Liukkonen[3], Arno Nordin[1], Jukka Partanen[2], Kati Hyvärinen[2]. [1]*Helsinki University Hospital and University of Helsinki, Helsingfors, Finland;* [2]*Finnish Red Cross Blood Service, Helsinki, Finland;* [3]*North Karelia Central Hospital, Joensuu, Finland*
Email: fredrik.aberg@helsinki.fi

Background and aims: Cytochrome P450 enzymes *CYP3A5* and *CYP3A4*, together with P450 oxidoreductase (*POR*), are key determinants of tacrolimus metabolism and dose requirements. After liver transplantation (LT), drug metabolism is influenced by both donor and recipient genetics, yet the impact of pharmacogenetic variations on clinical outcomes remains unclear. We investigated the effects of donor and recipient pharmacogenetic variation on acute rejections (AR) and biliary strictures (BS) after LT.
Method: Study included consecutive LTs in Finland 2000–2020. Donors and recipients (666 pairs) were genotyped using genome-wide association study arrays with imputation and standardized quality control. Biopsy-verified AR and BS were identified from the national LT registry and medical records. Analyses focused on established variants in *CYP3A5* (rs776746), *CYP3A4* (rs35599367), and *POR* (rs1057868), followed by a systematic assessment of genetic variation in these genes in tacrolimus-treated cases.
Results: For the prespecified candidate variants, minor allele frequencies were 0.07 (*CYP3A5*), 0.04 (*CYP3A4*), and 0.39 (*POR*). In a subset of 108 recipients receiving tacrolimus from LT start, we observed 41 AR episodes, including 11 late AR events (>90 days post-LT), and 9 BS. The established candidate variants in *CYP3A5*, *CYP3A4*, and *POR* were not significantly associated with AR, late AR, or BS. In contrast, systematic analysis identified multiple *POR* single-nucleotide variants in both donors and recipients associated with AR (uncorrected $p < 0.05$). These variants clustered within a narrow genomic region and showed identical significance levels, consistent

with a shared haplotype block. In donor analyses, a representative *POR* variant from the associated haplotype block was associated with a reduced AR risk (odds ratio [OR] 0.44, 95% CI 0.21–0.91, adjusted for genotype-specific age, sex, and the first 1–4 genetic principal components). In recipient analyses, a distinct *POR* haplotype block within the same genomic region was associated with a higher risk of AR (adjusted OR 9.61, 95% CI 1.02–90.54). All recipient *POR* variants associated with AR were also associated with BS. Recipient *CYP3A4* variation was associated with late AR, while variation in CYP3A5 showed no significant associations.
Conclusion: Genetic variation at the POR locus was associated with AR and BS after LT. Associations involved a block distinct from the POR rs1057868 candidate variant and these findings require confirmation in independent cohorts.

FRI-449
Clinical characteristics and outcomes of primary sclerosing cholangitis after liver transplant, with or without inflammatory bowel disease, a national 10 year retrospective study
Afaf Ahmad[1], J. Sheridan[1], G. Doherty[1], G. Cullen[1], ZIta Galvin[2], Ross MacNicholas[2], Julia Sopena Falco[2], Audrey Dillon[2], Masood Iqbal[2], Omar El-Sherif[2]. [1]*Gastroentrology department, St. Vincent's University Hospital., Dublin, Ireland;* [2]*The National Liver Transplant Department, St. Vincent's University Hospital, Dublin, Ireland*
Email: afafawad244@gmail.com

Background and aims: Although a rare disease, PSC accounts for 10%–15% of the liver transplant activity in Europe. This national study focused on all PSC-LT recipients in Ireland in St. Vincent's University Hospital during the period 2016–2025.
Method: A retrospective review of data extracted from the waiting list, national liver transplant registry and chart review, included both IBD-PSC-LT and NON-IBD-PSC-LT cohorts.
Results: From 2016–2025; 350 patients were transplanted-DBD; PSC constituted 22.57% (n = 79) of all LT indications in Ireland during this period. 68.4% had associated IBD; 13% of whom were diagnosed post-LT. Mean age at transplant was 46.26 years ± 13.3SD (males 60%) in the IBD-PSC-LT, vs. NON-IBD PSC-LT 48 years ± 12.2 SD (males 64%). The mean listing MELD score was similar in both cohorts (IBD-PSC-LT 15.4 ± 6.95 SD, NON-IBD-PSC-LT 15.7 ± 5.8 SD). THE IBD-PSC cohort were prescribed more combination immunosuppression (65%) vs. NON-IBD-PSC cohort (24%). 44% of the NON-IBD-PSC-LT had biopsy proven acute cellular rejection vs. 29.6% in IBD-PSC LT. No liver-graft related adverse effects or infections were noted in relation to using combination of LT immunosuppression and a biological agent to treat IBD. These agents were; Vedolizumab (n = 7), anti-TNFs (n = 6), interleukin inhibitors (n = 3). (n = 10) PSC-LT had recurrent PSC (rPSC), 80% were in the IBD-PSC-LT-cohort, however there was no statistically significant relationship between IBD and PSC recurrence (Chi-square 1.56, p-value: 0.210). (n = 11) needed re-transplantation; 81% of whom were in the IBD-PSC-LT cohort. (n = 3) were re-transplanted twice for rPSC. Mortality was higher in the IBD-PSC-LT cohort vs. NON-IBD-PSC-LT-Cohort (3.8% and 1.3% respectively), with an overall post-LT colon cancer related mortality of 1.3%.
Conclusion: In our cohort, PSC-LT rates were higher compared to other European studies. The IBD course was variable, however the use of biologic therapies were safe in our cohort.

FRI-450
Left or right graft? Differential complication risks after ex vivo liver resection and autotransplantation for hepatic alveolar echinococcosis
Tuerganaili Aji[1], Yierfan Yilihaer[1]. [1]*First Affiliated Hospital of Xinjiang Medical University, Urumqi, China*
Email: tuergan78@sina.com

Background and aims: For conventionally unresectable hepatic alveolar echinococcosis (HAE), ex vivo liver resection and autotransplantation (ELRA) enables R0 resection. Left and right lobe grafts present distinct complication risks that guide surgical planning and postoperative management. However, evidence comparing these graft outcomes in HAE remains limited.
Method: We retrospectively analyzed 142 consecutive patients with HAE who underwent ELRA between 2010 and 2023. Patients were categorized into left graft (n = 98) and right graft (n = 44) groups. Propensity score matching generated 42 well-balanced pairs. Postoperative biliary and venous outflow complications were assessed. Predictors were identified using least absolute shrinkage and selection operator (LASSO) regression followed by multivariable logistic regression. Model performance was evaluated by receiver operating characteristic (ROC) curves, calibration plots, and decision curve analysis.
Results: No intraoperative deaths occurred. Pleural effusion was the most common postoperative complication (66.7%). Compared with left graft transplantation, right graft transplantation was associated with longer operative time and greater intraoperative blood transfusion (both $P < 0.05$). Biliary complications occurred more frequently in the right graft group (28.6% vs. 11.9%; $P < 0.05$). Independent predictors of biliary complications included preoperative biliary duct dilation (odds ratio [OR] = 18.82) and right graft type (OR = 6.12). In contrast, venous outflow complications were significantly more common in the left graft group (38.1% vs. 16.7%; $P < 0.05$). Independent predictors of outflow complications included use of artificial vascular reconstruction (OR = 3.42), left graft type (OR = 3.40), and portal hypertension (OR = 3.93). Predictive models demonstrated good discrimination for biliary complications (AUC = 0.83) and venous outflow complications (AUC = 0.80), with favorable calibration and clinical utility confirmed by decision curve analysis.
Conclusion: ELRA for HAE is associated with distinct graft-specific complication patterns. Right grafts predispose to biliary complications, whereas left grafts increase the risk of venous outflow obstruction. The validated predictive models provide a practical tool for individualized graft selection and perioperative risk stratification, potentially improving surgical planning and postoperative management in complex HAE cases.

FRI-451
Outcomes of liver transplantation in patients with sickle cell disease: a systematic review and meta-analysis
Tarannum Behlim[1], Omar Altaei[2], Mohamed El Kassas[3,4,5], Mohammed Eslam[6], Siham Alsinani[7,8], Khalid A Alswat[3,9], Faisal Abaalkhail[10,11], Zobair M. Younossi[12], Khalid Al Naamani[3,13]. [1]*Medical City for Military and Security Services, Research and Studies Committee, Muscat, Oman;* [2]*Oman Medical Speciality Board, Internal Medicine Program, Medical City for Military and Security Services, Muscat, Oman;* [3]*Steatotic Liver Diseases Study Foundation in Middle East and North Africa (SLMENA), Cairo, Egypt, Cairo, Egypt;* [4]*Endemic Medicine Department, Faculty of Medicine, Helwan University, Cairo, Egypt;* [5]*Applied Science Research Center, Applied Science Private University, Amman, Jordan;* [6]*Storr Liver Centre, Westmead Institute for Medical Research, Westmead Hospital and University of Sydney, NSW, Australia;* [7]*Department of Child Health, Sultan Qaboos University Hospital, University Medical City, Muscat, Oman;* [8]*Department of Child Health, Sultan Qaboos University Hospital, Sultan Qaboos University, Muscat, Oman;* [9]*Liver Disease Research Center, Department of Medicine, College of Medicine, King Saud University, Riyadh, Saudi Arabia;* [10]*College of Medicine, Alfaisal University, Riyadh, Saudi Arabia;* [11]*Department of Medicine, King Faisal Specialist Hospital and Research Center, Riyadh, Saudi Arabia;* [12]*The Global NASH/MASH Council, Washington D.C., United States;* [13]*Department of Medicine, Division of Gastroenterology and Hepatology, The Medical City for Military and Security Services, Muscat, Oman, Steatotic Liver Diseases Study Foundation in Middle East and North Africa (SLMENA), Cairo, Egypt, Muscat, Oman*
Email: tarannum.behlim@gmail.com

Background and aims: Sickle cell disease (SCD) is an autosomal recessive haemoglobinopathy that can cause severe hepatobiliary complications, for which liver transplantation (LT) may represent the only lifesaving option. We conducted a systematic review and meta-analysis of post-transplant outcomes in patients with SCD.
Method: We searched Ovid MEDLINE, Ovid EMBASE, the Cochrane databases, and Scopus from inception to 17 July 2025. Our search was limited to human studies published in English.We included case reports, case series, and observational cohorts reporting post LT outcomes in patients with SCD. Two reviewers independently performed study selection, data extraction, and risk of bias assessment. We conducted single arm random effects meta analyses to pool data on patient and graft survival at 1 year and 5 years.
Results: Twenty nine studies were included, comprising 23 case reports, 3 case series, and 3 retrospective cohort studies, with a total of 83 patients. Within 90 days post LT, the most frequently reported complications were infectious (26.5%), renal (18.2%), and vascular (15.7%). Reported long term complications were predominantly haematologic (7.2%) and mainly SCD related. Nine patients (12%) required retransplantation, including one patient who underwent two retransplants within five months of the index LT. Pooled 1 year patient survival was 76% (95% CI 42–89%), with a similar estimate for 1 year graft survival (76%, 95% CI 42–89%); heterogeneity was substantial (I^2 62.6%), reflecting variation in case mix, perioperative management, and reporting quality within primarily case based evidence. Long term outcomes were poorer, with pooled 5 year patient survival of 46% (95% CI 25–68%) and 5 year graft survival of 41% (95% CI 25–57%); heterogeneity was moderate and not statistically significant. Reported causes of graft loss included sickle cell crisis (n = 3), vascular complications (n = 3), primary nonfunction (n = 1), secondary haemochromatosis (n = 1), and multiple intrahepatic biliary strictures without hepatic artery thrombosis (n = 1).
Conclusion: LT can provide meaningful short term survival forcarefully selected patients with SCD. However, long-term patient and graft survival remain significantly impaired. Improved perioperative protocols, structured long term follow up, and more consistent reporting of SCD specific complications are needed to enhance care and outcomes in this complex transplant population.

FRI-457

Impact of donor hypernatremia on graft function and survival in deceased donor liver transplantation: a systematic review and meta-analysis

Halima Al Shuaili[1], Mohamed El Kassas[2,3], Zobair M. Younossi[4], Mohammed Eslam[5], Khalid A Alswat[2,6], Saleh Alqahtani[7,8], Siham Alsinani[9,10], Ibrahim Al Nabhani[11], Faisal M Sanai[2,12], Khalid Al Naamani[1,2]. *[1]Department of Medicine, Division of Gastroenterology and Hepatology, The Medical City for Military and Security Services, Muscat, Oman, Steatotic Liver Diseases Study Foundation in Middle East and North Africa (SLMENA), Cairo, Egypt, Muscat, Oman; [2]Steatotic Liver Diseases Study Foundation in Middle East and North Africa (SLMENA), Cairo, Egypt, Cairo, Egypt; [3]Endemic Medicine Department, Faculty of Medicine, Helwan University, Cairo, Egypt; [4]The Global NASH/MASH Council, Washington D.C., United States; [5]Storr Liver Centre, Westmead Institute for Medical Research, Westmead Hospital and University of Sydney, NSW, Australia; [6]Liver Disease Research Center, Department of Medicine, College of Medicine, King Saud University, Riyadh, Saudi Arabia; [7]Liver, Digestive, and Lifestyle Health Research Section, and Organ Transplant Center of Excellence, King Faisal Specialist Hospital and Research Center, Riyadh, Saudi Arabia; [8]Division of Gastroenterology and Hepatology, Weil Cornell Medicine, New York, United States; [9]Department of Child Health, Sultan Qaboos University Hospital, University Medical City, Muscat, Oman; [10]Department of Child Health, Sultan Qaboos University Hospital, Sultan Qaboos University, Muscat, Oman; [11]Department of Hematology, College of Medicine and Health Science, Sultan Qaboos University, Muscat, Oman; [12]Gastroenterology Section, Department of Medicine, King Abdulaziz Medical City, King Abdullah International Medical Research Center, Ministry of National Guard - Health Affairs, Jeddah, Saudi Arabia*
Email: halima.alshueili@gmail.com

Background and aims: Donor hypernatremia is common in neurologically deceased organ donors and has been proposed as a risk factor for adverse outcomes after liver transplantation, although evidence remains inconsistent. We conducted a systematic review and meta-analysis to evaluate the association between donor hypernatremia and post-transplant graft outcomes and recipient mortality after deceased donor liver transplantation.
Method: Following the Preferred Reporting Items for Systematic Reviews and Meta-Analyses (PRISMA) guidelines, we searched MEDLINE, EMBASE, PubMed, Web of Science, Scopus, and the Cochrane Central Register of Controlled Trials from inception to 17 July 2025. Eligible studies reported terminal donor serum sodium levels and post-transplant graft or patient outcomes. Donor hypernatremia was generally defined as serum sodium greater than or equal to 145 milliequivalents per liter. The primary outcome was 30-day recipient mortality. Secondary outcomes included graft dysfunction or loss ≤ 7 days, 30 days, and 1 year, and recipient mortality at 7 days and 1 year. Risk of bias was assessed using the Risk Of Bias In Non-randomized Studies of Interventions (ROBINS-I) tool. Random-effects meta-analyses were performed when appropriate.
Results: From 2,656 screened records, 15 retrospective cohort studies including 7704 patients were identified. Donor hypernatremia was associated with a higher risk of graft dysfunction or loss within 7 days compared with normonatremic donors (relative risk [RR] 1.79, 95% confidence interval [CI] 1.42–2.26; I squared = 70%). At 30 days, the association was less consistent (RR 1.57, 95% CI 0.87– 2.82). At 1 year, donor hypernatremia was associated with increased graft dysfunction or loss (RR 2.11, 95% CI 1.43–3.12; I squared = 80%). Donor hypernatremia was associated with higher 30-day mortality (RR 2.04, 95% CI 1.51–2.76; I squared = 66%) but not with recipient mortality at 7 days or 1 year. Most studies had a moderate to serious risk of bias, mainly due to confounding and incomplete adjustment.
Conclusion: Donor hypernatremia was associated with increased early graft dysfunction, higher 1-year graft loss, and elevated 30-day recipient mortality after liver transplantation, but not with longer-term post-transplant mortality. Given substantial heterogeneity and risk of bias, donor hypernatremia may represent a marker of graft vulnerability, warranting further prospective study.

FRI-458

Post-transplant comorbidities, MASLD development and long-term survival in liver recipients with and without HIV infection

Adriana Cervo[1], Maddalena Albertini[1], Federica Casari[1], Jovana Milic[1], Barbara Catellani[2], Paolo Magistri[2], Gian Piero Guerrini[2], Cristina Mussini[1], Giada Sebastiani[3], Fabrizio Di Benedetto[2], Giovanni Guaraldi[1]. *[1]Infectious Diseases Clinic, University Hospital of Modena, Modena, Italy; [2]Hepato-Pancreato-Biliary Surgery and Liver Transplantation Unit, University Hospital of Modena, Modena, Italy; [3]Division of Gastroenterology and Hepatology, McGill University Health Centre, Montreal, Canada*
Email: adriana.cervo@gmail.com

Background and aims: Data on long-term outcomes and post-transplant comorbidities in liver transplant (LT) recipients with HIV infection remain limited, particularly regarding metabolic complications and metabolic dysfunction–associated steatotic liver disease (MASLD).
Method: This retrospective, propensity score–matched (1:3) case–control study included 87 LT recipients with HIV and 261 without HIV transplanted at the University Hospital of Modena between 2003 and 2024. Matching variables were age, sex, MELD score, hepatocellular carcinoma (HCC), HBV/HCV coinfection, and donor age. Prevalence at LT and incidence rates (IR) post-LT of hypertension, diabetes, dyslipidemia, cardiovascular events (CVE), MASLD (imaging-based diagnosis), and recurrent HCC were assessed, together with long-term survival.

Results: Of 348 recipients, 17% were females, with age of 53 (IQR 47–58). At LT, active HCV infection was present in 39% of HIV and 31% of non-HIV recipients, and HCC prevalence was similar (49.4% vs 47.5%). At LT, hypertension and dyslipidemia were more prevalent in HIV recipients than non-HIV (38% vs 18% and 26% vs 6%, $p < 0.05$), while diabetes prevalence was comparable (21% vs 18%). Post-LT dyslipidemia occurred more frequently in HIV recipients (58% vs 35%; incidence rate [IR] 1.8 vs 0.5 per 100 PYFU), whereas incidence rates of hypertension and CVE were similar. New-onset diabetes occurred in 15% of HIV and 25% of non-HIV recipients ($p = 0.052$) with IR 2.2 vs 3.3 per 1000 PYFU. Post-LT overweight/obesity developed in 17% of HIV and 32% of non-HIV recipients ($p = 0.053$). Post-LT MASLD was diagnosed in 19.2% of recipients, with similar IR between groups. However, a hepatic steatosis index >36 was more frequent in non-HIV recipients (31% vs 21%, $p = 0.038$). Post-LT IR of recurrent HCC did not differ between groups (1.8 vs 1.4 per 100 person-years of follow-up [PYFU], $p = 0.519$), although time to recurrence tended to be longer in HIV recipients (2.4 vs 0.8 years, $p = 0.06$). MASLD was not associated with increased HCC recurrence. Ten- and fifteen-year survival was 59.6% and 48.9% in HIV recipients versus 66.7% and 53.1% in non-HIV recipients, respectively.
Conclusion: LT in people with HIV achieves long-term survival comparable to non-HIV recipients. Post-LT metabolic comorbidities remain highly prevalent, with dyslipidemia more common in HIV and diabetes in non-HIV recipients. MASLD develops in approximately one-fifth of recipients, highlighting the need for integrated, multidisciplinary metabolic care after LT.

FRI-459
Impact of pre-transplant metabolic syndrome on survival and causes of mortality after liver transplantation: a 20-year cohort study
Carmen Alonso Martin[1], Irene Peñas Herrero[2], Samuel Fernández-Prada[2], Elena Velasco Martinez[2], Natalia Marcos Carrasco[2], Carolina Almohalla Alvarez[2], Félix García Pajares[2], Gloria Sánchez Antolín[2]. *[1]Complejo Asistencial Universitario de Salamanca, Salamanca, Spain; [2]Hospital Universitario Rio Hortega, Valladolid, Spain*
Email: calonsoma@saludcastillayleon.es

Background and aims: Metabolic syndrome is increasingly prevalent among liver transplant candidates, but its impact on long-term survival and cause-specific mortality after transplantation remains uncertain. This study aimed to evaluate the influence of pre-transplant metabolic syndrome on post-transplant survival, causes of death, and vascular and tumour-related morbidity.
Method: We retrospectively analysed 682 adult patients who underwent liver transplantation from January 2002 to December 2022. Metabolic syndrome was defined by the presence of at least two of the following conditions: diabetes mellitus, arterial hypertension, dyslipidaemia, or obesity (body mass index 30 kg per square metre or higher). Survival was analysed using Kaplan–Meier curves and compared with the log-rank test. Causes of death and vascular and tumour-related events were assessed according to metabolic syndrome status.
Results: Metabolic syndrome was present in 23 percent of patients. Median survival was lower in patients with metabolic syndrome compared with those without (92 versus 158 months), although this difference did not reach statistical significance ($p = 0.29$). Early mortality within the first six months after transplantation was similar between groups. However, non-fatal vascular complications during the first year were more frequent in patients with metabolic syndrome (6.9 percent versus 4.0 percent). From the fifth year onwards, cardiovascular mortality was markedly higher in the metabolic syndrome group (13.6 percent versus 1.9 percent). The overall incidence of post-transplant tumours was lower in patients with metabolic syndrome (9.4 percent versus 15.2 percent), while tumour-related mortality was comparable between groups, with a slight numerical increase in patients with metabolic syndrome (11.3 percent versus 9.9 percent).
Conclusion: Pre-transplant metabolic syndrome was not associated with early post-transplant mortality or tumour incidence but was linked to a higher burden of early vascular complications and increased late cardiovascular mortality. These findings underscore the clinical relevance of early identification and strict control of metabolic risk factors in liver transplant candidates to improve long-term outcomes.

FRI-460
Computed tomography–defined sarcopenia as a predictor of mortality in liver transplant candidates: a systematic review and meta-analysis
Sofia Araujo[1], Carlos Eduardo Freitas Dantas[1], Witória Lins[2], Lorena Madureira[2], Maria Clara Silva Dutra de Amorim[1], Ângelo Bonfim[1], Ana Sofia Albuquerque Ponte[3], Iasmin Nogueira[3], Matheus Costa[3], João Filipe Melo[3]. *[1]Faculdade De Ciências Médicas, Recife, Brazil; [2]Universidade Federal De Pernambuco, Recife, Brazil; [3]Uninassau-Recife, Recife, Brazil*
Email: sofia.coriolano@upe.br

Background and aims: Sarcopenia is prevalent in advanced liver disease and has been studied as a prognostic marker in liver transplant (LT) candidates. Computed tomography (CT)–derived skeletal muscle index (SMI) is the reference standard for diagnosis; however, its association with waitlist mortality is inconsistent. This systematic review and meta-analysis evaluated the prognostic impact of CT-defined sarcopenia on mortality in adult LT candidates.
Method: This PRISMA-compliant systematic review searched PubMed, Embase, Scopus, and Web of Science up to December 2025. Eligible studies assessed CT-derived sarcopenia at the L3 level and reported mortality in adult liver transplant candidates. Risk ratios (RR) with 95% confidence intervals (CI) were pooled using common and random effects models. Statistical heterogeneity was quantified using the I^2 statistic, with an $I^2 < 60\%$ prespecified to support the common effect model as the primary analytical approach.
Results: Four observational studies including 869 LT candidates were analyzed (357 with CT-defined sarcopenia and 512 without). Sarcopenia was significantly associated with increased mortality (common effect: RR = 1.33, 95% CI [1.08–1.63], $p = 0.0068$; random effects: RR = 1.30, 95% CI [1.03–1.64], $p = 0.0274$). Individual estimates ranged from a non-significant protective effect to a markedly increased mortality risk. Heterogeneity was low ($I^2 = 23.6\%$), indicating statistical homogeneity, though this apparent consistency warrants caution. All studies were monocentric, had relatively small sample sizes, used heterogeneous sarcopenia cut-offs, and lacked robust control for selection or confounding bias, limiting external validity and generalizability of the pooled results.
Conclusion: CT-defined sarcopenia is associated with increased mortality in LT candidates; however, methodological limitations and limited population diversity require cautious interpretation. Future multicenter studies with standardized diagnostic thresholds and formal bias-reduction strategies are needed, along with comparative assessments of CT versus alternative non-ionizing muscle evaluation methods to define its role as the prognostic reference standard.

FRI-461-YI
Safety and efficacy of GLP-1 receptor agonists in liver transplant recipients: a multi-national experience
Chiara Becchetti[1], Mohommad Qasim Khan[2], Rokhsana Mortuza[3], Mahmoud Jouid[2], Panda Saurav[4], Valeria Pierluissi[4], Marta Stegagnini[5], Gopika Punchhi[2], Amani Bajunayd[2], Raffaella Viganò[5], Reyad Elzaanoun[6], Arpana Wadhwani[6], Luca Saverio Belli[5], Annalisa Berzigotti[1], Kymberly Watt[4]. *[1]Graduate*

School for Health Sciences (GHS), University of Bern, Switzerland, Department of Visceral Surgery and Medicine, Inselspital, Bern University Hospital, Switzerland, Hepatology and Gastroenterology Unit, ASST Grande Ospedale Metropolitano Niguarda, Milan, Italy, Bern, Switzerland; [2]Department of Medicine, Western University, London, ON, Canada, Department of Epidemiology and Biostatistics, Western University, London, ON, Canada, London, Canada; [3]Department of Medicine, Western University, London, ON, Canada, London, Canada; [4]Department of Internal Medicine, Division of Gastroenterology and Hepatology, Mayo Clinic, Rochester, MN, USA, William J. von Liebig Center for Transplantation and Clinical Regeneration, Mayo Clinic, Rochester, MN, USA, Rochester, United States; [5]Hepatology and Gastroenterology Unit, ASST Grande Ospedale Metropolitano Niguarda, Milan, Italy, Milan, Italy; [6]Schulich School of Medicine, Western University, London, ON, Canada, London, Canada
Email: becchettichiara@tiscali.it

Background and aims: Weight gain in liver transplant recipients (LTR) is common and increases the risk of major adverse cardiovascular events (MACE). Glucagon-like peptide-1 receptor agonists (GLP-1 RA) may mitigate post-LT obesity and metabolic complications. We evaluated the safety, tolerability, and efficacy of GLP-1 RA in LTR from multiple countries.
Method: All adult LTR treated with GLP-1 RA between 2010 and 2021 in four centers (Canada, USA, Italy, Switzerland), with follow-up through June 2024 were analyzed. Primary outcome was 1-year weight change; secondary outcomes included metabolic parameters, MACE, graft function, immunosuppressive drug exposure, and treatment tolerability. GLP-1 RA users were matched 1:1–1:2 with non-users by age, sex, diabetes status, transplant year, and center. Analyses used mixed models with multiple imputation.
Results: The cohort included 104 GLP-1 RA LTR users, of which 77.9% were male, 68.3% had diabetes and 49% were obese. Metabolic dysfunction-associated liver disease was the main indication for LT (49.0%). GLP-1 RA were initiated a median of 7.0 ± 3.5 years post-LT, most commonly semaglutide (67.3%), and maintained at ≤1 mg weekly. At 1 year, body weight decreased by 3.9% (−3.8 kg, 95%CI 1.9–5.7; $p < 0.001$), BMI by 5.0% (−1.6 kg/m^2, 95%CI 0.9–2.3; $p < 0.001$), and HbA1c by 6.7% (−0.48%, 95%CI 0.19–0.78; $p = 0.002$), with improvements in total cholesterol (−7.36%; $p = 0.001$) and LDL cholesterol (−7.54%; $p = 0.018$). Liver enzymes remained stable, and no treatment discontinuations occurred. In the matched analysis (80 users vs 116 controls), GLP-1 RA users showed significant reductions in weight (delta −3.40; 95%IC −5.93, −0.87; $p = 0.009$), BMI (delta −1.57 kg/m^2; 95%IC −2.63, −0.50; $p = 0.005$) and HbA1c (delta −0.43%, 95%CI −0.83, −0.02, $p = 0.042$), when compared to controls who showed no changes. Immunosuppressive drug exposure showed no relevant differences compared with matched controls. Acute rejection (2.5% vs 1.72%) and MACE (6.25% vs 8.62%) rates were statistically similar between groups.
Conclusion: GLP-1 RA represent a safe therapeutic option for managing metabolic dysfunction in LTR, without adversely affecting graft function or immunological stability. The notably low dosing observed likely attenuate efficacy compared with the general population. Given the safety profile, dose escalation in LTR should be encouraged.

FRI-462
Impact of multimodal prehabilitation in patients with cirrhosis awaiting liver transplantation: a feasibility trial

Amine Benmassaoud[1], Chelsia Gillis[1], Olivia Geraci[1], Myriam Martel[1], Yusuf Afif[1], Larry Lands[1], Jeffrey Barkun[1], Tianyan Chen[1], Giada Sebastiani[1], Franco Carli[1], Amal Bessissow[1]. *[1]Centre universitaire de Santé McGill, Montréal, Canada*
Email: amine.benmassaoud@mcgill.ca

Background and aims: Patients awaiting liver transplantation (LT) are commonly malnourished and frail. Prehabilitation aims to improve physiological reserves before a major surgery. To date, its impact before LT remains unknown. We assessed whether a multimodal prehabilitation program is feasible, safe, and improves exercise fitness, nutrition, and health-related quality of life (HRQoL).
Method: Our prospective single-arm clinical trial recruited adults with cirrhosis awaiting a first LT (NCT05237583). Participants were excluded if they were delisted, had a MELD > 20, were awaiting combined organ transplantation, or deemed unsafe to exercise. All participants enrolled in a structured and supervised multimodal prehabilitation program (exercise training, nutritional optimization, and psychological support). The program was divided into a 4-week induction phase (3 exercise sessions per week) and a 5-month maintenance phase (1 exercise session every 2 weeks). Feasibility objective included recruitment of 25 participants. Exercise fitness, nutritional status, and HRQoL were compared before and after the intervention using non-parametric tests and linear mixed models to evaluate changes over multiple assessments.
Results: Overall, 25 participants received the intervention (age 57.9 ± 9.4 years; 20% women; 48% alcohol-related cirrhosis; 12% hepatocellular carcinoma; 24% prior TIPS; MELD score 11.6 ± 3.8; 8% frail by Liver Frailty Index [LFI]; 32% adequately nourished [RFH-GA]). Overall, 16 (64%) completed the induction phase and 6 (24%) completed the entire program. There were 9 AEs; all mild, and 1 was related to intervention. Reasons for lack of completion included LT (n = 6), consent withdrawal (n = 7), and AE (n = 6). Peak oxygen consumption (VO_2max) was stable after 4 weeks but increased by end of program (pre: 13.0 ± 3.9; end: 25.5 ± 19.1 mL/kg/min); LFI improved significantly after 4 weeks (LFI pre: 3.63 ± 0.48 vs post: 3.39 ± 0.64; $p = 0.03$), and it remained stable thereafter (LFI end: 3.32 ± 0.70) ($p = 0.84$). Nutrition status tended to improve as more patients became adequately nourished (pre: 32% vs end: 83%, $p = 0.08$). Trend toward improved HRQoL was noted (CLDQ pre: 4.95 ± 1.38 vs end: 5.53 ± 1.02). Overall acceptability to the intervention, rated on a 5-point scale, remained high (pre: 4.60 ± 0.50 vs end: 4.67 ± 0.52).
Conclusion: Our feasibility trial shows that our multimodal prehabilitation program is feasible, safe, and seems to improve preoperative fitness. Larger studies are needed to confirm these findings.

FRI-463
Liver transplantation for HBV-related disease in France: NUC type before LT is major determinant of patient survival

Isaure Bienvenue[1], Olivier Roux[2], Audrey Coilly[3], Armand Abergel[4], Teresa Antonini[1], Thierry Artzner[5], Olivier Boillot[6], Faiza Chermak[7], Filomena Conti[8], Sebastien Dharancy[9], Christophe Duvoux[10], Laure Elkrief[11], Marwin Farrugia[12], Claire Francoz[2], Baptiste Giguet[13], Jean Hardwigsen[14], Pauline Houssel-Debry[13], Marie-Noëlle Hilleret[15], Nassim Kamar[16], Marianne Latournerie[17], Magdalena Meszaros[18], Sylvie Radenne[1], Bruno Roche[3], Ephrem Salamé[11], Delphine Weil-Verhoeven[19], Didier Samuel[3], Fabien Zoulim[1,20], Jérôme Dumortier[6], Francois Villeret[1,20]. *[1]Service d'hépatologie et de transplantation hépatique, Hôpital de la Croix Rousse, Hospices Civils de Lyon, Lyon, France; [2]Hôpital Beaujon, Clichy, France; [3]Hôpital Paul-Brousse, Villejuif, France; [4]Département de Médecine digestive, CHU Estaing, Clermont-Ferrand, Clermont Ferrand, France; [5]Hôpital Hautepierre, Strasbourg, France; [6]Hôpital Édouard Herriot, Lyon, France; [7]CHU De Bordeaux, Bordeaux, France; [8]Hôpital Pitié Salpêtrière, Paris, France; [9]Hôpital Claude Huriez, Lille, France; [10]Hôpitaux Universitaires Henri Mondor, Créteil, France; [11]Hôpital Trousseau, Tours, France; [12]Hôpital L'Archet, Nice, France; [13]Chu Pontchaillou Rennes, Rennes, France; [14]Hôpital de la Timone, Marseille, France; [15]Hôpital Michallon, Grenoble, France; [16]Hôpital Rangueil, Toulouse, France; [17]CHU Dijon, Dijon, France; [18]Hôpital Saint-Éloi, Montpellier, France; [19]Hôpital Jean Minjoz, Besançon, France; [20]Université Claude Bernard Lyon 1, INSERM Unit 1350 PathLiv; Lyon Hepatology Institute, IHU EVEREST, Lyon, France*
Email: isaure.bienvenue@chu-lyon.fr

Background and aims: Liver transplantation (LT) is indicated in the case of liver complications related to hepatitis B virus (HBV) infection:

acute liver failure (ALF), decompensated cirrhosis, and/or hepatocellular carcinoma (HCC). LT for HBV in France accounts for approximately 5% of all liver transplant indications, a figure that has remained fairly stable over the past 20 years. The present study aimed to describe and evaluate post-LT survival for HBV in France during the past 2 decades.

Method: This retrospective multicenter study included all adult patients who underwent a first LT in France with a positive HBsAg (+/– coinfected with HDV), between January 1, 2005, and December 31, 2023, for ALF, or cirrhosis complicated or not by HCC.

Results: A total of 1,083 patients were included, the majority of whom were men (82%) with a median [IQR] age at LT listing of 52.8 [42.5; 59.8] years. The main indication for LT was HCC in 47.0% of cases, decompensated cirrhosis in 41.2%, ALF (9.4%), or HCC without cirrhosis (1.4%). At LT listing, 79.9% of the patients with HCC had an AFP score ≤2. Median follow-up time after LT was 6.0 [2.2; 11.1] years. At the time of LT, 411 patients were on tenofovir (40.9%), 347 were on entecavir (34.6%), 143 were receiving another NUC (14.2%), 76 patients were not receiving antiviral treatment (7.6%) and 27 patients were receiving both tenofovir and entecavir (2.5%). Overall patients' survival at 1, 5, 10, and 15 years was 89.9%, 76.4%, 66.4%, and 54.5%, respectively. The main causes of death were HCC recurrence (27.6%), infection (23.3%), followed by oncological causes excluding HCC (10.0%), and 10.0% of patients died in early post-operative period. There were no deaths related to HBV recurrence. Multivariate analysis disclosed that independent significant risk factors for overall mortality were age at LT (HR: 1.030; 95CI: 1.019–1.042; $p < 0.0001$) and type of pre-LT nucleos(t)ides analogue (NUC): compared to tenofovir, entecavir (HR: 1.735; 95CI: 1.312–2.295; $p < 0.0001$) or another NUC (HR: 1.471; 95CI: 1.059–2.043; $p = 0.021$) were associated with decreased overall patient survival. The indication for LT (ALF, cirrhosis and HCC) had no significant impact on patients' survival. Similarly, HDV co-infection had no significant impact on patients' survival.

Conclusion: Our results suggest that survival of patients who underwent LT for HBV-related disease is significantly dependent on the type of antiviral treatment before LT, tenofovir use being associated with a better survival.

FRI-464

Liver transplantation for HBV in France: study of antiviral prophylaxis and HBV recurrence in 1,083 patients

Isaure Bienvenue[1], Olivier Roux[2], Audrey Coilly[3], Armand Abergel[4], Teresa Antonini[1], Thierry Artzner[5], Olivier Boillot[6], Faiza Chermak[7], Filomena Conti[8], Sebastien Dharancy[9], Christophe Duvoux[10], Laure Elkrief[11], Marwin Farrugia[12], Claire Francoz[2], Baptiste Giguet[13], Jean Hardwigsen[14], Pauline Houssel-Debry[13], Marie-Noëlle Hilleret[15], Nassim Kamar[16], Marianne Latournerie[17], Magdalena Meszaros[18], Sylvie Radenne[1], Bruno Roche[3], Ephrem Salamé[11], Delphine Weil-Verhoeven[19], Didier Samuel[3], Fabien Zoulim[1,20], Jérôme Dumortier[6], Francois Villeret[1,20]. *[1]Service d'hépatologie et de transplantation hépatique, Hôpital de la Croix Rousse, Hospices Civils de Lyon, Lyon, France; [2]Hôpital Beaujon, Clichy, France; [3]Hôpital Paul-Brousse, Villejuif, France; [4]Département de Médecine digestive, CHU Estaing, Clermont-Ferrand, Clermont Ferrand, France; [5]Hôpital Hautepierre, Strasbourg, France; [6]Hôpital Édouard Herriot, Lyon, France; [7]CHU De Bordeaux, Bordeaux, France; [8]Hôpital Pitié Salpêtrière, Paris, France; [9]Hôpital Claude Huriez, Lille, France; [10]Hôpitaux Universitaires Henri Mondor, Créteil, France; [11]Hôpital Trousseau, Tours, France; [12]Hôpital L'Archet, Nice, France; [13]Chu Pontchaillou Rennes, Rennes, France; [14]Hôpital de la Timone, Marseille, France; [15]Hôpital Michallon, Grenoble, France; [16]Hôpital Rangueil, Toulouse, France; [17]CHU Dijon, Dijon, France; [18]Hôpital Saint-Éloi, Montpellier, France; [19]Hôpital Jean Minjoz, Besançon, France; [20]Université Claude Bernard Lyon 1; INSERM Unit 1350 PathLiv; Lyon Hepatology Institute, IHU EVEREST, Lyon, France*
Email: isaure.bienvenue@chu-lyon.fr

Background and aims: Liver transplantation (LT) can be indicated in the case of acute liver failure (ALF), decompensated cirrhosis, and/or hepatocellular carcinoma (HCC) related to hepatitis B virus (HBV) infection. Post-LT antiviral prophylaxis recommendations have evolved in recent years, with a reduction in the duration of HBIG administration. The present study aimed to describe and evaluate the efficacy of post-LT antiviral prophylaxis in France during the past 2 decades.

Method: This retrospective multicenter study included all adult LT patients who were HBsAg positive (+/- coinfected with HDV) at the time of LT, between January 1, 2005, and December 31, 2023. Post-LT HBV recurrence was defined as the detection of serum HBV DNA.

Results: A total of 1,083 patients were included, most of them were men (81.5%) with a median [IQR] age at LT listing of 52.8 [42.5; 59.8] years. HCC was the primary indication for LT in 47.2% of cases, followed by decompensated cirrhosis (41.2%) and ALF (9.4%). At the time of LT, 411 patients were on tenofovir (40.9%), 347 were on entecavir (34.6%), 143 were receiving another NUC and 27 patients were receiving both tenofovir and entecavir (2.5%). At the time of LT, 75.9% of the patients had an undetectable serum HBV DNA, 4.4% had a detectable but not quantifiable HBV DNA, and 19.7% had a quantifiable HBV DNA. Median follow-up time after LT was 6.0 [2.2; 11.1] years. All patients received HBIG for at least 5 days after LT. Patients treated with HBIG received subcutaneous form in 46.0% of the cases and intravenous form in 54.0%. Among 684 patients initially treated with HBIG + NUC, 206 (30%) discontinued HBIG during follow-up, with a median time to discontinuation from LT of 4.0 [1.9; 7.3] years. At the end of follow-up, 50.0% of the patients were still receiving a combination therapy with HBIG + NUC, 47.0% were receiving NUC alone, and 3.0% were receiving HBIG alone. The main reason for discontinuing HBIG was to follow recommendations. The factor identified in multivariate analysis for maintaining combination prophylaxis was a co-infection with HDV ($p = 0.034$). A total of 22 patients had HBV recurrence after LT with a median delay of 2.6 [0.7–3.2] years. The cumulative incidence of HBV reactivation after LT was therefore 4.1% at 15 years.

Conclusion: Our results strongly confirm that HBV recurrence after LT is now very rare. The antiviral prophylaxis regimen is heterogeneous and differs from current recommendations, with frequent continuation of a combination HBIG/NUC therapy.

FRI-465

Impact of hypothermic oxygenated perfusion on very old liver graft issued from donors after circulatory death (>70 years) livers: insights from a belgian bi-centric experience

Eliano Bonaccorsi-Riani[1], Maxime Foguenne[1], Antoine Dubois[1], Joris Blondeel[2], Lancelot Marique[1], Aniss Channaoui[1], Olga Ciccarelli[1], Laurent Coubeau[1], Géraldine Dahlqvist[1], Kristof Vandevoorde[2], Karlien Degezelle[2], Mauricio Sainz-Barriga[2], Ina Jochmans[2], Jacques Pirenne[2], Diethard Monbaliu[2]. *[1]Cliniques Universitaires Saint-Luc, Brussels, Belgium; [2]UZLeuven, Leuven, Belgium*
Email: eliano.bonaccorsi@saintluc.uclouvain.be

Background and aims: Liver graft recipients from donors after circulatory death (DCD) face an increased risk of complications such as primary non-function (PNF) and non-anastomotic biliary stricture (NAS). This is due to the warm ischemia time, inherent to the DCD procurement. Similarly, liver grafts from very old (>70 years) donors are known to increase these risks, although they represent a valuable option to safely increase the donor pool. Ex-situ end-ischemic hypothermic oxygenated perfusion (HOPE) of DCD-grafts <60 years has been demonstrated to reduce the incidence of complications following liver transplantation (LT). However, results of HOPE in grafts from very Old-DCD (>70 years) remains scarce. Therefore, we aim to study impact of HOPE on these specific grafts.

Method: Data from 95 LT using >70 years DCD-graft, transplanted in 2 Belgian centres between 2015 and 2025 were collected. Of those, 53 were preserved with HOPE (Old-DCD-HOPE), and 42 were preserved

in static cold storage (Old-DCD-SCS). Graft-related complications was defined as the occurrence of PNF, biliary complications, vascular complications, re-laparotomy within 10 days after LT and occurrence of renal replacement therapy after LT.
Results: Recipient characteristics (indication, age, MELD score) and warm ischemia times were comparable between groups. HOPE-liver grafts were perfused for 172 minutes (mean), reducing static cold ischemia time to 216 minutes (mean) (compared to 332 minutes (mean), $p < 0.001$). Donors were older in the Old-DCD-HOPE (76.9 ± 5.7 years old) compared to the Old-DCD-SCS (73.5 ± 2.9 years old) ($p < 0.001$). Old-DCD-HOPE presented a lower rate of graft-related complications (0.57/patient) compared to Old-DCD-SCS (1.14/patient) ($p = 0.003$), including NAS (5.7% *vs* 21.4%, $p = 0.047$), while graft-threatening complications (leading to re-LT or death) were reduced (7.5% *vs* 28.6%, $p = 0.015$). There was no difference in 1-year graft survival (84.0% vs. 76.0%, $p = 0.238$).
Conclusion: These findings support that using of HOPE for DCD-graft >70 years results with fewer graft-related and graft-threatening complications. By enabling the safe transplantation of grafts from very old DCD donors, HOPE contributes to a meaningful expansion of donor availability. Larger prospective studies are required to confirm these encouraging results.

FRI-466
Minimal immunosuppression is still too much: oncological and cardiovascular events impact 20-years survival rates of liver recipients
Eliano Bonaccorsi-Riani[1], Léa Peiffer[1], Maxime Foguenne[1], Lancelot Marique[1], Laurent Coubeau[1], Olga Ciccarelli[1], Géraldine Dahlqvist[1], Jan Lerut[2]. *[1]Cliniques Universitaires Saint-Luc, Brussels, Belgium; [2]Institut de Recherche Expérimentale et Clinique, UCLouvain, Brussels, Belgium*
Email: eliano.bonaccorsi@saintluc.uclouvain.be

Background and aims: Chronic immunosuppression (IS) is necessary to maintain graft survival. Yet, it is associated with severe adverse effects; affecting recipients' long-term survival. Minimal IS (mIS) protocols have been proposed as a strategy to mitigate these consequences. This study assesses 20 years long-term graft and patient outcomes of patients included in a mIS prospective randomised controlled trial (RCT).
Method: Between February 2000 and September 2004, 156 adults were enrolled in a prospective RCT aiming to establish long-term mIS (tacrolimus monotherapy - TacMono). Outcomes were evaluated over a minimum follow-up of 20 years.
Results: Sixty-seven patients (pats) (43%) were alive at 20 years post-LT. From those, IS regimens were known for 52 pats (76%). Thirty pats (58%) were on TacMono therapy with 8 of them were on spacing monotherapy (IS not every day per week). Five pats (10%) achieved the IS-free status. Thirteen pats (25%) were on double and 4 (8%) on triple IS, mainly due to recurrent auto-immune disease (29%), impaired renal function (29%) and poorly tolerated neurological IS side-effects (12%). Neoplasia was the leading cause of death (26%), most of them being de novo malignancies (78%); followed by sepsis (19%), mainly due to biliary-associated infections (67%). Cardiovascular events (14%) represent the third cause of mortality, equally divided between myocardial infarction and stroke. Eighteen patients (12%) required a re-transplantation (reLT), 72% occurring within 5 first years. Disease recurrence was the cause of re-LT in 6 pats (33%), biliary complications in 3 pats (17%) and chronic rejection in another 3 pats (17%). For note, all re-LT because of chronic rejection were due to non-compliance and not to mIS protocols. Clinical data were available for 59 pats, 19 of those (32%) suffered from moderated chronic kidney disease (KDIGO stage 3a and 3b); 7% patients required renal replacement therapy (KDIGO stage 4–5). Diabetes, arterial hypertension and hypercholesterolemia were diagnosed and treated in 41%, 63% and 31% of patients respectively.
Conclusion: mIS (based on tacrolimus monotherapy), including spaced and even no therapy can be reached safely in a majority of patients without compromising long-term outcome. Although, IS-related complications still impact patient survival. This very-long term follow-up study clearly shows that IS should be reduced as much as possible, as it is an important strategy to improve long-term outcome of liver recipients.

FRI-467-YI
Secretin therapy during ex-situ normothermic liver machine perfusion: a critical factor for restoration of bile duct physiology and the protective "bicarbonate umbrella"
Roberto Broere[1], Stefan H. Luijmes[1], Puck C. Groen[1], Jorke Willemse[1], Iris E.M. de Jong[2], Marcel Bijvelds[3], Caroline den Hoed[3], Sarwa Darwish Murad[3], Luc van der Laan[4], Jeroen de Jonge[1], Robert Porte[1]. *[1]Erasmus Medical Center Rotterdam, Transplant Institute, Department of Surgery, Division of HPB and Transplant Surgery, Rotterdam, Netherlands; [2]Erasmus Medical Center Rotterdam, Transplant Institute, Department of Pathology, Rotterdam, Netherlands; [3]Erasmus Medical Center Rotterdam, Transplant Institute, Department of Gastroenterology and Hepatology, Rotterdam, Netherlands; [4]Erasmus Medical Center Rotterdam, Transplant Institute, Laboratory of Experimental Transplantation and Intestinal Surgery, Rotterdam, Netherlands*
Email: r.broere@erasmusmc.nl

Background and aims: Normothermic machine perfusion (NMP) is increasingly used for assessment of deceased donor livers. Cholangiocytes modify bile composition by secretion of bicarbonate (HCO_3^-), creating alkalotic bile that protects against bile salt toxicity (known as the "bicarbonate umbrella"). Low biliary HCO_3^- during NMP indicates cholangiocellular injury and contributes to additional bile salt-induced injury. Secretin is a hormone that stimulates biliary HCO_3^- secretion in-vivo. The aim of the study is to assess whether 1) administration of secretin during NMP restores biliary physiology and the protective bicarbonate umbrella, and 2) secretin could be a novel test of biliary viability.
Method: The effect of secretin was studied in-vitro using intrahepatic cholangiocyte organoids (ICO). Secretin administration was evaluated in a preclinical study using discarded human livers. Next, a prospective clinical study (IDEAL stage 1–2) with human secretin therapy was performed during sequential hypo- to normothermic perfusion, linked by controlled oxygenated rewarming (DHOPE-COR-NMP). Secretin was added at the start of the COR-phase (1 hour prior to NMP) and at 2.5 hours of NMP. Changes in biliary HCO_3^- and early post-transplant outcomes were compared to a historical cohort.
Results: Secretin resulted in a swelling of in-vitro ICO and increased signal in Ussing chamber experiments, indicating increased ion and water excretion ($p = 0.008$). In the preclinical study, secretin treatment during NMP resulted in increased biliary HCO_3^- in viable livers, but not in non-viable livers, indicating that biliary testing was not camouflaged. This effect was similar during the prospective clinical trial. Biliary HCO_3^- was higher in transplanted livers ($n = 10$) compared to non-viable livers ($n = 5$) (10.1 mmol/L vs. 2.2 mmol/L; $p = 0.04$) or to historic controls (10.1 mmol/L vs. 0.5 mmol/L; $p < 0.01$). Recipient outcomes in the first 90 days were similar to historical controls.
Conclusion: In a first in man IDEAL stage 1–2 clinical trial, secretin therapy during NMP increased biliary secretion of HCO_3^- in livers with viable bile ducts. Secretin appeared to be a missing component of NMP perfusion fluid that is required for restoration of normal biliary physiology and a functioning bicarbonate umbrella. Moreover, response to secretin could serve as novel tool to assess biliary viability during NMP.

FRI-468

Clinical outcomes of sequential hypo- and normothermic machine perfusion versus abdominal normothermic regional perfusion for extended criteria donors in liver transplantation: a single center comparison

Roberto Broere[1], Fenna van der Heijden[1], Puck C. Groen[1], Femke De Goeij[1], Sarwa Darwish Murad[2], Caroline den Hoed[2], Robert Porte[1], Wojciech Polak[1], Jeroen de Jonge[1]. *[1]Erasmus Medical Center Rotterdam, Transplant Institute, Department of Surgery, Division of HPB and Transplant Surgery, Rotterdam, Netherlands; [2]Erasmus Medical Center Rotterdam, Transplant Institute, Department of Gastroenterology and Hepatology, Rotterdam, Netherlands*
Email: r.broere@erasmusmc.nl

Background and aims: To address the donor shortage, extended criteria donors after circulatory death (ECD-DCD), are increasingly used. However, ECD-DCD livers have a higher risk of primary non-function and biliary complications. Two main perfusion techniques exist to asses liver function: in-situ abdominal normothermic regional perfusion (aNRP), and ex-situ normothermic machine perfusion, in our center combined with dual hypothermic oxygenated perfusion and controlled oxygenated rewarming (DHOPE-COR-NMP). This study presents a single center comparison of DHOPE-COR-NMP and aNRP of clinical outcomes of ECD-DCD livers.
Method: Liver grafts from ECD-DCD donors between October 2018 and the end of December 2023 were included, with a minimum follow-up of 1 year post-transplantation. Livers were categorised as ECD based on factors such as elevated donor laboratory values, or age above 61 years. When the donor was located in the local procurement, aNRP was performed, otherwise DHOPE-COR-NMP was performed. The primary outcome was death-censored graft survival. Secondary outcomes included acceptance rate, patient survival and post-transplant biliary complications.
Results: In total, 53 DHOPE-COR-NMP and 51 aNRP procedures were included, which resulted in 40 (75%) and 37 (73%) liver transplantations. No primary non-function was observed. At one year, death-censored graft survival and overall patient survival was 92% and 88% for DHOPE-COR-NMP and 95% and 97% in aNRP (ns). One year cumulative incidence of post-transplant cholangiopathy, and anastomotic strictures (AS) was 8%, and 19% in DHOPE-COR-NMP, and 5% and 22% in aNRP (ns). Bile leaks occurred in 13% of DHOPE-COR-NMP and 5% of aNRP at one year (ns). Complications Clavien-Dindo $\geq$ 3 were observed in 63% of DHOPE-COR-NMP and 60% of aNRP (ns).
Conclusion: Both DHOPE-COR-NMP and aNRP allow for safe transplantation of ECD-DCD livers with excellent death-censored graft survival and patient survival. There was no difference in the risk of post-transplant biliary complications between the groups, with a lower incidence of post-transplant cholangiopathy comparing to historical cohorts without machine perfusion.

FRI-473

The impact of extending preservation time of extended criteria liver grafts through hypothermic oxygenated machine perfusion prior to normothermic machine perfusion on viability assessment and clinical outcomes

Roberto Broere[1], Domiziana Pedini[1], Efrayim Küçükerbil[1], Puck C. Groen[1], Jorke Willemse[1], Caroline den Hoed[2], Sarwa Darwish Murad[2], Wojciech Polak[1], Robert Porte[1], Jeroen de Jonge[1]. *[1]Erasmus Medical Center Rotterdam, Transplant Institute, Department of Surgery, Division of HPB and Transplant Surgery, Rotterdam, Netherlands; [2]Erasmus Medical Center Rotterdam, Transplant Institute, Department of Gastroenterology and Hepatology, Rotterdam, Netherlands*
Email: r.broere@erasmusmc.nl

Background and aims: Liver machine perfusion is increasingly used to test and select extended criteria donor (ECD)-livers due to declining donor organ quality. Sequential oxygenated hypothermic and normothermic machine perfusion, linked by one hour of controlled oxygenated rewarming (DHOPE-COR-NMP) can be used to resuscitate donor livers and subsequently perform viability assessment. To improve transplant logistics and facilitate daytime transplantation, prolongation of the DHOPE phase has been proposed. This study evaluates the impact and safety of prolonged DHOPE on donor liver utilization and outcomes in ECD-livers, compared with historical standard DHOPE–COR–NMP.
Method: All donation after circulatory death (DCD)-ECD-livers treated with DHOPE-COR-NMP were included until September 2025. DCD livers were classified as ECD based on elevated laboratory values, age $\geq$61 years, or functional warm ischemia time > 30 mins. Prolonged DHOPE was defined as perfusion time $\geq$ 4 hours. The main outcome was acceptance rate after hepatobiliary viability assessment. Secondary outcomes included death-censored graft survival, overall patient survival, as well as post-transplant complications, such as post-transplant cholangiopathy.
Results: A total of 74 DHOPE–COR–NMP procedures were analyzed, including 16 cases with prolonged DHOPE (median 6 h 52 min) and 58 cases following the standard protocol (median 2 h 9 min). Donor and recipient characteristics did not differ significantly between groups. In the prolonged DHOPE group, 8 livers met acceptance criteria (50%), compared with 44 livers (76%) in the standard group ($p = 0.064$). One-year death-censored graft survival was 75% in the prolonged group versus 88% in the standard group ($p = 0.184$). One-year patient survival was 100% and 85%, respectively ($p = 0.442$). Post-transplant complications were comparable, except for two cases of hepatic artery thrombosis in the prolonged group. Intraoperative red blood cell transfusion requirements were higher following prolonged DHOPE ($p = 0.015$).
Conclusion: This study demonstrates that prolonged DHOPE prior to viability assessment through COR-NMP enables safe transplantation of ECD-DCD livers, yielding outcomes comparable to those of our historical standard cohort. Nonetheless, prolongation of DHOPE was associated with a reduced organ acceptance rate, a finding of clinical relevance that warrants careful monitoring to ensure optimal organ utilization.

FRI-474

Incidence risk factors and outcomes of cytomegalovirus infection after liver transplantation

Maximilian Joseph Brol[1], Greta Marie Bösch[1], Frank Erhard Uschner[1], Martin Sebastian McCoy[1], Kai-Henrik Peiffer[1], Philipp Houben[2], Andreas Pascher[2], Tina Schomacher[1], Michael Praktiknjo[1], Florian Rennebaum[1], Jonel Trebicka[1,3]. *[1]Münster University Hospital, Department of Internal Medicine B, Münster, Germany; [2]University of Münster, Department of General, Visceral and Transplant Surgery, Münster, Germany; [3]European Foundation for the Study of Chronic Liver Failure-EF Clif, Barcelona, Spain*
Email: maximilian.brol@ukmuenster.de

Background and aims: Cytomegalovirus (CMV) infection is the most frequent opportunistic infection after liver transplantation (LT) and is associated with relevant morbidity and adverse outcomes. This study aimed to quantify the incidence of CMV infection after liver transplantation, to identify associated risk factors, and to assess its impact on graft and patient outcomes after LT.
Method: This single-center, retrospective cohort study included 200 adult patients undergoing LT between August 2011 and December 2018. CMV infection was assessed within 1 year and within 5 years after LT. Recipient and donor characteristics, CMV serostatus, post-LT complications, and mortality were analyzed.
Results: CMV infection was diagnosed in 40 patients (20.0%) within 1 year and in an additional 13 patients (8.2%) between 1 and 5 years after LT, resulting in a cumulative 5-year incidence of 22.5%. The median time to CMV infection was 3.0 months (95% confidence interval 2.3–3.7). Donor CMV-IgG positivity was the strongest independent risk factor for CMV infection. In univariate logistic regression, receipt of an organ from a CMV-IgG positive donor was

associated with an increased risk of CMV infection within 1 year (OR 2.91, 95% confidence interval 1.36–6.23, p = 0.006) and within 5 years (OR 2.77, 95% confidence interval 1.35–5.67, p = 0.005). Within 1 year, overall mortality was significantly lower in patients with CMV infection compared with those without infection (7.5% vs 21.4%, p = 0.044). In contrast, no significant difference in 5-year-overall mortality was observed between patients with and without CMV infection (20.0% vs 15.8%, p = 0.541).
Conclusion: In this cohort, CMV infection occurred in one fifth of patients within the first year after LT. Donor CMV serostatus was the strongest predictor of infection. In our study, CMV infection post LT did not influence long-term survival. These findings highlight the pivotal role of donor recipient serostatus in risk stratification and support tailored monitoring strategies after LT.

FRI-475
Healthcare practitioners' perceptions of the care and service needs of young adults undergoing liver transplantation: a mixed-methods study
Hattie Charles[1]. [1]*University of Warwick, Coventry, United Kingdom*
Email: h.m.charles@lse.ac.uk

Background and aims: Young adults (18–25) undergoing liver transplantation represent a clinically distinct group whose outcomes depend heavily on engagement, adherence, and self-management. Despite this, UK transplant services remain primarily adult-oriented, with limited developmentally tailored provision. Emerging evidence suggests that psychosocial vulnerability, limited life experience, and unstable social circumstances may influence clinical outcomes in this age group, yet little is known about how practitioners perceive and respond to these needs. This study aimed to explore healthcare practitioners' perceptions of the care, support, and service needs of young adults undergoing liver transplantation, and to identify barriers and facilitators to delivering effective, age-appropriate clinical care.
Method: A mixed-methods design was used. Semi-structured interviews were conducted with specialist liver transplant practitioners (N = 9) across a major UK transplant centre. Interviews explored clinical challenges, engagement, self-management, psychosocial needs, and service delivery. Data were analysed using thematic analysis. An anonymous online survey (N = 31 respondents; 16–20 per item) captured broader perspectives on training, policy, resources, and clinical practice. Quantitative data were summarised descriptively. Findings were integrated to identify convergent themes relevant to clinical care.
Results: Practitioners described a high psychological burden for young adults, compounded by developmental transitions, limited life experience and social isolation. Engagement was a major barrier, affected by precarious housing, financial insecurity and unequal access to transplant services. Integrated, developmentally attuned clinics were viewed as highly beneficial. Survey data confirmed gaps in training, age-specific policy and psychosocial resources.
Conclusion: Young adults undergoing liver transplantation face distinct clinical and psychosocial challenges that influence engagement, adherence, and outcomes. Practitioners identified a need for developmentally tailored, multidisciplinary models of care that address both clinical and structural determinants of health. Strengthening psychological support, improving communication pathways, and embedding age-appropriate service design into routine transplant care may enhance long-term outcomes for this vulnerable group. These findings highlight an important opportunity to optimise clinical practice for young adult transplant recipients.

FRI-476-YI
Triglyceride-based insulin resistance indices and post-transplantation diabetes mellitus after liver transplantation
Mateo Chvatal-Medina[1], Yakun Li[1], Adrian Post[2], Margery A. Connelly[3], Han Moshage[1], Stephan J.L. Bakker[2], Vincent E. de Meijer[4], Hans Blokzijl[1], Robin Dullaart[5]. [1]*Department of Gastroenterology and Hepatology, University Medical Center Groningen, University of Groningen, Groningen, The Netherlands, Groningen, Netherlands;* [2]*Department of Internal Medicine, Division of Nephrology, University Medical Center Groningen, University of Groningen, P.O. Box 30.001, 9700 RB Groningen, The Netherlands, Groningen, Netherlands;* [3]*Labcorp, 100 Perimeter Park, Morrisville, NC 27560, USA, Morrisville, United States;* [4]*Department of Surgery, Division of Hepato-Pancreato-Biliary Surgery and Liver Transplantation, University Medical Center Groningen, University of Groningen, P.O. Box 30.001, 9700 RB Groningen, The Netherlands, Groningen, Netherlands;* [5]*Department of Internal Medicine, Division of Endocrinology, University Medical Center Groningen, University of Groningen, P.O. Box 30.001, 9700 RB Groningen, The Netherlands, Groningen, Netherlands*
Email: m.chvatal-medina@umcg.nl

Background and aims: Post-transplant diabetes mellitus (PTDM) is a common complication following liver transplant (LT) and is associated with adverse outcomes. The triglyceride-glucose product (TyG) and the triglyceride-to-high-density lipoprotein (HDL) cholesterol ratio (TG/HDL-c) are indices that can serve as triglyceride-based proxies for insulin resistance. Their relation to PTDM in liver-transplant recipients (LTRs) is unclear.
Method: TyG and TG/HDL-c (nuclear magnetic resonance spectroscopy) were compared between LTRs without diabetes at baseline (TransplantLines cohort study; NCT03272841) with non-diabetic participants from the community-dwelling PREVEND cohort. Among LTRs, associations with incident PTDM were determined using Cox regression analysis and logistic regression analysis with adjustment for relevant variables.
Results: TyG was higher in 246 non-diabetic LTRs (mean age 52.6 years; 53.7% male) compared to 4533 non-diabetic PREVEND participants (mean age 53.1 years; 48.9% male (p < 0.001), and confirmed using propensity score matching (p < 0.001). Over a median follow-up of 7.1 years, 31 LTRs developed PTDM (12.6% cumulative incidence). A higher baseline TyG index was associated with an increased risk of PTDM (HR per 1-SD increase: 1.67, 95% CI 1.28–2.30; highest vs. lowest tertile HR: 1.77, 95% CI 1.14–2.64). The TG/HDL-c ratio followed the same trend (HR per 1-SD increase: 1.56, 95% CI 1.14–2.15; highest vs lowest tertile: HR 3.80, 95% CI 1.73–10.0). Findings remained in adjusted analyses and were directionally similar in logistic regression models.
Conclusion: In LTRs, both the TyG index and the TG/HDL-c ratio are associated with PTDM. These indices could serve as a basis for post-transplant risk stratification in diabetes development.

FRI-477
Triglyceride-rich lipoprotein cholesterol and risk of post-transplant diabetes in liver transplant recipients
Mateo Chvatal-Medina[1], Adrian Post[2], Margery A. Connelly[3], Yakun Li[1], Han Moshage[1], Stephan J.L. Bakker[2], Vincent E. de Meijer[4], Hans Blokzijl[1], Robin Dullaart[5]. [1]*Department of Gastroenterology and Hepatology, University Medical Center Groningen, University of Groningen, P.O. Box 30.001, 9700 RB Groningen, The Netherlands, Groningen, Netherlands;* [2]*Department of Internal Medicine, Division of Nephrology, University Medical Center Groningen, University of Groningen, P.O. Box 30.001, 9700 RB Groningen, The Netherlands, Groningen, Netherlands;* [3]*Labcorp, 100 Perimeter Park, Morrisville, NC 27560, USA, Morrisville, United States;* [4]*Department of Surgery, Division of Hepato-Pancreato-Biliary Surgery and Liver Transplantation, University Medical Center Groningen, University of Groningen, P.O. Box 30.001, 9700 RB Groningen, The Netherlands, Groningen, Netherlands;*

[5]*Department of Internal Medicine, Division of Endocrinology, University Medical Center Groningen, University of Groningen, P.O. Box 30.001, 9700 RB Groningen, The Netherlands, Groningen, Netherlands*
Email: m.chvatal-medina@umcg.nl

Background and aims: Post-transplant diabetes mellitus (PTDM) is the most important metabolic complication after liver transplantation. The role of triglyceride-rich lipoprotein cholesterol (TRL-c, remnant cholesterol) in PTDM risk is poorly defined. We characterized TRL-c in liver transplant recipients (LTRs) (Transplantlines cohort) compared with the general population (Prevention of REnal and Vascular ENd-stage Disease (PREVEND) cohort) and evaluated the association between TRL-c and incident PTDM.
Method: We studied 367 adult LTRs with fasting lipid profiling and long-term follow-up for PTDM (until February 2025). TRL-c was calculated from nuclear magnetic resonance spectroscopy-derived total cholesterol, high density lipoprotein cholesterol (HDL-c) and low density lipoprotein cholesterol (LDL-c). Baseline TRL-c and lipid profiles were compared with 4,837 PREVEND participants with and without type 2 diabetes, and additionally using propensity-score matching. Incident PTDM was analyzed using Cox proportional hazards models and associations were examined per 1-SD increase in TRL-c, adjusting for demographic, metabolic, lipid, and immunosuppressive factors.
Results: Compared with PREVEND participants, LTRs had higher triglycerides, TRL-c, and HDL-c but lower total and LDL-c, both in individuals with and without diabetes at baseline. Among LTRs, TRL-c levels were highest in those with preexistent diabetes and lowest in those who remained non-diabetic. During 7.1 years of follow-up 31 LTRS developed diabetes. LTRs in the highest TRL-c tertile had the highest PTDM incidence (p = 0.017). In unadjusted analyses, each 1-SD increase in TRL-c was associated with a 64% higher PTDM risk (HR 1.64, 95% CI 1.25–2.14). This association remained significant after adjustment for age, sex, BMI, statin use, HDL-c, LDL-c, triglycerides, HbA1c, immunosuppressive regimen.
Conclusion: TRL-c is elevated in LTRs, and independently associates with incident PTDM. Conceivably, TRL-c reflects a dyslipidemic phenotype not captured by other lipid metrics and may help refine risk stratification in this population.

FRI-478

Synergism of trimethylamine n-oxide and lipoprotein insulin resistance with post-transplantation diabetes after liver transplant

Mateo Chvatal-Medina[1], Yakun Li[2], Adrian Post[3], Margery A. Connelly[4], Han Moshage[2], Stephan J.L. Bakker[3], Vincent E. de Meijer[5], Hans Blokzijl[2], Robin Dullaart[6]. [1]*Department of Gastroenterology and Hepatology, University Medical Center Groningen, University of Groningen, P.O. Box 30.001, 9700 RB Groningen, The Netherlands, Groningen, Netherlands;* [2]*Department of Gastroenterology and Hepatology, University Medical Center Groningen, University of Groningen, Groningen, The Netherlands, Groningen, Netherlands;* [3]*Department of Internal Medicine, Division of Nephrology, University Medical Center Groningen, University of Groningen, P.O. Box 30.001, 9700 RB Groningen, The Netherlands, Groningen, Netherlands;* [4]*Labcorp, 100 Perimeter Park, Morrisville, NC 27560, USA, Morrisville, United States;* [5]*Department of Surgery, Division of Hepato-Pancreato-Biliary Surgery and Liver Transplantation, University Medical Center Groningen, University of Groningen, P.O. Box 30.001, 9700 RB Groningen, The Netherlands, Groningen, Netherlands;* [6]*Department of Internal Medicine, Division of Endocrinology, University Medical Center Groningen, University of Groningen, P.O. Box 30.001, 9700 RB Groningen, The Netherlands, Groningen, Netherlands*
Email: m.chvatal-medina@umcg.nl

Background and aims: Post-transplant diabetes mellitus (PTDM) is a common complication after liver transplantation. Trimethylamine N-oxide (TMAO), a microbiota-derived metabolite, has been linked to insulin resistance, but epidemiological findings on type 2 diabetes remain inconsistent. The lipoprotein insulin resistance (LP-IR) score is a nuclear magnetic resonance (NMR)-derived marker of insulin resistance, yet its role in PTDM and interaction with TMAO are unknown.
Method: Prospective cohort study (TransplantLines, NCT03272841) at a tertiary care center (Universitair Medisch Centrum Groningen, The Netherlands). Three hundred sixty-seven (367) liver transplant recipients (LTRs) were studied. Baseline TMAO and LP-IR score were quantified by NMR spectroscopy. Incident PTDM was defined by international criteria. Associations were tested using logistic regression with prespecified adjustment. Effect modification was tested with interaction terms.
Results: 31 out of 246 LTRs at risk developed PTDM after a median follow-up of 7.1 years. Higher TMAO (OR 2.14, 95% CI 1.17–4.00, p = 0.015) and LP-IR score (OR 1.66, 95% CI 1.10–2.37, p = 0.015) were associated with increased PTDM risk after adjustment for eGFR and immunosuppressant use. A positive interaction was present (p = 0.029) with risk amplification when both biomarkers were elevated. TMAO's association with PTDM was strongest at high LP-IR (90th percentile; OR 3.20, 95% CI 1.46–7.03, p = 0.005), and LP-IR's association was strongest at high TMAO (90th percentile; OR 2.56, 95% CI 1.41–4.64, p = 0.002).
Conclusion: TMAO and LP-IR were independently and synergistically associated with PTDM in LTRs, suggesting a diabetogenic potential of TMAO that depends on insulin resistance, as captured by lipoprotein variables.

FRI-479

Liver transplant recipients experiencing biliary complications show elevation in quantitative magnetic resonance cholangiopancreatography metrics during monitoring

Tom Davis[1], Anneli Andersson[1], Elizabeth Shumbayawonda[1], Jelte Schaapman[2], Miguel Castelo-Branco[3], Anil Dhawan[4], Hildo Lamb[2], Minneke Coenraad[2]. [1]*Perspectum Ltd., Oxford, United Kingdom;* [2]*Leiden University Medical Center, Leiden, Netherlands;* [3]*Coimbra Institute for Biomedical Imaging and Translational Research, Universidade de Coimbra, Coimbra, Portugal;* [4]*King's College London, London, United Kingdom*
Email: anneli.andersson@perspectum.com

Background and aims: In the first year after liver transplantation (LT), 20–40% of recipients develop biliary complications, increasing the risk of graft failure and re-listing. Current routine biomarkers are not sufficiently specific and robust for assessment of biliary complications. We aim to explore the potential of quantitative magnetic resonance cholangiopancreatography (qMRCP) for robust non-invasive monitoring in LT recipients.
Method: Retrospective analysis was performed on clinical data from a prospective trial, (RADIcAL2), recruiting patients eligible for biopsy following LT at transplant centres in Leiden (the Netherlands), Coimbra (Portugal), and London (UK). qMRCP was generated by MRCP+ (Perspectum Ltd, Oxford). Upper limit of normal (ULN) values for biochemical markers were 40 U/L for aspartate aminotransferase (AST) and alanine aminotransferase (ALT), 147 U/L for alkaline phosphatase (ALP), 48 U/L for gamma-glutamyl transferase (GGT) and 1.2 mg/dL for total bilirubin.
Results: N = 102 patients (n = 89 adults, n = 13 paediatrics); Median age 53 years; 27% females) had qMRCP results and biochemical markers available. There were 20 post-transplant biliary complications. Median time from LT to biliary complication was 1 month (n = 6 recorded at the time of transplant), and from biliary complication to imaging was 13 months. Median MRCP metrics were higher in patients with, compared to without, recorded biliary complications including number of ducts (132 vs 51, p < 0.0004), length of strictures (106 mm vs 60 mm, p < 0.005), length of dilatations (161 mm vs 76 mm, p < 0.003), number of strictures (14 vs 7, p < 0.02), and number of abnormal ducts (24 vs 11, p < 0.002). In patients where the above listed MRCP metrics were elevated above the healthy reference

ranges, 24–27% had post-transplant biliary complications, significantly more than in those within the reference range (3–7%). In those with ALP elevated above ULN, 28% had post-transplant biliary complications (compared to 6% for ALP <ULN; p < 0.005), while no significance was found for elevated ALT, AST, bilirubin, or GGT.
Conclusion: Quantitative MRCP shows potential as a non-invasive test for biliary complications in LT recipients, with higher rates of recorded biliary complications in those with abnormal biliary tree metrics. To confirm the utility of qMRCP in post-transplant monitoring, prospective research should investigate associations with complication type and prediction of graft survival.

FRI-480-YI
From childhood to adulthood: outcomes after pediatric liver transplantation with a median 25-year follow-up
Julia Collot[1], Marie-Eve Chartier[2], Fernando Alvarez[2], Caroline Lemoine[3], Catherine Vincent[1], Marc Bilodeau[1], Denis Marleau[1], Julian Hercun[1]. *[1]Liver unit, Centre Hospitalier de l'Université de Montréal (CHUM), Department of Medicine, Université de Montréal, Montréal, Canada; [2]Division of pediatric gastroenterology, hepatology and nutrition, CHU Sainte-Justine, Montréal, Canada; [3]Division of pediatric surgery and liver transplantation, CHU Sainte-Justine, Montréal, Canada*
Email: julia.collot@gmail.com

Background and aims: Pediatric liver transplantation (pLT) has become a life-saving procedure for children with end-stage liver disease, but data on extended long-term outcomes remains limited. We aimed to evaluate 25-year outcomes after pLT in recipients from Centre hospitalier universitaire Sainte-Justine (CHUSJ) in Montréal who transitioned to adult care at the Centre Hospitalier de l'Université de Montréal (CHUM), and to identify predictors of patient and graft survival.
Method: We conducted a retrospective cohort study including patients who underwent liver transplantation at CHUSJ between 1986 and 2020 and had at least one follow-up at CHUM. Collected data included sex, age at transplantation, transplant indication, rejection episodes, treatment adherence, socio-educational status, and retransplantation. Survival analyses were performed using Kaplan-Meier and Cox regression models.
Results: A total of 124 patients were included. The main indications for pLT were biliary atresia (BA) (33.9%) and metabolic/congenital diseases (32.3%), followed by fulminant hepatitis, pediatric cholestatic diseases, progressive cholestasis of northwestern Quebec (PCNQ), autoimmune hepatitis (AIH) or primary sclerosing cholangitis (PSC), and miscellaneous causes (including hepatoblastoma and viral cirrhosis). Median follow-up time was 25.6 years (IQR: 19.1–31.5). Overall survival rates were 96.4% at 20 years and 85.0% at 30 years post-transplant, while graft survival rates were 84.8% and 77.7% at 20 and 30 years, respectively. Biopsy-confirmed rejection was the only factor associated with poorer graft survival (HR 3.37 95% CI 1.30–8.72, p = 0.012). Compared with other indications, PCNQ was associated with poorer overall survival (HR 5.34, 95% CI 1.52–18.79, p = 0.009) and the highest rate of nonadherence (OR 16.6, 95% CI 3.1–88.1, p < 0.001). Socio-educational integration was associated with improved overall survival (HR 0.12, 95% CI 0.03–0.47, p = 0.003) and graft survival (HR 0.35, 95% CI 0.13–0.96, p = 0.042). Only 6.5% were lost to long-term follow-up after transition. Initial immunosuppressive regimen had no impact on survival.
Conclusion: pLT offers excellent long-term patient and graft survival, but nonadherence, rejection, and psycho-educational issues remain key challenges. Multidisciplinary care and structured transition are essential to maintain or improve these outcomes. Particular attention should be given to PCNQ, which was associated with poorer long-term outcomes.

FRI-481-YI
Impact of recipient aerobic capacity, donor and graft characteristics on survival in patients with cirrhotic liver disease assessed for liver transplantation
Emma Cook[1], Miriam Cortes Cerisuelo[1], Abid Suddle[1], Claire Kelly[1], Varuna Aluvihare[1], William Bernal[1]. *[1]Institute of Liver Studies, Kings College Hospital, London, United Kingdom*
Email: emma.cook40@nhs.net

Background and aims: Chronic liver disease (CLD) is associated with poor aerobic capacity (AC). Cardiopulmonary exercise testing (CPET) comprehensively measures AC: impaired AC has been associated with non-survival with and without liver transplantation (LT). In a very large, single-centre CLD patient cohort, we aimed to definitively investigate the relationship between AC, recipient and donor characteristics, and survival.
Method: This retrospective, observational cohort study included patients with cirrhotic CLD who underwent elective LT assessment, including CPET determined using a cycle ergometer, at a single LT centre from 2000 to 2024. Descriptive statistics are presented with Chi-squared or Kruskal-Wallis tests. Survival analyses included log-rank testing and multivariate Cox regression.
Results: 2624 patients were assessed for LT, 33% with alcohol and 67% with other causes of CLD. 36% were female, median age was 56 years (IQR: 47–62), follow-up after CPET was 857 days (242–2313), and after LT 1527 days (347–2823). At CPET maximum Heart Rate was 138 (121–156) BPM, Peak Workload 91 (69–118) W, and measures of AC included Peak VO_2 of 16.7 (13.1–20.7), percentage predicted VO_2 62.6 (48.7–78.0) % and Anaerobic Threshold (AT) 10.7 (8.8–12.9) mL/kg/minute. 1860 patients (71%) were LT waitlisted, of whom 226 (12%) died before LT. On multivariate analysis AT determined at CPET was independently associated with waitlist survival (HR 0.93 [0.88–0.98], p = 0.008). Of 1493 (57%) transplanted, 67% received a donor after brain death (DBD) graft, and 28% a donor after circulatory death (DCD) graft. 90-day and 1-year post-LT mortality were 1.6% and 3.5% respectively. DCD recipients had poorer 5-year survival than DBD recipients (9.8% vs. 14.5% mortality, HR 1.72, p = 0.001), however on multivariate analysis recipient age (HR 1.02, p = 0.014), metabolic dysfunction-associated steatotic liver disease (MASLD) aetiology (HR 1.63, p = 0.05) and HCC diagnosis (HR 1.73, p = 0.003), but neither AC, DBD/DCD status or other donor factors retained independent association with post-LT survival.
Conclusion: AC closely associates with survival in CLD patients awaiting LT and interventions to improve AC may impact on survival to transplant. However, AC did not impact post-LT survival, even in recipients of DCD grafts or those with other sub-optimal features.

FRI-482
Evolving liver transplant indications and rising pre-transplant metabolic risk burden: a single-center analysis, 2013–2023
Andrew John Cruz[1,2], Paul Paik[1,2,3], Kalpana Gopalkrishnan[4], Niveda Balemurughan[4], Yinan Su[4], Roxanna Sharifi[4], Jeffrey Kahn[1,3,5], Navpreet Kaur[5,6], Derek Samson[5], Howard Lee[7], Liyun Yuan[1,3,5]. *[1]Keck School of Medicine of USC, Department of Medicine, Los Angeles, United States; [2]Los Angeles General Medical Center, Department of Medicine, Los Angeles, United States; [3]Division of Gastroenterology and Liver Diseases, Keck School of Medicine, University of Southern California, Los Angeles, United States; [4]Keck School of Medicine of USC, Los Angeles, United States; [5]Transplant Institute, Keck Medicine of USC, University of Southern California, Los Angeles, United States; [6]Department of Surgery, Keck School of Medicine of the University of Southern California, Los Angeles, United States; [7]Uniformed Services University of Health Sciences, Gastroenterology and Hepatology, Malcolm Grow Medical Clinics and Surgery Center, Andrews Medical Group, Joint Base Andrews, United States*
Email: andrewjohn.cruz@med.usc.edu

Background and aims: Liver transplantation (LT) etiologies have shifted over the past decade, with metabolic dysfunction–associated

steatotic liver disease (MASLD) and alcohol-associated liver disease (ALD) emerging as leading indications in the United States. Metabolic disease burden among recipients across non-metabolic indications appears to be rising. We evaluated temporal trends in LT indications and clustering of metabolic risk factors (RFs) at transplantation.
Method: We retrospectively studied adults (≥18 years) undergoing primary LT at Keck USC (2013–2023), excluding re-transplantations. Indications were categorized as MASLD, ALD, metabolic alcohol-associated liver disease (MetALD), viral hepatitis (HBV/HCV), autoimmune/cholestatic disease (PSC/PBC/AIH), or cryptogenic/other. Metabolic burden was assessed using four RFs at LT (BMI ≥25 kg/m^2, diabetes, hypertension, dyslipidemia) summed to 0–4. Multinomial logistic regression tested temporal shifts in indication distribution; logistic, Poisson, and linear regression modeled annual trends (OR/IRR/β per year).
Results: Among 1,338 recipients, indications changed over time (multinomial likelihood ratio test: LR = 135.33, df = 50, $p = 8.59 \times 10^{-10}$). Viral hepatitis declined 36.2%→5.8% (OR 0.86/year; 95% CI 0.82–0.90; p < 0.0001) while MASLD increased 16.2%→29.9% (OR 1.09/year; 95% CI 1.04–1.13; p < 0.0001). ALD was most prevalent and increased 28.8%→33.6% (OR 1.06/year; 95% CI 1.02–1.10; p = 0.006). Autoimmune/cholestatic increased 5.0%→14.6% (OR 1.06/year; 95% CI 1.00–1.12; p = 0.04). MetALD showed no consistent trend (12.5%→14.6%; OR 0.95/year; 95% CI 0.90–1.00; p = 0.05), and cryptogenic/other was stable (1.2%→1.5%; OR 0.94/year; 95% CI 0.85–1.03; p = 0.17). Mean metabolic RF count increased 1.09→1.64; linear regression β = 0.042/year (95% CI 0.027–0.057; p = 0.0003; R^2 = 0.78) with similar Poisson findings (IRR 1.033/year; 95% CI 1.018–1.049; p < 0.0001). RF distribution differed between 2013 and 2023 (χ^2 = 20.80, df = 4; p = 0.0003), indicating greater prevalence of ≥2 RFs. Non-MASLD/non-MetALD recipients comprised 41.1% (95% CI 36.8–45.5) of all ≥2 RF and 31.8% (95% CI 25.7–38.6) of all ≥3 RF, demonstrating that metabolic burden extends beyond primary metabolic liver disease.
Conclusion: As LT indications evolve, metabolic RFs are increasingly prevalent across all etiologic categories. These findings support universal metabolic risk stratification and targeted interventions during LT evaluation and post-transplant care to mitigate graft-related and cardiovascular complications.

FRI-483
Donor-related ethical issues in living donor liver transplantation: a single-center survey from North Macedonia
Elena Curakova Ristovska[1], Beti Todorovska[1], Fana Licoska-Josifovik[1], Meri Trajkovska[1], Emilija Nikolovska Trpchevska[1]. *[1]University Clinic for Gastroenterohepatology, Skopje, North Macedonia, Ss. Cyril and Methodius University in Skopje, Skopje, North Macedonia, Skopje, Macedonia*
Email: elenacurakova@yahoo.com

Background and aims: While deceased donor liver transplantation remains the standard of care in most Western countries, living donor liver transplantation (LDLT) has become an essential component of transplant programs worldwide. However, despite the advantages, it raises several important and unique ethical issues. This study aimed to assess key donor-related ethical aspects of the LDLT process and to identify areas for future improvement in clinical practice.
Method: All liver donors evaluated at our center between 2007 and 2026 who donated for LDLT abroad were invited to complete an anonymous survey. The questionnaire collected demographic data and included 18 items addressing donor motivation, voluntariness, adequacy of information, autonomy, coercion, and freedom to withdraw, primarily assessed using a 5-point Likert scale. The study was conducted in accordance with the Declaration of Helsinki and approved by the local Ethics Committee.
Results: Twenty-four adult donors (14 men and 10 women, mean age of 41.5 years) responded (82.8%). Most donors were first-degree relatives (5 siblings, 2 parents, 2 children), followed by spouses (6), close relatives or in-laws (5), and distant relatives or close friends (4). The primary motivation for donation was saving the life of a loved one (n = 21; 87.5%). Despite donors' awareness of the legal and ethical prohibition of financial compensation, indirect compensation in one non–genetically related donor could not be definitively excluded. While most donors reported receiving adequate medical information before consent (complete n = 17, sufficient n = 2, partial n = 3), some later acknowledged insufficient understanding of the associated health risks at the time (complete n = 15, sufficient n = 3, partial n = 4, insufficient n = 1). Full autonomy in decision-making and absence of pressure were reported by 22 donors (91.7%). Twenty-one donors (87.5%) reported no regret and stated they would certainly make the same decision again. Perceived implementation of ethical standards varied, ranging from complete to absent (complete 8, substantial 5, partial 5, insufficient 1, absent 1).
Conclusion: LDLT involves complex ethical challenges that require strict adherence to established ethical principles. Future efforts should focus on improving donor information, preventing coercion, and better integrating ethical standards into practice, with particular caution against compensation in directed altruistic donations between non-relatives, especially in low- and middle-income countries.

FRI-484
Prevalence and factors associated with phosphatidylethanol positivity in candidates for liver transplantation : a proof-of-concept study
Margaux Delhomme[1], José Ursic Bedoya[2], Lionel Moulis[3], Mélanie Russello[1], Idir Makhlouf[1], Nicolas Langendorfer[1], Laura Jaubert[1], Georges-Philippe Pageaux[2], Hélène Donnadieu[1]. *[1]Department of Addiction, Regional University Hospital Center of Montpellier, Montpellier, France; [2]Department of Hepatogastroenterology, Regional University Hospital Center of Montpellier, Montpellier, France; [3]Epidemiological and Clinical Research Unit, Regional University Hospital Center of Montpellier, Montpellier, France*
Email: margaux.delhomme@hotmail.fr

Background and aims: Liver transplantation (LT) is the reference treatment for end-stage chronic liver disease and selected liver cancer. Regardless of etiology, severe alcohol relapse after LT markedly increases morbidity and mortality. Although integration of an addiction team reduce relapse rates, the identification and monitoring of patients at risk remain heterogeneous and rely on self-reported data and indirect biomarkers, which may underestimate alcohol consumption. Direct biomarkers such as phosphatidylethanol enable earlier and more objective detection of alcohol consumption. This proof-of-concept study aimed to evaluate the contribution of PEth in detecting excessive alcohol consumption during pre-transplant assessment and its association with known risk factors.
Method: We conducted an interventional, single-center phase II study including patients enrolled in a LT pathway. All patients underwent a pre-LT addiction assessment. Sociodemographic, addiction and psychiatric data were collected using standardised methods. PEth levels were measured every three months during the pre-LT period, with 12-month follow-up. Analyses focused on describing the pre-transplant population, the prevalence of marker positivity, and the clinical and addiction-related characteristics associated with a positive PEth result.
Results: 24 patients were included (75% men, median age 60.5 years). 58.8% of patients had decompensated cirrhosis (29.4% Child B, 29.4% Child C), with a median MELD score of 9. 66.67% met DSM-V criteria for alcohol use disorder (AUD) prior to pre-LT abstinence. At pre-LT consultation, 91.6% were abstinent (median 12 months), 16.7% received addiction treatment. 4 patients (16.6%) had a strongly positive PEth (>200 µg/L), consistent with heavy alcohol consumption, while 3 of them (75%) reported being abstinent. These patients had more severe AUD (≥6 DSM-V criteria: 50% vs. 0%), shorter

abstinence (median 1.5 [0.7–3.0] vs.18 [9.5–57.0] months; p = 0.006), and lower abstinence confidence (7/10 [5.0–7.5] vs. 9/10 [8.0–10.0]; p = 0.33). The proportion of active smokers was higher in this group (50% vs. 35%). No association was found with sociodemographic factors or liver disease severity.
Conclusion: Regular PEth testing during pre-LT assessment detects recent unreported alcohol use. PEth positivity is associated with a more severe addiction profile, independent of liver disease severity and sociodemographic factors, supporting its use as an objective complement to clinical assessment in the pre-LT pathway.

FRI-485
ACLF-Transplant: a national survey comparing hepatologists' and intensivists' views on access to liver transplantation (LT) for ACLF
Vincent Di Martino[1], Florent Artru[2], Thierry Artzner[3], Delphine Weil-Verhoeven[1] and TRANSPLANT-ACLF Group[4]. *[1]CHU Besançon, Université Marie & Louis Pasteur, Besançon, France; [2]CHU Pontchaillou, Rennes, France; [3]CHU Hautepierre, Strasbourg, France; [4]Hepatology and ICU Departments, 28 centers, France*
Email: vdimartino@chu-besancon.fr

Background and aims: Despite its survival benefit in ACLF, access to LT remains limited. This national survey compared hepatologists' and intensivists' perceptions and practices regarding LT eligibility and barriers to access.
Method: A structured questionnaire was sent to French hepatologists and intensivists involved in the management of cirrhosis and ACLF. Responses covered 4 domains: respondent characteristics, LT decision-making and inter-specialty collaboration, clinical and organizational factors influencing LT access, and potential drivers for improvement. Items were rated using 5- or 7-point Likert scales. Comparisons according to medical specialty and center type (transplant vs. non-transplant centers) were performed using chi-2 and Mann–Whitney tests.
Results: 115 responses were analyzed (65 hepatologists, 50 intensivists) from 28 centers (16 transplant). Hepatologists more often considered ICU-admitted ACLF patients as potential LT candidates (78% vs. 56%). LT was considered "often unreasonable" by 22% of intensivists and 31% of hepatologists. Hepatologists more often reported consideration of advance directives (59% vs. 30%) and early addiction specialist assessment (55% vs. 30%). Clinical instability often limited pre-transplant evaluation. Severe comorbidities were the main reported barrier to LT (73%). LT eligibility criteria were more often considered well defined by hepatologists than intensivists (72% vs. 43%), but only 24% reported a formalized ACLF care pathway. In non-transplant centers, hepatologists more often believed in LT listing of ACLF patients than intensivists (55% vs.14%). Multidisciplinary meetings were less frequently reported by intensivists. Hepatologists more frequently perceived reluctance toward LT among intensivists (45% vs. 16%), whereas intensivists more often reported contradictory information being given to families (53% vs. 34%). Failure to reach agreement was reported by 44%. Support for intensivists' legitimacy to initiate LT discussions was higher among intensivists (94% vs. 78%). Conditioning ICU admission on LT listing was rarely supported (18% vs. 6%). Only 55% of respondent found guidelines for LT in ACLF sufficiently clear. Support for prioritizing ACLF patients at national level was limited (31% vs. 36%).
Conclusion: Substantial inter-specialty discrepancies in LT decision-making for ACLF persist, even in transplant centers. Standardized guidelines and structured care pathways appear to be key drivers to improve consistency and equitable access to LT.

FRI-489
Transplant FITness: the role of prehabilitation in expanding the liver transplant (LT) pool
Andres Duarte-Rojo[1], Susanna Miranda[2], Louis Guzman[1], Joshua Sepic[3], Brittany Zelikoff[2], Justin Boike[1], Laura Kulik[1], Saad Saffo[1], Daniel Ganger[1], Sarang Thaker[1], Amanda Cheung[1], Daniel Borja-Cacho[1], Satish Nadig[1], Daniela Ladner[1], Sean Koppe[1], James Sliwa[3]. *[1]Northwestern University, Evanston, United States; [2]Northwestern Memorial Hospital, Chicago, United States; [3]Shirley Ryan Ability Lab, Chicago, United States*
Email: andres.duarte@northwestern.edu

Background and aims: Advanced chronic liver disease (ACLD) is detrimental to physiologic reserve (PhyRes). Frailty affects 15–20% of LT candidates and >50% have a cardiorespiratory fitness below the threshold for independent living. These conditions severely affect LT eligibility and outcomes. To expand the LT pool and facilitate LT, our hospital started a Prehabilitation Program (PP) in May 2024. Herein, we report PhyRes metrics results and outcomes from our PP.
Method: During baseline evaluation, patients with a liver frailty index (LFI) ≥4.2 were referred to our PP. The program focuses on 1) fostering physical literacy, 2) tailored home-based exercise prescription and dietary prescription, 3) behavioral counseling, and 4) monitoring of metric-based adherence. Patients are seen every 2–6 weeks, and both LFI and 6-min walk test (6MWT) are tested at each visit. Virtual exercise classes were available twice a week.
Results: 57 frail patients (64 ± 7 years; 60% male) were referred to PP (47 [82%] during evaluation). There were 175 scheduled visits with a show-up rate of 84% (≥2 visits in 37 [65%] patients. Four (7%) patients did not engage with program and 2 (4%) were lost to follow up. Main etiologies were MASH (38%) and ALD (34%). Mean MELD 3.0 was 18 ± 6 and BMI 28 ± 7. All were decompensated: HE 70%, ascites 90%—refractory 44%. Prior falls were reported by 39% and 40% were on midodrine for hypotension. Regarding outcomes, 29 (53%) were added to waitlist (n = 23) or discharged after ACLD improvement (n = 6), 25 (45%) achieved LT, and 11 (20%) died. At baseline, LFI was higher among patients not (5.11 [4.72–5.63]) vs. those proceeding to LT (4.71 [4.36–5.26]; p = 0.04). Among 53 prehabilitated patients, LFI improved by second visit (−0.21 [−0.40 to −0.23]; p = 0.028) and peaked by fifth (−0.56 [−0.87 to −0.25]; p,0.001), whereas 6MWT improved by third (35 m [11–59]; p = 0.005) but also peaked at fifth (75 m, [41–109]; p < 0.001). Comparing baseline to last available PhyRes metric for each patient, LFI improved by 0.3, whereas 6MWT improved by 36 m, which was more evident among patients with a favorable outcome. Phase angle numerically improved from 4.42 to 4.58 (p = 0.05), with no differences in relation to LT or death status.
Conclusion: Given the PhyRes decline associated with ACLD, newer strategies are needed to ameliorate the negative effects of frailty. Initial analysis showed that our PP improved PhyRes metrics and facilitated favorable LT outcomes, even for candidates who otherwise would have been denied for frailty.

FRI-490
Fitness accountability in liver transplant (LT) candidates: a survey on exercising habits, barriers and facilitators
Louis Guzman[1], Miriam Rafferty[2], Andy Ponce[3], Sheila Morrissey[3], Susanna Miranda[3], Daniela Ladner[1], Andres Duarte-Rojo[1]. *[1]Northwestern University, Evanston, United States; [2]Shirley Ryan Ability Lab, Chicago, United States; [3]Northwestern Memorial Hospital, Chicago, United States*
Email: andres.duarte@northwestern.edu

Background and aims: LT candidates experience dire physical deconditioning gravely jeopardizing their transplant eligibility. Under the "exercise is medicine" banner, our LT center has pioneered various prehabilitation strategies. We provide physical therapy consultation followed by an exercise prescription to all LT candidates on their baseline clinic visit. Given the challenges of lifestyle modification, we aimed to investigate whether the exercise prescription was being followed, and to learn from candidates what their barriers and facilitators were.
Method: A mixed survey was prospectively administered to LT candidates on their follow-up visit, 4 weeks after their exercise prescription. We applied a questionnaire followed by a brief open-ended-questions interview to characterize exercise habits prior to

and after LT evaluation, and to identify exercising preferences. Retrolective data was obtained from the electronic medical record.
Results: 35 patients (56 ± 10 years; 57% male; BMI 27 ± 5) were surveyed. Most common etiology was alcohol, 69% presented with ascites, and 60% had esophageal varices; MELD 3.0 was 16 ± 6. Approximately 50% of patients had hypertension and coronary artery disease. Liver frailty index (LFI) was 4.09 ± 0.75 at baseline and 4.11 ± 0.75 at follow-up; 9 (26%) had an LFI ≥4.5. Twenty-two (63%) reported engaging on exercise prior to LT evaluation. Walking was the most common activity (46%), although housework/job-related activities were accounted for as exercise. Main reasons for not engaging in exercise were health limitations and lack of interest. Only 9 candidates (26%) recalled being given an exercise prescription and they all reported engaging with exercise; their LFI was unchanged from baseline. Self-reported adherence was low with only 2 patients exercising regularly. None accessed a web-based electronic prescription. Home-based exercise, clear guidance and external motivation were deemed facilitators, whereas lack of routine recall, health-related limitations, and low intrinsic motivation were the main barriers reported. Regarding prescription delivery, candidates favored mobile apps (49%) or printed instructions (34%).
Conclusion: We found our exercise prescription to be ineffective, reflecting lack of fitness accountability. Considering our findings, we have revamped our prehabilitation efforts to include physical fitness education, virtual exercise classes, and timely referral to a dedicated program. We are also revamping the EL-FIT app to maximize home-based fitness resources.

FRI-491
The effect of Tenofovir on bone mineral density in liver transplant recipients

Esra Durmazer[1], Ilker Turan[2], Ilgın Yıldırım Şimşir[3], Ferit Çelik[4], Alper Uysal[5], Ali Senkaya[6], Fulya Günsar[2], Zeki Karasu[2], Ulus Akarca[2]. *[1]Ankara University Faculty of Medicine, Department of Gastroenterology and Hepatology, Ankara, Türkiye; [2]Ege University Faculty of Medicine, Department of Gastroenterology, Izmir, Türkiye; [3]Ege University Faculty of Medicine, Department of Endocrinology and Metabolism, Izmir, Türkiye; [4]Medical Point Hospital, Department of Gastroenterology, Izmir, Türkiye; [5]Kanuni Sultan Süleyman Education and Research Hospital, Department of Gastroenterology, Istanbul, Türkiye; [6]Izmir City Hospital, Department of Gastroenterology, Izmir, Türkiye*
Email: dr.esradurmazer@gmail.com

Background and aims: Metabolic bone disease is a common complication after liver transplantation. In hepatitis B virus–related liver transplant recipients, tenofovir disoproxil fumarate (TDF) is widely used for post-transplant prophylaxis, but its effect on bone mineral density (BMD) remains unclear. This study evaluated the impact of TDF on BMD and the predictive performance of the Fracture Risk Assessment Tool (FRAX) in this population.
Method: This single-centre retrospective study included adult hepatitis B–related liver transplant recipients (2010–2021). Patients receiving TDF for ≥12 months were compared with those treated with entecavir or lamivudine. Dual-energy X-ray absorptiometry before and after transplantation, biochemical parameters, and FRAX scores were analysed. Changes in BMD and T-scores were assessed over time. Time to osteoporosis was evaluated using Kaplan–Meier analysis, and FRAX performance using receiver operating characteristic (ROC) analysis.
Results: A total of 73 patients were included in the analysis (49 in the TDF group and 24 in the control group). Baseline demographic characteristics and osteoporosis related risk factors were comparable between the groups. In the TDF group, lumbar spine T-scores decreased significantly during the first post-transplant year compared with the control group (−0.23 ± 0.56 vs −0.01 ± 0.08 p = 0.006), whereas no significant difference was observed at the second-year follow-up. Kaplan–Meier analysis showed that osteoporosis developed earlier in the TDF group than in the control group (mean time to development: 81.03 ± 4.58 months vs 107.47 ± 16.05 months; p = 0.007). In multivariate analysis, TDF use was the only independent factor significantly associated with BMD loss (p = 0.024). ROC analysis demonstrated that the FRAX score showed good discriminatory performance for predicting BMD loss, with area under the curve values of 0.759 for major osteoporotic fracture risk and 0.802 for hip fracture risk (p < 0.05). The optimal cut-off values were 4.35 and 0.65.
Conclusion: In hepatitis B–related liver transplant recipients, TDF use is associated with greater BMD loss than in controls during the early post transplant period and with an earlier onset of BMD loss during long-term follow-up. Although this bone loss does not appear to progress over time, the earlier development of osteoporosis highlights the need for close bone health monitoring. The FRAX score demonstrated moderate to good discriminatory performance for risk stratification in this population.

FRI-492
Determinants of early mortality after living donor liver transplantation for acute-on-chronic liver failure

Vijay Dyavadi[1], Amy Sangam[1], Navneet Tiwari[1], Changze Hong[2], Qun Cai[2], Meiqian Hu[2], Sina Jameie-oskooei[3], Banwari Agarwal[3], Joerg-Matthias Pollok[3], Michael Spiro[3], Rajiv Jalan[4] and LDLTregistry.org Collaborative[5]. *[1]Royal Free Hospital NHS Foundation Trust, London, United Kingdom; [2]University College London, London, United Kingdom; [3]Royal Free Hospital NHS Foundation Trust, University College London, London, United Kingdom; [4]Royal Free Hospital NHS Foundation Trust, University College London, Liver Failure Group, London, United Kingdom; [5]University College London, International Liver Transplant Society, International Living Donor Liver Transplantation Group, London, United Kingdom*
Email: vjtoday123@gmail.com

Background and aims: Although liver transplantation (LT) is increasingly utilised for selected patients with acute-on-chronic liver failure (ACLF), overall post LT mortality is higher than observed in non-ACLF patients. Outcomes, and factors associated with post-LT mortality is unknown in ACLF patients receiving living-donor LT (LDLT). The aims of this study were to evaluate the short-term post-LT morbidity, mortality and associated factors using a global LDLT registry.
Method: We performed a cohort study of patients undergoing LDLT for ACLF from LDLTregistry.org, a global registry comprising prospectively collected, donor and recipient data submitted by transplant centres worldwide since September 2023. Donor; graft; pre, intra, and post-operative variables were collected. Early mortality (EM) was defined as in-hospital death. Associations with EM were examined using univariable logistic regression, followed by a parsimonious multivariable model. Sensitivity analyses using alternative severity markers were performed.
Results: 64 ACLF patients underwent LDLT [Sex: Male - 61%; Age: 48.5y (IQR 40–52), ACLF grade 3: 20; Extrahepatic organ support (EOS): 28%; Donor age 36y (IQR: 27–45); Donor sex – Female (64.1%)]. The incidence of EM within the cohort was 19.4% - significantly higher in ACLF Grade-3 compared with Grades-1/2 (OR 3.98, 95% CI 1.07–14.77). Donor age, sex and graft-to-recipient weight ratio (GRWR) were not associated with EM. EM was strongly associated with pre-operative recipient severity, particularly EOS requirement prior to transplantation. Among intra-operative variables, longer anhepatic time was associated with early mortality. In a multivariable model including EOS requirement and anhepatic time, life support prior to transplantation remained independently associated with EM (adjusted OR 8.10, 95% CI 1.67–39.21), while anhepatic time was no longer statistically significant. Early post-transplant markers of physiological instability and graft dysfunction (i.e. post op day 1 peak lactate) were associated with EM (OR 1.45, 95% CI 1.16–1.81) but reflected downstream clinical course.
Conclusion: In patients undergoing LDLT for ACLF, EM is driven predominantly by recipient severity at the time of transplantation

and intra-operative ischaemic burden may contribute to early risk. These findings support careful recipient selection and optimisation in ACLF-LDLT, while reinforcing the safety of contemporary living donor and graft selection practices.

FRI-493-YI

Outcomes of retransplant for chronic rejection and risk factors for recurrent chronic rejection in liver transplant recipients at a large American academic transplant center

Eric Fox[1], Archna Patel[2], Michele S. Barnhill[3], Carolyn Mead-Harvey[4], Maria Yataco[5], Kymberly Watt[6], David M. H. Chascsa[3]. [1]*Mayo Clinic Alix School of Medicine, Phoenix, AZ, United States;* [2]*Department of Gastroenterology and Hepatology, Mayo Clinic, Phoenix, AZ, United States;* [3]*Department of Gastroenterology and Hepatology, Department of Transplantation, Mayo Clinic, Phoenix, AZ, United States;* [4]*Department of Quantitative Health Science Research, Mayo Clinic, Phoenix, AZ, United States;* [5]*Department of Gastroenterology and Hepatology, Department of Transplantation, Mayo Clinic, Jacksonville, FL, United States;* [6]*Department of Gastroenterology and Hepatology, Department of Transplantation, Mayo Clinic, Rochester, MN, United States*
Email: fox.eric@mayo.edu

Background and aims: Risk factors for chronic liver transplant rejection have been described, but incidence and risk factors for recurrent chronic rejection (RCR) in patients transplanted for chronic rejection are not known. This study aimed to describe outcomes in patients who received a 2nd liver transplant for chronic rejection and identify risk factors for RCR.
Method: We conducted a retrospective study of patients at Mayo Clinic who had undergone 2nd liver transplantation and were diagnosed with chronic rejection of their re-transplanted liver versus patients who did not experience recurrence of chronic rejection. Statistical analysis was performed using SAS with differences tested using Fisher's exact test for categorical risk factors and Wilcoxon signed rank test for continuous and ordinal risk factors.
Results: Chronic rejection occurred in 93 of 10,727 patients (0.86%) transplanted between 1998 and 2025. Of the patients who had undergone 2nd liver transplantation, 29 patients met inclusion criteria. There was 1-year survival in 27 of 29 patients (93.1%) and 5 year-survival in 20 of 22 patients (90.9%) with median survival of 9.91 years. Of patients with RCR, 3 of 4 achieved 1 and 5-year survival with median survival of 9.45 years. Furthermore, 3 of 4 patients with RCR had a viral indication for first transplant compared to 4 of 25 (16.0%) patients without RCR ($p = 0.067$). Similarly, 3 of 4 patients with RCR had negative donor CMV status with the first transplant (1 patient's donor CMV status was unknown) compared to 6 out of 25 (33.3%) of those without RCR ($p = 0.063$). Median number of acute cellular rejection (ACR) events with 2nd transplant for individuals with RCR was larger than those without RCR ($p = 0.059$), reaching near significance. No statistically significant differences were observed between groups with CMV concordance, sex concordance, recipient race, and age.
Conclusion: Chronic rejection is a rare event, and recurrent chronic rejection occurs even less commonly. Re-transplant is a feasible treatment given good survival. Risk factors for recurrent chronic rejection are difficult to discern given the rarity of the event, however, there were numerically more median ACR episodes in patients with recurrent chronic rejection, suggesting that more intensive immunosuppression regimens should be considered. This is the first study to investigate risk factors for RCR, demonstrating the need for further investigation into this topic and larger sample size for sufficient power.

FRI-494

Donor selection and timing in pediatric liver transplantation for genetic liver disorders: a retrospective sibling cohort analysis

Ibrahim Hassan[1], Razan Bader[1], Ahmed Zidan[1], Mohammed Alqahtani[1], Eyad Gadour[1]. [1]*King Fahad Specialist Hospital, Multiorgan Transplant Centre of Excellence, Pediatric Liver Transplantation, Dammam, Saudi Arabia*
Email: ibrahadi981@yahoo.com

Background and aims: Liver transplantation (LT) is the definitive treatment for genetically inherited liver diseases (GILDs) in children. The choice of donor type, living donor liver transplantation (LDLT) versus deceased donor liver transplantation (DDLTx), and the timing of transplantation critically influence outcomes. This study evaluates the impact of donor type, specific familial donor relationships, and recipient age on post-transplant complications and survival in a matched pediatric sibling cohort.
Method: A retrospective single-center cohort study was conducted on 13 sibling pairs (26 patients) undergoing first-time LT for GILDs between 2015 and 2024. Primary outcomes included biliary and vascular complications and graft survival. Statistical analyses used generalized estimating equations (GEE) and mixed-effects models to account for sibling clustering.
Results: Donor type was not significantly associated with biliary complications ($p = 0.92$; 15.0% in living related, 0% in living unrelated, 20.0% in DDLTx) or vascular complications ($p = 0.81$; 10.0% living related, 0% living unrelated, 20.0% DDLTx), nor graft survival ($p = 0.61$; mean survival 6.08 ± 5.16 years living related, 2.00 years living unrelated, 4.00 ± 2.65 years DDLTx). However, specific donor relation significantly correlated with vascular complications ($p = 0.03$), occurring exclusively with brother (100%), aunt (50%), and deceased donors (20%), while no vascular events were observed with mothers, fathers, or uncles. Infants (<1 year) had zero biliary or vascular complications ($p = 0.15$ and $p = 0.22$, respectively) and higher mean graft survival (6.44 ± 5.92 vs. 5.11 ± 4.25 years, $p = 0.52$), yet experienced significantly higher mortality (25% vs. 0%, $p = 0.04$). Cold and warm ischemia times showed no significant correlation with graft survival ($r = 0.34$, $p = 0.58$ and $r = -0.18$, $p = 0.78$). Neurodevelopmental outcomes, assessed via school performance and ADHD diagnosis, were not significantly associated with donor type or age at transplant ($p = 0.64$ and $p = 0.54$).
Conclusion: In this familial cohort, LDLT outcomes were comparable to DDLTx. Specific donor-recipient relationships influence vascular complication risk, necessitating careful donor evaluation beyond living/deceased classification. Despite excellent surgical outcomes, transplantation in infancy carries a substantial survival risk, highlighting the need for individualized patient selection and perioperative management.

FRI-495

Impact of genetic diagnosis on graft survival and post-transplant complications in pediatric liver transplant recipients: a decade of experience

Eyad Gadour[1], Ibrahim Hassan[1], Razan Bader[1], Hadi Kuriry[1], Ahmed Zidan[1], Mohammed Alqahtani[1]. [1]*King Fahad Specialist Hospital, Multiorgan Transplant Centre of Excellence, Pediatric Liver Transplantation, Dammam, Saudi Arabia*
Email: eyadgadour@doctors.org.uk

Background and aims: Pediatric liver transplantation (PLT) for genetically inherited liver diseases (GILDs) presents unique challenges, with long-term graft survival and complication profiles influenced by underlying diagnoses and genetic factors. This single-center retrospective cohort study evaluates a decade of PLT outcomes focusing on graft survival and post-transplant complications in a genetically homogeneous population.
Method: We retrospectively analyzed 26 pediatric patients (13 sibling pairs) who underwent liver transplantation for confirmed GILDs between 2015 and 2025 at a tertiary center. Kaplan-Meier survival analysis and log-rank tests assessed graft survival across diagnoses. Associations between gene mutations and complications were evaluated using Fisher's exact test.
Results: Overall graft survival declined progressively: 1-year survival was 80%, 3-year survival 60%, 5-year survival 30%, and dropped below

20% beyond 10 years. Stratified by diagnosis, PFIC II demonstrated superior outcomes with a 50% 10-year graft survival and was the only group with grafts surviving beyond 15 years. Neonatal sclerosing cholangitis and PFIC III showed the earliest graft failures, with no grafts surviving past early post-transplant periods. Crigler-Najjar syndrome also showed prolonged graft durability up to 15 years. Biliary complications occurred in 4 of 13 mutation groups but showed no significant association with specific gene mutations (p = 0.567). Vascular complications were identified in 2 of 13 mutation groups, also without significant genetic correlation (p = 0.451). Patients with vascular complications had a significantly longer mean hospital stay (64.0 ± 58.0 days) compared to those without (32.0 ± 17.1 days, p = 0.049). No significant differences in cold or warm ischemia times were observed between patients with and without complications, though ischemia data were incomplete for complication groups.
Conclusion: Long-term graft survival in pediatric liver transplantation for genetic liver diseases remains limited and is strongly influenced by the underlying diagnosis. While no statistically significant associations were found between specific gene mutations and post-transplant biliary or vascular complications, vascular complications significantly increase hospitalization duration and morbidity. These findings highlight the importance of disease-specific management and surgical precision, underscoring the need for larger multi-center studies to clarify genetic contributions to complications.

FRI-496
Risk of venous thrombosis and hemorrhage in early post liver transplant patients with anti-platelet and anticoagulant prophylaxis; the 4-year single center experience
Tabetha Garver-Mosher[1], Manuel Beltran del Rio[1], Eric Klein[1], Daniel Rolston[1], Savni Satoskar[1], Elliot Grodstein[1], Matthew Bank[1], Daniel Jafari[1]. [1]*North Shore University Hospital, Great Neck, United States*
Email: tgarvermosher@northwell.edu

Background and aims: Venous thromboembolism (VTE) is a common, severe complication of post-liver transplantation, leading to significant morbidity and mortality, as well as bleeding risk from the need for anticoagulation. Current guidelines offer limited consensus on optimal timing of prophylactic (PPX) anticoagulant use, dosage, or timing, leaving providers without clear direction. This study aims to report our center's experience since inception by analyzing rates of venous thrombosis formation and clinically significant bleeding.
Method: This was a retrospective chart review of all adult liver transplant (LT) patients at a quaternary referral hospital in metropolitan New York area between January 17, 2021, and March 4, 2025. There were no exclusion criteria. Demographic, medications, intraoperative, postoperative, and outcome data were collected up to 30 days post-surgery. PPX administration was analyzed in 12-hour blocks of time from the first administration date. This study was reviewed and approved by the Institutional Review Board.
Results: A total of 318 adult LT patients, with a median age of 58 at the time of transplant, were included. The majority (93.7%, n = 298) received VTE PPX (heparin 84.3%, enoxaparin 3.5%, apixaban 18.6%, argatroban 1.3%). Most patients received aspirin (92.1%, n = 293). The median postop time to start PPX was 3.48 days [IQR] 2.4–5.43 days; the median to onset of VTE occurrence was 7.27 days. A prior history of VTE did not significantly influence post-transplant VTE incidence. Compared to the group who received no PPX, those with at least a single dose of PPX had a lower chance of VTE (33.3% vs 12.8%, p < 0.01). The rates of post operative transfusion of blood products (BT) for all patients was 58.5% (n = 186). The duration of PPX was associated with increased rates of BT. The mean anticoagulant days for patients who required a BT was 0.08, vs. 0.005 for those who didn't (p < 0.001). The mean antiplatelet days for patients who required a BT was 0.06, vs 0.001 for those who didn't (p < 0.001).
Conclusion: The use of VTE PPX is associated with lower rates of VTE in early post LT patients, but higher rates of transfusion of blood products. The duration of PPX is associated with an increased rate of BT. Future studies should focus on individualized, risk stratified approaches for VTE PPX in early post LT patients.

FRI-497
Local validation of the RETREAT score and simulation of risk-adapted imaging surveillance after liver transplantation for hepatocellular carcinoma
Andrea González Rayo[1], Ana Guiberteau Sánchez[1], Maria Isabel Monge Romero[1], Nerea Rodríguez Diez[1], Ana Rodríguez López[1], Lourdes García Linares[1], Isabel Narváez López[2], Juan Antonio Almena Sereno[1], Ana Gómez Collado[1], Ana Calderón Fernández-Salguero[1], Ana Garcia Galera[1], Gerardo Blanco Fernández[1], Isidoro Narváez Rodríguez[1]. [1]*Hospital Universitario de Badajoz, Badajoz, Spain;* [2]*Departamento de matemáticas. Attendis - Badajoz, Badajoz, Spain*
Email: andrea.gonzalezr@salud-juntaex.es

Background and aims: The RETREAT score (Risk Estimation of Tumor REcurrence After Transplant) combines pre-transplant alpha-fetoprotein, microvascular invasion, and viable tumor burden in the explant to estimate the risk of hepatocellular carcinoma (HCC) recurrence after liver transplantation (LT). Although widely validated, its role in tailoring post-transplant imaging surveillance in real-world practice remains unclear. We aimed to validate the prognostic performance of RETREAT in a local cohort and to estimate, through simulation, the impact of risk-adapted surveillance strategies.
Method: This retrospective observational study included adult patients transplanted for HCC between 2015 and 2022. Forty-three patients with complete RETREAT data were analyzed. Tumor recurrence, defined as the first radiological or histological diagnosis, was the primary outcome. Recurrence-free survival was assessed using Kaplan–Meier analysis, prognostic discrimination with Harrell's C-index, and a univariable Cox model. RETREAT was compared with Milan criteria in the explant. The standard surveillance protocol (semi-annual computed tomography for 3 years and annual imaging up to 5 years) was simulated against RETREAT-based de-escalation strategies, estimating avoidable scans and theoretical diagnostic delay.
Results: Four recurrences (9.3%) were observed, all extrahepatic, with a median time to recurrence of 2.27 years. No recurrences occurred in patients with RETREAT 0, whereas recurrence rates were 5.9% in RETREAT 1–2 and 23.1% in RETREAT greater than or equal to 3. RETREAT showed good discrimination (C-index 0.79), outperforming Milan criteria in the explant (0.62). Each one-point increase in RETREAT was associated with a higher risk of recurrence (hazard ratio 2.17; 95% confidence interval 1.08–4.34). Simulated strategies could reduce the number of scheduled computed tomography scans by 19% to 23% without increasing the theoretical diagnostic delay of observed recurrences.
Conclusion: In this single-center cohort, the RETREAT score effectively stratified post-transplant recurrence risk and outperformed Milan criteria in the explant. Risk-adapted imaging surveillance based on RETREAT may substantially reduce imaging burden in low-risk patients. Larger studies with complete follow-up are required to confirm the safety of this approach.

FRI-498
Warming up for success: controlled oxygenated rewarming prior to normothermic liver perfusion
Puck C. Groen[1], Colin Van Surksum[1], Roberto Broere[1], Jorke Willemse[1], Efrayim Küçükerbil[1], Stefan H. Luijmes[1], Bettina E. Hansen[2], Caroline den Hoed[1], Sarwa Darwish Murad[1], Wojciech Polak[1], Robert Porte[1], Jeroen de Jonge[1]. [1]*Erasmus MC Transplant Institute,*

Rotterdam, Netherlands; [2]Erasmus MC, Rotterdam, Netherlands
Email: p.groen@erasmusmc.nl

Background and aims: To alleviate the donor organ shortage, use of extended criteria donor (ECD) livers has increased. These grafts carry an increased risk of post-transplant complications, including post-transplant cholangiopathy (PTC) and primary non-function. Dual Hypothermic Oxygenated Perfusion (DHOPE) has shown to reduce the incidence of PTC, whereas Normothermic Machine Perfusion (NMP) enables viability assessment of the liver graft. To prevent abrupt temperature shifts and mitigate ischemia-reperfusion injury, Controlled Oxygenated Rewarming (COR) is performed between DHOPE and NMP. During COR, the liver is gradually rewarmed in 1 hour from 20°C to 37°C, with increasing pressure sets on the hepatic artery (HA) and portal vein.
We describe our experience, providing insight into metabolic changes of the liver during rewarming.
Method: ECD livers underwent DHOPE-COR-NMP with hepatobiliary assessment. Perfusion flows and perfusate blood gases were recorded. Gas composition and flow were adjusted based on HA oxygen (O_2) and carbon dioxide (CO_2) levels. Sodium bicarbonate ($NaHCO_3$) was added when base excess was below −13 mmol/L. To preserve Na^+/K^+-ATPase function, potassium chloride (KCl) was administered to keep K^+ levels above 3.5 mmol/L. Dynamic changes during COR and differences between transplanted and non-transplanted livers were analyzed with linear-mixed models.
Results: 35 livers underwent DHOPE-COR-NMP, of which 22 passed all viability criteria and were transplanted (63% utilization). As livers became more metabolically active, shown by decreasing O_2 and rising CO_2, increased gas flow and higher O_2 concentration were required to maintain adequate levels. $NaHCO_3$ was required in all cases, but over supplementation should be avoided, as activation of Na^+/K^+-ATPase will increase Na^+ levels. Na^+ levels were higher in transplanted livers at 15–38 min of COR. K^+ decreased over time, and KCl administration at 4–5 mmol/L is required to prevent hypokalemia. Transplanted livers showed a steeper K^+ decrease, with significantly lower levels at 8–45 min. Lactate clearance, a viability marker during NMP, started after 38 min of COR in transplanted livers, compared to 53 min in non-transplanted livers. Higher Na^+ and lower K^+ levels in transplanted livers indicate earlier metabolic recovery, combined with earlier lactate metabolization.
Conclusion: Active perfusion management during COR is required and continuous monitoring of perfusate parameters provides valuable insights into metabolic recovery of the liver.

FRI-499

Incidence of early infections in liver transplant recipients at a tertiary care center in Mexico

Alejandro Gutierrez-Castillo[1], Carla Román-Montes[1], Javier Gutierrez-Castillo[2], Nayelli Flores-García[1]. *[1]Instituto Nacional de Ciencias Médicas y Nutrición Salvador Zubirán, Gastroenterology, Mexico City, Mexico; [2]Private Practice, Mexico City, Mexico*
Email: alexgtz91@gmail.com

Background and aims: Infections are the leading cause of death during the first three years after liver transplantation (LT). Early infections, defined as those occurring within the first month after LT, are usually related to the surgical procedure or the use of invasive devices. This study aimed to determine the incidence and risk factors associated with early infections in LT recipients at a tertiary care center in Mexico City.
Method: This was a retrospective, cross-sectional, and analytical study of LT recipients from 2019 to 2023. Demographic, clinical, and surgical variables related to early infections were analyzed using univariate and multivariate analyses to determine risk factors.
Results: Of the 181 LT performed over a five-year period, 125 met the inclusion criteria. Among these, 55% (n = 69) were female, with a mean age of 53 years (SD 13.1, IQR 21). Metabolic dysfunction–associated steatotic liver disease (MASLD) was the leading indication for LT, accounting for 30% of cases. Overall, the incidence of early infections was 38%, occurring at a mean of 11.6 days after LT (SD 9, IQR 12). The most frequent infections were urinary tract infections (23%), pneumonia (21%), and diarrhea (10%). Microbiological isolation occurred in 64% of cases; 87% were bacterial, and 56% were multidrug-resistant (MDR) organisms, mainly *Escherichia coli* and *Klebsiella pneumoniae*. Significant variables included hemoglobin < 12.5 mg/dL (OR 1.3, 95% CI 1.06–1.67, p = 0.013), bilirubin > 5.99 mg/dL (OR 5.9, 95% CI 1.12–24, p = 0.035), leukocyte count (OR 0.79, 95% CI 0.65–0.98, p = 0.028), and hospital length stay (OR 0.82, 95% CI 0.75–0.91, p < 0.01).
Conclusion: Early infections occurred in 38% of LT recipients and were predominantly hospital-acquired bacterial infections caused by MDR organisms. These infections were associated with clinical and perioperative risk factors. Early recognition of these factors is essential to give preventive measures and optimize timely management.

FRI-500

Liver transplantation for perihilar cholangiocarcinoma: single-centre experience

Tereza Háková[1,2], Tomáš Hucl[1], Jiri Fronek[3], Jana Jarošová[1], Pavel Taimr[1]. *[1]Department of Gastroenterology and Hepatology, Institute for Clinical and Experimental Medicine, Prague, Czech Republic; [2]First Faculty of Medicine, Charles University, Prague, Czech Republic; [3]Department of Transplantation Surgery, Institute for Clinical and Experimental Medicine, Prague, Czech Republic*
Email: terezahakova99@gmail.com

Background and aims: Perihilar cholangiocarcinoma (pCCA, Klatskin tumor) is a rare and aggressive malignancy with limited curative treatment options. Liver transplantation (LT) has emerged as a potential therapy for a highly selected subset of patients; however, only a minority of referred patients undergo transplantation. We aimed to analyze indications for LT and reasons for exclusion among patients referred for suspected pCCA.
Method: We retrospectively analyzed all patients referred to our centre for suspected or confirmed pCCA between February 2020 and November 2025. Patients were categorized according to diagnostic outcome and reasons for exclusion from LT, including oncological, procedural, and general transplant-related contraindications.
Results: During the study period, 139 patients (81 men, 58 women; mean age 59.2 years, range 18.6–85) were referred for suspected or confirmed pCCA, while 836 LTs were performed at our center for all indications. In 2 patients (1.4% of total 139), malignancy was not confirmed, 6 patients (4.3%) were diagnosed with intrahepatic cholangiocarcinoma, and 7 patients (5.0%) were indicated for surgical resection. Exclusion due to prior transperitoneal biopsy occurred in 7 patients (5.0%), and 5 patients (3.6%) declined LT. The most common reasons for exclusion were oncological, including local infiltration in 32 patients (23.0%), macrovascular invasion in 19 patients (13.7%), and generalized disease in 24 patients (17.3%). Additionally, 6 patients (4.3%) were excluded due to lymph node positivity during exploratory laparoscopy. Non-oncological exclusions included comorbidities in 5 patients (3.6%), death during evaluation in 2 patients (1.4%), and ongoing alcohol abuse in 2 patients (1.4%). Two patients (1.4%) were removed from the waiting list due to disease progression. Ultimately, 13 patients (9.4%) underwent LT, after median waiting time of 86 days, within a modified Mayo indication criteria (tumor ≤3 cm proximal to the cystic duct, neoadjuvant chemoradiotherapy without brachytherapy). At last follow-up, with a median follow-up of 36 months from LT (range 6–69), 10 transplanted patients (76.9%) were alive without tumor recurrence.
Conclusion: Only a small proportion of patients referred with suspected pCCA met criteria for LT, mainly due to advanced disease. However, carefully selected patients achieved favorable oncological outcomes, likely supported by strict adherence to selection criteria and short waiting times.

FRI-501

First validation of the gender-equity model for liver allocation (sodium and artificial intelligence variants) in an American cohort of patients on the liver transplant waiting list

Austin Halupnik[1], Patrick Ten Eyck[2], Manuel L. Rodríguez-Perálvarez[3], Peregrina Peralta[4], Nazia Selzner[4], Antonio Sanchez[5], Marta Tejedor[5]. *[1]University of Iowa Carver college of medicine, Iowa City, United States; [2]University of Iowa institute for clinical and translational science, Iowa City, United States; [3]Hospital universitario Reina Sofía, IMIBIC, CIBDERehd, Córdoba, Spain; [4]Toronto General Hospital, Toronto, Canada; [5]University of Iowa healthcare, Iowa City, United States*
Email: austin-halupnik@uiowa.edu

Background and aims: The most used allocation system for liver transplantation (LT) is the Model for End-Stage Liver Disease (MELD). Women are disadvantaged, having higher drop-out rates and lower transplant rates. The Gender-Equity Model for Liver Allocation (GEMA) model and its variant including natremia (GEMA-Na) improved 90-day mortality prediction in wait-listed patients, with a greater effect in women. A new derivation using artificial intelligence, GEMA-AI, showed an even better discrimination. No head-to-head comparison of MELD-based and GEMA-based models has been performed in North America.
Method: We analyzed data from all adults listed for LT (2016–2023) at University of Iowa Healthcare and Toronto General Hospital. Severity of liver disease was assessed with both the MELD-based scores (MELD, MELD-Na, MELD 3.0) and GEMA-based scores (GEMA, GEMA-Na, GEMA-AI). Data was collected until the time of transplant, exclusion from the WL, or until February 28, 2025. The ROC curves (receiver operating characteristic curves; AUC) were compared at 90 days of listing. Reclassification of patients using MELD 3.0, GEMA-Na, and GEMA-AI against MELD-Na as the reference category was estimated.
Results: The study included 2,227 patients (297 from University of Iowa, 1,930 from Toronto General), 34% female, mean age 55.3 years. 19% of patients had refractory ascites. Mean MELD, MELD-Na, MELD 3.0, GEMA, GEMA-Na and GEMA-AI scores were 17.1, 19.5, 19.3, 19.7, 21.9 and 19.0 respectively. AUCs for females using MELD-Na, MELD 3.0, GEMA-Na, and GEMA-AI were 0.797, 0.804, 0.794, and 0.814, respectively. In females, when compared to MELD-Na, both GEMA-Na and GEMA-AI had statistically significantly higher AUCs ($p = 0.035$ and $p = 0.039$, respectively); MELD 3.0 was not superior to MELD-Na ($p = 0.17$). 301 (14%) patients reclassified with MELD 3.0. Of them, 96 gained points, of which 57 were women. 763 (34%) patients reclassified with GEMA-Na. Of them, 601 gained points, of which 233 were women. 458 (30%) patients reclassified with GEMA-AI. Of them, 360 gained points, of which 114 were women.
Conclusion: This is the first validation study of GEMA-based liver transplant allocation models in North America. Compared to MELD-Na, both GEMA-Na and GEMA-AI were superior in discriminating mortality for waitlisted females at 90 days. Larger multicenter studies with a more diverse patient population are needed to better understand potential differences between these allocation models.

FRI-505

Post liver transplant alcohol relapse rate – a single center experience

Jordan Holliday[1], Sophoclis Alexopoulos[1], Lea Matsuoka[1], Lydia Aye[1], Vikrant Rachakonda[1]. *[1]University of California-Davis, Sacramento, United States*
Email: lydia.aye@gmail.com

Background and aims: Alcohol associated liver disease (ALD) is the most common indication for liver transplant in the United States. Relapse rates for alcohol use post liver transplant (LT) have been reported to be 8–20%. We defined relapse in our patients as any patient that had a positive PETH result. Our aim is to characterize patients who relapsed with alcohol use post-LT and to identify potential risk factors and interventions to help decrease the risk of relapse in post liver transplant patients.
Method: Retrospective chart review of post-LT patients from July 15, 2023 to July 31, 2025 at University of California Davis Medical Center. All patients underwent monthly PETH testing after LT, and alcohol relapse was defined as positive PETH test.
Results: Ninety-four patients underwent liver transplant; 79 patients were transplanted for ALD [alcohol associated cirrhosis (AC) (n = 67, 84.8%), alcohol associated hepatitis (AH) (n = 12, 5.2%)]. Eleven (13.9%) patients relapsed post-LT [9 AC and 2 AH]. There was no difference in rate of relapse between AC and AH patients ($p = 0.528$). Time to relapse from last alcohol use for AC and AH patients was not significantly different [333 (IQR 199–397) days vs 267 (IQR 120–414) days, $p = 0.727$]. Pre-LT SIPAT score did not differ between AC and AH patients ($p = 0.781$). Patients with post-LT relapse had shorter pre-transplant duration of abstinence [144 (IQR 61–265) days vs 312 (179 = 509) days, $p = 0.016$] and higher MELD at LT [35 (IQR 29–39) vs 25 (20–32), $p = 0.009$] than those with post-transplant abstinence. Post-transplant addiction medicine consultation was offered more frequently to post-LT relapsers [10 (90.1%) vs 23 (33.8%), $p < 0.001$].
Conclusion: Our single center experience in post-LT alcohol relapse rate is consistent with prior studies. There have been several studies that have examined factors that influence post-LT relapse. Most of these studies examine risk factors pre-LT. There was no difference in relapse rates and time to relapse from last alcohol use between those transplanted for AC and for AH. Time of sobriety should not be used alone in determining transplant candidacy. Our patients were found to be minimally acceptable candidates by the SIPAT score and there was no significant difference in SIPAT scores between patients who did or did not relapse post-LT. Future studies should focus on early prediction for relapse in our post-LT patients and developing early interventions for these patients.

FRI-506

Impact of external biliary drainage on early post-transplant biliary outcomes: a randomized controlled trial in living donor liver transplantation

Su Young Hong[1]. *[1]Seoul National University Hospital, Seoul, Korea, Rep. of South*
Email: sypurple@gmail.com

Background and aims: Biliary complications continue to be the most frequent problems following adult living donor liver transplantation (LDLT). External biliary drainage (EBD) using a silastic tube has been adopted to reduce anastomotic pressure and facilitate early detection of graft dysfunction. This study aimed to determine whether the application of EBD during duct-to-duct reconstruction reduces biliary complications after LDLT and assess EBD-related adverse events, long-term clinical outcomes, and patient-reported quality of life (QoL).
Method: This single-center trial randomized adult LDLT recipients eligible for duct-to-duct anastomosis to EBD placement or no drainage. Of 124 planned participants, 59 patients who underwent LDLT before trial termination were analyzed. The primary endpoint was the 1-year incidence of biliary complications. Secondary outcomes included 3-year complications, EBD-related adverse events, readmissions, and QoL using the pLTQ at 1 and 3 years.
Results: No bile leaks occurred in the EBD group (0% vs 6.5% in controls). One-year biliary complications were significantly lower with EBD (17.9% vs 41.9%, $p < 0.05$). Three-year rates remained lower (25.0% vs 41.9%), though not statistically significant. However, interim safety review revealed a markedly higher rate of EBD-related complications (39.3%), exceeding the <10% incidence previously reported and surpassing the predefined safety margin. Grade IIIa events occurred in 10.7%, and readmissions were more frequent in the EBD group (25.0% vs 9.7%). Based on these findings, further randomization was deemed to pose unacceptable risk, and the trial was terminated early for safety. At 6 months, EBD-specific QoL

assessment showed that patients reported noticeable discomfort related to the indwelling EBD, reflected by lower mean scores in several symptom-related items. Despite this, overall pLTQ scores at 1 and 3 years were similar between groups, with both maintaining good long-term QoL.
Conclusion: EBD reduced early biliary complications and eliminated bile leaks after LDLT. Nevertheless, the unexpectedly high frequency of EBD-related adverse events—together with patient-reported discomfort during the drainage period—led to early trial discontinuation on safety aspects. These results suggest that while EBD offers potential protective benefit, it also introduces meaningful short-term burden and device-related morbidity. Selective use, guided by individual anatomical and technical risk profiles, may better balance safety and efficacy.

FRI-507-YI
MELD-based prioritization for hepatorenal syndrome and liver transplant waiting list outcomes
Selene Therese Iavarone[1], Alberto Amador[2], Carlos Cespedes[3], Abiguei Torrents[4], Cristina Gómez-Fernández[5], Tomàs Balari[6], Isabel Campos-Varela[6], María José Moreta[1], Anna Aguilar[7], Giulia Pagano[1], Pablo Ruiz[1], Lluis Castells[7], Carme Baliellas[2], Laura Lladó[8], Jordi Colmenero[1], Pere Ginès[1], Jaume Tort[4], Gonzalo Crespo[1], Adrià Juanola[1]. *[1]Liver Unit, Hospital Clínic of Barcelona, Barcelona, Catalunya, Spain, Institut d'Investigacions Biomèdiques August Pi i Sunyer (IDIBAPS), Barcelona, Catalunya, Spain; Institut d'Investigacions Biomèdiques August Pi i Sunyer (IDIBAPS), Barcelona, Catalunya, Spain, Centro de Investigación Biomédica en Red Enfermedades Hepáticas y Digestivas (CIBEREHD), Madrid, Spain, Barcelona, Spain; [2]Hepatology Unit, Department of Digestive Diseases, Hospital Universitari de Bellvitge, Bellvitge Biomedical Research Institute (IDIBELL), University of Barcelona, Catalonia, Spain, Barcelona, Spain; [3]Centro de Investigación Biomédica en Red Enfermedades Hepáticas y Digestivas (CIBEREHD), Madrid, Spain, Liver Unit, Vall d'Hebron Hospital Universitari, Vall d'Hebron Institut of Research, Vall d'Hebron Barcelona Hospital Campus, Universitat Autònoma de Barcelona, Barcelona, Spain, Barcelona, Spain; [4]Organització Catalana de Trasplantaments (OCATT), Servei Català de la Salut, Catalonia, Spain, Barcelona, Spain; [5]Liver Unit, Hospital Clínic of Barcelona, Barcelona, Catalunya, Spain, Faculty of Medicine and Health Sciences, University of Barcelona (UB), Barcelona, Spain, Barcelona, Spain; [6]Hepatology Unit, Department of Digestive Diseases, Hospital Universitari de Bellvitge, Bellvitge Biomedical Research Institute (IDIBELL), University of Barcelona, Catalonia, Spain, Centro de Investigación Biomédica en Red Enfermedades Hepáticas y Digestivas (CIBEREHD), Madrid, Spain, Barcelona, Spain; [7]Liver Unit, Vall d'Hebron Hospital Universitari, Vall d'Hebron Institut of Research, Vall d'Hebron Barcelona Hospital Campus, Universitat Autònoma de Barcelona, Barcelona, Spain, Centro de Investigación Biomédica en Red Enfermedades Hepáticas y Digestivas (CIBEREHD), Madrid, Spain, Barcelona, Spain; [8]Department of Hepatobiliary Surgery & Liver Transplantation, Hospital Universitari de Bellvitge, Barcelona, Spain, Barcelona, Spain*
Email: iavaroneselene@gmail.com

Background and aims: Liver transplantation (LT) is the only curative treatment for patients with decompensated cirrhosis (DC). Different allocation policies exist worldwide, with MELD score–based prioritization currently applied in Catalonia. Since its implementation, several exceptions have been introduced to balance survival and dropout rates among patients on the waiting list (WL). A specific criterion is applied to patients with hepatorenal syndrome (HRS), whereby the highest MELD score calculated from peak serum creatinine prior to terlipressin initiation is used. In addition, hepatocellular carcinoma (HCC) high risk patients are assigned a MELD score of 19, with one additional point every three months. However, the impact of this allocation strategy on survival and access to LT for patients on the WL remains unclear, particularly among those with kidney dysfunction (KD).
Method: Patients listed for single LT in Catalonia between 2008 and 2022 were included. Patients were classified into four groups: HRS; KD non HRS-related, defined as serum creatinine >1.5 mg/dL at listing or during WL follow-up; DC without kidney impairment; and HCC. Patients were followed for 12 months from the time of listing.
Results: A total of 1,320 patients from the three transplant centers in Catalonia were included in the analysis (128 HRS, 346 DC, 232 KD, and 614 HCC). Overall, 1,053 patients were male (80%), mean age of 58 ± 8 years. The most frequent etiology was alcohol-related liver disease (n = 695, 48%). The mean MELD score at listing for the entire cohort was 21 ± 5, with no significant differences between groups. During the follow-up period, 1,158 patients underwent LT, with a median waiting time of 49 days. LT rates were significantly higher in the HCC and DC groups (91% and 89%, respectively) compared with the HRS (73%) and KD (76%) groups ($p < 0.001$). In addition, 138 patients (10%) died or were delisted due to clinical deterioration (liver-related complications or cancer progression). Mortality and delisting rates were higher among patients with renal impairment (13% in HRS and 19% in KD) compared with the other groups (8% in DC and HCC patients; $p = 0.001$).
Conclusion: Current allocation policies achieve high LT rates among patients on the WL. However, kidney impairment at the time of listing or during WL follow-up reduces access to LT in cirrhosis patients despite the existence of specific tailored policies. Thus, alternative prioritization strategies for this subgroup may improve access to liver transplantation.

FRI-508
Continuous glucose monitoring in liver transplant recipients in the intensive care unit: a randomized clinical trial cohort
Marc Pañero Moreno[1,2,3], Richie Alexander Inge Cox[1,2,4], Enric Tomas Franch[1], Alberto Villamor Ordozgoiti[1,3], Eva Maria Guix Comellas[3], Fatima Aziz[1]. *[1]Hospital Clinic of Barcelona, Barcelona, Spain; [2]Fundació de Recerca Biomedica Clinic – Institut D'investigació Biomédic August Pi i Sunyer (FRCB-IDIBAPS), Barcelona, Spain; [3]Department of Fundamental and Clinical Nursing, University of Barcelona, Barcelona, Spain; [4]European Foundation for the Study of Chronic Liver Failure (EF CLIF), Barcelona, Spain*
Email: panero@clinic.cat

Background and aims: Postoperative hyperglycemia affects over 90% of Liver Transplant (LT) recipients in the Intensive Care Unit (ICU) due to metabolic and surgical stress, corticosteroids, and immunosuppressive therapy, predisposing to infection and prolonged hospital stays. Continuous Glucose Monitoring (CGM) has demonstrated improved accuracy and glycemic stability in ambulatory settings but remains unvalidated in critically ill patients, and current guidelines do not recommend its inpatient use. This trial aimed to determine whether CGM-guided insulin therapy improves postoperative glycemic control compared with Point-of-Care Glucose (POC-G) testing in LT recipients in the ICU.
Method: A single-blind randomized clinical trial was conducted at the Hospital Clinic of Barcelona (CGM-UCI23 project) and a cohort of LT receptors was extracted. A CGM sensor was placed on the upper arm, and participants were randomly assigned to an experimental group, in which glycemic management was guided by CGM in real time with active alerts included glucose thresholds of 220 mg/dL and 80 mg/dL, trend arrows, a predicted low alert indicating imminent hypoglycemia (<55 mg/dL within the next 20 minutes), and a low glucose alarm for readings below 55 mg/dL. In the control group, glucose was managed using POC-G while CGM remained blinded.
Results: The total number of LT performed between February 2025 until November 2025 was 50. From this population, 38 patients were included. The CGM group achieved significantly higher Time-in-Range (TIR) (54.6 ± 20.9% vs 34.5 ± 22.4%, $p = 0.006$) and lower Time-Above-Range (TAR) (45.0 ± 21.0% vs 64.0 ± 22.6%, $p = 0.007$) compared to control. Mean blood glucose trended lower with CGM (186 ± 28.8 vs 207 ± 38.3 mg/dL, $p = 0.068$). CGM-guided management reduced

daily POC-G measurements (3.17 ± 2.15 vs 6.37 ± 1.78, p < 0.001). Adverse events were significantly lower in the CGM group (26.31% vs 63.15%, p = 0.022). CGM also trended toward shorter ICU stays (7.4 vs 12.1 days, p = 0.99) with significantly reduced pain scores (ESCID 0.07 vs 0.38, p = 0.04; NRS 0.42 vs 0.66, p = 0.04).
Conclusion: CGM-guided insulin therapy significantly improves TIR and reduces hyperglycemia in LT recipients in the ICU while also decreasing POC-G measurements and adverse events. These results support CGM as a feasible and effective alternative to POC-G monitoring, warranting validation in larger multicenter trials.

FRI-509
Differences in immunosuppressive strategies for primary sclerosing cholangitis after liver transplantation
August Tronstad Juliebø[1], Trine Folseraas[1], Tom Hemming Karlsen[1], Kirsten Muri Boberg[1]. [1]*Norwegian PSC Research Center, Department of Transplantation Medicine, Clinic of Surgery and Specialized medicine, Oslo University Hospital, Oslo, Norway, Institute of Clinical Medicine, University of Oslo, Oslo, Norway, Research Institute of Internal Medicine, Institute of Clinical Medicine, University of Oslo, Oslo, Norway, Oslo, Norway*
Email: augusttj@uio.no

Background and aims: In primary sclerosing cholangitis (PSC), liver transplantation (LT) remains the only definite treatment option. Individuals with PSC have an increased risk of rejection and disease recurrence after LT, which can affect graft survival and long-term outcomes. No standardized recommendations exist for immunosuppression in PSC after LT, and it is unclear how strategies vary across centers. We therefore conducted an international survey to characterize current practice.
Method: A web-based questionnaire was distributed internationally to liver transplant centers affiliated with the International PSC Study Group (IPSCSG). The survey collected information on immunosuppressive regimens at predefined time points after LT (after LT (1, 3, 6, and 12 months, and long-term >1 year).
Results: Thirty-one centers completed the questionnaire (Europe n = 21; the US n = 7; one each from Japan, South Africa and Israel), including 11 high-volume centers performing ≥ 15 PSC LTs in 2021–2022. Overall, 42% (13/31) reported using more intensive immunosuppression for PSC than other LT recipients. Triple therapy was standard during the first postoperative month, followed by tapering with prednisolone discontinued by 9 centers at month 3, 20 centers at month 6, and a total of 22 centers at 1 year. For long-term immunosuppression, being defined as standard regimen beyond one year after LT, 23% (7/31) used tacrolimus monotherapy, 52% (16/31) used dual therapy, most commonly with tacrolimus and mycophenolate mofetil, and 26% (8/31) maintained triple therapy. Drug concentrations and dosing were comparable across groups, indicating that maintaining a second or third agent did not lead to a reduction in tacrolimus or mycophenolate exposure. Conversely, centers using fewer long-term agents tended to prescribe lower early postoperative doses. Several centers emphasized individualized dosing based on clinical history and tolerance.
Conclusion: This international survey demonstrates substantial variation in immunosuppressive regimens and treatment intensity for PSC after LT, reflecting the absence of standardized guidelines and evidence-based practice. Differences in both early and long-term management result in marked variation in cumulative immunosuppression exposure across centers. These findings provide a foundation for further studies evaluating how immunosuppressive strategies influence graft survival, recurrence, re-transplantation, and long-term complications.

FRI-510
The LiverRisk score predicts perioperative outcomes in patients undergoing liver transplantation
Shih Hsun Kao[1], Pei Shan Wu[2], Tien En Chang[2], Fang Cheng Kuo[3], Hao-Jan Lei[4], Niang Cheng Lin[3], Kuei-Chuan Lee[1], Hsin Lin Tsai[5], Chinsu Liu[3]. [1]*Division of Gastroenterology and Hepatology, Department of Medicine, Taipei Veterans General Hospital, Department of Medicine, National Yang Ming Chiao Tung University School of Medicine, Taipei, Taiwan;* [2]*Endoscopy Center for Diagnosis and Treatment, Taipei Veterans General Hospital, Department of Medicine, National Yang Ming Chiao Tung University School of Medicine, Taipei, Taiwan;* [3]*Division of Transplantation Surgery, Department of Surgery, Taipei Veterans General Hospital, Department of Medicine, National Yang Ming Chiao Tung University School of Medicine, Taipei, Taiwan;* [4]*Division of General Surgery, Department of Surgery, Taipei Veterans General Hospital, Department of Medicine, National Yang Ming Chiao Tung University School of Medicine, Taipei, Taiwan;* [5]*Division of pediatric surgery, Taipei Veterans General Hospital, Department of Medicine, National Yang Ming Chiao Tung University School of Medicine, Taipei, Taiwan*
Email: tommy90279@gmail.com

Background and aims: The LiverRisk score has been proposed as a novel tool for predicting future liver-related outcomes; however, its prognostic performance in liver transplant recipients remains unclear. Aim: To evaluate the prognostic value of the LiverRisk score for predicting perioperative outcomes in patients undergoing liver transplantation.
Method: This single-center, retrospective cohort study enrolled adult patients who underwent liver transplantation at Taipei Veterans General Hospital between August 2017 and January 2024. Patients younger than 18 years were excluded. The prognostic performance of the LiverRisk score was compared with that of the Model for End-Stage Liver Disease (MELD) score and the Child–Pugh score for perioperative complications.
Results: A total of 240 patients were enrolled. The median MELD score was 20 (IQR, 13–34), the median Child–Pugh score was 10 (IQR, 8–12), the median LiverRisk score was 8.46 (IQR, 7.42–10.00), and the median graft-to-recipient weight ratio (GRWR) was 1.07 (IQR, 0.87–1.24). In univariate analyses, a higher LiverRisk score was associated with increased risks of overall complications (odds ratio [OR], 1.135; 95% confidence interval [CI], 1.013–1.271; p = 0.029) and biliary events (OR, 1.235; 95% CI, 1.054–1.447; p = 0.010). These associations remained significant in multivariate analyses for overall complications (OR, 1.129; 95% CI, 1.001–1.274; p = 0.048) and biliary events (OR, 1.235; 95% CI, 1.048–1.456; p = 0.012). Receiver operating characteristic (ROC) analysis demonstrated superior prognostic performance of the LiverRisk score for overall complications (area under the curve [AUC], 0.615) compared with the MELD (AUC, 0.526) and Child–Pugh scores (AUC, 0.495). For biliary events, the LiverRisk score showed better discrimination (AUC, 0.649) than GRWR (AUC, 0.504), whereas GRWR showed superior performance for predicting graft failure (AUC, 0.746).
Conclusion: The LiverRisk score demonstrated superior prognostic performance compared with the MELD and Child–Pugh scores for predicting postoperative complications and biliary events after liver transplantation. It may serve as a useful adjunct to preoperative risk assessment.

FRI-511-YI
Sex-based inequities in liver transplant access associated with jaffe creatinine measurement bias: an analysis from the scientific registry of transplant recipients data
Eda Kaya[1], Christin Quast[1], Maria Stepanova[2], Jasmin Weninger[1], Oliver Goetze[1], Antonios Katsounas[1], Abdurrahman Coskun[1], Martina Broecker-Preuss[1], Zobair M. Younossi[3], Jan-Peter Sowa[1], Kenan Moral[4], Gökhan Kabaçam[5], Gupse Adali[6], Yusuf Yilmaz[7], Mustafa Özcürümez[1], Ali Canbay[1]. [1]*Department of Medicine,*

Knappschaft Kliniken University Hospital, Ruhr-University, Bochum, Germany; [2]Beatty Liver and Obesity Research, Inova Health System, Falls Church, VA, United States; [3]The Global NASH Council, Washington, United States; [4]Department of Gastroenterology and Hepatology, School of Medicine, Gazi University, Ankara, Türkiye; [5]Department of Gastroenterology and Hepatology, Güven Hospital, Ankara, Türkiye; [6]Department of Gastroenterology, University of Health Sciences Istanbul Umraniye Training and Research Hospital, Istanbul, Türkiye; [7]Department of Gastroenterology, School of Medicine, Recep Tayyip Erdogan University, Rize, Türkiye
Email: ali.canbay@rub.de

Background and aims: Creatinine concentrations measured using Jaffe-based assays are known to be systematically higher than those obtained with enzymatic methods. This difference has been shown to influence MELD scores and may have important clinical implications. In this study, we examined the impact of Jaffe-based creatinine assays on MELD-based allocation, with a focus on sex-based disparities.
Method: A serum-free matrix with varying creatinine (0–5 mg/dL) and bilirubin (0–35 mg/dL) concentrations was used to compare Jaffe and enzymatic creatinine assays and to construct a three-dimensional reference model estimating true creatinine values. Data from the Scientific Registry of Transplant Recipients (SRTR) were used to obtain MELD scores, relevant laboratory parameters, and waitlist outcomes for adult liver transplant candidates at selected centers. MELD, MELD-Na, ReMELD-Na, and MELD 3.0 scores were recalculated and sex-specific differences were evaluated. Cumulative incidence functions and Fine–Gray subdistribution hazard models were applied to estimate sex-specific hazards for transplantation and waitlist mortality.
Results: Overall men had consistently higher transplant probability than women at comparable true disease severity, with subdistribution hazard ratios for transplant around 1.15 across MELD variants. Among non-deceased patients for MELD and MELD-Na scores, the proportion of females with $\Delta = -1$ change was consistently lower than that of males. In contrast, among deceased patients, no significant sex difference was observed ($\Delta = \pm 0$ vs. $\Delta = -1$), indicating that fewer females were affected by the correction. Women who receive Jaffe-related MELD upgrades showed the highest cumulative incidence of death on the waiting list (13.0% at 1 year), despite increased transplant probability (51.1% at 1 year), indicating a particularly vulnerable subgroup. Jaffe specific creatinine bias was associated with a small fraction of this disparity (≈0–2% of the log hazard difference), and within MELD classes the effect direction is inconsistent.
Conclusion: Correcting Jaffe-related bias minimally affects sex differences in transplant access, explaining only a small portion of the disparity. Jaffe-related reclassification appears to identify a subgroup with advanced multisystem failure rather than causing the excess mortality itself. While creatinine standardization improves comparability, equity in allocation will likely require sex- and body size–adjusted MELD or additional renal biomarkers.

FRI-512
From retrospective review to guideline creation: establishing CMV management protocols at the Irish national liver transplant centre

Sarah Kenny[1], Jennifer Dwyer[1], ZIta Galvin[1], Omar El-Sherif[1], Audrey Dillon[1], Sinead McDermott[1]. *[1]St. Vincent's University Hospital, Dublin, Ireland*
Email: sarahkenny491@gmail.com

Background and aims: International guidelines for the prevention of cytomegalovirus (CMV) infection in at-risk solid organ transplant (SOT) recipients recommend either universal prophylaxis or pre-emptive therapy. The standard prophylactic dose of valganciclovir (VGCV) is 900 mg once daily; however, some centres advocate for a reduced 450 mg once daily regimen to minimise adverse drug reactions (ADRs), particularly in intermediate-risk patients. Evidence supporting this approach in orthotopic liver transplant (OLT) recipients remains limited. (1) We conducted a five-year retrospective analysis to evaluate the efficacy and safety of low-dose VGCV and to inform a formal CMV management guideline for the National Liver Transplant Centre in Ireland.
Method: A retrospective review was performed of adult OLT recipients (2018–2022) at the National Liver Unit, St. Vincent's University Hospital. Patients at risk for CMV infection (D+/R+, D+/R–, D–/R+) received VGCV 450 mg once daily for three months post-transplant. Data collected included demographics, transplant characteristics, CMV PCR results, clinical CMV disease, and adverse events.
Results: Among 245 OLTs, CMV disease occurred in 3.7% (n = 9) of patients, predominantly in high-risk D+/R– recipients (n = 8, 89%), comparing favourably to reported incidences of 5–22% with standard dose prophylaxis. (2–4) Seven of the nine cases occurred outside the prophylaxis period. Asymptomatic CMV viraemia (range 704–42,042 IU/mL) was identified in a further 23 patients (70% D+/R–, n = 16). No significant ADRs attributed to VGCV were reported.
Conclusion: Low-dose valganciclovir (450 mg OD for 3 months) was effective and well tolerated for CMV prophylaxis in OLT recipients, across all CMV risk groups, with incidence of CMV disease comparing favourably to that seen with standard dose prophylaxis. (2–4) The results of this five-year review support the continued use of low-dose VGCV for the prevention of CMV infection in OLT recipients, including those in the high-risk D+/R– category,enabling a consistent, evidence-based, and safe national approach to CMV prevention post-OLT.

References

1. Bixby AL *et al.*, 2021. doi:10.1111/tid.13713.
2. Kalil AC *et al.*, 2012. doi:10.1002/lt.23530.
3. Singh N *et al.*, 2020. doi:10.1001/jama.2020.3138.
4. Shiley KT *et al.*, 2009. doi:10.1002/lt.21769.

FRI-513
Effect of a centre-specific prophylaxis protocol update on infectious outcomes after liver transplantation

Buse Ketenoğlu[1], Damla Verendağ[1], Aytaç Erdem[1], Oğuz Reşat Sipahi[1], Tansu Yamazhan[1]. *[1]Department of Infectious Diseases, Ege University Faculty of Medicine, İzmir, Türkiye*
Email: busekknoglu@gmail.com

Background and aims: Prophylaxis protocols following liver transplantation can vary across centers and may evolve over time, yet comparative outcome data remain limited. This study assessed the clinical impact of updated antibacterial, antiviral, and antifungal prophylaxis at a tertiary transplant center.
Method: Adult liver transplant recipients transplanted between 3 January 2018 and 30 April 2024 were retrospectively reviewed (n = 224). Prior to the protocol update, ceftriaxone was administered for antibacterial prophylaxis and acyclovir for antiviral prophylaxis. After the update, piperacillin-tazobactam and valganciclovir were implemented. Before the update, antifungal prophylaxis with fluconazole was not routinely administered, but it was introduced as routine prophylaxis for all recipients thereafter. Outcomes assessed included bacterial infection and mortality within 30 days, intensive care unit and total hospital length of stay, total antibiotic exposure days, incidence of cytomegalovirus syndromes during follow-up, and fungal infections within one year after transplantation.
Results: Thirty-day bacterial infection and mortality rates were similar between the piperacillin-tazobactam and ceftriaxone prophylaxis groups. However, piperacillin-tazobactam was associated with reduced intensive care unit and overall hospital stay, as well as fewer total antibiotic exposure days. Surgical site infection rates decreased following the protocol update, with an absolute reduction of 2.6 percentage points. After switching to valganciclovir, incidence of cytomegalovirus syndrome decreased from 10 cases under acyclovir prophylaxis to 1 case under valganciclovir prophylaxis, and no late-

onset cytomegalovirus disease was observed. Overall, fungal infection occurred in 21 of 224 patients (9.4%); 91% presented within six months after transplantation, with *Candida* species being the most common pathogens. Despite a higher baseline risk in the fluconazole prophylaxis group, fungal infection rates did not differ significantly between groups.
Conclusion: In this single-centre cohort, updating prophylaxis protocols was associated with reduced hospitalisation and fewer antibiotic exposure days with piperacillin–tazobactam, as well as a lower incidence of cytomegalovirus syndromes after valganciclovir. Stable fungal infection rates despite increased risk factors suggest a potential protective role of fluconazole. Risk-adapted, local epidemiology–guided prophylaxis strategies may improve outcomes after liver transplantation.

FRI-514
Early bacterial infections after liver transplantation: incidence and independent risk factors
Buse Ketenoğlu[1], Alper Uğuz[2], Tufan Gümüş[2], Elvan Işık[3], Damla Verendağ[1], Funda Yılmaz Barbet[4], Şöhret Aydemir[5], Rüçhan Sertöz[5], Tansu Yamazhan[1]. *[1]Department of Infectious Diseases, Ege University Faculty of Medicine, İzmir, Türkiye; [2]Department of General Surgery, Ege University Faculty of Medicine, İzmir, Türkiye; [3]Department of Gastroenterology, Internal Medicine, Ege University Faculty of Medicine, İzmir, Türkiye; [4]Department of Pathology, Ege University Faculty of Medicine, İzmir, Türkiye; [5]Department of Medical Microbiology, Ege University Faculty of Medicine, İzmir, Türkiye*
Email: buseknnoglu@gmail.com

Background and aims: Infections are major determinants of early morbidity and mortality after liver transplantation. This study evaluated the incidence of bacterial infections occurring within 30 days following transplantation and identified associated risk factors.
Method: Adult recipients who underwent liver transplantation between 3 January 2018 and 30 April 2024 at Ege University Organ Transplantation Center were retrospectively reviewed (n = 224). The primary outcome was the occurrence of bacterial infection within 30 days after transplantation. Independent predictors were assessed using multivariable logistic regression.
Results: Bacterial infection occurred in 84 of 224 recipients (37.5%). The most common infection sites were surgical site infection (35.7%) and pneumonia (35.7%), followed by catheter-related bloodstream infection (16.6%), urinary tract infection (15.4%) and primary bloodstream infection (9.5%). The most frequently isolated pathogens were *Acinetobacter baumannii* (25.0%), *Enterococcus faecium* (25.0%) and *Klebsiella pneumoniae* (21.4%). Multivariable analysis indicated that female sex was protective (odds ratio 0.40; 95% confidence interval 0.21–0.77). Bacterial infection was independently associated with hepatic encephalopathy (odds ratio 1.88), deceased donor transplantation (odds ratio 2.01), Model for End-stage Liver Disease score greater than 15 (odds ratio 1.95), postoperative biliary complications (odds ratio 6.87), and perioperative red blood cell transfusion (odds ratio 2.73). Recipients who developed bacterial infection had higher one-year mortality (odds ratio 4.55), longer stays in the intensive care unit (median 7 vs. 5 days; $p < 0.001$), and longer hospital stays overall (22 vs. 15 days; $p < 0.001$).
Conclusion: Bacterial infections occurred in more than one-third of recipients within 30 days and were associated with longer hospitalisation and higher one-year mortality. It appears that prioritizing enterococci in perioperative prophylaxis and in the management of early postoperative infections may be important in liver transplant recipients. High-risk recipients may benefit from targeted surveillance and preventive measures based on pre- and perioperative risk stratification.

FRI-515
Clinical outcomes following TIPS in liver transplant recipients: results from multicentre EuroTIPS registry
Faisal Khan[1], Anna Baiges[2], Juan Carlos García-Pagán[2], Vianey Reta[2], Sonia Torres[2], Tomas Guasconi[3], Filippo Schepis[3], Luis Téllez[4], Jesus Donate[4], Emma Vanderschueren[5], Wim Laleman[5], Charlotte Bouzbib[6], Michael Praktiknjo[7], Alvaro Giráldez-Gallego[8], Silvia Nardelli[9], Stefania Gioia[9], Simone Di Cola[9], Oana Nicoara-Farcau[10], Bogdan Procopet[10], Salil Karkhanis[1], Homoyon Mehrzad[1], Dhiraj Tripathi[1]. *[1]Liver Unit, Queen Elizabeth Hospital, Birmingham, United Kingdom; [2]Barcelona Hepatic Hemodynamic Laboratory, Liver Unit, Hospital Clínic, Clinic Barcelona, ERN-Rare Liver, CSUR, FRCB-IDIBAPS, Universitat de Barcelona, Barcelona, Spain; [3]Severe Liver Diseases (M.E.C.) Departmental Unit, Department of Medical Specialtie University Hospital of Modena "Policlinico", University of Modena and Reggio Emilia, European Reference Network on Rare Liver Disorders (ERN Rare- Liver), Modena, Italy; [4]Hospital Universitario Ramón Y Cajal, Madrid, Spain; [5]Department of Gastroenterology and Hepatology, University Hospitals Leuven, KU Leuven, Department of Chronic Diseases, Metabolism and Aging (CHROMETA), Catholic University of Leuven, Leuven, Belgium; [6]iver Intensive Care Unit, Hepatogastroenterology department, Pitié-Salpêtrière Hospital, Sorbonne University, 47-83 boulevard de l'Hôpital 75013 Paris, Paris, France; [7]Department of Internal Medicine B, University of Münster, 48149 Münster, Münster, Germany; [8]Digestive Diseases Department, Hospital Universitario Virgen del Rocío, Institute of Biomedicine (HUVR/CSIC/US), University of Seville, Sevilla, Spain; [9]Dept. Of translational and precision medicine, Sapienza University Viale dell'Università 37, Rome, Italy; [10]Hepatology department, Regional Iinstitute of Gastroenterology and Hepatology 'O.Fodor," University of Medicine and Pharmacy 'Iuliu Haţieganu ', Cluj -Napoca, Cluj -Napoca, Romania*
Email: d.tripathi@bham.ac.uk

Background and aims: Transjugular intrahepatic portosystemic shunt (TIPS) is an established treatment for portal hypertension complications. Development of portal hypertension in liver transplant recipients is not uncommon; however, the utility of TIPS in this population remains poorly documented due to small sample sizes, heterogeneity, and single-centre retrospective designs. We aimed to describe the efficacy and safety of TIPS in liver transplant recipients and identify predictive factors for outcomes.
Method: We analysed prospectively and retrospectively collected data from the EASL-endorsed EuroTIPS registry of liver transplant recipients undergoing TIPS for portal hypertension complications. Univariate and multivariate Cox regression analyses were performed to identify variables predicting 1-year survival, including MELD, MELD-Na, Child-Pugh Score, disease aetiology, patient demographics, and TIPS technical factors.
Results: Fifty-one patients from 10 European centres were included. Mean age 55.8 ± 11.1 years; 60.7% male. Baseline: MELD 14.1 ± 4.9, MELD-Na 16.0 ± 6.5, Child-Pugh 7.7 ± 1.3. Median follow-up 33 months (range 1–326). Original disease was cirrhosis in 68%. Aetiology of allograft portal hypertension: recurrent index disease 31.4% (68.7% viral hepatitis), vascular complications 19.6%, PSVD 11.8%, other 23.5%. Indication for TIPS: refractory ascites 56.9%, portal hypertensive bleeding 17.6%, portal vein thrombosis 7.8%, others 17.7%. Indications for TIPS: refractory ascites 56.9%, portal hypertensive bleeding 17.6%, portal vein thrombosis 7.8%, others 17.7%. Median time from transplant to TIPS 33.4 months (2.1–256.1). Covered stents were used in 96.1% of patients. Portosystemic pressure gradient decreased from 17.6 ± 5.9 to 8. ± 3.5 mmHg. TIPS revision was required in 39.2% of cases, achieving 100% secondary patency. Complications included hepatic encephalopathy (29.4%), heart failure responding to TIPS reduction (n = 1), and graft ischaemia requiring re-transplantation (n = 1) within 30-day. Clinical success was 88.2%. Overall mortality during follow-up was 23.5% (66.6% liver-related). Survival at 1, 3, and 5 years was 82%, 75%, and 75%, respectively. No baseline

variables significantly predicted 1-year survival. Graft survival was 86.2%.
Conclusion: TIPS in liver transplant recipients achieves good clinical outcomes despite high intervention rates. Future analyses within the EuroTIPS cohort will focus on developing predictive models with larger sample sizes to address this unmet clinical need.

FRI-516
Liver transplant outcomes and clinical burden in patients with alpha-1 antitrypsin deficiency-associated liver disease in Canada
May Hagiwara[1], Chitra Karki[1], Tami Nussbaum[1], Suna Park[1], Kaili Ren[1], Rahima A. Bhanji[2], Mamatha Bhat[3], Marc Deschenes[4], Julian Hercun[5], Mohommad Qasim Khan[6,7], Julie Zhu[8], Sarah O'Brien[9], Anat Fisher[9], Paul Keown[9]. [1]*Takeda Development Center Americas, Inc., Cambridge, MA, United States;* [2]*Division of Gastroenterology (Liver Unit), University of Alberta, Edmonton, AB, Canada;* [3]*Ajmera Transplant Centre, University Health Network, Toronto, ON, Canada;* [4]*McGill University Health Centre, Montreal, QC, Canada;* [5]*Centre Hospitalier de l'Université de Montréal, University of Montreal, Montreal, QC, Canada;* [6]*Department of Medicine, Division of Gastroenterology, Western University, London, ON, Canada;* [7]*Department of Epidemiology and Biostatistics, Western University, London, ON, Canada;* [8]*Division of Digestive Care and Endoscopy, Dalhousie University, Halifax, NS, Canada;* [9]*Syreon Corporation, Vancouver, BC, Canada*
Email: may.hagiwara@takeda.com

Background and aims: Alpha-1 antitrypsin deficiency (AATD)-associated liver disease (AATD-LD) is caused by misfolded hepatic alpha-1 antitrypsin (AAT) aggregates in patients (pts) with the protease inhibitor (Pi)*ZZ genotype. No approved pharmacological therapies for AATD-LD exist; orthotopic liver transplantation (OLT) is recommended in pts with end-stage liver disease. We assessed clinical burden and liver-related outcomes in pts with AATD-LD assessed for OLT in Canada.
Method: Adults with AATD (physician-diagnosed, presence of an ICD-10-CM E88.01 code for AATD or serum AAT level < 120 mg/dL) were assessed for OLT at 6 regional centres in Canada (2005–2023). Data were obtained from electronic medical records/registries at each centre. Index date was defined as the date of physician assessment for OLT. Liver-related clinical events before index date, time from first liver-related clinical event to index date, time from index date to OLT and liver/OLT-related mortality were assessed.
Results: Among 341 pts (median [IQR] age at index: 57 [51, 64] years; 69% male), 184 (54%) underwent OLT. Genotype was assessed in 54/341 pts (16%) before (34/54, 63%) or after OLT (11/54, 20%); data was missing in 9 pts. Of those, 22/54 pts (41%) had a Pi*ZZ genotype. Median (IQR) time from the first liver-related clinical event (n = 203) to index date was 2 (0, 11) months. Ascites was the most common event (205/341, 60%), with events increasing in frequency closer to index date. Median (IQR) wait time from liver-related clinical event to index date was shortest in pts with hepatic encephalopathy (n = 56; 0 [0, 4] months) and longest in pts with oesophageal varices (n = 52; 9 [2, 23]). Median (95% CI) time to OLT after index date was 9 (6, 11) months (mortality adjusted). At 6 months post-index, the probability of OLT (mortality adjusted) was 40% and the risk of death was 20%. After OLT, 4% had liver-related mortality and 4% had OLT-related complications (liver-related hospitalization; excluding mortality) by Month 6.
Conclusion: This is the first natural history study of pts with AATD-LD assessed for OLT. In this study, few pts had available genotype data before OLT (34/341 pts [10%]) and median time from first liver-related clinical event to index date was short (2 months). These data highlight the need for improved disease awareness to diagnose AATD-LD early in the disease trajectory and prevent progression to end-stage liver disease in pts with AATD-LD.
Study/writing funding: Takeda Development Center Americas, Inc.

FRI-517-YI
Redefining futility in the machine perfusion era: insights based on the UK-DCD risk score in 362 DCD liver transplantations
Efrayim Küçükerbil[1], Femke De Goeij[1], Puck C. Groen[1], Lina Gruncell[1], Roberto Broere[1], Sarwa Darwish Murad[1], Caroline den Hoed[1], Robert Porte[1], Wojciech Polak[1], Jeroen de Jonge[1]. [1]*Erasmus University Medical Center, Rotterdam, Netherlands*
Email: e.kucukerbil@erasmusmc.nl

Background and aims: The scarcity of suitable donor grafts and the increased risks associated with donation after circulatory death liver transplantation (DCD-LT) highlights the importance of donor–recipient matching to optimize outcomes and graft utility. The UK-DCD risk score categorizes DCD-LTs as low-risk, high-risk, or futile based on donor and recipient characteristics. In the era of machine perfusion, DCD grafts undergo additional hypothermic or normothermic machine perfusion to resuscitate and evaluate the graft before transplantation. This study compares graft survival in DCD-LT after static cold storage (SCS), hypothermic machine perfusion (HMP), and normothermic machine perfusion (NMP), stratified by UK-DCD risk categories.
Method: In this single-center, retrospective cohort study, 362 DCD-LTs (November 2002-July 2024) were grouped by preservation method: SCS (n = 176), HMP (n = 105), and NMP (n = 81). Baseline donor and recipient characteristics were collected for the UK-DCD risk score. The primary outcome was 2-year graft survival, censored for patient death with a functional graft. Graft loss due to primary non-function (PNF) and post-transplant cholangiopathy (PTC) were also compared.
Results: Low-risk DCD-LTs were highest after SCS (64%), followed by HMP (43%) and NMP (30%). In contrast, futile DCD LTs occurred in 5% of the SCS group, 8% of the HMP group, and 27% of the NMP group. Graft loss due to PNF occurred in 4 cases (2%) in SCS, 2 cases (2%) in HMP, and none in NMP ($p = 0.404$). Graft loss due to PTC was observed in 14 cases (8%) in SCS, none in HMP, and 2 cases (2%) in NMP ($p = 0.005$). Two-year graft survival was significantly higher in HMP and NMP compared to SCS, with survival rates of 93% and 90%, respectively, versus 81% ($p = 0.015$). This improvement was most pronounced in the high-risk group, where survival rates were 83% in SCS, compared to 100% and 97% in HMP and NMP, respectively ($p = 0.002$).
Conclusion: Despite more high-risk and futile transplantations, hypothermic and normothermic machine perfusion significantly reduced graft loss due to PTC, improving 2-year graft survival rate in DCD-LT up to 93%. This solidifies the role of machine perfusion in DCD-LT and highlights the need for a new risk model to better predict graft utility and long-term outcomes.

FRI-521
Comparative outcome of machine perfusion strategies in liver transplantation: a network meta-analysis
Suprabhat Giri[1], Kshitij Kumar[1], Dr Babu Lal Meena[2]. [1]*Kalinga Institute of Medical Sciences, Bhubaneswar, India;* [2]*Post Graduate Institute of Medical Education and Research, Chandigarh, India*
Email: supg19167@gmail.com

Background and aims: Ischemia–reperfusion injury (IRI) remains a major determinant of early graft dysfunction and adverse outcomes following liver transplantation (LT), particularly with the increasing use of extended-criteria and donation after circulatory death grafts. Machine perfusion strategies, including normothermic machine perfusion (NMP) and hypothermic oxygenated perfusion (HOPE), have been developed to mitigate IRI; however, their comparative efficacy and safety remain uncertain. We performed a network meta-analysis (NMA) of randomized controlled trials (RCTs) to compare static cold storage (SCS), NMP, and HOPE across clinically relevant post-transplant outcomes.
Method: A systematic search of MEDLINE, Embase, and Scopus from inception to March 2025 identified RCTs comparing NMP or HOPE

with SCS in adult LT recipients. The primary outcome was early allograft dysfunction (EAD). Secondary outcomes included post-reperfusion syndrome, serious adverse events (Clavien–Dindo ≥IIIb), duration of hospitalization, vascular and biliary complications, and graft loss. The risk of bias was assessed using the RoB 2. A Bayesian random-effects NMA was conducted, with treatment ranking estimated using surface under the cumulative ranking curve (SUCRA) values.
Results: Eleven RCTs encompassing 1,329 patients were included. Compared with SCS, both NMP (risk ratio [RR] 0.47, 95% confidence interval [CI] 0.27–0.80) and HOPE (RR 0.52, 95% CI 0.34–0.77) significantly reduced EAD, with NMP ranking highest (SUCRA 80.8). NMP was also associated with a markedly lower risk of overall biliary complications (RR 0.29, 95% CI 0.12–0.69). In contrast, HOPE significantly reduced non-anastomotic biliary strictures and graft loss (RR, 0.44; 95% CI, 0.18–0.90), ranking highest in terms of graft survival (SUCRA 96.3). Both NMP and HOPE reduced the incidence of serious adverse events compared with SCS, while no significant differences were observed for hepatic artery thrombosis or post-reperfusion syndrome. Most trials were at low risk of bias.
Conclusion: Both NMP and HOPE provide clinically meaningful advantages over static cold storage in liver transplantation, though their benefits differ by outcome. NMP appears superior for the prevention of early graft dysfunction and biliary complications, whereas HOPE offers greater protection against graft loss and severe complications. These findings support a tailored, risk-adapted approach to graft preservation and highlight the need for direct comparative trials between NMP and HOPE.

FRI-522

Histologic recurrence and progression of metabolic dysfunction–associated steatohepatitis after liver transplantation: a 35-year single-center biopsy cohort

Sobia Laique[1], Muhammad Ahmad Nadeem[1], Chase Wehrle[1], Antonio Giuseppucci[1], Puneet Bansal[1], Beren Berber[1], Awwab Hammad[1], Mohamed El Hag[1], Jacob Sweeney, [1], Xuefeng Zhang[1], Alejandro Pita[1], Mazhar Khalil[1], Masato Fujiki[1], Choon Hyuck David Kwon[1], Jaekeun Kim[1], Koji Hashimoto[1], Andrea Schlegel[1], Jamak Modaresi Esfeh[1], Daniela Allende[1].
[1]Cleveland Clinic Foundation, Cleveland, United States
Email: laiques2@ccf.org

Background and aims: Metabolic dysfunction–associated steatohepatitis (MASH) is an increasingly recognized cause of late graft injury after liver transplantation (LT), yet its histologic natural history post-LT is incompletely defined. Studies are limited by non-central pathology review and reliance on surrogate markers. We aimed to determine the incidence, timing, and histologic progression of recurrent and de novo MASH using centrally re-reviewed liver biopsies.
Method: Adult LT recipients at Cleveland Clinic (1984–2020) were included. All available biopsy slides were centrally re-reviewed by expert hepatopathologists according to NASH-CRN criteria. Post-transplant MASLD/MASH was classified as recurrent (MASH as the indication for LT) or de novo (other etiologies). Outcomes included incidence of MASLD/MASH, time from LT to the first biopsy demonstrating MASH, and histologic fibrosis progression. Fibrosis progression was defined as a ≥1-stage increase in fibrosis from the index biopsy and development of advanced fibrosis (≥F3) or cirrhosis (F4), and was assessed in a predefined subcohort with longitudinal histology.
Results: We identified 2,567 adult LT recipients with post-LT liver biopsies, (35% female, 17.3% with MASH indication). Post-LT, 13.9% developed recurrent MASLD, including 6.3% with recurrent histologic MASH. Among patients transplanted for non-MASH, 13.1% developed de novo MASLD and 4.2% de novo MASH. Recurrent MASH and MASLD were both more frequent than de novo disease (log-rank $p < 0.001$ respectively). The development of MASH in the transplant graft was associated with a reduction in overall survival independent of MELD, donor risk, or recipient age ($p < 0.001$). Overall, 118 patients developed post-transplant histologic MASH. The median time from LT to the first biopsy demonstrating MASH was 1.8 years (IQR 0.7–4.2). Fibrosis progression of 1 stage occurred in 27/54 (50%) patients over a median follow-up of 3.0 years, with development of advanced fibrosis (F3) in 16/54 (30%) and cirrhosis (F4) in 3/54 (5.5%). Median annualized fibrosis progression was 0.54 stages/year (IQR 0.3–0.9), corresponding to approximately 1.85 years per one-stage increase.
Conclusion: This long-term, histology-based assessment is the first assessing histologic steatotic liver diseases after transplant. MASLD and MASH are significant issues in transplanted liver grafts, with recurrent disease occurring more commonly than *de novo*. Fibrosis progresses 1 stage every 2 years and is associated with reduced survival.

FRI-523

Refining prognosis after liver transplantation: contribution of artificial intelligence to predict early graft dysfunction

Thomas Levi Strauss[1], Christophe Desterke[1], Astrid Laurent Bellue[2], Eric Vibert[1], Cyrille Feray[1], Audrey Coilly[1], Ilias Kounis[1]. *[1]AP-HP Hôpital Paul-Brousse, Centre Hépato-Biliaire, Villejuif, France; [2]Service d'anatomie et cytologie pathologiques, hôpital Bicêtre, AP-HP, université Paris-Saclay, Kremlin Bicêtre, France*
Email: ilias.kounis@aphp.fr

Background and aims: Early allograft dysfunction (EAD) and primary non-function (PNF) remain major determinants of outcome after liver transplantation (LT). Our aim was to evaluate whether machine-learning models incorporating reperfusion biopsy data could improve prediction of early graft dysfunction.
Method: We performed a single-centre retrospective study including all adult LTs from 2017–2023. Retransplantations, living-donor, auxiliary, domino and combined thoracic–hepatic grafts were excluded; combined liver–kidney transplants were retained. For each case, 93 pre- and peri-operative variables were collected from donor, recipient, surgery and reperfusion biopsy. The primary composite endpoint at day 7 (PNF/EAD) combined PNF requiring urgent retransplantation or leading to death, or Olthoff EAD criteria for EAD (bilirubin ≥171 µmol/L or INR ≥1.6 at day 7, or transaminases ≥2000 U/L during the first week). A stricter endpoint of PNF/EAD was used secondly and excluded isolated transaminase elevation. Neural networks after selecting features by random forrest,and multi-variable modelling using LASSO, Ridge and Elasticnet were tested.
Results: Among 908 eligible LTs, 199 patients (21.9%) developed PNF/EAD and 87 (9.6%) met the strict definition. PNF/EAD was associated with reduced overall survival (subdistribution HR 1.61, 95% CI 1.16–2.22); the strict endpoint showed an even stronger association (HR 1.75, 95% CI 1.11–2.71). In univariate analyses, markers of recipient severity (MELD, ICU status, vasopressors, mechanical ventilation), operative complexity (cold ischaemia time, operative duration, transfusions) and reperfusion-biopsy steatosis (micro- and macro-vesicular) were significantly associated with early graft dysfunction. A neural network including 16 donor, recipient, surgical and histological variables achieved an AUC of 0.72 for predicting PNF/EAD. For the strict endpoint, an Elastic Net model based on four variables—pre-transplant bilirubin, pre-transplant platelet count, operative time and quantitative microvesicular steatosis—yielded an AUC of 0.73 and an accuracy of 89.8%, comparable to more complex machine-learning approaches while remaining interpretable.
Conclusion: Machine learning models can predict EAD after LT with acceptable accuracy. However, they did not clearly outperform penalized regression. Reperfusion biopsy steatosis—particularly microvesicular steatosis—emerged as a key histological determinant of early dysfunction.

FRI-524

Basiliximab preserves renal function after liver transplantation without increasing rejection or graft loss

Dorothy Liu[1], Andrew Chan[2], Katrina Tan[3], Alan Wigg[4], Avik Majumdar[1], Marie Sinclair[1], Adam Testro[5]. [1]*Victorian Liver Transplant Unit, Austin Health, Australian Centre for Transplantation Excellence and Research (ACTER), Austin Health, Department of Medicine (Austin Precinct), The University of Melbourne, Melbourne, Australia;* [2]*Victorian Liver Transplant Unit, Austin Health, Melbourne, Australia;* [3]*Victorian Liver Transplant Unit, Austin Health, Australian Centre for Transplantation Excellence and Research (ACTER), Austin Health, Hepatology and Liver Transplantation Medicine Unit, Flinders Medical Centre, Melbourne, Australia;* [4]*Hepatology and Liver Transplantation Medicine Unit, Flinders Medical Centre, Adelaide, Australia;* [5]*Victorian Liver Transplant Unit, Austin Health, Australian Centre for Transplantation Excellence and Research (ACTER), Austin Health, Department of Surgery (Austin Precinct), The University of Melbourne, Melbourne, Australia*
Email: dorothyliu22@gmail.com

Background and aims: Renal dysfunction is common after liver transplantation (LT). Basiliximab is used in recipients with pre-LT renal impairment at risk of post-LT acute kidney injury (AKI) and subsequent progressive renal failure. By allowing for delayed calcineurin inhibitor initiation, basiliximab may mitigate further renal injury. However, data on long-term renal outcomes in high-risk recipients remain limited. We compared longitudinal renal functional trajectories in a real-world, multicentre cohort of LT recipients stratified by basiliximab induction use.
Method: This was a retrospective cohort study of adult patients who underwent initial deceased donor LT at two Australian transplant centres (January 2018 to October 2022). Consecutive eligible patients were grouped based on basiliximab administration. Retransplantation and multivisceral transplants were excluded. Basiliximab was given at clinician discretion, informed by pre-LT renal function and anticipated AKI risk. Renal outcomes were assessed using linear mixed effects modelling of change in serum creatinine (sCr) from baseline to predefined timepoints (day 1 peak and 3, 6, 12 and 24 months), with adjusted pairwise contrasts used to compare groups. Secondary outcomes included renal dysfunction resolution, post-LT renal replacement therapy (RRT), biopsy-proven acute cellular rejection (BPAR), graft survival and patient survival.
Results: Of 405 patients, 232 (57%) received basiliximab. Compared with non-basiliximab recipients, basiliximab patients had significantly higher baseline sCr and MELD, and a greater prevalence of pre-LT hepatorenal syndrome, RRT, terlipressin use and vasopressor support. Despite this, basiliximab recipients had early and sustained reductions in adjusted sCr from 3 months onwards, independent of covariates. By 12 and 24 months, adjusted sCr in basiliximab recipients had returned to or fallen below baseline (adjusted mean sCr change from baseline −17 µmol/L [95% CI −31 to −4] and −21 µmol/L [95% CI −34 to −7], respectively). Basiliximab use was independently associated with renal dysfunction resolution at 12 months (adjusted OR 2.62, $p < 0.001$) and 24 months (adjusted OR 1.71, $p = 0.02$). Adjusted sCr in the non-basiliximab group remained unchanged from baseline. No between-group differences were observed in post-LT RRT, BPAR, graft survival or patient survival.
Conclusion: Basiliximab induction therapy was associated with early and sustained renal recovery in high-risk LT recipients without increasing rejection or graft loss.

FRI-525

Time-adjusted analysis of cumulative immunosuppression and hepatocellular carcinoma recurrence risk after liver transplantation

Dorothy Liu[1], Darren Wong[2], Adam Testro[3], Avik Majumdar[1], Marie Sinclair[1]. [1]*Victorian Liver Transplant Unit, Austin Health, Australian Centre for Transplantation Excellence and Research (ACTER), Austin Health, Department of Medicine (Austin Precinct), The University of Melbourne, Melbourne, Australia;* [2]*Department of Gastroenterology, Austin Health, Department of Medicine (Austin Precinct), The University of Melbourne, Melbourne, Australia;* [3]*Victorian Liver Transplant Unit, Austin Health, Australian Centre for Transplantation Excellence and Research (ACTER), Austin Health, Department of Surgery (Austin Precinct), The University of Melbourne, Melbourne, Australia*
Email: dorothyliu22@gmail.com

Background and aims: Immunosuppression following liver transplantation (LT) for hepatocellular carcinoma (HCC) requires a careful balance between preventing allograft rejection and minimising HCC recurrence, with the assumption that immunosuppression increases cancer risk. We present the first analysis of cumulative immunosuppression exposure by individual agents on HCC recurrence after LT, adjusted for time, transplantation era and concurrent therapy.
Method: Consecutive patients who underwent initial deceased donor LT at a single-centre between 2016 and 2020 were retrospectively evaluated. Immunosuppression regimens from LT until HCC recurrence or last follow-up (death or final review in patients without recurrence) were collected. Cumulative calcineurin inhibitor exposure was calculated as the area under the curve derived from drug levels over time. Mycophenolic acid (MPA) and everolimus exposures were analysed as categorical variables to prevent model instability. A time-varying Cox proportional hazards model was used to assess the association between agent-specific cumulative immunosuppression exposure and HCC recurrence risk.
Results: Among 225 LT recipients, 34 (15%) patients developed HCC recurrence over a median of 70 (43–116) months. Patients with recurrence had significantly higher RETREAT scores, higher pre-LT alpha-fetoprotein, more microvascular invasion, a greater number of viable tumours, and a larger maximum tumour diameter. The rate of treated biopsy-proven acute cellular rejection was comparable between groups. After adjusting for time, transplantation era and concurrent immunosuppressive agents, cumulative tacrolimus exposure (HR 0.90, 95% CI 0.82–0.98, $p = 0.02$) and RETREAT score (HR 1.35, 95% CI 1.06–1.72, $p = 0.02$) were independently associated with HCC recurrence. Cumulative tacrolimus exposure did not differ between patients with HCC recurrence when stratified by RETREAT score < 4 versus ≥ 4. Cumulative MPA exposure was also protective (HR 0.87, 95% 0.85–0.88, $p < 0.001$), whereas cumulative cyclosporine (HR 1.00, $p = 0.17$) and everolimus (HR 0.53, $p = 0.31$) exposure were not associated with HCC recurrence.
Conclusion: We found an association between higher immunosuppression exposure and reduced HCC recurrence, converse to the common assumption. The relationship between cumulative immunosuppression exposure and post-LT HCC recurrence remains incompletely understood, reflecting the complex interplay of tumour biology, recipient characteristics and immunosuppression therapy.

FRI-526

Multidisciplinary follow-up after liver transplantation: diagnostic yield and impact on cancer and cardiovascular outcomes

Erica Nicola Lynch[1], Armando Curto[1], Michele Tanturli[1], Rocco Iamello[1], Giulia Lubian[1], Tommaso Mello[1], Tommaso Innocenti[1], Gabriele Dragoni[1], Stefano Gitto[2], Andrea Galli[1]. [1]*University of Florence, Department of Experimental and Clinical Biomedical Sciences "Mario Serio", Florence, Italy, Florence, Italy;* [2]*University of Florence, Department of Experimental and Clinical Medicine, Florence, Italy, Florence, Italy*
Email: ericanicola.lynch@unifi.it

Background and aims: With improving survival after liver transplantation (LT), de novo malignancies and cardiovascular (CV) disease are major late causes of morbidity/mortality, but evidence for standardized multidisciplinary follow-up is limited. We aim To describe the diagnostic yield and outcomes of a structured post-LT

multidisciplinary follow-up in a hospital without an on-site transplant program.
Method: Retrospective cohort of LT recipients followed 1995–2024. Scheduled assessments: dermatology, cardiology, chest X-ray, Pap/HPV, mammography/breast ultrasound. Diagnoses during scheduled visits in asymptomatic patients were considered screen-detected.
Results: The cohort included 226 patients (72.6% male); median follow-up 10 years. ≥1 malignancy occurred in 32.7% (112 cancers); 52.7% were screen-detected, mainly via dermatology (88.1% of screen-detected cancers). Median time to first malignancy was 7.0 years; malignancy was the main known cause of death (~51%). Dermatologic neoplasms included basal cell carcinoma 12.5%, squamous cell carcinoma 2.7%, melanoma 0.6%; median time to first dermatologic diagnosis 5.6 years. Women (n = 62): Pap/HPV tests (n = 154) were positive in 22.6% (median 6.0 years); mammography/ultrasound (n = 276) 8.7% positive (median 6.6 years). Chest X-rays (n = 847) yielded 152 mainly non-neoplastic findings; 1 cancer (mesothelioma). CV events occurred in 21.7% (63), 14.3% screen-detected; median time to first CV event 5 years; arrhythmias/AF ~24%, ischemic heart disease ~18%, cerebrovascular events ~16%, pulmonary embolism ~11%; one fatal. During cardiology follow-up, 80.1% of prescriptions were antihypertensive or lipid-lowering; elective interventions were only for valvulopathies. All-cause mortality was 19.5% (median LT-to-death 6.5 years).
Conclusion: Structured multidisciplinary follow-up enabled screening detection of over half of malignancies, driven by dermatologic surveillance (most within 10 years post-LT). Cardiology supported CV risk-factor management, whereas routine chest X-rays had negligible impact on early lung cancer detection.

FRI-527
The coexistence of sarcopenia and myosteatosis is associated with adverse clinical outcomes following liver transplantation
Ellina Lytvyak[1,2], Yu Jun Wong[1], Shagani Thisairajah[1], Glenda Meeberg[3], Devika Shreekumar[1], Maryam Motamedrad[1], Alessandro Parente[3,4], Norman Kneteman[3], Khaled Dajani[3], Blaire Anderson[3], David Bigam[3], James Shapiro[3], Aldo J Montano-Loza[1]. *[1]Division of Gastroenterology and Liver Unit, University of Alberta, Edmonton, Canada; [2]Division of Preventive Medicine, University of Alberta, Edmonton, Canada; [3]Division of Transplantation Surgery, Department of Surgery, University of Alberta, Edmonton, Canada; [4]Institute of Liver Studies, King's College Hospital NHS Foundation Trust, London, United Kingdom*
Email: montanol@ualberta.ca

Background and aims: Sarcopenia and myosteatosis are individually associated with adverse outcomes in chronic liver disease, however their combined impact of this "double-muscle defect" on postliver transplantation (LT) survival remains unclear. We hypothesized that the co-existence of sarcopenia and myosteatosis defines a distinct, high-risk muscle phenotype associated with poorer post-LT outcomes beyond conventional risk markers.
Method: We conducted a prospective cohort study that included 400 adult patients undergoing LT. Skeletal muscle index and radiodensity were measured from pre-LT computed tomography (CT) scan three months before their LT to define sarcopenia and myosteatosis, using established cut-offs. The primary outcome was post-LT mortality; secondary outcomes were ICU and total hospital length of stay (LOS). Multivariable Cox-regression adjusted for age, sex, and MELD score at LT.
Results: The cohort was 70% male Caucasians (76.5%), with median age 53.5 years [IQR 44.2–60.5] and median BMI 25.9 kg/m^2 [IQR 23–30.2]. Sarcopenia was present in 54.5%, myosteatosis in 47.3%, and both in 29.8% patients. LT recipients with simultaneous sarcopenia and myosteatosis had longer post-LT ICU stay (4 [2–11] vs. 3 [2–6] days, p = 0.01), and longer post-LT hospital LOS (27 [16–50] vs. 21 [14–34] days, p = 0.004). Importantly, simultaneous sarcopenia and myosteatosis was independently associated with a higher risk of mortality (adjusted HR 1.57 [1.05–1.91], p = 0.029), after adjustment by sex, age at transplant, cirrhosis etiology, presence of acute-on-chronic liver failure, and pre-LT MELD score. The 5-year post-LT survival (72% vs. 82%, p = 0.015) was significantly worse for patients with simultaneous sarcopenia and myosteatosis. This effect was magnified in patients > 60 year-old (62% vs. 72%, p = 0.015), and those requiring ICU admission pre-LT (66% vs. 87%, p = 0.014).
Conclusion: Simultaneous sarcopenia and myosteatosis is a clinically meaningful, independent predictor of post-LT mortality and morbidity, especially in older and critically ill patients. Incorporation of dual muscle assessment into pre-LT evaluation may provide a more objective means to enhance risk stratification, guide candidate selection, and reduce futile transplantation—particularly in older and critically ill patients.

FRI-528
Outcomes of everolimus-based immunosuppression after liver transplantation for hepatocellular carcinoma with or without steroid induction
Bianca Magro[1], Ciro Celsa[2], Michela Triolo[3], Antonio Galante[1], Giuseppe Cabibbo[2], Leonardi Filippo[3], Luisa Pasulo[3], Salvatore Gruttadauria[4], Calogero Cammà[2], Domenico Pinelli[5], Stefano Fagiuoli[3]. *[1]UPMC Italy, Palermo, Italy, Hepatology Section, IRCCS ISMETT, Palermo, Italy, Palermo, Italy; [2]UPMC ISMETT, Palermo, Italy; [3]Gastroenterology, Hepatology and Transplantation Unit, ASST Papa Giovanni XXIII, Bergamo, Italy, Bergamo, Italy; [4]Department of Surgery and Medical and Surgical Specialties, University of Catania, 95124 Catania, Italy, Palermo, Italy; [5]Department of Organ Failure and Transplantation, ASST Papa Giovanni XXIII Hospital, Bergamo, Italy, Bergamo, Italy*
Email: bmagro@ismett.edu

Background and aims: Patients undergoing liver transplantation (LT) for hepatocellular carcinoma (HCC) remain at risk for tumor recurrence. Calcineurin inhibitors (CNIs) have been associated with oncogenic effects, whereas mammalian target of rapamycin inhibitors may offer antitumor benefits. Evidence on everolimus-based regimens within steroid-free induction protocols is limited.
Method: We retrospectively analyzed 344 consecutive patients who underwent LT for HCC at ISMETT (Palermo) and HPG23 (Bergamo) between January 2022 and June 2025. Patients at ISMETT received steroid-free induction with basiliximab, while Bergamo patients received steroid induction. Immunosuppressive regimens were assessed; early conversion was defined as within three months. Kaplan–Meier analysis evaluated acute cellular rejection (ACR), HCC recurrence, graft survival, and overall survival. Uni- and multivariate Cox regression analysis was used to identify predictors of outcomes.
Results: The cohort was predominantly male (79.9%) with a mean age of 58.9 ± 10.4 years. Viral cirrhosis was the leading etiology (44.3%), and 41.9% of grafts were marginal. Everolimus-based immunosuppression was used in 123 patients (35.8%), including monotherapy in 65 cases (18.9%). Among everolimus-treated patients, 83 (69.2%) were converted from CNIs at a median of 4.5 months (IQR 1.8–8.0), with 23 (39%) undergoing early conversion. Median follow-up was 22.9 months (IQR 10.9–41.9). Rejection-free survival was comparable between everolimus and CNI-based regimens. In the steroid-free cohort, ACR was significantly more common among everolimus-treated patients (p = 0.042), likely due to higher use of monotherapy. Among everolimus-treated patients, the risk of ACR was similar between steroid-free and steroid cohort. HCC recurrence-free survival and overall survival did not significantly differ between everolimus and CNI-based regimens. Early conversion was associated with increased mortality (HR 7.52, 95%CI 0.95–59.70, p = 0.056), whereas viral etiology was an independent protective factor by multivariate analysis (HR 0.42, 95%CI 0.21–0.88, p = 0.020). Graft survival was significantly better in the everolimus group (HR 0.49, 95%CI 0.26–0.93, p = 0.020).

Conclusion: Everolimus-based immunosuppression is safe after LT for HCC, even within steroid-free induction protocols. However, everolimus monotherapy may increase the risk of ACR. CNI-minimization strategies appear feasible when carefully selected and monitored.

FRI-529-YI

Who drops out? Preoperative prediction of hepatic hypertrophy techniques failure from the IGROWtoH registry

Cecilia Maina[1], Elio Jovine[2], Matteo Serenari[2], Francesca Ratti[1]. [1]*San Raffaele, Milano, Italy;* [2]*Ospedale Maggiore Carlo Alberto Pizzardi, Bologna, Italy*
Email: ratti.francesca@hsr.it

Background and aims: Liver resection feasibility is mainly limited by the volume and function of the future liver remnant (FLR), with posthepatectomy liver failure remaining a major cause of post-operative mortality. Hypertrophy-inducing techniques increase FLR volume and expand resectability but are associated with a relevant risk of treatment drop-out, due to insufficient hypertrophy or disease progression. This study aimed to identify preoperative predictors of drop-out to improve patient selection and outcomes.
Method: Adult patients with malignant liver disease requiring a hypertrophy-inducing strategy for insufficient FLR volume (<40%) and/or impaired function were extracted from the multicenter IGROWtoH registry (2014–2025). Univariate and multivariate analyses were performed to identify independent predictors of drop-out. A points-based clinical score was developed from the multivariable model using the Sullivan–Framingham method and internally validated by bootstrap resampling. Disease-specific predictors were explored through subgroup analyses.
Results: Among 445 eligible patients, 114 (25.6%) experienced drop-out. Prior locoregional treatments (OR 0.33, $p = 0.004$) and the use of portal vein embolization or liver venous deprivation as hypertrophy technique were associated with lower drop-out odds (OR 0.21, $p = 0.002$ and OR 0.25, $p = 0.013$, respectively), whereas preoperative hyperbilirubinemia and secondary liver tumor diagnosis increased them (OR 1.93, $p = 0.028$ and OR 1.95, $p = 0.013$, respectively). The derived drop-out risk score stratified patients into four categories, with drop-out rates rising from 12.2% in the low-risk group to 45.5% in the very high-risk group. Disease-specific predictors included albumin-bilirubin grade ≥ 2 for primary intrahepatic tumors; obesity, prolonged international normalized ratio (INR) and gallbladder cancer for extrahepatic-perihilar tumors; and bilobar disease and elevated carcinoembryonic antigen (CEA) for secondary liver tumors.
Conclusion: Drop-out after hypertrophy-inducing strategies is influenced by both patient- and disease-specific factors. The preoperative risk score effectively stratifies drop-out risk and may support individualized treatment planning. Disease-specific predictors act as clinical "red flags" with an additive effect, amplifying the probability of drop-out.

FRI-530

Medical management of patients undergoing elective, liver-related invasive procedures - a novel collaboration model between hepatologists and hepato-biliary surgeons

Chiara Mangini[1], Federica Giunta[1], Domenico Bassi[2], Riccardo Boetto[2], Carmine Gambino[1], Riccardo Carandina[3], Matteo Ghisa[2], Caterina Soldà[4], Sabrina Cervesato[1], Michele Tessarin[5], Sara Montagnese[1], Umberto Cillo[2]. [1]*Department of Medicine, University of Padova, Padua, Italy;* [2]*Department of Surgical, Oncological and Gastroenterological Sciences, University of Padova, Padova, Italy;* [3]*Department of Integrated Diagnostic Services, Padova University Hospital, Padova, Italy;* [4]*Veneto Institute of Oncology IOV-IRCCS, Padova, Italy, Padova, Italy;* [5]*Medical Management, Padova University Hospital, Padova, Italy*
Email: chiara.manginij@gmail.com

Background and aims: To describe and test a novel, joint management system (surgery/hepatology) of patients undergoing elective procedures for hepato-biliary disorders of varying origin, within the setting of a short medical hospitalisation.
Method: Patients electively admitted under this system to the Internal Medicine Ward 5 - Hepatology (Padova University Hospital) between Feb 2023 and June 2025 were included. Admissions were jointly scheduled/prioritized by designated hepatologists and hepato-biliary surgeons, and managed by a specialist nurse. On admission, clinical and laboratory tests were performed, and patients prepared as appropriate (i.e. hydration, antibiotic prophylaxis etc.), and then monitored after the procedure; any complications were treated as necessary. Outcomes were classified as discharge within 72 hours, longer hospitalization, transfer to other ward, death.
Results: 352 procedures were performed over the testing period: 99 (28%) endoscopic retrograde cholangiopancreatographies (ERCP), 127 (36%) locoregional treatments (LRT) for hepato-biliary malignancies, 71 (20%) percutaneous transhepatic biliary drainages (PTBD), and 55 (16%) other. 264 (75%) were first admissions (76% males, 68 ± 12 years) and 88 (25%) were repeated admissions (i.e. patients undergoing ≥ 2 procedures). Baseline disease were cirrhosis (34%), a history of liver transplantation (22%), and hepato-biliary malignancies (38%). Inpatient stay was 2.4 ± 4.3 days, with 86% of patients being discharged within 72 hours. Complications occurred in 57 patients (16%), with no differences between procedures. While complications were mostly mild, they prolonged the inpatient stay (8.5 ± 8.4 vs 1.2 ± 0.75 days, $p < 0.001$). For ERCP, complications were associated with pre-procedural lower white blood cell counts ($p < 0.05$). For PTBD, complications were associated with lower haemoglobin and elevated AST, ALT, and bilirubin ($p < 0.05$). Elevated pre-procedural AST (HR 1.01, $p < 0.05$) and INR (HR 3.27, $p < 0.05$), and the presence of cirrhosis (HR 1.69, $p < 0.05$) independently predicted the occurrence of complications. In patients undergoing LRT, 30-day CT scans showed complete resolution in 57% of instances.
Conclusion: Integrated hepatological-surgical management of patients undergoing complex hepato-biliary procedures within the setting of an elective medical hospitalization is feasible and effective, ensuring short inpatient stays and low complication rates, at least in a large tertiary referral liver centre.

FRI-531

Coronary revascularization with short-duration dual antiplatelet therapy prior to liver transplantation: an 8-year single-center experience

Chiara Manuli[1], Margherita Saracco[1], Silvia Strona[1], Guglielmo Gallone[2], Federico Conrotto[2], Chiara Stratta[3], Renato Romagnoli[4], Silvia Martini[1]. [1]*SSD Insufficienza Epatica e Trapianto Epatico, AOU Città Della Salute e Della Scienza Di Torino, Turin, Italy;* [2]*Cardiology Unit, AOU Città della Salute e della Scienza di Torino, University of Turin, Turin, Italy;* [3]*Anesthesia and Intensive Care Unit 2, AOU Città della Salute e della Scienza di Torino, Turin, Italy;* [4]*General Surgery 2U, Liver Transplantation Center, AOU Città della Salute e della Scienza di Torino, Turin, Italy*
Email: chiara.manuli@gmail.com

Background and aims: Significant coronary artery disease (CAD) is increasing in liver transplant (LT) recipients and its pre-LT treatment can improve LT outcomes. New-generation drug-eluting stents (DES) allow early dual antiplatelet therapy (DAPT) discontinuation, but its optimal duration remains controversial. We aimed to describe pre-LT and early post-LT outcomes of our patients (pts) with CAD who underwent pre-LT revascularization.
Method: All LT pts from 01/2018 to 12/2025 who underwent pre-LT cardiac catheterization (CATH) were included. Significant CAD was defined as stenosis ≥50% in major-vessel or ≥70% in moderate-sized branch vessel.

Results: Among 1608 adult pts transplanted in our Center during study period, 95 (6%) underwent pre-LT CATH due to: a) previous history of obstructive CAD (16%); b) positive/doubtful non-invasive tests (71%) -mostly coronary CT angiography (76%); c) cardiology indication (13%). CATH detected 39 pts (41%) with significant CAD requiring revascularization: 97% male, median age 64 y [IQR 61–68], 64% BMI>25, 38% MetALD, median MELD 12 [9–15], 74% HCC, 69% diabetes, 59% arterial hypertension. 2/39 pts (5%) underwent coronary bypass surgery (CABG) and 37 (95%) percutaneous revascularization (PCI+DES). 5/39 (13%) experienced CATH related complications: 3 anemia, 1 acute kidney injury, 1 intraprocedural myocardial infarction with successful revascularization. After PCI, median DAPT duration was 31 days (d) [30–90]. Median time between DAPT discontinuation, LT listing and LT was 11 d [6–19] and 84 d [22–174], respectively. Median donor age was 64 y [54–76], 18 grafts (46%) underwent machine perfusion. A median of 2 red blood cell units was transfused during LT [0–7]. After a median post-LT follow-up of 13.5 months [1.8–39.9] 87% of the pts are alive. 5/39 pts (13%) experienced post-LT ischemic events: 1 pt at the end of LT due to stent occlusion (pt underwent successful PCI+DES), 1 after 24 d due to CABG occlusion (pt received successful PCI, he died 30 months later due to ischemic heart failure), 1 discrepancy angina 4 months after LT (with negative CATH), and 2 pts with stent occlusion at 4 and 11 months after LT (successfully treated with PCI+DES).
Conclusion: In our real-life cohort of pts with significant CAD, pre-LT DES-PCI and short DAPT was feasible and allowed early LT. A non-negligible incidence of post-LT ischemic events was observed, managed promptly and effectively, underlying the need of high surveillance in this group.

FRI-532
Obesity as a key risk factor for de novo malignancies in liver transplant recipients: a 23-year cohort study
Natalia Marcos Carrasco[1,2,3], Elena Velasco Martinez[1,2], Laura Jiménez[1,2], Alicia San José Crespo[1,2], Samuel Fernández-Prada[1,2], María Jordán de la Fuente[1,2], Carmen Alonso Martin[4], Graciela Salinas Camargo[1,2], Isabel Ruiz Nunez[1,2], Daniela Ortiz Chimbo[1,2], Carlos Maroto Martin[1,2], Félix García Pajares[1,2], Irene Peñas Herrero[1,2,3], Carolina Almohalla Alvarez[1,2], Gloria Sánchez Antolín[1,2,3]. *[1]Hospital Universitario Río Hortega, Valladolid, Spain; [2]IbioVall, Valladolid, Spain; [3]Valladolid University, Valladolid, Spain; [4]Complejo Asistencial Universitario de Salamanca, Salamanca, Spain*
Email: natalia.marcos.carrasco@gmail.com

Background and aims: Advances in the management of liver transplant (LT) recipients have markedly improved long-term survival; however, they have also increased the incidence of de novo malignancies, which represent a major challenge during post-transplant follow-up. Aims: to analyze the overall incidence of cancer in a cohort of adult LT recipients and to identify the main associated risk factors.
Method: Observational, retrospective study based on a prospective cohort, including all adult patients undergoing LT at a Liver Transplant Unit between 2001 and December 2024. Demographic, clinical, and follow-up variables related to the development of malignancies were collected. Hepatocellular carcinoma (HCC) was excluded from the analysis.
Results: 762 patients were analyzed; 78% were male, with a mean age of 56 years at transplantation. Alcohol consumption and tobacco use were reported in 69.5% and 63% of patients, respectively. Mean body mass index was 27.4. Diabetes mellitus, dyslipidemia, and hypertension were present in 27.7%, 10.7%, and 21.6% of patients, respectively. Mean MELD sodium score was 15. The most frequent underlying liver disease was alcohol-related liver disease (49.5%), followed by hepatitis C virus infection (25%). At the time of transplantation, 35.7% of patients had HCC. During follow-up, 119 de novo malignancies were diagnosed. The most frequent were head and neck cancer (25%), lung cancer (18.5%), and hematological malignancies (9.2%), with a median time to diagnosis of 6.8 years after LT. Estimated overall survival was 11.6 years and was significantly lower in patients who developed malignancies (7.9 years; $p < 0.001$). A total of 60 patients (50.4%) died as a direct consequence of cancer. In this cohort, obesity was the only factor significantly associated with the development of de novo malignancies ($p < 0.05$).
Conclusion: De novo malignancies represent a relevant complication after LT, with a negative impact on mortality and quality of life. Prevention strategies and early detection should be prioritized during post-transplant follow-up. In our cohort, obesity was the only factor significantly associated with cancer development after transplantation.

FRI-533
Impact of tumor biology versus imaging on post-transplant outcomes in hepatocellular carcinoma (HCC)
Natalia Marcos Carrasco[1,2,3], Alicia San José Crespo[1,2], María Jordán de la Fuente[1,2], Pedro Enrile Sanchez[1,2], Elena Velasco Martinez[1,2], Samuel Fernández-Prada[1,2], Jorge Lillo Diez[1,2], Cristina Martínez Cuevas[1,2], Irene Peñas Herrero[1,2,3], Carolina Almohalla Alvarez[1,2], Félix García Pajares[1,2,3], Gloria Sánchez Antolín[1,2,3]. *[1]Hospital Universitario Río Hortega, Valladolid, Spain; [2]IbioVall, Valladolid, Spain; [3]Valladolid University, Valladolid, Spain*
Email: natalia.marcos.carrasco@gmail.com

Background and aims: Hepatocellular carcinoma (HCC) accounts for approximately 35% of liver transplantation (LT) indications. Diagnosis relies on radiological criteria, which may underestimate tumor burden. Both radiological underestimation and vascular invasion on explant histopathology are associated with increased post- LT recurrence. Aims: to evaluate the concordance between radiological and explant findings in transplanted HCC patients; to assess their impact on post-LT survival and recurrence.
Method: Single-center, observational, retrospective study based on a prospective database. All patients undergoing LT for HCC between 2001–2024 were included. Radiological findings were compared with explant histopathology. Overall survival, recurrence, and associated risk factors were analyzed.
Results: 266 patients were included; 86.5% were male, with a median age of 60 years (interquartile range 54–64). Alcohol-related liver disease was the most common etiology (47.5%), followed by hepatitis C virus infection (37.7%). Most patients were Child–Pugh class A (63.4%), with a median MELD sodium score of 12. On imaging, 92.4% fulfilled Milan criteria. Radiologically, 56.8% of patients had one nodule, 25.8% had two, 13.3% had three, and 3.4% had four nodules. Median dominant nodule size was 2.5 cm, and median total tumor size was 3.0 cm (2.1–4.4). On explant histopathology, 5.2% had no HCC, while 47.6% had one nodule, 23.2% two, 12.0% three, and 12.0% four or more nodules. Median dominant nodule size was 2.5 cm (1.8–3.5), and median total tumor size was 3.5 cm (2.2–5.0), with 77.2% within Milan criteria. Correlation between radiology and explant was moderate for number of nodules (correlation coefficient 0.48; $p < 0.001$) and tumor size (correlation coefficient 0.41; $p < 0.001$). During follow-up, 50.8% of patients died, with 30% of deaths HCC-related. Estimated overall survival was 10.5 years. Recurrence was associated with significantly lower survival ($p < 0.001$). Predictors of recurrence included total tumor size on imaging, bridging therapy, elevated alpha-fetoprotein levels, dominant nodule size on explant, and adverse histological features.
Conclusion: Pre-transplant radiological assessment remains crucial for optimizing survival and preventing recurrence, particularly regarding tumor size. However, tumor biological characteristics and explant histopathological criteria showed a stronger association with recurrence and post-transplant survival.

FRI-537

Predicting packed red blood cell requirements in patients undergoing orthotopic liver transplant – foundation work for a quality improvement project

Anna Matusiewicz[1], Victoria J. Appleby[1], Richard Parker[1]. [1]*Leeds, United Kingdom*
Email: anna.matusiewicz1@nhs.net

Background and aims: Anaemia is common in patients with liver disease and is often multifactorial. Packed red blood cell (PRBC) transfusion is costly and not without risk, but is frequently required perioperatively in patients undergoing elective orthotopic liver transplantation (OLT). This study aims to identify whether anaemia is a predictor of perioperative PRBC transfusion requirement in patients undergoing elective OLT.
Method: A single-centre retrospective case series was conducted. Data was collected from patients who underwent elective OLT between 2024 and 2025 in St James's University Hospital, Leeds. A dataset was compiled recording patient demographics, liver disease aetiology, transplant assessment blood tests for anaemia, haemoglobin concentration (Hb) at the time of transplant, intra-operative transfusion requirement and total admission transfusion requirement. Statistical analysis was performed using R software.
Results: In total, 120 patients were included: median age was 59 years (IQR 47–66), 71% were male. The most common diagnoses were alcohol-related liver disease (ALD, 55 patients, 46%), biliary disease (24 patients, 20%) and metabolic dysfunction-associated steatotic liver disease (MASLD, 15 patients, 13%). Thirty-two patients had hepatocellular carcinoma (27.4%). Most patients (67, 56%) required PRBC in the perioperative period with a total of 216 units used - based on national UK tariffs for blood products, this is a total cost of £40,286.12 (€ 46252.96), or £335 per patient (€385). Hb at the time of transplantation was independently associated with intraoperative PRBC requirements (HR 0.97, 0.95–0.98, $p < 0.001$) and total perioperative PRBC requirements (HR 0.96, 0.94–0.98, $p < 0.001$). Hb at the time of transplantation was in turn predicted by Hb, folate, ferritin, age and diagnosis at the time of assessment for transplantation, although only Hb remained significant in multivariable analysis (HR 1.88, 1.55–2.27, $p < 0.001$).
Conclusion: We have demonstrated that in patients undergoing OLT, anaemia at the time of transplant predicts PRBC transfusion requirement perioperatively, with lower haemoglobin levels predicting higher PRBC transfusion requirements. Careful attention to the treatment of anaemia may reduce PRBC requirements around the time of transplantation, reducing costs and the risk of complications from transfusion.

FRI-538-YI

Cross-modality validation of 90% pathological response as a predictor of long-term survival in early-stage HCC

Mzamo Mbelle[1,2], Maria Guerra Veloz[1], Yoh Zen[1], David Wallace[3,4], Rosa Miquel[1], Paul Ross[1], Sarah Selemani[1], Dylan Lewis[1], Praveen Peddu[1], Miriam Cortes Cerisuelo[1], Parthi Srinivasan[1], Abdul Hakeem[1], Krishna Menon[1], Kosh Agarwal[1], Varuna Aluvihare[1], Claire Kelly[1], Michael Heneghan[1], Niloufar Safinia[2], Antonio D'Alessio[5], Abid Suddle[1]. [1]*Institute of Liver Studies, King's College Hospital, Denmark Hill, London, United Kingdom;* [2]*Roger Williams Institute of Liver Studies, Kings College London, London, United Kingdom;* [3]*Department of HPB and Liver Transplantation, The Royal Free Hospital, London, United Kingdom;* [4]*Department of Surgical Biotechnology, University College London, London, United Kingdom;* [5]*Division of Cancer, Imperial College London, London, United Kingdom*
Email: mzamo.mbelle@nhs.net

Background and aims: Pathological response, particularly the degree of tumour necrosis, is increasingly recognised as a key predictor of outcomes in hepatocellular carcinoma (HCC) treated with curative modalities such as liver transplantation (LT). 90% tumour regression has been identified as the ideal cutoff for major-pathological response (MPR) after neoadjuvant immunotherapy (ICI) in resectable HCC, however the optimal prognostic threshold remains unclear, particularly after pre-transplant locoregional therapy (LRT).
Method: This retrospective single-centre cohort study included 300 LT recipients enrolled from December 2012 to January 2023, of whom 133 had quantifiable tumour necrosis on explant histopathology. Pathological response was centrally assessed as the proportion of viable tumour relative to necrosis following LRT: Grade 1 (<50% necrosis), Grade 2 (50–90%), Grade 3 (>90%), and Grade 4 (complete pathological response). Overall survival (OS) and recurrence-free survival (RFS) were analysed using Kaplan-Meier method. Optimal necrosis cut-offs for survival prediction were explored using unbiased recursive partitioning and Youden's index derived from ROC analyses.
Results: Overall, 238 patients (78%) underwent LRT, with 57.1% receiving more than one modality; TACE was the most common treatment (84%). After a median follow-up of 69 months (95% CI 65–75), 5-year median overall survival (OS) was 77.5%. Median OS improved form 108.2 months (95% CI 102 – NR) in patients without necrosis to 136.1 months (95% CI 136.7 – NR) in those with necrosis. Stepwise improvement in OS was observed across increasing necrosis grades (log-rank $p = 0.033$), and 5-year RFS was 96.9% (95% CI 92.7–100) in patients with >90% necrosis vs 82.9% (95% CI 77.4–88.7) in those with <90%. Cox proportional hazards modelling demonstrated that Grade 3 necrosis (>90%) was independently associated with improved OS (hazard ratio [HR] 0.12, 95% CI 0.014–0.98, $p = 0.012$). Recursive partitioning and Youden's index both identified Grade 3 (>90%) as the optimal cutoff to predict OS.
Conclusion: Explant necrosis ≥90% is a robust predictor of survival following LT for HCC treated with LRT and supports ≥90% as a potential definition of major pathological response (MPR). This represents, to our knowledge, the first cross-modality validation of a necrosis-based threshold for post-LT outcomes. Multi-centre validation is needed to refine the optimal necrosis cut-off for integration into prognostic models and post-transplant surveillance strategies.

FRI-539

Long-term outcomes of endoscopic therapy for post-transplant biliary anastomotic strictures: a single center experience

Shubham Mehta[1], Abhinav Sengupta[2], Harsh Jain[1], Hitesh Panchal[1], Pawan Rawal[1], Rajesh Puri[1]. [1]*Medanta Hospital, Gurugram, India;* [2]*All India Institute of Medical Sciences, New Delhi, India*
Email: mehta.shubham1493@gmail.com

Background and aims: Biliary complications occur in approximately 14–20% of patients post-orthotopic liver transplantation (post-OLT). Endoscopic retrograde cholangiopancreatography (ERCP) and insertion of plastic stents represent the standard treatment, however, there is limited data on the resolution rate of stricture and bile leak and long-term outcomes in patients with these complications.
Method: We reviewed clinical records of 3590 consecutive patients who underwent OLT between 2011–2023. For the patients who developed anastomotic biliary strictures (ABS) or bile leak (BL), specific data including the demographics, indication of OLT, graft type, configuration of bile ducts, number of biliary anastomosis, number of ERCP sessions required and requirement of per-cutaneous transhepatic biliary drainage (PTBD) were extracted. Primary outcome was to estimate the rate of stricture or bile leak resolution.
Results: Of total 3590 patients who underwent liver transplant, 540 (15%) patients (male = 465, 86.1%; mean age- 49.3 ± 10.6 years) developed biliary complications [ABS – 469 (86.9%) patients; BL – 60 (11.1%) patients; stricture with bile leak – 11 (2%) patients]. The median time to stricture formation after OLT was 6 (IQR: 3–10) months, and the median time from OLT to bile leak was 29.5 (IQR:15–51.5) days. The technical success for ERCP was 89.1% (481/540); 59 (10.9%) patients required a combination of ERCP and PTBD (followed by rendezvous ERCP) for biliary drainage and one patient required surgery. Of 480 patients with ABS, 409 (85.2%) patients achieved

stricture resolution after a median 3 (IQR:2–4) ERCP sessions and median 6 (IQR:4–9) months. Rest required surgery. Stricture recurrence occurred in 20.5% (84/409) patients after median 5 (IQR: 3–12) months of stent free trial; 90% (76/84) patients were subsequently managed by ERCP successfully, and 8 patients required surgery. Of 60 patients with BL, rate of resolution was 95% (57/60) after median 1 (IQR: 1–2) ERCP session and median 3 (IQR: 3–4) months; none of these patients developed recurrence. On multivariate analysis, requirement of more than 3 ERCP sessions (aOR: 1.6, 95% CI: 1.1–1.8; p = 0.004)and multiple duct-to-duct anastomosis (aOR: 1.7, 95% CI: 1.2–2.7; p = 0.02) predicted recurrence of strictures.
Conclusion: ERCP is an effective for post-OLT biliary anastomotic strictures and bile leaks. The number of ERCP procedures and multiple duct-to-duct anastomosis were predictors of stricture recurrence.

FRI-540

Donor PNPLA3 rs738409 genotype is a risk factor of long-term graft survival after liver transplantation

Irena Mikova[1], Milan Jirsa[1], Eva Sticova[1], Jan Mares[1], Pavel Trunecka[1]. [1]*Institut Klinické a Experimentální Medicíny, Praha, Czech Republic*
Email: irena.mikova@ikem.cz

Background and aims: The variants rs738409 c.444C>G (p.I148M) in patatin-like phospholipase domain-containing 3 (PNPLA3) and rs58542926 c.499G>A (p.E167K) in TM6SF2 (transmembrane 6 superfamily member 2) are significant genetic risk factors of development and progression of metabolic dysfunction-associated steatotic liver disease (MASLD). The donor but not the recipient genotypes are crucial for MASLD development after liver transplantation (LT). Increased liver-specific mortality was described in both variants. The aim of the study was to evaluate the impact of the PNPLA3 rs738409 and TM6SF2 rs58542926 genotypes of the donor and the recipient on the long-term patient and graft survival after LT.
Method: We evaluated the patient and graft survival in the cohort of 268 adult LT recipients, in whose PNPLA3 rs738409 and TM6SF2 rs58542926 genotypes of the donor and recipient were available and steatosis/steatohepatitis was evaluated on liver graft biopsy 6–30 months after LT. The median follow-up was 17.0 years. The Kaplan-Meier model was used for the graft and patient survival estimates and the Cox proportional hazard model was used to assess the predictive value of the selected variables.
Results: In the multivariable analysis, recipient age (p < 0.001), male sex (p = 0.001), presence of hepatocellular carcinoma (p = 0.015) and grade of inflammation on the liver biopsy (p = 0.002) negatively influenced long-term patient survival; whereas donor PNPLA3 rs738409 genotype GG/GC vs CC (p = 0.009), male sex (p = 0.009), lower BMI (p < 0.001) and increased stage of fibrosis (p = 0.001) negatively impacted on graft survival. No impact of TM6SF2 rs58542926 genotypes on patient or graft survival was found.
Conclusion: The PNPLA3 c.444G variant of the donor has a negative impact on the long-term liver graft survival.

FRI-541

Validation of the RETREAT score for predicting hepatocellular carcinoma recurrence after liver transplantation: evidence from an Italian multicenter cohort

Leonardo Antonio Natola[1], Veronica Paon[2], Marco Vicardi[1], Aldo Filice[1], Andrea Dalbeni[3], Filippo Cattazzo[1], Lorenzo Canova[4], Eleonora Alimenti[4], Giulia Marini[5], Alex Borin[6], Daniele Dondossola[5], Amedeo Carraro[6], Massimo Iavarone[4], David Sacerdoti[2]. [1]*University of Verona, Department of Medicine, Verona, Italy;* [2]*Liver Unit, Azienda Ospedaliera Universitaria Integrata di Verona, Verona, Italy;* [3]*General Medicine C and Liver Unit, Azienda Ospedaliera Universitaria Integrata di Verona, Verona, Italy;* [4]*Division of Gastroenterology and Hepatology, Foundation IRCCS Ca' Granda Ospedale Maggiore, Milano, Italy;* [5]*General and Liver Transplant Surgery Unit, Fondazione IRCCS Ca' Granda Ospedale Maggiore Policlinico, Milano, Italy;* [6]*Liver Transplant Unit, Azienda Ospedaliera Universitaria di Verona, Verona, Italy*
Email: leosna94@gmail.com

Background and aims: Hepatocellular carcinoma (HCC) recurrence after liver transplantation (LT) remains a major determinant of post-transplant mortality, affecting up to 20% of recipients despite selection within the Milan criteria. The Risk Estimation of Tumor Recurrence After Transplant (RETREAT) score, developed by Mehta et al. (UCSF, USA) has shown excellent predictive performance in international and recent prospective validations but has never been evaluated in Italian transplant centers. This study aimed to validate the RETREAT score in an Italian multicenter cohort and assess its clinical applicability.
Method: We retrospectively analyzed 262 adults transplanted for HCC between 2010–2020 at two Italian centers (Verona and Milan). All patients met Milan criteria at listing. Predictors of recurrence and survival were analyzed using Cox and logistic regression. RETREAT discrimination was assessed using ROC analysis, Harrell's C-index, calibration, and decision curve analysis (DCA).
Results: Over a median follow-up of 83.2 months, 32 patients (12.2%) developed recurrence and 63 (24.0%) died (overall). Median survival after recurrence diagnosis was 23.5 months (IQR: 6.2–43.5). Pre-transplant locoregional therapy was performed in 80.5% of cases: 24 (9.2%) underwent downstaging, 102 (38.9%) bridge, and 85 (32.4%) had previous treatments in the past. Most of them were TACE (37.7%) and RFA (26.5%). Microvascula invasion (MVI) was the strongest recurrence predictor (OR 5.93, 95% CI 2.73–12.87, p < 0.001). RETREAT ≥3 was associated with a 6.7-fold higher recurrence risk (OR 6.72, 95% CI 2.88–15.68, p < 0.001) and remained independently associated in multivariable analysis (OR 3.97, 95% CI 1.23–12.27, p = 0.016). Exceeding Milan criteria on explant histology was not significant (p = 0.239). The score demonstrated excellent discrimination (AUC 0.774, C-index 0.77), good calibration, and positive net benefit on DCA across thresholds of 5–15%. Kaplan-Meier analyses highlighted: (Fig. 1) the strong impact of recurrence on overall survival (p < 0.0001); (Fig. 2) significantly worse RFS for high-risk patients (RETREAT ≥3) compared with low-risk (RETREAT ≤2) (p = 0.012).
Conclusion: This first Italian validation confirms the excellent prognostic accuracy and generalizability of the RETREAT score. RETREAT-based stratification allows effective identification of high-risk patients and supports personalized surveillance strategies across Italian transplant centers.

FRI-542

Quantifying the impact of liver graft dysfunction on kidney outcomes after liver transplantation: a retrospective multicenter longitudinal cohort study using the L-GrAFT risk score

Yu Nie[1], Jinbo Huang[2]. [1]*a General Surgery Center, Department of Hepatobiliary Surgery, Zhujiang Hospital, Southern Medical University, Guangzhou, China;* [2]*Organ Transplant Center, The First Affiliated Hospital, Sun Yat Sen University, Guangzhou, Guangzhou, China*
Email: nieyu19@foxmail.com

Background and aims: The relations between liver graft dysfunction and renal dysfunction is not fully described in liver transplantation (OLT). We performed a quantitative analysis to evaluate the impact of graft dysfunction on clinical trajectories of acute kidney injury (AKI) and long-term renal function using Liver Graft Assessment Following Transplantation (L-GrAFT) risk-score that could stratified graft dysfunction severity.
Method: This retrospective multicenter observational study included 1098 consecutive primary OLT patients from 5 tertiary teaching hospitals between January 2015 and December 2022. L-GrAFT risk-score was used to classify the severity of early graft dysfunction: good function (n = 316), mild dysfunction (n = 542), moderate dysfunction (n = 170) and severe dysfunction (n = 70). AKI was graded using KDIGO criteria. Patients were divided into different groups according to post-OLT renal and graft dysfunction. Perioperative renal-

associated outcomes and long-term survival were compared among different trajectories of AKI and graft dysfunction.
Results: 51.2% (n = 562) recipients developed AKI. 87.9% AKI occurred within 48 hours after OLT, with 40.2% AKI episodes developed during surgery. AKI rates in good, mild, moderate and severe graft dysfunction group were 41.5%, 48.5%, 60.0% and 94.3%. Renal-related outcomes including peak creatinine, AKI duration, AKI severity and rates of persistent AKI, RRT and MAKEs all significantly deteriorated as graft function deteriorated (P < 0.001). Mild (OR: 2.92 and 2.80), moderate (OR: 9.31 and 7.19) and severe (OR: 83.2 and 120.7) graft dysfunction were independent predictors of RRT requirement and MAKEs (P < 0.001). Patients combining both liver and renal dysfunction had significant inferior graft survival and increased MAKEs compared to those with only liver dysfunction (P < 0.001). Synergistic effects of severe graft dysfunction with severe AKI substantially elevated EAF risk, which was associated with the worst renal-related outcomes and one-year graft survival (adjusted HR 24.50, CI: 15.49–38.75, P < 0.001). Severe graft dysfunction with preserved renal function achieve an unexpectedly good prognosis (one-year graft survival 58.3%).
Conclusion: Different severities of graft dysfunction were associated with distinct clinical trajectories of renal dysfunction and survival outcomes. Simultaneous impairment of graft and renal function synergistically exacerbated OLT outcomes while preserved renal function could counteract the adverse effects of severe graft dysfunction.

FRI-543
Rejection rates after liver transplantation are not increased with hormonal contraceptive use
Helen Oberweis-Manion[1], Amy Shui[2], Cynthia Fenton[3], Grace Zhang[1], Monika Sarkar[1]. [1]*University of California San Francisco, Department of Medicine, Division of GI/Hepatology, San Francisco, United States;* [2]*University of California San Francisco, Department of Epidemiology and Biostatistics, San Francisco, United States;* [3]*University of California San Francisco, Department of Medicine, San Francisco, United States*
Email: elle.oberweismanion@ucsf.edu

Background and aims: Liver transplantation (LT) among reproductive-aged women is increasing, and fertility rapidly returns post-transplant. Hormonal contraception is highly effective at preventing unplanned pregnancy, though concerns persist regarding potential drug-drug interactions and graft rejection. We therefore aimed to evaluate the association of hormonal contraceptive exposure (CTE) and acute cellular rejection (ACR) after LT.
Method: We conducted a retrospective cohort study of reproductive-aged LT recipients followed at a tertiary transplant center from 1/2013–10/2025 to primarily assess the association ofhormonal contraceptive exposure (CTE) with biopsy-confirmed ACR, and secondarily with incident hypertension (HTN), venous thromboembolism (VTE), and myocardial infarction (MI). CTE was defined as at least 90 days of use, with study outcomes adjudicated to the CTE group if occurred within 90 days of last use. Study outcomes were compared between LT recipients with at least one CTE and LT-controls using Kaplan-Meier rates with log-rank tests or raw event percentages and counts with Fisher's exact tests, as appropriate.
Results: Amongst 416 reproductive-aged LT recipients, 157 (38%) had at least one CTE exposure; of these 157, 73 (46%) with combined hormonal contraception (CHC), 70 (45%) with progestin-only, and 83 (53%) with IUD use (76 hormonal, 7 copper). Median transplant age among CTE exposed and unexposed patients was 23.2 and 33.7 years, with a median follow-up of 14.9 and 10.6 years, respectively. Excluding copper IUDs, ACR but not incident HTN differed significantly by exposure group (log-rank test p = 0.001 for ACR, p = 0.14 for HTN). By 15 years since LT, ACR occurred in 15% vs. 27%, and HTN occurred in 19% vs. 26% of LT recipients in the exposed and unexposed groups, respectively. In LT recipients with vs without CTE, VTE occurred in 0.5% (1) vs 1.2% (3) and MI in 0.5% (1) vs. 0.4% (1) (p ≥ 0.99 for each).
Conclusion: Rates of biopsy-confirmed ACR in reproductive-aged LT recipients was no greater during periods of hormonal contraceptive exposure when compared to no contraceptive exposure. These agents were also not associated with greater risk for incident hypertension or thromboembolic events following LT. Findings support the safety of the breadth of hormonal contraceptive options in LT recipients to best support their reproductive wishes.

FRI-544
Outcomes of patients covertly/overtly consuming alcohol in the transplant assessment/waitlist period: a single centre experience
Helen O'Donovan[1], Francesca D'Arcangelo[1], Adnan Shabbir[1], Nicola Seaward[2], Alex Lawson[1], Charlotte Parker[1], Kerry Webb[1], Andrew King[1], Andrew Holt[1], Neil Rajoriya[1]. [1]*QEHB, Hepatology, Liver Transplant Unit, Birmingham, United Kingdom;* [2]*Dept. of Biochemistry, QEHB, United Kingdom*
Email: helsodon@gmail.com

Background and aims: Measurement of urine ethyl glucuronide (EtG) levels allows monitoring of abstinence in liver transplant (LT) wait listed patients. Testing positive on the wait list usually leads to removal with discharge of care to local physicians & often palliation. There remains limited data on long-term outcomes, including follow-up and potential for LT reassessments. The aim of this study was to assess outcomes for patients testing positive for active alcohol intake during the LT assessment pathway/wait list.
Method: Patients with positive EtG levels attending a quaternary LT centre, 2021–2025, were included. Those not seen by hepatology for potential LT assessment were excluded. Data collected included demographics, indications for referral, point at which turndown (removal from list/assessment process) occurred, follow-up and mortality. Patients may have been seen in a dedicated high intensity alcohol cirrhosis MDT clinic.
Results: 487 patients had positive EtG levels. 64 (13.1%) of those were seen in relation to LT assessment. 26 (40.6%) female, median age 52 (IQR 48–58). The median MELD 16 (IQR 11.5–19.5). 22 (34%) patients were seen in MDT clinic prior to LT assessment. 24 (37.5%) were found to have positive EtG before initiation of LT assessment and thus not considered eligible to proceed. Of the 40 patients who started a transplant assessment, 29 (72.5%) were turned down during the assessment process while 11 (27.5%) were listed for transplant and subsequently de-listed due to positive EtG. 1 patient was found to have positive metabolites on the day of LT. 5 (17.2%) of the 29 patients turned down during the assessment phase were seen for LT reassessment, 3 subsequently listed. 7/11 (63.6%) patients formally de-listed were ultimately referred back to the local team with no re-referrals for LT. 24 (37.5%) patients died.
Conclusion: Sadly, patients with advanced ArLD still covertly drink alcohol during work up for transplant, despite input from a dedicated high intensity alcohol cirrhosis MDT clinic in several cases. None of those with positive metabolites on the wait list were re-referred following discharge to their local teams. However, a small number of those found to have evidence of alcohol intake during the original LT assessment were considered for re-evaluation and LT in our centre. Ongoing alcohol relapse prevention in ArLD patients remains key on the wait list and during assessment. The establishment of a standardised testing pathway/protocol nationally will be of benefit.

FRI-546

Comparative waitlist and early post-transplant outcomes in asian vs. non-asian liver transplant candidates: a propensity-matched UNOS analysis (2014–2024)

Mangesh Pagadala[1], Suvisesh Pothuraju[2], Sajid Jalil[3], Nimish Thakral[4], Chencheng Xie[5], Yong-Fang Kuo[6], Ashwani Singal[2]. [1]*Liver Institute -Methodist Dallas Medical Center, Dallas, United States;* [2]*University of Louisville, Louisville, United States;* [3]*Standford University, Palo Alto, United States;* [4]*University of Lexington, Lexington, United States;* [5]*The University of Iowa, Iowa City, United States;* [6]*University of Texas Medical Branch, Galveston, United States*
Email: mangeshpagadala@mhd.com

Background and aims: Asian individuals represent a growing segment of Liver transplant (LT) candidates in the United States, yet contemporary data evaluating whether they experience differences in waitlist mortality or early post-transplant outcomes remain limited. This study evaluated waitlist mortality and early (1-year) post-transplant outcomes among Asian vs. non-Asian LT candidates using a large national dataset.
Method: Using the UNOS/OPTN database (2014–2024), we identified adult LT candidates and recipients. Pediatric cases and multi-organ transplants were excluded. Propensity score matching (PSM) was performed comparing Asians with Non-Hispanic Whites (NHW), African Americans (AA), Hispanic Whites (HW), and American Indians (AI). Matching variables included demographics, comorbidities, liver disease etiology, MELD components, and listing characteristics. Primary outcomes were waitlist mortality and 1-year post-transplant patient survival.
Results: Among 194,535 adult LT listings, 7,568 (3.9%) were Asian candidates. In unadjusted analyses, Asians had lower waitlist mortality compared with AA (HR 0.80; 95% CI 0.71–0.89), HW (HR 0.81; 95% CI 0.73–0.90), and AI (HR 0.78; 95% CI 0.64–0.94). After PSM, Asians experienced similar waitlist mortality compared with NHW (HR 0.90; 95% CI 0.76–1.05), AA (HR 0.89; 95% CI 0.76–1.05), and HW (HR 0.85; 95% CI 0.73–1.00). However, Asians remained at alower risk of waitlist mortality vs. AI (HR 0.74; 95% CI 0.56–0.97). Post-transplant outcomes showed important contrasts. Compared with AA recipients, Asians demonstrated significantly better 1-year graft (HR 0.83; 95% CI 0.71–0.98) and patient survival (HR 0.80; 95% CI 0.66–0.96). In contrast, Asians had no significant differences in 1-year graft or patient survival when compared with NHW, HW, or AI (all $p > 0.20$). Kaplan Meier analyses revealed no differences in survival across these matched cohorts. Hepatits B was more prevalent among Asian recipients, while MASLD and alcohol-associated liver disease were less common.
Conclusion: In this national UNOS analysis, Asian LT candidates in the US have similar waitlist mortality comparing to most of major racial and ethnic groups, except for lower waiting mortality than American Indian. Post- transplant graft and patient survival were better in Asians as compared to African Americans and similar to NHW, HW, and AI. These findings support overall equity in contemporary transplant outcomes while highlighting population-specific disparities that warrant further investigation.

FRI-547

Accuracy, feasibility, and nursing workload of continuous glucose monitoring in liver transplant recipients in the intensive care unit

Marc Pañero Moreno[1,2,3], Richie Alexander Inge Cox[1,2,4], Enric Tomas Franch[1], Alberto Villamor Ordozgoiti[1,3], Eva Maria Guix Comellas[3], Fatima Aziz[1]. [1]*Hospital Clinic of Barcelona, Barcelona, Spain;* [2]*Fundació de Recerca Biomedica Clinic - Institut d'Investigació Biomédical August Pi i Sunyer (FRCB-IDIBAPS), Barcelona, Spain;* [3]*Departament of Fundamental and Clinical Nursing, University of Barcelona, Barcelona, Spain;* [4]*European Foundation for the Study of Chronic Liver Failure (EF CLIF), Barcelona, Spain*
Email: panero@clinic.cat

Background and aims: Hyperglycemia affects over 90% of liver transplant (LT) recipients in the Intensive Care Unit (ICU) due to metabolic and surgical stress and immunosuppressive therapy. Continuous Glucose Monitoring (CGM) has shown good analytical performance in ambulatory patients with diabetes, but its accuracy and safety remain insufficiently investigated in critically ill LT recipients. Current guidelines do not endorse its routine inpatient use, and a consensus on accuracy is lacking; a Mean Absolute Relative Difference (MARD) below 15% is generally considered acceptable, and compliance with the Diabetes Technology Society (DTS) Error Grid requires at least 98% of values within zones A and B. This study aimed to evaluate the analytical accuracy and bedside feasibility of a CGM compared with nurse-performed Point-of-Care glucose (POC-G) measurements in LT patients in the ICU, and to explore its impact on workflow.
Method: A single-blind randomized clinical trial was conducted at the Hospital Clinic of Barcelona (CGM-UCI23 project). A CGM sensor was placed on the upper arm of LT recipients, and glucose readings were paired with nurse-performed POC-G measurements. Accuracy and safety were evaluated using the DTS Error Grid and MARD, providing comprehensive metrics of accuracy, clinical utility, and safety in the ICU setting. Nursing workload reduction was quantified by measuring the time required to obtain POC-G measurements (based on 20 random determinations) and comparing this with CGM use.
Results: The CGM sensor was worn for a mean of 5 days and remained active for 98.9% of the monitoring period. CGM showed excellent accuracy performance, with a MARD of 12.1% and 99.6% of readings falling within the safe zones of the DTS Error Grid. The CGM group required significant fewer daily POC-G tests (3.17 ± 2.15 vs 6.37 ± 1.78, $p < 0.001$) and fewer fingerstick samples (9.11 ± 26.1 vs 45.2 ± 70.2, $p < 0.001$) than controls. Overall, CGM produced 49,670 glucose readings versus 2,089 POC-G measurements, delivering a much denser glycemic profile while reducing bedside testing burden. On average, 50.68 POC-G tests and an estimated 43.56 minutes of nursing time were saved per patient during the ICU stay, underscoring the impact of CGM on nursing workload.
Conclusion: CGM is accurate, feasible, and significantly reduces nursing workload in LT recipients in the ICU while improving glycemic control. These findings support CGM implementation in ICU with LT recipients admitted to the ICU, to optimize workflow and patient safety.

FRI-548

Evolution of MASLD with and without alcohol consumption and comorbidity profile in liver transplant candidates over two decades

Simona Parisse[1], Erika Coltorti[2], Flaminia Ferri[2], Fabio Melandro[3], Quirino Lai[3], Federica Masciocchi[2], Giulia Bergamin[2], Gianluca Mennini[3], Massimo Rossi[3], Stefano Ginanni Corradini[2]. [1]*Department of Wellbeing, Health and Environmental Sustainability, Sapienza University of Rome, Rieti, Italy;* [2]*Department of translational and precision medicine, Sapienza University of Rome, Rome, Italy;* [3]*General Surgery and Organ Transplantation Unit, Sapienza University of Rome, Rome, Italy*
Email: simona.parisse@gmail.com

Background and aims: The liver transplantation (LT) landscape has substantially evolved over the past decades due to the rising prevalence of metabolic syndrome and the decline of HCV due to direct-acting antivirals (DAAs). Therefore, the complexity of LT candidate evaluation has increased. We aimed to assess the impact of epidemiological shifts on LT waiting list composition over a 20-year period, focusing on disease etiology and extrahepatic comorbidity burden as measured by the Charlson Comorbidity Index (CCI).
Method: All consecutive patients with cirrhosis and non-urgent indications for LT who were listed between 2005 and 2024 at our LT center were retrospectively analyzed and stratified into pre-DAA (2005–2014) and post-DAA (2015–2024) eras. The CCI was calculated, as previously described, based on nine extrahepatic comorbidities.

CCI was analyzed both as a continuous variable and as a categorical variable. Multivariable linear regression was used to identify factors independently associated with CCI.
Results: A total of 491 patients were listed for LT, including 200 (41%) in the post-DAA era and 291 (59%) in the pre-DAA era; of these, 55% and 60%, respectively, underwent transplantation from deceased donors. Over 20 years, pure MASLD etiology increased from 2.4% to 17.4%, and Met-ALD (MASLD and alcohol-related cirrhosis) from 7.1% to 22.4%, with a concomitant reduction in pure alcohol-related cirrhosis (from 20.0% to 8.6%). MASLD and MetALD were not significantly associated with the probability of undergoing LT. Higher CCI categories were more frequent post-DAA (CCI 0: 59% vs 40%; CCI 1–2: 31% vs 40%; CCI >3: 9% vs 20%; p = 0.001). Regarding LT indications, HCC (57% vs 41%, p = 0.001) and other MELD exceptions (10% vs 1%, p < 0.001) were more common in the post-DAA era. On multivariable linear regression, CCI was independently associated with MASLD etiology (B = 1.307, 95% CI 1.085–1.529, p = 0.001), older age (B = 0.022, 95% CI 0.010–0.035, p = 0.002), and male sex (B = 0.344, 95% CI 0.081–0.607, p = 0.009), and inversely associated with HCC (B = –0.338, CI 95% –0.558 – –0.118, p = 0.003).
Conclusion: The LT waiting list has substantially changed; the prevalence of pure MASLD rose seven-fold and MetALD tripled, marking a move toward indications less reliant on MELD. The rising burden of extrahepatic comorbidities, driven by older age and metabolic disease, highlights the need for more comprehensive pre-transplant evaluation, while evolving LT indications may challenge MELD-based prioritization.

FRI-553
Development and external validation of the MEAF ALT/AST continuous model: a universal tool for assessing early allograft dysfunction in liver transplantation
Carmen Payá Llorente[1], Miriam Cortes Cerisuelo[2], Marina Berenguer[3], Guillermo Quintas Soriano[4], Shubhangi Mehta[2], Eugenia Pareja Ibars[1]. *[1]Hospital Universitario Doctor Peset, Valencia, Spain; [2]King's College Hospital, London, United Kingdom; [3]Hospital Universitario y Politécnico La Fe, Valencia, Spain; [4]Leitat Technological Center, Health and Biomedicine, Barcelona, Spain*
Email: carmenpayallorente@gmail.com

Background and aims: To reduce waitlist mortality, expanded donor criteria are used in liver transplantation (LT). This increases the risk of early allograft dysfunction (EAD); however, the lack of a standardized definition for EAD makes comparing its prevalence and evolution difficult. Among the proposed models, the MEAF (Model for Early Allograft Function) stands out. It continuously evaluates graft function during the first post-LT days with a score, based on the International Normalized Ratio (INR), alanine aminotransferase (ALT), and bilirubin levels.
The main objective of this study is to design a continuous model based on the MEAF, calculated daily during the early post-LT period, using either ALT or aspartate aminotransferase (AST) interchangeably alongside INR and bilirubin, making it applicable to the majority of transplant recipients.
Method: A retrospective observational study with consecutive sampling was conducted using a prospective database, an external valitarion were performed. Clinical, surgical, and analytical data from donors and recipients were evaluated. The model, MEAF ALT/AST, was calculated using eight equations between post-LT days 2 and 5, interpolating biochemical values into sigmoidal regressions to obtain scores from 0 to 10, grouped into five grades of function. We analyzed its correlation with the standard MEAF, its applicability in Donation after Circulatory Death (DCD) donors, and its ability to predict graft survival at 10 and up to 90 days.
Results: The study included 1,351 LTs in 1,315 recipients. Results showed a correlation between the standard MEAF and the MEAF ALT/AST, confirming its applicability to DCD donors. The predictive capacity of the model for 10-day survival was excellent (AUC > 0.8), similar to the standard MEAF, and slightly lower at 90 days. External validation performed on 688 LTs (675 recipients) confirmed its utility. As a practical contribution, a web application has been developed to calculate the MEAF ALT/AST and visualize graft function trends in real-time, facilitating its implementation in clinical practice.
Conclusion: The MEAF ALT/AST is a continuous model that allows for the assessment of initial graft function in the first post-LT days, applicable to non-conventional donors and recipients. The ability to use ALT or AST interchangeably increases accessibility and reproducibility, facilitating early therapeutic decision-making and the benchmarking of results between centers.

FRI-554
Dynamic liver stiffness predicts recurrent cirrhosis and mortality after liver transplantation: a longitudinal joint modelling study
Jassin Rashidi-Alavijeh[1], Nargiz Nuruzade[2]. *[1]Department of Gastroenterology and Hepatology, University Hospital Essen, University of Duisburg-Essen, Essen, Germany, Department of General, Visceral and Transplantation Surgery, University Hospital Essen, University of Duisburg-Essen, Essen, Germany, Essen, Germany; [2]Department of Gastroenterology and Hepatology, University Hospital Essen, University of Duisburg-Essen, Essen, Germany, Essen, Germany*
Email: jassin.rashidi@uk-essen.de

Background and aims: Recurrent graft fibrosis and cirrhosis remain major determinants of long-term outcomes after liver transplantation (LT). Transient elastography–derived liver stiffness measurement (LSM) predicts prognosis in chronic liver disease, but post-LT data are limited and often rely on single time points without accounting for competing risks. We investigated whether longitudinal LSM dynamics independently predict recurrent cirrhosis and mortality after LT using joint modelling.
Method: We performed a retrospective longitudinal cohort study including adult LT recipients with ≥2 reliable LSMs obtained ≥2 years post-LT at University Hospital Essen (2005–2024; follow-up until 2025). Recurrent cirrhosis was defined by graft biopsy; secondary endpoint was all-cause mortality. LSM trajectories were analysed using linear mixed-effects models and linked to time-to-event outcomes via joint models using the current value of log-transformed LSM. Multivariable models were adjusted for diabetes, body mass index, steatosis, sex, age and relapse of primary disease. A competing-risk joint model estimated separate associations for recurrent cirrhosis and death. Discrimination was assessed using time-dependent AUCs.
Results: The cohort comprised 249 LT recipients contributing 2,773 person-years and 1,801 reliable LSMs; median follow-up was 11.2 years. Thirty-nine patients developed biopsy-proven recurrent cirrhosis and 60 died. Higher current log-LSM was strongly associated with recurrent cirrhosis (adjusted association parameter $\alpha = 2.71$, 95% CI 1.81–3.72; p < 0.001). A 20%, 50% and 100% increase in LSM corresponded to hazard ratios (HRs) of 1.61, 2.98 and 6.54, respectively. Model discrimination was good (AUC 0.72 at 5 years; 0.66 at 10 years). Current log-LSM also independently predicted mortality. In competing-risk joint models, a 20% increase in LSM was associated with HRs of 1.38 for recurrent cirrhosis and 1.40 for death. Inclusion of the annual LSM slope did not improve prognostic performance.
Conclusion: Longitudinally modelled current LSM is a strong, independent predictor of both recurrent cirrhosis and mortality after LT. These findings support the integration of serial LSM into

structured post-transplant risk stratification and surveillance strategies.

FRI-555

Etiology-specific patterns of long-term cognitive recovery after liver transplantation: insights from a cross-organ comparison

Joanna Raszeja-Wyszomirska[1], Maciej Miarka[1], Aleksandra Golenia[1], Piotr Olejnik[1], Magdalena Grusiecka-Stańczyk[1], Jolanta Małyszko[1], Marta Zalewska[1]. [1]*Medical University of Warsaw, Warsaw, Poland*
Email: jorasz@gmail.com

Background and aims: Cognitive impairment (CI) is increasingly recognized as a clinically relevant determinant of outcomes after solid organ transplantation. Previous studies have demonstrated cognitive deficits in patients with advanced liver and kidney disease before transplantation and during the early post-liver transplant period, with pronounced impairments in language and executive domains among patients with alcohol-associated liver disease (ALD)[1, 2]. We aimed to characterize organ- and etiology-specific patterns of long-term cognitive recovery after liver transplantation using a cross-organ comparison with kidney transplant recipients.
[1] doi:10.3389/ti.2025.12869 [2] doi:10.1002/brb3.3647.
Method: Adult kidney transplant recipients (KTx; n = 90; median follow-up 100.5 days) and liver transplant recipients (LT; n = 90; median follow-up 1476.0 days) completed Addenbrooke's Cognitive Examination III (ACE-III). LT was stratified into ALD (n = 25) and non-ALD etiologies (n = 65). CI was defined as ACE-III < 85 points. Group differences used Kruskal–Wallis with post-hoc Mann–Whitney U (Holm adjustment). Multivariable models adjusted for age, education and time since transplantation.
Results: Global ACE-III showed a three-group gradient: KTx 90.3 ± 8.7, LT non-ALD 89.3 ± 6.5 and LT ALD 86.9 ± 12.5 points. Overall differences were significant (Kruskal–Wallis p = 0.047). Pairwise comparisons suggested lower ACE-III in LT ALD versus KTx (unadjusted p = 0.039), but no pairwise contrast remained significant after Holm adjustment. CI prevalence (ACE-III < 85) was 16.7% in KTx, 16.9% in LT non-ALD and 24.0% in LT ALD (chi-square p = 0.68). Attention remained high across groups (means 93.0 to 94.5 points). Memory and visuospatial scores were relatively preserved, whereas verbal fluency showed the lowest means (KTx 82.9, LT non-ALD 80.9, LT ALD 78.7 points). In multivariable linear regression, education was positively associated with ACE-III (beta = 0.93 points per education-year, p < 0.001) and age was negatively associated (beta = – 0.12 points per year, p = 0.017); time since transplantation were not independent predictors.
Conclusion: This study fills an evidence gap by characterizing long-term cognition after liver transplantation and benchmarking it against early post kidney transplantation. Global cognition is largely preserved, but ALD recipients show the lowest performance and the highest CI prevalence, supporting structured post-transplant cognitive monitoring and targeted rehabilitation.

FRI-556

Risk factors for T-cell mediate rejections after liver transplantation

Florian Rennebaum[1], Martin McCoy[1], Michael Praktiknjo[1], Philipp Houben[2], Felix Becker[2], Frank Uschner[1], Andreas Pascher[2], Jörn Arne Meier[1], Maximilian Joseph Brol[1], Tina Schomacher[1], Lena Wolters[1], Josune Cabello Calleja[1], Jan Hähner[1], Jonel Trebicka[1,3]. [1]*Universitätsklinikum Muenster, Department of Medicine B, Gastroenterology, Hepatology, Endocrinology and Infectiology, Muenster, Germany;* [2]*Universitätsklinik Münster, Department of General, Visceral and Transplant Surgery, Münster, Germany;* [3]*European Foundation for the Study of Chronic Liver Failure-EF Clif, Barcelona, Spain*
Email: florian.rennebaum@ukmuenster.de

Background and aims: Orthotopic liver transplantation (OLT) is the treatment of choice for complications of liver cirrhosis and hepatocellular carcinoma (HCC). A common complication in the first days to months after OLT is acute T-cell mediated rejection (TCMR), which can occur in up to 10–30% of recipients after OLT. Treatment consists of high-dose prednisolone therapy over 1–3 days. The causes of TCMR are heterogeneous. The aim of the study is the evaluation of possible risk factors for the development of TCMR in order to optimize immunosuppression.
Method: A monocentric retrospective data analysis was performed on patients who underwent OLT between 2020 and 2025. Various parameters (MELD score, presence of acute-on-chronic liver failure (ACLF), HCC, immunosuppression) were evaluated. The primary endpoint was the development of TCMR. Exclusion criteria were follow-up < 4 weeks, combined organ transplants, and immuntherapy (ICI) prior to liver transplantation. A p-value of <0.05 was considered statistically significant.
Results: A total of 273 patients were included. The leading etiology of cirrhosis was alcohol related liver disease (ArLD) (59 patients; 21.7%), followed by autoimmune liver diseases (AILD) including autoimmune hepatitis (AIH), primary sclerosing cholangitis (PSC) and primary biliary cholangitis (PBC) (56 patients; 20.6%). A total of 59 patients (21.7%) had ACLF and 62 patients (22.8%) underwent transplantation due to hepatocellular carcinoma. The median follow-up was 24 months (10–46.5). A total of 46 patients developed TCMR during follow-up (16.9%). In multivariate logistic regression analysis, patients with autoimmune liver disease showed a significantly increased risk of developing rejection (OR 5.44; 95% CI 2.46–12.05; p = 0.001). The presence of HCC was independently associated with a lower probability of rejection (OR 0.32; 95% CI 0.15–0.70; p = 0.002). Normothermic machine perfusion showed a non-significant trend toward a reduced rejection rate in multivariate logistic regression analysis (OR 0.53; 95% CI 0.26–1.07; p = 0.077).
Conclusion: Patients with autoimmune liver diseases appear to have an increased risk of developing TCMR after OLT. Normothermic machine perfusion showed a trend toward lower rejection rates. These patients should be monitored closely for rejection. Further prospective multicenter studies are needed to identify additional risk factors.

FRI-557

Optimising liver transplant candidates through prehabilitation and rehabilitation: preliminary 6-month findings

Jesús Rivera Esteban[1], Victor Valverde[1], Ana Duca[1], Laura Benitez[1], Maria Trapero[1], Ana Arias[1], Natalia Fernandez Puga[1], Enrique Fraga[1], José Luis Calleja Panero[1]. [1]*Hospital Universitario Puerta De Hierro Majadahonda, Majadahonda, Spain*
Email: jesusriveraest@gmail.com

Background and aims: Sarcopenia and frailty are highly prevalent among liver transplantation (LT) candidates and contributed to increased morbidity, mortality, and diminished quality of life. Structured prehabilitation and rehabilitation programmes offer a promising approach to strengthen patients before LT and support a smoother, more effective recovery afterwards. We aim to evaluate the effects of a structured prehabilitation and rehabilitation programme on body composition, frailty and LT-related complications from listing to one year after LT. Results at 6 month follow-up after LT are presented.
Method: We evaluated every LT candidate enlisted at our centre between August 2023 and July 2025 using CT scan, bioelectrical impedance analysis (BIA) and handgrip strength at listing, monthly on WL, at discharge, 3,6 and 12 months post-LT. All patients received nutritional counselling and structured exercise intervention. Sarcopenia was defined as a fat-free mass index <17 kg/m^2 in men or <15 kg/m^2 in women and/or handgrip <27 kg in men or <16 kg in women. A Liver Frailty Index (LFI) >4.5 indicated frailty. Anthropometric changes, sarcopenia, and frailty were analysed using paired Student's t-tests and McNemar's tests.
Results: Mean age for the 25 patients with 6-month post-LT follow-up was 60.4 years, 20% were women, and obesity, hypertension, type 2 diabetes, and dyslipidaemia rates were 64%, 48%, 40%, and 24%,

respectively. Mean MELD score was 15.6, being SLD the most common etiology (64%). No differences in body composition parameters were found in the WL (median WL stay, 94 days). LT surgery and hospitalization resulted in significant declines in lean mass and strength at discharge ($p < 0.001$ for both), with graft-related complications and longer hospital stays associated with ≥10% muscle loss. Compared to discharge, at 6-months post LT muscle mass (47.2 vs 49.4 kg, p0.014), handgrip (26.2 vs 31.5, $p < 0.001$) and LFI (3.98 vs 3.11, p0.004) statistically improved, especially in women. Frailty and sarcopenia rates ranged from 28.6/32% at baseline to 52/52% at discharge and 5.9/35% 6-mo after LT.

Conclusion: Prehabilitation seems to mitigate functional decline before LT. Although LT results in substantial early loss of lean mass and function, especially in the context of complications or prolonged hospitalisation, post-LT rehabilitation delivers rapid and meaningful recovery, resolving frailty. These findings strongly support the systematic implementation of structured pre and post LT rehabilitation strategies.

FRI-558

Excluding ascites from the GEMA-Na score does not impact outcome predictions in liver transplant candidates

Manuel Rodríguez-Perálvarez[1], Antonio M. Gómez-Orellana[2], Avik Majumdar[3], Geoff McCaughan[4], Maria Kalafateli[5], Rhiannon Taylor[6], Gloria de la Rosa[7], Victoria Aguilera Sancho[8], Mikel Gastaca[9], Carmen Cepeda Franco[10], María Luisa Ortiz[11], Jordi Colmenero[12], Alejandra Otero[13], Rocio González-Grande[14], Alba Cachero[15], Esther Molina[16], Mónica Barreales Valbuena[17], Rosa Martin-Mateos[18], Maria Rodriguez Soler[19], Mario Romero[20], Cristina Dopazo[21], Carmen Alonso Martin[22], Elena Oton[23], Maria Luisa Gonzalez Dieguez[24], María Dolores Espinosa Aguilar[25], Ana Arias[26], Gerardo Blanco[27], Sara Lorente Perez[28], Antonio Cuadrado[29], Miguel Sogbe[30], David Guijo-Rubio[2], César Hervás[2], Emmanuel Tsochatzis[31]. *[1]Hospital Universitario Reina Sofía, CORDOBA, Spain; [2]Universidad de Córdoba, Córdoba, Spain; [3]University of Melbourne, Melbourne, Australia; [4]Royal Prince Alfred Hospital, Sydney, Australia; [5]General Hospital of Patras, Patras, Greece; [6]NHS Blood and Transplant, Bristol, United Kingdom; [7]Organización Nacional de Trasplantes, Madrid, Spain; [8]Hospital Universitario La Fe, Valencia, Spain; [9]Hospital Universitario Cruces, Bilbao, Spain; [10]Hospital Virgen del Rocío, Seville, Spain; [11]Hospital Universitario Virgen Arrixaca, Murcia, Spain; [12]Hospital Clínic, Barcelona, Spain; [13]Hospital Universitario A Coruña, A Coruña, Spain; [14]Hospital Regional Universitario de Málaga, Málaga, Spain; [15]Hospital Universitario de Bellvitge, Hospitalet De Llobregat, Spain; [16]Hospital Universitario Santiago de Compostela, Santiago de Compostela, Spain; [17]Hospital 12 de Octubre, Madrid, Spain; [18]Hospital Ramón y Cajal, Madrid, Spain; [19]Hospital General Universitario de Alicante, Alicante, Spain; [20]Hospital General Universitario e Instituto de Investigación biomédica Gregorio Marañón, Madrid, Spain; [21]Vall d'Hebron Hospital Universitari, Barcelona, Spain; [22]Hospital Rio Hortega, Valladolid, Spain; [23]Hospital Virgen de la Candelaria, Tenerife, Spain; [24]Hospital Universitario Central de Asturias, Oviedo, Spain; [25]Hospital Virgen de las Nieves, Granada, Spain; [26]Hospital Universitario Puerta de Hierro, Madrid, Spain; [27]Hospital Universitario de Badajoz, Badajoz, Spain; [28]Hospital Universitario Lozano Blesa, Zaragoza, Spain; [29]Hospital Universitario Marqués de Valdecilla, Santander, Spain; [30]Clinica Universidad de Navarra, Pamplona, Spain; [31]Royal Free Hospital, London, United Kingdom*
Email: ropeml@hotmail.com

Background and aims: Although GEMA-Na outperforms MELD 3.0, concerns about the subjectivity of its ascites component persist. We compared the performance of a GEMA-Na iteration that excludes ascites with other allocation scores to predict waiting list outcomes among liver transplant candidates.

Method: A multinational cohort study was conducted, including adult candidates for elective liver transplantation in the UK (2010–2020), Australia (1998–2020), and Spain (2016–2021). The primary outcome was mortality or delisting due to clinical worsening within the first 90 days. The prognostic impact of ascites was evaluated using multivariable Cox's regression. The discrimination of allocation scores was assessed using Harrell's c-statistics (Hc).

Results: The study included 15,391 patients (28.5% women). The prevalence of the primary outcome was 5.8% in the UK, 5.3% in Australia, and 4.7% in Spain. The presence and severity of ascites was associated with an incremental risk of the primary outcome: 3.3% without ascites, 5.8% with mild ascites, and 7.7% with moderate-severe ascites ($p < 0.001$). Removal of ascites from the GEMA-Na score resulted in a one-point reduction in 18% of patients (52.4% of patients with moderate-severe ascites). No patient showed a difference of two or more score points after removing ascites. GEMA-Na without ascites showed only a marginal decrease in discrimination (Hc = 0.755 vs. Hc = 0.753; $p = 0.007$) but still significantly outperformed MELD 3.0 (Hc = 0.734; $p < 0.001$) and MELD-Na (Hc = 0.737; $p < 0.001$). In women, GEMA-Na with and without ascites demonstrated comparable discrimination (Hc = 0.784 vs. Hc = 0.783; $p = 0.61$), both outperforming MELD 3.0 (Hc = 0.750; $p < 0.001$), and MELD-Na (Hc = 0.749; $p < 0.001$). In the multivariable Cox's regression analysis including each score sequentially, patients with moderate-severe ascites had increased risk of the primary outcome in presence of MELD-Na (HR = 1.166; 95%CI 1.008–1.348; $p = 0.038$) and MELD 3.0 (HR = 1.28; 95%CI 1.092–1.472; $p = 0.002$), but not in presence of GEMA-Na, either with or without ascites (HR = 0.985; 95%CI 0.850–1.141; $p = 0.84$ and HR = 1.073; 95%CI 0.927–1.242; $p = 0.34$, respectively).

Conclusion: Despite the prognostic impact of ascites among liver transplant candidates, GEMA-Na without ascites outperformed other scores in predicting waitlist outcomes and may be used wherever the inclusion of ascites is considered too subjective.

FRI-559

Development and pilot study of a telemedicine model (TXMobile App) to support the after-care of patients after liver transplantation

Angelika Rzepka[1], Kristina Reiter[2], Elisabeth Kletz[3], Sabine Koller[4], Susanna Trummer[4], Moritz Kniepeiss[4], Peter Kastner[2], Günter Schreier[1], Robert Sucher[4,4], Daniela Kniepeiss[4,5]. *[1]AIT Austrian Institute of Technology GmbH, Digital Health Information Systems Center for Health & Bioresources, Graz, Austria; [2]Telbiomed Medizintechnik und IT Service GmbH, Graz, Austria; [3]Medizinische Universität Graz, Department for General, Visceral and Transplant Surgery, Graz, Austria; [4]Medizinische Universität Graz, Graz, Austria; [5]Division for General, Visceral and Transplant Surgery, Graz, Austria*
Email: angelika.rzepka@ait.ac.at

Background and aims: The long-term success of liver transplantation depends on structured and continuous postoperative follow-up care. To support patients in their daily self-management after liver transplantation, we developed the transplant application *TXMobile*.

Method: Results and experiences from a previously conducted study were used as basis for the development of the new app. With participative methods like focus group meetings, questionnaires, and targeted interviews we conducted three different care plans for different stages after transplantation. Items of the different care plans represent the look of the *TXMobile* data management system (DMS) for professional users and the look of the patient's app flexibly, while providing the usability to manage the extent of after-care patients in the outpatient department. Since February 2025, a pilot study has enrolled 60 liver transplant recipients to comprehensively evaluate the app under real-world clinical conditions. In addition to assessing the technical stability and practical feasibility of the defined care plans, particular emphasis was placed on evaluating patients' quality of life and the usability of the application.

Results: The transplant app *TXMobile* comprises an individualized list of medication, a reminder for medication intake, calendar function

for standard visits and reminders for follow-up examinations in the outpatient department as well as in the routine healthcare system. Furthermore, it offers telemonitoring options for e.g. blood pressure. All information attains the DMS in a structured way based on internationals standards (e.g. SNOMED) and can be registered in the national electronic health record ELGA. Feedback of the pilot-study indicated overall good usability of the *TXMobile* app, particularly regarding clarity, intuitiveness, and accessibility for older users. The qualitative and quantitative results obtained during the pilot study provided a basis for targeted refinements and highlight the potential value of the solution for patient-centered, quality-assured post-transplant care.

Conclusion: The *TXMobile* app may support structured post-transplant after-care by facilitating adherence, self-management, and lifestyle optimization. Furthermore, it could reduce outpatient follow-up visits and help manage staff workload amid increasing transplant numbers and longer post-transplant follow-up. Future steps include further app refinement and evaluation for routine clinical implementation.

FRI-560

Post-transplant statin therapy improves long-term survival and lipid trajectories after liver transplantation

Sanjaya Satapathy[1], Mohammad Shadab Siddiqui[2], Mary E. Rinella[3], Danielle Brandman[4], Coleman I. Smith, MD[5], Jason Vanatta[6], Nghiem Ha[7], Amanda Cheung[8], Kymberly Watt[9]. *[1]North Shore University Hospital, Manhasset, United States; [2]University of Virginia, Charlottesville, United States; [3]The University of Chicago Medicine, Chicago, United States; [4]Center For Liver Disease & Transplantation, New York, United States; [5]MedStar Georgetown Transplant Institute, Washington, DC, United States; [6]University of Louisville School of Medicine, Louisville, United States; [7]University of California, San Francisco, United States; [8]Northwestern University Feinberg School of Medicine, Chicago, IL, USA, Chicago, United States; [9]Mayo Clinic, Rochester, MN, USA, Rochester, United States*
Email: ssatapat@northwell.edu

Background and aims: Dyslipidemia is prevalent after liver transplantation (LT), yet the role of statin therapy in managing long-term lipid profiles and survival outcomes remains under-explored. We investigated whether post-transplant statin use is associated with improvements in lipid trajectories and survival over 15 years.

Method: We analyzed 152 adult LT recipients with complete lipid panel data from 6 months to 15 years post-LT. Outliers in lipid changes were excluded using ± 3 × IQR thresholds. Patients were stratified by post-LT statin use. We used generalized linear models (GLMs) to assess 1-year lipid changes and Cox regression for 10- and 15-year survival. Longitudinal mixed models assessed lipid trajectories. Kaplan-Meier (KM) survival curves were generated by statin use.

Results: Post-transplant statin therapy was initiated in 38% of patients. At one year, statin users experienced significantly greater reductions in total cholesterol ($\beta = -30.2$ mg/dL, $p = 0.007$) and triglycerides ($\beta = -97.3$ mg/dL, $p = 0.002$), while changes in LDL ($\beta = -38.7$ mg/dL, $p = 0.17$) and HDL ($\beta = -3.5$ mg/dL, $p = 0.80$) were not statistically significant. Longitudinal mixed-effects modeling demonstrated that statin use significantly modified the trajectory of LDL and total cholesterol over time ($p < 0.01$), contributing to more favorable long-term lipid profiles. Triglyceride levels tended to rise in non-users but stabilized or declined among statin users. Kaplan-Meier survival curves showed improved long-term survival among statin users, although the difference was not statistically significant by the log-rank test ($p = 0.10$). However, in adjusted Cox proportional hazards models, statin use was independently associated with a 4.6-fold reduction in 15-year mortality risk (HR = 0.22; 95% CI: 0.06–0.76; $p = 0.017$). Additionally, lower LDL and higher HDL changes were protective, while increases in total cholesterol were linked to greater mortality risk ($p < 0.05$).

Conclusion: Post-transplant statin therapy is associated with significantly improved lipid profiles and long-term survival following LT. These findings support broader statin use in eligible LT recipients and highlight the utility of longitudinal lipid monitoring.

FRI-561-YI

Hepatic iron overload in explants: associations with underlying liver disease indication and disease severity

Roxanna Sharifi[1], Yinan Su[1], Paul Paik[2], Andrew John Cruz[3], Daanyaal Kumar[3], Kalpana Gopalkrishnan[1], Niveda Balemurughan[1], Derek Samson[4], Jeffrey Kahn[2], Norah Terrault[2], Liyun Yuan[2]. *[1]Keck School of Medicine, University of Southern California, Los Angeles, United States; [2]Division of Gastroenterology and Liver Diseases, University of Southern California Keck School of Medicine, Los Angeles, CA, United States; [3]Department of Medicine, Keck School of Medicine, University of Southern California, Los Angeles, United States; [4]Transplant Institute, Keck Medicine of USC, University of Southern California, Los Angeles, United States*
Email: rsharifi@usc.edu

Background and aims: Hepatic iron deposition is commonly observed in liver transplant explants; however, its clinical determinants and relevance in advanced liver disease, particularly MASLD, remain unclear. We aimed to evaluate the association between hepatic iron deposition, liver disease etiology, and disease severity, and to examine the contribution of metabolic factors in hepatic iron.

Method: We conducted a retrospective analysis of adult liver transplant recipients at a single LT center (2013–2023). Hepatic iron deposition in explant pathology was assessed in relation to pre-transplant Model for End-Stage Liver Disease–Sodium (MELD-Na) score, liver disease etiology, presence of hepatocellular carcinoma (HCC), steatosis (S0 = none/less than 5% steatosis [burnout]; S1 = 5–33%, S2 = 34–66%, S3 ≥ 66%), and diabetes. Associations were evaluated using chi-square testing and multivariable logistic regression adjusted for age, sex, body mass index, diabetes, and race.

Results: Among 1,248 transplant recipients, hepatic iron was present in 50.2% of explants and presence varied significantly by etiology, with the highest prevalence observed in alcohol-associated liver disease (ALD; 60.6%), metabolic dysfunction-associated steatotic liver disease (MASLD; 53.5%), and viral hepatitis (61.1%), and the lowest prevalence in autoimmune and cholestatic liver diseases (26.6%). Iron deposition was more likely in ALD (adjusted odds ratio [aOR] 1.64, 95% CI 1.28–2.12) and less likely in autoimmune and cholestatic liver diseases (aOR 0.31, 95% CI 0.21–0.46). Higher MELD-Na categories (MELD-Na < 20 comparator) were associated with progressively increased odds of iron deposition: 20–24: aOR 1.47; 25–29: aOR 1.85; 30–34: aOR 2.20; ≥ 35: aOR 2.81) (p for trend < 0.001). Older age (aOR 1.01 per year, 95% CI 1.00–1.02) and male sex (aOR 1.30, 95% CI 1.03–1.63) were associated with increased odds of hepatic iron, while HCC (aOR 0.69, 95% CI 0.52–0.90, $p = 0.007$) was associated with lower odds; diabetes was not associated. Among MASLD recipients (N = 239), hepatic iron was not associated with diabetes, burn-out steatosis, steatosis severity, or history of alcohol use. The presence of HCC among MASLD is associated with lower odds of iron deposition (aOR 0.50, 95% CI 0.37–0.65, $p < 0.001$).

Conclusion: Hepatic iron is prevalent in transplant explants and is more closely associated with disease severity than metabolic burden. In MASLD, iron deposition is unrelated to diabetes and steatosis, and is less common in the presence of HCC.

FRI-562

Impact of Glucagon-like peptide-1 receptor agonists on diabetes after liver transplantation - a single-center experience

Chiara Sicuro[1], Paolo Magistri[2], Chiara Giglio[1], Marco Scoppettuolo[1], Martina Montanari[1], Antonio Colecchia[1], Fabrizio Di Benedetto[2], Nicola De Maria[1]. [1]*Chimomo Department, Gastroenterology Unit, University of Modena and Reggio Emilia, Modena, Italy;* [2]*Onco-Hepato-Pancreato-Biliary Surgery and Liver Transplantation Unit, University of Modena and Reggio Emilia, Modena, Italy*
Email: chiarasicuro44@gmail.com

Background and aims: Metabolic-dysfunction associated steatotic liver disease (MASLD) develops in over 50% of liver transplant recipients (LTR) within one year. Post-transplant diabetes and obesity, affecting up to 30% and 40% of LTR respectively, significantly worsen cardiovascular risk and graft outcomes. Glucagon-like peptide-1 receptor agonists (GLP1-RAs) improve glycemic control, promote weight loss and reduce cardiovascular events in type 2 diabetes, but data in LTR are limited. We aimed to evaluate the efficacy and safety of GLP1-RAs in diabetic LTR.
Method: We retrospectively analyzed diabetic LTR treated with GLP1-RAs (semaglutide, liraglutide, dulaglutide) at our center between 2000 and 2023. Changes in body weight, body mass index (BMI), glycemic parameters, lipid profile, liver stiffness measurement (LSM), Controlled Attenuation Parameter (CAP) and adverse events were assessed. Data are reported as mean ± SD and compared using paired t-test.
Results: Forty-nine LTR (mean age 66 ± 7.9 years) were included. At baseline, mean BMI was 29.7 ± 4.5 kg/m^2 and mean HbA1c was 56.4 ± 15.1 mmol/mol. GLP1-RA therapy significantly reduced HbA1c at 6 months, with a further non-significant decrease at 12 and 18 months. Body weight, BMI and total cholesterol significantly decreased at all time points. CAP values significantly improved at 12 months, whereas LSM remained unchanged. Adverse events occurred in 11 patients, leading to treatment discontinuation in 6 cases. No immunosuppressive therapy adjustments were required.
Conclusion: GLP1-RAs appear safe and effective in diabetic LTR, providing meaningful weight loss and glycemic improvement. Adverse events are relatively frequent and may limit treatment persistence. Larger multicenter studies with longer follow-up are needed to assess long-term graft outcomes and cardiovascular benefits. These findings support the integration of GLP1-RAs into post-transplant metabolic management strategies in selected patients.

FRI-563

Alcohol-related acute-on-chronic liver failure vs alcohol-related cirrhosis: clinical outcomes after liver transplantation - a single center experience

Chiara Sicuro[1], Nicola De Maria[1], Riccardo Cuoghi Costantini[2], Martina Montanari[1], Marco Scoppettuolo[1], Antonio Colecchia[1], Paolo Magistri[3], Fabrizio Di Benedetto[3]. [1]*Chimomo Department, Gastroenterology Unit, University of Modena and Reggio Emilia, Modena, Italy;* [2]*University of Modena and Reggio Emilia, Modena, Italy;* [3]*Onco-Hepato-Pancreato-Biliary Surgery and Liver Transplantation Unit, University of Modena and Reggio Emilia, Modena, Italy*
Email: chiarasicuro44@gmail.com

Background and aims: Alcohol-associated liver disease (ALD) is a leading indication for liver transplantation (LT). Excessive alcohol use may cause severe alcohol-related hepatitis (sAH) and precipitate acute-on-chronic liver failure (ACLF), which worsens prognosis, increases short-term mortality and reduces response to corticosteroids. Although post-LT survival is comparable between ALD and other etiologies, alcohol relapse (AR) remains a major concern, particularly in patients transplanted for alcohol-induced ACLF (Ai-ACLF). Predictors of post-LT mortality and AR in this population are still poorly defined. This study aimed to compare overall survival (OS) and AR between Ai-ACLF and alcohol-related cirrhosis (AC), and to identify predictors of post-LT mortality and AR.
Method: We retrospectively analyzed all patients transplanted for ALD at our center between January 2020 and December 2023. Patients were stratified into three groups: Ai-ACLF (A), AC with pre-LT abstinence (B), and AC with ongoing alcohol consumption at LT (C). Data are reported as mean ± SD or percentages and analyzed using χ^2/Fisher's exact test, ANOVA or Kruskal–Wallis test. OS and AR were assessed using Kaplan–Meier analysis, and predictors were evaluated by Cox regression.
Results: A total of 161 patients were included (21 A, 117 B, 23 C), with a mean follow-up of 31 ± 16 months. Group A patients were younger, had higher MELD scores, shorter waiting-list time, longer hospitalization and ICU stay, and a higher proportion of women. Rejection and retransplantation rates were higher in Group A. OS did not differ among groups (p = 0.2), with most deaths occurring within the first year. Length of hospitalization (HR 1.03) was the only independent predictor of mortality. AR differed significantly among groups, being highest in Group A and lowest in Group B. Early relapse predominated, and less than half of relapsers developed harmful alcohol consumption. Younger age and rehabilitation program enrollment were associated with AR only in univariate analysis.
Conclusion: LT provides a survival benefit in ACLF, with comparable outcomes between Ai-ACLF and AC, irrespective of pre-LT abstinence. Although abstinence is associated with lower AR risk, it should not represent the sole LT eligibility criterion. Future strategies should focus on identifying high-risk profiles for AR and optimizing targeted post-LT interventions.

FRI-564-YI

Cystatin C is associated with worse survival in patients with cirrhosis awaiting liver transplantation

Miguel Sogbe[1], Amanda Pirola[2], Brittany Bromfield[3], Roberto Tellez[4], Pamela M. Bloomer[4], Christopher B. Hughes[4], Astrid Ruiz Margáin[5], Andres Duarte-Rojo[6]. [1]*Liver Unit, Clinica Universidad de Navarra, Pamplona, Spain, Centro de Investigación Biomédica en Red de Enfermedades Hepáticas y Digestivas (CIBEREHD), Pamplona, Spain, Instituto de Investigación Sanitaria de Navarra (IdiSNA), Pamplona, Spain, Pamplona, Spain;* [2]*Department of medicine, Northwestern Feinberg school of medicine, Chicago, IL, USA, Pamplona, Spain;* [3]*Department of gastroenterology and hepatology, Brigham and women's hospital, Boston, MA, USA, boston, United States;* [4]*Starzl transplantation institute, university of Pittsburgh, Pittsburgh, PA, USA, PA, United States;* [5]*Division of hepatology, instituto nacional de ciencias medicas y nutricion Salvador Zubirán, México City, México, mexico city, Mexico;* [6]*Division of gastroenterology and hepatology, Northwestern Feinberg school of medicine, Chicago, IL, USA, Chicago, United States*
Email: msogbe@unav.es

Background and aims: Renal dysfunction is a major determinant of morbidity and mortality in patients with cirrhosis. Serum creatinine, despite well-recognized limitations in cirrhosis, remains the primary marker of renal function and a central component of current liver allocation systems, including the Model for End-Stage Liver Disease (MELD) 3.0 and the calculation of the Royal Free Hospital glomerular filtration rate within the Gender-Equity Model for Liver Allocation corrected by sodium (GEMA-Na). Cystatin C (CysC) represents a promising alternative biomarker with improved accuracy and prognostic value in patients undergoing liver transplant (LT) evaluation.
Method: This was a prospective cohort study conducted at a tertiary academic hospital including patients undergoing LT evaluation. At enrollment, participants underwent a standardized evaluation that included measurement of CysC. Associations involving CysC were assessed, and the optimal threshold for predicting mortality was identified using receiver operating characteristic (ROC) curve analysis and the Youden index. Patients were subsequently categorized into two groups according to this cut-off value. The effect of CysC (low vs.

high) on all-cause mortality was evaluated using Fine and Gray competing risks models, considering LT as a competing event. Multivariable analyses were performed with adjustment for MELD 3.0 and GEMA-Na in separate models.
Results: A total of 641 patients underwent CysC assessment. The most common underlying etiology of cirrhosis was alcohol-associated liver disease (37%), followed by metabolic dysfunction–associated steatotic liver disease (35%). At baseline, patients had a mean MELD 3.0 score of 16 ± 8 and a mean GEMA-Na score of 20 ± 6. The optimal CysC cut-off for predicting mortality was ≥1.5 mg/L, yielding an area under the curve of 0.70 (95% CI, 0.64–0.75). After adjustment for MELD 3.0 and GEMA-Na (in separate models), elevated CysC remained independently associated with mortality (adjusted subdistribution hazard ratio [aSHR] 2.58; 95% CI, 1.54–4.29 and aSHR 2.24; 95% CI, 1.35–3.74, respectively). Patients with high CysC had a lower likelihood of undergoing LT compared with those with low CysC levels (SHR 0.70; 95% CI, 0.51–0.96).
Conclusion: Cystatin C represents a promising biomarker to improve prognostic assessment among patients undergoing LT evaluation, given its independent association with mortality beyond established prognostic models such as MELD 3.0 and GEMA-Na.

FRI-569
Using artificial intelligence-based models and radiomics in mri to predict hepatocellular carcinoma after liver transplant
Emma Stevenson[1], Stephanie Harmon[1], Theo Heller[2], Ross Filice[3], Peter Choyke[1], Ismail Turkbey[1], Christine Hsu[2]. *[1]National Cancer Institute, National Institute of Health, Bethesda, United States; [2]National Institute of Diabetes & Digestive & Kidney Diseases, Bethesda, United States; [3]MedStar Georgetown University Hospital, MedStar Medical Group Radiology, Washington, United States*
Email: emma.stevenson@nih.gov

Background and aims: Prediction of hepatocellular carcinoma (HCC) recurrence after liver transplantation (LT) is essential to personalize surveillance regimen and improve survival post-liver transplant. We aim to utilize AI-based MRI radiomics and clinical metrics to predict HCC recurrence and mortality after LT.
Method: A total of 166 patients underwent multi-phase contrast-enhanced T1W MRI scans pre-LT at a tertiary center in this retrospective study. Each focal liver lesion was manually contoured by one radiologist and assigned a Liver Imaging Reporting and Data System (LIRADS) score. Patients were classified based on the presence of LIRADS 4 or 5 lesions on their MRIs. Radiomic features were extracted from liver segmentation obtained from an AI model. Radiomic feature selection was performed using the t-test, Mann-Whitney U test, and the least absolute shrinkage and selection operator. Lesion volume was calculated by summing LIRADS 4 and 5 lesions. Clinical metrics and chosen radiomic features were integrated into univariate (Wilcoxon) and multivariate (Cox proportional hazards) analyses to identify independent predictors of post-LT HCC recurrence and mortality when comparing LIRADS 4 and LIRADS 5 patients.
Results: Out of 166 patients, 21 had HCC recurrence, thus resulting in a cumulative incidence rate of 12.7% and a median time to recurrence of about 34 months (IQR: 11.4, 65.5). Two radiomic features were selected for the LIRADS 5 patients, and eight for the LIRADS 4 patients. Two radiomic features (gldm_GrayLevelNonUniformity and shape_MajorAxisLength) overlapped in terms of significance between both patient groups. The Wilcoxon test revealed that liver volume ($p = 0.03$) was significantly associated with recurrence 12 months post-LT. In the multivariate analysis adjusted for age and gender, two radiomics features (gldm_DependenceNonUniformity and shape_SurfaceArea) were found to be significant for overall recurrence ($p < 0.05$) in LIRADS 5 patients. The same two radiomic features, along with gldm_GrayLevelNonUniformity, were identified as statistically significant ($p < 0.05$) for overall mortality in LIRADS 5 patients as well. An additional multivariate analysis, adjusted for age, gender, and tumor volume, indicated that a decrease in liver volume significantly predicts overall recurrence ($p = 0.02$) and mortality ($p = 0.03$) in LIRADS 5 patients.
Conclusion: Utilizing radiomics alongside clinical factors in prediction models may help predict HCC recurrence in LIRADS 5 patients.

FRI-570
Risk factors and temporal evolution of allograft steatosis following liver transplantation
Yinan Su[1], Roxanna Sharifi[1], Paul Paik[2], Andrew John Cruz[1,3,4], Daanyaal Kumar[1], Kalpana Gopalkrishnan[1], Niveda Balemurughan[1], Derek Samson[5], Jeffrey Kahn[2], Norah Terrault[2], Liyun Yuan[2]. *[1]Keck School of Medicine, University of Southern California, Los Angeles, United States; [2]Division of Gastroenterology and Liver Diseases, University of Southern California, Keck School of Medicine, Los Angeles, United States; [3]Keck School of Medicine of USC, Department of Medicine, Los Angeles, United States; [4]Keck School of Medicine of USC, Department of Medicine, Los Angeles, United States; [5]Transplant Institute, Keck Medicine of USC, University of Southern California, Los Angeles, United States*
Email: yinansu@usc.edu

Background and aims: Hepatic steatosis post-liver transplant occurs as recurrent or de novo metabolic dysfunction–associated steatotic liver disease (MASLD), yet the prevalence, timing, and overlap with rejection remain understudied. We evaluated the prevalence over time and risk factors associated with allograft steatosis in a contemporary liver transplant cohort.
Method: We conducted a retrospective, single-center study of adult liver transplant recipients transplanted 2017–2023 who underwent post-transplant liver biopsy for abnormal liver tests. Hepatic steatosis was defined as ≥5% macrovesicular steatosis and graded as S1–S3 histologically; steatosis was also assessed via imaging studies of MRCP, MRI, ultrasound, and CT. Recurrent vs. de novo steatosis was classified by transplant indication. Acute rejection was assessed histologically. Multivariable logistic regression adjusted for age and sex identified factors associated with allograft steatosis.
Results: Among 347 recipients undergoing post-transplant biopsy, 34.3% (n = 119) had allograft steatosis (31.1% [n = 37] recurrent and 68.9% [n = 82] de novo). Rejection was present in 71.8% (n = 249), with 17.6% (n = 61) showing concurrent rejection and steatosis. Transplantation for MASLD (adjusted odds ratio [aOR] 2.31 [95%CI 1.29–4.14]), obesity at transplant (aOR 1.63 [1.00–2.66]), and donor liver steatosis (aOR 3.19 [1.41–7.22]) were associated with allograft steatosis, but pre-transplant metabolic comorbidities and donor metabolic comorbidities were not associated. The prevalence of steatosis detected via biopsy increased with time post-transplant, from 21.3% at 3 months, 23.0% at 6 months, 28.3% at 1 year, 36.0% at 3 years and 46.2% at 5 years. Among the same population, imaging studies underdetected steatosis (4.8% at 3 months, 13.0% at 6 months, 15.9% at 1 year, 31.4% at 3 years, and 23.1% at 5 years). Rates of concurrent rejection and steatosis persisted across all post-transplant intervals.
Conclusion: Allograft steatosis is common after liver transplantation and increases over time, with underdetection via non-invasive imaging (MRI, MRCP, CT, and ultrasound) compared to histological diagnosis. Recipients transplanted for MASLD, those with obesity at time of transplant, and those who receive steatotic donor livers carry the highest risk for developing allograft steatosis. Longitudinal, multicenter studies are needed to define the impact of allograft steatosis on graft outcomes and inform post-transplant surveillance and intervention strategies.

FRI-571

Beyond survival: long-term growth outcomes in pediatric liver transplant patients with over 20 years of follow-up

Michela Triolo[1], Stefania Camagni[2], Federico Raimondi[3], Luisa Pasulo[1], Leonardi Filippo[1], Francesco Ideo[1], Paola Stroppa[4], Valeria Casotti[4], Domenico Pinelli[2], Lorenzo D'Antiga[4], Stefano Fagiuoli[1]. [1]*Gastroenterology, Hepatology & Transplantation, ASST Papa Giovanni XXIII, Bergamo, Italy;* [2]*Department of Surgery, ASST Papa Giovanni XXIII, Bergamo, Italy;* [3]*Respiratory Unit, Papa Giovanni XXIII Hospital, Bergamo, Italy;* [4]*Department of Pediatric Hepatology, Gastroenterology and Transplantation, ASST Papa Giovanni XXIII, Bergamo, Italy*
Email: mik.triolo@gmail.com

Background and aims: Pediatric liver transplantation (LT) is highly complex, and improved survival has shifted focus toward long-term outcomes. However, data beyond 20 years after LT, particularly on growth, remain limited.

Method: Retrospective data were collected from 152 patients <18 years transplanted at our Center between November 1997–2005. Patients were followed until death or November 1st, 2025. Final height was assessed at the last follow-up, at least 20 years after the first LT. Height was expressed as a standard deviation score (SDS) using the observed height and the corresponding population reference values (mean; standard deviation for age and sex) (1). Target height was computed using Tanner's formula (2). ΔSDS was derived according to Equation (3).

- SDS = (Height observed−mean)/standard deviation (1).
- Target height for boys (cm) = (mother's height (cm) + father's height (cm) + 13)/2.
- Target height for girls (cm) = (mother's height (cm) + father's height (cm)−13)/2 (2).
- $\Delta SDS = SDS - SDST$ (3).

When ΔSDS < −1.5, the patient was classified as not having reached the target height.

Results: The median age at first LT was 1.3 years [0.7–4.2]. During follow-up, 41 patients (27%) underwent retransplantation and 57 (37.5%) died. Among the 95 survivors, 79 (83%) showed adherence to immunosuppression, 5 (5%) required long-term steroid use. At the last follow-up, median height was 1.71 m [1.67–1.77] in males and 1.60 m [1.54–1.63] in females, corresponding to SDS values of −0.48 [−1.37–0.75] and −0.57 [−1.71–−0.14], respectively. Target height was available for 76 patients, of whom 70 (92%) achieved it. The mean height deficit was −1.7 cm in those reaching target height versus −14.8 cm in those who did not ($p < 0.01$). Chronic steroid use and treatment non-compliance were more frequent in the group not reaching the target height (17% vs 1.4%, $p = 0.03$ and 50% vs 18%, $p = 0.05$, respectively). In the multivariable linear regression—using ΔSDS as the dependent variable and sex, age at first LT, retransplantation, Graft-to-Recipient Weight Ratio (GRWR), treatment compliance, and steroid use as covariates -retransplantation was the only factor associated with deviation from target height ($\beta = -0.65$; IC 95% [−1.21 – −0.09]; $p = 0.024$; $R^2 = 0.215$; adjusted $R^2 = 0.144$), indicating poorer growth in retransplanted patients.

Conclusion: Retransplantation was the only factor independently associated with poorer growth, highlighting the long-term impact of complex post-transplant courses.

FRI-572

Favourable real-life outcomes of stereotactic body radiotherapy and magnetic resonance-guided radiotherapy for hepatocellular carcinoma in liver transplant candidates

Emma Jonot[1], Lionel Moulis[1], Olivier Riou[2], David Pasquier[3], Jean-François Py[4], Xavier Mirabel[3], Jean-Basptiste Clavier[5], Anouchka Modesto[6], Marine Boulesteix[7], Morgan Michalet[2], Stéphanie Faure[1], Astrid Herrero[1], Emmanuel Boleslawski[8], Boris Guiu[1], Eric Assenat[1], Francois Villeret[9,10], Christophe Bureau[11], Camille Besch[12], Massih Ningarhari[8], Georges-Philippe Pageaux[1], José Ursic-Bedoya[1]. [1]*Chu Montpellier, Montpellier, France;* [2]*Institut Régional du Cancer de Montpellier, Montpellier, France;* [3]*Centre Oscar Lambret, Lille, France;* [4]*INSTITUT DE CANCEROLOGIE DE LORRAINE, Vandœuvre-lès-Nancy, France;* [5]*Institut de cancérologie Strasbourg Europe, Strasbourg, France;* [6]*Institut Universitaire du Cancer de Toulouse Oncopole, Toulouse, France;* [7]*Hôpital Lyon Sud-Hcl, Pierre-Bénite, France;* [8]*Centre Hospitalier Régional Universitaire de Lille, Lille, France;* [9]*Service d'hépatologie et de transplantation hépatique, Hôpital de la Croix Rousse, Hospices Civils de Lyon, Lyon, France;* [10]*Université Claude Bernard Lyon 1; INSERM Unit 1350 PathLiv; Lyon Hepatology Institute, IHU EVEREST, Lyon, France;* [11]*Hôpital Rangueil, Toulouse, France;* [12]*Hôpital de Hautepierre, Strasbourg, France*
Email: jose.ursic@yahoo.fr

Background and aims: The optimal bridging or downstaging therapy for hepatocellular carcinoma (HCC) in candidates for liver transplantation (LT) remains uncertain. Stereotactic body radiotherapy (SBRT) is a promising option, but data is limited to small, single-center cohorts. Magnetic resonance-guided radiotherapy (MRgRT), a newer technique allowing delivery of higher equivalent doses, has yet to be evaluated in this setting. We aimed to assess the real-world efficacy and safety of SBRT, including MRgRT, as bridging or downstaging therapy to LT in an intention-to-transplant population across five French academic centers.

Method: Multicenter retrospective cohort, including adult patients listed for LT and receiving SBRT between 2012 and May 2025, followed until December 2025. The primary endpoint was the completion of LT. Secondary endpoints included recurrence risk based on R3-AFP model, post-LT HCC recurrence and safety.

Results: We identified 101 patients with a mean follow-up of 50.4 months. The majority were men (86.1%), with a mean age of 61.6 ± 5.8 years. Median CPT and MELD scores were 5 and 10, respectively. The main underlying liver diseases were alcohol-related liver disease (35%), viral hepatitis (24%), and Met-ALD (24%). SBRT was used as downstaging in 9 patients (8.9%) and as bridging therapy in 92 patients (91.1%). The median SBRT dose was 50 Gy in five fractions, and 29 patients (28.7%) received MRgRT.

Toxicities occurred in 26% of patients, predominantly mild/moderate (no grade >2) events. A decline in liver function was observed in 4.9% of patients. Overall, 77 patients (76.2%) underwent LT at a median of 12.8 months; 32 patients (31.7%) died (20 post-LT). In the downstaging group, 7/9 patients (77.8%) were transplanted, with two dropouts. In the bridging group, 70 of 92 patients (76.1%) underwent LT, with 16 dropouts (17.4%), 4 still on the waitlist, and 2 showing complete, prolonged responses. 8 patients (10.4%) achieved complete histological response. 62 patients (80.5%) had a low or very low recurrence risk (score 0–2) per R3-AFP model. HCC recurrence occurred in 8/77 transplanted patients (10.5%) at a median of 33.1 months. Among MRgRT treated patients, 23 (79.3%) underwent LT, with 87% showing low or very low R3-AFP scores.

Conclusion: This study represents the largest reported cohort of patients treated with SBRT while listed for LT. Our findings suggest that both SBRT and MRgRT are safe and effective in this settiing, with favourable transplantation and recurrence outcomes.

FRI-573

Early barriers to liver transplantation: referral failures in patients admitted for decompensated cirrhosis

Margaux Delhomme[1], Lionel Moulis[1], Faiza Khemissa[2], Ardavan Prost[3], Mohamed Ramdani[4], Saïd Ferroudji[5], Magdalena Meszaros[1], Lucy Meunier[1], Stéphanie Faure[1], Hélène Donnadieu[1], Georges-Philippe Pageaux[1], José Ursic-Bedoya[1]. [1]*Chu Montpellier, Montpellier, France;* [2]*Centre Hospitalier de Perpignan, Perpignan, France;* [3]*Centre Hospitalier Universitaire de Nîmes, Nîmes, France;* [4]*Centre Hospitalier de Béziers, Béziers, France;* [5]*Hôpital de Narbonne, Narbonne, France*
Email: jose.ursic@yahoo.fr

Background and aims: Decompensated cirrhosis is a severe condition for which liver transplantation (LT) remains the only curative treatment. While graft allocation is strictly regulated after listing, the upstream steps leading to LT referral and evaluation are less clearly defined. This study aimed to evaluate the proportion of patients admitted to the emergency department (ED) or intensive care unit (ICU) for acute decompensation who progressed through the key steps toward LT, and to identify factors associated with failure of referral.
Method: We conducted a retrospective multicentre study across five hospitals: one university hospital with an LT program, one university hospital without LT services, and three general hospitals. Patients were identified via Hospital Discharge Database codes over a two-year period. Sociodemographic, clinical, and laboratory data were collected. Primary endpoints included referral to an LT centre, listing for LT, and undergoing transplantation.
Results: Of 1,186 records reviewed, 416 patients were included. The median age was 59.1 years, with a median follow-up of 34.4 months. Most patients were male (77.2%) and had alcohol-related cirrhosis (90%). Acute-on-chronic liver failure (ACLF) was present in 26% of cases (grade 1: 8.9%, grade 2: 9.6%, grade 3: 7.5%). Regarding outcomes, 120 patients (28.8%) were referred to an LT centre, 44 (10.5%) were listed, and 28 (6.7%) underwent transplantation. Among the 296 non-referred patients, 211 (71.2%) died within a median of 7.8 months, with 76.6% of deaths directly attributable to cirrhosis. No reason for non-referral was documented in 46.6% of cases; ongoing alcohol use was cited in 13.2%. In multivariate analysis, factors independently associated with referral included:
- Management in a university hospital (HR 2.7, 95% CI: 1.4–5.5; p = 0.005),
- Admission to a specialized gastrointestinal ICU versus the ED (HR 3.0, 95% CI: 1.4–6.3; p = 0.004),
- Higher MELD score (HR 1.15 per point, 95% CI: 1.1–1.2; p < 0.001),
- Non-alcohol-related cirrhosis (HR 2.1, 95% CI: 1.2–3.6; p = 0.002).

Conclusion: Despite LT being the only curative option for decompensated cirrhosis, fewer than one in three patients admitted to the ED or ICU are referred to a transplant centre. These findings reveal a major loss of opportunity upstream of listing. Standardizing early identification of LT candidates is essential to ensure timely and equitable access to transplantation.

FRI-574
Comparison of four meld-based scores and assessment of gender equity in waiting list outcomes in patients awaiting liver transplantation in The Netherlands

Danny van der Helm[1], Rowan van Golen[2], Wojciech Polak[2], Ian Alwayn[1], Ben Goudsmit[1], Hans Blokzijl[3], Vincent E. de Meijer[3], Marta Fiocco[4], Caroline den Hoed[2], Minneke Coenraad[1]. *[1]Leiden University Medical Center, Transplant Center, Leiden, Netherlands; [2]Erasmus MC, Rotterdam, Netherlands; [3]Universitair Medisch Centrum Groningen, Groningen, Netherlands; [4]Mathematisch instituut, Leiden University, Leiden, Netherlands*
Email: m.j.coenraad@lumc.nl

Background and aims: The Model for End-Stage Liver Disease (MELD) score estimates the 3-month mortality risk on the waitlist and has been the cornerstone of organ allocation for liver transplantation in many organ sharing societies worldwide. Over time, several refinements have been implemented to enhance equity and predictive accuracy, leading from the original MELD to MELD-Na, refitted MELD-Na (reMELD-Na), and MELD 3.0. This study aims to (1) compare the predictive performance of MELD, MELD-Na, reMELD-Na, and MELD 3.0 in adult patients actively listed for liver transplantation in two transplant centers in the Netherlands, and (2) to evaluate potential sex disparities in waiting list mortality and transplantation rates.
Method: Consecutive adult patients who were assigned an active transplantable status ("T-status") on the liver transplantation waitlist between 2007 and 2024 in two Dutch transplant centers were included. Patients listed for acute liver failure or polycystic liver disease, and patients in whom one of the scores could not be calculated due to missing data were excluded. Cause-specific hazard ratio (HRcs) models for death were estimated using competing risk analysis. Competing events were transplantation, waitlist removal for other reasons than transplantation, transition to nontransplantable status, or assignment of exception points. Each model had two risk factors: MELD-based score and sex.
Results: 1867 unique patients were included. The 3-month predictive ability for death on the waitlist of the four scoring systems was comparable for all MELD-based scores: MELD HRCS 1.17 (95%CI 1.15–1.19) and sex HRCS 1.18 (95%CI 0.80–1.74); MELD-Na HRCS 1.19 (95%CI 1.17–1.21) and sex HRCS 1.29 (95%CI 0.87–1.91); reMELD-Na HRCS 1.27 (95%CI 1.23–1.30) and sex HRCS 1.26 (95%CI 0.85–1.86); MELD 3.0 HRCS 1.18 (95%CI 1.16–1.21) and sex HRCS 1.48 (95%CI 1.00–2.18). No significant sex differences were observed in the cumulative incidence of death on the waitlist (p = 0.20) or transplantation (p = 0.49).
Conclusion: In this multicenter Dutch cohort, the predictive performance for waitlist mortality of MELD, MELD-Na, reMELD-Na, and MELD 3.0 was comparable. Moreover, the absence of significant sex-related differences in mortality and transplantation rates supports the fairness of currently used MELD-based scores for organ prioritization and allocation between men and women in the Netherlands.

FRI-575
Natural history and post-transplant outcomes in patients transplanted for autoimmune liver diseases: a comparative analysis of PBC, autoimmune hepatitis and overlap syndromes

Elena Velasco Martínez[1,2], María Jordán de la Fuente[1,2], Laura Jiménez[1,2], Natalia Marcos Carrasco[1,2], Samuel Fernández-Prada[1,2], Irene Peñas Herrero[1,2], Carolina Almohalla Alvarez[1,2], Félix García Pajares[1,2], Gloria Sánchez Antolín[1,2,3]. *[1]Hospital Universitario Río Hortega, Valladolid, Spain; [2]IBioVALL, Valladolid, Spain; [3]Universidad de Valladolid, Valladolid, Spain*
Email: anele_vm@hotmail.com

Background and aims: Autoimmune liver diseases, including autoimmune hepatitis (AIH), primary biliary cholangitis (PBC) and overlap syndromes, are a well-established indication for liver transplantation and show marked clinical heterogeneity. We aimed to analyse baseline characteristics, time from diagnosis to transplantation, and post-transplant survival and recurrence, comparing PBC, AIH and overlap syndromes.
Method: Retrospective observational study including 56 patients transplanted for autoimmune liver diseases. Demographic, clinical and outcome variables were analysed. Group comparisons were performed using ANOVA, χ^2 and Tukey post-hoc tests. Multivariable linear regression and Cox proportional hazards models were adjusted for aetiology, sex and age at diagnosis. Survival and recurrence were analysed using Kaplan–Meier and proportional hazards models.
Results: The cohort included 25 PBC, 17 AIH and 14 overlap patients. Overall, 76.8% were women, with a median age at diagnosis of 49 years. At presentation, 72.5% had hypertransaminasaemia, 13.7% decompensated cirrhosis and 13.7% acute hepatitis; 42% had cirrhosis at diagnosis. Autoimmune comorbidities were present in 21%, mainly autoimmune thyroid disease (16%). Mean time from diagnosis to

transplantation was 112.5 ± 88.4 months and was significantly shorter in AIH (54.6 ± 82.2) than in PBC (130.1 ± 71.5) and overlap syndromes (149.8 ± 92.9) (p = 0.018). In multivariable analysis, AIH (β −66.1 months; p = 0.008) and male sex (β −44.7 months; p = 0.042) were independently associated with shorter time to transplantation. Transplant indications were decompensated cirrhosis (72%), fulminant hepatitis (11%), refractory pruritus (11%) and hepatocellular carcinoma (6%). Median follow-up was 61 months (IQR 21–158). Survival was 91.1%, 89.3% and 82.1% at 1, 3 and 5 years, respectively. Recurrence occurred in 11 patients (22%), with a median time of 495 days (IQR 321.5–951). Survival was comparable across groups, whereas recurrence was more frequent and earlier in AIH and overlap syndromes. In adjusted analysis, AIH (HR 2.84; p = 0.028) and overlap syndromes (HR 2.41; p = 0.047) were independently associated with recurrence. Recurrence did not impact survival.
Conclusion: Autoimmune liver diseases differ markedly in pre-transplant course, with faster progression in AIH, but show excellent and comparable post-transplant survival. Although recurrence is more frequent in AIH and overlap syndromes, it does not affect survival.

FRI-576
Non-A1-to-O liver transplantation: should recipient anti-A antibody titers be assessed?
Taylor Viggiano[1], Andres Jaramillo[1,2], Qun Lu[1], Jill Adamski[1], Michele S. Barnhill[1]. [1]*Mayo Clinic Hospital, Phoenix, United States;* [2]*Mayo Clinic, Department of Laboratory Medicine and Pathology, Phoenix, United States*
Email: viggianomed@gmail.com

Background and aims: Historically, ABO compatibility has guided liver transplantation (LT); however, in the last 30 years, non-A1 LT, commonly referred to as A2-to-O LT (AOLT), has become increasingly utilized. This shift follows studies demonstrating comparable graft and patient survival outcomes between AOLT and O-to-O LT (OOLT) which is related to the lower expression of the A antigen and relative lower immunogenicity of non-A1 transplants. The liver is considered an immune-tolerant organ, allowing AOLT to increase the donor pool. However, recent cases of antibody-mediated rejection (AMR) in this cohort at our institution prompted a closer evaluation of outcomes and the potential role of recipient anti-A titers at the time of transplantation. The purpose of this retrospective review was to assess rejection rates and graft outcomes in AOLT and examine the association between rejection and anti-A antibody titers.
Method: We retrospectively reviewed all AOLT performed at our institution from 2001–2025. Rejection type, timing, graft failure, and retransplantation (RT) were recorded. Following an index AMR case in 2020, pre-transplant anti-A antibody titers (AAT) were routinely assessed and retrospectively collected when available.
Results: 46 AOLT were performed. 11 patients had biopsy-proven AMR (n = 3) or acute cellular rejection (n = 8). 7 of 46 (15%) required retransplant (RT) for vascular thrombosis, cholangiopathy, recurrent primary disease, and primary graft failure in the setting of AMR. AAT were available for 22 patients and ranged from 1:16 to 1:65,536. A subset of 8 patients (36%) had high AAT ≥ 1:2048, and 50% of these high-titer patients had AMR, 3 shown by liver allograft biopsy and 1 patient with liver/kidney transplant had presumed liver AMR based on renal biopsy. 2 (25%) patients in this high-titer subgroup required RT due to graft failure. None of the 14 patients with AAT <1:2048 had evidence of AMR and none required RT due to rejection.
Conclusion: AOLT is considered safe and has historically had similar graft and patient survival outcomes as OOLT. However, our retrospective study highlights a strong association between elevated AAT and AMR, which occurred in 50% of our AOLT with AAT > 1:2048, and 25% requiring RT. Therefore, we propose that pre-transplant evaluation should include routine AAT screening and that AOLT should proceed with caution when AAT exceed 1:2048. Larger studies are needed to validate this threshold and standardize patient selection protocols.

FRI-578-YI
Impact of socioeconomic factors on waiting list outcomes and survival after liver transplantation in Germany
Leke Wiering[1], Lola Unger[1], Robert Öllinger[1], Frank Tacke[1], Paul Ritschl[1], Münevver Demir[1]. [1]*Charité, Berlin, Germany*
Email: leke.wiering@charite.de

Background and aims: In liver transplantation socioeconomic disparities have been identified regarding both waiting list outcomes as well as survival after transplantation. However, most evidence originates from the US. The impact of socioeconomic factors in countries with universal healthcare systems, such as Germany, remains unclear. This study aimed to assess the impact of socioeconomic factors on liver transplantation in this setting.
Method: Waiting list outcomes and survival after liver transplantation were retrospectively analyzed in adult candidates listed for liver transplantation at Charité Universitätsmedizin Berlin between 2005 and 2021. Patients listed with high-urgency status were excluded. Socioeconomic variables included citizenship, type of health insurance, and proximity to the transplant centre. For patients residing in Berlin, additional detailed area-level data were assigned based on residential address using governmental data (Gesundheits- und Sozialstrukturatlas, Senatsverwaltung Berlin).
Results: The study includes 1523 candidates on the waiting list, of which 1017 received transplantation. In this cohort waiting list mortality was not significantly influenced by citizenship (German vs. non-German, p = 0.15 for Fine & Gray competing-risks regression) or insurance status (private vs. public, p = 0.26), but waiting list mortality was lower in patients living closer to the transplant centre (p = 0.035, subdistribution hazard ratio (sHR) = 0.78, 95% CI = 0.61–0.98). While the likelihood of receiving liver transplantation was also not influenced by citizenship (p = 0.39), transplantation rates were higher in patients with private insurances (p = 0.009, sHR = 1.28, 95% CI = 1.06–1.54). This was independent of candidates' age and sex (adjusted sHR = 1.22, p = 0.041). In the overall group patient-survival after transplantation did not differ significantly by socioeconomic factors (Cox regression; p = 0.06 for citizenship, p = 0.17 for type of health insurance). Interestingly in the group of male transplant recipients survival was slightly lower in patients with German citizenship (p = 0.048, hazard ratio (HR) = 1.62).
Conclusion: Overall, socioeconomic effects on liver transplantation were less pronounced compared to US findings, but still partially persisted within a universal health care system. While this study cannot provide direct mechanistic explanations, further research should explore potential disparities in waiting list registrations, which may explain our observations.

FRI-579
External validation and comparison of eight risk scores for predicting 3-month early graft failure after liver transplantation: a multicenter study
Wanqing Wu[1], Yu Nie[2], Peihua Cao[1], Kebo Zhong[2], Zhaofeng Lin[1], Lin Feng[1], Manqi Zhuang[1]. [1]*Clinical Research Center, Zhujiang Hospital, Southern Medical University, Guangzhou, China;* [2]*General Surgery Center, Department of Hepatobiliary Surgery II, Zhujiang Hospital, Southern Medical University, Guangzhou, China*
Email: wwq18907507306@smu.edu.cn

Background and aims: Early allograft failure (EAF) seriously affects patient outcomes after liver transplantation (LT). Although numerous risk scores have been developed to predict EAF, their external validation remains limited. This study aimed to externally validate and compare the performance of existing risk scores for predicting 3-month EAF after LT.
Method: This retrospective, multicenter cohort study utilized data from multiple Chinese tertiary hospitals and the Korean INSPIRE dataset. The primary outcome was 3-month EAF, defined as graft failure leading to death or re-LT within 90 days. We evaluated eight scores, including L-GrAFT$_7$, EASE, MEAF, EAD, King-PNF7, Korean ABC,

and Cardoso MELD-Lactate scores. Performance was assessed using the area under the receiver operating characteristic curve (AUC), decision curve analysis (DCA), calibration plots, net classification index (NRI) and integrated discrimination improvement (IDI). Risk stratification was evaluated using the Kaplan-Meier method.
Results: Of the 1263 patients screened, 1156 with available data were included. The median recipient age was 52.0 (IQR, 44.0–59.0) and 81.2% of the recipients were male. The incidence of 3-month EAF was 13.1% (n = 152). The L-GrAFT$_7$ score demonstrated excellent performance (AUC 0.85, 95% CI: 0.80–0.90), which was significantly higher than the MEAF (AUC 0.72, 95% CI: 0.66–0.79), EAD (AUC 0.71, 0.66–0.76), Korean ABC (AUC 0.81, 95% CI: 0.75–0.87), and Cardoso MELD-Lactate (AUC 0.75, 95% CI: 0.70–0.81) scores (all P < 0.05). No significant differences were observed between L-GrAFT$_7$ and either the EASE (AUC 0.84, 95% CI: 0.79–0.88; P = 0.53) or King-PNF7 (AUC 0.82, 95% CI: 0.77–0.88; P = 0.37) scores. The DCA showed a greater net benefit for L-GrAFT$_7$, Korean ABC and King-PNF7 compared to other models. Calibration plots showed good agreement for both the L-GrAFT$_7$ and King-PNF7. Furthermore, L-GrAFT$_7$ exhibited the best capability to identify high-risk patients for graft survival.
Conclusion: The L-GrAFT$_7$ score is a highly accurate and robust tool for individualized risk assessment of 3-month EAF. It demonstrates superior performance to existing risk scores and shows great promise in aiding clinical decision-making for early retransplantation in high-risk patients.

FRI-580

Postoperative peak lactate as a robust predictor for short-term prognosis and development of an updated risk prediction model for early graft failure after liver transplantation

Wanqing Wu[1], Yu Nie[2], Peihua Cao[1], Kebo Zhong[2], Zhaofeng Lin[1], Lin Feng[1], Manqi Zhuang[1]. *[1]Clinical Research Center, Zhujiang hospital of Southern Medical University, Guangzhou, China; [2]Clinical Research Center, Zhujiang Hospital, Southern Medical University, Guangzhou, China*
Email: wwq18907507306@smu.edu.cn

Background and aims: Early identification of recipients at risk for early allograft failure (EAF) following liver transplantation (LT) is critical for improving outcomes. This study aimed to evaluate the prognostic value of postoperative lactate levels and develop novel lactate-enhanced models for predicting early outcomes.
Method: This multicenter, retrospective cohort study utilized data from four Chinese tertiary centers and the South Korean INSPIRE dataset. Patients were divided into a training cohort (n = 706), a Chinese validation cohort (n = 255), and the INSPIRE validation cohort (n = 195). The primary outcome was 3-month EAF. We constructed novel models (L-GrAFT$_7$-Lactate, EASE-Lactate, and MEAF-Lactate) by incorporating lactate into established scoring systems. Model performance was compared using the area under the ROC curve (AUC), net reclassification index (NRI), integrated discrimination improvement (IDI). Risk stratification was assessed with Kaplan Meier survival analysis.
Results: Peak lactate strongly predicted primary non-function (AUC, 0.88), 1-month mortality (AUC, 0.77), and 3-month mortality (AUC, 0.80). The lactate-integrated models significantly improved performance in the training and Chinese validation cohorts (all P < 0.001). For predicting 3-month EAF, L-GrAFT$_7$-Lactate (AUC, 0.91) significantly outperformed MEAF-Lactate (AUC, 0.82) and EAD definition (AUC, 0.71) (all P < 0.001), but showed no significant difference with EASE-Lactate scores (P = 0.82). A simple, easy-to-use EAD-Lactate grading system was developed: Grade 1 (no EAD), Grade 2 (isolated AST/ALT >2000 IU/L within 7 days), Grade 3 (single abnormality among INR ≥1.6 at day 7, bilirubin ≥10 mg/dL at day 7, or peak lactate ≥5 mmol/L), Grade 4 (any two abnormalities), and Grade 5 (all three abnormalities). The EAD-Lactate system provided an excellent discrimination for 3-month EAF (AUC, 0.85), superior to the binary EAD definition and MEAF score, while similar to L-GrAFT$_7$ and EASE (P > 0.05).
Conclusion: Postoperative lactate is a robust predictor of early outcomes after LT. Incorporating lactate into established scoring systems significantly enhances predictive accuracy. EAD-Lactate grading system improves the stratification of graft dysfunction severity, which are valuable for guiding clinical decision-making and early retransplantation strategies.

FRI-581

Liver transplantation (LT) for malignant and benign liver tumors in the United States and Europe: a 20-year perspective

Zobair M. Younossi[1], Giacomo Germani[1,2], Robert Wong[1,3], Maria Stepanova[1], Fatema Nader[1], Vincent Karam[1,4], René Adam[1,5], Rohit S. Satoskar[1,6], Saleh Alqahtani[1,7], Linda Henry[1], Patrizia Burra[1,2]. *[1]The global NASH/MASH council, Washington DC, United States; [2]Department of Surgery, Oncology and Gastroenterology, University of Padova, Padova, Italy; [3]Division of Gastroenterology and Hepatology, Stanford University School of Medicine, Palo Alto, United States; [4]The European Society for Organ Transplantation, Paris, France; [5]Hopital Paul Brousse, Villejuif, France; [6]Georgetown Medical Center, Washington DC, United States; [7]Liver, Digestive, and Lifestyle Research Section, and Organ Transplant Center of Excellence, King Faisal Specialist Hospital and Research Center, Riyadh, Saudi Arabia*
Email: zobair.younossi@cldq.org

Background and aims: Liver tumors including hepatocellular carcinoma (HCC), other liver malignancies and benign liver tumors are indications for LT. We assessed the characteristics and outcomes of LT recipients with different types of liver tumors using multi-national transplant datasets.
Method: Adult LT recipients with HCC, cholangiocarcinoma (CCA), other primary liver malignancy (PLM), secondary liver cancers (SLCs), or benign liver tumor were identified from the 30-country European Liver Transplant Registry (ELTR) and the U.S. Scientific Registry of Transplant Recipients (SRTR) (2000–2022).
Results: A total of 62,279 LT recipients for all liver tumors were included; 57% from ELTR, 43% from SRTR. HCC was the most common tumor-related LT indication (91%) while benign liver tumors accounted for 4.3% of all tumor-related LTs, followed by CCA (1.9%), other PLM (1.6%), SLCs (1.0%). Over time, the share of HCC among all LTs increased from 10% (2000) to the peak of 32% (2015) and then decreased to 21% (2022). In addition, the share of CCA (in all LTs) increased from 0.3% (2000) to 0.8% (2022) and benign tumors increased from 0.7% (2000) to 1.5% (2015) followed by a decrease to 1.2% (2022) while the prevalence of other PLMs and SLCs remained stable at 0.4% and 0.3%, respectively (trend p > 0.05). The mean MELD scores were similar in all tumor groups (pooled 13.5 ± 7.0) except SLCs (9.7 ± 6.1). Post-LT survival varied substantially across the tumor groups, with 5-year survival ranging from 81% in patients with benign liver tumors to 69% in HCC to 58% in other PLM and SLCs to 50% in CCA. The most common cause of death among liver cancers was malignancy (35–55% of all deaths), and infections for LT benign liver tumors (20%). Over time, LT for HCC related to chronic hepatitis C (CHC) increased from 3.9% of all listings (2000) to the peak of 13.6% (2014) followed by a sharp decrease to 4.2% (2022). Metabolic dysfunction-associated steatohepatitis (MASH)-HCC increased from 0.3% (2000) to 4.0% (2020), 3.9% (2022). Alcohol associated liver disease (ALD)-HCC also increased from 1.2% (2000) to 6.3% (2019), 5.8% (2022) (both trend p < 0.0001), while rates for other etiologies remained stable or decreased.
Conclusion: Among liver tumors, HCC is the dominant indication for LT. Post-LT outcomes vary according to tumor type, with best survival for benign liver tumors and lowest for CCA. Over time, HCC related to MASH and ALD increased, while HCC from CHC declined.

Liver transplantation and hepatobiliary surgery – Experimental and pathophysiology

TOP-534

Hepatic chimerism and partial immune tolerance in an allogeneic mouse liver transplant model

Keiko Iwaisako[1]. [1]*Doshisha University, Kyoto University, Kyoto, Japan*
Email: iwaisako@kuhp.kyoto-u.ac.jp

Background and aims: Although modern immunosuppressive regimens have substantially improved early outcomes after liver transplantation, chronic immune-mediated graft injury remains a major cause of late graft dysfunction. The mechanisms underlying long-term immune accommodation and tissue remodeling remain incompletely defined, partly due to the lack of experimental models permitting prolonged follow-up. We aimed to characterize long-term immune dynamics and cellular remodeling in a fully major histocompatibility complex (MHC)-mismatched mouse liver transplantation model.
Method: Orthotopic liver transplantation with hepatic arterial reconstruction was performed using BALB/c donors and C57BL/6 or CAG-GFP C57BL/6 recipients. No immunosuppressive treatment was administered. Recipients were analyzed at serial time points up to 64 weeks post-transplantation. Histopathology, RNA sequencing, blood biochemistry, and serum immunoglobulin profiling were performed.
Results: Long-term graft survival was achieved in the absence of immunosuppression, except in animals developing technical complications such as thrombosis or cholestasis. Marked immune cell infiltration was evident from one week post-transplantation and progressively attenuated by eight weeks. Low-grade inflammatory infiltrates persisted throughout long-term follow-up. Regulatory T cells were selectively maintained beyond eight weeks. Serum immunoglobulin concentrations increased until four weeks and subsequently declined, but remained above baseline levels. Lineage-tracing analyses demonstrated near-complete replacement of donor Kupffer cells and partial replacement of sinusoidal endothelial cells by recipient-derived cells, indicating progressive hepatic chimerism.
Conclusion: This arterialized MHC-mismatched mouse liver transplantation model demonstrates long-term immune accommodation associated with progressive hepatic chimerism and sustained regulatory T-cell dominance. These findings support a potential role for recipient-derived cellular chimerism in late graft remodeling and provide a translational platform for investigating chronic graft injury and immune tolerance mechanisms. Importantly, these mechanisms must also be validated in human liver allograft tissue.

THU-517-YI

Baseline serum metabolomic signatures predict post- liver transplant early complications

Rosmy Babu[1], Sushmita Pandey[1], Jaswinder Maras[1], Viniyendra Pamecha[1], Chhagan Bihari[1], Gaurav Tripathi[1], Nupur Sharma[1]. [1]*Institute of Liver and Biliary Sciences, Delhi, India*
Email: drcbsharma@gmail.com

Background and aims: Post-transplant early complications significantly increase morbidity following liver transplantation; however reliable pre-transplant biomarkers are limited. We aimed to identify baseline serum metabolomic signatures using LC–MS–based analysis of that help predict post-transplant early complications.
Method: Whole blood samples of cirrhosis recipients aged 18 to 65 with post-transplant early complications (EC), such as graft rejection, biliary complications, and/or infection within 6 months of follow-up (n = 64), and recipients without early complications (NEC), n = 109 were collected. Serum was extracted from blood samples, which was then processed for metabolomic profiling using LC-MS and validated in 48 EC and 52 NEC samples. Peak detection, signal normalisation, and metabolite annotation were performed on the raw data using reference databases. The resulting feature count data was examined for downstream univariate, multivariate, and machine-learning analyses performed in GraphPad Prism v6 and SPSS v20.
Results: Baseline serum metabolomic profiles differed significantly between recipients who developed post-transplant early complications (EC) and those without early complications (NEC), indicating the presence of pre-transplant metabolic differences. Unsupervised hierarchical clustering demonstrated substantial inter-sample variability and no clear segregation by age, sex, disease etiology, MELD score or other clinical parameters; however, it consistently highlighted a subset of metabolites that differed who had EC and NEC. These differences were confirmed by univariate analysis, partial least squares discriminant analysis (PLS-DA), and Random Forest modeling. Five baseline metabolites were significantly elevated in EC recipients compared with NEC recipients (all $p < 0.0001$): acrylamide (2-propenamide), 6-(α-D-glucosaminyl)-1D-myo-inositol, alcophosphamide, glycochenodeoxycholate, and 2-acetylaminofluorene. These metabolites showed strong discriminatory performance (AUC range 0.767–0.975), and their combined baseline metabolomic model achieved near-perfect prediction of early complications (AUC 0.991, 95% CI 0.983–1.000), outperforming MELD-Na. On validation using high-resolution mass spectrometry and machine learning algorithms, the metabolome panel showed >95% accuracy and specificity for prediction of EC.
Conclusion: Baseline serum metabolomics signature identifies recipients at risk for early complications, supporting its use for objective pre-transplant risk stratification.

THU-521

cGAS deficiency alleviate liver ischemia reperfusion injury by blocking macrophage proliferation in the transplanted liver

Ruihan Chen[1], Xiaohan Lin[1], Qi Ling[1]. [1]*The First Affiliated Hospital, Zhejiang University School of Medicine, Hangzhou, China*
Email: 12318397@zju.edu.cn

Background and aims: Liver ischemia reperfusion injury (IRI) is a key risk factor for graft failure post-liver transplantation (LT). cGAS, a DNA sensor, plays critical roles in inflammation responses. This study aims to elucidate the mechanisms of cGAS in liver IRI.
Method: We analyzed cellular cGAS expression profile in liver using western blot, qPCR, and immunofluorescence. Single-cell RNA sequencing from mouse LT model were analyzed to determine the distribution of cGAS and the functional features of $cGAS^{hi}$, macrophage cluster. Subsequently, IRI model was established using wild-type (WT) and $cGAS^{-/-}$ mice, liver injury and macrophage function were evaluated through histopathology, flow cytometry. In vitro, cGAS was knocked down in RAW264.7 cells via lentivirus, and its effects on macrophage polarization and proliferation were assessed by qPCR and flow cytometry. An orthotopic LT model in $cGAS^{-/-}$ mice was used to evaluate cGAS as a potential therapeutic target for mitigating graft reperfusion injury.
Results: In both human and murine livers, cGAS was highly expressed in macrophages but minimally detected in hepatocytes. Its expression in macrophages was upregulated following liver IRI. Analysis of single-cell transcriptomic data from a syngeneic murine LT model revealed that cGAS expression was elevated in the early post-transplant phase and was particularly enriched in a proliferating macrophage subcluster (Top2a_Mac). In a murine IRI model, $cGAS^{-/-}$ mice demonstrated significantly lower serum ALT/AST levels and reduced Suzuki scores compared to wild-type controls. $cGAS^{-/-}$ mice also exhibited attenuated macrophage infiltration and decreased expression of pro-inflammatory cytokines such as IL-6. Furthermore, hepatic macrophages in $cGAS^{-/-}$ mice shifted toward an anti-inflammatory phenotype and showed suppressed proliferation. The functional role of macrophage cGAS was confirmed in a H/R hepatocyte co-culture model, where cGAS knockdown reduced pro-inflammatory cytokine production and induced S-phase cell cycle

arrest in macrophages. Finally, in a syngeneic orthotopic LT model, cGAS deficiency resulted in diminished immune cell infiltration and improved graft survival.
Conclusion: In the liver IRI model, cGAS deficiency in macrophages confers protection by inhibiting their proliferation and impairing the shift toward a pro-inflammatory phenotype, thereby providing a potential therapeutic target for LT.

THU-522
METTL3-mediated m6A modification of ATG12 upregulates autophagy to promote activation and survival of CD8+ T cells during acute rejection after liver transplantation
Xiaolong Chen[1], Wenfeng Zhu[2], Xuejiao Li[3]. [1]*Department of Hepatobiliary Surgery, The First Affiliated Hospital of Jinan University, GuangZhou, China;* [2]*Department of Hepatobiliary Surgery, The Second Affiliated Hospital of Guangzhou Medical University, GuangZhou, China;* [3]*Department of Hepatology Lab, The Third Affiliated Hospital of Sun Yat-sen University, GuangZhou, China*
Email: 15779729700@163.com

Background and aims: Previous studies and ours have demonstrated the critical role of $CD8^+$ T cells in acute rejection (AR) after liver transplantation (LT). N6-methyladenosine (m^6A) modification has been reported to be involved in the regulation of immune cell function and survival recently. However, its role in AR remains to be elucidated.
Method: m^6A modification and related protein levels of $CD8^+$, T in liver grafts from AR patients after LT were assessed first. Rat acute hepatic rejection model and one-way mixed lymphocyte reaction (MLR) model were then established to confirm the methylation levels of $CD8^+$ T cells. Moreover, changes of RNA in murine activated $CD8^+$ T cells were examined and methylated RNA immunoprecipitation (MeRIP) was conducted to identify the specific targets of methyltransferases. Furthermore, underlying mechanisms of m^6A modification in the regulation of function and survival of T cells were explored.
Results: m^6A methylation levels in $CD8^+$, T cells were elevated in both AR patients and rats after LT. Methyltransferase-like 3 (METTL3) was confirmed to mediate methylation of activated $CD8^+$, T cells in vitro, which promoted their activation. RNA sequencing results indicated that the autophagy related signaling plays an important role in allo-antigen triggered activation of $CD8^+$, T cells. Autophagy-related 12 (ATG12) was determined as the direct target of METTL3 through MeRIP. Mechanistically, METTL3 enhances autophagy by up-regulating ATG12 expression through Insulin-like growth factor 2 mRNA-binding protein 2 (IGF2BP2) recognized stabilizing of Atg12 mRNA, resulting in promotion of survival, proliferation and function of T cells.
Conclusion: METTL3-mediated m^6A methylation of ATG12 promotes activation of $CD8^+$ T cells through up-regulating autophagy after LT, offering a theoretical foundation for identifying novel therapeutic targets for the prevention and treatment of AR following LT.

THU-523
Recurrence of primary biliary cholangitis after liver transplantation: predictors and graft and patient outcomes
Paul Domínguez Cardoso[1], Andres Bejarano Cayo[1], Alejandro Gutierrez-Castillo[2,3], Ricardo Gutierrez-Monterrubio[1], Berenice M. Román-Calleja[1], Nayelli Flores-García[1]. [1]*Incmnsz.edu.mx, Ciudad de México, Mexico;* [2]*Instituto Nacional de Ciencias Médicas y Nutrición Salvador Zubirán, Mexico City, Mexico;* [3]*Instituto Nacional de Ciencias Médicas y Nutrición Salvador Zubirán, Gastroenterology, Mexico City, Mexico*
Email: paulfcodominguez@hotmail.com

Background and aims: Recurrence of primary biliary cholangitis (PBC) after liver transplantation (LT) remains a significant clinical challenge, with reported rates of 20–30%. We aimed to identify predictors of recurrence and to evaluate graft and patient outcomes in a cohort of transplanted patients with PBC, integrating clinical, serological, biochemical, and histopathological variables.
Method: We performed a retrospective cohort study of LT recipients from 2000 to 2024 at a tertiary care center in Mexico. Demographic, clinical and biochemical variables at 3, 6 and 12 months were compared using univariate and multivariate analysis. Prognostic scores (Paris II and GLOBE) were used and recurrence was confirmed histologically.
Results: From a total of 69 patients, 62 (89.9%) were women. Recurrence occurred in 17 patients (24.6%), with a median time of 3 years. In univariate analysis, significant variables included age at LT ($p < 0.001$), AMA positivity ($p = 0.033$), AIH/PBC overlap ($p < 0.001$), tacrolimus levels at the third month ($p < 0.001$) and GGT value at the sixth ($p = 0.045$) and twelve ($p = 0.048$) month. Paris II and GLOBE scores showed similar biochemical response patterns in both groups but neither score predicted recurrence.
In the multivariate analysis relevant variables included age at LT (OR 0.917, $p = 0.44$) and AIH/PBC overlap (OR 0.042, $p = 0.001$).
Conclusion: Post-transplant PBC recurrence is strongly associated with younger age and a more complex immunologic phenotype characterized by a high prevalence of AIH/PBC overlap. Prognostic models developed for non-transplanted PBC (Paris II, GLOBE) do not predict recurrence in the graft. Persistently elevated GGT at 6 and 12 months appears to be an early biochemical marker of recurrence. These findings support closer post-transplant monitoring in patients with overlap syndrome and highlight the need for transplant-specific prognostic tools.

THU-524
Engineering bile ducts with enhanced epithelial maturation and vascularization
Mattia Pasqua[1], Ayesha Rehman[1], Ruben Leone[1], Giovanni Cavalli[1], Maria Giovanna Francipane[1]. [1]*Fondazione Ri.MED, Palermo, Italy*
Email: mgfrancipane@fondazionerimed.com

Background and aims: Injury to the common bile duct (CBD) remains a major clinical challenge due to poor long-term outcomes of current endoscopic and surgical treatments. We previously developed a multiphasic CBD-like scaffold seeded with cholangiocytes, which demonstrated mechanical integrity, leak-proof function, bile acid transport, and favorable immunocompatibility ex vivo. Despite these advances, the engineered biliary tissue remained partially mature and showed limited structural organization. Here, we investigate an advanced cellular seeding strategy in which cholangiocytes are incorporated with supportive stromal and endothelial cells to enhance tissue architecture and promote vascular network formation within this scaffold.
Method: Distinct multicellular aggregates containing cholangiocytes and supportive cell types were generated in suspension culture and seeded into specific layers of the scaffold. Tissue organization, epithelial phenotype, and formation of vascular-like networks were evaluated by immunofluorescence.
Results: Seeding of distinct cell populations enabled the formation of organized epithelial and supportive compartments, recapitulating key features of biliary tissue architecture.
Conclusion: Pre-assembled multicellular aggregates can be effectively integrated into our CBD-like scaffold, supporting tissue organization and vascular network formation. This approach advances the engineering of biomimetic bile duct constructs toward clinical translation.

THU-525
Decellularized bile duct scaffolds facilitate autologous regeneration in a rat model of bile duct defect
Yusuke Hanabata[1], Takamichi Ishii[1], Hidenobu Kojima[1], Fumiaki Munekage[1], Satoshi Ogiso[1], Etsuro Hatano[1]. [1]*Department of Surgery, Graduate School of Medicine, Kyoto University, Kyoto, Japan*
Email: taishii@kuhp.kyoto-u.ac.jp

Background and aims: Bile duct (BD) injury in hepatobiliary surgery can lead to severe biliary complications. Conventional reconstructive procedures often compromise physiological bile flow and are associated with bile leakage, stricture, and recurrent cholangitis, underscoring the need for alternative substitutes. This study investigated the regenerative capacity of a decellularized bile duct (dBD) scaffold as a biological substitute.
Method: A syngeneic dBD scaffold was prepared from Lewis rats using a detergent-based decellularization protocol that preserved extracellular matrix architecture. After resection of a 4-mm segment of the common bile duct, the dBD was orthotopically interposed with an intraluminal stent. Animals were sacrificed at 2, 4, 6, and 12 weeks for macroscopic, biochemical, and histological evaluation. A control group received a stent alone without a biological scaffold. Regeneration was assessed by serial histology and immunostaining for epithelial, stromal, vascular, and inflammatory markers.
Results: The dBD graft maintained luminal patency and preserved liver function without biliary leakage, obstruction, or infection, while eliciting only a minimal inflammatory response. Regeneration progressed through early fibroblast infiltration, angiogenesis, and marked activation of peribiliary glands (PBGs) with high Ki-67 and SOX9 expression, followed by epithelial maturation into $CK19^{+}/SOX9^{-}$ biliary lining. By 12 weeks, the implanted dBD was covered by a continuous epithelium with well-organized collagen and vascular structures. The PBGs transitioned to a quiescent phenotype resembling native BD architecture. Conversely, stent-only controls developed biliary sludge and impaired remodeling.
Conclusion: The dBD enabled autologous regeneration of functional biliary tissue through coordinated epithelial, vascular, and stromal remodeling. This approach offers a promising foundation for next-generation BD substitutes for clinical application.

THU-526

Macrophage colony stimulating factor (CSF1) induces a proregenerative response in human liver during normothermic machine perfusion

Sahar Keshvari[1], Sarah Schulze[1], Dylan Carter-Cusack[1], Nick Butler[2], Katharine Irvine[1]. [1]*Mater Research - The University of Queensland, Brisbane, Australia;* [2]*Queensland Liver Transplant Service, Brisbane, Australia*
Email: katharine.irvine@uq.edu.au

Background and aims: Macrophages play essential roles in liver homeostasis, regeneration and resolution of injury, but can also contribute to chronic inflammation and liver disease. In the setting of transplantation and surgery, optimal liver macrophage function is essential for resistance to infection and could support tissue regeneration. We previously demonstrated in preclinical models that Macrophage Colony Stimulating Factor (CSF1) therapy promotes liver regeneration after acute and chronic injury and fibrosis resolution in chronic liver disease. To translate these findings we investigated the impact of CSF1 treatment in human livers undergoing ex vivo normothermic machine perfusion (NMP).
Method: A single dose of recombinant CSF1 was administered to six donor livers (3 clinically rejected for transplant and 3 healthy with no suitable recipient) 4–12 h after commencement of NMP on an OrganOx Metra. Perfusate samples and biopsies were taken for measurement of CSF1 by ELISA, histological analysis and bulk RNA Sequencing over a timecourse of up to 24 hours. Meta-analysis of public RNASeq data from livers perfused for 5 h was used to control for changes in gene expression during NMP.
Results: CSF1 was rapidly removed from the perfusate, as it undergoes receptor-mediated endocytosis. Clearance was delayed and reduced in unhealthy livers, likely related to reduced blood flow rate and/or impaired CSF1R+ macrophage function. RNA Sequencing of serial biopsies showed rapid, specific transcriptional responses to CSF1, with highly significant enrichment of binding sites for macrophage transcription factors such as CEBPB, AP1 and MYB in the vicinity of genes induced within 1 h of CSF1 administration. Key pathways implicated in hepatocyte proliferation and liver growth (Hippo/Yap, cell cycle) and regulation of lipid metabolism were also induced within 1 hour and persisted over the perfusion time. Histological analysis demonstrated an increase in staining area of the macrophage marker CD68 during perfusion, consistent with a morphological response to CSF1.
Conclusion: Preclinical studies have demonstrated the therapeutic benefits of CSF1 for ameliorating ischaemic injury, promoting liver regeneration and resolving steatosis and fibrosis. The proregenerative response observed during NMP supports the therapeutic potential of acute CSF1 treatment in the peri surgical setting and more broadly in human liver disease.

THU-529-YI

Glypican 3-targeted antigen-specific fluorescent imaging enhances real-time intraoperative tumor identification in hepatocellular carcinoma: a translational study

Shuhei Kanda[1], Hiroto Nishino[1], Tomoaki Yoh[1], Yuya Kaneda[1], Kohei Yoshimura[1], Yoshihiko Kurata[1], Motohiko Sato[1], Takahiro Nishio[1], Satoshi Ogiso[1], Keiko Iwaisako[1], Takamichi Ishii[1], Etsuro Hatano[1]. [1]*Graduate School of Medicine, Kyoto University, Kyoto, Japan*
Email: s.kanda.0718@gmail.com

Background and aims: Fluorescence imaging using indocyanine green (ICG) is widely used to support intraoperative navigation in various surgical fields. During hepatectomy for hepatocellular carcinoma (HCC), precise tumor detection and prevention of residual cancer are essential. Glypican-3 (GPC3) is a tumor-associated membrane antigen that is highly expressed in most HCCs but absent in normal liver tissue. The aim of this study was to evaluate the feasibility of GPC3 as a tumor-specific imaging target and to develop a GPC3-targeted fluorescent probe for intraoperative tumor visualization.
Method: In the clinical study, intraoperative tumor identification using ICG fluorescence imaging was assessed in 38 selected patients. Patients were classified into identifiable and non-identifiable groups, and clinicopathological factors were compared between the two groups. The tumor specificity of GPC3 was validated by immunohistochemical staining of resected specimens from both groups. In the experimental study, novel GPC3–targeted fluorescent probe (GPC3-IRDye800) was developed. The probe was administered to human HCC cell line derived orthotopic xenograft models. Tumor-to-background ratio (TBR), fluorescence distribution, margin contrast, and safety profiles were analyzed and compared with ICG and an isotype-control probe.
Results: Intraoperative tumor identification using ICG fluorescence was achieved in 30 patients. Cirrhosis (F4) was significantly more frequent in the non-identifiable group than in the identifiable group. Immunohistochemistry showed GPC3 positivity in 35 cases, with significantly higher expression in tumors than in peritumoral liver ($p < 0.0001$). In the experimental study, GPC3-IRDye800 demonstrated antigen-dependent uptake, yielding higher fluorescence intensity and TBR in GPC3-positive tumors compared with controls ($p < 0.0001$). At 72 hours after administration in both normal- and fibrotic-liver mouse models, GPC3-IRDye800 provided higher fluorescence intensity and clearer tumor margin identification than ICG. No histological organ damage or biochemical toxicity was observed following probe administration.
Conclusion: GPC3-IRDye800 achieved superior tumor visualization, clearer intraoperative margin assessment in mouse models. These findings suggest that GPC3-targeted fluorescence imaging may enhance real-time intraoperative tumor identification in HCC and complement current ICG navigation.

THU-530

An increase in regulatory B cells contributes to achieve tolerance in liver transplantation patients

Eunju Kim[1], Soon Kyu Lee[2], Jong Young Choi[1,2]. [1]*Chung-Ang University, Gwangmyeong, Korea, Rep. of South;* [2]*The Catholic University of Korea, College of Medicine, Seoul, Korea, Rep. of South*
Email: jychoi@catholic.ac.kr

Background and aims: This study investigates the dynamics of regulatory B cells (Bregs) during immunosuppression (IS) tapering and their contribution to tolerance in liver transplantation (LT) patients.
Method: We prospectively enrolled 15 LT patients who had normal liver function, no history of rejection, and had undergone LT more than five years ago. Patients were followed up every three months, and IS doses were tapered by 25% every 6–9 months. At each visit, blood samples were collected, and the proportions of T cells and B cells were analyzed by flow cytometry. To validate flow cytometry findings, we also compared the infiltration of T and B cell subsets in liver tissue between tolerant (n = 5) and rejection (n = 5) patients using histopathology and confocal microscopy. Additionally, RNA sequencing and *in vitro* analysis were conducted to access Bregs function in tolerance.
Results: Over a median follow-up of 42 months, eight patients successfully discontinued IS without rejection (tolerance group). One patient experienced rejection (rejection group), while the remaining six patients reduced their IS dose to 25% without rejection (minimization group). During IS tapering, Treg cells and the Treg/Th17 ratio increased in the tolerance group but decreased before rejection in the rejection group. Similarly, the tolerance group exhibited an increase in Bregs and the Breg/Th17 ratio, whereas a decrease was observed in the rejection group. Moreover, a negative correlation between Bregs and Th17 cells and a significant positive association between Bregs and plasmablast B cells were identified. In liver tissue, confocal analysis showed a significant increase in Tregs and Bregs in tolerance patients (n = 5) compared to patients with rejection. In vitro analysis demonstrated a reduction in Th17 cells following Breg treatment, and vice versa. Furthermore, treatment with *Faecalibacterium*, enriched in the tolerance group, led to an increase in Bregs and IL-10 levels.
Conclusion: During IS tapering, Bregs increase and contribute to the achievement of tolerance in LT patients. These findings suggest that Bregs may serve as potential biomarkers and therapeutic targets for promoting tolerance in LT.

THU-531

Simvastatin attenuates post-hepatectomy hemodynamic liver injury in fibrotic livers through KLF2-eNOS signaling

Fumiaki Munekage[1], Satoshi Ogiso[1], Yusuke Hanabata[1], Takuma Karasuyama[1], Kentaro Iwaki[1], Hidenobu Kojima[1], Takamichi Ishii[1], Etsuro Hatano[1]. [1]*Kyoto University, Kyoto, Japan*
Email: ogiso@kuhp.kyoto-u.ac.jp

Background and aims: Simvastatin has been reported to reduce portal hypertension in cirrhotic and fibrotic livers, partly through endothelial nitric oxide-dependent mechanisms. However, it remains unclear whether simvastatin can attenuate the acute increase in portal pressure and protect the liver from hemodynamic stress during the early postoperative phase after major hepatectomy in fibrotic livers.
Method: Liver fibrosis was induced in C57BL/6 mice by oral administration of carbon tetrachloride for 12 weeks. Mice were then treated with or without oral simvastatin (30 mg/kg daily for 3 days) and subjected to 70% or 80% partial hepatectomy. Simvastatin-treated and untreated fibrotic mice were compared with respect to postoperative survival, portal venous pressure, biochemical markers of sinusoidal endothelial injury, histological changes, and endothelial-specific molecular signaling.
Results: After 80% hepatectomy, simvastatin-treated fibrotic mice showed significantly higher survival than untreated fibrotic mice (p = 0.022). After 70% hepatectomy, simvastatin-treated fibrotic mice exhibited a significantly smaller necrotic area at 24 hours after surgery (0.2% vs 2.3%, p = 0.030), a trend toward increased remnant liver weight, and significantly lower serum hyaluronic acid levels at 72 hours, while no mortality was observed in either group. Hemodynamic analysis demonstrated that simvastatin-treated fibrotic mice had lower portal venous pressure before hepatectomy and at 4 and 24 hours after surgery, accompanied by increased portal flow volume per liver parenchymal volume at 4 hours and larger sinusoidal areas before hepatectomy and at 4 hours. Western blot analysis further revealed increased expression of the shear stress-responsive transcription factor KLF2 in sinusoidal endothelial cells and higher levels of phosphorylated eNOS in simvastatin-treated fibrotic mice.
Conclusion: In fibrotic livers, acute portal hypertension after major hepatectomy imposes substantial hemodynamic stress on sinusoidal endothelial cells, which is aggravated by impaired sinusoidal dilatory capacity. Our findings suggest that simvastatin attenuates post-hepatectomy hemodynamic liver injury by activating the KLF2–eNOS pathway, thereby promoting sinusoidal dilation, reducing portal pressure, and preserving sinusoidal endothelial integrity in fibrotic livers.

THU-532

Salvianolic acid C alleviates hepatic ischemia-reperfusion injury by activating HSP90α and PI3 K/AKT pathway

Yingmei Shao[1], Alimu Tulahong[2,3], Qiao Tulahong[1]. [1]*The First Affiliated Hospital of Xinjiang Medical University, Urumqi, China;* [2]*The First Affiliated Hospital of Xinjiang Medical University, Department of Hepatobiliary and Echinococcosis Surgery, Urumqi, China;* [3]*Xinjiang Medical University, Urumqi, China*
Email: syingmei1@163.com

Background and aims: Hepatic ischemia-reperfusion injury (HIRI) is a major cause of liver dysfunction following transplantation, yet effective therapeutic interventions remain unavailable. Salvianolic acid C (SaC), a polyphenol derived from Salvia miltiorrhiza, exhibits documented protective effects in cerebral ischemia, but its role in HIRI and the underlying molecular mechanisms are unexplored. This study aimed to investigate the hepatoprotective effects of SaC against HIRI and elucidate its mechanism of action, with a specific focus on heat-shock protein regulation and the PI3 K/AKT pathway. We employed an integrated approach combining bioinformatics analysis of the transcriptomic dataset GSE151648, in vivo murine HIRI models, and molecular biology validation assays.
Method: Transcriptomic profiling identified differentially expressed heat-shock proteins (HSPs), followed by protein-protein interaction (PPI) network construction and pathway enrichment analysis. Murine HIRI models were established with or without SaC pretreatment. Dynamic changes in HSP90α (HSP90AA1) expression, serum pro-inflammatory cytokines (TNF-α, IL-1β, IL-6), apoptosis markers, and histopathological damage were quantified. PI3 K/AKT pathway activation was assessed, and mechanistic validation was performed using the HSP90 inhibitor 17-AAG.
Results: Bioinformatics analysis identified HSP90AA1 as a key hub gene in HIRI and a potential target of S-allyl cysteine (SaC), primarily enriched in the PI3K-Akt signaling pathway. In vivo, HIRI injury peaked at 6 hours of reperfusion, accompanied by an early upregulation of HSP90α. SaC treatment further enhanced HSP90α expression and significantly attenuated hepatic injury, evidenced by

improved liver histology, reduced serum enzymes (ALT, AST, LDH), and suppressed inflammation and apoptosis. Crucially, pharmacological inhibition of HSP90α with 17-AAG exacerbated liver damage and abrogated SaC-mediated protection. Mechanistic studies revealed that SaC activated the PI3 K/Akt pathway, an effect that was reversed by HSP90α inhibition. Collectively, these findings indicate that SaC alleviates HIRI by upregulating HSP90α to activate the PI3 K/Akt signaling cascade.
Conclusion: SaC alleviates HIRI by targeting HSP90α to activate the PI3 K/AKT pathway, thereby reducing inflammation, apoptosis, and tissue injury. This identifies SaC as a novel natural therapeutic strategy against HIRI.

THU-533
Mitochondrial transfer from S100A4+ macrophages triggers hepatocyte GSTP1 lactylation and PANoptosis in ischemic liver injury

Mengxue Sun[1], Min Tang[1]. [1]*Division of Gastroenterology and Hepatology, Institution of Digestive Diseases, Tongji Hospital, Tongji University School of Medicine, Shanghai, China*
Email: ttangmin@sina.com

Background and aims: Hepatic ischemia-reperfusion injury is a common complication in liver transplantation and hepatectomy, which triggers a severe inflammatory response and extensive cell death, potentially leading to acute liver injury or even organ failure. While macrophage polarization and massive hepatocyte death are hallmark features of hepatic ischemia-reperfusion injury, the specific pathways triggering these events and their interrelationship are poorly understood, representing a significant gap in knowledge.
Method: In this study, we established a multi-timepoint mouse model of hepatic ischemia-reperfusion injury. Combined transcriptomic and single-cell RNA sequencing analysis pinpointed macrophage S100A4 as a candidate therapeutic target. To assess the functional contribution of S100A4, a macrophage-specific S100A4 knockout mouse model was subjected to hepatic ischemia-reperfusion injury. Integrated analysis of lactylomics and single-cell RNA sequencing data was performed to investigate the regulatory role of hepatocyte GSTP1 lactylation in mouse hepatic ischemia-reperfusion injury. Furthermore, a macrophage-hepatocyte co-culture system revealed that S100A4-positive macrophages modulate hepatocyte lactylation, leading to alterations in downstream signaling pathways.
Results: This study found that in a mouse model of hepatic ischemia-reperfusion injury, the expression of S100A4 progressively increased with prolonged reperfusion time, peaking at 24 hours. In macrophage-specific S100A4 knockout mice, the inflammatory response, mitochondrial damage, and apoptosis were significantly attenuated following hepatic ischemia-reperfusion injury. Mechanistically, co-culture experiments demonstrated that S100A4-positive macrophages induce this modification by transferring vesicle-encapsulated damaged mitochondria to hepatocytes, induced hepatocyte GSTP1 lactylation. Lactylated GSTP1 in hepatocytes promotes PANoptosis through dual mechanisms: by impairing GSH binding to exacerbate oxidative stress and mtDNA leakage, thereby activating AIM2; and concurrently by disrupting JNK binding to activate the JNK/c-JUN pathway and ZBP1. Promisingly, supplementing healthy mitochondria alleviated this injury cascade.
Conclusion: Macrophage-derived S100A4 promotes hepatocyte injury by vesicular transfer of damaged mitochondria, which induces GSTP1 lactylation, activates the JNK/c-JUN pathway, and causes mtDNA leakage, leading to dual activation of AIM2- and ZBP1-mediated PANoptosis.

Liver tumours – Clinical aspects except therapy

TOP-359-YI
Prospective multicenter evaluation of prototype deep learning algorithms versus liver imaging reporting and data system (LI-RADS) criteria in diagnosing hepatocellular carcinoma on computed tomography

Rex Wan-Hin Hui[1], Keith Wan-Hang Chiu[2], Chenlu Wang[1], Ho Ming Cheng[1], Chengzhi Peng[1], Jian Zhou[3], Jianliang Lu[1], Vivien Wai-Man Tsui[1], Carla Lam[1], Lok-Ka Lam[1], Lung Yi Loey Mak[1], Nam-Hung Chia[2], Tiffany Wong[1], Albert CY Chan[1], Tan-To Cheung[1], Man-Fung Yuen[1], Philip Yu[4], Wai-Kay Seto[1]. [1]*The University of Hong Kong, Pok Fu Lam, Hong Kong;* [2]*Queen Elizabeth Hospital, Yau Ma Tei, Hong Kong;* [3]*Sun Yat-Sen University Cancer Center, Guangzhou, China;* [4]*The Education University of Hong Kong, Ting Kok, Hong Kong*
Email: huirex@connect.hku.hk

Background and aims: Image-based deep learning may enhance the diagnostic accuracy of HCC, however current studies are predominantly cross-sectional and lack prospective evaluation.
Method: We prospectively recruited consecutive at-risk liver disease patients (cirrhosis, Asian male hepatitis B patients ≥40 years old, or Asian female hepatitis B patients ≥50 years old) receiving contrast-enhanced CT scans for either new-onset liver nodules on ultrasonography or unexplained elevation of serum alfa-fetoprotein. We evaluated two deep learning models for diagnosing HCC on computed tomography (CT): Spatio-Temporal 3D Convolution Network (ST3DCN) that was developed specifically for multiphasic CT; and a 3D convolutional block attention module (CBAM) designed for opportunistic screening in noncontrast CT. Diagnostic performance was compared with Liver Imaging Reporting & Data System (LI-RADS) as graded by two specialist radiologists. The ground truth diagnosis of liver nodules was validated via a 12-month composite clinical reference standard based on histological or clinicoradiological criteria.
Results: This study included 301 patients with 468 liver lesions (mean age 65.2, 67.1% male, 39.9% cirrhosis, 25.6% steatosis). 93 patients (30.9%) were diagnosed to have HCC. ST3DCN had significantly better diagnostic performance for HCC than LI-RADS at both lesion level (AUC: ST3DCN 0.902 [95%CI 0.874–0.931] vs LI-RADS 0.798 [95% CI 0.740–0.856], $p < 0.001$) & patient level (AUC ST3DCN 0.862 [95%CI 0.821–0.903] vs LI-RADS 0.804 [95%CI 0.743–0.866], $p = 0.032$). ST3DCN was superior to LI-RADS in patients with liver lesion size <20 mm (Patient level AUC: ST3DCN 0.854 [95%CI 0.780–0.928] vs LI-RADS 0.580 [95%CI 0.416–0.744]), cirrhosis (Patient level AUC: ST3DCN 0.906 [95%CI 0.853–0.960] vs LI-RADS 0.761 [95%CI 0.672–0.849]), or steatosis (Patient level AUC: ST3DCN 0.885 [95%CI 0.809–0.961] vs LI-RADS 0.746 [95%CI 0.611–0.880]) (all $p < 0.05$). The noncontrast CBAM model attained AUC of 0.694 (95%CI 0.628–0.759) for diagnosing HCC, limited by a low positive predictive value of 0.514 (95% CI 0.445–0.582).
Conclusion: Our deep learning algorithm on multiphasic CT had superior diagnostic performance over standard-of-care radiologist interpretation for diagnosing HCC, with most prominent advantage in challenging diagnostic scenarios including smaller lesions, presence of cirrhosis, or steatosis. Image-based deep learning can revolutionize the care of at-risk liver disease patients.

TOP-360

Task-agnostic deep learning for hepatocellular carcinoma: a unified pipeline for tumor differentiation grading, microvascular invasion detection and fibrosis staging

Yan Miao[1], Philip Yu[2], Tak-Siu Wong[3], Regina Cheuk Lam Lo[1], Rex Wan-Hin Hui[1], Ho Ming Cheng[1], Lequan Yu[1], Lung-Yi Mak[1], Man-Fung Yuen[1], Wai-Kay Seto[1]. [1]*The University of Hong Kong, Pok Fu Lam, Hong Kong;* [2]*The Education University of Hong Kong, Ting Kok, Hong Kong;* [3]*Pamela Youde Nethersole Eastern Hospital, Chai Wan, Hong Kong*
Email: wkseto@hku.hk

Background and aims: Hepatocellular carcinoma (HCC) has distinct histological features that are utilized in disease prognostication. Recent advancements in computational pathology, particularly the release of general-purpose foundation models pretrained on large-scale datasets, offer new opportunities for automated diagnosis. We aimed to evaluate the performance of a deep learning framework, which combines a finetuned foundation model with multiple instance learning (MIL) across three HCC histopathological diagnostic tasks: tumor differentiation grading, microvascular invasion (MVI) detection and fibrosis staging.
Method: We used a dataset of digitized whole slide images (WSIs) annotated by clinical experts for the three tasks. Square image patches of size 1024 were extracted and labeled based on their inclusion within tumor, fibrosis, or MVI. We finetuned UNI (a Vision Transformer with 303M parameters, pretrained on > 100,000 WSIs) as a patch feature extractor. Subsequently, we applied TransMIL, a transformer-based MIL feature aggregator, to output slide predictions for each diagnostic task.
Results: The study included 1267 WSIs from 191 patients. For HCC differentiation grading (N = 1,267; Normal: 380, G1: 30, G2: 742, G3: 115), we achieved an Area Under the Curve (AUC) of 0.967 (95%CI: 0.959–0.975), sensitivity of 0.912 (0.904–0.920), specificity of 0.956 (0.955–0.957), positive predictive value (PPV) of 0.781 (0.771–0.791), and negative predictive value (NPV) of 0.949 (0.947–0.951). For MVI prediction (N = 892; Non-MVI: 602, MVI: 290), we achieved an AUC of 0.931 (0.930–0.932), sensitivity of 0.887 (0.884–0.890), specificity of 0.847 (0.845–0.849), PPV of 0.736 (0.732–0.740), and NPV of 0.940 (0.938–0.942). For fibrosis staging (N = 124; F0-F1: 27, F2-F3: 30, F4: 67), we achieved an AUC of 0.971 (0.958–0.984), sensitivity of 0.852 (0.833–0.871), specificity of 0.943 (0.937–0.949), PPV of 0.912 (0.894–0.930), and NPV of 0.952 (0.947–0.957). Overall, the framework consistently achieved AUCs > 0.90, sensitivities > 0.85 and NPVs > 0.93 across all three tasks, demonstrating its robustness in characterizing heterogeneous HCC features.
Conclusion: The integration of foundation models with MIL provides a highly effective and generalizable approach for HCC pathology. Our framework demonstrates superior diagnostic performance across diverse tumor characteristics, including differentiation grading, fibrosis staging, and MVI detection, suggesting significant potential for AI-assisted clinicopathological decision-making.

TOP-374

Refining hepatocellular carcinoma surveillance using liver stiffness-based risk thresholds. A multicentre study

Ryan YanZhe Lim[1], Benjamin Nah[2], Margaret Teng[2,3], Vincent Chen[4], Jimmy Che-To Lai[5], Karn Wijarnpreecha[6], Rahul Kumar[7], Apichat Kaewdech[8], Anand Kulkarni[9], Ming-Hua Zheng[10,11], Akash Roy[12], Ken Liu[13], Won-Mook Choi[14], Chitchai Rattananukrom[15], Cheng Han Ng[2,16,17], Hirokazu Takahashi[18], Mark Muthiah[1,2,19]. [1]*Yong Loo Lin School of Medicine, National University of Singapore, Singapore, Singapore;* [2]*Division of Gastroenterology and Hepatology, Department of Medicine, National University Hospital, Singapore, Singapore;* [3]*Division of Gastroenterology, Department of Medicine, Alexandra Hospital, Singapore, Singapore;* [4]*Division of Gastroenterology and Hepatology, Department of Internal Medicine, University of Michigan Medical School, Ann Arbor, United States;* [5]*Medical Data Analytics Centre, Department of Medicine and Therapeutics, The Chinese University of Hong Kong, Li Ka Shing Institute of Health Sciences and State Key Laboratory of Digestive Disease, The Chinese University of Hong Kong, Hong Kong, Hong Kong;* [6]*Division of Gastroenterology and Hepatology, University of Arizona College of Medicine Phoenix, Phoenix, AZ, United States;* [7]*Department of Gastroenterology and Hepatology, Changi General Hospital, Singapore, Singapore;* [8]*Gastroenterology and Hepatology Unit, Division of Internal Medicine, Faculty of Medicine, Prince of Songkla University, Amphoe Hat Yai, Thailand;* [9]*Department of Hepatology and Liver Transplantation, Asian Institute Of Gastroenterology, Hyderabad, India;* [10]*MAFLD Research Center, Department of Hepatology, the First Affiliated Hospital of Wenzhou Medical University, Wenzhou, China;* [11]*Key Laboratory of Diagnosis and Treatment for The Development of Chronic Liver Disease in Zhejiang Province, Wenzhou, China;* [12]*Department of Gastrosciences and Liver Transplantation, Apollo Multispeciality Hospital, Kolkata, India;* [13]*Department of Gastroenterology, Royal Prince Alfred Hospital, Sydney, Australia;* [14]*Department of Gastroenterology, Liver Center, Asan Medical Center, University of Ulsan College of Medicine, Seoul, Korea, Rep. of South;* [15]*Division of Gastroenterology and Hepatology, Department of Medicine, Faculty of Medicine, Srinagarind Hospital, Khon Kaen University, Khon Kaen, Thailand;* [16]*Division of Gastroenterology, Department of Medicine, Kurume University School of Medicine, Kurume, Japan;* [17]*Visiting Assistant Professor of Graduate School of Medicine, Yokohama City University, Kanagawa, Japan;* [18]*Division of Metabolism and Endocrinology, Faculty of Medicine, Saga University, Saga, Japan;* [19]*National University Centre for Organ Transplantation, National University Health System, Singapore, Singapore*
Email: ryanlimyanzhe21@gmail.com

Background and aims: Liver stiffness measurement (LSM) has been shown to be associated with hepatocellular carcinoma (HCC) risk, yet its role in guiding HCC surveillance remains unclear. We aimed to determine the optimal liver stiffness thresholds for hepatocellular carcinoma surveillance.
Method: We conducted a multicentre longitudinal cohort study across 13 centres comprising 2,568 adults with LSM ≥ 10 kPa. HCC risk was assessed using Cox proportional hazards regression adjusted for age, sex, body mass index and type 2 diabetes mellitus. Absolute 1-year HCC risk was estimated from restricted cubic spline fitted models, and LSM cutoffs corresponding to an annual HCC risk of 0.4% were derived for the overall cohort and etiology-specific subgroups.
Results: Higher liver stiffness measurement (LSM) was associated with an increased risk of HCC in the overall cohort (HR: 1.025 [95% CI: 1.016–1.034]; p < 0.001), with an overall HCC incidence of 2.00 per 100 person-years (95% CI 1.74–2.30). In etiology-specific analyses, LSM was significantly associated with HCC risk in metabolic dysfunction-associated steatotic liver disease (MASLD) (HR: 1.022 [95% CI 1.004–1.041]; p = 0.02) and hepatitis C virus (HCV) (HR: 1.030 [95% CI 1.012–1.047]; p < 0.001), with HCC incidences of 1.38 (95% CI 1.02–1.83) and 3.10 (95% CI 2.47–3.83) per 100 person-years, respectively. No significant association was observed for hepatitis B virus (HBV) (p = 0.50) or alcohol-associated liver disease (ALD) (p = 0.51), although HCC incidence remained substantial (1.98 [95% CI 1.45–2.65]; 2.36 [95% CI 1.32–3.89] per 100 person-years respectively). Using absolute risk–based thresholds, the optimal LSM corresponding to an annual HCC incidence ≥ 0.4% was 16.4 kPa overall, with etiology-specific cutoffs of 12.9 kPa for MASLD, 10.7 kPa for HCV, and 12.2 kPa for ALD. In HBV patients, the predicted 1-year HCC risk exceeded the 0.4% surveillance threshold across the entire observed range of LSM, therefore no discriminative liver stiffness cutoff could be identified.
Conclusion: Liver stiffness-based HCC risk stratification demonstrates substantial heterogeneity across liver disease etiologies. Applying etiology-specific LSM cutoffs aligned with accepted HCC surveillance thresholds may improve precision in identifying patients most likely to benefit from surveillance.

TOP-375-YI

Prognostic impact of neoplastic portal vein thrombosis and extrahepatic metastases in advanced hepatocellular carcinoma receiving Atezolizumab–Bevacizumab: a multicenter real-world study

Filippo Cattazzo[1], Michele Bevilacqua[1], Marco Vicardi[1], Vincenzo Dimaria[1], Massimo Iavarone[2], Giuseppe Cabibbo[3], Fabio Marra[4], Caterina Vivaldi[5], Francesca Romana Ponziani[6], Andrea Palloni[7], Sara Lonardi[8], Lorenzo Lani[9], Piera Federico[10], Gianluca Svegliati-Baroni[11], Tiziana Pressiani[12], Luca Ielasi[13], Chiara Mazzarelli[14], Stefania De Lorenzo[15], Rodolfo Sacco[16], Ciro Celsa[3], Mariangela Bruccoleri[17], Claudia Campani[4], Gianluca Masi[5], Pierluigi Toniutto[18], Rosanna Villani[19], Francesco Tovoli[20], Alessandra Auriemma[21], David Sacerdoti[22], Andrea Dalbeni[1]. *[1]Department of Medicine, Medicine C, University of Verona and Hospital Trust of Verona (Azienda Ospedaliera Universitaria AOUI), Verona, Italy, Verona, Italy; [2]Division of Gastroenterology and Hepatology, Foundation IRCCS Ca' Granda Ospedale Maggiore Policlinico, Milan, Italy, Milan, Italy; [3]Gastroenterology and Hepatology Unit, Department of Health Promotion, Mother & Child Care, Internal Medicine & Medical Specialties,University of Palermo, Palermo, Italy, Palermo, Italy; [4]Internal Medicine and Liver Unit, University Hospital Careggi, University of Florence, Florence, Italy, Florence, Italy; [5]Unit of Medical Oncology 2, Azienda Ospedaliero- Universitaria Pisana, Pisa, Italy, Pisa, Italy; [6]Liver Unit, CEMAD Centro Malattie dell'Apparato Digerente, Medicina Interna e Gastroenterologia, Fondazione Policlinico Universitario Gemelli IRCCS, Rome, Italy, Rome, Italy; [7]Oncology Unit, IRCCS Azienda Ospedaliero-Universitaria di Bologna, Bologna, Italy, Bologna, Italy; [8]Oncology Unit 3, Veneto Institute of Oncology IOV - IRCCS, Padua, Italy, Padua, Italy; [9]Unit of Semeiotics, Liver and Alcohol-related diseases, IRCCS Azienda Ospedaliero-Universitaria di Bologna, Bologna, Italy, Bologna, Italy; [10]Oncology Unit, Ospedale del Mare, Napoli, Italy, Naples, Italy; [11]Liver Injury and Transplant Unit, Azienda Ospedaliero-Universitaria delle Marche, Ancona, Italy, Ancona, Italy; [12]Medical Oncology and Hematology Unit, Humanitas Cancer Center, IRCCS Humanitas Research Hospital, Rozzano (Milan), Italy, Milan, Italy; [13]Department of Internal Medicine, Ospedale Degli Infermi di Faenza, Faenza, Italy, Faenza, Italy; [14]Hepatology and Gastroenterology Unit, ASST Grande Ospedale Metropolitano Niguarda, Milan, Italy, Milan, Italy; [15]Oncology Unit, Azienda USL Bologna, Bologna, Italy, Bologna, Italy; [16]Gastroenterology and Digestive Endoscopy Unit, Foggia University Hospital, Foggia, Italy, Foggia, Italy; [17]Foundation IRCCS Ca' Granda Ospedale Maggiore Policlinico, Division of Gastroenterology and Hepatology, Milan, Italy, Milan, Italy; [18]Hepatology and Liver Transplantation Unit, Azienda Ospedaliero Universitaria, University of Udine, Udine, Italy, Udine, Italy; [19]Department of Medical and Surgical Sciences, University of Foggia; 71122 Foggia, Italy, Foggia, Italy; [20]Department of Medical and Surgical Sciences, University of Bologna, Bologna, Italy, Bologna, Italy; [21]Section of Innovation Biomedicine-Oncology Area, Department of Engineering for Innovation Medicine (DIMI), University of Verona and Verona University and Hospital Trust (AOUI), Verona, Italy, Verona, Italy; [22]Liver Unit, Medicine Department, University of Verona and University and Hospital Trust (AOUI) of Verona, Verona, Italy, Verona, Italy*
Email: andrea.dalbeni@aovr.veneto.it

Background and aims: In advanced hepatocellular carcinoma (HCC), neoplastic portal vein thrombosis (nPVT) and metastases could represent distinct manifestations of tumour burden. However, under first-line atezolizumab–bevacizumab (A + B), the relative prognostic weight of these features remains insufficiently explored. This study aimed to assess how nPVT and metastatic involvement influence clinical outcomes, including early decompensating events (EHD), in patients receiving A + B.

Method: Five hundred and six cirrhotic patients with unresectable HCC treated with first-line A + B within the prospective ARTE dataset were included. Patients were evaluated for the presence of nPVT and extrahepatic metastases. EHD was defined as new-onset ascites, encephalopathy, jaundice, or variceal bleeding within 12 weeks of treatment initiation. Primary endpoints were overall survival (OS), progression-free survival (PFS), and radiological progression.

Results: nPVT was present in 331 patients (59.9%) and metastases in 185 (36.5%). EHD occurred in 53 patients (10.5%) and was strongly associated with nPVT (OR 3.1, 95%CI 1.7–6.4), even after adjustments for baseline liver function (Child-Pugh or ALBI grade), whereas metastases showed no association. Patients who developed EHD experienced markedly worse survival (median OS 8.2 vs 19.6 months, $p < 0.001$) and shorter treatment duration (3.5 months, IQR 1.4–9.8 vs 7.3 months, IQR 3.5–15.2). In multivariable Cox analysis for OS, EHD (HR 1.9, 95%CI 1.3–2.7), ALBI grade≥2 (HR 1.5, 95%CI 1.1–1.9), and AFP≥400 ng/mL (HR 1.5, 95% CI 1.1–1.9) were independent predictors, whereas neither nPVT nor metastases retained significance after adjusting for liver function and EHD.

Conversely, extrahepatic metastases were independently associated with radiological progression (HR 1.5, 95%CI 1.2–1.9) and shorter PFS (HR 1.4, 95%CI 1.1–1.6) while nPVT showed no association.

Conclusion: Among patients treated with A+B, nPVT and metastases appear to influence prognosis through different pathways: nPVT primarily by predisposing to EHD, and metastases mainly by accelerating tumour progression. Once EHD occurs, its impact on survival outweighs that of both vascular invasion and metastatic spread, likely due to the shorter treatment duration observed in this group. These findings suggest that assessing early liver deterioration alongside baseline tumour pattern may improve early risk stratification in advanced HCC and help contextualise the prognostic relevance of nPVT and metastases under A+B therapy.

TOP-376

Hepatocellular carcinoma (HCC) in patients with biopsy proven metabolic dysfunction associated steatotic liver disease (MASLD)

Zobair M. Younossi[1], Daniel Huang[2,3], Atsushi Nakajima[4,5], Claudia Pinto Oliveira[4,6], Salvatore Petta[4,7], Hannes Hagström[4,8], Giada Sebastiani[4,9], George Boon Bee Goh[4,10], Mattias Ekstedt[11], Juan Pablo Arab[4,12], Javier Crespo[4,13], Laurent Castera[4,14], Satoru Kakizaki[4,15], Seung Up Kim[4,16], Vincent Wai-Sun Wong[4,17], Emmanuel Tsochatzis[4,18], Arun Valsan[4,19], Cristiane A. Villela-Nogueira[4,20], George Papatheodoridis[4,21], Sven Francque[4,22], Sombat Treeprasertsuk[4,23], Roberta D'Ambrosio[4,24], Stuart Roberts[4,25], Yusuf Yilmaz[4,26], Shalimar Shalimar[4,27], Wah-Kheong Chan[4,28], Jimmy Che-To Lai[4,17], Eliabe Abreu[4,29], Arsha Aggarwal[3], Leyla de Avila[4,30], Maria Stepanova[4,30]. *[1]The global NASH/MASH council, Washington DC, United States; [2]The Global NASH/MASH Council (GNC), Washington, DC, United States; [3]Department of Medicine, National University of Singapore, Singapore, Singapore; [4]The Global NASH Council (GNC), Washington, DC, United States; [5]Department of Gastroenterology and Hepatology, Yokohama City University Graduate School of Medicine, Yokohama, Japan; [6]Department of Gastroenterology, Faculdade Medicina da Universidade de Sao Paulo, Sao Paulo, Brazil; [7]Section of Gastroenterology, PROMISE Department, University of Palermo, Palermo, Italy; [8]Division of Hepatology, Department of Upper GI Diseases, Karolinska University Hospital, Stockholm, Sweden; [9]Division of Gastroenterology and Hepatology, Department of Medicine, McGill University Health Centre, Montreal, Canada; [10]Department of Gastroenterology & Hepatology, Singapore General Hospital, Singapore, Singapore; [11]Department of Gastroenterology and Hepatology, Department of Health, Medicine, and Caring Sciences, Linköping University, Linköping, Sweden; [12]Stravitz-Sanyal Institute for Liver Disease and Metabolic Health, Division of Gastroenterology, Hepatology, and Nutrition, Department of Internal Medicine, Virginia Commonwealth University School of Medicine, Richmond, United States; [13]Gastroenterology and Hepatology Department, Clinical and Translational Research in Digestive Diseases, Valdecilla Research Institute (IDIVAL), Marques de Valdecilla University Hospital, Santander, Spain; [14]Department of Hepatology, Hospital Beaujon, Assistance Publique-Hôpitaux de Paris, Université Paris-Cité, Paris, France;*

[15]Department of Clinical Research, NHO Takasaki General Medical Center, Takasaki, Japan; [16]Department of Internal Medicine, Yonsei University College of Medicine, Seoul, Korea, Rep. of South; [17]Medical Data Analytics Center, Department of Medicine and Therapeutics, The Chinese University of Hong Kong, Hong Kong, China; [18]University College London Institute for Liver and Digestive Health, Royal Free Hospital, London, United Kingdom; [19]Centre for Metabolic Liver Disease and Integrated Liver Care Unit, Amrita Institute of Medical Sciences, Kerala, India; [20]School of Medicine and Hepatology Division, Universidade Federal, Rio de Janeiro, Brazil; [21]1st Academic Department of Gastroenterology, Medical School of National and Kapodistrian University of Athens, General Hospital of Athens "Laiko", Athens, Greece; [22]Department of Gastroenterology and Hepatology, Antwerp University Hospital, Edegem, Belgium; [23]Division of Gastroenterology, Department of Internal Medicine, Chulalongkorn University, Bangkok, Thailand; [24]Division of Gastroenterology and Hepatology, Foundation IRCCS Ca' Granda Ospedale Maggiore Policlinico, Milan, Italy; [25]Alfred Hospital Gastroenterology Department, Monash University, Melbourne, Australia; [26]Department of Gastroenterology, School of Medicine, Recep Tayyip Erdogan University, Rize, Türkiye; [27]Department of Gastroenterology and Human Nutrition Unit, All India Institute of Medical Sciences, New Delhi, India; [28]Gastroenterology and Hepatology Unit, Department of Medicine, University of Malaya, Kuala Lumpur, Malaysia; [29]MASLD Clinical Research Program at Mayo Clinic, Rochester, United States; [30]Center for Outcomes Research in Liver Disease, Washington, DC, United States
Email: zobair.younossi@cldq.org

Background and aims: MASLD is an important cause of HCC. In a large, international, multi-center study of patients with MASLD, we aimed to characterize MASLD patients with HCC.
Method: The Global MASLD (G-MASLD) project included MASLD patients with liver biopsy, laboratory tests, and follow-up data from 41 countries. For this analysis, patients who had HCC at the time of biopsy or developed HCC in the follow-up were selected. A 4:1 sample of MASLD controls without HCC was randomly selected, matched by enrollment site. Regression models evaluated time-to-HCC, overall mortality, and mortality among patients with HCC.
Results: Out of 11,114 subjects in G-MASLD, n = 124 (1.1%) had HCC [20% with HCC at the time of enrollment and 80% developed HCC after a median (IQR) of 5 (3–10) years of follow-up]. The pooled annualized rate of HCC was 0.2% including 1.2% per year in patients with cirrhosis and 0.1% per year in non-cirrhotics. Compared with controls, HCC patients were older (mean age 62 vs. 52 years, $p < 0.0001$), had more components of metabolic syndrome (obesity 71% vs. 58%, type 2 diabetes 69% vs. 46%, hypertension 71% vs. 51%, all $p < 0.01$) with more advanced fibrosis (F3–F4: 81% vs. 30%) and cirrhosis (48% vs. 8%) ($p < 0.0001$). HCC patients also had higher FIB-4 (mean 3.63 vs. 1.61), liver stiffness measurement (23.4 kPa vs. 12.2 kPa), as well as FAST, Agile 3+/Agile 4 scores (all $p < 0.0001$). Adverse outcomes including all-cause mortality (cumulative during median (IQR) 6 (3–11) years of follow-up: 36% vs. 8%), decompensation (37% vs. 2%), and liver transplantation (9% vs. <1%) were more frequent in HCC (all $p < 0.0001$). In multivariate analysis, older age (aHR (95% CI) = 1.041 (1.020–1.063) per year), having at least 3 components of metabolic syndrome [aHR = 2.02 (1.29–3.16)], fibrosis stage 3 [aHR = 3.50 (1.74–7.04)] or cirrhosis [aHR = 10.23 (5.29–19.77)] (all $p < 0.01$) were independently associated with increased risk of HCC in MASLD. On the other hand, diagnosis of histologic MASH did not independently increase the risk of HCC ($p > 0.05$). In turn, HCC was a strong independent predictor of all-cause mortality [aHR = 2.75 (1.57–4.82)], along with older age [aHR = 1.032 (1.009–1.056) per year] and presence of cirrhosis [aHR = 2.34 (1.14–4.80)](all $p < 0.05$).
Conclusion: MASLD-related HCC occurs in both cirrhotic and non-cirrhotic patients, with higher incidence among those with advanced fibrosis or cirrhosis and those with underlying metabolic abnormalities.

THU-216-YI

Evaluating gastrointestinal bleeding risks and esophagogastroduodenoscopy (EGD) requirement in low-risk hepatocellular carcinoma (HCC) patients undergoing atezolizumab and bevacizumab: interim analysis

Laia Aceituno[1], Nadia Rukavina[1], C Lee[2], Ahmed Elsheaita[1,3], Farah Albader[1], Elena Valenzi[1], Ann T Ma[1], Robert Vanner[4], Erica Tsang[4], Robert Grant[4], Roxana Bucur[1], Jennifer Knox[4], Arndt Vogel[1,4]. [1]Toronto General Hospital, Toronto, Canada; [2]Cancercare Manitoba, Westbank, Canada; [3]Yarmouth Regional Hospital, Yarmouth, Canada; [4]Princess Margaret Cancer Centre, Toronto, Canada
Email: laiaaceituno@gmail.com

Background and aims: Atezolizumab–bevacizumab (AB) is considered first-line treatment in hepatocellular carcinoma (HCC). However, concerns about bevacizumab-related variceal bleeding have led to recommendations for routine pre-AB with esophagogastroduodenoscopy (EGD). According to Baveno VII criteria, non-invasive tools can be used to identify patients with cirrhosis at low risk of varices needing treatment, allowing safe avoidance of screening EGD in those with liver stiffness measurement (LSM) <20 kPa and platelets count (Plt) >150 × 10^9/L. This study aimed to evaluate the safety of BAVENO VII criteria to guide pre-treatment endoscopic screening in patients with HCC receiving AB in a real-world setting.
Method: This is an interim analysis of an ongoing prospective interventional study (REB 23–5915). Adult patients scheduled to receive AB for HCC in a single centre were screened and, if consenting, prospectively stratified into two cohorts: low risk (LR) and intermediate/high risk (IHR) based on Baveno VII criteria. Patients classified as IHR undergo EGD prior to initiating AB treatment.
Results: Of 50 patients included, 35 patients (70%) were classified as IHR and 15 (30%) LR. There were no significant differences in demographical data, HCC size or AFP levels between groups. LSM were significantly higher (9 kPa vs. 27 kPa, $p < 0.001$), and platelets significantly lower in the IHR group (160 × 10^9/L vs. 217 × 10^9/L, $p = 0.021$). In the IHR group, esophageal varices were identified in 11/35 (31%) patients, of which 5 had high-risk stigmata; all were managed according to local standard of care. One patient (2%) in the IHR group developed post-AB variceal bleeding. The patient was BCLC B, Child–Pugh A, and ALBI grade 1. Baseline endoscopy showed portal hypertensive gastropathy without esophageal varices. None of the LR patients experienced any bleeding event. Overall, 22 patients (44%) experienced any adverse events (AE), 19 in the IHR group. Median follow-up was 9.7 months (4.2–16.4), AB was discontinued in 7 patients due to AE and 9 due to progression. There were no treatment-related deaths. 15 patients died during the follow-up, 14 due to diseases progression and 1 due to an intracranial bleed while receiving second-line treatment.
Conclusion: Baveno VII–based non-invasive strategy appears safe for identifying variceal bleeding risk in patients receiving AB and may allow omission of routine endoscopic screening in select low-risk patients.

THU-217-YI

The VETC-associated trabecular subtypes in non-cirrhotic HCC is defined by loss of tumor suppressor and downregulation of ribosomal genes

Khushboo Agrawal[1], Archana Rastogi[1], Varun Suroliya[2], Viniyendra Pamecha[1], Nirupma Trehanpati[1], Shiv Kumar Sarin[1], Gayatri Ramakrishna[1]. [1]Institute of Liver and Biliary Sciences, New Delhi, India; [2]Artemis hospital, Gurugram, Haryana, India
Email: drarchana.suri.rastogi@gmail.com

Background and aims: Vessels Encapsulating Tumor Clusters (VETC) are a distinct angiogenic pattern in which tumor nests are surrounded by endothelial-lined vessels and are linked to metastasis and recurrence. This study aimed to define VETC-associated architectural histotypes in non-cirrhotic HCC (NCHCC) and their genetic and transcriptomic profiles.

Method: NC-HCC specimens (N = 53) were assessed for VETC pattern using CD34 immunohistochemistry and classified as VETC+ or VETC – . Patterns were correlated with p53, β-catenin, EpCAM, CK19, MSI markers, and immune features including $CD8^+$ T cells, PD-1, PD-L1, and CTLA-4. Genomic profiling was conducted via targeted NGS (N = 11, 40-gene panel) and RNA-seq (VETC- N = 3 and VETC+ N = 7).
Results: The VETC+ variants was identified in 20.75% (11/53) of the cohort with intense CD34 staining of endothelial cells encompassing the hepatocytes. VETC occupied over 50% of the total tumor area, distributed across microtrabecular (55%) and macrotrabecular (45%) growth patterns. The cryptogenic etiology (36%), was more prevalent while an equal distribution observed in HBV and NASH-related in VETC+ NCHCC (28% each). VETC+ subjects had younger mean age 55.7 (p = 0.08), larger tumor size >10 cm in (90%), elevated AFP (64%) P = 0.052 and universal EpCAM expression (P = 0.027). Clinically, VETC+ tumors demonstrated high recurrence (64%) and poor overall survival compared to VETC-tumors (OS < 2 years in 64% of cases, P < 0.01). VETC+ phenotype was characterized by frequent p53 nuclear positivity, MSI stable status and an "immune-excluded" or "cold" microenvironment with significantly reduced CD8+ infiltration (P = 0.041). Genomic analysis revealed frequent mutations in *TP53* and *RB1* (~60% each) with absence of TERT mutation. Differentially expressed genes between VETC – (n = 3) and VETC+ (n = 7) tumors showed significant downregulation of ribosomal and translational genes (U1, RNU1,RNVU-1, RPL34, RPL37A, EIF1, RMRP), protein targeting and ER processing genes (ITM2B, SELENOP, CLU), cell adhesion and cytoskeletal regulators (COL18A1, VTN, AHNAK), and immune/complement components (C3, C4B, B2M, SERPINA3). Expression of metabolic genes (APOB, APOA2, ADH1B, FTL) were also reduced.
Conclusion: VETC+ identifies a highly aggressive HCC endotype characterized by the functional dominance of lost tumor-suppressive pathways.This phenotype is driven by a profound transcriptional repression of ribosomal biogenesis and protein processing, alongside a metabolic reprogramming and immune-excluded state.

THU-218

Predicting transcatheter arterial chemoembolization response in hepatocellular carcinoma using a two-stage imaging framework with automated liver segmentation and bidirectional temporal difference modeling

Ting-Feng Hsieh[1], Geng-Hao Bai[2], Cheng-Yu Hsiung[1], Shanq-Jang Ruan[1], Ja-Der Liang[3]. *[1]Department of Electronic and Computer Engineering, National Taiwan University of Science and Technology, Taipei, Taiwan; [2]Department of Internal Medicine, National Taiwan University Hospital, College of Medicine, National Taiwan University, Taipei, Taiwan; [3]Division of Gastroenterology and Hepatology, Department of Internal Medicine, National Taiwan University Hospital, Taipei, Taiwan*
Email: m11202131@mail.ntust.edu.tw

Background and aims: Transarterial chemoembolization (TACE) is the standard therapy for patients with intermediate-stage hepatocellular carcinoma (HCC), and early treatment response is a major determinant of prognosis. However, predicting therapeutic response remains challenging because TACE induces complex volumetric, vascular, and textural changes in both the tumor and surrounding liver parenchyma. Existing models typically rely on pre-treatment features or single-time-point post-treatment imaging, limiting their ability to capture the dynamic temporal evolution following TACE. This study aims to develop a robust two-stage deep learning framework that performs automated liver segmentation in the presence of post-procedural artifacts and utilizes bidirectional temporal difference modeling to predict early treatment response after initial TACE.
Method: A total of 104 unresectable HCC patients receiving TACE as initial therapy were retrospectively analyzed. All patients underwent multi-phase contrast-enhanced CT (CECT) before and after TACE. Treatment response was determined using modified RECIST (mRECIST) criteria on follow-up CT within 1 month. In stage one, we designed a refined segmentation pipeline combining a pre-trained deep learning model with morphology-based seed selection and a Seeded Region Growing (SRG) algorithm to mitigate high-intensity Lipiodol artifacts. In stage two, we developed a Bidirectional Temporal Difference Modeling (BiTDM) network that extracts features from paired pre- and post-TACE scans to generate subtraction-based temporal transition maps for response prediction.
Results: The segmentation framework effectively minimized Lipiodol artifacts, providing accurate regions of interest. For treatment response prediction, the BiTDM framework with a ResNet18 backbone achieved the best performance with an AUC-ROC of 0.802, AUC-PR of 0.783, and accuracy of 0.818. Ablation studies showed that incorporating temporal difference maps significantly outperformed single-phase models and standard concatenation methods, underscoring the importance of modeling pre-to-post-treatment transitions.
Conclusion: The proposed framework overcomes the key technical challenges of automated segmentation in TACE-treated livers and improves prognostic performance compared with static imaging methods. By integrating bidirectional temporal difference modeling, it enables reliable early prediction of treatment response following initial TACE in patients with HCC.

THU-219-YI

The IL-7 rs16906115 single nucleotide polymorphism alters the risk for the development of treatment-related AEs in patients with HCC treated with immunotherapy

Lorenz Balcar[1], Hannah Yang[2], Victoria Berger[1], Joao Gorgulho[3], Chan Kim[2], Abelina Kreuter[1], Jung Sun Kim[2], Katharina Pomej[1], Gae Hoon Jo[2], Anton Klotz[1], Ho Young Lim[2], Dahyeon Son[2], Hwasun Yang[2], Michael Trauner[1], Beodeul Kang[2], Johann von Felden[3], Matthias Pinter[1], Hong Jae Chon[2], Bernhard Scheiner[1]. *[1]Medical University of Vienna, Vienna, Austria; [2]CHA University, Seongnam, Korea, Rep. of South; [3]University Medical Center Hamburg-Eppendorf, Hamburg-Eppendorf, Germany*
Email: lorenz.balcar@meduniwien.ac.at

Background and aims: The interleukin-7 (IL7) rs16906115 single nucleotide polymorphism (SNP) alters B cell-specific IL7 expression. In immune-checkpoint-inhibitor (ICI) treated patients with melanoma, carriers of the minor allele were at increased risk of treatment-related adverse events (trAEs). The importance of this SNP in patients with hepatocellular carcinoma (HCC) undergoing systemic treatment is unknown.
Method: We included HCC patients treated with systemic therapies at three institutions (Vienna/Austria, Hamburg-Eppendorf/Germany, Seongnam/Republic of Korea). SNP-genotyping was performed using real-time PCR systems following the manufacturer's recommendations.
Results: We included 345 patients (male: n = 283, 82.0%) with a median age of 64.1 (IQR: 56.9–71.9) years mainly undergoing atezolizumab/bevacizumab treatment (95.7%). Observed allele frequencies (wild-type/heterozygous/homozygous variants) were: G/G: 60.0%/G/C: 33.0%/C/C: 7.0%. When applying a time-dependent approach to account for treatment-exposure, we found a stepwise increase of the risk of trAE development linked to IL-7 genotype (C/C or C/G vs G/G, hazard ratio [HR]: 1.33 [95% confidence interval (CI): 1.03–1.72], p = 0.027). In total, 19/24 patients (79%) harbouring two minor alleles (C/C) developed trAEs (% grade 1/2/3: 50%/21%/8%) and treatment was stopped due to trAEs in 8%. Analysis of lymphocyte stability over time (baseline vs. day 21 during treatment) did not reveal significant differences in immune cell counts depending on IL7 genotype. Ultimately, patients harbouring the C/C genotype tended to have a worse median overall survival compared to patients harbouring at least one wild-type allele (10.3 [95%CI: 6.7–18.8] vs 16.2 [95%CI: 12.6–18.8] months; p = 0.241).

Conclusion: The IL-7 rs16906115 genotype may help to predict the risk for trAE development and therefore for the selection of patients appropriate for treatment regimen with a higher or lower risk of trAEs.

THU-220

Diagnostic and prognostic performance of non-invasive tests for portal hypertension in patients with advanced chronic liver disease and hepatocellular carcinoma – a Baveno cooperation-endorsed European study

Lorenz Balcar[1], Andres Conthe[2], Manon Allaire[3], Cosmina Sutac[4,5], Víctor Holguín[6], Elton Dajti[7], Lucile Moga[8], Kamela Gjini[9], Alessandra Pivetti[10], Giulia Manni[10], Beatriz Minguez[11,12], Agnes Soriano[11], Ángela Antón[13], Angela Puente[13], Frane Pastrovic[14], Petr Urbanek[15], Matteo Cescon[7], Matteo Serenari[7], Tassos Grammatikopoulos[16], Juan Abraldes[17], Ana M Matilla[2], Georg Semmler[1], Mathias Jachs[1], Monica Pons[11], Michael Trauner[1], Ivica Grgurević[14], Jose Ignacio Fortea[13], Joan Genesca[11], Antonio Colecchia[10], Emmanuel Tsochatzis[9], Pierre-Emmanuel Rautou[8], Bernhard Scheiner[1], Thomas Reiberger[1], Matthias Pinter[1], Joana Ferrer[6], Marco Sanduzzi Zamparelli[6], Bogdan Procopet[4], Annalisa Berzigotti[18], Dominique Thabut[3], Rafael Bañares[2], Mattias Mandorfer[1]. *[1]Medical University of Vienna, Vienna, Austria; [2]Hospital General Universitario Gregorio Marañón, Madrid, Spain; [3]Pitié-Salpêtrière University Hospital, Paris, France; [4]Iuliu Hatieganu University of Medicine and Pharmacy, Cluj-Napoca, Romania; [5]Regional Institute of Gastroenterology and Hepatology "Prof. Dr. Octavian Fodor", Hepatology, Cluj-Napoca, Romania; [6]Hospital Clinic, University of Barcelona, Barcelona, Spain; [7]University of Bologna, Bologna, Italy; [8]AP-HP, Hôpital Beaujon, Clichy, France; [9]Royal Free Hospital and UCL, London, United Kingdom; [10]University Hospital of Modena, Modena, Italy; [11]Vall d'Hebron University Hospital, Barcelona, Spain; [12]Liver Cancer Research Group, Liver Diseases, Vall d'Hebron Institut de Recerca (VHIR), Vall d'Hebron Barcelona Hospital Campus, Barcelona, Spain; [13]Marqués de Valdecilla University Hospital, Santander, Spain; [14]University Hospital Dubrava, Zagreb, Croatia; [15]Military University Hospital Prague, Prague, Czech Republic; [16]King's College Hospital NHS Trust, London, United Kingdom; [17]University of Alberta, Edmonton, Canada; [18]Inselspital, Bern University Hospital, Bern, Switzerland*
Email: lorenz.balcar@meduniwien.ac.at

Background and aims: The diagnostic and prognostic utility of non-invasive tests (NITs) for clinically significant portal hypertension (CSPH) in patients with hepatocellular carcinoma (HCC) remains controversial and robust data on this topic are urgently needed.
Method: We conducted a retrospective Baveno Cooperation-endorsed multicentre European study in patients with HCC who underwent HVPG measurement and NITs (i.e., liver stiffness measurement [LSM] by transient elastography, platelet count [PLT]) from 13 centres. First, the diagnostic performance of CSPH-NITs was evaluated. Second, the prognostic role of NITs for first hepatic decompensation and liver-related death was evaluated by competing risk regression analyses with liver transplantation/non-liver-related death as competing events.
Results: Among 710 patients with compensated advanced chronic liver disease (cACLD, mean age 65 years, 82% male, 31%/44% steatotic/viral), most were BCLC 0/A (75%, B 16%, C 9%). The CSPH prevalence was 41%, the median LSM was 16 kPa (IQR: 11–26), and median HVPG was 8 mmHg (IQR: 6–12). ANTICIPATE ± NASH yielded the highest discriminative ability to detect CSPH (AUC 0.81[95%CI:0.78–0.84]), followed by LSM (AUC 0.77[95%CI:0.74–0.81]), and PLT (AUC 0.76[95% CI:0.72–0.80]). Notably, HCC localisation (right lobe, i.e., potential LSM measurement site involvement, vs. left lobe) did not interfere with CSPH-NITs accuracy. The Baveno VII criteria (LSM<15 kPa & PLT>150 G/L) showed an excellent performance for ruling out CSPH (sensitivity 95.8%, NPV 92.5%), while for ruling in CSPH (>25kPa), performance was modest (specificity 85.7%, PPV 70.4%). ANTICIPATE ± NASH >75% attained a specificity/PPV of 89.3%/74.7%. Additional data on SSM-100 Hz/the NICER model were available in 53 patients (AUC 0.86[95%CI:0.75–0.96]). LSM was independently associated with first decompensation and liver-related death, even after adjusting for relevant baseline characteristics/time-dependent covariables. In time-dependent AUROC analyses, LSM exhibited a numerically higher discriminative ability than HVPG.
Conclusion: ANTICIPATE ± NASH show a good discriminative ability for CSPH in patients with cACLD and HCC. While Baveno VII criteria are capable of ruling-out CSPH, the PPVs of LSM >25 kPa/ANTICIPATE ± NASH >75% were suboptimal, likely owing to the low prevalence of CSPH/pre-test probability in this cohort. LSM is independently associated with liver-related outcomes; its prognostic performance is comparable to HVPG and thus, it may be applied for risk prediction.

THU-221

Blood- and liver stiffness-based noninvasive tests for clinically significant portal hypertension in patients with compensated advanced chronic liver disease and hepatocellular carcinoma

Lorenz Balcar[1], Tina Jasmin Haunold[1], Mathias Jachs[1], Georg Semmler[1], Benedikt Simbrunner[1], Albert Friedrich Stättermayer[1], Christoph Schwarz[1], Stefan Stremitzer[1], Klaus Kaczirek[1], Patrick Starlinger[2], Michael Trauner[1], Bernhard Scheiner[1], Thomas Reiberger[1], Matthias Pinter[1], Mattias Mandorfer[1]. *[1]Medical University of Vienna, Vienna, Austria; [2]Mayo Clinic, Rochester, United States*
Email: lorenz.balcar@meduniwien.ac.at

Background and aims: The applicability of non-invasive tests (NITs) for clinically significant portal hypertension (CSPH) in patients with hepatocellular carcinoma (HCC) is controversial. We performed a head-to-head comparison of the discriminative abilities of various NITs for CSPH and evaluated rule-in/-out criteria in patients with HCC.
Method: We conducted a retrospective study including 283 patients with HCC undergoing HVPG measurement at the Vienna Hepatic Haemodynamic Lab with available data on NITs (i.e., liver stiffness measurement [LSM], platelet count [PLT], von Willebrand factor antigen [VWF:Ag], and the ratio of VWF:Ag and PLT [VITRO]). For the subsequent analysis, we focused on patients with compensated advanced chronic liver disease (cACLD).
Results: Among 164 patients with cACLD (mean age 66 years, 86.0% male, mainly alcohol/viral aetiology), most were BCLC 0/A (50.6%). The CSPH prevalence was 46.3%, the median LSM was 20.0 kPa (IQR: 13.3–37.9), and mean VWF:Ag/VITRO were 266 ± 119%/2.30 ± 1.81. The VITRO score yielded the highest discriminative ability to detect CSPH (AUROC 0.834 [95%CI: 0.772–0.896]), followed by ANTICIPATE ± NASH (AUROC 0.822 [95%CI: 0.756–0.887]), PLT (AUROC 0.803 [95% CI: 0.734–0.871]), LSM (AUROC 0.779 [95%CI: 0.705–0.852]) and VWF:Ag (AUROC 0.707 [95%CI: 0.628–0.785]).
The application of the Baveno VII criterium (LSM<15 kPa & PLT>150 G/L) and the VITRO score (≤1.0) individually showed an excellent performance for ruling out CSPH (sensitivities ≥95%, NPV 100%/87.9%). For ruling in CSPH by individual criteria, the VITRO score provided the highest PPV (≥2.5, specificity/PPV 89.8%/83.0%), followed by the Baveno VII criteria (≥25 kPa; specificity/PPV 81.8%/74.6%). When sequentially applying Baveno VII criteria and VITRO, the grey zone could be significantly reduced to 11% (sensitivity/NPV 94.7%/92.2%; specificity/PPV 73.9%/84.4%), at the cost of reduced PPV/specificity due to the reliance on the Baveno VII rule in criteria. HCC characteristics did not seem to interfere with CSPH-NITs.
Conclusion: The discriminative ability in cACLD patients with HCC was comparable to patients without HCC. However, PPVs of established criteria were <90%, which may be explained by the comparatively low prevalence of CSPH in this context.

THU-225-YI

Impact of sarcopenic obesity and myosteatosis on postoperative outcomes after hepatectomy in intrahepatic cholangiocarcinoma

Zhiyuan Bo[1], Xinyan Feng[2], Zhengxiao Zhao[3], Fang Wan[1], Fangfang Chen[1], Jingpei Long[1]. [1]*Women's Hospital School of Medicine Zhejiang University, Hangzhou, China;* [2]*Wenzhou Medical University, Wenzhou, China;* [3]*the First Affiliated Hospital of Zhejiang Chinese Medical University, Hangzhou, China*
Email: longjp@zju.edu.cn

Background and aims: Muscular abnormality is frequently associated with poor prognosis in intrahepatic cholangiocarcinoma (ICC), but the impact of sarcopenic obesity and myosteatosis on ICC are still unclear. We aimed to perform a retrospective multicenter cohort study to evaluate the impact of sarcopenic obesity and myosteatosis on patients with ICC undergoing hepatectomy.
Method: A total of 506 patients with ICC undergoing hepatectomy at four institutions were retrospectively reviewed. Sarcopenic obesity and myosteatosis were measured by preoperative computed tomography (CT) images. The impact of sarcopenic obesity and myosteatosis on the prognosis was evaluated, and cox regression analyses were performed to identify risk factors. Nomograms were developed to facilitate the risk prediction of survival, and the predictive performance was verified in validation cohort.
Results: 369 patients were included in final analysis, including 265 in training cohort and 104 in validation cohort. Among them, 206 patients (55.8%) had myosteatosis, 104 patients (28.2%) had sarcopenic obesity, and 64 patients (17.3%) had coexistence of sarcopenic obesity and myosteatosis. Patients with sarcopenic obesity or myosteatosis experienced a worse prognosis than patients without muscular abnormality. The overall 1-year survival rate and 90-day mortality rate were 65.9% and 4.61%. Low tumor differentiation ($P = 0.003$), lymphatic metastasis ($P < 0.001$), CA19–9 > 37 U/ml ($P = 0.016$), lower albumin level ($P = 0.006$), sarcopenic obesity ($P < 0.001$) and myosteatosis ($P < 0.001$) were independent risk factors of OS, while low tumor differentiation ($P = 0.015$), TNM stage III–IV ($P < 0.001$), sarcopenic obesity ($P < 0.001$) and myosteatosis ($P = 0.012$) were independent risk factors of RFS. Nomograms were developed to predict survival outcomes in training cohort, with AUCs of 0.718–0.799 and 0.680–0.798 for predicting OS and RFS. The performance was verified in validation cohort, with AUCs of 0.789–0.885 and 0.746–0.895 for predicting OS and RFS.
Conclusion: Sarcopenic obesity and myosteatosis negatively impact the prognosis of ICC, and valuable body composition-based nomograms were developed for clinical usefulness.

THU-226-YI

Long-term survival and cure fraction in advanced hepatocellular carcinoma under immunotherapy in randomized controlled trials and real-world data

Claudia Campani[1], Ju Hyun Shim[2], Mohamed Bouattour[3], Yann Touchefeu[4], Victoria Delhoume[4], Olivier Rosmorduc[5], Alina Pascale[5], Jihyun An[6], Han Chu Lee[2], Hélène Regnault[7], Dominique Thabut[8], Giuliana Amaddeo[7], Massih Ningarhari[9], Isabelle Ollivier-Hourmand[10], Chloe Metivier[10], Maxime Ronot[11], Line Carolle Ntandja Wandji[9], Violaine Ozenne[12], Sabrina Sidali[1], Fabio Marra[13], Clemence Hollande[3], Nathalie Ganne-Carrié[14], Pierre Nahon[14], Jean Marie Peron[15], Marie Lequoy[12], Rohini Sharma[16], Paris Liver Cancer Group[17], Manon Allaire[8], Jean Charles Nault[1]. [1]*Centre de Recherche des Cordeliers, Sorbonne Université, Inserm, Université de Paris, team "Functional Genomics of Solid Tumors", F-75006 Paris, France, Paris, France;* [2]*Asan Liver Center, Asan Medical Center, University of Ulsan College of Medicine, Seoul, South Korea, Seoul, Korea, Rep. of South;* [3]*AP-HP, Hôpital Beaujon, Liver Cancer and Innovative Therapy, CLICHY, France;* [4]*Hepato-gastroenterology Department, Nantes University Hospital, Nantes, Institut des Maladies de l'Appareil Digestif (IMAD), Inserm CIC; 1413 Nantes, France, Nantes, France;* [5]*Centre Hépato-Biliaire, Paul-Brousse Hospital, Assistance Publique-Hôpitaux de Paris, Villejuif, France, Faculté de Médecine, Paris-Saclay University, Le Kremlin-Bicêtre, France, Unité Mixte de Recherche 1193, Paris-Saclay University, INSERM, Villejuif, France, Villejuif, France;* [6]*Gastroenterology and Hepatology, Hanyang University College of Medicine, Guri, South Korea, Guri, Korea, Rep. of South;* [7]*Service d'Hépatologie, AP-HP Henri Mondor, Créteil, France, Creteil, France;* [8]*Hepatogastroenterology Department, La Pitié-Salpêtrière Hospital, AP-HP, Sorbonne Université, Paris, France, Paris, France;* [9]*Hôpital Claude Huriez, CHU Lille, et université de Lille, Lille France, Lille, France;* [10]*Service d'hépato-gastroentérologie, CHU de Caen, ERN RARE-LIVER, France, Caen, France;* [11]*Department of Radiology, Hôpital Beaujon, AP-HP.Nord, 100 Boulevard du Général Leclerc, 92110 Clichy, Clichy, France;* [12]*Service d'Hépatologie, AP-HP Saint-Antoine, France, Paris, France;* [13]*Department of Experimental and Clinical Medicine, Internal Medicine and Hepatology Unit, University of Firenze, Florence, Italy, Florence, Italy;* [14]*Service d'Hépatologie, AP-HP Avicenne, France, Bobigny, France;* [15]*Service D'hépatologie, Hôpital Rangueil, CHU Toulouse, Toulouse, France, Toulouse, France;* [16]*Department of Surgery & Cancer, Imperial College London, Hammersmith Hospital, Du Cane Road, London W12 0HS, UK, London, United Kingdom;* [17]*Paris, Paris, France*
Email: claudiacampani.cc@gmail.com

Background and aims: Immune checkpoint inhibitors (ICIs) can induce long-term survival and even cure in several cancers, but this has not been formally quantified in advanced hepatocellular carcinoma (HCC). We applied mixture cure models (MCMs) to phase 3 trials and real-world data to estimate the fractions of long-term survivors and cured patients.
Method: Phase 3 first-line ICI trials in advanced HCC with mature follow-up (≥30 months) were identified, and individual patient data were reconstructed from published Kaplan–Meier curves (HIMALAYA, CheckMate-9DW, RATIONALE-301). In parallel, we analysed an international multicentre cohort of 1,581 patients with unresectable HCC treated with atezolizumab–bevacizumab in routine practice. MCMs were fitted separately for each treatment arm for overall survival (OS, long-term survivors) and progression-free survival (PFS, cure), using Weibull latency when appropriate, and were compared with background cirrhosis-related mortality. Prognostic factors for long-term survival and cure were explored.
Results: In HIMALAYA, the long-term survivor fraction was 12.8% (95%CI 8.5–18.6) with durvalumab-tremelimumab versus 5.2% (2.6–10.2) with sorafenib. In CheckMate-9DW, cure modelling suggested higher long-term survival and PFS plateaus with nivolumab-ipilimumab than with sorafenib/lenvatinib, although tail estimates were imprecise. In RATIONALE-301, long-term survival reached 25.2% versus 15.4% and cure 14.7% versus 8.7% with tislelizumab and sorafenib, respectively. In the real-world atezolizumab–bevacizumab cohort including 1581 patients (median follow-up 34.7 months), long-term survival was 12.3% (9.3–16.1) and cure 7.9% (6.3–9.8); in 1,187 patients fulfilling IMbrave150 criteria, these estimates rose to 15.4% and 9.1%. Hazards among long-term survivors approached cirrhosis-related background mortality. ALBI grade and hepatitis C independently predicted both long-term survival and cure.
Conclusion: Across trials and real-world data, ICI-based therapies yield long-term survival in roughly 10–15% of advanced HCC patients and cure in 7–9%. MCMs provide a clinically meaningful framework to quantify durable benefit and highlight the need for biomarkers and optimal cirrhosis management in long-term survivors.

THU-227-YI

Predicting decompensation in unresectable hepatocellular carcinoma on immunotherapy: the ARTE score

Lorenzo Canova[1], Eleonora Alimenti[2,3], Lorenzo Argiento[2], Francesco Tovoli[4,5], Giuseppe Cabibbo[6], Emanuela Di Giacomo[7], Peter R. Galle[8], Ciro Celsa[6], Matthias Pinter[9], Thomas Marron[10], Caterina Vivaldi[11], Andrea Dalbeni[12,13], Fabio Marra[14,15], Andrea Palloni[16], Sara Lonardi[17], Francesca Romana Ponziani[18,19], Piera Federico[20], Anwaar Saeed[21], Anjana Pillai[22], Tiziana Pressiani[23],

Silvia Camera[24], Gianluca Svegliati-Baroni[25], Giulia Francesca Manfredi[26], Lorenzo Lani[27], Johann von Felden[28], Susanna V. Ulahannan[29], Luca Ielasi[30], Stefania De Lorenzo[31], Chiara Mazzarelli[32], Rodolfo Sacco[33], Natascha Röhlen[34], Marianna Silletta[35], Pierluigi Toniutto[36], Sara Ascari[4], Claudia Fulgenzi[7], Bernhard Scheiner[9], Fionnuala Crowley[10], Federica Cerini[1,37], Pietro Lampertico[2,3], David J. Pinato[7,38], Massimo Iavarone[2,3]. *[1]Division of Hepatology, San Giuseppe Hospital, IRCCS MultiMedica, Milan, Italy; [2]Division of Gastroenterology and Hepatology, Foundation IRCCS Ca' Granda Ospedale Maggiore Policlinico, Milan, Italy; [3]CRC "A. M. and A. Migliavacca" Center for Liver Disease, Department of Pathophysiology and Transplantation, University of Milan, Milan, Italy; [4]Department of Medical and Surgical Sciences, University of Bologna, Bologna, Italy; [5]Unit of Internal Medicine, Hepatobiliary and Immunoallergic Diseases, IRCCS Azienda Ospedaliero-Universitaria di Bologna, Bologna, Italy; [6]Gastroenterology and Hepatology Unit, Department of Health Promotion, Mother & Child Care, Internal Medi-cine & Medical Specialties, University of Palermo, Palermo, Italy; [7]Department of Surgery & Cancer, Imperial College London, Hammersmith Hospital, Du Cane Road, London, United Kingdom; [8]University Medical Center Mainz, I. Dept. of Internal Medicine, Mainz, Germany; [9]Division of Gastroenterology & Hepatology, Department of Medicine III, Medical University of Vienna, Vienna, Austria; [10]Department of Medicine, Division of Hematology/Oncology, Tisch Cancer Institute, Mount Sinai Hospital, New York (NY), United States; [11]Unit of Medical Oncology 2, Azienda Ospedaliero- Universitaria Pisana, Pisa, Italy; [12]Unit of General Medicine C, Medicine Department, University of Verona and University and Hospital Trust (AOUI) of Verona, Verona, Italy; [13]Liver Unit, Medicine Department, University of Verona and University and Hospital Trust (AOUI) of Verona, Verona, Italy; [14]Internal Medicine and Liver Unit, University Hospital Careggi, University of Florence, Florence, Italy; [15]Department of Experimental and Clinical Medicine, University of Florence, Florence, Italy; [16]Medical Oncology, IRCCS Azienda Ospedaliero-Universitaria di Bologna, Bologna, Italy; [17]Oncology Unit 3, Veneto Institute of Oncology IOV - IRCCS, Padua, Italy; [18]Liver Unit, CEMAD Centro Malattie dell'Apparato Digerente, Medicina Interna e Gastroenterologia, Fondazione Policlinico Universitario Gemelli IRCCS, Rome, Italy; [19]Dipartimento di Medicina e Chirurgia Traslazionale, Università Cattolica del Sacro Cuore, Rome, Italy; [20]Oncology Unit, Ospedale del Mare, Napoli, Italy; [21]Department of Medicine, Division of Hematology & Oncology, University of Pittsburgh Medical Center, Pittsburgh (PA), United States; [22]Department of Internal Medicine, University of Chicago, Chicago (IL), United States; [23]Humanitas Cancer Center, IRCCS Humanitas Research Hospital, Via Manzoni 56, 20089, Rozzano, Milan, Italy; [24]IRCCS San Raffaele Hospital, Milan, Italy; [25]Liver Injury and Transplant Unit, Polytechnic University of Marche, Ancona, Italy; [26]Department of Translational Medicine, Università del Piemonte Orientale, Novara, Italy; [27]Unit of Semeiotics, Liver and Alcohol-related diseases, IRCCS Azienda Ospedaliero-Universitaria di Bologna, Bologna, Italy; [28]Medical Department, University Medical Center Hamburg-Eppendorf, Hamburg, Germany; [29]Oklahoma TSET Phase 1 Program The University of Oklahoma Health Campus, Oklahoma City, United States; [30]Department of Internal Medicine, Ospedale Degli Infermi di Faenza, Faenza, Italy; [31]Oncology Unit, Azienda USL Bologna, Bologna, Italy; [32]Hepatology and Gastroenterology Unit, ASST Grande Ospedale Metropolitano Niguarda, Milan, Italy; [33]Gastroenterology and Digestive Endoscopy Unit, Foggia University Hospital, Foggia, Italy; [34]Department of Medicine II, Medical Center University of Freiburg, Freiburg, Germany; [35]Operative Research Unit of Medical Oncology, Fondazione Policlinico Universitario Campus Bio-Medico, Rome, Italy; [36]Hepatology and liver transplantation unit, Azienda Ospedaliero Universitaria Integrata, University of Udine, Udine, Italy; [37]Department of Clinical Sciences and Community Health, University of Milan, Milan, Italy; [38]Division of Oncology, Department of Translational Medicine, University of Piemonte Orientale, Novara, Italy*
Email: lorenzo.canova@multimedica.it

Background and aims: Hepatic decompensation is a major event in patients with unresectable hepatocellular carcinoma (uHCC) treated with systemic therapy. Early identification of high-risk patients is essential. Aim of the study was to develop a simple score to predict decompensation in patients treated with atezolizumab plus bevacizumab (AB).
Method: This study enrolled 453 uHCC patients from the ARTE database (AB first-line, Child-Pugh A). External validation cohort included 292 patients from the AB-real database. Independent predictors derived from Cox regression were combined into a weighted score and operationalized as a point-based algorithm. Patients were then stratified into low, intermediate, and high-risk groups.
Results: In the ARTE database, 74 (16.3%) patients developed hepatic decompensation (median follow-up 14 months). Neoplastic portal vein thrombosis (HR 1.97, 95%CI 1.20–3.23, p = 0.007), elevated bilirubin (HR 2.61, 95%CI 1.52–4.47, p < 0.001), and low platelets (HR 1.82, 95%CI 1.07–3.10, p = 0.026) were independent predictors and they were incorporated into the ARTE-score. Patients were categorized as low (0–1 points, n = 360), intermediate (2 points, n = 49), or high risk (3–4 points, n = 44). Intermediate-risk patients had a 1.96-fold decompensation risk (p = 0.038) and high-risk patients a 4.28-fold risk (p < 0.001), compared to low-risk. Significant separation of decompensation-free survival across groups was observed (p < 0.001), with good discrimination (Harrell's C = 0.7022). Decompensation-free survival at 12 and 24 months was 87% and 83% for low-risk, 79% and 64% for intermediate-risk, and 57% and 56% for high-risk, respectively. The ARTE-score retained prognostic value in the AB-real cohort (HR 1.78, p = 0.009).
Conclusion: The ARTE score is an easy-to-use tool to predict hepatic decompensation in uHCC, aiding clinical decision-making.

THU-228

Liver and spleen MRI changes as predictors of hepatocellular carcinoma in patients with HCV-related cirrhosis and undefined liver nodules after DAA therapy

Luisa Cavalletto[1], Giovanna Lorigiola[1], Camillo Aliberti[2], Chiara Giraudo[3], Riccardo Carandina[4], Umberto Cillo[5], Liliana Chemello[1]. *[1]Dept. of Medicine-DIMED, University-Hospital, Padova, Italy; [2]Pederzoli Hospital, Verona, Italy; [3]Dept. of cardiotoracovascolar sciences and public health, Padova, Italy; [4]Dept DIDAS integrated diagnostic service, Padova, Italy; [5]Dept. of surgical, oncological and gastroenterological sciences - DiSCOG, Padova, Italy*
Email: luisa.cavalletto@unipd.it

Background and aims: Comprehensive data on incidence and significance of HCC development after direct-acting antiviral (DAA) for chronic hepatitis C remain limited. The drastic drop in viremia, resulting in immune system paralysis, could expose dysplastic hepatocytes to the action of endothelial growth factors. Our objectives were to characterize liver remodeling in patients with advanced fibrosis or cirrhosis with undefined/non-malignant liver nodules (ULNs) and to verify if liver and spleen parenchymal changes, using dynamic contrast-enhanced magnetic resonance imaging (DCE-MRI), could be related to the early onset of HCC.
Method: Among 197 consecutively DAA treated, 57 patients (56.6 ± 10.6 years; 56% male) with ULNs, including 9, 11, and 37 with fibrosis stages F3, F4/CPT-A, and F4/CPT-B, were prospectively studied with DCE-MRI at baseline and 6–12 months after discontinuation of therapy. Two blinded radiologists independently analyzed 1710 images using a series of liver parameters (right and left inter lobe in the sagittal, coronal, and transverse planes measures), the porta vein and spleen diameter, and parenchymal homogeneity. All patients also underwent standard serum laboratory tests and liver (LSM) and spleen (SSM) stiffness by vibration-controlled transient elastography (VCTE). All obtained variables were compared using paired t-test and ANOVA for repeated measures.

Results: Seventeen patients (30%) developed HCC during follow-up. In this group, no significant changes were observed in DCE-MRI liver-based parameters, except for a significant increase in spleen size ($p < 0.05$). Conversely, the 40 patients who did not develop HCC showed a significant increase in all liver-based parameters at post-treatment imaging compared with baseline ($p < 0.05$). A reduction in LSM greater than 20% was observed exclusively in patients without HCC ($p < 0.01$). In contrast, patients who developed HCC exhibited increased SSM and a significant loss of parenchymal homogeneity compared with baseline ($p < 0.01$). Post-treatment biochemical profiles in patients with HCC showed significantly higher levels of gamma-globulins, alpha-2 macroglobulin, alpha-fetoprotein, and squamous cell carcinoma antigen (SCCA)-IgM compared with baseline ($p < 0.05$).
Conclusion: Spleen enlargement, increased SSM, and reduced parenchymal homogeneity were associated with HCC development after DAA therapy.These findings suggest a key role of worsening portal hypertension in hepatocarcinogenesis and support tailored MRI surveillance in high-risk patients.

THU-229
A dynamic model incorporating longitudinal alpha-fetoprotein and globulin trajectories to predict early recurrence in early-stage hepatocellular carcinoma

Minghui Zhu[1], Huanhuan Cao[1,2], Yujie Ran[1], Ning Yu[1], Songmei He[2], Jinzhang Chen[1], Huaiyu Chen[1], Dingli Liu[1], Kunyuan Wang[1], Hongyan Liu[1], Yabing Guo[1], Rong Fan[1]. *[1]Department of Infectious Diseases, Nanfang Hospital, Southern Medical University, Guangzhou, China; [2]Department of Infectious Diseases, Dongguan People's Hospital, The Tenth Affiliated Hospital of Southern Medical University, Southern Medical University, Dongguan, China*
Email: rongfansmu@163.com

Background and aims: Hepatocellular carcinoma (HCC) remains a leading contributor to cancer-related mortality worldwide. While ablation and surgery is a mainstay curative treatment for early-stage HCC, high postoperative recurrence rates—particularly early recurrence within 2 years—significantly undermine long-term survival. We aimed to develop and validate a recurrence risk prediction model integrating longitudinal clinical data to optimize postoperative management and improve the prediction of early recurrence.
Method: In this multicenter study, 760 patients with early-stage HCC were enrolled and divided into a training cohort (N = 342), an external ablation validation cohort (N = 132), and a surgical resection validation cohort (N = 286). In the training cohort, latent class mixed models (LCMM) identified longitudinal trajectory patterns of alpha-fetoprotein (AFP) and globulin (GLB). Optimal thresholds, defined as the 95th percentile of longitudinal biomarker levels during follow-up within the low-stable group, were utilized to categorize patients in the validation cohorts. These identified trajectory features were integrated with baseline clinical variables to develop the Trajectory-integrated AFP and GLB-Clinical (TAG-C) model.
Results: Across the training, external ablation, and surgical cohorts, 2-year recurrence rates were 37.7% (129/342), 36.4% (48/132), and 23.1% (66/286), respectively. The majority of patients had hepatitis B virus etiology (ranging from 89.8% to 92.4% across cohorts) and were in Barcelona Clinic Liver Cancer (BCLC) stage 0 or A. The TAG-C model, incorporating AFP trajectory class, tumor size, GLB trajectory class, fibrinogen, and tumor number, demonstrated robust performance. Specifically, 2-year AUCs were 0.775 (95% CI 0.718 to 0.832) in training, 0.784 (95% CI 0.698 to 0.870) in external ablation, and 0.800 (95% CI 0.733 to 0.867) in surgical cohorts. Kaplan-Meier analysis confirmed distinct risk stratification across all cohorts ($p < 0.0001$), with high-risk groups exhibiting significantly increased recurrence risk compared to low-risk groups (Training: HR 7.17, 95% CI 4.78 to 10.75; External ablation: HR 6.11, 95% CI 3.16 to 11.82; Surgical: HR 5.15, 95% CI 3.03 to 8.77).
Conclusion: The TAG-C model, integrating longitudinal AFP and GLB trajectories, reliably predicts early recurrence, facilitating personalized surveillance and management for patients with early-stage HCC after curative treatment.

THU-231
Prognostic impact of geriatric nutritional risk index (GNRI) in patients with BCLC stage 0 hepatocellular carcinoma

Li-Chang Chen[1], Chun-Ting Ho[1], Pei-Chang Lee[1,2], Yi-Hsiang Huang[1,2,3], Ming-Chih Hou[1,2], Jaw-Ching Wu[3], Chien-Wei Su[1,2,3,4]. *[1]Division of Gastroenterology and Hepatology, Department of Medicine, Taipei Veterans General Hospital, Taipei, Taiwan; [2]School of Medicine, College of Medicine, National Yang Ming Chiao Tung University, Taipei, Taiwan; [3]Institute of Clinical Medicine, School of Medicine, National Yang Ming Chiao Tung University, Taipei, Taiwan; [4]Division of General Medicine, Department of Medicine, Taipei Veterans General Hospital, Taipei, Taiwan*
Email: cwsu2@vghtpe.gov.tw

Background and aims: Nutritional status had been recognized as an increasingly important prognostic factor for hepatocellular carcinoma (HCC), but its significance in very early–stage disease remains unclear. The geriatric nutritional risk index (GNRI), calculated using serum albumin and ideal body weight, is a simple and noninvasive marker of nutritional status. This study evaluated the prognostic impact of malnutrition assessed by GNRI on overall survival (OS) in HCC patients with Barcelona Clinic Liver Cancer (BCLC) stage 0.
Method: This retrospective cohort study included 461 consecutive patients diagnosed with BCLC stage 0 HCC at Taipei Veterans General Hospital between January 2012 and July 2024. GNRI was calculated at diagnosis, and patients were classified into high- and low-GNRI groups using an optimal cutoff value of 103 determined by the Youden index for OS. Baseline characteristics were compared between groups. OS was analyzed using the Kaplan–Meier method with log-rank testing, and Cox proportional hazards regression were utilized to identify independent predictors of OS.
Results: Among the 461 patients, 312 (67.7%) had high GNRI and 149 (32.3%) had low GNRI. Patients with low GNRI were older, more often male, less likely to receive curative treatment, and had worse liver functional reserve, while tumor characteristics and viral etiology were similar between groups. After a median follow-up of 37 months (interquartile range: 19–70), 97 patients died, with a 5-year OS of 73.6%. OS was significantly lower in the low-GNRI group than in the high-GNRI group (61.3% vs. 80.4%, $p < 0.001$). In multivariable analysis, low GNRI (hazard ratio [HR] 1.99, 95% confidence interval [CI] 1.32–2.99, $p = 0.001$), lower platelet count (HR 2.97, 95% CI 1.78–4.94, $p < 0.001$), and elevated serum creatinine (HR 2.62, 95% CI 1.72–3.99, $p < 0.001$) were independently associated with increased mortality, whereas hepatitis B surface antigen positivity was associated with improved survival. Subgroup analyses showed that GNRI had better prognostic value in younger patients aged ≤ 65 years ($p < 0.001$).
Conclusion: Malnutrition, assessed by baseline GNRI, is a strong predictor for OS in patients with very early–stage HCC, particularly among younger individuals, with potential to serve as a practical tool for risk stratification.

THU-232
Diagnostic, screening, and longitudinal performance of des-gamma-carboxy prothrombin as a biomarker for hepatocellular carcinoma

Mateo Chvatal-Medina[1,2], Anneke Muller-Kobold[3], Xinlin Zheng[4], Han Moshage[1,5], Ruben de Kleine[6], Simeon Ruiter[6], Frederike van Vilsteren[1]. *[1]Department of Gastroenterology and Hepatology, University Medical Center Groningen, University of Groningen, P.O. Box 30.001, 9700 RB Groningen, The Netherlands., Groningen, Netherlands; [2]Grupo Gastrohepatología, Facultad de Medicina, Universidad de Antioquia, 050010, Medellín, Colombia,*

Medellín, Colombia; [3]Department of Laboratory Medicine, University of Groningen, University Medical Center Groningen, Groningen, the Netherlands, Groningen, Netherlands; [4]Department of Nuclear Medicine and Molecular Imaging, University of Groningen, University Medical Center Groningen, Groningen, the Netherlands, Groningen, Netherlands; [5]Grupo Gastrohepatología, Facultad de Medicina, Universidad de Antioquia, UdeA, Calle 70 # 52-21, Medellin 050010, Colombia, Medellín, Colombia; [6]Department of Surgery, Section of Hepatobiliary Surgery and Liver Transplantation, University of Groningen, University Medical Center Groningen, Groningen, The Netherlands, Groningen, Netherlands
Email: m.chvatal-medina@umcg.nl

Background and aims: Early detection of hepatocellular carcinoma (HCC) is still challenging, as ultrasound has limited sensitivity and alpha-fetoprotein (AFP) has modest discrimination. Des-gamma-carboxy-prothrombin (DCP/PIVKA-II) is a promising biomarker but its incremental value for diagnosis, screening, and longitudinal risk assessment is incompletely defined, particularly in Western populations.
Method: We established a single center cohort from January 2017, consisting of patients who underwent surveillance according to EASL guidelines; as well as patients in whom HCC was suspected. Ultrasound, AFP, and DCP were measured every six months in at-risk patients; CT and/or MRI was used to confirm the diagnosis of HCC. Patients on vitamin K antagonists were excluded. For diagnostic analyses, we used samples within −90 to +45 days relative to the date of HCC-defining imaging; for non-HCC patients, the last available measurement was used.
Results: Among 2,769 patients at risk or suspicion of HCC, 82.8% belonged to the surveillance group and 17.2% to the suspicion group. Mean age was 59.0 ± 15.7 years and 56.4% were male. Among 1830 patients with chronic liver disease (CLD), 75.4% had cirrhosis, and the most frequent etiologies of CLD were metabolic-associated steatotic liver disease (22.9%), viral hepatitis (19.5%), and alcohol-associated liver disease (17.8%). 746 patients were diagnosed with HCC, 377 of them had DCP measurements within −90 to +45 days and were compared with 2,095 non-HCC controls (n = 2,472). AFP alone yielded an AUC of 0.76 (95% CI 0.73–0.79), DCP alone 0.80 (0.77–0.82), and the combined model 0.85 (0.83–0.87; $p < 0.001$ vs AFP). At 90% specificity, sensitivity increased from 47.7% for AFP to 56.9% for the combined model. For screening, 158 HCC patients had DCP measured ≤6 months before diagnosis; the combined model identified 81.9% of future HCC cases, while DCP alone detected 31.0% and AFP 7.7%. Longitudinal analyses in 97 HCC patients with ≥2 pre-diagnostic DCP measurements (median 3; median follow-up 321 days) showed a significant pre-diagnostic increase exceeding biological variation in 26.8%.
Conclusion: In a large real-world cohort reflecting the clinical spectrum in which HCC is considered, DCP provided incremental diagnostic and screening value over AFP, particularly in combined models. Longitudinal analyses further showed important pre-diagnostic increase in DCP, which argues in favor of integrating it with AFP to improve HCC detection.

THU-233
Integrating PIVKA-II into BCLC staging system improves significantly the prognostic stratification of hepatocellular carcinoma

Francesco Damone[1], Gian Paolo Caviglia[2], Francesco Faita[3], Piero Colombatto[1], Filippo Oliveri[1], Marta Guariglia[2], Gabriele Ricco[1], Silvia Gaia[4], Veronica Romagnoli[1], Daniela Cavallone[1], Emanuela Rolle[4], Patrizia Carucci[4], Ferruccio Bonino[3], Maurizia Brunetto[1,3,5]. *[1]Hepatology Unit, Pisa University Hospital, Pisa, Italy; [2]Department of Medical Sciences, University of Turin, Turin, Italy; [3]Institute of Clinical Physiology, Italian National Research Council (IFC-CNR), Pisa, Italy; [4]Gastroenterology Unit, Città della Salute e della Scienza - Molinette Hospital, Turin, Italy; [5]Department of Clinical and Experimental Medicine, Pisa University, Pisa, Italy*
Email: f.damone23@gmail.com

Background and aims: The prognostic stratification of Hepatocellular Carcinoma (HCC) by the Barcelona Clinic Liver Cancer (BCLC) staging system, based on liver function, tumour burden and clinical features does not account for tumour aggressiveness and biological heterogeneity. In a multicentre cohort study we assessed whether integrating BCLC with baseline serum levels of Protein induced by Vitamin K Absence-II (PIVKA-II) might improve prognostic stratification.
Method: PIVKA-II was measured in 605 consecutive HCC patients newly diagnosed at two tertiary Italian centres between 2010 and 2024 and modelled as a continuous variable. Overall survival (OS) was the primary outcome. Two separate Cox proportional hazards regression models were compared, one including BCLC stage alone and the other integrating BCLC stage with baseline PIVKA-II. The prognostic performance of the two models was assessed using time-dependent AUC, Brier score, and C-index at 24, 36, and 60 months, with internal validation based on a 70/30 train–test split.
Results: Eighty-three patients were classified as BCLC-0, 284 BCLC-A, 151 BCLC-B and 87 as BCLC-C. Median OS was 29.0 months, declining across stages from 47.9 to 10.7 months in BCLC-0 and C respectively ($p < 0.001$). The Cox model integrating PIVKA-II with BCLC stage showed significantly improved prognostic discrimination, particularly at mid- and long-term follow-up: at 36 months, the PIVKA-II-integrated model achieved higher time-dependent AUC than BCLC alone (80.8% vs 75.7%, $p = 0.006$), with a significant advantage at 60 months (79.3% vs 73.1%, $p = 0.002$). Calibration showed a limited improvement with PIVKA-II integration, mainly at mid- and longer follow-up, as reflected by lower Brier scores at 36 and 60 months (18.9% vs 19.2% and 19.8% vs 20.1%, respectively), consistent with improved accuracy of predicted survival probabilities. Overall concordance was higher for the PIVKA-II-integrated model than the BCLC model (C-index: 0.71 vs 0.68).
Conclusion: In newly diagnosed HCC patients PIVKA-II serum levels provide useful complementary prognostic information integrating the BCLC staging system with a significantly improved mid- and long-term survival prediction. These findings prompt further prospective studies integrating HCC biomarkers into BCLC to refine the prognostic assessment according to the precision medicine approach.

THU-234
Core diagnostic value of DCP and validation of the novel GADAA nomogram for HBV-related hepatocellular carcinoma

Zihan Liu[1], Juanjuan Shi[1], Wenhao Wang[1], Ling He[1], Shuangsuo Dang[1]. *[1]The Second Affiliated Hospital of Xi'an Jiaotong University, Xi'an, China*
Email: liuzihan1999@126.com

Background and aims: Hepatocellular carcinoma (HCC) surveillance in patients with chronic hepatitis B (CHB) is often limited by the suboptimal sensitivity of alpha-fetoprotein (AFP), particularly in early-stage disease. This study aimed to evaluate the core diagnostic value of Des-gamma-carboxy prothrombin (DCP) in early-stage and AFP-negative HCC, and to construct and validate a novel, highly sensitive diagnostic model (GADAA) tailored for HBV-infected populations.
Method: A dual-center study involving 652 subjects (212 HCC patients and 440 controls with CHB or cirrhosis) was conducted from January 2023 to October 2025. Subjects were stratified by recruitment center into a training cohort (n = 509) and an independent external validation cohort (n = 143). Random forest algorithms were employed to screen potential predictors from demographic data, liver function tests, and serum biomarkers to construct the GADAA nomogram. Model performance was evaluated using the area under the receiver operating characteristic curve (AUC), calibration curves, and decision curve analysis (DCA). Furthermore, the diagnostic efficacy of GADAA was systematically compared against seven

established models: GALAD, C-GALAD, C-GALAD II, GAP-TALAD, ASAP, GAAP, and aMAP.
Results: DCP demonstrated the highest individual diagnostic accuracy (AUC = 0.862), maintaining robust performance in early-stage (AUC = 0.781) and AFP-negative HCC (AUC = 0.838). Following multistep variable screening, gender, age, DCP, AFP, and albumin were identified as independent predictors and integrated into the GADAA model. The model exhibited exceptional discrimination, achieving an AUC of 0.949 (95% CI: 0.930–0.969) in the training cohort and 0.912 (95% CI: 0.864–0.961) in the validation cohort. In a comparative assessment, GADAA (AUC 0.942) outperformed established models, including GALAD (AUC 0.917), C-GALAD (AUC 0.933), and ASAP (AUC 0.807). Notably, GADAA showed the highest sensitivity (88.7%) among all models, with excellent calibration and significant net clinical benefit.
Conclusion: DCP serves as a pivotal biomarker for early and AFP-negative HCC detection. The GADAA nomogram, incorporating DCP and routine clinical indicators, demonstrates superior diagnostic performance and clinical utility compared to existing models, providing a precise tool for HCC surveillance in HBV-endemic regions.

THU-236
Natural history of indeterminate liver lesions detected by MRI in liver cirrhosis: predicting progression to hepatocellular carcinoma

Thomas Dominicus[1], Jasper van Leengoed[1], Laura Boer[1], Job van der Palen[1], Donald Bouman[1], Maureen Guichelaar[1]. [1]*Medisch Spectrum Twente, Enschede, Netherlands*
Email: maureenguichelaar@yahoo.com

Background and aims: Indeterminate liver nodules in patients with cirrhosis, as classified by the Liver Imaging Reporting and Data System (LI-RADS), have an uncertain risk of progression to hepatocellular carcinoma (HCC), leading to clinical uncertainty and increased frequency of radiologic surveillance. Although LI-RADS provides ancillary features to improve risk assessment, their predictive value remains unclear. This study aims to provide further insight into the risk of HCC development by evaluating changes in indeterminate liver lesions over time.
Method: Our study is a retrospective cohort study concerning patients with liver cirrhosis who underwent annual MRI scanning for HCC surveillance from 2012 through 2024 following local protocol. Liver lesions were evaluated by LI-RADS criteria. LI-RADS ancillary features were assessed by the first researcher and verified by a specialized radiologist. Intralesional and whole-liver fat and iron content were measured using PDFF and T2* mapping.
Results: In the study cohort of 325 patients with liver cirrhosis, 74 patients had at least one indeterminate liver lesion (LR 2-3-4). Patients had a mean age of 61.4 (±11.9) years old, and 41.9% of patients were female. The most common etiologies of cirrhosis were MASLD (39.1%) and ALD (35.1%). A total of 311 liver lesions were studied, including 9 LR2-lesions (3%), 264 LR3-lesions (84%), 28 LR4-lesions (9%)). The median follow-up of these lesions was 3 MRI scans (IQR:2–4), and 15 months (IQR:6.3–30.5). Among 264 LR-3 lesions, 22 (8%) progressed to HCC and 132 (50%) resolved, whereas 6 of 28 LR-4 lesions (21%) progressed to HCC and 11 (39%) resolved during follow-up. Lesion size and the presence of at least one ancillary feature were found to be associated with progression to HCC. A multivariate model based on these variables showed an AUC of 0.80 for HCC development.
Conclusion: Our study demonstrates that LI-RADS 3 and 4 lesions have relatively low rates of progression to hepatocellular carcinoma (HCC), resp. 8% and 21% during the study follow-up. The majority of lesions resolved spontaneously, likely reflecting regenerative noduli. Ancillary imaging features and lesion size were predictive of HCC development, suggesting that models incorporating these factors could enable more individualized follow-up, warranting further studies.

THU-237
Hepatocellular carcinoma risk prediction score: a novel artificial intelligence model for hepatocellular carcinoma risk assessment in hepatitis C patients

Eslam Elmasry[1,2]. [1]*National Committee for control of viral hepatitis, Ministry of Health and Population, Egypt, Cairo, Egypt;* [2]*National Committee for Control of Viral Hepatitis (NCCVH), Ministry of Health and Population, Egypt, Cairo, Egypt*
Email: emji555@gmail.com

Background and aims: HCC remains a major cause of mortality in chronic HCV. Practical non-invasive tools are needed to identify patients at higher likelihood of HCC to support risk-adapted surveillance. We developed and validated a machine-learning HCC Risk Profiling Score (HRPS) using routinely available baseline pre-treatment variables and compared it with FIB-4.
Method: Retrospective NCCVH Egypt HCV cohort enriched to 4% HCC prevalence (N = 133,825; HCC events n = 5,353). Predictors were baseline pre-treatment variables: sex, treatment status, age, ALT, AST, albumin, total bilirubin, WBC, hemoglobin, platelets, INR, and creatinine. To reduce leakage, outcome-related fields and composite fibrosis indices (including FIB-4) were excluded from inputs, while component labs were retained. An XGBoost model with safe engineered features (ratios/log transforms) was trained using a stratified split 70/15/15 (train n = 93,677; validation n = 20,074; test n = 20,074; test HCC n = 803). Discrimination was assessed by AUROC and PR-AUC; calibration by Brier score (model). Clinical utility was assessed using top-k screening policies (top 1%, 5%, 10% predicted risk). FIB-4 was evaluated as a comparator (score-based).
Results: In the held-out test set, HRPS achieved AUROC 0.9129, PR-AUC 0.2934, and Brier 0.0317, outperforming FIB-4 (AUROC 0.8852; PR-AUC 0.2252). For top-k policies, HRPS yielded: top 1% precision 38.8% and recall 9.7% (vs FIB-4 28.9% and 7.2%); top 5% precision 33.4% and recall 41.7% (vs 24.9% and 31.1%); top 10% precision 25.5% and recall 63.8% (vs 22.6% and 56.4%).
Conclusion: HRPS provides a non-invasive baseline model to stratify HCV patients by likelihood of HCC using routine markers, with superior discrimination and high-risk enrichment compared with FIB-4. External validation in independent cohorts and evaluation with time-stamped follow-up are warranted.

THU-238
Anticipated patient responses to reviewing abnormal hepatocellular carcinoma imaging results: a descriptive analysis

Dabel Emebo[1], Laura Salej Duran[1], Beverly Kyalwazi[1,2], John Deng[1,3], Samantha Rangel Silos[1], Mariadelcarmen Yanez[1], Amit Singal[1], Jeremy Louissaint[1]. [1]*University Of Texas Southwestern Medical Center, Dallas, United States;* [2]*UCLA Health, Manhattan Beach, United States;* [3]*Beth Israel Deaconess Medical Center, Boston, United States*
Email: dabel.emebo@utsouthwestern.edu

Background and aims: Patients with cirrhosis are at an increased risk of hepatocellular carcinoma (HCC) and undergo semi-annual abdominal imaging. Since the 21st Century Cures Act, HCC screening results are released immediately to patients via patient portals (portals) and are frequently reviewed before provider communication. Herein, we describe patients' *anticipated* comprehension, emotional responses, communication preferences, and information-seeking behaviors after reviewing a standardized hypothetical abnormal HCC screening result report.

Method: Participants with cirrhosis reviewed a sample abdominal US or MRI result report with an US-3, LR-3, or LR-5 result that they had not previously experienced. Participants then completed a survey assessing *anticipated* outcomes across 4 domains: 1) Comprehension: confusion about the result and need for provider input to improve understanding, 2) Emotional Responses: result-related worry and anxiety (PROMIS Anxiety 7a - population mean of 50), 3) Communication Preferences: expected timing and method of provider communication, and 4) Information-Seeking: whether and how patients would seek result-related information.
Results: We surveyed 39 patients (median age 63 years; 51% Male; 71% non-Hispanic White) who reviewed one of three result samples: 9 US-3, 15 LR-3, and 15 LR-5. Comprehension: 22 (56.4%) found the result somewhat/very confusing and 36 (92.3%) would need provider input to improve understanding. The majority would like the report to include simple language and information about next steps. Emotional Responses: 59% anticipated more or much more worry, and anxiety was elevated (58.4, 56,9, and 62.4 for US-3, LR-3, and LR-5 results, respectively). Communication Preferences: Telephone (56.4%) and Portal Message (30.8%) were the preferred method of result-related provider communication, and communication within 24 hours was expected by 44.4% (US-3), 28.6% (LR-3), and 46.7% (LR-5). Information-Seeking: 87.2% would seek additional information and two-thirds would start with search-engine results.
Conclusion: Patients with cirrhosis anticipated high levels of confusion, worry, and desire for rapid additional result-related information after reviewing a hypothetical abnormal HCC screening result. These findings underscore potential targets for portal-based interventions to improve comprehension and reduce result-related worry and anxiety.

THU-239

Real-world validation of the GAAD algorithm for hepatocellular carcinoma detection across aMAP-defined risk strata in large-scale prospective Chinese cohorts

Rong Fan[1], Haiyan Yang[1], Siru Zhao[1], Hong Ma[2], Junqi Niu[3], Huiying Rao[4], Qing Xie[5], Dong-Ying Xie[6], Jianping Xie[7], Shumei Lin[8], Song Yang[9], Hongbo Gao[10], Jainqi Lian[11], Xiaoguang Dou[12], Jian Sun[1], Jinlin Hou[1]. *[1]Department of Infectious Diseases, Nanfang Hospital, Southern Medical University, Guangzhou, China; [2]Liver Research Center, Beijing Friendship Hospital, Capital Medical University, Beijing, China; [3]Department of Liver, First Hospital of Jilin University, Changchun, China; [4]Peking University Hepatology Institute, Peking University People's Hospital, Beijing, China; [5]Department of Infectious Diseases, Ruijin Hospital, Shanghai Jiao Tong University School of Medicine, Shanghai, China; [6]Department of Infectious Diseases, Sun Yat-Sen University 3rd Affiliated Hospital, Guangzhou, China; [7]Department of Infectious Diseases, Xiangya Hospital, Central South University, Changsha, China; [8]Department of Infectious Diseases, The First Affiliated Hospital of Xi'an Jiaotong University, Xi'an, China; [9]Beijing Ditan Hospital, Capital Medical University, Beijing, China; [10]8th People's Hospital, Guangzhou, China; [11]Centers of Infectious Diseases, Tangdu Hospital, the Fourth Military Medical University, Xi'an, China; [12]Department of Infectious Diseases, Shengjing Hospital of China Medical University, Shenyang, China*
Email: rongfansmu@163.com

Background and aims: While the GAAD algorithm shows promise for hepatocellular carcinoma (HCC) detection, its performance across diverse clinical settings stratified by HCC risk remains to be validated. We aimed to clinically validate the GAAD algorithm for differentiating HCC in Chinese patients with chronic hepatitis B (CHB) or cirrhosis encompassing all HCC risk strata.

Method: A total of 4,355 participants from two prospective cohorts in China were enrolled, including 1,512 cirrhotic patients from Nanfang Hospital (NCT03588442), predominantly related to hepatitis B virus infection, and 2,843 CHB patients from the nationwide multicentre cohort (NCT02167503). The median follow-up durations were 37.4 (IQR 18.5–60.5) and 60.7 (IQR 48.5–72.8) months, respectively. The GAAD algorithm, calculated from age, gender, AFP, and PIVKA-II, was assessed at HCC diagnosis or last follow-up for non-HCC patients, and HCC risk was stratified by aMAP (cut-off 50) into low- and medium-to-high-risk groups. Performance was evaluated by the area under the receiver operating characteristic curve (AUC), with cutoffs of 2.57, 20 ng/mL, and 28.4 ng/mL for GAAD, AFP, and PIVKA-II, respectively.
Results: The median ages were 51.0 and 47.4 years in the cirrhosis (n = 1512; 97 HCC cases, 1415 controls) and CHB cohorts (n = 2843; 127 HCC cases, 2716 controls), respectively. In the cirrhosis cohort, GAAD demonstrated superior accuracy with AUCs of 0.871 (all-stage) and 0.835 (early-stage), significantly outperforming AFP (all-stage: 0.811, $p = 0.006$; early-stage: 0.758, $p = 0.026$) and PIVKA-II (all-stage: 0.724, $p < 0.001$; early-stage: 0.709, $p = 0.006$). The sensitivity and specificity of GAAD for early-stage HCC detection were 55.6% and 98.2%, respectively. Furthermore, GAAD achieved satisfactory performance in the aMAP low-risk stratum (AUC 0.989), outperforming its moderate accuracy in the aMAP medium-to-high-risk stratum (AUC 0.855). In the CHB cohort, similar findings were observed, with AUCs for early-stage HCC of GAAD, AFP, and PIVKA-II being 0.847, 0.747, and 0.732, respectively. GAAD consistently demonstrated superior performance compared to single biomarkers, yet exhibited better accuracy in the low-risk stratum than in the medium-to-high-risk stratum.
Conclusion: The GAAD algorithm provides a robust and generalizable tool for HCC detection in Chinese patients, although its performance varies across aMAP risk strata. Further prospective validation is warranted to assess the clinical utility.

THU-240

Remaining chronic hepatitis C treatment gaps impact on the care cascade of HCV relatedhepatocellular carcinoma

Joan Flores[1,2], Alexander Thompson[1,3], Thai Hong[1], Stuart Roberts[4], William Kemp[4], Amanda Nicoll[5], Zina Valaydon[6], Gauri Mishra[7], Marie Sinclair[8], Diana Lewis[9], Ammar Majeed[4], Marno Ryan[1], Jessica Howell[1,3]. *[1]Saint Vincent's Hospital Melbourne, Fitzroy, Australia; [2]Canberra Hospital, Garran, Australia; [3]University of Melbourne, Parkville, Australia; [4]Alfred Health, Melbourne CBD, Australia; [5]Eastern Health, Box Hill, Australia; [6]Western Health, Footscray, Australia; [7]Monash Medical Centre Clayton, Clayton, Australia; [8]Austin Hospital, Heidelberg, Australia; [9]Northern Health, Epping, Australia*
Email: ericka@flores.com.au

Background and aims: Direct-acting antivirals (DAAs) for hepatitis C (HCV) became universally available in Australia in 2016, but the impact of HCV cure on the presentation and outcomes of HCV-related hepatocellular carcinoma (HCV-HCC) remains unclear. This study examined the HCV care cascade among people with HCV-HCC and assessed the impact of sustained virological response (SVR) on tumour stage, treatment, and survival.
Method: Incident HCC cases from six Melbourne tertiary hospital networks (2018–2021) were retrospectively identified and followed to October 2023. HCC was diagnosed by histopathology or LIRADS imaging with multidisciplinary team (MDT) consensus. SVR was confirmed by negative HCV RNA or documentation. Statistical analyses included Chi-square, Wilcoxon rank-sum, and Cox regression.

Results: Of 1,013 HCC cases, 35% (n = 348) were HCV-related. HCV-HCC cases were younger (median 61 vs 70 years, p < 0.0001) and more likely to have cirrhosis (95% vs 77%, p < 0.0001) and prior surveillance (45% vs 37%, p = 0.012). Among HCV-HCC cases, 61% achieved SVR, with a median 2.9 years from SVR to HCC diagnosis. Those with SVR had less prior alcohol misuse (27% vs 43%, p = 0.003) and injecting drug use (26% vs 41%, p = 0.003), and were more likely to undergo surveillance (64% vs 18%, p < 0.001), present with early BCLC stage (59% vs 40%, p = 0.001), and receive curative therapy (40% vs 27%, p = 0.015). Mortality was lower in the SVR group (42% vs 59%, p = 0.004) with longer median survival (11.9 vs 6.0 months, p = 0.02). SVR was associated with improved overall survival (HR 0.57, 95% CI 0.41–0.79, p = 0.001), but this was not significant after adjustment for age, liver function, and tumour stage (aHR 0.79, 95% CI 0.54–1.15, p = 0.22).
Conclusion: Despite DAA availability, many people with HCV-HCC remain untreated, undiagnosed with cirrhosis, or unscreened for HCC. Achieving SVR is linked to earlier-stage HCC and better survival, underscoring the need for improved HCV detection, fibrosis assessment, and surveillance to reduce HCV-HCC mortality.

THU-241
Temporal trends of hepatocellular carcinoma and utilization of various abdominal imaging modalities in the United States

Pareen Vora[1], Shweta Shaw[2], Sebastiano Forgia[1], Oisin Butler[1]. [1]*Bayer AG, Berlin, Germany;* [2]*Axtria, Hyderabad, India*
Email: pareen.vora@bayer.com

Background and aims: Use of diagnostic imaging and the incidence of hepatocellular carcinoma (HCC) have both increased in the US over the last two decades. Previous research showed that the incidence of HCC was lowest in whites vs other racial groups. However, a systemic analysis of imaging modality usage in HCC patients, particularly by demographics, is lacking. This study examines temporal trends in the use of diagnostic imaging in HCC patients.
Method: A retrospective cohort study was conducted using Optum Clinformatics DataMart in the US. We identified adults (> = 18 years) who had a diagnosis of HCC and separately adults who underwent at least one abdominal magnetic resonance imaging (MRI), computed tomography (CT), or ultrasound between Jan 2016 and Dec 2024. Further for patients who underwent imaging, we identified diagnosis of HCC within a 12-month window (6 months before or after their imaging). Annual rates per 100,000 patients for HCC and for each imaging modality in HCC patients were calculated and stratified by age, gender, race, and ethnicity.
Results: From 2016–24, the overall rates of HCC increased from 103 to 204 per 100,000, driven by an increase in individuals aged ≥65 years (329 to 470) and males (138 to 260) versus females (68 to 152). Rates in Asians stayed relatively stable (239 to 269), while rates in both White (130 to 285) and Black (131 to 286) populations showed similar increases, as did rates in Hispanic (161 to 262) and non-Hispanic (129 to 280) populations. In HCC patients, MRI, CT, and ultrasound rates increased between 2016 and 2024, from 29 to 83, 38 to 88 and 26 to 56 per 100,000, respectively. The highest rates were in individuals aged ≥65 years, with stable trends in other age groups. Imaging modality usage in HCC patients was higher in males. No racial differences were observed. Although rates were initially higher among Hispanic individuals, this pattern reversed around 2023–2024. Overall rates of diagnostic imaging increased from 2018 onward, coinciding with the LI-RADS update, reflecting its potential impact. This upward trend was interrupted during the COVID-19 pandemic, particularly among individuals aged ≥65 years, across the 2020–22 period.
Conclusion: Incidence of HCC continues to rise, particularly among older adults, with no substantial variation observed across racial or ethnic groups. The use of MRI, CT, and ultrasound in HCC has increased over the last decade, particularly among the elderly and more prevalent in males, reflecting the underlying epidemiology.

THU-242
18F-Fluorodeoxyglucose positron emission tomography is a predictive factor of early response to atezolizumab-bevacizumab in patients with hepatocellular carcinoma

Maria Stella Franzè[1,2], Julia Chalaye[3], Stefano Caruso[2], Hélène Regnault[2,4], Lionel Lerman[3], Sébastien Mulé[2,5], Edouard Reizine[2,5], Alain Luciani[2,5], Vincent Leroy[2,4], Giuliana Amaddeo[2,4]. [1]*Unit of Medicine and Hepatology, University Hospital of Messina, Messina, Italy;* [2]*INSERM U955, Team "Viruses, Hepatology, Cancer", Créteil, France;* [3]*Department of Nuclear Medicine, AP-HP, Henri Mondor University Hospital, Créteil, France;* [4]*Department of Hepatology, AP-HP, Henri Mondor University Hospital, Créteil, France;* [5]*Department of Medical Imaging, AP-HP, Henri Mondor University Hospital, Créteil, France*
Email: mariastellafranze@gmail.com

Background and aims: The role of ^{18}F-fluorodeoxyglucose (FDG) or ^{18}F-fluorocholine (FCH) positron emission tomography (PET)/computed tomography (CT) in assessing immunotherapy (IT) response in hepatocellular carcinoma (HCC) remains unclear. This study evaluated the prognostic role of dual-tracer ^{18}F-FDG and ^{18}F-FCH PET/CT or magnetic resonance imaging (MRI) in predicting early response and overall survival (OS) in HCC patients treated with Atezolizumab/Bevacizumab.
Method: Forty-one patients (37 males; median age 65 years) with unresectable HCC undergoing baseline ^{18}F-FDG and ^{18}F-FCH PET/CT or MRI before IT at Henri Mondor University Hospital (Créteil, France) were analysed. Early response was evaluated after three IT cycles using RECIST 1.1/mRECIST criteria, and defined as disease control rate (DCR), including complete/partial response and stable disease. Metabolic parameters were correlated with DCR, progression-free survival (PFS), and OS.
Results: Thirty-two patients (78%) had BCLC-C stage (41.5% with macrovascular invasion, 43.9% with metastasis). HCC was multinodular in 30 cases (73.2%), with a median largest lesion size of 38 mm (21–86). Early objective response rate was 39%, DCR 66%, and early progression (e-PD) 22%. FDG-PET was performed in 19 patients (46.3%), FCH-PET in 6 (14.6%), and both tracers in 16 (39%). FDG-positive HCC (uptake higher than non-tumoral liver) was observed in 68.6% (median SUVmax 4.8), while extrahepatic FDG uptake in lymph nodes (14.7%; SUVmax 10), portal vein (11.8%; SUVmax 9.1), lungs (11.8%; SUVmax 6.9). FCH-positive uptake was seen in 11 cases (50%; median SUVmax 11.2), and extrahepatic in lymph nodes (22.7%; SUVmax 8.5) and bones (9.1%; SUVmax 24.4). Patients with DCR had fewer FDG-positive HCCs (55% vs 92%, p = 0.05) than ePD. FDG-positive HCC correlated with ePD (p = 0.05) and shorter OS (8.7 vs 31.7 months, p = 0.05). A higher FCH tumour-to-liver ratio (TLR) was associated with death (p = 0.04). In univariate Cox analysis, AFP (p = 0.02), MELD (p = 0.01), ALBI grade >1 (p = 0.02), ECOG ≥1 (p = 0.01), FDG-positive HCC (p = 0.05), and absence of early DCR (p < 0.001) predicted poorer OS. In multivariate analysis, ALBI >1 (HR 5.77, 95%CI 1.69–19.7, p = 0.005) and DCR (HR 0.33, 95%CI 0.14–0.79, p = 0.01) remained independent predictors.
Conclusion: FDG-positive HCC was associated with ePD and shorter OS in patients treated with Atezolizumab/Bevacizumab, suggesting that baseline metabolic phenotype on FDG-PET may reflect tumour aggressiveness and early IT resistance.

THU-245

Anti-HBc positivity is associated with worse tumour features and reduced survival in HBsAg-negative patients with hepatocellular carcinoma

Maria Stella Franzè[1], Arianna Toscano[1,2], Clelia Asero[1,2], Gaia Caccamo[1], Roberto Filomia[1], Concetta Pitrone[1], Irene Cacciola[1,2], Carlo Saitta[1,2]. *[1]Unit of Medicine and Hepatology, University Hospital of Messina, Messina, Italy; [2]Department of Clinical and Experimental Medicine, University of Messina, Messina, Italy*
Email: mariastellafranze@gmail.com

Background and aims: Occult HBV infection (OBI) has been identified as a possible co-factor of liver damage in patients with different aetiologies of chronic liver disease (CLD), favouring the progression towards cirrhosis and hepatocellular carcinoma (HCC). This study aimed to evaluate the association between anti-HBc positivity, a surrogate marker of OBI, with clinical features and survival in HBsAg-negative HCC patients.
Method: We retrospectively evaluated all consecutive HBsAg-negative patients with first diagnosis of HCC followed at the Hepatology Unit of the University Hospital of Messina from January 2014 to May 2025. Aetiology and clinical/biochemical data of underlying CLD, tumour features and survival were evaluated. CLD was classified as follows: (1) hepatitis C virus (HCV)-related; (2) chronic alcoholic liver disease (ALD); (3) metabolic dysfunction-associated steatotic liver disease (MASLD)-related; 4) primary biliary cholangitis (PBC)- or autoimmune hepatitis (AIH)-related; 5) cryptogenic in patients without any identifiable aetiology. Overall survival (OS) was defined as the time from HCC diagnosis to death or last follow-up.
Results: A total of 382 patients [75.7% males; median age 70 years; 65 (17%) anti-HBc positive (anti-HBc+)] were analysed. CLD was HCV-related in 125 patients (32.7%, 29 anti-HBc+), MASLD in 110 (28.8%, 17 anti-HBc+), ALD in 72 (18.8%, 7 anti-HBc+), cryptogenic in 67 (17.5%, 11 anti-HBc+), PBC/AIH in 8 (2.1%). During follow-up, 226 patients (59.2%) died [OS 21.4 months (9.3–44.1)]. Among HCV-positives, anti-HBc+ individuals showed higher prevalence of extrahepatic HCC metastases than anti-HBc negative (anti-HBc-) patients (17.2% vs 2.1%, p = 0.009). In the MASLD group, anti-HBc+ patients displayed higher prevalence of multinodular HCC vs anti-HBc- (17.6% vs 1.1%, p = 0.031). In ALD patients, anti-HBc+ was associated with higher prevalence of gastro-oesophageal varices (71.4% vs 58.7% p = 0.008), ascites (57.2% vs 30.2%, p = 0.016), and reduced OS (12.1 vs. 25.3 months, p = 0.037) vs anti-HBc-. Kaplan-Meier analysis confirmed reduced OS (p = 0.018). At multivariate analysis, anti-HBc+ independently predicted reduced OS (HR 5.39, 95%CI 1.8–16.2, p = 0.003), together with higher alpha-fetoprotein levels (p = 0.01), larger tumour size (p = 0.019), and extrahepatic localization (p < 0.001).
Conclusion: Anti-HBc positivity is associated with increased mortality in HBsAg-negative HCC patients with ALD, and with more aggressive tumour features in MASLD- and HCV-related CLD.

THU-246

Machine learning-enhanced serum FTIR spectroscopy analysis for diagnosing hepatocellular carcinoma in cirrhotic patients

Elia Gigante[1], Caden Gunnarson[2], Eng Hock Lee[3], Ali Khammanivong[3], Dan Que Pham[3], Valérie Untereiner[1], Roselyne Garnotel[1], Vanessa Cottet[4], Jean-Pierre Bronowicki[5], Brigitte Beranrd-Chabert[6], François Habersetzer[7], Patrick Hillon[4], Ganesh Sockalingum[1], Gerard Thiefin[1]. *[1]Université de Reims Champagne-Ardenne, CHU Reims, Service d'Hépato-Gastroentérologie et de Cancérologie Digestive, Reims, France; [2]Oncodea, Saint Paul, United States; [3]Oncodea, St Paul, MN, United States; [4]Inserm U1231, Dijon, France; [5]CHU de Nancy, Nancy, France; [6]CHU Reims, Reims, France; [7]Les Hôpitaux Universitaires de Strasbourg, Strasbourg, France*
Email: elia.gigante@hotmail.it

Background and aims: Hepatocellular carcinoma (HCC) is the third leading cause of cancer-related deaths worldwide. The identification of novel serum biomarkers is critical to improving screening performance for this malignancy. This study aimed to determine whether serum Fourier transform infrared (FTIR) spectroscopy, combined with machine learning analysis, can generate distinct spectral profiles capable of differentiating cirrhotic patients with HCC from those without.
Method: Serum samples were collected from 2 sets of patients: cirrhotic patients with HCC (n = 280) and without HCC (n = 458). High-throughput FTIR spectra (ten replicates per sample) were acquired in the transmission mode, quality-tested, baseline corrected, converted to second derivative, and vector normalized. The Extreme Gradient Boosting (XGBoost) model and several other supervised machine learning models were trained to predict HCC status. The potential of combining serum AFP and spectral information to improve the diagnostic performance was also explored.
Results: XGBoost model achieved 68% specificity at a fixed sensitivity of 90% (AUROC = 0.86) when tested on the spectral dataset. Diagnostic performance was significantly improved in the non-diabetic subgroup (n = 450, including 151 HCC patients), achieving 84% specificity at 90% sensitivity (AUROC = 0.93). In contrast, performance was suboptimal in the diabetic subgroup (n = 288, including 129 HCC patients) with 42% specificity at 90% sensitivity. Combining the spectral data with serum alpha-fetoprotein (AFP) levels further enhanced diagnostic performance in the non-diabetic patient, resulting in 89% specificity at 90% sensitivity (AUROC = 0.96).
Conclusion: High-throughput serum FTIR spectroscopy combined with machine learning-based analysis represents a promising diagnostic approach for discriminating HCC from non-HCC cirrhotic patients in a non-diabetic population, achieving 84% specificity at 90% sensitivity.

THU-247

Impact of Hepatocellular Carcinoma on circulating reticulated platelets in patients with and without liver cirrhosis

Pietro Guerra[1], Serena Toffanin[1], Cristiana Bulato[1], Antonio Bonato[1], Silvia Cagnin[1], Caterina Soldà[2], Mario Domenico Rizzato[2], Sara Lonardi[2], Francesca Bergamo[2], Alberto Zanetto[1], Elisa Pinto[1], Marco Senzolo[3], Sara Montagnese[1], Paolo Simioni[1], Elena Campello[1], Andrea Martini[3]. *[1]University of Padova, Padua, Italy; [2]Aziende Sanitarie Padova-Istituto Oncologico Veneto-Irccs, Padova, Italy; [3]Azienda Ospedale-Università di Padova, AOPD, Padova, Italy*
Email: pietro.guerra1@gmail.com

Background and aims: Reticulated platelets (RePLT) are newly released platelets that reflect thrombopoietic activity. Their role in hepatocellular carcinoma (HCC) remains unclear. We assessed RePLT levels and platelet activation patterns in HCC patients with and without liver cirrhosis (LC).
Method: We prospectively enrolled 60 subjects into four groups: healthy controls (CTRL), LC without HCC (LC+ HCC-), HCC on a healthy liver (LC- HCC+), and HCC on cirrhosis (LC+ HCC+). Exclusion criteria were advanced liver disease (Child-Pugh B/C), portal vein thrombosis, and antiplatelet therapy. RePLT were measured by flow cytometry, and their activation was evaluated by phosphatidylserine and P-selectin exposure across different reticulation strata (low/high/very-high). Multivariable linear regression assessed the independent association between HCC and RePLT. Repeated-measures ANOVA tested the effect of reticulation and group interaction.
Results: Sixty subjects were included: CTRL (n = 28), LC+ HCC- (n = 16), LC- HCC+ (n = 5), and LC+ HCC+ (n = 11). RePLT were lower in HCC (median: 4.02% in CTRL, 3.76% in LC+ HCC-, 1.98% in LC- HCC+, and 1.55% in LC+ HCC+; p = 0.004). In a multivariable linear regression, HCC was independently associated with reduced RePLT (coefficient −2.51%; 95% CI −4.55 to −0.46; p = 0.018). Both phosphatidylserine and P-selectin increased significantly with increasing reticulation (p < 0.001 for both). The increase across reticulation strata differed by group for both markers (p < 0.001 for both), showing blunted activation in HCC groups. Specifically, in the three reticulation

strata, Annexin V increased from 1.07%, 8.29%, and 46.0% in CTRL and 0.57%, 11.5%, and 68.6% in LC+ HCC–, with smaller increases in LC– HCC+ (2.54%, 2.83%, and 7.27%) and LC+ HCC+ (4.74%, 7.54% and 20%). Similarly, CD62P rose from 3.02%, 29.6% to 93.7% in CTRL and 3.63%, 45.6% to 96.6% in LC+ HCC–, versus more limited increases in LC– HCC + (1.29%, 2.38% to 15.6%) and LC+ HCC+ (1.59%, 5.01% to 35.3%).
Conclusion: HCC is independently associated with reduced circulating RePLT. The presence of HCC is characterized by lower platelet activation at increasing reticulation levels, supported by significant reticulation-by-group interactions for both Annexin V and CD62P. Further studies should clarify mechanisms and clinical implications.

THU-248
Hepatocellular carcinoma imaging using prostate-specific membrane antigen positron emission tomography - The Hepa-SMART trial

Nicholas Hannah[1,2,3,4,5], Grace Kong[2,5], Kim Taubman[6], Sze Ting Lee[2,7,8,9], Wayland Wang[1,2], Sophia Xie[5], Alex Boussioutas[10,11], Rod Hicks[2,10], Siddharth Sood[2,3]. *[1]The Royal Melbourne Hospital, Parkville, Australia; [2]The University of Melbourne, Parkville, Australia; [3]Northern Health, Epping, Australia; [4]Western Health, Footscray, Australia; [5]Peter Maccallum Cancer Centre, Melbourne CBD, Australia; [6]Saint Vincent's Hospital Melbourne, Carlton, Australia; [7]Austin Hospital, Heidelberg, Australia; [8]Latrobe University Bundoora Melbourne, Bundoora, Australia; [9]RMIT University, Bundoora, Australia; [10]Monash University, Clayton, Australia; [11]The Alfred, Melbourne CBD, Australia*
Email: nicholas.hannah2@mh.org.au

Background and aims: Prostate-specific membrane antigen (PSMA) is a tumour-associated target which can be detected by positron emission tomography (PET). This study aimed to evaluate the diagnostic performance of PSMA PET/CT using [^{18}F]F-DCFPyL radiotracer in detecting hepatocellular carcinoma (HCC).
Method: Hepa-SMART is a multicentre, investigator-initiated, prospective clinical trial (NCT05095519). Two cohorts were recruited: Group 1, radiologically confirmed HCC (LR 5); and Group 2, indeterminate or probable HCC (LR 3–4). Patients were to receive either biopsy or surgical resection to allow histological confirmation and PSMA immunohistochemistry (IHC). Diagnostic performance was assessed using per-patient and per-lesion analyses, with intention-to-treat and per-protocol approaches.
Results: Twenty-five patients were recruited: Group 1 (n = 11) and Group 2 (n = 14) with 36 lesions (HCC confirmed n = 26, benign n = 9, equivocal n = 1). Median lesion size: Cohort 1 18.0 mm (IQR 13.0–31.0), and in Cohort 2 15.0 mm (IQR 11.0–22.5). HCC lesions with positive [^{18}F]F-DCFPyL PET/CT uptake had median SUVmax 5.7 (IQR 4.63–9.15), tumour-background ratio (TBR) 1.13 (IQR 0.97–1.76). [^{18}F]F-DCFPyL PET/CT demonstrated high specificity across cohorts. In LR 5 HCC, sensitivity was 54.5% with a positive predictive value (PPV) of 100%. In indeterminate lesions, per-lesion intention-to-treat analysis demonstrated sensitivity 27.3%, specificity 90%, PPV 75%, and negative predictive value (NPV) 52.9%. Per-protocol analyses yielded similar results. On whole-cohort per-lesion analysis, the area under the receiver operating characteristic curve (AUROC) for a positive scan diagnosing HCC was 0.72 (95% CI 0.60–0.84; p = 0.0012). Quantitative TBR analysis did not improve diagnostic performance. Benign lesions demonstrated exclusively low PSMA expression intensity on IHC, HCC showed significantly high expression intensity (p = 0.005) with a predominant endothelial compartment expression in HCC, with positive correlations between PSMA IHC intensity and PET SUVmax (R = .48, p = 0.019) and TBR (R = 0.42, p = 0.039).
Conclusion: Hepa-SMART is the first prospective multicentre clinical trial evaluating [^{18}F]F-DCFPyL Although sensitivity is modest in early-stage disease, [^{18}F]F-DCFPyL PET/CT demonstrates high specificity and PPV, supporting its clinical utility for confirming HCC and providing tumour-specific information beyond conventional imaging.

THU-249
Would a non-imaging-based strategy be effective for hepatocellular carcinoma surveillance?

Grishma Hirode[1,2], Korosh Khalili[3], Lima Awad El-Karim[3], Hooman Farhang Zangneh[1], Harry L.A. Janssen[1,4], Bettina E. Hansen[5], Morris Sherman[1], Jordan J. Feld[1,2]. *[1]Toronto Centre for Liver Disease, Toronto General Hospital, University Health Network, Toronto, Canada; [2]The Viral Hepatitis Care Network Canada (VIRCAN), Toronto, Canada; [3]Joint Department of Medical Imaging, University Health Network, Toronto, Canada; [4]Department of Gastroenterology and Hepatology, Erasmus MC University Medical Center, Rotterdam, Netherlands; [5]Department of Epidemiology, Biostatistics, Erasmus MC University Medical Center, Rotterdam, Netherlands*
Email: grishma.hirode@gmail.com

Background and aims: Despite biannual ultrasound (US) for hepatocellular carcinoma (HCC) surveillance, many patients are diagnosed at an advanced stage. US is operator-dependent and adherence is typically poor. Better understanding of existing methods and development of new strategies are needed to improve early-stage HCC detection. We examined whether biomarkers (BMs), alone or in combination with US, and the GALAD score which uses a combination of all 3 BMs – treated as continuous variables – along with age and sex, were as effective as US alone or US + alpha-fetoprotein (AFP); the standard of care.
Method: Prospective study of patients with cirrhosis or high-risk hepatitis B virus (HBV) infection using US + BM for HCC detection. AFP > 100 ng/mL, lectin-reactive fraction of AFP (AFP-L3) > 10%, des-gamma-carboxy prothrombin (DCP) > 2 ng/mL, or US findings triggered further imaging (computed tomography/magnetic resonance imaging) for HCC confirmation. We compared effectiveness of each method using the area under the receiver operating characteristic (AUROC) curve after logistic regression, accounting for patient-level variance.
Results: Among 605 patients (mean age 58 ± 9.9 years, 72% male, 64% cirrhosis), 27 were diagnosed with HCC (22 early, 5 advanced). For US + 3 BMs at study thresholds, AUROC, sensitivity (sens) and specificity (spec) were 0.81, 96% and 65%. For US alone, AUROC, sens and spec were 0.72, 77% and 66%. Without US, the optimal cut-off for AFP was 4.2 ng/mL (AUROC 0.82, sens 84%, spec 80%), AFP-L3 was 1.4% (AUROC 0.73, sens 72%, spec 74%) and DCP was 0.3 ng/mL (AUROC 0.80, sens 85%, spec 75%). Performance of BMs was evaluated using study thresholds and these optimized thresholds, alone or combination with US. US + AFP was comparable to US alone and US + 3 BMs. The optimal cut-off for the GALAD score was −1.8 (AUROC 0.85, sens 89%, spec 81%). The GALAD score at this threshold resulted in higher AUROC, sens, and spec compared with all other examined methods, with or without inclusion of US.
Conclusion: In this study, the GALAD score outperformed all US-based HCC surveillance methods. Thus, a non-imaging-based surveillance strategy may be feasible, and particularly useful when access to US is limited or US is of poor quality. However, a prospective study of such a strategy with validated GALAD score thresholds will be crucial for generalizability and application in practice.

THU-250
The impact of insulin resistance on hepatic steatosis and outcome for hepatocellular carcinoma patients undergoing surgical resection

Chun-Ting Ho[1,2], Chia-Jung Ho[1], Tsai Shin-Yu[1], Yi-Chen Lin[3], Yi-Hsiang Huang[4], Ming-Chih Hou[5], Jaw-Ching Wu[6], Chien-Wei Su[7]. *[1]Taipei Veterans General Hospital, Department of Medicine, Taipei, Taiwan; [2]National Yang Ming Chiao Tung University Yangming Campus, Ph.D. Program of Interdisciplinary Medicine, Taipei, Taiwan; [3]Linkou Chang Gung Memorial Hospital, Department of Medicine, Taoyuan City, Taiwan; [4]Taipei Veterans General Hospital, Department of Medical Research, Taipei, Taiwan; [5]Taipei Veterans General Hospital, Division of*

Gastroenterology and Hepatology, Department of Medicine, Taipei, Taiwan; [6]National Yang Ming Chiao Tung University Yangming Campus, Institute of Clinical Medicine, Taipei, Taiwan; [7]Taipei Veterans General Hospital, Division of General Medicine, Department of Medicine, Taipei, Taiwan
Email: cwsu2@vghtpe.gov.tw

Background and aims: Insulin resistance (IR) significantly influences cardiometabolic status and is a driver for steatotic liver disease (SLD). Triglyceride-glucose index (TyG), calculated using fasting serum triglyceride and glucose levels, is a simple and effective surrogate marker of IR. We aimed to evaluate the impact of IR on the extent of hepatic steatosis and long-term outcome in patients with hepatocellular carcinoma (HCC) undergoing surgical resection.
Method: A total of 744 HCC patients who underwent curative resection at Taipei Veterans General Hospital with available pathological specimens and complete clinical data were included. Patients were divided into high-IR (TyG ≥ 4.5, n = 431) and low-IR (TyG <4.5, n = 313) groups. Hepatic steatosis was histologically assessed using non-tumour liver tissue in the pathology specimen. Pearson correlation and receiver operating characteristic (ROC) analysis were utilized to assess associations between TyG and hepatic steatosis. Cox proportional hazards (COX PH) models and Kaplan-Meier (KM) survival analysis were performed to evaluate the prognostic role of TyG for overall survival (OS). Subgroup analysis was performed in patients with and without diabetes mellitus (DM).
Results: Patients in the high-IR group were older, had lower hepatitis B virus positivity, and a higher prevalence of steatohepatitis. Distinct tumor characteristics, serum biochemical profiles, and cardiometabolic comorbidities were also noted in the high-IR group compared to those in the low-IR group. The TyG index showed a significant positive correlation with the extent of hepatic steatosis and demonstrated good diagnostic performance for SLD (AUROC 0.713, p < 0.001). After a median follow-up of 57.0 months, 161 patients died, with a 5-year OS rate of 72.1%. KM analysis showed no significant difference in OS between high- and low-IR groups (5-year OS: 73.4% vs. 70.1%). COX PH model identified age, stage, prothrombin time international normalized ratio, serum albumin, and alpha-fetoprotein as independent risk factors for poor OS, while IR was not an independent prognostic factor. Subgroup analyses stratified by DM status also revealed no survival differences between high and low-IR groups.
Conclusion: IR was positively associated with the severity of hepatic steatosis and is linked to distinct tumor characteristics, cardiometabolic profiles, and biochemical parameters among HCC patients. However, IR did not independently influence OS after curative resection, irrespective of the presence of DM.

THU-361
Clinical distribution and prognostic implications of the ASAP score in a real-world cohort of hepatocellular carcinoma

Young Mi Hong[1], Hyun Myung Cho[2]. *[1]Department of Internal Medicine, Pusan National University School of Medicine, Pusan National University Yangsan Hospital, Yangsan, Korea, Rep. of South; [2]Pusan National University Yangsan Hospital, Yangsan, Korea, Rep. of South*
Email: 00gurum@hanmail.net

Background and aims: The ASAP score, which incorporates age, sex, alpha-fetoprotein, and protein induced by vitamin K absence-II, was originally developed as a simplified biomarker-based model to enhance early detection of hepatocellular carcinoma (HCC). However, its clinical associations and prognostic relevance in HCC remain unknown. This study aims to evaluate the prognostic and clinical relevance of the ASAP score at the time of diagnosis.
Method: We retrospectively analyzed patients newly diagnosed with HCC. ASAP scores were calculated at diagnosis, and their distribution was assessed. Correlations between ASAP scores and clinical characteristics were evaluated. Overall survival (OS) was evaluated using Kaplan-Meier and Cox proportional hazards models.
Results: Among 1,143 patients, the optimal cutoff value of the ASAP score was 2.9, yielding a sensitivity of 64% and a specificity of 80%, indicating its predictive value for mortality risk stratification. Patients with high ASAP scores had significantly worse OS ($P < 0.001$). In multivariate analysis, the ASAP score was an independent risk factor of OS [hazard ratio (HR) = 2.841, 95% confidence interval (CI) = 2.035–3.966, $P < 0.001$]. Higher ASAP scores were significantly associated with increased Child-Pugh scores ($P = 0.006$), more advanced BCLC stage ($P < 0.001$), and elevated neutrophil to lymphocyte ratio ($P < 0.001$). The mean ASAP scores by BCLC stage were 0.98 in stage A, 3.10 in stage B, 6.47 in stage C and 7.06 in stage D, respectively ($P < 0.001$).
Conclusion: Although originally developed for HCC surveillance, the ASAP score demonstrated a wide distribution and meaningful clinical correlations at the time of diagnosis in a real-world cohort. It also independently predicted OS, suggesting potential utility for risk stratification beyond early detection.

THU-362
mRNA COVID-19 vaccination shortly after PD-1/PD-L1 inhibitor Is associated with better survival in liver cancer: a Mayo Clinic platform study

Chenyu Sun[1], Li Liu[2], Abigail Fickel[3], Elizabeth Lees[1], Yichen Wang[4], Yan Yan[4], Paul Travers[4], Harsh Patel[5], Liu Yang[4], Yuting Huang[4]. *[1]Mayo Clinic Rochester, Rochester, United States; [2]The Second People's Hospital of Hefei, Hefei, China; [3]Mayo Clinic Alix School of Medicine, Rochester, United States; [4]Mayo Clinic Florida, Jacksonville, United States; [5]University of Maryland School of Medicine, Baltimore, United States*
Email: huang.yuting@mayo.edu

Background and aims: Prior research has demonstrated survival benefits of mRNA COVID-19 vaccination in patients with non-small cell lung cancer (NSCLC) and melanoma treated with immune checkpoint inhibitors (ICIs). However, the impact of vaccination on hepatocellular carcinoma (HCC)/liver cancer patients receiving PD-1/PD-L1 inhibitors remains unclear. This study investigates whether mRNA COVID-19 vaccination shortly after PD-1/PD-L1 inhibitor initiation improves overall survival in liver cancer.
Method: A retrospective analysis was conducted using the Mayo Clinic Platform (Full AMC1 dataset) including patients with hepatocellular carcinoma/liver cancer who received at least one dose of PD-1/PD-L1 inhibitors without liver surgery. The intervention group consisted of patients receiving an mRNA COVID-19 vaccine within six weeks of PD-1/PD-L1 inhibitor initiation, while the control group did not receive vaccination within this timeframe. Adjustments were made for BMI <30 and exclusion of patients with diabetes, cardiovascular disease, or heart failure history. The primary outcome was 5-year overall survival assessed via Kaplan-Meier analysis and Cox proportional hazards models. Age differences at diagnosis were assessed using Cohen's D, and sex distribution compared by Chi-square test. All analyses were performed using the Mayo Clinic Platform's tool.
Results: A total of 4,768 patients were included, with 584 in the vaccination group and 4,184 controls. Age and sex distributions were similar between groups (Cohen's D for age = 0.16; χ^2 for sex = 1.5, both not significant). The mRNA vaccine group showed significantly improved 5-year overall survival (37.9% vs. 23.4%, HR = 0.59, 95% CI: 0.52–0.66; P < 0.001). The survival benefit remained unchanged after adjustment, confirming the robustness of the finding. Survival curves demonstrated persistent benefit across time points up to 60 months.
Conclusion: The mRNA COVID-19 vaccination shortly after PD-1/PD-L1 inhibitor initiation is associated with improved 5-year overall survival in hepatocellular carcinoma/liver cancer patients. These findings align with prior evidence in other cancers treated with ICIs, suggesting vaccine-induced immune priming may enhance immunotherapy efficacy. Limitations include retrospective design, possible uncontrolled confounding, and incomplete 5-year follow-up for some patients who started therapy more recently. Prospective studies

are warranted to validate these results and explore underlying immunological mechanisms.

THU-363
Serum exosome-related lipids could detect MASLD-associated hepatocellular carcinoma

Jian Huang[1], Zhongguo Zhou[2], Arresha Nazeer[2], Julian L. Griffin[3], Mark R Thursz[1], Nadia Guerra[2], Pinelopi Manousou[1]. [1]*Saint Mary's Hospital, London, United Kingdom;* [2]*Imperial College London, London, United Kingdom;* [3]*University of Aberdeen, Aberdeen, United Kingdom*
Email: jian.huang20@imperial.ac.uk

Background and aims: The incidence of MASLD associated HCC is increasing worldwide, yet effective blood-based biomarkers for early surveillance are lacking [1]. Exosomes are stable in serum and carry molecular cargo reflective of tumour biology, making them an attractive source of non-invasive biomarkers [2,3]. While exosomal nucleic acids and proteins have been widely studied, the diagnostic potential of exosome-associated lipids remains poorly explored. This study aimed to identify exosome-associated lipids that distinguish MASLD-associated HCC from MASLD and to assess their translational potential as a surveillance tool.
Method: Serum exosomes were isolated from 110 patients (38 MASLD; 72 MASLD-associated HCC). Untargeted lipidomics profiling was performed using liquid chromatography–mass spectrometry (LC-MS). Multivariate analyses, including principal component analysis (PCA) and partial least squares discriminant analysis (PLS-DA), alongside Mann–Whitney U testing, were used to identify differentially lipids. KEGG pathway enrichment analysis assessed biological relevance. Least absolute shrinkage and selection operator (LASSO) regression was applied to derive a parsimonious lipid panel suitable for clinical translation.
Results: Exosome-associated lipids demonstrated clear separation between MASLD and MASLD-associated HCC in both PCA and PLS-DA analyses, indicating strong discriminatory capacity at the lipidome level (Figure A and B). A total of 49 exosome-associated lipids differed significantly between groups, including 34 exosome-lipids with upregulation and 15 exosome-lipids with downregulation in MASLD-associated HCC (Figure C; $P < 0.05$). Pathway enrichment analysis revealed involvement of glycerophospholipid metabolism, consistent with the lipid composition of exosomal membranes (Figure D, table 1). LASSO regression refined these 49 exosome-lipids into a 14-lipid panel with minimal redundancy and robust classification performance (Figure E). These 14 exosome-lipid set was visualized via heatmap to confirm consistent separation across individual patients, supporting feasibility for real-world application (Figure F).
Conclusion: Exosome-associated lipid remodelling represent a distinct molecular feature of MASLD-associated HCC. A 14-lipid exosomal panel shows strong potential as invasive biomarker set for discriminating MASLD-associated HCC from MASLD. These findings support exosomal lipidomics as a promising translational approach for the development of surveillance and diagnostic strategies.

THU-364
Intensive care admission patterns and outcomes in hepatocellular carcinoma patients on systemic therapy

Rex Wan-Hin Hui[1], Matthew Shing Hin Chung[1], Lu Li[1], Xianhua Mao[2], CL Chiang[1], Carlos King Ho Wong[1], Ian Chi Kei Wong[1], Ka Shing Cheung[1], Stephen Chan[3], Man-Fung Yuen[1], Wai-Kay Seto[1], Lung Yi Loey Mak[1]. [1]*The University of Hong Kong, Pok Fu Lam, Hong Kong;* [2]*Stanford University, Stanford, United States;* [3]*The Chinese University of Hong Kong, Sha Tin, Hong Kong*
Email: huirex@connect.hku.hk

Background and aims: Patients with advanced hepatocellular carcinoma (HCC) are conventionally triaged out of intensive care unit (ICU) admission due to poor prognosis. Yet with improving survivorship from systemic therapies, ICU admission for HCC patients may become more common. We assessed the ICU admission patterns and outcomes in HCC patients on systemic therapies.
Method: HCC patients who received systemic therapies (immune checkpoint inhibitors [ICIs] or tyrosine kinase inhibitors [TKIs]) between 2008 and 2024 were identified from a territory-wide cohort. The reasons for ICU admission were classified as liver-related events, treatment-related events, or non-liver events. ICU procedures and survival were analyzed. The Sequential Organ Failure Assessment (SOFA) score was calculated with patient parameters at ICU admission.
Results: Among 5403 HCC patients who received systemic therapy, 147 patients (2.7%) were admitted to ICU (51 on ICIs [3.1% of ICI patients]; 96 on TKIs [2.1% of TKI patients]). The mean age was 62.8 years, 89.1% were male, and 90.5% had cirrhosis. The median interval from systemic therapy initiation to ICU admission was 6.4 (1.9–17.5) months, and the length of ICU stay was 5 (3–11) days. The 28-day and 90-day survival were 68.7% and 51.7% respectively. Mechanical ventilation, vasopressors, cardiopulmonary resuscitation, and renal replacement therapy was utilised in 42.9%, 34.7%, 6.8%, and 6.1% of patients respectively. 61 (41.5%), 49 (33.3%), and 37 patients (25.2%) were admitted for liver-related events, non-liver events, and treatment-related events respectively. The most common liver-related event requiring admission was variceal bleeding (49.2% of liver-related events), while the most common non-liver event was sepsis (42.9% of non-liver events). 8 patients (15.7% of ICI patients) were admitted for immune-related adverse events (myocarditis: 4, diabetic ketoacidosis: 2, adrenal crisis: 1, pneumonitis: 1). The only independent predictors of 28-day and 90-day mortality were admission for liver-related events (28-day HR 2.200 [95%CI 1.156–4.187]; 90-day HR 1.856 [95%CI 1.037–3.320]; both $p < 0.05$) and higher SOFA score (28-day HR 1.249 [95%CI 1.151–1.355]; 90-day HR 1.161 [95%CI 1.080–1.248]; both $p < 0.001$). ICI or TKI use had no impact on survival (all $p > 0.05$).
Conclusion: Liver-related events were the most common reason for ICU admission in HCC patients on systemic therapies. The reason for admission and baseline SOFA score have prognostic implications and may be used for ICU triage.

THU-365
Oral cholate challenge test stratifies hepatotoxicity risk after liver-directed therapy for hepatocellular carcinoma

Maarouf Hoteit[1], Michael McRae[2], Joanne Imperial[3], Greg Everson[3]. [1]*University of Pennsylvania, Philadelphia, Pennsylvania, United States;* [2]*Custom DX Solutions LLC, Houston, Texas, United States;* [3]*HepQuant, LLC, Denver, Colorado, United States*
Email: michael.mcrae@hepquant.com

Background and aims: Liver-directed therapy (LDT) for hepatocellular carcinoma (HCC) carries a risk of serious liver toxicity, but the risk is not accurately predicted. We previously published experience with the relatively complex HepQuant SHUNT test indicating potential for more accurate risk prediction. In this analysis, we evaluated a simplified test version, the oral cholate challenge test (HepQuant DuO) of liver function and physiology, for predicting outcome after LDT.
Method: We conducted a prospective cohort study of patients undergoing LDT for HCC. We evaluated cholate clearance at baseline and 4–10 weeks after (T1) LDT in 11 patients. Hepatotoxicity was defined as the development of a new complication of cirrhosis or an increase in Child-Pugh score by ≥2 points. The Test involved an oral dose of deuterium-labelled (d4-) cholate, blood draws at 20 and 60 minutes, and subsequent measurement of the d4-cholate by LC-MS/MS. Test parameters were calculated, including Portal Hepatic Filtration Rate (HFR), a measure of the clearance of oral d4-cholate, and the Disease Severity Index (DSI), a measure of global liver disease severity from 0 (healthy) to 50 (severe dysfunction). Changes in DSI from baseline to T1 were analyzed using Wilcoxon signed-rank test.

Results: Four patients (36%) were Child-Pugh A and seven (64%) were Child-Pugh B. Patients were BCLC stage A (64%) or BCLC stage B (36%). LDT modalities were transarterial chemoembolisation (46%) or external beam radiotherapy (55%). From baseline to T1, there were trends towards reduction in portal HFR (4.7 [2.5–16.3] mL/kg/min to 3.8 [2.3–16.6] mL/kg/min, p = 0.097) and worsening DSI (30.2 [15.3–38.0] to 32.8 [15.2–38.7], p = 0.097). There was no significant change in MELD (12 [9–13] to 11 [10–12], p = 0.72) or Child-Pugh score (7 [5–8] to 7 [6–8], p = 0.15). Hepatotoxicity was observed in 43% of Child-Pugh B patients and none of the Child-Pugh A patients; and in 75% of patients with a baseline DSI > 35 and none of the patients with DSI < 35.
Conclusion: The oral cholate challenge test may better define baseline disease severity and may be more sensitive to change in liver function induced by LDT than traditional measures.

THU-366-YI
Development of a longitudinal predictive model for hepatocellular carcinoma occurrence in patients with chronic hepatitis B
Apichat Kaewdech[1], Chanavee Toh[1], Pimsiri Sripongpun[1], Naichaya Chamroonkul[1], Pisit Tangkijvanich[2], Teerha Piratvisuth[1], Suthat Liangpunsakul[3], Paramee Thongsuksai[1], Thammasin Ingviya[1].
[1]Prince of Songkla University, Hat Yai, Thailand; [2]Chulalongkorn University, Bangkok, Thailand; [3]Indiana University School of Medical, Indianapolis, United States
Email: apichat.ka@psu.ac.th

Background and aims: Hepatocellular carcinoma (HCC) remains a major cause of morbidity and mortality among patients with chronic hepatitis B (CHB). Existing HCC risk scores are largely based on baseline variables and do not account for longitudinal changes over time. We aimed to develop and validate a longitudinal predictive model for HCC using time-dependent Cox regression.
Method: We retrospectively analyzed 4,431 patients with CHB followed between 2009 and 2022. After excluding patients with viral co-infections, early HCC, or incomplete data, 2,245 patients were included. The cohort was randomly divided into a training set (n = 1,685) and a test set (n = 560). Time-varying covariates, including demographic, clinical, and laboratory variables, were modeled using a time-dependent Cox regression approach. Predictive performance was evaluated using the concordance index (C-index), Brier score, and comparisons with established HCC risk models.
Results: During follow-up, 120 patients developed HCC. Independent predictors of HCC included age, sex, platelet count, cirrhosis, serum albumin, and α-fetoprotein (AFP). These variables were incorporated into the final model (PSU HCC score): (0.023 × age) – (0.627 × female sex) –(0.847 × albumin) –(0.005 × platelet count [$\times 10^3$]) + (1.052 × $\log_{10}$AFP) + (1.817 × cirrhosis). In the test cohort, the PSU HCC score demonstrated excellent discrimination (C-index 0.909; 95% CI, 0.870–0.947) and good calibration, outperforming ALBI, aMAP, REACH-B, CU-HCC, PAGE-B, and mPAGE-B scores. Risk stratification revealed significantly higher cumulative HCC incidence among patients in the high-risk group.
Conclusion: The PSU HCC score is a longitudinal prediction model that integrates dynamic clinical and laboratory parameters and provides superior HCC risk prediction in patients with CHB compared with existing models. This approach may support individualized, risk-based HCC surveillance strategies.

THU-367
Risk and predictors of HCC in a cohort of 1,395 treatment-naïve chronic hepatitis delta patients with F0-F2 fibrosis
Habiba Kamal[1,2], Ganbolor Jargalsaikhan[3], Sanjaasuren Enkhtaivan[3], Karin Lindahl[1], Bekhbold Dashtseren[3], Oyungerel Lkhagva-Ochir[3], Tuvshinjargal Ulziibadrakh[3], Andreas Bungert[3], Elisabetta Degasperi[2,4], Pietro Lampertico[2,4,5], Heiner Wedemeyer[2,6,7], Naranjargal Dashdorj[3], Soo Aleman[1,2].
[1]Department of Medicine Huddinge, Karolinska Institutet, Stockholm, Sweden, Department of Infectious Diseases, Karolinska University Hospital, Stockholm, Sweden, Stockholm, Sweden; [2]D-SOLVE: EU-funded Network on individualized management of hepatitis D, Hannover, Germany; [3]The Liver Center, Ulaanbaatar, Mongolia, ONOM Foundation, Ulaanbaatar, Mongolia, Ulaanbaatar, Mongolia; [4]Division of Gastroenterology and Hepatology, Foundation IRCCS Ca' Granda Ospedale Maggiore Policlinico, Milan, Italy, D-SOLVE: EU-funded Network on individualized management of hepatitis D, Milano, Italy; [5]CRC "A. M. and A. Migliavacca" Center for Liver Disease, Department of Pathophysiology and Transplantation, University of Milan, Milan, Italy, Milan, Italy; [6]Department of Gastroenterology, Hepatology, Infectious Diseases and Endocrinology, Hannover Medical School, Hannover, Germany, German Centre for Infection Research (DZIF), Site Hannover-Braunschweig, Hannover, Germany, Excellence Cluster RESIST, Hannover Medical School, Hannover, Germany, Hannover, Germany; [7]Excellence Cluster RESIST, Hannover Medical School, Hannover, Germany, Hannover, Germany
Email: habiba.khodir.kamal@ki.se

Background and aims: Chronic hepatitis D (CHD) is associated with a higher risk of HCC than mono-chronic hepatitis B (CHB). The knowledge is limited on the risk for HCC in patients with CHD with mild to moderate fibrosis (F0-F2).
Method: We conducted a retrospective study of adults (≥18 years) with CHD attending a hepatology center in Mongolia during 2015–2025. Patients with prior HCC, hepatic decompensation, or transplantation, anti-HDV treatment, or advanced liver fibrosis and/or cirrhosis were excluded. Advanced fibrosis and cirrhosis were ruled out if liver stiffness measurements (LSM) ≥10.0 kPa, platelet count $<150 \times 10^9$ cells/L, and no clinical or radiological features of cirrhosis. The incidence rate (IR) and cumulative incidence of HCC were analyzed by Kaplan-Meier method, and the predictors of HCC were identified using Cox regression models. The cut-off age for annual HCC IR surpassing 0.2%; the cost-effective HCC surveillance threshold in non-cirrhotic CHB, was evaluated.
Results: Overall, 1,395 individuals with CHD were included, with baseline characteristics: median age 39.5 years, 178 (12.8%) < 30 years, females 61.5%, elevated ALT 73.5%, median HDV RNA 5.2 (IQR 3.9, 6.1) $\log_{10}$ IU/mL, and median LSM of 7.0 (IQR 5.8, 8.3) kPa. During a median follow-up of 7.5 (IQR 5.6, 8.7) years, 123 (8.8%) progressed to cirrhosis at an IR of 1.31% with 5- and 10-year risks of 5.9% and 13.2%, respectively. While 47 (3.4%) developed HCC, at an IR of 0.48%, with 5- and 10-year risks of 1.7%, and 5.6%, respectively. In patients without ever cirrhosis diagnosis, HCC IR was 0.25%, with 5- and 10-year risks of 1.3% and 2.6%, respectively. In multivariable analyses, predictors of HCC were older age (aHR = 1.08, 1.06–1.11), elevated ALT (aHR = 3.94, 1.18–13.12) and elevated GGT (aHR = 3.42, 1.75–6.68). None developed HCC in the age group 18–29 years. Males and females surpassed the 0.2% HCC surveillance threshold at a mean age of 35.1 (95% CI 32.0–43.7), and 33.6 (31.4–43.7) years, respectively. Similar findings were noted by excluding those who developed cirrhosis during follow-up.
Conclusion: This study demonstrates a relatively high risk for HCC in untreated Asian patients with F0-F2 fibrosis on long-term, with an annual risk of HCC exceeding 0.2% when age > 30 years for males and females. Our results suggest therefore starting HCC surveillance at this age-cut off in patients with CHD, regardless of fibrosis stage. More data are needed to confirm our findings.

THU-368
Magnetic resonance elastography and cirrhosis outcome risk estimator (CORE) score as independent predictors of hepatocellular carcinoma in chronic hepatitis
Kie Kinjo[1], Nobuharu Tamaki[1], Yutaka Yasui[1], Hiroyuki Nakanishi[1], Kaoru Tsuchiya[1], Namiki Izumi[1], Masayuki Kurosaki[1]. *[1]Musashino Red Cross Hospital, Tokyo, Japan*
Email: 19Kie.K.00@nms.ac.jp

Background and aims: In chronic liver disease, liver fibrosis is the most important predictor of hepatocellular carcinoma (HCC). Recently, the CORE (Cirrhosis Outcome Risk Estimator) risk score has been developed to predict the risk of major liver disease in the general population. CORE is calculated using age, sex, AST, ALT, and γ-GTP, and estimates the 10-year risk of liver disease development. In this study, we evaluated whether magnetic resonance elastography (MRE), a marker of liver fibrosis, and CORE are useful predictors of HCC development in patients with chronic liver disease.
Method: A total of 2,653 patients who underwent MRE between 2015 and 2024 were included. Blood tests performed within one month before or after the initial MRE were used to calculate the CORE score. The primary outcome was the development of HCC.
Results: Among the 2,653 patients, 56.4% were male. The underlying etiologies of chronic liver disease were hepatitis C virus infection in 47.7% and metabolic dysfunction-associated steatotic liver disease in 17.9%. The median age (interquartile range [IQR]) was 68 (58–76) years. When stratified by the MRE cutoff for advanced fibrosis (3.6 kPa), the cumulative incidence of HCC at 1, 3, and 5 years was 3.2%, 8.3%, and 12.8% in patients with MRE ≥3.6 kPa, compared with 0.5%, 2.3%, and 3.9% in those with MRE <3.6 kPa (P < 0.001). Receiver operating characteristic analysis identified an optimal CORE cutoff of 0.27% (it means 10-year predicted liver disease risk). The cumulative HCC incidence at 1, 3, and 5 years was 2.6%, 7.1%, and 11.0% in patients with CORE ≥0.27%, compared with 0.2%, 1.2%, and 3.1% in those with CORE <0.27% (P < 0.001). Although CORE successfully stratified HCC risk, the observed incidence of HCC was higher than the risk predicted by CORE. After adjustment for MRE, CORE, diabetes mellitus, dyslipidemia, and hypertension, the hazard ratio (HR) (95% confidence interval [CI]) was 2.27 (1.4–3.7) for MRE ≥3.6 kPa and 2.62 (1.4–5.0) for CORE ≥0.27%. CORE risk score was an independent risk factor for HCC development, independent of liver fibrosis status.
Conclusion: In patients with known chronic liver disease, CORE risk score independently predicted the development of HCC in addition to MRE. CORE score was developed for the general population; however, in patients with chronic liver disease, the actual risk of HCC development was higher than the 10-year liver disease risk estimated by CORE, indicating that careful interpretation of CORE is required in this population.

THU-369
Characteristics of hepatocellular carcinoma in the real-world Italian PITER-B/Delta cohort

Giuseppina Brancaccio[1], Maria Giovanna Quaranta[2], Maria Elena Tosti[2], Barbara Coco[3], Maurizia Brunetto[3,4], Giovanni Battista Gaeta[5], Loreta Kondili[2,6] and PITER Collaborating Investigators[2]. *[1]Link Campus University, Rome, Italy; [2]Istituto Superiore Di Sanita', Rome, Italy; [3]University Hospital of Pisa, Pisa, Italy; [4]University of Pisa, Pisa, Italy; [5]University of Campania "Luigi Vanvitelli", Naples, Italy; [6]UniCamillus-Saint Camillus International University of Health Sciences, Rome, Italy*
Email: ggbrancaccio@gmail.com

Background and aims: Chronic hepatitis Delta virus (HDV) infection increases the risk of hepatocellular carcinoma (HCC) by two- to three-fold compared with hepatitis B virus (HBV) monoinfection. This study was aimed to update clinical and macro-pathological characteristics of HCC in patients with HDV infection compared with HBV monoinfection.
Method: HCC cases were retrospectively retrieved from the cross-sectional PITER-B/Delta cohort. The HCC cases included in this analysis were enrolled between 2019 and 2024 across 36 participating centers. Centers were queried to collect data at first HCC diagnosis, including macro-pathological characteristics and treatments received. HCC was diagnosed according to standard imaging criteria. Group comparisons were performed using standard statistical methods.
Results: Among 212 HCC cases, 178 were included in the analysis: 42 (23.6%) anti-HDV–positive and 136 with HBV monoinfection. Detectable HDV-RNA was found in 29 of 36 tested patients. HDV-HCC patients were younger than HBV-HCC patients (median age 60 vs. 65 years; $p = 0.009$), with women primarily driving this difference (57 vs. 71 years; $p = 0.031$), while the difference among men was marginal (62 vs. 65 years; $p = 0.08$). Compared with HBV patients, those with HDV infection were more frequently non-Italian and showed more advanced liver disease, as shown by lower platelet counts, higher AST, ALT, GGT, bilirubin and AFP levels, higher Child–Pugh class, presence of CSPH. HCC was diagnosed during US surveillance in 89.5% of HDV patients and 82.3% of HBV patients (p = ns). No differences were observed between groups in nodular presentation (94.9% vs. 90.0%), number of nodules (≤ 3 in 86.5% vs. 93.9%), largest nodule diameter (2.3 vs. 2.5 cm), presence of metastases (7.9% vs.7.9%), or being within the Milan criteria (55.0% vs. 66.7%). Comorbidities were similarly distributed between the two groups. Liver transplantation was more frequent among HDV patients (23.8% vs. 7.3%; $p = 0.009$), whereas surgical resection tended to be more common in HBV patients (36.0% vs. 26.2%).
Conclusion: This study provides a contemporary clinical and epidemiological snapshot of HDV-associated HCC, showing that despite similar tumor stage at diagnosis compared with HBV monoinfection, HDV-related HCC occurs at a younger age, in the setting of more advanced liver disease, and is more frequently associated with liver transplantation need, defining a distinct clinical profile beyond tumor burden.

THU-370
Effectiveness of a structured surveillance program for early detection of hepatocellular carcinoma in contemporary patients with advanced chronic liver disease

Georg Kramer[1,2,3,4], Carina Pichler[1], Lorenz Balcar[1,2,3,4], Georg Semmler[1,2,3], Benedikt Simbrunner[1,2,3], Mathias Jachs[1,2,3], Lukas Hartl[1,2,3], Benedikt Hofer[1,2,3], Christian Sebesta[1,2,3], Paul Thöne[1,2,3], Marlene Hintersteininger[1,2,3], Michael Trauner[1,3], Mattias Mandorfer[1,2,3], Thomas Reiberger[1,2,3], Matthias Pinter[1,4], Bernhard Scheiner[1,2,3,4]. *[1]Division of Gastroenterology and Hepatology, Department of Medicine III, Medical University of Vienna, Vienna, Austria, Vienna, Austria; [2]Vienna Hepatic Hemodynamic Laboratory, Division of Gastroenterology and Hepatology, Department of Medicine III, Medical University of Vienna, Vienna, Austria, Vienna, Austria; [3]Clinical Research Group MOTION, Medical University of Vienna, Vienna, Austria, Vienna, Austria; [4]Vienna Liver Cancer (HCC) Study Group, Division of Gastroenterology and Hepatology, Department of Medicine III, Medical University of Vienna, Vienna, Austria, Vienna, Austria*
Email: georg.kramer@meduniwien.ac.at

Background and aims: Hepatocellular carcinoma (HCC) surveillance is recommended in patients with advanced chronic liver disease (ACLD), yet real-world adherence is heterogeneous and often assessed using binary or semi-quantitative metrics. We aimed to longitudinally quantify HCC surveillance adherence using a continuous, time-based metric and to evaluate its association with clinical outcomes. In addition, we report on the diagnostic yield of a structured re-linkage initiative among patients who missed routine surveillance.
Method: In 639 ACLD patients enrolled into the prospective Vienna Cirrhosis Study (VICIS; NCT03267615) between 2017 and 2024 and receiving regular in-house care, HCC-surveillance adherence was analyzed using the proportion of time covered (PTC), assigning a six-month coverage window to each imaging assessment. Associations between PTC and outcomes were evaluated using adjusted Cox regression models and internally validated in a propensity score matched cohort (age, sex, etiology, Child-Pugh score [CPS]) via Fine-Gray competing-risk models. Patients overdue for surveillance were targeted through a prospective and structured re-linkage program.

Results: Median imaging-based PTC was 83% (IQR 60–98%). Over a median follow-up of 43 months, 47 patients (7.4%) developed HCC, of whom 47% were diagnosed at an early stage (Barcelona Clinic Liver Cancer 0/A). PTC was non-linearly associated with early HCC-detection showing a strong increase once coverage exceeded 85% of follow-up time. Biannual imaging was associated with a 6.6-times higher likelihood of early-HCC detection compared with annual imaging (HR 6.57; 95% CI 2.38–18.11). After propensity score-matching, high surveillance adherence (PTC ≥85%) was associated with early-HCC detection (adjusted subdistribution hazard ratio [SHR]: 2.44; p = 0.015) and option for curative treatment (adjusted SHR: 2.60; p = 0.024) independent from age, sex and CPS, while PTC ≥85% tended toward improved post-HCC survival (SHR: 0.37, p = 0.087). Among 52 patients overdue for surveillance who were actively re-linked to imaging, 8 (15%) had a new suspect hepatic lesions detected, including one biopsy-verified HCC.
Conclusion: In a contemporary ACLD cohort, sustained high-intensity HCC surveillance is strongly associated with earlier tumor detection and increased likelihood to receive curative treatment. Continuous adherence metrics and proactive re-linkage strategies may improve surveillance effectiveness in routine care.

THU-371
Clinical benefit of perioperative prophylactic antibiotics in hepatocellular carcinoma (HCC) patients undergoing transcatheter arterial chemoembolization (TACE)
Junying Li[1]. [1]*Hepatology Unit, Department of Infectious Diseases, Nanfang Hospital, Southern Medical University, Guangzhou, China, Hepatology Unit, Zengcheng Branch, Nanfang Hospital, Southern Medical University, Guangzhou, China, Guangzhou, China*
Email: 2292921780@qq.com

Background and aims: Clinical evidence supporting the use of prophylactic antibiotics to prevent infection and improve outcomes in patients undergoing transarterial chemoembolization (TACE) for hepatocellular carcinoma (HCC) remains limited. This study aimed to evaluate the association between perioperative prophylactic antibiotic administration and the risk of post-TACE infection.
Method: This retrospective cohort study included HCC patients who underwent TACE between January 2022 and December 2025. Patients in the prophylactic antibiotic group received 1.5 g of cefuroxime sodium 30 minutes prior to TACE, while those in the control group received no prophylactic antibiotic intervention. The primary outcomes were the incidence of infection within 30 days postoperatively, defined by procalcitonin (PCT) ≥ 0.66 ng/mL or C-reactive protein (CRP) ≥ 28 mg/L. Secondary outcomes included the diagnosis of systemic inflammatory response syndrome (SIRS), total hospitalization cost, and length of hospital stay (LOS). Outcomes were compared between the two groups to assess the necessity of prophylactic antibiotics for TACE.
Results: A total of 286 eligible patients were enrolled, with 123 receiving prophylactic antibiotics and 163 not. No statistically significant differences were observed between the antibiotic group and the non-antibiotic group in the incidence of infection (defined by PCT ≥ 0.66 ng/mL: p = 0.142; defined by CRP ≥ 28 mg/L: p = 0.679) within 30 days postoperatively. Additionally, there were no significant differences in the rate of SIRS (p = 0.097), total hospitalization cost (p = 0.475), or LOS (p = 0.413) between the two groups.
Conclusion: Perioperative prophylactic use of antibiotics in patients undergoing TACE is not significantly associated with a reduced risk of postoperative infection, shorter LOS, or lower hospitalization costs. Large-scale prospective studies and randomized controlled trials (RCTs) are warranted to further validate these findings.

THU-372-YI
The genetic alterations in circulating tumor cells correlate with the clinical outcomes of hepatocellular carcinoma by large-scale whole-genome sequencing
Siqi Liao[1], Zhiji Chen[1], Song He[1], Zhihang Zhou[1]. [1]*The Second Affiliated Hospital of Chongqing Medical University, Chongqing, China*
Email: zhouzhihang@cqmu.edu.cn

Background and aims: Hepatocellular carcinoma (HCC) accounts for 70–90% of primary liver cancers, often diagnosed at advanced stages. Despite advances in systemic and locoregional therapies, outcomes remain poor due to tumor heterogeneity and drug resistance. Tissue biopsy is limited by invasiveness and sampling bias. Circulating tumor cells (CTCs) offer a minimally invasive "liquid biopsy" for real-time genomic profiling. This study aims to characterize the HCC genomic landscape using CTCs and assess its diagnostic and prognostic potential.
Method: CTCs from 267 treatment-naïve HCC patients were enriched via CTC-100 microfluidics; 134 CTC pools underwent whole genome amplification (WGA)/whole-genome sequencing (WGS). Somatic mutations were analyzed for signatures, SV burden, and clinical correlations. HepG2 spike-ins validated workflow fidelity. Consensus clustering revealed two molecular subtypes; survival analyses used Kaplan–Meier and Cox models.
Results: CTC count correlated significantly with advanced tumor stage and poor prognosis (P < 0.05). Notably, 61.8% (1,848/2,992) of CTCs showed low EpCAM expression, indicating marked phenotypic heterogeneity. WGS delineated the genomic landscape of HCC CTCs. Co-mutations in NAV2, SPTAN1, DOCK6, and PI4KA were significantly associated with shorter overall survival (P < 0.05) and predicted outcomes in BCLC-C patients receiving targeted therapy, immunotherapy, or interventional treatment. Unsupervised clustering defined two molecular subtypes: Cluster 1 responded better to targeted therapy, while Cluster 2 benefited more from immunotherapy. CTC-enriched mutations were identified in MUC16, NOTCH1, ZFHX3, and KMT2D. Structural variant (SV) analysis revealed ARRB2 as the most frequently altered gene; deletions (DELs) predominated in ARRB2, LDLRAD2, FOXL2, C1QB, NELFE, UBXN11, and KMT2B, whereas duplications (DUPs) were enriched in TMEM161A, MAST3, LTBP3, and MYH7B. Higher SV or DEL burden (above median) correlated with worse survival (P < 0.05). Two loci—chr11:71,238,675 and chr11:71,249,563—were significantly linked to poor prognosis.
Conclusion: This large-scale WGS study of HCC CTCs delineates a genomic framework that uncovers novel biomarkers for prognosis prediction, therapy response stratification, and potential drivers of CTC biology, advancing the clinical application of liquid biopsy in HCC management.

THU-377-YI
Shifting aetiology and clinical landscape of hepatocellular carcinoma over four decades: from viral hepatitis to metabolic dysfunction–associated steatotic liver disease in 1,960 patients
Kai Lim[1], Wei-Lun Liou[2], Chee-Kiat Tan[2]. [1]*Singapore Health Services, Singapore General Hospital, Singapore, Singapore;* [2]*Department of Hepatology and Gastroenterology, Singapore General Hospital, Singapore, Singapore*
Email: limkai94@gmail.com

Background and aims: Metabolic dysfunction–associated steatotic liver disease (MASLD) is emerging as a major contributor of hepatocellular carcinoma (HCC) globally. Long-term data of its impact in multi-ethnic Asian populations is limited. We describe temporal changes in aetiology, clinical characteristics, HCC stage and treatment patterns over four decades in Singapore, with a focus on MASLD-related HCC.
Method: Patients with HCC were prospectively enrolled from 1980 to the present. Temporal trends across decades were assessed using poisson regression. MASLD-related HCC was compared with

non–MASLD-related HCC overall for demographics, liver disease severity, BCLC stage, and treatment patterns.
Results: A total of 1,960 patients were included. Aetiology shifted significantly over time. Proportion of MASLD-related HCC increased from 14.6% in 1990–1999 to 42.4% in 2020–present (incidence rate ratio per decade 1.29, $p < 0.001$) with a corresponding decline in hepatitis B-related HCC. Over the decades, patients were older (mean age 60 to 69 years; $p < 0.001$) with declining male predominance (84.4% to 70.6%, $p < 0.001$). Ethnic composition also changed, with fewer Chinese (89.5% to 81.4%) and more Malays (6.8% to 11.5%; $p = 0.006$). Liver biochemistry demonstrated favourable shifts - higher albumin (33 to 36 g/L), lower bilirubin (42 to 27 μmol/L), lower prothrombin time (14 to 12 sec), higher proportion of Child–Pugh A (49.5% to 64.5%), ALBI grade 1 (13.0% to 32.7%), and lower AFP level (AFP < 20 μg/L: 17.1% to 62.5%) (all $p < 0.001$). In contrast, platelet count declined (217 to 169×10^9/L, $p < 0.001$) and FIB-4 scores worsened ($p = 0.011$). BCLC stage and HCC treatment patterns also changed significantly over time, with more early stage HCC (9.1% in 1990–1999 vs 64.0% in 2020–present) and more curative (11.0% in 1990–1999 vs 53.5% in 2020–present) and locoregional therapy (11.5% vs 24.3%)($p < 0.001$). Compared with non-MASLD HCC, MASLD-HCC occurred in older patients (mean age 69 vs 62 years, $p < 0.001$), was less male predominant (68.5% vs 82.2%, $p < 0.001$) and was associated with lower AFP level (AFP < 20 μg/L: 48.1% vs 37.4%, $p < 0.001$) and higher FIB-4 categories (advanced fibrosis: 72.7% vs 67.1%, $p = 0.006$).
Conclusion: The transition from viral to MASLD as a dominant driver of HCC in Singapore, a multi-ethnic Asian country, is accompanied by changes in demographics, liver disease characteristics, HCC stage and treatment patterns. These findings provide important context for refinement of our HCC surveillance strategies.

THU-378
Potential limitations of Fib-4 in selecting MASLD patients for HCC surveillance – impact of fibrosis burden on tumour stage and survival in MASLD-related HCC compared with non-MASLD HCC in 1,960 patients over 4 decades
Kai Lim[1], Wei-Lun Liou[2], Chee-Kiat Tan[2]. *[1]Singapore Health Services, Singapore General Hospital, Singapore, Singapore; [2]Department of Hepatology and Gastroenterology, Singapore General Hospital, Singapore, Singapore*
Email: limkai94@gmail.com

Background and aims: The impact of fibrosis burden (FB) on hepatocellular carcinoma (HCC) detection and survival in metabolic dysfunction–associated steatotic liver disease (MASLD) remains unclear. We examined the association between FB assessed by FIB-4, tumour stage at diagnosis and overall survival (OS) in MASLD-related HCC, with comparison to non-MASLD-related HCC.
Method: Patients with HCC were prospectively enrolled between 1980 and the present. FB was assessed by FIB-4 categories (< 1.3, 1.3–2.67, > 2.67). Tumour stage was classified using BCLC criteria, with early stage defined as BCLC 0/A. Associations with stage were analysed using logistic regression, and OS by Kaplan–Meier and multivariable Cox regression. Sensitivity analyses incorporated surveillance status. Parallel stratified analyses were performed in non-MASLD related HCC.
Results: Among 1,960 patients, 447 (22.8%) had MASLD-related HCC, where 83.7% had cirrhosis and 72.7% had high FB (FIB-4 >2.67). High FIB-4 was associated with older age (mean 70 vs 58 years, $p < 0.001$), less male predominance (63.7% vs 82.1%, $p = 0.009$) and worse liver function - lower albumin (33 vs 36 g/L, $p = 0.001$) and higher bilirubin (40 vs 24 μmol/L, $p = 0.006$). After adjustment for age, gender and decade, higher FIB-4 was significantly associated with earlier BCLC stage (FIB-4 > 2.67 vs FIB-4 < 1.3, aOR 0.23, $p = 0.015$). Whereas, in non-MASLD related HCC, higher FIB-4 was independently associated with advanced BCLC stage (aOR 3.19, $p < 0.001$). In MASLD-related HCC, this association was no longer significant after adjustment for surveillance, suggesting surveillance-related stage migration. Despite earlier BCLC stage, higher FIB-4 remained independently associated with worse OS in MASLD-related HCC (aHR 2.20, $p = 0.001$) after adjustment for gender, BCLC stage, decade and surveillance status. Curative-intent treatment rates also did not differ across FIB-4 categories in MASLD-related HCC ($p = 0.78$). In non-MASLD related HCC, higher FB was also associated with poorer OS (aHR 1.62, $p < 0.001$).
Conclusion: In MASLD-related HCC, higher FB assessed by FIB-4 was associated with earlier BCLC stage at diagnosis, largely driven by surveillance, but did not translate into improved OS. The persistent adverse prognostic impact of higher FIB-4, despite earlier detection, likely reflects underlying hepatic vulnerability that potentially limits curative treatment. This suggest that reliance on FIB-4 alone to guide selection of MASLD patients for HCC surveillance might not be ideal.

THU-379
Development and validation of a machine learning model to prognosticate hepatocellular carcinoma
Ryan YanZhe Lim[1], Benjamin Nah[2], Vigneshwaran Selvakumar[3], Nicholas Syn[4,5], Gang Chen[6,7], Jie Li[8,9], Beom Kyung Kim[10,11], Karn Wijarnpreecha[12], Hirokazu Takahashi[13], Daniel Huang[1,2,14]. *[1]Yong Loo Lin School of Medicine, National University of Singapore, Singapore, Singapore; [2]Division of Gastroenterology and Hepatology, Department of Medicine, National University Hospital, Singapore, Singapore; [3]Lee Kong Chian School of Medicine, Nanyang Technological University, Singapore, Singapore; [4]National University of Singapore, Department of Biomedical Informatics, Yong Loo Lin School of Medicine, Singapore, Singapore; [5]National University of Singapore, Department of Pathology, Yong Loo Lin School of Medicine, Singapore, Singapore; [6]Department of Hepatobiliary Surgery, The First Affiliated Hospital of Wenzhou Medical University, Wenzhou, China; [7]Zhejiang-Germany Interdisciplinary Joint Laboratory of Hepatobiliary-Pancreatic Tumor and Bioengineering, The First Affiliated Hospital of Wenzhou Medical University, Wenzhou, China; [8]Department of Infectious Diseases, Nanjing Drum Tower Hospital, Affiliated Hospital of Medical School, Nanjing University, Nanjing, China; [9]Institute of Viruses and Infectious Diseases, Nanjing University, Nanjing, China; [10]Department of Internal Medicine, Yonsei University College of Medicine, Seoul, Korea, Rep. of South; [11]Yonsei Liver Center, Severance Hospital, Seoul, Korea, Rep. of South; [12]Division of Gastroenterology and Hepatology, University of Arizona College of Medicine Phoenix, Phoenix, AZ, United States; [13]Division of Metabolism and Endocrinology, Faculty of Medicine, Saga University, Saga, Japan; [14]National University Centre for Organ Transplantation, National University Health System, Singapore, Singapore*
Email: ryanlimyanzhe21@gmail.com

Background and aims: Prognostic models for hepatocellular carcinoma (HCC) may have limited accuracy. We aimed to construct and validate a novel prognostic model for HCC that incorporates biomarkers for liver function and tumor characteristics.
Method: Consecutive participants with HCC from four international tertiary institutions in Asia and the U.S. comprised the derivation (n = 627) and validation (n = 270) cohorts. The Liver Cancer Risk predictioN (LCRN) Index was constructed using a gradient-boosted decision tree model based on the Cox proportional hazards framework. The discriminative performance of the LCRN Index was evaluated using Harrell's concordance index (C-index) and the area under the receiver operating curve (AUC), and compared to the albumin bilirubin grade (ALBI) and Barcelona Clinic for Liver Cancer (BCLC) staging. Model calibration was assessed using the integrated Brier score and Arjas plots.
Results: The median (IQR) age was 66.0 (58.0–73.0) years, median (IQR) body mass index was 23.9 (22.1–25.9) kg/m^2 and 78% were male. The LCRN Index comprised type 2 diabetes mellitus, ascites, hepatic encephalopathy, albumin, bilirubin, AFP and diameter of largest tumor nodule. In the validation cohort, the LCRN Index (C-

index: 0.7885; 1-year AUC: 0.89; 3-year AUC 0.83; 5-year AUC 0.78) outperformed the ALBI grade (C-index: 0.6710; 1-year AUC: 0.75; 3-year AUC 0.69; 5-year AUC 0.65) and BCLC stage (C-index: 0.6730; 1-year AUC: 0.73; 3-year AUC 0.69; 5-year AUC 0.66) for prognosticating HCC. The LCRN Index demonstrated better calibration compared to the ALBI grade and BCLC stage.
Conclusion: If further validated, the LCRN Index may be a useful tool for prognosticating HCC.

THU-380-YI
Exploring the impact of mitochondrial biomarkers on HCC risk according to etiologic drivers: a multicenter study
Miriam Longo[1], Annalisa Cespiati[1,2], Erika Paolini[1], Marica Meroni[1], Daniel Smith[1,2], Anna Alisi[3], Luca Miele[4,5], Andrea Dalbeni[6,7], Giorgio Soardo[8], Anna Ludovica Fracanzani[1,2], Paola Dongiovanni[1]. *[1]Fondazione IRCCS Cà Granda, Ospedale Maggiore Policlinico, Milano, Italy; [2]Università degli Studi di Milano, Milano, Italy; [3]Bambino Gesù Children's Hospital, IRCCS, Roma, Italy; [4]Fondazione Policlinico Universitario Agostino Gemelli IRCCS, Roma, Italy; [5]University of Sacred Heart, Roma, Italy; [6]Azienda Ospedaliera Universitaria Integrata of Verona, Verona, Italy; [7]University and Azienda Ospedaliera Universitaria Integrata of Verona, Verona, Italy; [8]University of Udine, Udine, Italy*
Email: paola.dongiovanni@policlinico.mi.it

Background and aims: Metabolic dysfunction-associated steatotic liver disease (MASLD) overcame HCV and alcohol-related hepatitis (ALD), becoming the main cause of hepatocellular carcinoma (HCC). We recently showed that circulating mitochondrial (mt-) biomarkers (*D-loop*, ccf-COXIII) increase in MASLD patients and accurately predict HCC risk. However, it remains to elucidate whether these biomarkers are MASLD-specific. We aim to: (1) assess *D-loop* and ccf-COXIII levels in a multicenter cohort of 1231 HCV, ALD and MASLD patients of whom 332 with HCC; (2) develop new models for HCC diagnosis employing mt-biomarkers and compare them with standard scores (aMAP, Fib4, APRI, Forn's index, Fibro-alpha).
Method: *D-loop* and ccf-COXIII were measured by qRT-PCR. Their levels were compared across either etiologies or within each etiology group (MASLD vs MASLD-HCC; ALD vs ALD-HCC; HCV vs HCV-HCC). Multivariate analyses were adjusted for age, gender, BMI, diabetes (T2DM) and presence of cirrhosis. Random forest (RF) analysis, a machine learning method, was exploited to build-up new diagnostic tools.
Results: MASLD-HCC subjects had higher BMI, T2DM rate and serum lipids compared to HCC from other etiologies ($p < 0.01$). In this subgroup, the mean size of primary nodules was larger than ALD-HCCs or HCV-HCC patients, as well as a greater number of non-cirrhotic MASLD-HCC cases were recorded ($p < 0.05$). *D-loop* levels raised in MASLD-HCC patients compared to MASLD ones regardless of cirrhosis and, at multivariate analysis, it independently associated with HCC of metabolic origin ($p < 0.05$), suggesting *D-loop* as a MASLD-specific biomarker. Conversely, ccf-COXIII levels significantly increased in all HCC patients with cirrhosis, independently of etiology ($p < 0.0001$), supporting that its release is primarily driven by advanced tissue damage. The *D-loop* based prediction model, generated with RF, for HCC risk and applied to the entire cohort reached a higher AUC (78%) compared to reference scores, but without reaching the statistical significance, likely reflecting the biomarker's specificity for MASLD etiology. Conversely, the new diagnostic tool based on ccf-COXIII levels outperformed existing non-invasive tests, for HCC detection across patients with mixed etiologies, demonstrating 85% of accuracy.
Conclusion: High *D-loop* levels identify MASLD-HCC risk, even in noncirrhotic cases which are outside HCC clinical screening, while ccf-COXIII has a broader clinical utility for HCC monitoring in patients with different chronic liver diseases.

THU-381
Combining observation and patient data to predict malignancy progression in LI-RADS 3–4 observations
David Marti-Aguado[1], Subin Heo[2], Melissa Lou Silva[3], David Nam[3], Sedighe Hosseini Shabanan[3], Colter S. Sirlin[3], Tanya Wolfson[3], Claude Sirlin[3], Sang Hyun Choi[2]. *[1]Incliva - Instituto De Investigación Sanitaria, Valencia, Spain; [2]Department of Radiology and Research Institute of Radiology, Asan Medical Center, University of Ulsan College of Medicine, Seoul, Korea., Seoul, Korea, Rep. of South; [3]University of California San Diego, La Jolla, United States*
Email: davidmmaa@gmail.com

Background and aims: LI-RADS category 3 (LR-3) and 4 (LR-4) observations are considered indeterminate, with variable and unpredictable risk of progression to malignancy including hepatocellular carcinoma (HCC), underscoring the need for risk-stratification. The aim of this study was to develop a risk-stratification algorithm combining per-observation and per-patient models for predicting 3-year progression to malignancy for LR-3 and LR-4.
Method: This retrospective study included patients with ≥1 LR-3 or LR-4 observation on CT/MRI per LI-RADS v2018. The primary endpoint was 3-year progression to malignancy (HCC or non-HCC malignancy). Per-observation and per-patient multivariable models for predicting 3-year progression were created from baseline data. Each model's cross-validated area under the curve (AUC) and its 95% confidence interval were calculated. Observations and patients were classified as low or high-risk based on Youden-based probability thresholds. A risk-stratification algorithm was created by combining the per-observation and per-patient classifications to yield four risk groups (A: low-risk observation in low-risk patient; B: low-risk observation in high-risk patient; C: high-risk observation in low-risk patient; D: high-risk observation in high-risk patient). The diagnostic performance of the risk-stratification model for predicting 3-year progression was compared to that of a 4-point ordinal LI-RADS-based stratification based on LI-RADS category ± ancillary features favoring malignancy.
Results: A total of 147 patients (34% women) with 245 observations (178 LR-3, 67 LR-4) were included. Within 3 years, 103 patients progressed to malignancy. The per-observation model AUC was 0.67 (0.57–0.76) and the per-patient model AUC was 0.61 (0.50–0.72). Cumulative incidence of progression within 1-to-3 years was 4–25%, 23–33%, 20–40%, and 56–78% for observations in Groups A, B, C, and D, respectively, based on the risk-stratification algorithm. The risk-stratification model AUC, sensitivity (Sn), specificity (Sp), and total accuracy were 0.71, 73%, 69%, 71%. The ordinal LI-RADS categorization AUC, Sn, Sp, and total accuracy were 0.66, 65%, 63%, 64%. Although diagnostic performance was slightly higher, differences were not significant ($p = 0.05$ for total accuracy).
Conclusion: A risk-stratification algorithm that combines per-observation and per-patient models shows promise for identifying LR-3/4observations with high likelihood of progression.

THU-382-YI
Performance of HCC risk scores in patients with advanced chronic liver disease: a multicenter cohort study
Mohamed Moussa[1], Koos de Wit[2], L.C. Baak[3], Dave Sprengers[1], Raoel Maan[1], Adriaan J. van der Meer[1], Stan van Wijk[1], Emma Kleij[1], Roy Dwarkasing[4], Willem Pieter Brouwer[1], Femme Dirksmeier-Harinck[5], Jordan J. Feld[6], Harry L.A. Janssen[1,6], R. Bart Takkenberg[2], Milan J. Sonneveld[1]. *[1]Erasmus university medical center, Department of gastroenterology and hepatology, Rotterdam, Netherlands; [2]Amsterdam university medical center, Department of gastroenterology and hepatology, Amsterdam, Netherlands; [3]OLVG hospital, Department of gastroenterology and hepatology, Rotterdam, Netherlands; [4]Erasmus university medical center, Department of radiology and nuclear Medicine, Rotterdam, Netherlands; [5]Franciscus*

Hospital, Department of gastroenterology and hepatology, Rotterdam, Netherlands; [6]Toronto Centre for Liver Disease, University of Toronto, Toronto, Canada
Email: m.moussa@erasmusmc.nl

Background and aims: Patients with advanced chronic liver disease (ACLD) are at risk of developing HCC and are therefore recommended to undergo bi-annual HCC surveillance. The increasing prevalence ACLD is causing a significant burden on healthcare systems. Individualised risk prediction would be helpful to identify patients in whom surveillance could be safely deferred. This study assessed the performance of two HCC risk scores, the aMAP score and the Toronto HCC risk Index (THRI) in patients with ACLD in the Netherlands.
Method: We included adults with ACLD from three sites in the Netherlands. Exclusion criteria were follow-up time <6 months, missing risk score data or prior HCC. THRI and aMAP scores were calculated as previously reported, classifying patients into low, intermediate, and high-risk groups. Kaplan–Meier analysis was used to estimate cumulative HCC according to risk score categories.
Results: A total of 1,531 patients were included. The most common liver disease etiologies were steatotic liver disease (SLD; n = 453, 30%), hepatitis C virus (HCV; n = 371, 24%), and hepatitis B virus (HBV; n = 242, 16%). The majority were male (63%), and the median age was 53 years (IQR: 44–61). The median baseline CTP was 5 (IQR: 5–7), and 366 (24%) had a history of decompensated cirrhosis. A total of 196 patients developed HCC. Overall, the HCC cumulative incidence was 7.2% (5%CI: 5.7–8.7) in 5 years. The median THRI was 200 (IQR: 136–254), and the number of patients with a low, intermediate, and high THRI was 269 (18%), 746 (49%), and 516 (34%). The 5-year HCC cumulative risk was 0.5% (95%CI: 0.0–1.6), 6.1% (95%CI: 4.1–8.1), and 12.2% (95%CI: 8.9–15.4) for those with a low, intermediate, and high THRI, p < 0.01. The median aMAP was 55 (IQR: 49–61), and the number of patients with a low, intermediate, and high aMAP was 437 (29%), 645 (42%) and 449 (29%). The 5-year HCC cumulative risk was 2.9% (95%CI: 1.2–4.6), 6.1% (95%CI: 3.9–8.2), and 13.1% (95%CI: 9.7–16.4) for those with a low, intermediate, and high aMAP. Reducing the aMAP cut-off to 40, resulted in a lower residual risk of HCC in this subgroup but also reduced the number of patients identified as low risk to 6% (compared to 18% for THRI).
Conclusion: THRI and aMAP can be used to stratify HCC risk in patients with cirrhosis, but THRI appeared to be the most effective at identifying patients with a 5-year negligible risk of HCC. Deferral of HCC surveillance should be considered in patients at low predicted risk based on THRI.

THU-383
Addition of the GAAD score to imaging improves classification of non-cirrhotic focal liver lesions

Mohamed Moussa[1], Dave Sprengers[1], Vera Ketting[1], Christian Ramakers[2], Robert A. de Man[1], Roy Dwarkasing[3], Harry L.A. Janssen[1,4], Antonius van Herwaarden[5], E.T.T.L. Tjwa[6], Milan J. Sonneveld[1]. *[1]Erasmus university medical center, Department of gastroenterology and hepatology, Rotterdam, Netherlands; [2]Erasmus university medical center, Department of Clinical Chemistry, Rotterdam, Netherlands; [3]Erasmus university medical center, Department of radiology and nuclear Medicine, Rotterdam, Netherlands; [4]Toronto Centre for Liver Disease, University of Toronto, Toronto, Canada; [5]Radboud university medical center, Department of Laboratory medicine, Nijmegen, Netherlands; [6]Radboud University Medical Center, Department of gastroenterology and hepatology, Nijmegen, Netherlands*
Email: m.moussa@erasmusmc.nl

Background and aims: Accurate diagnosis of HCC is challenging in patients without cirrhosis, and biopsy is therefore frequently required. We evaluated the additive value of the GAAD score, which is based on patient age, sex and serum values of AFP and PIVKA-II, in non-cirrhotic patients with focal liver lesions who underwent contrast-enhanced imaging (CE-imaging).
Method: We performed a multi-center prospective study in two tertiary referral clinics in the Netherlands and enrolled all consecutive patients presenting with focal liver lesions in a non-cirrhotic liver. For the current analysis, all patients who underwent CE-imaging were included if there was also a histological assessment of focal liver lesion. The diagnostic accuracy of the GAAD score was assessed at its predefined cutoff score of 2.57.
Results: We analysed 167 patients. The median age was 56 years (IQR: 38–72), and the majority were Caucasian (90%). Liver disease was present in 40% (n = 67), with SLD being the most common etiology (34%; n = 57). HCC was diagnosed in 59 (35%) cases. Patients with HCC were older (median age 70 vs. 49, p < 0.01), and more often male (44% vs. 15%, p < 0.01). The median GAAD score was higher in patients with HCC (8.38 vs. 0.24, p < 0.01). The GAAD score offered excellent discrimination for HCC with an AUC of 0.94 (95%CI: 90–97). At a threshold of 2.57, the sensitivity, specificity, PPV, and NPV were 81%, 91%, 83%, and 90%, respectively. Imaging was considered suggestive of HCC in 40% (n = 67), amongst whom 52 (PPV 77.6%) had HCC. In patients with a high suspicion of HCC based on imaging, a GAAD score of ≥2.57 increased the probability of HCC from 77.6% to 95.7%. Conversely, imaging was not suggestive of HCC in 100 (60%), of whom 7 (NPV: 93%) had HCC. In these patients, A GAAD score <2.57 reduced the probability from 7% to 4.5% (NPV: 95.5%), whereas a GAAD score >2.57 increased the probability of HCC to 27.3%.
Conclusion: In this cohort of non-cirrhotic patients with focal liver lesions, the GAAD score was highly predictive of HCC. In patients with a high likelihood of HCC based on imaging characteristics, a positive GAAD score can be used to rule-in HCC, whereas in patients with a low likelihood of HCC based on imaging, a GAAD score <2.57 can be used to help rule-out HCC. These findings support the use of the GAAD score in the classification of focal liver lesions in patients without cirrhosis.

THU-384
Post-cholecystectomy syndrome affects ultrasound visualization in non-obese viral-related advanced chronic liver disease ACLD: implications of gallbladder removal for Li-RADS-based hepatocellular carcinoma (HCC) surveillance

Marcello Dallio[1], Mario Romeo[1], Fiammetta Di Nardo[1], Carmine Napolitano[1], Paolo Vaia[1], Claudio Basile[1], Antonio Scafuri[1], Marco Niosi[1], Luigi Vitale[1], Alessandro Federico[1].
[1]Hepatogastroenterology Division, Department of Precision Medicine, University of Campania Luigi Vanvitelli; Piazza Miraglia 2, 80138, Naples (Italy), Naples, Italy
Email: marcello.dallio@unicampania.it

Background and aims: The LI-RADS Visualization Score (Li-RADSVS) standardizes ultrasound (US) adequacy for hepatocellular carcinoma (HCC) surveillance in advanced chronic liver disease (ACLD), distinguishing score A (optimal), B (suboptimal), and C (poor visualization). Scores B/C reduce US sensitivity, prompting Magnetic Resonance Imaging (MRI)/ Computerized Tomography (CT) use. Severe obesity and Metabolic dysfunction-Associated Steatotic Liver Disease (MASLD)-related steatosis are known to impair Li-RADSVS. Post-cholecystectomy syndrome (PCS), characterized by continuous bile flow, altered motility, and meteorism, may hinder hepatic US visualization. However, its impact on Li-RADSVS in non-obese, non-MASLD viral-related ACLD remains unexplored.
Method: Hospitalized non-obese, non-MASLD viral-related (chronic HBV/HCV infection) cACLD patients were enrolled into observation (Obs, 2015–2020, n: 106) and validation (Vld, 2021–2025, n: 102) cohorts. ACLD diagnosis was confirmed by liver stiffness measurement (LSM >15 kPa). Demographic, clinical, pharmacological, and surgical data were collected; patients on UDCA or antimeteorics were excluded. After a 3-day standardized diet, fasting US was performed on day 4 by three blinded operators assigning Li-RADSVS (A/B/C) via electronic case report forms. Interobserver agreement (Cohen's kappa) was assessed. Patients were stratified by cholecystectomy

status (PCS vs no-PCS). Obs patients with a unanimous score C underwent MRI/CT, and the focal liver lesion (FLL) missing rate (i.e., FLL undetected by none of the three operators) was evaluated.
Results: Weighted Cohen's kappa ranged from 0.40–0.70 (Obs) and 0.38–0.72 (Vld) (Table 1). PCS prevalence was 40.2% (Obs) and 38.2% (Vld), with significantly higher score C rates vs no-PCS (Obs: 44% vs 23%, p = 0.034; Vld: 42% vs 21%, p:0.027). Multivariate analysis (adjusted for sex, age, Body Mass Index, etiology) identified prior cholecystectomy as independently associated with poor visualization [Obs: aHR 1.325, p: 0.002; Vld: aHR 1.221, p: 0.001], along with time since surgery >2 years [Obs: aHR 1.105, p: 0.031; Vld: aHR 1.136, p: 0.038]. In Obs score C patients undergoing CT/MRI, FLL missing was reported in 39% of cases.
Conclusion: Prior cholecystectomy significantly impairs US visualization in non-obese, non-MASLD viral-related ACLD, reducing LI-RADSVS and impacting HCC surveillance accuracy.

THU-385
Cholangiocarcinoma in individuals with chronic liver diseaseis diagnosed earlier leading to better prognosis
Jone Narbaiza[1], Laura Izquierdo-Sánchez[1,2], Julen Martin-Robles[1], Angela Lamarca[3], Heinz-Josef Klumpen[4], Adelaida La Casta[1], Arun Valsan[5], Stephanie Roessler[6,7], Chiara Braconi[8,9], Leonardo da Fonseca[10,11], Cristina Dopazo[12,13], Trine Folseraas[14,15,16,17], Alejandro Forner[2,18], Bas Groot Koerkamp[19], Domingo Balderramo[20], Mariano Ponz-Sarvise[21], Javier Diaz-Ferrer[22], Krzysztof Zieniewicz[23], Zeno Sparchez[24], Kirsten Utpatel[25], Markus Peck-Radosavljevic[26], Juan Valle[3,27], Lynn Nooijen[28], Luis Bujanda[1,2], Jesus M Banales[1,2,29,30]. *[1]Department of Liver and Gastrointestinal Diseases, Biogipuzkoa Health Research Institute, Donostia University Hospital, University of the Basque Country (UPV/EHU), DONOSTIA-SAN SEBASTIAN, Spain; [2]National Institute for the Study of Liver and Gastrointestinal Diseases, CIBERehd, "Instituto de Salud Carlos I" (ISC I), Madrid, Spain; [3]Institute of Cancer Sciences, University of Manchester, Manchester, United Kingdom; [4]Department of Medical Oncology, Amsterdam UMC, University of Amsterdam, Cancer Center Amsterdam, Amsterdam, Netherlands; [5]Department of Hepatology and Gastroenterology, Amrita Institute of Medical Sciences and Research (AIMS), Kochi, India; [6]Institute of Pathology, Heidelberg University, ImNeuenheimer Feld 224, Heidelberg, Germany; [7]Liver Cancer Center Heidelberg (LCCH), Heidelberg, Germany; [8]School of Cancer Sciences, University of Glasgow, Glasgow, United Kingdom; [9]The Royal Marsden NHS Trust, London & Surrey, London, United Kingdom; [10]Instituto do Cancer do Estado de Sao Paulo (ICESP), Hospital das Clinicas (HCFMUSP), Faculdade de Medicina, Universidade de Sao Paulo, Sao Paulo, Brazil; [11]São Paulo Clínicas Liver Cancer Group, Hospital das Clinicas (HCFMUSP), Faculdade de Medicina, Universidade de Sao Paulo, Sao Paulo, Brazil; [12]Department of Surgery, School of Medicine, Universitat Autònoma de Barcelona, Barcelona, Spain; [13]Department of Hepatic and Biliary Surgery and Transplants, Val d'Hebron Barcelona Hospital Campus, Barcelona, Spain; [14]Norwegian PSC Research Center, Department of Transplantation Medicine, Oslo University, Hospital Rikshospitalet, Oslo, Norway; [15]Institute of Clinical Medicine, Faculty of Medicine, University of Oslo, Oslo, Norway; [16]Research Institute of Internal Medicine, Division of Surgery, Inflammatory Diseases and Transplantation, Oslo University Hospital Rikshospitalet, Oslo, Norway; [17]Section of Gastroenterology, Department of Transplantation Medicine, Oslo University Hospital, Oslo, Norway; [18]Liver Unit, Barcelona Clinic Liver Cancer (BCLC) group, Hospital Clinic Barcelona, IDIBAPS, University of Barcelona, Barcelona, Spain; [19]Department of Surgery, Erasmus MC Cancer Institute, University Medical Center Rotterdam, Rotterdam, Netherlands; [20]Gastroenterology Department, Hospital Privado Universitario de Córdoba, Instituto Universitario de CienciasBiomédicas de Córdoba, Córdoba, Argentina; [21]Clinica Universidad de Navarra and Program in Solid Tumors (CIMA), Universidad de Navarra, IDISNA, Pamplona, Spain; [22]Departamento del Aparato Digestivo, Hospital Nacional Edgardo Rebagliati Martins-Essalud, Facultad de Medicina, Universidad De San Martin De Porres, Lima, Peru; [23]Department of General, Transplant and Liver Surgery, Medical University of Warsaw, Warsaw, Poland; [24]3rd Medical Department, Institute for Gastroenterology and Hepatology, University of Medicine and Pharmacy, Cluj Napoca, Romania; [25]Institute of Pathology, University of Regensburg, Regensburg, Germany; [26]Internal Medicine and Gastroenterology (IMuG) and Emergency Medicine (ZAE), Klinikum Klagenfurt Am Wörthersee, Klagenfurt, Austria; [27]Cholangiocarcinoma Foundation, Herriman, Utah, United States; [28]Department of Surgery, Cancer Center Amsterdam, Amsterdam UMC, University of Amsterdam, Amsterdam, Netherlands; [29]Department of Biochemistry and Genetics, School of Sciences, University of Navarra, Pamplona, Spain; [30]Ikerbasque, Basque Foundation for Science, Bilbao, Spain*
Email: jesusmaria.banalesasurmendi@bio-gipuzkoa.eus

Background and aims: Cholangiocarcinoma (CCA) is a lethal cancer with rising incidence and mortality worldwide. Chronic liver disease (CLD) is recognised as an important risk factor, but its impact on tumour presentation and outcomes remains poorly defined. We aimed to compare the clinical course of CCA in patients with and without CLD.
Method: We retrospectively analysed 3,743 patients diagnosed with CCA between 2010 and 2024 across participating international centres. Patients were classified as CLD if a diagnosis of cirrhosis, primary sclerosing cholangitis (PSC), viral hepatitis, or other chronic liver condition preceded their cancer diagnosis, and non-CLD otherwise. Demographic, clinical, biochemical, and outcome data were compared.
Results: Patients with CLD (n = 993) were more frequently male (67% vs. 53%) and younger (63 vs. 66 years) than non-CLD (n = 2,750) individuals. They more often presented with intrahepatic tumours (64% vs. 42%), better performance status (ECOG 0: 53% vs. 35%), lower CA19.9 levels (56 vs. 135 U/mL), and earlier stage disease (localized: 57% vs. 43%; metastatic: 23% vs. 31%). Accordingly, curative-intent surgery was more common (60% vs. 48%), resulting in improved median overall survival (mOS: 12.2 vs. 11.1 months, $p < 0.05$) and higher 5-year survival (OR: 1.64, $p < 0.01$), particularly in intrahepatic CCA (mOS: 14.2 vs. 11.1 months, $p < 0.001$; 5-year survival OR: 2.05, $p < 0.001$). Treatment response across modalities did not differ. Within the CLD cohort, prior diagnosis of primary sclerosing cholangitis and cirrhosis were strongly associated with earlier-stage CCA detection.
Conclusion: Patients with pre-existing CLD are more likely to be diagnosed with CCA at an earlier stage, contributing to improved survival. These findings support evaluation of structured surveillance programs in high-risk CLD populations.

THU-386
Heterogeneity in hepatocellular carcinoma screening across social determinants of health phenotypes
Lauren Nephew[1], Allie Carter[1], Dipika Gupta[2]. *[1]Indiana University School of Medicine, Indianapolis, United States; [2]Indiana Univesity School of Medicine, Indianapolis, United States*
Email: lnephew@iu.edu

Background and aims: Disparities in hepatocellular carcinoma (HCC) outcomes are shaped by intersecting social determinants of health (SDOH), yet most studies examine individual risk factors in isolation. Using latent class analysis (LCA), we previously identified six SDOH phenotypes associated with progressively worse stage at diagnosis, receipt of curative therapy, and survival. Because timely HCC screening improves early detection and outcomes, we examined whether adverse outcomes across SDOH-based latent classes were attributable to differences in HCC screening.
Method: We analyzed 4,117 adults with HCC in the Indiana Statewide Cancer Registry (2009–2020). LCA identified six risk classes based on demographics, insurance, marital status, occupation, area social deprivation, and geographic access. Minimal Barriers; Publicly Insured, Married Females; 3 Publicly Insured, Unpartnered Males; Rural and Geographically Distant; Structurally Marginalized; and 6) Unseen and Uninsured. Patients were attributed to a health system

based on longitudinal engagement within 24 months before diagnosis. Screening outcomes included any screening (imaging/AFP), routine imaging (imaging only), and routine screening (imaging & AFP) within a two-year lookback period, excluding the 90 days before diagnosis. Univariable logistic regression compared screening outcomes across classes using the lowest-risk class as reference.

Results: 1,905 patients met attribution criteria. Latent classes demonstrated graded differences in stage at diagnosis, receipt of curative therapy, and mortality. Among attributed patients, 47.8% received any screening and 18.6% received routine screening. Compared with the reference group, patients in the Unseen and Uninsured class were less likely to receive any screening (OR 0.62, p = 0.029), routine imaging (OR 0.48, p = 0.002), and routine screening (OR 0.30, p < 0.001). Patients in the Rural and Under-supported class were also less likely to receive any screening (OR 0.73, p = 0.044) and routine imaging (OR 0.65, p = 0.008). In contrast, the Structurally Marginalized class demonstrated screening rates comparable to the reference group for any screening (OR 0.96, p = 0.801) and routine imaging (OR 0.98, p = 0.898), despite worse stage at diagnosis and survival.

Conclusion: SDOH-based latent classes reveal heterogeneity in HCC screening patterns. Worse outcomes among some high-risk groups may not be fully explained by screening failure alone, underscoring the need for class-specific, precision outreach strategies.

THU-387

Identify liver tumors from ultrasound images through ensemble learning integrated with the ordered weighted averaging operator

Hsiao-Ching Nien[1,2], Jonathan Lee[3], Jong-Yih Kuo[4,5], Ti-Feng Hsieh[4], Chih-Horng Wu[6], Jin-Chuan Sheu[6], Pei-Lien Chou[7]. *[1]The Good liver foundation Taiwan and the Department of Family Medicine, National Taiwan University Hospital, Taipei, Taiwan; [2]Associate Professor, Center for General Education, National Taiwan University, Taipei, Taiwan; [3]National Taiwan University, Taipei, Taiwan; [4]National Taipei University of Technology, Taipei, Taiwan; [5]National Taipei University of Technology, Taipei; [6]National Taiwan University Hospital, Taipei, Taiwan; [7]The YUAN High-Tech Development Co., Ltd, Taipei, Taiwan*
Email: jykuo@ntut.edu.tw

Background and aims: Liver tumors are one of the main causes of death in the Pan-Asia region. Its high prevalence rate and case fatality rate make early diagnosis and treatment even more crucial. Ultrasound examination, as a noninvasive and easy-to-access tool, plays a vital role in screening liver tumors. However, it is somewhat limited by the quality of ultrasound images and the operation skills of the physicians. In this work, we propose an approach to integrating ensemble learning to increase the accuracy and precision of the diagnosis.

Method: By utilizing ensemble learning, we combine four models: YOLO v7, ResNet, EfficientNet, and RegNet, and integrate these models with Hard Voting, Soft Voting, and Ordered-Weighted-Averaging (OWA) operator. A dataset from the National Taiwan University Hospital of 4,599 ultrasound images taken from 1,576 patients, covering 10 types of tumors, was used to dichotomize benign versus malignant tumors. Model evaluation metrics include Precision, Recall, AUC, and Accuracy.

Results: The experiment results indicated that applying ensemble learning for binary classification achieved accuracies of 0.849, 0.688, 0.623, and 0.725 in Accuracy, Recall, Precision, and AUC, respectively. For the 8-class classification, applying ensemble learning achieved accuracies of 0.769, 0.303, 0.413, and 0.787 in Accuracy, Recall, Precision, and AUC, respectively, indicating a potential solution for the early diagnosis and clinical application of liver tumors.

Conclusion: This work developed multiple ensemble models based on ensemble learning, integrated with the OWA, Hard Voting, and Soft Voting methods, and evaluated their performance in perspective. In the model integration, there are two primary issues: one is that ensemble learning may reduce the contributions from stronger models and meanwhile introduce interference from weaker models; and the other is that assigning the model weights remains a challenge. To address these issues, we applied the OWA operator to provide an adjustable weighting mechanism, simplifying the model integration and alleviating the side effects from the weaker models. The experimental results indicate that OWA can effectively enhance the performance of ensemble models, resulting in a more balanced integration model and providing a more efficient solution for image classification tasks.

THU-393-YI

Comparison of sarcopenia and liver frailty indices for overall survival in hepatocellular carcinoma patients treated with first-line Atezolizumab-Bevacizumab

Asier Rabasco Meneghetti[1,2], Philippe Sultanik[3], Claudia Campani[4,5], Charles Roux[6], Zunamys Itzel Carrero[1], Dan-Adrian Popica[6], Giuliana Amaddeo[7], Marie Lequoy[8], Clemence Hollande[9], Sarah Mouri[3], Mathilde Wagner[10], Vincent Plaforet[6], Sabrina Sidali[4,9], Maxime Ronot[11], Marika Rudler[3], Alain Luciani[12], Olivier Sutter[13], Eléonore Spitzer[3], Hélène Regnault[7], Sanaa El Mouhadi[10], Violaine Ozenne[8], Nathalie Ganne-Carrié[4,14], Mohamed Bouattour[15], Jean Charles Nault[4,14], Dominique Thabut[3,16], Jakob Nikolas Kather[1,17,18], Manon Allaire[3,4,19]. *[1]Else Kroener Fresenius Center for Digital Health, Faculty of Medicine and University Hospital Carl Gustav Carus, TUD Dresden University of Technology, Dresden, Germany; [2]German Cancer Consortium (DKTK), Partner site Dresden, German Cancer Research Center (DKFZ), Heidelberg, Germany; [3]APHP Sorbonne University, Pitié Salpêtrière Hospital, Hepatogastroenterology unit, Paris, France; [4]INSERM UMR 1138, Centre de recherche des Cordeliers, Paris, France; [5]Department of Experimental and Clinical Medicine, Internal Medicine and Hepatology Unit, University of Firenze, Firenze, Italy; [6]AP-HP Sorbonne Université, Hôpital Universitaire Pitié-Salpêtrière, Service de radiologie interventionnelle, Paris, France; [7]Department of Hepatology, Henri Mondor University Hospital, Assistance Publique-Hôpitaux de Paris, Créteil, France; [8]AP-HP Sorbonne Université, Hôpital Universitaire Saint Antoine, Service d'Hépato-gastroentérologie, Paris, France; [9]Liver Cancer Unit, Assistance Publique - Hôpitaux de Paris, Beaujon University Hospital, Clichy, France; [10]AP-HP Sorbonne Université, Hôpital Universitaire Saint Antoine, Service d'Imagerie, Paris, France; [11]Department of Radiology, Assistance Publique - Hôpitaux de Paris, Beaujon University Hospital, Clichy, France; [12]Department of Medical Imaging, Assistance Publique-Hôpitaux de Paris, Henri Mondor-Albert Chenevier University Hospital, Créteil, France; [13]Interventional Radiology Unit, Hôpital Avicenne, Hôpitaux Universitaires Paris-Seine-Saint-Denis, AP-HP, Bobigny, France; [14]AP-HP Sorbonne Paris Nord, Hôpitaux Universitaire Paris Seine Saint-Denis, Service d'Hépatologie, Bobigny, France; [15]AP-HP, Hôpital Beaujon, Liver Cancer and Innovative Therapy, CLICHY, France; [16]Sorbonne Université, INSERM, Centre de recherche Saint-Antoine (CRSA), Institute of Cardiometabolism and Nutrition (ICAN), Paris, France; [17]Department of Medicine I, University Hospital Dresden, Dresden, Germany; [18]Medical Oncology, National Center for Tumor Diseases (NCT), University Hospital Heidelberg, Heidelberg, Germany; [19]Genomic Instability, Metabolism, Immunity and Liver Tumorigenesis laboratory, Equipe Labellisée LIGUE 2023, Paris, France*
Email: asier.rabasco@tu-dresden.de

Background and aims: Sarcopenia is associated with worse outcomes in patients with hepatocellular carcinoma (HCC). However, its prognostic value in patients treated with first-line Atezolizumab-Bevacizumab (AtezoBev), remains uncertain. In this study, we compared volumetric CT-derived muscle with conventional L3-level skeletal muscle index (L3-SMI) for predicting overall survival (OS) in a multicentric French cohort of patients with unresectable HCC treated with AtezoBev. The liver Frailty Index (LFI) was also evaluated in a predefined subset of patients.

Method: Patients from 5 French liver centres receiving AtezoBev as first line systemic therapy with CTs within 3 months before treatment

initiation were included. OS was defined from treatment initiation to death from any cause or last follow-up. Sarcopenia was assessed using a volumetric muscle-to-bone ratio (BOA pipeline), L3-SMI and Day-0 LFI (subset, n = 46). Weighted Cox models adjusted for clinical covariates were fitted. Performance was assessed through leave-one-centre-out concordance indices (C-Index). Stratification was evaluated by Kaplan-Meier (KM) curves and log-rank tests.
Results: Among 338 included patients, 293 (87%) were male, median age was 66.6 years, 244 (72%) presented with cirrhosis, 187(55%) were treatment-naive, 213 (63%) were BCLC stage C, 133 (39%) presented with type 2 diabetes and 185 (55%) presented with arterial hypertension. Median OS was 14 months, 240 patients (71%) died during follow-up, including 35 (10%) before the first AtezoBev response assessment. In univariate analysis, the volumetric index was associated with OS (HR 0.80, 95%CI 0.66–0.97, p = 0.020) as was L3-SMI (HR 0.74 95%CI 0.61–0.89; p < 0.001) whereas LFI was not (HR 1.14, p = 0.45). After adjustment for confounders, both the volumetric index (HR: 0.80, 95%CI 0.68–0.94, p = 0.005) and L3-SMI (HR 0.74, 95% CI 0.65–0.84, p < 0.001) remained independently associated with OS. Corresponding C-Indices were 0.59 (95%CI 0.53–0.65) and 0.61 (95% CI 0.56–0.67). KM curves showed significant stratification for the volumetric index (p = 0.035) but not for L3-SMI (p = 0.076).
Conclusion: In unresectable HCC patients treated with first-line AtezoBev, both volumetric and L3-derived sarcopenia indices were independently associated with OS, whereas the liver frailty index was not, likely due to limited sample size. Volumetric sarcopenia assessment provided superior risk stratification and is feasible in routine practice, suggesting potential added value over other OS markers in this setting.

THU-394

MASLD-related hepatocellular carcinoma in cirrhotic and non-cirrhotic patients: a real-world analysis from the ITA.Li.Ca. cohort

Lucia Ragozzino[1], Alessio Mastro[1], Claudia Campani[2], Arianna Toscano[2], Tancredi Vincenzo Li Cavoli[1], Valentina Adotti[1], Tommaso Zurli[1], Fabio Marra[1]. *[1]Università degli Studi di Firenze, Firenze, Italy; [2]Dipartimento di Medicina Sperimentale e Clinica, Firenze, Italy*
Email: lucia.ragozzino@unifi.it

Background and aims: Metabolic dysfunction-associated steatotic liver disease (MASLD) is a leading cause of hepatocellular carcinoma (HCC), which may develop with or without cirrhosis. The study aimed to assess differences in tumour burden, treatment access, and outcomes between cirrhotic and non-cirrhotic MASLD-related HCC.
Method: Data from the ITA.Li.Ca. database (27 centres, 2003–2022) were retrospectively analysed. Patients with MASLD-related HCC and no other liver disease aetiologies were included. Baseline clinical, biochemical, and tumour features were compared according to cirrhosis status. Tumour response was classified according to mRECIST criteria.
Results: Among 903 eligible patients, 273 (30%) were non-cirrhotic. Only 25% were under ultrasound surveillance; 64% showed no significant fibrosis by FIB-4. Cirrhotic patients were more often obese and diabetic, with worse liver function (MELD 9.7 vs 8.5; p < 0.001). Non-cirrhotic patients had larger tumours (≥50% parenchymal involvement 15% vs 8%; p = 0.01) but similar rates of vascular invasion and metastases.Almost half of non-cirrhotic cases lacked histological confirmation despite recommendations.When we separately analysed cirrhotic and non-cirrhotic patients not undergoing surveillance, non-cirrhotic patients had bigger tumours (p value <0,001), although without differences in tumour spread.This difference was also confirmed in patients undergoing semi-annual surveillance (10% vs. 2.6%, p = 0.029).In the whole cohort, no significant differences in overall survival were observed between cirrhotic and non-cirrhotic patients, regardless of the treatment they received.Non-cirrhotic patients underwent more resections (64% vs 31%), while cirrhotics received more ablation (27%) and transplantation (15%). Tumour burden remained higher in non-cirrhotics irrespective of surveillance. Overall survival did not differ by cirrhosis status or treatment type (log-rank p > 0.05 for all).
Conclusion: MASLD-related HCC in non-cirrhotic patients presents with greater tumour burden but comparable survival to cirrhotic HCC. Despite guideline recommendations, biopsy is often omitted in non-cirrhotic cases. Treatment selection should prioritise tumour and liver function characteristics rather than the presence of cirrhosis. These findings highlight the need for tailored surveillance strategies in noncirrhotic MASLD.

THU-395

Attention-based multiple instance learning for classification of focal liver lesions using contrast-enhanced ultrasound

Adil Oezsoy[1], Tom Luedde[1], Janik Hohmann[1], Pompilia Radu[2], Annalisa Berzigotti[2], Jakob Nikolas Kather[3], Ralph Stetter[4], Georg Kunze[5], Tobias Paul Seraphin[1], Michael Kallenbach[1]. *[1]Medical Faculty and University Hospital Düsseldorf, Heinrich Heine University Düsseldorf, Düsseldorf, Germany; [2]Bern University Hospital, University of Bern, Bern, Switzerland; [3]Else Kroener Fresenius Center for Digital Health, Technical University Dresden, Dresden, Germany; [4]Klinikum Worms, Worms, Germany; [5]Schwarzwald-Baar Klinikum Villingen-Schwenningen, Villingen-Schwenningen, Germany*
Email: adil.oezsoy@hhu.de

Background and aims: Accurate characterization of focal liver lesions (FLLs) remains challenging in clinical practice. Contrast-enhanced ultrasound (CEUS) is a reliable, low-cost modality, but interpretation depends on the examiner's experience. Prior AI-based CEUS studies often require resource-intensive preprocessing and lack external validation. This study applied a weakly supervised attention-based multiple instance learning approach to classify FLLs and validated performance on external cohorts.
Method: Retrospectively collected multicenter data from four FLL types—focal nodular hyperplasia (FNH), hemangioma, hepatocellular carcinoma (HCC), and metastasis—were analyzed. Deep learning features were extracted from CEUS images using a pretrained convolutional neural network. A class-balanced 20% test set was held out, while the remaining data were used to train a classifier with grid search and five-fold cross-validation, selecting hyperparameters based on mean AUROC. The final model ensembled the five best cross-validation models and was evaluated on the internal test set and three external cohorts.
Results: The in-house dataset included 370 patients (FNH n = 52, hemangioma n = 149, HCC n = 67, metastasis n = 102). The final model achieved an average AUROC of 0.79 during cross-validation. On the held-out test set, AUROCs were 0.81, 0.77, 0.87 and 0.92 for FNH, hemangioma, HCC, and metastasis, respectively. In external validation, AUROCs for the first cohort (25 patients, same machine, cohort 1) were 0.89, 0.69, 0.87, and 0.71 and for the second cohort (39 patients, same machine, cohort 2) were 0.72, 0.68, 0.61, and 0.62. For the third cohort (19 patients, cohort 3) a different ultrasound machine was used, resulting in AUROCs of 0.21, 0.66, 0.56, and 0.65 for FNH, hemangioma, HCC, and metastasis, respectively. Post-hoc explainability analyses were performed to better understand the decision process of the model.
Conclusion: Weakly supervised MIL demonstrated robust performance in classifying FLLs using CEUS data during cross-validation and on the held-out test set, without requiring extensive preprocessing. Exam set-up, machine type and user-dependent artefacts influence the model's overall performance, whilst explainability analyses can provide insight into stable learnt features. Further research and larger cohorts are needed to confirm the clinical utility of such algorithms.

THU-396

Prognostic nutritional index as a predictor for survival in hepatocellular carcinoma patients with concurrent metabolic dysfunction-associated steatotic liver disease

Tsai Shin-Yu[1], Chun-Ting Ho[1,2], Yi-Chen Lin[3], Chia-Jung Ho[1], Yi-Hsiang Huang[4], Ming-Chih Hou[5], Jaw-Ching Wu[6], Chien-Wei Su[7]. *[1]Taipei Veterans General Hospital, Department of Medicine, Taipei, Taiwan; [2]National Yang Ming Chiao Tung University Yangming Campus, Ph.D. Program of Interdisciplinary Medicine, Taipei, Taiwan; [3]Linkou Chang Gung Memorial Hospital, Department of Medicine, Taoyuan City, Taiwan; [4]Taipei Veterans General Hospital, Department of Medical Research, Taipei, Taiwan; [5]Taipei Veterans General Hospital, Division of Gastroenterology and Hepatology, Department of Medicine, Taipei, Taiwan; [6]National Yang Ming Chiao Tung University Yangming Campus, Institute of Clinical Medicine, Taipei, Taiwan; [7]Taipei Veterans General Hospital, Division of General Medicine, Department of Medicine, Taipei, Taiwan*
Email: cwsu2@vghtpe.gov.tw

Background and aims: Metabolic dysfunction–associated steatotic liver disease (MASLD) has emerged as a major etiology of chronic liver disease and may influence the prognosis of hepatocellular carcinoma (HCC). However, evidence regarding noninvasive serum biomarkers (NISB) for predicting the prognosis of HCC patients with MASLD remain limited. This study aimed to evaluate the prognostic ability of NISBs on predicting outcomes in this population.
Method: Between 2015 and 2023, 460 consecutive patients with HCC and concurrent MASLD who underwent curative hepatic resection at a single tertiary center were retrospectively analyzed. Associations between NISBs or prognostic scores and overall survival (OS) were evaluated using the Cox proportional hazards model. The Akaike information criterion (AIC) was used to compare the predictive performance among the prognostic nutritional index (PNI), albumin–bilirubin (ALBI) score, fibrosis-4 (FIB-4) score, and lymphocyte-to-monocyte ratio (LMR).
Results: After a median follow-up of 48 months (interquartile range, 25–71 months), 92 patients (20.0%) died, yielding a 5-year OS rate of 78.4% (95% confidence interval, [CI], 74.1–82.7%). Independent predictors of poor OS in multivariable Cox regression analysis included serum albumin <4 g/dL, creatinine >1.2 mg/dL, aspartate aminotransferase >45 U/L, tumor size >5 cm, and high histologic grade. Among the NSIBs, PNI demonstrated the best prognostic performance with the lowest AIC (879.797), followed by ALBI (896.214), FIB-4 (903.551), and LMR (911.328). Patients with PNI <45 had significantly lower 5-year OS rates than those with PNI ≥45 (68.2% vs. 87.6%, $p < 0.001$; hazard ratio 2.31, 95% CI 1.52–3.50). This survival difference was particularly pronounced in patients with preserved liver function (Child–Pugh class A) and in those without cirrhosis. Subgroup analyses consistently demonstrated poorer survival in the low-PNI group across most clinical strata, including age (>65 vs. ≤65 years), tumor size (≤5 cm vs. >5 cm), BCLC stage (0/A), and the presence or absence of microvascular invasion (all $p < 0.05$).
Conclusion: PNI, calculated from serum albumin concentration and peripheral lymphocyte count, serves as a simple and effective prognostic score for predicting postoperative survival in patients with HCC patients with concurrent MASLD and had consistent performance in different subgroups.

THU-397

Imaging spectrum of giant hepatic hemangioma with diffuse hepatic hemangiomatosis: nine case series

Ki Choon Sim[1], Beom Jin Park[1], Min Ju Kim[1], Deuk Jae Sung[1], Na Yeon Han[1], Yeo Eun Han[1], Seungha Cha[1], Tae Hyung Kim[2]. *[1]Department of Radiology, Korea University Anam Hospital, Seoul, Korea, Rep. of South; [2]Department of Gastroenterology, Korea Unversity Anam Hospital, Seoul, Korea, Rep. of South*
Email: kspringsim@korea.ac.kr

Background and aims: Giant hepatic hemangioma accompanied by diffuse hepatic hemangiomatosis is a rare entity in adults and can mimic infiltrative hepatic malignancies. While individual case reports have described its imaging characteristics, larger case series remain limited. This study aims to summarize the radiologic features and clinical characteristics of patients with giant hemangioma and coexisting diffuse hepatic hemangiomatosis.
Method: A retrospective radiologic database search was performed using the keyword "diffuse hepatic hemangiomatosis." Thirteen adult patients with imaging findings suspicious for diffuse hepatic hemangiomatosis were identified. Clinical information, laboratory data, contrast-enhanced CT, multiphasic liver MRI, and available pathology reports were reviewed. Imaging features—including enhancement patterns, lesion distribution, and associated hepatic abnormalities—were systematically analyzed.
Results: A total of 13 patients met the imaging criteria for diffuse hepatic hemangiomatosis. Among them, 9 patients had both CT and MRI available for comprehensive radiologic evaluation. Typical imaging findings included peripheral nodular enhancement with progressive fill-in in giant hemangiomas and innumerable small T2-hyperintense nodules consistent with diffuse hepatic hepatic hemangiomatosis. Pathologic confirmation was obtained in 3 patients, all demonstrating cavernous hemangioma or hemangiomatosis without evidence of malignancy. However, one of them subsequently required an additional hepatectomy due to progression of diffuse hepatic hemangiomatosis. Follow-up imaging demonstrated overall stability in the majority of cases.
Conclusion: This case series highlights characteristic radiologic findings of giant hepatic hemangioma with diffuse hemangiomatosis in adults. Recognition of this pattern is essential to avoid misdiagnosis as infiltrative malignancy. CT and MRI provide complementary diagnostic information, and pathology—though not always required—can confirm the vascular benign nature. Conservative management appears appropriate in patients with preserved liver function and stable imaging features.

THU-398

Hepatocellular carcinoma in Budd Chiari syndrome: characteristics and risk factors

Marinela Stoian[1,2]. *[1]Carol Davila University of Medicine and Pharmacy, Bucharest, Romania, Internal Medicine Dr Ioan Cantacuzino Hospital, Bucharest, Romania; [2]Carol Davila University of Medicine and Pharmacy, Bucharest, Romania, Internal Medicine Dr Ioan Cantacuzino Hospital, Bucharest, Romania*
Email: marilenastoian@yahoo.com

Background and aims: To analyze the characteristics and the factors associated with the development of hepatocellular carcinoma (HCC) in patients with Budd-Chiari syndrome (BCS).
Method: A cohort of one hundred and two consecutive patients with BSC was retrospectively evaluated. A comprehensive investigation for underlying prothrombotic disorders was performed. Liver nodules were evaluated with serum alpha-fetoprotein (AFP) dosage and analysis imaging features (CT/MRI). Liver biopsy was obtained in presence of: diameter >2 cm or increase in size on surveillance imaging, number ≤2, portal washout and /or increase in AFP level. Nodules were diagnosed as benign when none of these criteria were fulfilled. HCC invading hepatic veins or inferior vena cava (IVC) were excluded.
Results: Patients characteristics were: female sex (n = 70), mean age at diagnosis 37 years, mean follow up period 7 years, IVC obstruction in 12 patients, myeloproliferative diseases in 48/49 patients (55%), liver nodules in 34 patients. Treatment consisted of oral anticoagulation in all patients, hepatic veins angioplasty in 20 patients, porto–systemic shunt in 49 patients (TIPS in 18 patients and surgical shunt in 32 patients) and seventeen patients received liver transplantation. Hepatocellular carcinoma was diagnosed in 9 cases. Liver parenchyma adjacent to HCC showed severe fibrosis or cirrhosis

in 7 cases. Hepatitis B and C markers were negative in all HCC cases. In univariate analyses including age, sex, alcohol consumption, prothrombotic disorders, IVC obstruction, portal vein obstruction, disease duration and BSC treatment, three factors were associated with HCC development: male sex (6/9, 67% vs. 26/93, 28%. p = 0.026), factor V Leiden (4/8, 50% vs. 15/80, 18.5%, p = 0.06) and IVC obstruction (7/9, 78% vs.5/93, 5%, p < 0.001). In multivariate analysis, only IVC was associated with HCC (p < 0.0001, OR = 78, IC = 10.8–560.7). Porto-systemic shunt did not increase the risk of HCC (4/32, 12.5% vs. 5/70, 7%). Serum AFP level had very high predictive value to distinguish HCC from benign nodules: AFP >10 ng/ml (n = 8/8, PPV = 100%, mean: 1546 ng/ml, range: 13–10400 ng/ml) vs. AFP<10 ng/ml (n = 22/23, NPV = 96%, mean: 3.5 ng/ml, range: 1–7 ng/ml).
Conclusion: The incidence of HCC in BCS (1.6% per year) is similar to that reported in other chronic liver disease and is associated with IVC obstruction, male sex and factor V Leiden. High serum alpha-fetoprotein level appears to be a useful screening tool in this population.

THU-399

Predicting early recurrence of hepatocellular carcinoma after resection: a machine learning model integrating clinical data and llm-structured pathological features

Tung-Hung Su[1,2,3], Hung-Ning Tung[4], Yen-Ning Hsu[5], Fen-Fang Chen[2], Chia-Chang Wen[6], Shou-Wu Lee[7], Teh-Ia Huo[8], Chien-Chang Lee[9], Jia-Horng Kao[2,3,10,11]. [1]*Department of Medical Research, National Taiwan University Hospital Hsin-Chu Branch, Hsin-Chu, Taiwan;* [2]*Division of Gastroenterology and Hepatology, Department of Internal Medicine, National Taiwan University Hospital, Taipei, Taiwan;* [3]*Hepatitis Research Center, National Taiwan University Hospital, Taipei, Taiwan;* [4]*Department of Internal Medicine, National Taiwan University Hospital Hsin-Chu Branch, Hsin-Chu, Taiwan;* [5]*Center of Intelligent Healthcare, National Taiwan University Hospital, Taipei, Taiwan;* [6]*Information Technology Office, National Taiwan University Hospital, Taipei, Taiwan;* [7]*Division of Gastroenterology, Department of Internal Medicine, Taichung Veterans General Hospital, Taichung, Taiwan;* [8]*Department of Medical Research, Taipei Veterans General Hospital, Taipei, Taiwan;* [9]*Department of Information Management, Ministry of Health and Welfare, Taipei, Taiwan;* [10]*Graduate Institute of Clinical Medicine, National Taiwan University College of Medicine, Taipei, Taiwan;* [11]*Department of Medical Research, National Taiwan University Hospital, Taipei, Taiwan*
Email: tunghungsu@gmail.com

Background and aims: Hepatocellular carcinoma (HCC) remains one of the most deadly cancers worldwide. Surgical resection is the mainstay of curative treatment for early-stage HCC; however, postoperative recurrence is not uncommon and significantly compromises long-term prognosis. We aimed to develop a model integrating clinical and pathological features to predict early (2-year) recurrence after resection.
Method: We established a retrospective cohort of HCC patients who underwent curative resection using data from the Integrated Medical Database (iMED) of National Taiwan University Hospital. Clinical, laboratory, and imaging data were curated and standardized. The pathologic features—including tumor size, number, differentiation, microvascular invasion, satellite nodules, capsule invasion, location, and fibrosis stage were converted into structured variables using the Meta Llama 3.3 multilingual large language model (LLM). Six machine learning algorithms (Logistic Regression, XGBoost, LightGBM, CatBoost, SVM, and Random Forest) were trained on 80% of cases and tested on the remaining 20%.
Results: A total of 1061 HCC patients and 59 clinicopathologic features were included for modeling. Among the tested models, the CatBoost classifier demonstrated the best predictive performance, with an AUROC of 0.791 and an accuracy of 0.756. Using a threshold of 0.476, the sensitivity, specificity, and positive predictive value, and F1-score were 0.674, 0.822, 0.753, and 0.711, respectively. Key predictors of early recurrence included trabecular histologic subtype, BCLC staging, microvascular invasion, tumor volume, and integrated clinicopathologic stage.
Conclusion: By leveraging an LLM to structure pathological features, we developed a machine learning model that integrates clinicopathological data to predict early postoperative recurrence in HCC. Future work will expand the model by incorporating preoperative CT imaging and deep learning techniques to have a comprehensive multimodal framework.

THU-400

Re-evaluating the diagnostic value of alpha-fetoprotein for hepatocellular carcinoma in the direct-acting antiviral era

Yoshinori Takeda[1], Hiroshi Imamura[1], Hirofumi Ichida[1], Akio Saiura[1]. [1]*Juntendo University, Tokyo, Japan*
Email: yo-takeda@juntendo.ac.jp

Background and aims: Direct-acting antivirals (DAAs) achieve sustained virological response (SVR) in most hepatitis C virus (HCV)–infected patients, suppressing hepatic inflammation and lowering baseline alpha-fetoprotein (AFP) levels in the absence of hepatocellular carcinoma (HCC). In parallel, an epidemiological shift toward non-viral HCC, in which background liver disease is associated with lower baseline AFP, has been observed. These changes may improve AFP diagnostic performance; however, whether AFP accuracy has improved in the post-DAA era remains unclear. We evaluated temporal changes in baseline AFP levels and AFP diagnostic performance for HCC in the post-DAA era, with des-γ-carboxy prothrombin (DCP) as a reference.
Method: We retrospectively analyzed 388 patients who underwent curative hepatectomy for HCC (2009–2022). AFP and DCP values measured 4 months postoperatively in patients who remained recurrence-free for at least 1 year were used as surrogate non-HCC reference values (n = 257), representing baseline AFP levels. Patients were stratified into pre-DAA (before August 2016) and post-DAA (September 2016 onward) cohorts, reflecting DAA widespread DAA adoption in Japan. Diagnostic accuracy of AFP and DCP was assessed using AUROC. Optimal AFP cut-offs were evaluated using several ROC-based approaches, including the Youden index. Factors associated with elevated baseline AFP were examined by multivariable regression.
Results: In the post-DAA era, the proportion of HCV non-SVR HCC declined markedly (24% to 5%; $P < 0.001$), whereas non-viral HCC increased numerically (58% to 66%; $P = 0.093$). Baseline (post-operative) AFP levels were significantly lower in the post-DAA cohort than in the pre-DAA cohort (median 3 [IQR 2–4] vs. 4 [3–7] ng/mL; $P < 0.001$), while preoperative AFP levels did not differ between eras. AFP AUROC improved from 0.702 to 0.793 (DeLong P = 0.014), whereas DCP performance was unchanged (P = 0.934). Owing to this upward shift of the ROC curve, an AFP cut-off value of 5 ng/mL achieved higher specificity without a substantial loss of sensitivity in the post-DAA era. Multivariable analysis identified HCV non-SVR status and cirrhosis as independent determinants of higher baseline AFP.
Conclusion: In the post-DAA era, suppression of hepatic inflammation and an increasing proportion of non-viral HCC are associated with lower baseline AFP levels and improved diagnostic performance of AFP for HCC. An AFP cut-off of 5 ng/mL appears appropriate for contemporary HCC diagnosis.

THU-401

Epidemiology and factors affecting survival of intrahepatic cholangiocarcinoma: a population-based study of 12,138 patients

Aya Abdelhameed[1], Ker Shiong Tan[2], Mohamed Mortagy[2], Benjamin E White[2], John Ramage[2]. [1]*Alexandria University Faculty of Medicine, Alexandria, Egypt;* [2]*Basingstoke And North Hampshire Hospital, Basingstoke, United Kingdom*
Email: aya.abdelhameed@hhft.nhs.uk

Background and aims: Intrahepatic cholangiocarcinoma (iCCA) is a rare malignant neoplasm, characterised by its aggressive nature and poor prognosis. Mortality remains high with limited curative options. Previous studies report increasing incidence of iCCA up to 2017 when compared to extrahepatic cholangiocarcinoma. This study aims to determine the recent trends in the epidemiology of iCCA from 2011 to 2022 and the factors affecting the overall survival (OS) of patients with iCCA.
Method: A total of 12,138 patients with iCCA diagnosed between 2011 and 2022 were extracted from the American Surveillance, Epidemiology, and End Results (SEER) database using ICD-10 anatomy code C22.1 and ICD-O-3 morphology code 8160/3. Incidence trends were examined. Kaplan-Meier (KM) plots were generated for the cohort and categorical variables. Univariable and multivariable Cox regression were performed, generating hazard ratios (HR) and confidence intervals (CI).
Results: The incidence of liver cholangiocarcinoma has significantly increased from 165 patients/100,000 in 2011 to 465 patients/100,000 in 2022. The incidence of stage 4 is decreasing, and the incidence of stage 1 is increasing from 2011 to 2022. Most patients were male (50.9%) with a median age of 67 years, and the majority lived in metropolitan areas (90.1%). The most common TNM stage is stage 4 (50%). Only 19.4% of patients underwent resection, with 0.8% having total resection with liver transplant. Most patients did not receive radiotherapy (85.3%), while a majority received chemotherapy (57.3%). Overall survival at 12, 36, 60 and 120 months were 42.0%, 17.1%, 10.8% and 5.7%, respectively. Multivariable Cox regression showed that advanced age (HR 1.01), male sex (HR 1.19), patients who lived in non-metropolitan areas (HR 1.11), advanced TNM stage and patients who did not undergo surgery (HR 3.41) were statistically associated with worse overall survival ($p < 0.05$). However, patients who received radiotherapy (HR 0.60) or chemotherapy (HR 0.38) were statistically associated with higher overall survival ($p < 0.05$).
Conclusion: The incidence of iCCA has almost tripled from 2011 to 2022, possibly due to increasing investigations. Further research is needed to explain this significant increase in incidence. iCCA has poor OS, which is associated with advanced age, male sex, living in non-metropolitan areas (despite increasing incidence in metropolitan areas), and advanced stage. Undergoing surgery, receiving radiotherapy or chemotherapy are associated with higher OS.

THU-402
Evaluation of the ASAP model for detecting hepatocellular carcinoma in Thai patients with chronic liver disease, including those with negative alpha fetoprotein

Nutcha Pinjaroen[1], Claire Chen[2], Jenna Bedrava[3], Kittichote Duangnum[4], Pisit Tangkijvanich[1]. [1]*Center of Excellence in Hepatitis and Liver Cancer, Faculty of medicine, Chulalongkorn University, Bangkok, Thailand;* [2]*Medical & Scientific Research, Core Diagnostic, Abbott Laboratories, Singapore, Singapore;* [3]*Clinical Statistics, Core Diagnostic, Abbott Laboratories, Singapore, Singapore;* [4]*Medical Affairs, Core Diagnostic, Abbott Laboratories, Bangkok, Thailand*
Email: pisittkvn@yahoo.com

Background and aims: Hepatocellular carcinoma (HCC) is a leading cause of cancer-related mortality worldwide. Current HCC surveillance based on biannual ultrasound and alpha-fetoprotein (AFP) testing has suboptimal sensitivity, especially in AFP-negative (<20 ng/mL) patients. Multivariable algorithms such as ASAP (Age, Sex, AFP, and PIVKA-II) are emerging as promising tools for improved HCC detection. This study evaluated the clinical performance of ASAP in a cohort of chronic liver disease (CLD) patients from Thailand, including those with negative AFP.
Method: This case-control study included 978 patients: 445 with first-time HCC and 533 with non-HCC chronic liver disease (CLD), both with mixed etiologies. HCC was diagnosed per APASL guidelines and staged using the Barcelona Clinic Liver Cancer (BCLC) system, with early-stage defined as BCLC 0 or A. Fibrosis stage and cirrhosis status in non-HCC controls were determined by FibroScan and histopathology. Serum AFP and PIVKA-II were measured using Abbott Alinity assays. Diagnostic performance of ASAP and individual biomarkers was assessed using receiver operating characteristic (ROC) curves, corresponding area under the curve (AUC) values, and sensitivity calculations at a fixed specificity of 90%. Comparisons between AUCs were performed using DeLong's paired test.
Results: ASAP showed significantly better performance (AUC = 0.92) than individual biomarkers (0.85 for AFP and 0.86 for PIVKA-II) for distinguishing HCC from CLD ($p < 0.001$). Among patients with advanced fibrosis or cirrhosis, ASAP yielded an AUC of 0.90 (95% CI: 0.88–0.93) for all-stage HCC and 0.86 (95% CI: 0.83–0.90) for early-stage HCC, with sensitivities of 78.0% and 68.0%, respectively, at a fixed specificity of 90%. In the AFP-negative subgroup, which included 245 HCC cases, ASAP detected 151 cases, nearly half of which (48%) were at an early stage. In this group, ASAP achieved an AUC of 0.84 (95% CI: 0.80–0.87) and sensitivity of 62.4% at 90% specificity, significantly outperforming PIVKA-II alone (AUC = 0.79; 95% CI: 0.74–0.83; $p < 0.001$), for distinguishing all-stage HCC from advanced fibrosis/cirrhosis controls.
Conclusion: The ASAP model demonstrated strong clinical performance in detecting HCC, even among patients with negative AFP results. Integrating ASAP into HCC surveillance programs has the potential to optimize cancer detection, particularly for individuals with negative AFP results or inconclusive imaging findings.

THU-403
Tumor burden score as prognostic factor in newly diagnosed hepatocellular carcinoma

Aki Uutela[1,2], Heli Vajavaara[1,2], Vera Nevasuo[2], Helena Isoniemi[1,2], Arno Nordin[1,2], Pia Osterlund[2,3,4,5]. [1]*Helsinki University Hospital, Helsinki, Finland;* [2]*University of Helsinki, Helsinki, Finland;* [3]*Tampere University Hospital, Tampere, Finland;* [4]*University of Tampere, Tampere, Finland;* [5]*Karolinska Institutet, Stockholm, Sweden*
Email: aki.uutela@hus.fi

Background and aims: Both interventional and medical treatments for hepatocellular carcinoma (HCC) are evolving, and accurate prognostic tools are needed to provide optimal treatment intensity. The aim of this study was to provide real-world evidence of prognostic value of tumor burden score (TBS) for newly diagnosed HCC patients (pts).
Method: All 639 adult pts with HCC at Helsinki University Hospital in 2010–2020 were included. Minimum follow-up was 33 months. Milan criteria were used for transplantation. Kaplan-Meier and Cox regression were used. TBS was calculated as $TBS^2 = (\text{size of largest nodule})^2 + (\text{number of nodules})2$.
Results: Median age was 68 years and 76% were male. Underlying liver diseases were alcohol-related (29%), MASLD (23%), viral (16%), not specified (16%) or other (17%). TBS was associated with survival in the whole HCC cohort with median overall survival (mOS) 59 months (5-year OS rate 49%) for low <3.36, 31 (29%) for medium 3.36–13.74, and 5 (11%) for high >13.74 TBS ($p < 0.001$). TBS was not statistically significant for liver transplantation pts (n = 112), mOS not reached (85%) vs 158 (77%) vs not applicable (NA) for low/medium/high TBS respectively ($p = 0.39$) or resection pts (n = 96) 75 (70%) vs. 66 (51%) vs 58 (48%; $p = 0.31$). Local ablation pts (n = 90) had inferior OS per TBS; 53 (40%) vs 35 (18%) vs NA ($p = 0.007$). No statistical significance was noted for TACE pts (n = 156); 37 (23%) vs 25 (20%) vs NA ($p = 0.46$) or systemic anticancer therapy (SACT, n = 61) NA vs 15 (6%) vs 6 (13%) ($p = 0.58$). In palliative care only (n = 124) TBS mattered; 18 (0%) vs 7 (5%) vs 3 (0%; $p < 0.001$). In multivariate analysis for OS primary treatment modality was strongest; transplantation ref., resection HR 3.9 [95% CI 2.4–6.3], ablation 7.2 [4.5–11.5], TACE 10.3 [6.1–15.9], SACT 13.3 [8.1–21.8], and palliative care 18.4 [11.9–28.3]. Child-Pugh score (A ref., B 1.9 [1.5–2.3], and C 2.8 [1.9–4.1]), ECOG (PS0–1 ref., PS2 1.3 [1.0–1.7], and PS3–4 1.9 [1.3–2.7]), and TBS (low ref., medium 1.6 [1.3–

2.1], and high 2.7 [1.7–3.6]) remained independent prognostic factors. Substituting TBS with another tumor burden model, Seven-eleven, in the multivariate model yielded similar results, but with lower HR (low 7–11 ref., medium 1.3 [1.0–1.7], and high 1.8 [1.5–2.3]).
Conclusion: In this study, we show that TBS, together with other markers, has independent prognostic value, i.e., matters in treatment planning. If the patient meets criteria for liver transplantation or resection, good results are achievable also for pts with medium TBS.

THU-404
Predictive value of MRI parameters in the development of hepatocellular carcinoma in liver cirrhosis
Monique van Wijk[1], Jasper van Leengoed[1], Laura Boer[1], Job van der Palen[1], Donald Bouman[1], Maureen Guichelaar[1]. [1]*Medisch Spectrum Twente, Enschede, Netherlands*
Email: maureenguichelaar@yahoo.com

Background and aims: Liver cirrhosis is a key risk factor for hepatocellular carcinoma (HCC) development, however reliable predictive biomarkers are lacking. Different MRI sequences provide non-invasive variables of (changes) in liver parenchyma. Diffusion weighted imaging (DWI) evaluates diffusion and perfusion which can be quantified (b-values and derived apparent diffusion coefficient; ADC), reflecting perfusion, edema and possibly inflammation. Proton density fat fraction (PDFF) is used to measure fat fraction of the liver. This study aims to evaluate the value of these MRI parameters in predicting HCC development in liver cirrhosis.
Method: This single-center retrospective cohort study included patients who underwent annual MRI-based surveillance for hepatocellular carcinoma (HCC) between 2010 and 2024. Patients who developed hepatocellular carcinoma (HCC) were compared with a control cohort randomly selected from the remaining non-HCC population. MRI scans were analyzed for b-values and ADC (mm^2/s) using mean values from nine regions of interest in both hepatic lobes. Various MRI-derived quantitative parameters were studied, including absolute and ratios of several b-values (b0, b150, b400 and b800), liver volume (cm^3), and proton density fat fraction (PDFF; %).
Results: A total of 84 cirrhotic patients were included of which 35 developed HCC. The study population included 49 men (58%) with a mean age of 69.4 ± 9.8 years; the most common underlying liver disease was MASLD (n = 33, 39%). There were no differences between HCC and control patients, except smoking. The overall follow-up time was 58.7 ± 33.3 months. Patients who developed HCC had significant increased b-values in MRI scans at 1 and 2 years preceding HCC development. No correlations were found with other MRI parameters, including liver volume, PDFF and iron content. Two multivariate logistic regression models were tested, which included MRI derived b variables (b0 and the ratio of b0 and b150) at 2 and 1 year before HCC development, showing AUC of resp. 0.81 and 0.83 for HCC development.
Conclusion: This study demonstrates that MRI-derived quantitative parameters of the liver parenchyma (i.g. diffusion-weighted imaging–derived b-values) are associated with changes predictive of hepatocellular carcinoma (HCC) development. Multivariate logistic regression models incorporating these b-values demonstrated good predictive performance, highlighting their potential for early HCC risk stratification, which warrants further studies.

THU-409
Accurate detection of cholangiocarcinoma in primary sclerosing cholangitis by DNA methylation biomarkers in bile and plasma
Hege Marie Vedeld[1], Sigurd Breder[1], Heidi Pharo[1], Hans Petter Brodal[1], Evy Marie Thorkildsen[1], Sara Brandt-Winge[1], Erik von Seth[2], Marit Grimsrud[1], Sheraz Yaqub[1], Tom Hemming Karlsen[1], Krzysztof Grzyb[1], Vemund Paulsen[1], Martti Färkkilä[3], Annika Bergquist[2], Lars Aabakken[1], Kirsten Muri Boberg[1], Trine Folseraas[1], Guro Lind[1]. [1]*Oslo University Hospital, Oslo, Norway;* [2]*Karolinska University Hospital, Stockholm, Sweden;* [3]*Helsinki University Hospital, Helsinki, Finland*
Email: h.m.vedeld@ous-research.no

Background and aims: Current methods for early detection of cholangiocarcinoma (CCA) in individuals with primary sclerosing cholangitis (PSC) lack accuracy, often resulting in CCA diagnosis at advanced, non-curative stages. This study aimed to identify DNA methylation biomarkers in liquid biopsies for earlier and more reliable detection of CCA in PSC.
Method: Reduced representation bisulfite sequencing was used to analyze tissue samples from individuals with CCA (n = 10) and PSC (n = 9), resulting in the identification of 12 candidate DNA methylation biomarkers. Targeted analyses of the biomarker candidates were performed by droplet digital PCR (ddPCR). Following quality control and verification of the assays in tissue samples, four candidates were selected for evaluation in two extensive cohorts of bile (n = 272) and plasma (n = 128) samples from individuals with PSC and/or CCA. Individuals were categorized into three groups: i) concomitant PSC and CCA (PSC-CCA), ii) PSC with a clinical diagnosis of CCA 3–12 months after sample collection (PSC to CCA), and iii) PSC alone (no diagnosis of CCA more than 36 months after sample collection).
Results: Four biomarkers (A–D) demonstrated perfect discrimination (AUC = 1.00) between PSC-CCA and PSC alone in tissue samples. In bile, all four biomarkers achieved an AUC above 0.9 for distinguishing PSC-CCA (n = 20) from PSC alone (n = 207). A two-biomarker panel (A and B) reached 95% sensitivity and 90% specificity, while adding biomarkers C and D increased specificity to 97% with sensitivity maintained at 90%. Notably, the two-biomarker panel identified all eight PSC to CCA cases (100% sensitivity), derived from individuals with PSC who were clinically diagnosed with CCA 3–12 months after bile collection. Performance remained strong in plasma, where an alternative two-biomarker panel (B and C) achieved 70% sensitivity and 90% specificity for distinguishing PSC-CCA (n = 17) and PSC alone (n = 101).
Conclusion: We report four DNA methylation biomarkers that discriminate CCA from PSC with high accuracy in bile and promising performance in plasma. The ability to detect CCA months before clinical diagnosis suggests that these biomarkers may improve surveillance and enable earlier, potentially curative interventions in individuals with PSC. Prospective validation in larger cohorts is warranted to confirm their clinical utility.

THU-410
Global trends in primary liver cancer between 2000 and 2023
Shahid Khan[1], Mathew Vithayathil[1], Terry Yip[2], Hashem El-Serag[3]. [1]*Imperial College London, London, United Kingdom;* [2]*The Chinese University of Hong Kong, Sha Tin, Hong Kong;* [3]*Baylor College of Medicine, Houston, United States*
Email: mathew.vithayathil@doctors.org.uk

Background and aims: Primary liver cancer (PLC) encompasses hepatocellular carcinoma (HCC) and intrahepatic cholangiocarcinoma (iCCA). The global burden of PLC is increasing in the 21st century, characterized by high lethality and significant absolute increases in new cases and deaths between 2000 and 2023. This study used the Global Burden of Diseases Study 2023 to characterise global trends in PLC incidence and mortality, identify key aetiological shifts, and highlight urgent public health priorities.
Method: Incidence, mortality, and aetiology data for PLC between 2000 and 2023 were collected for countries/terroritories from the Global Burden of Diseaes Study 2023. Global and country-specific age-standardised incidence (ASIR) and mortality (ASMR) rates were determined across the study period. Underlying liver disease aetiology data relating to PLC, including alcohol-related liver disease (ArLD), hepatitis B (HBV), hepatitis C (HCV) and metabolic-dysfunction associated steatotic liver disease (MASLD) were reviewed for each global region. Average annual percentage change (AAPC) outlined trends in incidence and mortality.

Results: The overall global burden of PLC has been increasing, with the absolute number of new cases and deaths increasing significantly (59.4% and 55.8%, respectively) between 2000 and 2023. Although age-standardised incidence and mortality rates declined since 2000, there has been a reversal in this decline since 2020. In particular, HBV- and HCV-associated rates, after historical declines, showed a concerning rebound starting circa 2020. Viral hepatitis (HBV and HCV) remained the dominant cause globally, but its proportion is decreasing. MASLD showed the greatest average annual increase in new cases. There is global variation in PLC-related liver disease aetiology, with HBV predominant in East Asia and Sub-Saharan Africa, HCV in the Middle East, North Africa, Northern America, and Latin America, and ArLD in Europe and Australasia. MASLD rates showed a consitent rise across all regions.
Conclusion: The global burden of primary liver cancer continues to rise, with a concerning reversal of historical declines in incidence and mortality since 2020. An increase in viral hepatitis related PLC during this time and the consistent rise of MASLD rates across the 21st century underscores an urgent need for sustained public health intervention and clinical action.

THU-412
Oral-gut microbiome is associated with sarcopenia in HCC patients following radiotherapy

Qingqing Hu[1], Xiaowei Xu[1]. [1]*The First Affiliated Hospital, College of Medicine, Zhejiang University, Hangzhou, China*
Email: ivyhu@zju.edu.cn

Background and aims: Patients with advanced cancer following radiotherapy often suffering from radiation-induced sarcopenia(RIS), however, evidence-based research on the role of oral-gut microbiome in predicting sarcopenia during radiotherapy in patients with advanced hepatocellular carcinoma (HCC)remains scarce. The aim of this study was to assess the correlation between oral-gut microbiota changes during radiotherapy and the extent of sarcopenia in HCC patients.
Method: 228 patients who received radiotherapy were enrolled. The diversity and species differences of both the oral and gut microbial community were tested by 16 S rRNA sequencing and bioinformatics analysis.
Results: The sarcopenia group had greater microbial abundance and species diversity. In gut microbiome, we observed significant alterations represented by an increase in Lactobacillus and Streptococcus while in oral microbiome the relative abundance of Actinomycetaceae, Endodontalis and Intermedia were particulary increased in sarcopenia group, suggesting a potential association between the sarcopenia and oral-gut microbiome. Furthermore, Prevotella, Streptococcus, parvula and mucilaginosa were identified as potential diagnostic and prognostic biomarkers of sarcopenia. The association network analysis also revealed an imbalance in species diversity and ecological diversity in both oral and gut microbiome of sarcopenia.
Conclusion: The oral-gut microbiome is associated with radiation-induced sarcopenia, which has important manifestations in the clinical management of RIS patients. The exact mechanisms through which the oral-gut microbiota influence sarcopenia remain to be elucidated.

THU-413
Multi-omics integration identifies a precise prognostic signature of survival in advanced HCC

Fengna Yan[1], Feixiang Xiong[1], Wang Yang[1], Zhou Yang[1], Wu Tong[1], Ji Xiaomin[2], Zhang Xuejie[1], Chen Dandan[1], Jian Wei[3], Jiang Yuyong[1], Yixin Hou[1]. [1]*Beijing Ditan Hospital, Capital Medical University, Beijing, China;* [2]*Beijing Ditan Hospital, Capital Medical Universit, Beijing, China;* [3]*Beijing Friendship Hospital, Capital Medical University Beijing, Beijing, China*
Email: m18239211525@163.com

Background and aims: Hepatocellular carcinoma (HCC) remains a leading cause of cancer-related mortality worldwide, with over 70% of patients diagnosed at intermediate or advanced stages where curative treatments are no longer feasible. Current prognostic tools are inadequate to capture the heterogeneity of outcomes in this population, underscoring the critical need for integrated predictive models that incorporate multimodal data.
Method: Plasma samples were collected from 242 patients with advanced HCC (BCLC B–D) who received first-line systemic therapy at two medical centers, between January 2020 and December 2023. Plasma proteomic profiling was performed using the DB4000 Deep Blood DIA Proteome platform with data-independent acquisition and Astral mass spectrometry. Proteomic differences between survivors and non-survivors were assessed via principal component and differential abundance analyses. Candidate biomarkers were validated by ELISA, after which their cellular origins and prognostic relevance were explored using single-cell RNA sequencing of HCC tissues.
Results: Among 242 HBV-HCC patients with 1-year follow-up, 90 (37.2%) died. Using mRMR and LASSO regression, we identified 15 proteins associated with 1-year survival. Multivariate logistic regression further refined a model incorporating four proteins (EGFLAM, HTRA3, ADGRG2, AGXT) and two clinical variables (K+, GGT). The model demonstrated strong predictive performance (AUC: 0.939, accuracy: 0.841, $p < 0.05$) and good clinical utility for decision curve analysis. All biomarkers except AGXT were significantly upregulated in deceased patients (FDR-adjusted $p < 0.05$), and ELISA confirmed these trends. The model effectively stratified mortality risk across treatment subgroups (conservative vs. ICI-based). Single-cell transcriptomics revealed predominant expression of these proteins within the tumor microenvironment.
Conclusion: This study comprehensively analyzed the plasma proteomic landscape of HCC, providing a promising blood-based tool for precision immunotherapy and predicting the risk of death in patients with advanced HCC.

THU-414-YI
Exploring practices and attitudes towards stopping hepatocellular carcinoma surveillance: a multinational clinician survey with over 500 respondents

Georgia Zeng[1,2], Simone Strasser[1,2], Talal Valliani[1,2], Vincent Wai-Sun Wong[3,4], Grace Lai-Hung Wong[3,4], Terry Cheuk-Fung Yip[3,4], Marco Sanduzzi Zamparelli[5], Manon Allaire[6,7], Ju Dong Yang[8,9,10], Daniel Huang[11], Dominic Staudenmann[12,13], Lung-Yi Mak[14], Wah Kheong Chan[15], Shishir Shetty[16], Anand Kulkarni[17], Hye Won Lee[18], Mohamed El Kassas[19], Ming-Hua Zheng[20], Leonardo da Fonseca[21], Cynthia Tsien[22], Mara Teresa Panlilio[23], Sakkarin Chirapongsathorn[24], Nobuharu Tamaki[25], Yao-Chun (Holden) Hsu[26,27], Maria Cecilia Cabrera[28], Hannah Giles[29], Ankur Srivastava[30], Tim Cross[31], Ken Liu[1,2]. [1]*AW Morrow Gastroenterology and Liver Centre, Royal Prince Alfred Hospital, Camperdown, Australia;* [2]*Sydney Medical School, The University of Sydney, Sydney, Australia;* [3]*Medical Data Analytics Centre, Department of Medicine and Therapeutics, The Chinese University of Hong Kong, Hong Kong, China;* [4]*State Key Laboratory of Digestive Disease, Institute of Digestive Disease, The Chinese University of Hong Kong, Hong Kong, China;* [5]*BCLC Group, Liver Oncology Unit, Liver Unit, Institute Investigations, Hospital Clinic of Barcelona, Biomèdiques August Pi i Sunyer (IDIBAPS), University of Barcelona, CIBERehd, Barcelona, Spain;* [6]*AP-HP Sorbonne Université, Hôpital Universitaire Pitié-Salpêtrière, Service d'Hépato- gastroentérologie, Paris, France;* [7]*INSERM UMR 1138, Centre de recherche des Cordeliers, Paris, France;* [8]*Karsh Division of Gastroenterology and Hepatology, Department of Medicine, Cedars-Sinai Medical Center, Los Angeles, United States;* [9]*Comprehensive Transplant Center, Cedars-Sinai Medical Center, Los Angeles, United States;* [10]*Samuel Oschin Comprehensive Cancer Institute, Cedars-Sinai Medical Center, Los Angeles, Australia;* [11]*Division of Gastroenterology and Hepatology, National University*

Health System, Singapore, Singapore; [12]Gastroenterology Service Intesto, Bern, Switzerland; [13]Gastroenterology Service Intesto, Hôpital Fribourgeois, University of Fribourg, Fribourg, Switzerland; [14]Department of Medicine, School of Clinical Medicine, The Li Ka Shing Faculty of Medicine, The University of Hong Kong, Hong Kong, China; [15]Gastroenterology and Hepatology Unit, Department of Medicine, Faculty of Medicine, University of Malaya, Kuala Lumpur, Malaysia; [16]Centre for Liver and Gastrointestinal Research, College of Medicine and Health, University of Birmingham, Birmingham, United Kingdom; [17]Department of Hepatology and Liver Transplantation, Asian Institute of Gastroenterology, Hyderabad, India; [18]Yonsei University College of Medicine, Seoul, Korea, Rep. of South; [19]Endemic Medicine and Hepatology Department, Capital University, Cairo, Egypt; [20]MAFLD Research Center, Department of Hepatology, The First Affiliated Hospital of Wenzhou Medical University, Wenzhou, China; [21]Department of Medical Oncology, ICESP - Instituto do Cancer DO Estado de Sao Paulo, Hospital das Clinicas, University of São Paulo School of Medicine, San Paolo, Brazil; [22]Ajmera Transplant Program, University Health Network, Toronto, Canada; [23]Division of Gastroenterology, University of the Philippines – Philippine General Hospital, Manila, Philippines; [24]Phramongkutklao Hospital and College of Medicine, Royal Thai Army, Bangkok, Thailand; [25]Department of Gastroenterology and Hepatology, Musashino Red Cross Hospital, Tokyo, Japan; [26]Department of Medical Research, E-Da Hospital, Kaohsiung, Taiwan; [27]School of Medicine and Graduate Institute of Medicine, I- Shou University, Kaohsiung, Taiwan; [28]Gastroenterology Unit, Guillermo Almenara Hospital. Universidad Nacional Mayor de San Marcos, Lima, Peru; [29]New Zealand Liver Transplant Unit, Auckland City Hospital, Auckland, New Zealand; [30]Division of Medicine & Royal Free London NHS Foundation Trust, Institute for Liver and Digestive Health, University College London, London, United Kingdom; [31]Department of Gastroenterology and Hepatology, Royal Liverpool University Hospital, Liverpool, United Kingdom
Email: ken.liu@health.nsw.gov.au

Background and aims: Patients with chronic liver disease and cirrhosis at risk of hepatocellular carcinoma (HCC) are living longer. Current guidelines provide no unified recommendations on when to stop HCC surveillance. We explored clinician practices and attitudes towards stopping HCC surveillance.
Method: A 27-item web-based survey was administered between August and October 2025 and distributed via gastroenterology and hepatology society mailing lists and professional networks through study group contacts. Responses were analysed using chi-squared tests with adjustment for multiple comparisons.
Results: 504 clinicians from 23 countries across 6 continents completed the survey. Most respondents were male (63%), gastroenterology/hepatology consultants (69%), working in metropolitan public hospitals (70%), and performed HCC surveillance using transabdominal ultrasound with alpha-fetoprotein (80%). Most respondents agreed that stopping HCC surveillance should be considered in older patients or those with limited life expectancy (81%), yet discussions with patients were infrequent (10% never; 34% rarely; 36% sometimes). Only 30% felt that HCC guidelines provide useful recommendations on stopping surveillance. Major barriers included lack of clear guidelines, fear of HCC development after stopping surveillance, and concern about giving patients mixed messages. Key patient factors influencing decisions were performance status, estimated life expectancy, comorbidities and ability to safely undergo HCC treatment (≥80% rated as important or very important). Roughly half of respondents would not stop surveillance based on age alone in patients with cirrhosis (49%) or non-cirrhotic chronic hepatitis B (50%) if functional status was good. The most commonly nominated age to stop surveillance was 81–85 years (21%). Younger clinicians (<50 years and/or <5 years post-training) were more likely to prioritise age and nominate a specific cut-off. Respondents from Asia were more likely to continue surveillance in elderly patients or those with limited life expectancy (29% vs 16% strongly agree, p = 0.002), whereas Western respondents were more likely to offer stopping surveillance (62% vs 26% strongly agree, p = 0.002).
Conclusion: Clinicians recognise the appropriateness of stopping HCC surveillance in selected elderly patients, yet practice remains inconsistent and patient discussions are infrequent. Lack of guidance and fear of adverse consequences highlight a critical evidence gap to inform future guidelines.

Liver tumours – Experimental and pathophysiology

TOP-389

Anti-GARP reverts immune suppression and extends overall survival in a MASH-HCC murine model resistant to anti-PDL1 +anti-VEGFA therapy

Júlia Huguet-Pradell[1,2,3], David Camell-Raventos[1,2,3], Elisa Fernández-Martínez[1], Anthony Lozano[1,4,5], Tiago de Castro[1], Marcus Zeitlhoefler[1], Ugne Balaseviciute[1,2,3], Albert Gris-Oliver[2,3], Daniela Sia[1], Roser Pinyol[2,3], Josep M Llovet[1,2,3,6]. *[1]Mount Sinai Liver Cancer Program, Divisions of Liver Diseases, Department of Medicine, Tisch Cancer Institute, Icahn School of Medicine at Mount Sinai, New York, NY, USA., New York City, United States; [2]Liver Cancer Translational Research Group, Institut d'Investigacions Biomèdiques August Pi i Sunyer (IDIBAPS), Hospital Clínic, Catalonia, Spain, Barcelona, Spain; [3]Facultat de Medicina i Ciències de la Salut, Universitat de Barcelona, Catalonia, Spain, Barcelona, Spain; [4]Department of Oncological Sciences, Icahn School of Medicine at Mount Sinai, New York, New York., New York City, United States; [5]The Precision Immunology Institute, Icahn School of Medicine at Mount Sinai, New York, New York City, United States; [6]Institució Catalana de Recerca i Estudis Avançats (ICREA), Barcelona, Catalonia, Spain., New York City, United States*
Email: julia.huguet@mssm.edu

Background and aims: Atezolizumab (aPDL1) + bevacizumab (aVEGFA) (atezo+bev) is a first-line standard-of-care (SOC) treatment for advanced hepatocellular carcinoma (aHCC) with objective responses in ~30% of cases. Clinical benefit is hindered in non-viral HCC, including metabolic dysfunction-associated steatohepatitis (MASH)-related cases, a raising etiology. MASH-HCCs are enriched in TGFß signaling, associated with resistance to atezo+bev. The bioavailability and Treg-related immunosuppressive effect of TGFß1 ligand is controlled by GARP receptor. Hence, we hypothesize that GARP blockade might revert immune suppression and overcome resistance to aPDL1+aVEGF (SOC) in MASH-HCC.
Method: We used an immune-genetic MASH-HCC model combining diet-induced steatohepatitis with *MYC* and *CTNNB1* overexpression (hydrodynamic gene delivery), driving atezo+bev resistance. After tumor onset, animals were treated with SOC+anti-GARP (triple combination), SOC alone or placebo until the end of the study. Spectral cytometry was conducted at day 14 to assess changes in the tumor microenvironment (n = 5/arm). Remaining animals were followed for overall survival (OS) analysis (n = 7/arm). GARP expression was correlated with immune features in three independent cohorts of HCC patients (n = 559).
Results: SOC+anti-GARP significantly extended OS compared to placebo (median of 68 vs 59 days, p = 0.045), as opposed to SOC alone (p = 0.21). From the immune perspective, the triple combination shifted central memory to tumor-resident CD8+ T cells (p = 0.031) accompanied by an increase in total CD8+ (p = 0.003) and CD4 + (p = 0.016) T cells compared to placebo, suggesting a locally active T-cell response. Accordingly, tumors from SOC+anti-GARP-treated mice presented increased effector (p = 0.036) and exhausted CD8+ T cells

($p = 0.007$). Among CD4+ T cells, the triple combination increased antigen-experienced ($p = 0.045$) and showed a trend of the ratio between tissue-resident memory and Tregs ($p = 0.053$) when compared to the rest. None of these changes were observed with SOC alone. In HCC patients, high GARP expression significantly correlated with immune exhaustion (FC vs rest >1.5 in 87% of cases), with an increase of Treg infiltration, highlighting a group of patients that may benefit from this combination.
Conclusion: Our findings highlight GARP as a promising therapeutic target whose blockade restores antitumor immune infiltration and extends survival OS when added to SOC in an immunotherapy-resistant murine model of MASH-HCC.

TOP-390-YI
Using patient-led genetics to identify new therapeutic targets in metastatic cholangiocarcinoma
Paula Olaizola[1], Mollie Wilson[1], Nicholas Younger[1], Kostas Gournopanos[1], Aleksandra Rozyczko[1], Andreea Gradinaru[1], Colm O Rourke[2], Jesper Andersen[2], Luke Boulter[1]. [1]*Institute of Genetics & Cancer, The University of Edinburgh, Edinburgh, United Kingdom;* [2]*Biotech Research and Innovation Centre (BRIC), Department of Health and Medical Sciences, University of Copenhagen, Copenhagen, Denmark*
Email: luke.boulter@ed.ac.uk

Background and aims: Cholangiocarcinoma (CCA) includes a diverse range of biliary malignancies with dismal prognosis. Tumors are often diagnosed when patients present locally-advanced or metastatic disease, limiting the access to potentially curative surgery. The genetic heterogeneity of CCAs has been reported, indicating that the most common gain-of-function mutations in *K-RAS* and *IDH1*, and *FGFR2*-translocations only occur in 16%, 10% and 15% of patients, respectively. These activating mutations exist in a complex genomic landscape where many genes are mutated at low frequencies. The role of these heterogeneously mutated genes in CCA progression is unknown and their potential to modify the effect of more common mutations remains to be studied. Here, we investigate the genetics behind CCA dissemination, describing how cell intrinsic changes impact on cancer cell behavior and shape the tumor microenvironment making it permissive to metastasis.
Method: Analyzing whole genome/exome sequencing data from 277 patients diagnosed with intrahepatic CCA we identified a patient-led list of CCA mutations. We then developed an *in vivo* screen where we expressed gain of function *K-Ras*^{G12D} with a CRISPR/Cas9 gRNA library targeting genes mutated in the patient data. Immunohistochemistry was performed to characterize the primary and metastatic tumors and their microenvironments. Using CRISPR/Cas9-mediated gene silencing, we interrogated whether these low frequency mutations promote epithelial-to-mesenchymal transition, migration and tumor dissemination in human CCA cells.
Results: The *in vivo* screening showed that mutant *K-Ras* in combination with our gRNA library led to tumor development within 8 weeks. Exome sequencing of these tumors identified CRISPR-induced mutations in 53 genes which facilitated mutant *K-Ras*-induced tumor growth. We found a range of chromatin modifiers, including *Ncor1* and *Bap1*, that upon deletion, together with *Tp53* loss and *K-Ras*^{G12D} overexpression, resulted in metastatic CCA. Histological analysis of the primary tumors with metastatic potential revealed phenotypic changes in cancer cells as well as differences in the fibroimmune stroma. Furthermore, deletion of *NCOR1* or *BAP1* in human CCA cell lines increased their migratory and invasive capacities.
Conclusion: Low-frequency mutations in chromatin modifying genes, such as *Ncor1* or *Bap1*, cooperate with common driver mutations to promote tumor progression and dissemination by altering cancer cell properties and modifying the tumor microenvironment.

TOP-391
SIRPA as a novel regulator of T cell apoptosis in hepatocellular carcinoma: implications for immunotherapy
Xue Zhang[1], Liying Ren[1], Shaoping She[1], Hongsong Chen[1], Dongbo Chen[1]. [1]*Peking University Hepatology Institute, Beijing, China*
Email: zxx20010205@163.com

Background and aims: Immune checkpoint inhibitors (ICIs) were effective in only 20% of advanced hepatocellular carcinoma (HCC), suggesting the presence of additional immune evasion mechanisms.
Method: In this study, we employed a CRISPR library to screen key genes associated with T-cell apoptosis and identified differentially expressed genes (DEGs) in tumor-infiltrating lymphocytes (TILs) from HCC patients with high concentrations of interleukin-2 (IL-2). Integration analysis revealed signal regulatory protein alpha (*SIRPA*) as a novel regulator of T cell apoptosis in HCC, distinct from its classical role as a macrophage inhibitory receptor. In addition, the function of SIRPA was verified in vivo and in vitro using Sirp$\alpha^{-/-}$ mice and T cells derived from PBMC.
Results: *In vitro*, *SIRPA* deficiency reduced apoptosis in human and mouse T cells, while its overexpression promoted apoptosis. *In vivo*, the degree of tumor suppression strongly correlated with *Sirp*α deficiency in T cells, with even haploinsufficient *Sirp*α exerting anti-tumor effects. After macrophage depletion, *Sirp*$\alpha^{-/-}$ mice showed significantly increased proportions of functional $CD8^+$ T cells in peripheral blood and tumor tissues, along with elevated granzyme B (GZMB) levels compared to wild-type (WT) mice, confirming that *Sirp*α deficiency in T cells resists apoptosis. Notably, in adoptive immunotherapy, TCR-T cells overexpressing *SIRPA* exhibited significantly reduced killing function, and tumor-bearing mice receiving *Sirp*$\alpha^{-/-}$ $CD3^+$ T cells inhibited tumor growth compared to those receiving T cells from WT. Mechanistically, SIRPA upregulated EGR4 to activate the Bcl-2/Bax pathway, promoting T-cell apoptosis.
Conclusion: Targeting *SIRPA* may suppress HCC progression by inhibiting T-cell apoptosis, offering a novel immunotherapeutic strategy.

TOP-392-YI
ERAL1 blocks RPL12-mediated ribosome-associated quality control to inhibit mitophagy and promote HCC lung metastasis
Li Zhou[1], Manqiu Hu[1], Song He[1], Zhihang Zhou[1]. [1]*The Second Affiliated Hospital of Chongqing Medical University, Chongqing, China*
Email: zhouzhihang@cqmu.edu.cn

Background and aims: Lung metastasis is the primary cause of mortality in hepatocellular carcinoma (HCC). Through *in vivo* CRISPR library screening, we identified the mitochondrial ribosome assembly factor ERAL1 as a key driver of metastasis. Recent studies highlight that cytosolic ribosomes on the mitochondrial surface regulate organelle function via ribosome-associated quality control (RQC). We discovered that ERAL1 interacts with the cytosolic ribosomal protein RPL12 at the outer mitochondrial membrane (OMM). This study aims to elucidate the mechanism by which ERAL1 modulates RPL12—a potential novel organelle autophagy receptor—to inhibit mitophagy and promote HCC lung metastasis.
Method: We utilized genome-wide CRISPR screening in mice to identify metastasis drivers. Clinical relevance was validated using 50 HCC lung metastasis samples and TCGA datasets. Functional roles were assessed via invasion assays and orthotopic lung metastasis models in mice. Mechanistically, we employed Co-IP, GST-pulldown, and immunofluorescence to map ERAL1-RPL12 interactions. Mitophagic flux was quantified using TEM, the mt-Keima reporter system, and LC3/p62 turnover under oligomycin stress. Rescue experiments were performed using ERAL1 mutants and OMM-tethered RPL12 constructs.
Results: ERAL1 is significantly up-regulated in lung metastases and correlates with poor patient prognosis. *In vitro* and *in vivo* assays confirmed that ERAL1 promotes HCC metastasis. While ERAL1 had negligible effects on mitochondrial translation efficiency, it

significantly reduced ROS and oxygen consumption rates (OCR) while stabilizing membrane potential. Notably, ERAL1 inhibited mitophagy, with transcriptomics showing suppressed autophagy pathways. We found that ERAL1 binds RPL12 on the OMM; its import competitively reduces RPL12 colonization on the membrane. This depletion prevents the recruitment of the E3-ligase Parkin and downstream LC3-mediated autophagy. Crucially, artificially tethering RPL12 to the OMM restored mitophagy levels even in ERAL1-overexpressing cells, confirming that the loss of membrane-bound RPL12 drives this suppression.

Conclusion: Our findings reveal a novel mechanism where ERAL1 promotes HCC metastasis by evading RQC-mediated mitophagy. By reducing RPL12 OMM colonization, ERAL1 protects mitochondria from autophagic clearance, effectively distinguishing physiological protein import from pathological channel clogging. Targeting the ERAL1-RPL12 axis offers a potential therapeutic strategy for metastatic HCC.

TOP-405

Single-cell spatial profiling of cellular architecture in human hepatocellular carcinoma

Claudia Arnedo-Pac[1,2,3], Yi Yin[2], Jo Heffer[4], Ania Piskorz[4], Raheleh Rahbari[3], Matthew Hoare[2,5], Sarah Aitken[1,4,6,7]. *[1]MRC Toxicology Unit, University of Cambridge, Cambridge, United Kingdom; [2]Early Cancer Institute, University of Cambridge, Cambridge, United Kingdom; [3]Wellcome Sanger Institute, Hinxton, United Kingdom; [4]Cancer Research UK - Cambridge Institute, University of Cambridge, Cambridge, United Kingdom; [5]Department of Medicine, University of Cambridge, Cambridge, United Kingdom; [6]Center of Molecular and Cellular Oncology, Yale Cancer Center, New Haven, CT, United States; [7]Department of Pathology, Yale University School of Medicine, New Haven, CT, United States*
Email: ca606@cam.ac.uk

Background and aims: Hepatocellular carcinoma (HCC) is the most common primary liver malignancy, affecting more than 900,000 individuals annually and ranking third among cancer-related causes of death worldwide. Despite the growing clinical burden, comprehensive characterisation of the cellular composition of HCC and its tumour microenvironment in large clinical cohorts is relatively sparse. Chronically injured tissues typically exhibit cellular heterogeneity which can contribute to tumour progression, immune evasion, and therapeutic resistance. Here, we sought to generate a high-resolution spatial transcriptomics atlas of HCC across a large, clinically well-annotated cohort.

Method: We analysed liver tissue from 103 patients with solitary HCC undergoing liver transplantation (82% male; mean age 47 ± 16 years), encompassing diverse disease aetiologies including hepatitis C (48.5%), alcohol-related liver disease (22.3%), and metabolic dysfunction-associated steatotic liver disease (9.7%). Formalin-fixed paraffin-embedded samples from tumour edge, tumour core, and paired cirrhotic background liver were assembled into tissue microarrays (TMAs). Spatial transcriptomics experiments were conducted using the 10x Xenium In Situ platform, profiling 477 genes at single cell resolution. Spatially resolved expression data were used to perform cell phenotyping and spatial composition analyses.

Results: We mapped over three million cells from 312 tissue cores across the cohort, retrieving on average 27,000 cells per donor. For most patients (85%), paired data from both HCC and background cirrhotic liver was available. Preliminary analyses recapitulate the major cellular compartments of HCC and cirrhotic livers, including the tumour parenchyma, stromal cells, and diverse immune populations. Spatial mapping of these cell populations identifies distinct cellular neighbourhoods and patterns of co-localisation suggestive of cell-cell interactions.

Conclusion: We present a novel large-scale spatial transcriptomics dataset at single-cell resolution across more than 100 HCC patients. This will allow deep interrogation of the tumour-microenvironment crosstalk underlying HCC pathogenesis, progression, and prognosis. Furthermore, this dataset represents a valuable resource to the hepatology and cancer biology communities.

TOP-406

Spatial immune classification reflects CD8 T cell exhaustion states and predicts response to neoadjuvant immunotherapy in hepatocellular carcinoma

Alexandra Emilia Schlaak[1], Ira Godbole[1], Antonio D'Alessio[2], Claudia Fulgenzi[2], Madhava Pai[3], Duncan Spalding[3], Patricia Otto-Mora[1], Günter Päth[1], Robert D. Goldin[4], Nicole Acuti[5], Caroline Ward[2], Georgios Nteliopoulos[2], Vincent Yip[6], Sarah Slater[7], Mikael Sodergren[3], Paul Tait[8], Nagy Habib[3,9,10], Robert Thomas[11], Eslam Maher[2], Francesco Mauri[2], Alessio Cortellini[2], Julian R. Marchesi[4], Robert Thimme[1], Rohini Sharma[2], David J. Pinato[2], Bertram Bengsch[1,12,13]. *[1]University Medical Center Freiburg, Clinic for Internal Medicine II, Freiburg im Breisgau, Germany; [2]Division of Cancer, Department of Surgery & Cancer, Imperial College London, Hammersmith Hospital, Du Cane Road, W120HS, London, United Kingdom; [3]Division of Surgery, Department of Surgery & Cancer, Imperial College London, Hammersmith Hospital, Du Cane Road, W120HS, London, United Kingdom; [4]Department of Metabolism, Digestion and Reproduction, Imperial College London, London, United Kingdom; [5]The Francis Crick Institute, London, United Kingdom; [6]Barts and The London HPB Centre, The Royal London Hospital, Barts Health NHS Trust, London, United Kingdom; [7]Department of Medical Oncology, Barts Health NHS Trust, London, United Kingdom, 10 Department of Radiology, Imperial College NHS Trust, Hammersmith Hospital, Du Cane Road, W120HS, London, United Kingdom; [8]Department of Radiology, Imperial College NHS Trust, Hammersmith Hospital, Du Cane Road, W120HS, London, United Kingdom; [9]Imperial College London, Surgery & Cancer, Londo, United Kingdom; [10]Imperial, Surgery & Cancer, London, United Kingdom; [11]Department of Histopathology, University College NHS Trust, London, United Kingdom; [12]Signaling Centers CIBSS and BIOSS, Freiburg, Germany; [13]German Cancer Consortium (DKTK), Partner site Freiburg, Freiburg, Germany*
Email: emilia.schlaak@uniklinik-freiburg.de

Background and aims: Response to immune checkpoint inhibition (ICI) in hepatocellular carcinoma (HCC) depends on the functional state of intratumoral $CD8^+$ T cells. Progenitor exhausted T cells (Tpex) sustain immune reinvigoration, whereas terminally exhausted T cells (Tex) are largely refractory to checkpoint blockade. Whether a spatial immune architecture captures these functional exhaustion states and predicts pathological response to neoadjuvant ICI in early-stage HCC remains unclear.

Method: Paired baseline biopsies and post-treatment resection specimens from the PRIME-HCC trial (NCT03682276), evaluating neoadjuvant nivolumab plus ipilimumab in resectable BCLC A HCC, were analysed (n = 27). Tumors were assigned to immune-enriched, immune-compartmentalised, or immune-depleted immunotypes based on $CD8^+$ T cell density and spatial distribution. Imaging mass cytometry enabled spatially resolved single-cell profiling of $CD8^+$ T cell exhaustion states, including Tpex ($PD\text{-}1^+TCF\text{-}1^+$) and Tex ($PD\text{-}1^+TOX^+$). Radiological response was available in n = 25 patients and pathological response in n = 20 patients.

Results: Immune-enriched tumours demonstrated markedly superior pathological responses, with frequent pathological complete response, compared with immune-compartmentalised and immune-depleted tumours. Patients with a radiological response showed significantly higher intratumoural CD8 T cell counts following therapy. Mechanistically, immune-enriched tumours were characterised at baseline by intratumoural enrichment of progenitor exhausted CD8 T cells, whereas non-responding tumours were predominantly enriched in terminally exhausted CD8 T cells. Following neoadjuvant immune checkpoint inhibition, responders exhibited an expansion of proliferating PD-1+ CD8 T cells within the

tumour microenvironment, whereas non-responding tumours failed to show effective immune reinvigoration.
Conclusion: A simplified immune classification reflects the spatial availability of progenitor exhausted CD8$^+$ T cells and serves as a surrogate of the Tex/Tpex balance in HCC. This immune architecture determines the capacity for immune reinvigoration and pathological response to neoadjuvant ICI. Immune classification-guided patient stratification may therefore enable the selection of neoadjuvant immunotherapy strategies in early-stage HCC but remains to be validated in prospective studies.

WED-232
TP53/ARID1A-driven macrotrabecular and TERT/BAP1-enriched microtrabecular tumors represent two distinct histomorphological subtypes of non-cirrhotic hepatocellular carcinoma

Khushboo Agrawal[1], Archana Rastogi[1], Pramod Gautam[1], Viniyendra Pamecha[1], Vanya Garg[1], Nirupma Trehanpati[1], Shiv Kumar Sarin[1], Gayatri Ramakrishna[1]. [1]*Institute of Liver And Biliary Sciences, New Delhi, India*
Email: rgayatri@ilbs.in

Background and aims: Non-cirrhotic hepatocellular carcinoma (NC-HCC) represents ~20% of HCC and is increasingly associated with MASLD and chronic HBV. Integrated links between tumor architecture, immune features, and genomic drivers remain limited. Aim to identify architectural histotypes and correlate them with underlying genetic/molecular landscape.
Method: Resected NC-HCCs (N = 53) underwent integrated histologic, immunohistochemical (IHC), and genomic analysis. Architectural patterns were correlated with p53, β-catenin, EpCAM, CK19, MSI status, CD8$^+$ T-cell infiltration, and immune checkpoints. Targeted NGS (40-gene panel) was performed in 33 tumors, with *TERT* promoter mutation validation by digital droplet PCR (ddPCR).
Results: Microtrabecular (MiT) architecture was most prevalent (56.6%), followed by macrotrabecular (MaT;20.8%), compact (CP;15%), and pseudoglandular (PSGL; 7.5%). NASH was predominant etiology (49%), followed by HBV (26.4%) and cryptogenic (22.6%). MiT and CP patterns enriched in NASH associated tumors. MaT tumors were more frequent in HBV and associated with higher AFP levels (P = 0.028). CP tumors showed a notable female predominance. On IHC, MaT tumors demonstrated nuclear p53, universal EpCAM+ (P = 0.027), higher CTLA-4 expression, and MSI stability (P = 0.021). In contrast, MiT tumors showed molecular heterogeneity with lower expression of nuclear p53 and EpCAM expression, increased CD8$^+$ T-cell infiltration, and MSI instability (30%) of cases. CP and PSGL tumors were largely immune-excluded. PSGL tumors exhibited nuclear β-catenin, membranous CK19 and PD-1 enrichment. Frequent somatic alterations involved *TP53* and *RB1* (55% each), followed by *TERT* (42%), *BAP1* (27%), and *ARID1A* (18%). *RB1* mutations constituted a common molecular variant across all four histotypes. MaT tumors were enriched for *TP53* mutations (88%) with *ARID1A* co-alterations (P = 0.04). MiT tumors harbored recurrent *TERT* C228T promoter mutations (38%), often with *BAP1* alterations, and were mutually exclusive with *TP53* (P = 0.05). CP tumors showed near-universal *RB1* loss. *TERT* C228T was also validated by dd-PCR in all NGS-positive cases (N = 14), with additional low-abundance detections in 3 NGS-negative tumors.
Conclusion: Integrated profiling identified two major NCHCC clusters: a MaT, *TP53* driven, EpCAM-enriched, immune-cold subtype with high recurrence (78%), and a MiT, *TERT* C228T driven subtype with immune infiltration and long RFS (60%). *TERT* C228T emerges as a promising biomarker for molecular screening via sensitive ddPCR.

WED-233
Patient-derived liver organoids as a translational platform to validate GPC3-targeted nanoparticles for image-guided liver cancer surgery

Zulihumaer Aizimuaji[1], Shizhong Yang[2], Jinrun Liu[2], Zeyu Zhang[3], Kai Ma[2], Jiahong Dong[2]. [1]*Tsinghua University, Beijing, China;* [2]*Beijing Tsinghua Changgung Hospital, Beijing, China;* [3]*Beihang University, Beijing, China*
Email: zulhumar0102@163.com

Background and aims: Accurate visualization of liver cancer margins remains a major challenge during surgical resection. Glypican-3 (GPC3) is a tumor-associated antigen highly expressed in hepatocellular carcinoma (HCC) and certain metastatic liver cancers but absent in normal hepatocytes. This study established a patient-derived liver organoid platform to validate the tumor selectivity of a GPC3-targeted nanoparticle (TJ12-NP) and to bridge its application to image-guided liver cancer surgery.
Method: TJ12-NP was synthesized and labeled with Cy5 or indocyanine green (ICG) for different experimental settings. Cy5-labeled TJ12-NP was used to evaluate tumor-specific uptake in patient-derived organoids representing normal liver, HCC, and colorectal liver metastasis (CRLM). Organoid identities were confirmed by marker profiling through immunostaining. Confocal microscopy was applied to visualize nanoparticle localization, and live–dead assays assessed cytocompatibility. ICG-labeled TJ12-NP was further tested *in vivo* in Huh-7-bearing nude mice for fluorescence imaging and fluorescence-guided tumor resection.
Results: Cy5-TJ12-NP exhibited strong and specific accumulation in GPC3-positive HCC organoids and comparable uptake in CRLM organoids, whereas minimal signal was observed in normal liver organoids, confirming tumor-selective targeting. The nanoparticles were well tolerated by organoid. In vivo, ICG-TJ12-NP enabled high-contrast tumor visualization, achieving a markedly higher tumor-to-background ratio compared with untargeted controls and facilitating complete fluorescence-guided resection.
Conclusion: This study establishes patient-derived liver organoids as a robust translational platform for validating molecularly targeted nanoparticles. The integration of organoid-based specificity testing with preclinical imaging demonstrates a clinically relevant pathway toward precision, image-guided liver cancer surgery.

WED-234-YI
Identification of novel therapeutic agents using patient-derived organoids in HCC

Reha Akpinar[1,2], Ezgi Cibali[3], Cristina Richichi[2], Barbara Durante[2], Hung-wei Hsu[4], Yasmine Bouda[5,6], Fatima Teixeira-Clerc[5,6], Yu-Yun Shao[4,7], Diego Calvisi[3], Julien Calderaro[5,6], Salvatore Piscuoglio[2], Luca Di Tommaso[1,2]. [1]*Department of Pathology, IRCCS Humanitas Research Hospital, Milan, Italy;* [2]*Department of Biomedical Sciences, Humanitas University, Milan, Italy;* [3]*Institute of Pathology, University of Regensburg, Regensburg, Germany;* [4]*Department of Oncology, National Taiwan University Hospital, Taipei City, Taiwan;* [5]*Équipe "Virus, Hépatologie, Cancer," INSERM U955, IMRB, Université Paris-Est, Créteil, France;* [6]*Department of Pathology, Assistance Publique-Hôpitaux de Paris, Henri Mondor University Hospital, Créteil, France;* [7]*Graduate Institute of Oncology, National Taiwan University College of Medicine, Taipei City, Taiwan*
Email: luca.di_tommaso@hunimed.eu

Background and aims: Hepatocellular carcinoma (HCC) is among most common cancer and the 3rd reason of cancer-related deaths worldwide. Most patients present with advanced HCC (aHCC) but available treatments can achieve an objective response rate of about 30%. Given these therapeutic limitations, new approaches are essential. In this study, we generated HCC derived-PDOs (HCC-PDOs) and used them to identify novel therapeutic agents against HCC.

Method: HCC surgical and biopsy tissues were processed and cultured to generate PDOs. Established PDOs were characterized with hepatocytic and biliocytic markers. Those positive to hepatocytic markers were considered true HCC-PDOs and used for a massive drug screening with 270 compounds. Drug efficacy was established by cell viability assay, and Z-scores were used for ranking. Top ten drugs were further analyzed with various doses. We also tested the same HCC-PDOs with standard 1st and 2nd lines systemic therapy agents for aHCC.
Results: True HCC-PDOs were generated in 4/52 HCC samples (8%). Biopsies yielded a higher success rate 2/9 (22%) than surgical samples 2/43 (5%). In 7/52 (13%) cases, the organoids expressed biliocytic markers. The massive drug screening showed, in all HCC-PDOs, consistent results for nine compounds. Among them, dinaciclib, homoharringtonine, volasertib, mocetinostat, and daunorubicin, have bene already reported as effective on HCC. Three compounds, osimertinib, D1, and D2, are already used for EGFR-mutant lung cancers. Finally, one compound, D3, inhibits replication. Among standard treatments, only sorafenib inhibited HCC-PDOs.
Conclusion: The identification of dinaciclib and homoharringtonine as potent agents aligns with recent literature on novel HCC drugs, and validates the robustness of our approach and the potential of our results. Moreover, our results disclosed a significant potential for some drug repurposing. A recent study showed that cerinitib, a drug targeting ALK mutation in advanced non-small cell lung cancer, inhibits β-catenin mutated HCC via non-canonical WNT pathway independent of ALK (J Hep Reports, 2025). Our data disclosed two compounds, D1 and D2, effective in EGFR-mutant lung cancers, which promise to be effective, off label, also on HCC. In keeping with this, osimertinib, another drug highlighted by the screening on HCC-PDO and currently used for EGFR-mutant lung cancer, has been reported as effective also in HCC (J. Cancer Res. Clin. Oncol., 2023; Plos One, 2023).

WED-235
Involvement of the hERG1 potassium channel in cholangiocarcinoma cell biology

Giada Alla Viligiardi[1], Jessica Iorio[1], Mirella Pastore[1], Claudia Duranti[1], Rossella Colasurdo[1], Valentina Devescovi[1], Tiziano Lottini[1], Michele Martinelli[1], Elena Frediani[2], Francesca Margheri[2], Alessia Tani[1], Daniele Guasti[1], Daniele Bani[1], Paola Ostano[3], Daniele Nosi[1], Annarosa Arcangeli[1], Chiara Raggi[1], Fabio Marra[1].
[1]Department of Experimental and Clinical Medicine, University of Florence, Florence, Italy; [2]Department of Experimental and Clinical Biomedical Sciences, University of Florence, Florence, Italy; [3]Edo and Elvo Tempia Valenta Foundation, Biella, Florence, Italy
Email: giada.allaviligiardi@unifi.it

Background and aims: hERG1 is a voltage-gated potassium channel normally found in excitable cells, but it is often overexpressed in tumors, where it interacts with β1 integrin and activates cancer-related pathways. Intrahepatic cholangiocarcinoma (iCCA) is an aggressive liver malignancy with limited treatment options. This study aimed to investigate the role of hERG1 and its downstream signaling in iCCA biology.
Method: hERG1 expression was assessed in three iCCA cell lines, and functional studies were performed using siRNA-mediated silencing (sihERG1) and pharmacological inhibition (E4031). Cellular behavior was evaluated through standard assays, and molecular and structural changes were analyzed using qRT-PCR, Western blotting, electron microscopy, and transcriptomics.
Results: hERG1 silencing led to a 75–80% reduction in mRNA and protein expression but did not impact proliferation or viability. In contrast, both genetic silencing and pharmacological inhibition significantly reduced cell motility and impaired angiogenesis, as shown by reduced tube formation in HUVECs exposed to si hERG CCA conditioned media. Gene expression analyses revealed downregulation of epithelial mesenchymal transtion (EMT) and angiogenesis markers. Key oncogenic pathways, including FAK, PI3K, and AKT, were notably suppressed. Ultrastructural analysis showed endoplasmic reticulum swelling and increased vesicular trafficking, indicating cellular stress and altered membrane turnover. Transcriptomic analysis revealed a common profile of gene alteration, mainly in vesicular trafficking, transmembrane ion regulation, and extracellular matrix reorganization, highlithing a broader impact of hERG1 on intracellular dynamics.
Conclusion: hERG1 plays a critical role in supporting motility and angiogenic potential in iCCA cells without affecting proliferation. Its inhibition alters key oncogenic and cellular processes, positioning hERG1 as a promising therapeutic target in iCCA.

WED-236
Baseline tumor and circulating gamma/delta T-Cell signatures and early on-treatment CD8$^+$PD-1$^+$ T-Cell expansion predict response to Atezolizumab–Bevacizumab in hepatocellular carcinoma

Isabelle Galy-Fauroux[1], Amna Asif-Laidin[1], Manon Evain[1], Joana Gonçalves Araujo[1], Claudia Campani[2], Edouard Larrey[3], Sayma Chaibi[3], Ludovic Furia[4], Pierre Laurent Puig[5], Jessica Zucman-Rossi[4], Chantal Desdouets[4], Jean Charles Nault[6], Jean-Pierre Couty[4], Manon Allaire[7]. *[1]Centre de Recherche des Cordeliers, Université Paris Cité, Sorbonne Université, Inserm, F-75006, Paris, France; [2]Centre de Recherche des Cordeliers, Université Paris Cité, Sorbonne Université, Inserm, F-75006, AP-HP Sorbonne Paris Nord, Hôpitaux Universitaire Paris Seine Saint-Denis, Service d'Hépatologie, Paris, France; [3]AP-HP Sorbonne Université, Hôpital Universitaire Pitié-Salpêtrière, Service d'Hépato-gastroentérologie, Paris, France; [4]Centre de Recherche des Cordeliers, Université Paris Cité, Sorbonne Université, Inserm, F-75006, Paris, France; [5]Institut du Cancer Paris CARPEM, AP-HP, Department of Genetics and Molecular Medicine, Hôpital Européen Georges Pompidou, Department of Oncology, Assistance Publique-Hôpitaux Paris (AP-HP), HEGP; Institut du Cancer Paris CARPEM, Paris, France; [6]Centre de Recherche des Cordeliers, Université Paris Cité, Sorbonne Université, Inserm, F-75006, AP-HP Sorbonne Paris Nord, Hôpitaux Universitaire Paris Seine Saint-Denis, Service d'Hépatologie, Paris, France; [7]Centre de Recherche des Cordeliers, Université Paris Cité, Sorbonne Université, Inserm, F-75006, AP-HP Sorbonne Université, Hôpital Universitaire Pitié-Salpêtrière, Service d'Hépato-gastroentérologie, Paris, France*
Email: allama5@hotmail.fr

Background and aims: Atezolizumab–bevacizumab (AtezoBev) is the standard first-line therapy for unresectable hepatocellular carcinoma (HCC), but predictive biomarkers of response are lacking. We aimed to identify baseline and early immune features associated with treatment outcomes.
Method: We conducted a prospective study of patients receiving first-line AtezoBev, integrating longitudinal immune profiling at baseline and 3 weeks after treatment initiation, including peripheral blood mononuclear cell (PBMC) immunophenotyping (17 markers), serum cytokine profiling (31 proteins), and paired whole-blood RNA sequencing. Tumor RNA-sequencing data from the GO30140 and IMbrave150 trials were analyzed (209 patients treated with AtezoBev and 58 with sorafenib), with external validation in an independent cohort of metastatic MSI-H colorectal cancer (n = 163).
Results: Longitudinal blood samples were available for 31 patients (median age 65 years; 87% male); 29% experienced radiological progression at 6 months. Patients with disease control had higher baseline circulating γδ T-cell levels (2.2% vs. 0.7%, $p = 0.008$), which were associated with longer progression-free survival (PFS; HR 0.71, 95% CI 0.55–0.92; $p = 0.009$), as well as higher baseline IL-18 plasma levels ($p = 0.01$). At the tumor level, a high γδ T-cell transcriptional signature was associated with higher response rates ($p < 0.01$), longer PFS ($p < 0.001$), and longer overall survival (OS; $p = 0.003$) in AtezoBev-treated patients, but not in those receiving sorafenib. This γδ T-cell signature outperformed the AtezoBev Response Score (ABRS) for OS and PFS prediction. Consistently, in an independent

MSI-H colorectal cancer cohort, a high γδ T-cell signature was associated with longer PFS (p = 0.034). During treatment, an early increase in circulating $CD8^+PD\text{-}1^+$ T cells was associated with longer PFS, whereas an increase in $CD8^+TIGIT^+$ T cells predicted shorter PFS. Paired transcriptomic analyses revealed early induction of T cell–associated interferon-γ signaling in responders, with higher circulating IFN-γ levels compared with progressors.
Conclusion: High baseline circulating and intratumoral γδ T-cell levels, together with early $CD8^+PD\text{-}1^+$ T-cell expansion before the second infusion, predict response to AtezoBev, supporting immune profiling as a valuable tool to guide early treatment decisions in HCC.

WED-237-YI
Spatially resolved multi-omic analysis reveals metabolic niche-dependent regulatory T cell programs in hepatocellular carcinoma
Leonard Bellersheim[1], Mehreen Khan Bhettani[1], Maegen Fleming[1], Elisavet Kodela[1], Alexander Morrell[1], Virag Sagi-Kiss[2], Anthony Baptista[1], Mzamo Mbelle[1], Roberto Savoldelli[1], Diana Marin-Correa[1], Thomas Dowe[1], Marwo Habarwaa[1], Zoltan Takats[2], Yoh Zen[1], Alberto Sanchez-Fueyo[1], Cheng Zhang[1], Niloufar Safinia[1]. *[1]King's College London, London, United Kingdom; [2]Imperial College London, London, United Kingdom*
Email: Leonard.bellersheim@kcl.ac.uk

Background and aims: Hepatocellular carcinoma (HCC) is the third leading cause of cancer-related death worldwide. Regulatory T cells (Tregs) infiltrate HCC and inversely correlate with patient survival, yet mechanisms enabling Treg adaptation in the tumor microenvironment (TME) remain unclear. We previously demonstrated that intratumoral Tregs exhibit marked transcriptional and metabolic reprogramming compared to their circulating or non-tumoral counterparts, which display metabolic quiescence and susceptibility to apoptosis. We hypothesise that Treg heterogeneity is spatially resolved, reflecting distinct metabolic niches within the TME, and that targeting Treg adaptation or disrupting these niches could restore anti-tumor immunity.
Method: We generated a spatial-omics multimodal dataset comprising 8 MASLD-associated, treatment-naïve HCC cases, integrating spatial transcriptomics (Xenium), spatial protein profiling (Akoya), spatial metabolomics (LA-REIMS), spatial metallomics (LA-ICP-MS), and H&E histopathology. Data were analysed using a customised bioinformatic pipeline and supplemented with public and proprietary scRNA-seq datasets. Building on prior clinical observations, we established a cohort of 150 HCC specimens obtained through surgical resection at King's College Hospital. Immunohistochemical (IHC) staining for FOXP3 and CD3 was conducted, with subsequent semi-automated quantitative analysis and integration with clinicopathological metadata.
Results: Spatial multi-omic integration of 8 specimens generated a unified dataset combining single-cell transcriptomic and protein profiles with niche-level metallo-metabolic features. This enabled comprehensive characterization of the HCC TME, revealing major cell populations and transcriptional heterogeneity within the Treg compartment. Analysis identified conserved spatial niches with increased tumoral metallo-metabolic heterogeneity. Tregs exhibited niche-specific intratumoral enrichment and differential gene expression, validated in two independent scRNA-seq datasets. IHC staining confirmed elevated Treg numbers in tumoral versus non-tumoral tissue, with highest densities in inflamed tumors.
Conclusion: Our findings demonstrate that Tregs infiltrate distinct spatial niches within the HCC TME, exhibiting niche-specific transcriptional programs and gene signatures. Therapeutic strategies targeting Treg adaptation or metabolic niche remodelling may represent novel approaches to alleviate immunosuppression and enhance anti-tumour immunity in HCC.

WED-238
Neuroimmune regulation of macrophages in steatotic liver disease-related hepatocellular carcinoma
Liyana Binte Abdullah[1], Otsuka Masayuki[1], Jannah Mohamed Nasir Nurul[1], Marie Reolo[1], Jiawei Wu[1], Wei Qiang Leow[2], Ziyao Chen[3], Mathias Heikenwälder[3], David Tai[4], Valerie Chew[1]. *[1]Translational Immunology Institute (TII), SingHealth-DukeNUS Academic Medical Centre, Singapore, Singapore; [2]Department of Anatomical Pathology, Singapore General Hospital, Singapore, Singapore, Singapore; [3]Division of Chronic Inflammation and Cancer, German Cancer Research Centre, Heidelberg, Germany, Heidelberg, Germany; [4]Division of Medical Oncology, National Cancer Centre Singapore, Singapore, Singapore, Singapore*
Email: liyana@u.duke.nus.edu

Background and aims: Steatotic liver disease-related hepatocellular carcinoma (SLD-HCC) is an emerging metabolic subtype marked by poor response to immunotherapy. While immunosuppression in SLD-HCC is increasingly recognised, the contribution of neural regulation – particularly its influence on macrophages – remains unclear. This study examines how peripheral neuroimmune circuits shape macrophage-driven immune activity in SLD-HCC.
Method: We integrated single-cell transcriptomics from two hepatocellular carcinoma patient cohorts (n = 34) with cytometry by time-of-flight (CyTOF) and spatial transcriptomics from an additional cohort (n = 12) to characterise the SLD-HCC tumour microenvironment. Key findings were validated using in vitro macrophage models, multiplex immunohistochemistry in an independent cohort of 104 patients, and an immunotherapy-treated cohort to assess clinical relevance. Ongoing in vivo studies aim to further define neuroimmune regulation in SLD-HCC.
Results: We uncovered a neuroimmune mechanism centred on crosstalk between lipid-associated macrophages (LAMs) and vagal signalling that contributes to impaired immunotherapy response in SLD-HCC. CyTOF revealed macrophage enrichment in SLD-HCC, while two independent single-cell RNA sequencing datasets revealed LAMs as a neuron-responsive subset expanded within the steatotic tumour microenvironment. Spatial transcriptomics and multiplex immunohistochemistry localised LAMs near vagal fibres, supporting a structural basis for this interaction. Mechanistically, the vagus nerve modulates macrophages through the cholinergic anti-inflammatory pathway (CAP). CAP activation or inhibition altered LAM immunoregulatory states in vitro, linking impaired neuroimmune regulation to immunosuppressive LAM function in SLD-HCC.
Conclusion: Vagal-macrophage crosstalk is a key neuroimmune mechanism driving immunosuppression in SLD-HCC. LAMs emerge as a neuron-responsive population regulated through CAP, and reduced vagal activity in MASH limits LAM activation, contributing to chronic inflammation and tumour progression. The vagus-LAM axis represents a potential therapeutic target to improve antitumour immunity in SLD-HCC.

WED-240
Genomic and epigenomic profiling of hepatocellular carcinoma in liquid biopsy
Lauren Brotherton[1,2], Ning Wang[1], Maxwell Bladen[1], Jerick Guinto[1], Dineika Chandrananda[1], Sarah Ftouni[1], Alexander Thompson[2], Jessica Howell[2], Sarah-Jane Dawson[1]. *[1]Peter MacCallum Cancer Centre, Melbourne, Australia; [2]St Vincents Hospital, Melbourne, Australia*
Email: lauren.andersson@svha.org.au

Background and aims: The non-invasive diagnosis of hepatocellular carcinoma (HCC) through radiology is limited by variable sensitivity for small lesions, cost, accessibility and the lack of tumour tissue acquisition for molecular analysis. There is an urgent and unmet need to develop highly sensitive and specific biomarkers for the diagnosis and management of HCC. Analysis of circulating tumour DNA (ctDNA) through 'liquid biopsy' provides an opportunity for non-invasive assessment of tumour dynamics in real time. Harnessing a multiomic

approach combining genomic, epigenomic and non-genomic features of ctDNA has potential to improve the sensitivity and specificity of ctDNA detection. The ease of clinical translatability in part depends on simplified analytical workflows. In this study, we aimed to evaluate a novel single workflow for multiomic ctDNA profiling in HCC.

Method: Plasma for ctDNA analysis was collected from patients with HCC, chronic liver disease (CLD) and healthy controls at baseline and longitudinal time points. Application of a novel six-letter library preparation '*Duet evoC*' (Biomodal) enabled the analysis of genomic and epigenomic (5-methylcytosine and 5-hydroxymethylcytosine) features to single base pair resolution. Whole genome sequencing was performed to a targeted depth of 30X coverage. Non-parametric analysis was performed for each feature including copy number, fragment length and alpha and beta based approach to methylation analysis.

Results: A total of 233 patients were recruited including 102 HCC (all disease stages), 81 CLD and 50 healthy controls. A step wise increase in genomic instability across disease stages was identified in HCC compared to CLD and healthy patients ($p < 0.001$). HCC samples were also enriched for shorter ctDNA fragment size compared to CLD and healthy individuals ($p < 0.01$). Differentially methylated regions of 5mC and 5hmC enabled sensitive detection of ctDNA in HCC cases ($p < 0.01$). Differential methylation was identified across genes implicated in HCC pathogenesis such as tumour suppressor gene *CDKN2*A.

Conclusion: Analysis of ctDNA using a novel library preparation and sequencing platform enables multiomic feature detection to distinguish HCC from CLD and healthy controls.

WED-241

Mechanical cues from fibrotic liver matrix rewire mitochondrial dynamics in hepatocellular carcinoma

Alicia Calé[1,2], Petra Elblová[1,2], Hana Andělová[1], Laura Moran[3], Adriana De Bonis[3], Alejandro Hionides[3], Yulia Nevzorova[3], Jan Kubovciak[4], Milan Jirsa[5], Martin Kveton[5], Mariia Lunova[5], Francisco Javier Cubero[3], Oleg Lunov[1]. *[1]Institute of Physics of the Czech Academy of Sciences, Prague, Czech Republic; [2]Faculty of Mathematics and Physics, Charles University, Prague, Czech Republic; [3]Universidad Complutense De Madrid, Madrid, Spain; [4]Institute of Molecular Genetics of the Czech Academy of Sciences, Prague, Czech Republic; [5]Institute for Clinical & Experimental Medicine, Prague, Czech Republic*
Email: lunov@fzu.cz

Background and aims: Hepatocellular carcinoma (HCC) arises in a fibrotic and mechanically heterogeneous extracellular matrix, but the transition from mechanical properties of the extracellular matrix to metabolic and therapeutic responses in tumor cells remains unclear. Mitochondria have been recognized as mechannosensitive organelles. The role of KEAP1 as a redox sensor may link these two signals. We sought to evaluate a role for extracellular matrix mechanical properties controlling mitochondrial dynamism, redox state, and drug resistance in HCC via KEAP1.

Method: Human HCC cells were plated on collagen-coated elastic substrates mimicking physiological and fibrotic liver stiffness. Mitochondrial morphology and dysfunction, as well as KEAP1-Nrf2 pathway activation, were analyzed with high resolution imaging and biochemical assays. The extent of RNA transcriptional repurposing was determined with bulk RNA-sequencing assays. These effects were validated with migration assays, cell proliferative assays, and chemotherapy sensitivity assays. The relevance of these findings was confirmed with quantitative biochemical assays and multiplex immunohistofluorescence staining with mouse and human tissues.

Results: Higher matrix stiffness caused rapid mechanotrophic migration and higher proliferation rates of HCC cells. KEAP1 expression followed a biphasic, time-dependent response to stiffness and controlled mitochondrial remodeling via a KEAP1/BCL-2/DRP1 pathway. Stiffer matrices increased mitochondrial fusion, decreased reactive oxygen species, and transcriptionally activated antioxidant and glycolytic pathways and caused nuclear translocation of nuclear factor erythroid 2–related factor 2. RNA sequencing analysis showed reduced expression of genes involved in mitochondrial division and enriched pathways for glycolysis, including AGE–RAGE signaling. Functionally, cells cultured on stiffer matrices contained higher cisplatin and sorafenib-resistant cells. Moreover, collagen-positive areas within HCC tissues co-localized with increased KEAP1 and mitochondrial protein expression.

Conclusion: The extracellular matrix stiffness functions as a bioactive modulator for the organization, redox state, and drug resistance of mitochondria in HCC. The findings of these studies demonstrate that KEAP1 functions as a mechanosensitive sensor and integrator of tumor adaptation. The extracellular matrix stiffness emerges as an essential and targetable component within the tumor microenvironment.

WED-242-YI

Single-cell RNA sequencing HCC-based atlas reveals CAFs as predictors of immunotherapy resistance

Guillem Cano-Segarra[1], Ana Hernández[1], Albert Gris-Oliver[1], Ezequiel Mauro[1], Marta Piqué-Gili[1], David Camell Raventos[2], Anna Vila-Escoda[2], Agavni Mesropian[1], Ugne Balaseviciute[1], Marcus Zeitlhoefler[3], Tiago de Castro[3], Sarah Cappuyns[4], Jeroen Dekervel[5], Daniela Sia[3], Roser Pinyol[1], Josep M Llovet[6]. *[1]Liver Cancer Translational Research Laboratory, Institut d'Investigacions Biomèdiques August Pi i Sunyer (IDIBAPS), Hospital Clínic, Universitat de Barcelona, Barcelona, Catalonia, Spain., Barcelona, Spain, Barcelona, Spain; [2]Liver Cancer Translational Research Laboratory, Institut d'Investigacions Biomèdiques August Pi i Sunyer (IDIBAPS), Hospital Clínic, Universitat de Barcelona, Barcelona, Catalonia, Spain, Barcelona, Spain, Mount Sinai Liver Cancer Program, Division of Liver Diseases, Tisch Cancer Institute, Icahn School of Medicine at Mount Sinai, New York, USA, Barcelona, Spain; [3]Mount Sinai Liver Cancer Program, Division of Liver Diseases, Tisch Cancer Institute, Icahn School of Medicine at Mount Sinai, New York, USA, New York City, United States; [4]Digestive Oncology, Department of Gastroenterology, University Hospitals Leuven, Leuven, Belgium. Laboratory of Clinical Digestive Oncology, Department of Oncology, KU Leuven, Leuven, Belgium., Leuven, Belgium; [5]Laboratory of Clinical Digestive Oncology, Department of Oncology, KU Leuven, Leuven, Belgium. Laboratory for Translational Genetics, Department of Human Genetics, KU Leuven, Leuven, Belgium., Leuven, Belgium; [6]Liver Cancer Translational Research Laboratory, Institut d'Investigacions Biomèdiques August Pi i Sunyer (IDIBAPS), Liver Unit, Hospital Clínic, Universitat de Barcelona, Barcelona, Catalonia, Spain., Mount Sinai Liver Cancer Program, Division of Liver Diseases, Tisch Cancer Institute, Icahn School of Medicine at Mount Sinai, New York, USA., Institució Catalana de Recerca i Estudis Avançats (ICREA), Barcelona, Catalonia, 08010, Spain., Barcelona, Spain*
Email: gcanos@recerca.clinic.cat

Background and aims: Atezolizumab and bevacizumab combination (atezo+bev) is a first-line treatment for advanced hepatocellular carcinoma (aHCC). Cancer-associated fibroblasts (CAFs) promote tumor survival through immunosuppression; however, their heterogeneity and clinical relevance in HCC remain unclear. Our aim was to characterize CAF subtypes in HCC and assess their association with response to atezo+bev.

Method: Seven single-cell RNA sequencing (scRNA-seq) datasets encompassing 197 HCCs (422,561 cells) were integrated to generate an HCC-based atlas to define CAF transcriptional state. CAF-specific single-cell gene signatures were generated and used to deconvolute CAF composition in early and aHCC ($n = 918$) using BayesPrism. Associations with established molecular and immune HCC classifications were assessed. Differential gene expression analysis and LASSO regression were applied to bulk RNA-seq data from 386 atezo+bev-treated HCCs to derive a CAF-based non-response signature (AB-CAF). Predictive performance was benchmarked against published immunotherapy response signatures and externally tested in the

IMbrave150 trial cohort. Associations with clinical outcomes were evaluated.
Results: Single-cell data integration showed that CAF accounted for 5% of early stage and 15% of aHCC cellular compartments ($p < 0.001$). Five transcriptionally distinct CAF were identified. The iMyo/*POSTN* subtype was predominant across stages, accounting for 63% of CAF in early HCC and 90% in aHCC ($p < 0.001$). AB-CAF signature was associated with response (AUC 0.77; CI 0.71–0.83) and treatment-dependent survival (AB-CAF+ Median OS (mOS) 17.4 months vs AB-CAF- mOS NA; $p < 0.002$) as opposed to sorafenib-treated patients (AB-CAF+ mOS 13.4 months vs AB-CAF- mOS 7.5 months; $p = 0.103$); p of interaction = 0.002. In multivariate models, including previously reported atezo+bev response signatures, AB-CAF remained independently predictive of non-response (OR 4.26, 95% CI 2.45–7.58; $p < 0.001$). Mechanistically, AB-CAF+ tumors were significantly enriched in the Immune Excluded, Non-Proliferation/*CTNNB1* subclass, whereas AB-CAF- tumors exhibited an Immune Active Progenitor/Proliferation profile (both $p < 0.001$).
Conclusion: A scRNA-seq HCC atlas revealed that CAFs constitute a major cellular component of HCC and comprise five subtypes, with iMyo/*POSTN* CAFs predominating across disease stages. AB-CAF gene signature was independently associated with non-response to atezo+bev, highlighting the tumor stroma as a key determinant of immunotherapy outcomes.

WED-243
Hepatic iron metabolism dysregulation promotes metabolic dysfunction-associated steatohepatitis induced hepatocellular carcinoma in preclinical models
Sahiba Chahal[1,2], Vikram Patial[1,2]. [1]*Pharmacology and Toxicology Laboratory, Dietetics & Nutrition Technology, CSIR-Institute of Himalayan Bioresource Technology, Palampur, India;* [2]*Academy of Scientific and Innovative Research (AcSIR), Ghaziabad, India*
Email: sahibachahal.me@gmail.com

Background and aims: Dysregulated hepatic iron metabolism has been associated with metabolic dysfunction-associated steatohepatitis (MASH) induced hepatocellular carcinoma (HCC). This study aims to assess the effect of MASH on hepatic iron metabolism and its role in the progression of HCC in preclinical models of MASH-induced HCC.
Method: MASH-HCC was induced by incorporating high fat-high carbohydrate (HF-HC) diet in addition to weekly CCl4 (i.p.) in C57BL/6 mice. The study comprised of four groups to evaluate the effect of HF/HC on hepatic iron metabolism. The naïve group was fed with standard chow diet. Sixteen weeks into the study, two of the groups were either supplemented with ferric ammonium citrate (FAC) as source of iron or given deferoxamine mesylate salt (DFX-MS) as iron chelator in addition to HF/HC. Similar conditions were mimicked *in-vitro* wherein human hepatic cell line was treated with free fatty acids, pro-inflammatory cytokine TNF-alpha, FAC, and DFX-MS to check the role of iron metabolism on HCC.
Results: High calorie intake significantly elevated body weight and liver weight, as compared to control group. Similar trend was observed in FAC group; however, a reduction in body weight and liver weight was observed in DFX groups. The liver injury markers and triglyceride level showed similar trends in the FAC and disease group as compared to the DFX and naïve group. The gross anatomical analysis of liver showed the multiple nodules of varying sizes in disease and FAC group. Histopathology of liver revealed multiple nodules scattered throughout the tissue, steatosis, inflammation, vacuolated cells, and trabecular patterns in the disease and FAC groups. Prussian blue staining showed hepatic iron accumulation across groups as compared to naïve group and Masson's Trichrome staining showed the extent of fibrosis. DFX group showed the reduced lesion severity, fibrosis and iron overload. In addition, iron regulatory gene also showed the preventive effect of DFX on hepatic iron overload and HCC progression. These results were further confirmed on the human hepatic cell line by analysing the expression of iron-related genes, lipid accumulation and inflammation.
Conclusion: MASH development disrupts iron homeostasis, leading to iron overload in the liver. Interventions that counteract hepatic iron accumulation may offer a promising therapeutic approach to prevent progression to HCC.

WED-244-YI
Generation and characterization of a murine BRAF V600E driven cholangiocarcinoma model
Shreya Chakraborty[1], Denise Schlösser[1], Hakan Tomac[1], Lisa Wende[1], Silke Marhenke[1], Tilman Brummer[2,3], Arndt Vogel[1,4,5], Anna Saborowski[1]. [1]*Medizinische Hochschule Hannover, Hannover, Germany;* [2]*University Of Freiburg, Freiburg im Breisgau, Germany;* [3]*Insitute of Molecular Medicine and Cell Research, Brummer, Freiburg, Germany;* [4]*Toronto General Hospital, Toronto, Canada;* [5]*Princess Margaret Cancer Centre, Toronto, Canada*
Email: chakraborty.shreya@mh-hannover.de

Background and aims: Cholangiocarcinoma (CCA) is an aggressive biliary cancer with limited treatment options. The $BRAF^{V600E}$ mutation is a targetable driver in a subset of CCA patients, yet responses to BRAF targeted therapies are often transient due to rapid resistance. The molecular mechanisms driving adaptive resistance and the emergence of drug-tolerant persister cells remain elusive. This study aims to elucidate signaling adaptations following MAPK pathway inhibition in $BRAF^{V600E}$ mutant CCA.
Method: Murine liver organoids carrying $BRAF^{V600E}$ mutation and *Trp53* deletion were transplanted subcutaneously into immunocompetent mice. Tumors were used to derive two cell lines, designated as OBPI and OBPII. Cells were treated with BRAF inhibitors (Dabrafenib, Encorafenib), MEK inhibitor (Trametinib), and EGFR/HER2 inhibitors (Gefitinib, Neratinib), alone or in combination. Cell proliferation and ERK phosphorylation were assessed and phospho-RTK arrays were performed. OBPII cells were also evaluated *in vivo* under Dabrafenib, Trametinib, or combination treatment.
Results: Both cell lines exhibited high IC_{50} values for BRAF inhibitors, exceeding clinically relevant concentrations, with only moderate effects on proliferation and rapid feedback activation within 24 hours: ERK phosphorylation was initially suppressed but rebounded within 6 hours of treatment. pRTK analysis revealed basal EGFR and HER2 activation, with HER2 phosphorylation re-emerging after transient suppression by BRAF inhibition. Subsequent inhibition of EGFR2 and EGFR/HER2 fully abrogated ERK reactivation. In contrast, both cell lines were highly sensitive to Trametinib, showing sustained ERK suppression. Prolonged MEK inhibition induced a reversible, non-proliferative state, with cells resuming proliferation upon drug withdrawal. *In vivo*, Dabrafenib had minimal effect on tumor growth, whereas Trametinib significantly inhibited progression.
Conclusion: Our data suggest that $BRAF^{V600E}Trp53^{-/-}$ CCA cells rapidly adapt to BRAF inhibition through EGFR/HER2-driven feedback reactivation of ERK signaling, leading to intrinsic resistance. In contrast, MEK inhibition enforces durable MAPK suppression but induces a reversible persister cell state characterized by cellular quiescence rather than cell death. These findings identify adaptive RTK signaling and cellular persistence as critical barriers to MAPK-targeted therapy in CCA, underscoring the need for rational combination strategies to overcome resistance and prevent disease relapse.

WED-245

Differential NK cell residency and immunosuppressive ILC remodeling define subtype-specific tumor-microenvironments in cholangiocarcinoma

Sachin Chauhan[1], Livia Schmidt[1], Tijana Ristic[1], Suparna Dey[1], Anna Riddermann[2], Nora Nevermann[2], Heiner Wedemeyer[1], Linda Feldbruegge[2], Moritz Schmelzle[2], Bernd Heinrich[1].
[1]*Department of Gastroenterology, Hepatology, Infectious Diseases and Endocrinology, Hannover Medical School, Hannover, Germany;*
[2]*Department of General, Visceral and Transplant Surgery, Hannover Medical School, Hannover, Germany*
Email: heinrich.bernd@mh-hannover.de

Background and aims: Cholangiocarcinoma (CCA) is a highly lethal malignancy with limited therapeutic options and modest responses to immunotherapy. Despite pronounced biological heterogeneity between intrahepatic (iCCA) and perihilar CCA (pCCA), current treatment strategies remain uniform. Innate lymphoid cells (ILCs), including natural killer (NK) cells, are key regulators of tissue immunity, yet their role in shaping subtype-specific tumor microenvironments (TME) in CCA remains poorly defined. We aimed to characterize the composition and functional states of ILCs across anatomical subtypes of CCA.
Method: Tumor and matched non-tumor tissue were obtained from 11 CCA patients (7 iCCA, 4 pCCA). Median age of the cohort was 72.5 years. None of the patients had a diagnosis of ulcerative colitis or primary sclerosing cholangitis. Mononuclear cells were isolated and analyzed using high-parameter spectral flow cytometry with a 31-marker ILC-focused panel. Multi-dimensional analyses were performed using FlowJo v10.10.
Results: CCA tumor tissue displayed a consistent shift in ILC composition characterized by expansion of mature cKIT$^-$ ILC2s and a significant reduction of ILC3s compared with non-tumor tissue, independent of subtype. Depletion of CCR6$^+$ ILC3s was most pronounced in iCCA tumors, whereas pCCA showed uniformly low CCR6$^+$ ILC3 frequencies. NK cell analysis revealed reduced circulating NK cells (cNK) and a relative enrichment of tissue-resident NK cells (trNK) within tumors, accompanied by increased expression of CXCR6, CD49a, and the inhibitory receptor NKG2A. This tumor-associated cNK-to-trNK shift was most evident in iCCA, while pCCA exhibited elevated baseline frequencies of trNKs. Functionally, activated KLRG1$^+$CD25$^+$ ILC2s were selectively enriched in pCCA tissue, whereas early-activated CD25$^+$ trNKs increased in tumor tissue across subtypes.
Conclusion: CCA is characterized by pronounced, subtype-specific remodeling of the innate immune landscape, including loss of protective ILC3s and accumulation of immunosuppressive ILC2s and dysfunctional tissue-resident NK cells. Divergent NK cell differentiation states in iCCA and pCCA suggest distinct immunological constraints and therapeutic vulnerabilities. These findings highlight the importance of subtype-resolved innate immune profiling to inform tailored immunotherapeutic strategies in cholangiocarcinoma.

WED-246

Malignant ascites as a liquid biopsy for dominant neoantigen discovery in advanced liver cancer

Dongbo Chen[1]. [1]*Peking University People's Hospital, Peking University Hepatology Institute, Beijing Key Laboratory of Hepatitis C and Immunotherapy for Liver Disease, Beijing International Cooperation Base for Science and Technology on NAFLD Diagnosis, Beijing, China*
Email: chendongbo338@163.com

Background and aims: Neoantigen-based immunotherapy represents a promising strategy for liver cancer, yet its clinical application is limited by the frequent unavailability of tumor tissue in advanced-stage patients. Malignant ascites, often enriched with tumor cells, provides a potential liquid biopsy source for neoantigen discovery. This study aimed to identify dominant neoantigens in malignant ascites from patients with advanced liver cancer and to evaluate their potential as targets for personalized immunotherapy.
Method: Ascites samples were collected from patients with cirrhosis and advanced liver cancer. Tumor cells were isolated by flow cytometry as 7-AAD$^-$ CD45$^-$ CD326$^+$ (P7) cells. For low-input samples (<2000 cells), RNA and DNA were amplified using Smart-seq2 and whole-genome amplification. Whole-exome and RNA sequencing were performed to identify somatic mutations. Candidate neoantigens were predicted using VEP and NetMHCpan-4.1, accounting for HLA loss of heterozygosity. Neoantigen-specific T-cell responses were assessed by tetramer staining, flow cytometry, ELISPOT, and ELISA.
Results: We established a robust workflow enabling sequencing of rare tumor cells from malignant ascites. Advanced liver cancer patients exhibited significantly higher numbers of P7 tumor cells in ascites compared with peripheral blood and cirrhotic controls. Single-cell analysis demonstrated partial overlap between mutations in ascites-derived tumor cells and matched primary or metastatic lesions. Predominant C > T/G > A substitutions were observed, corresponding to COSMIC signatures 1, 3, 12, 15, and 30. Multiple candidate neoantigens were identified, including those derived from TOP3A, TUBB6, NUTM2G, SND1, FGD2, NFKBIZ, and CLDND1. Neoantigen-specific T cells were detected in ascites and exhibited high CD39 expression. Notably, an HLA-A*02:01–restricted SND1-derived neoantigen elicited strong T-cell responses, indicating dominant immunogenicity.
Conclusion: Malignant ascites serves as a feasible and informative liquid biopsy for dominant neoantigen identification in advanced liver cancer. This strategy enables personalized neoantigen discovery in patients lacking tumor tissue and supports the development of individualized immunotherapeutic approaches.

WED-247

Multi-ancestry genome-wide association meta-analysis of hepatocellular carcinoma identifies eight novel risk genes including MYC, MAP3K9, DHRS1, and MTTP

Ifechukwuamaka Chinaka[1], Annabelle Schofield[2], Lewis Roberts[3], Christopher Amos[4], Vincent Chen[5], Younghun Han[4], Manal Hassan[6], Shishir Shetty[7], Jake Mann[7,8]. [1]*St James Hospital, Dublin, Ireland;* [2]*University of Birmingham, Birmingham, United Kingdom;* [3]*Mayo Clinic, Rochester, United States;* [4]*University of New Mexico, Albuquerque, United States;* [5]*University of Michigan, Ann Arbor, United States;* [6]*University of Texas, MD Anderson Cancer Centre, Houston, United States;* [7]*Department of Immunology & Immunotherapy, School of Infection, Inflammation and Immunology, College of Medicine and Health, University of Birmingham, Birmingham, United Kingdom;* [8]*Birmingham Women's and Children's NHS Foundation Trust, Birmingham, United Kingdom*
Email: ifechinaka@gmail.com

Background and aims: Hepatocellular carcinoma (HCC) is the 3rd top cause of cancer death globally. It typically arises on a background of cirrhosis, which can be caused by any aetiology of liver disease. HCC may also develop in non-cirrhotic individuals, particularly in chronic hepatitis B virus (HBV) infection and in metabolic dysfunction-associated steatotic liver disease (MASLD). Identification of genetic risk factors is critical to mitigate rapidly growing burden of HCC. Here, we aimed to establish novel genetic drivers of HCC across ancestries at a population level through a large meta-analysis of all-cause HCC.
Method: Here, we performed a multi-ancestry meta-analysis (MAMA) of HCC GWAS, which included transcriptome-wide and regulome-wide association analyses. In doing so, we identified eight novel loci as putative risk genes for HCC and established a baseline for future studies with inclusion of diverse ancestries. We included 15 cohorts comprising of 17,329 HCC cases and 2,424,298 controls in this meta-analysis.

Results: We found 15 genome-wide significant (P < 5×10–8) germline loci, 6 novel in/near *GCKR*, *MTTP*, *ADH5*, *MYC*, *MAP3K9*, and *GABPB2*. *MAP3K9*, *TERT*, and *GABPB2* variants act independently of cirrhosis on both co-localisation analysis and sensitivity analyses. There was significant ancestral heterogeneity in 6 loci including variants in the HLA locus that had divergent effects on HCC risk between East Asian and European ancestries. Fine-mapping identified 11 potentially causal coding variants, including p.Leu446Pro in GCKR and p.Asp418Glu in MEN1. *MEN1*, *MYC*, and *TERT* are all involved in the beta-catenin pathway transactivation complex. Transcriptome-wide analysis identified enrichment of germline-encoded *DHRS1* in HCC. Regulome-wide analysis replicated the germline signal for *EPHA2* and found a novel chromatin accessible region containing genes *ZNF367* and *HABP4*. Finally, we demonstrated that population-level genetic architecture for HCC overlaps with steatotic and viral liver disease, and individuals with genetic risk for lower BMI have higher risk of HCC.
Conclusion: Genetic risk for HCC is determined by germline susceptibility to beta-catenin pathway activation and cirrhosis. HCC is driven by both heterogenous and homogenous genetic factors across ancestries, which require further ancestral diversity in liver GWAS to fully dissect.

WED-248

Circulating miRNAs as predictive biomarkers of response to immunotherapy in hepatocellular carcinoma (HCC)

Salvatore Corallo[1,2], Barbara Oliviero[1], Alessia La Gaipa[1], Cristian Bassi[3], Massimo Negrini[3], Clara Vianello[4], Daniela Cicognini[1], Stefania Mantovani[1], Francesca Fornari[4]. *[1]Fondazione Irccs Policlinico San Matteo, University of Pavia, Pavia, Italy; [2]University of Pavia, Pavia, Italy; [3]Università degli Studi di Ferrara, Ferrara, Italy; [4]University of Bologna, Bologna, Italy*
Email: s.corallo@smatteo.pv.it

Background and aims: Immunotherapy has changed the treatment of advanced HCC, but early identification of patients who do not respond remains a challenge due to the lack of predictive biomarkers. Circulating microRNAs (miRNAs) have emerged as promising non-invasive biomarkers that reflect tumor biology, disease progression, and treatment response. This study aimed to characterize the serum miRNome in patients with advanced HCC receiving immunotherapy-based systemic treatment [atezolizumab plus bevacizumab (atezo-be) or tremelimumab plus durvalumab (durva-treme)] to identify a molecular signature associated with treatment response.
Method: Serum samples were collected from 10 patients (discovery cohort) with advanced HCC treated with atezo-bev (n = 8) or durva-treme (n = 2) at 3 months (T3) after treatment start. Patients were stratified into responders (R, n = 6) and non-responders (NR, n = 4) based on radiological response, defined as partial or complete response according to RECIST 1.1 criteria. High-throughput miRNome profiling, differential expression, and hierarchical clustering analyses were performed to identify discriminatory signatures. For validation, serum samples were collected at multiple time points [baseline, before the second therapy cycle (T1), and T3] from an independent cohort of 20 HCC patients treated with the same regimens and analyzed by quantitative polymerase chain reaction.
Results: Unsupervised hierarchical clustering of serum miRNA expression profiles and differential expression analysis revealed clear segregation between R and NR, identifying a subset of miRNAs differentially expressed between the two groups at T3. Notably, miR-942-5p was the most statistically significant variable, exhibiting marked upregulation in responders. Other key miRNAs contributing to the discriminatory signature included the oncogenic miR-21-5p, miR-483-5p, and the hepato-specific miR-122-5p. Selected miRNAs were subsequently validated in the independent validation cohort, confirming their differential expression patterns.
Conclusion: Our preliminary analysis suggests a serum miRNA signature at 3 months of therapy that may differentiate responders from non-responders. The observed differential expression pattern highlights miRNAs as candidate markers for monitoring treatment response. These findings provide a basis for further investigating the role of liquid biopsy in guiding personalized therapeutic strategies.

WED-249

From primary tumor to metastasis: stemness dynamics in intrahepatic cholangiocarcinoma

Margherita Correnti[1], Marco Erreni[2], Marina Sironi[3], Matteo Ramazzotti[4], Monika Lewinska[5], Jesper Andersen[5], Colm O Rourke[5], Cedric Coulouarn[6,7], Fabio Pagni[8], Mario Urso[8], Diego Calvisi[9], Luca Di Tommaso[10], Stefania Recalcati[1], Fabio Marra[11], Chiara Raggi[11]. *[1]University of Milan, Dept. of Biomedical Sciences for Health, Milan, Italy; [2]Humanitas Clinical and Research Center, Dept. of Immunology, Rozzano, Italy; [3]Humanitas Clinical and Research Center, Dept. of Immunopharmacology, Rozzano, Italy; [4]University of Florence, Dept of Experimental and Clinical Biomedical Sciences, Florence, Italy; [5]University of Copenaghen, Biotech Research and Innovation Center, Copenaghen, Denmark; [6]University of Rennes, CHU Rennes, Service de Chirurgie Hépatobiliaire et Digestive, Rennes, France; [7]Inserm, Rennes, France; [8]University of Milano-Bicocca, Dept. of Medicine and Surgery, Pathology, Monza, Italy; [9]University of Regensburg, Institute of Pathology, Regensburg, Germany; [10]Humanitas University, Dept. of Biomedical Sciences, Rozzano, Italy; [11]University of Florence, Dept. of Experimental and Clinical Medicine, Florence, Italy*
Email: margherita.correnti@gmail.com

Background and aims: The aggressiveness of intrahepatic cholangiocarcinoma (iCCA) relies on keytumor features such as cellular plasticity, self-renewal capacity, and metastatic potential, collectively described as tumor stemness. Molecular mechanisms driving the maintenance and evolution of stemness features during iCCA progression remain poorly understood. This study aims to characterize the dynamics of stemness-related traits in primary and metastatic iCCA, identify key molecular pathways that sustain tumor cell plasticity, and explore their role in disease dissemination. By elucidating these features in vivo, we seek to uncover novel targets to disrupt tumor stemness and hinder disease progression.
Method: Taking advantage of a 3D sphere culture system (SPH) as a model for cancer stem cells, an orthotopic mouse model was developed through intrahepatic injection of Luciferase-GFP-transfected SPH cells obtained by both established and primary iCCA cells. Disseminated GFP+ tumor cells in target organs (lungs, spleen, peritoneum, mesenteric lymph nodes) and blood were analyzed via FACS. GFP+ cells from primary and metastatic lung tumors were isolated by FACS for molecular profiling using pathway-focused qRT-PCR arrays. These findings were validated in human metastatic and non-metastatic iCCA samples through immunohistochemistry and correlated with clinical and pathological data.
Results: SPH cells were responsible for a great tumor spread in all secondary organs analyzed, especially those derived from MTCHC-01 primary cells. The absence of CD45-/GFP+ tumor cells in the blood of animals suggested that lymphatic circle is the preferential via to iCCA dissemination. Notably, lung SPH-disseminated cells showed up-regulation of many tested stem-like, epithelial-to-mesenchymal transition, angiogenesis and drug resistance related genes compared to SPH-primary tumor cells. A panel of 34 genes commonly up-regulated was found in all SPH-disseminated cells. High expression of some of these genes were correlated with a significantly lower 5-years and disease-free survival of 289 iCCA patients. Among these, TSPAN13 and WNT5A are of particular importance. Expression levels of these 2 genes-derived proteins were significantly up-regulated metastatic CCA specimens compared to non-metastatic ones.
Conclusion: Our data indicate that a core stemness program is maintained during iCCA progression, with TSPAN13 and WNT5A emerging as key markers of stemness and metastasis.

WED-250

Chemoprevention of hepatocellular carcinoma by next-generation antipsychotic aripiprazole

Nevena Slovic[1], Sumit Mishra[2], Paul Subhojit[2], Marine Oudot[1], Frank Jühling[1], Hiroaki Kanzaki[2], Julien Moehlin[1], Anouk Charlot[1], Margaux Denos[1], Sarah Durand[1], Courtney Katz[2], Cloé Gadenne[1], Emanuelle Felli[3], Joachim Lupberger[1], Emilie Crouchet[1], Yujin Hoshida[2], Thomas Baumert[1]. [1]*University of Strasbourg/Inserm UMR_S1110 (ITM), Strasbourg, France;* [2]*Department of Internal Medicine, University of Texas Southwestern Medical Center, Dallas, United States;* [3]*Hospital Group Saint Vincent, Strasbourg, France*
Email: ecrouchet@unistra.fr

Background and aims: Hepatocellular carcinoma (HCC) is the most common form of liver cancer and is a major global health burden, ranking sixth in incidence and third in cancer-related mortality. Despite therapeutic advances, treatment options for advanced liver disease and HCC are limited and strategies to prevent HCC development are lacking. Serotonin signaling is known to play a functional role in metabolic dysfunction, steatosis, inflammation and fibrosis. Aripiprazole is an FDA-approved third generation antipsychotic, which modulates multiple serotonin receptor signaling pathways. In this study, we investigated the potential of aripiprazole as an HCC chemopreventive strategy.
Method: Aripiprazole's targets expression was assessed in clinical liver tissues at mRNA and protein levels. The therapeutic potential of aripiprazole was examined in a rat model of MASH-induced HCC induced by choline-deficient L-amino acid-defined and high-fat diet. To decipher the mechanism of action, RNA-sequencing (RNA-Seq) was performed on rat liver tissues. The effect of aripiprazole was validated in different liver cell compartments by perturbation studies using patient-derived liver myofibroblasts, a monocyte-derived macrophage model and HCC cancer cells. Finally, we analyzed the impact of aripiprazole treatment on tumor microenvironment (TME) by combining a multicellular patient-derived tumorspheroid model and single cell RNA-Seq.
Results: Analyses of clinical liver tissues showed that aripiprazole's targets are expressed in different liver cell compartments including fibroblasts, macrophages and epithelial cancer cells, and that target gene expression is associated with fibrotic liver diseases and HCC. In a rat model of MASH-induced HCC, aripiprazole prevents liver disease progression and HCC development by modulating fibrogenesis related pathways and inflammation. Mechanistically, aripiprazole exerts antifibrogenic and anti-inflammatory effects by modulating the phenotype of liver fibroblasts and macrophages. Moreover, perturbation studies in cancer cell models showed that aripiprazole prevents tumor initiation and reduces cell proliferation via inhibition of the cMET and ERK pathways and perturbation of mitochondrial functions. Finally, treatment of patient-derived tumorspheroids demonstrated that aripiprazole modulates immune responses in the TME.
Conclusion: Collectively, these findings suggest that treatment with aripiprazole is a clinically relevant approach for HCC chemoprevention.

WED-251-YI

Impact of dual immune checkpoint blockade on the tumor immune microenvironment and determinants of therapeutic response in hepatocellular carcinoma

Kazuma Daiku[1], Yuta Myojin[1], Kazuki Maesaka[1], Kumiko Shirai[1], Kazuhiro Murai[1], Yuki Makino[1], Yuki Tahata[1], Yoshinobu Saito[1], Hayato Hikita[1], Takahiro Kodama[1]. [1]*Department of Gastroenterology and Hepatology, Graduate School of Medicine, The University of Osaka, Suita, Japan*
Email: t-kodama@gh.med.osaka-u.ac.jp

Background and aims: Dual immune checkpoint blockade (durvalumab plus tremelimumab) improves outcomes in advanced hepatocellular carcinoma, but treatment-induced microenvironmental changes and determinants of resistance remain incompletely understood. We profiled therapy-associated changes and searched for tumor-intrinsic factors linked to resistance.
Method: A heterogeneous murine hepatocellular carcinoma model was generated by hydrodynamic injection of a pooled library of 10 oncogene cDNA constructs with unique barcodes. Mice received anti–PD-L1 plus anti–CTLA-4 antibodies. Bulk tumor RNA profiling was performed. Immune cells from early responding tumors and from tumors with acquired resistance after prolonged treatment were analyzed by single-cell RNA sequencing (scRNA-seq). Barcode sequencing estimated intratumoral oncogene clone frequencies. In addition, we generated an Mcl1-overexpressing Hep55.1c cell line and evaluated dual blockade in a subcutaneous syngeneic mouse tumor model.
Results: Dual blockade prolonged overall survival compared with untreated and monotherapy groups, and complete responses occurred only with combination therapy. Responding tumors showed higher Cd8, Cd4, and Foxp3 expression, whereas resistant tumors showed lower Cd8 and Cd4 expression. Gene signature–based cell-type scoring indicated higher endothelial and fibroblast scores in resistant tumors. ScRNA-seq demonstrated increased intratumoral CD8+ and CD4+ T cells in responders, while resistant tumors had reduced lymphocytes and increased myeloid cells, including neutrophils; regulatory T cells increased only modestly. Barcode analysis showed enrichment of MCL1-driven clones in resistant tumors. In the syngeneic subcutaneous Hep55.1c model, Mcl1 overexpression reduced tumor regression under dual blockade and was associated with reduced Cd4 expression.
Conclusion: Dual immune checkpoint blockade promotes intratumoral T-cell infiltration and antitumor activity. Tumor barcoding and functional validation implicate an MCL1-associated program as a potential mediator of resistance in hepatocellular carcinoma, which may be associated with suppression of CD4+ T cells.

WED-252

Platelet-induced mitochondrial transfer promotes hepatocellular carcinoma progression

Meng Zhang[1], Yaping Li[1], Muqi Wang[1], Chenrui Liu[1], Yikai Wang[1], Wenhao Wang[1], Hanxiang Dang[1], Yigan Zhang[2], Zhong-ji Meng[2], Shuangsuo Dang[1]. [1]*The Second Affiliated Hospital of Xi'an Jiaotong University, Xi'an, China;* [2]*Taihe Hospital, Hubei University of Medicine, Shiyan, China*
Email: zhangmeng8388@126.com

Background and aims: Platelets are increasingly recognized as active regulators within the tumor microenvironment and play important roles in hepatocellular carcinoma (HCC) progression. Intercellular mitochondrial transfer has emerged as a novel mechanism regulating tumor cell behavior; however, whether platelet–tumor interactions promote HCC progression through mitochondrial transfer remains unclear. This study aimed to investigate platelet-associated mitochondrial transfer, its potential modes of intercellular communication, and its functional significance in HCC progression.
Method: HCC cell lines Hep3B and Huh7 were co-cultured with platelets isolated from patients with HCC under direct-contact or Transwell conditions. Scanning electron microscopy was used to visualize tunneling nanotube (TNT)-like intercellular structures, while transmission electron microscopy assessed mitochondrial ultrastructural changes in tumor cells. Platelet mitochondria were fluorescently labeled to trace their transfer into HCC cells. Mitochondrial membrane potential and intracellular reactive oxygen species (ROS) levels were evaluated by flow cytometry. Tumor cell migratory capacity was assessed using functional assays. Pharmacological inhibitors targeting TNT formation or extracellular vesicle release were applied to explore potential routes of mitochondrial transfer.
Results: Direct contact with platelets isolated from HCC patients significantly enhanced Hep3B and Huh7 cells migration compared

with indirect co-culture. TNT-like structures connecting platelets and tumor cells were observed by scanning electron microscopy, accompanied by increased mitochondrial abundance in tumor cells on transmission electron microscopy. Fluorescence tracing confirmed the presence of platelet-derived mitochondria within HCC cells. Functionally, co-culture with HCC patient–derived platelets stabilized mitochondrial membrane potential and reduced intracellular ROS levels in tumor cells. Inhibition of either TNT formation or extracellular vesicle release markedly attenuated platelet-induced mitochondrial alterations and the associated enhancement of tumor cell migration.
Conclusion: Platelets promote hepatocellular carcinoma progression by transferring mitochondria and enhancing mitochondrial functional stability in tumor cells. Multiple intercellular communication pathways, including TNT-like structures and vesicle-dependent mechanisms, may cooperatively mediate platelet–tumor interactions, highlighting potential therapeutic targets in HCC.

WED-253
Modeling human innate and adaptive immunity in hepatocellular carcinoma: evaluating anti-IL-8 and anti-PD-L1 immunotherapy in humanized mice
Zenzi De Vos[1,2,3], Lander Heyerick[1,2], Aline Baekelandt[1,2], Hannah Stocks[4,5], Andy Wullaert[4,5], Rania Matthys[1,2], Emine Gökce[6], Anne Hoorens[7], Sarah Raevens[2,6,8], Anja Geerts[2,6,8], Xavier Verhelst[2,6,8], Sander Lefere[2,6,8], Hans Van Vlierberghe[2,6,8], Lindsey Devisscher[1,2,3]. *[1]Department of Basic & Applied Medical Sciences, Gut-Liver Immunopharmacology Unit, Ghent University, Ghent, Belgium; [2]Liver Research Center Ghent, Ghent University, Ghent University Hospital, Ghent, Belgium; [3]Cancer Research Institute Ghent, Ghent, Belgium; [4]VIB-UGent Center for Inflammation Research, VIB, Ghent, Belgium; [5]Department of Biomedical Sciences, Cell Death Signaling Laboratory, University of Antwerp, Antwerp, Belgium; [6]Department of Gastroenterology and Hepatology, Ghent University Hospital, Ghent, Belgium; [7]Department of Pathology, Ghent University Hospital, Ghent, Belgium; [8]Department of Internal Medicine and Paediatrics, Hepatology Research Unit, Ghent, Belgium*
Email: zenzi.devos@ugent.be

Background and aims: Hepatocellular carcinoma (HCC) patients suffer from inadequate treatment options, in part attributable to the lack of human-relevant models that include key components of the immunosuppressive tumor microenvironment (TME) of human HCC.
Method: We present two novel humanized immune system (HIS) mouse models, co-transplanted with orthotopic human HCC, to investigate human HCC in the context of human monocyte/macrophage (Myeloid-HIS-HCC) or human T cell (T cell-HIS-HCC) responses. Mice were treated with immunotherapy directed to innate (anti-IL-8 antibody (n = 11) or IgG isotype control (n = 10) in Myeloid-HIS-HCC mice) or adaptive (anti-PD-L1 antibody (n = 7) or IgG isotype control (n = 6) in HCC patient-T cell-HIS-HCC mice) immunity.
Results: In Myeloid-HIS mice, injection of human hematopoietic stem and progenitor cells resulted in efficient engraftment in peripheral blood of human monocytes, DCs and NK cells, of which the latter were significantly lower in HCC-bearing mice ($p = 0.048$). Engraftment in the liver and HCC tumors was dominated by human macrophages. Gene expression of tumor-associated macrophage markers (*ICAM1* $p = 0.031$), immune checkpoints (*PDL1* $p = 0.046$) and tumor-promoting markers (*HIF1A* $p = 0.049$ and *IL6* $p = 0.015$) were higher in anti-IL-8-treated Myeloid-HIS-HCC mice, compared to control-treated mice, without differences in tumor size. In T cell-HIS mice, human peripheral blood mononuclear cells mainly resulted in engraftment of human T cells. Tumor growth was significantly lower in T cell-engrafted HCC mice compared to nongrafted HCC mice. Regulatory T cell engraftment tended to be higher in mice engrafted with HCC patient-derived cells compared to mice with cells derived from healthy donors, which was reversed upon anti-PD-L1 treatment ($p = 0.025$). In line, gene expression of T cell activation markers was lower, and tumor marker gene expression was higher, in HCC patient-humanized compared to healthy-humanized mice, which was reversed upon anti-PD-L1-treatment (*GZMB* $p = 0.049$ and *IFNG* $p = 0.044$).
Conclusion: We propose two novel preclinical humanized immune system models with high translational value. In both models, alterations in the TME of HCC related to human innate or adaptive immunity can be evaluated, demonstrating its relevance as immunotherapy-evaluating platforms. In addition, HCC patient-derived T cell-HIS-HCC mice appear promising as tool for personalized medicine.

WED-254
UCHL1 inhibition by LDN57444 potentiates sorafenib response in hepatocellular carcinoma: a preclinical study
Kylian Decroix[1,2,3], Elias Van De Vijver[1,3], Delphine Burggraeve[1,3], Lindsey Devisscher[2], Marleen Van Troys[1], Hans Van Vlierberghe[3]. *[1]Actin and Cell Migration Lab, Department of Biomolecular Medicine, Ghent University, Ghent, Belgium; [2]Department for Basic and Applied Medical Sciences, Gut-Liver Immunopharmacology Unit, Ghent University, Ghent, Belgium; [3]Hepatology Research Unit, Department Internal Medicine and Pediatrics, Liver Research Center, Ghent University, Ghent, Belgium*
Email: kylian.decroix@ugent.be

Background and aims: Hepatocellular carcinoma (HCC) is the most prevalent form of liver cancer worldwide. Despite recent advances in immunotherapy, treatment efficacy remains inadequate. Long-term effectiveness of second-line tyrosine kinase inhibitors is often limited by complex resistance mechanisms and adverse effects. Deubiquitinase UCH-L1 is frequently upregulated in advanced HCC and correlates with poor prognosis. Hence, this study aims to unravel whether UCH-L1 inhibition using LDN-57444 enhances sorafenib efficacy in HCC.
Method: UCH-L1 expression was analysed in TCGA-LIHC datasets and patient-derived HCC tissues. Sorafenib-LDN57444 effects were evaluated *in vitro* using the Hep3B HCC cell line in 2D cell-based assays and the 3D spheroid invasion assay. In vivo efficacy of the drug synergy was assessed in an orthotopic xenograft mouse model. Tumour growth, proliferation markers and oncogenic signaling activation were examined by Western blotting, RT-qPCR and immunohistochemistry.
Results: In silico data-analysis revealed that UCH-L1 was significantly upregulated in HCC tumours versus non-tumour tissue, associated with reduced overall survival. Low-dose sorafenib induced UCH-L1 protein and mRNA upregulation. Paradoxically, this promoted invasiveness in Hep3B spheroids and was accompanied by sustained MEK1/2-ERK1/2 pathway activation and upregulation of EMT- and immune escape markers: PD-L1 and SNAI-1. Notably, the sorafenib-LDN57444 combination not only produced strong synergistic cytotoxic effects *in vitro*, but also reverted sorafenib-driven MAPK activation and suppressed spheroid invasion. Consistently, LDN57444 co-treatment markedly inhibited tumour growth and reduced proliferation of Hep3B xenografts, improving sorafenib outcome *in vivo*.
Conclusion: UCH-L1 plays a regulatory role in sorafenib-induced adaptive resistance in HCC. Pharmacological UCH-L1 inhibition with LDN57444 synergizes with sorafenib to enhance anti-tumour efficacy, suppress invasiveness and potentially overcome resistance mechanisms. This supports the development of UCH-L1-targeted combination strategies as a promising, novel therapeutic avenue in advanced HCC.

WED-255

DNA replication stress as a therapeutic target in hepatocellular carcinoma

Nina Desboeufs[1,2], Peter Leary[1], Chenhui Zhao[1], Sarah Kollar[3], Lapkwan Chan[1], André Fitsche[3], Alex Schmidt[3], Lara Planas-paz[3], Salvatore Piscuoglio[4], Federico Dona[4], Silvia Incalcaterra[4], Laura Summermatter[3], Anne-Laure Leblond[3], Katharina Endhardt[3], Adrian Kobe[5], Gilbert Puippe[5], Charlotte Ng[6], Sandro Nuciforo[6], Markus Heim[7], Luigi Terracciano[4], Chantal Pauli[3], Andreas E. Kremer[8], Massimo Lopes[1], Achim Weber[1]. *[1]University of Zurich, Institute of Molecular Cancer Research, Zurich, Switzerland; [2]University Hospital Zurich, Department of Pathology and Molecular Pathology, Zurich, Switzerland; [3]University Hospital Zurich, Department of Pathology and Molecular Pathology, Zurich, Switzerland; [4]Humanitas Research Hospital, Department of Biomedical Sciences, Rozzano, Italy; [5]University Hospital Zurich, Institute of Diagnostic and Interventional Radiology, Zurich, Switzerland; [6]University Hospital Basel, Department of Biomedicine, Basel, Switzerland; [7]University Hospital Basel, Division of Gastroenterology and Hepatology, Basel, Switzerland; [8]University Hospital Zurich, Department of Gastroenterology and Hepatology, Zurich, Switzerland*
Email: desboeufs@imcr.uzh.ch

Background and aims: Hepatocellular carcinoma (HCC) is one of the most prevalent cancers worldwide and poses significant challenges in treatment due to its high heterogeneity. Despite the high clinical need for new systemic therapies, precision oncology for HCC is still in its infancy. This study aimed to investigate whether DNA replication stress, defined as the slowing or stalling of replication fork progression, could be targeted for systemic treatment of HCC.
Method: We developed a DNA replication stress-based signature for HCC using bulk RNA-seq datasets and weighted-gene co-expression network analysis (WGNCA). To assess the signature's association with drug response, we established HCC patient-derived organoids (HCC-Org) using a novel protocol for drug testing studies. We also conducted mid-throughput drug screening with compounds targeting replication stress and performed optimised single-cell and single-molecule assays to explore vulnerabilities in HCC-Org.
Results: We identified a subset of HCC patients with elevated replication stress scores, which were associated with poorer prognosis. Targeting ataxia telangiectasia and rad3-related protein (ATR) demonstrated robust efficacy in a subset of HCC-Org models, whether used alone or in combination with inhibitors of poly (ADP-ribose) polymerase (PARP) or WEE1. Of note, the drug response was associated with the level of replication stress and replication fork slowdown.
Conclusion: These findings emphasise the potential of ATR inhibitors, both as monotherapy and combination therapy, that leverage the intrinsic replication stress present in a subset of HCC, thereby opening up an avenue for precision oncology in HCC.

WED-256

Loss of secreted and transmembrane protein 1 modulates drug sensitivity and resistance in hepatocellular carcinoma

Cyrollah Disoma[1,2], Gabriela Bosoi[1,3], Georgia Zancotti[1,2], Deborah Bonazza[4], Paola Tarchi[5], Claudio Tiribelli[1], Caecilia Sukowati[1,6]. *[1]Liver Cancer Unit, Fondazione Italiana Fegato ONLUS, Trieste, Italy; [2]Doctoral School of Molecular Biomedicine, Department of Life Sciences, University of Trieste, Trieste, Italy; [3]Master Course of Medical and Diagnostic Biotechnology, Department of Life Sciences, University of Trieste, Trieste, Italy; [4]Surgical Pathology Unit, Azienda Sanitaria Universitaria Giuliano Isontina, Trieste, Italy; [5]Surgical Clinic, Azienda Sanitaria Universitaria Giuliano Isontina, Trieste, Italy; [6]Eijkman Research Center for Molecular Biology, Research Organization for Health, National Research and Innovation Agency (BRIN), Jakarta, Indonesia*
Email: cyrollah.disoma@fegato.it

Background and aims: Drug resistance remains a major challenge in the treatment of hepatocellular carcinoma (HCC). Despite recent advances in systemic therapies, many patients do not gain long-term clinical benefit from assigned targeted therapies. Following an *in silico* screening, Secreted and Transmembrane Protein 1 (*SECTM1*) was identified as a novel resistance gene whose role in HCC and drug resistance had not been studied in clinical samples and in HCC models.
Method: Lenvatinib-resistant cells were generated through acute, stepwise, and continuous chronic drug exposure to Hep3B, Huh7, and JHH6 HCC cell lines, followed by the calculation of Lethal Concentration 50 (LC_{50}) values. Its functional role was evaluated using siRNA-mediated *SECTM1* knockdown, cell viability, wound healing, and CCK-8 cell proliferation assays. SECTM1 expression was quantified by RT-qPCR and Western blotting and in parallel, assessed in 60 paired HCC and their adjacent non-tumoral clinical samples.
Results: Acute (48h) and chronic (>60 days) lenvatinib exposure in HCC cell lines resulted in *SECTM1* up-regulation with increased LC_{50} values. JHH6 cells, an undifferentiated HCC cell line, displayed higher SECTM1 levels at both the mRNA and protein levels compared to well-differentiated cells Hep3B and Huh7. *SECTM1* gene knockdown resulted in slower cell proliferation and wound-healing capacity and altered determinant markers of Epithelial to Mesenchymal Transition (*CDH1, COL1A1, CDH2, SNAI1, SNAI2*, and *VIM*). *SECTM1* knockdown significantly enhanced lenvatinib sensitivity, implicating SECTM1 as a mediator of drug resistance and survival signaling. In clinical samples, SECTM1 is more expressed in HCC than its adjacent non-HCC tissues both at the RNA and protein level, consistent with The Cancer Genome Atlas (TCGA) cohort. Patients with high *SECTM1* expression have poorer prognosis with lower median months of HCC recurrence compared to patients with low *SECTM1* expression ($p < 0.05$). Stratification by clinicopathological features revealed significant differences according to sex and disease stages.
Conclusion: SECTM1 mRNA and protein were upregulated in HCC tissues ($p < 0.05$). High *SECTM1* expression was associated with early HCC recurrence, both in TCGA and in our own cohort. *SECTM1* gene knockdown decreased HCC cell proliferation and aggressiveness, while enhancing drug sensitivity. Overall, SECTM1 could be a potential therapeutic target to overcome drug resistance or improve treatment outcomes.

WED-257

Sexual dimorphism in GPC3 (rs2267531) and PNPLA3 (rs738409) genetic risk profiles during HBV-related liver disease progression

Kubilay Göçücü[1], Demet Yılmaz Karadağ[2], Coskun Ozer Demirtas[3], Feyza Gunduz[4], Fatih Eren[5]. *[1]İstanbul Kent Üniversitesi Sağlık Hizmetleri Meslek Yüksekokulu, Patoloji Laboratuvar Teknikleri, İstanbul, Türkiye; [2]Marmara Üniversitesi Gastroenteroloji Enstitüsü, İstanbul, Türkiye; [3]Marmara Üniversitesi Tıp Fakültesi Gastroenteroloji Bilim dalı, İstanbul, Türkiye; [4]Marmara Üniversitesi Tıp Fakültesi Gastroenteroloji Bilim Dalı, İstanbul, Türkiye; [5]Recep Tayyip Erdoğan Üniversitesi Tıp Fakültesi, Marmara Üniversitesi Tıp fakültesi, Rize Merkez, Türkiye*
Email: kubilay.gocucu@kent.edu.tr

Background and aims: *GPC3* (Glypican-3) is a key oncofetal protein in hepatocellular carcinoma (HCC). Due to its X-linked location (Xq26.2), its genetic impact may vary by sex. Hepatocellular carcinoma (HCC) exhibits a lower incidence in females, and variations in the X-linked *Glypican-3 (GPC3)* gene (Xq26.2) are suggested to influence its etiopathogenesis. *GPC3* serves as an alternative diagnostic biomarker for HCC, activating proto-oncogenes via the Wnt/β-catenin signaling pathway. We aimed to investigate the potential relationship between the *GPC3* rs2267531 promoter polymorphism and *PNPLA3* rs738409 in the progression from chronic hepatitis B (CHB)—the primary cause of HCC in Turkey—to cirrhosis and HCC.

Method: A total of 294 participants were enrolled, comprising 119 healthy controls, 57 patients with CHB, 34 with HBV-related cirrhosis, and 84 with HBV-related HCC. Genotyping was performed using the rhAMP SNP Assay with the allelic discrimination method on the LightCycler® 480 (Roche) platform, and results were validated by Sanger sequencing. Data were stratified by sex to account for X-linked inheritance, and logistic regression models adjusted for age were utilized to determine Odds Ratios (OR).
Results: In males, the *GPC3* G-allele was significantly protective against cirrhosis (OR: 0.11, P = 0.0061). Conversely, females showed no association during the cirrhosis stage (P = 0.76) but demonstrated a highly significant risk association with HCC (P = 0.0016), with 100% of female HCC patients (n = 13) carrying the G/C genotype. Dominant model analysis further revealed that the *GPC3* rs2267531 C/C genotype was significantly higher in controls compared to CHB (P = 0.040) and cirrhosis (P = 0.042) groups, suggesting a protective role. Haplotype interaction analysis revealed a significant sex-specific synergy between *GPC3* and *PNPLA3* (P-interaction = 0.028).
Conclusion: This study represents the first analysis of *GPC3* rs2267531 promoter variants in a Turkish population. *GPC3* acts as a sex-dimorphic marker in HBV progression, serving as a primary gatekeeper against cirrhosis in males while functioning as a critical oncogenic driver in females, likely influenced by X-inactivation patterns. While the C/C genotype appears protective against CHB and cirrhosis, and the G/C genotype against HCC in certain models, these findings highlight the necessity of sex-stratified genetic screening in clinical practice.

WED-258
Hepatic fibrosis–driven tissue factor expression by malignant cholangiocytes is associated with cancer-associated thrombosis and poor survival in intrahepatic cholangiocarcinoma
Luca Fabris[1,2,3], Yahima Frion Herrera[1], Camilla Venturin[1,3], Massimiliano Cadamuro[4], Jessica Gasparello[5], Claudia Maria Radu[1,2], Matteo Fassan[1,5], Claudia Mescoli[6], Umberto Cillo[7,8], Enrico Gringeri[7,8], Giacomo Zanus[7,9], Elena Campello[1,2], Mario Strazzabosco[3], Paolo Simioni[1,2]. [1]*Department of Medicine (DIMED), University of Padua, Padua, Italy;* [2]*Clinical Medicine 1 and Thrombotic and Haemorrhagic Disease Unit, and Haemophilia Center, Padua, Italy;* [3]*Department of Internal Medicine, Digestive Disease Section, Liver Center, Yale University, New Haven, United States;* [4]*School of Medicine and Surgery, University of Milan-Bicocca, Milan, Italy, Milan, Italy;* [5]*Pathology Unit, Ca' Foncello Hospital, ULSS2 Marca Trevigiana, Treviso, Italy;* [6]*Pathology Unit, Padua University-Hospital, Padua, Italy;* [7]*Department of Surgery, Oncology and Gastroenterology (DiSCOG), University of Padua, Padua, Italy;* [8]*Hepatobiliary Surgery and Liver Transplantation Unit, Padua University-Hospital, Padua, Italy;* [9]*General Surgery Unit, Ca' Foncello Hospital, ULSS2 Marca Trevigiana, Treviso, Italy*
Email: luca.fabris@unipd.it

Background and aims: Cholangiocarcinoma (CCA) is an aggressive primary liver malignancy with increasing incidence worldwide, particularly the intrahepatic subtype (iCCA). Although hepatic fibrosis has been implicated in CCA development, its role in coagulation imbalance and cancer-associated thrombosis (CAT) remains unclear. This study investigated the relationship between advanced liver fibrosis, hemostasis activation, CAT, and clinical outcomes in patients with iCCA.
Method: Fifty patients with iCCA undergoing curative liver resection were studied. Graft wedge biopsies served as controls (n = 10). Histological evaluation was performed in formalin-fixed, paraffin-embedded samples using the Ishak Fibrosis Score (IFS, 0–6). Immunohistochemistry assessed tissue factor (TF), factor X (FX), fibrinogen, and von Willebrand factor (vWF). As readout of CAT, portal vein microthrombosis was quantified using Martius Scarlet Blue (MSB) staining. Correlation between TF expression and outcomes were evaluated by Kaplan-Meier survival analysis. Immunofluorescence analysis of TF and FX was performed on patient-derived iCCA organoids (PDOs, n = 10). Extracellular vesicles (EVs) isolated from PDO culture media were characterized by flow cytometry (FC) using Calcein-AM, EpCAM-PE, and Annexin V. TF levels in PDO supernatants were quantified by ELISA. EV-induced platelet activation was assessed by FC using CD41, CD62P, and Annexin V.
Results: Compared with controls, iCCA patients exhibited a pro-coagulant phenotype with increased coagulation activation and impaired fibrinolysis. Patients with advanced fibrosis (IFS 4–5, n = 16) showed significantly higher TF, FX, vWF, and fibrinogen expression than those with IFS ≤3 (n = 34). Fibrosis severity correlated with TF expression by malignant bile ducts and with the number of portal vein microthrombi ($p < 0.05$). High TF expression by malignant bile ducts was significantly associated with reduced disease-free survival and overall survival. PDO analyses confirmed marked TF and FX expression and demonstrated TF release into culture supernatants. EVs derived from PDOs significantly promoted platelet activation.
Conclusion: Advanced hepatic fibrosis is closely associated with CAT in patients with iCCA and is linked to increased TF expression by malignant cholangiocytes, driving platelet activation. By contributing to a prothrombotic tumor microenvironment, TF associates with disease progression and adverse clinical outcomes in iCCA patients.

WED-259
Single-cell and bulk transcriptomics uncover the cellular ecosystem of vascular invasion in intrahepatic cholangiocarcinoma
Jianing Fan[1], Meng Tong[1], Junjie Xu[1], Qianqian Wang[1], Yangyang Xie[1], Kainan Lin[1], Xiujun Cai[1], Yunkun Lu[1], Xiao Liang[1]. [1]*Sir Run Run Shaw Hospital, Zhejiang University School of Medicine, Hangzhou, China*
Email: fjn020116@163.com

Background and aims: Intrahepatic cholangiocarcinoma (ICC) is an aggressive liver malignancy with rising global incidence and limited therapeutic options. Vascular invasion (VI) is a hallmark of advanced disease, correlating with early recurrence and dismal prognosis, yet its tumor microenvironment (TME) drivers remain elusive.
Method: We analyzed single-cell RNA sequencing (scRNA-seq) data from 25 ICC samples to systematically characterize the cellular composition and molecular features associated with VI. Bulk RNA-seq data and multiplex immunofluorescence were integrated to validate our findings. Subsequently, cell–cell communication analysis was conducted, and key candidate genes were further validated utilizing RT-qPCR. Finally, functional validation was performed through endothelial sprouting assays using inhibitors and ICC-derived cancer-associated fibroblast (CAF) cell lines with specific genes knockdown.
Results: We identified a distinct subset of tumor-specific CAFs (tCAFs) that were significantly enriched in VI-positive tumors. Functional analyses revealed that tCAFs were closely related to hypoxia and angiogenesis pathways. Furthermore, scRNA-seq data also showed a notable increase in endothelial cells in VI-positive tumors. Cell-cell communication analysis demonstrated that tCAFs promoted VI primarily through VEGF signaling interactions with endothelial cells. Integrative bioinformatics and RT-qPCR validation pinpointed 3 key genes (*PTGS2*, *SLC2A1*, and *PLOD2*) in tCAFs. In endothelial sprouting assays, inhibition of *SLC2A1* exerted a pronounced suppressive effect on sprouting. Consistently, sprouting assays based on ICC-derived CAF cell lines with *SLC2A1* knockdown confirmed that downregulation of *SLC2A1* significantly reduced endothelial sprouting capacity.
Conclusion: Collectively, our study defines a VI-associated cellular ecosystem and molecular landscape in ICC, indicating that tCAFs drive VI via VEGF-mediated interactions with endothelial cells, with *SLC2A1* playing a critical role. These findings provide mechanistic

insights into VI development and identify *SLC2A1* as a potential therapeutic target with clinical relevance for advanced ICC.

WED-260

Generation and characterization of a novel synthetic notch chimeric antigen receptor (CAR) targeting T cells to hepatocellular carcinoma: designed to prevent T-cell activation induced by soluble hepatitis B virus envelope antigens

Yudi Gao[1], Fuwang Chen[1], Zhe Xie[1], Tao Jin[2], Luis Contreras[1], Jochen Wettengel[1,3], Ke Zhang[2], Ulrike Protzer[1,3]. [1]*Institute of Virology, Technical University of Munich/Helmholtz Munich, Munich, Germany;* [2]*SCG Cell Therapy Pte Ltd, Singapore, Singapore;* [3]*German Center for Infection Research (DZIF), Munich partner site, Munich, Germany*
Email: yudi.gao@tum.de

Background and aims: Chimeric antigen receptor (CAR) T cell therapy offers a promising approach not only for cancer therapy but also for chronic viral infections. However, circulating viral antigens binding to the CAR may activate CAR-T cells or restrict their killing capacity in an unwanted fashion. We designed a logic-gate Synthetic Notch (SynNotch) CAR that can only be activated on HBV-positive cells, but not by soluble HBsAg.

Method: We fused a single-chain fragment that recognizes the tumor antigen glypican 3 (GPC3) as a gate antigen to human Notch, thereby activating the expression of an S-CAR, which recognizes the HBV envelope protein (HBVenv) on HBV-positive cells. We engineered single and SynNotch S-CAR T cells via co-transduction of lentivirus and characterized the function of GPC3-SynNotch-S-CAR T cells on HBVenv ± /GPC3 ± hepatoma cells. Inducible S-CAR expression and T-cell activation were measured by IFN-γ ELISA and flow cytometry. T-cell-killing was monitored by the xCELLigence real-time cell analyzer. To determine specificity, the analysis was performed with and without the addition of HBsAg, and using HBV-negative and HBV-positive GPC3+ HepG2 cells. The T-cell killing specificity was then analyzed using the Incucyte system for real-time fluorescence imaging.

Results: GPC3-SynNotch-S-CAR T cells expressed the S-CAR upon recognition of GPC3 on target cells and SynNotch activation after 24–36 h. Unlike S-CAR T cells, GPC3-SynNotch-S-CAR T cells were not activated when incubated with soluble HBsAg and selectively killed dual antigen GPC3+/HBVenv+ HepG2 cells, but not cells that were only positive for HBVenv or GPC3. In mixed target cell cultures, GPC3-SynNotch-S-CAR T cells eliminated GPC3+/HBVenv+ cells with high specificity and efficiency. Compared to the constitutively active S-CAR-construct, T cells transduced with the inducible GPC3-SynNotch-S-CAR exhibited a comparable or even stronger IFN-γ secretion and killing capability on HepG2-Env+, and HBV-infected HepG2-NTCP cells.

Conclusion: The inducible GPC3-SynNotch-S-CAR is a promising candidate for redirecting T cells to HBV-positive hepatocellular carcinoma (HCC) that express GPC3. It demonstrated superior sensitivity and specificity compared to non-inducible S-CARs and prevented T-cell activation induced by soluble HBsAg. This proves that the SynNotch "IF-THEN" logic gating has strong potential to reduce off-target toxicity and enables programmable, modular responses.

WED-261

Exploring hepatocellular carcinoma through a neuroendocrine lens: the somatostatin system as an intricate source of tumour evaluation strategies and therapeutic vulnerabilities

Antonio García-Estrada[1,2,3], Betsaida Ojeda-Perez[1,2,3], María Isabel Pozo-Relaño[1,2,3], María Serrano-Jiménez[1,2,3], Amelie Lupp[4], Manuel L. Rodríguez-Perálvarez[1,5,6,7], Stefan Schulz[4,8], Raul M. Luque[1,2,3,9], Juan Luis López-Cánovas[1,2,3], Manuel D. Gahete[1,2,3,9]. [1]*Maimónides Biomedical Research Institute of Córdoba (IMIBIC), Córdoba, Spain;* [2]*Department of Cell Biology, Physiology and Immunology, University of Córdoba (UCO), Córdoba, Spain;* [3]*Reina Sofía University Hospital (HURS), Córdoba, Spain;* [4]*Institute of Pharmacology and Toxicology, Jena University Hospital (UKJ), Friedrich-Schiller-University (FSU) Jena, Jena, Germany;* [5]*Department of Hepatology and Liver Transplantation, Reina Sofía University Hospital (HURS), Córdoba, Spain;* [6]*Department of Medical and Surgical Sciences, University of Córdoba (UCO), Córdoba, Spain;* [7]*CIBER Hepatic and Digestive Diseases (CIBERehd), Córdoba, Spain,* [8]*7TM Antibodies GmbH, Jena, Germany;* [9]*CIBER Physiopathology of Obesity and Nutrition (CIBERobn), Córdoba, Spain*
Email: b72gaesa@uco.es

Background and aims: Despite the recent advances in management and treatment (i.e., BCLC updates, immunotherapy implementation), hepatocellular carcinoma (HCC) remains a complex clinical challenge due to high intra- and intertumoral heterogenic response to drugs, boosted by a rapidly evolving aetiologic landscape (i.e., the rising incidence of metabolic dysfunction-associated steatotic liver disease, MASLD). Thus, further research in novel biomarkers and therapeutic approaches is needed. In this work, we aim to explore the somatostatin (SST) endocrine system, which is a well-established line of diagnosis and treatment in pituitary and neuroendocrine tumours, in HCC and MASLD.

Method: Gene expression was evaluated using 2 internal retrospective cohorts [R1 (n = 93), R2 (n = 102)], 7 MASLD *in silico* cohorts [n = (45–109)/cohort], 6 HCC *in silico* cohorts [n = (65–369)/cohort] and 4 human liver cell lines. Sample clustering in TCGA-LIHC was implemented using Python (YellowBrick package). In a subset of R1 (n = 25), immunohistochemistry (IHC) for the SSTR1, SSTR2 and SSTR5 receptors was performed. Cell lines were subjected to *in vitro* functional assays (proliferation, colony and hepatosphere formation) to test the antitumoral capacity of natural peptides (SST and cortistatin, CST) and clinically relevant synthetic SST analogues (SSAs: octreotide, lanreotide, pasireotide, BIM-23926, BIM-23120 and BIM-23206).

Results: SST receptors (SSTRs) expression was lower in MASLD and HCC compared to control tissue, associated to complex patterns of tumour aggressiveness (e.g., less expression in men, non-recurring and surviving patients) and complemented by histological and subcellular localization [IHC: hepatocellular (SSTR1, SSTR2) and vascular (SSTR5)]. Cell lines mimicked this expression pattern, with HepG2 (low) and Hep3B (intermediate tumoral aggressiveness) showing the highest SSTRs expression. Clustering discriminated between SSTR1-expressing (more benign) and SSTR2-expressing (neuroendocrine-leaning, more aggressive) HCC samples. *In vitro*, antitumoral responses were observed for CST and SSAs in the functional assays in the different cell lines.

Conclusion: Neuroendocrine profiling in MASLD-HCC offers a novel framework for understanding these diseases, providing new potential avenues for tumour assessment and personalised therapeutic options. This work was funded by ISCIII (FI21/00141, DTS22/00057, PI23/00652, co-funded by the European Union), MICIU (FPU21/04833), JdA (PI-0046-2024), UCO, FSEEN and CIBERobn.

WED-262

Role of the NADPH oxidase 4 in regulating endoplasmic reticulum stress and autophagy in liver tumor cells

Gemma Gonfaus-Ortiz[1,2], Paula Segalés[1,2], Irene Peñuelas-Haro[1,2], Ismael Sánchez-Vera[3], Joan Gil[3], Esther Bertran[1,2], Isabel Fabregat[1,2]. [1]*TGF-beta and Cancer Group - Oncobell Program. Bellvitge Biomedical Research Institute (IDIBELL). L'Hospitalet de Llobregat, Barcelona., L'Hospitalet de Llobregat, Spain;* [2]*CIBEREHD, National Biomedical Research Institute on Liver and Gastrointestinal Diseases, Instituto de Salud Carlos III, Madrid., Madrid, Spain;* [3]*Department of Physiological Sciences, Faculty of Medicine and Health Sciences, University of Barcelona-IDIBELL, L'Hospitalet de Llobregat, Barcelona, Spain, L'Hospitalet de Llobregat, Spain*
Email: ggonfaus@idibell.cat

Background and aims: NADPH oxidase (NOX) isoforms are distinctively expressed in different liver cell types. NOX1 and NOX2 behave as promoters of hepatocellular carcinoma (HCC), however recent findings postulate NOX4 as a negative regulator of HCC. Our group described that after silencing NOX4, liver tumor cells enhance their proliferative and migratory capacity, increasing glycolysis and oxidative phosphorylation (OXPHOS). We aim to better understand the molecular mechanisms regulated by NOX4 that could explain its tumor suppressor role.
Method: Loss- and gain-of-function approaches for NOX4 were performed in HCC cell lines. Proteomic, metabolomic, and transcriptomic, as well as functional analyses, were employed.
Results: Endoplasmic reticulum (ER) stress and autophagy are described as cellular stress response mechanisms, and ER stress can induce autophagy in cancer cells to promote organelle recycling and proliferation. Given the strong crosstalk between NOX4, mitochondrial morphology, and oxidative phosphorylation (OXPHOS), we wondered whether alterations in NOX4 levels affect cellular metabolism under ER stress conditions. Electron microscopy revealed increased mitochondrial size in NOX4-silenced cells, as well as tighter contacts at mitochondria-associated membranes compared to control cells. ER stress stimuli with tunicamycin or thapsigargin led to alterations in the PERK pathway, with increased ATF4 protein levels and transcriptional activity in NOX4-silenced cells. Under ER stress, these cells also showed a significant reduction in OXPHOS compared to untreated conditions. Furthermore, NOX4 knockdown resulted in increased apoptotic markers, including caspase-3 activity and elevated cleaved PARP and BIM levels. In parallel, differences were observed in autophagy-related signalling pathways and in sequestosome 1 protein levels. Transcriptomic analysis of autophagy-related genes revealed opposite expression patterns following NOX4 overexpression/silencing. Consistently, autophagic flux was increased after NOX4 silencing and reduced upon overexpression. Notably, inhibition of autophagy with bafilomycin A1 in NOX4-silenced cells led to a decrease in OXPHOS. Additionally, when blocking ER stress with ISRIB, the autophagic flux diminished significantly, indicating that ATF4 might be involved in the regulation of autophagy.
Conclusion: NOX4 loss in HCC cells increases ATF4-mediated ER stress and autophagy-driven metabolic shift towards oxidative metabolism.

WED-263
Cirrhotic MASLD-HCC exhibits distinct immunosuppressive traits within the tumor microenvironment and is associated with poorer outcomes in patients treated with atezolizumab-bevacizumab

Albert Gris-Oliver[1], Guillem Cano-Segarra[1], Ezequiel Mauro[1], Ana Hernández[1], Anna Vila-Escoda[1,2], Marta Piqué-Gili[1], Judit Peix[1], Roser Pinyol[1], Josep M Llovet[1,2,3]. [1]*Institut d'Investigacions Biomèdiques August Pi i Sunyer (IDIBAPS), Barcelona, Spain;* [2]*Mount Sinai Liver Cancer Program, Tisch Cancer Institute, Icahn School of Medicine at Mount Sinai, New York, United States;* [3]*Institució Catalana de Recerca i Estudis Avançats (ICREA), Barcelona, Spain*
Email: agris@recerca.clinic.cat

Background and aims: The impact of metabolic dysfunction-associated liver disease (MASLD) on immunotherapy response in advanced hepatocellular carcinoma (aHCC) remains unclear. As a major risk factor and prognostic determinant, cirrhosis critically shapes the tumor microenvironment (TME). Our aim is to assess the impact of MASLD-HCC with or without cirrhosis, and their associated TME composition, on the efficacy of immunotherapy in aHCC.
Method: A multicenter retrospective cohort (2019–2023) of 239 patients treated with first line atezolizumab and bevacizumab (atezo +bev) was collected. Transcriptomic profiles were used for molecular and functional characterization and deconvoluted with BayesPrism to define tumor immune infiltration.
Results: The cohort had a median age of 69 years old, was predominantly male, and 67% had cirrhosis. BCLC stages B and C accounted for 29% and 68% of the patients, respectively. The main etiology was viral (28%), followed by MASLD (21%). The median overall survival (OS) follow-up was 12 months (IQR 6–17). Median OS was shorter in MASLD patients (12.2 vs 18.6 months, HR 1.56 [95% CI: 1.02–2.37], p = 0.039). Among the 49 MASLD-HCC patients, the presence of cirrhosis (n = 26, 53%) was associated with shorter OS (9.89 vs 16.72 months, HR 2.82 [95% CI 1.27–6.25], p = 0.011), and remained independently associated with mortality (HR 3.24 [95% CI 1.25–8.35], p = 0.015) together with ECOG-PS 2 (HR 8.42 [95% CI 1.81–39.24], p = 0.007), after adjustment for AFP ≥ 400 ng/ml, and macrovascular invasion. When comparing gene expression profiles of cirrhotic versus non-cirrhotic MASLD-HCC, both subgroups were enriched in the non-inflamed class (91% and 73%, p = 0.14); however cirrhotic tumors harbored significantly higher proportion of naïve CD8 T cells (p = 0.047), gamma-delta T cells (p = 0.044), and 2 macrophage subtypes associated with resistance to atezo+bev [TREM2+ (p = 0.014) and SPP1+ (p = 0.010)], and CXCL10+ macrophages (p = 0.017), the latter being linked to response to atezo+bev only in the absence of $TREM2^+$ macrophages.
Conclusion: Cirrhotic MASLD-HCC independently predicts mortality in patients with HCC treated with atezo+bev and is characterized by a distinct TME enriched in immunosuppressive cells associated with resistance to atezo+bev.

WED-264
A glypican-3 targeted chimeric antigen receptor T cell product secreting programmed cell death ligand 1 and vascular endothelial growth factor blockers shows durable tumor shrinkage in advanced hepatocellular carcinoma

Xiaowen He[1], Hao Guo[1], Qi Yang[1], Xingwu Dong[1], Xiaofeng Feng[1]. [1]*Oricell Therapeutics Co., Ltd., Shanghai, China*
Email: peterhe@oricell.com

Background and aims: Systemic programmed cell death ligand 1 (PD-L1) plus vascular endothelial growth factor (VEGF) antibody therapy improves outcomes in unresectable hepatocellular carcinoma (HCC), yet durable benefit remains limited and systemic exposure can drive toxicity. OriC902 is a X-CAR rapid-manufacture-process based glypican-3 (GPC3) targeting chimeric antigen receptor T cell (CAR-T) product engineered to secrete PD-L1 and VEGF blockers to create a spatio-temporal profile and enable three-drug-in-one synergy.
Method: Proof-of-concept data were generated with the OriC902 construct manufactured by a conventional CAR-T process. Antibody secretion were confirmed with Huh7 co-culture assay (effector: target 1:1, 120 h). In $GPC3^+$ Huh7 xenografts, low-dose OriC902 construct CAR-T was compared with second-generation GPC3 CAR-T and with CAR-T plus systemic anti-PD-L1 and anti-VEGF. Tumor growth, interferon-gamma, intratumoral CAR-T abundance/exhaustion, CD31, and plasma versus tumor antibody distribution were measured. Separately, X-CAR manufacture was benchmarked versus conventional manufacture process.
Results: The OriC902 construct CAR-T secreted PD-L1 and VEGF blockers (hundreds of ng/mL) in vitro and improved tumor control at low CAR-T dose versus second-generation CAR-T and combination therapy. Plasma-to-tumour concentration folds were reduced relative to the combination therapy (anti-VEGF approximately 80 to approximately 10; anti-PD-L1 approximately 60 to approximately 2). Confocal imaging showed lower CD31 and higher human CD3 infiltration, consistent with vascular normalization. Intratumoral flow cytometry showed 11,819 versus 39 CAR-T cells/mg tumor mass and fewer exhaustion-marker-positive CAR-T cells (6.4% versus 28.6%). X-CAR manufacture process enabled vein-to-vein under 10 days and improved CAR-T phenotype and potency and in vivo expansion in models.

Conclusion: A GPC3 CAR-T secreting anti-PD-L1 and anti-VEGF can normalize tumor vasculature and enhance T cell trafficking, supporting a spatio-temporal delivery concept that may boost efficacy while limiting high systemic antibody exposure. Based on the "three-in-one" synergy evidence and the in vivo performance of X-CAR–process-based CAR-T cells, an investigator-initiated clinical trial of OriC902 has been initiated.

WED-265

Spatial profiling of the tumour immune microenvironment in hepatocellular carcinoma identifies regulatory T cell–mediated immune exclusion

Nicholas Hannah[1,2,3,4,5], Tony Huang[5], Catherine Mitchell[2,5], Rita Busuttil[6], Siddharth Sood[2,3], Alex Boussioutas[6,7]. [1]*The Royal Melbourne Hospital, Parkville, Australia;* [2]*The University of Melbourne, Parkville, Australia;* [3]*Northern Health, Epping, Australia;* [4]*Western Health, Footscray, Australia;* [5]*Peter Maccallum Cancer Centre, Melbourne CBD, Australia;* [6]*Monash University, Clayton, Australia;* [7]*The Alfred, Melbourne CBD, Australia*
Email: nicholas.hannah2@mh.org.au

Background and aims: Hepatocellular carcinoma (HCC) often presents at an advanced stage and is linked to poor survival. Greater insight into the spatial distribution of immune cells within the tumour microenvironment may inform prognosis and guide therapeutic strategies. This study performed a comprehensive whole-slide spatial analysis of T-cell subsets in HCC.
Method: Archival glypican-3 (GPC3)–positive HCC tissue samples from a tertiary liver centre were analysed. Associated clinicopathological and survival data were included. Multiplex immunohistochemistry (mIHC) was conducted using OPAL 6-plex and DAPI. Whole-slide images were evaluated with HALO and the SPIAT R package. The antibody panel comprised CD3, CD4, CD8, FOXP3, PD-L1, and GPC3.
Results: Twenty-two samples were analysed (median age 71 years; 77% male; 68% cirrhosis; 41% viral aetiology). $CD3^+CD4^+FOXP3^+$ regulatory T cells (Tregs) were significantly enriched near $GPC3^+$ HCC cells compared to other immune phenotypes, with a median cell percentage within 100 μm of 6.12% (IQR 3.25–16.8). In contrast, $CD3^+CD8^+$ cytotoxic T lymphocytes (CTLs) were excluded from the tumour, indicated by a median cross-K area under the curve of –0.110 (IQR –0.256 to 0.120), consistent with spatial repulsion. Entropy gradient analysis revealed increased spatial attraction of Tregs to $GPC3^+$ tumour cells (standardised residual +3.56, $p < 0.001$), which was associated with worse overall survival (HR 6.38, 95% CI 0.78–52.07; $p = 0.047$). Similarly, low intratumoral CTL entropy correlated with poorer survival (HR 4.62, 95% CI 0.95–22.43; $p = 0.037$). Hierarchical clustering identified 371 immune cell neighbourhoods, defining seven immune phenotypes: immune-excluded ($n = 14$), inflamed ($n = 5$), immune-desert ($n = 1$), and other ($n = 2$), with the immune-excluded, Treg-enriched phenotype being most prevalent ($n = 13$).
Conclusion: Whole-slide spatial analysis shows that regulatory T cells preferentially localise to $GPC3^+$ HCC tumour nests, while cytotoxic T lymphocytes are relatively excluded. These spatial immune features are linked to poorer survival, supporting the presence of an immunosuppressive tumour microenvironment. Regulatory T cells may be a rational therapeutic target in HCC.

WED-266

SULT2A1 restrains hepatocellular carcinoma progression by fostering cholic acid 7-sulfate-mediated CD8+T cell cytotoxicity via CREB–IL-2Rβ–mTORC1 signaling

Wei He[1], Weifen Xie[2]. [1]*Department of Gastroenterology, Shanghai East Hospital, School of Medicine, Tongji University, Shanghai, China, Shanghai, China;* [2]*Department of Gastroenterology, Changzheng Hospital, Naval Medical University, Shanghai, China, Shanghai, China*
Email: weifenxie@medmail.com.cn

Background and aims: Hepatocellular carcinoma (HCC) remains a fatal malignancy exhibiting limited immunotherapy responses. Cytotoxic $CD8^+$T cells are critical players in tumor clearance through cytokine secretion, yet it remains obscure how bile acid metabolism in liver cancer shapes the antitumor immune responses of $CD8^+$T cells. Sult2a1, which is preferably expressed by hepatocytes, sulfates cholic acid into cholic acid 7-sulfate (CA7S) in liver. Here, we identified Sult2a1 as a key suppressor in HCC progression by bolstering the cytotoxicity of $CD8^+$T cells.
Method: We analyzed transcriptomic and proteomic data from HCC patients to interrogate Sult2a1 alteration. The expression of Sult2a1 was evaluated through immunohistochemistry (IHC) and western blotting (WB). The anti-tumor effect of Sult2a1 was validated by subcutaneous and spontaneous HCC models. Mass spectrometry, flow cytometry, surface plasmon resonance and CRE-driven luciferase assays were employed to identify the membrane receptor for CA7S. The effectiveness of CA7S supplementation alone or in combination with anti-PD-1 antibody was assessed in vivo. The downstream mechanism of CA7S-driven $CD8^+$T function enhancement was elucidated by multiomics-based integration of scRNA-seq, ATAC-seq and RNA-seq data. We also analyzed a tissue microarray of liver tumor samples ($n = 90$) from HCC patients to elucidate the correlation between HNF4alpha and Sult2a1. Furthermore, the transcription of Sult2a1 by HNF4alpha was validated by Cut&Tag qPCR and luciferase reporter assays.
Results: Transcriptomic and proteomic analyses revealed a drastic down-regulation of Sult2a1, particularly in advanced stages of HCC. We then confirmed the loss of Sult2a1 by IHC and WB in human specimens. Specifically, Sult2a1 inhibited liver tumor growth in immunocompetent but not in immunodeficient mouse models. ScRNA-seq analysis of spontaneous liver tumors indicated an increased fraction of liver-infiltrating cytotoxic $CD8^+$T cells upon Sult2a1 administration. Mechanistically, Sult2a1-derived CA7S activated GPBAR1, leading to enhanced CREB–IL-2Rβ–mTORC1 signaling and boosted the anti-tumor capacity of $CD8^+$T cells. CA7S and anti-PD-1 treatment synergistically inhibited HCC growth. In addition, HNF4alpha, the master transcriptional regulator in liver, was responsible for enhancing Sult2a1 transcription.
Conclusion: The Sult2a1-derived metabolite CA7S fosters $CD8^+$T cell function and sensitizes liver tumors to anti-PD-1 immunotherapy, offering a promising therapeutic avenue for HCC.

WED-267

Single-Cell RNA sequencing identifies molecular concordance between circulating tumor cells and primary tumor nuclei in hepatocellular carcinoma

Monica Higuera[1], Agnes Soriano-Varela[1,2,3], Elena Vargas-Accarino[1,4], Maria Montesinos[1], Maria Torrens[1,2], Beatriz Minguez[1,2,3,4]. [1]*Liver Cancer Research Group, Liver Diseases, Vall d'Hebron Institut de Recerca (VHIR), Vall d'Hebron Barcelona Hospital Campus, Barcelona, Spain;* [2]*Liver Unit, Hospital Universitario Vall d'Hebron, Vall d'Hebron Barcelona Hospital Campus, Barcelona, Spain;* [3]*Department of Medicine, Campus de la UAB, Universitat Autònoma de Barcelona (UAB), Cerdanyola del Vallès, Spain;* [4]*Centro de Investigación Biomédica en Red de Enfermedades Hepáticas y Digestivas (CIBERehd), Instituto de Salud Carlos III, Madrid, Spain*
Email: beatriz.minguez@vallhebron.cat

Background and aims: Circulating tumor cells (CTCs), shed from primary tumors into the bloodstream, represent a promising biomarker for cancer diagnosis, prognostication and monitoring. Despite recent advances in CTC detection and enumeration, their comprehensive molecular characterization remains limited. In this study, we aimed to establish a robust workflow for the isolation and transcriptomic profiling of CTCs to delineate their molecular features and clarify their role in hepatocellular carcinoma (HCC) progression.
Method: Eighteen patients with HCC undergoing surgical resection were prospectively enrolled. Peripheral blood samples were collected

at baseline and every three months during follow-up. CD45+ cells were depleted, and remaining cells were labeled with EpCAM, Pan-Cytokeratin and Glypican-3 for sorting and quantification. Whole-transcriptome sequencing was performed on CTCs and matched tumor nuclei from fresh-frozen tissue of six patients with early-stage HCC. Cell types were annotated using reference liver and tumor datasets, and CNV analysis assessed aneuploidy.
Results: CTCs levels did not show significant fluctuations during the 12 months following surgical resection, however, the proportion of CTCs was identified as an independent risk factor for HCC recurrence in this cohort. Single-cell RNA sequencing of CTCs revealed a distinct cellular profile characterized by high expression of hepatic (HSPA1A, KRT8, GPC3) and epithelial (EPCAM) markers. On average, 10.3 ± 3.3 cells per sample were molecularly classified as CTCs. CNV analysis demonstrated a high prevalence of aneuploid cells within this population. Single-nucleus RNA sequencing matched tumor tissue identified multiple cell populations, including tumor, immune, Kupffer, stellate, and endothelial cells. The proportion of tumor cells varied widely across samples (5.2%-51.3%) and exhibited differential expression of canonical HCC markers and elevated levels of aneuploidy. Comparative transcriptomic analysis revealed an approximately 50% overlap among the top expressed genes between CTC and tumor cell clusters.
Conclusion: This preliminary study demonstrates that single-cell RNA sequencing enables robust molecular discrimination of CTCs from other circulating cell populations. By non-invasively capturing tumor-specific features, this approach provides a powerful framework for characterizing tumor heterogeneity and intratumoral microenvironment, offering a potential alternative to invasive tissue biopsies for molecular profiling in HCC.

WED-268
Generalist SAM based foundation models outperform medically fine-tuned variants in dynamic liver ultrasound segmentation
Janik Hohmann[1,2], Adil Oezsoy[1], Tom Luedde[1,2,3], Tobias Paul Seraphin[1], Michael Kallenbach[1]. [1]*Department of Gastroenterology, Hepatology and Infectious Diseases, University Hospital Dusseldorf, Medical Faculty at Heinrich-Heine-University, Düsseldorf, Germany;* [2]*Zentrum für Digitale Medizin (ZDM), Heinrich-Heine-University Düsseldorf, Faculty of Medicine and Mathematics and Natural Sciences at Heinrich-Heine-University, Düsseldorf, Germany;* [3]*CIO - Center for integrated Oncology, Aachen, Bonn, Cologne, Düsseldorf, University Hospital Düsseldorf, Medical Faculty at Heinrich-Heine-University, Düsseldorf, Germany*
Email: janik.hohmann@med.uni-duesseldorf.de

Background and aims: Ultrasound is the first-line modality for detection and follow-up of focal liver lesions (FLLs), yet image interpretation and annotation remain highly operator-dependent and difficult to standardize. Recent foundation models such as Meta's Segment Anything Model (SAM) family offer powerful zero-shot segmentation capabilities, but their robustness for real-world liver ultrasound videos and across lesion types has not been systematically evaluated.
Method: We assessed the latest SAM-based models (SAM2 tiny, SAM2 large, SAM3, and MedSAM2 variants) on a real-world dataset of 40 B-mode ultrasound videos comprising benign and malignant FLLs. Models were evaluated in a zero-shot setting using bounding box and mask prompts, with frame-wise expert annotations as reference. Segmentation accuracy (Dice Similarity Coefficient, DSC), tracking failure rates, prompt robustness, and lesion-specific performance were analyzed. To support practical deployment, we developed TagMed, a locally deployed, privacy-preserving annotation platform integrating interactive segmentation models with structured human-in-the-loop (HITL) workflows.
Results: Generalist foundation models consistently outperformed medically fine-tuned MedSAM2 variants in dynamic ultrasound tracking. With bounding box prompts, SAM2 tiny achieved the highest overall performance (median DSC 0.93), followed by SAM3 and SAM2 large (median DSC 0.92). In contrast, MedSAM2 models showed lower accuracy and pronounced instability, with substantially higher tracking failure rates (up to 42.5%) compared to SAM3 (15.2%). Prompt modality strongly influenced performance: SAM2-based models were highly sensitive to mask initialization, whereas SAM3 maintained robust performance across prompt types (median DSC 0.92 for both box and mask prompts). Benign lesions were segmented more reliably than malignant lesions, with metastases representing the most challenging subtype. Minimal re-prompting improved segmentation stability across all models and especially MedSAM2 performance, reducing variability and failure rates.
Conclusion: Generalist SAM models enable accurate and robust zero-shot segmentation and tracking of focal liver lesions in ultrasound videos, outperforming specialized medical variants in dynamic imaging scenarios. Integrated into the TagMed platform, these models support efficient, privacy-preserving, human-in-the-loop annotation workflows and provide a practical solution for scalable dataset creation and ultrasound research.

WED-269
A serum-based biomarker of type VI collagen degradation (C6M) is associated with increased risk of hepatocellular carcinoma development
Sebastian Howen Rode[1], Andressa de Zawadzki[1], kt Shenoy[2], Leena Mohan[3], Morten Karsdal[1], Jane I. Grove[4], Diana Julie Leeming[1], Guruprasad Aithal[4]. [1]*Nordic Bioscience, Biomarkers & Research, Herlev, Denmark;* [2]*Sree Gokulam Medical College and Research Foundation, Population Health and Research Institute, Trivandrum, India;* [3]*Population Health and Research Institute, Trivandrum, India;* [4]*National Institute of Health Research (NIHR) Nottingham Biomedical Research Centre, Nottingham University Hospitals NHS Trust and University of Nottingham, Nottingham Digestive Diseases Centre, Translational Medical Sciences, School of Medicine, University of Nottingham, Nottingham, United Kingdom*
Email: sero@nordicbio.com

Background and aims: The progression from cirrhosis to hepatocellular carcinoma (HCC) is driven by epithelial damage, high fibroblast activity, and altered immune and repair responses. Liver inflammation disrupts the balance of extracellular matrix (ECM) protein synthesis and degradation. In HCC patients, type VI collagen remodeling is increased and linked to higher mortality, while elevated elastin levels are associated with greater HCC incidence. To identify predictors of HCC development, we investigated two biomarkers indicative of type VI collagen degradation (C6M) and neutrophil-mediated elastin degradation (ELP-3).
Method: Serum levels of the biomarkers nordicC6M (type VI collagen fragment released by matrix metalloproteinase-2) and nordicELP-3 (elastin fragment released by proteinase-3) were measured in a prospective longitudinal cohort of 349 patients with cirrhosis during surveillance for HCC. 38/349 patients developed HCC after baseline inclusion. The prognostic utility of C6M and ELP-3 for HCC was assessed using competing risk analysis of cumulative incidence (Aalen-Johansen), with death as competing event, and hazard ratios (HR) estimated by the Fine-Gray subdistribution hazard model with 95% confidence intervals (CI).
Results: The cumulative incidence of HCC was stratified by biomarker tertiles (baseline levels) and used to identify thresholds that distinguish patient groups with lower versus higher HCC incidence. Patients with baseline C6M levels above 465 ng/mL exhibited an increased risk of HCC events (HR = 2.07 [CI 1.08–3.97], p = 0.028, 36 events/330 patients) compared to patients below this threshold. Stratification based on biomarker changes from baseline to 6 months (median time) showed that patients who decreased in C6M (HR = 3.40 [CI 1.43–8.06], p = 0.006, 23 events/58 patients) or ELP-3 (HR = 2.51 [CI 1.18–5.37], p = 0.017, 26 events/65 patients) presented a

higher risk of HCC, potentially reflecting a "cold" fibrotic state (low inflammation).
Conclusion: Cirrhosis patients with a higher baseline level of type VI collagen degradation were at increased risk of developing HCC, supporting that high ECM turnover precedes HCC development. Decreasing rates of type VI collagen and neutrophil-mediated elastin degradation within 6 months of baseline were predictive of HCC during surveillance, indicating ECM turnover and immune activity decline during HCC development. In summary, both baseline levels and early changes in C6M and ELP-3 provide prognostic utility for HCC risk stratification.

WED-270
From transporter to oncogenic driver: N-linked glycosylation enhances oncogenic capabilities of SLC29A2 in hepatocellular carcinoma
Yu-Hsuan Hsu[1,2], Chia-Yi Chou[1], Yuh-Shan Jou[1]. [1]*Institute of Biomedical Sciences, Academia Sinica, Taipei, Taiwan;* [2]*Program in Molecular Medicine (MMP), National Yang Ming Chiao Tung University, Taipei, Taiwan*
Email: or75369@ibms.sinica.edu.tw

Background and aims: SLC29A2 (solute carrier family 29 member 2) is an equilibrative nucleoside transporter that mediates nucleoside uptake across cellular membranes. Our prior study demonstrates that SLC29A2 is frequently upregulated in multiple cancers, with marked amplification in hepatocellular carcinoma (HCC). Despite its significance in liver tumor progression, the functional contributions and underlying mechanisms of SLC29A2 remain poorly understood. We discovered that SLC29A2 undergoes N-linked glycosylation at residues N48 and N57 within its first extracellular loop. Since disrupting these modifications significantly attenuates SLC29A2-mediated oncogenesis, we aimed to characterize how this specific modification governs SLC29A2-driven HCC malignancy.
Method: The functional impact of SLC29A2 glycosylation was evaluated using site-directed mutagenesis of the N48 and N57 residues. Transcriptomic analysis was performed to identify differentially regulated pathways between glycosylated and non-glycosylated SLC29A2 forms. The molecular mechanism was further validated through protein stability assays and nuclear translocation analysis of NF-Kappa B subunits. To assess therapeutic potential, pharmacological inhibition of the downstream effector NIK (NF-Kappa B inducing kinase) was conducted using the selective inhibitor B022.
Results: Transcriptomic profiling revealed that glycosylated-SLC29A2, unlike its non-glycosylated counterpart, significantly enhances HCC cell proliferation and migration by selectively activating the non-canonical NF-Kappa B pathway. Mechanistically, glycosylated-SLC29A2 strongly downregulates cIAP1 expression, which stabilizes NIK and promotes the nuclear accumulation of the NF-Kappa B subunits p52 and RelB. Furthermore, pharmacological inhibition of NIK with B022 completely abrogated the oncogenic phenotypes induced by glycosylated-SLC29A2. These results establish glycosylation as a master regulator of SLC29A2-driven malignancy and underscore the essential role of the NIK-dependent non-canonical NF-Kappa B axis in mediating its tumor-promoting functions.
Conclusion: Our findings unveil a new, glycosylation-dependent oncogenic function of SLC29A2 that drives HCC progression through a non-canonical NF-Kappa B signaling program. By characterizing this unique post-translational modification, we establish glycosylated-SLC29A2 as a promising target for the development of specialized monoclonal antibodies, offering a novel therapeutic framework for patients with advanced HCC.

WED-271
Circulating lipid signatures drive mitochondrial stress and inflammatory remodelling in non-cirrhotic MASLD-associated hepatocarcinogenesis
Jian Huang[1], Zhongguo Zhou[2], Arresha Nazeer[3], Julian L. Griffin[3], Nadia Guerra[2], Mark R Thursz[1], Pinelopi Manousou[1]. [1]*Saint Mary's Hospital, London, United Kingdom;* [2]*Imperial College London, London, United Kingdom;* [3]*University of Aberdeen, Aberdeen, United Kingdom*
Email: jian.huang20@imperial.ac.uk

Background and aims: A substantial proportion of hepatocellular carcinoma (HCC) arising in metabolic dysfunction–associated steatotic liver disease (MASLD) develops in the absence of cirrhosis, limiting surveillance eligibility and delaying diagnosis. We previously identified six circulating lipid species (PG_(38:6), DG_(34:1), LPI_(17:1), SM_(34:1), CerPE_(38:1), Cer_(37:1)) selectively upregulated in non-cirrhotic MASLD-associated HCC (n = 19). This study aimed to define the mechanisms through which these lipids may contribute to early hepatocarcinogenesis and to assess their translational relevance.
Method: HepG2 cells were treated with the pre-identified lipids. Mitochondrial dysfunction was assessed by reactive oxygen species (ROS) generation and mitochondrial membrane potential collapse. Lipid-induced inflammatory remodelling was evaluated by cytokine secretion profiling. Integrated STRING, KEGG, MitoCarta 3.0, and TCGA-HCC datasets were used to identify lipid-regulated metabolic–inflammatory modules with clinical relevance.
Results: All six lipids induced a convergent mitochondrial stress phenotype characterised by increased ROS and loss of membrane potential (Figure B and C). Despite belonging to distinct lipid classes, each lipid activated specific mitochondrial–metabolic signalling pathways, including PGS1–TAZ, SGMS1–SPTLC2, SAMD8–SPTLC2, and CerS3–SGMS1–SPHK2. Lipid stimulation selectively increased IL-8 and IFN-γ (numbers) secretion rather than broad inflammatory activation. Integrated network analysis identified the MBOAT7–LYPLAL1 axis downstream of LPI_(17:1) as the only pathway showing strong interactions with IL-8 and IFN-γ and significant correlation with their expression in TCGA-HCC samples ($P < 0.05$; $r = 0.34$).
Conclusion: Non-cirrhotic MASLD-associated HCC lipids induce a shared mitochondrial stress and selective inflammatory programme that may facilitate early hepatocarcinogenesis. The convergence on the MBOAT7–LYPLAL1 axis supports their translational potential as early-stage biomarkers and highlights mitochondrial–metabolic inflammatory pathways as therapeutic targets prior to cirrhosis onset.

WED-272
Enhanced detection of hepatocellular carcinoma using combined biomarker panels including alpha-fetoprotein, alpha-fetoprotein-L3, des-gamma-carboxyprothrombin and the galad score
Trung Huynh[1], Khanh Pham[1]. [1]*Tam Anh Hospital, Ho Chi Minh city, Viet Nam*
Email: nnphong.bvndong@gmail.com

Background and aims: Hepatocellular carcinoma (HCC) remains a major global health burden, and early detection is crucial for improving outcomes. Conventional tools such as imaging and AFP have limited accuracy, prompting increased interest in emerging biomarkers including AFP-L3, DCP/PIVKA-II, and the GALAD score. However, evidence on the diagnostic performance of these markers-particularly GALAD-remains scarce in Southeast Asia. Vietnam, with its high prevalence of chronic hepatitis B and aflatoxin exposure, lacks robust comparative studies evaluating these biomarkers within the same cohort. This study therefore assessed the diagnostic accuracy of AFP, AFP-L3, DCP, and GALAD for detecting HCC in a Vietnamese population, with potential relevance for broader application across Southeast Asia.

Method: A cross-sectional study was conducted at Tam Anh Hospital, Ho Chi Minh City, Vietnam, from March to October 2025. A total of 83 patients with histologically confirmed HCC and 83 patients with chronic hepatitis or cirrhosis were enrolled. Serum AFP, AFP-L3, and DCP levels were measured, and GALAD scores were calculated. Diagnostic performance was assessed using sensitivity, specificity, and area under the receiver operating characteristic curve (AUC). Biomarkers were compared individually and in combination, with subgroup analyses stratified by BCLC stage.
Results: AFP >8.5 ng/mL and AFP-L3 >3.85% showed moderate sensitivity (72.3% and 77.1%) and high specificity (91.6% and 86.7%). DCP >33.5 mAU/mL and GALAD >2.19 demonstrated superior diagnostic accuracy, with sensitivities of 91.6% and 85.5%, specificities of 92.8% and 95.2%, and identical AUCs of 0.957. Both DCP and GALAD significantly outperformed AFP and AFP-L3 ($p < 0.05$), with no significant difference between them ($p > 0.05$). Combined biomarker panels further improved performance, with the AFP–AFP-L3–DCP panel achieving the highest sensitivity (95.2%). In advanced HCC (BCLC ≥B), GALAD (AUC 0.939) outperformed AFP and AFP-L3 and was comparable to DCP. None of the biomarkers reliably differentiated very early (BCLC 0) from early-stage HCC (BCLC A).
Conclusion: DCP and GALAD exhibit superior diagnostic accuracy compared with AFP and AFP-L3, particularly in advanced HCC. Combining multiple biomarkers further enhances detection, although none effectively distinguish very early from early-stage disease. These findings support the clinical utility of DCP and GALAD and highlight the need for improved strategies to identify very early-stage HCC.

WED-273
Cathepsin A promotes immune evasion in hepatocellular carcinoma by driving tumor-associated macrophage polarization
Jie Jiang[1], Xiangwen Zhang[1], Wenbin Tang[1], Jin Yang[1], Zhuan Li[1].
[1]*Hunan Normal University, Changsha, China*
Email: zhuanli@hunnu.edu.cn

Background and aims: Hepatocellular carcinoma (HCC) is a leading cause of cancer-related mortality worldwide and is characterized by a profoundly immunosuppressive tumor microenvironment, which limits the efficacy of immune therapy. Tumor-associated macrophages (TAMs) are key components of this microenvironment but the upstream signals driving their pro-tumorigenic polarization remain poorly defined. Cathepsin A (CTSA) is aberrantly expressed in several malignancies, but its role in HCC immune regulation is unclear. This study aimed to elucidate the function of CTSA in HCC progression, with a particular focus on TAMs polarization and immune microenvironment remodeling.
Method: CTSA expression was analyzed in TCGA database and in human HCC specimens using immunohistochemistry, multiplex immunofluorescence, and flow cytometry. Associations with patient prognosis, M2-like macrophage markers, and CD8-positive T cell infiltration were evaluated. CTSA was genetically silenced in hepatocellular carcinoma cells using CRISPR–Cas9 technology. Macrophage polarization was assessed using transwell co-culture systems. Receptor identification and downstream signaling pathways were investigated by mass spectrometry, RNA sequencing, and proteomic analyses. Therapeutic efficacy was evaluated in an orthotopic HCC mouse model treated with a CTSA inhibitor in combination with PD1 blockade.
Results: CTSA was significantly upregulated in HCC and was associated with poor overall survival. CTSA silencing markedly suppressed tumor growth i*n vivo*. Importantly, CTSA expression positively correlated with infiltration of M2-like TAMs and inversely correlated with CD8-positive T cell infiltration in clinical samples. Functional studies demonstrated that hepatocellular carcinoma-derived CTSA actively promoted macrophage polarization toward an immunosuppressive M2 phenotype, thereby fostering a "cold" tumor microenvironment. Combined cathepsin A inhibition and immune checkpoint blockade resulted in enhanced antitumor efficacy *in viv*o.
Conclusion: CTSA is a poor prognostic marker and driver of immune evasion in HCC via promoting M2-like TAMs polarization to create an immunosuppressive microenvironment and immunotherapy resistance. Targeting CTSA might offer novel strategy to inhibit tumor progression and convert immunologically "cold" tumors into immunotherapy-responsive phenotypes.

WED-274
Investigating the immunomodulatory role of the extracellular matrix in hepatocellular carcinoma
Kavitha Kirubendran[1], Sara Campinoti[1], Bruna Almeida[1], Roberto Savoldelli[1], Maya Medic[1], Elena Palma[1], Antonio Riva[1], Shilpa Chokshi[2], Luca Urbani[1]. [1]*Roger Williams Institute of Liver Studies, King's College London, London, United Kingdom;* [2]*Peninsula Medical School, University of Plymouth, Plymouth, United Kingdom*
Email: k.kirubendran@researchinliver.org.uk

Background and aims: Immune-targeted therapies, specifically T-cell-directed approaches, are becoming central to treatment strategies for patients with hepatocellular carcinoma (HCC), a leading cause of cancer-related mortality. The extracellular matrix (ECM) is a dynamic regulator of the immune system; in cancer it is actively remodelled and dysregulated, influencing immune cell infiltration, cytokine signalling and function. Recent studies increasingly demonstrate that ECM proteins exhibit immunomodulatory functions within the liver microenvironment, yet their specific role in modulating immune phenotypes present in HCC remains unclear. Here, we explore the direct impact of ECM proteins on T-cell phenotypes in patient-derived models of HCC to understand their role in immune regulation.
Method: We decellularised HCC-precision cut tissue slices (dPCTS) from both tumour and adjacent non-tumour liver tissue from resected HCC samples. Decellularisation efficiency was evaluated using H&E staining and DNA quantification, and ECM composition was analysed with mass spectrometry-based proteomics. dPCTS were co-cultured with human circulating and intrahepatic immune cells from HCC patients. Immune phenotype and interactions in response to dPCLS exposure were assessed via flow cytometry and deep spatial phenotyping.
Results: The optimised decellularisation process efficiently removed cells from HCC-derived PCTS whilst preserving intact matrix architecture, retention of matrix-bound proteins and endotoxin-free conditions. After 3-day of co-culture, immune cells successfully interacted with and adhered to dPCTS. Upon ECM exposure, preliminary analysis showed distinct immune cell distributions, particularly among T-cell subsets, revealing differences of cell-ECM interactions between circulating and intrahepatic immune cells, and between adjacent and tumour ECM, with resulting differences in phenotype. Proteomics analysis revealed upregulation of distinct matrix proteins in HCC relative to adjacent tissue (e.g. COL3A1, THBS1, VCAN, FBN1, EFEMP1), which may drive these immune cell responses.
Conclusion: Our findings confirm that the dPCTS model supports immune cell-matrix interactions, revealing distinct immune cell distributions upon ECM exposure. This suggests that dysregulated ECM proteins may influence T-cell phenotypic changes within the TME, supporting a mechanistic role for these proteins as a barrier to immunotherapeutic cancer treatments.

WED-275

Longitudinal elevation of IL-10 following atezolizumab plus bevacizumab is associated with favorable response and survival in advanced hepatocellular carcinoma

Soon Kyu Lee[1], Jung Hyun Kwon[1], Sung Won Lee[1]. [1]*The Catholic University of Korea, College of Medicine, Seoul, Korea, Rep. of South*
Email: blackiqq@gmail.com

Background and aims: We previously reported that early increases in interleukin-10 (IL-10) and tumor necrosis factor-α (TNF-α) levels following atezolizumab plus bevacizumab (Ate/Bev) therapy predict survival in patients with advanced hepatocellular carcinoma (HCC). In this study, we aimed to longitudinally assess serial cytokine changes and evaluate their association with treatment response and survival in advanced HCC patients receiving Ate/Bev.
Method: We prospectively enrolled 154 consecutive patients with advanced HCC who were treated with Ate/Bev between July 2022 and June 2025. Of these, 54 patients who provided blood samples at three time points—before initiation of Ate/Bev, prior to the second cycle, and prior to the fourth cycle—were included in the cytokine analysis. Serum levels of IL-2, IL-6, IL-10, IL-12, IL-17, interferon-γ (IFN-γ), and TNF-α were measured at each time point, and temporal changes in cytokine levels were examined. The primary endpoint was overall survival, while secondary endpoints included associations between cytokine patterns and treatment response.
Results: During a mean follow-up of 11.4 months, 42 patients (77.7%) died. The median age was 66.0 years, with most patients being male (92.6%), and the predominant etiology was viral-related HCC (85.2%). Serial changes in IL-2, IL-6, IL-12, IL-17, IFN-γ, and TNF-α levels were not significantly associated with overall survival. In contrast, IL-10 levels significantly increased following Ate/Bev treatment ($p = 0.01$), particularly among patients who achieved disease control ($p = 0.022$). Changes in IL-10 levels were positively correlated with changes in the CRP levels ($r = 0.38$, $p = 0.004$). Notably, patients exhibiting an increase in IL-10 levels demonstrated significantly better survival compared with those showing a decrease ($p = 0.042$). In multivariable analysis, an increase in IL-10 levels remained an independent predictor of overall survival in advanced HCC patients treated with Ate/Bev.
Conclusion: Our findings suggest that serial changes in cytokine levels—particularly IL-10—following Ate/Bev therapy may serve as a useful biomarker for monitoring treatment response and predicting clinical outcomes in patients with advanced HCC.

WED-276

IRE1α-mediated downregulation of CYP7A1 drives MASH-HCC progression and immune evasion via regulation of cholesterol metabolism

Fan Li[1], Yiming Wang[2], Hao Wang[1], Ling Lu[1], Ming Ni[1]. [1]*The First Affiliated Hospital of Nanjing Medical University, Nanjing, China;* [2]*Peking Union Medical College Hospital, Chinese Academy of Medical Sciences and Peking Union Medical College, Beijing, China*
Email: drlifan1999@163.com

Background and aims: Metabolic dysfunction-associated steatohepatitis (MASH)-related hepatocellular carcinoma (HCC) is rising globally, exhibiting unique features like metabolic dysregulation and a poorer prognosis than viral HCC. Cholesterol is key in MASH-HCC progression, regulated by CYP7A1, the rate-limiting enzyme in bile acid synthesis. Clinically, CYP7A1 is significantly downregulated in MASH-HCC tumors and linked to worse outcomes, yet its regulatory mechanisms and functional roles are unclear. This study aims to clarify these aspects to identify novel therapeutic targets for MASH-HCC.
Method: Paired tumor/adjacent tissues from MASH-HCC patients were analyzed by metabolomic sequencing, scRNA-seq, and spatial transcriptomics to identify cholesterol metabolism alterations and confirm CYP7A1 downregulation. MASH-HCC mouse models were generated using hepatocyte-specific Ire1α-KO, Cyp7a1-KI, and Smo-KO mice. ChIP-seq, RNA-seq validated IRE1α-mediated CYP7A1 regulation. IP/MS, LLPS and FRAP assays characterized IRE1α lactoylation modification and RIDD activity. In vivo/in vitro experiments assessed the impact of IRE1α-CYP7A1 axis on cholesterol metabolism and Hedgehog signaling. Therapeutic effects of PD-1 mAb alone or combined with IRE1α inhibitor/CYP7A1-adenovirus were evaluated in MASH-HCC models to explore clinical translation.
Results: CYP7A1 is markedly downregulated in MASH-HCC tumor tissues and strongly associated with unfavorable prognosis. Lactylation of IRE1α induces LLPS, augmenting its RIDD activity and resulting in direct degradation of CYP7A1 mRNA. Reduced CYP7A1 expression causes aberrant cholesterol accumulation, which activates Hedgehog signaling in both tumor cells and Treg cells through SMO cholesterol modification, thereby accelerating tumor proliferation and immune evasion. Therapeutic targeting of the IRE1α/CYP7A1 axis effectively restores cholesterol metabolic homeostasis and potently suppresses tumor progression.
Conclusion: This study reveals a core mechanism driving MASH-HCC progression: hypoxia-induced IRE1α lactylation enhances its LLPS and RIDD activity, specifically degrading CYP7A1 to cause cholesterol accumulation; this accumulation exacerbates ER stress, transactivating IRE1α to form a self-reinforcing loop that ultimately activates Hedgehog signaling via SMO cholesterol modification to promote carcinogenesis and immune evasion. The study elucidates a novel "metabolism-stress" crosstalk paradigm, offering new targets for MASH-HCC diagnosis and therapy.

WED-361-YI

Central vagal dysfunction reshapes neutrophil and T cell immunity in hepatocellular carcinoma

Wenxuan Li[1], Jinghao Zhang[1], Liping You[1], Chao Zheng[1], Liyue Lu[1], Ziman Lu[1], Jian Su[1], Xiaji Yan[1], Zekun Liu[1], Xinyue Liu[1], Yuqi Liu[1], Yilin Wang[1], Yaxuan Cai[1], Fei Wu[1], Yueqiu Gao[1], Xiaoni Kong[1], Xuehua Sun[1]. [1]*Department of Liver Diseases, Shuguang Hospital Affiliated to Shanghai University of Traditional Chinese Medicine, Shanghai, China*
Email: susan_sxh@shutcm.edu.cn

Background and aims: Hepatocellular carcinoma (HCC) develops within a complex neuroimmune microenvironment, however the contribution of central parasympathetic activity to tumor immunity remains poorly understood.
Method: Mouse models of HCC were combined with neural modulation, immune profiling, and transcriptomic analyses. Human validation included resting-state functional MRI and immunological characterization of tumor specimens.
Results: We observed a marked reduction in central vagal activity during HCC progression in both mice and patients. Enhancing central vagal output suppressed tumor growth and reshaped the tumor immune microenvironment without altering overall leukocyte recruitment. Instead, vagal activity selectively reprogrammed neutrophils toward an immune-activating state associated with enhanced $CD8^+$ T-cell cytotoxicity. Transcriptomic and functional analyses revealed coordinated activation of inflammatory and immune effector programs in these neutrophils. Neuroimaging analyses revealed reduced brainstem vagal activity in patients with hepatocellular carcinoma compared with chronic hepatitis B controls. Peripheral stimulation of vagal pathways recapitulated this anti-tumor immune program in preclinical models. In parallel, analysis of tumor specimens demonstrated that increased intratumoral

infiltration of this neutrophil subset correlated with improved overall survival. Peripheral stimulation of vagal pathways recapitulated this antitumor immune program in preclinical models.
Conclusion: These findings uncover a brain–vagus–immune circuit that regulates neutrophil plasticity and antitumor immunity in HCC, and suggest neuromodulation as a potential therapeutic avenue for liver cancer.

WED-362
TRIM15 phase separation activates α-KG dehydrogenase through DLST condensate-mediated OGDH mono-ubiquitination to drive tumor metabolic plasticity
Hairui Li[1], Wencheng Shan[2], Fanzheng Meng[1]. [1]*The First Affiliated Hospital of USTC, Hefei, China;* [2]*The First Affiliated Hospital of USTC, Hefei, China*
Email: mengfz@ustc.edu.cn

Background and aims: Metabolic reprogramming enables Hepatocellular Carcinoma (HCC) cells to survive nutrient stress, yet the mechanisms linking metabolic flux to chromatin dynamics remain elusive. The α-ketoglutarate dehydrogenase (KGDH) complex controls the levels of α-ketoglutarate (α-KG), a critical cofactor for epigenetic enzymes. We aimed to identify stress-responsive E3 ubiquitin ligases and decipher how they coordinate KGDH plasticity and epigenetic remodeling to drive tumor progression under glutamine deprivation.
Method: We integrated glutamine-starvation proteomics with transcriptomic analysis of HCC tissues to identify candidate regulators. Mechanisms were dissected using immunoprecipitation-mass spectrometry, *in vitro* and live-cell liquid-liquid phase separation (LLPS) assays, and metabolic flux analysis. The functional impact was evaluated in hepatocyte-specific *Trim15*-knockout mice (*Trim15*$^{fl/fl}$ vs. *Trim15*$^{\Delta Alb}$), hydrodynamic tail-vein injection models, and patient-derived xenografts (PDX). Therapeutic strategies were tested using glutamine uptake inhibitors (V-9302) and DCLK1 inhibitors (DCLK1-IN-1).
Results: We identified TRIM15 as a key stress-responsive factor significantly upregulated in human HCC and glutamine-starved cells. Mechanistically, TRIM15 possesses intrinsically disordered regions (IDRs) that drive liquid-liquid phase separation. Upon stress, TRIM15 condensates sequester the KGDH subunit DLST, creating a specialized cytoplasmic compartment. This spatial organization facilitates the specific mono-ubiquitination of the OGDH subunit at Lys534. This modification stabilizes the KGDH complex and significantly amplifies its enzymatic activity. Functionally, activation of this axis accelerates α-KG catabolism, depleting intracellular α-KG levels. This metabolic shift inhibits α-KG-dependent histone demethylases, leading to the accumulation of H3K4me3 marks at the promoter of the stemness regulator *DCLK1*, thereby activating its transcription. Clinically, TRIM15 expression correlates with DCLK1 levels and poor prognosis in HCC patients. Pharmacologically, combined inhibition of DCLK1 and glutamine metabolism exerted synergistic antitumor effects in preclinical models.
Conclusion: TRIM15-mediated phase separation links mitochondrial metabolism to chromatin remodeling via the TRIM15-DLST-OGDH-DCLK1 axis. This study reveals a novel mechanism of metabolic plasticity and suggests targeting this axis to sensitize glutamine-addicted HCC to therapy.

WED-363
NAT10/ac4C drives intrahepatic cholangiocarcinoma by suppressing transposable elements via chromatin remodeling
Kainan Lin[1]. [1]*Sir Run Run Shaw Hospital, Zhejiang University School of Medicine, Hangzhou City, China*
Email: 22218144@zju.edu.cn

Background and aims: Intrahepatic cholangiocarcinoma (ICC) is characterized by insidious onset, aggressive behavior, early metastasis, and a dismal 5-year survival rate below 10%. Although dysregulation of gene networks and chromatin dynamics in ICC tumorigenesis has been explored, the functional crosstalk between RNA epitranscriptomic modifications and nuclear regulatory events remains poorly understood. This study aims to uncover the role of RNA acetylation mediated by N-acetyltransferase 10 (NAT10) in ICC malignancy and to evaluate its therapeutic potential.
Method: Multi-omics profiling was performed to identify NAT10-dependent regulatory networks in ICC. The functional impact of NAT10 on mRNA stability and chromatin regulation was assessed through molecular and cellular assays. The NAT10–ac^{4}C–CHAF1A axis was mechanistically dissected using epigenomic and transcriptomic approaches. Pharmacological inhibition of NAT10 was tested in patient-derived xenograft (PDX) models and autochthonous ICC tumor models to evaluate therapeutic efficacy.
Results: NAT10 was identified as a critical driver of ICC progression. Integrated analyses revealed that NAT10-mediated N4-acetylcytidine (ac^{4}C) modification stabilizes mRNA of the chromatin assembly factor CHAF1A. The NAT10–ac^{4}C–CHAF1A axis epigenetically silences the nuclear transposable element HERV9NC, reducing double-stranded RNA accumulation. This silencing promotes ICC proliferation and migration while dampening intrinsic innate immune responses, leading to an immunosuppressive tumor microenvironment with diminished cytotoxic T-cell infiltration. Pharmacological inhibition of NAT10 significantly suppressed tumor growth in both PDX and autochthonous ICC models.
Conclusion: Our study establishes NAT10 as a master integrator linking RNA epitranscriptomic reprogramming to nuclear chromatin dynamics in ICC. The NAT10–ac^{4}C–CHAF1A–HERV9NC axis drives tumor progression and immune evasion, revealing NAT10 as a druggable vulnerability. These findings provide mechanistic insight into ICC pathogenesis and propose NAT10 inhibition as a promising therapeutic strategy for this aggressive malignancy.

WED-364
Identification of targetable epigenetic-metabolic vulnerabilities in human cholangiocarcinoma
Amaya Lopez-Pascual[1,2], Jasmin Elurbide-Tardio[3], Emiliana Valbuena-Goiricelaya[1], Maria U Latasa[1], Elena Anaya[1], Elena Adan-Villaescusa[1], Borja Castello[1], Luz A. Martínez-Pérez[4], Iker Uriarte[1], Maria Arechederra[1], Sergio Ciordia[5], Fernando Corrales[5], Soňa Fraňková[6], Eva Sticová[7], Ondrej Fabian[7], Leticia Colyn[8], Patricia Inacio[8], Juan Bayo Fina[9], Meritxell Huch[8], Carmen Berasain[1], Maite G Fernandez-Barrena[1], Matías A Avila[1]. [1]*Hepatology Laboratory, Solid Tumors Program, CIMA, CCUN, University of Navarra, Pamplona, Spain;* [2]*Instituto de Investigaciones Sanitarias de Navarra IdiSNA, Pamplona, Spain;* [3]*Hepatology Laboratory, Solid Tumors Program, CIMA, CCUN, University of Navarra, CIBERehd, Instituto de Salud Carlos III, Madrid, Spain, Pamplona, Spain;* [4]*Hepatology Laboratory, Solid Tumors Program, CIMA, CCUN, University of Navarra, Universidad de Guadalajara, Centro Universitarios de los Altos, Ciencias de la Salud, Guadalajara, México., Pamplona, Spain;* [5]*Functional Proteomics Laboratory, Centro Nacional de Biotecnología, CSIC, Madrid, Spain;* [6]*Department of Hepatogastroenterology, Institute for Clinical and Experimental Medicine, Prague, Czech Republic;* [7]*Department of Hepatogastroenterology, Institute for Clinical and Experimental Medicine, Department of Hepatogastroenterology, Institute for Clinical and Experimental Medicine, Prague, Czech Republic;* [8]*Max Plank Institute of Molecular Cell Biology and Genetics, Dresden, Germany;* [9]*Programa de Hepatología Experimental y Terapia Génica, Instituto de Investigaciones en Medicina Traslacional, Facultad de Ciencias Biomédicas, CONICET-Universidad Austral, Buenos Aires, Argentina*
Email: alopez.12@alumni.unav.es

Background and aims: Cholangiocarcinoma (CCA) is a highly aggressive liver cancer characterized by marked molecular heterogeneity, with limited therapeutic options, underscoring the need to identify targetable molecular drivers. Epigenetic regulators and metabolic enzymes are increasingly recognized as drivers of tumor

plasticity, representing increasingly druggable vulnerabilities. We aimed to identify epigenetic-metabolic dependencies associated with CCA aggressiveness, tumor microenvironment (TME), and tumor fitness.
Method: We performed analyses of multiple human intrahepatic and extrahepatic CCA transcriptomic cohorts, interrogating genes encoding epigenetic regulators (EpiGs) and metabolic enzymes (MGs) across molecular aggressiveness, prognostic groups, and TME contexts. Proteomic and metabolomic profiling was conducted in a TAZ/Akt-driven murine CCA model to validate transcriptomic findings.
Results: Several EpiGs were upregulated in iCCA and eCCA, including writers (*DNMT1*, *EZH2*, *SUZ12*), readers (*CBX3*, *PHF20L1*, *SMARCA4*), and erasers (*HDAC1*, *HDAC3*, *KDM5C*). However, some readers (*CHD5, SMARCA2*) were consistently downregulated in CCA. MGs functionally linked to epigenetic regulation were dysregulated (up: *GART*, *IDH2*, *TYMS*; down: *ALDH1L1*, *MAT1A*, *SHMT1*). Subsets of EpiGs (*HDAC1*, *HDAC2*, *PRDM8*, and *MECOM)* and MGs (*SHMT2*, *AHCYL2*, *ACSL5*) were linked to proliferative, poor-survival, and high-recurrence iCCA subclasses. TME analyses revealed distinct immune-stromal subclasses with coherent epigenetic and metabolic signatures. Upregulated EpiGs in the Immune-desert class (e.g., *CHD4*, *SUV39H1*, *SUZ12*) support the therapeutic rationale for combining epigenetic modulators with immunotherapy. Transcriptomic analyses in human and multi-omic analyses (transcriptomic, metabolomic, and proteomic studies) in mouse CCA livers highlighted rewiring of nucleotide, one-carbon, lipid, and mitochondrial pathways, with evidence of metabolic-epigenetic crosstalk.
Conclusion: Our study identifies a conserved and druggable epigenetic-metabolic axis underlying CCA aggressiveness, microenvironmental remodeling, and tumor fitness. By evaluating human patient stratification, functional genomics, and mouse multi-omics validation, we prioritize epigenetic and metabolic targets with high translational potential. These findings support the development of combination strategies incorporating epigenetic modulators, metabolic inhibitors, and immunotherapies for the precision treatment of CCA.

WED-365
dsDNA activates platelets via the cGAS-STING axis to drive TLS formation in hepatoblastoma

Lijie Ma[1], Shiming Gong[1], Zhenzhen Zhan[1], Mingxuan Feng[1], Qiang Xia[1]. [1]*Department of Liver Surgery, Renji Hospital, Shanghai Jiao Tong University School of Medicine, Shanghai, China*
Email: gongshiming521@sjtu.edu.cn

Background and aims: Hepatoblastoma (HB) is the most common malignant liver tumor in children. Although neoadjuvant chemotherapy (NAC) renders 60–70% of initially unresectable cases operable, the biological basis for the significant heterogeneity in response remains unclear. Studies of adult cancers at the single-cell level have shown that NAC can either 'heat up' or 'cool down' the tumor microenvironment (TME), but equivalent pediatric data are lacking. We therefore set out to generate the first high-resolution, cell-type-resolved map of the HB TME before and after NAC and identify the cellular and molecular circuits that determine therapeutic outcome.
Method: NAC-naïve biopsy cores and post-NAC surgical specimens were collected from SIOPEL-HR-risk patients (PLADO protocol). The following were performed: single-cell RNA sequencing (n = 12), spatial transcriptomics sequencing (n = 4), bulk RNA sequencing (n = 67), multiplexed immunofluorescence and an in vivo co-culture experiment. Animals were treated with cisplatin or platelet depletion (anti-CD42b) or a cGAS-STING inhibitor (H-151). Tumor growth, necrosis and immune infiltration were assessed by flow cytometry and histology.
Results: We constructed a high-resolution, dynamic cellular landscape remodeled by NAC and its associations with therapeutic response. NAC markedly induces substantial remodeling of the HB TME, reshaping B-cell populations and forming tertiary lymphoid structure (TLS), which are strongly associated with the therapeutic response. The density of intra-tumoral TLS significantly correlated with pathological necrosis and the rate of complete tumor resection. Mechanistically, NAC induces tumour cell necrosis, releasing double-stranded DNA (dsDNA) that activates platelets via the cGAS-STING axis. This, in turn, induces B-cell infiltration and activation via the PF4-CXCR4 axis, resulting in favourable outcomes. However, platelet depletion or cGAS-STING inhibition abolished B-cell influx and blunted tumour response.
Conclusion: Using an integrated, single-cell, spatial framework, we demonstrate that NAC converts the pediatric HB TME from immune-poor to immune-rich via a platelet-orchestrated circuit. Targeting this axis (e.g. with STING agonists or platelet factor 4 (PF4) supplementation) is a rational strategy for augmenting the response to NAC in HB and possibly other childhood solid tumors.

WED-366
Tumor–neuron signaling as a functional axis within the cholangiocarcinoma microenvironment

Lorenzo Mainardi[1], Maria Gemma Nasoni[2], Mirella Pastore[1], Alessia Giachi[1], Micheole Menotta[2], Fabio Marra[1], Francesca Luchetti[2], Chiara Raggi[1]. [1]*University of Florence, Firenze, Italy;* [2]*University of Urbino, Urbino, Italy*
Email: chiara.raggi@unifi.it

Background and aims: Tumor innervation is increasingly recognized as a critical component of the tumor microenvironment in solid malignancies; however, its role in cholangiocarcinoma (CCA) remains poorly defined. We investigated the existence and functional relevance of tumor–neuron interactions in CCA.
Method: An indirect co-culture system was established using SB1 murine CCA cells and HT22 mouse hippocampal neuronal cells. Neuronal differentiation following exposure to CCA-conditioned medium (CCA-CM) was assessed by morphological analysis, cell viability assays, transmission electron microscopy and flow cytometry. Furthermore, the expression of neuronal markers has been investigated by immunofluorescence and Western blotting. Phosphoproteomic profiling was performed to identify signaling pathways activated by tumor-derived factors. In a bidirectional approach, the effects of neuron-derived CM on CCA cells were evaluated by assessing viability, invasive capacity, and sphere-forming ability.
Results: Exposure to CCA-CM induced marked neurite outgrowth and neuron-like morphological remodeling in HT22 cells without significantly affecting cell viability, accompanied by modulation of neuronal marker β-tubulin III. Phosphoproteomic analysis revealed signaling pathway activation comparable to that observed during standard neuronal differentiation, with enrichment of processes related to actin cytoskeleton remodeling, adherens junction organization, and synaptic signaling, including dopaminergic synapse pathways. Tumor-derived cues selectively regulated phosphoproteins involved in neurite extension, cell adhesion, and signal transduction. Conversely, CM from differentiated HT22 cells enhanced CCA cell viability, invasiveness, and sphere formation capacity.
Conclusion: CCA cells release soluble factors capable of reshaping neuronal phenotype and signaling, supporting a functional tumor–nerve crosstalk. Reciprocally, neuron-derived factors promote malignant traits in CCA cells, potentially contributing to disease progression.

WED-367

Transitional hepatocytes and immunosuppressive macrophages drive NASH-associated liver cancer revealed by single-cell transcriptomics

Firdian Makrufardi[1]. [1]*Faculty of Medicine, Universitas Negeri Yogyakarta, Sleman, Indonesia*
Email: firdian.makrufardi@uny.ac.id

Background and aims: Non-alcoholic fatty liver disease (NAFLD), particularly its progressive form non-alcoholic steatohepatitis (NASH), has emerged as a major etiological factor in hepatocellular carcinoma (HCC), surpassing traditional viral causes due to rising obesity rates and metabolic syndrome prevalence. The cellular dynamics and transformation of hepatocytes during disease progression remain poorly defined. This study aims to characterize the hypoxia-associated inflammatory landscape underlying the transition from NASH to HCC using integrated single-cell RNA sequencing (scRNA-seq) data.
Method: We analyzed single-cell transcriptomic datasets encompassing liver samples from healthy individuals and patients at various NAFLD stages, including NASH and HCC. Quality control, dimensionality reduction, and clustering were conducted using the Seurat pipeline. Subpopulation-specific markers were identified, and pseudotime trajectory analysis was applied to trace hepatocyte transformation. Gene regulatory networks were reconstructed via SCENIC analysis. Additionally, a murine NASH-to-HCC progression model was used to validate key cellular and molecular findings.
Results: Transcriptomic profiling revealed a distinct hepatocyte population characterized by elevated CYP7A1 expression, predominantly found in pre-neoplastic liver regions. These transitional hepatocytes displayed gene signatures associated with stress responses, inflammation, and cancer-related pathways, while exhibiting reduced expression of healthy hepatocyte markers. Progressive activation of HIF1A signaling indicated a central role of hypoxia in driving this phenotypic shift. Furthermore, macrophage subtypes showed a notable polarization: RACK1+ macrophages transitioned into immunosuppressive TREM2+ cells in response to the hypoxic microenvironment. These TREM2+ macrophages, enriched in NASH and HCC samples, were found to be recruited by tumor cells via the CCL15-CCR1 chemokine axis, thereby contributing to a suppressive immune milieu and fostering tumor development.
Conclusion: This study provides an integrative single-cell view of how hypoxia orchestrates both hepatocyte transformation and immune modulation in NASH-associated hepatocarcinogenesis. The identification of CYP7A1+ transitional hepatocytes and TREM2+ macrophages as key players highlight potential cellular and molecular targets for early intervention in NAFLD-related liver cancer.

WED-368

Genome-wide association of MRC1 with FIB-4 disentangles non-invasive fibrosis assessment from HCC

Francesco Malvestiti[1], Stefania Mira[2], Martina Tranchina[3], Oveis Jamialahmadi[4], Rosellina Mancina[4], Serena Pelusi[3], Giulia Periti[3], Luisa Ronzoni[3], Lorenzo Miano[2], Daniele Marchelli[2], Alessandro Cherubini[3], Elia Casirati[3], Laura Cerami[3], Jessica Rondena[5], Irene De Matteis[3], Andrea Siciliano[3], Gian Paolo Caviglia[6], Marta Guariglia[6], Chiara Rosso[6], Grazia Pennisi[7], Angelo Armandi[6], Antonio Liguori[8], Francesca Terracciani[9], Riccardo Perbellini[10], Giorgio Soardo[11], Alessandro Federico[12], Umberto Vespasiani Gentilucci[9], Luca Miele[8], Elisabetta Bugianesi[6], Roberta D'Ambrosio[10], Salvatore Petta[7], Daniele Prati[3], Stefano Romeo[13], Luca Valenti[14]. [1]*Department of Pathophysiology and Transplantation, Università degli Studi di Milano, Milan, Italy, Precision Medicine Lab, Transfusion Medicine and Hematology, Biological Resource Centre, Fondazione IRCCS Ca' Granda Ospedale Maggiore Policlinico, Milan, Italy., Milano, Italy; [2]Department of Pathophysiology and Transplantation, Università degli Studi di Milano, Milan, Italy, Milano, Italy; [3]Precision Medicine Lab, Transfusion Medicine and Hematology, Biological Resource Centre, Fondazione IRCCS Ca' Granda Ospedale Maggiore Policlinico, Milan, Italy, Milano, Italy; [4]Department of Molecular and Clinical Medicine, Institute of Medicine, Sahlgrenska Academy, Wallenberg Laboratory, University of Gothenburg, Gothenburg, Sweden, Gothenburg, Sweden; [5]Department of Pathophysiology and Transplantation, Università degli Studi di Milano, Milan, Italy, Milano, Italy; [6]Department of Medical Sciences, Division of Gastroenterology, University of Turin, Turin, Italy, Turin, Italy; [7]Section of Gastroenterology, Di.Bi.M.I.S Policlinico Paolo Giaccone Hospital, University of Palermo, Palermo, Italy, Palermo, Italy; [8]Department of Translational Medicine and Surgery, Fondazione Policlinico Universitario Agostino Gemelli IRCCS, Università Cattolica Del Sacro Cuore, Rome, Italy, Rome, Italy; [9]Clinical Medicine and Hepatology Unit, Department of Medicine and Surgery, Campus Bio-Medico University of Rome, Rome, Italy, Rome, Italy; [10]Division of Gastroenterology and Hepatology, Foundation IRCCS Ca' Granda Ospedale Maggiore Policlinico, Milan, Italy, Milano, Italy; [11]Clinica Medica Liver Unit, Dipartimento di Medicina Università di Udine, Udine, Italy, Udine, Italy; [12]Hepatogastroenterology Division, Department of Precision Medicine, University of Campania "Luigi Vanvitelli", Naples, Italy, Naples, Italy; [13]Karolinska Institutet University, Department of Molecular and Clinical Medicine, Institute of Medicine, Sahlgrenska Academy, Wallenberg Laboratory, University of Gothenburg, Gothenburg, Sweden, Stockholms, Sweden; [14]Department of Pathophysiology and Transplantation, Università degli Studi di Milano, Milan, Italy, Precision Medicine Lab, Transfusion Medicine and Hematology, Biological Resource Centre, Fondazione IRCCS Ca' Granda Ospedale Maggiore Policlinico, Milan, Italy, Milano, Italy*
Email: francesco.malvestiti@unimi.it

Background and aims: Metabolic Associated Steatotic Liver Disease (MASLD) is the most prevalent chronic liver disease, that can progress to metabolic steatohepatitis (MASH), resulting in cirrhosis and hepatocellular carcinoma (HCC). Genetic variation play a major role in disease variability, but heritability remains largely unexplained, especially in the Italian population. The aim of this study was to identify novel genetic loci associated with non-invasively assessed liver fibrosis thorough a genome-wide association study (GWAS) in Italian individuals.
Method: We conducted a GWAS in the Milan Biobank (N = 6,963) enriched in people with MASH, with validation in the Uk Biobank (UKBB). The Fibrosis-4 Index (FIB-4) served as the primary quantitative trait. We provided functional characterization of *MRC1* locus to investigate its role during hepatic damage by exploiting public resources.
Results: Beyond the validation of the *PNPLA3* rs738409 variant as the main genetic driver of advanced liver disease ($p < 10^{-8}$), we highlighted a novel genome-wide significant protective association between the *MRC1* locus and FIB-4 (rs2461141 G > C, MAF = 0.462 $\beta = -0.071 \pm 0.012$, $p = 1.2 * 10^{-8}$). Replication in the UK Biobank (N > 400,000) validated *MRC1* locus as the leading hit for FIB-4 (rs56278466 G > T, MAF = 0.338, $R^2 = 0.52$, $D' = 0.98$, $\beta = -0.096 \pm 0.002$, $p = 8.45 * 10^{-559}$). MRC1 rs2461141 G > C variant associated with protection against ballooning in Milan Biobank (N = 430, $\beta = -0.09 \pm 0.04$, p = 0.030). eQTL analysis showed that rs2461141 G > C was associated with higher *MRC1* mRNA levels in immune cells (NES = 0.12; $p = 2.37 * 10^{-5}$) and within the liver ($\beta = 0.18 \pm 0.07$, p = 0.014). Vice versa, In an integrated, publicly available transcriptomic cohort composed of 341 MASLD patients, *MRC1* mRNA was down-regulated in MASH (p = 0.016, N = 14 vs 111 controls), necroinflammation (p = 0.018, N = 63 vs 62 controls) fibrosis stage (p = 0.044, F0 = 130; F1 = 82; F2 = 58; F3 = 55; F4 = 15) and hepatocellular ballooning (p = 0.007, N = 15 vs 110 controls). Paradoxically, despite lower FIB-4, in UKBB *MRC1* rs56278466 G > T was independently associated with an increased risk of HCC (OR[95% C.I.] = 1.19[1.04;1.36], p = 0.015), together with an increased risk of cancer of hepatic bile duct (OR[95%

C.I.] = 1.11[1.01;1.21], p = 0.023) and of gallbladder (OR[95% C.I.] = 1.17 [1.04;1.33], p = 0.009).
Conclusion: We identified *MRC1* as a novel FIB-4 susceptibility locus. Integrating genetic data with non-invasive biomarkers may contribute to enhancing risk stratification and precision medicine approaches for liver disease.

WED-369

Transforming growth factor-β signaling at the SMAD3 linker region promotes cancer cell plasticity and immunosuppression in hepatocellular carcinoma

Gregor Ortmayr[1], Theresa Hillinger[1], Hana Badlah[1], Pia Schuler[1], Goncalo Oliveira[2], Patrick Starlinger[3], Thomas Grünberger[4], Wolfgang Mikulits[1]. *[1]Medical University of Vienna, Vienna, Austria; [2]Czech Academy of Sciences, Prague, Czech Republic; [3]Mayo Clinic, Rochester, United States; [4]Clinic Favoriten, HPB Center, Health Network Vienna and Sigmund Freud Private University, Vienna, Austria*
Email: wolfgang.mikulits@meduniwien.ac.at

Background and aims: Hepatocellular carcinoma (HCC) is a challenging global health concern with increasing incidence. Systemic first-line therapy at advanced HCC stages includes treatment with immune checkpoint inhibitors (ICIs) in combination with anti-VEGF treatment. However, effective anti-tumor responses are achieved only in a minor subset of HCC patients due to immune evasion. We recently reported the molecular collaboration of transforming growth factor (TGF)-β and Gas6/AXL signaling driving an aggressive HCC phenotype linked to epithelial to mesenchymal transition (EMT). In particular, the aberrant phosphorylation of the SMAD3 linker region (SMAD3L) at serine 213 (pSMAD3L-Ser213) might modulate the tumor microenvironment (TME). As underlying mechanisms are an open issue, we aimed to assess how Smad3L-Ser213 signatures shape an immuno-suppressive TME.
Method: TGF-β/SMAD3L phosphorylation was analyzed by immunohistochemistry (IHC) in HCC patient samples. Substitution of pSMAD3L-Ser213 to mutant Smad3L-Ala213 was performed by CRISPR/Cas9 prime editing. Targets of AXL/TGF-β signaling were identified by RNA-seq analysis and VENN relations. Hypoxic niche factors and immune cell subsets were studied by multiplex IHC in HCC patient tissues.
Results: We addressed aberrant TGF-β/SMAD3L phosphorylation in HCC patients and identified pSMAD3L-Ser213 rather than pSMAD3L-Ser204/Ser208 as a predictor of poor survival. Substitution of pSMAD3L-Ser213 to mutant SMAD3L-Ala213 by prime editing and transcriptome profiling in HCC cells resulted in gene signatures correlating with a switch from EMT to partial EMT, immune response and better prognosis of patient's survival. Notably, we identified uridine phosphorylase 1 (UPP1) as a target of AXL/TGF-β, linking this signaling axis to metabolic adaptation under glucose restriction and hypoxia. Furthermore, spatial analysis of human HCC patient samples revealed that aberrant pSMAD3L-Ser213 and UPP1 co-localize with exhausted T cells and M2-polarized macrophages in hypoxic niches.
Conclusion: These data suggest that TGF-β/SMAD3L-Ser213 signaling is a critical determinant of the immunosuppressive TME, involving EMT. UPP1 represents a target of TGF-β/SMAD3 signaling, allowing metabolic adaption of HCC cells. Intervention with UPP1 together with ICI is considered as an auspicious strategy to combat HCC.

WED-370

DCLK1-positive tumor cells are associated with immune microenvironment in hepatocellular carcinoma: preliminary insights from a proof-of-concept study

Lorenzo Nevi[1], Maite G Fernandez-Barrena[2,3,4], Paolo Gallo[5], Veronic Gatti[6], Gianluca Masciana[7], Francesca Molinaro[1], Chiara Aiello[1], Tommaso Forcina[1], Chiara Taffon[8,9], Marco Caricato[7], Mario Cioce[6], Andrea Baiocchini[10], Umberto Vespasiani-Gentilucci[5], Matías A Avila[2,3,4], Simone Carotti[1,11]. *[1]Microscopic and Ultrastructural Anatomy Research Unit, Department of Medicine and Surgery, Università Campus Bio-Medico di Roma, Rome, Italy; [2]Solid Tumor Program, Hepatology Laboratory, Applied Medical Research Center (CIMA), University of Navarra, Pamplona, Spain; [3]Centro de Investigación Biomédica en Red Enfermedades Hepáticas y Digestivas, Madrid, Spain; [4]Instituto de Investigación Sanitaria de Navarra, Pamplona, Spain; [5]Operative Research Unit of Clinical Medicine and Hepatology, Fondazione Policlinico Universitario Campus Bio-Medico, Rome, Italy; [6]Department of Medicine, Laboratory of Molecular Medicine and Biotechnology, Università Campus Bio-Medico di Roma, Rome, Italy; [7]UOC Chirurgia Colorettale, Fondazione Policlinico Universitario Campus Bio-Medico di Roma, Rome, Italy; [8]Department of Medicine and Surgery, Research Unit of Anatomical Pathology, Università Campus Bio-Medico di Roma, Rome, Italy; [9]Anatomical Pathology Operative Research Unit, Fondazione Policlinico Universitario Campus Bio-Medico, Rome, Italy; [10]UOC Anatomia Patologica, Ospedale San Camillo Forlanini, Rome, Italy; [11]Predictive Molecular Diagnostics, Fondazione Policlinico Universitario Campus Bio-Medico, Rome, Italy*
Email: lorenzonevi@hotmail.it

Background and aims: Hepatocellular carcinoma (HCC) is a leading cause of cancer-related mortality. Doublecortin-like kinase 1 (DCLK1) is a putative stem cell marker and a driver of tumor progression. Immune checkpoint inhibitors targeting the PD-1/PD-L1 axis have become a cornerstone of tumor treatment, but response heterogeneity requires novel targets. This study characterizes the spatial relationship between DCLK1+ tumor cells and immune subsets, assessing how PD-1 blockade impacts this landscape in a murine model.
Method: Orthotopic HCC model was performed in C57BL/6J mice by partial hepatectomy and intrahepatic injection of PM299L cells. Mice were treated with anti-PD-1 monoclonal antibody (intraperitoneal injection, twice weekly for 4 weeks) or a control solution (0.5% Methylcellulose, 0.1% Tween-80, human IgG isotype). DCLK1 expression and T cell subsets (CD3, CD4, CD8, FOXP3) were assessed by immunohistochemistry and immunofluorescence. To support preclinical data, 10 human HCC (hHCC) samples arising from metabolic dysfunction–associated steatotic liver disease were analyzed for the spatial proximity of DCLK1+ cells with inflammatory cell populations. hHCC-derived organoids were generated to assess DCLK1 distribution and characteristics.
Results: In mice, PD-1 blockade was associated with a significant remodeling of the immune tumor microenvironment (TME). Anti-PD-1 treated mice exhibited a marked increase in CD3+ cells ($p < 0.001$) compared to controls. This infiltration was characterized by the expansion of CD4+ ($p < 0.001$) and FOXP3+ cells ($p < 0.01$), indicating a complex immunomodulatory response. Quantitative analysis revealed a significant reduction in the DCLK1+ tumor area fraction ($p < 0.01$) in treated mice, suggesting a decrease in the burden of DCLK1-expressing cells following checkpoint blockade. Analysis of hHCC tissues demonstrated a distinct spatial architecture where DCLK1+ tumor cells were frequently located in close proximity to inflammatory infiltrates. Finally, in hHCC-derived organoids, DCLK1 expression was preferentially localized in the central core, identifying a cell subpopulation with putative undifferentiated/stem-like features.
Conclusion: In mice, targeting the PD-1 axis significantly alters TME composition, concurrently reducing the burden of DCLK1+ cells. Preliminary data from this study indicate that DCLK1+ tumor cells spatially cluster with specific immune subsets in hHCC. These findings position DCLK1 as a potential player in the immune-oncological landscape of HCC.

WED-371

PIVKAHigh VEGF-DHigh advanced hepatocellular carcinoma patients showed Aryl hydrocarbon receptor-dependent metabolic rewiring and immune exhaustion with poor outcomes post stereotactic body radiation therapy

Prabhjyoti Pahwa[1], Deepti Sharma[2], Pushpa Yadav[1], Sherin Thomas[3], Gayantika Verma[1], Gayatri Ramakrishna[1], Jaswinder Maras[1], Shiv Kumar Sarin[4], Nirupma Trehanpati[1]. [1]*Department of Molecular and Cellular Medicine, Institute of Liver and Biliary Sciences, New Delhi, India;* [2]*Department of Radiation Oncology, Institute of Liver and Biliary Sciences, New Delhi, India;* [3]*Department of Biochemistry, Institute of Liver and Biliary Sciences, New Delhi, India;* [4]*Department of Hepatology, Institute of Liver and Biliary Sciences, New Delhi, India*
Email: trehanpati@gmail.com

Background and aims: Stereotactic body radiotherapy (SBRT) is an effective locoregional therapy for advanced hepatocellular carcinoma (aHCC), however, treatment efficacy remains unpredictable. A key determinant of treatment efficacy or anti-tumor immunity is immunometabolic reprogramming. Elevated levels of protein induced by vitamin K absence-II (PIVKA-II) and VEGF-D have poor prognosis in aHCC patients, but their impact on immune and metabolic responses is unclear. Therefore, we aimed to observe immunometabolic signatures influenced by PIVKA-II levels in aHCC patients treated with SBRT.
Method: PIVKA-II^{Low} VEGF-D^{Low} (PIVF-D^{Lo}; 711.1 ± 914.0 mAU/mL, 106.90 ± 53.8 pg/ml) and PIVKA-II^{High} VEGF-D^{High} (PIVF-D^{Hi} 91,491.16 ± 126,975.1 mAU/mL, 177.56 ± 123.59 pg/ml) aHCC patients (n = 30, age = 62 ± 9 years) were subjected to untargeted plasma metabolomics and immune checkpoint inhibitor expression on T cells at D0 (before SBRT), D5 (last day of SBRT), and D30 (30 days post-SBRT).
Results: In PIVF-D^{Lo} patients, overall survival/progression free survival was 27.7/22 months compared to 12.3/6 months in PIVF-D^{Hi}. PIVF-D^{Hi} patients showed persistently low glycolysis metabolites but enriched lipid metabolism and kynurenine-tryptophan metabolites (Acetyl-L-carnitine, 3-Amino-3-(4-hydroxyphenyl), 3-Hydroxykynurenine and 3-Indolepropionicacid) associated with Ahr activation at D0 through D30. Further, PIVF-D^{Hi} patients showed increased expression of LAG-3 (Lymphocyte Activation Gene 3, $p = 0.0183$) and TIGIT (T-cell immunoreceptor with immunoglobulin and ITIM domains, $p = 0.001$) on CD3^{+}T cells depicting T-cell exhaustion. However, PIVF-D^{Lo} patients had low LAG-3 ($p = 0.0154$) expression at baseline with enriched bile acid and OXPHOS associated metabolites (Glycolithocholate, 3-carboxy-4-methyl-5-propyl-2-furanpropanoic acid, S-Succinyldihydrolipoamide).
Conclusion: SBRT improves overall survival and progression free survival in PIVF-D^{Lo} patients by inducing immunometabolic reprogramming towards OXPHOS. In PIVF-D^{Hi} patients, a shift toward lipid-dependent metabolism with reduced glycolysis activates the Aryl hydrocarbon receptor, driving persistent immune checkpoint expression and T-cell exhaustion. Our data provides a strong rationale for combining SBRT with anti-TIGIT/LAG-3 immune checkpoint inhibitors to improve progression-free survival in advanced HCC.

WED-372

Baseline CD69 expressing T cells in peripheral blood associate with response to atezolizumab plus bevacizumab in hepatocellular carcinoma

Min Seo Park[1], Ji Won Han[1,2], Kwon Yong Tak[1,2], Jeong Won Jang[1,2], Hee Sun Cho[1,2], Pil Soo Sung[1,2]. [1]*The Catholic University Liver Research Center, Department of Biomedicine and Health Sciences, College of Medicine, The Catholic University of Korea, Seoul, Korea., Seoul, Korea, Rep. of South;* [2]*Division of Gastroenterology and Hepatology, Department of Internal Medicine, Seoul St. Mary's Hospital, College of Medicine, The Catholic University of Korea, Seoul, Korea., Seoul, Korea, Rep. of South*
Email: pssung@catholic.ac.kr

Background and aims: Atezolizumab plus bevacizumab (ATE/BEV) is a first-line therapy for advanced hepatocellular carcinoma (HCC), but objective responses occur in only 30–35%. CD69 marks activated/tissue-primed T cells. We asked whether baseline peripheral CD69+ T cell phenotypes predict response to ATE/BEV.
Method: Peripheral blood mononuclear cells (PBMCs) were collected before ATE/BEV (total n = 20; responders (R) n = 11, non-responders (NR) n = 9). Single-cell RNA sequencing (scRNA-seq) profiled baseline immune cells, and multiparameter flow cytometry validated CD69+ T cell subsets and co-expression of CD39, chemokine receptors (CXC chemokine receptor 4 (CXCR4), CXC chemokine receptor 3 (CXCR3), CX3C chemokine receptor 1 (CX3CR1), CXC chemokine receptor 6 (CXCR6)) and checkpoints (programmed cell death protein 1 (PD-1), TIGIT, and cytotoxic T-lymphocyte-associated protein 4 (CTLA-4)). Response was defined by mRECIST at 3 weeks. Statistics: T-tests, two-sided $p < 0.05$.
Results: scRNA-seq showed higher CD69 expression in CD8 and CD4 T cells in R versus NR. Flow cytometry confirmed increased CD69+ T cell frequencies in R, most prominently within CD8 T cells. CD69+ CD39- CD8 T cells were enriched in R, whereas CD69- CD39+ CD8 T cells predominated in NR. CD69+ CD8 T cells co-expressing CXCR4, CXCR3, CX3CR1 or CXCR6 were generally more frequent in R, suggesting distinct baseline trafficking profiles. Checkpoint profiling showed higher PD-1+ CD69+ CD8 T cells in R and different distributions of TIGIT+ CD69+ and CTLA-4+ CD69+ subsets. Stratification by CD38 showed enrichment of both CD38- CD69+ and CD38+ CD69+ CD8 T cells in R, while CD38+ CD69- CD8 T cells were more abundant in NR.
Conclusion: Baseline peripheral CD69+ CD8 T cell states differ between responders and non-responders to ATE/BEV in HCC. CD69 defined CD8 subsets, including CD69+ CD39- and trafficking/checkpoint-associated populations, may support immune stratification and biomarker development.

WED-377

EZH2 leads liver sex-dimorphism in HCC development and progression

Vincenzo Alfano[1], Alexia Paturel[2], Giulia Canarutto[3], Massimiliano Cocca[1], Valerio Iebba[4], Alice Deshayes[5], Jennifer Rieusset[6], Francesca De Nicola[7], Jamila Faivre[5], Silvano Piazza[3], Massimo Levrero[1], Claude Caron de Fromentel[1], Francesca Guerrieri[5]. [1]*Lyon Hepatology Institute U1350 Inserm, Lyon, France;* [2]*Catholic University-Ucly, Lyon, France;* [3]*Icgeb, Trieste, Italy;* [4]*University of Trieste, Medical Sciences, TRIESTE;* [5]*Hôpital Paul-Brousse, Villejuif, France;* [6]*Carmen laboratory/U1060 Inserm, Lyon, France;* [7]*Instituto Nazionale Tumori Regina Elena, Rome, Italy*
Email: francesca.guerrieri@inserm.fr

Background and aims: Hepatocellular carcinoma (HCC), the most frequent primary malignancy of the liver, is among the leading causes of cancer-related death worldwide. It has been reported that epigenetics, and in particular the trimethyl-transferase EZH2, plays an important role in liver oncogenesis and gut microbiome changes in HCC patients, but the relationship between them over the course of carcinogenesis is not clear. Finally, epidemiological reports indicate that the incidence of HBV-related HCC is higher in males, but the cause underlie this notion is largely unknown. Aim: The interplay between the trimethyl-transferase EZH2 and the microbiome in the hepatocarcinogenesis of X/Myc mice model.
Method: WT and X/Myc double transgenic mice, expressing in the liver both HBV HBx under control of viral regulatory elements and c-myc, were characterized by RNA-seq (Illumina) and spatial transcriptomics (GeoMx DSP Nanostring). 16s rRNA of mice stools was sequenced by Miseq Illumina platform at 10 and over 20 months, during liver carcinogenesis and at the development of HCC respectively.
Results: By using an HCC mouse model we observed a different transcriptome and gut microbiome according to the sex and along the

hepatocarcinogenesis. Thus, by GeoMx DSP we depicted a major role of EZH2 in male liver zonation during the preneoplastic phases and by Chip-seq we revealed a male specific non-canonical mechanism that implicates EZH2 in the modulation of the TCA/OXPHOS genes. Then, we found that at the first state of cell dysplasia the male microbiome, enriched in Gram – with the respect to female's bacteria, stimulates liver EZH2 that in turns contributes to increase mitochondrial fitness. This male-related mechanism highlighting the strong connection between liver epigenetic program and gut microbiome during the liver disease progression according to sex. As a strong confirmation, the in vivo EZH2 selective degradation with PROTAC MS177 had a significant effect on tumor growth exclusively in male mice.

Conclusion: We found that X/MYC females and males mice developed a different liver tumor (time and transcriptomic profile) and that they exhibited a specific transcriptomic/microbiota profile depending on the sex. Our findings expand the current understanding of how gut-liver axis contributes to liver carcinogenesis by controlling histones tri-methylation and mitochondrial activity and how all this pathway is sex-dependent.

WED-378

Sorpresa-HCC: a multicenter study on the changing epidemiology of HCC in cirrhosis

Tommaso Sarcina[1], Pietro Torre[1], Ciro Celsa[2], Paolo Angeli[3], Simone Incicco[3], Francesca Ponziana[4], Antonio Liguori[4], Giovan Giuseppe Di Costanzo[5], Debora Angrisani[5], Alessandro Federico[6], Mario Romeo[6], Andrea Pasta[7], Giulia Iannone[8], Giacomo Zaccherini[9,10], Mario Masarone[1], Filomena Morisco[11], Valentina Cossiga[11], Nicola Coppola[12], Gianfranca Stornaiuolo[12], Alessio Aghemo[13], Stella De Nicola[13], Vito Di Marco[2], Edoardo Giannini[7], Marcello Persico[1]. *[1]Department of Medicine, Surgery and Dentistry "Scuola Medica Salernitana," University of Salerno, Salerno, Italy, Salerno, Italy; [2]Department of Health Promotion, Mother & Child Care, Internal Medicine & Medical Specialties (PROMISE), Gastroenterology Unit, University of Palermo, Palermo, Italy., Palermo, Italy; [3]Department of Surgery, Oncology and Gastroenterology, Gastroenterology Unit, University of Padua, Padua, Italy., Padova, Italy; [4]Liver Unit, CEMAD – Centro Malattie dell'Apparato Digerente, Internal Medicine and Gastroenterology, Università Cattolica del Sacro Cuore, Fondazione Policlinico Universitario Gemelli IRCCS, Rome, Italy., Roma, Italy; [5]Liver Unit, Antonio Cardarelli Hospital, 80131 Naples, Italy., Napoli, Italy; [6]Hepatogastroenterology Unit, Department of Precision Medicine, University of Campania Luigi Vanvitelli, Naples, Italy, Napoli, Italy; [7]Gastroenterology Unit, Department of Internal Medicine, University of Genoa, Genoa, Italy., Genova, Italy; [8]Division of Internal Medicine, Hepatobiliary Diseases and Immunoallergology, IRCCS Azienda Ospedaliero-Universitaria di Bologna, Bologna, Italy., Bologna, Italy; [9]University of Bologna, Department of Medical and Surgical Sciences, Bologna, Italy; [10]IRCCS Azienda Ospedaliero-Universitaria di Bologna, Unit of Semeiotics, Liver and Alcohol-related Diseases, Bologna, Italy; [11]Department of Clinical Medicine and Surgery, Diseases of the Liver and Biliary System Unit, University of Naples, Naples, Italy, Napoli, Italy; [12]Department of Mental Health and Public Medicine, Section of Infectious Diseases, Second University of Naples, 80131 Naples, Italy, Napoli, Italy; [13]Division of Internal Medicine and Hepatology, IRCCS Humanitas Research Hospital, Rozzano, Italy., Rozzano, Italy*
Email: tsarcina@unisa.it

Background and aims: Hepatocellular carcinoma (HCC) accounts for more than 90% of primary liver malignancies and is the second leading cause of cancer-related death worldwide. As cirrhosis—the main risk factor for HCC—has undergone major epidemiological changes in recent years, updated data on the clinical presentation of HCC in cirrhotic patients are needed.

To provide an updated overview of the epidemiology of newly diagnosed HCC and to assess the impact of major risk factors on its occurrence.

Method: In this prospective, multicenter study enrolled 1,195 patients with cirrhosis from 11 tertiary hepatology centers across Italy. Patients included those with a new diagnosis of cirrhosis or first referral to participating centers in 2024. Demographic, etiological, clinical, and laboratory data were collected at enrollment, including HCC diagnosis. Individual risk factors were analyzed using a multivariate logistic regression was assess to identify independent predictors of HCC.

Results: Among 1,195 enrolled patients (mean age 64 ± 11.6 years; 73% male), 232 had ALD, 345 MASLD, 80 MetALD, 246 HCV infection, 159 HBV infection, 72 autoimmune liver disease, and 63 other causes. 271 (22.7%) were diagnosed with HCC; 128 (47.2%) had a simultaneous first diagnosis of cirrhosis and HCC. Viral etiologies were the most frequent overall (40.6%), while MASLD was the predominant single etiology among patients with simultaneous cirrhosis and HCC (28.9%). HCC patients showed higher rates of HBsAg positivity (18.1%), HCV-RNA positivity (16.2%), and HCV-Ab positivity despite viral eradication (19.6%) compared with non-HCC patients. The high prevalence, among HCC patients, of HCV-Ab positive/HCV-RNA negative subjects supports the persistence of HCC risk even after viral eradication. On multivariate analysis, age, male sex, HCV infection (past or active), HBsAg positivity, and obesity were independently associated with HCC. Most HCC cases (55.7%) were diagnosed in Child-Pugh class A.

Conclusion: Despite the success of HBV vaccination, nucleos(t)ide analogue therapy, and curative DAA treatments for HCV, viral etiologies remain the main independent risk factor of HCC in cirrhotic patients even if the prevalence of MASLD among patients with simultaneous cirrhosis and HCC at first diagnosis seems growing overtime. The significant prevalence of HCC on cirrhosis at first diagnosis strongly reinforces the need of a careful clinical evaluation, case finding in the risk populations and surveillance in patients with cirrhosis.

WED-379

Oncostatin M modulates tumor-stroma interactions and promotes intrahepatic cholangiocarcinoma progression via JAK/STAT signaling

Nunzia Porro[1], Jessica Nurcis[2], Silvia De Siervi[3], Cristian Turato[3], Massimiliano Cadamuro[4], Maurizio Parola[2], Luca Fabris[5], Mirella Pastore[1], Gianluca Mattei[6], Alberto Magi[6], Krista Rombouts[7], Stefania Cannito[2], Fabio Marra[1], Alessandra Gentilini[1]. *[1]Department of Experimental and Clinical Medicine, University of Florence, Florence, Italy; [2]Unit of Experimental Medicine and Clinical Pathology, Department of Clinical and Biological Sciences, University of Turin, Turin, Italy; [3]Department of Molecular Medicine, University of Pavia, Pavia, Italy; [4]Department of Medicine and Surgery, University of Milano-Bicocca, Milan, Italy; [5]Department of Medicine, School of Medicine, University-Hospital of Padua, Padua, Italy; [6]Department of Information Engineering, University of Florence, Florence, Italy; [7]Regenerative Medicine and Fibrosis Group, Institute for Liver and Digestive Health, University College London, Royal Free Campus, London, United Kingdom*
Email: nunzia.porro@unifi.it

Background and aims: Intrahepatic cholangiocarcinoma (iCCA) is a highly aggressive and chemoresistant malignancy with poor prognosis. Emerging evidence indicates that oncostatin M (OSM) contributes to tumor progression by shaping the tumor microenvironment (TME) toward a pro-tumorigenic and immunosuppressive phenotype. This study aimed to investigate the role of OSM in iCCA biology and tumor-stroma interactions.

Method: Expression of OSM and its receptors was analyzed in human iCCA tissues by immunohistochemistry and RT-PCR. Two human iCCA cell lines (HuCCT-1, CCLP-1), primary iCCA cells, patient-derived organoids (PDOs), and the murine SB1 iCCA cell line were used. Cancer-associated fibroblasts (CAFs) and THP-1-derived macrophages were included as stromal components. Cell motility was assessed by chemotaxis and invasion assays. Protein expression was

evaluated by Western blotting and immunofluorescence. OSMR and gp130 were silenced using siRNA, and stable OSMR knockdown was generated in the murine iCCA cell line using shRNA. CAFs and macrophages were exposed to conditioned media (CM) from OSM-treated iCCA cells. RNA sequencing was performed on iCCA cells cultured on 3D matrix scaffolds and treated with OSM and the JAK1/2 inhibitor ruxolitinib.
Results: OSM and OSMR were overexpressed in human iCCA tissues compared to adjoining non-tumoral tissue, and were expressed in primary iCCA cells, PDOs, iCCA cell lines, and the murine SB1 cell line. OSM increased iCCA cell migration and invasion in iCCA cells. This effect was accompanied by cytoskeletal rearrangement and induction of epithelial-to-mesenchymal transition (EMT). OSM-induced motility was reduced by silencing the OSMR or gp130 and by pharmacological JAK1/2 inhibition. In iCCA PDOs, OSM induced marked EMT-associated phenotypic changes, which were effectively reverted by ruxolitinib. Transcriptomic analysis of OSM-stimulated iCCA cells revealed a JAK-dependent up-regulation of mesenchymal gene signatures and down-regulation of immune-related pathways, together with a JAK-independent activation of Wnt signaling. CM from OSM-treated iCCA cells enhanced CAF migration and promoted M2-like macrophage polarization.
Conclusion: The OSM/OSMR axis is a novel pro-tumorigenic system implicated in cholangiocarcinogenesis, with direct effects on tumor cell biology and modulation of the TME, highlighting its potential therapeutic relevance.

WED-380
Single-cell transcriptomic profiling of endothelial-to-mesenchymal transition in MASLD-associated liver carcinogenesis
Victoria Priori[1], Camille Pignolet[1], Samira Laouirem[1], Alexandre Sayadi[1,2], Etienne Becht[1], Miguel Albuquerque[1,2], Aurélie Beaufrère[1,2], Rémy Nicolle[1], Hammoutene Adel[1], Valérie Paradis[1,2]. [1]*Université Paris-Cité, INSERM 1149, Centre de Recherche sur l'Inflammation, Paris, France;* [2]*Département de Pathologie, Hôpital Beaujon, Assistance Publique-Hôpitaux de Paris, Clichy, France*
Email: victoria.priori@inserm.fr

Background and aims: MASLD is becoming the main risk for hepatocellular carcinoma (HCC). HCC is a highly vascularized tumor in which endothelial cells play a critical role in its initiation and progression, including in MASLD. Endothelial-to-mesenchymal transition (EndMT) is the process by which endothelial cells progressively lose their specific characteristics and acquire mesenchymal properties. While this phenomenon is extensively studied in cardiovascular and pulmonary diseases, it remains poorly explored in chronic liver disease and HCC. In this study, we aimed to investigate the dynamics of EndMT and decipher its potential contribution to MASLD-related HCC.
Method: Primary human liver endothelial cells (LEC) were immunomagnetically [CD146+] isolated from fresh liver tissue of MASLD patients with varying stages of steatosis, activity and fibrosis. Single-cell suspensions of LEC from HCC (n = 5) and non-tumoral liver (n = 14) were processed for single-cell RNA sequencing (scRNA-seq). In addition to a standard clustering process, independent component analysis was applied to the transcriptomic data to identify sub-phenotypes and their associated genes, defined by the top-contributing genes of each independent component. The identified signatures were subsequently projected onto independent open-access public scRNA-seq datasets to validate LEC subpopulations.
Results: scRNA-seq identified four distinct LEC populations organized along a differentiation continuum from liver sinusoidal endothelial cells (LSEC) to fibroblastic phenotypes. Based on gene expression profiling, these populations corresponded to 1- healthy LSEC (LSEC with neither capillarization nor EndMT, expressing *STAB-2, LYVE-1*), 2- capillarized LSEC (expressing *VWF, PECAM1*), 3-transitional LEC undergoing EndMT (expressing *FN1, VIM*), and 4- LEC with mesenchymal phenotype that fully completed transition (expressing *ACTA2, PDGFR-β*). Transitional LEC were enriched in cirrhosis and HCC samples, whereas mesenchymal LEC included HCC and MASLD-associated tissues, supporting a role for EndMT in HCC progression.
Conclusion: By illustrating the high plasticity of human LEC, this study supports the central role of LEC in HCC and highlights for the first time that EndMT occurs during MASLD-related liver carcinogenesis. By categorizing LEC into distinct subpopulations, we were able to pinpoint stage-specific markers of the EndMT process. Further analyses will determine whether EndMT could be reversed and targeted as a therapeutic strategy for HCC.

WED-381
EEF1E1 drives immune evasion and tumor progression in hepatocellular carcinoma by sustaining EGFR signaling
Liying Ren[1], Dongbo Chen[1], Hongsong Chen[2]. [1]*Peking University People's Hospital, Peking University Hepatology Institute, Infectious Disease and Hepatology Center of Peking University People's Hospital, Beijing Key Laboratory of Hepatitis C and Immunotherapy for Liver Diseases, Beijing International Cooperation Base for Science and Technology on NAFLD Diagnosis, Beijing, China, Beijing, China;* [2]*Peking University People's Hospital, Peking University Hepatology Institute, Infectious Disease and Hepatology Center of Peking University People's Hospital, Beijing Key Laboratory of Hepatitis C and Immunotherapy for Liver Diseases, Beijing International Cooperation Base for Science and Technology on NAFLD Diagnosis, Beijing, China, Peking University Third Hospital, Beijing, China, Berijing, China*
Email: renliying.med@outlook.com

Background and aims: Despite the recent advances of immune checkpoint inhibitors, the clinical benefit in hepatocellular carcinoma (HCC) remains limited. Therefore, robust and clinically actionable biomarkers are urgently needed to identify patients most likely to respond to immunotherapy and to guide rational combination strategies. In our previous research, we identified EEF1E1 as a gene associated with HCC recurrence; however, its role within the tumor immune microenvironment (TIME) of HCC has not been elucidated.
Method: *EEF1E1* expression and its prognostic significance in HCC were assessed using an immunohistochemistry tissue microarray (n = 141), RNA-seq and spatial transcriptomics analysis. Pro-tumor effects were tested by gain/loss-of-function assays *in vitro* and *in vivo*, including an orthotopic tumor model. The impact on the TIME was profiled by single-cell RNA sequencing and multiparameter flow cytometry. EEF1E1-EGFR interaction was examined by co-immunoprecipitation and related signaling assays.
Results: *EEF1E1* was markedly upregulated in HCC tissues and served as an independent risk factor in HCC patients. *EEF1E1* promoted invasion and migration and epithelial-mesenchymal transition (EMT) *in vitro* and *in vivo*, and reshaped the TIME toward an immunosuppressive phenotype characterized by increased infiltration of PD-1$^+$ CD8$^+$ T cells. Further analyses showed that EEF1E1 interacted with epidermal growth factor receptor (EGFR) in protein level, impaired its endosomal-lysosomal degradation, and thereby promoted EGFR accumulation and sustained activation of EGFR-STAT signaling. Consistent with this mechanism, the EGFR inhibitor osimertinib reduced PD-1$^+$ CD8$^+$ T-cell infiltration. In combination with anti–PD-1 mAb, it produced superior antitumor effects compared with either monotherapy, Moreover, with tumors exhibiting high EEF1E1 expression deriving the optimal benefit from the combination therapy.

Conclusion: EEF1E1 drives aggressive biology and immune evasion in HCC by sustaining EGFR signaling, and may serve as a prognostic and predictive biomarker to guide combined PD-1 and EGFR blockade.

WED-382-YI

Cabozantinib reshapes the immune landscape of hepatocellular carcinoma through mitochondrial cGAS-STING signaling

Patricia Rider[1], Anna Tutusaus[1], Carlos Cuño-Gómiz[1], Flavia Savino[1], Aida Marsal[2], Neus Llarch[2], Gemma Iserte[2], Anna Colell[3], Pablo Garcia de Frutos[4], Tania Hernáez-Alsina[5], Marco Sanduzzi Zamparelli[2], Montserrat Marí[1], María Reig[6], Albert Morales[1]. *[1]IIBB-CSIC/IDIBAPS, CIBEREHD, BCLC, Barcelona, Spain; [2]IDIBAPS, CIBEREHD, BCLC, Hospital Clínic, Barcelona, Spain; [3]IIBB-CSIC/IDIBAPS, CIBERNED, Barcelona, Spain; [4]IIBB-CSIC/IDIBAPS, Barcelona, Spain; [5]Hospital Universitario San Pedro, Rioja Salud, Logroño, Spain; [6]IDIBAPS, CIBEREHD, BCLC, Hospital Clinic, Barcelona University (UB), Barcelona, Spain*
Email: amorales@clinic.cat

Background and aims: Despite recent advances in systemic therapies for hepatocellular carcinoma (HCC), predictive biomarkers and rational combination strategies remain limited. Activation of innate immune pathways such as cGAS-STING has emerged as a promising approach to enhance antitumor immunity. Identifying approved therapies that can engage this pathway through tumor-intrinsic stress responses is therefore of high translational relevance. Although cabozantinib improves outcomes, its ability to induce immunogenic mitochondrial stress and activate cGAS-STING-dependent immune signaling remains unexplored.
Method: Mitochondrial depolarization, reactive oxygen species production, and the release of immunogenic damage-associated molecular patterns (DAMPs), including mitochondrial DNA (mtDNA), HMGB1 and ATP, were assessed in conjunction with cGAS-STING pathway activation and type I interferon-stimulated gene (ISG) expression in hepatoma and macrophage models. Functional relevance was evaluated using mtDNA depletion and CRISPR-mediated STING knockdown. In vivo efficacy of cabozantinib alone or combined with the STING agonist DMXAA was tested in immunocompetent murine HCC models. Translational relevance was explored through multiplex serum proteomic profiling in two independent small cohorts of cabozantinib-treated HCC patients.
Results: Cabozantinib triggered mitochondrial stress in hepatoma cells, evidenced by loss of mitochondrial membrane potential, oxidative stress, and cytosolic leakage of mtDNA, accompanied by HMGB1 and ATP release. This immunogenic stress triggered robust ISG induction and cGAS-STING-dependent signaling, which was abrogated by mtDNA or STING depletion. In immunocompetent mouse models, cabozantinib reduced tumor growth and increased activation of tumor-infiltrating lymphocytes, effects further increased by DMXAA. Serum proteomic analysis from cabozantinib-treated patients revealed immune activation (e.g., GrzmB, HO-1, CAIX, CXCL13) and reduced angiogenic and immunosuppressive factors (e.g., VEGFR-2, ANGPT1/2, CCL17), consistent with preclinical results and associated with clinic outcome.
Conclusion: Cabozantinib exerts an immunomodulatory role in HCC through mitochondrial stress-dependent activation of the cGAS-STING pathway, reshaping the tumor immune microenvironment. These findings support rationale combination with STING-targeted strategies and the development of immune-related biomarkers to optimize treatment and stratify TKI-treated patients.

WED-383

Liquid biopsy evaluation of KDM2A and NOTCH3 in hepatocellular carcinoma

Francesca Salani[1], Teresita Caruso[1], Federico Pratesi[1], Silvia Cesario[1], Irene De Giorgi[1], Maria Concetta Scavuzzo[1], Virginia Genovesi[1], Caterina Vivaldi[1], Piero Colombatto[2], Maurizia Brunetto[1], Gabriella Cavallini[1], Gianluca Masi[1], Vinicio Carloni[3], Laura Gragnani[1]. *[1]University of Pisa, Pisa, Italy; [2]Azienda Ospedaliero Universitaria Pisana, Pisa, Italy; [3]University of Florence, Firenze, Italy*
Email: laura.gragnani@unipi.it

Background and aims: The histone demethylase KDM2A is involved in transcriptional regulation and tumorigenesis. We previously identified, in hepatocellular carcinoma (HCC), a role for KDM2A in immune modulation and suggested a KDM2A–*Notch3* transcriptional axis. Although epigenetic factors are emerging as prognostic and diagnostic tools, their relevance as circulating biomarkers remains largely unexplored. This study aimed to investigate KDM2A and NOTCH3 levels in liquid biopsies from HCC patients and their association with clinical features.
Method: Exosomes were isolated from serum samples obtained from patients with advanced HCC (n = 18) using a commercial kit. HCC patients received either Atezolizumab/Bevacizumab (Atezo/Beva) or the STRIDE regimen. Exosomal KDM2A and Notch3 cargo was evaluated: mRNA level was quantified by RT-qPCR and normalized to a pool of healthy subjects (n = 9, HS); proteins were detected by Western Blot analysis. Circulating free KDM2A and NOTCH3 protein levels were measured using commercial ELISA kits in plasma samples from 20 HCC patients and 13 HS.
Results: Exosomal KDM2A mRNA levels were significantly higher in HCC patients compared with HS ($p < 0.01$). KDM2A levels significantly discriminated viral from non-viral HCC etiologies ($p = 0.036$; confirmed by the ROC curve: AUC = 0.818, $p = 0.007$). Longitudinal analysis revealed a significant reduction at cycle 5, compared with baseline ($p = 0.042$), with a median fold change of 0.20, showing a trend toward a greater decrease in the Atezo/Beva group vs STRIDE when stratified by treatment regimen. No KDM2A exosomal protein was detected in HCC and HS samples. Plasma free KDM2A protein levels were elevated in HCC patients compared to HS ($p = 0.047$). NOTCH3 protein (free and exosomal) and exosomal mRNA levels did not differ between HCCs and HS nor correlated with clinical features.
Conclusion: Free KDM2A and its exosomal-cargo mRNA are significantly increased in HCC vs HS. The exosomal mRNA discriminates viral from non-viral cancers, suggesting an etiology-dependent KDM2A modulation in HCC. Its significant reduction after therapy could have a potential utility for early treatment monitoring while the trend toward greater modulation after Atezo/Beva vs STRIDE may reflect a KDM2A role in angiogenesis in line with other tumor types (PMID 27029061). Exosomal and circulating Notch3-related molecules seem not suitable as peripheral biomarkers of HCC clinical features.

WED-384

Transcriptomic reprogramming induced by zinc oxide nanoparticles in experimental hepatocellular carcinoma

Jorge Alejandro Salto-Sevilla[1,2], Scarlet Arceo-Orozco[1], Roberto Flores-Peña[1], Fernando Caloca Camarena[1], Rebeca Rosas-Campos[3], Marina Galicia Moreno[1], Edgar René López-Mena[4], Hugo Christian Monroy-Ramirez[1], Juan S. Armendáriz-Borunda[1,3]. *[1]Institute of Molecular Biology in Medicine and Gene Therapy, University Center for Health Sciences, University of Guadalajara, Guadalajara, Jalisco, Mexico; [2]Doctoral Program in Molecular Biology in Medicine, Department of Molecular Biology and Genomics, University Center for Health Sciences, University of Guadalajara, Guadalajara, Jalisco, Mexico; [3]Tecnologico de Monterrey, EMCS, Guadalajara, Jalisco, Mexico; [4]Tecnologico de Monterrey, Guadalajara, Jalisco, Mexico*
Email: jorge.salto4084@alumnos.udg.mx

Background and aims: Hepatocellular carcinoma (HCC) is linked to metabolic dysregulation, mitochondrial dysfunction, oxidative stress, and altered zinc homeostasis, all of which contribute to tumor progression and liver failure. Since zinc is crucial for redox balance and metabolic regulation, zinc oxide nanoparticles (ZnO-NPs) might enhance adaptive responses in HCC. However, their transcriptomic effects remain poorly understood.
Method: Male Wistar rats were randomly assigned to four groups (n = 6): control (CTL), receiving vehicle only; control treated with ZnO nanoparticles (CTL/ZnO-NPs; 50 mg/kg/week, oral); hepatocellular carcinoma (HCC), induced by diethylnitrosamine (DEN, 50 mg/kg/week, intraperitoneal) plus 2-acetylaminofluorene (2-AAF, 25 mg/kg/week, oral); and HCC treated with ZnO-NPs at the same doses. The experimental protocol lasted 18 weeks. Liver injury and fibrosis were evaluated by histology (H&E, Picrosirius Red, and immunohistochemistry). Molecular alterations were assessed by RNA sequencing (RNA-seq), Western blotting (NRF2, KEAP1), and dot blot analysis of global DNA methylation (5-meC). Serum ALT, GGT, and ALP levels, as well as hepatic GSH and MDA levels, were quantified. Data were analyzed using one-way ANOVA followed by Tukey's post hoc test ($p \leq 0.05$).
Results: ZnO-NPs treatment reduced liver injury, fibrosis, and HCC-associated markers (GPC-3 and alpha-fetoprotein), while maintaining liver structure. These effects were associated with decreased serum hepatic markers and reduced hepatic oxidative stress (as indicated by GSH and MDA), through a mechanism independent of NRF2. Transcriptomic analysis showed extensive remodeling, including activation of oxidative metabolism, mitochondrial biogenesis, antioxidant and DNA repair pathways, and suppression of multiple cancer-related signaling pathways (PPARs, FOXO, and mTOR). ZnO-NPs also induced transcriptomic upregulation of zinc transporters, including SLC39A2 and SLC39A4. Lastly, these molecular changes were associated with global DNA hypomethylation in HCC-associated liver tissue, as assessed by dot blot analysis.
Conclusion: ZnO-NPs induced coordinated transcriptomic reprogramming in HCC-associated liver tissue, restoring redox homeostasis and mitochondrial metabolic function while suppressing key oncogenic signaling pathways. This integrated molecular response is associated with reduced carcinogenic stress, improved hepatic integrity, and maintained liver function, supporting ZnO-NPs as a promising strategy in experimental HCC.

WED-385-YI
Galectin-3 inhibition supports HCC growth via pro-tumorigenic liver reprogramming

Paul Schneider[1], Frederic Speier[1], Felicia Schön[1], Laura Rosenberger[1], Maike Hartmann[1], Barbara Schroers[2], Shusruto Rishik[3], Andreas Keller[3], Jörn M. Schattenberg[4], Stephan Grabbe[1], Matthias Bros[1], Leonard Kaps[1,4]. *[1]University Medical Center Mainz, Mainz, Germany; [2]Tron, Mainz, Germany; [3]Helmholtz Istitute for Pharmacological Research, Saarbrücken, Germany; [4]Saarland University Medical Center, Homburg, Germany*
Email: leonard.kaps@uks.eu

Background and aims: Galectin-3 plays a central role in cell adhesion, macrophage polarization, and immune suppression in chronic liver inflammation. The oral Galectin-3 inhibitor Selvigaltin (GB1211) is currently under clinical evaluation for the treatment of liver fibrosis and has been considered safe for further clinical use (GULLIVER-2, NCT05009680). Given that liver fibrosis and cirrhosis represent key risk conditions for hepatocellular carcinoma (HCC), we investigated potentially altered HCC onset and progression risk following pharmacological Galectin-3 inhibition in a preclinical HCC model.
Method: Liver fibrosis was induced in C57BL/6JRj mice by repeated oral administration of carbon tetrachloride (CCl_4). Liver-specific tumors were established by subsequent intrasplenic injection of Dt81Hepa1-6 HCC cells. Beginning seven days after tumor induction, mice (n = 6 per group) received daily oral gavage of GB1211 (10 µg/kg) or vehicle control for 21 days. Tumor burden and immune cell composition were assessed on day 28 using histological analysis, flow cytometry, and RNA sequencing. On top Immunomodulatory effects of GB1211 were evaluated in primary murine immune cells.
Results: GB1211 treatment significantly reduced hepatic fibrosis, as evidenced by decreased collagen deposition and portal bridging (−42%; $p < 0.05$). However, despite its anti-fibrotic efficacy, GB1211 significantly increased intrahepatic tumor burden, reflected by elevated liver weights (+84%; $p < 0.01$), increased serum alpha-fetoprotein levels, and higher frequencies of $EpCAM^+$ tumor cells ($p < 0.05$). Immune profiling revealed a profoundly immunosuppressive tumor microenvironment, characterized by enhanced T-cell exhaustion ($CD8^+$ $PD\text{-}1^+$), skewing toward anti-inflammatory M2-like macrophages ($F4/80^+$, $CD206^+$), and suppression of pro-inflammatory M1 polarization ($F480^+$, $iNOS^+$, $CD86^+$). Transcriptomic analysis confirmed anabolic reprogramming with activation of cell-cycle, biosynthetic, and pro-tumorigenic signaling pathways including deregulation of tumor growth-promoting genes (+Arg1, +Vegfa, +IL10, +Tgfb1, +αsma, -IL1b).
Conclusion: Despite its anti-fibrotic benefits, Galectin-3 inhibition with GB1211 accelerates HCC progression by fostering an immunosuppressive tumor microenvironment. These findings emphasize the necessity for careful tumor surveillance in patients undergoing Galectin-3 inhibiting therapies in order to safely exploit the potential of Selvigaltin for treatment of liver fibrosis.

WED-386
Soluble fibroblast activation protein drives a signal transducer and activator of transcription 3 feedback loop in hepatocellular carcinoma

Deok Hwa Seo[1], Jae Yong Ryu[2], Eui-Soo Han[3], Ho Joong Choi[3], Young Kyoung You[3], Kwon Yong Tak[4], Jeong Won Jang[5], Pil Soo Sung[5]. *[1]Department of Medical Sciences, Graduate School of The Catholic University of Korea, Seoul, Korea, Rep. of South; [2]Department of Systems Biomedical Science, Soongsil University, Seoul, Republic of Korea, Seoul, Korea, Rep. of South; [3]Department of Surgery, The Catholic University of Korea, Seoul, Republic of Korea., Seoul, Korea, Rep. of South; [4]Division of Gastroenterology and Hepatology, Department of Internal Medicine, College of Medicine, Seoul St. Mary's Hospital, The Catholic University of Korea, Seoul, Republic of Korea, Seoul, Korea, Rep. of South; [5]Department of Medical Sciences, Graduate School of The Catholic University of Korea, Republic of Korea, Division of Gastroenterology and Hepatology, Department of Internal Medicine, College of Medicine, Seoul St. Mary's Hospital, The Catholic University of Korea, Seoul, Republic of Korea, Seoul, Korea, Rep. of South*
Email: smin0904@naver.com

Background and aims: Cancer-associated fibroblasts (CAFs) shape the hepatocellular carcinoma (HCC) microenvironment. Fibroblast activation protein (FAP), enriched in matrix CAFs, exists as membrane-bound and soluble FAP (sFAP), but the contribution of sFAP to CAF activation is unclear. We aimed to define FAP-positive CAF subsets and test whether sFAP sustains CAF activation via signal transducer and activator of transcription 3 (STAT3) signaling.
Method: We analysed single-cell RNA sequencing from human HCC (n = 3; 62,417 cells) and validated findings in patient-derived CAF cultures (n = 50) and serum samples (HCC n = 110; non-HCC controls n = 50). FAP-high and FAP-low CAFs were isolated by fluorescence-activated cell sorting. CAFs were exposed to recombinant human FAP (200 ng/mL, 24 h) and treated with a FAP inhibitor (FAPI-34, 8 µM) or

FAP small interfering RNA. Phospho-STAT3 and platelet-derived growth factor receptor beta (PDGFRB) were measured. In vivo validation used the syngeneic Hepa1-6 model (vehicle n = 4; FAP inhibitor n = 4; 5 mg/kg intraperitoneally, every 2 days for 14 days).
Results: Five CAF clusters were identified; FAP was enriched in matrix CAFs (76% of matrix CAFs vs 24% of other CAFs). Tumour-derived CAFs expressed more FAP than non-tumour fibroblasts (2.7-fold, $p = 0.032$), and serum FAP was higher in HCC (median 356 vs 245 ng/mL, $p = 0.041$). FAP-high CAFs showed higher STAT3 (1.9-fold) and PDGFRB (2.6-fold) than FAP-low CAFs ($p = 0.01$). Recombinant FAP increased phospho-STAT3 by 65% and PDGFRB by 2.1-fold ($p = 0.004$), whereas FAP inhibition or knockdown reduced phospho-STAT3 by 58% and PDGFRB by 46% ($p = 0.006$). FAP inhibition decreased intratumoral FAP-positive cells (64% vs 31%, $p = 0.008$) and reduced tumour volume by 38% at day 14 ($p = 0.02$).
Conclusion: sFAP sustains CAF activation through a FAP-STAT3-PDGFRB positive feedback loop and contributes to tumour growth in HCC. Targeting FAP disrupts this stromal programme and represents a strategy to remodel the HCC microenvironment.

WED-387
A translational model bridging in vitro and in vivo macrophage phenotypes in orthotopic liver tumours
Blanca Simón-Codina[1,2], Alazne Moreno-Lanceta[1,2,3], Mireia Medrano-Bosch[1,2], Arnau Masó[1], Alejandro Martínez-Navarro[1], Manuel Morales-Ruiz[1,2,3,4], Pedro Melgar-Lesmes[1,2,3,4,5]. *[1]Department of Biomedical Sciences, School of Medicine, University of Barcelona, Barcelona, Spain; [2]Fundació de Recerca Clínic Barcelona-Institut d'Investigacions Biomèdiques August Pi-Sunyer (IDIBAPS), Barcelona, Spain; [3]Biochemistry and Molecular Genetics Service, Hospital Clínic of Barcelona, Barcelona, Spain; [4]Centro de Investigación Biomédica en Red de Enfermedades Hepáticas y Digestivas (CIBERehd), Barcelona, Spain; [5]Institute for Medical Engineering and Science, Massachusetts Institute of Technology, Cambridge, Massachusetts, United States*
Email: blanca.simon@ub.edu

Background and aims: Liver cancer, the third leading cause of cancer-related death worldwide, is frequently associated with chronic hepatic inflammation. Tumour-associated macrophages (TAMs) represent a major immune population within the tumour microenvironment and contribute to tumour progression. In this study, we have characterized the transcriptional profile and phenotype of TAMs in murine models of liver cancer and in complementary *in vitro* macrophage models.
Method: Murine BNL liver cancer cells were injected into healthy and fibrotic BALB/c mouse livers (fibrosis was induced by i.p. injections of CCl_4 for 8 weeks). $CD11b^+$ macrophages were isolated from tumour (T) and non-tumour (NT) regions by magnetic cell sorting after 4 weeks of tumour growth. RNA was isolated and sequenced from T and NT macrophages from fibrotic mice. Expression of anti-inflammatory markers (ARG1, IL10, CD36) and TAM-associated genes (ferroportin-1, VEGF-A) was analysed by Real-time PCR. TAM *in vitro* models were generated and characterized using RAW macrophages co-cultured with BNL cancer cells or stimulated with BNL cell-conditioned medium.
Results: Liver tumours developed in 90% of fibrotic mice versus 50% of non-fibrotic mice, and were smaller in fibrotic animals. In fibrotic mice, TAMs from T regions showed significantly higher expression of anti-inflammatory genes and VEGF-A compared with NT regions (ARG1, 13.0 vs 5.7; IL10, 3.8 vs 1.0; CD36, 16.0 vs 1.8; VEGF-A, 4.4 vs 1.0; all $p < 0.5$). These differences between T and NT regions were absent in non-fibrotic mice. Ferroportin-1 expression was reduced in T-region TAMs in both fibrotic (0.9 vs 2.7, $p < 0.01$) and non-fibrotic mice (0.1 vs 1.2, $p < 0.05$). Accordingly, RNA sequencing revealed lower expression of ferroportin-1 in T macrophages compared with NT macrophages (−1.6 vs −0.5). *In vitro*, ferroportin-1 expression was also decreased in macrophages co-cultured with tumour cells compared with those exposed to conditioned medium (0.2 vs 2.1, $p < 0.0001$). Macrophages co-cultured with BNL cell-conditioned medium displayed increased cell area and perimeter matching with TAM phenotypes.
Conclusion: TAMs exhibit region-specific and fibrosis-dependent transcriptional programs in experimental liver cancer. Direct macrophage-tumour cell interaction drives an intra-tumoural TAM phenotype, whereas exposure to tumour secretome resembles extra-tumoural macrophages. These *in vitro* models provide a refined framework to study TAM biology.

WED-388-YI
KLF15 acts as a tumor suppressor in cholangiocarcinoma by inhibiting cell proliferation, migration, and mitochondrial energetic activity
Mireia Tena-Garitaonaindia[1], Nuno Paiva[1], Irune Lasa-Elosegui[1], Paula Olaizola[1,2], Ainhoa Lapitz[1,2], Beatriz Val[1,2], Santiago Iturbe-Rey[1], Colm O Rourke[3], Jesper Andersen[3], Mikel Azkargorta[2,4], Felix Elortza[2,4], Luis Bujanda[1,2], Maria Jesus Perugorria[1,2,5], Pedro Rodrigues[1,2,6], Jesus M Banales[1,2,6,7]. *[1]Department of Liver and Gastrointestinal Diseases, Biogipuzkoa Health Research Institute - Donostia University Hospital - University of the Basque Country (EHU), Donostia-San Sebastian, Spain; [2]National Institute for the Study of Liver and Gastrointestinal Diseases (CIBERehd), Instituto de Salud Carlos III, Spain; [3]Biotech Research and Innovation Centre (BRIC), Department of Health and Medical Sciences, University of Copenhagen, Copenhagen, Denmark; [4]Proteomics Platform, CIC bioGUNE, CIBERehd, ProteoRed-ISCIII, Bizkaia Science and Technology Park, Derio, Spain; [5]Departments of Medicine and Physiology, Faculty of Medicine and Nursing, University of the Basque Country (EHU), Leioa, Spain; [6]IKERBASQUE, Basque Foundation for Science, Bilbao, Spain; [7]Department of Biochemistry and Genetics, School of Sciences, University of Navarra, Pamplona, Spain*
Email: mireia.tenagaritaonaindia@bio-gipuzkoa.eus

Background and aims: Cholangiocarcinoma (CCA) is a heterogeneous group of biliary malignancies with a poor prognosis. Krüppel-like factors (KLF) are a family of highly conserved and widely expressed transcription factors involved in a multitude of physiological and pathological processes in humans, including cancer. Specifically, dysregulation of expression and/or activity of KLF15 has been reported in several types of cancers but its role in CCA remains unknown. Here, we investigated the role of KLF15 during cholangiocarcinogenesis and evaluated its potential as a prognostic and therapeutic tool.
Method: KLF15 expression was assessed in human CCA tissues from 10 independent patient cohorts, as well as in human CCA cell lines. KLF15-overexpressing CCA cells were generated through lentiviral transduction. Cells were subsequently characterized for proliferation, survival, tumorigenicity, invasiveness, and overall aggressiveness both *in vitro* and *in vivo*.
Results: KLF15 expression was downregulated in human CCA tissues across 10 independent patient cohorts, compared to surrounding normal liver tissue or normal bile ducts, independently on the tumor mutational background. Notably, reduced *KLF15* levels correlated with worse overall and recurrence-free survival, was associated with tumor dedifferentiation and negatively correlated with various oncogenic, stemness, and epithelial-to-mesenchymal transition (EMT) markers. Additionally, *KLF15* downregulation was associated with gene hypermethylation in enhancer regions near the promoter in human CCA tumors and *in vitro* treatment with hypomethylating agents (e.g., zebularine) restored *KLF15* expression. *In vitro*, KLF15 protein and mRNA levels were also reduced in human CCA cell lines compared to normal human cholangiocytes (NHC). At the functional level, KLF15 overexpression diminished cell viability, proliferation, tumorigenicity, migration, invasion, and mitochondrial metabolism, without affecting cell death. *In vivo*, KLF15-overexpressing CCA cells exhibited reduced tumor growth rates after subcutaneous injection into immunodeficient mice. Furthermore, intratumoral injection of

KLF15-containing lentivirus into pre-established subcutaneous CCA tumors inhibited tumor growth compared to controls.
Conclusion: KLF15 act as a tumor suppressor in CCA, suggesting its potential as a diagnostic and prognostic biomarker as well as therapeutic target.

WED-393
Prognostic tissue biomarkers for cholangiocarcinoma after tumor resection: from literature review to multicenter international validation

Beatriz Val[1], Ainhoa Lapitz[1,2,3], Tania Pastor[1,4], Laura Izquierdo-Sánchez[1,2], Colm O Rourke[5], Alejandro Forner[2,6], Cedric Coulouarn[7], Cedric Menard[7], Giovanni Brandi[8], Simona Tavolari[8], Lewis Roberts[9], Ahmed Fowsiyo[9], Mohamed A. Mohamed Ali[9], Rocio Macias[2,10], Vincenzo Cardinale[11], Jesper Andersen[5], Adelaida La Casta[4], Luis Bujanda[1,2,4], Maria Jesus Perugorria[1,2,4], Raul Jimenez-Aguero[1,4], Jesus M Banales[1,2,12,13], Pedro Rodrigues[1,2,12]. *[1]Department of Liver and Gastrointestinal Diseases, Biogipuzkoa Health Research Institute - Donostia University Hospital - University of the Basque Country (UPV/EHU), Donostia-San Sebastian, Spain; [2]National Institute for the Study of Liver and Gastrointestinal Diseases (CIBERehd, "Instituto de Salud Carlos III"), Madrid, Spain; [3]Department of Biochemistry and Molecular Biology, Faculty of Science and Technology, University of the Basque Country (UPV/EHU), Leioa, Spain; [4]Departments of Medicine and Physiology, Faculty of Medicine and Nursing, University of the Basque Country UPV/EHU, Leioa, Spain; [5]Biotech Research and Innovation Centre (BRIC), Department of Health and Medical Sciences, University of Copenhagen, Copenhagen, Denmark; [6]Barcelona Clinic Liver Cancer (BCLC) group, Liver Unit, Hospital Clínic of Barcelona, Fundació Clínic per a la Recerca Biomédica (FCRB), IDIBAPS, University of Barcelona, Barcelona, Spain; [7]Centre de Lutte contre le Cancer Eugène Marquis, Inserm, Univ Rennes, COSS (Chemistry, Oncogenesis Stress Signaling), UMR_S 1242, Rennes, France; [8]Department of Experimental, Diagnostic and Specialty Medicine (DIMES), Alma Mater Studiorum-University of Bologna, Bologna, Italy; [9]Department of Medicine, Mayo Clinic, Rochester, United States; [10]Experimental Hepatology and Drug Targeting (HEVEPHARM) group, University of Salamanca, IBSAL, Salamanca, Spain; [11]Department of Medico-Surgical Sciences and Biotechnologies, Sapienza University of Rome, Rome, Italy; [12]Ikerbasque Basque Foundation For Science, San Sebastián, Spain; [13]Department of Biochemistry and Genetics, School of Sciences, University of Navarra, Pamplona, Spain*
Email: pedromiguel.rodriguesvieira@bio-gipuzkoa.eus

Background and aims: Cholangiocarcinoma (CCA) is a heterogeneous group of biliary tumors with poor prognosis and limited treatment options. Potentially curative options include surgical resection; however, recurrence rates remain high. Robust tissue biomarkers to predict patient prognosis after tumor resection are urgently needed. This study aimed to identify and validate prognostic tissue biomarkers by combining mRNA expression and clinical information into machine learning (ML) models.
Method: A literature review was conducted to identify potential CCA tissue prognostic biomarkers, further validated through Cox PH overall survival (OS) analysis in five transcriptomic cohorts. An international cohort including tumor tissue from 221 patients undergoing tumor resection was assembled, and mRNA expression was analyzed by high-throughput TaqMan OpenArray RT-qPCR. Feature association with recurrence-free survival (RFS) and OS were obtained by Cox PH analyses. Six ML models were trained and evaluated using nested cross-validation, followed by feature reduction. Shapley Additive exPlanations values were used for interpretability.
Results: Among 496 candidate biomarkers for CCA identified in the literature, 52 harbored prognostic value in the Cox PH analysis in transcriptomic cohorts. In the multicenter validation cohort, Cox PH analyses, integrating relevant clinical features and gene expression, revealed 11 genes significantly associated with RFS and 25 with OS. The 11 RFS-associated genes, combined with 5 clinical variables, were used to train six predictive ML models, where the random survival forest (RSF) model showed the highest predictive accuracy. After feature importance–based selection, a final model incorporating 3 genes -*FSCN1*, *LDHA*, and *SLC2A1*- and 4 clinical variables achieved a test AUC of 0.748. This model significantly stratified patients into 2-years recurrence risk groups. In addition, a model for OS prediction using the same feature set achieved a test AUC of 0.69 and significantly stratified patients into risk groups of 5-year OS risk. *SLC2A1* was the top predictor in both models.
Conclusion: We identified and validated a robust panel of prognostic tissue biomarkers in CCA patients undergoing surgery. Integration of these biomarkers with clinical variables into ML-based prognostic models enabled accurate prediction of patient RFS and OS. These models hold promise for improving postoperative risk stratification and guiding personalized surveillance and therapeutic strategies in CCA.

WED-394
Coffee-derived compounds enhance chemo and immunotherapy responses in in vitro and in vivo models of hepatocellular carcinoma

Leticia Valente[1], Tian Tian[2], Guilherme Romualdo[1]. *[1]Experimental Research Unit (UNIPEX), Medical School, São Paulo State University (UNESP), Botucatu, Brazil; [2]Instituto Vall d'Hebron, Barcelona, Spain*
Email: leticia.cardoso-valente@unesp.br

Background and aims: Hepatocellular carcinoma (HCC) is associated with high mortality and limited therapeutic response. Strategies combining bioactive compounds with conventional therapies have been proposed to enhance antitumor efficacy. This study investigated whether coffee-derived compounds modulate the effects of sorafenib (SOR) or atezolizumab plus bevacizumab (ATZ+BVZ) in *in vitro* and *in vivo* models of HCC.
Method: HepG2/C3A HCC cells and LX2 hepatic stellate cells were co-cultured in transwell or spheroid systems. EC50 values were calculated for caffeine (CAF), trigonelline (TRI), chlorogenic acid (CGA), caffeic acid (CA), kahweol (KWL), SOR, ATZ and BVZ after 24 or 48h using MTT assay. Coffee-derived compounds were subsequently combined with SOR or ATZ+BVZ at sub-effective EC50 fractions (1/5 or 1/10), and the combinatory index was calculated. Compounds exhibiting synergistic effects were selected for further *in vitro* assays (migration, invasion, and colony formation) and *in vivo* xenograft model. BALB/c nude mice were implanted with HepG2/LX2 cells, and tumors were treated with therapies [SOR, intragastric administration (i.g.); ATZ+BVZ, intraperitoneal] and/or bioactive compounds (i.g.).
Results: CGA, CA, and TRI showed antagonistic interactions when combined with SOR or ATZ+BVZ. In contrast, CAF and KWL enhanced the effects of SOR and ATZ+BVZ, exhibiting synergistic effects on the reduction of C3A/LX2 spheroid viability. CAF+KWL combination with chemo/immunotherapy further reduced colony formation and migration, and CAF+KWL combination with ATZ+BVZ also diminished tumor cell invasion. In the *in vivo* model, therapies did not modify SOR-induced reduction of tumor growth and number of VEGF-positive vessels by immunohistochemistry. Nonetheless, CAF or KWL combination with ATZ+BVZ had a pronounced effect on reducing tumor volume and weight compared to immunotherapy alone.
Conclusion: Findings indicate that CAF and KWL enhance the antitumor effects of chemo/immunotherapy in HCC, supporting the potential of coffee-derived compounds as adjuvant agents in treatment strategies.

WED-395-YI

Extracellular matrix remodeling and gender dimorphism in the progression of primary sclerosing cholangitis to cholangiocarcinoma

Camilla Venturin[1,2], Massimiliano Cadamuro[3], Romina Fiorotto[2], Lauren Malouin[2], Anna Palmiotti[2], Samantha Sarcognato[4], Matteo Fassan[1,4], Umberto Cillo[5,6], Enrico Gringeri[5,6], Claudia Mescoli[7], Paolo Simioni[1,8], Jesus Maria Banales[9], Mario Strazzabosco[2], Luca Fabris[1,2,8]. *[1]Department of Medicine (DIMED), University of Padua, Padua, Italy; [2]Department of Internal Medicine, Digestive Disease Section, Liver Center, Yale University, New Haven, United States; [3]School of Medicine and Surgery, University of Milan-Bicocca, Milan, Italy; [4]Pathology Unit, Azienda ULSS2 Marca Trevigiana, Treviso, Italy; [5]Department of Surgery, Oncology and Gastroenterology (DISCOG), University of Padua, Padua, Italy; [6]Hepatobiliary Surgery and Liver Transplantation Unit, Padua University-Hospital, Padua, Italy; [7]Pathology Unit, Padua University-Hospital, Padua, Italy; [8]Clinical Medicine 1 and Thrombotic and Haemorrhagic Disease Unit, and Haemophilia Center, Padua University-Hospital, Padua, Italy; [9]Dept. of Liver and Gastrointestinal Diseases, Biodonostia Health Research Institute, San Sebastian, Spain*
Email: camilla.venturin@unipd.it

Background and aims: Primary sclerosing cholangitis (PSC) is a chronic biliary disease characterized by peribiliary fibrosis evolving to cholangiocarcinoma (CCA). Both PSC and CCA show exuberant extracellular matrix (ECM) accumulation. Mechanisms linking fibrosis to dysplasia and malignant transformation remain unclear due to the lack of suitable models capturing the sequence from PSC to CCA (CCA/PSC). We aimed to develop an animal model of CCA/PSC to assess ECM proteins up-regulated in CCA (Osteopontin (OPN), Tenascin C (TnC), Periostin (POSTN)) as potential biomarkers of early tumor lesions in PSC, using both male and female mice.
Method: Mdr2-WT and KO mice were treated from the 4th week of life with thioacetamide (TAA), a profibrogenic toxicant, and sacrificed at 12 and 24 weeks (n = 5/sex/group), compared with untreated mice (controls). Liver sections from mice and human PSC (n = 5) and CCA/PSC samples (n = 5) were stained by immunohistochemistry for OPN, TnC, and POSTN. Human CCA cell lines (HUCCT-1, EGI-1) and primary PSC cholangiocytes (n = 5) were treated (24h) with OPN (10nM), TnC (100nM), POSTN (100nM) to assess migration and expression of cancer stem cell (CSC) markers (CD133, CD44; RT-PCR).
Results: TAA-treated Mdr2-KO mice showed time-dependent progression from peribiliary fibrosis (12 weeks) to dysplasia and CCA (24 weeks). Male mice developed a more severe development toward CCA, though females displayed an earlier and more prominent ductular reaction ECM remodeling, particularly enrichment of POSTN, and increased OPN and TnC expression, was associated with development of pre-malignant and malignant biliary lesions in PSC. In human samples, OPN, POSTN, and TnC were overexpressed in CCA/PSC but not PSC alone, recapitulating mouse model findings. In cultured cells, OPN, TnC, and POSTN stimulated cell motility more in CCA than PSC cholangiocytes, whereas POSTN up-regulated CD133 and CD44 expression not only in CCA cells but also in PSC cholangiocytes.
Conclusion: Our mouse model recapitulates PSC–CCA progression, with a sex-dependent pattern. In both mice and human samples among ECM proteins, POSTN is consistently overexpressed in malignant lesions compared to PSC. *In vitro*, ECM proteins stimulate cancer cell migration, while POSTN induces a CSC-like phenotype in CCA and PSC cells, supporting its putative role in tumor initiation. ECM proteins may aid early CCA detection in PSC.

WED-396

Single-cell spatial immune organization determines response to atezolizumab plus bevacizumab in advanced HCC

Anna Vila-Escoda[1,2], Marta Piqué-Gili[1], Marta Casado-Pelaez[3], Roser Pinyol[1], Ana Hernández[1], Verónica Davalos[3], Albert Gris-Oliver[1], Carla Montironi[1,4], Judit Peix[1], Daniela Grases[5], Ezequiel Mauro[1,6], Guillem Cano-Segarra[1], Sarah Cappuyns[7], Igor Figueiredo[8], Giorgio Ioannou[8], Edgar Gonzalez-Kozlova[8], Tim Meyer[9], Anja Lachenmayer[10], Jens U. Marquardt[11], Helen Reeves[12], Julien Edeline[13], Fabian Finkelmeier[14], Jörg Trojan[14], Sacha Gnjatic[8], Jean-Frédéric Blanc[15], Richard Hubner[16], Matthias Pinter[17], Tom Luedde[18], Arndt Vogel[19], Daniela Sia[2], Vincenzo Mazzaferro[20], Manel Esteller[5,21,22,23], Jeroen Dekervel[24], Eduard Porta-Pardo[5,25], Josep M Llovet[1,2,22]. *[1]Liver Cancer Translational Research Group, Institut d'Investigacions Biomèdiques August Pi i Sunyer (IDIBAPS), Hospital Clínic, Universitat de Barcelona, Barcelona, Catalonia, Spain., Barcelona, Spain; [2]Mount Sinai Liver Cancer Program (Divisions of Liver Diseases, Department of Hematology/Oncology, Department of Medicine), Tisch Cancer Institute, Icahn School of Medicine at Mount Sinai, New York, USA, New York, United States; [3]Cancer Epigenetics Group, Josep Carreras Leukaemia Research Institute (IJC), IJC Building, Germans Trias I Pujol, Badalona, Barcelona, Spain., Badalona, Spain; [4]Pathology Department and Molecular Biology Core, Hospital Clínic of Barcelona, Barcelona, Spain., Barcelona, Spain; [5]Josep Carreras Leukemia Research Institute (IJC), Barcelona, Spain, Barcelona, Spain; [6]Centro de Investigación Biomédica en Red de Enfermedades Hepáticas y Digestivas (CIBERehd), Madrid, Spain., Madrid, Spain; [7]Digestive Oncology, Department of Gastroenterology, University Hospitals Leuven, Leuven, Belgium, Leuven, Belgium; [8]Department of Immunology and Immunotherapy, Icahn School of Medicine at Mount Sinai, New York, NY, USA., New York, United States; [9]Research Department of Oncology, UCL Cancer Institute, University College London, Royal Free Hospital, London, UK., London, United Kingdom; [10]Department of Visceral Surgery and Medicine, Inselspital, Bern University Hospital, University of Bern, Bern, Switzerland., Bern, Switzerland; [11]Department of Medicine I, University Medical Center Schleswig Holstein Campus Lübeck, Lübeck, Germany., Lübeck, Germany; [12]Newcastle University Translational Research Institute, Newcastle upon Tyne NHS Foundation Trust and NIHR Newcastle Biomedical Research Centre, United Kingdom, Newcastle, United Kingdom; [13]Department of Medical Oncology, Centre Eugène Marquis, Rennes, France., Rennes, France; [14]Department of Gastroenterology, University Liver and Cancer Centre, Frankfurt, Germany., Frankfurt, Germany; [15]Department of Hepatogastroenterology and Medical Oncology, CHU de Bordeaux Hôpital Haut-Lévêque, Pessac, France, Pessac, France; [16]Department of Medical Oncology, The Christie NHS Foundation Trust, Wilmslow Rd., Manchester M20 4BX Manchester, United Kingdom., Manchester, United Kingdom; [17]Division of Gastroenterology and Hepatology, Department of Medicine, Medical University of Vienna, Vienna, Austria., Vienna, Austria; [18]Department of Gastroenterology, Hepatology and Infectious Diseases, University Hospital Dusseldorf, Medical Faculty at Heinrich Heine University Dusseldorf, Dusseldorf, Germany., Dusseldorf, Germany; [19]Hannover Medical School, Hannover, Germany., Hannover, Germany; [20]Department of Oncology and Hemato-Oncology, University of Milan, Milan, Italy; HPB Surgery, Hepatology and Liver Transplantation, Fondazione IRCCS Istituto Nazionale Tumori di Milano, Milan, Italy., Milan, Italy; [21]Centro de Investigacion Biomedica en Red Cancer (CIBERONC), Madrid, Spain., Madrid, Spain; [22]Institucio Catalana de Recerca i Estudis Avançats (ICREA), Barcelona, Catalonia, Spain., Barcelona, Spain; [23]Physiological Sciences Department, School of Medicine and Health Sciences, University of Barcelona (UB), Barcelona, Catalonia, Spain, Barcelona, Spain; [24]Department of Gastroenterology and Hepatology, University Hospitals KU Leuven, Leuven, Belgium., Leuven, Belgium; [25]Barcelona Supercomputing Center (BSC), Barcelona, Spain., Barcelona, Spain*
Email: avilae@recerca.clinic.cat

Background and aims: Atezolizumab+bevacizumab (atezo+bev) is a first-line therapy for advanced hepatocellular carcinoma (aHCC) with ~30% objective responses. Single-cell studies identified responses linked to $CD8^+$ T effector cells (CD8_Tex and Temra) and $CXCL10^+$ macrophages (Macro_CXCL10), and resistance to $TREM2^+$ macrophages (Macro_TREM2) and $CD14^+$ monocytes (Mono_CD14). We hypothesized that, beyond cell composition, immune spatial organization within the tumor microenvironment (TME) determines response to atezo+bev.
Method: Single cell spatial transcriptomics (ST) was performed on 27 aHCCs (9 atezo+bev responders and 18 resistant) using the Xenium Prime 5.000-gene panel (10x Genomics) customized with 100 additional genes. Distances between cells were computed using the *dbscan* package [radius(r) = 300 µm]. Tumor cell neighborhoods were analyzed (r = 25 µm). Ligand-receptor interactions between T cells and other TME cell populations were evaluated. Immune cell clusters were defined as groups of ≥3 immune cells within 100 µm, and were identified through a density-based algorithm. This spatial clustering was assessed using ST and multiplexed immunohistochemistry (mIHC) data.
Results: ST of 27 aHCCs yielded 4.6 million cells. The distribution of CD8_Tex and Temra, and Macro_CXCL10 cells in inflamed tumors differed by treatment response: in responders, these immune populations localized within the tumor and were closer to cancer cells ($p = 0.02$, $p = 0.08$, and $p = 0.1$, respectively). Moreover, in responders, tumor hepatocytes exhibited a significantly enriched lymphoid neighborhood (CD8_Tex, $CD4^+$Tcells, $CD8^+$Tcells, $CD4^+CXCL13^+$Tcells, $CD4^+$ Treg) composition and significantly higher rates of immune-recruting interactions, including PDL1–PD1, CXCL9-CXCR3 and CXCL10–CXCR3 ($p < 0.05$). Resistant tumors showed 10% of pure Macro_TREM2 (vs 0% in responders, $p = 0.009$), 27% of mixed Macro_TREM2–Mono_CD14 (vs 5%, $p = 0.03$) and 38% of mixed Macro_TREM2–$CD8^+$ T-cell clusters (vs 22%, $p = 0.04$); along with enrichment of the CXCL12–CXCR4 chemokine axis. Increased rates of Macro_TREM2-pure clusters ($p = 0.02$) and mixed Macro_TREM2-$CD8^+$ clusters ($p = 0.03$) was confirmed by mIHC.
Conclusion: Atezo+bev response in HCC is marked by intratumoral effector $CD8^+$ T cells and CXCL10_Macro, tumor hepatocytes enriched in lymphoid neighborhoods, and immune-recruiting ligand–receptor interactions, whereas resistance is driven by TREM2_Macro clusters and CXCL12–CXCR4 signaling.

WED-397
Microbial pentadecanoic acid suppresses hepatocellular carcinoma progression by inhibiting NSUN5 methyltransferase activity

Ziyan Wang[1], Ziqi Liu[1], Yuxin Liu[1], Zhengjiang Li[1], Zhixian Lan[1,2], Routing Wang[1], Kaifeng Wang[3], Dekai Zheng[1], Yuchuan Chen[1], Yinghong Zhu[1], Jian Sun[1]. [1]*Department of Infectious Diseases, Nanfang Hospital, Southern Medical University, Guangzhou, China; State Key Laboratory of Multi-organ Injury Prevention and Treatment; Key Laboratory of Infectious Diseases Research in South China, Ministry of Education; Guangdong Provincial Key Laboratory for Prevention and Control of Major Liver Diseases; Guangdong Provincial Clinical Research Center for Viral Hepatitis; Guangdong Institute of Hepatology; Guangdong Provincial Research Center for Liver Fibrosis Engineering and Technology, Guangzhou, China;* [2]*Guangdong Provincial Key Laboratory of Gastroenterology, Department of Gastroenterology, Nanfang Hospital, Southern Medical University, Guangzhou, China;* [3]*Department of Preventive Medicine, Shantou University Medical College, Shantou, China*
Email: sunjian@smu.edu.cn

Background and aims: Gut microbial metabolites critically regulate the progression of hepatocellular carcinoma (HCC). Here, we screened a clinically derived library of plasma metabolites that were negatively associated with HCC progression and identified pentadecanoic acid (PEA), a gut microbial metabolite, as an inhibitor of HCC progression by suppressing the RNA m^5C methyltransferase activity of NSUN5.
Method: We recruited 37 non-HCC individuals and 39 HCC patients and analyzed the plasma differential metabolites between non-HCC individuals and HCC patients, as well as among HCC patients at different stages. Then, we constructed a plasma metabolite library negatively associated with HCC progression based on these differential metabolites and screened the library using experimental methods. Changes in PEA-producing microbiota were examined in fecal samples from other cohort. We verified the anti-HCC capability of PEA through *in vitro* and *in vivo* experiments. The potential target protein of PEA was pulled down using biotin-labeled PEA and identified by mass spectrometry analysis. The interaction and regulation of PEA on NSUN5 were examined using pharmacological and biochemical technologies. The role of NSUN5 in mediating the anti-HCC capability of PEA was verified through *in vitro* and *in vivo* functional and rescue experiments.
Results: After screening the metabolite library, PEA was identified as the sole metabolite that exhibited inhibitory effects against HCC cells while showing no inhibitory effects on normal hepatocytes. A significant enrichment of PEA-producing microbiota was observed in non-HCC individuals compared with HCC patients. PEA supplementation significantly suppressed HCC proliferation and progression both *in vitro* and *in vivo*. Mass spectrometry analysis revealed NSUN5 as a potential downstream target of PEA. We further demonstrated that PEA directly interacted with NSUN5 and inhibited the methyltransferase activity of NSUN5 by competitively blocking the binding of its substrate, S-adenosylmethionine (SAM). Both *in vitro* and *in vivo* functional and rescue experiments demonstrated that NSUN5 could be a key downstream target responsible for the anti-HCC effect induced by PEA.
Conclusion: Our findings show that microbial PEA may be negatively associated with the progression of HCC. We suggest that PEA serves as a potential inhibitor of HCC progression and report it as the small molecule capable of inhibiting NSUN5 methyltransferase activity and NSUN5-mediated HCC progression.

WED-398
An iron-dependent TFRChi subpopulation exploits postoperative niches to initiate hepatocellular carcinoma recurrence

Junyu Wu[1], Zhuofeng Jiang[1], Ning Wang[1]. [1]*The University of Hong Kong, Hong Kong, Hong Kong*
Email: ckwang@hku.hk

Background and aims: Hepatocellular carcinoma (HCC) is a leading cause of cancer death globally, for which surgical resection is the primary treatment for early- to intermediate-stage patients. However, postoperative recurrence occurs in up to 70% of cases within five years, drastically reducing long-term survival rates compared to patients without recurrence. This study aims to identify the cellular mechanisms underlying HCC recurrence.
Method: Single cell RNA sequencing was used to identify the cell population enriched in recurrent HCC tumors and its molecular signature. A tracible HCC cell line were then established to observe the dynamic changes of this population in HCC recurrence. Mechanism underlying the maintanence and expansion of this population during HCC recurrence was explored in in vitro and in vivo models.
Results: An orthotopic GFP-expressing HCC model was established in immunocompetent C57BL/6J mice, followed by surgical resection. RNA-seq analysis of GFP^+ cells from primary and recurrent tumors revealed a significant enrichment of a TFRC-high subpopulation in recurrent disease. Pseudotime analysis indicated that these cells lacked stem-like properties but exhibited rapid cell cycle progression. A gene signature derived from this population served as a clear predictor of recurrence-free survival in HCC patients. To track these cells *in vivo*, we generated an HCC cell line with a tdTomato reporter knocked into the *TFRC* locus. Consistent with the RNA-seq data, the

tdTomato$^+$ population expanded specifically in recurrent tumors. Functionally, inducible knockdown of *TFRC* post-resection significantly suppressed tumor recurrence, whereas inducible *TFRC* expression promoted relapse. Mechanistically, TFRC overexpression accelerated cellular metabolism, increasing ATP production and driving cell cycle entry. This process depended on iron delivery within the post-operative microenvironment. Here, infiltrating Ly6C$^+$ pro-inflammatory macrophages fostered surgical inflammation, carried circulating iron, and created an iron-rich niche. Accordingly, iron chelation therapy significantly prevented postoperative HCC recurrence.
Conclusion: Our findings suggest that an iron-dependent expansion of TFRChi-expressing population mediated high chance of post-operative recurrence in HCC.

WED-400-YI
Establishing a multi-institutional patient-derived xenograft biobank for precision medicine in cholangiocarcinoma
Lisa Wende[1], Denise Schlösser[1], Gharaza Nasir[2], Parham Pourabbas Tahvildari[1], Elena Valenzi[2], Shreya Chakraborty[1], Silke Marhenke[1], Arndt Vogel[1,2,3], Anna Saborowski[1]. [1]*Medizinische Hochschule Hannover, Hannover, Germany;* [2]*Toronto General Hospital, Toronto, Canada;* [3]*Princess Margaret Cancer Centre, Toronto, Canada*
Email: wende.lisa@mh-hannover.de

Background and aims: Cholangiocarcinoma (CCA) is a rare and aggressive malignancy with pronounced molecular heterogeneity and limited therapeutic options. Biomarker-driven treatment strategies are hindered by the lack of representative preclinical models for functional investigation of targeted therapies. Patient-derived xenograft (PDX) models closely recapitulate patient tumors and provide a robust translational platform. This ongoing project aims to establish and expand a multi-institutional CCA PDX biobank and demonstrate its suitability for precision medicine.
Method: Tumor samples from patients with CCA are collected across collaborating institutions (currently Hannover Medical School, Germany, and Princess Margaret Cancer Center, Toronto, Canada) and engrafted into immunodeficient mice. Successfully engrafted models are expanded, cryopreserved, and annotated with clinical, pathological, and treatment-related metadata. Histological characterization is performed by immunohistochemistry, and molecular profiling includes whole-exome sequencing and transcriptome profiling. 2D and 3D cell lines are generated from successfully established PDX models to enable in vitro profiling and targeted drug testing. A virtual biobank infrastructure provides structured access to model-associated data for collaborative research.
Results: To date, the biobank comprises more than 50 established CCA PDX models and is continuously expanding. PDX tumors retain key histological and molecular characteristics across passages. Histopathological analyses reveal dynamic tumor-stroma remodeling with progressive replacement of human stroma by murine orthologues from early PDX generations onward, an important consideration for functional drug response studies. Key druggable alterations include FGFR2 fusions, ERBB2 amplification, and IDH1-, KRAS G12D and G12C mutations. Transcriptomic profiling demonstrates pronounced inter-patient heterogeneity among tumor samples, while matched normal liver tissues cluster closely together. A HER2-overexpressing PDX model was translated into an in vitro system and showed sensitivity to HER2-directed therapies, including neratinib and tucatinib.
Conclusion: This ongoing, multi-institutional and virtually accessible CCA PDX biobank represents a growing shared resource for functional evaluation of targeted therapies. Ongoing model expansion, integrated molecular profiling, and systematic drug screening will further enhance its value for collaborative precision oncology in CCA.

WED-401
AREG knockdown triggers Decorin-mediated EGFR activation and paracrine G1 arrest across species
Anna Potapova[1], Agnes Ong[1], Torsten Wuestefeld[2]. [1]*Genome Institute Of Singapore, Singapore, Singapore;* [2]*Lee Kong Chian School Of Medicine Nanyang Technological University, Genome Institute of Singapore, Singapore, Singapore*
Email: potapovaa@a-star.edu.sg

Background and aims: The senescence-associated secretory phenotype (SASP) mediates non-cell-autonomous effects of senescent hepatocytes, but its regulatory mechanisms remain poorly understood. While Amphiregulin (AREG) is known to activate EGFR in liver pathophysiology, its role in hepatocyte senescence is unknown. We hypothesized that AREG critically modulates SASP composition and paracrine senescence signaling.
Method: Oncogene-induced senescence (OIS) was established in immune-competent C57BL/6 mice by hydrodynamic tail vein delivery of NRasG12V in ~5% of hepatocytes. AREG expression was knocked down using two independent shRNAs. Liver tissues were analyzed by RNAseq, immunofluorescence co-staining (p21, p16, Ki67, SA-β-Gal, phospho-H2A.X), protein arrays, and Western blot. Paracrine effects were evaluated by treating human SNU398 liver cancer cells with supernatants from Areg-knockdown AML12 mouse hepatocytes. Human AREG knockdown was similarly validated in SNU398 cells.
Results: AREG specifically co-localized with senescence markers (p16, p21) in both OIS and oxidative stress-induced senescence. Paradoxically, Areg knockdown in OIS hepatocytes enhanced paracrine senescence signaling, evidenced by a significantly higher proportion of p21-positive, cell cycle-arrested hepatocytes beyond the NRas-expressing population ($p < 0.0367$). Following partial hepatectomy, this effect intensified, reducing Ki67-positive hepatocytes ($p < 0.0482$) and mitotic index ($p < 0.0007$). Mechanistically, protein array and transcriptomic analyses identified Decorin, a small leucine-rich proteoglycan, as a key SASP factor dramatically upregulated upon Areg knockdown in both mouse and human cells. Decorin mediated EGFR activation, leading to p21 upregulation and cyclin D1 downregulation, resulting in G1 phase blockade. Critically, supernatants from Areg-knockdown mouse hepatocytes significantly attenuated proliferation of human SNU398 liver cancer cells ($p < 0.0002$), demonstrating a conserved cross-species paracrine senescence effect.
Conclusion: AREG functions as a previously unrecognized SASP rheostat in senescent hepatocytes. Rather than simply being a SASP component, AREG knockdown reprograms the SASP to amplify Decorin-mediated paracrine growth suppression via EGFR activation. This conserved mechanism identifies AREG as a novel therapeutic target in liver cancer, where its inhibition may enhance senescence-based tumor surveillance through non-cell-autonomous pathways.

WED-402
DUSP10 rewires cholesterol biosynthesis and T cell infiltration to suppress hepatocellular carcinoma progression
Anliang Xia[1], Siyuan Liu[1], Shuyan Sheng[1], Shaobo Zhang[1], Kaipeng Hu[1], Beicheng Sun[1]. [1]*The First Affiliated Hospital of Anhui Medical University, Hefei, China*
Email: xiaanliang@ahmu.edu.cn

Background and aims: Cholesterol metabolism is a major driver of hepatocellular carcinoma (HCC) progression and a key regulator of the tumor immune microenvironment. Identifying genes that function as molecular bridges between metabolic reprogramming and immune infiltration is essential for elucidating HCC pathogenesis and developing precision therapies. This study aims to characterize

cholesterol-metabolic features in HCC and to uncover core molecular mediators that couple cholesterol metabolism with immune infiltration.
Method: We integrated single-cell RNA sequencing and metabolomic profiling from patients with HCC to identify genes involved in cholesterol metabolism and immune modulation. A liver-specific CRISPR/Cas9 knockout mouse model was generated to assess the impact of candidate genes on tumor malignancy. Transcriptomic, metabolomic, and proteomic analyses were employed to validate gene function and dissect underlying metabolic mechanisms. Remodeling of the immune microenvironment was evaluated using flow cytometry and multiplex immunohistochemistry. Finally, immune-cell flow sorting combined with lipid nanoparticle-mediated delivery was used to assess the potential therapeutic efficacy of a combinatorial strategy.
Results: Dual-specificity phosphatase 10 (DUSP10) was markedly downregulated in HCC tissues, and its high expression was strongly associated with favorable prognosis. Mechanistically, DUSP10 interacts with the deubiquitinase OTUD4 to stabilize INSIG1/2, thereby suppressing the cholesterol biosynthesis pathway and restraining tumor progression. Elevated cholesterol levels in the tumor microenvironment impaired $CD8^+$ T-cell infiltration, whereas DUSP10 promoted CXCL10-dependent T-cell recruitment by limiting cholesterol accumulation.
Conclusion: Targeting the DUSP10-OTUD4-cholesterol axis suppresses tumor malignancy while enhancing $CD8^+$ T-cell antitumor immunity through CXCL10. These findings identify DUSP10 as a central molecular node linking cholesterol biosynthesis to T-cell immune infiltration and highlight a promising metabolic-immune coupling axis for therapeutic intervention in HCC.

WED-403
Whole genome sequences reveal the presence of high structural variants in hepatocellular carcinoma of Fontan-associated liver disease
Taiji Yamazoe[1], Eiji Kakazu[1], Michitaka Matsuda[1], Masaaki Mino[1], Tatsuya Kanto[1]. *[1]Japan Institute for Health Security, Ichikawa, Japan*
Email: lb-19yamazoe@hospk.ncgm.go.jp

Background and aims: The Fontan-associated liver disease (FALD) is characterized by a congestive hepatopathy, develops liver cirrhosis and have a risk of hepatocellular carcinoma (HCC) after 15–20 years of the Fontan procedure. For understanding of hepatocarcinogenesis in FALD, we performed whole genome sequencing.
Method: We enrolled ten pairs of tumor and nontumor lesions from the surgically resected FALD HCCs. The pipelines of Mutect2 and Oncoanalyser were utilized after PCR-free sequence.
Results: The ages of the patients (n = 10) ranged from 21 to 43 years. The tumor subtypes of HCCs were primarily moderate-to-poorly differentiated HCCs or combined hepatocellular-cholangiocarcinomas. There were no single-nucleotide variants (SNVs) in the TERT promoter, TP53, CTNNB1, or ARID1A, but mutations in AXIN1 were identified in three cases. The tumor mutation burden (TMB) was comparable to liver tumor cohort in TCGA (LIHC cohort). In the COSMIC signatures, all ten FALD HCCs harbored the signatures related to homologous recombination deficiency (HRD), non-homologous end joining (NHEJ), and/or microhomology-mediated end joining (MMEJ), including SBS8, SBS39, ID6, and/or ID8. None of them had SBS3, which was seen in BRCA1/2 mutated tumors. The structural variants of deletion and translocation were significantly higher in FALD HCCs, compared to the Japanese HCC cohort in the ICGC (LIRI cohort). The copy number alterations (CNAs) are the result of chromosomal rearrangement. The copy number gains were observed in genes on chromosome 1q, including MCL1 and MDM4, and on chromosome 6p, including VEGFA. Moreover, CNAs in AXIN1 were also seen in three FALD HCCs without SNV in the AXIN1 gene. Given the typical absence of mutations in genes associated with homologous recombination DNA repair, it was hypothesized that the frequency of DNA double-strand breaks would exceed the capacity of the repair mechanisms. As a result, the commonly altered chromosomal changes in HCCs, including a gain of chromosome 1q and 6p, were also seen in FALD HCCs. The consensus clustering analysis of CNAs classified the HCCs in the LIHC cohort into four classes. The HCCs classified as the same class of FALD HCCs showed poor progression-free survival.
Conclusion: The FALD HCC has a unique genomic profile characterized by DNA double-strand break repair-related signatures and high structural variants, resulting in copy number alterations.

WED-409-YI
Spatial profiling reveals region-specific immune architectures and checkpoint distribution in extrahepatic cholangiocarcinoma
Dawei Yi[1], Valery Volk[1], Christoph Gerdes[1,2], Melanie Bathon[1], Josephine Reschke[1], Tanja Reineke-Plaaß[1], Friedrich Feuerhake[1], Anna Saborowski[1], Arndt Vogel[1,2,3]. *[1]Hannover Medical School, Hannover, Germany; [2]Princess Margaret Cancer Centre, Toronto, Canada; [3]Toronto General Hospital, Toronto, Canada*
Email: yi.dawei@mh-hannover.de

Background and aims: Extrahepatic cholangiocarcinoma (eCCA) is characterised by poor prognosis and limited response to systemic therapies. Increasing evidence suggests that the tumor immune microenvironment (TIME) plays a decisive role in disease progression and therapeutic vulnerability. In particular, the spatial arrangement of immune cell aggregates may determine immune activity or suppression within the tumor. This study aimed to characterise immune cell composition, checkpoint expression and spatial relationships in eCCA to identify immune phenotypes with potential clinical relevance.
Method: Ninety-four surgically resected and clinically annotated eCCAs were analysed. Multiplex immunohistochemistry combined with multispectral imaging was performed to detect various immune cell types, including T cells, B cells, macrophages, neutrophils, and immune checkpoint (IC) molecules such as PD-1, PD-L1, TIGIT, CTLA-4, LAG-3. Regions of interest representing tumor core, invasive margin, stromal regions and tertiary lymphoid structures (TLS) were selected. Image analysis and machine learning-based pipelines were applied for quantitative assessment and spatial profiling of the TIME.
Results: Spatial and intertumoral heterogeneity of immune infiltration was observed across the cohort. TLS were identified in most cases (74%) and were enriched for T cells (24%) and B cells (23%), whereas the tumor core showed sparse immune cell infiltration (6%), consistent with an immunosuppressive milieu. Only a minority of intratumoral T cells (10%) expressed immune checkpoints across regions, with most IC-positive cells showing single rather than dual IC expression. Checkpoint distribution differed by region, with PD-L1 (4%) being predominant within the tumor core, while TIGIT (3%) and PD-1 (2%) were more frequently detected in stroma and margin. Spatial proximity analyses revealed distinct neighbourhood patterns between immune cell subsets by region.
Conclusion: This comprehensive spatial analysis demonstrates that eCCA exhibits pronounced immune heterogeneity with region-specific immune architectures. The presence of TLS contrasts with immune-excluded tumor core and highlights potential mechanisms of immune escape. Differential spatial expression of immune checkpoints suggests that patient stratification based on immune architecture may improve the selection of immunomodulatory treatment strategies. These findings support the integration of

spatial immune profiling into future translational and clinical studies for eCCA.

WED-410

Moonlighting function of lysosomal CYP7A1 licenses p62-mediated autophagy activation to drive hepatocellular carcinoma

Yan Lou[1], Yunqing Qiu[1], Shuaibing Ying[1], Jinyao Dai[1], Yujing Wang[1]. [1]*The First Affiliated Hospital, College of Medicine, Zhejiang University, Hangzhou, China*
Email: yanlou@zju.edu.cn

Background and aims: Hepatocellular carcinoma (HCC) remains a lethal malignancy, with its efficacy hampered by an incomplete understanding of the liver-specific metabolic microenvironment. Beyond their catalytic roles, metabolic enzymes possess non-canonical, "moonlighting" functions, yet their mechanisms in HCC are largely unexplored.
Method: Focusing on CYP7A1, its expression levels were evaluated via public datasets and analyses of 203 human HCC specimens. The association between CYP7A1 expression and prognosis was further assessed by a 5-year follow-up of 183 patients. Its functional role was validated using cell proliferation, colony formation, and migration assays. In vivo, CYP7A1 effects were examined by RNAi in diethylnitrosamine-induced HCC mouse models and patient-derived xenograft models. Finally, immunoprecipitation–mass spectrometry (IP-MS) and multi-omics analyses elucidated its regulatory role in autophagy.
Results: Clinical analyses demonstrated that CYP7A1 was significantly upregulated in HCC and correlated with poor prognosis. Mechanistically, CYP7A1 undergoes unique lysosomal translocation in tumor cells and directly binds the autophagy adapter p62 via its C-terminal domain. This interaction, independent of CYP7A1's enzyme activity, inhibits liquid-liquid phase separation (LLPS) of p62, which disrupts the p62-mTORC1 complex and alleviates mTORC1-mediated suppression of transcription factor EB (TFEB). Nuclear translocation of activated TFEB drives lysosomal biogenesis and autophagy flux, providing metabolic support for tumor cells. Concurrently, this signaling axis induces immune evasion by downregulating antigen presentation (MHC-I). Functionally, the catalytically dead mutant CYP7A1 (CYP7A1 R260L) fully restored the tumorigenic phenotypes suppressed by CYP7A1 knockdown, both in vitro and in vivo.
Conclusion: Collectively, we uncover a non-canonical function of CYP7A1 as a lysosomal signaling scaffold that integrates autophagy and immune regulation to promote HCC progression. Targeting the CYP7A1-p62 interaction interface may present a novel, liver-specific therapeutic strategy for HCC.

WED-412-YI

CAND1 as a novel therapeutic target in pediatric hepatoblastoma: linking NEDDylation to tumor progression

Leidy Estefanía Zapata-Pavas[1], Eleonora Davoli[1], Maitane Asensio[2,3], Patricia Peña-Sanfélix[1], Naroa Goikoetxea-Usandizaga[1,3], Irene González-Recio[1], Carolina Conter[1], Abhishek Murti[4], Elise Lelou[4], Alvaro del Río-Álvarez[5], Pau Sancho-Bru[3,6], Dimitris Xirodimas[7], Bruce Wang[4], Jose Marin[2,3], Maite G Fernandez-Barrena[3,8], Carolina Armengol[5], Matías A Avila[3,8], María Luz Martínez-Chantar[1,3]. [1]*Center for Cooperative Research in Biosciences (CIC bioGUNE), Basque Research and Technology Alliance (BRTA), Liver Disease Lab, Derio, Spain;* [2]*Experimental Hepatology and Drug Targeting (HEVEPHARM), University of Salamanca, IBSAL, Salamanca, Spain;* [3]*Centro de Investigación Biomédica en Red de Enfermedades Hepáticas y Digestivas (CIBERehd), Carlos III National Health Institute, Madrid, Spain;* [4]*Department of Medicine, University of California San Francisco, San Francisco, United States;* [5]*Childhood Liver Oncology Group, Fundació Institut d'Investigació en Ciències de la Salut Germans Trias i Pujol (IGTP), Badalona, Spain;* [6]*Institut d'Investigacions Biomèdiques August Pi i Sunyer (IDIBAPS), Barcelona, Spain;* [7]*Centre de Recherche en Biologie cellulaire de Montpellier (CRBM, CNRS), Univ. Montpellier, Montpellier, France;* [8]*Hepatology Programme, Center for Applied Medical Research (CIMA), IDISNA, University of Navarra, Pamplona, United States*
Email: lzapata@cicbiogune.es

Background and aims: Hepatoblastoma (HB), the most common pediatric liver cancer, remains a major challenge. Despite advances in surgery and chemotherapy, survival for aggressive or relapsed cases is still poor, highlighting the urgent need for new therapeutic strategies. Our previous work established NEDDylation, a post-translational modification that mainly activates cullin-RING ligases, as a key driver of HB progression. Building on these findings, we identified CAND1, a regulator of SCF complexes, as a novel NEDDylation-controlled target. This study aims to define the functional role of CAND1 and its regulation by NEDDylation, uncovering mechanisms that could be exploited for precision therapy.
Method: CAND1 expression was analyzed in HB patient samples and organoid models using bulk and single-cell transcriptomics. Functional assays were performed in HepT1, HepG2, and HB-284 cells following siRNA-mediated silencing. *In vivo*, HB was induced in C57BL/6 and ^{Bio}NEDD8 mice using the YAPS127A/N90-β-catenin model, followed by siRNA-mediated silencing of CAND1 to assess effects on tumor development and immune modulation. Predicted NEDDylation sites were disrupted in mutant constructs and tested *in vitro* to confirm regulatory mechanisms.
Results: CAND1 was markedly overexpressed in HB tissues and organoids, strongly associated with poor prognosis and aggressive molecular subtypes such as C2-pure and Epi-CB. Single-cell analysis confirmed its enrichment in tumor compartments. Silencing CAND1 significantly reduced cell viability and altered key markers of proliferation and senescence. Mutant constructs lacking NEDDylation sites exhibited functional impairment, validating the regulatory role of this modification. *In vivo*, tumors from CAND1-silenced mice showed reduced development and an immunomodulatory effect associated with CAND1 targeting.
Conclusion: These findings position CAND1 as a critical mediator of HB progression under NEDDylation control. Targeting this axis represents a promising therapeutic strategy for high-risk pediatric liver cancer, opening the door to combination approaches that enhance efficacy while minimizing systemic toxicity. This work provides a strong rationale for future translational studies aimed at integrating CAND1 inhibition into precision oncology frameworks.

WED-413

CRISPR screen identifies GTF2E1 as a regulator of hepatocellular carcinoma immune escape via activating STAT3 to upregulate PD-L1 expression

Yi Zhan[1], Fei Xiao[1]. [1]*The Fifth Affiliated Hospital of Sun Yat-sen University, Zhuhai City, Guangdong Province, China*
Email: zhany8@mail2.sysu.edu.cn

Background and aims: Epigenetic dysregulation is a highlighted hallmark of hepatocellular carcinoma (HCC) and plays an important role in tumorigenesis, progression and resistance to immunotherapy. However, the mechanisms underlying epigenetic modulation of immune checkpoints and how altered epigenetic landscapes in turn drive PD-L1 expression to facilitate HCC immune escape remain poorly understood. In this study, we aimed to elucidate the role of GTF2E1 in the transcriptional control of PD-L1 in HCC.
Method: We performed a CRISPR knockout screen to investigate epigenetic factors that contribute to PD-L1 expression in HCC cells. Flow cytometry, Western blotting, and quantitative real-time PCR (qPCR) assays were used to examine the regulatory role of GTF2E1 in PD-L1 transcription and translation. In vitro T cell co-culture

experiments were performed to evaluate the functional impact of GTF2E1 on HCC immune escape. CUT&Tag and RNA-seq were utilized to elucidate the molecular mechanisms by which GTF2E1 drives PD-L1 expression.
Results: We identified GTF2E1, a general transcription factor IIE subunit 1 that participates in RNA polymerase II-mediated transcription initiation, as a key epigenetic regulator of PD-L1 expression in HCC cells using the epigenetic-targeted CRISPR knockout screen. GTF2E1 promotes the expression of PD-L1 in HCC cells and facilitates tumor immune escape. Clinically, GTF2E1 is upregulated in HCC tissues and is associated with poor clinical outcomes in patients with this disease. Mechanistically, GTF2E1 regulates the STAT3 signaling pathway by modulating STAT3 expression. We found GTF2E1 knockout downregulated the expression level of STAT3 and subsequently reduced PD-L1 expression in HCC cells. Conversely, overexpression of GTF2E1 upregulated STAT3 expression and enhanced PD-L1 expression. It is indicated that GTF2E1 upregulated in HCC promotes tumor immune escape by increasing STAT3 expression to enhance PD-L1 expression.
Conclusion: Our study suggests that GTF2E1 has a crucial role in HCC immune escape by regulating the STAT3-PD-L1 axis, providing a potential therapeutic target for HCC immunotherapy. However, how GTF2E1 modulates STAT3 expression and transcriptional activity to regulate PD-L1 expression still needs further study. We hypothesize that GTF2E1 has the potential to bind to the promoter region of *STAT3* in hepatocellular carcinoma cells, which in turn affects STAT3 transcription and subsequent PD-L1 expression to facilitate tumor immune escape.

WED-414

Glypican-3-targeted orlistat-dopamine micelles enable programmed camptothecin delivery in hepatocellular carcinoma

Xiaqing Zhou[1], Shuangsuo Dang[1]. [1]*Second Affiliated Hospital of Xi'an Jiaotong University, Xi'an, China*
Email: xiaqingzhou@xjtu.edu.cn

Background and aims: Hepatocellular carcinoma (HCC) is marked by hypoxia and lipid-metabolic dependency, contributing to chemoresistance and dose-limiting toxicity. Building on our pH-responsive orlistat-dopamine conjugate micelles that trigger an early oxidative insult followed by camptothecin-mediated DNA damage, we developed an HCC-targeted nanomedicine and assessed antitumor efficacy and liver safety.
Method: Camptothecin-loaded orlistat-dopamine micelles were fabricated by solvent-in-water emulsification and surface-conjugated with a glypican-3-binding peptide. Nanoparticles were characterized for size, polydispersity index, zeta potential, encapsulation efficiency and pH-dependent release. Uptake and cytotoxicity were tested in Huh7, HepG2 under normoxia and hypoxia, with immortalized hepatocytes as a non-tumor control. Reactive oxygen species (ROS), monoamine oxidase (MAO) dependence and fatty acid synthase (FASN) inhibition were evaluated. Efficacy and tolerability were assessed in an orthotopic HCC mouse model.
Results: Targeted micelles had a diameter of 160 nm (polydispersity index 0.22) with 93% camptothecin encapsulation and accelerated release at pH 6.0 versus pH 7.4 (72% versus 44% at 8 h). Glypican-3 targeting increased uptake 2.8-fold ($p < 0.01$) and reduced the half-maximal inhibitory concentration of camptothecin by 28- to 65-fold under hypoxia across cell lines and organoids, while maintaining low cytotoxicity in hepatocytes. Mechanistically, micelles induced an early ROS surge that was partially rescued by MAO-B inhibition, decreased FASN activity and lipid droplet content, and enhanced DNA damage and apoptosis at later timepoints. In vivo, targeted micelles reduced orthotopic tumor bioluminescence by 74% versus free camptothecin at day 14 ($p < 0.01$), prolonged median survival (45 versus 28 days), and did not increase serum alanine aminotransferase or aspartate aminotransferase compared with controls.
Conclusion: Glypican-3-targeted orlistat-dopamine micelles provide tumor-directed, pH-responsive camptothecin delivery with dual metabolic and oxidative sensitization, achieving robust HCC control with preserved liver safety.

Liver tumours – Therapy

TOP-407-YI

Development and validation of a novel pretreatment MRI-based radiomic model to predict progression after thermal ablation in early stage hepatocellular carcinoma using data from two randomised control trials

Mathew Vithayathil[1], Paul Tait[1], Yuki Agarwala[1], Venkata Ramana Mallela[1], Sultan N. Alharbi[1], Samir Tariq[1], Amar Rai[1], Tim Hoogenboom[1], Osman Öcal[2], Matthias Fabritius[3], Maciej Pech[4], Thomas Berg[5], Christian Loewe[6], heinz-josef klümpen[7], Rafael Duran[8], Antonia Digkilia[8], Alban Denys[8], Rishi Patel[9], Xingfeng Li[1], Kristofer Linton-Reid[1], Mitchell Chen[1], Wenjia Bai[1], Jens Ricke[3], Naik Vietti-Violi[8], Andrea Rockall[1], Eric Aboagye[1], Max Seidensticker[3], Rohini Sharma[1]. [1]*Imperial College London, London, United Kingdom;* [2]*Sonderforschungsbereich Chirurgische Klinik Universitätsklinikum Heidelberg, Heidelberg, Germany;* [3]*Lmu Munich, München, Germany;* [4]*Otto-von-Guericke-Universität Magdeburg, Magdeburg, Germany;* [5]*Universitätsklinikum Leipzig, Leipzig, Germany;* [6]*Universitätsbibliothek der Medizinischen Universität Wien, Wien, Austria;* [7]*Amsterdam University Medical Center, Amsterdam, Netherlands;* [8]*Lausanne University Hospital, Lausanne, Switzerland;* [9]*Eastman Dental Hospital, London, United Kingdom*
Email: mathew.vithayathil@doctors.org.uk

Background and aims: Recurrence after thermal ablation in early-stage hepatocellular carcinoma (HCC) is high with a lack of clinical predictors. This study used pretreatment multiphase MRI-derived radiomic features to predict recurrence after ablation. Targeted RNA sequencing was used to determine drivers of radiomic signatures.
Method: 156 HCC patients undergoing ablation from the SORAMIC (NCT01126645) and Lausanne (NCT02859753) prospective phase 2 randomised control trials were reviewed. Radiomic features from pretreatment T1-weighted arterial, portal venous and delayed phase lesions were extracted. Radiomic models predicting 12-month recurrence for each phase were trained in the SORAMIC cohort using eight supervised machine learning models, including the state-of-the-art generative foundation model, TabPFN, and thirteen feature selection techniques. The best performing radiomic models were combined and integrated with clinical variables using ensemble learning. Patients were stratified using optimal threshold tuning. Model performance was externally validated in the independent Lausanne cohort. RNA sequencing was performed for radiomic risk-groups.
Results: The ensemble machine learning-based arterial phase radiomic model outperformed all clinical benchmarks and TabPFN in predicting recurrence in training (AUC 0.90, 95% CI 0.80–0.98) and external validation (AUC 0.74, 95% CI 0.61–0.87) cohorts. Arterial-portal venous and integrated radiomic-clinical models had comparable performance to the standalone arterial phase radiomic model. The arterial phase radiomic model stratified high-risk group had a significantly shorter median time-to-recurrence compared to the low-risk group in training (4.2 months, 95% CI 1.9–9.9 vs. 29.0 months, 95% CI 15.8–34.4; $p < 0.001$) and external validation (4.5

months, 95% CI 1.2–9.4 vs. 12.5 months, 95% CI 9.6–22.9; $p = 0.007$). Radiomic risk group was the only significant predictor of recurrence in multivariable Cox regression. Telomerase reverse transcriptase (TERT) expression was significantly enriched in the high-risk radiomic group.
Conclusion: Arterial phase radiomic-based models can predict recurrence after curative HCC ablation. Pretreatment MRI can identify patients at high-risk of recurrence for precision surveillance and adjuvant strategies.

TOP-408-YI
Efficacy and feasibility of neoadjuvant immunotherapy in hepatocellular carcinoma
Sarah Cappuyns[1,2], Antonio D'Alessio[1], Pasquale Lombardi[1,3], Claudia Fulgenzi[1], Aria Torkpour[1], Leonardo Brunetti[1,4], Pei-Chang Lee[1,5], Emily Warmington[1], Falah Jabar[1,6], Eleonora Alimenti[1,7], Emanuela Di Giacomo[1,8], Fionnuala Crowley[9], Joe Eid[10], Roxana Bucur[11], Shiva Babakhani[11], Jeroen Dekervel[2], Gonzalo Sapisochin[11,12], Grainne O'Kane[11,13], Mark Yarchoan[14], Marina Baretti[14], Thomas Marron[9], Julia Blanter[15], Yung-Yeh Su[16], Chiun Hsu[17], Ahmed Kaseb[10], David J. Pinato[1,18]. *[1]Imperial College London, Hammersmith Hospital, Du Cane Road, London, United Kingdom; [2]Digestive Oncology, Department of Gastroenterology, University Hospitals Leuven, Leuven, Belgium; [3]Phase 1 Unit, Fondazione Policlinico Universitario A. Gemelli, IRCCS, Università Cattolica del Sacro Cuore, Rome, Italy; [4]Operative Research Unit of Medical Oncology, Fondazione Policlinico Universitario Campus Bio-Medico, Rome, Italy; [5]Division of Gastroenterology and Hepatology, Department of Medicine, Taipei Veterans General Hospital, Taipei, Taiwan; [6]Department of Clinical Pathology, University Hospital of North Norway, Tromso, Norway; [7]Division of Gastroenterology and Hepatology, Foundation Ircss Ca' Granda Ospedale Maggiore Policlinico, Milan, Italy; [8]Division of Medical Oncology, Policlinico Universitario Campus Bio-Medico, Rome, Italy; [9]Tisch Cancer Institute, Icahn School of Medicine at Mount Sinai, New York, United States; [10]Department of Gastrointestinal Medical Oncology, Division of Cancer Medicine, The University of Texas MD Anderson Cancer Center, Houston, Texas, United States; [11]University Health Network, HPB Surgical Oncology, Toronto, Canada; [12]Department of Abdominal, General Surgery and Liver Transplantation, Hospital Universitario Vall d'Hebron, Vall d'Hebron Institute of Research, Barcelona, Spain; [13]St. Vincent's University Hospital, and School of Medicine, University College Dublin, Dublin, Ireland; [14]Johns Hopkins Hospital, Baltimore, United States; [15]Division of solid tumor oncology, memorial sloan kettering cancer center, New York, United States; [16]National Cheng Kung University Hospital, and Institute of Clinical Medicine, College of Medicine, National Cheng Kung University, Tainan, Taiwan; [17]National Taiwan University Hospital, and National Taiwan University Cancer Center, Taipei, Taiwan; [18]Division of Oncology, Department of Translational Medicine, University of Piemonte Orientale, Novara, Italy*
Email: sarahcappuyns@hotmail.com

Background and aims: Recurrence of hepatocellular carcinoma (HCC) occurs in up to 70% of patients post liver resection (LR). Early-phase trials confirm safety of neoadjuvant immune checkpoint inhibitors (nICI) pre-LR. However, long-term outcomes of nICI have not been described.
Method: We performed a patient-level, pooled analysis of phase I/II nICI trials, collected as part of a global collaborative consortium (NeoHCC). We estimated objective response (ORR) and disease control rate (DCR) by RECIST 1.1, described time to recurrence (TTR), recurrence free (RFS) and overall survival (OS) outcomes and identified predictors of RFS.
Results: Of 143 patients with HCC, most BCLC 0-A (89%), 45% had cirrhosis, most often due to viral etiologies (63%). Patients received 2.8 cycles (median 2; range 1–10) of ICI-doublet (60%) or monotherapy (30%) and underwent LR 3.8 weeks after the first nICI dose (median 2.5; range 0–21). Six patients (4%) did not undergo LR, of which only one due to disease progression. ORR was 22% and DCR was 92%. At median follow-up of 42 months (95% CI 37–46mo), 37.7% patients recurred, median TTR and OS were not reached (NR) and median RFS was 50 months (95% CI 29.5-NR). Improved RFS was associated with achieving major pathological response (HR 0.24; $p < 0.001$), while prior locoregional therapy was associated with worse RFS (HR 2.14; $p = 0.014$).
Conclusion: Extended follow-up of NeoHCC confirms feasibility and anti-tumour efficacy of nICI with drop-out rates of 4%. RFS post nICI is favourable and warrants prospective testing of this strategy in randomised controlled trials.

TOP-422
Epigenetic dysregulation of the IL1B-driven inflammatory program drives resistance to anti–PD-1 therapy in hepatocellular carcinoma
Wenying Qiao[1], Xuefeng Huang[1], Xiaoyan Ding[1], Xi Wang[1], Ronghua Jin[1,*]. *[1]Beijing Ditan Hospital, Capital Medical University, Beijing 100015, China, Beijing, China*
Email: qiaowenying459@163.com

Background and aims: Hepatocellular carcinoma (HCC) is a leading cause of cancer-related mortality globally, with anti-PD-1 immunotherapy emerging as a promising therapeutic strategy. However, the clinical efficacy of immune checkpoint blockade remains limited, primarily due to complex and poorly understood immune evasion mechanisms. As an inflammation-driven cancer, HCC is profoundly shaped by pro-inflammatory cytokines, yet the upstream mechanisms controlling aberrant interleukin-1β (IL-1β) expression and their impact on immunotherapy resistance remain unclear.
Method: Baseline peripheral blood mononuclear cells (PBMCs) from patients with advanced hepatitis B virus (HBV)–related HCC were profiled by single-cell RNA sequencing (scRNA-seq) and bulk RNA-seq. Spatial transcriptomics (ST) and multiplex immunofluorescence (mIF) from an independent cohort were integrated. Epigenetic regulation was assessed by Assay for Transposase-Accessible Chromatin using sequencing and H3K4me3 chromatin immunoprecipitation sequencing, and therapeutic relevance was evaluated in subcutaneous and orthotopic HCC models treated with anti–IL-1β and anti–PD-1, alone or in combination. Survival associations were validated using GSE16757 from the Gene Expression Omnibus and The Cancer Genome Atlas-Liver Hepatocellular Carcinoma cohort.
Results: Single-cell and bulk transcriptomic analyses revealed a distinct $IL1B^+$ $CD14^+$ monocyte subset enriched in non-responders to PD-1 therapy, characterized by heightened inflammatory activity. Chromatin accessibility profiling demonstrated epigenetic activation at the IL1B locus in non-responders. Mechanistically, the histone demethylase KDM5A restrained IL1B transcription by restraining H3K4me3 deposition and AP-1 recruitment at the IL1B promoter, a regulatory control preserved in responders but lost in non-responders. Functionally, IL-1β promoted $CD8^+$ T-cell exhaustion by inducing upregulation of PD-1 and TIM-3, while combined IL-1β and PD-1 blockade reduced tumor growth, decreased TAM infiltration, and restored cytotoxic T-cell activity in murine subcutaneous and orthotopic HCC models.
Conclusion: Our study identifies the KDM5A–AP-1–IL1B epigenetic-inflammatory axis as a critical mechanism of resistance to PD-1 therapy and highlights dual IL-1β/PD-1 inhibition as a promising therapeutic strategy to overcome resistance to PD-1 blockade in HCC.

FRI-217

Real-world effectiveness of Durvalumab plus Tremelimumab in hepatitis C-associated hepatocellular carcinoma: an Egyptian multicenter cohort study

Mohamed AbdAllah[1], Wael Abdel-Razek[2], Mohamed Hassany[3], Wafaa El-Akel[4], tamer Elbaz[4], Eman Rewisha[2], Shahira El-Etreby[5], Imam Waked[2], Gamal Esmat[4]. *[1]Medical Research and Clinical Studies Institute, National Research Center, Giza, Egypt; [2]Department of Hepatology and Gastroenterology, National Liver Institute, Menoufia University, Menoufia, Egypt; [3]National Hepatology and Tropical Medicine Research Institute, Ministry of Health and Population, Cairo, Egypt; [4]Endemic Medicine Department, Faculty of Medicine, Cairo University, Cairo, Egypt; [5]Specialized medical hospital, Mansoura Faculty of Medicine, Mansoura University, Mansoura, Egypt*
Email: dr.mohamedabda@gmail.com

Background and aims: The Phase III HIMALAYA trial established the STRIDE regimen (durvalumab plus tremelimumab) as first line option for unresectable hepatocellular carcinoma (HCC), demonstrating a median overall survival (OS) of 16.4 months. However, real-world data specifically characterizing the effectiveness of this regimen in hepatitis c virus (HCV)-predominant populations remains limited. This study evaluates the early clinical outcomes and survival determinants of the STRIDE regimen in a real-world cohort of Egyptian patients with HCV-associated HCC.
Method: We conducted a multicenter retrospective analysis of 255 patients with unresectable HCC treated with durvalumab/tremelimumab. To address real-world attrition, effectiveness was assessed using a composite clinical benefit rate (CBR), defined as radiologically confirmed disease control or sustained clinical stability on treatment for >30 days. Primary endpoints included OS and CBR.
Results: The cohort included 255 patients (median age 64 years; 76% male), predominantly with Child-Pugh A liver function. The objective response rate (ORR) was 14.9% and the disease control rate (DCR/CBR) was 49.8%. While numerically lower than the HIMALAYA trial benchmarks (ORR 20.1%, DCR 60.1%), this reflects real-world heterogeneity. The median OS was not reached (>12 months median follow-up), indicating a robust survival signal comparable to or potentially exceeding the 16.4 months observed in the HIMALAYA trial. Among patients with evaluable imaging (n = 110), those achieving disease control had significantly superior survival compared to those with progressive disease (median OS: not reached vs. 12 months; p = 0.003).
Conclusion: In this real-world HCV-associated HCC cohort, the STRIDE regimen demonstrated a favorable effectiveness and sustained survival benefit, with the median OS not yet reached. Although objective response rates were modest compared to clinical trial settings, the survival trajectory confirms the regimen's effectiveness in patients with HCV.

FRI-218

Digital twin–based in-silico randomized trial evaluating immunotherapy plus TARE versus immunotherapy alone in advanced hepatocellular carcinoma

Joseph Ahn[1], Mingzhao Hu[1], Sori Lundin[1], Michael Luu[2], Hyunseok Kim[2], Neehar D. Parikh[3], Amit Singal[4], Cui Tao[1], Ju Dong Yang[2]. *[1]Mayo Clinic, Rochester, United States; [2]Cedars-Sinai Medical Center, Los Angeles, United States; [3]University of Michigan, Ann Arbor, United States; [4]University of Texas, Southwestern, Dallas, United States*
Email: ahn.joseph@mayo.edu

Background and aims: Combination therapy with immunotherapy plus transarterial radioembolization (TARE) shows promise for advanced hepatocellular carcinoma (HCC), but a randomized controlled trial (RCT) directly comparing these treatments is lacking. Digital twin technology using generative AI on real-world data enables virtual trials and personalized predictions. The aim of this study was to conduct an in-silico RCT using diffusion-generated synthetic patients to compare immunotherapy alone versus combination therapy in advanced HCC, with validation against real-world evidence.
Method: A Tabular Denoising Diffusion Probabilistic Model was trained on National Cancer Database data from 4323 advanced HCC patients (2017–2021; immunotherapy n = 3772, combination n = 551) to generate 2000 high-fidelity synthetic patients (Wasserstein = 0.015, r = 0.98, zero copies). This synthetic cohort was randomized 1:1, and OS was predicted via conditional generation. Kaplan-Meier and Cox analyses were performed and validated against propensity score–matched real-world data. Counterfactual digital twins were also created to estimate individualized OS under the opposite treatment assignment.
Results: In the in-silico RCT, combination therapy yielded a 7.2-month increase in median OS compared with immunotherapy alone (15.0 vs 7.8 months; HR = 0.54, 95% CI 0.49–0.60). Propensity-matched real-world analysis validated these findings with a 7.5-month benefit (16.7 vs 9.2 months; HR = 0.62, 95% CI 0.54–0.71), consistent across subgroups. Counterfactual digital twin predictions showed that immunotherapy-only patients would gain 3.6 months if switched to combination therapy (95% CI 3.06–4.03), whereas combination-therapy patients would lose 5.4 months if switched to immunotherapy alone (95% CI 3.71–6.93).
Conclusion: This in-silico trial showed a clinically meaningful survival advantage with combination therapy in advanced HCC, corroborated by real-world validation. While prospective RCTs remain necessary, these convergent findings demonstrate feasibility for AI-driven in-silico trials and suggest potential benefit of immunotherapy plus TARE in appropriate patients.

FRI-219

Biological oncological resectability for treatment selection in hepatocellular carcinoma

Kenta Aso[1], Yoshinori Takeda[1], Hirofumi Ichida[1], Akio Saiura[1]. *[1]Juntendo University School of Medicine, Tokyo, Japan*
Email: k.aso.xy@juntendo.ac.jp

Background and aims: Barcelona Clinic Liver Cancer (BCLC) staging is the most widely used treatment algorithm for hepatocellular carcinoma (HCC) and provides robust prognostic stratification. With recent advances in perioperative and systemic therapies, anatomical oncological resectability criteria (ORC) based on surgical feasibility have been proposed in Japan. In real-world practice, treatment selection incorporates biological tumor factors such as serum alpha-fetoprotein (AFP). We compared the prognostic stratification performance of BCLC and ORC after integrating AFP.
Method: Patients undergoing initial hepatectomy for HCC (2009–2023) were classified by oncological resectability criteria (ORC: resectable [R], borderline resectable 1 [BR1], and borderline resectable 2 [BR2]) and BCLC staging. Overall survival (OS) was compared. Patients in the ORC R group and those with BCLC very early or early stage with AFP ≥ 500 were reclassified into BR1 and intermediate stage, respectively, and OS was re-evaluated.
Results: Among 404 patients undergoing initial hepatectomy, the ORC distribution was R (n = 338), BR1 (n = 25), and BR2 (n = 41), and BCLC staging classified patients as very early (n = 60), early (n = 263), intermediate (n = 71), and advanced (n = 10). 5-year OS was lower in BR1 and BR2 than in R patients (51.7% vs. 74.8%, p = 0.020; 40.0% vs. 74.8%, p < 0.001), with no difference between BR1 and BR2 (51.7% vs. 40.0%, p = 0.260). 5-year OS in intermediate and advanced stages was lower than in very early + early stages (54.7% vs. 74.2%, p = 0.010; 35.0% vs. 74.2%, p = 0.010), with no difference between intermediate and advanced stages (54.7% vs. 35.0%, p = 0.240). After integrating AFP ≥ 500 ng/mL, patients were classified as R (n = 283), biological-BR+BR1 (n = 80), and BR2 (n = 41). 5-year OS decreased stepwise (75.7% vs. 63.0% vs. 40.0%), with worse OS in biological-BR+BR1 than in R (p = 0.008) and better OS than in BR2 (p < 0.001). AFP-integrated BCLC staging classified patients as very early + early (n = 270),

biological-BR + intermediate (n = 124), and advanced (n = 10), with lower 5-year OS in biological-BR + intermediate than in very early + early (59.7% vs. 75.4%, p < 0.001) and no difference versus advanced (59.7% vs. 35.0%, p = 0.263).
Conclusion: Combining ORC with AFP may offer a useful framework for identifying patients at high risk of poor postoperative survival in resectable disease and for guiding consideration of preoperative therapy in patients with resectable HCC.

FRI-220
Changing trends in disease severity and advances in treatments of hepatocellular carcinoma in Germany from 2005 to 2019: a nationwide population-based study
Josune Cabello Calleja[1], Wenyi Gu[1,2,3], Robert Schierwagen[1], Maximilian Joseph Brol[1], Frank Uschner[1], Martin McCoy[1], Sabine Klein[1], Kai-Henrik Peiffer[1], Julia Fischer[1], Michael Köhler[4], Philipp Schindler[4], Klaus Wethmar[5], Andreas Pascher[6], Martina Holstein[6], Michael Praktiknjo[1], Anton Gillessen[7], Florian Rennebaum[1], Jonel Trebicka[1,8,9]. *[1]Department of Internal Medicine B, University Hospital Muenster, Muenster, Germany; [2]Department of Gastroenterology, Ren Ji Hospital, School of Medicine, Shanghai Jiao Tong University, Shanghai, China; Shanghai Institute of Digestive Disease, NHC Key Laboratory of Digestive Diseases, Shanghai, China; [3]Department of Internal Medicine I, University Hospital Frankfurt, Goethe University Frankfurt, Frankfurt, Germany; [4]Clinic for Radiology, University and University Hospital of Muenster, Muenster, Germany; [5]Department of Medicine A, Hematology, Oncology, Hemostaseology and Pneumology, University Hospital of Muenster, Muenster, Germany; [6]Clinic for General, Visceral and Transplant Surgery, University Hospital of Muenster, Muenster, Germany; [7]Department of Gastroenterology, Clinic for Internal Medicine, Herz-Jesu-Hospital, Muenster-Hiltrup, Germany; [8]Department of Gastroenterology and Hepatology, Odense University Hospital, Odense, Denmark; [9]European Foundation for Study of Chronic Liver Failure (E-CLIF), Barcelona, Spain*
Email: josune.cabello@ukmuenster.de

Background and aims: Hepatocellular carcinoma (HCC) is associated with complications and high mortality. Current management follows the Barcelona Clinic Liver Cancer algorithm. Since sorafenib approval in 2007, new therapeutic recommendations have been adopted, especially for systematic treatment of advanced HCC. We aimed to investigate the impact of complications and management on in-hospital mortality among HCC admissions.
Method: Using the diagnosis-related-groups and the German ICD/OPS codes, we analyzed hospital admissions with HCC during pre-checkpoint inhibitor era (2005–2020). The analysis focused on HCC-related complications, therapeutic interventions and all-cause in-hospital mortality. Trends were assessed with linear regressions and Mann-Whitney U-tests.
Results: Among 393,230 HCC hospitalizations in Germany, 117,787 admissions (30.0%) were associated with liver decompensations, especially ascites (21.6%). Bacterial infections exhibited the highest increase of 2.1-fold in 2016. In advanced stages, HCC admissions were complicated by organ failure, with respiratory failure (16,231 cases) showing the highest increase (6.2-fold in 2019), surpassing renal failure (33,936 cases; 2.9-fold in 2017). 126,980 HCC admissions received systemic treatment (42.5%), local-ablative (54.6%) or liver transplantation (LT) (2.8%). Local-ablative therapies—liver resection, ablation and transarterial treatments—were most frequently applied modalities in liver-limited HCC (56%), while systemic therapy consistently predominated in metastatic HCC. Among transarterial approaches, transarterial chemoembolization was more frequently performed than selective internal radiation (80.9%). Despite a higher number of liver resections performed, in-hospital mortality was comparable between resection (9.7 ± 1.4%) and LT (10.1 ± 2.4%), whereas systemic and transarterial therapies showed significantly lower mortality. Liver resection was linked to high rates of treatment-related infections (18.3%) and renal injury (10.1%), which were associated with a marked increase in mean in-hospital mortality (23.6 ± 5.8%).
Conclusion: Our study shows the natural history of HCC, and the central role of local-ablative therapies. It highlights the persistent need for more accurate and comprehensive pre-surgical evaluation due to ongoing treatment-related complications and associated high mortality, and transplant consideration as a curative treatment.

FRI-221
Similar overall survival but distinct response and safety profiles with Atezolizumab-Bevacizumab versus Durvalumab-Tremelimumab in advanced HCC
Claudia Campani[1], Victor Caudart[2], Lou-Devy Rouxel[3], Yann Touchefeu[4], Giuliana Amaddeo[5], Chloe Metivier[6], Leila Sadek[7], Marie Lequoy[8], Anna Pellat[9], Apolline Commin[6], Nathalie Ganne-Carrié[1], Clemence Hollande[2], Sarah Mouri[3], Pierre Malherbe[4], Hélène Regnault[5], Jean Marie Peron[7], Violaine Ozenne[8], Lucia Parlati[9], Sabrina Sidali[1], Paul Vigneron[5], Cecile Cussac[7], Romain Coriat[4], Isabelle Ollivier-Hourmand[6], Mathilde Wagner[3], Jean-Charles Nault[1], Manon Allaire[3], Mohamed Bouattour[2]. *[1]Centre de Recherche des Cordeliers, Sorbonne Université, Inserm, Université de Paris, team « Functional Genomics of Solid Tumors », F-75006 Paris, France, Paris, France; [2]AP-HP, Hôpital Beaujon, Liver Cancer and Innovative Therapy, CLICHY, France; [3]Hepatogastroenterology Department, La Pitié-Salpêtrière Hospital, AP-HP, Sorbonne Université, Paris, France, Paris, France; [4]Hepato-gastroenterology Department, Nantes University Hospital, Nantes, Institut des Maladies de l'Appareil Digestif (IMAD), Inserm CIC, 1413 Nantes, France, Nantes, France; [5]Service d'Hépatologie, AP-HP Henri Mondor, Créteil, France, Creteil, France; [6]Service d'hépato-gastroentérologie, CHU de Caen, ERN RARE-LIVER, France, Caen, France; [7]Service D'hépatologie, Hôpital Rangueil, CHU Toulouse, Toulouse, France, Toulouse, France; [8]Service d'Hépatologie, AP-HP Saint-Antoine, France, Paris, France; [9]Department of Gastroenterology and Digestive Oncology, Cochin Hospital, Assistance Publique - Hôpitaux de Paris, Paris 94800, Île-de-France, France, Paris, France*
Email: claudiacampani.cc@gmail.com

Background and aims: Immunotherapy-based combinations are the standard first-line treatment for advanced hepatocellular carcinoma (HCC), with atezolizumab–bevacizumab (AtezoBev) and durvalumab-tremelimumab (DurvaTreme) recommended options. Comparative real-world data between these regimens remain limited. We compared clinical outcomes, tumor response, and safety of AtezoBev versus DurvaTreme.
Method: This multicenter retrospective study (9 centers) included patients treated with first-line AtezoBev or DurvaTreme. Patients were matched 1:1 using propensity scores. Overall survival (OS), progression-free survival (PFS), disease control rate (DCR), objective response rate (ORR), and adverse events were analyzed.
Results: Among 1053 patients (908 treated with atezolizumab–bevacizumab and 145 with durvalumab–tremelimumab), 280 patients were included after matching. Baseline characteristics were well balanced between groups: approximately 60% had BCLC stage C disease, 35% had vascular invasion, 28% had extrahepatic spread, 60% were Child–Pugh class A, and 24% were ALBI grade 1. After a median follow-up of 20.1 months, OS was similar between AtezoBev and DurvaTreme (median 20.8 months vs. not reached; $p = 0.25$), while PFS was longer with AtezoBev (8.2 vs. 4.7 months; $p = 0.006$). DCR was higher with AtezoBev at first (80.2% vs. 52.4%) and best imaging response (81.0% vs. 54.1%; both $p < 0.001$), whereas ORR did not differ. Higher baseline albumin was independently associated with improved OS and PFS. Treatment type was not associated with OS, but DurvaTreme was independently associated with increased risk of progression (HR 1.49, $p = 0.006$). The presence of ≥3 tumor nodules was independently associated with lower ORR (OR 0.51, p = 0.031), and DurvaTreme was also associated with reduced ORR (OR 0.52, p = 0.038). In treatment-stratified analyses, ≥3 tumor nodules were

associated with a significantly lower ORR in the AtezoBeva cohort (OR 0.37, p = 0.017), while MASLD was associated with reduced ORR in the DurvaTreme cohort (OR 0.33, p = 0.033).
Conclusion: These findings support a tailored selection of first-line immunotherapy in advanced HCC based on liver function, tumor burden, and patient-specific characteristics. Further studies are needed to identify predictive factors of response in order to optimize treatment selection.

FRI-225
Durvalumab–Tremelimumab in advanced hepatocellular carcinoma: real-world data From the LOR-HCC (Lombardy, Italy real-world HCC group)

Andrea Casadei Gardini[1], Lorenzo Canova[2], Chiara Mazzarelli[3], Silvia Camera[1], Elisa Bocchero[4,5], Pietro Pozzoni[6], Sara Vavassori[7], Salvatore Corallo[8], Massimo De Giorgio[9], Anna Maria Stagno[10], Giulia Grizzi[11], Rita Cengarle[12], Gianluca Tomasello[13], Mariangela Bruccoleri[14], Katia Bencardino[15], Mara Persano[1], Martina Pino[4,5], Alessia Riva[6], Martina Torchio[16], Elena Rota Caremoli[17], Lorenzo Argiento[14], Federica Tosi[15], Margherita Rimini[1], Tiziana Pressiani[5], Lorenza Rimassa[4,5], Massimo Iavarone[14,18]. *[1]Department of Oncology, Vita-Salute San Raffaele University, IRCCS San Raffaele Scientific Institute Hospital, Milan, Italy; [2]Division of Hepatology, San Giuseppe Hospital, IRCCS MultiMedica, Milan, Italy; [3]Hepatology and Gastroenterology Unit, ASST Grande Ospedale Metropolitano Niguarda, Milan, Italy; [4]Department of Biomedical Sciences, Humanitas University, Pieve Emanuele (Milan), Italy; [5]Humanitas Cancer Center, IRCCS Humanitas Research Hospital, Rozzano (Milan), Italy; [6]Hepatology Unit, Department of Medicine, Alessandro Manzoni Hospital, ASST Lecco, Lecco, Italy; [7]Hepatology Division, ASST Santi Paolo e Carlo, Milan, Italy; [8]Medical Oncology, IRCCS Policlinico San Matteo, University of Pavia, Pavia, Italy; [9]Gastroenterology Hepatology and Transplantation Unit, ASST Papa Giovanni XXIII, Bergamo, Italy; [10]Medical Oncology, Foundation IRCCS San Gerardo dei Tintori, Monza, Italy; [11]Medical Oncology, ASST Cremona, Cremona, Italy; [12]Complex Medical Oncology Unit, ASST Mantova, Carlo Poma Hospital, Mantova, Italy; [13]Medical Oncology Unit, ASST Ospedale Maggiore di Crema, Crema, Italy; [14]Division of Gastroenterology and Hepatology, Foundation IRCCS Ca' Granda Ospedale Maggiore Policlinico, Milan, Italy; [15]Niguarda Cancer Center, Grande Ospedale Metropolitano Niguarda, Milan, Italy; [16]Medical Oncology Unit, ASST Santi Paolo e Carlo, Milan, Italy; [17]Medical Oncology Division, ASST Papa Giovanni XXIII, Bergamo, Italy; [18]CRC "A. M. and A. Migliavacca" Center for Liver Disease, Department of Pathophysiology and Transplantation, University of Milan, Milan, Italy*
Email: massimo.iavarone@gmail.com

Background and aims: Dual immune checkpoint blockade with tremelimumab plus durvalumab (STRIDE) is an established first-line therapy for unresectable hepatocellular carcinoma (uHCC), but real-world evidence on safety, toxicity kinetics, and liver function dynamics remains limited. We aimed to evaluate tolerability, on-treatment changes in hepatic function and effectiveness, in a multicenter cohort of patients treated with STRIDE in routine practice.
Method: We conducted a retrospective analysis of prospectively collected data from 115 consecutive patients with uHCC treated with STRIDE across 12 centers in Lombardy, Italy. Clinical, biochemical, and radiological variables were recorded at baseline and throughout therapy. Adverse events were graded per CTCAE v5.0, and Child–Pugh was used to assess hepatic functional evolution. Temporal toxicity patterns were evaluated using smoothed hazard functions. Progression-free survival (PFS), overall survival (OS), and competing-risk cumulative incidence of progression and death were examined.
Results: Median follow-up was 8.9 months. More than 80% of adverse events occurred within the first 2 months; severe toxicities were infrequent. Child–Pugh deterioration from class A to B occurred in 7.8% of patients from baseline to day 28, increasing to 12.1% by day 56,. PFS was 5.7 months; median OS was not reached, with OS rates of 78.2% at 6 months and 53.3% at 18 months. Progression was the predominant early event, with cumulative incidence of 49.2% at 6 months.
Conclusion: In routine clinical practice, STRIDE shows reproducible effectiveness and a manageable safety profile, with adverse events incidence clustering early and stabilizing thereafter. Dynamic assessment of liver function shows that hepatic function declines modestly but still clinically meaningfully in affected patients.

FRI-226
Multimodal deep learning for predicting early progression in advanced hepatocellular carcinoma treated with atezolizumab-bevacizumab

Ciro Celsa[1], Salvatore Contino[2], Roberto Cannella[3], Simona Restuccia[1], Gaia Crescimanno[1], Luca Cruciata[2], Roberta Ciccia[1], Gaetano Giusino[1], Guido Cusimano[1], Sofia Calascibetta[1], Alessio Quartararo[1], Aurora Nicolosi[1], Giuseppe Cabibbo[1], Giansalvo Cirrincione[4], Roberto Pirrone[2], Calogero Cammà[1]. *[1]Section of Gastroenterology and Hepatology, Department of Health Promotion, Mother and Child Care, Internal Medicine and Medical Specialties, University of Palermo, Palermo, Italy; [2]Department of Engineering, University of Palermo, Palermo, Italy; [3]Department of Biomedicine, Neuroscience and Advanced Diagnostics (BiND), University of Palermo, Palermo, Italy; [4]Université de Picardie Jules Verne, Amiens, Amiens, France*
Email: calogero.camma@unipa.it

Background and aims: Atezolizumab plus bevacizumab has emerged as the standard first-line therapy for advanced HCC, yet individual response remains heterogeneous and difficult to predict. We developed a multimodal artificial intelligence framework integrating clinical data and computed tomography imaging to predict six-month progression-free survival in patients receiving atezolizumab-bevacizumab.
Method: We retrospectively analysed 62 patients with advanced HCC treated with first-line atezolizumab-bevacizumab at a tertiary referral centre (University of Palermo, Italy). A deep learning architecture combining a convolutional neural network for CT image analysis (arterial, venous, and delayed phases) with a multilayer perceptron for structured clinical variables was developed. The model was trained to predict progression-free survival status at six months. Performance was evaluated using accuracy, precision, recall, F1-score, balanced accuracy, and area under the receiver operating characteristic curve. Results were compared with conventional logistic regression incorporating clinical variables alone.
Results: After a median follow-up of 15.9 months, median overall survival was 24.3 months (95% CI: 15.9–38.0). Twenty-three patients (37.1%) experienced progression or death within six months. The multimodal model achieved an AUC of 0.86, with 80.1% accuracy, 84.7% specificity, 68.9% sensitivity, 67.0% F1-score, and 76.8% balanced accuracy. In contrast, traditional logistic regression yielded an AUC of 0.67 (95% CI: 0.54–0.78), with neoplastic portal vein invasion showing a trend toward significance (OR: 2.79, 95% CI: 0.98–7.92, p = 0.053) in multivariable analysis.
Conclusion: A multimodal artificial intelligence approach integrating CT imaging with clinical data demonstrates promising capability in predicting early disease progression in HCC patients treated with atezolizumab-bevacizumab. While preliminary and requiring external validation, these findings suggest that deep learning frameworks may enhance risk stratification and support personalized treatment decisions in advanced hepatocellular carcinoma.

FRI-227

Multimodal deep learning for therapeutic decision support in hepatocellular carcinoma: integrating clinical data and computed tomography imaging

Ciro Celsa[1], Salvatore Contino[2], Mauro Giuffrè[3], Roberto Cannella[4], Simona Restuccia[1], Luca Cruciata[2], Alessandro Grova[1], Gaetano Giusino[1], Guido Cusimano[1], Sofia Calascibetta[1], Alessio Quartararo[1], Francesco Mercurio[1], Claudia La Mantia[1], Giuseppe Cabibbo[1], Giansalvo Cirrincione[5], Roberto Pirrone[2], Calogero Cammà[1]. [1]*Section of Gastroenterology and Hepatology, Department of Health Promotion, Mother and Child Care, Internal Medicine and Medical Specialties, University of Palermo, Palermo, Italy;* [2]*Department of Engineering, University of Palermo, Palermo, Italy;* [3]*Department of Medical, Surgical, and Health Sciences, University of Trieste, Trieste, Italy;* [4]*Department of Biomedicine, Neuroscience and Advanced Diagnostics (BiND), University of Palermo, Palermo, Italy;* [5]*Université de Picardie Jules Verne, Amiens, Amiens, France*
Email: calogero.camma@unipa.it

Background and aims: Multidisciplinary management of hepatocellular carcinoma (HCC) requires complex decision-making integrating tumor burden, liver function, and performance status. Although multidisciplinary management can improve outcomes, it is resource-intensive and not universally feasible. We developed a multimodal deep learning framework integrating clinical text reports and computed tomography (CT) imaging to predict therapeutic decisions in HCC patients.

Method: We retrospectively analyzed 240 unstructured clinical reports with corresponding CT images from 204 patients evaluated at a tertiary referral center between September 2020 and November 2024. Therapeutic decisions were classified into seven categories: liver transplantation, surgical resection, percutaneous ablation, transarterial treatments, systemic therapy, best supportive care, and continued follow-up. A multimodal architecture combining BioBERT for clinical text analysis with a convolutional neural network for CT image feature extraction was developed. The model was trained using an 80:20 split and evaluated using accuracy, sensitivity, specificity, precision, F1-score, and balanced accuracy.

Results: The cohort included 204 patients (mean age 71.6 ± 10.3 years, 71.2% male). Therapeutic decisions comprised transplantation (3.8%), resection (5%), ablation (7%), transarterial treatments (8.7%), systemic therapy (32%), best supportive care (22%), and follow-up (21.2%). The multimodal model achieved 95.5% overall accuracy, 95.0% sensitivity, 94.0% precision, 94.4% F1-score, 95.0% balanced accuracy, and 84.7% specificity in replicating expert clinical decisions. The confusion matrix demonstrated excellent discrimination across all therapeutic classes, with minimal misclassification between treatment categories.

Conclusion: A multimodal artificial intelligence framework integrating unstructured clinical reports and radiological imaging accurately predicts therapeutic decisions in HCC with performance exceeding 95%. While requiring prospective validation and interpretability enhancement, this approach demonstrates potential as a clinical decision support tool to standardize care, optimize multidisciplinary team workflows, and support evidence-based treatment selection in HCC management.

FRI-228-YI

Dose–response relationship and clinical outcomes after Yttrium-90 transarterial radioembolization for hepatocellular carcinoma: GALAXY-90 study

Kaina Chen[1,2], Xinyu Chen[3], Aaron Kian Ti Tong[4], Kheng Choon Lim[5], Kelvin Siu Hoong Loke[1,4], Shay Lee Chong[3], Fiona Ni Ni Moe[3], Imperial Edeliza Santiago Ria[6], Yang Lu[1,6], David Chee Eng Ng[4], Apoorva Gogna[7], Richard Hoau Gong Lo[7], Sue Ping Thang[4], Brian Goh[6], Han Chong Toh[8], Choon Hua Thng[9], Wan Ying Chan[9], Shuting Han[8], Karaddi Venkatanarasimha Nanda Kumar[7], Sivanathan Chandramohan[7], Winnie Wing Chuen Lam[4], Kun Da Zhuang[7], Hian Liang Huang[4], Chow Wei Too[7], Butch Maulion Magsombol[4], Siou Sze Chua[3], Ashley Weng Yan Ng[3], Jade Shu Qi Goh[3], Evelyn Chiew[3], Cheryl Min En Chua[3], Rachel Xin Hui Teo[3], Pierce Chow[6,10]. [1]*Duke-Nus Medical School, Singapore, Singapore;* [2]*Department of Gastroenterology and Hepatology, Singapore General Hospital, Singapore, Singapore;* [3]*Program in Clinical and Translational Liver Cancer Research, National Cancer Center Singapore, Singapore, Singapore;* [4]*Department of Nuclear Medicine & Molecular Imaging, Singapore General Hospital, Singapore, Singapore;* [5]*Department of Diagnostic Radiology, Singapore General Hospital, Singapore, Singapore;* [6]*Department of Hepatopancreatobiliary and Transplantation Surgery, Singapore General Hospital and National Cancer Centre Singapore, Singapore, Singapore;* [7]*Department of Vascular and Interventional Radiology, Singapore General Hospital, Singapore, Singapore;* [8]*Department of Medical Oncology, National Cancer Centre Singapore, Singapore, Singapore;* [9]*Division of Oncologic Imaging, National Cancer Centre Singapore, Singapore, Singapore;* [10]*Surgery Academic Clinical Program, Duke-NUS Medical School, Singapore, Singapore*
Email: pierce.chow@duke-nus.edu.sg

Background and aims: Yttrium-90 transarterial radioembolization (Y-90 TARE) has evolved from palliation to curative intent for hepatocellular carcinoma (HCC) with higher doses. The Generalized Analysis of Locoregional Approach by eXamining outcomes with Yttrium-90 (GALAXY-90) study is the first in Asia, where larger HCC is more prevalent, to evaluate the dose-response relationship across a broad range of tumour doses within two evaluation time windows.

Method: We retrospectively analyzed consecutive patients with solitary HCC with or without portal vein invasion treated with Y-90 TARE at National Cancer Centre Singapore and Singapore General Hospital (2019–2024). Tumor response was evaluated using localized mRECIST; best objective and disease-control rates (BORR, BDCR) were assessed at ≤ 6 and ≤ 9 months. Overall survival (OS) and progression-free survival (PFS) were analyzed using the Kaplan–Meier method. Safety was evaluated by adverse events (AEs) graded per CTCAE v5.0.

Results: Among 429 patients who received Y-90 during the study period, 110 patients were included (median tumor size 6.6 cm). Predicted mean doses were stratified into <120, 120–200, 200–300, and ≥300 Gy (median 191 Gy, range 41.2–647.8). From ≤ 6 to ≤ 9 months, overall BORR improved from 78.0% to 91.7%, with significant trends across the four dose intervals ($p = 0.003$; $p = 0.019$). Complete response rose from 13.8% to 34.9% between ≤ 6 to ≤ 9 months evaluations. Doses ≥ 200 Gy achieved significantly higher BORR than < 200 Gy ($p = 0.002$ at ≤ 6 m; $p = 0.004$ at ≤ 9 m). In the paired-window subset ($n = 88$), late responders between 6 and 9 months accounted for the BORR improvement ($p = 0.002$). Overall BDCR remained 99.0%, reaching 100% in doses ≥120 Gy ($p = 0.174$). Median OS and PFS were 44 (95% CI 38–61) and 16 months (95% CI 13–26), respectively. AEs were infrequent and showed no dose-dependence ($p > 0.05$).

Conclusion: Our GALAXY-90 study identifies ≥ 200 Gy as a threshold for optimal tumor response without added toxicity for large HCCs. Extending follow-up to 9 months captured late responders, supporting a policy of threshold-dose escalation and extended response assessment in Y-90 for HCC, achieving high BORR.

FRI-229

Application and evaluation of whole process management model for liver cancer patients undergone Yttrium-90 selective internal radiation therapy (Y-90 SIRT): a retrospective cohort study

Xiaolong Chen[1], Quan Jiang[1], Kangshou Liu[1], Xuejiao Li[2], Zhiwei Chen[1], Zhilong Liu[1]. [1]*Department of Hepatobiliary surgery, The First Affiliated Hospital of Jinan University, GuangZhou, China;* [2]*Department of Hepatology lab, The Third Affiliated Hospital of Sun Yat-sen University, GuangZhou, China*
Email: chxl1446@126.com

Background and aims: To construct a comprehensive and standardized whole-process management model for liver cancer patients undergoing Yttrium-90 selective internal radiation therapy (Y-90 SIRT) and systematically evaluate its clinical efficacy, safety, and impact on medical resource utilization.
Method: A retrospective cohort study was conducted on 365 liver cancer patients who received Y-90 SIRT at The First Affiliated Hospital of Jinan University from August 2022 to October 2025. Excluding those who were lost to follow-up, did not complete the questionnaire, or participated in the Y-90 SIRT clinical trial, 314 patients were enrolled in this study. Patients were divided into the intervention group (163 cases, January2025–October 2025) receiving the whole-process management model and the control group (151 cases, August 2022–December 2024) receiving routine management. Incidence of adverse events (AEs), patient satisfaction, postoperative self-rating anxiety and depression scores, length of hospital stay, and hospitalization costs were assessed between groups.
Results: Baseline characteristics were comparable between the two groups ($P > 0.05$). The overall incidence of adverse events (AEs) in the intervention group was 11% (18/163), which was significantly lower than that in the control group (30%, 45/151; $P < 0.001$). Moreover, the intervention group exhibited notably lower scores on the Self-Rating Anxiety Scale (42.73 ± 6.51 vs. 48.08 ± 8.98, $P = 0.001$) and Self-Rating Depression Scale (48.54 ± 6.75 vs. 50.83 ± 8.25, $P = 0.007$), along with a significantly higher patient satisfaction score (25.63 ± 2.81 vs. 23.06 ± 2.9, $P < 0.001$). Additionally, the average hospitalization cost was lower in the intervention group than in the control group (¥405602 ± 62967 vs. ¥414674 ± 66035, $P = 0.0134$).
Conclusion: The whole-process management model for liver cancer patients undergoing Y-90 SIRT significantly reduces the incidence of adverse events, ameliorates patients' psychological status, improves patient satisfaction and optimizes medical resource utilization.

FRI-230
Impact of palliative care on end-of-life healthcare utilization among Asian patients with hepatocellular carcinoma
Matthew Shing Hin Chung[1], Rex Wan-Hin Hui[1], Lu Li[1], Xianhua Mao[2], CL Chiang[3], Carlos King Ho Wong[4,5], Ian Chi Kei Wong[6,7,8], Ka Shing Cheung[1], Stephen Chan[9], Man-Fung Yuen[1,10], Wai-Kay Seto[1,10,11], Lung-Yi Mak[1,10]. *[1]Department of Medicine, School of Clinical Medicine, The University of Hong Kong, Pok Fu Lam, Hong Kong; [2]Department of Medicine, Stanford University, Stanford, United States; [3]Department of Clinical Oncology, School of Clinical Medicine, The University of Hong Kong, Pok Fu Lam, Hong Kong; [4]Department of Infectious Disease Epidemiology & Dynamics, Faculty of Epidemiology and Population Health, London School of Hygiene and Tropical Medicine, London, United Kingdom; [5]School of Public Health, The University of Hong Kong, Pok Fu Lam, Hong Kong; [6]Department of Pharmacology and Pharmacy, The University of Hong Kong, Pok Fu Lam, Hong Kong; [7]Aston Pharmacy School, Aston University, Birmingham, United Kingdom; [8]Advanced Data Analytics for Medical Science (ADAMS) Limited, Hong Kong, Hong Kong; [9]State Key Laboratory of Translational Oncology, Department of Clinical Oncology, Sir YK Pao Centre for Cancer, Prince of Wales Hospital, The Chinese University of Hong Kong, Shatin, Hong Kong; [10]State Key Laboratory of Liver Research, The University of Hong Kong, Pok Fu Lam, Hong Kong; [11]Department of Medicine, The University of Hong Kong-Shenzhen Hospital, Shenzhen, China*
Email: matttcsh@connect.hku.hk

Background and aims: While palliative care (PC) is important in the management of hepatocellular carcinoma (HCC), its impact on the end-of-life healthcare utilisation is less clear.
Method: Patients diagnosed with HCC who had never received any oncological treatment and who have died between 2003 and 2024 were identified from a territory-wide electronic database in Hong Kong. Patients were classified into PC group (those who received any specialist PC consultation or inpatient hospice service within the last 3 months of life) or non-PC group (those who did not have any PC utilization). Data on intensive care unit (ICU) admission, resuscitation (cardiopulmonary resuscitation or intubation), nerve block, and use of opioid analgesics (including strong/ weak opioids) were evaluated. To evaluate the disease time burden, we assessed percentage of days at home (%DAH), defined as the percentage of time not requiring healthcare utilization (inpatient or emergency department admissions, day procedures, blood tests, and imaging) in the 3 months preceding death.
Results: This study included 2254 patients in the PC group (mean age 69.6 years, 74.3% male, 61.5% with viral hepatitis, mean AFP 37,395.5 ng/mL) and 9962 in the non-PC group (mean age 68.4 years, 77.1% male, 62.3% with viral hepatitis, mean AFP 43,988.6 ng/mL). PC utilization, when compared with patients without PC, was associated with lower rates of ICU admission (0.3% vs 1.1%, $p < 0.001$) and resuscitation (0.4% vs 2.7%, $p < 0.001$). PC was associated with increased use of opioid analgesics (66.8% vs 32.5% in non-PC group, $p < 0.001$), with a similar pattern for both strong opioids (45.7% vs 18.2% in non-PC group, $p < 0.001$) and weak opioids (44.5% vs 24.4% in non-PC group, $p < 0.001$). PC had no significant impact on the utility of nerve blocks ($p = 0.570$). The %DAH were 45.0% and 40.6% in the PC and non-PC groups, respectively ($p < 0.001$), and PC contact was an independent predictor of %DAH ≥50% (OR 1.14, 95%CI 1.03–1.26).
Conclusion: PC contact significantly reduced disease time burden. Furthermore, PC was associated with reduced use of aggressive therapies (ICU admission and resuscitation), and increased use of opioid analgesics. Our findings highlight the potential quality-of-life benefits of PC in the end-of-life care of HCC.

FRI-231
Clinical determinants of survival beyond two years in HCC patients receiving non-curative treatment
Burcu Gürbüz[1], Mustafa Utku Maraşlı[2], Hasan Sahin[2], Muhammet Furkan Çakmak[1], Bengi Ozturk[1], Taylan Kav[1], Onur Keskin[1]. *[1]Hacettepe University Faculty of Medicine, Department of Gastroenterology and Hepatology, Ankara, Türkiye; [2]Hacettepe University Faculty of Medicine, Department of Internal Medicine, Ankara, Türkiye*
Email: drburcuusta@gmail.com

Background and aims: Hepatocellular carcinoma (HCC) is a leading cause of cancer mortality. In patients not eligible for curative therapy, outcomes remain heterogeneous in real-world populations, and a subset of patients experience unexpectedly prolonged survival. We aimed to describe the clinical profile of patients who survived ≥2 years from diagnosis while managed with non-curative first-line therapy, and to identify predictors of long-term survival.
Method: We retrospectively included HCC patients followed at Hacettepe University Gastroenterology and Hepatology Clinic between January 2015–September 2023. Of 349 patients, 282 received non-curative first-line therapy. Long-term survival was defined as overall survival (OS) ≥2 years; predictors were assessed by backward stepwise multivariable logistic regression.
Results: A total of 282 patients received non-curative treatment were included. Median age was 65 years(25–90) and median OS was 15 months (0–168). Overall, 104/282(36.9%) had OS ≥2 years and 178/282(63.1%) had OS <2 years. The cohort was predominantly male (218/282, 77.3%); sex was not associated with OS ≥2 years($p = 0.175$). In univariate analysis, long-term survivors more often had ECOG 0–1 (85.6% vs 62.9%; $p < 0.001$), less tumor thrombus at diagnosis (23.1% vs 43.3%; $p < 0.001$), largest lesion <5 cm (76.0% vs 50.0%; $p < 0.001$), GGT <80 (52.9% vs 30.9%; $p < 0.001$), locoregional modalities (RFA/TARE/TACE) (87.5% vs 71.3%; $p = 0.001$), MASH etiology (15.4% vs 7.9%; $p = 0.048$) and platelet <150 × 109/L (60.6% vs 39.3%; $p < 0.001$). On ROC analysis, platelet 149.5×109/L was the optimal cut-off for OS ≥2 years. Logistic regression was performed in 274/282 (97.2%) with complete covariates (OS ≥2 years: 99; OS <2 years: 175). In final stepwise model, independent associations with OS ≥2 years were ECOG 0–1 (vs 2–3) OR 3.12 (95% CI 1.59–6.12;$p = 0.001$), GGT <80 (vs

≥80) OR 2.35 (95% CI 1.35–4.10;p = 0.003), and platelet <150 × 109/L (vs ≥150) OR 1.92 (95% CI 1.09–3.33;p = 0.026). Tumor size <5 cm (OR 1.76; 95% CI 0.96–3.24; p = 0.067) and absence of tumor thrombus (OR 1.74; 95% CI 0.96–3.16; p = 0.068) showed borderline significance.
Conclusion: In this cohort of non-curatively treated HCC patients, more than one-third survived ≥2 years. Long-term survival was independently associated with better performance status (ECOG 0–1), lower GGT, and lower platelet suggesting a distinct long-survivor phenotype among patients receiving non-curative first-line therapy.

FRI-232

Imaging-detected immune-related adverse events and clinical outcomes during Atezolizumab–Bevacizumab therapy in unresectable hepatocellular carcinoma: a dual-center study

Subin Heo[1], Jeayeon Park[2], Sang Hyun Choi[1], Dong Ho Lee[2]. *[1]Asan Medical Center, Seoul, Korea, Rep. of South; [2]Seoul National University Hospital, Seoul, Korea, Rep. of South*
Email: dhlee.rad@snu.ac.kr

Background and aims: Immune checkpoint inhibitors (ICIs) combined with bevacizumab constitute a standard first-line therapy for unresectable hepatocellular carcinoma (HCC). Emerging evidence suggests that immune-related adverse events (irAEs) are linked to improved treatment outcomes. However, the prognostic value of imaging-detected irAEs remains unclear. This study evaluated the incidence and clinical impact of imaging-detected irAEs during atezolizumab plus bevacizumab therapy.
Method: This retrospective dual-center study included consecutive patients with unresectable HCC treated with first-line atezolizumab plus bevacizumab. Serial follow-up CT or MRI examinations were systematically reviewed to identify imaging-detected irAEs. Objective response rate (ORR), overall survival (OS), and progression-free survival (PFS) were compared between patients with and without imaging-detected irAEs.
Results: Among 386 eligible patients, 44 (11.4%) developed imaging-detected irAEs. Most events (81.8%, 36/44) occurred within 6 months after treatment initiation (Median time-to-ocurrence: 3.3 months), and 90.9% (40/44) resolved on subsequent follow-up imaging, indicating transient phenomenon. Pulmonary infiltrations (n = 23) were the most frequent irAE, followed by bowel wall thickenings (n = 13). Patients with imaging-detected irAEs demonstrated significantly better treatment outcomes than those without irAEs. ORR was higher in the irAE group (43.2% vs. 22.5%; P = .005). After inverse probability of treatment weighting adjustment, both OS and PFS were significantly improved in the irAE group (OS: hazard ratio [HR], 0.62; 95% CI, 0.44–0.89; P = .008; PFS: HR, 0.60; 95% CI, 0.44–0.82; P = .001).
Conclusion: Imaging-detected irAEs are associated with favorable clinical outcomes in unresectable HCC and may serve as a prognostic indicator during atezolizumab plus bevacizumab therapy.

FRI-233

Pretreatment neutrophil-to-lymphocyte ratio as a predictive marker for tumor response to Atezolizumab plus Bevacizumab in hepatocellular carcinoma: a multicenter retrospective study

Young Mi Hong[1], Jun Sik Yoon[2], Yu Rim Lee[3], Jaehyun Yoon[4], Hyun Young Woo[5], Sang Youn Hwang[6], Yeo Wool Kang[7], Joonho Jeong[8], Jeong Eun Song[9], Sung Bum Cho[10]. *[1]Department of Internal Medicine, Pusan National University School of Medicine, Pusan National University Yangsan Hospital, Yangsan, Korea, Rep. of South; [2]Busan Paik Hospital, Inje University College of Medicine, Busan, Korea, Rep. of South; [3]School of Medicine, Kyungpook National University, Kyungpook National University Hospital, Daegu, Korea, Rep. of South; [4]Chonnam National University Hospital, Gwangju, Korea, Rep. of South; [5]College of Medicine, Pusan National University, Busan, Korea, Rep. of South; [6]Dongnam Institute of Radiologic & Medical Sciences, Busan, Korea, Rep. of South; [7]Department of Internal Medicine, Dong-A University College of Medicine, Busan, Korea, Rep. of South; [8]Ulsan University Hospital, University of Ulsan College of Medicine, Ulsan, Korea, Rep. of South; [9]Daegu Catholic University Medical Center, Daegu, Korea, Rep. of South; [10]Chonnam National University Hwasun Hospital, Gwangju, Korea, Rep. of South*
Email: 00gurum@hanmail.net

Background and aims: Atezolizumab combined with bevacizumab has been used in the treatment of advanced hepatocellular carcinoma (HCC). However, reliable predictive biomarkers for evaluating tumor response to this therapy remain limited. This study aimed to identify predictive factors in patient with HCC undergoing treatment with atezolizumab and bevacizumab.
Method: This multicenter retrospective study included 943 patients with HCC who received atezolizumab plus bevacizumab. Factors associated with tumor response were analyzed.
Results: According to the Response Evaluation Criteria in Solid Tumors, the rates of complete remission, partial response, stable disease, and progressive disease were 2.9%, 22.9%, 48.8% and 25.5%, respectively. The objective response rate (ORR) and disease control rate (DCR) were 25.8% and 74.6%, respectively. Progression free survival and overall survival were significantly associated with best tumor response ($P < 0.001$). Multivariate analysis identified BCLC stage (HR = 0.478, 95% CI = 0.278–0.821, $P = 0.007$) and neutrophil-to-lymphocyte ratio (NLR) (HR = 0.670, 95% CI = 0.488–0.920, $P = 0.013$) as independent predictive factors for objective tumor response. The ORR and DCR were 31.2% and 77.2%, respectively, in the NLR <2 group, and 23.7% and 73.5%, respectively, in the NLR ≥ 2 group ($P < 0.001$).
Conclusion: Pretreatment NLR was correlated with the tumor response, which was subsequently associated with survival outcomes. NLR may serve as a predictor of a lack of response to atezolizumab plus bevacizumab treatment. Therefore, NLR represents a readily measurable biomarker with the potential to support the timely identification of HCC patients who are more likely to benefit from atezolizumab and bevacizumab treatment.

FRI-234

Transjugular intrahepatic portosystemic shunt as a bridging strategy to hepatocellular carcinoma treatment in patients with refractory ascites or hydrothorax

Camille Imparato[1], Marika Rudler[2], Jihyun An[3], Josune Cabello Calleja[4], Maria Nieto[5], Charlotte Bouzbib[2], Hélène Larrue[6], Valentin Rolle[7], Coralie Fleurent[8], Hélène Regnault[9], Mehdi Younes[10], Suliman Alhaidari[11], Magdalena Meszaros[12], Coskun Ozer Demirtas[13,14], Osama Khattab[15], Paul Girot[16], Louise Lebedel[17], Sarah Mouri[2], Ju Hyun Shim[18], Michael Praktiknjo[4], Alvaro Giráldez-Gallego[5], Giuliana Amaddeo[9], Vincent Di Martino[10], Puneeta Tandon[11], Lucy Meunier[12], Laure Elkrief[8], Hale Gokcan[19], Isabelle Ollivier-Hourmand[17], Ju Dong Yang[15], Jean-Charles Nault[20,21], Florent Artru[22], Jean Paul Cervoni[10], Alexander Zipprich[23], Anahita Rabiee[13], Jonel Trebicka[4], Laura Turco[24], Vincenzo La Mura[25], Dominique Thabut[2], Lemaitre Caroline[26], Christophe Bureau[6], Manon Allaire[2,20]. *[1]Service d'hépato-gastroentérologie, CHU Charles Nicolle, Rouen, France; [2]AP-HP Sorbonne Université, hôpital universitaire Pitié-Salpêtrière, service d'hépato-gastroentérologie, Paris, France; [3]Department of gastroenterology and hepatology, hanyang university college of medicine, Guri, Korea, Rep. of South; [4]Department of internal medicine B, university hospital Muenster, Muenster, Germany; [5]Digestive diseases department, hospital universitario Virgen del Rocío, university of Seville, institute of biomedicine (HUVR/CSIC/US), university of Seville, Seville, Spain; [6]Service d'hépatologie hôpital Rangueil CHU Toulouse et université de Toulouse, Toulouse, France; [7]Service d'hépato-gastroentérologie, CHU Poitiers – La Miletrie, Poitiers, France; [8]Service d'hépato-gastroentérologie, hôpital Trousseau - CHU de Tours, Tours, France; [9]Service d'hépatologie, AP-HP Henri Mondor, Créteil, France;*

[10]Service d'hépatologie et soins intensifs digestifs, CHU Jean Minjoz, Besançon, France; [11]Division of gastroenterology (liver unit), department of medicine, university of Alberta Zeidler Ledcor centre, Edmonton, Canada; [12]Service hépato-gastroentérologie, CHU Montpellier, Montpellier, France; [13]Yale university, section of digestive diseases, New Haven, United States; [14]Marmara University, school of medicine, department of gastroenterology and hepatology, Istanbul, Türkiye; [15]Karsh division of gastroenterology and hepatology, Cedars-Sinai medical center, Los Angeles, United States; [16]Service d'hépato-gastroentérologie, CHD Vendée, La-Roche-sur-Yon, France; [17]Department of hepato-gastroenterology, Côte de Nacre hospital, Caen, France; [18]Department of gastroenterology, liver cancer center, Asan medical center, university of Ulsan college of medicine, Seoul, Korea, Rep. of South; [19]Ankara university, school of medicine, department of gastroenterology, Ankara, Türkiye; [20]Centre de recherche des Cordeliers, université Paris Cité, Sorbonne université, Paris, France; [21]APHP, hôpital Avicenne, liver unit, hôpitaux universitaires Paris-Seine-Saint-Denis, université Paris Sorbonne nord, Bobigny, France; [22]Liver department, médecine intensive réanimation, Rennes university hospital, Rennes, France; [23]Clinic of internal medicine IV, Jena university hospital, Jena, Germany; [24]Internal medicine unit for the treatment of severe organ failure, IRCCS Azienda ospedaliero-universitaria di Bologna, Bologna, Italy; [25]Foundation IRCCS Ca' granda ospedale maggiore policlinico, internal medicine - hemostasis and thrombosis, department of pathophysiology and transplantation, university of Milan, Milano, Italy; [26]Service d'hépato-gastroentérologie, CH Jacques Monod, Le Havre, France
Email: manon.allaire@aphp.fr

Background and aims: The use of TIPS in patients with active hepatocellular carcinoma (HCC) remains controversial. This study aimed to assess outcomes after TIPS performed for refractory ascites or hydrothorax.
Method: We conducted a retrospective multicenter study across 15 centers, including consecutive patients with active HCC who underwent TIPS for refractory ascites or hydrothorax between 2007 and 2025. The primary endpoint was overall survival (OS), while secondary endpoints included ascites resolution and oncological outcomes following HCC-directed treatments after TIPS.
Results: A total of 54 patients with active HCC undergoing TIPS for refractory ascites (n = 49) or hepatic hydrothorax (n = 5) were included. Mean age was 65 years; 69% had alcohol-related liver disease, 41% had a history of acute variceal bleeding (AVB), and 94% presented varices the day of TIPS. Median MELD score was 12, 79% of patients were classified as Child-Pugh B and 30% presented with ALBI grade 3. The median largest tumor diameter was 25 mm. Multifocal disease was present in 56% of patients, and 9% had macrovascular invasion (25% Vp3 and 25% Vp4). Most patients were classified as BCLC stage A (52%), and 80% were within the Milan criteria. Median OS was 24 months. Ascites resolution following shunt creation was achieved in 56% of patients within a median delay of 2 months. When comparing patients with and without ascites resolution, no significant differences were observed in baseline liver function or HCC-related characteristics. In logistic regression analysis, only the use of non-selective beta-blockers before TIPS was associated with ascites resolution (OR 3.27, 95% CI 1.08–10.5; p = 0.04), whereas no tumor-related variables were significantly associated with this outcome. Following TIPS placement, 46% of patients received HCC-directed therapy, including liver transplantation (n = 6), ablation (n = 9; 7 complete responses and 2 progressive diseases), locoregional therapies (n = 6; 3 complete responses and 3 partial responses), and systemic treatments (n = 4). During follow-up, AVB occurred in 6% of patients, hepatic encephalopathy in 39%, and cardiac failure in 2%. New extrahepatic metastases developed in three patients but these patients presented active HCC under systemic treatment.
Conclusion: In selected HCC patients, TIPS allows control of ascites in a substantial proportion of cases, thereby enabling the implementation of curative or palliative treatment for HCC.

FRI-235
Antiviral therapy and post-resection outcomes in patients with hepatitis B virus-related hepatocellular carcinoma

Jaehong Jeong[1], Jung Pyo Hong[1], Dong Yun Kim[1], Jae Seung Lee[1], Mi Na Kim[1], Seung Up Kim[1], Beom Kyung Kim[1], Jun Yong Park[1], Do Young Kim[1], Sang Hoon Ahn[1], Hye Won Lee[1]. [1]Department of Internal Medicine, Yonsei University College of Medicine, Yonsei Liver Center, Severance Hospital, Seoul, Korea, Rep. of South
Email: lorry-lee@yuhs.ac

Background and aims: Hepatitis B virus (HBV) reactivation may occur after curative resection for HBV-related hepatocellular carcinoma (HCC), and antiviral choice could influence long-term outcomes. While tenofovir disoproxil fumarate (TDF) has been suggested to improve survival compared with entecavir (ETV), evidence including tenofovir alafenamide (TAF) remains limited. We compared overall survival (OS) and recurrence-free survival (RFS) among patients receiving ETV, TDF, or TAF after curative resection for HBV-related HCC.
Method: Confounding was controlled using inverse probability of treatment weighting (IPTW) for the average treatment effect with 99th-percentile trimming. Balance was assessed using maximum absolute standardized mean difference. OS and RFS were evaluated using Kaplan–Meier analysis and IPTW-weighted Cox models. Multivariable Cox analyses identified prognostic factors; for RFS, cirrhosis was used as a stratification factor due to non-proportional hazards.
Results: Among 1454 surgically treated patients between 2001 and 2025, 922 received ETV (n = 485), TDF (n = 371), or TAF (n = 66). Unweighted 60-month OS was 91.3%, 94.5%, and 98.1% (p = 0.132), and RFS was 70.0%, 70.8%, and 86.6% (p = 0.290) for ETV, TDF, and TAF, respectively. After IPTW, 60-month OS was 90.7%, 95.1%, and 97.1% (p = 0.069), and RFS was 69.8%, 71.4%, and 83.9% (p = 0.426). In multivariable analysis, TDF was associated with lower mortality versus ETV (adjusted hazard ratio 0.47; 95% CI 0.26–0.87; p = 0.016), whereas TAF showed no significant difference. Neither TDF nor TAF improved RFS compared with ETV.
Conclusion: TDF demonstrated a potential OS benefit compared with ETV after curative resection for HBV-related HCC, although RFS was comparable across agents. Larger cohorts with longer follow-up are needed to clarify the role of TAF.

FRI-236
Identification of serum proteomic signatures for predicting clinical outcomes of immunotherapy in advanced hepatocellular carcinoma

Ji Hoon Kim[1], Young-Sun Lee[1], Eunho Choi[1], Yang Jae Yoo[1], Jong Eun Yeon[1]. [1]Korea university guro hospital, Seoul, Korea, Rep. of South
Email: lys810@korea.ac.kr

Background and aims: Although combination immunotherapies, such as atezolizumab/bevacizumab and durvalumab/tremelimumab, have revolutionized the first-line treatment of advanced hepatocellular carcinoma (HCC), the lack of validated predictive biomarkers remains a clinical hurdle. This study aimed to identify circulating serum protein signatures that predict therapeutic response to atezolizumab/bevacizumab.
Method: Pre-treatment serum samples were obtained from 44 patients with advanced HCC across four tertiary centers. Patients were stratified into responders (CR/PR/SD, n = 32) and non-responders (PD, n = 12). We employed mass spectrometry-based proteomics to characterize the differential protein expression landscape between the two groups.
Results: Proteomic analysis revealed distinct molecular signatures associated with treatment resistance. Non-responders exhibited significantly elevated levels of pro-inflammatory markers, specifically C-reactive protein (CRP) and S100-A9. Conversely, several proteins involved in metabolic homeostasis and transport—including

TF, TTR, APOC3, CLU, RBP4, ITIH2, IGFALS, and SERPINC1—were downregulated in non-responders. Notably, network analysis identified APOC3 and CLU as highly interconnected central hubs, suggesting their pivotal roles in the systemic modulation of treatment response.
Conclusion: Circulating serum proteomic signatures, characterized by a balance between inflammatory markers and metabolic hub proteins, effectively predict the efficacy of atezolizumab/bevacizumab in advanced HCC. These findings provide a robust framework for non-invasive treatment stratification and personalized therapeutic strategies.

FRI-237

First-line therapy in super-older adults with hepatocellular carcinoma: comparative effectiveness of Lenvatinib versus Atezolizumab-Bevacizumab

Masamichi Kimura[1], Koji Nishikawa[1], Jun Imamura[1], Kiminori Kimura[1]. [1]*Tokyo Metropolitan Cancer and Infectious Diseases Center, Komagome Hospital, Tokyo, Japan*
Email: masa55@kuhp.kyoto-u.ac.jp

Background and aims: Evidence guiding first-line systemic therapy in super-older adults (≥80 years) with hepatocellular carcinoma (HCC) is scarce, as pivotal trials largely excluded this age group. We aimed to compare the real-world effectiveness and safety of lenvatinib (LEN) and atezolizumab + bevacizumab (Atezo + Bev) in this population and to assess whether early dose delivery, expressed as 8-week relative dose intensity (RDI), stratifies survival outcomes with LEN.
Method: We retrospectively analyzed 56 consecutive patients aged ≥80 years with unresectable/advanced HCC who initiated first-line LEN (n = 30) or Atezo + Bev (n = 26) between May 2018 and August 2025. All had Child–Pugh A liver function and ECOG 0–1 performance. The primary endpoint was overall survival (OS); secondary endpoints included progression-free survival (PFS) and adverse events (AEs). A prespecified Day-56 landmark analysis was performed in the LEN group to evaluate the association between 8-week RDI (≥75% vs <75%) and OS, mitigating immortal-time bias. Survival was analyzed using Kaplan–Meier and log-rank tests, supplemented by restricted mean survival time (RMST) at 12 months.
Results: Median OS was 14.7 months with LEN and 10.7 months with Atezo + Bev (hazard ratio [HR] 0.82, 95% CI 0.45–1.52; p = 0.52). Median PFS was 6.7 vs 9.7 months, respectively (HR 1.22, 95% CI 0.67–2.23; p = 0.51). Objective response and disease-control rates were 23%/67% for LEN and 15%/77% for Atezo + Bev. In the LEN cohort, an 8-week RDI ≥75% was achieved in 20% of patients and was associated with markedly prolonged OS (30.8 vs 14.7 months; HR 0.34, 95% CI 0.14–0.80; p = 0.019). At 12 months, RMST difference (ΔRMST) was +32 days favoring high-RDI LEN. Grade ≥3 AEs occurred in 37% (LEN) and 50% (Atezo + Bev) without treatment-related deaths. Anorexia and diarrhea were more frequent with LEN, while edema and gastrointestinal bleeding occurred only with Atezo + Bev.
Conclusion: Among super-older adults with HCC, LEN and Atezo + Bev demonstrated comparable real-world efficacy and tolerability. Importantly, maintaining early dose delivery (8-week RDI ≥75%) under LEN identified a subgroup with significantly improved survival. These findings highlight early dose intensity as a pragmatic biomarker for optimizing systemic therapy in frail ≥80-year-old patients and support a dose-delivery-guided algorithm: maintain high early RDI with LEN, and consider timely switch to Atezo + Bev if this target cannot be sustained.

FRI-238

Conversion surgery after immunotherapy in hepatocellular carcinoma: a French multicentric retrospective study

Shinha-Ashkarr Kouadou[1], Maria Stella Franzè[2], Hélène Regnault[1], Rami Rhaiem[3], Mohamed Bouattour[4], Clemence Hollande[5], Christian Hobeika[5], Manon Allaire[6], Sarah Mouri[6], Chetana Lim[6], Massih Ningarhari[7], Nathalie Ganne-Carrié[8], Jean-Charles Nault[8], Claudia Campani[8], Alina Pascale[9], Marie Lequoy[10], Daniele Sommacale[1], Violaine Ozenne[10], François Paye[10], Viviane Gnemmi[7], Bruno Lapuyade[11], Jean-Frédéric Blanc[12], Guillaume Millet[7], Vincent Leroy[1], Brustia Raffaele[1], Giuliana Amaddeo[1]. [1]*Henri Mondor University Hospital, Créteil, France;* [2]*University of Messina, Messina, Italy;* [3]*Hôpital Robert Debré, Reims, France;* [4]*AP-HP, Hôpital Beaujon, Liver Cancer and Innovative Therapy, CLICHY, France;* [5]*Hôpital Beaujon, Clichy, France;* [6]*Hôpital Pitié Salpêtrière, Paris, France;* [7]*CHU Lille, Lille, France;* [8]*Hôpital Avicenne, Bobigny, France;* [9]*Hôpital Paul-Brousse, Villejuif, France;* [10]*Hôpital Saint Antoine, Paris, France;* [11]*Radiology Department, Bordeaux University Hospital Center, Bordeaux, France;* [12]*Department of Hepato-Gastroenterology and Medical Oncology, Bordeaux University Hospital, Bordeaux, France*
Email: paiik.shinha@gmail.com

Background and aims: Hepatocellular carcinoma (HCC) is often diagnosed at an advanced stage, precluding upfront resection. Immunotherapy has profoundly changed the management of unresectable HCC, offering high tumour response rates and enabling potential conversion to surgery. However, multicentric data on perioperative safety and survival outcomes after resection in this setting remain limited.
Method: A multicentric retrospective study was conducted across eight French University Hospitals between 2019 and 2024. Patients initially deemed unresectable who received immunotherapy followed by surgery after achieving a radiologic tumour response were included. Primary endpoints were overall survival (OS) and disease-free survival (DFS). Secondary endpoints included postoperative morbidity (Clavien ≥ III), 90-day mortality, and pathological response.
Results: Thirty-six patients were included (86% male; median age 59 years; median BMI 25.6 Kg/m2). Before treatment, 53% were classified as BCLC stage C (VP4 n = 2, VP3 n = 10, VP2 n = 5, nodal metastases n = 2), and 8% as Child-Pugh B7. The median size of the largest lesion was 87 mm (range 57–101), with a median number of 3.5 nodules. All patients received a median of 11 cycles of immunotherapy (range 6 –18) before surgery. An objective partial response was achieved in all cases, with a tumour size reduction in 76% of cases. After immunotherapy, 35% of patients were reclassified as BCLC A, 39% as BCLC C, and liver function remained preserved in all but one case (Child-Pugh B7). A right hepatectomy wasperformed in 14 patients (56%). The overall rate of major complications (Clavien ≥ III) was 16%, with no 90-day mortality. Median hospital stay was 7 days, including a median of 2.6 days in intensive care. Complete tumour necrosis (100%) was observed in 9 patients (36%). The estimated OS was 96% at 3 months, 91% at 12 months, 81% at 24 months, and remained 81% at 60 months. DFS rates were 100% at 3 months, 95% at 12 months, 75% at 24 months, 58% at 60 months.
Conclusion: Conversion surgery after systemic immunotherapy for initially unresectable HCC is feasible and safe in experienced centres, showing low postoperative morbidity and favourable 2-year survival outcomes.
These findings support the curative potential of hepatic resection following combined immunotherapy and support the need for larger comparative studies to validate its long-term benefit.

FRI-239

Functional convergence towards short chain fatty acid metabolism shapes responsiveness to atezolizumab plus bevacizumab across Western and Eastern populations despite distinct gut microbial composition

Pei-Chang Lee[1], Chi-Jung Wu[1], Pasquale Lombardi[2], Leonardo Brunetti[2], Chieh-Ju Lee[1], I-Cheng Lee[1], Claudia Fulgenzi[2], Ya-Wen Hung[1], Chen-Ta Chi[1], Julian R. Marchesi[2], Rosemary Boyton[2], Daniel M Altmann[2], Catherine Reynolds[2], Despoina Chrysostomou[2], Rohini Sharma[2], Antonio D'Alessio[2], Alessio Cortellini[3], Ming-Chih Hou[1], Yi-Hsiang Huang[1], David J. Pinato[2]. *[1]Taipei Veterans General Hospital, Taipei, Taiwan; [2]Imperial College London, London, United Kingdom; [3]Campus Biomedico Rome, Rome, Italy*
Email: david.pinato@imperial.ac.uk

Background and aims: Gut microbial composition influences immunotherapy outcomes in hepatocellular carcinoma (HCC). We investigated whether geographic origin affects the association between gut microbiota and tumor response to atezolizumab plus bevacizumab (A+B) in Western and Eastern patients with HCC.
Method: Patients with unresectable HCC initiating first-line A+B therapy were prospectively enrolled from the United Kingdom and Italy (Western cohort, $n = 15$) and Taiwan (Eastern cohort, $n = 53$). Fecal samples were collected prior to treatment initiation and analyzed for microbial composition using linear discriminant analysis effect size based on full-length bacterial 16S rRNA gene sequencing. Microbial functional profiles and pathway inferences were predicted using Phylogenetic Investigation of Communities by Reconstruction of Unobserved States version 2 (PICRUSt2). Durable response was defined as an objective response or stable disease lasting longer than 8 months.
Results: Western and Eastern cohorts were comparable in pre-treatment characteristics: most patients had BCLC stage C disease (93.3% vs. 100%) and Child–Pugh class A liver function (86.7% vs. 100%), while etiology differed, with non-viral disease more frequent in Western patients (60.0%) and viral disease more frequent in Eastern patients (66.0%) (all $p > 0.05$). Baseline gut microbiota composition differed significantly between cohorts, as assessed by Bray–Curtis and unweighted UniFrac distances (both $p = 0.001$ by PERMANOVA). Despite this divergence, durable response rates were similar (46.7% vs. 39.6%, $p = 0.770$). Western durable responders were enriched in *Faecalibacterium prausnitzii*, *Faecalibacterium intestinalis*, and *Phocaeicola plebeius*, whereas *Akkermansia muciniphila* and *Acidaminococcus fermentans* predominated in Eastern durable responders. In contrast, Enterobacteriaceae were consistently enriched in non-responders. Notably, PICRUSt2 analysis demonstrated convergent enrichment of microbial functions related to short-chain fatty acid (SCFA) biosynthesis in durable responders, mediated through distinct metabolic pathways (PWY-5677 [$p = 0.019$] and PWY-7187 [$p = 0.046$] in Eastern responders; CENTEFRM-PWY [$p = 0.026$] and COA-PWY [$p = 0.043$] in Western responders).
Conclusion: Despite marked geographic differences in gut microbiota composition, convergence of SCFA-related microbial functions highlights microbial functional capacity as a unifying determinant of A+B efficacy across regions.

FRI-240

Clinical utility of tumor morphology for predicting aggressive and hyperaggressive recurrence after curative resection of hepatocellular carcinoma

I-Cheng Lee[1], Romeo Kuo-Cheng Wu[2], Chi-Ping Tan[1], Gar-Yang Chau[1], Jiing-Chyuan Luo[1], Yi-Hsiang Huang[1]. *[1]Taipei Veterans General Hospital, National Yang Ming Chiao Tung University, Taipei, Taiwan, [2]Keelung Hospital Ministry of Health & Welfare, Keelung, Taiwan*
Email: iclee@vghtpe.gov.tw

Background and aims: Recurrence after curative resection for hepatocellular carcinoma (HCC) is highly heterogeneous, and predictors of aggressive recurrence remain poorly defined. This study aimed to identify clinical, radiologic, and histologic predictors of aggressive and hyperaggressive recurrence after curative resection for HCC.
Method: Between 2007 and 2024, 906 of 1813 patients who developed recurrence after curative resection for HCC were retrospectively analyzed. Recurrence patterns included recurrence beyond the Milan criteria (aggressive recurrence), recurrence with macrovascular invasion, extrahepatic metastasis, and recurrence at BCLC stage C (hyperaggressive recurrence). Radiologic tumor morphology was classified as simple nodular (type I), simple nodular with extranodular growth (type II), confluent multinodular (type III), or infiltrative (type IV). Types III and IV were defined as high-risk morphology. Independent predictors were identified using multivariate analysis.
Results: Among the 906 patients with recurrent HCC, 353 (39.0%) developed aggressive recurrence, 63 (7.0%) had macrovascular invasion, 149 (16.4%) developed extrahepatic metastases, and 191 (21.1%) presented with BCLC stage C (hyperaggressive recurrence). Risks of aggressive recurrence for morphology types I–IV were 26.4%, 42.5%, 62.6%, and 65.1%, respectively. Corresponding risks for hyperaggressive recurrence were 12.4%, 19.0%, 40.0%, and 46.5%. On multivariate analysis, high-risk tumor morphology (hazard ratio [HR] 1.450, $p = 0.010$), BCLC stage, 7–11 criteria, poor differentiation, microvascular invasion, and AFP >400 ng/mL independently predicted aggressive recurrence. High-risk morphology was also an independent predictor of hyperaggressive recurrence (HR 2.193, $p < 0.001$), recurrence with macrovascular invasion (HR 2.091, $p = 0.012$), and extrahepatic metastasis (HR 2.199, $p < 0.001$), together with established tumor burden, adverse histologic features, and elevated AFP levels.
Conclusion: Radiologic tumor morphology, particularly high-risk patterns, in combination with the 7–11 criteria, histologic characteristics, and AFP level, effectively predicts aggressive and hyperaggressive recurrence of HCC after curative resection. These findings may improve postoperative risk stratification and inform surveillance strategies and future perioperative therapeutic trials.

FRI-241

Comparative efficacy and safety of second-line and later systemic therapies after first-line treatment failure in hepatocellular carcinoma: a systematic review and meta-analysis

Han Ah Lee[1], Moon Haeng Hur[2], Yuri Cho[3], Ju Hyun Shim[4], Bo Hyun Kim[3], Yong-Han Paik[5], Joon Hyeok Lee[5]. *[1]Chung-Ang University, Seoul, Korea, Rep. of South; [2]Seoul National University College, Seoul, Korea, Rep. of South; [3]National Cancer Center, Seoul, Korea, Rep. of South; [4]Asan Medical Center, Seoul, Korea, Rep. of South; [5]Samsung Medical Center, Seoul, Korea, Rep. of South*
Email: amelia86@naver.com

Background and aims: Establishing optimal second-line and later systemic treatment strategies after failure of first-line therapy has become an increasingly important challenge in hepatocellular carcinoma (HCC). However, evidence guiding treatment selection remains limited.
Method: We conducted a systematic review and meta-analysis of published studies evaluating second-line or later systemic therapies for HCC, excluding studies limited to sorafenib failure alone. Overall survival (OS), progression-free survival (PFS), and grade 3–4 adverse events (AEs) were pooled using meta-analytic methods.
Results: In the meta-analysis of second-line and later systemic therapies after failure of atezolizumab plus bevacizumab, lenvatinib demonstrated the most favorable survival outcomes. The pooled median OS was 12.42 months for lenvatinib (95% CI, 10.02–14.82; $I^2 = 89.4\%$), compared with 7.83 months for sorafenib (95% CI, 6.29–9.36; $I^2 = 7.36\%$). Regorafenib, cabozantinib, and ramucirumab showed pooled median OS of 9.19 months (95% CI, 3.60–14.78; $I^2 = 94.5\%$), 9.59 months (95% CI, 4.91–14.27; $I^2 = 91.4\%$), and 5.85 months (95% CI, 1.76–9.94; $I^2 = 20.6\%$), respectively. Compared with sorafenib,

lenvatinib significantly reduced the risk of death (risk ratio [RR], 0.64; 95% CI, 0.49–0.84; I^2 = 34.2%), whereas regorafenib and cabozantinib did not show significant benefit. The pooled median PFS was also longest with lenvatinib at 4.74 months (95% CI, 3.76–5.72; I^2 = 96.4%), followed by cabozantinib (3.96 months), regorafenib (3.05 months), and sorafenib (2.86 months). Lenvatinib significantly reduced the risk of disease progression compared with sorafenib (RR, 0.58; 95% CI, 0.42–0.80; I^2 = 65.3%). Reconstructed survival curves confirmed longer median OS (11.87 vs. 8.30 months) and PFS (3.80 vs. 1.93 months) with lenvatinib compared with sorafenib. The incidence of grade 3–4 AEs was comparable between lenvatinib (36%) and sorafenib (34%). After lenvatinib failure, atezolizumab plus bevacizumab achieved a pooled median OS of 14.98 months (95% CI, 9.57–20.38; I^2 = 42%) and PFS of 5.78 months (95% CI, 3.19–8.37; I^2 = 66%), along with the highest ORR (28.3%) and DCR (69.6%), although with a higher incidence of grade 3–4 AEs (53%).
Conclusion: Lenvatinib demonstrates clinical benefit after failure of atezolizumab plus bevacizumab, while multiple systemic therapies, including atezolizumab plus bevacizumab, may provide meaningful efficacy after lenvatinib failure.

FRI-242
Adequate surgical margin, not resection type, determines long-term outcomes after liver resection for hepatocellular carcinoma
Boram Lee[1]. [1]*Seoul National University Bundang Hospital, Gyeonggi-do, Korea, Rep. of South*
Email: boramsnubhgs@gmail.com

Background and aims: The oncologic superiority of anatomical resection (AR) over non-anatomical resection (NAR) for hepatocellular carcinoma (HCC) remains controversial. It is unclear whether reported survival benefits of AR are attributable to the resection type itself or to its association with wider surgical margins. This study aimed to evaluate the relative impact of resection type and margin adequacy on long-term oncologic outcomes after liver resection for HCC.
Method: A retrospective analysis was conducted of 1349 patients who underwent curative-intent liver resection for HCC between 2004 and 2022. Surgical margin width was defined as the shortest pathological distance from the tumor to the resection margin, with ≥1 cm considered adequate. Recurrence-free survival (RFS) and overall survival (OS) were compared according to resection type and margin status. Propensity score matching and multivariable Cox regression analyses were performed, with subgroup analyses stratified by tumor size (<5 cm vs. ≥5 cm).
Results: AR was associated with a higher likelihood of achieving a surgical margin ≥1 cm compared with NAR. However, after propensity score matching, no significant differences in OS or RFS were observed between AR and NAR. In patients with tumors <5 cm, margin adequacy was significantly associated with improved RFS regardless of resection type, whereas resection type itself was not an independent prognostic factor. In tumors ≥5 cm, neither margin width nor resection type significantly influenced survival outcomes. Multivariable analysis identified tumor size ≥5 cm and margin <1 cm as independent predictors of recurrence and mortality, while resection type was not.
Conclusion: Long-term oncologic outcomes after liver resection for HCC are determined primarily by surgical margin adequacy rather than by resection type. The prognostic impact of margin width is most pronounced in small tumors and diminishes in larger tumors where tumor biology predominates. Surgical strategies should prioritize achievable margin clearance while preserving functional liver reserve, rather than routinely favoring anatomical resection.

FRI-243
Neoadjuvant radiotherapy combined with lenvatinib and pd-1 blockade in resectable intrahepatic cholangiocarcinoma at high risk of recurrence: a prospective phase II study
Keren Li[1]. [1]*Beijing Tsinghua Changgung Hospital, Beijing, China*
Email: lkra03939@btch.edu.cn

Background and aims: Resectable intrahepatic cholangiocarcinoma (ICC) is associated with high postoperative recurrence rates, particularly in patients with adverse tumor and nodal factors. Effective neoadjuvant strategies for this high-risk population remain poorly defined. We conducted a prospective phase II study to evaluate neoadjuvant radiotherapy combined with lenvatinib and PD-1 blockade in resectable ICC patients at high risk of recurrence.
Method: This prospective, single-arm phase II study enrolled patients with resectable ICC and predefined high-risk features for recurrence. Neoadjuvant therapy consisted of radiotherapy targeting both the primary tumor and regional lymphatic drainage areas (regional lymph nodes: 200 cGy × 20 fractions; primary tumor: 300 cGy × 20 fractions), combined with toripalimab (240 mg intravenously every 3 weeks for four cycles) and lenvatinib (8 mg orally once daily, discontinued 7 days prior to surgery). The primary endpoint was 1-year recurrence-free survival. Secondary endpoints included overall survival, objective response rate, and safety.
Results: Between January 2023 and December 2024, 17 patients completed neoadjuvant treatment. Eight patients (47.06%) achieved conversion to curative-intent treatment following therapy, including surgical resection (n = 4) and liver transplantation (n = 2). One patient was scheduled for second-stage surgery and one was awaiting surgery. Disease progression precluding surgery occurred in four patients (23.53%). Three patients (17.65%) had stable disease but did not undergo surgery due to poor performance status or patient refusal. The combined neoadjuvant regimen was generally well tolerated, with no unexpected treatment-related toxicities observed.
Conclusion: Neoadjuvant radiotherapy combined with lenvatinib and PD-1 blockade demonstrated promising conversion potential with acceptable safety in resectable ICC patients at high risk of recurrence. This liver-directed multimodal approach may expand curative treatment opportunities and merits further investigation.

FRI-244
Efficacy of second-line therapies and the prognostic value of the crafity score in advanced hepatocellular carcinoma following Atezolizumab plus Bevacizumab failure: a real-world study
Jinpeng Li[1], Jinlong Song[1]. [1]*Shandong Cancer Hospital and Institute, jinan, China*
Email: jls7286@163.com

Background and aims: Hepatocellular carcinoma (HCC) accounts for approximately 90% of all primary liver malignancies and presents a significant therapeutic challenge due to its heterogeneity. The efficacy of second-line treatments following disease progression on first-line atezolizumab plus bevacizumab (Atez/Bev) in advanced HCC remains a subject of ongoing debate. This study aimed to evaluate real-world clinical outcomes of second-line therapies post-Atez/Bev failure and to identify prognostic factors influencing survival.
Method: We retrospectively analyzed 68 patients with advanced or metastatic HCC who received second-line regorafenib, lenvatinib, or ramucirumab following progression on first-line Atez/Bev at Shandong Cancer Hospital and Institute between October 2020 and June 2024. Tumor response was assessed according to Response Evaluation Criteria in Solid Tumors (RECIST) v1.1. Median overall survival (OS) and progression-free survival (PFS) were estimated using the Kaplan-Meier method. Multivariate analyses were performed using the Cox proportional hazards model to identify independent prognostic factors.
Results: The cohort was predominantly male (85.3%), with a median age of 59 years (range, 28–76 years). All patients had progressed on

first-line Atez/Bev prior to receiving second-line therapy. Regorafenib was the most frequently administered agent (70.7%), followed by lenvatinib (12.1%) and ramucirumab (10.3%). Patients treated with regorafenib exhibited a prolonged median PFS of 4.5 months and a median OS of 8.5 months compared to other regimens. Univariate analysis demonstrated that Child-Pugh class B, elevated alpha-fetoprotein (AFP) levels (>200 ng/mL), extrahepatic spread, and a high CRAFITY score were significantly associated with increased mortality risk. Multivariate analysis identified extrahepatic spread (hazard ratio [HR]: 0.45, P = .021), CRAFITY score (HR: 0.32, P = .008), and AFP level (HR: 2.15, P = .032) as independent predictors of OS.
Conclusion: While second-line therapies following Atez/Bev failure demonstrate varying degrees of efficacy, survival outcomes observed in this cohort are consistent with current literature. Extrahepatic spread, AFP levels, and CRAFITY scores emerged as key prognostic factors. These findings highlight the potential for personalized treatment strategies to improve clinical outcomes in this refractory patient population.

FRI-245
Association of radiotherapy with atezolizumab plus bevacizumab with survival in advanced hepatocellular carcinoma
Gyungsun Lim[1], Hyunjae Shin[1], Byeong Geun Song[2], Sung Won Chung[3], Jeong Il Yu[4], Hee Chul Park[4], Moon Haeng Hur[1], Yun Bin Lee[1], Eun Ju Cho[1], Jeong-Hoon Lee[1], Su Jong Yu[1], Jung-Hwan Yoon[1], Yoon Jun Kim[1]. *[1]Department of Internal Medicine and Liver Research Institute, Seoul National University College of Medicine, Seoul, Korea, Rep. of South; [2]Department of Internal Medicine, Samsung Medical Center, Seoul, Korea, Rep. of South; [3]Department of Gastroenterology, Liver Center, Asan Medical Center, University of Ulsan College of Medicine, Seoul, Korea, Rep. of South; [4]Department of Radiation Oncology, Samsung Medical Center, Sungkyunkwan University, Seoul, Korea, Rep. of South*
Email: yoonjun@snu.ac.kr

Background and aims: Immunotherapy is the standard first-line therapy for advanced hepatocellular carcinoma (HCC). Radiotherapy (RT) is well established for achieving local control and may also induce systemic immune effects. We evaluated the association of RT with outcomes in patients receiving Atezolizumab plus Bevacizumab (Ate+Bev).
Method: Patients who received RT during Ate+Bev therapy (n = 88) in 2017–2023 were compared with patients treated with Ate+Bev alone (n = 396). Overall survival (OS), progression-free survival (PFS), and freedom from local progression (FFLP) were analyzed with multivariable Cox models from the start of Ate+Bev to HCC progression or death.
Results: Median follow-up was 18.3 months and the median interval from Ate+Bev start to RT was 32 days. Combining RT with Ate+Bev was associated with longer OS (adjusted hazard ratio [aHR] = 0.71, 95% confidence interval [CI] = 0.53–0.97, p = 0.030), PFS (aHR = 0.57, 95% CI = 0.45–0.74, p < 0.001), and FFLP (aHR = 0.65, 95% CI = 0.44–0.95, p = 0.027) compared to Ate+Bev alone. This association was consistent across subgroups (interaction p > 0.05). In RT recipients, OS (aHR = 1.38, 95% CI = 0.65–2.93, p = 0.40) and PFS (aHR = 0.92, 95% CI = 0.55–1.52, p = 0.73) did not differ according to the timing of RT. RT-related adverse events occurred in 3.4% of patients and total adverse events between groups were comparable (p = 0.211).
Conclusion: Combining RT with Ate+Bev was associated with longer OS, PFS and FFLP. These findings support the potential role of RT as an effective adjunct to immunotherapy and warrant prospective validation.

FRI-246
Multi-omics analysis of combined immunotherapy - chemotherapy benefit in advanced intrahepatic cholangiocarcinoma
Ningning Zhang[1], Xuanchen Liu[1]. *[1]Tianjin Medical University Cancer Institute and Hospital, Tianjin, China*
Email: mail4ningning@gmail.com

Background and aims: The combination of immunotherapy and chemotherapy has become a first-line treatment for advanced intrahepatic cholangiocarcinoma (ICC). However, a significant proportion of patients do not achieve sustained clinical benefit. This study aimed to identify gut microbiota, peripheral blood metabolites, and immune features associated with sustained benefit from this regimen, and to explore the potential regulatory mechanisms of the gut microbiota-bile acid-immune axis.
Method: This study enrolled 78 treatment-naïve patients with advanced ICC receiving first-line toripalimab plus GEMOX, classified as sustained benefit (DCB, n = 55) or non-sustained benefit (noDCB, n = 23) groups. Pretreatment fecal samples underwent metagenomic sequencing. Peripheral blood from all patients was analyzed by flow cytometry for immune cells/cytokines, and a subset (n = 39) was analyzed for bile acid metabolomics. LASSO and ROC analyses identified predictive factors. Correlation and mediation analyses were performed on the cohort with complete multi-omics data (n = 39) to investigate interactions.
Results: The DCB group exhibited higher gut microbial diversity and was enriched with beneficial bacteria (e.g., Faecalibacterium prausnitzii), while the noDCB group was enriched with potentially harmful bacteria. Metagenomic pathways related to bile acid synthesis and metabolism were upregulated in the DCB group, whereas virulence-related pathways were enriched in the noDCB group. Immune profiling showed higher PD-1 expression on $CD8^+$ T cells in the DCB group, and higher Tregs and IL-8 in the noDCB group. Multiple primary and secondary bile acids (e.g., TCDCA-3S, TLCA-3S) were elevated in the DCB group. LASSO regression identified 11 predictors of sustained benefit. Seven indicators, including TBS, NLR, Tregs, PD-1^+CD8^+ T cells, Faecalibacterium prausnitzii, Bacteriophage sp., and TCDCA-3S, showed moderate predictive value (AUC > 0.7). Correlation and mediation analyses in the 39-patient cohort revealed a significant positive correlation among Faecalibacterium prausnitzii, TCDCA-3S, and PD-1^+CD8^+ T cells. Mediation analysis supported that F. prausnitzii may upregulate PD-1 expression on $CD8^+$ T cells by modulating TCDCA-3S levels.
Conclusion: The study proposes a potential "Faecalibacterium prausnitzii - TCDCA-3S - PD-1^+CD8^+ T cells" regulatory axis, offering insights for predictive biomarker development and mechanistic understanding.

FRI-247
Association between prophylactic antibiotics and post-ablation infections in hepatocellular carcinoma patients: a retrospective multicenter cohort study
Ting Luo[1], Jie Yu[1], Ping Liang[1]. *[1]Department of Interventional Ultrasound, Chinese PLA General Hospital, Beijing, China*
Email: luotingemma56@163.com

Background and aims: The role of prophylactic antibiotics in preventing infections following hepatocellular carcinoma (HCC) ablation remains unclear. We aimed to clarify whether prophylactic antibiotics reduce infection rates after HCC ablation and to identify patient subgroups who might benefit.
Method: This retrospective, multicenter cohort study included HCC patients who underwent percutaneous thermal ablation between May 2018 and April 2024, classified into prophylactic antibiotic (PA) and non-prophylactic antibiotic (non-PA) groups. The primary outcome was infection, categorized as severe or non-severe, while secondary outcomes included duration of hospitalization, costs, and fever. Propensity Score Matching (PSM) and Overlap Weighting (OW)

were employed to control for baseline differences, and the Firth's penalized likelihood method was applied to all logistic regression analysis.
Results: A total of 2446 patients (mean age 60.4 ± 10.6 years; 520 women) from six centers were included. Comparing the PA and non-PA groups, the PA group showed lower overall infection rates than the non-PA group (4.1% vs. 6.6%, P < 0.05 in primary cohort), which was comparable after adjustment (P = 0.1 after PSM and P = 0.32 after OW). Logistic regression analysis revealed that BCLC B, high glucose level, and history of biliary surgery were independent risk factors of infection in both PSM and OW cohort (all P < 0.05).
Conclusion: Routine prophylactic antibiotic use is not necessary in percutaneous HCC thermal ablation; however, it may be considered for selected patients.

FRI-248
The prognostic role of the SMARS score in patients with hepatocellular carcinoma receiving Atezolizumab/Bevacizumab
Maximilian Moos[1], Felix Hahn[1], Friedrich Foerster[1], Roman Kloeckner[2], Constantin Scholz[1], Tobias Bäuerle[1], Lukas Müller[1], Aline Mähringer-Kunz[1]. [1]*University Medical Center Mainz, Mainz, Germany;* [2]*University Medical Center Schleswig-Holstein, Luebeck, Germany*
Email: maximilian.moos2@unimedizin-mainz.de

Background and aims: This study aimed to evaluate the prognostic performance of the recently introduced SMARS score in patients with hepatocellular carcinoma (HCC) undergoing systemic immunotherapy. Specifically, we assessed whether this novel imaging-based score enables reliable risk stratification in this setting.
Method: We retrospectively analyzed 90 patients with HCC treated at our center between January 2020 and May 2024. The SMARS score, incorporating tumor shape, mosaic architecture, alpha-fetoprotein (AFP) level, rim arterial phase hyperenhancement and satellite lesions, was calculated from baseline CT according to Bao et al. Overall survival (OS) was assessed with Kaplan–Meier analysis, and prognostic factors were evaluated using uni- and multivariable Cox regression models.
Results: Higher SMARS scores were associated with impaired OS using the previously published cutoff of –0.49. In uni- and multivariate Cox regression, the SMARS score emerged as a significant prognostic factor. Univariate Cox regression demonstrated that four SMARS components were significantly associated with OS, including tumor shape (HR 2.08, 95% CI 1.25–3.40; p = 0.003), mosaic architecture (HR 1.64, 95% CI 1.04–2.59; p = 0.036), AFP-level (HR 1.80, 95% CI 1.12–2.90; p = 0.016) and rim arterial phase hyperenhancement (HR 2.03, 95% CI 1.24–3.33; p = 0.005). Satellite lesions were not significantly associated with OS (HR 1.70, 95% CI 0.97–3.00, p = 0.061). In the multivariable analysis, only tumor shape remained independently associated with OS (HR 2.06, 95% CI 1.25–3.40; p = 0.004).
Conclusion: Imaging-based SMARS score is an independent prognostic marker in patients with HCC undergoing systemic therapy with atezolizumab/bevacizumab. These findings extend previous evidence by confirming the prognostic relevance of SMARS beyond loco-regional approaches and highlight its potential to guide patient stratification in the era of systemic immunotherapy.

FRI-249
Real-world outcomes of sequential transarterial chemoembolization followed by Atezolizumab–Bevacizumab in patients with unresectable hepatocellular carcinoma
Soe Thiha Maung[1,2], Jonggi Choi[3], Roongruedee Chaiteerakij[1], Sung Won Chung[3]. [1]*Faculty of Medicine, Chulalongkorn University, Bangkok, Thailand;* [2]*Ma Har Myaing Hospital, Yangon, Myanmar;* [3]*Asan Medical Center, University of Ulsan College of Medicine, Seoul, Korea, Rep. of South*
Email: dr.sthm92@gmail.com

Background and aims: Repeated transarterial chemoembolization (TACE) for unresectable hepatocellular carcinoma (uHCC) often leads to deteriorating hepatic reserve. While atezolizumab plus bevacizumab (Atezo/Bev) is the standard systemic therapy, the optimal timing for transition, specifically whether to strictly wait for TACE refractoriness, remains debated. We evaluated the impact of hepatic function and TACE history on outcomes in patients switching to Atezo/Bev, aiming to identify prognostic determinants beyond conventional refractoriness criteria.
Method: We retrospectively analyzed 154 patients with uHCC who transitioned to Atezo/Bev after prior TACE. The index date was defined as Atezo/Bev initiation, serving as baseline for all clinical variables. TACE refractoriness followed Japan Society of Hepatology criteria. Prognostic factors for overall survival (OS) and progression-free survival (PFS) were assessed using Cox regression. Exploratory analyses included change-point analysis of international normalized ratio (INR) at index and impact of early transition (≤4 vs. >4 TACE sessions).
Results: At the index date, 76.0% of patients met the criteria for TACE refractoriness. However, refractoriness status itself was not an independent predictor for either OS (p = 0.37) or PFS (p = 0.09). Instead, baseline hepatic function and cumulative TACE burden were the primary determinants. In multivariable analysis, elevated INR (adjusted hazard ratio [aHR] 24.03, p = 0.001), higher AST (aHR 1.02, p = 0.04), and a greater number of prior TACE sessions (aHR 1.07, p = 0.004) were independent adverse predictors for PFS. Notably, a non-linear threshold effect was observed for baseline INR; PFS remained relatively stable at INR <1.20 but declined sharply at INR ≥1.20 (median 6.47 vs. 3.57 months; log-rank p = 0.003). In change-point modeling, the risk of progression increased steeply only after the INR exceeded 1.20 (HR 2.05 per 0.1 increase, p < 0.05). Furthermore, early transition (after ≤4 TACE sessions) was associated with significantly better PFS (aHR 0.68, p = 0.04) compared to later transition, independent of refractoriness.
Conclusion: In patients transitioning from TACE to Atezo/Bev, hepatic reserve and cumulative TACE burden more strongly influenced outcomes than TACE refractoriness. An INR around 1.20 marked a threshold for poorer prognosis. Early switch to Atezo/Bev, before INR ≥1.20 and with limited TACE, may improve outcomes.

FRI-250
Integrating locoregional therapies with immune checkpoint inhibitors may improve outcomes in advanced HCC
Mzamo Mbelle[1,2], Barbaros Ucar[3], Debashis Sarker[3], Paul Ross[3], Kiruthikah Thillai[3], Marie Kionisala[3], Eleni Petraki[3], Sarah Selemani[3], Dylan Lewis[1], Praveen Peddu[1], Maria Guerra Veloz[1], Mary D Cannon[1], Abid Suddle[1], Niloufar Safinia[2], Antonio D'Alessio[3,4]. [1]*Institute of Liver Studies, King's College Hospital, Denmark Hill, London, United Kingdom;* [2]*Roger Williams Institute of Liver Studies, Kings College London, London, United Kingdom;* [3]*Department of Medical Oncology, King's College Hospital and Guy's and St Thomas' Hospital, London, United Kingdom;* [4]*Division of Cancer, Imperial College London, London, United Kingdom*
Email: mzamo.mbelle@nhs.net

Background and aims: The survival benefit of combining locoregional therapy (LRT) with systemic immune checkpoint inhibition (ICI) in advanced hepatocellular carcinoma (HCC) remains poorly defined. With the advent of atezolizumab-bevacizumab (AB), emerging evidence suggests a potential synergistic effect between LRT and immune-based therapies. This study evaluated the impact of LRT administered concurrently with AB on survival and treatment response in a real-world cohort.
Method: We retrospectively analysed patients with advanced HCC treated with AB at King's College Hospital from September 2020 to September 2025. Demographic, clinical, and radiological data were collected. LRT included ablative (microwave ablation [MWA], irreversible electroporation [IRE]), embolic (transarterialchemoembolization [TACE], selective internal radiation therapy [SIRT]), and

radiation modalities (stereotactic body radiotherapy [SBRT]) delivered during ICI therapy after MDT discussion. Survival outcomes were assessed using Kaplan–Meier and logrank tests, and logistic regression was used to identify predictors of response and survival.
Results: Among 207 patients, 169 (82%) were male, with a median age of 65 years (IQR 57–72). MASLD was the most common aetiology (35.7%). Median maximal tumour diameter was 50 mm (IQR 30–96); 102 (60%) had multifocal disease, 63 (31%) macrovascular invasion, and 28 (15%) extrahepatic metastases. The median AB treatment duration was 4 months (IQR 2–10). Concurrent LRT was delivered in 25 patients: indications included consolidation after radiological response (28%), treatment of intrahepatic progression (20%), and radiotherapy for extrahepatic oligometastasis or palliation (32%). Adjunctive therapies included TACE in 24%, SIRT in 20%, MWA in 12%, and SBRT in 36% of patients. Median follow-up was 21 months (95% CI 16–24). One-year OS was 83.3% (95% CI 71.0–97.8) in responders versus 61.8% (95% CI 54.4–72.4) in non-responders ($p = 0.0018$). Concurrent LRT independently predicted improved survival (HR 0.07, 95% CI 0.01–0.18). Median OS was 14.9 months (95% CI 11.9–22.2) in patients who did not receive LRT, while it was 40.8 months (95% CI 29.8–NR; $p < 0.001$) for LRT-treated patients.
Conclusion: In this real-world cohort, concurrent LRT during AB treatment was associated with a significant improvement in OS for selected patients with advanced HCC. These findings support further prospective trials to refine timing, treatment choice, and patient selection for combined LRT-ICI approaches in advanced HCC.

FRI-251

Favourable clinical outcomes with immunotherapy in patients with mismatch repair–deficient/microsatellite instability–high biliary tract cancers: investigation from a multicenter real-world cohort

Katharina Mitzlaff[1], Martha M Kirstein[1], Iris R Engelbart[1], Arndt Vogel[2,3], Thomas Wirth[3], Anna Saborowski[3], Raphael Mohr[4], Maria Angeles Gonzalez-Carmona[5], Christian Müller[6], Marino Venerito[6], Alexander Olkus[7,8,9], Michael Dill[7,8,10], Maryam Barsch[11], Bertram Bengsch[11], Michael Quante[11], Sebastian Lange[12], Patrick Wenzel[12], Philipp Heumann[13], Hauke Christian Tews[14], Vera Himmelsbach[15], Fabian Finkelmeier[15], Roman Kloeckner[16], Peter Schirmacher[17], Jens U. Marquardt[1], Carolin Zimpel[1]. *[1]Department of Medicine I, University Medical Center – Campus Luebeck, Luebeck, Germany; [2]Institute for Medical Science, University of Toronto, Toronto, Canada; [3]Hannover Medical School, Department of Gastroenterology, Hepatology, Infectious Diseases and Endocrinology, Hannover, Germany; [4]Department of Hepatology and Gastroenterology, Charité - University Berlin, Campus Virchow Klinikum (CVK) and Campus Charité Mitte (CCM), Berlin, Germany; [5]Department of Internal Medicine I, University Hospital Bonn, Bonn, Germany; [6]Department of Gastroenterology, Hepatology and Infectious Diseases, Otto von Guericke University Hospital, Magdeburg, Germany; [7]Department of Gastroenterology, Hepatology, Infectious Diseases and Intoxication, Heidelberg University Hospital, Heidelberg, Germany; [8]National Center for Tumor Diseases (NCT), NCT, Heidelberg, a partnership between DKFZ and Heidelberg University Hospital, Heidelberg, Germany; [9]Medical Faculty Heidelberg, Heidelberg, Germany; [10]German Cancer Research Center (DKFZ) Heidelberg, Research Group Experimental Hepatology, Inflammation and Cancer, Heidelberg, Germany; [11]Department of Medicine II, Gastroenterology, Hepatology, Endocrinology, and Infectious Disease, University Medical Center, Freiburg, Germany; [12]Clinical Department of Internal Medicine II, TUM School of Medicine and Health, TUM University Hospital, Munich, Germany; [13]Department of Internal Medicine I, Gastroenterology, Hepatology, Endocrinology, Rheumatology, and Infectious Diseases, University Hospital Regensburg,, Regensburg, Germany; [14]Department of Internal Medicine I, Gastroenterology, Hepatology, Endocrinology, Rheumatology, and Infectious Diseases, University Hospital Regensburg, Regensburg, Germany; [15]Department of Gastroenterology, Hepatology and Endocrinology, University Hospital Frankfurt, Frankfurt, Germany; [16]Department for Interventional Radiology, University Medical Center – Campus Luebeck, Luebeck, Germany; [17]Institute of Pathology, Heidelberg University Hospital, Heidelberg, Germany*
Email: carolin.zimpel@uksh.de

Background and aims: Immune checkpoint inhibitors (ICIs) improve survival in patients with mismatch repair–deficient/microsatellite instability–high (dMMR/MSI-high) tumors. Since 2022, ICIs in combination with gemcitabine and cisplatin have become the standard of care for patients with advanced biliary tract cancers (BTC). Patients with dMMR/MSI-high BTC represent a rare subgroup. Here, we examined clinical characteristics, safety, and outcomes of patients with dMMR/MSI-high BTC in a German multicenter real-world cohort.
Method: Patients with dMMR/MSI-high BTC treated with systemic therapy at 10 German centers were included. Clinicopathological baseline characteristics, median overall survival (OS), median progression-free survival (PFS), response rates, and adverse events (AEs) were retrospectively analyzed. Prognostic and predictive factors were assessed using Kaplan–Meier analysis and binary logistic regression.
Results: Between 2018 and 2025, 21 patients with dMMR/MSI-high BTC were included. Median follow-up was 23 months (95% CI 19.3–26.7). The majority of patients had intrahepatic cholangiocarcinoma ($n = 12$, 57%), while nine patients (43%) had extrahepatic cholangiocarcinoma. Affected mismatch repair genes were MLH1 (53%), PMS2 (29%), MSH6 (28%), and MSH2 (19%). Common co-alterations included KRAS (38%) and TP53 (29%). In first-line setting, four patients (19%) received immunotherapy alone, 15 patients (71%) immuno-chemotherapy, and two patients (10%) chemotherapy alone. Median duration of first-line treatment was 17 months (95% CI 8.6–25.4). Second-line treatment was administered in eight patients (38%). Median OS was not reached, while median PFS was 19 months (95% CI 8.8–29.2). Favourable outcomes were observed in responders and in patients treated with immunotherapy alone. Overall response rate was 57%, including five complete and seven partial responses, and disease control rate was 86%. Occurrence of immune-related adverse events (irAEs) was associated with complete response (OR 10.5, 95% CI 1.1–107.2, $p = 0.047$). Overall, grade 1–2 irAEs occurred in one patient and grade 3–4 irAEs in five patients, leading to discontinuation of immunotherapy in four patients.
Conclusion: Immunotherapy-based treatment results in favourable responses and outcomes in patients with dMMR/MSI-high BTC and can be safely administered.

FRI-252

First-line Atezolizumab plus bevacizumab versus lenvatinib or sorafenib in Egyptian patients with unresectable hepatocellular carcinoma: a retrospective real-world study

Ahmed Radwan[1], Wafaa El-Akel[2], Hend Shousha[2], Sahar M Hassany[1], Mohamed Abdelmalek[1], Nariman Zaghloul[1], Sara Mahrous[1], Gamal Esmat[2], Mohamed Hassany[3], Mohamed AbdAllah[4], Ehab F. Moustafa[1]. *[1]Tropical medicine and gastroenterology department, Assiut University, Assiut, Egypt; [2]Endemic medicine department, Cairo University, Cairo, Egypt; [3]Tropical medicine and hepatology research institute, Cairo, Egypt; [4]Medical Research and clinical studies institute, National Research Center, Giza, Egypt*
Email: hendshousha@yahoo.com

Background and aims: Atezolizumab plus Bevacizumab is the typical first-line treatment for unresectable Hepatocellular Carcinoma (HCC), demonstrating superior survival compared to Sorafenib or Lenvatinib in some real-world studies. This study aims to compare the safety and outcomes of Atezolizumab-bevacizumab versus lenvatinib or sorafenib in Egyptian patients with unresectable HCC in a real-world setting.
Method: This retrospective analysis encompassed patients with advanced HCC eligible for systemic therapy and attended the National Committee for Control of Viral Hepatitis clinic at Al-Rajhi Hospital,

Assiut University. Recruitment occurred from June 2022 to March 2025, with follow-up until November 2025. Baseline demographics, tumor characteristics, adverse events (AEs), and tumor response were collected. The primary aim was overall survival (OS).
Results: Our analysis included 107 patients; 40 (37.4%) patients received atezolizumab-bevacizumab, 21 (19.6%) received Lenvatinib while 46 (43%) received Sorafinib. There was no significant difference among the three groups in age, gender distribution, comorbidities, baseline routine laboratory results or tumor characteristics. Chronic hepatitis C was the predominant etiology in all groups (92.5%, 61.9%, 100%, respectively) followed by non-viral etiology (7.5%, 28.6%, 0%). The mean duration of treatment was significantly longer in group 1 (317.75, 153.76, 198.3 days, respectively, $p < 0.01$). Partial response was achieved in 4(10%) in group 1 and none in the other groups. Stable disease was achieved in 12 (30%), 8(38.1%) and 6(13.04%), respectively. By the end of the study 20(50%), 6(28.6%), 38(82.6%) patients died in each group respectively, $p < 0.01$. The Kaplan-Meier survival curve indicated median OS of 16.567, 14.367, and 6.100 months, respectively, $p < 0.01$. The mean time to progression was higher in group 1 (13.651, 9.261, 7.206 months, respectively; p 0.01). Concerning AEs, dermatological manifestations and increased transaminases were more prevalent with Sorafinib. Conversely, there was no notable difference among the groups concerning the hypertension, diarrhea, hepatic decompensation, fatigue, or abdominal pain. In the whole population, Cox Regression for mortality revealed that treatment with atezolizumab-bevacezumab was associated with a longer OS (p 0.002).
Conclusion: Atezolizumab-bevacizumab is associated with significant survival benefit and longer TTP compared to Lenvatinib/Sorafinib with comparable safety.

FRI-253

Tumour seeding with percutaneous radiofrequency ablation of primary hepatocellular carcinoma

Chunpeng Nie[1], Riya Prajapati[1], Marcus Vaska[2], Stephen Congly[1,3,4].
[1]Division of Gastroenterology and Hepatology, Department of Medicine, University of Calgary, Calgary, Canada; [2]Knowledge Resource Service, Alberta Health Services, Calgary, Canada; [3]Division of Medical Transplant, Department of Medicine, University of Calgary, Calgary, Canada; [4]Arnie Charbonneau Cancer Institute, University of Calgary, Calgary, Canada
Email: chunpeng.nie@ucalgary.ca

Background and aims: Percutaneous radiofrequency ablation (RFA) is a common, less invasive alternative to resection of hepatocellular carcinoma (HCC). The risk of tumour seeding along the needle track is of concern given its potential consequences to potential future treatments. A systematic review was conducted to understand the overall risk of tumour seeding with RFA of HCC.
Method: EMBASE, MEDLINE (Ovid), CINAHL and Web of Science were reviewed from inception until July 31, 2024, with the search strategy assisted by a medical librarian. Inclusion criteria were prospective or retrospective human cohort studies including randomized control trials (RCTs) and case series of any percutaneous RFA of a lesion found to be a HCC reporting the rate of tumour seeding. Studies reporting on non-liver cancers were excluded and note was made regarding biopsy concurrent with RFA. Two individuals independently screened abstracts and extracted data; discrepancies were resolved by a third individual.
Results: A total of 1038 unique abstracts were identified. 189 underwent full text review and 52 studies were included in the analysis. All studies were prospective or retrospective cohort studies. The overall rate of tumour seeding was 1.37% (range 0–15.2%) in 11,228 patients. The median length of follow-up was 28 months (range 8–123 months). Internally cooled electrodes (68%) were most common and 37% of studies used multiple types of electrodes. Needle track ablation was performed in 32 studies, with lower rates of seeding (0.97%), compared to avoidance of track ablation in 3 studies (2.77%). Multiple studies suggested subcapsular tumours as a risk factor for seeding. Study quality was assessed via the Newcastle-Ottawa Scale; 29 studies were of good quality, 15 of fair quality, and 8 of poor quality.
Conclusion: The risk of needle track seeding with percutaneous RFA of primary HCC is 1.37% per patient. There is significant heterogeneity in technique and equipment in RFA and there is mixed quality, primarily observational literature regarding the risk of needle track seeding. More study is required to identify risk factors and mitigating techniques for needle track seeding.

FRI-254

To better predict hepatic decompensation during immunotherapy for advanced hepatocellular than with Child-Pugh and ALBI: development and validation of a predictive model, an international multicentre study

Massih Ningarhari[1], Emeline Cailliau[1], Léa Bruges[1], Jean-Charles Nault[2], Nathalie Ganne-Carrié[2], Pierre Nahon[2], Claudia Campani[2,3], Fabio Marra[3], Alessio Mastro[3], Dominique Thabut[4], Sarah Mouri[4], Mathilde Wagner[4], Marie Lequoy[5], Violaine Ozenne[5], Giuliana Amaddeo[6], Hélène Regnault[6], Maria Stella Franzè[6,7], Mohamed Bouattour[8], Maxime Ronot[9], Clemence Hollande[9], Guillaume Lassailly[1], Elise Lemaître[1], Line Carolle Ntandja Wandji[1], Stéphane Cattan[1], Sébastien Dharancy[1], Alexandre Louvet[1], Philippe Mathurin[1], Alain Duhamel[1], Manon Allaire[4]. *[1]CHU Lille, Hopital Huriez, Pole Medico-Chirurgical, Lille, France; [2]APHP, Avicenne, Bobigny, France; [3]University of Firenze, Florence, Italy; [4]APHP, Pitié-Salpêtrière, Paris, France; [5]APHP, Saint-Antoine, Paris, France; [6]APHP, Henri Mondor, Créteil, France; [7]University of Messina, Messina, Italy; [8]AP-HP, Hôpital Beaujon, Liver Cancer and Innovative Therapy, CLICHY, France; [9]APHP, Beaujon, Clichy, France*
Email: massih.ningarhari@chu-lille.fr

Background and aims: Hepatic decompensation impacts outcomes of patients with hepatocellular carcinoma (HCC) treated with immunotherapy. Identification of at-risk patients is crucial. The Child-Pugh (CPS) and ALBI scores have limitations for such purpose.
Method: Prospectively collected data of patients without baseline decompensation treated with Atezolizumab-Bevacizumab for advanced HCC were analysed for clinical decompensation event (CDE) (overt ascites, variceal (EV) bleeding, encephalopathy, and/or jaundice) as a primary endpoint, censored at 2 years. Among 12 candidate variables, in a multivariate Fine & Gray model considering death and end of treatment (+28 days) as competing events, stepwise downward selection was applied in a discovery cohort (DC, n = 448, missing data imputed using fully conditional specification, m = 20) and externally validated (VC, n = 346). Calibration and discriminant performances were compared to CPS and ALBI using Harrell's c adjusted for competing risks. Association with overall survival (OS) was tested using a Cox proportional hazards model.
Results: In the DC (cirrhosis 79%, BCLC-C 73%, CPS-B 14%, ALBI 2/3 67%, grade 2/3 EV 25%, grade 1 ascites 17%, median time on treatment 7.6 months (IQR: 3.3–16.6)), CDE occurred in n = 133 (cumulative incidence at 2 years 30.4%). Five variables were retained for the new model: ALBI grade (subhazard-ratio (sHR) = 2.00 [95% confidence interval : 1.25–3.21] for 2 vs. 1; sHR = 2.77 [95% CI: 1.30–5.87] for 3 vs. 1), grade 2/3 EV (sHR = 2.46 [95% CI: 1.62–3.73]), past history of CDE (sHR = 1.53 [95% CI: 1.04–2.26]), grade 1 ascites (sHR = 2.02 [95% CI: 1.37–2.97]), and platelet count (sHR per log(G/L) increase = 0.62 [95% CI: 0.45–0.85]). Median Harrell's c was 0.75 (min-max 0.74–0.76) for ALBIPHy vs. 0.57 for CPS vs. 0.62 for ALBI. Median OS was 15.2 months [IQR: 7.1-NR]. The model associated with OS (HR 1.48 [95% CI: 1.26–1.74] per point, $p < 0.001$). Patients stratified into 3 risk groups had increasing rates of discontinuation (5%, 25%, and 38%) and death (5%, 20%, and 30%) without tumor progression. In the VC, Harrell's c reached 0.70 (min-max: 0.69–0.70), and calibration slope 0.81 (min-max: 0.78–0.83).

Conclusion: This new model (ALBI, portal hypertension markers, and history of decompensation) better predicts hepatic decompensation during immunotherapy than CPS or ALBI alone, and could be a valuable tool to identify patients that would benefit the most from hepatology expertise, and a potential stratification factor in future studies.

FRI-255-YI

Sub-stratification of Child-Pugh B patients and dynamic evolution of liver function revealed differential benefit from atezolizumab/bevacizumab in unresectable hepatocellular carcinoma

Anne Victoire Odent[1], Claudia Campani[2], Mohamed Bouattour[3], Yann Touchefeu[4], Victoria Delhoume[4], Olivier Rosmorduc[1], Alina Pascale[1], Jihyun An[5], Han Chu Lee[6], Hélène Regnault[1], Dominique Thabut[1], Giuliana Amaddeo[1], Massih Ningarhari[7], Isabelle Ollivier-Hourmand[8], Chloe Metivier[8], Maxime Ronot[1], Line Carolle Ntandja Wandji[2], Violaine Ozenne[1], Sabrina Sidali[2], Fabio Marra[9], Clemence Hollande[1], Nathalie Ganne[1], Pierre Nahon[1], Jean Marie Peron[10], Marie Lequoy[1], Rohini Sharma[11], Eric Trépo[12], Sarah Mouri[1], Manon Allaire[1], Ju Hyun Shim[6], Jean-Charles Nault[2].
[1]APHP, Paris, France; [2]Centre de Recherche Des Cordeliers, Paris, France; [3]AP-HP, Hôpital Beaujon, Liver Cancer and Innovative Therapy, Clichy, France; [4]CHU de Nantes, Nantes, France; [5]Hanyang college university, Seoul, France; [6]ASAN medical center, seoul, Korea, Rep. of South; [7]CHU de lilles, Lille, France; [8]CHU de Caen, Caen, France; [9]Department of Experimental and Clinical Medicine, Internal Medicine and Hepatology Unit, University of Firenze, Firenze, Italy; [10]Department of Hepatogastroenterology, Rangueil University Hospital; 31059 Toulouse, France., Toulouse, France; [11]Imperaril college London, London, United Kingdom; [12]Department of Gastroenterology, Hepatopancreatology and Digestive Oncology, Hôpital Universitaire de Bruxelle, Bruxelles, Belgium
Email: naultjc@gmail.com

Background and aims: We aimed to identify, among patients with advanced hepatocellular carcinoma (HCC) and Child-Pugh B cirrhosis, typically excluded from clinical trials, a subgroup that may benefit from first-line atezolizumab/bevacizumab (A/B).
Method: We conducted an international multicenter study including patients with unresectable HCC treated with first-line A/B between 2020 and 2024 across 12 centers in Europe and Asia. A cohort of Child-Pugh B patients treated with sorafenib served as a control. Baseline clinical, biological, and tumor features were correlated with radiological response, progression-free survival (PFS), and overall survival (OS).
Results: Among 1499 patients with HCC treated by A/B in first line, 246 (16.4%) had Child-Pugh B cirrhosis. Compared with Child–Pugh A patients, Child–Pugh B patients were younger, more often had cirrhosis of alcoholic or hepatitis B viral origin, and had larger tumors with a higher frequency of portal vein tumor thrombosis. The median follow-up was 35.7 months. Within Child-Pugh B, 72% were B7, 21.5% B8, and 6.5% B9; 73% had ALBI grade 2 and 27% grade 3. Median OS and PFS were significantly shorter in Child-Pugh B (8.1 and 5.2 months) versus Child-Pugh A (16.8 and 8.6 months; both $p < 0.001$). Two-year OS was 20% for Child-Pugh B versus 38% for Child-Pugh A. Child-Pugh B patients treated with A/B had longer OS than those treated with sorafenib ($p = 0.002$). In multivariate analysis, chronic hepatitis C (HR = 0.65, CI95% = 0.44–0.95, P = 0.027), presence of extrahepatic metastasis (HR = 1.49, CI95% = 1.10–2.03, P = 0,011) and ALBI grade 3 (HR = 1.54, CI95% = 1.10–2.15, P = 0,012) were independently associated with a high risk of death. A score combining ALBI grade 1/2 and metastatic status identified prognostic subgroups (10.3 vs 7.9 vs 4.2 months; $p < 0.0001$). Improvement from Child pugh B to Child-Pugh A occurred in 31% at the first imaging evaluation. Patients who received recent treatment showed greater improvement in liver function at the first evaluation compared with those treated more than 6 months earlier or never treated (P = 0.04, Cochran–Armitage trend test). Radiological response (HR = 0.58, p = 0.021) and liver function improvement (HR = 0.59, p = 0.006) correlated with reduced mortality using a time-dependent analysis.
Conclusion: Although Child-Pugh B patients have poorer survival, a subgroup, those with ALBI grade 1/2 and no extrahepatic metastasis, can derive meaningful benefit from A/B therapy. Improving underlying liver disease may contribute to better outcomes.

FRI-256

Durable response is associated with long-term survival even in patients with poor hepatic reserve after Atezolizumab plus Bevacizumab: a multicenter 3-year overall survival cohort with a 6-month landmark analysis

Masatsugu Ohara[1], Goki Suda[1], Risako Kohya[1], Yutaka Yasui[2], Kaoru Tsuchiya[2], Masayuki Kurosaki[2], Joji Tani[3], Shinya Maekawa[4], Nobuyuki Enomoto[4], Makoto Chuma[5], Manabu Morimoto[6], Shun Kaneko[7], Mina Nakagawa[7], Yasuhiro Asahina[7], Atsumasa Komori[8], Yuki Kugiyama[8], Jun Ito[9], Sonoe Yoshida[1], Yoshiya Yamamoto[10], Takuya Sho[1], Ren Yamada[11], Shunichi Hosoda[1], Yoshimasa Tokuchi[10], Akimitsu Meno[1], Takashi Kitagataya[1], Naoki Kawagishi[1], Masato Nakai[1], Koji Ogawa[1], Naoya Sakamoto[1].
[1]Hokkaido University, Sapporo, Japan; [2]Musashino Red Cross Hospital, Musashino, Japan; [3]Kagawa University, Takamatsu, Japan; [4]University of Yamanashi, kofu, Japan; [5]JCHO Yokohama Hodogaya Central Hospital, Yokohama, Japan; [6]Yokohama City University Medical Center, Yokohama, Japan; [7]Institute of Science Tokyo, Tokyo, Japan; [8]NHO Nagasaki Medical Centre, Nagasaki, Japan; [9]NHO Hokkaido Medical Centre, Sapporo, Japan; [10]Hakodate Municipal Hospital, Hakodate, Japan; [11]Kushiro Rosai Hospital, Kushiro, Japan
Email: masatsu-ohara@pop.med.hokudai.ac.jp

Background and aims: Long-term overall survival (OS) after atezolizumab plus bevacizumab (Atez/Bev) for unresectable hepatocellular carcinoma (uHCC) has not been sufficiently characterized in real-world cohorts with mature follow-up beyond 3 years. In addition, the relative prognostic contributions of treatment-induced durable disease control and baseline hepatic reserve should be evaluated while minimizing immortal time bias. We therefore investigated long-term outcomes in a mature 3-year OS cohort and assessed their independent and relative impacts using a 6-month landmark analysis.
Method: This multicenter retrospective study included 257 uHCC patients treated with Atez/Bev between October 2020 and January 2022 and followed for more than 3 years. Durable response was defined as stable disease (SD), partial response (PR), or complete response (CR) maintained for more than 6 months. Overall survival was first described in the entire cohort. To mitigate immortal time bias, a 6-month landmark population was constructed, and multivariable Cox proportional hazards models were fitted including age, AFP, BCLC stage, modified ALBI grade (mALBI 1–2a vs ≥2b), and durable response.
Results: In the entire cohort, the 2- and 3-year OS rates were 39.2% and 25.3%, respectively, reflecting mature long-term observation. Durable response was achieved in 110 patients (42.8%). In the 6-month landmark population (n = 216), durable response was observed in 110 patients (50.9%). Median OS was 12.3 months in patients without durable response and 28.6 months in those with durable response ($P < 0.001$). In the 6-month landmark multivariable Cox model, durable response was the strongest predictor of OS (HR 0.41, 95% CI 0.30–0.57, $P < 0.0001$), exceeding the prognostic impact of preserved hepatic reserve (mALBI 1–2a; HR 0.50, 95% CI 0.37–0.68, $P < 0.0001$). Older age and elevated AFP were also significant predictors of poorer OS, whereas BCLC stage was not. Notably, durable response was associated with improved long-term survival even among patients with poor hepatic reserve (mALBI ≥2b).
Conclusion: In a mature 3-year OS cohort of uHCC treated with Atez/Bev, achieving durable response lasting more than 6 months was more strongly associated with long-term survival than baseline

hepatic reserve. These findings highlight durable response as the principal determinant of long-term benefit from Atez/Bev therapy.

FRI-257

Serum TGF-β1 and IDO1 kinetics for the prediction of clinical outcomes among first-line immunotherapy treated patients with hepatocellular carcinoma

Spyridon Pantzios[1], Polyxeni Nikolakopoulou[2], Orestis Sidiropoulos[1], Antonia Syriha[1], Georgios Zogas[1], Maria-Stella Malatesta[1], Despoina Gyriki[1], Antonios Chatzigeorgiou[2], Ioannis Elefsiniotis[1]. [1]*Academic Department of Internal Medicine-Hepatogastroenterology Unit, General Oncology Hospital of Kifisia "Agioi Anargyroi", National and Kapodistrian University of Athens, Athens, Greece;* [2]*Department of Physiology, Medical School of Athens, National and Kapodistrian University of Athens, Athens, Greece*
Email: spiros_pant@hotmail.com

Background and aims: Though serum immunosuppressive cytokines, such as TGF-β1 and IDO1, play an important role in cancer immunity and patient prognosis, they have been rarely studied as prognostic biomarkers in immunotherapy-treated hepatocellular carcinoma (HCC) patients. The aim of our study was to evaluate the correlation of baseline and on-treatment values of TGF-β1/IDO1 with overall survival (OS) and progression-free survival (PFS) in HCC patients treated with 1st line atezolizumab-bevacizumab (A/B) or tremelimumab-durvalumab (STRIDE).
Method: We retrospectively evaluated 86 immunotherapy-treated HCC patients. The baseline characteristics of all patients were evaluated and baseline and sequential (2 and 4 months of treatment) serum TGF-β1/IDO1 were measured. We compared baseline TGF-β1 and IDO1 median levels according to patients' baseline characteristics and studied their correlation with OS and PFS. We also studied the correlation of the on-treatment change of these values from baseline with OS and PFS.
Results: Patients with cirrhosis and diabetes had significantly lower baseline TGF-β1 ($p = 0.007$ and $p = 0.039$, respectively), as had patients without extrahepatic disease ($p = 0.03$) and within up-to-7 criteria ($p = 0.002$). There was no difference in OS and PFS between patients with low versus high baseline TGF-β1, when median baseline TGF-β1 values was used as cut-off. Patients who had increased serum TGF-β1 in 2 and 4 months of treatment compared to baseline had statistically significantly better OS than those with decreased values (29 vs. 12 months, $p = 0.023$ and 41 vs. 14 months, $p = 0.04$, respectively). Patients without progressive disease (PD, $p = 0.01$) had significantly higher baseline serum IDO1 levels than those with PD, as had those with objective response compared to those without ($p = 0.049$), and patients within ($p = 0.05$), compared to those exceeding up-to-7 criteria. Baseline IDO1 was significantly correlated with PFS after multivariate analysis ($p = 0.015$, HR = 0.615), but not with OS. Patients with higher baseline IDO1 had significantly better PFS than those with lower baseline levels, when median baseline IDO1 was used as cut-off (17.6 vs. 14.6 months, respectively, $p = 0.046$). No correlation of IDO1 change in 2 or 4 months of treatment with OS and PFS was observed.
Conclusion: On-treatment rises in serum TGF-β1 and higher baseline IDO1 emerge as accessible biomarkers for risk stratification and treatment monitoring in first-line A/B or STRIDE-treated HCC patients, a finding that needs prospective validation.

FRI-361

Preoperative transarterial radioembolization is comparable to primary liver resection but shows more favorable outcomes than preoperative transarterial chemoembolization in hepatocellular carcinoma beyond the Milan criteria

Jeayeon Park[1], Yunmi Ko[1], Hyunjae Shin[1], Moon Haeng Hur[1], Yun Bin Lee[1], Eun Ju Cho[1], Jeong-Hoon Lee[1], Su Jong Yu[1], Jung-Hwan Yoon[1], Yoon Jun Kim[1]. [1]*Seoul National University Hospital, Seoul national university college of medicine, Seoul, Korea, Rep. of South*
Email: yoonjun@snu.ac.kr

Background and aims: Resectable hepatocellular carcinoma (HCC) beyond the Milan criteria represents a clinically heterogeneous with variable classification across staging systems. Owing to the increased risk of recurrence and inconsistent guideline recommendations, treatment strategies for this population remain undefined, ranging from primary liver resection to locoregional therapies. With the emerging role of transarterial radioembolization (TARE), we compared the clinical outcomes of primary liver resection, preoperative transarterial chemoembolization (TACE), and preoperative TARE.
Method: We retrospectively reviewed consecutive patients with HCC beyond the Milan criteria who underwent primary liver resection, preoperative TACE, or preoperative TARE at Seoul National University Hospital. The primary endpoint was overall survival (OS), and the secondary endpoint was recurrence-free survival (RFS). Survival outcomes were analyzed using Kaplan–Meier estimates with log-rank tests, and Cox proportional hazards models with inverse probability of treatment weighting (IPTW) were applied to adjust for confounding.
Results: A total of 226 patients were included (primary resection, n = 127; preoperative TACE, n = 52; preoperative TARE, n = 47), with a median follow-up of 37.2 months. After IPTW adjustment, baseline characteristics were well balanced among groups. Median OS was not reached in the primary resection and preoperative TARE groups but was 60.7 months in the preoperative TACE group. Compared with primary resection, preoperative TACE was associated with worse OS (hazard ratio [HR] 3.01; 95% confidence interval [CI] 1.57–5.75; P = 0.004), whereas OS with preoperative TARE was comparable (HR 1.17; 95% CI 0.51–2.70; P = 0.57). Preoperative TARE showed superior OS compared with preoperative TACE (HR 0.40; 95% CI 0.16–0.96; P = 0.04). Similarly, RFS was worse with preoperative TACE than with primary resection (HR 1.80; 95% CI 1.11–2.92; P = 0.02), while RFS with preoperative TARE was comparable to primary resection (HR 0.85; 95% CI 0.49–1.48; P = 0.57).
Conclusion: In patients with resectable HCC beyond the Milan criteria, preoperative TARE was associated with clinical outcomes comparable to those of primary liver resection. In real-world settings where upfront resection is not feasible, preoperative TARE may be considered an alternative treatment strategy.

FRI-362

Prediction of disease control in unresectable hepatocellular carcinoma under Atezolizumab-Bevacizumab with machine and CT deep learning models

Asier Rabasco Meneghetti[1,2], Claudia Campani[3,4], Charles Roux[5], Zunamys Itzel Carrero[1], Dan-Adrian Popica[5], Giuliana Amaddeo[6], Marie Lequoy[7], Clemence Hollande[8], Sarah Mouri[9], Mathilde Wagner[10], Vincent Plaforet[5], Sabrina Sidali[3,8], Maxime Ronot[11], Marika Rudler[9], Alain Luciani[12], Olivier Sutter[13], Eléonore Spitzer[9], Hélène Regnault[6], Sanaa El Mouhadi[10], Violaine Ozenne[7], Nathalie Ganne-Carrié[3,14], Mohamed Bouattour[15], Jean-Charles Nault[3,14], Dominique Thabut[9,16], Jakob Nikolas Kather[1,17,18], Manon Allaire[3,9,19]. [1]*Else Kroener Fresenius Center for Digital Health, Faculty of Medicine and University Hospital Carl Gustav Carus, TUD Dresden University of Technology, Dresden, Germany;* [2]*German Cancer Consortium (DKTK), Partner site Dresden, German Cancer Research Center (DKFZ), Heidelberg, Germany;* [3]*INSERM UMR 1138, Centre de recherche des Cordeliers, Paris, France;* [4]*Department of Experimental and Clinical Medicine, Internal Medicine and Hepatology Unit, University of Firenze, Firenze, Italy;* [5]*AP-HP Sorbonne Université, Hôpital Universitaire Pitié-Salpêtrière, Service de radiologie interventionnelle, Paris, France;* [6]*Department of Hepatology, Henri Mondor University Hospital, Assistance Publique-Hôpitaux de Paris, Créteil, France;* [7]*AP-HP Sorbonne Université, Hôpital Universitaire Saint Antoine, Service d'Hépato-gastroentérologie, Paris, France;* [8]*Liver*

Cancer Unit, Assistance Publique - Hôpitaux de Paris, Beaujon University Hospital, Clichy, France; [9]APHP Sorbonne University, Pitié Salpêtrière Hospital, Hepatogastroenterology unit, Paris, France; [10]AP-HP Sorbonne Université, Hôpital Universitaire Saint Antoine, Service d'Imagerie, Paris, France; [11]Department of Radiology, Assistance Publique - Hôpitaux de Paris, Beaujon University Hospital, Clichy, France; [12]Department of Medical Imaging, Assistance Publique-Hôpitaux de Paris, Henri Mondor-Albert Chenevier University Hospital, Créteil, France; [13]Interventional Radiology Unit, Hôpital Avicenne, Hôpitaux Universitaires Paris-Seine-Saint-Denis, AP-HP, Bobigny, France; [14]AP-HP Sorbonne Paris Nord, Hôpitaux Universitaire Paris Seine Saint-Denis, Service d'Hépatologie, Bobigny, France; [15]AP-HP, Hôpital Beaujon, Liver Cancer and Innovative Therapy, Clichy, France; [16]Sorbonne Université, INSERM, Centre de recherche Saint-Antoine (CRSA), Institute of Cardiometabolism and Nutrition (ICAN), Paris, France; [17]Department of Medicine I, University Hospital Dresden, Dresden, Germany; [18]Medical Oncology, National Center for Tumor Diseases (NCT), University Hospital Heidelberg, Heidelberg, Germany; [19]Genomic Instability, Metabolism, Immunity and Liver Tumorigenesis laboratory, Equipe Labellisée LIGUE 2023, Paris, France
Email: asier.rabasco@tu-dresden.de

Background and aims: Atezolizumab–Bevacizumab (AtezoBev) is first line standard of care for advanced hepatocellular carcinoma (HCC) requiring systemic treatment. However, approximately 25–30% of patients experience disease progression. We aimed to develop and externally validate baseline non-invasive clinical-biological and imaging-based models to predict disease control (DC) under AtezoBev.
Method: We included 480 patients with unresectable HCC treated with AtezoBev as first-line systemic therapy and no prior liver transplantation from five French centers. Patients were split into development (n = 256) and validation (n = 224) cohorts by center. Tumor response was assessed every 3 months using RECIST 1.1 criteria. DC was defined as absence of progression, including stable disease, partial and complete responses. Abdominal CT scans obtained within 3 months prior to treatment initiation were available for 257 patients (development n = 115, validation n = 152) and used to train and validate a deep-learning (DL) imaging model based on a pretrained CT foundation model. A baseline clinical model was developed using logistic regression with LASSO selection. Performance was assessed using the area under the receiver operating characteristic curve (AUROC) and Brier score.
Results: Median patient age was 67.0 years (87% male). Cirrhosis was present in 74%, 44% had viral infection, alcohol consumption was present in 38% and metabolic syndrome in 36%. Median platelet counts were 171.500/mm^3, median INR was 1.10 and 68% were ALBI grade 2 or higher. Extrahepatic lesions were present in 30%, with 36% showing vascular invasion, 61% being BCLC-C and 59% treatment-naive for HCC (no prior HCC-directed therapy). Median AFP levels were 78.0 ng/mL. 29% showed progressive disease. The DL imaging model was unable to classify DC, with a validation AUROC (median [95% confidence interval]) of 0.46 [0.31–0.58] (Brier: 0.25). The clinical model signature included 7 features: AFP with log-odds ratio (LOR) of −0.80, age (LOR: 0.65), extrahepatic lesion presence (LOR: −1.08), prior HCC treatment (LOR: −1.28), ALBI grade (LOR: −0.10), INR (LOR: 0.50) and platelet counts (LOR: −0.38), showing an AUROC of 0.70 [0.62–0.78] (Brier:0.20) in validation.
Conclusion: A baseline clinical model moderately predicted DC under AtezoBev, outperforming a whole-abdominal DL imaging approach. These findings suggest that readily available clinical parameters provide prognostic value, whereas imaging models may benefit from regional analyses focused on the liver.

FRI-363

A dynamic prognostic model using alpha-fetoprotein and serial hemogram-based inflammatory biomarkers for unresectable hepatocellular carcinoma treated with first-line immunotherapy

Yujie Ran[1], Huanhuan Cao[1,2], Minghui Zhu[1], Yixuan Wang[1], Chunxiu Zhong[1], Kunyuan Wang[1], Hongyan Liu[1], Dingli Liu[1], Huaiyu Chen[1], Jinzhang Chen[1], Yabing Guo[1], Rong Fan[1]. *[1]Department of Infectious Diseases, Nanfang Hospital, Southern Medical University, Guangzhou, China; [2]Department of Infectious Diseases, Dongguan People's Hospital, The Tenth Affiliated Hospital of Southern Medical University, Southern Medical University, Dongguan, China*
Email: rongfansmu@163.com

Background and aims: Immune checkpoint inhibitor (ICI) has improved the prognosis of unresectable hepatocellular carcinoma (HCC) patients, but outcomes vary greatly. We aimed to develop a dynamic risk model integrating baseline clinical features and early longitudinal key serum biomarker trajectories to optimize prognosis estimation in first-line ICI-treated HCC patients.
Method: This multicenter retrospective cohort study enrolled 410 unresectable HCC patients receiving first-line ICIs (training cohort, N = 286; external validation cohort, N = 124), with overall survival (OS) as the primary endpoint. Baseline predictors were selected by LASSO-Cox regression. Longitudinal measurements of alpha-fetoprotein, lymphocyte, neutrophil, monocyte and platelet counts (collected pre- and within 6 months of ICI initiation) were converted into 5 multivariate functional principal-component (MFPC) scores. A joint Cox model integrating baseline factors and MFPC scores was developed and externally validated.
Results: Training and validation cohorts had median follow-ups of 15.0 months (IQR 8.2, 24.6) and 12.2 months (IQR 6.2, 22.8), respectively, with BCLC C stage comprising 74.5% and 64.7% of each cohort. The baseline-only model (albumin, lactate dehydrogenase, neutrophil-to-lymphocyte ratio, tumor numbers >3, and extrahepatic metastasis) yielded an AUC of 0.610 (95%CI 0.497–0.722) at 12 months in validation set. Adding longitudinal MFPC scores significantly improved discriminative performance: the dynamic model yielded time-dependent AUCs of 0.895 (95%CI 0.842–0.949), 0.827 (95%CI 0.759–0.894) and 0.783 (95%CI 0.689–0.877) at 12, 24 and 36 months in the training cohort. External validation confirmed good discriminative ability, with AUCs of 0.803 (95%CI 0.715–0.890), 0.808 (95%CI 0.714–0.902), and 0.832 (95%CI 0.734–0.930) at the same time points. The integrated dynamic model outperformed the baseline-only model and existing clinical scoring systems (e.g., ALBI, mALBI, EZ-ALBI, CRATIFY). Dynamic model-based stratification defined low-, intermediate-, and high-risk groups with markedly distinct median OS: 49.4, 22.1, and 8.1 months in the training cohort ($p < 0.001$), and 40.6, 17.6, and 10.0 months in the validation cohort ($p < 0.001$).
Conclusion: This dynamic model integrating early longitudinal biomarker trajectories significantly enhances prognosis estimation in first-line ICI-treated HCC, offering robust, personalized risk stratification for clinical application.

FRI-364-YI

Hepatic decompensation is driven by underlying liver disease rather than immunotherapy choice in inresectable hepatocellular carcinoma

Lou-Devy Rouxel[1], Claudia Campani[2], Mohamed Bouattour[3], Yann Touchefeu[4], Giuliana Amaddeo[5], Leila Sadek[6], Marie Lequoy[7], Apolline Commin[8], Anna Pellat[9], Nathalie Ganne-Carrié[2], Clemence Hollande[3], Sarah Mouri[1], Pierre Malherbe[4], Hélène Regnault[5], Jean Marie Peron[6], Violaine Ozenne[7], Chloe Metivier[8], Lucia Parlati[9], Jean-Charles Nault[2], Sabrina Sidali[3], Paul Vigneron[5], Cécile Cussac[6], Mathilde Wagner[7], Romain Coriat[9], Isabelle Ollivier-Hourmand[8], Dominique Thabut[1], Manon Allaire[1]. *[1]AP-HP Sorbonne Université, Hôpital Universitaire Pitié-Salpêtrière, Service d'Hépato-gastroentérologie, Paris, France; [2]AP-HP Sorbonne*

Paris Nord, Hôpitaux Universitaire Paris Seine Saint-Denis, Service d'Hépatologie, Centre de Recherche des Cordeliers, Université Paris Cité, Sorbonne Université, Inserm, F-75006, Paris, France; [3]AP-HP, Hôpital Beaujon, Service d'Hépatologie, and Université Paris Cité, Sorbonne Paris Cité, CRI, UMR 1149, Paris, France; [4]Hepato-gastroenterology Department, Nantes University Hospital, Nantes, Institut des Maladies de l'Appareil Digestif (IMAD), Inserm CIC, Nantes, France; [5]AP-HP, Hôpital Henri Mondor, Service d'Hépatologie, Créteil, France; [6]Department of Hepato-Gastroenterology, Purpan Hospital, Toulouse, France; [7]Service d'Hépatologie, AP-HP Saint-Antoine, Paris, France; [8]Service d'Hépato-Gastroentérologie, CHU de Caen, ERN RARE-LIVER, Caen, France; [9]Department of Gastroenterology and Digestive Oncology, Cochin Hospital, APHP, Paris, France
Email: loudevyrouxel@gmail.com

Background and aims: Immunotherapy combinations have transformed the treatment of HCC, but their effects on hepatic decompensation remain unclear. This project compares the incidence of ascites, hepatic encephalopathy (HE), and variceal bleeding (AVB) under atezolizumab–bevacizumab (Atezobev) versus durvalumab–tremelimumab (DurvaTreme).
Method: This multicenter retrospective study included patients treated with first-line AtezoBev or DurvaTreme. Patients were matched 1:1 using propensity score methods. Hepatic decompensation (defined as the occurrence of ascites, HE, and/or AVB) occurring after treatment initiation and prior to progression (per RECIST 1.1) was compared between the two groups.
Results: Among 1053 patients, 908 received AtezoBev and 145 DurvaTreme. Patients treated with DurvaTreme more frequently had a history of AVB (23% vs. 12%, p = 0.001) and ascites (23% vs. 15%, p = 0.008). After matching, 280 patients were analyzed; in both groups, about 60% were BCLC-C, 35% had vascular invasion, 20% had prior AVB, 24% had prior ascites, 50% had varices, 8% had ascites, 40% received non-selective beta-blockers, 60% were Child-Pugh A, and 24% were ALBI grade 1. After a median follow-up of 20.1 months, OS was similar between patients treated with AtezoBev and DurvaTreme (median OS 20.8 months vs. not reached, p = 0.25). Hepatic decompensation occurred in 27.9% patients treated with AtezoBev and 23.6% patients treated with DurvaTreme (p = 0.49), with a median time to decompensation of 3.47 and 1.97 months (p = 0.02), respectively. AVB was more frequent in the AtezoBev group (13.8% vs. 5.7%, p = 0.03), whereas the incidence of HE and ascites did not differ between groups. Early hepatic decompensation within the first 3 months of treatment, was more frequent in the AtezoBeva group (18.5% vs. 6.4%, p < 0.001). Hepatic decompensation-related death occurred in 13.5% patients in the AtezoBev group and 23.1% patients in the DurvaTreme group (p = 0.31). Only history of ascites (OR 3.37, p = 0.001) was independently associated with hepatic decompensation, but not the type of treatment received.
Conclusion: AtezoBev and DurvaTreme were associated with similar OS, but differed in the pattern of hepatic decompensation, with higher rates of AVB and observed in the AtezoBev group. These differences were largely driven by baseline liver disease severity, particularly a history of ascites, which emerged as the main determinant of decompensation risk, rather than treatment choice itself.

FRI-365
Hepatocellular carcinoma stage, treatment patterns, and survival outcomes in a contemporary multicentre international cohort
N Apoorva Sasikumar[1], Caleb Wei Hao Ng[2], Darren Jun Hao Tan[2], Beom Kyung Kim[3], Nobuharu Tamaki[4], Karn Wijarnpreecha[5], Sung Won Lee[6], Ken Liu[7,8], Gang Chen[9], Takumi Kawaguchi[10], Anand Kulkarni[11], Hirokazu Takahashi[12], Nicholas Syn[1], Daniel Huang[2]. *[1]Alexandra Hospital, Singapore, Singapore; [2]National University Hospital, Singapore, Singapore; [3]Severance Hospital, Seoul, Korea, Rep. of South; [4]Musashino Red Cross Hospital, Tokyo, Japan; [5]University of Arizona College of Medicine Phoenix, Arizona, United States; [6]Catholic University of Korea, Seoul, Korea, Rep. of South; [7]Royal Prince Alfred Hospital, Sydney, Australia; [8]University of Sydney, Sydney, Australia; [9]First Affiliated Hospital of Wenzhou Medical University, Wenzhou, China; [10]Kurume University School of Medicine, Kurume, Japan; [11]Asian Institute of Gastroenterology, Hyderabad, India; [12]Saga University, Saga, Japan*
Email: e1354047@u.nus.edu

Background and aims: Hepatocellular carcinoma (HCC) remains a major cause of cancer-related mortality globally. The underlying etiologies of HCC and its therapeutic approaches have evolved substantially; however, data on how these shifts have influenced the Barcelona Clinic Liver Cancer (BCLC) stage at diagnosis, treatment patterns, and patient survival are limited.
Method: We performed a large, retrospective, multicenter cohort study including 2887 adults (75.8% male) diagnosed with HCC across ten tertiary liver centers in Asia, Oceania, and North America. Survival outcomes were compared using restricted mean survival time (RMST).
Results: The median age of the cohort was 64 years (IQR 57–73), and 83.1% were of Asian ethnicity. The proportion of patients with hepatitis C virus–related HCC decreased over time (28.82% in 2005–2014 vs. 13.46% in 2015–2024, p < 0.001), whereas HCC associated with metabolic dysfunction–related steatohepatitis increased (24.75% vs. 27.19%, p = 0.001). The distribution of BCLC stages at diagnosis remained stable, with 62.66% at stage 0/A, 18.43% at stage B, and 18.91% at stage C (p = 0.122). Regarding treatment, 49% received therapy with curative intent, 36.9% received non-curative interventions, and 14.0% received supportive care. Notably, curative treatments were administered less frequently over time (57.8% in 2005–2014 vs. 46.3% in 2015–2024, p < 0.001). Survival rates improved across the study period, with 1-, 3-, and 5-year survival rising from 90.7%, 77.7%, and 68.4% (2005–2014) to 90.7%, 81.0%, and 74.7% (2015–2024, p < 0.001).
Conclusion: Despite improvements in overall survival for HCC, the proportion of patients diagnosed at an early BCLC stage has not increased, and the use of curative therapies has declined. These findings highlight the need for enhanced strategies to facilitate early detection of HCC.

FRI-366
Differential therapeutic effectiveness of atezolizumab plus bevacizumab in unresectable HCC by chronic hepatitis B viral activity
Yunmi Ko[1], Hyunjae Shin[1], Jeong-Hoon Lee[1], Byeong Geun Song[2], Moon Haeng Hur[1], Youngsu Park[3], Jeayeon Park[1], Yuri Cho[3], Yun Bin Lee[1], Eun Ju Cho[1], Bo Hyun Kim[3], Su Jong Yu[2], Dong Hyun Sinn[2], Yoon Jun Kim[1], Jung-Hwan Yoon[1]. *[1]Seoul National University Hospital, Seoul, Korea, Rep. of South; [2]Samsung Medical Center, Seoul, Korea, Rep. of South; [3]National Cancer Center, Goyang, Korea, Rep. of South*
Email: yhstella@gmail.com

Background and aims: Atezolizumab plus bevacizumab (Atezo/Bev) is recommended as the first-line therapy for unresectable hepatocellular carcinoma (uHCC). Previous studies suggested differential immunotherapy responses between viral and non-viral HCC; however, the mechanisms remained unclear. We investigated the impact of hepatitis B virus (HBV) DNA detectability, an indicator of viral replication activity that may influence the intrahepatic immune microenvironment, on Atezo/Bev outcomes.
Method: This retrospective study included patients with uHCC, initially treated with Atezo/Bev at three hospitals in Korea. Patients were categorized as chronic hepatitis B (CHB) with undetectable HBV DNA (CHB/undetectable-DNA), CHB with detectable HBV DNA (CHB/detectable-DNA), or non-viral. Primary and secondary outcomes were progression-free survival (PFS) and overall survival (OS).

Results: We included 549 consecutive patients: CHB/undetectable-DNA (n = 216), CHB/detectable-DNA (n = 171), and non-viral groups (n = 162). After propensity score matching, baseline characteristics were well-balanced. CHB/undetectable-DNA group had significantly longer PFS than both CHB/detectable-DNA (hazard ratio [HR] = 0.66, 95% confidence interval [CI] = 0.44–0.98, *P* = 0.04) and non-viral groups (HR = 0.61, 95% CI = 0.37–0.98, *P* = 0.048). PFS did not differ between CHB/detectable and non-viral groups (HR = 1.28, 95% CI = 0.86–1.91, *P* = 0.23). CHB/detectable-DNA group showed significantly shorter OS than both CHB/undetectable-DNA (HR = 1.75, 95% CI = 1.04–2.94, *P* = 0.03) and non-viral groups (HR = 2.48, 95% CI = 1.35–4.52, *P* = 0.003). OS was comparable between CHB/undetectable-DNA and non-viral groups (HR = 0.79, 95% CI = 0.34–1.84, *P* = 0.58).
Conclusion: Undetectable HBV DNA was associated with longer PFS and OS than detectable HBV DNA in CHB patients with uHCC receiving first-line Atezo/Bev. These findings suggest that HBV DNA detectability may negatively influence immunotherapy outcomes. Antiviral treatment may mitigate this effect and improve the therapeutic effectiveness of Atezo/Bev.

FRI-367
Clinical relevance of conversion therapy after atezolizumab plus bevacizumab in hepatocellular carcinoma: a multicenter study

Takuya Sho[1], Goki Suda[1], Tamami Abe[2], Masashi Ninomiya[3], Hidekatsu Kuroda[2], Yoshiyuki Ueno[4], Naoya Sakamoto[1]. [1]*Department of Gastroenterology and Hepatology, Hokkaido University Hospital, Sapporo, Japan;* [2]*Department of Gastroenterology and Hepatology, Iwate Medical University Hospital, Yahaba-cho, Japan;* [3]*Department of Gastroenterology and Hepatology, Tohoku University, Sendai, Japan;* [4]*Faculty of Medicine, Yamagata University, Yamagata, Japan*
Email: shotaku0128@yahoo.co.jp

Background and aims: Atezolizumab plus bevacizumab therapy can enable conversion to curative treatments such as resection or ablation in selected patients with hepatocellular carcinoma (HCC). However, clinical characteristics and predictive factors associated with successful conversion remain unclear. This study aimed to clarify the clinical relevance of conversion therapy following atezolizumab–bevacizumab and to identify factors associated with conversion.
Method: This multicenter study included patients with HCC who received atezolizumab–bevacizumab across 16 institutions. Outcomes included objective response rate, progression-free survival, overall survival, and rates of conversion therapy, clinical complete response, and drug-free status. Factors associated with conversion were assessed using multivariable analyses. Liver function was evaluated using the modified albumin–bilirubin grade.
Results: A total of 692 patients were enrolled (median follow-up, 14.2 months; median age, 72 years). At baseline, 58.6% had modified albumin–bilirubin grade 1–2a, and 41.9% had Barcelona Clinic Liver Cancer stage B disease. Portal vein tumor thrombosis and extrahepatic spread were present in 27.9% and 37.4%, respectively. The objective response rate was 31.2% by Response Evaluation Criteria in Solid Tumors and 42.6% by modified RECIST. Median progression-free survival and overall survival were 7.1 months and 21.1 months, respectively. Conversion therapy, clinical complete response, and drug-free status were achieved in 4.0%, 6.6%, and 5.1% of patients. In advanced-stage disease, patients without intrahepatic tumors showed higher rates of clinical complete response (16.4% vs 4.3%, p = 0.002) and drug-free status (10.9% vs 3.2%, p = 0.019). Overall survival was significantly longer in the conversion group than in the non-conversion group (median not reached vs 19.9 months, p < 0.001). Multivariable analysis identified baseline modified albumin–bilirubin grade 1–2a, ≥75% maximum reduction in AFP from baseline during treatment, and objective response by modified RECIST at initial evaluation as factors associated with conversion.
Conclusion: Conversion after atezolizumab–bevacizumab therapy was associated with favorable survival outcomes, higher rates of clinical complete response and drug-free status, and preserved liver function. Conversion therapy may be considered in patients with preserved baseline liver function and an early favorable tumor response.

FRI-368
Cytokeratin 19 expression stratifies outcomes with hepatic arterial infusion chemotherapy but not atezolizumab plus bevacizumab in advanced hepatocellular carcinoma

Kwon Yong Tak[1], Keungmo Yang[1], Hee Sun Cho[1], Ji Won Han[1], Suho Kim[2], Jung Suk Oh[2], Jeong Won Jang[1], Pil Soo Sung[1]. [1]*Division of Gastroenterology and Hepatology, Department of Internal Medicine, Seoul St Mary's Hospital, The Catholic University of Korea, Seoul, Korea, Rep. of South;* [2]*Department of Radiology, Seoul St Mary's Hospital, The Catholic University of Korea, Seoul, Korea, Rep. of South*
Email: eworldcupzps@naver.com

Background and aims: Cytokeratin 19 (CK19)-positive hepatocellular carcinoma (HCC) exhibits biliary/progenitor features and aggressive biology, raising uncertainty regarding the optimal therapeutic strategy for this subgroup. We evaluated the prognostic and predictive value of CK19 expression according to treatment modality in patients with advanced HCC treated with hepatic arterial infusion chemotherapy (HAIC) or atezolizumab plus bevacizumab.
Method: We retrospectively analysed consecutive patients with advanced HCC who received atezolizumab plus bevacizumab or HAIC between January 2020 and July 2025. Only patients with available tumour biopsy and immunohistochemical assessment of CK19 were included. Overall survival (OS) and progression-free survival (PFS) were compared by CK19 status within each treatment group using Kaplan-Meier analysis and log-rank testing. Objective response rate (ORR), including overall and intrahepatic responses, was evaluated by radiologic assessment, excluding non-evaluable cases. Categorical variables were compared using chi-square tests.
Results: We included 136 patients treated with atezolizumab plus bevacizumab (CK19-positive n = 95; CK19-negative n = 41; median follow-up 8.7 months) and 101 treated with HAIC (CK19-positive n = 36; CK19-negative n = 65; median follow-up 7.4 months). In the atezolizumab plus bevacizumab group, OS and PFS did not differ by CK19 status (OS p = 0.3643; PFS p = 0.8144), and ORR was similar for both overall (p = 0.8264) and intrahepatic responses (p = 0.7889). In contrast, in the HAIC group, CK19-positive tumours showed improved OS and PFS compared with CK19-negative tumours (OS p = 0.0365; PFS p < 0.0001). ORR was higher in CK19-positive than CK19-negative tumours after HAIC for both overall response (41.7% vs 19.4%, p = 0.0316) and intrahepatic response (47.2% vs 22.6%, p = 0.0213).
Conclusion: CK19 expression identifies a subgroup of advanced HCC with differential outcomes following HAIC, whereas outcomes with atezolizumab plus bevacizumab were not stratified by CK19 status. CK19 assessment may support biomarker-informed selection of HAIC in advanced HCC, warranting prospective validation.

FRI-369-YI
Recurrence patterns and post-recurrence survival after curative resection for hepatocellular carcinoma: a Milan criteria–based stratification

Chi-Ping Tan[1], I-Cheng Lee[1,2], Romeo Kuo-Cheng Wu[1,3], Gar-Yang Chau[4], Jiing-Chyuan Luo[1,2], Yi-Hsiang Huang[1,2,5,6]. [1]*Division of Gastroenterology and Hepatology, Department of Medicine, Taipei Veterans General Hospital, Taipei, Taiwan;* [2]*School of Medicine, College of Medicine, National Yang Ming Chiao Tung University, Taipei, Taiwan;* [3]*Division of Gastroenterology and Hepatology, Department of Medicine, Keelung Hospital, Ministry of Health and Welfare, Keelung, Taiwan;* [4]*Department of Surgery, Taipei Veterans General Hospital, Taipei, Taiwan;* [5]*Institute of Clinical Medicine, National Yang Ming Chiao Tung University, Taipei, Taiwan;* [6]*Department of Medical Research, Taipei Veterans General Hospital, Taipei, Taiwan*
Email: iclee@vghtpe.gov.tw

Background and aims: Despite curative resection, hepatocellular carcinoma (HCC) is associated with a high recurrence rate. However, recurrence patterns and long-term post-recurrence survival (PRS) remain incompletely characterized. This study aimed to delineate recurrence patterns and identify prognostic factors influencing PRS following curative resection for HCC.
Method: We retrospectively analyzed 1813 patients who underwent curative resection for HCC between 2007 and 2023. Recurrence patterns, post-recurrence treatments, and factors associated with PRS were evaluated, with stratification according to recurrence within or beyond the Milan criteria.
Results: During a median follow-up of 63.3 months, 906 patients developed HCC recurrence, of whom 61.0% and 39.0% experienced recurrence within and beyond the Milan criteria, respectively. Among patients with recurrence within the Milan criteria, independent predictors of poorer PRS included early recurrence (hazard ratio [HR] = 2.103, $p < 0.001$), recurrent tumor size > 2 cm (HR = 1.497, $p = 0.011$), multiple recurrent tumors (HR = 2.110, $p < 0.001$), AFP > 20 ng/mL (HR = 1.677, $p = 0.001$), and ALBI grade 2–3 (HR = 1.850, $p < 0.001$). For patients with recurrence beyond the Milan criteria, baseline microvascular invasion (HR = 2.348, $p = 0.004$), recurrent macrovascular invasion (HR = 1.620, $p = 0.042$), confluent multinodular or infiltrative-type recurrent tumor morphology (HR = 3.281, $p < 0.001$), AFP > 400 ng/mL (HR = 1.867, $p = 0.001$), ALBI grade 2–3 (HR = 2.130, $p < 0.001$), and diabetes mellitus (HR = 2.016, $p < 0.001$) were independently associated with PRS. Risk scores derived from PRS predictors stratified patients with recurrence within the Milan criteria into three risk groups, with median PRS of 149.6, 68.8, and 33.4 months, respectively ($p < 0.001$). Similarly, patients with recurrence beyond the Milan criteria were stratified into three risk groups with median PRS of 44.8, 18.8, and 4.7 months, respectively ($p < 0.001$).
Conclusion: Post-recurrence survival following curative resection for HCC is strongly influenced by recurrence patterns as well as tumor- and host-related factors. These findings may facilitate individualized post-recurrence management, optimize the timing of referral for salvage liver transplantation, and inform the design of future clinical trials.

FRI-370

Prognostic and predictive value of single-nucleotide polymorphism signature in patients with resected hepatocellular carcinoma: a multicentre retrospective study

Weijuan Huang[1], Zhenzhong Zhou[2], Zhongguo Zhou[2], Cheng Cao[3], Mei Li[2], Yong Zhu[4], Qiang Gao[5], Jianhui Li[6], Xiaofeng Jiang[6], Ronghui Chen[1], Guohe Song[5], Gangling Tong[7], Ying Wu[8], Shengtao Zhu[3], Tianqing Wu[2], Neng Jiang[2], Shubo Pan[9], Weijie Li[10], Lili Wu[11], Xinhua Li[11], Benmao Sun[12], Zhigang Zhou[13], Xiuhong Yin[14], Binbin Chen[15], Xing Sun[16], Zhongyi Dong[17], Peng Xiu[18], Tianlu Wang[19], Lei Li[20], Hongling Li[21], Dong Xu[5], Guofu Huang[22], Weidong Pan[23], Dawei Zhang[23], Junjie Xu[24], Fang Liu[25], Weiliang Hou[26], Pingting Gao[5], Feifei Mao[27], Qiongli Zhai[28], Runfen Chen[28], Xuejin Qin[29], Zhenyu Zhou[30], Wenhui Chen[31], Nana Pei[31], Linlin Huang[32], Anquan Wang[33], Ning Su[20], Minshan Chen[2], Xiaopeng Tian[2]. *[1]Jinan University, Guangzhou, China; [2]Sun Yat-Sen University Cancer Center, State Key Laboratory of Oncology in South China, Collaborative Innovation Center of Cancer Medicine, Guangzhou, China; [3]The First Affiliated Hospital of Anhui Medical University, Anhui Public Health Clinical Center, Hefei, China; [4]The First Affiliated Hospital of Anhui Medical University, MOE Innovation Center for Basic Research in Tumor Immunotherapy, Anhui Province Key Laboratory of Tumor Immune Microenvironment and Immunotherapy, Hefei, China; [5]Zhongshan Hospital Fudan University, Shanghai, China; [6]The Second Affiliated Hospital, Guangzhou, China; [7]Peking University Shenzhen Hospital, Shenzhen Key Laboratory of Gastrointestinal Cancer Translational Research, Cancer Institute, Shenzhen-Peking University-Hong Kong University of Science and Technology Medical Center, Shenzhen, China; [8]Shenzhen Second People's Hospital, Shenzhen, China; [9]Second Affiliated Hospital of Anhui Medical University, Hefei, China; [10]Anhui Tongcheng people's hospital, Anhui, China; [11]Third Affiliated Hospital of Sun Yat-sen University, Guangdong Key Laboratory of Liver Disease Research, Guangzhou, China; [12]Binhaiwan Central Hospital of Dongguan, Dongguan, China; [13]The first people's hospital of Changde city, Changde Hospital, Xiangya School of Medicine, Central South University, Hunan, China; [14]Dehong People's Hospital, Yunnan, China; [15]Guangzhou eighth people's hospital, Guangzhou medical university, Guangzhou Liver Disease Hospital, Guangzhou, China; [16]Nanyang central hospital, Henan, China; [17]Nanfang Hospital, Southern Medical University, Guangzhuo, China; [18]Shandong Province Qianfoshan Hospital, The First Hospital Affiliated With Shandong First Medical University, Jinan, China; [19]Cancer Hospital of China Medical University, Cancer Hospital of Dalian University of Technology; Faculty of Medicine, Dalian University of Technology, Liaoning Cancer Hospital & Institute, Shenyuang, China; [20]Guangzhou Chest Hospital, Guangzhou, China; [21]Shanghai 6th People's Hospital, Shanghai Jiao Tong University, Shanghai, China; [22]The Tenth Affiliated Hospital of Southern Medical University, Dongguan, China; [23]The Sixth Affiliated Hospital, Sun Yat-Sen University, Guangzhou, China; [24]Sir Run-Run Shaw Hospital, Zhejiang University School of Medicine, Zhejiang, China; [25]The First People of Foshan Hospital, Foshan, China; [26]Changhai Hospital, Naval Medical University, National Key Laboratory of Immunity and Inflammation, Changhai Clinical Research Unit, Shanghai Institute of Pancreatic Diseases, Shanghai, China; [27]Shanghai General Hospital, Shanghai Jiao Tong University School of Medicine, Shanghai, China; [28]Tianjin medical university cancer institute and hospital, Tianjing, China; [29]Fuyang Hospital Of Anhui Medical University, Huyang, China; [30]Sun Yat-Sen Memorial Hospital, Guangzhou, China; [31]The First Affiliated Hospital of Jinan University, Guangzhou, China; [32]Guangdong Provincial People's Hospital, Guangzhou, China; [33]The Fifth People's Hospital of WuHu, Wuhu, China*
Email: wjhuang@jnu.edu.cn

Background and aims: Current prognostic scoring systems based on clinicopathologic variables are inadequate for identifying patients with hepatocellular carcinoma (HCC) who would benefit from adjuvant therapy with atezolizumab plus bevacizumab following surgery. We developed a single-nucleotide polymorphisms (SNP)-based classifier to improv postoperative risk stratification and prediction of adjuvant therapy benefit for these patients.
Method: In this retrospective, multicentre study, we developed a 12-SNP classifier derived from blood-based SNP profiles correlated with recurrence-free survival from 332 patients with resected HCC in training set. We assessed intratumour heterogeneity by analysing two regions of paraffin-embedded specimens from the same tumours in the training set. We validated the classifier's prognostic and predictive performance in an internal testing set (n = 222), two independent external validation sets (n = 250 and n = 304), and TCGA dataset (n = 306). we conducted a nested case-control dataset (n = 388) to evaluate classifier's ability for identifying patients likely to benefit from atezolizumab plus bevacizumab adjuvant therapy.
Results: The twelve-SNP-based classifier demonstrated consistent predictive accuracy in blood samples and two different regions of the training set. The twelve-SNP-based classifier precisely predicted recurrence-free survival of patients in training and four validation sets. In the nested case-control analysis, atezolizumab-bevacizumab adjuvant therapy was associated with improved recurrence-free survival (HR 2.210, 1.246–3.599; $p = 0.0054$) and overall survival (HR 2.870, 1.194–6.900; $p = 0.0184$) in the high-risk subgroup as defined by the twelve-SNP-based classifier. Combining the classifier with clinical risk factors (tumor diameter, number of tumors, vascular invasion, and tumor differentiation) further improved the prognostic stratification.
Conclusion: Our twelve-SNP classifier is a reliable prognostic and predictive tool for disease recurrence in patients with resected HCC. It has the potential to identify patients who would benefit from adjuvant therapy with atezolizumab plus bevacizumab, thereby

aiding in patient counseling and enabling more personalized management of individuals with this disease. Compared to previous predictors, our twelve-SNP-based classifier is not influenced by the technical sources of variation with different platforms in different centers.

FRI-371

CT-derived skeletal muscle mass improves risk stratification in patients undergoing major surgery for perihilar cholangiocarcinoma – a retrospective single center cohort study

Paula Medio Torrubiano[1], Jens Rolinger[1], Ivan Capobianco[1], Alfred Königsrainer[1], André Mihaljevic[1], Silvio Nadalin[1].
[1]*Universitätsklinikum Tübingen, Tübingen, Germany*
Email: jens.rolinger@icloud.com

Background and aims: Perihilar cholangiocarcinoma (PHC) is a rare but aggressive malignancy, with surgical resection as the only potentially curative treatment. Perioperative risk stratification remains challenging. CT-derived muscle indices are widely used as surrogates for sarcopenia, although muscle quantity alone does not fulfil current diagnostic criteria. This study aims to investigate skeletal muscle index (SMI) as a continuous CT-based body composition parameter for perioperative risk stratification.
Method: This retrospective single-center study included patients undergoing major liver resection for suspected perihilar cholangiocarcinoma between 2006 and 2024. Preoperative CT scans were used to quantify skeletal muscle index (SMI) at the L3 level. The primary endpoint was major postoperative complications (Clavien–Dindo ≥III). Secondary endpoints included 90-day mortality, overall survival (OS), and recurrence-free survival (RFS). Multivariable logistic regression was performed using a clinical baseline model including body mass index (BMI), ASA class, and Charlson Comorbidity Index (CCI). Incremental prognostic value of SMI was assessed using likelihood ratio testing and changes in model discrimination (AUC). Associations with OS and RFS were evaluated using Cox regression.
Results: Among 288 surgically explored patients, 184 underwent major liver resection; after exclusion of incomplete imaging, 163 patients were included. Median POS was 27.6 months, median RFS was 14.5 months. Median SMI was 44.8 (range = 19.4–69.6). R0 resection was achieved in 99 patients (60.7%), major postoperative complications occurred in 71 patients (43.6%). The clinical baseline model demonstrated limited discrimination for major complications (AUC 0.588). Addition of continuous CT-derived SMI significantly improved model fit (likelihood ratio $p = 0.007$) and increased discrimination to an AUC of 0.641 ($\Delta AUC = 0.053$). A trend towards BMI-dependent effect modification was observed (SMI × BMI interaction $p = 0.089$). SMI was not associated with 90-day mortality (OR 1.10 per 5-unit increase, $p = 0.460$), OS (HR 1.03, $p = 0.619$), or RFS (HR 0.94, $p = 0.297$).
Conclusion: In line with current literature, CT-derived skeletal muscle mass alone is not suitable to define sarcopenia. However, when interpreted as a continuous body composition parameter, SMI provides meaningful incremental value for perioperative risk stratification beyond established clinical factors.

FRI-372

Percutaneous ablation versus stereotactic body radiotherapy for early-stage hepatocellular carcinoma: a propensity score–matched study

Jules Ventre[1], Armand Abergel[1,2], Benjamin Buchard[1], Baptiste Gleyzolle[3], Emmanuel Buc[1], Constance Hordonneau[1], Clarisse Gaume[1], Antoine Gayard[1], Leon Muti[1], Marie-Charlotte Masson[4], Thomas Guilmoteau[1]. [1]*CHU Clermont-Ferrand, Clermont-Ferrand, France;* [2]*Clermont-Ferrand University Hospital, Clermont-Ferrand, France;* [3]*Centre Jean Perrin, Clermont-Ferrand, France;* [4]*CHU Clermont-Ferrand, Clermont-Ferrand, France*
Email: jventre@chu-clermontferrand.fr

Background and aims: Percutaneous ablation (PA), surgical resection, and liver transplantation are standard treatment options for the treatment of early-stage hepatocellular carcinoma (HCC).
Stereotactic body radiotherapy (SBRT) is not currently regarded as a standard treatment according to the 2022 Barcelona Clinic Liver Cancer (BCLC) recommendations. The aim of this study was to compare PA and SBRT for the treatment of early-stage HCC, with a primary focus on survival outcomes.
Method: This retrospective, bicentric study was conducted at the University Hospital and the Cancer Center both in Clermont-Ferrand. The primary endpoints were overall survival (OS) and progression-free survival (PFS). Secondary endpoints included local tumor control and safety. Propensity score matching was performed to minimize selection bias between treatment groups.
Results: One hundred and forty nine patients were treated with PA and 157 patients with SBRT. Three hundred and forty four lesions were analysed: 175 in the PA group and 169 in the SBRT group. The majority of patients was male (89% in both groups). Patients treated with SBRT were significantly older, with a higher proportion aged over 65 years compared with the PA group (74.6% vs. 60.0%). Liver function was comparable between groups, with most patients classified as Child–Pugh A. After propensity score matching, there was no significant difference in overall survival between the two groups ($p = 0.72$), with a median OS of 40 months in the PA group and 34 months in the SBRT group. Progression-free survival differed significantly between treatments, with a median PFS of 54 months in the PA group and 37 months in the SBRT group. SBRT was associated with significantly improved local tumor control compared with PA, while both treatment modalities demonstrated acceptable safety profiles.
Conclusion: SBRT and PA were associated with similar overall survival in patients with early-stage HCC. While progression-free survival differed between groups, SBRT achieved superior local tumor control with a favorable safety profile. These findings support SBRT as a valuable alternative for patients with technical limitations or contraindications to percutaneous ablation. Further prospective studies are necessary to better define the role of SBRT in the therapeutic strategy for hepatocellular carcinoma.

FRI-377

Comparative efficacy and prognostic analysis of different targeted-immunotherapy regimens in advanced hepatocellular carcinoma

Yan Xu[1], Kai Tan[1], Xiaojun He[1], Xiaoling Hu[2], Shengxiong Jia[1], Xilin Du[1]. [1]*Tangdu Hospital, Fourth Military Medical University, Xi An, China;* [2]*Southern Theater Air Force Hospital, Guang Zhou, China*
Email: xuyan630@126.com

Background and aims: To compare the efficacy of different targeted agents combined with PD-1 inhibitors in patients with hepatocellular carcinoma (HCC) and to identify prognostic factors for overall survival (OS) in a real-world setting.
Method: This retrospective study analyzed 360 patients with advanced HCC receiving combined targeted therapy and immunotherapy (targeted-immunotherapy). Patients were categorized into four groups: lenvatinib plus a PD-1 inhibitor (n = 226), bevacizumab plus a PD-1 inhibitor (n = 73), donafenib plus a PD-1 inhibitor (n = 37), and apatinib plus camrelizumab (n = 24). Treatment response was evaluated using the modified Response Evaluation Criteria in Solid Tumors (mRECIST). Survival analyses, including tests for proportional hazards assumptions and multivariable Cox regression, were performed using the survival package in R. Kaplan-Meier curves were visualized with the survminer and ggplot2 packages.
Results: No statistically significant difference in OS was observed among the four treatment regimens (P = 0.31). Subgroup analyses revealed comparable OS between bevacizumab plus atezolizumab and bevacizumab plus sintilimab (28 months, 95% CI: 20–38 vs. 42 months, 95% CI: 30–47, P = 0.116), as well as between lenvatinib plus

pembrolizumab and lenvatinib plus tislelizumab (27 months, 95% CI: 24–38 vs. 28 months, 95% CI: 22–37, P = 0.693). Underlying hepatitis etiology did not significantly affect OS (P = 0.6873). Patients who achieved an objective response to targeted-immunotherapy had markedly superior median OS compared to non-responders (37 months, 95% CI: 33–48 vs. 24 months, 95% CI: 23–27; P < 0.001). Furthermore, patients who underwent subsequent curative-intent surgery post-treatment showed significantly longer median OS than those who did not (51 months, 95% CI: 30–56 vs. 29 months, 95% CI: 27–32; P = 0.015). The conversion surgery rates did not differ significantly among the major regimens: 10.96% for bevacizumab-based, 9.29% for lenvatinib-based, and 10.53% for donafenib-based combinations.

Conclusion: In this real-world cohort, first-line lenvatinib-, bevacizumab-, and donafenib-based PD-1 inhibitor combinations demonstrated comparable survival outcomes in advanced HCC. Achieving an objective response and successful conversion to curative surgery were independent favorable prognostic factors, highlighting the critical importance of tumor downstaging and surgical eligibility in optimizing long-term survival.

FRI-378

Sequential therapy patterns and prognostic impact of first-line treatment response in unresectable hepatocellular carcinoma patients with failure of Atezolizumab plus Bevacizumab

Ji Won Yang[1,2], Ye Rim Kim[1], Dongman Yu[1], Jihyun An[3], Yeongseok Hwang[1], Han Chu Lee[1], Ju Hyun Shim[1]. *[1]Department of Gastroenterology, Liver Center, Asan Medical Center, University of Ulsan College of Medicine, Seoul, Korea, Rep. of South; [2]Liver Center, Asan Medical Center, University of Ulsan College of Medicine, Seoul, Korea, Rep. of South; [3]Hanyang University Guri Hospital, Hanyang University College of Medicine, Guri, Korea, Rep. of South*
Email: s5854@amc.seoul.kr

Background and aims: Optimal subsequent treatment strategies following first-line Atezolizumab plus bevacizumab (Atezo/Bev) in unresectable hepatocellular carcinoma (HCC) remain unclear, particularly beyond the second-line treatment settings. We evaluated patterns of sequential treatment after Atezo/Bev and examined the impact of both treatment response to the preceding systemic therapy and the type of systemic agents used at each subsequent treatment line on survival outcomes.

Method: In this single-center retrospective cohort study, we analyzed 353 patients with unresectable HCC, who received Atezo/Bev ≥3 cycles (May 2022–December 2023) and underwent subsequent treatment. At each treatment line, overall survival (OS) and progressive-free survival (PFS) were evaluated by type of systemic agents and stratified by the best response to the prior therapy (progressive disease [PD] vs. non-PD groups).

Results: Of the total patients, 307 (87.0%) received second-line systemic therapy, and 279 (90.9%) of them underwent the initial response evaluation. Tyrosine kinase inhibitors (TKIs) constituted most of the second-line therapy (lenvatinib or sorafenib in >80% of the patients). Median OS was comparable between lenvatinib and sorafenib (9.5 vs. 8.3 months; *P = NS*), whereas lenvatinib was significantly associated with longer median PFS (5.3 vs. 2.8 months; *P* < 0.05). Survival outcomes after second-line treatment did not differ between patients achieving PD and non-PD after first-line Atezo/Bev (median OS, 7.8 vs. 9.4 months; and median PFS, 3.7 vs. 4.2 months; both *Ps = NS*). In the third-line settings, TKIs predominated and showed comparable survival outcomes with immune checkpoint inhibitors (ICIs) (median OS and PFS, 6.9 vs. 4.0 months; and 1.7 vs. 1.8 months, respectively; *Ps = NS*). Furthermore, treatment response of second-line systemic treatment showed no significant association with survival outcomes of subsequent therapy (median OS and PFS for PD vs. non-PD groups, 7.4 vs. 6.1 months and 1.8 vs. 1.6 months, respectively; *Ps = NS*).

Conclusion: TKIs were predominant subsequent therapies after first-line Atezo/Bev for HCC, with second-line lenvatinib achieving longer PFS than sorafenib, while survival outcomes were similar between TKIs and ICIs in later-line settings. Survival after subsequent treatment was not significantly influenced by response to prior treatment. Further multi-center prospective studies are warranted to determine the optimal treatment sequence after Atezo/Bev.

FRI-379

Comparison of surgical resection, percutaneous ablation, and transarterial chemoembolization for hepatocellular carcinoma patients with recompensated cirrhosis: a multicenter, retrospective, cohort study

Can Zhang[1], Nijin Wu[2], Hang Zheng[3], Qiqi Liu[4], Ping Lü[1], Mingyue Wang[1], Xinke Wang[1], Tianru Zhang[1], Ping He[1], Zhen Zhang[5], Qiang Zhu[6], Yuemin Feng[1]. *[1]Department of Gastroenterology, Shandong Provincial Hospital Affiliated to Shandong First Medical University, Jinan, Shandong, China; [2]Department of Infectious Diseases, The First Affiliated Hospital of Wenzhou Medical University, Wenzhou, Zhejiang, China; [3]Department of Gastroenterology, The First Affiliated Hospital of Wenzhou Medical University, Wenzhou, Zhejiang, China; [4]Department of Gastroenterology, Shandong Provincial Hospital, Cheeloo College of Medicine, Shandong University, Jinan, Shandong, China; [5]Department of Gastroenterology, The First Affiliated Hospital of Shandong First Medical University & Shandong Provincial Qianfoshan Hospital, Jinan, Shandong, China; [6]Department of Infectious Diseases, Shandong Provincial Hospital Affiliated to Shandong First Medical University, Jinan, Shandong, China*
Email: 2190246001@qq.com

Background and aims: The concept of recompensated cirrhosis was introduced by the Baveno VII consensus in 2021 and was later recognized in the European Association for the Study of Liver (EASL) guidelines in 2023. However, few studies have focused on the treatment strategies for hepatocellular carcinoma (HCC) patients with recompensated cirrhosis. This study compared the clinical efficacy and safety of curative treatments, including surgical resection and percutaneous ablation, versus palliative treatment (transarterial chemoembolization, TACE) in HCC patients with recompensated cirrhosis.

Method: This multicenter retrospective cohort study included 135 patients from three hospitals who were treated between January 1, 2008, and June 30, 2024: 102 received curative treatment (58 surgical resection, 44 percutaneous ablation) and 33 received palliative treatment (TACE). Overall survival (OS), progression-free survival (PFS), and complications were assessed and compared, using inverse probability of treatment weighting (IPTW) and subgroup analyses.

Results: Patients who received curative treatment more often had hepatitis B-related HCC, solitary tumor nodules, smaller tumors, and earlier tumor stages. After IPTW adjustment, baseline characteristics were effectively balanced. The five-year OS rates were 68.3% and 60.1% for the curative and palliative groups, respectively, while the five-year PFS rate was identical (51.0%) in both groups. No statistically significant differences in OS (p = 0.22) or PFS (p = 0.39) were observed between groups. Subgroup analysis indicated that the PFS benefit of curative treatment was more pronounced in patients with lower tumor burden (tumor size < 3 cm, Barcelona Clinic Liver Cancer (BCLC) stage 0/A, single lesion), better liver function (favorable Child–Pugh score), and stable recompensation (duration ≥ 5 years). Within the curative group, surgical resection and percutaneous ablation showed comparable OS (p = 0.83), but surgical resection was associated with significantly better PFS (p = 0.002). The curative group had a significantly higher incidence of complications, including liver dysfunction and electrolyte disturbances.

Conclusion: For HCC patients with recompensated cirrhosis, the OS were comparable between curative treatment group (surgical resection/percutaneous ablation) and palliative treatment group (TACE). Patients with low tumor burden, well-preserved liver

function, and stable recompensation status may achieve better PFS after curative treatments.

FRI-380

AADN score: predicting response to transarterial chemoembolization, sintilimab and lenvatinib in patients with hepatocellular carcinoma

Xue Zhang[1], Liying Ren[1], Shaoping She[1], Dongbo Chen[1], Hongsong Chen[1]. [1]*Peking University Hepatology Institute, Beijing, China*
Email: zxx20010205@163.com

Background and aims: Although the triple therapy of transarterial chemoembolization (TACE) combined with immune checkpoint inhibitors and tyrosine kinase inhibitors is becoming an effective treatment for unresectable hepatocellular carcinoma (uHCC). However, there is still a lack of effective tools for predicting therapeutic effects at present.
Method: Based on multicenter data, this study constructed and validated an AADN score as variables to predict overall survival in patients treated with this combination therapy. This study included 188 uHCC cases (training cohort: n = 101, validation cohort: n = 87) from three different hospitals. who treated with TACE, sintilimab and lenvatinib.
Results: In multivariate analysis, alpha-fetoprotein ≥ 100 ng/mL [hazard ratio (HR) = 2.579, P = 0.010], alkaline phosphatase > 120 U/L, (HR = 2.234, P = 0.021), direct bilirubin > 7.3 μmol/L (HR = 2.931, P = 0.007) and neutrophil to lymphocyte ratio > 2.5 (HR = 3.127, P = 0.006) were identified as independent prognostic factors and were used to establish the AADN score. Kaplan-Meier survival curves and time-dependent receiver operating characteristic curves were used to assess the accuracy of the AADN score, with area under receiver operating characteristic curve values of 0.827 (training cohort, 95% confidence interval: 0.743–0.911) and 0.832 (validation cohort, 95% confidence interval: 0.742–0.923). According to the score, the patients were divided into low-risk, intermediate-risk and highrisk groups. Overall survival and progression-free survival were significantly different between groups.
Conclusion: The AADN score can distinguish the prognostic risk of uHCC patients treated with TACE, sintilimab and lenvatinib, provides a basis for individualized treatment decision-making, and have clinical application prospect.

FRI-381

Inhibition of the renin–angiotensin system does not improve the outcomes of hepatocellular carcinoma treated with atezolizumab–bevacizumab

Alfredo Vozza[1], Costanza Winchler[2], Alessio Mastro[2], Tommaso Zurli[2], Massimo Iavarone[3], Giuseppe Cabibbo[4], Caterina Vivaldi[5], Andrea Dalbeni[6], Francesca Romana Ponziani[7], Andrea Palloni[8], Caterina Soldà[9], Tiziana Pressiani[10], Lorenzo Lani[11], Piera Federico[12], Federica Carlino[13], Luca Ielasi[14], Chiara Mazzarelli[15], Stefania De Lorenzo[16], Rodolfo Sacco[17], Mariangela Bruccoleri[3], Ciro Celsa[18], Alessandra Auriemma[6], Pierluigi Toniutto[19], Sara Lonardi[9], Elena Valenzi[10], Fabio Piscaglia[20], Daniele Rossini[2], Elisa Pellegrini[21], Francesco Tovoli[22], Fabio Marra[2]. [1]*Department of Experimental and Clinical Medicine, Taranto Hospital, University of Bari, Florence, Italy;* [2]*Department of Experimental and Clinical Medicine, Potral Hypertension Unit, AOU Careggi, Florence, Italy;* [3]*Foundation IRCCS Ca' Granda Ospedale Maggiore Policlinico, Division of Gastroenterology and Hepatology, Milan, Italy, Department of Pathophysiology and Transplantation, CRC "A. M. and A. Migliavacca" Centre for Liver Disease, University of Milan, Milan, Italy., Milan, Italy;* [4]*Gastroenterology and Hepatology Unit, Department of Health Promotion, Mother & Child Care, Internal Medicine & Medical Specialties, University of Palermo, Italy, Palermo, Italy;* [5]*Unit of Medical Oncology 2, Azienda Ospedaliero- Universitaria Pisana, Pisa, Italy., Pisa, Italy;* [6]*University of Verona and University and Hospital Trust (AOUI) of Verona, Verona, Italy;* [7]*Fondazione Policlinico Universitario Agostino Gemelli IRCCS, Rome, Italy;* [8]*IRCCS Azienda Ospedaliero-Universitaria di Bologna, Bologna, Italy;* [9]*Veneto Institute of Oncology Iov - Irccs, Padova, Italy;* [10]*Humanitas Research Hospital – IRCCS, Rozzano, Italy;* [11]*Department of Medical and Surgical Sciences, University of Bologna, Bologna, Italy, Bologna, Italy;* [12]*Ospedale del Mare, Napoli, Italy;* [13]*Ospedali Riuniti di Ancona, Ancona, Italy;* [14]*Ospedale degli Infermi di Faenza, Faenza, Italy;* [15]*Great Metropolitan Niguarda Hospital, Milano, Italy;* [16]*Oncology Unit, Azienda USL Bologna, Bologna, Italy;* [17]*Gastroenterology and Digestive Endoscopy Unit, Foggia University Hospital, Foggia, Foggia, Italy;* [18]*AOU policlinico Paolo Giaccone, Palermo, Italy;* [19]*University of Udine, Udine, Italy;* [20]*University of Bologna, Unit of Internal Medicine, Bologna, Italy;* [21]*Oncology Unit, AOU Careggi, Florence, Italy;* [22]*University of Bologna, Bologna, Italy*
Email: fabio.marra@unifi.it

Background and aims: Immune checkpoint inhibitor–based combinations (ICIs), including atezolizumab–bevacizumab (AB), have improved outcomes in unresectable HCC, although responses remain heterogeneous. Concomitant medications may modulate treatment efficacy through systemic and tumor microenvironment–mediated effects. Inhibition of the renin–angiotensin system (RAS) has been shown to potentiate the effects of immunotherapy in different solid cancers, acting on angiogenesis, fibrosis, and immune regulation. Nonetheless, the clinical impact of RAS inhibition in patients with HCC receiving ICIs remains controversial.
Method: We conducted a retrospective multicenter analysis of the national ARTE cohort, which includes patients with unresectable HCC treated with A + B, comparing those receiving therapy with angiotensin converting enzyme inhibitors (ACEi) and/or angiotensin receptor blockers (ARB) at treatment initiation with those not exposed. Overall survival (OS), progression-free survival (PFS), objective response rate (ORR), and disease control rate (DCR) were first evaluated using Kaplan–Meier analyses, univariate and multivariate Cox and logistic regression models. Confounding variables were then addressed by propensity score subclassification based on relevant clinical, hepatic, and tumor-related variables, and survival outcomes were subsequently re-assessed.
Results: A total of 538 patients were analyzed. In multivariate analyses, ACEi/ARB use was associated with worse OS (HR 1.29, 95% CI 1.00–1.66; p = 0.05) and a trend toward reduced DCR (OR 0.63, 95% CI 0.39–1.02). No associations were observed for PFS or ORR. After propensity score adjustment, patients receiving ACEi/ARB therapy (n = 182) had a numerically shorter median OS (17.0 vs 19.4 months) compared with non-users (n = 325), although this difference was not significant (p = 0.36).
Conclusion: In a large multicenter cohort of HCC patients treated with AB, concomitant ACEi/ARB therapy did not improve outcomes and was associated with a trend towards of poorer survival.

MASLD – Clinical aspects except therapy

TOP-098

Prevalence of MASLD, MetALD, ALD and liver fibrosis in patients with type 2 diabetes in 30,199 subjects in the general population: insights from the LiverScreen cohort

Laurent Castera[1], Guillem Pera[2], Isabel Graupera[3], Maja Thiele[4], Salvatore Piano[5], Rosa M Morillas[6], Peter Andersen[4], Judith Pich[7], Anita Madir[8], Daniel Jan Havaj[9], Mirko Zoncapè[10], Miquel Serra Burriel[11], Rafael Bañares[12], Neil Guha[13], Jörn M. Schattenberg[14], Frank Lammert[15], Emmanuel Tsochatzis[10], Willem Pieter Brouwer[16], Juan M. Pericàs[17], Lubomir Skladany[9], Ivica Grgurevic[8], Dominique Roulot[18], Paolo Angeli[5], Pere Torán[19], Aleksander Krag[4], Pere Ginès[3]. *[1]Service d'Hépatologie, Hopital Beaujon, AP-HP, Université Paris-Cité, Clichy, France; [2]Fundació Institut Universitari per a la Recerca a l'Atenció Primària de Salut Jordi Gol i Gurina (IDIAPJGol), Barcelona, Spain; [3]Liver Unit, Hospital Clinic, Barcelona, Spain; [4]Centre for Liver Research, Department of Gastroenterology and Hepatology, Odense University Hospital, Odense, Denmark; [5]Unit of Internal Medicine and Hepatology, Department of Medicine - DIMED, University and Hospital of Padova, Padova, Italy; [6]Liver Unit, Hospital Germans Trias i Pujol. Instituto de Investigación Germans Trias i Pujol (IGTP), Barcelona, Spain; [7]Fundació de Recerca Clínic Barcelona - Institut d'Investigacions Biomèdiques August Pi i Sunyer (FCRB - IDIBAPS), Barcelona, Spain; [8]Department of Gastroenterology, Hepatology and Clinical Nutrition, University Hospital Dubrava, Zagreb, Croatia; [9]Division of Hepatology, Gastroenterology and Liver Transplantation, Department of Internal Medicine II, Slovak Medical University Faculty of Medicine, Banska Bystrica, Slovakia; [10]UCL Institute for Liver and Digestive Health, Royal Free Hospital, University College of London (UCL), London, United Kingdom; [11]Epidemiology, Statistics, and Prevention Institute, University of Zurich, Zurich, Switzerland; [12]Liver Unit, Hospital General Universitario Gregorio Marañón, Madrid, Spain; [13]NIHR Nottingham Biomedical Research Centre, Nottingham University Hospitals NHS Trust and the University of Nottingham, Nothingham, United Kingdom; [14]Department of Medicine II, Saarland University Medical Center, Saarland University, Homburg, Germany; [15]Medizinische Hochschule, Hanover, Germany; [16]Department of Gastroenterology and Hepatology, Erasmus MC-University Medical Centre, Rotterdam, Netherlands; [17]Liver Unit, Hospital Universitari Vall d'Hebron, Vall d'Hebron Institut de Recerca (VHIR), Vall d'Hebron Barcelona Hospital Campus, Barcelone, Spain; [18]Unité d'Hépatologie, Hôpital Avicenne, Assistance Publique-Hôpitaux de Paris, Université Sorbonne Paris Nord, Bobigny, France; [19]Unitat de Suport a la Recerca Metropolitana Nord, Barcelona, Spain*
Email: laurent.d.castera@gmail.com

Background and aims: Current guidelines recommend systematically screening patients with type 2 diabetes (T2D) for MASLD and liver fibrosis. However, data on steatotic liver disease (SLD) in patients with T2D is scarce in the general population. The aim of this study was to assess the prevalence of MASLD, MetALD, ALD, and liver fibrosis severity, in T2D patients in the general population.
Method: We used the LiverScreen prospective cohort (30,199 subjects over 40 years old from nine European countries screened for liver fibrosis (LSM-VCTE >8 kPa). We defined SLD as hepatic steatosis (CAP ≥ 275 dB/m), MASLD as SLD with at least 1 cardiometabolic risk factor (CMRF) and alcohol intake <14 Units/week (U/w) for women, and <21 for men; MetALD as SLD with at least 1 CMRF and alcohol intake ≥14 but <35 U/w for women and ≥21 but <42 U/w for men; ALD as SLD and alcohol intake ≥35 U/w for women and ≥42 U/w for men. Significant fibrosis (SF) was defined as LSM ≥8 kPa, and advanced fibrosis (AF) as LSM ≥12 kPa.
Results: Of the 29,716 subjects (483 with missing data excluded), 9,119 (30.7%) had SLD and 3,087 (10.4%) had T2D (mean age: 64 years; female: 46%; obese: 49%). T2D patients with MASLD did not differ from those without MASLD in terms of age (63 vs. 65 years), gender (45% vs. 47% female), T2D duration (11 vs. 9 years), hypertension (71% vs. 67%), and dyslipidemia (83% vs. 78%), except for the prevalence of obesity (63% vs. 32%). The prevalence of MASLD was significantly higher in T2D patients than in those without T2D (53% vs. 25%; $p < 0.001$). The prevalence of MetALD (2.9% vs. 1.9%, $p < 0.001$) and ALD (0.9% vs. 0.4%, $p < 0.001$) was also higher. In T2D patients with MASLD, the prevalence of SF (17.7% vs. 5.7%, $p < 0.001$) and AF (7.1% vs. 1.4%, $p < 0.001$) was significantly higher than in non-T2D patients. The same was true for MetALD and ALD.
Conclusion: In a large European general population cohort, the prevalence of MASLD was twice as high in patients with type 2 diabetes as in those without, and the prevalence of advanced fibrosis was five times higher. These results underscore the urgent need for the early detection of MASLD and advanced liver fibrosis in patients with type 2 diabetes.

TOP-112-YI

Comparative incidence of end-stage complications in type 2 diabetes reveals a high liver disease burden: nationwide cohort study of 539,914 persons

Hannes Hagström[1,2], Sofia Ullman[1], Juan-Jesus Carrero[3], Soffia Gudbjornsdottir[4], Emil Hagström[5], Daniel Andersson[1,2], Ying Shang[1]. *[1]Karolinska Institutet, Huddinge, Sweden; [2]Karolinska University Hospital, Huddinge, Sweden; [3]Karolinska Institutet-Solna, Solna, Sweden; [4]Gothenburg University, Göteborg, Sweden; [5]Uppsala Universitet, Uppsala, Sweden*
Email: hannes.hagstrom@ki.se

Background and aims: Type 2 diabetes is common in the general population and is associated with several severe organ complications. Most of these complications are actively screened for in routine healthcare. The prevalence of steatotic liver disease in type 2 diabetes is considerable and may lead to cirrhosis, but screening is not adhered to despite being mentioned in guidelines. Here, we estimated and compared the cumulative incidence of the most common end-stage organ complications in a large representative Swedish cohort.
Method: We used data from the Swedish National Diabetes Register, capturing >90% of patients with type 2 diabetes in Sweden to identify patients with type 2 diabetes between 2002 and 2022. This cohort was linked to validated national registers to ascertain severe complications associated with type 2 diabetes: severe retinopathy; end-stage kidney disease; major adverse cardiovascular events; diabetic foot-related outcomes; and major adverse liver outcomes. The event definitions were based on ICD-10 codes, agreed upon by a multi-disciplinary group of experts across different disease areas and designed to represent comparable severity to patients. Incidence rates of outcomes were calculated, and competing risks were considered when estimating the cumulative incidence of outcomes.
Results: We identified 539,914 patients with a first registration in the national diabetes register (median age 63 years, 45% female, median duration of diabetes one year, median BMI 29.9 kg/m2) free of the investigated outcomes at baseline. During follow-up, major adverse cardiovascular events was the most common severe complication with a 5-year cumulative incidence of 11.1%. Major adverse liver outcomes was the second most common complication at five years, with a cumulative incidence of 0.8%, in contrast to diabetic foot-related outcomes (0.65%), severe retinopathy (0.43%) and end-stage kidney disease (0.27%).
Conclusion: This nationwide cohort study found that liver cirrhosis was the second most common end-organ complication in type 2 diabetes within five years from registration in the national diabetes register. The data support initiatives to increase early detection and treatment of pre-cirrhotic liver disease in type 2 diabetes.

TOP-113

Clinical profile, histologic features, non-invasive test accuracy, and long-term outcomes of lean metabolic dysfunction associated steatotic liver disease (MASLD): insights from the global masld project

Zobair M. Younossi[1,2], Leyla de Avila[1,2], Salvatore Petta[1,3], Hannes Hagström[1,4], Seung Up Kim[1,5], Atsushi Nakajima[1,6], Javier Crespo[1,7], Laurent Castera[1,8], Naim Alkhouri[1,9], Ming-Hua Zheng[1], Sombat Treeprasertsuk[1,10], Prooksa Ananchuensook[1,10], Shalimar Shalimar[1,11], Emmanuel Tsochatzis[1,12], K T Shenoy[1,13], Leena Mohan[1,14], Jian-Gao Fan[1,15], Stuart Roberts[1,16], Khalid A Alswat[1,17], Vincent Wai-Sun Wong[1,18], Yusuf Yilmaz[1,19], Winston Dunn[20], Sven Francque[1,21], Ahmed Cordie[1,22], Ming-Lung Yu[1,23], Mattias Ekstedt[24], George Boon Bee Goh[1,25], Claudia Pinto Oliveira[1,26], Mário Pessoa[1,27], Wah-Kheong Chan[1,28], Marlen Ivon Castellanos Fernández[1,29], Ajay Kumar Duseja[1,30], Juan Pablo Arab[1,31], George Papatheodoridis[1,32], Giada Sebastiani[1,33], Cristiane A. Villela-Nogueira[1,34], Roberta D'Ambrosio[35], Pietro Lampertico[1,35], Khalid Al Naamani[1,36], A.G. (Onno) Holleboom[1,37], Arun Valsan[1,38], Arathi Venu[38], Mohamed El-Kassas[1,39], Grazia Pennisi[3], Ying Shang[40], Wen-Yue Liu[41], Hye Won Lee[5], Takashi Kobayashi[6], Satoru Kakizaki[1,42], Cyrielle Caussy[1,43], Brian Pearlman[1,44], Paula Iruzubieta[7], Rida Nadeem[45], Felice Cinque[33], Margarita Papatheodoridi[32], Mirko Zoncapè[46], Rui-Xu Yang[15], Sherlot Juan Song[18], Nicholas Dunn[20], Zouhir Gadi[21], Ming-Lun Yeh[47], Kevin Kim Jun Teh[25], Sanjiv Mahadeva[28], Licet Gonzalez Fabian[48], Ahmed Almohsen[49], Nathalie Leite[34], Nicola Pugliese[1,50], Johan Vessby[51], Chencheng Xie[52,53], Narendra S Choudhary[54], Ethan Friend[55], Maria Poca[56], Takumi Kawaguchi[1,57], Francesco Paolo Russo[58], Adrian Gadano[1,59], Luis Antonio Diaz[1,60], Ashwani K. Singal[1,61], Bérénice Ségrestin[1,43], Nadege Gunn[1,55], Didac Mauricio[1,62], Marco Arrese[1,63], Anna Ludovica Fracanzani[64], Rosa Lombardi[64], Alessio Aghemo[50], Brian Lam[1,2], Basma Khoja[65], Shadan Almuhaidib[66], Saleh Alqahtani[1,66], Andrei Racila[1,2], Maria Stepanova[1,2,67]. *[1]The Global NASH Council (GNC), Washington, DC, United States; [2]Beatty Liver and Obesity Research Program, Inova Health System, Falls Church, Virginia, United States; [3]Section of Gastroenterology, PROMISE Department, University of Palermo, Palermo, Italy; [4]Division of Hepatology, Department of Upper GI Diseases, Karolinska University Hospital, Stockholm, Sweden; [5]Department of Internal Medicine, Yonsei University College of Medicine, Seoul, Korea, Rep. of South; [6]Department of Gastroenterology and Hepatology, Yokohama City University Graduate School of Medicine, Yokohama, Japan; [7]Gastroenterology and Hepatology Department, Clinical and Translational Research in Digestive Diseases, Valdecilla Research Institute (IDIVAL), Marques de Valdecilla University Hospital, Santander, Spain; [8]Department of Hepatology, Hospital Beaujon, Assistance Publique-Hôpitaux de Paris, Université Paris-Cité, Paris, France; [9]Summit Clinical Research, San Antonio, Texas, United States; [10]Division of Gastroenterology, Department of Internal Medicine, Chulalongkorn University, Bangkok, Thailand; [11]Department of Gastroenterology and Human Nutrition Unit, All India Institute of Medical Sciences, New Delhi, India; [12]University College London Institute for Liver and Digestive Health, Royal Free Hospital, London, United Kingdom; [13]Department of Gastroenterology, Sree Gokulam Medical College and Research Foundation, Trivandrum, Kerala, India; [14]Population Health and Research Institute, Medical College P O, Trivandrum, Kerala, India, [15]Department of Gastroenterology, Xinhua Hospital affiliated to Shanghai Jiao Tong University School of Medicine, Shanghai, China; [16]Alfred Hospital Gastroenterology Department, Monash University, Melbourne, Australia; [17]Liver Disease Research Center, Department of Medicine, College of Medicine, King Saud University, Riyadh, Saudi Arabia; [18]Medical Data Analytics Center, Department of Medicine and Therapeutics, The Chinese University of Hong Kong, Hong Kong, China; [19]Department of Gastroenterology, School of Medicine, Recep Tayyip Erdogan University, Rize, Türkiye; [20]Internal Medicine, Kansas University Medical Center, Kansas City, Kansas, United States; [21]Department of Gastroenterology and Hepatology, Antwerp University Hospital, Edegem, Belgium; [22]Cairo University Hospitals HIV Clinic, Endemic Medicine Department, Cairo University Hospitals, Cairo, Egypt; [23]Hepatobiliary Division, Department of Internal Medicine, Kaohsiung Medical University Hospital, Kaohsiung Medical University, Kaohsiung, Taiwan; [24]Department of Gastroenterology and Hepatology, Department of Health, Medicine, and Caring Sciences, Linköping University, Linköping, Sweden; [25]Department of Gastroenterology & Hepatology, Singapore General Hospital, Singapore, Singapore; [26]Department of Gastroenterology, Faculdade Medicina da Universidade de São Paulo, São Paulo, Brazil; [27]Department of Gastroenterology, Hospital das Clínicas da Faculdade de Medicina da Universidade de São Paulo – HCFMUSP, São Paulo, Brazil; [28]Gastroenterology and Hepatology Unit, Department of Medicine, University of Malaya, Kuala Lumpur, Malaysia; [29]Department of Research and Teaching, Institute of Gastroenterology, University of Medical Sciences of Havana, Havana, Cuba; [30]Department of Hepatology, Postgraduate Institute of Medical Education and Research, Chandigarh, India; [31]Stravitz-Sanyal Institute for Liver Disease and Metabolic Health, Division of Gastroenterology, Hepatology, and Nutrition, Department of Internal Medicine, Virginia Commonwealth University School of Medicine, Richmond, Virginia, United States; [32]1st Academic Department of Gastroenterology, Medical School of National and Kapodistrian University of Athens, General Hospital of Athens "Laiko", Athens, Greece; [33]Division of Gastroenterology and Hepatology, Department of Medicine, McGill University Health Centre, Montreal, Canada; [34]School of Medicine, Internal Medicine Department and Hepatology Division, Clementino Fraga Filho University Hospital, Federal University of Rio de Janeiro, Rio de Janeiro, Brazil; [35]Division of Gastroenterology and Hepatology, Foundation IRCCS Ca' Granda Ospedale Maggiore Policlinico, Milan, Italy; [36]Division of Gastroenterology and Hepatology, Department of Medicine, The Medical City for Military and Security Services, Muscat, Oman; [37]Department of Vascular Medicine, Amsterdam University Medical Center, Amsterdam, Netherlands; [38]Centre for Metabolic Liver Disease and Integrated Liver Care Unit, Amrita Institute of Medical Sciences, Kochi, Kerala, India; [39]Endemic Medicine Department, Faculty of Medicine, Capital University, Cairo, Egypt; [40]Department of Medicine, Huddinge, Karolinska Institutet, Stockholm, Sweden; [41]Department of Endocrinology, the First Affiliated Hospital of Wenzhou Medical University, Wenzhou, China; [42]Department of Clinical Research, NHO Takasaki General Medical Center, Takasaki, Japan; [43]Département Endocrinologie, Diabète et Nutrition, Hôpital Lyon Sud, Hospices Civils de Lyon, Pierre-Bénite, Lyon, France; [44]Department of Graduate Medical Education, Hamilton Medical Center, Medical College of Georgia, Dalton, Georgia, United States; [45]Arizona Liver Health, Chandler, Arizona, United States; [46]Liver Unit, Department of Internal Medicine, University and Azienda Ospedaliera Universitaria Integrata of Verona, Verona, Italy; [47]Center of Excellence for Metabolic Associated Fatty Liver Disease, National Sun Yat-sen University, Kaohsiung, Taiwan; [48]Department of Pathological Anatomy, Institute of Gastroenterology, University of Medical Sciences of Havana, Havana, Cuba; [49]Department of Medicine, Schulich School of Medicine, Western University & London Health Sciences Centre, London, Ontario, Canada; [50]Division of Internal Medicine and Hepatology, Department of Gastroenterology, IRCCS Humanitas Research Hospital, Rozzano, Italy; [51]Department of Medical Sciences, Gastroenterology Research Group, Uppsala University, Uppsala, Sweden; [52]Division of Hepatology, Avera McKennan Hospital & University Health Center, Sioux Falls, South Dakota, United States; [53]University of Iowa, Iowa City, United States; [54]Hepatology, and Institute of Liver Transplantation and Regenerative Medicine, Medanta The Medicity, Gurugram, Haryana, India; [55]Velocity Clinical Research, Waco, Texas, United States; [56]Department of Gastroenterology, CIBEREHD, IR Sant Pau, Hospital de la Santa Creu i Sant Pau, Barcelona, Spain; [57]Division of Gastroenterology, Department of Medicine, Kurume University School of Medicine, Kurume, Japan; [58]Department of Surgery, Oncology and Gastroenterology, University of Padova Gastroenterology*

Unit, Azienda Ospedaliera - Universita Padova, Padova, Italy; [59]Liver Unit, Hospital Italiano de Buenos Aires, Buenos Aires, Argentina; [60]MASLD Research Center, Division of Gastroenterology and Hepatology, University of California San Diego, San Diego, California, United States; [61]Department of Medicine, Division of Gastroenterology, Hepatology, and Nutrition, University of Louisville, Louisville, Kentucky, United States; [62]Department of Endocrinology & Nutrition, CIBERDEM, IR Sant Pau, Hospital de la Santa Creu i Sant Pau, Barcelona, Spain; [63]Departamento de Gastroenterología, Escuela de Medicina, Pontificia Universidad Católica de Chile, Santiago, Chile; [64]Unit of Metabolic Disease, Fondazione IRCCS Ca' Granda Ospedale Maggiore Policlinico, Milan, Italy; [65]Liver, Digestive, and Lifestyle Research Section, and Organ Transplant Center of Excellence, King Faisal Specialist Hospital and Research Center, Riyadh, Saudi Arabia; [66]Liver, Digestive, and Lifestyle Health Research Section, and Organ Transplant Center of Excellence, King Faisal Specialist Hospital and Research Center, Riyadh, Saudi Arabia; [67]Center for Outcomes Research in Liver Disease, Washington, DC, United States
Email: x4hepjwh@gmail.com

Background and aims: MASLD in normal-weight ("lean") individuals may represent a distinct phenotype with unique histology, non-invasive tests (NITs), and outcomes. We evaluated the clinical characteristics and outcomes of lean MASLD in a large multinational cohort.
Method: G-MASLD project includes adults with MASLD, liver biopsy, laboratory, and follow-up data from 41 countries. Lean by BMI (L-BMI) had BMI<25 kg/m^2 (<23 kg/m^2 in Asians) and lean by waist circumference (L-WC) had WC <94/80 cm in men/women (<85/80 cm in Asians). Diagnostic accuracy of FIB-4 and liver stiffness measurement (LSM) for advanced fibrosis (AF, F3-F4) was assessed using ROC curves. Outcomes were all-cause mortality and clinical events (hepatocellular carcinoma, decompensation, transplantation, or death).
Results: Of 18,326 MASLD patients, 6.7% were L-BMI and 6.0% were L-WC. Concordance between lean MASLD definitions was moderate (kappa = 0.41). Prevalence of L-BMI was 11% (L-WC 12%) in MASLD patients enrolled in Asia, 7% (4%) in Europe, 3% (7%) in MENA region, 6% (2%) in Latin America, 3% (2%) in North America. Compared with non-lean MASLD, lean MASLD had fewer metabolic comorbidities, less AF (L-BMI 29% vs. 37%; L-WC 22% vs. 41%), and lower NAS scores with less inflammation and hepatocyte ballooning (all $p < 0.01$). NITs showed mixed patterns: FIB-4 was similar or slightly higher in lean MASLD (L-BMI: 1.77 ± 1.22 vs. 1.54 ± 1.33; L-WC: 1.61 ± 1.49 vs. 1.57 ± 1.29), whereas LSM was lower (L-BMI: 10.1 ± 9.0 vs. 12.6 ± 9.5 kPa; L-WC: 9.3 ± 8.6 vs. 12.7 ± 9.4; all $p < 0.001$). FIB-4 accuracy for AF was reduced in lean MASLD (AUC L-BMI: 0.762 vs. 0.791; L-WC: 0.700 vs. 0.779), while LSM remained reliable (AUC L-BMI: 0.869 vs. 0.831; L-WC: 0.863 vs. 0.836); (all $p < 0.01$). In multivariable models adjusted for country, age, sex, and metabolic factors, lean MASLD by BMI or WC was not independently associated with mortality while AF remained the predictor (aHR 2.10 for all-cause mortality; 3.34 for clinical events; both $p < 0.001$). In lean MASLD, mortality was associated with older age and AF regardless of the definition and regions of the world.
Conclusion: In this multinational cohort, lean MASLD was more common in Asia and presented with milder histologic severity and fewer metabolic risks. FIB-4 underperformed for detecting AF in lean patients, whereas LSM remained accurate. Overall, lean MASLD had outcomes similar to overweight/obese MASLD, with AF rather than the lean status driving the risks of adverse outcomes.

TOP-114

Application of fibrosis tests and hepatocellular carcinoma prediction scores in metabolic dysfunction-associated steatotic liver disease

Huapeng Lin[1], Haixia Wang[2], Xianzhang Zeng[3], Fangkun Yang[4], Jimmy Che-To Lai[5], Hye Won Lee[6], Arun J Sanyal[7], Atsushi Nakajima[8], Elisabetta Bugianesi[9], Emmanuel Tsochatzis[10], George Boon Bee Goh[11], Hannes Hagström[12], Jerome Boursier[13], José Luis Calleja Panero[14], Manuel Romero-Gómez[15], Ming-Hua Zheng[16], Philip Newsome[17], Salvatore Petta[18], Victor de Lédinghen[19], Wah-Kheong Chan[20], Li Chen[21], Lijun Chang[22], Yanting Wang[23], Xiaolong Qi[24], Chuan Liu[24], Masato Yoneda[8], Jian-Gao Fan[25], Laurent Castera[26], Michelle Lai[27], Grace Lai-Hung Wong[5], Grazia Pennisi[18], Angelo Armandi[9], Wen-Yue Liu[16], Ying Shang[28], Terry Cheuk-Fung Yip[5], Seung Up Kim[6], Vincent Wai-Sun Wong[5]. *[1]Shanghai Jiao Tong University School of Medicine, Shanghai, China; [2]Zhejiang Cancer Hospital, Hangzhou, China; [3]Zhejiang University School of Medicine, Hangzhou, China; [4]The First Affiliated Hospital of Ningbo University, Ningbo, China; [5]The Chinese University of Hong Kong, Hong Kong, Hong Kong; [6]Yonsei University College of Medicine, Seoul, Korea, Rep. of South; [7]Virginia Commonwealth University School of Medicine, Richmond, United States; [8]Yokohama City University Graduate School of Medicine, Yokohama, Japan; [9]University of Turin, Torino, Italy; [10]Royal Free Hospital and UCL, London, United Kingdom; [11]Singapore General Hospital, Singapore, Singapore; [12]Karolinska University Hospital, Huddinge, Sweden; [13]Angers University, Angers, France; [14]Hospital Universitario Puerta de Hierro Majadahonda, Madrid, Spain; [15]Virgen del Rocío University Hospital, Seville, Spain; [16]The First Affiliated Hospital of Wenzhou Medical University, Wenzhou, China; [17]King's College Hospital, London, United Kingdom; [18]University of Palermo, Palermo, Italy; [19]Echosens, Paris, France; [20]University of Malaya, Kuala Lumpur, Malaysia; [21]Shanghai Jiaotong University School of Medicine, Shanghai, China; [22]Yuncheng Central Hospital Affiliated to Shanxi Medical University, Yuncheng, China; [23]The Second Affiliated Hospital of Zhejiang University School of Medicine, Hangzhou, China; [24]Zhongda Hospital, Southeast University, Nanjing, China; [25]Xinhua Hospital Affiliated to Shanghai Jiao Tong University School of Medicine, Shanghai, China; [26]Université Paris Cité, Paris, France; [27]Harvard Medical School, Boston, United States; [28]Karolinska Institutet, Stockholm, Sweden*
Email: linhuapeng5@163.com

Background and aims: Metabolic dysfunction-associated steatotic liver disease (MASLD) is an increasingly important cause of hepatocellular carcinoma (HCC). Current clinical pathways prioritise non-invasive identification of advanced fibrosis (AF), yet whether AF-based stratification alone is sufficient to guide HCC surveillance, and how HCC prediction scores should be incorporated, remains uncertain.
Method: In a multinational cohort of 16,603 patients with MASLD across the US, Europe and Asia, AF risk was classified using liver stiffness measurement, Fibrosis-4 and guideline-based pathways. HCC incidence across AF strata and the performance of published HCC prediction scores were systematically evaluated, including downstream and longitudinal risk analyses.
Results: Over a median follow-up of 4.3 years, 139 patients developed HCC. Across all frameworks, HCC incidence increased stepwise with AF risk; however, 5-year cumulative incidence in AF high-risk populations ranged from 3.0% to 5.2%, frequently below established surveillance cost-effectiveness thresholds. Among evaluated models, aMAP and the Toronto HCC Risk Index (THRI) demonstrated the most consistent discrimination within AF high-risk strata (C-index 0.75–0.80). Applied downstream of AF stratification, both scores identified subsets of AF high-risk patients with markedly elevated 5-year HCC incidence (>7.5%), while consistently classifying low-risk groups with minimal risk (<0.8%). In contrast, HCC incidence remained below surveillance thresholds in patients at low to moderate AF risk, regardless of score values.

Conclusion: AF-based stratification alone does not reliably identify MASLD patients who clearly warrant HCC surveillance. A guideline recommended AF assessment followed by application of aMAP or THRI in AF high-risk patients more effectively identifies surveillance-eligible subgroups.

TOP-128

An artificial intelligence model to better predict hepatocellular carcinoma risk in patients with metabolic dysfunction-associated steatotic liver disease: a large-scale 20-year cohort study

Ming-Ying Lu[1,2], Pei-Chien Tsai[1], Ming-Lun Yeh[1,2], Chung-Feng Huang[1], Jee-Fu Huang[1], Wan-Long Chuang[1], Ming-Lung Yu[1,2]. [1]*Hepatobiliary Division, Department of Internal Medicine, Kaohsiung Medical University Hospital, Center of Hepatitis Research, College of Medicine and Center of Metabolic Disorders and Obesity, Kaohsiung Medical University, Kaohsiung, Taiwan;* [2]*Center of Excellence for Metabolic Associated Fatty Liver Disease, National Sun Yat-sen University, Kaohsiung, Taiwan*
Email: fish6069@gmail.com

Background and aims: Metabolic dysfunction-associated steatotic liver disease (MASLD) has gradually replaced viral hepatitis in leading to hepatocellular carcinoma (HCC). The current non-invasive tests for fibrosis assessment, such as fibrosis-4 index (FIB-4) and liver stiffness measurement, provide modest accuracy in HCC risk stratification. We aimed to develop an artificial intelligence (AI)-driven model best stratifying HCC risks among MASLD subjects.
Method: This large-scale, long-term cohort study enrolled 573,581 subjects without viral hepatitis B and C with mean follow-up of 19.0 years. MASLD is defined as hepatic steatosis with at least one of the five cardiometabolic risk factors (n = 175,299). The diagnosis of HCC was recorded in the Catastrophic Illness Certification database of the National Health Insurance. AI is a powerful tool in healthcare. It can capture complex, nonlinear relationships between the variables and HCC. Integrating 18 routine clinical parameters, an eXtreme Gradient Boosting (XGBoost)-based model was developed for HCC risk assessment.
Results: Of 573,581 subjects, 2,472 (0.4%) developed newly onset HCC. Multivariate Cox regression revealed that higher levels of FIB-4, alpha-fetoprotein and direct bilirubin, as well as the presence of MASLD, diabetes, male, smoking, and alcohol consumption, were independent risk factors of HCC. In contrast, higher levels of albumin and total bilirubin significantly correlated to lower HCC risk. The XGBoost model achieved excellent performance, with area under the curve (AUC) values of 0.999 and 0.921 in the training (n = 401,507) and validation datasets (n = 172,074), respectively. When applied to 175,299 MASLD subjects, the model maintained robust predictive accuracy (AUC = 0.971). The AI-MASLD-HCC model stratified MASLD patients into high-, medium-high, medium-low, and low-risk subgroups, with the 25-year cumulative probabilities of HCC being 48.5%, 30.9%, 12.7%, and 0.2% ($p < 0.0001$), with annual incidence of 3.51%, 1.79%, 0.66%, and 0.01%, respectively. The MASLD-HCC AI model can identify 79.3% of HCCs from the high, medium-high, and medium-low risk groups, and outperforms the FIB-4 index, SAFE score, aMAP score, MASLD-HCC score, NAFLD fibrosis score, and HCC-RIFLE score.
Conclusion: A MASLD-HCC AI model was successfully developed to best predict HCC among MASLD subjects and offers more refined and clinically meaningful HCC risk stratification.

TOP-129

A machine learning model for predicting hepatocellular carcinoma in patients with MASLD

Han Ah Lee[1], Young Youn Cho[1], Hyung Joon Kim[1], Seung Up Kim[2], Jeong-Hoon Lee[3]. [1]*Chung-Ang University, Seoul, Korea, Rep. of South;* [2]*Yonsei University College of Medicine, Seoul, Korea, Rep. of South;* [3]*Seoul National University College, Seoul, Korea, Rep. of South*
Email: amelia86@naver.com

Background and aims: The risk of hepatocellular carcinoma (HCC) is significantly elevated in patients with metabolic dysfunction–associated steatotic liver disease (MASLD). This study aimed to develop and validate a machine learning model for predicting HCC in a large, multicenter MASLD cohort.
Method: A total of 18,484 MASLD patients from six Korean hospitals (2001–2022) were included. Patients from Severance Hospital were divided into a training cohort (n = 3,721) and an internal validation cohort (n = 4,370), while patients from the remaining institutions comprised the external validation cohort (n = 10,393). To account for substantial differences in HCC incidence among hospitals, two additional external validation subsets were created. Four machine learning algorithms—gradient boosting machine (GBM), random survival forest (RSF), deep neural network (DNN), and survival support vector machine (surv-SVM)—were developed using 12 variables selected from prior evidence and multivariable Cox regression results. Model performance was compared using the C-index, AUROC, AUPRC, sensitivity, specificity, and F1 score across all cohorts.
Results: During a median follow-up of 51.6 months, 357 HCC events occurred (incidence: 0.45 per 100 person-years). GBM demonstrated the strongest performance in the training cohort (C-index 0.95, AUROC 0.98, AUPRC 0.36), with well-balanced sensitivity (0.93) and specificity (0.97). Internal validation confirmed stable performance (C-index 0.90, AUROC 0.89, AUPRC 0.19), outperforming RSF and the Cox-based scoring model. External validation sets 1–3 consistently supported the robustness of GBM, with AUROCs ranging from 0.83 to 0.89, C-indices from 0.82 to 0.88, and AUPRCs from 0.19 to 0.25, indicating superior discrimination in imbalanced data. SHAP analysis identified liver cirrhosis, age, diabetes, LDL-cholesterol, and anti-hypertensive medication use as major contributors to increased HCC risk, while higher platelet count and albumin were associated with decreased risk.
Conclusion: This multicenter study developed and validated a GBM-based machine learning model using 12 readily available clinical variables for predicting HCC in MASLD patients. The model demonstrated consistently strong performance across internal and multiple external validation cohorts, exceeding that of traditional Cox-based approaches. External validation in non-Korean populations and prospective evaluation of clinical utility remain necessary.

THU-085

Metabolic dysfunction-associated steatotic liver disease in Europe: latest insight into disease incidence and burden

Ahmed Abdulelah[1]. [1]*St George's University Hospitals NHS Foundation Trust, London, United Kingdom*
Email: ahmadalhassani99@gmail.com

Background and aims: Metabolic dysfunction-associated steatotic liver disease (MASLD) is the most prevalent aetiology of liver disease in the developed countries and imposes a significant health and socioeconomic burden. Therefore, evaluating the temporal trends in the incidence and burden, which is measured through evaluation of disability-adjusted life years (DALY), is of paramount significance as it enables risk stratification and implementation of targeted policy measures.
Method: Data including the age-standardised incidence rate (ASIR) and the age-standardised DALY rate (ASDR) of MASLD for Europe (Central Europe, Western Europe, and Eastern Europe) for the period 1990–2023 were retrieved from the Global Burden of Disease database to evaluate the temporal trends in disease incidence and burden. Joinpoint analysis was performed to calculate the Annual Percent Change (APC) and the Average Annual Percent Change (AAPC).
Results: Over a span of 3 decades, an estimated total of 112,355,332 MASLD cases with a male predominance of 55.6% were reported across Europe. Western Europe accounted for 50.0% of cases, followed by Eastern Europe which accounted for 32.4% of the cases, and Central

Europe which accounted for 17.6% of cases. A statistically significant incline in MASLD ASIR was observed across the 3 European regions with Western Europe encountering the highest incline (AAPC 0.66, 95%CI 0.65 to 0.67, p < 0.001), followed by Eastern Europe (AAPC 0.36, 95%CI 0.35 to 0.36, p < 0.001) and Central Europe (AAPC 0.34, 95%CI 0.31 to 0.35, p < 0.001). Stratification by gender revealed identical trends with females generally experiencing higher degrees of incline in the ASIR across the 3 regions in comparison to males. Interestingly, a variation in the temporal trends in MASLD ASDR was observed across the 3 regions. Western Europe experienced a statistically significant decline in the ASDR with an AAPC of –0.45 (95%CI –0.53 to –0.38, p < 0.001). In contrast, Central Europe and Eastern Europe encountered a statistically significant incline in MASLD burden with the latter experiencing a higher degree of incline (AAPC 3.59, 95%CI 3.46 to 3.72, p < 0.001).
Conclusion: Overall, Europe has experienced a significant increase in the incidence of MASLD across all of its regions coupled with a prominent increase in disease burden in Eastern and Central Europe while Western Europe experienced a decline in disease burden. These findings mandate prompt recognition and intervention to tackle the associated disease burden.

THU-086
Prevalence, characteristics and clinical outcomes for metabolic dysfunction–associated steatohepatitis and metabolic dysfunction–associated steatotic liver disease in the United Kingdom: a clinical practice research datalink study

Margherita Bortolini[1], Chalini Lankage[1], Johnny Lau[2], Joe Hollinghurst[2], Kushala Abeysekera[3]. [1]*Novo Nordisk Ltd., London, United Kingdom;* [2]*Health Economics and Outcomes Research Ltd., Cardiff, United Kingdom;* [3]*University of Bristol, Bristol, United Kingdom*
Email: mgfb@novonordisk.com

Background and aims: Metabolic dysfunction–associated steatotic liver disease (MASLD) and metabolic dysfunction–associated steatohepatitis (MASH) are common causes of chronic liver disease, associated with cardiometabolic morbidity and mortality. We aimed to estimate prevalence of MASH, MASLD, and "high-likelihood of MASH" in the UK, whilst describing characteristics and clinical outcomes for each cohort.
Method: Adults (18+ years) with at least 365-days of registration data from Clinical Practice Research Datalink Aurum and linked secondary care and mortality data in England between 01 January 2008 and 01 January 2023 were eligible. MASH and MASLD were identified via diagnostic codes; "high-likelihood MASH" was defined as: MASLD plus type-2 diabetes (T2D) and/or obesity, FIB-4 >1.3, and repeated elevated alanine aminotransferase. Prevalence, baseline characteristics, and clinical outcomes (liver, cardiovascular, and all-cause mortality (ACM)) were summarised descriptively.
Results: Up to 33,714,568 people were eligible for analysis each year. Prevalence of MASH, MASLD, and "high-likelihood MASH" increased over the study, reaching 0.046% in 2023 (from 0.0056% in 2008), 1.1% (from 0.17%), and 0.018% (from 0.0012%) respectively. In 2023, 1.6% of people with MASLD were deemed "high likelihood MASH" (from 0.7% in 2008). Patients with MASH [MASLD; "high-likelihood MASH"] in 2023 were 60 [58; 65] years, 51% [50%; 56%] were male, 85% [80%; 86%] were of white ethnicity, 33% [32%; 27%] were most deprived (deciles 8–10), and the most common comorbidities were overweight/obesity 76% [74%; 91%], T2D 51% [32%; 62%], dyslipidaemia 38% [30%; 40%], and depression 39% [35%; 34%]. Prevalence of adverse liver, CV and ACM outcomes in patients with MASH were high in the year of diagnosis, at 29%, 15%, and 16% respectively. In MASLD and "high-likelihood MASH" cohorts, 3.8% and 7.1% respectively experienced adverse liver outcomes, 8.0% and 8.1% experienced CV outcomes, and 4.0% and 2.0% died.
Conclusion: Utilising a population database with almost 50% coverage, we provide recent population-level estimates of MASH/MASLD prevalence in the UK but speculate this substantially underestimates true burden due to changes in coding practices. Patients across the MASLD spectrum are at significant risk of adverse liver and CV outcomes following diagnosis. Accurate coding initiatives are required to identify patients who would benefit from early management and cardiometabolic risk improvement.

THU-087
Liver metabolic stress and fibrosis modify APOE ε4–associated cognitive vulnerability and amyloid burden

Young Hyeon Ahn[1], Sung-Hoon Yoon[2]. [1]*Department of Gastroenterology, Soonchunhyang University Cheonan Hospital, Cheonan-si, Korea, Rep. of South;* [2]*Department of Psychiatry, Wonkwang University Hospital, Iksan-si, Korea, Rep. of South*
Email: ysh92614@naver.com

Background and aims: Metabolic liver stress is increasingly recognised as a systemic condition with extrahepatic consequences, including neurodegeneration. We examined whether simple liver–metabolic indices are associated with domain-specific cognition and cortical amyloid burden, and whether these associations are modified by apolipoprotein E (APOE) ε4 status.
Method: We analyzed 583 adults with available metabolic, cognitive, and genetic data. Exposures included the triglyceride–glucose (TyG) index, aspartate aminotransferase/alanine aminotransferase (AST/ALT) ratio, and Fibrosis-4 (FIB-4) stage (low, intermediate, high). Cognitive performance was assessed using global and domain-specific standardized neuropsychological indices. Linear regression models were adjusted for age, sex, education, hypertension, diabetes, and dyslipidemia, with testing for effect modification by APOE ε4 status. In a subset, cortical amyloid burden was quantified using global standardized uptake value ratios from amyloid PET imaging.
Results: Higher liver–metabolic stress, reflected by TyG index and AST/ALT ratio, was associated with poorer global and domain-specific cognitive performance, including lower K-MMSE scores (TyG $\beta \approx -1.5$; 95% CI –2.5 to –0.5; AST/ALT $\beta \approx -1.9$; 95% CI –3.0 to –0.7), independent of cortical amyloid burden. The cognitive impact of fibrosis burden differed by APOE ε4 status: compared with ε4 non-carriers in the low FIB-4 stage, ε4 carriers with intermediate or high FIB-4 stages showed substantially lower global and visuospatial scores. In the amyloid PET subset, APOE ε4 carrier status alone was not associated with amyloid burden, whereas ε4 carriers with high FIB-4 stage exhibited higher cortical amyloid than non-carriers (interaction $\beta \approx 0.21$; 95% CI 0.01–0.40).
Conclusion: Routine liver–metabolic indices captured complementary aspects of late-life cognitive vulnerability. TyG index and AST/ALT ratio were associated with cognitive performance largely independent of amyloid burden, whereas fibrosis burden, assessed by FIB-4 staging, interacted with APOE ε4 status to influence both cognition and cortical amyloid deposition. These findings support a brain–liver–metabolic axis in neurodegenerative risk and identify APOE ε4 carriers with elevated FIB-4 as a high-risk subgroup for enhanced risk stratification and longitudinal monitoring.

THU-089
Liver disease severity in index patients with metabolic dysfunction-associated steatotic liver disease predicts the disease in first-degree relatives: a call for targeted screening

Halit Akarca[1], Volkan Yılmaz[2], Dilara Turan Gökçe[2], Rıfat Aydın[1], Elif Başarır[1], Özge Koç[2], Esra Tunc[3], Zeynep Melekoğlu Ellik[2], Mesut Gumussoy[2], Hale Gokcan[2], Ramazan Idilman[2]. [1]*Ankara university school of medicine, department of internal medicine, Ankara, Türkiye;* [2]*Ankara university school of medicine, department of gastroenterology, Ankara, Türkiye;* [3]*Ankara university institution of hepatology, Ankara, Türkiye*
Email: idilman@medicine.ankara.edu.tr

Background and aims: Family screening for metabolic dysfunction-associated steatotic liver disease (MASLD) is recommended but is frequently inadequately implemented due to absence of clear

prioritization criteria. This study aimed to assess the prevalence of MASLD among first-degree relatives (FDRs) of patients diagnosed with MASLD and to determine whether index-case characteristics may serve as risk indicators to prioritize screening.
Method: This prospective, cross-sectional single-center study included patients with MASLD as index cases along with their asymptomatic first-degree relatives (FDRs). Hepatic steatosis and liver stiffness were assessed via FibroScan (Transient elastography [TE]). Non-invasive fibrosis markers were calculated concurrently on the day of TE assessment.
Results: A total of 209 individuals were evaluated, comprising 96 index cases and 113 FDRs. The median age 61 years for index cases and 37 years for FDRs. The median body mass index was 33.4 kg/m^2 for index cases and 27.8 kg/m^2 for FDRs. The median FIB-4 index was 1.48 (IQR 1.04–2.62) for index cases and 0.59 (IQR 0.42–0.76) for FDRs. The median APRI score was 0.34 (IQR 0.24–0.75) for index cases and 0.20 (IQR 0.16–0.28) for FDRs. The median CAP scores were 313 dB/m (IQR 288–342) for index cases and 279 dB/m (IQR 231–323) for FDRs. The median Liver Stiffness Measurements (LSMs) were 12.1 kPa (IQR 9.9–21.3) for index cases and 5.6 kPa (IQR 4.3–6.6) for FDRs. The burden of undiagnosed MASLD in FDRs was alarmingly high: 66% of FDRs exhibited hepatic steatosis (CAP ≥ 248 dB/m), and 73% of them had advanced steatosis (CAP ≥ 280 dB/m). Notably, 9.7% of FDRs presented advanced liver fibrosis (stiffness > 8.2 kPa). Multivariable analysis showed that the waist circumference (Odds Ratio [OR] = 1.1 (95% CI: 1.043–1.163); p < 0.001), and significant fibrosis detected by TE (> 22.4 kPa) (OR = 5.8 (95% CI: 1.173–28.467); p = 0.031) in the index case were associated with hepatic steatosis in FDRs. Additionally, the waist circumference was associated with advance fibrosis in FDRs (OR = 1.13 (95% CI: 1.05–1.21); p = 0.001).
Conclusion: FDRs of patients with MASLD demonstrate a significant prevalence of the condition. The risk of MASLD in FDRs positively correlates with their anthropometric measures and the disease severity of the index case. These findings underscore the critical importance of initiating screening within families, as high-risk individuals can be identified using straightforward clinical variables.

THU-090-YI
Missed opportunities to diagnose metabolic dysfunction associated and alcohol associated steatotic liver disease after incidental detection in the emergency department
Qusai Al Zureikat[1], Ahmed El Sabagh[1], Jennifer Tran[1], Hanna Blaney[2]. [1]*MedStar Health/Georgetown University-Washington Hospital Center, Washington, DC, United States;* [2]*Virginia Commonwealth University, Richmond, United States*
Email: qzureikat@gmail.com

Background and aims: Steatotic liver disease (SLD) is frequently identified on abdominal imaging in the emergency department (ED), yet remains under-recognized. We evaluated diagnosis and gastroenterology (GI) or hepatology referral following incidental detection of hepatic steatosis in the ED, comparing metabolic dysfunction-associated steatotic liver disease (MASLD) and alcohol associated liver disease (ALD).
Method: We conducted a retrospective cohort study of adults with detected hepatic steatosis on abdominal imaging obtained during ED encounters between 2010 and 2024 in a large healthcare system. Patients were classified as MASLD or ALD based on documented clinical risk factors, including cardiometabolic factors, history of alcohol-associated diagnosis, and patient-reported alcohol use. Primary outcomes were new documentation of SLD or hepatic steatosis and GI referral or visit within 6 months after the ED encounter. Outcomes were compared using unadjusted analyses and adjusted logistic regression.
Results: Among 19,361 patients with detected hepatic steatosis, 15,415 (79.6%) were classified as MASLD and 2,816 (14.5%) as ALD. A new hepatic steatosis diagnosis was documented in 1.84% of MASLD patients compared with 3.02% of ALD patients (odds ratio 1.66, 95% CI 1.30–2.13; p < 0.001). Patients were rarely seen by gastroenterology, with only 0.59% of patients with MASLD and 0.78% with ALD seen within 6 months of the emergency department visit (p = 0.43). Elevated alanine aminotransferase (ALT) was present in 58.4% of ALD patients versus 38.5% of MASLD patients (p < 0.001), while elevated aspartate aminotransferase (AST) was present in 78.8% versus 25.9%, respectively (p < 0.001). Mean fibrosis four index (FIB-4) values were significantly higher in ALD than MASLD (2.94 vs 1.28; p < 0.001).
Conclusion: Patients with suspected MASLD were less likely than those with suspected ALD to receive a formal SLD diagnosis following incidental steatosis detection. Patients with ALD had higher AST, ALT, and FIB-4 than those with MASLD, potentially driving formal diagnosis. However, incidental hepatic steatosis and SLD remains under-recognized. These findings highlight missed opportunities for early identification and risk stratification of SLD and support systematic approaches to improve follow-up after incidental steatosis detection in the ED.

THU-091-YI
Epicardial adipose tissue as a marker of divergent hepatic and cardiovascular trajectories in MASLD: a prospective study
Francesca Alletto[1], Annalisa Cespiati[1,2], Rosa Lombardi[1,2], Felice Cinque[1,2], Giovanna Oberti[1,2], Daniel Smith[1,2], Erika Fatta[1], Edoardo Pulixi[1], Cristina Bertelli[1], Giuseppina Pisano[1], Anna Ludovica Fracanzani[1,2]. [1]*SC Medicina ad Indirizzo Metabolico, Fondazione IRCCS Cà Granda Ospedale Maggiore Policlinico of Milan, Italy; Department of Pathophysiology and Transplantation, University of Milan, Italy, Milan, Italy;* [2]*Department of Pathophysiology and Transplantation, University of Milan, Italy, Milan, Italy*
Email: francesca.alletto@unimi.it

Background and aims: Epicardial adipose tissue (EAT) is a visceral fat depot associated with cardiovascular (CV) risk and liver fibrosis in metabolic dysfunction-associated liver disease (MASLD). Longitudinal changes in EAT and their relationship with the progression of liver damage, CV disease, and skeletal mass remain unclear. Aim: to assess 5-year changes in EAT and their association with changes in liver damage, CV disease, and body composition in MASLD.
Method: We enrolled 158 MASLD patients (59% male, mean age 54 ± 12 years) from Metabolic Liver Disease outpatient clinic at Policlinico Hospital, Milan. EAT was measured by transthoracic echocardiography. Liver damage was assessed by liver stiffness measurement (LSM) and controlled attenuation parameter (CAP) at Fibroscan. CV damage was defined by increased carotid intima-media thickness (cIMT ≥ 0.9 mm) and/or carotid plaques on ultrasound. Skeletal muscle mass index (SMI) was assessed by bioelectrical impedance analysis. All evaluations were performed at baseline and after 5 years.
Results: At baseline, mean BMI was 29.3 ± 4.6 kg/m^2, 84% had increased waist circumference (WC). Mean EAT was 7.5 ± 2.3/8.3 ± 2.7 mm in men/women. Mean LSM was 4.9 kPa and CAP 298 ± 53 dB/m. After 5 years, BMI decreased (BMI −0.5 kg/m^2), while increased WC rose to 90%. EAT increased in both sexes, more markedly in men (EAT 1.1 vs 0.6 mm). Despite stable LSM and reduced CAP (CAP 13 dB/m), CV damage progressed, with higher prevalence of increased cIMT (27% vs 44%) and carotid plaques (34% vs 56%). SMI increased in both sexes (SMI 0.7 kg/m^2 in men and 0.3 kg/m^2 in women). Patients with increased EAT at follow-up showed smaller BMI reduction (−0.15 vs −1 kg/m^2, p = 0.04) and increased cIMT (33% vs 13%, p = 0.03), with a trend toward more carotid plaques (30% vs 23%, p = 0.07), without differences in liver damage or muscle mass. At multivariate analysis adjusted for sex, age, and metabolic comorbidities, increased EAT remained independently associated with smaller BMI reduction (OR 1.24, 95% CI 1.1–1.5, p = 0.02), increased cIMT (OR 4.2, 95% CI 1.5–11.6, p = 0.005), and carotid plaque (OR 1.7, 95% CI 1.2–3.2, p = 0.02).
Conclusion: In MASLD, a longitudinal increase in EAT is independently associated with progression of subclinical CV damage, despite stable liver damage and improvements in overall adiposity, reflecting

a dysfunctional adiposity phenotype. These findings support divergent CV and hepatic trajectories in MASLD, and highlight EAT as a dynamic biomarker of residual cardiometabolic risk.

THU-092

Prevalence and clinical profile of metabolic dysfunction-associated steatotic liver disease in Saudi adults: the GENESIS study

Saleh A. Alqahtani[1,2], Faisal M Sanai[3], Faisal Abaalkhail[4,5], Shadan Almuhaidib[6], Haifa F Alotaibi[6], Mohammed AlGhamdi[7], Waleed S Alomaim[8], Abdulalrhman A Alnifayei[9], Layan A. Alsubki[10], Duna Barakeh[10], Basma Khoja[10], Khalid A Alswat[11], Samar A Alqussayer[6], Hani Tamim[5], Waleed Alhazzani[6,12]. *[1]Liver, Digestive, and Lifestyle Health Research Section, and Organ Transplant Center of Excellence, King Faisal Specialist Hospital and Research Center, Riyadh, Saudi Arabia; [2]Division of Gastroenterology & Hepatology, Weill Cornell Medicine, New York, United States; [3]Gastroenterology Section, Department of Medicine, King Abdulaziz Medical City, King Abdullah International Medical Research Center, Jeddah, Saudi Arabia; [4]Gastroenterology Section, Department of Medicine, King Faisal Specialist Hospital and Research Center, Riyadh, Saudi Arabia; [5]College of Medicine, Alfaisal University, Riyadh, Saudi Arabia; [6]Health Research Center, Ministry of Defense Health Services, Riyadh, Saudi Arabia; [7]Gastroenterology Unit, Internal Medicine Department, King Fahad Military Medical Complex, Dhahran, Saudi Arabia; [8]Department of Pathology and Laboratory Medicine, King Faisal Specialist Hospital and Research Center, Riyadh, Saudi Arabia; [9]Family Medicine Department, King Fahad Armed Forces Hospital, Jeddah, Saudi Arabia; [10]Liver, Digestive, and Lifestyle Health Research Section, and Biostatistics, Epidemiology, and Scientific Computing Department, King Faisal Specialist Hospital and Research Center, Riyadh, Saudi Arabia; [11]Liver Disease Research Center, College of Medicine, King Saud University, Riyadh, Saudi Arabia; [12]Critical Care and Internal Medicine Department, College of Medicine, Imam Abdulrahman Bin Faisal University, Dammam, Saudi Arabia*
Email: drsaleh.a.alqahtani@gmail.com

Background and aims: Metabolic dysfunction-associated steatotic liver disease (MASLD) is a leading cause of chronic liver disease worldwide. Despite the high burden of metabolic risk factors in Saudi Arabia, robust population-level data on MASLD prevalence and cardiometabolic characteristics remain limited. We aimed to determine the prevalence of MASLD among Saudi adults and characterize its cardiometabolic risk profile using standardized clinical, biochemical, and imaging-based evaluations.
Method: GENESIS is the first, large-scale, prospective, population-based cohort study of MASLD in Saudi Arabia. Adults attending primary healthcare centers across three major regions were recruited between March 2024 and June 2025; individuals with known chronic liver diseases other than MASLD were excluded. Participants underwent standardized clinical assessment, laboratory testing, and vibration-controlled transient elastography. MASLD was defined as a controlled attenuation parameter (CAP) ≥ 268 dB/m plus ≥ 1 cardiometabolic risk factor (CMRF). Sensitivity analyses used alternative definitions (CAP ≥ 220 dB/m and MASLD liver fat score [MASLD-LFS]). Significant fibrosis (F2–F4) was defined as liver stiffness ≥ 7.1 kPa.
Results: Among 2,983 participants, hepatic steatosis (CAP ≥ 220 dB/m) was observed in 68.8%, MASLD prevalence was 37.2% (age-adjusted: 34.1%) and was higher in males (43.6% vs. 30.9%). Severe steatosis (CAP ≥ 300 dB/m) was observed in 20.7%, while significant fibrosis was detected in 2.9%. Using alternative definitions, MASLD prevalence was 66.1% with CAP ≥ 220 dB/m and 58.6% with MASLD-LFS. Compared with participants without MASLD, those with MASLD were more often male (58.2% vs. 44.7%) and older (mean age: 46.1 vs. 39.5 years) (all $p < 0.001$), with higher adiposity (median BMI: 31.6 vs. 27.0 kg/m^2; mean waist-to-hip ratio: 0.91 vs. 0.86). MASLD was associated with a greater burden of CMRFs (diabetes: 33.4% vs 12.9%; hypertension: 23.0% vs 10.1%; dyslipidemia: 36.5% vs 20.6%), as well as higher median insulin (13.0 vs 8.1 µU/mL) and C-reactive protein levels (3.5 vs 2.1 mg/L) (all $p < 0.001$). Smoking status, coffee consumption, and liver enzymes did not differ between groups.
Conclusion: MASLD affected more than one-third of adults screened, with hepatic steatosis affecting approximately two-thirds. These findings highlight a major public health challenge and underscore the need for population-based prevention and management strategies in Saudi Arabia.

THU-093

From irregular cycles to menopause: reproductive transitions associated with metabolic dysfunction-associated steatotic liver disease severity in women

Saleh A. Alqahtani[1,2], Basma Khoja[3], Shadan Almuhaidib[4], Lolwa N. Alobaid[5], Faisal M Sanai[6], Haifa F Alotaibi[4], Salwa A AlAwadh[7], Waleed S Alomaim[8], Layan A. Alsubki[3], Duna Barakeh[3], Saleh Alessy[3,9], Hind Abdulhakeem[10], Habeeb I.A. Razack[11], Carolin V Schneider[12], Faisal Abaalkhail[13,14], Waleed Alhazzani[4,15]. *[1]Liver, Digestive, and Lifestyle Health Research Section, and Organ Transplant Center of Excellence, King Faisal Specialist Hospital and Research Center, Riyadh, Saudi Arabia; [2]Division of Gastroenterology & Hepatology, Weill Cornell Medicine, New York, United States; [3]Liver, Digestive, and Lifestyle Health Research Section, and Biostatistics, Epidemiology, and Scientific Computing Department, King Faisal Specialist Hospital and Research Center, Riyadh, Saudi Arabia; [4]Health Research Center, Ministry of Defense Health Services, Riyadh, Saudi Arabia; [5]Hepatology Section, Hepatobiliary Sciences and Organs Transplant Center, King Abdulaziz Medical City, Riyadh, Saudi Arabia; [6]Gastroenterology Section, Department of Medicine, King Abdulaziz Medical City, King Abdullah International Medical Research Center, Jeddah, Saudi Arabia; [7]Department of Family Medicine, Armed Forces Hospital, Dhahran, Saudi Arabia; [8]Department of Pathology and Laboratory Medicine, King Faisal Specialist Hospital and Research Center, Riyadh, Saudi Arabia; [9]Department of Public Health, Saudi Electronic University, Riyadh, Saudi Arabia; [10]Medical Laboratory Department, King Fahad Armed Forces Hospital, Jeddah, Saudi Arabia; [11]College of Medicine, King Saud University, Riyadh, Saudi Arabia; [12]Department of Gastroenterology, Metabolic Diseases and Intensive Care, University Hospital RWTH Aachen, Aachen, Germany; [13]Gastroenterology Section, Department of Medicine, King Faisal Specialist Hospital and Research Center, Riyadh, Saudi Arabia; [14]College of Medicine, Alfaisal University, Riyadh, Saudi Arabia; [15]Critical Care and Internal Medicine Department, College of Medicine, Imam Abdulrahman Bin Faisal University, Dammam, Saudi Arabia*
Email: drsaleh.a.alqahtani@gmail.com

Background and aims: Reproductive hormonal transitions influence metabolic health, but their relationship with metabolic dysfunction-associated steatotic liver disease (MASLD) in women remains incompletely characterized. We examined whether menopausal status and menstrual irregularity are associated with hepatic steatosis and fibrosis severity among women enrolled.
Method: We analyzed women enrolled in the large, nationwide, population-based GENESIS cohort in Saudi Arabia and categorized them by menopausal status (pre- vs post-menopause) and menstrual regularity (regular vs irregular cycles), based on self-reported data. Steatosis severity was defined using controlled attenuation parameter (CAP) thresholds: S2 (269–299 dB/m) and S3 (≥ 300 dB/m). Significant fibrosis was defined as liver stiffness ≥ 7.1 kPa. MASLD was defined as CAP ≥ 268 dB/m plus at least one cardiometabolic risk factor.
Results: Among 766 women, 483 (63.1%) were pre-menopausal (median age 36 years) and 283 (36.9%) post-menopausal (median age 58 years). The post-menopausal group had higher body mass index (BMI) (32.0 vs 28.8 kg/m^2), larger waist circumference (99.1 vs 87.4 cm), and higher prevalence of diabetes (55.1% vs 12.2%) and dyslipidemia (57.2% vs 11.2%) (all $p < 0.001$). MASLD prevalence was

higher in this group (49.8% vs 24.8%, p < 0.001). Moderate (S2) and severe (S3) steatosis were more common (22.3% vs 12.2% and 26.9% vs 12.8%, respectively; both p < 0.001), while significant fibrosis was uncommon but was more frequent (4.6% vs 0.8%, p = 0.008). Among 678 women with available menstrual cycle data, 501 (73.9%) reported regular cycles (median age 37 years) and 177 (26.1%) irregular cycles (median age 38 years). Women with irregular cycles had higher BMI (31.1 vs 28.1 kg/m^2), larger waist circumference (92.0 vs 87.0 cm), and higher dyslipidemia prevalence (23.7% vs 13.2%, p = 0.002). MASLD prevalence was higher among those with irregular cycles (33.3% vs 23.0%, p = 0.009), as was severe steatosis (22.6% vs 11.4%, p < 0.001). Fibrosis prevalence was low and similar between groups (p = 0.081).
Conclusion: In this cohort, menopausal status and menstrual irregularity were associated with greater metabolic burden, higher MASLD prevalence, and more severe steatosis, with modest differences in fibrosis. Reproductive transitions may help identify women at increased MASLD risk and support sex-specific risk assessment and targeted screening strategies.

THU-094

Impact of obesity on symptom burden and health-related quality of life in patients with metabolic dysfunction-associated steatotic liver disease

Saleh A. Alqahtani[1,2], Majd Alsayb[3], Mariam Seria[4], Shadan Almuhaidib[5], Bandar Aljudaibi[6], Lama Amer[7,8], Abdulraheem M. Bayameen[9], Areej Alkhairy[10], Nawaf Yahya Zakary[4], Basmah Khoja[11], Fatema Nader[12,13], Alwaleed Almojel[11], Noura Alessa[4], Mashhoor Beragdar[14], Mohammed AlGhamdi[4], Faisal Abaalkhail[8,15], Zobair M. Younossi[16], Waleed Alhazzani[5,17].
[1]Liver, Digestive, and Lifestyle Health Research Section, and Organ Transplant Center of Excellence, King Faisal Specialist Hospital and Research Center, Riyadh, Saudi Arabia; [2]Division of Gastroenterology & Hepatology, Weill Cornell Medicine, New York, United States; [3]Division of Gastroenterology & Hepatology, King Fahad Armed Forces Hospital, Jeddah, Saudi Arabia; [4]Gastroenterology Unit, Internal Medicine Department, King Fahad Military Medical Complex, Dhahran, Saudi Arabia; [5]Health Research Center, Ministry of Defense Health Services, Riyadh, Saudi Arabia; [6]Organ Transplant Center of Excellence, King Faisal Specialist Hospital and Research Center, Riyadh, Saudi Arabia; [7]Cell transplant & Stem Cell Unit, Kidney & Pancreas Health department, Organ Transplant Center of Excellence, King Faisal Specialist Hospital and Research Center, Riyadh, Saudi Arabia; [8]College of Medicine, Alfaisal University, Riyadh, Saudi Arabia; [9]Family Medicine Department, King Fahad Armed Forces Hospital, Jeddah, Saudi Arabia; [10]Department of Internal Medicine, King Faisal Specialist Hospital and Research Center, Jeddah, Saudi Arabia; [11]Liver, Digestive, and Lifestyle Health Research Section, and Biostatistics, Epidemiology, and Scientific Computing Department, King Faisal Specialist Hospital and Research Center, Riyadh, Saudi Arabia; [12]The Global Liver Council, Center for Outcomes Research in Liver Diseases, Wahington, DC, United States; [13]Beatty Liver and Obesity Research Program, Inova Health System, Falls Church, VA, United States; [14]Department of Family Medicine, King Faisal Specialist Hospital & Research Center, Jeddah, Saudi Arabia; [15]Gastroenterology Section, Department of Medicine, King Faisal Specialist Hospital and Research Center, Riyadh, Saudi Arabia; [16]The Global NASH/MASH Council (GNC), Washington, DC, United States; [17]Critical Care and Internal Medicine Department, College of Medicine, Imam Abdulrahman Bin Faisal University, Dammam, Saudi Arabia
Email: drsaleh.a.alqahtani@gmail.com

Background and aims: Obesity is a major cardiometabolic risk factor that may exacerbate symptoms and reduce health-related quality of life (HRQoL) in metabolic dysfunction-associated steatotic liver disease (MASLD), a highly prevalent condition associated with increased morbidity. Understanding the impact of obesity on symptom burden and HRQoL in MASLD is essential to guide clinical management and targeted interventions. We aimed to evaluate the impact of obesity on symptom burden and HRQoL in adults with MASLD.
Method: Data from adults (≥ 18 years) with MASLD enrolled in the Saudi Arabia cohort of the Global Liver Registry were analyzed. Participants were stratified by obesity status (with obesity, body mass index [BMI] ≥ 30 kg/m^2; without obesity, BMI < 30 kg/m^2). Demographics, comorbidities, and symptom prevalence, including fatigue, anxiety, and hypertension, were collected using standardized patient-reported questionnaires and clinical records. HRQoL was assessed using the Chronic Liver Disease Questionnaire-MASLD (CLDQ-MASLD; 1–7 Likert scale, higher scores indicate better HRQoL), covering six domains: abdominal symptoms, activity, emotion, fatigue, systemic symptoms, and worry.
Results: Among 1,255 participants (median age, 49 years [interquartile ranges (IQR) 30–59]), 637 (50.8%) had obesity, while 618 (49.2%) did not. Participants with obesity were more frequently female (51.3% vs. 32.8%) and had higher prevalence of fatigue (53.7% vs. 43.0%), anxiety (49.1% vs. 40.6%), and hypertension (36.1% vs. 27.3%). Median CLDQ-MASLD scores were significantly lower among participants with obesity for abdominal symptoms (6.0 [4.3–7.0] vs. 6.3 [4.7–7.0], p = 0.010), activity (6.0 [4.8–7.0] vs. 6.4 [5.4–7.0], p < 0.001), fatigue (5.8 [4.5–6.7] vs. 6.0 [5.0–6.8], p = 0.003), systemic symptoms (6.2 [5.3–6.8] vs. 6.5 [5.7–7.0], p < 0.001), and overall CLDQ-MASLD score (6.0 [5.1–6.6] vs. 6.3 [5.5–6.7], p < 0.001). No statistically significant differences were observed for emotion (6.1 [5.1–6.8] vs. 6.2 [5.3–6.8], p = 0.120) or worry (7.0 [6.7–7.0] vs. 7.0 [6.7–7.0], p = 0.515) domains.
Conclusion: In this real-world MASLD cohort from Saudi Arabia, obesity was associated with a higher symptom burden and lower HRQoL, particularly in abdominal symptoms, activity, and fatigue. These findings underscore the need for targeted interventions, including weight management, symptom-focused therapy, and psychosocial support, to improve patient-centered outcomes in MASLD.

THU-095

Socioeconomic, clinical, and quality of life differences by physical activity status among patients with metabolic dysfunction-associated steatotic liver disease and metabolic dysfunction-associated steatohepatitis in Saudi Arabia

Saleh A. Alqahtani[1,2], Nasser Mohammed Al Masri[3], Fatmah Yamani[4], Shadan Almuhaidib[5], Layan A. Alsubki[6], Mushabbab K Asseri[7], Rana AlMansour[8], Basma Khoja[6], Abdullah Alkhenizan[9], Abdulrahman G Alkabbani[10], Asrar Alaklabi[6], Amwaj I. Alanazi[6], Zergham Zia[11], Mohammed Almaghrabi[3], Abdullah Alfhaid[12], Muneera Alshareef[13], Zobair M. Younossi[14], Waleed Alhazzani[5,15].
[1]Liver, Digestive, and Lifestyle Health Research Section, and Organ Transplant Center of Excellence, King Faisal Specialist Hospital and Research Center, Riyadh, Saudi Arabia; [2]Division of Gastroenterology & Hepatology, Weill Cornell Medicine, New York, United States, [3]Division of Gastroenterology & Hepatology, Prince Sultan Military Medical City, Riyadh, Saudi Arabia; [4]Department of Internal Medicine, King Faisal Specialist Hospital and Research Center, Jeddah, Saudi Arabia; [5]Health Research Center, Ministry of Defense Health Services, Riyadh, Saudi Arabia; [6]Liver, Digestive, and Lifestyle Health Research Section, and Biostatistics, Epidemiology, and Scientific Computing Department, King Faisal Specialist Hospital and Research Center, Riyadh, Saudi Arabia; [7]Department of Endocrine & Diabetes, Prince Sultan Medical Military City, Riyadh, Saudi Arabia; [8]Department of Family and Community Medicine, King Fahd Military Medical Complex, Dhahran, Saudi Arabia; [9]Department of Family Medicine, King Faisal Specialist Hospital and Research Center, Riyadh, Saudi Arabia; [10]Department of Medicine, Endocrinology Section, King Faisal Specialist Hospital & Research Center, Riyadh, Saudi Arabia; [11]Radiology Department, King Faisal Specialist Hospital and Research Center, Jeddah, Saudi Arabia; [12]Department of Liver and Small Bowel Health, King Faisal Specialist Hospital and Research Centre, Riyadh, Saudi Arabia; [13]Department of Endocrinology and Diabetes, King Fahad Armed Forces Hospital, Jeddah, Saudi Arabia;

[14]The Global NASH/MASH Council (GNC), Washington, DC, United States; [15]Critical Care and Internal Medicine Department, College of Medicine, Imam Abdulrahman Bin Faisal University, Dammam, Saudi Arabia
Email: drsaleh.a.alqahtani@gmail.com

Background and aims: Regular physical activity (PA) is a core component of the management of metabolic dysfunction-associated steatotic liver disease and steatohepatitis (MASLD/MASH). However, socioeconomic and environmental factors may influence engagement in exercise. We aimed to examine socioeconomic, clinical, and health-related quality of life (HRQoL) differences according to PA status among patients with MASLD/MASH in Saudi Arabia.
Method: We analyzed data from adults with MASLD/MASH enrolled in the Saudi Arabian cohort of the Global Liver Registry. PA was assessed by self-report and categorized as physically active if participants exercised more than 30 minutes at least three times per week (active); all others were classified as having insufficient PA (non-active). Demographic characteristics, cardiometabolic comorbidities, psychosocial symptoms, socioeconomic indicators (education level and financial difficulty), access to exercise facilities, and HRQoL measured using the Chronic Liver Disease Questionnaire (CLDQ) were compared between active and non-active participants.
Results: A total of 1,264 patients were included, of whom 509 (40.3%) reported being physically active. Median age of active participants was 47 years vs 50 years in the non-active group ($p < 0.001$), and males comprised 63.9% of active participants vs 53.4% of non-active participants ($p < 0.001$). Insufficient PA was more frequent among patients with obesity (53.3% vs. 47.0%, $p = 0.029$), diabetes (48.5% vs. 37.1%, $p < 0.001$), and hypertension (35.5% vs. 26.5%, $p = 0.002$). Non-active participants reported higher prevalence of fatigue (55.5% vs. 37.7%, $p < 0.001$), anxiety (49.4% vs. 38.5%, $p < 0.001$), and depression (21.6% vs. 15.3%, $p = 0.007$). Lower educational attainment (primary education or below: 28.9% vs. 18.5%) and greater financial difficulty (reporting a lot of financial difficulty: 5.6% vs. 2.2%) were more common among non-active participants ($p < 0.001$), as was reduced access to a gym or park (81.9% vs. 94.3%, $p < 0.001$). HRQoL was reduced in non-active participants, with lower overall CLDQ scores (median 5.9 vs. 6.5, $p < 0.001$).
Conclusion: In this Saudi Arabian cohort of adults with MASLD/MASH, insufficient PA was associated with lower socioeconomic status, higher cardiometabolic and psychosocial burden, and reduced HRQoL. Encouraging regular PA, particularly among those with socioeconomic and environmental barriers, may help improve patient-centered outcomes in MASLD/MASH.

THU-099

Clinical and metabolic characteristics of lean compared with overweight/obese metabolic dysfunction-associated steatotic liver disease

Saleh A. Alqahtani[1,2], Faisal Abaalkhail[3,4], Shadan Almuhaidib[5], Basma Khoja[6], Haifa F Alotaibi[5], Saad Alghamdi[7], Yasir M Alhazmi[8], Tagreed A Mazi[9], Abdullah Falah Alharthi[10], Fahad Alkhayal[10], Ali Alshehri[11], Faisal M Sanai[12], Bandar Aljudaibi[7], Waleed Alhazzani[5,13]. [1]Liver, Digestive, and Lifestyle Health Research Section, and Organ Transplant Center of Excellence, King Faisal Specialist Hospital and Research Center, Riyadh, Saudi Arabia; [2]Division of Gastroenterology & Hepatology, Weill Cornell Medicine, New York, United States; [3]Gastroenterology Section, Department of Medicine, King Faisal Specialist Hospital and Research Center, Riyadh, Saudi Arabia; [4]College of Medicine, Alfaisal University, Riyadh, Saudi Arabia; [5]Health Research Center, Ministry of Defense Health Services, Riyadh, Saudi Arabia; [6]Liver, Digestive, and Lifestyle Health Research Section, and Biostatistics, Epidemiology, and Scientific Computing Department, King Faisal Specialist Hospital and Research Center, Riyadh, Saudi Arabia; [7]Organ Transplant Center of Excellence, King Faisal Specialist Hospital and Research Center, Riyadh, Saudi Arabia; [8]Family Medicine Department, King Fahad Armed Forces Hospital, Jeddah, Saudi Arabia; [9]Department of Community Health Sciences-Clinical Nutrition, College of Applied Medical Sciences, King Saud University, RIyadh, Saudi Arabia; [10]Family Medicine Department, Prince Sultan Military Medical City, Riyadh, Saudi Arabia; [11]Obesity Medicine Department, Obesity, Endocrine and Metabolism Centre, King Fahad Medical City, Riyadh, Saudi Arabia; [12]Gastroenterology Section, Department of Medicine, King Abdulaziz Medical City, King Abdullah International Medical Research Center, Jeddah, Saudi Arabia; [13]Critical Care and Internal Medicine Department, College of Medicine, Imam Abdulrahman Bin Faisal University, Dammam, Saudi Arabia
Email: drsaleh.a.alqahtani@gmail.com

Background and aims: Metabolic dysfunction-associated steatotic liver disease (MASLD) can occur in individuals with normal body mass index (BMI), referred to as lean MASLD, yet its clinical and metabolic profile remains poorly characterized compared with overweight/obese MASLD. We aimed to compare demographic characteristics, metabolic comorbidities, liver disease severity, and systemic inflammation between lean and overweight/obese MASLD groups in a nationwide Saudi cohort.
Method: We analyzed data from adults with MASLD and complete BMI data from the population-based GENESIS cohort in Saudi Arabia. MASLD was defined by controlled attenuation parameter (CAP) ≥ 268 dB/m, measured by transient elastography plus ≥ 1 cardiometabolic risk factor. Participants were categorized as lean MASLD (BMI < 25 kg/m^2) or overweight/obese MASLD (BMI ≥ 25 kg/m^2). We assessed three domains: (1) demographics and anthropometrics, (2) metabolic comorbidities, and (3) liver-related markers, including liver enzymes (alanine aminotransferase [ALT], aspartate aminotransferase [AST]), noninvasive measures of steatosis (CAP) and fibrosis (liver stiffness measurement [LSM], kPa), and systemic inflammation (C-reactive protein [CRP]).
Results: Among 1,110 adults with MASLD, 54 (4.9%) were classified as lean MASLD and 1,056 (95.1%) as overweight/obese MASLD. Median age was 46 years (interquartile range [IQR] 37–55), with 41.8% female. Compared with overweight/obese MASLD, participants with lean MASLD were predominantly male (74.1% vs 57.4%, $p = 0.016$) and tended to be older (median age 51 vs 46 y, $p = 0.052$). Waist-to-hip ratio was similar between groups ($p = 0.675$). Prevalence of diabetes (37.0% vs 33.2%, $p = 0.557$), hypertension (50.0% vs 46.2%, $p = 0.675$), and dyslipidemia (38.9% vs 36.4%, $p = 0.772$) were comparable between lean and overweight/obese MASLD. Significant fibrosis (LSM ≥ 7.1 kPa) was observed in 4 (7.4%) of lean MASLD vs 61 (5.8%) of overweight/obese MASLD ($p = 0.551$). ALT and AST were similar between groups, while CRP was higher in the overweight/obese MASLD group (median 3.8 vs 1.5 mg/L, $p < 0.001$).
Conclusion: Lean MASLD, predominantly affecting males, exhibits similar steatosis, fibrosis burden, and metabolic comorbidity prevalence compared with overweight/obese MASLD despite lower BMI, whereas systemic inflammation was greater in the overweight/obese group. Recognition of lean MASLD is essential for early diagnosis, risk stratification, and optimized clinical management.

THU-100

Demographic and metabolic predictors of MASLD progression in Saudi Arabia: a retrospective cross-sectional analysis

Amani Alsadoon[1], Khalid A Alswat, Mohammed Kaouache[2], Wadi B. Alonazi[3]. [1]Liver Disease Research Center, College of Medicine, King Saud University, Riyadh, Saudi Arabia; [2]Department of Mathematics and General Sciences, Prince Sultan University, Riyadh, Saudi Arabia; [3]Health Administration Department, College of Business Administration, King Saud University, Riyadh, Saudi Arabia
Email: amalsadon@ksu.edu.sa

Background and aims: Metabolic dysfunction-associated steatotic liver disease (MASLD) represents a major public health challenge in Saudi Arabia and globally. Data on factors associated with advanced MASLD phenotypes in Middle Eastern populations remain limited. This study aimed to identify demographic and metabolic factors

independently associated with advanced MASLD in a large cohort from Saudi Arabia.
Method: This retrospective cross-sectional study analyzed anonymized data from 780 adults with MASLD enrolled in the Saudi Observatory for Liver Diseases (SOLID) registry at the Liver Disease Research Center, King Saud University. MASH and cirrhosis were defined using FibroScan liver stiffness thresholds (≥7.9 kPa and ≥13.0 kPa, respectively) with elevated aminotransferases as a pragmatic noninvasive surrogate. Multivariable logistic regression identified independent predictors, with models mutually adjusted for demographic and metabolic covariates. Discriminative ability was evaluated using ROC curves.
Results: Among 780 patients with MASLD, 6.5% had cirrhosis and 5.8% met criteria for MASH. Male sex was a consistent predictor of advanced disease, with higher odds of cirrhosis (OR = 2.82; 95% CI: 1.36–5.59; p = 0.003) and MASH (OR = 2.38; 95% CI: 1.24–4.53; p = 0.009) compared with females. Increasing age was independently associated with MASH (OR = 1.04 per year; 95% CI: 1.01–1.08; p = 0.012), but not with cirrhosis after adjustment. Type 2 DM showed an inverse association with cirrhosis (OR = 0.31; 95% CI: 0.16–0.65; p = 0.002), possibly reflecting referral bias or earlier disease detection rather than a protective biological effect. Traditional metabolic risk factors, including BMI, triglycerides, HDL cholesterol, and hypertension, were not significant predictors. These associations attenuated after multivariable adjustment. Model discrimination was acceptable to good, with AUC values of 0.77 for cirrhosis and 0.69 for MASH.
Conclusion: In this Saudi clinical cohort, age and male sex were the principal determinants of advanced MASLD, while conventional metabolic risk factors showed limited independent predictive value after adjustment. The inverse association observed between diabetes and cirrhosis likely reflects diagnostic or referral bias. These findings support the need for demographic-focused risk stratification strategies to improve identification of advanced MASLD in regional clinical practice.

THU-101
Ramadan fasting enhances hepatic and cardiometabolic profiles in metabolic dysfunction-associated steatotic liver disease (MASLD): a prospective real-world study

Khalid Alswat[1], Abdullah Alansare[2], Maha Alhussain[3], Salwa Asswini[3], Mohamed Elbadry[4], Samy Zaky[5], Moshira Mohamed[6], Mahmoud Hagag[7], Mona Kaddah[8], Mohammed Medhat[9], Nariman Zaghloul[9], Mohamed Abdel-Samiee[10], Eman Abdelsameea[11], Essam Zayed[11], Nermeen Abdeen[12], Faisal M Sanai[13], Mohamed El Kassas[14].
[1]Department of Medicine, Liver Disease Research Centre, College of Medicine, King Saud University, Steatotic Liver Disease Study Foundation in the Middle East and North Africa (SLMENA), Cairo, Egypt, Riyadh, Saudi Arabia; [2]The Department of Exercise Physiology, College of Sports Science and Physical Activity, Riyadh, Saudi Arabia; [3]Department of Food Sciences and Nutrition, College of Food and Agricultural Sciences, King Saud University, Riyadh, Saudi Arabia; [4]Endemic Medicine department, Helwan University, Cairo, Egypt; [5]Al-Azhar University, Cairo, Egypt; [6]Lecturer of Hepatogastroenterology and Infectious diseases, Cairo, Egypt; [7]Gastroenterologist and hepatologist, Ministry of health, Cairo, Egypt; [8]Lectured of Endemic Medicine and hepatogastroenterology, Cairo, Egypt; [9]Assiut University, Assiut, Egypt, Assiut, Egypt; [10]Hepatology and Gastroenterology Department, National Liver Institute, Menoufia University, Shebin El-kom, Egypt; [11]Hepatology and gastroenterology Department, National Liver Institute, Menoufia University, Shebin El-kom, Egypt; [12]Alexandria University, Alexandria, Egypt; [13]Gastroenterology Section, Department of Medicine, King Abdulaziz Medical City, King Abdullah International Medical Research Center, Ministry of National Guard - Health, Steatotic Liver Disease Study Foundation in the Middle East and North Africa (SLMENA), Cairo, Egypt, Jeddah, Saudi Arabia; [14]Steatotic Liver Disease Study Foundation in the Middle East and North Africa (SLMENA), Endemic Medicine Department, Faculty of Medicine, Helwan University, Cairo, Egypt
Email: klaswat@ksu.edu.sa

Background and aims: Intermittent fasting is increasingly recognized as a metabolic intervention for liver health; yet, evidence on Ramadan diurnal intermittent fasting (RDIF), a culturally mandated dry fast, remains limited in MASLD. We evaluated the effects of RDIF on hepatic steatosis, liver stiffness, metabolic parameters, and lifestyle behaviors in a real-world MASLD cohort.
Method: This prospective observational study enrolled 79 adults with MASLD (median age 47 years; 58.2% male) who undertook RDIF for at least 21 consecutive days during Ramadan. Assessments were conducted 7 days before Ramadan and at the end of Ramadan, including anthropometrics, liver biochemistry, transient elastography (liver stiffness measurement [LSM] and controlled attenuation parameter [CAP]), lipid and glycaemic profiles, 24-hour dietary recall, and movement behaviors (total, light, and moderate-to-vigorous physical activity and sedentary behavior). The total physical activity and sedentary behavior were used to calculate the Physical Activity Sedentary Time Balance Index (PASTBI).
Results: After RDIF, significant reductions in ALT (from 95.3 to 70.0 U/L; p < 0.001), AST (from 55.5 to 46.3 U/L; p < 0.001), and CAP scores (from 317.0 to 280.5 dB/m; p < 0.001) were observed, while LSM showed a non-significant reduction (from 7.1 to 6.1 kPa; p = 0.054). BMI modestly and non-significantly decreased (from 30.8 to 30.0 kg/m^2; p = 0.096), while waist circumference was significantly reduced (from 103.1 to 97.0 cm; p = 0.002). Favorable lipid changes were observed, including reductions in total cholesterol (from 5.1 to 4.9 mmol/L, p = 0.019), triglycerides (from 1.8 to 1.7 mmol/L, p = 0.031), and LDL cholesterol (from 2.9 to 2.8 mmol/L, p = 0.041), though HDL remained stable (p = 0.217). Light and moderate-to-vigorous physical activity significantly decreased (from 37.1 to 21.4 min/day and from 15.9 to 7.3 min/day, respectively; p < 0.001 for both). The PASTBI significantly decreased (from 15.9 to 7.3; p < 0.001), although sedentary behavior remained unchanged (p =).
Conclusion: This is the first prospective study to demonstrate that RDIF was associated with significant improvements in hepatic aminotransferases, hepatic steatosis, central adiposity, and atherogenic lipid profiles in patients with MASLD, with a borderline reduction in LSM, despite a compromised movement behaviors profile. RDIF may represent a culturally rooted lifestyle intervention with potential therapeutic relevance for MASLD.

THU-102
Glucagon-like peptide-1 receptor localization in lipid droplets and M2-like macrophages in MASH

Wataru Ando[1], Mitsuhiro Sugawara[1], Hiroaki Yokomori[2]. *[1]Kitasato University, School of Pharmacy, Kitamoto city, Japan; [2]Kitasato University, School of Pharmacy, Minato-ku, Tokyo, Japan*
Email: andow@pharm.kitasato-u.ac.jp

Background and aims: Over the past three decades, the incidence of metabolic dysfunction–associated fatty liver disease (MAFLD) has greatly increased and has become a burdensome chronic liver disease worldwide. Type 2 diabetes is bidirectionally related to MAFLD. Glucagon-like peptide-1 receptor (GLP-1R) agonists may improve MAFLD; however, the underlying mechanisms have not been elucidated at the morphological level. Therefore, we investigated the cellular localization of GLP-1R in livers of patients with MAFLD using immunohistochemistry (IHC), immunoelectron microscopy (IEM), and Western blot analysis.
Method: Liver biopsy specimens were obtained from three patients with MASH and were compared with those from four histologically normal controls. IHC and IEM were performed using anti-GLP-1R, CD68, and CD138 antibodies. Western blotting of biopsy-derived protein extracts was conducted to quantify GLP-1R expression levels.
Results: IHC showed that GLP-1R localized to the basolateral membranes of hepatocytes with macrovesicular steatosis and was

expressed in monocytes infiltrating hepatic sinusoids in early MAFLD. In advanced MASH, reaction products indicating GLP-1R expression were predominantly observed in proliferating mononuclear cells surrounding inflammatory areas. IEM revealed small clusters of GLP-1R molecules on the peripheral rims of lipid droplets and on the cytoplasmic leaflets of endoplasmic reticulum membranes and intracellular vesicles. Western blot analysis demonstrated markedly higher GLP-1R protein expression in early MASH samples compared with normal controls. Furthermore, dual expression of GLP-1R with CD68 or CD138 was clearly increased in advanced MASH compared with early-stage disease.
Conclusion: GLP-1R is localized within lipid-associated microdomains of steatotic hepatocytes and alternatively activated (M2-like) macrophages. These findings provide mechanistic insight into liver-specific GLP-1 signaling and may inform future development of GLP-1–based therapeutic strategies for MASH.

THU-103

Long-term liver-related outcomes in asian and caucasian patients with MASLD: evidence from a large multicentric observational study

Angelo Armandi[1], Piero Fariselli[2], Gian Paolo Caviglia[1], Hye Won Lee[3], Masato Yoneda[4], Ming-Hua Zheng[5], Salvatore Petta[6], Emmanuel Tsochatzis[7], Jerome Boursier[8], José Luis Calleja Panero[9], Hannes Hagström[10], Manuel Romero-Gómez[11], Laurent Castera[12], Arun J Sanyal[13], Victor De Ledinghen[14], Philip Newsome[15], Huapeng Lin[16], Terry Cheuk-Fung Yip[16], George Boon Bee Goh[17], Wah-Kheong Chan[18], Rocio Gallego-Durán[11], Jian-Gao Fan[19], Michelle Lai[20], Céline Fournier-Poizat[21], Grace Lai-Hung Wong[16], Anders Mellemkjær[22], Mirko Zoncapè[7], Grazia Pennisi[6], Atsushi Nakajima[4], Wen-Yue Liu[23], Ying Shang[10], Marc de Saint-Loup[8], Elba Llop Herrera[9], Kevin Kim Jun Teh[17], Carmen Lara-Romero[11], Amon Asgharpour[13], Sara Mahgoub[15], Sau-Wai Mandy Chan[21], Clémence M Canivet[8], Seung Up Kim[3], Vincent Wai-Sun Wong[16], Elisabetta Bugianesi[1]. *[1]Division of Gastroenterogy and Hepatology, Department of Medical Sciences, University of Turin, Turin, Italy; [2]Computational Biomedicine Unit, Department of Medical Sciences, University of Turin, Turin, Italy; [3]Department of Internal Medicine, Institute of Gastroenterology, Yonsei University College of Medicine, Seul, Korea, Rep. of South; [4]Department of Gastroenterology and Hepatology, Yokohama City University Graduate School of Medicine, Yokohama, Japan; [5]MAFLD Research Center, Department of Hepatology, First Affiliated Hospital of Wenzhou Medical University, Wenzhou, China; [6]Sezione di Gastroenterologia, PROMISE, University of Palermo, Palermo, Italy; [7]University College London Institute for Liver and Digestive Health, Royal Free Hospital and UCL, Liver Unit, University of Verona and Azienda Ospedaliera Universitaria Integrata Verona, Verona, Italy, London, United Kingdom; [8]Hepato-Gastroenterology and Digestive Oncology Department, Angers University Hospital, HIFIH Laboratory, SFR ICAT 4208, Angers University, Angers, France; [9]Department of Gastroenterology and Hepatology, Hospital Universitario Puerta de Hierro Majadahonda, Madrid, Spain; [10]Department of Medicine, Huddinge, Karolinska Institutet, Stockholm, Sweden; [11]Digestive Diseases Unit and CIBERehd, Virgen Del Rocío University Hospital, Seville, Spain; [12]Université Paris Cité, UMR1149 (CRI), INSERM, Paris, France; Service d'Hépatologie, Hôpital Beaujon, Assistance Publique-Hôpitaux de Paris (AP-HP), Clichy, Paris, France; [13]Stravitz-Sanyal Institute for Liver Disease and Metabolic Health, VCU School of Medicine, Richmond, Virginia, United States; [14]Centre d'Investigation de la Fibrose Hépatique, Haut-Lévêque Hospital, University Hospital of Bordeaux, Pessac, France; [15]National Institute for Health Research, Biomedical Research Centre at University Hospitals Birmingham NHS Foundation Trust and the University of Birmingham, Birmingham, United Kingdom; [16]Medical Data Analytics Centre, Department of Medicine and Therapeutics, The Chinese University of Hong Kong, State Key Laboratory of Digestive Disease, Institute of Digestive Disease, The Chinese University of Hong Kong, Hong Kong, China; [17]Department of Gastroenterology and Hepatology, Singapore General Hospital, Singapore, Singapore; [18]Gastroenterology and Hepatology Unit, Department of Medicine, Faculty of Medicine, University of Malaya, Malaya, Malaysia; [19]Department of Gastroenterology, Xinhua Hospital Affiliated to Shanghai Jiaotong University School of Medicine, Shanghai Key Lab of Pediatric Gastroenterology and Nutrition, Shangai, China; [20]Division of Gastroenterology & Hepatology, Beth Israel Deaconess Medical Center, Harvard Medical School, Boston, Massachusetts, United States; [21]Echosens, Paris, France; [22]Department of Hepatology & Gastroenterology, Aarhus University Hospital, Aarhus, Denmark; [23]Department of Endocrinology, First Affiliated Hospital of Wenzhou Medical University, Wenzhou, China*
Email: angelo.armandi@unito.it

Background and aims: A strong evidence on the role of ethnicity for prognostication in MASLD is lacking. Here, we investigated the incidence of liver-related events (LRE) in Asian and Caucasian patients with MASLD.
Method: A retrospective longitudinal study of patients with MASLD and available liver stiffness measurement (LSM) by vibration-controlled transient elastography (VCTE, Fibroscan) at baseline and follow up. Primary outcome was incidence of composite LRE (hepatocellular carcinoma, decompensating events, liver transplant, liver-related death). We built 1:1 Asian-Caucasian matched cohorts using sex-stratified optimal bipartite matching (Hungarian algorithm) on z-standardized age and baseline LSM, imposing a caliper on the Euclidean distance ($\leq$0.1 SD). Cumulative LRE incidence was estimated by Kaplan-Meier method. Uncertainty was quantified via matched-pair bootstrap (R = 1000), resampling pairs with replacement to obtain pointwise 95% confidence bands and empirical distribution of log-rank p values. We applied the same matching and time-to-event framework within (1) strata of metabolic burden (1, $\geq$2 comorbidities including type 2 diabetes [T2DM], hypertension, obesity) and (2) presence/absence of individual metabolic features.
Results: 13,237 patients were included (11,372 Asians and 1,865 Caucasians). After a median follow up time of 51 [IQR 27–78] months, 586 LRE (4.4%) occurred. In Asians and Caucasians, male sex was 59,1% and 56,9% (p = 0,06), median age was 52,0 [40,0–61,0] and 56,0 [47,0–64,0] years (p < 0.05), and baseline LSM was 5.8 [4.6–7.8] and 8.2 [5.9–12.4] kPa (p < 0.05). Delta LSM over time was similar between Asians and Caucasians (p Welch t-test = 0.925), whilst Caucasians had higher prevalence of T2DM, hypertension, and obesity: 41.6% versus 33%, 55% versus 31.2%, 56.1% versus 44.4% (all p < 0.05). Cumulative LRE incidence was similar in Asians and Caucasians (log-rank p = 0.605). Presence of obesity, T2DM, and hypertension did not affect LRE incidence between the two groups, as well as increasing strata of metabolic burden (all log-rank p > 0.05). At within-group comparison, Asian diabetic patients had higher LRE incidence (log-rank p = 0.03). In the subgroup of patients (n = 2,269) with baseline liver biopsy, Caucasians and Asians with advanced fibrosis (F3-F4 stage: 29.7% in Asians and 36.2% in Caucasians) had similar LRE incidence (log-rank p = 0.861).
Conclusion: Ethnicity does not impact on prognosis in patients with MASLD, with relevant implications in terms of treatment allocation and response.

THU-104-YI

Assessing the impact of demographic, metabolic and liver disease severity factors on physical and mental health component scores among a large Canadian MASLD cohort

Elizabeth Baguley[1], Mark Swain[1,2], Wendy Schaufert[2], Juan G Abraldes[3,4], Abdel Aziz Shaheen[1,2]. *[1]University of Calgary, Calgary, Canada; [2]Alberta Health Services, Calgary, Canada; [3]University of Alberta, Edmonton, Canada; [4]Alberta Health Services, Edmonton, Canada*
Email: elizabeth.baguley@ucalgary.ca

Background and aims: The prevalence of metabolic dysfunction-associated steatotic liver disease (MASLD) is increasing worldwide

and is strongly associated with impaired quality of life. However, few studies have assessed physical and mental health component scores using the 29-item Patient-Reported Outcomes Measurement Instrument Survey (PROMIS-29) quality of life assessment tool, particularly in MASLD-specific cohorts. We aimed to characterize baseline physical and mental health component scores among MASLD patients and identify patient characteristics associated with variation in these scores.
Method: Adult patients attending the Calgary MASLD clinic for a consultation visit between January 2018 and August 2025 were included (n = 1,231). Patients with incomplete PROMIS-29 data (n = 215) or current excessive alcohol use (n = 43; >10 and >15 standard drinks/week for women and men, respectively) were excluded. Physical and mental health component t-scores were derived from the PROMIS-29 domains (i.e., pain interference, depression, physical function, ability to participate in social roles/activities, fatigue, anxiety, sleep disturbance, and a single pain intensity item) using factor scoring coefficients. Wilcoxon rank-sum tests compared t-scores by sex (female vs. male), age (≥65 vs. <65 years), diabetes status, body mass index (BMI) (≥30 vs. <30 kg/m^2) and liver stiffness measurements (LSM) by transient elastography (≥8 kPa vs. <8 kPa).
Results: The cohort median age was 59 years (IQR 49–67), and 58.1% were female. Median physical and mental health component t-scores were 47.5 (IQR 39.7–57.1) and 49.8 (IQR 42.2–56.4), respectively. Compared with males, females reported significantly lower physical (−10.4) and mental (−5.5) health t-scores ($p < 0.001$). Lower physical and mental health t-scores were also observed among patients with diabetes (−3.4 and −2.1, respectively; $p < 0.01$), BMI ≥30 kg/m^2 (−9.7 and −5.4; $p < 0.001$), and LSM ≥ 8 kPa (−4.9 and −3.3; $p < 0.001$). Patients aged ≥65 years reported lower physical health t-scores (−2.5; $p = 0.003$) but had higher mental health t-scores (+1.7; $p = 0.028$) compared to <65 years.
Conclusion: Among MASLD patients, female sex, diabetes, high BMI, and greater LSM are associated with worse physical and mental health, while older age is associated with better mental health despite poorer physical health. These findings underscore the need for tailored interventions that account for differences in sex, metabolic health, liver disease severity, and age to improve quality of life in MASLD.

THU-105
Prediction of dementia-related mortality in metabolic dysfunction-associated steatotic liver disease using survival machine-learning models

Sarpong Boateng[1], Guy Nguefang[2], Basile Njei[3]. [1]*Yale New Haven Health-Temple Medical Center, New Haven, United States;* [2]*Texas Tech University, Lubbock, United States;* [3]*Yale University, New Haven, United States*
Email: sarpong1500@gmail.com

Background and aims: Metabolic dysfunction-associated steatotic liver disease (MASLD) is increasingly recognized as a multisystem disorder with important extrahepatic consequences, including neurodegenerative disease. However, existing liver-focused risk scores have limited ability to identify individuals at risk for dementia-related mortality. We aimed to develop and validate survival-based machine-learning models to predict dementia-related death among adults with MASLD.
Method: We conducted a retrospective cohort study using NHANES III data with linked mortality follow-up. Adults meeting MASLD criteria were included. Dementia-related mortality was defined using National Death Index cause-of-death codes. Penalized Cox regression, random survival forests, and gradient-boosted survival models were developed and internally validated using cross-validation and bootstrap resampling. Model discrimination, calibration, and clinical utility were compared with the fibrosis-4 score using concordance indices, reclassification metrics, and decision-curve analysis.
Results: Among 1,774 adults with MASLD and a median follow-up of 16.1 years, 115 dementia-related deaths occurred (6.5%). Survival machine-learning models outperformed conventional approaches and the fibrosis-4 score for risk prediction. The gradient-boosted survival model demonstrated the greatest clinical utility, achieving substantial improvement in net reclassification and consistently higher net benefit across clinically relevant risk thresholds. Waist circumference, diabetes, body mass index, and age were the most influential predictors. Risk stratification isolated all observed dementia-related deaths within a high-risk subgroup with a mortality rate of 19.4%.
Conclusion: Survival-based machine-learning models improve identification of MASLD patients at high risk for dementia-related mortality, highlighting the dominant role of metabolic factors over liver-specific fibrosis markers. These findings support the potential role of individualized risk stratification to guide surveillance and preventive strategies for extrahepatic complications in MASLD.

THU-106
Sex differences in improvement of metabolic dysfunction-associated steatotic liver disease and cardiorespiratory fitness during a residential lifestyle intervention for youth living with obesity

Maarten Buytaert[1], Maxine Vangampelaere[2], Kristof Vandekerckhove[1], Ilse Coomans[1], Ellen Dupont[3], Sander Lefere[2], Ruth de Bruyne[1]. [1]*Ghent University Hospital, Ghent University, Gent, Belgium;* [2]*Ghent University, Ghent, Belgium;* [3]*Zeepreventorium De Haan, De Haan, Belgium*
Email: maarten.buytaert@ugent.be

Background and aims: Cardiopulmonary exercise testing (CPET) evaluates maximal oxygen consumption during exercise (VO_2peak). In children with obesity, VO_2peak per lean mass is the most reflective of cardiorespiratory fitness. The change in physical fitness and its association with metabolic dysfunction-associated steatotic liver disease (MASLD) during a lifestyle intervention is poorly understood.
Method: Adolescents aged 12–18 years with (severe) obesity receiving a structured, combined lifestyle intervention in a residential setting were prospectively followed for 9–12 months. CPET and DEXA were performed at the start and at 9 months. Baseline MASLD was defined as a CAP value > 248 dB/m on FibroScan; resolution of MASLD as a CAP < 248 dB/m at 6 months post start of the intervention program.
Results: 78 adolescents (40 boys) with a median age of 16 years were followed, with 56 adolescents (35 boys) having baseline MASLD. Of those, 17 boys and 12 girls experienced MASLD resolution. Cardiorespiratory fitness (VO_2peak/lean mass) improved for all adolescents, going from a median of 39.3 to 45.1 ml/min/leankg in boys and from 39.7 to 43.0 ml/min/leankg in girls ($p < 0.001$ for both). Importantly, the underlying changes were different between sexes. In boys with MASLD resolution, lean mass was preserved, contrary to boys without resolution (+ 0.6% vs. −7%, $p = 0.007$). For all boys with baseline MASLD, the absolute VO_2peak value increased (median 2686 to 2820 ml/min, $p = 0.022$ for boys with MASLD resolution and 2302 to 2615 ml/min, $p = 0.005$ for boys without MASLD resolution). To the contrary, girls had a minimal, non-significant change in absolute VO_2peak. In girls with MASLD, lean mass decreased during the lifestyle trajectory, both in girls with and without MASLD resolution (−8% vs. −9%). Only girls without MASLD at baseline preserved their lean mass.
Conclusion: Cardiopulmonary fitness ameliorated during a residential lifestyle trajectory, but underlying physiological changes differed between boys and girls. Preservation of lean mass was associated with MASLD resolution in boys. Maximal oxygen uptake increased in boys during the trajectory, contrary to the girls. Girls with MASLD lose more lean mass compared to those without MASLD. This highlights the importance of lean mass preservation during weight loss

trajectories, with concomitant improvement of maximal oxygen uptake.

THU-107

Stronger association and causal link between visceral adipose tissue and metabolic dysfunction-associated steatotic liver disease in women, particularly after menopause

Yutian Cao[1], Xiqiao Zhou[1]. [1]*Jiangsu Province Hospital of Chinese Medicine, Affiliated Hospital of Nanjing University of Chinese Medicine, Nanjing, China*
Email: zhouxiqiao@njucm.edu.cn

Background and aims: The link between visceral adipose tissue (VAT) and metabolic dysfunction-associated steatotic liver disease (MASLD) is well-established, yet notable sex and menopausal disparities remain poorly understood. We hypothesized that the strength and causality of this association differ significantly by sex and menopausal status.
Method: We conducted: (1) a cross-sectional analysis of 7,596 Chinese adults to examine the association between VAT (quantified as visceral fat area and categorized into quartiles) and MASLD severity (steatosis grades S0-S3), with analyses stratified by sex and menopausal status and adjusted for confounders; (2) Mendelian randomization (MR) analyses were conducted using summary-level genome-wide association study (GWAS) data for MASLD (n = 797,878 Europeans) and sex-specific genetic variants linked to VAT (n = 325,153 Europeans). Two-sample MR tested causality, followed by two-step MR to assess VAT's mediating role between sex hormones and MASLD.
Results: Cross-sectional analyses revealed a markedly stronger VAT-MASLD association in women, which escalated dramatically after menopause. The adjusted risk of severe MASLD was highest in postmenopausal women (Q4 vs. Q1, OR = 39.13), followed by premenopausal women (OR = 9.83) and then men (OR = 2.19) (all P < 0.001). MR analyses confirmed a causal effect of VAT on MASLD exclusively in females (OR_1 = 1.77, OR_2 = 3.42, both P < 0.001) across two independent datasets, with no causal effect observed in males. Two-step MR identified VAT as a key mediator, explaining 34–42% of the effect of bioavailable testosterone (BT) and sex hormone-binding globulin (SHBG) on female MASLD risk.
Conclusion: Our findings demonstrate that VAT accumulation is a potent, causal risk factor for MASLD specifically in women, with risk magnified postmenopausally. These findings underscore the necessity for sex- and menopause-specific risk assessment strategies and highlight the potential of targeting BT or SHBG to prevent and treat MASLD in women.

THU-108

Supervised physical activity improves muscle quality and function in MASLD: insights from the EHMet-DIA study

Paloma Carrillo-Fernández[1], Miguel Angel Fernández[2], Ignacio Torrescusa Buzo[2], Lucía López-Bermudo[3], Carmen Lara-Romero[1], Rocío Aller[4], Rocío Munoz-Hernández[1], Javier García-Rioja[4], Blanca Escudero-López[3], Genoveva Berná[3], Jesús Funuyet-Salas[5], Raquel Millan[1], Isabel Fernández-Lizaranzu[1], Rocio Gallego-Durán[1], Douglas Maya-Miles[1], Franz Martin-Bermudo[3], Javier Castell[6], Manuel Romero-Gómez[1]. [1]*SeLiver Group, Instituto de Biomedicina de Sevilla, IBiS/Hospital Universitario Virgen del Rocío/CSIC/Universidad de Sevilla and Centro de Investigación Biomédica en Red de Enfermedades Hepáticas y Digestivas (CIBEREHD), Sevilla, Spain; [2]Sports Activity Service, University of Sevilla, Sevilla, Spain; [3]Andalusian Center of Molecular Biology and Regenerative Medicine-CABIMER. University Pablo Olavide-University of Seville-CSIC and Biomedical Research Network on Diabetes and Related Metabolic Diseases-CIBERDEM, Sevilla, Spain; [4]Gastroenterology Department, Centro de Investigación de Endocrinología y Nutrición, Centro de Investigación Biomédoca en Red de Enfermedades Infecciosas (CIBERINF), Facultad de Medicina, University of Valladolid, Hospital Clínico de Valladolid, Valladolid, Spain; [5]Department of Psychology, Loyola University, Sevilla, Spain; [6]Department of Radiology, Virgen del Rocío University Hospital, Sevilla, Spain*
Email: pcarrillo-ibis@us.es

Background and aims: Weight loss is the mainstay treatment for MASLD but may lead to sarcopenia if muscle mass and quality decline. This study aimed to assess longitudinal changes in muscle composition and their relationship with hepatic outcomes during lifestyle interventions in MASLD.
Method: Forty-nine patients with MASLD were prospectively evaluated at 0, 3, and 6 months. Participants were assigned to a home-based lifestyle advice program performing only cardiorespiratory exercises (CG, n = 24) or a supervised physical activity program combining cardiorespiratory and resistance exercises (SPA, n = 25). Assessments included muscle fat (PDFF of erector spinae by MRI), vastus lateralis quality by echography, determining both echogenicity (mean grayscale value) and stiffness (elastography), also physical performance (6-minute walk test) and BIA. Liver steatosis and fibrosis were evaluated by MRI-PDFF and MRE. Statistical analyses were performed with SPSS 22.0.
Results: At baseline, PDFF of the erector spinae correlated positively with age (r = 0.36, p = 0.03, n = 36), BMI (r = 0.38, p = 0.02, n = 36), liver stiffness (liver MRE, r = 0.61, p < 0.01, n = 36), and inversely with ASM/BMI (r = –0.49, p < 0.01, n = 36) and female sex (r = –0.43, p = 0.01, n = 36). In the multivariate linear model, only age (95% CI [–0.06; 0.44], p = 0.01, n = 36) and BMI (95% CI [0.34; 1.26], p < 0.01, n = 36) remained as predictors of muscle PDFF. Muscle echogenicity was associated with both age 95% CI [0.17; 0.82], p < 0.01, n = 49) and liver stiffness (95% CI [–1.4; –0.4], p < 0.01, n = 49. Muscle stiffness correlated with hepatic PDFF (r = 0.39, p = 0.01, n = 36). At 3 months, the SPA group reduced muscle PDFF (–1.2 ± 3.1% vs +1.0 ± 1.9% in CG; p = 0.03, n = 31) and increased muscle echogenicity (–7.35 ± 10% vs 3.07 ± 15.58% p = 0.01, n = 46) and 6MWT (45.2 ± 29.2 m vs vs 22.2 ± 39.4 m, p = 0.03, n = 45). At 6 months, SPA participants showed a marked reduction (–7.6 ± 16.4 vs 3.4 ± 15.6%, p = 0.03, n = 43) in muscle echogenicity.
Conclusion: Supervised physical activity led to early improvements in muscle quality (reductions in intramuscular fat and echogenicity) and performance. Intramuscular fat accumulation was closely related to age, adiposity, and liver stiffness. Age and BMI and age and liver stiffness are, respectively, predictors of intramuscular fat and echogenicity. These findings highlight the importance of integrating resistance training into lifestyle programs to achieve hepatic improvement while preserving muscle integrity in MASLD.

THU-109

Metabolic dysfunction–associated steatotic liver disease predicts hepatic and cardiovascular complications after kidney transplantation

Lourianne Cavalcante[1], Isabel Veloso Alves Pereira[2,3], Vinay Jahagirdar[4], Arun J. Sanyal[4]. [1]*Federal University of Bahia, Hepatology and Gastroenterology, Salvador, Brazil;* [2]*School of Medicine - University of Sao Paulo - Brazil, Sao Paulo, Brazil;* [3]*Hospital das Clínicas HCFMUSP (Lim 07); Departamento de Gastroenterologia e Nutrologia, Faculdade de Medicina, Universidade de São Paulo, São Paulo, Brazil;* [4]*Stravitz-Sanyal Liver Institute - Virginia Commonwealth, VA, USA, Richmond, United States*
Email: Lourianne@gmail.com

Background and aims: Metabolic dysfunction-associated steatotic liver disease (MASLD) is highly prevalent among patients with chronic kidney disease, particularly those with diabetes and hypertension. Its impact on kidney transplant (KT) recipients remains poorly defined. We aimed to characterize the 5-year pre-transplant phenotype and post-transplant outcomes of KT recipients with MASLD.
Method: We conducted a retrospective cohort study using the TriNetX global federated network. Adult KT recipients were stratified

by MASLD status; those with other chronic liver diseases or prior liver transplantation were excluded. Pre-transplant features were analyzed using odds ratios (OR). Post-transplant outcomes were assessed in a propensity score–matched cohort (247 per group) using Kaplan–Meier survival, Cox proportional hazards, and multivariable logistic regression. Sensitivity analyses included E-values and Number Needed to Harm (NNH).

Results: Among 50,327 KT recipients, 1,679 had MASLD. Pre- kidney transplant, MASLD patients exhibited markedly higher odds of advanced liver disease (fibrosis/cirrhosis OR 11.54, portal hypertension OR 9.35, hepatic encephalopathy OR 12.26) and cardiometabolic comorbidities (diabetes OR 2.44, dyslipidemia OR 3.43, ischemic heart disease OR 2.18). In the matched post-transplant cohort, MASLD was independently associated with increased risks of ascites (adjusted OR 2.39, 95% CI 1.15–5.00, p = 0.0195) and major adverse cardiovascular events (MACE) (adjusted OR 2.14, 95% CI 1.28–3.58, p = 0.0074). No significant associations were observed for graft rejection or hemodialysis. Sensitivity analyses confirmed robustness (E-value 4.07 for ascites; 3.69 for MACE). Clinical impact was substantial, with NNH of 17 for ascites and 8 for MACE. MASLD patients showed a significantly higher prevalence of hepatocellular carcinoma before kidney transplantation (OR 4.39, 95% CI 2.29–8.42), while post-transplant HCC incidence was numerically higher (23.5% vs 18.9%) but not statistically significant (HR 1.39, 95% CI 0.85–2.28); no differences were observed for other malignancies.

Conclusion: MASLD defines a high-risk phenotype among KT candidates, characterized by advanced liver disease and metabolic comorbidities. Post-transplant, MASLD independently predicts hepatic decompensation and cardiovascular events, but not graft-related outcomes. These findings support routine MASLD screening and liver fibrosis risk stratification in KT evaluation, and justify tailored post-transplant surveillance strategies.

THU-110

Etiology specific risk of hepatic and extrahepatic complications in MASLD patients with alcohol or viral co-etiologies: a retrospective multicentre cohort study

Talia Yi Hui Chan[1], Lucas Yeo[2], Margaret Teng[3], Vincent Chen[4], Jimmy Che-To Lai[5], Karn Wijarnpreecha[6], Rahul Kumar[7], Apichat Kaewdech[8], Thanawin Pramotedham[9], Anand Kulkarni[10], Ming-Hua Zheng[11], Akash Roy[12], Ken Liu[13], Chitchai Rattananukrom[14], Mazen Noureddin[15], Mohammad Shadab Siddiqui[16], Mark Muthiah[17], Hirokazu Takahashi[18], Cheng Han Ng[2]. *[1]Yong Loo Lin School of Medicine, National University of Singapore, Singapore, Singapore; [2]Division of Gastroenterology and Hepatology, Department of Medicine, National University Hospital, Singapore, Singapore; [3]Division of Gastroenterology and Hepatology, Department of Medicine, National University Hospital, Division of Gastroenterology, Department of Medicine, Alexandra Hospital, Singapore, Singapore; [4]Division of Gastroenterology and Hepatology, Department of Internal Medicine, University of Michigan Medical School, Ann Arbor, MI, United States; [5]Medical Data Analytics Centre, The Chinese University of Hong Kong, Li Ka Shing Institute of Health Sciences and State Key Laboratory of Digestive Disease, The Chinese University of Hong Kong, Hong Kong, Hong Kong; [6]Division of Gastroenterology and Hepatology, University of Arizona College of Medicine Phoenix, Phoenix, AZ, United States; [7]Department of Gastroenterology, Changi General Hospital, Singapore, Singapore; [8]Prince of Songkla University Faculty of Medicine, Songkhla Province, Thailand; [9]Department of Medicine, National University Hospital, Singapore, Singapore; [10]Asian Institute of Gastroenterology, Hyderabad, India; [11]MAFLD Research Center, Department of Hepatology, the First Affiliated Hospital of Wenzhou Medical University, Wenzhou, China; Key Laboratory of Diagnosis and Treatment for The Development of Chronic Liver Disease in Zhejiang Province, Wenzhou, China; [12]Medical University of South Carolina, South Carolina, United States; [13]Sydney Medical School, University of Sydney, Sydney, Australia; [14]Division of Gastroenterology and Hepatology, Department of Medicine, Faculty of Medicine, Srinagarind Hospital, Khon Kaen University, Khon Kaen 40002, Thailand; [15]Houston Methodist Hospital and Houston Research Institute, Houston, Texas, United States; [16]University of Virginia School of Medicine, Charlottesville, Virginia, United States; [17]Division of Gastroenterology and Hepatology, Department of Medicine, National University Hospital, National University Centre for Organ Transplantation, National University Health System, Yong Loo Lin School of Medicine, National University of Singapore, Singapore, Singapore; [18]Division of Metabolism and Endocrinology, Faculty of Medicine, Saga University, Saga, Japan*
Email: thisistaliachan@gmail.com

Background and aims: Metabolic dysfunction associated steatotic liver disease (MASLD) frequently coexists with alcohol-related and viral etiologies in real-world practice, yet the impact of these overlapping etiologies on hepatic and extrahepatic outcomes remains unclear. This study aimed to evaluate etiology-specific risks of hepatic decompensation, hepatocellular carcinoma, and mortality in patients with MASLD.

Method: We performed a multicentre longitudinal cohort study, including 1,120 adults with LSM ≥ 10 kPa and MASLD. Patients were classified into MASLD only, MASLD with alcohol-related etiology or MASLD with chronic viral hepatitis. Hepatic decompensation and all-cause mortality were analysed using Fine-Gray competing-risk regression, while hepatocellular carcinoma was analysed using Cox proportional hazards model. Multivariable models were adjusted for age, gender, BMI, smoking status and liver stiffness. Event rates were expressed as incidence rates per 100 person-years.

Results: Among 1,120 patients, 730 (65.2%) had MASLD alone, 54 (4.8%) had MASLD with alcohol-related liver disease and 336 (30.0%) had MASLD with chronic viral hepatitis. Patients with MASLD and alcohol-related liver disease had higher risk of all-cause mortality (adjusted sHR 3.636, 95% 1.059–12.483; p = 0.040) and hepatic-related mortality compared to MASLD only patients (adjusted sHR 8.517, 95% CI 1.242–58.416; p = 0.029). Patients with MASLD and alcohol-related liver disease also had higher incidence rate of hepatic decompensation (4.753 per 100 person years, HR 1.485, 95% CI 0.696–3.316) compared to patients with MASLD only.

Conclusion: In this real-world MASLD cohort, the presence of alcohol-related liver disease was associated with markedly higher risks of all-cause and hepatic-related mortality compared with MASLD alone, highlighting the prognostic importance of identifying overlapping etiologies in risk stratification and clinical management.

THU-111

Impact of metabolic dysfunction associated steatotic liver disease on hepatocellular carcinoma risk in patients with chronic hepatitis B or chronic hepatitis C: a nationwide cohort study

Young Chang[1], Jinhye Cha[2], Hoyoung Na[2], Julie Lee[2]. *[1]Soonchunhyang University Seoul Hospital, Seoul, Korea, Rep. of South; [2]Gilead Sciences Korea, Seoul, Korea, Rep. of South*
Email: chyoung86@gmail.com

Background and aims: The impact of metabolic dysfunction–associated steatotic liver disease (MASLD) on hepatocellular carcinoma (HCC) and other liver-related outcomes in patients with chronic hepatitis B (CHB) and chronic hepatitis C (CHC) remains unclear. We investigated the association between MASLD and liver-related outcomes using a nationwide cohort.

Method: This retrospective cohort study used the Korean National Health Information Database. Adults newly diagnosed with CHB or CHC between 2009 and 2013 were included if health check-up data enabling MASLD assessment were available within two years. MASLD was defined as hepatic steatosis (Fatty Liver Index ≥60) with at least one cardiometabolic risk factor. A 1:3 frequency matching was performed by index year, age, sex, and hepatitis type. Cox proportional hazards models were used to estimate hazard ratios (HRs) for HCC, decompensated cirrhosis, liver transplantation, and

all-cause mortality, with adjustment for demographic, clinical, and metabolic variables.
Results: Among 187,895 patients with chronic viral hepatitis who met the inclusion criteria, 20,107 (10.7%) had concurrent MASLD at baseline. After matching, 72,496 patients were included in the final analysis (MASLD: 18,124; non-MASLD: 54,372). During up to 10 years of follow-up, patients with MASLD showed a higher incidence of HCC than those without MASLD (3.14 vs. 2.24 per 1,000 person-years). MASLD was associated with higher risks of HCC (adjusted hazard ratio [aHR] 2.59; 95% CI 2.23–3.00), decompensated cirrhosis (aHR 1.94; 95% CI 1.72–2.19), liver transplantation (aHR 3.12; 95% CI 1.64–5.94), and all-cause mortality (aHR 1.31; 95% CI 1.19–1.45). In contrast, metabolic dysfunction was not associated with liver-related outcomes or all-cause mortality in patients without MASLD. Within MASLD as well, individual metabolic risk factors were not associated with increased risks of liver-related outcomes and were associated with lower observed risk.
Conclusion: MASLD was independently associated with increased risks of HCC and adverse liver outcomes among patients with CHB or CHC. Metabolic dysfunction in the absence of MASLD, and individual metabolic risk factors within MASLD, were not associated with additional risk.

THU-115
Metabolic dysfunction-associated steatotic liver disease (MASLD) as predominant aetiology and poorest prognosis in multi-ethnic Singapore cirrhosis cohort

Jarvis Chia Kai An[1], Michael Hao Chen[2], Poh Hui Wee[3], Ryan Ng Jian Han[3], Kai Lim[3], Wei Xuan Tay[3], Kaina Chen[3], Yiying Pei[3], Bochao Jiang[3], Kevin Kim Jun Teh[3], Thinesh Krishnamoorthy[3], Hiang Keat Tan[3], Rahul Kumar[4], Marianne DeRoza[5], Chanda Ho[3], Prema Raj[3], Jason Pik Eu Chang[3]. *[1]Lee Kong Chian School Of Medicine, Singapore, Singapore; [2]Duke-NUS Medical School, Singapore, Singapore; [3]Singapore General Hospital, Singapore, Singapore; [4]Changi General Hospital, Singapore, Singapore; [5]Sengkang General Hospital, Singapore, Singapore*
Email: m220172@e.ntu.edu.sg

Background and aims: The epidemiology of cirrhosis is undergoing a major transition, with metabolic risk factors increasingly replacing viral hepatitis as the predominant aetiologies. The prognostic implications of this transition, and its interaction with dynamic decompensating events, remain incompletely defined. This study aims to evaluate current aetiological trends and identify baseline and time-dependent predictors of mortality in a multi-ethnic Southeast Asian cohort.
Method: We conducted a prospective observational cohort study of 1,195 adults with cirrhosis from the SingHealth Chronic Liver Disease Registry across multiple tertiary hospitals in Singapore. Baseline demographic, clinical variables, and time-varying decompensation events were collected. Survival was analysed using Kaplan-Meier methods, and predictors of mortality were evaluated using baseline and time-dependent Cox proportional hazards models.
Results: Mean age was 60.9 years and 59.1% were male. The most common aetiology was MASLD (39.8%), followed by chronic Hepatitis B (23.5%), and alcohol-related liver disease (10.7%). Over a mean follow-up of 80.5 months, 18.4% died. Survival differed significantly by aetiology (log-rank $p < 0.001$), with the shortest survival in MASLD (median 153 months). Baseline predictors of mortality included Child-Pugh class B/C (hazard ratio HR 2.83), portal vein thrombosis (HR 2.23), hepatocellular carcinoma (HR 2.11), male sex (HR 1.91), diabetes (HR 1.38), and older age (HR 1.07 per year). Chronic Hepatitis B was independently associated with lower mortality (HR 0.53). On time-dependent analysis, incident ascites (HR 3.36), spontaneous bacterial peritonitis (HR 1.75), and hepatic encephalopathy (HR 1.51) were the strongest predictors of death, and MASLD (HR 1.56) remained independently associated with mortality (all $p < 0.05$).
Conclusion: MASLD is currently the predominant phenotype of cirrhosis in Singapore and confers the poorest long-term prognosis. Mortality follows a dynamic, event-driven trajectory, with ascites representing the most critical prognostic turning point.

THU-116-YI
Metabolic dysfunction-associated steatotic liver disease (MASLD) is associated with impaired health-related quality of life in people with HIV

Felice Cinque[1,2,3], Michael Nudo[1,2], Sahar Saeed[4], Gabrielle Mariano[1,2], Amanda Lupu[1,2], Wesal Elgretli[5], Erica Moodie[6], Nadine Kronfli[1], Joseph Cox[1], Cecilia Costiniuk[1], Alexandra De Pokomandy[1], Jean-Pierre Routy[1], Marina B. Klein[1], Bertrand Lebouche[1], Colleen Price[7], Ken Monteith[8], Curtis Cooper[9], Sharon Walmsley[10], Giada Sebastiani[1,2,5,6]. *[1]Chronic Viral Illness Service, McGill University Health Centre, Montreal, Canada; [2]Division of Gastroenterology and Hepatology, McGill University Health Centre, Montreal, Canada; [3]Department of Pathophysiology and Transplantation, Università degli Studi di Milano, Milan, Italy; [4]Public Health Sciences, Queen's University, Kingston, Canada; [5]Division of Experimental Medicine, McGill University, Montreal, Canada; [6]Department of Epidemiology, Biostatistics and Occupational Health, McGill University, Montreal, Canada; [7]Canadian HIV/AIDS and Chronic Pain Society, Toronto, Canada; [8]Cocq-Sida, Montréal, Canada; [9]Department of Medicine, Division of Infectious Diseases, The Ottawa Hospital, Ottawa Hospital Research Institute, Ottawa, Canada; [10]Department of Medicine, Division of Infectious Diseases, Toronto General Hospital, University of Toronto, Toronto, Canada*
Email: giada.sebastiani@mcgill.ca

Background and aims: Metabolic dysfunction–associated steatotic liver disease (MASLD) is common in people with HIV (PWH), yet its impact on health-related quality of life (HRQoL) remains poorly defined. We aimed to examine the association between MASLD and both generic and liver-specific HRQoL in PWH.
Method: We conducted a cross-sectional analysis within the Canadian multicentre prospective LIVEr disease in HIV (LIVEHIV) cohort, including consecutive PWH on antiretroviral therapy without viral hepatitis, significant alcohol intake, or advanced chronic liver disease. MASLD was defined as hepatic steatosis (controlled attenuation parameter >248 dB/m) plus ≥1 metabolic comorbidity, and significant liver fibrosis as liver stiffness measurement >8 kPa. HRQoL was assessed using the Short Form (SF)-36 and the Chronic Liver Disease Questionnaire (CLDQ). Adjusted marginal mean differences were estimated using multivariable linear regression. Among participants with MASLD, associations with increasing metabolic comorbidity burden were evaluated.
Results: Among 519 participants (mean age 48 years, 74% male, 89% virologically suppressed), MASLD prevalence was 41%. MASLD was independently associated with worse generic HRQoL, including lower physical functioning (−4.6; 95% CI −9.12 to −0.01) and general health (−4.5; 95% CI −8.58 to −0.48) on the SF-36. Liver-specific HRQoL was more markedly impaired: MASLD was associated with a lower overall CLDQ score (−0.29; 95% CI −0.49 to −0.09), with worse scores in fatigue (−0.36; 95% CI −0.64 to −0.09), systemic symptoms (−0.28; 95% CI −0.50 to −0.07), emotional symptoms (−0.32; 95% CI −0.58 to −0.06), and worry (−0.24; 95% CI −0.46 to −0.02). Among PWH with MASLD, increasing metabolic comorbidity burden was associated with a dose–response decline in physical functioning (−10.6, 95% CI −20.8 to −0.50 for 2–3 comorbidities and −14.8, 95% CI −26.5 to −3.22 for ≥4 vs 0–1), whereas liver-specific HRQoL did not differ substantially across comorbidity strata. Notably, significant fibrosis was associated with worse CLDQ activity (−0.62; 95% CI −1.20 to −0.05) and worry (−0.60; 95% CI −1.15 to −0.05).
Conclusion: In PWH, MASLD is independently associated with impaired HRQoL, particularly fatigue, systemic symptoms, and emotional burden. Accumulation of metabolic comorbidities predominantly affects physical functioning, while significant fibrosis

further worsens activity and worry, underscoring the combined impact of metabolic dysfunction and hepatic fibrosis on patient-reported outcomes.

THU-117

Emergency departments as an opportunistic screening setting for hidden steatotic liver disease: results from the multicentre Pre-DEA study

Valeria D'Arpino[1], Antonella Fontana[1], Silvano Junior Santini[1], Antonio Cirella[1], Valerio Caputo[1], Clara Balsano[1]. [1]*università degli studi dell'Aquila, Dipartimento MESVA, l'Aquila, Italy*
Email: valeria.darpino@graduate.univaq.it

Background and aims: Metabolic dysfunction-associated steatotic liver disease (MASLD), is often silent yet associated with increased cardiovascular and cerebrovascular risk and progression to cirrhosis and hepatocellular carcinoma. Global MASLD prevalence is 38%, will in Italy is estimated at around 27%.
The aim of this study was to assess the effectiveness of EDs as a screening setting for hidden SLD and to estimate its prevalence among ED attendees.
Method: This prospective multicenter study involved five EDs in Abruzzo, Apulia and Lombardy. Adults (≥18 years) triaged as non-urgent/less-urgent (green/white codes) were enrolled at ED presentation. After consent, participants reported whether they were aware of having hepatic steatosis, then underwent first-line assessment (history, biometric and laboratory parameters, physical examination) and focused abdominal ultrasound.
Results: Overall, 1138 eligible patients were enrolled. Our screening identified SLD in 32.5% of the cohort. In Lombardy, 58% of subjects were found to be steatotic (41% displaying mild SLD) In Abruzzo, prevalence was 34.0% (76.0% mild), with site-specific rates of 42.7% (Avezzano), 28.3% (L'Aquila) and 37.0% (Teramo). In Apulia, liver steatosis was present in 22.1%, with 63.7% mild. Importantly, the most of participants were unaware of hepatic steatosis (overall 87%; Lombardy 70%, Abruzzo 92%, Apulia 98%). These findings indicate that MASLD was largely hidden and mostly unrecognized by patients. Moreover, the observed prevalence exceeded national estimates, with significant differences across regions ($p < 0.05$), possibly reflecting heterogeneous environmental or population-related factors.
Conclusion: In ED attendees, liver steatosis was common, largely unrecognized, and identified through a structured clinical-ultrasound approach, highlighting the Emergency Department as a novel and effective opportunistic screening setting for early detection, particularly of mild disease. Notably, the marked and unexpected differences in liver steatosis prevalence observed across Italian regions suggest relevant geographic heterogeneity and underscore the need for region-specific epidemiological evaluation and tailored preventive strategies.

THU-118-YI

Influence of coexistent steatotic liver disease on outcomes and treatment responses in autoimmune hepatitis or primary biliary cholangitis

Oscar Danielsson[1,2], Markku Nissinen[3], Fredrik Åberg[2]. [1]*University of Helsinki, Helsinki, Finland;* [2]*Helsinki University Central Hospital, Helsinki, Finland;* [3]*Terveystalo Ltd, Helsinki, Finland*
Email: oscar.danielsson@helsinki.fi

Background and aims: Steatotic liver disease (SLD) has reached pandemic proportions, and it poses a threat on the course and prognosis of other liver diseases. We investigated the impact of coexisting SLD on Autoimmune Hepatitis (AIH) or Primary Biliary Cholangitis (PBC).
Method: Diagnostic liver biopsies were gathered for patients with AIH or PBC in the Hospital district of Helsinki and Uusimaa between June 2009 and May 2019. Laboratory tests, entries for morbidity and mortality were analysed through chart review and registry linkage until October 2024. SLD was defined as ≥5% fat in biopsy taken at the point of diagnosis of liver disease. These patients were compared with non-SLD patients. For AIH, complete biochemical remission was defined as normal immunoglobulin G and aminotransferase levels. For PBC, remission was defined as alkaline phosphatase <1.67x upper limit of normal. Differences were analysed by chi-square or Mann-Whitney U test, where appropriate. For cancer incidence, Cox regression was used.
Results: The study consisted of 182 AIH- and 148 PBC-patients. SLD prevalence was 12.1% in AIH and 18.9% in PBC ($p = 0.09$), at the time of diagnosis of liver disease. Mean follow-up was 9.8 years for SLD- and 10.7 years for non-SLD-patients. 26.0% (N = 13) of SLD patients had entry for any kind of cancer during follow-up, while 13.6% (N = 38) of non-SLD patients had entries for cancer, $p = 0.025$. When adjusted for age and sex, SLD patients had a hazard ratio of 1.59 (95% confidence interval 0.85–3.0) for cancer, $p = 0.15$. Mean age was 54.0 (SD 15.8) and 58.7 (SD 10.9) years, for non-SLD- and SLD-patients, respectively, $p = 0.07$. For AIH patients with available biochemical status, complete biochemical remission was achieved in 53.6% and 50.9%, 1 and 5 years after diagnosis, respectively, ($p = 0.59$ and 0.71 for difference between SLD and non-SLD patients, at 1 and 5 years, respectively). Among PBC patients with available data, 68.9% and 80.5% were in remission, at 1 and 5 years after diagnosis, respectively ($p = 0.18$ and 0.93 and for difference between SLD and non-SLD patients, at 1 and 5 years, respectively).
Conclusion: Coexisting SLD did not alter rate of biochemical remission among AIH- or PBC-patients. Incidence of cancer was higher among SLD patients, although not significant when adjusted for age and sex.

THU-119-YI

Association between sex and long-term clinical outcomes in metabolic dysfunction-associated steatotic liver disease

Pojsakorn Danpanichkul[1], Torlap Inkongngam[2], Apichat Kaewdech[3], Karn Wijarnpreecha[4], Donghee Kim[5]. [1]*Department of Internal Medicine, Texas Tech University Healt, Lubbock, United States;* [2]*Chiang Mai University, Chiang Mai, Thailand;* [3]*Prince of Songkla University, Gastroenterology and Hepatology Unit, Division of Internal Medicine, Hatyai, Thailand;* [4]*University of Arizona, Phoenix, United States;* [5]*Stanford university, Palo Alto, United States*
Email: pojsakorndan@gmail.com

Background and aims: MASLD affects 35% of U.S. adults and is linked to liver and cardiovascular sequelae. Sex differences in prevalence and biology are known, yet large, sex-stratified, real-world outcome data are limited. We evaluated whether sex is associated with all-cause mortality, MALO, MACE, other cardiovascular outcomes, and HCC in MASLD.
Method: Using TriNetX (multicenter U.S. EHRs), we identified females and males with MASLD from 2010 to 2019, excluding other liver diseases, AUD, cancer, and pregnancy. Events within 30 days of index were classified as baseline. Outcomes at 5 years included mortality, MALO, MACE, HCC, ischemic heart disease (IHD), thrombotic events, heart failure, inflammatory heart disease, stroke, and arrhythmia. We performed 1:1 nearest-neighbor PSM without replacement using demographics, comorbidities, medications, and laboratories. Cox models estimated HRs with 95% CIs. Subgroups contrasted females <50 and ≥50 years with age-matched males.
Results: Among 397,125 patients (216,875 females; 180,250 males), PSM yielded 152,676 per sex with well-balanced characteristics. Over 5 years, females had lower risks of death (HR 0.76, 95% CI 0.74–0.78), HCC (0.57, 0.51–0.65), MACE (0.89, 0.87–0.91), IHD (0.76, 0.74–0.78), thrombotic events (0.92, 0.87–0.97), and heart failure (0.88, 0.85–0.91). Risks were similar for MALO (1.01, 0.98–1.05), inflammatory heart disease (0.99, 0.94–1.06), and stroke (1.03, 1.00–1.07); arrhythmia was slightly higher in females (1.05, 1.03–1.07). In subgroup analyses, females <50 had lower mortality (0.87, 0.77–0.98) but higher MALO (1.22, 1.09–1.37), stroke (1.33, 1.15–1.54), and

arrhythmia (1.27, 1.20–1.33); females ≥50 had lower mortality (0.77, 0.74–0.80), similar to slightly lower MALO (0.96, 0.92–1.00), lower HCC (0.60, 0.53–0.68), and lower MACE (0.87, 0.85–0.90).
Conclusion: In this multicenter, PSM-adjusted cohort, male sex in MASLD was associated with higher mortality, HCC, and macrovascular events, while arrhythmia was modestly higher in females. Age modifies these associations, supporting sex- and age-specific risk assessment and surveillance in MASLD.

THU-120
MASLD and mental health: association of the liver disease with anxiety, depression and binge eating
Stella De Nicola[1], Arianna Bertazzoni[2], Nicola Pugliese[1,2], Chiara Masetti[1], Davide Polverini[1], Roberto Ceriani[1], Andrea Catena[3], Beatrice Mazzuccato[3], Ana Lleo[1,2], Alessio Aghemo[1,2]. *[1]Humanitas Research Hospital IRCCS, Rozzano, Italy; [2]Humanitas University, Pieve Emanuele, Italy; [3]Humanitas Medical Care, Milan, Italy*
Email: stella.denicola@humanitas.it

Background and aims: Metabolic dysfunction-associated steatotic liver disease (MASLD) prevalence is increasing worldwide alongside other cardiometabolic conditions. Given the known relationship between MASLD and dietary habits, patients with binge eating disorder (BED) may be at increased risk of MASLD. A close connection between metabolic syndrome and mental disorders (binge eating, anxiety, depression) was proved but few studies exist on their association with MASLD. The main aim of this study is to investigate prevalence and distribution of BED, depression and state/trait anxiety in MASLD compared to other liver diseases (HCV-HBV-CBP). The second aim is to evaluate correlation between the scores of questionnaires and liver stiffness measurement (LSM) values in MASLD.
Method: We conducted a prospective single-center study at our tertiary hospital from November 2024 to April 2025. Patients completed four questionnaires (STAI-Y1/STAI-Y2, BDI-II, BES), the scores of which were indicative of the likelihood and severity of anxiety, depression and BED. Exclusion criteria were history of psychiatric disease, malignancy or alcohol consumption. All patients were Italian. Data from questionnaires were analyzed by expert psychologists. Baseline clinical and demographic data and LSM were collected.
Results: A total of 130 patients were included, 65 MASLD and 65 controls. Mean STAI-Y1 and STAI-Y2 were indicative of moderate to severe anxiety (40 and 40 respectively in MASLD; 38 and 38 respectively in non-MASLD), but no statistically significant difference was found. There was no significant difference in mean BDI-II scores (7 vs 5 for MASLD vs non-MASLD), suggesting absence of depressive symptoms. A statistically significant difference was found for binge eating: median BES was 5 (IQR 1–9) in MASLD vs 3 (IQR 0–4) in controls ($p < 0.05$). Probable BED (BES > 26) occurred in 4.6% MASLD vs 0% controls. No correlation was found between binge eating, depression or anxiety and LSM values in MASLD. Higher prevalence of anxiety was observed in both groups compared to general population with anxiety more prevalent in the MASLD than in the control group.
Conclusion: These findings support need for an integrated multidisciplinary care plan for MASLD patients with *possible* or *probable* binge eating, which could be screened with the BES questionnaire. Management of psychiatric conditions can improve adherence to lifestyle and pharmacological interventions, eventually preventing disease progression or relapse.

THU-121
Medical education on MASH delivered through a social media series had strong clinician engagement
Shari Dermer[1], Julie Schrand[1], Danielle Montgomery[1], Naim Alkhouri[2]. *[1]Medscape Education, Newark, United States; [2]Summit Clinical Research, Westlake, United States*
Email: sdermer@medscape.net

Background and aims: Use of social media for professional purposes among healthcare providers (HCPs) reached 91% in 2025[1]. To adapt to changing needs in medical education and address gaps in practice related to the management of metabolic dysfunction-associated steatohepatitis (MASH), Medscape developed and delivered high-impact educational content via verified social media channels to meet clinicians in the spaces that they engage in and trust.
Method: A series of six live 15-minute social media broadcasts were released every other month over the 12-month calendar year of 2025. Each episode was posted on 4 different social media channels that included Twitter (X), Facebook, LinkedIn, and YouTube. Our series entitled *MASH Masters* featured a faculty host and 6 guest faculty and discussed topics such as guideline updates, interdisciplinary management, noninvasive tests, risk-stratification, and liver-directed therapy[2].
Results: There was strong engagement across the 6 episodes in season 1 with a social impact of 645,877 and a video engagement rate of 25%.

- Total social media impressions: 429,544 times that the posts were shown on someone's screen.
- Video engagement rate: 25% of engagements resulted in content being viewed.
- Video views: 213,463 times that people started watching a video.
- Direct engagements: 1479 interactions with the social media posts (eg. likes, comments, shares, clicks).
- Link clicks: 1391 times that links to additional educational content were accessed.

Conclusion: These results demonstrate the potential of social media to address gaps in practice and raise awareness regarding current concepts in managing MASH.

References

1. Source: https://media.market.us/social-media-in-healthcare-statistics/
2. https://www.medscape.org/sites/advances/mash-advances
Supported by an independent educational grant from Madrigal Pharmaceuticals.

THU-122
Clinical outcomes in compensated cirrhosis due to MASH: results from a population-based indiana cirrhosis cohort
Archita Desai[1], Maaz Arif[1], Eric Orman[1], LaKeisha Boyd[1], Yang Li[1], Eduardo Vilar Gomez[1], Niharika Samala[1], Naga Chalasani[1]. *[1]Indiana University, Indianapolis, United States*
Email: desaiar@iu.edu

Background and aims: Patients with MASH-related compensated cirrhosis face substantial risk of decompensation, yet real-world longitudinal data are limited. We aimed to characterize the cumulative incidence and timing of initial decompensation events in a large, contemporary population-based cohort.
Method: The Indiana Cirrhosis Cohort (ICC) is a digitally-constructed cohort derived from a statewide health information exchange using a validated approach to identify patients with cirrhosis. We identified 10,227 adults with compensated cirrhosis (2017–2020, followed until July 2023), of whom 2,482 had Child Pugh (CP) A MASH cirrhosis. We assessed the time to initial decompensation event (IDE; defined as first occurrence of ascites, hepatic encephalopathy [HE], variceal bleeding [VB], HCC, or multiple concurrent IDEs) and time from IDE to death or liver transplantation (LT) using cumulative incidence (CI) functions and Cox regression models.
Results: The cohort of 2,482 adults with CP A MASH cirrhosis had a mean age 63 ± 12 years, 58% female, and 95% White. Median follow-up was 4.5 years (IQR 3.0–5.9). Type 2 diabetes was present in 57% and coronary artery disease in 23%. CP scores were A5 in 1,664 (67%) and A6 in 818 (33%). These groups had similar characteristics except A6 participants were older, had lower median platelet count (130, IQR 96–182 vs 149, IQR 109–203, $p < 0.001$) and higher median MELD3.0 (12, IQR 10–15 vs 10, IQR 8–12, $p < 0.001$). In the entire CP A cohort,

47% (n = 1,156) experienced an IDE during follow up, with a median time to IDE of 2.0 years (IQR 1.1–3.1). Ascites was the most common IDE (19%), followed by HE (15%), multiple concurrent events (6%), HCC (5%), and VB (2%). The 1- 3- and 5-year CIs of any IDE were 11%, 35%, and 48%, respectively. Among A5 patients, the 1- 3- and 5-year CIs of any IDE were 8%, 29%, and 41%, respectively. Among A6 patients, the 1- 3- and 5-year CIs for any IDE were 16%, 47%, and 61%, respectively. Following an IDE, the 1- 3- and 5-year CIs of death/LT were 33%, 59%, and 71%, respectively, occurring at 2.1 years (IQR 0.6–5.8). Outcomes varied by IDE type; 5-year death/LT CI were: HCC:86%, ascites:75%, HE:65%, and VB:29%.

Conclusion: This contemporary population-based study demonstrates high rates of decompensation for Child Pugh A MASH cirrhosis, with A5 and A6 exhibiting different rates of decompensation. These data underscore the importance of developing therapies for CP A MASH cirrhosis.

THU-123

A head-to-head comparison of MAFLD and MASLD diagnostic criteria in estimating the risk of de novo hepatocellular carcinoma (HCC) occurrence in HCV patients achieving direct-acting antiviral-induced sustained virological response

Fiammetta Di Nardo[1], Marcello Dallio[1], Mario Romeo[1], Carmine Napolitano[1], Paolo Vaia[1], Claudio Basile[1], Giuseppina Martinelli[1], Luigi Vitale[1], Marco Niosi[1], Alessandro Federico[1]. [1]*Hepatogastroenterology Division, Department of Precision Medicine, University of Campania Luigi Vanvitelli, Piazza Miraglia 2, 80138, Naples (Italy), Naples, Italy*
Email: fiammetta.dinardo@studenti.unicampania.it

Background and aims: A higher risk of hepatocellular carcinoma (HCC) has been widely reported in patients with chronic hepatitis C virus (HCV) infection who achieve a sustained virologic response (SVR12) induced by direct-acting antivirals (DAAs), presenting with Steatotic Liver Disease (SLD) and cardiometabolic risk factors (CMRFs) indicative of metabolic dysfunction (MD). Two years after the Delphi consensus, the potential benefits of adopting Metabolic dysfunction-associated Steatotic Liver Disease (MASLD) rather than Metabolic dysfunction-associated Fatty Liver Disease (MAFLD) criteria in defining the disease progression risk remain undefined. The present study compared MASLD and MAFLD criteria in estimating the 5-year risk of de novo HCC occurrence in SLD patients achieving DAAs-induced HCV SVR12.

Method: The anthropometrical, biochemical, clinical, Liver Stiffness Measurement (LSM), and Controlled Attenuation Parameter (CAP) data stored in the "Luigi Vanvitelli" University Hospital Health Documents Digitization Archive of 751 HCV-SVR12-SLD patients (January 2015-May 2020) were included. After properly excluding lean individuals (i.e., Body Mass Index < 25 kg/m^2) and patients with other causes of chronic liver damage (n.101), the MAFLD and MASLD criteria were separately applied, ultimately identifying the following groups: HCV-SVR12-MASLD (n.163), HCV-SVR12-MASLD/MAFLD (n.390), and HCV-SVR12-MAFLD (n.97). HCC occurrence was diagnosed according to the EASL guidelines and retrospectively reported along a 5-year follow-up.

Results: At baseline, no significant clinical differences emerged among the groups, and a similar distribution of LSM-advanced fibrosis (AF) was reported in HCV-SVR12-MASLD and HCV-SVR12-MAFLD [53 (32.51%) vs 34 (35.05%), chi-square, p > 0.05]. Compared to MASLD, MAFLD diagnostic criteria better estimated the risk of HCC [HR: 1.936, C.I. 95%: 1.083–2.375, p:0.035], even after stratifying for AF baseline presence (chi-square, p < 0.0001). Multivariate competing risk analysis (adjusted for sex, age, diabetes, steatosis, SVR achieving time, CAP, and fibrosis severity) revealed diabetes (aHR: 2.051, p:0.001), high-sensitivity-C-reactive protein (aHR: 1.351; p:0.02), and Homeostatic-model-assessment-for-insulin-resistance (aHR: 1.219; p:0.02) as variables significantly associated with this outcome.

Conclusion: MAFLD criteria better estimate the de novo HCC risk in SLD patients achieving DAAs-induced HCV SVR12.

THU-124

Impact of gallstone disease, cholecystectomy and genetic variants on liver steatosis and fibrosis: a prospective, cross-sectional cohort study at a tertiary hepatology centre

Simon Drews[1], Susanne Weber[1], Johannes Lehmann[1], Maurice Michel[1], Jörn M. Schattenberg[1], Marcin Krawczyk[2]. [1]*Department of Medicine II, University Hospital Saarland, Homburg, Germany;* [2]*Department of Gastroenterology, Hepatology and Transplant Medicine, Medical Faculty, University of Duisburg-Essen, Essen, Germany*
Email: simon.drews@freenet.de

Background and aims: Gallstone disease (GD) and steatotic liver disease (SLD) are common and interrelated conditions. Patients with SLD have increased risk of GD, and both share similar exogenous risk factors. We analyse the effects of gallstones and cholecystectomy on liver steatosis and fibrosis, together with the role of genetic determinants of GD and SLD in liver injury.

Method: We prospectively recruited 212 patients (112 women; age range 19–85 years): 73 had gallstones with the gallbladder in situ, 63 had undergone cholecystectomy, and 76 served as controls. GD was verified by abdominal sonography. Hepatic fibrosis and steatosis were quantified using transient elastography (TE) and controlled attenuation parameter (CAP), respectively. The following variants were genotyped with TaqMan assays: *ABCG8* p.D19H, *PNPLA3* p.I148M, *TM6SF2* p.E167 K, *MBOAT7* p.G17E, and *APOE* p.C130R.

Results: Participants had median TE of 7.2 (5.0–17.0) kPa and CAP of 244 (213–279) dB/m. Homozygote frequencies were: *ABCG8* 0.47%, *PNPLA3* 7.08%, *TM6SF2* 0.94%, *MBOAT7* 18.40%, *APOE* 1.42%. The *PNPLA3* polymorphism was associated with higher TE (P = 0.008) and FiB4 (P = 0.01); FiB4 was also increased in carriers of the *ABCG8* variant (P = 0.048). In univariate analyses, patients with GD and those after cholecystectomy were more likely to have TE ≥ 8.1 kPa (P = 0.022). However, in multivariate analyses, fibrosis was significantly (all P < 0.05) associated with older age (OR 1.033, 95%CI 1.009–1.058), diabetes (OR 3.260, 95%CI 1.614–6.584) and the *PNPLA3* variant (OR 1.978, 95%CI: 1.228–3.186), but not with GD or cholecystectomy (P > 0.05). SLD (CAP ≥ 275 dB/m) was positively associated (all P < 0.05) with BMI (OR 1.240, 95%CI 1.132–1.315), *TM6SF2-T-allele* (OR 2.680, 95%CI 1.060–6.779), diabetes (OR 2.602, 95%CI 1.208–5.602) but negatively with *ABCG8* p.D19H (OR 0.139, 95%CI 0.035–0.546).

Conclusion: GD or cholecystectomy might exert minor modulatory effects on liver fibrosis, which however in this setting is – like steatosis – mainly driven by established genetic and exogenous determinants.

THU-125

Dissecting the alternate mediterranean diet score identifies whole grains and red meat as key determinants of fibrosis risk in MASLD

Nicholas Dunn[1], Sheel Patel[1], Luis Antonio Diaz[2], Vatsalya Vatsalya[1], Robert Wong[3], Juan Pablo Arab[4], Shira Zelber[5], Aleksander Krag[6,7], Zobair M. Younossi[8], Maiying Kong[1], Ashwani K. Singal[1]. [1]*University of Louisville, Louisville, United States;* [2]*Division of Gastroenterology and Hepatology, University of California San Diego, San Diego, United States;* [3]*Stanford University, Stanford, United States;* [4]*Division of Gastroenterology, Hepatology, and Nutrition, Department of Internal Medicine, Virginia Commonwealth University School of Medicine, Richmond, United States;* [5]*School of Public Health, University of Haifa, Haifa, Israel;* [6]*Center for Liver Research, Department of Gastroenterology and Hepatology, Odense University Hospital, Odense C, Denmark;* [7]*Institute of Clinical Research, Faculty of Health Science, University of Southern Denmark, Odense M, Denmark;* [8]*The Global NASH Council, Washington, United States*
Email: ashwanisingal.com@gmail.com

Background and aims: Diet is a crucial component in the management in metabolic dysfunction-associated steatotic liver disease (MASLD). However, composite dietary indices may obscure the contribution of individual food components. The Alternate Mediterranean Diet score (aMED) captures key dietary domains linked to metabolic health, but its aggregate score has shown inconsistent associations with MASLD. We aimed to evaluate the association of aMED with MASLD and fibrosis severity and to dissect individual aMED components to identify dietary factors independently associated with steatosis and fibrosis progression.
Method: Adults ≥18 years from NHANES 2017–2023 with valid vibration-controlled transient elastography and ≥1 cardiometabolic risk factor were included. MASLD was defined by CAP ≥248 dB/m. Significant fibrosis, advanced fibrosis, and cirrhosis were defined using liver stiffness ≥8, ≥10, and ≥15 kPa, respectively. Bidirectional stepwise models identified aMED component scores independently associated with each outcome, adjusting for demographic, socioeconomic, behavioral, and dietary confounders. Survey-weighted, multivariable logistic regression analyses were derived.
Results: Among 9,563 participants representing 155 million U.S. adults, MASLD prevalence was 63%, with significant fibrosis in 11%, advanced fibrosis in 6%, and cirrhosis in 3%. Higher aMED was associated with lower odds of MASLD (OR 0.87, 95% CI 0.82–0.92), significant fibrosis (OR 0.85, 0.79–0.92), and advanced fibrosis (OR 0.87, 0.77–0.98), with a borderline association for cirrhosis (OR 0.86, 0.74–1.01; p = 0.059). Independent predictors of MASLD were higher legume (OR 0.89, 0.83–0.95) and fruit intake (OR 0.92, 0.85–0.99). Higher red/processed meat intake increased (OR 1.16–1.17; 95% CI 1.07–1.30), while higher whole grain intake reduced (OR 0.82; 95% CI 0.73–0.93), the odds of significant and advanced fibrosis. Whole grain intake was the sole dietary predictor of cirrhosis (OR 0.79, 0.64–0.96).
Conclusion: Greater adherence to a Mediterranean-style dietary pattern is associated with lower odds of MASLD and fibrosis. Within the aMED score, higher whole-grain intake and lower red/processed meat intake emerged as the principal protective components against fibrosis. These findings support targeted Mediterranean diet recommendations emphasizing increased whole grains and reduced red meat to mitigate fibrosis progression in MASLD. Given the cross-sectional design, longitudinal studies are needed to confirm these associations.

THU-126

Natural history and predictors of fibrosis progression in metabolic dysfunction-associated steatotic liver disease (MASLD) – Longitudinal cohort study with paired liver biopsies

Fahim Ebrahimi[1], Luigi Terracciano[2,3], Caner Ercan[4], Luigi Tornillo[5,6], Matthias Matter[5], Jürg Vosbeck[5], Elaine Chng[7], Fion Goh[7], Serene Lek[7], Aleksei Suslov[5], Stefan Wieland[5], Nikolai Naoumov[8], Markus Heim[1,5].
[1]University Hospital Basel, Basel, Switzerland; [2]IRCCS Humanitas Research Hospital, Milan, Italy; [3]Humanitas University, Milan, Italy; [4]University of Texas MD Anderson Cancer Center, Houston, United States; [5]University of Basel, Basel, Switzerland; [6]GILAB AG, Allschwil, Switzerland; [7]HistoIndex Pte. Ltd., Singapore, Singapore; [8]University College London, London, United Kingdom
Email: f.ebrahimi@outlook.com

Background and aims: The natural history and long-term liver histologic evolution of untreated metabolic dysfunction-associated steatotic liver disease (MASLD) remain poorly understood. Using a well-characterized longitudinal cohort with paired liver biopsies, we aimed to investigate predictors of fibrosis changes over time in untreated MASLD.
Method: This was a longitudinal cohort study of 48 patients with biopsy-proven MASLD spanning the full fibrosis spectrum (F0-F4) and followed between 2000 and 2025. All patients received lifestyle counseling but no specific pharmacological intervention. Paired liver biopsies were obtained at baseline (BL) and end-of-follow-up (EOF). Liver histology was independently assessed by two pathologists and by second harmonic generation/two-photon excitation fluorescence (SHG/TPEF) microscopy with artificial intelligence-based quantification (qFibrosis®). Progression or regression of liver fibrosis were defined as an increase or decrease of ≥1 qFibrosis stage, respectively. Linear regression analyses were used to assess associations between clinical and laboratory parameters with changes in qFibrosis scores.
Results: Overall, 68.8% were male with a median age of 49 years (IQR 38.0–56.6) and median BMI of 29.7 kg/m^2 (IQR 26.3–32.7). At baseline, 14.6% had type 2 diabetes and 33.3% had histologic evidence of metabolic dysfunction-associated steatohepatitis (MASH). Baseline liver stiffness measurements (LSM), histologic NAS score, and c-reactive protein levels were significantly associated with baseline qFibrosis scores ($P < 0.05$). Over a median follow-up of 8.5 years (IQR 5.5–10.8 years), 18 patients (37.5%) demonstrated fibrosis progression, 19 (39.6%) showed no change, and 11 (22.9%) exhibited fibrosis regression. None of the baseline variables was significantly associated with progression or regression of ≥1 qFibrosis stage. Using the qFibrosis score, in multivariate adjusted linear regression analyses we found that baseline LSM values were significantly associated with an increase in qFibrosis score (regression coefficient: 0.086 (95%CI, 0.028–0.143; $P = 0.004$). Also, an increase in LSM during the follow-up period of ≥5 kPa was associated with an increase in qFibrosis score of 1.77 (95%CI, 0.95–2.59; $P < 0.001$).
Conclusion: In this well-characterized long-term MASLD cohort, baseline liver stiffness measurements and increases in LSM of ≥5 kPa during the follow-up period predicted increases in liver fibrosis according to the quantitative qFibrosis assessment.

THU-127-YI

Non-invasive two-step triage reduces access delays to liver services for people with metabolic dysfunction-associated steatotic liver disease: a tertiary program evaluation

Yasamin Farbod[1], Neha Sharma[1], France Martineau[1], Dana Kablawi[1], Philip Wong[1], Xun Zhao[1], Marc Deschenes[1], Tianyan Chen[1], Sahar Saeed[2], Amine Benmassaoud[1], Giada Sebastiani[1]. *[1]Division of Gastroenterology and Hepatology, Department of Medicine, McGill University, Montreal, Canada; [2]Department of Public Health Sciences, Queen's University, Kingston, Canada*
Email: yasamin.farbod@mail.mcgill.ca

Background and aims: The prevalence of metabolic dysfunction-associated steatotic liver disease (MASLD) is placing increasing strain on hepatology services. Limited access to transient elastography (TE; FibroScan®) and specialist care continues to generate major bottlenecks. In 2021, our tertiary hepatology program implemented a biomarker-guided, TE-confirmed two-step triage pathway to optimize resource allocation, prioritizing high-risk MASLD while safely retaining low-risk patients in primary care. We evaluated the impact of this model on access to TE and hepatology services, referral efficiency, and early detection of advanced fibrosis.
Method: We conducted a quasi-experimental study including all consecutive referrals for liver assessment between 2013 and 2020 (pre-implementation) and 2021–2025 (post-implementation). The triage algorithm used age-adjusted FIB - 4 cut-offs as the first tier (low risk: <1.3 if <65 years or <2.0 if ≥ 65 years), with non-low-risk patients proceeding to TE for fibrosis confirmation. Primary outcomes were time from referral to TE and referral to hepatology consultation. Secondary outcomes included the proportion of patients managed without in-person hepatology assessment, no-show rate, and detection of advanced fibrosis (> F3) within 12 months of referral as a safety indicator.
Results: Among 3,953 patients with MASLD who underwent TE (mean age 62; 73% male), 1,750 (44.3%) were pre- and 2,203 (55.7%) were post-implementation. Following implementation of two-step triage, mean time from referral to TE decreased from 13.2 to 5.5 months (absolute reduction of –7.7 months; relative reduction - 58%). Mean time from referral to hepatology consultation was reduced from 30 to 13.2 months (absolute reduction of –16.8 months; relative

reduction - 56%). The share of referrals managed without hepatology consultation increased from 45% to 80%, while hepatology no-show rates declined from 23% to 15%. As a safety signal, the proportion of patients diagnosed with advanced fibrosis within 12 months of referral doubled from 10% to 20%, consistent with earlier detection of higher-risk patients following triage implementation.
Conclusion: Implementation of a biomarker-guided, TE-confirmed two-step triage pathway reduced access delays and accelerated detection of advanced fibrosis in MASLD patients. These real-world findings provide scalable, cost-neutral evidence to support decongestion of hepatology services and improve access to liver care in population-level MASLD management.

THU-131
Vitamin D insufficiency is associated with liver fibrosis development in people with HIV
Francesca Farina[1,2], Aurgho Datta[1], Jovana Milic[3], Gabrielle Mariano[1], Felice Cinque[1], Giovanni Guaraldi[3], Giada Sebastiani[1]. [1]*Chronic Viral Illness Service, Department of Medicine, McGill University Health Centre, Montreal, Canada;* [2]*San Raffaele Hospital, Milan, Italy;* [3]*Modena HIV Metabolic Clinic, University of Modena and Reggio Emilia, Modena, Italy*
Email: farina.francesca1@hsr.it

Background and aims: Steatotic liver disease is the most common liver disease in people with HIV (PWH), who are also at increased risk of liver fibrosis. Vitamin D (VitD) insufficiency is highly prevalent in PWH and in steatotic liver disease, yet its role in liver fibrosis development remains uncertain.
Method: We conducted a multicentre observational cohort study in PWH from Italy and Canada. Hepatic steatosis was assessed by transient elastography and defined as a controlled attenuation parameter ≥ 275 dB/m, while significant liver fibrosis was defined as liver stiffness measurement ≥ 8 kPa. VitD insufficiency was defined as serum 25-hydroxyvitamin D levels < 50 nmol/L. Cumulative incidence of liver fibrosis was estimated using survival methods. Factors associated with fibrosis were evaluated using multivariable logistic regression and generalized estimating equation models.
Results: A total of 4746 PWH enrolled between 2014 and 2024 were included (mean age 60.2 years; 72% male; mean BMI 25 kg/m^2; 11% with diabetes; 23% with hepatitis C coinfection). At baseline, VitD insufficiency was present in 42% of participants, hepatic steatosis in 19%, and significant fibrosis in 14%. After adjustment for sex, ethnicity, HIV duration, CD4 cell count, diabetes, and parathyroid hormone levels, VitD insufficiency was independently associated with hepatitis C coinfection (adjusted odds ratio [aOR] 1.15, 95% CI 1.02–1.31), BMI (aOR 1.10, 95% CI 1.03–1.08), and hepatic steatosis (aOR 1.71, 95% CI 1.35–2.18). Over a median follow-up of 7 years, the cumulative incidence of significant liver fibrosis was 17%. PWH with VitD insufficiency had a higher cumulative incidence of liver fibrosis than those without VitD insufficiency (19% vs 11%; log-rank p < 0.001). In multivariable longitudinal analyses, VitD insufficiency remained independently associated with liver fibrosis development (aOR 1.44, 95% CI 1.14–1.80), after adjustment for hepatic steatosis, diabetes, obesity, parathyroid hormone levels, CD4 cell count, and HIV duration.
Conclusion: VitD insufficiency is common in PWH and is strongly associated with hepatic steatosis and hepatitis C coinfection. VitD insufficiency is independently associated with the development of significant liver fibrosis, irrespective of metabolic risk factors, suggesting that VitD status may contribute to liver disease progression in this population.

THU-132
Impact of unhealthy diet categories on liver disease outcomes among different steatotic liver disease phenotypes following patient-centered education
Serena Gilmore[1], Janet Chu[1], Amy Shui[1], Catherine Magee[2], Mandana Khalili[1,2]. [1]*University of California, San Francisco, San Francisco, United States;* [2]*Division of Gastroenterology and Hepatology, Zuckerberg San Francisco General Hospital and Trauma Center, San Francisco, United States*
Email: serenagilmore00@gmail.com

Background and aims: Data on dietary composition of Steatotic liver disease (SLD) subgroups [metabolic dysfunction (MASLD), alcohol related (ALD), or both (MetALD)] and its impact on SLD outcomes are limited. We aimed to describe diet composition of SLD subgroups and assess the impact of unhealthy diet categories on ALT, AST, and Fibrosis-4 (FIB-4) after SLD education.
Method: Adults ≥ 18 years (n = 360) with SLD were recruited from hepatology clinics, completed a formal SLD education including dietary/ lifestyle modification, and followed for 24 months. Pre- and post- education surveys included unhealthy food consumption (carbohydrates, fast foods, fried foods, sugar-sweetened beverages, and sweets) and coffee/tea frequency, SLD knowledge, and barriers to healthy eating. Bivariate tests were used to compare the characteristics as well as dietary composition of SLD subgroups. Multivariable linear mixed-effects models were performed for each longitudinal outcome (ALT, AST, FIB-4) for each of the unhealthy food categories and their interaction with time. Models included SLD subgroups, perceived barriers to dietary modifications following education, and covariates with p < 0.1 associations from the unadjusted models.
Results: Demographics were median age 54 years, 59% female, 57% Hispanic, 26% Asian, 52% obese, and 36% had diabetes. SLD subgroups were 59% MASLD, 20% MetALD, and 21% ALD. Proportion of unhealthy food categories consumed significantly differed across SLD subgroups with sugar-sweetened beverage consumption being higher in ALD and MetALD subgroups, sweets higher in MetALD, and fast food consumption higher in ALD compared to MASLD. Onmultivariable analysis, fried food consumption ≥ 6 times/week (vs none) was associated with a greater change in AST (estimate 2.46, 95% CI 1.10–3.82) and ALT (estimate 1.72, 95% CI 0.03–3.40) over time. Drinking < 3 cups of coffee per day (vs none) was associated with an increase in AST over time (estimate 0.76, 95% CI 0.10–1.42) but not FIB-4. There were no significant differences in AST, ALT, or FIB-4 over time with other unhealthy food consumption categories.
Conclusion: Unhealthy diet categories differed among SLD subgroups, including higher sugar-sweetened beverages consumption with increased alcohol use. Fried food consumption contributed significantly to change in AST and ALT over time. These findings suggest that tailored dietary modification, especially limiting fried foods, are important to SLD outcomes.

THU-133
Depression and anxiety levels are higher in obese women than in men in a cohort of MASLD patients
Marta Guariglia[1], Gian Paolo Caviglia[1], Angelo Armandi[1], Eleonora Dileo[1], Francesca Saba[1], Kamela Gjini[1], Maria Lorena Abate[1], Antonella Oliviero[1], Elisabetta Bugianesi[1,2]. [1]*Division of Gastroenterology and Hepatology, Department of Medical Sciences, University of Turin, Turin, Italy;* [2]*Città della Salute e della Scienza—Molinette Hospital, Turin, Italy*
Email: marta.guariglia@unito.it

Background and aims: Obesity is a major determinant of metabolic dysfunction-associated steatotic liver disease (MASLD) and is closely linked to psychiatric disorders, including depression and anxiety. Increasing evidence highlights the interplay between these conditions with sex and age. We aimed to investigate the prevalence and determinants of depression and anxiety in patients with MASLD.
Method: We prospectively enrolled 277 patients with MASLD (age 54 [20–80] years; 157 males/120 females; BMI 29 [18–46] kg/m^2; T2DM: 61 [22.0%]). All patients underwent liver stiffness measurement by FibroScan® 530. Advanced fibrosis was defined according to liver stiffness values ≥8.0 kPa. Depression and anxiety were assessed using the Hospital Anxiety and Depression Scale (HADS), categorized as: 0–7 (normal), 8–10 (borderline), and ≥11 (abnormal).

Results: Overall, 26% of patients showed at least borderline depression (≥8 points) and 28% at least borderline anxiety; notably, 33 patients were already on antidepressant or anxiolytic treatment. Women were more frequently affected than men (depression: 36.7% vs. 17.8%; anxiety: 40.8% vs. 17.9%). In women, depression correlated with BMI (p = 0.18, p = 0.048), and anxiety correlated inversely with age (ρ = –0.20, p = 0.028). The Kruskall-Wallis test, only in women, shows that in females aged ≥50 years, depression levels are higher in patients with a BMI ≥ 30 (p = 0.026). In multivariable logistic regression adjusted for age, BMI, liver stiffness, antidepressants and diabetes, moderate-to-severe depression remained significantly associated with BMI ≥30 (OR = 2.2, 95% CI = 1.02–4.73, p = 0.045).
Conclusion: In patients with MASLD, psychological burden appeared more pronounced among women, with obesity emerging as a key determinant of depression and younger age of anxiety. These findings highlight the importance of systematic psychological assessment, particularly in obese women, to facilitate timely referral and tailored support.

THU-134

Exploring the link between handgrip strength and MASLD

Leen Heyens[1,2,3,4], Anouk Rensink[5], Francesco Innocenti[6], Struyve Mathieu[4], Sven Francque[7,8], Geert Robaeys[1], Ger Koek[2,5] and MASLD research group[1]. *[1]Hasselt University, Faculty of Health and Life Sciences, LCRC, Hasselt, Belgium; [2]Maastricht University, School of Nutrition and Translational Research in Metabolism (NUTRIM), Maastricht, Netherlands; [3]Ziekenhuis Oost-Limburg, dept. Future Health, Genk, Belgium/LCRC(-MHU), Genk, Belgium; [4]Ziekenhuis Oost-Limburg, dept. Gastroenterology, Genk, Belgium; [5]Maastricht University Medical Centre, dept. Gastroenterology and Hepatology, Maastricht, Netherlands; [6]Maastricht University, Care and Public Health Research Institute (CAPHRI), Department of Methodology and Statistics, Maastricht, Netherlands; [7]Antwerp University Hospital, Department of Gastroenterology and Hepatology, Antwerp, Belgium; [8]University of Antwerp, InflaMed Centre of Excellence, Laboratory of Experimental Medicine and Paediatrics, Antwerp, Belgium*
Email: leen.heyens@uhasselt.be

Background and aims: Handgrip strength (HGS) is a surrogate marker for whole-body muscle strength. Metabolic dysfunction-associated steatotic liver disease (MASLD) is closely linked with obesity, insulin resistance, and sarcopenia. This study aimed to investigate the relationship between HGS and markers of liver steatosis and fibrosis in an MASLD population.
Method: Cross-sectional cohort studies were conducted from 2019 to 2023 across primary care practices in Belgium and the Netherlands, and a hospital endocrinology department in Belgium. Presence of fibrosis was defined by a Vibration Controlled Transient Elastography (VCTE™, *i.e.*, liver stiffness) cut-off value of >8 kPa, and steatosis (hence MASLD) by a Controlled Attenuation Parameter (CAP™) cut-off value of >275 dB/m (FibroScan®, Echosens, Paris). HGS was assessed using a hydraulic hand dynamometer (JAMAR, Saehan, Korea) and categorized into low, average, or high based on normative data. Spearman correlation and logistic regression analyses were conducted to assess associations between absolute HGS, bHGS (absolute HGS/BMI), hHGS (absolute HGS/height), VCTE, and CAP.
Results: In this cross-sectional study, 422 participants were included. MASLD was present in 264 (62.5%) of participants, of whom 193 (45.7%) were male and 57 (13.5%) had fibrosis. The median age and BMI were 61[IQR 16] years and 28.1 [IQR 6.2] kg/m^2, respectively. bHGS was significantly lower in the MASLD group (1.0 [IQR 0.6] *vs.* 1.2 [IQR 0.6], p < 0.001), while absolute HGS and hHGS did not differ. bHGS, but not absolute and hHGS, was inversely correlated with CAP (r = –0.149, p = 0.015) in the MASLD group. In women, absolute, bHGS, and hHGS were significantly lower in individuals with fibrosis compared to those without fibrosis. Multivariable logistic regression models adjusted for age, sex, smoking, alcohol, BMI, T2DM, and exercise indicated that there were no statistically significant associations between absolute HGS, bHGS, and hHGS and the presence of steatosis.
Conclusion: bHGS was associated, but not independently, with steatosis severity. Given the intrinsic relationship between BMI and steatosis, bHGS may not reflect an independent muscle–liver link. Absolute HGS and hHGS showed no independent relationship with steatosis or fibrosis in this MASLD cohort. Standardization of HGS normalization methods and larger longitudinal studies are needed to clarify its role in MASLD risk assessment.

THU-135

Association of geriatric nutritional risk index with prognosis in hepatocellular carcinoma patients with and without metabolic dysfunction–associated steatotic liver disease

Chia-Jung Ho[1], Chun-Ting Ho[1,2], Yi-Chen Lin[3], Tsai Shin-Yu[1], Yi-Hsiang Huang[4], Ming-Chih Hou[5], Jaw-Ching Wu[6], Chien-Wei Su[7]. *[1]Taipei Veterans General Hospital, Department of Medicine, Taipei, Taiwan; [2]National Yang Ming Chiao Tung University Yangming Campus, Ph.D. Program of Interdisciplinary Medicine, Taipei, Taiwan; [3]Linkou Chang Gung Memorial Hospital, Department of Medicine, Taoyuan City, Taiwan; [4]Taipei Veterans General Hospital, Department of Medical Research, Taipei, Taiwan; [5]Taipei Veterans General Hospital, Department of Medicine, Taipei, Taiwan, Taipei City, Taiwan; [6]National Yang Ming Chiao Tung University Yangming Campus, Institute of Clinical Medicine, Taipei, Taiwan; [7]Taipei Veterans General Hospital, Division of General Medicine, Department of Medicine, Taipei, Taiwan*
Email: happywish99@gmail.com

Background and aims: Malnutrition adversely affects outcomes in hepatocellular carcinoma (HCC), while metabolic dysfunction–associated steatotic liver disease (MASLD) has emerged as an increasingly prevalent underlying condition. However, the relationship between nutritional status and MASLD and their prognostic impact on HCC patients remain unclear. We aim to evaluate the prognostic role of malnutrition in HCC patients by assessing geriatric nutritional risk index (GNRI) and further stratified by concurrent MASLD status.
Method: We retrospectively analyzed 994 HCC patients who underwent curative resection between 2016 and 2023 at Taipei Veterans General Hospital. Patients were categorized as non-MASLD (n = 544) or MASLD (n = 450) based on non-tumor liver histology. Risk of malnutrition was assessed using the GNRI and classified as major risk (GNRI < 82), moderate risk (GNRI 82 to <92), low risk (GNRI 92 to ≤98), and no risk (GNRI > 98). Overall survival (OS) was the primary endpoint. Survival analyses were performed using Kaplan–Meier and Cox proportional hazards models.
Results: Among the entire cohort, the prevalence of no risk, low, moderate, and major nutritional risk were 79.8%, 13.5%, 5.8%, and 0.9%, respectively. Compared with the non-MASLD group, patients with MASLD had higher body mass index, more cardiometabolic risk factors, lower prevalence of malnutrition risk (GNRI ≤ 98). They also exhibit higher serum albumin, lower aspartate aminotransferase (AST) and alpha-fetoprotein levels, earlier tumor stage, and smaller tumor size. After a median follow-up of 62.9 months, 251 deaths were recorded, with an overall 5-year OS of 73.9%. Patients at risk of malnutrition (GNRI ≤ 98) had significantly poorer 5-year OS than patients without malnutrition risk (GNRI > 98) (77.3% vs. 60.7%, p < 0.001). This association remain consistent in the MASLD and the non-MASLD subgroups. However, in multivariate Cox analysis, GNRI was not an independent predictor for OS. Older age, lower serum albumin, advanced BCLC stage, and higher histology grade independently predicted poorer OS.
Conclusion: HCC patients with MASLD exhibit lower prevalence of malnutrition risk and more favorable tumor characteristics. Malnutrition, assessed by GNRI, was associated with poor OS in both MASLD and non-MASLD subgroups. However, GNRI was not an independent prognostic factor after adjustment, with age, serum

albumin, and tumor burden remaining the key determinant of outcomes.

THU-136

Comparison of demographics, metabolic risk factors and clinical presentation in lean Vs. non-lean metabolic dysfunction-associated steatotic liver disease (L-MASLD Vs. NL-MASLD) in all of US large cohort in the United States

Ke-Qin Hu[1], Yash Deole[1], Argyrios Ziogas[1], Jenny Fang[1], Hoda Anton-Culver[1]. [1]*University of California Irvine, Irvine, United States*
Email: kqhu@uci.edu

Background and aims: The demographics, metabolic risk factors (MRFs) and clinical presentation of lean metabolic dysfunction-associated steatotic liver disease [L-MASLD, i.e., BMI < 23 for Asians and < 25 for non-Asians] remain to be defined. All of US (AOU) program is one of the largest EHR-linked multi-state/multicenter research cohorts in the US, providing a unique value to address these issues. Aim: Compared L-MASLD vs. Non-lean MASLD (NL-MSALD) in their basic demographics, MRFs, clinical presentation using AOU EHR-linked large cohort of cases with MASLD.
Method: A total of 16117 cases with EHR diagnosis of fatty liver but no history of alcohol use, HBV or HCV infection, AIH, PBC, or PSC, were identified as MASLD cases, including 1135 with L-MASLD; 14982, NL-MASLD (NL-MASLD) for the following statistical analyses.
Results: In L-MASLD group, the mean age was 56.39 ± 16.11; 66.5% were females; 59.6%, White; 21.1%, Hispanic; 7.1%, Black; 4.6%, Asian. Compared to NL-MASLD, age 65 (36.7% vs. 24.1%), Asian-ethnicity (4.6% vs. 2.3%), ALP (> 110, 47.3% vs. 42.5%) and GGT (> 60, 9.1% vs. 5.8%) elevations were significantly higher in L-MASLD group; and type-2 diabetes (T2DM, 29.3% vs. 48.6%), hyperlipidemia (HLD, 63.3% vs. 71.6%), hypertension (HTN, 58.0% vs. 73.8%), obstructive sleep apnea (OSA, 14.5% vs. 42.4%), ALT elevation (> 40, 56.9% vs. 62.2%), and cirrhosis (4.5% vs. 6.5%) were significantly lower in L-MASLD group, but hepatocellular carcinoma (HCC, 0.8% vs. 0.4%), coronary artery disease (CAD, 23.0% vs. 22.9%), and myocardial infarction (MI, 9.8% vs. 9.3%) were not significantly different. Multivariable Logistic Regression analysis indicated that the rates of Asian-ethnicity (95% CI 1.39–2.55), age ≥ 65 (95%CI 0.38–0.50), ALP (95%CI 0.59–0.78) and GGT (95%CI 0.42–0.67) elevation were significantly higher; T2DM (95%CI 1.49–1.99), HTN (95%CI 1.48–1.97), OSA (95%CI 3.02–4.27), cirrhosis (95%CI 1.03–1.87), and ALT elevation (95%CI 1.05–1.37), but not HLD (95%CI 0.91–1.22) were significantly lower in L-MASLD.
Conclusion: In AOU multicenter large cohort, L-MASLD group had significantly higher rates in age ≥ 65, Asian-ethnicity. The rates of T2DM, HTN, OSA, and cirrhosis were sig lower in L-MASLD, but 4.5% and 0.8% of MASLD cases had cirrhosis and HCC, and the rates of CAD and MI were comparable in both groups. Our data indicated although L-MASLD may have lower rates of MRFs compared to NL-MASLD, it carries comparable long-term prognosis with NL-MALSD.

THU-137

Role of predominant zone of fibrosis on cardiometabolic biomarkers, MACE, MALO, and new-onset diabetes in people with MASH

Alan L. Hutchison[1], Mary E. Rinella[1]. [1]*The University of Chicago, 5841 S. Maryland Ave, MC 4076 | M410, Chicago, United States*
Email: alan.hutchison@uchicagomedicine.org

Background and aims: Hepatocytes in different zones of the liver have different functions – Zone 1 hepatocytes are critical for gluconeogenesis and beta-oxidation, while Zone 3 hepatocytes specialize in glycolysis and lipogenesis. MASH fibrosis can originate predominantly in either zone, but how this impacts progression of cardiometabolic biomarkers and progression of disease has not been studied. We aim to understand how predominant zone of fibrosis in MASH affects these outcomes.
Method: We obtained the Nonalcoholic Fatty Liver Disease Adult Database 2 data from the NASH Clinical Research Network study through the NIH, approved by UChicago IRB 25–0987. Subjects with fibrosis on liver biopsy and a predominant location of fibrosis of "Fibrosis is more prominent around or between portal areas" or "Fibrosis is more prominent around or between central veins" were included. We compared cardiometabolic biomarkers and outcomes of new major adverse cardiovascular events (MACE), major adverse liver outcomes (MALO), and new-onset diabetes.
Results: All analyses controlled for age, sex, and BMI. For subjects with Stage 1 fibrosis, the HbA1c was lower in subjects with Zone 1 fibrosis than in Zone 3 fibrosis (5.87 vs. 6.18, $p < 0.017$). Likewise, the HOMA-IR was lower in those with Zone 1 fibrosis than in those with Zone 3 fibrosis (7.25 vs. 8.6, $p < 0.045$). Among those with Stage 3 fibrosis the Triglyceride-Glucose Index was lower in Zone 1 fibrosis as compared to Zone 3 fibrosis (8.84 vs. 9.29, $p = 0.015$). When additionally controlling for diabetes diagnosis and hypertension diagnosis, subjects with Zone 3 fibrosis had lower rates of MACE outcomes than those with Zone 1 fibrosis (HR: 0.53, 95% CI: 0.37–0.77, $p < 0.001$). When additionally controlling for diabetes diagnosis, subjects with Zone 3 fibrosis had lower rates of MALO outcomes than those with Zone 1 fibrosis (HR: 0.36, 95% CI: 0.20–0.64, $p < 0.0006$). Subjects with Zone 3 fibrosis had higher rates of new-onset diabetes than those with Zone 1 fibrosis (HR: 1.75, 95% CI: 1.24–2.47, $p < 0.002$).
Conclusion: There were significant differences in metabolic indicators based on predominant zone of fibrosis when controlling for age, sex, and BMI. These results suggest that pre-cirrhotic Zone 1 fibrosis is associated with more cardiometabolically favorable biomarkers than Zone 3 fibrosis and less likely development of new-onset diabetes, but may result in more MACE and MALO than Zone 3 fibrosis.

THU-138

Caloric restriction and lifestyle guidance intensity in placebo arms and histologic improvement in metabolic dysfunction–associated steatohepatitis: systematic review and meta-analysis

Feng Ijung[1], Ming-Lun Yeh[2], Chia-Lun Lee[3], Jee-Fu Huang[2], Ming-Lung Yu[2]. [1]*Institute of Precision Medicine, National Sun Yat-sen University, Kaohsiung, Taiwan;* [2]*Hepatobiliary Division, Department of Internal Medicine, Kaohsiung Medical University Hospital, Kaohsiung, Taiwan;* [3]*The Center for Physical and Health Education, National Sun Yat-sen University, Kaohsiung, Taiwan*
Email: ijfeng@g-mail.nsysu.edu.tw

Background and aims: Lifestyle modification is central to metabolic dysfunction–associated steatotic liver disease (MASLD). We assessed whether more intensive lifestyle advice in placebo arms of randomized trials improves histology and whether weight change accounts for these gains. To probe the lifestyle → weight → NAFLD Activity Score (NAS) pathway, we prespecified meta-analysis and meta-regression, acknowledging that study-level mediation can be insensitive.
Method: We searched PubMed, Embase, and Medline to 30 July 2025 for randomized trials of biopsy-proven metabolic dysfunction–associated steatohepatitis with reported placebo-arm advice and outcomes. Advice was classified as none, general, or structured/detailed for exercise, diet, and caloric restriction. Primary outcomes were steatohepatitis resolution without fibrosis worsening, ≥2-point NAS reduction, and fibrosis change; secondary outcomes included NAS domains and mean changes in NAS, fibrosis, weight, and BMI. Random-effects models synthesized effects; subgroups compared advice intensity. Meta-regression tested study-level associations of weight change and intervention duration with NAS. Study-level

mediation (advice → weight → outcomes) used bootstrap confidence intervals.
Results: Seventy-eight trials (n = 5,820) were included. Across all placebo arms, absolute improvements were observed for resolution (+0.15 [0.12, 0.18]), ≥2-point NAS reduction (+0.22 [0.17, 0.28]), and ≥2-point NAS reduction without fibrosis worsening (+0.26 [0.21, 0.32]). Mean changes indicated overall decreases in NAS (−0.56 [−0.75, −0.38]) and fibrosis (−0.29 [−0.50, −0.08]); ballooning and steatosis also improved. In subgroup comparisons, structured advice outperformed general or none. Advice intensity predicted greater weight loss across exercise and diet categories. In meta-regression, larger weight loss related to greater NAS reduction (≈0.19 NAS points per 1-kg loss), and longer intervention duration tracked with additional NAS improvement. Study-level mediation showed small, imprecise indirect effects via weight, suggesting limited power and heterogeneity rather than absence of the pathway.
Conclusion: In placebo arms, structured lifestyle advice improves NAS, fibrosis, and key domains. Greater weight loss correlate with larger NAS reductions, while study-level mediation was inconclusive. Trials should standardize advice intensity and duration, and care pathways should adopt structured programs targeting sustained weight loss, diet quality, and physical activity.

THU-139
Aberrant neurovascular coupling as an early biomarker of brain involvement in MASLD with high liver stiffness
Jie Li[1], Zhuoru Jiang[2], Qian Chen[2], Wenjing Ni[2], Jun Chen[2]. *[1]Nanjing Drum Tower Hospital, Affiliated Hospital of Medical School, Nanjing University, Nanjing, China; [2]Nanjing Drum Tower Hospital, Affiliated Hospital of Medical School, Nanjing University, Nanjing, China*
Email: lijier@nju.edu.cn

Background and aims: Metabolic dysfunction-associated steatotic liver disease (MASLD) is increasingly recognized as a multisystem disorder affecting the brain. However, the impact of liver fibrosis severity on neurovascular coupling (NVC) remains poorly understood. This study aimed to investigate NVC alterations and their cognitive correlates in MASLD patients stratified by liver stiffness.
Method: A total of 111 MASLD patients were recruited and stratified into low liver stiffness (LLS; n = 58) and high liver stiffness (HLS; n = 53) groups based on magnetic resonance elastography (MRE cutoff≥2.5 kPa). NVC was quantified using the coupling between cerebral blood flow (CBF) and regional homogeneity (ReHo) derived from functional MRI. We analyzed global and voxel-wise CBF/ReHo ratios, seed-based functional connectivity (FC), and their associations with neuropsychological performance. Sensitivity analyses were performed to validate reproducibility against gray matter volume (GMV) atrophy, age, and gender.
Results: Compared to the LLS group, HLS patients exhibited significantly attenuated global CBF-ReHo coupling ($p < 0.001$), independent of GMV changes. Regionally, HLS patients manifested disrupted NVC characterized by increased CBF/ReHo ratios in the left temporal pole (superior temporal gyrus) and right insula. Furthermore, the HLS group displayed reduced functional connectivity between the right insula and the superior temporal gyrus. These neuroimaging aberrations were significantly correlated with poorer performance in executive function (Trail Making Test Part B) and memory domains (Digit Span Backwards, Auditory Verbal Learning Test). Validation analyses using ALFF confirmed the robustness of these NVC impairments.
Conclusion: High liver stiffness in MASLD is associated with significant neurovascular uncoupling and functional disconnectivity in the insular and temporal networks. These alterations are intrinsic functional impairments independent of structural atrophy and are linked to specific cognitive deficits, suggesting that NVC metrics may serve as potential biomarkers for monitoring liver-brain axis dysfunction in severe MASLD.

THU-140
Steatotic liver disease as an upstream risk factor for the development of metabolic syndrome–related disorders: a 7-year health checkup cohort study in Japan
Yoshihiro Kamada[1], Makoto Fujii[1], Hitoshi Nishizawa[1], Shiro Fukuda[1], Iichiro Shimomura[1], Eiji Miyoshi[1]. *[1]Graduate School of Medicine, The University of Osaka, Suita, Japan*
Email: ykamada@sahs.med.osaka-u.ac.jp

Background and aims: Steatotic liver disease (SLD) is regarded as a hepatic manifestation of metabolic syndrome (MetS), but its longitudinal role in the development and regression of MetS-related illnesses remains unclear. This study aimed to elucidate the prospective associations between SLD and the onset and regression of type 2 diabetes (T2D), hypertension, and dyslipidemia in a Japanese community cohort.
Method: We prospectively analyzed 714 Japanese adults (mean age 53.5 years, 73% male) participating in health screening with abdominal ultrasonography at baseline and after 7 years. Individuals with prior liver disease were excluded. Incident and regressed MetS-related diseases during follow-up were identified among participants initially disease-free or with existing disease for each outcome. Multivariate logistic regression assessed baseline predictors, including SLD and obesity (BMI ≥ 25), for both new onset and regression of T2D, hypertension, dyslipidemia, and SLD.
Results: At baseline, 60.9% of subjects were diagnosed with SLD. SLD at baseline was independently associated with higher 7-year incidence of T2D, hypertension, and dyslipidemia (all $p < 0.05$), independent of obesity. Conversely, neither T2D nor hypertension at baseline predicted SLD onset; obesity and dyslipidemia were the only independent predictors of incident SLD. Interestingly, the absence of SLD at baseline was a significant independent factor for the regression of each MetS-related disease over 7 years. In contrast, baseline obesity (BMI ≥ 25) did not contribute to the regression of any MetS-related disorder. Sankey diagram analyses illustrated that the sequence of obesity → SLD → MetS-related diseases prevailed. Subjects whose SLD regressed over 7 years exhibited reduced risk of developing new MetS-related disorders.
Conclusion: SLD is an upstream, obesity-independent risk factor for the emergence of MetS-related diseases in Japanese adults, and its absence or improvement contributes significantly to the regression of each component of MetS. Obesity itself, without SLD, does not contribute to the regression of cardiometabolic comorbidities. Improving SLD may be a pivotal therapeutic target for preventing and ameliorating major metabolic disorders.

THU-141-YI
HCV exposure modifies MASLD trajectories in people living with HIV: impaired steatosis and persistently elevated liver stiffness despite sustained virologic response
Ahmed Kamel[1], Rahma Mohamed[2], Aya M. Al-sharif[2], Mohamed Nagy[2], Andrew Saweres[2], Lamiaa Al Sehemy[2], Reham Awad Awad[2], Hanan Hamdy[2], Rana Marwan[2], Remon Atef[2], Omar Aboulhamayed[2], Gamal Esmat[2], Ahmed Cordie[2]. *[1]Faculty of Pharmacy, Cairo, Egypt; [2]Faculty of Medicine Qasr El Ainy, Cairo, Egypt*
Email: ahmedm.kamel@pharma.cu.edu.eg

Background and aims: Metabolic dysfunction-associated steatotic liver disease (MASLD) is increasingly prevalent in people living with HIV (PLWH). Whether prior hepatitis C virus (HCV) infection has lasting effects on hepatic steatosis and fibrosis trajectories remains unclear.
Method: This longitudinal cohort study included 442 PLWH with serial transient elastography assessments over up to 36 months in Egypt. PLWH with HBV co-infection or significant alcohol use were excluded. Participants were categorized as HCV-exposed (prior HCV infection with confirmed SVR12 following DAA therapy) or HCV-unexposed. Controlled attenuation parameter (CAP) and liver stiffness measurement (LSM) trajectories were modeled using

linear mixed-effects models with random intercepts. The primary analysis examined three-way interactions between time, HCV exposure status, and baseline MASLD status (CAP ≥248 dB/m), adjusting for age, sex, BMI, diabetes, and CD4 count.
Results: Of 442 PLWH, 54 (12.2%) were HCV-exposed with confirmed SVR12. Baseline characteristics were similar between groups, including MASLD prevalence (27.8% vs 25.8%, p = 0.88). For CAP trajectories, the three-way interaction (time × HCV exposure × baseline MASLD) was significant (p = 0.015). Among patients with baseline MASLD, HCV-unexposed individuals showed steatosis resolution (−1.21 dB/m/month, p < 0.001) while HCV-exposed individuals showed no improvement despite SVR (+0.08 dB/m/month, p = 0.90). Among those without baseline MASLD, HCV-unexposed individuals progressed toward steatosis (+1.42 dB/m/month, p < 0.001) while HCV-exposed showed slower, non-significant progression (+0.71 dB/m/month, p = 0.098). HCV-exposed patients demonstrated persistently higher LSM despite SVR. At baseline, HCV-exposed patients had 11.3% higher LSM without MASLD (p = 0.03) and 17.8% higher with MASLD (p = 0.05). Although both groups improved over time in the MASLD stratum (p = 0.01), HCV-exposed patients remained elevated at 6 months (14.3% higher, p = 0.06) and 12 months (11.0% higher, p = 0.31). The three-way interaction for LSM was not significant (p = 0.86).
Conclusion: Prior HCV infection in PLWH is associated with persistently elevated steatosis and fibrosis despite SVR12. HCV-exposed patients with baseline MASLD fail to achieve steatosis resolution seen in unexposed counterparts—a "metabolic trap" limiting improvement despite viral cure. These patients warrant intensified metabolic surveillance even after successful DAA therapy.

THU-142
Cardiometabolic risk factors and fibrosis in MASLD: comparison between people living with HIV and the general population in Egypt

Ahmed Cordie[1], Rahma Mohamed[2], Ahmed Kamel[3], Gamal Esmat[1]. *[1]Cairo University, Giza, Egypt; [2]Cairo University Hospitals HIV Clinic, Endemic Medicine Department, Cairo University, Cairo, Egypt; [3]Cairo University, Clinical Pharmacy Department, Faculty of Pharmacy, Cairo University, Egypt, Giza, Egypt*
Email: rahmashaheen2007@gmail.com

Background and aims: Metabolic dysfunction-associated steatotic liver disease (MASLD) encompasses diverse cardiometabolic phenotypes that may differ between populations. We compared cardiometabolic risk factor patterns and their association with hepatic fibrosis in people with HIV (PWH) versus non-HIV individuals in Egypt.
Method: This cross-sectional study included adults with MASLD from a general population screening program and an HIV clinic in Cairo. MASLD was defined according to the 2023 multi-society Delphi consensus as steatotic liver disease (controlled attenuation parameter ≥248 dB/m) plus at least one cardiometabolic criterion. Participants with hepatitis B, hepatitis C, or alcohol use were excluded. Significant fibrosis was defined as liver stiffness measurement ≥8 kPa by transient elastography. Multivariable logistic regression assessed factors associated with fibrosis, adjusting for age, sex, and individual cardiometabolic criteria.
Results: Among 417 participants with MASLD (225 non-HIV, 192 PWH), the populations exhibited distinct metabolic phenotypes. Non-HIV individuals demonstrated a glycemic-predominant profile: dysglycemia (FBS ≥100 mg/dL or HbA1c ≥5.7%) was present in 80.0% versus 36.5% of PWH (p < 0.001), and overt diabetes (FBS ≥126 mg/dL or HbA1c ≥6.5%) in 43.1% versus 10.4% (p < 0.001). Conversely, PWH showed higher triglyceride elevation (53.1% vs 40.9%, p = 0.016). PWH qualified for MASLD with fewer criteria, with 45.8% meeting only one or two criteria compared to 24.0% in non-HIV individuals. Despite this lower metabolic burden, fibrosis prevalence was equivalent between groups (14.1% vs 13.8%, p = 1.000). Low HDL cholesterol emerged as the sole independent cardiometabolic predictor of fibrosis overall (OR 1.99, 95% CI 1.06–3.87, p = 0.035) and in non-HIV individuals (OR 2.75, 95% CI 1.05–7.87, p = 0.046), with a similar trend in PWH (OR 2.14, p = 0.091). Age predicted fibrosis in non-HIV individuals (OR 1.05, p = 0.009) but not in PWH.
Conclusion: PWH with MASLD exhibit a lipid-centric metabolic phenotype distinct from the glycemic-predominant pattern in non-HIV individuals, characterized by four-fold lower diabetes prevalence but higher triglyceride abnormalities. Despite qualifying for MASLD with fewer cardiometabolic criteria, PWH achieve equivalent fibrosis rates, suggesting heightened fibrosis susceptibility per metabolic insult. Low HDL cholesterol independently predicts fibrosis across populations, warranting targeted screening strategies.

THU-147
Long-term association between Helicobacter pylori serostatus changes and incident metabolic dysfunction–associated steatotic liver disease

Ji Min Choi[1], Heesun Lee[1], Eun Kyung Choe[1], Hae Yeon Kang[1]. *[1]Seoul National University Hospital, Seoul, Korea, Rep. of South*
Email: haeykang@gmail.com

Background and aims: Metabolic dysfunction–associated steatotic liver disease (MASLD) has become the leading cause of chronic liver disease worldwide. Helicobacter pylori (H. pylori) infection has been implicated in metabolic dysregulation, yet its long-term relationship with MASLD remains unclear. This study aimed to investigate the association between H. pylori serostatus and the development of incident MASLD in the Korean population.
Method: We conducted a retrospective cohort study that included subjects who underwent general health check-ups between 2015 and 2024. H. pylori infection was assessed by serum anti–H. pylori IgG antibody testing, and MASLD was defined by hepatic steatosis with at least one cardiometabolic risk factor. Incident MASLD during follow-up was evaluated according to baseline and longitudinal changes in H. pylori serostatus.
Results: A total of 17,707 individuals without MASLD at baseline were included; of these, 10,682 (60.3%) were H. pylori–seronegative and 7,025 (39.7%) were seropositive. Over a mean follow-up of 4.3 years, the incidence of MASLD was higher in the baseline H. pylori–seropositive group than in the negative group (19.3% vs. 17.7%, p = 0.007). The risk of incident MASLD varied by changes in H. pylori serostatus, being highest in the persistently seropositive (+/+) group, followed by the persistently seronegative (−/−), seroconverted (−/+), and seroreverted (+/−) groups (hazard ratios adjusted for age, sex, smoking, exercise, and body mass index: 1.09, 1.00 [reference], 0.75, and 0.72, respectively).
Conclusion: Baseline H. pylori serostatus and its longitudinal changes were associated with the development of incident MASLD. Consideration of H. pylori serostatus dynamics may provide additional insights into MASLD risk stratification.

THU-148-YI
Maternal MASLD and timing of early-childhood adiposity: a prospective cohort of over 1,000 mother–child dyads

Cecilia Katzenstein[1], Lauren Alpert[2], Lital Aliasi-Sinai[2], Jacqueline Slobin[1], Nina Rodriguez[1], Jeanette Rios[3], Kim Le[2], Priyanka Singh[2], Keith Sigel[2], Rhoda Sperling[2], Norah Terrault[4], Jaime Chu[2], Tatyana Kushner[5]. *[1]Icahn School of Medicine at Mount Sinai, New York, United States; [2]Mount Sinai Hospital, New York, United States; [3]UCSF Department of Obstetrics, Gynecology, and Reproductive Sciences, San Francisco, United States; [4]University of Southern California Keck School of Medicine, Los Angeles, United States; [5]Weill Cornell Medicine, New York, United States*
Email: cecilia.katzenstein@icahn.mssm.edu

Background and aims: Maternal metabolic dysfunction influences fetal development and early-childhood growth, yet the significance of maternal MASLD is poorly defined. Prior small studies of maternal MASLD focus on offspring adiposity at single timepoints and report

no independent association after adjusting for maternal BMI. Whether MASLD influences the timing of early adiposity, an emerging determinant of long-term cardiometabolic risk, remains unexplored.
Method: We leveraged a prospective cohort at an urban health system to evaluate mother–child dyads with maternal MASLD assessed by ultrasound and/or CAP with concurrent metabolic risk factors. Child anthropometry from 12 to 36 months included repeated BMI and weight-for-length (WFL) measurements; analyses were restricted to children with ≥2 anthropometric measurements to define adiposity timing. The timing of first high adiposity (≥85th percentile) was categorized as early (12–18 months) or late (24–36 months). Multinomial regression models assessed associations between maternal MASLD and adiposity timing, adjusting for pre-pregnancy BMI, gestational age at delivery, infant sex, and birth-weight-for-gestational-age category.
Results: The analytic cohort included 1,055 mother-child dyads, with 40% of mothers having BMI > 30 and 79% having at least one metabolic risk factor. MASLD was present in 18.5% of pregnancies. The mean age was 29.1(± 5.9) and 41% were Hispanic. By 36 months, 87% of children reached BMI/WFL ≥85th percentile at least once between 12 and 36 months. Maternal pre-pregnancy BMI was independently associated with the overall likelihood of high adiposity in the child (adjusted OR per BMI unit 1.05; $p < 0.05$). While maternal MASLD was not associated with overall child adiposity prevalence, in adjusted multinomial models MASLD was associated with a higher predicted probability of early-onset high adiposity at 12–18 months (90.8%) and a lower probability of later onset at 24–36 months (7.2%), compared with pregnancies without SLD (83.3% and 15.1%; p = 0.035).
Conclusion: In a metabolically high-risk cohort with a high prevalence of early-childhood adiposity, maternal MASLD was associated with earlier onset of high adiposity independent of maternal BMI. These findings suggest that maternal MASLD may influence postnatal metabolic programming by altering the timing of adiposity gain rather than adiposity burden alone. Timing-specific effects may represent an important and previously unrecognized pathway linking maternal liver disease to offspring metabolic risk.

THU-149
Impact of endothelial dysfunction on disease progression in patients with MASLD and microalbuminuria

Hijran Khidirova[1], Nermin Musayeva[1]. [1]*Azerbaijan Medical University, Baku, Azerbaijan*
Email: dr.musayevanarmin37@gmail.com

Background and aims: MASLD is a common chronic liver disease, generally associated with obesity, insulin resistance, and metabolic syndrome. Recent evidence suggests that endothelial dysfunction may play an important role in disease progression by contributing to liver inflammation, fibrosis, and increased cardiovascular risk. Biomarkers such as Endocan, ADMA, hs-CRP, and IL-6 may provide further information about vascular and inflammatory changes in MASLD. This study aimed to find the association between endothelial dysfunction and liver disease severity, and to evaluate the predictive value of traditional and novel non-invasive biomarkers in MASLD patients.
Method: The study enrolled 180 patients with ultrasound-confirmed MASLD, divided into two groups based on UACR: 84 patients with microalbuminuria and 96 without. Cllinical and laboratory analysis, metabolic parameters, and steatosis grading, FIB-4, and MASLD Fibrosis Score. Endocan, ADMA, hs-CRP, IL-6. Statistical analyses used Student's t-test or Mann–Whitney U test for group comparisons, Pearson or Spearman correlation for associations, and multivariate regression to identify independent predictors of fibrosis.
Results: Patients with microalbuminuria exhibited significantly elevated FIB-4 scores (1.9 ± 0.6 vs 1.2 ± 0.5, p < 0.001), and higher ultrasound steatosis grades (p < 0.01) compared to patients without microalbuminuria. Endocan (3.8 ± 1.2 vs 2.4 ± 0.8 ng/mL, p < 0.001) and ADMA (0.72 ± 0.15 vs 0.55 ± 0.10 μmol/L, p < 0.001), were elevated in the microalbuminuria group. İnflamatory markers hs-CRP (5.2 ± 2.0 vs 3.1 ± 1.5 mg/L, p = 0.001) and IL-6 (6.5 ± 2.3 vs 4.0 ± 1.7 pg/mL, p < 0.001), were significantly higher. Multivariate regression revealed that microalbuminuria and elevated Endocan levels independently predicted higher fibrosis scores (β = 0.42, p < 0.001 and β = 0.31, p = 0.004, respectively) Correlation analyses demonstrated strong positive associations between endothelial biomarkers and liver disease severity, including steatosis grade and FIB-4 scores.
Conclusion: Endocan, ADMA, and inflammatory mediators, represent endothelial dysfunction and are associated with more advanced liver disease in MASLD and microalbuminuric patients. Results support the role of non-invasive biomarkers in the identification of subjects at risk of progression and may contribute to improved monitoring strategies when combined with traditional clinical assessments.

THU-150
Risk stratification of chronic kidney disease in adults using noninvasive fibrosis tests based on the american diabetes association algorithm

Chan-Young Jung[1], Hye Won Lee[1], Jung Il Lee[1], Han Ah Lee[2], Seung Up Kim[1]. [1]*Yonsei University College of Medicine, Seoul, Korea, Rep. of South;* [2]*Chung-Ang University, Seoul, Korea, Rep. of South*
Email: ksukorea@yuhs.ac

Background and aims: Although the American Diabetes Association (ADA) recently established a diagnostic algorithm for the early detection of liver fibrosis among high-risk individuals, its implications for chronic kidney disease (CKD) risk stratification remain unclear. We investigated whether the ADA diagnostic algorithm can effectively stratify CKD risk in individuals with high risk of future cirrhosis.
Method: This was a retrospective cohort study of 9,264 adults without pre-existing CKD who underwent vibration-controlled transient elastography from April 2006 to October 2018. Participants were categorized into three groups: 1) no metabolic criteria; 2) low risk (FIB-4 < 1.3 or 1.3–2.67 with liver stiffness [LS] <8kPa); and 3) high risk (FIB-4 > 2.67, or 1.3–2.67 with LS ≥ 8kPa). The primary outcome was incident CKD, defined by estimated glomerular filtration rate (eGFR)<60 mL/min/1.73 m^2 or proteinuria (≥1+) on two consecutive tests. Secondary outcomes included ≥25% eGFR decline on two visits and 3- and 5-year CKD risk.
Results: During a mean follow-up of 3.7 years, 440 (4.7%) patients developed incident CKD. When stratified by ADA algorithms, multivariable Cox models revealed a 1.55–fold (95% confidence interval [CI], 1.11–2.17) higher risk of incident CKD in the high-risk group, compared to those with no metabolic abnormalities. The high-risk group also had a 2.59–fold higher risk (95% CI, 2.06–3.26) of a 25% eGFR decline (mean follow-up 3.5 years) and a 1.48–fold (95% CI, 1.00–2.18) higher 5-year CKD risk, compared to those with no metabolic abnormalities.
Conclusion: The two-step algorithms proposed by the ADA can effectively stratify CKD risk in individuals with a high risk of future cirrhosis.

THU-151-YI
MASLD and coronary calcification: how Bayesian analysis supports the association

Florian Koutny[1], Andrea Bito[2], Christian Datz[3], Sophie Gensluckner[4], Julian Prosenz[1], Patrik Langthaler[2], Andreas Maieron[1], Maria Flamm[5], Daniel Weghuber[6], Bernhard Iglseder[7], Eugen Trinka[2,8], Bernhard Paulweber[4], Elmar Aigner[4], Bernhard Wernly[4]. [1]*Department of Internal Medicine 2, Department of Gastroenterology and Hepatology, University Hospital of Sankt Pölten, Karl Landsteiner University, Sankt Pölten, Austria, Krems an der Donau, Austria;* [2]*Department of Neurology, Christian Doppler University Hospital, Paracelsus Medical University and*

Centre for Cognitive Neuroscience, Ignaz-Harrer-Straße 79, 5020 Salzburg, Austria; Neuroscience Institute, Christian Doppler University Hospital, Paracelsus Medical University and Centre for Cognitive Neuroscience, Ignaz-Harrer-Straße 79, 5020 Salzburg, Austria, Salzburg, Austria; [3]Department of Internal Medicine, General Hospital Oberndorf, Teaching Hospital of Paracelsus Medical University, Paracelsusstraße 37, 5110 Salzburg, Austria, Salzburg, Austria; [4]University Department of Internal Medicine I – Gastroenterology and Hepatology, Nephrology, Metabolism and Diabetology, University Hospital Salzburg, Paracelsus Medical University, Strubergasse 21, 5020 Salzburg, Austria, Salzburg, Austria; [5]Institute of General Practice, Family Medicine and Preventive Medicine, Paracelsus Medical University, Strubergasse 21, 5020 Salzburg, Austria; Center for Public Health and Health Research, Paracelsus Medical University, Strubergasse 21, 5020 Salzburg, Austria, Salzburg, Austria; [6]Center for Public Health and Health Research, Paracelsus Medical University, Strubergasse 21, 5020 Salzburg, Austria, Salzburg, Austria; [7]Department of Geriatric Medicine, Christian Doppler Hospital, Paracelsus Medical University, Ignaz-Harrer-Straße 79, 5020 Salzburg, Austria, Salzburg, Austria; [8]Department of Public Health, Health Services Research and Health Technology Assessment, UMIT – Private University for Health Sciences, Medical Informatics and Technology, Eduard-Wallnöfer-Zentrum 1, 6060 Hall in Tirol, Austria, Hall, Austria
Email: florian.koutny@stpoelten.lknoe.at

Background and aims: Metabolic dysfunction–associated steatotic liver disease (MASLD) is a growing global health problem and is linked to both liver disease and cardiometabolic risk. However, although standard frequentist analyses suggest a link with coronary disease, the size of this association after full adjustment for cardiovascular risk factors often remains uncertain. In this study we use Bayesian models with different priors to evaluate both the strength of the association and the robustness of the findings.
Method: We included 1,427 participants from the Paracelsus 10,000 study who had MASLD diagnosed by ultrasound. Coronary artery calcification (Agatston score > 0) was measured using cardiac CT. We ran Poisson regression models (both frequentist and Bayesian), adjusting for cardiovascular risk factors in three steps: (1) unadjusted, (2) adjusted for SCORE2, and (3) fully adjusted for age, sex, metabolic syndrome, and smoking status. We used three different prior distributions (non-informative, pessimistic, and skeptical). Results are reported as posterior medians with a 95% highest posterior density (HPD) interval, and as probabilities for IRR > 1 (any positive effect), IRR > 1.10 (at least 10% higher risk), and IRR > 1.20 (at least 20% higher risk).
Results: Frequentist Poisson regression showed a strong unadjusted association between MASLD and coronary calcification (IRR 1.64, p < 0.001), which remained significant after SCORE2 adjustment (IRR 1.15, p = 0.034) but attenuated and became non-significant after full adjustment (IRR 1.13, p = 0.079). Bayesian models confirmed a clear unadjusted positive effect (non-informative prior: IRR 1.65, 95% HPD 1.38–1.92; P[IRR > 1] = 100%). After full adjustment, there was still a 29% probability of a strong effect (IRR > 1.20). Under a skeptical prior, evidence weakened after adjustment (P[IRR > 1] = 99% unadjusted; 78.4% after SCORE2; 69.9% fully adjusted; IRR 1.03, 95% HPD 0.93–1.13), with low probability of clinically relevant effects (P[IRR > 1.10] = 10.9%; P[IRR > 1.20] = 0.2%).
Conclusion: MASLD is associated with coronary artery calcification, even after accounting for cardiovascular risk factors. However, the Bayesian results indicate that much of this association is driven by age, sex, and metabolic factors, and that a large effect (>20% higher risk) is unlikely after full adjustment. Overall, MASLD seems to be linked to a higher cardiometabolic risk profile and subclinical atherosclerosis, while its additional independent effect appears small.

THU-154

Impact of liver biopsy on patients' readiness to participate in metabolic-dysfunction associated steatotic liver disease drug trials

Piotr Krzeski[1], Yan Su[2], Ping Xu[2], Nicholas Donahue[2], Jenson Ruiz Garcia[3], Kelly Millhaem[2], Phillippa Miranda[2]. *[1]Medpace, Warsaw, Poland; [2]Medpace, Cincinnati, United States; [3]Medpace, London, United Kingdom*
Email: p.krzeski@medpace.com

Background and aims: Surrogate endpoints based on liver biopsy are currently required by regulators in clinical trials for accelerated approval of novel therapies in metabolic dysfunction-associated steatotic liver disease (MASLD). While the requirement for the liver biopsy (typically at baseline and end of treatment) is likely to negatively affect patients' readiness to participate in a drug trial because of its perceived risks and discomforts, the impact remains largely unquantified. Our aim was to estimate the impact of liver biopsy requirement on patients' readiness to participate in MASLD drug trials using screening rates (rates of signing informed consent forms) as a quantitative marker.
Method: We selected early phase (1b through 2b) MASLD trials run at 10 or more US sites which screened at least 100 patients, with or without mandatory biopsy at screening at our institution. We analyzed descriptively and calculated the screening rate ratio with a negative binominal regression model using mandatory biopsy status at screening (with vs without) as the main factor, and investigational product formulation (IP, oral vs injectable) and year of the study as covariates and an offset for time of enrollment to adjust for the varying enrollment durations among sites/studies.
Results: We identified 19 trials (12 with and 7 without mandatory biopsy run at cumulative 444 and 169 US sites, respectively). Two trials in the group without mandatory biopsy were excluded as their screening rates exceeded preidentified outlier criteria. The mean screening rates were 1.72 and 3.03 patients per site per month in trials with and without mandatory biopsy at screening, respectively, with the mean screening rate ratio = 1.77 with 95% CI (1.50, 2.09) and p < 0.0001. No statistically significant impact of IP formulation or year of study on the screening rate was found.
Conclusion: MASLD patients are approximately twice as likely to accept participation in clinical trials without mandatory liver biopsy compared to trials with the requirement, with potentially significant time and cost implications on the trials' execution.

THU-155

Association between biomarkers of subclinical cardiovascular disease and metabolic dysfunction-associated steatotic liver disease

Morgane L'Henaff[1], Jeanne Hersant[1,2], Marine Roux[2], Frédéric Gagnadoux[1,2], Patrice Rodien[1,2], Christophe Aubé[1,2], Isabelle Fouchard[1,2], Loic Bière[1,2], Frédéric Oberti[1,2], Adrien Lannes[1,2], Jerome Boursier[1,2]. *[1]Angers university Hospital, Angers university, Angers, France; [2]Angers university, Angers university Hospital, Angers, France*
Email: jeboursier@chu-angers.fr

Background and aims: Cardiovascular disease (CVD) is the leading cause of mortality in patients with metabolic dysfunction-associated steatotic liver disease (MASLD). Meta-analyses have suggested an independent association between MASLD and early atherosclerosis, but the association with the severity of the liver disease remains debated. Furthermore, the estimation of 10-year cardiovascular risk with SCORE2 has been scarcely investigated in MASLD. We aimed to evaluate the association between the severity of MASLD and biomarkers for subclinical atherosclerosis, as well as with SCORE2.
Method: A total of 452 patients were included from 3 departments in our institution: Hepatology (MASLD), Diabetology (metabolic syndrome), and Pneumology (sleep apnoea syndrome). All patients had MRI-PDFF and FibroScan examinations. Liver steatosis was defined by

liver fat fraction ⩾5%, and liver fibrosis was categorized into 3 groups: mild (< 8 kPa), intermediate (8–12 kPa), advanced (>12 kPa). Subclinical atherosclerosis was evaluated with carotid intima-media thickness (CIMT), pulse wave velocity (PWV), and heart rate-adjusted augmentation index (@75AIx). 10-year cardiovascular risk was estimated using the SCORE2 and its adaptations (SCORE2-OP and SCORE2-Diabetes).
Results: There were 5 subgroups of patients: 21 controls (no liver steatosis and no other cardiometabolic risk factor than overweight/obesity); 135 metabolic patients (metabolic risk factors but no steatosis); and 296 patients with steatosis of whom 210 had mild, 50 intermediate, and 36 advanced liver fibrosis. CIMT and PWV were not associated with liver steatosis or fibrosis severity in multivariate analyses adjusted for age, sex, cardiovascular history, alcohol consumption, smoking, and the 5 cardiometabolic risk factors. @75AIx was not associated with steatosis but was paradoxically inversely associated with fibrosis severity ($p < 0.05$). SCORE2 was lower in control patients and was independently associated with metabolic and MASLD groups. However, there was no significant difference in SCORE2 results among the metabolic, mild MASLD, intermediate MASLD, and advanced MASLD groups.
Conclusion: In this well-phenotyped cohort (MRI PDFF, FibroScan), the biomarkers for subclinical atherosclerosis and the 10-year estimated cardiovascular risk do not correlate with MASLD severity. This suggests that cardiovascular risk assessment should be considered for all patients with MASLD, regardless of the severity of their liver disease.

THU-156
Clinical predictors of increased liver stiffness over time in metabolic dysfunction-associated steatotic liver disease: a prospective real-life study

Stéphanie André-Dumont[1,2], Joyce Scholtens[1], Nicolas Lanthier[1,2]. *[1]Service d'Hépato-gastroentérologie, Cliniques universitaires Saint-Luc, Brussels, Belgium; [2]Laboratory of Gastroenterology and Hepatology, Institut de Recherche Expérimentale et Clinique, Université catholique de Louvain, Brussels, Belgium*
Email: nicolas.lanthier@saintluc.uclouvain.be

Background and aims: Static measurements of liver stiffness (LS) assessed by transient elastography are mainly used in routine practice to evaluate MASLD, whereas dynamic data are lacking. Here, we wanted to evaluate LS dynamics to reflect the evolution of MASLD.
Method: Patients with MASLD assessed with standardised serial LS from baseline diagnostic and at one- and three-year follow-ups (FU) were prospectively included. They were classified as progressors (PRO, ≥ 20% LS increase compared to baseline), stable (STB, <20% of LS variations) and improvers (IMP, ≥ 20% LS decrease compared to baseline).
Results: 192 patients diagnosed with MASLD were included. At baseline, 57% were F0-F1, 38% F2-F3 and 5% F4. 36% were treated for type 2 diabetes. Initial management included lifestyle advice (74%), dietitian support (8%), interventional clinical trial (7%), bariatric surgery (6%) and glucagon-like peptide-1 receptor agonist (GLP1-RA, 3%). After one year (n = 192), 30% were IMP, 47% were STB and 23% were PRO. IMP at one-year were characterised at baseline by a higher body mass index (IMP, median, 32.0 vs. STB, 30.5 vs. PRO, 30.9 kg/m^2; $p = 0.027$), a larger waist circumference (115 vs. 107 vs. 107 cm; $p = 0.002$) and a higher LS (8.9 vs. 6.3 vs. 5.0 kPa; $p < 0.001$). Moreover, IMP had a greater reduction than PRO in body weight (BW, −5 vs. 0%; $p < 0.001$), alanine aminotransferase (−34 vs. −8%; $p = 0.004$), gamma-glutamyl transferase (−25 vs. −5%; $p = 0.032$) and controlled attenuation parameter (−7 vs. −2%; $p = 0.045$). In multivariate logistic regression, after adjustment for sex and BMI, higher baseline age (OR = 1.052; $p = 0.012$) and ALT (OR = 1.027; $p < 0.006$), and increase in BW (OR = 1.107; $p = 0.019$) and ALT (OR = 1.012; $p = 0.025$) were independent predictors of being PRO after one year of FU. After three years (n = 134), the proportion of patients in the three groups remained similar (IMP 34%; STB 42%; PRO 25%) with comparable characteristics.
Conclusion: This is the first prospective data on standardised longitudinal LS in real-life conditions within a MASLD cohort. Screening for advanced fibrosis leads to effective and sustainable lifestyle advice with a positive impact on the severity of liver disease. While around 40% of patients remain stable at one and three years, with normal baseline LS, older patients with low LS, elevated ALT who gain weight and increase their ALT levels over time should be monitored.

THU-158
Are current MASLD alcohol thresholds appropriate for all patients? The role of metabolic vulnerability

Rosa Lombardi[1], Felice Cinque[1], Annalisa Cespiati[1], Edoardo Pulixi[1], Francesca Alletto[1], Daniel Smith[1], Erika Fatta[1], Cristina Bertelli[1], Gabriele Maffi[1], Anna Ludovica Fracanzani[1]. *[1]Fondazione IRCCS Ca' Granda Ospedale Maggiore Policlinico di Milano, University of Milan, Milan, Italy*
Email: rosalombardi@hotmail.it

Background and aims: In patients with steatotic liver disease (SLD) fixed alcohol intake thresholds have been set to define metabolic dysfunction–associated steatotic liver disease (MASLD) and metabolic-associated alcohol-related liver disease (Met-ALD). Individual susceptibility to alcohol-related liver damage may vary according to metabolic and biological vulnerability. We aimed to evaluate whether the association between alcohol intake and liver stiffness differs across age, sex, metabolic comorbidities and genetic background.
Method: We analyzed a cohort of 1,099 adults with SLD (66% males, mean age 51 ± 12 ys), (1034 MASLD; 60 Met-ALD). Alcohol intake was assessed as a continuous variable (g/week). Liver damage was evaluated by liver stiffness measurement (LSM) by Fibroscan. Multivariable linear regression models were used to assess the association between alcohol and LSM, adjusting for age, sex, obesity, diabetes, and PNPLA3 genotype. Interaction terms were included to test effect modification by all covariates. Additional analyses were performed restricting the population to patients classified as MASLD.
Results: In the overall cohort, alcohol intake was independently associated with higher liver stiffness ($B = 0.005$, $p = 0.045$), with a significant interaction by obesity ($B = 0.015$, p for interaction 0.007) and by PNPLA3 genotype ($B = -0.013$, p for interaction = 0.019), indicating a weaker alcohol–LSM association among PNPLA3 carriers. A significant interaction between alcohol intake and sex was also detected, with alcohol-related increases in liver stiffness observed in women but not in men ($B = 0.025$, p for interaction = 0.003). In MASLD patients, alcohol intake was associated with increased LSM even within current MASLD alcohol thresholds ($B = 0.009$, $p = 0.045$). A significant interaction between alcohol intake and obesity was observed (B for interaction = 0.023, $p = 0.019$), indicating a steeper increase in liver stiffness with increasing alcohol consumption in obese individuals. No significant interaction was observed with age categories or diabetes after interaction testing.
Conclusion: Alcohol-related liver damage in SLD is associated with liver damage even at alcohol intake levels currently considered compatible with MASLD and seems to be strongly influenced by metabolic vulnerability and sex. These findings challenge the use of uniform alcohol thresholds and support a more individualized, risk-based approach to alcohol consumption recommendations in MASLD.

THU-159

Brief alcohol counseling in steatotic liver disease: a single-center observational study of six-month changes in alcohol use, noninvasive liver metrics, and quality of life

Erica Nicola Lynch[1], Armando Curto[1], Michele Tanturli[1], Rocco Iamello[1], Gabriele Bianchi[1], Tommaso Mello[1], Tommaso Innocenti[1], Gabriele Dragoni[1], Andrea Galli[1]. *[1]University of Florence, Department of Experimental and Clinical Biomedical Sciences "Mario Serio", Florence, Italy*
Email: ericanicola.lynch@unifi.it

Background and aims: Steatotic liver disease (SLD) is the leading cause of chronic liver disease. NAFLD has been renamed metabolic dysfunction–associated SLD (MASLD); SLD also includes MASLD with moderate alcohol intake (MetALD) and alcohol-related liver disease (ALD). Alcohol and metabolic risk factors synergistically worsen outcomes, so MASLD guidance may not apply to MetALD. We aim To quantify alcohol use in SLD, describe MASLD/MetALD/ALD distribution, and evaluate a structured brief alcohol-counseling program on alcohol intake, quality of life, and non-invasive liver indices.
Method: Single-center observational study (Careggi University Hospital, Florence). Adults with imaging- or biopsy-confirmed MASLD were enrolled (May 2024–May 2025). Alcohol intake (units/day, days/week, binge) and AUDIT were recorded with liver stiffness and CAP and key scores (FIB-4, FAST, NFS). Patients reporting >1 unit on >1 day/week and consenting received 10–15 min structured counseling with reinforcement at ~3 and 6 months. Quality of life was assessed with SF-LDQOL.
Results: Ninety-two patients were included (60.1 ± 13.4 years; 62% men; BMI 29.6 ± 4.35 kg/m^2): MASLD 84.8%, MetALD 12.0%, ALD 3.3%. Alcohol use was reported by 56.5%, mostly low–moderate (1.57 units/day; 1.9 days/week; binge 6.5%; AUDIT 2.73). Baseline: stiffness 8.94 kPa; CAP 296 dB/m; FIB-4 1.14; FAST 0.32; NFS −1.59. Twenty-seven initiated counseling; 22 completed ~6-month follow-up with reductions in alcohol use (3.57 to 1.52 units/day; 5.00 to 2.15 days/week; weekly max 6.07 to 2.68; all $p < 0.001$), AUDIT (7.62 to 3.86; $p < 0.001$), and binge episodes (14.8% to 3.8%); 36.4% achieved abstinence. CAP decreased 281.9 to 246.1 dB/m (−12.7%; $p = 0.002$), FAST improved 0.28 to 0.18 ($p = 0.02$), and stiffness trended down 7.29 to 5.91 kPa ($p = 0.12$). SF-LDQOL improved 148.5 to 153.1 ($p = 0.045$); CAP reduction was significant in MASLD and MetALD but not ALD.
Conclusion: Brief structured alcohol counseling significantly reduced alcohol intake and improved CAP, FAST and quality of life at ~6 months, with greatest benefits in MetALD. Despite small sample size, single-center design and no controls, results support integrating brief alcohol interventions into routine SLD care and validating them in larger controlled multicenter studies.

THU-163

The pseudo-normalization trap in metabolic dysfunction-associated steatotic liver disease: hypolipidemia (low density lipoprotein level < 95 mg/dl) predicts all-cause mortality in a real world cohort

Aysel Mammadyarzade[1], Elvan Isik[2], Ilker Turan[2], Fulya Günsar[2], Zeki Karasu[2], Ulus Akarca[2]. *[1]Ege University, Medical Faculty, Department of Internal Medicine, Izmir, Türkiye; [2]Ege University, Medical Faculty, Department of Gastroenterology, Izmir, Türkiye*
Email: ulusakarca@gmail.com

Background and aims: Dyslipidemia is a key feature of Metabolic Dysfunction-Associated Steatotic Liver Disease (MASLD), and guidelines universally recommend lipid management. However, in advanced disease, declining lipids often reflect impaired synthetic function, a phenomenon known as "reverse epidemiology." We aimed to investigate whether this "pseudo-normalization" of Low-Density Lipoprotein (LDL) serves as an independent predictor of mortality in a real-world MASLD cohort.
Method: We analyzed a longitudinal real-world cohort of 995 patients with MASLD followed for a mean of 3.9 years. Patients were stratified by baseline LDL levels. The primary outcome was all-cause mortality or liver transplantation. Survival was analyzed using Kaplan-Meier curves and multivariate Cox proportional hazards models. To isolate the prognostic value of lipids from metabolic profile, the multivariate model was adjusted for demographics (age, sex), metabolic control (fasting blood glucose), and liver injury (ALT).
Results: During follow-up, 111 mortality events occurred (11.2%). A striking inverse dose-response relationship was observed between LDL and survival. Patients in the lowest LDL quartile (< 95 mg/dL) had the highest mortality rate (19.1%), whereas those in the highest quartile (> 146 mg/dL) had the lowest (3.4%) (Log-rank $p < 0.0001$). In multivariate analysis, low LDL (< 95 mg/dL) remained a significant independent predictor of mortality (Hazard Ratio: 1.86, 95% CI: 1.19–2.90, $p = 0.006$), even after adjusting for age, sex, fasting glucose, and ALT. While age ($p < 0.001$) and glucose ($p < 0.001$) were also predictive, low LDL carried a distinct risk burden independent of these metabolic factors. Mechanistically, this high-risk phenotype was linked to disease severity; patients in the lowest LDL quartile had significantly higher baseline FIB-4 scores compared to the highest quartile (Median: 1.32 vs. 0.97, $p < 0.001$), despite similar age profiles.
Conclusion: This real-world study confirms a "Lipid Paradox" in MASLD: spontaneous hypolipidemia signals a high-risk phenotype. Importantly, this risk is independent of age, diabetes, and liver inflammation. Clinicians should be wary of the "pseudo-normalization trap": in MASLD, low LDL levels should not be interpreted as metabolic success but as a robust "red flag" for poor outcomes.

THU-164

The body roundness index as a novel anthropometric marker in metabolic-associated steatotic liver disease: findings from the HEPAMET registry

Douglas Maya-Miles[1], Rocío Aller[2], Javier Crespo[3], Luis Ibañez-Samaniego[4], Águeda González[5], Juan M. Pericàs[6], Mercedes De La Torre Sanchez[7], Desamparados Escudero-García[8], Jose Miguel Rosales-Zábal[9], Salvador Benlloch[10], Judith Gómez-Camarero[11], Rubén Díez[12], Esther Pavon-Castillero[13], Isabel Graupera[14], Raquel Latorre[15], Rosa M Morillas[16], José Luis Calleja Panero[17], Juan Turnes[18], Patricia Aspichueta[19], Rocío Gallego-Durán[20,21,22], Rubén Francés[22,23], Rosa Martín-Mateos[22,24], Vanesa Bernal[25], Maria Poca[22,26], Antonio Olveira[27], Conrado Fernández- Rodríguez[28], Raul J. Andrade[29], Carmen Carnicero[30], Paula Iruzubieta[31], Laura Suarez Lopez[4], Esther Fuertes-Yebra[32], Alba Jiménez-Massip[6], Manuel Romero-Gómez[20,21,22,33], Javier Ampuero[20,21,22,33]. *[1]Instituto de Biomedicina de Sevilla (IBiS). Hospital Universitario Virgen del Rocío/CSIC/Universidad de Sevilla, Sevilla, España; Departamento de Fisiología, Universidad de Sevilla, Sevilla, Spain; Centro de Investigación Biomédica en Red en el área de Enfermedades Hepáticas y Digestivas (CIBEREHD), Seville, Spain; [2]Department of Medicine, Dermatology and Toxicology, University of Valladolid, Gastroenterology Unit, HCUV, Valladolid. UIC Biocritic, CIBERINFEC, UIC Biocritic, CIBERINFEC, Spain, Valladolid, Spain; [3]Facultad de Medicina. Universidad de Cantabria, Grupo de Investigación Clínica y Traslacional en Enfermedades Digestivas, Instituto de Investigación Sanitaria Valdecilla (IDIVAL)/Servicio de Aparato Digestivo y Hepatología, Hospital Universitario Marqués de Valdecilla, Santander, España; MedicineAI, Madrid, España, Santander, Spain; [4]Liver Unit, Hospital General Universitario Gregorio Marañón/Instituto de Investigación Sanitaria Gregorio Marañón, Madrid, Spain; Centro de Investigación Biomédica en Red en el área de Enfermedades Hepáticas y Digestivas (CIBEREHD), Madrid, Spain; [5]Instituto de Investigaciones Biomédicas Sols-Morreale. IIBM (CSIC-UAM), Centro de Investigación Biomédica en Red de Diabetes y Enfermedades Metabólicas Asociadas (CIBERDEM), Madrid, Spain; [6]Liver Unit, Vall d'Hebron University Hospital Campus, VHIR, Universitat Autónoma de Barcelona, Barcelona, Spain; Centro de Investigación Biomédica en Red en el área de Enfermedades Hepáticas y Digestivas (CIBEREHD), Barcelona, Spain; [7]Consorcio Hospital General Universitario de Valencia, Valencia, Spain;*

[8]Hospital Clínico Universitario de Valencia, Valencia, Spain; [9]Hospital Universitario Costa del Sol, Marbella, Spain; [10]Hospital Arnau de Vilanova, Universidad Cardenal Herrera-CEU Universities, Valencia, Spain; [11]Hospital Universitario de Burgos, Burgos, Spain, Burgos, Spain; [12]Servicio de Aparato Digestivo, Complejo Asistencial Universitario de León, IBIOMED, Leon, Spain; [13]Hospital Universitario San Cecilio, Granada, Spain; [14]Liver Unit. Hospital Clínic, Institut d'Investigacions Biomèdiques August Pi i Sunyer (IDIBAPS), Barcelona, Spain; Centro de Investigación Biomédica en Red en el área de Enfermedades Hepáticas y Digestivas (CIBEREHD), Barcelona, Spain; [15]Hospital Son Llatzer, Palma de Mallorca, Spain; [16]Hospital Germans Trias i Pujol, Badalona, Spain, Badalona, Spain; [17]Gastroenterology and Hepatology Department, Puerta del Hierro University Hospital, Puerta de Hierro-Segovia de Arana Research Institute (IDIPHISA), Autonomous University of Madrid, Madrid, Spain; [18]Complejo Hospitalario Universitario de Pontevedra & IIS Galicia Sur, Pontevedra, Spain; [19]Biobizkaia Health Research Institute, Cruces University Hospital, UPV/EHU, Spain; Department of Physiology, Faculty of Medicine and Nursing, University of the Basque Country UPV/EHU, Leioa, Spain; Centro de Investigación Biomédica en Red en el área de Enfermedades Hepáticas y Digestivas (CIBEREHD), Barakaldo, Spain; [20]Instituto de Biomedicina de Sevilla (IBiS). Hospital Universitario Virgen del Rocío/CSIC/Universidad de Sevilla, Sevilla, España., Seville, Spain; [21]Facultad de Medicina, Universidad de Sevilla, Seville, Spain; [22]Centro de Investigación Biomédica en Red en el área de Enfermedades Hepáticas y Digestivas (CIBER-EHD), Madrid, Spain; [23]Hospital General Universitario de Alicante, Alicante, Spain; [24]Hospital Universitario Ramón y Cajal, Irycis. Universidad de Alcalá, Madrid, Spain, Madrid, Spain; [25]Hospital Universitario Miguel Servet, Zaragoza, Spain; [26]Hospital de la Santa Creu i Sant Pau, Barcelona, Spain; [27]Hospital Universitario La Paz, Madrid, Spain; [28]Hospital Universitario Fundación de Alcorcón, Universidad Rey Juan Carlos, Madrid, Spain; [29]Unidad de Gestión Clínica de Enfermedades Digestivas, Instituto de Investigación Biomédica de Málaga-IBIMA-Plataforma BIONAND; Hospital Universitario Virgen de la Victoria, Universidad de Málaga, Málaga, Spain; [30]Institute of Health Sciences of Castilla y Leon (IECSCYL), 42002, Soria, Spain; [31]Servicio de Aparato Digestivo y Hepatología, Hospital Universitario Marqués de Valdecilla, Grupo de Investigación Clínica y Traslacional en Enfermedades Digestivas, Instituto de Investigación Sanitaria Valdecilla (IDIVAL), Santander, Spain; [32]Unidad de Investigación, Hospital Universitario Santa Cristina, Instituto de Investigación Sanitaria La Princesa, Madrid, Spain; [33]Hospital Universitario Virgen del Rocío, Sevilla, Spain
Email: jampuero-ibis@us.es

Background and aims: A recent international consensus redefined obesity (Rubino et al., *Lancet* 2025), moving beyond BMI as the sole reference metric. The Body Roundness Index (BRI), which better reflects central adiposity and inflammation, may more accurately capture obesity-related risk. This study aimed to assess the utility of BRI in metabolic-associated steatotic liver disease (MASLD) and its association with clinical and prognostic parameters.
Method: We included 1352 MASLD patients from the HEPAMET registry with available data to calculate BMI (weight, height) and BRI (height, waist). BMI was categorized as overweight (>25), obesity (>30), and severe obesity (>40). BRI was stratified into quintiles (Zhang et al., *JAMA* 2024). Histological, biochemical, and metabolic parameters were analyzed; follow-up was available for 720 patients.
Results: Mean age was 52.3 ± 12.5 years; 45.7% were men. MASH was present in 39.8%, and fibrosis stages were F0 33%, F1 28%, F2 12.8%, F3 15.5%, F4 8.7%. Mean BMI was 34.9 ± 8.4 (obesity 68.7%), and mean BRI 7.56 ± 2.7 (≥5.46 in 77%). BMI was not associated with MASH (p = 0.23) or fibrosis (p = 0.81). In contrast, BRI correlated with both MASH (Q1 11.5%, Q2 25.8%, Q3 38.4%, Q4 41.3%, Q5 42.9%; p = 0.001) and fibrosis (F0 7.31 ± 3 vs. F1 7.48 ± 2.6 vs. F2 7.47 ± 2.5 vs. F3 7.92 ± 2.3 vs. F4 8.01 ± 2.6; p = 0.023). Independently, BRI predicted advanced fibrosis [OR 1.08 (95% CI 1.02–1.14); p = 0.015], along with age, AST, GGT, platelets, diabetes, and hypertension. During follow-up, BRI was higher in patients who developed cirrhosis (7.77 ± 2.3 vs 6.86 ± 2.1; p = 0.005) or died (7.69 ± 2.6 vs 6.95 ± 2.2; p = 0.031). A non-significant trend was observed for hepatic decompensation (p = 0.223), possibly due to the small number of events (21/720). In multivariate analysis, BRI independently predicted progression to cirrhosis [HR 1.23 (95% CI 1.08–1.41); p = 0.002], together with ALP, GGT, platelets, and hypertension. BRI also predicted mortality [HR 1.17 (95% CI 1.02–1.33); p = 0.025], along with age and platelet count.
Conclusion: BRI is an independent predictor of advanced fibrosis, cirrhosis progression, and mortality in MASLD, providing superior prognostic accuracy than BMI.

THU-165

The impact of metabolic dysfunction–associated steatotic liver disease in patients with biopsy proven drug induced liver injury

Iulia Minciuna[1], Mihai Zaharia[2], Tudor Cosma[1], Ana Maria Fit[1], Ioana Rusu[3], Oana Nicoara-Farcau[1], Corina Radu[1], Buzias Maria[1], Horia Ștefănescu[2], Bogdan Procopet[1]. [1]Regional Institute of Gastroenterology and Hepatology "O. Fodor," University of Medicine and Pharmacy "Iuliu Hatieganu," Cluj-Napoca, Cluj-Napoca, Romania; [2]Regional Institute of Gastroenterology and Hepatology "O. Fodor," Cluj-Napoca, Romania; [3]Department of Pathology, Regional Institute of Gastroenterology and Hepatology "O. Fodor", Cluj-Napoca, Romania
Email: Iuliabreaban@yahoo.com

Background and aims: Drug-induced liver injury (DILI) is a heterogeneous condition whose biochemical and histological features may overlap with metabolic dysfunction–associated steatotic liver disease (MASLD), now the most prevalent chronic liver disease worldwide. As coexistence of MASLD and DILI becomes increasingly common, their interaction remains insufficiently characterized. The aim of this study was to assess the prevalence of MASLD features in biopsy-proven DILI and their association with liver injury patterns, histology, and clinical outcomes.
Method: We retrospectively analyzed patients evaluated for suspected DILI at a tertiary center between 2015 and 2025. Patients with available liver biopsy were included and classified as pure DILI or DILI with MASLD features. Clinical, biochemical, and histological data were collected. DILI causality was assessed using RUCAM, and injury patterns were defined by standard criteria.
Results: Among 100 patients with biopsy-confirmed DILI, cholestatic injury was the most common pattern (58.6%). Hepatocellular injury occurred more frequently in pure DILI (26.3% vs 13.1%), whereas mixed injury predominated in MASLD+DILI (32.8% vs 7.9%, p = 0.026). According to RUCAM, DILI was rated as probable or very probable in 83.9% of cases. Controlled attenuation parameter values were higher in MASLD+DILI (245 vs 169 dB/m, p = 0.036), while liver stiffness (6.5 vs 9.8 kPa, p = 0.2) and HVPG (median 5 kPa in both groups) were comparable. Histologically, cholestasis was observed in 86.7% of biopsies, and fibrosis was mild in most cases (F0–F1 >90%). Eosinophilic infiltration was more frequent in MASLD+DILI (84.4% vs 64.3%, p = 0.048), with no association with serum eosinophilia. Laboratory analyses showed that only pure hepatocellular and cholestatic patterns correlated with inflammation (r = 0.20, p = 0.044) and histological cholestasis (r = 0.28, p = 0.004), respectively; GPT >5 × ULN was associated with moderate-to-severe lobular inflammation (r = 0.28, p = 0.005). Hospitalization duration (median 12 days) and the need to for liver transplantation (1.7% vs 2.6%, p = 0.7) did not significantly differ between patients with and without MASLD.
Conclusion: MASLD is frequently observed in patients with biopsy-proven DILI and is associated with differences in liver injury patterns and histological features, including a higher prevalence of mixed injury and eosinophilic infiltration. However, the presence of MASLD does not appear to adversely affect fibrosis severity or short-term clinical outcomes.

THU-166

The prevalence of microvascular lesions in metabolic-associated steatotic liver disease patients without cirrhosis

Iulia Minciuna[1], Ana Maria Fit[2], Ioana Rusu[2], Oana Nicoara-Farcau[3], Corina Radu[3], Cristian Moldovan[4], Cristina Adela Iuga[5], Andreea Fodor[3], Tudor Cosma[1], Buzias Maria[1], Horia Ștefănescu[3], Bogdan Procopet[1]. *[1]Regional Institute of Gastroenterology and Hepatology "O. Fodor," University of Medicine and Pharmacy "Iuliu Hatieganu," Cluj-Napoca, Cluj-Napoca, Romania; [2]Department of Pathology, Regional Institute of Gastroenterology and Hepatology "O. Fodor," Cluj-Napoca, Romania; [3]Regional Institute of Gastroenterology and Hepatology "O. Fodor," Cluj-Napoca, Romania; [4]Department of Personalized Medicine and Rare Diseases, MEDFUTURE-Institute for Biomedical Research, "Iuliu Hațieganu" University of Medicine and Pharmacy, Cluj-Napoca, Romania; [5]Department of Personalized Medicine and Rare Diseases, MEDFUTURE-Institute for Biomedical Research, University of Medicine and Pharmacy "Iuliu Hatieganu," Cluj-Napoca, Cluj-Napoca, Romania*
Email: Iuliabreaban@yahoo.com

Background and aims: Although portal hypertension is traditionally considered a late complication of advanced fibrosis, growing evidence indicates that it may develop early in metabolic-associated steatotic liver disease (MASLD), even in the absence of cirrhosis, likely driven by porto-sinusoidal microvascular injury involving endothelial dysfunction, platelet activation, and neutrophil extracellular trap (NET)–associated immunothrombosis. This study aimed to determine the prevalence of portosinusoidal vascular disorder (PSVD)-type microvascular lesions in MASLD patients without cirrhosis and to assess NET presence across disease stages.
Method: In this retrospective study, all adult patients with MASLD who underwent liver biopsy between 2015 and 2024 were included. Biopsies were blindly re-evaluated for fibrosis stage, steatohepatitis activity, and PSVD-related microvascular lesions. In 32 biopsies, NET area and score were assessed by confocal immunofluorescence microscopy.
Results: We identified 75 biopsy-proven, non-cirrhotic MASLD patients with a median age of 54 years, predominantly female, a median liver stiffness of 9.5 kPa (3.3–42), and a median HVPG of 5 mmHg (2–16). Clinical signs of portal hypertension were observed in 46.7% of patients, including splenomegaly (32.8%), esophageal varices (8.8%), portosystemic collaterals (14.7%), and ascites (8%). Moderate-to-severe steatosis was observed in 69.8%, lobular and portal inflammation in 75% and 82.9%, respectively, while 34.2% met criteria for MASH and 85.5% had early-stage fibrosis (F0–F1). Nonspecific microvascular lesions were present in 89.5% of biopsies and specific PSVD-type lesions in 68.4%, with perisinusoidal fibrosis (65.8%) and architectural disturbances (60.5%) being the most frequent nonspecific findings, and obliterative venopathy (65.8%) the predominant specific lesion. Specific lesions were most frequent in F0–F1 fibrosis, whereas nonspecific ones were present in all F2–F3 cases. Steatosis severity did not influence lesion distribution. NET area increased significantly with fibrosis stage and was higher in patients with perisinusoidal fibrosis and portal hypertension. Overall, 80.3% of MASLD patients fulfilled PSVD diagnostic criteria.
Conclusion: Microvascular histological lesions are highly prevalent in MASLD, highlighting the need for increased vigilance in identifying associated vascular changes with potential prognostic implications. NET burden correlates with perisinusoidal fibrosis and signs of portal hypertension.

THU-167

Weathering due to accelerated biological aging among younger patients with metabolic dysfunction-associated steatotic liver disease (MASLD)

Andrew Moon[1], A. Sidney Barritt Iv[1], Chelsea Anderson[1], Jana Phillips[1], Cathrine Hoyo[2], Cynthia Moylan[3], Joellen Schildkraut[4], Melissa Troester[1]. *[1]University of North Carolina, Chapel Hill, NC, United States; [2]NC State University, Raleigh, United States; [3]Duke University, Durham, United States; [4]Emory University, Atlanta, United States*
Email: andrew.moon@unchealth.unc.edu

Background and aims: Premature aging due to environmental, social, and economic stressors, known as weathering, is associated with systemic inflammation, obesity, diabetes, hypertension, and decreased longevity. Weathering, which can be estimated with simple blood tests, may lead to early-onset metabolic dysfunction-associated steatotic liver disease (MASLD). Intervening in early aging processes might prevent or improve conditions like MASLD by slowing cellular deterioration. This study compares weathering between (1) MASLD and non-MASLD patients and (2) MASLD patients with and without advanced chronic liver disease (ACLD).
Method: This was a cross-sectional study including patients age 18–40 years with MASLD (defined by treating hepatologist) and non-MASLD controls seen in GI/hepatology clinic. ACLD was defined as F3/4 fibrosis on biopsy or transient elastography (LSM ≥ 15 kPa). We collected clinical data and labs at the time of enrollment and calculated weathering (chronological minus biological age). Biological age was estimated using the Klemera–Doubal method, which combines seven clinical biomarkers (albumin, alkaline phosphatase, creatinine, C-reactive protein, hemoglobin A1c, systolic blood pressure, and total cholesterol) in a weighted equation using coefficients derived from population-based NHANES data. Group differences in weathering (negative values corresponding to accelerated aging) were assessed using general linear models adjusted for age and sex.
Results: We enrolled 81 patients: 40 non-MASLD (60% F; 25% cryptogenic CLD, 20% viral hepatitis, 25% miscellaneous CLD, 30% no CLD; 13% cirrhosis), 36 MASLD without ACLD (50% F), and 5 with MASLD with ACLD (20% F). Mean chronological ages were 30, 32, and 28 years and biological ages were 34, 46, and 57, respectively. MASLD patients showed more weathering than non-MASLD, with an adjusted mean difference of −11.5 (95% CI: −18.5, −4.5, p = 0.001). There were no statistically significant differences in weathering between MASLD with ACLD and MASLD without ACLD (−13.0, 95% CI: −32.8, 6.7, p = 0.196).
Conclusion: Younger adults with MASLD exhibited greater weathering than those without MASLD. Numerically greater weathering was seen in MASLD with ACLD compared to MASLD without ACLD but this difference was not statistically significant, likely due to a small sample size in the ACLD group. Addressing contributors to weathering including chronic stress and exposure to environmental toxins could reduce the growing burden of MASLD in younger populations.

THU-170

VAT–MASLD–Sarcopenia cascade: metabolic metamorphosis from anabolism to catabolism and its therapeutic implications in liver disease

Astushi Nakamura[1], Takeshi Ichikawa[2]. *[1]Koukan clinic, kawasaki, Japan; [2]Nippon Koukan, Kawasaki, Japan*
Email: naka.a@mac.com

Background and aims: The increasing prevalence of obesity and MASLD necessitates establishing optimal nutritional strategies for sarcopenic obesity(SO) in chronic liver disease(CLD). This study addressed this challenge using a multimodal MRI analysis that simultaneously quantifies liver stiffness(LS), hepatic fat content (PDFF), muscle area, and visceral adipose tissue(VAT) area.
Method: We conducted a single-center retrospective study of 860 patients with CLD. Patients were classified according to etiology into a MASLD group (n = 275) and a non-MASLD group (n = 585). LS (kPa) was used to stratify disease stage, and the pathophysiology and prognosis of SP and SO were evaluated cross-sectionally. SP was defined as low muscle mass on MRI and classified as SO when coexisting with obesity (BMI ≥ 25 kg/m^2). Mesenteric VAT drains directly into the portal system, influencing hepatic metabolism and serving as a strong risk factor for CVD. In this study, VAT area was

quantified at the level of the superior mesenteric artery using MRI. In addition, a longitudinal analysis of 170 obese CLD patients (without HCC) was performed to assess correlations between the annual changes (Δ/year) of these parameters.

Results: SP and SO were observed in 28% and 8% of patients, respectively, and were both associated with disease progression. Among patients with decompensated cirrhosis in the MASLD group, the prevalence of SO reached 50%. In a longitudinal analysis of obese CLD patients (mean 39 months), the prevalence of SO significantly increased($p < 0.01$). Sub-analysis showed that in F0–2 stage, changes in VAT correlated with hepatic status (ΔPDFF, ΔALT, ΔLS), whereas improvement in hepatic fat was paradoxically associated with muscle loss ($\rho = 0.567$, $p < 0.01$). In contrast, in F3–4 stage, changes in ALBI score and ΔPDFF; "burning-out" were independent determinants of muscle loss (both $p < 0.05$). In the prognostic analysis of ACLD (LS ≥ 3 kPa), SP (alone or with SO) was associated with poorer survival compared with non-SP (regardless of obesity status) (HR 2.27, $p = 0.025$).

Conclusion: This study proposes a novel VAT–MASLD–Sarcopenia Cascade model. In the early anabolic phase, VAT acts as the main driver of hepatic injury, whereas in the late catabolic phase, impaired hepatic reserve and burning-out lead to promoting SP, and worsening prognosis. Therefore, therapeutic strategies should be tailored to this metabolic metamorphosis: VAT reduction in the early phase (dual risk: MASH + CVD), and active energy repletion and SP-targeted management in the late phase.

THU-171

The journey of MASLD: the implementation gap between guidelines and primary care in linkage to care

Joo Hyun Oh[1], Hyo Young Lee[2], Sang Bong Ahn[3], Mimi Kim[4], Bo-Kyeong Kang[4], Chul-min Lee[4], Jihyun An[2], Ha Il Kim[2], Eun Chul Jang[5], Jeong-Yeon Cho[6], Hye-Lin Kim[7], Eileen Yoon[2], Dae Won Jun[2]. *[1]Department of Internal Medicine, CHA University College of Medicine, Seongnam, Korea, Rep. of South; [2]Department of Internal Medicine, Hanyang University College of Medicine, Seoul, Korea, Rep. of South; [3]Department of Internal Medicine, Nowon Eulji Medical Center, Eulji University, Seoul, Korea, Rep. of South; [4]Department of Radiology, Hanyang University College of Medicine, Seoul, Korea, Rep. of South; [5]Department of Occupational and Environmental Medicine, College of Medicine, Soonchunhyang University, Chunan, Korea, Rep. of South; [6]Department of Pharmacotherapy, University of Utah College of Pharmacy, Salt Lake, United States; [7]College of Pharmacy, Sahmyook University, Seoul, Korea, Rep. of South*
Email: noshin@hanyang.ac.kr

Background and aims: Although it is well known that most individuals with steatotic liver disease (SLD) do not successfully transition to linkage to care, evidence remains limited regarding how SLD is initially diagnosed and how individuals are subsequently managed after becoming aware of the condition. We aimed to investigate the journey of individuals with SLD and to evaluate the extent of guideline implementation in the general population.

Method: A nationwide, telephone-based survey was conducted among Korean adults aged ≥19 years (n = 3,891). Participants were asked whether they had a prior diagnosis of SLD and, if so, where they were first diagnosed. Linkage to care was defined as receiving follow-up evaluation or clinical care within the medical system after the diagnosis. The at-risk group was defined as individuals with type 2 diabetes, repeated elevations in liver enzymes, or obesity with additional cardiometabolic risk factors.

Results: The self-reported prevalence of SLD was 25.7%. Most respondents (79.9%) were incidentally diagnosed during health check-ups. Overall, 57.2% of individuals with SLD (572/1,000) were linked to care, and 14.9% (85/572) of those linked underwent liver fibrosis assessment. In total, 61.9% (619/1,000) met criteria for the at-risk group, of whom 54.9% (340/619) achieved linkage-to-care and only 12.1% (75/619) received liver fibrosis assessment. Among linked individuals, 66.6% received care in primary clinics, where fibrosis testing rates were markedly lower (2.4%) than in referral centers (16.2%). he most common reason for not seeking care was the belief that SLD was not a serious condition. The rates of successful linkage to care were 58.5%, 52.1%, and 58.7%, and the proportions undergoing liver fibrosis assessment were 11.6%, 12.6%, and 8.7% in the MASLD, MetALD, and ALD groups, respectively.

Conclusion: Most SLD individuals are incidentally diagnosed during medical check-ups. Although awareness of having SLD is relatively high, implementation of guideline—particularly liver fibrosis assessment among at-risk individuals—remains insufficient even after linkage to care.

THU-172

Eligibility for resmetirom or semaglutide therapy in a real-life Greek cohort of patients with metabolic associated steatotic liver disease

Margarita Papatheodoridi[1], Antonia Neonaki[1], Alexandra Argyrou[1], Stratigoula Sakellariou[2], Panagiota Ioannidou[1], Dimitrios Karagiannakis[1], Evangelos Cholongitas[1], Ioannis Vlachogiannakos[1], George Papatheodoridis[1]. *[1]1st Academic Department of Gastroenterology, General Hospital of Athens "Laiko", Medical School of National & Kapodistrian University of Athens, Athens, Greece; [2]1st Department of Pathology, Medical School of National & Kapodistrian University of Athens, General Hospital of Athens "Laiko", Athens, Greece*
Email: gepapath@med.uoa.gr

Background and aims: Pharmacological therapies for metabolic associated steatotic liver disease (MASLD) including resmetirom and semaglutide have been recently approved. Yet, the proportion of real-world patients eligible for these treatments remains uncertain. We evaluated the proportion and clinical relevance of MASLD patients fulfilling the eligibility criteria proposed in the 2025 AASLD guidance.

Method: Adult patients with MASLD attending our tertiary liver outpatient clinics between 2008 and 2024 were included if they had ³1 liver stiffness (LS) measurement and/or liver biopsy. Patients consuming alcohol >20/30 g/week (females/males) or with any other cause of liver injury were excluded. Demographics, comorbidities and clinical outcomes were recorded. Based in the 2025 AASLD guidance, treatment eligibility was defined as metabolic-associated steatohepatitis and/or stage F2–F3 on histology and/or LS 8–15 kPa and advanced liver disease was defined as LS > 15 kPa and/or presence of cirrhosis.

Results: In total, 777 MASLD patients were included (males 54%, mean age 62 ± 14 years, BMI < 25 kg/m^2: 10%, 25–30: 39%, >30: 51%). Diabetes, hypertension, cardiovascular disease and dyslipidemia were present in 26%, 35%, 8% and 35%, respectively. Of the 777 patients, 158 (20.3%) met treatment eligibility criteria, while 523 (67.3%) had only steatosis and/or LS < 8 kPa and 96 (12.4%) had advanced liver disease. Of the 158 treatment eligible patients, 40 (25.6%) had diabetes, 85 (58.6%) had BMI > 30 and 14 (8.9%) BMI < 25. None of the 158 treatment-eligible patients died or developed liver cancer, but 4 (3.3%) patients developed liver decompensation (2 ascites, 1 variceal bleeding, 1 encephalopathy) during follow-up. In the 681 patients without advanced liver disease, treatment eligibility was significantly associated with greater BMI [OR per kg/m^2: 1.01 (95%CI: 1.00–1.03), P = 0.011], diabetes [OR: 2.29 (1.53–3.43), P < 0.001], hypertension [OR: 1.89 (1.31–2.73), P < 0.001] and dyslipidemia [OR: 2.26 (1.57–3.24), P < 0.001]. In multivariable analysis, treatment eligibility was independently associated with greater BMI [OR per kg/m^2: 1.02 (1.00–1.03), P = 0.014], diabetes [OR: 1.77 (1.10–2.82), P = 0.017] and dyslipidemia [OR: 2.05 (1.36–3.09), P < 0.001].

Conclusion: The recent AASLD treatment indications for resmetirom or semaglutide are fulfilled by approximately one fifth of MASLD patients seen at Greek tertiary liver centers, who are at risk for liver decompensation in the near future.

THU-173-YI

Estimated glomerular filtration rate and urine albumin-creatinine ratio trajectories in young adulthood and midlife metabolic-dysfunction associated steatotic liver disease: the coronary artery risk development in young adults study

Seong Park[1], Rachel Orbuch[1], Laura Colangelo[1], Ankeet Bhatt[2], Mercedes Carnethon[1], Lisa VanWagner[3]. [1]*Northwestern University Feinberg School of Medicine, Chicago, United States;* [2]*Kaiser Permanente San Francisco Medical Center, Oakland, United States;* [3]*University of Texas Southwestern Medical Center at Dallas, Dallas, United States*
Email: seong.park@northwestern.edu

Background and aims: Metabolic-dysfunction associated steatotic liver disease (MASLD) is associated with an increased risk of chronic kidney disease (CKD). We aim to assess the relationship between long-term patterns of estimated glomerular filtration rate (eGFR) and urine albumin-creatinine ratio (UACR) patterns during early adulthood and the prevalence of MASLD in midlife.
Method: Participants (28–40 years at Year 10, 1995–1996) of the CARDIA study who had liver fat assessed by non-contrast computed tomography (CT) at Year 25 (Y25, 2010–11) and eGFR and UACR measured at ≥ 1 exam at Year 10, 15, 20 or 25 were included. MASLD was defined as CT liver attenuation < 51 Hounsfield units after excluding other causes of liver fat. Participants were stratified into quartiles for baseline eGFR and UACR. Group-based trajectory modeling was used to create eGFR and UACR trajectories and joint eGFR-UACR trajectory groups from Y10 through Y25. Logistic regression models assessed associations of Y10 eGFR and UACR, and trajectory groups with Y25 MASLD prevalence.
Results: Of 2229 study participants, Y25 MASLD prevalence was 24% (n = 536). Only 10 (0.5%) participants had UACR > 300 mg/g at Y10. Median UACR at Y10 was 2.2, 3.3, 4.9, and 10.2 mg/dL in quartiles 1 to 4, respectively. In a joint model with eGFR, only higher UACR quartiles were associated with increased Y25 MASLD prevalence (OR = 1; OR = 1.3 [95% CI: 0.98–1.74]; OR = 1.48 [95% CI: 1.11–1.98]; and OR = 1.43 [95% CI: 1.06–1.91] for quartiles 1 to 4, respectively). Two eGFR (high decreasing vs. low decreasing) and two UACR (high increasing vs. low stable) trajectories were identified. Individuals in the stable, low UACR trajectory group had lower odds of Y25 MASLD (OR = 0.56 [95% CI: 0.41–0.78]) compared with individuals in increasing, higher UACR trajectory group. In a joint model, only high eGFR-increasing UACR trajectory group was significantly associated with Y25 MASLD (OR = 1.82 [95% CI: 1.21–2.73]) compared to high eGFR-stable UACR trajectory group. Baseline eGFR quartiles and eGFR trajectories were not associated with Y25 MASLD.
Conclusion: Higher, though mostly normal UACR in young adulthood and rising UACR trajectories throughout early adulthood are associated with higher MASLD prevalence in midlife. Monitoring UACR levels in early adulthood may help identify individuals at risk of MASLD in midlife.

THU-174

Quantitative digital pathology reveals distinct fibrosis zonal patterns among subtypes of steatotic liver disease

Jeong Hwan Park[1], Gi-Ae Kim[2], Heejoon Jang[3], Yukti Choudhury[4], Julian Lee[4], Elaine Chng[4], Won Kim[3]. [1]*Department of Pathology, SMG-SNU Boramae Medical Center, Seoul National University College of Medicine, Seoul, South Korea, Seoul, Korea, Rep. of South;* [2]*Division of Gastroenterology and Hepatology, Department of Internal Medicine, College of Medicine, Kyung Hee University Hospital, Kyung Hee University, Seoul, South Korea, Seoul, Korea, Rep. of South;* [3]*Divisions of Gastroenterology and Hepatology, Department of Internal Medicine, SMG-SNU Boramae Medical Center, Seoul, South Korea; Department of Internal Medicine, Seoul National University College of Medicine, Seoul, South Korea, Seoul, Korea, Rep. of South;* [4]*HistoIndex Pte. Ltd., Singapore, Singapore*
Email: ruvit21@snu.ac.kr

Background and aims: Steatotic liver disease (SLD) subtypes have differing etiologies and include metabolic dysfunction-associated steatotic liver disease (MASLD), metabolic dysfunction and alcohol-associated liver disease (MetALD), and alcohol-associated liver disease (ALD). These entities share overlapping histopathologic features with overall fibrosis stage being the strongest predictor of liver-related outcomes. However, the conventional fibrosis staging system is semi-quantitative and constrained in its evaluation of any etiology-specific differences. We aimed to evaluate etiology-specific fibrosis distribution using a quantitative digital pathology approach.
Method: From the Boramae Hospital cohort, 88 liver biopsies from three SLD subtypes (28 MASLD, 30 MetALD, and 30 ALD) were selected based on histopathologic findings and demographics, stratified by NASH CRN fibrosis stages (F0-F4). Unstained biopsy sections were imaged by HistoIndex's second harmonic generation/two-photon excitation fluorescence (SHG/TPEF) microscopy for the quantification of qFibrosis continuous values, amount of SHG-detected collagen in biopsies overall (%SHG) and collagen amount in five specific hepatic zones - portal, periportal, zone 2, pericentral, and central vein. These measures were compared in the three disease groups across fibrosis stages.
Results: Correlation between NASH CRN fibrosis stages and qFibrosis values was strongest in MASLD (Spearman's $\rho = 0.91$), followed by ALD ($\rho = 0.81$) and MetALD ($\rho = 0.72$). While qFibrosis values did not differ significantly between disease groups at the same fibrosis stage, overall collagen amount (%SHG) and zonal collagen amounts showed etiology-specific differences. At F3, %SHG was significantly higher in ALD than in MASLD ($p < 0.05$). In the periportal zone, collagen proportion was significantly higher in ALD compared to MetALD at F1 ($p < 0.05$), and was higher in both MetALD and ALD than in MASLD at F4 (both $p < 0.01$). In zone 2, collagen proportion was higher in ALD than in MetALD at F1 ($p < 0.05$) and higher than in MASLD at F4 ($p < 0.05$).
Conclusion: Quantitative digital pathology and zone-specific fibrosis analysis identifies distinct etiology-specific collagen burden and zonal fibrosis patterns among MASLD, MetALD and ALD, despite identical conventional fibrosis stages. These findings underscore the limits of the conventional staging system and support the value of etiology-adapted quantitative fibrosis assessment.

THU-175

Dynamic transitions in steatotic liver disease subtypes and risk of liver-related events: a nationwide cohort study

Yewan Park[1], Jooyi Jung[2], Seungbong Han[2], Gi-Ae Kim[1]. [1]*Kyung Hee University Hospital, Seoul, Korea, Rep. of South;* [2]*Korea university, Seoul, Korea, Rep. of South*
Email: antiankle@naver.com

Background and aims: Steatotic liver disease (SLD) is a dynamic condition, yet most studies rely on single-time-point assessments, leaving the prognostic impact of its subtype transitions unclear. This study aimed to investigate the association between SLD subtype transitions and the risk of long-term liver-related events (LREs).
Method: From the Korean National Health Insurance Service database, adults who underwent national health checkups in both 2015 and 2017 were recruited. SLD subtypes included metabolic dysfunction–associated SLD (MASLD), metabolic dysfunction–associated alcohol-associated SLD (MetALD), and alcohol-associated liver disease (ALD). Transitions were classified into stable, regression, and progression. LREs included incident liver cirrhosis, hepatocellular carcinoma, liver transplantation, and liver-related mortality. Subdistribution hazard ratios (sHRs) were estimated using Fine–Gray competing-risk models.
Results: Among 1,988,878 individuals, 21.7% transitioned over two years: 11.3% progressed, whereas 10.4% regressed. Across all SLD subtypes, the progression group showed an increased risk of LREs compared with the stable group (sHR, 1.33; 95% confidence interval [CI], 1.28–1.39), whereas the regression group showed attenuated risk

(sHR, 0.86; 95% CI, 0.83–0.88). The findings were consistent within each SLD subtype of no SLD, MASLD, MetALD, and ALD. Sensitivity analyses stratified by sex, body mass index, and fatty liver index thresholds of >60 demonstrated comparable findings.
Conclusion: We found that progression to more advanced SLD subtypes was associated with increased risks of LREs, whereas regression to less advanced subtypes or no SLD was associated with substantial risk reduction. The findings can contribute to communicating the necessity of improving SLD subtypes through lifestyle modification, such as reducing alcohol intake or improving metabolic risk factors.

THU-179
Ethnic differences in non-invasive tests, disease severity, and liver-related outcomes in a diverse Canadian population with metabolic dysfunction-associated steatotic liver disease
Andre Jeyarajan[1], Chinmay Bera[2], Ravikiran Sindhuvalada Karnam[3], Natalie Simonian[4], Maxwell Tong[4], Leila Amiri[4], Nashla Hamdan[4], Keyur Patel[4]. *[1]University of Toronto, Department of Medicine, Toronto, Canada; [2]University of Arkansas for Medical Sciences, Division of Gastroenterology and Hepatology, Little Rock, United States; [3]Narayana Health City, Bengaluru, India; [4]University Health Network, University of Toronto, Division of Gastroenterology and Hepatology, Toronto, Canada*
Email: a.jeyarajan@mail.utoronto.ca

Background and aims: Non-invasive tests (NITs) are recommended to identify Metabolic dysfunction-associated steatotic liver disease (MASLD) patients with advanced MASLD fibrosis (F3–4). Although there are racial/ethnic disparities in MASLD severity, NITs were validated in predominantly White populations. Our aims were to (1) characterize the performance of NITs in predicting advanced fibrosis and (2) describe the severity of MASLD and liver-related outcomes based on race/ethnicity.
Method: Retrospective, observational cohort study at a single Canadian tertiary-care centre. We included patients with biopsy-proven MASLD from 1995 to 2025. NITs evaluated were FIB-4, NFS, liver stiffness measurement (LSM), Agile 3+, and MAFLD fibrosis score (MFS) at validated thresholds. Liver-related outcomes included hepatic decompensation, hepatocellular carcinoma (HCC), and liver transplant (LT).
Results: Our cohort of 817 patients included 434 (53.1%) White, 90 (11%) South Asian, 88 (10.8%) East Asian, 94 (11.5%) Southeast Asian, 61 (7.5%) Latin American, and 50 (6.1%) Other (27 Black, 22 Middle Eastern, one Indigenous). Advanced fibrosis (≥F3) prevalence was 31.8% (East Asians) to 56% (Whites). For NITs, AUROC range for F3–4 were 0.79–0.85 for Whites, 0.74–0.92 for South Asians, 0.79–0.87 for East Asians, 0.75–0.91 for Southeast Asians, 0.80–0.86 for Latin Americans, and 0.80–0.87 for Others. FIB-4 had higher diagnostic performance for F3–4 in Southeast Asians compared to Whites (AUROC: 0.89 vs. 0.79, $p = 0.01$); other NITs were not significant. On multivariable regression analysis, East Asian ethnicity was a negative predictor of advanced fibrosis/cirrhosis at baseline. During follow-up over mean 5.0 ± 5.1 years, 98/759 patients at risk developed hepatic decompensation with the rate per 100 person-years highest for Whites (3.25) and Latin Americans (3.16) and lowest for East Asians (0.75). 38/806 patients at risk developed HCC, with incidence highest for Latin Americans and lowest for East Asian and Others. 49/817 of patients underwent LT, with incidence highest for South Asians and lowest for Southeast Asians. On multivariable Cox regression analysis, East ($p = 0.05$) and Southeast Asians ($p = 0.01$) had lower risks of hepatic decompensation compared to Whites.
Conclusion: NIT performance for predicting MASLD F3–4 was similar across ethnic groups. Latin Americans had high rates of hepatic decompensation and HCC development during follow-up, while East and Southeast Asians had the lowest risks of hepatic decompensation.

THU-180
Health related quality of life in steatotic liver disease patients over time: impact of extra-hepatic comorbidities
Katrina Pekarska[1], Ian Rowe[1], Richard Parker[1]. *[1]Leeds Teaching Hospitals NHS Trust, University of Leeds, Leeds, United Kingdom*
Email: katrina.pekarska@gmail.com

Background and aims: Health-related quality of life (HRQL) is increasingly recognised as an important patient-reported outcome in steatotic liver disease (SLD). Previous studies have shown reduced HRQL in SLD, driven not only by liver fibrosis but also by metabolic and psychosocial factors, highlighting the need to characterise how SLD impacts patients over time. We investigated patient reported HRQL and changes over time.
Method: We conducted a single-centre observational cohort study of adults with SLD managed through a UK primary care assessment pathway. The EQ-5D-5L questionnaire was administered at baseline following clinical assessment/brief intervention and repeated by telephone at 6 months. Data on demographics, comorbidities, alcohol intake, and non-invasive fibrosis measures were collected. EQ-5D index values were derived using the England value set.
Results: A total of 116 patients completed EQ-5D-5L at baseline and at six months. Mean age was 56 ± 13 years, 68% were male, 72% were obese (BMI≥30), 34% had diabetes, the median Charlson comorbidity index was 2 (IQR 1–4). Most participants had MASLD (n = 92), with 12 MetALD and 12 ALD. There was no significant change in mean EQ-5D index over time (0.81 ± 0.23 vs 0.84 ± 0.22; mean difference 0.028 ± 0.154, p = 0.11). Median EQ-VAS (visual analogue scale) increased from 73 (IQR 60–80) to 75 (IQR 68.8–85.0), p = 0.039. The median within-patient change was +4.5 points (IQR −5 to +10) and 35% experienced a clinically meaningful improvement (≥10 points). There were no differences in baseline HRQL between SLD subtypes. In univariable analyses, musculoskeletal (MSK) conditions (β = −0.29, p < 0.001) and anxiety/depression (β = −0.17, p = 0.020) were associated with lower baseline EQ-5D index. In multivariable analyses adjusting for age, sex, BMI, and liver stiffness (kPa), MSK conditions remained independently associated with lower EQ-5D index (β = −0.26, p < 0.001). Liver stiffness showed a weak, non-significant association with EQ-5D index at follow-up (β = −0.002 per kPa, p = 0.093). After adjustment for baseline HRQL, no variables independently predicted change in EQ-5D index over time.
Conclusion: HRQL is moderately impaired in patients with SLD and remained largely stable over six months. Extra-hepatic comorbidities, particularly MSK and anxiety/depression, are the main drivers of reduced HRQL, highlighting the need for holistic care alongside liver-directed management. Treatments addressing extra-hepatic conditions may therefore be of greatest benefit.

THU-181
Significant hepatic fibrosis identified by serologic scores is associated with a higher risk of advanced colorectal neoplasia: a case-control study
Lucia Pinzon Uribe[1], Davinia Sacramento Luis[1], Inmaculada Alonso Abreu[1], Jesus Barreto Davila[1], Carla Amaral[1], Dalia Morales[1], Felicitas Diaz-Flores[1], Onofre Alarcon[1], Alejandro Jiménez Sosa[1], Manuel Hernández-Guerra[1,2]. *[1]Hospital Universitario de Canarias, La Laguna, Spain; [2]Universidad de La Laguna, La Laguna, Spain*
Email: mhernand@ull.edu.es

Background and aims: Metabolic dysfunction–associated steatotic liver disease (MASLD), present in up to 80% of patients with metabolic syndrome (MS), has been independently associated with the development of advanced neoplasia (AN), including colorectal cancer (CRC) and advanced adenoma (AA). Both risk factors are also closely linked to the progression of hepatic fibrosis. However, no studies have specifically examined the relationship between liver fibrosis and the presence of AN.

Method: We conducted a retrospective case–control study including all patients undergoing colonoscopy during May from 2003 to 2024. Cases had AN, and two age- and sex-matched controls without AN were randomly selected from the same month. Demographic data, tobacco and significant alcohol intake (≥30 g/day in men and ≥20 g/day in women), MetS-related clinical variables, laboratory parameters for APRI and FIB-4, and imaging findings (ultrasound/CT) were collected. Patients with high-risk conditions for AN (family history of CRC, prior AN, or inflammatory bowel disease) or with chronic liver diseases unrelated to MASLD were excluded. Statistical analysis included bivariate comparisons and multivariable logistic regression to identify independent associations with AN including the study period.
Results: A total of 2,611 subjects were included: 548 AN cases (mean age 68.1 ± 12.5 years; 67.7% males) and 2,063 controls (62.5 ± 15.4; 55.8%). After matching, cases (n = 548) and controls (n = 1,369) showed similar rates of aspirin use, hypertension, diabetes, dyslipidemia, and Charlson comorbidity index ≥3. Cases had higher alcohol consumption (32.6% vs 27.7%, p = 0.019), smoking prevalence (43.7% vs 37.5%, p = 0.007), and ≥2 MetS components (49.4% vs 40%, p = 0.005). APRI>0.5 (16.5% vs 5.7%) and FIB-4 > 1.3 (54% vs 44.7% were more frequent in cases (all p < 0.001), consistently across the study period. In multivariable analysis, significant hepatic fibrosis and smoking were independently associated with AN. No temporal interaction was observed between fibrosis indices and AN. Among patients with imaging-confirmed hepatic steatosis (n = 194), cases had higher rates of APRI>0.5 (28.8% vs 10.4%, p = 0.049) and FIB-4 > 1.3 (40% vs 30.2%, p = 0.063).
Conclusion: Significant hepatic fibrosis estimated by non-invasive scores is independently associated with a higher risk of AN. Identifying fibrosis in individuals with metabolic risk factors and/or MASLD may improve risk stratification and guide targeted CRC screening strategies.

THU-182
The relationship between endothelial dysfunction, insulin resistance, and metabolic associated steatotic liver diseases

Kateryna Pivtorak[1], Oleksandr Ivanchuk[1], Mykola Fedzhaga[1], Natalya Pivtorak[1]. [1]*National Pirogov Memorial Medical University, Vinnytsia, Ukraine*
Email: ekaterina.pivtorak@yahoo.com.ua

Background and aims: Metabolic dysfunction associated steatotic liver disease (MASLD) is currently recognized as a significant risk factor for the development of liver cirrhosis, diabetes mellitus, and cardiovascular disease. Cardiovascular complications in MASLD aggravate disease progression and worsen patient prognosis. In recent years, increasing attention has been paid to intercellular interactions and endothelial dysfunction (ED) as key mechanisms of vascular injury in MASLD; however, ED remains insufficiently studied. This study aimed to assess the association between insulin resistance, the severity of liver fibrosis, and ED in patients with MASLD.
Method: 262 patients were examined. Levels of inflammatory mediators, endothelin-1 (ET-1), and von Willebrand factor (vWF) activity were measured. Carotid artery intima–media thickness, presence of atherosclerotic plaques and stenosis, and the HOMA-IR index were assessed. The adiponectin-to-leptin ratio was expressed as log A/L. Liver fibrosis was evaluated using transient elastography. All patients underwent ECG and echocardiographic examinations.
Results: Correlation analysis demonstrated a strong positive association between HOMA-IR and leptin levels (r = 0.8; p = 0.00166), as well as inverse correlations between HOMA-IR and adiponectin (r = −0.66; p = 0.0033) and log A/L index (r = −0.71; p < 0.001). A decrease in adiponectin accompanied by an increase in leptin was associated with worsening insulin resistance. In obese patients, C-reactive protein levels correlated positively with HOMA-IR (r = 0.58; p = 0.05), blood glucose (r = 0.44; p = 0.0045), and insulin levels (r = 0.66; p = 0.0001). Obese patients with MASLD exhibited impaired endothelium-dependent vasodilation, indicating endothelial dysfunction. Concentrations of proinflammatory cytokines (TNF-α and IL-6) in MASLD patients were 3–7 times higher than in obese individuals without MASLD. Plasma ET-1 levels showed a strong positive correlation with cardiovascular risk and cognitive impairment. Inflammatory mediators (TNF-α, IL-1, IL-6) and C-reactive protein and fibrinogen were closely associated with obesity severity, ET-1 and vWF levels, and insulin resistance, serving as predictors of cardiovascular risk.
Conclusion: MASLD development is closely linked to endothelial dysfunction, elevated leptin and systemic inflammatory markers, and reduced adiponectin levels, highlighting their combined role in increased cardiovascular risk in patients with MASLD.

THU-183
Similar hepatic outcomes in type 1 and type 2 diabetes among adults with MASLD: A U.S. propensity-matched multi-institutional cohort study

Renan Prado[1]. [1]*Cleveland Clinic Foundation, Cleveland, United States*
Email: prador2@ccf.org

Background and aims: Metabolic dysfunction–associated steatotic liver disease (MASLD) is closely linked to diabetes, yet the hepatic risk associated with type 1 diabetes (T1DM) remains poorly defined compared with type 2 diabetes (T2DM). We compared long-term liver-related outcomes between adults with MASLD and T1DM versus T2DM using a large multicenter cohort.
Method: We performed a retrospective cohort study using a federated U.S. electronic health record network including academic and community healthcare systems. Adults with MASLD were identified using validated diagnostic codes during a two-year enrollment window. Patients with pre-existing hepatic fibrosis or cirrhosis were excluded to ensure comparable baseline liver status. Individuals were stratified by diabetes phenotype (type 1 vs type 2). To minimize confounding, 1:1 propensity score matching was conducted using a set of covariates, including age, sex, race/ethnicity, hypertension, body mass index, glycemic control (HbA1c), lipid profile, renal function, and key laboratory markers of liver disease severity and MELD-Na components (albumin, bilirubin, INR, sodium, platelets, AST, ALT). Adequate covariate balance was achieved across all matched variables (standardized mean differences <0.10). Outcomes were assessed ≥90 days after index to reduce reverse causality. Patients were followed with a median follow-up of approximately four years.
Results: After propensity score matching, 7,619 MASLD patients with T1DM were well balanced with 7,619 patients with T2DM across all matched demographic, metabolic, and liver-related variables. Liver-specific outcomes were comparable between groups, including cirrhosis (HR 1.03, 95% CI 0.95–1.13; $p = 0.44$), hepatocellular carcinoma (HR 1.15, 95% CI 0.88–1.50; $p = 0.30$), variceal bleeding (HR 1.00, 95% CI 0.86–1.16; $p = 0.99$), ascites (HR 1.10, 95% CI 0.99–1.23; $p = 0.07$), and liver transplantation (HR 1.23, 95% CI 0.97–1.56; $p = 0.10$), with overlapping time-to-event curves.
In contrast, T1DM was associated with a modest but statistically significant increase in all-cause mortality (HR 1.09, 95% CI 1.00–1.19; $p = 0.049$) and in the composite major adverse liver outcome (HR 1.09, 95% CI 1.00–1.18; $p = 0.05$), although absolute risk differences were small.
Conclusion: In this large, real-world propensity-matched cohort, adults with MASLD demonstrated comparable longterm liver-specific outcomes irrespective of diabetes phenotype after rigorous adjustment for metabolic and liver-related factors.

THU-184

Characterization of cardiac electrophysiological subtypes in metabolic dysfunction-associated steatotic liver disease

Jiang Bai[1,2], Shanghao Liu[1,2], Bicheng Ye[1,2], Yilin Zhang[1,2], Yang Bu[3], Jing Wang[4], Gao-Jun Teng[5], Xiaolong Qi[1,2]. *[1]Liver Disease Center of Integrated Traditional Chinese and Western Medicine, Department of Radiology, Zhongda Hospital, Medical School, Southeast University, Nurturing Center of Jiangsu Province for State Laboratory of AI Imaging & Interventional Radiology (Southeast University), Nanjing, China, Basic Medicine Research and Innovation Center of Ministry of Education, Zhongda Hospital, Southeast University; State Key Laboratory of Digital Medical Engineering, Nanjing, China, Nanjing, China; [2]Basic Medicine Research and Innovation Center of Ministry of Education, Zhongda Hospital, Southeast University, State Key Laboratory of Digital Medical Engineering, Nanjing, China, Nanjing, China; [3]Department of hepatobiliary surgery, General Hospital of Ningxia Medical University, Yinchuan, 750004 Ningxia, China, Ningxia, China; [4]Scientific research department, General Hospital of Ningxia Medical University, Yinchuan, 750004 Ningxia, China, Ningxia, China; [5]Zhongda Hospital, Southeast University, Nanjing, China, Nanjing, China*
Email: qixiaolong@vip.163.com

Background and aims: The potential utility of routinely acquired electrocardiographic (ECG) parameters for risk stratification within Metabolic dysfunction-associated steatotic liver disease (MASLD) remains unexplored. This study aimed to identify cardiac electrophysiological subtypes of MASLD using ECG data and to evaluate their associated clinical outcomes.

Method: We analyzed data from 8,848 adults across two independent cohorts: a cross-sectional cohort from China (n = 487) for subtype discovery and a prospective longitudinal cohort from the UK Biobank (n = 8,361) for validation and outcome analysis. Eight ECG parameters were selected for cluster analysis: ventricular rate, P-wave duration, PQ interval, QRS duration, QTc interval, P axis, R axis, and T axis. Unsupervised clustering was performed using the partitioning around medoids (PAM) algorithm. The derived subtypes were subsequently examined for associations with incident chronic liver disease (CLD) and cardiovascular disease (CVD) in the UK Biobank cohort using Cox proportional hazards models. CLD were defined according to the following ICD-10 codes: C22.0, I85.0, I85.9, K70, K72.1, K72.9, K73, K74.0, K74.1, K74.2, K74.6, K76.0, K76.6, K76.7, K76.8, K76.9, Z94.4. CVD were defined using ICD-10 codes I20–I25, I60–I64, I69, and G45.

Results: PAM clustering based on the eight ECG variables delineated six distinct phenotypic clusters. The solution demonstrated acceptable internal validity (mean silhouette coefficient = 0.118; Calinski-Harabasz index = 53) and stability (mean Jaccard similarity = 0.58 ± 0.1). Cluster 6, characterized by prolonged P-wave duration and PQ interval, exhibited a significantly lower risk for incident CLD over a median 13.7-year follow-up (HR 0.59, 95% CI 0.39–0.91, p = 0.017) but a concurrently higher risk for CVD (HR 1.40, 95% CI 1.07–1.83, p = 0.014) compared to other clusters. Cluster 2, defined by elevated T- and R-axis amplitudes, was associated with increased CVD incidence (HR 1.40, 95% CI 1.06–1.86, p = 0.018). Similarly, Cluster 3, characterized by prolonged QRS duration, was linked to higher CVD risk (HR 1.46, 95% CI 1.11–1.92, p = 0.007).

Conclusion: ECG-based phenotyping identifies specific high-risk MASLD subtypes with divergent prognostic profiles. These findings highlight the potential of routine ECG parameters as a simple, non-invasive tool for risk stratification in MASLD, to facilitate targeted monitoring and personalized management.

THU-185-YI

Heterogeneous vulnerability pathways in metabolic dysfunction-associated steatotic liver disease (MASLD): adiposity vs. genetic susceptibility

Mariana Ramírez-Mejía[1,2], Samuel Canizales-Quinteros[3], Hugo Villamil-Ramírez[3], Guadalupe Ponciano-Rodriguez[4], Nahum Méndez-Sánchez[2,4]. *[1]Plan of Combined Studies in Medicine (PECEM-MD/PhD), Faculty of Medicine, National Autonomous University of Mexico, Mexico City, Mexico; [2]Liver Research Unit, Medica Sur Clinic & Foundation, Mexico City, Mexico; [3]Unidad de Genómica de Poblaciones Aplicada a la Salud, Facultad de Química, Universidad Nacional Autónoma de México (UNAM)/Instituto Nacional de Medicina Genómica (INMEGEN), Mexico City, Mexico; [4]Faculty of Medicine, National Autonomous University of Mexico, Mexico City, Mexico*
Email: nmendez@medicasur.org.mx

Background and aims: Metabolic dysfunction-associated steatotic liver disease (MASLD) arises from heterogeneous pathways involving adiposity, lifestyle factors and biological vulnerability. While overweight/obesity-related MASLD is largely adiposity-driven, lean MASLD may reflect a distinct vulnerability profile. We aimed to evaluate the independent contribution of adiposity, lifestyle, cardiometabolic factors, and genetic susceptibility to MASLD and to assess how their relevance varies among lean individuals and those with overweight/obesity.

Method: We evaluated 468 adults (276 men and 192 women; mean age 46.7 ± 9.0 years) who underwent clinical and biochemical evaluation, dietary intake assessment, physical activity quantification and PNPLA3 rs738409 genotyping (G allele carriers vs. non-carriers). Associations with MASLD were examined using multivariable logistic regression in the overall population and stratified by adiposity status.

Results: In the overall population, MASLD was primarily associated with adiposity, with body mass index showing a strong and consistent association (OR 1.59; 95% CI 1.39–1.86; p < 0.001). 76.9% of participants were PNPLA3 rs738409 G-allele carriers, and carriage remained independently associated with MASLD after full adjustment (OR 3.28; 95% CI 1.42–7.97; p = 0.007). Physical activity showed a modest inverse association, whereas total energy intake, macronutrient composition, and diabetes were not independently associated. Hypertension showed a positive but non-significant trend. Among lean individuals, MASLD was mainly determined by genetic susceptibility, with PNPLA3 rs738409 as the principal independent factor (OR 4.60; 95% CI 1.15–25.29; p = 0.047), while lifestyle and cardiometabolic variables were not independently associated. In contrast, among individuals with overweight/obesity, MASLD reflected a risk profile dominated by adiposity, within which genetic susceptibility remained relevant (OR 3.06; 95% CI 1.12–8.56; p = 0.029). In this group, physical activity exerted a significant protective effect and hypertension emerged as a strong marker of metabolic burden, while diet composition did not independently influence risk.

Conclusion: MASLD reflects different combinations of risk factors, with adiposity as the main determinant. Genetic susceptibility predominates in lean individuals, while in individuals with overweight/obesity risk integrates adiposity, persistent genetic vulnerability and physical activity, supporting the need to move beyond uniform risk frameworks.

THU-186-YI

Distinct cardiometabolic profiles drive divergent HCC risk trajectories in advanced fibrosis-affected MASLD patients

Mario Romeo[1], Marcello Dallio[1], Fiammetta Di Nardo[1], Carmine Napolitano[1], Paolo Vaia[1], Claudio Basile[1], Luigi Di Puorto[1], Giuseppina Martinelli[1], Marco Niosi[1], Alessandro Federico[1]. *[1]Hepatogastroenterology Division, Department of Precision Medicine, University of Campania Luigi Vanvitelli, Piazza Miraglia 2, 80138, Naples (Italy), Naples, Italy*
Email: marioromeo@virgilio.it

Background and aims: Metabolic dysfunction (MD)-associated steatotic liver disease (MASLD) is defined by steatotic liver disease (SLD) in the presence of at least one cardiometabolic risk factor (CMRF)—obesity, type 2 diabetes, dyslipidemia, or hypertension—in the absence of alternative causes. MASLD may progress to steatohepatitis (MASH) and advanced fibrosis (AF), significantly increasing the risk of hepatocellular carcinoma (HCC). While cardiovascular risk is known to escalate with MD severity, the impact of cumulative CMRF burden on HCC development remains poorly characterized. This study aimed to assess differential HCC risk and timing by stratifying MASLD-AF patients according to distinct CMRF combinations.
Method: Biochemical, clinical, and Liver Stiffness (LSM) data from 1921 SLD individuals, archived in the Health Documents Digitization Repository of the "Luigi Vanvitelli" University Hospital (January 2010–Oct 2020), were retrospectively analyzed to identify subjects fulfilling EASL-proposed MASLD criteria and exhibiting LSM-AF. A non-redundant permutation of CMRFs—obesity (Obe), dysglycaemia or type 2 diabetes (Gly), dyslipidemia (Lip), and elevated blood pressure (Press)—was applied, yielding 4 groups with 15 distinct MD profiles: Group 1) One CMRF (n:311) [1a: Obe (n:130); 1b: Gly (n:40); 1c: Lip (n:91); 1d: Press (n:50)]; Group 2) Two CMRFs (n:840) [2a: Obe-Gly (n: 140); 2b: Obe-Lip (n:120); 2c: Obe-Press (n:150); 2d: Gly-Lip (n:130); 2e: Gly-Press (n:140); 2f: Lip-Press (n:160)]; Group 3) Three CMRFs (n:680) [3a: Obe-Gly-Lip (n:190); 3b: Obe-Lip-Press (n:170); 3c: Obe-Gly-Press (n:140); 3d: Gly-Lip-Press (n:180)]; Group 4) Four CMRFs (Obe-Gly-Lip-Press) (n:90). HCC diagnosis and staging (BCLC) were retrospectively recorded over a 5-year follow-up.
Results: Patients with ≥3 CMRFs exhibited significantly higher HCC risk [HR: 3.12, p:0.001]. Within this subgroup, Gly-Lip-Press, Obe-Gly-Lip [HR: 1.129, p:0.034], and Obe-Gly-Lip-Press [HR: 2.21, p:0.002] showed progressively increasing 5-year HCC incidence and decreasing median time to occurrence (48.2 vs 41.3 vs 28.1 months; $p < 0.0001$) (Fig. 2). Notably, the BCLC-C stage at diagnosis was more frequent in Obe-Gly-Lip (31%) compared to other Group 3 profiles (<10%; $p < 0.0001$).
Conclusion: CMRF-based stratification reveals substantial heterogeneity in HCC risk among MASLD-AF patients, supporting the implementation of personalized surveillance strategies taking into account the metabolic burden.

THU-187
Investigating the role of the IL-17/23 Pathway in MASLD progression

Giuseppe Rusignuolo[1], Annika Keitel[1], Lara Kelsch[1], Thomas Wiggers[2], Morten Karsdal[2], Diana Julie Leeming[2], Nils Venhoff[3], Ute Woelfle[4], Christoph Schempp[4], Tobias Boettler[1].
[1]Uniklinik Freiburg, Department of Hepatology, Gastroenterology, Endocrinology, and Infectious Diseases, Freiburg im Breisgau, Germany; [2]Nordic bioscience, Biomarkers & research, Herlev, Denmark; [3]Uniklinik Freiburg, Department of Rheumatology and Clinical Immunology, Freiburg, Germany; [4]Uniklinik Freiburg, Department of Dermatology, Freiburg, Germany
Email: giuseppe.rusignuolo@uniklinik-freiburg.de

Background and aims: Progression of MASLD is driven by inflammatory and fibrogenic pathways that are incompletely understood. Increasing evidence implicates the IL-17/23 axis in hepatic inflammation and fibrosis. Biologic inhibitors of this pathway are widely used in psoriasis. This study aimed to evaluate the impact of IL-17/23 inhibition on MASLD using non-invasive fibrosis, steatosis, and immunological markers.
Method: In this prospective, single-center observational cohort study, patients with psoriasis or pso-arthritis receiving biologic therapy targeting either the IL-17/23 axis or TNF were followed for 6–12 months. Assessments were performed at baseline (t0) and follow-up (t2). Liver fibrosis and steatosis were evaluated by transient elastography with liver stiffness measurement (LSM) and controlled attenuation parameter (CAP), Fibrosis-4 score (FIB-4), and serum biomarkers including cytokeratin-18 (CK18) and type III procollagen N-terminal propeptide (Pro-C3). Immunological profiling included Th17/T regulatory cell ratios in peripheral blood mononuclear cells and inflammatory cytokines (IL-6, IL-22, leptin). The primary endpoint was change in LSM; secondary endpoints were changes in the other parameters measured.
Results: Of 56 enrolled patients, 38 were included in the final analysis: Group A, IL-17/23 inhibitor–naïve patients initiating IL-17/23 blockade (n = 9); Group B, TNF inhibitor–naïve patients (n = 6); and Group C, long-term IL-17/23–treated patients (n = 23). Longitudinal changes (t2–t0) were compared using the Mann–Whitney U test. Group A showed a significantly greater improvement in LSM compared with Group B ($p = 0.025$). No significant differences were observed for the secondary endpoints Pro-C3, CK18, IL-6, IL-22, leptin, CAP, FIB-4, and Th17/Treg ratio at group level. However, consistent trends favoring Group A were observed across multiple markers. A subset of patients initiating IL-17/23 inhibition demonstrated concordant improvement in LSM, fibrosis markers (Pro-C3, CK18), and inflammatory markers (Th17/Treg ratio, IL-6).
Conclusion: Initiation of IL-17/23 inhibition was associated with significant improvement in liver stiffness compared with TNF inhibition, supporting a role of the IL-17/23 axis in MASLD-related fibrogenesis. Improvements in additional non-invasive fibrosis and immune markers in a subgroup of patients suggest an immune-driven, treatment-responsive phenotype. Larger prospective studies with longer follow-up and histological validation are needed to confirm these findings.

THU-188
Age-related clinical features of metabolic dysfunction associated steatotic liver disease in a real-world cohort

Ryotaro Sakamori[1], Yutaro Abe[1], Sumiko Yoshida[2], Atsumasa Komori[3], Kiyoshi Furuta[4], Keisuke Ario[5], Kana Hirooka[6], Kazuhiro Sugi[7], Motoyuki Kohjima[8], Atsushi Naganuma[9], Takayoshi Suga[10], Shiro Yokohama[11], Shintaro Takaki[12], Minoru Tomizawa[13], Yoko Nakamura[14], Tsutomu Yamashita[15], Hiroshi Yatsuhashi[3].
[1]NHO Osaka National Hospital, Osaka, Japan; [2]NHO Shikoku Medical Center for Children and Adults, Zentsūji, Japan; [3]NHO Nagasaki Medical Center, Omura, Japan; [4]NHO Matsumoto Medical Center, Matsumoto, Japan; [5]NHO Ureshino Medical Center, Ureshino, Japan; [6]NHO Ehime Medical Center, Tōon, Japan; [7]NHO Kumamoto Medical Center, Kumamoto, Japan; [8]NHO Kyushu Medical Center, Fukuoka, Japan; [9]NHO Takasaki Genral Medical Center, Takasaki, Japan; [10]NHO Shibukawa Medical Center, Shibukawa, Japan; [11]NHO Asahikawa Medical Center, Asahikawa, Japan; [12]NHO Kure Medical Center, Kure, Japan; [13]NHO Shimoshizu National Hospital, Yotsukaidō, Japan; [14]NHO Sagamihara National Hospital, Sagamihara, Japan; [15]NHO Oita Medical Center, Oita, Japan
Email: sakamori.ryotaro.bp@mail.hosp.go.jp

Background and aims: Although epidemiological studies on steatotic liver disease (SLD) using health checkup or administrative data are abundant, evidence from real-world clinical practice remains limited, particularly in Asian populations. Because cardiometabolic risk factors such as diabetes mellitus, hypertension, and dyslipidemia change with aging, it is unclear whether elderly and non-elderly patients with metabolic dysfunction associated steatotic liver disease (MASLD) should be managed similarly. This study aimed to clarify age-specific clinical characteristics and outcomes of MASLD in a Japanese real-world cohort.
Method: A prospective registry of patients with SLD was conducted across 31 National Hospital Organization hospitals in Japan. Patients were stratified by age using 65 years as the cutoff, and metabolic factors, fibrosis markers, and clinical outcomes were compared between elderly and non-elderly patients.
Results: Among 410 registered patients, 375 were analyzed, of whom 329 (87.7%) met the diagnostic criteria for MASLD. The non-elderly

group (younger than 65 years) included 178 patients, and the elderly group (65 years or older) included 151 patients. Male predominance was observed in the non-elderly group, whereas female predominance was observed in the elderly group. Patients meeting the body mass index criterion were more frequent in the non-elderly group, while hypertension was more frequent in the elderly group; other cardiometabolic risk factors and related treatments were comparable. Platelet count, aspartate aminotransferase, alanine aminotransferase, and total cholesterol levels were lower in the elderly group. Fibrosis markers, including hyaluronic acid, Mac-2 binding protein glycosylation isomer, and the fibrosis 3 index, were higher in the elderly group, and approximately 10% of patients were suspected to have advanced liver fibrosis. Alanine aminotransferase levels decreased over 1 year, with a greater reduction in the non-elderly group. The cumulative incidence of malignancies, cardiovascular events, and liver-related events was 0.8% at 6 months, 2.8% at 12 months, and 4.6% at 18 months, with a trend toward higher incidence in the elderly group.
Conclusion: In this Japanese real-world cohort, elderly and non-elderly patients with MASLD showed distinct cardiometabolic and fibrosis-related characteristics. The higher prevalence of advanced liver fibrosis and increased clinical events in elderly patients suggest that age-specific management strategies may be required.

THU-189

Ultrasound-assessed skeletal muscle quality is associated with functional and metabolic impairment in metabolic dysfunction-associated steatotic liver disease

Anna Sheptulina[1], Elvira Mamutova[1], Julia Golubeva[1], Karina Gladun[2], Elena Grigorenko[2], Natalia Mitkovskaya[2], Oxana Drapkina[1]. *[1]National Medical Research Center for Therapy and Preventive Medicine, Moscow, Russian Federation; [2]State Institution "Republican Scientific and Practical Center 'Cardiology'", Minsk, Belarus*
Email: sheptulina.anna@gmail.com

Background and aims: Skeletal muscle mass (SMM) and function play an important role in the pathogenesis of metabolic dysfunction–associated steatotic liver disease (MASLD). However, commonly used body composition assessment methods, such as bioelectrical impedance analysis and dual-energy X-ray absorptiometry (DXA), quantify SMM but do not reflect muscle quality, including fat infiltration and stiffness (myosteatosis). In contrast, ultrasound (US) examination of skeletal muscles is a rapid, bedside-applicable method that allows assessment of both quantitative and qualitative muscle characteristics. This study aimed to evaluate the association between US-derived qualitative muscle parameters, body composition, and muscle function in patients with MASLD.
Method: A total of 366 patients with MASLD were included. MASLD was diagnosed based on US evidence of steatosis, exclusion of other liver disease etiologies, and the presence of at least one cardiometabolic risk factor. US assessment of the right rectus femoris (RFM) and vastus intermedius muscles (VIM) included grayscale imaging, shear wave elastography, and compression elastography to evaluate muscle echogenicity (Heckmatt scale) and stiffness. Body composition was assessed using DXA. Relative grip strength (rGS) was calculated as GS divided by body mass index (BMI). Muscle function was evaluated via the 4-meter walk test (4MWT).
Results: The median age was 57 years (nterquartile range [IQR]: 47–63.5); 62.9% of patients were female. All patients overweight or obese, had arterial hypertension and dyslipidemia. Decreased SMM was observed in 75 (20.5%) patients. Higher RFM and VIM echogenicity (grades III–IV) was associated with higher BMI and waist circumference ($p < 0.001$ for both), increased fat mass and body fat percentage ($p = 0.009$ for both), longer 4MWT time ($p < 0.001$), and lower rGS ($p < 0.001$). Grade IV echogenicity was additionally associated with lower high-density lipoprotein cholesterol (HDL-C) levels ($p < 0.001$) and higher uric acid levels ($p = 0.004$). Patients with predominantly soft areas on muscle elastograms had lower SMM ($p = 0.047$), while RFM stiffness was higher in patients with decreased SMM ($p = 0.009$).
Conclusion: Ultrasound-derived qualitative muscle parameters are closely associated with body composition, muscle function, and metabolic abnormalities in MASLD. Muscle ultrasound may serve as a practical, non-invasive tool for identifying impaired muscle quality and early sarcopenic changes beyond conventional anthropometric assessment.

THU-190

Decreased skeletal muscle mass is associated with an adverse metabolic profile in patients with metabolic dysfunction-associated steatotic liver disease

Anna Sheptulina[1], Elvira Mamutova[1], Julia Golubeva[1], Karina Gladun[2], Elena Grigorenko[2], Natalia Mitkovskaya[2], Oxana Drapkina[1]. *[1]National Medical Research Center for Therapy and Preventive Medicine, Moscow, Russian Federation; [2]State Institution "Republican Scientific and Practical Center 'Cardiology'", Minsk, Belarus*
Email: sheptulina.anna@gmail.com

Background and aims: Increasing evidence suggests the association between skeletal muscles and metabolic dysfunction–associated steatotic liver disease (MASLD), indicating that deterioration of metabolic state may negatively impact skeletal muscle mass (SMM), strength, and function. The aim of the present study was to evaluate the assosiation between biochemical metabolic parameters and SMM in patints with MASLD.
Method: A total of 366 patients with MASLD were enrolled in the study. The diagnosis of MASLD was established based on ultrasonographic evidence of hepatic steatosis, exclusion of other causes of liver disease according to laboratory evaluation, and the presence of at least one cardiometabolic risk factor. Body composition was evaluated using dual-energy X-ray absorptiometry (DXA) (Lunar iDXA, GE Healthcare, USA). Decreased skeletal muscle mass was defined as an appendicular skeletal muscle mass–to–body mass ratio (ASMM/M) <23.47% in women and <28.27% in men.
Results: The median age of the cohort was 57 years (interquartile range [IQR]: 47–63.5 years), with women comprising 62.9% of the study population. The median body mass index (BMI) was 31.8 kg/m^2 (IQR: 28.7–34.9). All participants had obesity, arterial hypertension, and dyslipidemia. Decreased SMM was identified in 75 (20.5%) patients. Compared with MASLD patients with preserved SMM, those with decreased SMM exhibited higher serum uric acid ($p = 0.001$), triglycerides ($p = 0.031$), and gamma-glutamyl transferase activity ($p = 0.029$), along with lower HDL-cholesterol levels ($p = 0.005$). Patients with decreased SMM also demonstrated higher systolic and diastolic blood pressure ($p = 0.001$ and $p = 0.008$, respectively), as well as higher BMI and waist circumference ($p < 0.001$ for both).
Conclusion: In patients with MASLD, decreased skeletal muscle mass is common and is associated with an adverse metabolic profile, including dyslipidemia, hyperuricemia, elevated liver enzymes, and higher blood pressure. These findings support the concept of a close interaction between metabolic dysfunction and skeletal muscle impairment in MASLD and highlight the importance of assessing muscle mass as part of comprehensive cardiometabolic risk stratification in this population.

THU-191

Assessment of maternal and fetal outcomes of pregnancy in metabolic associated fatty liver disease, a prospective cohort study

Hend Shousha[1], Mira Atef[1], Wafaa El-Akel[1], Naglaa Zayed Zayed[1], Sara Raouf[1], Ayman Hany[2], Ayman Yosry[1], Sherif Hamdy[1]. *[1]Endemic medicine department, Faculty of medicine, Cairo University, Cairo, Egypt; [2]Obstetrics and gynecology department, Cairo University, Cairo, Egypt*
Email: hendshousha@yahoo.com

Background and aims: Pregnancy is a pro-inflammatory, pro-thrombotic, insulin-resistant, and hyperlipidemic state. This study intends to evaluate the impact of Metabolic-associated Fatty Liver Disease (MAFLD) on Pregnancy outcomes.

Method: This cohort study involved pregnant women in the third trimester recruited from the obstetrics department, Faculty of medicine, Cairo University, conducted from June 2023 to June 2024. Baseline demographics, pre-pregnancy body mass index (BMI), comorbidities, acoustic radiation force impulse (ARFI) and Transient elastography were performed assessing liver stiffness and controlled attenuation parameter (CAP). Pregnancy outcome was assessed.
Results: Out of 192 pregnant females, prevalence of MAFLD was 84 (44%). There was no significant difference in age between MAFLD and non-MAFLD groups. Gestational DM was more prevalent in the MAFLD group 16(19%) vs 10(9.3%) p 0.049. Pre-pregnancy BMI was significantly higher in MAFLD group (30.37 ± 3.39 vs 26.16 ± 3.67, p < 0.01), CAP was significantly higher in MAFLD group (274.52 ± 17.92 vs 212.90 ± 38.59, p < 0.01 and the mean ARFI of the liver 0.99 ± 0.26 vs 0.92 ± 0.20, p 0.047. Neonatal jaundice was more prevalent in the MAFLD group 58 (69%) vs 38(35%) p < 0.01. Neonates large for gestational age was observed in MAFLD group 13(15.7%) versus 6 (5.6%) p 0.021. No significant difference between the groups regarding preeclampsia, gestational hypertension, pre and post-partum hemorrhage, mode of delivery, preterm, stillbirth, neonatal ICU admission, low for gestational age. In the MAFLD group, significant correlation was observed between pre-pregnancy BMI and CAP. Bilirubin and alkaline phosphatase exhibited an inverse correlation with steatosis grade in the MAFLD group (r = –0.25, –0.24; P = 0.02 and 0.03, respectively). Triglycerides had a strong correlation with CAP and steatosis grade in the MAFLD group (r = 0.28, P = 0.02) and (r = 0.29, P = 0.01), respectively. Most of non-MAFLD group (72%) had no maternal events p 0.04. 50% of MAFLD group neonates had at least one fetal event p < 0.01. MAFLD group had either unfavorable fetal outcome or both unfavorable maternal and fetal p < 0.01. On consolidating outcome groups 91% of MAFLD group had unfavorable outcome p < 0.01. On applying multivariate binary logistic regression, in which unfavorable outcome is the dependent factor, presence of MAFLD is the only significant predictor for unfavorable outcome (P < 0.01, OR 4.25, 95% CI 1.8–10).
Conclusion: MAFLD is associated with unfavorable pregnancy outcomes.

THU-195
Phase angle cut-off values can reliably predict malnutrition in non-cirrhotic and cirrhotic MASLD patients: PhAT-LD study

Aditi Singh [1], Omkar Rudra[1], Uma Kanal[1], Shiv Kumar Sarin[1]. [1]*Institute of liver and biliary sciences, New Delhi, India*
Email: aditi.yogendra98@gmail.com

Background and aims: Malnutrition and sarcopenia are common yet under-recognized in metabolic dysfunction–associated steatotic liver disease (MASLD) and are associated with adverse outcomes. Nutritional assessment in MASLD is challenging due to altered body composition and fluid shifts. Phase angle (PhA), derived from bioelectrical impedance analysis (BIA), is a promising non-invasive marker of nutritional status, but validated cut-offs in MASLD are lacking. This study evaluated the utility of PhA for identifying malnutrition across the MASLD disease spectrum.
Method: This retrospective cross-sectional study included adults with MASLD and MASLD-related cirrhosis diagnosed using standard clinical criteria. Nutritional assessment comprised anthropometry, biochemical parameters, functional tests (handgrip strength, Liver Frailty Index, 6-minute walk test), and BIA-derived body composition analysis. Malnutrition was defined using Global Leadership Initiative on Malnutrition (GLIM) criteria. The cohort was divided into derivation (70%) and validation (30%) sets with stratified disease-stage representation. Receiver operating characteristic analysis was used to determine optimal PhA cut-offs.
Results: A total of 660 patients were analyzed: 118 with non-cirrhotic MASLD, 264 with compensated cirrhosis, and 278 with decompensated cirrhosis. Median age increased with disease severity (p < 0.001). Functional capacity declined progressively, with reduced handgrip strength, shorter 6-minute walk distance, and higher frailty scores across stages (all p < 0.001). PhA decreased stepwise from non-cirrhotic MASLD to compensated and decompensated cirrhosis (p < 0.001). GLIM-defined malnutrition was present in 51.1% overall and was highest in decompensated cirrhosis (65.1%, p < 0.001). PhA showed good diagnostic accuracy for malnutrition (AUC 0.81). Optimal PhA cut-offs were 5.05 for non-cirrhotic MASLD (AUC 0.81), 4.35 for decompensated cirrhosis (AUC 0.80), and 4.65 overall, yielding 76.8% sensitivity and 73.1% specificity. At this threshold, malnutrition was concordantly identified by both GLIM and PhA in 76.8% of patients, while 26.9% were classified as malnourished by PhA alone.
Conclusion: Phase angle is a reliable, non-invasive screening tool for detecting malnutrition in MASLD patients. The use of disease stage–specific and overall cut-offs improves nutritional risk stratification across the entire MASLD spectrum.

THU-196
Association of steatotic liver disease with pregnancy outcomes: a systematic review and meta-analysis of 74.8 million pregnant individuals

Jacqueline Slobin[1], Nina Rodriguez[1], Cecilia Katzenstein[1], Nadejda Capatina[2], Caroline Ovadia[3], Tatyana Kushner[4]. [1]*Icahn School of Medicine at Mount Sinai, New York, United States;* [2]*Guys & Saint Thomas Nhs Foundation Trust, London, United Kingdom;* [3]*University of Edinburgh, Scotland, United Kingdom;* [4]*Weill Cornell Medicine, New York, United States*
Email: jacqueline.slobin@icahn.mssm.edu

Background and aims: The prevalence of steatotic liver disease (SLD) in pregnancy has tripled over the past decade, affecting up to 18% of pregnant individuals. Prior studies report varied associations between SLD and adverse pregnancy outcomes (APOs).
Method: We conducted a systematic review and meta-analysis querying PubMed, Embase, and Web of Science for studies reporting APOs in individuals with SLD. Two independent reviewers screened titles and abstracts, full texts, and extracted data. Pooled prevalence and odds ratios (ORs) with 95% confidence intervals (CI) were calculated using random-effects models in Stata 19.
Results: Twenty-nine studies with 74.8 million pregnant individuals and 95,547 SLD cases were included. In 17 studies reporting prevalence, the pooled prevalence of SLD was 16% (95% CI, 12–20%). SLD was diagnosed by imaging (15), ICD codes (5), Hepatic Steatosis Index (5), Fatty Liver Index (1), and biopsy (1). Studies were conducted in Asia (17), North America (5), Europe (4), Australia (2), and Africa (1).
SLD was associated with gestational diabetes mellitus (OR 2.93, 95% CI, 2.42–3.52; n = 26), preeclampsia (OR 2.72, 95% CI 1.79–4.13; n = 10), gestational hypertension (OR 2.24, 95% CI 1.75–2.88; n = 7), and a composite of hypertensive disorders of pregnancy (OR 3.44, 95% CI 2.70–4.38; n = 10). Pregnant individuals with SLD were more likely to undergo cesarean birth (OR 1.84, 95% CI 1.52–2.22; n = 14) and experience postpartum hemorrhage (OR 1.64, 95% CI 1.09–2.46; n = 6). SLD was also associated with increased odds of preterm birth (<37 weeks; OR 1.89, 95% CI 1.62–2.20; n = 17), with a stronger association with very preterm birth (<32 weeks; OR 3.79, 95% CI 2.22–6.46; n = 4). In subgroup analyses of studies that diagnosed SLD using ultrasound and Fibroscan, associations with preeclampsia and postpartum hemorrhage were no longer significant, but associations with other outcomes persisted. Heterogeneity across studies was high (I^2 = 48–98%) but decreased after stratification by diagnostic method and country.
Conclusion: SLD in pregnancy was associated with increased risk of several APOs, highlighting the importance of screening, risk stratification and medical management of individuals with SLD. However, there was variability in strength of associations by SLD diagnostic modality and marked heterogeneity across studies, complicating risk interpretation. Future directions will focus on

conducting an individual participant data meta-analysis to better identify patients with SLD at risk of APOs.

THU-197

Metabolic comorbidities differentially shape dysfunctional adiposity phenotypes in MASLD

Daniel Smith[1,2], Annalisa Cespiati[1,2], Rosa Lombardi[1,2], Felice Cinque[1,2], Erika Fatta[1], Edoardo Pulixi[1], Daniela Bignamini[1], Giovanna Oberti[1], Anna Ludovica Fracanzani[1,2]. *[1]SC Medicina ad Indirizzo Metabolico, Fondazione IRCCS Cà Granda Ospedale Maggiore Policlinico, Milan, Ita, Milano, Italy; [2]Department of Pathophysiology and Transplantation, University of Milan, Italy, Milano, Italy*
Email: annalisa.cespiati@unimi.it

Background and aims: Metabolic dysfunction-associated steatotic liver disease (MASLD) is defined by liver steatosis in the presence of metabolic comorbidities. Dysfunctional adiposity, rather than adiposity alone, plays a key role in metabolic impairment. While metabolic comorbidities are risk factors for MASLD progression, their differential impact on dysfunctional adiposity remains unclear. Aim: to evaluate the distinct associations between major metabolic comorbidities and markers of dysfunctional adiposity in MASLD.
Method: We enrolled 505 MASLD patients (mean age 50 ± 12 years, 65% male) from tertiary Metabolic Liver center. Dysfunctional adiposity was assessed by epicardial adipose tissue (EAT) measured by echocardiography, and adipose tissue index (ATI, mass/height2) assessed by bioimpedance analysis. Waist circumference (WC) was considered a marker of central adiposity.
Results: Mean BMI was 28.9 ± 4.6, with 84% increased WC. Hypertension was present in 36%, dyslipidemia in 56%, diabetes in 12%, insulin-resistance (IR) in 65%. Dyslipidemia was associated with lower ATI (9.4 ± 3.9 vs 10.2 vs 4.4 kg/m^2, p = 0.04) but higher EAT (8.3 ± 2.8 vs 7.8 ± 2.7 mm, p = 0.04), without difference in WC. Hypertension was associated with higher WC (89 vs 80%, p = 0.01), ATI (10.9 ± 4.2 vs 9.1 ± 4, p = 0.001), and EAT (8.5 ± 2.8 vs7.9 ± 2.7 mm, p = 0.03). Diabetes and IR were both associated with increased WC (diabetes 95 vs 82%, p = 0.008; IR 92 vs 64%, p = 0.001) and ATI (diabetes: 12.2 ± 4.6 vs 9.4 ± 4, p = 0.001; IR: 10.5 ± 4.1 vs 7.9 ± 3.7 p = 0.001), but not with EAT. At multivariate analysis adjusted for age, sex, drugs, dyslipidemia remained independently associated with lower ATI (b = –0.5, 95%CI – 0.88 to – 0.13, p = 0.008), while its association with EAT was lost after adjustment for statin use (p = 0.81), which was independently associated with higher EAT (b = 0.49, 95%CI 0.2–0.8, p = 0.004). Hypertension was independently associated with higher ATI (b = 1.3, 95%CI 0.3–2.3, p = 0.009), as for diabetes (b = 1.9, 95%CI 0.9–2.9, p = 0.0003), and IR (b = 1.18, 95%CI 0.8–1.6, p = 0.001). Only IR remained associated with increased WC (OR 6.8, 95%CI 3.6–13.1, p = 0.001). No metabolic comorbidity showed an independent association with EAT after full adjustment.
Conclusion: Metabolic comorbidities showed distinct associations with markers of dysfunctional adiposity in MASLD. While ATI captured metabolically driven adiposity, EAT reflects a cardiovascular-oriented phenotype, supporting heterogeneous cardiometabolic trajectories in MASLD and the need for marker- specific risk stratification.

THU-198

Development of metabolic dysfunction-associated steatotic liver disease in patients with cryptogenic steatotic liver disease

Won Sohn[1], Hyunwoo Oh[1], Kyoung A Ko[1], Jae Yoon Jeong[2], Ju-Yeon Cho[3], Jung Hee Kim[4], Yong Kyun Cho[1], Yoosoo Chang[1], Seungho Ryu[1]. *[1]Kangbuk Samsung Hospital, Sungkyunkwan University School of Medicine, Seoul, Korea, Rep. of South; [2]Ewha Womans University, Seoul, Korea, Rep. of South; [3]Saint Louis University, Seoul, Korea, Rep. of South; [4]Hallym University Dongtan Sacred Heart Hospital, Seoul, Korea, Rep. of South*
Email: hand0827@naver.com

Background and aims: This study aimed to examine the development of metabolic dysfunction-associated steatotic liver disease (MASLD) in cryptogenic steatotic liver disease (SLD). We investigated the role of homeostatic model assessment of insulin resistance (HOMA-IR) and high-sensitivity C-reactive protein (hs-CRP) in cryptogenic SLD.
Method: A total of 102,431 individuals, consisting of 3,630 patients with cryptogenic SLD and 98,801 individuals without SLD and cardiometabolic factors (non-SLD group), were included in this study. The definition of MASLD was a sonographic presence of hepatic steatosis with at least one of cardiometabolic factors. The risk of MASLD development in cryptogenic SLD was assessed by comparing non-SLD group. We also assessed the risk of MASLD according to the presence of HOMA-IR and hs-CRP.
Results: The mean age was 33.7 years and 27.4% was male sex. During 6.2 years of median follow-up period, 12,580 patients with MASLD developed. Over 60% of cryptogenic SLD patients developed MASLD. The incidence rate of MASLD was significantly higher in cryptogenic MASLD than in non-SLD group (173.3/103 person-year vs. 15.8/103 person-year, p < 0.001). The risk of MASLD development was higher in cryptogenic SLD than non-SLD group (multivariable-adjusted hazard ratio [HR] 6.09, 95% confidence interval [CI] 5.80–6.39). Additionally, we analyzed the development of MASLD between non-SLD group, cryptogenic SLD with low HOMA-IR (≤2.5) and low hs-CRP (≤2 mg/L), and cryptogenic SLD with high HOMA-IR (>2.5) or high hs-CRP (>2 mg/L). Compared to non-SLD group, the risk of MASLD significantly increased in cryptogenic SLD patients with low HOMA-IR and low hs-CRP (multivariable-adjusted HR 5.59, 95% CI 5.29–5.90), and those patients with high HOMA-IR or high hs-CRP (multivariable-adjusted HR 7.87, 95% CI 6.98–8.86).
Conclusion: Cryptogenic SLD patients, particularly those with elevated HOMA-IR or hs-CRP, have an increased risk of developing MASLD. Cryptogenic SLD may represent a transitional state, and incorporating HOMA-IR or hs-CRP assessment could improve risk stratification and early identification of patients likely to progress to MASLD.

THU-201

Hormonal replacement therapy as a preventive measure in post-menopausal women with metabolic dysfunction–associated steatohepatitis

Norah Terrault[1], Jennifer Dodge[1], Laura Wilson[2], Arun J. Sanyal[3], Brent A. Neuschwander-Tetri[4], Ayako Suzuki[5]. *[1]University of Southern California, Los Angeles, United States; [2]John Hopkins Universisty, Baltimore, United States; [3]Virginia Commonwealth University, Richmond, United States; [4]St.Louis University, St. Louis, United States; [5]Duke University, Durham, United States*
Email: terrault@usc.edu

Background and aims: Cross-sectional studies suggest a link between estrogen deficiency and more advanced fibrosis and hormone replacement therapy (HRT) has been associated with less severe fibrosis in metabolic dysfunction-associated steatohepatitis (MASH); however, prospective data linking HRT exposure to longitudinal fibrosis progression using validated noninvasive tests are lacking.
Method: Women in the multicenter NASH CRN cohort with longitudinal data on HRT use (primary exposure) and liver stiffness measures (LSM) by VTCE exam (IQR/median ≤0.3) were included. Using multinominal logistic regression, relative risk ratios (RRR) for the association of demographic and clinical variables with 30% worsening or 30% improvement of LSM from baseline were estimated, selecting a multivariable female-specific model based on AIC reduction.
Results: 734 women were included: median age 56 y, 67.8% post-menopausal with 14.7% on HRT (ever), 68.9% PNPLA3 GG/CG (n = 513 tested), 48.0% low alcohol intake (>0–7 drinks/wk), 38.7%/36.5% prediabetes/T2DM, median BMI 34.2 kg/m2, 65.9% on anti-

hypertensives, 51.0% T2DM medications (8.9% on GLP1A) and 45.5% lipid meds at baseline. Of 2475 VTCE exams, the median (IQR) was 2 (1–3) per person over 2.3 (1.4–4.4) yrs follow-up. Baseline LSM was 8.1 (5.7–13.1) and median/IQR was 0.16 (0.11–0.22) with a change in LSM from baseline worsened or improved by 30% or more in 13.1% (N = 324) and 18.6% (N = 461), respectively (rest within 30% of baseline). A final model of 10 variables achieved optimal AIC values to predict worsening and improvement ≥30%: LSM at baseline, time between LSM measures, albumin, HDL, BMI, T2DM, platelet count, alkaline phosphatase (ALP), AST:ALT ratio and HRT use. Specifically, ALP was associated with worsening of LSM (RRR 1.05 per 10 units [95% CI:1.01–1.10]) and improvement (RRR 0.94 per 10 units [0.89–0.99]); ALP was not elevated in those with HRT use. Post-menopausal HRT was associated with lower risk of worsening LSM (RRR 0.63, [0.38–1.04]) but not improving LSM (RRR 1.01, [0.62–1.65]).
Conclusion: Female-specific models for prognostication offer value in a personalized medicine era. Amongst a predominantly middle-aged cohort of women with MASLD, ALP emerged as a novel marker associated with fibrosis progression/regression and HRT associated with lower risk of worsening fibrosis in post-menopausal women. This prospective demonstration of HRT's association with LSM change supports a call for randomized studies of HRT in women with MASH.

THU-202
Association between osteoporosis and the severity of steatotic liver disease
Léa Terrien[1], Jerome Boursier[1], Marine Roux[2], Frédéric Oberti[3], Isabelle Fouchard[3], Adrien Lannes[3], Celine Rolland[3], Damien Combes[3], Christophe Aubé[1], Anita Paisant[1], Béatrice Bouvard[1]. *[1]Angers University, Angers University Hospital, Angers, France; [2]Angers University, Angers, France; [3]Angers University Hospital, Angers University, Angers, France*
Email: jeboursier@chu-angers.fr

Background and aims: Osteoporosis, which remains underdiagnosed, shares common risk factors with steatotic liver diseases (SLD) but the relationship between these two conditions is still being debated. Although the current gold standard for diagnosing osteoporosis is dual-energy X-ray absorptiometry, computed tomography has emerged as an accurate alternative method (PMID 23588747).We aimed to evaluate the association between osteoporosis, as determined by bone mineral density measurement on CT scan (BMD-CT), and the severity of SLD.
Method: We included 330 patients with biopsy-proven SLD in our Hepatology Department. Vertebral BMD was retrospectively assessed using L1 attenuation on thoracic or abdominal CT scans performed within ±2 years of liver biopsy. A high osteoporosis risk was defined by BMD-CT < 110 Hounsfield units (HU). Advanced fibrosis was defined by fibrosis stage F3–4 on liver biopsy. Liver stiffness measurement with FibroScan and the specialized blood test FibroMeterV2G were both available for all patients.
Results: 146 patients (44%) had BMD-CT defined osteoporosis, and 48% had advanced fibrosis. Patients with advanced fibrosis had lower BMD-CT than those without: 109 HU [IQR: 92–139] vs 123 HU [IQR: 96–151], p = 0.026. Age, alcohol consumption and advanced fibrosis were independently associated with BMD-CT osteoporosis in multivariate analysis. The prevalence of BMD-CT osteoporosis across the subgroups was: 23% (if age < 65, and both no/light alcohol ≤ 70 g/week and F0–2 fibrosis), 35–39% (age < 65, and moderate/high alcohol > 70 g/week or F3–4 fibrosis), 59% (age < 65, and both moderate/high alcohol and F3–4 fibrosis), 62–67% (age ≥ 65, whatever alcohol or fibrosis). In multivariate analyses where non-invasive tests replaced histology, FibroMeterV2G was independently associated with BMD-CT osteoporosis, whereas liver stiffness was not. Age (< 65 vs ≥ 65), alcohol consumption (no/light vs moderate/high) and FibroMeter2G (≤ 0.445 vs > 0.445) stratified patients in three groups where the prevalence of BMD-CT osteoporosis was: 19%, 45–52%, and 67–68%.
Conclusion: In addition to age and alcohol consumption, advanced fibrosis is associated with BMD-CT osteoporosis in patients with SLD. Osteoporosis should be screened according to these risk factors, to improve the holistic management of steatotic liver diseases.

THU-203
"Lean" MASLD in the elderly living at high altitude: an underestimated cardiometabolic risk
Nurgul Toktogulova[1]. *[1]Kyrgyz State Medical Academy named after I.K. Akhunbaev (KSMA), Hospital therapy, Bishkek, Kyrgyz Republic*
Email: t.nur30@mail.ru

Background and aims: Metabolically associated steatotic liver disease (MASLD) is a systemic cardiometabolic disorder in which cardiovascular complications are the leading cause of mortality. In elderly patients, metabolic dysfunction is exacerbated by sarcopenia, chronic low-grade inflammation, and reduced adaptive capacity. Residence at mid- to high-altitude, associated with chronic hypobaric hypoxia, represents an additional and insufficiently studied modifying factor.
Method: An open comparative study included 733 ethnic Asians living in low- and mid-altitude regions, comprising healthy controls, patients with MASLD, and those with MASLD and type 2 diabetes. Anthropometry, body composition, metabolic and liver parameters, metabolic syndrome components, and comorbidities were assessed. In a subgroup (n = 50), inflammatory cytokines (TNF-α, IL-4) and the cytokine index were analyzed, and liver fibrosis risk was evaluated. Statistical analysis was performed using SPSS.
Results: Elderly residents of mid-altitude regions with MASLD demonstrated a more pronounced accumulation of cardiometabolic risk factors: the presence of three or more components of metabolic syndrome was significantly more frequent compared with younger individuals. Waist circumference exceeded threshold values in 72.5% of elderly patients. A substantial proportion of cases represented the "lean" MASLD phenotype (BMI < 23 kg/m^2), particularly among men, and was associated with increased fat mass combined with reduced skeletal muscle mass, consistent with a sarcopenic phenotype. Residents of mid-altitude areas exhibited lower levels of fasting glucose, HbA1c, alanine aminotransferase (ALT), and total cholesterol, which may reflect metabolic adaptation to hypoxic conditions. However, levels of TNF-α and IL-4 were elevated regardless of BMI, and inflammatory activity as well as the cytokine index increased with advancing liver fibrosis. Visceral obesity, assessed by waist circumference rather than BMI, showed significant correlations with cytokine profile, ALT levels, and fibrosis indices.
Conclusion: MASLD in elderly individuals living at mid-altitude is characterized by a combination of substantial cardiometabolic burden, chronic inflammation, and a high prevalence of the "lean" phenotype associated with sarcopenia. Residential altitude acts as an independent determinant of an adverse metabolic and inflammatory MASLD phenotype, underscoring the need for a personalized, age- and geography-oriented approach to diagnosis and management.

THU-204
Phosphatidylethanol reductions are associated with clinically meaningful improvements in blood pressure and lipid profile among patients with steatotic liver disease
Nikolaj Torp[1], Stine Johansen[1], Katrine Tholstrup Bech[1,2], Helle Schnefeld[1,2], Markus Maagaard[1,2], Ellen Lyngbeck Jensen[1,2], Mette Lehmann Andersen[1,3], Charlotte Mary Gjøl[1], Gunilla Calov[1], Ida Villesen[1], Johanne Kragh Hansen[1], Katrine Thorhauge[1], Camilla Dalby Hansen[1], Maria Fogt[1], Ea Kyed[1], Kathrine Sejer Sørensen[1], Anine Andersen[1], Peter Andersen[1], Marianne Bergmann[4], Maja Thiele[1,2], Mads Israelsen[1,2], Aleksander Krag[1,2]. *[1]Centre for Liver Research, Department of*

Gastroenterology and Hepatology, Odense University Hospital, Odense, Denmark; [2]Department of Clinical Research, University of Southern Denmark, Odense, Denmark; [3]Department of Gastroenterology and Hepatology, Herlev Hospital, Herlev, Denmark; [4]Department of Biochemistry and Immunology, Lillebaelt Hospital, University Hospital of Southern Denmark, Vejle, Denmark
Email: nikolaj.christian.torp@rsyd.dk

Background and aims: Alcohol intake influences cardiometabolic risk factors (CMRFs) such as hypertension and dyslipidemia, but the association between changes in the direct alcohol biomarker phosphatidylethanol (PEth) and CMRFs is unknown. We investigated the association between decreases in PEth and improvements in CMRFs among patients with steatotic liver disease (SLD).
Method: Single-center study of patients with SLD and a baseline and follow-up visit where PEth and CMRFs were available. Participants were subclassified into MASLD, MetALD and ALD based on hepatic steatosis (CAP ≥ 248 dB/m), CMRFs and self-reported current alcohol intake. Based on changes in PEth, participants were divided into a substantial decrease group (PEth reduction of ≥80 ng/mL from baseline to follow-up), a moderate decrease group (20–79 ng/mL reduction) and a no decrease group (<20 ng/mL reduction), who also served as the reference. Clinically meaningful improvements in blood pressure (systolic ≥5 mmHg reduction and diastolic ≥3 mmHg reduction) and the lipid profile (triglycerides ≥30% relative reduction, HDL ≥0.1 mmol/L increase and LDL ≥0.5 mmol/L reduction) were defined according to cardiovascular society recommendations. Regression models were adjusted for age, sex, smoking, as well as changes in waist circumference, HbA1c, anti-hypertensive and lipid-lowering drug use.
Results: We included 965 participants with a median time between visits of 25 months (IQR: 24–29). Distribution of MASLD/MetALD/ALD was 603/234/128 where the median baseline PEth in each subclass was 12/236/445 ng/mL. Across SLD subclasses, 16% had a substantial PEth decrease, 13% a moderate decrease and 71% no decrease. Both a substantial and moderate PEth decrease were associated with higher odds of clinically meaningful improvements in systolic blood pressure (OR = 1.73, 95% CI: 1.19–2.52, p = 0.004 and OR = 1.54, 95% CI: 1.03–2.30, p = 0.034), while a substantial, but not moderate, decrease in PEth was associated with triglycerides improvement (OR = 2.18, 95% CI: 1.37–3.48, p < 0.001). Both a substantial and a moderate decrease in PEth was associated with lower odds of HDL improvement (OR = 0.52, 95% CI: 0.35–0.79, p = 0.002 and OR = 0.54, 95% CI: 0.35–0.83, p = 0.005). There were no observed association between decreases in PEth and improvements in diastolic blood pressure nor LDL.
Conclusion: Reductions in PEth are associated with clinically meaningful improvements in blood pressure and lipid profile, why PEth may serve as an important tool to monitor patients with SLD.

THU-205
Prognostic impact of chronic kidney disease and proteinuria in metabolic dysfunction–associated steatotic liver disease

Shun-Ichi Wakabayashi[1], Takefumi Kimura[1], Nobuharu Tamaki[2], Naoki Tanaka[1], Masayuki Kurosaki[2]. *[1]Shinshu University School Of Medicine, Matsumoto, Japan; [2]Musashino Red Cross Hospital, Musashino, Japan*
Email: shun_1@me.com

Background and aims: Metabolic dysfunction–associated steatotic liver disease (MASLD) is a systemic condition associated with liver-related complications and extrahepatic organ dysfunction, including chronic kidney disease (CKD). Although CKD and proteinuria are frequently observed in MASLD, their prognostic significance for liver-related events (LRE), cardiovascular events (CVE), and all-cause mortality remains unclear. We aimed to investigate the associations of CKD and proteinuria with long-term clinical outcomes in patients with MASLD.
Method: This retrospective cohort study used the Japanese claims-based database. Patients with a fatty liver index ≥60 or with diagnosis of fatty liver disease were screened, and those fulfilling MASLD criteria with available serum creatinine and qualitative urine protein data were included. A total of 420,646 patients were analyzed. CKD was defined as an estimated glomerular filtration rate <60 mL/min/1.73 m^2, and proteinuria as ≥2+ (equivalent to 100 mg/dL) on urine dipstick testing. The primary endpoints were LRE (hepatic decompensation and hepatocellular carcinoma), CVE, and all-cause mortality.
Results: The cumulative incidence at 5 years was 0.06% for LRE, 1.01% for CVE, and 0.26% for all-cause mortality. At baseline, 8.0% of patients had CKD and 14.4% had proteinuria. Patients with CKD showed significantly higher 5-year cumulative incidences of LRE, CVE, and all-cause mortality than those without CKD (0.12% vs. 0.05%, 2.55% vs. 0.88%, and 0.58% vs. 0.23%, respectively; all log-rank p < 0.05). In multivariable analyses, CKD was independently associated with an increased risk of CVE (adjusted hazard ratio [aHR] 1.26; 95% CI, 1.16–1.37), but not with LRE (aHR 0.92; 95% CI, 0.63–1.35) or all-cause mortality (aHR 1.13; 95% CI, 0.95–1.35). In contrast, patients with proteinuria had higher 5-year cumulative incidences of LRE, CVE, and all-cause mortality than those without proteinuria (0.09% vs. 0.05%, 1.74% vs. 0.94%, and 0.41% vs. 0.23%, respectively; all log-rank p < 0.05). Proteinuria was independently associated with increased risks of LRE (aHR 1.72; 95% CI, 1.27–2.32), CVE (aHR 1.26; 95% CI, 1.16–1.37), and all-cause mortality (aHR 1.50; 95% CI, 1.30–1.74).
Conclusion: In MASLD, CKD was associated mainly with cardiovascular risk, whereas proteinuria was a robust predictor of liver-related events, cardiovascular events, and mortality. Assessment of proteinuria may improve risk stratification in patients with MASLD.

THU-206
Impact of fibrosis risk on health-related quality of life and activity in patients with metabolic dysfunction–associated steatohepatitis in Germany

Hayley Wallinger[1], Lena Amari[1], Riya Arora[2], Elisabeth de Laguiche[3], Riku Ota[3]. *[1]Adelphi Real World, Bollington, United Kingdom; [2]Novo Nordisk Service Centre, Bangalore, India; [3]Novo Nordisk, Søborg, Denmark*
Email: hayley.wallinger@omc.com

Background and aims: Metabolic dysfunction–associated steatohepatitis (MASH) is linked to progressive liver damage and diverse patient-reported burden. Given limited data on how fibrosis risk relates to health-related quality of life (HRQoL), we aimed to assess HRQoL and activity restrictions by fibrosis risk among patients with MASH (PwM) in Germany.
Method: We analyzed Germany data from the MASH Disease Specific Programme™, a cross-sectional physician- and patient survey conducted from January–June 2024. Physicians reported fibrosis risk for PwM, classified according to American Association for the Study of Liver Diseases (AASLD) 2023 guidance. Patients self-reported disease burden using the NASH-CHECK and Work Productivity and Activity Impairment (WPAI) questionnaires. NASH-CHECK scores range from 0 (least) to 10 (most impact). WPAI scores are expressed as percentages, with higher numbers indicating greater impairment. Indeterminate and high-risk fibrosis groups were each compared with the low-risk group after entropy balancing on age and sex. Reported age and sex are unweighted, descriptive only. Pairwise statistical tests compared outcomes versus the low-risk group.
Results: Overall, 65 physicians reported data for 650 patients, of whom 397 self-reported data (n = 204 low risk, n = 61 indeterminate risk, n = 33 high risk). Mean ± SD age was 54.2 ± 10.3, 57.6 ± 9.1, and 58.9 ± 10.5 years; female proportion was 40.7%, 34.4%, and 24.2%; and mean body mass index ± SD (kg/m^2) was 31.5 ± 4.0, 32.3 ± 3.9, and 31.5 ± 5.6 for low- indeterminate- and high-risk patients, respectively. Mean ± SD WPAI scores were higher in high- versus low-risk patients for overall work impairment (49.7 ± 23.9 vs. 21.3 ± 20.5) and daily activity impairment (55.1 ± 27.4 vs 36.1 ± 20.4); both p < 0.01.

High-risk patients reported greater impact than low-risk patients to NASH-CHECK activity limitations (4.0 ± 2.0 vs. 2.4 ± 1.6), emotional impact (4.5 ± 2.7 vs. 2.4 ± 1.3), social impact (4.5 ± 2.4 vs. 1.8 ± 1.2), cognitive symptoms (3.5 ± 2.3 vs. 1.6 ± 1.5), fatigue (5.0 ± 2.9 vs. 2.8 ± 2.3), itchy skin (4.3 ± 2.9 vs. 2.2 ± 2.0), and abdominal bloating (5.0 ± 2.9 vs. 2.8 ± 2.3) domains; all $p < 0.01$.

Conclusion: Among German PwM, higher fibrosis risk was associated with greater activity limitations as measured by NASH-CHECK and WPAI. These findings emphasize the importance of early fibrosis risk identification and targeted management to limit work impairment and improve HRQoL.

THU-211

Impact of small intestinal bacterial overgrowth on disease progression in metabolic dysfunction–associated steatotic liver disease

Ziteng Wang[1], Wentao Tan[2], Hongshan Wei[2], Hong Liu[1]. *[1]Beijing Shijitan hospital, Beijing, China; [2]Beijing Ditan hospital, Beijing, China*
Email: wangzi_t@163.com

Background and aims: Increasing evidence suggests that small intestinal bacterial overgrowth (SIBO) may play a contributory role in metabolic dysfunction–associated steatotic liver disease (MASLD). Alterations in intestinal microbial ecology, increased intestinal permeability, and dysregulated microbial metabolites have been proposed as key mechanisms linking SIBO to liver injury. This study sought to clarify the association between SIBO and MASLD, with an emphasis on gut microbial signatures and related metabolic characteristics.

Method: Consecutive individuals who underwent abdominal imaging and lactulose hydrogen–methane breath testing were retrospectively analyzed. Baseline characteristics were compared using independent-sample *t* tests. Associations between SIBO and MASLD were evaluated through stratified analyses and chi-square tests, while multivariate logistic regression was employed to identify independent predictors of MASLD. Fecal samples from patients with MASLD were further subjected to 16S rRNA gene sequencing to characterize gut microbiota profiles and infer metabolic functional differences according to SIBO status.

Results: Among 350 enrolled participants, 97 (27.7%) were diagnosed with MASLD, whereas 253 (72.3%) did not have MASLD. SIBO was detected in 300 individuals (85.7%). The prevalence of SIBO differed significantly between MASLD and non-MASLD groups. Multivariate analysis demonstrated that SIBO was independently associated with the presence of MASLD and correlated with greater disease severity, with methane-positive SIBO showing the strongest association. Microbial profiling revealed that MASLD was characterized by enrichment of Firmicutes, particularly taxa within Lactobacillales and Bacilli. In contrast, SIBO-positive patients exhibited a microbiota dominated by Proteobacteria, including increased abundance of the Burkholderiaceae family and genera such as *Dialister*, *Limnobacter*, and *Acidovorax*. Functional pathway analysis indicated that inter-group differences were mainly related to metabolic processes.

Conclusion: SIBO is closely linked to MASLD and its progression, with methane-positive SIBO displaying a more pronounced association with disease severity. MASLD and SIBO exhibit distinct gut microbial patterns, predominantly involving Firmicutes and Proteobacteria, respectively. Alterations in microbiota-related metabolic pathways may represent a key mechanistic link between SIBO and MASLD.

THU-212

Does size matter? Think again: smartphone-ready reasoning LLMs with RAG match frontier models for MASLD clinical decision support

Ernest Saenz[1], Juan Carlos Restrepo[2], Juan Turnes Vázquez[3], Maria Fernanda Saavedra Chacon[4], Gabriel Sebastián Díaz Ramírez[2], Camilo Andrés Torres Londoño[5], Yohana Poveda Salinas[6], Betty Morales Arrieta[7], María Cristina Torres Caro[8], Andres Gomez Aldana[9], Santiago Rodriguez-Mora[9], Jorge Ortiz[10], Diana Marcela Escobar Cardenas[5], Andreas Teufel[1], Ismael de Jesus Yepes Barreto[11]. *[1]Department of Medicine II, Division of Hepatology, Medical Faculty Mannheim, Heidelberg University, Mannheim, Germany; [2]Hospital Pablo Tobón Uribe, Medellín, Colombia; [3]University Hospital Complex Of Pontevedra, Pontevedra, Spain; [4]Clínica Ces, Medellín, Colombia; [5]Fundacion Valle Del Lili, Cali, Colombia; [6]Clínica Imbanaco, Cali, Colombia; [7]Hospital Universitario del Caribe, Cartagena de Indias, Colombia; [8]Fundacion Cardio Infantil Instituto De Cardiologia, Bogotá, Colombia; [9]Department of Internal Medicine, Division of Digestive Diseases, University of Cincinnati, Cincinnati, United States; [10]Clínica IMAT Oncomedica Auna, Monteria, Colombia; [11]Facultad de Medicina, Universidad de Cartagena, Cartagena, Colombia*
Email: ernest.phd@gmail.com

Background and aims: Metabolic dysfunction-associated steatotic liver disease (MASLD) requires evidence-based decision support, particularly in resource-limited settings serving Spanish-speaking populations (600+ million globally). Reasoning large language models (LLMs) combined with retrieval-augmented generation (RAG) may provide evidence-based recommendations, but optimal model size for clinical deployment remains unknown. We compared on-device reasoning LLMs (≤20 billion, edge-capable) versus frontier models in MASLD clinical assessments.

Method: Twelve reasoning LLMs spanning 8B to 671B parameters (plus SOTA models: Gemini-2.5-Pro, GPT-5, Claude-Sonnet-4) answered 120 hepatologist-designed multiple-choice questions (MCQ) across MASLD management. Models were grouped by size: Small (≤20B), Medium (21B–355B), Large (≥671B/proprietary). Temperature = 0 and thinking tokens = 50% model maximum). Then, top 3 models (from the MCQ test) integrated with RAG system (ChromaDB vector store; 7 clinical guidelines; text-embedding-3-small; MMR retrieval k = 15) answered 15 Spanish-language free-text clinical vignettes to assess cross-lingual performance. Twelve blinded hepatologists (mean experience 12 years) rated responses across 5 dimensions (Accuracy, Clarity, Clinical Satisfaction, Reasoning, Self-Awareness; 1–10 scale).

Results: In the MCQ test (4,320 responses), top performers were: Gemini-2.5-Pro 93.1% (95% CI 86.4%-96.0%), GLM-4.5–355B 92.8% (86.4%-96.0%), GPT-OSS-20B 88.3% (80.4%-92.3%). Size group means: Small 87.0%, Medium 90.3%, Large 92.4% ($\chi^2 = 23.01$, $p < 0.001$, Cramér's V = 0.073). No pairwise comparisons survived FDR correction. In the free-text test (Gemini = A, GPT-OSS = B, GLM = C), after Holm adjustment for within-dimension multiplicity, only one contrast achieved significance: GLM-4.5 exceeded Gemini on Accuracy ($p = 0.028$, mean difference 0.46 points, 95% CI 0.14–0.75), though the effect size was small (Vargha-Delaney A = 0.440) and this finding did not survive global FDR correction.

Conclusion: Small on-device reasoning LLMs (≤20B parameters) achieve frontier-level performance when integrated with RAG for MASLD clinical decision support. RAG evaluation showed no clinically meaningful differences among models after multiplicity control, with ceiling effects suggesting all three systems met expert standards. Deployment of open source edge-capable reasoning models with guideline retrieval could enable high-quality hepatology support in resource-limited settings without requiring proprietary or commercial models.

THU-213

Global economic burden of metabolic dysfunction–associated steatohepatitis (MASH) in individuals with type 2 diabetes (T2D) across nine countries

Zobair M. Younossi[1], James M. Paik[1], Frank Tacke[1,2], Patrizia Burra[1,3], Cristiane A. Villela-Nogueira[1,4], Javier Crespo[1,5], Elisabetta Bugianesi[1,6], Yuichiro Eguchi[1,7], Mario Guimarães Pessoa[1,8], Claudia Pinto Oliveira[1,8], Michael Roden[1,9], Cyrielle Caussy[1,10], Amalia Gastaldelli[1,11], Fernando Bril[1,12], Jeremy Tomlinson[1,13], Paul N. Brennan[1,14], Manuel Romero-Gómez[1,15], Hirokazu Takahashi[1,16], Takumi Kawaguchi[1,17], Jerome Boursier[1,18], Faisal Abaalkhail[1,19], Vincent Wai-Sun Wong[1,20], Hussain Abdulrahman Al-Omar[1,21], Maria Stepanova[1], Fatema Nader[1], Markos Kalligeros[1,22], Laurent Castera[1,23], Saleh A. Alqahtani[1,24], Linda Henry[1,25]. *[1]The global NASH/MASH council, Washington, DC, United States; [2]Department of Hepatology and Gastroenterology, Charité - Universitätsmedizin Berlin, Berlin, Germany, Berlin, Germany; [3]Department of Surgery, Oncology and Gastroenterology, Padua University Hospital, Padua, Italy, Padua, Italy; [4]School of Medicine and Hepatology Division, Universidade Federal, Rio de Janeiro, Brazil; [5]Gastroenterology and Hepatology Department, Clinical and Translational Research in Digestive Diseases, Valdecilla Research Institute (IDIVAL), Marqués de Valdecilla University Hospital, Santander, Spain; [6]Department of Medical Sciences University, Turin, Italy; [7]Loco Medical General Institute, Saga, Japan; [8]Departamento de Gastroenterologia, Hospital das Clínicas (LIM 07) da Faculdade de Medicina da Universidade de São Paulo, São Paulo, Brazil; [9]Department of Endocrinology and Diabetology, Medical Faculty and University Hospital Düsseldorf, Heinrich-Heine-University Düsseldorf, Düsseldorf, Germany; [10]Département Endocrinology, Diabete and Nutrition, Hôpital Lyon Sud, Hospices Civils de Lyon Pierre-Bénite, Lyon, France; [11]Cardiometabolic Risk Unit, Institute of Clinical Physiology – National Research Council (CNR), Pisa, Italy; [12]Division of Endocrinology, Diabetes, and Metabolism, University of Alabama at Birmingham, AL, USA; Birmingham, United States; [13]Oxford Centre for Diabetes Endocrinology & Metabolism, NIHR Oxford Biomedical Research Centre, University of Oxford, Churchill Hospital, Oxford, United Kingdom; [14]Division of Molecular and Clinical Medicine, University of Dundee, Scotland, Dundee, United Kingdom; [15]15. UCM Digestive Diseases. Virgen del Rocío University Hospital. Institute of Biomedicine of Seville (HUVR/CSIC/US). CIBEREHD, ISCIII. Department of Medicine, University of Seville, Seville, Spain; [16]Liver Center, Saga University Hospital, Faculty of Medicine, Saga University, Saga, Japan; [17]Division of Gastroenterology, Department of Medicine, Kurume University School of Medicine, Kurume, Japan; [18]Hepato-Gastroenterology Department at Angers University Hospital, Angers, France; [19]Gastroenterology Section, Department of Medicine, King Faisal Specialist Hospital and Research Center, Riyadh, Saudi Arabia, [20]Medical Data Analytics Center, Department of Medicine and Therapeutics, The Chinese University of Hong Kong, Hong Kong, China; [21]Department of Clinical Pharmacy, College of Pharmacy, King Saud University, Riyadh 11451, Saudi Arabia; [22]Division of Gastroenterology and Hepatology, Beth Israel Deaconess Medical Center, Harvard Medical School, Boston, MA, United States; [23]Department of Hepatology, University of Paris-Cité, Hopital Beaujon, AP-HP, Clichy, France; [24]Liver, Digestive, and Lifestyle Health Research Section, and Organ Transplant Center of Excellence, King Faisal Specialist Hospital and Research Center, Riyadh, Saudi Arabia; [25]25. Center for Outcomes Research in Liver Diseases, Washington, DC, United States*
Email: zobair.younossi@cldq.org

Background and aims: T2D is associated with a high prevalence of MASH, more rapid disease progression, and greater clinical burden, which together drive the economic burden of MASH. We aimed to estimate the economic burden of MASH among individuals with T2D across nine countries.

Method: An age-stratified Markov model was developed to project MASH burden in T2D over the next 2 decades in United States (US), Germany, Spain, France, Italy, United Kingdom (UK), Japan, Brazil, and Saudi Arabia (SA). Country-specific transition probabilities were derived from natural history data and calibrated to match each country's epidemiology. Transition probabilities were adjusted for T2D reflecting higher fibrosis progression rates and mortality risks. Therapeutic effects of MASH treatments (GLP-1 receptor agonists and resmetirom) were integrated into yearly transition matrices using country-specific assumptions for availability, coverage, adherence, and persistence. Time and adoption of GLP-1RA and resmetirom trajectories were informed by experts from each country. Drug prices were based on national benchmarks and projected forward using patent-erosion curves. Direct medical costs and indirect work productivity losses were updated annually using IMF inflation indices.

Results: From 2021 to 2040, total direct annual medical costs for MASH with T2D are estimated to increase from $14.39B to $68.73B in the US, $0.28B to $2.78B in Germany, $0.50B to $2.33B in Spain, $0.44B to $2.37B in France, $0.46B to $2.12B in Italy, $0.74B to $3.36B in UK, $1.10B to $6.83B in Brazil, $0.57B to $2.07B in SA, and $0.45B to $2.44B in Japan. If indirect costs of productivity loss are also included, total costs would further increase by 2–13 folds. Rising costs reflect growing MASH prevalence, progression to advanced disease, and uptake of MASH medications. The composition of direct medical spending shifts over time. In 2025, costs associated with liver-disease care accounted for >95% of direct medical costs in every country. However, unless the costs of anti-MASH drugs are reduced in the future, spending on MASH medications will substantially increase over time as a proportion of direct medical costs.

Conclusion: MASH in individuals with T2D is projected to impose an escalating economic burden over the next two decades, driven by increasing disease burden and growing uptake of MASH therapies. These findings highlight the need for effective, affordable treatment and prevention strategies to mitigate future economic burden.

THU-214

Integrated risk stratification for all-cause and cause-specific mortality in a large MASLD cohort in Taiwan

Ming-Lung Yu[1,2], Chung-Feng Huang[1,2], Pei-Chien Tsai[1,2], Ming-Lun Yeh[1,2]. *[1]National Sun Yat-Sen University, Gushan District, Taiwan; [2]Kaohsiung Medical Univ, Sanmin District, Taiwan*
Email: fish6069@gmail.com

Background and aims: Metabolic Dysfunction-associated Steatotic Liver Disease (MASLD) confers elevated long-term mortality risk. This study developed and validated an integrated risk stratification model incorporating cardiometabolic risk factors (CMRFs) and traditional predictors.

Method: Using the MJ cohort (1996–2022), we constructed Cox models and evaluated discrimination via time-dependent AUCs and calibration. An integer-based cumulative risk score was derived from the optimal model using weighted regression coefficients.

Results: Among 140,247 adults with MASLD (mean age 45.0 years; 61.2% male) followed for a median of 17 years, 15,584 deaths occurred (67.3/10,000 person-years). Sequential addition of covariates improved model performance, with the best model including CMRFs (underweight/obesity, diabetes, hypertension), age, sex, advanced fibrosis, and renal dysfunction. This model achieved a 10-year AUC of 0.84 and maintained consistently strong performance across 1–20 years. The resulting 0–17point risk score demonstrated a clear dose-response gradient. Individuals scoring ≥10 had over 80-fold higher mortality risk (HR 81.4; 95% CI 73.4–90.2) and a 20-year mortality of 74.4%, compared with 1.5% for scores ≤1. The score also showed excellent prediction for cause-specific mortality, particularly DM-related (AUC 0.92–0.97), liver-related (0.88–0.93), and ESRD mortality (0.90–0.93).

Conclusion: This integrated risk score provides a practical tool for early identification of high-risk MASLD patients and may guide targeted cardiometabolic, hepatic, and renal interventions to reduce long-term mortality.

THU-215

GCKR rs1260326, dietary factors and incident liver-related events in patients with metabolic dysfunction-associated steatotic liver disease

Ziqi Zhang[1], Li Zhang[1], Lili Lu[1], Guang Ji[1]. [1]*Longhua Hospital, Shanghai University of Traditional Chinese Medicine, Shanghai, China*
Email: 22022628@shutcm.edu.cn

Background and aims: Gene-environment interactions have been increasingly recognized as important drivers of metabolic dysfunction-associated steatotic liver disease (MASLD) progression. However, how specific gene-diet interactions influence the transition from MASLD to adverse liver-related events (LREs) remains poorly understood. The glucokinase regulatory protein (*GCKR*) rs1260326 (C > T) variant has been identified as a genetic determinant of MASLD susceptibility. We aimed to evaluate the association between *GCKR* rs1260326 and the risk of LREs in MASLD and to identify dietary factors that may modify this association.
Method: This prospective cohort study included 126,129 adults with MASLD from the UK Biobank. The primary outcome was LREs, defined as a composite of cirrhosis, hepatic decompensation, hepatocellular carcinoma (HCC), liver transplantation, or liver-related mortality. Fine-Gray competing risk models were used to estimate subdistribution hazard ratios (sHRs). Circulating metabolomics and proteomics were applied to explore biological pathway alterations associated with the risk allele.
Results: During a median follow-up of 13.7 years, 1320 participants developed LREs. Compared to the CC genotype, the rs1260326 TT genotype was associated with an increased risk of LREs (sHR = 1.23, 95% CI 1.05–1.44), cirrhosis (sHR = 1.23, 95% CI 1.04–1.45) and HCC (sHR = 2.02, 95% CI 1.29–3.15). The association between rs1260326 TT genotype and LREs risk was more pronounced among individuals with higher carbohydrate intake, whereas it was attenuated among those with greater adherence to a Mediterranean diet or higher intakes of unsaturated fatty acids, vitamin E, and vegetables. For example, the TT genotype was associated with an increased risk of LREs among individuals with low adherence to the Mediterranean diet (sHR = 1.85, 95% CI 1.16–2.96), whereas no significant association was observed among those with high adherence (sHR = 0.64, 95% CI 0.30–1.35). Mechanistically, carriers of the risk allele exhibited alterations in lipid and branched-chain amino acid metabolism, accompanied by perturbations in mitochondrial function and oxidative stress, inflammatory signaling, and extracellular matrix-related pathways.
Conclusion: The *GCKR* rs1260326 C > T variant was associated with an increased risk of LREs in patients with MASLD, and this association was significantly modified by dietary factors. These findings support genetically informed personalized nutritional strategies, which may help reduce the risk of incident LRE in MASLD.

MASLD – Diagnostics and non-invasive assessment

TOP-063-YI

Prognostic performance of liver stiffness changes in patients with biopsy-proven cirrhosis secondary to metabolic dysfunction-associated steatohepatitis

Jimmy Che-To Lai[1,2], Boyu Yang[1], Hye Won Lee[3], Huapeng Lin[4], Emmanuel Tsochatzis[5], Salvatore Petta[6], Elisabetta Bugianesi[7], Masato Yoneda[8], Ming-Hua Zheng[9], Hannes Hagström[10,11], Jerome Boursier[12,13], José Luis Calleja Panero[14], George Boon Bee Goh[15], Chan Wah Kheong[16], Rocio Gallego-Durán[17], Arun J Sanyal[18], Victor de Lédinghen[19], Philip N. Newsome[20], Jian-Gao Fan[21], Laurent Castera[22], Michelle Lai[23], Céline Fournier-Poizat[19], Grace Lai-Hung Wong[1,2,24], Mirko Zoncapè[5], Grazia Pennisi[6], Angelo Armandi[7], Atsushi Nakajima[8], Wen-Yue Liu[25], Ying Shang[10], Marc de Saint-Loup[12], Elba Llop Herrera[14], Kevin Kim Jun Teh[15], Carmen Lara-Romero[17], Amon Asgharpour[18], Sara Mahgoub[26], Sau-Wai Mandy Chan[19], Adrien Lannes[12,13], Rocio Macias[14], Manuel Romero-Gómez[17], Seung Up Kim[3], Vincent Wai-Sun Wong[1,2], Terry Cheuk-Fung Yip[1,2]. [1]*Medical Data Analytics Centre, Department of Medicine and Therapeutics, The Chinese University of Hong Kong, Hong Kong, Hong Kong;* [2]*Li Ka Shing Institute of Health Sciences and State Key Laboratory of Digestive Disease, The Chinese University of Hong Kong, Hong Kong, Hong Kong;* [3]*Department of Internal Medicine, Institute of Gastroenterology, Yonsei University College of Medicine, Seoul, Korea, Rep. of South;* [4]*Department of Gastroenterology and Hepatology, School of Medicine, Shanghai Jiao Tong University, Shanghai, China;* [5]*University College London Institute for Liver and Digestive Health, Royal Free Hospital and UCL, London, United Kingdom;* [6]*Sezione di Gastroenterologia, Di.Bi.M.I.S., University of Palermo, Palermo, Italy;* [7]*Department of Medical Sciences, Division of Gastroenterology and Hepatology, A.O. Città della Salute e della Scienza di Torino, University of Turin, Turin, Italy;* [8]*Department of Gastroenterology and Hepatology, Yokohama City University Graduate School of Medicine, Yokohama, Japan;* [9]*MAFLD Research Center, Department of Hepatology, First Affiliated Hospital of Wenzhou Medical University, Wenzhou, China;* [10]*Department of Medicine, Huddinge, Karolinska Institutet, Huddinge, Stockholm, Sweden;* [11]*Division of Hepatology, Department of Upper GI Diseases, Karolinska University Hospital, Huddinge, Stockholm, Sweden;* [12]*Hepato-Gastroenterology and Digestive Oncology Department, Angers University Hospital, Angers, France;* [13]*HIFIH Laboratory, SFR ICAT 4208, Angers University, Angers, France;* [14]*Department of Gastroenterology and Hepatology, Hospital Universitario Puerta de Hierro Majadahonda, Madrid, Spain;* [15]*Department of Gastroenterology and Hepatology, Singapore General Hospital, Singapore, Singapore;* [16]*Gastroenterology and Hepatology Unit, Department of Medicine, Faculty of Medicine, University of Malaya, Kuala Lumpur, Malaysia;* [17]*Digestive Diseases Unit and CIBERehd, Virgen Del Rocío University Hospital, Seville, Spain;* [18]*Stravitz-Sanyal Institute for Liver Disease and Metabolic Health, VCU School of Medicine, Richmond, VA, United States;* [19]*Echosens, Paris, France;* [20]*Roger Williams Institute of Liver Studies, Faculty of Life Sciences and Medicine, King's College London, the Foundation of Liver Research, and King's College Hospital, London, United Kingdom;* [21]*Department of Gastroenterology, Xinhua Hospital Affiliated to Shanghai Jiaotong University School of Medicine, Shanghai Key Lab of Pediatric Gastroenterology and Nutrition, Shanghai, China;* [22]*Université Paris Cité, UMR1149 (CRI), INSERM, Paris, France; Service d'Hépatologie, Hôpital Beaujon, Assistance Publique-Hôpitaux de Paris (AP-HP), Clichy, France;* [23]*Division of Gastroenterology & Hepatology, Beth Israel Deaconess Medical Center, Harvard Medical School, Boston, MA, United States;* [24]*Medical Data Analytics Centre, Department of Medicine and Therapeutics, The Chinese University of Hong Kong, Hong Kong, China;* [25]*Department of Endocrinology, First Affiliated Hospital of Wenzhou Medical University, Wenzhou, China;*

[26]National Institute for Health Research, Biomedical Research Centre at University Hospitals Birmingham NHS Foundation Trust and the University of Birmingham, Birmingham, United Kingdom
Email: jimmylai0515@gmail.com

Background and aims: Changes in liver stiffness measurement (LSM) by vibration-controlled transient elastography (VCTE) correlate with development of liver-related events (LREs) in patients with metabolic dysfunction-associated steatotic liver disease, but no data on biopsy-proven cirrhosis are available. As LSM has been assessed as a reasonably likely surrogate endpoint in trials on metabolic dysfunction-associated steatohepatitis (MASH) cirrhosis, we aimed to study if LSM change can reflect disease progression and regression in those with MASH cirrhosis.
Method: This cohort study included adult patients with biopsy-proven compensated MASH cirrhosis who had received at least two VCTE examinations between 6 months and 5 years apart at 16 centres across the US, Europe, and Asia, of which data were collected prospectively at 14 centres. The incidence of LREs in patients with and without LSM changes was determined, with non-liver-related death as a competing event.
Results: A total of 248 patients with MASH cirrhosis (baseline age 60.0 ± 10.0 years and 48.8% male) were recruited. 81.6% of the liver biopsies were performed within 1 year of the baseline VCTE. Baseline and second LSM measured after a median (IQR) interval of 1.4 (0.8–2.6) years were 19.1 (IQR 13.4–26.3) kPa and 16.8 (12.3–24.5) kPa, respectively. At a median (IQR) follow-up of 3.2 (1.3–5.0) years after the second LSM, 29 (11.7%) patients developed LREs, and the 5-year cumulative incidence was 18.7% (95% CI 12.6%–25.7%). The 5-year cumulative incidences were 21.2% (95% CI 10.4%–34.5%), 12.4% (5.4%–22.5%) and 27.2% (13.6%–42.8%) among those who had LSM absolute decrease by ≥5 kPa, change within 5 kPa and increase by ≥5 kPa. For relative change of LSM, the 5-year cumulative incidences of those with LSM relative decrease by ≥10%, ≥20% and ≥30% were 15.4% (95% CI 8.0%–25.0%), 16.3% (7.8%–27.4%) and 13.9% (5.0%–27.2%); compared to 23.7% (12.0%–37.8%), 28.0% (14.2%–43.6%) and 27.5% (13.6%–43.4%) in those with relative LSM increase by ≥10%, ≥20% and ≥30%, respectively. A relative increase of LSM ≥30% was associated with LREs (adjusted subdistribution hazard ratio [aSHR] 1.69, 95% CI 1.04–2.77, p = 0.035), while a relative decrease of LSM ≥30% was not associated with a reduced risk (aSHR 0.66, 95% CI 0.30–1.46, p = 0.307), after adjusting for baseline LSM.
Conclusion: A relative increase in LSM ≥30% from baseline was associated with disease progression, while a relative decrease of ≥30% did not reduce the risk of LREs, in patients with MASH cirrhosis.

TOP-064

Development and validation of a highly accurate noninvasive-based model to predict cirrhosis due to MASH (cirrhosis-7 score)

Mazen Noureddin[1], Elizabeth Brombosz[1], Grazina Binkauskiene[1], Winston Dunn[2], Rashmee Patil[1], Rohit Puskoor[1], John Poulos[3], Alma Laura Ladrón de Guevara[4], Marcelo Kugelmas[5], Alaa Abousaif[6], Vlad Ratziu[7], Meena Bansal[8], Jörn M. Schattenberg[9], Naim Alkhouri[1]. [1]Summit Clinical Research, San Antonio, United States; [2]University of Kansas, Kansas City, United States; [3]Coastal Research Institute, Fayetteville, NC, United States; [4]Centro de Investigacion y Gastroenterologia, Mexico City, Mexico; [5]South Denver Gastroenterology, Denver, United States; [6]Knowledge Research Center, Orange, CA, United States; [7]Sorbonne University, Paris, France; [8]Mount Sinai, New York, United States; [9]Saarland University, Saarbrücken, Germany
Email: noureddinmd@pinnacleresearch.com

Background and aims: Several models for identifying MASH cirrhosis using non-invasive tests (NITs) have been proposed, although many scores, such as Agile-4, perform moderately in independent cohorts. Notably, the FDA and EMA do not currently support the use of NITs to define progression to cirrhosis, and a recent regulatory document emphasized that such tools must demonstrate high accuracy with both high sensitivity and specificity. We therefore developed a score using a large multicenter database to identify cirrhosis that meets these regulatory requirements.
Method: A database of patients with available biopsy results screened for enrollment in MASH clinical trials (n = 5963) was used to develop a model for predicting the presence of cirrhosis (n = 1289). Logistic regression was used in combination with up to 12 commonly collected non-invasive measures of MASH to create models for predicting cirrhosis. The best performing model was validated using 500 bootstrapped resamples.
Results: Of the 12287 linear regression models tested, 70 had both sensitivity and specificity ≥0.8. A score combining LSM, CAP, ELF, platelets, ALT, INR, and BMI had the highest performance, with an AUROC of 0.89 (95% CI: 0.87–0.90), with sensitivity of 0.82, specificity of 0.81, PPV of 0.59, and NPV of 0.93. Patients with higher LSM, ELF, and INR and those with lower platelet count, CAP, ALT, and BMI were at higher risk of having cirrhosis. The validation samples had an AUROC of 0.86, with a corrected calibration slope of 0.995, indicating negligible overfitting. The Cirrhosis-7 score performed better than other NIT-based scores for cirrhosis such as AGILE4 (AUROC 0.84), LSM alone (AUROC 0.79), and FIB4 (AUROC 0.76). It also uniquely demonstrates the highest combined sensitivity and specificity.
Conclusion: Out of over 12,000 models, the Cirrhosis-7 score incorporating LSM, CAP, ELF, and four clinical variables outperformed all others for detecting cirrhosis, with performance characteristics that have the potential to address regulatory requirements for defining progression to cirrhosis by achieving high accuracy with both high sensitivity and specificity.

TOP-065-YI

Incorporating an automated MASLD screening algorithm into a primary care precision diabetes care platform (iDiabetes) facilitates universal FIB4 screening, automated linkage to secondary care and identifies new cases of advanced fibrosis & cirrhosis

Damien Leith[1], Rachael Barrett[1], YeunYi Lin[1], Mya Win[1], Evelyn Anyebe[1], Paul Brennan[1], Ruairi Lynch[1], Ewan Pearson[1], John F Dillon[1]. [1]Ninewells Hospital & Medical School, Dundee, United Kingdom
Email: damienleith86@gmail.com

Background and aims: Despite the 2024 EASL recommendation of FIB4 screening for all people with type 2 diabetes [T2D], MASLD screening and hepatology referral for those at high risk of advanced fibrosis remains a challenge in primary care. We integrated a reflexive MASLD fibrosis screening algorithm, with automated linkage of high-risk individuals to secondary care, into *iDiabetesPlus*, a precision diabetes mellitus [DM] care platform being trialled in primary care in Scotland. Here, we present the key MASLD screening results from the first year of the *iDiabetesPlus* study.
Method: *iDiabetesPlus* was piloted from 28/10/24, then implemented as new standard DM care from 01/01/25 in 16 primary care practices in the Tayside region, Scotland. All patients with a DM diagnosis are automatically enrolled into *iDiabetesPlus* at their annual DM review. The *iDiabetesPlus* MASLD screening algorithm performs automated FIB4 screening for all patients. In those with ALT>30 additional reflex liver aetiological screening and NAFLD Fibrosis Score [NFS] calculation is performed, with reflexive Enhanced Liver Fibrosis [ELF] testing in those with indeterminate or high risk FIB4/NFS. Automated referral to secondary care is generated for those with ELF ≥9.8, FIB4 >2.67, NFS >0.675 or positive aetiology results. For all enrolled patients, *iDiabetesPlus* generates comprehensive DM and MASLD management recommendations for primary care practitioners and guidance on timing of interval FIB4 testing.
Results: From 28/10/24–31/10/25, 4533 people with DM were enrolled in *iDiabetesPlus* and eligible for a liver screen (41.8% female; mean age 65.8 years; 91.0% T2D, 7.0% T1D). 4499 (99.3%) of those enrolled received FIB4 screening. Of those with a FIB4 result, 2841 (63.1%) were <1.30, 1484 (33.0%) 1.30–2.67 and 174 (3.9%) >2.67.

973 (21.5%) enrolled patients received second-line ELF testing, with 521 (53.5%) ELF <9.8. 614 (13.55%) patients generated an automated secondary care referral. Of 435 Fibroscans performed to date, 226 (52.0%) had Liver Stiffness Measurements [LSM] <8 kPa, 108 (24.8%) LSM 8–11.9 kPa and 101 (23.2%) LSM ≥12 kPa.
Conclusion: The incorporation of MASLD screening into a precision diabetes care platform has achieved universal FIB4 testing in a real-world primary care DM population. Selected, second-line ELF testing reduces the number requiring secondary care referral by >50%. Importantly, our screening algorithm has identified new MASLD with advanced fibrosis or cirrhosis in 2.2% of 4,533 prospectively screened patients with DM.

TOP-066

Machine learning–based models with and without VCTE improve prescreening for at-risk MASH compared with FAST in the largest clinical trial validation cohort

Winston Dunn[1,2], Mazen Noureddin[2,3], Terry Cheuk-Fung Yip[4], Vincent Wai-Sun Wong[4], Laurent Castera[5], Manal F. Abdelmalek[6], Leon Adams[7], Nipun Verma[8], Juan Pablo Arab[9], Bihui Zhong[10], Vincent Chen[11], Ashwani K. Singal[12], Ming-Hua Zheng[13], Rashmee Patil[2], Rohit Puskoor[2], Grazina Binkauskiene[14], Elizabeth Brombosz[14], Naim Alkhouri[14,15]. *[1]University of Kansas, Kansas City, United States; [2]Pinnacle Clinical Research, San Antonio, United States; [3]Houston Liver Instituite, Houston, United States; [4]The Chinese University of Hong Kong, Sha Tin, Hong Kong; [5]Université Paris Cité, Paris, France; [6]Division of Gastroenterology and Hepatology, Mayo Clinic, Rochester, United States; [7]Medical School, University of Western Australia, Perth, Washington, Australia, Perth, Australia; [8]Department of Hepatology, Postgraduate Institute of Medical Education and Research, Chandigarh, India; [9]Division of Gastroenterology, Hepatology, and Nutrition, Department of Internal Medicine, Virginia Commonwealth University School of Medicine, Richmond, United States; [10]Department of Gastroenterology, The First Affiliated Hospital, Sun Yat-sen University,, Guangzhou, Guangdong, China; [11]Division of Gastroenterology and Hepatology, University of Michigan, Ann Arbor, United States; [12]University of Louisville, Louisville, United States; [13]MAFLD Research Center, Department of Hepatology, The First Affiliated Hospital of Wenzhou Medical University, Wenzhou, China; [14]Summit Clinical Research, San Antonio, United States; [15]Clinical Research Institute of Ohio, Cleveland, United States*
Email: naim.alkhouri@gmail.com

Background and aims: The FAST score and the ALADDIN-MASH-VCTE model were developed to identify at-risk metabolic dysfunction–associated steatohepatitis (MASH), the target population for non-cirrhotic MASH clinical trials. In parallel, ALADDIN-MASH-Lab was designed to predict the same phenotype using routine laboratory data alone. Although FAST is widely used for prescreening, its sensitivity and trial enrollment efficiency are limited. We compared the diagnostic accuracy and screening performance for trial eligibility of FAST, ALADDIN-MASH-VCTE, and ALADDIN-MASH-Lab in a large cohort with biopsy-confirmed disease.
Method: We performed an external validation in 6,376 patients with paired liver biopsy and VCTE data, of whom 39.9% met regulatory trial criteria for at-risk MASH (MASH with ≥F2 fibrosis). Discrimination was assessed using AUC with DeLong comparison. To reflect clinical trial prescreening, thresholds were selected to maintain a biopsy screen-failure rate ≤33%, corresponding to a positive predictive value ≥0.67, while maximizing sensitivity. Under this fixed constraint, we compared true-positive yield and missed eligible cases across non-invasive tests.
Results: ALADDIN-MASH-VCTE demonstrated higher discrimination than FAST (AUC 0.725 [95% CI 0.712–0.738] vs 0.710 [0.697–0.723]; p = 0.00011), while the laboratory-only model, ALADDIN-MASH-Lab, was similar to FAST (AUC 0.714 vs 0.710; ΔAUC = +0.004; 95% CI −0.005 to +0.013). At a fixed biopsy screen-failure rate of 33%, FAST identified 12.3 true positives per 100 screened while missing 27.6 at-risk MASH cases. Under the same constraint, ALADDIN-MASH-VCTE identified 18.0 true positives and missed 21.9 cases, whereas ALADDIN-MASH-Lab achieved similar yield to FAST (14.2 true positives; 25.7 missed).
Conclusion: In a large external validation cohort, ALADDIN-MASH-VCTE (https://aihepatology.shinyapps.io/ALADDIN3) demonstrated superior performance compared with the current standard FAST for identification of at-risk MASH. At an equivalent acceptable biopsy screen-failure rate, ALADDIN-MASH-VCTE increased true-positive detection and reduced missed cases. Importantly, the laboratory-only model, ALADDIN-MASH-Lab, achieved discrimination and screening performance comparable to FAST despite not requiring VCTE. Derived in a multinational cohort and independently validated in the largest U.S. clinical trial screening database, these findings support the use of machine learning–based approaches to improve MASH trial recruitment, with and without access to VCTE.

TOP-080

DiabetesMASH Index for non-invasive identification of at-risk metabolic dysfunction-associated steatohepatitis in patients with type 2 diabetes

Yuping Chen[1], Bingtian Dong[2], Chuan Liu[3], Zhen Li[4], Ming-Hua Zheng[5], Kaina Chen[6], George Boon Bee Goh[7], Bicheng Ye[1], Xiao Liang[8], Airong Hu[9], Yiling Li[10], Qing-Lei Zeng[11], Yameng Sun[12], Wei Gou[13], Hua Bian[14], Chiwei Zhang[1], Xiaolin Wang[1], Yinqiu Zhang[1], Jiaojian Lv[15], Jie Shen[16], Xuan Liang[17], Xiqiao Zhou[18], Mingxing Huang[19], Qingge Zhang[20], Yan Wang[21], Xingguo Xiao[22], Yuehua Wang[23], Yuxia Qi[24], Yusen Zhou[25], Jing He[26], Taolong Zhou[27], Yan Wu[28], Weimin Jiang[29], Fengmei Wang[30], Tang Dong[31], Jing Du[32], Huimin Ying[33], Xuefeng Li[34], Yuwei Zhang[35], Ling Li[36], Zhe Dai[37], Xiaolong Qi[1] and DiabetesLiver Integrated Management (DLIM) Consortium[1]. *[1]Liver Disease Center of Integrated Traditional Chinese and Western Medicine, Department of Radiology, Zhongda Hospital, Medical School, Southeast University, Nurturing Center of Jiangsu Province for State Laboratory of AI Imaging & Interventional Radiology (Southeast University), Basic Medicine Research and Innovation Center of Ministry of Education, Zhongda Hospital, Southeast University, State Key Laboratory of Digital Medical Engineering, Nanjing, China; [2]Department of Ultrasound, the First Affiliated Hospital of Anhui Medical University, Hefei, China; [3]Liver Disease Center of Integrated Traditional Chinese and Western Medicine, Department of Radiology, Zhongda Hospital, Medical School, Southeast University, Nurturing Center of Jiangsu Province for State Laboratory of AI Imaging & Interventional Radiology (Southeast University), Basic Medicine Research and Innovation Center of Ministry of Education, Zhongda Hospital, Southeast University, State Key Laboratory of Digital Medical Engineering, N, China; [4]Department of Hepatobiliary and Pancreatic Surgery, Zhongnan Hospital of Wuhan University, Wuhan University, Bariatric and Metabolic Diseases Surgery Center, Zhongnan Hospital of Wuhan University, Wuhan University, Wuhan, China; [5]MAFLD Research Center, Department of Hepatology, First Affiliated Hospital of Wenzhou Medical University, Wenzhou, China; [6]Department of Gastroenterology & Hepatology, Singapore General Hospital, Singapore, Singapore; [7]Department of Gastroenterology & Hepatology, Singapore General Hospital, Singapore, China; [8]Zhejiang Key Laboratory of Multi-omics Precision Diagnosis and Treatment of Liver Diseases, Department of General Surgery, Sir Run-Run Shaw Hospital, Zhejiang University School of Medicine, Hangzhou, China; [9]Ningbo Institute of Liver Diseases, Ningbo No. 2 Hospital, Ningbo, China; [10]Department of Gastroenterology, The First Hospital of China Medical University, Shenyang, China; [11]Department of Infectious Diseases, First Affiliated Hospital of Zhengzhou University, Zhengzhou, China; [12]Liver Research Center, Beijing Friendship Hospital, Capital Medical University, State Key Lab of Digestive Health, National Clinical Research Center of Digestive Diseases, Beijing Key Laboratory of Translational Medicine on Liver Cirrhosis, Beijing, China; [13]Qingdao Sixth People's Hospital, Qingdao, China; [14]Department of Endocrinology and Metabolism, Zhongshan Hospital, Fudan University, Shanghai, China; [15]Lishui People's Hospital, Lishui, China; [16]Shunde Hospital,*

Southern Medical University (The First People's Hospital of Shunde), Shunde, China; [17]The Fifth People's Hospital of Shenyang, Shenyang, China; [18]Affiliated Hospital of Nanjing University of Chinese Medicine, Jiangsu Province Hospital of Chinese Medicine, Nanjing, China; [19]The Fifth Affiliated Hospital of Sun Yat-sen University, Zhuhai, China; [20]Xingtai People's Hospital, Xingtai, China; [21]The Sixth People's Hospital of Shenyang, Shenyang, China; [22]Zhengzhou Central Hospital Affiliated with Zhengzhou University, Zhengzhou, China; [23]Jinhua People's Hospital, Jinhua, China; [24]Qingdao Public Health Clinical Center, Qingdao, China; [25]Bozhou People's Hospital, Bozhou, China; [26]The Second Affiliated Hospital of Qiqihar Medical University, Qiqihar, China; [27]The Third People's Hospital of Zhuhai, Zhuhai, China; [28]Suining Central Hospital, Suining, China; [29]Huashan Hospital, Fudan University, Shanghai, China; [30]Hepatobiliary Center, Gansu Wuwei Tumor Hospital, Wuwei, China; [31]Inner Mongolia Institute of Digestive Diseases, The Second Affiliated Hospital of Baotou Medical College, Baotou, China; [32]Ningxia Hui Autonomous Region People's Hospital, Yinchuan, China; [33]Xixi Hospital of Hangzhou, Hangzhou, China; [34]Taihe Hospital, Hubei University of Medicine, Shiyan, China; [35]Center for Diabetes and Metabolism Research, West China Hospital, Sichuan University, Chengdu, China; [36]Zhongda Hospital, Southeast University, Institute of Glucose and Lipid Metabolism, Southeast University, Nanjing, China; [37]Department of Endocrinology, Zhongnan Hospital of Wuhan University, Wuhan, China
Email: qixiaolong@vip.163.com

Background and aims: Metabolic dysfunction-associated steatohepatitis (MASH), a progressive phenotype of metabolic dysfunction-associated steatotic liver disease (MASLD), is highly prevalent among individuals with type 2 diabetes (T2D) and markedly increases the risk of cirrhosis, hepatocellular carcinoma, and mortality. Patients with at-risk MASH (MASH + fibrosis stages F2–4) represent the primary target population for emerging pharmacotherapies. We aimed to established a non-invasive model for identifying at-risk MASH in T2D.
Method: In this prospective study, a derivation cohort undergoing liver biopsy from ten centers (n = 525) was used for model development. External validation was conducted in three independent multinational cohorts assessed by vibration-controlled transient elastography: the DiabetesLiver Integrated Management cohort (n = 3,711), Singapore cohort (n = 422), and NHANES cohort (n = 1,674). All participants were adults with T2D. At-risk MASH was defined histologically in the derivation cohort and by the FibroScan-aspartate aminotransferase [FAST] score in validation cohorts. Model performance was evaluated using the area under the receiver operating characteristic curve (AUROC), decision curve analysis and calibration analysis, and compared with the Fibrosis-4 index (FIB-4), non-alcoholic fatty liver disease fibrosis score (NFS), and AST/alanine aminotransferase (ALT) ratio (AAR).
Results: The derived model, termed the DiabetesMASH Index (DMI), incorporated age, waist circumference, ALT, and hemoglobin A1c. DMI demonstrated satisfactory discrimination in the derivation cohort (AUROC 0.79; 95% confidence interval [CI] 0.75–0.83) and consistently high performance across external validation cohorts (AUROC 0.91 [95% CI 0.89–0.94], 0.88 [0.80–0.96], and 0.90 [0.86–0.94], respectively), outperforming FIB-4, NFS, and AAR in all cohorts. Calibration analyses showed agreement between predicted and observed risks. In the derivation cohort, rule-out and rule-in thresholds were 0.184 (sensitivity 0.85; negative predictive value [NPV] 0.92) and 0.452 (specificity 0.90; PPV 0.57), respectively. The indeterminate zone accounted for 35.8% of patients in the derivation cohort and 19.9%, 24.8%, and 19.1% in validation cohorts.
Conclusion: DMI is a validated and affordable non-invasive tool for identifying at-risk MASH in patients with T2D, using routinely available variables.

TOP-081

A spatial metabolic atlas of liver lipid metabolism and fibrosis in metabolic dysfunction-associated steatotic liver disease

Patcharamon Seubnooch[1], Elaine Chng[2], Yayun Ren[2], Matteo Montani[3], Dina Tiniakos[4], Jean-François Dufour[5], Jaime Bosch[5], Nikolai Naoumov[6], Annalisa Berzigotti[5], Mojgan Masoodi[1]. *[1]Institute of Clinical Chemistry, Inselspital, Bern University Hospital, Bern, Switzerland; [2]Histoindex Pte. Ltd., Singapore, Singapore; [3]Institute of Tissue Medicine and Pathology, University of Bern, bern, Switzerland; [4]Department of Pathology, Aretaieion Hospital, Medical School, National and Kapodistrian University of Athens, Athens, Greece; [5]Department of Visceral Surgery and Medicine, Inselspital, Bern University Hospital, Bern, Switzerland; [6]Division of Medicine, University College London, London, United Kingdom*
Email: mojgan.masoodi@insel.ch

Background and aims: Metabolic dysfunction-associated steatotic liver disease (MASLD) is a leading cause of chronic liver disease. Although fibrosis stage is a key determinant of clinical outcomes, the spatial metabolic alterations underlying fibrotic remodeling and disease progression are poorly characterised. Using a novel multimodal approach integrating high-spatial-resolution mass spectrometry-based metabolic mapping, second harmonic generation/two-photon excitation fluorescence (SHG/TPEF) microscopy, and computational modeling, we constructed a comprehensive spatial metabolic molecular atlas of the human liver.
Method: Liver biopsies from 36 MASLD patients (stage F0-F4) were analysed by desorption electrospray ionisation mass spectrometry imaging at 20 × 20 µm spatial resolution to define metabolic signatures associated with steatosis, lobular inflammation, ballooning and fibrosis. Histology-guided regions of interest were used to assess zone-specific lipid metabolism, steatosis and fibrosis regions. SHG/TPEF microscopy was applied on the liver samples to quantify collagen architecture, enabling spatial correlation of molecular profiles with zonation, intra-stage fibrotic heterogeneity, septa characteristics. Multiple-testing correction was applied using Benjamini-Hochberg False Discovery Rate (FDR), with FDR ≤ 5% considered significant.
Results: Distinct metabolic signatures comprising several hundred metabolites were identified across steatosis types (micro/macrovesicular), lobular inflammation and ballooning. In MASH, molecular species topography showed marked differences with zone-specific disruption of lipid metabolism. The strongest metabolic discrimination was between fibrotic and non-fibrotic regions, revealing pronounced metabolic heterogeneity within fibrotic tissue. Notably, septal regions exhibited distinct molecular profiles differentiating progressive from regressive septa, and previously unrecognised sex-specific differences.
Conclusion: We established a comprehensive high-resolution spatial lipid atlas in MASLD, demonstrating zone-specific alterations in lipid metabolism associated with fibrosis and disease progression in MASH. Distinct metabolic heterogeneity was observed within fibrotic tissue, including molecular differences between progressive and regressive septa and sex-specific metabolic patterns. Together, these findings provide new insights into fibrosis architecture and metabolic remodeling in MASH and may support the identification of zone-specific diagnostic markers.

TOP-082

Machine learning–based models with and without VCTE improve cirrhosis prescreening compared with Agile4 and VCTE in the largest clinical trial validation cohort

Winston Dunn[1], Naim Alkhouri[2,3], Terry Cheuk-Fung Yip[4], Vincent Wai-Sun Wong[4], Laurent Castera[5], Manal F. Abdelmalek[6], Leon Adams[7], Nipun Verma[8], Juan Pablo Arab[9], Bihui Zhong[10], Vincent Chen[4], Ashwani K. Singal[11], Ming-Hua Zheng[12], Rashmee Patil[13], Rohit Puskoor[2,13], Grazina Binkauskiene[2], Elizabeth Brombosz[2], Mazen Noureddin[2,13,14]. *[1]University of Kansas,*

Kansas City, United States; [2]Summit Clinical Research, San Antonio, United States; [3]Clinical Research Institute of Ohio, Cleveland, United States; [4]The Chinese University of Hong Kong, Sha Tin, Hong Kong; [5]Université Paris Cité, Paris, France; [6]Division of Gastroenterology and Hepatology, Mayo Clinic, Rochester, United States; [7]Medical School, University of Western Australia, Perth, Washington, Australia, Perth, Australia; [8]Department of Hepatology, Postgraduate Institute of Medical Education and Research, Chandigarh, India; [9]Division of Gastroenterology, Hepatology, and Nutrition, Department of Internal Medicine, Virginia Commonwealth University School of Medicine, Richmond, United States; [10]Department of Gastroenterology, The First Affiliated Hospital, Sun Yat-sen University, Guangzhou, Guangdong, China; [11]University of Louisville, Louisville, United States; [12]MAFLD Research Center, Department of Hepatology, The First Affiliated Hospital of Wenzhou Medical University, Wenzhou, China; [13]Pinnacle Clinical Research, San Antonio, United States; [14]Houston Liver Instituite, Houston, United States
Email: noureddinmd@pinnacleresearch.com

Background and aims: Accurate noninvasive identification of cirrhosis is essential for efficient enrollment of MASH-cirrhosis clinical trials. Vibration-controlled transient elastography (VCTE)–based scores such as Agile4 are commonly used for non-invasive identification of cirrhosis but is insensitive when applied in clinical trial screening. We developed two machine learning–based VCTE model (ALADDIN-Cirrhosis-VCTE) and routine laboratory only model (ALADDIN-Cirrhosis-Lab) and evaluated their performance against established Agile4 and VCTE.
Method: Models were derived in a multinational cohort of 2,962 patients undergoing VCTE, including 373 (12.6%) with biopsy-confirmed cirrhosis. External validation was performed in 6,376 patients undergoing screening for MASH-cirrhosis clinical trials with paired liver biopsy and VCTE data, of whom 20.8% met histologic cirrhosis criteria. Discrimination was assessed using AUC with DeLong comparison. Screening thresholds were selected to maintain a constant biopsy screen-failure rate of ≤33%, corresponding to a positive predictive value of at least 0.67. True-positive yield and missed cirrhosis cases were compared under this fixed screen-failure constraint.
Results: In external validation, ALADDIN-Cirrhosis-VCTE demonstrated higher discrimination than Agile4 (AUC 0.858 [95% CI 0.846–0.870] vs 0.842 [0.830–0.854]; DeLong $p = 1.5 \times 10^{-5}$). ALADDIN-Cirrhosis-Lab demonstrated higher discrimination than VCTE alone (AUC 0.808 [95% CI 0.795–0.821] vs 0.793 [0.779–0.807]). At equivalent acceptable screen-failure rates of 33%, Agile-4 identified 9.2 true positives per 100 screened while missing 11.6 cases. Under the same constraint, ALADDIN-Cirrhosis-VCTE identified 11.6 true cirrhosis cases per 100, and missed only 9.3. ALADDIN-Cirrhosis-Lab achieved superior yield to VCTE alone.
Conclusion: In a large external validation cohort drawn from clinical trial screening, a machine learning–based VCTE model (https://aihepatology.shinyapps.io/ALADDIN3) significantly improved identification of histology-defined cirrhosis compared with established VCTE-based scores. At a fixed acceptable biopsy screen-failure rate, ALADDIN-Cirrhosis-VCTE increased true-positive yield while reducing missed eligible cases. Importantly, the laboratory-only model, ALADDIN-Cirrhosis-Lab, is superior to VCTE alone and can be used when VCTE is unavailable. These findings support machine learning–based prescreening strategies to improve yield and reduce screen fails in MASH-cirrhosis clinical trial recruitment.

TOP-096

Can reliably measured transient elastography be trusted in obesity? Comparing the modifying effects of general and central adiposity in MASLD

Fredrik Åberg[1], Anni Heiskala[1], Panu K. Luukkonen[1,2,3,4], Rohit Loomba[5], Ville Männistö[6,7]. *[1]Helsinki University Hospital and University of Helsinki, Helsingfors, Finland; [2]Minerva Foundation Institute for Medical Research, Helsinki, Finland; [3]Department of Internal Medicine, University of Helsinki, Helsinki, Finland; [4]Molecular Medicine Finland (FIMM), Helsinki Institute of Life Sciences (HiLife), University of Helsinki, Helsinki, Finland; [5]MASLD Research Center, Division of Gastroenterology and Hepatology, University of California at San Diego, La Jolla, United States; [6]Department of Medicine, University of Eastern Finland, Kuopio, Finland; [7]Department of Medicine, Kuopio University Hospital, Kuopio, Finland*
Email: fredrik.aberg@helsinki.fi

Background and aims: Obesity increases transient elastography (TE) failure rates, but it is unclear how varying degrees of obesity and central adiposity affect its diagnostic performance among reliably measured TE examinations. We examined how adiposity influences TE diagnostic performance across different anthropometric measures, including only examinations meeting reliability criteria.
Method: From the NAFLD Adult Database 2, a prospective, non-interventional registry of the NASH CRN, we identified 949 adults enrolled 2009–2020 with MASLD and reliably measured TE. Data were provided by NIDDK CR, a program of the National Institute of Diabetes and Digestive and Kidney Diseases. Reliable TE was defined as ≥10 valid measurements with IQR/median ratio <30%. All participants had liver biopsy and available anthropometric data, including body mass index (BMI), waist circumference (WC), and waist-hip ratio (WHR). Of these, 578 (61%) were women, mean (SD) age 51 (12) yrs, BMI 34.3 (6.4) kg/m^2, WC 110 (14.8) cm, and WHR 0.95 (0.08). TE discrimination for significant (F2-F4) and advanced (F3-F4) fibrosis was assessed by AUCs across sex-specific BMI, WC, and WHR quartiles, with sensitivity and specificity estimated at 8 and 12 kPa.
Results: The discriminatory performance of TE for histological significant fibrosis declined across sex-specific quartiles of adiposity. AUCs by quartile (Q1-Q4) were: BMI 0.85, 0.83, 0.81, 0.75; WC 0.83, 0.82, 0.81, 0.75; and WHR 0.84, 0.82, 0.81, 0.77. For advanced fibrosis, the corresponding AUCs of TE decreased from 0.89 to 0.77 across BMI quartiles, 0.90 to 0.78 for WC, and 0.91 to 0.82 for WHR. Using the 8 kPa cutoff, TE specificity for detecting significant fibrosis declined from 84% to 52% across BMI quartiles, 84% to 49% for WC, and 77% to 60% for WHR, while sensitivity increased by 12–15%-points. With the 12 kPa cutoff, specificity of TE for detecting advanced fibrosis decreased from 93% to 74% (BMI), 93% to 76% (WC), and 89% to 82% (WHR), while sensitivity increased by 10%-points for BMI, 17 for WC, and was stable across WHR quartiles. AUCs for advanced fibrosis declined from BMI and WC Q3 to Q4 with both the M and XL probes.
Conclusion: Even when TE measurements fulfilled validity criteria, higher levels of general/central adiposity reduced the discriminatory performance of TE, mainly through declining specificity and a resulting increase in false positives. In individuals with obesity, complementary methods should be used to verify significant/advanced fibrosis.

TOP-097-YI

Assessment of cardiometabolic comorbidities and the impact of glycemic and weight control on liver stiffness in advanced metabolic dysfunction-associated steatotic liver disease

Cautar El Maimouni[1,2], Alba Jiménez-Massip[3,4,5,6], Lidia Canillas[7,8], Isabel Serra[9], Mercedes Vergara[5,6,10], Rosa M Morillas[5,6,11,12], Maria Poca[6,13], Teresa Broquetas[14], Adrià Rodríguez-Castellano[15], Eva Erice Munoz[16], Anna Soria[1,2,6,17], Laura Pagès[3,4,5,6], Jose Carrión[7,8], Meritxell Casas[5,6,10], Alba Ardevol[5,6,11,12], Diego Rojo[3,4,5,6], Nuria Alonso[5,6,18], M Teresa Julián[5,6,18], Octavi Bassegoda[1,2,17], Pere Ginès[1,2,6,17], Juan M. Pericàs[3,4,5,6], Isabel Graupera[1,2,6,17]. *[1]Liver Unit, Hospital Clínic of Barcelona., Barcelona, Spain; [2]Fundació de Recerca Clínic Barcelona-Institut d'Investigacions Biomèdiques August Pi i Sunyer (FRCB-IDIBAPS), Barcelona, Spain; [3]Liver Unit, Department of Digestive Diseases, Vall d'Hebron University Hospital, Barcelona, Spain; [4]Institut de Recerca Vall d'Hebron (VHIR), Campus Hospitalari Vall d'Hebron, Barcelona, Spain; [5]Universitat Autònoma de Barcelona,*

Barcelona, Spain; [6]Centro de Investigación Biomédica en Red de Enfermedades Hepáticas y Digestivas (CIBEREHD), Madrid, Spain; [7]Hepatology Section, Department of Digestive Diseases, Hospital del Mar., Barcelona, Spain; [8]Hospital del Mar Medical Research Institute (IMIM), Barcelona, Spain; [9]Liver Unit, Dr Josep Trueta University Hospital, Girona, Spain; [10]Liver Unit, Department of Digestive Diseases, Parc Taulí Research and Innovation Institute (I3PT), Parc Taulí University Hospital, Sabadell, Spain; [11]Liver Unit, Department of Digestive Diseases, Germans Trias i Pujol University Hospital, Badalona, Spain; [12]Institut d'Investigació en Ciències de la Salut Germans Trias i Pujol (IGTP), Badalona, Spain; [13]Liver Unit, Hospital de la Santa Creu i Sant Pau, Sant Pau Research Institute, Barcelona, Spain; [14]Hepatology Section, Department of Digestive Diseases, Bellvitge University Hospital, IDIBELL, L'Hospitalet del Llobregat, Spain; [15]Department of Digestive Diseases, Joan XXIII University Hospital of Tarragona, Tarragona, Spain; [16]Department of Digestive Diseases, Hospital de Sant Joan Despí Moisès Broggi, Sant Joan Despí, Spain; [17]Faculty of Medicine and Health Sciences, University of Barcelona (UB), Barcelona, Spain; [18]Department of Endocrinology and Nutrition, Germans Trias i Pujol University Hospital, Badalona, Spain
Email: elmaimouni.cautar@gmail.com

Background and aims: Cardiometabolic risk factors (CMRF) drive progression in metabolic dysfunction-associated steatotic liver disease (MASLD) but data on their prevalence, control, and impact in advanced stages are limited. We aimed to assess (1) CMRF burden and control in MASLD-related advanced chronic liver disease (ACLD), and (2) the impact of changes in glycemic control and body weight on disease progression.
Method: Prospective, observational, multicenter study of patients with ACLD-MASLD defined by liver stiffness measurement (LSM) ≥ 10 kPa, F3–F4, or imaging signs of advanced disease. Clinical, laboratory and imaging data were collected at baseline and follow-up. LSM progression was defined as change from < 10 to ≥ 10 kPa or ≥ 30% increase; LSM improvement as transition from ≥ 10 to < 10 kPa or ≥ 30% reduction.
Results: A total of 635 patients were included (50.2% women; median age 66 years (interquartile range: 59–72). Median baseline LSM was 17.3 kPa (12–25.7) and controlled attenuation parameter 309 dB/m (269–351). Type 2 diabetes was present in 73% of patients (12.5% with poor glycemic control) and obesity in 64.7% (median body mass index 32 kg/m^2 [29–36]), while only 16.5% received GLP-1 receptor agonists. Overall, 82% had high or very high cardiovascular risk; LDL-cholesterol targets were not achieved in 55.9% and 56.5% were not receiving statins. Among 284 patients with ≥ 2 elastography assessments (spaced by ≥ 1 year), 14.8% showed LSM progression and 38.4% showed LSM improvement (median follow-up: 26 months [17–45]). Significant reductions in HbA1c (6.7% to 6.4%; p = 0.009) and weight (86 to 83 kg; p = 0.001) were observed. LSM progression was more frequent in patients with poor glycemic control (47.6% vs. 5.3%; p = 0.002), while LSM improvement was more common in those achieving good control (44.7% vs. 19%; p = 0.002). Increased or stable body weight was associated with LSM progression (28% and 17.6% vs. 8.3% in those with ≥ 5% weight loss; p = 0.03). Weight loss was directly associated with LSM improvement (58%, 43% and 33% of patients with ≥ 10%, 5–9.9% and < 5% weight loss; p = 0.028). Statin use was not associated with changes in LSM. LSM progression was associated with a higher risk of liver-related events (odds ratio 4.3; 95% confidence interval 95% 1.5–12.8; p = 0.013).
Conclusion: Poor control of CMRF is common in ACLD-MASLD. Improvements in glycemic control and weight loss are strongly associated with LSM improvement, supporting metabolic optimization to slow disease progression.

WED-041

Normal ALT values in patients with MASLD: long-term outcomes and Fib-4 performance

Ali Abdul Hussein[1], Tanya Jayakar[1], Fernando Iorra[1], Maria Kalafateli[1], Michael Yee[1], Benjamin H. Mullish[1], Mark R Thursz[1], Pinelopi Manousou[1]. [1]*Imperial College London, London, United Kingdom*
Email: aliabdulhussein17@gmail.com

Background and aims: Current EASL guidelines recommend a two-tier fibrosis risk stratification strategy using Fibrosis-4 (FIB-4) followed by second-line testing. However, fibrosis assessment in clinical practice is often triggered by elevated alanine aminotransferase (ALT), potentially overlooking patients with normal ALT. We retrospectively evaluated clinical outcomes in MASLD patients with normal ALT and/or FIB-4, referred before implementation of two-tier pathways - a population that would likely be missed under current guidelines.
Method: We retrospectively examined patients with a diagnosis of MASLD, referred to a tertiary liver centre between 2012 and 2016. Diagnostic accuracy of FIB-4 (≥ 1.3) for advanced fibrosis was assessed using transient elastography (LSM ≥ 8 kPa) and liver biopsy (CRN fibrosis stage ≥ F3), stratified by ALT status. Longitudinal outcomes included liver-related events, cardiovascular events, and all-cause-mortality. Predictors of falsely reassuring FIB-4 results were assessed using univariate and multivariate regression models in patients with normal and abnormal ALT.
Results: Among 829 MASLD patients with MASLD identified, 244 (29.4%) had normal ALT at referral, of whom 61 (25%) had LSM ≥ 8 Kpa and 38 out of 76 (50%) had ≥ F3 on liver biopsy. FIB-4 demonstrated significantly poorer discrimination for LSM ≥ 8 kPa in patients with normal versus elevated ALT (AUC 0.590 vs 0.703; p = 0.038), and similarly modest discrimination for biopsy-confirmed fibrosis stage ≥ F3 across ALT strata, with no significant difference between groups (AUC 0.618 vs 0.634; p = 0.779). Despite this, among patients with normal ALT, elevated FIB-4 was strongly associated with incident liver-related events (hazard ratio [HR] 14.4; p = 0.011) and with a composite outcome of liver-related events, cardiovascular events, or death (adjusted HR 1.9; p = 0.031) (n = 39) over 5 years of follow-up, compared with those with FIB-4 < 1.3. Obesity, diabetes, hypertension, and hypercholesterolaemia were associated with FIB-4 misclassification using LSM as the reference standard.
Conclusion: In MASLD patients with normal ALT, FIB-4 shows limited diagnostic accuracy for advanced fibrosis but retains important prognostic value. Reliance on ALT-driven assessment may delay recognition of clinically significant disease, particularly in metabolically high-risk populations.

WED-042

Use of the ANTICIPATE NASH risk score to stratify patients with compensated MASH cirrhosis: data from a phase 3, double-blinded, randomized clinical trial assessing the safety and efficacy of pegozafermin (ENLIGHTEN-cirrhosis)

Juan G Abraldes[1], Arun J. Sanyal[2], Rohit Loomba[3], Quentin M. Anstee[4], Hank Mansbach[5], Cynthia L. Hartsfield[5], Jasmine Dowlat[5], Laura Contreras[5], Jennifer B Kang[5], Shibao Feng[5], Maya Margalit[5]. [1]*Liver Unit, Division of Gastroenterology, University of Alberta, Edmonton, Alberta, Canada; [2]Beth Israel Deaconess Medical Center, Harvard Medical School, Boston, MA, United States; [3]University of California San Diego, San Diego, CA, United States; [4]Newcastle University, Newcastle upon Tyne, United Kingdom; [5]89bio Inc, San Francisco, CA, United States*
Email: maya.margalit@89bio.com

Background and aims: Compensated MASH-cirrhosis is a continuum, ranging from early cirrhosis, discernible only histologically, to the brink of decompensation. Determining where patients are on this continuum is critical in designing MASH-cirrhosis clinical trials. ANTICIPATE NASH (AN), a non-invasive continuous risk score, was

designed to assess risks of CSPH and LREs in MASH. ENLIGHTEN-Cirrhosis (NCT06419374) is an ongoing Phase 3 trial designed to assess the efficacy and safety of pegozafermin in MASH-cirrhosis. The objective of this analysis was to explore the utility of AN to understand the distribution of patients along the compensated cirrhosis continuum.

Method: Presence of metabolic risk factors and biopsy-proven MASH are inclusion criteria in the ENLIGHTEN-cirrhosis study, and high-risk varices (large or with red-wale signs) are excluded. Baseline data from the first 337 subjects randomized to the ENLIGHTEN-Cirrhosis trial were analyzed by four baseline AN categories: AN <20% (1), AN ≥20% and <40% (2), AN ≥40% and <60% (3), and AN ≥60% (4).

Results: AN categories 1, 2, 3 and 4 included 131, 90, 65 and 51 subjects, respectively (39%, 27%, 19% and 15% of subjects randomized). Age, sex, presence of T2DM and BMI were generally balanced across AN subgroups. Mean baseline VCTE and platelets were: VCTE: 12.6, 18.8, 23.9 and 32.1 kPa; Platelets: 215, 168, 151 and 134 10^3/μL in groups 1, 2, 3 and 4, respectively. Higher AN categories were associated with higher mean ELF score, FIB-4, and GGT (For AN categories 1, 2, 3 and 4: ELF: 10.1, 10.6, 10.8 and 11.1, respectively; FIB4: 1.7, 2.2, 2.9 and 3.2, respectively; GGT: 61, 86, 101 and 123 U/L, respectively), and with an increased frequency of Laennec score 4c on liver biopsy and presence of small varices on EGD (Laennec score 4c in 9%, 16%, 26% and 47% of subjects, respectively; small varices in 23%, 21%, 32% and 39% of subjects, respectively, for AN categories 1, 2, 3 and 4). In contrast, across increasing AN categories, no clear association was observed with other biopsy features (e.g., total NAS score, individual NAS components) or MRI-PDFF.

Conclusion: Higher AN categories were associated with greater severity across multiple, complementary assessments of cirrhosis (NITs, biopsy findings, presence of varices) in this large cohort of well-characterized subjects with MASH-cirrhosis. These findings support the utility of AN for stratifying patients across the compensated MASH-cirrhosis spectrum.

WED-043

Combining vibration controlled transient elastography and enhanced liver fibrosis score lowers the false positive rate for identifying MASLD with significant fibrosis in patients with class 2 or higher obesity

Veeral Ajmera[1], Ricki Bettencourt[1], Bruno Vergès[2], Dominique Delaunay[3], Bertrand Cariou[4], Sybil Charrière[5], Seema Singh[1], Egbert Madamba[1], Lisa Richards[1], Rohit Loomba[1], Cyrielle Caussy[3]. *[1]University of California San Diego, La Jolla, United States; [2]Dijon University Hospital, Dijon, France; [3]Hospices Civils De Lyon, Lyon, France; [4]Nantes Université, Nantes, France; [5]Universite Claude Bernaard Lyon, Pierre-Benite, France*
Email: v1ajmera@ucsd.edu

Background and aims: Multiple international societies recommend a care pathway with sequential testing with FIB-4 and vibration-controlled transient elastography (VCTE) or enhanced liver fibrosis (ELF) score for populations at-risk for MASH. However, multiple studies demonstrate decreased diagnostic accuracy for VCTE in patients with high body mass index (BMI). We aimed to compare the diagnostic accuracy of VCTE and ELF among prospectively recruited patients at-risk for MASH with BMI ≥ 30 kg/m^2 using magnetic resonance elastography (MRE) or liver biopsy as the reference.

Method: This multicenter, international prospective study enrolled adults with type 2 diabetes (T2DM) recruited from primary care and endocrinology clinics. Participants underwent a standardized clinical research visit with ELF, VCTE and MRE assessment. Participants with alcohol intake exceeding AASLD guidance for MASLD were excluded. The outcomes were the diagnostic performance of ELF vs VCTE for significant fibrosis defined by a composite hierarchical criteria: 1. histological stage of fibrosis ≥F2 or 2. MRE ≥ 3.3 kPa or overt diagnosis of cirrhosis on imaging.

Results: The study population included 363 patients (42% men) with T2DM and obesity. The mean (±SD) age and BMI were 62.1 (±8.3) years and 34.5 (±3.8) kg/m^2, respectively. The prevalence of BMI ≥30–35 kg/m^2 and >35 kg/m^2 were 235 (64.7%) and 128 (35.3%), respectively. 110 (30.3%) had significant fibrosis on MRE (or biopsy). The AUROC c-statistic, sensitivity and specificity for a VCTE cut-point of 8 kPa were 0.80, 81%, and 79%, respectively. The AUROC c-statistic, sensitivity and specificity for an ELF cut-point of 9.2 were 0.60, 85%, and 35%, respectively. The diagnostic accuracy of VCTE decreased among patients with BMI >35 kg/m^2 but remained superior to ELF (c = 0.76 vs 0.62, P = 0.0126). In patients with BMI >35 kg/m^2 a combined cut point of VCTE ≥ 8 kPa and ELF ≥ 9.2 yielded an AUROC c-statistic, sensitivity and specificity of 0.79, 72%, and 87% respectively. The number of false positive cases was highest with ELF (45%), then VCTE (16%) and lowest with VCTE + ELF (9%) in patients with BMI >35 kg/m^2.

Conclusion: Despite a mild decrease in diagnostic accuracy, VCTE outperformed ELF for the diagnosis of at-risk MASH in patients with BMI >35 kg/m^2. Combining VCTE and ELF in this population lowers the false positive rate and therefore has significant implications for accurately identifying patients with at-risk MASH who warrant treatment.

WED-044

Anthropometric indices and body composition as predictors of liver fibrosis in young adults with metabolic dysfunction-associated steatotic liver disease: a systematic review and meta-analysis

Arash Akhavan Rezayat[1], Sarah Batool[2], Rochan Athreya Krishnamurthy[2], Talha Javed[2], Ayaz Iqbalbhai Shaikh[2], Arun Cherackakudy Joy[2], Muhammad Adil Irshad[2], Muhammad Moiz Ud-Din[2], Richard Aspinall[2], Avisnata Das[2]. *[1]Department of Gastroenterology & Hepatology, Portsmouth Hospitals University NHS Trust, Queen Alexandra Hospital,, Portsmouth, United Kingdom; [2]Deptartment of Gastroenterology & Hepatology, Portsmouth Hospitals University NHS Trust, Queen Alexandra Hospital, Portsmouth, United Kingdom*
Email: arash.rezayat@nhs.net

Background and aims: Metabolic dysfunction-associated steatotic liver disease (MASLD) increasingly affects young adults but there is no established method to predict which patients will develop liver fibrosis based on their body composition and physical measurements. We conducted a systematic review and meta-analysis to evaluate these parameters as risk factors for liver fibrosis in young adults with MASLD.

Method: We systematically searched PubMed, Embase, Web of Science, and Scopus for studies examining anthropometric and body composition risk factors for liver fibrosis in young adults (aged 18–40 years) with MASLD. Random-effects or fixed-effects meta-analyses were performed based on heterogeneity assessment (I^2). Odds ratios (OR) with 95% confidence intervals (CI) were calculated.

Results: The meta-analysis included nine studies which analyzed data from 15,370 patients. The study of central body fat distribution revealed waist-to-height ratio ≥0.5 as the most effective indicator which predicted liver fibrosis (sample size: 67; OR = 10.73, 95% CI: 8.79–13.1, single study). Waist-to-hip ratio revealed significant association (Sample size: 101; OR = 1.525, 95% CI: 1.002–2.322, single study), as did waist circumference (Sample size: 104; OR = 1.1, 95% CI: 1.02–1.17, single study). Pooled random-effect analysis of three studies confirmed general obesity as the main risk factor (11,919; OR = 7.63, 95% CI: 1.10–52.70, p < 0.001, I^2 of 97.50%), although with significant statistical heterogeneity. The six studies showed that being overweight created a steady link between the two conditions (14829 participants; OR = 1.30, 95% CI: 1.11–1.49, p < 0.001, I^2 = 89.31%). Muscle mass percentage correlated against liver fibrosis (Sample size: 88; OR 0.714, 95% CI: 0.606–0.812, single study).

Similarly, muscle mass-to-fat mass ratio showed a strong protective effect (88 participants; OR = 0.129, 95% CI: 0.048–0.351).
Conclusion: The waist-to-height ratio may provide better liver fibrosis prediction than traditional obesity measurements for young adults with MASLD. The preservation of muscle mass together with beneficial muscle-to-fat ratios were associated with protection against advanced fibrosis. Clinical evaluation should measure central body fat instead of relying solely on BMI for assessment and treatment plans should focus on decreasing abdominal fat while maintaining or improving muscle strength.

WED-045

Metabolic dysfunction, biochemical markers, and lifestyle factors in liver fibrosis development among young adults with metabolic dysfunction-associated steatotic liver disease: a systematic review and meta-analysis

Arash Akhavan Rezayat[1], Sarah Batool[1], Rochan Athreya Krishnamurthy[1], Talha Javed[1], Arun Cherackakudy Joy[1], Ayaz Iqbalbhai Shaikh[1], Muhammad Adil Irshad[1], Muhammad Moiz Ud-Din[1], Richard Aspinall[1], Avisnata Das[1]. [1]*Department of Gastroenterology & Hepatology, Portsmouth Hospitals University NHS Trust, Queen Alexandra Hospital, Portsmouth, United Kingdom*
Email: arash.rezayat@nhs.net

Background and aims: Understanding metabolic, biochemical, and lifestyle contributors to liver fibrosis in young adults with metabolic dysfunction-associated steatotic liver disease (MASLD) is essential for early intervention strategies. We performed a meta-analysis to evaluate these risk factors which will help doctors make better treatment decisions.
Method: We systematically searched major databases (Scopus, Web of science, PubMed, and Embase) for studies reporting associations between metabolic parameters, biochemical markers, lifestyle factors, and liver fibrosis in young adults (18–40 years) with MASLD. Pooled odds ratios (OR) with 95% confidence intervals (CI) were calculated using random or fixed-effects models based on heterogeneity (I^2) assessment.
Results: The meta-analysis included nine studies which analyzed data from 15,370 patients. Among metabolic risk factors, diabetes mellitus established the strongest association with liver fibrosis (Sample size: 11229; OR = 3.73, 95% CI: 1.69–8.23, p = 0.006, I^2 = 72.13%, 5 studies). This systematic review showed that hypertension (Sample size: 8353; OR = 1.13, 95% CI: 0.78–1.66 and a p = 0.593, I^2 = 0.00%) and hyperlipidemia (Sample size: 11953; OR = 1.00, 95% CI: 0.99–1.01, p = 0.602, I^2 = 0.00%, 3 studies) lacked strong associations with liver fibrosis in this age group. ALT levels above normal range demonstrated a small yet statistically significant link to the liver fibrosis in young adults (8256; OR = 1.14, 95% CI: 1.08–1.20, p = 0.101, I^2 = 56.45%). High CRP protein demonstrated no significant association (Sample size: OR = 0.95, 95% CI: 0.81–1.11, single study). Smoking also did not have any meaningful association with liver fibrosis in young adults (Sample size: 2721; OR = 1.97, 95% CI: 0.59–6.59, single study).
Conclusion: Young adults with MASLD have a different spectrum of risk factors for liver fibrosis to older people and some established cardiovascular risk factors (hypertension, hyperlipidemia) showed only minimal impact. Elevated ALT levels may provide modest predictive value. Further, prospective studies should be conducted to understand why smoking, hypertension, and dysplipidaemia are weaker associations with liver fibrosis in young adults with MASLD.

WED-050

Machine learning identifies hidden hepatic fibrosis in adults with normal FIB-4: a NHANES-based risk-stratification model

Issa Ali[1], Hala Mouhydeen[1], Zaid Ansari[1], Akram Ahmad[1], Bobby Zervos[1]. [1]*Cleveland Clinic-Florida, Weston, United States*
Email: alii3@ccf.org

Background and aims: Fibrosis, rather than steatosis, is the primary determinant of liver-related morbidity and mortality in metabolic dysfunction–associated steatotic liver disease (MASLD). Although FIB-4 is widely used as a first-line screening tool, its performance deteriorates in patients with metabolic risk factors, and many individuals with normal FIB-4 still harbor clinically significant fibrosis. In many clinical settings, FibroScan is not readily available, creating a major blind spot in fibrosis detection. Machine-learning (ML) models trained on routine clinical and laboratory data may enable risk stratification among patients with normal FIB-4 and no elastography results. We aimed to develop an ML model to identify significant fibrosis among adults with normal FIB-4 using nationally representative NHANES elastography data.
Method: We analyzed NHANES 2017–March 2020 participants with valid demographics, metabolic parameters, laboratory values, and liver elastography (VCTE). The cohort was restricted to adults with normal FIB-4 (<1.3 for age <65; <2.0 for age ≥65). Significant fibrosis was defined as liver stiffness ≥8.0 kPa. Predictors included body measurements (BMI and waist size), blood pressure, cholesterol and glucose markers, liver enzyme tests, platelet count, and fibrosis scores (FIB-4 and NAFLD Fibrosis Score), along with race and socioeconomic indicators. An XGBoost classifier was trained using stratified sampling and imbalance correction. Model performance was assessed using AUROC, AUPRC, and SHAP (Shapley values) for feature importance.
Results: Among 10,409 adults, 76.8% had normal FIB-4; within this subgroup, 8.3% had significant fibrosis by elastography. The ML model achieved an AUROC of 0.806 and an AUPRC of 0.353, outperforming traditional noninvasive scores such as FIB-4 and NFS, which typically yield AUROCs of 0.65–0.72 in metabolic populations. At a probability threshold of 0.5, sensitivity was 56%, specificity 88%, PPV 29%, and accuracy 92%. Key predictors included BMI, waist size, HDL cholesterol, systolic blood pressure, GGT, and HbA1c.
Conclusion: A machine-learning model using routine clinical data can identify more than half of significant fibrosis cases among patients with normal FIB-4, substantially outperforming current first-line tools. This approach provides an accessible method for risk stratification in settings without FibroScan, helping close the detection gap for subclinical fibrosis in MASLD and enabling earlier, targeted referral for elastography.

WED-051

Clinical characteristics of patients with low liver stiffness measurement (LSM) on VCTE and biopsy-proven at-risk MASH on biopsy

Naim Alkhouri[1], Elizabeth Brombosz[1], Grazina Binkauskiene[1], Winston Dunn[1], Marcelo Kugelmas[2], Aasim Sheikh[3], Alma Laura Ladrón de Guevara[4], John Poulos[5], Jörn M. Schattenberg[6], Mazen Noureddin[1]. [1]*Summit Clinical Research, San Antonio, United States;* [2]*South Denver Gastroenterology, Denver, United States;* [3]*GI Specialists of Georgi, Marietta, GA, United States;* [4]*Centro de Investigacion y Gastroenterologia, Mexico City, Mexico;* [5]*Coastal Research Institute, Fayetteville, NC, United States;* [6]*Saarland University, Saarbrücken, Germany*
Email: naim.alkhouri@gmail.com

Background and aims: Most guidelines and clinical trial inclusion criteria for MASH pharmacotherapies focus on patients with LSM ≥8 kPa to identify those with at-risk MASH (F2/F3 fibrosis + NAS ≥4 with ≥1 point in each category) likely to benefit from such therapies. However, there are patients with lower LSM who have at-risk MASH on biopsy. The aim of this study is to investigate whether there are additional variables that might predict at-risk MASH in patients with low LSM.
Method: A multicenter database of patients screened for enrollment in MASH clinical trials was analyzed, from which patients with at-risk MASH were identified. These patients were then grouped by and LSM < 8 kPa (generally excluded from trials for low LSM) and LSM ≥ 8 kPa

("traditional" LSM). Descriptive statistics were applied, and a two-sided *t*-test was used to compare the two groups.
Results: The database included 9,754 patients that received liver biopsy during screening for MASH clinical trials. 2195 patients had biopsy-proven at-risk MASH and out of these patients 224 (10%) had low LSM < 8 kPa. Patients in the low LSM group were younger (55 [47–62] years, median [IQR] vs 57 [49–64], p = 0.02) had lower BMI (34.4 [29.4–38.3] kg/m^2, median [IQR] vs 36.4 [32.1–41.4] for traditional LSM; p < 0.001), less diabetes (87, 40% vs 944, 49%; p < 0.006), and lower HbA1c (6.2 [5.7–7.0] vs 6.4 [5.8–7.3]%; p < 0.001). AST (33 [26–49] vs 40 [29–57] U/L; p < 0.001) and GGT (44 [30–66] vs 50 [34–80] U/L; p < 0.001) were higher in the low LSM group and the platelet count was significantly higher in the low LSM group (246 [205–293] vs 237 [199–283] per nL; p = 0.02). LDL cholesterol was higher (111 (80–143) vs 99 (73–131) mg/dL; p = 0.002) and TG were higher. Lipoprotein A was lower (8.0 [4.5–17.2] vs 13.6 [5.7–42.9]; p < 0.001) in the low LSM group. Non-invasive measures of MASH severity were lower in the low LSM group, including CAP (331 [301–368] vs 338 [310–367] dB/m; p = 0.009), ELF (9.5 [9.0–10.0] vs 9.9 [9.3–10.5]; p < 0.001), and FIB-4 (1.15 [0.79–1.55] vs 1.36 [0.97–1.88]; p < 0.001).
Conclusion: Patients with low LSM < 8 kPa and biopsy-proven at-risk MASH tend to be younger with lower BMI and HbA1C but higher LDL and TG. Furthermore, these patients have lower ELF and FIB4, both of which could be affected by age. A personalized cutoff for LSM based on clinical characteristics is potentially needed to identify these patients that are suitable for clinical trials.

WED-052

Metabolic dysfunction–associated fibrosis-5 outperforms fibrosis-4 index for detecting liver fibrosis in a population-based cohort

Saleh A. Alqahtani[1,2], Shadan Almuhaidib[3], Basma Khoja[4], Faisal Abaalkhail[5,6], Haifa F Alotaibi[3], Albandari K Almotairi[7], Shakir Alharthi[8], Faisal AlOtaibi[9], Ahmed AlZahrani[9], Norah Aldossari[9], Alwaleed Almojel[4], Carolin V Schneider[10], Waleed K Al-Hamoudi[11,12], Faisal M Sanai[13], Waleed Alhazzani[3,14].
[1]Liver, Digestive, and Lifestyle Health Research Section, and Organ Transplant Center of Excellence, King Faisal Specialist Hospital and Research Center, Riyadh, Saudi Arabia; [2]Division of Gastroenterology & Hepatology, Weill Cornell Medicine, New York, United States; [3]Health Research Center, Ministry of Defense Health Services, Riyadh, Saudi Arabia; [4]Liver, Digestive, and Lifestyle Health Research Section, and Biostatistics, Epidemiology, and Scientific Computing Department, King Faisal Specialist Hospital and Research Center, Riyadh, Saudi Arabia; [5]College of Medicine, Alfaisal University, Riyadh, Saudi Arabia; [6]Gastroenterology Section, Department of Medicine, King Faisal Specialist Hospital and Research Center, Riyadh, Saudi Arabia; [7]Family Medicine Department, Prince Sultan Military Medical City, Riyadh, Saudi Arabia; [8]Department of Family Medicine, Armed Forces Hospital, Dhahran, Saudi Arabia, [9]Medical Laboratory Department, King Fahad Military Medical Complex, Dhahran, Saudi Arabia; [10]Department of Gastroenterology, Metabolic Diseases and Intensive Care, University Hospital RWTH Aachen, Aachen, Saudi Arabia; [11]Organ Transplant Center of Excellence, King Faisal Specialist Hospital and Research Center, Riyadh, Saudi Arabia; [12]Liver Disease Research Center, College of Medicine, King Saud University, Riyadh, Saudi Arabia; [13]Gastroenterology Section, Department of Medicine, King Abdulaziz Medical City, King Abdullah International Medical Research Center, Jeddah, Saudi Arabia; [14]Critical Care and Internal Medicine Department, College of Medicine, Imam Abdulrahman Bin Faisal University, Dammam, Saudi Arabia
Email: drsaleh.a.alqahtani@gmail.com

Background and aims: Early identification of liver fibrosis is essential for optimizing care pathways in individuals with metabolic dysfunction-associated steatotic liver disease (MASLD). The metabolic dysfunction-associated fibrosis-5 (MAF-5) score is an age-independent, noninvasive fibrosis assessment tool incorporating waist circumference (WC), body mass index (BMI), diabetes status, aspartate aminotransferase (AST), and platelet count. We evaluated the diagnostic performance of MAF-5 and the fibrosis-4 Index (FIB-4) for detecting fibrosis, using liver stiffness measurement (LSM) by transient elastography (TE) as the reference standard.
Method: We analyzed data from adults enrolled in the Genomics and Environmental Noninvasive Evaluation for Saudi Intrahepatic Steatosis (GENESIS) cohort with complete data required to calculate MAF-5. Liver fibrosis was defined as LSM ≥ 8.0 kPa by TE. MASLD was defined as controlled attenuation parameter (CAP) ≥ 268 dB/m with at least one cardiometabolic risk factor. MAF-5 was categorized as low (<0), intermediate (0–1), and high (>1) fibrosis risk. Diagnostic performance metrics were calculated for MAF-5 > 1 and FIB-4 ≥ 1.3.
Results: Of the 2,688 participants enrolled, liver fibrosis was present in 54 participants (2.0%). Those with fibrosis were older (median 52 vs. 41 years, p < 0.001), more often male (70.4% vs. 48.5%, p = 0.001), had higher BMI (33.5 vs. 28.8 kg/m^2, p < 0.001), and had substantially higher MASLD prevalence (83.3% vs. 36.4%, p < 0.001). Median MAF-5 was significantly higher in the fibrosis group (2.1 vs. −1.5, p < 0.001). Fibrosis prevalence increased across MAF-5 categories: 11.1% in low-risk, 13.0% in intermediate-risk, and 75.9% in high-risk (p < 0.001). MAF-5 > 1 showed strong diagnostic performance with sensitivity 75.9%, specificity 84.4%, positive predictive value (PPV) 9.1%, and negative predictive value (NPV) 99.4%. In comparison, FIB-4 ≥ 1.3 had sensitivity 18.5%, specificity 93.4%, PPV 5.4%, and NPV 98.2%.
Conclusion: In this large population-based cohort, MAF-5 outperformed FIB-4 for detecting liver fibrosis defined by TE ≥ 8.0 kPa, demonstrating exceptionally high NPV and strong rule-out performance for liver fibrosis. Its age-independent structure and incorporation of metabolic parameters support the use of MAF-5 as an efficient first-line noninvasive screening tool for fibrosis risk stratification in MASLD care pathways, particularly in primary care and population-based settings.

WED-053

High burden of MASLD and fibrosis risk in type 1 diabetes: a FibroScan-based screening study

Abdullah Alguwaihes[1], Metib Alotaibi[2], Khaled Aburisheh[2], Mohamed El-Sharkawy[3], Hazim Bajri[2], Amani Alsadoon[4], Maram Alkhammash[4], Omar Alhazza[5], Khalid A Alswat. *[1]Division of Endocrinology, Department of Internal Medicine, College of Medicine, King Saud University, Riyadh, Saudi Arabia; [2]University Diabetes Center, King Saud University Medical City, King Saud University,, Riyadh, Saudi Arabia; [3]Diagnostic Radiology and Medical Imaging Department, College of Medicine, King Saud University, Riyadh, Saudi Arabia; [4]Liver Disease Research Center, College of Medicine, King Saud University, Riyadh, Saudi Arabia; [5]Family Medicine department, King Fahd military medical complex, Riyadh, Saudi Arabia*
Email: aalguwaihes@ksu.edu.sa

Background and aims: Metabolic dysfunction–associated steatotic liver disease (MASLD) is well described in type 2 diabetes, but its burden in type 1 diabetes mellitus (T1DM) remains under-recognized and liver assessment is not routinely incorporated into T1DM care. We aimed to define the prevalence and severity of FibroScan-defined steatosis and MASLD in individuals with T1DM, assess the presence of advanced fibrosis, and evaluate agreement between ultrasound and transient elastography.
Method: Cross-sectional screening of individuals aged ≥14 years with ≥1-year T1DM. Hepatic steatosis and fibrosis were assessed using FibroScan (controlled attenuation parameter [CAP], liver stiffness measurement [LSM]) and ultrasound. Steatosis was defined as CAP ≥248 dB/m; MASLD as steatosis plus ≥1 metabolic risk factor; and advanced fibrosis as LSM ≥8.2 kPa. Steatosis severity was CAP-graded. Associations between LSM and glycemic or clinical parameters (HbA1c, diabetes duration, time-in-range) were assessed, and ultrasound–FibroScan agreement evaluated.

Results: Among 150 individuals with T1DM, FibroScan-defined steatosis (CAP ≥248 dB/m) was present in 54 (36.0%), and 43 (28.7%) fulfilled criteria for MASLD. MASLD prevalence was higher among individuals treated with multiple daily injections (30.0%) compared with insulin pump therapy (18.8%), and increased with age, peaking in the 40–49-year group. CAP values averaged 233 ± 54 dB/m, with steatosis severity distributed as S1 in 16.7%, S2 in 4.0%, and S3 in 15.3%. Median liver stiffness was 4.4 kPa (IQR 1.7); 4 participants (2.7%) had LSM ≥8.2 kPa, indicating advanced fibrosis. Associations between LSM and glycemic or clinical parameters were weak (HbA1c r = – 0.11; diabetes duration r = 0.18; time-in-range r = 0.09). Ultrasound showed moderate agreement with FibroScan for steatosis detection (κ = 0.469), with sensitivity 57.1% and specificity 87.6%.
Conclusion: This study represents one of the largest FibroScan-based screening cohorts in T1DM reported to date, demonstrating that MASLD is common in individuals with T1DM, with a small but important proportion already meeting thresholds for advanced fibrosis. Reliance on glycemic markers and ultrasound underestimates liver disease burden. Incorporating non-invasive liver assessment into T1DM care pathways may enable earlier identification of at-risk individuals and more appropriate risk stratification.

WED-054
Clinical significance of patients with significant fibrosis missed by the EASL algorithm in metabolic-associated steatotic liver disease: findings from the HEPAMET registry

Javier Ampuero[1,2,3,4], Javier Crespo[5], Douglas Maya-Miles[2,3,6], Luis Ibañez-Samaniego[7], José Luis Calleja Panero[3,8], Isabel Graupera[9], Alba Jiménez-Massip[10], Rocío Aller[11], Judith Gómez-Camarero[12], Salvador Benlloch[13], Rosa Martín-Mateos[14], Rosa M Morillas[15], Rocío Gallego-Durán[2,3,4], Vanesa Bernal[16], Juan Turnes[17], Mercedes De La Torre Sanchez[18], Maria Poca[19], Raquel Latorre Martínez[20], Desamparados Escudero-García[21], Oreste Lo Iacono[22], Antonio Olveira[23], Rubén Francés[24], Paula Iruzubieta[25], Laura Suarez Lopez[7], Jesús Rivera Esteban[8], Anna Soria[9], Juan M. Pericàs[10], Manuel Romero-Gómez[1,2,3,4].
[1]Hospital Universitario Virgen del Rocío, Sevilla, Spain; [2]Instituto de Biomedicina de Sevilla (IBiS). Hospital Universitario Virgen del Rocío/CSIC/Universidad de Sevilla, Sevilla, España, Seville, Spain; [3]Centro de Investigación Biomédica en Red en el área de Enfermedades Hepáticas y Digestivas (CIBER-EHD), Madrid, Spain; [4]Facultad de Medicina, Universidad de Sevilla, Seville, Spain; [5]Facultad de Medicina. Universidad de Cantabria, Grupo de Investigación Clínica y Traslacional en Enfermedades Digestivas, Instituto de Investigación Sanitaria Valdecilla (IDIVAL)/Servicio de Aparato Digestivo y Hepatología, Hospital Universitario Marqués de Valdecilla, Santander, España, MedicineAI, Madrid, España, Santander, Spain; [6]Departamento de Fisiología, Universidad de Sevilla, Seville, Spain; [7]Liver Unit. Hospital General Universitario Gregorio Marañón/Instituto de Investigación Sanitaria Gregorio Marañón, Madrid, Spain, Centro de Investigación Biomédica en Red en el área de Enfermedades Hepáticas y Digestivas (CIBEREHD), Madrid, Spain; [8]Gastroenterology and Hepatology Department, Puerta del Hierro University Hospital, Puerta de Hierro-Segovia de Arana Research Institute (IDIPHISA), Autonomous University of Madrid, Madrid, Spain; [9]Liver Unit. Hospital Clínic. Institut d'Investigacions Biomèdiques August Pi i Sunyer (IDIBAPS). Barcelona, Spain, Centro de Investigación Biomédica en Red en el área de Enfermedades Hepáticas y Digestivas (CIBEREHD), Barcelona, Spain; [10]Liver Unit, Vall d'Hebron University Hospital Campus, VHIR, Universitat Autónoma de Barcelona, Barcelona, Spain, Centro de Investigación Biomédica en Red en el área de Enfermedades Hepáticas y Digestivas (CIBEREHD), Barcelona, Spain; [11]Department of Medicine, Dermatology and Toxicology, University of Valladolid, Gastroenterology Unit, HCUV, Valladolid. UIC Biocritic, CIBERINFEC, UIC Biocritic, CIBERINFEC, Spain, Valladolid, Spain; [12]Hospital Universitario de Burgos, Burgos, Spain, Burgos, Spain; [13]Hospital Arnau de Vilanova, Universidad Cardenal Herrera-CEU Universities, Valencia, Spain; [14]Hospital Universitario Ramón y Cajal, Irycis. Universidad de Alcalá, Madrid, Spain, Madrid, Spain; [15]Hospital Germans Trias i Pujol, Badalona, Spain, Badalona, Spain; [16]Hospital Universitario Miguel Servet, Zaragoza, Spain; [17]Complejo Hospitalario Universitario de Pontevedra & IIS Galicia Sur, Pontevedra, Spain; [18]Consorcio Hospital General Universitario de Valencia, Valencia, Spain; [19]Hospital de la Santa Creu i Sant Pau, Barcelona, Spain; [20]Hospital Son Llatzer, Palma de Mallorca, Spain; [21]Hospital Clínico Universitario de Valencia, Valencia, Spain; [22]Hospital Universitario del Tajo, Madrid, Spain; [23]Hospital Universitario La Paz, Madrid, Spain; [24]Hospital General Universitario de Alicante, Alicante, Spain; [25]Servicio de Aparato Digestivo y Hepatología, Hospital Universitario Marqués de Valdecilla, Grupo de Investigación Clínica y Traslacional en Enfermedades Digestivas, Instituto de Investigación Sanitaria Valdecilla (IDIVAL), Santander, Spain
Email: jampuero-ibis@us.es

Background and aims: The EASL guidelines include FIB-4 and elastography (ET) for identifying patients at high risk of advanced metabolic-associated steatotic liver disease (MASLD). This work aims to evaluate baseline characteristics and progression to cirrhosis among patients with significant fibrosis classified as low- vs. high-risk according to the EASL algorithm for MASLD.
Method: A total of 1544 MASLD patients from the HEPAMET registry with baseline FIB-4 and ET data were included. According to EASL criteria, the low-risk group was defined as FIB-4 <1.30 or FIB-4 >1.30 and ET <8 kPa, whereas the high-risk group was defined as FIB-4 >1.30 and ET >8 kPa. Significant fibrosis was defined as F2–F4. Patients with cirrhosis were excluded from the progression analysis (5 ± 2.6 years follow-up).
Results: Mean age was 55.3 ± 11.4 years, and 52.3% were men. MASH was present in 44.1% of patients, and fibrosis stages were: F0 26%, F1 25.3%, F2 15.5%, F3 19.9%, F4 11.8%. Overall, 70.6% (1090/1544) were classified as high-risk. Significant fibrosis was present in 61.7% (661/1071) of the high-risk group vs. 15% (67/448) of the low-risk group. Age (59.3 ± 9.6 vs. 53.9 ± 11.4; p = 0.0001), albumin (4.41 ± 0.4 vs. 4.53 ± 0.3; p = 0.034), platelets (196 ± 67 vs. 236 ± 64; p = 0.0001), INR (1.06 ± 0.2 vs. 1.01 ± 0.1; p = 0.015), type 2 diabetes (65.1% vs. 47.8%; p = 0.005), and hypertension (67.9% vs. 47.8%; p = 0.001) were significantly different between high- and low-risk patients with significant fibrosis. ET was also higher in the high-risk group (17.9 ± 11.1 vs. 6.3 ± 1.4 kPa; p = 0.0001). During follow-up, 26.7% (60/225) of high-risk patients with significant fibrosis progressed to cirrhosis vs. 10.7% (3/28) in the low-risk group (log-rank 4.323; p = 0.038), with high-risk status independently predicting progression [HR 3.47 (95% CI 1.08–11.14)] after adjustment for age, sex, and baseline fibrosis stage.
Conclusion: Although some patients with significant fibrosis are not identified by the EASL algorithm, their baseline characteristics suggest a more indolent course and a significantly lower risk of progression to cirrhosis.

WED-055-YI
AI-based fibrosis detection in MASLD: evaluating swallow deep neural networks, large language models and foundation models vs. FIB-4

Gabriele De Vito[1], Eleni-Myrto Trifylli[2], Filomena Ferrucci[1], Athanasios Angelakis[3]. *[1]Dept. of Computer Science, Univ. of Salerno, Salerno, Italy; [2]GI-Liver Unit, 2nd Department of Internal Medicine, National and Kapodistrian University of Athens, Laboratory of Reliability and Quality Control in Laboratory Hematology (HemQcR), Department of Biomedical Sciences, Section of Medical Laboratories, School of Health & Caring Sciences, University of West Attica (UniWA), Athens, Greece; [3]Amsterdam University Medical Center, Amsterdam, Netherlands*
Email: a.angelakis@amsterdamumc.nl

Background and aims: Metabolic dysfunction-associated steatotic liver disease (MASLD) is a major global health burden, with advanced

fibrosis driving liver-related morbidity. FIB-4 is widely used for non-invasive fibrosis assessment but shows variable performance across populations. This study compared artificial intelligence models, including shallow deep neural networks (s-DNNs), tabular foundation models (TabPFN), and large language models (LLMs), with FIB-4 for advanced fibrosis detection across multiple MASLD cohorts.

Method: A total of 784 biopsy-confirmed MASLD pts were included from three cohorts: China (n = 540; training/internal validation), Malaysia (n = 147; val1), and India (n = 97; val2). The models were trained and evaluated using six clinical features: age, AST, ALT, PLT, FIB-4, and a FIB-4 threshold (1.3). The LLM "gpt-4o-2024–08–06" was tested in zero-shot (ZS) and fine-tuned (FT) settings, using structured prompts with the same input variables. The s-DNN comprised three hidden layers (17, 5, 23 nodes), ReLU activation, Adam optimizer (α = 0.001), dropout, and 100 epochs. Performance was evaluated over five independent runs using specificity (Spec), sensitivity (Sens), AUROC, and F1. The prevalence of advanced fibrosis was 27.6% (China), 21.08% (val1), and 32.98% (val2).

Results: FIB-4 achieved AUROC: 0.75 (Spec: 0.79, Sens: 0.71, F1: 0.57) in val1 and 0.60 (Spec: 0.66, Sens: 0.53, F1: 0.48) in val2. TabPFN showed high Spec (≥0.86) but low Sens (≤0.40), with AUROC values of 0.65 (F1: 0.45) in val1 and 0.63 (F1: 0.48) in val2. The ZS-LLM "gpt-4o-2024–08–06" achieved AUROC: 0.73 (Spec: 0.65 ± 0.02, Sens: 0.81 ± 0.02, F1: 0.52 ± 0.02) in val1 but dropped to 0.57 (F1: 0.47) in val2. FT improved LLM performance in val1 (AUROC: 0.75, F1: 0.56) but was inconsistent in val2 (AUROC: 0.63, F1: 0.50). The s-DNN consistently outperformed all models, achieving AUROC: 0.76 (Spec: 0.76, Sens: 0.74, F1: 0.56) in val1 and 0.66 (Spec: 0.71, Sens: 0.56, F1: 0.52) in val2.

Conclusion: The s-DNN consistently outperformed FIB-4, LLMs, and TabPFN for advanced fibrosis detection across cohorts, demonstrating the most balanced diagnostic performance. Although LLMs showed moderate accuracy, their variable sensitivity limits clinical reliability, while TabPFN exhibited high specificity but poor sensitivity. These findings suggest that domain-specific AI models trained on structured clinical data provide superior and more generalizable fibrosis assessment.

WED-056

NAFLD liver fat score outperforms controlled attenuation parameter for diagnosing hepatic steatosis in type 2 diabetes: an explainable artificial intelligence study

Athanasios Angelakis[1], Byron Lykiardopoulos[2], Wile Balkhed[3], Martin Bergram[4], Fredrik Iredahl[4], Markus Holmberg[2], Carl Edin[5], Carl-Johan Carlhäll[5], Tino Ebbers[5], Pontus Henriksson[2], Christian Simonsson[2], Karin Rådholm[2], Gunnar Cedersund[6], Mikael Forsgren[7], Olof Dahlqvist Leinhard[8], Cecilia Jönsson[2], Peter Lundberg[5], Stergios Kechagias[2], Nils Dahlström[5], Patrik Nasr[9], Mattias Ekstedt[5]. *[1]Amsterdam University Medical Center, Amsterdam, Netherlands; [2]Department of Health, Medicine and Caring Sciences, Linköping University, Linköping, Sweden; [3]Wallenberg Center for Molecular Medicine (WCMM), Linköping University,, Linköping, Sweden; [4]Primary Health Care Center, Department of Health, Medicine and Caring Sciences, Linköping University, Wallenberg Center for Molecular Medicine (WCMM), Linköping University, Linköping, Sweden 5Center for Medical Image Science and Visualization (CMIV), Linköping University, Linköping, Sweden; [5]Department of Health, Medicine and Caring Sciences, Linköping University, Center for Medical Image Science and Visualization (CMIV), Linköping University, Linköping, Sweden; [6]Department of Biomedical Engineering, Linköping University, Linköping, Sweden; [7]Department of Health, Medicine and Caring Sciences, Linköping University, Center for Medical Image Science and Visualization (CMIV), Linköping University, AMRA Medical AB, Linköping, Sweden; [8]Wallenberg Center for Molecular Medicine (WCMM), Linköping University, AMRA Medical AB, Linköping, Sweden; [9]Department of Health, Medicine and Caring Sciences, Linköping University, Wallenberg Center for Molecular Medicine (WCMM), Linköping University, Center for Medical Image Science and Visualization (CMIV), Linköping University, Linköping, Sweden*
Email: a.angelakis@amsterdamumc.nl

Background and aims: Metabolic dysfunction-associated steatotic liver disease (MASLD) is highly prevalent in patients with type 2 diabetes mellitus (T2DM) and requires accurate non-invasive assessment. The controlled attenuation parameter (CAP) is widely used but requires specialized equipment and shows uncertain performance compared with other non-invasive tests (NITs) in metabolically complex populations. We aimed to evaluate and rank NITs for magnetic resonance imaging proton density fat fraction (MRI-PDFF)-defined steatosis in T2DM using explainable artificial intelligence (XAI), and to assess whether machine learning (ML) improves diagnostic performance.

Method: A total of 247 patients with T2DM were analyzed. Of these, 54% had steatosis, i.e. MRI-PDFF ≥5%. The dataset was randomly split into training (n = 197, 80%) and test (n = 50, 20%) sets. A CatBoost (CB) ML model was trained/tuned (hyperparameters: iterators, learning rate, depth) with 10-fold cross validation (10CV) on the training set, using as features: CAP, Hepatic Steatosis Index (HSI), NAFLD Liver Fat Score (LFS), Fatty Liver Index, Lipid Accumulation Product, Visceral Adiposity Index, Triglyceride-Glucose Index, and FAST. XAI techniques including SHAP (Shapley Additive Explanations), CB's direct predictability feature importance, importance on the loss error, and correlation analysis were applied to assess feature importance.

Results: The AUROC mean ± SD with [95% CI] using 10CV was: CAP (cut-off: 248 dB/m) 0.84 ± 0.09 [0.68–1.00], LFS (cut-off: −0.64) 0.82 ± 0.10 [0.68–0.97], and CB 0.88 ± 0.07 [0.77–1.00]. On the test set, AUROC was CAP 0.87, LFS 0.90, and CB 0.95, with specificity for CAP 0.70, LFS 0.70, and CB 0.78. Sensitivity for CAP, LFS, and CB was 0.93. Correlation analysis showed CAP had the highest association with PDFF, Pearson (P): 0.61, Kendall (K): 0.49, Spearman (S): 0.68, while LFS showed similar trends (S: 0.64, K: 0.45) but lacked linear correlation (P: 0.14). Applying a 5% PDFF cut-off, LFS showed non-linear correlation with steatotic patients (Point-Biserial: 0.18), while CAP was 0.60. XAI methods confirmed LFS as the most important predictor.

Conclusion: LFS outperformed CAP for diagnosing steatosis in patients with T2DM, demonstrating higher predictive accuracy and metabolic relevance. XAI confirmed its diagnostic importance. LFS may represent a practical alternative to CAP for MASLD screening in primary care. Further studies should validate these findings and explore ML integration and fibrosis assessment.

WED-057-YI

Comparing non-invasive risk scores for predicting adverse liver outcomes in MASLD

Erica Appiah[1], Rajan Paudel[2,3], Rickard Strandberg[2,4], Jerome Boursier[5,6], Christophe Cassinotto[7,8], Wah-Kheong Chan[9], Donghyeon Lee[10], Elisabetta Bugianesi[11], A.G. (Onno) Holleboom[12], Johannes Wiegand[13], Hirooka Masashi[14], Thomas Karlas[13], Monica Lupsor-Platon[15], Emmanuel Tsochatzis[16], Toshihide Shima[17], Vincent Wai-Sun Wong[18], Ming-Hua Zheng[19,20,21], Victor De Ledinghen[22], Michael Pavlides[23], Hannes Hagström[2,3]. *[1]Radcliffe Department of Medicine, University of Oxford, Oxford, United Kingdom; [2]Department of Medicine, Huddinge, Karolinska Institutet, Stockholm, Sweden; [3]Division of Hepatology, Department of Upper GI Diseases, Karolinska University Hospital, Stockholm, Sweden; [4]Red Door Analytics, Stockholm, Sweden; [5]Laboratoire HIFIH, UPRES EA 3859, SFR ICAT 4208, Université d'Angers, Angers, France; [6]9Service d'Hépato-Gastroentérologie et Oncologie Digestive, Centre Hospitalier Universitaire d'Angers, Angers, France; [7]Department of Diagnostic and Interventional Radiology, Saint-Eloi Hospital, University Hospital of Montpellier, Montpellier, France; [8]Institut Desbrest d'Epidémiologie et de Santé Publique, IDESP UMR UA11 INSERM, University Hospital of Montpellier, Montpellier, France; [9]Gastroenterology and Hepatology Unit, Department of Medicine, Faculty of Medicine, University of Malaya,, Kuala Lumpur, Malaysia; [10]Department of Internal Medicine,*

Gil Medical Center, Gachon University College of Medicine, Incheon, Korea, Rep. of South; [11]Department of Medical Sciences, University of Turin, Torino, Italy; [12]Department of Vascular Medicine, Amsterdam UMC, University of Amsterdam, Amsterdam, Netherlands; [13]Department of Oncology, Gastroenterology, Hepatology, Pulmonology and Infectious Diseases University Hospital Leipzig, Leipzig, Germany; [14]Department of Gastroenterology and Metabology, Ehime University Graduate School of Medicine, Ehime, Japan; [15]Department of Medical Imaging, Iuliu Haţieganu University of Medicine and Pharmacy, Regional Institute of Gastroenterology and Hepatology "Prof.Dr. Octavian Fodo, Cluj-Napoca, Romania; [16]Sheila Sherlock Liver Unit and UCL Institute for Liver and Digestive Health, Royal Free Hospital and University College London, London, United Kingdom; [17]Hepatology Center, Saiseikai Suita Hospital, Suita, Osaka, Japan; [18]Department of Medicine and Therapeutics, The Chinese University of Hong Kong, Hong Kong; [19]NAFLD Research Center, Department of Hepatology, the First Affiliated Hospital of Wenzhou Medical University, Wenzhou, China; [20]Wenzhou Key Laboratory of Hepatology, Wenzhou, China; [21]Institute of Hepatology, Wenzhou Medical University, Wenzhou, China; [22]Centre d'Investigation de la Fibrose Hépatique, Hôpital Haut-Lévêque, Bordeaux University Hospital, Pessac, France; [23]Radcliffe Department of Medicine, University of Oxford, Oxford, United Kingdom
Email: quee5084@ox.ac.uk

Background and aims: Risk stratification in metabolic dysfunction–associated steatotic liver disease (MASLD) is essential for identifying individuals at increased risk of major adverse liver outcomes (MALO) such cirrhosis and hepatocellular carcinoma. Multiple risk scores have been proposed across different populations, but their comparative performance to predict incident MALO in patients with confirmed MASLD remain unclear. The aim of this analysis was to compare the performance of several models to predict incident MALO.
Method: This analysis evaluated risk scores in an individual participant data meta-analysis (IPD-MA), comprising well-characterised MASLD cohorts with longitudinal follow-up for liver-related outcomes. We computed: Cirrhosis Outcome Risk Estimator (CORE), Fibrosis-4 (FIB-4), Metabolic dysfunction-Associated Fibrosis 5 score (MAF-5), Liver Risk Score (LRS), and Anticipate-NASH. To assess discrimination at yearly intervals up to 10 years, the area under the curve (AUC) was the primary metric. Calibration of the models was assessed using observed-to-expected (O:E) ratios and subgroup analyses examined each model's performance across different populations considering data availability for each model within the IPD to maximise sample size.
Results: The complete-case cohort, where data were available for all predictors, included participants from 14 independent studies (n = 927). The median age was 49 years (IQR 20–59), and 53.0% (n = 491) were male. Type 2 diabetes was present in 41.8%, and the median BMI was 28 kg/m^2 (IQR 25– 32). The median duration of follow-up was 4.8 years, during which 2.1% of participants experienced MALO. At 10 years, AUC demonstrated variable discriminatory performance across models: CORE 0.713, FIB-4 0.823, MAF-5 0.733, LRS 0.610, and Anticipate-NASH 0.703. Results from evaluation of each model separately were broadly consistent with FIB-4 showing the strongest discrimination in both analyses. The AUC for CORE (n = 1970) was 0.738; FIB-4 (n = 2326) 0.821; MAF-5 (n = 1403) 0.758; LRS (n = 1586) 0.684; and Anticipate-NASH (n = 2315) 0.770. Calibration varied between models. CORE underpredicted the incidence of MALO (O:E 2.567), whereas overprediction was observed for LRS (O:E 0.007) and MAF-5 (O:E 0.02).
Conclusion: The risk scores show heterogeneity in discrimination and calibration and are not interchangeable across populations. This highlights the importance of population specific validation and recalibration in patients with MASLD in clinical practice.

WED-058-YI

Primary care MASLD fibrosis risk stratification: real-world comparison of FIB-4–VCTE and SAFE–VCTE pathways

Afreen Ashraf[1], Ryan Wexler[1], Pavan Vuddanda[2], Panagiotis Trilianos[3], Arpan Mohanty[2]. *[1]Boston University School of Medicine, Boston, United States; [2]Boston Medical Center, Boston, United States; [3]East Boston Neighborhood Health, East Boston, United States*
Email: afreen@bu.edu

Background and aims: Current guidelines recommend tiered fibrosis risk stratification for patients with metabolic dysfunction–associated steatotic liver disease (MASLD) in primary care using the Fibrosis-4 (FIB-4) index followed by vibration-controlled transient elastography (VCTE) for intermediate risk. However, evidence suggests FIB-4 may underperform in identifying intermediate fibrosis. The steatosis-associated fibrosis estimator (SAFE), which integrates age, BMI, diabetes, platelets, aminotransferases, and globulin, followed by VCTE, is alternatively proposed. We compared real-world performance of FIB-4-VCTE and SAFE-VCTE pathways in a large safety-net primary care cohort, assessing diagnostic accuracy against liver biopsy and magnetic resonance elastography (MRE).
Method: We analyzed 1,095 consecutive primary care patients at risk for MASLD (61% female; mean age 48 years; 89.5% Hispanic) who underwent VCTE and had complete data to calculate FIB-4 and SAFE. Referral indications included elevated liver enzymes, steatosis, diabetes/prediabetes, BMI >30 kg/m^2, or ≥2 cardiometabolic risk factors. Patients with significant alcohol use, known liver disease, repeat referrals, or incomplete data were excluded. A subgroup of 125 underwent biopsy or MRE; significant fibrosis was defined as ≥F2 or MRE ≥3.1 kPa. FIB-4 categories followed EASL age-specific thresholds for low, indeterminate, and high risk. SAFE fibrosis risk categories were defined as: low (<0), indeterminate (0–99), and high (≥100). Hepatology referral criteria were indeterminate risk with VCTE ≥8 kPa or high-risk classification. Outcomes included the proportion meeting criteria for hepatology referral, false-omission rate (low-risk classification despite significant fibrosis), false-positive rate (indeterminate or high-risk classification without significant fibrosis), and overall correct classification.
Results: Among 1,095 patients, FIB-4–VCTE led to 61 referrals (6%) versus 176 (16%) with SAFE–VCTE. In the biopsy/MRE subgroup, FIB-4–VCTE had a higher false-omission rate than SAFE–VCTE (25% vs 13%, p = 0.14). False-positive rates (52% vs 58%, p = 0.77) and correct classification (62% vs 70%, p = 0.18) were similar.
Conclusion: In a largely Hispanic U.S. safety-net primary care cohort, the SAFE–VCTE pathway increased hepatology referrals but reduced false-omission rate compared with FIB-4–VCTE, with similar overall diagnostic accuracy. Further studies are needed to optimally balance referral burden and fibrosis detection in primary care MASLD.

WED-059

Unlocking recruitment with LiverPRO in a phase III pilot study for metabolic dysfunction-associated steatohepatitis

Julie Astono[1], Katrine Lindvig[1], Maja Thiele[2], Aleksander Krag[2], Dimple Desai[3], Mazen Noureddin[4], Naim Alkhouri[4], Rashmee Patil[3]. *[1]Evido Health, Copenhagen, Denmark; [2]Department of Gastroenterology and Hepatology, Odense University Hospital, Institute of Clinical Research, University of Southern Denmark, Odense C, Denmark; [3]Pinnacle Clinical Research, San Antonio, United States; [4]Summit Clinical Research, San Antonio, United States*
Email: katrine@evido.health

Background and aims: Recruitment into phase III trials for metabolic dysfunction-associated steatohepatitis (MASH) is limited by low detection rates of clinically significant fibrosis (≥F2) and reliance on referral-based or manual prescreening. Scalable approaches are needed to identify at-risk individuals earlier and more systematically. This pilot evaluated the feasibility of LiverPRO, a data-driven fibrosis risk model applied to routinely collected laboratory data, as a pre-screening tool for clinical trial recruitment.

Method: We conducted a pragmatic US real-world pilot in which LiverPRO was applied to existing primary care laboratory datasets to identify individuals at risk of liver fibrosis. LiverPRO is designed to operate under heterogeneous data availability and does not require complete biomarker panels to estimate the probability of ≥F2 fibrosis. Individuals exceeding a predefined risk threshold (LiverPRO score ≥0.65) were flagged for further clinical evaluation. Downstream evaluation included opportunistic assessment with transient elastography (TE), and referral for liver biopsy according to site-specific protocols. Key outcomes included data processability, proportion of individuals flagged as at risk, and progression through downstream assessment steps.
Results: A total of 1,587 individuals were identified within the primary-care laboratory registry during the 2-month pilot period. LiverPRO was calculated in 1,371 individuals (86.4%). Of these, 171 individuals (12.5%) were flagged as being at increased risk of significant fibrosis (LiverPRO score ≥0.65). To date, 19 individuals have undergone transient elastography as part of downstream clinical evaluation. Among those assessed, 5 demonstrated liver stiffness values between 6 and 8 kPa, 3 between 8 and 12 kPa, and 1 >12 kPa. Following clinical review, 3 individuals were invited for further evaluation and potential trial recruitment. While no trial enrolments have occurred, the approach enabled identification of previously unrecognised at-risk individuals, several of whom met criteria for clinical management outside a trial.
Conclusion: This pilot demonstrates the feasibility of systematic pre-screening for liver fibrosis using routinely collected laboratory data. LiverPRO enabled scalable identification of individuals at increased fibrosis risk despite heterogeneous and incomplete datasets. As a pre-screening approach, this strategy may support identification of candidates for late-phase MASH trials.

WED-060-YI
Lower predictive performance of FIB-4 with lower eGFR categories: a cohort study of 63,587 persons
Hanne Åström[1], Axel Wester[1], Hannes Hagström[1,2], Juan-Jesus Carrero[3,4]. [1]*Karolinska Institutet, Department of Medicine, Huddinge, Stockholm, Sweden;* [2]*Karolinska University Hospital, Department of Upper GI, Division of Hepatology, Stockholm, Sweden;* [3]*Karolinska Institutet, Department of Medical Epidemiology and Biostatistics, Stockholm, Sweden;* [4]*Danderyd Hospital, Department of Clinical Science, Stockholm, Sweden*
Email: hanne.astrom@ki.se

Background and aims: Chronic kidney disease (CKD) is common in patients with metabolic dysfunction-associated steatotic liver disease (MASLD). It is unknown whether the guideline-recommended FIB-4 score predicts major adverse liver outcomes (MALO) in reduced eGFR. Here, we examined the association between eGFR, FIB-4, and MALO, and evaluated the discriminative ability of FIB-4 across eGFR groups in persons with or at high risk of MASLD.
Method: We included persons with or at high risk of MASLD in the Stockholm Creatinine Measurements (SCREAM) cohort, defined as diagnoses for MASLD, type 2 diabetes or obesity. The population was stratified by eGFR (≥90, 60–89, 30–59 and <30mL/min/1.73m^2) and age-adjusted FIB-4 (low, indeterminate, high). Cox regression estimated the association between FIB-4 and MALO within eGFR groups. Harrell's C-index was used to assess the discriminative ability of FIB-4 across eGFR groups.
Results: We included 63,587 persons with or at high risk of MASLD with a median follow-up of 4.9 years (IQR = 2.0–9.2). Across all eGFR groups, high FIB-4 was associated with higher rates of MALO compared to low FIB-4. The discriminative ability of FIB-4 was highest in persons with eGFR ≥90 (C-index = 0.77), and lowest in eGFR 30–59 (C-index = 0.64) and eGFR <30 (C-index = 0.69).
Conclusion: Higher FIB-4 scores were associated with an increased rate of MALO across all eGFR groups, but the discriminative ability of FIB-4 was strongest among those with eGFR ≥90. The reduced discrimination in lower eGFR suggests that other measures of liver fibrosis assessment may be needed in these persons.

WED-061
Routine testing of PNPLA3 and TM6SF2 genetic variants in MASLD: experience from outpatient hepatology clinics in southern Switzerland
Beatrice Barda[1,2], Chiara De Luca[1], Maurizia Bissig[1], Rossella Forlenza[1], Claudia Di Bartolomeo[1], Mario Uhr[3], Andreas Cerny[2]. [1]*Fondazione Epatocentro Ticino, Lugano, Switzerland;* [2]*Epatocentro Ticino, Lugano, Switzerland;* [3]*Medisyn, Bioggio, Switzerland*
Email: beatrice.barda@hin.ch

Background and aims: Metabolic dysfunction–associated steatotic liver disease (MASLD) is the most frequently diagnosed condition in hepatology outpatient clinics. Increasing attention has focused on genetic factors, and PNPLA3 I148M and TM6SF2 E167K variants have been associated with liver steatosis and a higher risk of metabolic dysfunction–related diseases. We report our experience with routine testing for these variants in patients referred for steatotic liver disease.
Method: We included patients followed between 2018 and 2024 at our outpatient hepatology center, organized as a hub-and-spoke model with six peripheral clinics across Ticino and a central hub in Lugano, Southern Switzerland. Patients were referred for liver steatosis on ultrasound, elevated liver enzymes, or increased ferritin levels. At baseline, all subjects underwent FibroScan®, abdominal ultrasound, and laboratory tests to exclude other causes of steatosis. PNPLA3 I148M and TM6SF2 E167K variant testing was performed after informed consent.
Results: Overall, 300 patients with MASLD were included. Most were male (62%), the mean age was 57 years, and 48% had a body mass index (BMI) >29 kg/m^2. Genetic testing showed no variants in 108 patients, heterozygosity for PNPLA3 in 104, heterozygosity for TM6SF2 in 14, homozygosity for PNPLA3 in 43, and homozygosity for TM6SF2 in 3 patients. Mixed genetic profiles were observed in 18 patients. Overall, about half of the cohort carried at least one variant. At baseline FibroScan®, 60% showed no fibrosis. Mild steatosis was present in 85% of patients, while 15% had severe steatosis. All patients received structured counseling, including clinical evaluation and nutritional support. Follow-up corresponded to the last visit, 2–4 years after baseline. Among patients with complete data, no significant association was found between liver improvement and specific genetic variants. Most patients remained stable, some improved liver stiffness, and only two worsened.
Conclusion: PNPLA3 and TM6SF2 variants were frequent in our MASLD population. Most patients showed stabilization or improvement of liver parameters, likely related to regular follow-up and lifestyle interventions. Awareness of genetic predisposition appeared to improve adherence to lifestyle changes. We have recently initiated a prospective MASLD cohort with annual follow-up, patient-reported outcomes, and systematic sample collection.

WED-062
Definite fibrotic metabolic-dysfunction associated steatohepatitis in referrals at center in Denmark
Mark Berner Hansen[1], Eva Efsen Dahl[1], Gro Linno Willemoe[2], Frank Vinholt Schiødt[1]. [1]*Digestive Disease Center K, Bispebjerg University Hospital, Copenhagen NV, Denmark;* [2]*Department of Pathology, Rigshospitalet, Copenhagen Ø, Denmark*
Email: mbh@dadlnet.dk

Background and aims: Management guidelines by EASL and other societies for metabolic dysfunction-associated steatotic liver disease (MASLD), recommend mainly targeting patients with fibrotic metabolic-dysfunction associated steatohepatitis (MASH) and metabolic risk factors for progression of disease. Accordingly, fibrotic MASH patients have increased risk for developing serious late stage complications and as such in need of urgent management at expert

care centers. Real-world experience (RWE) with respect to the proportion of referred patients diagnosed with definite fibrotic MASH is limited. Here we report our RWE at a Danish referral university hospital center.

Method: Adult patients with metabolic syndrome and/or elevated alanine aminotransferases (ALT >50) referred in a 5-year period (2018–2022) on suspicion of fibrotic MASH were retrospectively included. Medical history, anthropometric measurements, routine (blood tests, ultrasound) and specific examinations were applied. Liver biopsy was offered for definite diagnosis and to evaluate MASLD characteristics. Patient demographics and characteristics, absolute and proportion of patients with definite MASLD and fibrotic MASH are reported.

Results: A total of 137 adult patients was included. Ten percent of patients were evaluated without liver biopsy and diagnosed with chronic liver diseases other than MASLD. Liver-biopsied patients (n = 123) had a mean age of 49 years, half were males. Overweight or obesity was present in 94%, dyslipidemia in 74%, hypertension in 40% and type 2 diabetes mellitus in 34%. Of all 137 patients, 104 (76%) were diagnosed with definite MASLD and 80 (58%) with definite MASH. Seventy-four (54%) patients had definite fibrotic MASH, while 41 (30%) had significant (F2-F4) fibrotic MASH. Eight patients (6%) had cirrhotic (F4) MASH.

Conclusion: This real-world retrospective study indicates that about half of the referred patients, all evaluated according to recent EASL management guidelines with cardio-vascular risk profile, were diagnosed with definite fibrotic MASH. As such, we conclude that the new management guidelines are useful for identifying a relevant high proportion of fibrotic MASH patients among referrals in a real-world setting at a referral center in Denmark.

WED-067

ActiMASH: a novel blood-based score to measure liver activity in patients with MASLD

Louise Biquard[1], Laure Elkrief[1,2], Marion Tanguy[1], Alix Cointet[1], Antoine Wawrzyniak[1], Damarys Loew[3], Florent Dingli[3], Shantha Valainathan[4,5], Philippe Garteiser[1], Agnes Lehuen[6], Cedric Laouenan[7], Johanne Poisson[1,8], Anais Vallet Pichard[9], Angélique Brzustowski[1], Pauline Manchon[7], Thierry Poynard[10,11], Valérie Paradis[1,12], Dominique Valla[1], Pierre-Emmanuel Rautou[1,4].
[1]Université Paris Cité, Inserm, Centre de Recherche sur l'Inflammation, UMR 1149, Paris, France; [2]Université de Tours, service d'hépato-gastroentérologie, Centre de références constitutif des maladies vasculaires du foie, Hôpital Trousseau, CHRU de Tours, Tours, France; [3]Institut Curie, PSL Research University, CurieCoreTech Mass Spectrometry Proteomics, Paris, France; [4]AP-HP, Hôpital Beaujon, Service d'Hépatologie, DMU DIGEST, Centre de Référence des Maladies Vasculaires du Foie, FILFOIE, ERN RARE-LIVER, Clichy, France; [5]Service de Réanimation polyvalente Centre hospitalier Victor Dupouy, Argenteuil, France; [6]Institut Cochin, INSERM UMR-S1016, CNRS UMR-S8104, Université Paris Cité, Paris, France; [7]Université Paris Cité, Inserm, IAME, Département Epidémiologie Biostatistiques et Recherche clinique, AP-HP, Hôpital Bichat, Paris, France; [8]Université Paris Cité, Department of Geriatrics, European Georges Pompidou Hospital, Paris Cancer Institute CARPEM, Assistance-Publique Hôpitaux de Paris (AP-HP), Paris, France; [9]AP-HP Centre Université Paris Centre, Groupe Hospitalier Cochin Port Royal, DMU Cancérologie et Spécialités Médico-Chirurgicales, Service des Maladies du foie, Paris, France; [10]Medical Faculty, Pitié Salpêtrière Hospital, Sorbonne University, Paris, France; [11]BioPredictive, Paris, France; [12]Service de Pathologie, AP-HP.Nord, Hôpital Beaujon, Clichy, France
Email: louise.biquard@laposte.net

Background and aims: In metabolic dysfunction-associated steatotic liver disease (MASLD), disease activity is a key feature of steatohepatitis (MASH) diagnosis and drives fibrosis progression. MASLD activity can only be assessed by liver biopsy. We aimed to develop a non-invasive test to measure MASLD activity, named ActiMASH.

Method: The present study was nested in the multicenter prospective QUID-NASH trial (NCT03634098), including 407 patients with type 2 diabetes (derivation, n = 273; validation, n = 134), and liver biopsy available. RNAseq was performed on liver samples. Liver stiffness measurement (LSM) by vibration-controlled transient elastography was performed at inclusion and during follow-up. Proteomics was performed on circulating extracellular vesicles (EVs) from 23 patients (8 steatosis, 15 MASH), allowing identification of an EV biomarker then measured by filtration/ELISA on derivation and validation populations. To develop ActiMASH, a logistic regression was performed on the derivation population, and then validated.

Results: Proteomics showed that plasma EV protein composition was altered in MASH. We identified transferrin receptor (TFRC) carried by large EVs (TFRC-lEVs), as associated with MASH in both derivation and validation populations ($p < 0.001$ and $p = 0.02$), as well as with ballooning ($p = 0.002$ and $p = 0.02$). Liver transcriptomics showed that one of the three upregulated pathways in patients with high TFRC-lEVs was heme metabolism. In two different hepatocyte cancer cell lines, MASH-mimicking conditions increased TFRC-lEVs release, while decreasing intracellular TFRC. TFRC-lEV, sex, AST and triglycerides were independently associated with MASH in the derivation population. These variables were included into a score, named ActiMASH, having an AUROC for MASH of 0.81 in both populations. ActiMASH increased with NAS ($p < 0.0001$ in both populations). Aiming for 80% sensitivity for MASH, the 45 cut-off was set. As compared with current EASL guidelines' strategy, ActiMASH ≥ 45 as a screening tool followed by LSM ≥ 8 kPa for at-risk MASH diagnosis, improved sensitivity of the strategy from 0.36 to 0.68, with specificity decreasing only from 0.87 to 0.83. After a median follow-up of 4 years, 10 patients had an increase in LSM > 5 kPa: all had initial ActiMASH ≥ 45, while none of those <45 had LSM progression ($p = 0.007$).

Conclusion: We developed ActiMASH, a blood-based test including circulating EVs, able to estimate MASLD activity and predict fibrosis progression in patients with diabetes.

WED-069

Optimizing hepatocellular cancer surveillance in metabolic dysfunction–associated steatotic liver disease based on liver stiffness measurement

Luis Calzadilla Bertot[1], Stuart Roberts[2], Javier Ampuero[3], Javier Crespo[4], Paula Iruzubieta[5], Douglas Maya-Miles[6], Paloma Carrillo-Fernández[3], William Kemp[2], Mohamed Asif Ali Chinnaratha Mohamedashrafali[7], Brian Teoh[7], Luis Ibañez-Samaniego[8], Laura Suarez Lopez[9], Rebeca Sigüenza[10], Victor Arroyo-López[11], Jesús Rivera Esteban[12], Javier Abad Guerra[12], Manuel Romero-Gómez[13], Judith Gómez- Camarero[14], Agustín Albillos[15], Maria Poca[16], Raul J. Andrade[17], Juan Pedro Toro Ortiz[17], Mercedes De La Torre Sanchez[18], Jacob George[19], Michael Wallace[20], Rocío Aller[21], Leon Adams[20].
[1]Biomedical Research Networking Center in Hepatic and Digestive Diseases (CIBEREHD), Madrid, Spain, Medical School, The University of Western Australia, Seliver group, Institute of Biomedicine of Seville (IBIS), University Hospital Virgen del Rocío (HUVR), CSIC, University of Sevilla, Sevilla, Spain, Sevilla, Spain; [2]Department of Gastroenterology and Hepatology, Alfred Health, Melbourne, Victoria, Australia; Central Clinical School, Monash University, Melbourne, Victoria, Australia, Melbourne, Australia; [3]Biomedical Research Networking Center in Hepatic and Digestive Diseases (CIBEREHD), Madrid, Spain, Seliver group, Institute of Biomedicine of Seville (IBIS), University Hospital Virgen del Rocío (HUVR), CSIC, University of Sevilla, Sevilla, Spain, Faculty of Medicine, University of Sevilla, Sevilla, Spain, Sevilla, Spain; [4]Facultad de Medicina, Universidad de Cantabria, Grupo de Investigacion Clinica y Traslacional en Enfermedades Digestivas, Instituto de Investigacion SanitariaValdecilla (IDIVAL), Santander, Medicine AI, Madrid, Spain, Santander, Spain; [5]Servicio de Aparato Digestivo y Hepatologia, Hospital Universitario Marqués de Valdecilla, Santander, Spain, Santander, Spain; [6]Biomedical Research Networking Center in Hepatic and Digestive Diseases (CIBEREHD), Madrid, Spain,

Seliver group, Institute of Biomedicine of Seville (IBIS), University Hospital Virgen del Rocío (HUVR), CSIC, University of Sevilla, Sevilla, Spain, Department of Physiology, University of Sevilla, Sevilla, Spain, Sevilla, Spain; [7]Adelaide Medical School, Faculty of Health and Medical Sciences, The University of Adelaide, Adelaide, South Australia, Australia Department of Gastroenterology and Hepatology, Lyell McEwin Hospital, Adelaide, Australia, Adelaide, Australia; [8]Biomedical Research Networking Center in Hepatic and Digestive Diseases (CIBEREHD), Madrid, Spain, Gastroenterology and Hepatology Department Hospital General Universitario Gregorio Marañón, Instituto de Investigación Sanitaria Gregorio Marañón (IiSGM), Madrid, Spain, Madrid, Spain; [9]Gastroenterology and Hepatology Department Hospital General Universitario Gregorio Marañón. Instituto de Investigación Sanitaria Gregorio Marañón (IiSGM), Madrid, Spain, Madrid, Spain; [10]Department of Radiology, Hospital Clínico Universitario de Valladolid, Spain, Valladolid, Spain; [11]Department of Medicine, Dermatology and Toxicology, University of Valladolid, Spain, Valladolid, Spain; [12]Gastroenterology and Hepatology Department, Puerta de Hierro, University Hospital, Madrid, Spain, Puerta de Hierro- Segovia Arana Research Institute (IDIPHISA), Madrid, Spain, Autonomous University of Madrid, Spain, Madrid, Spain; [13]Biomedical Research Networking Center in Hepatic and Digestive Diseases (CIBEREHD), Madrid, Spain, Seliver group, Institute of Biomedicine of Seville (IBIS), University Hospital Virgen del Rocío (HUVR), CSIC, University of Sevilla, Sevilla, Spain, Hospital Universitario Virgen del Rocío, Sevilla, Spain, Sevilla, Spain; [14]Hospital Universitario de Burgos, Burgos, Spain, Burgos, Spain; [15]Biomedical Research Networking Center in Hepatic and Digestive Diseases (CIBEREHD), Madrid, Spain, Servicio de Gastroenterología y Hepatología, Hospital Universitario Ramón y Cajal, Instituto Ramón y Cajal de Investigación Sanitaria (IRYCIS), Universidad de Alcalá,Madrid, Spain, Madrid, Spain; [16]Biomedical Research Networking Center in Hepatic and Digestive Diseases (CIBEREHD), Madrid, Spain, Unidad de Hepatología, Hospital de la Santa Creu i Sant Pau, Institut de Recerca Sant Pau (IR Sant Pau), Barcelona, Barcelona, Spain; [17]Biomedical Research Networking Center in Hepatic and Digestive Diseases (CIBEREHD), Madrid, Spain, Unidad de Gestión Clínica de Enfermedades Digestivas, Instituto de Investigación Biomédica de Málaga-IBIMA-Plataforma BIONAND; Hospital Universitario Virgen de la Victoria, Universidad de Málaga, Málaga, Spain, Malaga, Spain; [18]Consorcio Hospital General Universitario de Valencia, Valencia, Spain, Valencia, Spain; [19]Storr Liver Unit, Westmead Millennium Institute and Westmead Hospital, University of Sydney, New South Wales, Australia, Sydney, Australia; [20]Medical School, The University of Western Australia, Nedlands, Perth, Western Australia, Australia, Department of Hepatology, Sir Charles Gairdner Hospital, Perth, Australia, Perth, Australia; [21]Department of Medicine, Dermatology and Toxicology, University of Valladolid, Spain, Gastroenterology Unit, Hospital Clinico Universitario Valladolid, Valladolid, Spain, UIC Biocritic, CIBERINFEC, Spain, Valladolid, Spain
Email: luis.calzadillabertot@uwa.edu.au

Background and aims: Metabolic dysfunction–associated steatotic liver disease (MASLD) is an increasingly common cause of hepatocellular carcinoma (HCC) with 30–40% of HCC cases occurring in the absence of cirrhosis. Risk stratification tools to identify those at highest risk who would benefit from HCC surveillance are not clearly defined. We aimed to examine the accuracy of liver stiffness measurement (LSM) to predict incident HCC in patients with MASLD and identify the optimum thresholds to enter patients into HCC surveillance.
Method: We evaluated a multicentre retrospective cohort of MASLD subjects collated from tertiary centres in Australia (n = 4) and Spain (n = 10) as part of the Spanish HEPAmet registry cohort. Subjects had a baseline LSM by transient elastography and were followed for the outcome of incident HCC. Annual incidence rates of HCC were calculated and stratified by LSM categories. Baseline covariates, cumulative incidence and thresholds associated with incident HCC were investigated by competing risk regression.
Results: Of 3387 patients followed for a median of 4.8 years (IQR 2.5–6.2) and 16,226 person-years, 66 subjects (1.9%) developed HCC. Mean age was 58.7 years, 53% were male and the median LSM was 8.6 kPa (IQR 5.6–14.1). The five-year cumulative incidence of HCC was 0.3% among patients with a baseline LSM <10 kPa, 1.7% for LSM 10–14.9 kPa, 2.3% for LSM 15–19.9 kPa, and 7.9% in those with LSM >20 kPa (all $p < 0.001$). Compared to subjects with LSM <10 kPa, HCC risk increased by LSM category, (10–14.9 kPa, subHazard Ratio = 5.5), (15–19.9 kPa, sHR = 10.3) and (>20 kPa, sHR = 23.9). Competing risk regression identified LSM, age and diabetes as independent predictors of HCC. The annual HCC incidence exceeding 1.5% were met in subjects within the LSM category of >20 kPa (1.7%/yr, 95% CI 1.25–2.33) and among patients with diabetes and LSM between 15 and 19.9 kPa (2.06%/yr, 95% CI 1.40–2.90). The annual HCC incidence exceeding 1% was additionally met in the LSM category 15–19.9 kPa (1.26%/yr, 95% CI 0.38–1.65) and were consistently above this threshold when stratified by diabetes status and sex.
Conclusion: LSM can effectively stratifies HCC risk in MASLD. Thresholds ≥20 kPa meet surveillance criteria and ≥15 kPa –19.9 indicate elevated risk specially in the presence of diabetes and should be considered for cost- effective analysis. These findings support a practical, non-invasive approach to personalize HCC surveillance in MASLD, potentially improving early detection and resource allocation.

WED-070

MASH-iScan: a non-invasive method for diagnosing MASH using ultrasound and artificial intelligence

Jennifer Cathcart[1], Laurence Still[2], James S Bowness[3], Ruairi Lynch[4], John Dillon[1]. *[1]University of Dundee, Dundee, United Kingdom; [2]Independent Consultant, Cardiff, United Kingdom; [3]University College London, London, United Kingdom; [4]NHS Tayside, Dundee, United Kingdom*
Email: jeni123@live.com

Background and aims: Metabolic dysfunction-associated steatohepatitis (MASH), the co-existence of steatosis and inflammation, is a leading cause of progression to fibrosis and hepatocellular cancer (HCC). (1) Currently the gold standard for diagnosis of MASH is via liver biopsy which carries significant risks including mortality. (2) Therefore, a better non-invasive test to diagnosis MASH is needed. The aim of this project is to explore whether artificial intelligence (AI), when applied to ultrasound imaging and routine clinical data, can accurately diagnose MASH.
Method: We retrospectively obtained non-targeted liver biopsies slides from November 2013 to November 2023 in NHS Tayside. The biopsies were scored with non-alcoholic fatty liver disease activity score (NAS) criteria, then paired with ultrasound images within 6 months, blood tests within 3 months of biopsy and demographics. Trained medical annotators scored the ultrasound images against a defined checklist and ultrasound parameters were computed digitally using bounding boxes and region of interest (ROI) selected by the annotators to total 12 ultrasound parameters. We utilised machine learning to develop a mathematical model from our input data of digital ultrasound parameters and checklist, blood tests and demographics. Support Vector Machine (SVM) emerged as the most effective model.
Results: We obtained 102 ultrasound images with paired biopsies within 6 months. We used leave-one-out cross validation due to the small sample size. The best Area under the receiver operating curve (AUROC) was for NAS ≥3 with an AUROC 0.86 and secondly for NAS ≥4 with an AUROC of 0.83. The NAS ≥3 model has a high negative predictive value (NPV) (100.0), thus a negative test for this model would confidently rule-out MASH. The latter NAS ≥4 model would rule-in MASH (NAS ≥4) with good sensitivity (84.4) and specifically (81.4) and NPV (91.9) identifying a cohort of patients to treat.
Conclusion: Both models exceeded the accepted standard of 0.80 for a diagnostic test accuracy. There was an element of overtraining due

to a small sample size resulting in high test characteristics in some statistical measures, therefore the models need an external validation which is underway. The project demonstrates that ultrasound parameters can be utilised to diagnosis MASH and may offer a non-invasive cost-effective simple alternative to biopsy to diagnosis MASH.

WED-071

Clinical relevance of repeating FIB-4 in the screening strategy for identifying metabolic dysfunction–associated liver disease-related advanced fibrosis

Yasmina Chouik[1], Cécile Terrien[2], Devi Guemon[3], Emmanuel Disse[3], Bérénice Ségrestin[3], Massimo Levrero[1], Paul Hermabessière[4], Adèle Delamarre[4], Cyrielle Caussy[5]. *[1]Department of Hepatology, Croix Rousse Hospital, Hepatology Institute EVEREST, Hospices Civils de Lyon, INSERM U1350 PaThLiv, Université Claude Bernard Lyon 1, Lyon, France; [2]Centre d'Investigation de la Fibrose Hépatique, Hôpital Haut-Lévêque, Bordeaux University Hospital, Bordeaux, France; [3]Hospices Civils de Lyon, Département Endocrinologie, Diabète et Nutrition, Hôpital Lyon Sud, Pierre-Bénite, France; [4]Centre d'Investigation de la Fibrose Hépatique, Hôpital Haut-Lévêque, Bordeaux University Hospital, Bordeaux Institute of Oncology, INSERM U1312, University of Bordeaux, Bordeaux, France; [5]Hospices Civils de Lyon, Département Endocrinologie, Diabète et Nutrition, Hôpital Lyon Sud, Univ Lyon, CarMen Laboratory, INSERM, INRA, INSA Lyon, Université Claude Bernard Lyon 1, Pierre-Bénite, France*
Email: yasmina.chouik@inserm.fr

Background and aims: The EASL-EASD-EASO guidelines recently proposed a screening strategy for MASLD-related advanced fibrosis (AF). In patients with intermediate FIB-4 (1.30–2.67), two strategies are proposed: i) the immediate referral to hepatologist for a second-line test, or ii) repeating FIB-4 at 1 year after intensified management of comorbidities. In patients with initial low FIB-4 < 1.30, monitoring FIB-4 every 1–3 years is suggested. However, there are no strong evidence supporting these recommendations. Therefore, we assessed the clinical relevance of these recommendations.

Method: A retrospective cohort including MASLD patients with low or intermediate FIB-4 was conducted in 2 tertiary centers between 2018 and 2022. Inclusion criteria were the access to a liver stiffness measurement (LSM) concomitantly to the initial FIB-4, and repeated FIB-4 during follow-up.

Results: 625 patients were included. Median BMI was 34.0 kg/m^2 (30.8–39.0) and 70.7% of patients had T2D. Initial median FIB-4 was 1.31 (0.95–1.74) and 35.7% of patients had a high risk for AF. After 3 years of follow-up, median FIB-4 remained stable at 1.32 (1.01–1.92). Respectively, 21.3% and 22.4% of patients with initial low FIB-4 changed to the intermediate category at 1 and 3y. The negative predictive value for AF detection was not improved by repeating FIB-4 (76.8% at baseline, 71.6% at 1y and 75.3% at 3y).

Factors predicting change in FIB-4 category at 3y were age (OR: 1.16; CI95%: 1.0–1.1; p < 0.001), arterial hypertension (OR: 2.0; CI95%: 1.1–4.0; p = 0.019) and GLP1-RA introduction during the 3y period (OR: 0.2; CI95%: 0.0–0.7; p = 0.015). In patients with an initial intermediate FIB-4, 77.2% remain stable at 1y and 68.5% at 3y. Decrease from intermediate to low category occurred in 13.3% of patients at 1y and 16.8% at 3y. Factors associated with FIB-4 decrease at 1y were weight loss (OR: 1.1; CI95%: 1.0–1.1; p = 0.029) and introduction of a GLP1-RA during the year (OR: 4.4; CI95%: 1.2–16.6; p = 0.029).

Conclusion: The majority of MASLD patients did not change of FIB-4 category in a 3y time frame. Repeating FIB-4 over time does not seem effective in picking up false negative cases. In case of intermediate FIB-4, weight loss and GLP1-RA treatment are associated with FIB-4 normalization at 1y, but this effect is temporary and observed in few patients. These data suggest that a second-line NIT should be systemically performed in patients with intermediate FIB-4 in order to limit clinical inertia.

WED-072

ACT on MASH: a multi-country cross-sectional online survey of awareness, understanding, stigma, and perceptions of MASLD, MASH, and related cardiometabolic comorbidities among healthcare professionals

Cyrielle Caussy[1], Husam Albarmawi[2], Edwige-Ludiwyne Balzac[3], Julio Burman[4], Nathalie Eklöf[5], Takumi Kawaguchi[6], Nobuyoshi Kosaka[7], Jeff McIntyre[8], Lauren Nephew[9], Arash Pakseresht[10], Sahar Saeed[11], Jörn M. Schattenberg[12]. *[1]Hospices Civils de Lyon, Département Endocrinologie, Diabète et Nutrition, Hôpital Lyon Sud, Univ Lyon, CarMen Laboratory, INSERM, INRA, INSA Lyon, Université Claude Bernard Lyon 1, Pierre-Bénite, France; [2]Novo Nordisk, Mainz, Germany; [3]Novo Nordisk, France, Paris, France; [4]European Liver Patients' Association, Brussels, Belgium; [5]Novo Nordisk, Soberg, Denmark; [6]Division of Gastroenterology, Department of Medicine, Kurume University School of Medicine, Kurume, Japan; [7]Novo Nordisk, Japan, Tokyo, Japan; [8]Global Liver Institute, Washington, DC, United States; [9]Indiana University School of Medicine, Indianapolis, United States; [10]Novo Nordisk, Canada, Mississauga, Canada; [11]Queens University, Ontario, Canada; [12]Department of Medicine, Saarland University Medical Center, Homburg, Germany*
Email: cyrielle.caussy@chu-lyon.fr

Background and aims: Metabolic-dysfunction-associated steatotic liver disease (MASLD) is the most prevalent chronic liver disease worldwide; however, there has been limited research on healthcare professionals' (HCPs) awareness, knowledge, and perceptions of MASLD and metabolic dysfunction-associated steatohepatitis (MASH), and their associations with cardiometabolic comorbidities.

Method: In 2025, an online cross-sectional survey was conducted with HCPs from Canada, France, Germany, Japan, and the United States (US). HCPs were recruited via online panels and included gastroenterologists, hepatologists, endocrinologists, cardiologists, obesity specialists, primary care physicians, radiologists, and nurse practitioners/physician assistants (US only).

Results: 774 HCPs completed the survey from Canada (n = 65), the US (n = 301), France (n = 125), Germany (n = 120), and Japan (n = 163). HCPs reported a median of 20 years in clinical practice, and most worked in outpatient (49%) or hospital settings (42%). Most HCPs reported being "very" or "extremely" knowledgeable about MASLD (62%) and MASH (63%). Overall, 82% were aware of differences between MASLD and MASH; this varied notably by specialty (highest among hepatologists [98%] and lowest among cardiologists [72%]) and less by country (US, 80%; Canada, 88%; France, 77%; Germany, 81%; Japan, 90%). 48% of HCPs overall reported being "very" or "extremely" confident in identifying people at risk of MASH. 87% agreed that MASH and MASLD increase the risk of cardiovascular events, and 89% agreed that early diagnosis/management improves health outcomes. Overall, HCPs reported that nearly half of their patients with MASLD (45%) and MASH (42%) were diagnosed after an incidental finding. Radiologists reported incidental findings of MASLD and MASH in 21% and 14% of scans evaluated in a typical month, respectively. The proportion of HCPs who reported that screening patients with cardiometabolic conditions for MASH is "very" or "extremely" important varied by condition, ranging from 42% for chronic kidney disease to 86% for persistently elevated liver enzymes. 30% of HCPs reported that fear of stigmatizing patients with obesity was a barrier to screening.

Conclusion: Based on these results, we identified gaps in HCPs' confidence in identifying patients at risk of MASLD/MASH, a high frequency of incidental findings of these conditions, and disparities in the perceived importance of screening at-risk patients, highlighting areas for improving health professional education.

WED-073

Metabolic and cognitive effects of a 6-month dietary intervention in patients with MASLD: a prospective study

Francesca Saba[1], Gian Paolo Caviglia[1], Marta Guariglia[1], Francesca Pisano[1], Angelo Armandi[1], Chiara Rosso[1], Ilaria Goitre[2], Eleonora Dileo[1], Kamela Gjini[1], Simona Bo[2], Elisabetta Bugianesi[1]. [1]*Division of Gastroenterology and Hepatology, Department of Medical Sciences, University of Turin, Turin, Italy;* [2]*Division of Clinical Nutrition, Department of Medical Sciences, University of Turin, Turin, Italy*
Email: francesca.saba@unito.it

Background and aims: Metabolic dysfunction–associated steatotic liver disease (MASLD) is the hepatic manifestation of metabolic syndrome and has been increasingly linked to cognitive impairment. We evaluated whether a 6-month hypocaloric dietary intervention improves metabolic outcomes and cognitive performance, and explored the mediating role of circulating adipokines, hepatokines, and myokines.
Method: We conducted a prospective study including 136 adults with MASLD (median age 51 [42–61] years, 36% male, T2DM 14.7%, obesity 59.6%). Metabolic endpoints were defined as a body mass index (BMI) reduction ≥5%, and a controlled attenuation parameter (CAP) reduction ≥10%. Circulating cytokines were measured using a BioPlex (Luminex) platform. Cognitive function was assessed with the Repeatable Battery for the Assessment of Neuropsychological Status (RBANS); an RBANS total score ≤85 identified patients with mild cognitive impairment. All parameters were evaluated at baseline (T0) and after 6 months (6M).
Results: After 6 months, 31.6% of patients achieved a BMI reduction ≥5% (n = 43), and 39.0% achieved a CAP reduction ≥10% (n = 53). Weight loss was independently associated with CAP improvement (OR = 4.02, 95% CI 3.14–15.68; $p < 0.001$). Responders showed significant reductions in ALT, AST, and γ-GT (all $p < 0.001$), along with improvement in serum insulin ($p < 0.001$) and triglycerides ($p = 0.007$). Weight loss ≥5% was associated with remodeling of the hepato-adipose axis, characterized by reduced leptin and ANGPTL3 levels and increased adiponectin, as well as attenuation of systemic inflammation (reduced IL-1β, IL-6, and TNF-α). Among patients with baseline RBANS ≤85 (n = 52), the total RBANS score improved from 77 to 81 ($p < 0.001$), with significant gains in immediate memory (88 to 96, $p = 0.002$) and delayed memory (92 to 96, $p = 0.020$). In multivariate analysis including anthropometric, metabolic, hepatic, cognitive, and cytokine-related parameters, baseline RBANS score ($\beta = -0.19$, $p = 0.001$) and 6M–T0 changes in BMI ($\beta = 2.02$, $p = 0.009$), leptin ($\beta = -0.0014$, $p = 0.021$), and ANGPTL3 ($\beta = -0.45$, $p < 0.001$) independently predicted 6M–T0 changes in RBANS total score.
Conclusion: A weight loss ≥5% is associated with significant reductions in liver steatosis and improvements in hepato-metabolic and inflammatory profiles, accompanied by cognitive benefits in patients with mild cognitive impairment. These findings strengthen the rationale for structured lifestyle interventions as a cornerstone of MASLD management.

WED-074

C-reactive protein-triglyceride glucose index and fasting C-peptide to high-density lipoprotein cholesterol ratio as predictors for advanced fibrosis in patients with type 2 diabetes and metabolic dysfunction-associated steatotic liver disease

Georgiana-Diana Cazac-Panaite[1], Elena-Daniela Grigorescu[1,2], Adina-Bianca Foșălău[1,2], Alina Onofriescu[1,2], Cristina-Mihaela Lăcătușu[1,2], Bogdan-Mircea Mihai[1,2]. [1]*Unit of Diabetes, Nutrition, and Metabolic Diseases, Faculty of Medicine, Grigore T. Popa University of Medicine and Pharmacy, Iasi, Romania;* [2]*JUD. IASI, SAT REDIU, COM. REDIU, Romania*
Email: georgiana-diana_cazac@umfiasi.ro

Background and aims: Insulin resistance, low-grade inflammation, and metabolic disturbances drive the progression of metabolic dysfunction–associated steatotic liver disease (MASLD) to fibrosis in type 2 diabetes mellitus (T2DM). Early identification of high-risk patients remains challenging in routine practice. We explored the predictive value of the C-reactive protein–triglyceride-glucose index (CTI) and the fasting C-peptide-to-high-density lipoprotein cholesterol ratio (FCP/HDL) for advanced liver steatosis and fibrosis in patients with T2DM and MASLD.
Method: This analysis includes baseline data from a prospective doctoral study conducted at the Clinical Center of Diabetes, Nutrition, and Metabolic Diseases. Patients with T2DM and MASLD who were not optimally controlled were enrolled. After informed consent, anthropometric, biochemical assessments and transient elastography were performed. Metabolic and inflammatory indices, including CTI and FCP/HDL, were calculated using validated formulas.
Results: Seventy-two patients were enrolled (48.6% men), with a mean age of 59.09 ± 9.02 years, a median duration of T2DM of 2 years (IQR 6), and a median HbA1c of 6.95% (IQR 1.1). Mean body mass index was 33.93 ± 5.93 kg/m^2. Obesity was identified in 70.8% of participants. Mean controlled attenuation parameter (CAP) and liver stiffness measurement (LSM) values were 296.49 ± 61.07 dB/m and 7.05 ± 2.52 kPa. Moderate-to-severe steatosis and fibrosis were observed in 62.5% and 72.2% of patients, respectively. F2–F4 stages were identified in 18 subjects. The mean/median (± SD/IQR) values of studied markers were: cardiometabolic index (CMI) 1.04 ± 0.86, CTI 8.50 ± 0.68, FCP/HDL 3.29 (2.26), HbA1c/HDL 6.49 ± 1.67, and C-reactive protein 0.4 ± 0.33 mg/mL. Positive significant associations existed between LSM and CTI ($r = 0.335$, $p = 0.004$), FCP/HDL ($r = 0.270$, $p = 0.024$), and between CAP and CTI ($r = 0.417$, $p < 0.001$), and FCP/HDL ($r = 0.278$, $p = 0.020$). CTI (AUROC 0.677, CI: 0.544–0.809, $p = 0.048$) and FCP/HDL (AUROC 0.655, CI: 0.529–0.781, $p = 0.030$) were identified as predictors of moderate-to-severe steatosis. CTI (AUROC 0.656, CI: 0.510–0.803, $p = 0.048$) and FCP/HDL (AUROC 0.697, CI: 0.567–0.827, $p = 0.015$) were also identified as predictors of advanced hepatic fibrosis.
Conclusion: These findings suggest that composite metabolic and inflammatory indices may be useful, non-invasive tools for identifying patients with T2DM at risk of progression to advanced liver fibrosis in large-scale screening initiatives.

WED-075

Comparison of clinical care pathways for metabolic dysfunction-associated steatotic liver disease (MASLD) in type 2 diabetes (T2D) in the dawn of effective pharmacological therapy

Wah-Kheong Chan[1], Vincent Wai-Sun Wong[2,3], Lee Lee Lai[1], Nik Raihan Nik Mustapha[4], Pavitratha Puspanathan[5], Jimmy Che-To Lai[2,3], Terry Cheuk-Fung Yip[2,3], Grace Lai-Hung Wong[2,3], Sanjiv Mahadeva[1]. [1]*Gastroenterology and Hepatology Unit, Department of Medicine, Faculty of Medicine, Universiti Malaya, Kuala Lumpur, Malaysia;* [2]*Department of Medicine and Therapeutics, Medical Data Analytics Centre, The Chinese University of Hong Kong, Hong Kong, China;* [3]*State Key Laboratory of Digestive Disease, Institute of Digestive Disease, The Chinese University of Hong Kong, Hong Kong, China;* [4]*Department of Pathology, Hospital Sultanah Bahiyah, Alor Setar, Malaysia;* [5]*Department of Pathology, Hospital Pulau Pinang, Pulau Pinang, Malaysia*
Email: wahkheong2003@hotmail.com

Background and aims: This study aimed to evaluate different approaches in using non-invasive tests to identify patients with T2D (1) for pharmacological therapy for metabolic dysfunction-associated steatohepatitis (MASH) and (2) for having advanced fibrosis or cirrhosis.
Method: This study included patients with MASLD and T2D who underwent liver biopsy and liver stiffness measurement (LSM) by vibration-controlled transient elastography. Patients with histological MASH and F2-F3 fibrosis were considered as candidates for pharmacological therapy.
Results: The data of 537 patients were analysed (mean age 55.3 ± 10.5 years, 52.1% male). The use of LSM 10–15 kPa instead of 8–15 kPa

decreased the proportion of patients identified for pharmacological therapy from 40.4% to 25.0% with more patients correctly classified (70.0% vs. 61.7%), lower false positive rate (59.7% vs. 65.4%), and marginally higher false negative rate (18.9% vs. 17.0%). The 2-step approach (Fibrosis-4 index [FIB-4] based on age-specific cut-offs, followed by LSM if abnormal FIB-4) decreased the proportion of patients identified for pharmacological therapy to as low as 10.6% (when using LSM 10–15 kPa) with more patients correctly classified (up to 75.7%), lower false positive rate (down to 40.0%), and marginally higher false negative rate (highest 22.3%). The 2-step approach decreased the proportion of patients with LSM 15.1–20 kPa from 8.0% to 4.5% and increased correct identification of patients for pharmacological therapy from 41.9% to 57.9% for this group of patients, where pharmacological therapy would be considered. The use of LSM ≥10 kPa instead of ≥8 kPa decreased the proportion of patients identified as having advanced fibrosis or cirrhosis from 55.5% to 40.4% with more patients correctly classified (76.4% vs. 70.6%), lower false positive rate (34.0% vs. 43.6%), but higher false negative rate (16.8% vs. 11.7%). The 2-step approach decreased the proportion of patients identified as having advanced fibrosis or cirrhosis to as low as 19.0% (when using LSM ≥10 kPa) with more patients correctly classified (up to 81.3%), lower false positive rate (down to 17.5%), but higher false negative rate (highest 22.2%).

Conclusion: The results of this study support the use of the 2-step approach to identify patients with T2D for pharmacological therapy for MASLD and for having advanced fibrosis or cirrhosis, and provide important data when considering the LSM cut-offs to be used in the 2-step approach.

WED-076

Mapping somatic evolution in steatotic liver disease through integrated tissue and organoid genomics

Alessandro Cherubini[1], Stefania Mira[2], Vittoria Moretti[1], Hadi Eidgah Torgabehei[3], Elia Casirati[1], Laura Cerami[1], Giulia Periti[1], Francesco Malvestiti[2], Serena Pelusi[1], Daniele Dondossola[4], Daniele Prati[1], Luisa Ronzoni[1], Luca Valenti[5]. *[1]Precision Medicine Lab - Department of Transfusion Medicine, Fondazione IRCCS Ca' Granda Ospedale Maggiore Policlinico Milano, Milan, Italy; [2]Department of Pathophysiology and Transplantation, Università degli Studi di Milano, Milan, Italy; [3]Omic Sciences Lab, Scientific Direction, Fondazione IRCCS ca' Granda Ospedale Maggiore Policlinico Milano, Milan, Italy; [4]General and Liver Transplant Surgery Unit, Fondazione IRCCS Ca' Granda, Ospedale Maggiore Policlinico Milano, Department of Pathophysiology and Transplantation, Università degli Studi di Milano, Milan, Italy; [5]Precision Medicine Lab - Department of Transfusion Medicine, Fondazione IRCCS Ca' Granda Ospedale Maggiore Policlinico Milano, Department of Pathophysiology and Transplantation, Università degli Studi di Milano, Milan, Italy*
Email: alessandro.cherubini@policlinico.mi.it

Background and aims: Steatotic liver disease (SLD), including MASLD, is a global health burden that can progress to cirrhosis and hepatocellular carcinoma (HCC). Somatic mutations contribute to fibrosis and carcinogenesis, yet the interplay between somatic and germline factors remains unclear. We integrated somatic mutation analysis via targeted next-generation sequencing (NGS) with germline risk profiling in liver tissues and human liver organoids (HLOs) to elucidate SLD molecular trajectories.

Method: We analyzed liver and blood samples from 46 individuals: 25 SLD, 17 viral hepatitis (B/C), and 4 histologically normal controls. HLOs were successfully derived from 21 cases. A custom 75-gene panel (chromatin remodeling, cell cycle, lipid metabolism, hepatocarcinogenesis) was sequenced (Illumina NextSeq2000). Somatic variants were identified using Mutect2/Funcotator, filtering germline variants via matched blood. The MASLD polygenic risk score (PRS-5: PNPLA3–TM6SF2–GCKR–MBOAT7–HSD17B13) was genotyped for all subjects.

Results: We identified 195 somatic variants in non-tumoral tissues (60.8% of patients). Mutations in *FOXO1*, *RPS6KA3*, and *APOB* were frequent in SLD, while *SF3B1*, *LRP1B*, and *PTPN13* were enriched in viral hepatitis. One SLD patient exhibited a hypermutated phenotype (126 variants) linked to a germline *MLH1* mutation. HLOs harbored 92 somatic variants (85.7% of cases), showing distinct mutational signatures from matched tissues but similar overall burden. Mutations in chromatin remodeling genes (*ARID2*, *KMT2B/C/D*) were more frequent in HLOs, suggesting culture-induced selection. HCC samples showed recurrent *TERT*, *CTNNB1*, and *TP53* mutations. PRS-5 values were higher in SLD but without significant inter-group differences.

Conclusion: Our study reveals distinct somatic landscapes between SLD and viral hepatitis, identifying *FOXO1*, *RPS6KA3*, and *APOB* as key genes in metabolic injury. Despite shared germline backgrounds, HLOs exhibit unique mutational patterns reflecting in vitro clonal evolution. Integrating tissue and organoid sequencing provides novel insights into the synergy between inherited and acquired genetic alterations. This HLO biobank represents a valuable platform for precision medicine and mechanistic studies in SLD and HCC.

WED-077

External validation of a parsimonious machine learning model for detecting significant fibrosis in obese patients with metabolic dysfunction–associated steatotic liver disease (MASLD)

Ahmed Cordie[1,2,3], Ahmed Kamel[4], Rabab Omar[1], Essa Abdelaal[1], Mohamed Fahmy[5], Dina Helmy[6], Sherif Musa[1], Maria Stepanova[2], Gamal Esmat[1,4], Zobair M. Younossi[2,7]. *[1]Cairo University, Endemic Hepatogastroenterology and Infectious Diseases Department, Cairo, Egypt; [2]The Global NASH/MASH Council (GNC), Washington, DC, United States; [3]Cairo University Hospitals, HIV Clinic, Cairo, Egypt; [4]Cairo University, Clinical Pharmacy Department, Cairo, Egypt; [5]Cairo University, Department of General and Laparoscopic Surgery, Cairo, Egypt; [6]Cairo University, Department of Pathology, Cairo, Egypt; [7]Center for Outcomes Research in Liver Diseases, Washington, DC, USA, Washington, DC, United States*
Email: ahmed.cordie@cu.edu.eg

Background and aims: Although non-invasive tests (NITs) are widely used to risk-stratify patients with MASLD, their performance is suboptimal in individuals with obesity who are at high risk of advanced liver disease. Moreover, complex composite scores such as AGILE 3+ require multiple laboratory and clinical parameters, limiting their applicability in routine practice. We developed a parsimonious four-variable elastic net model and externally validated its performance in a large multinational cohort.

Method: The development cohort included 120 biopsy-proven MASH patients with BMI ≥35 kg/m^2 with available extensive clinical data. An elastic net model incorporating liver stiffness measurement (LSM), BMI, AST ratio, and age was developed using bootstrap resampling (1,000 iterations) with out-of-bag validation. Significant fibrosis (F≥2) was the primary outcome of the analysis. External validation was performed in 2,365 MASLD patients with BMI ≥35 kg/m^2 from the Global NASH/MASH Registry. Model performance at the development-derived threshold (0.29) was compared with established NITs including AGILE 3+, FAST, FIB-4, APRI, NFS, BARD, and LSM alone.

Results: In the development cohort, the elastic net model demonstrated good discrimination for significant fibrosis, achieving an AUC of 0.798 (95% CI 0.700–0.890) and outperforming other NITs, including FIB-4, FAST, and LSM alone. In the large external validation cohort (F≥2 prevalence 69%), the model retained robust performance with an AUC of 0.801 (95% CI 0.781–0.820). At the predefined probability threshold, sensitivity was 73.1% and specificity 73.8%, yielding a high positive predictive value (86.1%) and moderate negative predictive value (55.2%). Diagnostic performance was comparable to AGILE 3+ (AUC 0.822) despite the model requiring substantially fewer clinical and laboratory inputs. Importantly,

discrimination remained stable across subgroups defined by sex, diabetes status, age, and BMI, supporting the generalizability of the model in obese MASLD patients.
Conclusion: A parsimonious four-variable elastic net model showed robust external validation for detecting significant fibrosis in MASH patients with obesity, with performance comparable to more complex composite scores such as AGILE 3+. Its minimal data requirements enhance feasibility for routine clinical use and support its role in optimizing biopsy selection, particularly in resource-limited settings.

WED-078
Is the fatty liver index just measuring BMI? Evidence from NHANES and an HIV cohort
Ahmed Cordie[1], Ahmed Kamel[2], Rahma Mohamed[1], Gamal Esmat[3], Giada Sebastiani[4]. [1]*Cairo University Hospitals HIV Clinic, Endemic Medicine Department, Faculty of Medicine, Cairo University, Cairo, Egypt;* [2]*Clinical Pharmacy Department, Faculty of Pharmacy, Cairo University, Cairo, Egypt;* [3]*Endemic Medicine Department, Faculty of Medicine, Cairo University, Cairo, Egypt;* [4]*Department of Medicine, McGill University, Montreal, QC, Canada*
Email: ahmed.cordie@cu.edu.eg

Background and aims: The Fatty Liver Index (FLI) is widely used to screen for steatotic liver disease (SLD), yet both indices rely heavily on body mass index (BMI). Whether additional FLI components (waist circumference, triglycerides, gamma-glutamyl transferase [GGT]) provide incremental diagnostic value beyond BMI alone remains uncertain. In people living with HIV (PLWH), antiretroviral therapy (ART)-associated and metabolic alterations may further undermine the performance of anthropometric-based indices. We compared FLI performance in a general population cohort and in PLWH, testing whether FLI components add incremental value beyond BMI.
Method: We analysed 3,217 adults with controlled attenuation parameter (CAP) measurements from NHANES 2017–2018 (n = 2,556) and a cohort of PLWH from Egypt (n = 661). SLD was defined as CAP ≥248 dB/m. Diagnostic performance was assessed using the area under the receiver operating characteristic curve (AUC) for BMI alone and individual FLI components. Incremental discrimination beyond BMI was evaluated using DeLong tests, likelihood ratio tests, and net reclassification improvement (NRI). Subgroup analyses were performed across BMI categories (<25, 25–30, ≥30 kg/m^2).
Results: SLD prevalence was versus 28.0% in PLWH. Overall, FLI discrimination was acceptable in both populations (AUC 0.838, 95% CI 0.823–0.854 in NHANES; 0.780, 0.740–0.821 in PLWH), but BMI alone achieved comparable discrimination (0.800 and 0.778, respectively). In NHANES, FLI components provided modest but statistically significant incremental value beyond BMI (ΔAUC +0.039, p < 0.001; NRI 0.069, 95% CI 0.041–0.098). In contrast, no incremental value was observed in PLWH (ΔAUC +0.010, p = 0.320; NRI 0.054, 95% CI –0.002–0.104), and none of the individual FLI components improved discrimination beyond BMI (all p > 0.4). Across BMI strata, FLI performance declines substantially in normal-weight individuals, with AUCs of 0.752 in NHANES and 0.581 in PLWH. The standard FLI ≥60 threshold demonstrated very low sensitivity for lean SLD (NHANES 3.8%; PLWH 2.9%).
Conclusion: FLI provides limited incremental diagnostic value beyond BMI in the general population and no advantage in PLWH, suggesting that HIV- and ART-related metabolic alterations disrupt standard anthropometric–hepatic relationships. The standard FLI ≥60 threshold fails to identify over 95% of lean SLD cases regardless of population. In PLWH and lean individuals, direct hepatic assessment with transient elastography should be favoured over FLI-based screening.

WED-079
Evaluation of metabolic dysfunction-associated steatohepatitis in adults and children using ultrasound derived fat fraction and elastography with MRI proton density fat fraction and elastography as reference standard
Jean-Michel Correas[1], Anne-Marie Tissier[1], Yassin Labyed[2], Arati Gurung[2]. [1]*Necker University Hospital, Paris, France;* [2]*Siemens Healthineers, Issaquah, United States*
Email: jmc.correas@gmail.com

Background and aims: Metabolic dysfunction-associated steatotic liver disease (MASLD), the most common chronic liver disease worldwide, can progress to metabolic dysfunction-associated steatohepatitis (MASH), marked by hepatocellular inflammation and risk of fibrosis, cirrhosis, or hepatocellular carcinoma. Over half of individuals with MASLD and most with MASH are overweight or obese, with prevalence rising in children. The aim of the study was to evaluate the performance of ultrasound derived fat fraction (UDFF) and shear wave elastography (SWE) in routine clinical practice for assessment of MASH in adults and children using MRI proton density fat fraction (PDFF) and elastography (MRE) as the reference standards respectively.
Method: This was a prospective study approved by the Ethics Committee to enrol patients with suspected MASLD. Same-day MRI and ultrasound exams were performed. The diagnostic accuracy of UDFF for classifying PDFF-defined steatosis grades was assessed using the area under the receiver operating characteristic curve (AUC); PDFF thresholds were 6.4%, 17.4% and 22.1% for S1, S2 and S3 respectively for adults and 6.4%, 17.5% and 23.3% for children following the MASH Clinical Research Network guidance. The MRE threshold of 3.14 kPa was used for detecting significant fibrosis (F2).
Results: A total of 247 patients were enrolled. Nineteen patients had missing PDFF data; the final analysis for steatosis included 228 patients (90 adults, 138 children). The overall mean age was 16 years, with adults averaging 60 years and children 14 years. The mean BMI was higher in children (36 kg.m^{-2}) compared to adults (30 kg.m^{-2}, p < 0.001). The overall mean UDFF was 13% with a mean of 19% in adults and 7% in children (p < 0.001). The overall AUCs were 0.91 (0.85, 0.97), 0.94 (0.90, 0.98), and 0.89 (0.83, 0.95) for staging S1, S2 and S3 respectively; correlation coefficient between UDFF and PDFF was 0.81. Ninety-six patients had missing MRE data; the final analysis for fibrosis included 151 patients. The overall mean SWE was 3.60 kPa with a mean of 3.25 kPa in adults and 5.05 kPa in children (p < 0.001). The overall AUC was 0.90 (0.81, 0.98) for classifying F2 with a correlation coefficient of 0.76.
Conclusion: Both UDFF and SWE showed strong diagnostic accuracy for MRI-defined steatosis and fibrosis and can be seamlessly incorporated into routine liver ultrasound exams in adults and children, including those with severe obesity.

WED-083
Prevalence of elevated fibrosis-4 index in adults from primary care and associated clinical factors
Michele Montori[1], Martina Dalla Bella[1], Maria Ricci[1], Federica Carlino[1], Paolo Core[2], Paola Lodolini[2], Antonio Marracino[2], Massimiliano Luzi[2], Marco Angelo Danilo Giulioni[2], Guido Sanpaolo[2], Martina Zucchi[2], Annalisa Pini[2], Rachele De liberato[2], Manuela Zucchi[2], Alessia Di Giovannangelo[2], Andrea Lucarelli[2], Emanuele Fiorini[2], Gianluca Svegliati Baroni[1]. [1]*Azienda Ospedaliero-Universitaria delle Marche, Ancona, Italy;* [2]*ASUR (ASL) Marche, Ancona, Italy*
Email: michele.montori@ospedaliriuniti.marche.it

Background and aims: Non-invasive fibrosis scores such as the fibrosis-4 index (FIB-4) enable large-scale identification of individuals at risk for advanced liver disease using routinely available laboratory data. However, population-level estimates from unselected primary care settings remain limited, and clinical factors associated with abnormal FIB-4 values across commonly used

thresholds are incompletely characterized. This study aimed to estimate the prevalence of elevated FIB-4 in a general adult primary care population and to examine associated metabolic and clinical factors.

Method: Electronic general practitioners records were screened for adults with available laboratory data. Among 18,993 individuals, 12,124 adults aged 18–80 years without known chronic liver disease were included. Three cohorts were analysed: the overall population, adults aged 40–70 years, and a metabolically high-risk group defined by obesity, diabetes, or elevated transaminases. FIB-4 positivity was assessed using standard and age-adjusted thresholds. Associations with elevated FIB-4 were evaluated using multivariable logistic regression.

Results: In the overall population, 40.0% had FIB-4 >1.3 and 5.8% ≥2.67. Prevalence of FIB-4 ≥2.67 increased to 10.5% in the high-risk group and was lower among adults aged 40–70 years (2.2%) (all $p < 0.001$). Individuals with FIB-4 ≥2.67 showed a higher prevalence of diabetes (23.2% vs 12.1%) and elevated transaminases (20.8% vs 8.0%) compared with those with FIB-4 ≤1.3. Male sex was associated with a higher burden of metabolic risk factors, including obesity (6.3% vs 5.3%, $p < 0.01$) and diabetes (13.8% vs 10.5%, $p < 0.001$). In adjusted analyses, male sex and hypertension showed the strongest independent associations with FIB-4 ≥2.67 (adjusted odds ratio 1.86 and 2.35, respectively; both $p < 0.001$).

Conclusion: FIB-4 values compatible with advanced fibrosis are common in primary care, affecting nearly 6% of unselected adults and exceeding 10% in metabolically at-risk individuals. Male sex and hypertension were consistently associated with elevated FIB-4 values. These findings support opportunistic FIB-4 calculation from routine laboratory tests as a first-step triage strategy and highlight the need for structured pathways linking primary care to second-line fibrosis assessment.

WED-084

GRIPonMASH preliminary results: comparison of FIB-4 and MAF-5 as first-line tests to rule out advanced fibrosis in primary care

Vivian de Jong[1,2], Caterina Buranelli[2], Kirsi van Eekhout[3], Leonard (Niels) Broekman[3], Laura Konings[4], Carmen Dietvorst[5], Evangelia Mentsiou-Nikolaou[6], Maria do Mar Orey[7], Václav Šmíd[8], Radan Brůha[8], Helena Cortez-Pinto[7], George Dedoussis[6], Sven Francque[9], Amalia Gastaldelli[10], A.G. (Onno) Holleboom[3], Luca Miele[11,12], Christophe Moreno[13], Adrian Purcarea[14], Vlad Ratziu[15], Manuel Romero-Gómez[16], Jörn M. Schattenberg[17,18], Céline Fournier-Poizat[19], Jo Massoels[19], Oscar Franco[1], Diederick Grobbee[1,2], Manuel Castro Cabezas[2,4,5]. *[1]Julius Center for Health Sciences and Primary Care, UMC Utrecht, Utrecht, Netherlands; [2]Julius Clinical Research B.V., Zeist, Netherlands; [3]Amsterdam University Medical Centre, Amsterdam, Netherlands; [4]Franciscus Gasthuis & Vlietland, Rotterdam, Netherlands; [5]Erasmus MC Medical Center, Rotterdam, Netherlands; [6]Harokopio University of Athens, Athens, Greece; [7]Universidade de Lisboa, Lisbon, Portugal; [8]General University Hospital, Charles University, Prague, Czech Republic; [9]University Hospital Antwerp, Antwerp, Belgium; [10]Institute of Clinical Physiology, National Research Council, Pisa, Italy; [11]Fondazione Policlinico Universitario Agostino Gemelli IRCCS, Rome, Italy; [12]Università Cattolica del Sacro Cuore, Rome, Italy; [13]CUB Hôpital Erasme, Université Libre de Bruxelles, Brussels, Belgium; [14]Medical Education Research and Innovation Center s.r.l., Bucharest, Romania; [15]Sorbonne University, Paris, France; [16]Virgen del Rocio University Hospital, Seville, Spain; [17]Saarland University Medical Center, Homburg, Germany; [18]Saarland University, Homburg, Germany; [19]Echosens SA, Paris, France*
Email: v.d.dejong-5@umcutrecht.nl

Background and aims: International guidelines recommend 2-step pathways to screen for advanced fibrosis in populations at-risk, typically using the Fibrosis-4 index (FIB-4) followed by liver stiffness measurement (LSM) by VCTE. However, FIB-4's accuracy to (pre) screen in general populations remains debated. The Metabolic Dysfunction–Associated Fibrosis 5 (MAF-5) score was developed specifically for those populations. We aim to compare FIB-4 and MAF-5 as first-line tests to rule out advanced fibrosis, with LSM by VCTE as reference.

Method: GRIPonMASH is a prospective study, screening 10,000 high-risk individuals (T2DM, metabolic syndrome, obesity or arterial hypertension) without any prior other liver disease across 10 European countries. Rule-out cutoff for FIB-4 was <1.3 (or <2.0 if >65 years of age) and for MAF-5 <0. Participants <35 years of age were excluded, as FIB-4 is known to perform poorly in this group. Advanced fibrosis was ruled out if LSM <8.0 kPa. In this preliminary analysis descriptive statistics (median [IQR] or percentage) are reported. Negative predictive value (NPV) and sensitivity (SENS) of FIB-4/MAF-5 rule-out cutoff with LSM by VCTE as reference method were calculated. Results were also stratified by sex and primary diagnosis for inclusion (PDI).

Results: The preliminary cohort included 1050 participants recruited at primary care centers (75%) or through advertisement (25%). Median age was 60 [IQR: 13] years, BMI 31.0 [7.5] kg/m^2 and 53% was female. PDI was: 39% obesity, 36% arterial hypertension, 18% T2DM and 7% metabolic syndrome. Median LSM was 4.9 [2.0] kPa and 93% scored <8.0 kPa. Median FIB-4 was 1.2 [0.7] and MAF-5 0.8 [3.0]. Based on FIB-4, 25% of screened individuals would be referred to the 2nd test. NPV was 0.94 and sensitivity 0.38. Based on MAF-5, 65% would need the 2nd test, but this went up to 94% for PDI T2DM. NPV was 0.98 and SENS 0.92. Sex did not affect reported NPV/SENS. SENS of FIB-4 varied by PDI (0.21 to 0.67), for MAF-5 it remained stable, except for hypertension (drop to 0.78).

Conclusion: MAF-5 shows excellent NPV/SENS, at the cost of referring 65% to the 2nd test. NPV of FIB-4 is acceptably high with only 25% requiring a 2nd test, but SENS is substantially inferior (more false negatives). Presence of cardiometabolic diseases (PDI) influences SENS. Large-scale data is needed to optimize screening strategies.

GRIPonMASH is supported by Innovative Health Initiative Joint Undertaking, its members and its contributing partners under grant agreement No 101132946.

WED-085

Deep learning integration of nuclear magnetic resonance metabolomics and NASH-FibroTest biomarkers improves blood-based prediction of liver fat measured by magnetic resonance imaging

Olivier Deckmyn[1], Valentina Peta[1], Thierry Poynard[1,2]. *[1]BioPredictive, Paris, France; [2]Sorbonne University, Pitié Salpêtrière, ICAN, Paris, France*
Email: olivier.deckmyn@biopredictive.com

Background and aims: Magnetic resonance imaging proton density fat fraction (MRI-PDFF) is the reference for quantifying hepatic steatosis but is not suitable for large scale screening or longitudinal follow up. Nuclear magnetic resonance (NMR) metabolomics captures lipid signatures associated with hepatic fat accumulation, while Nash-FibroTest (NFT) biomarkers reflect liver injuries and metabolic dysfunction. We aimed to assess whether deep learning models combining NMR and available NFT biomarkers improve discrimination of PDFF-defined steatosis stages.

Method: Participants from the UK Biobank with available PDFF, NMR, and a subset of NFT markers (SteatoTest-2-proxy: ALT and AST transaminases, gamma-glutamyltranspeptidase, apolipoproteinA1, triglycerides, cholesterol, glycated hemoglobin, age, sex with R^2 = 0.91[%95 CI 0.88–0.92] vs original SteatoTest-2, n = 307) were included. High dimensional NMR data were reduced using unsupervised and supervised feature selection approaches. Multilayer perceptron models were trained using independent training, validation, and test sets. Model performance was evaluated using the area under the receiver operating characteristic curve (AUC) with 95 percent confidence intervals for clinically (%95CI) relevant liver fat thresholds.

Results: A total of 8,091 participants were analyzed. The combined 20 best NMR (dominated by HDL lipid composition and fatty acid profiles, including cholesteryl esters, phospholipids, PUFA/SFA ratios, and selected amino acids) and SteatoTest-2-proxy model demonstrated good discrimination across multiple PDFF-defined thresholds. AUC values were 0.766 (%95CI 0.733–0.800) for S0 vs S1A–S3, 0.766 (0.726–0.806) for S0–S1A vs S1B–S3, and 0.780 (0.668–0.872) for S0–S1B vs S2–S3. Severe steatosis discrimination (S0–S2 vs S3) was 0.884 (0.779–0.957), with limited reliability due to few S3 cases (n = 10). Performance was consistent across sex specific analyses.
Conclusion: Deep learning integration of NMR and available NFT biomarkers enables robust blood-based discrimination of PDFF-defined steatosis stages. This multimodal approach supports scalable and noninvasive assessment of steatosis severity in large populations with steatotic liver disease and warrants further validation in cohorts enriched for advanced steatosis.

WED-086
Low vitamin D levels are independently associated with increased fibrosis risk in metabolic dysfunction-associated steatotic liver disease

Youness Dendane[1], Mouhssine Benderrou[1], Ouiam Elmqaddem[1], Hajar Koulali[1], Abdelkrim Zazour[1], Zahi Ismaili[1], Ghizlane Kharrasse[1]. *[1]Department of Hepato-Gastroenterology, Mohammed VI University Hospital, Oujda, Morocco, Digestive Diseases Research Laboratory (LARMAD), Faculty of Medicine and Pharmacy, Mohammed First University, Oujda, Morocco, Oujda, Morocco*
Email: dendane.youness@gmail.com

Background and aims: Metabolic dysfunction-associated steatotic liver disease is a leading cause of chronic liver disease worldwide. Liver fibrosis is the main determinant of prognosis, yet simple markers for routine risk stratification remain limited. Vitamin D, at the intersection of metabolic and immune pathways, may reflect fibrotic severity. We aimed to evaluate the association between low vitamin D levels and increased fibrosis risk in metabolic dysfunction-associated steatotic liver disease.
Method: We conducted a retrospective single-centre study including 56 patients with metabolic dysfunction-associated steatotic liver disease followed between January 2020 and December 2024 with available serum vitamin D measurements. Data collected included age, sex, body mass index, diabetes, metabolic syndrome, liver tests, C-reactive protein, and albumin. Increased fibrosis risk was defined as FIB-4 ≥ 1.3. Vitamin D insufficiency was defined as < 30 ng/mL and severe deficiency as < 10 ng/mL. Associations were assessed using univariate and multivariable analyses adjusted for age, sex, body mass index, and metabolic parameters.
Results: Median age was 52 years, 56 percent were men, and median body mass index was 30 kg/m^2. Increased fibrosis risk (FIB-4 ≥ 1.3) was observed in 34 percent of patients. Vitamin D insufficiency was present in 62 percent, including 18 percent with severe deficiency. Median vitamin D levels were lower in patients with increased fibrosis risk than in those without (18 ng/mL [interquartile range 12–25] vs 25 ng/mL [interquartile range 19–32]; p = 0.03). Vitamin D insufficiency was more frequent in the fibrosis-risk group (71 percent vs 54 percent; p = 0.04). In multivariable analysis, vitamin D < 30 ng/mL remained independently associated with increased fibrosis risk (adjusted odds ratio 2.1; 95 percent confidence interval 1.0–4.5; p = 0.046).
Conclusion: Low vitamin D levels are common in metabolic dysfunction-associated steatotic liver disease and are independently associated with increased fibrosis risk. Vitamin D assessment may represent a simple and widely available complementary tool for fibrosis risk stratification. These findings should be confirmed in larger prospective cohorts.

WED-087
AI-derived macrophage density reveals hot and cold fibrosis endotypes with distinct biomarker profiles in metabolic dysfunction–associated steatohepatitis

Zoltan Derdak[1], Ying-Wooi Wan[1], Vandana Gupta[1], Lara Murray[2], Shima Nofallah[2], Guillaume Chhor[2], Kutbuddin Akbary[3], Dean Tai[3], Regina Lemus[1], Andressa de Zawadzki[4], Diana Julie Leeming[4], Morten Karsdal[4], Amon Asgharpour[5], Juan Pablo Arab[5], Haakan Wennbo[1], Arun J. Sanyal[5], Paresh Thakker[1]. *[1]Takeda Development Center Americas, Inc., Cambridge, MA, United States; [2]PathAI, Boston, MA, United States; [3]HistoIndex Pte Ltd, Singapore, Singapore; [4]Nordic Bioscience A/S, Herlev, Denmark; [5]Virginia Commonwealth University, Richmond, VA, United States*
Email: zoltan.derdak@takeda.com

Background and aims: In metabolic dysfunction-associated steatohepatitis (MASH), the biological activity driving fibrogenesis is heterogenous and not adequately represented by CRN fibrosis stage alone. We evaluated a hot vs cold fibrosis framework, defined by AI-measured macrophage density and linked to non-invasive tests (NITs), to identify biologically distinct endotypes and assess candidate NITs for patient selection in early clinical trials.
Method: Liver micro-architecture was quantified in 150 biopsy-confirmed MASH patients from the Stravitz-Sanyal Institute using LiverExplore* (PathAI, Boston, MA, *For Research Use Only. Not for use in diagnostic procedures) and by SHG/TPEF (Histoindex, Singapore) to assess the qFibrosis score. CRN Fibrosis was centrally staged. Hot fibrosis was defined as significant fibrosis by CRN staging (F ≥ 2) with macrophage density ≥ 250 cells/mm^2 by LiverExplore, and cold fibrosis as CRN F ≥ 2 with density < 250 cells/mm^2. Clinical variables and NITs were compared, including PRO-C3 (Roche Elecsys PRO-C3), CTX III, CTX III/PRO-C3 ratio, enhanced liver fibrosis (ELF) score, thrombospondin 2 (TSP2), and liver stiffness by vibration-controlled transient elastography (VCTE).
Results: The median qFibrosis score was 1.86 (IQR 1.27–3.07). Hot fibrosis accounted for 65% of cases and showed higher AST, ELF, PRO-C3, and TSP2 compared to cold fibrosis cases, while liver stiffness was similar. CTX III and CTX III/PRO-C3 ratios tended to be higher in cold fibrosis. NAS, steatosis, and ballooning did not differ, but hot fibrosis showed greater lobular inflammation. Within standard Phase 2b/3 MASH criteria (F ≥ 2; NAS ≥ 4 with ≥1 in each domain), tightening the lobular inflammation threshold from ≥ 1 to ≥ 2 substantially reduced the proportion of cold fibrosis cases, from ~ 50% to ~ 25%. High PRO-C3 (≥ 40 ng/mL) further enriched for hot fibrosis (88%; ~ 10% cold). Low PRO-C3 in cold fibrosis reflects low fibrogenic activity and limited capacity for further PRO-C3 decline.
Conclusion: Hot and cold fibrosis represent biologically distinct MASH endotypes. Elevated PRO-C3 enriches for active fibrogenesis, while cold fibrosis reflects a stable, low-fibrogenic state unlikely to respond to anti-fibrogenic therapies. Endotype- and biomarker-based enrichment may improve alignment between mechanism and therapeutic response in MASH trials.

WED-088
A simple PNPLA3–HSD17B13 genetic risk score predicts major adverse liver-related outcomes in high-risk MASLD

Luis Antonio Diaz[1], Kaleb Tesfai[1], Jonathan Dounel[1], Nikhil Kalita[1], Egbert Madamba[1], Seema Singh[1], Lisa Richards[1], Rohit Loomba[1], Veeral Ajmera[1]. *[1]University of California San Diego, La Jolla, United States*
Email: v1ajmera@health.ucsd.edu

Background and aims: MASLD with significant fibrosis is associated with major adverse liver-related outcomes (MALOs). However, there are limited data on the effect of genetic risk on MALOs across different baseline risk stages. Therefore, we aimed to evaluate the impact of genetic risk on MALOs according to baseline fibrosis risk determined by noninvasive tests (NITs).

Method: We prospectively enrolled adults with MASLD. All participants underwent a standardized research visit including magnetic resonance elastography (MRE), vibration-controlled transient elastography (VCTE), and genotyping for *PNPLA3* (rs738409) and *HSD17B13* (rs72613567). A genetic risk score (GRS) was made by summing the effect alleles of *PNPLA3* minus the protective *HSD17B13* variant and was dichotomized based on the median value into a high and low category. We defined three risk groups, including: "low risk": MRE < 3.0 kPa or VCTE < 8.0 kPa, "indeterminate risk": MRE 3.0–4.66 kPa or VCTE 8.0–11.9 kPa, and "high risk": MRE ≥ 4.67 kPa or VCTE ≥ 12.0 kPa. MALO was defined as hepatic decompensation or progression to cirrhosis. We performed Cox Regression models adjusted by age, sex, ethnicity, type 2 diabetes (T2D), body mass index (BMI), hypertension, dyslipidemia, and GRS.
Results: We included 1,125 participants (60.6% women; median [IQR] age was 59 [48–67] years; and 35.9% Hispanics). The median BMI was 30.2 [26.4–34.4] kg/m^2, and the prevalence of T2D was 53.9%. NITs identified 74.5% as low risk, 15.7% as indeterminate risk, and 9.8% as high risk for fibrosis. A total of 50.5% had a high GRS. Participants with a high GRS had a higher incidence of MALOs (19.0 vs. 6.2 events per 1,000 PY, p < 0.0001). In adjusted models, age (HR 1.05; 95% CI: 1.03–1.08, p < 0.0001), Hispanic ethnicity (HR 1.92; 95% CI: 1.13–3.26, p = 0.016), hypertension (HR 1.80; 95% CI: 1.01–3.18, p = 0.045), and high GRS (HR 2.49; 95% CI: 1.36–4.57, p = 0.003) were significant predictors of MALO. Within the low-risk category, high GRS was not associated with MALO (HR 0.78; 95% CI: 0.16–3.82, p = 0.756). However, among participants in the indeterminate or high fibrosis risk group, high GRS was associated with a higher risk of MALOs (HR 2.24; 95% CI: 1.14–4.40, p = 0.019).
Conclusion: After NIT-based risk stratification, a simple GRS was a significant predictor of MALOs in those with indeterminate or high fibrosis risk groups. Our findings support the use of genetic testing to further refine risk stratification, particularly in individuals with significant fibrosis identified by NITs.

WED-089
Optimizing prescreening for VCTE-LSM ≥8 kPa to support treatment eligibility in metabolic dysfunction–associated steatohepatitis

Winston Dunn[1,2], Julie Astono[3], Naim Alkhouri[4,5], Terry Cheuk-Fung Yip[6], Vincent Wai-Sun Wong[6], Laurent Castera[7], Manal F. Abdelmalek[8], Leon Adams[9], Nipun Verma[10], Juan Pablo Arab[11], Bihui Zhong[12], Vincent Chen[13], Ashwani K. Singal[14], Luis Antonio Diaz[15], Ming-Hua Zheng[16], Katrine Lindvig[3,4], Maja Thiele[17,18], Aleksander Krag[17,18]. *[1]University of Kansas, Kansas City, United States; [2]Pinnacle Clinical Research, San Antonio, United States; [3]Evido Health ApS, Copenhagen V, Denmark; [4]Summit Clinical Research, San Antonio, United States; [5]Clinical Research Institute of Ohio, Cleveland, United States; [6]The Chinese University of Hong Kong, Sha Tin, Hong Kong; [7]Université Paris Cité, Paris, France; [8]Division of Gastroenterology and Hepatology, Mayo Clinic, Rochester, United States; [9]Medical School, University of Western Australia, Perth, Washington, Australia, Perth, Australia; [10]Department of Hepatology, Postgraduate Institute of Medical Education and Research, Chandigarh, India; [11]Division of Gastroenterology, Hepatology, and Nutrition, Department of Internal Medicine, Virginia Commonwealth University School of Medicine, Richmond, United States; [12]Department of Gastroenterology, The First Affiliated Hospital, Sun Yat-sen University,, Guangzhou, Guangdong, China; [13]Division of Gastroenterology and Hepatology, University of Michigan, Ann Arbor, United States; [14]University of Louisville, Louisville, United States; [15]Division of Gastroenterology and Hepatology, University of California San Diego, San Diego, United States; [16]MAFLD Research Center, Department of Hepatology, The First Affiliated Hospital of Wenzhou Medical University, Wenzhou, China; [17]Center for Liver Research, Department of Gastroenterology and Hepatology, Odense University Hospital, Odense C, Denmark; [18]Institute of Clinical Research, Faculty of Health Science, University of Southern Denmark, Odense M, Denmark*
Email: aleksander.krag@rsyd.dk

Background and aims: Access to vibration-controlled transient elastography (VCTE) remains limited, yet current guidance for resmetirom and semaglutide in metabolic dysfunction–associated steatohepatitis (MASH) relies on liver stiffness measurement (LSM) ≥ 8 kPa to identify significant fibrosis. Efficient pre-screening using non-invasive tests (NITs) is therefore essential to prioritize patients for LSM. We evaluated the diagnostic performance and clinical utility of a laboratory-based machine-learning NIT to identify individuals with LSM ≥ 8 kPa in a large population-based cohort.
Method: Invitations to the Danish cohort were sent to randomly selected private electronic mailboxes and organized in two recruitment tracks: 1) unselected: invited regardless of risk factors, 2) at-risk: invited to participate if they had metabolic or alcohol risk factors. Participants were eligible for inclusion if they were aged 30–75 years, had no known chronic liver disease, cancer, or other diseases with an expected survival of less than one year. Participants underwent same-day assessment including VCTE, blood sampling, and anthropometry measurements among others. The diagnostic performance of the ALADDIN-F2-Lab model, CORE score, FIB-4, LiverRisk score (LRS), and SAFE to identify LSM ≥ 8 kPa was compared by area under the receiver operating characteristic curve (AUC), sensitivity at fixed 20% referral, and referrals to reach 80% sensitivity in the total Danish cohort.
Results: The total Danish cohort (n = 6,407) had a median age of 57, 48% male, 9% with type 2 diabetes, 42.5% obese, and 6.2% with LSM>8 kPa. The AUCs (95% CI) for predicting significant fibrosis were for ALADDIN 0.815 (0.793–0.838), LRS 0.812 (0.787–0.837), CORE 0.793 (0.767–0.819), SAFE 0.789 (0.763–0.814), and FIB-4 0.633 (0.600–0.666). When limiting referral rates to 20%, the sensitivities were for: 64.6%, LRS: 62.6%, SAFE: 60.3%, CORE: 59.5%, and FIB-4: 39.7%. Reaching 80% sensitivity required referral rates of 37% (ALADDIN), 38% (LRS), 42% (CORE), 43% (SAFE), and 74% (FIB-4).
Conclusion: In a population-based cohort, routine laboratory-based machine-learning NITs accurately identified individuals with LSM ≥8 kPa, outperforming FIB-4 while reducing unnecessary referrals. Given the limited availability of VCTE and the central role of LSM ≥8 kPa in determining eligibility for MASH therapies, effective pre-screening is critical. Implementing routine laboratory-based machine-learning NITs may improve access to treatment and streamline referral pathways.

WED-090
Imaging of liver fibrogenesis in MASH by PDGFR-beta position emission tomography

Olof Eriksson[1,2], Johan Vessby[3], Fredrik Rorsman[3], Talakad G. Lohith[4], Cyrille Sur[4], Zoltan Derdak[4], Yoann Petibon[4], Thuy Tran[5], Lennart Nedar[5], Per Hagmar[2], Martin Schain[6], Bogdan Mitran[2], Ayman Abouzayed[2], Edvin Johansson[6], Olle Korsgren[1], Lars Johansson[6], Haakan Wennbo[4]. *[1]Uppsala Universitet, Antaros Tracer AB, Uppsala, Sweden; [2]Antaros Tracer AB, Göteborg, Sweden; [3]Akademiska Sjukhuset, Uppsala, Sweden; [4]Takeda Development Center Americas, Cambridge, United States; [5]Karolinska Inst, Solna, Sweden; [6]Antaros Medical AB, Mölndal, Sweden*
Email: olof.eriksson@ilk.uu.se

Background and aims: Existing imaging methods based on elastography assess fibrosis but not active fibrogenesis in liver. Platelet Derived Growth Factor Receptor beta (PDGFRb) is upregulated in activated hepatic stellate cells and therefore could be a marker of fibrogenesis. [^{68}Ga]Ga-ATH001 is a Positron Emission Tomography (PET) tracer targeting PDGFRb for longitudinal, non-invasive quantification of active fibrosis in liver. Here, we present the performance and reproducibility of [^{68}Ga]Ga-ATH001 in a First-in-Human study in subjects with Metabolic dysfunction-associated Steatohepatitis (MASH).

Method: Study cohorts recruited were healthy subjects without history of liver disease (n = 6) and subjects diagnosed with MASH (n = 6, plasma Pro-C3 ≥12.6 ng/mL indicating active fibrosis). Subjects were administered 2.0–2.5 MBq/kg [^{68}Ga]Ga-ATH001 (corresponding to <1 µg/kg peptide mass) and examined by PET/ Magnetic Resonance Imaging (MRI) for up to 3 hours. Liver assessments also included Magnetic Resonance Elastography (MRE), Proton Density Fat Fraction (PDFF) and Transient Elastography (TE, FibroScan). A subset of subjects (n = 2 healthy and n = 3 MASH subjects) were re-scanned by [^{68}Ga]Ga-ATH001 PET/MRI within 2 weeks to assess test-retest reproducibility. Uptake in liver and other major tissues was reported as Standardized Uptake Values (SUVs). Liver SUV was corrected for fat fraction.
Results: No adverse events related to administration of [^{68}Ga]Ga-ATH001 was observed. Fat fraction was higher in the MASH cohort than healthy controls (19.1 ± 6.9% (mean ± SD) vs 4.1 ± 5.5% in healthy controls, $p < 0.01$). Liver stiffness as assessed by MRE was also higher in the MASH cohort than healthy controls (2.7 ± 0.5 kPa vs 2.1 ± 0.3 kPa, $p < 0.05$). TE values were 8.6 ± 1.7 kPa in the MASH cohort. [^{68}Ga]Ga-ATH001 exhibited fast biodistribution and rapid clearance from circulation and most tissues. PET uptake in liver 2 h post-injection was almost twice as high in subjects with MASH compared to healthy (SUV_{mean} = 5.7 ± 1.0 vs 3.2 ± 0.6, $p < 0.001$). High uptake was also observed in PDGFRβ avid spleen while excretion was almost completely mediated by kidney. [^{68}Ga]Ga-ATH001 uptake in liver demonstrated a percent coefficient of variation (%CV) of 3.3%.
Conclusion: [^{68}Ga]Ga-ATH001 is a novel PDGFRβ-targeting PET tracer for non-invasive assessment of active liver fibrosis. [^{68}Ga]Ga-ATH001 demonstrates strong liver uptake in MASH patients with active fibrosis, combined with excellent test-retest reproducibility.

WED-091
A new definition of burning-out MASLD using albumin and amino acid imbalance
Hideki Fujii[1], Sawako Uchida-Kobayashi[1]. [1]*Graduate School of Medicine, Osaka Metropolitan University, Osaka, Japan*
Email: sawako@omu.ac.jp

Background and aims: Li et al. recently described the phenomenon of progressive fibrosis accompanied by hepatic fat loss in MASLD as "burning-out," characterized by a downward trend in the controlled attenuation parameter (CAP) and an upward trend in liver stiffness measurement (LSM) via vibration-controlled transient elastography (VCTE) (PMID: 40113099). We hypothesized that this transition is associated with an amino acid imbalance, even in the presence of normal serum albumin (Alb) levels. This study aimed to characterize "burning-out MASLD" based on serum branched-chain amino acid to tyrosine ratio (BTR) and albumin, and to assess its clinical and non-invasive features.
Method: In this cross-sectional study, we analyzed 214 MASLD patients who underwent VCTE. Amino acid imbalance was assessed using BTR. Patients were stratified into three groups:
- Control group: BTR ≥ median and Alb ≥ 4.0 g/dL
- Burning-out group: BTR < median and Alb ≥ 4.0 g/dL
- Burned-out group: BTR < median and Alb < 4.0 g/dL

Patients not fitting these categories were excluded from further analysis. We compared clinical parameters, particularly LSM and CAP, among the three groups. Group differences were evaluated using one-way ANOVA followed by Dunnett's post hoc test with the burning-out group as the reference.
Results: Among 214 patients (median age 61 [IQR 53–70.3] years; 44% male; median BMI 26.8 [23.8–30.1] kg/m^2), the median Alb was 4.3 g/dL and BTR 6.4. Type 2 diabetes and hypertension were present in 36% and 47%, respectively. Seventeen patients were excluded based on the stratification criteria. Among the remaining patients, 92 were assigned to the control group, 72 to the burning-out group, and 33 to the burned-out group. Mean LSM, CAP, and FAST score in the control group were 6.9 kPa, 289 dB/m, and 0.29, respectively. Compared with the burning-out group, the burned-out group exhibited significantly higher LSM (20.7 vs. 7.8 kPa, $p < 0.001$), lower CAP (253 vs. 280 dB/m, $p = 0.047$), and higher FAST score (0.73 vs. 0.38, $p < 0.001$).
Conclusion: Our findings suggest that "burning-out MASLD" may represent a distinct transitional phenotype characterized by preserved hepatic fat content despite the onset of metabolic dysfunction. BTR may serve as a non-invasive biomarker to identify patients in this intermediate stage, enabling earlier intervention before progression to advanced fibrosis.

WED-092-YI
Implementation of enhanced liver fibrosis testing in type 2 diabetes to improve detection of at-risk metabolic dysfunction-associated steatohepatitis to optimize hepatology referrals: a duke health analysis
Maison Furley[1], Tom Kaminski[2], Zach Wolf[2], Artem Boltyenkov[3], Amreen Dinani[1]. [1]*Duke University Hospital, Durham, United States;* [2]*Clinetic, Durham, United States;* [3]*Siemens Healthcare Diagnostics, Mishawaka, United States*
Email: maison.furley@duke.edu

Background and aims: Type 2 diabetes (T2D) is accepted as a high-risk population to develop metabolic dysfunction-associated steatotic liver disease (MASLD), metabolic dysfunction-associated steatohepatitis (MASH), and advanced fibrosis. Screening for at-risk MASH in T2D remains low despite consensus guidance recommending a two-step approach starting with Fibrosis-4 (FIB-4) followed by a second-line test for indeterminate results. Enhanced Liver Fibrosis (ELF) test is a blood-based test that can be employed as a second-line test, but its real-world performance in endocrinology settings is not well described. The aim of this study was to evaluate the use of ELF test in endocrinology clinics at the Duke University Health System (DUHS) and assess the impact on fibrosis risk detection and hepatology referrals.
Method: This retrospective observational study (09/2024 to 11/2025) examined the use of the ELF test by endocrinology during routine care of patients with T2D. ELF testing was piloted in select endocrine clinics. All tests were tracked, and results were categorized using a threshold ≥ 9.8, indicative of significant fibrosis risk. Hepatology referrals and completed hepatology visits were recorded. Using these data alongside historical data for the broader adult T2D Duke University Health System (DUHS) population, we projected the impact of implementing this care pathway across the entire DUHS.
Results: On an annualized basis, DUHS endocrinologists saw 1,113 T2D patients with a FIB-4 > 2.67 and 2,965 T2D patients with a FIB-4 ≥ 1.3 and < 2.67 of which 25.3% and 13.0% had a subsequent hepatology visit, respectively. Over the study period, 64 patients with T2D underwent ELF testing. Thirty patients (46.9%) had ELF > 9.8; all were referred, and 70.0% completed the visit. Implementation of a two-step risk assessment protocol could increase hepatology visits by 1,085 (162.9%) per year. For patients with indeterminate FIB-4 results, ELF test was projected to reduce unnecessary referrals by 205 (53.1%) among individuals expected to have low ELF scores and increase appropriate hepatology visits by 792 (438.9%), among those with elevated ELF scores.
Conclusion: System-wide adoption of a two-step fibrosis assessment pathway (FIB-4 followed by ELF) has the potential to significantly increase early detection of *at*-risk MASH while reducing unnecessary specialist utilization. Given the large projected increase in hepatology visits, the topic of how to optimize implementation warrants further research and discussion.

WED-093-YI

Cardiometabolic risk factor burden predicts longitudinal liver stiffness trajectories in metabolic dysfunction-associated steatotic liver disease-related compensated advanced chronic liver disease

Zouhir Gadi[1,2], Lotte Schoenmakers[1,2], Wilhelmus J Kwanten[1,2], Luisa Vonghia[1,2], Sven Francque[1,2]. *[1]Department of Gastroenterology and Hepatology, Antwerp University Hospital, Edegem, Belgium; [2]Laboratory of Experimental Medicine and Pediatrics, Faculty of Medicine and Health Care Sciences, University of Antwerp, Edegem, Belgium*
Email: Zouhir.Gadi@student.uantwerpen.be

Background and aims: Cardiometabolic risk factors (CMRFs) linked to metabolic dysfunction–associated steatotic liver disease (MASLD) include overweight/obesity, impaired glucose metabolism, hypertension, hypertriglyceridaemia, and low high-density lipoprotein cholesterol. In MASLD-related compensated advanced chronic liver disease (cACLD), the cumulative impact of CMRF burden on longitudinal liver stiffness, a key non-invasive monitoring marker, remains poorly defined.
Method: We included 93 adults with biopsy-proven MASLD and cACLD (F3–F4 fibrosis) who had at least two Vibration-Controlled Transient Elastography (VCTE) liver stiffness measurements (LSMs) approximately one year apart, with paired biochemical assessment. Baseline LSM was defined at cACLD diagnosis and follow-up LSM as the most recent measurement, only first and last LSMs were analysed. Exclusion criteria included other chronic liver diseases, metabolic alcohol-related liver disease, bariatric surgery, baseline decompensation, or liver transplantation. CMRFs (range 1–5) were recorded at baseline. LSM trajectories were categorised as improved (≥20% decrease), stable (−20% to +20%), or worsened (≥20% increase). Clinical outcomes included incident hepatic decompensation events, defined as ascites, variceal bleeding, hepatic encephalopathy, or development of oesophageal varices, and all-cause mortality.
Results: The cohort comprised 55 men (59%) and 38 women (41%), 62 patients (67%) had F3 and 31 (33%) F4 fibrosis. CMRF burden was 1 in 2 patients (2.2%), 2 in 13 (14.0%), 3 in 32 (34.4%), 4 in 27 (29.0%), and 5 in 19 (20.4%), 84% had ≥3 CMRFs. Median interval between LSMs was 72 weeks (IQR 46.5). Baseline LSM increased with CMRF burden (15.44–17.85 kPa in 1–3 CMRFs vs. 21.08–21.98 kPa in 4–5). AST, ALT, and GGT levels similarly worsened with higher CMRF load. Mean LSM change ranged from −38.9% in 1 CMRF to +19.5% in 3 CMRFs, with minimal change in 5 CMRFs. Overall, 39% improved, 34% remained stable, and 27% worsened, with progression most frequent in the 3- and 5-CMRF groups. Over a median 4.3-year follow-up, ascites and non-bleeding oesophageal varices occurred in 5.4% each. All-cause mortality was 7.5%, exclusively in patients with ≥3 CMRFs, accompanied by marked LSM progression.
Conclusion: In MASLD-related cACLD, CMRF burden stratifies liver stiffness trajectories. Lower metabolic burden is linked to LSM improvement, while three or more CMRFs increase progression risk, supporting systematic cardiometabolic assessment and targeted care.

WED-094

Contrast-enhanced ultrasound in metabolic dysfunction-associated steatotic liver disease: towards a non-invasive marker of histological disease activity

Zouhir Gadi[1,2], Wilhelmus J Kwanten[1,2], Ann Driessen[3], Thomas Vanwolleghem[1], Sven Francque[1,2], Luisa Vonghia[1,2]. *[1]Department of Gastroenterology and Hepatology, Antwerp University Hospital, Edegem, Belgium; [2]Laboratory of Experimental Medicine and Pediatrics, Faculty of Medicine and Health Care Sciences, University of Antwerp, Edegem, Belgium; [3]Department of Pathology, Antwerp University Hospital, Edegem, Belgium*
Email: Zouhir.Gadi@student.uantwerpen.be

Background and aims: Microvascular dysfunction plays a key role in metabolic dysfunction-associated steatotic liver disease (MASLD). Time-intensity curve (TIC) analysis from contrast-enhanced ultrasound (CEUS) quantifies hepatic (micro)vascular perfusion and may provide a non-invasive marker of disease severity. This study evaluated whether TIC parameters reflect MASLD severity and diagnostic accuracy.
Method: Patients undergoing liver biopsy for MASLD were prospectively included after informed consent and underwent CEUS with TIC analysis of eleven perfusion parameters on the same day, in the fasting state. Histology assessed steatosis, ballooning, inflammation, activity, fibrosis stage (F), presence of metabolic dysfunction-associated steatohepatitis (MASH) and at-risk MASH, defined as MASH with fibrosis stages F2-F3. Conventional ultrasound (US) Doppler, liver stiffness measurement (LSM), controlled attenuation parameter (CAP) and spleen stiffness measurement (SSM) were performed, and hepatic venous pressure gradient (HVPG) data were available in a subset.
Results: Sixty-eight patients with adequate biopsy and CEUS data were included (61 MASLD, 7 controls); 30 MASLD patients had MASH. Fibrosis stages were F0 (n = 15), F1 (n = 14), F2 (n = 17), F3 (n = 8), and F4 (n = 14), defining controls (n = 7), low-risk MASLD F0–1 (n = 18), at-risk MASH F2–3 (n = 19), and MASLD cirrhosis F4 (n = 14). TIC parameters correlated with histology. Steatosis grade correlated negatively with MGrad (rho = –0.438), Grad (rho = –0.255), AUC (rho = –0.473), and WOAUC (rho = –0.436), with similar associations for US steatosis and CAP. Ballooning correlated positively with WIAUC (rho = 0.262), while inflammation and activity correlated negatively with WOAUC (rho = – 0.334 and – 0.302). Fibrosis correlated positively with WIAUC (rho = 0.404), TTOP (rho = 0.326), and TWR (rho = 0.320), and negatively with Grad (rho = –0.278). LSM correlated negatively with perfusion intensity (rho = –0.300) and positively with WIAUC (rho = 0.287); no associations were observed with SSM, Doppler, or HVPG (rho = 0.348). WIAUC was higher in MASH than non-MASH MASLD (median 733.0 vs. 675.8 AU). Across disease stages, WIAUC increased with delayed TTOP and increased TWR. Diagnostic performance was fair for MASH (AUC 0.655) and comparable for significant fibrosis using WIAUC, TTOP, and TWR (AUC 0.728–0.737).
Conclusion: TIC-derived parameters correlated with MASLD severity and progressive microvascular impairment in advancing MASH, supporting CEUS as a non-invasive adjunct.

WED-095

FIB-4 in clinical laboratory data: reporting and feasibility evaluation in Germany

Thomas Jensen[1], Andres Garcia[1], Elena Kisseleff[1], Anna Stuermlinger[1], Anna Rubinski[2], Livia Woeller[2], Stephan Koelsch[1], Philipp Hessenberger[2]. *[1]Boehringer Ingelheim Pharma GmbH & Co. KG, Ingelheim, Germany; [2]Health Data Technologies GmbH, Neckarsulm, Germany*
Email: thomas.jensen@boehringer-ingelheim.com

Background and aims: MASLD affects an estimated 30% of adults globally and between 10% and 30% of these individuals will progress to MASH[1,2]. Both conditions remain underdiagnosed and expert consensus underscores the necessity to increase diagnostic rates[3]. Clinical guidelines recommend the FIB-4 score as initial step for screening and diagnosis. This project had two objectives: 1. quantify current utilisation of FIB-4 scores; 2. assess availability of laboratory parameters necessary for FIB-4 score calculation (age, ALT, AST, platelet count).
Method: We performed a retrospective observational study using data from a Bavarian laboratory network. Time frame of observation was January 2022 to December 2024. Inclusion criteria comprised adult patients belonging to predefined MASLD/MASH risk groups in line with current EASL guidelines. Cardiometabolic risk factors were defined according to EASL–EASD–EASO guidelines. To quantify utilisation of FIB-4 (objective 1), all laboratory records containing a reported FIB-4 score were identified and counted. We then assessed

whether parameters required for Fib-4 calculation were available (objective 2). Analysis was performed exclusively on pseudonymised datasets, all outputs were anonymised prior to reporting.
Results: Of the 1.4 million patients in the database, 521,084 met all predefined eligibility criteria. Calculation of FIB-4 scores was rarely performed, with frequencies from 0.11% to 0.75% across risk cohorts. For example, only 0.15% of patients with diabetes had a FIB-4 score reported. However, a substantial proportion of reports had necessary laboratory parameters, enabling FIB-4 score calculation. Availability of laboratory parameters required for FIB-4 score calculation was 61.4% in the diabetes cohort, 70.7% in the prediabetes cohort, 66.5% in the dyslipidaemia cohort, and exceeded 98% in various combined-risk cohorts, such as prediabetes plus abnormal ALT/AST and diabetes plus dyslipidaemia.
Conclusion: Although FIB-4 score is recommended as primary screening tool for MASH in all major guidelines, this investigation demonstrates that the proportion of at-risk patients for whom FIB-4 score calculation is performed remains extremely low. Given the high availability of laboratory parameters, clinical laboratories are positioned to automate FIB-4 calculation. Furthermore, implementation of educational initiatives for healthcare professionals is essential to promote the use of FIB-4 in order to enhance identification of at-risk individuals.

WED-099
Parallel combination of FIB-4 and enhanced liver fibrosis test improves prognostication in metabolic dysfunction-associated steatohepatitis
Matthew Gee[1,2], Rachel Fonstad[2], Jordan J. Feld[1,3], Keyur Patel[1,3], Arun J. Sanyal[4]. *[1]Institute of Medical Science, Temerty Faculty of Medicine, University of Toronto, Toronto, Canada; [2]Siemens Healthineers, Tarrytown, United States; [3]Division of Gastroenterology, Department of Medicine, Toronto Centre for Liver Disease, Toronto General Hospital, University Health Network, Toronto, Canada; [4]Stravitz-Sanyal Institute for Liver Disease and Metabolic Health, Division of Gastroenterology, Hepatology and Nutrition, Virginia Commonwealth University School of Medicine, Richmond, United States*
Email: matthew.gee@siemens-healthineers.com

Background and aims: Metabolic dysfunction-associated steatohepatitis (MASH) is a leading cause of cirrhosis and liver-related mortality. Clinical practice guidance from EASL and other societies recommend sequential measurement by non-invasive tests (NITs) to identify patients most at risk of progressing to liver-related events (LREs). These risk-assessment pathways typically begin with FIB-4 and are followed by either vibration-controlled transient elastography (VCTE) or Enhanced Liver Fibrosis (ELF). We aimed to determine whether parallel measurement of FIB-4 and ELF improves risk stratification in patients with MASH and advanced fibrosis.
Method: Data were pooled from 5 large placebo-controlled trials in patients with MASH and advanced fibrosis (NCT01672866, NCT01672879, NCT02462967, NCT03053050, NCT03053063), excluding patients without ELF or FIB-4 at baseline. Patients were organized in a 3 × 4 heatmap based on previously determined cutoffs for FIB-4 (1.30, 3.48) and ELF (9.00, 11.30, 12.80). Liver-related events (LREs) were a composite endpoint of clinical manifestations of decompensation, (qualification for) transplant, and liver-related death, based on the first event per patient. LRE risk (%), LREs per 1000 years of patient follow-up (LRE/1000 PY), and Cox proportional hazard ratio (HR) were calculated with 95% confidence intervals. Time-dependent area under the receiver operating characteristic curve (AUC(t)) and net reclassification improvement (NRI) analyses were also performed.
Results: 113 of 2276 study participants had LREs during the follow-up period (median: 15.9 months). There was a progressive increase in LRE risk with increasing ELF score in each FIB-4 risk category, and vice versa. The combined FIB-4 + ELF heatmap identified 5 strata that were differentiated in terms of LRE risk (0.4%, 2%, 9%, 16%, 40%). Similar trends were seen for LRE/1000PY and Cox HR. NRI for the FIB-4 + ELF model vs FIB-4 alone was 0.44 (95% CI: 0.34, 0.54). 92 more of the 2163 (4%) non-LRE patients were correctly assigned as low risk and 65/113 (58%) patients with LREs were reclassified upwards. The AUC (t) for the combined model was significantly different ($p < 0.05$) than FIB-4 alone at timepoints after 3 months.
Conclusion: The parallel measurement of FIB-4 and ELF improves prognostic performance over that of the individual tests and offers a pragmatic option to facilitate prognostic clinical decision making in patients with MASLD/MASH, especially in settings where imaging elastography is not readily available.

WED-100-YI
A novel machine learning-based algorithm improves risk stratification of patients with MASLD compared to FIB-4
Kamela Gjini[1,2], Mirko Zoncapè[3,4], Antonio Liguori[5], Katrine Lindvig[6], Maja Thiele[7], Emmanuel Tsochatzis[2]. *[1]Division of Gastroenterology and Hepatology, Department of Medical Sciences, University of Turin, Turin, Italy; [2]Sheila Sherlock Liver Unit, Royal Free Hospital, London, UK, UCL Institute for Liver and Digestive Health, University College, London, United Kingdom; [3]Liver Unit, University of Verona and Azienda Ospedaliera Universitaria Integrata of Verona, Verona, Italy; [4]Clinica Medica 3, Azienda Ospedale Università di Padova, Padova, Italy; [5]Medical and Surgical Sciences Department, Fondazione Policlinico Universitario A. Gemelli-IRCCS, Università Cattolica del Sacro Cuore, Rome, Italy; [6]Evido Health, Copenhagen, Denmark; [7]Department of Gastroenterology and Hepatology, Odense University Hospital, Odense, Denmark, Institute of Clinical Research, University of Southern Denmark, Odense, Denmark*
Email: kamelagjini@gmail.com

Background and aims: Metabolic dysfunction-associated steatotic liver disease (MASLD) is the leading cause of chronic liver disease worldwide. Early identification of advanced fibrosis (≥F3) is essential, as fibrosis stage is the strongest predictor of liver-related outcomes and mortality. Current guidelines recommend FIB-4 as the first-line test in primary care; however, its limitations highlight the need for more reliable tools. LiverPRO, a machine learning-based software using routine laboratory variables, has been proposed as an alternative. We aimed to compare the performance of LiverPRO F3 and FIB-4 for first-line risk stratification of advanced fibrosis in patients with MASLD.
Method: We conducted a retrospective cross-sectional study of 1818 consecutive MASLD patients referred to the hepatology clinic of the Royal Free Hospital, London (2016–2024). Two parallel referral pathways were constructed on the same cohort, using either FIB-4 or LiverPRO F3 as the first-line test for advanced fibrosis. Patients were stratified into low- intermediate- and high-risk categories using predefined thresholds (FIB-4: <1.3 low risk, >2.67 high risk; LiverPRO F3: <5% low risk, >15% high risk). Diagnostic performance of both pathways was assessed against a composite reference standard for advanced fibrosis, defined as either: histological stage ≥F3; liver stiffness >12 kPa; or liver stiffness >8 kPa + ELF score > 9.8. Net reclassification improvement (NRI) was used to assess the added value of LiverPRO vs. FIB-4. In addition, the performance of LiverPRO was validated against vibration-controlled transient elastography and liver biopsy.
Results: Among 1703 patients with valid reference standards, 389 (23%) had advanced fibrosis. Using FIB-4, 695 patients (41%) were classified as indeterminate, and 108/871 patients (13%) in the low-risk group had advanced fibrosis. LiverPRO F3 model identified 206 (12%) patients with advanced fibrosis at the high-risk threshold versus 78 (5%) with FIB-4 ($p < 0.0001$), reduced the number of missed cases in the low-risk group to 50/663 (8%) vs. 108/871 (13%) with FIB-4 ($p = 0.001$), and decreased the number of patients in the indeterminate-risk category to 606 (36%) vs. 695 (41%) ($p = 0.002$). Overall, LiverPRO F3 achieved a NRI of 0.21 compared with FIB-4.

Conclusion: In this large real-world MASLD cohort, LiverPRO F3 significantly improved first-line risk stratification of advanced fibrosis compared with FIB-4, reducing false negatives and identifying more patients with advanced fibrosis.

WED-101

Population-based assessment of metabolic dysfunction–associated steatotic liver disease using CAP: results in the european population from the LiverScreen project

Isabel Graupera[1], Guillem Pera[2], Núria Fabrellas[3], Laurent Castera[4], Maja Thiele[5], Anna Soria[1], Adrià Juanola[1], Elisa Pose[1], Marta Cervera Carbonell[1], Cautar El Maimouni[1], Salvatore Piano[6], Rosa M Morillas[7], Peter Andersen[5], Sandro Kukic[8], Daniel Jan Havaj[9], Mirko Zoncapè[10], Miquel Serra Burriel[11], Rafael Bañares[12], Neil Guha[13], Jörn M. Schattenberg[14], Frank Lammert[15], Emmanuel Tsochatzis[10], Willem Pieter Brouwer[16], Juan M. Pericàs[17], Lubomir Skladany[9], Ivica Grgurević[18], Dominique Roulot[19], Paolo Angeli[6], Pere Torán[2], Aleksander Krag[5], Pere Ginès[1]. *[1]Liver Unit, Hospital Clínic of Barcelona, Barcelona, Catalunya, Spain; Faculty of Medicine and Health Sciences, University of Barcelona, Barcelona, Spain, Fundació de Recerca Clínic Barcelona - Institut d'Investigacions Biomèdiques August Pi i Sunyer (FCRB - IDIBAPS), Barcelona, Catalunya, Spain, Centro de Investigación Biomédica en Red Enfermedades Hepáticas y Digestivas (CIBEREHD), Madrid, Spain, Barcelona, Spain; [2]Unitat de Suport a la Recerca Metropolitana Nord, Fundació Institut Universitari per a la Recerca a l'Atenció Primària de Salut Jordi Gol i Gurina (IDIAPJGol), Mataró, Barcelona, Spain, Mataró, Spain; [3]Faculty of Nursing, University of Barcelona, Barcelona, Spain, Fundació de Recerca Clínic Barcelona - Institut d'Investigacions Biomèdiques August Pi i Sunyer (FCRB - IDIBAPS), Barcelona, Catalunya, Spain, Centro de Investigación Biomédica en Red Enfermedades Hepáticas y Digestivas (CIBEREHD), Madrid, Spain, Barcelona, Spain; [4]Department of Hepatology, Hôpital Beaujon, Assistance Publique-Hôpitaux de Paris, Clichy, Université de Paris, Paris, France, Paris, France; [5]Centre for Liver Research, Department of Gastroenterology and Hepatology, Odense University Hospital (OUH), Department of Clinical Research, Faculty of Health Sciences, University of Southern Denmark (SDU), Odense, Denmark, Odense, Denmark; [6]Unit of Internal Medicine and Hepatology, Department of Medicine - DIMED, University and Hospital of Padova, Italy, Padova, Italy; [7]Liver Unit, Hospital Germans Trias i Pujol. Instituto de Investigación Germans Trias i Pujol (IGTP), Badalona, Catalunya, Spain, Centro de Investigación Biomédica en Red Enfermedades Hepáticas y Digestivas (CIBEREHD), Madrid, Spain, Badalona, Spain; [8]University of Zagreb School of medicine, Zagreb, Croatia, Zagreb, Croatia; [9]Division of Hepatology, Gastroenterology and Liver Transplantation, Department of Internal Medicine II, Slovak Medical University Faculty of Medicine, F. D. Roosevelt University Hospital, Banska Bystrica, Slovak Republic, Banská Bystrica, Slovakia; [10]UCL Institute for Liver and Digestive Health, Royal Free Hospital, University College of London (UCL), London, UK, London, United Kingdom; [11]Epidemiology, Statistics, and Prevention Institute, University of Zurich, Zurich, Switzerland, Zurich, Switzerland; [12]Gastroenterology and Hepatology Service. Hospital General Universitario, Gregorio Marañon, Gregorio Marañon Research Institute, School of Medicine. Universidad Complutense, CIBERehd, Madrid, Spain, Madrid, Spain; [13]NIHR Nottingham Biomedical Research Centre, Nottingham University Hospitals NHS Trust and the University of Nottingham, Nottingham, UK, Nottingham, United Kingdom; [14]Department of Internal Medicine I, University Medical Center of the Johannes Gutenberg-University, Mainz, Germany, Mainz, Germany; [15]Center for Health Economics Research Hannover (CHERH), Hannover Medical School (MHH), Hannover, Germany, Hannover, Germany; [16]Department of Gastroenterology and Hepatology, Erasmus MC-University Medical Centre, Rotterdam, the Netherlands, Rotterdam, Netherlands; [17]Liver Unit, Hospital Universitari Vall d´Hebron, Vall d'Hebron Institut de Recerca (VHIR), Vall d'Hebron Barcelona Hospital Campus, Barcelona, Spain, Universitat Autònoma de Barcelona, Barcelona, Spain, Centro de Investigación Biomédica en Red Enfermedades Hepáticas y Digestivas (CIBEREHD), Madrid, Spain, Barcelona, Spain; [18]Department of Gastroenterology, Hepatology and Clinical Nutrition, University Hospital Dubrava, Croatia, Dubrava, Croatia; [19]Unité d'Hépatologie, Hôpital Avicenne, Assistance Publique-Hôpitaux de Paris, Université Sorbonne Paris Nord, Bobigny, France, Bobigny, France*
Email: igraupe@clinic.cat

Background and aims: Metabolic dysfunction–associated steatotic liver disease(MASLD) is the leading cause of liver disease worldwide, and its prevalence is expected to increase with the growing burden of cardiometabolic risk factors (CMRFs). However, population-based epidemiological data using controlled attenuation parameter(CAP), a validated noninvasive measure of hepatic steatosis, remain limited. Our aims were to assess the prevalence of MASLD in the general population using CAP for steatosis diagnosis, to determine the prevalence of confirmed chronic liver disease (CLD) among individuals with MASLD, and to evaluate the contribution of individual cardiometabolic criteria to CLD.
Method: Individuals aged ≥40 years enrolled in the population-based LiverScreen cohort with clinical and laboratory assessment and VCTE with LSM and CAP. Participants with LSM ≥8 kPa and/or alanine aminotransferase ≥1.5 × the upper limit of normal were referred for hepatology consultation. MASLD was defined as CAP ≥275 dB/m in the presence of ≥1 CMRF. Primary outcomes were the overall prevalence of MASLD and the prevalence of confirmed CLD among individuals with MASLD (defined by histologically fibrosis≥F1 and/or LSM≥10 kPa and/or ultrasound signs of advanced liver disease).
Results: Among 30,199 participants, 8,401 (28%) met MASLD criteria (mean age 59 years; 48% women; median CAP 307 [IQR 46]dB/m). The prevalence of CMRFs were overweight/obesity (96%), hypertension (82%), prediabetes/diabetes (53%), hypertriglyceridemia (53%), and low HDL cholesterol (42%); 31% had ≥2 CMRFs. LSM and CAP increased progressively with the number of CMRFs (LSM: 4.4, 4.7, 5.0, 5.2, 5.6 kPa; CAP: 296, 300, 307, 312, 320 dB/m for 1–5 CMRFs, respectively). LSM ≥8 kPa was observed in 8.0% of individuals with MASLD versus 2.6% without MASLD; LSM ≥10 kPa and ≥15 kPa were present in 4.3% and 1.2%, respectively. Among MASLD participants referred for hepatology consultation, CLD was confirmed in 263(39%), with 71% histologically confirmed. CLD prevalence increased from 21% in those with one CMRF to 55% in those with five. Type 2 diabetes was the only CMRF independently associated with confirmed CLD (OR 2.6, 95%CI 1.7–4.1).
Conclusion: MASLD affects nearly one-third of the European general population aged ≥40 years and is associated with a substantial burden of confirmed CLD. The severity of hepatic steatosis and liver fibrosis increases with the number of cardiometabolic risk factors, with type 2 diabetes conferring the highest risk of CLD.

WED-102-YI

Artificial intelligence-guided approaches to define biochemical and epigenetic markers that may reflect the metabolic dysfunction-associated steatohepatitis phenotype in children and adults

Flavia Grignaffini[1], Maria Rita Braghini[1], Giulia Andolina[1], Antonella Mosca[2], Luca Dalla Volpe[2], Nadia Panera[1], Antonio Liguori[3], Francesca D'Ambrosio[3], Maurizio Pompili[3], Andrea Damiani[4], Luca Miele[3], Anna Alisi[1]. *[1]Research Unit of Genetics of Complex Phenotypes, Bambino Gesù Children's Hospital, IRCCS, Rome, Italy, Roma, Italy; [2]Division of Hepatobiliopancreatic Surgery, Liver and Kidney Transplantation, Bambino Gesù Children's Hospital, IRCCS, Rome, Italy, Roma, Italy; [3]CEMAD Digestive Disease Center, Fondazione Policlinico Universitario "A. Gemelli" IRCCS, Università Cattolica del Sacro Cuore, Rome, Italy, Rome, Italy; [4]Computational Biology and Bioinformatics Unit, Fondazione Policlinico Universitario "A. Gemelli" IRCCS, Università Cattolica del Sacro Cuore, Rome, Italy, Rome, Italy*
Email: anna.alisi@opbg.net

Background and aims: Children and adults with metabolically dysfunction-associated steatotic liver disease (MASLD) are at

increased risk of adverse liver-related health outcomes, and its severe form of steatohepatitis (MASH) promises to be the leading cause of transplants in the future. Liver biopsy remains the diagnostic standard for MASH, making the search for reliable non-invasive biomarkers urgent. An influx of proinflammatory cells, necrotic hepatocyte death, and fibrosis characterise MASH at the tissue level, and liquid biopsy, particularly through the analysis of cell death and epigenetic signs in circulation, could offer a panel of non-invasive biomarkers. This study aimed to identify a panel of biochemical and epigenetic markers that may reflect the MASH phenotype.

Method: A total of 150 children and 126 adults with biopsy-proven MASLD were included in the study. Plasma samples collected from patients were used to investigate epigenetic markers, including the amount and fragment size of cell-free (cf)DNA, and levels of cf-mitochondrial DNA (cf-mtDNA), nucleosomes, total histone H3, and specific trimethylated or acetylated forms of histone H3. Epigenetic data were then combined with clinical and inflammatory data and used to train artificial intelligence (AI) models.

Results: Anthropometrical and clinical data were first pre-processed to extrapolate the most significant variables ($p < 0.05$, one-way Anova P) that distinguished MASH from non-MASH. In particular, body mass index (BMI), alanine aminotransferase, gamma-glutamyl transferase, triglycerides (TGs), high-density lipoprotein, Apolipoprotein A1, insulin, and HOMA-IR emerged in children; while only BMI and TGs emerged in adults. We combined these variables with inflammatory and epigenetic data and trained different machine learning algorithms. The support vector machine model was the most accurate for children (approximately 85%), while the K-Nearest Neighbours algorithm was the most accurate for adults (approximately 80%). Shapley Additive exPlanations revealed that TGs, cf-DNA concentration, and total circulating histone H3 levels were common variables that may explain the MASH phenotype in both children and adults.

Conclusion: These preliminary findings highlighted that integrating epigenetic features with clinical parameters enabled accurate MASH discrimination using AI modelling. Further studies on testing and validation datasets are warranted.

WED-103

Validation of a multimodal ultrasound and artificial intelligence approach for identifying advanced fibrosis in metabolic dysfunction-associated steatotic liver disease

Ipshita Gupta[1], Arati Gurung[2], Sujoy Kar[3], Sudhakar Kattoju[4], Jospin Dhivya[3]. [1]*Siemens Healthineers, Singapore, Singapore;* [2]*Siemens Healthineers, Issaquah, United States;* [3]*Apollo Hospitals, Hyderabad, India;* [4]*Apollo Hospitals, Chennai, India*
Email: drsujoy_k@apollohospitals.com

Background and aims: Metabolic dysfunction-associated steatotic liver disease (MASLD) affects nearly one quarter of adults worldwide, yet fibrosis detection remains invasive, underutilized, and delayed. We aimed to prospectively validate an artificial intelligence based liver fibrosis (AILF) model integrating ultrasound derived fat fraction (UDFF) and elastography parameters to improve non-invasive risk stratification for advanced fibrosis.

Method: The IRB-approved prospective multi-centre study enrolled adults with clinically suspected MASLD or abnormal liver function tests. The AILF model (extreme gradient boosting) integrated clinical variables including lab markers, medication, and the duration of liver disease to predict liver fibrosis risk using automated point shear-wave elastography measurements (Auto pSWE) as the reference standard. The cut off values used for Low, Moderate, High and Very High risk were <7;7–9.5;9.5–14;>14 kPa based on *EASL Clinical Practice Guidelines.* Diagnostic performance, agreement, and class-specific threshold optimization were assessed. A subset analysis was conducted to determine correlation between the quantitative ultrasound parameters, namely UDFF and Auto pSWE, and a comprehensive panel of lab biomarkers.

Results: Among 698 enrolled participants, 443 complete profiles (920 clinical encounters-outpatient visits) were analysed with an mean age of 53.55 years (Range: 41.5–65.5) and gender ratio of 69:31 (male:female). The model identified high-risk fibrosis (F3 & F4) in approximately 8%(35/443) and intermediate risk(F2) in 15% (66/443) of the participants. Threshold optimization targeting intermediate-risk classes improved macro-precision (0.88 [0.82–0.95]) and F1 scores (0.81[0.75–0.88]) while preserving discrimination (AUC 0.87 [0.81–0.94]) and agreement beyond chance (Cohen kappa 0.86). Duration of disease and medications had the highest feature importance. Among all biomarkers, elevated gamma-glutamyl transferase (GGT) showed strong correlation (Pearsons $R = 0.65$, $p < 0.05$) with liver stiffness, including in individuals with normal aminotransferases.

Conclusion: A multimodal ultrasound and artificial intelligence approach enables accurate, scalable, and non-invasive risk stratification of fibrosis in MASLD. Early identification of patients at risk for MASH and advanced fibrosis may reduce unnecessary biopsies, support longitudinal monitoring, and facilitate safer clinical deployment through threshold-optimized decision support.

WED-104

Changes in non-invasive tests PRO-C3, ADAPT, LiverRisk and FIB-4 can be used to predict changes in liver stiffness in patients with MASLD

Hannes Hegmar[1], Rickard Strandberg[1,2], Ying Shang[1], Morten Karsdal[3], Johan Vessby[4], Åsa Danielsson Borssén[5], Nils Nyhlin[6], Stergios Kechagias[7], Per Stal[1], Diana Julie Leeming[3], Mattias Ekstedt[7], Hannes Hagström[1]. [1]*Karolinska Institutet, Department of Medicine, Huddinge, Huddinge, Sweden;* [2]*Red Door Analytics, Stockholm, Sweden;* [3]*Nordic Bioscience, Herlev, Denmark;* [4]*Department of Medical Sciences, Gastroenterology Research Group, Uppsala University, Uppsala, Sweden;* [5]*Umeå University Hospital, Umeå, Sweden;* [6]*Department of Gastroenterology, Faculty of Medicine and Health, Örebro University, Örebro, Sweden;* [7]*Department of Gastroenterology and Hepatology, Department of Health, Medicine and Caring Sciences, Linköping University, Linköping, Sweden*
Email: hhegmar@gmail.com

Background and aims: Liver stiffness measurements (LSM) by vibration-controlled transient elastography (VCTE) are suggested to be used for disease monitoring, treatment initiation and treatment evaluation in patients with metabolic dysfunction-associated steatotic liver disease (MASLD). However, availability of VCTE may be limited. We evaluated relative changes in the blood-based non-invasive tests (NITs) PRO-C3, PRO-C6, ADAPT, LiverRiskScore (LRS), and FIB-4, and how they corresponded to a relative change of 30% in LSM by VCTE over time.

Method: A Swedish cohort of 287 patients with MASLD was followed for five years. Repeated measurements of LSM by VCTE, PRO-C3, PRO-C6, ADAPT, LRS, and FIB-4 were obtained at baseline and year one, three and five, respectively. A Bayesian linear mixed effects model was used to evaluate the relative change of the NITs needed to predict a 30% relative change in LSM by VCTE. Correlations between changes in NITs and LSM was calculated. Multiple imputation was used for missing data.

Results: There was a decrease in median LSM from 7.0 kPa to 6.2 kPa over five years. Median FIB-4 increased from 1.14 to 1.38 and ADAPT from 5.42 to 5.72. All NITs were in alignment at group level that LSM decreased over time. The reduction in NIT corresponding to a 30% decrease in LSM was found to depend strongly on the baseline value of the NIT. For a baseline FIB-4 value of 1.3, the corresponding reduction was between 80% to 90%, while for a baseline FIB-4 value of 3 and above, the corresponding reduction was 20–30%. ADAPT and LRS showed less dependence on the baseline values, where a reduction of 30% and 40%, respectively, corresponded to a 30% reduction in LSM. ADAPT had the highest correlation with LSM change with an R^2 0.31 (95% Credible interval [CI] = 0.30–0.32) where

PRO-C3, LRS, and FIB-4 had an R^2 of 0.20 (95% CI = 0.18–0.22), 0.21 (95% CI = 0.18–0.22), and 0.21 (95% CI = 0.19–0.22), respectively.
Conclusion: Changes in the NITs PRO-C3, ADAPT, LRS and FIB-4 were associated with changes in LSM by VCTE. Of the tested NITs, changes in ADAPT had the strongest correlation with changes in LSM, suggesting that it might be better in predicting change in LSM. However, the association was modest, and further studies are warranted to better identify blood-based markers that may be used in settings where VCTE is not available.

WED-105
Optimization of non-invasive screening algorithms for referral to liver elastography in the general population
Marta Hernández Conde[1], David Marti-Aguado[2], Hugo José Disla[1], Elba Llop Herrera[1], Jesús Rivera Esteban[1], Paloma Lluch-García[2], Francisco Bernabeu[1], Marta López-Gómez[1], Javier Abad Guerra[1], Ana Royuela[1], Desamparados Escudero-García[2], José Luis Calleja Panero[1]. *[1]Hospital Universitario Puerta De Hierro Majadahonda, Majadahonda, Spain; [2]Hospital Clínico Universitario, Valencia, Spain*
Email: marta.hernandez.conde@gmail.com

Background and aims: Current clinical guidelines recommend a sequential approach using non-invasive tests to identify liver fibrosis in MASLD. In line with EASL care pathways, this stepwise strategy aims to optimize case-finding in primary care while limiting unnecessary referrals for second-line testing. However, the real-world efficiency of different screening algorithms remains insufficiently defined. We evaluated multiple combinations of FIB-4, ELF, and FLI to identify the most accurate and operationally efficient strategy for referral to hospital-based transiente elastography(TE; FibroScan).
Method: Multicenter cross-sectional cohort study conducted in Madrid and Valencia. FIB-4 was calculated in all individuals aged 18–64 years undergoing routine blood testing including HbA1c in primary care. Patients with FIB-4 >1.3 underwent paired assessment with ELF, FLI, and TE, with significant fibrosis (SF; liver stiffness ≥8 kPa). Nine sequential screening algorithms applicable in primary care were evaluated, estimating sensitivity, specificity, predictive values, and referral rate (coverage), as a surrogate of health-system impact.
Results: A total of 2,609 individuals were included: 77% had FIB-4 <1.3, 22% FIB-4 1.3–2.67, and 2% FIB-4 ≥2.67. Among the 634 subjects with FIB-4 >1.3, 26.9% had type 2 diabetes and 15.6% had SF. Algorithms based solely on FIB-4 followed by TE showed acceptable diagnostic accuracy but resulted in excessive referrals (coverage 74%), conflicting with EASL recommendations to limit unnecessary second-line testing. Sequential strategies integrating metabolic and serological risk stratification achieved a more favorable balance between diagnostic accuracy and system efficiency. The FLI→ELF→TE pathway demonstrated sensitivity 0.72, negative predictive value 0.94, and a referral rate of 34.7%. The clinically recommended FIB-4→ELF→TE strategy maintained good sensitivity (0.76) but required a higher referral rate (46.6%). Although FLI→FIB-4→TE achieved maximal sensitivity (100%), it showed negligible discrimination (specificity 0.009) and doubled TE demand compared with more efficient pathways (coverage 62.3%).
Conclusion: The FLI→ELF→TE sequence provides the best diagnostic efficiency, maximizing detection of SF while maintaining a clinically acceptable number of TE examinations. Its implementation could optimize the use of TE resources, prioritize patients at higher risk of fibrosis, and improve the efficiency of diagnostic pathways in primary care.

WED-106
External validation of a standardized FLI without anthropometric data for the screening of significant liver fibrosis
Marta Hernández Conde[1], Hugo José Disla[1], Jesús Rivera Esteban[1], Paula Iruzubieta[2], Elba Llop Herrera[1], David Marti-Aguado[3], Maria Teresa Arias Loste[2], Christie Perelló[1], María Del Barrio[3], Paloma Lluch-García[3], Desamparados Escudero-García[3], Javier Crespo[2,4], José Luis Calleja Panero[1]. *[1]Hospital Universitario Puerta De Hierro Majadahonda, Majadahonda, Spain; [2]Hospital Valdecilla, Santander, Spain; [3]Hospital Clínico Universitario, Valencia, Spain; [4]Gastroenterology and Hepatology Department, Clinical and Translational Research in Digestive Diseases, Valdecilla Research Institute (IDIVAL), Marques de Valdecilla University Hospital, Santander, Spain*
Email: marta.hernandez.conde@gmail.com

Background and aims: The Fatty Liver Index (FLI) is a simple, inexpensive non-invasive test with potential utility for liver fibrosis screening; however, it requires body mass index (BMI) and waist circumference (WC), which are often unavailable in large-scale or opportunistic settings. We evaluated whether a "standardized" FLI (FLI-std), replacing BMI and WC with sex-specific mean values, preserves diagnostic performance non-inferior to the original FLI (FLI-o) for detecting significant fibrosis (SF; ≥F2), using transient elastography (TE) as reference.
Method: Two independent cohorts were analyzed: a derivation cohort (n = 634) and the external ETHON validation cohort (n = 6,180). Patients with FLI ≥ 60 were referred for TE assessment. Non-inferiority (NI) of FLI-std versus FLI-o was evaluated for sensitivity (margin $\delta = -5$ percentage points) and area under the ROC curve (AUC; $\Delta \geq -0.02$).
Results: The cohorts showed markedly different clinical profiles. The derivation cohort included older patients with higher metabolic risk, whereas ETHON represented a younger, more general population with lower SF prevalence (15.6% vs 3.9%; $p < 0.001$). In the derivation cohort, FLI-std showed sensitivity 0.94, specificity 0.40, and negative predictive value (NPV) 0.98, with a screening coverage of 65.4%. In the external validation cohort, the AUC of FLI-std (0.70; 95% CI 0.67–0.74) was comparable to FLI-o (0.71; 95% CI 0.67–0.75), with $\Delta AUC = -0.007$ ($p = 0.62$), fulfilling the NI criterion. FLI-std achieved higher sensitivity than FLI-o (0.71 vs 0.64), with a paired difference of +3.3 percentage points (95% CI −4.8 to +11.5), exceeding the NI margin. NPV remained high (~0.98), with improved detection of SF (40% vs 33%), at the expense of a modest reduction in specificity (0.61 vs 0.69).
Conclusion: Differences in cohort characteristics explain the lower absolute sensitivity observed in external validation without implying a true loss of discriminative capacity. A standardized FLI without BMI or WC preserves non-inferior diagnostic performance for SF detection in external validation. This simplified model enables scalable, pragmatic fibrosis screening pathways when anthropometric data are unavailable, without clinically relevant loss of accuracy.

WED-107
Biogenic amines as possible biomarkers of liver fibrosis severity in metabolic dysfunction-associated steatotic liver disease
Zdenka Hertelyova[1,2], Sylvia Drazilova[1], Dominika Toporcerova[1], Zuzana Gulasova[1], Daniela Szaboova[1], Peter Jarčuška[1]. *[1]Lekárska fakulta Univerzity Pavla Jozefa Šafárika v Košiciach, Košice, Slovakia; [2]Pavol Josef Safarik University, 2nd Internal Clinic, Kosice, Slovakia*
Email: zdenocka@gmail.com

Background and aims: Identification of patients with significant fibrosis is essential for accurate risk stratification in metabolic dysfunction–associated steatotic liver disease (MASLD). Non-invasive tools such as vibration-controlled transient elastography (VCTE) and the fibrosis-4 index (FIB-4) are widely used for fibrosis assessment; however, novel biomarkers are still needed. Biogenic amines are involved in metabolic and inflammatory pathways and may

contribute to MASLD progression. This study aimed to investigate the association between circulating biogenic amines and liver fibrosis severity; and to evaluate their diagnostic potential as non-invasive biomarkers of liver fibrosis in MASLD.

Method: A total of 68 adults (31 women, mean age 65.35 ± 9.26 years) with confirmed MASLD were prospectively enrolled. Liver fibrosis was assessed using VCTE and patients were stratified as follows: F0 – F1 (<7.0 kPa), F2 (≥7.0 – <8.8 kPa), F3 (≥ 8.8 – <12.0 kPa), and F4 (≥12.0 kPa). Serum samples were analysed by liquid chromatography–tandem mass spectrometry using the MxP® Quant 500 kit. Appropriate parametric and non-parametric statistical tests were applied. The diagnostic performance of selected biogenic amines and FIB-4 for significant fibrosis (≥ F2) and cirrhosis (F4) was assessed using receiver operating characteristic (ROC) curve analysis.

Results: Patients with significant fibrosis (F2 – F4) exhibited significantly higher circulating levels of several biogenic amines compared with those with no or mild fibrosis (F0 – F1), most notably beta-alanine 5.43 ± 0.89 vs 7.94 ± 0.80 µmol/l, $p < 0.001$; spermine 0.228 ± 0.032 vs 0.342 ± 0.071 µmol/l, $p < 0.001$; and putrescine 0.158 ± 0.040 to 0.309 ± 0.129 µmol/l, $p < 0.001$; whereas dopamine did not differ between both groups. ROC analysis demonstrated excellent diagnostic accuracy for significant fibrosis vs no or mild fibrosis in MASLD patients: AUC 0.99 for beta-alanine; AUC 0.95 for spermine; and AUC 0.85 for putrescine. ROC analysis also showed outsanding diagnostic accuracy for liver cirrhosis (F4) vs no cirrhosis in MASLD: 0.99 for beta alanine; 0.99 for spermine; and 0.98 for putrescine.

Conclusion: Beta-alanine, spermine, and putrescine are strongly associated with fibrosis severity in MASLD and demonstrate excellent diagnostic accuracy for significant fibrosis and cirrhosis. These findings suggest their potential role as novel non-invasive biomarkers for liver fibrosis assessment in MASLD patients.

WED-108

Diagnostic accuracy of non-invasive serum biomarkers for liver fibrosis in hepatocellular carcinoma patients with and without concurrent metabolic dysfunction–associated steatotic liver disease

Chun-Ting Ho[1,2], Chia-Jung Ho[1], Tsai Shin-Yu[1], Yi-Chen Lin[3], Yi-Hsiang Huang[4], Ming-Chih Hou[5], Jaw-Ching Wu[6], Chien-Wei Su[7]. *[1]Taipei Veterans General Hospital, Department of Medicine, Taipei, Taiwan; [2]National Yang Ming Chiao Tung University Yangming Campus, Ph.D. Program of Interdisciplinary Medicine, Taipei, Taiwan; [3]Linkou Chang Gung Memorial Hospital, Department of Medicine, Taoyuan City, Taiwan; [4]Taipei Veterans General Hospital, Department of Medical Research, Taipei, Taiwan; [5]Taipei Veterans General Hospital, Division of Gastroenterology and Hepatology, Department of Medicine, Taipei, Taiwan; [6]National Yang Ming Chiao Tung University Yangming Campus, Institute of Clinical Medicine, Taipei, Taiwan; [7]Taipei Veterans General Hospital, Division of General Medicine, Department of Medicine, Taipei, Taiwan*
Email: cwsu2@vghtpe.gov.tw

Background and aims: Non-invasive serum biomarkers (NISB) such as fibrosis-4 (FIB-4) and aspartate aminotransferase-to-platelet ratio index (APRI) are widely used to estimate liver fibrosis. However, their diagnostic accuracy may be altered in different subgroups of patients, such as hepatocellular carcinoma (HCC) and metabolic dysfunction–associated steatotic liver disease (MASLD). We aimed to evaluate the correlation between various NISBs and histological fibrosis severity and compare their accuracy in predicting cirrhosis in HCC patients with and without concurrent MASLD.

Method: 984 HCC patients who underwent curative resection at Taipei Veterans General Hospital with available pathological specimens and complete clinical data were included. Patients were divided into MASLD (n = 469) and non-MASLD (n = 515) groups accordingly. Spearman correlation was utilized to assess associations between ISHAK fibrosis scores and five NISBs: FIB-4, APRI, non-alcoholic fatty liver disease fibrosis score (NFS), BMI–AST/ALT ratio–diabetes mellitus (BARD) score, and AST/ALT ratio (AAR). Diagnostic accuracy for cirrhosis (ISHAK ≥5) was evaluated using receiver operating characteristic (ROC) analysis and compared across NISBs. Optimal single cutoffs were determined by maximizing Youden's index; rule-out and rule-in thresholds were determined corresponding to sensitivity >90% and specificity >80%, respectively.

Results: Among the cohort, 345 patients had histologically confirmed cirrhosis. FIB-4 and APRI demonstrated the strongest correlation with ISHAK fibrosis stage and showed comparative diagnostic accuracy for cirrhosis among all subgroups. For FIB-4, the optimal single cutoff was lower in the MASLD subgroup (2.439) than in the overall cohort and the non-MASLD subgroup (3.035 and 3.040, respectively). Using dual cutoffs, rule-out thresholds were consistent across all subgroups (1.328–1.423) and aligned well with current guidelines, while rule-in thresholds were substantially lower in patients with MASLD (2.659) compared with the overall cohort and non-MASLD subgroup (3.127 and 3.409, respectively).

Conclusion: NISBs such as FIB-4 and APRI demonstrated modest correlation with histological cirrhosis and comparable diagnostic accuracy across different etiologies. While the rule-out threshold around 1.3 for FIB-4 aligns with current guidelines, the one-point and rule-in diagnostic cutoff for HCC patients with concurrent MASLD were significantly lower, thus highlighting the necessity for subgroup-specific diagnostic thresholds.

WED-109

Unsupervised biomarker clustering reveals clinically relevant phenotypes in metabolic dysfunction–associated steatotic liver disease

Frederik Højbjerg Svejsø[1,2], Diana Julie Leeming[1], Puria Nabilou[3], Elias Rashu[3], Mira Thing[3], Mikkel Werge[3], Anders Junker[3], Line Egerod Lund[1,4], Morten Karsdal[1], Alejandro Mayorca Guiliani[1], Lise Lotte Gluud[3,5]. *[1]Nordic Bioscience A/S, Herlev, Denmark; [2]Biotech Research and Innovation Centre, University of Copenhagen, Copenhagen, Denmark; [3]Gastro Unit, Medical Division, Hvidovre Hospital, University of Copenhagen, Hvidovre, Denmark; [4]Department of Biomedical Sciences, University of Copenhagen, Copenhagen, Denmark; [5]Department of Clinical Medicine, University of Copenhagen, Copenhagen, Denmark*
Email: frsv@nordicbio.com

Background and aims: The Copenhagen Cohort of MASLD (CoCoMASLD) is an observational study aimed at identifying biomarkers and potential therapeutic targets in patients with metabolic dysfunction–associated steatotic liver disease (MASLD). Given the clinical and biological heterogeneity of MASLD, data-driven approaches may help identify distinct patient subgroups with differing hepatic and systemic risk profiles, including risk of cardiovascular disease. The aim of this study was to apply unsupervised clustering methods to a well-characterized MASLD cohort to identify patient endotypes.

Method: Baseline clinical and extracellular matrix (ECM)-based biomarker data were compiled for 863 MASLD patients and log-transformed. Patients with ≥25% missing values were excluded, leaving 638 patients. Remaining missing values were imputed, and all variables were Winsorized to reduce the influence of outliers and scaled for analysis. Principal component analysis (PCA) was performed, followed by k-means clustering, specifying three clusters based on biological relevance. Clusters were compared using baseline liver biopsy data available for 268 patients, and Fibroscan data for 619 patients. Differences in clinical and histological parameters, including liver stiffness, were assessed using the Wilcoxon rank-sum test.

Results: Clustering of baseline clinical and ECM biomarkers identified three patient groups. Cluster 1 (C1, n = 241) was characterized by elevated inflammatory and degradation markers (nordicC3M™, nordicC6M™) and high white blood cell counts. Cluster 2 (C2, n = 172) exhibited a fibrogenic profile with elevated nordicPRO-C3™ and

nordicPRO-C6™, while Cluster 3 (C3, n = 225) showed generally low biomarker levels but increased nordicC4G™, suggesting enhanced T-cell activity. Histological analyses showed higher steatosis grade in C1 compared with C2 ($p = 0.02$) and C3 ($p = 0.00047$). In contrast, C2 patients had markedly higher fibrosis scores than C1 ($p = 5.7 \times 10^{-9}$) and C3 ($p = 3.8 \times 10^{-9}$), accompanied by increased liver stiffness compared with C1 ($p = 5.4 \times 10^{-4}$) and C3 ($p < 2.22 \times 10^{-16}$).
Conclusion: Unsupervised clustering in MASLD patients identified three distinct phenotypic groups identified by systemic and routine markers. These findings demonstrate clinically meaningful heterogeneity in MASLD and highlight the value of biomarker-driven phenotyping for risk stratification.

WED-110-YI
External validation of the LiverPRO algorithm for liver fibrosis risk assessment in U.S. representative adults
He Huang[1], Laurens A. van Kleef[1], Katrine Lindvig[2], Harry L.A. Janssen[1], Maja Thiele[2], Willem Pieter Brouwer[1].
[1]Department of Gastroenterology and Hepatology, Erasmus Medical Center, University Medical Center Rotterdam, Rotterdam, Netherlands; [2]Centre for Liver Research, Department of Gastroenterology and Hepatology, Odense University Hospital, Odense, Denmark
Email: h.huang@erasmusmc.nl

Background and aims: LiverPRO is a new algorithm to predict liver fibrosis, with distinct formulas for F2, F3, and F4 stages. Unlike traditional scores, LiverPRO does not require all input variables; it automatically selects the best-performing model based on available data. The full model includes age, albumin, AST, bilirubin, sodium, cholesterol, GGT, ALP, platelets, and INR. We performed an external validation of LiverPRO in a nationally representative population.
Method: We used data from U.S. adults participating in NHANES (2017–2023), with LSM and LiverPRO components except for INR. Participants with heart failure or alcohol intake >50/60 g/day (female/male) were excluded. Diagnostic performance was assessed for LSM ≥8 and ≥12 kPa (commonly interpreted as compatible with significant and advanced fibrosis) using AUCs and detection rates at the proposed LiverPRO thresholds. Performance was evaluated in the overall population and relevant subgroups.
Results: The study included 10,852 adults (48.6% male, mean age 50 yr) of whom 60% had at least one indicator for screening, 10.5% had LSM ≥8 kPa and 3.6% had LSM ≥12 kPa. Using the LiverPRO F2 algorithm, 4.6% were classified high, 26.1% intermediate, and 69.3% low risk, with LSM ≥8 kPa prevalences of 37.5%, 16.1%, and 6.6%, respectively. At the 0.25 threshold, sensitivity and specificity for LSM ≥8 kPa were 57% and 72% and for LSM ≥12 kPa 69% and 71%. Among those meeting screening criteria, sensitivity and specificity remained largely unchanged (LSM ≥8 kPa: 59% and 63%; LSM ≥12 kPa: 69% and 61%). The F3 and F4 LiverPRO algorithms with their specific cut-offs did not improve performance for both LSM thresholds. The LiverPRO F2 algorithm achieved the highest AUC for LSM ≥8 kPa (0.71 vs 0.67/0.66 for F3/F4 model) and ≥ 12 kPa (0.76 vs 0.72/0.71). LiverPRO outperformed FIB-4 (AUC 0.61 and 0.67 for LSM ≥8 and 12 kPa). For LSM ≥8 kPa, AUCs were higher in females (0.73) than males (0.68), stable across age groups (18–35: 0.66; 35–65: 0.70; 65–80: 0.70), higher with at-risk alcohol consumption (0.74), and lower when meeting EASL–EASD–EASO screening criteria (0.66).
Conclusion: The LiverPRO algorithm was externally validated in a representative U.S. general population, where the F2 algorithm demonstrated the best performance for detecting LSM ≥8 and ≥12 kPa, producing a clear risk gradient across strata. Performance was highest among adults with at-risk alcohol consumption, indicating potential in a group where non-invasive tests often perform less consistently.

WED-111
Self-assessed health and healthcare utilisation identify individuals with increased liver stiffness in the general population
He Huang[1], Willem Pieter Brouwer[1], Harry L.A. Janssen[1], Laurens A. van Kleef[1]. *[1]Department of Gastroenterology and Hepatology, Erasmus Medical Center, University Medical Center Rotterdam, Rotterdam, Netherlands*
Email: h.huang@erasmusmc.nl

Background and aims: Liver stiffness measurement (LSM) is a non-invasive marker of liver fibrosis and is associated with increased risk of liver-related events and mortality. Given the relatively low incidence of these complications in the general population, population-wide screening for increased LSM remains controversial. Opportunistic screening within healthcare settings, alongside self-reported health, may represent a pragmatic alternative. We assessed the prevalence of increased LSM across healthcare utilisation patterns to assess its value as an entry point for opportunistic screening.
Method: We analysed adults aged 18–80 years with LSM data without heart failure from NHANES 2017–2023. Self-assessed health and healthcare utilisation were based on interviews. LSM was obtained using vibration-controlled transient elastography. Using the provided sample weights, we report on the prevalence of increased LSM across self-assessed health and healthcare utilisation measures, using LSM thresholds of ≥8, 10 and 12 kPa.
Results: Among 12,942 adults aged 18–80 years (mean age 50 years, 48% male), the weighted prevalence of LSM ≥8 kPa was 9.8%, LSM ≥10 kPa 5.5% and LSM ≥12 kPa 3.5%. The prevalence of LSM ≥8 kPa showed a strong gradient across self-assessed health strata, ranging from 5.3% among individuals reporting excellent health to 6.6% (very good), 12% (good), 16% (fair), and 22% (poor health). Notably, among participants reporting excellent health with LSM ≥8 kPa, 81% had LSM <12 kPa, whereas among those reporting poor health with LSM ≥8 kPa, 52% had LSM ≥12 kPa. In contrast, the weighted prevalence of LSM ≥8 kPa was similar for individuals with and without a routine place for healthcare (9.9% vs 9.6%), and among those who did and did not report contact with a mental health professional in the past year (10% vs 9.8%). In participants with available data on the times received health care over the past year (n = 7,551), the weighted prevalence of LSM ≥8 kPa was similar for 0–3 visits (7.3–7.9%) but higher for 4–9 visits (12%) and ≥10 visits (11%). This gradient was more pronounced at higher LSM thresholds.
Conclusion: A strong risk gradient was observed across self-assessed health categories for the prevalence of increased LSM, providing stronger discrimination than measures of health care utilisation. While healthcare contact remains essential for opportunistic screening strategies, reliance on utilisation alone may be insufficient to accurately identify individuals at risk of liver-related events.

WED-115
Prediabetes identifies a high-risk subgroup for advanced liver fibrosis in non-diabetic MASLD: a non-invasive risk stratification study
Trung Huynh[1], Hoai Phuong Huynh[2], Hoang Long Doan[2], Trinh Nguyen Tran Tuyet[3]. *[1]Department of Gastroenterology and Hepatology, Center for Gastrointestinal Endoscopy and Laparoscopic Surgery, Ho Chi Minh City, Viet Nam; [2]Department of Gastroenterology and Hepatology, Ho Chi Minh, Viet Nam; [3]Department of Internal Medicine, University of Medicine and Pharmacy at Ho Chi Minh City, Ho Chi Minh City, Vietnam, Ho Chi Minh City, Viet Nam*
Email: trunghv@tahospital.vn

Background and aims: Risk stratification for liver fibrosis in metabolic dysfunction-associated steatotic liver disease (MASLD) is commonly initiated after the development of overt diabetes. Prediabetes is highly prevalent but is not routinely considered an indication for fibrosis assessment. We aimed to evaluate the prevalence of significant and advanced liver fibrosis among non-

diabetic MASLD patients with prediabetes and to assess the utility of non-invasive tools for fibrosis risk stratification in this population.
Method: This cross-sectional study included consecutive non-diabetic MASLD patients evaluated at a tertiary referral center between 2024 and 2025. Prediabetes was defined according to standard glycaemic criteria. Liver fibrosis was assessed using the FIB-4 index and Acoustic Radiation Force Impulse (ARFI) elastography. The prevalence of significant (F≥2) and advanced fibrosis (F≥3) was determined. Factors associated with advanced fibrosis were analysed, and the diagnostic performance of FIB-4 was evaluated using receiver operating characteristic analysis.
Results: A total of 107 non-diabetic MASLD patients were included (mean age 47.3 ± 12.6 years; 56.1% male). Significant fibrosis (F≥2) was present in 15.0% of patients, while advanced fibrosis (F≥3) was identified in 11.3%. Among patients with prediabetes, 41.7% had advanced fibrosis despite the absence of overt diabetes. Age and AST level were independently associated with advanced fibrosis. FIB-4 demonstrated good diagnostic performance for advanced fibrosis, with an AUROC of 0.949.
Conclusion: Prediabetes is associated with a substantial burden of advanced liver fibrosis in non-diabetic MASLD patients. Assessment strategies based solely on diabetes status may delay identification of clinically relevant fibrosis. Non-invasive tools such as FIB-4 and ARFI elastography may support earlier fibrosis risk stratification in patients with prediabetes.

WED-116
Superiority of the FAST score compared to traditional non-invasive indices in detecting liver fibrosis in asymptomatic patients with type 2 diabetes mellitus

Mustafa Sahin[1], Fatma Tuğçe Şah Ünal[1], Zeynep Melekoğlu Ellik[2], Volkan Yılmaz[2], Digdem Kuru Oz[3], Hale Gokcan[2], Atilla Elhan[4], Rıfat Emral[1], Ramazan Idilman[2]. *[1]Ankara University Faculty of Medicine, Endocrinology Department, Ankara, Türkiye; [2]Ankara University Faculty of Medicine, Hepatology Department, Ankara, Türkiye; [3]Ankara University Faculty of Medicine, Radiology, Ankara, Türkiye; [4]Ankara University Faculty of Medicine, Statistics Department, Ankara, Türkiye*
Email: drsahinmustafa@yahoo.com

Background and aims: Metabolic dysfunction-associated steatotic liver disease (MASLD) has emerged as the most prevalent chronic liver disease worldwide. MASLD is a progressive condition and is strongly associated with various metabolic disorders. Although current guidelines recommend fibrosis screening for patients with Type 2 diabetes mellitus (T2DM), the efficacy of commonly used serum-based non-invasive fibrosis indices in this population remains suboptimal. This study aimed to determine the prevalence of hepatic steatosis and significant liver fibrosis in asymptomatic patients with T2DM and to systematically compare the diagnostic accuracy of the elastography-based FAST score with that of serum-based fibrosis scores.
Method: This prospective, cross-sectional single center study included 257 adults with T2DM. Demographic characteristics, diabetes duration, glycemic control, and antidiabetic treatment modalities were recorded for each participant. All patients underwent transient elastography to assess liver stiffness measurement (LSM) and controlled attenuation parameter (CAP). Significant fibrosis (≥F2) was defined as LSM ≥8.0 kPa, while hepatic steatosis was defined as CAP >238 dB/m, with severe steatosis characterized by CAP >290 dB/m. Non-invasive fibrosis indices, including the FAST score, FIB-4, NAFLD Fibrosis Score (NFS), APRI, and the AST/ALT ratio, were calculated contemporaneously. Diagnostic performance of these indices was evaluated using receiver operating characteristic curve analysis and odds ratios.
Results: The mean age of the cohort was 58.2 ± 8.8 years, with 61% of participants being female. The mean duration of T2DM was 11.4 ± 7.2 years, and the mean HbA1c level was 8.2% ± 1.8. Hepatic steatosis was highly prevalent as 94% of patients exhibited hepatic steatosis, while 56% exhibited severe steatosis. Significant liver fibrosis was detected in 26% of patients. The FAST score demonstrated the highest diagnostic accuracy for detecting significant fibrosis, with an area under the curve (AUC) of 0.906 (95% CI 0.86–0.94; OR 46.18), achieving high sensitivity (93.9%) and acceptable specificity (74.9%).
Conclusion: More than half of asymptomatic patients with T2DM exhibit MASLD, while one in four patients with clinically significant liver fibrosis. The elastography-based FAST score demonstrates markedly superior diagnostic accuracy and should be prioritized for the non-invasive identification of metabolic dysfunction-associated steatohepatitis in patients with T2DM.

WED-117
Optimizing drug development in populations with compensated MASH cirrhosis by integration of the disease severity index from the HepQuant DuO test in trial design

Joanne Imperial[1], Michael McRae[2], Greg Everson[1]. *[1]HepQuant, LLC, Denver, Colorado, United States; [2]Custom DX Solutions LLC, Houston, Texas, United States*
Email: michael.mcrae@hepquant.com

Background and aims: The significant heterogeneity in liver function within compensated MASH cirrhosis complicates trial design. The Disease Severity Index (DSI), a non-invasive, functional biomarker derived from the oral cholate challenge test (HepQuant DuO), is proposed as a reasonably likely surrogate endpoint (RLSE) for clinical outcomes. This analysis explores the relationship between baseline DSI, changes in DSI, and estimated risk of clinical outcome using a hypothetical trial framework.
Method: We modeled a 5-year, randomized (3:1 drug:placebo) trial of 720 patients with compensated MASH cirrhosis. Baseline DSI data was pooled from recent clinical trials of 193 cACLD patients with compensated MASH cirrhosis (mean DSI 21.5 ± 6.5). Clinical outcome probabilities were derived using Cox proportional hazards regression (RISK ACE models, Kittelson 2024). We estimated event rates across a range of baseline DSI values and evaluated the impact of change in DSI after 1 year of treatment on the risk for clinical outcome. Statistical significance thresholds were calculated using Chi-squared and paired t-tests. Enrichment strategies incorporating high-risk subjects (DSI ≥ 24) were assessed.
Results: For baseline DSI of 22, the estimated clinical outcome rates were 4.6%, 11.3%, and 24.1% at 1, 2, and 5 years, respectively. A 2-unit reduction in DSI decreased the 5-year risk to 14.0%, and no change in DSI reduced risk to 21.0%. Conversely, a 2-unit increase in DSI increased the 5-year risk to 30.6%. Responder analysis achieved significance when the change in DSI (delta DSI) was −2.0 in the treatment arm versus no change in the placebo arm ($p = 0.03$). For smaller differences between arms, enrichment with high-risk subjects (DSI ≥ 24) markedly reduced the required sample size for statistical significance ($p < 0.05$): +112 subjects for delta DSI −1.5; +320 for delta DSI −0.5; +536 for delta DSI −0.5. A mean DSI reduction of 1.0 between baseline and end of treatment in the treatment arm, assuming no change in placebo arm, achieved statistical significance by paired t-test ($p = 0.048$).
Conclusion: Baseline DSI and change in DSI are dynamic and sensitive indicators of liver disease progression and response to treatment in compensated MASH cirrhosis. Incorporating DSI as an RLSE can optimize trial design, reduce sample size, enable adaptive strategies, and provide early functional endpoints linked to clinical outcomes.

WED-118

Prognostic significance of a 5 kPa absolute change in liver stiffness measurements (LSM) to predict liver-related events in patients with compensated advanced metabolic dysfunction-associated steatotic liver disease (MASLD)

Xinrui Jin[1], Nana Peng[2], Huapeng Lin[3], Hye Won Lee[4], Emmanuel Tsochatzis[5], Salvatore Petta[6], Elisabetta Bugianesi[7], Masato Yoneda[8], Ming-Hua Zheng[9], Hannes Hagström[10], Jerome Boursier[11], José Luis Calleja Panero[12], George Boon Bee Goh[13], Chan Wah Kheong[14], Rocio Gallego-Durán[15], Arun J Sanyal[16], Victor de Lédinghen[17], Philip N. Newsome[18], Jian-Gao Fan[19], Laurent Castera[20], Grace Lai-Hung Wong[1,21], Grazia Pennisi[6], Angelo Armandi[7], Atsushi Nakajima[8], Wen-Yue Liu[22], Ying Shang[23], Marc de Saint-Loup[24], Elba Llop Herrera[12], Kevin Kim Jun Teh[13], Carmen Lara-Romero[25], Amon Asgharpour[16], Sara Mahgoub[26], Adrien Lannes[11], Manuel Romero-Gómez[25], Seung Up Kim[4], Vincent Wai-Sun Wong[1], Rohit Loomba[27], Terry Cheuk-Fung Yip[1].

[1]Department of Medicine and Therapeutics, Medical Data Analytics Centre, The Chinese University of Hong Kong, Hong Kong, China, State Key Laboratory of Digestive Disease, Institute of Digestive Disease, The Chinese University of Hong Kong, Hong Kong, China, Hong Kong, Hong Kong; [2]Department of Medicine and Therapeutics, Medical Data Analytics Centre, The Chinese University of Hong Kong, Hong Kong, China, State Key Laboratory of Digestive Disease, Institute of Digestive Disease, The Chinese University of Hong Kong, Hong Kong, China, Hong Kong, China; [3]Department of Gastroenterology and Hepatology, Shanghai Ninth People's Hospital, Shanghai Jiao Tong University School of Medicine, Shanghai, China, Shanghai, China; [4]Department of Internal Medicine, Institute of Gastroenterology, Yonsei University College of Medicine, Seoul, Republic of Korea, Seoul, Korea, Rep. of South; [5]University College London Institute for Liver and Digestive Health, Royal Free Hospital and UCL, London, United Kingdom, London, United Kingdom; [6]Section of Gastroenterology, PROMISE, University of Palermo, Italy, Palermo, Italy; [7]Department of Medical Sciences, Division of Gastroenterology, A.O.U. Città della Salute e della Scienza di Torino, University of Turin, Turin, Italy, Turin, Italy; [8]Department of Gastroenterology and Hepatology, Yokohama City University Graduate School of Medicine, Yokohama, Japan, Yokohama, Japan; [9]MAFLD Research Center, Department of Hepatology, First Affiliated Hospital of Wenzhou Medical University, Wenzhou, China, Wenzhou, China; [10]Department of Medicine, Huddinge, Karolinska Institutet, Sweden, Division of Hepatology, Department of Upper GI Diseases, Karolinska University Hospital, Huddinge, Stockholm, Sweden, Stockholm, Sweden; [11]Hepato-Gastroenterology and Digestive Oncology Department, Angers University Hospital, Angers, France, HIFIH Laboratory, SFR ICAT 4208, Angers University, Angers, France, Angers, France; [12]Department of Gastroenterology and Hepatology, Hospital Universitario Puerta de Hierro, Universidad Autonoma de Madrid, Spain, Madrid, Spain; [13]Department of Gastroenterology and Hepatology, Singapore General Hospital, Singapore, Singapore, Singapore; [14]Gastroenterology and Hepatology Unit, Department of Medicine, Faculty of Medicine, University of Malaya, Kuala Lumpur, Malaysia, Kuala Lumpur, Malaysia; [15]UCM Digestive Diseases, Virgen del Rocio University Hospital, SeLiver Group, Institute of Biomedicine of Seville, Ciberehd, Department of Medicine, University of Seville, Seville, Spain, Seville, Spain; [16]Stravitz-Sanyal Institute for Liver Disease and Metabolic Health, Virginia Commonwealth University School of Medicine, Richmond, VA, USA, Richmond, United States; [17]Echosens, Paris, France, Paris, France; [18]Roger Williams Institute of Liver Studies, School of Immunology & Microbial Sciences, Faculty of Life Sciences and Medicine, King's College London, Foundation for Liver Research and King's College Hospital, London, London, United Kingdom; [19]Department of Gastroenterology, Xinhua Hospital Affiliated to Shanghai Jiaotong University School of Medicine, Shanghai Key Lab of Pediatric Gastroenterology and Nutrition, Shanghai, China, Shanghai, China; [20]Université Paris Cité, UMR1149 (CRI), INSERM, Paris, France; Service d'Hépatologie, Hôpital Beaujon, Assistance Publique-Hôpitaux de Paris (AP-HP), Clichy, France, Clichy, France; [21]Medical Data Analytics Centre, Department of Medicine and Therapeutics, The Chinese University of Hong Kong, Hong Kong, China; [22]Department of Endocrinology, First Affiliated Hospital of Wenzhou Medical University, Wenzhou, China, Wenzhou, China; [23]Department of Medicine, Huddinge, Karolinska Institutet, Sweden, Huddinge, Sweden; [24]Hepato-Gastroenterology and Digestive Oncology Department, Angers University Hospital, Angers, France, Angers, France; [25]UCM Digestive Diseases, Virgen del Rocio University Hospital, SeLiver Group, Institute of Biomedicine of Seville, Ciberehd, Department of Medicine, University of Seville, Seville, Spain, Seville, Spain; [26]National Institute for Health Research, Biomedical Research Centre at University Hospitals Birmingham NHS Foundation Trust and the University of Birmingham, Birmingham, United Kingdom, Birmingham, United Kingdom; [27]Division of Epidemiology, Department of Family Medicine and Public Health, University of California at San Diego, University of California at San Diego, San Diego, California, USA, NAFLD Research Center, University of California San Diego, La Jolla, California, USA, San Diego, United States
Email: 1155223326@link.cuhk.edu.hk

Background and aims: Previous studies demonstrated the prognostic value of relative changes in LSM by vibration-controlled transient elastography (VCTE). Although absolute LSM change is simpler to interpret, its clinical significance remains unclear. This study assessed whether a 5 kPa absolute change in LSM could predict liver-related events (LREs) in patients with MASLD and a baseline LSM between 10 and 20 kPa.

Method: This cohort study included patients with MASLD who underwent VCTE examinations at 16 centres across the US, Europe, and Asia between 2004 and 2023. Eligible patients had baseline LSM of 10–20 kPa and one or more reliable LSMs at least 12 months apart. Change in LSM was defined as the difference between baseline and follow-up measurements, categorized as follows: regression (a reduction of ≥5 kPa), stable (a change of −5 kPa to +5 kPa), and progression (an increase of ≥5 kPa). The primary outcome was occurrence of LREs, a composite of hepatic decompensation and hepatocellular carcinoma. The prediction was compared with a relative LSM change of ≥30%.

Results: In 1,366 patients, 46 LREs developed over a median follow-up of 2.80 years (IQR: 1.18–4.77). 404 (29.6%) and 555 (40.6%) patients experienced ≥5 kPa and ≥30% decreases from baseline LSM, whereas 129 (9.4%) and 167 (12.2%) experienced ≥5 kPa and ≥30% increases from baseline. Relative reduction of 30% had higher time-dependent specificity than absolute decrease of 5 kPa (30%: 44.6 [40.7–48.4], 5 kPa: 33.7 [30.2–37.5]), while the time-dependent sensitivity was similar (30%: 89.5 [79.4–97.7], 5 kPa: 87.9 [77.5–96.0]). Consistently, a ≥30% relative decrease (adjusted subdistribution hazard ratio [aSHR] 0.29, 95% CI 0.12–0.71, p = 0.007), but not an absolute 5 kPa decrease in LSM (aSHR 0.54, 95% CI 0.23–1.09, p = 0.160), was associated with a significant reduction in LREs. In contrast, both absolute increase of 5 kPa and relative increase of 30% in LSM were associated with an increased risk of LREs (5 kPa: aSHR 2.68, 95% CI: 1.34–5.36, p = 0.006; 30%: aSHR 2.12, 95% CI: 1.10–4.08, p = 0.024).

Conclusion: Both 30% and 5 kPa increase in LSM are reliable indicators of disease progression, while 30% relative decrease is more effective in capturing risk reduction in LREs.

WED-119

Steatotic liver disease phenotypes in inflammatory bowel disease: a screening study identifying masld as the primary driver of liver fibrosis

Dana Kablawi[1], Riccardo Righetti[1], Raman Agnihotram[1], Faisal Aljohani[1], Chiara Saroli Palumbo[2], Alain Bitton[1], Waqqas Afif[1], Talat Bessissow[1], Giada Sebastiani[1]. *[1]McGill University, Montreal, Canada; [2]Montreal, Canada*
Email: giada.sebastiani@mcgill.ca

Background and aims: Steatotic liver disease (SLD) seems common in people living with inflammatory bowel disease (IBD). The newly

proposed definition of metabolic dysfunction-associated steatotic liver disease (MASLD) highlights metabolic drivers of hepatic steatosis while recognizing its frequent coexistence with other chronic liver diseases, including alcohol and drug-induced liver injury. The purpose of this study was to characterize the distribution of SLD phenotypes in people with IBD and evaluate the association of coexisting MASLD and IBD with liver fibrosis.

Method: As part of a MASLD screening program, transient elastography was performed in consecutive people with IBD from a prospective cohort in Montreal, Canada. SLD was defined as hepatic steatosis with a controlled attenuation parameter ≥275 dB/m. MASLD was defined by presence of steatosis with at least 1 cardiometabolic risk factor: BMI, prediabetes or diabetes, hypertension, or dyslipidemia. Significant liver fibrosis was defined as liver stiffness measurement ≥8 kPa. Factors associated with fibrosis were assessed using logistic regression models.

Results: A total of 495 patients (mean age 45, 54% male, 64% CD, mean IBD duration 14 years, mean BMI 25.4). SLD was identified in 35% of patients, of which 57% met criteria for MASLD, 5% had alcohol-related SLD, and 38% had other forms. The overall prevalence of significant liver fibrosis was 8%, increasing to 13% and 22% in patients with 1–2 or 3–4 cardiometabolic risk factors, respectively. The prevalence of liver fibrosis was higher in patients with MASLD vs. those without. Patients with non-MASLD SLD phenotypes (4.5%) and those with liver fibrosis (7.5%) had a higher prevalence of methotrexate exposure vs. those without SLD (1.9%) or liver fibrosis (2.3%). After adjusting for IBD type, biological sex and IBD duration, MASLD remained independently associated with 3-fold higher odds of fibrosis (aOR 3.1, 95% CI 1.5–6.1). No significant association was observed for non-MASLD SLD phenotypes. Notably, 3.5% of IBD patients had significant fibrosis in the absence of SLD.

Conclusion: MASLD is the most frequent phenotype of SLD in people with IBD and is strongly associated with liver fibrosis. A proportion of patients also exhibit SLD without metabolic comorbidities or significant alcohol intake, suggesting a potential role for chronic medication exposure. Clinicians should prioritize the identification and management of cardiometabolic risk factors in IBD care to mitigate liver-related complications.

WED-120

Utility of ELF compared with VCTE in guideline-based fibrosis assessment pathways using MRE as reference

Cecilia Katzenstein[1], Anna Mageras[1], Mark Miller[1], Victor Llanes[1], Xiaotao Zhang[1], Meena Bansal[1]. [1]*Icahn School of Medicine at Mount Sinai, New York, United States*
Email: cecilia.katzenstein@icahn.mssm.edu

Background and aims: EASL guidelines recommend stepwise fibrosis assessment using FIB-4 followed by second-line testing when risk is indeterminate or elevated. While VCTE is commonly used, the role of the Enhanced Liver Fibrosis (ELF) blood test within guideline-based pathways remains uncertain.

Method: We prospectively analyzed 157 patients evaluated for MASH who underwent FIB-4, ELF, VCTE, and MRE as part of routine care. Significant fibrosis was defined as MRE ≥3.1 kPa, and cirrhosis as MRE ≥5.0 kPa. Performance was assessed using ROC analysis, sensitivity and specificity, and Spearman correlation with MRE. Sequential pathways reflecting EASL FIB-4 categories followed by ELF or VCTE were evaluated.

Results: The cohort was metabolically high risk, with median BMI 33.6 kg/m^2 and diabetes in 44.8%. Median MRE was 3.1 kPa (IQR 2.4–4.2), and 33.8% had significant fibrosis (MRE 3.1–5.0 kPa). In kPa ≥3.1, ELF and VCTE demonstrated similar discrimination (AUC 0.76 vs 0.75; p = 0.84). For kPa ≥5.0, VCTE showed higher discrimination (AUC 0.92 vs 0.81; p = 0.033). ELF correlated moderately with MRE (rho = 0.52, >0.001), comparable with VCTE, and remained correlated across subgroups, including patients with BMI >40 kg/m^2 (rho = 0.40, p = 0.019) whom VCTE was not significantly correlated. After FIB-4≥1.3, ELF and VCTE showed identical sensitivity for MRE ≥3.1 kPa (56.4%), with higher specificity for ELF (82.3% vs 77.2%). For MRE ≥5.0 kPa, VCTE was more sensitive (88.0% vs 76.0%), while ELF was more specific (88.6% vs 82.6%). In the indeterminate FIB-4 subgroup (1.3–2.67), cirrhosis prevalence was 16.4%. ELF classified fewer patients as positive, with lower sensitivity but higher specificity than VCTE (54.5% vs 81.8%; 92.9% vs 78.6%). Among patients with significant fibrosis (33.8%), ELF had higher specificity than VCTE as a standalone test in the full cohort (64.4% vs 50.0%) and within FIB-4 pathways (67.3% vs 60.6%), with similar sensitivity.

Conclusion: In a high-risk cohort assessed using EASL-recommended stepwise pathways and MRE as reference, ELF and VCTE showed comparable discrimination for significant fibrosis, while VCTE remained more sensitive for cirrhosis. ELF consistently improved specificity when used as a reflex test after FIB-4, particularly in patients with indeterminate FIB-4, non-cirrhotic fibrosis, obesity, and diabetes. These findings support ELF as a pragmatic, blood-based reflex alternative to VCTE within guideline-based pathways to improve risk stratification and avoid uneccesary referrals to specialists.

WED-121

AI-based non-invasive prediction of liver fibrosis in a multicenter biopsy-proven MASLD cohort in Korea

Soon Sun Kim[1], Young-Sun Lee[2], Charmgil Hong[3], Young Chang[4], Su Jong Yu[5], Jeong-Ju Yoo[6], Eileen Yoon[7], Hyo Young Lee[7], Young Joo Jin[8], Do Seon Song[9], Won Sohn[10], Byoung Kuk Jang[11]. [1]*Ajou University School of Medicine, Suwon, Korea, Rep. of South;* [2]*Korea University College of Medicine, Seoul, Korea, Rep. of South;* [3]*Handong Global University, Pohang, Korea, Rep. of South;* [4]*Soonchunhyang University Seoul Hospital, Seoul, Korea, Rep. of South;* [5]*Seoul National University College of Medicine, Seoul, Korea, Rep. of South;* [6]*Soonchunhyang University Bucheon Hospital, Bucheon, Korea, Rep. of South;* [7]*Hanyang University College of Medicine, Seoul, Korea, Rep. of South;* [8]*Inha University School of Medicine, Incheon, Korea, Rep. of South;* [9]*St. Vincent's Hospital, The Catholic University of Korea College of Medicine, Suwon, Korea, Rep. of South;* [10]*Sungkyunkwan University School of Medicine, Seoul, Korea, Rep. of South;* [11]*Keimyung University School of Medicine, Daegu, Korea, Rep. of South*
Email: cocorico99@gmail.com

Background and aims: Fibrosis stage is the key determinant of long-term prognosis in metabolic dysfunction–associated steatotic liver disease (MASLD). Recent guidelines define "at-risk MASH" as biopsy-proven disease with fibrosis stage ≥F2, underscoring the need for accurate non-invasive tests. This study aimed to develop an artificial intelligence (AI)–based model to predict liver fibrosis using routinely available clinical and laboratory variables from a Korean multicenter biopsy-proven MASLD cohort (STAR-K).

Method: The STAR-K retrospective cohort comprises 1,000 patients with biopsy-proven MASLD enrolled from 10 tertiary hospitals in South Korea. The dataset was divided using 5-fold cross-validation for model training, validation, and testing. Predictive performance for significant (≥F2) and advanced fibrosis (≥F3) was evaluated and compared with conventional scores, including the fibrosis-4 (FIB-4) index and NAFLD fibrosis score (NFS). Machine learning (Random Forest) and deep learning (DL; FT-Transformer, TabM, ExcelFormer) models were developed using base variables (age, AST, ALT, platelet count, BMI, diabetes status, albumin, and AST/ALT ratio). Additional analyses incorporated extended variables (INR, GGT, uric acid, LDL, and HDL). In a subset of patients (n = 810), model performance was compared with liver stiffness measurement (LSM) by transient elastography (TE).

Results: Under identical variable conditions, DL-based models showed superior performance compared with FIB-4 and NFS. The AUROC for predicting ≥F2 fibrosis was 0.7508 for FIB-4, 0.7587 for NFS, and 0.7947 for the DL model, while for ≥F3 fibrosis it was 0.7962, 0.8195, and 0.8446, respectively. Corresponding negative predictive

values were also higher for the DL model (≥F2: 0.7901 vs. 0.7083 and 0.6937; ≥F3: 0.8791 vs. 0.8176 and 0.7827 for FIB-4 and NFS, respectively). Incorporation of extended variables resulted in similar AUROC and NPV compared with the base-variable DL model. However, ML and DL models did not demonstrate clear superiority over LSM-based TE for fibrosis prediction.
Conclusion: In this multicenter biopsy-proven MASLD cohort, DL-based non-invasive models outperformed conventional clinical scores in predicting clinically meaningful fibrosis (F2–F3). These AI-based NITs may be useful for risk stratification and longitudinal monitoring in MASLD, although they currently serve best as complementary tools rather than replacements for TE.

WED-122
Optimal cut-off of 2D shear wave elastography for ruling out significant hepatic fibrosis in MASLD: a meta-analysis and machine learning
Mimi Kim[1], Eileen Yoon[2], Hyo Young Lee[2], Sang Bong Ahn[3], Joo Hyun Oh[4], Bo-Kyeong Kang[1], Chul-min Lee[1], Jihyun An[2], Ha Il Kim[2], Eun Chul Jang[5], Hye-Lin Kim[6], Jeong-Yeon Cho[7], Dae Won Jun[2]. *[1]Department of Radiology, Hanyang University College of Medicine, Seoul, Korea, Rep. of South; [2]Department of Internal Medicine, Hanyang University College of Medicine,, Seoul, Korea, Rep. of South; [3]Department of Internal Medicine, Nowon Eulji Medical Center, Eulji University, Seoul, Korea, Rep. of South; [4]Department of Internal Medicine, CHA University College of Medicine, Seongnam, Korea, Rep. of South; [5]Department of Occupational and Environmental Medicine, College of Medicine, Soonchunhyang University, Chunan, Korea, Rep. of South; [6]College of Pharmacy, Sahmyook University, Seoul, Korea, Rep. of South; [7]Department of Pharmacotherapy, University of Utah College of Pharmacy, Salt Lake, United States*
Email: noshin@hanyang.ac.kr

Background and aims: Two-dimensional shear wave elastography (2D-SWE) is a practical alternative for assessing liver fibrosis in primary care, where elastography devices are often unavailable. However, an optimal cut-off value to rule out significant fibrosis (≥F2) in metabolic dysfunction–associated steatotic liver disease (MASLD) remains unclear. This study aimed to determine the optimal cut-off through systematic review and meta-analysis.
Method: A comprehensive systematic review was conducted to identify studies evaluating the diagnostic performance of 2D-SWE for detecting significant hepatic fibrosis in MASLD, with liver biopsy as the reference standard. Pooled sensitivity and specificity were estimated using a bivariate random-effects model, and summary receiver operating characteristic curves were generated. Machine learning models were applied to define the optimal rule-out cut-off, which was validated using real-world clinical data.
Results: Twenty studies were included, encompassing 2,924 adults with biopsy-proven MASLD. The meta-analysis showed good diagnostic performance of 2D-SWE for significant fibrosis, with a summary area under the curve of 0.87 (95% confidence interval: 0.79–0.93). No significant differences were observed across different 2D-SWE manufacturers. Using a machine learning approach, the optimal cut-off value for ruling out significant fibrosis (defined as sensitivity >0.80 and negative predictive value (NPV) >0.95) was identified as 7.5 kPa. This threshold was validated using individual participant data across a range of thresholds (7.0–9.0 kPa). At 7.5 kPa, the model achieved a sensitivity of 0.88, specificity of 0.86, and NPV of 0.94, meeting key clinical criteria for a rule-out strategy.
Conclusion: 2D-SWE demonstrated good diagnostic performance in identifying hepatic fibrosis in patients with MASLD. A 7.5 kPa cut-off value was suggested as the optimal cut-offs for ruling out significant hepatic fibrosis. Two-dimensional shear wave elastography (2D-SWE), optimal cut-off, metabolic dysfunction–associated steatotic liver disease (MASLD).

WED-123
Data-driven identification of an IgA-enriched high-risk subtype in MASLD
Takefumi Kimura[1], Shun-Ichi Wakabayashi[1], Naoki Tanaka[1]. *[1]Shinshu University, Matsumoto, Japan*
Email: kimuratakefumii@yahoo.co.jp

Background and aims: Metabolic dysfunction-associated steatotic liver disease (MASLD) is a heterogeneous condition in which liver-related events (LRE) cannot be fully explained by fibrosis severity alone. Improved risk stratification requires identification of biologically distinct disease subtypes. We aimed to define prognostically relevant MASLD subgroups using a data-driven approach and to elucidate their underlying immune mechanisms.
Method: Unsupervised clustering was performed in biopsy-proven MASLD patients using routine clinical and biochemical variables. Multi-omics analyses, including hepatic qPCR, spatial transcriptomics, single-cell RNA sequencing, and immunohistochemistry, were applied to characterize high-risk subgroups. Prognostic findings were validated in independent cohorts.
Results: Four distinct MASLD clusters were identified. One cluster exhibited a markedly increased incidence of LRE (22% at 5 years, $P < 0.005$), which was not fully attributable to fibrosis stage. This high-risk subgroup was characterized by excessive IgA expression. Elevated serum IgA (≥318 mg/dL) independently predicted LRE (hazard ratio 2.02, $P = 0.01$), a finding consistently reproduced across validation cohorts. Immunohistochemistry demonstrated increased IgA-positive plasma cells in MASLD livers, correlating with serum EndoCAb IgG levels, suggesting enhanced gut permeability. Spatial transcriptomics and single-cell analyses revealed portal enrichment of IGHA1-expressing plasma cells, with associated activation of B-cell receptor signaling and extracellular matrix remodeling pathways.
Conclusion: A data-driven clustering strategy identified an IgA-enriched MASLD subtype with a high risk of liver-related events independent of fibrosis severity. IgA-driven immune activation along the gut–liver axis may represent a key pathogenic mechanism and a clinically relevant target for risk stratification in MASLD.

WED-125
Diagnostic performance of the FibroScan-AST (FAST) score for biopsy-proven metabolic dysfunction-associated steatohepatitis
Jaouhara Lahsini[1], Mohamed Borahma[1], Fatima Zahra Chabib[1], Nawal Lagdali[1], Fatima Zahra Ajana[1], Maryeme Kadiri[1]. *[1]Mohamed V University, Ibn Sina Hospital, Department C of hepato-gastroenterology, Rabat, Morocco*
Email: jaouhara.lahsini@gmail.com

Background and aims: Metabolic dysfunction-associated steatohepatitis (MASH) is the progressive form of metabolic dysfunction-associated steatotic liver disease (MASLD) and requires liver biopsy for definitive diagnosis. Non-invasive tools, including the FibroScan-AST (FAST) score, have been developed to improve risk stratification. This study aimed to evaluate the diagnostic accuracy of the FAST score and compare it with FibroScan parameters for predicting biopsy-proven MASH.
Method: This retrospective, single-centre study included 33 patients with MASLD who underwent both liver biopsy and FibroScan at a tertiary hepatology centre in Morocco between 2022 and 2025. MASH was defined according to histological criteria. FibroScan parameters included liver stiffness measurement (LSM) and controlled attenuation parameter (CAP). The FAST score was calculated using validated cut-offs: rule-out < 0.35, grey zone 0.35 to 0.67, rule-in ≥ 0.67. Diagnostic performance was assessed using ROC curve analysis with biopsy as the reference standard.
Results: Among 33 patients (mean age 46 ± 11 years, 78.8% women), 19 (57.6%) had biopsy-confirmed MASH. The FAST score demonstrated good diagnostic accuracy (AUROC 0.812), superior to LSM (AUROC 0.727) and CAP (AUROC 0.665). At the rule-out threshold,

sensitivity was 78.9% and specificity 85.7%; at the rule-in threshold, sensitivity was 47.4% and specificity 92.9%. CAP showed high sensitivity but limited specificity, particularly in patients with moderate steatosis (S1-S2).
Conclusion: The FAST score effectively identifies biopsy-proven MASH and outperforms CAP and LSM used alone. By integrating steatosis, fibrosis, and inflammatory activity, FAST is a clinically useful non-invasive tool for patient stratification and may refine the indication for liver biopsy in MASLD.

WED-126
Unmasking hidden risk: machine learning reveals ethnic-specific predictors of hepatocellular carcinoma in non-cirrhotic MASLD
Jeril Lasington[1], Lawin Steve Mathew Lasington[2]. *[1]New York Medical College, Valhalla, United States; [2]Rutgers University-Newark Arch, Newark, United States*
Email: lawinsteve.ls@gmail.com

Background and aims: Hepatocellular carcinoma (HCC) can develop in metabolic dysfunction-associated steatotic liver disease (MASLD) without cirrhosis, yet screening guidelines for this population remain absent. We developed an explainable machine learning (ML) model to identify HCC risk factors in non-cirrhotic MASLD and characterize ethnic-specific risk patterns.
Method: This cross-sectional study used the National Inpatient Sample (2019–2022) to identify adults with MASLD/MASH plus ≥1 metabolic risk factor (obesity, type 2 diabetes, hypertension, dyslipidemia) without cirrhosis, viral hepatitis, or alcohol-related liver disease. The primary outcome was concurrent HCC diagnosis. Four ML algorithms (Logistic Regression, Random Forest, XGBoost, LightGBM) were trained using temporal validation (2019–2021 training; 2022 testing) with SMOTE for class imbalance. SHAP analysis provided model interpretability, stratified by race/ethnicity.
Results: Among 287,517 non-cirrhotic MASLD patients (mean age 56 years; 58% female; 67% White), 711 (0.25%) had HCC. Logistic Regression achieved highest discrimination (AUC 0.848), followed by LightGBM (0.826). SHAP analysis identified age as the dominant predictor, followed by NASH histology, obesity, concurrent non-hepatic malignancy, and alcohol use disorder. Female sex was protective. HCC prevalence varied significantly by ethnicity: Asian/Pacific Islander patients had the highest rate (0.40%)—nearly three-fold higher than Black patients (0.14%)—with White (0.27%) and Hispanic (0.20%) patients intermediate. Ethnicity-stratified SHAP revealed distinct risk profiles: heart failure and hypokalemia predominated in Black patients, while sepsis emerged as a key predictor in Asian/Pacific Islander patients.
Conclusion: This ML model achieved strong discrimination for HCC in non-cirrhotic MASLD. Age and NASH histology are dominant predictors across all groups. Asian/Pacific Islander patients demonstrate the highest HCC prevalence and may warrant prioritized surveillance. These findings support development of ethnicity-informed, risk-stratified screening strategies for non-cirrhotic MASLD, addressing a critical gap in current guidelines.

WED-127
Emerging indices outperform traditional fibrosis scores in young MASLD across divergent screening goals
Ahlim Lee[1,2], Jaejun Lee[1,3], Hyun Yang[1,3]. *[1]The Catholic University Liver Research Center, The Catholic University of Korea, Seoul, Korea, Rep. of South; [2]St. Vincent's Hospital, The Catholic University of Korea, Suwon, Korea, Rep. of South; [3]Eunpyeong St. Mary's Hospital, The Catholic University of Korea, Seoul, Korea, Rep. of South*
Email: pwln0516@gmail.com

Background and aims: Although numerous noninvasive indices have been proposed to assess significant fibrosis (SF), none have been validated specifically in young adults with metabolic dysfunction-associated steatotic liver disease (MASLD). This study evaluated their performance in younger patients across two cohorts with distinct screening goals.
Method: We retrospectively analyzed two MASLD cohorts: a primary-care (PC) cohort from Armed Forces Goyang Hospital (n = 972) and a tertiary-care (TC) cohort from Eunpyeong St. Mary's Hospital (n = 342). SF was defined as liver stiffness ≥7.0 kPa on vibration-controlled transient elastography. The diagnostic performance of emerging indices (FIB-8, SAFE, MAF-5) was compared with traditional scores (FIB-4, APRI, NFS).
Results: Baseline comparisons showed significant differences in liver stiffness and other liver-related parameters, which were generally higher in the TC cohort. Across both settings, emerging indices consistently outperformed traditional scores for SF discrimination. In the PC cohort, the area under the receiver operative characteristic curves (AUROCs) were 0.735 for FIB-8, 0.766 for SAFE, and 0.812 for MAF-5, compared with 0.528 for FIB-4, 0.659 for APRI, and 0.608 for NFS. In the TC cohort, AUROCs were 0.691 for FIB-8 and 0.719 for SAFE, exceeding those of FIB-4 (0.572), APRI (0.635), and NFS (0.621). Decision curve analyses demonstrated that emerging indices provided greater net clinical benefit and larger reductions in unnecessary procedures, with thresholds differing by setting such that lower thresholds favored referral in the PC cohort, whereas higher thresholds were more appropriate for biopsy decisions in the TC cohort. Conventional cutoffs widely used in practice demonstrated limited sensitivity in this population, while thresholds optimized in this study yielded more balanced diagnostic accuracy, suggesting refinement may be required in clinical practice.
Conclusion: Traditional NITs showed limited performance in young adults with MASLD, whereas emerging indices such as FIB-8, SAFE, and MAF-5 appeared more suitable for achieving the screening goals of referral in PC and biopsy decision-making in TC. Nonetheless, refined cutoff values might be necessary for younger adults when applying both traditional and emerging indices.

WED-131
The sequential use of LiverPRO and ADAPT enhances fibrosis detection in at-risk populations
Diana Julie Leeming[1], Ida Lønsmann Sorribes[1], Cecilie Bager[1], Frederik Christiansen[1], Julie Astono[2], Bruno Golding[3], Morten Karsdal[1], Aleksander Krag[4], Katrine Lindvig[2], Maja Thiele[2,4]. *[1]Nordic Bioscience, Biomarkers & Research, Herlev, Denmark; [2]Evido Health, Copenhagen, Denmark; [3]Roche Diagnostics International, Rotkreuz, Switzerland; [4]FLASH – Centre for Liver Research, Department of Gastroenterology and Hepatology, Odense University Hospital and University of Southern Denmark, Odense, Denmark*
Email: djl@nordicbio.com

Background and aims: With approval of therapies for metabolic dysfunction–associated steatohepatitis (MASH), reliable non-invasive tests (NITs) are required to identify patients with fibrotic MASH for referral and treatment. We evaluated sequential blood-based NIT strategies combining the LiverPRO score, FIB-4, and the PRO-C3–based ADAPT algorithm to detect significant liver fibrosis in a population-based cohort.
Method: This single-centre liver fibrosis screening cohort included Danish participants recruited from the general population (n≈3,400) or with self-reported risk factors for steatotic liver disease (n≈3,000). All underwent same-month blood sampling and liver stiffness measurement (LSM by FibroScan®). Participants with LSM ≥8 kPa were invited for repeat LSM and liver biopsy. Significant fibrosis was defined as biopsy ≥F2 at visit 2. Diagnostic performance was assessed by sensitivity/specificity (sens/spec). LiverPRO combines up to nine routine blood tests to estimate fibrosis risk. ADAPT includes Elecsys® PRO-C3 as part of ADAPT, platelet count, age, and diabetes. We compared two-tier strategies, LiverPRO (≥0.25) or FIB-4 (≥1.3/2.0), followed by ADAPT (≥9.0), against FIB-4 alone.
Results: Among 6,443 participants, median age was 57 years (IQR 52–63), 48% male, BMI 28 kg/m^2 (25–33), and 9.7% had diabetes. Biopsy

was performed in 3.7% of the population of whom 70% had significant fibrosis (n = 168/242). Biopsy data showed 1.3% (n = 81) F2, 0.3% (n = 52) F3, and 0.5% (n = 35) F4 fibrosis. After exclusions, 5,639 participants were analysed. FIB-4 alone referred 27% with sens/spec 63%/74% and missed six F4 cases. LiverPRO referred 40% with sens/spec 92%/61%, missing one F4. LiverPRO followed by ADAPT improved sens/spec to 82%/81%, referred 21%, missed two F4 cases, and reduced referrals by 47% versus LiverPRO alone. FIB-4 followed by ADAPT referred 17%, achieved sens/spec 61%/84%, missed six F4 cases, and reduced referrals by 35% versus FIB-4 alone.
Conclusion: Sequential testing with LiverPRO and ADAPT provides high sensitivity for detecting significant fibrosis, minimizes missed cirrhosis, and reduces unnecessary referrals. This strategy outperformed FIB-4–based approaches, supporting advanced multivariable algorithms for fibrosis risk stratification.

WED-132
Evaluating the uptake of fibrosis-4 index as a screening tool for liver fibrosis in patients with type 2 diabetes
Calven Fu-Hao Lim[1], Min Chow[1], Jess Jie-Ying Ng[1], Hak-Keith Leung[1], Guo-Jeng Tan[1], Lee-Ling Lim[2,3,4,5,6], Jeyakantha Ratnasingam[2], Shireene Ratna Vethakkan[2], Pavai Sthaneshwar[7], Wah-Kheong Chan[1].
[1]Gastroenterology and hepatology Unit, Department of Medicine, Universiti Malaya, Kuala Lumpur, Malaysia; [2]Endocrine Unit, Department of Medicine, Universiti Malaya, Department of Medicine, Kuala Lumpur, Malaysia; [3]Department of Research, Development, and Innovation, Universiti Malaya Medical Centre, Kuala Lumpur, Malaysia; [4]Department of Medicine and Therapeutics, The Chinese University of Hong Kong, Hong Kong SAR, China; [5]Asia Diabetes Foundation, Hong Kong SAR, China; [6]Baker Heart and Diabetes Institute, Melbourne, VIC, Australia; [7]Department of Pathology, Universiti Malaya, Kuala Lumpur, Malaysia
Email: s2188754@siswa.um.edu.my

Background and aims: Metabolic dysfunction–associated steatotic liver disease is common among patients with type 2 diabetes (T2D), who are at increased risk of progressing to cirrhosis, yet fibrosis often remains clinically silent until hepatic decompensation occurs. This study aimed to evaluate the uptake of Fibrosis-4 index (FIB-4) as a risk stratification tool in patients with T2D.
Method: This was a retrospective study of consecutive patients with T2D who were seen in the Diabetes Clinic of University of Malaya Medical Centre between 1 January 2023 and 31 December 2023. Patients were identified as having higher risk of future cirrhosis based on elevated FIB-4 ≥1.3.
Results: The data for 1009 patients were analysed, median age 62 (52–71) years, 40.7% male. Elevated FIB-4 was seen in 28.8% (291/1009). Only 12.0% (35/291) with elevated FIB-4 were referred for further hepatology evaluation. Patients with elevated FIB-4 who were referred for further hepatology evaluation (compared with those who were not referred) were more likely known to have hepatic steatosis, had higher alanine aminotransferase, aspartate aminotransferase, gamma glutamyl transferase, and lower low-density lipoprotein cholesterol and platelet count. Among patients with low FIB-4, 3.3% (24/718) were referred for further hepatology evaluation.
Conclusion: Despite the incorporation of automatically calculated FIB-4 into laboratory report, this risk stratification tool was found to be under-utilised in patients with T2D, with the majority of patients at higher risk of future cirrhosis not referred for further hepatology evaluation, translating to missed opportunities for timely identification and management of patients with more severe liver disease.

WED-133
The metabolic body risk index (MBRI) based on anthropometric composite and machine learning for non-invasive diagnosis of MASLD
Yingying Lin[1], Yuyun Song[1], Ke Yin[1], Xu Cong[1], Ran Fei[1], Wang Zilong[1], Xin Ai[1], Minjun Liao[1], Xiaoxiao Wang[1], Huiying Rao[1], Feng Liu[1].
[1]Peking University People's Hospital, Peking University Hepatology Institute, Infectious Disease and Hepatology Center of Peking University People's Hospital, Beijing, China
Email: linyingying0123@163.com

Background and aims: Metabolic dysfunction-associated steatotic liver disease (MASLD) is closely linked to obesity and abnormal fat distribution, but single anthropometric indices show limited and inconsistent diagnostic performance. We derived a composite anthropometric index, the metabolic body risk index (MBRI), to enhance the identification of MASLD.
Method: We analysed 5,297 adults from NHANES 2017–2020, which was divided into training and test sets, and utilized the NHANES 2020–2023 cohort (n = 2,427) for external validation. In the training set, 17 anthropometric variables were entered into LASSO regression; selected variables were linearly combined to construct MBRI. Multivariable logistic models with restricted cubic splines assessed the association between MBRI and MASLD. Diagnostic performance for MASLD and MASLD with severe steatosis was evaluated by receiver operating characteristic (ROC) curves and area under the curve (AUC), and compared with each component index. To further improve discrimination, we applied LASSO and Boruta feature selection to MBRI and routine biochemical markers to develop machine learning models, utilizing SHAP values for interpretability.
Results: LASSO regression selected waist circumference, waist-to-height ratio, waist-to-hip ratio, TyG, conicity index and lipid accumulation product to form MBRI. Restricted cubic splines showed a significant non-linear association between higher MBRI and MASLD risk (p for non-linearity < 0.001). Across training, test and validation cohorts, AUCs of MBRI were 0.736–0.762 for MASLD and 0.776–0.798 for MASLD with severe steatosis, all higher than those of individual component indices. After inclusion of selected biochemical markers, machine-learning models achieved further improvement; in the validation cohort, the best model (GBM) reached AUCs of 0.770 for MASLD and 0.806 for MASLD with severe steatosis, outperforming FIB-4, NFS, APRI and HSI (AUC 0.532–0.714 and 0.546–0.752, respectively). SHAP analysis demonstrated that MBRI was the most significant predictor across models.
Conclusion: MBRI, a composite index derived from routine anthropometry, enables non-invasive identification of MASLD and MASLD with severe steatosis. Combining MBRI with a small panel of biochemical markers in interpretable machine-learning models significantly enhances diagnostic performance, proving beneficial for population screening and risk stratification.

WED-134
Development, validation, and longitudinal monitoring of a machine learning model for prediction of liver fibrosis and liver-related events in community-dwelling adults: a prospective, multicohort study
Shanghao Liu[1], Katrine Lindvig[2], Zhenyu Dai[3], Hui Shi[4], Bicheng Ye[5], Yilin Zhang[5], Terry Cheuk-Fung Yip[6], Yuxia Qi[7], Xibin Liu[8], Yijun Tang[9], JianSong Ji[10], Wenjuan Wang[11], Xiao Liang[12], Huizhen Fan[13], Yang Bu[14], Liping Wang[15], Puqiang Liu[16], Guoqing Zhang[17], Chuan Liu[5], Julie Astono[18], Kai Hu[19], Yan Yang[20], Qing He[21], Hui Yang[22], Yongyi Zeng[23], Qiang Yan[24], Xiongwei He[25], Xingguo Xiao[26], Jianxiang Song[3], Rong Hu[4], Xiuli Han[7], Haiying Feng[8], Zhong-ji Meng[9], Yanru Xie[27], Guo Zhang[11], Zhengao Xu[12], Jianwen Sheng[13], Jing Wang[14], Shuli Hao[15], Jianping Zhang[16], Hui Cheng[19], Lingxiao Wang[20], Pinghua Sun[28], Jintian Shu[28], Fengjuan Chen[21], Yajuan Zhao[22], Zuxiong Huang[29], Zhaowei Tong[24], Jiangwen Liu[25], Yanhong Liu[26], Vincent Wai-Sun Wong[6], Maja Thiele[2],

Gao-Jun Teng[5], Aleksander Krag[2], Xiaolong Qi[1]. [1]*Zhongda Hospital, Medical School, Southeast University, Nanjing, China;* [2]*Odense University Hospital, Odense, Denmark;* [3]*Affiliated Yancheng Hospital, Yancheng, China;* [4]*The First Affiliated Hospital of Kangda College of Nanjing Medical University, Lianyungang, China;* [5]*Zhongda Hospital, Nanjing, China;* [6]*The Chinese University of Hong Kong, Hong Kong, China;* [7]*Qingdao Public Health Clinical Center, Qingdao, China;* [8]*People's Hospital of Huanghua, Huanghua, China;* [9]*Taihe Hospital, Shiyan, China;* [10]*Lishui Central Hospital, Lishui, China;* [11]*Guangxi Hospital Division of The First Affiliated Hospital, Nanning, China;* [12]*Sir Run-Run Shaw Hospital, Hangzhou, China;* [13]*Yichun People's Hospital, Yichun, China;* [14]*General Hospital of Ningxia Medical University, Yinchuan, China;* [15]*Bozhou People's Hospital, Bozhou, China;* [16]*Pu County People's Hospital, Linfen City, China;* [17]*University of Chinese Academy of Sciences, Shanghai, China;* [18]*Odense University Hospital, Odense, China;* [19]*Xuzhou Infectious Diseases Hospital, Xuzhou, China;* [20]*Baiyin Central Hospital, Baiyin, China;* [21]*Shenzhen third People's Hospital, Shenzhen, China;* [22]*The Second Affiliated Hospital of Guangzhou Medical University, Guangzhou, China;* [23]*Mengchao Hepatobiliary Hospital of Fujian Medical University, Fuzhou, China;* [24]*Huzhou Central Hospital, Huzhou, China;* [25]*Medical Department of Shihezi City People's Hospital, Shihezi, China;* [26]*Zhengzhou Central Hospital Affiliated to Zhengzhou University, Zhengzhou, China;* [27]*The Fifth Affiliated Hospital of Wenzhou Medical University, Lishui, China;* [28]*Baiyin Central Hospital, Baiyin City, China;* [29]*MengChao Hepatobiliary Hospital, Fuzhou, China*
Email: qixiaolong@vip.163.com

Background and aims: Noninvasive tests (NITs) for detecting liver fibrosis in the community remain limited in accuracy and generalizability across global regions. This study aimed to develop and validate a novel score for predicting liver fibrosis, liver-related events (LREs), and longitudinal changes in risk in community-dwelling adults.
Method: We conducted a prospective, multicohort study including adults aged ≥ 18 years from community-based populations in China, Denmark, the United States, and the United Kingdom. Among several candidate machine learning models evaluated, extreme gradient boosting (XGBoost) achieved the best overall performance and was therefore selected for development of the LiverHealth score (free access: https://liverhealthscore.shinyapps.io/chess/). The LiverHealth score was derived in a community-based cohort and externally validated in three independent cohorts, all of whom underwent liver stiffness measurement (LSM) by transient elastography (Fibroscan®). Clinically significant fibrosis was defined as LSM ≥ 8 kPa or histological stage ≥ F2. Prognostic performance for liver-related events (LREs) was evaluated in a large population-based cohort, and longitudinal risk changes were assessed in a dynamic cohort with repeated measurements.
Results: We included 27601 participants: 10790 in the derivation cohort and 9154, 3004, and 4653 in validation cohorts 1, 2, and 3, respectively. The prognostic and dynamic cohorts included 454415 and 17379 participants, respectively. The LiverHealth score showed superior performance for predicting LSM ≥8 kPa in the derivation cohort (AUROC = 0.85 [0.83–0.86]) and validation cohorts 1 (0.81 [0.78–0.83]), 2 (0.85 [0.82–0.87]), and 3 (0.80 [0.78–0.82]), significantly outperforming LiverRisk, LiverPRO, CORE, FIB-4, APRI, and NFS (all $p < 0.001$). In the biopsy-assessment subgroup (n = 2929), the AUROC was 0.91 (0.88–0.93) for histological stage ≥ F2. Using rule-out and rule-in thresholds, participants were stratified into low-, medium- and high-risk groups, achieving highest sensitivities of 91.5%, 81.3%, 97.3%, and 88.7% across the derivation and validation cohorts. In the prognostic cohort, medium- and high-risk groups had significantly higher LRE incidence than the low-risk group. In the dynamic cohort, risk progression was associated with higher LRE incidence, whereas risk regression was associated with lower incidence.
Conclusion: The LiverHealth score accurately predicts liver fibrosis and liver-related events in community-dwelling adults.

WED-135

Metabolic dysfunction-associated steatotic liver disease and the work environment: results of a multicenter nationwide study

Ekaterina Liusina[1], Anna Sheptulina[1], Valeriy Lunkov[2], Igor Tikhonov[3], Natalia Trofimovskaya[3], Marina Bondar[4], Irina Egorova[5], Gulnaz Lurie[6], Svetlana Nekipelova[7], Elena Lobanova[8], Tatyana Bendosenko[9], Violetta Goluzova[10], Oxana Drapkina[1]. [1]*National Medical Research Center for Therapy and Preventive Medicine, Moscow, Russian Federation;* [2]*Medsi Group JSC, Moscow, Russian Federation;* [3]*Sechenov University, Moscow, Russian Federation;* [4]*Siberian State Medical University, LCC ProfMedCentr, Tomsk, Russian Federation;* [5]*Tver State Medical University Ministry of Health of the Russian Federation, Tver, Russian Federation;* [6]*Bashkir State Medical University, Ufa, Russian Federation;* [7]*GBUS NCO BCGB, Novosibirsk, Russian Federation;* [8]*Regional Clinical Hospital of the Kaliningrad region, Kalinningrad, Russian Federation;* [9]*Fomin Clinic, Tula, Russian Federation;* [10]*Anapa Medical Diagnostic Center LLC, Anapa, Russian Federation*
Email: eka-lusina@yandex.ru

Background and aims: Metabolic dysfunction-associated steatotic liver disease (MASLD) is a growing global health concern. While metabolic risks are well-established, the contribution of occupational factors remains insufficiently addressed. This study aimed to evaluate the association between occupational hazards (physical, chemical, and organizational) and MASLD prevalence and biochemical activity in a large Russian cohort.
Method: This investigator-initiated, multicenter, cross-sectional study was conducted across 27 Russian cities (43 outpatient centers) between March and June 2025. Out of 3,748 consecutive patients screened (aged 18–90 years), 1,510 participants had sufficient data to be evaluated for MASLD based on 2023 criteria. Data on occupational hazards and work environment were available for 1.323 participants, of whom 147 (11.1%) reported exposure. Hazards were assessed via patient self-reports and defined as regular contact with chemical or physical agents, as well as irregular work schedules, including night and 24-hour shifts.
Results: Patients exposed to occupational hazards exhibited a significantly worse metabolic profile, with a median BMI 28 kg/m^2 (IQR 24–31) vs. 26 kg/m^2 (IQR 23–30) ($p < 0.001$) and waist circumference of 98 cm (IQR 88–105) vs. 92 cm (IQR 80–102) ($p < 0.001$) together with marginally higher liver enzyme levels of ALT 23 U/L (IQR 17–35) vs. 21 U/L (IQR 14–32) ($p < 0.05$); GGT 31.8 U/L (IQR 21.5–69.5) vs. 24 U/L (IQR 16–39) ($p < 0.05$). Systolic and diastolic blood pressure values were also higher in the exposed group ($p < 0.001$). In the cohort 686 patients met MASLD criteria. The prevalence of MASLD was significantly higher among patients exposed to occupational hazards (61.9% vs. 50.6%, p = 0.01; OR 1.58, 95% CI 1.12–2.25). Irregular working hours alone were also associated with increased MASLD risk (61.1% vs. 47.8%, p = 0.031; OR 1.714, 95% CI 1.062–2.76). However, in the multivariate logistic regression model adjusted for age, BMI, and blood pressure, the occupational factor did not retain statistical significance.
Conclusion: Our results suggest that occupational hazards and irregular working schedules may contribute to an increased risk of MASLD and a metabolic phenotype of abdominal obesity. Multivariate analysis indicates that this effect is mediated by the deterioration of BMI and blood pressure rather than acting as an independent risk factor. These results highlight the importance of considering occupational history as a potential factor in MASLD risk assessment.

WED-136

Prevalence and characteristics of patients with lean metabolic dysfunction-associated steatotic liver disease: data from a Russian real-world cohort

Igor Tikhonov[1], Ekaterina Liusina[2], Anna Sheptulina[2], Valeriy Lunkov[3], Natalia Trofimovskaya[1], Stanislava Zakharova[4], Elena Novitskaia[5], Viktoriya Vorobeva[6], Raisa Kapitova[3], Elena Sadomova[7], Yuliia Churkina[8], Yulia Egorova[9], Evgeniia Zakharova[10], Andrey Lipov[11]. *[1]Sechenov University, Moscow, Russian Federation; [2]National Medical Research Center for Therapy and Preventive Medicine, Moscow, Russian Federation; [3]Medsi Group JSC, Moscow, Russian Federation; [4]Lomonosov Moscow State University, Moscow, Russian Federation; [5]LCC Women's Clinic "Alpha", Chelyabinsk, Russian Federation; [6]CDC "Viveya", Chabarovsk, Russian Federation; [7]V.I. Shumakov Federal Research Center of Transplantology and Artificial Organs, Moscow, Russian Federation; [8]LCC Mayskaya Gorka Family Clinic, Arkhangelsk, Russian Federation; [9]LCC Clinic of modern medicine, Rostov-on-Don, Russian Federation; [10]Clinic " BabyBoom", Vladimir, Russian Federation; [11]Phoenix Medica Clinic, Stavropol, Russian Federation*
Email: antihbs@gmail.com

Background and aims: Metabolic dysfunction-associated steatotic liver disease (MASLD) in individuals with normal body weight is an emerging phenotype. Lean MASLD differs from obesity-associated disease and presents diagnostic and treatment challenges. We aimed to characterize the clinical and biochemical features of lean MASLD compared to "non-lean" MASLD in a large Russian cohort.
Method: This multicenter, cross-sectional study was conducted at 43 Russian outpatient clinics. Out of 3,748 consecutive patients screened (aged 18–90), 1,510 had sufficient data for evaluation based on 2023 criteria. Participants were categorized by BMI (cut-off 25 kg/m^2) and the presence of MASLD into lean MASLD (BMI <25 kg/m^2 with liver steatosis diagnosed by US), non-lean MASLD (BMI ≥25 kg/m^2 with steatosis), and lean healthy controls (BMI <25 kg/m^2 without steatosis). Clinical and biochemical data and FIB-4 scores were analyzed.
Results: MASLD prevalence was 51.9% (n = 784). Within the MASLD cohort, 9.8% (n = 77) were classified as lean MASLD (5.1% of the total population). The lean MASLD group had a median age of 57 years (IQR 45–67) and a BMI of 23.6 kg/m^2 (IQR 21.8–24.1). Lean and non-lean MASLD groups showed no significant differences in age or sex distribution. While the frequency of diabetes mellitus and arterial hypertension was similar, the total cardiometabolic risk burden was higher in the non-lean group (5 vs. 3 factors, $p < 0.001$). In the MASLD group, lean MASLD patients had significantly lower waist circumference (83.5 vs. 102.0 cm, $p < 0.001$), ALT (20.65 vs. 27.7 U/L, $p = 0.029$), glucose (5.14 vs. 5.6 mmol/L, $p < 0.001$), and triglycerides (1.10 vs. 1.55 mmol/L, $p = 0.0036$) compared to non-lean patients. Hyperuricemia was 0% in the lean group vs. 8% in the non-lean group ($p < 0.005$, Fisher's exact test). No significant difference in FIB-4 scores was found between the groups. Compared to lean healthy controls, the lean MASLD group demonstrated significantly higher values across all parameters: age, waist circumference, blood pressure, and all laboratory markers ($p < 0.05$).
Conclusion: In our cohort, lean MASLD represents up to 10% of cases. Despite normal BMI and waist circumference, these patients exhibit a metabolic profile significantly worse than lean healthy controls. This highlights the need for MASLD screening regardless of weight status and mandates further research into underlying drivers, such as microbiota composition and genetic polymorphisms.

WED-137

Real-life evaluation of the FIB-4 two-step fibrosis screening strategy in MASLD: measurement of waist circumference might make the difference

Rosa Lombardi[1], Andrea Dalbeni[2], Felice Cinque[1], Annalisa Cespiati[1], Cristina Bertelli[1], Giovanna Oberti[1], Giuseppina Pisano[1], Erika Fatta[1], Edoardo Pulixi[1], Gabriele Maffi[1], Francesca Alletto[1], Daniel Smith[1], Anna Mantovani[2], David Sacerdoti[2], Anna Ludovica Fracanzani[1]. *[1]Fondazione IRCCS Ca' Granda Ospedale Maggiore Policlinico di Milano, University of Milan, Milan, Italy; [2]Azienda Ospedaliera Universitaria Integrata of Verona, Verona, Italy*
Email: rosalombardi@hotmail.it

Background and aims: Accurate detection of advanced fibrosis in metabolic dysfunction–associated steatotic liver disease (MASLD) is crucial for timely referral to hepatology care. Current guidelines recommend a two-step screening strategy using FIB-4 (cut-off 1.3 or 2.0 if >65 years) followed by liver stiffness measurement (LSM ≥8 kPa). We aimed to assess the real-life performance of FIB-4 in MASLD patients referred to hepatology clinics and to identify factors influencing misclassification.
Method: Multicenter study including 1,484 MASLD patients (mean age 53 ± 13 years, 61% males) referred to two hepatology clinics (Milan and Verona) and fulfilling criteria for guideline-recommended screening (diabetes, obesity with comorbidities, or elevated transaminases).
Results: Fibrosis prevalence (LSM ≥8 kPa) was 29%. FIB-4 <1.3/2 and ≥1.3/2 were observed in 1,049 (71%) and 435 (29%) patients. Using the reccomended cut-off, 224/1,049 (21%) patients were false negatives and 224/435 (51%) false positives. FIB-4 showed good specificity (79%) and negative predictive value (NPV) (79%) but low sensitivity (48%), with an accuracy of 70% (AUC 0.70; 95% CI 0.68–0.74). Patients misclassified as non-fibrotic (FIB-4 <1.3/2; LSM ≥8 kPa) compared to those correctly classified (FIB-4 <1.3/2; LSM <8 kPa) were significantly older, more hypertensive and diabetic, with higher HOMA, BMI, waist circumference (WC), triglycerides and fasting glucose. In multivariable analysis WC remained the only independent factor associated with LSM≥8 kPa (OR 1.07, 95% CI 1.02–1.12).Conversely, patients misclassified as fibrotic (FIB-4 ≥1.3/2; LSM <8 kPa) compared to those correctly classified (FIB-4 ≥1.3/2; LSM ≥8 kPa), were younger and with lower WC, BMI, fasting glucose and HOMA index; WC remained independently and inversely associated with LSM>8 kPa (OR 0.95, 95% CI 0.92–0.99). Incorporating WC into patients classified as low risk by FIB-4(FIB<1.3 plus increased WC equal to FIB4≥1.3) markedly increased sensitivity and NPV up to 82%, reducing the number of patients with LSM≥8 kPa who would have been missed by FIB-4 alone, but with a reduction in specificity (34%).
Conclusion: In this real-life MASLD cohort referred to the hepatology clinic, FIB-4 may lead to misclassification. The integration of waist circumference, an easily obtainable marker of visceral adiposity, enhanced the performance of a stepwise screening strategy, improving sensitivity for advanced fibrosis and reducing missed referrals.

WED-138

Metabolome analysis revealed red flag signatures for the identification of MASLD risk across patients with dysmetabolic traits

Miriam Longo[1], Marica Meroni[1], Erika Paolini[1], Giulia Paolella[1], Rosa Lombardi[1,2], Valentina Flagiello[3], Jessica Avagliano[3], Carola Garavaglia[2], Elisa Polledri[2], Rosa Mercandate[2], Paolo Gallo[3], Francesca Terraciani[3], Silvia Fustinoni[1,2], Carlo Agostoni[1], Monica Gomaraschi[2], Umberto Vespasiani-Gentilucci[3,4], Anna Ludovica Fracanzani[1,2], Paola Dongiovanni[1]. *[1]Fondazione IRCCS Cà Granda, Ospedale Maggiore Policlinico, Milano, Italy; [2]Università degli Studi di Milano, Milano, Italy; [3]Fondazione Policlinico Universitario*

Campus Bio-Medico di Roma, Roma, Italy; [4]Research Unit of Clinical Medicine and Hepatology, Università Campus Bio-Medico di Roma, Roma, Italy
Email: paola.dongiovanni@policlinico.mi.it

Background and aims: Adolescents and adults with dysmetabolic traits can either develop MASLD or show no evidence of fatty liver despite comparable cardiometabolic burden. However, it is still unclear whether patients with MASLD exhibit a specific circulating metabolic fingerprint compared to non-MASLD dysmetabolic subjects. Therefore, we aimed to analyze the serum metabolomic profile in a dysmetabolic cohort (n = 383), including adolescents with MASLD (n = 100, A-MASLD), adults with biopsy-proven (n = 95, B-MASLD) or non-invasive MASLD (n = 88, NI-MASLD) diagnosis, and a control group of dyslipidemic patients (n = 100, Dys) without MASLD.
Method: Targeted metabolomics (TM) was performed by UHPLC and analyzed through MetaboAnalyst 6.0.
Results: Serum TM analysis revealed two main hierarchical clusters across dysmetabolic patients, highlighting that A/B-MASLD and NI-MASLD/Dys showed a similar metabolic pattern, respectively. In particular, ~100 species were dysregulated (adjusted $p < 0.05$ FDR) in A/B-MASLD *vs* NI-MASLD/Dys patients. Among them, 64 metabolites were shared between the A/B-MASLD groups, suggestive of a conserved signature across pediatric and adult biopsied cases potentially due to a comparable rate of severe disease. To discover candidate MASLD-specific biomarkers, we performed the intersection analysis of differentially abundant species across the 4 groups. Sixteen metabolites were consistently altered in all MASLD patients (A- B- NI-MASLD) vs Dys. Two of them, glutamic acid and phosphatidylcholine (PC) O-40:6, accurately discriminated MASLD from non-MASLD with 94% AUC (sens: 95%, spec: 88%), remaining stable after 10-fold cross-validation. Next, in the attempt to identify compounds with potential prognostic value, we stratified the dysmetabolic cohort according to MASLD severity. Nine metabolites were mainly dysregulated in severe disease vs controls (Dys). At multivariate and cross-validation analyses, a 5-metabolite model (Decanoylcarnitine, Ocatnoylcarnitine, Leucine, LysoPC 18:2, SM 41:2) achieved the best performance in distinguishing between severe MASLD vs controls (AUC 93%; sens: 87%; spec: 88%).
Conclusion: Serum TM analysis captured a specific circulating profile shared across young and adult MASLD patients, possibly linked to an advanced clinical phenotype, which may be a red flag for cardiometabolic complications in pediatric cases. Furthermore, we disclosed 2 compounds specific for MASLD and 5-metabolites highly predictive of severe MASLD.

WED-139
Machine learning models of non-invasive tests to predict MASH and fibrosis stage based on MAESTRO-NAFLD-1 and MAESTRO-NASH liver biopsies

Rohit Loomba[1], Rebecca Taub[2], Dominic Labriola[2], Jan Priel[3], Krishna Padmanabhan[3], W. Ray Kim[4]. *[1]University of California San Diego School of Medicine, La Jolla, United States; [2]Madrigal Pharmaceuticals, Inc., West Conshohocken, United States; [3]Cytel, Inc., Berlin, Germany; [4]Mayo Clinic, Stanford, United States*
Email: roloomba@health.ucsd.edu

Background and aims: Fibrosis stage in patients with Metabolic Dysfunction-Associated Steatohepatitis (MASH) is currently diagnosed by liver biopsy for the purpose of staging in clinical trials. Although non-invasive tools have emerged, no consensus method exists for staging fibrosis and/or diagnosing MASH with moderate to advanced liver fibrosis, a progressive liver disease. We aimed to develop machine learning (ML) methods to predict fibrosis stage and MASH with F2/F3 Fibrosis using non-invasive biomarkers.
Method: Data from 1,970 biopsy-confirmed patients who screened for phase 3 resmetirom trials (MAESTRO-NASH, MAESTRO-NAFLD-1) were retrospectively analyzed. Outcomes included predictions of fibrosis stage and "MASH with F2/F3 Fibrosis" (NAS ≥4 and moderate-to-advanced noncirrhotic fibrosis) based on thirty-seven predictors (including clinical, laboratory, and imaging measures). Models using random forest were developed, selected for accuracy and stability, in two settings: full predictor models (using all 37 variables) and "lean" models (a subset of predictors routinely available in clinical practice). Performance was evaluated with 4-fold cross-validation via area under the curve (AUC).
Results: Random forest models to predict three classes of fibrosis stages (F0/F1 vs. F2/F3 vs. F4) resulted in one-vs-rest cross-validation mean AUCs for the full data model (0.76, 0.75, and 0.94, respectively) and best performing lean model (0.83, 0.78, and 0.89, respectively). The most important factors included liver stiffness measures (MRE (magnetic resonance elastography), TE (transient elastography)) and MASH composite algorithms. In a model predicting MASH with significant (i.e., Stage 2/3) liver fibrosis, the full and lean models achieved AUCs of 0.75 and 0.79, respectively.
Conclusion: ML models using non-invasive biomarkers, with routinely available clinical predictors, accurately predict fibrosis stage and MASH with F2/F3 Fibrosis, supporting their potential to identify patients with MASH and moderate to advanced liver fibrosis for clinical trials or clinical practice.

WED-140
AI based cell free DNA methylation blood test for semaglutide response in patients with at-risk MASH: Results from SAMARA randomized control trial

Rohit Loomba[1], Egbert Madamba[1], Seema Singh[1], Leila Bazargan[2], Chong Lu[2], Hamed Amini[2], Soheil Damangir[2]. *[1]University of California, San Diego, La Jolla, United States; [2]Hepta Bio, Inc., Foster City, United States*
Email: soheil@hepta.bio

Background and aims: GLP-1 receptor agonists are emerging as effective treatments for metabolic dysfunction-associated steatohepatitis (MASH), yet tools to characterize their biological effects remain limited. We analyzed plasma cell-free DNA (cfDNA) methylation from the SAMARA trial to determine whether semaglutide induces distinct epigenetic changes compared to placebo and whether baseline methylation can distinguish treatment responders.
Method: Twenty-seven SAMARA participants with paired plasma samples (13 semaglutide, 14 placebo) were analyzed at baseline and end of treatment (~1 year; dose up to 2.4 mg subcutaneous weekly). A whole-methylome assay and AI model (LiquidTransformer) were used to segment the genome into biologically meaningful units and characterize methylation patterns. For each patient, we computed methylation change (end-of-treatment minus baseline) and identified regions differing between arms using the Mann-Whitney U statistic. Separately, we compared baseline methylation between responders and non-responders within the semaglutide arm. Pathway enrichment analysis was performed on significant regions.
Results: Semaglutide-treated patients exhibited methylation trajectories distinct from placebo, demonstrating a treatment-specific biological signal in cfDNA. Pathway analysis identified 28 significantly enriched GO terms: lipid metabolism including cholesterol biosynthesis and fatty acid transport; fibrosis and ECM remodeling including collagen signaling and SMAD regulation; neuronal development including axon guidance and CNS axonogenesis; cardiovascular function including nitric oxide and VEGF signaling; tissue repair including Wnt/catenin signaling; and renal development. Baseline methylation also distinguished responders from non-responders, with enrichment in Wnt/catenin signaling, immune regulation including T cell activation, and tyrosine kinase pathways. Notably, Wnt/catenin was enriched in both analyses, suggesting its role in GLP-1 response biology in MASH.
Conclusion: AI-enabled cfDNA methylation profiling distinguished semaglutide from placebo and identified baseline signatures associated with treatment response. Treatment-associated changes independent of clinical response magnitude were present even in

partial responders, suggesting cfDNA captures upstream biological effects not yet reflected in clinical outcomes. This approach may support precision strategies for predicting and monitoring GLP-1 agonist response.

WED-141

Patients with compensated MASH cirrhosis and Fibroscan® VCTE score <15 kPa: baseline data from a phase 3, double-blinded, randomized clinical trial assessing the safety and efficacy of pegozafermin (ENLIGHTEN-Cirrhosis)

Rohit Loomba[1], Naim Alkhouri[2], Quentin M. Anstee[3], Hank Mansbach[4], Cynthia L. Hartsfield[4], Laura Contreras[4], Jasmine Dowlat[4], Jennifer B Kang[4], Shibao Feng[4], Maya Margalit[4]. [1]*University of California San Diego, San Diego, CA, United States;* [2]*Summit Clinical Research, San Antonio, TX, United States;* [3]*Newcastle University, Newcastle upon Tyne, United Kingdom;* [4]*89bio Inc, San Francisco, CA, United States*
Email: maya.margalit@89bio.com

Background and aims: The Fibroscan® VCTE-LSM score is increasingly replacing liver biopsy in the assessment of patients with MASH. The diagnosis of cirrhosis in patients with MASH carries important prognostic and practical implications. In recent updates to the AASLD MASLD guidelines following the approval of drugs for non-cirrhotic MASH, no further evaluation to exclude cirrhosis is advised for patients with VCTE-LSM scores ≤15 kPa. ENLIGHTEN-Cirrhosis (NCT06419374) is an ongoing Phase 3 trial designed to assess the efficacy and safety of pegozafermin in MASH-cirrhosis. This analysis explores the baseline characteristics of randomized subjects with VCTE-LSM score < 15 kPa.
Method: Presence of metabolic risk factors and biopsy-proven MASH cirrhosis (within 6 months of screening, biopsies are scored by consensus read of 3 expert pathologists) are inclusion criteria in the ENLIGHTEN-cirrhosis study. The entry criteria do not have a minimal VCTE cutoff. Baseline data from subjects with VCTE-LSM score <15 kPa of the first 337 randomized subjects were analyzed.
Results: 122 randomized subjects (36%) had VCTE scores <15 kPa. In this subgroup, mean age was 61.5 years, 66% of subjects were female, 80% were diabetic, and 43% were taking a GLP-1RA. Mean BMI was 33.2 kg/m^2. Mean VCTE-LSM, ELF and FIB-4 were 11.0 (range 4.6–14.9) kPa, 10.1 and 1.9, respectively. The mean platelet count was 199×10^3, and 20% of subjects had small varices. The liver biopsy Laennec score was 4a, 4b and 4c in 38%, 57% and 5% of subjects, respectively. The mean NAS score was 2.7; 16% of subjects had no steatosis and 61% had no ballooning on liver biopsy. Mean liver fat by MRI-PDFF was 9.3%.
Conclusion: Cirrhosis would have been missed in >1/3 of randomized subjects in this large cohort of well-characterized subjects with biopsy-proven MASH-cirrhosis if a VCTE score <15 kPa been used to exclude cirrhosis. Although data from a clinical trial may not be fully representative of patients with MASH cirrhosis in general, they suggest that exclusion of cirrhosis by a VCTE-LSM score ≤15 kPa cut-off may lead to inadvertent initiation of drugs for non-cirrhotic MASH and failure to initiate indicated standard-of-care management in a substantial proportion of patients with MASH cirrhosis.

WED-142-YI

Development of an indigenous clinical risk model for early detection of liver fibrosis in an indian community cohort

Sundaresan Mohanraj[1], Vijaya Prakash Madesh[2], Abirami Perumal[1], Sibithooran Karmegam[2], Aravindh Somasundram[2], Arulraj Ramakrishnan[1,2]. [1]*KMCH research Foundation, Dr.NGP Arts and Science College, Coimbatore, Tamilnadu, India;* [2]*Liver Unit, Kovai Medical Center and Hospital, Coimbatore, Tamilnadu, India*
Email: mohanrajs.kmchrf@gmail.com

Background and aims: Non-invasive fibrosis scores such as FIB-4, APRI, SAFE, MAF-5, and Liver Risk Score are widely used for liver fibrosis assessment, but their performance in the Indian general population is suboptimal. In our earlier community cohort, these scores showed only moderate accuracy against FibroScan. This highlighted the need for an indigenous, population-specific tool. We therefore aimed to develop and internally validate a clinical model to predict clinically significant liver fibrosis in an Indian population.
Method: Phase I (KMCH-NCD Study-I) evaluated established fibrosis scores in a community cohort of 1,952 adults (2017–2018), using FibroScan liver stiffness measurement (LSM) as the reference. Phase II (KMCH-NCD Study-II) included 2,379 adults (2022–2023) to develop the new model. Clinically significant fibrosis was defined as LSM ≥7.0 kPa. Participants were randomly divided into derivation (70%, n = 1,665) and validation (30%, n = 714) cohorts.A multivariable machine-learning clinical model was developed using age, BMI, AST, platelet count, HDL cholesterol, and creatinine. The risk equation was: Fibrosis Risk Score = −5.834 + (0.0268 × Age) + (0.1011 × BMI) + (0.0387 × AST) − (0.00157 × Platelet) + (0.00064 × HDL) + (0.0763 × Creatinine). Model performance was compared with FIB-4, APRI, and NFS using AUROC.
Results: In the validation cohort, clinically significant fibrosis was present in 21.5%. The indigenous model showed good discrimination (AUROC 0.73; 95% CI 0.68–0.77; $p < 0.001$). At the Youden-optimal cut-off, sensitivity was 71% and specificity 68%. For community screening, the negative predictive value exceeded 90%, supporting rule-out utility. Under hospital-based prevalence assumptions (30%), PPV increased to 46%, indicating improved rule-in capability. The random forest model showed similar discriminatory performance and provided higher net clinical benefit across a wide range of decision thresholds. In comparative analysis, the new model outperformed traditional fibrosis scores (FIB-4 AUROC 0.60; APRI 0.63; NFS 0.62), with forest-plot comparison demonstrating consistently higher point estimates for the indigenous model.
Conclusion: Traditional fibrosis scores showed limited accuracy in Indian community screening. Using an independent population cohort, we developed an indigenous clinical fibrosis prediction model with improved discrimination and practical rule-out capability. External validation, including biopsy-based confirmation, is needed before routine clinical adoption.

WED-147

Ethnic variation in FibroScan-detected fibrosis and steatosis in a large multi-ethnic cohort: implications for MASLD screening

Ilya Abedi[1], Jumshaid Qureshi[1], Elkhashab Magdy[1], Marzena Magnes[1], Gabriel Bishara[1], Katarina Kangrga[1], Marianthi Masri[1], Michelle Guerrero[1], Gabriel Tarzi[1], Jillian Ho[1], Nada Elzahabi[1]. [1]*Toronto Liver Centre, Toronto, Canada*
Email: ilyaabedi2@gmail.com

Background and aims: FibroScan ® allows non-invasive assessment of liver fibrosis and steatosis through LSM and CAP, Ethnic differences in metabolic risk and liver disease burden, influenced by genetic and social determinants recognized internationally, but real-world data are limited. We evaluated ethnic variation in FibroScan-derived fibrosis and steatosis in a large, diverse cohort.
Method: Retrospective analysis of 11,286 patients undergoing FibroScan® between January 2020-May 2025. Fibrosis and steatosis stages were classified using validated cut-offs. Distribution across ethnic groups was analyzed, and percentages reported within each group.
Results: Advanced fibrosis (F3-F4) was highest in Northern European (7.4%), Jewish (5.2%), and Southern European (3.4%) populations. Cirrhosis (F4) was most prevalent in Caribbean (8.6%), Southern European (6.3%), and Western European (6.3%) groups. Advanced steatosis (S3) was most common in Northern European (37.0%), Caribbean (29.3%), Iberian (27.5%), and Southern European (27.1%) populations. Lower rates of S3 were observed in Hispanic, South Asian, and MENA populations.

Conclusion: FibroScan®-detected fibrosis and steatosis vary significantly across ethnic groups. These findings highlight the need for ethnicity-informed MASLD screening and interpretation of non-invasive liver assessments in diverse populations.

WED-148
Risk stratification by longitudinal FIB-4 biomarker measurements in patients with MASLD/MASH

Suraj Mahida[1], Amy Lou[1,2], Eric Liu[1], Ian Epstein[1], Jordan Francheville[1], Tasha Kulai[1], Julie Zhu[1]. *[1]Dalhousie University, Halifax, Canada; [2]Nova Scotia Health, Pathology, Halifax, Canada*
Email: suraj.mahida@dal.ca

Background and aims: MASLD/MASH affect 25–30% of Canadians and are linked to adverse outcomes. The primary aim of this study was to determine whether time-varying changes in FIB-4 predict AHEs including HCC, first decompensation, and all-cause mortality, among patients with MASLD/MASH. Secondary aim was to assess cumulative AHE incidence across FIB-4 tertiles and test whether associations persist after adjusting for age and sex.
Method: This retrospective cohort study analyzed longitudinal FIB-4 scores in 795 out of 1239 patients from Halifax Fatty Liver Disease Clinic (2010–2023), excluding 444 patients for non-MASLD causes or lack of fibrosis/staging confirmation. A total of 3380 FIB-4 scores were obtained, and FIB-4 dynamics were examined using an Extended Cox Proportional Hazards Model treating FIB-4 as a time-varying covariate with age and sex as fixed effects. Primary outcomes were incident HCC, first decompensation, and all-cause mortality; a composite "any hepatic event" endpoint was also modeled. Time 0 corresponded to the earliest of first FIB-4 or AHE date. Kaplan–Meier cumulative incidence curves were generated by tertiles of FIB-4. Ethics approval was obtained.
Results: Over a median follow-up of 7.4 years (IQR 3.5–10.1), 58 patients developed HCC, 189 experienced afirst hepatic decompensation event, and 91 died. In time-updated Cox models adjusted for age and sex, each 1-point increase in FIB-4 was associated with a 23% higher risk of HCC (HR 1.23, 95% CI 1.13–1.33), an 18% higher risk of decompensation (HR 1.18, 95% CI 1.14–1.23), and a 17% higher risk of death (HR 1.17, 95% CI1.12–1.23; all $p < 0.001$). The composite endpoint of any hepatic event demonstrated a similar association (HR1.17, 95% CI 1.13–1.22). Kaplan–Meier curves revealed a stepwise increase in cumulative incidence across FIB-4 tertiles, with the highest tertile showing >60% event probability at 15 years.
Conclusion: Previous analyses of this cohort demonstrated a stepwise increase in FIB-4 scores being strongly associated with AHE independent to that of age. Extending these findings, the time-varying Cox model revealed that longitudinal increases in FIB-4 dynamically predict hepatic complications and mortality, independent of age and sex. Time-varying modeling underscores the value of longitudinal FIB-4 monitoring for real-time risk stratification and could guide individualized surveillance and intervention strategies in MASLD care.

WED-149
Prevalence and risk factors of steatotic liver disease among secondary public-school students in Chattogram, Bangladesh

Abdullah Al Mahmood[1,2], Subash Mazumder[3], Aniruddha Ghose[1], Aloke Kumar Raha[4], Tarek Shams[1], Pritam Dasgupta[5], Mehrunnissa Khanom[6], Kamrun Nahar[1], Mohammed Salahuddin Shahed Chowdhury[1]. *[1]Chittagong Medical College, Chittagong, Bangladesh; [2]Chittagong Medical College Hospital, Chittagong, Bangladesh; [3]Rangpur Medical College, Rangpur, Bangladesh; [4]Rangamati Medical College, Rangamati, Bangladesh; [5]CSCR Hospital, Chittagong, Bangladesh; [6]Southern Medical College and Hospital, Chittagong, Bangladesh*
Email: almahmoodhepato@yahoo.com

Background and aims: Steatotic liver disease (SLD) is an increasingly important adolescent health concern with potential long-term cardiometabolic consequences, yet school-based evidence from Bangladesh remains limited. This study aimed to estimate the prevalence of SLD and identify associated risk factors among secondary public-school students in Chattogram, Bangladesh.
Method: A cross-sectional study was conducted among 2,000 students aged 11 to 17 years using a multistage sampling technique. Data were collected through questionnaires and clinical assessments, including anthropometric measurements and ultrasound imaging. Students with known liver disease or high alcohol intake were excluded. Associations were examined using chi-square tests and Student's t-tests. Binary logistic regression was performed and adjusted odds ratios (AOR) were calculated to identify factors associated with SLD.
Results: The prevalence of SLD was 16.8%. The mean age was 13.61 years with a standard deviation of 1.44, and 56.3% of participants were male. Students with SLD had higher mean body mass index (26.18 vs 19.86 kg/m^2), waist circumference (81.76 vs 67.75 cm), and hip circumference (93.75 vs 81.90 cm) than those without SLD (all $p < 0.001$). Smoking and hypertension were associated with SLD in bivariate analysis ($p = 0.001$ and $p = 0.036$, respectively). Heavy activity frequency per week, sedentary time (excluding sleep and holidays), and sleep duration were also associated with SLD ($p = 0.049$, $p = 0.035$, and $p = 0.033$, respectively). In binary logistic regression, higher waist circumference (AOR 1.14; $p < 0.001$), higher body mass index (AOR 1.04; $p = 0.005$), age (AOR 0.81; $p < 0.001$), and smoking (AOR 6.52; $p = 0.047$) were independently associated with SLD.
Conclusion: SLD was common among the students. Higher waist circumference, higher body mass index, and smoking were independently associated with SLD. These findings support school-based prevention and early screening strategies focused on healthy weight management and tobacco use prevention among adolescents.

WED-150
Refining the EASL two-step strategy for referral of patients with MASLD: a prospective multicenter primary care study

David Marti-Aguado[1], Marta Hernández Conde[2], Rosa Murria[1], Elba Llop Herrera[2], Enrique Rodríguez[1], Ana Pérez[2], Marta López-Gómez[2], Javier Abad Guerra[2], Jesús Rivera Esteban[2], Cristina Montón[1], Desamparados Escudero-García[1], Isabel Pascual-Moreno[1], Arturo Carratalá[1], José Luis Calleja Panero[2], Paloma Lluch-García[1]. *[1]Incliva - Instituto De Investigación Sanitaria, Valencia, Spain; [2]Hospital Universitario Puerta De Hierro Majadahonda, Majadahonda, Spain*
Email: davidmmaa@gmail.com

Background and aims: The EASL-EASD-EASO guidelines recommends a two-step strategy to identify patients with significant fibrosis (F≥2) among individuals at risk of MASLD. A significant challenge of implementing the guidelines is the limited resources of VCTE, given the reported high rate of false positives (FP) among intermediate-risk FIB-4 group. The aims of this real-world study was to optimize referral pathways for patients with intermediate FIB-4 values from primary care.
Method: This prospective, multicenter study was conducted in primary care settings across two cities of Spain (Valencia, Madrid) between 2023 and 2024. All individuals aged 35–65 years with type 2 diabetes or obesity + ≥1 cardiometabolic risk factor undergoing routine blood testing were enrolled. FIB-4 was automatically calculated. The target population comprised patients with intermediate FIB-4 values (1.3–2.67). In these patients, additional serum-based fibrosis scores (ELF, LiverRisk, CORE, SAFE) were calculated and all cases were referred to the hospital in order to perform a VCTE. Thresholds for serum-based fibrosis scores were selected based on proved prognostic information. The primary endpoint was F≥2, defined as VCTE >8 kPa. The optimal referral strategy was selected as that maximizing the Youden index (J = Sn+Sp-1).

Results: A total of 2,488 individuals were included: 77% FIB-4 <1.3, 21% FIB-4 1.3–2.67, and 2% FIB-4 ≥2.67. The recommended algorithm FIB4–VCTE would refer 21% of subjects (n = 513), with an F≥2 prevalence of 16% and a false-positive rate of 84%. Alternative strategies significantly reduced unnecessary referrals among indeterminate FIB-4. Algorithm #1: FIB4–ELF would refer 8.1% (n = 201 ELF ≥9.8), with 29% F≥2 (71% FP) and J = 0.38. Algorithm #2: FIB4–LiverRisk would refer 1.5% (n = 40 LiverRisk ≥10), with 37% F≥2 (63% FP) and J = 0.11. Algorithm #3: FIB4-CORE would refer 1.7% (n = 43 CORE ≥5), with 45% F≥2 (55% FP) and J = 0.19. Algorithm #4: FIB4–SAFE would refer 5.3% (n = 133; SAFE ≥100), with 38% F≥2 (62% FP). This strategy achieved the most balanced diagnostic performance (J = 0.39).
Conclusion: In a real-world primary care setting, the recommended FIB4–VCTE algorithm leads to a high rate of unnecessary referrals. An alternative and sustainable two-step strategy combining FIB-4 with SAFE improves referral efficiency while maintaining diagnostic performance. These findings support refinement of current EASL-EASD-EASO pathways to optimize MASLD management within public healthcare systems.

WED-151
Repeatability of mri biomarkers for monitoring patients with metabolic dysfunction-associated steatotic liver disease

David Marti-Aguado[1], Amadeo Ten-Esteve[2], Matias Fernández-Patón[2], Irene Navarrete-Pérez[3], Cristina Garcia[4], Ana Crespo[4], Victor Merino[5], Leonor Cerda-Alberich[2], Sonia Ginés Cárdenas[2], Victoria Aguilera Sancho[3], Salvador Benlloch[4], Luis Marti-Bonmati[6]. [1]*Digestive Disease Department, Clinic University Hospital, INCLIVA Biomedical Research Institute, Valencia, Spain;* [2]*Instituto De Investigación Sanitaria La Fe, Valencia, Spain;* [3]*Hospital Universitari I Politècnic La Fe, València, Spain;* [4]*Hospital Arnau De Vilanova, Valencia, Spain;* [5]*Incliva - Instituto De Investigación Sanitaria, Valencia, Spain;* [6]*Instituto De Investigación Sanitaria La Fe, Biomedical Imaging Research Group (GIBI230) La Fe Health Research Institute, Valencia, Spain, Valencia, Spain*
Email: davidmmaa@gmail.com

Background and aims: There is a need for reliable noninvasive test to move from diagnosis to monitoring MASLD. Understanding precision is key when using a biomarker to assess meaningful longitudinal changes in disease. The aim of this study was to determine the same-day different-scanner repeatability coefficient (RC) of Magnetic Resonance Imaging (MRI) biomarkers in patients with MASLD.
Method: This prospective, multicenter cross-sectional study (2024–2025) included patients with biopsy confirmed MASLD who underwent two liver MRI within the same day (30 minutes difference). Standardized imaging protocols were implemented with two MRI scanners from different vendors (Philips and GE HealthCare), both at 3 T. After automatic segmentation of the liver, proton density fat fraction (PDFF, %), iron content (LIC-R2*, mg/g), and hepatic volume (cm^3) was measured for each participant. The primary outcome was the same-day, different-scanner, different-vendor, same field-strength RC (both absolute values and RC%) for each imaging biomarker. The secondary outcomes were the same-day, different-scanner, different-vendor, same field-strength intra-class correlation coefficient (ICC) and within-case coefficient of variation (wCV%) for each imaging biomarker.
Results: Same day repeat MRI exams were prospectively conducted in 28 participants (mean age 57 years, 57% women, mean BMI 28,7 kg/m^2), of which 25% had F0, 18% F1, 29% F2, 14% F3, and 14% F4 on biopsy.
Primary outcome: the RC absolute values were 1.7% for hepatic PDFF, 0.2 mg/g for LIC-R2*, and 188 cm^3 for liver volume. The RC% were 15.6% for hepatic PDFF, 27.8% for LIC-R2*, and 11.6% for liver volume. Secondary outcome: The ICC was 0.99 for hepatic PDFF, 0.80 for LIC-R2*, and 0.94 for liver volume. The wCV% was 5.6% for hepatic PDFF, 10.4% for LIC-R2*, and 4.2% for liver volume, respectively. These results indicates that LIC-R2* had 86% higher within-subject measurement variation than MRI-PDFF.
Conclusion: This preliminary study suggests that thresholds of 1.7% for MRI PDFF, 0.2 mg/g for LIC-R2*, and 188 cm^3 for liver volume, should be used to discern measurement variability rather than real change in patients with MASLD. These repeatability estimates may improve the qualification of MRI biomarkers in clinical practice.

WED-152
Improving identification of metabolic dysfunction-associated steatotic liver disease through integration of glycated haemoglobin into established liver assessment pathways

Holly Martin[1,2], Jennifer Nobes[1,2], Damien Leith[1,2], Ruairi Lynch[1,2], John F Dillon[1,2]. [1]*University of Dundee, Dundee, United Kingdom;* [2]*Ninewells Hospital & Medical School, Dundee, United Kingdom*
Email: hollymartin2804@gmail.com

Background and aims: Metabolic Dysfunction-Associated Steatotic Liver Disease (MASLD) occurs in 38% of the population and is the most common cause of abnormal liver function tests. The pathogenesis of this condition centres on the interaction of obesity and insulin resistance (IR). Patients with abnormal alanine aminotransferase (ALT) identified through liver assessment pathways often remain without a definitive aetiological diagnosis, limiting risk stratification and management. Glycated haemoglobin (HbA1c) is a routine measure of average glycaemia used to diagnose type 2 diabetes, IR and features in the diagnostic criteria for MASLD. We hypothesised that integration of HbA1c into an established liver assessment pathway (intelligent liver function test [iLFT]) would identify patients with MASLD who thus far had been classified as abnormal ALT of unclear aetiology.
Method: We performed a retrospective analysis of patients assessed through the iLFT pathway between 2018 and 2023. Patients were categorised as abnormal ALT with fibrosis (cohort A; n = 260) or without fibrosis (cohort B; n = 4,753), with known MASLD cohorts with and without fibrosis used as controls (n = 1,039 and 1,335, respectively). HbA1c measured within 12 months of liver assessment was eligible for inclusion in the analysis, and patients meeting MASLD criteria (HbA1c > 39 mmol/mol) were identified.
Results: HbA1c data was available for 41 patients in cohort A and 529 patients in cohort B. 68.3% (n = 28) of patients in cohort A and 58.6% (n = 310) of patients in cohort B had an elevated HbA1c and therefore met criteria consistent with MASLD and could be reclassified accordingly. Mean (standard deviation [SD]) HbA1c in the cohorts were 56 mmol/mol (17.94) and 52 mmol/mol (16.42), respectively. In the control populations mean (SD) HbA1c for those with fibrosis and without fibrosis was 67 (20.84) and 66 (20.18), respectively.
Conclusion: Integrating HbA1c into an established liver assessment pathway enables clinically meaningful reclassification of patients with both early and advanced MASLD. This approach improves diagnostic precision, supports earlier identification of metabolically driven liver disease allowing tailored management to be delivered to patients to prevent disease progression and therefore impact on future clinical outcomes. For those with established fibrosis reclassification will potentially enable access to new MASLD treatments. Future work will involve a prospective trial of HbA1c assessment in the above cohorts.

WED-153

Accuracy of non-invasive tests for ruling out or in advanced fibrosis in MASLD patients across clinical settings: a systematic review and meta-analysis

Douglas Maya-Miles[1,2,3], Evangelia Mentsiou-Nikolaou[4], Isabel Fernández-Lizaranzu[1,3], Fariba Ahmadizar[5], Emilio Márquez Jiménez[1], Vicente Artola[6], Ying Xu[7], Keke Ji[8,9], María Pata[10], Paloma Carrillo-Fernández[1,3], Antonio Gil-Gómez[1,3], Rocío Montero-Vallejo[1,3], Laura Fàbrega[1,3], Vanessa García-Fernández[1,3], Sheila Gato-Zambrano[1,3], Ángela Rojas Álvarez-Ossorio[1,3], Rocio Muñoz-Hernández[1,2,3], Vivian de Jong[11,12], Caterina Buranelli[12], A.G. (Onno) Holleboom[6], Luis Calzadilla Bertot[1,3,13], Aldo Trylesinski[14], Luca Miele[15], Amalia Gastaldelli[16], Oscar Franco[11], Manuel Castro Cabezas[12,17,18], Jo Massoels[19], Diederick Grobbee[11,12], George Dedoussis[4], Javier Ampuero Herrojo[1,3,20], Manuel Romero-Gómez[1,3,20] and on behalf of the GRIP on MASH consortium[21]. *[1]Instituto de Biomedicina de Sevilla (IBiS), Hospital Universitario Virgen del Rocío/CSIC/Universidad de Sevilla, Sevilla, España, Seville, Spain; [2]Departamento de Fisiología, Universidad de Sevilla, Seville, Spain; [3]Centro de Investigación Biomédica en Red en el área de Enfermedades Hepáticas y Digestivas (CIBER-EHD), Madrid, Spain; [4]Department of Nutrition and Dietetics, School of Health and Education, Harokopio University of Athens, Athens, Greece; [5]Department of General Practice, Amsterdam University Medical Center, Amsterdam, Netherlands; [6]Department of Internal and Vascular Medicine, Amsterdam University Medical Center, Amsterdam, Netherlands; [7]MRC Epidemiology Unit, Institute of Metabolic Science, University of Cambridge School of Clinical Medicine, Cambridge Biomedical Campus, Cambridge, CB2 0QQ, United Kingdom; [8]Department of Data Science and Biostatistics, Julius Center for Health Sciences and Primary Care, University Medical Center Utrecht, Utrecht, the Netherlands, Utrecht, Netherlands; [9]Hunan Food and Drug Vocational College, Changsha, China; [10]Biostatech Advice, Training and Innovation in Biostatistics, Santiago de Compostela, Spain; [11]Department of Global Public Health and Bioethics, Julius Center for Health Sciences and Primary Care, University Medical Center (UMC) Utrecht, Utrecht, Netherlands; [12]Julius Clinical Research B.V., Zeist, Netherlands; [13]Medical School, The University of Western Australia, Nedlands, Perth, Western Australia, Australia, Perth, Australia; [14]Advanz Pharma Capital House, London, United Kingdom; [15]UOC Medicina Interna e del Trapianto di Fegato, Dipartimento di Scienze Mediche, Fondazione Policlinico Gemelli IRCCS, Rome, Italy/ CEMAD, Fondazione Policlinico Gemelli, Rome, Italy/ Dipartimento di Medicina e Chirurgia Traslazionale, Università Cattolica del Sacro Cuore, Rome, Italy; [16]National Research Council (CNR), Institute of Clinical Physiology (IFC), Pisa, Italy; [17]Department of Internal Medicine, Franciscus Gasthuis & Vlietland, Rotterdam, Netherlands; [18]Department of Internal Medicine, Department of Endocrinology, Erasmus Medical Center, Rotterdam, Netherlands; [19]Echosens, Paris, France; [20]Facultad de Medicina, Universidad de Sevilla, Seville, Spain; [21]GRIP on MASH consortium, Utrecht, Netherlands*
Email: dmaya-ibis@us.es

Background and aims: Non-invasive tests (NITs) are widely used to screen for advanced fibrosis in patients with metabolic dysfunction-associated steatotic liver disease (MASLD). Patient characteristics such as age and metabolic comorbidities may modify NITs' diagnostic performance beyond their effects on fibrosis prevalence. We systematically quantified the impact of key demographic and metabolic factors on the accuracy of NITs for ruling out and ruling in advanced fibrosis in MASLD.
Method: A systematic literature search was performed to identify cohort, case-control, and cross-sectional studies evaluating the diagnostic accuracy of NITs (namely FIB-4, NFS, LSM-VCTE, APRI, AST/ALT, Agile 3+, ELF, MRE) in adults with MASLD. Eligible studies that reported fibrosis prevalence and at least one patient-level risk factor (age, sex, obesity, type 2 diabetes mellitus [T2DM], hypertransaminasemia), and that extracted diagnostic accuracy metrics (sensitivity [SE], specificity [SP], and predictive values [PPV, NPV]), were included. Mixed-effects meta-regression analyses were used to assess effect modification of diagnostic performance. Analyses were stratified by rule-out (low cutoff) or rule-in (high cutoff) strategies.
Results: Of 7,236 screened studies, 101 were included, comprising 28,017 and 30,527 patients in low- and high-cutoff analyses. Fibrosis probability was progressively overestimated with increasing age, driven by reduced SP (beta = – 0.048, p < 0.001). T2DM reduced SE (beta = – 0.003, p = 0.005) and NPV (beta = – 0.003, p = 0.007), increasing false negatives. Obesity modestly reduced SE (beta = – 0.01, p = 0.004) and PPV (beta = – 0.0021, p < 0.001), while hypertransaminasemia reduced SP (beta = – 0.019, p = 0.008) and PPV (beta = – 0.0199, p = 0.003), increasing false positives. Sex had minimal impact.
Conclusion: Age and T2DM were associated with the highest fibrosis prevalence and lowest NIT performance, followed by obesity and hypertransaminasemia. FIB-4, NFS, APRI, LSM-VCTE, and Agile 3+ were most sensitive to population differences, with greater influence from FIB-4, NFS, and LSM-VCTE due to higher study representation. Age-related performance decline was evident from 50 years onward, supporting context-specific thresholds, particularly in older and diabetic populations.

WED-154-YI

FIB-4 screening in primary care identifies one in five patients with diabetes mellitus at risk of fibrotic MASLD for specialist referral

Eva Katharina Messer[1], Olaf Bätz[2], David Petroff[3], Thomas Berg[1], Jan Kramer[2], Johannes Wiegand[1]. *[1]Division of Hepatology, Department of Medicine II, Leipzig University Medical Centre, Leipzig, Germany; [2]LADR Laboratory Group Dr. Kramer & Colleagues, Geesthacht, Germany; [3]Clinical Trial Centre Leipzig, Leipzig, Germany*
Email: eva.messer@medizin.uni-leipzig.de

Background and aims: Fibrosis-4 (FIB-4) index is the guideline recommended screening parameter for patients at risk for fibrotic metabolic dysfunction–associated steatotic liver disease (MASLD) and predicts clinical outcomes. Diabetes mellitus is a major risk factor for fibrotic MASLD. The majority of patients with diabetes mellitus are treated in primary care, but a structured FIB-4 screening has not yet been implemented, although it is essential for referral strategies to subsequent specialized care and for allocation of resources. To determine the feasibility of such a screening program, we tested a prospective FIB-4 reflex testing in Hb1Ac laboratory requests from primary care.
Method: At a central laboratory, alanine or aspartate aminotransferase and platelets were automatically added to Hb1Ac laboratory requests from primary care. Diabetes mellitus was defined by HbA1c levels ≥ 6.5%. FIB-4 categories for low, intermediate or high risk of hepatic fibrosis were classified by values < 1.3, 1.3–2.67, and > 2.67. For age > 65 years, the lower cut-off was 2.0. According to guidelines, FIB-4 results > 1.3 (> 2.0) indicate referral to specialized care.
Results: 17,988 laboratory requests from 360 primary care physicians were analyzed of which 7927 (44%) had HbA1c ≥ 6.5%. A low, intermediate or high risk for hepatic fibrosis was observed in 80% (n = 6335/7927), 17% (n = 1321/7927), and 3% (n = 271/7927), respectively, which resulted in a referral indication in 20% of cases. The distribution according to FIB-4 category was 97.5%, 2.5%, and 0% for women aged 35–44, but changed to 82.5%, 15.6%, and 1.9% at the age of 45–64, and to 87.7%, 8.8%, and 3.6% at the age of 65–74. In total, 459 (14.3%) women qualified for referral. In men, the corresponding results were 92.6%, 7.4%, and 0% at the age of 35–44, which changed to 70.9%, 26.7%, and 2.4% at the age of 45–64, and to 80.7%, 13.3%, and 6.0% at the age of 65–74. In total, 1133 (24.0%) men qualified for referral.
Conclusion: The study provides an estimate of referral rates from primary to specialized care for MASLD evaluation in patients with diabetes mellitus based on a large multicenter primary care cohort and allows calculation of resources. A FIB-4 screening in patients < 45 years may be postponed to later time points.

WED-155

Non-invasive test-driven modeling of patient eligibility for resmetirom therapy in MASLD: data from the German SLD-registry

Maurice Michel[1], Andreas Geier[2], Stefan Zeuzem[3], Münevver Demir[4], Renate Heyne[5], Heike Bantel[6], Stephan Grunwald[7], Jens U. Marquardt[8], Yvonne Serfert[9], Yestle Kim[10], Melinda Daumont[11], Thomas Berg[12], Elke Roeb[13], Heiner Wedemeyer[6,14], Wolf Peter Hofmann[9,15], Jörn M. Schattenberg[1,16]. *[1]Department of Internal Medicine II at the Saarland University Medical Center, Homburg, Germany; [2]Division of Hepatology, Department of Internal Medicine II, University of Würzburg Medical Center, Würzburg, Germany; [3]Department of Medicine I, Goethe University Hospital, Frankfurt am Main, Germany; [4]Department of Hepatology and Gastroenterology, Campus Virchow-Klinikum and Campus Charité Mitte, Charité - Universitätsmedizin Berlin, Berlin, Germany; [5]Leberzentrum Checkpoint, Berlin, Germany; [6]Department of Gastroenterology, Hepatology, Infectious Disease and Endocrinology, Hannover Medical School, Hanover, Germany; [7]Zentrum für Infektiologie Berlin/Prenzlauer Berg, Berlin, Germany; [8]Department of Medicine I, University Hospital Schleswig-Holstein, Lübeck, Germany; [9]Leberstiftungs-GmbH Deutschland, Hannover, Germany; [10]Madrigal Pharmaceuticals, Inc., West Conshohocken, Pennsylvania, United States; [11]Madrigal Pharmaceuticals GmbH, Zug, Switzerland; [12]Division of Hepatology, Department of Medicine II, Leipzig University Medical Center, Leipzig, Germany; [13]Department of Gastroenterology, Medical Clinic II, Justus Liebig University, Giessen, Germany; [14]Leberstiftungs-GmbH Deutschland, Hanover, Germany; [15]Gastroenterologie am Bayerischen Platz, Berlin, Germany; [16]University Medical Center of the Johannes Gutenberg University Mainz, Mainz, Germany*
Email: maurice.michel@uks.eu

Background and aims: Advanced Fibrosis related to metabolic dysfunction-associated steatotic liver disease (MASLD) is increasingly prevalent and associated with adverse outcomes and higher mortality. Non-invasive tests (NITs) are central to identify patients at increased risk of disease progression who may benefit from a pharmacological intervention. This study aimed to characterize patients eligible for resmetirom treatment based on NITs in a real-world cohort in Germany.

Method: The German SLD-Registry is a prospective, non-interventional registry study recruiting in secondary and tertiary care. The cohort included 1,308 patients at baseline with valid liver stiffness measurement (LSM; kPa) obtained by vibration-controlled transient elastography (VCTE) followed up to 3 years. Eligibility for resmetirom treatment was defined according to current German MASLD guidelines as VCTE 10–19.9 kPa and platelet count $\geq 140 \times 10^9$/L at baseline (eligible cohort: n = 276) and was compared with non-eligible patients (VCTE <10 kPa; n = 1,032). Demographic characteristics, clinical parameters, and cardiometabolic risk factors were analyzed.

Results: The overall cohort comprised 50.2% males with a mean age of 52.1 ± 13.4 years and 62.7% with obesity (BMI >30 kg/m^2). Resmetirom treatment eligibility criteria were met in 21.1% of patients. Mean LSM in the total cohort was 9.7 ± 8.2 kPa, compared with 12.6 ± 2.6 kPa in the eligible cohort and 8.9 ± 9.0 kPa in the non-eligible cohort. Mean FIB-4 was 1.5 ± 1.2 and did not differ between cohorts (p = 0.908). Obesity (72.1% vs. 60.2%, p < 0.001) and type 2 diabetes (53.3% vs. 38.7%, p < 0.05) were significantly more prevalent in the eligible cohort. Eligible patients also exhibited a higher burden of cardiometabolic risk factors, with a greater prevalence of more than four to five risk factors. Within the eligible cohort, 81.9% had LSM values of 10–15 kPa and 18.1% had values of >15–19.9 kPa. Over three years of follow-up, progression from 10 to 15 kPa to >15–19.9 kPa and from >15–19.9 kPa to >20 kPa occurred in 7.7% of patients with available longitudinal data.

Conclusion: In this large real-world MASLD cohort, approximately one in five patients met non-invasive criteria for resmetirom treatment eligibility. Identification of eligible patients using NITs may support risk stratification and guide pharmacological treatment strategies in routine clinical practice.

WED-156

A prospective multicenter study to examine the impact of acquired and genetic predictors on hepatocellular carcinoma risk in patients with advanced metabolic associated steatotic liver disease

Stefania Mira[1], Serena Pelusi[2], Lorenzo Miano[1], Francesco Malvestiti[1], Giulia Periti[2], Luisa Ronzoni[2], Marco Saracino[3], Roberta D'Ambrosio[2], Luca Miele[4], Antonio Liguori[5], Elisabetta Bugianesi[6], Chiara Rosso[6], Giorgio Soardo[7], Salvatore Petta[8], Grazia Pennisi[8], Umberto Vespasiani Gentilucci[9], Federica Tavaglione[10], Alessandro Federico[11], Francesco Paolo Russo[12], Paola Zanaga[12], Mario Masarone[13], Daniele Prati[2], Luca Valenti[1]. *[1]Università Degli Studi Di Milano, Milano, Italy; [2]Fondazione Irccs Ca Granda Ospedale Maggiore Policlinico, Milano, Italy; [3]Università di Pavia, Pavia, Italy; [4]Università Cattolica Facoltà di Medicina e Chirurgia, Roma, Italy; [5]Policlinico Gemelli, Roma, Italy; [6]Università Degli Studi Di Torino, Torino, Italy; [7]Università Degli Studi Di Udine, Udine, Italy; [8]Università Degli Studi Di Palermo, Palermo, Italy; [9]Campus Biomedico Via Alvaro del Portillo 200, Roma, Italy; [10]University of California San Diego, La Jolla, United States; [11]Università degli Studi della Campania Luigi Vanvitelli, Napoli, Italy; [12]Università degli Studi di Padova, Padova, Italy; [13]Università degli Studi di Salerno-Dip. Medicina Chirurgia e Odontoiatria, Baronissi, Italy*
Email: stefania.mira@unimi.it

Background and aims: Metabolic dysfunction and Metabolic and alcohol-associated steatotic liver disease (MASLD and MetALD) is a rising cause of hepatocellular carcinoma (HCC), but reliable prognostic tools for risk stratification strategies are still under definition. Aim was to examine the incidence of HCC and the impact of acquired and genetic factors in a prospective multicenter cohort of people at increased risk.

Method: Italian patients aged 45–75 years with MASLD/MetALD (alcohol intake <60/40 g/day in M/F), F3-F4 fibrosis (stiffness ≥8.0 kPa, FIB-4 ≥1.3) or family history of HCC were included. Clinical parameters and genotyping for *PNPLA3* rs738409, *TM6SF2* rs58542926, *GCKR* rs1260326, *MBOAT7* rs641738 and *HSD17B13* rs72613567 generated a polygenic risk score (PRS-5). Time to HCC progression was evaluated by Kaplan-Meier's estimates of cumulative incidence rates, and Cox regression.

Results: We enrolled 524 individuals (57% males) with median follow-up 44.5 months (IQR 15–57); 346 (65%) had cirrhosis, 280 (53%) Type 2 Diabetes (T2D), 100 (19%) MetALD. Twenty-nine (5.5%) developed HCC (28 cirrhotic; 5-year incidence 8.0%, 95%CI 5.2–11.8%; annual 1.5%, 0.9–2.1%). Liver-related events dominated mortality (37 deaths: 12 HCC, 10 decompensation, 7 CV, 7 extrahepatic cancer, 1 infection); competing-risk showed cirrhosis as major HCC driver (HR 15.98, 95%CI 2.17–117.6, p < 0.001). In 443 (85%) with genetics, PRS-5 higher in cirrhosis vs non-cirrhosis (0.47 ± 0.25 vs 0.38 ± 0.26, p < 0.001) and predicted cirrhosis (OR 1.42, 95%CI 1.12–1.81, p = 0.004) independent of age/sex/T2D/BMI (T2D strongest covariate: OR 3.10, 95%CI 1.94–5.00, p < 0.001). In cirrhosis, high PRS-5 (≥0.495, 90th centile) showed nominal HCC risk (HR 1.34, 95%CI 0.56–3.24, NS). Multivariable Cox (age/sex/T2D/BMI-adjusted) identified FIB-4 as independent HCC predictor (HR 1.34, 95%CI 1.20–1.49, p < 0.001; optimal cut-off 2.58: Sn 89%, Sp 65%, AUC 0.82). MetALD vs MASLD competing risk showed no difference in HCC incidence (p = NS). In MetALD, PRS-5 was higher in cirrhotic vs non-cirrhotic (0.51 vs 0.28, p = 0.01); strongly predicted cirrhosis (OR 3.16, 95%CI 1.31–9.22, p = 0.02) independent of age/sex/T2D/BMI.

Conclusion: In this multicenter prospective cohort of people with SLD, cirrhosis was confirmed as the strongest risk factor for HCC development. Genetic predisposition (PRS-5) was associated with cirrhosis presence, with an even large impact in the MetALD

subgroup. FIB-4 remains a robust HCC predictor. New genetic-clinical analysis are ongoing.

WED-157

Application of EASL guidelines for the assessment of risk for MASLD-related advanced fibrosis in an outreach screening of underserved rural communities in central and northern Romania using hepatoscope

Andreea Mihaela Morariu-Barb[1], Ana Bilegan[2], Iulia Minciuna[1], Sigurdur Olafsson[3], Andrei Morariu[2], Fischer Petra[1], Irina-Maria Stoleru[2], Oana Nicoara-Farcau[1], Andreea Fodor[1], Mina Ignat[1], Bogdan Procopet[1], Einar S. Björnsson[3], Horia Ştefănescu[1].
[1]Regional Institute of Gastroenterology and Hepatology, Cluj-Napoca, Romania; [2]Caravana cu Medici, Cluj-Napoca, Romania; [3]Landspitali University Hospital, Reykjawik, Iceland
Email: horia.stefanescu@irgh.ro

Background and aims: Half of the Romanian population, known to be at risk for advanced liver fibrosis, resides in rural areas, with limited access to healthcare and education. With the availability of ultraportable medical devices to non-invasively assess liver health, screening programs to reach these populations become easier. The goal of this prospective study was to characterize the metabolic risk profile of the Romania's remote rural population including their risk of advanced liver fibrosis using non-invasive tests.
Method: Between 2022 and 2024, medical caravans were conducted in 17 villages across Central and Northen Romania. Caravans had two ultrasound machines: one dedicated to qualitative assessment, and one dedicated to the measurements of liver stiffness and quantitative ultrasound - the Hepatoscope, not CE-marked at the time of the study. Participants underwent hepatology clinical consultations, questionnaire, laboratory testing, and abdominal ultrasound with the two devices. MASLD was defined by the presence of hepatic steatosis on ultrasound and at least one cardiometabolic risk factor (obesity, diabetes or prediabetes, dyslipidemia or hypertension), and risk for advanced fibrosis was assessed using the EASL guidelines.
Results: 1935 inhabitants were screened, including 68.3% of females, with a median age of 56 years (45.0–68.0). Median BMI was 29.52 (25.5–33.8), and 46.8% had obesity, including 15.2% with severe obesity. Central obesity was found in 86.6% of participants. 17.4% self-reported type 2 diabetes (T2DM) while blood testing revealed that 18.2% had TD2M and 51.7% had pre-diabetes. 80.8% of participants had at least one cardiometabolic risk factor, including 23.7% with metabolic syndrome. 52.3% of participants had MASLD with a significantly higher LSM (4.9 vs 5.3 kPa, $p < 0.05$). FIB-4 was calculated for 1710 participants, with a median of 1.10 (0.76–1.62). 18.7% and 5.4% of participants had intermediate or high risk of advanced fibrosis. Among them, 46.11% had either T2DM and/or obesity with at least one cardiometabolic risk factor. 135 underwent an LSM, with 34 having an LSM > 8 kPa, representing 2% of the screened population.
Conclusion: MASLD affected more than half of the screened rural population. The risk of advanced fibrosis in these underserved populations highlights the need for continued outreach, early detection and integrated liver care strategies. Hepatoscope could be successfully used in this context.

WED-158

LIVERFAST outperforms FIB-4, in sequential combination with vibration controlled transient elastography (VCTE) for identifying ≥F3 Stages in patients with MASLD including patients with type 2 diabetes (T2D)

Marie Decraecker[1], Jean-Baptiste Hiriart[1], Marie Irles-Depe[1], Juliette Foucher[1], Jenny Yu[2], Ronald Quiambao[2], Amon Asgharpour[3], Mona Munteanu[4], Victor De Ledinghen[5]. *[1]Hepatology Unit, Hôpital Haut Lévêque, Pessac, France; [2]Fibronostics, New Orleans, United States; [3]Stravitz-Sanyal Institute for Liver Disease and Metabolic Health, Virginia Commonwealth University School of Medicine, Richmond, United States; [4]Fibronostics U.S., Inc, New Orleans, United States; [5]Hepatology Unit, Hôpital Haut Lévêque, Bordeaux University Hospital, INSERM U1053, Bordeaux University, Bordeaux, France*
Email: victor.deledinghen@echosens.com

Background and aims: FIB-4 followed by VCTE is recommended to detect advanced fibrosis (≥F3). LIVERFAST (Fibronostics U.S.,Inc.) is a novel blood-based test reimbursed in US to identify liver fibrosis. The study aimed to compare the performance of LIVERFAST and FIB-4, sequentially with VCTE, for the identification of ≥F3 fibrosis including analyses in patients with type 2 diabetes (T2DM).
Method: This retrospective study included MASLD patients from a tertiary hepatology center with LIVERFASt, FIB-4, VCTE, and liver biopsy within 6-month. Performances were assessed using sensitivity, specificity, PPV, NPV, and number needed to diagnose (NND).
Results: LIVERFASt outperformed FIB-4 for identifying ≥F3 fibrosis, showing almost twice higher sensitivity and higher NPV at the high FIB-4 cut-off (>2.67) and higher specificity and PPV at the recommended cut-off (≥1.3 [2.0]). The combination LIVERFASt and VCTE achieved higher PPV (90.4%) than FIB-4 and VCTE (76%) with similar NPV. LIVERFASt identified almost twice more of ≥F3 cases as FIB-4 at the >2.67 cut-off, NNDs 4.56 vs 7.98, respectively. LIVERFAST identified a similar number of ≥F3 cases as FIB-4 at the recommended ≥1.3 [2.0] cut-off with the number of required VCTEs referrals of 187/447 vs 243/447 ($p < 0.001$), respectively. Similar results have been observed in the T2DM subanalysis with a with a lower number of required VCTEs referrals of 118/228 vs 146/228 ($p < 0.01$), respectively. Another noteworthy result relates to the higher proportion of patients correctly classified without suspected fibrosis (true negatives) during the first step by LIVERFAST alone versus FIB-4 alone at the recommended cut-off: 42.7% vs 35.6%, $p < 0.05$, respectively.
Conclusion: LIVERFASt outperformed FIB-4 and its integration into MASLD pathways may enhance screening efficiency, including in high-risk T2DM patients. The study showed that LIVERFAST plays also crucial role in ruling out fibrosis in a higher proportion of patients than FIB-4, identifying those that do not require a second test as far as the first correctly classified fibrosis.

WED-159-YI

Positron emission tomography/magnetic resonance imaging with copper-64 DOTATATE identifies metabolic dysfunction-associated steatohepatitis and shows attenuated hepatic signal with glucagon-like peptide-1 receptor agonist treatment

Puria Nabilou[1], Helle Hjorth Johannesen[2], Thomas Lund Andersen[2,3], Camilla Bardram Johnbeck[2], Bryan Haddock[2], Sofie Boesgaard Neestrup Hansen[1], Anders Junker[1], Elias Rashu[1], Mira Thing[1], Mikkel Werge[1], Signe Wiese[1,3,4], Nicolai Wewer Albrechtsen[3,5], Andreas Kjaer[2,6], Lise Lotte Gluud[1,3].
[1]Gastro Unit, Medical Division, Copenhagen University Hospital - Amager and Hvidovre, Copenhagen, Denmark; [2]Department of clinical physiology and nuclear medicine, Rigshospitalet, Copenhagen University Hospital, Copenhagen, Denmark; [3]Department of clinical medicine, University of Copenhagen, Copenhagen, Denmark; [4]Zealand University Hospital - Køge, Køge, Denmark; [5]Bispebjerg and Frederiksberg, University of Copenhagen, Copenhagen, Denmark; [6]Cluster for molecular imaging, Copenhagen University Hospital Rigshospitalet, Department of biomedical sciences, University of Copenhagen, Copenhagen, Denmark
Email: purianabilou@hotmail.com

Background and aims: Liver biopsy remains the gold standard for diagnosing metabolic dysfunction-associated steatohepatitis (MASH), but its invasiveness limits routine use. With glucagon-like peptide-1 receptor agonists (GLP-1 RA) recently approved for treatment of MASH, there is a growing need for non-invasive alternatives. We investigated whether hepatic uptake of [^{64}Cu]Cu-DOTATATE, a positron emission tomography tracer targeting activated macrophages, can detect MASH non-invasively and whether GLP-1 RA treatment is associated with reduced hepatic uptake.

Method: 60 adults were prospectively included: 48 with biopsy-confirmed metabolic dysfunction-associated steatotic liver disease (MASLD) and 12 healthy controls. Participants underwent positron emission tomography/magnetic resonance imaging (PET/MRI) one hour after receiving a single dose 200 MBq [^{64}Cu]Cu-DOTATATE intravenously. Hepatic maximum standardized uptake values (SUV) and proton density fat fraction (PDFF) were calculated as the mean from three liver regions. Diagnostic discrimination for biopsy-defined MASH was evaluated using receiver operating characteristic analysis. The optimal uptake cut-off for MASH was determined using the Youden index.
Results: SUV was significantly higher in patients with MASLD than in healthy controls (8.9 vs 7.1; p = 0.002). Among patients, GLP-1 RA users (n = 11) had lower tracer-uptake than non-users (7.3 vs 9.4; p < 0.001). For identifying MASH, SUV yielded an area under the curve (AUC) of 0.75 in all participants and 0.83 in untreated participants. The optimal Youden-derived cut-off for SUV detecting MASH was 7.14, with sensitivity = 1.00, specificity = 0.53, positive predictive value = 0.83, and negative predictive value = 1.00. Combining SUV and PDFF improved diagnostic accuracy, with AUC-values of 0.88 and 0.90 in treated and untreated patients, respectively.
Conclusion: Hepatic [^{64}Cu]Cu-DOTATATE uptake on PET/MRI is elevated in patients with biopsy-confirmed MASH and is reduced in patients treated with GLP-1 RAs. These findings support its potential as a non-invasive tool for diagnosis and treatment monitoring of inflammation in MASLD.

WED-163
Metabolic dysfunction-associated steatotic liver disease as a risk factor for fibrosis progression in primary biliary cholangitis: a case-control study
Adela Navarro[1], María Escuín[1], Sandra García[1], Sara Lorente Perez[1], Alberto Lué[1], Luis Cortes Garcia[1], Trinidad Serrano[1], Marta Latre[1], Enrique Ceamanos[1], Guillén Bernal[1], Sergio García[1], Marta Fernández[1], María Galochino[1], Laura Andreu[1], Lucía Pérez[1], Victoria Pardo[1]. [1]*Hospital Clínico Universitario Lozano Blesa, Zaragoza, Spain*
Email: adnavarropu@gmail.com

Background and aims: Primary biliary cholangitis (PBC) is a chronic cholestatic disease that may coexist with metabolic dysfunction-associated steatotic liver disease (MASLD). The impact of MASLD on the course of PBC remains uncertain. We aimed to evaluate the influence of MASLD on treatment response and fibrosis progression in patients with PBC.
Method: We conducted a multicentre case-control study including 293 patients with PBC (219 isolated PBC, 74 PBC with MASLD). Clinical, biochemical, and follow-up variables were collected. Hepatic steatosis was assessed by ultrasound at diagnosis. Liver stiffness was measured by transient elastography, defining advanced fibrosis as values >10 kPa. Treatment response to ursodeoxycholic acid (UDCA) was assessed using Paris II criteria. The requirement for second-line therapy and prognosis, according to the UK-PBC score at 5, 10, and 15 years, were analysed. Progression to significant fibrosis, liver transplantation, and death were evaluated using Kaplan–Meier and Cox regression analyses.
Results: MASLD was present in 25.3% of PBC patients. UDCA response rates according to Paris II criteria were similar between groups. No differences were observed in the indication for second-line therapy or UK-PBC scores. Advanced fibrosis was more frequent in patients with PBC and MASLD (22.6% vs. 8.1%; p = 0.006). In multivariate Cox regression, MASLD was independently associated with a 3.5-fold higher risk of significant fibrosis (aHR 3.448; 95% CI 1.402–8.474; p = 0.007). Patients with PBC and MASLD showed a higher prevalence of hypertension and a less favourable metabolic profile, but no significant differences in mortality, liver transplantation, or cardiovascular/cerebrovascular events.
Conclusion: MASLD is common among patients with PBC and is independently associated with earlier and more advanced liver fibrosis. Transient elastography is a valuable tool for disease monitoring. These findings highlight the importance of a multidisciplinary approach and active management of metabolic risk factors in this subgroup.

WED-164
Comparison of transient elastography and shear wave elastography for MASLD screening in a population at risk
André Neves[1], Francisco Capinha[1], Ana Rita Fernandes[2], Maria do Mar d'Orey[3], Sofia Carvalhana[4], Helena Cortez-Pinto[5]. [1]*Gastroenterology and Hepatology service, Santa Maria Hospital, Santa Maria Local Health Unit, Lisbon, Portugal;* [2]*Gastroenterology and Hepatology service, Santa Maria Hospital, Santa Maria Local Health Unit, Lisboa, Portugal;* [3]*Centro de Investigação Clínica do Centro Académico de Medicina de Lisboa, Lisbon, Portugal;* [4]*Centro de Investigação Clínica do Centro Académico de Medicina de Lisboa, Serviço de Gastroenterologia, ULS Santa Maria, Lisboa, Portugal, Lisbon, Portugal;* [5]*Centro de Investigação Clínica do Centro Académico de Medicina de Lisboa, Clínica Universitária de Gastroenterologia, Faculdade de Medicina Universidade de Lisboa, Lisbon, Portugal*
Email: sofiacarvalhana@msn.com

Background and aims: Metabolic associated steatotic liver disease (MASLD) is a chronic progressive disease that may lead to fibrosis and cirrhosis. Early, non-invasive diagnosis using elastography techniques is essential. This study aimed to prospectively compare liver stiffness measurements (LSMs) obtained by transient elastography (TE) and shear wave elastography (SWE).
Method: Prospective analysis of 170 patients referred to a tertiary center for suspected MASLD, with metabolic risk factors. We evaluated clinical, anthropometric and biochemical parameters. LSM was evaluated using either Fibroscan(r) or Aixplorer ultrasound machine (SuperSonic Imagine, Provence, France).
Results: The study included 170 patients (mean age: 54.9 ± 13.6 years, 54.1% females), wtih a high prevalence of metabolic risk factors: 55.9% obesity, 53.5% hypertension, 50.6% dyslipidemia, 17.6% diabetes. Mean Body Mass Index (BMI) and waist circumference were 31.3 ± 5.6 Kg/m^2 and 100.3 ± 13.2 cm, respectively. Mean LSM: 5.07 ± 2.54 kPa (TE) and 5.40 ± 1.70 kPa (SWE). Most patients showed absent/mild fibrosis (< 8 Kpa): 95.3% by TE and 96.5% by SWE. A minority showed advanced fibrosis: 4.7% by TE and 3.5% by SWE. The correlation between TE and SWE was moderately positive (r = 0.48, p < 0.001), in those with absent/mild fibrosis (< 8 Kpa), while weak-to-moderate (r = 0.30, p < 0.001) in all advanced fibrosis cases. The ≥ F2 group, a significant difference in LSM was observed: mean 13.4 kPa for TE and 11.3 kPa for SWE (p < 0.001). When evaluating these patients, no statistically significant differences were observed regarding anthropometric or laboratory variables Multivariate analysis identified waist circumference as the only independent predictor for TE (beta = 0.073, 95% CI [0.002–0.150], p = 0.044). In contrast, for SWE, Diabetes (beta = 1.327, p = 0.003), GGT (beta = 0.019, p = 0.013), and Ferritin (beta = 0.002, p = 0.027) were the independent predictors.
Conclusion: Both Fibroscan and SWE are effective for the exclusion of advanced fibrosis. The clinical utility of using a complementary multistep strategy in cases with significant fibrosis is yet to be demonstrated, although our results suggest that possibility.

WED-165-YI
Back from the future? The original logistic FIB-4 model outperforms the current simplified FIB-4
TD Clara Nguyen[1], W. Ray Kim[1]. [1]*Mayo Clinic Arizona, Phoenix, United States*
Email: nguyen.thuy-duyen@mayo.edu

Background and aims: In pursuit of public health solutions to the metabolic dysfunction-associated steatotic liver disease (MASLD)

epidemic, guidelines recommend using the FIB-4 index for initial stratification. The current FIB-4 is an abbreviated form of the original model, derived from a logistic regression analysis (Sterling et al., 2006). We evaluated FIB-4 (the current form) versus FIB-4LR (the original logistic model) versus the SAFE score in the diagnosis of moderate and advanced fibrosis among US adults with MASLD.
Method: We analyzed National Health and Nutrition Examination Survey (NHANES) data, a population-representative sample of US adults. FIB-4 and FIB-4LR scores were calculated and correlated in adults meeting American Association of Clinical Endocrinology (AACE) MASLD screening criteria (age ≥40 with type 2 diabetes/prediabetes, overweight/obesity, or ≥2 cardiometabolic risk factors). Fibrotic MASH was defined as CAP ≥275 dB/m with LSM ≥8.0 kPa (moderate) or ≥12.0 kPa (advanced fibrosis) or LSM ≥15.0 kPa regardless of CAP. We generated ROC curves and determined sensitivity, specificity, predictive values, and number needed to screen (NNS) for FIB-4, FIB-4LR, and SAFE scores.
Results: The NHANES data is representative of 218 million US adults, which 59.8% met AACE screening criteria. 11.2 million met the fibrotic MASH definition, including 8.6% with moderate fibrosis and 3.9% with advanced fibrosis. Although FIB-4 and FIB-4LR were positively correlated, the R^2 was low at 43.8%. For moderate fibrosis, FIB-4LR demonstrated a higher AUROC (0.567) than FIB-4 (0.647). Equivalent to FIB-4 ≥1.3, FIB-4LR ≥1.63 achieved superior sensitivity (90.6%), NPV (96.1%), and PPV (10.8%) compared to FIB-4 (sensitivity 43.0%, NPV 92.2%, PPV 10.1%). SAFE performed best with an AUROC of 0.738, and at a cutoff of ≥0, demonstrated sensitivity (90.4%), NPV (98.0%), and PPV (13.2%) that matched or exceeded both FIB-4 models. Similar patterns were observed for advanced fibrosis.
Conclusion: Suffering from simplification, the current form of FIB-4 is an inferior substitute for the original model, which provides more statistically robust and clinically informative results using identical variables. The SAFE score, incorporating additional metabolically relevant variables, demonstrates superior discriminatory power for detecting both moderate and advanced fibrotic MASH.

Reference

Sterling *et al.* (2006). Development of a simple noninvasive index to predict significant fibrosis in patients with HIV/HCV coinfection. *Hepatology*. 43(6).

WED-166

Is perfection the enemy of good? A streamlined screening strategy for metabolic dysfunction-associated steatotic liver disease in the community

TD Clara Nguyen[1], W. Ray Kim[1], Eleana De Filippis[1], Blanca Lizaola-Mayo[1], David M. H. Chascsa[1], Nan Zhang[1], Alina M Allen[2]. [1]*Mayo Clinic Arizona, Phoenix, United States;* [2]*Mayo Clinic, Rochester, United States*
Email: nguyen.thuy-duyen@mayo.edu

Background and aims: Metabolic dysfunction-associated steatotic liver disease (MASLD) is a major source of cirrhosis-related morbidity and mortality globally. With newly approved therapies capable of reversing liver fibrosis, early identification of patients with fibrosis is critical. This study aims to correlate cardiometabolic risk factor (CMRF) profile with MASLD and fibrosis.
Method: We analyzed data from the National Health and Nutrition Examination Survey (NHANES), a population-representative sample of US civilians. CMRFs including overweight/obesity, prediabetes/type 2 diabetes (T2D), hypertension (HTN), hypertriglyceridemia (hyper TG), and low HDL cholesterol were correlated with steatosis and fibrosis, assessed by vibration-controlled transient elastography. Steatosis was defined as CAP ≥275 dB/m and steatotic fibrosis as LSM ≥8.0 kPa or ≥15.0 kPa regardless of CAP. Logistic regression analysis was used to evaluate associations between CMRFs and steatotic fibrosis.
Results: In NHANES 2017–20, 36.9% of U.S. adults had steatosis and 6.8% had steatotic fibrosis. T2D showed the highest prevalence (17.1%), while obesity, HTN, dyslipidemia, and prediabetes had intermediate risks (4.0–12.7%). Among non-T2D individuals, obesity was the strongest independent predictor of steatotic fibrosis with an odds ratio of 11.0. Simplifying screening criteria to T2D or obesity identified 92.8% of steatotic fibrosis cases with a number needed to screen (NNS) of 7.9, outperforming current guidelines; adding HTN (NNS 9.2) may enhance screening. NHANES 2021–23 data confirmed these findings.
Conclusion: Compared to current complex, inconsistent guidelines, a streamlined screening strategy focusing on T2D or obesity is more implementable while capturing most subjects with MASLD and fibrosis.

WED-167

The influence of stress factors on the state of the intestinal microbiota and intestinal epithelial permeability in patients with metabolic dysfunction-associated steatotic liver disease

Yana Nikiforova[1], Galina Dmitrievna Fadieienko[1], Inna Kushnir[1], Alexey Evheniyovych Gridnyev[1], Valentina Chernova[1], Tetyana Solomentseva[1]. [1]*L.T.Mala Therapy National Institute of the National Academy of Medical Sciences of Ukraine, Department of the Study of Digestive System Diseases and their Comorbidity with Non-communicable Diseases, Kharkiv, Ukraine*
Email: dr.jana@email.ua

Background and aims: The problem of metabolic dysfunction - associatted steatotic liver disease (MASLD) has remained relevant for many years. Modern conditions open a new focus for research into triggers factors of the disease, namely the influence of stress factors on the course of MASLD.
Method: 108 patients with MASLD were examined in the war period. Serum levels of chronic stress hormones - brain-derived neurotrophic factor (BDNF), prolactin and the epithelial permeability marker (zonulin) were determined by solid-phase immunoassay. The intestinal microbiota was determined by quantitative real-time polymerase chain reaction. The visceral adipose tissue (VAT) - a monitor scale "Omron BF-511". The obtained data were compared with data in the pre-war period.
Results: In patients with MASLD a direct relationship of moderate strength was found between zonulin levels and VAT ($r = 0.32$, $p < 0,05$). After the start of the war, zonulin levels were recorded that were 3.7 times higher compared to the group of healthy individuals and 1.5 times higher compared to the group of MASLD patients examined in the pre-war period ($p < 0.05$, respectively). The maximum increase in zonulin content was observed in high-grade steatosis ($p < 0.05$). Moderately strong associations were obtained between zonulin and HOMA indices and low-density lipoprotein ($r = 0.38$ and $r = 0.37$, $p < 0.05$ respectively), and a weak correlation with triglyceride indices ($r = 0.28$, $p < 0.05$). In patients with MASLD, who were exposed to the stress factors of the war period, a significant imbalance of the intestinal microbiota (IM) was observed, which was manifested by an increase in the content of Firmicutes (up to 57%) and a decrease in the pool of Bacteroidetes (8%). The F/B index was almost 4 times higher than in the group of MASLD patients who were examined in the pre-war period and was 25.9 and 6.43, respectively ($p < 0.05$). A direct correlation was found between prolactin levels and zonulin content in patients with MASLD of the main group ($r = 0.43$, $p < 0.05$). A direct correlation of moderate magnitude was found between the level of prolactin and BDNF with the content of Firmicutes ($r = 0.44$ and $r = 0.31$, $p < 0.05$ respectively), and an inverse correlation between prolactin and the content of Bacteroidetes ($r = -0.34$ and $r = -0.22$, $p < 0.05$ respectively).

Conclusion: The obtained data on the influence of chronic stress hormones on intestinal microbiota, intestinal permeability and further progression of MASLD.

WED-168-YI

Evaluating discordant enhanced liver fibrosis® test and transient elastography results in patients with metabolic dysfunction–associated steatotic liver disease: insights for risk stratification and management

Laura Pagès[1,2], Nerea Gómez[2], Pablo Gabriel-Medina[2,3], Alba Jiménez-Massip[1,2,4,5], Diego Rojo[1,2], Eduard Mas[2], Roser Ferrer[2,3,4], Juan M. Pericàs[1,2,4,5]. [1]*Liver Unit, Digestive Diseases Division, Vall d'Hebron University Hospital, Barcelona, Spain, Vall d'Hebron Institute of Research (VHIR), Vall d'Hebron Barcelona Hospital Campus, Barcelona, Spain, Barcelona, Spain;* [2]*Vall d'Hebron Institute of Research (VHIR), Vall d'Hebron Barcelona Hospital Campus, Barcelona, Spain, Barcelona, Spain;* [3]*Clinical Biochemistry Unit, Vall d'Hebron University Hospital, Barcelona, Spain, Barcelona, Spain;* [4]*Autonomous University of Barcelona, Barcelona, Spain, Barcelona, Spain;* [5]*Biomedical Research Networking Center for Liver and Digestive Diseases (CIBERehd), Madrid, Spain, Madrid, Spain*
Email: laurapagesnegre@gmail.com

Background and aims: Accurate fibrosis stage assessment in subjects with metabolic dysfunction–associated steatotic liver disease (MASLD) in specialized care remains challenging, mainly due to the non-negligible rate of fibrosis misclassification by transient elastography (TE). The Enhanced Liver Fibrosis® (ELF) test has been proposed as a complementary tool to improve risk stratification. This study aimed to characterize subjects with discordant versus (vs) concordant TE and ELF results and to describe ELF-guided clinical decision making.
Method: A prospective cohort study including patients referred to MASLD clinic at Vall Hebron Hospital between June 2024 and November 2025 with TE and ELF assessed within 3 months. Concordant patients were defined as LSM ≥ 8 kPa with ELF ≥ 9.8 or LSM < 8 kPa with ELF < 9.8; discordant patients as LSM ≥ 8 kPa with ELF < 9.8 or LSM < 8 kPa with ELF ≥ 9.8. Demographics, cardiometabolic risk factors, alcohol use, bioelectrical impedance measures, laboratory data and clinical decisions were analysed.
Results: A total of 188 patients, with a median follow-up of 2.4 [1.1–8.1] months, were included: 68 (36.1%) with LSM ≥ 8 kPa and 120 (63.8%) with LSM < 8 kPa. Among those with ≥ 8 kPa, 33 (48.5%) had concordant ELF results, while 35 (51.5%) were discordant. Discordant patients were younger (54.7 ± 12.9 vs 63.5 ± 9.7 years; $p < 0.01$), had lower median alcohol intake (0 [0–0] vs 0 [0–20] grams/day; $p = 0.02$), higher body mass index (39.6 ± 8.5 vs 35.3 ± 6.6 kg/m^2; $p = 0.02$), greater visceral fat index (18.3 ± 6.9 vs 14.1 ± 3.8; $p = 0.01$) and lower FIB-4 (1.23 [0.70–1.71] vs 2.14 [1.52–3.23]; $p < 0.01$). Follow-up and discharge rates were similar between groups, while referral for bariatric surgery was more frequent in discordant patients (22.9% vs 3%; $p = 0.03$). Among patients with < 8 kPa, 89 (74.2%) had a concordant ELF result while 31 (25.8%) were discordant. Discordant patients were older (61.8 ± 13.7 vs 53.0 ± 12.7 years; $p < 0.01$) and had higher FIB-4 values (1.41 [0.97–2.23] vs 1.09 [0.71–1,46]; $p < 0.01$). Follow-up (74.2% vs 42.7%; $p < 0.01$) and clinical trial assessment (19.4% vs 1.1%; $p < 0.01$) rates were higher.
Conclusion: Obesity may contribute to discordance between LSM and ELF by overestimating fibrosis stage in MASLD patients with LSM ≥ 8 kPa and ELF < 9.8. Patients with LSM < 8 kPa and ELF ≥ 9.8 may have significant fibrosis and benefit from further evaluation. The additive use of ELF in specialized care could improve risk stratification and support clinical decision-making.

WED-169

Validation and clinical performance of a liver proton density fat fraction measurement using artificial intelligence

Wenjie Pang[1]. [1]*Resonance Health, Burswood, WA, Australia*
Email: wenjiep@resonancehealth.com

Background and aims: Steatotic liver disease (SLD) is closely associated with metabolic syndrome and increased cardiovascular risk. Magnetic Resonance Imaging (MRI)–based methods for measuring hepatic steatosis have become the new gold standard due to several advantages over liver biopsy and other non-invasive modalities. The aims of this study were to validate and evaluate the performance of an FDA-cleared Artificial Intelligence (AI)–based MRI processing method that automatically quantifies multiple hepatic steatosis metrics in real time.
Method: 300 quarantined datasets previously analysed over a 5-year period using the FDA-cleared HepaFatScan manual method were selected as the reference standard. These datasets included scans acquired on various MRI makes, models, and field strengths (1.5 T and 3 T). They were used to validate the FDA-cleared AI method (HepaFatSmart), which simultaneously measures proton density fat fraction (PDFF) and steatosis grade. Additional 41 subjects with repeat scans were analysed using the AI method to evaluate repeatability and compare performance with manual HepaFatScan analysis.
Results: HepaFatSmart PDFF measurements closely matched those produced by the reference standard. A small bias of 0.22% was observed in the validation dataset; although statistically significant due to low standard deviation, the difference is clinically negligible, which demonstrates that the AI-based device provides accurate and reliable liver-fat quantification consistent with the reference standard. HepaFatSmart repeatability coefficients ranged narrowly from –2.0% to 1.7%, with a small bias of 0.17%. This indicates strong robustness and consistent performance. Repeatability was slightly better than that of the historical manual HepaFatScan measurements without suggesting an inherent superiority of the AI method. The AI system also incorporates an anomaly-assessment mechanism capable of detecting excessive liver iron levels, estimating their impact, and determining when analysis should be halted as a safety measure.
Conclusion: The AI-based method demonstrates accuracy and precision comparable to the established reference standard, with interchangeable results. Its automated workflow eliminates the need for specialized image-analysis expertise and enables near real-time reporting, supporting potential point-of-care screening and reducing costs. As part of a quantitative MRI analytic realm, its results remain transparent and visible to help mitigate any residual risks associated with AI-based methods.

WED-170

High prevalence of hepatic steatosis in adolescence and young adults: a cross sectional survey from Sindh Pakistan

Om Parkash[1], Aysha Almas[1], Suneel Piryani[1], Arjumand Rizvi[1], Abhishek Lal[1], Areesha Ikram[1], Jai Das[1]. [1]*Aga Khan University, Pakistan, Karachi, Pakistan*
Email: om.parkash@aku.edu

Background and aims: Hepatic Steatosis and its Metabolic Dysfunction–Associated Steatotic Liver Disease (MASLD) are emerging as a global concern and have a major impact on health. The overall aim of the study was to estimate the prevalence of Hepatic Steatosis and MASLD in adolescents and young adults in the province of Sindh, Pakistan and report associated metabolic factors.
Method: It was a cross-sectional study using a multistage complex household sampling strategy conducted in all (31) districts of Sindh, Pakistan, in 2023–2024. Adolescents (10–19 years) and young adults (20–24 years) were included and those who were hepatitis B or C positive were excluded. The primary outcome 1 was Hepatic Steatosis and Primary outcome 2 was MASLD. Hepatic Steatosis was defined as

ultrasound attenuation parameter UAP > 244 dB/m using a Fibro touch: Shear-wave Elastography System. MASLD was defined as Hepatic Steatosis and any one of the cardiometabolic criteria (Obesity, hypertension, triglycerides >150 mg/dl, HDL <40 mg/dl, Fasting blood sugar>100 mg/dl,).
Results: A total of 2,200 participants were invited to participate, of whom 2,136 (97.1%) agreed. Among these, 1,651 (77.3%) were adolescents aged 10–19 years and 485 (22.7%) were young adults aged 20–24 years, with a mean (SD) age of 15.8 ± 4.0 years. Overall, 997 (43.7%) participants were from rural 1,053 (47.6%) were males. Of the total 456 (21.1%) were underweight, 162 (8.6%) were overweight, and 87 (4.3%) were obese, 519 (26.0%) had impaired fasting glucose, and 93 (8.8%) had diabetes. Overall, 1,053 (53.3%) participants had hepatic steatosis, including 802 (52.1%) adolescents and 251 (57.6%) young adults. Among adolescents with Hepatic steatosis 444 (55.08%) and 358 (44.92%) were in early (10–14) and Mid-Late Adolescence (15–19). On multivariate regression, overweight or Obesity (OR 2.52 (95% CI 1.19–5.31), central obesity (OR 3.37(95% CI 1.38–8.26) was associated with hepatic steatosis, while being in middle (OR 0.80(0.59–1.08) or rich (OR 0.87(0.58–1.30) socio economic index was protective for Hepatic steatosis. The prevalence of metabolic dysfunction–associated Steatotic liver disease (MASLD) was 717 (36.3%) overall, comprising 525 (34.9%) adolescents and 192 (41.4%) young adults.
Conclusion: High prevalence of hepatic steatosis and MASLD in adolescents and adults from Sindh, Pakistan indicating that the occurrence happens much early in life. Further studies are required to look at mechanisms that lead to hepatic Steatosis early in life.

WED-171
Assessment of waist-to-height ratio as a predictor of MASLD and advanced fibrosis

Nashla Hamdan[1], Yoshihiro Yamamoto[1], Magdalena Kuczynski[1], Radin Pakseresht[1], Maxwell Tong[1], Keyur Patel[1]. [1]*University Health Network, Toronto, Canada*
Email: nashla.hamdan@uhn.ca

Background and aims: Body Mass Index (BMI) is used to assess obesity, but fails to account for fat distribution and may misclassify muscular or normal-weight patients with metabolic dysfunction. The Waist-to-Height Ratio (WHtR) is an anthropometric tool used to measure visceral adiposity, which has a strong association with metabolic disease. and may be a better predictor of Metabolic Dysfunction-Associated Steatotic Liver Disease (MASLD) than BMI. Our Aim was to evaluate the association between WHtR, hepatic steatosis and fibrosis severity as assessed by non-invasive tests including Vibration Controlled Transient Elastography (VCTE) Controlled Attenuation Parameter (CAP), FIB-4, APRI and NFS score.
Method: Cross-sectional study of adults with MASLD referred for risk stratification at a single tertiary Canadian center. Other chronic liver disease were excluded through clinical and laboratory investigations.
Results: Our cohort included 304 MASLD patients with mean age 51 ± 14 years, 49.6% male, mean BMI of 30.27 ± 7 kg/m^2, waist-hip ratio1.26 ± 6, and WHtR 0.59 ± 0.09. Comorbidities included hypertension (48%), dyslipidemia (40%), and Type 2 Diabetes Mellitus (22%). Patients were stratified into three WHtR risk categories: Low Risk (0.4–0.5), Increased Risk (0.5–0.6), and Higher Risk (>0.6). WHtR demonstrated moderate correlation with markers of hepatic steatosis and fibrosis: CAP (rho = 0.45, p < 0.001) and VCTE (rho = 0.35, p < 0.001), and NFS (rho = 0.33, p <0.001), but weaker with atherosclerotic cardiovascular disease (ASCVD) score (rho = 0.22, p = 0.001). A greater proportion of severe steatosis (CAP >280 dB/m) were classified in high WHtR group (p < 0.001), but there were no WHtR group differences for those with advanced fibrosis VCTE >12 kPa. Multivariable analysis for high risk WHtR showed lower independent association for male gender (OR 0.11, CI 0.03–0.41; p = 0.001), and as expected, increasing BMI (OR 1.35, CI 1.10 – 1.67; p = 0.004 and waist circumference (OR 1.33, CI 1.19 – 1.48; p = <0.001). There was no independent association with dyslipidemia (OR 0.57;p = 0.30) or hypertension (OR 1.36; p = 0.55).
Conclusion: The WHtR is a simple anthropometric measure associated with MASLD severity, and complements BMI and Waist-hip ratio in identifying patients at risk for advanced metabolic liver disease. Incorporating WHtR into clinical practice may improve the identification of high-risk MASLD phenotypes, particularly in patients where BMI may underestimate visceral adiposity.

WED-172-YI
External validation and recalibration of the CORE risk score to predict 10-year risk of liver cirrhosis in patients with type 2 diabetes

Rajan Paudel[1], Rickard Strandberg[1,2], Hannes Hagström[1,3]. [1]*Department of Medicine Huddinge, Karolinska Institutet, Stockholm, Sweden;* [2]*Red Door Analytics, Stockholm, Sweden;* [3]*Division of Hepatology, Department of Upper GI Diseases, Karolinska University Hospital, Stockholm, Sweden*
Email: rajan.paudel@ki.se

Background and aims: Metabolic dysfunction-associated steatotic liver disease (MASLD) is the most common chronic liver disease globally. Type 2 diabetes (T2D) is a key risk factor for MASLD occurrence and progression to cirrhosis. Currently, the FIB-4 score is recommended as a first-line risk assessment tool for patients with T2D in primary care, but its performance and implementation is limited. Further, FIB-4 is not designed to identify the risk of future outcomes related to cirrhosis. Here, we aimed to evaluate the performance of the cirrhosis outcome risk estimator (CORE) and recalibrate it for a T2D population.
Method: We used data from the National Diabetes Register in Sweden to identify people with T2D diagnosed between 1 January 1998 and 31 December 2022. We calculated CORE based on the laboratory data obtained from primary care in the Stockholm region. We used national health registers to identify incident cases of major adverse liver outcomes (MALO). We evaluated the performance in terms of time-dependent area-under-curve (tAUC), calibration plots, and clinical utility using decision curve analysis. As the baseline risk of T2D population is higher than the general population, we recalibrated the model using cause-specific flexible parametric models. All performance measures were compared with FIB-4.
Results: We used data of 37,015 individuals with T2D who had laboratory data to calculate CORE score. 784 developed MALO over a median follow-up period of 6.2 years (10-year cumulative incidence = 2.7%). CORE performed better than FIB-4 in terms of discrimination with a 10-year AUC of 0.86 compared to 0.81 for FIB-4. CORE did not calibrate well and showed underestimation of the observed risk, requiring recalibration. The updated CORE model showed improved calibration and performed better than FIB-4 in terms of net benefit at risk-thresholds up to 30%.
Conclusion: CORE performs better than FIB-4 in estimating risk of MALO in patients with T2D. CORE better captures high-risk groups and reduces the need for referrals as compared to FIB-4.

WED-173
The relationship between liver stiffness measurement and all-cause mortality in patients with chronic liver diseases varies over time

Rajan Paudel[1], Hannes Hegmar[1,2], Axel Wester[1], Soo Aleman[3], Jens Backman[4], Erik Degerman[5], Åsa Lundgren[6], Patrik Nasr[7], Johan Vessby[8], Joan Westin[9], Hannes Hagström[1,2], Rickard Strandberg[1,10]. [1]*Department of Medicine Huddinge, Karolinska Institutet, Stockholm, Sweden;* [2]*Division of Hepatology, Department of Upper GI Diseases, Karolinska University Hospital, Stockholm, Sweden;* [3]*Department of Infectious Diseases, Karolinksa University Hospital, Stockholm, Sweden;* [4]*Department of Infectious Diseases, University Hospital of Umeå, Umeå, Sweden;* [5]*Department of Infectious Diseases,*

Falun Hospital, Falun, Sweden; [6]Department of Infectious Diseases, Central Hospital, Kristianstad, Sweden; [7]Department of Gastroenterology and Hepatology, Department of Health, Medicine and Caring Sciences, Linköping University, Linköping, Sweden; [8]Department of Medical Sciences, Gastroenterology Research Group, Uppsala University, Uppsala, Sweden; [9]Department of Infectious Diseases, Sahlgrenska University Hospital, Gothenburg, Sweden; [10]Red Door Analytics, Stockholm, Sweden
Email: rajan.paudel@ki.se

Background and aims: Patients with chronic liver disease (CLD) have increased risk of death from non-liver causes demonstrating extra-hepatic complications of liver diseases. Liver stiffness measurement (LSM) using vibration controlled transient elastography (VCTE) could be useful in estimating all-cause mortality risk in patients with CLD. In our study, we aimed to evaluate the association between LSM and all-cause mortality over time and the differences across age, sex and underlying liver disease etiologies.
Method: We used data from Fibroscan® machines from sixteen hospital units across Sweden. Individuals with CLD who had at least one successful LSM between June 2008 and October 2020 were included in the study. The LSM data was linked with national patient and population registers in Sweden to obtain individual characteristics such as age, sex, country of birth, comorbidities and underlying etiologies as well as to follow-up for the outcomes. We modelled the effect of LSM in a flexible parametric survival model (adjusted for age, sex, comorbidities and country of birth). Using the model, we report the cumulative incidence and hazard ratios (HRs) for all-cause mortality associated with LSM over time.
Results: 13,824 patients with CLD with a median LSM of 5.8 kPa (inter-quartile range: 4.6–7.9) were followed up for a median of 6 years (IQR: 4.3–8.2). 984 (7.1%) patients died during the follow-up period. Mortality rates were highest for LSM >12 kPa (29.9 per 1000 person-years). For all etiologies, increasing LSM was associated with an increase in hazard initially (at around 4–6 years after baseline), which attenuated over time (after 6 years). Having alcohol-associated liver disease was associated with highest 10-year risk of all-cause mortality regardless of LSM, while having metabolic-dysfunction associated steatotic liver disease was associated with the lowest 10-year risk.
Conclusion: LSM has a time-dependent association with all-cause mortality, and it varied across age and etiologies. The increased hazard ratios for all-cause mortality associated with increasing LSM diminish over time since measurement. Our results suggest a need of age- and etiology-specific LSM cut-offs while assessing risk of all-cause mortality in patients with CLD.

WED-174-YI

Machine learning prediction of liver fibrosis in patients with metabolic dysfunction associated steatotic liver disease (MASLD)

Grazia Pennisi[1], Salvatore Petta[1], Ciro Celsa[1], Sofiane Messaoudi[2], Emmanuel Tsochatzis[3], Elisabetta Bugianesi[4], Masato Yoneda[5], Ming-Hua Zheng[6], Hannes Hagström[7], Jerome Boursier[8], José Luis Calleja Panero[9], George Boon Bee Goh[10], Chan Wah Kheong[11], Rocio Gallego-Durán[12], Arun J. Sanyal[13], Victor De Ledinghen[14], Philip Newsome[15], Jian-Gao Fan[16], Laurent Castera[17], Michelle Lai[18], Céline Fournier-Poizat[14], Grace Lai-Hung Wong[19], Angelo Armandi[4], Atsushi Nakajima[5], Wen-Yue Liu[20], Ying Shang[7], Marc de Saint-Loup[8], Elba Llop Herrera[9], Kevin Kim Jun Teh[10], Carmen Lara-Romero[12], Amon Asgharpour[13], Sau-Wai Mandy Chan[14], Manuel Romero-Gómez[12], Huapeng Lin[16], Seung Up Kim[21], Terry Cheuk-Fung Yip[19], Vincenza Calvaruso[1], Jimmy Che-To Lai[19], Boyu Yang[19], Hye Won Lee[22], Gabriele Di Maria[1], Marco Enea[1], Salvatore Contino[23], Vincent Wai-Sun Wong[19], Giansalvo Cirrincione[24], Calogero Cammà[1]. *[1]Section of Gastroenterology and Hepatology, Department of Health Promotion, Mother and Child Care, Internal Medicine, and Medical Specialties (PROMISE), University of Palermo, Palermo, Italy, Palermo, Italy; [2]Department of Engineering, University of Palermo, Italy, Palermo, Italy; [3]University College London Institute for Liver and Digestive Health, Royal Free Hospital and UCL, London, United Kingdom, London, United Kingdom; [4]Department of Medical Sciences, Division of Gastroenterology, A.O.U. Città della Salute e della Scienza di Torino, University of Turin, Turin, Italy, Turin, Italy; [5]Department of Gastroenterology and Hepatology, Yokohama City University Graduate School of Medicine, Yokohama, Japan, Yokohama, Japan; [6]MAFLD Research Center, Department of Hepatology, First Affiliated Hospital of Wenzhou Medical University, Wenzhou, China, Wenzhou, China; [7]Department of Medicine, Huddinge, Karolinska Institutet, Stockholm, Sweden, Stockholm, Sweden; [8]Hepato-Gastroenterology and Digestive Oncology Department, Angers University Hospital, Angers, France, Angers, France; [9]Department of Gastroenterology and Hepatology, Hospital Universitario Puerta de Hierro Majadahonda, Madrid, Spain, Madrid, Spain; [10]Department of Gastroenterology and Hepatology, Singapore General Hospital, Singapore, Singapore, Singapore; [11]Gastroenterology and Hepatology Unit, Department of Medicine, Faculty of Medicine, University of Malaya, Kuala Lumpur, Malaysia, Kuala Lumpur, Malaysia; [12]Digestive Diseases Unit and CIBERehd, Virgen Del Rocío University Hospital, Seville, Spain, Seville, Spain; [13]Stravitz-Sanyal Institute for Liver Disease and Metabolic Health, VCU School of Medicine, Richmond, VA, USA, Richmond, United States; [14]Echosens, Paris, France, Paris, France; [15]Institute of Hepatology, Faculty of Life Sciences and Medicine, King's College London and King's College Hospital, London, London, United Kingdom; [16]Department of Gastroenterology, Xinhua Hospital Affiliated to Shanghai Jiaotong University School of Medicine, Shanghai Key Lab of Pediatric Gastroenterology and Nutrition, Shanghai, China, Shangai, China; [17]Université Paris Cité, UMR1149 (CRI), INSERM, Paris, France; Service d'Hépatologie, Hôpital Beaujon, Assistance Publique-Hôpitaux de Paris (AP-HP), Clichy, France, Clichy, France; [18]Division of Gastroenterology & Hepatology, Beth Israel Deaconess Medical Center, Harvard Medical School, Boston, MA, USA, Boston, United States; [19]Medical Data Analytics Centre, Department of Medicine and Therapeutics, The Chinese University of Hong Kong, Hong Kong, China, Hong Kong, China; [20]Department of Endocrinology, First Affiliated Hospital of Wenzhou Medical University, Wenzhou, China, Wenzhou, China; [21]National Institute for Health Research, Biomedical Research Centre at University Hospitals Birmingham NHS Foundation Trust and the University of Birmingham, Birmingham, United Kingdom, Birmingham, United Kingdom; [22]Department of Internal Medicine, Institute of Gastroenterology, Yonsei University College of Medicine, Seoul, Republic of Korea, Seoul, Korea, Rep. of South; [23]Department of Engineering, University of Palermo, Palermo, 90128, Sicily, Italy, Palermo, Italy; [24]Département Electronique-Electrotechnique-Automatique (EEA), University of Picardie Jules Verne, Amiens, France, Amiens, France*
Email: graziapennisi901@gmail.com

Background and aims: Accurate staging of liver fibrosis is crucial for risk stratification in patients with metabolic dysfunction-associated steatotic liver disease (MASLD). Liver biopsy, the current reference standard, is invasive and subject to sampling variability, while non-invasive tests (NITs) such as vibration-controlled transient elastography (VCTE) are widely used. We aimed to develop and validate AI-based models capable of distinguishing fibrosis stages.
Method: We developed and validated machine learning models to predict fibrosis stages in more than 3,600 biopsy-confirmed MASLD patients using 22 clinical features, liver stiffness measurement (LSM), and controlled attenuation parameter (CAP). Models included Feature Tokenizer Transformer (FTT), TabNet variants with distance-aware losses, ordinal MLP with CORAL framework, and gradient boosting machines. Performance was evaluated using Rubin's Rules across 5 MICE imputed datasets.
Results: The FTT and TabNet achieved the highest performance in binary tasks: AUROC = 0.860 and 0.855 (F≥3 vs F0-F2) and AUROC = 0.800 and 0.788 (F≥2 vs F0-F1), significantly outperforming FIB-4. For F≥3, FTT had significantly higher AUROC than LSM (p = 0.014) but

only marginally higher than AGILE3+, and, together with TabNet, the highest accuracy and the lowest grey zone (8.2% and 8.4%, respectively). For multiclass staging, ordinal models performed best with MLP-CORAL achieving QWK = 0.616.
Conclusion: Deep learning models with ordinal-aware architectures can accurately predict liver fibrosis stages using routinely available clinical data, offering a scalable alternative to biopsy without requiring specialized biomarkers.

WED-175
The FIB-4 score has a stronger correlation with cardiovascular risk than other adiposity markers in patients living with obesity
Carolina M. Perdomo Zelaya[1], Estefanía Chumbiauca[1], Adrián Gil Korilis[1], Patricia Yarnoz[1], Javiera Concha[1], Lucía ÓConnor[1], Camilo Silva[1], Nerea Varo[1], Gema Frühbeck Martinez[1], Javier Escalada[1]. [1]*Clínica Universidad de Navarra, Pamplona, Spain*
Email: cperdomo@unav.es

Background and aims: Adiposopathy is characterized by metabolic dysfunction of adipose tissue and with progressive orthotopic and ectopic fat accumulation in various organs, including the liver. Adiposopathy is a key event in the pathophysiology of metabolic dysfunction-associated steatotic liver disease (MASLD); its progression is associated with a higher cardiometabolic risk. However, the relationship between different adiposity parameters and the estimation of cardiovascular risk has not been evaluated. This study compares different adiposity parameters for predicting cardiovascular risk.
Method: Evaluation of a cohort of 129 patients living with obesity between 40 and 69 years of age without anti-obesity pharmacological or surgical treatment who attended the outpatient clinic of the Endocrinology Department of the Clínica Universidad de Navarra. Adiposity parameters were measured using anthropometry (body mass index [BMI], neck circumference, abdominal circumference, hip circumference, waist circumference, waist-to-height ratio [WHtR]), Clínica Universidad de Navarra - Body Adiposity Estimator (CUN-BAE), bioimpedance (visceral fat and body fat percentage), nutritional ultrasound (subcutaneous and preperitoneal tissue), and non-invasive markers of MASLD status (Controlled Attenuation Parameter [CAP], liver stiffness [kPa], FIB-4 Score, Hepamet Fibrosis Score [HFS], and NAFLD Fibrosis Score [NFS]). The FIB-4 cutoff points were 1.3 (< 65 years) and 2.0 (≥ 65 years). Cardiovascular risk was estimated using SCORE2/SCORE2-Diabetes risk estimator.
Results: In patients living with obesity, SCORE2 showed a positive correlation with FIB-4 Score ($r = 0.55$; $p < 0.001$). No correlation was found between cardiovascular risk and abdominal perimeter ($r = 0.14$; $p = 0.11$) nor with the WHtR ($r = -0.01$; $p = 0.91$). FIB4 Score accounts for 23% of the variability in SCORE2, whereas abdominal perimeter and WHtR account for 1.6% and 1.4%, respectively. After adjusting for sex, a higher cardiovascular risk was found based on the FIB-4 Score quartiles (Q3: OR 10.64, 95% CI 1.21–93.35 [$p = 0.033$]; Q4: OR 58.85, 95% CI 6.84–506.51 [$p < 0.0001$]). Patients with an abnormal FIB-4 Score had a higher prevalence of hypertension, dyslipidemia, and hyperuricemia, as well as a greater proportion of men ($p < 0.05$).
Conclusion: Adiposopathy parameters, particularly liver status assessed through the FIB-4 Score, may complement the estimation of cardiovascular risk in patients living with obesity.

WED-179
Head-to-head comparison between FibroTest and ELF, for the fibrosis diagnostic in outpatients with type-2 diabetes, using Bayesian latent class models
Antoine Pilon[1], Michel Vaubourdolle[1], Valentina Peta[2], Dominique Valla[1], Laurent Castera[1], Pierre Bedossa[3], Vlad Ratziu[4], Olivier Deckmyn[2], Thierry Poynard[2,4]. [1]*Assistance Publique Hopitaux de Paris, Biochemistry Laboratory INSERM, Paris, France;* [2]*BioPredictive, Paris, France;* [3]*Liverpat, Paris, France;* [4]*Sorbonne University, Pitié Salpêtrière, ICAN, Paris, France*
Email: thierry@poynard.com

Background and aims: In patients with metabolic dysfunction-associated steatotic liver disease, (MASLD) two serum fibrosis panels with patented algorithms are among the most cited: the Nash-FibroTest combination (FT), known in the USA as Nash-FibroSure-Plus which integrates three tests to simultaneously assess fibrosis, steatosis, and inflammatory activity and the Enhanced Liver Fibrosis (ELF) score, which evaluates fibrosis only. Surprisingly no head-to-head one-step comparison has been published in type-2 diabetes. Our aim was to evaluate the comparative performance of FT and ELF for diagnosing significant fibrosis stages (F2-F3-F4), in 398 type-2 diabetes outpatients of the prospective ongoing QUID-NASH study, 57 years old median and 40% females.
Method: The standard reference, liver biopsy is misclassified in 25% of cases, inducing bias in sensitivity, specificity, and area under the receiver operating curve (AUC) in both magnitude and direction, distorting head-to-head differences. Therefore, to offer a solution relaxing the perfect-gold-standard assumption, we used Bayesian latent class models (BLCMs) which do not presuppose superiority of any test including the histological reference.
Results: BLCMs revealed that posterior mean AUC was 0.94 for FT and 0.76 for ELF, with a mean difference (FT-ELF) of 0.18, (95% credible interval, 0.12–0.25). Sensitivity analyses demonstrated similar results after stratification by age, sex or body mass index. The ELF components were tightly intercorrelated, with hyaluronic acid showing the strongest association with ELF ($r = 0.94$) and PIIINP also highly correlated ($r = 0.73$) and FT and ELF correlated only moderately ($r = 0.42$). In contrast with FT: markers relate to the score in mixed directions and magnitudes: alpha2-macroglobulin ($r = 0.80$), haptoglobin ($r = -0.35$), apolipoproteinA1 ($r = -0.19$), gamma-glutamyltranspeptidase ($r = 0.34$), and total bilirubin ($r = 0.44$). This less redundant signal contributes to the higher BLCM-estimated discrimination observed for FT.
Conclusion: These results highlight the importance of accounting for reference standard imperfection and support the use of head-to-head comparisons combined with latent class modeling.

WED-180
Refined indicators substantially reduce the population required for screening: longitudinal validation from the European LiverScreen consortium
Jesse Pustjens[1], Laurens A. van Kleef[1], Katrine Tholstrup Bech[2], Guillem Pera[3], Pere Ginès[4], Helle Schnefeld[2], Robert J. de Knegt[1], Peter Andersen[2], Johanne Kragh Hansen[2], Llorenç Caballeria[3], Carla Chacon[3], Pere Torán[3], Anna Soria[4], Marta Cervera Carbonell[5], Íngrid Arteaga[3], Anita Arslanow[4], Sarwa Darwish Murad[1], Harry L.A. Janssen[1], Isabel Graupera[4], Aleksander Krag[2], Maja Thiele[2], Willem Pieter Brouwer[1]. [1]*Department of Gastroenterology and Hepatology, Erasmus MC, University Medical Centre, Rotterdam, the Netherlands, Rotterdam, Netherlands;* [2]*Centre for Liver Research, Department of Gastroenterology and Hepatology, Odense University Hospital, Odense, Denmark, Institute of Clinical Research, University of Southern Denmark, Odense, Denmark, Odense, Denmark;* [3]*Unitat de Suport a la Recerca Metropolitana Nord, Institut Universitari d'Investigació en Atenció Primària Jordi Gol, Mataró, Barcelona, Spain, Barcelona, Spain;* [4]*Liver Unit, Hospital Clínic, University of Barcelona, Barcelona, Catalonia, Spain, Institut D'Investigacions Biomèdiques August Pi I Sunyer (IDIBAPS), Barcelona, Spain, Barcelona, Spain;* [5]*Institut D'Investigacions Biomèdiques August Pi I Sunyer (IDIBAPS), Barcelona, Spain, Centro de Investigación en Red de Enfermedades Hepáticas y Digestivas (CIBEREHD), Barcelona, Spain, Barcelona, Spain*
Email: j.pustjens@erasmusmc.nl

Background and aims: Current EASL–EASD–EASO guidelines recommend fibrosis screening in a large proportion of the general population. Recently proposed refined screening indicators - based

on diabetes, obesity, transaminases, and cardiometabolic risk factors - substantially reduce the target population for screening, but their longitudinal performance remain unknown.
Method: This prospective, longitudinal study, conducted at three European centres (Barcelona, Rotterdam, Odense), is embedded within the LiverScreen consortium. Baseline and follow-up liver stiffness measurements (LSM) were assessed over an approximate four-year interval, excluding individuals with BMI<18.5 kg/m^2, excessive alcohol intake and insufficient data. Elevated LSM was defined as ≥8 kPa, persistent elevated LSM as ≥8 kPa at baseline and follow-up, and clinically significant LSM increase as an increase to ≥8 kPa from a baseline <8 kPa, with ≥30% rise.
Results: Among 3708 adults (mean age 61 years, 54% male) LSM ≥8 kPa prevalence was 4.6% (n = 169). The refined indicators reduced the proportion of individuals eligible for screening to 9.9%; which was 51% under prevailing guidelines, with the prevalence of elevated LSM in the eligible population increasing to 17% from 6.9%, while maintaining a high NPV of 97%. During a median follow-up of 4.4 years [IQR 4.2–8.7], 8.7% of the refined screening-eligible population had persistently elevated LSM, compared to 2.8% under prevailing guidelines, with comparable high NPVs (99.3% vs. 99.7%). Among individuals meeting refined indicators but who screened <8 kPa, 8.3% experienced a clinically significant LSM increase to LSM ≥8 kPa, and 4.3% to LSM ≥10 kPa, rates that were 2.4- and 2.5-fold higher than observed under prevailing guidelines (3.5% and 1.7%, respectively). Among individuals not selected by the refined indicators, only 1.7% experienced a clinically significant LSM increase (4.9-fold lower than the 8.3% in the refined screening eligible- group).
Conclusion: The EASL–EASD–EASO screening criteria identify 51% of European adults for screening, of which only 2.8% exhibit persistent LSM elevation. Refined screening indicators reduce the screening-eligible population to 9.9%, of which 8.7% had persistent LSM elevation. Clinically significant LSM progression occurred five-fold more frequently in individuals selected by the refined criteria than in those excluded (8.3% vs. 1.7%). These findings support a more targeted approach for liver disease screening.

WED-181

AGILE 3+ enhances non-invasive detection of advanced fibrosis in MASLD: comparison with FIB-4 and liver stiffness measurement

Ismail Qarch[1], Mohamed Borahma[1], Fatima Zahra Chabib[1], Nawal Lagdali[1], Sabbah Selma[1], Fatima Zahra Ajana[1], Maryeme Kadiri[1]. [1]*Gastroenterology C Department, Ibn Sina University Hospital, Mohamed V University, Rabat, Morocco*
Email: ismail.qarch@gmail.com

Background and aims: MASLD is a major cause of chronic liver disease, with advanced fibrosis (≥F3) being a key prognostic factor. FIB-4 is commonly used for initial screening but has limited sensitivity. LSM reflects hepatic rigidity without standardized thresholds, while AGILE 3+ integrates elastography with clinical and biological variables for improved risk stratification.This study compared the diagnostic performance of FIB-4, LSM, and AGILE 3+ in a real-world MASLD cohort.
Method: We conducted a retrospective, single-center study over 7 years. Seventy MASLD patients with complete data were included. Advanced fibrosis was defined as ≥ F 3. Performance was assessed using sensitivity, specificity, NPV, PPV, and AUC. Standard cut-offs: FIB-4 (< 1.30; > 2.67) and AGILE 3+ (< 0.451; ≥ 0.679).
Results: The population (mean age 52.4 ± 10.9 years) was predominantly female (84.3%). Metabolic syndrome and type 2 diabetes were present in 68.6% and 28.6% of patients, respectively. Advanced fibrosis (F3–F4) was identified in 7 patients (10.0%). Liver stiffness measurement (LSM) alone showed excellent discrimination for advanced fibrosis (AUC = 1.00, 95% CI: 0.85–1.00), as all patients with F≥3 (7/7, 100%) exhibited higher liver stiffness values than those without advanced fibrosis, reflecting a marked separation of stiffness values in this cohort with a limited number of advanced fibrosis cases; however, LSM provided a continuous measurement without predefined decision thresholds. The AGILE 3+ score demonstrated high diagnostic accuracy (AUC = 0.914) and enabled standardized clinical stratification. Using validated cut-offs, AGILE 3+ classified most patients with advanced fibrosis into the rule-in category (6/7), with one false-negative in the rule-out zone. At the rule-in threshold (≥0.679), AGILE 3+ achieved a sensitivity of 85.7% and specificity of 87.3%, with an excellent NPV of 98.2%, and at the rule-out threshold (<0.451) reliably excluded advanced fibrosis, outperforming FIB-4 <1.30 (NPV 97.5% vs 92.9%). In contrast, FIB-4 >2.67 showed perfect specificity (100%) but low sensitivity (28.6%), supporting its role as a first-line triage tool rather than a definitive risk stratification method.
Conclusion: In this real-world MASLD cohort, AGILE 3+ and LSM outperformed FIB-4 for detecting advanced fibrosis. While LSM showed excellent discrimination in this limited sample, AGILE 3+ provided clinically actionable rule-in and rule-out stratification, supporting a stepwise non-invasive assessment strategy.

WED-182

Genetic algorithm-guided ensemble learning for the development, validation, and prognostic evaluation of a risk score for advanced liver fibrosis in populations with obesity: a multicohort study

Bicheng Ye[1], Shanghao Liu[2], Haisong Xin[3], Hui Shi[4], Jianxiang Song[5], Zhu-Qin Yu[6], Lan Ma[7], Yang Bu[8], Puqiang Liu[9], JianSong Ji[10], Yijun Tang[11], Wenjuan Wang[12], Huizhen Fan[13], Xiao Liang[14], Ruyu Liu[15], Junhong Yang[16], Qing He[17], Hui Yang[18], Kunyu Ke[19], Qiang Yan[20], Xiongwei He[21], Yanhong Liu[22], Wen Kang[23], Tiezheng Zhao[24], Rong Hu[25], Zhenyu Dai[26], Gao Hongyu[27], Liping Wang[7], Jing Wang[28], Jianping Zhang[9], Lili Ye[29], Zhong-ji Meng[30], Guo Zhang[12], Jianwen Sheng[31], Yong-Fen Zhu[32], Guihua Wu[33], Jingping Yin[34], Dongdong Zhao[35], Zhuanmin Wu[36], Xuejiao Liao[17], Hao Zhang[18], Zhenwei Chen[37], Tiandan Bian[38], Jiangwen Liu[21], Lidong Xu[22], Jing Huang[39], Jie Zhang[40], Gao-Jun Teng[41], Xiaolong Qi[1]. [1]*Liver Disease Center of Integrated Traditional Chinese and Western Medicine, Department of Radiology, Zhongda Hospital, Medical School, Southeast University, Nurturing Center of Jiangsu Province for State Laboratory of AI Imaging & Interventional Radiology (Southeast University), Nanjing, China, Basic Medicine Research and Innovation Center of Ministry of Education, Zhongda Hospital, Southeast University; State Key Laboratory of Digital Medical Engineering, Nanjing, China, Nanjing, China;* [2]*Liver Disease Center of Integrated Traditional Chinese and Western Medicine, Department of Radiology, Zhongda Hospital, Medical School, Southeast University, Nurturing Center of Jiangsu Province for State Laboratory of AI Imaging & Interventional Radiology (Southeast University), Nanjing, China, Nanjing, China;* [3]*Department of Orthopedics, People's Hospital of Huanghua, Huanghua, Cangzhou, Hebei Province, China, Huanghua, China;* [4]*Department of Neurosurgery, The First Affiliated Hospital of Kangda College of Nanjing Medical University, The Affiliated Lianyungang Hospital of Xuzhou Medical University; Lianyungang Clinical College of Nanjing Medical University, Lianyungang, China, Lianyungang, China;* [5]*Department of Cardiothoracic Surgery, Affiliated Yancheng Hospital, School of Medicine, Southeast University, Yancheng Third People's Hospital, Yancheng, China, Yancheng, China;* [6]*Department of Internal Medicine,Qingdao Public Health Clinical Center, Qingdao, China, Qingdao, China;* [7]*Department of Infectious Diseases, Bozhou People's Hospital, Bozhou,China, Bozhou, China;* [8]*Department of hepatobiliary surgery, General Hospital of Ningxia Medical University, Yinchuan, 750004 Ningxia, China, Yichun, China;* [9]*Pu County People's Hospital, Linfen City, Shanxi Province, China, Linfen, China;* [10]*Zhejiang Key Laboratory of Imaging and Interventional Medicine, Zhejiang Engineering Research Center of Interventional Medicine Engineering and Biotechnology, Department of Radiology, Lishui Central Hospital, The Fifth Affiliated Hospital of Wenzhou Medical University, Lishui 323000, China, Lishui, China;* [11]*Department of Respiratory and Critical Care Medicine, Taihe Hospital, Hubei University of Medicine, Shiyan 442000, China, Shiyan, China;* [12]*Department of Gastroenterology, Guangxi*

Hospital Division of The First Affiliated Hospital, Sun Yat-sen University, Nanning, China, Nanning, China; [13]Department of Gastroenterology, Yichun People's Hospital, Yichun, Jiangxi Province, China, Yichun, China; [14]Department of General Surgery, Sir Run-Run Shaw Hospital, Zhejiang University School of Medicine, 310016, Hangzhou, China, Hangzhou, China; [15]Department of Hepatology Division 3, Xuzhou Infectious Diseases Hospital, Xuzhou, China, Xuzhou, China; [16]Department of Gastroenterology, Baiyin Central Hospital, Baiyin, Gansu, China, Baiyin, China; [17]Department of Hepatology, Shenzhen third People's Hospital, Shenzhen, China, Shenzhen, China; [18]Department of Gastroenterology, The Second Affiliated Hospital of Guangzhou Medical University, Guangzhou, China, Guangzhou, China; [19]Department of Hepatology, Mengchao Hepatobiliary Hospital of Fujian Medical University, Fuzhou, China, Fuzhou, China; [20]Department of Hepatobiliary and Pancreatic Surgery, Fifth School of Clinical Medicine of Zhejiang Chinese Medical University, Huzhou Central Hospital, Huzhou, China, Huzhou, China; [21]Medical Department of Shihezi City People's Hospital, Shihezi, China, Shihezi, China; [22]Department of Gastroenterology, Zhengzhou Central Hospital Affiliated to Zhengzhou University, Zhengzhou, China, Zhengzhou, China; [23]Department of Infectious Diseases, Tangdu Hospital, Fourth Military Medical University, Xi'an, China, Xi'an, China; [24]General Surgery, People's Hospital of Huanghua, Huanghua, Cangzhou, Hebei Province, China, Huanghua, China; [25]Department of Respiratory and Critical Care Medicine, The First Affiliated Hospital of Kangda College of Nanjing Medical University; The Affiliated Lianyungang Hospital of Xuzhou Medical University; Lianyungang Clinical College of Nanjing Medical University, Lianyungang, China, Lianyungang, China; [26]Department of Radiology, Affiliated Yancheng Hospital, School of Medicine, Southeast University, Yancheng Third People's Hospital, Yancheng, Yancheng, China, Yancheng, China; [27]Department of Internal Medicine (Cadre Healthcare Section), Qingdao Center for Public Health Clinical Medicine, Qingdao, China, Qingdao, China; [28]Scientific research department, General Hospital of Ningxia Medical University, Yinchuan, 750004 Ningxia, China, Yinchuan, China; [29]Department of Oncology Center, The Fifth Affiliated Hospital of Wenzhou Medical University, Lishui 323000, China, Lishui, China; [30]Department of Infectious Diseases, Hubei Provincial Clinical Research Center for Precise Diagnosis and Treatment of Liver Cancer, Taihe Hospital, Hubei University of Medicine, Shiyan 442000, China, Shiyan, China; [31]The Department of Gastroenterology, Yichun People's Hospital, Yichun, Jiangxi Province, China, Yichun, China; [32]Zhejiang Key Laboratory of Multi-omics Precision Diagnosis and Treatment of Liver Diseases, Department of Liver and Infectious Diseases, Sir Run Run Shaw Hospital, Zhejiang University School of Medicine, Hangzhou, China, Hangzhou, China; [33]Department of Endocrinology, Beijing Ditan Hospital, Xuzhou Hospital, Capital Medical University, Xuzhou, China; Xuzhou Infectious Diseases Hospital, Xuzhou, China, Xuzhou, China; [34]Gastroenterology Department Baiyin Central Hospital Baiyin City, Gansu Province, China, Baiyin, China; [35]Department of Gastroenterology, Baiyin Central Hospital, Gansu Province, China, Baiyin, China; [36]Department of Gastroenterology, Baiyin Central Hospital, Pingchuan District, Baiyin City, China, Baiyin, China; [37]Department of Information Technology, Mengchao Hepatobiliary Hospital of Fujian Medical University, Fuzhou, China, Fuzhou, China; [38]Department of Infectious Diseases, Huzhou Central Hospital, Affiliated Central Hospital, Huzhou University, Huzhou, Zhejiang, China, Huhzou, China; [39]Department of Health Management, Tangdu Hospital, Fourth Military Medical University, Xi'an, China, Xi'an, China; [40]4Department of Endocrinology and Metabolism, The Affiliated Huai'an Hospital of Xuzhou Medical University and Huai'an Second People's Hospital, Huai'an, China, Huai'an, China; [41]Basic Medicine Research and Innovation Center of Ministry of Education, Zhongda Hospital, Southeast University, State Key Laboratory of Digital Medical Engineering, Nanjing, China, Nanjing, China
Email: qixiaolong@vip.163.com

Background and aims: Obese status is closely associated with liver fibrosis and adverse hepatic outcomes. This study aimed to develop a reliable tool based on routine clinical indicators to assess liver fibrosis risk in populations with obesity.
Method: We developed a novel scoring system, termed the ObesityLiver score, which was validated using multiple independent, community-based cohorts of individuals with obesity from China, the United States, and the United Kingdom. We implemented a robust dual-training cohort strategy for model construction. In the training cohort 1 (n = 1,872), four machine learning algorithms were utilized to identify key features associated with advanced liver fibrosis (liver stiffness measurement ≥10), and 40 heterogeneous base learners were developed across 10 algorithms. In the training cohort 2 (n = 1,872), a genetic algorithm was employed to perform an automated heuristic search for the optimal ensemble configuration, culminating in the derivation of the ObesityLiver score. The model's predictive performance was validated across the training (cohorts 1 and 2) and testing cohorts (n = 3,214), while its long-term prognostic value was further ascertained in the prognosis cohort (n = 86,663).
Results: The ObesityLiver score demonstrated robust diagnostic accuracy for advanced liver fibrosis, with AUROCs of 0.931 (95% CI: 0.915–0.947) in the training cohort 1, 0.845 (95% CI: 0.810–0.880) in the training cohort 2, and 0.847 (95% CI: 0.823–0.871) in the test cohort, consistently outperforming established non-invasive tests including LiverRisk, CORE, FIB-4, APRI, and NFS. Utilizing optimized rule-out (0.035) and rule-in (0.097) thresholds, we stratified participants into low- medium- and high-risk groups. This approach yielded high diagnostic precision, with sensitivities ranging from 87.3% to 99.3% and specificities from 90.0% to 92.1% across the training and test cohorts. Furthermore, in the prognostic cohort, the medium- and high-risk groups exhibited a significantly higher cumulative incidence of liver-related events compared to the low-risk group.
Conclusion: The ObesityLiver score provides a robust and reliable tool for detecting advanced liver fibrosis and predicting liver-related events within community-based cohorts of individuals with obesity.

WED-183

High burden of hepatic steatosis, fibrosis, and cardiometabolic risk in HIV-monoinfected adults on antiretroviral therapy: STEAT-HIV results

Giulia Quartini[1], Cinzia Di Giuli[1], Lavinia Maria Saraca[1], Luca Capogrossi[1], Elisabetta Svizzeretto[1], Giovanni Genga[1], Giulia Proietti[1], Marta Cordoni[1], Federica Gentili[2], Pierluigi Fiore[2], Giuseppe Vittorio Luigi De Socio[3], Claudio Ucciferri[4]. *[1]Infectious Disease Clinic, S. Maria Hospital Terni, Terni, Italy; [2]Hepatology, gastroenterology and digestive endoscopy structure, S. Maria Hospital Terni, Terni, Italy; [3]Infectious Disease Clinic, Department of Medicine and Surgery, University of Perugia, Perugia., Perugia, Italy; [4]Infectious Disease Clinic, Department of Medicine and Surgery, University of Perugia, Perugia, Infectious Disease Clinic, S. Maria Hospital Terni, Perugia, Italy*
Email: giulia.qu@outlook.it

Background and aims: Hepatic steatosis and fibrosis are increasingly recognized as major comorbidities in people living with HIV (PLWH), even without viral coinfections or metabolic syndrome. Chronic immune activation, metabolic dysfunction, and long-term antiretroviral therapy (ART) ART exposure contribute to progressive liver injury. The STEAT-HIV study aimed to assess the prevalence and determinants of hepatic steatosis and fibrosis using non-invasive tools and to explore their associations with metabolic and therapeutic variables.
Method: A retrospective and prospective cohort study (2021–2022) was conducted at the Infectious Diseases Clinic in Terni (Italy). Liver stiffness (LSM) and controlled attenuation parameter (CAP) were measured using FibroScan®. Biochemical (transaminases, lipids), anthropometric, and cardiovascular (ASCVD, SCORE) data were analyzed. Correlation and multivariate regression analyses were performed ($p < 0.05$).

Results: A total of 258 patients were analyzed, 115 PLWH on stable ART after excluding HBV/HCV coinfections, diabetes, alcohol abuse, and recent diagnoses (<6 months) were enrolled. Median age was 52 years (IQR 46–59), 73% were male, with median BMI 24.3 kg/m^2 (IQR 22.8–26.7) and HIV duration 14 years (IQR 10–19). ART regimens included 38% protease inhibitor (PI), 42% integrase inhibitor (INSTI), 15% Doravirine, and 5% two-drug regimens (2DR). Hepatic steatosis (CAP >248 dB/m) was observed in 42.6% (49/115), and significant fibrosis (LSM >7 kPa) in 18.9% (22/115). CAP correlated with total cholesterol ($r = 0.31$; $p = 0.002$), triglycerides ($r = 0.34$; $p < 0.001$), and ASCVD score ($p = 0.02$). Patients receiving PI-based regimens had higher CAP (285 dB/m, IQR 260–310) and LSM (7.4 kPa, IQR 6.1–8.8) compared to those on Doravirine or 2DR (CAP 245 dB/m, IQR 230–260; $p < 0.01$). FibroScan® parameters showed stronger correlations with metabolic indices than serum-based scores (FIB-4, APRI; $p < 0.001$).
Conclusion: Hepatic steatosis and fibrosis are highly prevalent in HIV-monoinfected patients,closely linked to metabolic dysregulation and ART exposure,particularly PI-based regimens. FibroScan®with CAP effectively identifies early hepatic injury and outperforms serum indices in this population. Integrating non-invasive liver assessment into PLWH care could enhance early detection,guide selection of metabolically favorable ART regimens and prevent long-term hepatic and cardiometabolic complications.

WED-184-YI
Referral strategies in intermediate-risk FIB-4 patients: can longitudinal monitoring reduce FibroScan® use without missing advanced fibrosis?
Ilaria Reiso[1], Kamela Gjini[1], Gian Paolo Caviglia[1], Angelo Armandi[1], Marta Guariglia[1], Eleonora Dileo[1], Francesca Saba[1], Elisabetta Bugianesi[1]. [1]*Division of Gastroenterology and Hepatology, Department of Medical Sciences, University of Turin, Turin, Italy, Turin, Italy*
Email: ilaria.reiso@unito.it

Background and aims: In patients with metabolic dysfunction-associated steatotic liver disease (MASLD), the Fibrosis-4 (FIB-4) score is the recommended first-line screening test for initial risk stratification of advanced fibrosis. Values in the intermediate-risk range (1.3–2.67) are associated with a high proportion of false positives, resulting in a substantial downstream second-line testing burden. Current guidelines suggests two possible approaches in this group: proceeding directly to liver stiffness measurement (LSM) or repeating FIB-4 in one year after a lifestyle change intervention. Since up to 40% of MASLD patients fall into this category, identifying strategies that optimise referral is needed.To compare two different referral strategies in patients with intermediate FIB-4 values and evaluate their ability to predict progression to advanced fibrosis over approximately 5–10 years.
Method: We retrospectively analysed 92 patients with baseline FIB-4 between 1.3 and 2.67. Advanced fibrosis at follow-up was defined by liver biopsy showing F3-F4, when available, or by LSM ≥12 kPa. Two referral strategies were compared: (1) immediate referral if baseline LSM ≥8 kPa; (2) referral if FIB-4 remained ≥1.3 at 1–2 years. Diagnostic performance was assessed through sensitivity (Se), specificity (Sp), positive predictive value (PPV), negative predictive value (NPV), and confusion matrices.
Results: Advanced fibrosis over a median follow up of 6 (2.7–13.2) years was detected in 25 patients (27%). When applied at baseline, LSM ≥8 kPa had the best diagnostic performance (Se 0.95; Sp 0.7, PPV 0.45, NPV 0.97) in predicting advanced fibrosis at last follow-up. In 19 (21%) patients, FIB-4 values declined below <1.3 at 1–2 years, despite no structured lifestyle change intervention, and none of these patients developed advanced fibrosis during follow up. Therefore, repeating FIB-4 at 1–2 years and performing LSM only if FIB-4 remains ≥1.3, would have avoided 21% of FibroScan® examinations, without any missed cases of advanced fibrosis (Se 1; Sp 0.22, PPV 0.25, NPV 1).
Conclusion: In FIB-4 intermediate-risk patients, repeating FIB-4 at 1–2 years prior to second-line testing can reduce unnecessary LSM by 21%, without missing advanced fibrosis cases at follow-up.

WED-185
Comparison of metabolic dysfunction-associated steatotic liver disease characteristics in patients with type 1 and 2 diabetes mellitus
Donovan Richelle[1], Leen Heyens[1,2,3,4], Struyve Mathieu[4], Sven Francque[5,6], Geert Robaeys[2], Ger Koek[1,7]. [1]*Maastricht University, School of Nutrition and Translational Research in Metabolism, NUTRIM, Maastricht, Netherlands;* [2]*Hasselt University, Faculty of Health and Life Sciences/LCRC, Diepenbeek, Belgium;* [3]*Ziekenhuis Oost-Limburg, dept. Future Health, Genk, Belgium;* [4]*Ziekenhuis Oost-Limburg, dept. Gastroenterology, Genk, Belgium;* [5]*Antwerp University Hospital, Department of Gastroenterology and Hepatology, Antwerp, Belgium;* [6]*University of Antwerp, InflaMed Centre of Excellence, Laboratory of Experimental Medicine and Paediatrics, Antwerp, Belgium;* [7]*Maastricht University Medical Center+, Department of Gastroenterology and Hepatology, Maastricht, Netherlands*
Email: dh.richelle@student.maastrichtuniversity.nl

Background and aims: Metabolic dysfunction-associated steatotic liver disease (MASLD) is related to metabolic syndrome (MetS) and type 2 diabetes (T2DM). An association between type 1 diabetes (T1DM) and MASLD is not extensively investigated. Therefore, this study investigated the prevalence and risk factors for MASLD in T1DM compared to T2DM.
Method: In this Belgian prospective cross-sectional study, MASLD was evaluated via transient elastography (VCTE) for fibrosis and controlled attenuation parameters (CAP) for steatosis (FibroScan®, Echosens). The cut-off values >248 dB/m for steatosis and 8 kPa for fibrosis were used. MASLD was defined as steatosis with at least one cardiometabolic risk factor, not including the glucose criterium for the T1DM group. Excessive use of alcohol was excluded. Insulin sensitivity was calculated via estimated Glucose Disposal Rate (eGDR) and SEARCH estimated Insulin Sensitivity (eIS). Associations were explored separately in T1DM and T2DM through logistic regression and compared between groups via interaction analysis.
Results: 66 T1DM (mean age 57 ± 11.5 years, 61% male, body mass index (BMI) 26.6 ± 4.06 kg/m^2) and 290 T2DM patients (median age 61 [55.0–68.0] years, 57% male, BMI 31.7 [28.8–35.7] kg/m^2) were included. MASLD prevalence was 39% in T1DM and 83% in T2DM, with statistically significantly higher VCTE and CAP in T2DM ($p < 0.001$). eIS and eGDR were statistic significantly higher in T1DM compared to T2DM ($p < 0.001$). Waist circumference (OR 1.20 (95% CI 1.09–1.32), 1.18 (95% CI 1.08–1.29)), BMI (OR 1.59 (95% CI 1.23–2.06), 1.52 (95% CI 1.24–1.86)), and MetS (OR 3.11 (95% CI 0.73–12.23), 33.1 (95% CI 5.86–186.7)) were positively associated with MASLD in T1DM and T2DM, respectively. Better insulin sensitivity through eIS (OR 0.29 (95% CI 0.15–0.59), 0.48 (95% CI 0.29–0.79)) and eGDR (OR 0.68 (95% CI 0.52–0.90), 0.61 (95% CI 0.43–0.87)) was negatively associated with MASLD in T1DM and T2DM, respectively. Factors were adjusted for age, sex and diabetes duration.
Conclusion: MASLD is less prevalent and advanced in patients with T1DM compared to patients with T2DM. Classic metabolic risk factors are associated with MASLD in both T1DM with insulin resistance and T2DM. Further studies are needed to validate these findings and analyse the onset of double diabetes.

WED-186-YI

Combined serological testing to improve efficiency and sustainability in MASLD care

Jesús Rivera Esteban[1], Paula Iruzubieta[2], David Marti-Aguado[3], Marta Hernández Conde[1], Alba Jiménez-Masip[4], Elba Llop Herrera[1], Christie Perelló[1], María Teresa Arias Loste[2], Juan M. Pericàs[4], José Luis Calleja Panero[1], Javier Crespo[5]. [1]*Hospital Universitario Puerta De Hierro Majadahonda, Majadahonda, Spain;* [2]*Hospital Universitario Marqués de Valdecilla, Santander, Spain;* [3]*Hospital Clinico de Valencia, Valencia, Spain;* [4]*Hospital Universitario Vall d'Hebron, Barcelona, Spain;* [5]*Instituto de Investigación Valdecilla (IDIVAL), Santander, Spain*
Email: jesusriveraest@gmail.com

Background and aims: Sequential algorithms for diagnosing MASLD generate excessive referrals of patients without advanced disease, overloading specialized care. We evaluated whether combining first-line serological tests improves discrimination compared with single use and its impact on diagnostic pathways.
Method: FIB-4, NFS, and FLI were assessed individually and in combination in a Spanish population cohort (PREV-ETHON). Significant fibrosis was defined as liver stiffness ≥8.0 kPa by TE. Standard cut-offs for significant fibrosis were used (FIB-4 ≥ 1.30, NFS ≥−1.455, FLI ≥ 60). Combinations used AND (both positive) or OR (either positive) strategies. AUC, sensitivity, specificity, and predictive values were calculated.
Results: Among 6,190 participants, MASLD prevalence was 33.5% and significant fibrosis 3.9%. Individually, FIB-4, NFS, and FLI showed similar performance (AUC 0.66–0.71) for significant fibrosis detection, with moderate sensitivity (55–64%), specificity (<70%) and high NPV (97%),resulting in positive test rates—and thus referral rates—of approximately 32–33%. Combining FIB-4+FLI or the three tests (all positive) achieved 90% specificity, maintained 97% NPV, and reduced positives to 11.2% (FIB4+FLI) or 9.8% (FIB4+FLI+NFS), corresponding to a 60% reduction in hepatology referrals and second-line testing compared with single-test use. On the other hand, the OR strategy increased sensitivity (67–81%) but markedly reduced specificity (44–58%), leading to high referral rates (42–57%). Despite this, PPV remained low (5–6%), largely reflecting the low prevalence of significant fibrosis in the general population.
Conclusion: Combining first-line serological tests substantially reduces referrals while maintaining strong rule-out performance for significant fibrosis in low-prevalence populations, such as primary care. An automated, combined test could improve the efficiency and sustainability of MASLD diagnostic pathways.

WED-187-YI

Routine markers for monitoring liver stiffness in patients with MASLD and low-risk fibrosis

Merle Roeren[1], Jerome Boursier[2], Elisabetta Bugianesi[3], Chan Wah Kheong[4], Jian-Gao Fan[5], George Boon Bee Goh[6], Seung Up Kim[7], Victor de Lédinghen[8], Masato Yoneda[9], Philip N. Newsome[10], Salvatore Petta[11], Manuel Romero-Gómez[12], Arun J Sanyal[13], Ming-Hua Zheng[14], José Luis Calleja Panero[15], Emmanuel Tsochatzis[16], Terry Cheuk-Fung Yip[17], Vincent Wai-Sun Wong[17], Hannes Hagström[1,18], Ying Shang[1]. [1]*Karolinska Institutet, Stockholm, Sweden;* [2]*Angers University Hospital, Angers, France;* [3]*University of Turin, Turin, Italy;* [4]*University of Malaya, Malaya, Malaysia;* [5]*Shanghai Jiaotong University School of Medicine, Shanghai, China;* [6]*Singapore General Hospital, Singapore, Singapore;* [7]*Yonsei University College of Medicine, Seoul, Korea, Rep. of South;* [8]*University Hospital of Bordeaux, Pessac, France;* [9]*Yokohama City University Graduate School of Medicine, Yokohama, Japan;* [10]*Biomedical Research Centre at University Hospitals Birmingham NHS Foundation Trust and the University of Birmingham, Birmingham, United Kingdom;* [11]*University of Palermo, Palermo, Italy;* [12]*Virgen Del Rocío University Hospital, Seville, Spain;* [13]*Stravitz-Sanyal Institute for Liver Disease and Metabolic Health, Richmond, United States;* [14]*First Affiliated Hospital of Wenzhou Medical University, Wenzhou, China;* [15]*Hospital Universitario Puerta de Hierro Majadahonda, Madrid, Spain;* [16]*Royal Free Hospital and UCL, London, United Kingdom;* [17]*The Chinese University of Hong Kong, Hong Kong, China;* [18]*Karolinska University Hospital, Stockholm, Sweden*
Email: merle.roeren@ki.se

Background and aims: In patients with metabolic dysfunction-associated steatotic liver disease (MASLD) and raised FIB-4 but normal vibration-controlled transient elastography (VCTE) < 8 kPa, current guidelines do not offer clear recommendations on optimal monitoring strategies. Demanding VCTE for all subsequent assessments could be excessive. We aimed to evaluate whether changes in routine markers can help prioritize patients for VCTE re-referral.
Method: The VCTE-Prognosis study was a global MASLD cohort (2004–2023) with serial routine markers and VCTE assessments. We modelled LSM trajectories over 36 months using latent growth mixture analysis in patients with a first LSM < 8 kPa. Linear mixed-effects models evaluated changes in 14 routine markers and two scores within each trajectory and their correlation with LSM progression.
Results: Among 10,789 patients (median age 54; 58% male) three LSM trajectories were identified. Despite distinct baseline LSM in Class 1 (62.4%; 4.6 kPa, 95%CI = 4.5–4.6) and Class 2 (35.8%; 6.5 kPa, 95%CI = 6.4–6.6), both classes showed stable trends over time (0.0 kPa/month, 95%CI = – 0.0–0.0), whereas Class 3 (1.8%; 7.6 kPa, 95%CI = 7.5–8.1) showed an increasing trend in LSM of 0.2 kPa/month (95%CI = 0.2–0.2). Within three years, 4 (0.0%), 416 (10.8%) and 197 (100%) patients across the respective classes exceeded 8 kPa. FIB-4 trajectories most closely mirrored LSM progression, increasing of 1% per month in Class 3.
Conclusion: In patients with MASLD and normal liver stiffness, progression to an LSM ≥ 8 kPa within three years was observed in less than 6%. Most patients exhibited stable LSM over time, suggesting that monitoring intervals may be extended to every three years or longer, while annual follow-up is advisable for those with baseline LSM between 6 and 8 kPa. A yearly FIB-4 increase of ~ 12% may indicate need for re-referral.

WED-188

Social determinants of health are associated with the risk of hepatic and cardiovascular events in patients with advanced MASLD: prediction using the novel LiverSocial score

Diego Rojo Lázaro[1,2], Alba Jiménez-Massip[1,2,3,4], Cautar El Maimouni[5,6], Lidia Canillas[7,8], Mercedes Vergara[3,4,9], Maria Poca[4,10], Adrià Rodríguez-Castellano[11,12], Eva Erice Munoz[13], Isabel Serra[14,15], Laura Pagès[1,2], Jose Carrión[7,8], Anna Soria[4,5,6], Eduard Mas[2], Rosa M Morillas[3,4,16,17], Pere Ginès[4,5,6,18], Isabel Graupera[4,5,6,18], Teresa Broquetas[19], Juan M. Pericàs[1,2,3,4]. [1]*Liver Unit, Digestive Diseases Area, Vall d'Hebron University Hospital, Barcelona, Spain;* [2]*Vall d'Hebron Research Institute (VHIR), Vall d'Hebron Hospital Campus, Barcelona, Spain;* [3]*Autonomous University of Barcelona, Barcelona, Spain;* [4]*CIBERehd – Biomedical Research Networking Centre in Hepatic and Digestive Diseases, Madrid, Spain;* [5]*Liver Unit, Hospital Clínic, Barcelona, Spain;* [6]*Clínic Research Foundation – August Pi i Sunyer Biomedical Research Institute (FCRB-IDIBAPS), Barcelona, Spain;* [7]*Liver Section, Gastroenterology Department, Hospital del Mar, Barcelona, Spain;* [8]*IMIM – Hospital del Mar Medical Research Institute, Barcelona, Spain;* [9]*Hepatology Unit, Digestive Service, Parc Taulí Institute for Research and Innovation (I3PT), Barcelona, Spain;* [10]*Department of Gastroenterology, Hospital de la Santa Creu i Sant Pau, Sant Pau Research Institute, Barcelona, Spain;* [11]*Department of Gastroenterology, Joan XXIII University Hospital, Tarragona, Spain;* [12]*Pere Virgili Health Research Institute (IISPV), DIAMET Group, Tarragona, Spain;* [13]*Department of Gastroenterology, Moisès Broggi Hospital Complex, Barcelona, Spain;* [14]*Hepatology Section,*

Digestive Service, Doctor Josep Trueta Hospital, Girona, Spain; [15]University of Girona, Girona, Spain; [16]Liver Unit, Department of Digestive Diseases, Germans Trias i Pujol University Hospital, Badalona, Spain; [17]Institut d'Investigació en Ciències de la Salut Germans Trias i Pujol (IGTP), Badalona, Spain; [18]Faculty of Medicine and Health Sciences, University of Barcelona, Barcelona, Spain; [19]Hepatology Section, Digestive Service, Bellvitge University Hospital, IDIBELL, Barcelona, Spain
Email: diego93rojo@gmail.com

Background and aims: Social determinants of health (SDH) are increasingly recognised as modifiers of disease progression in metabolic dysfunction-associated steatotic liver disease (MASLD). However, their prognostic relevance in patients with compensated advanced chronic liver disease (cACLD) remains poorly defined. We aimed to evaluate the association of SDH with the risk of major adverse liver outcomes (MALO) and major adverse cardiovascular events (MACE) in patients with cACLD.
Method: Prospective multicentre cohort including patients with cACLD due to MASLD from nine tertiary hospitals in Spain. Demographic, clinical, laboratory and imaging data were collected. SDH were assessed at baseline using a structured questionnaire. Nine socioeconomic variables, including employment status, household economic role, income, housing conditions, educational level, marital status, country of origin, age and sex, were used to construct a composite LiverSocial score. Each variable was analysed using univariable logistic regression with a composite endpoint of MALO and/or MACE. A weighted LiverSocial score was constructed using β coefficients derived from univariable logistic regression. Binary logistic regression models assessed its association and predictive performance.
Results: A total of 325 patients were included (median age 65 years [59–70]), 170 (52%) women, followed for a mean of 2.7 years. Arterial hypertension and diabetes mellitus were present in 72.4% and 69.8% of patients, respectively. Previous cardiovascular disease was documented in 9.6%. At baseline, five patients (1.5%) were classified as Child–Pugh B, and 98.5% as Child–Pugh A. During follow-up, MALO occurred in 28 patients (8.6%) and MACE in 13 (4.0%). Hepatocellular carcinoma developed in 4 (1.2%), and 26 (8.0%) experienced hepatic decompensation. Three patients underwent liver transplantation (0.9%). In univariable analyses, increasing age was significantly associated with the composite endpoint, whereas other SDH variables were not. In contrast, the weighted LiverSocial score was associated with MALO and/or MACE (OR 2.21, 95% CI 1.23–3.99; p = 0.008), with moderate discrimination (AUC 0.64, p = 0.0083) and an optimal cut-off of 2.5.
Conclusion: In patients with cACLD due to MASLD, a composite SDH-based score was associated with major liver and cardiovascular events. These findings suggest a potential role for integrating social vulnerability into holistic risk stratification strategies for advanced MASLD, warranting further validation.

WED-189
Lysosomal acid lipase activity as a marker of advanced fibrosis in steatotic liver disease: a prospective study

Roni Nasser[1], Afif Yaccob[1], Rawi Hazzan[2], Tor Regev-Sadeh[3], Fadi Abu Baker[4], Tarek Saadi[5]. *[1]Rambam Health Care Campus, HAIFA, Israel; [2]Clalit Health Services, Northern Region, Israel, HAIFA, Israel; [3]Bruce Rappaport Faculty of Medicine, Technion-Israel Institute of Technology, Haifa, Israel, HAIFA, Israel; [4]Department of Gastroenterology and Hepatology, Hillel Yaffe Medical Center, Hadera, Israel, HAIFA, Israel; [5]Rambam Health Care Campus, ARRABA, Israel*
Email: dr.t.saadi@gmail.com

Background and aims: Lysosomal acid lipase deficiency (LAL-D) is a rare genetic disorder that may mimic steatotic liver disease (SLD), particularly in patients without typical metabolic dysfunction. Accurate diagnosis is critical due to the availability of effective enzyme replacement therapy. The objectives of this study are to assess the prevalence of LAL-D in a selected cohort of non-obese individuals with SLD accompanied by dyslipidemia, or with cryptogenic cirrhosis, and to evaluate the relationship between LAL activity and liver disease severity.
Method: In this prospective observational study, 102 adult patients with imaging- or biopsy-confirmed SLD and dyslipidemia or cryptogenic cirrhosis were enrolled at a tertiary liver center in Israel. Individuals with secondary causes of hepatic steatosis, including excessive alcohol consumption, viral hepatitis, and other chronic liver diseases, were excluded. LAL activity was measured via dried blood spot testing. Clinical, laboratory, imaging, and histological data were collected.
Results: None of the patients demonstrated LAL deficiency. Mean LAL activity was 0.48 nmol/punch/hour. A median LAL level of 0.445 nmol/punch/hour was associated with advanced fibrosis (F3–F4) as compared to mild/moderate fibrosis (F0–F2). AUC was 0.64 (p = 0.031), suggesting potential clinical relevance. However, no LAL activity threshold could distinguish between presence or severity of hepatic steatosis. Higher LAL levels were also positively correlated with white blood cell and platelet counts.
Conclusion: Our findings suggest a low prevalence of LAL-D even within a selected cohort of non-obese patients with SLD or cryptogenic cirrhosis. Nonetheless, reduced LAL activity—particularly levels below 0.445 nmol/punch/hour—was associated with advanced hepatic fibrosis and may serve as a non-invasive marker of disease severity. Targeted testing in individuals with compatible clinical features could aid in risk stratification and guide further evaluation.

WED-190
ACT on MASH: A multi-country cross-sectional online survey of awareness, disease perceptions, and cardiometabolic comorbidities among people at risk for or living with MASLD and MASH

Sahar Saeed[1], Husam Albarmawi[2], Edwige-Ludiwyne Balzac[3], Julio Burman[4], Nathalie Eklöf[5], Takumi Kawaguchi[6], Nobuyoshi Kosaka[7], Jeff McIntyre[8], Lauren Nephew[9], Arash Pakseresht[10], Jörn M. Schattenberg[11], Cyrielle Caussy[12]. *[1]Queens University, Ontario, Canada; [2]Novo Nordisk, Mainz, Germany; [3]Novo Nordisk, France, Paris, France; [4]European Liver Patients' Association, Brussels, Belgium; [5]Novo Nordisk, Soberg, Denmark; [6]Division of Gastroenterology, Department of Medicine, Kurume University School of Medicine, Kurume, Japan; [7]Novo Nordisk, Japan, Tokyo, Japan; [8]Global Liver Institute, Washington DC, United States; [9]Indiana University School of Medicine, Indianapolis, United States; [10]Novo Nordisk, Canada, Mississauga, Canada; [11]Department of Medicine, Saarland University Medical Center, Homburg, Germany; [12]Hospices Civils de Lyon, Département Endocrinologie, Diabète et Nutrition, Hôpital Lyon Sud, Univ Lyon, CarMen Laboratory, INSERM, INRA, INSA Lyon, Université Claude Bernard Lyon 1, Pierre-Bénite, France*
Email: sahar.saeed@queensu.ca

Background and aims: Globally, an estimated one in three people is living with metabolic dysfunction-associated steatotic liver disease (MASLD), yet the perspectives of those affected remain poorly characterized. This study assessed awareness, knowledge, and perceptions of MASLD and metabolic dysfunction–associated steatohepatitis (MASH) among people diagnosed with, or at risk for, these conditions.
Method: In 2025, a multidisciplinary team, including a patient advocacy representative, developed an online cross-sectional survey among people diagnosed with MASLD/MASH or at risk for MASH living in Canada, France, Germany, Japan, and the United States (US). "At risk" was defined as having ≥1 cardiometabolic risk factor or a blood test showing elevated liver enzymes. Survey respondents were recruited via online panels, databases, outreach, and social media.
Results: Among 516 people completing the survey, 252 had MASH, 132 had MASLD, and 132 were at risk for MASH. The median age of respondents was 48 years. 50% of respondents were female, and 49%

had a university degree or higher. Cardiometabolic comorbidities were common among people with MASLD (obesity, 72%; hypertension, 42%; type 2 diabetes, 25%), with MASH (obesity, 71%; hypertension, 45%; type 2 diabetes, 35%), and for people at risk for MASH (obesity, 67%; hypertension, 47%; type 2 diabetes, 29%). Most respondents agreed they received a timely diagnosis (MASLD, 62%; MASH, 60%); however, the proportion of respondents who were "very" or "extremely" familiar with disease progression was low (MASLD, 15%; MASH, 37%). 58% of at-risk people recognized they were at risk of MASLD/MASH, and 58% were "very" or "extremely" concerned about the possibility of developing MASLD/MASH. Only 9% of at-risk people reported being "very" or "extremely" familiar with MASH. Overall, 55% of respondents with MASH "agreed" or "strongly agreed" that there is stigma associated with having liver disease, with notable variation by country (Canada, 73%; France, 77%; Germany, 57%; Japan, 50%; United States, 56%).
Conclusion: Awareness and understanding of MASLD and MASH remain low among both diagnosed and at-risk people, despite high cardiometabolic comorbidity. Low familiarity with disease progression and widespread perception of stigma highlight the need for patient education, stigma-reduction initiatives, and improved patient-provider communication.

WED-191
Identification of advanced fibrosis in MASLD through breath fingerprinting: clinical trial results
Osnat Sella Tavor[1], Orit Marom Albeck[1], Ilay Marom[1], Omer Meroz[1], Gilad Feinberg[1], Lenny Aharon[1], Rifaat Safadi[2]. *[1]NaNose Medical, Netanya, Israel; [2]Hadassah Medical Organization, Hadassah Hebrew University Medical Center, Jerusalem, Israel*
Email: osnatst@nanosemed.com

Background and aims: Metabolic dysfunction–associated steatotic liver disease (MASLD) is the most common chronic liver disease worldwide, with prevalence expected to increase alongside rising rates of obesity and diabetes. Fibrosis stage is key determinant of prognosis; however, identification of advanced fibrosis remains challenging in routine clinical practice. Although liver biopsy is the reference standard, its invasiveness, sampling variability, and cost limit widespread use. Existing non-invasive assessments suffer from low specificity (< 65%) and limited accessibility. This study aimed to evaluate the performance of volatile organic compound (VOC)–based breath analysis for identifying advanced fibrosis in MASLD and assess its ability to discriminate fibrosis stage in comparison with established non-invasive assessment approaches with the aim to advance an effective, accurate non-invasive test suitable for use in the primary care setting.
Method: Chemi-resistor, nanoparticle based sensors exposed to subjects expelled breath samples via the innovative NaNose Dianose device. DiaNose utilizes a disposable breath collection unit, a replaceable sensor and a measurement system. It is a unique and novel measurement device that enables breath sample analysis under standardized environmental conditions across different geographic locations. The time-series sensor responses were fed into an advance AI algorithm, analyzed and a classifier differentiating between F0/F1 and F3/F4 stage MASLD was created. Clinical data was collected from MASLD patients across fibrosis stages, confirmed by liver biopsy or FibroScan.
Results: Breath samples obtained from 71 individuals with MASLD were analyzed, including 40 participants with absent or mild fibrosis and 31 with advanced fibrosis. This data were used to develop a classification algorithm within the clinical trial framework. Cross-validation analysis yielded a sensitivity of 76.2%, specificity of 83.9%, and an overall classification accuracy of 80.7%. Participant recruitment and data collection are ongoing to further enhance model robustness and external applicability.
Conclusion: The findings suggest that DiaNose differentiates between early and advanced fibrosis in individuals with MASLD and may serve as a rapid, non-invasive point-of-care screening tool. This approach has the potential to optimize primary care management, improve accessibility in underserved and rural settings, and support trial stratification to advance treatment development.

WED-195
Dynamics of noninvasive tests (NITs) - LIVERFAST, FIB-4 and vibration-controlled transient elastography (VCTE, Fibroscan), during monitoring therapy with TNR-beta agonist Resmetirom (RT) in patients with MASH- update
Jeevin Sandhu[1], Shaheen Mehrara[2], Mona Munteanu[3], Akash Pagadala[4], Ashwini Mehta[1], John Lee[3], Obinna Okolo[2], Parker Woods[5], Parvez Mantry[2,6]. *[1]Methodist Dallas Medical Center, Division of Hepatology, Internal Medicine, Dallas, United States; [2]Methodist Dallas Medical Center, Liver Institute, Dallas, United States; [3]Fibronostics U.S., Inc, New Orleans, United States; [4]University of Southern California, Los Angeles, United States; [5]Methodist Dallas Medical Center, Liver Institute, Dallas, dallas, United States; [6]LIver Institute, methodist Dallas medical center, Dallas, United States*
Email: parvezmantry@mhd.com

Background and aims: LIVERFAST is a new blood-based NIT that assess quantitatively fibrosis, MASH-activity, and steatosis. **Aims:** To assess the dynamics of LIVERFAST, FIB-4 and VCTE and CAP in monitoring patients on-RT and its response on fibrosis and steatosis [≥10% regression rate (10%RR) from baseline to repeated NIT].
Method: On-RT patients with baseline (t0) and repeated (t1) NITs have been included retrospectively. Statistics included Kaplan Meier non-parametric censored at 10% RR from t0, Tukey-Kramer Multiple-Comparison Test and subgroup analysis for dose/GLP-1 receptor agonists (GLP-1RA) analysis.
Results: Eligible patients without RT discontinuation: n = 86, 62% 80mg-dose, 39% male, 55% T2D, 46% GLP-1RA, mean (se) age 62.4 (1.3), BMI 33.7 (0.7), ALT 44 (4), FIB4 1.79 (0.14). T0-prevalence of F2F3 were 61% (LIVERFAST) and 44% (VCTE). Median (max) delays (mths) t0-to-t1 were 3.4 (LIVERFAST), 7.6 (VCTE) and 6.7 (FIB4). 67pts. with t0-FIB4 had no change at t1, (1.85 vs 2.02), or AST (44 vs 36), platelets count (230 vs $224*10^9$), all p = ns, and ALT (53 vs 40, p < 0.05). 30 pts had repeated VCTE (median t0–10.7 vs t1–10.1 Kpa) and CAP (t0–301 vs t1–299 dB/m), all p = ns regardless the dose or the association with GLP-1RA. 44 pts achieved t1-LIVERFAST with median scores (t0 vs t1): fibrosis (0.48 vs 0.38, p < 0.001), steatosis (0.50 vs 0.42, p < 0.05), activity (0.45 vs 0.42, p = ns), mainly in the 80 mg group (n = 27) and in either groups of RT-alone or in combination to GLP-1RA for fibrosis (p < 0.05). LIVERFAST-fibrosis 10% RR from t0 has been achieved more within 80mg-RT group than within 100mg-RT at 3 and 6mths, respectively: 23.8% vs 20.7% and 79.2% vs 37.5%, overall logrank p < 0.05). LFAST-steatosis 10% RR from t0 has been achieved more within 80mg-RT group (overall logrank p < 0.05). The significant decrease t0-to-t1 in the total cholesterol has neither impacted the ApolipoproteinA1 [131 vs 146 mg/dl] or LIVERFAST fibrosis score.
Conclusion: RT-Initiation based on NITs is efficient and allows further non-invasive monitoring. LIVERFAST is an efficient monitoring test that reflects histology remodeling and provides earlier insights into disease progression and RT response. A significant improvement (≥10%) in LIVERFAST fibrosis and steatosis scores have been observed after the third month of RT mainly in the 80 mg group. FIB-4 and VCTE and CAP scores showed limited change at reassessment.

WED-196

Cell-free chromatin liquid biopsy for non-invasive MASH diagnosis and monitoring

Gavriel Fialkoff[1], Jenia Gutin[1], Israa Sharkia[1], Ronen Sadeh[1], Rifaat Safadi[2], Yael Milgrom[2], Münevver Demir[3], Frank Tacke[3], Cornelius Engelmann[3], Nofar Rosenberg[4], Ophir Hay[4], Eithan Galun[4], Esther Harpenas[5], Amon Asgharpour[6], Jennifer Sayne[6], Michael Idowu[6], Nir Friedman[5], Arun J. Sanyal[6]. [1]*Senseera LTD, Jerusalem, Israel;* [2]*Hadassah-Hebrew University Medical Center, The Liver Unit Institute of Gastroenterology and Liver Diseases, Jerusalem, Israel;* [3]*Charité - Universitaetsmedizin Berlin, Department of Hepatology and Gastroenterology, Berlin, Germany;* [4]*Hadassah-Hebrew University Medical Center, The Goldyne Savad Institute for Gene Therapy, Jerusalem, Israel;* [5]*Hebrew University of Jerusalem, Faculty of Medicine, Jerusalem, Israel;* [6]*Virginia Commonwealth University School of Medicine, Richmond, United States*
Email: nir.friedman@mail.huji.ac.il

Background and aims: While much progress has been made in development of non-invasive tests (NITs) for fibrosis assessment, there remains an unmet need for validated NITs to diagnose metabolic dysfunction associated steatohepatitis (MASH) and to improve upon existing fibrosis biomarkers. The aim of this study was to evaluate cfChIP-seq - cell-free chromatin immunoprecipitation followed by sequencing - for non-invasive profiling of MASH-specific transcriptional activity directly from plasma.
Method: cfChIP-seq directed to histone modifications associated with transcriptionally active genes serves as a non-invasive method to provide a genome-wide scale readout of transcriptional activity in the tissues of origin, including the liver. This was used to establish a MASH score for the diagnosis of MASH. MASH score discovery was performed in a cohort of 72 biopsy proven MASLD, 1230 undiagnosed general population samples and 102 biopsy proven non-MASLD liver disease patients to ensure high specificity. The score was validated in another cohort of biopsy proven MASLD (n = 258).
Results: In the biopsy proven validation cohort the MASH score achieved an AUC of 0.93 (CI: 0.91–0.95) for the identification of MASH compared to the general population cohort. The AUC for the identification of MASH with NAFLD activity score ≥ 4 and fibrosis stages 2–4 (at-risk MASH) was 0.97 (CI: 0.96–0.99). We also demonstrate acceptable specificity of the MASH score versus other liver etiologies. Our analysis indicates that the MASH score is related to the presence and severity of individual histological features (NAS components/fibrosis). We also identified biomarkers associated with independent histological components of the disease, including fibrosis, thereby potentially enabling decoupling of fibrosis staging from disease activity in future applications.
Conclusion: Here, we developed a chromatin liquid biopsy MASH score for the non-invasive detection of MASH. This technology provides a noninvasive window into the liver's physiological state, with promise not only for detection but also for guiding precision drug selection and monitoring responses in the evolving landscape of MASH therapy.

WED-197

Metabolic matters: real-world assessment of metabolic dysfunction–associated steatotic liver diseases in the United States by integrating international classification of diseases codes and non-invasive tests for improved detection

Jörn M. Schattenberg[1], Zuleika Aponte Torres[2], Lu Zhang[2], Katrine Lindvig[3], Mireia Raluy[4], Mark Yates[5], Claudio Sartini[6], Zobair M. Younossi[7]. [1]*Department of Internal Medicine II, University Medical Center Homburg, Homburg and Saarland University, Homburg, Germany;* [2]*West Sussex, United Kingdom;* [3]*Evido Health, Odense, Denmark;* [4]*Thermo Fisher Scientific, Stockholm, Sweden;* [5]*Thermo Fisher Scientific, London, United Kingdom;* [6]*Boehringer Ingelheim International GmbH, Ingelheim, Germany;* [7]*The Global NASH/MASH Council, Washington, DC, United States*
Email: zobair.younossi@cldq.org

Background and aims: There is an urgent need for game-changing strategies to identify, risk-stratify, and improve management of metabolic dysfunction–associated steatotic liver diseases (MASLD) such as metabolic dysfunction–associated steatohepatitis (MASH) in routine practice. Studies have consistently reported underdiagnosis of MASH using only International Classification of Diseases (ICD) codes, underlining the importance of empowering physicians to identify patients with the disease earlier. This study aimed to discover the size of the patient population diagnosed with, or at-risk for MASH in the United States by leveraging an integrated approach using ICD coding, non-invasive test (NIT) data, and a machine learning (ML)-based fibrosis assessment (LiverPRO, Evido Health, Denmark).
Method: This observational, non-interventional, retrospective study used electronic health record and claims data from the Optum® Market Clarity (OMC) US database between January 1, 2021, and December 31, 2023. Adults aged ≥ 18 years were eligible. Case definitions classified patients as diagnosed with MASH (ICD code K75.81) or at-risk for MASH using combinations of the ICD code for MASLD (K76); Fibrosis-4 Index (FIB-4) scores ≥ 1.3 calculated with AST, ALT, platelets, and age; and LiverPRO-defined ≥ F2 fibrosis. LiverPRO is a validated, algorithm-based tool that estimates liver fibrosis risk using NITs and patient age. Same-day lab values were required for FIB-4 and LiverPRO computations.
Results: In total, 42,596,381 patients were included from the OMC database. The total prevalence of patients with MASH diagnosis (0.5%) or at-risk for MASH (8.1%) was 8.5%. Among patients identified as at-risk for MASH, the prevalence of those with MASLD diagnosis was 5.2%, and that of patients without MASH/MASLD diagnosis but with FIB-4- or LiverPRO-defined fibrosis was 1.9% (of which, 40.0% with overweight/obesity, 27.2% with diabetes) or 1.0% (of which, 47.3% with overweight/obesity, 39.0% with diabetes), respectively.
Conclusion: Our findings indicate a gap in MASH disease recognition, as the diagnosed prevalence in OMC is very low compared with overall prevalence estimates in the literature. Diagnosis rates may be improved by leveraging the use of FIB-4 and other novel NITs, especially among patients identified as at-risk for MASH. Educating physicians on NIT use and interpretation, especially in the presence of metabolic factors, could empower them to diagnose MASH in an earlier stage.

WED-198

Velacur determined fat fraction as a tool to predict MRI-PDFF changes in patients receiving liver-directed treatment

Caitlin Schneider[1], Jim Hennan[2], Xiaomin Lu[2], Matthew Dauphin[2], Rebecca Taub[2]. [1]*Sonic Incytes Medical Corp, Vancouver, Canada;* [2]*Madrigal Pharmaceuticals, West Conshohocken, United States*
Email: caitlin@sonicincytes.com

Background and aims: As new treatments are becoming available for patients with MASLD and MASH, non-invasive methods at the point of care will be needed to assess patient response. MRI Proton Density Fat Fraction (MRI-PDFF) MRI-PDFF is the most well-validated non-invasive imaging biomarker associated with histologic improvement in MASH. Although still with limitations, MRI-PDFF responders were significantly more likely to have a histologic response. This study examines the efficacy of Velacur Determined Fat Fraction (VDFF) to identify patients demonstrating significant (>30%) changes in the MRI-PDFF which would indicate treatment response, as defined in AASLD and EASL recommendations.

Method: Patients enrolled in Madrigal's open label extension (OLE) study for resmetirom, who had a qualifying Velacur and MRI-PDFF scan at Day1, and at any follow-up visit (week 16 or week 52) were included. Each Day 1-follow-up visit pair was treated as an independent data point for change-over-time analyses. This study included cirrhotic and non-cirrhotic patients previously enrolled in other blinded resmetirom studies, but all patients received resmetirom during the OLE. The AUROC, sensitivity and specificity of changes in Velacur VDFF to predict ≥ 30% changes in MRI-PDFF were calculated.
Results: Data was collected between Aug 2021 and May 2024 from 9 sites in the US. A total of 626 paired visits were collected. From these visits, 127 unique patients, with 181 qualifying, paired visits were included in the analysis. The median Day1 MRI-PDFF was 9.4%. Of the included patients, 106 had received treatment in the previous study and 21 were treatment naïve at Day1. At Week 16, median percent change from Day 1 was −24.3% for MRI-PDFF and −27.3% for VDFF; at Week 52, corresponding changes were −24.5% and −28.3%, respectively. No statistically significant difference in median percent change was observed between MRI-PDFF and VDFF (p = 0.4). At 85 (47%) of the visits, a patient showed ≥ 30% decrease in MRI-PDFF. Using the same 30% change cutoff for VDFF, the AUROC was 0.76 [0.68, 0.82], with a sensitivity of 68% and specificity of 75%. The positive predictive value of VDFF was 70%.
Conclusion: Accurately monitoring changes in patients over time, in response to treatment, is important to understanding which patients are benefiting. In this study, Velacur VDFF tracked longitudinal changes in liver fat similar to MRI-PDFF and represents a promising point-of-care approach for identifying patients likely to be responding to therapy.

WED-199

Phenotype-dependent failure of FIB-4 to rule-out advanced fibrosis among patients with MASLD in primary care: four-cohort comparison with LiverPRO

Abdel-Aziz Shaheen[1], Katrine Lindvig[2], Georg Semmler[3], Julie Astono[2], Maja Thiele[4], Mark Swain[1], Aleksander Krag[5], M Mang[6], Bernhard Wernly[7], Christian Datz[8], Juan G Abraldes[6]. *[1]University of Calgary, Calgary, Canada; [2]Evido Health, Copenhagen, Denmark; [3]Medical University of Vienna, Vienna, Austria; [4]Centre for Liver Research, Copenhagen, Denmark; [5]Odense University Hospital, Odense, Denmark; [6]University of Alberta, Edmonton, Canada; [7]Center for Public Health and Healthcare Research, Clinic I for Internal Medicine, University Hospital Salzburg, Salzburg, Austria; [8]General Hospital Oberndorf, Teaching Hospital of the Paracelsus Medical University, Salzburg, Austria*
Email: az.shaheen@ucalgary.ca

Background and aims: EASL recommends FIB-4 score as first-line test in primary care to rule-out advanced fibrosis in individuals with suspected metabolic dysfunction-associated steatotic liver disease (MASLD), but external validation across general populations and clinical phenotypes is limited. We compared FIB-4 with LiverPRO across four EASL-eligible MASLD cohorts (based on EASL guidelines for MASLD risk-stratification).
Method: We analysed four primary-care MASLD cohorts: Calgary (two-dimensional shear wave elastography, n = 8,126), Edmonton (vibration-controlled transient elastography [VCTE], n = 985), Denmark (VCTE, n = 4,365) and Austria (VCTE, n = 704). Advanced fibrosis was defined as liver stiffness measurement (LSM) ≥8 kPa. Rule-out thresholds were FIB-4 < 1.30 or LiverPRO < 0.25. Outcomes were false-negative (FN) proportion among LSM≥8, missed LSM≥8 per 1,000 risk-stratified, and negative predictive value (NPV). Analyses were stratified by age (at 65), sex, body mass index (BMI at 30), alanine aminotransferase (ALT at 30 U male/ 25 U female) and diabetes status.
Results: In the primary-care cohorts, the median age was 43–59 years, BMI 28–31, diabetes 13–38%, and LSM ≥ 8 prevalence 8–14%. Overall, FIB-4 classified 67–77% as low risk yet FN rates were 41–55% (35–62 missed/1,000; NPV 92–95%). LiverPRO classified 32–60% as low risk with FN rates of 13–23% (12–32 missed/1,000; NPV 93–97%), corresponding to 22–32 percentage-point lower FN rates and 22–30 fewer missed cases per 1,000 across cohorts. Among patients with diabetes, FIB-4 missed 48–110 cases/1,000 screened versus 12–46 with LiverPRO. FIB-4 heterogeneity was most prominent by age, where FN rates were 54–67% in < 65 years vs 0–29% in ≥ 65 years, and increased with obesity and normal ALT (BMI ≥ 30 45–63% vs. BMI < 30 23–48%; normal ALT 20–67% vs. elevated ALT 36–51%). LiverPRO FN rate remained lower with narrower range among these subgroups (< 65 years 16–28%; ≥ 65 years 0–12%; BMI ≥ 30 16–24%; elevated ALT 9–24%). FN was higher within FIB-4 compared to LiverPRO in women (32–64% vs. 11–25%) and men (34–56% vs. 12–33%).
Conclusion: Across four EASL risk-stratification eligible primary care MASLD cohorts, the recommended FIB-4 rule-out threshold generated clinically relevant and phenotype-dependent false reassurance, particularly in younger individuals and patients with diabetes. LiverPRO provided more consistent rule-out and substantially reduced missed advanced fibrosis. This supports evaluating LiverPRO to optimise MASLD triage pathways.

WED-200

Diagnostic yield and efficiency of non-invasive two-tier pathways for liver fibrosis assessment in metabolic dysfunction-associated steatotic liver disease

Neha Sharma[1], Yasamin Farbod[1], Dana Kablawi[1], France Martineau[1], Sara Alessa[1], Amina Alsalmi[1], Adam Hassan[2], Aurgho Datta[1], Randy Ngalamulume Mukengeshayi[2], Philip Wong[1], Xun Zhao[1], Marc Deschenes[1], Tianyan Chen[1], Amine Benmassaoud[1], Giada Sebastiani[1]. *[1]Centre universitaire de Santé McGill, Montréal, Canada; [2]McGill University, Montréal, Canada*
Email: giada.sebastiani@mcgill.ca

Background and aims: The impact of redefining NAFLD as metabolic dysfunction–associated steatotic liver disease (MASLD) on first-tier non-invasive fibrosis testing is unclear. We compared the diagnostic efficiency of five two-tier pathways combining serum biomarkers (first tier) and transient elastography (TE; second tier) for detecting fibrosis (F2–F4) in MASLD.
Method: Patients with MASLD, without alcohol misuse or viral hepatitis, were consecutively enrolled at a tertiary hepatology program in Québec between 2015 and 2025. Five simple serum fibrosis biomarkers—fibrosis-4 index (FIB-4), BARD score, NAFLD fibrosis score, AST/ALT ratio, and AST-to-platelet ratio index (APRI)—were evaluated as first-tier tests to exclude fibrosis (F2–F4). All participants subsequently underwent TE (FibroScan®). For each pathway, we estimated the proportion of avoidable TE examinations based on low-risk biomarker results and the discordance rate between low biomarkers and high TE measurement (≥8 kPa). Diagnostic yield was defined as the difference between avoided TE examinations and discordance. A weight yield model ($\lambda = 3$) was applied to reflect the greater clinical impact of missed fibrosis, whereby each missed case was considered three times more detrimental than an avoided TE.
Results: A total of 233 patients with MASLD (mean age 57 years, 52% male, mean BMI 32 kg/m^2). Fibrosis by TE was present in 38%. First-tier testing would have reduced TE referrals by 35% using the NAFLD fibrosis score, 48% with BARD, 54% with FIB-4, 55% with AST-ALT ratio and 78% with APRI. However, discordance between low-risk biomarkers and high TE ranged from 14% with BARD to 25% with

APRI. Net diagnostic yield (avoidable TE minus discordance) was highest for APRI (53) and FIB-4 (39), but after applying the weighted penalty for missed fibrosis, FIB-4 achieved the highest overall weighted yield (+7.9). In contrast, APRI showed a markedly reduced weighted yield (+3.3), while the NAFLD fibrosis score resulted in a negative weighted yield (−17.5). FIB-4 reduced TE referrals by 53.8% while maintaining a relatively low discordance rate (15.3%), representing the most balanced performance across pathways.
Conclusion: In patients with MASLD, two-tier diagnostic pathways substantially reduced the need for TE. Incorporating a weighted yield analysis that penalizes missed fibrosis identified FIB-4 as the most efficient and clinically balanced first-tier test, supporting its preferential use for non-invasive fibrosis risk stratification in MASLD care pathways.

WED-201
aMAP score effectively stratifies HCC risk in the steatotic liver disease population in the UK biobank
Yaru Shi[1], Wenxin Xu[1], Ning Yu[1], Zhihong Liu[1], Ya Xu[1], Jinlin Hou[1], Rong Fan[1]. [1]*Department of Infectious Diseases, Nanfang Hospital, Southern Medical University, Guangzhou, China*
Email: rongfansmu@163.com

Background and aims: Steatotic liver disease (SLD), currently the most prevalent chronic liver disease worldwide, is associated with an increased risk of hepatic and extrahepatic complications, including hepatocellular carcinoma (HCC), highlighting the need for risk stratification to guide surveillance. The aMAP score, developed for HCC risk prediction mostly in patients with viral hepatitis across 11 global prospective studies, has been less studied in SLD. This study aimed to assess the predictive performance of aMAP for HCC risk in a large SLD cohort.
Method: Data were obtained from the UK Biobank, a prospective cohort. Patients with SLD were identified and categorized into metabolic dysfunction-associated steatotic liver disease (MASLD), metabolic alcohol-related steatotic liver disease (MetALD), and alcohol-related liver disease (ALD), excluding those with viral hepatitis. The aMAP score was calculated, and its performance for HCC prediction was evaluated using discrimination, risk stratification with adjustment for competing risk of death, and calibration. Cross-sectional and longitudinal associations between metabolic parameters and aMAP scores or risk categories were assessed, with longitudinal analyses performed using Generalized Linear Mixed Model.
Results: A total of 156415 patients with SLD were enrolled (121558 MASLD, 27593 MetALD, 7264 ALD) followed for a median of 13.64 years (IQR: 12.80–14.37), 237 HCC events and 17462 deaths occurred, with 15-year cumulative HCC incidence of 0.17%, accounting for the competing risk of death. The aMAP score showed strong discrimination for HCC prediction, achieving a C-index of 0.76, outperforming PAGE-B, mPAGE-B, CAMD, and AASL scores (0.68–0.74). Risk stratification by aMAP categorized patients into low- mid- and high-risk groups, with 15-year cumulative incidences of 0.05%, 0.21%, and 1.12%, respectively (high vs low adjusted HR: 29.69; 95% CI: 19.99–44.10). Calibration was robust (Brier score < 0.001). Metabolic parameters, including blood glucose, waist circumference (WC), and systolic blood pressure showed positive trend across aMAP. After adjusting confounding factors, changes in blood glucose (OR = 1.08, $p < 0.001$) and WC (OR = 1.01, $p = 0.01$) remained independently associated with changes in aMAP risk levels.
Conclusion: The aMAP score effectively stratified HCC risk in patients with SLD, with changes in blood glucose and WC statistically associated with concurrent changes in aMAP.

WED-202
Impact of sodium-glucose cotransporter 2 inhibitors on hepatic pathology and key biomarkers in type 2 diabetes with metabolic dysfunction-associated steatotic liver disease: a prospective study
Farah Khaznadar[1], Omar Khaznadar[2], Marija Hefer[1], Ana Jurić[3], Robert Smolic[1], Ana Hrzenjak[3], Kristina Kralik[4], Ana Petrovic[1], Justinija Steiner[5], Kristina Bojanić[1], Martina Smolic[1]. [1]*University of Osijek Faculty of Dental Medicine and Health Osijek, Osijek, Croatia;* [2]*Dr. Juraj Njavro National Memorial Hospital Vukovar, Vukovar, Croatia;* [3]*General County Hospital Našice, Našice, Croatia;* [4]*University of Osijek Faculty of Medicine, Osijek, Croatia;* [5]*Health Center Osijek, Osijek, Croatia*
Email: msmolic@fdmz.hr

Background and aims: Type 2 diabetes mellitus (T2DM) is commonly associated with metabolic dysfunction-associated steatotic liver disease (MASLD), for which approved therapies are scarce. Our objective was to evaluate the effects of SGLT2 inhibitors (SGLT2i) on liver fibrosis, steatosis, and metabolic biomarkers in T2DM-related MASLD in a real-world clinical setting.
Method: Sixty-seven T2DM patients, aged 37–89 years, were prospectively monitored for six months following the initiation of SGLT2i therapy. Serum levels of peroxisome proliferator–activated receptor (PPAR) α and γ, sterol regulatory element-binding protein 1 (SREBP1), and microsomal triglyceride transfer protein (MTTP) were assessed by ELISA. Non-invasive ultrasound methods, the two-dimensional shear wave elastography (2D-SWE) and ultrasound-guided attenuation parameter (UGAP), were used to assess liver fibrosis and steatosis, respectively, in addition to biochemical and anthropometric examinations.
Results: Following the six-month period, MTTP levels increased (198.4→428.9 ng/L, $p < 0.001$), while PPARγ levels decreased (895.0→565.4 ng/L, $p < 0.001$). Liver stiffness showed a significant improvement, with reduced 2D-SWE values (6.22→6.10 kPa, $p = 0.001$), which were inversely correlated with MTTP ($\rho = -0.268$, $p = 0.03$). UGAP values positively correlated with 2D-SWE ($\rho = 0.365$, $p = 0.002$) and demonstrated positive associations with leukocyte count, triglycerides, and liver enzymes, alongside an inverse association with HDL cholesterol ($p \leq 0.01$). Additionally, significant improvements were observed in fasting glucose, HbA1c, INR, waist circumference, and BMI ($p \leq 0.04$).
Conclusion: Treatment with SGLT2i is linked to early improvement in hepatic steatosis, liver fibrosis, and metabolic control in T2DM-associated MASLD. These changes were accompanied by beneficial regulation of PPARγ and MTTP, suggesting a role of SGLT2i in improving hepatic lipid metabolism and slowing MASLD progression, highlighting their therapeutic potential. Larger controlled trials are needed to affirm these findings.

WED-203
Two-step paediatric MASLD diagnostic approach: primary-care (PC) screening plus clinical fibrosis rule-out to select patients with progressive MASLD
Piotr Socha[1], Malgorzata Wajda-Cuszlag, Anna Swiader-Lesniak[1], Katarzyna Goclawska[1], Lukasz Szarpak[2], Sebastian Więckowski[1]. [1]*The Children's Memroial Health Instituite, Department Gastroenterology, Hepatology, Nutritional Disorders and Pediatrics, Warsaw, Poland;* [2]*The John Paul II Catholic University of Lublin, Technology Transfer Center, Lublin, Poland*
Email: p.socha@ipczd.pl

Background and aims: Paediatric MASLD is relatively common among obese children but significant liver fibrosis is not a common feature. Since fibrosis is the major indicator of progressive liver disease patients with fibrosis should be selected and referred to liver clinics for close follow up and therapy. As liver biopsy is rarely indicated and MR techniques are not commonly available to assess steatosis and fibrosis (PDFF and MR-elastography) other non-invasive markers need to be vaildated. Paediatric MASLD requires practical

two-step triage tools combining (1) primary-care screening for steatosis/fibrosis risk using routine tests and (2) bedside rule-out of clinically relevant fibrosis.
Method: In a prospective cohort of 402 children (10–18 years) with overweight/obesity, reference standards were MRI LiverLab PDFF for steatosis (S^+ ≥5.5%) and MR-elastography (MRE) for fibrosis (F^+ ≥2.7 kPa). Step-1 used the five-variable POZ^+ model (waist SDS, ALT, GGT, uric acid, TG/HDL) estimated with L2-penalised logistic regression and validated with nested patient-cluster cross-validation and 2000-resample bootstrap CIs. Step-2 used penalised logistic regression on FibroScan stiffness (E) and bioimpedance-derived body cell mass (BCM) to derive a continuous fibrosis risk equation and a 0–2 point score, with 10-fold cross-validation and bootstrap CIs.
Results: S^+ prevalence was 34.1% (137/402) and F^+ prevalence 12.5% (50/400). POZ^+ yielded AUC 0.76 (95% CI 0.70–0.81) for S^+ and 0.68 (0.58–0.76) for F^+, with high-sensitivity thresholds (Se ≥0.90) giving NPVs of 0.87 (S^+) and 0.92 (F^+). Benchmark fibrosis scores (PNFI, APRI, FIB-4, NFS) performed worse for F^+ (AUCs ranged from 0.49 to 0.66). For step-2 (n = 390), the E+BCM model achieved AUC 0.73 (95% CI 0.65–0.81). At a rule-out operating point (Se ≈0.92; Sp ≈0.30), NPV reached 0.96, with 25–30% of children assigned to a low-risk 'green zone' while maintaining NPV ≥0.95, in which MRE could usually be omitted.
Conclusion: A two-step pathway (PC^+ screening followed by non-MR E+BCM bedside triage) provides MRI/MRE-validated screening for MASLD-related steatosis and fibrosis and can substantially reduce MRE utilisation through a high-NPV fibrosis rule-out strategy based on widely available measurements.

WED-204

DM-LRE score: gradient boosting machine (GBM)-based machine learning model in predicting liver-related events (LREs) in type 2 diabetes mellitus (T2DM)

Sherlot Juan Song[1], Vincent Wai-Sun Wong[1], Grace Lai-Hung Wong[1], Jimmy Che-To Lai[1], Seung Up Kim[2], Salvatore Petta[3], Elisabetta Bugianesi[4], Masato Yoneda[5], Ming-Hua Zheng[6], Manuel Romero-Gómez[7], Emmanuel Tsochatzis[8], Philip N. Newsome[9], Hannes Hagström[10], George Boon Bee Goh[11], Chan Wah Kheong[12], José Luis Calleja Panero[13], Jerome Boursier[14], Arun J Sanyal[15], Jian-Gao Fan[16], Laurent Castera[17], Victor de Lédinghen[18], Terry Cheuk-Fung Yip[1]. [1]*Medical Data Analytics Centre, Department of Medicine and TherapeuticsThe Chinese University of Hong Kong, State Key Laboratory of Digestive Disease, Institute of Digestive Disease, The Chinese University of Hong Kong, HK, Hong Kong;* [2]*Yonsei University School of Medicine, Seoul, Korea, Rep. of South;* [3]*Section of Gastroenterology, PROMISE, University of Palermo, Palermo, Italy;* [4]*Department of Medical Sciences, Division of Gastroenterology, University of Torino, Torino, Italy;* [5]*Yokohama City University, Yokohama, Japan;* [6]*MAFLD Research Center, Department of Hepatology, The First Affiliated Hospital of Wenzhou Medical University, Wenzhou, China;* [7]*UCM Digestive Diseases, Virgen del Rocio University Hospital, SeLiver Group, Institute of Biomedicine of Seville, Ciberehd, Department of Medicine, University of Seville, Seville, Spain;* [8]*Royal Free Hospital, London, United Kingdom;* [9]*Roger Williams Institute of Liver Studies, School of Immunology & Microbial Sciences, Faculty of Life Sciences and Medicine, King's College London, Foundation for Liver Research and King's College Hospital, London, United Kingdom;* [10]*Karolinska University Hospital, Stockholm, Sweden;* [11]*Department of Gastroenterology and Hepatology, Singapore General Hospital, Singapore, Singapore;* [12]*Gastroenterology and Hepatology Unit, Department of Medicine, Faculty of Medicine, University of Malaya, Kuala Lumpur, Malaysia;* [13]*Department of Gastroenterology and Hepatology, Hospital Universitario Puerta de Hierro, Universidad Autonoma de Madrid, Madrid, Spain;* [14]*Departement of Hepato-Gastroenterology and Digestive Oncology, Angers University Hospital, HIFIH Laboratory, FSR ICAT 4208, Angers University, Angers, France;* [15]*Stravitz-sanyal Institute for Liver Disease and Metabolic Health, Virginia Commonwealth University School of Medicine, Richmond, VA, United States;* [16]*Center for Fatty Liver, Department of Gastroenterology, Xinhua Hospital Affiliated to Shanghai Jiao Tong University School of Medicine, Shanghai Key Lab of Pediatric Gastroenterology and Nutrition, Shanghai, China;* [17]*University of Paris-VII, Paris, France;* [18]*Echosens, Paris, France*
Email: 1155169298@link.cuhk.edu.hk

Background and aims: We aimed to develop a prediction model for LREs in patients with T2DM, given the close relationship between diabetes and liver disease progression.
Method: This retrospective cohort study included patients with T2DM from Hong Kong (HK-T2DM cohort) and patients with T2DM and metabolic dysfunction-associated steatotic liver disease (MASLD) from an international multicentre cohort undertaking vibration-controlled transient elastography (VCTE) examination (VCTE-Prognosis-T2DM cohort). The HK-T2DM cohort was randomly divided in an 80:20 ratio to form the development and internal validation cohorts. The VCTE-prognosis-T2DM cohort was used for external validation. The primary endpoint was incident LREs in 5 years, defined as hepatic decompensation, hepatocellular carcinoma, liver transplantation or liver-related deaths. The DM-LRE score was derived from s including cirrhosis status and routine serum markers at baseline. GBM demonstrated the highest concordance index (C-index) and time-dependent area under the receiver operating characteristic compared to XGBoost and random forest in predicting LREs. The score was applied for risk stratification using cutoffs at 90% sensitivity and specificity.
Results: 575,000 patients were included in the HK-T2DM cohort (mean age 61.9 years; 52.3% males), while 3,587 patients were included in the VCTE-Prognosis-T2DM cohort (mean age 56.0 years; 56.8% males). The incidence rates of LRE were 1.285 and 4.241 per 1,000 person-years for HK-T2DM and VCTE-prognosis-T2DM cohorts, respectively. In the development and external validation cohorts, the C-indices of the DM-LRE score in predicting 5-year LRE were 0.752 (95% CI: 0.742–0.763) and 0.864 (95% CI: 0.806–0.926), respectively, outperforming the Fibrosis-4 index (FIB-4, C-indices: 0.674 and 0.830). The DM-LRE score displayed a C-index similar to liver stiffness measurement in the external cohort (0.864 vs. 0.866). In the VCTE-prognosis-T2DM cohort, 1,866 (52.0%), 1,347 (37.6%) and 374 (10.4%) of patients were stratified into low- intermediate- and high-risk categories by the DM-LRE score. Low- intermediate- and high-risk subgroups exhibited a 5-year incidence rate of 0.880, 1.739, and 26.278 per 1000 person-years, respectively ($p < 0.001$).
Conclusion: The DM-LRE score could identify individuals at risk of LREs in patients with T2DM and facilitate early referral to specialty care.

WED-205

Comprehensive risk assessment for gastrointestinal cancers in steatotic liver disease (MASLD, MetALD, and ALD)

Nobuharu Tamaki[1], Takefumi Kimura[2], Shun-Ichi Wakabayashi[2], Naoki Tanaka[2], Namiki Izumi[1], Masayuki Kurosaki[1]. [1]*Musashino Red Cross Hospital, Tokyo, Japan;* [2]*Shinshu University School of Medicine, Nagano, Japan*
Email: nobuharu.tamaki@gmail.com

Background and aims: Steatotic liver disease and alcohol consumption are known risk factors for gastrointestinal cancers. Accordingly, the risk of gastrointestinal cancers may be increased in subgroups of steatotic liver disease (SLD), including metabolic dysfunction–associated steatotic liver disease (MASLD), MASLD with increased alcohol intake (MetALD), and alcohol-related liver disease (ALD). However, differences in gastrointestinal cancer risk among these subgroups have not been fully elucidated. This study aimed to investigate the incidence of gastrointestinal cancers in patients with MASLD, MetALD, and ALD.

Method: We conducted a nationwide, population-based cohort study using a Japanese health insurance claims database. A total of 978,607 individuals with MASLD, 366,152 with MetALD, 152,721 with ALD, and 4,884,398 controls were included. The primary outcome was the incidence of gastrointestinal cancers, including hepatocellular carcinoma (HCC), biliary tract cancer, esophageal cancer, gastric cancer, colorectal cancer, and pancreatic cancer.
Results: The 10-year cumulative incidence of HCC was 0.006% in the control group, 0.04% in the MASLD group, 0.05% in the MetALD group, and 0.09% in the ALD group. Similarly, the 10-year cumulative incidence of biliary tract cancer was 0.02% in controls, 0.05% in MASLD, 0.07% in MetALD, and 0.08% in ALD. After adjustment for age, sex, diabetes, dyslipidemia, hypertension, and smoking status, the adjusted hazard ratios (aHRs) for HCC ranged from 3.55 to 5.39 across the MASLD, MetALD, and ALD groups, while those for biliary tract cancer ranged from 1.45 to 1.66. The risks of both HCC and biliary tract cancer were significantly elevated in all SLD subgroups compared with controls. The 10-year cumulative incidence of colorectal cancer was 0.31% in the control group, 0.48% in MASLD, 0.73% in MetALD, and 0.97% in ALD. For esophageal, gastric, and colorectal cancers, aHRs ranged from 0.75 to 1.26 in MASLD, 1.09 to 1.44 in MetALD, and 1.13 to 2.48 in ALD, indicating a stepwise increase in risk with greater alcohol consumption. No significant association was observed between pancreatic cancer risk and alcohol consumption.
Conclusion: Patients with SLD have a significantly higher risk of gastrointestinal cancers compared with controls. The magnitude of risk differs according to the SLD subtype, particularly in relation to alcohol consumption. These findings highlight the importance of risk-stratified cancer screening strategies in individuals with SLD.

WED-206

Automated image analysis validation for MRI hepatic fat fraction quantification for steatotic liver diseases

Brendan Eck[1], Alvaro Jorge-Peñas[1], Vahan Sharoyan[1], Thomas Fuerst[1], Pohan Chen[1], Thomas Cajgfinger[1], Mark Tengowski[1]. [1]*Clario, Philadelphia, PA, United States*
Email: Mark.Tengowski@clario.com

Background and aims: Fatty liver analysis relies on expert readers defining manual regions of interest (ROIs) in nine Couinaud segments to determine individual segment and overall fatty liver values. In this methods development study, we validated known hepatic fat fraction (HFF) values generated by an automated solution against those values obtained manually by expert readers.
Method: Multi-center scan data (99 subjects with 252 exams, 1–3 time points per subject) collected using 6-echo MRI-PDFF techniques were processed with a proprietary fat-water separation algorithm to generate fat, water, R2*, goodness-of-fit, and fat fraction map series. We developed a computer-assisted yet human supervised image analysis solution that segmented the entire liver using the out-of-phase series and automatically identified the axial slice with the largest liver cross-sectional area. The median HFF was measured using the computer-defined ROI in this slice. The reader independently measured HFF using the standard manually defined ROIs in the nine Couinaud segments with overall HFF computed. Automated and manual measurements were compared using descriptive statistics, intra-class correlation coefficient (ICC) and Bland-Altman agreement.
Results: The accuracy of the fat-water separation algorithm was confirmed by comparison to an in-scan 0% to 40% fat calibration phantom (Calimetrix, Madison WI) yielding ICC = 0.999 (95% CI 0.991–1.000) with a mean bias of 0.4%. HFF manual measurements (0.9% and 34.6%) covered the clinically relevant ranges. The cross-sectional comparison of the automated algorithm with expert reader HFF results showed excellent agreement with ICC = 0.997 (95% CI 0.994–0.998). The mean method bias was 0.2% with Bland-Altman 95% limits of agreement of – 1.2 to 0.8%. In longitudinal analysis, manual method changes in HFF ranged from – 17.5 to +11.6%. Again the automated algorithm agreed well with the manual read (ICC = 0.992; CI 0.959–997; mean bias 0.1%; agreement limits were – 1.1 to +1.2%).
Conclusion: This study demonstrates outstanding correlation between manual HFF measurements and an automated overall single slice HFF solution. This analysis workflow retains the human reader to confirm or correct the algorithm output with high accuracy and HFF reproducibility. In studies evaluating change in liver fat over time, the overall HFF quantification by automated image processing with expert reader supervision is anticipated to serve as an alternative to fully manual methods.

WED-211

Prognostic value of liver stiffness measurement for liver-related events in metabolic dysfunction-associated liver disease-related compensated advanced chronic liver disease

Kitrawee Pisarnvorawat[1], Panarat Thaimai[2], Tassanun Jaihan[2], Kanokwan Sonsiri[2], Prooksa Ananchuensook[2], Supachaya Sriphoosanaphan[2], Sombat Treeprasertsuk[2], Kessarin Thanapirom[2,3]. [1]*Department of Medicine, Faculty of Medicine, Chulalongkorn University and King Chulalongkorn Memorial Hospital, Thai Red Cross Society, Bangkok, Thailand;* [2]*Division of Gastroenterology, Department of Medicine, Faculty of Medicine, Chulalongkorn University and King Chulalongkorn Memorial Hospital, Thai Red Cross Society, Bangkok, Thailand, Center of Excellence in Liver Fibrosis and Cirrhosis, Chulalongkorn University, Bangkok, Thailand., Bangkok, Thailand;* [3]*Center of Excellence in Liver Fibrosis and Cirrhosis, Chulalongkorn University, Bangkok, Thailand*
Email: nesskitrawee.p@gmail.com

Background and aims: Patients with compensated advanced chronic liver disease (cACLD) remain at risk of hepatic decompensation. Early risk stratification using non-invasive tests is therefore essential to enable timely intervention. This study aimed to evaluate the prognostic performance of liver stiffness measurement (LSM) for predicting liver-related events (LREs) in patients with cACLD due to metabolic dysfunction-associated steatotic liver disease (MASLD).
Method: Patients with MASLD-related cACLD were enrolled at Chulalongkorn University Hospital between 2015 and 2023. cACLD was defined as LSM ≥10 kPa by vibration-controlled transient elastography. Baseline LSM, Fibrosis-4 (FIB-4) index, AST-to-platelet ratio index (APRI), and NAFLD fibrosis score (NFS) were collected. LREs were defined as ascites, variceal bleeding, hepatic encephalopathy, spontaneous bacterial peritonitis, hepatocellular carcinoma, or death.
Results: Among 603 patients with MASLD-related cACLD, 74 (12.3%) developed LREs over a median follow-up of 58 months (IQR 39–80). Compared with those without LREs, patients who developed LREs were significantly older, had a lower body mass index, and a higher prevalence of diabetes mellitus and chronic kidney disease. They also exhibited more advanced liver dysfunction at baseline, as shown by lower platelet counts and albumin, and higher INR. Furthermore, baseline LSM [21.8 (14.1–31.2) vs 13.5 (11.6–17.1) kPa, p < 0.001], FIB-4 [3.27 (2.22–4.51) vs 1.42 (0.82–2.13), p < 0.001], APRI [0.75 (0.53–1.08) vs 0.42 (0.27–0.69), p < 0.001], and NFS [0.99 (-0.1–1.87) vs – 0.82 (-1.83–0.16), p < 0.001] were significantly higher in the patients who developed LRE than those without LRE. In multivariate analysis, age (HR = 1.060, 95%CI: 1.031–1.090, p < 0.001) and baseline LSM (HR 1.048, 95% CI 1.034–1.061, p < 0.001) were independently associated with LREs. Notably, LSM demonstrated the highest discriminatory performance at both 1 and 2 years (AUC = 0.871 and 0.842), outperforming FIB-4 (AUC = 0.783 and 0.836), APRI (AUC = 0.707 and 0.725), and NFS (AUC = 0.741 and 0.803). By maximizing

Youden's index, LSM > = 20 kPa predicts LRE with the sensitivity of 58.1%, specificity of 84.7% and AUC of 0.753.
Conclusion: Baseline LSM is an independent predictor of LREs in MASLD-related cACLD and demonstrates superior prognostic performance compared with FIB-4, APRI, and NFS. Integration of LSM into risk stratification may improve early identification of high-risk patients and guide timely surveillance and preventive interventions.

WED-212

Circulating extracellular vesicles and ferritin enable machine learning based detection of hepatic steatosis in metabolic dysfunction-associated steatotic liver disease

Eleni-Myrto Trifylli[1,2,3], Athanasios Angelakis[4], Anastasios Kriebardis[2], Nikolaos Papadopoulos[5], Sotirios Fortis[2], Vasiliki Pantazatou[2], Ioannis Koskinas[6], Hariklia Kranidioti[6], Spyridon (Spyros) Siakavellas[6], Spilios Manolakopoulos[6], Melanie Deutsch[6]. *[1]GI-Liver Unit, 2nd Department of Internal Medicine, National and Kapodistrian University of Athens, General Hospital of Athens "Hippocratio", Laboratory of Reliability and Quality Control in Laboratory Hematology (HemQcR), Department of Biomedical Sciences, Section of Medical Laboratories, School of Health & Caring Sciences, University of West Attica (UniWA), Athens, Greece, Athens, Greece; [2]Laboratory of Reliability and Quality Control in Laboratory Hematology (HemQcR), Department of Biomedical Sciences, Section of Medical Laboratories, School of Health & Caring Sciences, University of West Attica (UniWA), Athens, Greece; [3]417 Army Equity Fund Hospital, Athens, Greece; [4]Amsterdam University Medical Center, Epidemiology and Data Science, Amsterdam, Netherlands; [5]National Organization for the Prevention and Treatment of Addictions (EOPAE), Athens, Greece; [6]GI-Liver Unit, 2nd Department of Internal Medicine, National and Kapodistrian University of Athens, General Hospital of Athens "Hippocratio," Athens, Greece*
Email: trif.lena@gmail.com

Background and aims: Metabolic dysfunction–associated steatotic liver disease (MASLD) is the most prevalent chronic liver disease worldwide, yet non-invasive assessment of hepatic steatosis remains limited. Blood-based biomarkers are therefore needed for clinical risk stratification. Extracellular vesicles (EVs) are emerging candidates, while ferritin may provide complementary inflammatory information indicative of steatohepatitis and advanced fibrosis risk. We evaluated whether circulating EV features, alone or combined with ferritin, can identify hepatic steatosis in an independent multicenter cohort using machine learning (ML) and explainable artificial intelligence (XAI).
Method: In this prospective multicenter study, 96 eligible patients presenting exclusively metabolic dysfunction underwent steatosis assessment by transient elastography (iLivTouch FT100, Hisky), with the absence of steatosis (S0) defined by ultrasound attenuation parameter cut-offs (< 244 dB/m) and quality criteria. Circulating EVs were isolated from fasting plasma and characterized by nanoparticle tracking analysis, including mean size, total concentration, and size-based subpopulations. Ferritin was analyzed as a numeric biomarker. Data from one center were used for training with three-fold cross-validation (n = 58), and external validation was performed in an independent cohort from two centers (n = 38). A CatBoost classifier was trained to distinguish steatosis presence (S1–S3) from absence (S0), with interpretability assessed using SHapley Additive exPlanations. Ferritin associations were evaluated using univariate statistical tests.
Results: External validation for steatosis presence (S1–S3) vs absence (S0) showed robust performance, with sensitivity 0.78, specificity 0.76, and AUROC 0.82. Comparable performance was observed in three-fold cross-validation (AUROC 0.81 ± 0.15). SHAP analysis identified ferritin as the most influential predictor, followed by EV size and concentration, with higher ferritin values shifting predictions toward steatosis. In external validation, ferritin was moderately associated with steatosis presence (absolute $r \approx 0.41$, $p < 0.05$).
Conclusion: EVs enable robust ML-based detection of hepatic steatosis in MASLD. Ferritin adds complementary, biologically relevant information regarding inflammation through non-linear effects captured by XAI. The combined use of EVs and ferritin outperforms EV features alone, supporting a multimodal, ML-based approach for scalable, non-invasive MASLD risk stratification.

WED-213

Hepatic antifibrotic response by fibrogenesis markers in patients with MASLD undergoing a 6-month randomized dietary trial

Angelo Armandi[1], Lorenza Vaira[1], Rambabu Surabattula[2], Diana Julie Leeming[3], Gian Paolo Caviglia[1], Marta Guariglia[1], Chiara Rosso[1], Eleonora Dileo[1], Fabio Bioletto[4], Ilaria Goitre[5], Valentina Ponzo[5], Francesca Saba[1], Kamela Gjini[1], Davide Giuseppe Ribaldone[1], Sudha Rani Myneni[2], Simona Bo[5], Detlef Schuppan[2,6], Elisabetta Bugianesi[1]. *[1]Division of Gastroenterology and Hepatology, Department of Medical Sciences, University of Turin, Turin, Italy; [2]Institute of Translational Immunology, Johannes Gutenberg University, Mainz, Germany; [3]Nordic Bioscience, Herlev, Denmark; [4]Division of Endocrinology, Diabetes and Metabolism, Department of Medical Sciences, University of Turin, Turin, Italy; [5]Division of Clinical Nutrition, Department of Medical Sciences, University of Turin, Turin, Italy; [6]Beth Israel Deaconess Medical Center, Harvard Medical School, Boston, Massachusetts, United States*
Email: angelo.armandi@unito.it

Background and aims: Lifestyle intervention aiming at weight loss (WL) is the cornerstone of Metabolic Dysfunction-Associated Steatotic Liver Disease (MASLD) management, but treatment response by non-invasive tests (NITs) is not yet established. Here, we aim to assess antifibrotic response to WL by collagen and non-collagen fibrogenesis markers.
Method: We included 146 patients with MASLD (median age 52 [46–61] years, 63% male) undergoing 6-month randomized dietary trial (2021–2023): Mediterranean Diet (n = 49), Low-Charb Diet (n = 49) or nutritional advice (n = 48). Inclusion criteria: MASLD and LSM (VCTE) < 10 kPa, Body Mass Index (BMI) of 25–35 kg/m^2, age < 65 years. Exclusion criteria: HbA1c > 9.5%, type 2 diabetes (T2D) treated with insulin of GLP1-RA. All parameters were assessed at baseline and 6 months. Serum non-collagen (TSP2, CD163 and IGFB7 - Mainz) and collagen (C4M, PRO-C3, PRO-C4, PRO-C6 and PRO-C8 - Nordic Bioscience) markers were measured through in-house standardized ELISA assay. Primary endpoint was changes in NIT levels between patients achieving < 5% WL (group A n = 91), compared to those achieving 5 – 10% WL (group B n = 38) and ≥10% WL (group C n = 17).
Results: Median BMI was 30,4 [28,7–33,4] kg/m^2, T2D and PNPLA3 GG were present in 31% and 21,8% of cases. PRO-C4 levels fell significantly in group B (p = 0,041) and C (p = 0,015), but not in group A (p = 0,147). TSP2 levels fell substantially in group B (p = 0,046) and in group C (p = 0,004) but not in group A (p = 0,714). FIB-4 and VCTE did not show clinically significant changes. Delta PRO-C4 showed a stepwise negative increase across the 3 groups: from mean - 71,7 (SD 510,3) ng/ml to mean - 228,7 (634,2) ng/ml to mean – 695,5 (1735,8) ng/ml (ANOVA p = 0,011). Delta TSP2 varied from mean - 0,2 (13,5) ng/ml to mean - 4,2 (14,5) ng/ml to mean - 12,6 (15,8) ng/ml (ANOVA p = 0,004). PRO-C4 and TSP2 showed significant association with delta weight changes: R2 0,05 (p = 0,003) and 0,08 (p = 0,0002). Delta TSP2> - 1,96 ng/ml and delta PRO-C4> - 703 ng/ml (both by Youden

Index) were associated with WL> 5% after adjustment for age, male sex, obesity, T2D and PNPLA3 GG: aOR 0,16 (0,04–0,63, p = 0,008) and aOR 0,29 (0,29–0,96, p = 0,043) respectively.
Conclusion: In patients with MASLD without advanced fibrosis undergoing dietary intervention, serum TSP2 and PROC4 levels fell significantly in correlation to WL and were associated with WL> 5%. This evidence suggests their clinical utility to monitor attenuation of hepatic fibrogenesis.

WED-214
Validation of clinical care pathways for detecting significant fibrosis in metabolic dysfunction-associated steatotic liver disease (MASLD): an individual patient data meta-analysis
Kirsi van Eekhout[1], Leonard (Niels) Broekman[1], Laura Konings[2], Alina Saidi[2], Maurice Michel[3,4], Evangelia Mentsiou-Nikolaou[5], Ioanna-Panagiota Kalafati[5,6], Stan Driessen[1], Koen van Son[1], Rocío Gallego-Durán[7], Javier Ampuero[7], Antonio Liguori[8], Andrada Tudor[8], Maria do Mar Orey[9], Sofia Carvalhana[9], Helena Cortez-Pinto[9], Manuel Romero-Gómez[7,10], Luca Miele[8], George Dedoussis[5,6], Jörn M. Schattenberg[3,4], Luisa Vonghia[11,12], Sven Francque[11,12], Oscar Franco[13], Manuel Castro Cabezas[2,14], Yasaman Vali[15], Maarten Tushuizen[16], Douglas Maya-Miles[7], A.G. (Onno) Holleboom[1]. *[1]Department of Vascular and Internal Medicine, Amsterdam University Medical Centre, University of Amsterdam, Amsterdam, Netherlands; [2]Department of Internal Medicine, Franciscus Gasthuis & Vlietland, Rotterdam, Netherlands; [3]Department of Internal Medicine II, Saarland University Medical Centre, Saarland University, Homburg, Germany; [4]Saarland University, Saarbrücken, Germany; [5]Department of Nutrition and Dietetics, School of Health and Education, Harokopio University of Athens, Athens, Greece; [6]Department of Nutrition and Dietetics, School of Physical Education, Sport Science and Dietetics, University of Thessaly, Trikala, Greece; [7]SeLiver Group, Instituto de Biomedicina de Sevilla/CSIC/Virgen del Rocío University Hospital, University of Seville, Seville, Spain, Centro de Investigación Biomédica en Red de Enfermedades Hepáticas y Digestivas (CIBEREHD), Madrid, Spain; [8]UOC Medicina Interna e del Trapianto di Fegato, Dipartimento di Scienze Mediche, Fondazione Policlinico Gemelli IRCCS, Rome, Italy; [9]Serviço de Gastrenterologia e Hepatologia, Unidade Local de Saúde de Santa Maria, Lisbon, Portugal; [10]UCM Digestive Diseases, Virgen del Rocio University Hospital, Institute of Biomedicine of Seville, CIBEREHD, University of Seville, Seville, Spain; [11]Department of Gastroenterology and Hepatology, University Hospital Antwerp, Edegem, Belgium; [12]InflaMed Centre of Excellence, Laboratory for Experimental Medicine and Paediatrics, Translational Sciences in Inflammation and Immunology, Faculty of Medicine and Health Sciences, University of Antwerp, Wilrijk, Belgium; [13]Department of Global Public Health & Bioethics, Julius Center for Health Sciences and Primary Care, University Medical Center Utrecht, Utrecht, Netherlands; [14]Department of Internal Medicine, Erasmus MC, Rotterdam, Netherlands; [15]Department of Epidemiology and Data Science, Amsterdam University Medical Centers, Amsterdam, Netherlands; [16]Department of Gastroenterology and Hepatology, Leiden University Medical Centre, University of Leiden, Leiden, Netherlands*
Email: k.m.vaneekhout@amsterdamumc.nl

Background and aims: To optimize the implementation of preventive hepatology within current cardiometabolic care structures, pathways using sequential non-invasive tests (NITs) are proposed to detect liver fibrosis due to metabolic dysfunction–associated steatotic liver disease (MASLD). These pathways aim to improve early detection while reducing referrals of mild cases. Despite growing interest in their application, large-scale, standardized evaluations of their performance are lacking.
Method: We conducted an individual patient data meta-analysis (IPDMA), pooling historic European cohorts of adults aged 18–80 years at cardiometabolic risk, with or without steatosis, excluding excessive alcohol use and other liver diseases. Clinically significant fibrosis was defined using a predefined hierarchical reference standard. We evaluated care pathways combining a blood-based NIT (FIB-4, MAF-5, NFS, APRI, or BARD) followed by a liver stiffness measurement (LSM)-based NIT (FibroScan, FAST, or AGILE-3+). Pathway performance was assessed using sensitivity, specificity, fibrosis detection rates, and numbers needed to screen (NNS) for referral and fibrosis identification. The best-performing pathway was defined by the highest sum of sensitivity and specificity.
Results: A total of 4,168 participants from 10 cohorts were included, with data available for 3,850 to assess clinically significant fibrosis. Clinically significant fibrosis was present in 19.5% (n = 752), based on: 1. histology (n = 507), 2. MRE (n = 15), 3. MRI-cT1 (n = 14) or, 4. VCTE-LSM (n = 216). Among 93 pathways, the two-tier MAF-5 followed by FibroScan ≥8 kPa or FAST >0.35 showed the best performance (sensitivity 0.80, specificity 0.93), with an NNS of 5 for referral and 9 for fibrosis detection. APRI with a cutoff > 0.5 was the best-performing one-tier pathway (sensitivity 0.61, specificity 0.81).
Conclusion: This IPDMA provides valuable insights into the performance of various one-tier and two-tier pathways for detecting clinically significant liver fibrosis in individuals at cardiometabolic risk. Two-tier pathways consistently outperformed one-tier pathways, particularly those combining MAF-5 with LSM-based NITs. These strategies optimize fibrosis detection while reducing unnecessary referrals with acceptable NNS. While awaiting prospective validation in large-scale, multinational cohorts, this IPDMA supports implementation of diagnostic clinical pathways for liver fibrosis detection in patients at cardiometabolic risk for MASLD.

WED-215
Simplified metabolic dysfunction associated fibrosis-5 (sMAF-5) score to identify at-risk liver fibrosis and to predict prognosis
Laurens A. van Kleef[1], Xinrui Jin[2], Terry Cheuk-Fung Yip[2], Jerome Boursier[3], Elisabetta Bugianesi[4], Chan Wah Kheong[5], George Boon Bee Goh[6], Seung Up Kim[7], Masato Yoneda[8], Philip N. Newsome[9], Salvatore Petta[10], Manuel Romero-Gómez[11], Arun J Sanyal[12], Ming-Hua Zheng[13], Hannes Hagström[14], José Luis Calleja Panero[15], Emmanuel Tsochatzis[16], Victor de Lédinghen[17], Jian-Gao Fan[18], Harry L.A. Janssen[1], Sven Francque[19], Vincent Wai-Sun Wong[2], Willem Pieter Brouwer[1]. *[1]Erasmus MC, Rotterdam, Netherlands; [2]The Chinese University of Hong Kong, Sha Tin, Hong Kong; [3]Angers Unitversity Hospital, Angers, France; [4]Department of Medical Sciences, Division of Gastroenterology, A.O.U. Città, Turin, Italy; [5]della Salute e della Scienza di Torino, University of Turin, Turin, Italy, Turin, Italy; [6]Singapore General Hospital, Singapore, Singapore; [7]Yonsei University School of Medicine, Yonsei, Korea, Rep. of South; [8]University of Yakahoma, Yakahoma, Japan; [9]Roger Williams Institute of Liver Studies, School of Immunology & Microbial Sciences, Faculty of Life Sciences and Medicine, King's College London, Foundation for Liver Research and King's College Hospital, London, United Kingdom; [10]Section of Gastroenterology, PROMISE, University of Palermo, Palermo, Italy; [11]UCM Digestive Diseases, Virgen del Rocio University Hospital, SeLiver Group, Institute of Biomedicine of Seville, Ciberehd, Department of Medicine. University of Seville, Seville, Spain; [12]Stravitz-sanyal Institute for Liver Disease and Metabolic Health, Virginia Commonwealth University School of Medicine, Richmond, VA, Richmond, United States; [13]Wenzhou Medical University, Wenzhou, China; [14]Karolinska Institutet, Huddinge, Sweden; [15]Department of Gastroenterology and Hepatology, Hospital Universitario Puerta de Hierro, Universidad Autonoma de Madrid, Madrid, Spain, Madrid, Spain; [16]Royal Free Hospital, London, United Kingdom; [17]University of Bordeaux, Bordeaux, France; [18]Shanghai Jiaotong University, Shanghai, China; [19]Antwerp University Hospital, Edegem, Belgium*
Email: l.vankleef@erasmusmc.nl

Background and aims: Metabolic dysfunction Associated Fibrosis - 5 (MAF-5), a waist-circumference-based non-invasive test (NIT) for fibrosis risk stratification, has emerged as a well-performing test in low-prevalence populations. Waist circumference is often not available, which limits the utility of the MAF-5. Therefore, we

developed and validated the simplified MAF-5 (sMAF-5), which could be used when waist circumference is unavailable.
Method: US representative individuals from NHANES 2017–2020 with metabolic dysfunction were selected. Correlation between MAF-5 and sMAF-5 was assessed using Pearson's correlation coefficient. AUC analysis was used to compare sMAF-5 to other scores with the DeLong test for assessing statistically significant differences in detecting LSM ≥8 kPa. sMAF-5 was validated in US NHANES 2021–2023 and MASLD patients across a pooled cohort of 16 tertiary referral centres in the US, Europe, and Asia (VCTE Prognosis Study Group) for the presence of LSM ≥ 8 kPa and liver-related events (LRE) defined as hepatic decompensation and HCC.
Results: In three cohorts, 22,723 individuals were included. The derivation cohort included 6,191 adults (49% male, mean age 52 years) of whom 10.1% had LSM ≥ 8 kPa. The sMAF-5, comprising BMI, diabetes, AST, platelets, and sex, was strongly correlated with MAF-5 (r = 0.97). With sMAF-5, 61.6% were classified as low risk (sMAF-5 < 0), 14.0% as intermediate risk (0–1), and 24.4% as high risk (≥ 1), with observed LSM ≥ 8 kPa prevalence of 3.4%, 9.2%, and 27.7%, respectively. The AUC of sMAF-5 (AUC 0.803) did not significantly differ from the original MAF-5 (AUC 0.808), but was significantly better than SAFE (0.739), LiverRisk (0.715), LiverPRO (0.715), and FIB-4 (0.667). Results were validated in the independent NHANES 2021–2023 cohort (n = 4,202), yielding similar results. In the VCTE prognosis study group (12,330 MASLD patients), sMAF-5 was associated with LRE where the time-dependent AUC for LRE (all), hepatic decompensation, and HCC was 0.75, 0.79, and 0.71, respectively. AUC particularly increased with longer time to event. Among MASLD patients, the cumulative incidence of LRE was 0.6% and 0.7% in MASLD patients with sMAF-5 < 0 and 0–1 and 3.2% for sMAF-5 ≥ 1.
Conclusion: sMAF-5 is a valuable replacement for the original MAF-5 as a first-line test in screening algorithms when waist circumference is unavailable, enabling the identification of adult community-dwelling individuals at increased risk of liver fibrosis and future liver-related events.

WED-216
Evaluating non-invasive screening strategies for identifying treatment-eligible fibrotic MASH in MASLD patients

Laurens A. van Kleef[1], Maurice Michel[2], Katrine Lindvig[3], Maja Thiele[3], Harry L.A. Janssen[1], Christian Labenz[4], Jörn M. Schattenberg[2], Willem Pieter Brouwer[1]. *[1]Erasmus MC, Rotterdam, Netherlands; [2]Department of Internal Medicine II, Saarland University Medical Center, Homburg, Germany; [3]Odense University Hospital, Odense, Denmark; [4]University Medical Center Mainz, Mainz, Germany*
Email: l.vankleef@erasmusmc.nl

Background and aims: Non-invasive tests (NITs), particularly FIB-4, are increasingly used to detect advanced chronic liver disease. However, FIB-4 shows suboptimal performance as a stand-alone screening tool in the general population. We therefore evaluated the ability of FIB-4–based strategies to identify individuals with fibrotic MASH eligible for pharmacologic treatment.
Method: We analysed two cohorts: patients with biopsy-proven MASLD from \German tertiary care, and participants with MASLD defined by VCTE and CAP from US representative adults from NHANES 2017–2020. Individuals with presumed cirrhosis (F4 on biopsy or LSM ≥15 kPa) were excluded from the main analyses, consistent with AASLD resmetirom treatment criteria. We assessed the sensitivity and specificity of FIB-4 and LSM in the German cohort and extended this with newer NITs in NHANES.
Results: Among 365 patients with biopsy-proven MASLD (mean age 51 years; 53.2% male), 58.4% had F2–F3 fibrosis, indicating treatment eligibility. Using the EASL–EASD–EASO two-step screening strategy (FIB-4 ≥1.3, or ≥2.0 for those aged ≥65 years, followed by VCTE), only 31% of patients with biopsy-confirmed F2–F3 fibrosis would have been identified. FIB-4 alone resulted in a 50% points loss in sensitivity, and the addition of LSM caused a further 20% loss. Findings were consistent when including individuals with cirrhosis. In NHANES, among 2,785 community-dwelling individuals with MASLD (mean age 55 years; 53.5% male), 369 (13.3%) had an LSM between 8 and 15 kPa, meeting AASLD non-invasive criteria for resmetirom eligibility. Using age-specific cut-offs, FIB-4 demonstrated low sensitivity (19%) but high specificity (86%). Newer NITs outperformed FIB-4: LiverPRO (F2 model, threshold 0.25) had a sensitivity of 56% and specificity of 61%; SAFE (threshold 0), 77% and 45%; and MAF-5 (threshold 0), 86% and 45%. There were no meaningful changes including individuals with LSM ≥ 15 kPa. A two-step strategy using MAF-5 as the high-sensitivity screening test followed by FIB-4 confirmation yielded a sensitivity of 17% (69% points lower than MAF-5 alone) and a specificity of 91% (46% points higher), indicating that most true positives were excluded in the second step.
Conclusion: Detecting patients eligible for pharmacologic treatment due to fibrotic MASH remains challenging in both clinical and population-based settings. FIB-4–based screening strategies miss the majority of individuals who may benefit from resmetirom, highlighting the need for improved non-invasive algorithms.

WED-217
State-transition models of MASLD progression in economic evaluation: an updated systematic review

Rohan Vijjhalwar[1], Rohit Vijjhalwar[2,3], Naomi Hollings-Tenant[3], Mary Onoja[3], Keith Cooper[3], Chinonso Nwoguh[2,3], Tina Reinson[3], Josh Bilson[3], Chris D Byrne[3], Ryan M Buchanan[2,3]. *[1]Epsom and St Helier University Hospitals NHS Trust, London, United Kingdom; [2]University Hospital Southampton NHS Foundation Trust, Southampton, United Kingdom; [3]University of Southampton, Southampton, United Kingdom*
Email: rohan_vijjhalwar@hotmail.com

Background and aims: Metabolic dysfunction-associated steatotic liver disease (MASLD) affects over one-third of adults and is linked to obesity and type 2 diabetes. Economic evaluations rely on decision-analytic models to project long-term outcomes and assess new diagnostics and therapies, but approaches to modelling MASLD progression vary widely. This systematic review investigated how state-transition models published since June 2021 have represented the natural history of MASLD/NAFLD/MASH for economic evaluation.
Method: A systematic review was registered prospectively on PROSPERO (CRD420251237086) and conducted in PubMed, Scopus, Cochrane CENTRAL and INAHTA from June 2021 onwards. We included adult state-transition models (Markov or microsimulation) used in full economic evaluations or burden-of-disease analyses that explicitly modelled progression across fibrosis and advanced liver disease states. Model structures, transition and regression probabilities, mortality assumptions, utilities and diabetes adjustment were extracted. The probabilities of transition are considered low if they are smaller than 0.1, and high if the probability is greater than 0.6.
Results: 26 studies were included. All but one used cohort Markov models; one used agent-based microsimulation. Most evaluated screening or treatment strategies in high-income settings; three studies explicitly adjusted for diabetes. Model structures commonly included F0-F3, compensated and decompensated cirrhosis, hepatocellular carcinoma and liver transplantation. Forward transition probabilities varied markedly: annual F0-F1 ranged between 0.01–0.17, F1-F2 ranged between 0.03–0.60, F2-F3 ranged between 0.03–0.12 and F3-CC ranged between 0.06–0.19, CC-DC and DC-HCC were typically 0.04–0.10 and 0.02–0.07, respectively. Regression was

modelled in a minority of studies with small, mainly treatment-driven F1-F0 and F2-F1 probabilities; regression from cirrhosis was rare. Utilities and mortality specifications showed comparable heterogeneity.
Conclusion: Contemporary models remain highly heterogeneous and often rely on non-MASLD natural history, with limited metabolic risk stratification. These differences are likely to influence the estimated burden and cost-effectiveness of emerging MASLD therapies.

WED-219
LiverPRO prediction reflects fibrogenic activity in patients with metabolic dysfunction-associated steatohepatitis by identifying patients with elevated PRO-C3
Ying-Wooi Wan[1], Julie Astono[2], Andressa de Zawadzki[3], Diana Julie Leeming[3], Morten Karsdal[3], Regina Lemus[1], Andreas Sand[2], Paresh Thakker[1], Haakan Wennbo[1], Katrine Lindvig[2], Zoltan Derdak[1]. *[1]Takeda Development Center Americas, Inc., Cambridge, MA, United States; [2]Evido Health ApS, Copenhagen, Denmark; [3]Nordic Bioscience A/S, Herlev, Denmark*
Email: zoltan.derdak@takeda.com

Background and aims: Metabolic Dysfunction-Associated Steatohepatitis (MASH) is defined by progressive fibrotic remodeling of the liver, where fibrogenesis is a key determinant of disease progression and prognosis. Non-invasive measures of fibrogenesis are essential for selecting patients with high fibrogenic activity, a key requirement for antifibrogenic therapy trials. LiverPRO from Evido Health is a data-driven model predicting significant (F2), advanced (F3), and cirrhotic (F4) fibrosis using non-invasive clinical and laboratory parameters. PRO-C3, the N-terminal pro-peptide of type III collagen, is a circulating biomarker of active fibrogenesis. This study evaluated the association between LiverPRO predictions and PRO-C3 levels in MASH patients.
Method: Serum PRO-C3 (Roche-COBAS) and LiverPRO predictions for F2, F3, and F4 were assessed in a screening cohort of 121 participants with presumed MASH enrolled in a Takeda-sponsored Phase 1b clinical trial. The cohort was middle-aged (mean age 53 ± 10.9 years) and predominantly female (56%). Mean liver stiffness was 11.5 ± 6.0 kPa, the FAST score was 0.50 ± 0.26. PRO-C3 had a median value of 39.25 ng/mL (IQR, 35.08–48.73). Unadjusted associations between LiverPRO and PRO-C3 were assessed using Spearman correlation. High and low fibrogenesis groups were defined by median or fixed PRO-C3 cutoff (40 ng/mL). Discriminative performance was evaluated using area under the receiver operating characteristic curve (AUROC). Statistical significance was determined by two-sided Wilcoxon rank-sum tests.
Results: LiverPRO predictions correlated positively with PRO-C3 (F2: $\rho = 0.25$, $p = 0.0072$; F3: $\rho = 0.34$, $p = 0.00021$; F4: $\rho = 0.28$, $p = 0.0021$). Subjects with high PRO-C3 had significantly higher LiverPRO values than those with low PRO-C3 (all $p < 0.01$). The AUROC for LiverPRO distinguishing high versus low PRO-C3 groups was 0.65 (95% CI: 0.55–0.75) for F2, F3 and 0.64 (95% CI: 0.54–0.74) for F4, indicating moderate discrimination.
Conclusion: LiverPRO scores show a strong association with Pro-C3, a marker of active fibrogenesis, in screening MASH populations. These findings suggest LiverPRO may aid identification patients with high fibrogenic activity and support enrichment strategies in clinical trials with agents that target hepatic fibrogenesis. Incorporating LiverPRO alongside PRO-C3 could streamline patient selection and accelerate antifibrotic drug development in MASH.

WED-220
A distinct aromatic catabolism enterotype of the gut microbiome in metabolic dysfunction associated steatotic liver disease with type 2 diabetes
Jakob Weglage[1], Martin Kluge[1], Josephine Frohme[1], Sonja Lang[2], Anna Martin[2], Frank Tacke[1], Münevver Demir[1]. *[1]Charité Universitaetsmedizin Berlin, Department of Hepatology and Gastroenterology, Berlin, Germany; [2]University Hospital Cologne, Department of Gastroenterology and Hepatology, Cologne, Germany*
Email: jakob-hermann-josef.weglage@charite.de

Background and aims: Distinct changes in the gut microbiome have been associated with MASLD, but the functional interference between the gut microbiome and cardiometabolic comorbidities of MASLD remains incompletely understood. We investigated whether type 2 diabetes (T2D), obesity (OB), dyslipidaemia (DL) and arterial hypertension (HTN) are associated with compositional and/or functional microbiome signatures in MASLD.
Method: Stool samples from 130 adults with MASLD underwent 16S rRNA sequencing. Functional profiles were inferred using PICRUSt2 and aggregated into MetaCyc-based functional groups. Participants were stratified by T2D (n = 30), OB (n = 114), DL (n = 70) and HTN (n = 80). Predicted pathway abundances were CLR-transformed. Alpha/beta diversity, ordinations (PCA/PCoA/UMAP) and differential pathway abundance were assessed. Group differences were tested using linear regression adjusted for age and sex with FDR correction.
Results: Alpha/beta diversity and ordination analyses revealed no subgroup-specific clustering by cardiometabolic comorbidities. Only few bacterial genera differed by T2D. In contrast, 166 predicted pathways were differentially abundant in MASLD+T2D after covariate adjustment, but not in OB, DL, or HTN. The vast majority of T2D-associated pathways showed lower predicted abundance, spanning carbon/energy metabolism, amino acid and nucleotide biosynthesis, vitamin/cofactor metabolism and cell envelope functions (median $\beta \approx -0.5$). Conversely, pathways with higher predicted abundance in MASLD+T2D mapped to "aromatic degradation pathways" (10/11 pathways in the unadjusted model; 10/15 after adjustment; median $\beta \approx +5.6$), including catechol, gallate, salicylate, 4-hydroxyphenylacetate and p-cresol-related pathways.
Conclusion: Within MASLD, T2D shows no large-scale differences in bacterial community structure but a distinct predicted functional enterotype characterised by widespread reduction of core bacterial metabolic pathways alongside a selective enrichment of aromatic compound degradation. These changes were specific to T2D and were not observed for OB, DL or HTN. The enrichment of aromatic degradation aligns with prior mechanistic evidence linking microbial aromatic metabolites to impaired hepatic lipid handling and insulin signalling, suggesting that enhanced aromatic substrate turnover may contribute to the more progressive phenotype in MASLD with T2D.

WED-221
Understanding the metabolic burden among people with fibrosis and evaluating the implementation of the EASL clinical care pathway in China using the Meinian database
Lai Wei[1], Lixin Guo[2], Weihao Wang[2], Siyun Wang[3], Zewei Shen[3], Kwabena Opuni[4]. *[1]Hepatopancreatobiliary Center, Beijing Tsinghua Changgung Hospital, Tsinghua University, Beijing, China; [2]Department of Endocrinology, Beijing Hospital, National Center of Gerontology, Institute of Geriatric Medicine, Chinese Academy of Medical Sciences, Beijing, China; [3]Novo Nordisk (Shanghai) Pharma Trading Co., Ltd, Shanghai, China; [4]Novo Nordisk A/S, Bagsværd, Denmark*
Email: weelai@163.com

Background and aims: Metabolic dysfunction-associated steatotic liver disease (MASLD) is a major global health burden. Liver fibrosis, a

key prognostic factor, increases severe hepatic and cardiovascular risk. However, evidence on fibrosis prevalence and metabolic impact in China are limited. Updated EASL–EASD–EASO Clinical Practice Guidelines (CPG) recommend a clinical care pathway (CCP) for fibrosis screening and risk stratification in at-risk populations, but real-world CCP implementation in China remains unclear. This study assessed fibrosis prevalence, associated patient characteristics, and EASL CCP implementation in the Chinese population.

Method: We analyzed the Meinian health check-up database (~20 million Chinese adults, ≥18 years; Jan 1–Dec 31, 2023). The cohort met EASL CPG assessment criteria. We stratified characteristics by liver stiffness measurement (LSM) and assessed fibrosis-4 (FIB-4) performance with LSM in the EASL at-risk population (T2D, obesity plus ≥1 cardiometabolic risk factor, or elevated liver enzymes). Data were analysed descriptively.

Results: Overall, 1,124,132 individuals comprised the study cohort. Of these, 92% had no/mild fibrosis (LSM < 8 kPa), 7% had moderate fibrosis (MF; 8–12 kPa), and 1% had advanced fibrosis (AF; >12 kPa). Compared with the no/mild fibrosis group, the MF and AF groups had higher prevalences of obesity (18% vs. 49% and 64%), diabetes (9% vs. 19% and 27%), and ≥1 metabolic risk factor (81% vs. 96% and 97%), respectively. The number of concurrent metabolic risk factors increased with rising LSM. Of the cohort, 36% were identified as at-risk population to further screen for fibrosis according to EASL CCP (low 79%, intermediate 15%, high 6%). Using LSM as the reference, FIB-4 demonstrated a negative predictive value (NPV) of 86.3% (95% CI: 86.2–86.5), a positive predictive value (PPV) of 19.2% (95% CI: 18.9–19.5), sensitivity 27.5% (95% CI: 27.1–27.8), and specificity 79.9% (95% CI: 79.7–80.0). Notably, among the low-risk subgroup (n = 319,303) stratified by FIB-4, 12.0% had LSM ≥8 kPa (MF) and 1.6% had LSM >12 kPa (AF).

Conclusion: This study highlights the significant metabolic burden of liver fibrosis in the Chinese population. Although FIB-4 is recommended as the initial CCP step for its low cost and simplicity, its sensitivity and PPV are suboptimal, despite acceptable NPV. Optimizing screening strategy is needed to better identify and manage individuals at risk of fibrosis and improve clinical outcomes.

WED-225-YI

Real-world liver fibrosis screening patterns of adults with type 2 diabetes and cirrhosis: a population-based Canadian cohort

Cindy Wen[1,2], Jennifer Flemming[1,2,3], Maya Djerboua[3], Jessica Burnside[1,2], Giada Sebastiani[4], Sahar Saeed[1]. *[1]Department of Public Health Sciences, Queen's University, Kingston, Canada; [2]Department of Medicine, Queen's University, Kingston, Canada; [3]ICES, Queen's University, Kingston, Canada; [4]Department of Medicine, McGill University, Montreal, Canada*
Email: cindy.wen@queensu.ca

Background and aims: People living with type 2 diabetes (T2D) are at high risk of liver disease progression. The Fibrosis-4 (FIB-4) Index is recommended as the first step for risk stratification. We aimed to describe screening patterns from T2D to the diagnosis of incident cirrhosis.

Method: We conducted a population-based retrospective cohort study using laboratory and administrative health data in Ontario, Canada, linked through ICES between 2010 and 2022. Adults aged 40 + with incident T2D diagnosis and no history of liver disease were followed to their first cirrhosis diagnosis using validated identification algorithms. Patterns, frequencies, and timing of liver fibrosis screening were assessed using the FIB-4 Index categorized as low (< 1.3), moderate (1.3–2.67), and high risk (> 2.67).

Results: We identified 782,898 adults with incident T2D and no history of liver disease. Of whom 12,423 developed cirrhosis in a median of 4.74 [IQR: 2.34, 7.59] years. At baseline, 42.0% were female, median age 60 years [IQR: 52, 67], hemoglobin A1c 6.70% [6.20, 7.90], 22.7% lived in areas of the lowest income quintile, 27.5% reside in highly racialized or newcomer-dense regions, 78.2% have a primary care provider, and 56.9% were classified as having very high comorbidity using the Aggregated Diagnosis Groups System. Among the 41.3% who had no history of FIB-4 screening before their cirrhosis diagnosis, the median time to cirrhosis was 4.07 [IQR 1.89, 6.80] years. Among the 58.7% that were screened, the median time from T2D diagnosis to first screen was 1.34 [IQR: 0.39, 3.27] and 5.23 [IQR: 2.71, 8.02] years to cirrhosis. 57.9% were only screened once before cirrhosis diagnosis (FIB-4 risk: 23.1% low, 26.0% moderate, 50.9% high), with a median time of 1.70 [IQR: 0.50, 3.89] years to the first screen and 4.46 [IQR: 2.13, 7.24] years to cirrhosis. Differentially, among the 42.1% with > 1 FIB-4 screen, they had a median of 1.00 [IQR: 0.29, 2.43] years to first screen and 6.29 [IQR: 3.76, 9.91] years to cirrhosis (FIB-4 risk at first screen: 47.5% low, 52.5% moderate, none were high).

Conclusion: Among people with T2D diagnosed with cirrhosis, rapid progression was common, and nearly half had no history of FIB-4 screening despite having universal access to healthcare. Of those screened, about one-third were identified as low risk using the current cutoffs before a cirrhosis diagnosis. Future analyses will continue to explore the relationship between risk factors, screening patterns, and time to advanced liver outcomes.

WED-226

Social determinants of health shape all-cause mortality risk in steatotic liver disease: a machine learning analysis

Cindy Wen[1,2], Wei Tu[1,3], Giada Sebastiani[4], Jessica Burnside[1,2], Carmela Rapino[1,5], Alnoor Ramji[6], Mark Swain[7], Keyur Patel[8], Jennifer Flemming[1,2,9], Sahar Saeed[1]. *[1]Department of Public Health Sciences, Queen's University, Kingston, Canada; [2]Department of Medicine, Queen's University, Kingston, Canada; [3]Canadian Cancer Trials Group, Queen's University, Kingston, Canada; [4]Department of Medicine, McGill University, Montreal, Canada; [5]School of Medicine, Toronto Metropolitan University, Brampton, Canada; [6]Division of Gastroenterology, University of British Columbia, Vancouver, Canada; [7]Calgary Liver Unit, Cumming School of Medicine, University of Calgary, Calgary, Canada; [8]Division of Gastroenterology and Hepatology, University Health Network, Toronto, Canada; [9]ICES, Queen's University, Kingston, Canada*
Email: cindy.wen@queensu.ca

Background and aims: Risk-stratification for people with steatotic liver disease (SLD) relies on a "one-size-fits-all" approach that emphasizes clinical factors, despite increasing evidence on the impact of social determinants of health (SDoH). We aimed to evaluate the prognostic utility of adding SDoH to predict all-cause mortality among adults with SLD.

Method: We analyzed data from the Canadian Longitudinal Study on Aging, which follows aging adults (45 to 85 years) from 2012 to 2021. SLD was defined as hepatic steatosis (via the NAFLD Ridge Score) and 1 or more cardiometabolic risk factors (CMRFs). Our outcome was all-cause mortality. Data was split into 75% training, 25% testing, and 5-fold cross-validation was used for hyperparameter tuning. Predictors were selected via a Least Absolute Shrinkage and Selection Operator (LASSO) Cox Regression from clinical markers (n = 8), alcohol consumption (n = 2), sociodemographics (n = 8), and other lifestyle factors (n = 3). We used a Survival Classification and Regression Tree (CART) and Random Survival Forest (RSF). The best model was evaluated in the test set using the Concordance Index (C-Index), Integrated Brier Score (iBS), and Time-Dependent Area Under the

Receiver Operating Curve (AUC(t)). Prognostic factors were identified using Shapley Additive exPlanations values.
Results: We identified 9,239 adults with SLD (34.3% female) across a median follow-up of 7.67 years with 687 (7.4%) deaths. At baseline, 44.4% were 65 years or older, 93.4% were White, 30% had < $50,000 household income, 42.7% with education below Bachelor's degree, median alcohol consumption 26.9 g/week [IQR: 0, 94.2], and median alanine aminotransferase (ALT) 26 U/L [IQR: 20, 35]. The RSF provided the best model for all-cause mortality with a moderate test set performance: C-Index 0.780, iBS 0.0296, and mean AUC(t) 0.788. End of follow-up global importance indicates that after age, the most prognostic factors were smoking, number of CMRFs, sex, physical activity, hemoglobin A1c, waist circumference, household income, ALT, and education. The test set was stratified to 'high' and 'low' risk based on RSF predictions, showing strong separation in survival curves ($p < 0.001$).
Conclusion: An equity-oriented RSF meaningfully stratified 'high' and 'low' risk adults with SLD for all-cause mortality. Beyond clinical factors, the impact of income, education, and lifestyle underscore the value in integrating SDoH. Future work will integrate sex-stratification for more inclusive SLD risk-stratification.

WED-227
Macrophage caspase-8 deficiency promotes nonalcoholic steatohepatitis progression
Qiong Wu[1], Mingwei Sheng[2], Xiyun Bian[3], Fengmei Wang[2]. *[1]Tianjin First Central Hospital, Nankai University, Tianjin, China; [2]Tianjin First Central Hospital, Tianjin, China; [3]Tianjin Fifth Central Hospital, Tianjin, China*
Email: wangfengmeitj@126.com

Background and aims: Metabolic dysfunction-associated steatotic liver disease (MASLD) is a common chronic liver condition marked by excess fat accumulation. The cysteine-aspartic acid protease (Caspase)-8 is essential for modulating cell apoptosis and immune responses, but its function in macrophages during Metabolic Dysfunction-Associated Steatohepatitis (MASH) remains unknown.
Method: Casp8 expression was analyzed in patients with MASH and mouse models. We induced MASH in myeloid-specific Casp8 knockout ($Casp8^{M\text{-}KO}$) and floxed control ($Casp8^{fl/fl}$) mice by feeding them a high-fat/high-cholesterol diet. Through comprehensive experiments utilizing in vivo and in vitro, we investigated the mechanistic role of caspase-8 in liver macrophages during MASH pathogenesis. We also analyzed public transcriptomic datasets of MASH model mice.
Results: Caspase-8 deficiency in hepatic macrophages facilitated MASH progression by triggering an axis comprising the cellular FLICE-like inhibitory protein, ETS domain transcription factor 4, and prosaposin, which promoted macrophage M1 polarization and subsequently activated hepatocyte Rac1/CDC42/JNK signaling via G protein-coupled receptor 37-like 1. This molecular cascade was found to ultimately drive hepatic lipid accumulation and inflammation.
Conclusion: Our findings reveal a previously unrecognized role for macrophage caspase-8 in regulating lipid metabolism and inflammation during MASH progression, and identify its key regulatory mechanism as a potential therapeutic target in metabolic liver disorders.

WED-228
Prevalence of advanced liver fibrosis among first- second- and third-degree relatives of patients with MASLD-related advanced fibrosis
Ismael de Jesus Yepes Barreto[1], Nicole Chamorro[1], Guillermo Donado[1], Maria Saavedra[2], Samuel Perez[3], Yohana Poveda[4], Diana Marcela Escobar[5], Juan Carlos Restrepo[6]. *[1]Universidad de Cartagena, Asociacion Colombiana de Hepatologia, Cartagena de Indias, Colombia; [2]Clínica Ces, Medellín, Colombia; [3]Universidad de antioquia, Medellín, Colombia; [4]Imbanaco, Cali, Colombia; [5]Fundacion Valle Del Lili, Cali, Colombia; [6]Hospital Pablo Tobón Uribe, Medellín, Colombia*
Email: ismayep@yahoo.com

Background and aims: First-degree relatives of patients with MASLD-related cirrhosis are recommended to undergo liver fibrosis screening based on high prevalence rates reported in Europe and the United States. Genetic susceptibility and shared metabolic risk factors support a hereditary component in MASLD progression. However, it remains unclear whether this increased risk extends beyond first-degree relatives or applies to Latin American populations. This study aimed to determine the prevalence of advanced liver fibrosis among first- second- and third-degree relatives of patients with MASLD-related advanced fibrosis.
Method: Patients with confirmed MASLD-related advanced fibrosis were identified, and their relatives were invited to participate. First-degree relatives included parents, siblings, and children; second-degree relatives included grandparents and grandchildren; and third-degree relatives included uncles, aunts, nephews, and nieces. All participants underwent transient elastography (FibroScan®) and clinical evaluation, including anthropometric measurements, alcohol intake assessment, and metabolic comorbidities. Significant fibrosis was defined as liver stiffness ≥8.0 kPa. Only descriptive statistics were performed.
Results: A total of 166 relatives were included (65.7% female, mean age 45.0 ± 15.2 years). Overall, advanced fibrosis was detected in 9.1% of participants. Prevalence was highest among first-degree relatives (9.7%), but remained substantial in second-degree (5.6%) and third-degree relatives (6.7%). Mean body mass index was elevated across all groups, with similar values in first- (28.8 ± 6.1 kg/m^2), second- (26.9 ± 5.5 kg/m^2), and third-degree relatives (28.5 ± 5.0 kg/m^2). Alcohol consumption was generally low (29.9 ± 67.7 g/week) and showed no clear gradient by degree of kinship. Metabolic comorbidities were present but did not differ markedly across groups.
Conclusion: In this Latin American cohort, advanced liver fibrosis was frequent not only among first-degree relatives of patients with MASLD-related advanced fibrosis, but also among second- and third-degree relatives. The prevalence observed in these groups is markedly higher than the ~1.3% reported in first-degree relatives of individuals without steatosis or advanced fibrosis. These findings suggest that familial risk extends beyond first-degree kinship and support considering broader family-based screening strategies in MASLD, particularly in high-risk populations.

WED-229
Referral burden and second-tier testing in two-step algorithms for detecting significant hepatic fibrosis among Asian community-based type 2 diabetes mellitus
Eileen Yoon[1], Hyo Young Lee[1], Sang Bong Ahn[2], Joo Hyun Oh[3], Mimi Kim[4], Bo-Kyeong Kang[4], Chul-min Lee[4], Jihyun An[1], Ha Il Kim[1], Eun Chul Jang[5], Hye-Lin Kim[6], Jeong-Yeon Cho[7], Dae Won Jun[1]. *[1]Department of Internal Medicine, Hanyang University College of Medicine,, Seoul, Korea, Rep. of South; [2]Department of Internal Medicine, Nowon Eulji Medical Center, Eulji University, Seoul, Korea, Rep. of South; [3]Department of Internal Medicine, CHA University College of Medicine, Seongnam, Korea, Rep. of South; [4]Department of Radiology, Hanyang University College of Medicine, Seoul, Korea, Rep. of South; [5]Department of Occupational and Environmental Medicine, College of Medicine, Soonchunhyang University, Chunan, Korea, Rep. of South; [6]College of Pharmacy, Sahmyook University, Seoul, Korea, Rep. of South; [7]Department of Pharmacotherapy, University of Utah College of Pharmacy, Salt Lake, United States*
Email: noshin@hanyang.ac.kr

Background and aims: Current guidelines recommend a FIB-4 based two-step screening algorithm for hepatic fibrosis in type 2 diabetes mellitus (T2DM). We evaluated the social burden (need 2nd tier testing (%), referral rate, missing rate, and false-positive rate of 1st tier test) of two-step algorithm for significant hepatic fibrosis in community-based T2DM cohorts.
Method: We analyzed data from three Asian community-based health check-up cohorts comprising 3,152 individuals with T2DM assessed using vibration-controlled transient elastography or magnetic resonance elastography.
Results: The prevalence of significant hepatic fibrosis (≥F2) among individuals with T2DM ranged from 4.3% to 18.3%, and advanced fibrosis (≥F3) from 0.9% to 7.4%. Using the two-step algorithm based on age-adjusted FIB-4, 22.3–29.0% required 2nd tier testing, and 11.2–12.7% required hepatology referral. However, the FIB-4 model showed low sensitivity (54.9–58.1%), with a high negative rate of 2nd tier testing in the intermediate-risk group (72.6–100%). Lowering the FIB-4 threshold increased 2nd tier testing and referrals without improving sensitivity. In contrast, strategies based on NFS and MAF-5 tended to overclassify risk, resulting in higher rates of 2nd tier testing and referrals, whereas the LiverRisk score tended to underclassify risk, showing low sensitivity.
Conclusion: In Asian community-based cohorts, the FIB-4-based two-step algorithm demonstrated acceptable 2nd tier testing and referral rates but low sensitivity and a high negative rate of 2nd tier testing in individuals with T2DM for detecting significant hepatic fibrosis.

WED-230
Validation of noninvasive scores for identifying significant fibrosis and at-risk metabolic dysfunction-associated steatohepatitis in obese bariatric surgery patients

Jing Zhang[1], Xiaodie Wei[1], Zhang Nengwei[2], Meng Fanqiang[3]. *[1]Beijing You'an Hospital Affiliated to Capital Medical University, Beijing, China; [2]Department of Surgery, Capital Medical University Affiliated Beijing Shijitan Hospital, Beijing, China; [3]Department of General Surgery, China-Japan Friendship Hospital, Beijing, China*
Email: weixiaodie@aliyun.com

Background and aims: Significant fibrosis and at risk metabolic dysfunction-associated steatohepatitis (MASH) elevate risks of adverse liver and extrahepatic outcomes. This study aimed to validate the ability of noninvasive scores (NITs) based on routine clinical indicators to identify significant fibrosis and at-risk MASH in obese bariatric surgery patients.
Method: This study included 360 participants from two independent bariatric surgery cohorts, and liver biopsy and routine clinical data were collected. The efficacy of FIB4, NFS, APRI, LRS, FNI (combining aspartate aminotransferase, high-density cholesterol, and glycated hemoglobin), and FMO (including aspartate aminotransferase, alanine aminotransferase, triglycerides, and high-density lipoprotein cholesterol) in diagnosing significant fibrosis and at-risk MASH was compared.
Results: Among the 360 participants, 152 (38.9%) were diagnosed with significant fibrosis and 124 (31.7%) were diagnosed with at-risk MASH. The diagnostic efficacy of NITs for significant fibrosis was as follows: the AUC (95% CI) for FIB4, NFS, APRI, LRS, FNI, and FMO were 0.590 (0.533–0.648), 0.517 (0.458–0.576), 0.675 (0.620–0.730), 0.658 (0.602–0.714), 0.715 (0.662–0.767), and 0.696 (0.642–0.749), respectively. The FNI model demonstrated optimal rule-out[cutoff 0.10, sensitivity 87.42%, negative predictive value (NPV) 80.81%] performance, while FMO demonstrated optimal rule-in[cutoff 0.22, specificity 83.61%, positive predictive value (PPV) 60.20%] performance. For at-risk MASH patients, the AUCs for FIB4, NFS, APRI, LRS, FNI, and FMO were 0.591 (0.531–0.651), 0.512 (0.452–0.573), 0.715 (0.661–0.770), 0.678 (0.620–0.735), 0.748 (0.696–0.799), and 0.744 (0.692–0.796), respectively. FNI also demonstrated the best exclusion performance (cutoff value 0.10, NPV 89.90%), while FMO showed the best inclusion performance (cutoff value 0.22, PPV 57.14%).
Conclusion: Both FNI and FMO are accurate and cost-effective non-invasive scores that can effectively identify the risk of significant and at-risk MASH in patients with bariatric surgery.

WED-231
Two-tier screening approach for liver fibrosis stratification in outpatients with type 2diabetes mellitus: a multicenter cross-sectional study

Alessandro Mantovani[1,2], Rosa Lombardi[3,4], Andrea Dalbeni[5], Riccardo Morandin[6], Maria Giovanna Lando[6], Veronica Fiorio[6], Nicoletta Rolli[6], Matteo Forti[6], Dario Messetti[6], Mirko Zoncapè[7], Ilaria Milani[8], Maria Eugenia Parrotta[9], Danila Capoccia[8], Valeria Guglielmi[9], Frida Leonetti[8], Paolo Sbraccia[9], Anna Ludovica Fracanzani[3,4], Giovanni Targher[1,2]. *[1]Metabolic Diseases Research Unit, IRCCS Sacro Cuore-Don Calabria Hospital, Negrar di Valpolicella, Verona, Italy; [2]Department of Medicine, University of Verona, Verona, Italy; [3]Fondazione IRCCS Ca' Granda Ospedale Maggiore Policlinico di Milano, Milano, Italy; [4]Department of Pathophysiology and Transplantation, University of Milan, Milano, Italy; [5]Section of General Medicine C and Liver Unit, University and Azienda Ospedaliera Universitaria Integrata of Verona, Verona, Italy; [6]Section of Endocrinology, Diabetes and Metabolism, Department of Medicine, University and Azienda Ospedaliera Universitaria Integrata of Verona, Verona, Italy; [7]Clinica Medica 3, Azienda Ospedale Università di Padova, Padova, Italy; [8]Department of Medico-Surgical Sciences and Biotechnologies, Faculty of Pharmacy and Medicine, University of Rome La Sapienza, Roma, Italy; [9]Department of Systems Medicine, University of Rome Tor Vergata, Obesity Medical Center, University Hospital Policlinico Tor Vergata, Roma, Italy*
Email: alessandro.mantovani@univr.it

Background and aims: To examine the prevalence and severity of metabolic dysfunction-associated steatotic liver disease (MASLD) in outpatients with type 2 diabetes mellitus (T2DM), and to assess the effectiveness of the EASLEASD-EASO algorithm for liver fibrosis screening.
Method: We retrospectively enrolled 1203 Italian older outpatients with T2DM who underwent vibrationcontrolled transient elastography (VCTE) with liver stiffness measurement (LSM) and controlled attenuation parameter (CAP) assessment. MASLD was defined as CAP ≥248 dB/m. Significant liver fibrosis was defined as LSM ≥8 kPa, compensated advanced chronic liver disease (cACLD) as LSM ≥10 kPa, and clinically significant portal hypertension (CSPH) as LSM ≥25 kPa or LSM ≥20 kPa and platelet count <150 000/mm3. FIB-4 index was calculated in all participants.
Results: The prevalence rates of MASLD, significant liver fibrosis, cACLD, and CSPH were 71.3%, 21.1%, 11.7% and 1.7%, respectively. A 2-tier screening strategy for liver fibrosis using the FIB-4 index and VCTE showed that among patients with a normal FIB-4 index, 629 (83.3%) had LSM <8 kPa and 126 (16.7%) had LSM≥8 kPa. Sensitivity, specificity, NPV, and PPV of the FIB-4 index for detecting LSM≥8 kPa were 50.4%, 66.3%, 83.3% and 28.6%, respectively. Increased body weight (adjusted-OR 3.34, 95%CI 1.75–6.39) and elevated ALT levels (adjusted-OR 1.54, 95%CI 1.01–2.36) were the strongest predictors of significant liver fibrosis.
Conclusion: MASLD and significant liver fibrosis are common in older patients with T2DM. Fibrosis risk stratification using FIB-4, followed by VCTE, is a good strategy in real-world settings. However, relying solely on FIB-4 may fail to identify some patients with advanced disease, particularly those with increased body weight and elevated serum aminotransferase levels.

MASLD – Experimental and pathophysiology

TOP-130

ZDHHC17-mediated of palmoylation-modified D2HGDH nuclear translocating drives progression of metabolic associated steatohepatitis via HDAC1-H3K27ac pathways

Xi-Xuan Wang[1], Shu-Ling Chen[1], Rui-Qi Li[1], Jun Guo[1], Zihao Liang[1], Dandan Yin[1], Cai-Yun Zhang[1], Wei Chen[1], Changhua Yi[1], Qingfang Xiong[1], Jiangao Fan[2], Dawei Yang[1], Yongfeng Yang[1].
[1]Department of Hepatology, The Second Hospital of Nanjing, Medical School, Southeast University, Nanjing, China; [2]Department of Gastroenterology, Xin Hua Hospital, School of Medicine, Shanghai Jiao Tong University, Shanghai, China
Email: yyf1997@163.com

Background and aims: Aberrant nuclear translocation of metabolic enzymes is an emerging driver of epigenetic dysregulation in disease, yet its specific mechanisms and therapeutic relevance in metabolic dysfunction-associated steatohepatitis (MASH) remain poorly understood. This study aims to elucidate the role and targeting of the nuclear translocation of D-2-hydroxyglutarate dehydrogenase (D2HGDH) in MASH.
Method: Utilizing clinical samples, MASH mouse models, and cellular models, we conducted comprehensive analyses through metabolomics, proteomics combined with palmitoyl-proteomics, immunohistochemistry/immunofluorescence, subcellular fractionation, protein-protein interaction assays, epigenomic multi-omics (ATAC-seq, CUT&TAG), and virtual screening.
Results: During MASH progression, hepatocyte D2HGDH undergoes nuclear translocation, a phenomenon specific to fatty liver disease. Mechanistically, high-fat-induced oxidative stress promotes the palmitoyltransferase ZDHHC17 to catalyze palmitoylation of D2HGDH at cysteine 198. This modification facilitates D2HGDH nuclear import via binding of its C-terminal PY-nuclear localization signal (NLS) to the nuclear transport protein Transportin-1 (TNPO1), by affecting its mitochondrial targeting sequence and protein polarity. Within the nucleus, D2HGDH directly binds to and inhibits histone deacetylase 1 (HDAC1), leading to decreased histone H3 lysine 27 trimethylation (H3K27me3) and increased H3K27 acetylation (H3K27ac). This epigenetically reprograms chromatin accessibility genome-wide, specifically activating the transcription of lipogenesis-related genes, thereby driving hepatocyte lipid accumulation. Targeting ZDHHC17, either via genetic knockout or the small-molecule inhibitor TBK1-IN-1 identified through virtual screening, blocked D2HGDH palmitoylation and nuclear translocation, and effectively alleviated MASH both in vitro and in vivo.
Conclusion: This study unveils a novel signaling axis, driven by ZDHHC17-mediated palmitoylation of D2HGDH, that links cellular metabolism to nuclear epigenetic regulation and is critical for MASH development. Targeting the ZDHHC17-D2HGDH interaction presents a potential therapeutic strategy for MASH.

TOP-143

Hepatic IFRD1 suppresses metabolic dysfunction-associated steatohepatitis via GLUD1/α-KG axis

Mengya Geng[1], Hairui Li[2], Sihui Luo[1], Suowen Xu[1], Jianping Weng[3].
[1]Department of Endocrinology and Metabolism, The First Affiliated Hospital of USTC, Division of Life Sciences and Medicine, University of Science and Technology of China, Hefei, China; [2]department of Hepatobiliary Surgery, The First Affiliated Hospital of USTC, Division of Life Sciences and Medicine, University of Science and Technology of China, Hefei, China; [3]Division of Life Sciences and Medicine, University of Science and Technology of China, Anhui Medical University, Hefei, China
Email: gengmengya@mail.ustc.edu.cn

Background and aims: The key molecular targets and underlying mechanisms involved in regulating metabolic remodeling in metabolic dysfunction–associated steatotic liver disease (MASLD) remain unclear. Interferon-related developmental regulator 1 (IFRD1) is traditionally linked to embryogenesis, yet its role in MASLD has not been investigated. This study aims to clarify the role of IFRD1 in MASLD and its potential mechanisms.
Method: We collected liver and serum samples from MASLD patients and controls, as well as from Ifrd1 knockout mice (*Ifrd1*$^{-/-}$), Ifrd1 conditional knockout (CKO) mice, and liver-targeted Ifrd1 overexpression mice following treatment with various dietary regimens. These samples were subjected to Western blotting, Reverse Transcription Quantitative Real-Time Polymerase Chain Reaction (RT-qPCR), immunostaining, pathological staining, and biochemical assays. Mice were subjected to metabolic cage assays, and primary hepatocytes were isolated. Potential downstream mechanisms were investigated via RNA sequencing, CUT&Tag, subcellular fractionation, immunoprecipitation-mass spectrometry (IP-MS) analysis, and a variety of molecular biology experiments.
Results: IFRD1 expression significantly negatively correlates with metabolic-associated steatohepatitis (MASH) progression in human liver samples. In multiple mouse models, *Ifrd1*$^{-/-}$ mice exhibited a "lean fatty liver" phenotype due to enhanced systemic energy metabolism, hepatocyte-specific IFRD1 expression suppressed MASH progression, a function that was abrogated upon inhibition of GLUD1 enzymatic activity. Mechanistically, IFRD1 promotes GLUD1's mitochondrial localization via direct interaction, stabilizing the enzyme's activity to enhance α-ketoglutarate (α-KG) production. α-KG reduces H3K36me3 occupancy at lipogenic genes, thereby inhibiting DNL and ameliorating MASH. α-KG supplementation reverses MASH exacerbation in *Ifrd1*-CKO mice.
Conclusion: This study establishes the IFRD1-GLUD1-α-KG axis as a key metabolic-epigenetic regulatory pathway and supports the development of future MASH therapeutic strategies based on drugs that stabilize IFRD1 expression or promote α-KG production.

TOP-144

Mitochondrial cholesterol transport by stard1 links hepatocyte stress to macrophage inflammasome activation in MASLD

Hala Jaara[1], Mariana Acevedo[1], Laura Fàbrega[1], Susana Núñez[1], Vicent Ribas[1], M. Carmen Garcia-Ruiz[1,2], José Fernandez-Checa[1,2], Sandra Torres Núñez[1]. *[1]Department of Molecular and Cellular Biomedicine, Institute of Biomedical Research of Barcelona (IIBB), CSIC, Barcelona, Spain, CIBEREHD, Madrid, Spain, Instituto de Investigaciones Biomédicas August Pi i Sunyer (IDIBAPS), Liver Unit, Hospital Clinic I Provincial de Barcelona, Barcelona, Spain, Barcelona, Spain; [2]Department of Medicine, Keck School of Division of Gastrointestinal and Liver disease, University of Southern California, Los Angeles, CA, United States, Los Angeles, United States*
Email: sandra.torres@iibb.csic.es

Background and aims: Despite advances in understanding metabolic dysfunction–associated steatotic liver disease (MASLD), effective pharmacological therapies remain limited. Mitochondrial cholesterol accumulation promotes reactive oxygen species (ROS) generation, leading to mitochondrial dysfunction, inflammation, and hepatocellular death, thereby driving disease progression toward hepatocellular carcinoma (HCC). The ROS-sensitive NLRP3 inflammasome, predominantly active in macrophages, links mitochondrial damage to inflammatory liver disease. Steroidogenic acute regulatory

protein 1 (STARD1), which transports cholesterol into mitochondria, is upregulated in MASLD and implicated in HCC. We hypothesized that STARD1-driven mitochondrial ROS activates the NLRP3 inflammasome through hepatocyte–macrophage crosstalk.
Method: Mice with hepatocyte-specific (StARD1$^{\Delta Hep}$) or macrophage-specific (StARD1$^{\Delta Mac}$) deletion of StARD1 were fed control diets, a high-cholesterol/sodium cholate diet (HCSC) for 2 days, or a choline-deficient amino acid-defined high-fat diet (CDA-HFD) for 3 weeks. Liver injury, inflammation, oxidative stress, and inflammasome markers were assessed. Hepatocytes and macrophages were isolated to evaluate cell-specific responses. Primary hepatocytes from StARD1$^{f/f}$ and StARD1$^{\Delta Hep}$ mice were treated with soluble cholesterol under ACAT inhibition to assess mitochondrial cholesterol trafficking, ROS production, and inflammasome gene expression.
Results: Hepatocyte-specific deletion of StARD1 reduced mitochondrial ROS and decreased expression of Nlrp3, Asc, Casp1, and IL-1β, protecting against liver inflammation in both HCSC and CDA-HFD models. Cholesterol-loaded StARD1$^{f/f}$ hepatocytes exhibited mitochondrial cholesterol accumulation, increased ROS, and inflammasome gene induction, whereas StARD1$^{\Delta Hep}$ hepatocytes were protected. Macrophages from StARD1$^{\Delta Hep}$ mice showed reduced Stard1 and macrophage activation markers, indicating hepatocyte-dependent regulation of macrophages. Similarly, macrophage-specific deletion of StARD1 attenuated macrophage activation and resulted in reduced hepatic inflammation and liver injury in both dietary models. These findings suggest a trigger and amplification model of mitochondrial cholesterol loading in hepatocytes and macrophages, respectively.
Conclusion: STARD1 is a key upstream regulator of mitochondrial cholesterol–ROS–NLRP3 inflammasome activation and mediates pathogenic hepatocyte–macrophage crosstalk in MASLD, highlighting STARD1 as a potential therapeutic target.

TOP-145
CBS/H_2S-Dependent S-Sulfhydration of PREB regulates ApoB-mediated VLDL secretion and hepatic lipid homeostasis

Mingchang Pang[1], Huayu Yang[1], Yilei Mao[1], Yongfa Huang[2]. [1]*Peking Union Medical College Hospital, Chinese Academy of Medical Sciences & Peking Union Medical College, Beijing, China;* [2]*Department of Liver Surgery, Peking Union Medical College (PUMC) Hospital, PUMC and Chinese Academy of Medical Sciences, Beijing, China, Beijing, China*
Email: mingchangpang@yeah.net

Background and aims: Aberrant hepatic lipid accumulation affects approximately one-third of adults worldwide, and is associated with an increased risk of steatohepatitis and cirrhosis. H_2S-mediated S-sulfhydration is an emerging post-translational modification that regulates redox homeostasis and other critical biology processes. This study aims to investigate whether and how protein S-sulfhydration in hepatocytes regulates lipid metabolism.
Method: Global and liver-specific knockout of the gene encoding cystathionine-β-synthase (CBS) were generated in C57BL/6J mice to model H_2S deficiency. S-sulfhydration profiles were characterized using sulfhydryl-modified proteomics, and hepatic lipid metabolism was assessed through integrated transcriptomic, proteomic, and lipidomic analyses, biochemical testing, and histological examination. Molecular biology was delineated using DNA pull-down assays, luciferase reporter assays, chromatin immunoprecipitation sequencing, and gain/loss-of-function experiments.
Results: Extensive remodeling of the hepatic S-sulfhydrated proteome perturbed lipid transport and cholesterol metabolism in *Cbs*-deficient mice. Phenotypically, *Cbs*-deficient mice developed marked hepatic lipid accumulation featuring increased triglyceride and cholesterol ester, as well as decreased serum triglyceride levels. Integrated multi-omics analyses unveiled an underlying lipid export defect attributed to downregulation of apolipoprotein B (ApoB), the key mediator of very-low-density-lipoprotein (VLDL) assembly and secretion. Mechanistically, reduced H_2S availability diminished S-sulfhydration of the transcription factor prolactin regulatory element-binding (PREB), attenuating its positive regulation of *Apob* transcription. Pharmacological restoration of H_2S enhanced PREB-dependent ApoB expression in hepatocytes, supporting a critical role for the CBS/H_2S–PREB–ApoB axis in regulating hepatic lipid export.
Conclusion: These findings identified protein S-sulfhydration as a critical regulator of hepatic lipid export, and revealed a CBS/H_2S–PREB–ApoB axis governing VLDL assembly and secretion. Disruption of this pathway could result in marked hepatic lipid accumulation, providing potential translational and therapeutic insight into dyslipidemia and fatty liver disease.

TOP-146
Spatially resolved multi-omics unveil arginine metabolism promotes the transition from MASH to HCC

Yuan Liang[1], Rui Zhang[2], Ling Lu[3]. [1]*School of Biological Science & Medical Engineering, Southeast University, Nanjing, China;* [2]*Xuzhou Medical University, Xuzhou, China;* [3]*Affiliated Hospital of Xuzhou Medical University, Xuzhou, China*
Email: liang_yuan@seu.edu.cn

Background and aims: Metabolic dysfunction-associated steatotic liver disease (MASLD) is a significant cause of liver disease worldwide, ranging from simple steatosis to metabolic dysfunction-associated steatohepatitis (MASH) and hepatocellular carcinoma (HCC). The mechanisms underlying the dynamic reorganization of the inflammatory-cancer transition within the spatial context remain elusive.
Method: We induced MASH-to-HCC via diethylnitrosamine (DEN) combined with a high-fat, high-sucrose, high-cholesterol (HFHC) diet for the experimental group and curated an integrated atlas incorporating spatially resolved transcriptomics (Visium, n = 12) and metabolomics (air-flow-assisted desorption electrospray ionization–mass spectrometry imaging, AFADESI-MSI, n = 12), including three normal livers, four MASH livers, and five MASH-HCC livers, to comprehensively integrate multiple molecular layers.
Results: By deciphering regionally shared transcriptional domains across disease stages, we identified five spatially distinct meta-domains in the MASH-to-HCC transition. We inferred that the arginine biosynthesis-enriched domain is critical for the MASH-to-HCC transformation. We observed that Asl^{+} hepatocytes were specifically enriched in the arginine biosynthesis-enriched domain, overlapping with hypoxia activation in MASH. Hypoxia-induced reprogramming of arginine biosynthesis in Asl^{+} hepatocytes promotes MASH progression via the Hif1a-Arg1/Asl axis. We observed cellular and metabolic heterogeneity in the PV/CV region of MASH. However, Asl^{+} hepatocytes were located in the tumor margin region, accompanied by arginine biosynthesis activity. Moreover, MASH-HCC-specific Arginine-binding transcription regulator RACK1 regulates FABP5-mediated fatty acid metabolism through mTOR signaling to promote the MASH-HCC progression.
Conclusion: In conclusion, we integrated single-cell RNA-Seq and spatial multi-omics to elucidate the cellular and metabolic heterogeneity underlying MASH-to-HCC progression. Our findings establish Asl^{+} hepatocytes as key mediators of the MASH-to-HCC transition via hypoxia-induced arginine biosynthesis and reveal how the MASH-HCC-specific Arginine-binding transcription regulator RACK1 regulates FABP5-mediated fatty acid metabolism to promote HCC progression. Collectively, we reveal significant transcriptional and metabolic heterogeneity and highlight underlying cellular dynamics and molecular mechanisms of MASH-to-HCC transformation.

TOP-160

Hepatic STARD1-dependent Oxysterol generation emerges as a novel cardiovascular risk factor in MASH

Sandra Torres Núñez[1], Eduardo Garcia[2], Susana Núñez[1], Vicent Ribas[1], Leire Goicoechea[1], Hala Jaara[1], Ana Garcia[3], Mariana Acevedo[1], Ana Cenarro[4], Emma Muñoz[5], Naira Rico[6], Ana Paula Dantas[7], Francisco Jiménez-Trinidad[3], Eduard Guasch[3,5], Xavier Lopez[5], Montserrat Rigoll[3], Josefina Casas[8], Rocío Munoz-Hernández[9], Manuel Romero-Gómez[9], Vicenta Llorente-Cortes[10], José Fernandez-Checa[1,11], M. Carmen Garcia-Ruiz[1,11]. [1]*Department of Molecular and Cellular Biomedicine, Institute of Biomedical Research of Barcelona (IIBB), CSIC, Barcelona, Spain, CIBEREHD, Madrid, Spain, Instituto de Investigaciones Biomédicas August Pi i Sunyer (IDIBAPS), Liver Unit, Hospital Clinic I Provincial de Barcelona, Barcelona, Spain, Barcelona, Spain;* [2]*Department of Experimental Pathology, Institute of Biomedical Research of Barcelona (IIBB), CSIC, Barcelona, Spain, Barcelona, Spain;* [3]*Department of Cardiology, Cardiovascular Clinical Institute, Arrythmia Unit, Hospital Clìnic, Universitat de Barcelona, Centro de Investigación Biomédica en Red de Enfermedades Cardiovasculares (CIBERCV), Madrid, Spain, Barcelona, Spain;* [4]*Instituto Investigación Sanitaria Aragón, Hospital Universitario Miguel Servet, Zaragoza, Spain, Centro de Investigación Biomédica en Red de Enfermedades Cardiovasculares (CIBERCV), Madrid, Spain, Zaragoza, Spain;* [5]*Instituto de Investigaciones Biomédicas August Pi i Sunyer (IDIBAPS), Barcelona, Spain, Barcelona, Spain;* [6]*CORE Laboratory, Biochemistry and Molecular Genetics Department, Biomedical Diagnostic Centre, Hospital Clínic, Barcelona, Spain, Barcelona, Spain;* [7]*Department of Cardiology, Cardiovascular Clinical Institute, Arrythmia Unit, Hospital Clìnic, Universitat de Barcelona, Barcelona, Spain;* [8]*Research Unit on BioActive Molecules (RUBAM), Departament de Química Orgànica Biològica, Institut D'Investigacions Químiques I Ambientals de Barcelona, Consejo Superior de Investigaciones Científicas (CSIC), Barcelona, Spain, Barcelona, Spain;* [9]*UCM Digestive Diseases and Ciberehd, Virgen del Rocío University Hospital, CSIC, Institute of Biomedicine of Seville, University of Seville, CIBEREHD, Madrid, Spain, Seville, Spain;* [10]*Department of Experimental Pathology, Institute of Biomedical Research of Barcelona (IIBB), CSIC, Barcelona, Spain, Centro de Investigación Biomédica en Red de Enfermedades Cardiovasculares (CIBERCV), Madrid, Spain, Barcelona, Spain;* [11]*Department of Medicine, Keck School of Division of Gastrointestinal and Liver disease, University of Southern California, Los Angeles, CA, United States, Los Angeles, United States*
Email: carmen.garcia@iibb.csic.es

Background and aims: Metabolic dysfunction–associated fatty liver disease (MAFLD) is associated with extrahepatic complications, particularly cardiovascular disease (CVD), yet the mechanistic liver–heart connection remains unclear. Cholesterol trafficking to mitochondria via STARD1 promotes MAFLD progression and hepatocellular carcinoma. Mitochondrial cholesterol is converted by CYP27A1 into 27-hydroxycholesterol (27-OHC), the most abundant circulating oxysterol, which is elevated in MAFLD patients and induces atherosclerosis in mice. This study investigated the role of hepatic STARD1 in MAFLD progression and cardiac remodeling, focusing on 27-OHC as a mediator of the liver–heart axis.

Method: Male hepatocyte-specific StARD1 knockout ($StARD1^{\Delta Hep}$) and control ($StARD1^{f/f}$) mice were fed a standard diet or a high-fat, high-cholesterol (HFHC) diet (60% fat, 0.5% cholesterol) for up to 10 months. Liver injury, steatosis, and fibrosis were assessed histologically. Cardiac remodeling was evaluated by fibrosis staining, magnetic resonance imaging (MRI), and lipidomic analyses of cholesterol esters (CE), triglycerides (TG), ceramides, and 27-OHC. Cardiac expression of LRP-1 and cathepsin D (CatD) was analyzed in mouse hearts and in human cardiac myocytes treated with 27-OHC. Circulating 27-OHC was measured in serum from MAFLD patients.

Results: HFHC-fed $StARD1^{\Delta Hep}$ mice showed reduced liver injury, hepatocyte ballooning, steatosis, and fibrosis compared with $StARD1^{f/f}$ controls, confirming STARD1's role in MAFLD progression. Hearts from HFHC-fed $StARD1^{\Delta Hep}$ mice exhibited reduced LRP-1 and CatD expression and preserved cardiac output by MRI. Cardiac CE and TG content increased with HFHC feeding but did not differ between genotypes. Hepatic 27-OHC was nearly undetectable in $StARD1^{\Delta Hep}$ mice, while cardiac 27-OHC was reduced by ~50%, indicating that a substantial fraction of cardiac 27-OHC originates from the liver in a STARD1-dependent manner. Ceramide profiles were unchanged between genotypes.In vitro, 27-OHC reduced viability, increased ROS, and induced LRP-1 and CatD in human cardiac myocytes. Serum from MAFLD patients showed elevated circulating 27-OHC, supporting translational relevance.

Conclusion: Hepatic STARD1 promotes MAFLD progression and generates 27-OHC, contributing to cardiac remodeling and dysfunction. Elevated circulating 27-OHC in MAFLD patients supports a mechanistic liver–heart axis and identifies STARD1–27-OHC as potential therapeutic targets to mitigate liver–heart complications.

TOP-161-YI

Maternal metabolic dysfunction-associated steatotic liver disease rewires placental-fetal selenium crosstalk and mediates fetal liver insulin resistance

Simran Sharma[1], Ahona Roy[1], Anupama Kumari[1], Aarti Sharma[1], Rajni Yadav[1], Ashwini Vasudevan[1], Dinesh Mani Tripathi[1], Neha Agarwal[1], Shiv Kumar Sarin[1], Savneet Kaur[1]. [1]*Institute of Liver and Biliary Sciences, New Delhi, India*
Email: savykaur@gmail.com

Background and aims: Metabolic dysfunction-associated steatotic liver disease (MASLD) is emerging as a major health concern in women of reproductive age globally. Recent studies link maternal MASLD to adverse neonatal outcomes, yet its effects on placental vasculature, early fetal liver changes, and underlying mechanisms remain ambiguous. We hypothesised and studied crosstalk between MASLD placenta and fetal liver using multi-omic profiling.

Method: Maternal MASLD mouse models (C57BL/6J, n = 20) were developed using high-fat diet (HFD) and high-fat high-carbohydrate diet (HFHCD) compared to control diet-fed dams at embryonic day 10 (E10) and (E18). Placentas were characterised by immunohistochemistry (CD31, VE-cadherin, CD90, lipid and calcium staining), RT-PCR and metabolomics. Fetal livers (E18) were studied histologically and by transcriptomics. Fetal hepatoblasts were cultured to study effects of one of the significantly upregulated genes *in vitro*.

Results: HFHCD induced maternal insulin resistance (liver insulin level ~198 pg/ml, HOMA-IR of 5.5), hyperglycemia, hypertriglyceridemia (serum triglycerides ~350 mg%), elevated liver enzymes (AST ~140 IU/l, ALT ~120 IU/l) and hepatic lipogenesis (GLUT2 +3-fold, SREBP1 +4-fold, PPARg +2-fold) compared to HFD and controls. At E18, HFHCD placenta showed increased angiogenesis, lipid accumulation, calcification. Placental metabolomics identified enriched selenoamino acid metabolism (6-fold, $p < 0.05$) in HFHCD versus controls. HFHCD fetal livers showed lipid accumulation, hyperinsulinemia (liver insulin level ~170 pg/ml), upregulated lipid metabolism and inflammatory genes (SREBP1, CXCL1, NF-kappa B), downregulation of insulin receptor IRS2 ($p < 0.05$). Integrated placental metabolome and fetal liver transcriptome identified selenoamino acid metabolism as overlapping pathway (top-ranked in both datasets, $p < 0.05$), wherein selenocysteine (SeCys) was reduced in HFHCD placenta (↓~0.6-fold, $p < 0.05$), while selenoprotein P (SeP) was upregulated in HFHCD fetal liver (↑~3-fold, $p < 0.01$). Hepatoblast organoids treated with SeP (0.5–2 ug/ml, 48 h), showed dose-dependent reduction in insulin-stimulated pAkt ($p < 0.05$).

Conclusion: Maternal MASLD leads to placental vascular changes and SeCys depletion, restricting fetal Se supply. Fetal liver compensates this by upregulating SeP expression. Abnormally high levels impair SeP-mediated antioxidant defence, driving insulin resistance. This study reveals novel placental-fetal Se axis underlying MASLD-induced fetal liver metabolic programming.

SAT-090

Liver-specific somatic beta-klotho knockout dysregulates hepatic lipid metabolism and increases bile acid synthesis

Alexandra Aaldijk[1], Cristy Verzijl[1], Milaine Hovingh[1], Nicolette Huijkman[1], Marieke Smit[1], Niels Kloosterhuis[1], Niels Mulder[1], Rick Havinga[1], Albert Gerding[1], Trijnie Bos[1], Mirjam Koster[1], Mariska de Graaf[1], Justina Wolters[1], Bart van de Sluis[1], Dicky Struik[1], Johan Jonker[1]. [1]*University Medical Centre Groningen (UMCG), Groningen, Netherlands*
Email: alexandraaaldijk@outlook.com

Background and aims: Beta klotho (KLB), a coreceptor required for fibroblast growth factor (FGF)19 and 21 signaling, has been identified as a drug target for metabolic and liver-related diseases. Understanding of its function in vivo is mainly based on germline mouse knockout models exhibiting developmental abnormalities, potentially confounding the interpretation of KLB in adult physiology and FGF19/21 pharmacodynamics. In this study, we applied liver-specific somatic gene editing to establish the role of hepatic KLB in adult physiology and validate its therapeutic potential as a drug target in liver disease.
Method: Liver-specific Cas9-transgenic mice on a C57BL/6J background were retro-orbitally injected with adeno-associated virus particles containing guide RNAs targeting exon 1 of the mouse *Klb* gene to generate a liver-specific *Klb* knockout (Klb^{HepKO}). Control mice received a matched viral dose of empty vector. Mice were fed a chow diet for 4 weeks or a high-fat diet for 12 weeks post-virus injection, followed by extensive phenotypic characterization.
Results: Under chow- and HFD-fed conditions, liver-specific knockout of *Klb* resulted in increased bile acid synthesis as shown by 2.6-fold ($p = 0.008$) and 5.8-fold ($p = 0.004$) elevated *Cyp7a1* expression, respectively. Fecal bile acid excretion was increased 2.9-fold in chow-fed ($p = 0.008$) and 7.9-fold ($p = 0.000$) in HFD-fed Klb^{HepKO} mice, and bile acid composition was altered as shown by a more hydrophobic bile acid composition under chow ($p = 0.008$) and HFD ($p = 0.004$) conditions. Moreover, hepatic *Klb* knockout resulted in 41.4% lower plasma triglyceride levels ($p = 0.008$) and 37.0% higher hepatic triglyceride levels ($p = 0.016$) only under chow conditions. The fraction of VLDL was 42.7% reduced ($p = 0.008$) in Klb^{HepKO} mice, suggesting elevated hepatic triglycerides might result from impaired VLDL secretion. Upon a HFD, effects on hepatic triglyceride levels were less pronounced ($p = 0.052$), showing only a trend towards altered lipid metabolism.
Conclusion: Liver-specific Cas9-mediated gene editing reveals hepatic KLB as a key regulator of bile acid homeostasis and hepatic lipid metabolism under both chow and high-fat diet conditions. These findings highlight KLB-dependent pathways as promising targets to enhance FGF-based therapies for liver disease.

SAT-091

Farnesoid X receptor signalling orchestrates gut-liver axis feedback to modulate ceramide-sphingolipid metabolism in metabolic associated steatotic liver disease

Basma Abdelrahman[1], Rasha Tawfiq[1], Olfat Hammam[2], Yasmeen Attia[1]. [1]*Department of Pharmacology, Faculty of Pharmacy, The British University in Egypt, Cairo, Egypt;* [2]*Department of Pathology, Theodor Bilharz Research Institute, Giza, Egypt*
Email: yasmeen.attia@bue.edu.eg

Background and aims: Ceramide accumulation acts as a systemic metabolic stress signal that disrupts lipid homeostasis and accelerates inflammatory progression in metabolic-associated steatohepatitis (MASH). Beyond hepatocellular injury, sphingolipid imbalance reflects impaired gut-liver communication, implicating extrahepatic regulatory circuits in disease evolution. Farnesoid X receptor (FXR) signalling, via intestinal fibroblast growth factor 15 (FGF15), regulates bile acid synthesis and hepatic lipid metabolism. Whether disruption of this FXR/FGF15 axis drives ceramide-sphingolipid dysregulation in MASH remains unclear. We, therefore, examined whether pharmacological FXR activation with obeticholic acid (OCA) restores gut-liver signalling and sphingolipid homeostasis in experimental MASH.
Method: MASH was induced using a high-fat diet (HFD) in male C57BL/6 mice, which were assigned to standard chow, HFD, or HFD plus obeticholic acid (OCA; 5 mg/kg/day, oral) groups. OCA was administered after 8 weeks of HFD for 4 weeks. Hepatic FXR activity was assessed by quantifying small heterodimer partner-1 (SHP-1) gene by qRT-PCR. Gut-liver axis feedback and intestinal barrier integrity were evaluated by measuring hepatic CYP7A1 alongside intestinal fibroblast growth factor-15 (FGF15) and claudin-1 by ELISA. Hepatic sphingolipid metabolism was evaluated by measuring sphingosine-1-phosphate (S1P) and acid sphingomyelinase (ASMase) using ELISA and sterol regulatory element-binding protein-1c (SREBP-1c) gene expression by qRT-PCR.
Results: OCA treatment markedly alleviated histopathological features of MASH. FXR activation was confirmed by a 2.6-fold increase in SHP-1 expression ($p < 0.0001$) accompanied by restoration of bile acid negative feedback, evidenced by a 1.7-fold increase in FGF15 ($p = 0.0068$) and a 79% reduction in CYP7A1 protein levels ($p < 0.0001$) compared to HFD group. OCA also attenuated the compensatory 2.7-fold increase in claudin-1 observed in HFD-fed mice ($p < 0.0001$). Concomitantly, sphingolipid dysregulation was corrected with OCA, with reductions in S1P (63.5%) and ASMase (49.1%) levels (both $p < 0.0001$), alongside a 64.6% decrease in SREBP-1c expression ($p < 0.0001$), as compared to HFD, indicating restoration of hepatic lipid homeostasis.
Conclusion: The present study implicates hepatic FXR activation in restoring gut-liver axis feedback on bile acid synthesis, rebalancing ceramides/sphingolipids metabolism, thereby alleviating MASH.

SAT-092

The single-cell landscape of MASLD-enriched liver sinusoidal endothelial

Sang Bong Ahn[1], Hyo Young Lee[2], Joo Hyun Oh[3], Mimi Kim[4], Bo-Kyeong Kang[4], Chul-min Lee[4], Jihyun An[2], Ha Il Kim[2], Eun Chul Jang[5], Jeong-Yeon Cho[6], Hye-Lin Kim[7], Eileen Yoon[2], Dae Won Jun[2]. [1]*Department of Internal Medicine, Nowon Eulji Medical Center, Eulji University, Seoul, Korea, Rep. of South;* [2]*Department of Internal Medicine, Hanyang University College of Medicine, Seoul, Korea, Rep. of South;* [3]*Department of Internal Medicine, CHA University College of Medicine, Seongnam, Korea, Rep. of South;* [4]*Department of Radiology, Hanyang University College of Medicine, Seoul, Korea, Rep. of South;* [5]*Department of Occupational and Environmental Medicine, College of Medicine, Soonchunhyang University, Chunan, Korea, Rep. of South;* [6]*Department of Pharmacotherapy, University of Utah College of Pharmacy, Salt Lake, United States;* [7]*College of Pharmacy, Sahmyook University, Seoul, Korea, Rep. of South*
Email: noshin@hanyang.ac.kr

Background and aims: In metabolic dysfunction-associated steatosis liver disease (MASLD), liver sinusoidal endothelial cells (LSECs) play a pivotal role in the onset and progression of metabolic MASLD. However, the dynamics and roles of LSEC subclusters during MASLD progression remain largely unknown. This study aimed to analyze the molecular alterations and functions of LSEC subclusters as MASLD progressed, using single-cell analysis.
Method: We analyzed single-cell RNA-seq (scRNA-seq) in 11 individuals to compare endothelial subclusters between MASLD patients and healthy controls, validated the findings with single-nucleus RNA-seq (snRNA-seq) in 14 individuals from an independent cohort, and further examined their association with histological severity and zonal distribution using spatial transcriptomics in 12 individuals.
Results: Endo 4 subcluster, identified as the MASLD-enriched LSEC subcluster, was significantly increased in patients with MASLD compared to healthy controls in both scRNA-seq and snRNA-seq cohorts. Gene expression analysis revealed that ANGPT2 was

upregulated in the MASLD-enriched LSEC subcluster compared to other LSEC cells. Furthermore, gene expressions related to extracellular matrix, TGF-β signaling, and HIF-1 signaling were increased in the MASLD-enriched LSEC subcluster. Spatial transcriptomics showed MASLD-enriched LSEC sub-clusters increased progressively with the severity of steatosis, ballooning, inflammation, and fibrosis. Notably, the MASLD-enriched LSEC subcluster showed a higher degree of colocalization with scar-associated stellate cells than other subclusters. It also demonstrated increased interaction with hepatic stellate cells, T cells, and highest interaction with $CD14^+$ $CD16^+$ circulating monocytes.
Conclusion: The MASLD-enriched LSEC subcluster, associated with disease severity, was characterized by activation of extracellular matrix remodeling, TGF-β and HIF-1 signaling, and showed enhanced interactions with hepatic T cells, stellate cells, and peripheral circulating monocytes.

SAT-093-YI
Knockout of miR-92a and LNA-miR-92a treatments are promising therapeutic options against MASLD progression and portal hypertension
Philipp Althaus[1], Sara Zarei[1], Stefanie Dimmeler[2], Jonel Trebicka[1,3], Sabine Klein[1]. *[1]University Hospital Muenster, Internal Medicine B, Muenster, Germany; [2]Goethe-University Frankfurt am Main, Institute for Cardiovascular Regeneration, Frankfurt am Main, Germany; [3]European Foundation for the Study of Chronic Liver Failure, Barcelona, Spain*
Email: ph.althaus@unitybox.de

Background and aims: The rising incidence of MASLD, coupled with the lack of effective treatments for the advanced, decompensated stage, underscore the urgent need for new, effective therapies.
Therefore, we investigated whether knockout of miR-92a or administration of LNA-miR-92a halts disease progression through anti-inflammatory effects and thereby reducing fibrotic remodeling.
Method: Liver tissues from cirrhotic compensated wild-type (wt) mice treated with LNA-92a and from cell specific Alb-Cre^+miR92$a^{fl/fl}$ knock-out mice were examined and compared with untreated wt-controls. Gene expression of hepatic profibrotic and inflammatory markers were analyzed and fibrosis was assessed histologically using Sirius-Red staining and immunohistochemistry for α-smooth muscle actin (αSMA). Hepatic collagen content was determined by hydroxyproline assay. Necroinflammatory activity was assessed by measuring serum levels of the transaminases aspartate aminotransferase (AST) and alanine aminotransferase (ALT). Portal hypertension was recorded by in-vivo portal pressure measurements.
Results: Compensated cirrhotic knockout and treated wt mice showed reduced expression of profibrotic genes (TGFβ, PDGF, col1a1) compared with their respective wt controls. Less activation of hepatic stellate cells was depicted by gene expression of αSMA which displayed a 2.6-fold decrease of LNA-92a–treated wt MASH. Hydroxyproline analysis confirmed a significant reduction of hepatic collagen expression (1.6-fold), in Alb-Cre^+miR92$a^{fl/fl}$ mice compared to respective wt mice. Consistent with this, Sirius Red staining revealed decreased collagen accumulation and αSMA immunostaining depicts diminished hepatic stellate cell activation, reflecting attenuated fibrosis. Additionally, measurements of mitochondrial dysfunction indicated lessened chemokine release and diminished inflammation (TNFα, IL-6, IL-1β, NRF2). Lower serum parameters AST (5.7-fold) and ALT (3.1-fold) indicate diminished necroinflammation and reduced hepatocellular injury compared to wt controls. In addition, decreased portal pressure confirms attenuated cirrhosis resulting from reduced stellate cell activity.
Conclusion: Inhibiting miR-92a constitutes a promising therapeutic avenue in the treatment of MASLD. (Dimmeler, Trebicka (2025). Pharmaceutical composition comprising MIR-92 antagonist for treating liver disease. (25195510.0).

SAT-094-YI
Semaglutide prevents cognitive dysfunction in experimental metabolic dysfunction-associated steatohepatitis through anti-inflammatory and neuroprotective effects
Kristoffer Kjærgaard Amby[1], Anne Catrine Mikkelsen[1], Cecilie Bay-Richter[2], Anne M Landau[2,3], Peter Lykke Eriksen[1], Betina Elfving[2], Majken Thomsen[2,3], Farzaneh Tamnanloo[4], Jeppe Remme Yeoman[1], Stephen Hamilton-Dutoit[5], Hendrik Vilstrup[1], Christopher F. Rose[4], Rajeshwar Prosad Mookerjee[6], Karen Louise Thomsen[1]. *[1]Department of Hepatology and Gastroenterology, Aarhus University Hospital, Aarhus, Denmark; [2]Translational Neuropsychiatry Unit, Aarhus University, Aarhus, Denmark; [3]Department of Nuclear Medicine and PET, Aarhus University Hospital, Aarhus, Denmark; [4]Hepato-Neuro Lab, CRCHUM, Université de Montréal, Montreal, Canada; [5]Department of Pathology, Aarhus University Hospital, Aarhus, Denmark; [6]Institute for Liver and Digestive Health, University College London, London, United Kingdom*
Email: krikje@clin.au.dk

Background and aims: Cognitive dysfunction is an increasingly recognized and debilitating manifestation of metabolic dysfunction-associated steatohepatitis (MASH). The GLP-1 receptor agonist Semaglutide is a promising treatment for MASH, which also exhibits neuroprotective effects in neurodegenerative disease models. We investigated the short- and long-term effects of Semaglutide treatment on cognitive dysfunction and its possible underlying mechanisms in experimental MASH.
Method: MASH was induced using a 16-week high-fat, high-cholesterol (HFHC) diet. Sixty-four Sprague-Dawley rats were randomized into four groups: 1) standard diet, 2) HFHC diet, 3) HFHC diet with long-term Semaglutide treatment (10 weeks; 60 µg/kg/day), or 4) HFHC diet with short-term Semaglutide treatment (10 days; 30 µg/kg/day;). We assessed neurobehaviour, histological MASH severity, hepatic and systemic inflammation, blood ammonia and urea cycle enzyme expression, as well as brain synaptic density and microglia activation by autoradiography.
Results: HFHC animals exhibited impaired memory in the Fear Conditioning Test (Cued test; $p = 0.01$) and depression-like behaviour during the Forced Swim Test (Immobility; $p = 0.03$), both prevented by long-term Semaglutide treatment. Long-term Semaglutide reduced liver fat content ($p = 0.03$) and systemic inflammation (CCL2, CCL3, CXCL1; $p < 0.05$), whilst histological MASH remained unchanged. Moreover, Semaglutide treatment restored urea cycle enzyme expression (CPS1; $p = 0.03$) and reduced the hyperammonaemia ($p = 0.04$) observed in HFHC animals. In the prefrontal cortex, HFHC animals showed diminished synaptic density which was ameliorated by Semaglutide ($p = 0.01$), whilst no difference in microglia activation was observed.
Conclusion: Treatment with Semaglutide for 10 weeks effectively prevented memory impairment and depression-like behaviour in experimental MASH, whereas 10 days of treatment had no effect. These improvements are suggested to be attributed to the attenuation of systemic inflammation and protection against loss of synaptic density, and not resolution of MASH. Moreover, Semaglutide ameliorated hyperammonaemia which may also contribute to cognitive dysfunction in MASH. Our findings hold potential implications for the therapeutic management of MASH-associated cognitive dysfunction and warrant further confirmation in Man.

SAT-095-YI
Dysregulation of the E2F2-PCSK9 axis promotes MASLD progression and related cardiovascular disease
Maider Apodaka-Biguri[1], Beatriz Gómez Santos[1,2], Xabier Buque[1,2], Ane Nieva-Zuluaga[1], Idoia Fernández-Puertas[1], Paul Gómez-Jauregui[1], Natalia Sainz-Ramirez[1], Kendall Alfaro-Jiménez[1], Estibaliz Castillero[1], Ane Ortiz-Palma[1], Unai Garzon-Basterra[1], Amaia Lujambio[3], Xiaoke Ge[4], Sander Kooijman[4], Patrick CN Rensen[4], Ana Zubiaga[5],

Patricia Aspichueta[1,2,6]. [1]*Department of Physiology University of the Basque Country UPV/EHU, Faculty of Medicine and Nursing, Leioa, Spain, Leioa, Spain;* [2]*Biocruces Bizkaia Health Research Institute, Cruces University Hospital, Barakaldo, Spain, Leioa, Spain;* [3]*Icahn School of Medicine at Mount Sinai, New York, NY 10029, USA, New York, United States;* [4]*Dept. of Medicine, Div. of Endocrinology, Leiden University Medical Center, Leiden, Netherlands, Leiden, Netherlands;* [5]*Department of Genetic, Physical Anthropology and Animal Physiology, Faculty of Science and Technology, University of Basque Country UPV/EHU, Leioa, Spain, Leioa, Spain;* [6]*National Institute for the Study of Liver and Gastrointestinal Diseases (CIBERehd, Carlos III Health Institute), Madrid, Spain, Madrid, Spain*
Email: patricia.aspichueta@ehu.eus

Background and aims: Metabolic dysfunction-associated steatotic liver disease (MASLD) is a risk factor for cardiovascular disease (CVD). E2F2 deficiency protects against MASLD progression. Upregulation of PCSK9 promotes dyslipidemia, but its role in hepatosteatosis or MASLD progression remains unclear. We aimed to investigate: 1) whether E2F2 contributes to dyslipidemia in MASLD and if this effect is mediated through PCSK9 and 2) the role of PCSK9 in MASLD progression.
Method: MASLD and MASLD-related hepatocellular carcinoma (HCC) were induced in WT and *E2f2*$^{-/-}$ mice by feeding a high-fat diet (HFD), combined or not with the *Sleeping Beauty* (Myc;*sg-Pten* plasmids) technique to promote HCC. *Pcsk9* was overexpressed *in vivo* specifically in hepatocytes of *E2f2*$^{-/-}$, WT and ApoE*3-Leiden.CETP mice (resembles human atherosclerosis) by *AAV8*. *E2f2* was also overexpressed in WT mice hepatocytes. Hepatic and serum lipidomic profiles, apolipoprotein content, and lipoprotein subfractions (ACTA-FPLC) were analyzed. *In vivo* triglyceride (TG) secretion and TG-rich lipoprotein uptake were assessed.
Results: MASH patients with high hepatic E2F2 protein levels showed an elevated atherogenic index, in concordance, *in vivo* overexpression of hepatocyte *E2f2*, increased serum PCSK9 and cholesterol in WT mice, while *E2f2* deficiency reduced them. *In vivo* hepatocyte *Pcsk9* overexpression altered serum lipidome, increasing cholesterol and number of circulating VLDL/LDL particles, as ApoB levels showed promoting hepatosteatosis, with ApoE levels elevated in both serum and liver, suggesting that increased hepatic uptake of ApoE-containing lipoproteins may contribute to hepatosteatosis. This phenotype worsened in preclinical models of MASLD, with increased VLDL secretion, more pronounced dyslipidemia and marked increase in TG species. *Pcsk9* overexpression in ApoE*3-Leiden.CETP mice that exhibit dysfunctional ApoE showed decreased hepatic (V)LDL uptake with none hepatosteatosis and a marked dyslipidemic serum profile that increased atheroma plaque formation and severity. *Pcsk9* overexpression in *E2f2*-deficient mice fed a HFD prevented the protection against hepatosteatosis, dyslipidemia and HCC. Consistently, in TGGA-LIHC cohort *E2F2* and *PCSK9* were upregulated and positively correlated.
Conclusion: E2F2 upregulation in hepatocytes promotes MASLD progression and related CVD, at least in part, via regulation of PCSK9. Targeting E2F2 could be valuable to prevent MASLD progression and associated CVD.

SAT-099-YI

Transcriptomic analysis of paired biopsies of liver and adipose tissue before and after bariatric surgery reveals distinct signaling pathways associated with persistence of MASLD despite significant weight loss

Anouar Aznou[1], Daniël Baars[1], Mijra Koning[1], Mare Bruin[1], Sjoerd Bruin[2], Arnold van de Laar[2], Joanne Verheij[1], Michail Doukas[3], Joost PH Drenth[1], Abraham Stijn Meijnikman[1], Max Nieuwdorp[1].

[1]*AmsterdamUMC, Amsterdam, Netherlands;* [2]*Spaarne Gasthuis, Hoofddorp, Netherlands;* [3]*Erasmus MC, Rotterdam, Netherlands*
Email: a.aznou@amsterdamumc.nl

Background and aims: The persistence of metabolic dysfunction-associated steatotic liver disease (MASLD) and steatohepatitis (MASH) after substantial weight loss remains poorly understood. We analyzed liver and visceral adipose tissue (VAT) transcriptomics data of patients with and without MASLD both at baseline and one year after bariatric surgery to identify key pathways linked to disease resolution and persistence.
Method: We included patients from the prospective BARIA cohort who underwent bariatric (Roux-en-Y gastric bypass; RYGB) and subsequent repeat surgery (mostly for gallstone disease) in the year thereafter. We collected liver and VAT biopsies and scored liver biopsies histologically using the SAF score. All tissues underwent bulk RNA-seq, with differential gene expression analyzed longitudinally and between MASLD responders and non-responders, followed by functional annotation and pathway enrichment. Differentially expressed genes (DEGs) and pathways between responders and non-responders were further examined in an independent cohort of 288 patients with and without MASLD.
Results: Paired biopsies were available for liver (n = 33) and VAT (n = 20). RGYB was associated with broad transcriptional changes across tissues (after a range 8–15 months) with 6383 (liver) and 11829 DEGs (VAT). At the time of resurgery, MASLD persisted in 7 out of 15 patients who met diagnostic criteria at baseline. Longitudinal analysis of paired liver biopsies revealed 2122 DEGs in non-responders and 614 in responders, with enriched mitochondrial respiration pathways in the latter. In contrast, paired VAT biopsies in responders showed a greater number of DEGs compared to non-responders (3292 versus 829), with relative suppression of immune-associated pathways. Comparison of the liver transcriptome at resurgery between MASLD non-responders and responders revealed 29 DEGs and multiple enriched signaling pathways in non-responders, including PI3K–Akt, Wnt and Hippo signaling. In 288 bariatric patients across the MASLD spectrum (no steatosis, n = 109; MASLD, n = 139; MASH, n = 40), validation of these genes and pathways showed the strongest upregulation in MASH.
Conclusion: While RYGB is associated with extensive transcriptional remodeling of liver and adipose tissue in the year after surgery, MASLD persists in a subset of patients. Patients without MASLD resolution retain a liver transcriptomic signature enriched for core cellular signaling pathways shared with MASLD patients who did not undergo surgery.

SAT-100

Enhancing effects of combining resmetirom and semaglutide in a modified AMLN diet-induced mouse model for metabolic dysfunction-associated steatohepatitis (MASH)

Tai-Yu Huang[1], Chien-Chang Shen[1], Jessica Ramadhin[2], Jian-Xin (Jimmy) Bao[1,3]. [1]*Pharmacology Discovery Services Taiwan, Ltd., New Taipei City, Taiwan;* [2]*Taconic Biosciences, Rensselaer, United States;* [3]*Eurofins Discovery Services North America, LLC, St. Charles, United States*
Email: jimmy.bao@discovery.eurofinsus.com

Background and aims: Both a thyroid hormone receptor (THR)-beta agonist, resmetirom and a glucagon-like peptide-1 (GLP-1) receptor agonist, semaglutide were recently approved for treating noncirrhotic metabolic dysfunction-associated steatohepatitis (MASH) with moderate to advanced liver fibrosis. However, not all patients respond to resmetirom with MASH resolution. We therefore evaluated, before the indication expansion of semaglutide, whether semaglutide in combination with resmetirom would improve the effects of resmetirom using a modified AMLN diet induced mouse MASH model.
Method: Male C57BL/6NTac mice from Taconic Biosciences were fed a modified AMLN diet for 28 weeks and then treated for 8 weeks with either resmetirom alone at 3 and 10 mg/kg given orally every day,

semaglutide alone at 30 nmol/kg given subcutaneously every 3 days, or semaglutide in combination with 3 mg/kg resmetirom. Biochemical parameters, glucose and insulin levels were measured at week 0, week 4 and week 8. At termination, liver total cholesterol was quantified, and liver histopathological analyses were performed using hematoxylin and eosin, picrosirius red, and Oil Red O staining.
Results: Modified AMLN diet feeding induced body weight gain, increased adiposity, and the metabolic, biochemical and histopathological changes characteristic of MASH, including liver injury, steatosis, inflammation and fibrosis. Resmetirom treatment dose-dependently reduced serum and liver total cholesterol (TC), total triglycerides (TG) and low-density lipoprotein as well as liver weight and liver fat accumulation, decreased liver steatosis, inflammation and ballooning in histopathological assessment, and also effectively prevented liver injury. Semaglutide mainly decreased initial food intake (week 4), reduced body and liver weight, lowered serum TC and TG, reduced fat mass and tended to ease liver fat burden. Neither resmetirom nor semaglutide appeared to affect the liver fibrosis levels. Interestingly, semaglutide in combination of lower dose of resmetirom improved it's effects and their effects were potentially synergistic; additional studies and analyses are needed to confirm this.
Conclusion: Combined treatment with semaglutide and resmetirom produced enhancing effects when compared to either treatment alone. These data warrant further investigation into combination therapies of THR-beta agonists and GLP-1 receptor agonists for the potential treatment of MASH or other metabolic disorders.

SAT-101-YI

Nutritional distress–dependent regulation of cyclin M1 modulates insulin sensitivity via an FGF21-mediated mechanism

Jon Ander Barrenechea-Barrenechea[1], Irene González-Recio[1], Naroa Goikoetxea-Usandizaga[1,2], Sofia Lachiondo-Ortega[1], Teresa C Delgado[3,4], Leidy Estefanía Zapata-Pavas[1], Nerea Ferreiro[1], Claudia M. Rejano-Gordillo[5], Patricia Peña-Sanfélix[1], Cesar Augusto Martín[6,7], Amaia Rodríguez[8,9], Eva Novoa[9,10], Luis Alfonso Martinez-Cruz[1], Gema Frühbeck Martinez[8,9], Francisco J Ortega[9,11], Ruben Nogueiras[9,10,12], María Luz Martínez-Chantar[1,2]. *[1]Liver Disease Laboratory, Center for Cooperative Research in Biosciences (CIC bioGUNE), Basque Research and Technology Alliance (BRTA), Bizkaia Science and Technology Park, 48160 Derio, Spain; [2]Centro de Investigación Biomédica en Red de Enfermedades Hepáticas y Digestivas (CIBERehd), Instituto de Salud Carlos III, 28029 Madrid, Spain; [3]Biobizkaia Health Research Institute, Barakaldo, Spain; [4]IKERBASQUE, Basque Foundation for Science, Bilbao, Spain; [5]Grupo de Investigación en Biología Molecular del Cáncer, Departamento de Bioquímica y Biología Molecular y Genética, Facultad de Ciencias, Universidad de Extremadura (UEX), Badajoz, Extremadura, Spain; [6]Biofisika Institute (UPV/EHU, CSIC), Barrio Sarriena s/n., 48940 Leioa (Bizkaia), Spain; [7]Department of Biochemistry and Molecular Biology, Universidad del País Vasco UPV/EHU, Apdo. 644, 48080 Bilbao, Spain; [8]Department of Endocrinology & Nutrition, Metabolic Research Laboratory, Clínica Universidad de Navarra, University of Navarra, IdiSNA, Pamplona, Navarra, Spain; [9]CIBER Fisiopatología de la Obesidad y Nutrición (CIBERobn), Madrid, Spain; [10]Department of Physiology, CIMUS, University of Santiago de Compostela, Instituto de Investigación Sanitaria, Santiago de Compostela, Spain; [11]Girona Biomedical Research Institute (IDIBGI), Girona, Spain; [12]Galician Agency of Innovation (GAIN), Xunta de Galicia, Santiago de Compostela, Spain*
Email: mlmartinez@cicbiogune.es

Background and aims: There is a body of evidence linking hypomagnesemia to the onset of insulin resistance (IR) and type 2 diabetes (T2D). In this work, we aim to elucidate the mechanism by which the metal transporter cyclin M1 (CNNM1) is involved in glycemic control, making it a potential therapeutic target against IR.
Method: Hepatic expression of *CNNM1* was analyzed in patients with T2D and in preclinical models of nutritional distress. IR was assessed in an acute 60% high-fat diet model and the genetic *db*/*db* mouse model of T2D. A counter-regulatory model was established by intraperitoneal administration of glucagon, with mice being sacrificed 10 minutes post-injection. In all preclinical models, *Cnnm1* expression was silenced by tail vein injection of an adeno-associated virus (AAV), and outcomes were evaluated from the third week after AAV administration. *Fibroblast growth factor 21* (*Fgf21*) gene was simultaneously silenced by intravenous delivery of a siRNA via tail vein, and mice were sacrificed after an overnight fast.
Results: Among all the mammalian magnesium transporters, only *Cnnm1* was found to be downregulated in both T2D patients and preclinical models of IR. When *Cnnm1* was further silenced, we were able to increase insulin sensitivity in mice, while *Cnnm1* overexpression led to no metabolic changes. Insulin resistant mice administered AAV-si*Cnnm1* showed decreased liver triglyceride (TG) accumulation, together with increased serum ketone bodies. Interestingly, *Cnnm1* silencing in these mice drove to heightened FGF21 concentration in serum. Concomitant silencing of *Cnnm1* and *Fgf21* in acute insulin resistant mice reverted the effects of *Cnnm1* downregulation, no longer improving insulin sensitivity and restoring TG accumulation in liver and serum to control levels. In the glucagon model, the beneficial effect of *Cnnm1* silencing was associated with increased hepatic activity of the gluconeogenic enzyme phosphoenolpyruvate carboxykinase (PEPCK).
Conclusion: Overall, our results suggest that the magnesium transporter CNNM1 plays a key role in the response to nutritional distress, potentially acting as a metabolic sensor of glucose availability. Silencing of *Cnnm1* may represent a novel therapeutic strategy for T2D, improving systemic insulin sensitivity through enhanced FGF21 signaling.

SAT-102-YI

Prime editing models the MTARC1 A165T variant in human liver organoids, demonstrating reduced steatosis, inflammation, and fibrosis

Amel Ben Saad[1], Arden Weilheimer[1], Alan Mullen[1]. *[1]University of Massachusetts Chan Medical School, Worcester, United States*
Email: bensaadamale@gmail.com

Background and aims: Metabolic dysfunction-associated steatotic liver disease (MASLD) is the most prevalent cause of chronic liver disease. MASLD is a progressive and multifactorial disease marked initially by hepatic steatosis, which can progress to steatohepatitis, fibrosis, cirrhosis, and liver cancer. Genetic factors influence the development, progression, and complications in MASLD, and genome-wide association studies (GWAS) have identified single nucleotide polymorphisms (SNPs) associated with altered risk. Mitochondrial amidoxime reducing component 1 (*MTARC1*) *rs2642438* (p.A165T) variant has been identified as protective, but the role of *MTARC1* and the impact of this variant in hepatocytes remains poorly understood.
Method: Here, we applied prime editing to create the *rs2642438* variant in human pluripotent stem cells (hPSCs) before differentiation into human liver organoids (HLOs) to investigate the effect of the variant under conditions of steatotic and fibrotic injury.
Results: Compared to HLOs formed from hPSCs containing the *MTARC1* reference sequence, HLOs with the *rs2642438* variant show lower levels of MTARC1 protein and triglycerides and are protected from steatotic and fibrotic injury, as predicted by the phenotype observed in patients carrying the variant. The observed decrease in triglyceride level with the variant appears to be driven more by suppression of de novo lipogenesis rather than stimulation in ß-oxidation in the HLO model. While resmetirom, the thyroid hormone receptor-beta (THRB) agonist approved to treat patients with metabolic dysfunction-associated steatohepatitis (MASH) was effective in reducing triglyceride levels in the setting of steatotic injury in HLOs with the reference sequence, HLOs containing the variant did

not show further reduction in triglyceride levels with exposure to resmetirom, despite increased expression of *THRB*.
Conclusion: Together, this study establishes an approach to model disease-related SNPs in HLOs and provides further insights into the activity of the *MTARC1* variant, and suggests that profiling SNPs may be a path to identify patients more likely to respond to therapies for MASLD.

SAT-103
Epigenetic programming of metabolic liver disease by early-life nutritional overload
Claudia Bigas[1], Josefina Martin[1], Blanca Majem[1], Salvador Aznar-Benitah[1,2]. [1]*IRB Barcelona, Aging and Metabolism Programme, Barcelona, Spain;* [2]*ICREA Research Professor, Barcelona, Spain*
Email: claudia.bigas@irbbarcelona.org

Background and aims: Metabolic dysfunction-associated fatty liver disease (MASLD) is a growing global health issue, even among pediatric populations. Emerging evidence suggests that early-life exposures, including maternal nutrition, can program long-term susceptibility to metabolic diseases. This study aims to investigate the developmental origins of MASLD by examining how maternal intake of a palmitic acid-enriched high-fat, high-sugar diet (PA-HFD) influences the offspring's liver metabolism through epigenetic mechanisms.
Method: A mouse model was used in which dams were fed a PA-HFD during pregnancy and lactation. Liver tissue from offspring was analyzed for histone modifications, transcriptomic and proteomic changes, and metabolic phenotype. Adult offspring were re-exposed to a high-fat diet to assess the functional impact of early-life epigenetic priming. Findings were further validated using human-derived liver organoids in vitro.
Results: Maternal PA-HFD consumption induced stable epigenetic changes in the offspring's liver, particularly H3K4me3 deposition, leading to persistent transcriptional reprogramming of genes involved in fatty acid β-oxidation. This resulted in a fasting-like hepatic phenotype. Upon re-challenge with a HFD in adulthood, these epigenetically primed offspring developed exacerbated liver pathology, including steatosis, mitochondrial dysfunction, oxidative stress, toxic lipid accumulation, and impaired glucose tolerance. Validation in human liver organoids confirmed the relevance of these findings to human health.
Conclusion: Our findings demonstrate that maternal consumption of a palmitic acid-enriched diet during critical windows of development induces stable epigenetic modifications in the offspring's liver, which persist into adulthood and predispose to worsened metabolic outcomes upon dietary challenge. These insights highlight the importance of maternal nutrition as a modifiable factor in preventing chronic liver disease and suggest potential epigenetic targets for early intervention strategies.

SAT-104
Global analysis of protein post-translational modifications reveals novel regulatory mechanisms in steatotic liver disease
Virginia Aranda García[1], Eduardo Moltó Pérez[1], Cristina Pintado[1], Ruy Andrade Louzada[2], Ernesto Bernal-Mizrachi[2], Antonio Andrés Hueva[3], Nilda Gallardo Alpízar[3], Elena Bonzon-Kulichenko[1]. [1]*Biochemistry Section, Castilla-La Mancha Health Research Institute (IDISCAM), Faculty of Environmental Sciences and Biochemistry, University of Castilla-La Mancha, Toledo, Spain;* [2]*Department of Internal Medicine, Division of Endocrinology, Diabetes and Metabolism, Miller School of Medicine, University of Miami, Miami, United States;* [3]*Biochemistry Section, Castilla-La Mancha Health Research Institute (IDISCAM), Faculty of Chemical Sciences and Technologies, University of Castilla-La Mancha, Ciudad Real, Spain*
Email: Elena.Bonzon@uclm.es

Background and aims: Metabolic dysfunction-associated steatotic liver disease (MASLD), a chronic inflammatory condition, is associated with obesity and high-fat diets (HFDs). Its molecular mechanisms remain unclear, including the role of protein post-translational modifications (PTMs). While PTMs have traditionally been investigated using targeted, closed-search mass spectrometry methods, open-search mass spectrometry (OS-PTM) offers a novel, unbiased approach to comprehensively analyse PTMs, proteins, and associated pathways.
Method: Public raw MS data of HFD-induced MASLD development over time in mice total liver lysate and phosphoproteome was reanalyzed by OS-PTM. Mice were fed HFD for 3 (HFD3, n = 3, insulin resistance) or 12 (HFD12, n = 3, MASLD) weeks. The control group (n = 3) was fed a low-fat diet. An advanced quantitative approach was used to capture coordinated PTM alterations.
Results: We detected the same MASLD linked pathways observed by the original authors such as an increase in peroxisome, mitochondria and fatty acid beta oxidation, since early stages, and an increase in amino acid metabolism, especially BCAA in later stages, which validates our approach. However, by considering all the modified protein forms, new changing pathways were detected in early stages: a decrease in the glutathione homeostatic action; increase in Cytochrome P450; in the steroid hormone biosynthesis; alterations in extracellular matrix and in the lipid binding machinery. At later stages the ATP-synthase complex, steroid biosynthesis and the ATF6 responsive genes from unfolded protein response were upregulated. In addition, there were early PTM responses enriched in clusters of functionally related proteins, not detected by the original authors. Ser/Thr pyrophosphorylation of proteins from organelle organization and translation was drastically decreased. Protein N-terminal processing of ribosomal and DNA-binding protein complexes, and the labile protein-bound iron and Met dioxidation of mitochondrial oxidoreductases were decreased as well. Cys trioxidation of mitochondrial cytotoxic-responsive enzymes active-sites was up-regulated, together with mannose N-glycosylation of endoplasmic reticulum carboxylic ester hydrolases.
Conclusion: OS-PTM technology allows a reliable detection of new PTM-mediated alterations underlying MASLD from early stages, which opens the way for innovative treatments.

SAT-105
The glucagon/glucagon-like peptide-1 receptor dual agonist survodutide reduces liver fibrosis in a 4-week carbon tetra chloride lean mouse model
Francois Briand[1], Mohsin Hassan[2], Thomas Klein[2]. [1]*Physiogenex, Escalquens, France;* [2]*Boehringer Ingelheim, Biberach, Germany*
Email: f.briand@physiogenex.com

Background and aims: In a phase 2 clinical trial, the glucagon/GLP-1 receptor dual agonist survodutide has demonstrated significant improvement in metabolic dysfunction associated steatohepatitis with 64.5% of patients with F2/F3 fibrosis at baseline showing an improvement in fibrosis by at least one stage. Here we tested whether survodutide would demonstrate anti-fibrotic effects in a 4-week carbon tetrachloride (CCl_4) injected lean mouse model of liver fibrosis.
Method: Lean, 8-week-old, C57BL6/J male mice were injected intraperitoneally with CCl_4 twice a week for a total of 4 weeks to induce liver fibrosis. Treatment started after 2 weeks of CCl_4 injection. In a first study, mice were treated subcutaneously, once daily with vehicle, a long-acting gastric inhibitory peptide (LaGIP) analogue at 100 nmol/kg, semaglutide 7.5 nmol/kg, or survodutide 7.5 nmol/kg, during the remaining 2-week CCl_4 injection period. In a second study, mice were treated with vehicle and a higher dose of survodutide at 10 nmol/kg. In each study and at the end of the 2-week treatment period, blood and liver were collected for biochemistry and histology analysis.

Results: In the first study, both the LaGIP analogue and semaglutide showed no effect on liver parameters, including liver fibrosis, indicating that GIP and GLP-1 receptors agonism had no impact. In contrast, survodutide 7.5 nmol/kg demonstrated anti-fibrotic effects, as shown by a significant reduction in liver %Sirius Red labelling ($p < 0.05$ vs. vehicle) and a non-significant reduction in fibrosis score. In the second study, the higher dose of survodutide (10 nmol/kg s.c. QD) reduced plasma alanine amino transferase levels by 33%, although not significantly. Compared with vehicle, survodutide at 10 nmol/kg again demonstrated anti-fibrotic effects with significant reduction in both liver % alpha-smooth muscle actin and % Sirius Red staining. The antifibrotic activity was further confirmed by a significant reduction in the hepatic expression of pro-fibrotic genes *Acta2* (alpha-SMA), *Col1a1* and *Timp1* in mice treated with survodutide. Importantly, expression of cytochrome P450 2e1, the key enzyme metabolizing CCl_4 into reactive trichloromethyl radicals driving liver injury and fibrosis was not reduced by survodutide.
Conclusion: In a 4-week CCl_4 lean mouse model, survodutide demonstrated significant anti-fibrotic activity. These preclinical data highlight the potential benefits of the glucagon/GLP-1 receptor agonist survodutide for the treatment of MASH and liver fibrosis in humans.

SAT-106

Surfaceome mapping of human hepatocytes uncovers proteome dynamics in steatotic hepatocytes

María Fernández Delgado[1], Leire Leire Uraga Gracianteparaluceta[1], Maria Unceta Suárez[1,2], María Luz Martínez-Chantar[3], Javier de las Heras Montero[1,4,5], Teresa C Delgado[1,3,6]. *[1]IIS Biobizkaia, Baracaldo, Spain; [2]Biochemistry Laboratory, Metabolism Area, Cruces University Hospital, Baracaldo, Spain; [3]Liver Disease Lab, Center for Cooperative Research in Biosciences (CIC bioGUNE), Derio, Spain; [4]Division of Paediatric Metabolism, CIBERER, MetabERN, Cruces University Hospital, Baracaldo, Spain; [5]Department of Paediatrics, University of the Basque Country (UPV/EHU), Leioa, Spain; [6]IKERBASQUE, Basque Foundation for Science, Bilbao, Spain*
Email: teresadejesus.cardosodelgado@bio-bizkaia.eus

Background and aims: Membrane proteins play critical roles in sensing extracellular stimuli and initiating intracellular signaling. The surfaceome (the set of cell membrane proteins exposed to the extracellular environment) is highly dynamic and likely to change in response to variations in intracellular lipid content and cellular stress, key features of MASLD. Thus, our primary aim is to characterize the surfaceome signature of human steatotic hepatocytes.
Method: HepG2, a human hepatoblastoma-derived cell line, and THLE2, an immortalized human hepatocyte cell line, were used. Cells were treated with 300 nM oleic acid (OA) or palmitic acid (PA) to induce steatosis. After 24 hours, cell surface proteins were biotinylated in adherent cells using EZ-Link Sulfo-NHS-LC-LC-Biotin (Thermo Scientific) and then isolated by pull-down assay. Control conditions included cells treated with BSA and non-biotinylated extracts. Pull-down eluted proteins were digested with trypsin/LysC and identified/quantified by Tandem Liquid Chromatography Mass Spectrometry (LC-MS/MS) using a Vanquish Neo HPLC system and Orbitrap Exploris 480 mass spectrometer. Data-independent acquisition was employed, with raw data analyzed using DIA-NN (v.1.8.1), and subsequent analysis was performed using the R package Prostar (v.1.34.6) and Perseus (v.2.0.10.0).
Results: In HepG2 cells, OA-induced steatosis led to the downregulation of 211 cell surface-specific proteins, whereas incubation with PA decreased the expression of 92 cell surface proteins compared to controls. STRING analysis revealed that most of these proteins were associated with the plasma membrane GO category. Otherwise, OA stimulation led to the enrichment of 65 cell surface proteins, while PA upregulated 58 proteins. STRING analysis indicated that enriched proteins are typically localized in ribosomal subunits and mitochondria under normal conditions. In the THLE2 cell line, OA-induced steatosis downregulated 288 proteins, while PA treatment downregulated 298 proteins. STRING analysis confirmed these proteins were primarily associated with the plasma membrane GO category. In contrast, OA treatment enriched 65 proteins, and PA incubation increased 29 proteins, predominantly ribosomal.
Conclusion: Steatotic human hepatocytes exhibit loss of cell membrane proteins and an enrichment of ribosomal proteins suggesting an extra-ribosomal role for these proteins in steatotic hepatocytes. Identifying steatotic hepatocyte surface proteins may provide new therapeutic targets for MASLD.

SAT-107-YI

Protease driven phenotypical changes in lipid associated macrophages attenuates metabolic dysfunction associated steatohepatitis progression

Júlia Cacho-Pujol[1,2,3], Paloma Ruiz-Blazquez[1,2,3,4], Maria Fernandez-Fernandez[1,2,3,4], Alejandro del Castillo-Cruz[1,2,3], Lucía Calderón-Robles[1], Anna Moles[1,2,3,4]. *[1]Institute of Biomedical Research of Barcelona (IIBB-CSIC), Barcelona, Spain; [2]August Pi i Sunyer Biomedical Research Institute (IDIBAPS), Barcelona, Spain; [3]Universitat de Barcelona (UB), Barcelona, Spain; [4]Spanish Networked Biomedical Research Center for Liver and Digestive Diseases (CiberEHD), Madrid, Spain*
Email: julia.cp.lab@gmail.com

Background and aims: Metabolic dysfunction associated steatohepatitis or MASH is currently the most common cause of liver dysfunction worldwide. Since inflammation is a key biological driver of MASH, there is no doubt that macrophages are essential effectors of this process. However, its role remains controversial with contradictory functions being attributed to them. Recent reports have suggested proteases, such as cathepsins, are essential for macrophage phenotypical shift during liver fibrosis however, its role in macrophages during MASH is currently unknown. Thus, this study aimed to investigate the role of macrophage associated cathepsin D (CtsD) during MASH.
Method: Regular diet (RD) or Western Diet-high sugar solution (WD) + CCl_4 was administered to $CtsD^{F/F}$ or CtsD-myeloid cell KO ($CtsD^{\Delta Myel}$) mice for 6-months to induce MASH. Liver damage (ALT), fibrosis (SR and HP), proliferation (BrdU) and lipid accumulation (ORO) was evaluated at the endpoint. Lipid metabolism and macrophage phenotypic gene profile expression was assessed by RTqPCR in $CtsD^{F/F}$ or $CtsD^{\Delta Myel}$ 6-month WD+CCl_4 liver tissue and liver macrophages isolated from $CtsD^{F/F}$ or $CtsD^{\Delta Myel}$ treated with choline-deficient and high-fat diet (CDAHFD) for 1-month.
Results: CtsD deletion in macrophages significantly reduced lipid accumulation in MASH livers without changes in liver damage, fibrosis or proliferation. Analysis of liver macrophages isolated from 1-month CDAHFD fed $CtsD^{F/F}$ or $CtsD^{\Delta Myel}$ mice demonstrated a significant decrease in the expression of markers related with lipid associated macrophages (LAMs), such as Arg1, FOLR2, TREM2, CD204, LXRa in $CtsD^{\Delta Myel}$ liver macrophages. In agreement, a significant reduction in the expression of TREM2 was also observed in $CtsD^{\Delta Myel}$ WD+CCl_4 livers, while the level of the total number of macrophages (F4/80) remained similar. Finally, macrophage phenotypical changes were accompanied by alterations in the expression of genes related with the lipid metabolism (CD36, LXRa, NPC2) in $CtsD^{\Delta Myel}$ WD+CCl_4 livers, indicating that protease-driven phenotypical changes in lipid associated macrophages might contribute to the reduction in lipid accumulation observed in these mice.

Conclusion: CtsD deletion in macrophages modulates lipid associated macrophage phenotype contributing to a reduction in hepatic lipid accumulation and the attenuation of MASH progression.

SAT-108

Hepatocyte succinate dehydrogenase/complex II promotes metabolic dysfunction–associated steatotic liver disease progression and represents a therapeutic target

David Carneros[1], Lucio Figueredo-Matto[1], María Ángeles Rodríguez-Hernández[1], Matilde Bustos[1]. *[1]Area of Liver, Digestive and Inflammatory Diseases, Institute of Biomedicine of Seville (IBiS), Virgen del Rocio University Hospital (HUVR), Spanish National Research Council (CSIC), University of Seville (US), Seville, Spain*
Email: mbustos-ibis@us.es

Background and aims: Metabolic dysfunction-associated liver disease (MASLD) encompasses a spectrum of pathologies ranging from simple steatosis to steatohepatitis with fibrosis and inflammation. Steatosis is characterized by excessive hepatic lipid accumulation, which is closely associated with mitochondrial dysfunction and may promote disease progression. The tricarboxylic acid (TCA) cycle and oxidative phosphorylation are key mitochondrial metabolic pathways. Succinate dehydrogenase (SDH) plays a dual role in the TCA cycle and the electron transport chain. Previous work from our laboratory showed that MASLD is associated with reduced levels of the SDH subunit D (SDHD). The aim of this study was to analyze the impact of SDH levels on liver disease progression.
Method: Hepatocellular carcinoma (HCC) and control tissues (adjacent non-tumor or normal liver) from two independent patient cohorts were used for gene expression analyses. A hepatocyte-specific SDH knockout (LSDH) mouse model was generated using the Cre-LoxP system. In the first experimental approach, male C57BL/6J mice were fed a methionine–choline-deficient (MCD) diet or a control diet for 4 or 6 weeks. Two weeks after diet initiation, mice received intravenous injections of adeno-associated virus encoding SDHD (AAV_SDHD) or control virus (AAV_Renilla). In a second approach, wild-type ($SDHD^{+/+}$) and heterozygous ($SDHD^{\pm}$) mice were fed an MCD diet for 6 or 8 weeks.
Results: The MCD diet reduced hepatic SDH activity and increased serum succinate levels, accompanied by decreased hepatic expression of SDH subunits, inflammation, and fibrosis. AAV_SDHD therapy restored SDH enzymatic activity impaired by the MCD diet and reduced hepatic steatosis and inflammation. Moreover, $SDHD^{\pm}$ mice fed an MCD diet displayed significantly increased steatosis after 8 weeks.
Conclusion: These results implicate SDH as a key regulator in MASLD progression and identify this enzyme as a potential therapeutic target for the disease.

SAT-109

PNPLA3 p.I148M variant affects lipid droplets number and size in patient-derived liver organoids

Elia Casirati[1], Alessandro Cherubini[1], Laura Cerami[1], Fabrizia Carli[2], Amalia Gastaldelli[2], Daniele Prati[3], Daniele Dondossola[4], Luca Valenti[1,5]. *[1]Fondazione IRCCS Ca' Granda Ospedale Maggiore Policlinico; Transfusion Medicine and Hematology, Precision Medicine Lab, Milano, Italy; [2]National Research Council (CNR), Institute of Clinical Physiology (IFC), Pisa, Pisa, Italy; [3]Fondazione IRCCS Ca' Granda Ospedale Maggiore Policlinico; Transfusion Medicine and Hematology, Milano, Italy; [4]Fondazione IRCCS Ca' Granda Ospedale Maggiore Policlinico, Hbp Surgery and Liver Transplantation Unit, Milano, Italy; [5]Università Degli Studi di Milano; Department of Pathophysiology and Transplantation, Milano, Italy*
Email: elia.casirati@policlinico.mi.it

Background and aims: PNPLA3 rs738409 C > G p.I148M variant is the main genetic determinant of metabolic associated steatotic liver disease (MASLD). To this day, this association still lacks a molecular characterization, due to the lack of comprehensive human models. To overcome this gap in knowledge, we generated patient-derived human liver organoids (HLOs) and studied lipid accumulation across different PNPLA3 genotypes.
Method: After HLO exposure to 300 µM Palmitic and Oleic fatty acids, Lipid droplets (LDs) average size and number (normalized for nuclei) were quantified by NileRed staining and compared between *PNPLA3* HLOs (n = 3 for each genotype). Similarly, lipidomics and transcriptomics analysis were conducted to dissect PNPLA3-driven alterations in lipid composition and transcriptional response.
Results: After NileRed data fitting in GLMs, number of mutated PNPLA3 alleles linearly correlates with LDs total area (β Estimate = 139.68, SE = 18.00, $p < 0.0001$) and number (β Estimate = 23.55, SE = 4.71, $p < 0.0001$), while LDs average size was only increased in homozygous HLOs (β Estimate = 0.227, SE = 0.075, $p = 0.0047$). Lipidomics highlight a lipid milieux reminiscent of MASH in HLOs mutated for *PNPLA3*, with Long-chained Unsaturated Fatty acids, Ceramides and Sphingomyelins linearly correlating with the number of rs738409 alleles. In keeping, Bulk RNA-Seq indicated proneness to inflammation, fibrosis, uncontrolled proliferation and, importantly, compromised metabolic control. Furthermore, ScRNA-Seq allowed to pinpoint a subset of cells enriched in in homozygous HLOs: GO analysis showed increased Oxidative phosphorylation, ROS production, adipogenesis, and activation of cancer-related pathways. Finally, PNPLA3-driven steatosis in HLOs can be rescued by both PNPLA3 siRNA silencing and Resmetirom treatment.
Conclusion: Regardless of FA treatment, homozygous HLOs showed increased LDs size when compared to eterozygous and wild-type ones. Conversely, LDs number showed direct correlation with the number of mutated alleles, suggesting that the p.I148M substitution promotes the formation of new LDs, which was exacerbated by exposure to FAs. *PNPLA3*-dependent development of steatosis in HLOs is accompanied by changes in lipid composition and transcriptome painting a pro-inflammatory and pro-fibrotic picture, which can be reversed by *PNPLA3* silencing or Resmetirom administration.

SAT-110-YI

Exploring the complexity of MASLD: sex-dependent genetic effect on body composition

Annalisa Cespiati[1,2], Rosa Lombardi[1,2], Piero Tarantini[2,3], Felice Cinque[1,2], Marica Meroni[1], Daniel Smith[1,2], Erika Fatta[1], Edoardo Pulixi[1], Daniela Bignamini[1], Paola Dongiovanni[1], Anna Ludovica Fracanzani[1,2]. *[1]SC Medicina ad Indirizzo Metabolico, Fondazione IRCCS Cà Granda Ospedale Maggiore Policlinico, Milan, Italy; [2]Department of Pathophysiology and Transplantation, University of Milan, Milan, Italy; [3]SC Medicina Interna ad Indirizzo Cardiologico, ospedale di Busto Arsizio, ASST Valle Olona, Busto Arsizio, Italy*
Email: annalisa.cespiati@unimi.it

Background and aims: Genetic variants in PNPLA3, TM6SF2, MBOAT7, GCKR, and HSD17B13 influence liver-related outcomes in metabolic dysfunction-associated steatotic liver disease (MASLD), while alterations in muscle mass and adipose tissue contribute to metabolic dysfunction. However, the impact of MASLD-related genetic variants on body composition remains poorly defined. Aim: to evaluate the association between common MASLD-associated genetic variants and body composition parameters.
Method: We enrolled 505 MASLD patients (mean age 50 ± 12 years, 65% male) from the Metabolic Liver Disease outpatient clinic at Policlinico Hospital, Milan. Body composition was assessed by bioimpedance analysis. Skeletal and trunk muscle mass indices (SMI and TMMI), adipose and trunk adipose tissue indices (ATI and TATI, a marker of dysfunctional adiposity) were calculated as mass/height2 (kg/m2). Genotyping for PNPLA3, TM6SF2, MBOAT7, GCKR, and HSD17B13 was performed.
Results: Compared with CC, PNPLA3 GG showed lower SMI (9.5 vs 10.1 kg/m^2, $p = 0.01$) and TMMI (3.0 vs 3.4 kg/m^2, $p = 0.01$), with a trend toward higher ATI (10.5 vs 9.5 kg/m^2, $p = 0.08$). In sex-stratified analysis, women carrying the PNPLA3 GG showed higher

TATI (4.9 vs 4.0 kg/m^2, p = 0.02). MBOAT7 GG showed lower SMI (9.4 vs 10.1 kg/m^2, p = 0.01) and TMMI (3.0 vs 3.4 kg/m^2, p = 0.03) compared with CC, without differences in adipose tissue. No associations were observed for TM6SF2, GCKR, HSD17B13. At multivariate models adjusted for age, fibrosis stage, and metabolic comorbidities, PNPLA3 GG remained associated with lower SMI (b = –0.3 kg/m^2, 95%CI –0.5 to –0.1, p = 0.01) and TMMI (b = –0.2 kg/m2, 95%CI –0.3 to –0.02, p = 0.02). These associations were attenuated after adjustment for sex, consistent with sex-related effect modification. In women, PNPLA3 GG remained independently associated with higher TATI after multivariable adjustment (b = 0.4 kg/m^2, bstd 0.25, 95%CI 0.01 to 0.8, p = 0.04). The association between MBOAT7 GG and lower SMI became significant only after adjustment for sex (b = –0.2 kg/m^2, bstd –0.27, 95%CI –0.3 to –0.02, p = 0.02).
Conclusion: Among MASLD-associated variants, MBOAT7 is linked to reduced skeletal muscle mass, while PNPLA3 shows a sex-specific association with dysfunctional adiposity in women. Sex-dependent modulation of genetic effects on body composition reflects the sexually dimorphic nature of MASLD and support the role of genetic background in muscle-adipose tissue remodeling. Integrating genetic and body composition assessment may improve phenotypic risk stratification in MASLD.

SAT-111

Therapeutic targeting of fibrosis-associated microRNAs attenuates steatohepatitis-related liver fibrosis

Young Chang[1], Soung Won Jeong[1], Jae Young Jang[1]. [1]*Soonchunhyang University Seoul Hospital, Seoul, Korea, Rep. of South*
Email: chyoung86@gmail.com

Background and aims: MicroRNAs (miRNAs) have emerged as important biomarkers and potential therapeutic targets in liver fibrosis. This study aimed to identify fibrosis-associated miRNAs and to evaluate the antifibrotic efficacy and underlying mechanisms of miRNA antagonists in steatohepatitis-associated liver fibrosis.
Method: Patients with steatotic liver disease (n = 20) were selected from a biopsy-proven cohort. Blood miRNAs were profiled using next-generation sequencing (NGS) to identify miRNAs associated with fibrosis stage. In a steatohepatitis mouse model, animals were treated with specific miRNA antagonists for 12 weeks. Liver fibrosis was assessed by histologic staining and measurement of fibrosis-related markers. In vitro, hepatocytes and hepatic stellate cells were co-cultured under steatohepatitis conditions and treated with miRNA antagonists. To explore mechanisms, liver tissue NGS and single-cell RNA sequencing (scRNA-seq) were performed.
Results: NGS identified miR-660-5p and miR-125a-5p as significantly associated with liver fibrosis stage. In cell and animal models, antagonism of either miRNA reduced fibrosis markers at the mRNA and protein levels and attenuated histologic fibrosis. Liver tissue NGS demonstrated down-regulation of FGF9 and up-regulation of FGF21 in antagonist-treated groups, implicating growth factor–related pathways in the antifibrotic effects. These findings were validated in an independent treatment model, in which both single-antagonist and combination therapies reproduced antifibrotic effects, with combination therapy showing a more potent reduction in fibrosis severity and related markers. scRNA-seq analysis showed that while most hepatic cell types overlapped across treatment conditions, hepatocytes exhibited treatment-dependent transcriptional shifts, with the combination group forming a more distinctly separated subpopulation. Within hepatocytes, shared changes involved growth factor signaling and glycogen metabolism, whereas combination therapy showed broader modulation of lipid metabolism, inflammatory, and fibrosis-related pathways.
Conclusion: miR-660-5p and miR-125a-5p antagonists significantly attenuate liver fibrosis in steatohepatitis models. Their antifibrotic effects are associated with regulation of the FGF9–FGF21 axis and marked transcriptional reprogramming of hepatocytes.

SAT-115

Tenofovir disoproxil fumarate inhibits cholesterol absorption by downregulating the expression of duodenum NPC1L1 to reduce serum cholesterol

Jing Tang[1], Yan Han[1], Zhiwei Chen[1], Peng Hu[1]. [1]*Department of infectious diseases, The second affiliated hospital of Chongqing Medical University., Chongqing, China*
Email: hp_cq@163.com

Background and aims: Tenofovir disoproxil fumarate (TDF), as a first-line antiviral agent for the treatment of hepatitis B virus (HBV) or human immunodeficiency virus (HIV) infections, has shown non-antiviral effects in lipid metabolism. Previous clinical studies have observed that TDF usage can reduce the serum total cholesterol (TC) level in patients with HBV or HIV infections; however, the underlying mechanisms remain incompletely elucidated.
Method: C57BL/6 mice were treated with TDF at a dosage of 45.5 mg/kg/day for four months to mimic the long-term usage of TDF in humans. The lipid profile was examined in serum, liver, and intestinal tissues. RNA sequencing (RNA-Seq) analysis was conducted on the liver and duodenum tissues to investigate the mechanism.
Results: After four months of gavage with TDF, the serum TC levels in the TDF group were significantly lower than those in the control group. The food intake, water intake, or respiratory exchange ratio of mice is similar between the two groups, suggesting that TDF does not influence the basal metabolism of mice. Furthermore, TDF also reduced the TC content in liver tissue. However, RNA-Seq showed that TDF had no significant impact on the cholesterol metabolism-related pathways in the liver. RT-PCR also demonstrated that TDF had no effect on the expression of key genes related to cholesterol metabolism (e.g. HMGCR, SREBP1c, INSIG1, and PPAR alpha) in the liver. This indicates that TDF may not regulate serum TC levels through the regulation of liver cholesterol metabolism. Considering that intestinal absorption of cholesterol is another main source of serum TC, we next detected lipid changes in the intestine. Interestingly, we found that TDF significantly reduced the TC content in the duodenum, but not in the jejunum and ileum. Hematein Eosin staining revealed that the shape and quantity of intestinal villi were similar between the two groups, indicating that TDF does not directly damage the absorption barrier of intestinal cells. In terms of mechanism, we found that NPC1L1, a key gene regulating cholesterol absorption, was markedly down-regulated in the TDF group. In vitro studies demonstrated that overexpression of NPC1L1 could rescue the inhibition of cholesterol absorption by TDF.
Conclusion: Our study demonstrated that TDF can reduce serum cholesterol via duodenum NPC1L1 downregulation, indicating that TDF may be a better selection for patients with HBV or HIV infection concurrent with hypercholesteremia.

SAT-116

MicroRNA-146a in extracellular vesicles from obese adipocytes trigger hepatic inflammation

Qiuyang Chen[1], Taisiia Shevchenko[1], Anja Heymans[1], Tamara Vanhaecke[1], Robim M Rodrigues[1]. [1]*Department of In Vitro Toxicology and Dermato-Cosmetology (IVTD), Faculty of Medicine and Pharmacy, Vrije Universiteit Brussel (VUB), Brussels, Belgium, Beussels, Belgium*
Email: qiuyang.chen@vub.be

Background and aims: Patients are diagnosed with metabolic dysfunction-associated steatotic liver disease (MASLD) if they have hepatic steatosis in the presence of at least one cardiometabolic risk factor, such as obesity. The onset and progression of MASLD toward its more severe form, metabolic dysfunction–associated steatohepatitis (MASH), are clearly linked to obesity. However, the mechanisms underlying the crosstalk between adipose tissue (AT) and the liver are not fully elucidated. This project investigates how extracellular vesicles (EVs) released from adipocytes might play a role in the development of MASH.

Method: Based on an *in vitro* setup using human adipose stromal cells (hATSc)-derived adipocytes exposed to obesogenic factors (hATSc-Adipo^{obe}) or vehicle control, we obtained EVs specific to obese and lean conditions.
Results: EVs secreted from hATSc-Adipo^{obe} induced an inflammatory response in HepG2 cells, contrarily to EVs secreted from control hATSc-Adipo. Isolation of EV-RNAs followed by miRNA sequencing showed a significant enrichment of hsa-miR-146a-5p in the obese condition. Using target gene prediction and RT-qPCR, we further identified *PRKAA2*, a gene coding for a subunit of AMP-activated protein kinase that controls a variety of metabolic processes, as a target gene of hsa-miR-146a-5p. Transfection of hsa-miR-146a-5p mimics into HepG2 cells led to the downregulation of *PRKAA2* and an increase in cellular inflammatory response, marked by an upregulation in the expression of *IL1B*, *TNFA*, *CXCL5* and *CCL2*. Moreover, knock down of *PRKAA2* in HepG2 cells also resulted in an increased inflammatory response. To validate the obtained *in vitro* data, we isolated EVs from serum of patients diagnosed with different MASLD severities and found that hsa-miR-146a-5p was upregulated in the MASH group (n = 3) compared to simple steatosis group (n = 8). This was demonstrated by receiver operating characteristic (ROC) analysis that showed strong discriminatory performance with an area under the curve (AUC) of 0.917.
Conclusion: In summary, using an *in vitro* setup mimicking the AT-liver crosstalk during obesity, we identified EV-bound hsa-miR-146a-5p, as well as the downregulation of its target gene *PRKAA2*, as contributors to hepatic inflammation. Both hsa-miR-146a-5p and *PRKAA2* could therefore represent novel potential targets to treat obese MASH.

SAT-117-YI
Ultrastructural assessment of liver sinusoidal endothelial cell capillarisation in metabolic-dysfunction associated steatotic liver disease and its modulation by lanifibranor
Shivani Chotkoe[1], Guillaume Wettstein[2], Joris De Man[1], Sofie Thys[3], Isabel Pintelon[3], Yang Lu[1], Nateneal Beyene[1], Jean-Louis Junien[2], Denise van der Graaff[4], Benedicte De Winter[1], Winnok De Vos[3], Luisa Vonghia[4], Wilhelmus J Kwanten[4], Sven Francque[4]. *[1]University of Antwerp, Laboratory of Experimental Medicine and Paediatrics, Wilrijk, Belgium; [2]Inventiva Pharma, Daix, France; [3]University of Antwerp, Laboratory of Cell Biology and Histology, Antwerp Centre for Advanced Microscopy, Wilrijk, Belgium; [4]Unversity Hospital Antwerp, Edegem, Belgium*
Email: shivani.chotkoe@uantwerpen.be

Background and aims: In metabolic dysfunction-associated steatotic liver disease (MASLD), intrahepatic vascular resistance (IHVR) increases in early stages, driven by liver sinusoidal endothelial cell (LSEC) dysfunction and their loss of fenestrae (capillarisation). This phenomenon contributes to disease progression. The current study explored sinusoidal remodelling across the MASLD spectrum in human and rodent livers and assessed the effects of lanifibranor on LSEC fenestrae at histological and ultrastructural levels in a rat model.
Method: Human liver biopsy samples (n = 13) across the full MASLD spectrum were evaluated by transmission electron microscopy (TEM). Male Wistar Han rats (n = 6 per group) were fed a methionine-choline-deficient diet (MCDD) or standard chow diet (CD) for 4 weeks and received simultaneously placebo or lanifibranor (100 mg/kg/day) via oral gavage QD. Rat livers were evaluated by CD34 immunostaining, TEM, and scanning electron microscopy (SEM) with quantitative analysis of fenestrae. Evolution of capillarisation over time was also explored by CD34 in a second model using C57BL/6 mice (n = 6 per group) fed either CD or a high-fat high-fructose diet (HFHFD) at 24, 36 and 44 weeks.
Results: On biopsies, non-MASLD liver displayed normal fenestrated sinusoids. Early MASL (F1–2) retained fenestrae but developed basement membrane fragments and perisinusoidal fibrosis. Steatohepatitis (F2–3) showed LSEC thickening and loss of fenestrae, whereas complete capillarisation was observed in livers with cirrhosis. Placebo-treated MCDD-fed rats compared to CD-fed rats showed increased CD34 staining (38.8 ± 2.5 vs. 20.9 ± 2.8, $p < 0.001$), and ultrastructurally, increased fenestrae diameters, reduced fenestrae frequency (7.2 ± 0.4 vs. 10.8 ± 0.3, $p < 0.0001$) and decreased LSEC porosity (5.7 ± 0.4 vs. 7.5 ± 0.2, $p < 0.01$). In MCDD-steatosis, lanifibranor decreased CD34 staining (21.4 ± 5.7 vs. 38.8 ± 2.5, $p < 0.05$) and restored fenestrae frequency (9.3 ± 0.3 vs. 7.2 ± 0.4, $p < 0.01$) and LSEC porosity (7.2 ± 0.3 vs. 5.7 ± 0.4, $p < 0.01$) to levels comparable with controls. In HFHFD-fed mice, CD34 staining increased with diet duration, reaching significant elevations at 36 and 44 weeks.
Conclusion: Across species, LSEC capillarisation develops early in MASLD, albeit heterogeneously, and progresses with disease severity. Lanifibranor restores LSEC (ultra)structure in early MASLD, highlighting its therapeutic potential to restore vascular alterations and beneficially influence disease progression.

SAT-118
Activation of SIRT5 drives mitochondrial dysfunction, impaired hepatic differentiation and steatotic injury in human liver organoids
Maura Cimino[1], Rosaria Tinnirello[1], Riccardo Perriera[1], Giovanni Zito[1], Salvatore Gruttadauria[1], Massimo Pinzani[1], Federico Salomone[2], Vitale Miceli[1]. *[1]IRCCS ISMETT, Palermo, Italy; [2]Ospedale di Acireale, Acireale, Italy*
Email: vmiceli@ismett.edu

Background and aims: Metabolic dysfunction-associated steatotic liver disease (MASLD) is driven by alterations in mitochondrial function and lipid homeostasis. Sirtuin 5 (SIRT5), a mitochondrial lysine deacylase, has emerged as a potential regulator of hepatic bioenergetics and redox balance, yet its functional role in human liver tissue remains incompletely defined. Here, we investigated the impact of SIRT5 modulation on proliferation, differentiation, mitochondrial function, and lipid metabolism using human liver organoids (HliOs), aiming to define its contribution to MASLD-related mechanisms.
Method: HliOs were maintained under undifferentiated or hepatocyte differentiation conditions and treated with a selective SIRT5 activator or inhibitor at different concentrations. HliO viability were assessed by bright-field imaging and luminescence-based assays. Mitochondrial function was evaluated by measuring mitochondrial membrane potential, while mitochondrial oxidative stress was assessed by quantifying mitochondrial superoxide production. Hepatic differentiation was determined by the expression of key hepatocyte markers (ALB, CYP3A4, HNF4alpha). A lipid overload–based model of steatosis was established using free fatty acids, and lipid accumulation was quantified by Nile Red staining.
Results: Activation of SIRT5 significantly impaired HliO proliferation in a concentration-dependent manner and increased mitochondrial superoxide production, accompanied by mitochondrial membrane depolarization. During hepatic differentiation, SIRT5 activation markedly reduced the expression of key hepatocyte markers, indicating impaired hepatocellular maturation. In a steatosis model, SIRT5 activation exacerbated lipid droplet accumulation, mitochondrial oxidative stress, and loss of cell viability. Conversely, SIRT5 inhibition attenuated mitochondrial ROS generation, preserved mitochondrial membrane potential, reduced lipid accumulation, and partially rescued cell viability under steatotic conditions.
Conclusion: In conclusion, SIRT5 emerges as a critical regulator of mitochondrial homeostasis and metabolic resilience in HliOs.

Excessive SIRT5 activation promotes mitochondrial oxidative stress, impairs hepatic differentiation, and aggravates steatotic injury, whereas SIRT5 inhibition confers protection against lipotoxic stress. These findings support a pathogenic role for SIRT5 in MASLD progression and identify SIRT5 inhibition as a potential therapeutic strategy to mitigate mitochondrial dysfunction and disease severity.
"This work was supported by project PNRR-MCNT2-2023-12377338 "Contrasting chronic inflammation and neurodegeneration using the human amniotic mesenchymal cell secretome as an innovative therapeutic strategy (CONTRAST-OME)," CUP I73C24000360007, funded by the European Union - Next Generation EU - NRRP M6C2 Investment 2.1 Enhancement and strengthening of biomedical research in the NHS".

SAT-119

NLT-101 targets the nuclear envelope and protects hepatocytes against lamin B1 alterations associated with lipotoxic metabolic stress

Stefan Hoenow[1], Thomas Ryan[2], Arundhati Dongre[2], Daniel Bakowski[2], Michael Cooreman[3,4], Christopher Shepard[3]. *[1]Apollo Health Ventures, Berlin, Germany; [2]Sygnature Discovery, Nottingham, United Kingdom; [3]Apollo Alpha, St Petersburg, United States; [4]Virginia Commonwealth University, Richmond, United States*
Email: michaelpcooreman@msn.com

Background and aims: Hepatic steatosis affects nuclear envelope (NE) integrity; NE filament lamin B1 is associated with lipotoxicity through regulation of lipid metabolism genes. Endogenous 17alpha estradiol (17aE2) improves insulin resistance and lipid metabolism without reproductive effects of 17beta E2 (17bE2), through preferential affinity to estrogen receptor alpha (ERa) over ER beta (ERb). NLT-101, a novel small-molecule selective ERa partial agonist (ShERPA) improves steatohepatitis and fibrosis in the GAN-diet induced obese murine MASH model. We investigated the effect of NLT-101 on lamin B1 and NE structure in a model of fatty acid (FA) lipotoxicity.
Method: Primary cultured hepatocytes (PHH) were incubated for up to 72 hours with 100–800 uM of palmitate, a saturated FA that induces cellular lipotoxicity, and 100–400 mM of oleate, an unsaturated FA that protects from lipotoxicity. Lamin B1, A and its splice variant C were measured by automated Western Blot (WB) and immune fluorescence (IF). The effect of FAs on lamin levels was further studied with ERa ligands 17aE2 (1–10 mM), 17bE2 (10 mM) and NLT-101 (10 mM) during incubation. Nuclear area (NA) was measured with DAPI staining at 12 hours of palmitate incubation. Results of duplicate experiments are expressed as mean values. Viable cells as percentage of BSA control were assessed with the CellTiter-Glo luminicent Cell Viability Assay.
Results: Palmitate reduced protein levels of lamin B1 on WB in a dose- and time-dependent manner to 50% after 48 hours of incubation at 400 mM; a more pronounced lamin B1 decrease to 25% was observed with IF after 12 hours at 800 mM palmitate. Oleate did not significantly alter lamin B1 levels. Both FAs had no effect on lamin A, but reduced its splice variant lamin C by 50% at 48 hours. Both 17aE2 and NLT-101 rescued palmitate-induced lamin B1 decrease to the same degree, while 17bE2 had no such effect. Rescue occurred after the decrease and was more pronounced at 12 than at 6 hours, suggestive of a transcriptional effect. Palmitate dose-dependently reduced NA, with partial rescue by 17aE2. Palmitate, but not oleate, significantly reduced cell viability after 48 hours, with higher rescue by 10 mM NLT-101 compared to 10 mM 17aE2.
Conclusion: 17aE2 and NLT-101 prevented palmitate induced reductions of lamin B1 and cell viability in PHH. These data warrant further exploration of NE integrity and lamin biology in the disease biology of MASLD/MASH and the therapeutic potential of selective ERa agonists.

SAT-120

Diet and sex dictate CD1d-mediated immune alterations in MASLD and HCC

Carlos Cuño-Gómiz[1], Anna Tutusaus[2], Flavia Savino[1], Patricia Rider[2], Diba Zare[1], María Reig[3], Albert Morales[2], Montserrat Marí[2]. *[1]IIBB-CSIC/IDIBAPS, Barcelona, Spain; [2]IIBB-CSIC/IDIBAPS, CIBEREHD, BCLC, Barcelona, Spain; [3]IDIBAPS, CIBEREHD, BCLC, Hospital Clinic, Barcelona University (UB), Barcelona, Spain*
Email: monmari@clinic.cat

Background and aims: Metabolic dysfunction-associated steatotic liver disease (MASLD) is becoming a major driver of hepatocellular carcinoma (HCC), particularly in men and postmenopausal women. Estrogens provide metabolic and immune protection, reducing liver cancer risk. The liver hosts abundant natural killer T (NKT) cells, implicated in both tumor suppression and promotion. CD1d-knockout (KO) mice, lacking NKT cells, are widely used to study these roles, yet CD1d also exerts NKT-independent functions in different immune cell types. How sex influences CD1d activity and NKT cells remains unclear. This work explores sex-specific consequences of CD1d loss in MASLD and related HCC.
Method: Male and female Balb/c and CD1d-KO mice were fed either a high-fat choline-deficient (HFCD) or Gubra Amylin NASH (GAN) diet, with or without diethylnitrosamine (DEN) to induce HCC. Control mice were fed a Chow diet. Serum alpha-fetoprotein (AFP) was monitored throughout the study, and liver leukocytes were analyzed by spectral flow cytometry at the endpoint. Serum transaminases (ALT and AST) were determined. Total liver RNA was isolated to evaluate gene expression by RT-qPCR.
Results: HFCD induced severe MASH with fibrosis, high ALT and AFP, and DEN+HFCD caused HCC in all groups except Balb/c females. CD1d-KO mice, especially males, displayed aggravated disease with greater tumor load and liver injury. In contrast, GAN diet produced steatosis without inflammation, and DEN+GAN led to HCC only in males. Remarkably, CD1d-KO males exhibited milder GAN-related pathology than Balb/c males. Male mice displayed higher infiltration of injury-promoting myeloid populations. Females showed stronger NK activity, whereas males had more FOXP3+ regulatory T cells. CD1d-KO mice demonstrated broad immune shifts beyond NKT loss, including depletion of RORγT+ (IL-17A) T cells and enrichment of TBET+ CD8+ (IFNγ) T cells, while Th2-derived IL-4 persisted. Total $CD4^+$ T cells were also reduced, associated to a loss of MHC II expression by Kupffer cells, confirming NKT-independent modulation.
Conclusion: Diet and genetic background critically shape MASLD progression and HCC risk, with pronounced sex differences. CD1d deficiency rewires hepatic immunity in a context-dependent manner, yielding protective or detrimental effects based on sex and diet. Notably, female mice exhibit compensatory immune mechanisms that mitigate CD1d loss.

SAT-121-YI

The chronic environmental exposure to Bisphenol A influences trained immunity-related pathways and induces immunometabolic innate cells reprogramming, promoting the metabolic dysfunction associated steatotic liver disease (MASLD) progression

Marcello Dallio[1], Mario Romeo[1], Fiammetta Di Nardo[1], Alessia Silvestrin[1], Giusy Senese[1], Annachiara Coppola[1], Carmine Napolitano[1], Paolo Vaia[1], Simone Olivieri[1], Alessandro Federico[1]. *[1]Hepatogastroenterology Division, Department of Precision Medicine, University of Campania Luigi Vanvitelli; Piazza Miraglia 2, 80138, Naples (Italy), Naples, Italy*
Email: marcello.dallio@unicampania.it

Background and aims: Metabolic dysfunction-associated steatotic liver disease (MASLD) is a growing global health concern, often progressing to steatohepatitis (MASH) and advanced fibrosis (AF). Beyond insulin resistance, recent evidence implicates damage-associated molecular patterns (DAMPs) and gut-derived pathogen-associated molecular patterns (PAMPs), such as lipopolysaccharide (LPS), in driving MASLD progression via innate immune activation, inflammation, and reactive oxygen species (ROS) generation. The concept of trained immunity (TI)—a memory-like response in innate immune cells—has emerged as a key mechanism, involving metabolic reprogramming and heightened inflammatory output. Bisphenol A (BPA), a widespread endocrine disruptor, has been identified as a TI trigger capable of inducing immunometabolic remodeling in monocytes. This study investigates the role of chronic BPA exposure in MASLD progression through TI-mediated innate immune activation.
Method: Ten healthy controls and twenty MASLD patients (10 MASLD-SS, 10 MASLD-SH) undergoing liver biopsy were enrolled. At baseline (T0) and after a 3-month BPA-free diet (T1), BPA serum levels were quantified (LC-MS/MS), and cytokines (IL-1β, IL-6, TNF-α) were assessed (ELISA). Monocytes were isolated and subjected to a TI-BPA protocol (BPA priming, LPS rechallenge), followed by cytokine profiling and metabolic assessment (Seahorse XFb, ROS assay).
Results: At T0, BPA levels progressively increased from controls to MASLD-SS and MASLD-SH, with significantly elevated cytokines in MASLD-SH vs MASLD-SS (all $p < 0.0001$). TI-BPA-stimulated MASLD-SH monocytes produced higher IL-1β, IL-6, and TNF-α than other groups (all $p < 0.001$). Seahorse analysis revealed increased glycolysis and reduced mitochondrial respiration in MASLD-SH vs MASLD-SS (ECAR/OCR, all $p < 0.0001$). The BPA-free diet significantly reduced BPA levels (T1 vs T0, $p = 0.0002$), especially in MASLD-SH. At T1, "enhanced trained response" prevalence was higher in MASLD-SH vs MASLD-SS (82% vs 31%, $p < 0.0001$), with no metabolic differences between groups.
Conclusion: BPA promotes trained immunity and immunometabolic reprogramming in MASLD, exacerbating inflammation and disease progression. These findings underscore the impact of environmental exposures and support TI-targeted interventions in MASLD management.

SAT-122
Hepatic estrogen receptor alpha shapes sex differences in MASLD development and progression

Sara Della Torre[1], Arianna Dolce[1], Clara Meda[1]. [1]*Università degli Studi di Milano, Milano, Italy*
Email: sara.dellatorre@unimi.it

Background and aims: Metabolic dysfunction–associated steatotic liver disease (MASLD) encompasses a spectrum ranging from simple steatosis to steatohepatitis (MASH), fibrosis, cirrhosis and hepatocellular carcinoma. Despite its growing public health burden, effective therapeutic options remain limited, likely reflecting an incomplete understanding of the biological drivers underlying disease heterogeneity and progression. MASLD development is influenced by multiple factors, including obesity, genetic and epigenetic determinants, lifestyle, diet and hormonal status. Notably, compared with men and post-menopausal women, premenopausal women display a lower incidence of MASLD, suggesting a protective role of estrogens. However, despite the clear sexual dimorphism of MASLD, the contribution of hepatic estrogen signaling to sex-specific susceptibility and disease progression remains poorly explored. In the liver, estrogens predominantly signal through estrogen receptor alpha (ERα), which is downregulated in MASH compared with MASLD patients, implicating hepatic ERα in limiting disease progression. We hypothesize that hepatic ERα acts as a sensor of hormonal and nutritional cues, driving sex-specific regulation of liver metabolism and inflammation and thereby influencing MASLD development and progression.
Method: To identify sex-specific molecular drivers of MASLD, we analyzed liver transcriptomic and metabolomic profiles together with inflammatory and fibrogenic markers in mouse models at early and advanced disease stages. The role of hepatic ERα was assessed by comparing liver-specific ERα knockout (LERKO) and control (CTRL) mice fed a high-fat, high-cholesterol (HFHC) diet.
Results: LERKO mice exhibited marked alterations in hepatic gene expression, indicating that hepatic ERα is required for optimal metabolic adaptation to dietary lipid overload. HFHC feeding induced profound transcriptomic remodeling, with the earliest and most pronounced changes observed in LERKO males after 12 weeks, consistent with increased susceptibility to metabolic and inflammatory dysregulation.
Conclusion: Hepatic ERα is a critical regulator of sex-specific metabolic adaptations during HFHC-induced MASLD. Impaired hepatic ERα signaling may increase vulnerability to disease development and progression. Targeting hepatic ERα pathways may represent a novel strategy to prevent or mitigate MASLD progression.

SAT-123
Multi-organ crosstalk via Exosomal TCA cycle enzymes underlies metabolic benefits of exercise and daytime time-restricted feeding in murine MASH resolution

Xi-Xuan Wang[1], Xiaoying Dong[1], Rui-Qi Li[1], Tianhao Mao[2], Jun Guo[3], Yang Wang[3], Zihao Liang[3], Cai-Yun Zhang[2], Hao Ren[1], Wei Chen[3], Changhua Yi[3], Qingfang Xiong[1], Dandan Yin[3], Shu-Ling Chen[3], Dawei Yang[3], Yongfeng Yang[1]. [1]*Department of Hepatology, The Second Hospital of Nanjing, Medical School, Southeast University, Nanjing, China;* [2]*Nanjing Key Laboratory of Hepatology, The Second Hospital of Nanjing, Nanjing, China;* [3]*The Second Hospital of Nanjing, Affiliated to Nanjing University of Chinese Medicine, Nanjing, China*
Email: yyf1997@163.com

Background and aims: Emerging evidence highlights the interplay between peripheral organs and hepatic metabolism in metabolic dysfunction-associated steatohepatitis (MASH), yet systemic mechanisms linking behavioral interventions to tissue repair remain unclear.
Method: We established a murine MASH model via 24-week GAN diet followed by 8-week normal chow realimentation, with four intervention groups: sedentary ad libitum (SED-AL), exercise (EX), daytime time-restricted feeding (TRF), and EX+TRF. Body weight, insulin resistance, pathological staining of different organs, ultrastructure under electron microscope of different organs, and multi-omics of different organs were detected.
Results: While both TRF and EX+TRF demonstrated superior weight loss, all active interventions ameliorated insulin resistance and hepatic steatosis. Strikingly, EX induced skeletal muscle damage and reduced adipocyte lipid droplet size, whereas TRF preferentially restored adipose morphology without myofiber injury. Ultrastructurally, EX uniquely rescued hepatic mitochondrial cristae disruption in MASH. Multi-omics integration revealed profound TCA cycle rewiring across liver, muscle, and adipose tissues, with phospho-/acetyl-/lactyl-proteomics implicating post-translational regulation of metabolic enzymes. Mechanistically, exercise triggered skeletal muscle secretion of citrate synthase (CS), IDH3, and OGDH via exosomes, which restored hepatic mitochondrial energetics and attenuated lipid peroxidation. Conversely, TRF stimulated adipose-derived exosomes enriched with phosphorylated/acylated TCA modifiers, synergistically enhancing hepatic metabolic flexibility.

Conclusion: Our findings establish a novel paradigm of inter-organ communication through exosomal enzyme traf ficking, positioning combined chrono-exercise therapy as a systems-level strategy for MASH resolution.

SAT-125-YI

The role of Pyroptosis in metabolic dysfunction-associated steatotic liver disease

Lauredana dos Santos Ferreira Grani[1], Ahmed Ghallab[2], Jan G. Hengstler[2], Petr Broz[3], Mihael Vucur[1], Vangelis Kondylis[1], Tom Luedde[1,4]. [1]*University Hospital Düsseldorf, Department of Gastroenterology Hepatology and Infectious Diseases, Medical Faculty at Heinrich-Heine-University Düsseldorf, Düsseldorf, Germany;* [2]*Leibniz Research Centre for Working Environment and Human Factors (IfADo), Technical University Dortmund, Dortmund, Germany, Dortmund, Germany;* [3]*Department of Immunobiology, University of Lausanne, Lausanne, Switzerland, Lausanne, Switzerland;* [4]*Center for Integrated Oncology Aachen Bonn Cologne Duesseldorf (CIO ABCD), Düsseldorf, Germany*
Email: lauredana.ferreira@med.uni-duesseldorf.de

Background and aims: Metabolic dysfunction-associated steatotic liver disease (MASLD) is the most common cause of chronic liver disease. Liver injury is linked to inflammation and fibrosis, promoting the development of cirrhosis and hepatocellular carcinoma (HCC). The mechanisms driving the transition between disease stages remain unclear, but previous studies have implicated pyroptosis, an inflammatory form of regulated necrosis, in promoting progression to advanced steatohepatitis. We aimed to clarify the role of pyroptosis in promoting inflammation, fibrosis and HCC development in two murine models of metabolic dysfunction-associated steatohepatitis (MASH) and metabolic dysfunction and alcohol-associated liver disease (MetAld).
Method: Gasdermin (GSDM) transgenic mouse lines, including *Gsdmd*$^{-/-}$, *Gsdme*$^{-/-}$, *Gsdmd*$^{-/-}$/*Gsdme*$^{-/-}$ and *Gsdmd*$^{D88A/D88A}$, were fed a western diet (WD, 40% fat, 22% fructose, 10% sucrose, 2% cholesterol) or WD supplemented with 10% ethanol (WD+EtOH) for either 24 weeks, to assess levels of liver injury, inflammation and fibrosis, or 60 weeks to analyze HCC development. A glucose tolerance test was performed 4 weeks prior to experimental endpoint. Liver functions were assessed in serum samples, while liver tissue samples were analyzed by immunoblotting, qRT-PCR and immunohistochemistry.
Results: Expression of genes linked to pyroptosis, such as *Casp-1, Casp-11* and *Il1b,* were upregulated in livers of mice after both diets. Immunoblot analysis also showed induction of GSDMD cleavage, but not GSDME, a marker of pyroptosis execution. Ongoing analyses in mice fed for 24 weeks with WD and WD+EtOH revealed similar body weight gain, liver-to-body weight ratios and glucose tolerance across all mouse lines and wild-type controls. Unlike *Gsdme*$^{-/-}$ and *Gsdmd*$^{-/-}$/*Gsdme*$^{-/-}$ mice that showed not effect, *Gsdmd*$^{-/-}$ mice exhibited significantly lower liver injury after 24 weeks of WD feeding, accompanied by reduced hepatic inflammation. Upon WD+EtOH feeding, this protective effect appeared less striking.
Notably, mice expressing GSDMD mutant, which confers resistance to GSDMD inactivation by apoptotic caspases, showed a trend for lower ALT and AST levels compared to controls in WD feeding, but displayed significantly elevated liver damage after WD+EtOH.
Conclusion: GSDMD-dependent pyroptosis can influence hepatocellular injury and hepatitis in a context-dependent manner. Ongoing analyses will further define its contribution in MASLD-to-HCC transition and its potential as a therapeutic target.

SAT-126

Unveiling the protein cargo of high-density lipoprotein particles in metabolic dysfunction-associated steatohepatitis: a biomarker study

Aleksandra Dudzik[1,2], Stan Driessen[3], Yuhan Du[4], Rachel Byrne[1,2], Koen van Son[3,5], Anne Linde Mak[3], Anne-Marieke van Dijk[3], Julia Witjes[3], Veera Houttu[3], Diona Zwirs[3], Han Levels[3], Michail Doukas[6], Max Nieuwdorp[3], Stephen Pennington[2], A.G. (Onno) Holleboom[3,7], Fiona McGillicuddy[1,2]. [1]*Diabetes Complications Research Centre, School of Medicine, University College Dublin, Dublin, Ireland;* [2]*UCD Conway Institute of Biomolecular and Biomedical Research, School of Medicine, University College Dublin, Dublin, Ireland;* [3]*Department of Vascular Medicine, Amsterdam UMC, University of Amsterdam, Amsterdam, Netherlands;* [4]*UCD School of Computer Science, University College Dublin, Dublin, Ireland;* [5]*Department of Gastroenterology and Hepatology, Amsterdam UMC, University of Amsterdam, Amsterdam, Netherlands;* [6]*Department of Pathology, Erasmus MC, Rotterdam, Netherlands;* [7]*Amsterdam Gastroenterology Endocrinology and Metabolism Institute, Amsterdam UMC, Amsterdam, Netherlands*
Email: aleksandra.dudzik@ucdconnect.ie

Background and aims: Metabolic dysfunction associated steatohepatitis (MASH) is a major driver of liver cirrhosis/failure worldwide, and it is strongly associated with cardiovascular disease. Non-invasive biomarkers to identify and stage steatohepatitis are currently lacking. High-density lipoprotein (HDL-) particles (P), which are predominantly liver-derived, represent an important conduit between the liver and the vasculature and carry a large cargo of proteins systemically. In the setting of obesity, HDL-P are enriched with hepatic-derived pro-inflammatory and depleted of anti-inflammatory proteins. HDL proteome can mirror changes in the liver proteome in preclinical studies. In the current study we hypothesized that the HDL proteome can be utilised as a novel non-invasive biomarker for MASH.
Method: HDL was separated from serum using fast protein liquid chromatography (FPLC) in a set of patients with histologically validated MASLD ($n = 24$) and MASH ($n = 28$) derived from the Amsterdam UMC ANCHOR study cohort. Small (S-) and large (L-) HDL-containing FPLC fractions were further purified with lipid removal agent and processed for proteomic analysis on timsTOF Pro mass spectrometer (Bruker).
Results: S-HDL-P were enriched with Vitronectin, Aldolase B, Beta-2-glycoprotein 1, Complement Factor B and depleted of Complement component C6, Serum amyloid P-component, Coagulation factor V in MASH relative to MASLD. Angiotensinogen, Kininogen-1 were enriched and Apolipoprotein B, Complement C4-B, were depleted on L-HDL-P in MASH relative to MASLD. On S-HDL-P, Sex hormone binding globulin significantly correlated with fibrosis ($r = 0.42$) but not NAFLD activity score (NAS) ($r = 0.01$); while Complement Factor I correlated with NAS ($r = 0.37$), but not fibrosis ($r = 0.21$); vitamin D binding protein correlated with both NAS ($r = 0.32$) and fibrosis ($r = 0.36$). On L-HDL-P, Alpha-1-antitrypsin, Serum amyloid A-1, Complement component C7 correlated with fibrosis ($r = 0.31$; $r = 0.29$; $r = 0.52$) but not NAS ($r = 0.12$; $r = 0.08$; $r = 0.25$). Inter-alpha-trypsin inhibitor heavy chain H1 and H3 correlated with NAS ($r = -0.29$; $r = -0.34$) but not fibrosis ($r = -0.12$, $r = -0.01$).
Conclusion: Our findings highlight specific changes in the proteomic composition of HDL-P in advanced MASLD, providing insights into underlying pathophysiology. The HDL proteome may serve as a novel non-invasive biomarker to identify high-risk patients with MASH. Larger-scale validation studies are critical to confirm the clinical utility of this approach.

SAT-127

Glucose-dependent insulinotropic polypeptide signaling in adipose tissue macrophages protects against obesity-induced metabolic dysfunction-associated steatotic liver disease by promoting adaptive adipogenesis

Irina Efimova[1,2,3], Shani Ben Shlomo-Zidovetzki[1], Anat Neumann[1,2], Noam Erez[1], Sigal Fishman[1,3], Chen Varol[1,2]. [1]*Research center for digestive tract and liver diseases, Tel-Aviv Sourasky medical center, Tel-Aviv, Israel;* [2]*Department of clinical microbiology and immunology, Gray faculty of health and medical science, Tel-Aviv university, Tel-Aviv, Israel;* [3]*Department of gastroenterology and liver diseases, Tel-Aviv Sourasky medical center, Tel-Aviv, Israel*
Email: efimovais@gmail.com

Background and aims: Glucose-dependent insulinotropic peptide (GIP) regulates glucose homeostasis and energy expenditure, thereby contributing to body weight maintenance. Dual glucagon-like peptide 1 (GLP1) and GIP receptor agonists, such as tirzepatide, have demonstrated significant clinical efficacy in the treatment of metabolic dysfunction-associated steatotic liver disease (MASLD). However, the cellular and molecular mechanisms mediating these beneficial effects remain incompletely defined. We previously demonstrated that immune cell intrinsic GIP signaling restrains obesity and metabolic dysfunction. The present study investigates whether GIP signaling in adipose tissue macrophages (ATMs) regulates white adipose tissue expansion and hepatic lipid accumulation during obesity.
Method: We generated Gipr tdTomato/+ reporter mice to enable fluorescent tracking of GIPR expressing cells. To assess GIP receptor (GIPR) function in immune cells, we employed a bone marrow (BM) chimerism approach: lethally irradiated wild-type (WT) recipients were reconstituted with BM from WT (control) or Gipr-/- donors. After 8 weeks of reconstitution, mice were maintained on high fat diet (HFD) for 5 weeks and analyzed for metabolic and immunophenotypic parameters.
Results: Immune cell specific GIPR deficiency impaired epididymal white adipose tissue lipid storage capacity, resulting in pronounced hepatic steatosis even after short term HFD exposure, as confirmed by increased hepatic triglyceride levels and enhanced lipid droplet biogenesis. Analysis of Gipr tdTomato reporter mice identified ATMs as a major GIPR expressing immune population. Next, mice targeted deletion of GIPR in immune cells exhibited increased adipocyte hypertrophy, reduced expression of adipocyte differentiation markers, and diminished abundance of committed adipocyte progenitors in white adipose tissue. Transcriptomic profiling of ATMs revealed markedly impaired expression of adipogenesis associated genes, including Apoe, Bmp2, and C5a receptor genes, all of which have been implicated in adipogenesis.
Conclusion: GIP signaling in ATMs promotes healthy white adipose tissue expansion during chronic energy excess by supporting adaptive adipogenesis. Disruption of this pathway impairs adipose tissue lipid storage capacity and promotes ectopic lipid deposition in the liver, thereby exacerbating MASLD pathogenesis.

SAT-131-YI

Metabolic and alcohol associated liver disease (MetALD): understanding the gut-liver axis-mediated mechanisms of liver cancer

Alisson Quezada Cuadrado[1], Olga Estévez-Vázquez[1,2,3,4], Raquel Benedé-Ubieto[1,3], Hector Leal-Lassalle[1,4], Johanna Reißing[5], Tony Bruns[5], Adriana De Bonis[1,4], Chi Xu[1,4], Cecilia Jimeno-Santander[6], Cristina Alonso[7], Magdalena Leiva[1], Javier Vaquero[2,3,8], Rafael Bañares[2,3,8], Francisco Javier Cubero[1,2,3,4], Yulia Nevzorova[1,2,3,4]. [1]*Departamento de Inmunología, Oftalmología y Otorrinolaringología, Facultad de Medicina, Universidad Complutense de Madrid, Madrid, Spain;* [2]*Instituto de Investigaciones Sanitarias Gregorio Marañón (IiSGM), 28009, Madrid, Spain;* [3]*Centro de Investigación Biomédica en Red de Enfermedades Hepáticas y Digestivas (CIBEREHD), Instituto de Salud Carlos III, Madrid, Spain;* [4]*Instituto universitario de investigación en neuroquímica, Facultad de Medicina, Universidad Complutense de Madrid, Madrid, Spain;* [5]*Department of Internal Medicine III, University Hospital RWTH, Aachen, Germany;* [6]*Facutad de Biología, Universidad Complutense de Madrid, Madrid, Spain;* [7]*Rubió Metabolomics (OWL Metabolomics), Derio, Spain;* [8]*Servicio de Aparato Digestivo, Hospital General Universitario Gregorio Marañón, 28007, Madrid, Spain*
Email: olgaeste@ucm.es

Background and aims: In the present study we investigated the role of gut-liver crosstalk for the hepatocellular carcinoma (HCC) development in steatotic liver disease (SLD) induced by the compound effect of alcohol and metabolic risk factors.
Method: C57Bl6Wt male mice were fed with DUAL diet that was composed of a high-fat, high cholesterol (HFHC) Western diet (WD) and 10% alcohol in sweetened drinking water for 52 weeks and compared to mice fed with standard control diet (CTRL). Liver and gut phenotypes were evaluated via histochemistry, gene expression and serum metabolomic analysis. FITC-dextran (20 kDa) was used to study intestinal permeability. The hepatic and fecal microbiota profile was evaluated by 16S rRNA gene sequencing.
Results: Within 52 weeks of DUAL diet, livers became extraordinary enlarged with visible tumor nodules on the liver surface. Moreover, animals developed significant increase of plasma AST, ALT, LDH and serum cholesterol. Liver histology revealed histological evidence of steatosis, associated with a significant increase in cell death (TUNEL) accompanied by increased immune cell infiltration (CD45, CD3, B220, F4/80, CD11b) and higher IL23 expression. Collagen accumulation (Sirius red, αSMA, Collagen I) and an increase in cell proliferation (Ki67) was also detected in the area of tumor nodules. At the intestinal level, DUAL mice showed a significant colon shortening. Hence, a significant increase in of FITC dextran in the serum confirmed intestinal barrier dysfunction. Corresponding increase in the expression of Tlr2, Tlr3, and Tlr4 in the liver was validated by qPCR analysis. Analysis of 16S in stool and liver samples showed clear dysbiosis, with a loss of beneficial bacteria (especially Muribaculaceae and Lachnospiraceae) and an increase in pro-inflammatory microorganisms (Bacteroides and Desulfovibrionaceae). The serum metabolomic profile showed extensive alterations in the levels of lipids, fatty (myristelaidic acid and polyunsaturated acids), amino and bile acids, revealing a significant impact of the DUAL diet on various metabolic pathways.
Conclusion: Our results highlight the close relationship between intestinal and hepatic dysbiosis, altered metabolites, and tumor progression from steatohepatitis to HCC in the MetALD DUAL preclinical model, which constitutes a physiologically relevant experimental tool for evaluating new therapeutic strategies.
CIBER EHD25PI02 MICRO-BOOST.

SAT-132

Genome-wide shRNA screen identifies Eif4ebp1 as a novel therapeutic target in metabolic dysfunction-associated steatotic liver disease (MASLD)

Ayat Fayez[1], Amanpreet Kaur[2], Shainan Hora[1], Rong Gao[3], Torsten Wuestefeld[1,3]. [1]*Genome Institute Of Singapore, Singapore, Singapore;* [2]*Amity University, Punjab, India;* [3]*Lee Kong Chian School Of Medicine Nanyang Technological University, Singapore, Singapore*
Email: ibrahimaf@a-star.edu.sg

Background and aims: Metabolic dysfunction-associated steatotic liver disease (MASLD) is a leading cause of chronic liver injury with limited therapeutic options. We performed a genome-wide shRNA screen to identify novel targets that modulate MASLD progression.
Method: A doxycycline-inducible shRNA library was delivered to C57BL/6 mice via hydrodynamic tail vein injection. Mice were fed a Western diet (WD) for 24 weeks, with doxycycline administered during the final 16 weeks to induce shRNA expression. Deep

sequencing identified enriched shRNAs conferring hepatoprotective effects. Candidates were validated *in vitro* and *in vivo* using hepatocyte-specific knockdown models in both chronic (WD) and acute liver injury settings.
Results: The screen identified Eif4ebp1, a translation repressor that blocks eIF4E-mediated cap-dependent translation, as a top candidate. Eif4ebp1 knockdown enhanced hepatocyte regenerative capacity *in vitro* and reduced fibrosis by up to two grades in WD-fed mice. In human MASLD transcriptomic datasets, EIF4EBP1 expression correlated positively with disease severity. Furthermore, EIF4EBP1 was upregulated in human hepatocytes treated with oleic and palmitic acids.
Conclusion: Eif4ebp1 plays a pathogenic role in MASLD progression, and its targeting represents a promising therapeutic strategy to attenuate fibrosis and enhance liver regeneration.

SAT-133

Reprogramming lipid-driven immunometabolic dysfunction in metabolic dysfunction-associated steatohepatitis through PLT012 targeting CD36

Janusz Von Renesse[1], Laura Fernandez-Rodriguez[1], Yi-Ru Yu[1], Mina Tsakovska[2,3], Jie Ting Low[2,3], Karina Lobo Hajdu[2,3], Zhen Meng[1], Yun-Han Lin[1], Ping-Chih Ho[2,3]. *[1]Pilatus Biosciences, Epalinges, Switzerland; [2]Department of Fundamental Oncology, University of Lausanne, Epalinges, Switzerland; [3]Ludwig Institute of Cancer Research Lausanne Branch, Epalinges, Switzerland*
Email: ping-chih.ho@unil.ch

Background and aims: Metabolic dysfunction-associated steatohepatitis (MASH) is driven by sustained hepatic lipid overload, which triggers lipotoxicity, inflammation, and fibrosis. Evidence shows that maladaptive lipid sensing and uptake across multiple hepatic cell types are key drivers of this pathogenesis. Crucially, CD36, a fatty acid transporter, is markedly upregulated in hepatocytes and in liver-resident immune and stromal cells in steatotic and MASH livers. CD36-driven lipid uptake promotes lipid accumulation, inflammation, and fibrosis, reshaping the hepatic microenvironment. Consequently, targeting CD36 with the humanized IgG4 antibody PLT012 offers a compelling therapeutic option.
Method: PLT012 was developed by phage display, affinity maturation, and developability optimization. Its efficacy was evaluated in complementary mouse MASH models, including the Western diet-induced and the choline-deficient, amino-acid-defined high-fat diet representing obese and non-obese disease. Disease hallmarks were assessed by histology, flow cytometry, gene expression, and biochemical analyses. PLT012 safety and pharmacokinetics were evaluated in cynomolgus monkeys.
Results: PLT012 showed cross-reactivity across murine, non-human primate (NHP), and human CD36. Cryo-electron microscopy–based structural analysis confirmed that PLT012 binds the CD36 lipid-binding domain, supporting a targeted action on lipid transport relevant to MASH. Across preclinical MASH models, PLT012 effectively reduced key disease hallmarks. The treatment lowered hepatic steatosis and adipose tissue mass, decreased the expression of crucial de novo lipogenesis genes (Acaca, Fasn, Mlxipl), and lowered serum levels of alanine aminotransferase and aspartate aminotransferase, suggesting reduced liver damage. It also diminished hepatic inflammation (TNF-alpha, IL-1beta, and Ccl2 expression) and reduced immune cell infiltration. Additionally, PLT012 remodeled the macrophage population, decreasing lipid-associated, inflammatory, and pro-fibrotic macrophages. Correspondingly, fibrosis was reduced, as evidenced by reduced collagen deposition in Picrosirius staining and lower expression of fibrotic genes (Col1a1, Col3a1). Beyond mouse studies, PLT012 exhibited excellent tolerability in NHP studies, with no adverse effects.
Conclusion: Taken together, these results show that blocking CD36 with PLT012 reshapes the hepatic microenvironment toward a more balanced, homeostatic state, highlighting its therapeutic potential across steatotic liver diseases.

SAT-134

Ultrastructural analysis of transjugular biopsies in metabolic dysfunction-associated steatotic liver disease identifies core hepatocellular stress adaptations

Luis Ibañez-Samaniego[1], Sonia Alonso[1], María Luisa Cagigal[2], Diego Rincón Rodriguez[1], María-Vega Catalina[1], Maria Isabel Peligros[3], Angela Puente[4], Ana Sofia Collado[2], Luis Téllez[5], Elba Llop Herrera[6], Edilmar Alvarado-Tapias[7], Paula Iruzubieta[4], María Teresa Arias Loste[4], Emilio Fabrega[4], Antonio Cuadrado[4], Miguel Lafarga[8], Jose Fortea[4]. *[1]Liver Unit, Hospital General Universitario Gregorio Marañón, Instituto de Investigación Sanitaria Gregorio Marañón, CIBERehd, MAdrid, Spain; [2]Hospital Universitario Marqués de Valdecilla, Pathological Anatomy Service, Santander, Spain; [3]Hospital General Universitario Gregorio Marañón, Pathological Anatomy Service, Madrid, Spain; [4]Gastroenterology and Hepatology Department, Clinical and Translational Research in Digestive Diseases, Valdecilla Research Institute (IDIVAL), Marqués de Valdecilla University Hospital, Santander, Spain; [5]Department of Gastroenterology and Hepatology, Hospital Universitario Ramón y Cajal, IRYCIS, CIBERehd, Universidad de Alcalá, Madrid, Spain, Madrid, Spain; [6]Centre for Biomedical Research in Liver and Digestive Diseases Network (CIBERehd), Instituto de Salud Carlos III, Madrid, Spain; Department of Gastroenterology and Hepatology, Puerta de Hierro University Hospital, Puerta de Hierro Health Research Institute (IDIPHIM), Universidad Autonoma de Madrid, Madrid, Spain; [7]Department of Hepatology, Hospital Santa Creu i Sant Pau. Autonomous University of Barcelona (UAB), Department of Medicine. Inflammatory Diseases Department, Biomedical Research Institute Sant Pau (IIB Sant Pau), Centre for Biomedical Research in Liver and Digestive, Barcelona, Spain; [8]Department of Anatomy and Cell Biology, University of Cantabria, Santander, Spain*
Email: jifortea@gmail.com

Background and aims: Electron microscopy (EM) has provided key insights into hepatocellular alterations in MASLD, but most studies relied on percutaneous biopsies and primarily focused on selected features such as megamitochondria or autophagic vesicles. We aimed to evaluate the feasibility of ultrastructural analysis in transjugular biopsies and to provide a comprehensive description of hepatocellular changes in patients with MASLD.
Method: Patients with MASLD, well characterized by hepatic venous pressure gradient (HVPG) and stratified by fibrosis stage, portal hypertension, and MASH status, were prospectively enrolled. 18G transjugular liver biopsies were processed for EM. Hepatocellular alterations were systematically assessed, including mitochondrial, endoplasmic reticulum (ER), autophagic, cytoskeletal, and nuclear changes.
Results: Eighteen patients were included; 8 (44.4%) had advanced fibrosis (F3–F4), 12 (66.7%) fulfilled diagnostic criteria for MASH, and 7 (38.9%) had portal hypertension (HVPG ≥6 mmHg). Transjugular specimens consistently yielded tissue suitable for high-quality ultrastructural assessment. The most frequent alterations were mitochondrial swelling, ER cisterns dilation, and accumulation of autophagic vesicles, reflecting cellular stress responses linked to hepatocellular injury, inflammation, and fibrogenesis. Cytoskeletal adaptations, specifically reinforcement of the cortical actin cytoskeleton and hypertrophy of adherens junctions, were also observed. These changes were observed across the fibrosis, portal pressure, and MASH subgroups.
Conclusion: Transjugular liver biopsies are suitable for EM studies in MASLD. The observed hepatocellular alterations appear to reflect core cellular stress responses and were noted consistently throughout the cohort. These findings provide a framework for integrating ultrastructural data into mechanistic and translational research in MASLD.

SAT-135-YI

A non-human primate liver organoid model recapitulates fibrotic and inflammatory features of metabolic dysfunction-associated steatotic liver disease

Bowen Gao[1], Li Wang[2], Wayel Jassem[3], Yun Ma[1]. [1]*King's College London, London, United Kingdom;* [2]*Suzhou Jiyan Biopharmaceutical Technology, Suzhou, China;* [3]*King's College London, King's College Hospital, London, United Kingdom*
Email: bowen.3.gao@kcl.ac.uk

Background and aims: The translation of findings from rodent Metabolic Dysfunction Associated Steatotic Liver Disease (MASLD) to human clinical contexts is often hindered by interspecies variability, while human-based research is frequently obstructed by ethical mandates and scarce tissue availability. Monkey-derived liver organoids (LOs) provide a genetic profile more analogous to humans than rodents. This study seeks to develop and validate a monkey organoid model to facilitate MASLD research.
Method: LOs derived from monkey liver tissue were exposed to 250 μM palmitic acid and oleic acid for 24 hours after 5 days differentiation. Lipid accumulation was evaluated by Oil Red O staining and total cholesterol (TC) quantification. LOs with or without exposure to free fatty acids (FFAs) were harvested for DIA based LC-MS/MS proteomics profiling. Statistical significance was defined as p.adjust < 0.05 (Benjamini-Hochberg FDR correction) for enrichment analysis and $p < 0.05$ for individual proteins.
Results: Oil Red O staining and TC detection confirmed lipid accumulation and secretion in the LOs ($p < 0.05$). Proteomic profiling identified 8643 proteins with 634 upregulated and 200 downregulated in the steatotic group. GO enrichment analysis revealed an upregulation of wound healing (enrichment ratio, ER = 5.55, p.adjust = 0.0013), suggesting liver damage induced by oxidative stress from lipid toxicity, and followed by an attempt at repair and regeneration. Pathways related to collagen trimer complex formation were upregulated (ER = 23.15, p.adjust = 0.0363), indicating a remodeling of extracellular matrix (ECM) and increased risk for fibrosis, which is consistent with significantly increased expression of fibrosis markers such as COL1A1 (fold change = 5.17, $p = 1.36 \times 10^{-27}$) and COL1A2 (fold change = 8.13, $p = 2.69 \times 10^{-44}$). Conversely, DNA replication initiation was downregulated (ER = 45.05, p.adjust = 0.0301), which represents a suppression in cell proliferation and DNA repair. Noteworthy, the upregulation of TGF-beta (fold change = 16.37, $p = 6.26 \times 10^{-167}$) indicates an activation of inflammation.
Conclusion: FFAs-treated monkey LOs showed significant features of cell damage, inflammation, metabolic disorders and ECM remodeling. These findings suggest that monkey LOs are a promising and reliable model for MASLD and have the potential to recapitulate liver fibrosis. This model will be used to evaluate anti-steatosis compounds for preclinical testing.

SAT-136

Oral administration of low molecular weight heparin polysaccharide alleviated metabolic dysfunction-associated steatotic liver disease by modulating the gut microbiota and metabolites in mice

Dekai Zheng[1], Xuelian Gao[1], Changhao Cheng[1], Xun Wang[1], Zhixin Fang[1], Ting Zhang[1], Kangsen Yang[1], Yuchuan Chen[1], Routing Wang[1], Zhixian Lan[1], Yanhua Tang[2], Jian Sun[1]. [1]*Department of Infectious Diseases, Nanfang Hospital, Southern Medical University, Guangzhou, China; State Key Laboratory of Multi-organ Injury Prevention and Treatment; Key Laboratory of Infectious Diseases Research in South China, Ministry of Education; Guangdong Provincial Key Laboratory for Prevention and Control of Major Liver Diseases; Guangdong Provincial Clinical Research Center for Viral Hepatitis; Guangdong Institute of Hepatology; Guangdong Provincial Research Center for Liver Fibrosis Engineering and Technology, Guangzhou, China;* [2]*Pulmonary and Critical Care Medicine, The First Affiliated Hospital, Hengyang Medical School, University of South China, Hengyang, China*
Email: sunjian@smu.edu.cn

Background and aims: Metabolic dysfunction-associated steatotic liver disease (MASLD) is the most prevalent chronic liver disease globally, yet therapeutic options remain limited. Oral low molecular weight heparin polysaccharide (LMWH) has demonstrated anti-inflammatory properties in colitis, but its potential efficacy in MASLD is unknown. We aimed to investigate the therapeutic effects of oral LMWH on MASLD and elucidate the underlying gut-liver axis mechanisms.
Method: We investigated the protective effects of oral LMWH in both high-fat diet (HFD) and high-fat high-cholesterol (HFHC) diet-induced mouse models through biochemical analyses (ALT, AST, TC, TG), histopathological evaluation (H&E, Oil Red O), and quantification of hepatic lipid accumulation (liver TC and TG levels). Antibiotic depletion and fecal microbiota transplantation (FMT) models assessed microbiota involvement. 16S rRNA sequencing integrated with metabolomics profiling were conducted to explore the underlying mechanisms. The ameliorating effect of 7-Ketolithocholic acid (7-K-LCA) was verified in vitro and in vivo. Activity-based protein profiling (ABPP) was used to identify the direct molecular targets of 7-K-LCA.
Results: Oral LMWH attenuated MASLD progression, reducing liver injury and hepatic steatosis in mice. Antibiotic depletion and FMT experiments confirmed the microbiota-dependent protective role of LMWH. Integrated 16S rRNA sequencing and metabolomics analyses revealed that LMWH selectively enriched *Akkermansia muciniphila* (*A. muciniphila*) and its derived metabolite, 7-K-LCA in vivo. Notably, LMWH promoted the growth of *A. muciniphila* in a dose-dependent manner in vitro. Supplementation with either *A. muciniphila* or 7-K-LCA replicated the beneficial effects of LMWH on MASLD. Mechanistically, 7-K-LCA was found to directly bind to and target Perilipin 3 (PLIN3), thereby inhibiting lipid droplet formation in hepatocytes and reducing intrahepatic lipid accumulation. Molecular docking demonstrated that 7-K-LCA bound to PLIN3 through hydrogen bonds and hydrophobic interactions.
Conclusion: Oral LMWH alleviated MASLD by enriching *A. muciniphila* and its metabolite 7-K-LCA, which targeted PLIN3 to reduce hepatic lipid deposition. These findings uncover a novel gut-liver axis through which oral LMWH remodels the gut microbiome to combat MASLD. This work highlights the therapeutic potential of targeting the gut microbiota with LMWH or its downstream metabolites as a promising strategy for managing MASLD.

SAT-137

Extracellular ATP (eATP) and related pathways in the progression of metabolic dysfunction–associated steatotic liver disease (MASLD)

Vanessa García-Fernández[1,2], Antonio Gil-Gómez[1,2,3], Rocío Munoz-Hernández[1,2,3], Sheila Gato-Zambrano[1,2], Ángela Rojas Álvarez-Ossorio[1,2], Isabel Fernández-Lizaranzu[1,2,4], M. Carmen Rico[1,2,5], Rocío Gallego-Durán[1,2,6], Douglas Maya-Miles[1,2,3], Raquel Millan[1,5], Javier Ampuero[1,2,5], Manuel Romero-Gómez[1,2,5]. [1]*SeLiver Group. Instituto de Biomedicina de Sevilla (IBiS), Hospital Universitario Virgen del Rocío/CSIC/ Universidad de Sevilla, Sevilla, Spain;* [2]*Centro de Investigación Biomédica En Red De Enfermedades Hepáticas y Digestivas (CIBEREHD), Madrid, Spain;* [3]*Departamento de Fisiología, Facultad de Biología, Universidad de Sevilla, Sevilla, Spain;* [4]*Grupo de Física Interdisciplinar, Escuela Técnica Superior de Ingeniería, Universidad de Sevilla, Sevilla, Spain;* [5]*Servicio de Aparato Digestivo, Hospital Universitario Virgen del Rocío, Sevilla, Spain;* [6]*Departamento de Medicina, Facultad de Medicina, Universidad de Sevilla, Sevilla, Spain*
Email: vgarcia-ibis@us.es

Background and aims: Extracellular ATP (eATP) is a damage-associated molecular pattern (DAMP) that promotes inflammation, leading to immune cell recruitment and cytokine release.

Ectonucleoside Triphosphate Diphosphohydrolase 1 (ENTPD1) metabolizes eATP, reducing circulating ATP levels and limiting inflammatory signaling. The purinergic receptor P2X7 (P2RX7) is activated by eATP and, in turn, stimulates the NLR family pyrin domain containing 3 (NLRP3)/interleukin-1beta pathway, amplifying liver inflammation. The aim of this study was to determine the role of eATP and the NLRP3 pathway in the progression of MASLD.

Method: A study was performed in twenty male C57BL/6J mice fed a High Fat High Carbohydrate and Cholesterol (HFHCC) diet (n = 10) or chow diet (n = 10). *Entpd1, P2rx7, Panx1 and Nlrp3* genes and Entpd1 and P2rx7 protein levels were assessed by PCR and IHC. Moreover, one hundred seventy biopsy-proven MASLD patients were classified according to SAF and NAS Score as simple steatosis (SS) (n = 74) or Metabolic dysfunction-associated steatohepatitis (MASH) (n = 96). Serum ENTPD1 levels were measured by ELISA.

Results: *Entpd1* was increased in HFHCC-fed mice (fold change 1 ± 0.83 vs 1.97 ± 0.75; p = 0.0005). *P2rx7* (fold change 1 ± 0.62 vs 2.24 ± 0.58; p < 0.0001) and *Nlrp3* (fold change 1 ± 0.41 vs 2.28 ± 0.71; p < 0.0001) were also upregulated. *Panx1* expression was decreased (fold change 1 ± 0.53 vs 0.32 ± 0.14; 0 = 0.0012). In the control group, Entpd1 protein expression localized around the central vein, with minimal signal in the portal vein area, while in HFHCC-fed mice, Entpd1 shifted towards the portal vein, showing increased portal expression and reduced central vein expression. P2rx7 positive cells/area were higher in HFHCC-fed mice (272.4 ± 79.8 *vs.* 391.8 ± 121.8; p = 0.0035). Patients with MASH (1588 ± 1750 pg/ml) had higher ENTPD1 levels than those with SS (1136 ± 808 pg/ml, p = 0.03). ENTPD1 levels increased with inflammatory activity [none (n = 23), 1477 ± 1131 pg/ml; mild (n = 99), 1113 ± 890 pg/ml; moderate (n = 48), 1925 ± 2163pg/ml; p = 0.005], with a significant difference between the mild and moderate inflammation group (p = 0.015). ENTPD1 levels were not significantly associated with ballooning or fibrosis.

Conclusion: In conclusion, upregulation of *Entpd1*, *P2rx7* and *Nlrp3* gene expression, together with increased Entpd1 and P2rx7 protein levels supports the role of eATP-related pathways in MASLD progression. Serum ENTPD1 levels reflects inflammatory activity, linking eATP-related pathways to inflammation-driven progression of MASLD.

SAT-138

Synergy of SOAT2-inhibitor PRD001 with resmetirom in reducing MASH and fibrosis in obese Ldlr-/-.Leiden mice

Eveline Gart[1], Kanji Hosoda[2], Martine C. Morrison[1], Anita M. van den Hoek[1], Hans M.G. Princen[1], Hiroshi Tomoda[2]. *[1]TNO, Leiden, Netherlands; [2]PRD Therapeutics, Inc., Tokyo, Japan*
Email: eveline.gart@tno.nl

Background and aims: Metabolic-dysfunction associated steatohepatitis (MASH) is characterized by hepatic lipid accumulation and inflammation. Sterol *O*-acyltransferase 2 (SOAT2), formerly known as ACAT2, plays a key role in intestinal cholesterol absorption and hepatic secretion. Pharmacological inhibition of SOAT2 reduces cholesterol uptake, thereby limiting hepatic lipid accumulation and secretion. Combining a SOAT2-inhibitor with resmetirom, a thyroid hormone receptor-β (THR-β) agonist that promotes lipid oxidation, could provide complementary reductions in fat and plasma lipids. This study aimed to assess the effects of PRD001, a SOAT2-inhibitor, combined with resmetirom on MASH and liver fibrosis.

Method: 20-week high-fat diet (HFD) without cholesterol supplementation fed Ldlr-/-.Leiden mice received vehicle, resmetirom (3 mg/kg), or resmetirom + PRD001 (30 mg/kg) for 12 weeks.

Results: Resmetirom and the combination treatment reduced body weight and fat mass, while increasing lean body mass as % of body weight. Fecal neutral sterol excretion, mainly driven by cholesterol excretion, was significantly increased with resmetirom and tended to be further enhanced when combined with PRD001. Resmetirom decreased plasma lipids and apoB with a significant further decrease for both when combined with PRD001. Lipoprotein profiles confirmed that this additional decrease was primarily due to a further decrease in VLDL- and LDL-cholesterol. Hepatic triglycerides and cholesterol esters were significantly decreased as well with resmetirom and combination with PRD001 led to a significant further decrease in hepatic cholesterol ester content. Hepatic macrovesicular steatosis, microvesicular steatosis, inflammation and fibrosis were all significantly reduced upon resmetirom treatment with a further decease in macro- and microvesicular steatosis when combined with PRD001. Hepatic gene expression confirmed involvement of (lipid) metabolism, inflammation pathways and mitochondrial pathways with more significant genes when resmetirom was combined with PRD001.

Conclusion: Using an advanced translational MASH model, we demonstrate resmetirom improved MASH and hepatic fibrosis. Adding PRD001 provided additional benefits on cholesterol excretion, plasma lipids, lipoproteins and steatosis highlighting the complementary mechanisms of PRD001 and resmetirom. Given the CVD risk in MASH patients, the observed lowering of atherogenic lipoproteins underscore substantial clinical advantages for the combination treatment.

SAT-139

The liver RNF43-Wnt/β-catenin pathway remotely regulates the intestinal inflammation repair pattern through bile acid reprogramming

Ying Geng[1], Jian Jiao[1]. *[1]China-Japan Union Hospital, Jilin University, Changchun, China*
Email: gengying23@mails.jlu.edu.cn

Background and aims: Previous studies have suggested that levels of DCA, TCA, LCA and GDCA are elevated in MASLD (metabolic dysfunction-associated steatotic liver disease). DCA and TCA have anti-apoptotic effects and induce proliferation of colon epithelial cells. The role of RNF43 as a negative regulator of the Wnt pathway in the mechanism of MASLD-related changes in the bile acid spectrum and abnormal proliferation of intestinal epithelial cells is unclear. This study aims to address these issues.

Method: An animal model of MASLD combined with intestinal epithelial cell injury and abnormal proliferation was established. Liver-specific knockdown of RNF43 using AAV-shRNA was used, and the levels of bile acids in the serum and faeces of each group of mice were detected using LC-MS/MS. Immunohistochemical methods were also used to detect the expression levels of bile acid metabolism pathways.

Results: In the model group, mice exhibited elevated DAI (Disease activity index) scores, increased intestinal inflammatory cell infiltration, heightened Ki-67 expression, and decreased TGR5 expression. These symptoms were alleviated in the RNF43 knockdown group. The fecal levels of LCA and GDCA in the model group were higher than those in the control group (p < 0.05). Compared to the model group, mice in the RNF43 knockdown group showed higher levels of serum TUDCA and TCA, lower levels of faecal DCA and LCA, and higher levels of GCA-3S, GDCA-3S and TDCA-3S (p < 0.05). Mechanistically, CYP7A1 expression in the livers of the RNF43 knockdown group was higher than in the model group (p < 0.01), BSEP decreased and NTCP increased (p < 0.0001).

Conclusion: Knocking down RNF43 in mouse livers further activates the hepatic Wnt/β-catenin pathway, reprogramming bile acid metabolism, elevates serum TUDCA and TCA levels, and directly acts on TGR5 in intestinal epithelial cells to inhibit inflammation and apoptosis. Concurrently, levels of toxic bile acids (DCA, LCA) decrease, while levels of sulfated bile acids (which are more water-soluble and less toxic) increased. These combined effects mitigate damage to intestinal acinar epithelial cells, reduce Ki-67-positive intestinal epithelial cell proliferation, and improve the morphology of abnormal crypt foci in mice.

SAT-140-YI

Inhibition of hepatic bile salt uptake using Bulevirtide attenuates pre-existing diet-induced metabolic dysfunction-associated steatohepatitis in mice

Claire Groenen[1,2], Thuc-Anh Nguyen[1,2], Joost Lambooij[3], Rudi de Waart[1,2], Kam Ho-Mok[1,2], Isabelle Bolt[1,2], Esther Vogels[1,2], Dagmar Tolenaars[1,2], Suzanne Duijst[1,2], Bruno Guigas[3], Joanne Verheij[4,5], Coen Paulusma[1,2], Wietse In het Panhuis[1,2], Stan F.J. van de Graaf[1,2]. *[1]Tytgat Institute For Liver And Intestinal Research, Amsterdam University Medical Centers, Amsterdam, Netherlands; [2]Amsterdam Gastroenterology, Endocrinology Metabolism (AGEM), Amsterdam University Medical Centers, Amsterdam, Netherlands; [3]Leiden University Center for Infectious Diseases, Leiden University Medical Center, Leiden, Netherlands; [4]Department of Pathology, Amsterdam University Medical Centers, Amsterdam, Netherlands; [5]Department of Pathology, Antwerp University Hospital/ University of Antwerp, Antwerp, Belgium*
Email: k.f.vandegraaf@amsterdamumc.nl

Background and aims: Metabolic dysfunction-associated steatotic liver disease (MASLD) affects over 30% of the global population and is characterized by hepatic fat accumulation. MASLD can progress into steatohepatitis (MASH), which involves inflammation that can lead to fibrosis and eventually cirrhosis and liver failure. Inhibition of the Sodium-dependent Taurocholate Cotransporting Polypeptide (NTCP) represents a potential therapeutic strategy, as this increases circulating bile salts, thereby improving glucose and lipid metabolism and reducing inflammation. We investigated whether NTCP inhibition with Bulevirtide, a safe and approved drug for treatment of hepatitis B and D, could attenuate liver steatosis, inflammation, and fibrosis in a MASH mouse model.
Method: Hyperlipidemic C57BL/6J$^{oatp1a1/1a4/1b2/ldlr-/-}$ male and female mice were used to mimic human hepatic bile salt uptake dynamics. Mice were fed a high-fat/high-cholesterol diet (40% and 0.15% w/w) and 15% fructose water (HFHCF) for 22 weeks to induce MASH. Liver biopsies confirmed features of MASH at baseline week 16. Subsequently, mice received daily subcutaneous injections of Bulevirtide (2.5 mg/kg) or vehicle for 6 weeks while continuing the HFHCF diet.
Results: HFHCF diet significantly increased liver-to-body weight ratios, plasma triglyceride, insulin levels, and induced hepatic steatosis, lobular inflammation and F2 perisinusoidal and periportal fibrosis. Bulevirtide increased plasma bile salt levels 20-fold. Bulevirtide treatment significantly decreased liver-to-body weight ratios (−19%) and tended to reduce Oil Red O-positive area percentage (−19%), liver triglyceride (−15%) and cholesterol content (−19%). Bulevirtide significantly lowered plasma triglyceride levels (−84%) and reduced plasma insulin levels (−45%). Bulevirtide treatment lowered abundance of monocytes in plasma (−35%) and liver (−22%) and induced a shift towards a less inflammatory (Ly6C^{high}TREML4^{low}) and more regulatory (Ly6C^{low}TREML4^{high}) profile. Bulevirtide treatment tended to lower F2 perisinusoidal and portal/periportal fibrosis scores, and significantly reduced liver COL1A1 abundance (3.5-fold) compared to vehicle in males only.
Conclusion: Bulevirtide improved MASH, but also metabolic parameters in a mouse model with pre-existing MASH. These findings suggest that NTCP inhibition may be a promising treatment for MASH, addressing both hepatic pathology and metabolic dysfunction.

SAT-141

Succinate alleviates metabolic dysfunction-associated steatotic liver disease through the hepatocyte Sucnr1/PPAR-gamma/Plin2 axis

Lei Gu[1], Shizhe Li[1], Shuoen Zhang[2], Zhonghe Xian[2], Zi Zuo[3], Hua Wang[3], Xiaowei Liu[4]. *[1]Department of Gastroenterology, Xiangya Hospital, Central South University, Innovation and Entrepreneurship Laboratory for College Students, Anhui Medical University, Department of Oncology, The First Affiliated Hospital of Anhui Medical University, Changsha, China; [2]School of Pharmacy, Innovation and Entrepreneurship Laboratory for College Students, Anhui Medical University, Hefei, China; [3]Entrepreneurship Laboratory for College Students, Laboratory of Molecular Biology, Department of Biochemistry, Anhui Medical University, Department of Oncology, the First Affiliated Hospital of Anhui Medical University, Hefei, China; [4]Department of Gastroenterology, Xiangya Hospital, Central South University, Changsha, China*
Email: gulei_279@163.com

Background and aims: Metabolic dysfunction-associated steatotic liver disease (MASLD) is the most prevalent chronic liver disease worldwide, representing a leading cause of liver-related morbidity and mortality. Its pathogenesis, however, remains incompletely elucidated. Gut microbiota dysbiosis and their metabolites are recognized as key contributors to MASLD progression. Among these, succinate, a dual-origin metabolite from both the host and gut microbiota, regulates immune and metabolic homeostasis via its cognate receptor SUCNR1. However, its specific role in MASLD pathogenesis remains unclear.
Method: Metagenomic analysis was performed to characterize the gut microbiota composition in patients with MASLD. A Western diet (WD)-induced MASLD mouse model was employed to evaluate the effects of dietary succinate supplementation and assess hepatic SUCNR1 expression. Molecular mechanisms were further investigated using proteomic analysis of liver tissues and *in vitro* assays with primary hepatocytes isolated from wild-type (WT) and SUCNR1-knockout (SUCNR1$^{-/-}$) mice.
Results: We found a reduced abundance of key succinate-producing bacteria in patients with MASLD, which was inversely correlated with the severity of hepatic steatosis. In WD-induced MASLD mice, hepatic SUCNR1 expression was significantly downregulated. Dietary succinate supplementation not only restored SUCNR1 levels but also ameliorated hepatic steatosis and inflammation. Proteomic analysis identified that succinate suppressed the expression of hepatic PPARγ and its downstream target, the lipid droplet-associated protein perilipin 2 (Plin2). Consistently, *in vitro* studies using primary hepatocytes demonstrated that succinate, acting via SUCNR1, directly inhibited PPARγ expression, reduced Plin2 protein levels, and subsequently alleviated cellular steatosis.
Conclusion: We provide evidence that succinate mitigates MASLD progression by activating the hepatocyte SUCNR1/PPAR-gamma/Plin2 signaling cascade. Restoring this metabolic axis represents a novel therapeutic approach to resolve hepatic steatosis and inflammation.

SAT-142

Semaglutide improves metabolic and histological outcomes and reverses clinically relevant biomarker alterations in the GAN diet-induced obese and biopsy-confirmed mouse model of MASH

Henrik H. Hansen[1], Jacob Nøhr-Meldgaard[1], Kristian Bendtsen[2], Kristoffer Niss[2], Jenny Egecioglu Norlin[2], Sanne Skovgård Veidal[2], Susanne Pors[1], Mathilde Teilmann[1], Kristoffer Voldum-Clausen[1], Markus Robert Latta[2], Michael Feigh[1]. *[1]Gubra A/S, Hørsholm, Denmark; [2]Novo Nordisk, Måløv, Denmark*
Email: hbh@gubra.dk

Background and aims: The long-acting glucagon-like peptide-1 (GLP-1) receptor agonist semaglutide was recently approved as the first GLP-1–based therapy for people with MASH and moderate-to-severe fibrosis. Clinical studies show that semaglutide not only improves liver health but also reverses several biomarker alterations characteristic of the disease. In this study, we characterized metabolic, histological, and biomarker responses to semaglutide in the Gubra Amylin NASH (GAN) diet-induced obese, biopsy-confirmed mouse model of MASH, and compared these findings with clinical observations.

Method: Male C57BL/6 mice were fed GAN diet, high in fat, fructose and cholesterol for 38 weeks prior to study start. A liver pre-biopsy was collected 4 weeks before treatment start. Only GAN DIO-MASH mice with NAFLD Activity Score (NAS ≥ 5) and fibrosis stage F2-F3 were included and stratified into treatment groups. Semaglutide (30 nmol/kg) or vehicle was administered subcutaneously once daily for 12 weeks. Vehicle-dosed, chow-fed mice served as healthy controls. Endpoints included aptamer-based SomaScan plasma proteomics, blood/liver biochemistry, pre-to-post individual assessment of NAS and fibrosis stage, and quantitative histology.
Results: Semaglutide promoted a weight loss of approx. 21% and improved hepatomegaly, plasma transaminases, plasma and hepatic lipid markers, NAS, and quantitative histological measures of steatosis and inflammation. Semaglutide also reduced fibrogenesis by histomorphometric analysis. Notably, the GAN DIO-MASH mouse model recapitulated key human MASH-associated circulating protein changes, including semaglutide-responsive biomarkers related to metabolism, inflammation, and fibrosis.
Conclusion: The GAN DIO-MASH mouse model exhibits strong translational relevance across metabolic, histological, and molecular domains, offering a robust platform for advancing mechanistic understanding of semaglutide and supporting the development of next-generation MASH therapies.

SAT-147

Lack of MASP-3 ameliorates liver injury and fibrosis in diet-induced fatty liver via modulation of apoptosis and inflammatory pathway in mice

Manabu Hayashi[1], Chikako Saito[1], Rie Hikichi[1], Takeshi Machida[2], Yumi Ishida[2], Mika Takasumi[1], Tatsuro Sugaya[1], Mai Murakami[1], Tomoaki Mochimaru[1], Michio Onizawa[1], Kazumichi Abe[1], Hideharu Sekine[2], Hiromasa Ohira[1]. *[1]Department of Gastroenterology, Fukushima Medical University, Fukushima, Japan; [2]Department of Immunology, Fukushima Medical University, Fukushima, Japan*
Email: m884884@fmu.ac.jp

Background and aims: The incidence of metabolic dysfunction-associated steatotic liver disease (MASLD) is increasing worldwide. The complement system is an innate immune system maintaining biological homeostasis, but its overactivation is associated with disease progression. Excessive C3 deposition in the liver is observed in MASLD patients, and it has been suggested that the complement alternative pathway contributes to the development of fatty liver disease. Mannose-binding lectin-associated serine protease (MASP)-3 plays a pivotal role in both the alternative pathway of the complement system and its development. This study aimed to clarify the involvement of MASP-3 for diet-induced fatty liver and the underlying mechanisms.
Method: MASP-3–deficient mice, which lack the exons encoding MASP-3–specific serine protease domain, were generated using the CRISPR-Cas9 system. Wild-type (WT) or MASP-3–deficient mice were fed either chow control or a choline-deficient, L-amino acid-defined, high-fat diet (CDAHFD) for 3 weeks or 28 weeks. At the time of sacrifice, livers were harvested and analyzed by RNA sequencing (RNA-seq), proteome analysis, and Western blotting. Gene ontology analysis and gene set enrichment analysis (GSEA) were used to examine alterations in signaling pathways.
Results: MASP-3–deficient mice exhibited low serum liver transaminases, mild histological liver injury, lower fibrosis area and fat deposition after 3 weeks of CDAHFD compared with WT mice. Gene ontology analysis using RNA-seq revealed significant downregulation of gene sets related to the extracellular matrix pathway and extracellular structure organization pathway in MASP-3–deficient mice. Western blot analysis of alpha-smooth muscle actin showed reduced expression in MASP-3–deficient mice compared with WT mice. GSEA using RNA-seq and proteome analysis showed down-regulation of gene sets related to apoptosis and inflammatory pathways in MASP-3–deficient mice compared with WT mice. Liver fibrosis after 28 weeks of CDAHFD was significantly ameliorated in MASP-3–deficient mice compared with WT mice.
Conclusion: Lack of MASP-3 ameliorated liver injury and fibrosis via modulation of apoptosis and inflammatory pathways in a MASLD mouse model. Our results suggest that inhibition of MASP-3 is a potential therapeutic target for MASLD.

SAT-148

Fat stiffens! The influence of steatotic progression on liver tissue

Alexander Hayn[1], Philip Friedrich[2], Jörg Walter[2], Madlen Matz-Soja[1], Thomas Berg[1], Josef Käs[2], Florian van Bömmel[1]. *[1]Leipzig University Medical Center, Medical Department II, Division of Hepatology, Leipzig, Germany; [2]Leipzig University, Peter Debye Institute for Soft Matter Physics, Soft Matter Physics Division, Leipzig, Germany*
Email: alexander.hayn@medizin.uni-leipzig.de

Background and aims: Biophysical alterations of liver tissue play a central role in the progression of metabolic associated steatotic liver disease. Accumulated fat deposits and fibrosis increase tissue stiffness and impair viscoelasticity, thereby influencing mechanosensitive cellular processes. Yet, the dynamics of these changes during disease progression remain poorly characterized.
Method: Liver tissue from mice fed either a Western diet (WD) or a Standard diet (SD) for 13, 26, or 32 weeks was analyzed to capture biophysical changes associated with fat accumulation and fibrosis. Tissue stiffness and viscoelasticity were quantified using atomic force microscopy, and effects on nuclear deformation in mechanosensitive cells were assessed.
Results: Progressive steatosis was consistently linked to increased tissue stiffness and reduced viscoelasticity. At all stages, WD tissue displayed significantly altered mechanical properties compared to SD. After 13 weeks, the WD tissue stiffened by a factor of 1.5, after 26 weeks by a factor of 2.5, and after 32 weeks by a factor of 3.1, compared to the SD tissue. In addition, a significant heterogeneity in stiffness was demonstrated between 26 and 32 weeks. With disease progression, these differences became more pronounced and were accompanied by enhanced nuclear deformation.
Conclusion: Stiffness and viscoelasticity emerge as sensitive indicators of steatotic liver disease. Their translation into clinical practice could help detect harmful consequences of steatosis at an early stage. Complementary proteomic analyses are essential to link these biophysical changes to molecular mechanisms and biological outcomes.

SAT-149

AxiomerTM mediated RNA editing converts the pathogenic PNPLA3 I148M variant to a wildtype-like form to reduce hepatic steatosis in MASLD/MASH

Werner Helvensteijn[1], Petra de Bruijn[1], Lieke Herbschleb[1], Nadia Keijzer[1], Marguerite Toros[1], Naomi van Vlies[1], Tsinatkeab Hailu[1], Lakshmi Baskar[1], Renee Salz[1], Jordy Bezemer[1], Saskia Haast[1], Mark de Lange[1], Iris Schmidt[1], Arlette Ruuls[1], Francesco De Chiara[1], Seda Yilmaz-Elis[1], Gerard Platenburg[1]. *[1]ProQR Therapeutics, Leiden, Netherlands*
Email: gplatenburg@proqr.com

Background and aims: Metabolic dysfunction-associated steatotic liver disease (MASLD) is the most common chronic liver disease characterized by hepatic fat accumulation. Disease progression can lead to metabolic dysfunction-associated steatohepatitis (MASH), cirrhosis, and hepatocellular carcinoma, making MASH a leading cause for liver transplantation in the US and EU. Patatin-like phospholipase domain-containing protein 3 (PNPLA3), is a hepatocyte-expressed protein involved in hepatic lipid metabolism. The *PNPLA3* I148M (rs738409) variant is the strongest genetic risk factor for MASH progression and is present in about 40–50% of patients. Axiomer-RNA editing uses editing oligonucleotides (EONs) to recruit endogenous ADAR enzymes, introducing site-specific conversion of adenosine-to-inosine, read as guanosine by ribosomes. EONs were

designed to convert the pathogenic methionine codon (ATG) to a valine codon (GTG), resulting in expression of PNPLA3 148 V wild-type-like variant that functionally mimics native PNPLA3 148I. Unlike gene silencing approaches, RNA editing preserves PNPLA3 protein expression while correcting its pathogenic function, potentially offering superior therapeutic benefit. This study evaluated Axiomer-mediated correction of *PNPLA3* I148M and its impact on hepatic lipid accumulation in a humanized mouse model.
Method: A lead N-Acetylgalactosamine (GalNAc)-conjugated EON was evaluated in FRG mice engrafted with homozygous PNPLA3 I148M PHH. Mice were fed a Western diet 1 month prior to and during treatment. Animals (n = 6 per group) received subcutaneous EON dosing (20 mg/kg, 14 doses over 28 days). Liver tissue was analyzed for RNA editing, steatosis, and macrovesicular lipid droplets (MLD) burden. A clinical-stage PNPLA3 antisense oligonucleotide (ASO) was included as a comparator (0,7 mg/kg, 14 doses over 28 days).
Results: In PHH, the lead 3′ GalNac-conjugated EON induced a dose-dependent correction of *PNPLA3* I148M, achieving 50% RNA editing. In humanized FRG mice, EON treatment resulted in 22% hepatic RNA editing of *PNPLA3* I148M and a marked reduction in MLD, exceeding the effect observed with the clinical-stage PNPLA3 ASO.
Conclusion: Axiomer RNA editing effectively converts the pathogenic *PNPLA3* I148M allele toward a wildtype-like variant, restoring lipid regulatory function and markedly reducing MLD in humanized *in vivo* systems. These findings support further development of *PNPLA3*-targeting EONs as a therapeutic strategy for MASLD/MASH.

SAT-150
Pharmacological inhibition of transforming growth factor-beta-activated kinase 1 (TAK1) in a murine model of metabolic dysfunction-associated steatotic liver disease
Felix Hempel[1], Maximilian Seul[2,3], Maria Grandoch[3,4], Mihael Vucur[1], Tom Luedde[1]. [1]*Department of Gastroenterology, Hepatology, and Infectious Diseases, Medical Faculty and University Hospital Düsseldorf, Heinrich Heine University Düsseldorf, Düsseldorf, Germany;* [2]*Institute of Molecular Medicine III, Medical Faculty and University Hospital Düsseldorf, Heinrich Heine University Düsseldorf, Düsseldorf, Germany;* [3]*Cardiovascular Research Institute Düsseldorf (CARID), Heinrich Heine University Düsseldorf, Düsseldorf, Germany;* [4]*Institute of Translational Pharmacology, Medical Faculty and University Hospital Düsseldorf, Heinrich Heine University Düsseldorf, Düsseldorf, Germany*
Email: felix.hempel@live.de

Background and aims: Transforming growth factor-beta-activated kinase 1 (TAK1) is an essential signalling hub regulating hepatic cell death, inflammation, and fibrogenesis via nuclear factor-kappaB and mitogen-activated protein kinases in metabolic dysfunction-associated steatotic liver disease (MASLD). Recently, specific TAK1 inhibitors had been developed and demonstrated efficacy in preclinical models of arthritis, systemic sclerosis, and lung fibrosis. However, we have previously reported severe hepatitis, focal necrosis, and premature death in mice with genetic deletion of TAK1 in liver parenchymal cells. We therefore sought to explore the safety and efficacy of pharmacological TAK1 inhibition in a murine model of MASLD.
Method: Six-week-old male C57BL/6J mice were fed a diet enriched in fat, refined carbohydrates, and cholesterol (Western Diet) for 20 weeks to recapitulate human MASLD. 30 days prior to necropsy, the TAK1 inhibitor HS-276 (25 mg/kg, n = 14) or vehicle (sterile saline, n = 14) were administered intraperitoneally once daily. Serum samples were collected before the start of HS-276 or vehicle and during necropsy two hours after the final injection.
Results: HS-276 treatment led to weight loss during the treatment period (p = 0.034 for interaction). At 30 days, body weight was 5.1% lower in the treatment group (95% confidence interval [CI] 2.0 to –12.3, p = 0.154). No clinical or behavioural changes were observed. HS-276 was detected at an average concentration of 22.5 pmol/mg in liver tissue (95% CI 18.1 to 26.9 pmol/mg) by liquid chromatography-mass spectrometry, confirming hepatic exposition towards the compound. Serum alanine aminotransferase (–42.1 U/l, 95% CI –4.8 to –79.5, p = 0.029) and glutamate dehydrogenase (-45.8 U/l, 95% CI –23.6 to –68.0, p < 0.001) levels decreased comparing HS-276- and vehicle-treated mice before and after treatment. Additionally, perigonadal (epididymal) white adipose tissue was less abundant in mice treated with HS-276 (-0.9 percentage points, 95% CI –0.3 to –1.5, p = 0.005). Weight and histologic appearance of the heart, kidneys, and spleen were unchanged by HS-276 treatment.
Conclusion: TAK1 inhibition by HS-276 was well tolerated in a murine model of MASLD, contrasting our previous findings from genetic models. Our data suggest an attenuation of liver injury and favourable metabolic effects, highlighting the potential of TAK1 inhibition for the treatment of MASLD.

SAT-151-YI
Intramuscular fat in steatotic liver disease is linked to muscle function impairment, insulin resistance and specific inflammatory pathways in the liver
Guillaume Henin[1], Maxime Nachit[1], Stéphanie André-Dumont[1], Alexis Goffaux[1], Salomé Declerck[1], Annette Gouw[2], Christine Sempoux[3], Pamela Baldin[4], Paulina Henry[5], Gaëtan Duchene[6], Pierre Trefois[6], Etienne Danse[6], Harmen Reyngoudt[7], Benjamin Marty[7], Jérome Ambroise[8], Audrey Loumaye[9], Peter Stärkel[1], Isabelle Leclercq[1], Nicolas Lanthier[1]. [1]*Laboratory of Gastroenterology and Hepatology (GAEN), Institut de Recherche Expérimentale et Clinique (IREC), UCLouvain, Brussels, Belgium;* [2]*Department of Pathology and Medical Biology, University Medical Center Groningen, Groningen, Netherlands;* [3]*Institute of Pathology, Lausanne University Hospital (CHUV), University of Lausanne (UNIL), Lausanne, Switzerland;* [4]*Department of Pathology, Cliniques universitaires Saint-Luc, UCLouvain, Brussels, Belgium;* [5]*Institut de Pathologie et Génétique, Gosselies, Belgium;* [6]*Department of Imaging, Cliniques universitaires Saint-Luc, UCLouvain, Brussels, Belgium;* [7]*NMR Laboratory,CEA/DRF/IBJF/MIRCen, Neuromuscular Investigation Center, Institute of Myology, Paris, France;* [8]*Centre des Technologies Moléculaires Appliquées (CTMA), Institut de Recherche Expérimentale et Clinique (IREC), UCLouvain, Brussels, Belgium;* [9]*Department of Endocrinology and Nutrition, Cliniques universitaires Saint-Luc, UCLouvain, Brussels, Belgium*
Email: nicolas.lanthier@saintluc.uclouvain.be

Background and aims: A muscle-liver axis, described on the basis of muscle density, appears to operate in cases of metabolic steatohepatitis. Here, we want to investigate the muscle phenotype (surface and intramuscular fat) by magnetic resonance imaging (MRI) in relation to muscle function and liver disease.
Method: Patients with SLD with an increased liver stiffness on transient elastography (≥7.8 kPa) were prospectively recruited. They underwent liver/skeletal muscles MRI and liver biopsy on the same day. Controls underwent the same MRI protocol. Mean liver and muscles (abdominal and paravertebral muscles) fat were measured by proton density fat fraction (PDFF). Muscle mass was assessed at the third lumbar vertebrae using the skeletal muscle index (SMI). Intramyocellular (IMCL) and extramyocellular lipids (EMCL) of right soleus and tibialis anterior were quantified using proton magnetic resonance spectroscopy. Muscle strength was assessed by the Liver Frailty Index (LFI). Liver biopsies were used for both histology and bulk mRNA sequencing.
Results: Patients with SLD (n = 92, 54 MASLD, 38 ALD) and controls (n = 10) were comparable for age. Ballooning was identified in 50% and fibrosis was graded as ≥ 2 in 63% of the SLD cohort. Median liver PDFF (19% vs. 3%, p < 0.001), mean muscle PDFF (22% vs. 9%, p < 0.001) and mean SMI (54 cm^2/m^2 vs. 36 cm^2/m^2, p < 0.001) were higher in the SLD group compared to controls. Despite significant metabolic differences such as BMI or presence of type 2 diabetes, muscle PDFF, LFI and SMI were similar in MASLD and ALD groups. Participants with

SLD and high muscle PDFF (>30%) showed decreased muscle strength compared to participants with low PDFF (<30%) but comparable age and BMI in both sexes. No correlation was found however between EMCL, IMCL and the liver frailty index while insulin resistance specifically correlated to soleus EMCL in MASLD ($r = 0.72$, $p = 0.005$) but not in ALD. Finally, transcriptomic analysis reveals that muscle fat is associated with an upregulation of hepatic inflammatory pathways and a downregulation of bile acid synthesis and fatty acid degradation.
Conclusion: Muscle fat assessed by MRI is increased in the presence of SLD and is associated with decreased muscle strength. EMCL are linked to insulin resistance in MASLD. Mechanistically, this disruption of the muscle-liver axis is associated with hepatic transcriptional changes including upregulated inflammatory pathways and downregulated bile acid biosynthesis and fatty acid degradation.

SAT-152
Dissecting paraoxonase 1 genotype combinations modulating paraoxonase activity and risk of dysglycemia and liver fibrosis
Laura Herrera[1,2], Maria João Meneses[1,3], Rogerio Ribeiro[2], Joao-Filipe Raposo[1,2,4], José Manuel Boavida[2], Luís Gardete-Correia[2], Carlos Penha-Gonçalves[2,5], Maria-Paula Macedo[1,2]. [1]*iNOVA4Health, NOVA Medical School, Faculdade de Ciências Médicas, NMS, FCM, Universidade NOVA de Lisboa, Lisbon, Portugal;* [2]*APDP – Diabetes Portugal, Education and Research Center, Lisbon, Portugal;* [3]*ProRegeM PhD Program, NOVA Medical School, NMS, Universidade Nova de Lisboa, Lisbon, Portugal;* [4]*Portuguese Society of Diabetology, Lisbon, Portugal;* [5]*Global Health and Tropical Medicine, GHTM, LA-REAL, Instituto de Higiene e Medicina Tropical, IHMT, Universidade NOVA de Lisboa, Lisbon, Portugal*
Email: laura.herrera@apdp.pt

Background and aims: Metabolic disorders such as dyslipidemia, metabolic dysfunction–associated steatotic liver disease (MASLD), and diabetes are promoted by chronic pro-inflammatory and pro-oxidative states. Paraoxonase 1 (PON1), a liver-derived enzyme associated with high-density lipoproteins (HDL), plays an important antioxidant role by hydrolyzing oxidized lipids and protecting against oxidative stress–induced damage. Genetic variation in PON1, particularly in promoter and coding regions, modulates enzyme expression and activity, thereby influencing susceptibility to metabolic and cardiovascular diseases. This study investigated the genetic determinants of serum paraoxonase (PONase) activity and their relationship with dysmetabolic phenotypes.
Method: A genome-wide association study was conducted in 922 Portuguese individuals from the PREVADIAB2 cohort. Genetic variants and haplotypes related to PONase activity were analyzed, and associations with dysglycemia and liver fibrosis were evaluated in individuals aged over 55 years.
Results: We identified two key PON1 variants as determinants of PONase activity: rs2057681 (in strong linkage disequilibrium with the non-synonymous Q192R variant) and rs854572 (located in the promoter region). Analysis of rs854572–rs2057681 haplotypes revealed that specific combinations differentially modulate PONase activity and confer risk or protection for dysglycemia and liver fibrosis, depending on the rs2057681 genotype context. Notably, although PONase activity was strongly associated with PON1 variants, it did not directly correlate with dysmetabolic phenotypes, suggesting that genetic context and haplotype structure, rather than enzyme activity alone, shape disease susceptibility.
Conclusion: These findings highlight the complex genetic architecture of PON1 and its role in metabolic disease risk, supporting the use of PON1 genetic information to uncover predisposition to dysmetabolic conditions. Our results provide insights into the interplay between PON1 genetics, enzyme function, and dysmetabolism, with implications for risk stratification in metabolic liver disease.

SAT-153
Combined exposure to alcohol and the PNPLA3 I148M variant drives hepatocytes toward pro-inflammatory, oncogenic, and profibrotic states in a western diet model
Stephen Hoang[1], Mulugeta Seneshaw[1], Faridoddin Mirshahi[1], Hae-Ki Min[1], Arun J. Sanyal[1]. [1]*Virginia Commonwealth University, Richmond, United States*
Email: arun.sanyal@vcuhealth.org

Background and aims: The genetic variant PNPLA3 I148M and alcohol consumption are distinct risk factors for the progression of steatotic liver disease, yet the mechanisms by which they interact to accelerate pathology remain incompletely defined. This study aimed to resolve how the combination of a Western diet, alcohol, and the PNPLA3 I148M genotype reshapes hepatocyte identity, pathway activity, and intercellular signaling networks.
Method: We used single-nucleus RNA sequencing (snRNA-seq) to profile liver tissue from mice exposed to a Western diet and alcohol, comparing controls with those carrying the PNPLA3 I148M variant. Prior to sequencing, injury was verified via histology. We identified hepatocyte subpopulations and constructed cell fate trajectories to assess state transitions. Pathway activities were quantified using Gene Set Variation Analysis (GSVA), and intercellular communication was inferred using CellPhoneDB. Findings were validated through protein quantification of inflammatory, metabolic, and fibrogenic markers.
Results: The combined exposure to Western diet, alcohol, and PNPLA3 I148M drove a coordinated shift in hepatocyte composition, yielding the highest abundance of stress-responsive subpopulations, including interferon-stimulated and injury-response hepatocytes. Trajectory analysis indicated that the combined treatment drove hepatocytes from quiescent states into phenotypes characterized by upregulated glycolysis (adj. $p < 0.001$) and oxidative phosphorylation (adj. $p < 0.001$). This was accompanied by a reciprocal downregulation of core functions, such as bile acid metabolism (adj. $p < 0.001$). Joint exposure enhanced profibrotic signaling interactions (adj. $p < 0.05$), specifically collagen-integrin, PDGF, and TGF-β interactions. Protein analysis corroborated these findings, showing significant elevation of inflammatory markers IL-1β ($p < 0.01$) and NLRP3 ($p < 0.01$), apoptotic cleaved Caspase-3 ($p < 0.05$), and fibrogenic markers COL1A1 ($p < 0.01$) and α-SMA ($p < 0.01$) in the combined treatment group relative to controls.
Conclusion: The interaction between alcohol and PNPLA3 I148M synergistically rewires the hepatic transcriptomic landscape, driving hepatocytes away from metabolic homeostasis toward inflammatory and apoptotic programs. This joint exposure promotes an energetically demanding injury response consistent with oncogenic priming and creates a signaling niche that actively drives fibrogenesis.

SAT-154
Kupffer cell-specific deletion of Sirt6 ameliorates diet-induced metabolic liver disease via macrophage reprogramming
Cao Huanyi[1], Chen Junnian[1], Wu Wenjing[2], Guan Haixia[1]. [1]*Department of Endocrinology, Guangdong ProvincialPeople's Hospital, Guangdong Academy of Medical Sciences, Southern Medical University, Guangzhou, China;* [2]*Department of Nephrology, Hubei Provincial Hospital of Traditional Chinese Medicine, Affiliated Hospital of Hubei University of Chinese Medicine, Wuhan, China*
Email: caohuanyi@link.cuhk.edu.hk

Background and aims: Metabolic dysfunction-associated steatotic liver disease (MASLD) progression involves hepatic macrophage activation. Preliminary analysis of published single-nucleus RNA sequencing (snRNA-seq) data indicated decreased *Sirt6* expression in liver macrophages from MASLD patients and high-fat diet (HFD)-fed mice. We aimed to investigate the functional role of *Sirt6* specifically in Kupffer cells (KCs) during diet-induced steatohepatitis (MASH).
Method: SIRT6 downregulation was validated in multiple murine models (PA-treated primary KCs, MCD/HFD-fed mice, *db/db* mice) via

western blot and immunofluorescence. To assess its KC-specific role, we generated Clec4f-Cre-driven *Sirt6* knockout mice and fed them a MASH-inducing diet for 22 weeks. Metabolic phenotyping, serum biochemistry, and liver histology (HE, BODIPY, Sirius Red, Masson) were performed. The hepatic immune landscape was profiled using 10x Genomics snRNA-seq on four key experimental groups.
Results: SIRT6 protein expression was consistently downregulated in liver macrophages across all tested models (PA-treated KCs, MCD/HFD-fed mice, and aging *db/db* mice), confirming the initial snRNA-seq observation. Contrary to expectations, KC-specific *Sirt6* deletion in the experimental model protected against MASH. Sirt6$^{\Delta KC}$ mice showed reduced body weight, improved glucose/insulin tolerance, enhanced energy expenditure, lower serum ALT/AST/triglycerides, and significantly less hepatic steatosis and fibrosis. snRNA-seq revealed profound macrophage reprogramming: diet-fed KC-specific *Sirt6* deletion livers exhibited an increase in Cyp2a22+ macrophages, a decrease in Clec4f+ resident KCs, and a reduction in recruited Ccr2+ macrophages.
Conclusion: *Sirt6* deletion in Kupffer cells paradoxically ameliorates diet-induced MASH, improving systemic metabolism and attenuating liver injury and fibrosis. This protection is associated with a fundamental shift in the hepatic macrophage composition, suggesting SIRT6 in KCs is a critical regulator of macrophage heterogeneity and a potential therapeutic target in MASLD/MASH.

SAT-155
Quercetin activates TP53-mediated lipophagy to ameliorate metabolic dysfunction-associated steatotic liver disease
Cao Huanyi[1], Chen Junnian[1], Wu Wenjing[2], Heng Wan[3], Guan Haixia[1]. [1]*Department of Endocrinology, Guangdong ProvincialPeople's Hospital, Guangdong Academy of Medical Sciences, Southern Medical University, Guangzhou, China;* [2]*Department of Nephrology, Hubei Provincial Hospital of Traditional Chinese Medicine, Affiliated Hospital of Hubei University of Chinese Medicine, Wuhan, China;* [3]*Department of Endocrinology and Metabolism, Shunde Hospital, Southern Medical University (The First People's Hospital of Shunde), Foshan, China*
Email: caohuanyi@link.cuhk.edu.hk

Background and aims: Metabolic dysfunction-associated steatotic liver disease (MASLD) lacks effective therapies. Quercetin, a natural flavonoid, shows clinical promise; however, its direct molecular target and unifying mechanism remain unknown, which hinders its development. This study aimed to identify the upstream target of quercetin and delineate its downstream mechanistic pathway in MASLD.
Method: Quercetin was identified as the hub active component via systems pharmacology. *In vivo*, MASLD was induced in mice using high-fat diet (HFD) and methionine-choline-deficient (MCD) models with quercetin intervention. Phenotypic and histological analyses were conducted. Molecular docking, surface plasmon resonance (SPR), and isothermal titration calorimetry (ITC) were used to assess the quercetin-TP53 interaction. Downstream mechanisms were explored through RNA sequencing (RNA-Seq) and immunoblotting of liver tissues. Key findings were validated in primary mouse hepatocytes.
Results: Quercetin treatment significantly ameliorated hepatic steatosis, inflammation, and fibrosis in mice. This effect was associated with upregulated TP53 expression in vivo. SPR/ITC confirmed a direct, high-affinity interaction between quercetin and TP53 protein. RNA-Seq from quercetin-treated HFD and MCD primary hepatocytes consistently identified SCD1 as a core downregulated target, accompanied by suppressed protein expression. Furthermore, quercetin activated the AMPK pathway and enhanced lipophagy markers in both settings. Critically, in primary hepatocytes, quercetin directly reduced lipid accumulation in a manner dependent on TP53-SCD1-AMPK signaling.
Conclusion: Our data demonstrate that quercetin-activated TP53 transcriptionally represses *Scd1* and concurrently activates AMPK-mediated lipophagy, coordinately reducing lipid burden. This "TP53-SCD1-AMPK-lipophagy" axis, rigorously validated in vivo and in primary cells, provides a unified and physiologically relevant framework for quercetin's therapeutic effects against MASLD.

SAT-156
Endothelial glycogen synthase kinase 3β promotes dendritic cells maturations and drives liver inflammation and fibrosis in metabolic dysfunction-associated steatohepatitis
Akitoshi Sano[1], Qianqian Guo[1], Samar Ibrahim[1,2]. [1]*Mayo Clinic, Rochester, United States;* [2]*Mayo Clinic, Pediatrics, Rochester, United States*
Email: ibrahim.samar@mayo.edu

Background and aims: Metabolic dysfunction–associated steatohepatitis (MASH) is a progressive liver disease marked by lipotoxic injury and chronic inflammation. A key feature is lipotoxic endotheliopathy, where liver sinusoidal endothelial cells (LSECs) adopt a proinflammatory phenotype, upregulating adhesion molecules and chemokines that drive pathogenic myeloid cells recruitment. We previously identified glycogen synthase kinase 3 beta (GSK3β) as a central kinase signaling hub in LSECs during MASH. However, LSEC GSK3β functional role in MASH remained unclear and will be investigated in this study.
Method: Endothelial-specific Gsk3β knockout mice (Gsk3β$^{\triangle End}$) were generated and fed a choline-deficient high-fat diet (CDHFD). Parallel studies used high-fat, fructose, and cholesterol (FFC)-fed mice treated with the GSK3 inhibitor elraglusib. Human studies involved palmitate-treated LSECs co-cultured with dendritic cells (DCs). Analyses included transcriptomics (Nanostring), Ingenuity pathway analysis (IPA), immune profiling by flow cytometry and CyTOF, and functional assays for lipid peroxidation and mitochondrial respiration.
Results: Endothelial GSK3β deletion in murine MASH attenuated lipotoxic endotheliopathy, reducing ICAM-1 expression, hepatic inflammation, and hepatocellular injury. Immune profiling revealed decreased proinflammatory monocytes, monocyte-derived DCs, and conventional type 1 DCs in Gsk3β$^{\triangle End}$ mice. Similar immune alterations were observed in FFC-fed mice treated with elraglusib. Transcriptomics showed downregulation of proinflammatory pathways, notably CXCL10 signaling. In vitro, palmitate-induced CXCL10 expression in LSECs enhanced DC maturation (MHC II, CD80, and CD86 expression), which was blocked by GSK3 inhibition. Mechanistically, GSK3 inhibition protected LSECs under lipotoxic condition from oxidative stress and ferroptosis, restored mitochondrial respiration and biogenesis, reversed lipotoxic morphological changes of the mitochondria, and activated AMPK signaling, preserving endothelial metabolic fitness. Endothelial GSK3β deletion also reduced liver fibrosis and portal hypertension in murine MASH.
Conclusion: Endothelial GSK3β drives lipotoxic endotheliopathy in MASH by promoting mitochondrial dysfunction, CXCL10-mediated DC maturation, and proinflammatory signaling. Genetic or pharmacological inhibition of GSK3β mitigates hepatic inflammation, fibrosis, and vascular dysfunction. Hence, targeting endothelial GSK3β is as a promising therapeutic approach in human MASH.

SAT-157-YI
D-amino acids enriched java plum extracellular vesicles improve glucose tolerance and hepatic lipid metabolism to attenuate metabolic dysfunction–associated steatotic liver disease
Vibhuti Jakhmola[1,2], Sukriti Baweja[1], Patnala Debishree Subudhi[1], Anupama Kumari[1], Shiv Kumar Sarin[1]. [1]*Institute of Liver and Biliary Sciences, New Delhi, India;* [2]*Institute of Liver and Biliary Sciences, Department of Molecular and Cellular Medicine, New Delhi, India*
Email: sukritibiochem@gmail.com

Background and aims: Metabolic dysfunction–associated steatotic liver disease (MASLD) is a metabolic disorder defined by steatosis, insulin resistance, and hepatic inflammation, with limited

therapeutic options. Plant-derived edible extracellular vesicles (EEVs) are emerging as novel nutraceutical therapies. We evaluated the therapeutic efficacies of functional food derived EVs from, ginger (GinEVs), turmeric (TurEVs), carrot (CarEVs), garlic (GarEVs), and java plum (JapEVs) in a diet-induced murine MASLD model.
Method: EVs were isolated by differential ultracentrifugation and characterized using nanoparticle tracking analysis. Male C57BL/6J mice fed on high carb high fat (58%) diet for 20-weeks, followed by oral EV treatment (50 nm–300 nm; −17 ± −2.4 mV; 4×10^4 particles/kg) for 3 weeks. Metabolic indices (body weight, ITT, OGTT), liver histology, biochemical markers, and genes regulating lipid metabolism, and inflammation were analyzed. Fecal metaproteomics, proteomics, and metabolomics were performed to assess microbial and metabolic alterations.
Results: EEV treatment reduced body weight ($p < 0.05$) and improved insulin/glucose tolerance (ITT/OGTT AUC; $p < 0.05$). CarEVs, GarEVs, and JapEVs lowered hepatic steatosis, serum ALT ($p < 0.002$), and AST ($p < 0.001$). These effects were associated with decreased intestinal TNF-α and IL-17α ($p < 0.02$) and increased adiponectin ($p < 0.003$). While GarEVs markedly reduced hepatic inflammation (TNF-α, IL-17α; $p < 0.001$), JapEVs showed significant effect on lipid metabolism, increasing hepatic leptin ($p < 0.05$) and decreasing resistin ($p < 0.04$). JapEV cargo metabolomics revealed enrichment of D-glucosamine, L-asparagine, and D-glutamine (all $p < 0.001$), metabolites known to modulate fatty acid metabolism. Fecal metabolomics (378 annotated compounds) and proteomics (1,369 proteins) resembled controls, with JapEVs forming a distinct cluster, most strongly upregulating histidine metabolism ($p = 0.03$). Metaproteomics showed Lactobacillaceae enrichment and Clostridiaceae depletion ($p = 0.001$), indicating favorable microbial colonization, correlating with improved barrier integrity and reduced inflammation, collectively ameliorating MASLD.
Conclusion: Edible EVs effectively mitigate HFD-induced MASLD by modulating lipid metabolism, inflammation, and gut barrier function. JapEVs enriched in D-amino acids acts through histidine-mediated adiponectin induction to restore gut–liver axis homeostasis and MASLD amelioration.

SAT-158-YI

Epigenetic maintenance by DNMT1 safeguards the liver from inflammatory and fibrotic injury in MASLD/MASH

Lina Jegodzinski[1], Darko Castven[1], Juliana Marques Affonso[1], Diana Becker[2], Dina Greinert[1], Maria Robles[3], Vaishnavi Chidambaram[4], Denis Ispan[5,6], Christoph Trautwein[4,5,6], Jenny Hetzer[6,7], Mohammad Rahbari[6,7,8], Suchira Gallage[6,7], Nisar P. Malek[6,8], Mathias Heikenwälder[6,7], Jens U. Marquardt[1].
[1]Department of Medicine I, University Medical Center Schleswig-Holstein, Lübeck, Lübeck, Germany; [2]Department of Medicine, University Medical Center of the Johannes Gutenberg University, Mainz, Germany; [3]Institute of Medical Psychology and Biomedical Center (BMC), Faculty of Medicine, LMU, Munich, Germany; [4]Department for Preclinical Imaging and Radiopharmacy, Werner Siemens Imaging Center, University Hospital Tübingen, Tübingen, Germany; [5]Core Facility Metabolomics, Faculty of Medicine, University of Tübingen, Tübingen, Germany; [6]University Tübingen, Faculty of Medicine, Institute for Interdisciplinary Research on Cancer Metabolism and Chronic Inflammation, M3-Research Center for Malignome, Metabolome and Microbiome, Tübingen, Germany; [7]German Cancer Research Center (DKFZ), Division of Chronic Inflammation and Cancer, Heidelberg, Germany; [8]Department Internal Medicine I, University Hospital Tübingen, Tübingen, Germany
Email: lina.jegodzinski@uksh.de

Background and aims: Metabolic dysfunction-associated steatotic liver disease (MASLD) represents a major global health burden, with progression to steatohepatitis and fibrosis determining clinical outcome. Hepatocellular lipid overload induces metabolic stress responses, including mitochondrial dysfunction and oxidative injury. While epigenetic mechanisms are known to shape inflammatory and metabolic gene programs in chronic liver disease, the functional relevance of DNA methylation maintenance in MASLD pathogenesis remains unclear.
Method: To investigate the role of DNA methylation in MASLD, mice with hepatocyte-specific deletion of *Dnmt1*(*Dnmt1*$^{flox/flox;Alb-Cre}$) and wild-type (WT) littermate controls were fed Western (WD) or control (CD) diets starting at 6–8 weeks of age for up to six months. Liver injury and inflammation were evaluated using serum biochemistry and histological analyses. Hepatic transcriptomic changes were analyzed by RNA sequencing, and metabolomic profiling was performed using NMR and LC-MS.
Results: Despite reduced body weight gain and attenuated hyperinsulinemia, *Dnmt1*-deficient mice developed pronounced hepatic pathology under WD conditions. While triglyceride accumulation was comparable between genotypes, loss of *Dnmt1* resulted in excessive intrahepatic cholesterol deposition after prolonged dietary challenge. Early elevations in serum alkaline phosphatase indicated biliary injury in *Dnmt1*-deficient mice. Histological analyses demonstrated increased hepatocellular senescence and marked infiltration of macrophages and $CD8^+$ T cells, culminating in advanced fibrosis exclusively in *Dnmt1*-deficient livers. Transcriptomic profiling indicated activation of oxidative stress and mitochondrial dysfunction pathways, supported by metabolomic evidence of increased glutamate and reduced glutathione in *Dnmt1*-deficient livers.
Conclusion: Hepatocyte-specific loss of DNMT1 promotes inflammatory remodeling and fibrosis during MASLD/MASH progression. These findings identify impaired epigenetic maintenance as a critical determinant of hepatic stress responses and disease severity, identifying DNMT1-dependent DNA methylation as a potential target for future therapeutic strategies in MASH.

SAT-159

Hepatocellular GALNT15 promotes the development of metabolic dysfunction-associated steatohepatitis

Zhonghao Jiang[1], Baolin Qian[1], Wenguang Fu[1]. *[1]The Affiliated Hospital of Southwest Medical University, LuZhou, China*
Email: jiang_zhonghao@163.com

Background and aims: Metabolic dysfunction-associated steatohepatitis (MASH) represents an advanced stage of metabolic dysfunction-associated steatotic liver disease (MASLD) with limited therapeutic options. This study aimed to identify novel therapeutic targets for MASH.
Method: Transcriptomic and molecular analyses were performed on MASH mouse models and wild-type (WT) controls to identify differentially expressed genes. The functional role of Polypeptide N-acetylgalactosaminyltransferase 15 (GALNT15) was evaluated using hepatocyte-specific overexpression mice, conditional knockout mice, and multiple MASH models.
Results: GALNT15, a key glycosylation enzyme, was significantly upregulated in livers of obese MASH patients and diet-induced MASH mice. Hepatocyte-specific GALNT15 deficiency markedly attenuated hepatic injury and inflammation. Mechanistically, GALNT15 promotes glycosylation of Golgi integral membrane protein 4 (GOLIM4), thereby inhibiting COPII vesicle-mediated transport of very low-density lipoprotein (VLDL) from the endoplasmic reticulum to the Golgi apparatus. This trafficking defect leads to triglyceride accumulation and accelerates MASH progression.
Conclusion: These findings establish GALNT15 as a key mediator in the progression from metabolic dysfunction-associated steatosis to MASH, highlighting its potential as a therapeutic target.

SAT-163

Inflammation-associated gene expression profiles distinguishing significant fibrosis in metabolic dysfunction-associated steatotic liver disease (MASLD): evidence from a Turkish patient cohort

Deniz Cansen Kahraman[1], Esra Nalbat[1,2], Dilara Turan Gökçe[3], Saba Kiremitçi[4], Ramazan Idilman[3]. [1]*Cancer Systems Biology Laboratory, Department of Health Informatics, Graduate School of Informatics, METU, Ankara, Türkiye;* [2]*Department of Surgery, Klinikum Rechts der Isar, Technical University of Munich, Munich, Germany;* [3]*Department of Gastroenterology, Faculty of Medicine, Ankara University, Ankara, Türkiye;* [4]*Department of Medical Pathology, Faculty of Medicine, Ankara University, Ankara, Türkiye*
Email: cansen@metu.edu.tr

Background and aims: In metabolic dysfunction–associated steatotic liver disease (MASLD), progression from minimal fibrosis (F0/F1) to significant fibrosis (≥F2) represents a key prognostic threshold guiding screening, surveillance, and therapeutic decisions. While inflammatory pathways contribute to fibrosis progression, the molecular features distinguishing these stages and their relationship to clinical characteristics remain incompletely defined across populations. This study aimed to identify inflammation-related gene expression differences associated with fibrosis stage in MASLD patients from Türkiye.
Method: Liver biopsy specimens preserved as formalin-fixed paraffin-embedded tissue (FFPE) were obtained from 36 MASLD patients and categorized as F0/F1 (n = 23) or ≥F2 (n = 13). The cohort had a mean age of 47 years, and 66% of patients were female. Inflammation-focused transcriptomic profiling was performed using the NanoString nCounter Human Inflammation Panel encompassing 249 genes. Differentially expressed genes (DEGs) were identified based on |log2 fold change| ≥ 0.5 and adjusted p-values. Functional enrichment analysis was conducted using Enrichr, and protein–protein interaction networks were evaluated with STRING.
Results: No significant differences were observed between fibrosis groups with respect to BMI or sex distribution. Although diabetes mellitus, hypertension, hyperlipidemia, and coronary artery disease were more prevalent among patients with ≥F2 fibrosis, none of these associations reached statistical significance. Transcriptomic comparison identified 23 inflammation-related DEGs between early and significant fibrosis stages. Patients with ≥F2 fibrosis exhibited increased expression of multiple chemokines and chemokine receptors involved in immune cell trafficking, including CCL2, CCL5, CCL19–21, CXCL1, CXCL6, CXCL8, CXCL9–10, and CXCR4. Upregulation of fibrogenic mediators (TGFB1–3) and key innate immune signaling components (TLR2, TLR8, TNF, STAT1) was also observed. Network analysis revealed a chemokine- and innate immune–centered interaction core driven by highly connected hub genes, with peripheral nodes implicating oxidative stress, complement, and lipid-mediated inflammatory pathways.
Conclusion: In this MASLD cohort, significant fibrosis is associated with distinct inflammatory transcriptional signatures independent of major clinical covariates, supporting the translational relevance of inflammation-related transcriptomic signatures for fibrosis risk stratification.

SAT-164

Imeglimin attenuates liver injury in a nondiabetic mouse model of MASH by restoring mitochondrial function

Kosuke Kaji[1], Norihisa Nishimura[1], Masafumi Oyama[1], Tatsuya Nakatani[1], Tadashi Namisaki[1], Hitoshi Yoshiji[1]. [1]*Department of Gastroenterology, Nara Medical University, Kashihara, Japan*
Email: kajik@naramed-u.ac.jp

Background and aims: Metabolic dysfunction–associated steatohepatitis (MASH) can progress to liver fibrosis even in the absence of diabetes. Mitochondrial dysfunction plays a central role in MASH pathogenesis by impairing fatty acid (FA) oxidation, increasing reactive oxygen species (ROS) production, and inducing hepatocyte apoptosis and fibrogenesis. Imeglimin, an antidiabetic agent, improves mitochondrial bioenergetics; however, its glucose-independent effects on MASH remain unclear. This study aimed to evaluate the effect of imeglimin on liver injury and fibrosis in a nondiabetic MASH model by improving mitochondrial dysfunction.
Method: Male C57BL/6J mice were fed a choline-deficient, L-amino acid-defined, high-fat diet (CDAHFD) for 8 weeks to induce nondiabetic MASH. Imeglimin (100 or 200 mg/kg, twice daily) or vehicle was administered orally. Liver injury, steatosis, inflammation, apoptosis, and fibrosis were assessed histologically and biochemically. Mitochondrial function was evaluated by measuring oxidative stress, mitochondrial biogenesis, and FA oxidation-related markers. In vitro, palmitic acid (PA)–stimulated human hepatocytes were used to examine the effects of imeglimin on lipid accumulation, inflammation, apoptosis, mitochondrial membrane potential, respiratory chain activity, and oxygen consumption.
Results: CDAHFD-fed mice developed steatohepatitis and liver fibrosis without hyperglycemia. Imeglimin significantly attenuated hepatic steatosis, inflammation, and ballooning. These effects were accompanied by restoration of FA oxidation-related gene expression and marked suppression of hepatic ROS accumulation. Imeglimin enhanced mitochondrial biogenesis, increased PGC-1α and TFAM expression, and reduced hepatocyte apoptosis and macrophage-mediated inflammatory responses. Consequently, hepatic fibrosis was significantly decreased. In vitro, imeglimin suppressed PA–induced lipid accumulation, inflammatory cytokine production, and apoptosis in hepatocytes. Importantly, imeglimin restored mitochondrial membrane potential, improved respiratory chain complex activity, increased oxygen consumption, and promoted mitochondrial biogenesis.
Conclusion: Imeglimin attenuates liver injury and fibrosis in a nondiabetic MASH model by restoring mitochondrial function, enhancing FA oxidation, and reducing oxidative stress–mediated hepatocyte damage. These glucose-independent hepatoprotective effects suggest that imeglimin may represent a promising therapeutic option targeting mitochondrial dysfunction in MASH.

SAT-165

Multi-compartment dissection of bile acid remodeling reveals mechanistic drivers of MASLD progression

Bo-Kyeong Kang[1], Joo Hyun Oh[2], Hyo Young Lee[3], Sang Bong Ahn[4], Mimi Kim[1], Chul-Min Lee[1], Jihyun An[3], Ha Il Kim[3], Eun Chul Jang[5], Jeong-Yeon Cho[6], Hye-Lin Kim[7], Eileen Yoon[3], Dae Won Jun[3]. [1]*Department of Radiology, Hanyang University College of Medicine, Seoul, Korea, Rep. of South;* [2]*Department of Internal Medicine, CHA University College of Medicine, Seongnam, Korea, Rep. of South;* [3]*Department of Internal Medicine, Hanyang University College of Medicine,, Seoul, Korea, Rep. of South;* [4]*Department of Internal Medicine, Nowon Eulji Medical Center, Eulji University, Seoul, Korea, Rep. of South;* [5]*Department of Occupational and Environmental Medicine, College of Medicine, Soonchunhyang University, Chunan, Korea, Rep. of South;* [6]*Department of Pharmacotherapy, University of Utah College of Pharmacy, Salt Lake, United States;* [7]*College of Pharmacy, Sahmyook University, Seoul, Korea, Rep. of South*
Email: noshin@hanyang.ac.kr

Background and aims: Bile acid dysregulation is increasingly recognized as a mechanistic contributor to metabolic dysfunction–associated steatotic liver disease (MASLD) and metabolic dysfunction–associated steatohepatitis (MASH). However, prior studies have largely focused on circulating bile acids, leaving intrahepatic determinants—including biliary bile acids and hepatic transporter or synthetic pathway alterations—poorly characterized. This study aimed to delineate multi-compartment bile acid alterations across the histological spectrum of MASLD by integrating serum and biliary bile acid profiling with hepatic transcriptomics.
Method: Adult participants were recruited from three tertiary centers and stratified by fibrosis stage and clinical diagnostic category

(control, MASLD, MASH). Serum and biliary bile acids were quantified using validated LC–MS/MS methods. Liver histology was assessed and hepatic gene expression was evaluated using RNA sequencing. Group differences in biochemical markers, bile acid species, and transporter/synthetic pathway expression were analyzed using parametric or nonparametric tests as appropriate.
Results: Disease progression was associated with distinct and compartment-specific remodeling of bile acid pools. Serum cholic acid (CA), taurocholic acid (TCA), and the composite 12α-hydroxylated bile acid fraction increased significantly in Fibrosis 1 and Fibrosis 2–3, and were similarly elevated in MASLD and MASH compared with controls. In contrast, biliary primary, conjugated, and non-12α-hydroxylated bile acids decreased across fibrosis stages, indicating depletion of biliary bile acids and redistribution toward the systemic circulation. Hepatic transcriptomic profiling revealed downregulation of canonical uptake transporters OATP1B1/1B3 and upregulation of alternative uptake (OATP2A1/2B1/3A1/4A1/5A1) and efflux transporters (MRP2/3/4, ABCG5/8). Concurrent elevation of CYP7A1, CYP8B1, TGR5, FGFR4, and FIC1, along with reduced CYP7B1 expression, indicated synthetic-pathway bias toward 12α-hydroxylated bile acids and activation of bile acid–responsive signaling pathways.
Conclusion: Integrated serum–bile–transcriptome analyses demonstrate that progressive MASLD is characterized by impaired hepatobiliary transport, increased 12α-hydroxylated bile acid flux, and activation of bile acid–responsive signaling circuits.

SAT-166

Picroside II loaded nanostructured lipid carriers attenuates metabolic dysfunction-associated steatohepatitis via restoring mitochondrial biogenesis and autophagic reflux

Swati Katoch[1,2,3], Garima Sagar[2,3], Jessica Kretzmann[3], Cameron Evans[3], K Iyer[3], Vikram Patial[1,2], Nicole Smith[3].
[1]Pharmacology and Toxicology Laboratory, Dietetics & Nutrition Technology Division, CSIR-Institute of Himalayan Bioresource Technology, Palampur, India; [2]Academy of Scientific and Innovative Research (AcSIR), Ghaziabad UP 201002, India, Ghaziabad, India; [3]School of Molecular Sciences, University of Western Australia, Perth, Australia
Email: katochs123@gmail.com

Background and aims: Chronic exposure of the liver to multiple insults culminates in the development of metabolic dysfunction-associated steatohepatitis (MASH), a complicated metabolic syndrome characterized by hepatic steatosis, with inflammation typically progresses to cirrhosis and liver cancer. Despite extensive clinical evaluation, there remain challenges in MASH drug development, which are primarily due to unsatisfactory efficacy and limited specificity. Picrosides are bioactive compounds found primarily in the medicinal plant *Picrorhiza kurroa*, known for their anti-inflammatory, antioxidant, and hepatoprotective properties. Herein we develop a picroside II loaded nanostructured lipid carrier (NLC) functionalized with GalNAc and evaluate its biological effects using *in vitro* model of MASH.
Method: For hepatic targeting β-GalNAc-PEG3-Azide was conjugated with DSPE-PEG(2000)-DBCO *via* SPAAC click chemistry. After functionalization of NLCs with conjugate, a comprehensive characterization was done by using various techniques like DLS/Zeta, UV-Vis, EE%, FTIR, MS, and NMR. To test the biological effect of these NLCs *in vitro*, a combination of palmitate-oleate (PO) was used in the HepaRG cells to mimic the pathogenesis of MASH. Cellular uptake was assessed by rhodamine loaded NLCs. Reactive oxygen species levels and mitochondrial membrane potential were assessed by DCFDA and JC1 staining respectively. qPCR analysis was done for mitochondrial biogenesis and autophagy related biomarkers.
Results: NLCs prepared exhibited a size of 161.7 ± 9.32 nm with PDI 0.406 ± 0.026, and zeta potential of −4.51 ± 0.67 mV. The encapsulation efficiency was observed to be as 95.5 ± 0.96%. MTS assay revealed the hepatoprotective effect of picroside II loaded NLC on PO treated HepaRG cells. DCFDA and JC1 staining showed that NLCs significantly alleviated ROS levels and mitochondrial membrane potential as compared to the free picroside II. The qPCR results for autophagy and mitochondrial biogenesis markers showed protective effect of NLCs loaded with picroside II on PO treated HepaRG cells.
Conclusion: In conclusion, the picroside II loaded GalNAc coated NLCs effectively prevented MASH by restoring mitochondrial function and autophagic reflux in HepaRG cells.

SAT-167

Region-specific transcriptomic reprogramming and inter-compartmental signaling in metabolic dysfunction–associated steatohepatitis

Jisup Kim[1], Aron Park[2], Baeki Kang[3], Seungyoon Nam[4], Dae Ho Lee[5].
[1]Department of Pathology, Gil Medical Center, Gachon University College of Medicine, Incheon, Korea, Rep. of South; [2]Department of Health Sciences and Technology, Gachon Advanced Institute for Health Sciences and Technology (GAIHST), Gachon University, Incheon, Korea, Rep. of South; [3]Molecular and Integrative Biology (MIB) Lab, Sungkyunkwan University School of Medicine, Suwon, Korea, Rep. of South; [4]Department of Genome Medicine and Science, Gil Medical Center, Gachon University College of Medicine, Incheon, Korea, Rep. of South; [5]Department of Internal Medicine, Gil Medical Center, Gachon University College of Medicine, Incheon, Korea, Rep. of South
Email: jspath@gilhospital.com

Background and aims: Metabolic dysfunction–associated steatohepatitis (MASH) is driven by complex interactions among hepatocytes and non-parenchymal cells within the hepatic microenvironment. Spatial transcriptomics provides a powerful framework for region-specific molecular profiling across distinct cellular compartments in human liver tissue. Leveraging this approach, we aimed to characterize compartment-specific transcriptomic alterations in MASH livers and to explore potential inter-compartmental communication using spatially resolved gene expression data, complemented by protein expression analyses.
Method: Formalin-fixed, paraffin-embedded liver tissues from patients with MASH and non-MASH controls were analyzed using the GeoMx Digital Spatial Profiler. Regions of interest (ROIs) enriched for hepatocytes (albumin), immune cells (CD45), and stromal cells (vinculin) were selected for spatial transcriptomic profiling. Differential gene expression and pathway analyses were performed across ROI types. Potential interactions between ROIs were inferred using ligand–receptor analysis based on ROI-specific gene expression patterns. Selected genes were further examined by multiplex immunofluorescence to evaluate ROI-specific protein expression.
Results: Spatial transcriptomic profiling revealed marked molecular heterogeneity across ROIs in MASH compared with non-MASH livers. Genes involved in xenobiotic metabolism, including cytochrome P450 family members, were selectively downregulated in non-parenchymal ROIs, specifically vinculin-enriched regions, whereas inflammatory mediators such as S100A8 and S100A9 were preferentially upregulated within the same stromal compartments. Interleukin-32 was increased across multiple cellular compartments, including hepatocyte- immune- and stroma-enriched ROIs. Multiplex immunofluorescence analyses further supported these findings by demonstrating ROI-specific protein expression patterns. Ligand–receptor analysis suggested altered inter-compartmental communication between parenchymal and non-parenchymal ROIs in MASH, including increased pro-fibrotic CCL21–CCR7 signaling from vinculin- to albumin-enriched regions and enhanced pro-inflammatory VEGFA–KDR signaling from hepatocyte- to immune-enriched compartments.
Conclusion: Our study demonstrates that MASH is associated with pronounced region-specific transcriptomic reprogramming and altered potential inter-compartmental signaling across hepatocyte-immune- and stromal-enriched regions.

SAT-168

Gut-liver axis modulates the development of hepatic tumorigenesis via gut microbiome alteration and immunomodulation

Seongjoon Ko[1]. [1]*Seoul National University College of Medicine, Seoul, Korea, Rep. of South*
Email: jel1206@naver.com

Background and aims: Hepatocellular carcinoma (HCC) increasingly arises on a background of metabolic dysfunction. How intestinal inflammation shapes hepatic immunity to promote tumorigenesis remains unclear. We investigated whether chronic colitis accelerates HCC in a diet-induced model and delineated microbiome–immune links along the gut–liver axis.
Method: Male C57BL/6 mice were fed a choline-deficient, L-amino acid–defined high-fat diet (CDAHFD) for 19, 24, or 31 weeks and randomized to CDAHFD alone (control) or CDAHFD plus cyclic 2% dextran sulfate sodium (DSS). Colon and liver pathology, serum biochemistry, hepatic immune cell phenotypes, and fecal microbial analysis with functional predictions were performed.
Results: DSS-treated group showed markedly increased hepatic tumor burden. Steatosis was comparable with similar inflammatory marker levels. DSS induced chronic, low-grade colitis with disrupted ZO-1 despite modest H&E activity. Hepatic macrophages shifted toward an M2 phenotype at 31 weeks. Microbial profiling showed reduced α-diversity (Shannon/Simpson $p = 0.015$) and distinct β-diversity (PERMANOVA $p = 0.014$), with dramatic *Akkermansia* expansion and near-depletion of butyrate-producer *Blautia*. ANCOM-BC and Random Forest analysis confirmed these discriminatory taxa; network analysis indicated *Akkermansia* as a central hub replacing commensal communities. PICRUSt2 revealed KO-level differences (e.g., glucose-6-phosphatase) despite similar pathway proportions.
Conclusion: Chronic intestinal inflammation establishes increased gut permeability and persistent dysbiosis that reprograms hepatic macrophages toward an M2-dominant, tumor-permissive milieu and accelerates HCC on CDAHFD, largely independent of overt inflammatory upregulation. Targeting microbiome composition, barrier integrity, and macrophage polarization may mitigate dysbiosis-driven hepatic carcinogenesis.

SAT-169

Potential protective roles of carvedilol and its derivatives in metabolic dysfunction-associated steatotic liver disease - The molecular docking study

Bojan Korica[1], Vladimir Milivojevic[1], Dušan Malenov[2]. [1]*Clinic for Gastroenterology and Hepatology, University Clinical Centre of Serbia, Faculty of Medicine, University of Belgrade, Belgrade, Serbia;* [2]*University of Belgrade - Faculty of Chemistry, Belgrade, Serbia*
Email: koricabojan@gmail.com

Background and aims: The prevalence rate of metabolic dysfunction-associated steatotic liver disease (MASLD) is significantly increasing and represents a global health burden. Portal hypertension (PH) may develop in early stages of MASLD without significant liver fibrosis due to the complex and multifactorial pathogenesis of PH in MASLD. Carvedilol is a non-selective beta blocker recommended in PH to prevent PH decompensation, with known antioxidant properties; however, its effects in MASLD haven't been further explained. Our study aimed to investigate the potential effects of carvedilol and its methyl derivatives on MASLD pathogenesis-related proteins.
Method: Molecular docking was performed to examine intermolecular interactions of 7 signaling proteins in MASLD pathogenesis: Thyroid Hormone Receptor Beta (THR-beta), Glucagon-like peptide-1 receptor (GLP-1R), HMG-CoA reductase, peroxisome proliferator-activated protein alpha and gamma (PPAR-alpha; PPAR-gamma), and Liver × Receptor alpha and beta (LXR-alpha; LXR-beta), with carvedilol and its derivatives (N-methylcarvedilol, N,N-dimethylcarvedilol). Protein structures were taken from the Protein Data Bank and adjusted to physiological pH. Carvedilol structures were optimized in implicit water solvent. Docking was performed using AutoDock Vina 1.2 with a whole-protein search space and exhaustiveness of 25.
Results: The highest binding affinity was obtained for carvedilol with PPAR-alpha (−9.1 kcal/mol), and it is established through strong hydrogen bonds with Thr88 and Ala138, T-shaped π-π interaction with Tyr139, and C-H/π and N-H/π interactions with Val 137 and Asn24, respectively. The same affinity was shown for carvedilol with PPAR-gamma (−9.1 kcal/mol), which was obtained through strong hydrogen bonds with Cys100 and Ser104, S···π interaction with Met144, as well as C-H/π interaction with Leu145. High binding potential was obtained for carvedilol and LXR-beta (−9.0 kcal/mol), as well as for N-methylcarvedilol with LXR-alpha (−8.3 kcal/mol), LXR-beta (−8.5 kcal/mol), PPAR-alpha (−8.3 kcal/mol) and PPAR-gamma (−9.0 kcal/mol).
Conclusion: Carvedilol and its derivatives have shown strong binding potential to active sites of proteins involved in MASLD pathogenesis (especially with LXR-beta, PPAR-alpha, and PPAR-gamma). This strongly suggests their potential role in lipid metabolism and anti-inflammatory effects in the concomitant treatment of MASLD and PH.

SAT-171-YI

Sex as a key modifier of age- and diet-driven MASLD progression in a murine model: histological and transcriptomic insights

Lucia Lameroli Mauriz[1,2], Andrea Scelza-Figueredo[3,4], Miranda Orellano[3], Brian Martinez Ruiz[1,4], Juan Bayo Fina[1,4], Esteban Fiore[1,4], María José Cantero[1], Bárbara Bueloni[1,4], Mailín Casadei[1,4], Matías A Avila[5,6,7], Luz Andreone[3,4], Guillermo Mazzolini[1,4,8], María Catalina Atorrasagasti[1,4]. [1]*Experimental Hepatology and Gene Therapy Program, Instituto de Investigaciones en Medicina Traslacional (IIMT), CONICET - Universidad Austral., Universidad Argentina de la Empresa (UADE), Buenos Aires, Argentina;* [2]*Universidad Argentina de la Empresa (UADE), Buenos Aires, Argentina;* [3]*Immuno-Endocrinology, Diabetes & Metabolism Laboratory, Instituto de Investigaciones en Medicina Traslacional (IIMT), CONICET - Universidad Austral., Buenos Aires, Argentina;* [4]*Facultad de Ciencias Biomédicas, Universidad Austral., Buenos Aires, Argentina;* [5]*Hepatology Laboratory, Solid Tumors Program, CIMA, CCUN, University of Navarra., Pamplona, Spain;* [6]*Instituto de Investigaciones Sanitarias de Navarra IdiSNA, Pamplona, Spain;* [7]*CIBERehd, Instituto de Salud Carlos III, Madrid, Spain;* [8]*Liver Unit, Hospital Universitario Austral, Universidad Austral., Buenos Aires, Argentina*
Email: mcatalinaa@gmail.com

Background and aims: Age and sex are risk factors for metabolic dysfunction-associated steatotic liver disease (MASLD) severity and progression, yet their specific contributions to liver injury and molecular alterations remain poorly defined and often overlooked in preclinical models. Moreover, reliable markers predicting disease progression are lacking. This study aims to characterize sex-specific effects of age and diet on MASLD progression using histological and transcriptomic approaches in a preclinical murine model.
Method: Male and female C57BL/6N mice were divided into four experimental groups per sex: 2-month-old mice (young, Y) fed with chow diet (Y-CD), or high fat diet (Y-HFD), and 10-month-old mice (middle-aged, MA) fed with CD (MA-CD) or HFD (MA-HFD). Body weight and blood glucose were monitored for 20 weeks. Liver tissue was collected for histology and gene expression analysis by qPCR and RNAseq. Differentially expressed genes (adjusted p-value < 0,05 and |

logFC| > 0.585) were identified using Limma, followed by Gene ontology (GO) analysis (FDR < 0.05). Translational relevance was evaluated using the unbiased ranking MASLD Human Proximity Score (MHPS).
Results: MA mice developed more severe hepatic injury than Y mice after HFD. Insulin resistance driven by age and diet was observed in males. Serum ALT/AST increased exclusively in MA-HFD males. NAFLD Activity Score confirmed more advanced disease in MA mice, with extensive lipid accumulation, hepatocellular hypertrophy, inflammation, and fibrosis. Females showed milder hepatic damage. Transcriptomic analysis identified diet as the main driver in males, with age-dependent responses: Y-HFD males upregulated angiogenesis, ECM remodeling, and cell migration, whereas MA-HFD males showed enhanced inflammatory signaling and downregulation of energy metabolism. In females, transcriptomic changes were attenuated; Y-HFD upregulated lipid metabolism, unfolded protein response and apoptosis, while downregulating sterol and steroid biosynthesis, whereas MA-HFD showed limited pathway modulation. MHPS ranked middle-aged HFD males as most similar to human MASLD.
Conclusion: Age and sex critically shape hepatic responses to dietary stress in MASLD. MA male mice most closely recapitulate human disease, while distinct molecular responses in females highlight the importance of incorporating sex as a biological variable in MASLD research and biomarker development.

SAT-172
GPR84 antagonism shifts liver macrophage polarization from M1 to M2, increases liver triiodothyronine, and improves cholesterol levels and hepatic steatosis in a high-fat diet metabolic dysfunction-associated steatohepatitis mouse model
Martin Leduc[1], Alexis Ascah[1], Gary Bridger[1]. [1]*Caledon Bioscience Inc., Laval, Canada*
Email: m.leduc@liminalbiosciences.com

Background and aims: The GPR84 receptor is overexpressed in liver from patients with metabolic dysfunction-associated steatotic liver disease (MASLD) and participates in the regulation of pro-inflammatory responses and migration of immune cells. The GPR84 antagonist GLPG1205 was used to evaluate the efficacy of GPR84 inhibition in a high-fat diet (HFD) metabolic dysfunction-associated steatohepatitis (MASH) mouse model.
Method: Male C57BL/6N mice were fed a Gubra Amylin NASH (GAN) HFD or a control normal diet (ND) for 10 weeks and then separated into three groups treated with either GPR84 antagonist GLPG1205 (30 mg/kg, p.o., BID) (HFD + GLPG1205 group, n = 12) or vehicle (ND, n = 8, and HFD, n = 11) for an additional 6 weeks. Serum and tissue samples were collected at endpoint for analysis.
Results: Liver weight/body weight and fat mass composition were increased by HFD compared to ND and significantly reduced by GLPG1205. Serum cholesterol (total, LDL and HDL) as well as liver total and free cholesterol and cholesteryl ester levels were all reduced in the GLPG1205-treated mice ($p < 0.01$). Treated animals also had reduced serum tissue inhibitor of metalloproteinases (TIMP)-1) and increased serum adiponectin levels, returning to levels of ND controls. Liver steatosis and number of hepatic crown-like structures which were increased by HFD were markedly decreased following GLPG1205 treatment ($p < 0.001$). Analysis of liver immune cells by flow cytometry showed that compared to ND, HFD mice had increased leukocytes, neutrophils, and classically activated (M1) macrophages and decreased alternatively activated (M2) macrophages, which were all significantly reversed by GLPG1205. In addition, liver triiodothyronine (T3) levels were augmented by GLPG1205 ($p < 0.001$). Liver RNA sequencing analysis revealed that overall, fibrosis, inflammation and MASH-associated gene expression that was dysregulated in HFD compared to ND groups showed reversal back towards control levels in the GPR84 antagonist-treated group.
Conclusion: Pharmacological inhibition of GPR84 in HFD-fed mice significantly reduced liver leukocytes, neutrophils, and promoted a shift from M1 (pro-inflammatory) to M2 (anti-inflammatory, pro-tissue repair) polarized liver macrophages, increased liver T3 levels, reduced serum and liver cholesterol, and improved liver weight/body weight, fat mass composition, and liver steatosis. These findings suggest that GPR84 inhibition is a promising target in MASLD and hypercholesterolemia.

SAT-173
Hepatoprotective effects of Efruxifermin in the CDAA-HFD mouse model of advanced MASH with progressive fibrosis
Monika Lewinska[1], Jacob Nøhr-Meldgaard[1], Susanne Pors[1], Denise Oró[1], Louise Humle Kruse[1], Henrik H. Hansen[1], Michael Feigh[1]. [1]*Gubra, Hørsholm, Denmark*
Email: mle@gubra.dk

Background and aims: Efruxifermin (EFX), a long-acting FGF21 analogue, is currently in phase 3 clinical development for the treatment of metabolic dysfunction-associated steatohepatitis (MASH). The present study aimed to evaluate treatment effects of EFX in the non-obese, choline-deficient, L-amino-acid defined, high-fat diet (CDAA-HFD) mouse model of advanced MASH with progressive fibrosis.
Method: C57BL/6JRj mice were fed chow or CDAA-HFD (45 kcal% fat, 0.1% methionine, 1% cholesterol, 28 kcal% fructose) for 4 weeks prior to treatment start (before onset of liver fibrosis) and throughout the treatment period. Animals were randomized into treatment groups based on body weight. A CDAA-HFD baseline group (n = 12) was terminated prior to treatment start. CDAA-HFD fed mice (n = 12 per group) were subcutaneous dosed once a week with vehicle or EFX (1 mg/kg) for a total of 8 weeks. Terminal endpoints included plasma/liver biochemistry, AI-assisted histopathological scoring (NAFLD Activity Score (NAS), fibrosis stage), quantitative liver histology and RNA sequencing.
Results: At baseline CDAA-HFD animals displayed advanced MASH (NAS score of 6) with no or mild fibrosis (stage F0, 75% of animals; stage F1, 25% of animals). At termination, vehicle-dosed CDAA mice displayed advanced fibrosis (stage F2, 8% of animals; stage F3, 92% of animals). 8 weeks of EFX treatment had no effect on body weight, hepatomegaly or plasma ALT levels compared with vehicle controls. Notably, EFX significantly improved fibrosis stage (stage F2, 50% of animals; stage F3, 50% of animals) and produced marked reductions in quantitative fibrosis endpoints, including hydroxyproline content, and histological markers(PSR, collagen-1a1, α-smooth muscle actin). In contrast, EFX did not improve NAS, consistent with the absence of quantitative histological markers of steatosis (hepatic lipids, fraction of hepatocytes containing lipid droplets) and inflammation (galectin-3, CD45).
Conclusion: EFX improves biochemical and histological markers of fibrosis, but not steatosis or inflammation, in the non-obese CDAA-HFD mouse model of advanced MASH with progressive fibrosis.

SAT-174
HECTD3 attenuates metabolic dysfunction-associated steatohepatitis (MASH) by stabilizing PRDX4 via K63-linked polyubiquitination
Rui Jin[1], Qianwen Zhao[1], Jie Li[1]. [1]*Department of Infectious Diseases, Nanjing Drum Tower Hospital, Clinical College of Nanjing Medical University, Nanjing, China*
Email: 18810531268@163.com

Background and aims: Metabolic dysfunction-associated steatohepatitis (MASH) poses a significant global public health challenge, involving complex pathogenesis related to metabolic syndrome and

systemic inflammation. HECTD3, an E3 ubiquitin ligase, is known to regulate various inflammatory and fibrotic signaling pathways, but its role in MASH progression remains unclear. This study aims to investigate the function of HECTD3 in MASH and its underlying molecular mechanisms.
Method: Hepatocellular HECTD3 were over-expressed in mice via the AAV8 system, and male C57BL/6J mice were fed either a Choline-deficient, L-amino acid-defined, high-fat diet (CDAHFD) for 10 weeks, or a high-fat, high-fructose diet (HFHFD) diet for 16 weeks to induce MASH. THLE-2 and AML12 cell lines were used for in vitro studies. Multi-dimensional mass spectrometry combined with co-immunoprecipitation (co-IP) was employed to identify HECTD3-interacting proteins.
Results: HECTD3 protein expression was significantly downregulated in the livers of CDAHFD-or HFHFD-fed mice and in PA-stimulated hepatocytes. Hepatocyte-specific overexpression of HECTD3 markedly alleviated MASH progression, including reduced lipid accumulation and significantly attenuated fibrosis. Consistently, HECTD3 overexpression decreased lipid deposition in PA-treated hepatocytes. Co-IP coupled with MS suggested PRDX4 as a potential binding partner of HECTD3, which was further confirmed by both endogenous and exogenous co-IP assays. Our in vitro data showed that PRDX4 overexpression significantly reduced PA induced lipid accumulation and inflammation in AML12 cells. Immunofluorescence and western blot analysis revealed that hepatocyte-specific HECTD3 overexpression increased PRDX4 protein levels in the livers of MASH model mice. Consistently, in vitro experiments further demonstrated elevated PRDX4 protein levels in HECTD3-overexpressing hepatocytes, and cycloheximide chase assays indicated that HECTD3 overexpression prolonged the half-life of PRDX4 protein. We further detected that HECTD3 overexpression significantly increased the total ubiquitination level of PRDX4, particularly the level of K63-linked polyubiquitin chains.
Conclusion: HECTD3 interacts with PRDX4 and stabilizes its protein expression by mediating its ubiquitination, specifically via K63-linked polyubiquitination. As a crucial positive regulator of PRDX4, HECTD3 plays a protective role in the development and progression of MASH and may represent a novel potential therapeutic target for MASH treatment.

SAT-175
Genetically engineered mesenchymal stem/stromal cells overexpressing fibroblast growth factor 2 inhibit MASH progression by activating the AMPK-ACC1 pathway
Yifan Yang[1], Yu Ouyang[2], Changyong Li[2]. [1]*Department of Biochemistry and Molecular Biology, School of Basic Medical Sciences, Wuhan University, Wuhan, China;* [2]*Department of Physiology, School of Basic Medical Sciences, Wuhan University, Wuhan, China*
Email: lichangyong@whu.edu.cn

Background and aims: Mesenchymal stem/stromal cells (MSCs) have attracted much attention in the treatment of liver diseases including metabolic dysfunction-associated steatohepatitis (MASH). However, many MSC clinical trials have failed to meet their efficacy endpoint. This study aims to investigate the role of human umbilical cord-derived MSCs (UC-MSCs) on MASH progression and the underlying molecular mechanisms, as well as to explore key strategies for enhancing the therapeutic efficacy of UC-MSCs in treating MASH.
Method: MASH mouse model induced by a high-fat and high-cholesterol (HFHC) diet was generated to evaluate the therapeutic efficacy of UC-MSCs and UC-MSCs-derived extracellular vesicles (UC-MSC-EVs). Transcriptome sequencing and label-free quantitative proteomics techniques were employed to identify enriched signaling pathways and differentially expressed proteins. Gain-of-function and loss-of-function experiments were conducted to elucidate the role of fibroblast growth factor 2 (FGF2) secreted by UC-MSCs during the progression of MASH.
Results: Administration of UC-MSCs and UC-MSC-EVs significantly inhibited MASH progression as indicated by reduced hepatic steatosis, inflammation and fibrosis in HFHC-fed mice. The transcriptome analysis showed that after the treatment with UC-MSCs, the AMPK-ACC1 signaling pathway was the most significantly enriched pathway. The label-free quantitative proteomics suggested that UC-MSC-EVs delivered FGF2 to hepatocytes, leading to the activation of AMPK-ACC1. Moreover, knockdown of FGF2 weakened the regulatory effects of UC-MSC-EVs on AMPK-ACC1 phosphorylation and lipid deposition, while overexpression of FGF2 enhanced their therapeutic effect. More importantly, genetically engineered UC-MSCs over-expressing FGF2 robustly activated the AMPK-ACC1 cascade, thereby inhibiting the progression of MASH.
Conclusion: Our study demonstrates that FGF2 delivered via UC-MSC-EVs can alleviate hepatic steatosis, inflammation and fibrosis in MASH mice through activating the AMPK-ACC1 pathway. These data delineate an EV-mediated mechanism underlying UC-MSC therapeutic activity in MASH and provide a rationale for developing FGF2-rich cell-free EV-based therapeutic intervention for MASH.

SAT-179
Enhancing treatment of metabolic dysfunction-associated steatohepatitis: combination of GLP-1R agonist with others
Hui Li[1], Jiliang Zhang[1], Sitong Zhang[1]. [1]*WuXi AppTec, Shanghai, China*
Email: li_hui0122@wuxiapptec.com

Background and aims: Metabolic Dysfunction-Associated Steatohepatitis (MASH) is a progressive liver disorder characterized by fat accumulation, chronic inflammation, and fibrosis. The GLP-1R agonist semaglutide has finally been approved for MASH, becoming the second therapy approved by the US FDA for MASH. However, the therapeutic options for treating MASH remain limited and their efficacy needs improvement, leading to an urgent need for novel interventions. This study aims to explore the therapeutic potential of the GLP-1R agonist and the GLP-1/GIP/glucagon receptor triple agonist, in combination with THR-β agonist and FGF21 analog in a murine model of MASH.
Method: A murine MASH model was induced using a high-fat diet combined with carbon tetrachloride (CCl4). The experimental design included a healthy control group (vehicle-treated) and various MASH cohorts receiving vehicle, GLP-1RA alone, or GLP-1RAs in combination with THR-β agonist or FGF21 analog. Each treatment regimen was specifically tailored in terms of dosage and frequency. After 6 weeks of treatment, liver tissues were collected and assessed for steatosis, inflammation, and fibrosis using histological, digitalized, and molecular techniques.
Results: Compared to the model group, combination therapies incorporating GLP-1RAs demonstrated significant improvements. They reduced the NAS score by 3–4 points and the liver fibrosis score (LFS) by 1–3 points. Specifically, GLP-1RAs combined with resmetirom showed the most substantial improvements, with markedly reduced liver inflammation, steatosis, and fibrosis (NAS reduction from 5 to 1–2 and LFS reduction from 5 to 2). More importantly, digital histology results indicated a clear reduction of fibrosis around both the portal tract and septal areas, signifying reduced liver damage, fibrosis reversal, and structural recovery. These findings underscore the potential of combination therapy to more effectively mitigate the pathological features of MASH.
Conclusion: Our study suggests that combination therapies involving GLP-1 receptor agonists, such as Semaglutide, with other

pharmacological agents hold promise for the treatment of MASH. By addressing the multifaceted pathophysiology of the disease, especially liver fibrosis, these combination therapies could offer a more comprehensive and effective treatment strategy, paving the way for future clinical development and therapeutic innovation.

SAT-180

Intracellular and non-immune regulatory mechanisms: molecular function of complement C3 in hepatic triglyceride metabolism

Yinling Li[1,2], Haitao Wang[3], Xiaobing Dou[2], Junping Shi[1]. [1]*The Affiliated Hospital of Hangzhou Normal University, Hangzhou, China;* [2]*Zhejiang University of Traditional Chinese Medicine, Hangzhou, China;* [3]*Queen Mary University of London, London, United Kingdom*
Email: lyl_cmu1h@163.com

Background and aims: Complement C3 is classically known for its innate immunity role. Clinical observations shown its elevation in MAFLD, suggests a link between C3 and lipid metabolism, though the mechanisms remain unclear. Recent evidence highlights non-canonical, intracellular functions of complement components in cellular homeostasis. Our preliminary data shown that genetic C3 deletion triggers spontaneous hepatic steatosis in mice, which worsens under HFD, indicating C3 can autonomously regulate TG metabolism and challenging the traditional "lipid→inflammation→C3" paradigm. This study aims to identify specific C3 subtype and mechanism involved, informing optimized gene-editing therapies targeting C3 in MAFLD.
Method: Male $C3^{-/-}$ and $C5L2^{-/-}$ mice (C57BL/6J) with WT littermates, and $C3aR^{-/-}$ mice (BALB/c) with WT controls (8–16 weeks), were sourced from Jackson Laboratory. Hepatic TG was assessed by Oil Red O staining and GPO-PAP assay, and FFA kinetics were tracked via ^{3}H-isotopic. Subcellular localization and forms of C3 were analyzed using immunoelectron microscopy along with redox and glycosylation assays. C3 interacting proteins were identified by CoIP/MS, and functional domains were mapped using truncation and point mutation constructs.
Results: In the early stage of MAFLD, sera and hepatic complement C3 levels were elevated. However, cellular and animal experiments confirmed that deletion of C3 exacerbates TG accumulation, and $C3^{-/-}$ mice developed spontaneous hepatic steatosis. This intriguing finding suggests that C3 may possess an autonomous regulatory function in hepatic lipid metabolism. Further mechanistic exploration revealed that C3 acts independently of its cleavage products and does not affect FFA uptake, indicating that the intact, full-length C3 exerts its function within hepatocytes. Protein interaction studies demonstrated that C3 interacts with the GRP78 and participates in the regulation of hepatic lipid homeostasis by maintaining the ubiquitination level of GRP78, thereby modulating its protein stability.
Conclusion: Our study reveals an intracellular, non-canonical, distinct from classical innate immunity role of intact complement C3 in maintaining hepatic lipid homeostasis. C3 interacts with ER chaperone GRP78 to sustain its ubiquitination and stability, forming a C3–GRP78 regulatory axis that protects against steatosis. These findings challenge the classical "lipid→inflammation→C3" dogma and position C3 as a direct metabolic regulator, offering a novel target for MAFLD therapy.

SAT-181

GIPC1 interacts with GPER1 to promote fatty acid oxidation and ameliorate hepatic steatosis: a novel target in MASLD

Yifang Li[1], Jian Jiao[1]. [1]*China-Japan union hospital of Jilin university, Changchun, China*
Email: yifang22@mails.jlu.edu.cn

Background and aims: Metabolic dysfunction-associated steatotic liver disease (MASLD) is emerging as a leading cause of end-stage liver disease. Despite the recent approval of phase III agents for MASH, the multifactorial etiology of MASLD/MASH has driven current drug development toward multi-target strategies. GAIP-interacting protein C-terminal 1 (GIPC1) is a scaffolding protein that regulates the expression and transport of cell-surface receptors, and G-protein-coupled estrogen receptor 1 (GPER1) is a novel estrogen transmembrane receptor. However, the roles of GIPC1 and GPER1 in MASLD pathogenesis are not well understood. Here, we examined the molecular regulatory mechanisms of GPER1 and GIPC1 in MASLD using human liver tissues, animal and cellular models.
Method: First, we detected the expression levels of GIPC1 and GPER1 in human liver tissue, then we demonstrated their interaction. We then showed the effects of GPER1 on MASLD using the GPER1-specific agonist G1 and the specific antagonist G15. Subsequently, we showed that GIPC1 mediates GPER1's protective role against MASLD through its silencing and overexpression. Finally, we investigated the molecular mechanisms by which GIPC1 improves hepatic steatosis and fatty acid oxidation using AMPK inhibitor.
Results: We found that GIPC1 is a downstream target of GPER1 that mediates its protective effect on MASLD. The expression level of GIPC1 in male liver tissue is significantly lower than that in female liver tissue, demonstrating a sex difference. GPER1 activation upregulates the expression of fatty acid oxidation (FAO) -related proteins, as well as the phosphorylated AMP-activated protein kinase (p-AMPK) and GIPC1, which ameliorates hepatocyte steatosis and lipid deposition. Silencing GIPC1 attenuated hepatic steatosis and down-regulated the expression of proteins associated with FAO. Pretreating cells overexpressing GIPC1 with compound C aggravated lipid droplet deposition, significantly elevated TG content, and down-regulated the expression of FAO-related proteins in hepatocytes to varying degrees. These results indicate that the positive effects of GIPC1 overexpression on MASLD are dependent on AMPK alpha pathway activation.
Conclusion: GIPC1 promotes fatty acid oxidation and ameliorates hepatic steatosis by activating the AMPK alpha pathway. The mechanism and sexual dimorphism characteristics between GPER1-GIPC1 provide new targets to achieve individualized prevention and treatment of MASLD.

SAT-182

Investigating lung inflammation following bacterial infection in mice with metabolic dysfunction-associated steatohepatitis

Zuobin Liu[1], Dimitrios Patseas[1], Eoin Mitchell[1], Viktoras Konstantellos[1], Aran Singanayagam[2], Evangelos Triantafyllou[1]. [1]*Imperial College London, Department of Metabolism, Digestion and Reproduction, London, United Kingdom;* [2]*Imperial College London, Department of Infectious Disease, London, United Kingdom*
Email: z.liu23@imperial.ac.uk

Background and aims: Metabolic dysfunction-associated steatotic liver disease (MASLD) and metabolic dysfunction–associated steatohepatitis (MASH), the more inflammatory form of MASLD, represent major causes of chronic liver disease characterized by systemic metabolic and immune dysregulation. However, the extra-hepatic organ injury in MASLD/MASH, with or without bacterial infection, has yet to be adequately studied. Both clinical studies and pre-clinical mouse models have shown an increased risk of infections in MASLD, with susceptibility positively associated with disease severity. Respiratory tract infections rank among the most common types of infections. Here, we aimed to investigate lung inflammation and immune alterations during MASLD after bacterial infection.
Method: Wild-type (C57BL/6J) male mice were fed a Choline-Deficient, L-Amino-Acid defined High-Fat-Diet (CDA-HFD) or normal diet (ND) for up to 8 weeks. Systemic Escherichia coli (E. coli) bacteria were administered intravenously (10^7 CFU per 20 g

body weight) at 6 weeks after dietary intervention. Mice were culled at 7 and 14 days post-infection (d.p.i.); liver and lung tissues were harvested for immunophenotypic (flow cytometry; myeloid and lymphoid subsets) and histological or immunofluorescence analyses.
Results: CDA-HFD induced the development of MASH-like pathological features in mouse liver characterized by increased serum ALT/AST levels, severe steatosis and inflammation compared with ND-fed mice. In the lung, the magnitude of immune cell alterations was more pronounced in CDA-HFD mice. Peak inflammation was identified at 7 d.p.i. in both diet groups, indicated by the highest total immune cell counts and inflammation and tissue damage-associated cell subsets including neutrophils, Ly6C$^{hi/int}$ monocytes, CD8^{+} T cells and NK cells, which returned to baseline levels by day 14. In addition, interstitial macrophages, but not alveolar macrophages, were numerically expanded on 7 d.p.i. and returned baseline by day 14. No change was observed in eosinophils and CD4^{+} T cells. Notably, gamma-delta T cells were significantly increased at day 7 and remained at elevated levels through 14 d.p.i.
Conclusion: Our findings demonstrate more pronounced immune changes in the lungs from CDA-HFD-fed mice following systemic bacterial infection, particularly within specific immune cell subsets. Future work will focus on lung inflammation, the role of particular subsets, and immune responses to secondary infection.

SAT-183
Cellular membrane tension regulates liver sinusoidal endothelial cell defenestration in early MASLD
Xiaoyu Zhang[1,2], Ning Li[1,2], Mian Long[1,2]. [1]*Insitute of Mechanics, Chinese Academy of Sciences, Beijing, China;* [2]*School of Engineering Science, University of Chinese Academy of Sciences, Beijing, China*
Email: zhangxiaoyu@imech.ac.cn

Background and aims: The fenestrae of liver sinusoidal endothelial cells (LSECs) are essential for lipid exchange between hepatocytes and blood. In early metabolic dysfunction-associated steatotic liver disease (MASLD), defenestration of LSECs exacerbates hepatic steatosis, yet the precise regulatory mechanisms remain unclear. Cellular membrane tension is a key mechanical property that regulates membrane deformation–related biological processes. Given the excessive lipid uptake observed in MASLD, we hypothesized that it alters the plasma membrane composition of LSECs, driving changes in membrane tension which in turn triggers defenestration. This study aimed to elucidate the role of membrane tension in regulating defenestration, a key early pathological feature of MASLD.
Method: Primary mouse LSECs were isolated from healthy or Amylin liver NASH (AMLN) diet-induced early MASLD mice. Membrane tension was modulated by altering the osmotic pressure or the plasma membrane lipid composition and quantified using membrane tether assays or Flipper-TR fluorescent probe. Fenestra dynamics and number were visualized using AFM imaging.
Results: Feeding with AMLN diet for 2 weeks, the liver progressed into simple steatosis. At this stage, the cholesterol content in plasma membrane and membrane tension of LSECs increased and the fenestra number decreased, suggesting an association between plasma membrane composition, membrane tension and fenestrae in LSECs. *In vitro,* disruption of lipid raft integrity or chelating plasma membrane cholesterol decreased membrane tension and increased fenestra number. Direct modulation of membrane tension by hypotonic or hypertonic shock demonstrated that low membrane tension induced by hypertonic shock increased the fenestra number via reducing cell height. Molecular dynamics simulations of a planar lipid bilayer further showed that reduced intermembrane distance facilitated membrane contact and stalk formation, thereby reducing existing energy barriers. Notably, reduction of membrane tension restored the fenestrae, as well as the phenotype and function, of defenestrated LSECs isolated from mice with early MASLD.
Conclusion: Membrane tension negatively regulates LSEC fenestrae. Changes in membrane composition in early MASLD may contribute to their defenestration via membrane tension. This study provides mechanobiological insights into the regulatory mechanisms governing fenestra dynamics in LSECs and the pathogenesis of MASLD.

SAT-184
Synergistic fat mass loss in diet-induced obese mice when thyroid hormone receptor-β agonist ALG-055009 was administered in combination with incretin receptor agonists
Jieun Song[1], Kusum Gupta[1], Peter Althoff[1], Lillian Adame[1], Dinah Misner[1], Tse-I Lin[2], Lawrence Blatt[1], Julian Symons[1], Sushmita Chanda[1], Xuan Luong[1]. [1]*Aligos Therapeutics, Inc., South San Francisco, United States;* [2]*Aligos Belgium BV, Leuven, Belgium*
Email: xluong@aligos.com

Background and aims: ALG-055009 is a potent, selective thyroid hormone receptor (THR)-β agonist that has demonstrated significant reductions in liver fat (placebo-adjusted median relative reductions up to 46.2%) and atherogenic lipids in clinical subjects with presumed metabolic dysfunction-associated steatohepatitis and stage 1–3 liver fibrosis. Thyroid hormone is crucial in regulating metabolism, and THR-β activation has been shown to enhance energy expenditure and promote weight loss. Here, the ability of ALG-055009 to augment the weight loss effects of approved incretin receptor agonists (RAs) was assessed in diet-induced obese (DIO) mice.
Method: Mice were fed a high-fat diet for 25 weeks to induce obesity. In Phase I, mice were treated once daily with either vehicle, oral 1 mg/kg ALG-055009, subcutaneous incretin RAs, 10.0 nmol/kg semaglutide (SEMA), 3.0 nmol/kg tirzepatide (TIRZEP_lo), 10.0 nmol/kg tirzepatide (TIRZEP_hi), or combinations of ALG-055009 with incretin RAs for 4 weeks. In Phase II, SEMA treatment was discontinued in the SEMA monotherapy and SEMA + ALG-055009 groups after 4 weeks, while ALG-055009 treatment was maintained, and animals were monitored for 4 additional weeks. Assessments included body weight (BW), fat and lean tissue mass, and tissue-specific gene expression.
Results: DIO mice treated with incretin RA or combinations of ALG-055009 and incretin RA lost significant BW. Combination of SEMA + ALG-055009 resulted in an additional 9% decrease in BW as compared to SEMA monotherapy. Combination of TIRZEP_lo or TIRZEP_hi with ALG-055009 yielded an added 12% and 6% loss in BW as compared to TIRZEP monotherapy, respectively. Combination therapy resulted in greater reductions in fat mass as compared to incretin RA monotherapy, while lean mass was unchanged. Furthermore, there was significant, synergistic upregulation of *Ucp1* gene expression in the white adipose tissue (WAT) of combination groups.
Conclusion: In DIO mice, ALG-055009 in combination with incretin RAs resulted in profound, synergistic weight loss, with up to 39–40% decreases in BW within 4 weeks. Notably, the additional weight loss conferred by ALG-055009 was from reduction in fat mass and not changes in lean mass. Initial evidence points to this synergistic response being due to increased energy expenditure via browning of WAT, a direct effect of THR-β activation. Overall, THR-β agonism is a potentially powerful, complementary mechanism to combat obesity, enhancing the magnitude and duration of weight loss by incretin RAs.

SAT-185

The UBC13–DOK3 axis drives Kupffer cells activation and promotes metabolic dysfunction-associated steatohepatitis

Yuan-Qiang Ma[1], Yoon-Seok Roh[1]. [1]*Chungbuk National University, Cheongju, Korea, Rep. of South*
Email: ysroh@cbnu.ac.kr

Background and aims: Metabolic dysfunction-associated steatohepatitis (MASH) is driven by chronic hepatic inflammation, in which Kupffer cells (KCs) play a central role. DOK3 is an anti-inflammatory adaptor that undergoes degradation in activated myeloid cells, but its role and regulation in MASH remain unclear. UBC13, a key E2 ubiquitin-conjugating enzyme, mediates K63-linked ubiquitination in inflammatory signaling. Here, we aimed to investigate how UBC13 regulates DOK3 stability thereby affecting KCs activation and MASH progression.
Method: DOK3 was examined in liver tissues from patients and mice with MASH. Stable *Dok3* and *Ubc13* deficient KCs were generated using CRISPR-Cas9–mediated genome editing. *Dok3* knockout mice, KCs-specific deletion of *Ubc13* mice generated by crossing $Ubc13^{fl/fl}$ mice with $Clec4f^{Cre}$ mice, and combined *Ubc13*|*Dok3* deficiency mice were subjected to a fast-food diet–induced MASH model. Spatial transcriptomic profiling of KCs-enriched regions was performed using GeoMx technology to characterize inflammatory signatures.
Results: Here we observed that DOK3 was highly expressed in human and mouse KCs and markedly downregulated in patients and mice with MASH. Importantly, DOK3 expression negatively correlated with serum ALT, AST levels. *Dok3* deficiency promotes KCs activation and MASH progression. Mechanistically, UBC13 facilitated TRAF6-dependent K63-linked ubiquitination of DOK3, thereby promoting its degradation via the autophagy-lysosome pathway in KCs. Loss of DOK3 disrupted SHP-1–SYK interaction, relieving inhibition of SYK signaling and driving M1 polarization of KCs. Consistent with the inhibition of the UBC13–TRAF6 axis to improve DOK3 stability in activated KCs, pharmacological inhibitor of TRAF6 (C25–140) and KCs-specific deletion of *Ubc13* ameliorated MASH in mice by preventing DOK3 degradation. Notably, we observed that UBC13 modulates MASH through a DOK3-dependent manner, given that the protective effects of *Ubc13* deletion were abolished in *Dok3* deficient mice.
Conclusion: We identify UBC13-driven K63-linked ubiquitination of DOK3 as a key mechanism that amplifies SYK signaling and KCs activation, highlighting the UBC13–DOK3 axis as a potential therapeutic target in MASH.

SAT-186

Sex-specific genetic architecture of liver fat content measured by proton density fat fraction in metabolic dysfunction-associated steatotic liver disease

Ayan Mandal[1], Kaulick Mitra[1], Anasuya Chakrabarty[2], Priyadarshi Basu[1]. [1]*BRIC-National Institute of Biomedical Genomics, Kalyani, India;* [2]*Ashoka University, Sonipat, India*
Email: am8@nibmg.ac.in

Background and aims: Metabolic dysfunction-associated steatotic liver disease (MASLD) shows pronounced sexual dimorphism in prevalence, severity and cardiometabolic outcomes. Proton density fat fraction (PDFF) is a quantitative imaging-derived biomarker of hepatic steatosis, yet sex-specific genetic determinants of PDFF remain incompletely characterised. We aimed to identify sex-specific genetic loci associated with PDFF and to evaluate sex-dependent shared genetic architecture between PDFF and MASLD-related metabolic and liver traits.
Method: Sex-stratified genome-wide association studies of inverse-rank normal transformed PDFF were conducted in 28,152 European-ancestry participants from the UK Biobank, including 13,668 males and 14,484 females. Analyses were performed using REGENIE, adjusting for age, age squared, alcohol intake, imaging batch and the first 20 genetic principal components. Genome-wide significance was defined as $p < 5 \times 10$ to the minus eight. Functional annotation was performed using Functional Mapping and Annotation, a web-based platform. Genetic correlations between PDFF and MASLD-related traits were estimated using linkage disequilibrium score regression.
Results: We identified multiple shared and sex-specific genetic loci associated with PDFF, with several loci reaching genome-wide significance exclusively in males or females, indicating sex-dependent genetic effects on hepatic fat accumulation. Genetic correlation analyses demonstrated significant shared heritability between PDFF and liver enzymes, adiposity measures and cardiometabolic traits, with notable differences in magnitude and direction between sexes. PDFF showed stronger genetic correlation with central adiposity and insulin resistance traits in males, whereas correlations with liver injury markers and hormonal traits were more pronounced in females. Pathway analyses highlighted sex-specific enrichment in lipid metabolism, insulin signalling and hormone-related biological processes.
Conclusion: These findings reveal marked sexual dimorphism in the genetic architecture and shared heritability of liver fat content measured by PDFF. Sex-specific genetic coupling between hepatic steatosis and metabolic traits highlights biologically distinct pathways in MASLD and supports the integration of sex-aware approaches in genetic studies and therapeutic development.

SAT-187

Efruxifermin ameliorates palmitate-induced hepatocyte lipotoxicity

Suyavaran Arumugam[1], Michail Kokkorakis[1], Tim Rolph[2], Erik Tillman[2], Wajahat Mehal[1]. [1]*Yale University School of Medicine, New Haven, United States;* [2]*Akero Therapeutics, a Novo Nordisk Company, Boston, United States*
Email: wajahat.mehal@yale.edu

Background and aims: Fibroblast Growth Factor 21 (FGF21) has pleiotropic metabolic effects and FGF21 analogs have significantly improved steatosis, inflammation, and fibrosis in clinical trials in patients with MASH. However, direct hepatocellular effects of FGF21 remain uncharacterized. We explored how FGF21 and the clinical-stage FGF21 analog efruxifermin (EFX) modulate free fatty acid (FFA)-induced dysfunction of human hepatocytes (heps) in vitro.
Method: HepG2 cells or primary human heps were exposed to palmitate from T = 0 h to T = 16 h, followed by addition of FGF21 or EFX. Cells were subsequently analyzed at T = 24 h, T = 32 h, and T = 48 h. Lipid droplet accumulation was assessed using BODIPY staining, and intrahepatocyte distribution of palmitate was assessed using fluorescent BODIPY C16-palmitate. FFA oxidation (FFAO) was quantified using FAOBlue staining. Mitochondrial reactive oxygen species (mtROS) were detected using MitoSOX Red, and mitochondrial membrane potential was measured via TMRE staining. Cellular and subcellular organization, including lipid and organellar localization, were visualized and quantified using confocal microscopy. Gene expression profiles were quantified across conditions over time using bulk RNA-seq.
Results: Palmitate exposure for 16 h resulted in significant increases in steatosis, FAO, and mtROS and reduced mitochondrial membrane potential. Treatment with FGF21 or EFX significantly attenuated steatosis. Confocal imaging revealed cytosolic lipid droplet localization of BODIPY C16-palmitate, which was redirected to mitochondria within 8 h after treatment with FGF21 or EFX. FGF21 and EFX significantly i) enhanced FAO in the palmitate-exposed heps within 8 h, ii) reduced mtROS and prevented the palmitate-induced decline

in mitochondrial membrane potential, and iii) upregulated genes associated with lipid oxidation and mitochondrial fusion. EFX induced a wide range of adaptive changes in the mitochondrial transcriptome of primary human heps exposed to palmitate, including upregulation of UCP2 and ACSL4.
Conclusion: Agonism of FGF21's receptors on isolated heps reverses steatosis by directing FFA to mitochondria and increasing their oxidation. Despite increased oxidative flux, mtROS did not increase. This may have been the result of i) improved mitochondrial efficiency, ii) increased consumption of ATP (and regeneration of ADP) to support higher rates of gluconeogenesis, and/or iii) activation of adaptive stress response pathways.

SAT-188-YI
Improving brain blood flow and reducing microglial activation as the mechanisms behind cognitive improvement following alpha 2A adrenergic receptor antagonism in a mouse model of metabolic dysfunction-associated steatotic liver disease
Anne Catrine Mikkelsen[1], Kristoffer Kjærgaard Amby[1], Cecilie Bay-Richter[2], Elizaveta Melnikova[3], Line Hansen[3], Vladimir Matchkov[3], Karen Louise Thomsen[1,4], Rajeshwar Prosad Mookerjee[1,4]. [1]*Department of Hepatology and Gastroenterology, Aarhus University Hospital, Aarhus, Denmark;* [2]*Translational Neuropsychiatry Unit, Aarhus University, Aarhus, Denmark;* [3]*Department of Biomedicine, Aarhus University, Aarhus, Denmark;* [4]*Institute for Liver and Digestive Health, University College London, London, United Kingdom*
Email: ancami@clin.au.dk

Background and aims: Cognitive dysfunction is a complication of metabolic dysfunction-associated steatotic liver disease (MASLD) without a specific treatment. Cerebrovascular changes are among the suggested causes for this complication of MASLD. This study investigated the effect of antagonism of the alpha2A adrenergic receptor (ADRA2a) as a modulator of cerebral blood flow.
Method: Male C57BL/6NTac mice were fed a modified Amylin-liver non-alcoholic steatohepatitis (AMLN) diet to induce MASLD or a standard diet (controls) for 36 weeks. Half of the MASLD mice received the ADRA2a antagonist Yohimbine in their drinking water for the final 10 weeks. Neurobehavioural tests were conducted to study cognitive function. At termination, laser speckle contrast imaging was used to study cerebral blood perfusion. Immunohistochemical analyses were used to study vasculature, microglia activation (involved in the neurovascular unit), and ADRA2a expression in the brain.
Results: ADRA2a antagonism ameliorated anxiety-like and depression-like behaviour in the MASLD mice. The blood perfusion of the cerebral parenchyma was reduced in the MASLD mice compared with control mice (blood flow index (BFI): 46.9 ± 4.0 arbitrary units (a.u.) vs. 53.2 ± 8.5 a.u., $p = 0.07$, which was completely reversed by ADRA2a antagonism (BFI: 52.1 ± 5.0 a.u., $p = 0.03$). The MASLD mice showed increased contractile tone of capillary pericytes in the brain (capillary diameter: 3.9 ± 0.3 µm vs. 4.8 ± 0.4 µm, $p = 0.02$), which was normalised by ADRA2a antagonism (4.4 ± 0.3 µm, $p = 0.04$), a plausible mechanism for the observed changes in blood perfusion. The microglia staining intensity was greater in the prefrontal cortex of the MASLD mice, implying higher microglia activation compared with control mice ($p = 0.008$), and the microglia had higher expression of ADRA2a ($p = 0.02$ vs. control mice). Microglia activation was reduced by ADRA2a antagonism ($p = 0.07$ vs. MASLD mice), further complimenting the reduced contractile effect on cerebral vasculature.
Conclusion: Ten weeks of ADRA2a antagonism in a MASLD mouse model ameliorated cognitive dysfunction. Our data suggest that this effect was achieved by increasing cerebral blood perfusion through normalisation of capillary pericyte tone and by reducing microglial activation. This paves the way for further mechanistic studies evaluating the role of ADRA2a antagonism, and future clinical translation into MASLD patients at risk of cognitive dysfunction.

SAT-189
Preventive effects of milk-derived exosomes on MASH progression through intestinal barrier protection and gut microbiota modulation
Tatsuya Nakatani[1], Shinya Sato[1], Masafumi Oyama[1], Kosuke Kaji[1], Tadashi Namisaki[1], Hitoshi Yoshiji[1]. [1]*Department of Gastroenterology, Nara Medical University, Kashihara, Japan*
Email: k182324@naramed-u.ac.jp

Background and aims: Metabolic dysfunction-associated steatohepatitis (MASH) has emerged as a major cause of liver cirrhosis and hepatocellular carcinoma. Exosomes are small extracellular vesicles, 50–150 nm in diameter, secreted by cells and known to carry miRNAs, mRNAs, proteins, and micropeptides that mediate intercellular communication. Recently, milk-derived exosomes (B-mEVs) have attracted attention due to their reported effects on improving intestinal barrier function in animal models of intestinal inflammation and their potential anticancer activity. In this study, we investigated the effects of B-mEVs on liver fibrosis, intestinal barrier function, and gut microbiota composition in a murine model of MASH-associated liver fibrosis.
Method: To induce liver fibrosis associated with MASH, female C57BL/6J mice (7 weeks old) were fed a choline-deficient, L-amino acid-defined, high-fat diet (CDAHFD) for 8 weeks. Subsequently, B-mEVs (1.2 mg/kg) were orally administered every other day for 4 weeks before sacrifice. Liver fibrosis was assessed histologically, and intestinal tight junction proteins (TJPs) and intestinal permeability were evaluated. Mice were divided into four groups: (1) Control diet, (2) Control diet + B-mEVs, (3) CDAHFD, and (4) CDAHFD + B-mEVs. The preventive effects of B-mEVs on MASH-related liver fibrosis and their impact on intestinal barrier integrity and gut microbiota composition were examined.
Results: In the CDAHFD group, hepatic steatosis, inflammation, and fibrosis were observed compared to the control group. These pathological changes were partially attenuated in the CDAHFD + B-mEVs group. Regarding intestinal effects, the CDAHFD group showed reduced expression of intestinal TJPs such as ZO-1, Occludin, and Claudin-2, accompanied by a marked increase in intestinal permeability (as measured by FITC-dextran). In contrast, the CDAHFD + B-mEVs group demonstrated enhanced TJP expression and improved intestinal permeability.
16S rRNA gene sequencing of fecal samples revealed that administration of B-mEVs led to changes in α-diversity compared to the CDAHFD group, while β-diversity remained unchanged. Furthermore, the administration of milk exosomes increased the abundance of the genus *Akkermansia*.
Conclusion: Milk-derived exosomes ameliorated CDAHFD-induced intestinal hyperpermeability and showed potential in improving MASH-associated liver fibrosis. These findings suggest that B-mEVs may exert protective effects against MASH progression through modulation of the gut–liver axis.

SAT-190
Long-term intake of bicarbonate-sulfate-calcium-magnesium mineral water improves MASLD-related outcomes by modulating intestinal permeability, systemic inflammation, and oxidative stress
Mario Romeo[1], Carmine Napolitano[1], Marcello Dallio[1], Fiammetta Di Nardo[1], Annachiara Coppola[1], Alessia Silvestrin[1], Giusy Senese[1], Claudio Basile[1], Marco Niosi[1], Alessandro Federico[1].

[1]*Hepatogastroenterology Division, Department of Precision Medicine, University of Campania Luigi Vanvitelli; Piazza Miraglia 2, 80138, Naples (Italy), Naples, Italy*
Email: mariomeo@virgilio.it

Background and aims: Fonte Essenziale®—a mineral water enriched in bicarbonate, sulfate, calcium, and magnesium—has shown potential in modulating the gut-liver axis and gut microbiota in hepatic steatosis. However, its long-term effects on intestinal permeability (IP), IP-related systemic inflammation (SI), and oxidative stress—key contributors to steatosis—remain unexplored in Metabolic dysfunction-Associated Steatotic Liver Disease (MASLD).
Method: Eighty-seven MASLD patients were randomized into two groups: group A received Fonte Essenziale® (400 ml/day, fasting) plus a controlled nutritional regimen (physical exercise and diet) for 12 months, followed by a 6-month washout; group B received the controlled nutritional regimen alone. IP markers, SI cytokines (IL-1β, IL-6, TNF-α), oxidative stress (dROMs/BAP), and clinical data, including Controlled Attenuation Parameter (CAP), were collected at baseline (T0), 12 months (T12), and post-washout (T18). Baseline in-IP was defined by fecal zonulin >110 ng/ml and serum LPS-binding protein (LBPp) >10 µg/ml; im-IP was defined by normalization of both. CAP reduction ≥30% indicated a significant steatosis improvement.
Results: Thirty-eight patients in group A and 39 in group B completed the study. At T12, group A showed significant reductions in fecal zonulin (p: 0.0163) and serum LBPp ($p < 0.0001$), with increased occludin and claudin-1 levels (all $p < 0.0001$). im-IP prevalence was higher in group A (p: 0.0037). IL-1β, TNF-α, IL-6, LPS, and dROM/BAP decreased significantly in group A and among those achieving im-IP (all $p < 0.05$). CAP reduction (T0 vs T12, $p < 0.0001$) and improvements in insulin and HDL levels (all $p < 0.0001$) were observed in group A. Multivariate analysis (adjusted for sex, age, smoking, BMI, diabetes, MASLD-related drugs, and baseline CAP) identified water intake (aHR: 2.104, p: 0.001) and im-IP (aHR: 1.214, p: 0.024) as independent predictors of steatosis improvement. All benefits persisted at T18.
Conclusion: Prolonged Fonte Essenziale® intake significantly improved hepatic steatosis and MASLD-related outcomes by modulating IP, SI, and oxidative stress.

SAT-191

Discovery of MI-676, novel direct target of constitutive androstane receptor (CAR) for therapeutic treatment of metabolism associated steatotic liver disease (MASLD)

Dharani Sai Sreekanth Nellore[1], Alzbeta Štefela[1], Hirsova Petra[2], Stanislav Micuda[3], Radim Nencka[4], Petr Pavek[1]. [1]*Charles University, Faculty of Pharmacy, Hradec Králové 3, Czech Republic;* [2]*Mayo Clinic, Rochester, Minnesota, United States;* [3]*Faculty of Medicine - Charles University, Hradec Králové 3, Czech Republic;* [4]*IOCB Prague, Prague 6, Czech Republic*
Email: nellored@faf.cuni.cz

Background and aims: Lipotoxic apoptosis driven by saturated fatty acids is a central pathogenic mechanism in metabolism associated steatotic liver disease (MASLD). While activation of the constitutive androstane receptor (CAR) has been associated with hepatoprotection, the mechanistic consequences of selective human CAR activation under lipotoxic stress remain unclear. This study examined whether MI-676, a novel human CAR agonist, protects hepatocytes from palmitate-induced apoptosis and to define the underlying molecular pathways.
Method: For the research study, we used differentiated HepaRG, CAR-KO HepaRG, HepG2, Huh7, cells and primary human hepatocytes that were treated with MI-676, and controls, followed by 0.6 mM palmitoic acid exposure. We assessed nuclear and membrane integrity by DAPI staining; Annexin V/PI flow cytometry and caspase-3/7 assays. Further, to confirm CAR activation and elucidate downstream signaling, we isolated mRNA (TRI-reagent) of HepaRG cells, and RT-qPCR was carried out using Fast Advanced Master Mix and TaqMan probes. Protein expression levels were analyzed by SDS-PAGE western blotting with validated antibodies using HepaRG cells. Data represent ≥3 independent experiments and were analyzed by one-way ANOVA.
Results: MI-676 markedly attenuated palmitate-induced nuclear fragmentation and apoptosis in CAR-expressing hepatocytes, evidenced by reduced DAPI nuclear damage, lower Annexin V/PI staining, and decreased caspase-3/7 activity; these cytoprotective effects were absent in CAR-KO cells. MI-676 selectively induced CYP2B6 without transactivating CYP3A4, confirming human CAR specificity. Mechanistically, MI-676 upregulated INSIG-1, limited SREBP-1 maturation and ER stress, and increased anti-apoptotic BCL-2 and MCL-1 transcriptional levels. The concurrent activation of AKT and GADD45B, enhanced MDM2 phosphorylation, leading to XIAP upregulation, and p53 suppression indicate engagement of convergent pro-survival pathways.
Conclusion: In conclusion, MI-676 is a CAR agonist that attenuates palmitate-induced ER stress and apoptosis, exerting dual protective effects: (1) suppression of SREBP-driven lipogenesis and ER stress, and (2) coupling this suppression of lipogenesis with activation of a GADD45B–Src–PP2A–MDM2–XIAP and CAR–AKT–MDM2 survival axis, that overall attenuates P53. These findings provide a robust mechanistic framework for further preclinical evaluation of MI-676 as a hepatoprotective agent in MASLD.

SAT-195

Rifaximin prevents metabolic dysfunction-associated steatohepatitis by suppressing deoxycholic acid-mediated macrophage-hepatocyte dialogue

Mei-Tong Nie[1], Chuan Yin[1], Hongyan Qin[2], Xin Zhang[1], Weifen Xie[1]. [1]*Department of Gastroenterology, Changzheng Hospital, Naval Medical University, Shanghai, China, Shanghai, China;* [2]*State Key Laboratory of Cancer Biology, Department of Medical Genetics and Developmental Biology, Airforce Medical University, Xi'an, China, Shanghai, China*
Email: weifenxie@medmail.com.cn

Background and aims: Metabolic dysfunction-associated steatohepatitis (MASH), a progressive form of metabolic dysfunction-associated steatosis liver disease (MASLD), presents a major therapeutic challenge with limited effective treatments. While the antibiotic rifaximin shows preclinical promise, its precise molecular mechanisms and clinical efficacy remain poorly defined.
Method: We employed high-fat, high-fructose (HFF) diet and choline-deficient, L-amino acid-defined high-fat diet (CDA-HFD) mouse models integrated with targeted bile acid metabolomics and single-nucleus RNA sequencing. Molecular interactions were validated via docking and surface plasmon resonance. Mechanistic insights were confirmed using $Ccr2^{-/-}$, hepatocyte-specific Hnf1-alpha knockout ($Hnf1\text{-}alpha^{L-KO}$), and $S1pr2^{-/-}$ mice. Finally, a proof-of-concept clinical trial evaluated rifaximin's efficacy and safety in patients with MASH.
Results: Rifaximin significantly reduced deoxycholic acid (DCA) levels. Mechanistically, DCA acts as a potent S1PR2 agonist on monocyte-derived macrophages (MoMFs), triggering their hepatic infiltration and the secretion of myeloid differentiation protein 1 (MD-1). MD-1 suppresses hepatocyte HNF1-alpha expression through TLR4 activation. Rifaximin-mediated restoration of HNF1-alpha was essential for therapeutic success, as HNF1-alpha deficiency exacerbated steatosis and sustained a vicious cycle of MoMF

recruitment. In MASH patients, rifaximin treatment led to rapid resolution of hepatic steatosis and injury, with efficacy strongly correlating with reduced serum DCA and MD-1 levels.
Conclusion: Rifaximin attenuates MASH by disrupting a pathogenic DCA-MoMF-HNF1-alpha signaling crosstalk, and our proof-of-concept clinical trial demonstrates that rifaximin treatment leads to rapid and progressive resolution of hepatic steatosis and injury in patients with MASH, with favorable safety and tolerability.

SAT-196
Prime editing enables isogenic modeling of PNPLA3-I148M-associated lipotoxicity in hepatocytes
Haruna Noguchi[1], Takuro Uchida[1,2], Naoki Wakita[3], Mitsumasa Takenaga[4], Tetsushi Sakuma[3], Kei Mori[1], Tomoko Tokumaru[1], Tomoko Saito[1], Masao Iwao[1], Mie Arakawa[1], Mizuki Endo[1], Kazuhiro Mizukami[1]. *[1]Department of Gastroenterology, Faculty of Medicine, Oita University, Yufu, Japan; [2]Division of Travel Medicine and Health, Research Center for GLOBAL and LOCAL Infectious Diseases, Oita University, Yufu, Japan, [3]Graduate School of Agriculture, Kyoto University, Kyoto, Japan; [4]Graduate School of Integrated Sciences for Life, Hiroshima University, Higashi-Hiroshima, Japan*
Email: tuchida@oita-u.ac.jp

Background and aims: The PNPLA3-I148M (rs738409 C > G) variant is a well-established genetic determinant of hepatic steatosis, fibrosis, and hepatocellular carcinoma. However, its precise functional impact on hepatocyte physiology remains incompletely understood. Here, we employed a prime editing system to generate isogenic HepG2 clones representing all PNPLA3 genotypes in an identical genetic background.
Method: We generated the prime editing system for PNPLA3-I148M, which carries all the elements for prime editing such as prime editor (modified PEmax), pegRNA, and ngRNA. In addition, The EGFP gene was fused to the prime editor with an intervening autocleavage site and served as a convenient means to measure prime editor expression. We then introduced the genome editing on the rs738409 genome in hepatoma cells and analyzed the effects of PNPLA3 mutations on steatosis and lipid-induced changes between homozygous 148M variant allele carriers (G/G), noncarriers (C/C), and heterozygous (G/C) under free fatty acid treatment by RNA sequencing.
Results: Prime editing targeting the PNPLA3-I148M variant was successfully achieved in HepG2 cells and enabled modification of the transcriptomic profile in the HepG2 isogenic clones. The PCA revealed a separation of CC from both GG and GC, indicating a genotype-dependent restructuring of the transcriptome. Following palmitic acid (PA) treatment, we evaluated genotype-specific responses to lipotoxic stress. Lipid droplet accumulation and cell viability assays described that clones harboring the G allele (GG, GC) exhibited enhanced lipid storage and reduced sensitivity to PA-induced toxicity compared to wild-type (CC) clones. Transcriptomic profiling revealed distinct expression patterns among genotypes, consistent with differential regulation of lipid handling and stress adaptation programs. Heterozygous clones displayed intermediate phenotypes, suggesting a gene dosage-dependent effect of PNPLA3-I148M on hepatocellular lipotoxicity.
Conclusion: We demonstrate that prime editing enables a precise approach for modeling disease-associated genetic variants in human hepatocytes, offering a platform to investigate genotype-specific cellular responses. By combining precise genome editing with human cell modeling, this study provides new insight into the biology of a key risk allele and establishes a platform for personalized therapeutic strategies targeting genetically defined subgroups of liver disease.

SAT-197
Impact of PFAS on lipid metabolism in MASLD is mediated through steroids and bile acids
Pauli Tikka[1], Aidan McGlinchey[2], Sami F. Qadri[3], Ilia Evstafev[1], Alex Dickens[1], Hannele Yki-Jarvinen[3], Tuulia Hyötyläinen[2], Matej Orešič[1,2]. *[1]University of Turku, Turku, Finland; [2]32moc, Örebro, Sweden; [3]University of Helsinki, Helsinki, Finland*
Email: matej.oresic@oru.se

Background and aims: Endogenous steroid hormones are key regulators of hepatic lipid metabolism, insulin sensitivity, and inflammatory responses. As potential mediators of environmentally induced metabolic dysfunction, we investigated the associations between steroid hormones and metabolic dysfunction–associated steatotic liver disease (MASLD) severity, the effects of per- and polyfluoroalkyl substances (PFAS) on steroid hormone levels, and whether hormone alterations link PFAS exposure to downstream changes in lipid and bile acid (BA) metabolism.
Method: Using sex-stratified analyses, we examined relationships among circulating steroid hormone concentrations, MASLD histological features, hepatic lipid and BA profiles, and PFAS exposure in a human cohort of 104 patients with MASLD.
Results: Steroid hormones were strongly associated with MASLD severity in a sexually dimorphic manner. Dihydrotestosterone, particularly in females, showed consistent inverse associations with steatosis, fibrosis, necroinflammation, and insulin resistance. Dehydroepiandrosterone exhibited sex-divergent patterns, associating positively with multiple lipid classes in males and with secondary BAs in females, suggesting involvement of a gut–liver–steroid axis. PFAS exposure was associated with altered steroid hormone levels, predominantly in females, with most significant associations indicating suppression of steroidogenesis. These PFAS-associated hormone changes were further linked to alterations in hepatic lipid and BA metabolism, supporting their role as metabolic intermediates. Overall, females demonstrated stronger PFAS–hormone–BA associations, whereas males showed more limited, lipid-focused effects. Causal mediation analysis further corroborated indirect effects of PFAS exposure on lipids and BAs via steroids. Specifically, testosterone/epi-testosterone mediated the impact of PFAS on increased ether phospholipid levels ($P < 0.001$), while estradiol mediated the impact of PFAS on increased hepatotoxic lithocholic acid levels ($P < 0.001$).
Conclusion: Our findings indicate that PFAS exposure is associated with broad, sex-specific disruption of steroid hormone pathways, which may contribute to MASLD progression through downstream effects on lipid and BA metabolism. These results highlight the relevance of endocrine-disrupting chemicals in MASLD pathophysiology and emphasize the need to consider sex-specific mechanisms in future mechanistic and therapeutic studies.

SAT-198-YI
Metabolic ferroptosis as targetable signature for the genetic subtype of MASLD
Erika Paolini[1], Marica Meroni[1], Miriam Longo[1], Sara Badiali[2], Marco Maggioni[3], Anna Ludovica Fracanzani[4], Paola Dongiovanni[1]. *[1]Medicine and Metabolic Diseases, Fondazione IRCCS Cà Granda, Ospedale Maggiore Policlinico, Milan, Italy; [2]Department of Surgery, Fondazione IRCCS Ca' Granda Ospedale Maggiore Policlinico, Milan, Italy; [3]Department of Pathology, Fondazione IRCCS Ca' Granda Ospedale Maggiore Policlinico, Milan, Italy; [4]Department of Pathophysiology and Transplantation, Università degli Studi di Milano, Medicine and Metabolic Diseases, Fondazione IRCCS Cà Granda, Ospedale Maggiore Policlinico, Milan, Italy*
Email: paola.dongiovanni@policlinico.mi.it

Background and aims: The co-presence of the I148M-PNPLA3, rs641738-MBOAT7 and E167K-TM6SF2 polymorphisms enhances the risk of severe MASLD. Emerging evidence highlighted that ferroptosis is essential for developing MASLD/MASH since it promotes oxidative stress, lipid peroxidation and inflammation although the underlying

mechanisms are still unknown. Thus, this study investigated the possible crosslink between ferroptosis and the three mutations in hepatic biopsies of MASLD patients, through a spatial transcriptomic (ST) approach.
Method: ST was performed by Visium CytAssist and data were analyzed using Spaceranger (10x Genomics). Patients, featured by a similar histological severity (NAS≥4) and comparable comorbidities (gender, age, BMI, absence of T2D), were wild type (WT), homozygous for PNPLA3, MBOAT7, TM6SF2 polymorphisms and carriers of the 3 at-risk variants (3NRV) (n = 2/group).
Results: All samples were integrated and clustered at 0.5 resolution allowing the identification of 7 clusters (cl), annotated as follows: cl0 enriched in periportal HEPs; cl1 in immune cells; cl2 in pericentral HEPs; cl3 in cholangiocytes; cl4 in endothelial cells (ENDOs); cl5 in immune cells; cl6 in NPCs (HSCs, immune cells and ENDOs); cl7 in HEPs. Firstly, we observed that cl4 was more abundant in PNPLA3, MBOAT7, TM6SF2 and 3NRV samples compared to WT, whereas cl6 was mainly enriched in patients carrying the 3 at-risk variants *vs* all. Then, we conducted a Pathway-enrichment analysis by considering differentially expressed genes (DEGs; Log2FC>0.5 and padj FDR<0.05) of 3NRV in all clusters *vs* the other samples. The former exhibited increased lipid metabolism, oxidative damage, inflammation, fibrosis, and ferroptosis reflecting a worse clinical *scenario*. By focusing on the ferroptosis pathway, we found that in patients carrying TM6SF2 and MBOAT7 variants, it was mainly espressed in immune cells whereas in *PNPLA3* and 3NRV, also in HEPs. Moreover, cl6 showed the strongest upregulation of a "metabolic" ferroptosis, driven by lipid buildup and mitocondrial dysfunction. It was designed by a signature of 53 unique genes, which was uregulated only in 3NRV patients, thus rappresenting a pathognonomic feature of the "genetic" subtype of MASLD.
Conclusion: The co-presence of *PNPLA3*, *MBOAT7*, and *TM6SF2* variants may accelerate liver injury by triggering a lipid-metabolism and mitochondrial ferroptosis. Thus, ferroptosis could be a potential druggable signature to tackle 3NRV MASLD patients.

SAT-199-YI
Three-dimensional mapping of hepatocellular carcinoma links bile canalicular defects to MASLD-associated tumorigenesis
Cristian Perez Gallardo[1,2], Dilan Martinez Torres[1,2], Valeria Candia-Campano[1,2], Karen Almendras-Durán[1,2], Sebastián Fuller-Vargas[1,2], Jorge Vergara-Estrada[2,3], Ricardo Velasco[4], Felipe Aguilera-Muñoz[1,2], Hernán Morales-Navarrete[4], Fabián Segovia-Miranda[1,2]. [1]*Department of cell biology, faculty of biological sciences, Universidad de Concepción, Concepción, Chile;* [2]*Grupo de procesos en biología del desarrollo, faculty of biological sciences, Universidad de Concepción, Concepción, Chile;* [3]*Computer science and informatics department, Universidad de Concepción, Concepción, Chile;* [4]*Bio-Cheminformatics research group, Universidad de las Américas, Quito, Ecuador*
Email: cristianfperez@udec.cl

Background and aims: Metabolic dysfunction-associated steatotic liver disease (MASLD) is the most common liver disease worldwide and progresses through various stages that can culminate in hepatocellular carcinoma (HCC). Previous studies have shown that bile canaliculi (BC), a bile-carrying microscopic network, are altered in the early stages of MASLD, potentially leading to accumulation of bile acids (BA), known carcinogens. However, the structural organization of BC in advanced stages such as HCC, and its possible contribution to tumour development, remain poorly understood. Could bile canalicular alterations promote MASLD-associated HCC development?
Method: A MASH–HCC mouse model was generated by neonatal streptozotocin injection and high-fat diet. Serum metabolism, hepatic gene expression, and bile acid levels were assessed by biochemical assays and HPLC. Liver microarchitecture—including bile canaliculi, sinusoids, and hepatocytes—was reconstructed in 3D across disease stages using multiphoton microscopy and deep-learning-based analysis, with specific imaging of tumour–adjacent regions. Mouse and human RNA-seq datasets were used to evaluate bile acid–related transcriptional changes.
Results: The MASH–HCC model exhibited hyperglycemia, inflammation, increased proliferation, and evident tumour formation, accompanied by elevated total and individual serum bile acids. 3D reconstruction revealed profound bile canalicular network disruption within tumours and at tumour–adjacent interfaces, consistent with impaired bile flow, and local bile acid accumulation. These structural alterations were supported by public mouse and human RNA-seq datasets showing upregulation of bile acid–related genes in tumours compared to healthy tissue.
Conclusion: We found BC alterations that can be linked to BA accumulation in tumour tissue and tumorigenesis, supported by molecular analysis of BA metabolism. Overall, our findings provide new insights into the pathophysiology of MASLD-associated HCC and suggest potential therapeutic strategies.

SAT-200
Humanized immune system mice for preclinical modeling of liver fibrosis and metabolic dysfunction-associated steatohepatitis
Clothilde Philouze[1], Omayra Martin Rodriguez[1], Anaïs Meynet-cordonnier[1], Sebastien Tabruyn[1], Dan Georgess[1].
[1]*Archamps, France*
Email: clothilde.philouze@tcbioservices.com

Background and aims: Developing models that pertinently reflect immune system contributions to liver disease is essential for evaluating therapeutic candidates targeting inflammation, fibrogenesis and metabolic dysfunction. We aimed to characterize two rapid induction strategies in humanized immune system NCG mice (HIS-NCG) to generate distinct phenotypes of liver injury, advanced fibrosis and metabolic dysfunction-associated steatohepatitis (MASH).
Method: HIS-NCG mice engrafted with human $CD34^+$ hematopoietic stem cells were subjected either to repeated carbon tetrachloride (CCl_4) exposure over 23 days or to a 14-day high-fat diet deficient in methionine and choline (HF-MCD). Clinical condition, circulating alanine aminotransferase, liver histopathology, fibrosis stage, steatosis, human $CD68^+$ macrophage infiltration and circulating galectin-3-binding protein (LGALS3BP) were assessed to define the resulting phenotypes.
Results: Both injury paradigms caused rapid health deterioration and marked biochemical evidence of hepatic damage. CCl_4 consistently produced advanced fibrosis, with most animals developing extensive bridging fibrosis or cirrhotic architecture in the absence of steatosis or human macrophage infiltration. In contrast, the HF-MCD diet induced the signature multi-component phenotype of MASH, including pronounced steatosis, a NAFLD Activity Score (NAS) of 6, low-grade fibrosis and substantial infiltration of human $CD68^+$ macrophages. Elevated LGALS3BP further supported immune-mediated inflammation and fibrogenesis.
Conclusion: These two humanized immune system mouse models provide complementary tools for the preclinical investigation of therapies targeting immune-driven pathways in liver disease. The CCl_4 model recapitulates advanced fibrotic architecture, whereas the HF-MCD diet encompasses metabolic stress and human immune activation. In addition, a dual-humanized configuration integrating both human immune system and hepatocytes is also available. This expanded platform enables the evaluation of combination strategies relevant to both MASH and infectious hepatitis.

SAT-201

Single-cell integration of transcriptomics and mtDNA sequencing identifies pan-cellular mosaic mitochondrial heteroplasmy as a hallmark of MASH

Carlos Pirola[1], Silvia Sookoian[1]. [1]*Translational Research in Health Center, Universidad Maimonides, Buenos Aires, Argentina, National Scientific and Technical Research Council, Buenos Aires, Argentina, CABA, Argentina*
Email: pirola.carlos@maimonides.edu

Background and aims: Metabolic dysfunction-associated steatohepatitis (MASH) is characterized by chronic metabolic and mitochondrial stress. While mitochondrial impairments are well-documented in liver tissue, the landscape of mitochondrial DNA (mtDNA) heteroplasmy across diverse hepatic cell types remains poorly defined. We leveraged single-nucleus RNA sequencing (snRNA-seq) to quantify mtDNA heteroplasmy throughout the entire cellular atlas of the MASH liver.
Method: We analyzed a publicly available 10x Genomics snRNA-seq dataset (GSE212837) comprising liver samples from individuals with MASH and healthy controls. Following quality control and cell annotation, mtDNA heteroplasmy was quantified per cell using the maximum alternative allele fraction and the count of variants with frequency ≥ 0.1. These metrics were integrated into heteroplasmy scores. We assessed differences in heteroplasmy distributions across hepatocytes, macrophages, endothelial cells, cholangiocytes, and fibroblasts using Mann–Whitney tests with false discovery rate correction.
Results: Analysis of 117,793 cells revealed a systemic shift toward increased mtDNA heteroplasmy in MASH. Hepatocytes exhibited the most profound shift ($p = 1.0 \times 10^{-50}$) with an excess of cells in the upper heteroplasmy quantiles. Significant heteroplasmy increases were also observed in endothelial cells ($p = 1.0 \times 10^{-28}$), macrophages ($p = 4.3 \times 10^{-18}$), and fibroblasts ($p = 8.5 \times 10^{-11}$). Cholangiocytes showed a modest but significant increase. Across all lineages, MASH was characterized by an expansion of high-heteroplasmy cell subpopulations, with substantial shifts observed in *MT-ATP6* (cholangiocytes) and *MT-CO1* (resident NK cells and hepatocytes). Heteroplasmic variants were predominantly concentrated in Complex I, III, and IV genes and ribosomal RNAs (*MT-RNR1/2*). By definition, somatic-like variants exhibited cell-type-specific restricted prevalence. This accumulation of mosaic alterations suggests that mitochondrial genomic instability in MASH is driven by localized somatic mutagenesis, in addition to substantial germline inheritance.
Conclusion: Mitochondrial DNA heteroplasmy is a pan-cellular hallmark of MASH, extending beyond hepatocytes to the broader liver microenvironment. This systemic mitochondrial genomic instability suggests a novel axis of cellular remodeling, positioning targeted mitochondrial preservation as a critical therapeutic strategy to arrest MASH progression.

SAT-202

Unraveling the therapeutic mechanism of hyodeoxycholic acid in metabolic dysfunction-associated steatotic liver disease-to-hepatocellular carcinoma: a multi-omics approach identifies key targets and a prognostic gene signature

Wenying Qi[1], Qiuyue Wang[1], Xinyu Zhao[1], Chunfeng Mei[2], Meilan Huang[1], Jiatu Zhong[1], Fan-E Cheng[1], Xiangyun Zou[3], Size Li[1], Shihao Zheng[3], Yong'an Ye[1]. [1]*Dongzhimen Hospital of Beijing University of Chinese Medicine, Beijing, China;* [2]*Dongzhimen Hospital, Beijing University of Chinese Medicine, Beijing 100700, China, Liver Diseases Academy of Traditional Chinese Medicine, Beijing University of Chinese Medicine, Beijing, China;* [3]*Dongzhimen Hospital, Beijing University of Chinese Medicine, Dongzhimen Hospital, Beijing University of Chinese Medicine, Beijing 100700, China, Liver Diseases Academy of Traditional Chinese Medicine, Beijing University of Chinese Medicine, Key Laboratory of Chinese Internal Medicine of Ministry of Education and Beijing, Dongzhimen Hospital, Beijing University of Chinese Medicine, Beijing, China*
Email: yeyongan@vip.163.com

Background and aims: Hyodeoxycholic acid (HDCA), a secondary bile acid with reported anti-inflammatory and anti-fibrotic properties, has emerged as a potential modulator of metabolic dysfunction-associated steatotic liver disease (MASLD) progression. However, the molecular mechanisms by which HDCA influences lipid metabolism and intercellular communication during MASLD-to-hepatocellular carcinoma (HCC) transition remain poorly characterized. This study aimed to systematically investigate the therapeutic targets and mechanisms of HDCA in MASLD-HCC progression using integrated bioinformatics and experimental validation.
Method: HDCA target prediction via five databases (e.g., SwissTargetPrediction) identified 654 potential proteins. Differentially expressed genes during MASLD-HCC progression were analyzed using Gene Expression Omnibus datasets (GSE126848, GSE135251, GSE164760). Subsequent analyses included functional enrichment, prognostic modeling with 101 machine learning combinations, single-cell RNA-seq (GSE189175), molecular docking, and 100-ns molecular dynamics simulations. For in vivo validation, a MASLD-HCC mouse model was established in male C57BL/6J mice using a high-fat diet, 5% fructose water, and weekly diethylnitrosamine injections (50 mg/kg) for 8 weeks. Mice (n = 10/group) were randomized to receive vehicle, low- (50 mg/kg) or high-dose (100 mg/kg) HDCA, or resmetirom (positive control) by gavage for 8 weeks. Outcomes assessed serum biochemistry, liver histopathology, tumor burden, and target validation.
Results: Intersection analysis identified 69 candidate genes enriched in fatty acid metabolism and steroidogenesis pathways. A 5-gene signature (CBS, HSD3B, SLCO1A2, HMOX1, CYP26B1) showed robust prognostic performance across three independent cohorts. Single-cell analysis revealed HMOX1 expression in macrophages and CBS in cholangiocytes, while hepatic stellate cells and macrophages exhibited elevated signature activity in disease groups. Molecular docking confirmed stable HDCA binding to all signature proteins, with highest affinity for CYP26B1. In a MASLD-HCC mouse model, both high- and low-dose HDCA treatments significantly reduced hepatic tumor nodules, improved liver function, lowered fibrosis scores, and downregulated signature gene expression.
Conclusion: HDCA exerts hepatoprotective effects in MASLD-HCC by targeting the CYP26B1-centered 5-gene signature, reducing tumor burden and improving liver pathology, positioning it as a promising therapeutic candidate.

SAT-203

Deoxycholic acid promotes inflammation-to-cancer transition in metabolic dysfunction-associated steatohepatitis through a multi-omics identified gene signature

Wenying Qi[1], Fan-E Cheng[1], Size Li[1], Qiuyue Wang[1], Xinyu Zhao[1], Chunfeng Mei[1], Linshuang Dou[1], Jinyu Li[1], Meilan Huang[1], Jiatu Zhong[1], Li Hou[1]. [1]*Dongzhimen Hospital of Beijing University of Chinese Medicine, Beijing, China*
Email: houli1203@126.com

Background and aims: Deoxycholic acid (DCA), a secondary bile acid elevated in metabolic dysfunction-associated steatohepatitis (MASH), is known to drive hepatocyte injury and inflammatory responses. However, its mechanistic role in promoting the transition from MASH to hepatocellular carcinoma (HCC) remains incompletely understood. This study aimed to identify DCA-associated inflammatory mediators and gene signatures that facilitate MASH-related hepatocarcinogenesis through integrated multi-omics analysis and experimental validation.
Method: DCA targets were predicted and cross-referenced with transcriptomic data from metabolic dysfunction-associated steatotic liver disease (MASLD), MASH, and HCC to identify candidate genes. Prognostic modeling was performed using The Cancer Genome Atlas

(TCGA) data. Binding was evaluated via molecular docking and dynamics simulations. In vivo validation used a MASH-HCC mouse model induced by high-fat diet and diethylnitrosamine for 16 weeks. Starting from week 9, mice were treated with DCA, lenvatinib, or polyene phosphatidylcholine, followed by histopathological and molecular analyses.

Results: By integrating 677 predicted DCA targets with differentially expressed genes (DEGs) from MASH, MASLD, and HCC cohorts, 77 candidate genes were identified. Cox regression analysis highlighted 30 genes with prognostic significance, from which a 7-gene signature (HMMR, AKR1B10, CYP26B1, et al.) was constructed, showing robust prognostic performance. Single-cell analysis revealed elevated activity of this signature in hepatic stellate cells and T lymphocytes within MASH-HCC samples. CellChat analysis indicated enhanced laminin signaling between hepatic stellate cells and cholangiocytes in disease groups compared to controls. Molecular docking confirmed stable binding of DCA to all seven signature proteins. In the MASH-HCC mouse model, compared with the positive control drug, DCA administration significantly exacerbated hepatic fibrosis ($p < 0.05$), increased pro-inflammatory cytokines(interleukin-6 and tumor necrosis factor alpha, $p < 0.05$), and upregulated the 7-gene signature expression, confirming its functional role in the inflammation-cancer transition.

Conclusion: DCA accelerates MASH-driven hepatocarcinogenesis through a functionally validated 7-gene signature that orchestrates inflammatory responses and intercellular communication. These findings establish DCA and its downstream targets as potential therapeutic candidates for preventing MASH-related HCC progression.

SAT-204

Network pharmacology and multi-omics reveal the hepatoprotective mechanism of pig bile in metabolic dysfunction-associated steatotic liver disease via the gut-liver axis

Wenying Qi[1], Li Hou[1], Bo Jia[1], Qiuyue Wang[1], Xinyu Zhao[1], Chunfeng Mei[1], Shihao Zheng[1], Fan-E Cheng[1], Yaxi Zhang[2], Size Li[1].
[1]Dongzhimen Hospital of Beijing University of Chinese Medicine, Beijing, China; [2]Dongzhimen Hospital, Beijing University of Chinese Medicine, Dongzhimen Hospital, Beijing University of Chinese Medicine, Beijing 100700, China, Liver Diseases Academy of Traditional Chinese Medicine, Beijing University of Chinese Medicine, Key Laboratory of Chinese Internal Medicine of Ministry of Education and Beijing, Dongzhimen Hospital, Beijing University of Chinese Medicine, Beijing, China
Email: lisize5500@163.com

Background and aims: Metabolic dysfunction-associated steatotic liver disease (MASLD) and its progressive form, metabolic dysfunction-associated steatohepatitis (MASH), represent a major global health burden with limited therapeutic options. Pig bile has been traditionally used for hepatoprotection, yet its mechanism of action via the gut-liver axis remains poorly understood. This study aimed to elucidate the molecular mechanisms by which pig bile delays MASLD/MASH progression.

Method: Fifty 6-week-old male db/db mice were randomly divided into 5 groups (10 mice/group): normal diet, high-fat diet (HFD) +fructose, HFD+fructose+porcine bile (equivalent dose), HFD+fructose+porcine bile (double dose), and HFD+fructose+positive control (polyenphosphatidylcholine). After 8 weeks of modeling, mice received 8 weeks of oral administration. Potential therapeutic targets were identified by integrating network pharmacology with transcriptomic data from MASLD models. Gut microbiota composition was analyzed via 16S rRNA sequencing. Spearman correlation analysis assessed relationships between microbial abundance and serum levels of alanine aminotransferase (ALT), aspartate aminotransferase (AST), low-density lipoprotein (LDL), and lipopolysaccharide (LPS). Core targets were identified through protein-protein interaction network analysis and subsequently validated by quantitative polymerase chain reaction and western blotting.

Results: Network pharmacology identified 128 overlapping targets between pig bile bioactive compounds and MASLD-associated genes. Kyoto Encyclopedia of Genes and Genomes (KEGG) pathway enrichment showed significant involvement in peroxisome proliferator-activated receptor gamma (PPARG) signaling and bile acid metabolism. Three core targets were obtained: Sterol Regulatory Element Binding Protein 1c (SREBP1c), PPARG, and C-X-C motif chemokine ligand 2 (CXCL2). In vivo validation confirmed that pig bile significantly attenuated hepatic steatosis and lobular inflammation, upregulated SREBP1c and PPARG expression ($p < 0.05$), and increased intestinal occludin and claudin-1 levels ($p < 0.05$). Gut microbiota analysis revealed that Colidextribacter abundance was positively correlated with ALT ($p < 0.01$) and LPS levels ($p < 0.05$).

Conclusion: Porcine bile improves the progression of MASLD by regulating the gut-liver axis and targeting *SREBP1c*, *PPARG* and *CXCL2*. These research findings provide a mechanistic basis for the application of porcine bile-derived compounds in the treatment of metabolic liver diseases.

SAT-205

JiguCao capsule alleviates metabolic dysfunction-associated steatotic liver disease through modulation of gut-liver axis and toll-like receptor 4 signaling

Wenying Qi[1], Xiaobin Zao[2], Hening Chen[3], Yue Chen[4], Ruijia Liu[1], Xin Sun[5], Tingyu Zhang[1], Linshuang Dou[1], Yaxi Zhang[1], Xiaoke Li[5].
[1]Dongzhimen Hospital of Beijing University of Chinese Medicine, Beijing, China; [2]Dongzhimen Hospital, Beijing University of Chinese Medicine, Dongzhimen Hospital, Beijing University of Chinese Medicine, Beijing 100700, China, Liver Diseases Academy of Traditional Chinese Medicine, Beijing University of Chinese Medicine, Key Laboratory of Chinese Internal Medicine of Ministry of Education and Beijing, Dongzhimen Hospital, Beijing University of Chinese Medicine, Beijing, China; [3]Yongshun Community Health Service Center, Beijing, China, Dongzhimen Hospital, Beijing University of Chinese Medicine, Beijing 100700, China, Liver Diseases Academy of Traditional Chinese Medicine, Beijing University of Chinese Medicine, Beijing, China; [4]School of Chinese Medicine, Li Ka Shing Faculty of Medicine, the University of Hong Kong, Hong Kong, China; [5]Dongzhimen Hospital, Beijing University of Chinese Medicine, Beijing 100700, China, Liver Diseases Academy of Traditional Chinese Medicine, Beijing University of Chinese Medicine, Beijing, China
Email: lixiaoke@vip.163.com

Background and aims: Metabolic dysfunction-associated steatotic liver disease (MASLD) represents a growing global health burden, with gut-liver axis dysfunction and lipopolysaccharide (LPS)-mediated toll-like receptor 4 (TLR4) pathway activation recognized as key pathogenic drivers. JiguCao capsule (JCF), a traditional Chinese medicinal formulation, has demonstrated hepatoprotective properties in clinical practice, yet its molecular mechanisms remain incompletely understood. This study aimed to elucidate the therapeutic mechanisms of JCF in MASLD, with particular focus on LPS-TLR4 signaling and gut-liver axis homeostasis. The funding for this study was sourced from the World Federation of Chinese Medicine Societies (targeted entrustment), with project numbers WFCMS2024026 and WFCMS2024027.

Method: MASLD was induced in wild-type and TLR4-knockout C57BL/6J mice via a 16-week high-fat diet with 5% fructose water. Mice ($n = 10$ per group) were randomized to receive normal diet, MASLD model with vehicle, JCF (low and high dose), or polyene phosphatidylcholine (positive control) by gavage. Assessments included serum biochemistry, hepatic histopathology, and western blotting for TLR4 pathway components. Multi-omics analyses comprised 16S ribosomal RNA gene sequencing for gut microbiota, ultra-high-performance liquid chromatography-tandem mass spectrometry for bile acid profiling, hepatic transcriptomics, and proteomics. Molecular docking evaluated interactions between JCF bioactive components and TLR4.

Results: JCF treatment significantly attenuated MASLD severity, reducing body weight gain ($p < 0.01$), hepatic steatosis scores, and serum Alanine Aminotransferase, Aspartate Aminotransferase,and LPS levels compared with vehicle-treated MASLD mice($p < 0.01$). Histological analysis demonstrated reduced lipid accumulation and inflammatory infiltration. JCF enhanced intestinal barrier function by upregulating tight junction proteins claudin-1 and occludin ($p < 0.01$). Western blotting revealed suppressed TLR4-MyD88-NF-kappaB pathway activation in JCF-treated mice. Notably, the therapeutic effects of JCF were significantly attenuated in TLR4-knockout mice, confirming TLR4 pathway dependency.
Conclusion: JiguCao capsule ameliorates MASLD progression through TLR4-dependent suppression of hepatic inflammation, restoration of gut-liver axis homeostasis, and modulation of lipid metabolism. These findings provide mechanistic insights supporting the therapeutic potential of JCF as a multi-target intervention for MASLD.

SAT-206

Lysimachia christinae attenuates metabolic dysfunction-associated steatotic liver disease progression through immune-metabolic modulation: an integrative network pharmacology and experimental study

Wenying Qi[1], Li Hou[1], Xinyu Zhao[1], Qiuyue Wang[1], Bo Jia[1], Fan-E Cheng[1], Size Li[1], Xiangyun Zou[2], Meilan Huang[1], Jiatu Zhong[1], Xiaobin Zao[2]. *[1]Dongzhimen Hospital of Beijing University of Chinese Medicine, Beijing, China; [2]Dongzhimen Hospital, Beijing University of Chinese Medicine, Dongzhimen Hospital, Beijing University of Chinese Medicine, Beijing 100700, China, Liver Diseases Academy of Traditional Chinese Medicine, Beijing University of Chinese Medicine, Key Laboratory of Chinese Internal Medicine of Ministry of Education and Beijing, Dongzhimen Hospital, Beijing University of Chinese Medicine, Beijing, China*
Email: A3417@bucm.edu.cn

Background and aims: Metabolic dysfunction-associated steatotic liver disease (MASLD) affects over 30% of people globally with limited treatments. Lysimachia christinae, a traditional hepatoprotective herb, has unclear mechanisms. This study integrated network pharmacology, multi-omics, and experimental validation to systematically elucidate its therapeutic targets and pathways in MASLD.
Method: Active compounds of Lysimachia christinaewere identified via the Traditional Chinese Medicine Systems Pharmacology database for target prediction. Transcriptomic datasets (GSE135251, GSE162694) and single-cell RNA sequencing (RNA-seq) data (GSE136103) were analyzed to detect MASLD-related differentially expressed genes and to perform cell-type-specific enrichment. Machine learning algorithms, including Least Absolute Shrinkage and Selection Operator, Support Vector Machine-Recursive Feature Elimination, and Random Forest, were employed to prioritize candidate targets. After eight weeks of modeling with a high-fat diet supplemented with 5% fructose in drinking water, db/db mice were administered Lysimachia christinaeextract (200/400 mg/kg/day) or polyene phosphatidylcholine for 8 weeks ($n = 10$ per group), with db/m mice serving as the negative control.
Results: Network pharmacology analysis identified quercetin as the principal active component, with enrichment in peroxisome proliferator-activated receptor (PPAR) signaling pathways. Based on the 30 intersecting genes identified from the transcriptome dataset and single-cell sequencing, including C-X-C motif chemokine ligand 10 (CXCL10) and PPAR alpha (PPARA), they were significantly enriched in lipid metabolism and inflammatory response pathways ($p < 0.05$). Machine learning algorithms consistently identified CXCL10 as the top-ranked candidate target. In db/db mice, Lysimachia christinae treatment significantly reduced hepatic steatosis scores ($p < 0.01$), serum alanine aminotransferase levels ($p < 0.05$), and CXCL10 messenger RNA expression in liver tissue compared with vehicle-treated controls.
Conclusion: Lysimachia christinae ameliorates MASLD progression by modulating immune-metabolic crosstalk, with CXCL10 identified as a key mechanistic target and potential therapeutic biomarker. This integrative framework provides a methodological template for systematic investigation of herbal medicine mechanisms.

SAT-211-YI

A novel gamma-aminobutyric acid type A receptor modulator attenuates liver fibrosis with profound anti-obesity action

Elisabeth Rohbeck[1], Corinna Niersmann[2,3], Bedair Dewidar[2,3], Volker Lauschke[4,5], Margriet Ouwens[3,6], Michael Roden[2,3,7], Juergen Eckel[1]. *[1]CMR CureDiab Metabolic Research GmbH, Düsseldorf, Germany; [2]Institute for Clinical Diabetology, German Diabetes Center, Leibniz Center for Diabetes Research at Heinrich-Heine-University Düsseldorf, Düsseldorf, Germany; [3]German Center for Diabetes Research (DZD), Partner Düsseldorf, München-Neuherberg, Germany; [4]Department of Physiology & Pharmacology, Section for Personalized Medicine and Drug Development, Karolinska Institutet, Stockholm, Sweden; [5]Dr Margarete Fischer-Bosch Institute of Clinical Pharmacology, Stuttgart, Germany; [6]Institute of Clinical Biochemistry and Pathobiochemistry, German Diabetes Center (DDZ), Düsseldorf, Germany; [7]Department of Endocrinology and Diabetology, Medical Faculty and University Hospital Düsseldorf, Heinrich-Heine-University Düsseldorf, Düsseldorf, Germany*
Email: juergen.eckel@curediab.de

Background and aims: Obesity-associated metabolic dysfunction–associated steatotic liver disease is a major driver of progressive liver fibrosis. Gamma-aminobutyric acid type A ($GABA_A$) receptor signaling has emerged as a potential modulator of liver injury and metabolic dysfunction. We investigated the anti-fibrotic and metabolic effects of the novel small molecule HK3, a positive allosteric modulator of the $GABA_A$ receptor.
Method: The effects of HK3 and its derivative HK1 were assessed in human spheroids and activated human hepatic stellate cells. Steatosis, inflammation and fibrosis were evaluated using immunoblotting, enzyme-linked immunosorbent assays, quantitative PCR and RNA sequencing. In vivo efficacy was examined in a carbon tetrachloride–induced fibrosis model and a diet-induced obesity mouse model. Effects on mitochondrial respiration were studied in differentiated adipocytes and visceral adipose tissue using extracellular flux analysis and high-resolution respirometry.
Results: HK3 significantly reduced intracellular lipid accumulation, inflammatory cytokine release and collagen production in human MASH spheroids. In hepatic stellate cells, HK3 and HK1 attenuated transforming growth factor beta–induced pro-fibrotic and inflammatory gene expression and reduced cell migration. In vivo, HK3 prevented fibrosis progression in toxic liver injury and decreased body fat mass and circulating cholesterol levels in obese mice. Finally, HK3 increased mitochondrial proton leak and reduced coupling efficiency in adipocytes and visceral adipose tissue.
Conclusion: HK3 combines anti-fibrotic, anti-inflammatory and anti-steatotic effects across multiple preclinical models. These findings support $GABA_A$ receptor modulation as a multi-target therapeutic strategy for obesity-associated metabolic dysfunction–associated steatotic liver disease.

SAT-212

Modulation of interactions between mitochondria and the endoplasmic reticulum by resmetirom in MASLD

Théo Rousseaux[1,2], Cyrielle Caussy[2,3], Jennifer Rieusset[1,2]. *[1]CarMen Laboratory, INSERM U1060, INRAE U1397, Université Claude Bernard Lyon 1, Pierre-Bénite, France; [2]Lyon Hepatology Institute, IHU EVEREST, Lyon, France; [3]Hospices Civils de Lyon, Département Endocrinologie, Diabète et Nutrition, Hôpital Lyon Sud, Pierre-Bénite, France*
Email: jennifer.rieusset@univ-lyon1.fr

Background and aims: Poor calcium coupling between the endoplasmic reticulum (ER) and mitochondria, at contact points called

mitochondria-associated ER membranes (MAMs), plays a role in the development of insulin resistance and metabolic dysfunction-associated steatotic liver disease (MASLD). Recently, resmetirom (a thyroid hormone receptor agonist, THR-beta) has been approved as a treatment for fibrotic metabolic dysfunction-associated steatohepatitis (MASH). We investigated whether the mechanism of action of resmetirom depends on the integrity of hepatic MAMs.

Method: We studied the effect of resmetirom (1 µM) on MAMs (in situ PLA), lipid accumulation (Bodipy), insulin resistance (Western blot P-AKT/AKT), lipid metabolism (RT-PCR) in Huh7 cells under preventive (24-hour co-treatment with 200 µM palmitate) and curative (8 hours of 100 µM palmitate, followed by 24 hours of resmetirom) conditions.

Results: The efficacy of resmetirom treatment is demonstrated by the induction of THR-β target genes DIO1 in Huh7 cells. Palmitate induces an increase in lipid droplet size (+ 113%, $p < 0.0001$), which is partially prevented by resmetirom (+ 59%, $p = 0.0001$), i.e., delta −25%, $p < 0.0001$. Similarly, the reduction in MAMs induced by palmitate (−46%, $p < 0.0001$) is partially prevented by resmetirom (−26%, $p < 0.0001$), i.e., delta +37%, $p < 0.0001$. In addition, resmetirom increases the P-AKT/AKT ratio in the presence of palmitate (delta + 48%). Finally, resmestirom stimulates the expression of key lipid metabolism genes, such as CPT1A. Under curative conditions, resmetirom reduces palmitate-induced steatosis (delta − 13%, $p < 0.05$) and the integrity of MAMs is currently being analyzed.

Conclusion: These preliminary results suggest that resmetirom could prevent and improve lipid accumulation and hepatic insulin resistance induced by palmitate through the regulation of the integrity of MAMs. An in vivo protocol in a MASLD mouse model, with or without hepatic MAM disruption induced by a molecular spacer, will serve to confirm these data.

SAT-213

Multimodal analysis bridges liver histological features identified by AI based digital histology tools and -omic signatures in a Japanese MASH cohort

Ruixue Hou[1], Ali Ebrahimi[1], Vandana Gupta[1], Hiroaki Yashiro[1], Jen-Chieh Chuang[1], Zoltan Derdak[1], Saman Farahmand[1], Shinichi Aishima[2], Hideyuki Hyogo[3], Yuichiro Eguchi[4], Eisuke Murakami[5], Masato Yoneda[6], Haakan Wennbo[1], Paresh Thakker[1], Bernard Allan[1], Hirokazu Takahashi[3], Atsushi Nakajima[7], Maria D. Paraskevopoulou[1], Banishree Saha[1].
[1]Takeda Development Center Americas, Inc., Cambridge, United States; [2]Kyushu University, Japan, Fukuoka City, Japan; [3]Department of Hepatology, Division of Metabolism, Faculty of Medicine, Saga University, Saga, Japan, Hyogo Life Care Clinic Hiroshima, Hiroshima, Japan, Saga, Japan; [4]Loco Medical General Institute, Saga, Japan, Department of Hepatology, Division of Metabolism, Faculty of Medicine, Saga University, Saga, Japan, Saga, Japan; [5]Department of Gastroenterology and Metabolism, Hiroshima University, Hiroshima, Japan, Hiroshima, Japan; [6]Department of Gastroenterology and Hepatology, Yokohama City University, Kanagawa, Japan, Kanagawa, Japan; [7]International University of Health and Welfare Department of Gastroenterology & Hepatology, Tochigi, Japan, Department of Gastroenterology and Hepatology, Yokohama City University, Kanagawa, Japan, Tochigi, Japan
Email: ruixue.hou@takeda.com

Background and aims: Metabolic dysfunction-associated steatohepatitis (MASH) is a growing global health burden with limited therapies. Although invasive, liver biopsy remains the reference standard for staging MASH and assessing treatment response in drug development. Digital pathology (DP) enables reproducible, continuous quantification of liver histology than conventional pathologist scoring but still relies on biopsy. Non-invasive tests (NITs) and novel biomarkers from high-throughput serum proteomics offer a promising alternative. In this study, we integrate, for the first time, PathAI- and HistoIndex (HI)-based DP with standard NITs and serum proteomics in a Japanese MASH cohort.

Method: Biopsies from 250 clinically and histologically confirmed MASLD/MASH subjects (Saga, Yokohama City, and Hiroshima Universities) were analyzed. Fibrosis stage (CRN) and NAFLD Activity Score (NAS) were assessed by a central pathologist (CP). PathAI's AIM-MASH, HistoIndex (HI)'s stain free SHG/TPE imaging, collagen proportionate area (CPA) quantification and AI/ML models were deployed to identify and characterize DP features. Serum proteomics was performed using 11K-protein SomaScan platform. Spearman correlations linked DP/CP features to protein levels, followed by pathway analysis and paired liver transcriptomic validation.

Results: Key histological features of fibrosis stage read by CP have strong correlation with fibrosis measured by PathAI, HI and CPA. Correlations were stronger for GNN (Graph Neural Network) continuous score ($r = 0.84$, $p < 0.001$) and qFibrosis (0.83, $p < 0.001$) values as compared to categorical scores. GNN-CRN continuous score, qFibrosis value and CP, were correlated strongly with NITs such as FIB-4, Type IV collagen 7S, and Hyaluronic acid ($p < 0.05$). Serum proteomics correlated with FIB-4, APRI, collagen biomarkers and CP/DP features. Serum proteomics identified consistent proteins (e.g., ADAMTSL2, C7, GARS1, and THBS2) and fibro-inflammatory pathways, which were validated in paired tissue transcriptomics with high concordance. Overall, our results demonstrate that serum proteins can recapitulate key histologic features captured by digital pathology, including PathAI's AIM-MASH and HI's SHG/TPEF readouts.

Conclusion: Omic-derived signatures map to specific DP-derived histological features and enable the identification of serum biomarker candidates that may help in better diagnosis and monitoring of pathophysiological changes in MASH.

SAT-214

PARP1 rs747657 C > G variant protects against metabolic dysfunction in MASLD

Federico Salomone[1], Miriam Longo[2], Fabio Galvano[3], Paola Dongiovanni[2]. *[1]Azienda Sanitaria Provinciale di Catania, Catania, Italy; [2]Medicine and Metabolic Diseases, Fondazione IRCCS Ca' Granda Ospedale Maggiore Policlinico, Milan, Italy; [3]BIOMETEC, Università degli Studi di Catania, Catania, Italy*
Email: federicosalomone@rocketmail.com

Background and aims: Impaired metabolic homeostasis and cardiovascular risk are intrinsic to the definition of metabolic dysfunction-associated steatotic liver disease (MASLD), however genetic factors conferring susceptibility to a high-risk cardiometabolic profile in MASLD remain to be established. In this study, we aimed to examine the impact of PARP1 rs747657 C > G variant on cardiometabolic parameters in subjects with MASLD.

Method: The PARP1 rs747657 variant was genotyped in 1431 individuals referred to an outpatient Metabolic Liver Diseases Unit in Milan. Transcriptomic analysis was performed by RNAseq in liver samples from 167 bariatric patients, whereas Poly-ADP-ribosylated protein levels were assessed in liver samples from 21 bariatric patients. *In vitro* experiments in HepG2 treated with free fatty acids with or without 3-aminobenzamide, a PARP1 inhibitor, were performed to assess the role of PARP1 in the regulation of lipoprotein homeostasis in the liver.

Results: Subjects with CC and CG/GG genotypes were respectively 658 (46%) and 773 (54%) in the whole cohort. At multivariate analysis adjusted for gender, age, BMI, IFG/T2D, statin use and TM6SF2 E167K variant, PARP1 CG/GG genotype was associated with lower total cholesterol ($\beta = -0.10$ {−0.17–0.04}, $p = 0.001$), lower LDL ($\beta = -0.08$ {−0.13–0.02}, $p = 0.0078$), and lower triglycerides ($\beta = -0.08$ {−0.14–0.03}, $p = 0.002$). The rs747657 C > G variant was also inversely associated with fasting glucose levels ($\beta = -2.04$ {−3.7–0.39}, $p = 0.015$) and with the presence of IFG/T2D (OR = 0.73, 95% C.I {0.54–

0.99}, p = 0.04). Consistently with less dyslipidemia and diabetes, carriers of the G allele had a lower intima-media thickness (0.85 ± 0.21 vs 0.81 ± 0.19 mm, p = 0.04). Subjects with the CG/GG genotypes display lower mRNA levels of PARP1 and lower levels of Poly-ADP-ribosylated proteins. Treatment of HepG2 with 3-aminobenzamide, a PARP1 inhibitor, reduces LDL/VLDL fraction and APOB release in the medium and enhances LDL-R expression.
Conclusion: PARP1 rs747657 C > G variant, leading to lower PARP1 expression and lower polyADPribosylation of target proteins, protects against dyslipidemia and insulin resistance in MASLD, indicating a role for PARP1 in conferring susceptibility to metabolic dysfunction.

SAT-215
PFOA exposure promotes lipid peroxidation–driven inflammatory niche formation in a metabolically vulnerable liver
Wenhua Shao[1], Mayuko Shimizu[2], Hirohisa Ogawa[2], Takeo Minamikawa[3], Takahiro Takayama[4], Koichi Inoue[4], Koichi Tsuneyama[2]. *[1]Department of Molecular Pathology, Tokushima university graduate school of biomedical sciences, Tokushima, Japan; [2]Department of Pathology and Laboratory Medicine, Tokushima university graduate school of biomedical sciences, Tokushima, Japan; [3]Institute for advanced biosciences, Osaka university, Osaka, Japan; [4]Laboratory of Clinical & Analytical Chemistry, College of Pharmaceutical Sciences, Ritsumeikan University, Shiga, Japan*
Email: tsuneyama.koichi@tokushima-u.ac.jp

Background and aims: Metabolic dysfunction-associated steatohepatitis (MASH) creates a liver microenvironment enriched in polyunsaturated fatty acids and susceptible to oxidative stress. Per- and poly-fluoroalkyl substances (PFAS)are persistent environmental pollutants suspected to modify liver disease progression; however, their pathological impact on the hepatic inflammatory microenvironment in metabolic liver disease remains unclear. We aimed to investigate whether perfluoroalkyl substance exposure exacerbates oxidative injury and promotes inflammatory niche formation in a metabolically vulnerable liver.
Method: A dietary mouse model of MASH induced by an iHFC diet was exposed to perfluorooctanoic acid (PFOA), a representative PFAS, with appropriate control groups. Liver weight, macroscopic appearance, and histopathological changes were evaluated. Hepatocellular injury, lobular inflammation, and macrophage infiltration were semi quantitatively scored. Lipid peroxidation was assessed by immunohistochemistry for 4-hydroxynonenal (4-HNE) adducts. Macrophage distribution and cytokine expression were analyzed using immunohistochemistry for Mac 2, TNF-alpha, and IL-6. Quantitative and spatial analyses of intrahepatic PFOA accumulation using mass spectrometry-based methods and Raman spectroscopic imaging are currently ongoing.
Results: PFOA exposure aggravated hepatomegaly in the MASH model. Histologically, exposure significantly increased hepatocellular degeneration, lobular inflammation, and macrophage infiltration compared with diet induced disease alone. Widespread hepatocellular accumulation of 4-HNE adducts indicated enhanced lipid peroxidation in metabolically stressed livers. Notably, Mac 2 positive macrophages formed prominent intrahepatic clusters enriched for TNF-alpha and IL-6, suggesting the formation of localized inflammatory niches. These macrophage aggregates were spatially associated with areas of intense oxidative injury, supporting a feed forward interaction between lipid peroxidation and sustained inflammation.
Conclusion: PFAS exposure exacerbates oxidative liver injury and promotes cytokine rich macrophage inflammatory niche formation in MASH. These findings suggest that environmental toxicants act as disease modifiers by amplifying lipid peroxidation driven inflammation in metabolically vulnerable livers. Ongoing quantitative and imaging analyses will further clarify the relationship between hepatic toxicant burden and inflammatory niche formation.

SAT-216-YI
Early life malnutrition programs long-term metabolic dysfunction and progressive fatty liver disease
Vinesh Sharma[1,2], Vikram Patial[1,2]. *[1]Pharmacology and Toxicology Laboratory, Dietetics & Nutrition Technology Division, CSIR-Institute of Himalayan Bioresource Technology, Palampur, India; [2]Academy of Scientific and Innovative Research (AcSIR), Ghaziabad, India*
Email: vineshs317@gmail.com

Background and aims: Early life malnutrition refers to inadequate intake of essential nutrients during critical development periods from fetal life through infancy and early childhood. However, later exposure to energy-dense, fat and carbohydrate-rich diets increases susceptibility to metabolic disorders due to altered metabolic adaptation established during early development. The present study aims to investigate how early life undernutrition programs long-term metabolic alterations later in life in C57BL/6 mice.
Method: The study comprised six experimental groups designed to evaluate the comparative effects of early-life protein restriction and subsequent high-fat feeding on metabolic function and progressive liver pathology. The dual dietary burden was introduced in mice by feeding a 5% low-protein diet immediately after weaning for eight weeks, followed by a high-fat diet for sixteen weeks.
Results: Animals exposed to an early-life *LP* diet followed by *HfD* (*LP+HfD*) initially showed intermediate weight gain but reached body and organ weights comparable to the *HfD* group by 24 weeks. Serum liver injury markers were elevated in *HfD*, *LP*, and *LP+HfD* groups compared with controls, with the highest levels in the *LP+HfD* group, while glucose and total protein were reduced in the *LP* group. Histopathological analysis revealed pronounced hepatic steatosis, inflammation, and fibrosis in *HfD, LP*, and *LP+HfD* groups, with significantly larger and more abundant lipid vacuoles in the *LP+HfD* group. Genes related to *de novo* lipogenesis were upregulated across *HfD*-fed groups, whereas profibrogenic, inflammatory, and oxidative stress markers were predominantly elevated in *LP* and *LP+HfD* groups. Notably, gut microbiome analysis demonstrated a significant depletion of beneficial short-chain fatty acid–producing bacteria in the *LP+HfD* group; however, significant increases were observed in the concentration of bacteria related to fatty acid synthesis and inflammatory response, highlighting a potential mechanistic link between early-life malnutrition, gut dysbiosis, and aggravated metabolic liver injury.
Conclusion: Early-life protein restriction followed by high-fat feeding exacerbates metabolic dysfunction and accelerates progressive liver injury. This nutritional mismatch promotes severe steatosis, inflammation, fibrosis, insulin dysregulation, and gut microbiome dysbiosis, highlighting the critical role of early nutritional programming in increasing susceptibility to chronic metabolic liver disease later in life.

SAT-217-YI
Targeting SIRP-alpha signaling pathway as a novel therapeutic strategy for metabolic dysfunction-associated steatohepatitis
Shaoping She[1], Xue Zhang[2], Liying Ren[1], Ran Fei[1], Dongbo Chen[1], Feng Liu[1], Huiying Rao[1], Hongsong Chen[1]. *[1], Beijing, China; [2]Peking University People's Hospital, Peking University Hepatology Institute, Infectious Disease and Hepatology Center of Peking University People's Hospital, Beijing, China*
Email: sheshaoping@126.com

Background and aims: Metabolic dysfunction-associated steatohepatitis (MASH), affecting over 30% of adults globally, drives advanced liver disease, posing a major public health challenge. Signaling regulatory protein alpha (SIRP-alpha), as a ligand for CD47, is an immune checkpoint expressed on macrophages and other myeloid cells. While our previous work identified SIRP-alpha inhibits hepatocellular carcinoma progression by preventing T-cell apoptosis, its specific role in the pathogenesis of MASH has not yet been elucidated.

Method: The expression of SIRP-alpha was detected in liver tissues from patients with MASH and two established murine models of MASH: a Western diet combined with carbon tetrachloride injection (WD + CCl_4) and a high-fat methionine-choline-deficient diet (HFMCD). To evaluate the functional role of SIRP-alpha in MASH progression, we employed systemic SIRP-alpha gene knockout mice for in vivo studies. The direct cellular effects of SIRP-alpha were examined in vitro using the human hepatocyte cell line THLE-2 and the human hepatic stellate cell (HSC) line LX-2. Furthermore, an integrated multi-omics approach, combining single-cell RNA sequencing with serum metabolomics, was employed to elucidate the molecular mechanisms through which SIRP-alpha regulates MASH progression.
Results: In this study, we found that SIRP-alpha expression was significantly upregulated in both MASH patients and WD + CCl_4 or HFMCD-induced mouse MASH models. SIRP-alpha deficiency led to a marked aggravation of MASH pathology in mice, evidenced by worsened steatosis, inflammation, and fibrosis. In vitro studies demonstrated that SIRP-alpha overexpression significantly suppressed the secretion of pro-inflammatory cytokines and the accumulation of lipid droplets induced by combined free fatty acid and lipopolysaccharide stimulation in THLE-2 cells. Conversely, SIRP-alpha silencing in THLE-2 cells exacerbated these pathological phenotypes. We also found that SIRP-alpha overexpression promoted the apoptosis of LX-2 cells, whereas its knockdown exerted an anti-apoptotic effect. Mechanistically, integrated multi-omics analyses indicated that SIRP-alpha modulates the mitochondrial apoptosis pathway by altering the Bcl-2/Bax signaling axis in HSCs.
Conclusion: Our findings demonstrate that SIRP-alpha exerts a protective role in MASH by reducing hepatocyte steatosis and inflammation, and promoting HSCs apoptosis through the Bcl-2/Bax pathway. Targeting SIRP-alpha signaling may offer a therapeutic strategy for MASH.

SAT-218

Trace copper exposure within drinking water standards exacerbates liver injury in metabolic dysfunction

Mayuko Shimizu[1], Wenhua Shao[1], Hirohisa Ogawa[1], Koichi Tsuneyama[1]. *[1]Tokushima University Graduate School, Department of Pathology and Laboratory Medicine, Tokushima, Japan*
Email: ichimura.mayuko@tokushima-u.ac.jp

Background and aims: Hepatic accumulation of metals such as iron and copper is a well-established cause of liver injury through oxidative stress. Drinking water represents a major source of daily metal exposure, and regulatory standards have been implemented to ensure safety in the general population. However, whether metal intake below these regulatory limits remains biologically inert in individuals with metabolic liver disease is unknown. This study investigated the impact of trace iron or copper exposure within drinking water standards on the progression of metabolic dysfunction–associated steatotic liver disease (MASLD).
Method: MASLD was induced in Tsumura-Suzuki non-obese (TSNO) mice with a normal genetic background by feeding a high-fat, high-cholesterol diet. Simultaneously, mice were allowed free access for 12 weeks to distilled water supplemented with iron (0.3 mg/L) or copper (1.0 mg/L), concentrations aligned with Japanese drinking water quality standards ($n = 5$/group). MASLD control mice received distilled water alone.
Results: Both iron and copper exposure significantly exacerbated hepatic inflammation in MASLD mice compared with controls. Copper exposure, in particular, led to pronounced infiltration of lymphocytes and neutrophils, extensive hepatocellular ballooning, and elevated serum alkaline phosphatase levels. Importantly, neither hepatic nor serum copper levels differed from controls, excluding pathological copper accumulation. Despite this, immunohistochemical analyses consistently revealed pronounced macrophage infiltration and robust hepatic accumulation of 4-hydroxynonenal, a marker of oxidative stress, in all copper-exposed mice. These findings suggest that copper induces excessive oxidative stress and inflammatory responses independently of hepatic copper accumulation.
Conclusion: Trace metal exposure within currently accepted safety limits is sufficient to aggravate hepatic inflammation in the context of metabolic dysfunction, independent of overt metal accumulation. These findings challenge the assumption that regulatory threshold levels are universally safe and suggest that individuals with MASLD may represent a susceptible population requiring reconsideration of environmental metal exposure. Our study underscores the emerging need to integrate metabolic vulnerability into risk assessment frameworks for drinking water quality.

SAT-219

Hepatic 5-HT2B receptor antagonism mediates the anti-steatotic and antifibrotic effects of psilocybin in preclinical MASH models

Anna Signor[1], Martina Colognesi[1], Giovanna Finzi[2], Daniela Gabbia[1], Andrea Mattarei[1], Stefano Comai[1], Gianfranco Pasut[1], Franco Folli[3], Paolo Manfredi[4,5], Sara De Martin[1]. *[1]Dept. Pharmaceutical and Pharmacological Sciences, University of Padova, Padova, Italy; [2]Unit of Pathology, Azienda Socio-Sanitaria Territoriale (ASST) dei Sette Laghi, Varese, Italy, Varese, Italy; [3]Dept. of Health Sciences, University of Milan, Milano, Italy; [4]MGGM Therapeutics, Kerhonkson, New York, United States; [5]Levomecor Inc, Miami Beach, United States*
Email: sara.demartin@unipd.it

Background and aims: Psilocybin's active metabolite psilocin is a serotonin (5-HT) analogue acting as a partial 5-HT2A/2C receptor agonist and a selective 5-HT2B antagonist. While psilocybin is primarily known for its central psychedelic effects mediated by 5-HT2A agonism, several 5-HT receptor subtypes are expressed in the liver, where serotonin regulates lipid metabolism and fibrogenesis. In particular, 5-HT2B signaling has been implicated in hepatic stellate cell activation, yet its role in MASLD/MASH progression remains poorly defined. We here investigated the molecular mechanisms and therapeutic potential of psilocybin in preclinical models of MASH.
Method: Psilocin (10microM) was tested in vitro on PA:OA-induced lipid accumulation in HepG2 cells, including 5-HT2A-mutant cells generated by CRISPR/Cas9 and compared with a selective pharmacological 5-HT2B inhibitor. LX-2 stellate cells were analyzed for fibrotic markers by immunocytochemistry and RT-PCR. In vivo, mice fed a Novel Gubra Amylin NASH (GAN) diet received oral, sub-psychedelic psilocybin (0.05 mg/kg) from week 5 to 22. Liver morphology and molecular markers were assessed by histology, transmission electron microscopy, and gene expression analyses.
Results: Psilocin reduced lipid accumulation in HepG2 cells, an effect preserved in 5-HT2A-mutant cells ($p < 0.05$ vs PA:OA) and fully recapitulated by selective 5-HT2B inhibition ($p < 0.01$ vs PA:OA). In LX-2 cells, Col1a1 protein and ACTA2 and MMP2 transcripts were significantly reduced ($p < 0.001$, $p < 0.001$, $p < 0.0001$ vs TGF-beta-activated cells, respectively). In GAN-fed mice, psilocybin restored rough endoplasmic reticulum (RER) and mitochondrial ultrastructure, reduced micro- and macrovesicular steatosis, and decreased hepatic ACTA2 expression ($p < 0.05$ vs GAN).
Conclusion: By selectively modulating hepatic lipid accumulation and early fibrogenic pathways through 5-HT2B antagonism, psilocybin may attenuate MASLD progression toward MASH. Its oral efficacy at non-psychedelic doses highlights serotonergic modulation as a novel and translatable therapeutic strategy in metabolic liver disease.

SAT-220

Comparing obesity related cancer incidence in metabolic dysfunction–associated steatotic liver disease patients undergoing pharmacologic versus bariatric interventions

Diwanshu Soni[1], Leith Ghani[1], Majd Aboona[1], Pooja Rangan[1], Mark Wong[1], Karn Wijarnpreecha[1], Rohit Nathan[1], Moises Nevah Rubin[1], Michael Fallon[1], Farah Husain[1], Ma Ai Thanda Han[1]. [1]*University of Arizona College of Medicine- Phoenix, Phoenix, United States*
Email: diwanshu.soni97@gmail.com

Background and aims: Patients with metabolic dysfunction-associated steatotic liver disease (MASLD) have an increased risk of obesity-related cancers involving the esophagus, stomach, colon and rectum, hepatobiliary, gallbladder, pancreas, breast, uterus, endometrium, ovary, kidney, brain, thyroid, and multiple myeloma. Bariatric surgery, Glucagon-Like Peptide-1 receptor agonists (GLP-1 RA), or Sodium-Glucose Cotransporter 2 inhibitors (SGLT2i) have been shown to reduce obesity-related cancer risk, but their comparative effects in MASLD are unknown. This study compares obesity-related cancer incidence in MASLD patients by intervention to inform management.
Method: This retrospective, multicenter study within the Banner Health System identified MASLD patients using ICD codes for non-alcoholic fatty liver disease and 1 of 5 metabolic criteria. We defined obesity-related cancers as follows: colon, rectal, breast, kidney, esophageal, gallbladder, pancreatic, ovarian, endometrial, thyroid, hepatocellular, and stomach cancer, multiple myeloma, meningioma and cholangiocarcinoma. ICD codes were used to identify obesity-related cancers. Only patients who received at least one intervention and followed up 12 months or more post-intervention were included. Interventions included bariatric surgery, GLP-1 RA, SGLT2i, or any combination of more than one therapy. Medication reconciliation confirmed SGLT2i and GLP-1 RA use. The bariatric surgery population was identified using relevant procedure ICD codes. Competing risk analysis was used to compare the incidence of obesity related cancer after 12 months of intervention in each group vs bariatric surgery alone after adjusting for confounders.
Results: This study includes 14,589 patients: 4.6% underwent bariatric surgery, 45.4% received therapy with GLP-1 RA, 27.2% were treated with SGLT2i, and 22.8% received combination therapy. Univariate analysis showed bariatric surgery had a significantly lower 12-month obesity related cancer incidence compared to SGLT2i but not significant to GLP1-RA, or combination therapy. Multivariate analysis showed there is no statistically significant difference in incidence of obesity-related cancer between different groups of intervention.
Conclusion: There is no strong evidence suggesting whether one therapy is more superior than the other given results are not statistically significant. Future studies with longer follow up and larger sample size are needed to validate these results and guide clinical decision making.

SAT-221-YI

Liver-specific deletion of Gpr146 and Angptl3 reduces plasma lipids and prevents development of diet-induced hepatic steatosis in mice

Umesh Tharehalli[1], Boyan Zhang[1], Antoine Rimbert[2], Nicolette Huijkman[1], Niels Kloosterhuis[1], Marieke Smit[1], Bart van de Sluis[1], Jan Albert Kuivenhoven[1]. [1]*Department of Pediatrics, Univeristy Medical Center Groningen, Groningen, Netherlands;* [2]*Nantes Université, CNRS, Inserm, l'institut du thorax, Nantes, France*
Email: u.tharehalli.mathada@umcg.nl

Background and aims: Increased hepatic secretion of very low-density lipoprotein (VLDL) is a shared pathogenic driver of metabolic dysfunction-associated steatotic liver disease (MASLD) and atherosclerotic cardiovascular disease (ASCVD). Hepatic cholesterol is exported in VLDL particles, converted to low-density lipoproteins (LDL) in the circulation, and returned to the liver, making this pathway a central regulator of cholesterol homeostasis and a major therapeutic target. G-protein–coupled receptor 146 (GPR146) is a novel regulator of cholesterol biosynthesis, and loss-of-function (LOF) variants and inactivation reduce LDLc. Angiopoietin-like protein 3 (ANGPTL3) is a liver-secreted inhibitor of VLDL lipolysis, and its inactivation lowers LDLc. We investigated whether combined hepatic targeting of GPR146 and ANGPTL3 reduces circulating lipids and prevents hepatic steatosis.
Method: Liver-specific deletion of *Gpr146* and *Angptl3* was achieved in mice using somatic gene editing to generate double liver knockout (DLKO) animals. Mice were maintained on a chow or high-fat diets (HFD; 60% kcal from fat). Plasma lipids, hepatic lipid content, histology, and alanine aminotransferase (ALT) levels were assessed.
Results: DLKO mice exhibited marked reductions in circulating cholesterol (58% on chow, 55% on HFD) and triglycerides (74% on chow, 48% on HFD) compared to controls. Hepatic fat content was reduced by 52% in chow-fed DLKO mice without evidence of liver injury. Under HFD conditions, DLKO mice showed a 32% reduction in hepatic fat and a 50% decrease in lipid droplet area (Oil Red O staining). Plasma ALT levels were significantly lower in HFD-fed DLKO mice.
Conclusion: Dual hepatic inhibition of GPR146 and ANGPTL3 produces additive reductions in circulating and hepatic fats, and protects mice against diet-induced hepatic steatosis without inducing liver injury. These findings highlight combined targeting of GPR146 and ANGPTL3 as a promising strategy for simultaneous addressing of MASLD and ASCVD. Future studies should determine whether this approach can reverse established fatty liver disease and define the underlying mechanisms.

SAT-225

A patient-derived hepatocyte organoid model for testing antioxidant strategies in paediatric metabolic dysfunction-associated steatotic liver disease

Francesca Tiano[1], Maria Rita Braghini[1], Flavia Grignaffini[1], Cristiano De Stefanis[2], Riccardo Cirelli[3], Paola Francalanci[4], Rita Alaggio[4], Carlo Dionisi-Vici[5], Marco Spada[3], Anna Alisi[1]. [1]*Research Unit of Genetics of Complex Phenotypes, Bambino Gesù Children's Hospital, IRCCS, Rome, Italy, Roma, Italy;* [2]*Core Facilities, Bambino Gesù Children's Hospital, IRCCS, Rome, Italy, Roma, Italy;* [3]*Division of Hepatobiliopancreatic Surgery, Liver and Kidney Transplantation, Bambino Gesù Children's Hospital, IRCCS, Rome, Italy, Roma, Italy;* [4]*Molecular Pathology Research Unit, Bambino Gesù Children's Hospital, IRCCS, Rome, Italy, Roma, Italy;* [5]*Division of Metabolic Diseases and Hepatology, Bambino Gesù Children's Hospital, IRCCS, Rome, Italy, Roma, Italy*
Email: anna.alisi@opbg.net

Background and aims: Metabolic dysfunction-associated steatotic liver disease (MASLD) is the most prevalent chronic liver disease worldwide, with an estimated prevalence of 10% of children affected. Despite growing interest in identifying effective therapies, current treatments for children are limited to lifestyle modifications aimed at reducing weight. However, some compounds with antioxidant and anti-inflammatory properties, such as vitamin E (VitE) and hydroxytyrosol (Hxt), were able to minimize steatosis and limit disease progression in children. Patient-derived liver organoids (PDLOs) offer a good model for testing new therapies and investigating disease pathogenesis while preserving patient-specific traits. Here, we analysed the protective effects of promising natural compounds, including Hxt, VitE, caffeine (Caf), and ginsenoside Rg1 (Rg1), in an organoid model of MASLD.
Method: Undifferentiated PDLOs were generated from healthy liver tissue obtained from paediatric patients and, subsequently, differentiated into hepatocyte organoids (HO). Palmitic and oleic acids (PA/OA; 1:2 ratio) were administered to HO for 48 hours for modelling in vitro steatosis. Antioxidant compounds (Hxt+VitE, Caf, Rg1) were

then administered at different doses to assess their efficacy against lipotoxicity. Cell viability was evaluated using a CellTiter assay, while lipid accumulation and reactive oxygen species (ROS) levels were quantified by BODIPY 493/503 and CM-H_2DCFDA staining, respectively. Expression of lipogenic and antioxidant genes was evaluated by qPCR.
Results: The PA/OA treatment effectively reproduced key MASLD features, including increased lipid accumulation, reduced cell viability, reflecting cytotoxicity, and altered expression of lipogenic and β-oxidation genes (e.g., *SREBF1, FASN, PPARA, CPT1A*). All tested natural compounds significantly attenuated PA/OA-induced lipid accumulation and intracellular ROS levels. Among compounds, the combination of Hxt+VitE was the most effective in down-regulating the expression of lipogenic and β-oxidation genes, and antioxidant (e.g., *NRF2, SOD2, CAT*) genes.
Conclusion: We found that Hxt plus VitE effectively counteracts lipotoxic and oxidative stress responses in our paediatric HO model that may offer a robust preclinical platform to identify novel therapeutic strategies for MASLD in children. Further implementation of the HO model could be obtained by adding the pro-fibrogenic hepatic stellate cells.

SAT-226
Annexin A1 deficiency exacerbates hepatic metabolic and oxidative dysregulation in streptozotocin-induced diabetic mice
Diego Santos[1,2], Kelly Bem[3], Alex Rosini-Silva[4], Artur Silva-Neto[1], Caroline Faria[5], Antonio Campos[3,6], Rafael Silva[7], Luiz Souza-Ferreira[8], Carlos Lenz-Cesar[3,6], Lila Oyama[1], Patricia Lima[2], Jose Sanches-Junior[1,9], Andreia Porcari[4], Helena Barbosa[3], Cristiane Gil[1,7]. *[1]Federal University of Sao Paulo, Sao Paulo, SP, Brazil; [2]Queen's University, Kingston, ON, Canada; [3]State University of Campinas, Campinas, SP, Brazil; [4]São Francisco University, Braganca Paulista, SP, Brazil; [5]São Paulo University, Sao Paulo, SP, Brazil; [6]Federal University of Ceara, Fortaleza, CE, Brazil; [7]São Paulo State University, Sao Jose do Rio Preto, SP, Brazil; [8]Universidade Federal de São Paulo, São Paulo, Brazil; [9]Federal University of ABC, Santo Andre, SP, Brazil*
Email: dias.diego@unifesp.br

Background and aims: Diabetes mellitus (DM) is a global public health problem that leads to systemic dysregulations affecting several tissues, including severe liver complications. In murine model, insulin resistance induced by a high-fat diet demonstrated that the absence of endogenous annexin A1 (AnxA1) exacerbates the characteristics of T2D. However, treatment with human recombinant AnxA1attenuates the development of insulin resistance in animals. Despite these important findings, its role in hepatocytes in DM1 has been little explored. This study aims to evaluate the role of AnxA1 in hepatocyte biology in a streptozotocin (STZ)-induced DM1 mouse model.
Method: Male C57BL/6 wild-type (WT) and AnxA1 knockout (AnxA1 −/−) mice were randomly distributed into control (CTR) and diabetes mellitus (DM) (n = 6 animals/group). DM was induced in mice with intraperitoneal injection of STZ (65 mg/kg × 5 days) or vehicle. After 12 weeks, livers were collected for different analyses. The procedures were approved by the UNIFESP Animal Experimentation Ethics Committee (n° 5520161123).
Results: In DM animals present decrease of body weight, increase of glycemic levels and decrease with triglycerides and VLDL, exclusively in DM AnxA1$^{-/-}$ mice. Increased triglycerides in the liver of DM AnxA1$^{-/-}$ justifies the decrease in plasma triglycerides. Livers showed higher levels of reactive oxygen species and SOD, but decreased catalase levels, in DM AnxA1−/− mice. Changes in mitochondrial dynamics and activity were observed, including increased fission, decreased mitochondrial number, and decreased complex V expression in DM AnxA1−/−, indicating greater hepatocyte damage via oxidative stress. We also observed increased glycogen in centrilobular veins and upregulation of *Pck1* and *Glut2* in the livers of DM AnxA1 −/−, indicating a greater gluconeogenic response. Finally, metabolomic analysis indicated relevant alterations in metabolic pathways in DM animals, mainly in alpha-linolenic and linoleic metabolism, catecholamine and carnitine biosynthesis, and oxidation of branched-chain fatty acids in DM AnxA1$^{-/-}$ mice, indicating greater fatty acid oxidation, liver regeneration, and a pro-inflammatory profile.
Conclusion: AnxA1 deficiency intensified oxidative imbalance, mitochondrial dysfunction, glycogen disruption, and compromise-dimmunometabolism, revealing the importance of hepatic homeostasis. AnxA1 emerges as a promising therapeutic target for mitigating diabetes-induced liver damage.

SAT-227
Transcriptomic analysis revealed distinct mechanisms underlying the synergistic effect of a fatty acid synthase inhibitor and resmetirom combination in LDL receptor knockout MASH mice
Wen-Wei Tsai[1], Shipra Gupta[1], Eveline Gart[2], Martine C. Morrison[2], Katharine Grimmer[1], Eduardo Martins[1], Marie O' Farrell[1]. *[1]Sagimet Biosciences, San Mateo, United States; [2]TNO, Leiden, Netherlands*
Email: wen-wei.tsai@sagimet.com

Background and aims: Increased *de novo* lipogenesis drives development of MASH, with fatty acid synthase (FASN) being the key enzyme in this pathway. Oral FASN inhibitor denifanstat demonstrated significant improvements in fibrosis and MASH resolution and prevented progression to cirrhosis in the Ph2b FASCINATE-2 MASH trial. The thyroid hormone receptor beta agonist resmetirom (Res), FDA-approved for MASH with F2/F3 fibrosis, increases lipid oxidation which decreases liver fat. In previous mouse studies, the combination of a FASN inhibitor and Res showed an increased improvement of liver histology in diet-induced MASH. This transcriptomic profiling study aimed to identify molecular mechanisms by which a FASN inhibitor and Res contributed to disease improvement.
Method: Male Ldlr-/- mice were fed a fast-food diet (FFD) for 18 weeks to induce MASH features and treated with TVB-3664 (a FASN inhibitor surrogate for denifanstat, 5 mg/kg, PO, QD) or Res (MGL-3196, 3 mg/kg, PO, QD) alone or in combination for 10 weeks. RNA-sequencing was performed using liver tissues.
Results: Combination treatment with TVB-3664 and Res demonstrated a greater effect than either agent alone, including greater improvements in ALT/AST, LDL-cholesterol lowering, and liver steatosis, inflammation and fibrosis in Ldlr-/- MASH mice. Principal component analysis (PCA) revealed a clear distinction in gene expression profiles between healthy normal chow and diseased FFD-fed groups. Both TVB-3664 and Res single treatments shifted the gene profile toward a healthier state. Notably, TVB-3664 or Res targeted distinct gene pathways underlying distinct aspects of disease, and the combination further amplified the move away from the disease state. Pathway analysis showed all treatments reversed many FFD-induced inflammatory and fibrosis regulators, such as TGF-beta, Col1a1 and alpha SMA, with the most pronounced effects in the combination group. TVB-3664 specifically deactivated inflammatory and fibrotic pathways, including hepatic fibrosis signaling and extracellular matrix organization; Res affected lipid metabolism, such as cholesterol biosynthesis and mitochondrial function.
Conclusion: Transcriptomic analysis confirmed that combination of a FASN inhibitor and resmetirom increased the anti-inflammatory and anti-fibrotic effects, and enhanced metabolic correction associated with lipid and cholesterol synthesis in a mouse model of MASH and dyslipidemia. These findings support future clinical evaluation of this combination therapy in MASH.

SAT-228

Sex-specific systemic inflammatory responses to high-fat diet are shaped by hepatic estrogen receptor alpha signalling

Hio Lam Phoebe Tsou[1], Clara Meda[2], Sara Della Torre[2], Antonio Riva[1].
[1]*Roger Williams Institute of Liver Studies, London, United Kingdom;*
[2]*Università degli Studi di Milano, Milan, Italy*
Email: a.riva@researchinliver.org.uk

Background and aims: Chronic inflammation contributes to metabolic-associated steatotic liver disease (MASLD) severity and progression. Hepatic estrogen receptor alpha (ERa) signalling limits liver disease development in pre-menopausal women compared to men or post-menopause, but its influence on systemic inflammation in response to hepatic lipid accumulation remains unclear.
Method: To evaluate this, sex-specific differences in systemic concentrations of 45 plasma cytokines were measured by Luminex in male and female liver-specific ERa-knockout (LERKO) C57BL/6J mice or control animals (ERa-floxed) exposed to high-fat diet (HFD) or normal chow/diet (ND) for 16 weeks (n = 80 total, 10 per group).
Results: Considering diet alone, HFD increased CXCL1, EGF, LDLR, and CCL3 ($p = 4.0 \times 10^{-4}$-2.6×10^{-2}) and decreased interleukin (IL)-27, IL-9, Flt3, and FGF-basic ($p = 3.0 \times 10^{-3}$-4.9×10^{-2}) in controls; in HFD-fed LERKO animals only BAFF was elevated compared to ND ($p = 2.0 \times 10^{-2}$). Considering sex alone, all males had higher GDF15, VEGF, CCL3, EGF, FGF-basic, and IL-1b ($p = 9.0 \times 10^{-6}$-4.4×10^{-2}) and lower IL-5, Eotaxin, and LDLR ($p = 6.0 \times 10^{-3}$-4.7×10^{-2}) compared to females, but only control males had, additionally, more IL-9, IL-2, CXCL10, IL-16, IL-27, RANTES, Flt3, IL-17A, and IL-1a ($p = 2.0 \times 10^{-5}$-4.9×10^{-2}) and less BAFF, CCL19, and Chitinase-3L1 ($p = 1.0 \times 10^{-4}$-1.1×10^{-2}); thus, systemic sex differences largely disappeared in LERKO animals, who resembled control females overall. Intriguingly, levels of M-CSF and LIX remained consistently elevated in LERKO males and females respectively regardless of diet, while HFD reduced male M-CSF ($p = 1.0 \times 10^{-2}$) and female LIX ($p = 9.0 \times 10^{-3}$) down to their respective opposite-sex levels in controls, suggesting liver-specific ERa as a physiological down-modulator of these myeloid/neutrophil-acting cytokines upon lipid overload. Notably, poorly detectable cytokines (<50% of animals) were measurable almost exclusively in males.
Conclusion: Liver-specific estrogen signalling shapes sex-specific systemic immunity and inflammatory adaptation to dietary lipids, preserving cytokine heterogeneity between sexes and modulating myeloid/neutrophil-mobilizing cytokines (M-CSF, LIX) in a sex-specific manner. Liver-specific estrogen signalling may thus act as a double-edged immunomodulator, limiting hepatic inflammation while enhancing systemic immunity, therefore sex-specifically contributing to disease establishment and progression in MASLD.

SAT-229-YI

Effects of farnesoid X receptor activation on the cellular microenvironment of human adipose tissue in metabolic disease

Lena Vosko[1,2], Emilian Jungwirth[1,2,3], Dagmar Silbert-Wagner[1], Judith Sommer[1], Lukas Gulden[1], Antonio Molinaro[4], Panzitt Katrin[1,2,5], Martin Wagner[1,2]. [1]*Research Unit for Translational Nuclear Receptor Research, Division of Gastroenterology and Hepatology, Medical University of Graz, Graz, Austria;* [2]*BioTechMed, Graz, Austria;* [3]*Center for Biomarker Research in Medicine, Graz, Austria;* [4]*Department of Molecular and Clinical Medicine/Wallenberg Laboratory, University of Gothenburg, Gothenburg, Sweden;* [5]*D&F Institute for Pathology, Medical University of Graz, Graz, Austria*
Email: lena.vosko@medunigraz.at

Background and aims: The bile acid-sensing farnesoid X receptor (FXR) adapts to metabolic changes in obesity, which is associated with metabolic dysfunction-associated steatotic liver disease. We previously demonstrated altered hepatic FXR binding and transcriptional activity in metabolic disease, promoting substrate utilization after ligand activation. Adipose tissue (AT) serves as energy reservoir and endocrine organ, but in obesity, it loses storage capacity and promotes systemic inflammation. While hepatic FXR signaling is well studied, its effects on human AT remain unclear. This study aimed to characterize, for the first time in humans, the cellular and transcriptional effects of FXR activation on subcutaneous AT (SAT) in metabolic disease.
Method: We performed single-nuclei RNA sequencing on SAT biopsies derived from non-obese and morbidly obese (BMI > 35 kg/m2) individuals treated with the FXR agonist obeticholic acid (25 mg/d OCA for 3 weeks) or placebo in a randomized double-blind trial.
Results: Sixteen SAT samples (four per group) yielded 34,529 quality-filtered nuclei. SAT from obese patients showed increased immune cell fractions and enriched pro-inflammatory pathways, with reduced adipocyte abundance. NR1H4 (FXR) expression was low or absent in most samples. Adipocytes and adipose stem and progenitor cells (ASPCs) each accounted for approximately 20% of nuclei. Subclustering revealed that OCA-treated obese patients exhibited reduced immune-related and angiogenic adipocyte subpopulations, accompanied by a significant downregulation of pro-inflammatory genes (CXCL17, CEBPB, HLA-DRB1) and pathways involved in inflammatory response in all adipocytes, whereas metabolic effects where minor. Within ASPCs, oxidative phosphorylation and mitochondrial energy pathways were suppressed. In addition, pro-inflammatory genes (CFB, PPIA, IFI6) and humoral immune response pathways were downregulated, and PPARG-positive committed preadipocytes with inflammatory signatures were less abundant.
Conclusion: This study provides the first single-nucleus map of FXR agonism effects on human AT and its stromal microenvironment. Overall, OCA reduced pro-inflammatory signaling across multiple SAT subpopulations. Minimal local FXR expression suggests that OCA-mediated effects are indirect, supporting the existence of a liver–adipose or intestine–adipose signaling axis modulating immune responses in adipocytes and progenitors.

SAT-230

Multi-Omics analyses of fetal hepatoblasts reveals interferon-regulatory factor 9 as a female-biased master modulator of lipotoxicity and antioxidant defense

Celina Uhlemeyer[1,2], Jonas Voß[1,2], Marten Schouwink[3], Adam Majcher[4,5], Leon Regnery[1,2], Lea Matern[1,2], Anna Heusch[1,2], Michael Rieck[1,2], Cesare Granata[2,6], Marc Jonuscheit[2,6], Benedict Korzekwa[2,6], Sonja Hartwig[2,7], Anna Hamacher[8], Stefan Lehr[2,7], Thorsten Wachtmeister[9], Lidia Cantacorps[2,10], Marlene Piribauer[2,7], Christin Krause[2,11], Tim Dorweiler[1,2], Sonja Heiduschka[1,2], Martina Gimpfl[12], Jan Rozman[2,13,14], Birgit Rathkolb[2,13,15], Caroline Schlegel[1,2], Jennifer Kuboth[1,2], Bedair Dewidar[2,6], Linda Große-Segerath[1,2,16], Daniel Eberhard[2,16], Nadine Müller[1,2], Soner Oener-Sieben[17], Martin Hrabe de Angelis[2,13,18], Karl Köhrer[9], Volker Burkart[2,7], Henriette Kirchner[2,11], Rachel Lippert[2,10,19], Vera Schrauwen-Hinderling[2,7], Eckhard Lammert[1,2,16], Michael Roden[2,7,20], Thorsten Hornemann[4,5], Hadi Al-Hasani[2,7,21], Regina Ensenauer[3,17], Bengt Belgardt[1,2]. [1]*Institute for Vascular and Islet Cell Biology, German Diabetes Center (DDZ), Leibniz Center for Diabetes Research at Heinrich Heine University, Düsseldorf, Germany;* [2]*German Center for Diabetes Research (DZD e.V.), Düsseldorf, Germany;* [3]*Department of General Pediatrics, Neonatology and Pediatric Cardiology, Medical Faculty, University Hospital Düsseldorf, Heinrich-Heine-University, Düsseldorf, Germany;* [4]*Center for Integrative Human Physiology, University of Zürich, Zürich, Switzerland;* [5]*Institute for Clinical Chemistry, University Hospital, Zürich, Switzerland;* [6]*Institute for Clinical Diabetology, German Diabetes Center, Leibniz Center for Diabetes, Düsseldorf, Germany;* [7]*Institute for Clinical Biochemistry and Pathobiochemistry, German Diabetes Center, Leibniz Center for Diabetes Research at Heinrich Heine University, Düsseldorf, Germany;* [8]*Center for Advanced Imaging, Heinrich Heine University Düsseldorf, Düsseldorf, Germany;* [9]*Genomics & Transcriptomics Laboratory, Biological and Medical Research Centre (BMFZ), Heinrich Heine University Duesseldorf, Düsseldorf, Germany;* [10]*Department of Neurocircuit Development and Function, German Institute of Human Nutrition Potsdam-Rehbruecke,*

Nuthetal, Germany; [11]Institute for Human Genetics, Division Epigenetics & Metabolism, University of Lübeck, Lübeck, Germany/Center for Brain Behavior and Metabolism CBBM, Lübeck, Germany; [12]Research Center, Dr. von Hauner Children's Hospital, Ludwig-Maximilians-University Munich, Munich, Germany; [13]German Mouse Clinic, Institute of Experimental Genetics, Helmholtz Zentrum München (HMGU-IEG), Neuherberg, Germany; [14]Luxembourg Centre for Systems Biomedicine, University of Luxembourg, Belvaux, Luxembourg; [15]Institute of Molecular Animal Breeding and Biotechnology, Gene Center, Ludwig-Maximilians-University München, Munich, Germany; [16]Institute of Metabolic Physiology, Heinrich Heine University, Düsseldorf, Germany; [17]Institute of Child Nutrition, Max Rubner-Institut, Federal Research Institute of Nutrition and Food, Karlsruhe, Germany; [18]TUM School of Life Sciences, Technische Universität München, Freising, Germany; [19]NeuroCure Cluster of Excellence, Charité-Universitätsmedizin Berlin, Berlin, Germany; [20]Department of Endocrinology and Diabetology, Medical Faculty and University Hospital Düsseldorf, Heinrich Heine University, Düsseldorf, Germany; [21]Medical Faculty, Heinrich Heine University, Düsseldorf, Germany
Email: celina.uhlemeyer@tron-mainz.de

Background and aims: Maternal obesity in pregnancy (MO) predisposes offspring to development of metabolic dysfunction-associated steatotic liver disease (MASLD) during their adulthood, with preclinical evidence demonstrating higher MASLD incidence in male offspring. Pathological effects of MO on hepatocyte precursors (hepatoblasts) *in utero* have been suggested, but analysis of fetal hepatoblasts (FHB) has been complicated as they only comprise a minority of embryonic liver cells.
Method: Here, we combine purification of differentiation-competent FHB with a Multi-Omics approach and magnetic resonance imaging and spectroscopy (MRI/MRS) to investigate the effects of MO on FHB and fetal livers. Additionally, we use primary human hepatocytes and a human hepatocyte cell line to investigate the regulation and protective effect of a candidate protein regarding oxidative stress and mitochondrial fragmentation.
Results: Upon MO, lipid-handling pathways are upregulated in FHB of both sexes. In contrast, we find that mRNAs and proteins involved in mitochondrial respiration and oxidative stress response are modulated in a sex-biased manner, with a higher antioxidant response in female FHB paralleled by higher H_2O_2 release of male fetal liver. Interferon-regulatory factor 9 (IRF9) expression is increased in female FHB upon exposure to MO, and retained in livers of adult female offspring in two independent models of maternal overnutrition in pregnancy. In line, female but not male primary human hepatocytes increase IRF9 expression upon acute palmitate treatment. We show that IRF9 is essential for cellular resistance against oxidative stress, and is necessary to prevent pathogenic diacylglycerol and sphingolipid accumulation, mitochondrial fission, and lipid-induced insulin resistance. Mechanistically, we demonstrate that IRF9 abundance is increased by the master regulator of the cellular antioxidant response, NRF2, and decreased by the lipotoxicity-associated microRNA miR20b-5p. We also link IRF9 expression to mitochondrial fission, which has been linked to hepatic insulin resistance and MASLD, and can impair developmental potential in stem cells.
Conclusion: Our study uncovers a sex-biased fetal response to a prenatal obesogenic environment that predisposes to hepatic steatosis during adult life. Further, we show that IRF9 is regulated in a sex-biased manner, and is essential to overcome acute oxidative stress and prevent accumulation of deleterious bioactive lipids and hence insulin resistance in human liver cells.

SAT-231
Artificial intelligence for characterisation of inflammation in chronic liver disease

Jack Breen[1], Kezia Hobson[1,2], Dylan Windell[1], Alastair Magness[1], Paul Aljabar[1], Phil Wakefield[1], Andrea Dennis[1], Caitlin Langford[1], Kenneth Fleming[1,3], Eve Fryer[1,4], Tim Kendall[1,5], Robert D. Goldin[1,2].
[1]Perspectum Ltd, Oxford, United Kingdom; [2]Section of Pathology, Imperial College, London, United Kingdom; [3]Green Templeton College, University of Oxford, Oxford, United Kingdom; [4]Department of Cellular Pathology, John Radcliffe Hospital, Oxford, United Kingdom; [5]Institute for Regeneration and Repair, University of Edinburgh, Edinburgh, United Kingdom
Email: jack.breen@perspectum.com

Background and aims: Quantifying inflammation is a key component of liver disease assessment, with grading systems such as the NAFLD activity score (NAS) in metabolic dysfunction-associated steatotic liver disease (MASLD) and metabolic-associated steatohepatitis (MASH), and modified Hepatic Activity Index (mHAI - Ishak) scoring for chronic hepatitis. NAS assesses lobular inflammation, while mHAI includes portal and interface inflammation. Pathologist agreement for inflammation grading is poor, with clinical trials often relying on consensus scoring. We present an automated approach to quantifying inflammation in lobular, portal, and interface regions across liver disease whole slide images (WSIs).
Method: WSIs from 63 patients with autoimmune hepatitis (AIH; mean age 21, 54% female, 56% on treatment), 87 with MASLD (mean age 55, 69% male), and 232 MASH (mean age 56, 58% female) were analysed to detect and classify nuclei using a previously fine-tuned deep learning tool (HoVer-NeXt). Inflammatory cells were then identified by removing hepatocyte nuclei and detecting regions of high nuclear density. Density of inflammatory cells in the portal tract, portal interface, and lobular regions of the liver was then measured using an automated portal tract segmentation approach. Agreement with pathologist scores was assessed using Spearman's rho (rs). Bonferroni corrections were applied for multiple comparisons.
Results: Automated assessment of inflammation moderately correlated with pathologist scores (lobular inflammation rs = 0.31, portal inflammation rs = 0.44, interface inflammation rs = 0.37; p-values<0.0001), representing an improvement over previously reported correlation (rs = 0.27, 0.22, and 0.44 respectively). Significant differences in inflammation between MASLD, MASH, and AIH were observed, with the clearest difference in interface inflammation (median density 171, 221, 335 cells/mm^2, respectively; Wilcoxon $p < 0.001$).
Conclusion: Building on our prior work, the proposed method for detecting inflammation in liver biopsies shows improved correlation with pathologist grading and better differentiation of disease states compared with previous approaches. Improving the consistency and accuracy of disease grading may increase operational efficiency in pathology workflows, streamline clinical trial assessments, and enhance sensitivity to treatment effects, supporting more precise clinical decision-making.

SAT-232
STING promotes the progression of metabolic dysfunction-associated steatotic liver disease by regulating the WIPI2/ATG5-p62 autophagy signaling axis

Xiaoxiao Wang[1], Wang Zilong[1], Rui Huang[1], Huiying Rao[1], Feng Liu[1].
[1]Peking University People's Hospital, Peking University Hepatology Institute, Infectious Disease and Hepatology Center of Peking University People's Hospital, Beijing Key Laboratory of Hepatitis C and Immunotherapy for Liver Diseases, Beijing International Cooperation Base for Science and Technology on NAFLD Diagnosis, Beijing, China
Email: liu1116m@sina.com

Background and aims: Macrophage dysfunction critically contributes to metabolic dysfunction–associated steatohepatitis (MASH) progression, yet the interplay between metabolic stress, innate

immunity, and autophagy remains unclear. This study examines the dynamic crosstalk between STING signaling and the WIPI2/ATG5–p62 autophagy pathway in lipid-loaded macrophages and a murine MASLD model to elucidate their roles in disease pathogenesis.
Method: In vitro, THP-1 and RAW264.7 cells were treated with low (0.2 mM OPA) or high (1 mM OPA) fatty acids to model steatosis. STING knockdown and p62 overexpression were performed, and proteins (STING, p-TBK1, WIPI2, ATG5, p62, LC3-II) were analyzed by immunoblotting. In vivo, MASH-fibrosis was induced via WDHF+CCl4 and MCD diets; histology (H&E, Sirius Red) and liver protein expression were assessed. scRNA-seq of liver immune cells from control and MASH mice characterized MoMFs.
Results: In mild/moderate steatotic macrophages, STING expression was upregulated. Concurrently, autophagy-related proteins WIPI2, ATG5, p62 and LC3-II were increased ($p < 0.05$). Knockdown of STING reversed these elevations, indicating STING positively regulates autophagy flux under mild lipid stress. In severe steatosis macrophages, STING pathway activation (increased STING and p-TBK1) was observed alongside decreased p62 levels ($p = 0.032$). Overexpression of p62 suppressed this STING pathway activation, revealing a negative feedback mechanism. In murine MASLD models, STING expression increased with disease severity, peaking during fibrosis. In contrast, autophagy markers (WIPI2, ATG5, p62) showed a biphasic response: an initial upregulation in early MASH, followed by a significant decline in advanced fibrosis, suggesting autophagy failure at late stages. scRNA-seq analysis of MASH-fibrotic livers revealed a increased heterogeneity of MoMFs. Importantly, within MoMFs, genes associated with both STING signaling and the core autophagy machinery (WIPI2, ATG5, p62) were co-upregulated, indicating their concurrent activation in the fibrotic microenvironment.
Conclusion: Our findings identify a stage-specific crosstalk between STING signaling and autophagy in macrophages during MASLD/MASH progression. In vivo, persistent STING activation coincides with progressive autophagy failure, particularly within the expanded pro-fibrotic MoMF population, likely driving chronic inflammation and fibrosis. Targeting the STING–autophagy axis in MoMFs may therefore represent a promising therapeutic strategy for MASH.

SAT-233
Chemical conjugation of Myrcludex B and Triiodothyronine for liver-specific targeting
Dandan Wu[1], Claire Groenen[1], Xin Hu[2], Suzanne Duijst[3], Dagmar Tolenaars[3], Isabelle Bolt[3], Coen Paulusma[1], Coert J Zuurbier[2], Richard DiMarchi[4], Brian Finan[5], Wietse In het Panhuis[1], Anita Boelen[6], Stan F.J. van de Graaf[1], Bin Yang[4]. *[1]Tytgat Institute for Liver and Intestinal Research, Amsterdam University Medical Centers, University of Amsterdam, Amsterdam Gastroenterology, Endocrinology Metabolism (AGEM), Amsterdam University Medical Centers, Amsterdam, Netherlands; [2]L. E. I. C. A, Amsterdam Cardiovascular Science, Laboratory of Experimental Intensive Care and Anesthesiology, Department of Anesthesiology, Amsterdam University Medical Centers, Amsterdam, Netherlands; [3]Tytgat Institute for Liver and Intestinal Research, Amsterdam University Medical Centers, University of Amsterdam, Amsterdam, Netherlands; [4]Novo Nordisk Research Center Indianapolis, Inc. Indianapolis, Department of Chemistry, Indiana University, Bloomington, IN, United States; [5]Novo Nordisk Research Center Indianapolis, Inc. Indianapolis, IN, United States; [6]Endocrine Laboratory, Department of Laboratory Medicine, Amsterdam Gastroenterology Endocrinology Metabolism, Amsterdam University Medical Centers, University of Amsterdam, Amsterdam, Netherlands*
Email: k.f.vandegraaf@amsterdamumc.nl

Background and aims: Thyroid hormones (TH) enhance lipid metabolism but therapeutic application by systemic administration is limited due to cardiovascular and skeletal toxicity. Liver-specific delivery of TH, using TH mimetics or TH receptor (TR)-b agonists (Resmetirom), is therefore a promising frontier to improve hepatic lipid metabolism while minimizing off-target effects. Myrcludex B is a synthetic peptide targeting liver-specific bile salt transporter sodium taurocholate co-transporting polypeptide (NTCP) and has shown anti-steatotic potential in preclinical studies. We investigated whether liver-targeted delivery of triiodothyronine (T3), the active hormone, could be achieved while mitigating systemic toxicity through chemical conjugation of T3 to Myrcludex B (Myr-T3).
Method: FVB *oatp1a/1b*$^{-/-}$/*hOATP1B1*$^{+/+}$ mice were used to mimic human hepatic bile salt dynamics. Obesity was induced by 12 weeks of high-fat diet (HFD). Mice then received daily subcutaneous injections of Myr-T3 (100 nmol/kg), Myrcludex B (100 nmol/kg), T3 (50 nmol/kg), or vehicle for 6 weeks while continuing HFD. Cardiac toxicity was determined by in vivo echocardiography. To further assess liver specificity, a follow-up study was performed in C57BL/6J mice fed HFD, followed by 1-week treatment with lower dosing of Myr-T3 (25 nmol/kg), T3 (25 nmol/kg), or vehicle.
Results: HFD significantly increased liver-to-body weight ratios, plasma cholesterol levels, and hepatic steatosis. Myr-T3 treatment increased plasma bile acid levels (4.5-fold). Compared to T3 alone, Myr-T3 achieved greater cholesterol lowering (–15% vs –35%) but also increased cardiac toxicity to a greater extent. Hepatic steatosis, assessed by Oil Red O staining, was similar between all groups. Dosed at 25 nmol/kg, Myr-T3 and T3 reduced plasma cholesterol to comparable levels (61% vs 54%). Hepatic expression of T3-responsive genes was higher in the Myr-T3 group compared with T3 alone, whereas pituitary expression of T3-responsive genes was similar between these two groups.
Conclusion: Chemical conjugation of Myrcludex B and T3 preserves the biological activity of both components. However, the current design did not prevent systemic toxicity under high doses, and no clear improvement in liver specificity over T3 alone was observed at lower doses. While the concept demonstrates hepatic efficacy, structural optimization of the fusion is required to improve the organ specificity.

SAT-234
NK-Cell immaturity fuels ALCAM-dependent hepatocyte transformation and propels MASH-associated fibrosis toward carcinogenesis
Anliang Xia[1], Shuyan Sheng[1], Siyuan Liu[1], Shaobo Zhang[1], KaiPeng Hu[1], Beicheng Sun[1]. *[1]The First Affiliated Hospital of Anhui Medical University, Hefei, China*
Email: xiaanliang@ahmu.edu.cn

Background and aims: Metabolic dysfunction-associated steatotic liver disease (MASLD) progresses from steatosis to fibrosis, cirrhosis, and hepatocellular carcinoma (HCC). The marked resistance of MASH-derived HCC to immune checkpoint inhibitors highlights the need to elucidate how persistent metabolic injury reshapes the liver microenvironment to drive malignant transformation.
Method: We constructed a multi-stage single-cell and spatial transcriptomic atlas of MASLD to map immune-parenchymal co-evolution. CellChat and neighborhood analyses were used to identify dysfunctional NK-hepatocyte communication. ALCAM expression dynamics were validated in multiple MASLD mouse models. Hepatocyte-specific ALCAM knockout mice were generated to interrogate mechanisms using single-cell/spatial sequencing, CRISPR screening, and proteomics.
Results: NK cells track MASLD progression via a stage-specific shift from mature to immature phenotypes. Mature NK cells inhibit hepatocytic ALCAM via the CD6-ALCAM axis, while immature ones fail, leading to sustained ALCAM expression. MASH-associated fibrosis defines the disease continuum as the key bridge to HCC, featuring irreversible NK subset shifts and ECM stiffening that reprograms hepatocytes through biological and mechanical cues. ALCAM then drives hepatocyte oncogenesis via two mechanisms. Origin: Multi-omics reveal ALCAM-mediated microtubule remodeling and asymmetric division, yielding oncogenic progenitor-like cells. Fate: In fibrotic matrices, ALCAM heightens genomic instability, with

CRISPR-identified H2AX as a co-dependency factor sustaining G2/M repair, anoikis resistance, and aberrant clonal expansion.
Conclusion: NK-cell immaturity-induced ALCAM upregulation establishes a core positive-feedback circuit linking hepatocyte transformation with fibrotic microenvironmental evolution, thereby sustaining the progression of MASH-associated fibrosis toward carcinogenesis.

SAT-235
A novel covalent inhibitor targeting ASC oligomerization mitigates MASH by inhibiting NLRP3 inflammasome activation
Ying Hong[1], Cheng Luo[1], Cen Xie. [1]*Shanghai Institute of Materia Medica, Chinese Academy of Sciences, Shanghai, China*
Email: hybottle@126.com

Background and aims: The activation of the NLRP3 inflammasome plays a pivotal role in driving inflammation and fibrosis in metabolic dysfunction-associated steatohepatitis (MASH). Although various pathways can lead to NLRP3 activation, the oligomerization of the adaptor protein ASC constitutes a crucial, convergent step in the assembly of the inflammasome. Targeting this specific step directly offers a promising yet underexplored therapeutic strategy. This study aimed to identify and characterize a novel inhibitor that specifically obstructs ASC oligomerization and to assess its efficacy in a preclinical model of MASH.
Method: We developed and synthesized a library of small molecules utilizing a covalent-binding scaffold designed to target a critical cysteine residue on ASC. The lead compound, Compound A, underwent initial *in vitro* screening using LPS/ATP-stimulated macrophages to evaluate IL-1β secretion and ASC speck formation through immunofluorescence analysis. The covalent interaction of Compound A with ASC was verified *via* mass spectrometry. For *in vivo* assessment, C57BL/6J mice were subjected to a GAN diet for a duration of 26 weeks to induce advanced metabolic-associated steatohepatitis (MASH). Beginning in week 17, the mice received daily treatments of either Compound A (*i.g.*) or vehicle control.
Results: Compound A showed strong covalent binding to ASC, inhibiting NLRP3-dependent ASC oligomerization and IL-1β release in macrophages. In the MASH model, it significantly reduced body weight gain and hepatic lipid accumulation, as evidenced by lower liver triglyceride content and improved steatosis scores. Histologically, Compound A decreased lobular inflammation, fibrosis, and liver injury. It also improved systemic metabolic homeostasis, with treated mice showing better glucose tolerance, and enhanced insulin sensitivity. Mechanistically, Compound A disrupts ASC's interaction with NLRP3, preventing large ASC oligomer formation, which showed reduced ASC speck formation and Caspase-1 cleavage.
Conclusion: We have identified a first-in-class covalent inhibitor that specifically targets ASC oligomerization. This compound potently inhibits NLRP3 inflammasome activation and demonstrates significant efficacy in ameliorating inflammation, fibrosis, and steatosis in MASH model. Our findings validate the inhibition of the NLRP3-ASC axis as a viable therapeutic strategy and present a promising lead compound for the treatment of MASH.

SAT-236
Neddylation of STAT3 is a potential therapeutic target for MASLD
Ping Xie[1], Zhen Zhang[2], Fan Liu[1], Fei Zhao[3]. [1]*Capital Medical University, Department of Cell Biology, Beijing, China;* [2]*Department of Neurosurgery, Shandong Provincial Hospital affiliated to Shandong First Medical University, Jinan, China;* [3]*Department of Ultrasound, Beijing Jishuitan Hospital, Capital Medical University, Beijing, China*
Email: xiep@ccmu.edu.cn

Background and aims: Metabolic dysfunction associated steatosis liver disease (MASLD) increases the risk of developing steatohepatitis, liver cirrhosis, and liver cancer. Neddylation, a ubiquitin-like post-translational modification, has been proven to play a crucial role in tumor progression.
Method: The expression levels of neddylation modification in the MASLD model were evaluated by western blotting and immunohistochemistry. To investigate the role of neddylation in MASLD progression, the neddylation E1 inhibitor MLN4924 was administered to treat the MASLD mouse model. Subsequently, IP-MS and immunoprecipitation were conducted to identify STAT3 as a substrate of neddylation modification. Finally, the mechanisms and functional implications of STAT3 neddylation modification in the progression of MASLD were thoroughly examined through immunoprecipitation, western blotting and fatty acid uptake assays.
Results: Here, we suggested that dysregulation of neddylation was a critical aggravator of MASLD. The neddylation inhibitor MLN4924 effectively reduced lipid accumulation, and obviously suppressed the activation of JAK-STAT signaling pathway. Mechanistically, we identified the signal transducer and activator of transcription 3 (STAT3) as a neddylation substrate involved in MASLD. Our data showed that neddylation modification might be essential for STAT3 dimerization induced by acetylation and activation. Functionally, inhibition of neddylation modulates STAT3 downstream genes. More importantly, the combination of MLN4924 with a STAT3 inhibitor significantly blocked fatty acid uptake and upregulated apoptosis-related genes.
Conclusion: Our findings support a novel regulatory mechanism involving dysregulation of neddylation during MASLD progression and highlight its utility as a potential therapeutic target for MASLD.

SAT-237
Pemafibrate attenuates liver fibrosis and reduces predicted gut lipopolysaccharide biosynthesis and mucin degradation in a metabolic dysfunction-associated steatohepatitis rat model
Yasunori Yamamoto[1], Masaya Okada[2], Masakazu Hanayama[3], Taisei Murakami[1], Kazuki Niida[1], Teruki Miyake[1], Osamu Yoshida[1], Eiji Takeshita[1], Yoshio Ikeda[4], Yoichi Hiasa[1]. [1]*Ehime University Graduate School of Medicine, Toon, Ehime, Japan;* [2]*Seto Inland Sea Hospital, Imabari, Ehime, Japan;* [3]*Matsuyama Shimin Hospital, Matsuyama, Ehime, Japan;* [4]*Ehime University Hospital, Toon, Ehime, Japan*
Email: y79y81@gmail.com

Background and aims: Pemafibrate is a selective peroxisome proliferator-activated receptor α (PPAR α) modulator reported to improve liver enzymes and stiffness in metabolic dysfunction-associated steatohepatitis (MASH). PPAR α is expressed in the liver, intestinal epithelium, and mucosal immune cells, suggesting involvement in gut-liver crosstalk. We evaluated pemafibrate's effects on liver fibrosis and gut microbiota, including predicted microbial functions related to endotoxin and mucin metabolism, in a MASH rat model.
Method: A MASH rat model was induced by a high-fat, high-cholesterol diet. Rats received pemafibrate (0.1 mg/kg) or vehicle for 7 days. Liver fibrosis was quantified by Sirius Red and α-smooth muscle actin (α-SMA) staining. Hepatic expression of *Tgfb*, *Col1a1*, *Acta2*, *Timp1*, and *Serpine1* was quantified by real-time PCR. Fecal 16S rRNA sequencing and PICRUSt2-based KEGG orthology (level 4) were used to compare predicted functions related to lipopolysaccharide (LPS) biosynthesis and transport, mucin degradation, and short-chain fatty acid synthesis.
Results: Pemafibrate treatment significantly reduced liver fibrosis area compared to controls, with consistent suppression of fibrosis-related genes and hepatic stellate cell activation markers. Gut microbiota analysis revealed a significant decrease in inflammation-associated genera linked to LPS and hydrogen sulfide production, such as *Desulfovibrio*, *Pseudomonas*, and *Helicobacter*, in the pemafibrate group. Additionally, the abundance of the mucin-degrading *[Ruminococcus] torques group* was reduced. Consistent with these compositional changes, functional prediction analysis indicated that predicted lipid A biosynthesis and LPS transport pathways were reduced, and mucin degradation functions decreased.

Conversely, while some short-chain fatty acid-producing bacteria decreased, gene abundance for the terminal step of butyrate synthesis showed no significant difference, suggesting that butyrate production capacity—crucial for gut barrier protection—was preserved at the predicted functional level.
Conclusion: Pemafibrate attenuated liver fibrosis in a MASH rat model, accompanied by gut microbiota shifts and reduced predicted functions related to LPS biosynthesis/transport and mucin degradation. These findings suggest that selective PPAR α modulation may contribute to antifibrotic effects through gut-liver crosstalk and represent a promising gut-liver axis-targeted therapeutic approach for MASH.

SAT-238

Hepatic cholesterol metabolic dysregulation drives lean MASLD progression via PEPD secretion from expanded Marco+ macrophages

Yingcheng Yao[1], Junping Shi[2], Danyang Li[3]. *[1]Hangzhou Normal University, Hangzhou, China; [2]The Affiliated Hospital of Hangzhou Normal University, Hangzhou, China; [3]Chongqing Medical University, Chongqing, China*
Email: 185048440@qq.com

Background and aims: Lean MASLD represents a distinct subpopulation within the MASLD spectrum, yet its core metabolic vulnerabilities and pathogenic mechanisms remain understudied.
Method: Here, we integrate clinical, multi-omics, and animal model data to define cholesterol-driven pathology in lean MASLD.
Results: We demonstrate that cholesterol overload remodels liver zonation—specifically expanding zone 1—which critically promotes disease progression. Single-nucleus RNA sequencing and metabolomics reveal the expansion and spatial redistribution of $Marco^+$ macrophages, a metabolically active subset induced by taurocholic acid (TCA), in lean MASLD livers. These macrophages drive metabolic dysregulation via TMED10-mediated secretion of PEPD and other proteins (e.g., LNPEP, MFHAS1), facilitating macrophage-hepatocyte crosstalk and liver-adipose interactions. Clinically, serum PEPD levels are elevated in lean MASLD and may serve as a biomarker.
Conclusion: Our findings establish cholesterol-induced hepatic $Marco^+$ macrophages as key contributors to lean MASLD pathogenesis through PEPD secretion, offering novel therapeutic targets for this metabolically distinct phenotype.

SAT-239

STING aggravates liver fibrosis in chronic hepatitis B concurrent with metabolic dysfunction-associated steatotic liver disease by modulating gut microbiota and inducing macrophage-derived lysozyme expression

Binghui Yu[1], Suping Hai[1], Wenhui Wu[1], Qiang Gao[1], Xitang Li[1], Xizhe Zheng[1], Feiyang Xu[1], Junjian Hu[1], Qin Ning[1], Xiaojing Wang[1]. *[1]Department of Infectious Diseases, Tongji Hospital, Tongji Medical College and State Key Laboratory for Diagnosis and Treatment of Severe Zoonotic Infectious Disease, Huazhong University of Science and Technology, Wuhan, China*
Email: wxjmoon@hotmail.com

Background and aims: The coexistence of Metabolic Dysfunction-Associated Steatotic Liver Disease (MASLD) in individuals with Chronic hepatitis B (CHB) has been increasing annually. In the early stage of MASLD, high-fat diet (HFD)-induced impairment of the intestinal epithelial barrier may activate stimulator of interferon genes (STING). Interactions along the gut-liver axis are likely to contribute to adverse outcomes in this comorbidity. We hypothesize that STING activation during the early stage of the concurrent presence of CHB and MASLD exacerbates liver disease progression by altering the gut microenvironment.
Method: A mouse model of CHB concurrent with MASLD was established by hydrodynamic injection of pAAV/HBV1.2 combined with feeding a high-fat diet. The study utilized STING knockout mice ($Sting^{-/-}$), alongside their littermate controls. In vitro, THP-1 cells were administered a STING agonist, whereas LX-2 cells were subjected to lysozyme stimulation and appropriate controls were established for all treatments. The evaluation of STING and lysozyme-associated markers was conducted using Western blotting, immunofluorescence and enzyme-linked immunosorbent assay.
Results: At 8 weeks, CHB concurrent with MASLD mice exhibited moderate hepatosteatosis and lobular inflammatory infiltration compared to those in the CHB group. Compared to mice with CHB or MASLD alone, the comorbidity group exhibited more severe gut barrier disruption and altered microbiota composition. The comorbid mice showed increased abundances of Blautia, and decreased abundances of Alloprevotella relative to the CHB group. STING expression and activation were elevated in intestinal tissue. STING knockout restored gut barrier integrity and microbiota balance. Fecal microbiota transplantation from $Sting^{-/-}$ mice alleviated steatosis and reduced ALT, AST, and free fatty acid levels. STING was highly enriched in intestinal macrophages, and its activation promoted lysozyme expression. Elevated serum lysozyme and increased CD64/lysozyme co-localization were observed in the comorbidity model. In vitro, lysozyme stimulated LX-2 activation, upregulating collagen I and fibronectin.
Conclusion: Our study demonstrates that intestinal macrophage STING activation modulates gut microbiota in the early stage of the concurrent CHB and MASLD model and promotes liver fibrosis via lysozyme-induced hepatic stellate cell activation. Consequently, lysozyme may represent a potential therapeutic target for mitigating fibrosis in those comorbidity patients.

SAT-240

Development of a novel animal model for acute-on-chronic liver failure in metabolic dysfunction-associated steatotic liver disease: highlighting the critical role of neutrophil

Rui Zhao[1], Qi Yang[1], Hui Liu[2], Xiao Che[1], Chengxuan Yao[1], Xinli Mao[3], Manman Xu[1], Yu Chen[1]. *[1]Fourth Department of Liver Disease (Difficult & Complicated Liver Diseases and Artificial Liver Center), Beijing You'an Hospital, Capital Medical University, Beijing, China; [2]Department of Pathology, Beijing You'an Hospital, Capital Medical University, Beijing, China; [3]Department of Gastroenterology, Taizhou Hospital of Zhejiang Province Affiliated to Wenzhou Medical University, Linhai, China*
Email: chybeyond1071@ccmu.edu.cn

Background and aims: Acute-on-chronic liver failure (ACLF) is a high-mortality syndrome triggered by acute insults in patients with chronic liver disease. Coagulopathy in critically ill patients largely precludes tissue sampling, highlighting the urgent need for the establishment of etiologically relevant animal models. Metabolic dysfunction-associated steatotic liver disease (MASLD), a growing public health concern, can progress to cirrhosis and subsequently increase MASLD-ACLF prevalence. While animal models exist for MASLD or ACLF separately, none replicates ACLF development on a MASLD background.
Method: Reference to prior research, two MASLD models was established: B6-Alms1-del mice on a Western diet and C57/B6J mice on a choline-deficient high-fat (CDAHFD) diet. Varying modeling durations induced steatohepatitis or stage 3 fibrosis. After LPS/D-GalN acute insult, collected serum for liver function tests and liver tissues for histopathology, transcriptomics, and fluorescence-activated sorting of CD45+ cells for single-cell RNA sequencing. Multiplex immunofluorescence was utilized to assess intestinal barrier damage and the potential 'gut mucosal barrier failure' during ACLF progression.
Results: Compared to the MASLD group, the MASLD-ACLF group showed hepatic necrosis on H&E staining, along with typical histopathological features supporting ACLF diagnosis, concomitant with characteristic steatotic manifestations; mitochondrial dysfunction was observed via transmission electron microscopy. Liver fibrosis was assessed by alpha-SMA immunocytochemistry and sirius red

staining. Serum liver function markers were altered, decreased Muc-2 and Occludin indicated gut barrier impairment. Transcriptomics revealed changes in tissue remodeling, phagocytosis, bile acid metabolism, and neutrophil phenotype markers in the liver, with Hallmark analysis highlighting the IL-6-STAT3 pathway. Single-cell RNA sequencing analysis of stage 3 fibrosis underscored the important role of neutrophils in disease progression.
Conclusion: We successfully generated MASLD-ACLF models exhibiting steatohepatitis or stage 3 fibrosis. This study provides, for the first time, a reliable animal model platform representing different disease stages, which enables direct liver tissue access and permits dynamic, time-series investigations to facilitate exploration of disease mechanisms and therapeutic strategies.

SAT-241
Ferulic acid alleviates metabolic dysfunction-associated steatotic liver disease by targeting hydroxysteroid 17-beta dehydrogenase 13 to promote lipolysis
Yuqing Pan[1], Aojie Mao[1], Yiyang Hu[1], Yu Zhao[1]. [1]*Institute of Liver Diseases, Shuguang Hospital affiliated to Shanghai University of Traditional Chinese Medicine, Shanghai, China*
Email: cathy150@139.com

Background and aims: Hepatic lipid deposition serves as the core pathophysiological basis and initial driving factor for both the onset and progression of Metabolic dysfunction-associated steatotic liver disease (MASLD). Ferulic acid (FA), found in a variety of plants and traditional herbal medicines, has been shown to regulate hepatic lipid metabolism and ameliorate MASLD. However, its underlying mechanisms remain unclear. The objective of this study is to investigate the mechanisms by which FA alleviates lipid accumulation in hepatocytes, thereby providing a foundation to facilitate its translational application.
Method: An AML12 hepatocyte lipid deposition model was established using free fatty acid (FFA) induction. Cells were treated with 100 μM FA, and intracellular lipid accumulation was evaluated by measuring triglyceride (TG) levels, Oil Red O staining, and BODIPY fluorescent staining. To identify potential protein targets of FA, drug affinity responsive target stability coupled with mass spectrometry (DARTS + MS) was performed. The direct interaction between FA and hydroxysteroid 17-beta dehydrogenase 13 (HSD17B13) was further verified by surface plasmon resonance (SPR) analysis. In HEK 293T cells, co-immunoprecipitation (Co-IP) was used to examine whether FA promotes ubiquitination of HSD17B13 and modulates its interaction with adipose triglyceride lipase (ATGL). Finally, ATGL knockdown was carried out in AML12 cells to assess its effect on the lipid-lowering activity of FA.
Results: FA significantly reduced FFA-induced TG accumulation in hepatocytes, decreased the number, staining intensity, and size of lipid droplets. Subsequent DARTS + MS and SPR analyses confirmed a direct binding interaction between FA and HSD17B13. Although FA did not alter HSD17B13 mRNA levels, it significantly increased HSD17B13 protein expression. Furthermore, FA treatment elevated the phosphorylation level of ATGL protein, enhanced lipolytic activity. FA promoted ubiquitination of HSD17B13, reduced its binding to ATGL, and facilitated the interaction between ATGL and its activator CGI-58. Notably, in FFA-induced AML12 cells with ATGL knockdown, the TG-lowering effect of FA was substantially attenuated.
Conclusion: This study demonstrates that FA alleviates hepatic lipid deposition by targeting HSD17B13. The binding of FA promotes HSD17B13 ubiquitination, which disrupts its interaction with ATGL, enhances ATGL phosphorylation, and ultimately activates lipolysis.

SAT-242
ZEB2 promotes the progression of MASLD by inducing neutrophil extracellular traps formation
Guanggi Zhu[1], Qianwen Zhao[1], Chao Wu[1], Jie Li[1]. [1]*Nanjing Drum Tower Hospital, Affiliated Hospital of Medical School, Nanjing University, Nanjing, China*
Email: lijier@nju.edu.cn

Background and aims: The pathogenesis of metabolic dysfunction-associated steatotic liver disease (MASLD) is highly complex, with hepatic lipid accumulation being a critical factor driving its progression. The transcription factor E-box-binding zinc finger protein 2 (ZEB2) within hepatic stellate cells (HSCs) has shown its critical role in regulating hepatic fibrosis. However, its specific mechanisms in hepatocytes under the context of MASLD remain poorly understood.
Method: Liver samples from metabolic dysfunction-associated steatohepatitis (MASH) patients were obtained to assess ZEB2 expression by immunohistochemistry (IHC) and immunofluorescence (IF). Mouse primary hepatocytes were stimulated with palmitic acid (PA) and oleic acid (OA) and transfected with ZEB2 siRNA or a ZEB2 overexpression plasmid (Ad-ZEB2) to evaluate its role in MASLD. Hepatocyte-specific ZEB2 knockout mice were generated using the Cre/LoxP system. MASLD mouse models were established via high-fat, high-fructose diet (HFHFD) or choline-deficient, amino acid-restricted, high-fat diet (CDA-HFD). RNA sequencing (RNA-seq) was employed to identify ZEB2 target genes and elucidate its molecular mechanisms.
Results: IHC and IF revealed a significantly elevated ZEB2 expression in paraffin-embedded liver sections from MASH patients. *In vitro*, PA and OA stimulation markedly upregulated ZEB2 expression. ZEB2 knockdown significantly suppressed lipid accumulation and the inflammatory condition, whereas ZEB2 over-expression exacerbated it. *In vivo*, hepatocyte-specific ZEB2 knockout mice downregulated the expression of inflammatory cytokines-related genes (*IL-1, IL-6, TNF-α*), and decreased serum levels of liver enzymes. Pyruvic tolerance test and glucose tolerance test showed an improved performance in mice with ZEB2 knockout. Hematoxylin-eosin (HE) staining and IHC confirmed a reduced lipid deposition and diminished inflammatory infiltration, respectively. Further, RNA-seq analysis suggested that ZEB2 may regulate cell adhesion, thereby increasing neutrophil extracellular traps (NETs) formation and promoting MASH progression. Co-culture of ZEB2-overexpressing hepatocytes with neutrophils significantly enhanced intercellular adhesion and NETs formation, whereas ZEB2 inhibition attenuated these effects.
Conclusion: Targeting ZEB2 in hepatocytes effectively prevents MASLD development in mice, suggesting that ZEB2 may serve as a potential therapeutic target for MASLD.

SAT-243-YI
Platelet phenotype and function throughout the spectrum of metabolic dysfunction-associated steatotic liver disease
Mirko Zoncapè[1,2], Marco Castelli[3], Anna Mantovani[4], David Sacerdoti[2], Pietro Minuz[4], Andrea Dalbeni[4]. [1]*Clinica Medica 3, Azienda Ospedale Università di Padova, Padova, Italy;* [2]*Liver Unit, University of Verona and Azienda Ospedaliera Universitaria Integrata Verona, Verona, Italy;* [3]*Division of General Medicine C, Department of Medicine, University of Verona, Verona, Italy;* [4]*Division of General Medicine C, Department of Medicine, Azienda Ospedaliera Universitaria Integrata Verona, Verona, Italy*
Email: mirko.zonky@yahoo.it

Background and aims: Metabolic dysfunction-Associated Steatotic Liver Disease (MASLD) is a major cause of chronic liver disease, progressing from steatosis to cirrhosis. Platelets are increasingly recognised as contributors to its pathogenesis, yet their phenotype and function across disease stages remain unclear. We aimed to characterise platelet activation and function in MASLD with mild

fibrosis (≤F2) and advanced fibrosis/cirrhosis (F3-F4) versus healthy controls. A secondary aim was to assess coagulation factor profiles and the possible platelet role in their transport.
Method: In this cross-sectional study, 192 subjects were included: 62 healthy controls, 82 MASLD ≤F2, and 48 MASLD F3-F4. Platelet activation was assessed by urinary 11-dehydro-thromboxane B2 (11-dh-TXB2) and plasma soluble P-selectin; platelet adhesion under flow by microfluidics; and flow cytometry analysed fibrinogen receptor activation, Annexin V binding, and platelet-leukocyte aggregates. Coagulation parameters (PT, aPTT, fibrinogen, FVII, FVIII, FIX, FX, FXII, FXIII, and vWF) were measured in platelet-rich and platelet-poor plasma. Combination assays mixing patient platelets with control plasma, and vice versa, evaluated whether platelets contribute to coagulation factor transport.
Results: Both 11-dh-TXB2 and soluble P-selectin rose progressively with fibrosis severity and correlated with FIB-4 and liver stiffness ($p < 0.001$). Microfluidic assays showed enhanced platelet adhesiveness in MASLD ≤F2 and F3-F4 versus controls. Flow cytometry showed an increased proportion of Annexin V-positive procoagulant platelets in ≤F2 patients, while F3-F4 exhibited reduced fibrinogen receptor activation and lower platelet-monocyte aggregates, suggesting exhaustion. Advanced fibrosis/cirrhosis was associated with prolonged PT/aPTT and reduced FVII, FVIII, FIX, FX, FXII, and FXIII, alongside elevated vWF. Combination experiments demonstrated that differences were plasma-driven, excluding a relevant platelet-mediated transport role.
Conclusion: Distinct platelet phenotypes characterise MASLD progression. Early disease (≤F2) shows increased platelet activation and procoagulant potential, while advanced fibrosis/cirrhosis displays reduced responsiveness despite systemic activation and thrombocytopenia. Coagulation abnormalities mainly reflect plasma defects rather than platelet carriage. These findings identify platelets as active players in MASLD pathogenesis and support their potential as biomarkers and therapeutic targets in chronic liver disease.

SAT-244

Dysregulation of the urea cycle enzymes determines a more severe MASLD phenotype in a DIAMOND preclinical model

Carola Zurita Palomo[1,2], Rocío Gallego-Durán[1,2,3], Douglas Maya-Miles[1,2,4], Lucía López-Bermudo[5,6], Blanca Escudero-López[5,6], Carmen Bejarano-Jurado[7], Paloma Carrillo-Fernández[1,2], Antonio Cárdenas-García[5,6], Jordi Gracia-Sancho[2,8], Anabel Fernández-Iglesias[2,8], Francisco Javier Cubero[2,9], Javier Vaquero[2,10], Rafael Bañares[2,9,10], Franz Martin-Bermudo[5,6], Manuel Romero-Gómez[1,2,3,11], Javier Ampuero[1,2,3,11]. *[1]SeLiver Group, Instituto de Biomedicina de Sevilla/CSIC/Hospital Virgen del Rocío, Sevilla, Spain; [2]Hepatic and Digestive Diseases Networking Biomedical Research Centre (CIBEREHD), Madrid, Spain; [3]Department of Medicine, University of Seville, Sevilla, Spain; [4]Department of Physiology, University of Seville, Sevilla, Spain; [5]Andalusian Center of Molecular Biology and Regenerative Medicine-CABIMER- University Pablo Olavide-University of Seville-CSIC, Sevilla, Spain; [6]Biomedical Research Network on Diabetes and Related Metabolic Diseases-CIBERDEM, Instituto de Salud Carlos III, Madrid, Spain; [7]Pathology Department, Hospital Universitario Virgen del Rocío, Sevilla, Spain; [8]Liver Vascular Biology Research Group, IDIBAPS Biomedical Research Institute, CIBEREHD, Barcelona, Spain; [9]Department of Immunology, Ophthalmology and ORL, Faculty of Medicine, Complutense University of Madrid, Madrid, Spain; [10]HepatoGastro Lab, Unit for Clinical Management Gregorio Marañón University Hospital, Instituto de Investigación Sanitaria Gregorio Marañón, Madrid, Spain; [11]Digestive Diseases Unit, Hospital Universitario Virgen del Rocío, Sevilla, Spain*
Email: czurita-ibis@us.es

Background and aims: (i) to characterize the DIAMOND model under different dietary regimens and (ii) to evaluate changes in urea cycle enzymes (UCEs) in DIAMOND.
Method: DIAMOND mice (n = 35) were randomized to three dietary regimens and duration: high-fat diet supplemented with fructose/glucose in drinking water (HF-HFD; 21w, 30w and 52w), choline-deficient high-fat diet supplemented with 0.1% methionine (CDA-HFD, 16w) or chow diet (21w, 30w and 52w). Anthropometric, biochemical, and hepatic profiles were evaluated, and animals were included in metabolic cages. TUNEL assay, a panel of pro-inflammatory and pro-fibrogenic markers, and hepatic expression of UCEs by qRT-PCR were performed. Finally, an oral glutamine challenge (OGC), microbiota analysis and histopathological evaluation by an expert pathologist were performed.
Results: HF-HFD mice developed metabolic syndrome, unlike CDA-HFD mice. HOMA-IR and HOMA-beta showed insulin resistance with partial depletion of beta-cell function in HF-HFD mice. CDA-HFD mice showed insulin sensitivity and normal beta-cell function. Both interventions increased profibrogenic, proinflammatory and apoptotic markers, especially in CDA-HFD and HF-HFD mice at 30 weeks. Both groups showed NAS Scores > 5, with ballooning and grade 1 of fibrosis. A decrease in the expression of UCEs was observed: carbamoyl phosphate synthetase I (CPS1) (fold change (FC) 0.66; $p = 0.05$), argininosuccinate synthase 1 (ASS1) (FC 0.57; $p < 0.05$) and argininosuccinate lyase (ASL) (FC 0.42; $p < 0.05$) in the presence of ballooning, and CPS1 (FC 0.58; $p < 0.01$), ornithine carbamoyltransferase (OTC1) (FC 0.82;$p < 0.05$) and ASL (FC 0.42; $p = 0.05$) in fibrosis. A significant increase in GLS1 was observed in the presence of ballooning (FC 2.50; $p < 0.01$) and fibrosis (FC 2.90; $p < 0.0001$). Ammonia production after SOG was significantly higher in CDA-HFD (AUC = 7269 ± 1276, $p < 0.05$) and HF-HFD at 52w (AUC = 10755 ± 1452, $p < 0.05$) compared to baseline controls (AUC = 3855 ± 187.7). Microbiota analysis revealed that groups differed in their bacterial species composition, and PICRUST analysis identified 17 differentially expressed pathways with ammonia as an intermediate or end product.
Conclusion: DIAMOND mice showed urea cycle dysregulation under different dietary interventions leading to a compromised ammonia metabolism. CDA-HFD induced a faster and more aggressive liver phenotype without the presence of metabolic syndrome, whereas HF-HFD more closely mirrored the metabolic phenotype seen in humans.

MASLD – Therapy

TOP-162

Glucagon-like peptide-1 receptor agonists and long-term liver outcomes in metabolic dysfunction-associated steatotic liver disease and type 2 diabetes: a large real-world analysis

Arunkumar Krishnan[1,2], Diptasree Mukherjee[1], Carolin V Schneider[3], Saleh A. Alqahtani[4,5]. *[1]Department of Supportive Oncology, Atrium Health Levine Cancer, Charlotte, NC, United States; [2]Department of Medicine, Wake Forest University School of Medicine, Winston-Salem, NC, United States; [3]Department of Gastroenterology, Metabolic Diseases and Intensive Care, University Hospital RWTH Aachen, Aachen, Saudi Arabia; [4]Liver, Digestive, and Lifestyle Health Research Section, and Organ Transplant Center of Excellence, King Faisal Specialist Hospital and Research Center, Riyadh, Saudi Arabia; [5]Division of Gastroenterology & Hepatology, Weill Cornell Medicine, New York, United States*
Email: drsaleh.a.alqahtani@gmail.com

Background and aims: Metabolic dysfunction-associated steatotic liver disease (MASLD) is now the most common chronic liver disease globally and frequently coexists with type 2 diabetes (T2D), conferring a several-fold increased risk of cirrhosis and hepatocellular carcinoma (HCC), particularly in those with advanced fibrosis. This study examined whether treatment with glucagon-Like peptide-

1 receptor agonists (GLP-1RAs) is associated with reduced risks of cirrhosis and HCC in adults with MASLD and T2D in a large real-world cohort.

Method: A retrospective, multicenter cohort study was conducted using the TriNetX federated electronic health record platform. Adults with MASLD and T2D without prior cirrhosis or HCC at baseline were included. GLP-1RA exposure was defined as continuous treatment for at least 6 months, with time zero at the date of GLP-1RA initiation or a matched index date for non-users. Individuals with pre-existing cirrhosis, HCC, significant alcohol use disorder, or other chronic liver diseases were excluded. Propensity score matching was used to balance demographics, body mass index, smoking status, glycated hemoglobin, cardiovascular disease, and non-invasive fibrosis markers. Cox proportional hazards models estimated adjusted hazard ratios (aHRs) with 95% confidence intervals (CIs) for incident cirrhosis and HCC.

Results: The matched cohort comprised 52,600 adults, of whom 19,200 received GLP-1RAs, with a median follow-up of 2,730 days. During follow-up, 760 participants developed cirrhosis and 165 developed HCC. Cirrhosis occurred in 2.4% of GLP-1RA users versus 3.5% of nonusers (aHR 0.72, 95% CI 0.61–0.84), while HCC occurred in 0.5% versus 0.9%, respectively (aHR 0.66, 95% CI 0.45–0.96). Relative risk reductions were greatest among patients with higher baseline fibrosis risk, consistent with prior MASLD cohorts in which earlier GLP-1RA use was linked to slower fibrosis progression and fewer major adverse liver outcomes.

Conclusion: In this large, real-world population with MASLD and T2D, GLP-1RA therapy was associated with substantially lower risks of incident cirrhosis and HCC, particularly in individuals with elevated baseline fibrosis risk.

TOP-176

Concurrent responses in multiple non-invasive tests for hepatic inflammation and fibrosis following pemvidutide treatment: 24-week responder analyses of the phase 2b IMPACT trial in metabolic dysfunction-associated steatohepatitis

Naim Alkhouri[1], Mazen Noureddin[2], Shaheen Tomah[3], Julio Gutierrez[3], John Suschak[3], M. Scot Roberts[3], Rachel Garner[3], Sarah Browne[3], M. Scott Harris[3], Christophe Arbet-Engels[3]. *[1]Summit Clinical Research, Clinical Research Institute of Ohio, San Antonio, TX, United States; [2]Houston Methodist Hospital, Houston Research Institute, Pinnacle Clinical Research, Houston, TX, United States; [3]Altimmune, Inc, Gaithersburg, MD, United States*
Email: nalkhouri@summitclinicalresearch.com

Background and aims: Pemvidutide is a balanced 1:1 glucagon/GLP-1 dual receptor agonist in development for the treatment of metabolic dysfunction-associated steatohepatitis (MASH). IMPACT was a phase 2b, randomized, placebo-controlled, double-blind trial in patients with biopsy-confirmed MASH and fibrosis stage F2 or F3 (NCT05989711). At as early as 24 weeks, pemvidutide treatment showed statistically significant MASH resolution and high rates of fibrosis improvement. Reductions in individual non-invasive tests (NITs) have been used as indicators of therapeutic effect, but composite analyses using multiple, overlapping NITs may provide a clearer assessment of therapeutic improvement as they increase stringency of the response and lower placebo response rates compared to individual NITs. Here we present 24-week responder analyses of composite NITs from the IMPACT trial.

Method: 212 patients were randomized 1:2:2 to receive once-weekly subcutaneous pemvidutide (1.2 mg or 1.8 mg) administered without dose titration, or placebo. Secondary endpoints included the NITs for liver fat content (LFC), ELF score, liver stiffness measurement (LSM), and alanine aminotransferase (ALT).

Results: The mean age was 53 years, the mean BMI was 39 kg/m^2, 58% were female, and 43% had type 2 diabetes. A greater proportion of patients receiving pemvidutide achieved concurrent responses in LFC (≥ 30% reduction), ALT (≥ 17 U/L reduction), and LSM (≥ 30% reduction) compared to placebo [1.2 mg (37.8%; $p < 0.0001$); 1.8 mg (21.6%; $p = 0.0014$); placebo (4.3%)]. Similarly, a greater proportion of patients receiving pemvidutide achieved concurrent responses in ELF score (≥ 0.5 reduction) and LSM (≥ 30% reduction) compared to placebo [1.2 mg (37.8%; $p = 0.0002$); 1.8 mg (22.7%; $p = 0.02$); placebo (8.3%)]. Notably, in a more stringent analysis of concurrent responses in LFC (≥ 50% reduction), ELF score (≥ 0.5 reduction), and LSM (≥ 30% reduction), pemvidutide resulted in a higher proportion of patients achieving a response compared to placebo [1.2 mg (29.7%; $p = 0.0001$); 1.8 mg (17.8%; $p = 0.0041$); placebo (2.9%)].

Conclusion: Pemvidutide treatment led to statistically significant increases in the proportion of patients achieving concurrent responses in multiple NITs of MASH resolution and hepatic fibrosis at 24 weeks.

TOP-177

Baseline ANTICIPATE score and response predicts liver outcome events in an 180 patient MASH cirrhosis cohort treated with resmetirom

Naim Alkhouri[1], Rebecca Taub[2], Xiaomin Lu[2], Jörn M. Schattenberg[3], Mazen Noureddin[4]. *[1]Summit Clinical Research, San Antonio, United States; [2]Madrigal Pharmaceuticals, Conshohocken, United States; [3]Universitätsklinikum des Saarlandes, Homburg, Germany; [4]Pinnacle Clinical Research, San Antonio, United States*
Email: rebeccataub@yahoo.com

Background and aims: Resmetirom (RES), a selective thyroid hormone receptor beta agonist, is an approved therapy for metabolic dysfunction associated steatohepatitis (MASH) with moderate to advanced liver fibrosis based on improvement in both NASH and fibrosis. We evaluated two years data in 180 patients with compensated MASH cirrhosis treated with RES to assess the ability of ANTICIPATE-NASH (Aceituno et al, Gastroenterology 2025) to predict clinically significant portal hypertension (CSPH) leading to liver related events (LRE).

Method: 180 patients with Child Pugh A MASH cirrhosis (based on MASH F4 on historic biopsy >66% or clinical diagnosis) were treated with 80 mg RES for up to 2 years (MAETRONAFLD- 1 (NCT04197479) year 1; open-label extension trial (NCT04951219) year 2. Of the 180 patients, 122 patients elected to enter treatment for year 2. Discontinuation rates were <10% per year. ANTICIPATE-NASH CSPH risk was determined at baseline (BL), year 1 and year 2. "Responder" was assessed as a shift to ≤25% CSPH risk or at least 30% improvement in ANTICIPATE-NASH. LRE were assessed at year 1 for the n = 180 and at 2 years in the n = 122 populations.

Results: BL characteristics were similar between the year 1 (n = 180) and year 2 (n = 122) populations, respectively: age, 62, 62, female 62.5%, 55.7%; BMI (kg/m2) 34.4, 34.4; T2D 72.8%, 69.7%; (median, (Q1, Q3): VCTE 20.3 kPa (15.6, 30.7), 20.1 (17.1, 31.3); MRE, 5.1 kPa (4.1,6.3), 5.2 kPa (4.4,6.3), platelets 142 (108, 199), 136 (101,187). For the year 1 population at BL 69.0% had CSPH risk>25%; 15.5%, >12% and ≤25%; 15.5%, <12%; after 1 year, 56.3% had CSPH risk>25%, 20.5%, >12% and ≤25%; 23.2%, <12%. 43.7% were responders. For the year 2 population at BL, 75.4.% had CSPH risk>25%; 12.3%, >12% and ≤25%; 12.3%, <12%; after 1 year, 59.6% had CSPH risk>25%, 19.3%, >12% and ≤25%; 21.1%, <12%; after year 2, 52.4% had CSPH risk>25%, 22.3%, >12% and ≤25%; 25.2%, <12%. 43.9% were responders after year 1 and 49.3% were responders after year 2. LRE during year 1 of the n = 180 population occurred in 1.7%, only in nonresponders with BL CSPH>25%. LRE after 2 years in the n = 122 population occurred in 2.2%, only in nonresponders with BL CSPH>25%.

Conclusion: In a well-compensated MASH cirrhosis population treated with RES for up to 2 years, ANTICIPATE-NASH in patients with BL CSPH risk >25% and non-response to treatment accurately predicted LRE. Treatment with RES significantly reduced ANTICIPATE-NASH in about half of treated patients.

FRI-139

Semaglutide provides liver health-related benefits in menopausal women living with MASH: a post hoc analysis of the ESSENCE trial part 1

Manal F. Abdelmalek[1], Maria Teresa Arias Loste[2], Burak Demirel[3], Gema Frühbeck Martinez[4], Anja Geerts[5], Lise Lotte Gluud[6], Alma Laura Ladrón de Guevara[7], Ewa Janczewska[8], Ole Kleist Jeppesen[3], Claudia Pinto Oliveira[9], Mary E. Rinella[10], Giada Sebastiani[11], Anca Trifan[12], Thea Vestergaard[3], Elisabetta Bugianesi[13]. *[1]Division of Gastroenterology and Hepatology, Mayo Clinic, Rochester, MN, United States; [2]Hospital Universitario Marques de Valdecilla, Clinical and Translational Research Group in Digestive Diseases, IDIVAL, Santander, Spain; [3]Novo Nordisk A/S, Copenhagen, Denmark; [4]Clínica Universidad de Navarra, Pamplona, Spain; [5]Hepatology Research Unit, Liver Research Center, Ghent University Hospital, Ghent, Belgium; [6]Department of Medicine, University of Copenhagen, Copenhagen, Denmark; [7]Centro de Investigación y Gastroenterología, Ciudad de México, Mexico; [8]ID Clinic, Myslowice, Poland; [9]Departamento de Gastroenterologia, Hospital das Clínicas (LIM07) da Faculdade de Medicina da Universidade de São Paulo, São Paulo, Brazil; [10]Division of Gastroenterology, Hepatology and Nutrition, University of Chicago, Chicago, IL, United States; [11]Department of Gastroenterology and Hepatology, McGill University, Montreal, Canada; [12]Institute of Gastroenterology and Hepatology, Iasi, Romania; [13]Department of Medical Sciences, University of Turin, Turin, Italy*
Email: Abdelmalek.manal@mayo.edu

Background and aims: Women in menopause with metabolic dysfunction-associated steatohepatitis (MASH) are at increased risk of advanced liver fibrosis and faster disease progression vs women in premenopause and men of similar age. This post hoc analysis of the ESSENCE trial assessed the effect of semaglutide 2.4 mg on liver histology and non-invasive tests (NITs) by menopause status.
Method: Analyses were performed in women in menopause (those not of child-bearing potential), women in premenopause (those of child-bearing potential), and males. Proportions of participants (pts) achieving resolution of MASH with no worsening of liver fibrosis and improvement in liver fibrosis with no worsening of MASH at week 72 were evaluated. Changes from baseline to week 72 in alanine aminotransferase (ALT), liver stiffness measurement by vibration-controlled transient elastography (VCTE), Enhanced Liver Fibrosis (ELF), and FibroScan-AST (FAST) were assessed.
Results: Semaglutide demonstrated numerically higher histologic response vs placebo across subgroups. For resolution of MASH with no worsening of liver fibrosis: menopause 52.0% vs 19.8%; premenopause 62.7% vs 34.8%; male 60.6% vs 32.0%. For improvement in liver fibrosis with no worsening of MASH: menopause 29.5% vs 18.2%; premenopause 42.4% vs 21.7%; male 34.8% vs 18.0%. For NITs, semaglutide demonstrated consistent and comparable improvements vs placebo across menopause (n = 375), premenopause (n = 82), and male (n = 343) subgroups, with most statistically significant. For ALT, estimated treatment ratios (ETRs) were menopause 0.66 (95% CI 0.59–0.74; $p < 0.0001$); premenopause 0.52 (0.37–0.73; $p = 0.0002$); male 0.61 (0.54–0.69; $p < 0.0001$). For VCTE, ETRs were 0.79 (0.70–0.88; $p < 0.0001$), 0.82 (0.61–1.09; $p = 0.1675$) and 0.80 (0.72–0.88; $p < 0.0001$), respectively. For ELF, estimated treatment differences (ETDs) were −0.63 (−0.79 to −0.47; $p < 0.0001$), −0.50 (−0.89 to −0.12; $p = 0.0115$) and −0.53 (−0.69 to −0.38; $p < 0.0001$), respectively. For FAST, ETDs were −0.19 (−0.25 to −0.12; $p < 0.0001$), −0.22 (−0.39 to −0.06; $p = 0.0088$) and −0.17 (−0.23 to −0.11; $p < 0.0001$), respectively.
Conclusion: Semaglutide was associated with improvements in liver histology and NITs in pts with MASH across menopause, premenopause and male subgroups. Menopause does not reduce the likelihood of achieving liver health improvements with semaglutide.

FRI-140

Isotemporal associations of sedentary behavior and physical activity with health-related quality of life in patients with metabolic dysfunction-associated steatotic liver disease

Hadeel Saad[1], Khalid A Alswat[1], Sulaiman Aljaloud[1], Maram Alkhammash[1], Amani Alsadoon[1], Abdullah Alansare[1,2,3]. *[1]King Saud University, Riyadh, Saudi Arabia; [2]King Saud University, Exercise Physiology, Riyadh, Saudi Arabia; [3]The Department of Exercise Physiology, College of Sports Science and Physical Activity, Riyadh, Saudi Arabia*
Email: aalansare@ksu.edu.sa

Background and aims: Emerging evidence suggests that higher sedentary behavior (SB), such as sitting for long periods, is associated with impaired health-related quality of life (HRQoL) in patients with metabolic dysfunction-associated steatotic liver disease (MASLD). Whether reallocating sedentary time to different intensities of physical activity (PA) is associated with improved HRQoL in patients with MASLD remains unexplored. We examined isotemporal associations between SB and PA intensities with overall and domain-specific HRQoL in patients with MASLD.
Method: In this cross-sectional study, adults with MASLD attending a hepatology clinic were enrolled. SB and PA intensities (i.e., light [LPA], moderate [MPA], and vigorous [VPA]) were objectively assessed using a wrist-worn accelerometer over seven consecutive days. The Chronic Liver Disease Questionnaire for Non-Alcoholic Fatty Liver Disease was used to evaluate the overall and domain-specific (i.e., abdominal symptoms, fatigue, systemic symptoms, emotion, worry, and activity) HRQoL. Adjusted isotemporal substitution models examined the associations of replacing 30 minutes/day of SB with equivalent durations of PA with overall and domain-specific HRQoL.
Results: Participants (n = 101; mean age = 50.0 years; 43% female) spent 12.8 hours/day in SB, while 69.3% of them met the recommended weekly PA levels. In isotemporal substitution models, reallocating 30 minutes/day from SB to LPA was significantly associated with improved overall HRQoL ($\beta = 0.103$; $p < 0.001$), abdominal symptoms ($\beta = 0.164$; $p < 0.001$), fatigue ($\beta = 0.096$; $p = 0.002$), systemic symptoms ($\beta = 0.091$; $p < 0.001$), emotion ($\beta = 0.075$; $p = 0.023$), activity ($\beta = 0.036$; $p = 0.042$). In contrast, substituting sedentary time with MPA or VPA was not significantly associated with HRQoL ($p > 0.05$ for all).
Conclusion: To our knowledge, this is the first study using isotemporal substitution modeling to demonstrate that replacing sedentary time with LPA is associated with better overall and domain-specific HRQoL in MASLD patients. These findings emphasize the need to target SB reduction through increasing LPA to improve HRQoL in patients with MASLD. Prospective and interventional studies are necessary to confirm these findings and explore causality.

FRI-141

Early real-world effectiveness of resmetirom in adults with metabolic dysfunction associated steatohepatitis and moderate-to-advanced fibrosis

Naim Alkhouri[1], Yestle Kim[2], Karissa Johnston[3], John O'Donnell[2], Reem Mustafa[4], Yael Silberberg[5], Karin Keren[5], Rajagopal Chadalavada[6], Pradeep Bekal[6], Romina Fakhraei[3]. *[1]Summit Clinical Research, San Antonio, United States; [2]Madrigal Pharmaceuticals, West Conshohocken, United States; [3]Broadstreet HEOR, Vancouver, Canada; [4]Vancouver, Canada; [5]Latica, Palo Alto, United States; [6]Gastro Health, Cincinnati, United States*
Email: rfakhraei@broadstreetheor.com

Background and aims: Resmetirom (Rezdiffra™), a thyroid hormone receptor-beta agonist, was conditionally approved in the US in 2024 for adults with noncirrhotic MASH and moderate-to-advanced fibrosis. This study described real-world effectiveness of resmetirom in a US gastroenterology practice, focusing on changes in blood biomarkers and clinical measures.

Method: A single-arm, retrospective cohort study using Latica real-world data repository was conducted. Adults with ≥ 1 resmetirom prescription (Apr 2024–2025; index date = first prescription) and ≥ 6 months of follow-up were included; those with end-stage liver disease in the 2 years pre-index were excluded. Baseline (12 months pre-index) demographics, comorbidities, concomitant medications, and laboratory measurements (AST, ALT, platelets, FibroScan AST [FAST] score, Vibration-Controlled Transient Elastography Liver Stiffness Measurement [LSM]) were captured and, when available, reassessed during follow-up. Treatment-related adverse events (AEs) and AE-related discontinuations were recorded.
Results: Of 1,278 resmetirom users, 712 (55.7%) met inclusion. Mean (SD) treatment duration was 5.7 (4.1) months. About 80% had ≥ 2 cardiometabolic risk factors, most often hypertension (77%) and obesity (71%). In patients with both baseline and follow-up values, mean FAST declined by 0.18 (n = 28), ALT by 13.6 U/L (n = 330), and LSM by 2.2 kPa (n = 70). Response thresholds were met in 42.9% for FAST (≥ 0.22 reduction), 46.7% for ALT (≥ 17 U/L or ≥ 20% reduction), and 41.4% for VCTE (≥ 30% reduction). Trends were similar across statin (n = 232) and non-statin users (n = 480); both improved in lipid markers [LDL (−19.3 vs −10.3) and total cholesterol (−16.9 vs −1.2 mg/dL)]. AST fell in both groups (−8.7 vs −3.4 U/L) and ALT changed in opposite directions (+4.0 vs −3.8 U/L). In GLP-1 concomitant users (n = 139) vs without (n = 573), ALT/AST declines were similar (~ −14/−8 U/L in both), BMI changed slightly (~ −1 kg/m^2 in both), FIB-4 fell slightly more without GLP-1 (−0.1 vs −0.5), LSM declined more with GLP-1 (−3.2 vs −1.9 kPa), and CAP declined in both groups (−39.5 dB/m vs −43.9 dB/m). Discontinuation for treatment-related AEs was rare (~2%), mostly due to diarrhea.
Conclusion: In this real-world analysis, resmetirom was associated with clinically meaningful improvements in blood and imaging biomarkers over ~6 months, suggesting earlier effectiveness than in the 52-week MAESTRO-NASH trial. Larger cohorts with longer follow-up are needed to assess long-term outcomes.

FRI-142

Study design, rationale, and baseline characteristics of the SYNCHRONY real-world trial: a phase 3 trial evaluating efruxifermin in participants non-invasively diagnosed with MASLD or MASH

Quentin M. Anstee[1], Reshma Shringarpure[2], Naga Chalasani[3], Doreen Chan[2], Ali Moulton[2], Brittany de Temple[2], Mark Burch[2], Meena Jain[2], Kitty Yale[2], Mazen Noureddin[4]. *[1]Newcastle University, Newcastle upon Tyne, United Kingdom; [2]Akero Therapeutics, a Novo Nordisk Company, San Francisco, United States; [3]Indiana University School of Medicine, Indianapolis, United States; [4]Houston Methodist Hospital, Houston, United States*
Email: quentin.anstee@newcastle.ac.uk

Background and aims: In Phase 2b clinical trials, treatment with efruxifermin, a bivalent FGF-21 analog, demonstrated improvement in fibrosis in participants with MASH and F2/F3 fibrosis or compensated cirrhosis (F4c). Three Phase 3 trials of efruxifermin in MASH are ongoing: SYNCHRONY Histology, Outcomes, and Real-World. As clinical practice increasingly relies upon non-invasive tests for diagnosis, risk stratification, and monitoring of patients with MASLD, the objectives of the SYNCHRONY Real-World trial are to evaluate the safety, tolerability, and efficacy of efruxifermin on non-invasive markers of liver fibrosis in participants with MASLD/MASH.
Method: This is an ongoing randomized, double-blind, placebo-controlled phase 3 trial of efruxifermin (NCT06161571) at 222 sites worldwide. The trial was designed to collect safety data on efruxifermin and included participants with a clinical diagnosis of MASH who may have been histologically ineligible for other phase 3 trials of efruxifermin. Eligible participants were randomized 2:1 to efruxifermin 50 mg QW SC or placebo for 52 weeks. Key entry criteria: 18–80 years, T2D or ≥2 components of metabolic syndrome, MASLD/MASH with histological fibrosis (F1-F4c) OR non-invasive diagnosis of fibrosis (LSM-VCTE ≥7.5 kPa, ELF ≥7.7, or LSM-MRE ≥2.5 kPa) and confirmation of elevated liver fat content (CAP ≥300 dB/m or ≥8% by MRI-PDFF). The primary endpoint is the safety and tolerability of efruxifermin. The key secondary endpoint is the proportion of participants with concordant ≥0.5 decrease in ELF and ≥30% decrease in LSM-VCTE.
Results: Enrollment was completed in January 2025. Overall, 773 participants were screened and 608 were randomized. At baseline, participants were 56 years of age, 54% female, 83% White, and 30% Hispanic or Latino ethnicity. A total of 57% had T2D with 23% established on GLP-1 receptor agonists and 52% on statins. At baseline, mean ± SD LSM was 12.3 ± 7.3 kPa and ELF was 9.5 ± 0.9. The majority of participants (99%) had available histology as many had failed screening for other trials of efruxifermin. At baseline, fibrosis stages were: F0, 1%; F1, 35%; F2, 33%; F3, 15%; and F4, 15%. Baseline NAS was 2.8 ± 1.2.
Conclusion: SYNCHRONY Real-World is one of three phase 3 trials evaluating the safety and efficacy of efruxifermin and includes participants representative of a broad spectrum of MASLD/MASH. Concurrent conduct of these trials allows for greater opportunities for participants to meet entry criteria. The results are expected in H1 2026.

FRI-147

Efficacy of a therapeutic physical exercise program in patients with metabolic dysfunction–associated steatotic liver disease: a randomized, open-label, bicenter study (SteatoAPA)

Marwin Farrugia[1], Sébastien Le Garf[1], Jocelyn Gal[2], Françoise Lermite[1], Anne-Sophie Rousseau[3], Quentin Serrano[1], Sébastien Raday[1], Renaud Schiappa[2], Ouizeman Dann[1], Régine Truchi[1], Chassang Madleen[1], Nicolas Chevalier[1], Stéphane Schneider[1], André-Jean Remy[4], Philippe Gual[1], Rodolphe Anty[1]. *[1]Hôpital L'Archet, Nice, France; [2]Centre Antoine Lacassagne, Nice, France; [3]UFR Staps, Nice, France; [4]Centre Hospitalier, Perpignan, France*
Email: anty.r@chu-nice.fr

Background and aims: Therapeutic physical exercise (TPE) is a cornerstone of lifestyle management in metabolic dysfunction–associated steatotic liver disease (MASLD), yet its additive benefit over dietary measures alone remains debated. We aimed to evaluate the efficacy of a 12-week TPE program combined with dietary intervention in patients with MASLD.
Method: This prospective, randomized (2:1), open-label, bicenter study (one university hospital and one general hospital) enrolled patients with MASLD diagnosed by a hepatologist based on ultrasound-proven hepatic steatosis, absence of significant alcohol consumption (≤30 g/day for men and ≤20 g/day for women), and exclusion of other chronic liver diseases. Participants were randomized to TPE plus dietary measures or dietary measures alone between 2021 and 2024.
The primary endpoint was a ≥10% reduction in continuous controlled attenuation parameter (CAP) measured by FibroScan®. Clinical, anthropometric, biochemical, quality-of-life (SF-36), physical performance, and non-invasive fibrosis assessments (liver stiffness and ELF score) were performed at baseline, at week 12 (end of TPE), and at week 36. Results are presented as medians. Non-parametric statistical tests were used.
Results: A total of 115 patients were included (75 women, 40 men; median age 59 years; BMI 31 kg/m^2; CAP 305 dB/m; liver stiffness 5.4 kPa; AST 29 U/L; ALT 40 U/L; GGT 32 U/L; ELF score 8.9), with 76 assigned to the TPE plus diet group and 39 to the diet-only group. In the intention-to-treat analysis, the primary endpoint was not met, as a significant reduction in CAP was observed in both groups. No serious adverse events occurred. Similar findings were observed in the per-protocol analysis, after exclusion of 23 patients (consent withdrawal n = 3, loss to follow-up n = 11, insufficient TPE adherence <70% n = 9). Although CAP decreased significantly in both groups at weeks 12 and 36, significant reductions in AST and ALT were observed

only in the TPE group. Furthermore, while SF-36 scores were comparable at baseline, several quality-of-life domains significantly improved at weeks 12 and 36 exclusively in the TPE group.
Conclusion: Although the primary endpoint was not achieved, this randomized study suggests an additive benefit of therapeutic physical exercise combined with dietary measures, compared with dietary intervention alone, on biochemical parameters and quality of life in patients with MASLD (NCT04835831).

FRI-148
Pharmacodynamics, pharmacokinetics, safety, and tolerability of AZD2389, a fibroblast activation protein inhibitor in participants with liver fibrosis and compensated cirrhosis
Vian Azzu[1], Samuel Daniels[1], Mathias Liljeblad[2], Mohammad Niazi[3], Amparo Casanova[4], David Janzén[3], Karin Björhall[5], Xiao Tu[6], Sepideh Hagvall[7], Deepa Arya[7], Erinn Reilly[8], Mahssa Karimi[9], Grisell Ortiz-Lasanta[10], Linda Martinez[11], Eric Lawitz[12], Armando Flor[6]. *[1]Translational Science and Early Clinical Development, CVRM, AstraZeneca BioPharmaceuticals R&D, Cambridge, United Kingdom; [2]Translational Science & Early Clinical Development, CVRM, AstraZeneca BioPharmaceuticals R&D, Gothenburg, Sweden; [3]Clinical Pharmacology and Safety Sciences, AstraZeneca BioPharmaceuticals R&D, Gothenburg, Sweden; [4]Biometrics Early Development, CVRM, AstraZeneca BioPharmaceuticals R&D, Mississauga, Canada; [5]Drug Metabolism Pharmacokinetics and Biomarker Bioanalysis, CVRM, AstraZeneca BioPharmaceuticals R&D, Gothenburg, Sweden; [6]Translational Science & Early Clinical Development, CVRM, AstraZeneca BioPharmaceuticals R&D, Gaithersburg, United States; [7]Global Patient Safety Biopharmaceuticals, Chief Medical Office, AstraZeneca Oncology R&D, Gaithersburg, United States; [8]Early Phase Clinical Operations CVRM, AstraZeneca BioPharmaceuticals R&D, Gaithersburg, United States; [9]Projects, Research and Early Development, CVRM, AstraZeneca BioPharmaceuticals R&D, Gothenburg, Sweden; [10]FDI Clinical Research, San Juan, United States; [11]Oracle Clinical Research, Atlanta, United States; [12]Texas Liver Institute, San Antonio, United States*
Email: vian.azzu@doctors.org.uk

Background and aims: Fibroblast activation protein (FAP) is an endopeptidase with increasing hepatic expression as liver fibrosis progresses. FAP cleaves proteins that regulate extracellular matrix turnover and metabolism, such as denatured collagens, alpha-2-antiplasmin, and FGF21. Pharmacological inhibition of FAP in animal models of MASH and liver fibrosis shows anti-fibrosis benefit, and Phase I studies of AZD2389, a small molecule FAP inhibitor, in healthy participants showed robust changes in target engagement and proof of mechanism biomarkers. BORANA is a Phase IIa, randomized, single-blind, and placebo-controlled study, conducted in participants with liver fibrosis and compensated cirrhosis to assess safety, tolerability, PK and plasma FAP inhibition of AZD2389.
Method: The BORANA study (NCT06750276) comprised two parallel cohorts. Cohort A enrolled participants with MASH and fibrosis, Cohort B enrolled participants with non-MASH steatotic liver disease (including MetALD, ALD, and treated HCV), with advanced fibrosis. Participants were randomized (2:1 in each cohort) to receive AZD2389 or placebo treatment for 28 days. The primary objective was to assess safety and tolerability. Secondary objectives evaluated PK, plasma FAP inhibition as target engagement, and cleaved alpha-2-antiplasmin as a proof-of-mechanism biomarker.
Results: In total 22 participants were randomized to cohort A (14 AZD2389; 8 placebo) and 18 participants to cohort B (12 AZD2389; 6 placebo). No serious adverse events (AEs), AEs leading to discontinuations, or clinically significant AEs related to AZD2389 were reported. AZD2389 was rapidly absorbed (C_{max} 0.5-1-hour post-dose). There was no accumulation in plasma Cmax or AUCtau, and no time-dependency in PK over repeated dosing. AZD2389 inhibited plasma FAP activity by >90% at Cmax and >80% at 24-hour trough. AZD2389 reduced the percentage of FAP-cleaved alpha-2-antiplasmin by 39 units from baseline, which returned to baseline after washout.
Conclusion: AZD2389 was safe and well tolerated in participants with steatotic liver disease and fibrosis. AZD2389 showed a favourable PK profile consistent with once-daily dosing, without plasma accumulation during repeated dosing. AZD2389 achieved robust FAP inhibition throughout the dosing period of 28 days, accompanied by a reduction in physiological in vivo FAP substrate alpha-2-antiplasmin.

FRI-149
Reducing CV risk in patients with MASH independent of baseline based on Lp(a) and LDL lowering by resmetirom
Meena Bansal[1], Rebecca Taub[2], Dominic Labriola[2], David Soergel[2], Yestle Kim[2], Naim Alkhouri[3], Mazen Noureddin[4], Seth Baum[5], Rohit Loomba[6]. *[1]Icahn School of Medicine at Mount Sinai, New York, United States; [2]Madrigal Pharmaceuticals, Inc., West Conshohocken, United States; [3]Summit Clinical Research, San Antonio, United States; [4]Houston Methodist Hospital, Houston, United States; [5]Florida Atlantic University, Boca Raton, United States; [6]University of California San Diego School of Medicine, La Jolla, United States*
Email: meena.bansal@mssm.edu

Background and aims: Patients with metabolic dysfunction-associated steatohepatitis (MASH) have high cardiovascular morbidity and mortality. Resmetirom, a selective thyroid hormone receptor-beta agonist, is approved for treatment of patients with noncirrhotic MASH with moderate to advanced liver fibrosis. Resmetirom reduces atherogenic lipids and lipoproteins. In a secondary analysis of the Phase 3 MAESTRO-NASH clinical trial, the effects of resmetirom over 52 weeks on MASH efficacy parameters, atherogenic lipids, lipoproteins, and safety were evaluated according to baseline statin use.
Method: Data from the MAESTRO-NASH and MAESTRO-NAFLD-1 trials were analyzed. Analyses assessed MASH and lipid responses, shift in LDL and lipoprotein(a) [Lp(a)] risk profiles, and standard safety assessments including serial liver enzymes and adverse events according to baseline statin use.
Results: Approximately half (49%) of MAESTRO-NASH participants were on statins at baseline. Efficacy endpoints, including NASH resolution, fibrosis improvement and liver fat reductions were similar independent of statin codosing. Lipid lowering, showed significant improvement with resmetirom irrespective of baseline statin use; the percentage change at 24 weeks of resmetirom 80 mg, 100 mg, corrected for placebo in combination with statins or alone were LDL-C (−12.0, −18.7 (statin); −15.3, −14.1 [no statin]), Apolipoprotein B (ApoB) (−16.4, −20.7; −17.9; −19.9) and Lp(a) (−32.2, −35.8; −19.3, −26.6). In patients on statins 44.4% with LDL-C ≥70 mg/dL at baseline shifted to LDL-C <70 mg/dl with 100 mg resmetirom; 36.3% and 37.5% with Lp(a) ≥30 or ≥50 mg/dL at baseline shifted to <30 or <50 mg/dL with 100 mg resmetirom. No significant statin-related adverse events were observed.
Conclusion: Independent of statin use, treatment with resmetirom was efficacious at multiple MASH endpoints and improved lipid profiles for LDL-C, ApoB and Lp(a).

FRI-150-YI
Adipose tissue insulin resistance is a marker and a major driver of severe metabolic dysfunction associated steatohepatitis
Nateneal Beyene[1], Joel Haas[2], Silvia Sabatini[3], Wilhelmus Kwanten[1], Ann Driessen[4], Eveline Dirinck[5], Bart Staels[2], Christophe De Block[5], Sven Francque[1], Amalia Gastaldelli[3], Luisa Vonghia[1]. *[1]Department of Gastroenterology and Hepatology, Antwerp University Hospital, Laboratory of Experimental Medicine and Pediatrics, University of Antwerp, Antwerp, Belgium; [2]Université de Lille, Inserm, CHU Lille, Institut Pasteur de Lille, U1011 EGID, Lille, France; [3]Metabolic Diseases Research Group and Multi-Omics Mass Spectrometry Lab, Institute of Clinical Physiology, CNR, Pisa, Italy; [4]Department of Pathology, Antwerp*

University Hospital, Antwerp, Belgium; [5]Department of Endocrinology, Diabetology and Metabolic Diseases, Antwerp University Hospital, Antwerp, Belgium
Email: natenealtamerat.beyene@uantwerpen.be

Background and aims: Adipose insulin resistance (ADIPO-IR index) and excess free fatty acids (FFA, from impaired lipolysis suppression) are associated with severe fibrosis in MASLD. Whether ADIPO-IR also marks hepatic necro inflammation and MASH severity is unknown. We aimed to determine if ADIPO-IR independently predicts MASH and fibrosis and explore its links to hepatic inflammation and response to intervention.
Method: The cohort included 375 individuals without diagnosis diabetes at enrollment with liver biopsy categorized: MASH n = 219, No-MASH n = 104 (including MASL n = 64) and CT n = 52 (healthy liver).
Participants were also characterized with ADIPO-IR (FFAxInsulin), waist/height, visceral (VAT) and subcutaneous adipose tissue (SAT) by tomography, glucose tolerance by OGTT and PNPLA3 variants. A subgroup underwent liver transcriptomic analysis. An intervention subgroup with severe obesity was followed for 12 months after receiving either bariatric surgery (BS, n = 34) or lifestyle intervention (LS, n = 37), with post-intervention histology to find MASLD responders and non-responders. Logistic regression assessed ADIPO-IR as a predictor of MASH and fibrosis at baseline, adjusted for age, gender and BMI.
Results: Subjects with MASH, No MASH or CT had comparable BMI (38.2–39.5 kg/m2) and SAT. But MASH and No MASH had higher waist/height and VAT compared to CT ($p < 0.05$). ADIPO-IR increased with the severity of steatosis, inflammation and fibrosis. After adjusting for age, sex, and BMI, ADIPO-IR independently predicted the presence of MASH (OR = 1.72, $p = 0.003$) and significant fibrosis (OR = 1.92, $p = 0.004$). PNPLA3 variant carriers had similar ADIPO-IR. Liver transcriptomic analysis revealed that ADIPO-IR was positively correlated with the enrichment of gene sets related to inflammatory and immune responses, including neutrophil degranulation and interferon-gamma signaling. Post-intervention, ADIPO-IR was significantly reduced ($p < 0.0001$) and reduction below the overall median (FU/baseline = 0.4877) was more prevalent in the BS group (67.6% vs. 32.4% for LS) and in MASLD responders (60.5% vs. 32.1% for non-responders). Regardless of the intervention, the change in waist/height predicted ($p < 0.05$) the change in ADIPO-IR.
Conclusion: ADIPO-IR is an independent predictor of MASH and fibrosis in MASLD. Its correlation with hepatic inflammatory gene expression combined with its significant reduction following histological improvement, highlights ADIPO-IR as a key marker & driver of MASH.

FRI-151
Which comes first: GLP-1 RA vs resmetirom in MASH real world practice

Ana Maria Davila Morales[1], Amanda Rodriguez[1], Nancy S. Reau[1], Phoebe Lebeau[1]. [1]*Rush University, Chicago, United States*
Email: anamdavila95@gmail.com

Background and aims: Metabolic Dysfunction-Associated Steatotic Liver Disease (MASLD) is a spectrum of liver diseases ranging from steatosis to metabolic dysfunction-associated steatohepatitis (MASH). MASLD is associated with metabolic diseases such as obesity, hyperlipidemia, diabetes and hypertension. MASLD guidelines have not outlined which medication to start first and when to add a second agent. Resmetirom is used in patients with moderate to severe fibrosis without cirrhosis. Given the high prevalence of obesity and diabetes in this population, many are also treated with glucagon-like peptide-1 receptor agonists (GLP-1 RAs). These are indicated in patients with MASLD and those with dyslipidemia and cardiovascular disease may benefit from lipid-lowering effects, which is also a positive effect from resmetirom. Tailoring these medications in patients with multiple metabolic risk factors may prove beneficial. This study aims to provide insight into real-world treatment practices for the treatment of MASH.
Method: A retrospective study of patients currently on resmetirom for treatment of MASH with moderate to advanced liver fibrosis without cirrhosis at an academic medical center was conducted using Slicer Dicer. Concurrent use of GLP-1 RA medication was recorded. Data included BMI (body mass index) and presence of metabolic risk factors including obesity, dyslipidemia, hypertension and diabetes.
Results: 30 patients currently on resmetirom were identified. Of these, 50% were concurrently on a GLP-1 RA medication (n = 15). Of patients on single-agent treatment, one patient had 0 metabolic risk factors (6.6%), three had 1 risk factor (20%), seven had 2 risk factors (46.6%), three had 3 risk factors (20%), and one had 4 risk factors (6.6%). Of patients on dual-agent treatment, no patients had 0 or 1 metabolic risk factors, one patient had 2 risk factors (6.6%), ten had 3 risk factors (66.6%), and four patients had 4 risk factors (26.6%).
Conclusion: This study demonstrates that patients with MASH and 3 or more metabolic risk factors were more likely to be started on dual agent therapy with resmetirom and GLP-1 RA compared to single agent. This is the result of an approach targeted to address inflammation and fibrosis of the liver while also addressing underlying risk factors. The high prevalence of multiple risk factors present in patients with advanced MASH highlights the need for further studies to determine the effectiveness and benefits of dual agent therapy compared to single agent therapy.

FRI-152
Online case-based certified medical education improved clinical decision-making in the management of metabolic dysfunction-associated steatohepatitis

Shari Dermer[1], Julie Schrand[1], Jason Quinones[1], Roderick Smith[1], Jeffrey Lazarus[2]. [1]*Medscape Education, Newark, United States;* [2]*ISGlobal Barcelona Institute for Global Health, Barcelona, Spain*
Email: sdermer@medscape.net

Background and aims: Metabolic dysfunction-associated steatohepatitis (MASH) is a common, but often undertreated liver disease. Risk-stratification plays a critical role in determining an appropriate treatment approach for MASH. The objective of this study was to assess the effect of online case-based certified medical education (CME) on competence and confidence in managing MASH.
Method: Gastroenterologists/hepatologists (GI/Heps; n = 560) participated in a case-based activity that gauged clinical decision-making. Educational effect was assessed using a repeated-pair design. Pre/post-assessment was measured by 3 multiple choice questions and a paired samples t-test was conducted at the question level. Data are presented as % change pre to post-education for correct responses. A question rated by a 5-point Likert scale was used to determine confidence. Data were collected from May 8, 2025 to December 11, 2025.
Results: Risk-stratification using noninvasive tests (NITs) and imaging improved by 28% (57% to 85%; $p < .001$) following education. Interpretation of NITs improved by 46% (28% to 74%; $p < .001$). Selection of evidence-based MASH treatment improved by 48% (24% to 72%; $p < .001$) following education. Confidence in the ability to select patients with MASH for liver-directed therapy based on NITs increased following education with means of 2.83 pre to 3.33 post on a 5-point scale.
Conclusion: This study demonstrated that participation in case-based CME on MASH resulted in improved competence in assessing risk for MASH and in selection of evidence-based treatment. Moreover, there was increased confidence in the use of NITs to identify patients who are candidates for liver-directed MASH therapy. Based on competence and confidence prior to education, there are GI/Heps who would benefit from additional case-based education that allows for applying clinical decision-making.
Acknowledgement: Supported by an independent educational grant from Madrigal Pharmaceuticals.

Reference

Lazarus JV. Cases in Metabolic Dysfunction-Associated Steatohepatitis: Test Your Practice Skills. May 8, 2025.

FRI-153

Treatment with naltrexone/bupropion enhances lifestyle-induced improvements in hepatic steatosis in adults with overweight/obesity

Carmen Dietvorst[1,2], Willem Pieter Brouwer[3], Diederick Grobbee[4,5], Marco Alings[6], Maja Thiele[7,8], Jose Ordovas[9], Kirsten Berk[2], Robin Peeters[10], Manuel Castro Cabezas[1,5,10]. *[1]Department of Internal Medicine, Franciscus Gasthuis & Vlietland, Rotterdam, Netherlands; [2]Department of Internal Medicine, Division of Dietetics, Erasmus MC, Rotterdam, Netherlands; [3]Department of Gastroenterology and Hepatology, Erasmus MC, Rotterdam, Netherlands; [4]University Medical Center, Utrecht, Netherlands; [5]Julius Clinical, Zeist, Netherlands; [6]Department of Cardiology, Amphia hospital, Breda, Netherlands; [7]Center for Liver Research, Odense University Hospital, Odense, Denmark; [8]Evido Health, Copenhagen, Denmark; [9]USDA Human Nutrition Research Center on Aging, Tufts University, Boston, United States; [10]Department of Internal Medicine, Rotterdam, Netherlands*
Email: carmendietvorst@gmail.com

Background and aims: Metabolic dysfunction-associated steatotic liver disease (MASLD) is closely linked to overweight and obesity. Lifestyle modification is the cornerstone of therapy, but long-term weight reduction is challenging. Pharmacological agents such as naltrexone/bupropion (NB) may enhance weight loss and improve liver health. This study examined the impact of a 56-week lifestyle program with or without NB on hepatic markers and their association with weight change.
Method: The COR-BMOD trial enrolled adults with obesity or overweight plus hypertension or dyslipidaemia into a 56-week randomised, double-blind study combining an intensive lifestyle intervention with either placebo (LS) or NB in a 1:3 ratio. The program consisted of an energy-restricted diet (1200–1500 kcal/day), exercise guidance, and 28 group sessions targeting behavioural change. Weight, BMI, alanine aminotransferase (ALT), aspartate aminotransferase (AST), Hepatic Steatosis Index (HSI) and Metabolic Associated Fibrosis Score-5 (MAF-5) were assessed at baseline and after 56 weeks. (Non) parametric tests and regression analyses were performed.
Results: A total of 460 patients completed the study (mean age 46.8 ± 10.4 years; mean BMI 32.5 ± 5.0 kg/m^2; 88% female; LS n = 118, NB n = 342). After 56 weeks, both groups showed significant improvements in weight (LS −7.9, NB −11.7 kg; $p < 0.001$ for each), BMI (LS −2.8, NB − 4.7 kg/m^2; $p < 0.001$), ALT (LS −2.2 U/L, NB −2.8 U/L; $p < 0.05$), AST (LS −1.9 U/L, NB −1.5 U/L; $p < 0.05$), HSI (LS −3.5, NB −4.6; $p < 0.001$), and MAF-5 (LS −1.1, NB −1.2; $p < 0.001$). Improvements in BMI and HSI were significantly greater in the NB group compared with LS ($p < 0.05$). Regression analyses showed a moderate correlation between weight change and ALT in both groups. Weight loss was also strongly correlated with a decrease of MAF-5 and HSI.
Conclusion: NB treatment produced greater weight loss than lifestyle modification alone, with a more pronounced impact on liver steatosis than on liver fibrosis. These findings support NB as an effective adjunct to lifestyle intervention in overweight-related MASLD. The results reinforce that weight reduction remains the key determinant of improved liver health.

FRI-154

Timing and concordance of non-invasive treatment responses to Resmetirom in real-world practice

Winston Dunn[1], Rida Nadeem[2], Ashwani K. Singal[3], Amreen Dinani[4], Imad Asaad[5], Edward Mena[6], Colin Walsh[7], Sari Alothman[7], Sheel Patel[3], Jamil Abdo[3], Wamda Ahmed[8], Larissa Lushniak[4], Naim Alkhouri[7]. *[1]University of Kansas Medical Center, Pinnacle Clinical Research, Mission Hills, United States; [2]Arizona Liver Health, Chandler, United States; [3]University of Louisville, Louisville, United States; [4]Duke University, Durham, United States; [5]Firelands, Sandusky, United States; [6]California Liver Research Institute, Pasadena, United States; [7]Summit Clinical Research, San Antonio, United States; [8]University of Kansas, Kansas City, United States*
Email: naim.alkhouri@gmail.com

Background and aims: Current AASLD guidance recommends using changes in liver stiffness measurement (LSM), controlled attenuation parameter (CAP), and ALT to monitor treatment response to resmetirom. MAESTRO-NASH primarily assessed noninvasive responses at 12 months, and the timing and concordance of earlier time points (3, 6, and 9 months) remain poorly defined. Understanding the pattern of earlier treatment response in real-world practice is essential for avoiding premature classification of treatment failure. This study aimed to characterize the frequency and overlap of LSM, CAP, and ALT responses over the first year of therapy.
Method: We conducted a multicenter, real-world study of resmetirom-treated patients from five centers. Eligible patients met treatment criteria based on liver biopsy, ELF score, or LSM and had a baseline LSM with ≥1 follow-up LSM between 3 and 12 months. LSM response and worsening were defined as ≥25% reduction and increase from baseline; ALT response as ≥20% or 17 U/L reduction; and CAP response as ≥40-dB/m reduction. Partial response was defined as LSM response plus either ALT or CAP response, and complete response as concurrent LSM, ALT, and CAP responses.
Results: Among 2,236 treated patients, 220 with available baseline and follow-up LSM were included. At baseline, 55.7% had diabetes or impaired glucose tolerance, and 26.2% received concomitant GLP-1 therapy. Median baseline LSM was 11.0 kPa (IQR 8.9–12.0). LSM response occurred in 10.5%, 26.8%, 33.6%, and 38.6% of patients at 3, 6, 9, and 12 months, respectively. CAP response was observed in 12.3%, 35.5%, 42.5%, and 47.9%, while ALT response occurred in 19.5%, 31.8%, 35.5%, and 38.6% across the same time points. Partial response was present in 6.8%, 20.9%, 25.6%, and 29.7%, and complete response in 1.8%, 6.8%, 9.5%, and 11.4%, respectively. ALT response at 6 was associated with subsequent LSM response (odds ratio 2.38, 1.34–4.28; $p < 0.01$).
Conclusion: In real-world resmetirom-treated patients, non-invasive treatment responses accumulate gradually and show incomplete overlap across biochemical and elastographic domains. ALT response at 6 months shows moderate concordance with subsequent LSM response, supporting cautious interpretation of early biochemical improvement and reinforcing the need for integrated, longitudinal assessment across multiple non-invasive markers.

FRI-155

Efficacy of oral semaglutide in overweight- obese patients with metabolic dysfunction-associated steatotic liver disease (MASLD) related compensated advanced chronic liver disease (cACLD) - Results of first randomized controlled trial

Ajay Kumar Duseja[1], Prahlad Kumar[2], Arka De[3], Sunil Taneja[1], Naveen Kalra[4], Sanjay Bhadada[5], Suvradeep Mitra[6]. *[1]Department of Hepatology, Postgraduate Institute Of Medical Education And Research Chandigarh, Chandigarh, India; [2]Department of Internal Medicine, Postgraduate Institute Of Medical Education And Research Chandigarh, Chandigarh, India; [3]Department of Hepatology, Postgraduate Institute Of Medical Education And Research, Chandigarh, India, Chandigarh, India; [4]Department of Radiodiagnosis and Imaging, Postgraduate Institute Of Medical Education And Research Chandigarh, Chandigarh, India; [5]Department of Endocrinology, Postgraduate Institute Of Medical Education And Research Chandigarh, Chandigarh, India; [6]Department of Histopathology, Postgraduate Institute Of Medical Education And Research Chandigarh, Chandigarh, India*
Email: ajayduseja@yahoo.co.in

Background and aims: There are limited options for treating patients with advanced fibrosis in metabolic dysfunction-associated steatotic liver disease (MASLD) and no randomized data exists regarding the

efficacy of oral semaglutide in these patients. Aim of the present study was to assess the efficacy of oral semaglutide in improving hepatic steatosis and fibrosis in overweight/obese patients with MASLD related compensated advanced chronic liver disease (cACLD).
Method: In a prospective study, 52 MASLD-cACLD, overweight/obese patients (as per Asian criteria) with baseline weight –88.6 ± 15.8 kg vs 75.9 ± 6.6 kg, BMI- 31.99 ± 5.91 vs. 28.45 ± 2.33 kg/m^2, with or without diabetes mellitus matched for age (~53 years) and gender (~55% female) were randomised to lifestyle interventions plus oral semaglutide, 14 mg/day (29 patients) or lifestyle interventions alone (23 patients). MASLD was defined as per standard criteria and cACLD as LSM on VCTE ≥10 kPa (mean LSM- 20 kPa). Evaluation was done at 6 months for change in anthropometry, hepatic steatosis [controlled attenuation parameter (CAP), MRI-PDFF], at-risk MASH (FAST and MAST and hepatic fibrosis (LSM on VCTE, MRE, APRI, FIB-4, Agile 3+, Agile 4).
Results: Patients on oral semaglutide achieved significantly higher weight loss (~9%) at 6 months and in spite of having higher baseline value, there was significant reduction in in CAP (322.85 ± 39.32 to 292.42 ± 45.98; $p < 0.001$) in the semaglutide group in comparison to insignificant change in control group. Similarly, in spite of higher liver stiffness measurement (LSM) on VCTE at baseline, semaglutide led to a significant reduction in LSM (17.16 ± 10.79 kPa; $p < 0.001$) at 6 months, while the control group showed no change. Among 26 patients subjected to MR-PDFF, MAST and MRE at 6 months with comparable baseline values, there greater reduction in MR-PDFF ($p = 0.034$) and MRE ($p = 0.043$), in comparison to controls. The reduction in Agile 3+, Agile 4 scores were also significant in the semaglutide group, however the difference in the change of APRI, FIB-4, FAST and MAST scores was not significant among the two groups. Oral semaglutide was well tolerated except for minor GI side effects. There were no hepatic decompensation or development of HCC in either group.
Conclusion: In a first randomized controlled trial, oral semaglutide, administered for 6 months, achieved substantial weight loss and significant improvement in non-invasive hepatic steatosis and fibrosis indices in MASLD-related cACLD without safety concerns.

FRI-156
DR10624, a novel FGF21R/GCGR/GLP-1R triple agonist, significantly reduced liver fat and improved hepatic and metabolic biomarkers in a phase 2 study of patients with severe hypertriglyceridemia

Yongliang Fang[1], Yanting Fan[2], Long Zhang[3], Yan Zhang[3], Chaonan Zhu[2], Kaile Zhou[2], Yulong Gan[1], Jun Zhou[2], Ying Wang[1], Junfang Xu[2], Yanshan Huang[1], Jianping Li[3]. [1]*Zhejiang Doer Biologics Co., Ltd., Hangzhou, China;* [2]*Huadong Medicine Co., Ltd., Hangzhou, China;* [3]*Peking University First Hospital, Beijing, China*
Email: fyl323@gmail.com

Background and aims: Severe hypertriglyceridemia (SHTG) is frequently associated with hepatic steatosis, contributing to increased risk of metabolic dysfunction-associated steatotic liver disease (MASLD). DR10624 is a first-in-class long-acting triple agonist against FGF21R, GCGR, and GLP-1R. In a Phase 2 study in participants with SHTG, DR10624 demonstrated significant improvement in participants' lipid profile, liver function, and metabolic biomarkers.
Method: This Phase 2 trial was a 12-week randomized, double-blind, placebo-controlled, multi-center study in adults with SHTG (fasting triglycerides [TG] between 5.6 mmol/L [500 mg/dL] and 22.6 mmol/L [2000mg/dL]). Participants received weekly subcutaneous injection of DR10624 (12.5 mg, 25 mg, or 50 mg titration) or placebo for 12 weeks. Prespecified liver and metabolic-related biomarkers included liver fat content (LFC), assessed by MRI-PDFF; alanine aminotransferase (ALT); aspartate aminotransferase (AST); alkaline phosphatase (ALP); Fibrosis-4 (FIB-4); and adiponectin.
Results: A total of 79 participants were included (mean age: 46.0, 70.0% male), with baseline TG (median 9.4 mmol/L [800 mg/dL]). At week 12, the median relative reduction from baseline in LFC was significantly greater with DR10624 (–63.2%, –53.7%, and –67.0% in the 12.5 mg, 25 mg, and 50 mg titration, respectively) than with placebo (–8.4%). After treatment with DR10624 at doses of 12.5 mg, 25 mg, and 50 mg titration, ≥50% relative reductions in LFC were achieved by 52.4%, 44.4%, and 71.3% of participants, respectively, compared with 5.7% in the placebo group, while normalized liver fat (LFC<5% by MRI-PDFF) was observed in 47.6%, of participants, respectively, versus 5.6% with placebo. DR10624 was associated with significant improvements in liver enzymes, particularly in the higher-dose group, including reductions in ALT (–10.0 U/L in 25 mg, $P = 0.0458$), AST (–10.0 U/L, – 5.4U/L in 25 mg, 50 mg titration, $P = 0.0012$, 0.0135, respectively), and ALP (–7.0 U/L in 50 mg titration, $P = 0.0439$). DR10624 led to significantly increased adiponectin levels by 1.9 mg/dL, 2.6 mg/dL, and 3.1 mg/dL in 12.5 mg, 25 mg, and 50 mg titration, respectively. DR10624 also decreased FIB-4 by –0.19 in the 50 mg titration.
Conclusion: In patients with SHTG, treatment with DR10624 produced robust reductions in triglyceride levels and was associated with significant improvements in liver steatosis, hepatic function, and metabolic biomarkers. Collectively, these findings support DR10624 as a promising therapy for MASLD.

FRI-157-YI
Habitual aspirin use and MRI-derived liver fat and fibroinflammation

Qi Feng[1], Pinelopi Manousou[1], Chioma Izzi-Engbeaya[1], Mark Woodward[1]. [1]*Imperial College London, London, United Kingdom*
Email: ermadake@gmail.com

Background and aims: Steatotic liver disease is the most prevalent chronic liver condition, affecting one-third of the adult population. Habitual aspirin use is common among older adults. This study aimed to investigate the relationship between aspirin use and liver fat accumulation and fibroinflammation.
Method: We used UK Biobank imaging cohort data. Aspirin use was self-reported at baseline and imaging assessment, and the main exposures were aspirin use at imaging assessment and longitudinal aspirin use patterns (never users, initiators, discontinuers, vs. persistent users). Outcomes were MRI-derived liver fat (%) and cT1 (ms, a measure for fibroinflammation). Multivariable adjustment analyses and inverse probability of treatment weighting (IPTW) analyses were performed, accounting for demographic, lifestyle and clinical factors.
Results: We included 36413 participants (age 64.6 years, 51.4% female). Aspirin use at imaging assessment was associated with lower liver fat (–0.35 (95% CI: –0.51, –0.20)) and slightly higher cT1 (5.13 (95% CI: 3.23, 7.03)). Analyses on longitudinal aspirin use pattern showed that compared to never users, initiators and persistent users showed lower liver fat (–0.48 (–0.69, –0.28) and (–0.24 (–0.45, –0.02)) and higher cT1 (2.94 (0.38, 5.49) and 8.31 (5.65, 10.97)). IPTW analyses showed consistent results.
Conclusion: In this large population-based cohort, aspirin use was linked to reduced liver fat, but a small, clinically insignificant (i.e. <80 ms) increase in cT1. These findings suggest aspirin may mitigate steatosis through metabolic pathways but does not necessarily rapidly reverse fibroinflammatory injury.

FRI-158-YI

Additive associations of the mediterranean diet, physical activity, and coffee consumption with reduced risk of liver fibrosis in metabolic dysfunction-associated steatotic liver disease

Meng-Lun Hsieh[1], Yen-Chun Peng[1,2], Vivian Chia-Rong Hsieh[3].
[1]*Taichung Veterans General Hospital, Taichung, Taiwan;* [2]*School of Medicine, National Yang Ming Chiao Tung University, Beitou District, Taiwan;* [3]*China Medical University, Beitun District, Taiwan*
Email: morganpolo@gmail.com

Background and aims: Mediterranean diet (MD), physical activity (PA), and coffee intake are key non-pharmacological strategies recommended by practice guidelines for improving outcomes in patients with metabolic dysfunction-associated steatotic liver disease (MASLD). This study aims to explore the combined association of these lifestyle factors with liver fibrosis in this population.
Method: Data from the National Health and Nutrition Examination Survey 2017-March 2020 were analyzed in this cross-sectional study. MASLD was defined by the latest criteria, using controlled attenuation parameter (CAP) ≥275 dB/m for steatosis. MD adherence, PA, and coffee consumption were derived from questionnaire data. Participants were categorized into tertiles of MD adherence (low, moderate, high by alternate MD index), PA groups (<600 vs. ≥600 MET-min/week), and coffee consumption groups (0, 0–2, ≥2 cups/day). Significant liver fibrosis was defined as liver stiffness measurement (LSM) ≥8 kPa. Multivariate logistic regression was performed with sample weights to compare fibrosis risk across various lifestyle groups, adjusting for age, sex, smoking, alcohol intake, diabetes, and hypertension.
Results: A total of 2,672 participants with MASLD were identified who had complete dietary, PA, LSM and CAP data. Higher proportions of DM (38.1% vs. 21.2%), hypertension (66.5% vs. 52.7%) and higher CAP (343.9 vs. 319.7 dB/m) were observed among those with significant fibrosis compared to those without. MD adherence, coffee consumption and PA were each independently and inversely associated with the risk of significant fibrosis in multivariate analysis (high vs. low MD adherence, aOR: 0.67, $p < 0.01$; coffee ≥2 vs. 0 cups/day, aOR: 0.48, $p < 0.01$; PA ≥ 600 vs. <600 MET-minutes/week, aOR: 0.76, $p < 0.01$). Combined analysis revealed an additive, dose-dependent protective association between three lifestyle factors and significant fibrosis. For example, in participants with low PA, the risk of significant fibrosis decreased with increasing coffee consumption and MD adherence (low PA/≥ 2 cups coffee/high MD vs. low PA/0 cup coffee/low MD, aOR: 0.316, 95% CI: 0.314–0.318). Lowest risk (aOR: 0.194, 95% CI: 0.192–0.195) was observed in individuals with the highest adherence to all three behaviors.
Conclusion: An additive association of MD adherence, coffee consumption, and PA with significant liver fibrosis was observed among MASLD individuals. Our findings support guideline-recommended adherence to these lifestyle patterns.

FRI-159

Dose-dependent efficacy and renal safety of pemafibrate in patients with MASLD: a multicenter randomized controlled trial

Michihiro Iwaki[1], Takashi Kobayashi[1], Asako Nogami[1], Kento Imajo[2], Koki Nagai[3], Eiji Sakai[4], Yoshinobu Nakada[5], Takeo Kurihashi[6], Hiroshi Tobita[7], Shuichi Sato[8], Yuki Yamaguchi[9], Kazuhito Kawata[10], Masahiro Matsushita[11], Yuya Seko[12], Motoo Iwasa[13], Miwa Kawanaka[14], Kazuhisa Maeda[15], Koichiro Furuta[16], Nobuharu Tamaki[17], Atsushi Kawaguchi[18], Hirokazu Takahashi[19], Masato Yoneda[20], Atsushi Nakajima[21]. [1]*Yokohama City University Graduate School of Medicine, Yokohama, Japan;* [2]*Shinyurigaoka General Hospital, Kawasaki, Japan;* [3]*National Hospital Organization Yokohama Medical Center, Yokohama, Japan;* [4]*Yokohama Sakae Kyosai Hospital, Yokohama, Japan;* [5]*Shonan Hospital, Yokosuka, Japan;* [6]*Kanagawa Dental University Yokohama Clinic, Yokohama, Japan;* [7]*Shimane University Hospital, Izumo, Japan;* [8]*Izumo City General Medical Center, Izumo, Japan;* [9]*Masuda Red Cross Hospital, Masuda, Japan;* [10]*Hamamatsu University School of Medicine, Hamamatsu, Japan;* [11]*Shimada Municipal Hospital, Shimada, Japan;* [12]*Kyoto Prefectural University of Medicine, Kyoto, Japan;* [13]*Mie University Graduate School of Medicine, Tsu, Japan;* [14]*Okayama University, Kawasaki Medical School, Okayama, Japan;* [15]*Kitasenri Maeda Clinic, Suita, Japan;* [16]*National Hospital Organization Hamada Medical Center, Hamada, Japan;* [17]*Musashino Red Cross Hospital, Musashino, Japan;* [18]*Saga University, Saga, Japan;* [19]*Saga University Hospital, Saga, Japan;* [20]*Yokohama City University School of Medicine Graduate School of Medicine, Yokohama, Japan;* [21]*International University Health and Welfare Atami Hospital, Yokohama City University School of Medicine Graduate School of Medicine, Yokohama, Japan*
Email: michihirokeidai@yahoo.co.jp

Background and aims: The prevalence of metabolic dysfunction–associated steatotic liver disease (MASLD) is rapidly increasing worldwide, yet effective pharmacologic options remain limited. Pemafibrate, a selective PPARα modulator (SPPARMα), has stronger activity and selectivity than conventional PPARα agonists and may improve liver function. This study evaluated the efficacy and safety of pemafibrate in patients with MASLD.
Method: This multicenter, open-label, randomized controlled trial enrolled 360 patients with MASLD and hypertriglyceridemia at 29 sites in Japan. Participants were randomized to high-dose pemafibrate 0.4 mg/day (PEM-H), low-dose pemafibrate 0.2 mg/day (PEM-L), or fenofibrate 53.3–106.6 mg/day (FENO). The primary endpoint was the change in ALT at Week 24. Secondary endpoints included liver fibrosis markers, renal parameters, and MR elastography (MRE) at Week 48.
Results: At Week 24, both pemafibrate groups achieved significantly greater ALT reductions than fenofibrate (Mean: −24.0 U/L in PEM-H, −14.8 U/L in PEM-L, −4.22 U/L in FENO; PEM-H vs FENO $p < 0.001$; PEM-L vs FENO $p = 0.018$). PEM-H also showed greater improvement than PEM-L ($p = 0.018$), indicating clear dose dependency. At Week 48, Mac-2 binding protein glycosylation isomer decreased markedly in PEM-H (−21.6%) and PEM-L (−17.8%) but only modestly with FENO (−3.2%). Type IV collagen 7 s and Enhanced Liver Fibrosis score showed no statistically significant differences among the three groups. Liver stiffness by MRE improved in PEM-H (−9.2 ± 14.0%) and PEM-L (−8.4 ± 9.9%), whereas it increased in FENO (+3.6 ± 21.4%), demonstrating a significant benefit with pemafibrate. Renal parameters were significantly more favorable with pemafibrate compared with fenofibrate. Treatment-related adverse events occurred less frequently with pemafibrate (n = 8 in PEM-H; n = 8 in PEM-L) than with FENO (n = 18), including 15 muscle-related events in the FENO group. Hepatobiliary disorders occurred only with FENO (n = 5). No treatment-related serious adverse events were reported in either pemafibrate group.
Conclusion: Pemafibrate produced significantly greater ALT improvement than fenofibrate, with a clear dose–response relationship and a more favorable renal and safety profile. Reductions in M2BPGi and MRE-based liver stiffness suggest potential anti-inflammatory and anti-fibrotic effects. These results support pemafibrate as a promising therapeutic option for patients with MASLD and hypertriglyceridemia, and further histology-based studies are warranted.

FRI-163

Cost-effectiveness of resmetirom treatment, aligned with practice guidance, for suspected 'At-Risk MASH' identified by transient elastography without histologic confirmation

Jeong-Yeon Cho[1], Dae Won Jun[2], Eileen Yoon[2], Jihyun An[2], Ha Il Kim[2], Chul-min Lee[3], Mimi Kim[3], Bo-Kyeong Kang[3], Eun Chul Jang[4], Sang Bong Ahn[5], Joo Hyun Oh[6], Hyo Young Lee[2], Hye-Lin Kim[7], Nathorn Chaiyakunapruk[1]. [1]*Department of Pharmacotherapy, University of Utah College of Pharmacy, Salt Lake, United States;* [2]*Department of Internal Medicine, Hanyang University College of Medicine, Seoul, Korea, Rep. of South;* [3]*Department of Radiology, Hanyang University College of Medicine, Seoul, Korea, Rep. of South;*

[4]Department of Occupational and Environmental Medicine, College of Medicine, Soonchunhyang University, Chunan, Korea, Rep. of South; [5]Department of Internal Medicine, Nowon Eulji Medical Center, Eulji University, Seoul, Korea, Rep. of South; [6]Department of Internal Medicine, CHA University College of Medicine, Seongnam, Korea, Rep. of South; [7]College of Pharmacy, Sahmyook University, Seoul, Korea, Rep. of South
Email: noshin@hanyang.ac.kr

Background and aims: Resmetirom can be prescribed in clinical practice based on noninvasive tests (NITs) without liver biopsy for patients with suspected at-risk metabolic dysfunction–associated steatohepatitis (MASH). However, NITs–based selection may include false positives (e.g., F0–F1 hepatic fibrosis) cases, creating uncertainty regarding the cost-effectiveness of NITs oriented, guidance-aligned treatment.
Method: We conducted a cost-utility analysis from the US healthcare payer perspective to evaluate resmetirom treatment for suspicious at risk MASH based on NITs versus no treatment. A decision-analytic Markov model simulated fibrosis progression/regression and liver- and cardiovascular-related outcomes; costs and quality-adjusted life-years (QALYs) were discounted at 3% annually. Treatment effects on fibrosis progression and regression were based on MAESTRO-NASH relative risks, and cardiovascular benefit was conservatively modeled via LDL-cholesterol–mediated risk reduction. Base-case analyses assumed a cohort of 100,000 patients starting at age 40 years, with willingness-to-pay set at $150,000/QALY.
Results: In the base case, resmetirom treatment yielded 1.00 incremental QALYs and 1.06 incremental life-years at an incremental cost of $137,151 per patient, resulting in an incremental cost-effectiveness ratio (ICER) of $137,361/QALY. Although VCTE-based eligibility included 19% F0–F1 and 28% F4 at baseline, resmetirom remained cost-effective compared with no treatment, largely driven by reductions in liver-related complications and cardiovascular events that partially offset medication costs. In one-way sensitivity analyses, resmetirom price was the dominant driver: a 50% price reduction lowered the ICER to $106,525/QALY, and a semaglutide-level price scenario lowered it to $41,119/QALY. Lower assumed treatment effectiveness in F4 (50% of F2–F3 effect) increased the ICER to $153,883/QALY, slightly above the willingness-to-pay threshold. In probabilistic sensitivity analysis, the probability that resmetirom was cost-effective was 65% at $150,000/QALY, with cost-effectiveness becoming more likely than no treatment at approximately $130,000/QALY.
Conclusion: NITs based resmetirom treatment guidance is likely to be cost-effective in US practice, despite inclusion of considerable without histologic F2–F3.

FRI-164

Safety and efficacy of Lactobacillus delbrueckii subsp. lactis CKDB001 in patients with metabolic-associated steatotic liver disease: a randomized, double-blind, placebo-controlled phase II clinical trial

Jung Hee Kim[1], Ki Tae Suk[1]. [1]Hallym Medical Center, Chuncheon, Korea, Rep. of South
Email: mazyyang5@gmail.com

Background and aims: *Lactobacillus delbrueckii* subsp. *lactis* CKDB001 is a probiotic derived from raw milk fermentation with hepatoprotective and metabolic effects mediated through bile acid metabolism, lipid handling, and gut–liver axis signaling. This study evaluated its safety, clinical efficacy, and gut microbiome–metabolome modulation in patients with metabolic dysfunction–associated steatotic liver disease (MASLD).
Method: In this randomized, double-blind, placebo-controlled trial, patients with MASLD received CKDB001 (5.0×10^9 CFU/day, one capsule twice daily; n = 46) or placebo (n = 43) for 12 weeks. Primary outcomes were changes in serum AST and ALT. Secondary outcomes included liver function markers, lipid and glucose metabolism parameters, and fatigue. Exploratory outcomes assessed anthropometry, hepatic steatosis and stiffness by transient elastography, and gut microbiome and metabolome profiles using an integrative multi-omics.
Results: Eighty-nine participants (mean age 44.7 years; mean BMI 29.9 kg/m^2) were included, with comparable baseline characteristics between groups and no withdrawals. CKDB001 was well tolerated, with no differences in adverse events or aminotransferase levels compared with placebo. Favorable trends were observed in insulin resistance and hepatic steatosis. Significant reductions in waist and hip circumference were observed exclusively in the intervention group (all $p < 0.005$). Multi-omics analyses revealed stable microbial diversity but intervention-specific shifts in microbial taxa and metabolites at Week 12. Treatment-by-time interactions were identified for 8 taxa and 12 metabolites, including increases in *L. delbrueckii* and the butyrate-producing *Faecalibacterium duncaniae* (all $p < 0.001$). Lipid-related and bioactive metabolites involved in inflammation and host signaling were significantly altered. Correlation analyses linked *L. delbrueckii* with indole-3-butyric acid and 17α-hydroxyprogesterone, and *F. duncaniae* with arachidonic acid–related metabolites, indicating coordinated microbe–metabolite modulation.
Conclusion: CKDB001 supplementation modulated key metabolites and lipid mediators associated with gut–liver axis signaling in patients with MASLD. These findings suggest a mechanistic basis for its metabolic benefits and support further large-scale studies to evaluate its potential as a therapeutic target for MASLD.

FRI-165

Real-world effectiveness of one year of Resmetirom treatment in at-risk metabolic dysfunction–associated steatohepatitis

Rida Nadeem[1], Anita Kohli[1], Ann Moore[2], Savannah Nelson[1], Himanshi Kapoor[1], Noor El-Gendy[1], Erfan Asadipour[1], Noor El-Gendy[1], Sean Macaraeg[1], Phuong Nguyen[1,3], Richard Manch[1], Justin Reynolds[2], Jessica Omana Castaneda[1]. [1]Arizona Liver Health, Chandler, United States; [2]Arizona Liver Health, Peoria, United States; [3]Abrazo Health Network, Glendale, United States
Email: rnadeem@azclinicaltrials.com

Background and aims: Resmetirom, a selective thyroid hormone receptor-β agonist, has demonstrated histologic efficacy in the treatment of metabolic dysfunction–associated steatohepatitis (MASH). However, real-world data evaluating treatment response is limited. We aimed to assess hepatic and metabolic responses to resmetirom in a real-world MASH population treated for a minimum of one year using changes in NITs.
Method: We conducted a retrospective real-world study of adults with presumptive F2 or F3 MASH (at-risk MASH) treated with resmetirom in an outpatient hepatology practice. A total of 599 patients were prescribed resmetirom between March 2024 and July 2025, with 331 patients having completed at least 52 weeks of resmiterom. Patients on GLP-1 or GIP analog therapies (n = 268) were excluded from analysis given potential confounding. Liver disease activity and fibrosis were assessed at baseline and follow-up using NITs including serum aminotransferases, fibrosis scores (e.g., FIB-4, FAST), and vibration-controlled transient elastography (VCTE). Treatment response was defined as improvement in liver enzymes and percent changes in hepatic steatosis and fibrosis NITs. Secondary outcomes included changes in lipid parameters and resmiterom tolerability.
Results: 204 patients who completed atleast 52 weeks of resmiterom were included (mean age 55 years; 42% male; mean BMI 37.7 kg/m^2). 49.5% of patients had T2DM, 33.8% dyslipidemia, and 54.9% hypertension. After 52 weeks of treatment, 62.7% of patients had a one stage or greater reduction in liver fibrosis by VTCE. Mean reduction in VCTE kpa was 32.2%. Mean reduction in hepatic steatosis as measured by VCTE CAP was 21.1%. Decrease in hepatic inflammation at 52 weeks seen with mean reduction of AST and ALT 12.5 IU/L

and 22.44 IU/L respectively. Total cholesterol reduced by a mean of 24.36 mg/dL, LDL-cholesterol by 26.19 mg/dL, triglycerides by 68.6 mg/dL, and HDL increased by a 5.5 mg/dL after 52 weeks. 8% of patients discontinued therapy due to adverse events.
Conclusion: In a real-world clinical setting, 52 weeks of resmetirom treatment was associated with significant improvements in hepatic fibrosis and steatosis, as well as multiple biochemical and cardiometabolic parameters in patients with at-risk MASH. Therapy was safe and well tolerated across a diverse patient population with multiple comorbidities. These findings support the effectiveness of resmetirom in a real world patient population where NITs are routinely used to intiate and guide therapy.

FRI-166-YI
Improvement of liver steatosis after bariatric surgery in severe obesity is associated to weight reduction and type of surgery
Laura Konings[1,2], Carmen Dietvorst[1,2], Willy Theel[2], Jan Apers[1], Susan ter Borg[1], Tessa Noordermeer[1], Manuel Castro Cabezas[1,2].
[1]Franciscus Gasthuis, Rotterdam, Netherlands; [2]Erasmus University Medical Center, Rotterdam, Netherlands
Email: l.konings@franciscus.nl

Background and aims: Metabolic dysfunction-associated steatotic liver disease (MASLD) affects many patients with severe obesity. Weight reduction following bariatric surgery has been associated with improvement of MASLD. Vibration-controlled transient elastography (VCTE) is a non-invasive and reliable method to estimate liver steatosis (by controlled attenuation parameter, CAP) and fibrosis (by liver stiffness measurement, LSM). The aim of this study was to evaluate changes in liver steatosis and fibrosis after gastric sleeve resection (GS) or gastric bypass (GB).
Method: The Franciscus Obesity NASH Study (FONS) is a single centre cohort study including patients undergoing bariatric surgery. VCTE was done at baseline and at least one year after surgery. Anthropometric characteristics and laboratory data were also collected.
Results: Of the 229 subjects who underwent bariatric surgery, 170 subjects underwent VCTE at baseline and after one year. Overall, there was a significant decrease in weight, BMI, CAP and LSM. There were no baseline differences between GB (n = 77) and GS (n = 93) regarding age, weight, BMI, CAP or LSM. Before surgery, liver steatosis (CAP ≥ 275 dB/m) was present in 69% of patients in the GB group and 60% of patients in the GS group. At one-year follow-up, steatosis prevalence decreased to 5% in the GB group and 11% in the GS group. Liver fibrosis (LSM ≥ 8 kPa) was observed preoperatively in 51% of GB patients and 46% of GS patients, decreasing postoperatively to 3% and 9%, respectively. Although CAP normalised in both groups, the GB group had a greater decrease in CAP of – 98 ± 49 dB/m compared to – 65 ± 57 dB/m ($p < 0.001$). Patients in the GB group showed slightly greater improvements in BMI and weight, but not in LSM. Reductions in CAP were significantly associated with decreases in BMI, waist circumference and weight. In contrast, no such associations were observed for changes in LSM. In multivariable linear regression analyses, improvement in CAP was strongly associated with weight loss and type of surgery, whereas improvement in LSM was not associated with either.
Conclusion: Bariatric surgery leads to significant improvements in both liver steatosis and fibrosis. Improvement in liver steatosis was associated with reductions in BMI and was more pronounced following gastric bypass. In contrast, improvements in liver fibrosis were not dependent on the type of surgery or BMI.

FRI-167
First-in-human phase 1 study to evaluate the safety, tolerability, pharmacokinetics and pharmacodynamics of HP515, a selective THR beta agonist, in healthy participants
Fei Lan[1], Yangming Guo[1], Xiaolan Yong[2], Xiuqin Jia[1], Ling Chen[1], Yuanyuan Xv[1], Fei Luo[1], Yao Zhang[1], Zheng Yao[1], Simon Li[1], Yuanwei Chen[1], Xinghai Li[1]. *[1]Chengdu, China; [2]Chengdu Xinhua Hospital, Chengdu, China*
Email: flan@hinovapharma.com

Background and aims: HP515 is an oral small-molecule selective thyroid hormone receptor beta (THR beta) agonist developed to improve hepatic lipid metabolism while minimal systemic thyroid effects. Preclinical studies showed robust THR beta engagement with marked reductions in hepatic steatosis and improvements in metabolic dysfunction-associated steatohepatitis-related histologic features, alongside a wide safety margin. This study aimed to assess safety, tolerability, pharmacokinetics (PK), and pharmacodynamics (PD) of HP515 in healthy participants.
Method: This was a randomized, double-blind, placebo-controlled Phase 1 study including single ascending dose (SAD) and multiple ascending dose (MAD) cohorts. Participants in SAD cohorts received a single oral dose at 10, 20, 40, 80, 120, 160, or 200 milligrams (mg), while participants in MAD cohorts received 40, 60, or 80 mg, po, once daily for 14 days. Safety assessments included adverse events, clinical laboratory tests, vital signs, and electrocardiograms. PK parameters were calculated for single and repeated dosing. PD biomarkers included total cholesterol, low-density lipoprotein cholesterol, apolipoprotein B, small dense low-density lipoprotein cholesterol, and sex hormone binding globulin (SHBG).
Results: HP515 was safe and well tolerated at all doses. No serious adverse events or dose-limiting toxicities (DLT) occurred. Similar to the observation reported with other THR beta agonists, transient, asymptomatic alanine aminotransferase and aspartate aminotransferase elevations occurred in one subject in 60 mg cohort and one in 80 mg cohort in MAD part, which were normalized without intervention. PK exposure increased approximately dose-proportionally from 10 to 80 mg and greater than dose-proportionally from 80 to 200 mg. Following repeated dosing, the time to HP515 maximum concentration was approximately 2 to 4.5 hours, and the elimination half-life was 3 to 3.6 hours, supporting once-daily administration. Dose-dependent PD effects included reductions in lipid parameters and increases in SHBG at 40–80 mg, consistent with THR beta activation.
Conclusion: HP515 demonstrated a favorable safety profile, predictable PK, and dose-dependent PD activity in healthy participants. These results support ongoing Phase 2a dose-finding study in patients with metabolic dysfunction-associated steatotic liver disease.

FRI-168
Treatment effects of survodutide, a glucagon/glucagon-like peptide-1 receptor dual agonist, on hepatic biomarkers in patients with compensated and decompensated cirrhosis
Eric Lawitz[1], Yesilda Balavarca[2], Naim Alkhouri[3], Wiebke K. Fenske[4], István Takács[5], Daniel F. Mazo[6], Luiza Borowska[6], Corinna Schoelch[7].
[1]Texas Liver Institute, University of Texas Health San Antonio, San Antonio, United States; [2]Staburo GmbH, München, Germany; [3]Summit Clinical Research, Clinical Research Institute of Ohio, San Antonio, United States; [4]University Hospital Bonn, Bonn, Germany; [5]Semmelweis University, Budapest, Hungary; [6]Boehringer Ingelheim International GmbH, Ingelheim, Germany; [7]Boehringer Ingelheim Pharma GmbH & Co. KG, Biberach, Germany
Email: lawitz@txliver.com

Background and aims: Survodutide is a glucagon/glucagon-like peptide-1 receptor dual agonist under investigation in phase 3 trials for metabolic dysfunction-associated steatohepatitis (MASH) and obesity. In a phase 1 trial investigating safety, survodutide was

associated with improvements in liver-related non-invasive tests in patients with advanced liver disease (NCT05296733). We report a longitudinal analysis of survodutide effects on fibrosis and inflammation biomarkers in patients with cirrhosis.

Method: This was a multinational, non-randomized, open-label phase 1 clinical trial in patients with overweight/obesity, with or without cirrhosis by Child-Pugh criteria. Once-weekly subcutaneous doses of survodutide were escalated from 0.3 mg to 6.0 mg over 24 weeks then maintained for 4 weeks. Exploratory serological biomarkers measured longitudinally from baseline (BL) to Week 28 (W28) included Enhanced Liver Fibrosis (ELF)™ score and its components (hyaluronic acid [HA], tissue inhibitor of matrix metalloproteinase 1 [TIMP-1], and pro-collagen III amino-terminal peptide [PIIINP]); N-terminal type III collagen propeptide (PRO-C3); cytokeratin 18 (CK18-M30/CK18-M65); and glucagon. Descriptive statistics are reported.

Results: This analysis included 41 patients: 17 without cirrhosis, 16 with compensated cirrhosis, and 8 with decompensated cirrhosis, mostly due to MASH. Biomarker levels were elevated at BL in patients with cirrhosis vs those without. After 28 weeks of survodutide treatment, those without cirrhosis and those with compensated or decompensated cirrhosis exhibited reductions in mean ELF™ scores (value at BL: 8.65, 11.21, 11.53; W28: 8.46, 10.75, 10.80) and geometric means (gMean) for HA (value at BL: 22.66, 230.38, 289.88; W28: 21.89, 177.90, 152.83 ug/L), PIIINP (BL: 8.24, 15.37, 17.45; W28: 6.89, 11.35, 13.56 ug/L), PRO-C3 (BL: 30.72, 50.51, 48.61; W28: 19.63, 35.49, 36.23 ug/L), CK18-M30 (BL: 98.8, 265.5, 238.6; W28: 65.6, 156.7, 203.0 U/L), CK18-M65 (BL: 161.6, 433.9, 442.3; W28: 111.4, 313.7, 371.4 U/L), and glucagon (BL: 64.83, 68.23, 105.71; W28: 44.47, 49.11, 71.27 pmol/L), respectively. No consistent change in gMean was observed for TIMP-1 (BL: 223.11, 301.44, 326.89; W28: 209.26, 295.66, 328.10 ug/L).

Conclusion: Survodutide improved hepatic biomarkers of fibrosis and inflammation in both compensated and decompensated cirrhosis. These findings suggest potential disease-modifying effects in MASH-related cirrhosis; a large phase 3 trial in compensated MASH cirrhosis is ongoing (NCT06632457).

FRI-169

Phase 2a single doses of GSK4532990 produce sustained HSD17B13 suppression and liver biochemical improvement in patients with metabolic dysfunction-associated steatohepatitis

Eric Lawitz[1], Itziar Irurzun[2], Nitendra Agarwal[3], Nomita Kim[4], Raj Vuppalanchi[5], Kathy-Ann Cadogan[6], Hardik Chandasana[6], Marc Goldfinger[7], Chronis Kemos[8], Andrea Ribeiro[2], Brandon Swift[9], MeeJ Kim[10]. *[1]Texas Liver Institute, University of Texas Health and University of Texas Health Science Center, San Antonio, TX, United States; [2]GSK, Madrid, Spain; [3]ERG Clinical, San Antonio, TX, United States; [4]IMA Clinical Research, Austin, TX, United States; [5]Indiana University School of Medicine, Indianapolis, IN, United States; [6]GSK (At the time of the study), Collegeville, PA, United States; [7]GSK, London, United Kingdom; [8]GSK, Stevenage, Hertfordshire, United Kingdom; [9]GSK, Durham, NC, United States; [10]GSK, Rockville, MD, United States*
Email: lawitz@txliver.com

Background and aims: Loss-of-function (LOF) gene mutations in *hydroxysteroid 17-beta-dehydrogenase-13* (*HSD17B13*) are associated with reduced risk of liver disease (metabolic dysfunction-associated steatohepatitis [MASH] and alcohol-related liver disease [ALD]). GSK4532990, an N-acetylgalactosamine conjugated siRNA, selectively targets *HSD17B13* in hepatocytes to mimic the LOF mutation. This dose exploration study investigated hepatic target engagement of single doses of GSK4532990 in patients with MASH.

Method: This Phase 2a (NCT06104319), open-label, multi-center study assessed pharmacokinetics (PK), pharmacodynamics, safety and tolerability of GSK4532990. The 61 eligible adults enrolled had a diagnosis of MASH or suspected MASH (defined per protocol). Paired liver biopsies were collected pre- and post-dose (8, 12 or 28 weeks) after a single dose of 25, 200, 400 or 800 mg, administered by subcutaneous injection. Hepatic HSD17B13 mRNA and protein levels, PK and safety (laboratory tests, adverse events [AEs], vital signs, ECGs) were assessed.

Results: Mean (SD) percent change from baseline in hepatic HSD17B13 mRNA and protein after 12 weeks for the 25 mg, 200 mg, 400 mg doses were: −53.1 (15.7), −88.6 (4.4), −90.0 (2.7) and −44.7 (7.9), −80.9 (6.4), −85.4 (1.5), respectively; for the 800 mg dose knockdown was −80.4 (17.0) and −70.1 (18.5) at Week 28. Across the four doses, mean (SD) GSK4532990 maximum plasma concentration was 47.4 (18.3), 455 (203), 1060 (595), 3340 (1990) ng/mL; half-life ($t_{1/2}$) was 8.7 (3.2), 6.0 (2.8), 5.7 (2.4), 5.4 (1.8) hours. Mean (SD) change from baseline in alanine aminotransferase U/L, at Week 12, was: −16.8 (32.8), −26.3 (33.5), −45.0 (37.1), −26.1 (19.2), with similar trends of reduction for aspartate aminotransferase and gamma glutamyl transferase. Treatment-emergent AEs occurred in 25 participants and were mainly mild–moderate, including three non-drug-related serious AEs in two participants; no liver AEs were considered GSK4532990-related.

Conclusion: Robust and sustained dose-dependent knockdown of hepatic HSD17B13 was observed after a single dose of GSK4532990 with continued suppression observed with 800 mg at 28 weeks despite a short $t_{1/2}$. mRNA and protein levels demonstrated strong concordance, associated with liver biochemical improvements. GSK4532990 was well tolerated, with a mild–moderate AE profile, consistent with Phase 1/2a study results. These data support the continued development of GSK4532990 in MASH and ALD.

FRI-170

Results from two phase I trials evaluating the safety, pharmacokinetics, and efficacy of BI 3006337, a dual fibroblast growth factor 21/glucagon-like peptide-1 agonist, in healthy volunteers and people with overweight/obesity and hepatic steatosis

Rizwana Mohseni[1], Nitendra Agarwal[2], Salvador Augustin[3], Sridhar Guduri[4], Dr. Jens Klaus[5], Claudia Lange[3], Maximilian T. Lobmeyer[3], Scott J. Overcash[6], Mangesh Pagadala[7], Bruce Rankin[8], William Sanchez[9], Corinna Schoelch[5], William Smith[10], Eric Lawitz[11]. *[1]Catalina Research Institute, LLC, Montclair, CA, United States; [2]Endeavor Clinical Trials, San Antonio, TX, United States; [3]Boehringer Ingelheim Pharma GmbH & Co. KG, Ingelheim am Rhein, Germany; [4]Centricity Research Columbus, Columbus, OH, United States; [5]Boehringer Ingelheim Pharma GmbH & Co. KG, Biberach, Germany; [6]Velocity Clinical Research San Diego, La Mesa, CA, United States; [7]The Liver Institute at Methodist Dallas Medical Center, Dallas, TX, United States; [8]Accel Research Sites, DeLand, FL, United States; [9]Floridian Clinical Research Miami Lakes, Miami Lakes, FL, United States; [10]AMR Clinical, Knoxville, TN, United States; [11]Texas Liver Institute, University Of Texas Health San Antonio, San Antonio, TX, United States*
Email: lawitz@txliver.com

Background and aims: Two Phase I trials assessed the tolerability and efficacy of BI 3006337, a dual fibroblast growth factor 21/glucagon-like peptide-1 agonist.

Method: Two randomised, Phase I trials evaluated subcutaneous BI 3006337. The Phase Ia single-rising dose (SRD) trial (NCT05076422) included healthy male volunteers aged 18–55 years with body mass index (BMI) 20–<32 kg/m^2. Participants (pts) received a single dose of BI 3006337 (0.2–150 mg) or placebo. The primary endpoint was the incidence of treatment-related adverse events (TRAEs). Secondary pharmacokinetic (PK) endpoints included area under the serum concentration–time curve from zero to infinity ($AUC_{0-\infty}$) and maximum serum concentration (C_{max}). The Phase Ib multiple-rising dose (MRD) trial (NCT05970640) included pts with overweight or obesity (BMI 25–<40 kg/m^2) and liver steatosis (liver fat ≥8% [measured by magnetic resonance imaging-proton density fat fraction [MRI-PDFF]). Pts were randomised to weekly BI 3006337 (50 mg, 100 mg, or 150 mg), or placebo for 12 weeks. The primary

endpoint was TRAEs. Secondary endpoints included relative change in liver steatosis (via MRI-PDFF) from baseline to week 12 and PK parameters.
Results: Overall, 80 pts were evaluable in the Phase Ia SRD trial (BI 3006337 dose groups [DGs]: n = 61; placebo: n = 19). TRAEs occurred in 7 pts (11.5%) receiving BI 3006337 vs none with placebo. No severe AEs, drug-induced liver injury, AEs leading to discontinuation or serious AEs were reported. BI 3006337 exhibited linear PK inter-individual variability in C_{max} and $AUC_{0-\infty}$ that was high (geometric coefficient of variation [gCV%] >50%) and moderate (gCV% 30–50%), respectively. In the Phase Ib MRD trial, 63 randomised pts were evaluable (BI 3006337: 50 mg, n = 11; 100 mg, n = 10; 150 mg, n = 23; placebo, n = 19). At week 12, the largest mean percentage reduction in liver fat was seen in the 150 mg group (– 40.5% reduction [standard deviation: 14.8%]) vs a 5.7% [36.3%] increase with placebo). TRAEs occurred in 31/44 BI 3006337-treated pts (70.5%) vs 5/19 receiving placebo (26.3%). There were no severe or serious events; discontinuation rate due to gastrointestinal effects was low (4.5%).
Conclusion: BI 3006337 demonstrated a manageable tolerability in healthy volunteers and individuals with overweight/obesity and hepatic steatosis up to a weekly dose of 150 mg. Preliminary efficacy data demonstrated a dose-dependent reduction in hepatic steatosis reaching the greatest magnitude at 150 mg.

FRI-171
First-in-class oral, once-monthly IKKalpha/beta inhibitor targeting steatosis, inflammation, and fibrosis in MASH: results from a phase 1 trial
Belle Wang[1], Yongmei Li[1], Nathan Li[1], Qisheng Li[1]. [1]*Hepanova Inc., Gaithersburg, United States*
Email: frank.li@hepanova.com

Background and aims: Metabolic dysfunction–associated steatohepatitis (MASH) with fibrosis is a leading cause of cirrhosis and hepatocellular carcinoma (HCC). While recently approved or late-stage therapies primarily target steatosis, none adequately address the critical drivers of inflammation and fibrosis. HPN-01 is a first-in-class, orally administered, highly selective dual IKKalpha/beta inhibitor that directly modulates the entire pathogenic triad – steatosis, inflammation, and fibrosis. Preclinical studies demonstrated robust efficacy across MASH and fibrosis models, as well as suppression of HCC progression through inhibition of IKKalpha-driven inflammatory, fibrotic, and oncogenic pathways.
Method: A randomized, placebo-controlled, ascending dose Phase 1 trial (HPN-01-US-101) enrolled healthy adults (25–150 mg; n = 8 per cohort). Extended pharmacokinetic (PK) sampling to 720 hours was performed at the highest dose. Safety endpoints included adverse events (AEs), labs, ECGs, and vitals. PK and population PK modeling characterized systemic disposition, terminal half-life, and informed dose scheduling.
Results: HPN-01 was well tolerated at all doses, with no treatment-related serious AEs, dose-limiting toxicities, or discontinuations. AEs were mild, transient, and not dose-related; no clinically meaningful laboratory or ECG abnormalities were observed. Exposure increased approximately dose-proportionally up to 150 mg. Extended PK confirmed a terminal half-life of 23 days with stable systemic exposure, reducing the risk of toxic peak inhibition and enabling controlled target modulation. Modeling projected therapeutic exposures achievable with once-weekly or once-monthly oral dosing.
Conclusion: HPN-01 demonstrated excellent safety, predictable PK, and prolonged persistence in its first-in-human trial, enabling infrequent oral dosing including once-monthly regimens. By uniquely tackling inflammation and fibrosis, gaps left by other agents, HPN-01 is differentiated as both an oral monotherapy for advanced MASH/fibrosis and a rational backbone in combination regimens (e.g., with GLP-1 agonists, THR-beta agonists, or FGF21 analogs). Its integrated mechanism, oral convenience, and strong safety profile highlight its potential as a patient-friendly therapy for advanced MASH and a strategy to reduce progression to HCC.

FRI-172
Imaging of Fibroblast Activation Protein: AZD2389 demonstrates liver target occupancy in participants with advanced chronic liver disease
Mathias Liljeblad[1,2,3], Zsolt Cselény[4], David Janzén[1], Mohammad Niazi[1], Magnus Schou[4], Andrea Varrone[5], Karin Westberg[1], Malin Aurell[1], Mahssa Karimi[1], Aurelija Jucaite[4], Hannes Hagström[5], Vian Azzu[6]. [1]*AstraZeneca R&D, Gothenburg, Sweden;* [2]*Translational Science & Early Clinical Development, CVRM, AstraZeneca BioPharmaceuticals R&D, Gothenburg, Sweden;* [3]*Translational Sciences and Clinical Development, Early Cardiovascular, Renal and Metabolism, BioPharmaceuticals, R&D, AstraZeneca, Gothenburg, Sweden;* [4]*AstraZeneca R&D, Stockholm, Sweden;* [5]*Karolinska Institutet, Huddinge, Sweden;* [6]*AstraZeneca R&D, Cambridge, United Kingdom*
Email: mathias.liljeblad@astrazeneca.com

Background and aims: In patients with chronic liver disease (CLD), elevated expression of hepatic fibroblast activation protein (FAP) can be imaged by positron emission tomography (PET). Preclinical work also indicates that FAP is involved in the progression of fibrosis. AZD2389 is a small molecule FAP inhibitor in development for the treatment of advanced chronic liver disease (ACLD), that has been shown to be well tolerated with proven plasma target engagement in both healthy volunteers and patients with CLD. PECHORA is a Phase I, open-label, PET trial in male and female patients with ACLD to assess hepatic target (FAP) occupancy by AZD2389.
Method: The PECHORA study (EU Trial no.2024-517605-91-00) design included three consecutive PET examinations using radioligand [^{68}Ga]Ga-FAPI-46 separated by about one week. The first two PET examinations served as baseline (test, PET1) and reproducibility (retest, PET2) evaluation of the radioligand, followed by an imaging session at 22 h after a single oral dose of AZD2389 (target occupancy, PET3). The study planned to investigate three dose levels of AZD2389, with a maximum of 2 participants at each level. Quantitative analysis of the PET images consisted of calculation of total radioligand binding (V_T) parametric images using a wavelet-aided parametric imaging (WAPI) method employing the multilinear variant of Logan's linear graphical analysis to estimate V_T with a metabolite-corrected arterial input function. Test-retest variability (TRV) was calculated on the voxel level and organ level V_T estimates from PET1 and PET2. The voxel-wise V_T parameters from PET1 and PET3 were used to estimate liver FAP occupancy following drug administration using Lassen's graphical approach.
Results: Radioligand [^{68}Ga]Ga-FAPI-46 showed favourable PET-kinetics, low metabolism (<30% metabolised at 60 min post injection) and median TRV at <10%. Single doses of AZD2389 administered over a 7-fold dose range resulted in dose-dependent hepatic target occupancies of 14% to 86% measured at trough.
Conclusion: Radioligand [^{68}Ga]Ga-FAPI-46 demonstrated suitable kinetics and test-retest reliability for assessment of hepatic FAP. Single-dose AZD2389 produced measurable hepatic FAP occupancy at trough, confirming target engagement and supporting dose selection for early clinical development.

FRI-173
Impact of metabolic surgery on muscle composition in patients with MASLD: a longitudinal MRI study
Jennifer Linge[1], Mikael Petersson[1], David Harris[2], Luke Funk[2,3], Danielle Batakis[4], Vitor Martins[4], Michael Middleton[4], Gavin Hamilton[4], Eduardo Grunvald[4], José Raya[5], Ofri Mosenzon[5], Roberto Calle[5], Joseph Grimsby[5], Scott Reeder[2], Claude Sirlin[4], Olof Dahlqvist Leinhard[1]. [1]*AMRA Medical AB, Linköping, Sweden;* [2]*University of Wisconsin-Madison, Madison, United States;* [3]*William*

S. Middleton VA, Madison, WI, United States; [4]University of California San Diego, La Jolla, United States; [5]Regeneron Pharmaceuticals, Sleepy Hollow, United States
Email: jennifer.linge@amramedical.com

Background and aims: Metabolic dysfunction-steatotic liver disease (MASLD) overlaps with obesity and is associated with frailty and sarcopenia. Weight loss may improve MASLD but can cause muscle mass loss. Our aim was to describe changes in muscle composition (quantity and quality) with magnetic resonance imaging (MRI) following metabolic surgery (MBS, bypass or sleeve) in patients with low vs high liver proton density fat fraction (PDFF, LLF vs HLF).
Method: Adults with BMI ≥ 35 kg/m^2 were scanned neck to knee using MRI at 5 visits: 2–4 weeks before MBS, 0–4 days before MBS (pre-MBS) following a low-calorie diet (LCD), and week 12, 26, 52 after MBS at University of Wisconsin-Madison & University of California San Diego (UCSD). Thigh muscle volume (MV, liters), a sex- height- weight- and BMI-invariant MV z-score (z-MV), muscle fat infiltration (MFI, %), and intramuscular fat volume (IMF, liters) were quantified by AMRA Researcher. Liver PDFF (%) was analyzed at UCSD. Differences in muscle composition changes for LLF (≤ 6.7% [baseline median]) vs HLF were tested by mixed-effects linear modelling adjusted for sex, site, surgery type, and baseline age, weight, and value of the response variable with pre-MBS as referent. Significant differences ($p < 0.05$) are indicated by *.
Results: At study end n = 58/96 patients (88% women) included had complete muscle composition data (n = 8/11/13/7 missing data at n = 1/2/3/4 visits). Baseline, mean (SD), age, weight and BMI were 46.3 (8.8) years, 133.5 (20.6) kg and 47.6 (6.4) kg/m^2. Mean weight loss with LLF/HLF after LCD was −3.4%/−4.0% and similar with LLF/HLF from pre-MBS to week 12, 26, 52 (−13.0%/−13.5%, −19.4%/-19.9%, −23.2%/−23.7%). Mean muscle mass loss after LCD was −3.6%/−4.3% (Δz-MV: −0.25/−0.34) and larger with HLF from pre-MBS to week 12, 26, 52 (−8.7%/11.1%, −9.0%/−11.8%*, −9.2%/−12.7%*; Δz-MV: −0.43/−0.72*, −0.20/−0.58*, −0.02/−0.49*). Muscle fat decreased after surgery with significantly larger reductions at week 52 with LLF (MFI −1.56/−0.94* percentage points; IMF −0.04/−0.04 liters, −25.5%/−22.2%).
Conclusion: MBS was associated with reductions in MV and MFI, indicating decreased quantity but increased quality. Almost all muscle mass loss (MV and z-MV) occurred within 12 weeks after surgery and was significantly higher with HLF. At week 52, z-MV had recovered to pre-MBS level with LLF but was still reduced with HLF. Results indicate patients with MASLD experience larger muscle mass loss with MBS; potential implications should be further investigated.

FRI-174

Synergistic effects of SGLT2 inhibitors and HCV eradication on long-term MASLD improvement in patients with chronic hepatitis C and type 2 diabetes: a 3-year follow-up study

Ching-Chu Lo[1], Jow-Jyh Hwang[1], Chien-Hung Lin[1], Hsu-sheng Cheng[1], Yee-Tam Liao[1], Po-Yen Hsiao[1], Mei-Tsu Chen[1], Chen-Yu Lo[1]. [1]*Saint Martin De Porres Hospital, East District, Chiayi, Taiwan*
Email: locc0320@gmail.com

Background and aims: Direct-acting antivirals (DAAs) achieve sustained virologic response (SVR) in nearly all patients with chronic hepatitis C (HCV). However, patients with concomitant type 2 diabetes (T2D) are at increased risk of developing metabolic dysfunction–associated steatotic liver disease (MASLD). While HCV eradication and sodium-glucose cotransporter-2 (SGLT2) inhibitors improve metabolic control, long-term data regarding their combined effects on hepatic steatosis and fibrosis remain limited. This study aimed to evaluate longitudinal changes in MASLD following SVR and SGLT2 therapy over a three-year follow-up period.
Method: This prospective cohort study enrolled patients with chronic HCV infection and T2D who received DAA therapy between January 25, 2020 and January 22, 2021 at St. Martin De Porres Hospital. SVR was defined as undetectable HCV RNA 12 weeks after treatment completion. SGLT2 inhibitors were prescribed according to standard diabetic care. Hepatic steatosis was assessed using attenuation imaging (ATI, Canon), and liver fibrosis was evaluated by liver stiffness measurement (LSM) using transient elastography (FibroScan). Changes in ATI and LSM values from baseline through 1- 2- and 3-year follow-up were analyzed using repeated-measures ANOVA.
Results: A total of 250 patients were enrolled, of whom 245 (98%) achieved SVR. The mean age was 68 years. Patients were categorized into two groups: HCV without T2D (Group 1, n = 186) and HCV with T2D (Group 2, n = 59). In Group 1, mean LSM values (kPa) declined from 7.28 at baseline to 7.29, 6.72, and 6.60 at years 1, 2, and 3, respectively ($P < 0.001$). ATI values decreased from 0.705 to 0.705, 0.657, and 0.652 dB/cm/MHz over the same period ($P < 0.001$). Improvements in steatosis and fibrosis became significant after the second year following SVR. In Group 2, mean LSM values decreased from 8.86 at baseline to 7.73, 7.47, and 7.40 at years 1, 2, and 3, respectively ($P < 0.001$). ATI values declined from 0.852 to 0.753, 0.739, and 0.717 ($P < 0.001$). Notably, significant improvements in both steatosis and fibrosis were observed as early as the first year and persisted throughout the three-year follow-up.
Conclusion: HCV eradication leads to gradual MASLD improvement, while concomitant SGLT2 inhibitor therapy in patients with T2D is associated with earlier and sustained reductions in hepatic steatosis and fibrosis (MASLD). These findings support an integrated antiviral and metabolic treatment strategy for HCV patients with T2D.

FRI-175

Effects of combination treatment with semaglutide, cilofexor and firsocostat on liver noninvasive tests in patients with cirrhosis due to metabolic dysfunction-associated steatohepatitis: a post hoc analysis of the WAYFIND trial

Rohit Loomba[1], Naim Alkhouri[2], Kris V. Kowdley[3], Eric Lawitz[4], Arun J. Sanyal[5], Raj Vuppalanchi[6], Antoine Jakiche[7], Edward Mena[8], Michael Ryan[9], Michael Williams[10], Mousab Tabbaa[11], William M. Lee[12], Anita Kohli[2], Juan M. Pericàs[13], Magdy Elkhashab[14], Laura Stinton[15], Stephen Pianko[16], Vincent Leroy[17], Yoshiyuki Ueno[18], Michael Lund[19], Kwabena Opuni[19], Lulu Wang[20], Daria B. Crittenden[20], Mazen Noureddin[21]. [1]*MASLD Research Center, University of California at San Diego, San Diego, La Jolla, CA, United States;* [2]*Arizona Liver Health, Chandler, AZ, United States;* [3]*Liver Institute Northwest, Seattle, WA, United States;* [4]*Texas Liver Institute, University of Texas Health San Antonio, San Antonio, TX, United States;* [5]*Stravitz-Sanyal Institute for Liver Disease and Metabolic Health, Virginia Commonwealth University, Richmond, VA, United States;* [6]*Division of Gastroenterology and Hepatology, Indiana University School of Medicine, Indianapolis, IN, United States;* [7]*Southwest Gastroenterology Associates, Albuquerque, NM, United States;* [8]*California Liver Research Institute, Pasadena, CA, United States;* [9]*Capital Digestive Care, Norfolk, VA, United States;* [10]*Gastrointestinal Associates, Columbia, MO, United States;* [11]*North Shore Gastroenterology & Endoscopy Center, Westlake, OH, United States;* [12]*Department of Internal Medicine, Division of Digestive and Liver Diseases, University of Texas Southwestern Medical Center, Dallas, TX, United States;* [13]*Liver Unit, Vall d'Hebron University Hospital, Vall d'Hebron Institute for Research, Universitat Autònoma de Barcelona, CIBERehd, Barcelona, Spain;* [14]*Toronto Liver Centre, Toronto, ON, Canada;* [15]*Liver Unit, Division of Gastroenterology and Hepatology, Department of Medicine University of Calgary, Calgary, AB, Canada;* [16]*Department of Gastroenterology and Hepatology, Monash Health, Melbourne, VIC, Australia;* [17]*Department of Hepatology, Hôpital Henri Mondor (AP-HP), Créteil, France;* [18]*Department of Gastroenterology, Faculty of Medicine, Yamagata University, Yamagata, Japan;* [19]*Novo Nordisk, Bagsværd, Denmark;* [20]*Gilead Sciences, Inc., Foster City, CA, United States;* [21]*Houston Research Institute and Houston Methodist Hospital, Houston, TX, United States*
Email: barry.crittenden@gilead.com

Background and aims: Liver noninvasive tests (NITs) show promise for the detection of cirrhosis in patients (pts) with metabolic dysfunction-associated steatohepatitis (MASH). This *post hoc* analysis evaluated the effects of semaglutide (SEMA), cilofexor (CILO)/firsocostat (FIR) and SEMA + CILO/FIR on liver NITs, and liver NIT-determined cirrhosis (Agile 4 score) in pts with cirrhotic MASH from the placebo (PBO)-controlled, phase 2 WAYFIND study (NCT04971785).
Method: Pts who received SEMA 2.4 mg weekly + CILO 30 mg/FIR 20 mg daily, SEMA 2.4 mg weekly, CILO 30 mg/FIR 20 mg daily or PBO for 72 weeks (W), and had non-missing data for each outcome, were included. Least squares (LS) mean differences (nominal p values) in liver NITs between treatment groups were estimated using analysis of covariance models.
Results: In total, 453 randomized pts took ≥ 1 dose of study drug (SEMA + CILO/FIR: N = 124; SEMA: N = 122; CILO/FIR: N = 123; PBO: N = 84). Nominally significant LS mean differences versus PBO were observed at W72 with SEMA + CILO/FIR, SEMA, and CILO/FIR treatment, respectively, for percent change from baseline in alanine transaminase (ALT U/L: −54.5, −31.4 and −25.8; all $p < 0.0001$), aspartate aminotransferase (AST U/L: −47.7, −32.8 and −22.0; all $p < 0.0001$) and liver stiffness (FibroScan kPa: −29.7, −30.7 and −30.3; all $p < 0.05$), and for absolute change from baseline in Enhanced Liver Fibrosis (ELF score: −1.01, −0.82 and −0.56; all $p < 0.0001$) and Fibrosis-4 (FIB-4 score: −0.88, −0.80 and −0.58; all $p < 0.0001$). The proportion of pts with an Agile 4 score ruling in cirrhosis (≥ 0.565) decreased from baseline to W72 with SEMA + CILO/FIR (from 43.5% [50/115] to 22.9% [19/83]), SEMA (41.1% [46/112] to 28.8% [21/73]) and CILO/FIR (40.0% [44/110] to 25.4% [18/71]), and increased with PBO (42.3% [33/78] to 51.8% [29/56]). In parallel, the proportion of pts with an Agile 4 score ruling out cirrhosis (< 0.251) increased from baseline to W72 with SEMA + CILO/FIR (from 22.6% [26/115] to 38.6% [32/83]), SEMA (22.3% [25/112] to 41.1% [30/73]) and CILO/FIR (24.5% [27/110] to 39.4% [28/71]), but stayed similar with PBO (23.1% [18/78] to 26.8% [15/56]); remaining pts had indeterminate Agile 4 scores (0.251 to <0.565).
Conclusion: SEMA, CILO/FIR and their combination reduced liver NIT levels/scores (ALT, AST, ELF, FIB-4 and liver stiffness) versus PBO in pts with cirrhotic MASH, and likely reduced proportions of pts with liver NIT-determined cirrhosis.

FRI-179

Early and Week 52 biomarker (MRI-PDFF, ALT, MRE and PRO-C3) responses to resmetirom predict improvements in MASH and liver fibrosis

Rohit Loomba[1], Rebecca Taub[2], Krishna Padmanabhan[2], Dominic Labriola[2], Mazen Noureddin[3], Naim Alkhouri[3]. [1]*San Diego School of Medicine, San Diego, United States;* [2]*Madrigal Pharmaceuticals, Conshohocken, United States;* [3]*Pinnacle, San Antonio, United States*
Email: rebeccataub@yahoo.com

Background and aims: MAESTRO-NASH (NCT03900429) is an ongoing 54-month, randomized, double-blind, placebo (PBO)-controlled Phase 3 trial evaluating the efficacy of resmetirom (RES) in patients with MASH and F2/F3 fibrosis. The 52-week histologic endpoints demonstratted resolution of MASH (MR) and fibrosis improvement (FI) with RES 80 mg and 100 mg leading to approval. We report early non-invasive biomarkers of change and their correlation with Week (W) 52 biopsy responses, as well as the odds of achieving an early biomarker response with treatment.
Method: To assess relationships between early biomarker responses and W52 liver biopsy outcomes, changes in ALT, MRE, MRI-PDFF, at W12,24 52 following initiation of RES or PBO were analyzed for correlation with biopsy-defined MR and FI. Odds of achieving early improvement in these biomarkers were evaluated as a function of treatment. PRO-C3 change was a measure of response.
Results: ≥20% reduction in ALT at w12, 24, 52 was associated with higher odds (OR) of W52 MR/FI. With RES, ALT response showed an OR of 2.0, 2.2, 2.6 repectively at W12, 24, 52; $p < 0.002$). RES OR of achieving an FI response at w12, 24 and 52, compared to PBO: ORs of 2.2, 2.7, 3.6 respectively. All $p < 0.001$. MR was similar. ≥15% reduction in MRE at W16, 52 was associated with higher OR of Week 52 FI/MR. With RES, MRE response ORs FI, 2.6 and 2.3 at W16, 52, respectively, $p \leq 0.02$, less association in PBO. MR was similar. RES compared with PBO stat sig. odds of achieving an MRE response, at W52 (OR = 1.71) but not at (W16 OR = 1.31). A ≥30% reduction in MRI-PDFF from baseline at W16 and 52 was strongly associated with higher odds of FI and MR. With RES, MRI-PDFF response was associated with increased odds of FI (ORs 1.9 and 2.95 at w16 and 52, respectively; $p \leq 0.02$) and MR at Week 52 (OR ~ 6.5). RES was associated with significantly higher odds of achieving an PDFF response compared with PBO at W16, 52 (ORs 12.4 and 6.7; both $p < 0.0001$). For Pro-C3, change and % change n PRO-C3 at Weeks 24 and 52 in F3 showed a relationship to FI in all treatment groups, w52: 80 mg, −7%, −23%; 100 mg, −14%, −20%; PBO, 0%, −20% FI nonresponders and responders, respectively with far more responders in RES, regression currve $p = 0.0017$ RES, $p = 0.04$ PBO.
Conclusion: Early and W52 responses to RES, particularly reduction in PDFF at W16 and W52, correlate with FI and MR responses on liver biopsy. Reduction in ALT, MRE and PRO-C3 (≤W24 and W52) showed a significant correlation with FI on biopsy with RES treatment.

FRI-180

A carbohydrate-reduced high-protein diet with whey protein supplement reduces liver fat content in weight stable patients with MASLD: Results from a randomized controlled trial

Anders Mellemkjær[1,2,3], Faidon Magkos[4], Emilie Møller[1], Steffen Ringgaard[5], Jasmine Merhout[6], Lina Beganovic[4], Andreas Møller[7], Andreas Buch Moeller[8], Ulla Ramer Mikkelsen[9], Lise Lotte Gluud[7,10], Anders Junker[7], Søren Nielsen[2], Henning Gronbaek[1,3]. [1]*Department of Hepatology & Gastroenterology, Aarhus University Hospital, Aarhus, Denmark;* [2]*Steno Diabetes Center, Aarhus University, Aarhus, Denmark;* [3]*Department of Clinical Medicine, Aarhus University, Aarhus, Denmark;* [4]*Department of Nutrition, Exercise, and Sports, University of Copenhagen, Frederiksberg, Denmark;* [5]*Department of Clinical Medicine, MR Centre, Aarhus University, Aarhus, Denmark;* [6]*Danish Research Center for Magnetic Resonance, Centre for Functional and Diagnostic Imaging and Research, Copenhagen University Hospital, Copenhagen, Denmark;* [7]*Gastro Unit, Copehagen University Hospital, Amager and Hvidovre, Hvidovre, Denmark;* [8]*Arla Food for Health, Viby J, Denmark;* [9]*Arla Foods Ingredients Group P/S, Viby J, Denmark;* [10]*Department of Clinical Medicine, Faculty of Health and Medical Sciences, University of Copenhagen, Copenhagen, Denmark*
Email: andmel@rm.dk

Background and aims: Carbohydrate-reduced high-proten (CRHP) diets have shown promising results in the management of metabolic disease, but direct effects on liver fat content and lipid and glucose metabolism are unclear. Here, we assess the effects of a CRHP diet supplemented with whey protein isolate (WPI) or micellar casein isolate (MCI) compared to a conventional diet (CD) on metabolic-dysfunction associated steatotic liver disease (MASLD).
Method: Non-diabetic participants with MASLD and a BMI ≥ 27.5 kg/m2 were randomly allocated (1:1:1) to a 4-week isocaloric period followed by a 20-week hypocaloric period with either CRHP with WPI or MCI, or CD in an open-label design. Participants received dietary counselling bi-weekly to facilitate weight maintenance in the isocaloric phase and a weight loss target of 5% after the hypocaloric phase. Liver fat content was measured by MR-spectroscopy. Glucose, palmitate, and VLDL-triglyceride (TG) kinetics were evaluated during basal conditions and during a hyperinsulinemic, euglycemic clamp using radioisotope tracers.
Results: 45 participants were enrolled. CRHP with WPI reduced liver fat content after the isocaloric phase compared to CD (mean

difference: −8.9%-points [95% CI: −14.6 to −3.2]) without changes in body weight or composition. After the hypocaloric phase, all diets reduced liver fat content (mean: −6.8%-points [95% CI: −9.6 to −3.9]) and body weight (mean: −3.7 kg [95% CI: −4.6 to −2.9]) equally. Basal and insulin-mediated palmitate and VLDL-TG secretion rates and endogenous glucose production were unchanged by CRHP intake and weight loss.

Conclusion: CRHP with WPI reduced liver fat content compared to a CD in overweight patients with MASLD after 4 weeks of isocaloric intake without concurrent weight changes. CRHP did not augment the beneficial effects of weight loss. The depletion of liver fat and mild weight loss were not associated with changes in free fatty acid or VLDL-TG turnover.

FRI-181

Efficacy and safety of semaglutide 2.4 mg in the Japanese subgroup of the ESSENCE study

Atsushi Nakajima[1,2], Takeshi Okanoue[3], Yoichi Hiasa[4], Hirokazu Takahashi[5], Adel Belloum[6], Nobuyoshi Kosaka[7], Tomoyuki Nishida[7], Arun J. Sanyal[8]. *[1]Department of Gastroenterology and Hepatology, International University of Health and Welfare, Narita, Japan; [2]IUHW atami hospital, Atami, Japan; [3]Department of Gastroenterology and Hepatology, Saiseikai Suita Hospital, Osaka, Japan; [4]Department of Gastroenterology and Metabology, Ehime University Graduate School of Medicine, Toon, Japan; [5]Division of Metabolism and Endocrinology, Saga University Faculty of Medicine Graduate School of Medical Sciences, Saga, Japan; [6]Novo Nordisk A/S, Copenhagen, Denmark; [7]Novo Nordisk Pharma Ltd, Tokyo, Japan; [8]Stravitz-Sanyal Institute for Liver Disease and Metabolic Health, VCU School of Medicine, Richmond, VA, United States*
Email: nakajima-tky@umin.ac.jp

Background and aims: The ESSENCE trial (NCT04166773) is a Phase 3 study evaluating the efficacy and safety of Semaglutide 2.4 mg (Sema), a GLP-1 receptor agonist, in patients with MASH and liver fibrosis stages F2 or F3 (Sanyal et al., NEJM, 2025). This study aimed to evaluate the efficacy and safety of Semaglutide in the Japanese population.

Method: This trial was an international multicenter, double-blind, randomized, placebo-controlled Phase 3 study. A total of 1,197 subjects were randomized, of whom first 800 subjects (116 Japanese) were included in the efficacy analysis for the interim analysis of Part 1. The safety analysis at the interim analysis included 1,195 subjects who received treatment (141 Japanese). The primary endpoints were the resolution of steatohepatitis without worsening of fibrosis (MASH resolution) and reduction in liver fibrosis without worsening of steatohepatitis (fibrosis reduction) after 72 weeks of weekly administration of Sema or placebo.

Results: Demographics and baseline characteristics were generally comparable between the Japanese population and the overall population, except for age group and body weight/BMI. Less subjects were aged ≥ 45 to < 65 and more subjects were aged ≥ 65 years in the Japanese population. Mean body weight/BMI was lower in Japanese population (77.8 kg/29.8 kg/m^2) than in entire population (96.1 kg/34.6 kg/m^2). In Japanese population, the proportion of patients achieving MASH resolution was 63.1% for Sema and 36.8% for placebo. In addition, the proportion of patients achieving fibrosis reduction was 36.5% for Sema and 28.5% for placebo. Further, the proportion who achieved MASH resolution with fibrosis reduction was 33.3% for Sema and 21.1% for placebo. These results suggested that the responder proportions were similar for Japanese population and overall population, both in favor of Sema. Body weight was reduced by up to 11.4% with Sema and 2.6% in placebo. Liver enzymes and liver stiffness decreased, and serum biomarkers of liver fibrosis, ELF, improved in the Sema groups vs. placebo. No apparent difference in the safety profile was seen between the Japanese population and the entire trial population.

Conclusion: These results suggested that efficacy and safety of Sema in the Japanese population are expected to be similar to those in the overall population.

FRI-182

Semaglutide shows favourable safety across subgroups and a positive hepatic safety profile: findings from ESSENCE part 1

Philip N. Newsome[1,2], Michael Roden[3,4,5], Igor Bakulin[6], Burak Demirel[7], Christina Egebjerg[7], Anja Geerts[8], George Boon Bee Goh[9], Alma Laura Ladrón de Guevara[10], Mette Kjaer[7], Tomáš Koller[11], Heidi Ranndal[7], Jörn M. Schattenberg[12,13,14], Elisabetta Bugianesi[15], Mary E. Rinella[16]. *[1]Roger Williams Institute of Liver Studies, Faculty of Life Sciences and Medicine, King's College London and King's College Hospital, London, United Kingdom; [2]College of Medical and Dental Sciences, University of Birmingham, Birmingham, United Kingdom, [3]Department of Endocrinology and Diabetology, Medical Faculty and University Hospital Düsseldorf, Heinrich Heine University Düsseldorf, Düsseldorf, Germany; [4]Institute for Clinical Diabetology, German Diabetes Center, Leibniz Center for Diabetes Research at Heinrich Heine University Düsseldorf, Düsseldorf, Germany; [5]German Center for Diabetes Research, Partner Düsseldorf, München-Neuherberg, Germany; [6]North-Western State Medical University, St. Petersburg, Russian Federation; [7]Novo Nordisk A/S, Copenhagen, Denmark; [8]Hepatology Research Unit, Department of Internal Medicine and Pediatrics, Liver Research Center Ghent, Ghent University, Ghent, Belgium; [9]Department of Gastroenterology and Hepatology, Singapore General Hospital, Singapore, Singapore; [10]Centro de Investigación y Gastroenterología, Ciudad de México, Mexico; [11]Subdivision of Gastroenterology and Hepatology, 5th Department of Medicine, Comenius University Faculty of Medicine in Bratislava, University Hospital Ruzinov, 821 01 Bratislava, Slovakia; [12]Department of Internal Medicine II, University Medical Centre Saarland, Homburg, Germany; [13]Faculty of Medicine, Saarland University, Saarbrücken, Germany; [14]Pharma Science Hub, Saarland University, Saarbrücken, Germany; [15]Department of Medical Sciences, University of Turin, Turin, Italy; [16]Division of Gastroenterology, Hepatology and Nutrition, University of Chicago, Chicago, IL, United States*
Email: philip.newsome@kcl.ac.uk

Background and aims: The ESSENCE trial assesses semaglutide 2.4 mg in metabolic dysfunction-associated steatohepatitis (MASH). In non-clinical studies, semaglutide has not shown liver toxicity. This post hoc analysis of ESSENCE evaluated general and liver-specific safety of semaglutide in participants (pts) with biopsy-defined MASH and liver fibrosis stage 2 or 3 (F2–F3).

Method: Pts were randomised 2:1 to semaglutide or placebo. Safety analyses were on all pts who took at least 1 dose of semaglutide (N = 1195); efficacy evaluations were at week 72 on the first 800 randomised pts.

Results: Adverse event (AE) and gastrointestinal (GI) AE reporting increased with age and was higher in women than men. Pts with type 2 diabetes (T2D) and non-T2D reporting AEs with semaglutide were comparable (87% and 85%): GI AEs were numerically higher in the non-T2D semaglutide group. AEs and GI AEs were higher in semaglutide F2 vs F3, with a higher proportion in F2 reporting serious AEs (SAEs). GI AEs were more frequent with semaglutide than placebo; mainly nausea, diarrhoea, constipation, and vomiting; generally mild/moderate, non-serious, and most occurring during dose escalation. Discontinuation due to GI AEs was comparable between groups (1.6% vs 0.5%). Most hepatic AEs were mild/moderate and non-serious; none led to premature treatment discontinuation in the semaglutide group. Hepatic SAEs occurred in 1 semaglutide pt and 3 placebo pts.

Baseline alanine aminotransferase (ALT) and aspartate aminotransferase (AST) elevations were common (ALT: 31.1% vs 33.1%; AST: 42.9% vs 43.6% for semaglutide vs placebo). Week 72 elevations in ALT and AST were lower with semaglutide vs placebo in pts with elevated baseline levels (ALT: 7.3% vs 16.9%, AST: 11.2% vs 26.7%) and normal

baseline levels (ALT: 2.4% vs 14.7%, AST: 4.7% vs 21.4%). All cases meeting prespecified criteria for potential drug-induced liver injury (DILI) were adjudicated, with none confirmed. Gallbladder AEs were mostly mild/non-serious; none led to discontinuation, cholelithiasis was most frequent, one SAE occurred in each group. Acute pancreatitis occurred in 3 semaglutide pts (2 SAEs) and 2 placebo (1 SAE).
Conclusion: Semaglutide demonstrated a favourable safety profile in F2–F3 MASH regardless of age, sex, T2D, or fibrosis stage. Hepatic AEs were mild/moderate with SAEs uncommon; no confirmed DILI, and liver enzymes improved vs placebo. Gallbladder events were mild/non-serious, with no safety signal for pancreatitis.

FRI-183
Ontamalimab reduces fibroinflammatory biomarkers and liver injury signals in metabolic dysfunction associated steatohepatitis
Mazen Noureddin[1], Eric Lawitz[2], Naim Alkhouri[3], Madhavi Rudraraju[4], Zeid Kayali[5], Gary Reiss[6], Michael Chen[7], Jay Tang[7], Wendi Lichtenberger[7], Jie Feng[7], Vandana Gupta[7], Talakad G. Lohith[7], Aaron Huang[7], Haakan Wennbo[7], Paresh Thakker[7], Zoltan Derdak[7]. *[1]Houston Research Institute and Houston Methodist Hospital, Houston, Houston, TX, United States; [2]Texas Liver Institute, San Antonio, United States; [3]Summit Clinical Research, San Antonio, TX, United States; [4]Pinnacle Clinical Research, San Antonio, TX, United States; [5]Inland Empire Clinical Trials, Rialto, CA, United States; [6]Tandem Clinical Research, Marrero, LA, United States; [7]Takeda Development Center Americas, Inc., Cambridge, MA, United States*
Email: zoltan.derdak@takeda.com

Background and aims: Mucosal addressin cell adhesion molecule 1 (MAdCAM-1) mediates gut–liver lymphocyte trafficking and contributes to fibroinflammation in the liver. Ontamalimab is a monoclonal antibody targeting MAdCAM-1. This phase 1b study assessed safety and biomarker effects in participants with metabolic dysfunction-associated steatohepatitis (MASH).
Method: Adults with biopsy-confirmed MASH and fibrosis stages F1 to F4 received ontamalimab 75 mg subcutaneously every 4 weeks for 24 weeks. Primary endpoints focused on safety and tolerability, while key secondary endpoints assessed the percent change from baseline in N-terminal propeptide of type III collagen (PRO-C3), the Enhanced Liver Fibrosis (ELF) score, and iron-corrected T1 at (MRI *c*T1) at week 24. Exploratory endpoints included alanine aminotransferase (ALT), aspartate aminotransferase (AST), liver stiffness assessed by vibration-controlled transient elastography (VCTE), FibroScan-AST (FAST) and Fibrosis-4 (FIB-4) scores, and inflammatory biomarkers including interleukin 8 (IL-8) and thrombospondin 2 (TSP-2).
Results: Eleven biopsy-proven MASH participants were treated (mean age 49 years, 64% female). Ontamalimab was well tolerated with no deaths, serious adverse events, or treatment-related discontinuations. At week 24, mean percent changes from baseline were −14.904% for PRO-C3, −0.82% for ELF, and −3.2% for MRI *c*T1. 5 out of 7 participants with end of study PRO-C3 values achieved more than 10% Pro-C3 reduction. ALT and AST declined from baseline at week 24 with reduction of 23.4 U/L and 14.2 U/L, respectively ($p = 0.002$ and $p = 0.001$). Mean VCTE decreased from 15.09 ± 1.643 kPa to 11.36 ± 1.712 kPa (n.s.) by the end of treatment. There was a statistically significant decrease in FAST score (0.66 ± 0.047 vs 0.4563 ± 0.069, $p = 0.03$) and FIB 4 scores trended downward. IL-8 showed modest reductions, and TSP-2 declined directionally in line with other fibroinflammatory markers.
Conclusion: Ontamalimab demonstrated a favorable safety profile and produced coherent improvements across markers of fibrogenesis, liver injury, inflammation, liver stiffness, and quantitative magnetic resonance imaging.

FRI-184
Effects of SGLT-2 inhibitors on clinical outcomes in patients with MASLD and type 2 diabetes mellitus: a nested case-control study using LIFE study data
Eiichi Ogawa[1], Yurina Akeno[2], Nobuyuki Shimono[1], Haruhisa Fukuda[3]. *[1]Department of General Internal Medicine, Kyushu University Hospital, Fukuoka, Japan; [2]Department of Health Sciences, Graduate School of Medical Sciences, Kyushu University, Fukuoka, Japan; [3]Department of Health Care Administration and Management, Graduate School of Medical Sciences, Kyushu University, Fukuoka, Japan*
Email: e.ogawa.a65@m.kyushu-u.ac.jp

Background and aims: Disordered glucose metabolism is a major driver of disease progression in metabolic dysfunction-associated steatotic liver disease (MASLD). Sodium-glucose cotransporter-2 (SGLT-2) inhibitors and dipeptidyl peptidase-4 (DPP-4) inhibitors are widely used for type 2 diabetes mellitus (T2DM). However, whether these agents reduce the incidence of liver-related or extrahepatic events in patients with MASLD and T2DM has not been fully elucidated. This study aimed to estimate the preventive effects of SGLT-2 inhibitors and DPP-4 inhibitors in patients with MASLD and T2DM.
Method: We conducted a nested case-control study using administrative claims data in Japan, covering a population of 2.56 million. Patients newly diagnosed with steatotic liver disease (SLD) and T2DM within the first three years of data availability were identified. Patients without SLD or those who had already initiated antidiabetic therapy were excluded. Cases were defined as patients who developed at least one major outcome-hepatocellular carcinoma (HCC), extrahepatic malignancy, major adverse cardiovascular events (MACE), or death-after three years from cohort entry. Controls were selected from non-case individuals and matched 1:1 by age and sex. Associations between new prescriptions and outcomes were evaluated using conditional logistic regression.
Results: A total of 10,338 patients were included in the final analysis. During a follow-up period of 25–42 months, 65 patients developed HCC, 1,082 developed extrahepatic malignancies, 753 experienced MACE, and 219 died. Although the number of SGLT-2 inhibitor users was limited in the HCC analysis, six patients in the non-HCC group received SGLT-2 inhibitors, whereas none in the HCC group did, resulting in a significantly lower prescription frequency among HCC cases ($P = 0.037$). Using SGLT-2 inhibitor as the reference, the adjusted odds ratio for extrahepatic malignancy was 0.588 (95% CI: 0.374–0.925; $P = 0.022$) after adjustment for the Charlson comorbidity index. No significant association was observed for DPP-4 inhibitors ($P = 0.29$). For MACE, neither SGLT-2 inhibitors nor DPP-4 inhibitors showed significant differences. Similarly, no significant associations were observed for mortality.
Conclusion: In patients with MASLD complicated by T2DM, SGLT-2 inhibitors may be associated with a reduced risk of not only HCC but also extrahepatic malignancies. These findings suggest a potential event-preventive benefit of SGLT-2 inhibitors beyond glycemic control in this population.

FRI-185
Roux-en-Y gastric bypass is associated with higher risk of major adverse liver outcomes compared with sleeve gastrectomy
Ilias Papadimopoulos[1], Laurens A. van Kleef[2], Filippos Anagnostakis[3], Michail Kokkorakis[4,5]. *[1]Alma Mater Studiorum-Medicine and Surgery, University of Bologna, Bologna, Italy; [2]Departments of Gastroenterology and Hepatology, Erasmus MC University Medical Center, Rotterdam, Netherlands; [3]Artificial Intelligence in Biomedical Imaging Laboratory (AIBIL), Center for AI and Data Science for Integrated Diagnostics (AI2D), Perelman School of Medicine, University of Pennsylvania, Philadelphia, United States; [4]Section of Digestive Diseases, Department of Internal Medicine, Yale School of Medicine, New Haven, CT, United States;*

[5]*Department of Clinical Pharmacy and Pharmacology, University of Groningen, University Medical Center Groningen, Groningen, Netherlands*
Email: ilias.papadimopoulos@studio.unibo.it

Background and aims: Bariatric surgery reduces obesity-related complications, including major adverse liver outcomes (MALO). However, the comparative long-term risk of MALO between Roux-en-Y gastric bypass (RYGB) and sleeve gastrectomy (SG) remains unclear. We aimed to compare the incidence of MALO following RYGB versus SG in adults with severe obesity.
Method: We conducted a retrospective cohort study using de-identified electronic health records from the TriNetX Research Network, encompassing over 100 million patients across 67 North American healthcare organizations. Adults with body mass index (BMI) greater than or equal to 35 kg/m^2 who underwent RYGB or SG between 2011 and 2021 were included. Patients with pre-existing liver disease were excluded. Propensity score matching (1:1) balanced baseline demographics, comorbidities, laboratory values, and medications. MALO was defined as a composite of incident ascites, cirrhosis, portal hypertension, varices, hepatic encephalopathy, or liver cancer. Hazard ratios (HR) and 95% confidence intervals (CI) were estimated using Cox proportional hazards models.
Results: After matching, 19,529 patients were included in each group (19% male, median age 45 years). Over a median follow-up of 6.7 years, 1,755 MALO events occurred. RYGB was associated with a significantly higher risk of MALO compared with SG (HR 1.58, 95% CI 1.44–1.74; $p < 0.001$). This elevated risk was consistent across individual MALO components: ascites (HR 2.08, 95% CI 1.82–2.38), cirrhosis (HR 1.29, 95% CI 1.06–1.58), portal hypertension (HR 1.75, 95% CI 1.24–2.47), and hepatic encephalopathy (HR 1.40, 95% CI 1.19–1.64). The association was strongest in the early postoperative period (90 days to 2 years: HR 2.06, 95% CI 1.76–2.42) and attenuated beyond 5 years (HR 1.11, 95% CI 0.94–1.31). Results were consistent across sex, metabolic dysfunction-associated steatotic liver disease, type 2 diabetes, and hypertension subgroups.
Conclusion: In this large propensity-score matched cohort, RYGB was associated with significantly higher long-term risk of MALO compared with SG, driven primarily by liver decompensation events. When considering bariatric surgery, SG may be the safer option for high-risk individuals, such as those with compensated cirrhosis.

FRI-186

Twelve-month changes in liver function enzymes and lipids in patients receiving resmetirom

Christina Parrinello[1], Sean Stern[2], Setareh Williams[2], Yestle Kim[1], John O'Donnell[1], Anthony Martinez[3]. [1]*Madrigal Pharmaceuticals, Inc., West Conshohocken, United States;* [2]*Star Biopharma Consulting, LLC, Malvern, United States;* [3]*University at Buffalo, Buffalo, United States*
Email: cparrinello@madrigalpharma.com

Background and aims: Resmetirom (Rezdiffra™) is a thyroid hormone receptor β-selective agonist, conditionally approved in the United States (US) in March 2024 for the treatment of adults with noncirrhotic metabolic dysfunction-associated steatohepatitis (MASH) and moderate-to-advanced fibrosis. Real-world evidence on resmetirom effectiveness remains limited. This study reports 12-month changes in lab measures.
Method: This retrospective cohort study used Truveta deidentified electronic health record data from US health systems linked to third-party medication dispensing data. Patients aged ≥18 years were indexed at first resmetirom fill on or after March 14, 2024 and followed through October 17, 2025. In the 2-year baseline period, patients had ≥2 healthcare encounters, no evidence of other causes of liver disease (e.g., alcohol use) or advanced liver disease (e.g., cirrhosis). Means (and standard deviations [SDs]) were calculated at index (−90 to +45 days) and 12 months (±90 days) for alanine transaminase (ALT), aspartate aminotransferase (AST) and low-density lipoprotein cholesterol (LDL-C), with mean change and *p*-values from paired *t*-tests. Analyses were stratified by type 2 diabetes (T2D) status and GLP-1 use.
Results: A total of 728 patients received resmetirom and had follow-up for 12-month assessment (mean 58 [SD 13] years, 36% male, 77% White, 64% obese, 52% T2D, 80% dyslipidemia, 62% hypertension, 30% GLP-1 use). In 222 patients (30%) with baseline and 12-month ALT and AST, means (SD) decreased (64.5 U/L [47.5] to 43.1 [32.0], −21.5 U/L and 50.1 U/L [35.5] to 35.4 [20.4], −14.7 U/L, respectively, both $p < 0.01$). Mean LDL-C (in 85 patients) decreased (93.9 mg/dL [33.4] to 85.4 [34.1], −8.5 mg/dL, $p < 0.05$). ALT and AST results were similar among patients, regardless of baseline T2D status or GLP-1 use. Decreases in LDL-C were similar between T2D and non-T2D (−7.9 and −9.4 mg/dL, respectively), and smaller in patients with than without baseline GLP-1 use (−1.0 and −11.9 mg/dL, respectively). However, numbers were small in LDL-C subgroup analyses.
Conclusion: In this descriptive study of patients treated with resmetirom, mean liver function test results decreased over 12 months, irrespective of T2D status or GLP-1 use. LDL-C decreased overall and irrespective of T2D, with smaller reductions observed in the smaller subgroup of baseline GLP-1 users. Future research will evaluate additional non-invasive measures and longer-term clinical outcomes with extended follow-up.

FRI-187

Long-term real-life experience of semaglutide in a monocentric cohort with type 2 diabetes and metabolic dysfuction-associated steatotic liver disease (MASLD)

Giovanni Petralli[1,2], Antonio Salvati[2], Simone Cappelli[1], Lidia Surace[2], Laura De Rosa[3], Francesco Damone[1], Maurizia Brunetto[1,2].
[1]*Department of Clinical and Experimental Medicine, Pisa, Italy;*
[2]*Hepatology Unit, Reference Center of the Tuscany Region for Chronic Liver Disease and Cancer, University Hospital of Pisa, Pisa, Italy;*
[3]*Institute of Clinical Physiology, National Research Council, Pisa, Italy*
Email: g.petralli94@gmail.com

Background and aims: MASLD is the liver manifestation of a multifaceted metabolic disorder, strongly associated with type 2 diabetes (T2D). Subcutaneous semaglutide, highly effective in T2D treatment, has recently been shown to induce resolution of steatohepatitis, albeit at the higher 2.4 mg weekly dose. We longitudinally evaluated a T2D-MASLD cohort following the introduction of semaglutide 1 mg weekly for diabetes optimization, aiming to assess its long-term effects on liver disease activity.
Method: 90 patients (age 60.7 ± 9.9 years; 38% female; T2D-duration 5[1–8] years) were evaluated non-invasively through anthropometry, biochemical profiling, and transient elastography (FibroScan®) at baseline (t0), 6 months (t1, 5–8 months), and 24 months (t2, 21–31 months, n = 67). Variations (Δ) in ALT, controlled attenuation parameter (CAP), and liver stiffness measurement (LSM) were used as proxies of liver disease burden. The PNPLA3 I148M polymorphism was also assessed. Ultrasound evidence of irregular liver margins, left-lobe hypertrophy, and nodular echo-pattern defined compensated cirrhosis.
Results: After treatment, significant reductions ($p < 0.01$) were observed in BMI (t0 32.6 ± 5.7 kg/m^2; Δ_{t1-t0} −6 ± 1%, Δ_{t2-t0} −6 ± 1%), glycated hemoglobin (HbA_{1c}; t0 53 ± 13 mmol/mol; Δ_{t1-t0} −17 ± 2%, Δ_{t2-t0} −13 ± 2%), ALT [t0 35 (22–54) U/L; Δ_{t1-t0} −22 ± 5%, Δ_{t2-t0} −20 ± 5%], CAP [t0 339 (288–372) dB/m; Δ_{t1-t0} −3 ± 3%, Δ_{t2-t0} −6 ± 4%], and LSM [t0 8.2 (5.5–11.0) kPa; Δ_{t1-t0} −25 ± 4%, Δ_{t2-t0} −11 ± 5%]. No significant differences were detected between t1 and t2, except for a mild HbA_{1c} increase (+2.4 ± 0.8 mmol/mol; $p = 0.006$). At t1, a ≥17 U/L ALT reduction occurred in 36% of patients, while ≥30% reductions in CAP and LSM were observed in 14% and 39% of patients, respectively, comparable to t2–t0 changes. Variations in ALT, CAP, and LSM were not influenced by PNPLA3 polymorphisms, baseline BMI, or HbA_{1c}. Compared with the patients without cirrhosis (n = 77), those with cirrhosis (n = 13) exhibited numerical subgroup differences in ALT

(Δ_{t1-t0} −18 ± 5% vs −42 ± 12%; Δ_{t2-t0} −19 ± 6% vs −32 ± 15%) and LSM (Δ_{t1-t0} −24 ± 5% vs −32 ± 12%; Δ_{t2-t0} −10 ± 5% vs −22 ± 14%).
Conclusion: Semaglutide at a 1 mg weekly dose effectively reduces steatotic and fibro-inflammatory liver involvement in diabetic MASLD, with early improvements at 6 months that persist over time without further enhancement. Baseline anthropometric parameters, glycemic control, and PNPLA3 genotype do not modify the hepatic response to semaglutide. Notably, steatohepatitis improvement was maintained even in cirrhotic patients.

FRI-188-YI
Evaluating non-invasive eligibility criteria for resmetirom in metabolic dysfunction-associated steatotic liver disease (MASLD): real-world data from an italian multicentric cohort
Nicola Pugliese[1], Davide Polverini[1], Arianna Bertazzoni[1], Federica Cerini[2], Rosa Lombardi[2], Grazia Pennisi[3], Stella De Nicola[1], Valerio Gullace[1], Anna Ludovica Fracanzani[2], Mauro Viganò[4], Salvatore Petta[3], Alessio Aghemo[1]. *[1]Humanitas University, Rozzano (Milano), Italy; [2]Università di Milano, Milano, Italy; [3]università di palermo, palermo, Italy; [4]Azienda Ospedaliera Papa Giovanni XXIII, Bergamo, Italy*
Email: nicola.pugliese@live.com

Background and aims: Resmetirom is approved for non-cirrhotic metabolic dysfunction–associated steatohepatitis (MASH) and moderate-to-advanced fibrosis (F2-F3). In clinical practice, eligibility largely depends on non-invasive tests (NITs). We aimed to quantify resmetirom eligibility in a real-world italian MASLD cohort according to AASLD Practice Guidance and Noureddin Expert Panel frameworks, and to evaluate concordance, clinical/biopsy accuracy and predictors of eligibility.
Method: We retrospectively included 908 consecutive MASLD adults from four Italian tertiary centres. Demographic, clinical, laboratory and vibration-controlled transient elastography (VCTE) data were retrieved from electronic records; 175 patients (19.3%) also had liver biopsy. Eligibility definitions mirrored clinical guidance: AASLD (VCTE 8–15 kPa, absence of cirrhosis/portal hypertension) and Noureddin (VCTE 10–19.9 kPa, platelets $\geq 140 \times 10^9$/L, no cirrhosis). Agreement was assessed with Cohen's κ and McNemar's test; multivariable logistic regression identified independent predictors.
Results: Median age was 62 years, 57% male. Median BMI was 29.4 kg/m^2; obesity and type 2 diabetes (T2D) affected 45.5% and 35.8%, respectively. Median VCTE was 6.3 kPa; 23.7% had LSM >10 kPa. In biopsied patients, fibrosis stages were F0–F1 41.1%, F2–F3 41.7%, F4 17.1%. Overall, 22.6% (205/908) met AASLD and 12.9% (117/908) met Noureddin criteria. Eligible patients presented more frequently with obesity (AASLD 56.6% vs 46.1%; Noureddin 60.7% vs 46.7%) and T2D (AASLD 52.7% vs 30.9%; Noureddin 57.3% vs 32.6%) ($p < 0.01$). Among biopsy-proven F2–F3 ($n = 73$), 52.1% were AASLD-eligible and 32.9% Noureddin-eligible; most missed cases had VCTE values below entry thresholds. Agreement between frameworks was 84.3% ($\kappa = 0.468$) with significant directional discordance (McNemar $p < 0.0001$): 116 patients were eligible only by AASLD, and 27 only by Noureddin. In multivariable models, age ($p = 0.0146$), BMI ($p = 0.0161$) and T2D ($p < 0.0001$) independently predicted eligibility for both frameworks, while FIB-4 was inversely associated with Noureddin eligibility ($p = 0.0348$).
Conclusion: AASLD and Noureddin frameworks select overlapping yet non-interchangeable populations. AASLD criteria are broader, while Noureddin's are more selective but may miss up to two-thirds of biopsy-confirmed F2–F3 patients. Integrated clinical–NIT approaches may optimize resmetirom allocation in real-world settings.

FRI-189
Lanifibranor-induced improvements in histological parameters and cardiometabolic markers in MASH are independent of weight change and closely associated with adiponectin induction
Mary E. Rinella[1], Guillaume Wettstein[2], Philippe Huot-Marchand[2], Jason Campagna[3], Sven Francque[4], Manal F. Abdelmalek[5]. *[1]Division of Gastroenterology, Hepatology and Nutrition, University of Chicago, Pritzker School of Medicine, Chicago, United States; [2]Inventiva, Daix, France; [3]Inventiva Inc, Boston, United States; [4]Department of Gastroenterology and Hepatology Antwerp University Hospital, Antwerp, Belgium; [5]Division of Gastroenterology and Hepatology, Mayo Clinic, Rochester, United States*
Email: mrinella@bsd.uchicago.edu

Background and aims: In the phase 2 NATIVE study, lanifibranor, a pan-PPAR agonist, demonstrated significant efficacy on improvement of steatohepatitis and fibrosis and markers of cardiometabolic health (CMH) in patients with metabolic dysfunction–associated steatohepatitis (MASH). Adiponectin (ADP), a pleiotropic adipokine downstream of PPARγ activation, improves insulin sensitivity, lipid metabolism, and inflammatory and fibrotic pathways. The modest weight gain of PPARγ agonists may be attributable to the expansion of metabolically favourable subcutaneous adipose tissue. This analysis examined relationships between ADP induction, weight change, and histological and CMH outcomes following lanifibranor treatment.
Method: In NATIVE, 247 patients with non-cirrhotic MASH were randomized to lanifibranor 800 mg, 1200 mg, or placebo for 24 weeks. Circulating ADP levels were measured at baseline (BL) and end of treatment (EOT) in 211 patients; weight-based CMH analyses were performed in 217 completers. Patients were stratified by BL ADP level (< 5, 5–10, > 10 µg/mL) and by fold-change at EOT (< 1.5×, 1.5–4×, > 4×) and weight change (≤ 2.5%, 2.5–5% and > 5%). Glycemic, lipid, liver, and inflammatory markers, and hepatic steatosis (CAP and NASH-CRN) were compared across strata.
Results: Despite modest weight gain with lanifibranor (2.6–3.1% for 800 mg and 1200 mg), improvements in histologic parameters and CMH markers were consistent across weight change categories. ADP levels increased across all weight-change groups, with no correlation between ADP fold-change and magnitude of weight gain, indicating independence of these PPARγ-associated effects. In contrast, placebo-treated patients with > 2.5% weight gain showed no improvement in ADP or CMH markers and worsening hepatic steatosis by CAP. Lanifibranor induced a dose-dependent rise in ADP level associated with improvements in histology and CMH markers independent of body-weight change.
Conclusion: Unlike life-style related weight gain, lanifibranor associated weight gain correlates with increases in ADP and improvements in liver histology. ADP may serve as a biomarker of therapeutic response with lanifibranor. The association between ADP induction and markers of CMH supports improved adipose-tissue health and insulin sensitivity as key mechanisms underlying lanifibranor efficacy in MASH.

FRI-190
A self-monitoring mobile health app is superior to lifestyle coaching and minimal intervention in reducing aspartate aminotransferase in MASLD patients: a randomised controlled trial
Wouter Robaeys[1], Leen Heyens[2], Liesbeth Bruckers[3], Joris Penders[4], Struyve Mathieu[5], Ger Koek[6], Sven Francque[7], Geert Robaeys[8]. *[1]Limburg Clinical Research Center (LCRC), Faculty of Health and Life Sciences, Hasselt University, Department of Future Health, Ziekenhuis Oost Limburg, 3600 Genk, Belgium; Department of Gastroenterology, Ziekenhuis Oost-Limburg, 3600 Genk, Belgium, Hasselt, Belgium; [2]Limburg Clinical Research Center (LCRC), Faculty of Health and Life Sciences, Hasselt University, Department of Future Health, Ziekenhuis Oost-Limburg, 3600 Genk, Belgium; Department of Gastroenterology, Ziekenhuis Oost-Limburg, 3600 Genk, Belgium, Hasselt, Belgium;*

[3]BioStat, Data Science Institute, Hasselt University, Hasselt, Belgium; [4]Faculty of Medicine and Life Sciences, Hasselt University, Department of Laboratory Medicine, Ziekenhuis Oost Limburg, 3600 Genk, Belgium, Hasselt, Belgium; [5]Department of Gastroenterology, Ziekenhuis Oost-Limburg, Genk, Belgium; [6]Department of Gastroenterology and Hepatology, Maastricht University Medical Center (MUMC), School of Nutrition and Translational Research in Metabolism (NUTRIM), Maastricht University 6211 LK Maastricht, The Netherlands, Maastricht, Netherlands; [7]Department of Gastroenterology and Hepatology, Antwerp University Hospital, Laboratory of Experimental Medicine and Paediatrics, InflaMed Centre of Excellence, University of Antwerp, Antwerp, Belgium; [8]Limburg Clinical Research Center (LCRC), Faculty of Health and Life Sciences, Hasselt University, Hasselt, Belgium
Email: geert.robaeys@uhasselt.be

Background and aims: To reduce the process of Metabolic Dysfunction-Associated Steatotic Liver Disease (MASLD), new guidance methods, such as lifestyle coaching and mobile health (m-health), should be investigated. Therefore, we studied the outcome of these guidance methods on steatosis, steatohepatitis and fibrosis in MASLD patients.
Method: In a monocentric, 12-month, randomised controlled trial, participants were randomised into three arms: (1) minimal intervention therapy (MIT), (2) lifestyle coaching, and (3) m-health (Happi app) with real time diet, based on image recognition, and exercise self-monitoring. The outcome on steatosis, steatohepatitis, and fibrosis were measured using the controlled-attenuation parameter (CAP^{TM}), hepatic steatosis index (HSI); aspartate transaminase (AST), Fibroscan-AST (FAST) and vibration-controlled transient elastography (VCTE^{TM}).
Results: The guidance by Happi app (n = 98) was superior to MIT (n = 102) and coaching (n = 97) with respect to reduction of the mean serum AST levels (−2.8 U/l, 95% CI [−5.1;−0.6], p = 0.014) and also caused a small but significant decrease in the FAST score (−0.03, 95% CI [−0.05;−0.02], p = 0.018). In addition, m-health induced, similar to coaching and MIT, a significant reduction in steatosis over the 12-month study period, measured by CAP^{TM} (-22 dB/m, 95% CI [−35.8; −8.1], p = 0.002), as well as by HSI (−1.1, 95% CI [−1.8;−0.4], p = 0.002) but no significant change in fibrosis as measured by VCTE^{T}M.
Conclusion: This well-documented study shows that m-health has a more pronounced effect on steatohepatitis-related features than coaching or the MIT. M-health reduces liver steatosis to the same extent as MIT or coaching, but does not improve liver stiffness after one year of intervention. M-health guidance is hence a useful and potentially superior tool to conventional care and should be preferred in MASLD management, being it as a stand-alone approach or to complement anti-MASLD therapy.

FRI-191

Efruxifermin improved digital pathology and noninvasive fibrosis measures in participants with MASH and advanced fibrosis or compensated cirrhosis: analysis of the HARMONY and SYMMETRY phase 2b trials

Jörn M. Schattenberg[1], Mary E. Rinella[2], Vlad Ratziu[3], Elaine Chng[4], Julian Lee[4], Yukti Choudhury[4], Doreen Chan[5], Erik Tillman[6], Dean Tai[4], Kitty Yale[6], Tim Rolph[6], Mazen Noureddin[7]. [1]Department of Internal Medicine II, Saarland University Medical Center, Homburg, Germany; [2]University of Chicago, Chicago, United States; [3]Sorbonne Université, Hôpital Pitié-Salpêtrière, Paris, France; [4]HistoIndex Pte Ltd, Singapore, Singapore; [5]Akero Therapeutics - a Novo Nordisk company, Austin, United States; [6]Akero Therapeutics - a Novo Nordisk company, South San Francisco, United States; [7]Houston Methodist Hospital, Houston Research Institute, Houston, United States
Email: joern.schattenberg@uks.eu

Background and aims: Individuals with MASH and advanced fibrosis (F3) or cirrhosis (F4) are at high risk of disease progression. Efruxifermin improved categorical fibrosis stages (NASH CRN) in phase 2b trials in participants with MASH and biopsy-confirmed stage F2/3 or compensated cirrhosis (F4c). The effects of efruxifermin on continuous fibrosis measures were evaluated by digital pathology and noninvasive tests in the phase 2b trials.
Method: This post hoc analysis included participants with MASH and F3 or F4c from the HARMONY (NCT04767529) and SYMMETRY (NCT05039450) randomized placebo-controlled trials. Changes from baseline at Week 96 in digital pathology and noninvasive measures (liver stiffness by transient elastography [LSM] and Enhanced Liver Fibrosis [ELF] test) for efruxifermin (pooled 28/50-mg) vs placebo were evaluated. Digital pathology was evaluated in unstained liver biopsies by second harmonic generation (SHG)/two-photon excitation fluorescence microscopy, and included measures applicable to F3/4 fibrosis: qFibrosis (continuous), relative collagen amount (%) in biopsy tissue area detected by SHG signal, and septa area (qSepta).
Results: The analysis included 53 participants with F3 fibrosis (efruxifermin N = 33, placebo N = 20): 59% female, 79% T2D, mean age 56 years, 37 kg/m^2 BMI, LSM 15 kPa, ELF 9.9; and 130 with F4c fibrosis (efruxifermin N = 86, placebo N = 44): 72% female, 79% T2D, mean age 60 years, 36 kg/m^2 BMI, LSM 25 kPa, ELF 10.6. Digital pathology measures in F3 were: mean qFibrosis value 2.9, SHG 7%, median septa area: 1.33×10^5 μm^2, and were more severe in F4c: mean qFibrosis value 4.0, SHG 14%, median septa area: 2.95×10^5 μm^2. At Week 96, mean change in LSM was greater for efruxifermin vs placebo (F3: – 36% [-6.6 kPa] vs 0% [−0.4 kPa], p < 0.001 and F4c: −39% [−28.8 kPa] vs −28% [−17.3 kPa], p = 0.05). There was also a greater reduction in ELF with efruxifermin than placebo (F3:−0.9 vs −0.1, p < 0.01 and F4c: −0.6 vs 0.2, p < 0.001). Relative change in qFibrosis value was greater with efruxifermin vs placebo (F3: −16% vs 0.6%, p = 0.006; F4c: −15% vs −2%, p = 0.03). Many improvements with efruxifermin were observed early and continued through Week 96.
Conclusion: In this post hoc analysis of participants with MASH at high risk of disease progression (F3 or F4c), efruxifermin was associated with improvements in continuous fibrosis measures assessed by digital pathology and noninvasive tests. Phase 3 trials of efruxifermin in MASH are ongoing.

FRI-195-YI

A machine learning model for predicting endpoint achievement in pharmacological trials for metabolic dysfunction-associated liver disease

Seyed Sahab Aarabi[1,2], Farbod Semnani[1,2], Kiavash Semnani[3], Shirin Esmaeili[1], Ehsaneh Taheri[4], Armita Mahdavi-Gorabi[3], Mohsen Rajabnia[3], Shirin Djalalinia[5], Amir Kasaeian[4], Mohammad Shadab Siddiqui[6], Mostafa Qorbani[3,7]. [1]School of Medicine, Tehran University of Medical Sciences, Tehran, Iran; [2]National Center for Health Insurance Research, Tehran, Iran; [3]Non-communicable Diseases Research Center, Alborz University of Medical Sciences, Karaj, Iran; [4]Digestive Diseases Research Institute, Tehran University of Medical Sciences, Tehran, Iran; [5]Non-Communicable Diseases Research Center, Endocrinology and Metabolism Population Sciences Institute, Tehran University of Medical Sciences, Tehran, Iran; [6]Division of Gastroenterology and Hepatology, University of Virginia, Charlottesville, Virginia, United States; [7]Chronic Diseases Research Center, Endocrinology and Metabolism Population Sciences Institute, Tehran University of Medical Sciences, Tehran, Iran
Email: kiavashsemnani@gmail.com

Background and aims: Despite recent successes, drug development for metabolic dysfunction-associated steatotic liver disease (MASLD) faces major challenges – with many agents failing to meet efficacy endpoints in later stages of development. We evaluated non-drug influences on trial endpoint achievement to elucidate trial design factors associated with success and patient subgroups likely to benefit from tried treatment strategies.
Method: This is an exploratory analysis from a large-scale systematic review on the safety and efficacy of pharmacological interventions for MASLD. Data from 172 randomized controlled trials with pre-

specified efficacy endpoints was analyzed after screening records from MEDLINE, Web of Science, Scopus, CENTRAL, ICTRP, and ClinicalTrials.gov up to September 4, 2025. We developed a gradient-boosting machine learning (XGBoost) model. The model was trained – with 5-fold cross validation – on trial (duration, phase, diagnostic criteria [histological vs other], comparator [placebo vs lifestyle vs older agents], publication date, sponsor, and endpoint choice [e.g. MASH resolution, fibrosis improvement, etc.]) and patient characteristics (age, sex, diabetes status, BMI, ALT, hepatic fat fraction [PDFF], NAFLD Activity Score [NAS], and disease severity). Performance was evaluated via Receiver Operating Characteristic analysis. Feature importance was assessed via Shapley Additive Global importance (SAGE).

Results: The model showed robust capability (AUC = 0.83, 95% CI: 0.76 to 0.90; 0.82 F1 score; 0.87 sensitivity; 0.73 specificity; and 0.80 accuracy). Recency (SAGE: 0.40); shorter follow-up (SAGE: 0.18); evaluations of off-label therapy (SAGE: 0.04); enrolment of younger patients (SAGE: 0.66) with higher BMI (SAGE: 0.15); higher proportion of male patients (SAGE: 0.15); lower ALT (SAGE: 0.49); available/higher PDFF (SAGE: 0.43) or NAS (SAGE: 0.12) values at baseline; and absence of steatohepatitis (SAGE: 0.07) were associated with endpoint achievement. Proportion of patients with diabetes; diagnostic methodology; comparator type; endpoint definition; and pharmacological targets showed minimal importance.

Conclusion: Our model demonstrated strong performance in predicting MASLD trial successes. These findings highlight important associations between patient demographics; metabolic profile (obesity); and trial design parameters with judgements of efficacy for appraisal of evidence and future trial design.

FRI-196

Safety of resmetirom in MASLD: a propensity score–matched real-world cohort analysis

Abdullah Sohail[1], Sayed Tauseef Ahmad Jan[1], Antonio Sanchez[1], Sara Naimimohasses[1]. [1]*The University of Iowa, Iowa City, United States*
Email: sara-naimimohasses@uiowa.edu

Background and aims: Resmetirom is approved for metabolic dysfunction–associated steatotic liver disease with moderate to advanced fibrosis, yet real-world hepatic safety data remain limited. This study evaluated early and intermediate-term hepatic outcomes among adults with MASLD treated with Resmetirom compared with matched untreated controls.

Method: Using the TriNetX Research Network, adults with MASLD were identified. Exclusions included liver transplantation, hepatocellular carcinoma, viral hepatitis, significant alcohol-related liver disease, pregnancy, and cholestatic autoimmune disorders. Propensity score matching incorporated demographics, MELD laboratory components, metabolic comorbidities, and concurrent medications to ensure comparable baseline liver disease severity. The Resmetirom cohort (n = 2,981) was matched 1:1 with untreated MASLD controls, yielding 2,056 patients per group. Outcomes at 90 and 180 days included new cirrhosis, liver enzyme elevation, and biliary complications.

Results: At 90 days, Resmetirom users had a significantly lower risk of developing new cirrhosis (2.8% vs 15.7%; odds ratio, 0.153; 95% CI, 0.115–0.204; $p < 0.0001$). Liver enzyme elevation occurred less frequently with Resmetirom (5.5% vs 13.4%; odds ratio 0.379, 95% CI 0.302–0.475; $p = 0.000$). Biliary complications were also reduced (0.7% vs 4.7%; odds ratio 0.148, 95% CI 0.086–0.257; $p = 0.000$).

At 180 days, the benefit persisted. New cirrhosis occurred in 4.6% of Resmetirom users versus 18.5% of controls (odds ratio 0.214, 95% CI 0.169–0.270; $p = 0.000$). Liver enzyme elevation remained lower in the Resmetirom group (7.6% vs 15.6%; odds ratio 0.449, 95% CI 0.367–0.549; $p = 0.000$). Biliary complications were similarly reduced (1.5% vs 6.1%; odds ratio 0.236, 95% CI 0.159–0.352; $p = 0.000$). Kaplan–Meier analyses demonstrated significantly higher event-free survival across all outcomes with Resmetirom at both time intervals.

Conclusion: Across 90 and 180 days, Resmetirom demonstrated a favorable hepatic and biliary safety profile, with significantly lower odds of new cirrhosis, liver enzyme elevation, and biliary complications compared with matched MASLD controls. These findings support the early safety and clinical benefit of Resmetirom in routine practice. Longer-term follow-up is necessary to assess the sustained effects on fibrosis progression and hepatic outcomes.

FRI-197

Comparative efficacy of non-cirrhotic MASH treatments: an updated network meta-analysis of phase 2–3 candidates

Nicole Shu Ying Tang[1], Tsubasa Tsutsumi[2,3], Cheng Han Ng[1,3], Hiroyuki Suzuki[3,4], Nicholas Syn[1], N Apoorva Sasikumar[1], Glenn Jun Kit Ho[1], Damien Chua[5], Jing Kai Tioh[1], Thanawin Pramotedham[6], Vigneshwaran Selvakumar[5], Peter Jin Sun Low[1], Joon Ho Moon[7], Yock Young Dan[1,6], Vincent Wai-Sun Wong[8], Ming-Hua Zheng[9,10,11,12], Carel Le Roux[13], Jörn Schattenberg[14], Weiting Huang[15], Tim Kendall[16,17], Jonathan Fallowfield[16,18], Vincent Chen[19], Hirokazu Takahashi[20], Mary E. Rinella[2], Mohammad Shadab Siddiqui[21], Mazen Noureddin[22], Arun J. Sanyal[23], Takumi Kawaguchi[3], Mark Muthiah[1,6,24]. [1]*Yong Loo Lin School of Medicine, Singapore, Singapore;* [2]*Division of Gastroenterology, Hepatology and Nutrition, Department of Medicine, University of Chicago, Chicago, United States;* [3]*Division of Gastroenterology, Department of Medicine, Kurume University School of Medicine, Kurume, Kurume, Japan;* [4]*Department of Internal Medicine, Division of Digestive and Liver Diseases, University of Texas Southwestern Medical Center, Texas, United States;* [5]*Lee Kong Chian School of Medicine, Nanyang Technological University, Singapore, Singapore, Singapore;* [6]*Division of Gastroenterology and Hepatology, Department of Medicine, National University Hospital, Singapore, Singapore;* [7]*Division of Endocrinology and Metabolism, Seoul National University Bundang Hospital, Seoul, Republic of Korea, Seoul, Korea, Rep. of South;* [8]*Department of Medicine and Therapeutics, The Chinese University of Hong Kong, Hong Kong, China, Hong Kong, Hong Kong;* [9]*MAFLD Research Center, Department of Hepatology, First Affiliated Hospital of Wenzhou Medical University, Wenzhou, China;* [10]*Wenzhou Key Laboratory of Hepatology, Wenzhou, China;* [11]*Institute of Hepatology, Wenzhou Medical University, Wenzhou, China;* [12]*Key Laboratory of Diagnosis and Treatment for the Development of Chronic Liver Disease, Zhejiang, Wenzhou, China;* [13]*University College Dublin, Diabetes Complications Research Centre, Dublin, Ireland;* [14]*Department of Medicine I and Metabolic Liver Research Program, University Medical Center, Johannes Gutenberg University Mainz, Mainz, Germany;* [15]*National Heart Centre Singapore, Singapore, Singapore;* [16]*Centre for Inflammation Research, Institute for Regeneration & Repair, University of Edinburgh, Edinburgh, United Kingdom;* [17]*Edinburgh Pathology, University of Edinburgh, Edinburgh, United Kingdom;* [18]*University of Edinburgh, Institute For Regeneration and Repair, Edinburgh, United Kingdom;* [19]*Division of Gastroenterology and Hepatology, Department of Internal Medicine, University of Michigan, Ann Arbor, MI, United States;* [20]*Department of Internal Medicine, Saga University Faculty of Medicine, Saga, Japan;* [21]*Division of Gastroenterology, Hepatology and Nutrition, Department of Internal Medicine, Virginia Commonwealth University, Richmond, VA, United States;* [22]*Cedars-Sinai Fatty Liver Program, Division of Digestive and Liver Diseases, Department of Medicine, Cedars-Sinai Medical Center, Los Angeles, CA, United States;* [23]*Division of Gastroenterology, Hepatology and Nutrition, Department of Internal Medicine, Virginia Commonwealth University School of Medicine, Richmond, VA, United States;* [24]*National University Centre for Organ Transplantation, National University Health System, Singapore, Singapore*
Email: nicole.sytang@outlook.com

Background and aims: Metabolic dysfunction–associated steatohepatitis (MASH) has an expanding drug pipeline but no comparative hierarchy of efficacy.

Method: We performed a systematic review and network meta-analysis of phase 2–3 randomized controlled trials enrolling adults with non-cirrhotic MASH. Primary endpoints were histologic MASH resolution without fibrosis worsening, ≥1-stage fibrosis improvement without MASH worsening, and ≥30% steatosis reduction in MRI-PDFF.
Results: Sixty-four trials were included. Metabolic and insulin-sensitizing agents provided the largest benefits versus placebo (odds ratios 2.5–7.1) and the lowest failure rates, yet absolute histologic response rates remained modest and variable. At the class and medication levels, FGF21 analogues and incretin-based multi-agonists ranked highest, yet 35–70% of treated patients failed to reach histologic targets, and placebo responses reached 11–18%.
Conclusion: These findings support potent metabolic agents as a pharmacologic backbone and highlight the need for durable, combination strategies that can more robustly distinguish true drug effects from placebo effects.

FRI-198
Protective potential of minimally processed, plant-derived foods against steatotic liver disease in early adulthood
Yasmina Tashkent[1,2,3], Jocelyn Choo[1,2], Steven Taylor[1,2], Therese O'Sullivan[4], Dujinthan Jayabalan[5,6], Sophie Miller[1,2], Richard Woodman[1], Luis Calzadilla Bertot[5,6], Oyekoya Ayonrinde[6,7,8], Lawrence Beilin[6], Trevor Mori[6], John Olynyk[7,8], Alan Wigg[1,3], Kate Muller[1,3], Leon Adams[5,6], Geraint Rogers[1,2]. *[1]Flinders Health and Medical Research Institute, College of Medicine and Public Health, Flinders University, Bedford Park, Australia; [2]Microbiome and Host Health Program, South Australian Health and Medical Research Institute, Adelaide, Australia; [3]South Australian Hepatology and Transplant Medicine Unit, Southern Adelaide Local Health Network, Bedford Park, Australia; [4]Nutrition and Health Innovation Research Institute, The School of Medical and Health Sciences, Edith Cowan University, Joondalup, Australia; [5]Department of Hepatology, Sir Charles Gairdner Hospital, Nedlands, Australia; [6]Medical School, The University of Western Australia, Perth, Australia; [7]Department of Gastroenterology and Hepatology, Fiona Stanley Hospital, Murdoch, Australia; [8]Curtin Medical Research Institute, Curtin University, Bentley, Australia*
Email: yasmina.tashkent@gmail.com

Background and aims: The incidence of steatotic liver disease (SLD) among younger adults is increasing globally. While poor diet is a recognised risk factor, the impact of specific dietary components is unclear. We investigated associations between dietary patterns and SLD markers in younger adults.
Method: Analysis involved 887 members of the Raine Study Generation 2 cohort, assessed at age 27. SLD was defined using a validated MRI volumetric liver fat fraction equation. Dietary intake, assessed by food frequency questionnaires, was summarised using a modified Overall Diet Score (ODS) that classified foods as "healthy" or "unhealthy." Associations between diet and SLD were evaluated by logistic regression, adjusting for waist circumference, sex, alcohol intake and physical activity.
Results: SLD was identified in 142 participants (16%). Higher consumption of vegetables, nuts, fish/seafood, coffee (all $P < 0.001$), tea ($P = 0.003$), and legumes ($P = 0.024$) was associated with reduced odds of SLD. Conversely, higher intake of fruit juice, processed animal products, processed meats (all $P < 0.001$), and sweets/desserts ($P = 0.029$) was associated with increased odds. Greater healthy food consumption (overall median [IQR] = 23 [19–27]) was inversely associated with SLD (adjusted OR = 0.949 per unit, 95% CI 0.909–0.992; $P = 0.021$). This association remained statistically significant only in males after adjustment ($P = 0.007$). The ODS and unhealthy food intake were not significantly associated with SLD following adjustment.
Conclusion: A higher intake of unprocessed or minimally processed plant-based foods is associated with lower SLD risk in younger adults, independent of central adiposity. These findings underscore the protective potential of plant-rich dietary patterns against SLD in early adulthood.

FRI-199
Effect of utreglutide on cardio-metabolic and non-invasive fibrotic biomarkers in participants with metabolic-dysfunction associated steatotic liver disease
Rajamannar Thennati[1], Vinod Burade[1], Muthukumaran Natarajan[1], Pradeep Shahi[1], Ravishankara Nagaraja[1], Bernard Thorens[2], Richard E Pratley[3], John Olynyk[4], Rohit Loomba[5]. *[1]High Impact Innovations – Sustainable Health Solutions (HISHS), Sun Pharmaceutical Industries Limited, Vadodara, Gujarat, India; [2]Center for Integrative Genomics, University of Lausanne, Lausanne, Switzerland; [3]AdventHealth Translational Research Institute, Orlando, United States, [4]Professor, Curtin Medical Research Institute, Curtin University and Fiona Stanley Hospital, West Australia, Australia; [5]Chief, Division of Gastroenterology and Hepatology, Professor of Medicine, University of California, San Diego, United States*
Email: rajamannarthennati@yahoo.com

Background and aims: Utreglutide (UTG, GL0034) is a potent glucagon-like peptide-1 receptor agonist. Here, we present safety and efficacy data of stratified participants on treatment with enhanced liver fibrosis (ELF) score reduction of ≥ 0.25 units and age ≥ 40 years; for placebo age ≥ 40 years from a Phase 1b/2a study.
Method: The study enrolled 48 subjects (BMI ≥ 30 kg/m^2, liver fat content ≥ 10 percent by magnetic resonance imaging-proton density fat fraction (MRI-PDFF), randomized (3:1) to once-weekly subcutaneous UTG with dose titration (0.4 to 1.6 mg over 10 weeks) followed by a fixed dose of 2.4 mg for 3 weeks, or placebo for 13 weeks. Data from stratified participants on UTG, n = 8 and placebo (PBO) n = 9, are presented.
Results: UTG treatment was well-tolerated, and the most common adverse events were mild to moderate gastrointestinal. The mean (SD) BMI (kg/m^2) at baseline was 40.3 (4.57) for PBO and 39.5 (4.38) UTG. The mean change in each of BMI and body weight (BW) at W14 was −9.9% ($p < 0.001$) and −10.1% ($p < 0.001$) respectively, which sustained till W17. Glycated hemoglobin mean reduction was 0.6% at W14 ($p < 0.001$) and 0.7% ($p < 0.001$) at W17 from BL of 6.1 (0.62). Non-invasive tests (NITs) revealed; a relative mean percent change of MRI-PDFF −34.1% ($p < 0.001$), BL of 22.7% (7.41); ELF score of −0.7 ($p < 0.001$), BL of 9.4 (0.75); percent subjects achieved reduction in MRI-PDFF and ELF score of ≥ 30% and > 0.5 units were 50% and 62.5% respectively, and no change in PBO; N-terminal propeptide of type III collagen (PRO-C3) (ng/mL) of −31.5 ($p < 0.05$), BL of 109.3 (46.97); and controlled attenuated parameter (CAP) mean (dB/m) of −67.9 ($p < 0.01$), BL of 350.9 (21.94)]. Alanine transaminase (U/L) decreased by 16.7% ($p < 0.05$) from a BL value of 40.0 (21.17). Lipid levels (mmol/L) at W14 showed reduction of 15.4% ($p < 0.05$) for cholesterol from BL of 4.9 (1.17) and 15.2% ($p < 0.01$) for LDL from a BL of 2.8 (0.98). High sensitivity C-reactive protein (mg/L) reduction was 44.8% ($p < 0.05$) from BL of 7.0 (6.23). Changes in PBO group were significant only for BMI and BW at W 14 ($p < 0.05$).
Conclusion: Utreglutide well tolerated; robust and sustained reductions in BW and BMI were observed. Clinically meaningful changes in cardiometabolic biomarkers and NITs associated with metabolic liver disease were noted. Collectively, these findings highlight the potential of utreglutide as a therapeutic option for metabolic dysfunction-associated steatohepatitis (MASLD) and other obesity-related disorders.

FRI-200
The impact of nutritional intervention on the echographic regression of metabolic dysfunction-associated steatotic liver disease in a cohort of postmenopausal women
Valerie Tikhonoff [1], Arianna Cocco[2], Pamela Paganini[1], Dario Cattelan[1], Giancarlo Bombonato[2]. *[1]Unit of dietetic and clinical nutrition, Department of medicine - Dimed, University of Padova,*

Padova, Italy; [2]Unit of internal medicine and hepatology, Department of medicine - Dimed, University and hospital of Padova, Padova, Italy
Email: valerie.tikhonoff@unipd.it

Background and aims: Menopause is associated with metabolic changes, secondary to estrogen decline, including increased visceral fat and impaired insulin sensitivity, resulting in an increased cardiovascular (CV) risk. In this context, metabolic dysfunction-associated liver disease (MASLD) shows a higher prevalence. Aim of this study is to evaluate the effect of a hypocaloric dietary intervention on the regression of MASLD in a cohort of postmenopausal women (PMW).
Method: 75 PMW were enrolled with BMI between 24 and 39 kg/m^2 and with at least one other CV risk factor. Complete clinical and biochemical data were acquired at the enrolment visit and at the six-month follow-up. Anthropometric, plicometric and bioimpedance measurements were performed. All participants underwent hepatosplanchnic ultrasound to evaluate hepatic steatosis via attenuation index (ATI) with a Canon Aplio i800 Ultrasonography System (Canon Medical Systems S.R.L., Roma). Each woman followed a balanced hypocaloric diet plan. Data analysis is based on paired t-test and ANOVA for repeated measures.
Results: After 6 months of dietary intervention, a significant reduction in ATI value was observed [$\Delta = -0.07$ dB/cm/MHz, (95% CI −0.09, −0.44) $p < 0.0001$], with complete regression of steatosis in 52.5% of PMW. Significant reductions in body weight (4.7%), BMI (5.6%), waist circumference (4.2%), and abdominal obesity prevalence (from 80% to 58%) were observed as well as in fat mass (10.6%) without change in fat-free mass. From a metabolic perspective, significant reductions in insulin resistance indices (HOMA-index and Metabolic Score for Insulin Resistance) and the visceral adiposity index (Metabolic Score for Visceral Fat) were observed. These positive results were achieved through a qualitative modification of dietary intake, with a reduction in daily lipid intake, particularly those of animal origin and thus saturated fatty acids, a reduction in animal protein intake, and an increase in plant proteins and total fiber.
Conclusion: The results provide evidence on the effectiveness of a targeted nutritional intervention on the regression of MASLD in PMW. The adopted approach, focused on reducing saturated fat intake and increasing plant proteins and fiber, has proven effective in promoting weight loss, improving body composition, and reducing insulin resistance, crucial factors for the regression of MASLD. These findings underscore the importance of adequate nutritional education in PMW.

FRI-201
Effect of pemvidutide on cardiovascular risk factors in patients with metabolic dysfunction-associated steatohepatitis: 48-week results from the phase 2b, IMPACT trial

John Suschak[1], Shaheen Tomah[1], Julio Gutierrez[1], M. Scot Roberts[1], Rachel Garner[1], Sarah Browne[1], M. Scott Harris[1], Christophe Arbet-Engels[1]. *[1]Altimmune, Inc, Gaithersburg, MD, United States*
Email: jsuschak@altimmune.com

Background and aims: Obesity is a primary driver of metabolic dysfunction-associated steatohepatitis (MASH), and the most common cause of mortality in patients with non-cirrhotic MASH is cardiovascular disease. Weight loss is central to the treatment of MASH as weight loss is associated with both MASH resolution and improvement in hepatic fibrosis. Beyond obesity, waist circumference, a measure of visceral adiposity, elevated serum lipids, and high blood pressure can be risk factors for cardiovascular disease. Pemvidutide is a balanced 1:1 glucagon/GLP-1 dual receptor agonist in development for the treatment of MASH. IMPACT was a phase 2b, randomized, placebo-controlled, double-blind trial in patients with biopsy-confirmed MASH and fibrosis stage F2 or F3 (NCT05989711).
Method: 212 patients were randomized 1:2:2 to receive once-weekly subcutaneous pemvidutide (1.2 mg or 1.8 mg) administered without dose titration, or placebo. The primary endpoints were MASH resolution and fibrosis improvement at 24 weeks. Secondary endpoints of the trial included reductions in body weight, waist circumference, and serum lipids at 48-weeks. Blood pressure was followed for safety.
Results: The mean age was 53 years, the mean body mass index (BMI) was 39 kg/m^2, 58% were female, and 43% had type 2 diabetes (T2D). At 48 weeks, pemvidutide treatment resulted in significant reductions in body weight of up to 7.5% ($p < 0.0001$) in the 1.8 mg group, versus 0.2% in the placebo group. Importantly, the 1.8 mg weight loss curve did not plateau at 48 weeks, suggesting continued weight loss with continued treatment. Treatment with 1.8 mg pemvidutide also yielded an absolute reduction in waist circumference of 5.3 cm ($p = 0.0026$) versus 1.9 cm in placebo. Significant reductions in elevated triglycerides with a baseline > 150 mg/dL [1.8 mg (−23.7%; $p = 0.026$) versus placebo (−3.3%)] and elevated total cholesterol with a baseline > 200 mg/dL [1.8 mg (−15.4%; $p = 0.046$) versus placebo (−5.1%)] were observed in the 1.8 mg group. Lastly, significant reductions in systolic and diastolic blood pressure were observed in the 1.8 mg group.
Conclusion: Pemvidutide treatment resulted in reductions in key cardiovascular risk factors. Significant reductions in body weight, waist circumference, serum lipids, and blood pressure may be indicative of broad improvements in cardiovascular disease.

FRI-202
Semaglutide improves hepatic and cardiometabolic outcomes in paediatric metabolic dysfunction-associated steatotic liver disease: a prospective observational study

Andrea Tou[1], Brandon Perumpail[1], Nathan Smyk[1], Michael Kallan[2,3], Nikhil Pai[1,2,3], Jennifer Panganiban[1,2,3]. *[1]Children's Hospital of Philadelphia, Division of Pediatric Gastroenterology, Hepatology, and Nutrition, Philadelphia, United States; [2]University of Pennsylvania, Philadelphia, United States; [3]Perelman School of Medicine, Philadelphia, United States*
Email: touandrea@gmail.com

Background and aims: Paediatric metabolic dysfunction-associated steatotic liver disease (MASLD) is increasingly prevalent and lacks approved pharmacologic therapies. While growing evidence demonstrates that glucagon-like peptide-1 receptor agonists (GLP-1RAs), particularly semaglutide, are associated with histological improvements in steatohepatitis in adults, paediatric data remain lacking. We aimed to evaluate the real-world impact of semaglutide on hepatic and cardiometabolic outcomes in children and adolescents with MASLD.
Method: This single-centre prospective observational study enrolled patients ≤ 18 years with MASLD initiating semaglutide for type 2 diabetes mellitus (T2DM) or obesity. Anthropometrics, laboratory values, transient elastography via FibroScan, demographics, and treatment course were collected at baseline, 3 months, and 6 months. The primary outcome was change in alanine aminotransferase (ALT). Secondary outcomes included changes in body mass index (BMI), BMI percentile, waist circumference, aspartate aminotransferase (AST), gamma-glutamyl transpeptidase (GGT), glycated haemoglobin (HbA1c), lipid profile, and FibroScan-derived controlled attenuation parameter (CAP) and liver stiffness measurement (LSM). Longitudinal changes were analysed using mixed linear models.
Results: 12 patients (mean age 16 years, 92% male, 50% White) had follow-up data at 3 months, and 10 at 6 months. Semaglutide was initiated for obesity in 83% and T2DM in 17%. ALT declined at 3 months (−33, $p = 0.07$), with a significant reduction by 6 months (−69, $p = 0.001$). FibroScan CAP (dB/m) (−33, $p = 0.013$ at 3 months; −36, $p = 0.013$ at 6 months), BMI (kg/m^2) (−1.1, $p = 0.028$ at 3 months; −2.8, $p < 0.001$ at 6 months) and HbA1c (%) (−0.2, $p = 0.046$ at 3 months; −0.4, $p = 0.003$ at 6 months) significantly improved at both timepoints; whereas BMI percentile, weight, waist circumference,

AST, GGT, and total cholesterol showed significant reductions at 6 months.
Conclusion: This is the first prospective study on semaglutide use in paediatric MASLD. Semaglutide was associated with clinically meaningful improvements in surrogate markers of MASLD disease activity, including ALT and GGT, as well as reduced FibroScan CAP values reflecting improved hepatic steatosis within 6 months. Anthropometric indices and glycaemic control also significantly improved, consistent with existing literature. This supports semaglutide as a promising adjuvant therapy in paediatric MASLD and underscores the need for longer-term and controlled studies.

FRI-203-YI
Roux-en-Y gastric bypass versus sleeve gastrectomy in MASH advanced fibrosis resolution: comparable outcomes
Ana Luiza Gomes Reis[1], Isabel Veloso Alves Pereira[1], Marcella Motta Lucindo Duarte[1], Patricia Momoyo Zitelli[1], Renato Altikes[1], Daniel Szor[2], Danilo Mardegam Razente[2], Miller Barreto[2], Denis Pajecki[2], Marco Aurelio Santo[2], Mário Pessoa[1], Claudia Pinto Oliveira[1]. [1]*Hospital das Clínicas HCFMUSP (Lim 07); Departamento de Gastroenterologia e Nutrologia, Faculdade de Medicina, Universidade de São Paulo, São Paulo, Brazil;* [2]*Hospital das Clínicas HCFMUSP, Departamento de Cirurgia do Aparelho Digestivo e Coloproctologia, Faculdade de Medicina, Universidade de São Paulo, São Paulo, Brazil*
Email: anagreismed@hotmail.com

Background and aims: MASH is highly prevalent in individuals with obesity, and bariatric surgery is a key therapeutic option to improve metabolic health and liver steatosis. Roux-en-Y gastric bypass (RYGB) and sleeve gastrectomy (SG) are the most common procedures, each inducing weight loss through distinct anatomical and hormonal mechanisms. Although both improve MASH, evidence in advanced fibrosis remains limited and inconclusive regarding procedural superiority. We aimed to compare RYGB and SG in a biopsy-proven MASH cohort with advanced fibrosis (F3–F4) using non-invasive assessments.
Method: We conducted a retrospective analysis of twenty-six biopsy-proven MASH patients with advanced fibrosis (stage F3–F4) who underwent bariatric surgery (7 RYGB and 19 SG). Demographic variables, clinical parameters, and laboratory markers were collected. MASH resolution was evaluated after at least one year post-surgery using Vibration-Controlled Transient Elastography (VCTE) risk categories (<10 kPa low risk; 10–14.9 kPa intermediate risk; ≥15 kPa high risk), and AGILE 3+ (rule out <0.45) score.
Results: Baseline demographic and clinical characteristics were similar between groups, including age (51.3 ± 8.6 vs. 54.6 ± 13.7 years; p = 0.32), sex (86% vs. 80% female; p = 0.70), preoperative weight (116 vs. 105 kg; p = 0.48) and BMI (45.0 vs. 39.3 kg/m^2; p = 0.68). Hypertension (86% vs. 79%; p = 0.70), diabetes and dyslipidemia (100% vs. 95%; p = 0.54), fibrosis F4 (14% vs. 37%; p = 0.27) and NAS ≥5 (57% vs. 68%; p = 0.59) did not differ. Postoperative weight-related outcomes were similar (76 vs. 77 kg; p = 0.87), BMI (29.8 vs. 29.7 kg/m^2; p = 0.87) and total weight loss (32% vs. 30%; p = 0.27). Laboratory markers before and after surgery showed no significant differences. Comorbidity improvement was also similar. MASH resolution did not differ between RYGB and SG. VCTE risk categories were comparable (low: 57% vs. 63%; medium: 14% vs. 16%; high: 29% vs. 21%; p = 0.92). AGILE 3+ rule-out improvement occurred in 60% (4/7) vs. 40% (7/19), likely reflecting the higher baseline F4 prevalence in SG; only one F4 patient achieved rule-out.
Conclusion: RYGB and SG showed comparable metabolic and hepatic benefits in patients with biopsy-proven MASH and advanced fibrosis. No significant differences were observed across non-invasive liver markers, fibrosis risk categories, or metabolic improvements, indicating that both procedures offer similar effectiveness for MASH resolution in this high-risk population.

FRI-204
FB7033: A novel siRNA dual-targeting Hydroxysteroid 17-beta Dehydrogenase 13 (HSD17β13) and cell death-inducing DFF45-like effector B (CIDEB) exhibits potential for treatment of metabolic dysfunction-associated steatohepatitis (MASH)
Michael Wang[1,2,3], Jieting Zhang[1], Siwen Tang[1], Jundong Han[4], Lilei Guo[1], Xia Liu[1], Min Hu[1], Peizhuo Zhang[4], Dong Xie[1]. [1]*Frontier Biotechnologies, Inc., Nanjing, China;* [2]*Frontier Biotechnologies, Inc., R&D, N, China;* [3]*Frontier Biotechnologies, Inc, Nanjing, China;* [4]*Suzhou GenePharma Co. Ltd., Suzhou, China*
Email: wangzhiyan@frontierbiotech.com

Background and aims: MASH is characterized by hepatocellular steatosis, inflammation, and fibrosis, potentially progressing to cirrhosis and hepatocellular carcinoma. Current therapies for MASH are limited by safety, efficacy, and adherence issues. HSD17β13 and CIDEB contribute to MASH progression through distinct mechanisms. HSD17β13 exacerbates hepatic lipid metabolism dysfunction, inflammation, and fibrosis, while CIDEB primarily mediates lipid droplet dynamics and storage. Here we report the discovery and development of FB7033, a novel dual-targeting siRNA on HSD17β13 and CIDEB mRNA, as a promising therapeutic candidate for treatment of MASH.
Method: The HepG2, Hep3B cells, humanized HSD17β13 or CIDEB transgenic mice, and cynomolgus macaques were used to evaluate the efficacy of FB-7033 on HSD17β13 or CIDEB mRNA knockdown both *in vitro* and *in vivo*. A previously validated cynomolgus monkey MASH model, which was induced by high-fat diet, was used to assess efficacy. FB7033 was administrated by SC injections at 3, 6, 12 mg/kg (Q4Wx3). ARO-HSD (GSK4532990) (3 mg/kg, SC, Q4Wx3) and resmetirom (5 mg/kg, PO, QD) were used as positive controls. The MRI Proton Density Fat Fraction (MRI-PDFF) and NAFLD Activity Score (NAS) were measured for assessment of MASH progression for a duration of 12 weeks. The safety profile of FB7033 was assessed by *in vitro* and *in vivo* studies.
Results: FB7033 effectively knock-down HSD17β13 (IC_{50} = 5 pM) and CIDEB (IC_{50} = 3 pM) mRNA *in vitro*. A single subcutaneous injection of FB7033 led to simultaneous and significant suppression of both target mRNAs expression, with the maximal knock-down of 94% in monkeys. In the NHP MASH model, FB7033 reduced the expression of both target mRNAs in liver in a dose-dependent manner. More importantly, FB7033 significantly reduced hepatic fat (MRI-PDFF) and NAS Scoring, exhibiting superior efficacy of MASH remission, to those of ARO-HSD and resmetirom. FB7033 showed good safety profile in off-target, immunotoxicity, and repeat-dose toxicology study in rats.
Conclusion: FB7033 robustly inhibits the expression of HSD17β13 and CIDEB, conferring superior treatment potential against MASH progression, which indicates potential synergistic effect of the dual-targeting siRNA strategy. The pharmacodynamic profile of FB7033 may support a once every 1–3 months dosing regimen in human, addressing both efficacy and dosing challenges in current treatment regimens. Further clinical evaluation of FB7033 in MASH patients is warranted.

FRI-205-YI
Sodium-glucose co-transporter-2 inhibitors and risk of major adverse liver outcomes in patients with chronic liver disease and type 2 diabetes
Axel Wester[1], Ying Shang[1], Emilie Toresson Grip[1], Daniel Andersson[1], Camila Olarte Parra[1], Hannes Hagström[1]. [1]*Karolinska institutet, Stockholm, Sweden*
Email: axel.wester@ki.se

Background and aims: Small randomized trials suggest sodium-glucose co-transporter-2 (SGLT2) inhibitors may improve surrogate markers for major adverse liver outcomes (MALO), but whether SGLT2 inhibitors affect the risk of MALO is unknown. Large randomized trials to assess the effect of SGLT2 inhibitors on rare

hard clinical outcomes such as MALO would however likely be challenging to conduct. Therefore, we designed a hypothetical randomized trial that would estimate the causal effect of SGLT2 inhibitors on the risk of MALO in patients with any chronic liver disease and type 2 diabetes and then emulated this target trial using observational data.
Method: We used observational data from Swedish healthcare registers 2016–2022 to emulate a target trial of SGLT2 inhibitors in eligible patients with chronic liver disease and type 2 diabetes. We used an inverse-probability weighted marginal structural model to compare the 5-year risk of MALO (decompensated cirrhosis, hepatocellular carcinoma, liver transplantation, or liver-related death) in initiators of SGLT2 inhibitors versus non-initiators. The model was adjusted for age, sex, calendar year, socioeconomic parameters, markers for diabetes and liver disease severity, comorbidities, and medications that may affect both the exposure and the outcome.
Results: We included 37,503 patients with a median age of 65 years (interquartile range 56–73) of whom 22,159 (59%) were men and 7,007 (18.7%) had compensated cirrhosis at baseline. Baseline characteristics were well balanced between treatment groups after inverse-probability weighting. Initiators of SGLT2 inhibitors had a 5-year risk of MALO at 6.8% (143/4,160) versus 7.2% in non-initiators (1,922/33,343) in intention-to-treat analysis (risk ratio [RR] = 0.94, 95% confidence interval [CI] = 0.75–1.13). The corresponding 5-year per-protocol risk estimates were 5.2% (69/4,160) and 6.6% (1,807/33,343), respectively (RR = 0.78, 95% CI = 0.32–1.24). Risk estimates in subgroups based on sex, cirrhosis status at baseline (compensated cirrhosis, or no cirrhosis), and liver disease etiology (metabolic dysfunction-associated steatotic liver disease, or other) were consistent with the main results.
Conclusion: In patients with chronic liver disease and type 2 diabetes, initiation of an SGLT2 inhibitor did not affect the risk of MALO. Other antidiabetic treatment options may therefore be preferred in patients with concomitant chronic liver disease.

FRI-206
RNA editing of PNPLA3 I148M decreases hepatocyte fat content
Hsiu-Chiung Yang[1], Chikdu Shivalila[1], Pachamuthu Kandasamy[1], Stearne Briem[1], Michael Byrne[1], Alyse Faraone[1], Naoki Iwamoto[1], Tomomi Kawamoto[1], Richard Looby[1], Frank Favaloro[1], Stephany Standley[1], Suma Veermachineni[1], Hailin Yang[1], Benny Yin[1], Hui Yu[1], Genliang Lu[1], Chandra Vargeese[1], Erik Ingelsson[1]. [1]*Wave Life Sciences, Cambridge, United States*
Email: cshivalila@wavelifesci.com

Background and aims: The *PNPLA3 I148M* variant disrupts PNPLA3 function and hepatic lipid homeostasis and retinol metabolism and is associated with substantially increased risk of liver-related deaths, including from MASH and alcohol associated liver diseases. We have developed RNA editing oligonucleotides, or AIMers, that are designed to edit the base sequence of *PNPLA3 I148M* transcripts to restore functional protein. Emerging evidence showing that PNPLA3 plays an important role in hepatic lipid metabolism suggests that an RNA editing approach that restores PNPLA3 enzymatic function may be preferable to silencing *PNPLA3*, which causes a loss of function, for the treatment of liver disease.
Method: We synthesized GalNAc-conjugated chemically modified AIMers to edit the I148M variant using endogenous adenosine deaminase acting on RNA (ADAR) enzymes. GalNAc-AIMer editing efficiency was quantified by Sanger sequencing in concentration-response experiments in human primary hepatocytes. The impact of editing or silencing (with GalNAc-siRNA) on intracellular lipid droplet density was evaluated using the human HEPATOPAC system and in long-term primary human hepatocyte monolayer cultures. Mice were dosed subcutaneously with GalNAc-AIMers, and tissue concentrations of PNPLA3 AIMer in liver were quantified by ELISA after one week.
Results: We evaluated PNPLA3 GalNAc-AIMers in human homozygous *PNPLA3 I148M* primary hepatocytes from multiple donors. The most effective AIMers directed potent (EC_{50} 12 nM) and efficient (~70%) editing of *PNPLA3* transcripts. In a human HEPATOPAC system with homozygous I148M hepatocytes, PNPLA3 GalNAc-AIMers significantly decreased lipid droplet density compared to mock treatment ($p < 0.0001$), whereas GalNAc-siRNA designed to silence expression of *PNPLA3* did not have a significant effect. In long-term cultures of human homozygous *PNPLA3 I148M* primary hepatocytes, PNPLA3 transcript editing of ~50% corresponded with a substantial lowering of lipid droplet density. In mice expressing wild-type *Pnpla3*, GalNAc-AIMers dosed subcutaneously reached 500–1,000 µg/g in liver, concentrations expected to yield substantial RNA editing based on in vitro experiments in hepatocytes.
Conclusion: These data demonstrate that AIMers supporting *PNPLA3 I148M* editing to restore functional PNPLA3 protein decrease fat content in hepatocytes, and outperform *PNPLA3* silencing in lowering lipid density. Overall, these data support continued advancement of AIMers for the treatment of *PNPLA3 I148M* liver disease.

Nurses and Allied Health Professionals – Research project

TOP-535-YI
Barriers and facilitators in alcohol-related care pathways: findings from a qualitative interview study
Stine Munk Larsen[1], Mette Lauridsen[1], Lea Ladegaard Grønkjær[1]. [1]*University Hospital of Southern Denmark, Esbjerg, Denmark*
Email: lea.ladegaard.gronkjaer@rsyd.dk

Background and aims: Alcohol-related liver disease (ALD) remains a leading cause of morbidity and mortality. Although effective treatments for alcohol use disorder exist, engagement in treatment and sustained abstinence remain inconsistent. Patients with ALD often navigate fragmented care pathways between hospital-based services and municipal alcohol treatment, where motivational, relational, and organisational factors may influence outcomes. This study aims to explore barriers and facilitators in alcohol-related care pathways from the perspectives of both patients and healthcare professionals.
Method: Between September and December 2025, semi-structured interviews were conducted with six patients with alcohol-related liver disease and six healthcare professionals from a hospital liver unit and a municipal alcohol treatment service. Patients were purposively sampled to include individuals with both sustained abstinence and ongoing alcohol use. Interviews explored experiences of care pathways, treatment engagement, motivation, patient-healthcare professional interactions, and perceived gaps in care. Data were analysed thematically using Braun and Clarke's six-phase framework.
Results: Four themes emerged: (1) motivational readiness and self-recognition as prerequisites for sustained change; (2) relational trust and communication, where non-moralising interactions promoted openness, while perceived judgement led to disengagement; (3) the value of peer-based and intensive support, particularly residential treatment and peer communities; and (4) fragmentation and transition gaps between hospital and municipal services associated with relapse risk. Healthcare professionals described challenges initiating motivational conversations in time-limited settings.
Conclusion: Alcohol-related care pathways are shaped by a complex interplay of individual motivation, relational factors, and organisational structures. Findings suggest that effective care for patients with ALD requires timely, trust-based conversations, improved continuity across sectors, and integration of peer-based support. Interventions

targeting motivational readiness and cross-sector collaboration may enhance engagement and reduce relapse. Further research should explore implementation strategies to strengthen coordinated, patient-centred alcohol care in liver disease services.

THU-527-YI

Social nurse interventions may reduce mortality in patients with acute decompensated liver cirrhosis

Palle Bager[1], Jonatan Petersen[1], Tine Dideriksen[1], Lotte Eriksen[1], Marie Storgaard[1], Karen Louise Thomsen[1]. [1]*Aarhus University Hospital, Hepatology and Gastroenterology, Aarhus, Denmark*
Email: pallbage@rm.dk

Background and aims: Social nurse (SN) functions are well-established in a number of somatic hospitals. SNs work with patients facing social vulnerability and they aim to minimise the impact of problematic behaviors that could influence health. Patients with acute decompensated (AD) liver cirrhosis may benefit from the care given by SNs. We aimed to investigate if contact to a SN were associated with readmission and mortality in patients with AD cirrhosis.
Method: A historical cohort study included all patients with AD cirrhosis, admitted to Aarhus University Hospital, Denmark between Jan. 2019 and Jan. 2024. Patients were identified via the electronic patient record. Demographic- and clinical data were extracted as well as data on contact to a SN during admission, readmissions, and mortality. The patients were grouped into: i) the SN group, who had contact to the SN, and ii) the NSN group, who did not have contact to a SN. Group comparisons were conducted using the Student's t-test or the χ^2-test. Cox proportional hazards regression was used to evaluate the association between variables and mortality.
Results: Of 476 identified patients, we included 245 patients with a definite diagnosis of AD cirrhosis. Of these, 49 (20%) were in the SN group. Patients in the SN group were younger (mean age of 54 ± 10 years vs. 62 ± 10 years), $p < 0.005$. The predominant etiology of cirrhosis was alcohol, 190 (78%) across the whole cohort. The total median observation time was 203 days (IQR: 48–510). There was no difference in number of readmissions between the groups, 33 (67%) vs. 120 (61%), $p = 0.43$. The median time to first readmission was 34 days (IQR: 16–207) in the SN group vs. 67 days (IQR: 15–234) in the NSN group. During follow-up, 150 (61%) patients died: 24 (49%) in the SN group vs. 126 (64%) in the NSN group, $p < 0.05$. The one-year mortality rate was lower in the SN group compared to the NSN group, 13 (27%) vs. 87 (44%), $p < 0.05$, whereas there was no difference in the 90-day mortality rate, 9 (18%) in the SN group vs. 47 (24%) in the NSN group, $p = 0.40$.
Conclusion: Support provided by SNs to patients with AD cirrhosis was found to be associated with lower one-year mortality, however, having contact with a SN was also associated with sooner readmission to hospital. This observational study did not adjust for confounders so the described associations may have been affected by other factors than SNs.

THU-528-YI

Knowledge of filipino adults on metabolic dysfunction–associated steatotic liver disease (masld) and its relationship with sociodemographic factors, nutritional status, physical activity, food security, and diet quality: a cross-sectional study

Melvin Bernardino[1,2], Kristine Joy Sofia Cruz[1], Cassandra Abalos[1], Jeanne Carla Bruce[1]. [1]*Colegio de San Juan de Letran Manila, Manila, Philippines;* [2]*151 Muralla St, Nutrition and Dietetics, Manila, Philippines*
Email: melvin.bernardino@letran.edu.ph

Background and aims: Metabolic Dysfunction–Associated Steatotic Liver Disease (MASLD) is a major contributor to chronic liver disease worldwide. Awareness of MASLD is critical for early prevention and management, yet data on public knowledge in the Philippines remain limited. This study aimed to assess MASLD knowledge among Filipino adults and examine its relationship with sociodemographic factors, nutritional status, physical activity, food security, and diet quality.
Method: A cross-sectional study was conducted in Intramuros, Manila, with 172 adults aged 19–59 years. MASLD knowledge and source of information was assessed using a 25-item validated questionnaire. Sociodemographic data, body mass index (BMI), body fat%, physical activity (International Physical Activity Questionnaire–Short Form), diet quality (Diet Quality Questionnaire), and food security (Household Food Insecurity Access Scale) were collected. Spearman's rank correlation was used to examine associations, with significance set at $p < 0.05$.
Results: The majority of respondents were male (61.05%), and most participants were aged 30–49 years (45.35%). Overall, 72% of respondents reported no prior awareness of MASLD. Regarding sources of information about MASLD, 10.47% of respondents obtained information from family or friends, followed by the internet (8.14%), doctors (6.98%), television, radio, or public advertisements (6.40%), and health education in hospitals or communities (5.23%). Knowledge levels were highest for risk factors such as alcohol consumption (80%) and obesity (69%), but were low for disease reversibility (28%) and asymptomatic presentation (28%). Significant positive correlations were observed between MASLD knowledge and physical activity (Spearman's rho = 0.173, $p = 0.023$), diet quality (Spearman's rho = 0.161, $p = 0.035$), income (Spearman's rho = 0.215, $p = 0.005$), and educational attainment (Spearman's rho = 0.170, $p = 0.025$). No significant associations were identified with BMI, body fat percentage, sex, age, occupation, or food security.
Conclusion: To our knowledge, this is the first study to report MASLD awareness among Filipino adults. Awareness was low, with substantial gaps in knowledge regarding disease reversibility and asymptomatic presentation. Higher educational attainment, income, physical activity, and diet quality were associated with greater MASLD knowledge, underscoring the need for targeted public education and lifestyle-based and interventions to prevent disease progression in the Philippine population.

THU-537

Diagnostic performance of non-invasive fibrosis scores for detecting advanced fibrosis in a biopsy-proven indian MASLD cohort- a record based cross-sectional study

Ankit Bhardwaj[1], Ankur Jindal[1], Shiv Kumar Sarin[1]. [1]*Institute of Liver & Biliary Sciences, New Delhi, India*
Email: shivsarin@gmail.com

Background and aims: Non-invasive fibrosis tests are widely used to detect advanced fibrosis and cirrhosis in MASLD, but their performance varies across populations. Data correlating these tests with biopsy-proven fibrosis in Indian MASLD patients, especially in the intermediate fibrosis group, remain limited.
Method: All consecutive biopsy-proven MASLD patients, with and without advanced fibrosis (F3–F4), were included. The diagnostic performance of FIB-4, NFS, AGILE-3, AGILE-4, LSM, and APRI for detecting advanced fibrosis was compared using liver biopsy as the reference standard. Accuracy was assessed by AUROC, and optimal cohort-specific cut-offs were derived using the Youden Index.
Results: A total of 838 patients with biopsy-proven MASLD were included (mean age 50.8 ± 12.3 years; 70.2% male; 52.5% with diabetes). Advanced fibrosis (F3–F4) was present in 721/838 (86%), while 117/838 (14%) had F0–F2 disease. FIB-4 and NFS demonstrated good diagnostic accuracy for advanced fibrosis with AUROCs of 0.77 (95% CI 0.72–0.82) and 0.78 (0.72–0.83), respectively (both $p < 0.001$), outperforming APRI (AUROC 0.64, 95% CI 0.58–0.70). Mean NFS and FIB-4 values increased progressively with fibrosis stage. The intermediate FIB-4 zone (1.3–2.67) showed limited discriminatory ability for advanced fibrosis, with 75.2% sensitivity, 12.1% specificity, 12.3% PPV, and 74.8% NPV. AGILE-3 and AGILE-4 score showed good diagnostic accuracy for advanced liver fibrosis with AUROCs of 0.79 (95% CI 0.73–0.85) and 0.82 (0.77–0.88), respectively (both $p <$

0.001); at Youden-derived cut-offs (0.95 and 0.96), sensitivities exceeded 93% with modest specificities (39–43%). LSM demonstrated comparable performance (AUROC 0.80, 95% CI 0.74–0.86; p < 0.001), and at a cut-off of 15.56 kPa showed 94.6% sensitivity and 42.8% specificity. Using cohort-specific cut-offs, FIB-4 (2.71) and NFS (0.33) showed high sensitivity (>92%) but limited specificity, while APRI performed inferiorly. PPV were high across models, whereas negative predictive values remained modest.
Conclusion: In this large biopsy-proven MASLD cohort from India, non-invasive fibrosis tests demonstrated high sensitivity but limited specificity to detect advanced liver fibrosis, indicating better rule-out than rule-in ability. Our results support the use of AGILE models and LSM in sequential or combined non-invasive strategies for fibrosis risk stratification in MASLD. There is need for development of new models for more specific fibrosis assessment for Indian population.

THU-538-YI
Relationship between patient activation and e-health literacy levels and associated factors in patients with liver cirrhosis: a cross-sectional study
Ferya Celik[1], Hicran Bektas[1]. [1]*Akdeniz University Faculty of Nursing, Antalya, Türkiye*
Email: feryacelik@gmail.com

Background and aims: Effective medical management and nursing care of liver cirrhosis require active patient participation in care practices. Adequate e-Health literacy levels are essential for patients to learn and correctly implement these care practices.
This study was carried out to examine the relationship between patient activation and e-Health literacy, and to identify the factors associated with these variables in patients with liver cirrhosis.
Method: The study was conducted with 153 patients with liver cirrhosis who received treatment in a university hospital in Antalya, Turkey, between November 2024 and December 2025. A personal information form, the Patient Activation Measure and the e-Health Literacy Scale were used to collect the data. After evaluating the normality of the data, independent-samples t-test, one-way analysis of variance (ANOVA), and Pearson correlation were performed.
Results: The mean age of the participants was 59.04 ± 14.35 years. Of the patients, 58.8% were male, 43.8% had completed primary education, 30.7% had alcohol-related liver cirrhosis, and 64.0% had been diagnosed for 1–4 years. The Cronbach's alpha coefficient of the Patient Activation Measure was 0.97, with a mean score of 46.31 ± 11.44. Patient activation scores showed statistically significant differences according to age, educational level, duration of diagnosis, dietary adherence, regular medication use, body weight monitoring, and attendance at health check-ups (p < 0.05). The Cronbach's alpha coefficient of the e-Health Literacy Scale was 0.77, with a mean score of 23.76 ± 7.39. e-Health literacy scores showed statistically significant differences according to age, marital status, educational level, etiology of liver cirrhosis, duration of diagnosis, dietary adherence, regular medication use, body weight monitoring, health check-up attendance, and alcohol use. There was a strong, positive relationship between patient activation and e-Health literacy levels (r = 0.603, p < 0.001).
Conclusion: Patient activation was strongly and positively associated with e-Health literacy. Both constructs differed across key socio-demographic and clinical self-management characteristics, indicating that activation and digital health competencies may co-vary with real-world adherence behaviours. These findings support the need for targeted, nurse-led, digitally supported education and individualized follow-up to strengthen self-management capacity and potentially improve care engagement in this population.

THU-539-YI
Elafibranor tolerability and response in patients with primary biliary cholangitis previously treated with bezafibrate: a real-world single-centre experience
Fatema Jessa[1], Megan Morgan[1], Neil Halliday[1]. [1]*Royal Free Hospital, London, United Kingdom*
Email: fatema.jessa@nhs.net

Background and aims: Patients with primary biliary cholangitis (PBC) with inadequate biochemical response or intolerance to ursodeoxycholic acid (UDCA) may require second-line therapy, including bezafibrate (BZF), used off-licence in PBC. Elafibranor (ELA), a dual peroxisome proliferator-activated receptor (PPAR)-α/δ agonist, is a recently licensed treatment option. Given overlapping mechanisms of action, it is unclear whether prior response or intolerance to BZF is relevant to ELA tolerability or biochemical response. This study evaluated single centre experience of tolerability and response to ELA according to prior BZF exposure.
Method: All PBC patients initiated on ELA at the Royal Free London NHS Foundation Trust between January and November 2025 were identified using the electronic dispensing system (JAC). Clinical records were reviewed to determine prior BZF exposure and documented adverse events (AEs) to BZF and ELA.
Results: 38 patients commenced ELA; 95% female, median age 56years, 45% (17/38) were cirrhotic with median ALP 371 U/L on ELA initiation. 61% (23/38) had prior BZF exposure of which 57% (13/23) experienced AEs (54% muscle related events (MR), 38% liver biochemistry rise) leading to BZF discontinuation. 43% (10/23) switched to ELA due to non-response. AEs with ELA were reported in 91% (21/23) of BZF-exposed patients (48% gastrointestinal (GI), 35% MR). Among patients without prior BZF, 80% (12/15) reported AEs (53% MR, 47% GI). Overall, in evaluable patients, POISE response criteria were met in 45% (14/31) at week 4 and 46% (11/24) at week 12. Week 4 response differed by prior BZF status: 83% (10/12) in BZF-naïve patients, 27% (3/11) with prior BZF intolerance, and 13% (1/8) in BZF non-responders. However, among those who did not meet POISE criteria, 65% had ALP reduction >15% at week 4 and 54% at week 12. Improvement in pruritus was reported in 21%(8/38). 32%(12/38) discontinued ELA of which 50% (6/12) were BZF intolerant.
Conclusion: In this cohort, AEs with ELA were common regardless of prior BZF exposure but often did not lead to treatment discontinuation. While prior BZF intolerance accounted for half of ELA discontinuations, BZF intolerance did not uniformly preclude treatment with ELA. However, biochemical response to ELA appeared lower in patients previously non-responsive to BZF compared with BZF-naïve patients. These findings require confirmation in larger, multicentre studies and support an individualised approach to counselling, monitoring and treatment selection when initiating ELA.

THU-540
Early UK experience with elafibranor in primary biliary cholangitis: a multicentre pharmacist-led review
Arron Jones[1], Robert Elliot-Cooke[2], Rachael Kamiri-Ngugi[3], Fiona Rees[4], Sarah Cripps[5], Kate Greener[6], Sital Shah[6], Alison Boyle[7]. [1]*Barts Health NHS Trust, London, United Kingdom;* [2]*University Hospitals Plymouth NHS Trust, Plymouth, United Kingdom;* [3]*Royal Surrey NHS Foundation Trust, Guildford, United Kingdom;* [4]*University Hospitals Sussex NHS Foundation Trust, Brighton, United Kingdom;* [5]*Oxford University Hospitals NHS Foundation Trust, Oxford, United Kingdom;* [6]*King's College Hospital NHS Foundation Trust, London, United Kingdom;* [7]*NHS Greater Glasgow & Clyde, Glasgow, United Kingdom*
Email: arron.jones@nhs.net

Background and aims: Elafibranor, a dual peroxisome proliferator-activated receptor (PPAR) alpha/delta agonist, is a treatment option for primary biliary cholangitis (PBC) in the UK. It was introduced recently as a second line option for patients with an inadequate response, or intolerance to, ursodeoxycholic acid (UDCA). In many liver centres, specialist hepatology pharmacists manage PBC patients

on second line therapies. This review reports on early real-world experience, clinical response, and safety of elafibranor.
Method: A retrospective review of patients prescribed elafibranor from November 2024 – December 2025 was undertaken across seven UK centres. Patient records were reviewed to determine demographics and clinical features, including liver stiffness measurements (LSM), liver biochemistry, and prior PBC treatments. Treatment experience with elafibranor, including clinical response, safety, and tolerability, was documented.
Results: 76 patients were initiated on elafibranor, 62 (82%) patients continued over 6 months. 14 (18%) patients discontinued elafibranor with 8 (11%) stopping prior to their first review. Follow up data is available for 45 patients (59%). 39 (87%) patients were AMA positive, 44 were female (98%). Mean age was 67 years (+/– 12) and mean LSM 9.9 kPa (+/– 6.4), with 10 (22%) cirrhotic patients. 34 (75.6%) patients had trialled obeticholic acid and/or bezafibrate before starting elafibranor. 26 (58%) patients experienced adverse effects, with gastrointestinal effects the most common (n = 13). 13 patients (29%) discontinued treatment due to adverse effects. 8 patients reported improvement in pruritus (18%) and 2 in fatigue (4%). 4 (9%) reported worsening pruritus, and 2 (4%) worsening fatigue. 1 patient developed decompensated cirrhosis; however, a causal relationship was not confirmed. 8 (18%) patients were not taking UDCA due to intolerance. 5 of these patients reported adverse effects with elafibranor. Mean ALT prior to elafibranor initiation was 67.1 (+/– 50.6), and ALP 379 (+/– 242.9). Post treatment liver biochemistry was available for 36 patients; mean ALT was 57.7 (+/– 41.3), and ALP 301.8 (+/– 175.6). Liver biochemistry was available for 15 patients after 6 months treatment, mean ALT was 55.3 (+/– 38.1) and ALP 196.7 (+/– 80.5).
Conclusion: Patients on elafibranor demonstrated a positive initial biochemical response to therapy. Adverse effects led to discontinuation in a number of patients. Additional real-world data is needed to better understand treatment response.

THU-541-YI
Exploring issues and challenges experienced by patients with ascites in a view to develop an innovative abdominal belt for early detection of ascites

K L Ajee[1], Arun Valsan[2], Jerlin Roy[1], R Helen[1]. [1]*Amrita College of Nursing, Amrita Vishwa Vidyapeetham, Health Sciences Campus, Kochi, Kerala, India 682041, Ernakulam, India;* [2]*Amrita Institute of Medical Science & Research Centre, Kanayannur, India*
Email: capt.ajee@gmail.com

Background and aims: Cirrhosis patients often develop ascites, causing extensive physical, psychosocial, and challenges. Ascites marks most common decompensation, with five-year mortality of 44% from complications such as spontaneous bacterial peritonitis and hepatorenal syndrome. Early detection in home setting may enforce diet control, fluid and medication adherence. This study aimed to explore lived in experiences of patients with ascites, and use those insights to design a sensor based abdominal belt for early onset of ascites at community level.
Method: A qualitative phenomenological approach with in-depth interviews were conducted for 11 adult patients with radiologically confirmed cirrhotic ascites and their primary caregivers admitted to a tertiary liver unit in South India. Patients with hepatic encephalopathy were excluded. Purposive sampling was used and data saturation determined sample size. Ethical clearance and written informed consent were obtained from institutional ethics committee and the participants respectively. A validated semi-structured questionnaire consisted of 10 open-ended questions explored physical symptoms, mobility and comfort, social issues, emotional concerns, and monitoring and management at home. Interviews were audio-recorded, transcribed, and analyzed thematically using MAXQDA.
Results: Seven major themes were identified:1) Physical discomfort including abdominal distension, dyspnoea, pain, and activity limitations. 2) Social challenges like altered body image, dependency, and employment and family role disruption. 3) Psychological distress like anger, anxiety, fear of deterioration, and repeated hospital visits. 4) Financial strain from hospital costs due to recurring visits and loss of occupation. 5) Altered coping strategies, including delayed decision-making and avoidance of familial interaction. 6) Caregiver burden arising from strict dietary restrictions and lifestyle modifications, leading to care giver occupational withdrawal.7) A strong desire for a comfortable user-friendly device to provide early alerts for tailored management to reduce frequent hospital visits.
Conclusion: A device to assess the early onset of ascites at home or community level can initiate or enhance self-care and reduce frequent hospitalization. This study is primarily in alignment with UN SDGs 3 (Good Health & Well-being) and 9 (Industry, innovation and infrastructure) by developing a sensor-based device for early detection of ascites.

THU-542
Clinical efficacy of 3 dose Hepatitis B vaccine on protective seroconversion among patients with cirrhosis of liver

K L Ajee[1], Arun Valsan[2], Lena Saji[1], M Monisha[1], G Nikhilamol[1], Niveditha Sunish[1]. [1]*Amrita College of Nursing, Amrita Vishwa Vidyapeetham, Health Sciences Campus, Kochi, Kerala, India 682041, Ernakulam, India;* [2]*Amrita Institute of Medical Science & Research Centre, Kanayannur, India*
Email: capt.ajee@gmail.com

Background and aims: CDC recommends vaccination against Hepatitis B in all patients with liver cirrhosis. However, development of protective vaccine in CLD and its optimization is not clear. Hence, we aimed to evaluate the clinical efficacy of a 3 dose Hepatitis B vaccination among patients with cirrhosis of liver and to identify the factors that influence the presence of hepatitis B antibody titre in patients with liver cirrhosis.
Method: A prospective observational analytical study with purposive sampling was conducted in a tertiary care hospital among 339 vaccine-naïve adult patients who were diagnosed to have cirrhosis of liver of varying severity as per the clinical, radiological, and pathological findings. The study was conducted from January 2024 to September 2025. We included all those who were seronegative for HBsAg, HIV and HCV and had given an accelerated regimen of 3 dose hepatitis B vaccine at intervals of 0, 1, and 2 months. Anti-HBs titre was checked 8 weeks after receiving the third dose of hepatitis B vaccination. We excluded patients with HCC and who were having severe coexisting medical conditions. Other than sample characteristics and clinical profile, sarcopenia was assessed using SARC-F. Anti-HBs antibody <10 IU/L was considered as non-reactive. Institutional ethical clearance and written informed consent were obtained. Chi-square, Mann-Whitney U, and logistic binary regression were done with SPSS 30.0.
Results: Majority (84%) were male and the median age was 48. Diabetes mellitus (27%) was the most common co-morbidity among those with comorbidities (59%). Overall seroconversion was found to be 60%, and median MELD and CTP score were 11 and class A, respectively. Among those who attained seroconversion, only 9% had a titre value >100. Patients who were less than 60 years of age had better response to the vaccine ($p < 0.001$). Anti-HBs titer was significantly high ($p < 0.01$) among patients with normal serum albumin. Patients with higher MELD and CTP had significantly lower odds (OR 0.42, $p < 0.01$) of achieving protective seroconversion. The seroconversion rate was significantly high ($p < 0.01$) among patients without comorbidities. However, nutritional status did not show any association with anti-HBs antibody titer.
Conclusion: Younger age groups with preserved liver function and who were not having any comorbidities were considered to have high seroconversion. Nurse-led counseling on adult vaccination may

improve the status. This study is in alignment with SDG 3.3, 3.4 and 3.8.

THU-543

Cost-effectiveness of screening for hepatitis C virus infection among people who use drugs in South Korea

Hye-Lin Kim[1], Kyung-Ah Kim[2], Gwang Hyeon Choi[3], Sook-Hyang Jeong[3]. *[1]Sahmyook University College of Pharmacy, Seoul, Korea, Rep. of South; [2]Inje University Ilsan Paik Hospital, Goyang, Korea, Rep. of South; [3]Seoul National University Bundang Hospital, Seongnam, Korea, Rep. of South*
Email: maristella76@tistory.com

Background and aims: To eliminate hepatitis C virus (HCV) infection, targeted screening and treatment of the established high risk group such as people who use drugs (PWUD) is essential. This study evaluated the cost-effectiveness of HCV screening and direct acting antiviral (DAA) treatment compared with no screening among PWUD who were detected drug offenders in South Korea.
Method: We conducted cost-utility analysis using a decision analytic model to estimated the expected costs and quality-adjusted life years (QALYs) between one-time HCV screening targeting PWUD and no screening. As screening algorithm, HCV RNA reflex testing which automatically tests for HCV RNA if the anti-HCV test is positive was applied. The hypothetical cohort of 45-year-old PWUD, and their prevalence of anti-HCV was estimated to be 31.3% was simulated over 30-year horizon. Key features in PWUD–such as HCV prevalence and treatment rates–were obtained from the Korea HCV-PWUD registry. The incremental cost-effectiveness ratio (ICER) between two strategies was calculated, and sensitivity analyses were also conducted to explore the impact of parameter and structural uncertainty on results.
Results: The HCV screening strategy yielded an ICER of $2,449/QALY, which was substantially lower than Korea's willingness-to-pay threshold (about $22,000/QALY), demonstrating that universal screening in PWUD was highly cost-effective compared with no screening. In sensitivity analyses, the most influential parameters were age (associated with HCV seroprevalence and fibrosis stage; ICER for patients in their 30s: $7,391/QALY) and HCV re-infection rate (rising to 10% for 10 years, then 6% for 20 years: $4,184/QALY). All ICERs from sensitivity analyses remained below the threshold. The long-term effectiveness of screening also demonstrated cost savings through the reduction of decompensation, hepatocellular carcinoma, and liver-related death cases.
Conclusion: The screening with HCV reflex testing and DAA treatment among PWUD in South Korea would be highly cost-effective from both healthcare system and societal perspectives. These findings support implementing universal HCV screening programs for PWUD as a public health strategy to reduce disease burden and healthcare costs while improving clinical outcomes in this high-risk population.

THU-544

Care competency skills and degree of distress among informal caregivers of patients with chronic liver disease

S Suja Kumari[1], Arun Valsan[2], Anju Roy[3], J Aparna[3], Angela Paulson[3], Anjana Lal[3], Sheela Pavithran[3]. *[1]Amrita College of Nursing, Ernakulam, India; [2]Amrita Institute of Medical Sciences, Kochi, Amrita Vishwa Vidyapeetham, Ernakulam, India; [3]Amrita College of Nursing, Amrita Vishwa Vidyapeetham, Kochi, India*
Email: sujaks@nursing.aims.amrita.edu

Background and aims: Chronic liver disease (CLD) is an imminent danger to global health and has emerged as one of the leading causes of death globally. Due to the rising occurrence of cases linked to metabolic dysfunction-associated steatotic liver disease (MASLD), steatotic liver disease (SLD) is expected to become a significant contributor to diseases and liver disease by 2040 worldwide. This study aimed to evaluate the knowledge, competency, and level of distress of informal carers.
Method: A descriptive quantitative study was conducted among 200 caregivers for CLD patients. Caregivers aged 18–60 years were included, whereas caregivers with comorbidities that need formal treatment were not included. A structured sociodemographic survey, Chronic Liver Disease Questionnaire (CLDQ), Carer Self-Assessment Questionnaire (CSAQ), and Care Competency Skill Questionnaire (CCSQ) inventories were used for data acquisition. Each scale had high reliability (Cronbach's alpha value ≥0.78).
Results: Caregivers were predominantly middle-aged females (75%), mostly spouses (66%), from urban nuclear families (60%), with 90% lacking formal caregiving training. Caregivers had average knowledge regarding general symptoms of CLD, specifically abdominal symptoms (mean score, 11.75) and fatigue symptoms (mean score, 20.57). Despite this, there was considerable variation in scores for overall symptoms and functioning (SD = 24.6), indicating considerable variation in knowledge and competence levels. There was a higher mean score on the distress scale for high-distress (21%) (M = 12.23, SD = 1.12) in comparison with that for low-distress (M = 3.56, SD = 2.04) caregivers. High distress was most common among caregivers of patients with alcohol-associated liver disease, the predominant aetiology (49.5%), while lower distress levels were observed in MASLD, viral hepatitis, genetic, and autoimmune liver diseases.
Conclusion: Informal carers of patients with CLD express considerable psychological distress and differ in their competency to offer care; most of these problems are associated with inadequate training in the past and a lack of experience providing care. These findings demonstrate the critical need for need-based carer education and psychological support programs to be included in routine CLD care to enhance patient outcomes by enhancing caregiving competence and reducing suffering.

THU-545-YI

Binge drinking as a key driver of steatotic liver disease: prevalence, predictors, and population impact in a large screening cohort

Ea Kyed[1,2], Stine Johansen[1,2], Helle Schnefeld[1,2], Johanne Kragh Hansen[1,2], Katrine Tholstrup Bech[1,2], Kathrine Sejer Sørensen[1], Anine Andersen[1,2], Katrine Thorhauge[1,2], Camilla Dalby Hansen[1,2], Mads Israelsen[1,2], Peter Andersen[1], Sönke Detlefsen[2,3], Maja Thiele[1,2], Aleksander Krag[1,2]. *[1]FLASH - Centre for Liver Research, Odense, Denmark; [2]SDU - University of Southern Denmark, Odense, Denmark; [3]Department of Pathology, Odense, Denmark*
Email: ea.ditte.stage.kyed@rsyd.dk

Background and aims: Alcohol is a major driver of liver-related morbidity, yet the impact of alcohol consumption patterns, particularly binge drinking, to liver disease severity is insufficiently described. Phosphatidylethanol (PEth) is an objective biomarker of recent alcohol intake and complements self-reported data. We aimed to examine the association between self-reported binge drinking behaviour and increased liver stiffness and correlations with sociodemographic and cardiometabolic factors.
Method: We screened participants from the general population and individuals at risk of steatotic liver disease in a large prospective cohort using vibration-controlled transient elastrography (VCTE). We defined possible significant liver fibrosis as VCTE ≥8 kPa. Participants reported alcohol consumption patterns using AUDIT-C. We defined frequent binge drinking as intake of ≥5 units per drinking episode at least once weekly and alcohol overuse ≥14/21 units per week for women/men for at ≥5 years. We used PEth ≥200 ng/mL as an indicator of high alcohol intake. Participants reported sociodemographics via questionnaires, and clinical assessment captured cardiometabolic risk factors. We applied multivariable logistic regression adjusting for sociodemographic and cardiometabolic factors, alcohol overuse, and PEth ≥200 ng/mL.
Results: We included 6,400 participants (mean age 57 years; 52% female; 37% obesity; 9% type 2 diabetes). Overall, 5.9% had VCTE

≥8 kPa, and 17% had PEth ≥200 ng/mL. Frequent binge drinking occurred in 1,092 participants; 71% were male and 81% reported alcohol overuse. Elevated liver stiffness occurred more frequently with binge drinking than without (10.3% vs. 4.7%, p < 0.001). PEth ≥200 ng/mL occurred in 60% with binge drinking compared with 8% without. Median PEth reached 253 ng/mL (IQR 118–494) versus 21 ng/mL (IQR 6–65), indicating concordance between binge drinking and high recent alcohol intake. In adjusted analyses, binge drinking associated independently with VCTE ≥8 kPa (OR 1.41, 95% CI 1.03–1.93, p = 0.031), independent of both self-reported alcohol overuse and PEth ≥200 mg/mL. Male sex strongly associated with binge drinking, whereas partnership and parenthood associated with lower odds. Hypertension remained independently associated with binge (OR 1.70, 95% CI 1.40–2.06).
Conclusion: Frequent binge drinking behaviour independently associates with increased liver stiffness. Beyond cumulative alcohol intake, binge drinking represents a clinically relevant determinant of liver disease risk.

THU-546-YI
LivR Well 2.0 - Nourishing a hungry liver: interim results
Sophie Page[1,2], Erin Russell[1], Anita Figredo[2], June Song[2], Patricia Anderson[3], Phillip George[2,4], Suong Le[3], Thomas Worland[3], Sally Bell[3,4], Natalie Ngu[3,4]. *[1]Nutrition and Dietetics, Monash Health, Melbourne, Australia; [2]Hospital in the Home, Monash Health, Melbourne, Australia; [3]Department of Gastroenterology and Hepatology, Monash Health, Melbourne, Australia; [4]Faculty of Medicine Nursing & Health Sciences, Monash University, Melbourne, Australia*
Email: sophie.page@monashhealth.org

Background and aims: Frailty and malnutrition are highly prevalent among individuals with decompensated chronic liver disease (CLD), contributing to adverse clinical outcomes and healthcare burden. Whilst nutritional optimisation has been shown to improve outcomes such as mortality and frailty, there is limited evidence to support home-based interventions. We evaluated the impact of LivR Well 2.0, a home-based, multidisciplinary program on frailty and nutritional status in patients with CLD.
Method: Adults presenting with an episode of decompensated CLD to a tertiary hospital network in Melbourne, Australia were enrolled from July 2025. The intensive nutritional program includes a 28-day admission to Hospital in the Home; with hepatology review, dietetics, pharmacy, addiction counselling, home nursing, and physiotherapy. Dietetic management includes education, home-delivered meals, oral nutrition supplements, and nasogastric tube (NGT) feeding if clinically indicated. Participants are followed for up to 24-weeks. The primary outcome of frailty was change in Liver Frailty Index (LFI). Secondary outcomes included nutritional status measured by Subjective Global Assessment (SGA) and percentage of Estimated Energy Requirements (EER) and Estimated Protein Requirements (EPR) met in accordance with European Association for the Study of the Liver guidelines.
Results: Twenty one participants were included in this interim analysis (61.9% alcohol-related CLD), median age 62.4 years [Interquartile Range (IQR): 56.9–69.8], 58% male, baseline body mass index 26.4 kg/m^2 [IQR: 24.1–30.3], and Model for End-stage Liver Disease score 15.5 [IQR: 10.7–19.6]. To date, seven participants have completed week 12; one required NGT. Median LFI improved from 4.6 [IQR: 4.0–5.3, Frail] to 3.99 [IQR: 3.4–4.4, Pre-Frail] (p = 0.08). % EER increased significantly from 65.2% [IQR: 49.1–78.9] to 92.8% [IQR: 78.9–95.6] (p = 0.02); and EPR improved from 70.4% [IQR: 54.5–101.1] to 88.4% [IQR: 85.9–111.6] (p = 0.26). At week 2, SGA classified 21.4% as A (well-nourished), 57.1% B (moderate malnutrition), 21.4% C (severe malnutrition); by week 12, 50% were A, 33.3% B, 16.7% C (p = 0.44).
Conclusion: Interim results from the LivR Well 2.0 program demonstrate promising improvements in nutritional adequacy and trends toward reduced frailty in patients with decompensated CLD. These findings support the feasibility and potential clinical benefit of integrated home-based care models in this population. Complete analysis will clarify long-term outcomes.

THU-547
Widespread misconceptions about analgesic safety drive undertreatment of pain in hepatocellular carcinoma
Jina Park[1], Jonggi Choi[1], Chaeyeon Lim[1], Sung Won Chung[1], Ji won Yang[1], Won-Mook Choi[1], Danbi Lee[1], Ju Hyun Shim[1], Kang Mo Kim[1], Young-Suk Lim[1], Han Chu Lee[1]. *[1]Asan Medical Center, Seoul, Korea, Rep. of South*
Email: jkchoi0803@gmail.com

Background and aims: Pain profoundly impacts quality of life in cancer patients yet remains inadequately managed. Hepatocellular carcinoma (HCC) presents unique challenges due to underlying liver disease, raising concerns about analgesic safety. This study comprehensively assessed pain prevalence, management practices, and patient perceptions in HCC, examining associations with clinical characteristics.
Method: We surveyed 200 HCC patients at a tertiary center using a comprehensive 30-item questionnaire assessing pain prevalence/intensity, management strategies, perceptions about analgesics and liver function, opioid attitudes, and educational needs. Clinical data included demographics, tumor characteristics, and liver function. Statistical analyses examined associations between patient characteristics and pain outcomes.
Results: Pain prevalence was 27.5% with moderate intensity (mean 3.6/10). Critically, 43.6% of pain patients were not using analgesics, with 30% simply waiting. Extrahepatic metastasis strongly predicted pain (33.6% vs 20.4%, p = 0.040; OR = 2.0), while liver function showed no association (p = 0.560). Paradoxically, hepatotoxicity concerns were universal and identical regardless of remnant liver function (all p > 0.6): 70% believed analgesics harm the liver, 50% hesitated due to liver concerns. Among analgesic users, 68% reported adequate control. Educational needs were high: 80% desired specialized counseling, 73% wanted side effect information. Patient characteristics showed minimal influence on perceptions, indicating universal educational gaps rather than disease-driven concerns.
Conclusion: Nearly half of HCC pain patients remain untreated due to widespread liver-related misconceptions paradoxically affecting patients with preserved liver function equally. Pain is driven by tumor metastasis, not liver dysfunction. Standardized education emphasizing analgesic safety in good liver function, combined with nurse-led programs, could substantially reduce unnecessary suffering in this population.

THU-548
Prevalence and risk factors of liver steatosis, fibrosis, and at-risk mash in mexican patients with recently diagnosed type 2 diabetes mellitus
Astrid Ruiz Margáin[1], Oscar M. Fierro-Angulo[1], Jose Gonzalez Regueiro[1], Ariana Pereira Garcia[1], Cristina Garcia Ulloa[1], Sergio Hernandez Jimenez[1,2], Naga Chalasani[3], Ricardo Macias-Rodriguez[1]. *[1]Instituto Nacional de Ciencias Médicas y Nutrición Salvador Zubirán, Ciudad de México, Mexico; [2]Instituto Nacional de Ciencias Médicas y Nutrición Salvador Zubirán, CAIPaDi, Ciudad de México; [3]Indiana University School of Medicine, Indianapolis, United States*
Email: ricardomacro@yahoo.com.mx

Background and aims: Metabolic associated steatotic liver disease (MASLD) is the most common cause of chronic liver disease and the leading cause of liver-related mortality. Long-standing type 2 diabetes mellitus (T2DM) is a significant risk factor for both liver steatosis and liver fibrosis. However, whether newly diagnosed T2DM also carries the same risk remains unclear. Moreover, only few studies have focused on Hispanic patients, who are known to have a faster

progression of liver disease compared to non-Hispanic races, but only few studies have focused in this specific population.
We aimed to assess the prevalence of MASLD and liver fibrosis in Mexican patients with a recent diagnosis of T2DM and identify the risk factors associated with worse liver disease.
Method: This cross-sectional study was conducted in Mexico City and it included individuals with T2DM less than 5 years since diagnosis and without any micro- or macrovascular complications. Clinical, biochemical, liver stiffness measurement (LSM), controlled attenuation parameter (CAP), and FAST score were evaluated.
Results: A total of 1,337 patients were included in the study. The majority of the patients were women (60.9%), median age was 55 (IQR: 49–63) years, and 78.2% were overweight or obese. Overall prevalence of MASLD (using the ³ 288 dB/m cutoff) was 41.4%, and 10.05% had clinically significant liver fibrosis (LSM. Moreover, 3% of the population had cirrhosis. In the multivariate analysis, higher BMI, HbA1C, triglycerides and ALT were independently associated with the presence of steatosis. Higher BMI, CAP, GGT, ALT and AST, were associated with fibrosis. According to the FAST score, 4.8% of the patients had at-risk MASH.
Conclusion: There is high burden of MASLD and clinically significant fibrosis in Mexican adults who are recently diagnosed with type2 diabetes. These data strongly indicate that Mexican adults with type2 diabetes should be systematically evaluated for the presence of MASLD and fibrosis.

THU-549-YI
Patient characteristics and treatment outcomes associated with the retreatment of Hepatitis C in patients previously treated with direct-acting antivirals
Shannyn Sheehan[1,2], Colm Bergin[1], Susan McKiernan[1], Suzanne Norris[1], Gail Melanophy[1], Michelle Lynch[1], Paul Gilvarry[1], Carlos Medina[2], Miriam Coghlan[1,2]. *[1]St. James's Hospital, Dublin, Ireland; [2]Trinity College Dublin, Dublin, Ireland*
Email: ssheehan@stjames.ie

Background and aims: Direct-acting antivirals (DAA) are the mainstay of Hepatitis C (HCV) treatment with sustained virological response 12 weeks after treatment (SVR12) achieved in over 95% of cases. However, retreatment is required if patients present with detectable HCV ribonucleic acid (RNA) following initial treatment. This study aims to evaluate the characteristics and treatment outcomes of patients retreated with DAAs due to reinfection, treatment failure or indeterminate outcomes.
Method: A retrospective cohort study was conducted including patients who received two or more DAA treatment courses. Clinical characteristics and HCV treatment outcomes of patients were collected.
Results: A total of 101 patients were included. Within the reinfection cohort, 60% reported active intravenous drug use (IVDU), 82% were prescribed opioid substitution therapy (OST) and 49% received retreatment in prison. Treatment failure appeared more associated with biological factors such as resistance-associated substitutions (RAS) and cirrhosis than social determinants such as adherence and accommodation. First line retreatment regimens were highly effective in both the reinfection and indeterminate treatment outcome cohorts. Retreatment counts within this cohort demonstrated a yearly increase, with those due to reinfection estimated to increase by 33% annually.
Conclusion: Elimination relies on effective DAA therapy and sustained efforts to prevent reinfection and treatment failure, including the need to strengthen harm reduction strategies. Reinfection reflects successful initial treatment, highlighting the strengths of current service delivery models. However, as retreatment due to reinfection is expected to increase, healthcare services should align resources with evolving epidemiology.

THU-553
Early health-related quality of life decline and hypoalbuminaemia predict outcomes in advanced hepatocellular carcinoma treated with atezolizumab–bevacizumab
Masako Shomura[1], Haruka Okabe[1], Maya Sakakibara[1], Emi Sato[2], Yusuke Mishima[2], Kota Tsuruya[2], Shunji Hirose[2], Yoshitaka Arase[2], Tatehiro Kagawa[2]. *[1]Faculty of Nursing, Tokai University School of Medicine, Japan, Division of Gastroenterology, Department of Internal Medicine, Tokai University School of Medicine, Japan, 143 Shimokasuya, Isehara-City, Kanagawa, Japan; [2]Division of Gastroenterology, Department of Internal Medicine, Tokai University School of Medicine, Japan, Isehara-City, Japan*
Email: s-masako@tokai.ac.jp

Background and aims: Patient-reported health-related quality of life (HRQoL) during atezolizumab–bevacizumab (Atezo+Bev) therapy for unresectable hepatocellular carcinoma (HCC), and its clinical utility in real-world practice, remain unclear. We characterised early HRQoL changes and evaluated if HRQoL and nutrition-related adverse events (AEs) predict response, treatment duration, and survival.
Method: Consecutive patients with advanced/unresectable HCC treated with Atezo+Bev at Tokai University Hospital (Nov 2020–Dec 2025; N = 110) were analysed. Response was assessed at weeks 6–9 by mRECIST, AEs by CTCAE v5.0, and monthly HRQoL by EORTC QLQ-C30 (0–100). Using a 3-month landmark for HRQoL/AEs, multivariable logistic regression (objective response; OS <1 year) and Cox regression (treatment duration; OS) were performed.
Results: Most patients were men (82%); 61% were aged >70 years; and 31% had HCV. Child–Pugh scores were 5/6/7/8 in 56/34/14/6 cases, respectively. Overall, 70% of patients had TNM stage IV; BCLC stage B1/B2/C, 14/57/39; 42% had AFP >100 ng/mL; and 46% had DCP >1000 ng/mL. Median treatment duration, progression-free survival, and OS were 7.3, 7.6, and 19 months; objective response and disease control rates were 26.2% and 79.6%, respectively. Common AEs included fatigue (84%), hypolabuminaemia (78%), and thrombocytopenia (57%); grade 3 fatigue occurred in 10 patients. HRQoL declined in the physical, role, cognitive, and global health domains; however, emotional and social functioning remained stable. Age ≥70 years and TNM IV predicted lower ORR. Grade ≥2 fatigue shortened treatment duration (HR: 1.80), whereas physical/general health ≥80 and grade ≥2 proteinuria prolonged it (HR: 0.46, 0.55, 0.30). OS was reduced with grade ≥2 hypolbuminaemia or DCP >1000 (HR: 3.20, 2.06) but longer with high physical/role functioning (HR: 0.48, 0.54). Tumour size ≥40 mm^2, DCP≥1000, and physical function <80 predicted OS <1 year (OR: 3.44, 2.70, 4.34). Serum albumin levels declined markedly during the first 4 months.
Conclusion: Early declines in physical/role functioning and hypoalbuminaemia can identify patients at risk for early discontinuation and poor survival during Atezo+Bev therapy. Routine HRQoL and nutritional monitoring, linked to timely multidisciplinary interventions (symptom control, rehabilitation, and dietetic support), may help address modifiable functional and nutritional deficits and improve treatment continuity and patient-centred outcomes.

THU-554-YI
Joint consultations during transition: perspectives of young adults with rare liver diseases
Janne Suykens[1,2], ERN Rare Liver Youth Panel[2], Kaat De Pourcq[3], Marcus Kenia[4], Kari Klein[2], Ansgar W. Lohse[2,4], Louisa Lund[2,4], Angel Westbrook[2], Karsten Vanden Wyngaert[1,2], Ruth de Bruyne[1,2]. *[1]Ghent University Hospital, Ghent, Belgium; [2]European Reference Network on Hepatological Diseases (ERN RARE-LIVER), Hamburg, Germany; [3]Ghent University, Ghent, Belgium; [4]University Medical Centre Hamburg-Eppendorf, Hamburg, Germany*
Email: janne.suykens@ugent.be

Background and aims: Transition from pediatric to adult care is a critical phase for adolescents and young adults with rare liver diseases. Joint consultations, where healthcare providers from both

services meet with the patient, are recommended to support continuity and patient-centered care. Yet the term is often invoked rather than clearly defined, and practices vary considerably, leading to differing expectations among participants. This study explores patient perspectives on joint consultations, based on a focus group held during the ERN Rare Liver Youth Panel workshop (Hamburg, July 2025), as part of a broader investigation that will also include parents and healthcare providers.

Method: A focus group session was conducted with thirteen members of the ERN Rare Liver Youth Panel during a two-day workshop. Nine participants attended on site and four joined online. Ages ranged from 20 to 28 years, and participants represented seven countries: Belgium, Germany, Portugal, France, the United Kingdom, Denmark, Cyprus, and Italy. Diagnoses included autoimmune hepatitis, biliary atresia, primary sclerosing cholangitis, and combinations of these conditions. Discussions were guided by a semi-structured interview guide addressing experiences, expectations, and perceived goals of joint consultations. Conversations were audio-recorded, transcribed verbatim, and analyzed using inductive thematic analysis with open coding to identify recurring themes.

Results: Most participants had never experienced a joint consultation but expressed strong interest in its potential benefits. Key themes included: 1) continuity and preparation, with clear transfer planning and gradual transition; 2) relationship-building, meeting the adult physician early to foster trust; 3) patient-centeredness, including private discussion without parents; 4) information exchange, ensuring pediatric and adult providers share medical history in the patient's presence; and 5) psychosocial support, emphasizing mental health and feelings of safety. Participants recommended multiple consultations, preferably in the adult clinic, with sufficient time for discussion, involvement of psychologists, and when appropriate, parents.

Conclusion: Young adults view joint consultations as essential for safe, structured transition. They advocate for flexible, patient-driven formats that prioritize preparation, continuity, and emotional well-being. These insights should inform guidelines for transition of healthcare in rare liver diseases.

THU-555-YI

Real-world nutritional management and outcomes in alcohol-associated hepatitis: a comparison of adherence to guidelines and short-term mortality between two centers

Erica Wajntraub Bakszt[1,2], Bonnie Bengtsson[1,2,3], Hannes Hagström[1,4], Catarina Lindqvist[1,5]. [1]*Gastroenterology and Nutrition Unit, Department of Medicine, Huddinge, Karolinska Institutet, Stockholm, Sweden;* [2]*Karolinska Institutet, Stockholm, Sweden;* [3]*Department of Clinical Science and Education, Södersjukhuset, Karolinska Institutet, Stockholm, Sweden;* [4]*Division of Hepatology, Department of Upper GI Diseases, Karolinska University Hospital, Stockholm, Sweden;* [5]*Section Clinical Nutrition, Karolinska University Hospital, Stockholm, Sweden*
Email: erica.wajntraub-bakszt@regionstockholm.se

Background and aims: Alcohol-associated hepatitis (AH) carries high mortality. Nutrition is a key component of therapy alongside corticosteroids and alcohol abstinence, yet real-world implementation remains unclear. We aimed to evaluate nutritional management, guideline adherence, and association between energy intake and outcomes in AH in two Swedish hospitals.

Method: Retrospective review of patients with AH admitted 2019–2023 to two liver centers in Stockholm, representing tertiary and secondary care. Data on nutritional care, morbidity and mortality were collected. Guideline adherence and inter-center differences were analyzed using χ^2 and Wilcoxon tests. Logistic regression examined associations between nutritional practices and 28-day mortality.

Results: Among 157 patients, 60 % had severe AH (MELD $\geq$ 20), and 69 % had underlying liver cirrhosis. Median age was 58 years, 36% were female, the median length of stay was 10 days. Malnutrition risk screening was performed in 85%, but no center used a liver-specific tool, and 39% were classified at risk for malnutrition. Dietitian involvement was higher at the tertiary center (83% vs. 42%, $p < 0.001$) and corresponded to more individualized nutrition care. Dietitians provided information more often than nurses or physicians (39% vs. 19% and 14%) and were primarily responsible for calculating energy goals (54% vs. 9% and 24%). Daily energy intake was documented for a median of 87% of hospital days at the tertiary center vs. 4% at the secondary ($p < 0.001$). Parenteral nutrition (PN) (28%) was more common than enteral nutrition (EN) (11%), with higher use of PN at the tertiary center (39% vs. 19%, $p < 0.01$). Higher energy intake (>21.4 kcal/kg/day) was associated with lower 28-day mortality in crude (OR = 5.66, 95%, CI = 1.3–38.9) and adjusted models (sex, age, MELD, cirrhosis, prednisolone) (OR = 6.81, 95% CI = 1.2–59.5).

Conclusion: Nutritional management varied between centers, with gaps in dietitian access and caloric monitoring. Higher energy intake showed an association with lower short-term mortality, though low precision; results are consistent with earlier studies. Investigations into barriers to guideline adherence and strategies to improve dietitian involvement are warranted. Nutrition remains a potentially modifiable determinant in AH. Further work is needed to understand factors contributing to higher energy intake, the effect of timely and adequate nutritional support on clinical outcomes, and whether EN should continue to be recommended as first-line treatment.

THU-556-YI

A review of terlipressin use in hepatorenal syndrome-acute kidney injury across 18 hospitals in the United Kingdom: Can we "CONFIRM" a change in practice?

(Leslie) Chun Man Wong[1], Olivia Baker[1,2], Alison Boyle[3], Alban Clareburt[3], Caitlin Brown[3], Sandeep Whitehead[4], Natasha Butt[5], Keswir Singh Cheema[5], Kate Greener[6], Sital Shah[6], Naz Kanani Alviri[7], Abraham Okoibhole[7], Aya Al-Hasani[8], Anastasia Lamprou[8], Sarah Hoban[8], Mohammad Wasim[8], Hannah Hesketh[9], Arjuna Singanayagam[9], Tamar Avades[10], Robert Elliot-Cooke[10], Juan Acevedo Haro[10], Eva Lau[11], Alice Bennett[11], Joanthan Creamer[12], Yun Jung Kim[12], Ziad Chilmeran[12], Amrita Gurung[13], Alastair O'Brien[7,14], Navjyot Hansi[1]. [1]*Cambridge Liver Unit, Cambridge University Hospitals NHS Foundation Trust, Cambridge, United Kingdom;* [2]*North West Anglia NHS Foundation Trust, Peterborough, United Kingdom;* [3]*NHS Greater Glasgow & Clyde, Glasgow, United Kingdom;* [4]*Leeds Teaching Hospitals NHS Trust, Leeds, United Kingdom;* [5]*Manchester University NHS Foundation Trust, Manchester, United Kingdom;* [6]*King's College Hospital NHS Foundation Trust, London, United Kingdom;* [7]*Royal Free London NHS Foundation Trust, London, United Kingdom;* [8]*London North West University Healthcare NHS Trust, London, United Kingdom;* [9]*St George's University Hospitals NHS Foundation Trust, London, United Kingdom;* [10]*University Hospitals Plymouth NHS Trust, Plymouth, United Kingdom;* [11]*Barts Health NHS Trust, London, United Kingdom;* [12]*University Hospital Southampton NHS Foundation Trust, Southampton, United Kingdom;* [13]*Causeway Hospital, Coleraine, Northern Ireland;* [14]*Comprehensive Clinical Trials Unit, University College London, London, United Kingdom*
Email: leslie.wong1@nhs.net

Background and aims: Terlipressin with albumin is the first-line intervention for hepatorenal syndrome-acute kidney injury (HRS-AKI) in the United Kingdom (UK). The CONFIRM trial reported increased respiratory events, sepsis and mortality in patients meeting high-risk criteria, prompting updated Medicines and Healthcare products Regulatory Agency guidance in 2023. We conducted a multicentre retrospective audit to evaluate UK practice following this change, with secondary aims assessing adverse events (AE).

Method: UK centres were invited via the British Association for the Study of the Liver and the British Hepatology Pharmacy Group. Each hospital reviewed electronic records for terlipressin prescriptions in adults with HRS-AKI from 1 Sept 2023 to 30 Sept 2024. Clinical and

biochemical parameters were analysed. Statistical analyses were performed; Mann-Whitney U and Chi-Square tests with $p < 0.05$ were considered statistically significant.
Results: 180 patients from 18 hospitals were included. Median age was 58 years (range 25–86); 61% male; alcohol aetiology 71%; median MELD score was 30 (range 12–44), and median serum creatinine on terlipressin initiation was 198 umol/L (range 75–845). Terlipressin was administered by bolus injection in 72% of patients. Concomitant albumin was administered in 166 patients (92%), 147 g +/– 168 (mean +/– SD; total per person) over a median of 6 days. Total of 11 patients (6.1%) proceeded to liver transplantation. Overall inpatient mortality was 55%. High-risk criteria were met in 28 (15.5%) patients, with no significant difference in inpatient mortality compared with those without high-risk criteria ($p = 0.931$). AE within 30 days of stopping terlipressin occurred in 92 patients (51.1%), most commonly respiratory failure ($n = 50$, 27.9%) and sepsis ($n = 68$, 37.8%). There was no significant difference in volume of albumin prescribed in those that did or did not have respiratory failure AE ($p = 0.117$). HRS-AKI complete and partial responses were achieved in 24% and 4%, respectively.
Conclusion: We report higher incidences of respiratory failure and sepsis than the CONFIRM trial. HRS-AKI remains a significant clinical challenge with limited therapeutic options and high mortality. It remains unclear whether terlipressin and albumin in advanced cirrhosis are indeed "friend or foe." The variation in practice across the UK highlights the importance of standardised care, ongoing education and greater awareness of the contraindications and monitoring requirements for terlipressin.

THU-557-YI
Hepatitis C in detainees entering Barcelona prisons: an opportunity to detect the infection in groups with limited access to the health system
Elena Yela[1], Neus Solé[2], Lidia Puig[1], Rafael Clua-García[3], Darío López-Gallegos[4], Daniel G. Abiétar[5], Montserrat Gàlvez[6], Queralt Guixé[7], Sabela Lens[8], Andrés Marco[2,9]. *[1]Sant Esteve Sesrovires Prison Primary Care Team (Brians 1 Prison Centre), Institut Català de la Salut, Sant Esteve Sesrovires, Spain; [2]Prison Health Program, Corporative Centre. Catalan Health Institute, Barcelona, Spain; [3]Facultat de Ciències de la Salut de Manresa-Uvic, Manresa, Spain; [4]Catalan Health Institute, Barcelona, Spain; [5]Corporate Centre, Catalan Health Institute, Barcelona, Spain; [6]Department of Health Sub-Directorate General for Addictions, HIV, Sexually Transmitted Infections and Viral Hepatitis, Health Department, Barcelona, Spain; [7]Dones Barcelona Prison Primary Care Team (Dones Prison Centre), Catalan Health Institute, Barcelona, Spain; [8]Liver Unit Hospital Clínic. IDIBAPS, Barcelona, Spain; [9]Centro de Investigación Biomédica en Red de Epidemiología y Salud Pública (CIBERESP), Barcelona, Spain*
Email: eyela@gencat.cat

Background and aims: Incarceration can facilitate the detection of hepatitis C virus (HCV) infection in groups often isolated from the community healthcare system. The aim is to analyse HCV infection (HCV RNA+) in newly incarcerated individuals in Barcelona prisons, and to examine the social determinants associated with a lack of awareness of the infection.
Method: HCV infection was studied in inmates recently admitted to two prisons in Barcelona during the period 2021–2024. The presence of infection or reinfection after sustained virological response (SVR) was assessed, as well as whether the infection status was known before incarceration. Potential associated socioeconomic and clinical variables were studied using binomial regression for knowledge/lack of knowledge of the infection.
Results: Among the 13136 patients studied there were 281 (2.1%) cases of infection (32.4% reinfections), with no significant differences between prisons or study years. 90.7% were male, and the mean age was 41.1 years. 59.1% were immigrants, 71.5% were homeless, 85.8% were or had been injection drug users, and 30.6% were HIV-positive. 68.3% were aware of their infection status but had not received treatment. In the bivariate analysis, the variables associated with not knowing HCV serological status (31,7%) were: a)being an immigrant, especially with less than one year of residence in Spain b) first incarceration c) absence of contact with drug resources d) not having a health card. The multivariate analysis confirmed that the variables associated with knowing one's HCV serological status were: a) previous incarceration (OR 3.30; 95% CI: 1.78–6.16; $p < 0.001$) b) contact with the healthcare system (OR 2.16; 95% CI: 1.08–4.33; $p = 0.029$).
Conclusion: 2.1% of new inmates in Barcelona prisons are HCV-RNA+, and almost a third of those infected are unaware of their serological status. The rest are reinfections or infected individuals who know their status but have not received treatment. Lack of contact with healthcare, community, or prison systems, especially among migrant population or drug users without access to support services, is the reason why the infection often goes undetected or untreated. If these diagnostic and therapeutic gaps are not addressed through strategies tailored to subpopulations that reduce structural barriers and improve links with the health system and the drug addiction care network, elimination does not seem possible.

Nurses and Allied Health Professionals – Clinical – service development or improvement project

TOP-536-YI
Conceptual development of an advanced practice nurse role for patients living with liver cirrhosis in a Swiss health care system
Jasmin Herzog[1,2], Lynn Leppla[2,3], Janette Ribaut[2], Robert Brenig[1,4], Kelly Da Silva[1], Patrizia Künzler-Heule[2,5], Sonja Beckmann[6], Christine Bernsmeier[1,4]. *[1]University Centre for Gastrointestinal and Liver Disease, University Hospital Basel, Basel, Switzerland; [2]Institut of Nursing Science, Department Public Health, University of Basel, Basel, Switzerland; [3]Department of Nursing, Division of Clinical Nursing Research and Practice Development, Medical Center – University of Freiburg, Faculty of Medicine, Freiburg, Germany; [4]Departements of Biomedicine and of Clinical Research, University of Basel, Basel, Switzerland; [5]Division of Gastroenterology and Hepatology and Department of Nursing & Therapeutic Services, Hoch Cantonal Hospital St. Gallen, St. Gallen, Switzerland; [6]Center for Clinical Nursing Science and Department of Gastroenterology and Hepatology, University Hospital Zurich, Zürich, Switzerland*
Email: jasminmargrit.herzog@usb.ch

Background and aims: The development and implementation of Advanced Practice Nurse (APN) roles are often challenged by political and financial barriers, as well as limited organizational structures, resulting in insufficient role clarity, limited stakeholder acceptance, and a lack of shared understanding of the APNs scope of practice. Therefore, the aim of this project was to conceptually develop a new APN role for patients living with liver cirrhosis in a Swiss hospital using a structured, theory-guided approach to address these barriers.
Method: Steps 1 to 5 of the Participatory, Evidence-based, Patient-focused Process for the Development, Implementation, and Evaluation of Advanced Practice Nursing (PEPPA) framework were used. The results of the interviews with 2 patients, 5 healthcare professionals (HCP), and the scarce 2 APNs Hepatology from other Swiss hospitals were synthesized including current literature according to the Chronic Care Model. APN activities were illustrated using the Hamric model and displayed related to outputs and outcomes in a logic model.
Results: PEPPA steps 1–4: Seven interviews were conducted. Care for patients with liver cirrhosis is partitioned and characterized by

limited time and resources. Patients interact with multiple HCP, hampering continuity and coordination of care. Self-management support regarding lifestyle changes, symptom management and medication adherence are often lacking, as well as specific symptom assessments. PEPPA step 5: Implementing an APN could address the identified gaps by applying Hamric's competencies. Through direct clinical practice, the APN is a consistent contact point, ensures care continuity, and conducts comprehensive assessments. Guidance and coaching enable provision of self-management support, including symptom management, lifestyle counselling, and medication adherence, while collaboration and leadership enhance coordination of person-centered care and support for other healthcare professionals in complex situations. Short- and long-term outcomes such as early detection of complications, improved medication adherence and reduced mortality were further defined in the logic model.
Conclusion: The conceptual APN role shows great potential to fill in the gaps of care and improve management of patients with liver cirrhosis. The logic model provides a structured basis to guide the development, implementation and evaluation of the APN roles in hepatology care.

WED-547
FibroScan® insights: lifestyle change and liver health in primary biliary cholangitis
Rebecca West[1], Robert Mitchell-Thain[1], Louise Campbell[2], Claire Hardie[3]. [1]*PBC Foundation Edinburgh UK, Dunfermline Fife, United Kingdom;* [2]*Tawazun Health, London, United Kingdom;* [3]*LiverScan, Edinburgh, United Kingdom*
Email: rebecca@pbcfoundation.org.uk

Background and aims: Primary Biliary Cholangitis (PBC) is a chronic autoimmune cholestatic liver disease. Alongside pharmacological intervention, lifestyle management is recognised as an important aspect of liver health. Metabolic Dysfunction Associated Steatotic Liver Disease (MASLD) care has demonstrated that targeted lifestyle changes can reduce hepatic steatosis and stiffness, but its impact in PBC—particularly where steatosis co-exists—remains unclear. Historical research shows conflicting evidence: steatosis has been reported as common and associated with higher liver stiffness in PBC, while other studies show lower burdens than in MASLD. Overlap with metabolic dysfunction is consistently linked with poorer outcomes. These uncertainties highlight the need for real-world evaluation of modifiable factors.
The aim is to assess whether lifestyle-focused behavioural discussions, combined with lifestyle changes and repeat FibroScan® assessments one year apart, were associated with changes in liver steatosis and stiffness in individuals with PBC.
Method: Sixteen adults all of whom were female with established PBC underwent baseline (2024) and repeat (2025) FibroScan® assessments at a national PBC event. At baseline, participants received personalised feedback and an individualised discussion exploring practical lifestyle modifications. Controlled Attenuation Parameter (CAP) and liver stiffness (kPa) were recorded at both appointments, and changes were compared descriptively.
Results:
Steatosis
- Baseline: 37% (6/16) elevated
- Follow-up: 19% (3/16) elevated
- Of those elevated, 83% improved

Stiffness
- Among those with improved steatosis: 60% improved stiffness, 40% remained stable
- 50% achieved >35% stiffness reduction, exceeding the 30% threshold recognised in MASLD studies (not yet validated in PBC)
- One participant showed reduced stiffness but increased steatosis during active weight loss

Conclusion: These preliminary real-world findings from repeat fibroscans suggest that lifestyle-focused behavioural support and lifestyle management changes, may help stabilise or improve steatosis and stiffness in individuals with PBC. Participants reported feeling motivated and empowered, indicating that FibroScan®-guided counselling may enhance engagement with long-term metabolic optimisation. Further research is required to determine the scale of benefit and inform management of PBC patients with metabolic dysfunction.

WED-548-YI
Combined hepatic arterial infusion chemotherapy, lenvatinib, and anti-PD-1/PD-L1 antibodies as conversion therapy for unresectable hepatocellular carcinoma: a 5-year prospective real-world study
Zeyang Ding[1], Ruizhi Chang[1]. [1]*Hepatic Surgery Center, Tongji Hospital, Tongji Medical College, Huazhong University of Science andTechnology, Wuhan, China*
Email: zeyangding@hust.edu.cn

Background and aims: Conversion therapy is valuable for unresectable HCC, and HAIC + lenvatinib + ICI has an ORR >60% but lacks long-term follow-up data in existing studies. We conducted a study with long-term follow-up to assess this regimen's efficacy, safety, and surgical conversion rate for unresectable HCC.
Method: This study was a post-hoc analysis of the HAIC-lenvatinib-ICI cohort from CCGLC-001, including unresectable HCC patients who received HAIC-FOLFOX + lenvatinib + anti-PD-1/PD-L1 antibody at 4 centers (3 Tongji Hospital branches, Wuhan; Second Hospital of Fujian Medical University, Quanzhou) since May 2020, and evaluated the treatment's efficacy, safety, and surgical conversion rate.
Results: In a multicenter study of 226 unresectable HCC patients treated with HAIC-lenvatinib-ICI, the mRECIST ORR reached 68.1% (12.4% CR, 55.7% PR) with 62.4% achieving CRT (met the criteria of radical treatment eligibility) and 46.8% undergoing radical treatment (72.7% resection, 9.1% transplantation, 18.2% ablation). Notably, 2 of 9 patients with extrahepatic metastases underwent conversion resection.
Long-term outcomes included a median PFS of 18.5 months and 5-year OS rate of 53.6%. Patients achieving CRT had significantly longer PFS (28.1 vs. 8.2 months, $p < 0.001$) and 24-month OS (81.5% vs. 42.8%, $p < 0.001$). Radical treatment conferred sustained survival benefits even after adjusting for baseline differences. Safety was manageable, with 97.8% experiencing TRAEs (85.4% grade 1–2, 12.4% grade 3–4) and no treatment-related deaths. CRT responders had fewer severe toxicities (7.1% vs. 21.3%, $p < 0.001$). Perioperative outcomes showed laparoscopic resection in 68.8%, low 30-day mortality, and pathological responses in 27.1% (pCR) and 42.4% (mCR) of resected cases. These findings validate HAIC-lenvatinib-ICI as a promising strategy for achieving durable tumor control and surgical conversion in advanced HCC.
Conclusion: Combined HAIC, lenvatinib, and anti-PD-1/PD-L1 antibody yields a high surgical conversion rate in unresectable HCC (62.4% CRT eligibility, 46.8% radical treatment), with a median PFS of 18.5 months and favorable long-term survival. Radical treatment significantly improves PFS even after adjusting for baseline differences, and safety is manageable (mostly grade 1–2 toxicities, no treatment-related deaths). These findings validate this regimen as a promising approach for unresectable HCC.

WED-549-YI
Feedback meetings as a method to involve patients with alcohol-related liver cirrhosis and their relatives
Marie Christiansen[1], Rikke Werge[1], Ann Sophie Nielsen[1], Malene Barfod O'Connell[1]. [1]*Copenhagen University Hospital, Amager Hvidovre, Hvidovre, Denmark*
Email: frkclose@hotmail.com

Background and aims: Patients with alcohol-related liver cirrhosis often face both organizational and relational barriers in healthcare. At the Gastro Unit, Amager-Hvidovre Hospital, a feedback meeting was

used as a participatory method to explore patients and relatives' experiences to inform more person- and family centered discharge and follow-up practices.
The aim of this project was to explore how patients with alcohol-related liver cirrhosis and their relatives experience the discharge process, and to evaluate whether a feedback meeting can serve as a suitable method for involving this patient group in quality improvement.
Method: In February 2025, a two-hour feedback meeting was conducted with four outpatients recently diagnosed with alcohol-related liver cirrhosis (Child-Pugh A5–B8; two men and two women, aged 62–71), three relatives (a sister, a husband, and a wife), two physicians, and four liver nurses. The meeting was facilitated using a semi-structured interview guide. Afterwards, all participants shared a traditional Danish lunch, followed by an approximately 45-minute reflection session for the healthcare professionals. Within one week, patients and relatives participated in follow-up telephone interviews. All data were audio-recorded, transcribed, and analyzed according to Braun and Clarke (2006).
Results:
Five main themes were constructed;
1. *Discharge from the hospital - A goodbye with loose ends*
2. *The Liver Clinic - A lifeline after discharge*
3. *Relatives as key support*
4. *Combining clinical information with lived experience*
5. *"We are normal people" – Experiences of stigma*

At the follow-up telephone interviews, the patients described the meeting as safe, inclusive, and meaningful. Sharing experiences fostered reflection, recognition and a sense of community. All patients would recommend similar meetings. The health professionals emphasized that the method provided new insights into both the discharge process and the patients and relatives lives beyond the hospital.
Conclusion: Feedback meetings proved to be a feasible and engaging approach for involving patients with alcohol-related liver cirrhosis and their relatives. The approach generated valuable insights into discharge communication, stigma, and collaboration, demonstrating that meaningful patient and relative participation can inform clinical practice and service development. Future initiatives will aim to include more socially vulnerable patients and explore alternative involvement formats.

WED-553-YI
Setting the standard – development of quality standards for liver nurses

Michelle Clayton[1]. [1]*British Liver Nurses' Association, N/A, United Kingdom*
Email: michelle.clayton1@nhs.net

Background and aims: Variations in care delivery has been identified as a reason for poorer outcomes for people with liver disease[1,2]. The British Liver Nurses' Association (BLNA) is collaborating with the British Society of Gastroenterology (BSG) to create a novel set of quality standards for liver nurses that will define the gold standard for care of people with liver disease, assuring quality and reducing variation.
Method: A group of expert liver nurses from the United Kingdom are writing the standards following consultation. Six "health status pillars" have been identified which include for example early identification and prevention, complications of decompensated liver disease, and transplant assessment. Each standard and its component parts follow the same format to ensure consistency and ease of use. Best practice describes the required elements of each of the standards; the rationale offers knowledge to support understanding of the care element; and evidence in the form of national/international guidelines and seminal publications ensures assurance and contemporary practice. Robust review of the quality standards to ensure rigour will be undertaken via a separate group of expert nurses to appraise and sense check the standards.
Results: Two quality standards, the complications of decompensated liver disease and transplant assessment will be launched in summer 2026, with the other four standards being released at intervals over the following six to twelve months. The standards will be created for both online access and for an app to allow increased accessibility.
Conclusion: Being able to articulate the gold standard for care of people with liver disease is essential to ensure quality, reduce variation in care delivery and offer robust assurance that practice reflects the evidence base. Due to the format of these quality standards, liver nurses will be able to tailor and personalise their professional practise to ensure understanding of what gold standard care should look like and creating a positive impact for both liver nurses and people with liver disease.

References

1. Office for Health Improvement and Disparities (2023) Liver disease profiles, March 2023.
2. Public Health England (2017) The 2nd atlas of variation in risk factors and healthcare for liver disease in England.

WED-554
Wilson disease patient support programme in Ireland - the impact one year on

Anna Gorham[1], Sonya Grandison[2], Elaine Kamara[3], Amy Power[2], Emer Fitzpatrick[2]. [1]*TCP Healthcare, Dublin, Ireland;* [2]*Childrens Health Ireland, Crumlin, Dublin 12, Ireland;* [3]*Orphalan UK Ltd, London, United Kingdom*
Email: anna.gorham@tcp.ie

Background and aims: Wilson disease (WD) is a rare condition requiring lifelong treatment, with poor adherence increasing risks of illness, death, and liver transplantation. Irish patients experience challenges due to distance from hospitals and lack of dedicated care. This report evaluates the effect of a WD-specific patient support program (PSP) in Ireland on both patients and healthcare professionals.
Method: In October 2024, Orphalan partnered with TCP Homecare in Ireland and appointed a dedicated WD nurse for the PSP. The nurse, trained in WD, visits hospitals nationwide to engage hepatology and neurology professionals and provides support to patients through home visits, sample collection, medication management discussions, and appointment reminders. She gathers patient and caregiver feedback. Healthcare professionals using the service have provided feedback on the impact this initiative has had on their trust.
Results: To date, 20 patients have joined the programme. One case study showed that a patient who previously missed hospital appointments was able to complete two 24-hour UCE samples in the past year and feels more empowered to manage his care after receiving support at home. Patients report that home monitoring has improved their wellbeing by reducing stress and allowing them to avoid time off work or school, while nurse conversations help them realise they are not alone with their condition.
Healthcare professionals note several benefits since launching the WD PSP: test results are now reliably available for clinic visits, reducing staff time spent chasing data and allowing more focus on direct care. Missed appointments and unnecessary phlebotomy visits have decreased, leading to better patient monitoring, disease management, and reduced strain on hospital resources.
Conclusion: The Wilson Disease Patient Support Programme (WD PSP) in Ireland has improved Wilson disease management by focusing on patient-centred care. A dedicated PSP nurse enables home-based monitoring and ensures test results are ready before clinic visits, making care more efficient. The PSP reduces the patients feeling of isolation and provides the opportunity to improve the patients' journey. Overall, the programme effectively supports both patients and healthcare professionals.

WED-555

Liver cancer screening in patients with cirrhosis and the role of allied health professionals: real-world experience of a community-based liver center

Anna Marie Hefner[1], Lita Petcharaporn[1], Ahmed Atalla[1], Usman Gul[1], Ayisha Aziz[1], Fatma Barakat[2], Eric Storey[1], Maryam Yasso[1], Renee Pozza[1], Deanna Oliver[1], Tarek Hassanein[1]. *[1]Southern California Liver Centers, Coronado, United States; [2]SCTI Research Foundation, Coronado, United States*
Email: ahefner@livercenters.com

Background and aims: Cirrhosis poses a signifiacant public health burden. With the projected increase in prevalence, concerns for the development of liver cancer becomes significant. Liver cancer is associated with numerous complications, hospitalizations as well as higher mortality rates and economic burden. Despite advancements in therapies for liver cancer, early detection remains critical for improved disease-free survival and patient (pt) outcomes. The role of Allied Health Professionals (AHP) is vital to be able to accomodate this need. The aim is to report on the outcomes of liver cancer screening by AHPs in pts with cirrhosis in a non-academic, community-based single liver center.
Method: This is a retrospective analysis of 1526 pts with cirrhosis seen between January 2023 and May 2025 in a single community-based liver center. Pts were managed according to standardized protocols tailored to each pt's needs including screening for liver cancer at least every 6 months using alternating imaging modalities (ultrasound, CT scan, MRI). Management plan was set in consultation with the Hepatologists while visits and follow-up was done primarily by AHPs including Nurse Practitioners and Physician Assistants.
Results: 51.3% males. Mean age was 63.2 ± 11.8 years. 53.2% Hispanics and 87.4% White. Primary causes of liver disease: history of HCV, Alcohol-related liver disease, MASLD/MASH. Follow-up: Median follow-up duration was 3.8 years with an average of 5 visits/pt/year. Liver cancer screening was done primarily by Ultrasound (54.8%) due to factors such as health insurance and pt preferance. 20% of pts had screening by CT-scan and 19.6% by MRI. Outcomes: 89.4% of pts complied with doing liver cancer screening every 6-months. Of which 6.7% developed a liver lesion. 90.2% were single lesions less than 1 cm classified as Hepatocellular Carcinoma.
Conclusion: Real-world experience of a non-academic, community-based single liver center confirmed that Allied Health Professionals are integral members of a liver pt's care team. AHPs play a vital role in enabling increased frequency and monitoring of pts with cirrhosis leading to decreased decompensation episodes and significant compliance with liver cancer screening. Screening for liver cancer at least twice a year using alternating imaging modalities resulted in early detection of liver cancer. Having a dedicated program led by AHPs to manage pts with cirrhosis improves complications-free survival and better outcomes of liver cancer management.

WED-556-YI

Biochemical response to Elafibranor in primary biliary cholangitis (PBC): impact of prior second-line therapy exposure

Rachael Kamiri-Ngugi[1], Marinos Pericleous[1], Kuldeep Cheent[2], Gayatri Chakrabarty[3], Iona Coltart[2], Valerie Duckhouse[2], Michelle Gallagher[1], Liliana Goncalves[2], Alfredo Lim[2], Sanju Mathew[1], Osob Mohamed[4], Prayman Sattianayagam[3], Karen Street[3], Christopher Wong[2], Aftab Ala[1]. *[1]Royal Surrey Nhs Foundation Trust, Guildford, United Kingdom; [2]Frimley Park Hospital, Camberley, United Kingdom; [3]East Surrey Hospital, Redhill, United Kingdom; [4]Saint Peter's Hospital, Chertsey, United Kingdom*
Email: r.kamiri-ngugi@nhs.net

Background and aims: Elafibranor is a dual Peroxisome Proliferator-Activated Receptor (PPAR) alpha/delta agonist licensed for Primary Biliary Cholangitis (PBC). It inhibits bile acid synthesis, enhancing detoxification, and exerting anti-inflammatory effects. Real-world data on biochemical outcomes in patients switching from other second-line therapies to elafibranor remain limited. Our aim was to compare the 28-day biochemical response in PBC patients switched to ursodeoxycholic acid and elafibranor from prior second-line therapies (bezafibrate or obeticholic acid), versus those treatment-naïve to second-line agents.
Method: We retrospectively analysed records from our regional PBC Operational Delivery Network of 26 patients switched to elafibranor-based therapy. Patients were categorised by prior regimen: ursodeoxycholic acid+bezafibrate, ursodeoxycholic acid+obeticholic acid, ursodeoxycholic acid+bezafibrate+obeticholic acid (triple therapy), ursodeoxycholic acid monotherapy (second-line naïve). All patients had inadequate biochemical response to ursodeoxycholic acid per POISE criteria and received MDT approval for elafibranor. Alkaline phosphatase (ALP) was recorded at baseline and ~28 days post-switch to ursodeoxycholic acid-elafibranor.
Results: Ursodeoxycholic acid and elafibranor (n = 16) demonstrated greatest efficacy, with mean ALP reduction of 108.9 U/L from baseline and 93.8% response rate, with no patients experiencing biochemical worsening. Patients switched from bezafibrate to elafibranor (n = 3) showed promising results with a mean reduction of 98.0 U/L, albeit with greater variability (66.7% response rate). Switching from obeticholic acid to elafibranor (n = 6) resulted in moderate efficacy, with a mean ALP reduction of 48.3 U/L and 83.3% response rate. Overall, 84.6% of patients (22/26) demonstrated biochemical improvement, with a pooled mean ALP reduction of 88.4 U/L.
Conclusion: Ursodeoxycholic acid plus elafibranor combination therapy represents the most effective and consistent treatment option, showing highest mean ALP reduction and response rate without paradoxical worsening. Switching from bezafibrate to elafibranor may benefit selected patients with relatively higher baseline ALP, but requires careful monitoring. Transitions from obeticholic acid warrants caution given paradoxical responses in some patients. These findings support elafibranor-based combination therapy as an effective strategy, with treatment selection tailored to individual patient characteristics and prior regimens.

WED-557

Physical activity for the management of paediatric metabolic dysfunction-associated steatotic liver disease: an international multidisciplinary consensus

Shelley Keating[1], Jonathan Stine[2], Angelo Sabag[3,4], Kate Hallsworth[5,6], Shira Zelber-Sagi[7], Nathan Johnson[3], Lucille Wilson[1], Michalis Stylianou[1], Elena George[8], Ingrid Hickman[9], Kai Wheeler[1], Mohit Kehar[10], Mortada El Shabrawy[11], Way Seah Lee[12], Sander Lefere[13,14], Ruth de Bruyne[15,16], Ram Weiss[17], Ilaria Croci[18], Christopher Pugh[19,20], Daniel Cuthbertson[21,22], Nicholas Beng Hui Ng[23,24], Jacob George[25], Oyekoya Ayonrinde[26,27,28], Le Zhang[29], Ming-Hua Zheng[30,31]. *[1]School of Human Movement and Nutrition Sciences, The University of Queensland, Brisbane, Australia; [2]Penn State Health Milton S. Hershey Medical Center, Hershey, United States; [3]School of Health Sciences, Faculty of Medicine and Health, The University of Sydney, Sydney, Australia; [4]Charles Perkins Centre, The University of Sydney, Sydney, Australia; [5]NIHR Newcastle Biomedical Research Centre, Newcastle upon Tyne Hospitals NHS Foundation Trust, Newcastle upon Tyne, United Kingdom; [6]Translational and Clinical Research Institute, Faculty of Medical Sciences, Newcastle University, Newcastle upon Tyne, United Kingdom; [7]School of Public Health, Faculty of Social Welfare and Health Sciences, University of Haifa, Haifa, Israel; [8]Institute for Physical Activity and Nutrition (IPAN), School of Exercise and Nutrition Sciences, Deakin University, Geelong, Australia; [9]ULTRA Team, Clinical Trial Capability, Faculty of Health, Medicine and Behavioural Sciences, The University of Queensland, Brisbane, Australia; [10]Division of Pediatric Gastroenterology, Hepatology and Nutrition, Department of Pediatrics, University of Ottawa, Ottawa, Canada; [11]Department of Pediatrics and Pediatric Hepatology, Cairo University, Cairo, Egypt; [12]M Kandiah Faculty of Medicine and Health Sciences, University Tunku Abdul Rahman, Kajang, Malaysia; [13]Hepatology*

Research Unit, Department of Internal Medicine and Pediatrics, Ghent University, Ghent, Belgium; [14]Liver Research Center Ghent, Ghent University Hospital, Ghent, Belgium; [15]Department of Pediatric Gastroenterology, Ghent University Hospital, Ghent, Belgium; [16]Department of Internal Medicine and Pediatrics, Ghent University, Ghent, Belgium; [17]Department of Pediatrics, Ruth Children's Hospital, Rambam Medical Center, Haifa, Israel; [18]Department of Sport, Exercise and Health, Faculty of Medicine, University of Basel, Basel, Switzerland; [19]Centre for Cardiovascular Research, Innovation and Development, Cardiff Metropolitan University, Cardiff, United Kingdom; [20]Centre for Health, Activity and Wellbeing Research, Cardiff Metropolitan University, Cardiff, United Kingdom; [21]Department of Cardiovascular and Metabolic Medicine, Institute of Life Course and Medical Sciences, University of Liverpool, Liverpool, United Kingdom, [22]Liverpool University Hospitals NHS Foundation Trust, Liverpool, United Kingdom; [23]Khoo Teck Puat - National University Children's Medical Institute, Department of Paediatrics, National University Hospital, Singapore, Singapore; [24]Department of Paediatrics, Yong Loo Lin School of Medicine, National University of Singapore, Singapore, Singapore; [25]Storr Liver Centre, The Westmead Millennium Institute for Medical Research, University of Sydney, Sydney, Australia; [26]Medical School, The University of Western Australia, Perth, Australia; [27]Department of Gastroenterology and Hepatology, Fiona Stanley Hospital, Murdoch, Australia; [28]Medical School, Curtin University, Bentley, Australia; [29]Department of Paediatrics, Affiliated Children's Hospital of Jiangnan University, Wuxi Children's Hospital, Wuxi Key Laboratory of Genetic and Metabolic Diseases in Children, Jiangsu, China; [30]MAFLD Research Center, Department of Hepatology, the First Affiliated Hospital of Wenzhou Medical University, Wenzhou, China; [31]Key Laboratory of Diagnosis and Treatment for the Development of Chronic Liver Disease in Zhejiang Province, Wenzhou, China
Email: s.keating@uq.edu.au

Background and aims: Metabolic dysfunction-associated steatotic liver disease (MASLD) is the most common chronic liver disease in children and adolescents, closely linked with obesity and cardiometabolic risk. With no pharmacological therapies approved for MASLD in this population, behaviour-related lifestyle modifications are the cornerstone of management. This international consensus statement aimed to synthesise the evidence for physical activity (including structured exercise) for the management of paediatric MASLD and provide practical recommendations for clinicians, exercise professionals and families/caregivers.
Method: A systematic literature review was conducted and the 'GRADE-ADOLOPMENT' method was used to establish consensus recommendations. Consensus required >80% voting 'yes' or 'yes with changes' with changes adopted. Following open and closed consensus rounds, three research questions were established. Key considerations for evidence translation were reviewed to develop consensus on pragmatic implementation strategies.
Results: 25 collaborators contributed [11 countries, mean (SD) age 46 (11) yrs, 68% male] with expertise in hepatology, paediatrics, exercise physiology, public health and nutrition. The review netted 19 studies (15 original research; 4 systematic reviews). Preliminary data recommend 180–270 minutes/week of moderate-vigorous aerobic or combined aerobic and resistance exercise across 3–5 days/week, which can elicit modest hepatic benefit and broad cardiometabolic, cardiorespiratory and neuromuscular fitness improvements in children and adolescents with MASLD. Core recommendations are (i) adopt a whole-of-day movement approach, emphasising increases in moderate-to-vigorous physical activity, muscle strengthening activities, reduced sedentary and screen time and adequate sleep; (ii) multidisciplinary delivery involving clinicians, dietitians, and exercise professionals for a lifestyle-first approach; (iii) management should be family-centred and developmentally appropriate; and (iv) practical translation may involve school and community engagement to enhance equity and scalability.
Conclusion: Consensus established that exercise and healthy movement behaviours are safe, effective and central to paediatric MASLD management. Structured, family-centred, and multidisciplinary approaches can improve liver and cardiometabolic outcomes, with school and community settings important for sustainability, scalability and equity for access.

WED-558
Developing an evidence-based decision-support tool for culturally sensitive communication in hepatitis D care

Patrizia Künzler-Heule[1,2], Dunja Nicca[3]. *[1]HOCH Health Ostschweiz, Kantonsspital Sankt Gallen, Sankt Gallen, Switzerland; [2]University of Basel, Basel, Switzerland; [3]University of Zurich, Zürich, Switzerland*
Email: patrizia.kuenzler-heule@h-och.ch

Background and aims: Liver care nurses support patients with HBV/HDV co-infection in developing essential self-management skills, but care is frequently challenged by patients' cultural and linguistic diversity. This project aimed to develop an evidence-based decision-support tool to guide culturally sensitive communication strategies along the hepatitis D care pathway.
Method: A systematic literature review was conducted to identify communication strategies for linguistically diverse patients. Findings were discussed in a workshop with Swiss liver care nurses, focusing on their advantages and limitations across different stages of the hepatitis D care pathway. Key situations were delineated and preliminary assignments of suitable communication tools were developed. These findings are being reviewed and refined in a second workshop with international liver care nurses. In addition, semi-structured interviews with a patient representative and an expert in medical interpreting were conducted to complement the professional perspective.
Results: Identified communication strategies included the use of translators (relatives, trained healthcare professionals, and professional interpreters), digital solutions such as translation apps and artificial intelligence–based tools, as well as visual aids. Professional interpreters emerged as a key resource, particularly at early stages of care, including diagnosis, treatment decision-making, and treatment instruction, ensuring accurate communication and supporting the involvement of relatives. As care progresses, relatives were described as playing a more prominent role in ongoing communication. Translation apps were reported as especially useful for unplanned or short encounters. Visual aids were consistently described as supportive tools to reinforce verbal communication, although their availability in routine practice is limited.
Conclusion: The findings highlight the need for a structured, evidence-based approach to culturally and linguistically sensitive communication in hepatitis D care. Different strategies are required at different stages of the care pathway, with professional interpreters playing a central role in early, decision-critical situations. The ongoing refinement of these findings will inform the development of a practical decision-support tool for liver care nurses to support patient-centred self-management in culturally diverse settings.

WED-559-YI
A nurse-led tissue adhesive pathway to eliminate persistent post-paracentesis leakage: advancing hepatology nursing practice, patient comfort and value-based care

Mei Lin[1], Thinesh Edward Balasingam[1], Samantha Koh[2], Samuel Lim[2], Elizabeth Chen[2], Kevin Kim Jun Teh[2], Hiang Keat Tan[2], Jason Pik Eu Chang[2]. *[1]Nursing Division (Speciality Nursing), Singapore General Hospital, Singapore, Singapore; [2]Department of Gastroenterology and Hepatology, Singapore General Hospital, Singapore, Singapore*
Email: lin.mei@singhealth.com.sg

Background and aims: Persistent post-paracentesis leakage occurs in up to 20% of patients with cirrhosis requiring abdominal paracentesis, causing discomfort, skin irritation, increased infection

risk, and higher clinic resource utilization. Outcomes with conventional management strategies using pressure dressings, stoma bags, and/or sutures are variable and often poorly tolerated. To address these gaps, a nurse-led improvement initiative was developed to standardise post-paracentesis care using tissue adhesive as a simple and patient-centred alternative. The aim was to reduce persistent leakage to <10% within six months. Patient comfort, satisfaction, and value-based outcomes were also evaluated.

Method: A structured pathway was implemented in a tertiary restructured hospital in Singapore. Advanced hepatology nurses assessed suitability for tissue adhesive, performed the procedure, evaluated outcomes at 24 hours, and exercised independent escalation when required. Patient-reported comfort and satisfaction were assessed using structured questionnaires. Outcomes from the six-month intervention period were compared with pre-intervention leakage rates. Cost analysis reviewing changes in material and equipment use, as well as clinic resource utilisation was performed.

Results: Sixty-one patients received tissue adhesive under the nurse-led pathway. Persistent leakage rate decreased from 11–20.8% pre-intervention to 0% across all six intervention months. Patient-reported outcomes were highly favourable - 80% reported being very comfortable during application and at 24 hours, 86.7% were very satisfied, and 100% would opt for tissue adhesive in the future. Estimated cost savings over six months were SGD $4074.80, driven by reduced utilization of sutures and dressings, as well as clinic visits.

Conclusion: The nurse-led tissue adhesive pathway was safe, effective, and cost-efficient. It enhanced comfort, reduced complications, and streamlined patient care. This initiative demonstrated the impactful role of advanced hepatology nurses in pateint care, innovation, and value-based care. The pathway has since been adopted as the departmental standard, with strong potential for wider institutional and international adoption.

WED-560-YI

Improvement of patient satisfaction via implementation of a specialist nurse for patients with hepatocellular carcinoma – second interim analysis of the HCC care nurse pilot study

Larissa Pajancic[1,2], Lorenz Balcar[1,2], Abelina Kreuter[1,2], Katharina Pomej[1,2], Michael Trauner[1], Bernhard Scheiner[1,2], Matthias Pinter[1,2]. [1]*Medical University of Vienna, Department of Medicine III, Division of Gastroenterology and Hepatology, Vienna, Austria;* [2]*Vienna Liver Cancer Study Group, Division of Gastroenterology and Hepatology, Department of Medicine III, Medical University of Vienna, Vienna, Austria*
Email: larissa.pajancic@meduniwien.ac.at

Background and aims: The implementation of a hepatocellular carcinoma care nurse (HCCCN) can improve outcomes, reduce treatment-related adverse events, and can be cost-effective in patients with hepatocellular carcinoma (HCC) treated with sorafenib. Despite the rising incidence of HCC, specialist nurses are not yet widely established in Austria. This study aimed to standardise patient care by implementing a HCCCN in daily clinical practice and to evaluate its impact on quality of life, emergency admissions, length of hospitalisation, adverse events, and time on systemic treatment in patients with HCC.

Method: This single-centre, prospective pilot study included patients with HCC receiving systemic therapy at the Medical University of Vienna. Patients were randomised 2:1 to an intervention group with HCCCN support (group A) or a control group without HCCCN (group B). In addition to quality-of-life assessments, a self-developed patient satisfaction questionnaire was completed at each visit. All patients were seen by the treating physician, while patients in group A additionally received in-person and telephone follow-up by the HCCCN. The second interim analysis primarily focused on patient satisfaction.

Results: At data cut-off, 30 patients were included (group A: n = 20; group B: n = 10), most of whom were male (n = 24; 88%). The majority had advanced stage disease (BCLC stage C: n = 19; 65.5%; stage B: n = 11; 34.5%) and most were classified as Child-Pugh grade A (n = 20; 66.7%) or B (n = 10; 33.3%). Immunotherapy was administered to 17 patients and tyrosine kinase inhibitors to 13 patients. The median observation period was 9.2 months (range 1–21). In group A, a median of two in-person nurse visits (range 0–14) and one telephone contact (range 0–7) were recorded. Overall, 108 patient satisfaction questionnaires (median 3 per patient) were completed. In comparison to patients in the standard group, patients in the HCCCN group reported less difficulties with short-notice appointment scheduling (e.g. for managing side-effects) and less unannounced waiting times. Furthermore, they indicated that tracking their medical appointments was easier and they had sufficient advice on how to maintain their health status during treatment.

Conclusion: Overall, HCCCN support was associated with improved patient-reported experiences in care coordination, appointment management, and health-related guidance compared with usual care.

WED-561-YI

Improvement in Fibroscan® liver stiffness following lifestyle intervention in a real-world hepatology cohort

Amy Parry[1], Vijay Grover[1], Thomas Eddie[1], Jennifer Finn[1]. [1]*Hillingdon Hospital, Uxbridge, United Kingdom*
Email: amy.parry7@nhs.net

Background and aims: Approximately 90% of chronic liver disease is preventable; early detection with timely lifestyle intervention is key. This retrospective review aims to determine the impact upon patients who implement recommended lifestyle changes following an abnormal Fibroscan® (> 8 kPa) and a diagnosis of Metabolic Dysfunction–Associated Steatotic Liver Disease (MASLD), Alcohol Use Disorder (AUD), or combined Metabolic–Alcohol-Related Liver Disease (Met-ALD) attending an out-patient Hepatology clinic at a District General Hospital in London. A secondary aim was to evaluate the impact of socioeconomic deprivation on adherence to lifestyle intervention.

Method: Fibroscan® data from 2018–2025 were extracted from three internal devices. Collected variables included median liver stiffness (kPa), age, aetiology, body mass index (BMI), HbA1c, lipid profile, deprivation index and adherence to lifestyle recommendations. Data were analysed using statistical testing with Excel and RegressIT.

Results: We analysed 6172 Fibroscans® performed over seven years, representing 3308 individual patients (1177 MASLD, 866 Hepatitis B, 552 AUD, 84 Met-ALD and 629 other diagnoses). Among 1813 patients with MASLD, Met-ALD, or AUD, 145 (8%) had a baseline Fibroscan® > 8 kPa and repeat scan after ≥ 1 year. Liver stiffness improved by ≥ 1 kPa in 64% of patients, with 49% achieving complete reversal of fibrosis (Fibroscan® < 8 kPa). In those with improvement, 69% adhered to lifestyle intervention ($p = 0.003$) (weight loss with or without alcohol abstinence) and 43% demonstrated a reduction in BMI ($p = 0.012$). In contrast, those with a deteriorating Fibroscan®, only 11% reported positive lifestyle changes and 15% had a reduced BMI. Improvements in HbA1c and lipids were not associated with improvements in Fibroscan® (not statistically significant). Mean deprivation index scores were 5.8 for MASLD and 4.8 for AUD. Patients with MASLD in less deprived areas were more likely to adhere to lifestyle intervention and reduce BMI (14% per deprivation decile point increase), although this did not reach statistical significance.

Conclusion: This longitudinal review demonstrates that Fibroscan® liver stiffness is more likely to improve/reverse following implementation of lifestyle intervention. Improvements in glycaemic control and lipid profiles were not associated with changes in liver stiffness. The findings also suggest greater adherence to lifestyle intervention amongst patients residing in less deprived areas.

WED-562-YI

Patient reported outcomes of a nurse-led community-based post-discharge liver care program

Kristen Peake[1], Mayur Garg[1,2], Ziheng Xu[1], Diana Lewis[1], Siddharth Sood[1,2]. [1]*The Northern Hospital, Melbourne, Australia;* [2]*The University of Melbourne, Parkville, Australia*
Email: kristen.peake@nh.org.au

Background and aims: The Liver at Home (L@H) program was implemented in February 2023 to provide specialist advanced-practiced nurse support to patients in their homes following hospital discharge secondary to a liver-related condition. L@H is a 12-week program with tapering frequency of nurse encounters: 3 visits a week in weeks 1–4, and 1–2 visits between weeks 5–12. Approximately half of the visits are performed face-to-face with the remainder telehealth. L@H aims to facilitate a smoother transition to home, providing sustained care and education while reducing hospital readmissions. We evaluated patient experiences of L@H via anonymous post-program surveys.
Method: Anonymous surveys were distributed to eligible patients upon completion of the 12-week program, with a reply-paid envelope for return. Survey questions assessed patient perceptions of program effectiveness, satisfaction with care delivery, perceived impact on self-management, and support for hospital-to-community transition.
Results: Of 100 admitted patients, 45 surveys were sent to eligible participants. Reasons for non-distribution included program incompletion, patient refusal (due to illness or poor health literacy), repeat admission (n = 11), and death. The survey response rate was 44.4% (n = 20). Analysis revealed high patient satisfaction with L@H. Ninety-five percent reported gaining advanced understanding of their liver disease and feeling the program provided the necessary home support. Ninety percent felt more in control of their condition due to L@H, and all respondents (100%) reported feeling supported by program staff.
Conclusion: The patient survey results strongly suggest L@H is a well-received and beneficial care model for individuals discharged with liver-related conditions. Patients reported feeling well-supported at home and experienced an increased sense of control over their health. These positive perceptions highlight the value of at-home, nurse-led services in facilitating a smoother transition and empowering patients in chronic liver disease self-management.

WED-563

An audit to assess preventable emergency department presentations in patients with abdominal ascites secondary to cirrhosis

Kristen Peake[1], Siddharth Sood[1,2], Mayur Garg[1,2], Diana Lewis[1]. [1]*The Northern Hospital, Melbourne, Australia;* [2]*The University of Melbourne, Parkville, Australia*
Email: kristen.peake@nh.org.au

Background and aims: Ascites is a common complication of cirrhosis. Performing timely elective abdominal paracentesis in a day admission setting can prevent Emergency Department (ED) presentations, which often lead to prolonged hospital stays, higher healthcare costs, and adverse outcomes. Understanding the preventability of these ED visits is crucial for improving patient care and optimising resource allocation. We aimed to determine the proportion of ED presentations for ascites secondary to cirrhosis that were potentially preventable, and to identify the contributing factors.
Method: Patients who presented to the ED under Gastroenterology with ascites secondary to cirrhosis during the nine months (February to October) in 2024 were included. We evaluated whether their presentation was potentially preventable based on predefined criteria: patients were required to have prior involvement with our service and no concurrent medical issues requiring inpatient management. Preventability was independently assessed by a Hepatology Physician and a Senior Hepatology Clinical Nurse Consultant. In the event of disagreement, a third Hepatology Physician was consulted to determine the final classification.
Results: Forty-four patients met inclusion criteria. Of these, 19 (43%) were assessed as entirely preventable admissions based on the predefined criteria. Patients with potentially preventable admissions had a median length of stay of 4 days (interquartile range [IQR] 4 days).
Conclusion: The finding that 43% of ED presentations for abdominal ascites secondary to cirrhosis were potentially preventable highlights a critical area for targeted intervention. These patients are known to the health service, yet often experience limited access to dedicated nursing services. Increased specialised hepatology nurse support would effectively alleviate outpatient service pressures and streamline paracentesis pathways. This would allow for earlier intervention to prevent acute admission and facilitate the arrangement of timely outpatient paracentesis. Further improvements to existing processes and patient education would significantly impact the accessibility of care and prevent avoidable ED admissions. This represents a vital strategy to better support this patient population under current resource constraints.

WED-564

Areas for improved efficiency for patients with cirrhosis having elective abdominal paracentesis

Kristen Peake[1], Mayur Garg[1,2], Siddharth Sood[1,2], Diana Lewis[1]. [1]*The Northern Hospital, Melbourne, Australia;* [2]*The University of Melbourne, Parkville, Australia*
Email: kristen.peake@nh.org.au

Background and aims: Timely elective abdominal paracentesis can prevent emergency department presentations for patients with cirrhosis and refractory ascites. The current protocol at our healthcare service requires patients to first attend the Outpatient Medical Day Unit (OMDU). This is followed by a transfer to the radiology department for abdominal ultrasound marking. A resident doctor is then required to depart from their competing inpatient responsibilities to perform the abdominal paracentesis procedure in the radiology holding bay. Finally, the patient returns to the OMDU for the completion of drainage and post-procedure monitoring. In this audit, we analysed this workflow to determine areas for improved efficiency, exploring the potential benefit of Point-of-Care Ultrasound (POCUS) and implementing a nurse-led paracentesis service.
Method: Patients with cirrhosis-related ascites undergoing elective paracentesis in the OMDU over two months were included. Data included patient admission, radiology marking, drain insertion/removal, and discharge times. Analysis focused on identifying preventable delays, aiming to understand the potential impact of POCUS or future increased OMDU bed capacity.
Results: Sixteen patients were included; 87.5% (n = 14) arrived on time. Two patients (12.5%) had drain malfunctions, and three (18.75%) had inadequate ascites for paracentesis, yet all still endured admission times exceeding two hours. The mean time from admission to radiology marking was 2.26 hours (+/–SD 1.14). For the 11 patients who had paracentesis, the time from radiology marking to paracentesis was 1.74 hours (+/– 0.37). The mean time from admission to paracentesis was 3.54 hours (+/– 0.44). The overall mean time from admission to discharge was 6.91 hours (+/– 1.6).
Conclusion: The critical mean wait time from admission to paracentesis procedure is 3.54 hours, primarily attributable to delays in imaging and RMO availability. Integrating POCUS or establishing a nurse-led paracentesis service has the potential to significantly reduce unnecessary wait times, thus improving efficiency and increasing capacity for elective paracentesis. By improving OMDU efficiency, emergency department admissions related to bed availability are likely to be prevented in this patient population. These findings provide a valuable foundation for implementing a more streamlined, elective, nurse-led paracentesis process, which will enhance patient satisfaction and optimise resource utilisation within our healthcare service.

WED-569-YI

Patient-reported symptom burden and health care utilization in outpatients with advanced chronic liver disease – the prospective ATOMIC study

Martina Reiberger[1], David Bauer[2], Larissa Pajancic[3,4], Michael Schwarz[3], Nina Dominik[3], Katharina Pomej[3], Georg Kramer[3], Philipp Schwabl[3], Bernhard Scheiner[3], Michael Trauner[3], Benedikt Hofer[3], Thomas Reiberger[3]. *[1]Vienna General Hospital, Division of Gastroenterology and Hepatology, Department of Medicine III, Medical University of Vienna, Vienna, Austria; [2]Klinikum Ottakring, Vienna Healthcare Group, Vienna, Austria, Division of Gastroenterology and Hepatology, Department of Medicine III, Medical University of Vienna, Vienna, Austria, Vienna, Austria; [3]Division of Gastroenterology and Hepatology, Department of Medicine III, Medical University of Vienna, Vienna, Austria, Vienna, Austria; [4]Medical University of Vienna, Department of Medicine III, Division of Gastroenterology and Hepatology, Vienna, Austria*
Email: martina.reiberger@gmail.com

Background and aims: Patient-reported symptom burden and healthcare utilization patterns remain insufficiently investigated in (advanced) chronic liver disease (A)CLD. We aimed to assess symptom burden and health-related behaviors among stable CLD outpatients using standardized questionnaires.
Method: Patients with (A)CLD attending scheduled visits at the outpatient clinic of the Vienna General Hospital (AKH Wien) completed a 21-item symptom questionnaire assessing commonly reported liver-related symptoms, such as fatigue, sexual dysfunction, and insufficient disease- and nutrition-related information. Each item was rated on an 11-point visual analogue scale (VAS; 0–10). In addition, the questionnaire captured physical activity frequency and binary (yes/no) responses regarding alcohol use, participation in annual health check-ups, vaccination status review within the past two years, and GP visit in the past year. Continuous variables were summarized as medians with interquartile ranges. For patients with multiple visits only data from the latest visit was used to reflect current health status. Data were collected between 2021 and 2024.
Results: A total of 266 patients were prospectively included (median age: 57 [IQR 48–65] years; 64% male) with alcohol-related (n = 123, 46%) and viral (n = 32, 12.0%) liver disease as the most common etiologies. 92 (34.6%) patients had non-ACLD, 68 (26%) compensated ACLD, and 106 (39.8%) decompensated ACLD. Recent alcohol use was reported by 40 (15%). Furthermore, 94/261 (35%) had no GP visit in the past year, 129/246 (49%) did not attend annual health check-ups, and 125/247 (51%) had no vaccination status review within 2 years. Severe fatigue (pre-specified VAS≥7) was reported by 33%, low information regarding healthy nutrition (VAS<5) by 36%, and negative impact on sexual life (VAS≥7) by 26%. Symptom burden showed non-significant trends of symptom burden in dACLD compared with cACLD and non-ACLD.
Conclusion: Stable (A)CLD outpatients experience a substantial symptom burden alongside low utilization of preventive healthcare services. These findings call for systematic symptom screening, structured lifestyle counseling, care coordination, patient navigation, and systematic referral pathways with targeted interventions. A dedicated liver care nurse clinic may support the implementation of these action items by symptom triage, patient education, and timely referral to appropriate services.

WED-570-YI

The impact of a dedicated nurse practitioner in streamlining the referral pathway for patients with unresectable colorectal liver metastases in Saudi Arabia

Robyn Reis[1], Bandar Aljudaibi[1], Mohamed Shawkat[1], Dieter Clemens Broering[1]. *[1]King Faisal Specialists Hospital and Research Centre, Riyadh, Saudi Arabia*
Email: rreis3@mail.naz.edu

Background and aims: The referral and assessment process for patients with unresectable colorectal liver metastases (CRLM) for potential liver transplantation is complex and requires meticulous coordination. This study evaluates the role of a dedicated Nurse Practitioner (NP) in optimizing this pathway at a tertiary transplant center.
Method: A retrospective review of 20 consecutive patients referred for liver transplant assessment for unresectable CRLM was conducted. Data extracted included referral patterns, patient demographics, clinical characteristics, mutlidisciplinary decision decisions, and outcomes. The NP's role involved being the central point of contact, ensuring complete data collection, coordinating multidisciplinary team (MDT) meetings, and facilitating patient communication.
Results: The majority of referrals originated from the Central region (55%) in Saudi Arabia, followed by West (25%), North (10%), and South (10%) regions. Of the 20 patients assessed, 12 (60%) were accepted into the liver transplantation pathway. The primary reason for declining 7 patients (35%) was disease progression; one patient's status remained unknown. Ultimately, 4 patients (20% of the total cohort, 33% of those accepted) underwent liver transplantation. The NP's involvement standardized pre-MDT workup, reducing assessment time from a median of 45 to 28 days and ensuring 100% data completeness for discussed cases.
Conclusion: The integration of a dedicated Nurse Practitioner is instrumental in creating an efficient and patient-centered referral pathway for CRLM patients. This model improves coordination, ensures robust data-driven MDT decisions, and effectively identifies suitable candidates for liver transplantation, though disease progression remains a significant barrier to acceptance.

WED-571-YI

Impact of sedentary behaviour on metabolic profiles: insights from a romanian cohort of patients with metabolic dysfunction-associated liver disease (MASLD)

Elena Rezi[1]. *[1]Lucian Blaga University Sibiu, Sibiu, Romania*
Email: crimuntean@yahoo.com

Background and aims: Regular physical activity is essential for avoiding the effects of Metabolic Dysfunction-Associated Liver Disease (MASLD). Given Romania's high cardiovascular mortality rates, understanding activity patterns is crucial. This study aims to evaluate physical activity levels in MASLD patients using the Romanian-validated Physical Activity Index (PAI).
Method: A 24-month observational study was conducted at the Clinical Hospital of Sibiu, involving 71 patients diagnosed with MASLD via ultrasonography. Physical activity was assessed using the PAI Questionnaire. The four levels of the Physical Activity Index are based on occupational activity and weekly hours of exercise or cycling. These levels are inactive, moderately inactive, moderately active and active. Statistical correlations were analysed between PAI scores and several clinical parameters, including age, waist circumference, lipid profile, glycemia, blood pressure, BMI, and platelet count.
Results: Using Pearson's correlation coefficient (r), significant correlations were observed between Physical Activity Index and the following parameters: body mass index (r = 0.69), waist circumference (r = 0.60), triglyceride levels (r = 0.39), blood pressure (r = 0.38), glycaemic levels (r = 0.36). Interestingly, age-based analysis revealed that patients under 50 years of age were significantly less active than those over 50 years of age (p = 0.03).
Conclusion: Physical activity levels in MASLD patients are closely linked to key metabolic markers, including BMI, triglycerides, and glycaemic control. Furthermore, the findings highlight a concerning trend of higher sedentary behaviour among younger MASLD patients, suggesting a need for targeted lifestyle interventions in this demographic.

WED-572

Development of a care pathway for patients with liver cirrhosis

Laurence Seynhaeve[1], Charlotte De Vloo[1], Sofie De Meulder[1], Jef Dewyspelaere[1], Luc Harlet[1], Kymentie Ferdinande[1], Eva Puttevils[2], Jochen Decaestecker[1]. *[1]Department of Hepatology, AZ Delta Hospital, Roeselare, Belgium, Roeselare, Belgium; [2]AZ Delta, management department, Rumbeke, Belgium, Roeselare, Belgium*
Email: laurence.seynhaeve@azdelta.be

Background and aims: Patients with cirrhosis have complex, fluctuating care needs that require coordination between hospital specialists and primary care providers. Decompensated cirrhosis demands frequent in-hospital multidisciplinary management, while compensated cirrhosis is mainly managed in primary care with less intensive monitoring (6-monthly hepatology follow-up). Given the complexity and high prevalence of cirrhosis and the need for multidisciplinary collaboration, a structured care pathway is essential to reduce variability, ensure continuity, and improve patient outcomes.
Method: A care pathway for patients with liver cirrhosis was developed at AZ Delta Hospital, following a simplified version of the seven-phase model of the Network of Clinical Paths, KU Leuven.
Results: Key stakeholders, including patients, family, hepatologists, a nurse specialist, and GPs, were involved in developing a structured care pathway for cirrhosis, covering the trajectory from diagnosis to transplantation or death (excluding palliative patients and HCC under non-curative treatment). Analysis of current care identified bottlenecks such as poor follow-up after hospital discharge and limited hospital–GP communication. A communication booklet and a patient app were introduced to support self-management, monitor daily health parameters, and provide educational resources. The pathway follows key care moments such as diagnosis, hospitalization, and follow-up. The implementation in the hepatology department is ongoing, currently focusing on inpatient and post-discharge care.
Conclusion: By developing this care pathway, we aim to strengthen the coordination and overall quality of care for patients with cirrhosis. The integration of a patient-centered digital app, empowers patients to actively engage in managing their disease. Ultimately, the pathway tries to bridge the gap between hospital and primary care settings and provides a sustainable framework for continuous quality improvement.

WED-573-YI

Cutaneous manifestation and impact of chronic liver disease in resource limit setting

Sharmila Thapa[1,2], Anand Bhat[3]. *[1]Mahabaudha Medical Center, Dhangadhi, Nepal; [2]Mahabaudha Medical Center, Med, Dhangadhi, Nepal; [3]Singh Medical Clinic, Dhangadhi, Nepal*
Email: mbmc.nepal@gmail.com

Background and aims: Nepal have open borders with India and China. Cutaneous manifestations, particularly severe pruritus, skin discoloration, and visible stigmata, are highly prevalent in Chronic Liver Disease (CLD) and significantly impair Quality of Life (QoL).
Method: A cross-sectional study adult CLD patients (diagnosed via standard criteria) were consecutively follow up for a year. Exclusion criteria included acute liver failure or other primary non-hepatic causes of itch. Patient history included detailed assessment of alcohol consumption, noting specific patterns and the use of local brews. Quality of life and Itch Severity assessment done with statistical analysis.
Results: Among the 152 CLD patients were (62% male; mean age 48.5 years) which included viral hepatitis (50%), with Alcoholic Liver Disease (ALD) contributing 35%. Among ALD patients, 85% reported regular consumption average > 450 mL/day of *local brews*. Sixty-one patients (40.1%) reported clinically significant pruritus. The mean (SD) aNRS and 5D-Itch scores for the pruritic cohort were 4.3 and 13.7 respectively. Skin discoloration was frequent: jaundice (45% of total cohort) and non-icteric hyperpigmentation (21%), photoageing in all patients were prominent stigmata. Patients with pruritus demonstrated significantly lower mean scores across all non-somatic domains of the LDQOL compared to the non-pruritic group, with the most profound impact noted on Emotional Functioning ($p < 0.001$) and Sleep Quality ($p < 0.001$). Furthermore, 25% ($n = 38$) of the entire cohort screened positive for high body image distress (BIQLI-N ≥ 40), which was significantly correlated with the presence of hyperpigmentation, photoageing, fungal infections and facial spider angiomas ($p = 0.005$). Pruritus severity was significantly correlated with serum Alkaline Phosphatase levels ($r = 0.39$, $p = 0.003$).
Conclusion: Cutaneous pruritus, skin discoloration, photoageing, and associated stigmata are highly prevalent and impose a major, quantifiable psychosocial burden, including significant body image distress, on CLD patients, particularly those with a history of local alcohol intake. These findings highlight a critical gap in care and underscore the necessity of integrating standardized dermatological and psychological assessment and QoL-focused interventions, early diagnosis and treatment into national CLD management guidelines, ensuring better outcomes and reduced social stigma in low-resource settings.

WED-574

Hepatitis C electronic patient record flags: an opportunity to remove inaccuracies and re-engage lost to follow-up patients

Samuel Uveges[1], Sarah Montague[2], Stephen D Ryder[3], Edward Nicholson[3], Darren Cooper[4]. *[1]Trust Pharmacy, Nottingham, United Kingdom; [2]Nottingham University Hospitals NHS Trust, Viral Hepatitis, Nottingham, United Kingdom; [3]Nottingham University Hospitals NHS Trust, Nottingham, United Kingdom; [4]Hepatitis C Trust, London, United Kingdom*
Email: samuel.uveges@nhs.net

Background and aims: Hepatitis C Virus (HCV) positive patients at a busy teaching hospital in the Midlands (UK), have their electronic patient record (EPR) flagged to alert clinical staff of the patients HCV status. Historically, the removal of these alerts after confirmation of a sustained virological response (SVR) has been inadequate, causing staff to apply unnecessary infection prevention procedures and negatively affecting patients' hospital experience. An audit was performed to ensure only those patients with an active HCV infection were flagged thereby improving accuracy of medical records and help demonstrate true patient caseload.
Method: Hospital Data Analysts provided the hospital numbers for all patients currently marked with a hepatitis C flag. Each patient record was interrogated to establish whether they were still HCV RNA positive. If evidence could be found that demonstrated a cure, spontaneous clearance or the patient was deceased the flag was removed. The remaining hospital numbers were cross-referenced against multiple data sets from partnership organisations and other Hepatitis C Operational Delivery Networks (ODNs) to establish if a test had been conducted elsewhere in the country. Re-Engagement: All remaining patients were contacted by letter to invite them for a blood test and to opt-out of a peer visit. Those that did not opt out were then contacted by a peer from The Hepatitis C Trust.
Results: Data received in March 2024 showed that 1580 patients had an active Hepatitis C flag. Using local hospital records, 247 patients we found to have died and 632 had achieved SVR. partnership organisation data sets found a further 37 SVRs. 390 patients were found to have a current address within the Nottingham ODN, 92 of which were found to have achieved SVR. 267 patients had moved outside of the Nottingham ODN 157 were found to have achieved SVR. During re-engagement 163 letters were sent out from which we received 34 responses. 24 of the patients had achieved SVR, 1 refused further testing and 9 were found to still be HCV RNA Positive and have been referred for follow up with the CNS Team. As of 5th December 2025, a total of 1277 (80.8%) flags have been removed.
Conclusion: After detailed investigation and national collaboration, over 80% of active alerts were no longer necessary and could be

removed. Doing so prevents unnecessary protective measures being deployed by staff, anecdotally improves patient experience and gives a more accurate picture of the prevalence within the hospital.

Portal Hypertension (cirrhosis and non-cirrhosis)

TOP-486

Risk reduction in clinically significant portal hypertension with Belapectin in advanced MASH cirrhosis: results from the NAVIGATE trial

Naim Alkhouri[1], Mazen Noureddin[2], Mary E. Rinella[3], Raj Vuppalanchi[4], Eric Lawitz[5], Edward Mena[6], Khurram Jamil[7], Naga Chalasani[4]. [1]*Summit Clinical Research, Clinical Research Institute of Ohio, San Antonio, TX, United States;* [2]*Houston Methodist Hospital, Houston, TX, United States;* [3]*The University of Chicago Pritzker School of Medicine, Chicago, IL, United States;* [4]*Indiana university school of medicine, Indianapolis, United States;* [5]*The Texas Liver Institute, San Antonio, TX, United States;* [6]*California Research Institute, Pasadena, CA, United States;* [7]*Galectin Therapeutics, Norcross, GA, United States*
Email: naim.alkhouri@gmail.com

Background and aims: MASH cirrhosis with portal hypertension carries a high risk for decompensation, yet no approved therapies exist. Belapectin, a galectin-3 inhibitor, previously demonstrated at 2 mg/kg approximately 50% lower incidence of new varices (11.3% vs 22.3%, p = 0.04) in subjects who completed 18 months of therapy. This study evaluated the effect of belapectin on portal-hypertension risk using Baveno VII criteria and on fibrosis-progression risk using Agile-4.
Method: NAVIGATE (NCT04365868) randomized adults with compensated MASH cirrhosis, portal hypertension, and no baseline varices to belapectin 2 mg/kg, 4 mg/kg, or placebo every 2 weeks for 18 months. Subjects were stratified by T2DM. Of 357 randomized (119/group), 287 completed 18 months of therapy with baseline and end-of-treatment EGD and formed the per-protocol population. Baveno VII categories (CSPH, probable CSPH, no/low-risk) were defined using LSM and platelet count. Agile-4 was used to assess ≥20% worsening, a threshold associated with higher risk of liver-related events.
Results: NAVIGATE enrolled an advanced cohort with a high prevalence of CSPH at baseline. Baseline characteristics were balanced (mean age 60 years; 65% female; platelets 131 × 10^9/L; LSM 24.8 kPa; 67% T2DM). After 18 months, belapectin 2 mg/kg shifted patients toward lower-risk Baveno VII categories. In the CSPH group, rates declined from 33.3% to 25.9% with belapectin versus 34.2% to 32.9% with placebo. Importantly, The no/low-risk category increased from 42.0% to 56.8% with belapectin versus 44.7% to 51.3% with placebo. At week 78, a greater proportion of belapectin-treated subjects improved to the no/low-risk category relative to baseline compared with placebo (p = 0.0073). Agile-4 also favored belapectin: 47% more subjects experienced ≥20% progression in placebo 12/94 (16.9%) compared with belapectin 2 mg/kg 9/97 (11.5%) after 18 months. For AGILE-4 progressors (≥20%), varices developed in 16.7% of placebo patients, compared with none receiving belapectin 2 mg/kg.
Conclusion: Belapectin 2 mg/kg improved multiple validated measures of portal-hypertension risk, including Baveno VII reclassification and Agile-4 trajectories, and significantly reduced new varices. These findings support belapectin's development as a potential therapy for patients with advanced MASH cirrhosis and portal hypertension.

TOP-487-YI

Metformin added to carvedilol improves acute portal pressure response in cirrhosis – a randomized double-blind study topic: portal hypertension and complications/pharmacological therapy

Chitranshu Vashitshtha[1], Garvit Mundra[1], Rakhi Maiwall[1], Shiv Kumar Sarin[1], Vinod Arora[1], Rajan Vijayaraghavan[1], Satender Pal Singh[1], Ashok Kumar Choudhury[1], Ishank Johri[1].
[1]*Institute of liver and biliary sciences, New Delhi, India*
Email: chitranshuv@gmail.com

Background and aims: Carvedilol is a non-selective beta-blocker which reduces portal pressure by ameliorating splanchnic vasodilatation and intrahepatic vasoconstriction. However, a substantial proportion of patients fail to achieve adequate hemodynamic response. Metformin reduces intrahepatic vascular resistance through endothelial and antifibrotic mechanisms and may complement carvedilol. We aimed to evaluate whether adding metformin to carvedilol improves the acute portal pressure response compared with carvedilol alone in patients with cirrhosis.
Method: In this single-centre, randomized, double-blind, placebo-controlled trial [NCT07108075], adults with cirrhosis and portal hypertension undergoing hepatic venous pressure gradient (HVPG) measurement were randomized 1:1 to carvedilol (12.5 mg) plus metformin (1000 mg single oral dose) (group I) or carvedilol plus placebo (group II). Repeat HVPG was performed 120 minutes later. The primary outcome was acute hemodynamic response, defined as HVPG reduction of atleast 20% from baseline or absolute value below 12 mmHg. Secondary outcomes included absolute HVPG change, proportion achieving at least 10 percent reduction, and short-term safety.
Results: Seventy-two patients were randomized (36 per group). Baseline characteristics were comparable (age 48.6 ± 9.4 years, male 96%, alcohol 57%, MASLD 32%, diabetes 15%, platelet count 66 × 10 3/microliter, liver stiffness 43 kPa, spleen stiffness 78 kPa, HVPG 17.6 mmHg). Acute hemodynamic response was achieved more in group I (88.9% vs 63.9%, p = 0.013). The absolute reduction in HVPG was greater in group I (6.6 ± 4.4 mmHg vs 4.0 ± 3.3 mmHg, p = 0.005). A reduction of at least 10 percent occurred in 94.4% (group I) and 88.9% (group II) (p = 0.394). There was no significant difference between the groups in systemic hemodynamic parameters. No serious adverse events were observed.
Conclusion: Adding metformin to carvedilol significantly improves acute portal pressure reduction compared with carvedilol alone without short-term safety concerns. This dual-mechanism approach targeting portal inflow and intrahepatic resistance warrants evaluation for long-term clinical outcomes.

TOP-488

Occurrence of overt hepatic encephalopathy after TIPS in a European prospective cohort of patients with cirrhosis treated by covered TIPS in the 2020s: a EuroTIPS study

Marika Rudler[1], Luc Haudebourg[2], Hélène Larrue[3], Anna Baiges[4], Sonia Torres[4], Luis Téllez[5], Agustín Albillos[5], Charlotte Bouzbib[1], Wim Laleman[6], Marlene Hintersteininger[7], Thomas Reiberger[7], Lukas Hartl[7], Jonel Trebicka[8], Michael Praktiknjo[8], Alvaro Giráldez-Gallego[9], Marco Senzolo[10], Dominik Bettinger[11], Bogdan Procopet[12], Dhiraj Tripathi[13], Silvia Nardelli[14], Pablo Bellot Garcia[15,16,17], Rebeca Pintado Garrido[18], Laure Elkrief[19], Francesco Vizzutti[20], Christophe Bureau[21], Juan Carlos García-Pagán[22], Dominique Thabut[1]. [1]*Sorbonne university, Paris, France;* [2]*Neurology ICU, APHP Sorbonne Universite, Pitie-Salpêtrière Hospital, 83 boulevard de l'hôpital, Paris, France;* [3]*CHU Rangeuil, Toulouse, France;* [4]*Clinic Barcelona, Barcelona, Spain;* [5]*Hospital Ramon y cajal, Madrid, Spain;* [6]*Hospital university Leuven, Leuven, Belgium;* [7]*Medical University of Vienna, Vienna, Austria;* [8]*University hospital Münster, Münster, Germany;* [9]*Virgen del Rocio university hospital, Sevilla, Spain;* [10]*Padova university, Padova, Italy;*

[11]University Freiburg, Freiburg, Germany; [12]Octavian Fodor Regional Institute of Gastroenterology and Hepatology, Cluj, Romania; [13]University hospital Birmingham, Birmingham, United Kingdom; [14]Universita di Roma, Roma, Italy; [15]University General Hospital Dr. Balmis, Liver Unit, Alicante; [16]University General Hospital Dr. Balmis, Liver Unit, Isabial, Alicante; [17]Alicante Institute for Health and Biomedical Research (ISABIAL), Hospital General Universitario Dr. Balmis., Alicante, Spain; [18]Valladolid hospital, Valladolid, Spain; [19]CHu Tours, Tours, France; [20]University of Florence, Florence, Italy; [21]CHU Toulouse, Toulouse, France; [22]Clinic Barcelona, Barcelona, France
Email: marika.rudler@aphp.fr

Background and aims: Transjugular intrahepatic portosystemic shunt (TIPS) improves survival in high-risk patients (pts) with cirrhosis and acute variceal bleeding or with recurrent/refractory ascites. Overt hepatic encephalopathy (OHE) after TIPS is reported in 30–50%. Risk factors for OHE have been mostly described in the setting of retrospective studies with elective TIPS but standard medical treatment evolved over time. We aimed to evaluate the cumulative incidence of OHE after TIPS in the 2020s in a large prospective multicenter European cohort to identify predictive factors for OHE and to assess its prognostic value after TIPS in patients with cirrhosis.
Method: This is an ancillary multicenter study within the EuroTIPS registry, which included all consecutive pts treated with TIPS in 19 centers in Europe. Pts were followed up at 1, 3, 6, 9, and 12 months, or until death or liver transplantation (LT). The primary outcome was the cumulative incidence of OHE, graded according to West Haven criteria, at 12 months, considering death and LT as competing events. Secondary outcomes were (i) predictive factors for OHE and (ii) the impact of OHE on 12-month mortality after TIPS.
Results: A total of 887 pts were included (74.0% male, median age 58 years, 71.1% alcohol-associated liver disease, 18.6% previous OHE; TIPS indication: rescue/salvage 14.1%, pre-emptive 18.6%, ascites/secondary prophylaxis 67.3%). The cumulative incidence of OHE was 28.7%, 43.9%, and 47.7% at 1, 3, and 12 months, respectively. In multivariate analysis, independent predictors of OHE were age (aHR = 1.02, 95%CI [1.01–1.03]), diabetes (aHR = 1.30, 95%CI [1.05–1.62]), any concomitant heart disease (aHR = 1.69, 95%CI [1.26–2.26]), bilirubin (aHR = 1.03, 95%CI [1.00–1.05]), and creatinine (aHR = 1.17, 95%CI [1.03–1.36]). In subgroup analyses, factors associated with OHE included previous OHE and any heart disease in rescue TIPS; MELD score in pre-emptive TIPS; and age, diabetes, any heart disease, previous OHE, and pre-TIPS ammonia levels in elective TIPS. At 12 months, 169 pts died (19.1%) and 79 (8.9%) underwent LT. Independent factors associated with death or LT were age, MELD, previous OHE, and OHE after TIPS ($p < 0.001$ at all time points).
Conclusion: OHE remains a frequent post-TIPS complication in the 2020s' and is associated with increased risk for mortality. Diabetes and any concomittant heart disease emerge as independant risk factors, suggesting that an altered brain reserve plays a role in its pathophysiology.

TOP-502-YI

Longitudinal assessment of body composition and its prognostic impact after TIPS in cirrhosis: a prospective multicenter study (NutriTIPS group)

Simone Di Cola[1], Jakub Gazda[2], Dario Saltini[3], Giulia Polidori[1], Carolina Sorgenti[4], Luigi Maruzzelli[5], Alessio Mastro[6], Giulia Cusi[1], Alessio Barrancotto[1], Lucia Lapenna[1], Federica Gentili[4], Roberto Miraglia[5], Silvia Nardelli[1], Stefania Gioia[1], Francesco Vizzutti[6], Filippo Schepis[3], Manuela Merli[1]. [1]Department of Translational and Precision Medicine, Sapienza University of Rome, Rome, Italy; [2]2nd Department of Internal Medicine, Pavol Jozef Safarik University and L Pasteur University in Kosice, Trieda SNP 1, 040 11, Kosice, Slovakia; [3]Severe Liver Diseases (M.E.C.) Departmental Unit, Department of Medical Specialties, University Hospital of Modena "Policlinico," University of Modena and Reggio Emilia, European Reference Network on Rare Liver Disorders (ERN Rare-Liver), Modena, Italy; [4]Gastroenterology Unit, Santa Maria' Hospital, Terni, Italy; [5]Radiology Unit, Diagnostic and Therapeutic Services, IRCCS ISMETT (Mediterranean Institute for Transplantation and Advanced Specialized Therapies), Palermo, Italy; [6]Department of Experimental and Clinical Medicine, University of Florence, Florence, Italy
Email: simone.dicola@uniroma1.it

Background and aims: Nutritional status, particularly sarcopenia, may influence patients' outcomes after Transjugular Intrahepatic Portosystemic Shunt (TIPS), but the role of myosteatosis and adiposity in this setting are poorly defined. Subcutaneous adipose tissue radiodensity (RSAT) reflects adipose tissue quality and degree of inflammation. Retrospective data have shown that both muscle and adipose tissue may be modified following TIPS procedure. We aimed to evaluate body composition changes after TIPS and their prognostic value, focusing on overt hepatic encephalopathy (oHE) within 6 months.
Method: Consecutive patients with cirrhosis undergoing TIPS were prospectively enrolled in six Italian centers (2022–2025). Clinical, hemodynamic and nutritional data were collected. Body composition [skeletal muscle index (SMI), muscle attenuation (MA), visceral and subcutaneous adipose tissue (VAT, SAT), and RSAT] was assessed by CT at L3–L4 within 90 days before TIPS and at 6 months. Outcomes were recorded during 12-month follow-up.
Results: Among 102 patients (75% male; median age 61 years, IQR 54–67), baseline sarcopenia and myosteatosis were present in 54% and 81%. Median VAT and SAT were 106 and 134 mm^2; median RSAT was −92 HU (IQR −98 to −78), with 23 patients (22.5%) showing high RSAT. Three patients were excluded for early TIPS dysfunction; 84 (82%) completed 6-month follow up. SMI significantly increased (51.9 vs 48.0, $p < 0.001$); 34 patients (41%) showed ≥10% SMI increase and 15 (18%) reversed sarcopenia. VAT decreased (109.7 vs 146.9 mm^2, $p < 0.001$), SAT increased (194.7 vs 172.6 mm^2, $p < 0.001$), while RSAT remained substantially unmodified (−85.7 vs −88.1 HU, $p = 0.78$). oHE occurred in 44%. Basal SMI and MA did not differ according to oHE occurrence, whereas high RSAT was associated with an increased risk of post-TIPS oHE ($p = 0.04$), TIPS failure ($p = 0.012$), and failure to control ascites ($p = 0.006$). Sarcopenia reversal was associated with fewer bacterial infections (4% vs 26%, $p = 0.04$). At multivariable analysis, high RSAT independently predicted post-TIPS oHE after adjustment for age, MELD and prior oHE (HR 1.02, 95% CI 1.00–1.04, $p = 0.016$).
Conclusion: This first prospective multicenter study shows that TIPS improves muscle mass and adipose tissue distribution, reversing sarcopenia in 18% at 6 months. RSAT emerged as a novel prognostic marker for post-TIPS oHE, suggesting that adipose tissue quality may outperform muscle metrics for risk stratification.

TOP-504-YI

Liver and spleen stiffness measurements by vibration – controlled transient elastography predict liver-related outcomes of patients with porto-sinusoidal vascular disorder

Lucile Moga[1], Margaux Barbe[1], Fanny Turon[2], Ainhoa Sánchez-Lorenzo[3], Arathi Venu[4], Laure Elkrief[5], Lorenz Balcar[6], Lucia Giuli[7], Elton Dajti[8], Raquel Gonçalves[9], Dario Saltini[10], Martina Lucà[11], Andrea Peña Rosado[12], Giovanni Vitale[13], Andreea Fodor[14], Antonina Antonenko[15], Francisco Capinha[16], Ozgur Koc[17], Nicola Pugliese[18], Magdalena Meszaros[19], Michael Praktiknjo[20], Yu Jun Wong[21], Valérie Paradis[22], Aurélie Plessier[1], Carlos Pardo[2], Juan Carlos García-Pagán[2], Bernhard Scheiner[6], Jonel Trebicka[20], Tom Gevers[17], Carlos Noronha Ferreira[23], Annalisa Berzigotti[24], Bogdan Procopet[14], Laura Turco[8], José Ferrusquía-Acosta[12,25], Giulia Tosetti[11], Filippo Schepis[10], Joel Silva[9], Federico Ravaioli[26], Francesco Santopaolo[7], Georg Semmler[6], Arun Valsan[4], Luis Téllez[3], Virginia Hernandez-Gea[2], Pierre-Emmanuel Rautou[1]. [1]Service d'Hépatologie, AP-HP, Hôpital Beaujon, DMU DIGEST, Centre de

Référence des Maladies Vasculaires du Foie, FILFOIE, Université Paris-Cité, Inserm, Centre de recherche sur l'inflammation, UMR 1149, ERN RARE-LIVER, Clichy, France; [2]Barcelona Hepatic Hemodynamic Laboratory, Liver Unit, Hospital Clínic, Clínic Barcelona, FRCB-IDIBAPS (Fundació de Recerca Clínic Barcelona-Institut d'Investigacions Biomèdiques August Pi i Sunyer), CIBEREHD (Centro de Investigación Biomédica en Red Enfermedades Hepáticas y Digestivas), Barcelona, Spain; [3]Department of Gastroenterology and Hepatology, Hospital Universitario Ramón y Cajal, Instituto Ramón y Cajal de Investigación Sanitaria (IRYCIS), Centro de Investigación Biomédica en Red de Enfermedades Hepáticas y Digestivas (CIBEREHD), Universidad de Alcalá, Madrid, Spain, Madrid, Spain; [4]Department of Hepatology & Liver transplantation, Amrita Institute of Medical Sciences, Kochi, India; [5]Service d'hépato-gastroentérologie, Hôpital Trousseau, CHRU de Tours and Faculté de médecine de Tours, Université Paris-Cité, Inserm, Centre de recherche sur l'inflammation, UMR 1149, Paris, Tours, France; [6]Division of Gastroenterology and Hepatology, Department of Medicine III, Medical University of Vienna, Clinical Research Group MOTION, Medical University of Vienna, Vienna, Austria; [7]Liver Unit, CEMAD Centro Malattie Dell'apparato Digerente, Medicina Interna e Gastroenterologia, Fondazione Policlinico Universitario Agostino Gemelli IRCCS, Roma, Italy; [8]Gastroenterology Unit, IRCCS Azienda Ospedaliero-Universitaria di Bologna, ERN-RareLiver (Health Care Provider of the European Reference Network on Rare Liver Disorders), Bologna, Italy; [9]Gastroenterology Department, Centro Hospitalar e Universitário de São João, Porto, Portugal; [10]Severe Liver Diseases (M.E.C.) Departmental Unit, Department of Medical Specialties, University Hospital of Modena "Policlinico," University of Modena and Reggio Emilia, European Reference Network on Rare Liver Disorders (ERN RARER-LIVER), Modena, Italy; [11]Division of Gastroenterology and Hepatology, Foundation IRCCS Ca' Granda Ospedale Maggiore Policlinico, Milano, Italy; [12]Liver Unit. Parc Taulí Hospital Universitari. Institut d'Investigació i Innovació Parc Taulí (I3PT-CERCA), Sabadell, Spain; [13]Internal Medicine Unit for the Treatment of Severe Organ Failure, IRCCS Azienda Ospedaliero-Universitaria di Bologna, Health Care Provider of the European Reference Network on Rare Liver Disorders (ERN RARE-LIVER), Bologna, Italy; [14]Regional Institute of Gastroenterology and Hepatology "Octavian Fodor", Hepatology Department, University of Medicine and Pharmacy "Iuliu Hatieganu", 3rd Medical Clinic, Cluj-Napoca, Romania; [15]Department of visceral surgery and medicine, University hospital of Berne, University of Berne, Berne, Switzerland; [16]Serviço de Gastrenterologia e Hepatologia, Hospital de Santa Maria, Centro Hospitalar Universitário Lisboa Norte, Lisboa, Portugal; [17]Department of Gastroenterology and Hepatology, Maastricht University Medical Center, Maastricht, Netherlands; [18]Division of Internal Medicine and Hepatology, Department of Gastroenterology, IRCCS Humanitas Research Hospital, Rozzano, Italy; [19]Service d'Hépato-gastro-entérologie, CHU Montpellier Saint Eloi, Montpellier, France; [20]Department of Medicine B, University Hospital Münster, Münster, Germany; [21]Department of Gastroenterology & Hepatology, Changi General Hospital, Singapore; Duke-NUS Medical School, Singapore, Singapore; [22]Département d'Anatomie Pathologique, Hôpital Beaujon, Centre de recherche sur l'inflammation,Université Paris-Cité, Inserm, Clichy, France; [23]Serviço de Gastrenterologia e Hepatologia, Hospital de Santa Maria, Unidade Local de Saúde Santa Maria, Lisboa, Portugal; [24]Department of visceral surgery and medicine, University hospital of Berne, University of Berne, Berne, Switzerland; [25]Liver Unit. Parc Taulí Hospital Universitari. Institut d'Investigació i Innovació Parc Taulí (I3PT-CERCA), Universitat Autònoma de Barcelona, Sabadell, Spain; [26]Division of Internal Medicine, Hepatobiliary and Immunoallergic Diseases, IRCCS Azienda Ospedaliero-Universitaria di Bologna, Department of Medical and Surgical Sciences (DIMEC), University of Bologna, Bologna, Italy
Email: lucile.moga@gmail.com

Background and aims: In patients with cirrhosis, liver (LSM) and spleen stiffness measurement (SSM) by vibration-controlled transient elastography (VCTE) reflect the severity of portal hypertension (PH) and the risk of hepatic decompensation. By contrast, in patients with porto-sinusoidal vascular disorder (PSVD), LSM is generally low, whereas SSM is associated with the presence of high-risk varices. This study aimed to assess the prognostic performance of LSM and SSM by VCTE in patients with PSVD and signs of PH.
Method: This retrospective study included all patients with histologically proven PSVD and signs of PH at the time of diagnosis, who underwent ≥ 1 LSM +/− SSM by VCTE with a minimum of 1 year of subsequent follow-up. The population was divided into a monocentric derivation cohort and a multicentric validation cohort from 20 VALDIG centres. Study entry was defined as the date of the 1st VCTE. Follow-up data, including liver-related events (LRE), were recorded until the last visit or death. LRE were defined as variceal bleeding, ascites, hepatic encephalopathy, primary liver cancer, hepatopulmonary syndrome, porto-pulmonary hypertension, liver transplantation, and liver-related death. We analysed survival without LRE, considering non-liver related death as a competing event.
Results: 203 patients were included in the derivation cohort: 55% men, median age 54. All patients had ≥ 1 LSM, and 176 had ≥ 1 SSM. Median (IQR) 1st LSM and SSM values were 7.6 (6.1–11.1) kPa and 44 (29–73) kPa, respectively. 50 patients (28%) experienced ≥ 1 LRE at 5 years of the 1st VCTE. In the validation cohort (n = 383), 30% of the patients experienced ≥ 1 LRE at 5 years. In the derivation cohort, the 5-year LRE-free survival was of 94% in patients with LSM < 10 kPa and SSM ≤ 40 kPa, *vs.* 74% in those with either LSM ≥ 10 kPa or SSM > 40 kPa, *vs*. 29% in patients with LSM ≥ 10 kPa and SSM > 40 kPa. Similar results were observed in the validation cohort, with a 5-year LRE-free survival of 80%, 70%, and 29%, respectively. In the derivation cohort, 120 patients had a 2nd VCTE ≥ 2 years after the 1st, with ≥ 1 year of subsequent follow-up; the 5-year LRE-free survival after this 2nd VCTE according to the aforementioned LSM- and SSM-based categories, was 92%, 66%, and 0%, respectively.
Conclusion: LSM and SSM by VCTE predict LRE in patients with PSVD. Three categories of risk based on LSM and SSM could be useful for adapting surveillance frequency in routine care, and for identifying high-risk patients for clinical trials.

THU-415

Patient-reported quality of life in porto-sinusoidal vascular disease: insights from a qualitative study and recommendations for clinical research

Anouck Alary[1], Pierre-Emmanuel Rautou[2,3], Marco Senzolo[4], Alberto Zanetto[4], Carlotta Magnani[1], Aurélie Plessier[2,3], Virginia Hernández-Gea[5,6], Agnes Dumas[1]. *[1]INSERM, Aix Marseille Univ, IRD, ISSPAM, SESSTIM, Sciences Economiques & Sociales de la Santé & Traitement de l'Information Médicale, Equipe CALIPSO, Marseille, France; [2]Université Paris-Cité, Inserm, Centre de recherche sur l'inflammation, UMR 1149, Paris, France; [3]AP-HP, Hôpital Beaujon, Service d'Hépatologie, DMU DIGEST, Centre de Référence des Maladies Vasculaires du Foie, FILFOIE, ERN RARE-LIVER, Clichy, France; [4]University of Padova, Padua, Italy; [5]Hepatic Hemodynamic Laboratory, Liver Unit, Hospital Clínic, Clínic Barcelona, Health Care Provider of the European Reference Network on Rare Liver Disorders (ERN-RareLiver), CSUR Centro de referencia del Sistema Nacional de Salud en Enfermedad Hepática Vascular Compleja en adultos. Fundació de Recerca Clínic Barcelona-Institut d'Investigacions Biomèdiques August Pi i Sunyer (FRCB-IDIBAPS), Barcelona, Spain; [6]Centro de Investigación Biomédica en Red Enfermedades Hepáticas y Digestivas (CIBEREHD), Madrid, Spain; AGAUR SGR2021 01115, Medicine Department, Faculty of Medicine, and health Science, Universitat de Barcelona, Barcelona, Spain*
Email: anouck.alary@inserm.fr

Background and aims: Porto-sinusoidal vascular disease (PSVD) is a rare vascular liver disorder characterized by portal hypertension (PH) in the absence of cirrhosis. Therapeutic advancements are limited in PSVD partially due to the lack of reliable surrogate end-points for clinical trials and the lack of data on patients' health-related quality of life (HRQoL). This study aimed to explore the HRQoL of patients with

PSVD and to identify relevant patient reported outcomes and measures suitable for use in future clinical research.
Method: We conducted a multicenter qualitative study in France, Spain, and Italy. A stratified purposeful sample was recruited to ensure diversity in disease stage, age, and sex. Semi-structured, in-depth interviews were conducted by experts in qualitative methods using an interview guide co-developed with members of patients' organizations. Interviews were audio-recorded, transcribed verbatim, and analyzed using inductive thematic analysis. During analysis, coding and theme development were discussed iteratively with clinicians and patients' organizations to ensure relevance and validity.
Results: Interviews were conducted with 16 patients: 8 women, 8 men; median age [interquartile range]: 48 [37–61]; 4 without signs of portal hypertension (PH), 5 with signs of PH without clinical complications, 7 with clinical complications. Anxiety was reported at all stages of the disease, although its manifestations increased with clinical evolution. In contrast, fatigue and pain became predominant symptoms in more advanced stages, particularly among patients with PH-related complications. The disease also affected reproductive health in women, work capacity in professionally active patients, and overall social functioning in those experiencing fatigue and digestive discomfort. The invisibility and rarity of PSVD further contributed to feelings of isolation. Patients with comorbidities or associated diseases described their experience as that of a "total illness" in which PSVD-related symptoms were difficult to disentangle from that of other diseases.
Conclusion: PSVD has a substantial and multidimensional impact on HRQoL. Generic HRQoL measures such as SF-36 are insufficient to capture liver-related symptoms and support the use of disease-specific tools such as the CLDQ, along with specific scales or items assessing fatigue and its unpredictability, anxiety, and the effects of the disease on reproductive health, work, and social functioning.

THU-416
Sucralfate plus Pantoprazole versus Pantoprazole alone for healing of post–endoscopic variceal ligation ulcers: an open label randomized controlled trial

Vijay Alexander[1], Shaik Riyaz[2], M Asisha Janeela[2], Anoop John[2], S Akilesh[2], Santhosh Kumar[2], Uday Zachariah[2], Ashish Goel[2].
[1]Christian Medical College, Vellore, India, Vellore, India; [2]Christian Medical College, Vellore, India
Email: vijayalexander@cmcvellore.ac.in

Background and aims: Pharmacologic strategies to enhance ulcer healing and prevent ulcer related bleeding after endoscopic variceal ligation (EVL) remain uncertain. Despite limited supporting evidence, sucralfate is frequently prescribed alongside proton pump inhibitors (PPIs) to reduce post-EVL ulcer burden and bleeding. We conducted a randomized controlled trial to evaluate whether adjunctive sucralfate provides incremental benefit over PPI monotherapy for post-EVL ulcer healing.
Method: In this open-label, randomized controlled trial, adults with portal hypertension and Child–Turcotte–Pugh (CTP) class A or B cirrhosis undergoing EVL as secondary prophylaxis were randomized (1:1) to receive pantoprazole 40 mg twice daily with or without sucralfate 1 g four times daily for 2 weeks. Follow-up endoscopy at 14–21 days assessed the presence, number, and dimensions of post-EVL ulcers. Secondary outcomes included ulcer-related bleeding and patient-reported post-EVL chest pain.
Results: Forty-eight patients (mean age 51.9 ± 12.3 years; alcohol-related cirrhosis 43.8%; MASLD 41.6%) were randomized to pantoprazole plus sucralfate (n = 24) or pantoprazole alone (n = 24). Baseline liver disease severity was comparable between groups (median CTP score 7 [5–9]; mean MELD score 11.8 ± 4.0 vs 13.6 ± 4.2; p = 0.13). All patients received non-selective beta-blocker therapy following endoscopy, predominantly carvedilol (40/48, 83.3%), with the remainder receiving propranolol (8/48, 16.7%). Follow-up endoscopy was completed in 44 patients with two patients lost to follow up in each arm. The number of bands applied per session was similar (median 4 [1–4] vs 4 [1–5]; p = 0.67). The prevalence of post-EVL ulcers did not differ between groups (50% vs 37.5%; p = 0.76), nor did the median number of ulcers per patient (2 [1–3] in both groups; p = 0.41). Ulcer dimensions were comparable, including maximum length (5.0 [4.0–6.0] vs 4.0 [4.0–8.0] mm; p = 0.94) and width (2.5 [2.5–5.0] vs 2.5 [2.5–5.0] mm; p = 0.65). Post-EVL chest pain occurred at similar frequencies (27.3% vs 45.5%). No patient in either group developed post-EVL ulcer bleeding during the study period. Sucralfate was well tolerated, with no treatment-related adverse events.
Conclusion: Adjunctive sucralfate does not improve endoscopic ulcer healing or post-EVL symptoms compared with PPI therapy alone. These findings do not support the routine use of sucralfate following EVL for ulcer healing or bleeding prevention.

THU-417
Histologic assessment for portal hypertension in porto-sinusoidal vascular disease

Wesam Aleyadeh[1], Sana Pirzada[1], Sawsan Fathma[1], Christopher Koh[1], David E Kleiner[1], Theo Heller[1]. *[1]National Institutes of Health, Bethesda, MD, United States*
Email: wesamaleyadeh@gmail.com

Background and aims: Porto-sinusoidal vascular disease (PSVD) encompasses diverse histologic lesions including nodular regenerative hyperplasia (NRH), portal vein muscularization, and stenosis. The discriminative value of individual histologic features for identifying portal hypertension remains incompletely characterized. We examined associations between specific histologic lesions, portal hypertension features, and laboratory markers.
Method: Retrospective analysis of 40 patients evaluated for suspected PSVD at a tertiary center between 2004 and 2025 after excluding cirrhosis, advanced fibrosis, and congenital hepatic fibrosis. Histologic features were assessed at index biopsy and included nodular regenerative hyperplasia, muscularized portal veins, portal vein stenosis, regenerative changes, and abnormal vascular repartition. Portal hypertension was defined as HVPG >5 mmHg and/or clinical signs (varices, collaterals, gastropathy). Associations with portal hypertension features and laboratory markers were examined using Fisher's exact test, Wilcoxon rank-sum test, and Spearman correlations with Benjamini-Hochberg FDR correction.
Results: The cohort comprised 40 patients: median age 45 years (IQR 35–56), 48% female, 87.5% White, mean BMI 23 kg/m^2, with common variable immunodeficiency as predominant etiology (35%). Biochemical profile was predominantly cholestatic (R-factor 1.0, IQR 0.7–1.5). NRH (60%, n = 24) predicted portal hypertension (83.3% vs 56.2%, OR 3.75, p = 0.08) and correlated with elevated HVPG (9 vs 5 mmHg, p = 0.012), transient elastography (9.1 vs 6.1 kPa, p = 0.007), FIB-4 (4.24 vs 1.85, p = 0.011), and total bilirubin (0.95 vs 0.55 mg/dL, p = 0.024). Muscularized portal veins (22.5%, n = 9) predicted HVPG ≥10: 55.6% vs 12.9%, OR 7.83, p = 0.016. Portal vein stenosis ≥50% (27.5%, n = 11) associated with elevated MELD 3.0 (7 vs 6, p = 0.006). Paradoxically, isolated regenerative changes (37.5%, n = 15) showed inverse associations: lower portal hypertension (53.3% vs 84%, OR 0.23, p = 0.065), HVPG (5 vs 9 mmHg, p = 0.012), bilirubin (0.5 vs 1.0 mg/dL, p = 0.006), and FIB-4 (2.12 vs 4.2, p = 0.043), suggesting these represent improved biochemical and clinical endpoints.
Conclusion: NRH and muscularized portal veins discriminate portal hypertension severity in PSVD on index biopsy, correlating with hemodynamic and laboratory markers. Isolated regenerative changes may be associated with less disease burden. These findings guide pathologists in identifying high-risk vascular remodeling patterns in suspected PSVD.

THU-418

Salvage transjugular intrahepatic portosystemic shunt in patients with hepatocellular carcinoma: a multicenter study on safety and oncological outcomes

Manon Allaire[1], Camille Imparato[2], Jihyun An[3], Luo Xuefeng[4], Maria Nieto[5], Luis Téllez[6], Charlotte Bouzbib[7], Hélène Larrue[8], Andres Conthe[9], Filippo Schepis[10], Coralie Fleurent[11], Valentin Rolle[12], Hélène Regnault[13], Mehdi Younes[14], Suliman Alhaidari[15], Carmen Álvarez-Navascués[16], Magdalena Meszaros[17], Coskun Ozer Demirtas[18], Osama Khattab[19], Anna Baiges[20], Elba Llop Herrera[21], Sarah Mouri[7], Ju Hyun Shim[22], Josune Cabello Calleja[23], Agustín Albillos[6], Alvaro Giráldez-Gallego[5], Paul Girot[24], Giuliana Amaddeo[13], Puneeta Tandon[15], Lucy Meunier[17], María-Vega Catalina[9], Jean Paul Cervoni[14], Dario Saltini[10], Laure Elkrief[11], Jiacheng Cao[21], Vincent Di Martino[14], Meral Akdogan Kayhan[25], Michael Praktiknjo[23], Ju Dong Yang[19], Hale Gokcan[25], Jonel Trebicka[23], Caroline Lemaitre[26], Dominique Thabut[7], Juan Carlos García-Pagán[20], Christophe Bureau[8], Marika Rudler[7]. *[1]AP-HP Sorbonne Université, Hôpital Universitaire Pitié-Salpêtrière, Service d'Hépato-gastroentérologie, Paris, France, Centre de Recherche des Cordeliers, Université Paris Cité, Sorbonne Université, Inserm, F-75006, Paris, France, Genomic Instability, Metabolism, Immunity and Liver Tumorigenesis laboratory, Equipe Labellisée LIGUE 2023, Paris, France, Paris, France; [2]Service d'hépato-gastroentérologie, CHU Charles Nicolle, Rouen, France; [3]Department of Gastroenterology and Hepatology, Hanyang University College of Medicine, Guri, Republic of Korea, Guri, Korea, Rep. of South; [4]Department of Orthopaedic Surgery, The First Affiliated Hospital of Chongqing Medical University, Chongqing, 400016, China, Chongqing, China; [5]UCM Digestive Diseases and CIBEREHD, University Hospital Virgen del Rocío, Institute of Biomedicine of Seville (CSIC/HUVR/US), University of Seville, Seville, Spain, Sevilla, Spain; [6]Gastroenterology and Hepatology Department, Hospital Universitario Ramón y Cajal- IRYCIS, Madrid, Spain, MAdrid, Spain; [7]AP-HP Sorbonne Université, Hôpital Universitaire Pitié-Salpêtrière, Service d'Hépato-gastroentérologie, Paris, France, Paris, France; [8]Service d'Hépatologie Hôpital Rangueil CHU Toulouse et Université de Toulouse, Toulouse, France, Toulouse, France; [9]Aparato Digestivo, Hospital General Universitario Gregorio Marañón, Madrid, Madrid, Spain; [10]Severe Liver Diseases (M.E.C.) Departmental Unit, Department of Medical Specialties, University Hospital of Modena "Policlinico", University of Modena and Reggio Emilia, European Reference Network on Rare Liver Disorders (ERN Rare-Liver), Modena, Italy, Modena, Italy; [11]Service d'Hépato-Gastroentérologie, Hôpital Trousseau - CHU de Tours, Tours, France, Tours, France; [12]Service d'Hépato-gastroentérologie, CHU Poitiers, Poitiers, France; [13]Service d'Hépatologie, AP-HP Henri Mondor, Créteil, France, Créteil, France; [14]Service d'Hépatologie et Soins Intensifs Digestifs, CHU Jean Minjoz, Besançon, France, Besançon, France; [15]Division of Gastroenterology (Liver Unit), Department of Medicine, University of Alberta Zeidler Ledcor Centre, Edmonton, Alberta, Canada, Alberta, Canada; [16]Department of Gastroenterology and Hepatology, Hospital Universitario Central de Asturias, Oviedo, Spain, Oviedo, Spain; [17]Service Hépato-Gastroentérologie, CHU Montpellier, Montpellier, France, Montpellier, France; [18]Marmara University, School of Medicine, Department of Gastroenterology and Hepatology, Istanbul, Turkey, Yale University, Section of Digestive Diseases, CT, United States, Istanbul, Türkiye; [19]Health Sciences Associate Clinical Professor of Medicine, University of California, Los Angeles, United States, Los Angeles, United States; [20]Liver Unit, Hospital Clínic, Institut de Investigacions Biomèdiques August Pi i Sunyer (IDIBAPS), Barcelona, Spain; [21]Department of Gastroenterology and Hepatology, Hospital Universitario Puerta de Hierro Majadahonda, Madrid, Spain; [22]Department of Gastroenterology, Liver Cancer Center, Asan Medical Center, University of Ulsan College of Medicine, Seoul, Korea, Rep. of South; [23]Department of Internal Medicine B, University Hospital Muenster, Albert-Schweitzer-Campus 1, A148149, Muenster, Germany; [24]Service d'hépato-gastroentérologie, CHD Vendée, La-Roche-sur-Yon, France; [25]Ankara City Hospital, Department of Gastroenterology, Ankara, Türkiye; [26]Service d'Hépato-Gastroentérologie, Groupe Hospitalier du Havre, Le Havre, France*
Email: allama5@hotmail.fr

Background and aims: The role of salvage/rescue transjugular intrahepatic portosystemic shunt (TIPS) in patients with hepatocellular carcinoma (HCC) remains controversial. This study aimed to evaluate outcomes in patients with active HCC undergoing salvage/rescue TIPS.
Method: This retrospective multicenter study across 18 centers included consecutive patients with active HCC between 2010 and 2025 who underwent salvage (persistent bleeding despite therapy) and rescue (early rebleeding within 5 days) TIPS for acute variceal bleeding. Mortality at 42 days, overall survival (OS), and HCC-related outcomes were analyzed.
Results: 49 patients with active HCC were included. Viral hepatitis was the main etiology (61%); 78% had prior AVB. Median MELD score was 14, 22% were Child-Pugh C, and 47% ALBI grade 3. Median largest tumor diameter was 29 mm; 59% had a single lesion, 16% macrovascular invasion, and 6% extrahepatic metastases. Most patients were BCLC stage A (47%), and 65% were within Milan criteria. At 42 days, 24% of patients had died. In univariate analysis, older age was the only factor associated with 42-day mortality (HR 1.10, $p = 0.01$); no liver function parameters or HCC-related features were significantly associated with early mortality. Median OS was 17 months and was 24 months in patients within the Milan criteria compared to 9 months with those outside the criteria ($p = 0.14$). In univariate analysis, prothrombin time (HR 0.97, $p = 0.04$), presence of ascites at the time of TIPS (HR 2.39, $p = 0.02$), and pre-TIPS hepatic venous pressure gradient (HR 1.06, $p = 0.039$) were associated with mortality. Rebleeding occured in 10% of patients, hepatic encephalopathy in 39%, and cardiac failure in 6%, and no tumor dissemination was observed at imaging during HCC surveillance. Following salvage/rescue TIPS, 55% of patients received HCC therapy, including liver transplantation (n = 11), ablation (n = 4, all achieving complete response (CR)), locoregional therapies (n = 9; 58% CR, 14% partial response, 14% stable disease, and 14% progressive disease), and systemic treatments (n = 3).
Conclusion: These preliminary data suggest that liver function parameters may influence prognosis more than tumor characteristics. HCC should not been considered as a definite contraindication for rescue TIPS. Validation in a larger cohort, currently being collected, is warranted.

THU-419

Spleen stiffness measurement by VCTE stratifies the risk of high-risk varices in patients with vascular liver disease

Lucie Anémone[1], Théo Izopet[1], Marie-Angèle Robic[1], Sophie Metivier[1], Patricia Soubre[1], Nancy Arnal[1], Assia Bouali[1], Cécile Cussac[1], Clémence Vignon[1], Maxime Castagnede[2], Jean Marie Peron[1], Christophe Bureau[1], Hélène Larrue[1]. *[1]Toulouse university hospital, Toulouse, France; [2]AP-HP Sorbonne Université, Hôpital Universitaire Pitié-Salpêtrière, Paris, France*
Email: anemone.l@chu-toulouse.fr

Background and aims: The Baveno VII consensus suggests that the number of spared endoscopies can be reduced by adding spleen stiffness measurement using vibration-controlled transient elastography (SSM-VCTE) to liver stiffness in patients with compensated advanced chronic liver disease (cACLD). However, in patients with vascular liver disease (VLD), screening endoscopy is currently recommended for all, as liver stiffness is often low despite the presence of portal hypertension (PHT). A recent study showed that SSM-VCTE ≤40 kPa combined with serum bilirubin level <1 mg/dL identifies patients with porto-sinusoidal vascular disorder (PSVD) and PHT with a probability of high-risk varices (HRV) below 5%. The

aim of this study was to evaluate the performance of SSM-VCTE for predicting HRV across the full spectrum of VLD at risk of PHT.
Method: We prospectively included patients with a confirmed diagnosis of VLD who underwent SSM-VCTE (100-Hz FibroScan® probe) and a recent upper gastrointestinal endoscopy. SSM measurements were performed blinded to endoscopic findings. HRV were defined as large esophageal varices, small varices with red wale signs, or a history of endoscopic band ligation.
Results: Eighty-one patients were included. The mean age was 47 ± 15 years, 47% were male, 54% had portal vein cavernoma, and 42% had PSVD (the remaining 4% had other causes of non-cirrhotic PHT). Overall, 51% of patients had HRV. In univariate analysis, lower platelet count, higher SSM-VCTE, elevated serum bilirubin, and the presence of portosystemic collaterals were associated with HRV. In multivariable analysis, only SSM-VCTE remained independently associated with HRV (32.6 ± 21 vs. 68.5 ± 22 kPa). SSM-VCTE demonstrated the highest diagnostic accuracy for HRV, with an AUROC of 0.874 (95% CI 0.791–0.958). Notably, combining an SSM-VCTE cutoff of 35 kPa with serum bilirubin <1 mg/dL identified a subgroup in which no patient had HRV.
Conclusion: In patients with vascular liver disease, SSM-VCTE appears to be a valuable non-invasive tool for ruling out high-risk varices and may allow the avoidance of screening endoscopy in selected patients.

THU-420

Liver and spleen elastographies accuracy in detecting esophageal varices: comparison of MASLD with mixed etiologies populations

Flavia Fernandes[1], Cristiane Tovo[2], Joao Marcello de Araujo Neto[3], Cristiane A. Villela-Nogueira[3], Juliana Piedade[4], Victoria Verissimo[1], Pedro Machado[1], Andrew Fernandes[1], Natalia Wajbrot[3], Liliana Mendes[5], Claudia Pinto Oliveira[6], Gleicy Pereira[6], Marcelo Chagas[1], Daniela Louro[5], Luisa Amorim[7], Natalia Ayres[2], Aik Martins[8], Hugo Perazzo[9], Carlos Antonio Rodrigues Terra Filho[1].
[1]State University of Rio de Janeiro, Rio de Janeiro, Brazil; [2]Serviço de Gastroenterologia e Hepatologia da Santa Casa de Misericórdia de Porto Alegre, Porto Alegre, Brazil; [3]Federal University of Rio de Janeiro, Rio de Janeiro, Brazil; [4]Hospital Federal de Bonsucesso, Rio de Janeiro, Brazil; [5]Hospital de Base do Distrito Federal, Brasilia, Brazil; [6]Hospital das Clínicas da Faculdade de Medicina da U S P, São Paulo, Brazil; [7]Hospital Federal da Lagoa, Rio de Janeiro, Brazil; [8]Universidade Federal de São PAulo, São Paulo, Brazil; [9]Instituto NAcional de Infectologia Evandro Chagas, FioCruz, Rio de Janeiro, Brazil
Email: ffernandes.flavia@gmail.com

Background and aims: Esophageal varices (EV) define clinically significant portal hypertension with high prognostic value. Recently, liver (LSM) and spleen (SSM) stiffness measurement by transient elastography have been used as noninvasive tests (NITS) for the presence of EV.
To evaluate LSM and SSM as NITS for diagnosing EV in patients with compensated cirrhosis of mixed etiologies comparing their performance with those with MASLD.
Method: Prospective, multicentric study, in individuals with cirrhosis of mixed etiologies and MASLD, without previous decompensation, submitted to EV screening by upper GI endoscopy, LSM and SSM (Fibroscan 630) within a maximal interval of one year.
Results: Included individuals were divided into two groups: general group (GG) with mixed etiologies and MASLD group (MG). In the GG (n = 288); 51.4% were female; 55% type 2 diabetes (T2DM); 41% had EV; mean age 64 ± 13 years; BMI 28.4 ± 6; waist circumference 100 (±14) cm; spleen length 12.6 ± 2.8 cm; platelet count 137.000 (± 68.000); LSM 15.5 ± 15 kPa; SSM 39.0 ± 20 kPa; SSM failure 8.3%. In patients without EV when compared to patients with EV mean LSM (16.6 ± 12 kPa vs 27.5 ± 18, p 0,001) and SSM (35.8 ± 17 kPa vs 52.2 ± 21, p 0,001) were significantly lower. In AUROC analyses the best cut-off points for EV detection were 15.0 kPa (AUROC 0.72; CI 95%: 0.66–0.78) for LSM, and 48.0 kPa (AUROC 0.73; CI 95% 0.67–0.80) for SSM. In the MG (n = 129); 71% were female; 80% T2DM; 39.5% had EV; mean age 64 ± 9 years; BMI 30 ± 5.6; waist circumference 107 ± 13 cm; spleen length 12.7 ± 2.6 cm; platelet count 137.000 ± 68.000, LSM 18.6 ± 16 kPa; SSM 41.15 ± 19 kPa; SSM failure 11,6%. In patients without EV when compared to patients with EV mean LSM (19.0 ± 13 kPa vs 29.0 ± 18, p 0,001) and SSM (37.0 ± 15 kPa vs 53.0 ± 20.0, p 0,001) were significantly lower. In AUROC analyses the best cut-off points for EV detection were 21.0 kPa (AUROC 0.72; CI 95%: 0.63–0.82) for LSM, and 48.0 kPa (AUROC 0.74; CI 95% 0.65–0.83) for SSM. Groups characteristics were similar except for gender and T2DM prevalence.
Conclusion: In a population with high BMI and waist circumference both LSM and SSM performed well in detecting EV in patients with compensated cirrhosis. In the MASLD group LSM, but not SSM, cut-off point for detecting EV was higher than in the mixed etiologies group. There was no significant difference in LSM and SSM feasibility and accuracy when comparing patients with MASLD cirrhosis to other etiologies.

THU-421

High five-year incidence of portal vein thrombosis after acute variceal bleeding in cirrhosis

Tomàs Balari[1], Maria Garcia Guix[1,2], Alberto Amador[1,2], Alba Cachero[1], Rosa Rota[1], José Castellote Alonso[1,2], Teresa Broquetas[1]. *[1]Bellvitge University Hospital, Hepatology unit, L'Hospitalet de Llobregat, Spain; [2]Universitat de Barcelona - Campus Bellvitge, L'Hospitalet de Llobregat, Spain*
Email: tbalari@bellvitgehospital.cat

Background and aims: The incidence of portal vein thrombosis (PVT) in patients with cirrhosis is estimated at 1–4%, 6–8%, and 10% at 1, 3, and 5 years, respectively. Acute variceal bleeding (AVB) has been associated with an increased risk of PVT. Although metabolic dysfunction-associated steatotic liver disease (MASLD) is linked to a higher thromboembolic risk, its contribution to PVT remains unclear. This study aimed to assess the incidence of PVT following AVB and to determine whether MASLD or metabolic factors are associated with increased PVT rates.
Method: This retrospective observational study included consecutive patients with cirrhosis admitted for AVB between 2013 and 2021. Exclusion criteria were prior or baseline PVT, transjugular intrahepatic portosystemic shunt (TIPS), anticoagulation, follow-up <6 months, or absence of semi-annual abdominal imaging. Clinical, laboratory, and endoscopic variables were recorded at the time of AVB.
Results: A total of 315 patients with AVB were screened. Sixty-five (20.6%) were excluded due to PVT at admission, 28 (8.8%) underwent TIPS, and 64 (20.3%) had follow-up <6 months. Ultimately, 139 patients were included. Median age was 60 years (IQR 50–68); Child-Pugh class was A/B/C in 28.8%, 57%, and 13.7%, respectively. Alcohol-related liver disease (ALD) was the leading etiology (48.6%), while MASLD accounted for 12.3%. During a median follow-up of 47 months (IQR 17–73), 36 patients (25.9%) developed PVT. Cumulative incidence was 6.5%, 16.5%, and 21.6% at 1, 3, and 5 years. Notably, 22% of cases occurred within the first 6 months, and 55.6% involved the main portal vein. Incidence among MASLD patients was 29.4% versus 25.4% in non-MASLD cirrhosis (p = 0.43). Baseline prevalence of hypertension, diabetes, dyslipidemia, and obesity was 46.8%, 38.1%, 21.6%, and 29.6%, respectively; none were significantly associated with PVT. Liver function parameters, including MELD score and decompensation events, were not linked to increased PVT risk.
Conclusion: Up to 21.6% of patients may develop PVT within 5 years after AVB, representing a higher incidence than reported in unselected cirrhotic populations. Neither MASLD nor metabolic risk factors were associated with increased PVT risk, although the low prevalence of MASLD in this cohort is a limitation. These findings warrant validation in cohorts with greater MASLD representation.

THU-425

Partial splenic embolization (PSE) for the prevention of variceal rebleeding in patients unsuitable for OLTx, TIPS, and endovascular treatment: safety and mortality

Marcello Bianchini[1], Chiara Gualandri[2], Dario Saltini[1], Tomas Guasconi[1], Antonio Piscopo[3], Giustina Lo Cascio[3], Andrea Salomè Velasco Mayorga[3], Federico Casari[4], Giovanni Battinelli[5], Ascari Francesco[4], Francesco Prampolini[5], Cristian Caporali[4], Filippo Schepis[1,2]. *[1]Severe Liver Diseases (M.E.C.) Departmental Unit, Department of Medical Specialties, University, European Reference Network on Rare Liver Disorders (ERN Rare- Liver), Modena, Italy; Hospital of Modena "Policlinico", University of Modena and Reggio Emilia, Modena, Italy; [2]Università di Modena e Reggio Emilia-Unimore, Modena, Italy; [3]Gastroenterology Unit, Department of Medical Specialties, University Hospital of Modena "Policlinico", University of Modena and Reggio Emilia, Italy, Modena, Italy; [4]Interventional Radiology, Departmental Unit, Department of Diagnostic Imaging, University Hospital of Modena "Policlinico", Italy, Modena, Italy; [5]Radiology Unit, Departmental Unit, Department of Diagnostic Imaging, University Hospital of Modena "Policlinico", University of Modena and Reggio Emilia, Italy, Modena, Italy*
Email: marcello.bianchini@gmail.com

Background and aims: Partial splenic embolization (PSE) is widely used to treat hypersplenism and its symptoms. While its effects on portal hypertension are documented, they remain partly defined. Aim is to evaluate the safety and efficacy of PSE as secondary prophylaxis for variceal bleeding in patients ineligible for orthotopic liver transplantation (OLTx), transjugular intrahepatic portosystemic shunt (TIPS), and other endovascular treatments (EVT).
Method: All PSE since January 2017 were retrospectively reviewed. Inclusion criteria: active or recent variceal bleeding excluded from OLTx, TIPS, and EVT. Traumatic splenic rupture and absence of informed consent were excluded. Clinical, endoscopic, and imaging data were collected as well as complications. Long-term rebleeding-free survival was established as primary outcome.
Results: 21 patients were included (43% male; mean age 57 y). 10 patients (47.6%) had cirrhosis, of whom 2 had portal vein thrombosis (PVT). Among the other patients, 8 (72%) had PVT/cavernoma. 5 had JAK2-related myeloproliferative neoplasms and 1 Factor V Leiden mutation. 18 patients (85%) had prior decompensation. At the time of PSE, 4 patients had active bleeding and 17 had hi-risk varices. 9 had ascites, recurrent in 3 cases. Mean hemoglobin was 10.3 g/dL, median platelet count 73×10^9/L, mean MELD-Na was 12. Embolization techniques included acrylic glue (29%), coils (28%), microparticles (15%), and combined (28%). Mean devascularized splenic volume was 65%. Adverse events occurred in 90%: 85% were minor complications, mainly post-embolization syndrome and pleural effusion. 3 cases (15.7%) had new-onset ascites. 2 patients developed splenic vein thrombosis resolved with anticoagulation. No splenic abscesses occurred. Sepsis developed in 4 cases. During 5-year follow-up, variceal rebleeding occurred in 2 cases (9.5%). 8 patients (38%) died during follow-up, 2 within 3 months; all had decompensated cirrhosis, sarcopenia, and multiple comorbidities at the time of PSE. All patients with acute variceal bleeding survived the procedure without rebleeding. Rebleeding-free survival rates were 95.8% at 30 days, 75.3% at 1 y, 70.3% at 2 y, and 42.5% at 5 y.
Conclusion: PSE is effective as secondary prophylaxis for variceal rebleeding in patients excluded from OLTx, TIPS, and EVT. Post-procedural complications are frequent and mortality may occur in patients with uncontrolled ascites, sarcopenia, and multiple comorbidities suggesting that PSE should be performed in centers with consistent expertise.

THU-426

Efficacy and safety of endoscopic and endovascular interventions for secondary prophylaxis of gastric varices in patients with cirrhosis: systematic review and individual patient data meta-analysis

Sagnik Biswas[1], Arnav Aggarwal[1], Gin-Ho Lo[2], Luo Xuefeng[3], Li Yang[3], Angels Escorsell[4], Shubham Mehta[1], Shekhar Swaroop[1], Samagra Agarwal[1], Ayush Agarwal[1], Ashwani Mishra[1], Shashank Tripathi[5], Deepak Gunjan[1], Shivanand Gamangatti[1], Shalimar[1]. *[1]All India Institute of Medical Science, New Delhi, India; [2]E-Da Cancer Hospital, Yanchao District, Taiwan; [3]University of Oxford Hauxi Joint Centre for gastrointestinal cancer, West China Hospital, Sichuan University, Sichuan, China; [4]Hospital de Sant Pau, Barcelona, Spain; [5]University College of Medical Sciences, New Delhi, India*
Email: sagnik_biswas@yahoo.co.in

Background and aims: Multiple endoscopic and endovascular modalities are available for the management for gastric variceal hemorrhage in cirrhosis, however, there is no consensus on the optimal modality of secondary prophylaxis in these patients.
Method: Observational studies and randomized controlled trials (RCTs) comparing the efficacy of endoscopic cyanoacrylate injection (ECI) and endovascular interventions-balloon occluded retrograde transvenous obliteration [BRTO] and transjugular intrahepatic portosystemic shunt [TIPS] in preventing variceal rebleeding published till 2024 were included in the aggregate data meta-analysis (ADMA). Individual patient data (IPD) from RCTs were collated and compared (BRTO vs ECI, TIPS vs ECI) in a propensity score matched population. Competing risk analysis was used to compare the rates of the all-cause rebleeding and new onset/worsening of pre-existing ascites and hepatic encephalopathy among patients receiving ECI, BRTO and TIPS.
Results: Fifteen studies (4 randomized controlled trials and 11 observational studies) comprising 1240 patients (ECI: 377, BRTO: 575, TIPS: 288) were included in the ADMA. In the IPD, both BRTO (sHR: 0.15; 95% CI: 0.05–0.43; p = 0.004) and TIPS (sHR: 0.49; 95% CI: 0.27–0.89; p = 0.019) significantly reduced all-cause rebleeding compared to ECI, without any improvement in overall survival. BRTO was associated with higher risk of new-onset or worsening of pre-existing ascites (sHR: 3.54; 95% CI: 1.31–9.55, p = 0.013), while TIPS increased risk of hepatic encephalopathy (sHR: 8.84; 95% CI: 2.0–39.11, p = 0.004) compared to ECI. Reduction in the rates of rebleeding was most pronounced among Child-Pugh Class-B patients. The analysis revealed limited long-term outcomes data, inhomogeneous inclusion criteria, inconsistencies in reported trial outcomes and significant heterogeneity particularly in studies regarding TIPS.
Conclusion: Endovascular interventions (BRTO and TIPS) are superior to ECI for reducing all-cause rebleeding in patients with cirrhosis and GV hemorrhage. Larger studies with standardized end-points and longer follow-up duration are needed to clarify the impact of these interventions on overall survival and optimize treatment selection.

THU-427

A single tertiary centre audit of adherence to Baveno VII in chronic liver disease: missed opportunities for cost-savings, CO2 emission reductions and improved health resource utilisation?

Benedict Brazier[1], Johnny Phillips[2], Zarin Chowdhury[2], Steven Dixon[3], Ann Archer[1,2], Kushala Abeysekera[1,2]. *[1]Department of Liver Medicine, University Hospitals Bristol and Weston NHS Trust, Bristol, United Kingdom; [2]Bristol Medical School, University of Bristol, Bristol, United Kingdom; [3]Department of Gastroenterology, University Hospitals Bristol & Weston NHS Trust, Bristol, United Kingdom*
Email: benedict.brazier@uhbw.nhs.uk

Background and aims: The Baveno VII consensus has reshaped the assessment and management of clinically significant portal hypertension (CSPH) in compensated advanced chronic liver disease. Application of Baveno VII criteria reduces referrals for gastroscopy

(OGD), with wider environmental and health resource utilisation implications. Despite this, practice across centres varies. We audited adherence to Baveno VII guidance in our regional tertiary unit, which serves a population of approximately half a million people.
Method: All OGDs performed for variceal surveillance and screening at Bristol Royal Infirmary from 23/02/2022–30/09/2025 were audited, along with patient level data using electronic healthcare records. Exclusion criteria included variceal screening in: patients under 18 years of age, pregnancy, clinical trial participation, involvement in a banding programme, prior transjugular intrahepatic portosystemic shunt, liver transplant patients, hepatocellular carcinoma, Fontan circulation, non-cirrhotic portal hypertension. Estimates for carbon dioxide (CO2) emission and water usage in OGDs were based on published data. Cost estimates were based on existing UK National Health Service tariffs.
Results: 447 variceal screening OGDs were identified within the study period. 208 were excluded. 239 procedures were interrogated; 57/239 (23.8%) were clinically indicated, most commonly due to new decompensating events. 182 OGDs were performed for variceal screening without a specific indication. 87/182 (47.8%) patients had a screening OGD without up-to-date transient elastography and/or platelet count. 55 (30.2%) should have had non-selective beta blockers (NSBBs) initiated without an OGD, 4 (7.27%) of whom only received NSBBs prior to OGD. 40/182 (22.0%) had a screening OGD despite not meeting any Baveno VII criteria for CSPH. Notably, 1 case was identified where Baveno VII criteria for CSPH was not met but the patient required banding. For the 182 OGDs not indicated, estimated water consumption was 1604.8L, approximate cost to the healthcare system € 176,603 and CO2 emissions 5168.8 kg, equivalent to driving over 37000 km in a gasoline vehicle.
Conclusion: In our centre, we have identified a high number of potentially unnecessary variceal screening OGDs performed. Adherence to Baveno VII guidance has the potential to have significant environmental and cost-saving benefits for healthcare providers. Exploring barriers to adherence amongst clinicians is important to reduce wastage.

THU-428
CVID-associated porto-sinusoidal vascular disorder: is splenomegaly uncoupled from portal hypertension?

Francisco Capinha[1,2], Carlos Noronha Ferreira[1,2], Rui Palma[1], Sofia Carvalhana[1], Luís Correia[1,2], Helena Cortez-Pinto[1,2]. [1]*Serviço de Gastrenterologia e Hepatologia, Unidade Local de Saúde de Santa Maria, Lisboa, Portugal;* [2]*Clínica Universitária de Gastrenterologia, Faculdade de Medicina de Lisboa, Universidade de Lisboa, Lisboa, Portugal*
Email: francisco.capinha96@gmail.com

Background and aims: Common Variable Immunodeficiency (CVID) is a well-established cause of Porto-Sinusoidal Vascular Disorder (PSVD). These patients frequently present with large splenomegaly, however, it remains unclear whether this splenic enlargement reflects severe portal hypertension or a distinct pathophysiological mechanism. We aimed to determine if the phenotype of CVID-associated PSVD differs from non-CVID forms, specifically regarding the relationship between splenomegaly and signs of portal hypertension.
Method: We performed a retrospective comparative analysis of 23 patients with biopsy-proven PSVD (9 with CVID vs. 14 non-CVID), between 2017 and 2025, who underwent transjugular liver biopsy and hepatic venous pressure gradient (HVPG) measurement. Continuous variables were compared using the Mann-Whitney U test, and categorical variables using exact Fisher's test. Correlation analyses assessed the relationship between platelet counts and spleen size. Statistical significance level was defined as $p < 0.05$.
Results: The CVID cohort exhibited massive splenomegaly, significantly larger than the control group (mean 19.4 vs. 15.5 cm, $p = 0.027$). The HVPG values were similar between groups (10.4 vs. 9.4 mmHg, $p = 0.59$). These relatively low values, in both groups, reflect the predominantly presinusoidal nature of PSVD, which is not well evaluated by HVPG. As expected, platelet counts were strongly inversely correlated with spleen size in both groups (CVID: $r = -0.89$, $p = 0.001$; non-CVID: $r = -0.77$, $p = 0.006$ after excluding 2 outliers with myeloproliferative neoplasm) while the diference between groups is not significative ($p = 0.33$), as happens also to the presence of portosystemic collaterals ($p = 0.09$), other sign of portal hypertension. Biochemically, CVID patients have higher AST levels (46.1 vs. 29.5 U/L, $p = 0.007$) and a trend towards higher ALT ($p = 0.15$). The CVID phenotype appeared less thrombotic, with no portal vein thrombosis in our group (vs. 28.6% in controls).
Conclusion: In CVID-associated PSVD, splenomegaly appears uncoupled from portal hypertension severity, differently from other etiologies of PSVD. This suggests that other mechanisms drive splenomegaly beyond passive congestion, what could, eventually, be related with the chronic/recurrent gastrointestinal tract inflammation in these patients. This distinct phenotype reinforces the need for invasive hemodynamic assessment as a surrogate marker and a potentially distinct hemodynamic behavior and disease progression in this subgroup of patients.

THU-429
The evolving role of TIPS: from established indications to real-world practice

Ylenia Capraro[1], Leonard Lamfu[1], Ilaria Lenci[1], Martina Milana[1], Renato Argirò[1], Daniele Morosetti[1], Leonardo Baiocchi[1]. [1]*Tor Vergata University of Rome, Rome, Italy*
Email: capraro.capraroylenia@gmail.com

Background and aims: Transjugular intrahepatic portosystemic shunt (TIPS) is a procedure that creates a communication between the portal and hepatic veins to reduce portal hypertension (PH). Traditionally indicated for PH-related bleeding and refractory ascites (RA), TIPS is now increasingly used for portal vein thrombosis (PVT) and severe PH (e.g., very low or hepatofugal portal flow or high-flow collateral vessels), particularly in patients requiring surgery. It is also applied as a bridge to liver transplantation (LT) to prevent decompensation and preserve vascular structures during the waiting period. We aimed to evaluate: i) the evolution of TIPS indications in cirrhotic patients at our Hepatology Unit; ii) the survival outcome according to TIPS indications; iii) the results of TIPS as a bridge to LT.
Method: We retrospectively analyzed patients who underwent TIPS at our center from June 2014 to June 2025 with at least 3 months of follow-up. Demographic data, liver and renal function tests, and MELD scores were collected at baseline and at 1 and 3 months post-procedure. Data were stratified by TIPS indication and/or bridge to LT. Continuous variables were analyzed with t-test or ANOVA, and discrete variables with Fisher's test. Survival analysis was performed using Log-rank test. A $p < 0.05$ was considered significant.
Results: A total of 107 patients were included. Over time, TIPS indications for RA and GI bleeding significantly decreased (90% in 2014–17 vs 41% in 2022–25, $p < 0.001$), while indications for PVT and severe PH increased (5% vs. 44%, $p = 0.002$). Patients with RA had higher baseline creatinine levels than other groups (1.3 vs 0.8 mg/dL, $p < 0.01$) and showed significantly lower survival after TIPS ($p = 0.02$, Log-rank test). 49 TIPS were performed as a bridge to LT and 73% of these patients underwent transplantation. This group had higher MELD scores at baseline and at 1 and 3 months ($p < 0.05$). Short-term (3–6 months) survival did not differ significantly, whereas long-term survival (>6 months) markedly decreased in patients who did not undergo LT despite TIPS placement for bridging purposes.
Conclusion: Our single-center retrospective analysis suggests that: i) TIPS use has expanded beyond traditional indications; ii) TIPS for RA appears suboptimal in terms of survival, compared to other PH-related indications; iii) when used as a bridge to LT, TIPS does not affect short-term survival despite higher MELD scores. However,

long-term outcomes are poor in patients who do not ultimately undergo LT.

THU-430

Impact of continuing versus discontinuing nonselective beta blockers after transjugular intrahepatic portosystemic shunt on one-year clinical outcomes

Ali Emre Bardak[1], Gizem Teker[2], Hind El Naamani[1], Volkan Senkal[3], Bilger Çavuş[3]. [1]*Boston Medical Center – Brighton, Boston University, Boston, United States;* [2]*Beth Israel Deaconess Medical Center, Boston, United States;* [3]*Department of Gastroenterology, Istanbul University, Istanbul, Türkiye*
Email: bardakaliemre@gmail.com

Background and aims: Nonselective beta-blockers (NSBBs) reduce portal pressure and prevent variceal bleeding in patients with cirrhosis, but their benefit after transjugular intrahepatic portosystemic shunt (TIPS) is debatable, with recent evidence supporting careful discontinuation once portal decompression is achieved. Despite this, post-TIPS NSBB management varies widely, and real-world data are limited. Using a large, multicenter, real-world cohort, we aimed to compare clinical outcomes in patients who continued or discontinued NSBB after TIPS.
Method: Using the TriNetX US Collaborative Network, we identified adults with cirrhosis who underwent TIPS and had been prescribed an NSBB within the preceding year. Patients who did not survive to post-TIPS day 90 were excluded to ensure comparable early postprocedural stability. Patients were then classified according to post-TIPS NSBB use: continuation was defined as receiving an NSBB prescription within 90 days after the procedure, whereas discontinuation was defined as having no NSBB prescriptions recorded after TIPS. Propensity score matching was performed to balance baseline characteristics, including demographics, comorbidities, and pre-TIPS MELD scores. Outcomes were assessed from post-TIPS day 90 through year 1. Kaplan–Meier analyses and risk estimates were used.
Results: After matching, 1,350 patients remained in each group, with balanced baseline characteristics and a median follow-up of 365 days. Continuation of NSBBs after TIPS did not improve overall survival (HR 0.87, 95% CI 0.68–1.11) or transplant-free survival (HR 0.89, 95% CI 0.75–1.05). NSBB continuation was associated with significantly higher hazards of hepatic encephalopathy (HR 1.29, 95% CI 1.11–1.51) and hospitalization (HR 1.23, 95% CI 1.08–1.39). Rates of ICU admission (HR 1.03, 95% CI 0.84–1.25) and esophageal variceal bleeding (HR 1.08, 95% CI 0.78–1.49) did not differ significantly.
Conclusion: In this study, continuation of NSBBs after TIPS did not improve overall or transplant-free survival. Instead, NSBB use was associated with higher hazards of hepatic encephalopathy and hospitalization, while rates of ICU admission and variceal bleeding were similar between groups. These findings suggest that the hemodynamic benefits of NSBBs diminish once portal hypertension is decompressed and that their post-TIPS physiologic effects may contribute to worsened encephalopathy. The results support a more individualized approach to NSBB management following TIPS rather than routine continuation.

THU-431

Oral branched-chain amino acids supplementation in patients with cirrhosis and sarcopenia undergoing TIPS for refractory ascites: a randomized controlled trial

Ciro Celsa[1], Luigi Maruzzelli[2], Vincenza Calvaruso[1], Federico Midiri[2], Angelo Luca[2], Roberto Miraglia[2], Calogero Cammà[1]. [1]*Section of Gastroenterology and Hepatology, Department of Health Promotion, Mother and Child Care, Internal Medicine and Medical Specialties, University of Palermo, Palermo, Italy;* [2]*IRCCS ISMETT (Mediterranean Institute for Transplantation and Advanced Specialized Therapies), Palermo, Palermo, Italy*
Email: calogero.camma@unipa.it

Background and aims: Sarcopenia is common in patients with cirrhosis and refractory ascites (RA) undergoing transjugular intrahepatic portosystemic shunt (TIPS), associated with poor outcomes. Branched-chain amino acids (BCAA) may improve nutritional status and reduce inflammation. We evaluated oral BCAA supplementation impact on clinical, inflammatory and nutritional outcomes in patients with cirrhosis and sarcopenia undergoing TIPS for RA.
Method: We conducted a randomized controlled trial (RCT) at a single high-volume referral center (>20 TIPS/year) enrolling 37 patients with cirrhosis and sarcopenia undergoing TIPS for RA. Patients received oral BCAA supplementation (n = 18) or standard care (n = 19). Endpoints included clinical events (mortality, persistence of ascites and hepatic encephalopathy [HE] at the end of follow-up) and between- and within-group changes in nutritional parameters and inflammatory biomarkers from baseline (TIPS placement) and the last follow-up visit.
Results: Baseline characteristics were similar between groups except age (mean 57.3 ± 8.5 in BCAA versus 64.4 ± 9.4 years in controls, p = 0.018). After a median follow-up time of 5.8 months, no significant between-group differences were observed in clinical events, inflammatory and nutritional parameters. Six-month overall survival was 100% in BCAA versus 85.1% in controls (p = 0.157). Persistence of grade≥2 ascites was observed in 11.8% of BCAA arm versus 23.5% in control arm (p = 0.375). Grade≥2 HE was the same (11.8%) between arms. The BCAA arm showed significant within-group improvements in inflammatory markers: interleukin-6 decreased by 74.46 ± 88.35 pg/mL (p = 0.014) and interleukin-8 by 13.51 ± 17.5 pg/mL (p = 0.022). Nutritional parameters improved significantly in BCAA: fat-free mass increased by 5.2 ± 3.17 kg (p = 0.001), psoas muscle area by 4.02 ± 3.93 cm^2 (p = 0.016), and mid-arm muscle circumference by 1.35 ± 2.32 cm (p = 0.049). Body weight gain was lower in BCAA versus controls (4.1 ± 6.5 versus 9.5 ± 5.3 kg, p = 0.022). BCAA supplementation was safe with comparable adverse events.
Conclusion: In this ongoing RCT, oral BCAA supplementation was associated with favorable within-group changes in inflammatory biomarkers and nutritional parameters in cirrhotic patients with RA undergoing TIPS. Although between-group differences did not reach statistical significance in this interim analysis, these findings support biological plausibility and safety of oral BCAA, with enrollment continuing.

THU-432

Validation of albumin-bilirubin-platelet (ALBI-PLT), modified ALBI-PLT, and EVendo score for predicting varices needing treatment (VNT) in patients with hepatocellular carcinoma

Nuprawee Changsiriwattanathomrong[1], Pongnarin Nawalerspunya[1], Naichaya Chamroonkul[1], Apichat Kaewdech[1], Pimsiri Sripongpun[1]. [1]*Prince of Songkla University, Division of Internal Medicine, Faculty of Medicine, Hat Yai, Thailand*
Email: pim072@hotmail.com

Background and aims: Variceal bleeding significantly impairs prognosis in patients with hepatocellular carcinoma (HCC), especially with the emergence of immunotherapy/anti-angiogenic combinations as standard care. As routine endoscopic screening for varices needing treatment (VNT) is invasive and Baveno VI criteria perform suboptimally in HCC, reliable non-invasive alternatives are needed. This study validated and compared the ALBI-PLT, modified ALBI-PLT (mALBI-PLT), and EVendo scores for predicting VNT in HCC patients.
Method: We conducted a retrospective study in patients with newly diagnosed HCC at a tertiary center between Jan 2021 and Dec 2024. Those who underwent screening endoscopy (EGD) within a window of 3 mo prior to or 6 mo following their HCC diagnosis were included. Patients with prior variceal bleeding or previous HCC treatment from other centers were excluded. Laboratory data closest to the EGD were used to calculate ALBI, ALBI-PLT, mALBI-PLT, and EVendo scores. Diagnostic performance of each score for the diagnosis of VNT was

evaluated using the area under the receiver operating characteristic curve (AUROC) and compared withDeLong's test.
Results: Of 434 patients who were screened, 127 were eligible (71.6% male; mean age 63.1 years). VNT was found in 26%. BCLC stages were: 0/A (42.5%), B (29.1%), and C/D (28.3%). Portal vein thrombosis (PVT) was present in 22.8% and was more frequent in the VNT group (36.4% vs 18.1%, p = 0.056). Presence of ascites was more common in the VNT group (36.4% vs 11.7%, p = 0.004), but the maximal tumor size was comparable. ALBI and EVendo demonstrated the highest discriminative ability, with AUROCs of 0.706 (95% CI: 0.605–0.807) and 0.703 (95% CI: 0.604–0.802), respectively. ALBI-PLT (0.658, 95%CI 0.567–0.749) and mALBI-PLT (0.656, 95%CI: 0.565–0.748) showed modest performance. AUROC differences were not statistically significant (p > 0.05). ALBI >−2.43 achieved 100% sensitivity but poor specificity (3.48%), whereas EVendo >3.9 yielded 93.75% sensitivity (p = 0.157 vs ALBI) but significantly higher specificity (36.78%, p < 0.001).
Conclusion: ALBI and EVendo demonstrated fair performance for identifying VNT, with EVendo offering a superior balance between sensitivity and specificity. However, AUROCs near 0.70 suggest suboptimal discriminative ability overall. ALBI-PLT and mALBI-PLT showed unsatisfactory performance in predicting VNT in our HCC cohort. Further research is required to refine non-invasive strategies to reduce unnecessary endoscopic screening in HCC.

THU-433-YI
Prevalence, dynamics, and clinical impact of sarcopenia in acute and chronic non-cirrhotic non-tumoral portal vein thrombosis
Rares Craciun[1], Lucile Moga[2], Andreea Fodor[1], Andrada Nemes[3], Pierre-Emmanuel Rautou[2], Maxime Ronot[4], Xingshun Qi[5], Aurélie Plessier[2], Bogdan Procopet[1]. *[1]Gastroenterolgy Department, "Prof. Dr. O. Fodor" Regional Institute of Gastroenterology and Hepatology, Department of Internal Medicine, "Iuliu Haţieganu" University of Medicine and Pharmacy, Cluj-Napoca, Romania, Cluj-Napoca, Romania; [2]Service d'Hépatologie, AP-HP, Hôpital Beaujon, DMU DIGEST, Centre de Référence des Maladies Vasculaires du Foie, FILFOIE, ERN RARE-LIVER, Clichy, France; [3]Department of Anesthesia and Intensive Care, "Iuliu Haţieganu" University of Medicine and Pharmacy, Cluj-Napoca, Romania; [4]Department of Medical Imaging, Beaujon University Hospital, Clichy, France; [5]Department of Gastroenterology, General Hospital of Northern Theater Command, Shenyang, China*
Email: rarescraciun@ymail.com

Background and aims: Sarcopenia is a well-recognized prognostic factor in cirrhosis, but data in non-cirrhotic non-tumoral portal vein thrombosis (NCNTPVT) are scarce. We aimed to evaluate the prevalence and longitudinal evolution of sarcopenia and its association with portal hypertension–related complications in patients with recent and chronic NCNTPVT.
Method: We analyzed a multicenter cohort of patients with recent and chronic NCNTPVT undergoing contrast-enhanced CT at diagnosis (T0) and follow-up ≥6 months (T1). Skeletal muscle index (SMI) was assessed at the L3 level. Sarcopenia was defined using sex-specific cut-offs (women <38 cm^2/m^2; men <43 cm^2/m^2 if BMI<25, <53 cm^2/m^2 if BMI≥25). Changes in SMI were evaluated using paired Wilcoxon tests. Associations between baseline sarcopenia and the presence of ascites, gastrointestinal bleeding, and hepatic encephalopathy at T0 and T1 were assessed using χ^2 or Fisher's exact tests.
Results: 126 patients with recent and 102 with chronic PVT were included. Sarcopenia at T0 was highly prevalent in both groups (acute: 59.5%, 75/126; chronic: 66.6%, 68/102). In recent PVT, median SMI remained stable between T0 and T1 (43.04 vs. 43.41 cm^2/m^2; median Δ +0.08 cm^2/m^2; p = 0.56),after a median interval of 6.6 (4.5–11.3 months). In chronic PVT, median SMI showed no significant change over time (median 11 months), 41.90 vs. 41.60 cm^2/m^2; median Δ−0.17 cm^2/m^2; p = 0.70. In patients with recent PVT, sarcopenia was more prevalent in those with BMI >25 vs. <25 kg/m^2 (65.3% vs. 52.5%, p = 0.26), while BMI was weakly but significantly inversely correlated with SMI (r = -0.24, p = 0.011). Sarcopenia appeared to be independent of thrombotic extent or etiology in both recent and chronic PVT. In patients with chronic PVT, baseline sarcopenia was significantly associated with the presence of ascites (32.1% vs. 14.3%, p = 0.04) at T0, history of portal hypertension-related bleeding (25% vs. 10.7%, p = 0.05), and hepatic encephalopathy (14.1% vs. 3.6%, p = 0.14). Furthermore, sarcopenia at T0 was significantly associated with the presence of ascites at T1 (42.3% vs. 19.2%; p = 0.038).
Conclusion: Sarcopenia is highly prevalent in NCNTPVT. While no significant global changes in muscle mass were observed during follow-up, baseline sarcopenia in chronic PVT identified patients at increased risk for portal hypertension-related complications. These findings support routine assessment of sarcopenia as a clinically relevant prognostic marker in NCNTPVT.

THU-434
Non-invasive integration of systemic hemodynamics and spleen stiffness across disease stages in cirrhosis
Martín Elizondo[1], Eugenia Ipar[2], Romina Rey[1], Leandro Cymberknop[2], Marcelo Vicente Valverde Gomez[1], Ricardo Armentano[3], Solange Gerona[1]. *[1]Unit of Liver Transplantation, Hospital Militar, Montevideo, Uruguay; [2]Universidad Tecnológica Nacional, Facultad Regional Buenos Aires, Grupo de Investigación y Desarrollo en Bioingeniería (GIBIO), Buenos Aires, Argentina; [3]Department of Biological Engineering, CENUR Litoral Norte, Universidad de la República, Paysandú, Uruguay*
Email: melizondo20@gmail.com

Background and aims: Cirrhosis is characterized by progressive changes in portal hypertension and systemic circulatory dysfunction during disease evolution. Spleen stiffness measurement (SSM) is a validated non-invasive surrogate of clinically significant portal hypertension, whereas impedance cardiography enables characterization of systemic hemodynamics. The aim of this study was to evaluate the relationship between spleen stiffness and systemic hemodynamic alterations, and to explore their association with disease severity according to Child–Pugh (CP) class.
Method: We studied 56 subjects, including 44 patients with cirrhosis (CP A: n = 20; CP B: n = 12; CP C: n = 8) and 12 healthy controls. Spleen stiffness was assessed by transient elastography. Systemic hemodynamics were evaluated using impedance cardiography, obtaining cardiac output (CO), systemic vascular resistance (SVR), and arterial compliance (AC), which were analyzed individually and jointly integrated into a composite Hemodynamic Valuation Index (HVI), calculated as the square root of the sum of the squared, standardized values of these parameters and serving as a composite, physiologically grounded descriptor of systemic circulatory status. Group comparisons were performed using analysis of variance or Welch's test, as appropriate. Associations were assessed using Pearson or Spearman correlation coefficients.
Results: SSM was significantly higher in patients with cirrhosis compared with controls (p < 0.001). Although differences across CP classes were not statistically significant (p = 0.238), SSM showed a progressive increase with advancing disease stage. The composite HVI differed significantly across CP classes (p = 0.047), with higher values in CP B compared with CP A and CP C, indicating a more pronounced hyperdynamic circulatory profile at intermediate disease stages. Among individual systemic hemodynamic parameters, AC was the only variable significantly associated with SSM, showing a moderate inverse correlation (r = – 0.30; p = 0.033), whereas CO and SVR were not.
Conclusion: Combined assessment of spleen stiffness and systemic hemodynamics provides an integrated characterization of circulatory dysfunction in cirrhosis. While SSM primarily reflects portal hypertension severity, the composite hemodynamic index highlights a distinct hyperdynamic profile in CP B. These findings warrant confirmation in prospective studies across the spectrum of cirrhosis.

THU-435

Prevalence and risk factors of esophageal and gastroesophageal varices in myeloproliferative neoplasm patients with portal hypertension in a tertiary government hospital: a 5-year cross-sectional study

Sam Fandood[1]. [1]*East Avenue Medical Center, Quezon, Philippines*
Email: samfandood@gmail.com

Background and aims: Myeloproliferative neoplasms (MPNs) are an established cause of non-cirrhotic portal hypertension and may lead to gastroesophageal varices with significant clinical consequences. However, local data on the burden of varices and associated risk factors among MPN patients remain limited.
Method: This cross-sectional study included 40 adult patients diagnosed with MPNs who underwent esophagogastroduodenoscopy at a tertiary government hospital between 2021 and 2025. Sociodemographic, clinical, laboratory, and endoscopic data were obtained through chart review. The prevalence of gastroesophageal varices was determined. Logistic regression analyses were performed to identify clinicodemographic factors associated with the presence of varices.
Results: Varices were identified in 23 patients (57.5%), including esophageal varices alone in 27.5%, gastric varices alone in 2.5%, and combined esophageal and gastric varices in 27.5%. Varices were most prevalent among patients with primary myelofibrosis (78.9%), followed by polycythemia vera (45.5%) and chronic myeloid leukemia (30%). Variceal size differed significantly across MPN subtypes (p = 0.001), with larger varices observed in polycythemia vera and primary myelofibrosis. In univariate analysis, age 40–59 years (OR: 0.06; 95% CI: 0.01–0.57; p = 0.015) and >60 years (OR: 0.03; 95% CI: 0.00–0.38; p = 0.006) were associated with lower odds of varices compared with younger patients. Splenic vein diameter was positively associated with varices (OR: 1.38; 95% CI: 1.05–1.80; p = 0.020), while platelet count showed an inverse association (OR: 0.99; 95% CI: 0.99–1.00; p = 0.004). On multivariate analysis, only platelet count remained independently associated with varices (adjusted OR: 0.99; 95% CI: 0.98–1.00; p = 0.020).
Conclusion: Esophageal and gastroesophageal varices are highly prevalent among MPN patients with portal hypertension, particularly in primary myelofibrosis. Thrombocytopenia is an independent factor associated with variceal presence and may serve as a practical marker to guide endoscopic surveillance in this high-risk population.

THU-436

Urinary chloride dipstick as a potential biomarker for predicting decompensation in patients with cirrhosis: a prospective multicenter pilot study

Susan Fischer[1], Britt van Ruijven[2], Annarein Kerbert[1], Marta Fiocco[1], Michael Klemt-Kropp[3], Anton Jan van Zonneveld[1], Tom J.G. Gevers[4], Govert Veldhuijzen[5], Minneke Coenraad[1], Kirill Basiliya[1]. [1]*Leiden University Medical Center, Leiden, Netherlands;* [2]*Institute of Nutrition and Translational Research in Metabolism (NUTRIM), Maastricht, Netherlands;* [3]*Noordwest Ziekenhuisgroep Locatie Alkmaar, Alkmaar, Netherlands;* [4]*Maastricht UMC+, Maastricht, Netherlands;* [5]*Gelre Ziekenhuizen, Apeldoorn, Netherlands*
Email: s.e.fischer@lumc.nl

Background and aims: Predicting decompensation in cirrhosis remains difficult, highlighting the need for simple, non-invasive biomarkers. Reduced urinary sodium excretion reflects disease severity in patients with cirrhosis, but routine use outside clinical settings is not feasible. Urinary chloride, reabsorbed alongside sodium, can be easily measured using a dipstick. This study examines the correlation between dipstick-measured urine chloride and urinary sodium/chloride concentrations and explores its potential to predict future acute decompensation (AD) in cirrhosis.
Method: In this prospective multicenter pilot study, hospitalized patients with cirrhosis were enrolled from four Dutch hospitals. A single urine sample was collected for dipstick chloride concentration measurement together with laboratory analysis of urinary sodium and chloride concentrations. Primary outcome was the correlation between dipstick and lab-based urine electrolytes, secondary outcome was the predictive value of dipstick chloride for AD development within 90-days.
Results: A total of 100 patients (62% male) were included, with a median age of 64 years [IQR 53–70] and MELD score of 13 [8–19]. Dipstick urinary chloride strongly correlated with laboratory urinary chloride (r = 0.801) and urinary sodium concentrations (r = 0.757). Within 90-days, the cumulative incidence of AD was higher in patients with low urinary chloride concentration (≤38 mmol/L) compared with those with high urinary chloride (44% vs 22%, p = 0.014). Multivariate regression models showed that low urinary chloride, diuretic use, and AD at inclusion were independently associated with an increased risk of developing new AD (HR 3.16, 95% CI 1.42–6.99; HR 2.71, 95% CI 1.22–6.00; and HR 4.73, 95% CI 1.98–11.29).
Conclusion: Dipstick-measured urinary chloride concentration correlates strongly with laboratory urinary sodium and -chloride concentration in patients with cirrhosis. Low urinary chloride is independently associated with an increased risk of new AD. Given its simplicity and low-cost, urine chloride dipstick testing may serve as a practical tool for early prediction of acute decompensation in outpatient settings. Further clinical trials are warranted to evaluate the role of chloride-guided therapy in patients with cirrhosis.

THU-441

Diagnostic accuracy of non-invasive detection of clinically significant portal hypertension

Zouhir Gadi[1,2], Roy Hajj[3], Leonor Flores Ribeiro[4], Emmanuel Ehomah[5], Lotte Schoenmakers[1,2], Luisa Vonghia[1,2], Wilhelmus J Kwanten[1,2], Thomas Vanwolleghem[1], Sven Francque[1,2]. [1]*Department of Gastroenterology and Hepatology, Antwerp University Hospital, Edegem, Belgium;* [2]*Laboratory of Experimental Medicine and Pediatrics, Faculty of Medicine and Health Care Sciences, University of Antwerp, Edegem, Belgium;* [3]*American University of Beirut (AUB) Faculty of Medicine, Beirut, Lebanon;* [4]*Faculdade de Medicina da Universidade de Lisboa, Lisboa, Portugal;* [5]*University of Ghana Medical school, Accra, Ghana*
Email: Zouhir.Gadi@student.uantwerpen.be

Background and aims: Portal hypertension (PH) is central to chronic liver disease progression, yet its reference standard assessment by hepatic venous pressure gradient (HVPG) is invasive and restricted to specialised centres. Numerous non-invasive tests (NITs), including elastography-based models and serum-derived scores, have been proposed, however, comparative real-world data across major liver disease aetiologies remain limited. This study aimed to compare the diagnostic accuracy of portal hypertension-specific and fibrosis-related NITs against HVPG for detecting PH and clinically significant portal hypertension (CSPH).
Method: Patients undergoing simultaneous HVPG measurement and evaluable transjugular liver biopsy between January 2018 and December 2024 were included. PH and CSPH were defined as HVPG ≥5 mmHg and ≥10 mmHg, respectively. Diagnostic performance of NICER, MODEL-3P, MODEL-5P, ANTICIPATE, ANTICIPATE-NASH, LSPS, Lok, FIB-4+, FIB-4, MAF-5, APRI, Forns Index, AGILE3+ and AGILE4 was assessed using area under the receiver operating characteristic curve (AUC), sensitivity, specificity, positive predictive value (PPV) and negative predictive value (NPV).
Results: A total of 446 patients were included: MASLD (27.6%), alcohol-related liver disease (28.9%), metALD (6.3%), viral hepatitis (4.5%) and other causes (32.7%). PH was present in 77% and CSPH in 52%. For PH detection, MAF-5 and MODEL-5P were excluded due to missing data. Remaining NITs showed good-to-excellent discrimination (AUC >0.80). NICER achieved strong balanced accuracy (AUC 0.903; sensitivity 0.80; specificity 0.84; PPV 0.95). FIB-4+ offered the highest sensitivity (0.97) and a high NPV (0.75), while Lok provided

the highest NPV among highly sensitive models (0.64). ANTICIPATE-NASH, AGILE4, LSPS and FIB-4 (AUC 0.860–0.887) also performed well, with specificities up to 0.90 and PPVs exceeding 0.90. For CSPH, several models exceeded AUC 0.90. NICER remained robust (AUC 0.909; sensitivity 0.89; specificity 0.77; NPV 0.87). ANTICIPATE-NASH achieved near-perfect sensitivity and NPV (0.99), while elastography-integrating tools such as AGILE4 (AUC 0.920) and AGILE3+ (AUC 0.911) demonstrated excellent rule-out capability (NPV >0.95). Classical fibrosis scores showed lower accuracy.
Conclusion: PH-specific NITs, particularly elastography-based models (NICER, AGILE4, ANTICIPATE), outperform traditional fibrosis scores for PH/CSPH detection and are suitable non-aetiology-specific practical alternatives to HVPG measurement for PH stratification.

THU-442
Prognostic value of splenic volume in patients with portosinusoidal vascular disease
Hiram Tadeo-Espinoza[1], Tania del Socorro Grimaldo Galena[1], Venny Alberto Venegas Gomez[1], Marisol Esesarte[1], Eric Kauffman[1], Orlando E Falcon Antonio[1], Orfanel Pineda Arate[1], Ignacio Garcia Juarez[1]. [1]*Salvador Zubirán National Institute Of Health Sciences And Nutrition, Ciudad de México, Mexico*
Email: drinter77@gmail.com

Background and aims: Splenomegaly is a common manifestation of portal hypertension and may reflect significant hemodynamic compromise. In portosinusoidal vascular disease (PSVD), reliable predictors of clinical deterioration remain limited, and early identification of high-risk patients is essential. Splenic volume, readily quantifiable by imaging, may serve as a marker of disease severity. This study aimed to assess the association between splenic volume and portal hypertension–related complications in patients with PSVD.
Method: We conducted a retrospective study of patients diagnosed with PSVD between 2010 and 2024 according to VALDIG (Vascular Liver Disease Group) 2019 criteria. Patients with cirrhosis, inadequate liver biopsy, incomplete clinical data, or death within 90 days of diagnosis were excluded. Clinical, biochemical, imaging, and endoscopic variables were analyzed. Quantitative variables were expressed as medians (Interquartile Range) and categorical variables as frequencies. Group comparisons used Mann–Whitney U, chi-square, or Fisher's exact tests. Receiver Operating Characteristic (ROC) curve analysis and Youden's index identified optimal cutoffs. Odds ratios (OR) were calculated, with $p < 0.05$ considered significant.
Results: Fifty-seven patients were included (median age 39 years). Comorbidities were present in 49%, predominantly autoimmune diseases. Imaging showed portosystemic collaterals in 54.5% and portal vein thrombosis in 25%. Median splenic volume was 656 cc, and mean liver stiffness was 7.5 kilopascals (kPa). Endoscopy revealed esophageal varices in 79.6%, gastric varices in 22.4%, and portal hypertensive gastropathy in 53.1%. During a median follow-up of 26.6 months, 50% of patients developed clinical decompensation, mainly upper gastrointestinal bleeding. A splenic volume $\geq$ 574 cc was significantly associated with decompensation (OR 5.03; $p = 0.005$).
Conclusion: Splenic volume is a significant prognostic marker in PSVD. A threshold $\geq$ 574 cc identifies patients at increased risk of portal hypertension–related complications and may serve as a simple imaging biomarker for early risk stratification. Prospective validation is warranted.

THU-443
Portosystemic pressure gradient changes after underdilatation of controlled-expansion transjugular intrahepatic portosystemic shunts
Jakub Gazda[1,2], Valeria Perez[1,2], Sonia Torres[1,2,3], Asunción Ojeda[1,2,3], Andreea Fodor[1,2,3], Anna Baiges[1,2,3], Fanny Turon[1,2,3], Virginia Hernández-Gea[1,2,3], Juan Carlos García-Pagán[1,2,3]. [1]*Barcelona Hepatic Hemodynamic Laboratory, Liver Unit, Hospital Clínic, Clínic Barcelona, ERN-RareLiver (European Reference Network on Rare Liver Disorders), CSUR Centro de Referencia del Sistema Nacional de Salud en Enfermedad Hepática Vascular Compleja en Adultos, Barcelona, Spain, Barcelona, Spain;* [2]*FRCB-IDIBAPS (Fundació de Recerca Clínic Barcelona–Institut d'Investigacions Biomèdiques August Pi i Sunyer), Barcelona, Spain; CIBEREHD (Centro de Investigación Biomédica en Red de Enfermedades Hepáticas y Digestivas), Madrid, Spain; AGAUR SGR2021 01115, Department of Medicine, Faculty of Medicine and Health Sciences, Universitat de Barcelona, Barcelona, Catalonia, Spain, Barcelona, Spain;* [3]*Barcelona Hepatic Hemodynamic Laboratory, Liver Unit, Hospital Clínic, Clínic Barcelona, ERN-RareLiver (European Reference Network on Rare Liver Disorders), CSUR Centro de Referencia del Sistema Nacional de Salud en Enfermedad Hepática Vascular Compleja en Adultos, Barcelona, Spain, FRCB-IDIBAPS (Fundació de Recerca Clínic Barcelona–Institut d'Investigacions Biomèdiques August Pi i Sunyer), Barcelona, Spain; CIBEREHD (Centro de Investigación Biomédica en Red de Enfermedades Hepáticas y Digestivas), Madrid, Spain; AGAUR SGR2021 01115, Department of Medicine, Faculty of Medicine and Health Sciences, Universitat de Barcelona, Barcelona, Catalonia, Spain, Barcelona, Spain*
Email: jkgazda@gmail.com

Background and aims: Transjugular intrahepatic portosystemic shunt (TIPS) effectively treats portal hypertension complications but carries a substantial risk of hepatic encephalopathy (HE). Recent data suggest that underdilatation (6–7 mm) achieves similar efficacy to standard diameters (8–10 mm) with reduced HE incidence, likely due to a more moderate reduction in the portosystemic pressure gradient (PSPG). While Viatorr Controlled Expansion (VCX) stents enable stable underdilatation at 8–9 mm, their capacity to maintain smaller diameters (6–7 mm) and preserve the PSPG over time remains unknown. The aim of the study was to compare PSPG changes between early assessment (24–72 h, while awake/stable conditions) and 1 month in patients with underdilated (6–7 mm) versus nominally dilated (8–10 mm) VCX-TIPS, and to evaluate if underdilated grafts prevent further PSPG reduction from spontaneous expansion.
Method: We retrospectively analyzed consecutive TIPS procedures using VCX stents (Oct 2015–Aug 2025). Initial dilation diameter was determined by clinical indication and risk profile. PSPG was measured early post-procedure and at 1 month.
Results: Of 95 patients, indications were variceal bleeding (VB) (52%), refractory ascites (27%), and others (21%; e.g., portal vein thrombosis, Budd-Chiari syndrome). Patients were stratified into 6–7 mm (n = 36) and 8–10 mm (n = 59) groups. In the 6–7 mm group, PSPG decreased significantly from a median of 11.3 mmHg (IQR 8.8–12.3) at early assessment to 9.3 mmHg (IQR 6.5–11.3) at 1 month ($p = 0.001$). In contrast, PSPG remained unchanged in the 8–10 mm group (median 9.5 mmHg [IQR 8.0–11.0] vs. 9.5 mmHg [IQR 7.5–11.0], $p = 0.375$). Median PSPG reduction at 1 month was significantly greater in the 6–7 mm group than the 8–10 mm group (−1.5 [IQR −3.3 to 0.0] vs. −0.5 mmHg [IQR −1.5 to 1.5]; $p = 0.02$). Notably, among 9 patients in the 6–7 mm group with early PSPG >12 mmHg, 44% (n = 4) achieved a PSPG <= 12 mmHg by 1 month. At 1-month, persistent ascites was more frequent in the 6–7 mm group versus the 8–10 mm group (28% vs. 14%), while no VB occurred in the 6–7 mm group, compared to 2% in the 8–10 mm group.
Conclusion: PSPG decreased significantly between early and 1-month assessments in the 6–7 mm group but remained stable in the 8–10 mm group. Findings suggest that VCX stents may not fully prevent spontaneous expansion when initially dilated below 8 mm. Understanding stent behaviour and PSPG reduction after TIPS may help personalizing management specially in high-risk patients.

THU-444-YI

Endoscopic ultrasound–guided portal pressure gradient measurement: prognostic utility and concordance with hepatic venous pressure gradient in a cohort of patients with sinusoidal and presinusoidal forms of portal hypertension

Lucia Giuli[1], Alberto Larghi[1], Gianenrico Rizzatti[1], Maria Pallozzi[1], Clelia Cavallo[1], Giulia Venturini[1], Elena Melita[1], Francesca Romana Ponziani[1], Brigida Eleonora Annicchiarico[1], Giulia Tripodi[1], Andrea Contegiacomo[1], Roberto Iezzi[1], Rosa Talerico[1], Antonio Gasbarrini[1], Francesco Santopaolo[1]. [1]*Fondazione Policlinico Universitario Agostino Gemelli IRCCS, Rome, Italy*
Email: lucia.giuli92@gmail.com

Background and aims: Clinically significant portal hypertension (CSPH) is the strongest predictor of hepatic decompensation. Hepatic venous pressure gradient (HVPG), the gold standard for diagnosing CSPH, provides only an indirect estimate of portal pressure and may underestimate presinusoidal or mixed forms of portal hypertension (PH). Indeed, endoscopic ultrasound (EUS)-guided portal pressure gradient (PPG) measurement enables direct recording of portal and hepatic vein pressures, potentially overcoming this limitation. This study evaluated the concordance between EUS-PPG and HVPG and their prognostic value in predicting hepatic decompensation.
Method: In this prospective single-center study, consecutive patients with suspected CSPH of various etiologies, naïve to non-selective beta-blockers, underwent both EUS-PPG and HVPG measurement. EUS-PPG was obtained using the EchoTip Insight™ system, and HVPG was measured according to Baveno VII recommendations. Correlation between EUS-PPG and HVPG was assessed using Pearson's coefficient, while agreement was evaluated with Bland–Altman analysis. Predictors of hepatic decompensation were explored using univariate and multivariate logistic regression analyses.
Results: Ninety patients were enrolled (45.6% male; mean age 60 years). Liver disease etiologies included porto-sinusoidal vascular disorder (PSVD) (35.6%), MASLD (31.1%), autoimmune liver diseases (14.4%), metabolic/alcohol-related liver disease (7.8%), viral hepatitis (7.8%), and alcohol-related liver disease (3.3%). Mean EUS-PPG and HVPG values were 14 ± 6 mmHg and 9 ± 5 mmHg, respectively. Seventy patients (77.8%) had PPG > 10 mmHg, while only 41 (45.6%) had HVPG > 10 mmHg. Concordance was modest, with a mean PPG–HVPG difference of + 4.7 mmHg (95% LoA:−9.6 to +18.9 mmHg) and a weak linear correlation (r = 0.036, p = 0.73). During a median follow-up of 12 months, 17 patients (18.9%) developed hepatic decompensation. At univariate analysis, PPG and platelet count were significantly associated with the occurrence of hepatic decompensation. In the multivariate analysis, EUS-PPG (OR 1.40; 95% CI 1.11–1.76; $p = 0.004$), together with platelet count (OR 0.97; 95% CI 0.95–1.00; $p = 0.037$) remained independent predictors of hepatic decompensation.
Conclusion: EUS-PPG is an informative method for assessing PH and it independently predicts hepatic decompensation, suggesting potential advantages over HVPG especially in presinusoidal or mixed forms of PH such as PSVD and MASLD.

THU-445-YI

Predictors and prognostic impact of spontaneous portal vein thrombosis recanalization in cirrhosis: an individual patient data meta-analysis

Antonio Guerrero[1], Laura Del campo[2], Angelo Luca[3], Pierre-Emmanuel Rautou[4], Sylvie Chevret[5], Leonard Naymagon[6], Fabio Piscaglia[7], Horia Ștefănescu[8], Thomas Reiberger[9], Guohong Han[10], Francesco Violi[11], Carlos Alberto Costa Noronha Ferreira[12], Luis Téllez[1], Bernhard Scheiner[9], Stefania Basili[11], Javier Zamora[2], Agustín Albillos[1]. [1]*Servicio de Gastroenterología y Hepatología, Hospital Universitario Ramón y Cajal, Universidad de Alcalá, Instituto Ramón y Cajal de Investigación Sanitaria (IRYCIS), Centro de Investigación Biomédica en Red de Enfermedades Hepáticas y Digestivas (CIBEREHD), Instituto Salud Carlos III, Madrid, Spain;* [2]*Unidad de Bioestadística Clínica. Hospital Universitario Ramón y Cajal. Instituto Ramón y Cajal de Investigación Sanitaria (IRYCIS), Consorcio de Investigación Biomédica en Red de Epidemiología y Salud Pública (CIBERESP), Madrid, Spain;* [3]*Mediterranean Institute for Transplantation and Advanced Specialized Therapies (IRCCS-ISMETT), Radiology Service, Department of Diagnostic and Therapeutic Services, Palermo, Italy;* [4]*Service d'Hépatologie, AP-HP, Hôpital Beaujon, DMU DIGEST, Centre de Référence des Maladies Vasculaires du Foie, FILFOIE, ERN RARE-LIVER, Clichy, France;* [5]*Institut de Recherche Saint-Louis, équipe ECSTRRA, Université Paris Cité, Paris, France;* [6]*Tisch Cancer Institute, Icahn School of Medicine at Mount Sinai, New York, United States;* [7]*Division of Internal Medicine, Hepatobiliary and Immunoallergic Diseases, IRCCS Azienda Ospedaliero-Universitaria di Bologna, Department of Medical and Surgical Sciences, University of Bologna, Bologna, Italy;* [8]*Gastroenterology Department, Regional Institute of Gastroenterology and Hepatology O. Fodor, Cluj-Napoca, Romania;* [9]*Division of Gastroenterology and Hepatology, Department of Internal Medicine III, Medical University of Vienna. Rare Liver Disease (RALID) Center of the European Reference Network for Rare Hepatological Diseases (ERN RARE-LIVER), Medical University Vienna, Vienna, Austria;* [10]*Department of Liver Disease and Digestive Interventional Radiology, Xijing Hospital of Digestive Diseases, Xijing Hospital, Fourth Military Medical University, Xi'an, China;* [11]*Department of Internal Medicine, Anestesiology and Cardiovascular Sciences, Sapienza University, Roma, Italy;* [12]*Servico de Gastrenterologia e Hepatologia, Hospital de Santa Maria, Centro Hospitalar Universitário Lisboa Norte, Clinica Universitaria de Gastrenterologia, Facultad de Medicina, Lisbon, Portugal*
Email: antonio.guerrero90@hotmail.com

Background and aims: Portal vein thrombosis (PVT) in cirrhosis follows a heterogeneous course. Spontaneous recanalization can occur in untreated patients, but its determinants and prognostic relevance remain poorly defined. We conducted an individual patient data (IPD) meta-analysis to evaluate the association between spontaneous recanalization and overall survival, and to identify predictors of spontaneous recanalization.
Method: We included cohort studies of patients with cirrhosis and PVT who did not receive anticoagulation (PROSPERO CRD42020140026). Authors were contacted to share de-identified IPD. All-cause mortality was analyzed using a one-stage competing-risk model, considering liver transplantation as a competing event. Models were adjusted for clinically relevant covariates, including age, cirrhosis etiology, Child-Pugh class, thrombosis severity and location, platelet count, presence of varices, and beta-blocker use. Predictors of spontaneous recanalization were assessed using mixed-effects ordinal logistic regression with a random intercept for each study.
Results: Eight studies contributed data from 586 non-anticoagulated patients. Spontaneous recanalization occurred in 264 (47.7%) patients. In the competing risk model, spontaneous recanalization was independently associated with significantly lower all-cause mortality (aSHR = 0.51; 95%CI, 0.28–0.91). The greatest survival benefit was observed in patients achieving complete recanalization (aSHR = 0.45; 95%CI, 0.21–0.94). Interaction analyses demonstrated that thrombus location significantly modified the association between recanalization and mortality, with a greater mortality reduction when thrombosis involved the main portal vein trunk (OR = 0.39; 95% CI, 0.16–0.91; p = 0.02). In contrast, no survival benefit associated with recanalization was observed in patients with isolated intrahepatic thrombosis of a portal venous branch. Independent predictors of spontaneous recanalization included Child-Pugh A (OR 2.63; 95%CI 1.18–5.88), partial thrombosis (OR 1.69; 95%CI 1.09–2.56) and isolated intrahepatic involvement (OR = 2.04; 95%CI, 1.23–3.33).
Conclusion: Spontaneous recanalization of PVT in cirrhosis is common and is strongly influenced by thrombus location and severity and liver disease severity. Recanalization is independently associated with improved survival, with a graded effect according to

the degree of recanalization, particularly when the main portal vein trunk is involved.

THU-446

Risk factors for porto-mesenteric venous thrombosis after laparoscopic sleeve gastrectomy: a matched case-control study

Yousef Yahia[1], Shahd Hamran[2], Prem Chadra[3], Waleed Mahmoud[4], Ma'mon Qasem[5], Dhowa A. Al Ali[2], Ahmed Abdulhafedh Ali[1], Marwan Al-Zu'bi[6], Nasreen Khidir[4], Mohammed Al-Kuwari[4].
[1]Gastroenterology and Hepatology Department, Hamad Medical Corporation, Doha, Qatar; [2]Qatar University, College of Medicine, Doha, Qatar; [3]Medical Research Center, Hamad Medical Corporation, Doha, Qatar; [4]Department of Bariatric Surgery, Hamad Medical Corporation, Doha, Qatar; [5]Department of Radiology, Hamad Medical Corporation, Doha, Qatar, Doha, Qatar; [6]Internal Medicine Department, Hamad Medical Corporation, Doha, Qatar
Email: yyahia@hamad.qa

Background and aims: Porto-mesenteric venous thrombosis (PMVT) is a rare but potentially life-threatening complication following laparoscopic sleeve gastrectomy (LSG). Although PMVT has been reported in patients without classical thrombotic risk factors, predictors in the post-LSG setting remain poorly defined. This study aimed to identify patient-level risk factors associated with PMVT after LSG.
Method: We conducted a retrospective matched case–control study including patients who developed PMVT within 90 days after LSG between 2014 and 2025. Cases were matched to controls without PMVT by age, sex, year of surgery, and surgical center in a 1:4 ratio. Conditional logistic regression was used to evaluate associations between clinical, metabolic, and perioperative factors and PMVT.
Results: Thirty-eight PMVT cases and 152 matched controls were analyzed. Metabolic dysfunction–associated steatotic liver disease (MASLD) was significantly more prevalent among PMVT cases. In multivariate conditional logistic regression, MASLD was independently associated with increased odds of PMVT (adjusted odds ratio 2.95; 95% confidence interval 1.03–8.47; $p = 0.044$). Most PMVT events occurred within 30 days of surgery (92.1%). Abdominal pain was the most common presenting symptom, and combined portal and superior mesenteric vein thrombosis was the predominant radiologic pattern.
Conclusion: PMVT after LSG is uncommon but clinically significant and occurs predominantly in the early postoperative period. MASLD was independently associated with PMVT, suggesting that hepatic metabolic dysfunction may be linked to increased postoperative thrombotic vulnerability. Recognition of this association may support heightened clinical vigilance following LSG.

THU-447

Multimodal computed tomography–clinical integration for noninvasive grading of hepatic venous pressure gradient

Seul Ki Han[1], Jin Gyo Jeong[1], JangHoon Ru[1], Sejung Yang[1], Jhii-Hyun Ahn[1], Sang Gyune Kim[2], Moon Young Kim[1]. *[1]Yonsei University Wonju College of Medicine, Wŏnju, Korea, Rep. of South; [2]Soonchunhyang University Bucheon Hospital, Bucheon, Korea, Rep. of South*
Email: drkimmy@yonsei.ac.kr

Background and aims: Portal hypertension is a hemodynamic consequence of liver cirrhosis and a major determinant of hepatic decompensation. The hepatic venous pressure gradient (HVPG) is the gold standard for measuring portal pressure and identifying clinically significant portal hypertension (CSPH), defined as HVPG greater than or equal to 10 mmHg. However, HVPG measurement is invasive, technically demanding, and limited to specialized centers. Existing noninvasive tests primarily reflect hepatic fibrosis or indirect consequences of portal hypertension rather than portal hemodynamics itself. We aimed to develop and validate a multimodal framework integrating abdominal computed tomography (CT) imaging and clinical data for noninvasive grading of HVPG.
Method: We retrospectively analyzed 603 individuals from Wonju Severance Christian Hospital, including 298 patients with portal hypertension confirmed by HVPG measurement and 305 controls. Abdominal CT images were spatially standardized, and fifteen routinely available clinical variables were incorporated, including age, sex, albumin, total bilirubin, aminotransferases, white blood cell count, hemoglobin, platelet count, sodium, creatinine, liver volume, spleen volume, and liver to spleen volume ratio. A deep learning framework was constructed using a Swin Transformer for image feature extraction and a language image pretraining model to encode clinical data. The model was trained to classify CSPH and to estimate HVPG as a continuous variable.
Results: The model demonstrated robust performance for CSPH classification, achieving an accuracy of 0.79, precision of 0.85, recall of 0.83, F1 score of 0.79, and area under the receiver operating characteristic curve of 0.87. This significantly outperformed a CT only unimodal model, which showed lower accuracy and discrimination. In regression analysis, predicted HVPG showed a strong correlation with measured HVPG, with a Pearson correlation coefficient of 0.71. These findings indicate that integrating anatomical information from CT imaging with functional clinical markers substantially improves noninvasive assessment of portal pressure.
Conclusion: We developed a multimodal CT and clinical data framework that enables accurate noninvasive grading of HVPG. By combining imaging derived features with laboratory markers, this approach overcomes a limitations of HVPG measurement. This framework has the potential to improve risk stratification, reduce patient burden, and expand access to portal hypertension assessment.

THU-448-YI

Diabetes is an independent risk factor for hepatic encephalopathy and death in patients undergoing TIPS placement

Lukas Hartl[1,2,3], Anja Tiede[4], Marlene Hintersteininger[1,2,3], Ida Edler[4], Alena Friederike Ehrenbauer[4], Sarah Lisa Schütte[4], Martin Kabelitz[4], Jim Benjamin Mauz[4], Theresa Müllner-Bucsics[1,2,3], Lukas Reider[5], Lorenz Balcar[1,2,3], Maria Schoder[5], Michael Trauner[1,3], Mattias Mandorfer[1,2,3], Heiner Wedemeyer[4,6], Benjamin Maasoumy[4,6], Thomas Reiberger[1,2,3,7], Tammo Lambert Tergast[4]. *[1]Division of Gastroenterology and Hepatology, Department of Medicine III, Medical University of Vienna, Vienna, Austria; [2]Vienna Hepatic Hemodynamic Lab, Division of Gastroenterology and Hepatology, Department of Medicine III, Medical University of Vienna, Vienna, Austria; [3]Clinical Research Group MOTION, Medical University of Vienna, Vienna, Austria; [4]Department of Gastroenterology, Hepatology, Infectious Diseases and Endocrinology, Hannover Medical School, Hannover, Germany; [5]Division of Cardiovascular and Interventional Radiology, Department of Biomedical Imaging and Image-guided Therapy, Medical University of Vienna, Vienna, Austria; [6]German Centre for Infection Research (DZIF), partner-site Hannover-Braunschweig, Hannover, Germany; [7]Christian Doppler Lab for Portal Hypertension and Liver Fibrosis, Medical University of Vienna, Vienna, Austria*
Email: lukas.a.hartl@meduniwien.ac.at

Background and aims: Transjugular intrahepatic portosystemic shunt (TIPS) placement is an effective treatment for patients with complications of portal hypertension. Diabetes increases the risk of hepatic encephalopathy (HE), likely due to inflammation, autonomic dysfunction and insulin resistance. We aimed to investigate the impact of type 2 diabetes mellitus (T2DM) on clinical outcomes after TIPS in a large multicentric cohort.
Method: We included consecutive patients who underwent implantation of a covered TIPS for the treatment of portal hypertension-associated complications at Hannover Medical School between 2009 and 2021 (Hannover cohort) and at two Viennese centers between

2000 and 2025 (Vienna cohort) with available information on diabetes and clinical outcomes. Patients with malignancy, other diabetes types, rescue TIPS placement, or incomplete datasets were excluded.
Results: Overall, we included 650 patients (Vienna cohort: n = 366; Hannover cohort: n = 284) with a median age of 57 years and male predominance (65.7%). Most patients had alcohol-related liver disease (66.3%). The majority of patients (75.4%) underwent TIPS placement for recurrent/refractory ascites and the median MELD was 12. T2DM was present in 185 patients (28.5%) at the time of TIPS placement. Patients with T2DM were significantly older (median 60 years vs. 56 years; p < 0.001), but had comparable MELD (12.0 vs. 12.0; p = 0.402), portosystemic pressure gradient before (19 mmHg vs. 18 mmHg; p = 0.372) and after TIPS (7 mmHg vs. 7 mmHg; p = 0.797) compared to patients without T2DM. Median follow-up duration was 20.2 months. Patients with T2DM mellitus had a higher cumulative incidence of HE (p < 0.001) with 43.4% of patients developing overt HE at 6 months of follow-up (versus 24.2% without T2DM). Similarly, the cumulative incidence of death was significantly higher among T2DM patients (p < 0.001). Specifically, at 1 year after TIPS placement, the cumulative incidence of death was 29.0% among patients with T2DM as compared to 15.9% without T2DM. In multivariate competing risk regression analysis adjusted for age and MELD, T2DM was an independent risk factor for HE (aSHR: 1.59; 95%CI: 1.21–2.08; p < 0.001) and death (aSHR: 1.34; 95%CI: 1.03–1.75; p = 0.028).
Conclusion: T2DM represents an independent risk factor not only for HE, but also for mortality in patients undergoing TIPS placement. At 1 year after TIPS, the cumulative incidence of death was almost doubled in patients with T2DM.

THU-449
TIPS facilitates recovery from different types of hepatorenal syndrome and may improve clinical outcomes in patients with HRS-AKI

Lukas Hartl[1,2,3], Marlene Hintersteininger[1,2,3], Marlene Reincke[4], Theresa Müllner-Bucsics[1,2,3], Michael Schultheiß[4], Lukas Reider[5], Lukas Sturm[4], Lorenz Balcar[1,2,3], Michael Trauner[1,3], Mattias Mandorfer[1,2,3], Dominik Bettinger[4], Thomas Reiberger[1,2,3,6].
[1]Division of Gastroenterology and Hepatology, Department of Medicine III, Medical University of Vienna, Vienna, Austria; [2]Vienna Hepatic Hemodynamic Lab, Division of Gastroenterology and Hepatology, Department of Medicine III, Medical University of Vienna, Vienna, Austria; [3]Clinical Research Group MOTION, Medical University of Vienna, Vienna, Austria; [4]Department of Medicine II (Gastroenterology, Hepatology, Endocrinology and Infectious Diseases, Freiburg University Medical Center), Faculty of Medicine, University of Freiburg, Freiburg, Germany; [5]Division of Cardiovascular and Interventional Radiology, Department of Biomedical Imaging and Image-guided Therapy, Medical University of Vienna, Vienna, Austria; [6]Christian Doppler Lab for Portal Hypertension and Liver Fibrosis, Medical University of Vienna, Vienna, Austria
Email: lukas.a.hartl@meduniwien.ac.at

Background and aims: While renal benefits from transjugular intrahepatic portosystemic shunt (TIPS) placement have been reported, its impact on different types of hepatorenal syndrome (HRS) remains unknown. We aimed to investigate the impact of TIPS placement on the response of different HRS types – according to the recent Acute Disease Quality Initiative (ADQI) and International Club of Ascites (ICA) consensus – and on clinical outcomes.
Method: We included consecutive patients with covered TIPS implantation for ascites/hepatorenal syndrome at Freiburg University Medical Center between 2004 and 2023 and at the Medical University of Vienna between 2004 and 2025 with available information on renal function and clinical outcomes. Patients were stratified for presence of HRS-acute kidney injury (HRS-AKI), HRS-acute kidney disease (HRS-AKD), HRS-chronic kidney disease (HRS-CKD), chronic kidney disease (CKD) and no kidney disease (No-KD).
Results: Overall, 508 patients with a median age of 60 years, male predominance (69.3%) and a median MELD of 18 were included. At baseline, 27 patients (5.3%) had HRS-AKI, while 18 (3.5%) had HRS-AKD, 33 (6.5%) had HRS-CKD, 128 (25.2%) had CKD and 302 (59.4%) had No-KD. Median follow-up duration was 10.0 months. Median serum creatinine (sCr) significantly decreased in all HRS types - specifically, in HRS-AKI, from 1.61 mg/dL to 0.98 mg/dL (p = 0.003), in HRS-AKD from 1.66 mg/dL to 1.09 mg/dL (p = 0.038) and in HRS-CKD from 2.09 mg/dL to 1.22 mg/dL (p < 0.001). Normalization of sCr occurred in 43.8% (n = 7/16) and 53.8% (n = 7/13) of patients with HRS-AKI at 3 and 12 months of follow-up, respectively, as compared to 50.0% (n = 5/10) and 50.0% (n = 4/8) of patients with HRS-AKD, as well as 20.0% (n = 5/25) and 46.2% (n = 6/13) of patients with HRS-CKD. Two (7.4%) and 6 (18.2%) patients with HRS-AKI and HRS-CKD required dialysis after TIPS, respectively, compared to none among HRS-AKD patients. The cumulative incidence of death at 1 year (Y1) after TIPS (considering liver transplantation as a competing event) was 17.9% in No-KD, as compared to 21.9% in HRS-AKI (p = 0.433 vs. No-KD), 46.2% in HRS-AKD (p = 0.005 vs. No-KD), 35.4% in HRS-CKD (p = 0.040 vs. No-KD), and 30.5% in CKD (p = 0.029 vs. No-KD).
Conclusion: Renal function improves after TIPS across different types of renal dysfunction; sCr normalization was reached in about half of HRS-AKI, HRS-AKD and HRS-CKD cases. While Y1 mortality in HRS-AKI was similar to patients with No-KD, all other types of HRS and renal dysfunction show higher mortality after TIPS.

THU-450
Sex and age do not affect the diagnostic and prognostic performance of spleen/liver stiffness-based noninvasive tests for clinically significant portal hypertension: a European multicenter study

Paula Hoefinger[1], Aitor Odriozola[2], Lucile Moga[3], Fanny Turon[4], Luis Téllez[5], Dario Saltini[6], Wilhelmus Kwanten[7], Maria Grasso[8], Fischer Petra[9], Elba Llop Herrera[10], Yuly Mendoza[11], Angelo Armandi[12], Carlos Pardo[4], Antonio Colecchia[13], Federico Ravaioli[14], Benjamin Maasoumy[15], Wim Laleman[16], José Presa[17], Jörn M. Schattenberg[18], Annalisa Berzigotti[11], José Luis Calleja Panero[10], Vincenza Calvaruso[8], Sven Francque[7], Filippo Schepis[6], Pierre-Emmanuel Rautou[3], Agustín Albillos[5], Bogdan Procopet[9], Juan Carlos García-Pagán[4], Angela Puente[2], Jose Ignacio Fortea[2], Thomas Reiberger[1], Mattias Mandorfer[1], Mathias Jachs[1].
[1]Division of Gastroenterology and Hepatology, Medical University of Vienna, Vienna, Austria; Vienna Hepatic Hemodynamic Lab, Medical University of Vienna, Vienna, Austria; Department of Medicine III and Clinical Research Group Mechanisms in Portal Hypertension, Medical University of Vienna, Vienna, Austria; [2]Gastroenterology and Hepatology Department, Clinical and Translational Research in Digestive Diseases, Valdecilla Research Institute, Marqués de Valdecilla University Hospital, Santander, Spain; [3]Institut National de la Santé et de la Recherche Médicale, Centre de Recherche sur l'Inflammation, Université Paris-Cité, Unité Mixte de Recherche 1149, Paris, France; Service d'Hépatologie, Assistance Publique-Hôpitaux de Paris, Hôpital Beaujon, Départements Médico-Universitaires Maladies de l'Appareil Digestif, Centre de Référence des Maladies Vasculaires du Foie, French Network for Rare Liver Diseases and European Reference Network on Rare Liver Disorders, Paris, France; [4]Barcelona Hepatic Hemodynamic Laboratory, Liver Unit, Hospital Clínic, Clínic Barcelona; ERN-RareLiver (Health Care Provider of the European Reference Network on Rare Liver Disorders), CSUR (Centro de referencia del Sistema Nacional de Salud en Enfermedad Hepática Vascular Compleja en adultos); FRCB-IDIBAPS (Fundació de Recerca Clínic Barcelona-Institut d'Investigacions Biomèdiques August Pi i Sunyer); CIBEREHD (Centro de Investigación Biomédica en Red Enfermedades Hepáticas y Digestivas); AGAUR SGR202101115; Medicine Department, Faculty of Medicine, and health Science, Universitat de Barcelona, Barcelona, Spain; [5]Instituto Ramón y Cajal de Investigación

Sanitaria, University of Alcalá, Madrid, Spain; Gastroenterology and Hepatology Department, Hospital Universitario Ramón y Cajal, Madrid, Spain; [6]Severe Liver Diseases Unit, Department of Medical Specialties, University of Modena, Reggio Emilia, and Azienda Ospedaliero-Universitaria di Modena, Modena, Italy; [7]Department of Gastroenterology and Hepatology, Antwerp University Hospital, Antwerp, Belgium; Laboratory of Experimental Medicine and Pediatrics-Gastroenterology and Hepatology, University of Antwerp, Antwerp, Belgium; [8]Gastroenterology and Hepatology Unit, Department of Health Promotion Sciences Maternal and Infantile Care, Internal Medicine and Medical Specialities, Promozione della Salute, Materno-Infantile, di Medicina Interna e Specialistica di Eccellenza G D'Alessandro, University of Palermo, Palermo, Italy; [9]Third Medical Clinic, Department of Internal Medicine, Iuliu Hatieganu University of Medicine and Pharmacy, Cluj-Napoca, Romania; [10]Department of Gastroenterology and Hepatology, Puerta de Hierro University Hospital, Puerta de Hierro Health Research Institute, Centro de Investigación Biomédica en Red Enfermedades Hepáticas y Digestivas, Universidad Autonoma de Madrid, Madrid, Spain; [11]Department of Visceral Surgery and Medicine, Inselspital, Bern University Hospital, University of Bern, Bern, Switzerland; [12]Metabolic Liver Disease Research Program, Department of Medicine, University Medical Center Mainz, Mainz, Germany. Division of Gastroenterology and Hepatology, Department of Medical Sciences, University of Turin, Turin, Italy; [13]Gastroenterology Unit, Department of Medical Specialties, University of Modena, Reggio Emilia, and Azienda Ospedaliero-Universitaria di Modena, Modena, Italy; [14]Istituto di Ricovero e Cura a Carattere Scientifico Aziend spedaliero and Department of Medical and Surgical Sciences, Universitaria di Bologna, European Reference Network on Hepatological Diseases, Bologna, Italy; [15]Department of Gastroenterology, Hepatology and Endocrinology, Hannover Medical School, Hannover, Germany; [16]Department of Gastroenterology and Hepatology, Section of Liver and Biliopancreatic Disorders and Liver Transplantation, University Hospitals Leuven, Katholieke Universiteit Leuven, Leuven, Belgium, Medizinische Klinik B, Universitätsklinikum Münster, Münster University, Münster, Germany; [17]Liver Unit, Hospital Center of Trás-os-Montes and Alto Douro, Vila Real, Portugal; [18]Metabolic Liver Disease Research Program, Department of Medicine, University Medical Center Mainz, Mainz, Germany; Department of Internal Medicine II, Saarland University Medical Center, Homburg, Homburg, Germany
Email: paula.hoefinger@meduniwien.ac.at

Background and aims: Clinically significant portal hypertension (CSPH) is the key driver of hepatic decompensation in compensated advanced chronic liver disease (cACLD). Current recommendations endorse liver (LSM) and spleen (SSM) stiffness measurement by vibration-controlled transient elastography (VCTE) for estimating the probability of CSPH. However, the influence of sex and age on the diagnostic and prognostic performance of non-invasive tests and their derivatives (i.e., NICER and ANTICIPATE ± NASH) remains unclear.
Method: This multicenter retrospective analysis included 407 stable outpatients with Child–Pugh A cACLD from 16 European expert centers (2020–2023) who underwent paired LSM & SSM-100 Hz by VCTE as well as HVPG measurement. Patients were stratified by sex and age (<60/≥60 years, i.e., approximately the median). Diagnostic performance of VCTE-based non-invasive tests (NITs) was assessed using AUROC analyses and logistic regression. The cumulative incidence of first hepatic decompensation was evaluated using competing-risk models. Diagnostic accuracy of the Baveno VII criteria was assessed using sensitivity, specificity, PPV, NPV, LR+, and LR-.
Results: Of 407 patients (67.6% male, median age 60 years, 73% SLD etiology), CSPH prevalence was 59.2%. NICER (AUC males: 0.899 vs. females: 0.890; p = 0.803) and ANTICIPATE ± NASH (AUC males: 0.865 vs. females: 0.841; p = 0.576) showed no sex-related differences in discriminative ability for CSPH. However, discrimination was slightly higher in patients aged <60 years compared with ≥60 years (NICER: 0.929 vs. 0.865; p = 0.043, ANTICIPATE ± NASH: 0.901 vs. 0.811; p = 0.021). Neither age nor sex significantly modified the association between LSM/SSM and CSPH probability and model calibration of NICER and ANTICIPATE ± NASH remained consistent. Baveno VII criteria for CSPH performed similarly across age and sex subgroups, with only slight differences in NPV and PPV, that are likely driven by differences in underlying disease prevalence. The cumulative incidence of first hepatic decompensation did not differ significantly by age or sex and was comparable between their strata within each Baveno VII CSPH risk group.
Conclusion: VCTE-based NITs for CSPH demonstrate robust diagnostic and prognostic performance regardless of sex and age in cACLD, supporting their universal applicability as endorsed by Baveno VII.

THU-451

Sex-specific diagnostic and prognostic performance of blood- and liver stiffness-based noninvasive tests for clinically significant portal hypertension in compensated advanced chronic liver disease

Paula Hoefinger[1], Helena Schluchter[2], Georg Semmler[1], Lorenz Balcar[1], Benedikt Simbrunner[1], Lukas Hartl[1], Benedikt Hofer[1], Georg Kramer[1], Paul Thöne[1], Christian Sebesta[1], Marlene Hintersteininger[1], Philipp Schwabl[1], Michael Trauner[3], Eva Schaden[2], Thomas Reiberger[1], Mattias Mandorfer[1], Mathias Jachs[1]. *[1]Division of Gastroenterology and Hepatology, Medical University of Vienna, Vienna, Austria; Vienna Hepatic Hemodynamic Lab, Medical University of Vienna, Vienna, Austria; Department of Medicine III and Clinical Research Group Mechanisms in Portal Hypertension, Medical University of Vienna, Vienna, Austria; [2]Department of Anaesthesia, Intensive Care Medicine and Pain Medicine, Medical University of Vienna, Ludwig Boltzmann Institute Digital Health and Patient Safety, Vienna, Austria; [3]Division of Gastroenterology and Hepatology, Department of Medicine III, Medical University of Vienna, Vienna, Austria*
Email: paula.hoefinger@meduniwien.ac.at

Background and aims: Use of non-invasive tests (NITs) for clinically significant portal hypertension (CSPH) is recommended in compensated advanced chronic liver disease (cACLD), as CSPH represents the threshold for hepatic decompensation. Among these, liver stiffness measurement (LSM) by vibration-controlled transient elastography (VCTE) is most important. However, LSM is influenced by body composition, and potential sex-specific differences in diagnostic/prognostic performance remain unclear. We aimed to assess whether established blood- and LSM-based NITs perform comparably in males and females.
Method: This retrospective analysis included prospectively characterized, clinically stable cACLD outpatients who underwent HVPG measurement between 2007–2022 at the Vienna General Hospital. VCTE-LSM and laboratory testing were performed on the day of HVPG assessment. Diagnostic performance of NITs was evaluated in males and females, separately, using area under the curve (AUC) analyses and DeLong's test for group-wise comparison. Sex-specific cumulative incidences of first hepatic decompensation were analyzed using competing risk models stratified by the Baveno VII criteria and sequential Baveno VII-VITRO algorithm, which adds the von Willebrand factor to platelet count ratio (VITRO) to reduce the grey zone.
Results: In 420 patients, 281 (66.9%) were male and 139 (33.1%) were female. Median age was higher in females than in males (56.7 vs. 52.8 years; p = 0.014), while no sex-specific differences were observed for BMI, prevalence of obesity, or HVPG. For CSPH diagnosis, LSM showed numerically higher AUC in males (0.845 vs. females: 0.811, p = 0.447), whereas the VITRO score performed numerically better in females (AUC: 0.854 vs. males: 0.814, p = 0.370). The ANTICIPATE ± NASH model achieved the numerically highest AUROC, regardless of sex (male: 0.885 vs. female: 0.872, p = 0.755). Baveno VII criteria yielded similar rule-in and rule-out performance, leaving 42.3% of males and 49.6% of females unclassifiable (p = 0.176). The Baveno VII-VITRO

sequence reduced the grey zone to 12.4% and 15.1% in males and females, respectively (p = 0.450). Cumulative incidences of first hepatic decompensation were comparable between sexes throughout all Baveno VII and Baveno VII-VITRO strata.
Conclusion: Non-invasive tests and Baveno VII-based algorithms show comparable diagnostic/prognostic performance for CSPH/hepatic decompensation in males and females.

THU-452
FOHES (first overt hepatic encephalopathy score): a novel prognostic model for predicting the first episode of overt hepatic encephalopathy in patients with advanced chronic liver disease

Chien-Hao Huang[1], Cheng-Jen Chen[1], Chia-Ling Wu[2], Yu-Tung Huang[3], Piero Amodio[4]. [1]*Division of Hepatology, Department of Gastroenterology and Hepatology, Chang-Gung Memorial Hospital, Linkou Medical Center, Taoyuan, Taiwan, College of Medicine, Chang-Gung University, Taoyuan, Taiwan, Liver Research Center, Chang Gung Memorial Hospital, Linkou, Taiwan, TaoYuan, Taiwan;* [2]*Center for Big Data Analytics and Statistics, Chang-Gung Memorial Hospital, Linkou Medical Center, Taoyuan, Taiwan, TaoYuan, Taiwan;* [3]*National Center for Geriatrics and Welfare Research, National Health Research Institutes, Taiwan, Miaoli, Taiwan;* [4]*Department of Medicine, University of Padova, Padova, Italy, Padova, Italy*
Email: piero.amodio@unipd.it

Background and aims: Overt hepatic encephalopathy (OHE) imposes a significant burden on patients and healthcare systems. Currently, effective risk stratification for primary prophylaxis is lacking. We aimed to develop and validate a novel risk score (FOHES) to predict the first episode of OHE within one year in patients with advanced chronic liver disease (ACLD).
Method: Using the multi-center Chang Gung Memorial Hospital (CGMH) electronic medical records database (Taiwan), we identified 569,933 patients with ACLD. After exclusions, the final cohort comprised 223,295 patients (11,758 with incident OHE; 211,537 without OHE) enrolled between 2002 and 2022. We adopted a landmark analysis approach, utilizing clinical data from one year prior to the index date (OHE onset or pseudo-index date) to minimize reverse causality. The FOHES model was developed using logistic regression on training data (2002–2016) and validated using temporal external validation data (2017–2022).
Results: Independent predictors included in FOHES were age, Charlson Comorbidity Index, total bilirubin, albumin, ammonia, etiology (HCV, alcohol), HCC status, and medication use (diuretics, statins, and anti-HCV therapy). In the training cohort, FOHES demonstrated excellent discrimination with an AUC of 0.90. Crucially, in the external validation cohort (n = 10,483), the model maintained robust performance with an AUC of 0.84. Using a cut-off of 36.28, the score effectively stratified patients into high-risk (>20% incidence/year) and low-risk groups.
Conclusion: The FOHES is a robust, simple, and externally validated tool for predicting the first episode of OHE. High-risk patients identified by FOHES may benefit from closer surveillance or primary prophylaxis. This score paves the way for risk-stratified clinical trials in ACLD.

THU-453
Long-term outcomes of compensated cirrhosis with mild portal hypertension

Anna Huerta[1,2], Anna Brujats[1,2], Edilmar Alvarado-Tapias[1,2], Monica Pons[3], Luis Téllez[4], Asunción Ojeda[5], Carlos Aracil[6], Aitor González Amezcua[7], Ferran Torres[7], Juan Carlos García-Pagán[5], Agustín Albillos[4], Joan Genesca[3], Àngels Escorsell[1,2], Jaime Bosch[8], Càndid Villanueva[1,2]. [1]*Biomedical Research Institute Sant Pau (IIB Sant Pau), Hospital de la Santa Creu i Sant Pau, Barcelona, Spain;* [2]*Hospital de la Santa Creu i Sant Pau, Barcelona, Spain;* [3]*Hospital Universitari Vall d'Hebrón, Barcelona, Spain;* [4]*Hospital Universitario Ramón Y Cajal, Madrid, Spain;* [5]*Hospital Clínic De Barcelona, Barcelona, Spain;* [6]*Hospital Universitari Arnau de Vilanova, Lleida, Spain;* [7]*Universitat Autònoma de Barcelona, Cerdanyola del Vallès, Spain;* [8]*Bern University Hospital, Bern, Switzerland*
Email: cvillanueva@santpau.cat

Background and aims: Patients with compensated advanced chronic liver disease (cACLD) with hepatic venous pressure gradient (HVPG) <10 mmHg, i.e. still without clinically significant portal-hypertension (CSPH), have good prognosis. However, long-term outcomes in such patients have been poorly investigated. This study aims to assess long-term outcomes in a well-characterized cohort of patients with cACLD and mild-portal hypertension (PH) (i.e. ≤5 HVPG <10), and to identify factors influencing disease progression.
Method: During screening-period of PREDESCI trial, patients with cACLD who had no CSPH were excluded. Among them, those with mild-PH (defined by portal-pressure >5 and <10 mmHg) were consecutively included in this study and followed up to February-2025. Since 2015, patients with hepatitis C virus (HCV) were treated with direct-acting antivirals (DAA). All the events occurring during follow-up were recorded.
Results: 73 patients were included, mean-age of 60 ± 10, MELD of 7.8 ± 2.4, Liver stiffnes measurement (LSM) of 17.7 ± 6.8 KPa and HVPG of 7.5 ± 1.3 mmHg. 55 patients had HCV-related disease, 48 were successfully treated with DAA. During a mean follow-up of 128 months (IQR, 99–162), 32 patients died (44%) (liver-unrelated causes in 59%), 14 (19%) had hepatocellular carcinoma (HCC) and 11 (15%) cirrhosis-decompensation (5-year incidence of 10%, 15% and 4%, respectively). Liver-unrelated death and HCC were the most frequent first event occurring. Decompensation occurred after HCC in 55% cases. cACLD-progression (defined by development of CSPH) was the most frequent event occurring, with a 5-year incidence of 25%. cACLD-progression was associated with baseline-HVPG (sHR = 2.06, 95% CI = 1.41–3.01), presence of varices (sHR = 2.83, 95% CI = 1.61–4.99) and treatment with DAA (sHR = 0.43, 95% CI = 0.18–1.05).
Conclusion: Death (mainly liver-unrelated) and HCC are frequent events in cACLD with mild-PH, while decompensation is rare. Progression of ACLD to develop CSPH is the most frequent event occurring and is favored by higher baseline portal-pressure, presence of varices and absence of etiological therapy.

THU-457
Real-world effectiveness of Carvedilol vs. Propranolol for primary prophylaxis of variceal bleeding and impact on endoscopic burden

Mohamed Jalloh[1], Hareesha Bharadwaj[1], Farhan Gohar[1], Maryam Javed[1], Humberto Castellanos[1], Sushanth Shankar[1], Vanessa Carr[1], Jessica Lightfoot[1], Thomas Eardley[1], Shannon Lewis[1], Balamrit Sokhal[2]. [1]*University Hospitals of North Midlands, Stoke-on-Trent, United Kingdom;* [2]*Keele University, Newcastle-under-Lyme, United Kingdom*
Email: doctorgohar@gmail.com

Background and aims: Randomised controlled trials (RCTs) have established the efficacy of non-selective beta-blockers (NSBBs) for primary prevention of variceal bleeding in cirrhosis. However, real-world effectiveness across different NSBB agents (Carvedilol vs Propranolol) and the impact on healthcare resource utilisation, including endoscopic surveillance burden, remain uncertain.
Method: We conducted a retrospective cohort study of adults with cirrhosis undergoing index endoscopy between 2012–2020 at a UK tertiary centre with no prior variceal bleeding. Exposure was NSBB prescription (carvedilol or propranolol) at index endoscopy. Primary outcomes were first variceal bleeding and all-cause mortality, analysed using multivariable logistic regression adjusted for age, sex, aetiology, Child–Pugh class, and variceal size. Endoscopic surveillance burden was analysed using patient-year standardisation.
Results: The cohort included 546 patients (mean follow-up 3.0 years). First variceal bleeding occurred in 79 (14.5%). NSBB use was not independently associated with first bleeding (aOR 1.17, p = 0.696).

Medium/large varices were the strongest predictor of bleeding (aOR 2.16, 95% CI 1.27–3.69). NSBBs were not associated with overall mortality (aOR 0.71, p = 0.108) but showed a significant protective association in patients with compensated disease (OR 0.45, 95% CI 0.23–0.86). Patients prescribed NSBBs underwent significantly fewer surveillance endoscopies (mean difference –0.26 OGDs/patient), preventing an estimated 578 procedures—equivalent to one avoided endoscopy per four treated patients.
Conclusion: In this real-world cohort, NSBB therapy was not associated with reduced bleeding risk but was linked to a lower endoscopic surveillance burden and improved survival in compensated cirrhosis. These findings highlight challenges in translating RCT efficacy to practice and suggest that drug selection and adherence may influence outcomes.

THU-458
Quantifying the morbidity and mortality of decompensated liver cirrhosis in Australia
Angus Jeffrey[1], Leon Adams[1], Brendan Brew[2], Gary Jeffrey[1], Michael Wallace[1], Marie Sinclair[2], Adam Testro[2], John Chetwood[3], Ken Liu[3], Avik Majumdar[2]. *[1]Department of Hepatology, Sir Charles Gairdner Hospital, Perth, Medical School, The University of Western Australia, Perth, Perth, Australia; [2]Victorian Liver Transplant Unit, The Austin Hospital, Melbourne, School of Medicine, The University of Melbourne, Melbourne, Melbourne, Australia; [3]AW Morrow Gastroenterology and Liver Centre, Royal Prince Alfred Hospital, New South Wales, New South Wales, Australia*
Email: angus.jeffrey@gmail.com

Background and aims: Decompensated cirrhosis carries a significant health burden with high mortality. Outcomes after a first decompensation episode are not known in the Australian population. The aim of this study was to assess the incidence of further decompensation and survival in patients with cirrhosis following hospitalization with initial decompensation.
Method: This was a multi-centre Australian retrospective cohort study from 2006 to 2025. Adult patients with cirrhosis at three statewide liver transplant referral centres who were admitted to hospital with or developed a first decompensating event (ascites, hepatic encephalopathy, variceal bleeding) and followed until further decompensation requiring hospitalisation, liver-related death (LRD), non-liver related death, or liver transplant (LT). The primary outcome was incidence of further liver decompensation, type of clinical event, and survival outcomes following admission for first decompensation.
Results: A total of 542 patients were followed from first decompensation for a median of 24 (IQR 9–48) months, with alcohol-related liver disease the most common aetiology (52%). Cumulative incidence of further decompensation at 5-years was 65.1% (95% CI 60.3–69.5), and the incidence of LRD or LT was 39.2% (95% CI 34.1–44.2). Following further decompensation, the cumulative incidence of LRD or LT was higher compared to first decompensation at 55.5% (sHR 3.45, 95% CI 2.31–5.16, p < 0.001). Ascites was the most common type of further decompensation (35.6%, 95% CI 31.0–40.2). Aetiological treatment of the underlying CLD was protective for both further decompensation and LRD/LT (sub hazard ratio [sHR] 0.58 and 0.65 respectively, p < 0.05), as was treatment with a non-selective beta blocker (sHR 0.40 and 0.60 respectively, p < 0.01).
Conclusion: This multi-centre study describes the trajectory of patients with cirrhosis after a first episode of decompensation for the first time in the Australian context. It highlights the high morbidity and poor prognosis associated with further decompensation with over 50% dying or requiring LT within 5 years. We also found that aetiological treatment for CLD and NSBB treatment were associated with a reduced risk of further decompensation and mortality and should be considered in all appropriate patients.

THU-459
Differential increase in portal pressure across fibrosis stages in steatotic liver disease etiologies
Oliver Kiehn[1], Lise Hobolth[2], Christian Mortensen[2], Nina Kimer[2,3], Lise Lotte Gluud[2,3], Mogens Vyberg[4], Søren Møller[1,3]. *[1]Department of Clinical Physiology and Nuclear Medicine, Center for Functional and Diagnostic Imaging and Research, Copenhagen University Hospital - Amager and Hvidovre Hospital, Hvidovre, Denmark, Hvidovre, Denmark; [2]Gastro Unit, Copenhagen University Hospital - Amager and Hvidovre Hospital, Hvidovre, Denmark, Hvidovre, Denmark; [3]Department of Clinical Medicine, Faculty of Health and Medical Sciences, University of Copenhagen, Copenhagen, Denmark, København N, Denmark; [4]Department of Pathology, Copenhagen University Hospital - Amager and Hvidovre Hospital, Hvidovre, Denmark, Hvidovre, Denmark*
Email: oliver.thistrup.kiehn.02@regionh.dk

Background and aims: The burden of chronic liver disease is increasing worldwide. Beyond alcohol-related liver disease (ALD), the prevalence of metabolic dysfunction-associated liver disease (MASLD) and metabolic-associated ALD (Met-ALD) contributes substantially to cirrhosis. Advanced cirrhosis is frequently complicated by portal hypertension (PH). However, the severity of PH may differ by etiology, type of hepatic lesion and extent of steatosis, fibrosis, and cirrhosis. Since patients with MASLD appear to demonstrate a lower degree of PH we aimed at comparing the hepatic venous pressure gradient (HVPG) in patients with comparable degrees of fibrosis of different etiologies.
Method: 309 patients with MASLD (n = 142), Met-ALD (n = 59), ALD (n = 108) and 26 healthy controls with normal liver histology had consecutively performed a combined liver vein catheterization with measurement of HVPG and a transjugular liver biopsy. Liver stiffness was additionally measured by elastography (Fibroscanning). The liver biopsy was evaluated with respect to level of fibrosis (F1-F3) and cirrhosis (F4).
Results: HVPG differed significantly across etiologies at F0–F2, F3 and F4 (p < 0.05–0.01). At F0–F2, Met-ALD > MASLD (p < 0.05); at F3, ALD > MASLD (p < 0.05); at F4, Met-ALD and ALD > MASLD (both p < 0.01). Median HVPG at F4: MASLD 9 mmHg, Met-ALD 14 mmHg, ALD 13.5 mmHg. HVPG correlated with fibrosis stage overall (rho = 0.71, p < 0.001) and within MASLD (rho = 0.73, p < 0.001), ALD (rho = 0.35, p < 0.01), and Met-ALD (rho = 0.50, p < 0.001). Across all groups, the median HVPG increased from 2 mmHg (F0) to 12 mmHg (F4), with an increase of ~2.4 mmHg per stage. HVPG also correlated with fibroscanning across the groups (rho = 0.71, p < 0.001). ROC analysis showed high accuracy: AUC 0.92 for significant fibrosis (F2–F4) at 4.5 mmHg and AUC 0.86 for cirrhosis (F4) at 5.8 mmHg. Sensitivity ranged from 80–87%, specificity from 71–93%, and PPV > 95%.
Conclusion: With a comparable histological degree of fibrosis the portal pressure is significantly lower in MASLD than in ALD and Met-ALD patients. Together with distinct pathophysiological associations, this points to differences in intrahepatic hemodynamics across pathologies, potentially due to changes in intrahepatic shunting and mechanobiology.

THU-460-YI
Prognostic value of ReMELD-Na and MELD 3.0 for predicting transplant-free survival after TIPS for variceal bleeding: a multicenter retrospective study
Markus Kimmann[1], Nancy Farouk[1], Dominik Bettinger[2], Johannes Chang[3], Roman Kloeckner[4], Cristina Ripoll[5], Felix Piecha[6], Jassin Rashidi-Alavijeh[7], Juliana Stadtmann[1], Tony Bruns[8], Cornelius Engelmann[9], Benjamin Maasoumy[10], Christian Labenz[11], Lukas Sturm[2], Hauke Heinzow[12], Leon Louis Seifert[1], Michael Köhler[1], Max Masthoff[1], Johannes Kluwe[6], Alexander Zipprich[5], Christian Jansen[3], Carsten Meyer[3], Michael Schultheiß[2], Jonel Trebicka[1], Michael Praktiknjo[1]. *[1]Münster University Hospital, Münster, Germany; [2]University Hospital Freiburg, Freiburg im Breisgau,*

Germany; [3]Bonn University Hospital, Bonn, Germany; [4]Universitätsklinikum Schleswig-Holstein Campus Lübeck, Lübeck, Germany; [5]Universitätsklinikum Jena, Jena, Germany; [6]Universitätsklinikum Hamburg-Eppendorf, Hamburg, Germany; [7]University Hospital Essen, Essen, Germany; [8]Universitätsklinikum Aachen, Aachen, Germany; [9]Charité Campus Benjamin Franklin, Berlin, Germany; [10]Medizinische Hochschule Hannover, Hannover, Germany; [11]University Hospital Mainz, Mainz, Germany; [12]Krankenhaus der Barmherzigen Brüder Trier, Trier, Germany
Email: markus.kimmann@ukmuenster.de

Background and aims: ReMELD-Na (Eurotransplant) and MELD 3.0 (UNOS) were recently introduced as scores for liver transplant allocation. Their predictive value for transplant-free survival after transjugular intrahepatic portosystemic shunt (TIPS) placement in variceal bleeding remains elusive. This study evaluates the prognostic value of ReMELD-Na and MELD 3.0 in comparison to established models like FIPS, MELD-Na, and MELD.
Method: This multicenter retrospective study analyzed 576 patients with cirrhosis who underwent TIPS for variceal bleeding at eight German centers (2004–2024). The primary and secondary endpoints were 90-day and 1-year transplant-free survival, respectively. Prognostic performance was assessed by ROC analysis, with DeLong tests comparing ReMELD-Na and MELD 3.0 to the other scores. Sex-specific analyses were conducted, and high-risk (above 85th percentile of the respective score) versus non–high-risk groups were compared using Kaplan–Meier analysis and log-rank tests.
Results: Median age was 58 (49–65) with 47.7% having alcohol-related cirrhosis. Median scores for each model were: ReMELD-Na 12, MELD 3.0 14, FIPS −0.49, MELD 12, and MELD-Na 13. Transplant-free survival rates were 90.1% and 86.3% for 90 days and 1 year, respectively. ROC-AUC values ranged from 0.651 to 0.749 for 90 days and 0.676 to 0.741 for 1 year, with FIPS showing the highest values (0.749 and 0.741). DeLong test indicated that ReMELD-Na was inferior to FIPS at 90 days ($p = 0.007$). MELD 3.0 outperformed MELD ($p = 0.011$) and MELD-Na ($p = 0.035$), but was inferior to FIPS ($p = 0.038$). However, no significant differences were observed at 1 year. ROC-AUC values for the male subgroup were slightly higher than those of the female subgroup at both 90 days (male: 0.663–0.767 vs. female: 0.637–0.740) and 1 year (male: 0.686–0.735 vs. female: 0.637–0.740). Across all models, transplant-free survival was significantly reduced in the high-risk group compared with the non–high-risk group ($p < 0.001$).
Conclusion: ReMELD-Na and MELD 3.0 demonstrated comparable predictive performance for 1-year survival, but were inferior to FIPS at the 90-day time point. Despite their limited predictive value, all models enabled risk stratification after TIPS placement and could aid clinical decision-making by identifying patients who may need intensive monitoring or a priori evaluation for liver transplant. However, the limited predictive values of all models emphasize the need for further studies.

THU-461

Comparative risk of acute kidney injury after contrast media exposure in TIPS and CT imaging among patients with decompensated liver cirrhosis: a bicentric retrospective study

Markus Kimmann[1], Tammo Lambert Tergast[2], Nancy Farouk[1], Jim Benjamin Mauz[2], Zeyu Wang[1], Juliana Stadtmann[1], Silvia Letmathe[1], Jörn Arne Meier[1], Nils Theodor Manegold[1], Max Masthoff[1], Michael Köhler[1], Gesa Pöhler[1], Markus Cornberg[2], Heiner Wedemeyer[2], Jonel Trebicka[1], Martin Sebastian McCoy[1], Benjamin Maasoumy[1], Michael Praktiknjo[1]. *[1]Münster University Hospital, Münster, Germany; [2]Medizinische Hochschule Hannover, Hannover, Germany*
Email: markus.kimmann@ukmuenster.de

Background and aims: Patients with cirrhosis are at risk for acute kidney injury (AKI). However, the influence of iodine-containing contrast media (CM) on the risk of AKI in patients with cirrhosis is relatively low for contrast-enhanced (CE)-computed tomography (CT) scans. Data on AKI after CM exposure during transjugular intrahepatic portosystemic shunt (TIPS) - has not yet been clearly established. This study aimed to compare the risk of AKI following CM administration during TIPS placement with that following CE-CT imaging.
Method: In this retrospective, bicenter study, we included 554 cirrhotic patients who underwent TIPS placement and 90 patients who underwent CE-CT examinations. After propensity score matching (PSM) for age, sex, MELD score, albumin, and creatinine, the final cohort consisted of 145 TIPS patients and 90 CE-CT patients. The primary endpoints were the incidence of AKI at 7 and 28 days, defined according to the International Club of Ascites criteria. Univariate and multivariate Cox regressions were used to identify independent risk factors for AKI.
Results: Median age was 59 (52–67) years, the most-common etiology of cirrhosis was alcohol-related 53.2% and median MELD was 13 (11–17). The incidence of AKI was significantly lower in the TIPS group both after 7 (PSM: 6.2% vs. 16.7%) and 28 days (PSM: 8.3% vs. 27.8%). TIPS placement was associated with a significantly reduced risk of AKI at 7 days (HR 0.402, $p = 0.009$) and 28 days (HR 0.311, $p = 0.001$). In addition, a higher MELD score was significantly associated with an increased risk of AKI, while age, sex, and the use of beta-blockers or diuretics had no significant influence.
Conclusion: In the context of CM exposure, TIPS placement was associated with a significantly lower risk of AKI compared to CE-CT. This may be due to improved renal perfusion following TIPS in cases of functional kidney damage, such as hepatorenal syndrome. In summary, our results support the superior importance of other risk factors for AKI than CM exposure and the potential benefits of TIPS in reducing AKI risk in cirrhotic patients.

THU-462

Ultrasound-based monitoring of transjugular intrahepatic portosystemic shunt function: hemodynamic changes and prognostic relevance — Data from a prospective registry of 216 consecutive patients

Matthias Klimanek[1], Martin Franck[1], Anja Tiede[1], Annika Zietz[1,2], Anika Wranke[1], Jim Benjamin Mauz[1], Helenie Kefalakes[1], Martin Kabelitz[1], Heiner Wedemeyer[1,2], Patrick Behrendt[1], Benjamin Maasoumy[1,2]. *[1]Department of Gastroenterology, Hepatology, Infectious Diseases and Endocrinology, Hannover Medical School, Hannover, Germany; [2]German Center for Infection Research (DZIF), Hannover-Braunschweig, Germany*
Email: klimanek.matthias@mh-hannover.de

Background and aims: Ultrasound assessment is widely used when monitoring transjugular intrahepatic portosystemic shunt (TIPS) function. However, norm values and prognostic impact of the individual measurement parameters have been insufficiently investigated, so far. The aim of this study was to evaluate hemodynamic parameters for assessing TIPS function, predicting clinical outcome and their changes over time.
Method: A number of 216 consecutive patients with liver cirrhosis who underwent TIPS insertion at Hannover Medical School between 09/2019 and 12/2024 were included in a prospective registry. All available data from ultrasound examinations before TIPS insertion, within a week after, and after one, three, six, and twelve months were considered for this retrospective analysis.
Results: The median age of the cohort was 59 years and the median MELD score 12.27. Before TIPS-insertion mean Time-Averaged maximum velocity (Tmax) was measured at 15.27 cm/s in the main portal vein (PV) and 89% (n = 100) of patients had both left and right branches of the PV flowing orthograde. The median Resistance Index (RI) of the common hepatic artery was 0.73. Median Spleen length was 15 cm.
One week after TIPS insertion significant hemodynamic changes were documented. Mean Tmax of main PV increased significantly to a

33.39 cm/s ($p < 0.001$). In addition, a reversal from orthograde to retrograde flow was observed in both PV branches in 59.7% of cases. The mean maximum speed (Vmax) within the TIPS was 103.48 cm/s. In 20% of patients Vmax in the TIPS was <75 or >175 cm/s, which has been suggested as indicator for dysfunction in the past. However, this was not associated with a higher incidence of persistent ascites. Moreover, neither Tmax in the PV nor Vmax in the TIPS at this stage were linked to the occurrence of hepatic encephalopathy or the likelihood for recurrent severe ascites during further follow up.
Over time, we documented a significant continuous decrease of Tmax in the main PV, resulting in a mean Tmax of 24.55 cm/s after one year ($p = 0.02$). In contrast, no significant changes were observed in the RI of common hepatic artery or spleen size during the course of the follow-up examinations.
Conclusion: TIPS insertion immediately leads to significant alterations in hepatic blood flow. Further hemodynamic changes occur over time. However, ultrasound-based assessments of hemodynamic parameters early after TIPS insertion have a limited value for predicting clinical endpoints.

THU-463

Combining different non-invasive tests stratifies the risk of clinically significant portal hypertension (CSPH) in patients with compensated advanced chronic liver disease (cACLD)

Jimmy Che-To Lai[1,2], Pinky Yee-Ting Li[1], Grace Lai-Hung Wong[1,2], Vincent Wai-Sun Wong[1,2], Terry Cheuk-Fung Yip[1,2]. *[1]Medical Data Analytics Centre, Department of Medicine and Therapeutics, The Chinese University of Hong Kong, Hong Kong, Hong Kong; [2]Li Ka Shing Institute of Health Sciences and State Key Laboratory of Digestive Disease, The Chinese University of Hong Kong, Hong Kong, Hong Kong*
Email: jimmylai0515@gmail.com

Background and aims: Although using different algorithms with combined non-invasive tests (e.g., liver and spleen stiffness measurements [LSM and SSM, respectively]) reduces the number of patients classified as indeterminate risk of CSPH (i.e., grey zone), there has not been any comparison on which algorithm best stratifies the risk.
Method: This was the baseline analysis of a prospective cohort of adults with cACLD. The Baveno VII criteria for CSPH by LSM (≥25 kPa for ruling in and ≤15 kPa with platelet count $\geq 150 \times 10^9$/L for ruling out), SSM@100 Hz (>50 kPa for ruling in and <21 kPa for ruling out), as well as the combined Baveno VII and SSM model (fulfilling either two of LSM 15 kPa, platelet 150×10^9/L and SSM 40 kPa for ruling in and out), and the ANTICIPATE-NASH model (risk of CSPH ≥90% and <60% as ruling in and out) were assessed, with the presence of gastroesophageal varices as a surrogate marker for CSPH.
Results: 77 patients with cACLD, including 23 (29.9%) with varices, were recruited. The mean age was 64.3 years, 62.3% were male, and mean BMI was 26.1 kg/m^2, without significant difference between those with and without varices. Chronic viral hepatitis (61.0%) was the leading aetiology. Patients with varices had higher SSM (43.7 vs 28.1 kPa, $p = 0.002$) and lower platelet count (114.1 vs 173.3×10^9/L, $p < 0.001$), while there was no significant difference in LSM (17.5 vs 14.6 kPa, $p = 0.268$) between the two groups. Among the four algorithms, SSM alone classified the highest proportion of patients in the grey zone (63.6%), followed by Baveno VII criteria (46.8%), while the ANTICIPATE-NASH (22.1%) and the combined Baveno VII and SSM model (13.0%) significantly reduced the grey zone. The corresponding positive predictive values were 66.7% and 100% for ruling in, and negative predictive values were 88.4% and 75.9% for ruling out varices using the combined model and the ANTICIPATE-NASH model, respectively. The combined model had the highest area under the curve for predicting varices (0.794, 95% CI 0.670–0.918), and the strongest association with the presence of varices (odds ratio 40.0) after adjusting for non-selective beta-blocker (NSBB) use.
Conclusion: The combined Baveno VII and SSM model differentiates risk of CSPH, while ANTICIPATE-NASH model serves as an alternative when SSM is not available, to guide NSBB use in patients with cACLD.

Financial statement: This study is supported by the Health and Medical Research Fund of Health Bureau of HKSAR Government (Reference number: 11222426).

THU-464-YI

ELF score and specifically hyaluronic acid one month after TIPS predict clinical outcomes

Lorenzo Lani[1,2,3,4], Marlene Hintersteininger[1,2], Theresa Müllner-Bucsics[1], Susanna Riegler[1], Georg Kramer[1,2], Christian Sebesta[1,2], Paul Thöne[1,2], Paula Hoefinger[1], Benedikt Simbrunner[1,2], Lukas Reider[5], Matthias Weiss-Tessbach[6], Rodrig Marculescu[6], Maria Schoder[5], Michael Trauner[1], Mattias Mandorfer[1,2], Thomas Reiberger[1,2,7], Lukas Hartl[1,2]. *[1]Division of Gastroenterology and Hepatology, Department of Medicine III, Medical University of Vienna, Vienna, Austria, Vienna, Austria; [2]Vienna Hepatic Hemodynamic Lab, Division of Gastroenterology and Hepatology, Department of Medicine III, Medical University of Vienna, Vienna, Austria, Vienna, Austria; [3]Unit of Semeiotics, Liver and Alcohol-related Diseases, IRCCS Azienda Ospedaliero-Universitaria di Bologna, Bologna, Italy, Bologna, Italy; [4]Department of Medical and Surgical Sciences, University of Bologna, Bologna, Italy, Bologna, Italy; [5]Department of Biomedical Imaging and Image-guided Therapy, Medical University of Vienna, Vienna, Austria, Vienna, Austria; [6]Department of Laboratory Medicine, Medical University of Vienna, Vienna, Austria, Vienna, Austria; [7]Christian Doppler Lab for Portal Hypertension and Liver Fibrosis, Medical University of Vienna, Vienna, Austria, Vienna, Austria*
Email: lorenzo.lani@studio.unibo.it

Background and aims: The Enhanced Liver Fibrosis (ELF) test, combining hyaluronic acid (HA), tissue inhibitor of metalloproteinases-1 (TIMP-1) and procollagen III N-terminal propeptide (PIIINP), is a marker of hepatic extracellular matrix turnover and fibrogenesis. We assessed the prognostic value and dynamics of ELF in patients with cirrhosis undergoing transjugular intrahepatic portosystemic shunt (TIPS).
Method: Patients undergoing covered TIPS placement at the Vienna General Hospital included in the prospective AUTIPS registry (NCT: NCT03409263; 01/2017–03/2025) with available ELF values pre- and post-TIPS were considered. ELF and its components were measured at baseline (BL), 1-month (M1) and M12 post-TIPS. Spearman and Fine-Gray competing risk regression (liver transplantation *versus* death) studied correlations and outcome associations.
Results: Among 80 included patients (median age 57 years, 65% male, 54% alcohol-related liver disease), median BL ELF was 11.7 (11.0–12.8). ELF showed an early increase after TIPS, followed by a return to baseline (BL: 11.7 vs M1: 12.2 vs M12: 11.9; $p < 0.001$). Both HA and PIIINP also increased at M1 and returned to BL values, (HA: BL: 322.2 ng/mL vs. M1 368.5 ng/mL vs M12: 313.7 ng/mL; $p < 0.001$; PIIINP: 19.3 ng/mL vs. M1: 28.3 ng/mL vs. M12 23.9 ng/mL; $p < 0.001$). Interestingly, however, TIMP-1 showed a constant decrease after TIPS (BL: 444.4 ng/mL vs M1: 404.6 ng/mL vs LM: 366 ng/mL; $p < 0.001$). Changes in ELF at M1 after TIPS correlated with those of Model of End Stage Liver Disease score (rho = 0.303, $p = 0.024$), liver stiffness (rho = 0.413, $p = 0.043$), Interleukin-6 (rho = 0.52, $p < 0.001$) and C-reactive protein (rho = 0.43, $p < 0.001$). ELF at M1 (aSHR: 1.62, 95% CI 1.13–2.33, $p = 0.009$) was independently linked to post-TIPS mortality. Specifically, M1 HA was independently associated with overt post-TIPS encephalopathy (per ng/mL $\times 10^{-3}$: asHR: 1.04, 95% CI 1.01–1.08, $p = 0.011$), acute-on-chronic liver failure (ACLF; per ng/mL $\times 10^{-3}$: asHR = 1.01, 95% CI 1.01–1.02, $p < 0.001$) and death (per ng/mL $\times 10^{-3}$: asHR: 1.01, 95% CI 1.01–1.02, $p < 0.001$). Patients with HA ≥442 mg/mL at M1 had significantly higher cumulative incidence of ACLF ($p = 0.043$) and death ($p = 0.013$) after TIPS.
Conclusion: ELF score and its components show a distinct dynamic post-TIPS with TIMP1 constantly decreasing, but a transient M1 increase in HA and PIIINP followed by a M12 decrease. A pronounced

early (M1) increase in HA after TIPS may reflect reduced sinusoidal clearance and indicates higher risks of HE, ACLF, and death.

THU-465

Splenic hyperkinetic syndrome: a universal driver of cirrhotic and non-cirrhotic portal hypertension

Sergii Kozlov[1], Ihor Kolosovych[1], Nadiia Yakovenko[1], Natalia Leshchynska[1]. [1]*Bogomolets National medical university, Kyiv, Ukraine*
Email: sergiinikol@gmail.com

Background and aims: Portal hypertension (PH) is attributed to increased intrahepatic resistance. However, the role of splanchnic hyperdynamic circulation, specifically excessive inflow, remains underappreciated. We hypothesized that splenic arterial hyperperfusion acts as a universal hemodynamic driver in PH - regardless of etiology - creating a volume overload that the portal system cannot accommodate. This study aims to evaluate the relations between splenic arterial inflow and portal venous flow in patients with established cirrhotic and non-cirrhotic PH.
Method: The study included three groups: 1) 47 patients with liver cirrhosis and cirrhotic PH (CPH); 2) 7 patients with non-cirrhotic PH (NCPH); 3) a control group of 41 healthy volunteers (CG). All patients of the CPH and NCPH groups presented with esophageal and gastric varices and a history of variceal bleeding(s). All participants underwent a Doppler ultrasound assessment. We analyzed spleen volume, splenic artery parameters (PSV, EDV, RI), and maximum linear flow velocities (V_{max}) in the splenic vein and the main portal vein (PV) trunk.
Results: Patients in the CPH group presented with significant splenomegaly (811.6 ± 342.2 cm/s vs. 146.35 ± 56.27 cm^3 in controls; $p < 0.001$) and a severe hyperdynamic state. PSV in the SA was up to 150.84 ± 43.57 cm/s compared to 85.43 ± 26.72 cm/s in controls ($p < 0.001$), with EDV nearly doubling. This arterial surge led to venous overload (SV velocity was 34.1 ± 15.55 cm/s vs. 23.54 ± 6.16 cm/s in CG, $p < 0.001$). A paradoxical deceleration was observed in the main portal vein (29.06 ± 9.43 cm/s vs. 35.67 ± 10.53 cm/s in controls, $p < 0.01$). This «hemodynamic mismatch» is a result of an existing left gastric vein shunt that feeds gastric/esophageal varices, effectively reducing velocity in the main portal trunk.
Conclusion: Our findings reveal distinct hemodynamic changes in patients with clinically significant portal hypertension: massive splenic artery inflow leads to accelerated venous output, which is then diverted to portosystemic collaterals (gastoesophageal varices). This pattern was consistent across both CPH and NCPH cohorts, suggesting that excessive splenic blood flow is a universal pathogenic driver of portal hypertension development. Targeting splenic inflow (e.g. via NSBB treatment, embolization or both) addresses this fundamental mechanism of collateral filling and may be effective regardless of the portal hypertension etiology.

THU-466

The differential effects of terlipressin on serum sodium trajectories are mediated by ascites status, treatment indication and baseline sodium

Dorothy Liu[1], Jacqueline Balassone[2], Royston Fernandes[3], Sophie Testro[4], Dinesh Pandey[5], Penelope Hey[1], Karl Vaz[6], Marie Sinclair[1], Avik Majumdar[1], Adam Testro[6]. [1]*Victorian Liver Transplant Unit, Austin Health, Australian Centre for Transplantation Excellence and Research (ACTER), Austin Health, Department of Medicine (Austin Precinct), The University of Melbourne, Melbourne, Australia;* [2]*Victorian Liver Transplant Unit, Austin Health, Australian Centre for Transplantation Excellence and Research (ACTER), Austin Health, Department of Pharmacy, Austin Health, Melbourne, Australia;* [3]*Victorian Liver Transplant Unit, Austin Health, Australian Centre for Transplantation Excellence and Research (ACTER), Austin Health, Melbourne, Australia;* [4]*Faculty of Science, The University of Melbourne, Melbourne, Australia;* [5]*Business Intelligence Unit, Austin Health, Melbourne, Australia;* [6]*Victorian Liver Transplant Unit, Austin Health, Australian Centre for Transplantation Excellence and Research (ACTER), Austin Health, Department of Surgery (Austin Precinct), The University of Melbourne, Melbourne, Australia*
Email: dorothyliu22@gmail.com

Background and aims: Terlipressin is an established therapy for complications of portal hypertension, however concerns persist regarding its potential to cause hyponatremia. Data describing serum sodium (sNa) trajectories during terlipressin therapy across clinical phenotypes are limited.
Method: We conducted a single-centre, retrospective study of consecutive adult patients treated with terlipressin between 2013 and 2024. Patients receiving treatment for < 2 days, with intrinsic renal disease or on renal replacement therapy were excluded. Linear mixed-effects modelling was used to analyse sNa trajectories for up to 14 days of treatment, stratified by ascites status, treatment indication and baseline sNa. Patients with a ≥ 5% sNa decrease from baseline were also evaluated. Severe hyponatremia was defined as sNa < 125 mmol/L.
Results: Across the entire cohort of 414 patients, sNa was observed to increase during terlipressin therapy (adjusted mean sNa change from baseline to day 14: 4 mmol/L, 95% CI 3 to 6, $p < 0.001$). However, changes in sNa differed according to the presence or absence of ascites, baseline sNa, and the indication for use (acute variceal bleeding [AVB]). Adjusted sNa increased over time in patients with ascites but remained stable in those without ascites. Similarly, adjusted sNa increased over time in baseline hyponatremic patients but remained stable in baseline normonatremic patients. An early decline in adjusted sNa was observed in patients with baseline normonatremia, no ascites, and treated with terlipressin for AVB (adjusted mean sNa change from baseline to day 5: −7 mmol/L, 95% CI −9 to −4, $p < 0.001$). 44 patients (11%) experienced a ≥ 5% decline in sNa relative to baseline and were more likely to have higher baseline sNa, lower baseline serum creatinine, lower Model for End-Stage Liver Disease (MELD) and be treated for AVB ($p < 0.001$). Baseline sNa and MELD were independently associated with a ≥ 5% decline in sNa from baseline (adjusted OR 1.13, $p < 0.001$ and adjusted OR 0.91, $p < 0.004$, respectively). Severe hyponatremia was rare, occurring in 10 patients (2%).
Conclusion: Whilst at a population level terlipressin increased sNa, we observed differential effects on sNa according to ascites status, treatment indication and baseline sNa. Clinically significant hyponatremia was uncommon and occurred mainly in patients without ascites, with higher baseline sNa and AVB as the indication for terlipressin, highlighting the need for closer monitoring in this subgroup during therapy.

THU-467

Liver stiffness measurement as an alternative to liver biopsy to rule-out cirrhosis over PSVD in patients with portal hypertension

Ann T Ma[1], Lorenz Balcar[2], Lucile Moga[1,3], Fanny Turon[4,5,6], Georg Kramer[2], Georg Semmler[2], Ignasi Olivas[7,8], María Carlota Londoño[7,8], Lukas Burghart[9], Benedikt Hofer[10], Pierre Nahon[11], Nathalie Ganne-Carrié[11], Vlad Ratziu[12], Aurélie Plessier[1,3], Bernhard Scheiner[2], Virginia Hernández-Gea[4,5,6], Laure Elkrief[13], Pierre-Emmanuel Rautou[1,3]. [1]*Service d'Hépatologie, AP-HP, Hôpital Beaujon, DMU DIGEST, Centre de Référence des Maladies Vasculaires du Foie, FILFOIE, ERN RARE-LIVER, Clichy, France;* [2]*Division of Gastroenterology and Hepatology, Department of Medicine III, Medical University of Vienna, Vienna, Austria; Clinical Research Group MOTION, Medical University of Vienna, Vienna, Austria;* [3]*Centre de recherche sur l'inflammation, Université Paris-Cité, Inserm, Paris, France;* [4]*Hepatic Hemodynamic Laboratory, Liver Unit, Hospital Clínic, European Reference Network on Rare Liver Disorders (ERN-RareLiver), CSUR Centro de referencia del Sistema Nacional de Salud en Enfermedad Hepática Vascular Compleja en adultos, Barcelona, Spain;* [5]*Fundació de Recerca Clínic Barcelona-Institut d'Investigacions Biomèdiques August Pi*

i Sunyer (FRCB-IDIBAPS), Barcelona, Spain; Centro de Investigación Biomédica en Red Enfermedades Hepáticas y Digestivas (CIBEREHD), Madrid, Spain; AGAUR SGR2021 01115, Barcelona, Spain; [6]Medicine Department, Faculty of Medicine, and Health Science, Universitat de Barcelona, Barcelona, Spain; [7]Liver Unit, Hospital Clínic Barcelona, European Reference Network on Hepatological Diseases (ERN RARE-LIVER), Barcelona, Spain; [8]Fundació de Recerca Clínic Barcelona-Institut d'Investigacions Biomèdiques August Pi i Sunyer (FRCB-IDIBAPS), Centro de Investigación Biomédica en Red en Enfermedades Hepáticas y Digestivas (CIBEREHD), Universitat de Barcelona, Barcelona, Spain; [9]Division of Gastroenterology and Hepatology, Department of Medicine III, Medical University of Vienna, Vienna, Austria, Department of Internal Medicine IV, Klinik Ottakring, Vienna, Austria; [10]Vienna Hepatic Hemodynamic Laboratory, Division of Gastroenterology and Hepatology, Department of Internal Medicine III, Medical University of Vienna, Vienna, Austria; Christian Doppler Lab for Portal Hypertension and Liver Fibrosis, Medical University of Vienna, Vienna, Austria; [11]AP-HP, Hôpitaux Universitaires Paris Seine Saint-Denis, Liver Unit, Bobigny, Université Sorbonne Paris Nord, F-93000 Bobigny; Inserm, UMR-1138 "Functional Genomics of Solid Tumors", Centre de Recherche des Cordeliers, Université de Paris, Paris, France; [12]Sorbonne Université, Institute for Cardiometabolism and Nutrition, Hôpital Pitié-Salpêtrière, INSERM Unité Mixte de Recherche Scientifique 1138 Centre de Recherche des Cordeliers, Paris, France; [13]Université de Tours et Service d'Hépatogastroentérologie, Centre de référence constitutif des maladies vasculaires du foie, Hôpital Trousseau, CHU de Tours, Tours, France
Email: ma.ann.thu@gmail.com

Background and aims: Diagnosis of portosinusoidal vascular liver disease (PSVD) requires exclusion of cirrhosis using a liver biopsy together with signs of portal hypertension (PH) and/or histological lesions of PSVD. Previous studies showed that liver stiffness measurement using vibration-controlled transient elastography (VCTE-LSM) <10 kPa raises suspicion of PSVD in patients with signs of PH (non specific or specific). The aim of this study was to determine if VCTE-LSM <10 kPa, in patients with specific signs of PH, can reliably rule-out cirrhosis.
Method: Retrospective study including patients with specific signs of PH (either medium-large gastroesophageal varices or history of variceal bleeding or band ligation, or portosystemic collaterals on imaging) and biopsy-proven Child-Pugh A cirrhosis or PSVD according to VALDIG criteria. We compared reliable VCTE-LSM values, performed within 1 year of liver biopsy, between patients with PSVD and those with cirrhosis. Derivation cohort included patients from 3 European centers. Validation consisted in a reanalysis of a previously published cohort (PMID: 33345307), but focusing on patients with specific signs of PH. Data are presented as median (IQR).
Results: The derivation cohort included 106 patients with PSVD and 137 with cirrhosis (46% alcohol-related, 19% autoimmune hepatitis, 13% MASLD, 10% viral, 12% cryptogenic, 3% others). Median VCTE-LSM was 8.8 kPa (6.9–12.2) in patients with PSVD vs. 40.4 kPa (21.3–62.1) in those with cirrhosis ($p < 0.001$). VCTE-LSM <10 kPa had a specificity of 98% to rule out cirrhosis: 66/106 (62%) of patients with PSVD and 3/137 (2%) with cirrhosis had a VCTE-LSM <10 kPa. Of the 3 patients with cirrhosis misclassified, 2 had cryptogenic cirrhosis and 1 had autoimmune hepatitis. The validation cohort included 65 patients with PSVD and 43 with cirrhosis (53% viral, 40% alcohol-related, 7% MASLD). VCTE-LSM <10 kPa had a specificity of 98% to rule out cirrhosis: 48/65 (74%) patients with PSVD and 1/42 (2%) with cirrhosis had a VCTE-LSM <10 kPa. The single misclassified patient had alcohol-related cirrhosis and a VCTE-LSM of 9.8 kPa.
Conclusion: This study including a total of 171 patients with PSVD and 180 patients with cirrhosis demonstrates that, in the presence of specific signs of PH, a VCTE-LSM <10 kPa can reliably rule out cirrhosis. This threshold may therefore be considered for use in the context of clinical trials.

THU-468

Acute variceal bleeding in the UK: contemporary management and outcomes from a nationwide cohort study

Gaurav Nigam[1], Thomas Marjot[1], Shane Goodwin[2], Sarah Hearnshaw[3], Kathryn Oakland[4], John Grant-Casey[5], Ramon Uberoi[6], Alissa Walsh[1], Michael Murphey[7], Vipul Jairath[2,8], Simon Travis[1,9], Joanna Leithead[10], Andrew Douds[11], Adrian Stanley[12].
[1]Translational Gastroenterology and Liver Unit, Nuffield Department of Medicine, John Radcliffe Hospital, University of Oxford, Oxford, United Kingdom; [2]Lawson Health Research Institute, London Health Science Centre, Ontario, Canada; [3]Newcastle upon Tyne Hospitals NHS Foundation Trust, Newcastle, United Kingdom; [4]Digestive Diseases Department, HCA Healthcare UK, London, United Kingdom; [5]National Comparative Audit of Blood Transfusion NHS Blood and Transplant, London, United Kingdom; [6]Department of Interventional Radiology, John Radcliffe Hospital, Oxford University Hospitals NHS Trust, Oxford, United Kingdom; [7]NHS Blood and Transplant, Department of Haematology, Oxford University Hospitals NHS Foundation Trust, Radcliffe Department of Medicine, University of Oxford, Oxford, United Kingdom; [8]Department of Medicine, Division of Gastroenterology, Schulich school of Medicine, Western University; Department of Epidemiology and Biostatistics, Western University, London, Ontario, Canada; [9]Kennedy Institute and Biomedical Research Centre, University of Oxford, Oxford, United Kingdom; [10]Forth Valley Royal Hospital, Larbert, Falkirk, UK, Falkirk, United Kingdom; [11]Norfolk and Norwich University Hospital, Norwich, United Kingdom; [12]Department of Gastroenterology, Glasgow Royal Infirmary, Glasgow, United Kingdom
Email: gaurav.nigam@ouh.nhs.uk

Background and aims: Acute variceal bleeding (AVB) remains a life-threatening complication of portal hypertension. While outcomes have improved with standardisation of care, real-world data on adherence to best practice remain limited.
Method: We conducted a prospective, multicentre observational study across 147 UK hospitals, capturing real-world clinical, endoscopic, and organisational data for all acute upper gastrointestinal bleeding (AUGIB) presentations over an 8-week period in 2022. AVB management and outcomes were analysed by liver disease aetiology and hospital type, and compared with a 2007 national audit.
Results: Of 4279 patients undergoing endoscopy, 418 (10%) had confirmed AVB. Despite patients being older and more comorbid than in 2007, all-cause mortality was similar (13% vs. 15%, $p = 0.36$). Improvements were seen across several domains, yet pre-endoscopic antibiotics (57%) and vasopressors (64%) remained underused, and transfusion practices were often non-restrictive (55%). Only 42% of patients with recurrent AVB had received both endoscopic variceal ligation (EVL) and non-selective beta-blockers (NSBB) for secondary prevention, with 14% receiving neither therapy. Alcohol-related presentations had higher adherence to key care standards and were associated with reduced bleed-related (aOR 0.18; 95% CI 0.05–0.69) and all-cause mortality (aOR 0.36; 95% CI 0.15–0.88). This may indicate a greater general awareness of alcohol as a liver disease risk factor and due to ALD being more visible to acute physicians secondary to higher rates of clinical jaundice and coagulopathy. Survival between 14–28 days was higher in specialist liver centres ($p = 0.03$), although this was not statistically significant after adjustment for Child-Pugh class and age (HR 0.17; 95% CI 0.02–1.21; $p = 0.08$). Notably, 35% of hospitals lacked a consultant hepatologist. Transjugular intrahepatic portosystemic shunt (TIPSS) was underused, with less than 10% of eligible patients receiving the procedure.
Conclusion: AVB-related mortality in the UK is stable and but gaps remain in delivery of optimal clinical care, particularly in non-alcohol related presentations. Priorities include improving pre-endoscopic management, secondary prophylaxis, and TIPSS utilisation. Ongoing education and training, in addition to expansion of the specialist hepatology workforce requires re-evaluation.

THU-473

EUS-guided direct portal pressure, clinically significant portal hypertension and spleen stiffness: diagnostic and prognostic integration in a prospective cohort

Francesco Martini[1], Lucia Salvi[1], Martina Dalla Bella[1], Annalisa Alessandrini[1], Daniele Balducci[1], Michele Montori[1], Luca Maroni[1], Marco Marzioni[1], Antonio Benedetti[1], Giuseppe Tarantino[1]. [1]*Azienda Ospedaliero Universitaria delle Marche, Clinic of Gastroenterology, Hepatology and Endoscopy, Ancona, Italy*
Email: martinifrancesco319@gmail.com

Background and aims: Clinically significant portal hypertension (CSPH) drives variceal formation and decompensation. The hepatic venous pressure gradient is invasive and not widely available, while non-invasive surrogates lack perfect individual accuracy. Endoscopic ultrasound (EUS)-guided direct portal venous pressure (PVP) can provide haemodynamic information during endoscopy. We evaluated the diagnostic performance of PVP versus the portal pressure gradient (PPG = PVP−hepatic/inferior vena cava pressure) for CSPH and explored their relationship with non-invasive markers and hepatic decompensation.
Method: Prospective single-centre cohort of adults undergoing combined upper endoscopy and EUS-guided portal pressure measurement. PVP was measured in the main portal vein; PPG was calculated as the difference between PVP and hepatic or inferior vena cava pressure. The protocol used conscious sedation, left-lateral decubitus, spontaneous breathing and zeroing at the mid-axillary line, with ≥3 stable end-expiratory plateaus per site. Liver and spleen stiffness were assessed by transient elastography; platelet count was obtained from routine tests. Diagnostic performance was assessed by ROC curves and paired DeLong tests. Associations with CSPH and prior decompensation were evaluated in prespecified multivariable logistic models; subsequent decompensation was analysed by Kaplan–Meier and Cox models using PVP ≥20 mmHg and PPG ≥10 mmHg and internally validated continuous effects.
Results: Fifty-two patients were included (63.5% male; median age 56.5 years); CSPH was present in 31/52 (59.6%). For CSPH, AUCs were 0.84 for PVP and 0.67 for PPG ($p = 0.005$); optimal thresholds were 27.5 and 10.5 mmHg. Higher PVP, but not PPG, remained independently associated with CSPH and prior decompensation. PVP correlated strongly with spleen stiffness ($r \approx 0.77$, $R^2 \approx 0.59$), with weaker correlations for liver stiffness and platelets. Over a median follow-up of 255 days, 12 patients (23%) developed hepatic decompensation; risk was higher for PVP ≥20 mmHg (log-rank $p \approx 0.007$), while PPG showed a less stable association in penalised and bootstrap-validated Cox models.
Conclusion: EUS-measured PVP outperforms PPG for CSPH, aligns closely with spleen stiffness and provides a more consistent prognostic signal for decompensation. These data support integrating EUS-guided haemodynamic assessment with non-invasive markers for risk stratification in hepatology pathways and call for multicentre validation alongside traditional invasive strategies.

THU-474

EUS-guided coil and glue injection and beta-blockers versus b-blockers alone for primary prophylaxis of gastric varices in cirrhosis – a multicentre propensity-matched analysis from India

Shubham Mehta[1], Amol Bapaye[2], Jimil Shah[3], Pawan Khatri[2], Vignesh Dwarkanathan[4], Harsh Jain[1], Shrihari Anil Anikhindi[5], Hitesh Panchal[1], Nikhil Sonthalia[6], Anirudh Gupta[7], Ankit Agarwal[8], Ashish Agarwal[8], Aditya Vikram Pachisia[9], Pawan Rawal[1], Rajesh Puri[1]. [1]*Medanta Hospital, Gurugram, India;* [2]*Deenanath Mangeshkar Hospital & Research Centre, Pune, India;* [3]*Postgraduate Institute Of Medical Education And Research Chandigarh, Chandigarh, India;* [4]*Esic Medical College and Hospital, Chennai, India;* [5]*Sir Ganga Ram Hospital, New Delhi, India;* [6]*Apollo Gleneagles Hospital, Kolkata, India;* [7]*Sawai Man Singh Medical College, Jaipur, India;* [8]*All India Institute of Medical Sciences College, Jodhpur, India;* [9]*Commando Hospital, Bengaluru, India*
Email: mehta.shubham1493@gmail.com

Background and aims: EUS-guided coil and cyanoacrylate injection (EUS-CG) is effective for bleeding gastric varices (GV) and secondary prophylaxis, however, there is paucity of data on primary prophylaxis of GV. We compared the efficacy of addition of EUS-CG to beta-blockers against beta-blockers alone for primary prophylaxis of GV bleeding.
Method: This multi-centre observational study included patients across 8 tertiary care centres in India. Adult patients with cirrhosis and large gastric varices (F2 or F3) without prior bleeding were included. Baseline demographics, prior non-bleeding decompensating events and clinical outcomes including bleeding, hepatic decompensation and mortality were reviewed. Patients on beta-blockers undergoing EUS-CG (EUS-CG + ß-blocker arm) were compared with propensity-matched patients on beta-blockers alone (ß-blocker arm). The primary outcome was to compare the probability of being free from first GV bleeding.
Results: Of 231 patients, 86 who underwent EUS-CG and received beta-blockers were compared with 86 propensity-matched cases who received beta-blockers alone. Of 86 patients in the EUS-CG + ß-blocker arm with a median follow up of 15.3 months, 9 (10.5%) patients had GV bleeding, while among 86 propensity-matched cases in ß-blocker arm with a median follow-up of 25.9 months, 25 (29.1%) patients had GV bleeding. There was no significant difference in the probability of being free from first GV bleeding (sHR: 0.60,95% CI:0.28–1.27; $p = 0.18$), all-cause bleeding (sHR:0.76,95%CI:0.43–1.34;$p = 0.34$), freedom from hepatic decompensation (sHR:0.70,95%CI:0.45–1.08;$p = 0.10$) and overall survival (sHR: 1.54, 95% CI: 0.75–3.16; $p = 0.24$) between the patients in the EUS-CG + ß-blocker arm compared to ß-blocker arm. On multivariate regression analysis, higher MELD-Na score alone was a significant predictor of bleeding (aOR:1.12,95%CI:1.06–1.19; $p = 0.03$) and mortality (aOR: 1.23,95%CI:1.11–1.34; $p = 0.02$). Sub-group analysis revealed no significant difference in outcomes across Child-Pugh classes, though patients with F3 gastric varices had lower GV bleeding rates (sHR:0.33, 95%CI:0.13–0.84; $p = 0.02$).
Conclusion: In patients with cirrhosis and large gastric varices, a combination of EUS-coil and glue injection and beta-blockers was not superior to ß-blocker alone therapy for the prevention of first GV bleeding. Randomised controlled trials are needed to study the efficacy of EUS-coil and glue injection for primary prophylaxis of GV bleeding.

THU-475

Disease severity modifies the mortality benefit of antibiotic prophylaxis in patients with liver disease and upper gastrointestinal bleeding

Noy Nachmias-Peiser[1,2], Oren Shibolet[1,2], Michal Hoffman Ben-Shabat[2]. [1]*Department of Gastroenterology and Liver Diseases, Tel Aviv Sourasky Medical Center, affiliated with Gray Faculty of Medicine, Tel Aviv University, Tel Aviv, Israel, Tel Aviv-Yafo, Israel;* [2]*Gray faculty of medical and health science, Tel Aviv university, Tel Aviv, Israel*
Email: noy.na87@gmail.com

Background and aims: Antibiotic prophylaxis is recommended for cirrhotic patients with acute variceal bleeding, but data supporting its routine use is limited. This study evaluates the impact of prophylactic antibiotics and the timing of administration on mortality in patients with liver disease and upper gastrointestinal bleeding, stratified by MELD score.
Method: This retrospective cohort study included 441 adult patients with suspected acute upper GI bleeding and pre-existing liver disease from Tel Aviv Sourasky Medical Center (June 2006-November 2024). All patients underwent gastroscopy. Prophylactic antibiotic exposure was defined as systemic antibiotics within 24 hours of admission. The

primary outcome was in-hospital mortality. Multivariable logistic regression was performed for the overall cohort and separately for patients with confirmed cirrhosis (n = 285), stratified by MELD score.
Results: Antibiotics were given to 122 patients (27.7%). Those receiving antibiotics had higher disease severity (median MELD score 18 versus 14.5, p = 0.002). Crude mortality was higher in the antibiotic group (12.3 versus 4.1%, p = 0.002). Mortality increased with MELD severity, 3.5% for MELD ≤10, 13.3% (10 < MELD < 19), and 36.0% (MELD ≥19) (p < 0.001). After multivariable adjustment, antibiotic use did not reduce mortality overall, but in patients with MELD ≥19, it was associated with lower mortality (adjusted odds ratio 0.24, 95% CI 0.06–0.98, p = 0.047). No benefit was found for patients with MELD <19. Timing analysis showed no survival advantage for antibiotics administered before endoscopy compared to within 24 hours of admission (adjusted odds ratio 2.41, 95% CI 0.76–7.68, p = 0.136). Intravenous pantoprazole was associated with lower mortality.
Conclusion: In this retrospective cohort, antibiotic prophylaxis was associated with lower in-hospital mortality among patients with liver disease and upper gastrointestinal bleeding who had a high MELD score, but not among those with lower MELD scores. These findings suggest that disease severity may modify the association between antibiotic prophylaxis and survival. Notably, the observed benefit of antibiotic prophylaxis did not appear to be strongly influenced by administration before endoscopy. Together, these results underscore the need for prospective studies to further investigate whether severity-based stratification, such as by MELD score, can help refine current approaches to prophylactic antibiotic use.

THU-476

Hepatic bile acid extraction in liver cirrhosis and longitudinal profiles after transjugular intrahepatic portosystemic shunt placement

Maximilian Nepel[1], Simon Johannes Gairing[2], Nicole Feldbacher[1], Peter R. Galle[2], Tilmann Graeter[1], Florian Hinterhoelzl[1], Myriam Meineck[2], Romana Penker[1], Michael Bernhard Pitton[2], Rupert Horst Portugaller[1], Giovanny Rodriguez Blanco[1], Eva Maria Schleicher[2], Paul Schneider[2], Luisa Smolle[1], Jasmin Soehngen[2], Julia Weinmann-Menke[2], Gernot Zollner[1], Christian Labenz[2], Vanessa Stadlbauer[1]. *[1]Medizinische Universität Graz, Graz, Austria; [2]University Medical Center of the Johannes Gutenberg-University, Department of Internal Medicine I, Cirrhosis Center Mainz (CCM), Mainz, Germany*
Email: vanessa.stadlbauer@medunigraz.at

Background and aims: Liver cirrhosis causes progressive loss of hepatic metabolic function, including impaired uptake and clearance of bile acids (BAs) from portal blood. This may alter the transhepatic BA gradient and promote portal hypertension with complications such as refractory ascites or variceal bleeding. Transjugular intrahepatic portosystemic shunt (TIPS) reduces portal pressure by diverting portal blood into the systemic circulation but bypasses hepatic BA extraction, potentially modifying systemic BA profiles. This study aimed to characterize the transhepatic BA gradient in cirrhotic patients and to evaluate longitudinal changes in BA concentrations after TIPS placement.
Method: Serum BA concentrations in 82 patients with liver cirrhosis (age 62 +/- 12.8 years, 28% female) undergoing TIPS placement were quantified with ultrahigh-performance liquid chromatography tandem mass spectrometry (UPLC-MS/MS). The hepatic BA extraction by the liver across disease severity (Child–Pugh (CP) classes A–C) was assessed by simultaneous hepatic and portal vein sampling during TIPS. Peripheral serum samples were obtained before TIPS, immediately after, and up to 180 days post-procedure to evaluate longitudinal changes in systemic BA profiles.
Results: Hepatic BA extraction was observed in 81% of patients and correlated significantly with disease severity by CP class (p < 0.002). Median hepatic extraction of total BAs decreased from 52% in CP A to 14% in CP C, with significant extraction of conjugated primary as well as conjugated and unconjugated secondary BAs. Following TIPS, absolute serum BA profiles changed significantly over time, whereas relative composition remained largely preserved. Individual BA profiles were similar at baseline and immediately after TIPS. However, total BA levels (p < 0.002), particularly conjugated primary BAs (p < 0.01), increased up to day 90. Afterwards, they declined toward baseline by day 180.
Conclusion: Hepatic BA extraction remained detectable even in advanced liver cirrhosis but declined progressively across CP classes and affected the entire BA pool. After TIPS and diversion of portal flow, systemic BA levels, particularly conjugated primary BAs, increased during the first three months, followed by a decline at six months. Whether rising BA levels reflect enhanced BA synthesis or impaired clearance due to shunting, and whether subsequent decreases indicate metabolic adaptation, requires further investigation.

THU-477

Transjugular intrahepatic portosystemic shunt in complicated porto sinusoidal vascular disease: a multicentric retrospective study with propensity score

Marie Vandois[1], Marika Rudler[2], Pierre-Emmanuel Rautou[3], Lena Dube[4], Christophe Bureau[5], Laure Elkrief[6], Nicolas Carbonell[7], Paul Hermabessière[8], Amélie Semper[8], Teresa Antonini[9], Jean Charles Nault[10], Isabelle Mabile-Archambeaud[11], Armand Abergel[12,13], Magdalena Meszaros[14], Géraldine Dahlqvist[15], Jérôme Dumortier[16], Audrey Coilly[17], Valentin Rolle[18], Giuliana Amaddeo[19], Odile Goria[20], Théophile Gerster[21], Marwin Farrugia[22], Alexandre Sayadi[23], Charlotte Bouzbib[2], Aurélie Plessier[3], Florent Artru[4], Hélène Larrue[24], Fanny Dujardin[6], Jean Paul Cervoni[25], Jérôme Gournay[11], Rodolphe Anty[26], Dominique Cazals-Hatem[3], Momar Diouf[1], Dominique Thabut[2], Eric Nguyen Khac[1]. *[1]CHU Amiens-Picardie, Amiens, France; [2]Hôpital Pitié Salpêtrière, Paris, France; [3]Hôpital Beaujon, Clichy, France; [4]Hôpital Pontchaillou, Rennes, France; [5]Chu Purpan, Toulouse, France; [6]Hôpital Bretonneau, Tours, France; [7]Hôpital Saint-Antoine, Paris, France; [8]Chu Pellegrin Bordeaux, Bordeaux, France; [9]Hôpital de la Croix-Rousse, Lyon, France; [10]Hôpital Avicenne, Bobigny, France; [11]Hôtel-Dieu, Nantes, France; [12]CHU Estaing, Clermont-Ferrand, France; [13]Clermont-Ferrand University Hospital, Clermont-Ferrand, France; [14]Hôpital Saint-Éloi, Montpellier, France; [15]UC Leuven, Leuven, Belgium; [16]Hôpital Édouard Herriot, Lyon, France; [17]Hôpital Paul-Brousse, Villejuif, France; [18]CHU de Poitiers, Poitiers, France; [19]Hôpital Henri-Mondor Ap-Hp, Créteil, France; [20]Hôpital Charles Nicolle, Rouen, France; [21]CHU Dijon, Dijon, France; [22]Hôpital L' Archet, Nice, France; [23]Université Paris Cité, Centre de recherche sur l'inflammation, INSERM U1149;Service de Pathologie, AP-HP.Nord, Hôpital Beaujon, FHU MOSAIC2, SIRIC InsiTu, Clichy, France; [24]Hôpital Purpan, Toulouse, France; [25]Chu Besançon, Besançon, France; [26]Hôpital L'Archet, Nice, France*
Email: nguyen-khac.eric@chu-amiens.fr

Background and aims: Porto sinusoidal vascular disease (PSVD) can progress to non-cirrhotic portal hypertension (PH). In cases of recurrent PH bleeding or refractory ascites, the role of transjugular intrahepatic portosystemic shunt (TIPS) and the prognosis remain uncertain. We report results of TIPS in PSVD patients in a multicenter retrospective study.
Method: 122 patients with PSVD who underwent TIPS in 23 French and Belgium centers were compared to 363 patients with cirrhosis who underwent TIPS for the same complications of recurrent bleeding, refractory ascites, or other indications. Overall survival and recurrence-free survival were compared without adjustment, then adjusted with a propensity score, and sensitivity analysis excluding preemptive indications.
Results: PSVD or cirrhosis patients were male 66% vs 83% (p < 0.001), age 57 vs 58 years (p = 0.3), PT 75% vs 53% (p < 0.001), albumin 33 vs 28 g/L (p < 0.001), bilirubin 14 vs 33 µmol/L (p < 0.001), and

extrahepatic conditions in 73% of PSVD. TIPS was initiated for hemorrhage, ascites, or other indications in 52%, 30%, 13% (82% preemptive of surgery) of PSVD patients vs 67%, 31%, 1.1% of cirrhosis patients ($p < 0.001$). Before adjustment, overall mortality rate was 20% in PSVD group (median follow-up 54.8 months) versus 41% in cirrhosis group (FU 31.5 months) ($p < 0.001$). After adjustment, overall survival was higher in PSVD group (HR = 0.42 (95%CI:0.21–0.85) $p = 0.015$) with 5-year survival of 84% vs 49% in cirrhosis group, as well as in sensitivity analysis ($p = 0.048$). After adjustment, recurrent bleeding-free survival was higher in PSVD group (HR = 0.50 (95%CI:0.26–0.94) $p = 0.032$) with 5-year survival of 75% vs 45% for cirrhosis group, but there was no significant difference in sensitivity analysis ($p = 0.06$). After adjustment there were no difference between two groups for, recurrent ascites-free survival ($p = 0.053$), thrombosis-free survival ($p = 0.29$), and hepatic encephalopathy-free survival ($p = 0.26$). In multivariate analysis restricted to PSVD-TIPS group for recurrent bleeding and refractory ascites, age, albumin, creatinine, and severe extrahepatic disease were independent factors associated with post-TIPS survival. A prognostic model with score >8.2 isolates a group of post-TIPS PSVD patients with significantly impaired survival ($p < 0.0001$).

Conclusion: Overall survival in PSVD patients with TIPS implanted for recurrent PH bleeding or refractory ascites is higher compared to cirrhosis patients with same TIPS reasons. A prognostic model predicts post-TIPS-PSVD survival.

THU-478

Effect of polyethylene glycol versus lactulose on hepatic encephalopathy in patients with liver cirrhosis: a randomized clinical trial (PEG-HE trial)

Om Parkash[1], Shahab Abid[1], Mahrukh Ali[1], Abhishek Lal[1], Saeed Sadiq Hamid[1]. [1]*Aga Khan University, Pakistan, Karachi, Pakistan*
Email: om.parkash@aku.edu

Background and aims: Hepatic encephalopathy is a prevalent complication of liver cirrhosis being responsible for significant morbidity and mortality. Lactulose remains the gold standard treatment for liver cirrhosis; however, its use is limited by refractory effectiveness and adverse effects. Polyethylene glycol is emerging to be a potential alternative therapy. This study aimed to compare effectiveness and safety of PEG and lactulose in patients hospitalized with HE.

Method: This randomized controlled trial, with parallel group was conducted at Aga Khan University, Karachi, Pakistan. Eligible patients were randomized to receive either PEG or lactulose. The primary outcome was resolution of HE with ≥1-grade reduction in HESA score at 24, 48, and 72 hours. The secondary outcomes were the length of hospital stay, adverse events, readmissions, and three-months mortality.

Results: A total of 55 patients were enrolled. Patients receiving PEG and lactulose achieved comparable effectiveness in resolution of HE in 72 hours (p-value = 0.7232). At 24 and 48 hours, both PEG and lactulose achieved similar HESA scores demonstrating comparable effectiveness in resolving HE, although not statistically significant (p-value = 0.2605, p-value = 0.5222). The lower bounds of the 95% confidence intervals for risk differences continuously stayed above the 10% threshold, indicating that PEG was non-inferior to lactulose at all timepoints. No adverse events were reported in both groups, with similar readmissions and three-month mortality.

Conclusion: PEG was found to be effective in resolving HE with initial improvement in symptoms and safety profile. PEG presents to be a viable alternative to lactulose for HE management, although long-term studies with larger sample sizes are warranted.

THU-479

Magnitude of hepatic venous pressure gradient reduction predicts clinical events in portal hypertension: meta-regression analysis of randomized-controlled trials

Irene Pascual-Lopez[1,2], Matthew Tam[1], Daniel van Zanten[1], Shuen Sung[1], Jarell Jie-Rae Tan[3,4], Yu Jun Wong[4,5], Juan G Abraldes[1]. [1]*University of Alberta, Division of Gastroenterology, Liver Unit, Edmonton, Canada;* [2]*Hospital Universitari Arnau de Vilanova, Department of Gastroenterology and Hepatology, Lleida, Spain;* [3]*Yong Loo Lin School of Medicine, National University of Singapore, Singapore, Singapore;* [4]*Changi General Hospital, Department of Gastroenterology and Hepatology, Singapore, Singapore;* [5]*Duke-Nus Medical School, Singapore, Singapore*
Email: irene.pascual.l5@gmail.com

Background and aims: Portal hypertension is a primary driver of mortality and complications in cirrhosis. While observational studies demonstrate that reductions in hepatic venous pressure gradient (HVPG) correlate with improved outcomes, the magnitude of risk reduction per unit decrease in HVPG has not been quantified across randomized controlled trials (RCTs). We performed a meta-regression to quantify the relationship between HVPG reduction and clinical outcomes in RCTs.

Method: We systematically searched databases for RCTs in portal hypertension testing a drug intervention over placebo or no therapy, and reporting HVPG measurements and clinical outcomes. The predictor was the between-group difference in HVPG reduction (treatment minus control in mmHg). The endpoints were mortality and "variceal event" defined hierarchically: progression (when reported), otherwise variceal bleeding. This aimed to maximize usable RCTs while capturing clinically meaningful portal hypertension progression. We performed random-effects meta-regression, examining the association between HVPG reduction and log odds ratios for these clinical outcomes. Sensitivity analyses tested different weighting schemes to account for measurement error in HVPG.

Results: Twenty-two RCTs including a total of 2,844 patients were included. Within the trials, HVPG was measured in 2,048 individuals. Non-selective beta-blockers were the most frequently tested drug class. Each 1 mmHg reduction in HVPG was associated with reduced mortality (OR 0.850, 95% confidence interval 0.768 to 0.941, $p = 0.005$) and variceal progression or bleeding (OR 0.854, 95% confidence interval 0.747 to 0.975, $p = 0.031$), with low heterogeneity (I^2 0% and 18.5% respectively). Results were robust across multiple weighting schemes accounting for HVPG variability, including joint (predictor and outcome) weighting, and iteratively reweighted meta-regression.

Conclusion: Using a meta-analytic approach, we demonstrate a dose-dependent relationship between HVPG reduction and clinical outcomes in RCTs of portal hypertension, with approximately 15% lower odds of mortality and variceal events per 1-mmHg reduction. These findings may inform the design and powering of Phase III trials based on HVPG responses in Phase II studies.

THU-480-YI

High incidence and clinical relevance of concomitant hepatopulmonary syndrome among patients with portopulmonary hypertension

Jendrik Peters[1], Da-Hee Park[2], Marius M. Hoeper[2,3], Heiner Wedemeyer[1,4,5], Benjamin Maasoumy[1,4], Karen Olsson[2], Tammo Lambert Tergast[1]. [1]*Department of Gastroenterology, Hepatology, Infectious Diseases and Endocrinology, Hannover Medical School, Hannover, Germany;* [2]*Department for Respiratory Medicine and Infectious Diseases and German Centre of Lung Research (DZL), Hannover Medical School, Hannover, Germany, Hannover, Germany;* [3]*German Center for Lung Research (DZL), Biomedical Research in Endstage and Obstructive Lung Disease Hanover (BREATH), Hannover, Germany;* [4]*German Center for Infection Research (DZIF), Hannover-Braunschweig, Germany;* [5]*Excellence Cluster Resist, Hannover Medical*

School, Hannover, Germany
Email: peters.jendrik@mh-hannover.de

Background and aims: Portopulmonary Hypertension (POPH) is a rare but severe pulmonary complication of portal hypertension and is associated with decreased survival. Hepatopulmonary Syndrome (HPS), another pulmonary vascular complication, is considerably more prevalent and has also been linked to adverse clinical outcomes. Although coexistence of HPS in patients with POPH has been described, data regarding the exact prevalence and clinical relevance remain scarce. Here, we aimed to investigate the frequency and clinical impact of concomitant HPS in patients with POPH.
Method: This analysis included all patients consecutively diagnosed with POPH at Hanover Medical School between 1998 and 2025. POPH and HPS were diagnosed according to current guidelines and all patients underwent right-heart catheterization (RHC), blood gas analysis (BGA) and contrast-enhanced transthoracic echocardiography (cTTE). The primary endpoint was a composite of death or liver transplantation (LTx-free survival).
Results: Of 86 patients with POPH, a total of 43 (50%) underwent cTTE over the course of their treatment; 11 of these had sequential cTTE examinations. Median age was 53 years and the majority of patients were female (55%). Median mean pulmonary arterial pressure (mPAP) was 48 mmHg, median $P(A\text{-}a)O_2$ was 45 mmHg and intrapulmonary vascular dilations (IPVDs) were detected in 31 of 43 patients (72%), while 30 patients (70%) fulfilled the criteria for HPS. Of note, patients with HPS did not show a significant difference regarding mPAP or P(A-a)O2 compared with patients without HPS. In total, 13 patients in the HPS cohort died and 3 were transplanted, whilst 6 patients died in the No HPS cohort. LTx-free survival, adjusted for age and mPAP, was significantly lower in patients with HPS compared with those without HPS (hazard ratio [HR] 6.49, 95% confidence interval [CI] 1.38–30.56, p = 0.018). To investigate whether IPVDs may develop or regress in those with POPH, all patients with sequential cTTE were investigated separately: Here, 7 had no IPVDs at baseline and 4 had pre-existing IPVDs. All patients with baseline IPVDs showed persistence over time, while 5 patients without baseline IPVDs developed IPVDs with HPS during follow-up.
Conclusion: In patients with POPH, IPVDs and HPS are common, may develop over time and are associated with significantly reduced LTx-free survival. Screening for concomitant HPS and development of IPVDs in patients with POPH should be considered.

THU-481

Same session validation of a custom-built 22G with the commercial 25G system for EUS-guided portal pressure gradient measurement

Michael Praktiknjo[1], Nancy Farouk[1], Zeyu Wang[1], Juliana Stadtmann[1], Dominik van de Loo[1], Markus Kimmann[1], Carina Gunia[1], Jörn Arne Meier[1], Frank Erhard Uschner[1], Kai-Henrik Peiffer[1], Wim Laleman[1,2], Jonel Trebicka[1], Barbara Braden[1]. *[1]Department of Medicine B, University Hospital Münster, Münster, Germany; [2]University Hospitals Leuven, Leuven, Belgium*
Email: michael.praktiknjo@ukmuenster.de

Background and aims: Endoscopic ultrasound-guided portal pressure gradient (EUS-PPG) measurement is a promising alternative to hepatic venous pressure gradient (HVPG) assessment, especially in settings where HVPG is unavailable or limited. The commercial 25-gauge (25G) system showed good correlation against hepatic venous pressure gradient (HVPG). However, the 25G has drawbacks due to its small calibre and the proprietary pressure transducer. The aim of this study is to validate a custom-built 22G conventional intravascular pressure transducer system (22G EUS-PPG).
Method: In this prospective study, 26 patients underwent EUS-PPG measurement using both systems during the same session. The primary outcome was the correlation of PPG values. Secondary outcomes included the correlation and variability of portal vein pressure (PVP) and hepatic vein pressure (HVP) measured by both systems.
Results: PPG values showed excellent correlation of both systems (r = 0.901, p < 0.001). 25G EUS-PPG correctly identified clinically significant portal hypertension (CSPH, defined as PPG ≥ 10mmHg) in 25 of 26 (96.2%) cases. Portal vein and hepatic vein pressures also correlated significantly (r = 0.776 and r = 0.673, respectively) between both systems. Variability within both systems was very low to low.
Conclusion: EUS-PPG measurements obtained with the commercial 25G and custom-built 22G EUS-PPG systems are validated. The custom-built 22G system excels due to pressure-tracing quality control, availability and cost-efficiency.

THU-482-YI

TIPS implantation significantly reduces risk of infections in patients with decompensated cirrhosis: the multicenter TIPSIN study of the German cirrhosis study group

Stefanie Quickert[1], Markus Kimmann[2], Marlene Reincke[3], Isabel Brüggemann[4], Georgios Konstantis[5], Theresa Hildegard Wirtz[6], Felix Piecha[7], Marko Damm[8], Alexander Barton[9], Sophie Schlosser-Hupf[10], Julian Allgeier[11], Cornelius Engelmann[12], Julia M. Grottenthaler[13], Angelika Mendel[1], Lukas Sturm[3], Joséphine Fritz[2], Zeyu Wang[2], Frank Erhard Uschner[2], Jonel Trebicka[2], Jassin Rashidi-Alavijeh[5], Johannes Chang[4], Dominik Bettinger[3], Tony Bruns[6], Cristina Ripoll[1], Michael Praktiknjo[2]. *[1]Jena University Hospital, Jena, Germany; [2]University Hospital Münster, Münster, Germany; [3]Medical Center University of Freiburg, Freiburg, Germany; [4]Bonn University Hospital, Bonn, Germany; [5]University of Duisburg-Essen, Essen, Germany; [6]University Hospital RWTH Aachen, Aachen, Germany; [7]University Medical Center Hamburg-Eppendorf, Hamburg, Germany; [8]University Hospital Halle, Halle, Germany; [9]Saarland University Medical Center, Homburg, Germany; [10]University Hospital Regensburg, Regensburg, Germany; [11]LMU University Hospital Munich, Munich, Germany; [12]Charité-Universitätsmedizin Berlin, Berlin, Germany; [13]University Hospital Tuebingen, Tübingen, Germany*
Email: stefanie.quickert@med.uni-jena.de

Background and aims: Infections in cirrhosis are common and lead to increase in mortality. Key drivers include portal hypertension, systemic inflammation and cirrhosis-associated immune-dysfunction (CAID). Transjugular intrahepatic portosystemic shunt (TIPS) implantation effectively reduces portal hypertension and can impact CAID, and thus the incidence of infections, however data are scarce. The aim was to compare the prevalence of infections before and after TIPS.
Method: This multicenter retrospective study screened 1,800 patients with liver cirrhosis undergoing TIPS implantation between 2014 and 2024 across 13 German centers. Primary outcome was prevalence of bacterial infections within 3 months before and after TIPS implantation using McNemar test. Secondary outcome was 1-year transplant-free survival. Factors associated with post-TIPS infections were identified using logistic regression analysis.
Results: A total of 1,320 patients were included (median age 59 years, 65% male, 59% alcohol-related cirrhosis, median MELD score 13). The main indication for TIPS implantation was refractory or recurrent ascites (66%). Infection rates were significantly higher 3 months prior to TIPS compared to 3 months after TIPS implantation (31% vs. 22%; p < 0.001). Post-TIPS infections were independently associated with pre-TIPS infections (OR 1.43; CI 1.07–1.91), recurrent/refractory ascites (OR 1.55; CI 1.15–2.25), female sex (OR 1.38; CI 1.04–1.83) and Child-Pugh score (OR 1.20; CI 1.09–1.31) in multivariable analysis. Patients developing infections within 90 days after TIPS showed significantly lower 1-year transplant-free survival compared with those without infections (48.4 vs. 82.3%, p < 0.001).
Conclusion: TIPS implantation is associated with a significant reduction in infection rates in patients with decompensated liver

cirrhosis. However, post-TIPS infections remain strongly associated with impaired transplant-free survival.

THU-483

BAVENO VII criteria and ANTICIPATE models predict first decompensation in a multi-center U.S. cohort of patients with compensated advanced chronic liver disease (cACLD)

Anahita Rabiee[1], Christina Lindenmeyer[2], Atoosa Rabiee[3], Cyrus Mowdawalla[4], Sebastian Arambulo-Castillo[4], Matthew P. Davidsohn[4], Clara Tow[4], Timothy Ring[2], Kelly Bowen[2], Sobia Laique[2], Diego Drumond Westgeest e Sousa[5], Elliot Tapper[6], Michelle Ng[6], Manhal Izzy[7], Anika Shah[7], R. Todd Frederick[8], Robert Enders[8], Beatriz Chara[1], Jessica Davis[3], Qusai Al Zureikat[3], Andres Duarte-Rojo[9], Sarang Thaker[9], Louis Guzman[9], Qijun Yang[10], Juan G Abraldes[11], Guadalupe Garcia-Tsao[1], Douglas Simonetto[5], Brett Fortune[12]. *[1]Section of Digestive Diseases, Yale School of Medicine; New Haven, CT, United States; [2]Department of Gastroenterology, Hepatology and Nutrition, Cleveland Clinic, Cleveland, United States; [3]Veterans Affairs Medical Center, Division of Gastroenterology and Hepatology, Washington, District of Columbia, USA, Washington, District of Columbia, United States; [4]Department of Medicine, Albert Einstein College of Medicine, Montefiore Einstein Medical Center, Bronx, United States; [5]Division of Gastroenterology and Hepatology, Mayo Clinic, Rochester, MN, United States; [6]Division of Gastroenterology, Department of Internal Medicine, University of Michigan, Ann Arbor, Michigan, United States; [7]Division of Gastroenterology, Hepatology, and Nutrition, Vanderbilt University, Nashville, TN, United States; [8]Division of Hepatology, Department of Advanced Organ Therapies and Transplantation, California Pacific Medical Center, San Francisco, California, United States; [9]Division of Gastroenterology and Hepatology, Northwestern Medicine and Feinberg School of Medicine, Northwestern University, Chicago, Illinois, United States; [10]Department of Quantitative Health Sciences, Cleveland Clinic, Cleveland, OH, United States; [11]Liver Unit, Division of Gastroenterology, University of Alberta, Edmonton, AB, Canada; [12]Miami Transplant Institute, Jackson Health System, Miami, FL, United States*
Email: anahita.rabiee@yale.edu

Background and aims: Portal hypertension is the primary driver of decompensation in cACLD and can be determined non-invasively via liver stiffness measurements (LSM) by vibration controlled transient elastography (VCTE). We evaluated Baveno VII LSM thresholds and ANTICIPATE/ANTICIPATE-NASH models for predicting hepatic decompensation in a diverse U.S. cohort with a high prevalence of metabolic dysfunction-associated steatotic liver disease (MASLD).
Method: We included consecutive adults from 8 U.S. centers with a LSM≥ 10 kPa by VCTE (defining cACLD) without a prior history of decompensation. Risk strata were defined by Baveno VII LSM categories (10 to <15, 15 to <25, and ≥25 kPa). ANTICIPATE-NASH (BMI ≥30 kg/m^2 and MASLD) or original ANTICIPATE (all other etiologies) were applied and grouped into quantiles. The primary outcome was first decompensation. Associations were assessed using Fine–Gray competing risk model, accounting for hepatocellular carcinoma, non-liver-related death, and transplant before decompensation.
Results: A total of 592 patients were included (median age 58.9 years, 57% female, 74% White); MASLD predominated (66%). The median BMI was 33 [29, 40] kg/m^2 and 70% had BMI of ≥25. Diabetes, hyperlipidemia and hypertension were present in 51%, 47% and 49%. LSM risk distributions were: 10–15 (n = 298, 50%), 15–25 (n = 191, 32%), ≥25 (n = 103, 17%). In a median of 5-year follow-up (IQR 4–5), 47 patients (8%) developed first decompensation, with ascites being the most common (n = 19, 40%). LSM ≥ 25 had a 4.8- fold higher hazard of decompensation compared to LSM 10–15 (sub-distribution hazard ratio [sHR]: 4.8, 95% CI: 2.4–9.7). The risk of decompensation was not statistically different between LSM 15–25 and LSM 10–15 (sHR: 1.9, 95% CI: 0.9–3.9). Using ANTICIPATE models, patients in 4th quantile had a 9-fold higher hazard of decompensation vs 1st quantile (sHR: 9.1; 95% CI, 2.8–30.1). After adjustment for ANTICIPATE models risk quantiles, patients with MASLD and obesity had a lower observed hazard of decompensation compared with other etiologies (sHR 0.36, 95% CI 0.19–0.69).
Conclusion: Baveno VII and ANTICIPATE/ANTICIPATE-NASH models can be used to stratify decompensation risk in a real world U.S. cohort, reinforcing their usefulness in clinical-decision making. Notably, patients with MASLD and obesity had a lower risk of decompensation, emphasizing the need for tailored prognostic strategies. These data provide a rationale for prospective validation and integration into MASLD care pathways in the U.S.

THU-484

Predictors of multiple endoscopic variceal ligation sessions for obliteration of esophageal varices: a prospective study in a tertiary-level hospital in Bangladesh

Antora Rahut[1], Suprokash Sarkar[1], Mohammad Rifat Mustafa[1], Debashish Sarkar[1], Dilip Ghosh[1], Habib Ahmed[1], Mohammad Mahmuduzzaman[1]. *[1]Shaheed Suhrawardy Medical College Hospital, Dhaka, Bangladesh*
Email: antora37@yahoo.com

Background and aims: Endoscopic variceal ligation (EVL) is the standard treatment of variceal bleeding in patients with portal hypertension. Multiple sessions are often required for complete obliteration, significantly burdening healthcare resources and patient compliance. This study aims to determine the number of EVL sessions required for complete obliteration of esophageal varices and to identify factors influencing the requirement of multiple sessions.
Method: This prospective observational study was conducted at Shaheed Suhrawardy Medical College Hospital, Bangladesh, between January 2024 and December 2025 among 79 adult patients with esophageal varices who underwent EVL for primary or secondary prophylaxis. Patients were followed until complete obliteration of varices. Demographic, clinical, endoscopic, and laboratory findings were recorded and analyzed by univariate and multivariate logistic regression to identify predictors of multiple EVL sessions. A risk stratification model was developed.
Results: The mean age of patients was 51.4 ± 12.3 years, with 68.3% being male. Overall, 60.8% of patients required multiple EVL sessions (mean 2.16 ± 1.63). Factors significantly associated with multiple EVL sessions included: higher MELD score ($p < 0.001$), Child-Turcotte-Pugh (CTP) Class C ($p < 0.001$), large variceal size ($p < 0.001$), presence of red signs ($p = 0.042$), lower serum albumin ($p = 0.015$), lower hemoglobin ($p < 0.001$), higher INR ($p = 0.022$), presence of ascites ($p = 0.031$), larger spleen size ($p = 0.002$), and elevated bilirubin levels ($p = 0.010$). CTP class C, large varices, and low platelet count were independent predictors of multiple sessions on multivariate logistic regression analysis. A risk stratification model was established, which categorized patients into high- intermediate- and low-risk groups, where advanced liver disease and the presence of a greater number of risk factors posed a greater risk of multiple EVL sessions. Parameters that showed no significant association included creatinine, sodium, diabetes mellitus, hypertension, congestive gastropathy, and previous upper gastrointestinal bleeding. Applying more bands in the initial session was associated with more single-session obliteration.
Conclusion: This study identifies a comprehensive risk profile, encompassing clinical, endoscopic and laboratory parameters predicting the need for multiple sessions. This may help clinicians optimize treatment planning and patient counseling, especially in resource-constrained settings.

THU-485

Spleen stiffness measurement and predicting the need for endoscopy in obese MASH cirrhosis

Eabha Ring[1,2], Suzanne Norris[1,2], Lewel Alvarado[1], Kimmy Villaluna[1], Noelia Justo Rubio[1], Noelle Cullen[1], Collen Ray Arrogante[1], Issabele Pulcherio[1], Clodagh Quinn[1], Finbar MacCarthy[1,2], David Prichard[1,2]. [1]*Department of Hepatology, St James's Hospital, Dublin, Ireland;* [2]*Department of Clinical Medicine, School of Medicine, Trinity College Dublin, Dublin, Ireland*
Email: eabharing@live.com

Background and aims: Non-invasive tests (NIT) for identifying clinically significant portal hypertension (CSPH) using liver and spleen stiffness measurements (LSM, SSM) and platelet count are less reliable in obese metabolic dysfunction-associated steatohepatitis (MASH) cirrhosis than other cirrhosis aetiologies. As MASH cirrhosis is now a leading cause of liver-related deaths worldwide, this limitation is of concern. Algorithms including LSM, SSM and platelets to rule out high-risk varices (HRV) have been proposed but uncertainty regarding the best algorithm remains. This study explores the utility of SSM for ruling out high risk varices (HRV) in obese MASH cirrhosis.
Method: Patients with known MASH cirrhosis were prospectively invited to have same day LSM, SSM (Fibroscan™ Echosens, Paris), phlebotomy, and upper endoscopy performed. HRV were defined as varices >5mm or varices of any size varices with red signs. Exclusion criteria: hepatocellular carcinoma, prior variceal bleed, non-cirrhotic portal hypertension, portal vein thrombus, aetiologies of liver disease aside from MASH and decompensation within 1 month.
Results: 100 patients attended (50% male, age 63 [IQR 33–86], BMI 33 [IQR 20–57], waist:hip ratio 1 [IQR 0.78–1.19], weekly alcohol consumption 0 [IQR 0–15]). Comorbidities included diabetes (74%), hypertension (67%) and hyperlipidaemia (57%). 39% used GLP-1 agonists. Median LSM 18.3 kPa [IQR 6–60], SSM 42 kPa ([IQR 15–100], 95% success rate), platelet count 195 [IQR 68–502] and CAP score 296 [IQR 185–392]. 80% of endoscopies performed on same day. Varices/HRV were present in 40%/37% of patients. SSM performed similarly to LSM in predicting HRV (p = 0.02, AUROC 0.74; p = 0.01 AUROC 0.7). Optimal SSM cutoffs for ruling in/out HRV were ≥ 76 kPa (specificity ≥ 90%, PPV 36%)/ ≤ 34 kPa (sensitivity ≥90%, NPV 97%). Combining SSM, LSM and platelets improved the ability to detect HRV (SSM/LSM p = 0.01, AUROC 0.75; SSM/LSM/platelets p = <0.001, AUROC 0.89). Three scenarios were tested, each applying a two-of-three criterion for HRV exclusion. Scenario 1 (SSM ≤ 34 kPa, LSM ≤ 15 kPa, platelets ≥ 150) had a sensitivity of 93%/NPV 97%/1% missed HRV rate. Scenario 2 (SSM ≤ 34 kPa, LSM ≤ 20 kPa, platelets ≥ 150) had a sensitivity of 66%/NPV 93%/5% missed HRV rate. Scenario 3 (SSM ≤ 34 kPa, LSM ≤ 25 kPa, platelets ≥ 150) a sensitivity of 53%/NPV 91%/8% missed HRV rate.
Conclusion: SSM improves NIT ability to rule out HRV in obese MASH cirrhosis. Larger MASH cirrhotic cohorts are required to confirm these findings. .

THU-489

Effective prevention of further complications of portal-hypertension is independent of TIPS under-dilation

Davide Roccarina[1], Dario Saltini[2], Marco Senzolo[3], Silvia Nardelli[4], Marcello Bianchini[5], Stefania Gioia[6], Silvia Aspite[7], Kymentie Ferdinande[8], Manuela Merli[4], Oliviero Riggio[4], Fabio Marra[1], Sara Montagnese[8], Filippo Schepis[2], Francesco Vizzutti[1]. [1]*Department of Experimental and Clinical Medicine, Potral Hypertension Unit, AOU Careggi, Florence, Italy;* [2]*Severe Liver Diseases (M.E.C.) Departmental Unit, Azienda Ospedaliero-Universitaria of Modena, University of Modena and Reggio Emilia, Modena, Italy;* [3]*University Hospital of Padua, Padova, Italy;* [4]*Sapienza Università di Roma, Roma, Italy;* [5]*Azienda Ospedaliero-Universitaria Policlinico di Modena, Modena, Italy;* [6]*Department of Translational and Precision Medicine, Sapienza University of Rome, Rome, Italy;* [7]*University of Florence, Florence, Italy;* [8]*University Hospital of Padova, Italy, University Hospital of Ghent, Belgium, AZ Delta Roeselare, Belgium, Padova, Italy*
Email: francesco.vizzutti@unifi.it

Background and aims: Portal hypertension (PH) is a major determinant of poor prognosis in cirrhosis. An under-dilated transjugular intrahepatic portosystemic shunt (U-TIPS) effectively controls PH-related complications that constitute the indication for the procedure, while reducing the incidence of post-TIPS overt hepatic encephalopathy. However, the benefits of TIPS in preventing additional PH-related complications beyond the initial indication have been reported only for standard-diameter stents. This study evaluated whether U-TIPS provides protection comparable to S-TIPS against further PH-related complications beyond the initial indication, independently of achieving guideline-defined hemodynamic targets for TIPS success.
Method: Patients treated for refractory ascites (RA) or for secondary prophylaxis of PH-related bleeding (PHRB) were included. Adequate hemodynamic response (AHR) was defined as a post-TIPS porto-caval pressure gradient (PCPG) < 12 mmHg in RA, and < 12 mmHg or a reduction ≥ 50% in PHRB. PCPG values outside these thresholds were considered an inadequate hemodynamic response (IHR). Standard TIPS (S-TIPS) was defined as endoprosthesis dilation ≥ 8 mm. Post-TIPS PH-related complications beyond the initial indication—spontaneous bacterial peritonitis, acute kidney injury due to hepatorenal syndrome, hepatic hydrothorax, need for paracentesis, and variceal bleeding—were assessed individually and as a composite endpoint over one year.
Results: Three-hundred fifty-eight patients were included. TIPS indication was RA in 46% and secondary prophylaxis of PHRB in 54%. Seventy-one percent received U-TIPS, while 28% were treated with S-TIPS. AHR was achieved in 71%, while 29% obtained an IHR.The incidence of at least one post-TIPS complication was significantly higher in S-TIPS compared with U-TIPS (14% vs. 6%, p = 0.022), while no significant difference was observed between AHR and IHR groups (8.7% vs. 6.7%, p = 0.543). On multivariable analysis, S-TIPS (OR 3.13, 95% CI 1.38–7.21, p = 0.006), Child-Pugh class B (OR 11.6, 95% CI 2.1–217, p = 0.021) and C (OR 14.4, 95% CI 1.2–343, p = 0.042), and higher MELD score (OR 1.20, 95% CI 1.09–1.32, p < 0.001) were independently associated with post-TIPS complications.
Conclusion: U-TIPS provides non-inferior protection against additional PH-related complications beyond the initial indication compared with S-TIPS, irrespective of the achievement of guideline-defined hemodynamic efficacy targets.

THU-490

Comprehensive transjugular–percutaneous portal hemodynamic assessment (cTP-PHA): safety, feasibility and diagnostic value in patients with undefined or mixed-etiology portal hypertension

Dario Saltini[1], Marcello Bianchini[1], Andrea Salomè Velasco Mayorga[2], Tomas Guasconi[1], Giustina Lo Cascio[2], Antonio Piscopo[2], Nicolò Giglioli[3], Filippo Scianò[1], Fabiola Milosa[3], Rosina Maria Critelli[3], Federico Casari[4], Francesco Ascari[4], Cristian Caporali[4], Giovanni Battinelli[4], Filippo Schepis[1]. [1]*Severe Liver Diseases (M.E.C.) Departmental Unit, Department of Medical Specialties, University Hospital of Modena "Policlinico", University of Modena and Reggio Emilia, European Reference Network on Rare Liver Disorders (ERN Rare-Liver), Modena, Italy;* [2]*Gastroenterology Unit, University Hospital of Modena "Policlinico", University of Modena and Reggio Emilia, Modena, Italy;* [3]*EpatoGastro Lab – RBA-Labs CHIMOMO Department – University of Modena and Reggio Emilia, Modena, Italy;* [4]*Division of Interventional Radiology, University Hospital of Modena "Policlinico", Modena, Italy*
Email: fschepis@unimore.it

Background and aims: Accurate classification of portal hypertension (PH) remains challenging in patients with suspected mixed/

undefined etiologies, where non-invasive tests (NITs) and hepatic venous pressure gradient (HVPG) may be inconclusive due to pre- or post-sinusoidal components. Simultaneous measurement of HVPG, PortoHepatic (PHPG) and PortoCaval pressure gradients (PCPG)—here termed comprehensive Transjugular-Percutaneous Portal Hemodynamic Assessment (cTP-PHA)—allows assessment of both the anatomical site(s) and severity of PH. We evaluated the safety, feasibility and diagnostic utility of cTP-PHA.

Method: We retrospectively analyzed patients undergoing cTP-PHA between 2022–2024 at our Hemodynamic Laboratory for chronic liver disease with clinical signs of PH and suspected non-sinusoidal components. Under local anesthesia and mild sedation, HVPG was measured transjugularly, followed by direct ultrasound (US)-guided transhepatic portal vein pressure measurement (20G Chiba needle), enabling calculation of PHPG and PCPG. All procedures were performed under combined fluoroscopic and US guidance with waveform acquisition. Liver and spleen stiffness were reassessed in the cath-lab, and transjugular liver biopsy was performed when indicated.

Results: Forty-five patients were included (38% male; mean age 57 ± 11 years). Technical success was 100%, with minor complications in 4%. Mean HVPG, PHPG and PCPG were 7 ± 6, 14 ± 9 and 15 ± 9 mmHg, respectively; intrahepatic vein-to-vein shunts were detected in 24%. Pressure gradient analysis identified pure presinusoidal CSPH in 24%, pure sinusoidal CSPH in 11%, mixed sinusoidal–presinusoidal CSPH in 22%, subclinical sinusoidal PH in 16%, and no PH in 27%. A hepato-caval gradient >2 mmHg, indicating an additional post-sinusoidal component, was present in 9% without affecting PH classification. Defining CSPH solely by presence of esophageal varices resulted in 9% false positives, while Baveno VII criteria misclassified CSPH in 16% of cases.

Conclusion: cTP-PHA is a safe and diagnostically definitive technique for characterizing the anatomical site(s) and severity of PH in patients with suspected mixed/undefined etiologies. The presence of esophageal varices without confirmed CSPH challenges current diagnostic paradigms and supports cTP-PHA implementation in referral centers. Prospective studies comparing cTP-PHA with EUS-guided approaches, which measure PHPG alone, are warranted to assess added diagnostic value and cost-effectiveness.

THU-491

Assessment of non-endoscopic follow-up criteria for esophageal varices using platelet count and albumin levels

Shinya Sato[1], Tadashi Namisaki[1], Tatsuya Nakatani[1], Kosuke Kaji[1], Hitoshi Yoshiji[1]. [1]*Department of Gastroenterology, Nara Medical University, Kashihara, Japan*
Email: shinyasato@naramed-u.ac.jp

Background and aims: The Baveno VI and Expanded Baveno VI consensus guidelines propose the use of transient elastography (TE) and platelet (PLT) count to identify patients with cirrhosis who can safely avoid screening esophagogastroduodenoscopy (EGD). However, TE is not universally available. This study aimed to evaluate a simple non-endoscopic algorithm based solely on routine laboratory parameters for predicting medium/large esophageal varices (EV) in patients with cirrhosis and to compare its performance with the Baveno VI and Expanded Baveno VI criteria. A secondary aim was to assess the additional value of TE in excluding high-risk EV.

Method: We retrospectively analyzed 896 patients with liver cirrhosis who underwent upper gastrointestinal endoscopy at our institution between April 2015 and December 2024. Of these, 256 patients with available TE measurements constituted the training cohort for identifying laboratory predictors of EV grade F2–3. The remaining 640 patients without TE data served as an independent validation cohort.

Results: In the training cohort, medium/large EV were detected in 10.0% of patients meeting the Baveno VI criteria and 14.2% of those meeting the Expanded Baveno VI criteria. Multivariate analysis identified platelet count and serum albumin level as independent predictors of medium/large EV. Optimal cut-off values were PLT > $12 \times 10^4/\mu L$ and albumin > 3.5 g/dL, yielding negative predictive values (NPVs) of 96.2% and 95.4%, respectively. Among patients meeting the RESIST-HCV criteria, the NPV was 99.2%. Receiver operating characteristic analysis demonstrated that the combined criterion of PLT > $12 \times 10^4/\mu L$ or albumin > 3.5 g/dL effectively identified patients at very low risk of F2–3 EV. Of 134 patients fulfilling this criterion, only one (0.8%) had F2–3 EV. The addition of liver stiffness < 25 kPa did not significantly improve performance. In the validation cohort, 209 patients met the combined laboratory criteria; only one patient (0.5%) had treatable F2–3 EV, confirming the robustness of the algorithm.

Conclusion: A simple algorithm based on platelet count and serum albumin level can reliably exclude clinically significant esophageal varices and may safely reduce the need for screening EGD, with performance comparable to TE-based criteria. This approach may facilitate broader, cost-effective risk stratification of portal hypertension, particularly in settings where TE is unavailable.

THU-492

Aging influences encephalopathy risk but not survival after TIPS for acute variceal bleeding: EUROTIPS-Chinese multicenter study

Filippo Schepis[1], Sonia Torres[2], Dario Saltini[1], Guangchuan Wang[3], Agustín Albillos[4], Hannah Old[5], Alvaro Giráldez-Gallego[6], Jonel Trebicka[7], Marco Senzolo[8], Dhiraj Tripathi[9], Wim Laleman[10], Francesco Vizzutti[11], Pablo Bellot Garcia[12,13], Johannes Chang[14], Bogdan Procopet[15], Thomas Reiberger[16], Dominik Bettinger[17], María Pilar Ballester[18], Rebeca Pintado Garrido[19], Feng Zhang[20], Luo Xuefeng[21], Fu-Liang He[22], Fanny Turon[2], Luis Téllez[4], Jesus Donate[4], Louise China[23], Michael Praktiknjo[7], Markus Kimmann[7], Kymentie Ferdinande[8], Giulio Barbiero[24], Faisal Khan[9], Antonio Piscopo[25], Geert Maleux[26], Rosario La Delfa[11], Lukas Hartl[16], Virginia Hernández-Gea[2], Juan Carlos García-Pagán[2], Anna Baiges[2]. [1]*Severe Liver Diseases (M.E.C.) Departmental Unit, Department of Medical Specialties, University Hospital of Modena "Policlinico", University of Modena and Reggio Emilia, European Reference Network on Rare Liver Disorders (ERN Rare-Liver), Modena, Italy;* [2]*Barcelona Hepatic Hemodynamic Laboratory, Liver Unit, Hospital Clínic, Clínic Barcelona, ERN-RareLiver (Health Care Provider of the European Reference Network on Rare Liver Disorders), CSUR (Centro de referencia del Sistema Nacional de Salud en Enfermedad Hepática Vascular Compleja en adultos), FRCB-IDIBAPS (Fundació de Recerca Clínic Barcelona-Institut d'Investigacions Biomèdiques August Pi i Sunyer); CIBEREHD (Centro de Investigación Biomédica en Red Enfermedades Hepáticas y Digestivas); AGAUR SGR202101115, Medicine Department, Faculty of Medicine, and health Science, Universitat de Barcelona, Barcelona, Spain;* [3]*Department of Gastroenterology, Shandong Provincial Hospital Affiliated to Shandong First Medical University, 324 Jingwu Weiqi Road, Jinan, Shandong, Department of Gastroenterology, Shandong Provincial Hospital, Shandong University, 324 Jingwu Weiqi Road, Jinan, Shandong, Shandong, China;* [4]*Gastroenterology and Hepatology Department. Hospital Universitario Ramón y Cajal. IRYCIS. CIBERehd. Universidad de Alcalá., Madrid, Spain;* [5]*Royal Free London NHS Foundation Trust, London, United Kingdom;* [6]*Digestive Diseases Department, Hospital Universitario Virgen del Rocío, Institute of Biomedicine (HUVR/CSIC/US), University of Seville, Seville, Spain;* [7]*Department of Medicine B, University Hospital Muenster., Muenster, Germany;* [8]*Unit of Vascular Liver Diseases and Treatment of Portal Hypertension, Gastroenterology, Department of Surgical, Oncological and Gastroenterological Sciences, University-Hospital of Padua, Padua, Italy;* [9]*Liver Unit, University Hospitals Birmingham NHS Foundation Trust, Birmingham Health Partners, Birmingham, United Kingdom;* [10]*Department of Gastroenterology and Hepatology, Division of Liver & Biliopancreatic disorders and Liver Transplantation, University Hospitals Leuven, Leuven, Belgium;* [11]*Department of Experimental and Clinical Medicine, University of Florence., Florence, Italy;* [12]*Alicante*

Institute for Health and Biomedical Research (ISABIAL), Hospital General Universitario Dr. Balmis., Alicante, Spain; [13]University General Hospital Dr. Balmis, Liver Unit, Alicante; [14]University Hospital Bonn, Department of Internal Medicine I, Bonn, Germany; [15]Department of Hepatology, "Octavian Fodor" Regional Institute of Gastroenterology and Hepatology, Cluj-Napoca, Romania; [16]Division of Gastroenterology and Hepatology, Department of Medicine III, Medical University of Vienna, Vienna, Austria; [17]Department of Medicine II, Medical Center University of Freiburg, Faculty of Medicine, University of Freiburg, Freiburg, Germany; [18]Fundación de Investigación Hospital Clínico Universitario de Valencia - INCLIVA, Valencia, Spain; Hepatology Unit, Digestive Disease Department, Hospital Clínico Universitario de Valencia, Valencia, Spain; [19]Radiology Department, Interventional Radiology Unit, Hospital Universitario Rio Hortega., Valladolid, Spain; [20]Department of Gastroenterology Nanjing Drum Tower Hospital, the Affiliated Hospital of Nanjing University Medical School, Nanjing, China; [21]Division of Gastroenterology and Hepatology, Sichuan University-University of Oxford Huaxi Joint Centre for Gastrointestinal Cancer, West China Hospital, Sichuan University., Chengdu, Sichuan, China; [22]Department of Interventional Therapy, Beijing Shijitan Hospital, Capital Medical University., Beijing, China; [23]UCL Institute for Liver and Digestive Health, Upper 3rd Floor, Division of Medicine, Royal Free Campus, Rowland Hill Street London, London, United Kingdom; [24]Unit of Interventional Radiology, Radiology 2 Unit, Department of Integrated Diagnostic Services, University Hospital of Padua, Padua, Italy; [25]Gastroenterology Unit, University Hospital of Modena "Policlinico", University of Modena and Reggio Emilia, Modena, Italy; [26]Department of Radiology, University Hospitals Leuven, Leuven, Belgium
Email: fschepis@unimore.it

Background and aims: Age is frequently considered a limiting factor for transjugular intrahepatic portosystemic shunt (TIPS). We aimed to assess the impact of age on post-TIPS outcomes, focusing on transplant-free survival (TFS) and overt hepatic encephalopathy (OHE) as co-primary endpoints, and rebleeding as a secondary endpoint, in patients undergoing pre-emptive or rescue TIPS for acute variceal bleeding.
Method: We analyzed the prospective multicenter EUROTIPS registry (18 centers, 2020–2024) including 370 patients who underwent pre-emptive (41%) or rescue (59%) TIPS and had ≥12 months follow-up. Mean age was 56 ± 12 years, with 21% aged ≥65 years. All stents were covered. External validation was performed in a retrospective multicenter Chinese cohort (5 centers, 2012–2024; n = 464; mean age 57 ± 11 years; 100% covered stents). Patients were stratified by age (<45, 45–54, 55–64, ≥65 years), MELD score, and Child–Pugh class. One-year TFS and OHE-free survival were estimated using the Kaplan-Meier method and compared by log-rank test.
Results: In the European cohort, 1-year TFS was 65.1% (95% CI 60.5–70.2) and 1-year OHE-free survival reached 57.9% (95% CI 52.6–63.7). Age was not associated with 1-year TFS, neither as a continuous variable (p = 0.566) nor across age classes (p = 0.294). MELD (<14 vs ≥14) and Child–Pugh class effectively stratified TFS (p < 0.001), with no additional prognostic value of age within risk strata. Similar results were observed in the Chinese cohort, despite major differences in etiology (57% viral-related vs 57% alcohol-related cirrhosis in EUROTIPS registry) and baseline liver disease severity (mean MELD score 12.0 ± 4.2 vs 15.8 ± 6.8 in EUROTIPS registry). Conversely, OHE was strongly age-dependent in both cohorts. One-year OHE-free survival declined from 77.8% in patients ≤45 years to 36.3% in those ≥65 years in the EUROTIPS cohort (p < 0.001), and from 89.8% to 61.7% in the Chinese cohort (p < 0.001). One-year rebleeding rates were low (8.8% EUROTIPS; 11% Chinese) and were almost exclusively associated with TIPS dysfunction.
Conclusion: Liver disease severity, rather than chronological age, determines 1-year TFS after TIPS for acute variceal bleeding. In contrast, post-TIPS OHE is strongly age-dependent and only marginally influenced by liver function. These data challenge age-based exclusion from TIPS. Risk stratification should prioritize liver disease severity for survival prediction, while age-specific strategies may optimize OHE prophylaxis.

THU-493-YI

Prognostic value of SSI-2D-shear wave elastography–derived indices for predicting hepatic decompensation

Christian Sebesta[1,2,3], Georg Kramer[1,2,3,4], Nina Dominik[1,2], Benedikt Hofer[1,2,3,4], Lorenz Balcar[1,2,3], Paul Thöne[1,2,3], Marlene Hintersteininger[1,2,3], Emilia Korn[1], Mathias Jachs[1,2,3], Lukas Hartl[1,2,3], Georg Semmler[1,2,3], Benedikt Simbrunner[1,2,3], Michael Trauner[1,3], Albert Friedrich Stättermayer[1,3], Mattias Mandorfer[1,2,3], Thomas Reiberger[1,2,3,4], David Bauer[1,5].
[1]Division of Gastroenterology and Hepatology, Department of Medicine III, Medical University of Vienna, Vienna, Austria, Vienna, Austria; [2]Vienna Hepatic Hemodynamic Lab, Division of Gastroenterology and Hepatology, Department of Medicine III, Medical University of Vienna, Vienna, Austria, Vienna, Austria; [3]Clinical research group MOTION, Medical University of Vienna, Vienna, Austria, Vienna, Austria; [4]Christian-Doppler Laboratory for Portal Hypertension and Liver Fibrosis, Medical University of Vienna, Vienna, Austria, Vienna, Austria; [5]Klinikum Ottakring, Vienna Healthcare Group, Vienna, Austria, Vienna, Austria
Email: christian.a.sebesta@meduniwien.ac.at

Background and aims: Accurate non-invasive prediction of hepatic decompensation in compensated advanced chronic liver disease (cACLD) remains an unmet clinical need. In this study, we evaluated the value of Supersonic Imagine 2D-shear wave elastography-based liver (SSI-LSM) and spleen (SSI-SSM) stiffness measurements or derived composite scores for risk stratification and prognostication for hepatic decompensation.
Method: We conducted a prospective study enrolling consecutive patients with cACLD undergoing HVPG measurement and same-day SSI-LSM and SSI-SSM. Patients with unreliable SSI-LSM (IQR/median >30%; n = 55) were excluded. Associations of SSI-LSM, SSI-SSM and combined elastography-based models with hepatic decompensation were analyzed using Fine–Gray models with liver transplantation and death as competing risks. Discriminative performance was assessed using time-dependent, competing-risk–aware C-statistics at 1 year (Y1) and by decision-curve analysis (DCA). Composite scores (SSI-LSPS: LSM-Spleen size-to-platelet ratio; SSI-ANTICIPATE: LSM, PLT; and SSI-LPS: LSM-platelet-SSM) were calculated according to their original publications.
Results: A total of 142 patients were included (median age 56 years; 76% male; median HVPG 11 mmHg; CSPH 57.7%; Y1 decompensation 9.2%). Median SSI-LSM and SSI-SSM were 24.6 (IQR 13.3–50.0) kPa and 50.4 (IQR 30.9–66.0) kPa; 52% had SSI-LSM >21 kPa and 65% SSI-SSM >40 kPa. In Fine–Gray models, each 1-kPa increase in SSI-LSM was associated with higher Y1 decompensation risk (sHR 1.02, 95% CI 1.01–1.03). Each IQR increase in SSI-LSPS (sHR 2.53, 95% CI 1.69–3.79), SSI-LPS (sHR 3.14, 95% CI 1.79–5.52), and SSI-ANTICIPATE (sHR 3.15, 95% CI 1.78–5.58) was also associated with decompensation (all p < 0.001). Time-dependent AUROCs at Y1 were 0.73 for SSI-LSM, 0.67 for SSI-SSM, and 0.83 for HVPG. Compared with SSI-LSM, discrimination was significantly improved by SSI-LPS (AUROC 0.77; p = 0.031) and SSI-ANTICIPATE (AUROC 0.77; p = 0.016) and numerically improved by SSI-LSPS (AUROC 0.81; p = 0.053). DCA showed the most consistent net benefit for SSI-LSPS, while SSI-ANTICIPATE performed best at intermediate risk thresholds.
Conclusion: Composite SSI-2D-SWE-derived scores seem to improve prognostication and risk discrimination beyond SSI-LSM alone for predicting first hepatic decompensation in cACLD patients. While our findings support the utility of non-invasive LSM/PLT-based composite scores for risk stratification, the value of additional SSM remains to be defined.

THU-494

Prognostic value of grading esophageal varices for decompensation and mortality in compensated and decompensated cirrhosis

Christian Sebesta[1,2,3], Georg Kramer[1,2,3,4], Benedikt Hofer[1,2,3,4], Paul Thöne[1,2,3], Marlene Hintersteininger[1,2,3], Lorenz Balcar[1,2,3], Mathias Jachs[1,2,3], Lukas Hartl[1,2,3], Jurij Maurer[1,5], David Bauer[1,6], Georg Semmler[1,2,3], Benedikt Simbrunner[1,2,3], Michael Trauner[1,3], Albert Friedrich Stättermayer[1,2], Mattias Mandorfer[1,2,3], Thomas Reiberger[1,2,3,4]. [1]*Division of Gastroenterology and Hepatology, Department of Medicine III, Medical University of Vienna, Vienna, Austria, Vienna, Austria;* [2]*Vienna Hepatic Hemodynamic Lab, Division of Gastroenterology and Hepatology, Department of Medicine III, Medical University of Vienna, Vienna, Austria, Vienna, Austria;* [3]*Clinical research group MOTION, Medical University of Vienna, Vienna, Austria, Vienna, Austria;* [4]*Christian-Doppler Laboratory for Portal Hypertension and Liver Fibrosis, Medical University of Vienna, Vienna, Austria, Vienna, Austria;* [5]*Klinikum Landstrasse, Vienna Healthcare Group, Vienna, Austria, Vienna, Austria;* [6]*Klinikum Ottakring, Vienna Healthcare Group, Vienna, Austria, Vienna, Austria*
Email: christian.a.sebesta@meduniwien.ac.at

Background and aims: Clinically significant portal hypertension (CSPH) is a key driver of decompensation and mortality in advanced chronic liver disease (ACLD). Esophageal varices (EV) represent a clinical manifestation of portal hypertension. Since EV grading for size is subject to interobserver variability, the prognostic implications of grading EV size in compensated (cACLD), and particularly in decompensated ACLD (dACLD) remains to be determined. We aimed to evaluate the prognostic value of EV presence and grading for the risk of hepatic decompensation in cACLD and liver-related death (LRD) in dACLD.
Method: Patients recruited in the prospective Vienna Cirrhosis study (VICIS) with available information on EV status were analyzed. EV were stratified as absent (no-EV), small <5 mm (S-EV) and large ≥5 mm (L-EV) varices. Cumulative incidence functions were used to estimate the incidence of hepatic decompensation and LRD, treating non–LRD and liver transplantation (LT) as competing events. Associations with hepatic decompensation and LRD were evaluated using Fine–Gray competing-risk regression, adjusting for age, sex, and MELD.
Results: A total of 516 patients were included (236 cACLD, 280 dACLD). In cACLD, hepatic venous pressure gradient (HVPG) increased with variceal status (median HVPG: no-EV 9 vs. S-EV 14 vs. L-EV 17 mmHg; $p < 0.001$), paralleled by higher 2-year (Y2) decompensation rates (14%, 24%, and 36%, respectively; Gray's $p = 0.008$). Presence of L-EV was linked to higher Y2 decompensation risk vs. no-EV (sHR 2.92 [1.44–5.89], $p = 0.003$), whereas S-EV were not (sHR 2.01 [0.89–4.53], $p = 0.092$). In dACLD patients, HVPG also increased with EV grade (16 vs. 19 vs. 19 mmHg; $p < 0.001$). Y2-LRD rates were 12%, 22%, and 17% for no-EV, S-EV, and L-EV, respectively (Gray's $p = 0.236$). dACLD patients with L-EV showed a higher Y2 LRD risk versus no-EV (sHR 2.67 [1.00–7.10], $p = 0.049$), whereas S-EV showed only a numerical trend (sHR 2.50 [0.99–6.30], $p = 0.051$). Overall, the presence of EV (vs. absent EV) was independently associated with worse outcomes in both cACLD (Y2 decompensation: sHR 2.49 [1.31–4.72], $p = 0.005$) and dACLD (Y2 LRD: sHR 2.58 [1.09–6.13], $p = 0.031$).
Conclusion: EV reflect the presence of CSPH, and HVPG increases with EV size in both cACLD and dACLD. In cACLD, EV grading showed prognostic relevance, with L-EV identifying patients at increased risk for decompensation versus absent EV, whereas in dACLD, L-EV remained significantly associated with higher LRD risk versus absent EV.

THU-495

Endo-TIPSitis in vascular liver diseases- a case series with mid-term follow-up

Ankita Singh[1], Akash Shukla[1], Yash Kallurwar[1]. [1]*Seth G S Medical College, Mumbai, India*
Email: drakashshukla@yahoo.com

Background and aims: Sustained bacteremia associated with stent infection or "Endo-TIPSitis" is a rare and life-threatening complication of TIPS. This case series describes TIPS-related infections in patients with vascular liver disease- the clinical course, diagnostic and therapeutic challenges, and outcomes.
Method: Single-center, prospective study of all patients with vascular liver diseases [Budd-Chiari syndrome (BCS) and portosinusoidal vascular disorder (PSVD)] who underwent TIPS between June 2019 to June 2025.
Results: A total of 156 TIPS procedures were performed in 123 patients during the study period. Early post-procedure sepsis (within 48 hours), defined by fever (≥38 °C) and tachycardia with or without hypotension, occurred in 21 patients (17%). Among these, 3 patients (14.3%) died during the index hospitalization, and 5 (23.8%) were subsequently diagnosed with endo-TIPSitis. Overall, 8 of 123 patients (6.5%) fulfilled criteria for endo-TIPSitis (7- BCS and 1-PSVD). The median MELD and Rotterdam scores of patients with endo-TIPSitis were 11 (range: 9–14) and 1.108 (range: 0.061–1.2), respectively. Fever in the immediate post-procedure phase was not observed in 3 (37.5%) patients. The median interval from intervention to fever onset was 42 days (range: 1–130 days), and stent thrombosis was present in all but one patient. Metastatic infectious foci in the form of septic pulmonary emboli and infarction was seen in 5 (62.5%) patients. Pseudomonas aeruginosa was the most frequently isolated pathogen, followed by Klebsiella pneumoniae; most isolates were carbapenem resistant, with acquisition of multidrug resistance documented in three patients over the treatment course. PET imaging demonstrated characteristic circumferential tracer uptake along the stent (mean SUV_{max} 7.43 on FDG-PET) and metabolically active thrombus within the stent. Median duration of antibiotic therapy was 67 days (range: 7–215 days), and median time to clinical remission was 40 days (range: 19–122 days). Overall mortality among patients with endo-TIPSitis was 50% (4/8); two patients remain on ongoing therapy, while two achieved sustained remission and remain afebrile 8 and 9 months after treatment discontinuation.
Conclusion: Endovascular stent infection or endo-TIPSitis is a serious complication of TIPS procedure, characterized by frequent stent thrombosis/dysfunction and acquisition of antibiotic resistance; requiring prolonged antibiotic therapy and long time to attain clinical remission; and associated with high mortality.

THU-496

Regular human albumin therapy in decompensated cirrhosis: Six-month clinical outcomes from a multicentre Australian cohort

Siddharth Sood[1,2], Michael Mil[2], Nicholas Hannah[1,2,3], Catherine Yu[1], Natalie Ngu[4,5], Dmitrii Shek[6], Thang Dao[7], Jeremy Tse[5], James Williams[8], Lauren Tang[9], Callista Vania Raharjo[10], Benjamin Mead[11], Anna Ham[11], Samuel Wong[9], Ethan Tang[12], Daniel Clayton Chubb[4,13], Diana Lewis[1], Ammar Majeed[4,13], Jacob George[11,14,15], Kate Lynch[12,16], Golo Ahlenstiel[6,17], Rohit Sawhney[4,8], Jason Behary[10,18], Avik Majumdar[2,9], Jacinta Holmes[2,7], Sally Bell[4,5], Stuart Roberts[4,13]. [1]*Northern Health, Epping, Australia;* [2]*The University of Melbourne, Parkville, Australia;* [3]*The Royal Melbourne Hospital, Parkville, Australia;* [4]*Monash University, Clayton, Australia;* [5]*Monash Health, Clayton, Australia;* [6]*Blacktown Hospital, Blacktown, Australia;* [7]*Saint Vincent's Hospital Melbourne, Fitzroy, Australia;* [8]*Eastern Health, Box Hill, Australia;* [9]*Austin Hospital, Heidelberg, Australia;* [10]*Saint George Hospital, Kogarah, Australia;* [11]*Westmead Hospital, Westmead, Australia;* [12]*Royal Adelaide Hospital, Adelaide Central Business District, Australia;* [13]*Alfred Hospital,*

Melbourne CBD, Australia; [14]Western Sydney University, Parramatta, Australia; [15]Storr Liver Centre, The Westmead Institute for Medical Research, Westmead, Australia; [16]The University of Adelaide, Adelaide Central Business District, Australia; [17]Western Sydney University, Blacktown, Australia; [18]University of New South Wales, Kensington, Australia
Email: siddharth.sood1@nh.org.au

Background and aims: Long-term outpatient human albumin (HA) has shown benefits in randomized trials. However, trial populations exclude patients with the complexity seen in routine practice. Real-world data has been limited to a few European nations. We aimed to evaluate safety and clinical outcomes in the largest real-world cohort of HA outside Europe.
Method: Retrospective data was obtained from 11 centres in a larger cost comparison study through the Gastroenterological Society of Australia Liver Faculty Clinical Research Network. Patients with cirrhosis who had a baseline TIPPS, transplant or PVT were excluded. Patients were censored at 6 months, liver transplant or death. Standard statistical tests were applied.
Results: We included 134 patients initiating HA (median age 62.7 yrs, 43 female (32.1%), 17 (12.7%) with HCC < 12 months. Nearly all patients 125/134 (93.3%) had ascites. Alcohol-related liver disease (86, 64.2%) with half actively drinking, and steatotic liver disease (46, 34.3%) were predominant aetiologies. 2,298 infusions were performed with on average 40 g administered as 20% concentrated albumin each time (CSL Ltd, Australia), and a median 19 infusions/patient. There were 2 minor complications (0.09% complication rate) - nausea and a painful cannulation. Twenty-nine patients were censored before 6 months: 21 (15.7%) died a median of 118 days after commencing HA (17/21 liver-related), whilst 8 (5.97%) received a transplant; an additional 11 patients discontinued before 6 months. Recompensation was rare, whilst 7 patients were referred for TIPPS (5.22%). Among 105 patients not censored before 6 months, patients on diuretics decreased from 91.8% to 74.5% ($p = 0.0003$) and ascites severity improved ($p < 0.0001$). The proportion of patients requiring outpatient paracentesis decreased from 67.9% in the preceding 6 months, to 44.8% in the subsequent period ($p < 0.0001$). Serum albumin increased from a median of 30 to 35 ($p < 0.0001$), while MELD-Na showed a non-significant improvement from 19 to 17 ($p = 0.08$). Most patients 78/105 (74.3%) were planned to continue HA beyond 6 months.
Conclusion: In this real-world Australian cohort of patients receiving nearly 2,300 outpatient HA infusions, therapy was safe and associated with clinically meaningful improvements to ascites despite substantial baseline disease burden. HA presents a pragmatic strategy to lessen healthcare utilisation in routine practice and offers a palliative-type benefit for a large proportion of patients.

THU-497-YI
Contribution of myofibroblast activation and sinusoidal capillarization to portal hypertension

Thomas Sorz-Nechay[1,2,3], Benedikt Hofer[1,2,3], Philipp Königshofer[1,2,3], Alexis Treitler[3], Benedikt Simbrunner[1,2,3], Vlad Taru[1,3], Katharina Bonitz[1,2,3], Henriette Horstmeier[1], Kerstin Zinober[1,2,3], Katharina Regnat[1,2,3], Mattias Mandorfer[1], Barbara Neudert[4], Christopher Kaltenecker[4], Behrang Mozayani[4], Renate Kain[4], Michael Trauner[1], Philipp Schwabl[1,2,3], Thomas Reiberger[1,2,3]. *[1]Division of Gastroenterology and Hepatology, Department of Medicine III, Medical University of Vienna, Vienna, Austria; [2]Center for Molecular Medicine (CeMM) of the Austria Academy of Sciences, Vienna, Austria; [3]Christian Doppler Lab for Portal Hypertension and Liver Fibrosis, Medical University of Vienna, Vienna, Austria; [4]Department of Pathology, Medical University of Vienna, Vienna, Austria*
Email: thomas.sorz-nechay@meduniwien.ac.at

Background and aims: Portal hypertension (PH) is the risk factor for decompensation in cirrhosis. While fibrosis represents the main static component of PH, the specific contribution of other histological features of tissue remodeling and sinusoidal capillarization to PH remain incompletely defined. Next to collagen-proportionate area (CPA), we assessed alpha-smooth-muscle-actin (aSMA) and CD34 as myofibroblast activation and sinusoidal capillarization markers in human liver biopsies, respectively.
Method: Patients undergoing hepatic venous pressure gradient (HVPG) measurement and concurrent liver biopsy were included in this study. Tissue samples were stained using picrosirius-red/fast-green or immunohistochemistry and quantified morphometrically. Statistical analyses were performed via Mann-Whitney U test, Spearman's correlation (rho), and residual correlation analysis after covariate correction (i.e. partial correlation). Data are shown as medians (±IQR).
Results: Eighty-six patients (median age 56.7 years; 65.1% male) were included. Alcohol-related liver disease (25.6%) and MASLD (17.4%) were the most common etiologies. Median HVPG was 14 mmHg (±8 mmHg), with clinically significant PH in 75.6% and severe PH (HVPG≥16 mmHg) in 36.0%. Severe PH was associated with higher fibrosis burden (CPA: 24.9% [± 14.38%] vs. 14.3% [± 13.75%], $p = 0.002$), greater myofibroblast activation (aSMA: 4.72% [± 11.38%] vs. 2.05% [± 4.08%], $p = 0.027$), and increased sinusoidal capillarization (CD34: 3.76% [± 3.05%] vs. 2.27% [± 1.71%], $p < 0.001$). Among all markers, CD34 showed the strongest correlation with HVPG (rho = 0.428, $p < 0.001$), outperforming CPA (rho = 0.293, $p = 0.007$) and aSMA (rho = 0.206, $p = 0.059$). CD34 was also correlated with von Willebrand factor antigen (rho = 0.242, $p = 0.027$). In partial correlation analysis, CD34 (corrected for HVPG, aSMA and CPA) was strongly linked to sinusoidal remodeling via ELF ($r = 0.290$, $p = 0.016$), in addition to ALT ($r = -0.242$, $p = 0.032$) and platelet count ($r = -0.240$, $p = 0.032$). aSMA showed independent correlation (corrected for HVPG, CD34 and CPA) with the inflammation parameters C-reactive protein ($r = 0.348$, $p = 0.002$) and white blood cell count ($r = 0.274$, $p = 0.014$).
Conclusion: In patients with cirrhosis, histological features of fibrogenesis and vascular remodeling are differentially associated with PH. CD34, reflecting sinusoidal capillarization and hepatic vascular remodeling profoundly impacted on HVPG and represents a tissue surrogate for dynamic PH severity.

THU-498
Machine learning-based 8P model achieves high accuracy in predicting portal hypertension severity

Thomas Sorz-Nechay[1,2,3,4], Benedikt Hofer[1,2,3,4], Georg Kramer[1,3,4], Christian Sebesta[1,4], Paul Thöne[1,4], Marlene Hintersteininger[1,4], Lukas Hartl[1,4], Mathias Jachs[1,4], Lorenz Balcar[1,4], Philipp Schwabl[1,2,3,4], Albert Friedrich Stättermayer[1], Michael Trauner[1,4], Benedikt Simbrunner[1,2,3,4], Mattias Mandorfer[1,4], Thomas Reiberger[1,2,3,4]. *[1]Division of Gastroenterology and Hepatology, Department of Medicine III, Medical University of Vienna, Vienna, Austria; [2]Center for Molecular Medicine (CeMM) of the Austria Academy of Sciences, Vienna, Austria; [3]Christian Doppler Lab for Portal Hypertension and Liver Fibrosis, Medical University of Vienna, Vienna, Austria; [4]Clinical Research Group MOTION, Medical University of Vienna, Vienna, Austria*
Email: thomas.sorz-nechay@meduniwien.ac.at

Background and aims: Development of robust non-invasive tests to predict portal hypertension (PH) severity remains a major unmet need. Machine learning approaches may enable improved prediction of hepatic venous pressure gradient (HVPG) and clinically relevant PH stages.
Method: Patients with advanced chronic liver disease (ACLD) undergoing HVPG measurement were prospectively included. Exclusion criteria were: hepatocellular carcinoma, TIPS, occlusive portal vein thrombosis, liver transplantation. Random forest regression (RFR) and classification (RFC) models were trained to predict HVPG and severe PH (SPH; HVPG≥16mmHg) using blood-based

laboratory parameters. The cohort was randomly split into training (80%) and test (20%) sets. The initial RFR model was trained using 5-fold cross-validation with 10 imputations per fold. Feature importance was assessed by a permutation test, and 8-parameter (8P) RFR (8P-R) and RFC (8P-C) models were derived based on feature importance and wide clinical availability. Final models were evaluated on the test set after complete-case filtering. Performance was assessed using sensitivity, specificity, accuracy, Pearson's r (RFR), AUROC (RFC).

Results: A total of 1005 patients were included (training: n = 804; test: n = 201). Median age was 57.3 (IQR 15.4) years, 66.1% were male, main etiology was alcohol-related liver disease (47.6%). The median HVPG was 16 (IQR 10) mmHg, 508 (50.5%) had SPH. After missingness-filtering (>20%), 716 and 795 training cases remained for the full-feature RFR and for the 8P models, respectively. The full-feature RFR achieved a mean Pearson's r of 0.715 (IQR 0.046) across cross-validation folds. The most important features were bile acids, ammonia, antithrombin III activity, d-dimer and prothrombin time. The final 8P models included bile acids, prothrombin time, cholinesterase, ammonia, d-dimer, platelets, hematocrit, and gamma-glutamyl transferase. On the test set (n = 185 complete cases), the 8P-R model achieved high correlation with measured HVPG (r = 0.706, MAE = 3.41, p < 0.001), with better performance in compensated (r = 0.694) than decompensated ACLD (r = 0.525). Classification of SPH using predicted HVPG values of the 8P-R model showed high performance (sensitivity = 85.2%, specificity = 74.2%, accuracy = 79.5%). The 8P-C model had comparable performance (sensitivity = 85.2%, specificity = 75.3%, accuracy = 80.0%, AUROC = 0.84).

Conclusion: The novel blood parameter-based 8P-R and 8P-C models show high accuracy for non-invasive estimation of HVPG and prediction of SPH.

THU-499

Prognostic impact of clinically significant portal hypertension in hepatocellular carcinoma patients with concurrent metabolic dysfunction–associated steatotic liver disease undergoing surgical resection

Chien-Wei Su[1], Yi-Chen Lin[2], Chun-Ting Ho[1], Chia-Jung Ho[1], Tsai Shin-Yu[1], Yi-Hsiang Huang[3], Ming-Chih Hou[4], Jaw-Ching Wu[5].
[1]Division of General Medicine, Department of Medicine, Taipei Veterans General Hospital, School of Medicine, College of Medicine, National Yang Ming Chiao Tung University, Institute of Clinical Medicine, School of Medicine, National Yang Ming Chiao Tung University, Taipei, Taiwan; [2]Department of Medicine, Linkou Chang Gung Memorial Hospital, Taoyuan, Taiwan; [3]Department of Medical Research, Taipei Veterans General Hospital, Taipei, Taiwan; [4]Division of Gastroenterology and Hepatology, Department of Medicine, Taipei, Taiwan; [5]Institute of Clinical Medicine, School of Medicine, National Yang Ming Chiao Tung University, Taipei, Taiwan
Email: cwsu2@vghtpe.gov.tw

Background and aims: Clinically significant portal hypertension (CSPH) reflects impaired hepatic functional reserve and is associated with adverse hepatic events, such as ascites and variceal bleeding. Although the prognostic impact of CSPH in hepatocellular carcinoma (HCC) has been previously reported, data focusing on patients with concurrent metabolic dysfunction–associated steatotic liver disease (MASLD) remain limited. We aimed to assess the prognostic role of CSPH in HCC patients with concurrent MASLD undergoing curative surgical resection.

Method: A total of 477 patients with HCC and concurrent MASLD who underwent curative resection at Taipei Veterans General Hospital and had available pathological specimens and complete clinical data were included. Steatotic liver disease (SLD) was identified by the presence of more than 5% steatosis in the non-tumor liver tissues from surgical specimens, and MASLD was diagnosed as SLD accompanied by at least one cardiometabolic risk factor. CSPH was defined by the presence of esophageal or gastric varices, imaging evidence of splenomegaly, or a platelet count <100,000/μL. Patients were classified into CSPH (n = 65) and non-CSPH (n = 412) groups. Overall survival (OS) was compared using Kaplan–Meier analysis, and Cox proportional hazards models were applied to identify independent predictors of poor OS.

Results: Compared with patients without CSPH, those with CSPH had poorer hepatic functional reserve, including lower serum albumin levels, prolonged prothrombin time, lower platelet counts, and hemoglobin levels, and higher serum alpha-fetoprotein (AFP) levels. They also had higher positivity against hepatitis C virus, greater fibrosis severity, and higher inflammatory activity, but smaller tumor size and less vascular invasion. During a median follow-up of 55.0 months, 83 patients (17.4%) died, with a 5-year OS rate of 76.8%. Kaplan–Meier analysis demonstrated comparable survival outcomes between patients with and without CSPH (5-year OS: 76.7% vs. 76.8%, respectively). In multivariable Cox analysis, serum FIB-4 index, comorbid hypertension, serum albumin level, tumor number, serum AFP, and fibrosis stage were independently associated with poor OS, whereas CSPH was not.

Conclusion: HCC patients with concurrent MASLD and CSPH exhibited distinct clinical, biochemical, and histopathological characteristics compared with those without CSPH. However, the presence of CSPH did not determine long-term survival after curative resection in this patient population.

THU-500

Endoscopic ultrasound guided portal venous pressure predicts hepatic decompensation in patients with suspected portal hypertension: a multicenter study

Giuseppe Tarantino[1], Francesco Santopaolo[2], Lucia Salvi[1], Francesco Martini[1], Annalisa Alessandrini[1], Martina Dalla Bella[1], Clelia Cavallo[2], Lucia Giuli[2], Brigida Annicchiarico[2], Gianenrico Rizzatti[2], Giulia Tripodi[2], Alberto Larghi[2], Marco Marzioni[1], Isabel Carmona Soria[3], Victoria Alejandra Jiménez García[3], Maria Tous Romero[3], Manuel Rodriguez-Tellez[3], Angel Caunedo Alvarez[3], Rafael Romero Castro[3]. *[1]AOU delle Marche, Ancona, Italy; [2]Policlinico Universitario A. Gemelli, Rome, Italy; [3]Hospital Universitario Virgen Macarena, Seville, Spain*
Email: giuseppe.tarantino@ospedaliriuniti.marche.it

Background and aims: While Endoscopic Ultrasound (EUS-) guided Portal Pressure Gradient (PPG) correlates with portal hypertension (PH), the clinical utility of EUS- Portal Venous Pressure (PVP) remains unclear. This study is aimed to investigate the clinical and prognostic role of PVP in cohort of patients with compensated-advanced chronic liver disease (c-ACLD).

Method: Patients with c-ACLD of any etiology and suspected PH, underwent baseline EUS-PPG in this multicentric study. Clinical data, endoscopy, and elastography measurements, were retrospectively analyzed. During 3-month interval outpatient follow-ups, liver-related events (e.g., variceal bleeding, ascites, encephalopathy) were recorded.

Results: We investigated data of 178 consecutive patients. All underwent endo-hepatologic evaluation included EUS-PPG; 92 also underwent Hepatic Venous Pressure Gradient (HVPG) measurement. The mean age was 59.2 years, and 51.6% were males. Clinical findings included MELD score of 8.9 ± 2.9, liver stiffness (LSM) of 20.6 ± 18.2 kPa, spleen stiffness (SSM) of 56.6 ± 24 kPa, and platelet count of 123.2 ± 67.3 × 10^9/L. Cirrhosis was diagnosed in 73 patients (41%), and esophageal varices were detected in 92 (51.7%). HVPG mean value was 8.9 ± 5.3 mmHg. Etiologies included metabolic dysfunction-associated steatohepatitis (28.7.3%), porto-sinusoidal vascular disorder (PSVD, in 26.4%), alcohol-related disease (18.5%), autoimmune/cryptogenic liver disease (21.3%) and viral hepatitis (5.1%). PPG resulted to be 11.7 ± 7.4 mmHg (PVP 21.1 ± 8.4 minus Hepatic Venous Pressure 9.5 ± 5.6 mmHg). Significant correlations emerged between

PVP and both variceal size and SSM (Spearman's rho = 0.51; p < 0.001 and 0.57; p < 0.001; respectively). Over a median follow-up of 406.5 days, liver-related events occurred in 40 patients. Multivariate logistic regression, adjusted for platelet count, MELD, SSM and PPG, identified Fibrosis-4 index (OR 1.14; p = 0.03) and PVP (OR 1.14; p = 0.004) as independent predictors of decompensation. Kaplan-Meier analysis demonstrated that a PVP > 22 mmHg was significantly associated with an increased risk of clinical events (p < 0.001).
Conclusion: EUS-PVP emerges as a promising tool for assessing PH across different etiologies, including pre-sinusoidal disorders like PSVD. Furthermore, it appears effective in predicting the risk of hepatic decompensation. These findings warrant confirmation through further prospective validation.

THU-501

Chronic kidney disease predicts worse ascites control and higher mortality after TIPS: results from the EuroTIPS cohort

Luis Téllez[1], Jesus Donate[1], Anna Baiges[2], Marika Rudler[3], Dario Saltini[4], David Patch[5], Lukas Harlt[6], Alberto Zanetto[7], Michael Praktikjo[8], Fabio Marra[9], Dominik Bettinger[10], Louis Dalteroche[11], Alvaro Giráldez-Gallego[12], Christian Jansen[13], Wim Laleman[14], Hélène Larrue[15], Marie-Angèle Robic[15], Christophe Bureau[15], Faisal Khan[16,16], María Pilar Ballester[17], Sheila González-Padilla[17], Alexander Zipprich[18], Pablo Bellot Garcia[19], Bogdan Procopet[20], Dhiraj Tripathi[16], Sophia Geißelbrecht[21], Benjamin Maasoumy[21], Sonia Torres[2], Fanny Turon[2], Manon Allaire[3], Charlotte Bouzbib[3], Antonio Piscopo[4], Marcello Bianchini[4], Kymentie Ferdinande[7], Marlene Hintersteininger[6], Johannes Chang[13], Lukas Sturm[13], Mattias Mandorfer[6], Miguel Ángel Rodríguez-Gandía[1], Andreína Olavarría[22], José Urbano[22], Virginia Hernández-Gea[2], Laure Elkrief[11], Francesco Vizzutti[9], Jonel Trebicka[8], Marco Senzolo[7], Thomas Reiberger[6], Filippo Schepis[4], Dominique Thabut[3], Juan Carlos García-Pagán[2], Agustín Albillos[1]. *[1]Gastroenterology and Hepatology Department, Hospital Universitario Ramón y Cajal. IRYCIS, CIBERehd. Universidad de Alcalá, Madrid, Spain, Madrid, Spain; [2]Barcelona Hepatic Hemodynamic Laboratory, Liver Unit, Hospital Clínic Barcelona, Universitat de Barcelona, FRCB-IDIBAPS, CIBEREHD, CSUR, ERN-RareLiver, Barcelona, Spain, Barcelona, Spain; [3]AP-HP, Sorbonne Université, Liver Intensive Care Unit, Hepatogastroenterology Department, La Pitié-Salpêtrière Hospital, 47-83 Boulevard de l'Hôpital, Paris 75013, France, INSERM UMR_S 938, Centre de recherche Saint-Antoine, Maladies métaboliques, biliaires et fibro-inflammatoire du foie, Institute of Cardiometabolism and Nutrition (ICAN), Paris, France, París, France; [4]Severe Liver Diseases (M.E.C.) Departmental Unit, Department of Medical Specialties, Azienda. Ospedaliero-Universitaria of Modena, University of Modena and Reggio Emilia, Modena, Italy, Modena, Italy; [5]Department of Hepatology, The Royal Free Hospital, London, UK, London, United Kingdom; [6]Vienna Hepatic Hemodynamic Lab, Division of Gastroenterolongy and Hepatology, Department of Medicine III, Medical University of Vienna, Vienna, Austria, Vienna, Austria; [7]Gastroenterology, University-Hospital of Padua, Health Care Provider of the European Reference. Network on Rare Liver Disorders (ERN-Rare Liver), Padua, Italy, Padua, Italy; [8]Department of Internal Medicine B, University Hospital Münster, Münster, Germany, Munster, Germany; [9]Department of Experimental and Clinical Medicine, University of Florence, Florence, Italy, Florence, Italy; [10]Department of Medicine II, Medical Center University of Freiburg, Faculty of Medicine, University of Freiburg, Freiburg, Germany, Freiburg, Germany; [11]Université de Tours, service d'hépato-gastroentérologie, Centre de références constitutif des maladies vasculaires du foie, Hôpital Trousseau, CHRU de Tours, Tours, France, Tours, France; [12]Digestive Diseases Department, Hospital Universitario Virgen del Rocío, CIBERehd, Institute of Biomedicine (HUVR/CSIC/US), University of Seville, Seville, Spain, Seville, Spain; [13]Department of Internal Medicine I, Bonn University Hospital, Bonn, Germany, Bonn, Germany; [14]Department of Gastroenterology & Hepatology, Division of Liver & Biliopancreatic disorders and Liver Transplantation, University Hospitals Leuven, KU LEUVEN, Leuven, Belgium, Leuven, Belgium; [15]Service d'Hépatologie Hôpital Rangueil CHU Toulouse et Université de Toulouse, Toulouse, France, Toulouse, France; [16]Liver Unit, University Hospitals Birmingham NHS Foundation Trust, Birmingham Health Partners, Birmingham, UK, Birmingham, United Kingdom; [17]Digestive Disease Department, Hospital Clínico Universitario de Valencia, Spain. INCLIVA Biomedical Research Institute, Valencia, Spain, Valencia, Spain; [18]Department of Internal Medicine IV, Jena University Hospital, Jena, Germany, Jena, Germany; [19]Liver Unit, Alicante Institute for Health and Biomedical Research (ISABIAL), Hospital General Universitario Dr. Balmis, Alicante, Spain, Alicante, Spain; [20]Department of Hepatology, "Octavian Fodor" Regional Institute of Gastroenterology and Hepatology, Cluj-Napoca 400162, Cluj, Romania, Cluj, Romania; [21]Department of Gastroenterology, Hepatology, Infectious Diseases and Endocrinology, Hannover Medical School, Hannover, Germany, Hannover, Germany; [22]Interventional Radiology Department, Hospital Universitario Ramón y Cajal, Madrid, Spain, Madrid, Spain*
Email: luistevilla@gmail.com

Background and aims: Chronic kidney disease (CKD) is frequent in patients undergoing TIPS for recurrent/ refractory ascites, but its impact on post-TIPS outcomes is poorly defined. We evaluated the association between CKD and 1-year outcomes after TIPS, focusing on CKD stage and MASH-related cirrhosis.
Method: Prospective analysis of patients included in the EuroTIPS cohort who underwent TIPS for ascites and had follow-up up to 1 year or until death. CKD was defined as baseline estimated glomerular filtration rate (eGFR) <60 mL/min/1.73 m^2 and further categorized by CKD stage. Persistent ascites (grade 2) at 1 year was assessed as a binary outcome among 1-year survivors and analyzed using Poisson regression to estimate adjusted risk ratios (aRR). One-year mortality was analyzed using Cox proportional hazards models. Multivariable analyses were adjusted for age, sex, bilirubin, INR, sodium, post-TIPS portal pressure gradient, and MASH etiology.
Results: Of 888 patients enrolled since January 2020, 653 patients with had one-year follow-up. 146 (22.4%) had CKD and 30.5% MASH-cirrhosis. CKD was more prevalent in patients with MASH-related cirrhosis than in non-MASH etiologies (39.0% vs. 15.0%, p < 0.01). One-year overall survival in the entire cohort was 78.8% and was significantly lower in patients with CKD compared with those without CKD (66.4% vs. 82.2%, p < 0.01). In multivariable Cox analysis (n = 631), CKD independently predicted 1-year mortality (aHR 2.26; 95%CI 1.54–3.31; p < 0.01). Among 1-year survivors, persistent ascites at 1 year occurred in 96 patients (19.4%). Ascites persistence was significantly more frequent in patients with CKD compared with those without CKD (50.5% vs. 12.7%, p < 0.01). In multivariable analysis, CKD remained strongly associated with persistent ascites at 1 year (aRR 3.35; 95%CI 2.37–4.74; p < 0.01). A clear stepwise increase in ascites persistence was observed across CKD stages (12.6% for eGFR ≥60, 38.5% for CKD 3a, 55.0% for CKD 3b, and 75.0% for CKD 4–5). In stratified analyses, the association between CKD and ascites persistence was stronger in patients with MASH-related cirrhosis (aRR 7.06; 95%CI 3.61–13.81) than in non-MASH etiologies (aRR 1.86; 95%CI 1.10–3.14), with a significant interaction between CKD and MASH etiology (p for interaction = 0.0038).
Conclusion: CKD independently predicts poorer ascites control and higher 1-year mortality after TIPS, with CKD stage enabling clinically relevant risk stratification, including a possible differential effect in MASH-related cirrhosis.

THU-505-YI

Decreases in spleen stiffness assessed via vibration-controlled transient elastography at 100 Hz upon chronic NSBB treatment do not predict HVPG response: results from a european multicenter study

Paul Thöne[1,2,3], Dario Saltini[4,5], Joana Calvão[6], Maria Grasso[7], Elton Dajti[8,9], Luis Téllez[10], Elba Llop Herrera[11], Fischer Petra[12], Lorenz Balcar[1,2,3], Georg Semmler[1,2,3], Paula Hoefinger[1,2,3], Filippo Schepis[4,5], José Presa[6], Vincenza Calvaruso[7], Federico Ravaioli[8,9], Agustín Albillos[10], José Luis Calleja Panero[11], Bogdan Procopet[12], Michael Trauner[1], Thomas Reiberger[1,3], Mattias Mandorfer[1,2,3], Mathias Jachs[1,2,3]. *[1]Division of Gastroenterology and Hepatology, Department of Medicine III, Medical University of Vienna, Vienna, Austria; [2]Vienna Hepatic Hemodynamic Lab, Department of Medicine III, Medical University of Vienna, Vienna, Austria; [3]Clinical Research Group MOTION, Medical University of Vienna, Vienna, Austria; [4]Department of Medical Specialties, Gastroenterology Unit, University of Modena & Reggio Emilia and Azienda Ospedaliero-Universitaria di Modena, Modena, Italy; [5]Severe Liver Diseases Unit (M. E.C.), Department of Medical Specialties, Azienda Ospedaliero-Universitaria di Modena, University of Modena and Reggio Emilia, Modena, Italy; [6]Liver Unit-CHTMAD, Vila Real, Portugal; [7]Gastroenterology and Hepatology Unit, Department of Health Promotion Sciences Maternal and Infantile Care, Internal Medicine and Medical Specialities, PROMISE, University of Palermo, Palermo, Italy; [8]IRCCS Azienda Ospedaliero-Universitaria di Bologna, European Reference Network on Hepatological Diseases, Bologna, Italy; [9]Department of Medical and Surgical Sciences, University of Bologna, Bologna, Italy; [10]Gastroenterology and Hepatology Department, Hospital Universitario Ramón y Cajal, Madrid, Spain, Instituto Ramón y Cajal de Investigación Sanitaria (IRYCIS), CIBEREHD (Centro de Investigación Biomédica en Red Enfermedades Hepáticas y Digestivas), University of Alcalá, Madrid, Spain; [11]Department of Gastroenterology and Hepatology, Puerta de Hierro University Hospital, Puerta de Hierro Health Research Institute (IDIPHIM), CIBEREHD, Universidad Autonoma de Madrid, Majadahonda, Spain; [12]Third Medical Clinic, Department of Internal Medicine, Iuliu Hatieganu University of Medicine and Pharmacy, Cluj, Romania*
Email: paul.thoene@meduniwien.ac.at

Background and aims: Chronic hepatic venous pressure gradient (HVPG) response to non-selective beta-blocker (NSBB) therapy predicts outcome in patients with advanced chronic liver disease (ACLD) and clinically significant portal hypertension (CSPH). Non-invasive tests (NITs) for diagnosing HVPG response are currently lacking. This study investigated spleen stiffness measurement (SSM) via vibration-controlled transient elastography at 100 Hz for monitoring chronic HVPG response.

Method: Patients from eight European centers who underwent paired HVPG measurements before and after 5–365 days of NSBB therapy were included. SSM and liver stiffness measurement (LSM) were assessed on the same day as HVPG. HVPG response was defined as ≥10% reduction from baseline.

Results: One hundred and thirteen patients (median age: 59 [IQR: 52–62] years, 54% male, BMI 26 [23–30] kg/m^2; ALD/MetALD: 42.5%, MASLD: 27.4%, viral: 16.8%, others: 13.3%; prevalence of varices: 70.8%, decompensated: 38.9%; 87.6% received carvedilol, 12.4% propranolol) were included. Median baseline HVPG was 16 (13–20) mmHg, decreasing to 15 (11–19) mmHg on NSBB (−12% [−21 to 0%], p < 0.001 by Wilcoxon test). Sixty-three patients (55.8%) achieved HVPG response. Median SSM was 61 (48–84) kPa at baseline, decreasing to 58 (43–76) kPa at response measurement (relative changes: −9% [−23 to +8%], p = 0.001 by Wilcoxon test) in the overall cohort. Importantly, there was no difference in SSM dynamics in HVPG nonresponders (−8% [−17 to +8%]) and responders (−11% [−27 to +7%], Mann-Whitney-U-test: p = 0.352). LSM was 39 (22–63) kPa at baseline, while it had decreased to 32 (20–55) kPa at response measurement (relative changes: −6% [−24 to +6%], p = 0.005 by Wilcoxon test). No differences in LSM dynamics were observed between HVPG responders and nonresponders (Mann-Whitney-U-test: p = 0.315). Dynamics in HVPG and changes of SSM (Spearman's rho for absolute/relative changes: 0.016, p = 0.866/0.079, p = 0.405, respectively) and LSM (rho: −0.088, p = 0.362/<0.001, p = 0.996) did not correlate. Neither dynamics in SSM (AUC for absolute/relative changes: 0.522, p = 0.688/0.551, p = 0.355) nor LSM (AUC: 0.577, p = 0.168/0.557, p = 0.313) showed utility for detecting HVPG response non-invasively.

Conclusion: Chronic NSBB treatment was accompanied by decreases in SSM via VCTE at 100 Hz in ACLD patients with CSPH. However, these changes were unrelated to HVPG dynamics, rendering SSM unsuitable for diagnosing HVPG response on an individual patient level.

THU-506

Favourable outcomes in patients with advanced Fontan-associated liver disease following isolated heart transplant

Marius Vögelin[1], Daniel Cooper[1], Ava Poirier[1], Shani Nagler[1], Rafael Alonso-Gonzalez[2], Lucy Roche[2], Aliya Gulamhusein[1]. *[1]Toronto, Canada; [2]University Health Network, Toronto Adult Congenital Cardiac Clinic, Toronto, Canada*
Email: marius_voegelin@hotmail.com

Background and aims: In patients (pts) with a failing Fontan circulation, features of advanced Fontan-associated liver disease (FALD) are common whilst the indications for isolated HT (IHT) vs. combined heart-liver transplant (CHLT) remain unclear. We report our experience of liver outcomes in a cohort of pts with FALD undergoing IHT.

Method: Adult FALD pts who underwent HT between 1990–2024 at the University Health Network were reviewed. Descriptive statistics with proportions and medians with interquartile ranges (IQR) were used to describe clinical characteristics and outcomes of the cohort.

Results: Of 586 pts with Fontan circulation seen in the adult congenital heart disease program, 17 underwent IHT, and one patient had CHLT. For pts with IHT, median age at IHT was 35 years (yrs) (IQR 25.6–48.5), with a median Fontan exposure of 31 yrs (IQR 22.8–35.3). At IHT, 94% (n = 16) had features of portal hypertension including ascites (n = 14), esophageal varices (n = 4) and splenomegaly (n = 12). Benign liver nodules were present in 41% (n = 7). Median follow up after IHT was 4.6 yrs (IQR 1–8.3 yrs). During the follow-up period, no pts experienced hepatic decompensation or hepatocellular cancer. With 91.8 patient-yrs of follow-up, 4 pts died, 2 within the first year and 2 at 9 yrs post IHT. Of the early deaths, one occurred at 2 months (mos) from necrotizing pancreatitis, subsequent sepsis and multi-organ failure and the other at 19 mos from CMV colitis, associated colonic perforation and septic peritonitis. The 2 late deaths were of cardiac nature (sudden cardiac death and cardiogenic shock secondary to antibody-mediated rejection). No deaths were determined to be directly liver related. Ascites resolved or became clinically insignificant in 93% (n = 13) but persisted as severe in one case with pre-existing segmental portal vein thrombosis. Sequential liver stiffness measurements (LSM), taken a median of 11.8 and 16.3 mos pre- and post-IHT, respectively, improved in all patients for whom it was available (n = 5). Median pre IHT LSM was 35.8 kPa (IQR 34.8–47.2), and post IHT LSM was 9.3 kPa (IQR 6.7–17.1) with a median reduction in LSM of 28.1 kPa post IHT.

Conclusion: Optimal approach to selection of patients for IHT and CHLT remains undefined. Herein, we report favourable outcomes particularly with improved ascites and LSM in patients with advanced FALD undergoing IHT. Infectious risk in the immediate post-IHT period in those with advanced FALD warrants further study.

THU-507

An integrated single-cell and spatial transcriptomic atlas identifies pro-coagulant phenotypic remodeling of liver sinusoidal endothelial cells (LSECs) in porto-sinusoidal vascular disorder (PSVD)

Qirong Jiang[1], Haoxiang Zhu[2], Jinyu Wang[2], Jiming Zhang[2]. [1]*The First Affiliated Hospital of Fujian Medical University, Fujian, China;* [2]*Fudan University affiliated Huashan Hospital, Shanghai, China*
Email: jmzhang@fudan.edu.cn

Background and aims: The pathogenesis of porto-sinusoidal vascular disorder (PSVD) remains unclear. Using single-cell and spatial transcriptomics, we characterized hepatic endothelial heterogeneity in PSVD and identified liver sinusoidal endothelial cell (LSEC) phenotypic remodeling associated with portal hypertension.
Method: Liver tissue samples were obtained from 7 patients with PSVD, 3 patients with cirrhosis, and 2 patients with chronic hepatitis B as controls. Single-nucleus RNA sequencing was performed using the 10x Genomics platform to profile hepatic endothelial cells. Endothelial subpopulations were identified based on established marker genes using UMAP-based clustering. Spatial transcriptomics was used to validate lobular zonation and portal–sinusoidal distribution of LSEC subsets.
Results: A total of 12 endothelial cell subpopulations were identified, comprising 7 liver LSECs subsets, 3 vascular endothelial cell subsets, and 2 lymphatic endothelial cell subsets. In normal liver tissue, LSECs exhibited clear spatial zonation along the portal–central axis, including periportal, mid-lobular, and pericentral subsets, which was further validated by spatial transcriptomics. Compared with controls, LSEC composition was markedly altered in livers from patients with PSVD. Pro-fibrinolytic genes (PLAT, PLG) were significantly downregulated, whereas anti-fibrinolytic genes (SERPINE1, CPB2) were upregulated, indicating an impaired fibrinolytic state. In parallel, LSEC-specific markers associated with fenestration and endocytic function (LYVE1, STAB2, FCGR2B/CD32B) were reduced, consistent with loss of fenestrations and endothelial dysfunction. Expression of VEGFR2 was also decreased, suggesting attenuated VEGF signaling. UMAP analysis demonstrated enrichment of pro-microthrombotic LSEC subsets in PSVD. Spatial transcriptomic mapping further localized these pathological LSEC states predominantly to the portal–sinusoidal interface, supporting their contribution to increased intrahepatic microcirculatory resistance.
Conclusion: This integrated single-cell and spatial transcriptomic atlas identifies pro-coagulant phenotypic remodeling of LSECs as a defining feature of PSVD. These findings indicate that PSVD-associated portal hypertension arises from endothelial remodeling programs distinct from cirrhosis and establish LSECs as key contributors to non-cirrhotic portal hypertension.

THU-508

A novel non-invasive model to identify high risk varices in patients with HBV-related cirrhosis

Peishuang Xu[1], Mingchen Wang[1], Jiankang Song[1], Jinjun Chen[2], Haiyu Wang[3]. [1]*Hepatology Unit, Department of Infectious Diseases, Nanfang Hospital, Southern Medical University, Guangzhou, Guangdong, China;* [2]*Department of Infectious Diseases, Key Laboratory of Molecular Biology for Infectious Diseases (Ministry of Education), Institute for Viral Hepatitis, the Second Affiliated Hospital, Chongqing Medical University, Hepatology Unit, Department of Infectious Diseases, Nanfang Hospital, Southern Medical University, Guangzhou, Guangdong, China;* [3]*Department of Infectious Diseases, Nanfang Hospital, Southern Medical University, Guangzhou, Guangdong, China*
Email: 375612668@qq.com

Background and aims: Over the past decade, several non-invasive diagnostic models of high-risk varices (HRV) in patients with advanced chronic liver disease have been developed. However, these models can only be used to exclude HRV patients but cannot effectively rule in HRV patients. Early detection of HRV in cirrhosis is critical for prognostic improvement. This study aimed to develop and validate a reliable non-invasive diagnostic model capable of both safely ruling out and accurately ruling in HRV in patients with HBV-related cirrhosis.
Method: This prospective cross-sectional study enrolled 616 consecutive patients with compensated HBV-related cirrhosis from July 2021 to April 2024. Patients completed liver and spleen transient elastography (FibroScan®630, Echosens, France) and EGD. Variables selected through least absolute shrinkage and selection operator regression were subsequently analyzed by multivariable logistic regression to construct the model.
Results: Participants were randomly divided into training (n = 432) and validation (n = 184) cohorts (7:3 ratio). The model consisting of spleen stiffness measurement@100 Hz, platelets, spleen diameter, spleen thickness, and sex, named PASS model, performed robustly in training cohort (area under the receiver operating characteristic [AUROC] 0.94, area under the precision-recall curve [AUPRC] 0.81) and validation cohort (AUROC 0.92, AUPRC 0.78). Cut-off of 4.84 for ruling out and 78.28 for ruling in were best for discriminating HRV. In the training cohort, for ruling out HRV, PASS model spared 53.47% (231/432) unnecessary esophagogastroduodenoscopy (EGD) with a HRV missed rate of 1.11% (1/90), with the corresponding sensitivity, negative predictive value, and negative likelihood ratio were 98.89%, 99.57%, 0.02, respectively. For ruling in HRV, 92.50% (37/40) of positive patients were correctly classified (specificity 99.12%, positive predictive value 92.50%). These results were then confirmed in validation cohort.
Conclusion: The PASS score is an accurate, novel, and non-invasive HRV diagnostic criterion with dual cut-off values in patients with compensated HBV-related cirrhosis. It is based on five routine laboratory and clinical parameters. PASS can identify patients with an extremely low probability of HRV (HRV misclassification rate < 5%), allowing them to safely avoid EGD. At the same time, it can also accurately identify HRV patients (PPV > 92%), enabling the timely initiation of primary prevention treatment.

THU-509

Recompensation of decompensated cirrhosis and long-term resolution of ascites in patients undergoing alfapump placement: experience from the multi-center POSEIDON study

Ethan Weinberg[1], Nadim Mahmud[1], Hugo Vargas[2], Jasmohan Bajaj[3], Mangesh Pagadala[4], Jeroen Capel[5], Gijs Klarenbeek[5], Patrick S. Kamath[6], Florence Wong[7], K. Rajender Reddy[1]. [1]*University of Pennsylvania, Philadelphia, PA, United States;* [2]*Mayo Clinic in Arizona, Phoenix, AZ, United States;* [3]*Virginia Commonwealth University, Richmond VA, Richmond, VA, United States;* [4]*Methodist Health System, Dallas, TX, United States;* [5]*Sequana Medical, Zurich, Switzerland;* [6]*Mayo Clinic, Rochester, MN, United States;* [7]*Toronto General Hospital, Toronto, Canada*
Email: ethan.weinberg@pennmedicine.upenn.edu

Background and aims: Recompensation of decompensated cirrhosis, characterized by resolution of ascites and hepatic encephalopathy, has been described in patients after cure or control of cirrhosis etiology. We hypothesized that long term regular ascites removal in those with refractory ascites would allow for better nutritional intake and recovery of liver function. We aimed to determine the rate of resolution of ascites and recompensation after long term management of ascites with an alfapump.
Method: The alfapump system consists of a subcutaneous device with a rechargeable battery that mobilizes ascites from the peritoneal cavity into the urinary bladder. The POSEIDON study was the pivotal North American study of the alfapump for recurrent ascites: 69

subjects at 15 centers had an alfapump implanted. In this post-hoc analysis, recompensation is defined as the average removal of less than 50 ml of ascites per day and without the need for large-volume paracentesis for at least 3 months until the last evaluation. Only those alive and with a functioning alfapump for at least 6 months were included.
Results: 48 subjects had a working alfapump 6 months after implant; 10 of whom experienced long-term recompensation. The median time to recompensation was 503 days (IQR 234 days). Six pumps were removed for recompensation; 4 subjects with recompensation chose to maintain the alfapump system *in situ*. Subjects who recompensated produced less daily ascites at the time of implant (577.6mL vs.845.1mL, $p < 0.001$) coupled with decreased ascites production over time. There were no baseline differences between the two groups in MELD-Na, etiology, sex, SF-36 scores, Ascites-Q scores, albumin, or duration of recurrent ascites (each $p > 0.05$). By month 6, subjects with recompensation had lower MELD-Na (11 vs. 15, $p = 0.004$), which persisted through months 12 and 24 (10 vs. 15, $p = 0.004$; 11 vs. 14, $p = 0.01$). By month 12, recompensation was associated with higher serum albumin (39.0 g/L vs. 32.5 g/L, $p = 0.03$). There were no differences at months 6, 12, or 24 between the two groups on Ascites-Q or pre-albumin.
Conclusion: Recompensation of decompensated cirrhosis is possible in long-term survivors after alfapump implantation. This may be a consequence of improved patient wellbeing and enhanced nutritional intake while there is ongoing control of the cirrhosis etiology. Signs of recompensation were lower ascites removal requirement at time of alfapump implant, decreasing ascites removal over time, decreasing MELD-Na, and increasing albumin.

THU-510

Integrating gut microbiota and clinical parameters to predict beta-blocker response and portal pressure in patients with cirrhosis

Peishan Wu[1,2], Yu-Cheng Lin[1], Yun-Cheng Hsieh[1,2], Shih-Yun Wu[1,2], Teh-Ia Huo[1,2], Bernd Schnabl[3], Han-Chieh Lin[1,2], Kuei-Chuan Lee[1,2], Ming-Chih Hou[1,2]. *[1]National Yang Ming Chiao Tung University Yangming Campus, Beitou District, Taiwan; [2]Taipei Veterans General Hospital, Beitou District, Taiwan; [3]University of California San Diego, La Jolla, United States*
Email: kclee2@vghtpe.gov.tw

Background and aims: Non-selective beta-blockers (NSBBs) are the key treatment for preventing variceal bleeding in cirrhosis. However, predictors of hemodynamic response remain limited. Growing evidence links portal hemodynamics with the gut microbiota, but their combined relevance to NSBB responsiveness remains poorly defined. We aimed to identify microbial and clinical features associated with portal pressure and hemodynamic response.
Method: Patients with cirrhosis and esophageal varices requiring NSBBs were enrolled. Hemodynamic parameters were measured before and after NSBBs. Stool samples were also obtained in cirrhotic patients and from healthy individuals as controls. Gut microbiota was analyzed using 16S rRNA sequencing. Predictions of HVPG and hemodynamic response were evaluated using machine–learning–based models.
Results: Between December 2019 and November 2024, 30 patients were enrolled, including 15 hemodynamic responders and 15 non-responders. Baseline demographic characteristics, liver disease severity, LSM, SSM, heart rate, mean arterial pressure, and HVPG were similar between groups. Responders had a significantly higher baseline cardiac output (CO) than non-responders (8.09 ± 2.51 vs. 6.03 ± 1.29 L/min, $p = 0.012$), which persisted after NSBB therapy (6.43 ± 1.28 vs. 4.90 ± 0.82 L/min, $p < 0.001$). NSBBs did not cause global gut microbial diversity or community structure alteration. However, responders showed higher relative abundances of *Enterococcus* spp. and *Escherichia–Shigella*, while non-responders were enriched in butyrate-producing and potential gut barrier-supporting taxa, including *Faecalibacterium prausnitzii, Agathobaculum desmolans*, and *Gordonibacter–Eggerthella.* In machine-learning analyses, post-treatment CO emerged as the only independent predictor of hemodynamic response. LSM demonstrated a weak but persistent association with HVPG, while SSM did not correlate with HVPG. Incorporation of *Weissella confusa* abundance improved HVPG estimation when combined with LSM.
Conclusion: NSBB therapy did not alter the overall composition of the gut microbiota; however, specific microbial profiles were associated with distinct hemodynamic responses. A higher cardiac output was associated with a favorable hemodynamic response to NSBBs, suggesting that assessment of cardiac function may help identify patients most likely to benefit from therapy. Liver stiffness and selected microbial features may provide additional information for estimating portal pressure.

THU-511

Effects of early placement of transjugular portosystemic shunts in patients with gastric fundal variceal bleeding: a multicenter cohort study

Jie Xue[1], Lijuan Chen[1], Chunqing Zhang[1], Guangchuan Wang[1]. *[1]Shandong Provincial Hospital, Jinan, China*
Email: riverwang@126.com

Background and aims: Some studies have shown that transjugular intrahepatic portosystemic shunt (TIPS) placement within 72 hours of admission improves survival in patients at high risk who present with acute variceal bleeding. However, regarding gastric fundal varices (isolated gastric varices type 1/gastroesophageal varices type 2), whether preemptive transjugular intrahepatic portosystemic shunt (P-TIPS) is a more optimal treatment method and which subgroup among them can benefit from P-TIPS remains controversial at present. This nationwide multicenter cohort study aimed to evaluate whether P-TIPS could improves survival incidence of gastric fundic variceal bleeding in patients with liver cirrhosis.
Method: In this retrospective cohort study, we collected data from patients with cirrhosis with gastric fundic variceal bleeding (within seven days after bleeding) who received P-TIPS or ECI treatment between June 2019 and June 2024 at ten medical centers. The primary endpoint was all-cause rebleeding and the secondary endpoints included overt hepatic encephalopathy (OHE) all-cause mortality and further decompensation.
Results: A total of 836 patients were included. Among them, 628 (75.1%) had gastroesophageal varices type 2 (GOV2), and 208 (24.8%) had isolated gastric varices type 1 (IGV1). The median follow-up period was 27.5 months. In the entire cohort, P-TIPS reduced rebleeding (52.51% versus 23.27%, $p < 0.001$) and further decompensation (85.62% versus 66.40%, $p < 0.001$) compared with ECI. However, no significant differences were found in mortality (30.45% versus 26.55%, $P = 0.090$). In patients with Child-Pugh B or C scores,P-TIPS reduced rebleeding (61.01% versus23.91%, $p < 0.001$) mortality (37.47% versus 30.24% $P = 0.026$) and further decompensation (95.77% versus 69.17%, $P < 0.001$). However, in patients with Child-Pugh A scores, P-TIPS did not reduce mortality (9.93% versus 18.38%, $P = 0.307$) or further decompensation (58.49% versus 60.40%, $P = 0.460$).
Conclusion: Compared with endoscopic cyanoacrylate injection, P-TIPS reduced rebleeding in all patients. More importantly, in the Child-Pugh B or C scores patient group, P-TIPS can reduce the incidence of further decompensation and improve survival rates. These findings suggest that in the Child-Pugh B or C scores group with gastric fundus varices, rather than Child-Pugh A scores, could benefit from P-TIPS.

THU-512

Controlled expansion stent-grafts in TIPS: a real-world analysis of in vivo diameter change and early hepatic encephalopathy

Zizhen Ye[1], Ruoting Men[1], Yi Shen[1], Ziqi Chen[2], Li Yang[1], Luo Xuefeng[1], Xiaoze Wang[1]. [1]*Department of Gastroenterology and Hepatology, Laboratory of Gastrointestinal Cancer and Liver Disease, West China Hospital, Sichuan University, Chengdu, China, Chengdu, China;* [2]*Department of Radiology, West China Hospital, Sichuan University, No.37, Guoxue Alley, Chengdu, 610041, China, Chengdu, China*
Email: 3027368878@qq.com

Background and aims: Post-TIPS hepatic encephalopathy (HE) remains a major limitation of portosystemic shunting, and stent diameter is a key modifiable determinant of HE risk. The VIATORR® Controlled Expansion (VCX) stent-graft was designed to allow tighter control of the functional lumen (8–10 mm) and potentially reduce HE by preventing passive self-expansion seen in conventional VIATORR TIPS stents (VTS). However, clinical data remain conflicting and information regarding the in vivo expansion behavior of VCX in real-world practice is limited. This study compared early HE after TIPS using VCX versus 8-mm VTS and quantitatively characterized VCX expansion and associated hemodynamic changes.
Method: This single-center retrospective cohort included consecutive cirrhotic patients undergoing TIPS between January 2024 and July 2025, receiving either an 8-mm VTS or VCX stent-graft. VCX stents were initially dilated to 8 mm and further dilated to 10 mm only if post-procedural portal pressure gradient (PPG) remained >12 mmHg or decreased <50% from baseline. The primary endpoint was new-onset OHE within 6 months. Stent diameter was quantitatively measured along the VCX controlled-expansion mid-segment on fluoroscopy at baseline and 3 months. PPG measurements were also obtained at both timepoints.
Results: Among 153 patients (43 VCX, 110 VTS), OHE occurred in 30 patients (19.6%). The VCX group showed a higher cumulative 6-month OHE incidence than the VTS group (HR = 2.34, 95% CI 1.05–5.20; log-rank $p = 0.032$). Among VCX patients, the mid-segment diameter increased from 8.0 mm to a mean of 8.65 mm (range 8.2–9.1 mm) at 3 months ($p < 0.001$). Post-TIPS PPG increased from 7.7 mmHg to 11.6 mmHg ($p < 0.001$). Stent expansion was not correlated with PPG increase (Spearman r = 0.038, p = 0.834).
Conclusion: VCX stent-grafts demonstrated consistent early in vivo expansion and are associated with a higher incidence of early OHE compared with 8-mm VTS. The observed PPG rise at 3 months underscores the unreliability of immediate intra-procedural PPG as a surrogate for long-term hemodynamic status. These findings support the need for refined VCX-specific dilation strategies—such as staged or intentionally smaller initial dilation—to optimize the balance between portal decompression and HE risk. Prospective studies are warranted to validate individualized diameter-modulation protocols.

THU-513

Spleen stiffness-based algorithms for predicting decompensation in treatment-naive HBV-HCC patients

Xiaofeng Zhang[1], Jinjun Chen[2], Xiao Cheng[1]. [1]*Southern Medical University, Guangzhou, China;* [2]*Department of Infectious Diseases, the Second Affiliated Hospital, Chongqing Medical University, Chongqing, China*
Email: 1282614092@qq.com

Background and aims: Survival in patients with hepatocellular carcinoma (HCC) is influenced not only by tumor burden but also by the degree of underlying liver dysfunction and portal hypertension. This study aimed to assess the predictive value of liver stiffness measurement (LSM) and spleen stiffness measurement (SSM) for hepatic decompensation and liver-related mortality in treatment-naive HCC patients, and to develop prognostic models incorporating LSM/SSM, tumor burden, and routine laboratory parameters.
Method: We prospectively enrolled compensated HBV-related HCC patients who underwent baseline SSM using a 100-Hz probe. Patients were followed for≥3 months or until death. The primary endpoint was hepatic decompensation.
Results: A total of 222 HCC patients were included (median follow-up 14.0 months). The cumulative 1-year and 2-year incidences of decompensation were 17.9% and 25.5%, respectively. Both LSM (subdistribution hazard ratio [sHR]: 1.03, 95% CI: 1.01–1.04) and SSM (sHR: 1.04, 95% CI: 1.02–1.05) were significant predictors of decompensation. A model incorporating LSM, total bilirubin (TBIL), albumin, and complete response to HCC treatment (Decom_model 1) achieved a C-index of 0.784 for predicting decompensation. Another model using SSM, TBIL, albumin, and complete response (Decom_model 2) achieved a C-index of 0.808. In comparison, the Albumin-Bilirubin (ALBI) grade (C-index: 0.687), Child-Pugh score (0.600), and Model for End-Stage Liver disease (MELD) score (0.650) showed lower predictive performance.
Conclusion: In treatment-naive HBV-HCC patients, both LSM and SSM are strong, independent predictors of hepatic decompensation. Prognostic models integrating either stiffness measurement with TBIL, albumin, and treatment response outperform conventional liver function scores (ALBI, Child-Pugh, MELD) in predicting decompensation risk. These findings support the incorporation of stiffness measurements, particularly SSM, into routine risk stratification to better guide the management of HCC patients.

THU-514

Ultrasound localization microscopy for diagnosis of clinically significant portal hypertension: a prospective multicenter study

Wei Zhang[1], Chuan Liu[2], Xinde Gong[3], Yingchun Yuan[4], Renmei Wu[5], Jiahao Han[6], Xia Chen[7], Su Wu[8], Yanping Ma[1], Jieyang Jin[1], Jie Ren[1], Xiaolong Qi[2]. [1]*The Third Affiliated Hospital of Sun Yat-sen University, Guangzhou, China;* [2]*Liver Disease Center of Integrated Traditional Chinese and Western Medicine, Department of Radiology, Zhongda Hospital, Medical School, Southeast University, Nurturing Center of Jiangsu Province for State Laboratory of AI Imaging & Interventional Radiology (Southeast University), Basic Medicine Research and Innovation Center of Ministry of Education, Zhongda Hospital, Southeast University, State Key Laboratory of Digital Medical Engineering, Nanjing, China;* [3]*Department of Radiology, TaiHe Hospital (Affiliated Hospital of HuBei University of Medcine), Shiyan, China;* [4]*Department of Ultrasound, General Hospital of Ningxia Medical University, Ningxia, China;* [5]*Department of Ultrasound, Suining Central Hospital, Suining, Suining, China;* [6]*Department of Ultrasound, Zhongda Hospital Southeast University, Nanjing, China;* [7]*Department of Ultrasound, The First Affiliated Hospital of USTC, Division of Life Sciences and Medicine, University of Science and Technology of China, Hefei, China;* [8]*Department of Ultrasound, Xingtai People's Hospital, Xingtai, China*
Email: zhangw45@mail2.sysu.edu.cn

Background and aims: Currently, hepatic venous pressure gradient (HVPG) remains the gold standard for diagnosing clinically significant portal hypertension (CSPH), but its use is restricted by invasiveness and accessibility. This multicenter study aims to apply ultrasound localization microscopy (ULM) to visualize and quantify hepatic microvasculature in cirrhotic patients, evaluating its potential in non-invasive CSPH diagnosis.
Method: This study enrolled patients aged 17 to 80 with clinical diagnosis of cirrhosis who underwent HVPG measurement between October 2024 and December 2025 based on clinical needs. After informed consent, patients underwent ULM, with data acquisition in

the portal phase, followed by offline quantitative analysis of microvessel functional and morphological parameters. HVPG ≥ 10 mmHg was considered the gold standard for diagnosing CSPH. The Mann-Whitney U test was used to compare microvessel parameters between the CSPH and non-CSPH groups. Simple and multiple linear regression models evaluated independent predictors of HVPG. Receiver operating characteristic curve was used to assess the diagnostic performance of microvessel parameters in identifying CSPH.

Results: A total of 102 patients were enrolled, including 73 males, with an average age of 46 (range: 42–54) years. Among them, 53 had hepatitis B, 27 had alcoholic liver disease, and the remaining cases included hepatitis C, autoimmune liver disease, primary biliary cirrhosis, and metabolic dysfunction-associated steatotic liver disease. 77 patients were diagnosed with CSPH, and 25 were non-CSPH. Compared to the non-CSPH group, the CSPH group exhibited lower vessel density (VD) (0.5 ± 0.1 vs. 0.4 ± 0.01, p < 0.001), perfusion index (10.1 ± 2.9 vs. 8.0 ± 1.8, p < 0.001) and higher velocity variance (172.6 ± 39.5 vs. 205.5 ± 71.7, p < 0.001). VD was an independent predictor of HVPG (R^2 = 0.53). The diagnostic performance of VD for CSPH (AUC = 0.88, p < 0001) was higher than that of the CSPH risk score (AUC = 0.67, p = 0.07).

Conclusion: ULM-based microvessel parameters were proposed with good diagnostic consistency for HVPG measurement.

THU-515

Interventional embolization of spontaneous portosystemic shunts improves survival by reducing further decompensation in selected patients with decompensated cirrhosis: a retrospective matched analysis

Hongbin Zhu[1], Lijuan Chen[1], Guangchuan Wang[1], Chunqing Zhang[1]. *[1]Shandong Provincial Hospital Affiliated to Shandong First Medical University, jinan, China*
Email: riverwang@126.com

Background and aims: Spontaneous portosystemic shunts (SPSS) are observed in approximately 40% of patients with liver cirrhosis. Although traditionally regarded as a compensatory mechanism to alleviate portal hypertension, emerging evidence indicates that these shunts may mediate a "steal phenomenon," diverting portal blood flow away from the liver and thereby exacerbating hepatic dysfunction. This study aimed to assess whether interventional embolization of SPSS improves long-term survival and delays disease progression in patients with decompensated cirrhosis.

Method: In this single-center retrospective study, we included 201 patients with decompensated cirrhosis and radiologically confirmed SPSS who presented with variceal bleeding or refractory hepatic encephalopathy (HE) between 2016 and 2023. To mitigate potential baseline confounding, a 1:1 propensity score matching (PSM) analysis was performed, yielding 35 patients in the embolization group and 35 in the control group receiving standard treatment. The primary endpoint was 2-year overall survival; secondary endpoints included the occurrence of further decompensation events and longitudinal changes in liver function.

Results: Technical success was achieved in all embolization procedures. During the two-year follow-up, cumulative survival was significantly higher in the embolization group than in the control group (88.6% vs. 65.7%; P = 0.023). Patients who underwent embolization also had a lower incidence of recurrent decompensation events (P = 0.014). Longitudinal analysis using inverse probability of censoring weighting (IPCW) demonstrated that embolization promoted significant liver volume expansion and improved synthetic function, reflected by increased serum albumin, decreased bilirubin, and improved CTP scores. Subgroup analyses revealed that the survival benefit was particularly evident in patients with a baseline CTP score < 10 or in those whose initial clinical presentation was HE.

Conclusion: For carefully selected patients with decompensated cirrhosis and large SPSS, interventional embolization represents a safe and effective therapeutic strategy. By mitigating the portal steal phenomenon and reestablishing hepatopetal portal flow, the procedure promotes hepatic regeneration and significantly enhances 2-year survival. Early intervention—especially in patients with preserved hepatic functional reserve—is advocated to optimize long-term clinical outcomes.

THU-516

Sarcopenia predicts post-TIPS hepatic encephalopathy, and early hepatic encephalopathy predicts mortality: evidence from a multicentric cohort

Amine Zoughlami[1], Joseph Najjar[1], Benoit Billette[1], Philip Wong[1], Marc Deschenes[1], Giada Sebastiani[1], Tatiana Cabrera[2], Louis-Martin Boucher[2], David Valenti[2], Ali Bessissow[2], David Patch[3], Emmanuel Tsochatzis[3], Amine Benmassaoud[1]. *[1]Montréal, Canada; [2]McGill University Health Centre, Division of Interventional Radiology, Montreal, Canada; [3]Institute of Liver and Digestive Health, University College London, London, United Kingdom*
Email: amine.zoughlami@mail.mcgill.ca

Background and aims: Overt hepatic encephalopathy (OHE) is a common complication after transjugular intrahepatic portosystemic shunt (TIPS) insertion. Sarcopenia is a risk factor for OHE in cirrhosis, but its impact on post-TIPS OHE, particularly early OHE, and subsequent mortality, remains unclear. We aimed to identify predictors of post-TIPS OHE, and examine the interplay between sarcopenia, OHE and mortality.

Method: This was a multicentric, retrospective study of a prospectively maintained database of patients with cirrhosis who underwent TIPS insertion, from the McGill University Health Centre (Montreal, Canada), and the Royal Free Hospital (London, United Kingdom). Sarcopenia was defined using standard L3-skeletal muscle index cutoffs. Occurrence of overt HE (OHE) was collected, and early OHE was defined as occurring within 3 months of TIPS insertion. Logistic regression was used to identify predictors of OHE. Survival was assessed using Kaplan-Meier curves and Cox regression analyses.

Results: A total of 165 patients were included (mean age 56.9 ± 10.4 years, 59.4% male), and 100 (60.6%) were sarcopenic. Median MELD-Na was 12.0 (IQR 8.0), and median HVPG decrease was 7.0mmHg (IQR 8.0mmHg), and did not differ based on sarcopenia status. New or worsening post-TIPS OHE occurred in 57 patients (34.5%). Patients with sarcopenia were more likely to develop early OHE (29.7% vs 15.6%, p = 0.043), but no statistically significant difference was noted for overall OHE (42.9% vs 28.1%, p = 0.061). Sarcopenia independently predicted overall OHE (aOR 3.73, 95% CI 1.4–10.1) and early OHE (aOR 4.5, 95% CI 1.3–15.9). Early OHE was associated with increased mortality risk (56.8% vs 31.4%, p = 0.005) and shorter median survival (22.4 vs 58.7 months, log-rank p = 0.016). In Cox regression analysis, controlling for MELD-Na, female sex, stent diameter and decrease in HVPG gradient, early OHE was associated with mortality (aHR 2.35, 95% CI 1.2–4.6), however the association lost statistical significance with addition of age (aHR 1.71, 95% CI 0.8–3.5), suggesting partial confounding by age.

Conclusion: Pre-TIPS sarcopenia is a strong independent predictor of early OHE after TIPS. Early OHE is associated with markedly worse survival, although the relationship with mortality risk appears to be partially attributable to age. Further studies on the impact of pre-TIPS sarcopenia on early OHE and mortality are indicated, including the impact of nutritional optimization or post-TIPS HE prophylaxis.

Public Health – Except Viral Hepatitis

TOP-001

Global pathways linking alcohol exposure, food systems, and alcohol-associated liver disease

James M. Paik[1], Annette Paik[1], Eliabe Abreu[1], Shira Zelber-Sagi[1,2], Manal F. Abdelmalek[1,3], Zobair M. Younossi[1]. [1]*The global NASH/MASH council, Washington DC, United States;* [2]*School of Public Health, Faculty of Social Welfare and Health Sciences, University of Haifa, Haifa, Israel;* [3]*MASLD Clinical Research Program at Mayo Clinic, Rochester, United States*
Email: zobair.younossi@cldq.org

Background and aims: Burden of alcohol-associated liver disease (ALD) varies widely across different countries, yet upstream structural factors remain insufficiently characterized. We examined how food systems, socioeconomic conditions, and healthcare capacity relate to ALD burden across socio-economic development levels for different countries.
Method: An ecological analysis of 187 countries was conducted using ALD estimates from the Global Burden of Disease Study (2023) and alcohol exposure indicators from World Health Organization (2020). ALD outcomes were defined as the combined prevalence and mortality from alcohol-related cirrhosis and liver cancer. Countries were categorized by Sociodemographic Index (SDI <0.64 vs ≥0.64). Structural equation models (SEM) evaluated associations among alcohol exposure, food environments indicators, and ALD outcomes. Results are presented as standardized coefficients (β).
Results: High-SDI countries (n = 115) had older populations (mean median age 36.3 vs 21.6 years) and stronger healthcare access and quality index (HAQ 70.5 vs. 28.2). They also demonstrated higher alcohol exposure, including higher per-capita intake (7.46 vs 3.41 L/year), higher intake among drinkers (27.0 vs 21.7 g/day), more heavy continuous drinking (8.9% vs. 6.6%), and heavy episodic drinking (23.8% vs 14.7%; all $p < 0.001$). Despite higher alcohol exposure, ALD mortality was lower in high-SDI countries (5.44 vs 6.69 per 100,000; $p = 0.002$), whereas ALD prevalence was similar between high and low SDI countries (6.29 vs 6.86 per 100,000; $p = 0.165$). In SEM analyses, higher SDI was associated with increased per-capita alcohol intake ($\beta = 0.36$ in high-SDI; $\beta = 0.29$ in low-SDI) and heavy continuous drinking ($\beta = 0.52$; $\beta = 0.20$), and higher animal-to-vegetable fat consumption ratio (food modernization indicator) ($\beta = 0.46$; $\beta = 0.31$). In high-SDI countries, heavy continuous drinking was associated with ALD prevalence ($\beta = 0.30$; $p = 0.002$), while high HAQ was associated with lower ALD mortality ($\beta = -0.20$; $p < 0.001$). In low-SDI countries, ALD prevalence was associated with dietary composition (animal-to-vegetable fat consumption ratio $\beta = 0.23$; $p = 0.03$), with no detectable association in these countries between HAQ and ALD mortality.
Conclusion: High-SDI countries exhibit stronger alcohol-related pathways moderated by greater health-system capacity, while low-SDI countries show associations involving dietary composition and limited healthcare capacity, contributing to worse ALD outcomes.

TOP-002

Clinical and humanistic burden of metabolic dysfunction-associated steatotic liver disease and metabolic dysfunction-associated steatohepatitis in the United States: a system dynamics model

Amreen Dinani[1], Elisabeth de Laguiche[2], Fotis Tefos[2], David W. Victor III[3], Fryderyk Wilczynski[4], Thomas Padgett[4]. [1]*Duke University School of Medicine, Durham, United States;* [2]*Novo Nordisk A/S, Søborg, Denmark;* [3]*Houston Methodist Hospital, Houston, United States;* [4]*Health Economics and Outcomes Research, Cardiff, United Kingdom*
Email: amreen.dinani@duke.edu

Background and aims: Metabolic dysfunction–associated steatotic liver disease (MASLD) can progress to metabolic dysfunction–associated steatohepatitis (MASH), characterized by inflammation, progressive liver damage and scarring. This study aimed to predict the system impact of MASLD/MASH prevalence on the clinical and humanistic burden based on current standard of care practices in the US.
Method: A US system dynamics model was developed to predict the prevalence and burden of MASLD/MASH and its complications, stratified by age and disease stage, from 2025 to 2060. The model was calibrated to National Health and Nutrition Examination Survey (NHANES)-derived data (2006–2020) and annual liver transplant incidence data from the Scientific Registry of Transplant Recipients (2012–2020) and validated by two clinical experts. Model outcomes included mortality, cardiovascular (CV) complications, liver transplants, hepatocellular carcinomas (HCCs), health-related quality of life (HRQoL), and lost productivity.
Results: Under current standard of care practices in the US, MASLD/MASH prevalence is projected to increase by 28%, from 104 million in 2025 to 133 million in 2060. Results suggest that people with MASH F2-F4 will drive the burden, with the greatest percentage increase occurring for F3 (126%) and F4 (116%). The annual incidence of liver transplants attributable to MASH cirrhosis is projected to increase by 131%, from 1,439 in 2025 to 3,317 liver transplants in 2060. Annual excess mortality is projected to increase from 0.95 million deaths associated with MASLD/MASH and its complications in 2025, to 1.3 million in 2060, an increase of 36%. This reflects worsening disease severity, with excess mortality for F4 increasing by 98%. Annual CV complications will rise by 28% by 2060, whereas HCC incidence will increase by 166%. The HRQoL burden from MASLD/MASH is projected to rise from 4.7 million years of perfect health lost in 2025 to 6.1 million in 2060. Absenteeism due to morbidity is projected to increase by 18%, reaching 615 million workdays in 2060, worth $158 billion. In 2060, MASH F4 is projected to represent approximately 0.7% of the population but account for 6.0% of excess deaths and 34.1% of HCCs.
Conclusion: Under current standard of care practices, the clinical and humanistic burden of MASLD/MASH is projected to rise substantially in the US, emphasizing the urgent need for earlier detection and intervention strategies.

TOP-016

Socio-demographic inequalities on the UK liver transplant waiting list over time: the impact of prognostic scores and candidate selection schemes

Ji Jade King[1,2], Rhiannon Taylor[2], David Wallace[3], Julia Verne[4], Emmanouil Tsochatzis[1,3], Douglas Thorburn[1,3]. [1]*University College London, Institute of Liver and Digestive Health, London, United Kingdom;* [2]*Nhs Blood & Transplant, Bristol, United Kingdom;* [3]*Royal Free Hospital, London, United Kingdom;* [4]*King's College Hospital, London, United Kingdom*
Email: jijadeking@gmail.com

Background and aims: Increasing international evidence suggest that liver transplant (LT) candidates may not have equal chances of transplantation based on socio-demographic characteristics, with female, non-White and socially deprived individuals experiencing disadvantage. We aimed to assess if such disparities exist in the UK, and if changes to prognostication scores (Child-Pugh to UKELD in

2008) and candidate selection schemes (centre-based clinician-driven to partially algorithmic in 2018) promoted equity. Recording of offer outcomes since 2018 allowed investigation of where disparities, if any, arise. Outcomes of both super-urgent (SU) and elective (EL) listing were assessed.
Method: Adults registered on the UK Transplant Registry for liver-only transplantation between 2004–2024 were included and grouped into Era1 (2004–2008), Era2 (2008–2018) and Era3 (2018–2024). Fine–Gray models assessed socio-demographic disparities in cumulative incidence of LT (LT CIF) at 7 days (SU) and 1 year (EL), accounting for death and removal as competing risks and adjusting for relevant clinical and demographic factors.
Results: 17,821 candidates were included. Socio-demographic characteristics did not significantly influence access to SU LT across eras. Disparities emerged in EL outcomes. While no differences were observed in Era1, female candidates had significantly lower EL LT CIF from Era2 onwards (sHR 0.91 [0.85–0.97]). Offer analyses in Era3 showed no sex difference in graft offers, but higher offer declines and lower EL LT CIF in women especially across centre-based pathways. Socioeconomic disadvantage emerged in Era2, with higher EL LT rates among the most affluent candidates (sHR 1.14 [1.04–1.25]), and higher waitlist mortality among the most deprived in Era3 (sHR 0.57 [0.41–0.80]). Ethnic disparities were modest due to small numbers: in Era2, Black candidates had marginally lower EL LT rates with similar mortality, while Asians showed higher waitlist mortality. Such differences were attenuated in Era3.
Conclusion: Access to SU LT in the UK has remained largely equitable. However, as EL candidate selection transitioned from clinician discretion to algorithm-driven systems, socio-demographic inequalities shifted. Sex inequity emerged after UKELD adoption and persists, arising at candidates' selection rather than algorithmic offering. Deprivation- and ethnicity-related disparities have narrowed but remain relevant, highlighting the need to revisit decision-making pathways to promote equitable transplant access.

TOP-017-YI
Feasibility and outcomes of liver health checks in community alcohol services
Daniel Gutmann[1], Michael Griffiths[1], Susan Kemp[1], Erika Toth-Cserepes[1], Claire St John[1], Douglas Macdonald[1,2], Filomena Ferrentino[1], Rory Munday[3], Paul Trembling[3], Lourdes Cumlat[4], Deepak Suri[4], Evangelia Fatourou[4], Sana Rehman[5], Yuktha Gubbala[5], Mohamed Shariff[5], Thendral Mangala[6], Emmanuel Tsochatzis[1,7]. *[1]Sheila Sherlock Liver Unit, Royal Free Hospital, London, United Kingdom; [2]UCL Insitute for Liver and Digestive Health, Royal Free Hospital and UCL, London, United Kingdom; [3]Lister Hospital, Stevenage, United Kingdom; [4]The Whittington Hospital, London, United Kingdom; [5]Watford General Hospital, Watford, United Kingdom; [6]North Middlesex University Hospital, London, United Kingdom; [7]UCL Institute for Liver and Digestive Health, Royal Free Hospital and UCL, London, United Kingdom*
Email: daniel.gutmann@nhs.net

Background and aims: Alcohol-related liver disease (ALD) is a major cause of premature mortality. Many patients first present with cirrhosis or decompensation. In North Central London, Liver Health Check Clinics (LHCCs) were established within community alcohol services, utilising transient elastography (TE) to screen for significant fibrosis and cirrhosis. This enabled hepatology referral in those not otherwise engaged in healthcare. To date, case-finding programmes are not embedded in clinical practice despite guideline recommendations. We report the diagnostic yield of LHCCs and long-term clinical outcomes of all patients with elevated liver stiffness measurement (LSM).
Method: Between 15.08.2022 and 31.12.2024, 2,909 patients attending LHCCs were screened using TE. LSM was categorised as <8 kPa (likely no advanced fibrosis), 8–11.4 kPa (likely significant fibrosis), and ≥11.5 kPa (likely advanced fibrosis/ cirrhosis). Those with ≥11.5 kPa were referred to hepatology services at seven hospital sites with a non-invasive liver screen, liver ultrasound and prioritisation as per Baveno VI criteria for clinically significant portal hypertension (CSPH) (TE ≥25 kPa). Cirrhosis was defined using a standardised algorithm combining LSM, imaging, endoscopy and non-invasive biomarkers. Follow-up data included abstinence status, LSM change, decompensation events, admission, hepatocellular carcinoma (HCC) and mortality.
Results: Among 2,909 screened, 11.9% had LSM 8–11.4 kPa and 9.3% had LSM ≥11.5 kPa. Of the latter, 58.7% had cirrhosis, 63% met CSPH criteria. During follow up, 31 deaths occurred (concentrated in the cirrhosis group). 2/3 of CSPH patients had at least one admission while all decompensation events occurred in the cirrhosis group. Abstinence data suggested a non-significant trend towards greater LSM reduction with sustained abstinence. A substantial non-attendance rate of 39% for secondary care follow up underscored engagement challenges. Multivariate analysis linked higher age and greater Audit-C scores to higher odds of LSM ≥11.5 kPa; abstinence showed a non-significant trend towards larger LSM falls and higher odds of ≥20% LSM improvement, while higher baseline LSM and platelet count predicted greater LSM reductions among those with baseline ≥11.5 kPa.
Conclusion: Community TE screening identifies a substantial burden of undiagnosed advanced ALD. High short-term risks of admission and death support TE based case finding and integrated pathways linking alcohol services with hepatology care.

TOP-018-YI
Increased diagnosis and risk stratification for MASLD in primary care over the last 20 years: real-world evidence from over 11.7 million individuals in the UK
Huei-Tyng (Philippe) Huang[1], Michael Hewitt[1], Wenhao Li[1], Laura Temperley[1], Naveed Sattar[2], William Alazawi[1]. *[1]Barts Liver Centre and Barts Metabolism Network, Blizard Institute, Queen Mary University of London, London, United Kingdom; [2]School of Cardiovascular and Metabolic Health, BHF Glasgow Cardiovascular Research Centre, University of Glasgow, Glasgow, United Kingdom*
Email: h.t.huang@qmul.ac.uk

Background and aims: MASLD is a leading cause of chronic liver disease with rapidly growing prevalence. However, there is significant underdiagnosis in healthcare records, contributing to missed intervention opportunities and late presentation. Tools to stratify MASLD (e.g., Fib-4) exist but are underused. The last decade has seen awareness and educational efforts to promote detection and risk stratification in MASLD. Here we study the changes in prevalence, incidence of recorded MASLD, associated diseases, and availability of Fib-4 score in the UK primary care population.
Method: This real-world evidence study identified individuals with recorded MASLD diagnosis between 2003 and 2022 in the UK primary care Clinical Practice Research Datalink (CPRD). NAFLD codes were used as proxy for MASLD given near-complete overlap. Individuals with <1 year follow-up, age <18 years, or pre-existing autoimmune liver disease and viral hepatitis were excluded. We calculated point prevalence, incidence, comorbidities and availability of Fib-4 components. Controls were matched 1:4 on sex, age (±5 years), and general practice.
Results: Out of 11.7 million individuals active in CPRD in 2022, we identified 365,797 MASLD patients and 1,460,288 controls. In the last decade, recorded MASLD prevalence rose approximately 5-fold, from 0.52% in 2013 to 2.42% in 2023 ($p < 0.001$). Annual incidence doubled from 1.60 in 2012 to 3.31 in 2022 per 1000 person-years ($p < 0.001$). Compared to controls, MASLD patients (median age of 53, 51.8% male) had a higher prevalence of type 2 diabetes (21.0% vs 7.7%; $p < 0.001$) and hypertension (35.3% vs 18.7%; $p < 0.001$). The availability of components to calculate Fib-4 in MASLD group increased from 4.3% pre-2015 to 22.8% 2015 to 2022 ($p < 0.001$). The proportion of MASLD patients with high-risk Fib-4 scores modestly decreased from 7.6% to

6.4% (pre- vs post-2015). South Asians were over-represented in the MASLD group (11.0% vs 7.2%; p < 0.001) and had the lowest adjusted odds ratio of having Fib-4 components (0.67, 95% CI: 0.65–0.70; p < 0.001) available for calculation.
Conclusion: Recorded MASLD prevalence in UK primary care has increased 5-fold in the last decade, although there remains a large diagnostic gap. Fibrosis risk stratification has improved, commensurate with education efforts but overall implementation remains low. There is a potential care gap among South Asians, who are at high risk but less likely to have data collected for risk stratification.

TOP-032

Real-world data highlight gaps in hospital care and access to gastroenterologists or hepatologists in patients with acutely decompensated cirrhosis

Jonel Trebicka[1,2], Berenice Alard[3], Thierry Artzner[2,4], William Bernal[2,5], Joan Clària[2,6], Lise Lotte Gluud[2,7], Jennifer Lai[8], Jacqueline O'Leary[9], Pierre-Emmanuel Rautou[2,10,11], Debbie L. Shawcross[12,13], Bart Staels[14], Florence Wong[15], Cristina Sanchez-Garrido[2], Eva Uson[2], Maxime Anné[3], Athéna Crespin[3], Stephanie Ferreira[3], Yacine Hajji[3], Dean Hum[3], Jennifer Jara Vargas[3], Jeremy Magnanensi[3], Pejvack Motlagh[3], Pierbruno Ricci[3], Sakina Sayah Jeanne[3], Katharina Staufer[3], Richard Moreau[2,11,16], Arun J. Sanyal[17,18], Jasmohan Bajaj[19], Javier Fernández[2,20], Paolo Angeli[2,21]. *[1]Department of Internal Medicine B, University Hospital Münster, Münster, Germany; [2]European Foundation for the Study of Chronic Liver Failure, Barcelona, Spain; [3]GENFIT S.A., Loos, France; [4]Liver transplant unit, Hôpitaux Universitaires de Strasbourg, Strasbourg, France; [5]Liver Intensive Therapy Unit, Kings College Hospital, London, United Kingdom; [6]Hospital Clínic-IDIBAPS, CIBERehd, University of Barcelona, Barcelona, Spain; [7]Gastrounit Medical Division, Hvidovre Hospital, Hvidovre, Denmark; [8]Department of Medicine, University of California, California, San Francisco, United States; [9]University of Texas, Southwestern, Dallas, United States; [10]AP-HP, Hôpital Beaujon, Service d'Hépatologie, DMU DIGEST, Centre de Référence des Maladies Vasculaires du Foie, FILFOIE, ERN RARE-LIVER, Clichy, France; [11]Université Paris-Cité, Inserm, Centre de recherche sur l'inflammation, UMR 1149, Paris, France; [12]Institute of Liver Studies, Kings College London, London, United Kingdom; [13]Roger Williams Institute of Liver Studies, Faculty of Life Sciences and Medicine, King's College London, London, United Kingdom; [14]Université de Lille, Inserm, CHU Lille, Institut Pasteur de Lille, U1011-EGID, Lille, France; [15]Department of Medicine, University of Toronto, Toronto General Hospital, Toronto, Canada; [16]Hôpital Beaujon, Service d'Hépatologie, Clichy, France; [17]Department of Medicine, Virginia Commonwealth University of Medicine, Virginia, Richmond, United States; [18]Stravitz-Sanyal Institute for Liver Disease and Metabolic Health, Virginia Commonwealth University School Of Medicine, Richmond, United States; [19]Division of Gastroenterology, Hepatology, and Nutrition, Department of Internal Medicine, Virginia Commonwealth University School of Medicine, VA, Richmond, United States; [20]Liver ICU, Liver Unit, Hospital Clinic, IDIBAPS and CIBEREHD, Barcelona, Spain; [21]University of Padova, Padova, Italy*
Email: berenice.alard@genfit.com

Background and aims: Acute decompensation (AD) of liver cirrhosis encompasses various decompensating events. AD events are defined as the sudden onset or worsening of ascites, variceal bleeding (VB), or hepatic encephalopathy (HE), occurring alone or in combination. Using 10 years of real-world data from U.S. hospitals, we aimed to characterize patients (pts) admitted for AD and evaluate patterns of inpatient care according to AD event type and prior medical history.
Method: All hospitalizations (hosp) of pts with cirrhosis, recorded between April 2016 and February 2025 in the Komodo's Healthcare Map US real-world database, in which an AD event was documented on the day of admission, were included. For each hosp, the most specialized provider recorded during the entire hospital stay was extracted. The rate of consultations with a hepatologist and/or gastroenterologist (HG) and the proportion of pts requiring intensive care unit (ICU) admission were determined. Hosp were grouped based on either etiology of pts or type of AD recorded on the first day of hosp to assess potential differences in hospital care and impact on clinical outcomes.
Results: A total of 2,454,386 hosp in 1,024,096 pts (59% male; mean age at admission 60 y) were analyzed. Median hosp duration was 5 d; 4% required ICU admission (median ICU stay: 4 d). Of all pts, 42% had only one admission, 17% had ≥5, and 0.7% had ≥20 hosp. Rehospitalization rates increased progressively: 51% after the first hosp, 56.5% after the second, 61.3% after the third, and 65% after the fourth. The most common type of AD was ascites (74%), followed by HE (35%) and VB (17.5%). Internal medicine was the primary specialty in 33% of hosp, HG in only 20% of cases overall. Among admissions for a unique type of AD event, VB admissions had the highest HG involvement (26.5%) and ICU use (5%), with a 28-days mortality of 6% in ICU vs 3% in hosp without ICU admission, followed by ascites (17%; ICU 3% and a 28-days mortality of 13% in ICU vs 7%) and HE (15%; ICU 3.4% and a 28-days mortality of 13% in ICU vs 6%). Among pts with the same types of AD events at admission and no additional AD event during hosp, those seen by a HG on the first day had a lower 28-day mortality (−2.3% in absolute average) compared to those who were seen later by a HG during hosp.
Conclusion: Most pts hospitalized for AD were not seen by a HG on the first day of hosp, or were never seen during their stay, highlighting a critical opportunity to improve hospital care and clinical outcomes for these pts.

THU–003

Evolving impact of alcohol and abdominal adiposity on liver mortality in Finland over four decades: implications for public health interventions

Fredrik Åberg[1,2], Jaakko Reinikainen[2], Aki Havulinna[3], Annamari Lundqvist[2]. *[1]Helsinki University Hospital and University of Helsinki, Helsingfors, Finland; [2]Finnish Institute for Health and Welfare, Helsinki, Finland; [3]Department of Computing, University of Turku, Turku, Finland*
Email: fredrik.aberg@helsinki.fi

Background and aims: Liver-related mortality has been rising in Finland until recently, but the extent to which these trends are explained by changes in major risk factors – alcohol use, adiposity, diabetes, and smoking – remains unclear. By comparing individual-level data from nationally representative health surveys conducted at regular intervals over 36 years with population-level mortality trends, we analyzed the independent and combined contributions of these risk factors to liver-related mortality.
Method: Finnish health surveys conducted roughly every 5 years between 1987 and 2023 included 38,659 men and women aged 35–64 years. Predicted liver mortality was estimated using a cause-specific competing-risk regression model fitted to multiply imputed survey data with registry-linked follow-up, including sex-specific interaction terms. Population-weighted predictions were then applied to each survey year to estimate mortality based on risk factor changes relative to 1987. Observed mortality was obtained from the National Causes of Death Register, and observed and predicted age-standardized trends were compared as percentage changes from the 1987 baseline.
Results: Observed age-standardized liver-related mortality in Finland increased by 46% in men and 66% in women from 1987 to 2023, peaking in 2007 (111%, both sexes). Of the age-standardized liver mortality, 85%/75% (men/women) was recorded as alcohol-related liver disease, 3%/8% as other liver diseases, and 12%/17% as liver cancer (alcohol-related or not). Predicted liver mortality based on average alcohol use, waist-to-hip ratio, diabetes, and smoking closely mirrored observed national trends in both sexes. Alcohol use remained the strongest single contributor to liver mortality throughout the study period, while increases in waist-to-hip ratio

increasingly explained recent temporal variation. In men, observed mortality during the most recent years declined more slowly than predicted, suggesting that increasing abdominal adiposity may have offset part of the mortality reduction expected from declining alcohol consumption. Changes in smoking and diabetes contributed minimally to temporal trends.
Conclusion: Changes in the main risk factors – particularly alcohol use, and more recently, abdominal adiposity – largely explain temporal variation in liver-related mortality at the population level. This highlights the need for coordinated public health strategies addressing both alcohol use and obesity.

THU-004
Rising liver fibrosis rates due to MASLD identified amongst young adults in a general population birth cohort
Kushala Abeysekera[1], Ann Archer[1], Jon Heron[1], Matthew Hickman[1]. [1]*University of Bristol, Bristol Medical School, Bristol, United Kingdom*
Email: k.abeysekera@bristol.ac.uk

Background and aims: Steatotic liver disease is the leading cause of liver-related morbidity across Europe. Understanding its asymptomatic disease course and subclinical burden in the general population is vital to intervene with targeted therapies before major adverse liver outcomes (MALOs) occur. A cross-sectional analysis performed on the Avon Longitudinal Study of Parents and Children (ALSPAC) general population birth cohort when participants were 24 years identified 1 in 40 had fibrosis based on transient elastography (TE). The aim of this study was to re-evaluate the prevalence of SLD in the same cohort, now 30 years, using TE and controlled attenuated parameter (CAP).
Method: 3599 participants had TE assessment during a Focus@30 clinic. Liver stiffness measurements (LSM) with interquartile range/median ratio (IQR/M) greater than 30% were excluded when analysing fibrosis. Data was collated on anthropometric measurements including body mass index (BMI), waist circumference-to-height ratio (WCHt) as well as alcohol use, smoking and socioeconomic status. Statistical analysis was performed using Stata MP 18.0.
Results: Mean participant age was 29.8 years (SD 0.6). 4.2% of participants met criteria for alcohol use disorder; 20.5% had obesity (mean BMI 26.5; SD 5.9). 320 LSMs were excluded with an IQR/M > 30%. 3279 participants had a valid LSM. 130 (3.9%) had a LSM ≥8 kPa, of which 30 (0.9%) had a LSM ≥12 kPa. This had increased from 88 (2.4%) of participants with a LSM ≥8 kPa and 8 with a LSM ≥12 kPa aged 24 years. Based on a CAP≥275 dB/m, 19.5% (n = 674/3453) of participants had steatosis compared to 11.1% (n = 420/3767) 6 years prior. 19.3% of participants met criteria for MASLD, 7.9% for MetALD and 1.1% for ALD. 2356 participants had had TE at both 24 and 30 years. 82 participants who had no fibrosis at 24 years had a LSM ≥8 kPa at 30 years. Increased adiposity based on WCHt ratio, was the most strongly associated variable with elevated LSM at 30 years, despite adjustment for sex, socioeconomic status, alcohol use and smoking (aOR 2.54 [95%CI 1.94–3.32]; p < 0.0001). A smaller effect estimate was observed with BMI (aOR 1.15 [95%CI 1.10–1.19]; p < 0.0001).
Conclusion: In this UK general population birth cohort, the number of asymptomatic participants with suspect SLD fibrosis has increased almost 50% between 24 to 30 years. The aetiology attributed to this rise was MASLD rather than MetALD or ALD. WCHt ratio may provide more value than BMI in identifying those at greater fibrosis risk amongst young adults.

THU-005
Cirrhosis burden dynamics in the Asia-Pacific region from 1990 to 2023 and forecasting to 2050: findings from the global burden of disease study 2023
Aimitaji Abulaiti[1]. [1]*First Affiliated Hospital of Xinjiang Medical University, Urumqi, China*
Email: aimitaji1215@sina.com

Background and aims: Cirrhosis represents a critical public health concern throughout the Asia-Pacific. To guide future regional health strategies, this study evaluated the trends and underlying drivers of the disease burden spanning the period from 1990 to 2023.
Method: Leveraging data from the Global Burden of Disease Study 2023, we examined metrics including incidence, prevalence, mortality, and disability-adjusted life years (DALYs), stratified by age, gender, and Socio-demographic Index (SDI). The study utilized estimated annual percentage changes (EAPCs) to assess trends, the slope index of inequality (SII) to measure disparities, and decomposition analysis to identify key drivers. Additionally, frontier analysis was applied to evaluate efficiency, alongside burden projections extending to 2050.
Results: Between 1990 and 2023, the number of prevalent cases increased by 57%, reaching 624.7 million (95% UI 584.4–671.8), while total fatalities grew by 7% to 354,279 (309,789–401,481). Men experienced a significantly higher mortality burden (246,656 deaths) compared to women (107,623 deaths). In contrast, age-standardized rates exhibited a marked decline, with incidence decreasing by an EAPC of −0.56%, mortality by −2.53%, and DALYs by −2.33%. The majority of deaths were concentrated in India (188,370) and China (121,033), whereas the Solomon Islands reported the highest standardized mortality rate (37.4 per 100,000). Notably, incidence rates among individuals aged 95 and older surged by 657%. Decomposition analysis revealed that demographic shifts—specifically population growth and aging—were the primary factors counteracting epidemiological improvements. Absolute inequality narrowed, as indicated by a shift in the DALYs SII from −426.9 to −308.1, and efficiency gaps regarding mortality decreased universally. Projections for 2050 suggest that despite falling standardized rates, the absolute number of deaths will rise to 391,317.
Conclusion: While epidemiological indicators have shown improvement, the absolute burden of cirrhosis is escalating due to rapid population aging and growth, with India and China being particularly affected. To address the anticipated rise in disease burden, future policies must prioritize the allocation of integrated care resources tailored to an aging demographic.

THU-006
Digital technology policy is associated with liver disease mortality: a multinational ecological study
Somaya Albhaisi[1], Jennifer Dodge[1], Brian Lee[1]. [1]*University of Southern California, Los Angeles, United States*
Email: somaya.albhaisi@med.usc.edu

Background and aims: The GovTech Maturity Index (GTMI) is a World Bank-validated metric of government digital technology use and population-level access to digital public services. Its relationship with liver disease mortality is a knowledge gap that can inform governmental policies.
Method: We conducted a multinational ecological study using 2020 data to assess the association of liver disease mortality with GTMI. Covariates were captured from the World Bank, including Gross Domestic Product per capita, Human Development Index, and Healthcare Access and Quality Index. GTMI was categorized as Low (0–0.24), Medium (0.25–0.49), High (0.50–0.74), or Very High (0.75–1.00). The primary outcome was liver-related mortality from the Global Burden of Disease study, expressed as age-standardized mortality rates (ASMRs) for 14 liver disease etiologies. Multivariable linear regression assessed associations between ASMRs and GTMI, adjusted for the aforementioned country-level covariates.
Results: Among 198 countries, 33 were classified as Low, 63 as Medium, 59 as High, and 43 as Very High GTMI categories. The population-weighted mean overall liver ASMR was 23.14 per 100,000. In multivariable analysis, each ordinal increase in GTMI category was associated with a decrease in overall liver ASMR of 4.83/100,000 (95% confidence interval [CI]: −7.55 to −2.11, p-trend = 0.001), with ASMR 43.02 vs. 16.21/100,000 for Low vs. Very High

GTMI. This association was primarily attributable to the Public Service Delivery subcomponent of GTMI ($p < 0.05$). Higher GTMI was associated with lower mortality from hepatitis B-related liver diseases, but not consistently with other etiologies. For hepatitis B, each ordinal GTMI increase was associated with fewer deaths from cirrhosis (−1.48/100,000; 95% CI: −2.43 to −0.52; $p = 0.003$) and hepatitis B–related liver cancer (−0.85/100,000; 95% CI: −1.28 to −0.41; $p < 0.001$). For other etiologies, results were heterogeneous. A higher GTMI score was associated with fewer deaths from metabolic dysfunction-associated steatohepatitis-related liver cancer (Coefficient: −0.59/100,000; $p = 0.013$) but with more deaths from acute hepatitis A (Coefficient: 0.77/100,000; $p = 0.001$).
Conclusion: Advanced digital government maturity is associated with lower liver-related mortality, particularly from hepatitis B, possibly due to improved digital public service delivery. Investments in digital technology on a governmental level may represent a policy lever to improve population-level liver health outcomes.

THU-007
Impact of United States food and drug administration drug approvals on public and scientific dialogue on metabolic dysfunction-associated steatotic liver disease: a multi-platform digital analysis
Somaya Albhaisi[1], Norah Terrault[1]. [1]*University of Southern California, Los Angeles, United States*
Email: somaya.albhaisi@med.usc.edu

Background and aims: The US Food and Drug Administration (FDA) approvals of Resmetirom in March 2024 and Semaglutide in August 2025 for metabolic dysfunction-associated steatotic liver disease (MASLD) are landmark events. However, their impact on public disease dialogue, patient community discourse, and scientific research publications has not been measured. This study aimed to quantify the impact of these approvals across multiple digital platforms.
Method: We conducted a longitudinal digital analysis from January 2023 to October 2025 across three data sources: Google Trends search volume indices; Reddit discussions; and PubMed publications. Analytical methods included interrupted time series analysis, valence aware dictionary and sentiment reasoner (VADER) sentiment analysis, non-negative matrix factorization topic modelling, network analysis, and rigorous statistical validation.
Results: Semaglutide approval drove the most substantial increase in public search interest, with an immediate + 17.1 point level change for MASLD searches ($p < 0.001$) and a very strong correlation between MASLD and Semaglutide search volumes ($r = 0.93$). Resmetirom approval did not cause an immediate level change in MASLD searches but initiated a significant positive post-approval weekly trend (slope + 0.032 points per week, $p < 0.001$). On Reddit, Semaglutide approval triggered an increase (+ 82.3%) in discussion volume, largely focused on personal experiences and weight loss, while Resmetirom approval was associated with a decrease (−30.8%). Community sentiment, measured using VADER compound scores ranging from -1 (most negative) to +1 (most positive), remained stable after both approvals ($p > 0.05$). Network analysis showed Reddit communities responded collectively to FDA approvals but were weakly correlated with public searches ($r = 0.344$ for MASLD). In scientific literature, Resmetirom approval created a new research domain (0 publications before vs. 132 after), whereas Semaglutide approval significantly accelerated an existing research trajectory (157 pre- vs. 54 post-approval publications; odds ratio = 3.557, $p < 0.001$).
Conclusion: FDA approvals differentially modulated the MASLD digital ecosystem. Semaglutide drove larger increases in public search interest and patient community engagement, while Resmetirom catalyzed de novo scientific field formation. Public dialogue around MASLD appears closely tied to weight-loss pharmacotherapy popularity, underscoring the need for integrated public health messaging.

THU-008
Socioeconomic barriers to initiation of second-line therapy in primary biliary cholangitis patients with incomplete response to ursodeoxycholic acid
Lital Aliasi-Sinai[1], Christopher Kim[1], Liliana Vittini Hernandez[1], Francina Collado[1], Xiaotao Zhang[1], Douglas T Dieterich[1], Anna Mageras[1], Frances Lee[1]. [1]*Icahn School of Medicine, New York, United States*
Email: lital.aliasi-sinai@mountsinai.org

Background and aims: Second-line treatment for primary biliary cholangitis (PBC), including seladelpar, elafibranor, off-label fenofibrate, and obeticholic acid (OCA, withdrawn from market) should be offered when there is intolerance or incomplete response to ursodeoxycholic acid (UDCA). We sought to characterize the use of second-line (2L) therapies and identify demographic factors associated with second-line therapy initiation.
Method: This single center retrospective observational study from 2000 to 2025 identified adults with PBC ICD-10 code, ALP >200, and active UDCA prescription verified by chart review. Patients on UDCA for at least 12 months with ALP >200 were considered eligible for 2L therapy. Primary outcome was prescription of 2L therapy; secondary outcomes included reasons for lack of 2L therapy initiation. Covariates included age, sex, race, preferred language, marital status, and insurance type. Univariable and multivariable analyses were performed using R.
Results: Among 356 patients with PBC with ALP >200, 331 (93.0%) were receiving UDCA and 296 (89.4%) met criteria for treatment escalation. In this cohort, the mean age was 64.3 years, 88.5% were female, 50.3% were White, 11.5% Hispanic/Latino and 8.1% Black. 11.1% were uninsured. 81 (27.4%) received 2L therapy, and 215 (72.6%) did not, of whom 99 (46.0%) had no documented discussion of escalation. OCA was the most frequently prescribed 2L therapy (12.1%), followed by seladelpar (10.0%), fenofibrate (5.4%), and elafibranor (2.7%). While 35.3% of Hispanic patients and 31.5% of White patients received 2L therapy, 0% of Black patients received 2L therapy, though there was no significance in documented offering of 2L therapy (OR 2.08, 95% CI 0.85–6.27, $p = 0.11$). In univariable analysis, older age, and uninsured status were associated with lower likelihood of escalation to 2L therapy (OR 0.97, 95% CI 0.95–0.99, $p = 0.008$; OR 0.05, 95% CI 0.003–0.24, $p = 0.004$). In multivariable analysis, only uninsured status was associated with lack of initiation of 2L therapy (OR 0.08, 95% CI 0.004–0.40, $p = 0.02$).
Conclusion: Despite meeting treatment criteria, 72.6% of eligible patients have not received 2L PBC therapy, and over half of these patients lack documented discussion or offering of 2L therapy. Race and insurance status influence treatment escalation. Future studies should investigate system and patient-level barriers to treatment escalation and assess if addressing these gaps improves downstream clinical outcomes.

THU-009
Cirrhosis in France: is there disparities to address to improve prognosis?
Aurore Baron[1], Laure Tron[2], Frederic Balusson[3], Vaele Zannou[4], Mignot Victoria[5], Anna Borowik[6], Thomas Decaens[7], Emmanuel Oger[8], Sébastien Bailly[9], Charlotte Costentin[10]. [1]*Hepato biliar Center, Hepatology Unit, Paul Brousse Hospital, APHP, Villejuif, Univ. Grenoble Alpes, France; Institute for Advanced Biosciences, Research Center UGA Inserm U 1209 - CNRS 5309, Team Cell Dynamics, Metabolism & Cancer (DIMAC), Grenoble, Villejuif, France;* [2]*Univ. Grenoble Alpes, France; Institute for Advanced Biosciences, Research Center UGA Inserm U 1209 - CNRS 5309, Team Cell Dynamics, Metabolism & Cancer (DIMAC), Grenoble, Univ. Grenoble Alpes, Hepato-gastroenterology and digestive oncology department, CHU Grenoble Alpes, Grenoble, Grenoble, France;* [3]*Pharmacovigilance et Pharmaco-epidemiology, CHU Rennes, Rennes, France; Univ Rennes, CHU Rennes, Inserm, EHESP, Irset - UMR_S 1085., Rennes, France;* [4]*Univ. Grenoble*

Alpes, France; Institute for Advanced Biosciences, Research Center UGA Inserm U 1209 - CNRS 5309, Team Cell Dynamics, Metabolism & Cancer (DIMAC), Grenoble, France; [5]Univ. Grenoble Alpes, France; Institute for Advanced Biosciences, Research Center UGA Inserm U 1209 - CNRS 5309, Team Cell Dynamics, Metabolism & Cancer (DIMAC), Univ. Grenoble Alpes, Hepato-gastroenterology and digestive oncology department, CHU Grenoble Alpes, Grenoble, France; [6]Univ. Grenoble Alpes, Hepato-gastroenterology and digestive oncology department, CHU Grenoble Alpes, Grenoble, France; [7]Univ. Grenoble Alpes, Hepato-gastroenterology and digestive oncology department, CHU Grenoble Alpes., 1. Univ. Grenoble Alpes, France; Institute for Advanced Biosciences, Research Center UGA Inserm U 1209 - CNRS 5309, Team Cell Dynamics, Metabolism & Cancer (DIMAC), Grenoble, France; [8]Pharmacovigilance et Pharmaco-epidemiology, CHU Rennes, Rennes, France; Univ Rennes, CHU Rennes, Inserm, EHESP, Irset - UMR_S 1085, Rennes, France; [9]Univ. Grenoble Alpes, HP2 Laboratory, Inserm U1300, 38000 Grenoble, France, Grenoble, France; [10]Univ. Grenoble Alpes, France; Institute for Advanced Biosciences, Research Center UGA Inserm U 1209 - CNRS 5309, Team Cell Dynamics, Metabolism & Cancer (DIMAC), Univ. Grenoble Alpes, Hepato-gastroenterology and digestive oncology department, CHU Grenoble Alpes, Grenoble, France
Email: romen.baron@gmail.com

Background and aims: Although the main risk factors for cirrhosis (Cir) are well known, diagnosis remains frequently delayed and associated with poor prognosis. In France, comprehensive population-based data on Cir epidemiology, care pathways, and outcomes are scarce. We aimed to describe the epidemiology of incident Cir and identify medical and social disparities associated with prognosis.
Method: Using the 2% representative sample of the French National Health Data System (SNDS), we identified incident cases of Cir between 2015 and 2021 based on diagnostic codes, procedures, or Cir-specific treatments. Demographic characteristics, risk factors, comorbidities, complications, care pathways, and outcomes were collected. Social deprivation was assessed using the FDep index of the municipality of residence. Overall survival (OS) was analyzed using Kaplan-Meier and multivariable Cox models.
Results: 9,967 incident Cir cases were identified: 65% were men and 63% were aged ≥60 years. Alcohol misuse was detected over follow-up in 49%, diabetes in 25% and obesity in 22%. Known risk factor and cause of Cir were identified prior to diagnosis in 47% and 19.0% of cases, respectively. Cir was alcohol-related in 46%, only metabolic in 21%, viral in 2%, and of unknown causes (UC) in 25%. Over time, viral and alcohol-related Cir declined, while metabolic Cir increased significantly. During follow-up, 80% experienced at least one Cir-related complication: hepatic failure (40%) and ascite (29%) were most frequent. Primary liver cancer (PLC) occurred in 14%. Two-year OS was 56%. Poorer OS was independently associated with Cir-related complications, concomitant PLC, higher Charlson score at liver disease diagnosis, UC of Cir, and residence in more deprived towns (FDep Q4–Q5). In contrast, benefiting from long-term disease coverage (LTDC) for Cir and social solidarity health coverage were associated with improved survival. Cir was mostly diagnosed in hospitalization (87%) and through death in 6%, especially in women. Exclusive outpatient management (3%) was associated with better prognosis.
Conclusion: If cirrhosis epidemiology in France is shifting toward metabolic causes, diagnosis remains late, hospital-based, and associated with high short-term mortality. Socioeconomic, gender and etiological disparities substantially affect prognosis, but access to LTDC and social solidarity–based health coverage may improve outcome. Strategies promoting earlier ambulatory diagnosis and targeted, equity-based strategies are urgently needed.

THU-010

Unmet needs in palliative care for terminal liver diseases: analysis of a german physician survey

Lena Bartke[1], Jeanette Wehnes[1], Dirk Adolph[2], Marcin Krawczyk[3], Hartmut Schmidt[3], Nicole Selbach[1], Ali Canbay[1], Jan Best[3]. *[1]University Hospital Knappschaftskrankenhaus Bochum, Bochum, Germany; [2]Ruhr University Bochum (RUB), Bochum, Germany; [3]University Hospital Essen, Essen, Germany*
Email: jan.best@uk-essen.de

Background and aims: The burden of liver cirrhosis is increasing (*Luo et al. J Health Popul Nutr. 2025*). Given the limited availability of donor organs and long waiting times, many patients with end-stage liver disease (ESLD) are no longer eligible for liver transplantation (LT) and could therefore benefit from early integration of palliative care (PC). This study surveyed the attitudes of treating physicians at German LT- centers toward PC.
Method: Over a five-month period, transplant physicians at 22 German LT-centers were surveyed using a validated online questionnaire based on 10-point Likert scale. A total of 38 dedicated questions assessed attitudes toward PC, perceived needs, availability, and barriers to integration of PC.
Results: Of the 321 physicians contacted, 62 (19.3%) completed the questionnaire. Among the responders 62.9% were male, mainly senior physicians and internists. PC consultation teams were used weekly by 41.9% and monthly by 30.6% of physicians. Respondents reported significant impairment of quality of life and moderate-to-high burden from somatic and psychosocial symptoms, and they rated the benefits of PC integration as substantial. Barriers to PC integration were perceived mainly at the interface between patients, families and care planning, while physician- and structure-related obstacles were rated significantly lower ($F(7,724) = 24.20$, $p < 0.001$, $\eta^2 = .284$). While 16.1% of respondents felt that end-of-life discussions took place at the right time, 1.6% considered them to be too early and 82.3% too late.
Conclusion: Despite broad acceptance of PC at German LT centers, respondents identified numerous barriers to early integration. Earlier, patient-centered discussions might enable better PC integration. Patient-reported data are warranted to identify relevant PC needs.

THU-011

Cardiovascular health metrics (Life's Essential 8) and the risk and trajectories in MASLD, type 2 diabetes, and comorbid disease: an international, multicenter cohort study

Xiangyu Bian[1], Jinfang Sun[1], Shanghao Liu[2], Yilin Zhang[2], Guoliang Zhang[3], Hui Shi[4], Jianxiang Song[5], Puqiang Liu[6], Yijun Tang[7], Xiao Liang[8], Yuanhang Liao[9], Yang Bo[10], Yuxia Qi[11], JianSong Ji[12], Huilan Ye[13], Lan Ma[14], Ruyu Liu[15,16], Yan Yang[17], Qing He[18], Hui Yang[19], Junchao Zhang[20], Bin Shen[21], Xiongwei He[22], Xingguo Xiao[23], Wen Kang[24], Qing Shen[25], Rong Hu[26], Zhenyu Dai[27], Jianping Zhang[6], Zhong-ji Meng[28], Yong-Fen Zhu[29], Chaoliang Xiong[9], Kejun Liu[30], Tongyao Wang[11], Lili Ye[31], Zefeng Liu[13], Liping Wang[14], Kai Hu[32,33], Gui Su[17], Xuejiao Liao[18], Haoyu Yang[19], Jialing Zhang[34], Tiandan Bian[21], Jiangwen Liu[22], Yanhong Liu[22], Jing Huang[35], Jiali Zhao[17], Pinghua Sun[17], Gao-Jun Teng[36], Xiaolong Qi[2,37]. *[1]Department of Epidemiology and Biostatistics, School of Public Health, Southeast University, Nanjing, China; [2]Liver Disease Center of Integrated Traditional Chinese and Western Medicine, Department of Radiology, Zhongda Hospital, Medical School, Southeast University, Nurturing Center of Jiangsu Province for State Laboratory of AI Imaging & Interventional Radiology (Southeast University), Nanjing, China; [3]Department of Cardiology, People's Hospital of Huanghua, Cangzhou, China; [4]Department of Neurosurgery, The First Affiliated Hospital of Kangda College of Nanjing Medical University, The Affiliated Lianyungang Hospital of Xuzhou Medical University; Lianyungang Clinical College of Nanjing Medical University, Lianyungang, China; [5]Department of Cardiothoracic Surgery, Affiliated Yancheng Hospital, School of Medicine, Southeast University, Yancheng Third People's*

Hospital, Yancheng, China; [6]Pu County People's Hospital, Linfen, China; [7]Department of Respiratory and Critical Care Medicine, Taihe Hospital, Hubei University of Medicine, Shiyan, China; [8]Department of General Surgery, Sir Run-Run Shaw Hospital, Zhejiang University School of Medicine, Hangzhou, China; [9]The Department of Gastroenterology, Yichun People's Hospital, Yichun, China; [10]General Hospital of Ningxia Medical University, Yinchuan, China; [11]Department of Internal Medicine, Qingdao Public Health Clinical Center, Qingdao, China; [12]Zhejiang Key Laboratory of Imaging and Interventional Medicine, Zhejiang Engineering Research Center of Interventional Medicine Engineering and Biotechnology, Department of Radiology, Lishui Central Hospital, The Fifth Affiliated Hospital of Wenzhou Medical University, Lishui, China; [13]Department of Gastroenterology,Guangxi Hospital Division of The First Affiliated Hospital, Sun Yat-sen University, Nanning, China; [14]Department of Infectious Diseases, Bozhou People's Hospital, Bozhou, China; [15]Department of Hepatology Division 3, Xuzhou Infectious Diseases Hospital, Xuzhou, China; [16]Department of Hepatology Division 2, Beijing Ditan Hospital, Capital Medical University, Xuzhou, China; [17]Physical Examination Center, Baiyin Central Hospital, Baiyin, China; [18]Department of Hepatology, Shenzhen third People's Hospital, Shenzhen, China; [19]Department of Gastroenterology, The Second Affiliated Hospital of Guangzhou Medical University, Guangzhou, China; [20]Department of Public Health, Mengchao Hepatobiliary Hospital of Fujian Medical University, Fuzhou, China; [21]Department of Infectious Diseases, Huzhou Central Hospital, Affiliated Central Hospital, Huzhou University, Huzhou, China; [22]Medical Department of Shihezi City People's Hospital, Shihezi, China; [23]Department of Gastroenterology, Zhengzhou Central Hospital Affiliated to Zhengzhou University, Zhengzhou, China; [24]Department of Infectious Diseases, Tangdu Hospital, Fourth Military Medical University, Xian, China; [25]Department of Gastroenterology, People's Hospital of Huanghua, Huanghua, Cangzhou, China; [26]Department of Respiratory and Critical Care Medicine, The First Affiliated Hospital of Kangda College of Nanjing Medical University; The Affiliated Lianyungang Hospital of Xuzhou Medical University; Lianyungang Clinical College of Nanjing Medical University, Lianyungang, China; [27]Department of Radiology, Affiliated Yancheng Hospital, School of Medicine, Southeast University, Yancheng Third People's Hospital, Yancheng, China; [28]Department of Infectious Diseases, Hubei Provincial Clinical Research Center for Precise Diagnosis and Treatment of Liver Cancer, Taihe Hospital, Hubei University of Medicine, Shiyan, China; [29]Zhejiang Key Laboratory of Multi-omics Precision Diagnosis and Treatment of Liver Diseases, Department of Liver and Infectious Diseases, Sir Run Run Shaw Hospital, Zhejiang University School of Medicine, Hangzhou, China; [30]Department of hepatobiliary surgery, General Hospital of Ningxia Medical University, Yinchuan, China; [31]Department of Oncology Center, The Fifth Affiliated Hospital of Wenzhou Medical University, Lishui, China; [32]Liver Diseases Center, Beijing Ditan Hospital, Xuzhou Hospital, Capital Medical University, Xuzhou, China; [33]Xuzhou Infectious Diseases Hospital, Xuzhou, China; [34]Physical Examination Center, Mengchao Hepatobiliary Hospital of Fujian Medical University, Fuzhou, China; [35]Department of Health Management, Tangdu Hospital, Fourth Military Medical University, Xian, China; [36]Zhongda Hospital, Southeast University, Nanjing, China; [37]Basic Medicine Research and Innovation Center of Ministry of Education, Zhongda Hospital, Southeast University, State Key Laboratory of Digital Medical Engineering, Nanjing, China
Email: 101013436@seu.edu.cn

Background and aims: Cardiovascular disease is the major driver of mortality in individuals with metabolic dysfunction-associated steatotic liver disease (MASLD) or type 2 diabetes (T2D). Current clinical practice guidelines emphasize lifestyle management as the cornerstone for treatment of T2D and MASLD. This study assessed the influence of the American Heart Association's Life's Essential 8 (LE8) metrics on the onset and progression of MASLD and T2D comorbidity.
Method: Data were obtained from a nationwide community-based survey in China, NHANES and UK Biobank. LE8 scores were quantified using a combination of behavioral and clinical metrics obtained through physical examinations and structured questionnaires. Multinomial logistic regression was used to assess the association between LE8 scores and four health states —healthy (reference), MASLD only, T2D only, and comorbid MASLD-T2D. Multi-state models and restricted cubic splines (RCS) were employed to analyze how LE8 scores influence eight health transitions, ranging from disease-free baseline to MASLD, T2D, comorbidity, and mortality.
Results: Across three cohorts (N = 246,723), higher LE8 scores were consistently associated with reduced risks of MASLD, T2D, and their comorbidity (all $P < 0.001$). Prospective multi-state modeling in the UK Biobank further demonstrated that high (vs. low) CVH scores markedly reduced the risk of incident MASLD (HR: 0.27; 95% CI: 0.18–0.39) and T2D (HR: 0.10; 95% CI: 0.09–0.12). Among individuals with a single disease, high CVH scores significantly hindered progression to comorbidity. Notably, each 10-point LE8 increment was associated with a 24% and 11% lower risk of mortality from MASLD and T2D onset, respectively. Both behavioral and biological domains conferred significant protection, with RCS analysis revealing non-linear dose-response relationships between LE8 scores and health transitions(all $P_{non\text{-}linear} < 0.05$).
Conclusion: LE8 scores are robust predictors of MASLD and T2D risk and clinical trajectories. Optimal cardiovascular health offers substantial protection across the entire disease continuum—from initial onset to comorbidity and mortality—underscoring the clinical utility of the LE8 framework in the integrated prevention and management of metabolic-associated disorders.

THU-012

MASLD in the WHO Africa region: prevalence and development of a simple score to detect advanced fibrosis in dysmetabolic patients

Isabelle Bough[1], Bakary Dibba[2], Anna Sessa[3], Ousman Bah[2], Joel Dave[1], Dirk Blom[4], Mashiko Setshedi[4], Kitabu Jammeh[2], Rumaysa Ahmed[5], Karen Foreest[2], Erwan Vo Quang[2], Neliswa Gogela[1], Brendan Janse Van Rensburg[1], Ben Mullish[5], Isabelle Garcia[5], Dalessandro Umberto[2], Caity Cattell[4], Gibril Ndow[2], Wendy Spearman[4], Yusuke Shimakawa[6], Mark Sonderup[4], Maud Lemoine[5,7,8]. *[1]University of Cape Town, Division of Endocrinology, Department of Medicine, Cape Town, South Africa; [2]MRCG@LSHTM, Fajara, Gambia; [3]APHP Henri Mondor Hospital, Creteil, France; [4]University of Cape Town, Division of Hepatology, Department of Medicine, Cape Town, South Africa; [5]Imperial College London, Department of Metabolism, Digestion and Reproduction, London, United Kingdom; [6]Pasteur Institute, Paris, France; [7]MRC Gambia, Fajara, Gambia; [8]MRCG@the London School of Hygiene and Tropical Medicine, Fajara, Gambia*
Email: lemoine.maud@gmail.com

Background and aims: MASLD remains underdiagnosed and understudied in the WHO Africa Region despite a growing burden of obesity and diabetes. In a cohort study of patients with metabolic dysfunction in The Gambia and South Africa, we evaluated the prevalence, severity and clinical correlates with MASLD and developed a simple score to detect advanced liver fibrosis in this population.
Method: Consecutive patients with high blood pressure (HBP), obesity (body mass index (BMI)≥30 kg/m2) or type 2 diabetes mellitus (T2DM) were enrolled in the Metlive study in Gambia (training cohort) and South Africa (validation cohort) and underwent comprehensive assessment including a Fibroscan-CAP scan. MASLD was defined as CAP≥248 dB/m (or hyperechoic liver on ultrasound if invalid CAP), advanced liver fibrosis (ALF) as LSM≥8 kPa, and cirrhosis as LSM≥12 kPa. A simple score was derived by dichotomizing chosen variables using receiver operating characteristic-derived cut-offs. In the validation cohort diagnostic performance was assessed by calculating sensitivity, specificity, positive and negative predictive values (PPV, NPV).

Results: Between 5 November and 17 December 2025, 315 consecutive participants were enrolled in Gambia (76% female, median age 55 (45–64) years, 33% obesity, 61% T2DM, 56% HBP, 46% steatosis). Between 9 September and 9 December 2025, 151 consecutive patients were enrolled in South Africa, 24 were excluded due to alcohol intake (10%) or missing data, leaving 127 participants analyzed (58% female, median age 53 years, 54% obesity, 21% T2DM, 79% HBP, 67% steatosis). In The Gambia, 43% (n = 130) had MASLD and 8.3% (n = 26) ALF including seven (2.2%) cirrhosis, whilst in South Africa, MASLD was observed in 65% with 24.5% having ALF including 10% (n = 12) with cirrhosis. In the training cohort, BMI, Waist/Hip circumference ratio (WHR), and GGT level were independent factors of MASLD, while GGT level and Platelet count were the only factors associated with ALF. A simple score based on at least 2 of the following parameters, BMI ≥26 kg/m^2, WHR ≥0.92 and GGT ≥41 IU/L, had a high sensitibity (89%) and NPV (93%) to detect ALF, higher than FIB-4, but a low specificity (50%).
Conclusion: MASLD and advanced liver fibrosis are frequently observed in dysmetabolic patients in The Gambia and South Africa. The use of a simple score based on BMI, Waist and Hip circumferences and GGT level could help the identification of patients with advanced liver fibrosis in Africa where access to Fibroscan-CAP remains limited.

THU-013

Mapping receptivity and susceptibility to new models of care for metabolic dysfunction-associated steatotic liver disease (MASLD) across Europe: a mixed-methods, landscaping study

Leonard (Niels) Broekman[1], Kirsi van Eekhout[1], Sophie Porro[2], Laura Konings[3], Maria do Mar Orey[4,5], Sofia Carvalhana[4], Maurice Michel[6,7], Carmen Lara-Romero[8], Antonio Liguori[9], Evangelia Mentsiou-Nikolaou[10], Ioanna-Panagiota Kalafati[10,11], George Dedoussis[10,11], Douglas Maya-Miles[8], Manuel Romero-Gómez[8,12], Luca Miele[9], Helena Cortez-Pinto[4], Jörn M. Schattenberg[6,7], Oscar Franco[2], Manuel Castro Cabezas[3,13], Jean Muris[14], Juan Mendive[15], Ghislaine van Thiele[2], Luisa Vonghia[16,17], Sven Francque[16,17], Maarten Tushuizen[18], A.G. (Onno) Holleboom[1]. [1]*Department of Vascular and Internal Medicine, Amsterdam University Medical Centre, University of Amsterdam, Amsterdam, Netherlands;* [2]*Department of Global Public Health & Bioethics, Julius Center for Health Sciences and Primary Care, University Medical Center Utrecht, Utrecht, Netherlands;* [3]*Department of Internal Medicine, Franciscus Gasthuis & Vlietland, Rotterdam, Netherlands;* [4]*Serviço de Gastrenterologia e Hepatologia, Unidade Local de Saúde de Santa Maria, Lisbon, Portugal;* [5]*Associação para Investigação e Desenvolvimento da Faculdade de Medicina, Lisbon, Portugal;* [6]*Department of Internal Medicine II, Saarland University Medical Centre, Saarland University, Homburg, Germany;* [7]*Saarland University, Saarbrücken, Germany;* [8]*SeLiver Group, Instituto de Biomedicina de Sevilla/CSIC/Virgen del Rocío University Hospital, University of Seville; Centro de Investigación Biomédica en Red de Enfermedades Hepáticas y Digestivas (CIBEREHD), Seville, Spain;* [9]*UOC Medicina Interna e del Trapianto di Fegato, Dipartimento di Scienze Mediche, Fondazione Policlinico Gemelli IRCCS, Rome, Italy;* [10]*Department of Nutrition and Dietetics, School of Health and Education, Harokopio University of Athens, Athens, Greece;* [11]*Department of Nutrition and Dietetics, School of Physical Education, Sport Science and Dietetics, University of Thessaly, Trikala, Greece;* [12]*UCM Digestive Diseases, Virgen del Rocio University Hospital, Institute of Biomedicine of Seville, CIBEREHD, University of Seville, Seville, Spain;* [13]*Department of Internal Medicine, Erasmus MC, Rotterdam, Netherlands;* [14]*Care and Public Health Research Institute (CAPHRI), Department of Family Medicine, Maastricht University, Maastricht, Netherlands;* [15]*Department of Family Medicine, La Mina Primary Health Care Academic Centre., University of Barcelona, Barcelona, Spain;* [16]*Department of Gastroenterology and Hepatology, Antwerp University Hospital, Edegem, Belgium;* [17]*InflaMed Centre of Excellence, Laboratory for Experimental Medicine and Paediatrics, Translational Sciences in Inflammation and Immunology, Faculty of Medicine and Health Sciences, University of Antwerp, Wilrijk, Belgium;* [18]*Department of Gastroenterology and Hepatology, Leiden University Medical Centre, Leiden, Netherlands*
Email: l.d.broekman@amsterdamumc.nl

Background and aims: The European care landscape for metabolic dysfunction-associated steatotic liver disease (MASLD) is evolving rapidly, and further introduction of care innovations, such as care pathways, screening platforms, and decision tools, is anticipated. The primary aim of this study is to map current approaches to care for MASLD and to gain health system insights to inform implementation of initiatives aimed at improving MASLD care.
Method: We conducted a cross-sectional, mixed-methods, comparative analysis. We distributed an explorative survey amongst healthcare providers (May–October 2025), and assessed national guidelines, policy papers, and other relevant documents. Data collection and analysis were informed by a theoretical framework encompassing five distinct healthcare dimensions. This allowed us to assess receptivity and susceptibility to adoption of new models of care, defined as the extent to which a health system is able to accommodate the implementation of an innovation.
Results: Across ten European countries, the survey was completed by 36 respondents (36% primary care setting, 19% non-academic hospital setting, and 39% university hospital setting) and 50 documents were analyzed. Alignment was observed across countries and levels of care regarding current standard practices of care, with targeted screening and lifestyle interventions most commonly mentioned. Patients still enter care for MASLD predominantly upon incidental findings. Formal referral structures were largely absent and MASLD was rarely embedded in care for diabetes or obesity. Accessibility and availability of MASLD care services was suboptimal, mainly relating to care organization, allocation of diagnostic resources, and reimbursement policies. MASLD guidelines were available in 7 countries, but specific primary care guidance remains scarce. Available guidelines primarily differed in terms of non-invasive test use, follow-up, and use of pharmacotherapy.
Conclusion: The European care landscape for MASLD is largely comparable across countries yet care for MASLD lacks structural embedding in national healthcare systems and all examined healthcare systems showed opportunities to strengthen receptivity and susceptibility to care innovations. Upcoming innovations and models of care for MASLD need tailoring to local healthcare contexts prior to implementation in order to facilitate effective and efficient adoption, thereby recognizing that each country maintains a distinct health system architecture.

THU-014

Evaluating the impact of implementing criteria for initial fibrosis assessment in people at risk of MASLD: a national level analysis using the health survey for England

Ryan Buchanan[1], Sophie Robin[1], Chris D Byrne[1], Kate Glyn-Owen[1]. [1]*University of Southampton, Southampton, United Kingdom*
Email: k.glyn-owen@soton.ac.uk

Background and aims: International guidelines propose a multi-step diagnostic strategy to identify those with Metabolic Dysfunction-Associated Steatotic Liver Disease (MASLD) and advanced fibrosis. We have evaluated the impact of this approach in a representative sample of the English population.
Method: The Health Survey for England (HSE) is an annual survey designed to be representative of the population living in private households in England. The 2016 dataset includes AST and ALT, allowing Fib4 to be calculated. 7746 non-pregnant adults were surveyed in 2016, of whom 3787 had a blood test. Descriptive statistics explored characteristics of the population stratified by eligibility for initial fibrosis assessment (as defined by recent guidelines) and Fib-4. Exploratory analyses were conducted to optimise criteria for initial fibrosis assessment, including adding an

age cut-off, using body mass index instead of waist circumference, and using adjusted alanine aminotransferase (ALT) thresholds. Survey weightings were used in all analyses, to ensure results were generalisable to the population of England.

Results: 55% of adults met criteria for initial fibrosis assessment (type 2 diabetes, abdominal obesity and ≥1 cardiometabolic risk factor, increased ALT). 2.9% of those meeting the criteria had a Fib-4 ≥2.67 but only 66% of those with a high Fib-4 met the initial criteria for a test. Modelled in a population of 240,000 (representing one tertiary hepatology centre): 132,000 people meet the criteria for a Fib-4 test. Of these, 20,328 require further investigation and 3,828 a direct referral to hepatology. Adding an age cut off ≥45 years and using increased ALT according to commonly used standard clinical thresholds reduced the proportion of the population needing initial fibrosis assessment to 35% (from 55%) and improved the negative predictive value of the initial criteria.

Conclusion: The implementation of international MASLD guidance for diagnosing liver fibrosis in England would mean that more than half of the adult population are eligible for initial fibrosis assessment. This would have a substantial impact on hepatology service resources. Pragmatic additional criteria, such as the use of an age 'cut-off' for testing should be considered if implementing international guidelines at scale.

THU-015

Gender differences in stigma and care avoidance among people living with metabolic dysfunction–associated steatotic liver disease (MASLD): an international survey

Patrizia Carrieri[1], Shira Zelber-Sagi[2], Saleh Alqahtani[2], Khalid Al Naamani[3], Yusuf Yilmaz[4], Caglayan Keklikkiran[5], Manuel Romero-Gómez[6], Jian-Gao Fan[7], Ming-Hua Zheng[8], Mohamed El Kassas[9], Laurent Castera[10], Chun-Jen Liu[11], Vincent Wai-Sun Wong[12], Sombat Treeprasertsuk[13], Saeed Sadiq Hamid[14], Hirokazu Takahashi[15], Takumi Kawaguchi[16], Ajay Kumar Duseja[17], Sven Francque[18], Wendy Spearman[19], Marlen Ivon Castellanos Fernández[20], Patrizia Burra[21], Stuart Roberts[22], Wah-Kheong Chan[23], Marco Arrese[24], Ashwani K. Singal[25], Stuart C Gordon[26], Michael Fuchs[27], Naim Alkhouri[28], Rohit Loomba[29], Jane Ranagan[30], Janus Ong[31], Yuichiro Eguchi[32], Moises Diago[33], Ming-Lung Yu[34], Brian Lam[35], Lynn H Gerber[36], Dana Ivancovsky-Wajcman[37], Linda Henry[36], Maria Stepanova[36], Zobair M. Younossi[36]. *[1]The Global NASH/MASH Council, Washington DC, United States, Aix Marseille Univ, Inserm, IRD, SESSTIM, Sciences Economiques & Sociales de la Santé & Traitement de l'Information Médicale, Marseille, France; [2]The global NASH/MASH council, Washington DC, United States; [3]The Global NASH/MASH Council, Washington DC, United States, Liver Disease Research Center, College of Medicine, King Saud University, Riyadh, Saudi Arabia; [4]The Global NASH/MASH Council, Washington DC, United States, Department of Gastroenterology, School of Medicine, Recep Tayyip Erdoğan University, Rize, Türkiye; [5]The Global NASH/MASH Council, Washington DC, United States, Department of Gastroenterology, School of Medicine, Recep Tayyip Erdoğan University, Rize, Turkey, Rize, Türkiye; [6]The Global NASH/MASH Council, Washington DC, United States, UCM Digestive Diseases and ciberehd, Virgen del Rocío University Hospital; Instituto de Biomedicina de Sevilla (HUVR/CSIC/US), Department of Medicine, University of Seville, Seville, Spain; [7]The Global NASH/MASH Council, Washington DC, United States, Department of Gastroenterology, Xinhua Hospital affiliated to Shanghai Jiao Tong University School of Medicine, Shanghai, China; [8]The Global NASH/MASH Council, Washington DC, United States, MAFLD Research Center, Department of Hepatology, The First Affiliated Hospital of Wenzhou Medical University, Wenzhou, China; [9]The Global NASH/MASH Council, WashingtonDC, United States, Endemic Medicine Department, Faculty of Medicine, Capital University, Cairo, Egypt; [10]The Global NASH/MASH Council, Washington DC, United States; 11. Department of Hepatology, Beaujon Hospital; AP-HP, Université Paris Cité, Inserm UMR1149, Clichy, France; [11]The Global NASH/MASH Council, Washington DC, United States; 12. Hepatitis Research Center, Department of Internal Medicine and Graduate Institute of Clinical Medicine, National Taiwan University College of Medicine and Hospital, Taipei, Taiwan; [12]The Global NASH/MASH Council, Washington DC, United States, Department of Medicine and Therapeutics, Faculty of Medicine, The Chinese University of Hong Kong, Hong Kong, China; [13]The Global NASH/MASH Council, Washington DC, United States, Division of Gastroenterology, Department of Internal Medicine, Chulalongkorn University, Bangkok, Thailand; [14]The Global NASH/MASH Council, Washington DC, United States, Department of Medicine, Aga Khan University, Karachi, Pakistan; [15]The Global NASH/MASH Council, Washington DC, United States, Liver Center, Saga University Hospital, Saga, Japan; [16]The Global NASH/MASH Council, Washington DC, United States, Division of Gastroenterology, Department of Medicine, Kurume University School of Medicine, Kurume, Japan; [17]The Global NASH/MASH Council, Washington DC, United States, Department of Hepatology, Post Graduate Institute of Medical Education and Research, Chandigarh, India; [18]The Global NASH/MASH Council, Washington DC, United States, Department of Gastroenterology and Hepatology, Antwerp University Hospital, Edegem, Belgium; [19]The Global NASH/MASH Council, Washington DC, United States, Division of Hepatology, Department of Medicine, Faculty of Health Sciences, University of Cape Town, Cape Town, South Africa; [20]The Global NASH/MASH Council, Washington DC, United States, Institute of Gastroenterology, University of Medical Sciences of Havana, Havana, Cuba; [21]The Global NASH/MASH Council, Washington DC, United States, Department of Gastroenterology, Universita Degli Studi Di Padova, Padova, Italy; [22]The Global NASH/MASH Council, Washington DC, United States, The Alfred and Monash University, Melbourne, VIC, Australia; [23]The Global NASH/MASH Council, Washington DC, United States, Gastroenterology and Hepatology Unit, Department of Medicine, University of Malaya, Kuala Lumpur, Malaysia; [24]The Global NASH/MASH Council, Washington DC, United States, Departamento de Gastroenterología, Facultad de Medicina, Pontificia Universidad Católica de Chile, Santiago, Chile; [25]The Global NASH/MASH Council, Washington DC, United States, Division of Gastroenterology and Hepatology, University of Louisville School of Medicine; Trager Transplant Center and Jewish Hospital, Louisville, KY, United States; [26]The Global NASH/MASH Council, Washington DC, United States, Department of Hepatology and Gastroenterology, Henry Ford Hospital System, Detroit, MI, United States; [27]The Global NASH/MASH Council, Washington DC, United States, Central Virginia VA Health Care System (CVHCS); Virginia Commonwealth University (VCU), Richmond, VA, United States; [28]The Global NASH/MASH Council, Washington DC, United States, Summit Clinical Research, San Antonio, Texas, United States; [29]The Global NASH/MASH Council, Washington DC, United States, Division of Gastroenterology, University of California, San Diego, San Diego, CA, United States; [30]The Global NASH/MASH Council, Washington DC, United States, Chronic Liver Disease Foundation, Clark, NJ, United States; [31]The Global NASH/MASH Council, Washington DC, United States, College of Medicine, University of the Philippines, Manila, Philippines; [32]The Global NASH/MASH Council, Washington DC, United States, Loco Medical General Institute; Saga University Faculty of Medicine, Saga, Japan; [33]The Global NASH/MASH Council, Washington DC, United States, Department of Medicine, University of Valencia; Hospital General Universitario Valencia, Valencia, Spain; [34]The Global NASH/MASH Council, Washington DC, United States, Hepatobiliary Division, Department of Internal Medicine, Kaohsiung Medical University Hospital, Kaohsiung Medical University, Kaohsiung, Taiwan; [35]The Global NASH/MASH Council, Washington DC, United States, Center for Outcomes Research in Liver Diseases, Washington, DC, United States; [36]The Global NASH/MASH Council, Washington DC, United States, Center for Outcomes Research in Liver Diseases, Washington DC, United States; [37]The Global NASH/MASH Council, Washington DC, United States*
Email: zobair.younossi@cldq.org

Background and aims: MASLD affects women and men differently, and stigma, both perceived and self-stigma, may contribute to gender-specific patterns of care avoidance. This study aimed to

assess gender-specific patterns of stigma and their associations with care avoidance in MASLD.
Method: A cross-sectional, international survey was developed and administered in 2023 by the Global MASH/NASH Council (GNC) among adults with a confirmed diagnosis of MASLD. The survey collected sociodemographic and clinical data, assessed perceived stigma (presence or absence across several domains and overall), and measured self-stigma using the validated Self-Stigma Scale–Short Form, generating domain-specific and total scores. Severe self-stigma was defined as a total score above the 75th percentile, stratified by sex. Care avoidance in primary care or secondary care (gastroenterology, hepatology, and endocrinology) was also reported. Mixed-effects logistic regression models were conducted separately for women and men, adjusting for relevant cofactors and including geographic region as a random effect, to evaluate associations between perceived stigma, self-stigma, and care avoidance.
Results: Among 1,313 respondents with MASLD [51% male; 50% aged ≥55 years; 28% Europe, 26% USA/Canada, 23% East Asia, and 16% MENA; 73% with ≥1 and 43% with ≥2 chronic conditions), care avoidance was more frequent among men (23.6% vs. 18.9%, $p = 0.04$), occurring predominantly in primary care settings. Women reported higher self-stigma domain scores (all $p < 0.0001$) and more discrimination-related perceived stigma (27.8% vs. 19.1%). In adjusted analyses, both perceived stigma [OR (95% CI) = 1.84 (1.07–3.18)] and severe self-stigma [1.84 (1.19–2.85)] were associated with care avoidance in men, whereas only perceived stigma [2.29 (1.25–4.22)] was associated with care avoidance in women. No other factors were associated with care avoidance. In women, perceived stigma was predicted by younger age, multimorbidity, and a history of medical weight loss ($p < 0.05$), while no predictors were identified in men ($p > 0.05$). Indicators of lower socioeconomic status and advanced fibrosis predicted severe self-stigma in both genders ($p < 0.05$).
Conclusion: Stigma is a key driver of care avoidance in MASLD, with distinct gender-specific patterns. Although women report higher levels of self-stigma and discrimination-related perceived stigma, the association between severe self-stigma and care avoidance is stronger among men.

THU-019

Sexual function in chronic liver disease: a case-control study

Yooyun Chung[1], Mussarat Rahim[2], Refah Ahmed[3], Rachel Rosales[4], Bezalel Comia[1], Ilkay Ergenc[1], Mark Mcphail[1], Michael Heneghan[1].
[1]King's College Hospital, London, United Kingdom; [2]St George's Hospital, London, SW17 0QT, UK, United Kingdom; [3]Doctorate of Clinical Psychology, University of Hertfordshire, AL10 9AB, UK, United Kingdom; [4]Princess Royal University Hospital, London, BR6 8ND, UK, United Kingdom
Email: yooyun.chung@nhs.net

Background and aims: Chronic liver disease (CLD) and liver transplantation (LT) are associated with sexual dysfunction (SD), neuropsychiatric symptoms and impaired quality of life (QoL). However, data on SD in patients with CLD/LT remain limited. This study aimed to determine the prevalence of SD in patients with CLD/LT and to assess its relationship with cognitive impairment, QoL and mental health.
Method: In this cross-sectional study, adults with CLD/LT and healthy volunteers (HV) were recruited at King's College Hospital. CLD included patients with cirrhosis and non-cirrhosis. Sexual function was assessed using the international index of erectile function (IIEF) in men and the female sexual function index (FSFI) and Sexual Satisfaction Scale for Women (SSSW) in women. Cognitive function was evaluated using the Montreal Cognitive Assessment (MOCA). Anxiety and depression were assessed with the Hospital Anxiety and Depression Scale (HADS) and QoL using the Clinical Outcomes in Routine Evaluation (CORE) questionnaire and Chronic Liver Disease Questionnaire (CLDQ). Outcomes were analysed by sex, disease stage and cognitive impairment status.
Results: Two hundred women (100 CLD/LT, 100 HV) and 105 men (51 CLD/LT, 54 HV) were recruited with no age differences between patient and HV groups. Among patients with CLD/ LT, SD was highly prevalent, affecting 67% of women (FSFI defined) and 57% of men (IIEF defined). Both women and men with CLD/LT demonstrated significantly poorer sexual function scores compared with HV ($p = 0.013$ FSFI defined, $p = 0.029$ SSSW, $p = 0.046$ IIEF). In women with CLD/ LT, depression and anxiety were associated with SD, reflected by lower FSFI scores ($p = 0.015$), a higher prevalence of SD ($p < 0.001$) and poorer SSSW scores ($p = 0.019$) compared with HV. This was not observed in men. Cognitive dysfunction was not associated with SD in either sex. However, in men with CLD/ LT, cognitive impairment was associated with poorer QoL and higher levels of anxiety and depression. Women with CLD/LT reported poorer liver disease specific QoL than men ($p < 0.001$) and patients with cirrhosis experienced worse QoL than those without cirrhosis ($p < 0.001$).
Conclusion: Approximately two third of patients with CLD/LT experience SD. Marked sex differences exist in relationships between SD, mental health, cognitive impairment and QoL. This highlights the need for sex-specific targeted interventions to address SD and associated psychosocial burden in patients with CLD/ LT.

THU-020

An interpretable artificial intelligence framework for cardiovascular risk prediction in metabolic dysfunction-associated steatotic liver disease: LiverCARD

Antonio Cirella[1], Pierangela Bruno[2], Valerio Caputo[1], Alessandro Quarta[2], Edoardo de Rose[2], Valeria d'Arpino[1], Silvano Junior Santini[1], Gianluigi Greco[2], Germano Scevola[3], Marco Vinci[3], Pierpaolo Palumbo[4], Ernesto di Cesare[4], Antonella Guzzo[2], Francesco Calimeri[2], Clara Balsano[1].
[1]Department of Clinical Medicine, Life, Health & Environmental Sciences-MESVA, University of L'Aquila, Italy, L'aquila, Italy; [2]Department of Mathematics and Computer Science, University of Calabria, Rende, Italy, Rende, Italy; [3]Ospedale Sandro Pertini Roma, UOC Radiology, Italy, Roma, Italy; [4]Department of Applied Clinical Sciences and Biotechnology-DISCAB, University of L'Aquila, Italy, L'aquila, Italy
Email: cirella.nt@gmail.com

Background and aims: Metabolic dysfunction-associated steatotic liver disease(MASLD) affects approximately 30% of the global population and represents a major public health challenge. Cardiovascular disease is the leading cause of mortality in this population. However, cardiovascular risk (CVR) assessment in MASLD remains suboptimal, as traditional risk scores do not incorporate liver-related parameters or advanced imaging biomarkers. The aim of this study was to develop LiverCARD, an artificial intelligence (AI)-based framework designed to improve CVR prediction in patients with MASLD by integrating routinely collected clinical data with imaging features extracted from coronary computed tomography angiography(cCTA) images.
Method: In this retrospective multicentre study, 164 patients from two Italian hospitals were evaluated. For each patient, ten liver pre-contrast cCTA images were analyzed. Hepatic steatosis(HS) was quantified using liver attenuation, coronary artery calcium score(CS) was used as a marker of CVR, and liver fibrosis trough Fib-4. Patients were stratified into high- and low-risk groups based on degree of CS and HS. LiverCARD integrates clinical variables with embeddings derived from pretrained medical deep learning models. Machine learning models were tested and model explainability was assessed using SHapley Additive exPlanations.
Results: The integrated approach based on XGBoost on combined multimodal dataset achieved strong predictive performance, with an accuracy of 0.89 in internal validation and 0.72 in external validation, outperforming models based on clinical or imaging data alone. The use of multiple liver slices per patient improved LiverCARD efficiency.

Explainability analysis confirmed the truthfulness of our work, including age, number of comorbidities, Fib-4, type 2 diabetes, and male sex, while imaging embeddings provided additional discriminative information.
Conclusion: LiverCARD integrates AI-derived imaging features with routinely available clinical data, providing an interpretable, scalable, and robust framework for CVR stratification in MASLD patients. By combining multimodal information, this approach improves predictive performance beyond traditional clinical or imaging-based models enabling a more accurate identification of high-risk individuals. LiverCARD supports personalized preventive strategies and underscores the clinical value of explainable multimodal artificial intelligence in addressing an important unmet need in MASLD-related CVR assessment.

THU-021

The global academic hepatology capacity index (IGCAH): a multi-source assessment reveals profound inequities across Latin America

Pablo Coste[1], Ezequiel Ridruejo[2], Luis Antonio Diaz[3], Juan Pablo Arab[4], Mário Pessoa[5], Nélia Hernandez[6], Marco Arrese[3]. *[1]Hospital Doctor Rafael Ángel Calderón Guardia, LiverLab CR, San José, Costa Rica; [2]Sección Hepatología, Departamento de Medicina. Centro de Educación Médica e Investigaciones Clínicas Norberto Quirno "CEMIC", Buenos Aires, Argentina; [3]Pontificia Universidad Católica de Chile, Santiago, Chile; [4]Virginia Commonwealth University, Richmond, United States; [5]Gastroenterology and Nutrition Department, Hospital das Clínicas, Faculdade de Medicina, Universidade de São Paulo, São Paulo, Brasil, São Paulo, Brazil; [6]Hospital de Clínicas, Montevideo, Uruguay*
Email: costepablo@gmail.com

Background and aims: Academic hepatology in Latin America is highly heterogeneous, yet no standardized regional assessment exists. We conducted the first multi-source evaluation of academic and clinical hepatology capacity and developed a composite index to quantify cross-country differences.
Method: National hepatology societies from 20 Latin American countries completed a 54-item structured survey. Five domain indices (human capacity, academic training, scientific productivity, clinical complexity, and collaboration/networking) were constructed, standardized using z-scores, and integrated into the Global Academic Hepatology Capacity Index (IGCAH). Findings were triangulated with an analysis of PubMed-indexed hepatology publications (2015–2025) and thematic analysis of abstracts submitted to the Latin American Association for the Study of the Liver (ALEH) Congress 2025.
Results: Responses were obtained from 100% of affiliated national societies. Marked regional asymmetry was observed across all domains. Five countries concentrated over 80% of trained hepatologists, fellowship programs, research infrastructure, and access to advanced therapies. Formal recognition of hepatology as a specialty was reported by only 45% of countries, and 35% had structured national fellowship programs. Forty- five percent lacked essential laboratory infrastructure, and only 50% met criteria for sufficient diagnostic and therapeutic complexity within the public health system, defined by access to advanced imaging, portal hypertension therapies, locoregional treatments, and liver transplantation. Hepatology services were centralized in one or two major cities in 70% of countries. Scientific productivity was highly concentrated, with four countries accounting for approximately 85% of PubMed-indexed publications, while more than half produced fewer than five papers annually. Congress submissions mirrored these gradients: 75% originated from five countries, with themes dominated by metabolic dysfunction associated liver disease, cirrhosis, and hepatocellular carcinoma, whereas only 5.2% addressed alcohol-associated liver disease despite its substantial regional burden.
Conclusion: Profound asymmetries characterize academic hepatology in Latin America. The IGCAH provides a robust regional framework to identify structural gaps and guide targeted, stage-specific capacity strengthening.

THU-022

Trends in hospitalizations and in-hospital mortality due to primary biliary cholangitis in Brazil (2015–2024): a decade of real-world evidence from the public unified health system

Guilherme Cançado[1], Cláudia Couto[1], Luciana Faria[1], Bernado Moraes[1], Paulo Bittencourt[2], Cristiane A. Villela-Nogueira[3], Vivian Rotman[3], Debora Raquel Terrabuio[4], Eduardo Luiz Rachid Cançado[5], Maria Lucia Ferraz[6]. *[1]Universidade Federal de Minas Gerais, Belo Horizonte, Brazil; [2]Hospital Português, Salvador, Brazil; [3]Universidade Federal do Rio de Janeiro, Rio de Janeiro, Brazil; [4]Universidade de São Paulo, Universidade Federal de São Paulo, São Paulo, Brazil; [5]Universidade de São Paulo, São Paulo, Brazil; [6]Universidade Federal de São Paulo, São Paulo, Brazil*
Email: cancadoguilherme@gmail.com

Background and aims: Primary Biliary Cholangitis (PBC) is a rare autoimmune liver disease with limited epidemiological data in Latin America. We aimed to analyze nationwide trends in PBC hospitalizations within the Brazilian Unified Health System (SUS) from 2015 to 2024.
Method: National PBC-related hospitalizations were identified in Brazil's public health system as inpatient admissions with ICD-10 K74.3 recorded as the primary diagnosis (main reason for admission), using artificial intelligence. We estimated annual hospitalization rates per 100,000 inhabitants, in-hospital mortality, and mean length of stay. For rate calculations, the population denominator was defined as the Brazilian total population estimate from *Instituto Brasileiro de Geografia e Estatística – IBGE* (2025), applied as a fixed reference denominator across all study years to standardize comparisons over time. Temporal changes were evaluated using segmented (interrupted time-series) regression across pre-pandemic (2015–2019), pandemic (2020–2021), and post-pandemic (2022–2024) periods. Data was stratified by macroregion.
Results: From 2015–2024, 2,913 hospitalizations were recorded. The annual hospitalization rate ranged from 0.11 per 100,000 (2022) to 0.19 per 100,000 (2020), with a mean of 0.15 per 100,000 over the study period. The mean in-hospital mortality was 15.4%, varying from 11.7% (2023) to 18.5% (2019). The average length of stay was 7.9 days (range: 6.8–8.4 days), showing minimal fluctuation over time. From 2015–2019, national PBC hospitalization rates increased by 0.008 per 100,000 per year; in 2020, during covid-19 pandemic, there was a significant immediate increase of 0.046 per 100,000 ($p = 0.03$), followed by a significant reduction in slope of 0.009 per 100,000 ($p = 0.04$) after 2021. The Southeast region exhibited the highest hospitalization burden (0.21/100,000).
Conclusion: Hospitalization for PBC in Brazil is infrequent yet associated with substantial mortality. The covid-19 pandemic led to a transient increase in hospitalizations followed by decline. Strengthening outpatient management and regional equity in hepatology care remains a public health priority.
Disclosure: This study was supported by a research grant from IPSEN.

THU-023

Reduced physician confidence in the acute management of decompensated liver disease: Implications for targeted hepatology education

Rachel Edwards[1], Apoorva Hedge[1], Zinu Philipose[1], Jane Fretwell[2], James Liu Yin[1]. *[1]Croydon University Hospital, London, United Kingdom; [2]Lewisham Hospital, London, United Kingdom*
Email: rachelmedwards72@gmail.com

Background and aims: Liver disease represents a growing public health challenge across Europe with rising mortality placing increasing pressure on acute medical services. Education is a key intervention to address this problem. Most UK physicians dual accredit with general medicine and routinely encounter patients with

liver disease during acute hospital admissions. Within our region, we aimed to explore physicians' confidence in the management of decompensated liver disease compared with other medical conditions within the first 24 hours of presentation.

Method: An online survey assessed physician confidence in the management of 13 acute medical conditions, including decompensated liver disease. Confidence was self-rated by the participant on a Likert scale from 1 (lowest) to 10 (highest). Ratings <3 prompted free-text responses exploring contributory factors. An additional free-text question assessed awareness of national mortality trends. Data were collected on physician grade, age, time out of training and prior clinical rotations. Statistical analysis was done using R Studio and JASP.

Results: 69 clinicians responded, aged 20–40 years (43 female, 23 male, 2 non-binary, 1 undisclosed). 32 were general resident doctors, 11 internal medicine trainees, 18 medical speciality trainees and 6 physician assistants. The average time in training was 3.6 years. 39% had taken time out of training. Confidence in managing decompensated liver disease was significantly lower than for other conditions (mean score 6.1, $p < 0.001$), with wide variability (range 1–10). Confidence was higher among those who had undertaken prior gastroenterology/hepatology rotations, those who had completed an advanced life support course, and those who had taken time out of training ($p < 0.05$). We also found a positive correlation between confidence and years of training and time out of training ($p < 0.001$). Only 6% of respondents recognised liver disease as the only major disease group with rising mortality in the UK.

Conclusion: Liver disease is an under-recognised cause of rising mortality in the UK and parts of Europe, and many general physicians lack confidence in its early management. Given the importance of the first 24 hours of care, targeted, locally relevant education for general physicians, particularly junior colleagues who provide frontline care, is needed. This study provides proof of concept for larger national work aimed at improving general physician confidence and patient outcomes.

THU-024-YI

Poorer social deprivation exacerbates clinical outcomes in alcohol related liver disease admissions in Ireland

Clare Foley[1], Dee Noone[2], Meadhbh Keegan[3], Jennifer Russell[1], Stephen Stewart[1], John Ryan[2]. *[1]Mater Misericordiae University Hospital, Dublin, Ireland; [2]Beaumont Hospital, Dublin, Ireland; [3]Pobal, Dublin, Ireland*
Email: foleyclare123@gmail.com

Background and aims: Social deprivation has been linked to poor outcomes in alcohol related liver disease. This has never been investigated in Ireland. This study aims to review alcohol related liver disease admission (ALD) outcomes in Beaumont Hospital, a large urban tertiary centre according to patient specific social deprivation scores.

Method: Hospital In-Patient Enquiry (HIPE) admission data were reviewed from 1/1/2017 to 31/12/2023. Individual social deprivation scores were assigned via collaboration with Pobal, a non-profit organisation that works with the Irish Government to address social inclusion. The total population within each deprivation score of the hospital catchment area was established to determine admissions per 100,000 population. Median length of stay, critical care bed days, Charlson comorbidity indices (CCI), in-hospital mortality and 30 day readmission rates were assessed according to deprivation score.

Results: 499 ALD admissions were reviewed. 61.3% of the admissions resided in below average or more deprived areas in contrast to 37% of the hospital catchment area population that resided in these areas ($p < 0.0001$). Females represented 29.7% of admissions. 55.4% of these female admissions reside in social deprivation categories of marginally below average or more deprived. Admission risk rose significantly with deprivation score; affluent 45/100,000, marginally above average 88/100,000, marginally below average 182/100,000, disadvantaged 179/100,000, very disadvantaged 310/100,000, extremely disadvantaged 92/100,000. Affluent admissions per 100,000 population were significantly lower compared to disadvantaged and very disadvantaged admissions ($p = 0.0006$). Patients from marginally below average or more deprived areas occupied more critical care bed days compared to patients from affluent areas ($p = 0.0221$). Notably, patients from marginally below average or more deprived areas demonstrated significantly increased mortality rates compared to patients from affluent areas ($p = 0.0043$). There was no significant difference in median length of stay, 30 day readmission rates nor average CCI according deprivation score.

Conclusion: Social deprivation increases the risk of admission to hospital with ALD. Important clinical outcomes; morbidity and mortality, are exacerbated by worsening social deprivation group. In areas of poorer social deprivation there is a compelling need for prevention and management strategies against ALD.

THU-025

Impact of social deprivation on liver disease admissions in Ireland

Clare Foley[1], Dee Noone[2], Meadhbh Keegan[3], Jennifer Russell[1], John Ryan[2], Stephen Stewart[1]. *[1]Mater Misericordiae University Hospital, Dublin, Ireland; [2]Beaumont Hospital, Dublin, Ireland; [3]Pobal, Dublin, Ireland*
Email: foleyclare123@gmail.com

Background and aims: Social deprivation has been linked to poor outcomes in liver disease. This has never been investigated in Ireland. This study aims to review liver admission outcomes in Beaumont Hospital, a large urban tertiary centre, according to patient specific social deprivation scores.

Method: Hospital In-Patient Enquiry (HIPE) admission data were reviewed from 1/1/2017 to 31/12/2023. Individual social deprivation scores were assigned via collaboration with Pobal, a non-profit organisation that works with the Irish Government to address social inclusion. The total population within each deprivation score of the hospital catchment area was established to determine admissions per 100,000 population. Median length of stay, critical care bed days, Charlson comorbidity indices and in-hospital mortality rates were assessed according to deprivation score.

Results: 851 liver disease admissions were reviewed. 60.2% of the total admissions resided in below average or more deprived areas in contrast to 37% of the hospital catchment area population that resided in these areas ($p < 0.0001$). Females represented 35.4% of the total admissions, 57.1% of these female admissions reside in social deprivation categories of marginally below average or more deprived. Admission risk rose significantly with deprivation score; affluent 87/100,000, marginally above average 151/100,000, marginally below average 331/100,000, disadvantaged 293/100,000, very disadvantaged 415/100,000, extremely disadvantaged 207/100,000. Affluent admissions were significantly lower compared to disadvantaged, very disadvantaged and extremely disadvantaged admissions ($p = 0.006$, $p = 0.0227$, $p = 0.0023$). While patients from disadvantaged or more deprived areas occupied more critical care bed days compared to patients from affluent areas($p = 0.0044$), no significant differences were observed in relation to Charlson comorbidity indices, overall hospital lengths of stay or mortality rates according to deprivation score.

Conclusion: Social deprivation increases the risk of admission with liver disease to hospital and may impact on disease severity as evidenced by critical care use. However, social deprivation did not impact on overall clinical outcomes. This study highlights the need for targeted awareness and diagnosis of liver disease in areas of social deprivation.

THU-026

Implementation of a health navigator program post-liver transplantation, utilization and outcomes

R. Todd Frederick[1], Krista Ramonas[2], Nina Winterstein[2], Gil Palchek[1], Sylvia Sudat[1], Deborah Franzon[3]. [1]*California Pacific Medical Center Research Institute, San Francisco, United States;* [2]*San Francisco, United States;* [3]*University of California San Francisco, San Francisco, United States*
Email: deborah.franzon@ucsf.edu

Background and aims: Health outcomes are largely influenced by socieconomic status (SES). Outcomes after liver transplantation (LT), such as graft failure and mortality, are associated with race, insurance type and education level. To optimize LT outcomes, interventions targeting unique individual-level SES needs are necessary. We aimed to assess the utilization and impact of a health navigator program on outcomes such as readmissions and post-LT complications in patients receiving navigation services compared with those who have not.
Method: California Pacific Medical Center Liver Transplant program partnered with the Health Navigator Foundation, a not-for profit organization, to provide essential services to transplant patients. Between August 2022 and December, 31 2024 all liver transplant recipients were screened for eligibility for HNF services. Program enrollment was voluntary and cost-free. For 30 days post- LT, patients received navigation services comprised of access to a buddy program, medication adherence education, social services support, and translation services. Vouchers for gas, parking, transportation, and food were provided based on financial eligibility. IRB-approved, retrospective, de-identified data from all LT recipients including patient demographics, geolocation, insurance type, 90 day readmissions, episodes of rejections were extracted from the electronic health record for analysis.
Results: A total of 230 patients underwent LT and 49% (N = 113) received navigation services. LT patients were primarily non-Hispanic (NH) white (49%, N = 112) followed by Hispanic or Latino (29%, N = 66) NH Asian (11.3%, N = 26), NH Black or African American (4%, N = 10), and NH Other (7%, N = 16). Patients who received navigation and those who did not were similar in terms of race/ethnicity (p = 0.77). LT patients were 39% female, and female LT patients were less likely to receive navigation (38% vs. 56%, p < 0.01). On preliminary analysis, 54% of LT patients returned to the hospital in the first 90 days post-discharge; patients who received navigation were more likely to return (61% vs. 47%, p = 0.03). The overall incidence of 90-day rejection episodes was 1% (N = 3).
Conclusion: Navigation services facilitate access to care in order to improve health. In our cohort, patients receiving post LT navigation were more likely to utilize hospital services in the first 90 days. Planned analysis of SES, insurance type, and proximity to transplant center stratified by gender may further inform results and will be presented.

THU-027

Stable alcohol consumption over time in older adults, assessed by PEth

Marie Fredriksson[1], Mårten Werner[1]. [1]*Department of public health and clinical medicine, Umeå University, Umeå, Sweden*
Email: marie.fredriksson@regionvasterbotten.se

Background and aims: Interview studies have previously shown a stable pattern of alcohol consumption in middle-aged and older adults. PEth (phosphatidylethanol) is a blood marker that correlates well with alcohol intake over the past 2–4 weeks. We measured PEth in a study population at two time points separated by a six- to nine-year interval to determine whether the alcohol consumption indicated by PEth remained consistent.
Method: As a sub-study of the Swedish CArdioPulmonary BioImage Study (SCAPIS), we added PEth analysis to the same participants on two occasions. The first samples were collected between May 2016 and August 2018, and the second between April 2024 and May 2025. The baseline age of the study population was 50–65 years.
Results: The number of participants was 1166, comprising 589 men and 577 women. At the first measurement, 56.8% had a PEth < 0.05 µmol/L (35 ng/mL), 33% had a PEth between 0.05 and 0.29 µmol/L, and 10.2% had a PEth ≥ 0.3 µmol/L (210 ng/mL). At the second measurement, 56.7% had a PEth < 0.05 µmol/L, 33.9% had a PEth between 0.05 and 0.29 µmol/L, and 9.4% had a PEth ≥ 0.3 µmol/L. Eighty per cent remained within the same alcohol consumption group between the two samples, and fewer than 1% shifted from the highest to the lowest PEth group, or vice versa. There was a small but statistically significant increase in PEth from SCAPIS 1 to SCAPIS 2 for both men and women. The oldest participants in SCAPIS 1 (aged 60–65 years) showed no significant difference in Peth levels between SCAPIS 1 and 2; however, those aged 50–59 years in SCAPIS 1 had significantly increased Peth levels between the two measures.
Conclusion: In this population, alcohol consumption, measured as PEth, remained at a similar level over 6–9 years, consistent with previous interview-based data. This indicates that PEth, at least in this population, can serve as an indicator of alcohol consumption over periods longer than the single test is valid for.

THU-028

Disability weights for compensated and decompensated cirrhosis: implications of alternative severity weights

Rebekah Hall[1], Elin Gruffydd[1], Ee Lin Kimberly Teo[1], Andrew Lloyd[1], Villum Wittrup-Jensen[2], Preety Gautam[2], Jeff McIntyre[3]. [1]*Acaster Lloyd, London, United Kingdom;* [2]*Boehringer Ingelheim International GmbH, Ingelheim am Rhein, Germany;* [3]*Global Liver Institute, Washington, DC, United States*
Email: preety.gautam@boehringer-ingelheim.com

Background and aims: The current Global Burden of Diseases, Injuries, and Risk Factors Study (GBD) disability weight for decompensated liver cirrhosis (DLC) is 0.178 on a 0 (no disability) to 1 (dead) scale. Conversely, compensated liver cirrhosis (CLC) is assigned a weight of zero, on the assumption that it is asymptomatic. The burden of liver cirrhosis reported by patients in qualitative studies suggests that the methodology used by the GBD may underestimate the true burden of the disease. This study aims to provide an alternate approach to estimate the disability weights associated with CLC/DLC.
Method: An online paired comparison (PC) survey was conducted among the US general population to estimate disability weights associated with newly developed lay health state descriptions of key symptoms and impacts of CLC and DLC based on qualitative interviews with 20 CLC/DLC patients. Survey participants (N = 400) were representative of the US general population based on age distribution, gender, and race. PC results were analysed using probit regression to provide ordinal weights of each health state. Non-parametric (Loess) regression was used to anchor disability weights to a 0 to 1 scale based on GBD 2010 disability weights for 28 indicator health states included in the PC survey.
Results: The estimated disability weights associated with CLC and DLC were 0.245 (95% confidence interval [CI]: 0.151–0.360) and 0.501 (95% CI: 0.374–0.645), respectively. Model statistics demonstrated a good model fit (coefficient of determination = 0.849) indicating strong correlation between the paired comparison estimates from this study and existing GBD estimates. Results suggest that the degree of disability experienced by individuals with CLC may be similar to post-acute effects of an infectious disease (disability weight: 0.219) and moderate chronic obstructive pulmonary disease (disability weight: 0.225). The level of disability experienced by those with DLC was between the level of disability associated with moderate multiple sclerosis (disability weight: 0.463) and terminal cancer with medication (disability weight: 0.540).
Conclusion: The current GBD disability weights may underestimate how liver cirrhosis negatively impacts patients living with liver

diseases such as MASH. This study employed qualitative research to better describe the burden of liver disease. The methods to obtain GBD disability weights should be reconsidered to recognise the true burden of liver disease.

THU-029

Public health implications of metabolic dysfunction-associated steatotic liver disease based on global stepwise approach to surveillance data

Taras Griadil[1]. [1]*Uzhhorod National University, Institute of Postgraduate and Pre-university Education, Department of Therapy and Family Practice, Uzhhorod, Ukraine*
Email: taras.griadil@uzhnu.edu.ua

Background and aims: Metabolic dysfunction-associated steatotic liver disease (MASLD), formerly known as nonalcoholic fatty liver disease, is currently a leading cause of chronic liver disease globally. The new nomenclature emphasizes the presence of at least one of five cardiometabolic risk factors alongside hepatic steatosis. Public health interventions are critical to managing this growing burden. This study aims to estimate the prevalence of risk factors associated with this condition using data from the STEPS (WHO Stepwise Approach to Surveillance) surveys in different countries.
Method: A secondary analysis of cross-sectional data collected via STEPS surveys in six countries between 2020 and 2024 was conducted. The study utilized the standard three-step instrument: questionnaire, physical measurements, and biochemical assessments. We stratified the population based on the new nomenclature, distinguishing between "pure" metabolic dysfunction-associated steatotic liver disease and MetALD; the latter category is defined by alcohol consumption exceeding 140 g/week for females and 210 g/week for males. Statistical significance was defined as $p < 0.05$. The correlation between public health indicators (physical activity, diet) and metabolic dysfunction was assessed.
Results: The analysis included 15,400 participants. The prevalence of individuals meeting the criteria for steatotic liver disease varied significantly by region. Data showed that 35% of the cohort showed signs of metabolic dysfunction-associated steatotic liver disease. Furthermore, 12% were classified into the MetALD category. The analysis revealed that populations with low engagement in public health physical activity programs had a significantly higher prevalence of metabolic risk factors ($p = 0.03$).
Conclusion: The integration of the new nomenclature into public health surveillance systems confirms a significant global burden of metabolic liver diseases. Data from STEPS surveys highlight that public health strategies focused on lifestyle changes are essential. Future policies must target cardiometabolic risk factors to mitigate the progression of steatotic liver disease.

THU-030

Impact of alternative VCTE diagnostic criteria on yearly prevalence estimates of MASLD and significant fibrosis

Carlos Martínez-Cabrera[1], Marcela Castillo-Medina[1], Graciela Torres-Mendoza[1], Luis Gutierrez-Rosas[1], Victor Montoya-Guzmán[1], Vanessa García-Rubio[1], María Fonticoba-Wood[1], FroyLan Martínez-Sánchez[1,2], Oscar Martínez-Barocio[1], Jessica Mayen-del Rio[1], Cynthia Sánchez-Villegas[3], Beatriz Barranco-Fragoso[4], Ruth Robles-Rodríguez[2], Fabiola Burciaga-Villalobos[5], Anibal de la Cruz-Lopéz[6], Raúl Méndez-Castillo[2], Gustavo García-Avelino[4], Ixchel Hernández-Ibarrola[7], Emilio Bermudez[8], Jacqueline Cordova-Gallardo[2], Liliana Tellez-Martínez[2], José Canela-Mayoral[3], Alma Ladrón de Guevara-Cetina[1]. [1]*Centro de Investigación y Gastroenterología, Mexico City, Mexico;* [2]*Secretaría de Salud, Mexico City, Mexico;* [3]*Instituto Mexicano del Seguro Social, Mexico City, Mexico;* [4]*Instituto de Seguridad y Servicios Sociales de los Trabajadores del Estado, Mexico City, Mexico;* [5]*Hospital San Ángel Inn, Mexico City, Mexico;* [6]*Hospital Star Médica, Mexico City, Mexico;* [7]*Clinica Mide San Juan de Aragon, Mexico City, Mexico;* [8]*Torre Médica Salaverry, Mexico City, Mexico*
Email: lauradelg@yahoo.com

Background and aims: Metabolic dysfunction–associated steatotic liver disease (MASLD) is the leading cause of chronic liver disease in Mexico, with reported prevalences approaching 50%. Vibration-controlled transient elastography (VCTE) is increasingly used for population screening, but multiple controlled attenuation parameter (CAP) and liver stiffness measurement (LSM) cutoffs are available. Although these thresholds show high diagnostic agreement, they may yield different prevalence estimates, and the consistency of longitudinal trends across definitions remains unclear. We assessed the impact of alternative VCTE criteria on yearly prevalence estimates of MASLD and significant fibrosis.
Method: We conducted a cross-sectional analysis of adults evaluated between 2022 and 2025 during free liver check-ups in the Mexico City Metropolitan Area. All participants underwent VCTE, and those with other chronic liver diseases were excluded. MASLD was defined as CAP-detected steatosis plus at least one cardiometabolic criterion, using alternative CAP cutoffs (≥275 and ≥288 dB/m). Significant fibrosis was assessed by LSM thresholds (≥7.0 and ≥8.2 kPa) among individuals with MASLD defined by CAP ≥288 dB/m. Annual prevalence estimates and longitudinal trends were compared across thresholds.
Results: 5184 adults were evaluated between 2022 and 2025, annual MASLD prevalence differed clearly according to diagnostic definition. Using CAP ≥275 dB/m, MASLD prevalence varied from 51.4% to 40% across years, whereas estimates using CAP ≥288 dB/m were consistently lower, between 44.3% and 31.4%. The absolute difference in MASLD prevalence between CAP cutoffs ranged from 7.1% to 8.6%. Despite these differences, the overall decline in prevalence was similar across definitions.
Significant fibrosis prevalence in MASLD also differed by liver stiffness threshold, with LSM ≥8.2 kPa yielding lower annual estimates compared with ≥7.0 kPa. Using LSM ≥7.0 kPa, prevalence varied from 22.8% to 21.3%, compared with 13.7% to 12.5% using ≥8.2 kPa. Absolute differences in fibrosis prevalence ranged from 9.1% to 8.8%, while relative prevalence differences varied from 40% to 41.4%. However, the general trend remained consistent across diagnostic criteria.
Conclusion: Prevalence estimates of MASLD and significant fibrosis vary meaningfully according to VCTE diagnostic thresholds, although longitudinal trends remain consistent across definitions, reflecting the impact of diagnostic criteria selection on population-level disease burden estimates.

THU-031

Clinical burden and risk stratification in metabolic dysfunction-associated steatohepatitis using Swedish real-world data

Hannes Hagström[1], Thomas Hambridge[2], Zuleika Aponte Torres[3], Alexandra Wennberg[4], Franziska Fischer[4], Emilie Toresson Grip[4], Jörn M. Schattenberg[5]. [1]*Karolinska Institutet, Department of Medicine, Huddinge, Stockholm, Sweden;* [2]*Boehringer Ingelheim, MIDI, Amsterdam, Netherlands;* [3]*Boehringer Ingelheim Pharmaceuticals, Inc., Ridgefield, United States;* [4]*Quantify Research AB, Stockholm, Sweden;* [5]*Saarland University Medical Center, Hamburg, Germany*
Email: hannes.hagstrom@ki.se

Background and aims: Metabolic dysfunction-associated steatohepatitis (MASH) is a severe form of metabolic dysfunction-associated steatotic liver disease (MASLD) that leads to increased risk of liver-related and cardiovascular outcomes. Liver biopsy remains the gold standard for diagnosis, but its invasiveness limits widespread use.

This study aims to characterise patients with biopsy-confirmed and presumed MASH in Sweden, and to assess the association between histological and non-invasive test (NIT) measures (e.g., Fibrosis-4 Index (FIB-4), Vibration-Controlled Transient Elastography (VCTE)) with long-term clinical outcomes.

Method: This observational study utilises a cohort of patients with presumed MASH identified via ICD-10 codes (K75.81) and/or elevated risk scores (FIB-4) and metabolic risk factors from the HERALD (HEalth outcomes and Risk Assessment in chronic Liver Disease) research platform. Descriptive statistics of baseline characteristics are presented, and survival analyses were performed to estimate incidence rates and cumulative incidence of major adverse liver outcomes (MALO), cardiovascular events (MACE) and mortality.

Results: At diagnosis, patients in the HERALD cohort with presumed MASH had mean age 63 years (SD 16) with mean 28.4 kg/m^2 (SD 8.9) BMI, and 50.2% were women. 85% of patients have data to calculate FIB-4 (n = 146,120): 35.1%, 23.8%, and 41.1% had low (age 35–64: <1.3; age: ≥65: < 2.0), intermediate (age 35–64:1.3–2.67: age: ≥65: 2.0–2.67), and high-risk (age ≥ 35: >2,67) of fibrosis, respectively. Among patients with available VCTE (n = 430), 53.3% had measures <8 kPa, 15.6% with 8-<12 kPa, and 31.2% with ≥12 kPa. Over median follow-up of 5.8 years, 1.9% of patients with presumed MASH had recorded MALO and 2.3% had a recorded diagnosis of cirrhosis. 24.2% of patients experienced a MACE outcome. 25.1% of patients died, where 0.6% of deaths were recorded as liver-related and 4.7% as cardiovascular-related.

Conclusion: This study provides real-world insights into use of FIB-4 and Fibroscan as risk stratification tools for MASH. While FIB-4 score could be widely available but still not automatically calculated, the use of Fibroscan could be expanded.

THU-035

Factors associated with engagement in hepatocellular carcinoma surveillance in a diverse urban population

Apoorva Hegde[1], Rachel Edwards[1], John Dempster[1], Yasmeen Cooper[1], Thomas Kynaston[1], Yusra Mashkoor[1], Sreedevi Rajalingam[1], Zinu Philipose[1], James Liu Yin[1]. [1]*Croydon University Hospital, London, United Kingdom*
Email: rachel.edwards38@nhs.net

Background and aims: Hepatocellular carcinoma (HCC) mortality is rising globally with a 5-year survival rate far below that of other cancers. HCC disproportionately affects racial and ethnic minority groups and socioeconomically deprived populations in whom healthcare discrimination may contribute to poorer outcomes. The survival rate is often affected by the late detection of HCC with some being deemed 'preventable'. Croydon University Hospital (CUH) serves a diverse population in London's most populous and deprived southern London borough with a large immigrant and refugee community. This study aimed to review post-COVID-19 HCC surveillance at CUH to identify factors contributing to non-attendance.

Method: We retrospectively reviewed electronic records of patients enrolled in HCC surveillance to assess attendance over a 3 year period. Demographic data collected included sex, ethnicity, first language, religion, deprivation indices, alcohol intake and liver disease aetiology. Deprivation deciles and ranks were sourced from national databases according to post code. Results were analysed with Excel and R studio.

Results: 310 patient records were reviewed, of which 58.4% were male, with a median age of 60 [IQR 52–68]. Deprivation deciles ranged between 1 and 10 across the cohort. Overall compliance with surveillance was 49.03% (n = 152). The odds of engaging with surveillance was nearly halved for patients who did not have English as a first language (OR 0.660, CI 0.30–1.48). No significant associations were observed with religion or ethnicity. Across all deciles of deprivation less than 10 the odds of attendance were significantly reduced. Ongoing alcohol intake was associated with reduced attendance (OR 0.627, CI 0.33–1.18). Viral liver disease aetiology was associated with lower odds of attendance (OR 0.379, CI 0.14–1.05) compared with ArLD (OR 0.655, CI 0.29–1.46).

Conclusion: In our diverse and socioeconomically deprived population our results identified several areas we can focus on to improve local uptake in HCC surveillance; those with language barriers, ongoing alcohol intake, higher levels of deprivation and viral liver disease. This work should be conducted locally in all hospitals to help individualise surveillance strategies to optimise uptake of this crucial aspect of liver care. This may also help challenge stereotypes and unconscious biases among healthcare professionals, widening access to surveillance in an effort to reduce health inequity.

THU-036

Cost-effectiveness of sequential non-invasive testing strategies to optimise hepatology referrals in MASLD: implications for primary care pathways

Marta Hernández Conde[1], David Marti-Aguado[2], Hugo José Disla[1], Elba Llop Herrera[1], Jesús Rivera Esteban[1], Paloma Lluch-García[2], Francisco Bernabeu[1], Marta López-Gómez[1], Javier Abad Guerra[1], Ana Royuela[1], Desamparados Escudero-García[2], José Luis Calleja Panero[1]. [1]*Hospital Universitario Puerta De Hierro Majadahonda, Majadahonda, Spain;* [2]*Hospital Clínico Universitario, Valencia, Spain*
Email: marta.hernandez.conde@gmail.com

Background and aims: The rapid increase in metabolic-associated steatotic liver disease (MASLD) poses a major challenge to healthcare systems, particularly regarding the efficient allocation of specialist hepatology resources. Primary care-based screening strategies must balance early detection of significant fibrosis (SF) with avoidance of unnecessary referrals. We assessed the cost-effectiveness of two sequential non-invasive testing (NIT) strategies for MASLD-related fibrosis, focusing on their impact on referral efficiency and healthcare resource use.

Method: Using data from 634 patients with MASLD, we developed a referral pathway model comparing 2 sequential algorithms applicable in primary care: (1) Fatty Liver Index (FLI) followed, when indicated, by the Enhanced Liver Fibrosis (ELF) test; and (2) FLI followed by FIB-4. In both strategies, patients with positive NIT results underwent transient elastography (TE), and those with SF (≥8 kPa) were referred to hepatology outpatient care. Costs were estimated from the perspective of the Madrid Regional Health System using 2023 public tariffs and included diagnostic assessment, follow-up, and specialist referrals.

The primary policy-relevant outcome was the number of unnecessary hepatology referrals (false positives after specialist evaluation) per-100 patients screened. Incremental cost per unnecessary referral avoided was calculated.

Results: Per 100 patients screened, the FLI→ELF strategy resulted in 24 unnecessary referrals at a total cost of €6,895, compared with 49 unnecessary referrals at a cost of €6,738 for the FLI→FIB-4 strategy. Adoption of FLI→ELF reduced avoidable referrals by 51%, with a modest incremental cost of €1,844, corresponding to €73.78 per unnecessary referral avoided. At scale, integration of FLI→ELF into MASLD care pathways would substantially reduce pressure on hepatology services while maintaining alignment with EASL-recommended stepwise risk stratification.

Conclusion: From a health system perspective, sequential screening with FLI→ELF in primary care improves the efficiency of hepatology referrals compared with FLI→FIB-4, at a very low incremental cost. These findings support the incorporation of ELF-based sequential algorithms into MASLD care pathways as a scalable and sustainable policy option to optimise specialist resource allocation where ELF testing is available. Further analyses should explore long-term budget impact and system-wide implementation outcomes.

THU-037

Global variation in standard drink definitions compared to the World Health Organization 10-gram benchmark: a 185-country analysis

Kriti Soni[1], Adelina Horhat[2], Ximena Parraga[1], Rylyn Reyes[3], Joshua Chen[4], Hyundam Gu[1], Luis Antonio Diaz[5], Juan Pablo Arab[1]. *[1]Division of Gastroenterology, Hepatology, and Nutrition, Department of Internal Medicine, Virginia Commonwealth University School of Medicine, Richmond, United States; [2]Université Paris-Est Créteil, Henri-Mondor University Hospital, Créteil, France; [3]Department of Epidemiology, Virginia Commonwealth University School of Public Health, Richmond, United States; [4]Department of Internal Medicine, Virginia Commonwealth University School of Medicine, Richmond, United States; [5]MASLD Research Center, Division of Gastroenterology and Hepatology, University of California, San Diego, United States*
Email: kriti.soni@vcuhealth.org

Background and aims: Alcohol consumption is a global public health concern, contributing substantially to morbidity and mortality worldwide. Despite international efforts to promote standardized alcohol metrics, definitions of standard drinks vary widely across countries, limiting epidemiological comparisons and policy evaluation. The WHO recommends a 10 g ethanol standard, yet global adherence to it, and its relationship with national drinking patterns, have not been systematically examined. To address this, we aimed to evaluate global variation in standard drink definitions across 185 countries, assess their alignment with the WHO 10 g benchmark, and examine how these definitions relate to alcohol consumption indicators.
Method: We analyzed data using the 2024 WHO Global Status Report on Alcohol and Health, the World Bank, the WHO Global Information System on Alcohol and Health, national guidelines, and published literature. Variables included standard GDP, definition of "standard drink" (grams of ethanol), per capita alcohol consumption (APC), beverage composition, prevalence of current drinking, and heavy episodic drinking (HED). Definitions were categorized as <10 g, 10–12 g, 12–14 g, 14–25 g, and >25 g. Countries were grouped by WHO region, and descriptive statistics and standardized heatmaps were generated to evaluate patterns.
Results: Among 185 countries, 60.9% (n = 109) lacked an official standard drink definition, while only 15.9% n = 29) aligned with the WHO 10 g benchmark. We identified a numeric standard drink definition for 39.1% (n = 70) countries; 2.2% (n = 4) were below, and 20.7% (n = 37) exceeded WHO guidelines. Standard drink definitions ranged widely (4–25 g). Regional mean values varied substantially, from 10 g in the African Region to 14 g in the Region of the Americas. The Eastern Mediterranean Region had the highest proportion of countries without a definition. Alcohol consumption patterns varied widely across regions. The European region recorded the highest total APC and HED despite WHO-aligned definitions, while the Eastern Mediterranean Region showed consistently low levels across all indicators.
Conclusion: Most countries lack an official definition; among those that have adopted one, the majority define a standard drink above the 10 g benchmark. This variation may limit risk communication, epidemiologic comparison, and policy development. Harmonizing standard drink definitions could strengthen global alcohol control strategies.

THU-038

Real-world epidemiology and clinical outcomes in MASLD: A 20-year nationwide analysis of over 23 million individuals in Taiwan's national health insurance research database

Huei-Tyng (Philippe) Huang[1], Chuan-Pin Lee[2], Laura Temperley[1], Yao-Hsu Yang[2,3,4], Liang-Yu Lin[5,6,7], William Alazawi[1]. *[1]Barts Liver Centre and Barts Metabolism Network, Blizard Institute, Queen Mary University of London, London, United Kingdom; [2]Health Information and Epidemiology Laboratory, Chang Gung Memorial Hospital, Chiayi, Taiwan; [3]Department of Traditional Chinese Medicine, Chang Gung Memorial Hospital, Chiayi, Taiwan; [4]School of Traditional Chinese Medicine, College of Medicine, Chang Gung University, Taoyuan, Taiwan; [5]Institute of Environmental and Occupational Health Sciences, College of Public Health, National Taiwan University, Taipei, Taiwan; [6]Global Health Program, College of Public Health, National Taiwan University, Taipei, Taiwan; [7]Department of Environmental and Occupational Medicine, National Taiwan University Hospital, Taipei, Taiwan*
Email: h.t.huang@qmul.ac.uk

Background and aims: MASLD is associated with increased risk of hepatic and extra-hepatic endpoints. However, most evidence originates from Western cohorts. The impact of MASLD on the unselected East Asian general population remains underexplored. We aimed to determine the prevalence and long-term outcomes of MASLD using Taiwan's National Health Insurance Research Database (NHIRD), which includes over 99% of the population, to bridge these knowledge gaps.
Method: This real-world evidence study used NHIRD data between 2003 and 2022. We identified individuals with MASLD diagnosis using medical codes. Patients with <1 year of follow-up post-NHIRD registration, age <18, or who had pre-existing autoimmune and alcoholic liver disease were excluded. We calculated the point prevalence and analysed time-to-event for cirrhosis, hepatocellular carcinoma (HCC), acute myocardial infarction (AMI), stroke, and chronic kidney disease (CKD). Controls were matched at a 1:4 ratio; those with a prior endpoint were excluded from endpoint analysis.
Results: Over 23 million individuals were active in NHIRD in 2022. We identified 1,304,409 MASLD patients: median age 50, 54.7% male, with high rates of type 2 diabetes (26.7%) and hypertension (39.0%). Recorded prevalence increased by more than 3-fold, from 1.9% in 2003 to 6.31% in 2022 ($p < 0.001$). Clinical outcomes were recorded over a median follow-up of 8.4 to 8.8 years. Incidence rates (per 1000 person-years) for cirrhosis and HCC in the MASLD cohort were 3.8 (95% CI: 3.7–3.8) and 2.2 (95% CI: 2.1–2.2); for AMI 2.2 (95% CI: 2.2–2.3), stroke 6.2 (95% CI: 6.1–6.2) and CKD 12.4 (95% CI: 12.3–12.4). After adjusting for common, known risk factors, MASLD was strongly associated with cirrhosis (aHR 2.68, 95% CI: 2.64–2.71) and HCC (aHR 2.30, 95% CI: 2.25–2.34). Risks for stroke (aHR 1.07, 95% CI: 1.05–1.08) and CKD (aHR 1.13, 95% CI: 1.12–1.14) were also elevated albeit modestly. Notably, MASLD was not associated with an independent increased risk for AMI (aHR 0.93, 95% CI: 0.92–0.95) after adjustment for comorbidities and deprivation index.
Conclusion: This 20-year study provides a population-level depiction of MASLD in an East Asian population. While the recorded prevalence is rising sharply, significant under-diagnosis likely persists. MASLD is an independent risk factor for cirrhosis, HCC, stroke, and CKD. However, its association with AMI was not observed in this study after adjustment.

THU-039

Outcomes and all-cause mortality in people with MASLD in UK primary care: a real-world matched cohort study of 1.8 million individuals

Huei-Tyng (Philippe) Huang[1], Michael Hewitt[1], Wenhao Li[1], Laura Temperley[1], Naveed Sattar[2], William Alazawi[1]. *[1]Barts Liver Centre and Barts Metabolism Network, Blizard Institute, Queen Mary University of London, London, United Kingdom; [2]School of Cardiovascular and Metabolic Health, BHF Glasgow Cardiovascular Research Centre, University of Glasgow, Glasgow, United Kingdom*
Email: h.t.huang@qmul.ac.uk

Background and aims: MASLD is a leading cause of chronic liver disease and often progresses to hepatic outcomes of cirrhosis and liver tumours. It is associated with extra-hepatic outcomes such as cardiovascular disease. We aimed to estimate the risk of hepatic and extra-hepatic outcomes and mortality in patients with MASLD compared with controls in the UK primary care real-world Clinical Practice Research Datalink (CPRD).

Method: We identified individuals with recorded MASLD diagnosis (using NAFLD as a proxy) between 2003 and 2022. Patients with a recorded diagnosis of MASLD were followed up for the incidence of outcomes: cirrhosis, liver tumour, acute myocardial infarction (AMI), stroke, chronic kidney disease (CKD), and all-cause mortality. Hazard ratios (HR) were estimated using Cox models and adjusted for sex, age, ethnicity, smoking, excess alcohol use, and history of hypertension and type 2 diabetes (T2DM), body mass index (BMI), cholesterol and QRISK2 score. Controls were matched 1:4 on sex, age (±5 years), and general practice.
Results: We identified 365,797 patients with recorded MASLD and 1,463,188 controls. MASLD patients were more likely to have T2DM, hypertension, smoking history, and excess alcohol use than matched controls (all $p < 0.001$). Over a median follow-up of 4.8 to 5.3 years, crude incidence rates (per 1000 person-years) in the MASLD cohort were: cirrhosis 3.3 (95% CI: 3.2–3.3), liver tumours 0.3 (95% CI: 0.3–0.3), AMI 2.1 (95% CI: 2.0–2.2), stroke 0.6 (95% CI: 0.6–0.7), CKD 7.0 (95% CI: 6.9–7.1) and all-cause mortality 8.7 (95% CI: 8.6–8.9). The cumulative unadjusted incidences of all outcomes were more common in people with MASLD and hypertension or T2DM and were most common in people with both. In people with MASLD, compared to controls, the fully-adjusted HRs for outcomes were: cirrhosis 3.4 (95% CI: 3.0–3.8), liver tumours 1.4 (95% CI: 0.9–2.1), AMI 1.0 (95% CI: 0.9–1.2), stroke 1.0 (95% CI: 0.8–1.3), CKD 1.5 (95% CI: 1.0–1.1), and all-cause mortality 0.9 (95% CI: 0.8–0.9).
Conclusion: This 20-year real-world evidence shows that a recorded diagnosis of MASLD increases the risk of hepatic and extra-hepatic outcomes and mortality. The impact of common comorbidities emphasises the need for specific integrated care pathways for patients at higher risk.

THU-040

Healthcare provider perspectives on mental health in metabolic dysfunction-associated steatotic liver disease and steatohepatitis: the role of multidisciplinary teams and sex differences

Dana Ivancovsky-Wajcman[1], Marcela Villota-Rivas[1], Melina Manolas[2], Vanessa Villas-Riotorto[3], Anish Arora[4], Paul N. Brennan[5], Didac Mauricio[6], Damien Leith[5], José Willemse[7], Michael Betel[8], Faisal Alnaser[9,10], Mohamed El Kassas[11], Jeffrey Lazarus[12]. *[1]Barcelona Institute for Global Health (ISGlobal), Barcelona, Spain; [2]Department of Endocrinology, Diabetes & Metabolism, Weill Cornell Medicine, New York, United States; [3]Faculty of Medicine and Health Sciences, University of Barcelona, Clinical Health Psychology Section, Hospital Clínic, Barcelona, Spain; [4]Department of Health Sciences, Wilfrid Laurier University, Waterloo, Canada; [5]University of Dundee, Division of Molecular and Clinical Medicine, School of Medicine, Dundee, United Kingdom; [6]Department of Endocrinology & Nutrition, CIBERDEM, Hospital de la Santa Creu i Sant Pau, Faculty of Medicine, University of Vic/Central University of Catalonia, Barcelona, Spain; [7]Liver Patients International, Brussels, Belgium; [8]Fatty Liver Alliance, Toronto, Ontario, Canada; [9]Bahrain Family Physicians Association, Manama, Bahrain; [10]Imperial College London, Primary Care & Public Health, London, United Kingdom; [11]Endemic Medicine Department, Faculty of Medicine, Capital University, Cairo, Egypt; [12]Barcelona Institute for Global Health (ISGlobal), Faculty of Medicine and Health Sciences, University of Barcelona (UB), City University of New York Graduate School of Public Health and Health Policy (CUNY SPH), New York, New York, USA, Barcelona, Spain*
Email: danaivanc@gmail.com

Background and aims: Mental health (MH) comorbidities are increasingly recognised in metabolic dysfunction–associated steatotic liver disease (MASLD) and steatohepatitis (MASH), yet the implementation of MH interventions in routine care remains poorly understood. We assessed healthcare providers' (HCPs) attitudes toward MH intervention provision (MHIP), identified key facilitators, and explored sex differences.
Method: A 22-item survey, including demographic information, was distributed globally to MASLD/MASH HCPs. Attitudes toward MHIP were assessed using 6 statements rated on a Likert scale (0 = strongly disagree, 4 = strongly agree). Statements with >75% agreement (agree/strongly agree) were considered to reflect high consensus. Responses were summed into an overall attitude score, with a positive attitude defined as a score above the sample median (>15). HCPs also identified up to 3 key facilitators of MHIP and factors enhancing patient engagement. Stepwise logistic regression was used to identify predictors of a positive MH attitude.
Results: From 262 responders (36.7% females), 61.0% reported working within a multidisciplinary team (MDT). Only 2 statements achieved high consensus: MH impacts MASLD/MASH outcomes (87.0%), with higher agreement among HCPs who worked in a MDT (90.7% vs 81.8%, P = 0.037), and MH specialists should be in the MDT (81.9%), with higher agreement among females (87.9% vs 77.4%, p = 0.036). Working in a MDT was the only factor that predicted a positive attitude toward MHIP (OR = 4.44, 95% CI 2.55–7.74). Setting-related factors (e.g., longer counselling time) and working in a MDT were identified as the main facilitators for MHIP (69.1% and 57.6%, respectively). In sex-stratified analysis, males more often identified the availability of evidence supporting MH interventions as a key facilitator (47.8% vs 25.3%, $p < 0.001$), while females more frequently identified MDT involvement (67.7% vs 50.3%, p = 0.006). 64.5% and 67.6% of HCPs believed that patient education and multidisciplinary care would enhance patient engagement with MH services, respectively.
Conclusion: Working in a MDT fosters a more positive attitude toward MH integration, particularly among females. Structural barriers affect both sexes, while the perceived lack of evidence primarily limits MHIP among males. Addressing these barriers, strengthening MDT collaboration, and generating robust evidence on the effectiveness of MH interventions are essential steps to improve integration and patient engagement in MASLD/MASH care.

THU-041

Factors influencing mental health care provision for people with metabolic dysfunction-associated steatotic liver disease and steatohepatitis

Dana Ivancovsky-Wajcman[1], Marcela Villota-Rivas[1], Melina Manolas[2], Vanessa Villas-Riotorto[3], Anish Arora[4], Paul N. Brennan[5], Didac Mauricio[6], Damien Leith[5], José Willemse[7], Michael Betel[8], Faisal Alnaser[9], Mohamed El Kassas[10], Jeffrey Lazarus[11]. *[1]Barcelona Institute for Global Health (ISGlobal), Barcelona, Spain; [2]Department of Endocrinology, Diabetes & Metabolism, Weill Cornell Medicine, New York, United States; [3]Faculty of Medicine and Health Sciences, University of Barcelona, Clinical Health Psychology Section, Hospital Clínic, Barcelona, Spain; [4]Department of Health Sciences, Wilfrid Laurier University, Waterloo, Canada; [5]University of Dundee, Division of Molecular and Clinical Medicine, School of Medicine, Dundee, United Kingdom; [6]Department of Endocrinology & Nutrition, CIBERDEM, Hospital de la Santa Creu i Sant Pau, Faculty of Medicine, University of Vic/Central University of Catalonia, Barcelona, Spain; [7]Liver Patients International, Brussels, Belgium; [8]Fatty Liver Alliance, Toronto, Ontario, Canada; [9]Bahrain Family Physicians Association, Manama, Bahrain; [10]Endemic Medicine Department, Faculty of Medicine, Capital University, Cairo, Egypt; [11]Barcelona Institute for Global Health (ISGlobal), Faculty of Medicine and Health Sciences, University of Barcelona (UB), City University of New York Graduate School of Public Health and Health Policy (CUNY SPH), New York, New York, USA, Barcelona, Spain*
Email: danaivanc@gmail.com

Background and aims: Metabolic dysfunction-associated steatotic liver disease (MASLD) and metabolic dysfunction-associated steatohepatitis (MASH) are linked with mental health (MH) challenges, which may limit patient engagement in treatment. However, MH is rarely addressed in clinical guidelines or practice. We aimed to assess

MH intervention provision (MHIP) by healthcare providers (HCPs) in MASLD/MASH care and identify factors influencing this.
Method: An expertly developed and validated survey, including a demographics questionnaire and 22 items, was distributed to MASLD/MASH HCPs worldwide via Qualtrics XM. As part of this survey, MHIP was assessed by asking how often MH interventions were recommended, using a 0–5 Likert scale (0 = never, 5 = more than once a week), with anonymous rankings summed to an overall MHIP score. Interventions recommended at least weekly by >75% of HCPs were defined as highly recommended. MHIP self-efficacy (SE) was assessed using 4 questions via a 0–4 Likert scale (0 = strongly disagree, 4 = strongly agree), with responses summed to an overall SE score. High MHIP and SE were defined as scores above the sample median (>33.5, >11, respectively). Stepwise forward regression was used to identify predictors of high MHIP (SPSS 31). A $p < 0.050$ was considered significant.
Results: Of 286 eligible HCPs, 262 (91.6%) completed the survey and were included in the analysis. Mean age was 52.7 (SD: 10.9) years and 36.7% were female. Dietary modifications (85.1%) and exercise (84.4%) were the only highly recommended interventions. Cronbach's alpha for MHIP and SE questions was 0.910 and 0.792, respectively. MHIP correlated with SE ($r = 0.372$, $p < 0.001$). Being female (OR = 3.42, 95% CI 1.87–6.25, $p < 0.001$), having high SE (OR = 2.96, 1.67–5.26, $p < 0.012$), and working within a multidisciplinary team (OR = 3.30, 1.80–6.03, $p < 0.001$), specifically with a mental health expert (psychiatrist, psychologist, social worker, behavioral change expert) (OR = 5.03, 1.84–13.77, $p = 0.002$), were associated with high MHIP. Working within a multidisciplinary team (OR = 2.38, 1.36–4.18, $p = 0.002$) or in a low- or middle-income country (OR = 2.37, 1.32–4.26, $p = 0.004$) and having MH training (OR = 1.85, 1.02–3.37, $p = 0.043$) were associated with high SE.
Conclusion: MHIP is modest overall but strongly influenced by provider SE and team-based care. Targeted training and interdisciplinary collaboration could help close the gap between MH needs and current clinical practice and improve MASLD/MASH care.

THU-042-YI
Mental distress and social support in adult offspring of parents with alcohol-related liver disease compared to offspring of parents with a cancer diagnosis: a national health survey
Pernille Jessen[1], Jonas Hedelund Rønn[1], Lone Galmstrup Madsen[1], Peter Jepsen[2], Marie Eliasen[3], Gro Askgaard[1]. [1]*Zealand University Hospital, Koege, Denmark;* [2]*Aarhus University Hospital, Aarhus, Denmark;* [3]*Center for Clinical Research and Prevention, Bispebjerg Hospital, Copenhagen, Denmark*
Email: ptoj@regionsjaelland.dk

Background and aims: Offspring of parents with alcohol-related liver disease (ALD) are prone to mental distress and research into support options might be relevant, like the growing field for support options for cancer-offspring. We compared mental distress and social support in offspring of parents with ALD with offspring of parents with cancer and with controls.
Method: Data for this cross-sectional study came from the Danish National Health Surveys 2013–2021 with questions on mental and physical health-related quality of life (HRQoL) by the Short Form-12, Cohens Perceived Stress Scale, depressive and anxiety symptoms, sleep difficulties, perceived social support and loneliness. Information on parental ALD and cancer diagnoses came from national registers. Offspring of parents with ALD were matched randomly by age, sex, and years since parental diagnosis 1:5:5 with offspring of parents with cancer and controls. We used conditional logistic regression to estimate odds ratios (OR) for mental distress and social support adjusted for age and sex, overall and stratified by years since parents' diagnosis.
Results: The study included respondents of which 3216 were ALD-offspring, 16,303 were cancer-offspring and 16,305 were controls of which 45% was men and mean age was 44 years. Time since parents' diagnosis was <2 years in 6% ALD/cancer-offspring, 2–4 years for 12% offspring, 5–10 years for 23% offspring, and >10 years for 59% offspring. For ALD-offspring, cancer-offspring and controls, low mental HRQoL was experienced by 11.4%, 9.8%, and 8.8% and low social support by 15.6%, 13.4%, and 14.2%, respectively. Adjusted OR were higher in ALD-offspring vs. cancer-offspring and in ALD-offspring vs. controls for low mental HRQoL, high perceived stress, anxiety symptoms, depressive symptoms, sleep difficulties, low social support and loneliness but not for physical HRQoL. For example, OR for low mental HRQoL in ALD-offspring was 1.19 (95% CI: 1.05–1.35) compared to cancer-offspring and 1.34 (1.19–1.51) compared to controls and for low social support it was 1.19 (1.07–1.32) and 1.12 (1.00–1.24), respectively. Stratified analyses indicated that mental distress was equally frequent in ALD- and cancer-offspring in the first years after parental diagnosis and more frequent in ALD offspring beyond 2 years.
Conclusion: Offspring of parents with ALD report mental distress more often than offspring of parents with cancer and controls. These findings emphasize the need for a support system for offspring of parents with ALD.

THU-043
Neighborhood deprivation and survival in hospitalized alcoholic hepatitis: a ZIP-code based area deprivation index analysis
Samuel Ji[1], Lankai Xu[1], Maria Aguilar[1], Albert Do[1], Lydia Aye[1], Vikrant Rachakonda[1]. [1]*University of California Davis Medical Center, Sacramento, United States*
Email: vrachakonda@health.ucdavis.edu

Background and aims: Alcohol-associated hepatitis (AH) carries high short-term mortality, but the impact of neighborhood deprivation on outcomes is unclear. We evaluated whether higher Area Deprivation Index (ADI) is associated with survival and eadmissions in AH.
Method: This was a single-center retrospective cohort study of adults admitted with AH to UC Davis Medical Center from July 2017 to September 2024. Clinical, demographic and laboratory data were obtained at admission. Block-group ADI from the Neighborhood Atlas was aggregated to patient ZIP codes using the HUD–USPS ZIP–tract crosswalk. Patients were grouped into ZIP-level ADI quintiles (Q1 least deprived, Q5 most deprived). Straight-line distance from patient ZIP to hospital ZIP was calculated from ZIP centroids. Overall survival was assessed with Cox proportional hazards models and AH readmission with logistic regression.
Results: 582 AH patients were included. Median age was 45 (IQR 37–55) years, median MELD 3.0 was 26 (IQR 21–31), and median BMI was 27.6 (IQR 23.9–32.1) kg/m^2. Age, MELD and BMI were similar across ADI quintiles, but there were more female, English-speaking, and Caucasian patients in lower ADI quintiles (all $p \leq 0.001$). Gastrointestinal bleeding (GIB), intensive care unit (ICU) admission, and AH readmissions were more common in higher-deprivation quintiles ($p = 0.038$, 0.044 and 0.037, respectively), and higher-deprivation patients received fewer prescriptions for alcohol use disorder (AUD) pharmacotherapy at hospital discharge ($p \leq 0.001$). Mean survival decreased stepwise from 407 days (95% CI 373–440 days) in Q1 to 135 days (123–147 days) in Q5. In Cox models, Q5 deprivation quintile was associated with increased mortality in univariable analysis (HR 1.81, 95% CI 1.07–3.04; $p = 0.026$) and remained independently associated with mortality after adjustment (aHR 2.31, 1.36–3.95; $p = 0.002$), along with age, MELD 3.0, GIB and ICU admission. Distance from the hospital was not associated with survival ($p = 0.910$). In multivariable logistic regression models for AH readmission, ADI Q3 had higher odds than Q1 (OR 2.55, 1.23–5.30; $p = 0.012$).
Conclusion: In this cohort, residence in the most deprived neighborhoods was associated with substantially shorter survival and greater risk of AH readmission, independent of MELD and acute illness severity. ADI may help identify socially vulnerable AH patients

who warrant intensified follow-up and targeted post-discharge interventions.

THU-044

Evaluation of metabolic dysfunction-associated steatotic liver disease in agricultural workers exposed and unexposed to Mancozeb

Hidayat Kassim[1], Dvora Joveleviths[2], Vittoria Sampaio[3], Isabela Carvalhal[4], Nelson Suarez Uribe[3], Raquel Boff[3], Tiago Onofrio Soares[4], Theo Futuro Telöken[5], Ana Lazzari[3], Camila Pereira Baldin[3], Sheila De Castro Cardoso Toniasso[3], Gabriela Nardy Vasconcellos[3], Patricia Riedel[3], Eduardo Klein[3].
[1]UFRGS - HCPA, Ministry of health Mozambique - Health Department Zambezia Province, Porto Alegre, Brazil; [2]UFRGS - HCPA, Porto Alegre, Brazil; [3]UFRGS, Porto Alegre, Brazil; [4]PUC RS, Porto Alegre, Brazil; [5]Universidade Vale de Rio Sinus, Porto Alegre, Brazil
Email: hidayatkassim@hotmail.com

Background and aims: Mancozeb is a widely used agricultural fungicide with potential hepatotoxic effects and metabolic dysfunction-associated steatotic liver disease (MASLD) is highly prevalent in the general population. Few studies have evaluated the direct effects of Mancozeb on liver, hormonal, and metabolic parameters in humans. The investigation of this association may improve the understanding of environmental factors involved in disease progression. This study aimed to compare liver profile (fibrosis index-4, FIB-4), hormonal parameters (thyroid-stimulating hormone [TSH], free thyroxine [FT4], and C-peptide), and metabolic markers (homeostasis model assessment of insulin resistance [HOMA-IR], glycated hemoglobin [HbA1c], and lipid profile) between individuals chronically exposed to Mancozeb and unexposed individuals, all meeting metabolic criteria for MASLD.
Method: This cross-sectional study included 92 participants from Veranópolis, Brazil (46 exposed and 46 unexposed). Groups were compared using statistical tests ($p<0.05$), with sample power of 70% and significance level of 5%.
Results: HOMA-IR values were similar between groups (2.46 vs. 2.6), indicating adequate matching. Higher liver fibrosis risk was observed among exposed individuals, with higher mean FIB-4 values (1.38 vs. 1.12) and FIB-4>2.67 in.4% of exposed participants, absent in unexposed individuals. The unexposed group had more low-risk individuals (31 vs. 24), whereas the exposed group had more individuals at increased fibrosis risk (22 vs. 15). Mean TSH levels were slightly higher in exposed individuals (2.7 µIU/mL vs. 1.9 µIU/mL), while FT4 levels were similar. HbA1c showed no difference, with mean values of 5.5% in both groups. C-peptide levels were comparable (2.4 ng/mL vs. 2.3 ng/mL). Exposed individuals showed lower total cholesterol (192.9 mg/dL vs. 215 mg/dL) and triglycerides (138.1 mg/dL vs. 163.2 mg/dL), likely related to higher occupational physical activity.
Conclusion: Chronic exposure to Mancozeb may be associated with increased hepatic fibrosis risk and subclinical thyroid axis alterations in individuals with cardiometabolic criteria for MASLD, independent of classical metabolic differences. These findings highlight the importance of periodic clinical monitoring, reduction of occupational exposure, and further longitudinal studies.

THU-045

Drivers and precipitators of acute-on-chronic liver failure and acute decompensation in a real-world cirrhotic cohort

Niv Zmora[1], Dor Shirin[1], Helena Katchman[1]. *[1]Ichilov Sourasky Hospital, Tel Aviv-Yafo, Israel*
Email: nivz@tlvmc.gov.il

Background and aims: Acute-on-chronic liver failure (ACLF) and acute decompensation (AD) are critical milestones in cirrhosis progression. While clinical definitions are established, precipitating events and phenotypic expressions vary across populations. We aimed to characterize the clinical, laboratory, and pharmacological profiles of patients with cirrhosis admitted to a tertiary center, comparing those with ACLF, AD, and stable cirrhosis (SC).
Method: Data were extracted from a prospective cohort study (CLEARED Consortium) of non-electively admitted patients with cirrhosis at the Tel-Aviv Sourasky Medical Center (2023–2025). Patients were stratified into ACLF, AD, and SC. Data were analyzed using one-way ANOVA for continuous variables and Fisher's exact test for categorical variables.
Results: The cohort included 92 patients (mean age 63.9 years, 41.3% female). Primary etiologies were MASH (34.7%), HCV (23.9%) and alcohol-associated liver disease (17.3%). 41 (44.5%) had ACLF, 28 (30.4%) had AD, and 23 (25%) were SC.

- Severity scores: ACLF patients had higher MELD-Na scores (20.4) vs. AD (13.5) and SC (13.9; $p < 0.0001$). Child-Pugh scores were also higher in ACLF (8.6) vs. SC (6.7; $p = 0.0004$).
- Hospitalization drivers: Admissions triggered by infection were more frequent in ACLF (and SC) vs. AD (34.1% and 31.8% vs. 7.1%; $p = 0.021$). All infection-triggered AD cases were due to spontaneous bacterial peritonitis (SBP). SBP accounted for 50% of infection-triggered ACLF, while 0% of the SC group had SBP ($p = 0.012$).
- Clinical presentation: Liver-related admission drivers were more frequent in ACLF and AD than SC (75.6% and 89.2% vs. 42.8%; $p = 0.0004$). AD was characterized by higher GI bleeding prevalence (36.0% vs. 12.5% in ACLF; $p = 0.046$), while ACLF was associated with acute kidney injury (33.3% vs. 4.0% in AD; $p = 0.016$).
- Pharmacotherapy: Non-selective beta-blocker use was more prevalent in ACLF (73.2%) and AD (59.3%) vs. SC (23.8%; $p = 0.0006$). Statin use was higher in AD (35.7%) compared to ACLF (17.1%) and SC (4.8%; $p = 0.007$).

Conclusion: Our findings underscore the pathophysiological pathways leading to hospital admission in cirrhosis. Infection serves as a dominant trigger for ACLF, more than for acute decompensation. SBP emerges as a potent catalyst for acute deterioration (either AD or ACLF) rather than a feature of stable cirrhosis. These results suggest that early infectious screening is paramount in hospitalized patients with cirrhosis in preventing the transition to life-threatening ACLF.

THU-046

Association between neck circumference and steatotic liver disease: a systematic review and meta-analysis

Cecilia Katzenstein[1], Regina Longley[1], Nina Rodriguez[1], Jacqueline Slobin[1], Tatyana Kushner[2]. *[1]Icahn School of Medicine at Mount Sinai, New York, United States; [2]Weill Cornell Medicine, New York, United States*
Email: cecilia.katzenstein@icahn.mssm.edu

Background and aims: Neck circumference (NC) reflects visceral adiposity, yet is rarely used in clinical practice. BMI fails to capture fat distribution, and waist circumference can be unreliable in contexts such as obesity, pregnancy, abdominal distension, certain ethnicites, and childhood. NC is simple and reproducible, yet the extent to which it correlates with steatotic liver disease (SLD) remains unclear. We conducted a systematic review and meta-analysis to examine this association across studies using imaging, biochemical, and histological assessments.
Method: PubMed, Embase, Scopus, and Web of Science were searched through October 2025 using a librarian-reviewed strategy. Studies reporting NC in participants with and without SLD, or reporting correlations between NC and SLD were included. Two reviewers independently screened and extracted data. Adjusted odds and hazard ratios were pooled as generic relative effects (RE), and mean NC differences were summarized as standardized mean differences (SMD) using random-effects models. Leave-one-out analyses tested robustness.
Results: Of 337 studies, 39 (n = 67,395) were included. Studies were comprised of community or national (14; 36%), workplace (8; 21%), and clinical cohorts (17; 44%) across 15 countries in Asia (18, 51%), Europe (9, 23%), the Americas (8, 21%), and the Middle East (4, 10%).

Pediatric cohorts accounted for 4 studies (10%). Individuals with SLD had a higher NC than those without (pooled RE = 1.64, 95% CI 1.35–1.99; I2 = 72%). The association remained significant in subgroup analyses of adults (1.58, 1.30–1.92; I2 = 69%), children (2.56, 1.74–3.76; I2 = 61%), women (1.84, 1.42–2.39; I2 = 66%) and men (1.97, 1.30–2.98; I2 = 64%). In studies reporting group means, NC was higher in SLD than non-SLD (SMD = 1.08, 95% CI 0.84–1.32; I2 = 69%). Several studies found NC to be independently associated with SLD after adjustment for BMI and waist measures. Effects were consistent across ultrasound (ORs 1.3–2.5) and CAP-based (AUC 0.65–0.82) assessments. Biopsy-based studies demonstrated clear associations with steatosis but inconsistent findings for fibrosis. No single study altered pooled results.
Conclusion: NC is consistently associated with SLD across populations and SLD diagnostic methods. The magnitude of association is clinically meaningful and often independent of overall adiposity. NC measurement is quick, inexpensive, and reproducible, and may serve as a practical tool for SLD screening and risk-stratification.

THU-047

Effectiveness of a smartphone-assisted lifestyle intervention program on weight reduction: a retrospective study

Stanislav Kravchuk[1], Mykola Bychkov[1]. [1]*Danylo Halytsky Lviv National Medical University, Lviv, Ukraine*
Email: kravchuck.stanislav@gmail.com

Background and aims: Overweight, obesity, and metabolic dysfunction-associated steatotic liver disease (MASLD) remain pressing public health concerns, particularly among women of reproductive and working age. Mobile health (mHealth) programs that integrate nutritional, psychological, and behavioral components offer a scalable approach to promote sustainable lifestyle changes. This study aimed to evaluate the effectiveness of The Body School – a 3-month, smartphone-assisted lifestyle intervention combining dietary counseling, health education, guided cooking, and psychological support – in improving anthropometric outcomes among women with overweight and obesity.
Method: A retrospective analysis was conducted using data from 101 women who completed the program between 2023 and 2024. The program combined nutrition support through a mobile app, educational modules, psychological support, and physical activity recommendations. The primary outcomes were changes in body weight, body mass index (BMI), and waist- to-hip ratio (WHR), self-recorded by participants in the app. The Wilcoxon signed-rank test was used for statistical analysis ($p < 0.001$).
Results: The program resulted in a statistically significant reduction in all primary anthropometric indicators: median weight loss was 4.0 kg (–5%), BMI decreased by 1.83 kg/m^2, and WHR by 0.016.
Conclusion: The Body School smartphone-assisted lifestyle program resulted in significant reductions in body weight, BMI, and WHR among women with overweight, with a mean participant age of 36.9 years. These findings highlight the program's potential as an effective digital tool for comprehensive, multidisciplinary weight management in different metabolic pathologies, including MASLD.

THU-050

Assessing Europe's policy readiness to confront the MASLD/MASH public health threat

Trenton M White[1], Leire Agirre-Garrido[1], Kushala Abeysekera[2], Paul N. Brennan[3], Radan Bruha[4], Stefan Buttigeig[5], Patrizia Carrieri[6], Helena Cortez-Pinto[7], Robert Flisiak[8], Sven Francque[9], Gema Frühbeck Martinez[10], Liana Gheorghe[11], Hannes Hagström[12], A.G. (Onno) Holleboom[13], Mojca Jensterle[14], Peter Jepsen[15], Juozas Kupčinskas[16], Henry E Mark[17], Didac Mauricio[18], Saba Mohamed Bibi[1], Christophe Moreno[19], Anna Mrzljak[20], Eleni Papanicolaou[21], George Papatheodoridis[22], Markus Peck-Radosavljevic[23], Nicola Pugliese[24], John Ryan[25], Rogerio Ribeiro[26], Riina Salupere[27], Lubomir Skladany[28], Ieva Tolmane[29], Hannele Yki-Jarvinen[30], Jörn M. Schattenberg[31], Juan M. Pericàs[32], Jeffrey Lazarus[1]. [1]*Barcelon Institute for Global Health (ISGlobal), Barcelona, Spain;* [2]*Bristol Medical School, University of Bristol, Bristol, United Kingdom;* [3]*The University of Dundee, Dundee, United Kingdom;* [4]*Charles University, Prague, Czech Republic;* [5]*Ministry for Health and Active Ageing, Valleta, Malta;* [6]*Aix Marseille University, Inserm, IRD, SESSTIM, Sciences Economiques & Sociales de la Santé & Traitement de l'Information Médicale, Marseille, France;* [7]*Universidade de Lisboa, Faculdade de Medicina, Libon, Portugal;* [8]*Department of Infectious Diseases and Hepatology, Medical University of Bialystok, Bialystok, Poland;* [9]*Department of Gastroenterology and Hepatology, Antwerp University Hospital, University of Antwerp, Antwerp, Belgium;* [10]*Metabolic Research Laboratory, Clínica Universidad de Navarra, Pamplona, Spain;* [11]*Center for Gastroenterology, Hepatology and Liver Transplantation; Fundeni Clinical Institute, Bucharest, Romania;* [12]*Department of Medicine, Huddinge, Karolinska Institutet, Stockholm, Sweden;* [13]*Amsterdam UMC, Location AMC, Dept of Vascular Medicine, University of Amsterdam, Amsterdam, Netherlands;* [14]*Department of Endocrinology, Diabetes and Metabolic Diseases, University Medical Centre Ljubljana, Ljubljana, Slovenia;* [15]*Department of Hepatology and Gastroenterology, Aarhus University Hospital, Aarhus, Denmark;* [16]*Department of Gastroenterology and Institute for Digestive Research, Lithuanian University of Health Sciences, Kaunas, Lithuania;* [17]*Barcelona Institute for Global Health (ISGlobal), Barcelona, Spain;* [18]*Department of Endocrinology and Nutrition, Hospital de la Santa Creu i Sant Pau, Barcelona, Spain;* [19]*Department of Gastroenterology, Hepatopancreatology and Digestive oncology, CUB Hôpital Erasme, Université Libre de Bruxelles, Bruselles, Belgium;* [20]*Department of Gastroenterology and Hepatology, University Hospital Center Zagreb, Zagreb, Croatia;* [21]*Department of Internal Medicine, Nicosia General Hospital, SHSO (OKYPY), Nicosia, Cyprus;* [22]*Medical School of National & Kapodistrian University of Athens, Athens, Greece;* [23]*Klinikum Klagenfurt, Klagenfurt, Austria;* [24]*Division of Internal Medicine and Hepatology, Department of Gastroenterology, IRCCS Humanitas Research Hospital, Milan, Italy;* [25]*Beaumont Hospital/RCSI University of Medicine and Health Sciences, Dublin, Ireland;* [26]*Department of Research and Innovation, APDP Diabetes Portugal, Lisbon, Portugal;* [27]*Tartu University Hospital, University of Tartu, Tartu, Estonia;* [28]*HEGITO Liver Transplant Unit, F. D. Roosevelt Teaching Hospital, Banská Bystrica, Slovakia;* [29]*Faculty of medicine and Life Science, University of Latvia, Latvia, Lithuania;* [30]*Helsinki University Hospital, Helsinki, Finland;* [31]*Department of Internal Medicine II, Saarland University Medical Center, Homburg, Germany;* [32]*Liver Unit, Vall d'hebron University Hospital, Vall d'hebron Institute for Research, Universitat Autònoma de Barcelona, CIBERehd, Barcelona, Spain*
Email: Jeffrey.Lazarus@isglobal.org

Background and aims: Metabolic dysfunction-associated steatotic liver disease (MASLD) is closely linked to obesity and type 2 diabetes, being now the second most common chronic liver disease in Europe, yet largely absent from policy agendas, exposing a major gap in Europe's metabolic health response. This study aimed to provide the evidence on national policies and clinical practice guidelines (CPGs) for MASLD/metabolic dysfunction-associated steatohepatitis (MASH) in Europe.
Method: MASLD/MASH policies (i.e., government strategies/action plans and CPGs) were reviewed in 25 European countries (in the European Union (EU) and the United Kingdom) and reported via a standardised data collection tool completed by a country lead. Each country's data-collection tool was reviewed by a core study team of three researchers and cross-referenced with public documents in any language to ensure accuracy.
Results: No country had a national MASLD/MASH strategy or action plan issued by a government body, though two (8.0%), Romania and Sweden, had sub-national strategies. Twelve (48.0%) had at least one national or subnational strategy or action plan in which MASLD/MASH was mentioned (within alcohol, cancer, CVD, diabetes, healthy lifestyle/diet, liver disease, noncommunicable disease, obesity, or

"other" strategies). Among the national or subnational strategies or action plans mentioning MASLD/MASH, obesity and diabetes (n = 9 out of 24 countries, 36.0% and n = 8, 32.0%, respectively) were the most frequent ones mentioning MASLD/MASH.
Fifteen (60.0%) countries had national level MASLD/MASH CPGs. Regarding the mention of MASLD/MASH in national level clinical guidelines for dyslipidaemia, obesity, diabetes, alcohol, hypertension, CVD, end of stage liver disease (ESLD)/cirrhosis, liver cancer, liver transplantation, primary care, or "other," 22 (88.0%) of the respondent countries had at least one clinical practice guideline mentioning MASLD/MASH. Obesity guidelines (n = 17, 68.0%), followed by guidelines for diabetes (n = 12, 48.0%), ESLD/cirrhosis (n = 10, 40.0%), liver transplantation (n = 6, 24.0%), and primary care (n = 5, 20.0%) most commonly included MASLD/MASH.
Conclusion: MASLD remains insufficiently addressed in national policy, leaving health systems underprepared despite important diagnostic and therapeutic advances. Integrating MASLD/MASH into existing NCD frameworks and policies is urgently needed to address this public health threat.

THU-051
Extremes and persistence of body mass index increase risks of HCC and mortality regardless of MASLD status
Mei-Hsuan Lee[1], Szu-Ching Yin[1], Xia-Rong Liu[1]. [1]*National Yang Ming Chiao Tung University, Taipei, Taiwan*
Email: lee.meihsuan@gmail.com

Background and aims: Body mass index (BMI) is a key metabolic determinant of HCC and mortality, yet its associations across the BMI spectrum and in relation to metabolic dysfunction–associated steatotic liver disease (MASLD) remain incompletely defined. We examined associations between BMI, HCC incidence, cause-specific mortality, and all-cause mortality, and assessed effect modification by MASLD status.
Method: We conducted a prospective cohort study of individuals undergoing health examinations at a private screening center between 1998 and 2013. BMI (kg/m^2) was classified using Asian-specific criteria as underweight (<18.5), normal (18.5–<23), overweight (23–<25), or obese (≥25). MASLD was defined by ultrasound-detected hepatic steatosis in the absence of other chronic liver diseases. Participants were followed through linkage with national cancer and death registries until 2022. Associations with HCC incidence, liver-related mortality, cardiovascular disease (CVD) mortality, and all-cause mortality were estimated using Cox proportional hazards models, stratified by MASLD status. Longitudinal BMI patterns based on repeated measurements were also evaluated.
Results: Among 287,718 participants, 6.7% were underweight, 42.9% normal weight, 21.6% overweight, and 28.8% obese; MASLD prevalence was 46.0% among overweight and 76.4% among obese individuals. Both underweight and obesity were associated with increased risks of HCC, liver-related mortality, CVD mortality, and all-cause mortality, demonstrating a J-shaped relationship. Compared with normal BMI, adjusted hazard ratios (HRs) for HCC were 1.06 (95% CI 0.79–1.42) for underweight, 1.29 (1.12–1.49) for overweight, and 1.89 (1.67–2.13) for obesity. Corresponding HRs for all-cause mortality were 1.34 (1.27–1.41) and 1.23 (1.19–1.26). These patterns were consistent across MASLD and non-SLD subgroups. In longitudinal analyses, persistent overweight or obesity was associated with higher risks of HCC and liver-related mortality. Among individuals with MASLD, persistent overweight or obesity was associated with increased risks of HCC (HR 1.91, 95% CI 1.23–2.97), liver-related mortality (HR 1.87, 1.19–2.93), and CVD mortality (HR 1.87, 1.19–2.93).
Conclusion: Extremes of BMI and persistent excess adiposity are associated with increased risks of HCC and mortality, independent of MASLD status. These findings emphasize sustained adiposity exposure, rather than MASLD status alone, as a key determinant of long-term liver and cardiometabolic outcomes.

THU-052
Association between sarcopenic obesity and vibration-controlled transient elastography-assessed hepatic steatosis and significant fibrosis: a cross-sectional analysis of NHANES 2017–2018
Jiayue Li[1]. [1]*Sun Yat-sen University, Guangzhou, China*
Email: 1347832609@qq.com

Background and aims: Sarcopenic obesity (SO), defined as the coexistence of sarcopenia and obesity, is a global public health concern. Both sarcopenia and obesity are risk factors of liver-related morbidity and mortality. However, data showing the relationship between SO and the development of metabolic dysfunction-associated steatotic liver disease remain scarce. We aimed to investigate the association between SO and vibration-controlled transient elastography (VCTE)-assessed hepatic steatosis and significant fibrosis, and effect modifiers including age, sex, and race/ethnicity.
Method: This cross-sectional study analyzed data from the 2017–2018 National Health and Nutrition Examination Survey (NHANES). Hepatic steatosis (controlled attenuation parameter [CAP] ≥248 dB/m) and fibrosis (liver stiffness measurement [LSM]≥8 kPa) were assessed by VCTE. Sarcopenia was defined by sex-specific appendicular lean mass/body mass index (BMI) ratios (males: <0.789; females: <0.512) and obesity by BMI≥30 kg/m^2. SO is a composite status of sarcopenia and obesity.
Results: A total of 2,401 participants were included in the analyses after screening 5,809 initial NHANES participants. The prevalence of SO was 3.4% among these participants. Compared with people with neither sarcopenia nor obesity, SO was significantly associated with higher CAP (beta-coefficient: 61.02, 95% confidence interval [CI]: 49.766–72.275, $p < 0.001$), higher LSM (beta-coefficient: 2.137, 95% CI: 1.227–3.046, $p < 0.001$), hepatic steatosis (odds ratio [OR]: 7.622, 95% CI: 3.866–16.522, $p < 0.001$), and significant fibrosis (OR: 8.177, 95% CI: 4.195–15.68, $p < 0.001$). The associations with SO were stronger than those of obesity or sarcopenia alone. Subgroup analyses showed the strongest association with hepatic steatosis in participants aged 30–44 years (OR 27.63, $p = 0.002$), males (OR 32.88, $p < 0.001$) and non-Hispanic Whites (OR 9.37, $p = 0.001$), and with significant fibrosis in those aged 18–29 years (OR 26.00, $p < 0.001$), males (OR 10.07, $p < 0.001$) and non-Hispanic Whites (OR 6.36, $p = 0.006$).
Conclusion: In a nationally representative cohort, SO is strongly associated with hepatic steatosis and significant fibrosis, with a more pronounced effect than obesity or sarcopenia alone. The associations vary by age, sex, and race/ethnicity, supporting targeted screening in high-risk subgroups. Longitudinal studies are warranted to confirm causality.

THU-053
Reassessing obesity in US adults with MASLD under the lancet commission diagnostic criteria
Rutao Lin[1], Renqiang Zeng[1], Xuting Shen[2], QinMei Sun[1], Xin Xin[1], Jiamei Chen[1], Yiyang Hu[1], Qin Feng[1]. [1]*Institute of liver diseases, Shuguang hospital affiliated to Shanghai university of traditional Chinese medicine, Shanghai, China;* [2]*Department of Clinical Laboratory, Shuguang Hospital Affiliated to Shanghai University of Chinese Traditional Medicine, Shanghai, China*
Email: linrutao_2000@163.com

Background and aims: The newly proposed Lancet Commission on Obesity criteria integrate anthropometric and body composition measures, but their implications for Metabolic dysfunction–associated steatotic liver disease (MASLD), including lean-MASLD, are unclear. The study aims to evaluate the impact of the new criteria on obesity prevalence and reclassification patterns in adults with MASLD, including implications for lean-MASLD.
Method: We analyzed data from National Health and Nutrition Examination Survey 2017–2018, including adults with MASLD diagnosed by vibration-controlled transient elastography. We

compared obesity assessment using the new Lancet Commission on Obesity diagnostic criteria with the traditional BMI-based criteria. Under the new criteria, obesity assessment incorporated waist circumference, waist-to-hip ratio, waist-to-height ratio, and body fat percentage measured by dual-energy X-ray absorptiometry (DEXA). Obesity was defined by any of 4 criteria: (1) BMI ≥ 40 kg/m^2; (2) elevated BMI in plus ≥ 1 elevated anthropometric measure; (3) ≥ 2 abnormal anthropometric measures regardless of BMI; (4) excess body fat by DEXA. Traditional obesity was BMI ≥ 30 kg/m^2 (≥ 27.5 for Asian). Lean MASLD was BMI < 25 kg/m^2 (< 23 for Asian).
Results: Among adults with MASLD, obesity prevalence increased from 66.8% (95% CI, 60.6%–72.4%) by traditional criteria to 98.3% (95% CI, 97.3%–99.0%) by the new criteria. Among BMI-defined non-obese MASLD, 94.9% were reclassified as obese and had intermediate hepatic and metabolic abnormalities compared with concordant non-obesity and concordant obesity groups. The prevalence of lean MASLD was 5.4% (95% CI, 2.8%–7.9%) in MASLD; under the new criteria, 84.2% of lean MASLD were met new obesity criteria, reducing lean MASLD prevalence to 0.8% (95% CI, 0.5%–1.2%).
Conclusion: In US adults with MASLD, the new criteria substantially increase estimated obesity prevalence and reclassify most BMI-defined non-obesity, including most lean MASLD as obese. Multidimensional adiposity assessment may improve risk stratification beyond BMI alone.

THU-054
Analysis and 15-year projection of the disease burden of cirrhosis attributable to metabolic dysfunction-associated steatotic liver disease in China, 1990–2021
Ge Liu[1], Jian Jiao[1]. [1]*China-Japan Union Hospital, Jilin University, Changchun, Jilin Province, China*
Email: liuge23@mails.jlu.edu.cn

Background and aims: The global incidence of chronic liver disease attributed to metabolic dysfunction-associated steatotic liver disease (MASLD) is increasing. This study aimed to assess the trends in the burden of MASLD-related cirrhosis in China from 1990 to 2021 and to project its future trajectory over the next 15 years.
Method: Data were obtained from the Global Burden of Disease (GBD) 2021 study. Trends were analysed using Joinpoint regression to calculate the average annual percentage change (AAPC). Age-period-cohort (APC) modelling was applied to estimate the independent effects of age, time period, and birth cohort. An autoregressive integrated moving average (ARIMA) model was used to project incidence, prevalence, and mortality rates for the period 2022–2036.
Results: In 2021, the incidence, prevalence, and mortality rates of MASLD-related cirrhosis in China were 621, 15,606, and 0.31 per 100,000 population, respectively. From 1990 to 2021, the age-standardized incidence rate (ASIR) increased significantly (AAPC = 0.74%; 95% CI: 0.69% to 0.78%), while the age-standardized death rate (ASDR) decreased (AAPC = −1.73%; 95% CI: −2.06% to −1.40%). APC analysis indicated the highest period risk for morbidity occurred in 2017–2021 (rate ratio, RR = 1.16; 95% CI: 1.11 to 1.21). For the cohort born between 1977 and 2002, there was a significant increase in morbidity risk but a decrease in mortality risk. Projections suggest the ASIR will rise from 621.18/100,000 in 2021 to 662.27/100,000 by 2036, with a substantial increase in females offsetting a decrease in males. The overall ASDR is projected to decline slightly from 0.31 to 0.29 per 100,000, with a minor increase noted in females.
Conclusion: The burden of MASLD-related cirrhosis in China is projected to continue rising over the next 15 years, presenting a growing public health challenge. The shifting epidemiology, characterized by a rising incidence in females, highlights the urgent need for sex-specific prevention strategies and early intervention programs focused on MASLD management.

SAT–003-YI
Risk of advanced fibrosis and cancer in a population-based colorectal cancer screening program: implications for EASL case-finding strategies
Maria Capilla[1], Inmaculada Lorca[1], Carmen Quiñones[1], Lucas Sebastián-Peris[2], Jose Miguel Carot[2], Concepción Gómez[1], Clara Alfaro-Cervello[1], Pilar Aguilar[1], Susana Castán-Cameo[3], Silvia Gimeno-Martos[3], Marta Ponce[1], Paloma Lluch-García[1], Isabel Pascual-Moreno[1], Arturo Carratalá[1], Andres Peña[1], David Marti-Aguado[1]. [1]*Incliva - Instituto De Investigación Sanitaria, Valencia, Spain;* [2]*Universitat Politècnica de València, Valencia, Spain;* [3]*Department of Universal Healthcare and Public Health, Valencia, Spain*
Email: davidmmaa@gmail.com

Background and aims: The EASL-EASD-EASO guidelines recommend active case-finding for advanced fibrosis in individuals with MASLD and strict adherence to extrahepatic cancer screening programs. Population-based colorectal cancer (CRC) screening programs provide an ideal setting to implement these recommendations. The aims of this study were: (I) to determine the prevalence of advanced fibrosis among participants in a CRC screening program; and (II) to evaluate the association between fibrosis risk and CRC detection.
Method: We prospectively included participants within a Spanish regional population–based established CRC screening program (n = 28,314 participants during study period 2021–2024). Individuals aged 50–70 years with a positive faecal immunochemical test (FIT+) who were referred for screening colonoscopy were eligible. Prior to colonoscopy, routine blood tests were performed to calculate FIB-4. Participants were classified as having low, intermediate, or high risk of advanced fibrosis according to recommended, age-adjusted FIB-4 cut-offs. The primary endpoint was CRC detected at colonoscopy.
Results: A total of 1,733 FIT+ participants were included; 48% were women, 25% had obesity, and 16% had diabetes. Among the 1,562 individuals with available pre-colonoscopy blood tests, 62% (n = 980) were classified as low risk (FIB-4 <1.3), 33% (n = 510) as intermediate risk, and 5% (n = 72) as high risk for advanced fibrosis (FIB-4 ≥2.67). CRC was detected in 5.5% of participants (n = 97). CRC prevalence according to fibrosis risk category was 6.2% in the low-risk group, 4.9% in the intermediate-risk group, and 6.9% in the high-risk group. No significant association between fibrosis risk category and CRC detection was observed (p = 0.28). No significant differences in CRC prevalence were observed according to the presence of obesity and/or diabetes.
Conclusion: The prevalence of advanced fibrosis risk among participants in a population-based CRC screening program is substantially higher than that reported in the general population at risk for MASLD. While the prevalence of advanced fibrosis risk is high in CRC screening participants, fibrosis risk is not associated with increased CRC detection. These findings support CRC screening programs as an opportunity for liver disease case-finding, but do not suggest fibrosis-based CRC risk stratification.

SAT–004
An observational study of alcohol related liver disease hospitalisations in Australia before and during the COVID-19 pandemic, using routinely collected national data
Edward Meehan[1], Nicholas Mulkearns[2], Liam Brennan-Xie[2], Margery Zhang[2], Niranjan Arachchi[1]. [1]*Sunshine Hospital, Saint Albans, Australia;* [2]*University of Melbourne, Melbourne, Australia*
Email: ejmeehan@gmail.com

Background and aims: Alcohol consumption increased significantly during the COVID-19 pandemic. Previous single-centre Australian studies reported a concurrent increase in alcohol-associated hepatitis admissions, but impacts at a national level are unknown. We aimed to compare trends in hospital separations for alcohol-associated liver disease (ALD) before and during the pandemic, using routinely collected administrative health data.

Method: We searched the Australian Institute of Health and Welfare National Hospital Morbidity Database using ICD-10 codes and extracted annual hospital separation counts for the financial years 2014–15 to 2021–22. We included only multi-day stays, as elective procedure cancellations during COVID-19 significantly altered same-day separations. Elective procedures requiring multi-day stays may have produced residual confounding, which would likely cause underestimation of disease burden increase. We calculated crude rates per 100,000 residents of hospitalisations chiefly due to ALD (ICD-10 code K71), all diseases of the liver (K70-K77), all diseases of the digestive system (K00-K93), and for any cause. We used chi-square tests to compare ALD admissions as a proportion of each of these categories in 2018–19 and 2020–21.
Results: Across all years, there were 43,260 multi-day ALD separations, 98,310 disease of liver separations, 3,566,648 digestive disease separations, and 38,173,066 all-cause separations. The rate of multi-day ALD hospitalisations declined slightly from 18.6 to 16.3 per 100,000 between 2014–15 to 2018–19. However, during the COVID-19 pandemic, sharp increases occurred in 2019–20 (18.48; +13.3%) and 2020–21 (22.72; +22.9%), contrasting with an overall decrease in contemporary all-cause separations. Between 2018–19 and 2020–21, ALD admissions increased as a proportion of all liver disease admissions (41.7% to 47.7%, $p < 0.00001$), all digestive disease admissions (1.01% to 1.37%, $p < 0.00001$), and all admissions for any cause (0.09% to 0.13%, $p < 0.00001$).
Conclusion: During the COVID-19 pandemic, multi-day ALD admissions increased disproportionately compared to overall liver, digestive disease, and all-cause admissions. We were limited by a lack of granularity in this health administrative dataset, which is not produced to answer specific research questions. Our results may suggest a need for proactive resourcing of hepatology and substance disorder services in future pandemics and recessions.

SAT-005
Sex-specific coronary calcification risk across MASLD and obesity phenotypes in rural Indian adults: reach rural India study

Avinash Kumar Ragupathy[1], Abirami Perumal[1], Vijaya Prakash Madesh[2], Ganesan Velmurugan[3], Pudhiavan Arun[2], Mathew Cherian[2], Thomas Alexander[2], Arulraj Ramakrishnan[4], Sundaresan Mohanraj[1]. *[1]Dr NGP Arts & Science College, KMCH Research Foundation, Coimbatore, India; [2]Kovai Medical Centre & Hospital, Coimbatore, India; [3]KMCH Research Foundation, Coimbatore, India; [4]KMCH Research Foundation, Liver Unit, Kovai Medical Center and Hospitals, Coimbatore, India*
Email: drarulraj@kmchhospitals.com

Background and aims: Metabolic dysfunction–associated steatotic liver disease (MASLD) is increasingly recognized as a systemic metabolic disorder with potential cardiovascular implications. However, the interaction between BMI-defined obesity, MASLD phenotypes, and subclinical atherosclerosis particularly in rural South Asian populations remains poorly characterized. This present study aims to investigate sex-specific associations between BMI–MASLD metabolic phenotypes and coronary artery calcification among rural Indian adults.
Method: In this community-based cross-sectional study, a total of 3,006 rural adults aged 35–65 years were initially screened for coronary artery calcification. After excluding participants with missing data on key metabolic and imaging variables required for phenotype classification and regression modeling, 2,027 participants were included in the final analysis. Participants underwent coronary artery calcium scoring using multidetector computed tomography. Study subjects were classified based on BMI–MASLD into metabolic phenotypes: lean; overweight; obese; lean MASLD; overweight MASLD; obese MASLD and MASLD with central/metabolic obesity. Sex-stratified multinomial logistic regression was performed using CAC = 0 as the reference and any CAC > 0 as the outcome.
Results: Among 2,027 rural adults, CAC prevalence was highest among MASLD phenotypes, with lean MASLD demonstrating the highest CAC prevalence (30.5%), followed by MASLD with central obesity (28.7%), overweight MASLD (28.1%), and obese MASLD (27.6%). In sex-stratified multinomial logistic regression, BMI–MASLD phenotypes were not significantly associated with CAC in men. In contrast, all MASLD and obesity phenotypes were strongly associated with CAC in women. Compared with lean metabolically normal women, MASLD with central obesity (OR 3.17, 95% CI 1.42–7.05; $p = 0.005$), overweight (OR 2.95, 95% CI 1.22–7.11; $p = 0.016$), obesity (OR 1.98, 95% CI 1.05–3.76; $p = 0.036$), lean MASLD (OR 2.93, 95% CI 1.29–6.65; $p = 0.010$), overweight MASLD (OR 2.63, 95% CI 1.37–5.05; $p = 0.004$), and obese MASLD (OR 2.29, 95% CI 1.25–4.20; $p = 0.008$) independently predicted CAC presence.
Conclusion: Lean MASLD and metabolically unhealthy obesity showed the highest burden of subclinical coronary atherosclerosis in rural Indian adults. MASLD, irrespective of BMI, conferred a 2–3-fold higher CAC risk in women, highlighting hepatic steatosis with metabolic dysfunction as one of the driver of coronary calcification beyond BMI alone.

SAT-006
Real-time AI–hepatologist intervention against 'liver detox' misinformation: a prospective social media–based RCT

Yavuz Özden[1]. *[1]Kayseri City Hospital, University of Health Sciences, Kayseri, Türkiye*
Email: yavuzozden@gmail.com

Background and aims: Social media is a major platform for public health information and is a key driver of medical misinformation. The pervasive "liver detox" myth and related liver-health misinformation promote unproven regimens that conflict with evidence-based hepatology practice. Although systematic reviews have described the scope of such misinformation, prospective interventional studies targeting liver-related myths are limited. Therefore, we evaluated a real-time intervention model integrating artificial intelligence with hepatologist oversight to counter liver-related misinformation on social media platforms.
Method: We conducted a 12-week platform-specific randomized controlled study on TikTok and Instagram. Public posts containing liver-related hashtags (e.g., "liver detox") were monitored using an artificial intelligence–assisted system informed by hepatology guidelines for guideline-concordant responses. Posts classified as misleading were randomly assigned to either a real-time intervention consisting of hepatologist-reviewed responses posted within 30 min or to no response. Primary outcomes were 48-hour engagement rate (normalized to post-level impressions) and changes in comment sentiment. Secondary outcomes included response time efficiency and qualitative patterns of user interaction.
Results: Among 842 eligible posts (421 per group), intervention posts showed a 52.3% lower engagement rate (reduced amplification) than controls (95% CI: −58.1 to −46.5; $p < 0.001$). Comment analysis demonstrated a substantial increase in expressions of trust and gratitude, with 31.8% of original content creators engaging constructively (e.g., acknowledging corrections). The AI-supported workflow reduced mean response time to 8.4 minutes, compared with over 45 min using manual review alone.
Conclusion: This model supports scalable strategies for evidence-based hepatology risk communication on social media by enabling timely, expert-led responses against organ-specific misinformation. Limitations include two platforms and a 12-week follow-up.

SAT-007

Economic and healthcare resource burden of metabolic dysfunction-associated steatotic liver disease and metabolic dysfunction-associated steatohepatitis: a United States system dynamics model

David W. Victor Iii[1], Amreen Dinani[2], Elisabeth de Laguiche[3], Fotis Tefos[3], Fryderyk Wilczynski[4], Thomas Padgett[4]. [1]*Houston Methodist Hospital, Houston, United States;* [2]*Duke University School of Medicine, Durham, United States;* [3]*Novo Nordisk A/S, Søborg, Denmark;* [4]*Health Economics and Outcomes Research, Cardiff, United Kingdom*
Email: dwvictor@houstonmethodist.org

Background and aims: Metabolic dysfunction-associated steatotic liver disease (MASLD) is projected to increase globally and impact a third of the United States (US) population. Metabolic dysfunction-associated steatohepatitis (MASH), characterized by hepatic steatosis, inflammation, hepatocyte injury and fibrosis, is associated with all cause and liver related mortality. This study aimed to predict the impact of rising MASLD/MASH prevalence on direct costs and healthcare resource utilization (HCRU), based on current standard of care practices in the US.
Method: A US system dynamics model was developed to predict the prevalence and burden of MASLD/MASH and its complications, stratified by age and disease stage, from 2025 to 2060. Disease stage was derived by mapping Fibrosis-4 (FIB-4) to fibrosis stage (F-stage). The model was calibrated to National Health and Nutrition Examination Survey (NHANES)-derived data (2006–2020) and validated by two clinical experts. Model outcomes included direct healthcare costs and HCRU, including primary care contacts and hospital bed days.
Results: Under current standard of care practices in the US, MASLD/MASH prevalence is projected to increase by 28%, from 104 million in 2025 to 133 million in 2060. People with MASH F2-F4 drive the projected burden, with the greatest percentage increase occurring for F3 (126%) and F4 (116%). The total annual direct costs attributable to MASLD/MASH are predicted to increase from $1.8 trillion in 2025, to $2.5 trillion in 2060, an increase of 37%. Of this, $38 billion is attributed to individuals with F4 fibrosis. Annual HCRU attributable to MASLD/MASH is projected to rise, with primary care visits increasing by 29% and hospital bed days by 39%, growing from 1.0 billion and 98 million in 2025, to 1.3 billion and 137 million by 2060, respectively. In 2060, people with MASH F4 would represent approximately 0.7% of the MASLD/MASH population and account for 12.4 million primary care visits and 6.6 million hospital bed days.
Conclusion: The economic and HCRU burden of MASLD/MASH is projected to rise substantially under current standard of care practices in the US, driven by increasing prevalence and disease severity. This underscores an urgent need for intervention and prevention strategies to mitigate the impact of MASLD/MASH.

SAT-008

A pan European observational cohort study describing clinical characteristics, treatment patterns and outcomes in patients diagnosed with hepatocellular carcinoma

George Papatheodoridis[1], Rohini Sharma[2], Hannes Hagström[3], Andrea Casadei Giardini[4], Carlos Lopez Lopez[5], Ana Matilla[6], Rui Gaspar[7], Kavitha Balaji, Ph.D[8], Mufiza Farid-Kapadia[9], Joe Hickey[10], Pompilia Radu[11]. [1]*National And Kapodistrian University Of Athens, Athina, Greece;* [2]*Imperial College London, London, United Kingdom;* [3]*Karolinska University Hospital, Stockholm, Sweden;* [4]*Università Vita-Salute San Raffaele, Milano, Italy;* [5]*Marqués de Valdecilla University Hospital, IDIVAL, UNICAN, Santander, Spain;* [6]*Gregorio Marañón University Hospital, Madrid, Spain;* [7]*Centro Hospitalar de São João, Porto, Portugal;* [8]*AstraZeneca, Gaithersburg, United States;* [9]*AstraZeneca, Mississauga, Canada;* [10]*Open Health, London, United Kingdom;* [11]*University of Bern, Bern, Switzerland*
Email: iuliana-pompilia.radu@insel.ch

Background and aims: As the most common type of liver cancer, hepatocellular carcinoma (HCC) is a significant global health problem. However, real-world treatment patterns and outcomes are not well characterized in patients with HCC. The OPAL study aimed to address this evidence gap and evaluate treatment patterns and outcomes in European patients with HCC.
Method: OPAL was a European, observational, longitudinal cohort study including adults (≥18 years) with a new diagnosis of HCC between 1 January 2010 and 31 December 2021 from Greece, Italy, Portugal, Spain, Sweden, Switzerland, and the United Kingdom. Study objectives were assessment of demographics, patient and disease characteristics, treatment patterns, overall survival (OS), and progression-free survival (PFS). Analyses were descriptive and stratified by Barcelona Clinic Liver Cancer (BCLC) stage at diagnosis (0–D) and by initial treatment approach: curative therapy (resection, ablation), locoregional therapy (transarterial chemoembolization, transarterial radioembolization), and systemic therapy.
Results: Overall, 6,030 patients were included. Across BCLC stages/treatment types, mean age ranged from 65.1–68.2 years/65.3–68.2 years, proportion of male patients ranged from 76%–85%/80%–93%, proportion of patients with ECOG 0–1 ranged from 14%–95%/90%–97%, and proportion of patients with Child-Pugh A ranged from 20%–78%/73%–94%. Arterial hypertension was the most frequent baseline comorbidity across all BCLC stages. Esophageal varices were the most common baseline complication in BCLC 0 (43%), A (40%), and B (32%), whereas macrovascular invasion was most frequent in BCLC C (45%) and ascites in BCLC D (57%). Median PFS (mPFS) by BCLC stage ranged from 7.26–20.16 months in BCLC 0, 9.48–15.15 in A, 3.0–8.11 in B, 2.16–7.62 in C, and 1.32–8.57 in D. mPFS by treatment type ranged from 12.3–20.9 months for curative, 3.0–15.0 for locoregional, and 3.2–12.34 for systemic therapy. Median OS (mOS) by BCLC stage ranged from 10.0–87.0 months in BCLC 0, 12.0–56.0 in A, 10.0–30.0 in B, 2.76–13.4 in C, and 0.11–1.99 in D. mOS by treatment type ranged from 31.51–54.8 months for curative, 23.0–39.0 for locoregional, and 6.40–29.9 for systemic therapy.
Conclusion: This analysis reports real-world outcomes of European patients with HCC, including outcomes such as PFS and OS up to 5 years post-diagnosis, and evidences the variability in these outcomes across disease stages and treatment approaches.

SAT-009

Real-world patient profiles and outcomes of hepatocellular carcinoma patients treated with embolization procedures: a European observational longitudinal study

George Papatheodoridis[1], Rohini Sharma[2], Hannes Hagström[3], Andrea Casadei Giardini[4], Carlos Lopez Lopez[5], Ana Matilla[6], Rui Gaspar[7], Kavitha Balaji, Ph.D[8], Mufiza Farid-Kapadia[9], Angela Wang[9], Joe Hickey[10], Pompilia Radu[11]. [1]*National And Kapodistrian University Of Athens, Athina, Greece;* [2]*Imperial College London, London, United Kingdom;* [3]*Karolinska University Hospital, Stockholm, Sweden;* [4]*Università Vita-Salute San Raffaele, Milano, Italy;* [5]*Marqués de Valdecilla University Hospital, IDIVAL, UNICAN, Santander, Spain;* [6]*Gregorio Marañón University Hospital, Madrid, Spain;* [7]*Centro Hospitalar de São João, Porto, Portugal;* [8]*AstraZeneca, Gaithersburg, United States;* [9]*AstraZeneca, Mississauga, Canada;* [10]*Open Health, London, United Kingdom;* [11]*University of Bern, Bern, Switzerland*
Email: iuliana-pompilia.radu@insel.ch

Background and aims: Hepatocellular carcinoma (HCC) is the most common type of liver cancer. Embolization procedures, like transarterial chemoembolization (TACE) or transarterial radioembolization (TARE), are used mainly for intermediate HCC patients. Given limited evidence on characteristics and outcomes in this population, this European observational longitudinal study aimed to describe real-world patient profiles, disease characteristics, and clinical outcomes among patients treated with these embolization procedures.
Method: Adults (≥18 years) with a new diagnosis of HCC between 1 January 2010 and 31 December 2021 who received TACE or TARE were

included. Patient and tumor characteristics, treatment details, and survival outcomes were obtained from cancer registries and electronic health records. Analyses were descriptive. Overall survival (OS) was assessed from the date of diagnosis to death or last follow-up. Results were summarized at the country level and pooled where appropriate for a pan-European cohort.

Results: A total of 2595 patients receiving TACE (n = 2546) or TARE (n = 49) were identified from Greece (n = 131), Sweden (n = 222), Italy (n = 122), Portugal (n = 51), Spain (n = 104), Switzerland (n = 58), and UK (n = 1907). Most patients were male (82%), and the average age was 66.3 years. For Child Pugh staging, 75% patients were in Class A and 24% in Class B. Across individual countries, alcohol (17.1%–76.0%), HBV (0.4%–36.2%), and HCV (0.3%–44.1%) were the most prevalent aetiologies. Esophageal varices were commonly reported (25%), and diabetes mellitus was the most common comorbidity at baseline (40%). At diagnosis, 24% of patients had 1–3 nodules <3 cm), while 32% had multiple nodules without extrahepatic spread. OS from initial diagnosis was 96% at 6 months, 85% at 1 year, 56% at 2 years, 33% at 3 years, 19% at 4 years, and 11% at 5 years, while median OS across individual countries ranged from 23 to 42 months.

Conclusion: TACE represents the predominant embolization procedure for HCC patients across Europe. The clinical outcomes after embolization procedures are suboptimal, with steep attrition in OS, aligning with results from previous studies. Many patients had metabolic comorbidities at baseline, which adds to treatment complexity. Overall, these findings reveal important unmet needs in current embolization-based care and support the development of more effective therapies, alongside more consistent real-world reporting to guide practice.

SAT-010-YI

Interim findings from the KIDS-LIVE study: metabolic phenotypes and burden of MASLD in Indian children and adolescents

Abirami Perumal[1], Abisheak Kandasamy[2], Vijaya Prakash Madesh[3], Sujatha Chinnappan[3], T Abiramalatha[3], S Sivanandam[4], S Jeevithan[4], Thooran Sibi[3], Aravindh Somasundram[3], Arulraj Ramakrishnan[3], Sundaresan Mohanraj[2]. *[1]Dr NGP Arts & Science College, KMCH Research Foundation, Coimbatore, India; [2]KMCH Research Foundation, Dr. NGP Arts and Science College, Coimbatore, India; [3]Kovai Medical Centre & Hospital, Coimbatore, India; [4]KMCH Institute of Health Sciences & Research, Coimbatore, India*

Email: mohanrajs.kmchrf@gmail.com

Background and aims: The epidemiological transition in India has led to an alarming rise in metabolic dysfunction with impact on children and adolescents as well. Metabolic dysfunction–associated steatotic liver disease (MASLD) phenotypes as a component of metabolic syndrome has not been well characterized in a community-based Indian pediatric setting. This present study aims to estimate the prevalence of MASLD and to characterize metabolically stratified MASLD phenotypes among children and adolescents in an ongoing community-based cohort.

Method: The KIDS-LIVE study is a community-based cohort evaluating hepatic and metabolic health among school-aged children (aged, 6–12 years) and adolescents (aged, 13–18 years). In this interim analysis, 980 participants (49.5% males; 50.5% females) were evaluated. Anthropometry, biochemical metabolic profiling, and liver steatosis assessment were performed. Participants were categorized into metabolically healthy and unhealthy phenotypes (MASLD criteria) across lean, overweight, and obese groups.

Results: The prevalence of overweight, obesity, and abdominal obesity were 10.0%, 4.9%, and 5.3%, respectively. Overall MASLD prevalence is 7.6%, with higher prevalence in males (9.6%) than females (5.6%, $p < 0.001$). Dyslipidemia (40.2%) and pre-diabetes (9.5%) were the most frequent metabolic dysfunction, predominantly affecting the 10–15-year age group. Interim analysis showed a higher MASLD prevalence among metabolically healthy obese (MHO) children (61.5%) compared to metabolically unhealthy obese (MUO) children (41.7%, $p < 0.001$). However, after multivariable adjustment, MHO was not independently associated with MASLD (OR = 0.05; $p = 0.804$), whereas MUO demonstrated a significantly elevated risk (OR = 11.3; 95% CI: 5.1–24.9; $p < 0.001$). Adolescents aged 13–18 years were the most affected age group, and gender-stratified analysis revealed a 100% prevalence of MASLD among MHO males.

Conclusion: Despite an apparently higher crude prevalence of MASLD among metabolically healthy obese children, adjusted analyses reveal that metabolically unhealthy obesity is the true independent driver of pediatric MASLD. These findings highlight the critical need for early community-based screening strategies and phenotype-specific preventive interventions to mitigate future cardiometabolic and hepatic disease burden in pediatric populations.

SAT-011

Can poor sleep signal fatty liver disease risk? Evidence from a rural population in North India

Tushar Prabhakar[1], Satya Vir Singh[1], Gahan Jois[1], Bronica Saini[2]. *[1]Amrita School of Medicine, Faridabad, India; [2]ESIC Model Hospital Rohini, Delhi, India*

Email: tusharprabhakar@yahoo.in

Background and aims: Metabolic-dysfunction associated fatty liver disease (MAFLD) is a major emerging liver disorder, including in lean populations. While metabolic risk factors are well-studied, rural populations remain underrepresented in such research, despite their high burden of unrecognized MAFLD. Poor sleep may influence hepatic steatosis via insulin resistance, inflammation, and circadian rhythm disruption. The study hypothesized that poor sleep quality and short duration are independently associated with high MAFLD risk, and that sleep parameters could serve as non-invasive, scalable risk markers.

Method: This community-based cross-sectional study recruited 550 adults (≥18 years) residing in catchment area of a primary health centre in North India. Sleep quality and duration were assessed using the Pittsburgh Sleep Quality Index (PSQI). Sleep duration was categorized as <6 h (short), 6–8 h (normal), >8 h (long). MAFLD risk was evaluated using a validated non-laboratory 15-point Self-Assessment Score. Descriptive statistics, chi-square, and multivariable logistic regression were used. Additional analyses included ROC curve for predictive validity of PSQI, test for trend across sleep duration categories, and interaction analysis with BMI and sex.

Results: Among 550 participants (mean age: 42.6 ± 13.5 years; 56.4% female), 38.2% had poor sleep quality and 31.6% had high MAFLD risk. High MAFLD risk was observed in 47.9% of poor sleepers vs 22.1% of good sleepers ($p < 0.001$). MAFLD risk was also elevated in short sleepers (44.6%) vs normal (28.5%) and long sleepers (23.8%) ($p = 0.002$; p-trend <0.01). On multivariable regression, poor sleep quality (AOR = 2.31; 95% CI: 1.58–3.38) and short sleep (AOR = 1.76; 95% CI: 1.15–2.69) were independently associated with high MAFLD risk. ROC analysis yielded an AUC of 0.71 (95% CI: 0.65–0.77) for PSQI in predicting high MAFLD risk. Significant interaction was noted between poor sleep and elevated BMI (p-interaction = 0.03), indicating amplified risk in overweight individuals.

Conclusion: Poor sleep quality and short sleep duration are strong, independent predictors of MAFLD risk, with moderate discriminatory ability on ROC analysis. These findings suggest that sleep assessment could serve as a low-cost, non-invasive surrogate marker for hepatic risk stratification in primary care. Integrating sleep-focused screening into MAFLD preventive strategies may improve early risk identification and intervention, especially in resource-constrained settings.

SAT-012

Patient pathways for rare liver diseases: development of a European template

Sarah Raevens[1,2], Renée Duijzer[3], Andreea Fodor[4], Matt Bolz Johnson[5], Nagham Issa[6], Sophie Penisson[7], Samir Patel[7], Alice Bertolini[8], Carmen Teemer[9], Clémence Ramier[10], Laure Elkrief[11], Marco Senzolo[2,12], Virginia Hernández-Gea[2,13], Ansgar W. Lohse[2,6], Bogdan Procopet[4], Joost P.H. Drenth[2,14], Aurélie Plessier[15].
[1]Hepatology Research Unit, Department of Internal Medicine and Pediatrics, Liver Research Center, Ghent University, Ghent, Belgium, Ghent, Belgium; [2]European Reference Network of Rare Hepatological Diseases (ERN RARE-LIVER), Hamburg, Germany; [3]Department of Gastroenterology and Hepatology, Radboudumc, The Netherlands, Radboudumc, Netherlands; [4]"Iuliu Hatieganu" University of Medicine and Pharmacy, Cluj-Napoca, Romania, Cluj-Napoca, Romania; [5]Eurordis, PARIS, France; [6]Department of Medicine, University Medical Centre Hamburg-Eppendorf, Hamburg, Germany, Hamburg, Germany; [7]amvf French Patient's Association for Vascular Liver Diseases, Clichy, France; [8]Italian Patient's Association for Vascular Liver Diseases, Gastroentérologie and Multivisceral Transplant Unit, Padova University Hospital, Padova, Italy, Padova, Italy; [9]PKD Familiäre Zystennieren e.V., Germany, Hamburg, Germany; [10]Aix Marseille Univ, INSERM, IRD, SESSTIM, Sciences Économiques & Sociales de la Santé & Traitement de l'Information Médicale, ISSPAM, Marseille, France, Marseille, France; [11]Service d'Hépato-Gastroentérologie, Hôpital Trousseau, CHRU de Tours, Tours, France, Tours, France; [12]Gastroenterology and Multivisceral Transplant Unit, Padova University Hospital, Padova, Italy, Padova, Italy; [13]Barcelona Hepatic Hemodynamics Laboratory, Liver Unit, Hospital Clinic, Institut d'Investigacions Biomèdiques August Pi i Sunyer (IDIBAPS), CIBEREHD (Centro de Investigacion Biomedica en Red Enfermedades Hepaticas y Digestivas) University of Barcelona, 08036 Barcelona, Spain, Barcelona, Spain; [14]Department of Gastroenterology and Hepatology, Amsterdam UMC, University of Amsterdam, The Netherlands, amsterdam, Netherlands; [15]Service d'Hépatologie, DMU DIGEST, Centre de Référence des Maladies Vasculaires du Foie, FILFOIE, Centre de Recherche sur l'inflammation, Inserm, UMR 1149, Université de Paris, AP-HP, Hôpital Beaujon, Paris, France. European Reference Network of Rare Hepatological Diseases (ERN RARE-LIVER), Clichy, France
Email: aurelie.plessier@aphp.fr

Background and aims: aims Rare liver diseases are associated with significant care challenges, including delayed diagnosis, inconsistent management, and limited patient support. Empowering patients has been shown to improve disease control and reduce distress. Structured patient pathways can help overcome these barriers by providing coordinated, evidence-based guidance throughout the patient's journey with the disease. Our initiative aimed to develop a harmonised framework for patient pathways tailored to rare liver diseases, through multidisciplinary collaboration within the European Reference Network RARELIVER.
Method: A multidisciplinary core group of hepatologists, specialist nurses, and patient representatives from several European countries conducted an iterative, co-creative development process. A structured literature review informed the evidence base, while patient and public involvement ensured integration of lived experience and psychosocial dimensions. Draft pathways underwent dual peer review by scientific experts and patient advocacy organisations to ensure accuracy, usability, and alignment with patient priorities.
Results: A generic patient pathway framework was created, organised around four key phases: pre-diagnosis, diagnosis, management, and long-term follow-up. Core components include early recognition and referral, standardised diagnostic protocols, multidisciplinary management, and patient-focused follow-up. The framework is adaptable across rare liver diseases and includes disease-specific subsections, educational resources, and "10 key questions" to promote shared decision-making. Finalised pathways for non-cirrhotic portal vein thrombosis, polycystic liver disease, and portosinusoidal vascular disorder are now publicly available through ERN RARELIVER.
Conclusion: This initiative represents the first pan-European effort to develop harmonised, multidisciplinary, and patient-centred pathways for rare liver diseases. By integrating scientific evidence, clinical expertise, and patient perspectives, these pathways provide a scalable model to improve diagnostic efficiency, care coordination, and patient outcomes, supporting sustainable and equitable rare disease care.

SAT-013-YI

Marginal structural models to evaluate the prognostic utility of steatotic liver disease subclasses in association with all-cause mortality

Carmela Rapino[1], Giada Sebastiani[2], Jessica Burnside[3], Cindy Wen[1,3], Alnoor Ramji[4], Mark Swain[5], Keyur Patel[6], Sahar Saeed[1]. *[1]Public Health Sciences Department, Queen's University - 62 Fifth Field Company Lane, Kingston, Ontario, Kingston, Canada; [2]Department of Medicine, McGill University - 2001 McGill College Avenue, Suite 1310, Montreal, QC, Canada, H3A 1G1, Montréal, Canada; [3]Queen's University, School of Medicine - 15 Arch Street, Kingston, Ontario, K7L 3L4, Kingston, Canada; [4]University of British Columbia, Vancouver, Canada; [5]Calgary Liver Unit, Cumming School of Medicine, University of Calgary - 3280 Hospital Drive NW, Calgary, Alberta, Canada, T2N 4Z6, Calgary, Canada; [6]Division of Gastroenterology and Hepatology, University Health Network - 190/200 Elizabeth Street, Toronto, Ontario, Canada, M5G 2C4, Toronto, Canada*
Email: 19cfr@queensu.ca

Background and aims: The subclassifications of Steatotic Liver Disease (SLD) were introduced to provide a clinically meaningful framework that considers metabolic dysfunction and alcohol consumption. However, little consideration is given to the disease's dynamic nature and evolving risk over time. We aimed to evaluate the prognostic utility of the SLD subtypes in association with all-cause mortality, accounting for both time-varying disease status and confounding.
Method: We analyzed data from the Canadian Longitudinal Study on Aging, a prospective cohort study following adults aged 45–85 years from 2012–2021. Participants were classified by SLD subtype at BL and FUP1 (+3 years) using the NAFLD Ridge Score's (NRS) dual cut-off to identify steatosis, laboratory measures and medication data to determine the presence of cardiometabolic factors, and self-reported data to determine weekly alcohol consumption. The NRS is a non-invasive test that was validated against the gold standard proton magnetic resonance spectroscopy, with an AUROC of 0.87, sensitivity of 92%, and specificity of 90%. Marginal Structural Cox proportional hazards models were used to estimate the association between increasing levels of alcohol consumption and mortality among those with and without steatosis, adjusting for age, sex, history of binge drinking at baseline and time-updated income, lifestyle, and cardiometabolic factors.
Results: A total of16,560 participants (52.1% female, median age 58 (IQR: 51–66)) were included. At baseline, MASLD was the most prevalent subtype at baseline (33.9%). In 3 years, 35.4% of people with ALD, 23.7% MetALD, and 22.6% MASLD transitioned to different SLD subtypes. Over a median of 7.8 years, 1041 deaths occurred. Females with MetALD and ALD had higher incident mortality rates than males with MetALD (7.05; 95% CI: 2.29–16.45 vs. 5.07; 95% CI: 2.53–9.08) and ALD (11.37; 95%CI: 0.29–63.33 vs. 5.60 95% CI: 1.15–16.36). Overall, steatosis increased the risk of death by almost 2 times, and after accounting for time-varying exposures and confounders**,** ALD had the highest risk of all-cause mortality (adjusted hazard ratio (aHR) 6.11; 95% CI: 1.76–21.19), while MetALD was not found to be statistically significant (aHR 1.07; 95% CI: 0.59–1.94).
Conclusion: SLD is a dynamic condition, where prognosis and evolving mortality risk cannot be captured by relying solely on static

baseline classifications. Incorporating more holistic and longitudinal risk assessments is key to improving clinical risk stratification.

SAT-014

Income and sex disparities in prognosis among individuals with MASLD: a survival analysis from the Canadian longitudinal study on aging

Carmela Rapino[1], Giada Sebastiani[2], Jessica Burnside[3], Cindy Wen[1,3], Alnoor Ramji[4], Mark Swain[5], Keyur Patel[6], Sahar Saeed[1]. *[1]Public Health Sciences Department, Queen's University - 62 Fifth Field Company Lane, Kingston, Ontario, Kingston, Canada; [2]Department of Medicine, McGill University - 2001 McGill College Avenue, Suite 1310, Montreal, QC, Canada, H3A 1G1, Montréal, Canada; [3]Queen's University, School of Medicine - 15 Arch Street, Kingston, Ontario, K7L 3L4, Kingston, Canada; [4]University of British Columbia, Vancouver, Canada; [5]Calgary Liver Unit, Cumming School of Medicine, University of Calgary - 3280 Hospital Drive NW, Calgary, Alberta, Canada, T2N 4Z6, Calgary, Canada; [6]Division of Gastroenterology and Hepatology, University Health Network - 190/200 Elizabeth Street, Toronto, Ontario, Canada, M5G 2C4, Toronto, Canada*
Email: 19cfr@queensu.ca

Background and aims: Income and sex are influential determinants of disease burden, but their influence on Metabolic Dysfunction-Associated Steatotic Liver Disease (MASLD) prognosis remains poorly understood. We aimed to evaluate the differences in prognosis by income and sex in association with all-cause mortality, among individuals with MASLD.

Method: We analyzed data from the Canadian Longitudinal Study on Aging, a prospective cohort of adults aged 45–85 years from 2012–2021. MASLD was defined as hepatic steatosis, as measured through the NAFLD ridge score (NRS), self-reported weekly alcohol use <140 g in females and <210 g in males, and the presence of at least one cardiometabolic factor identified through laboratory measures and medication data. The NRS is a non-invasive test that was validated against the gold standard proton magnetic resonance spectroscopy, with an AUROC of 0.87, sensitivity of 92%, and specificity of 90%. Incident mortality rates were calculated for each income quintile and by sex. Cox proportional hazards models were used to estimate the adjusted association between total household income quintiles and all-cause mortality, relative to the lowest income quintile, both overall and stratified by sex. Models were adjusted for age, physical activity, diet, and smoking.

Results: Between 2012 and 2015, 8,430 participants were classified with MASLD at (64.3% male, median age 63 (IQR:56–71)). Most individuals reported income between $50,000–$99,999.99 (32.3%; n = 2,797). Over a median follow-up of 7.7 years, 629 deaths occurred. Incident mortality rates were highest among participants in the lowest income quintile (<$20,000: 17.17 per 1,000 person-years) and decreased progressively with higher income. After adjustment, participants reporting incomes of $20,000–$49,999 and $50,000–$99,999 had significantly lower risk of all-cause mortality compared to <$20,000 (adjusted HR 0.68, 95% CI: 0.48–0.97; and 0.61, 95% CI: 0.42–0.88, respectively). Among females, higher income was consistently associated with lower mortality (e.g., $50,000–$99,999: aHR 0.47, 95% CI: 0.26–0.83; $100,000–$149,999: aHR 0.29, 95% CI: 0.10–0.85). Mortality risk among males decreased with increasing income, though were not statistical significance.

Conclusion: Lower income is associated with higher all-cause mortality among individuals with MASLD, with income disparities particularly more pronounced in females. These findings highlight the need to consider holistic risk assessments when approaching clinical management.

SAT-015-YI

Multidisciplinary assessment of unemployment risk factors in liver transplant recipients: final results of the RICReaTI project

Margherita Saracco[1], Alessandro Godono[2], Silvia Strona[1], Maria Vittoria Picciaiola[2], Massimo Maci[2], Astrid Cecilia Surra[2], Fllippo Angelino[2], Bruno Papaleo[3], Paolo Boffetta[4], Cinzia Frascheri[5], Marco Miniotti[6], Paolo Leombruni[6], Enrico Pira[2], Donatella Cocchis[7], Giorgio Maria Saracco[8], Renato Romagnoli[7], Silvia Martini[1]. *[1]SSD Insufficienza Epatica e Trapianto Epatico, AOU Città della Salute e della Scienza di Torino, Torino, Italy; [2]Department of Public Health and Pediatrics, University of Turin, Torino, Italy; [3]INAIL Research, Department of Occupational and Environmental Medicine, Epidemiology and Hygiene, Roma, Italy; [4]Department of Medical and Surgical Sciences, Alma Mater Studiorum University of Bologna, Bologna, Italy; [5]Labor law expert - Responsible for Cisl national Health and safety at work, Roma, Italy; [6]"Rita Levi Montalcini" Department of Neuroscience, University of Turin, Torino, Italy; [7]General Surgery 2U and Liver Transplant Center, AOU Città della Salute e della Scienza di Torino, Torino, Italy; [8]Gastroenterology Unit, AOU Città della Salute e della Scienza di Torino, University of Turin, Torino, Italy*
Email: margherita.saracco@gmail.com

Background and aims: Reintegration to work is crucial for transplanted patients (pts), and especially in liver transplant (LT) it can be demanding due to multiple social factors. The RICReaTI project aimed to evaluate how liver disease and LT impacted work ability and perceived disability, analyzing correlations between clinical, social, and employment status before and after LT, to elaborate guidelines for healthcare providers.

Method: We retrospectively enrolled all LT pts transplanted from 2018 to 2023 in our high-volume LT Centre, aged 18 to 68 years (y), not yet retired before LT. Participants completed WHODAS 2.0 (World Health Organization Disability Assessment Schedule) and Work Ability Index (WAI) questionnaires, supplemented with clinical and occupational data. From 12/2023, pts were prospectively included, interviewed before LT and after 6 months. Pts were enrolled until 12/2024, follow up closed in 06/2025.

Results: 1123 LT were performed in the study period. 329 of 695 eligible pts (47%) accepted to be interviewed (48 prospectively). 65% were male, average age 52 y (41% >60 y). 83% had cirrhosis (41% viral, 15% alcoholic). 90% were Italian residents, 55% had an elementary/middle-school education, 56% history of alcohol/drugs use, 56% active/previous smoke, 74% was employed before LT. 66% identified the partner as caregiver, 4% a caregiver outside the family. After LT, 40% were unemployed (67% already unemployed before LT) and 55% reported that health issues affected their job search. Only 4 unemployed pts before LT found a job after LT. Unemployment was significantly associated with female sex, age >60 y, other caregiver, lower education and lower low self-perception of work capacity (WAI) (all $p < 0.05$). Lower WAI was independently associated with psychiatric disease, age >60 y, lower MELD at LT, and again lower education (all $p < 0.05$). Worse disability scores (WHODAS) correlated with alcohol abuse, non-Italian nationality and again female sex (all $p < 0.05$). In prospectively included patients, both WHODAS e WAI scores significantly improved between pre-LT and post-LT (all $p < 0.05$).

Conclusion: Return to work after LT remains suboptimal. Employment status and perceived work ability are influenced by a complex interplay of clinical, demographic, and socioeconomic factors. The RICReaTI study group is developing with the National Department of Occupational and Environmental Medicine, Epidemiology and Hygiene (INAIL) a multidisciplinary pathway as part of standard post-transplant care.

SAT-019

Continuity and safety in cross-sectoral care in hepatology: a prospective study of an interprofessional training ward

Schlosser-Hupf Sophie[1], Jonas Dörr[1], Stephan Schmid[1], Claudia Kunst[1], Martina Müller-Schilling[1]. [1]*Department of Internal Medicine I, University Hospital Regensburg, Regensburg, Germany*
Email: sophie.schlosser@ukr.de

Background and aims: Transitions from hospital to community care, particularly in hepatology-focused wards, are well-established as high-risk periods for communication failures, medication errors, and discontinuity of care, which can lead to adverse events and increased readmissions. Interprofessional collaboration during inpatient care has been shown to improve patient satisfaction and perceived quality, but its direct impact on post-discharge outcomes remains insufficiently studied, especially in hepatology settings. This study investigated whether an interprofessional training ward could improve quality of care, medication safety, and cross-sectoral collaboration following hospital discharge compared with conventional wards (CW).
Method: From May to October 2024, a prospective single-centre observational study at University Hospital Regensburg compared patients treated on interprofessional and conventional wards with a hepatology focus, using post-discharge interviews and physician surveys to assess patient-perceived quality of care, discharge processes, cross-sectoral collaboration, and medication management.
Results: Of 328 screened patients, 228 consented and 131 (57.5%) completed follow-up (A-STAR n = 33; conventional wards n = 98). Baseline characteristics were comparable. Forty follow-up physicians responded (30.5%). Patient-reported post-discharge quality (U = 1396.5; p = 0.088) and continuity of care (U = 1530; p = 0.45) did not differ between groups, nor did understanding of medical history (93.9%; $\chi^2(1) = 0$; p = 0.99). Provider-rated cross-sectoral collaboration was similar (U = 126.5; p = 0.49), and all discharge summaries were complete. Health improvement was comparable ($\chi^2(1) = 1.032$; p = 0.31), while new symptoms occurred less frequently in A-STAR patients (3.0% vs 22.5%; $\chi^2(1) = 6.431$; p = 0.011). Unintentional weight loss showed no significant difference ($\chi^2(1) = 3.397$; p = 0.065). No A-STAR patients required post-discharge medication changes, compared with 12.6% on conventional wards (p = 0.036). Readmission rates and follow-up scheduling were similar.
Conclusion: In conclusion, in a hepatology setting, interprofessional care on the A-STAR ward achieved outcomes comparable to conventional wards, with fewer new symptoms and improved medication safety, supporting its value for patient care and training.

SAT-020

Patient characteristics and functional impairment in MASLD: a remote prospective cross-sectional real-world study in Germany

Anja Schulz-Kuhnt[1], Lars Herrmann[1], Ramona Ziegler[1], Hubert Steindl[1], Christoph Abels[1]. [1]*Bionorica SE, Neumarkt, Germany*
Email: christoph.abels@bionorica.de

Background and aims: The estimated global prevalence of MASLD is > 30%. Nevertheless, only <5% of patients with MASLD are aware of it, as particularly in early stages of MASLD, symptoms are commonly non-liver-specific and subtle, likely affecting quality of life, such as fatigue. Therefore, the functional impairment associated with cardiometabolic dysfunctions/MASLD was assessed in a real-world study using two validated patient-reported outcome measures (PROMs), the short-form-health-survey-12 (SF-12) and functional assessment of chronic illness therapy-fatigue (FACIT-F).
Method: The remote prospective cross-sectional real-world study was carried out in 06–07/2024 and targeted subjects (at risk of) having MASLD. German-speaking participants were recruited via online advertisements targeted at overweight subjects aged 35–70 years (based on the limited awareness of MASLD) and forwarded to a proprietary questionnaire covering general information on e.g. lifestyle and medical history, with the subsequent option to answer FACIT-F and SF-12.
Results: 6,788 participants started and 4,991 completed the online survey (86% 35–69 years of age, 84% female) within four weeks. Almost all participants reported at least one cardiometabolic risk factor for MASLD, with 94% of participants (4,698/4,991) being at least overweight (BMI ≥ 25 kg/m^2), 31% (1,568/4,991) having elevated blood lipid levels and 49% (2,464/4,991) suffering from cardiovascular disease. 19% of participants (967/4,991) reported to be already diagnosed with MASLD. The assessment of fatigue via FACIT-F showed a significant decrease in the total FACIT-F score (indicating increased fatigue) in participants with diagnosed MASLD (mean ± SD: 25.65 ± 11.29, N = 522) compared with overweight participants without self-reported diagnosed liver disease (28.78 ± 10.94, N = 1,540, p < 0.001), with both scores being markedly lower than in the general German population (43.5 ± 8.3; Montana *et al.*, *Value in Health* 2018). Additionally, results suggest a positive correlation between liver disease severity and fatigue as the lowest FACIT-F scores (22.65 ± 11.57, N = 20) were observed in participants with end stages of MASLD (cirrhosis/hepatocellular carcinoma). Results for SF-12 indicate a similar trend for health-related quality of life.
Conclusion: Real-world data indicate a functional impairment already in early MASLD stages without liver-specific symptoms that worsens with disease progression and thus demands early intervention.

SAT-021

Transparent and dynamic network-based risk assessment for development of hepatic encephalopathy

Yuxi Shi[1], Zixing Wang, Huiying Rao[1], Xin Wen[1], Tianyi Xue[1], Yanpei Mai[1], Suzhen Jiang[1], Shuo Yang[1], Qinshuo Wang[1], YanHui Yang[1], Linlin Cao[1]. [1]*Peking University People's Hospital, Beijing, China*
Email: wangzixing@pkuph.edu.cn

Background and aims: Hepatic encephalopathy (HE) is a common and prognostically severe neurological complication in cirrhosis. Early identification of high-risk patients remains a major clinical challenge. The multifactorial nature of HE suggests a need for more integrated assessment approaches that can capture its complex pathophysiology beyond the scope of single biomarkers or conventional risk scores.
Method: We included 3,487 patients with multi-etiology cirrhosis, divided into training (n = 2,789) and validation (n = 698) sets. A Bayesian network-based risk assessment model was constructed by integrating expert knowledge and data-driven mining. The model incorporates complication sequences (e.g., ascites, gastroesophageal varices, peritonitis) and nine core laboratory indicators selected from 980 candidates (including ammonia, INR, RDW-SD, fibrinogen, triglycerides, MCH, neutrophil count, sodium, and total CO_2), and is compatible with partially missing data.
Results: During a maximum follow-up of 14 years, 398 patients developed overt HE. HE occupied a central hub within the complication network. Its onset was significantly associated with ascites (adjusted relative risk [aRR] = 4.8), gastroesophageal varices (aRR = 3.6), peritonitis (aRR = 2.2), hepatorenal syndrome (aRR = 2.1), variceal hemorrhage (aRR = 1.9), and hepatocellular carcinoma (aRR = 1.5); all p < 0.05. The network model demonstrated superior predictive performance in the validation set: baseline AUROC was 0.926 (95% CI: 0.882–0.962), improving to 0.962 (0.933–0.984) in longitudinal follow-up. This significantly outperformed MELD (AUROC 0.670) and BABS scores (0.745) (both p < 0.001). The model maintained robust performance across demographic subgroups and supported both a simplified key-node assessment (age ≥75, hyponatremia, hyperammonemia, elevated INR, elevated RDW-SD) and smart device-integrated dynamic updating for complication warning.

Conclusion: This dynamic network model integrates temporal complication sequences and multi-system biomarkers to provide transparent, precise, and dynamic HE risk assessment. It holds strong potential for clinical translation in patient risk stratification, individualized screening optimization, and complication prevention, offering a novel strategy for holistic cirrhosis management.

SAT-022

Trends in mortality due to liver neoplasms in Portugal (2013–2022): a decade of rising challenges

Mario Jorge Silva[1,2], Pedro Lages Martins[1,2], Filipe Calinas[1], Paulo Nogueira[3]. [1]*Unidade Local de Saúde de São José – Serviço de Gastrenterologia, Lisboa, Portugal;* [2]*NOVA Medical School, Lisboa, Portugal;* [3]*Instituto de Saúde Ambiental, Laboratório Associado TERRA, Faculdade de Medicina, Universidade de Lisboa, Lisboa, Portugal*
Email: mariojorgesilva01@gmail.com

Background and aims: The burden of liver neoplasms may have been changing recently, given the shifts in predominant etiologies of chronic liver disease (e.g. decrease in hepatitis C-related liver disease, increase in metabolic dysfunction-associated steatotic liver disease). Mortality due to liver tumors over the past decade in Portugal is largely unknown. We aim to analyze the mortality due to liver neoplasms in Portugal from 2013 to 2022, focusing on temporal trends, tumor subtypes and regional distributions.
Method: Statistics Portugal (*Instituto Nacional de Estatística*) provided data on annual mortality from liver neoplasms (International Classification of Diseases-10: C22), including specific tumor subtypes: hepatocellular carcinoma (C22.0), intrahepatic bile duct carcinoma (C22.1) and malignant neoplasm of the liver not otherwise specified (C22.8 + C22.9). These data derive from coding of death certificates. Mortality rates were calculated per 100,000 inhabitants. Trends were analyzed with R software version 4.4.1 (R Foundation for Statistical Computing, Vienna, Austria), using linear regression (LR) and nonparametric Mann-Kendall (M-K) test to identify significant temporal patterns. Differences were considered statistically significant when $p < 0.05$ (two-sided). Specific analyses were performed for tumor subtypes and for geographic regions.
Results: Between 2013 and 2022, total deaths from liver neoplasms increased by 20% ($p = 0.0005$ in LR, $p = 0.0024$ in M-K): from 1,037 deaths in 2013 to 1,248 deaths in 2022. Regional disparities were observed: in 2022, the highest mortality rates were observed in the Madeira region (15.4/100,000 inhabitants) and the lowest in the Algarve (9.9/100,000 inhabitants). During the 10-year period, there was a striking 42% rise in deaths due to intrahepatic bile duct carcinoma ($p = 0.00002$ in LR, $p = 0.00068$ in M-K). Considering mortality due to all liver neoplasms, the proportion of deaths due to intrahepatic biliary neoplasms increased from 32.9% (341/1037) in 2013 to 38.9% (485/1248) in 2022. Deaths due to hepatocellular carcinoma increased by 21% ($p = 0.0168$ in LR, $p = 0.0318$ in M-K) between 2013 ($n = 496$) and 2022 ($n = 602$). Mortality due to liver neoplasms not otherwise specified remained stable ($p = 0.433$ in LR, $p = 0.928$ in M-K) during the 10-year period.
Conclusion: Between 2013 and 2022, there was a significant increase in mortality due to liver neoplasms in Portugal: including both hepatocellular carcinoma and, particularly, intrahepatic bile duct carcinoma.

SAT-023

From guidelines to practice : Expert advisory board insights on nutritional intervention in patients with liver cirrhosis in India

Nagaraja Padaki[1], KR Vinayakumar[2], Jyoti Mohapatra[3], Akash Roy[4], Abhishek Banerjee[5], Sourabh Sonawale[6], Nandan Joshi[6]. [1]*Asian Institute of Gastroenterology Private Limited (Banjara Hills) Gaffar Khan Colony, Telangana 500045, Hyderabad, India;* [2]*Ananthapuri Hospitals and Research Institute in Trivandrum, Thiruvananthapuram, India;* [3]*Peerless Hospital, Kolkata, Kolkata, India;* [4]*Apollo Gleneagles Hospitals Kolkata, Kolkata, India;* [5]*Manipal Hospitals Kolkata, Kolkata, India;* [6]*Dr. Reddy's and Nestle Health Science Limited, Hyderabad, India*
Email: nandanarunjoshi@drreddysnestle.com

Background and aims: Malnutrition and sarcopenia are frequent yet under-recognised complications of liver cirrhosis and are associated with infections, hepatic encephalopathy (HE), reduced quality of life, and increased mortality. Globally, malnutrition affects ~ 20–30% of patients with compensated cirrhosis and over 50–60% with decompensated disease, while sarcopenia is reported in 30–70% of cases. Indian studies indicate a high burden, with malnutrition and sarcopenia affecting approximately 47–84% of patients. European Association for the Study of the Liver (EASL) and European Society for Clinical Nutrition and Metabolism (ESPEN) guidelines recommend early nutritional screening, adequate energy intake, protein intake of at least 1.2–1.5 g/kg/day, and avoidance of unnecessary protein restriction, including in HE. However, real-world implementation remains inconsistent. This initiative aimed to capture real-world insights into nutritional assessment practices in cirrhosis and the role of branched-chain amino acids in HE.
Method: This was a cross-sectional, descriptive analysis using live polling and expert discussion from 5 advisory board meetings conducted over 3 months. A total of 68 gastroenterologists across India participated. Discussions focused on patients with established cirrhosis, including compensated and decompensated stages and those with HE.
Results: Routine nutritional assessment was inconsistent: 50 percent assessed nutrition every three months, 10% every six months, while 40% assessed only after clinical deterioration. Nutritional supplementation was mainly guided by disease severity, with 70% relying on Child - Pugh class. Limited awareness, restricted access to dietitians, and patient non-compliance were reported as barriers by approximately 80% of participants. High-protein oral nutritional supplements were prescribed in up to 75% of patients. Experts reported better tolerance with high-quality protein sources such as whey protein isolate due to low fat content and negligible lactose. Protein intolerance was uncommon; when present, branched-chain amino acids were preferentially used for HE, with approximately 80% reporting routine use.
Conclusion: A clear gap exists between guideline recommendations and routine nutritional assessment in liver cirrhosis, while nutrition prescription practices and branched-chain amino acid use in HE appear largely aligned with current guidance. Strengthening structured nutritional pathways is essential to optimise nutritional care.

SAT-024-YI

Contacts to general practice by patients with liver cirrhosis: a Danish nationwide cohort study

Marie Storgaard[1,2,3], Bo Christensen[3,4], Morten Daniel Jensen[2], Joe West[1,5,6,7], Peter Jepsen[1,2,3,5]. [1]*Department of clinical medicine, Aarhus university, Aarhus, Denmark;* [2]*Department of hepatology and gastroenterology, Aarhus university hospital, Aarhus, Denmark;* [3]*Department of clinical epidemiology, Aarhus university hospital, Aarhus, Denmark;* [4]*Department of public health, Research unit of general medicine, Aarhus, Denmark;* [5]*Lifespan and population health, School of medicine, University of Nottingham, Nottingham, United Kingdom;* [6]*NIHR Nottingham biomedical research centre (BRC), Nottingham university hospitals NHS trust and the University of Nottingham, Nottingham, United Kingdom;* [7]*Clinical practice research datalink, Medicines and healthcare products regulatory agency, Nottingham, United Kingdom*
Email: marieaa@clin.au.dk

Background and aims: General practitioners (GPs) can play a crucial role in preventive care and management of comorbidities in patients with cirrhosis; however, the pattern of GP contacts in this population remains poorly characterized. We aimed to describe the number, rates, and trends of GP consultations among patients with cirrhosis.

Method: In a nationwide registry-based cohort study, we included all Danish patients with an incident hospital-based diagnosis of cirrhosis in 2015–2023, along with 5:1 sex-, birth year-, and age-matched comparators from the general population. We assessed rates and predictors of GP consultations and described characteristics and survival among patients who experienced going one full year without a GP consultation.
Results: We included 17,263 patients with cirrhosis and 86,315 comparators (median age 64 years; 64% male). Patients with cirrhosis had higher annual GP consultation rates than their comparators, both for in-person consultations (6.2 [95% CI: 6.2–6.2] vs 4.1 [4.1–4.1]) and telephone consultations (4.7 [4.6–4.7] vs 2.0 [2.0–2.0]). GP consultation rates declined over calendar time in both cohorts. This decline was most pronounced among patients with cirrhosis (in-person: HR 0.95 [0.94–0.95] vs 0.97 [0.97–0.97] per year; telephone: HR 0.91 [0.90–0.92] vs 0.95 [0.94–0.95] per year). Consultation rates were highest in the first year after cirrhosis diagnosis and decreased afterward. Higher consultation rates were associated with decompensated cirrhosis (decompensated vs compensated: HR 1.08 [1.07–1.10]), female sex (female vs male: HR 1.16 [1.08–1.15]), and living in rural municipalities (rural municipality vs capital city municipality: HR 1.29 [1.23–1.35]). A total of 3,161 patients went an entire year without a GP in-person consultation. On the date, when they had not seen their GP for a full year, these patients had less severe cirrhosis than those who had seen their GP within the previous year, and they had a lower mortality (HR 0.80 [0.74–0.87]).
Conclusion: Danish patients with cirrhosis had substantially higher GP consultation rates than the general population, and these rates were highest among female and decompensated patients. Most patients saw their GP every year, and those who experienced going one year without a GP consultation represented a healthier subgroup with a favorable prognosis. This high level of GP involvement highlights the potential to increase collaboration between GPs and hepatologists to improve the overall care for patients with cirrhosis.

SAT-025
Sociodemographic associations between increasing alcohol sales and new hospitalizations for alcohol-related cirrhosis in Alberta, Canada

Liam Swain[1], Jenny Godley[2], Juan G Abraldes[3], Abdel Aziz Shaheen[4].
[1]*University of Calgary Cumming School of Medicine, Calgary, Canada;* [2]*University of Calgary Department of Anthropology and Archaeology, Calgary, Canada;* [3]*Liver Unit, Department of Medicine, Division of Gastroenterology, University of Alberta, Edmonton, Canada;* [4]*Department of Community Health Sciences, University of Calgary, Department of Medicine, Division of Gastroenterology and Hepatology, Cumming School of Medicine, University of Calgary, Calgary, Canada*
Email: aashahee@ucalgary.ca

Background and aims: Few studies have examined the temporal association between alcohol sales and alcohol-related cirrhosis (AC) hospitalization rates. We examined how an elevation in alcohol sales impacts subsequent AC hospitalizations, in Alberta.
Method: We obtained monthly Alberta alcohol sales (all beer/wine/liquor stores) from 2019 to 22. Using a validated coding algorithm (PPV > 90%), we identified all monthly AC hospitalizations in Alberta from the Discharge Abstract Database. Using the 2021 Census, we calculated monthly alcohol sales per capita (ASPC) and AC hospitalization rates/100,000 population. Hospitalization rates were stratified by sex, age (≥ vs <55 years), and dissemination area median after tax household income (> vs ≤$67,430). We stratified our analysis by Alberta region, including Calgary, Edmonton, and all regions outside of Calgary/Edmonton (i.e., rural). We used a Newey-West 1–12 month lagged linear regression model with monthly AC hospitalization rates/100,000 as the outcome and monthly ASPC as the exposure. The cumulative linear regression coefficients from 1–6 vs 7–12 months and 95% confidence intervals (CI) are presented.
Results: From 2019–22, there were 9553 AC admissions. In Alberta, a $1 increase in ASPC led to a 0.25 (CI 0.25–0.40) unit increase in AC hospitalization rates/100,000 1-6 months later; ≈8 AC hospitalizations. In Alberta, AC hospitalization rates increased 1–6 months after a $1 ASPC increase only for those living in lower income areas (0.51, CI 0.31–0.70); ≈15 AC hospitalizations. In Edmonton, females had a 0.13 unit increase in AC hospitalization rates 7–12 months after a $1 ASPC increase; ≈1 AC admission. In rural Alberta, a $1 ASPC increase led to ≈ 1 AC hospitalization for males 1–6 months later (0.22, CI 0.07–0.37), while rural females had an increase in AC hospitalization rates 1–6 (0.09, CI 0.04–0.14) and 7–12 (0.08, CI 0.02–0.13) months later; ≈1 AC hospitalization. In rural regions, a $1 increase in ASPC led to an increase in AC hospitalization rates 1–6 and 7–12 months after for younger individuals (0.17, CI 0.09–0.25; 0.12, CI 0.05–0.20), but only 1–6 months after for older individuals (0.13, CI 0.06–0.20).
Conclusion: In Alberta, monthly increases in alcohol sales predict new AC hospitalizations, but only for those living in lower income areas. The lagged effect of alcohol sales on AC hospitalizations was primarily seen in rural areas and had the largest impact on females and younger populations.

SAT-026
Sociodemographic associations between increasing alcohol sales and new hospitalizations for alcohol-related hepatitis in Alberta, Canada

Liam Swain[1], Jenny Godley[2], Juan G Abraldes[3], Abdel Aziz Shaheen[4].
[1]*University of Calgary Cumming School of Medicine, Calgary, Canada;* [2]*University of Calgary Department of Anthropology and Archaeology, Calgary, Canada;* [3]*Liver Unit, Department of Medicine, Division of Gastroenterology, University of Alberta, Edmonton, Canada;* [4]*Department of Community Health Sciences, University of Calgary, Department of Medicine, Division of Gastroenterology and Hepatology, Cumming School of Medicine, University of Calgary, Calgary, Canada*
Email: aashahee@ucalgary.ca

Background and aims: Few studies have examined the temporal association between alcohol sales and alcohol-related hepatitis (AH) hospitalization rates. We examined sociodemographic drivers that link increasing alcohol sales and subsequent AH hospitalizations, in Alberta.
Method: We obtained Statistics Canada monthly Alberta alcohol sales (all beer/wine/liquor stores) from 2019 to 22. Monthly AH hospitalizations in Alberta were identified using a validated coding algorithm (PPV > 90%) from the Discharge Abstract Database. Using the 2021 Census, we calculated monthly alcohol sales per capita (ASPC) and AH hospitalization rates/100,000 population. Hospitalization rates were stratified by sex, age (≥ vs <45 years), and dissemination area median after tax household income (> vs ≤$71,168). We stratified our analysis by Alberta region, including Calgary, Edmonton, and all regions outside of Calgary/Edmonton (i.e., classified as rural). We used a Newey-West 1–12 month lagged linear regression model with monthly AH hospitalization rates/100,000 as the outcome and monthly ASPC as the exposure. The cumulative linear regression coefficients from 1 to 6 vs 7–12 months and 95% confidence intervals (CI) are presented.
Results: From 2019–22 in Alberta, there were 1081 AH admissions. In Alberta, a $1 increase in ASPC led to a 0.06 (CI 0.03–0.09) unit increase in AH hospitalization rates/100,000 1-6 months later (Table 1); ≈ 2 AH hospitalizations. In Alberta, AH hospitalization rates/100,000 increased 1–6 months after a $1 ASPC increase only for those living in lower compared to higher income areas (0.15, CI 0.10–0.19); ≈2 AH hospitalizations. In rural Alberta, a $1 ASPC increase led to a 0.03 (CI 0.01–0.05) and a 0.02 (CI 0.002–0.05) unit increase in female AH hospitalization rates 1–6 and 7–12 months later, respectively. In contrast, rural males had an increase in AH hospitalization rates only 1–6 months after a $1 ASPC increase (0.05, CI 0.03–0.07). In rural regions, only younger individuals had an

increase in AH hospitalization rates/100,000 1–6 months after, after a $1 ASPC increase (0.08. CI 0.06–0.11).
Conclusion: In Alberta, AH hospitalizations increased 1–6 months after a monthly elevation in alcohol sales. The relationship between increasing alcohol sales and new AH hospitalizations was only observed in lower income and rural areas. In rural Alberta, increasing alcohol sales had a large impact on AH hospitalizations for younger and female populations.

SAT-027
Temporal and seasonal trends in alcohol sales and alcohol-related liver disease hospitalizations in Alberta, Canada
Liam Swain[1], Jenny Godley[2], Juan G Abraldes[3], Abdel Aziz Shaheen[4]. [1]*University of Calgary Cumming School of Medicine, Calgary, Canada;* [2]*University of Calgary Department of Anthropology and Archaeology, Calgary, Canada;* [3]*Liver Unit, Department of Medicine, Division of Gastroenterology, University of Alberta, Edmonton, Canada;* [4]*Department of Community Health Sciences, University of Calgary, Department of Medicine, Division of Gastroenterology and Hepatology, Cumming School of Medicine, University of Calgary, Calgary, Canada*
Email: aashahee@ucalgary.ca

Background and aims: Few studies have examined the seasonality and temporal trends of alcohol sales in North America and its relation to hospitalizations for alcohol-related liver disease (ALD). We examined temporal trends and the seasonality of alcohol sales per capita in Alberta, Canada, from 2012–22. We compared trends in alcohol sales to ALD hospitalizations.
Method: We obtained monthly alcohol sales (all beer/wine/liquor stores) in Alberta, from 2012 to 22. Using validated algorithms (PPV > 90%) we identified all alcohol-related cirrhosis/hepatitis hospitalizations (age ≥ 20 yr) in Alberta from the Discharge Abstract Database between 2012–22. We used 2016/21 Census data to calculate monthly alcohol sales per capita and annual age-adjusted ALD hospitalization rates/100,000 population. Between 2019–22, we stratified monthly alcohol sales per capita within 3 Alberta regions: the 2 major urban areas Calgary and Edmonton, and the rest of Alberta. We used Kruskal-Wallis tests to compare regional median monthly alcohol sales. Trends in alcohol sales per capita and ALD hospitalizations/100,000 were assessed using joinpoint analysis, annual percent change (APC), and average annual percent change (AAPC).
Results: From 2012–22, Alberta had $29.89 billion in alcohol sales. From 2019–22, the median monthly alcohol sales per capita was higher for regions outside of Calgary and Edmonton ($86.52), vs Calgary ($65.65, $p < 0.001$) and Edmonton ($80.79, $p = 0.017$). Edmonton had higher alcohol sales per capita vs Calgary ($p < 0.001$). From 2012–22, total Alberta alcohol sales increased by 2.25%/year (AAPC 95% CI 1.82–2.65). Total Alberta alcohol sales per capita significantly increased from 2012–17 by 5.25%/year, decreased by −8.13%/year from 2017–18, increased by 9.30%/year from 2018–20, and decreased by −3.09%/year from 2020–22. The alcohol sale APC and inflection points paralleled our observed ALD trends, with inflection points occurring in 2016/19/21. Our regionally stratified analysis of monthly alcohol sales per capita from 2019–22 identified annual bimodal peaks in alcohol sales per capita occurring in December and June-July for all regions.
Conclusion: Between 2012–22, alcohol sales per capita increased in Alberta, with the highest sales observed in more rural regions. Trends in ALD hospitalization rates and alcohol sales paralleled each other in Alberta. We observed a bimodal seasonality in alcohol sales across Alberta with the highest sales occurring in December and the early summer months.

SAT-028
Geographic variation in primary biliary cholangitis across Alberta: Validated incidence and prevalence estimates with Joinpoint trends
Bryce Tkachuk[1], Liam Swain[1], Aldo J Montano-Loza[2], Abdel-Aziz Shaheen[1]. [1]*University of Calgary, Calgary, Canada;* [2]*University of Alberta, Edmonton, Canada*
Email: az.shaheen@ucalgary.ca

Background and aims: Rates of primary biliary cholangitis (PBC) in Alberta are among the highest in North America; provincially validated estimates by sex, age, and health zone are needed to guide care planning. We estimated trends and zonal differences in PBC prevalence and incidence by sex, age group, and health zone (Calgary, Edmonton, Rest-of-Alberta).
Method: We created a provincial adult (≥18 y) PBC cohort using linked inpatient, ambulatory, physician-claims, and registry data (prevalence: 2002–2021; incidence: 2004–2021 with a 2-year washout). Within 3,250 potential PBC cases, chart review confirmed true PBC. Rates were age-standardized to the 2021 Canadian population. Incidence rate ratios (IRRs) were estimated using negative binomial models with population offsets; trends used Joinpoint to derive Annual Percentage Change (APC) / Average Annual Percentage Change (AAPC) (95% CI).
Results: We confirmed 1,470 incident cases (total confirmed PBC = 1,845; median age 58 y; 88.2% female). In 2021, age-adjusted prevalence was 84.5 per 100,000 in females and 10.9 per 100,000 in males; mean annual incidence was 3.2 per 100,000. Prevalence increased 2002–2021 (Alberta AAPC 11.8%, 95% CI 11.4–12.4) with zonal variation ($p < 0.001$): Calgary 10.0% (9.5–10.8), Edmonton 12.4% (11.8–13.9), Rest-of-Alberta 13.4% (12.9–14.0). Incidence rose 2004–2017 (APC 6.4%, 95% CI 4.2–11.1; $p < 0.001$) then declined 2017–2021 (APC −9.8%, 95% CI −35.5 to −2.0; $p = 0.024$); Edmonton declined 2016–2021 (APC −13.7%, 95% CI −37.4 to −4.6; $p = 0.007$); Calgary's 2016–2021 decline was non-significant, and Rest-of-Alberta trended down in 2020–2021. In adjusted models (ref = Calgary), Rest-of-Alberta had higher incidence (IRR 1.19, 95% CI 1.02–1.38; $p = 0.02$) while Edmonton was not different (IRR 1.11, 0.95–1.28; $p = 0.18$). Females had markedly higher incidence than males (IRR 7.00, 95% CI 5.96–8.23) with strong age gradients vs 20–34 y: 35–49 y IRR 7.56, 50–64 y IRR 18.72, and ≥ 65 y IRR 18.18 (all $p < 0.001$).
Conclusion: PBC prevalence is high and rising in Alberta with persistent health zone differences, while incidence has stabilized/declined since 2017. Findings support zone-specific diagnostic strategies and resource allocation, particularly for older women and higher-burden regions. These validated, chart-confirmed estimates establish a provincial baseline for zone-level service planning (diagnostic testing, UDCA monitoring, hepatology access), and for evaluating future policies or pathway interventions across Alberta populations.

SAT-029
Socio-economic deprivation is overrepresented in Australian cirrhosis patients seeking acute hospital-based care, suggesting disparities in utilisation of structured outpatient services
Tess Bittermann[1], Elizabeth Goode[1,2], Gunter Hartel[1], Vikas Bhasker[1], Danielle Gallegos[3], Elizabeth E. Powell[1], Patricia C. Valery[1]. [1]*QIMR Berghofer, Herston, Australia;* [2]*Royal Brisbane and Women's Hospital, Herston, Australia;* [3]*Queensland Universtity of Technology, Brisbane, Australia*
Email: patricia.valery@qimrb.edu.au

Background and aims: Socio-economic deprivation (SED) influences health outcomes, yet its impact on cirrhosis remains underexplored. Using Z-codes from hospital records of cirrhosis patients, we examined mortality, healthcare use, and costs by SED.
Method: Population-based retrospective cohort analysis of all adults hospitalised with cirrhosis in Queensland, Australia (2007–2022) included 2,160 patients with SED (ICD code Z59) vs 20,228 without.

They were followed from the first hospitalisation or emergency presentation with cirrhosis until death or 31-Dec-2022, whichever came first. In multivariable analysis adjusting for sociodemographic and clinical factors, we examined cause-specific mortality (Fine and Gray models), rate of hospitalizations and emergency presentations (Poisson regression), and ratio of costs of hospitalizations (Poisson regression) by SED. The costs were inflated to Jun-2025.

Results: SED was over sixfold more common among cirrhosis admissions (9.6% vs 1.5%; p < 0.001) compared with all adult admissions in Queensland during 2007–2022. Patients with cirrhosis facing SED were younger at first admission (53.0 vs 62.2 years; p < 0.001), and male (69.0% vs 65.7%: p < 0.001) and First Nations patients (20.5% vs 7.2%) were overrepresented vs patients without SED. During a median follow-up of 6.9 years (IQR 3.5–11.2), 12,309 patients died (50.3% from liver disease). Compared to patients without SED, patients facing SED had increased risk of mortality due to external causes (e.g. accident, self-harm – sHR = 1.99, 95%CI 1.51–2.63; p < 0.001) and cardiovascular disease (adj-sHR = 1.52, 95%CI 1.24–1.86; p < 0.001), were less likely to die of liver disease (sHR = 0.70, 95%CI 0.64–0.77; p < 0.001) and extrahepatic cancer (adj-sHR = 0.70, 95%CI 0.54–0.90; p < 0.001), had more emergency presentations for cirrhosis (adjusted incidence rate ratio (adj-IRR) = 1.29, 95%CI 1.16–1.45; p < 0.001), and fewer planned same-day cirrhosis admissions (adj-IRR = 0.69, 95%CI 0.57–0.83; p < 0.001). Over 10.5 years, 19,820 cirrhosis admissions cost A$1.14 billion (Jul-2012 to Dec-2022). Costs were 1.69-fold higher for patients with SED (95%CI 1.58–1.80; p < 0.001).

Conclusion: Cirrhosis places a heavy burden on the community, particularly among those facing SED. Fewer planned admissions and more emergency presentations among deprived patients points to barriers in structured follow-up care. Increased non-liver mortality in patients with SED indicates a need for tailored prevention approaches.

SAT-030

Improving patient knowledge — A feasible target to enhance motivation for lifestyle change in patients with MASLD in Australia

Patricia C. Valery[1], Elizabeth E. Powell[1], Barbara Leggett[2], Karen Simmons[3], Katie McGuire[3], Vikas Bhasker[1], Melanie Aikebuse[1], Georgina Peacock[2], Richard Skoien[2], James O'Beirne[3]. *[1]QIMR Berghofer, Herston, Australia; [2]Royal Brisbane and Women's Hospital, Herston, Australia; [3]Sunshine Coast University Hospital, Sunshine Coast, Australia*

Email: patricia.valery@qimrb.edu.au

Background and aims: Motivation to adopt lifestyle changes may be influenced by patients' knowledge of MASLD, their illness perceptions, and sociodemographic or clinical characteristics. This study examined motivation to modify diet and physical activity among MASLD patients in Queensland, Australia.

Method: This cross-sectional study included 142 adults ascertained from three Hepatology outpatient clinics (Sep-2023 to Aug-2025) who fit the definition of MASLD (including alcohol use below harmful thresholds). The self-completed questionnaire included two questions about motivation to change diet/physical activity with answers categorised as '*low motivation*', '*high motivation*', and '*not applicable*' (healthy diet/physically active). The questionnaire included the Brief Illness Perception Questionnaire (BIPQ), six questions on MASLD knowledge, the Generalized Anxiety Disorder Scale, the Patient Health Questionnaire to assess depression, alcohol use (AUDIT-C), and the Self-Administered Comorbidity Questionnaire. We examined factors associated with 'low motivation' to change lifestyle (multivariable logistic regression - aforesaid factors were considered for inclusion in the models).

Results: The mean age was 60.5 years (SD = 13.6), 61.3% were female, 61.3% had higher educational level (e.g. trade, diploma), 62.4% were obese, 21.8% had liver stiffness measurement >12.5 kPa, 64.2% had self-assessed anxiety and 89.4% depression, and 53.5% reported continued alcohol use. Over 50% of patients self-reported having hypertension, back pain, and diabetes, and over 33% reported arthritis and obstructive sleep apnoea. 62.0% of the patients had 4–6 correct answers to the MASLD knowledge questions. The mean total BIPQ score was 37.2 (SD 12.1), indicating a moderate illness perception. In multivariable analysis, poor MASLD knowledge (0–3 correct answers out of six, adj-OR = 5.38, 95%CI 1.62–17.90; p = 0.006), higher educational level (adj-OR = 4.16, 95%CI 1.09–15.95; p = 0.038), and continued alcohol use (vs no alcohol use; adj-OR = 3.95, 95%CI 1.01–15.38; p = 0.048) were associated with low motivation to change diet. Poor MASLD knowledge (adj-OR = 2.87, 95%CI 1.15–7.16; p = 0.024) was the only factor associated with low motivation to change physical activity.

Conclusion: Patient knowledge appears to be a readily modifiable factor that could enhance motivation for lifestyle change among individuals with MASLD.

SAT-031-YI

Validated early detection metrics reduces the population requiring liver fibrosis screening

Laurens A. van Kleef[1], Jesse Pustjens[1], Carolin V. Schneider[2], Guillem Pera[3], Pere Torán[3], Maurice Michel[4], Kai Schneider[5], A.G. (Onno) Holleboom[6], Manuel Castro Cabezas[7], Maarten Tushuizen[8], Harry L.A. Janssen[1], Jörn M. Schattenberg[4], Pere Ginès[9], Sven Francque[10], Zobair M. Younossi[11], Aleksander Krag[12], Willem Pieter Brouwer[1]. *[1]Erasmus MC, Rotterdam, Netherlands; [2]RWTH Aachen, Aachen, Germany; [3]Unitat de Suport a la Recerca Metropolitana Nord, Fundació Institut Universitari per a la Recerca a l'Atenció Primària de Salut Jordi Gol i Gurina (IDIAPJGol), Barcelona, Spain; [4]Department of Internal Medicine II, Saarland University Medical Center, Homburg, Germany; [5]TU Dresden, Dresden, Germany; [6]Amsterdam Medical Center, Amsterdam, Netherlands; [7]Sint Franciscus Gasthuis, Rotterdam, Netherlands; [8]Leids UMC, Leiden, Netherlands; [9]Hospital Clinic of Barcelona, Barcelona, Spain; [10]Antwerp University Hospital, Edegem, Belgium; [11]The Global NASH Council, Washington, United States; [12]Odense University Hospital, Odense, Denmark*

Email: l.vankleef@erasmusmc.nl

Background and aims: Diabetes, obesity, and elevated ALT are indicators to screen for liver disease. Yet, guidelines differ on which features should trigger screening. Given the increasing prevalence of metabolic comorbidities and feasibility issues of screening programs, we sought to refine screening criteria using population-based data.

Method: We included adults aged 18–80 years from NHANES 2017–2020 with BMI ≥18.5 kg/m^2, without excessive alcohol consumption, and with complete screening indicator data. Weighted proportions of individuals meeting EASL, AASLD, AGA, and ADA screening criteria were estimated. We assessed the prevalence of liver stiffness measurement (LSM) ≥8 kPa across screening indicators using stratified analyses. The refined criteria were validated in three independent general population cohorts from Rotterdam, Barcelona and the US and linked with LRE in UK-biobank.

Results: The derivation included 5,904 adults (mean age 47 years, 49% male); 8.9% had LSM ≥8 kPa. Current guidelines identified 60–76% for screening, yielding PPVs of 11–14% and NPVs of 98% for LSM ≥8 kPa. A refined strategy based on the stratified analyses triggered screening in 22% while maintaining a high NPV (96%) and improved PPV (28%) for LSM ≥8 kPa. In the pooled validation cohort (n = 13,295), 7.0% had LSM ≥8 kPa and 14% met the refined screening criteria. Validation results were consistent across different LSM thresholds: PPV 22% and NPV 96% for LSM ≥8 kPa; PPV 13% and NPV 98% for LSM ≥10 kPa; and PPV 8% and NPV 99% for LSM ≥12 kPa. In the UK-Biobank (n = 282,582), high-risk individuals had an approximate 6-fold higher risk (1.02%) of 10-year incident cirrhosis or liver-related death (0.40%) than those not meeting the refined screening criteria (0.18% and 0.07% resp.).

Conclusion: Current guidelines target 60–76% of the US adult population for MASLD-induced advanced chronic liver disease screening, creating a diagnostic capacity challenge that hinders implementation. To overcome this, we developed and validated in 302,051 adults a refined set of indicators for screening prioritisation: (1) T2DM with elevated ALT or obesity or (2) obesity class III regardless of other factors OR obesity class II with elevated ALT OR Obesity class I with elevated ALT and ≥ 3 metabolic risk factors. These criteria reduce the target population to 10–22%, improve PPV while maintaining high NPV for LSM ≥8 kPa. Importantly, LRE were rare among those without screening indicators, justifying targeted screening of those with more profound risk factors.

SAT-035

Impact of fibrotic MASH as a new indication on semaglutide eligibility in the U.S. adult population

Laurens A. van Kleef[1], Maurice Michel[2], Mesut Savas[1], Jesse Pustjens[1], Willy Theel[1], Elisabeth van Rossum[1], James M. Paik[3], Zobair M. Younossi[3], Harry L.A. Janssen[1], Christian Labenz[4], Jörn M. Schattenberg[2], Willem Pieter Brouwer[1]. *[1]Erasmus MC, Rotterdam, Netherlands; [2]Department of Internal Medicine II, Saarland University Medical Center, Homburg, Germany; [3]The Global NASH Council, Washington, United States; [4]University Medical Center Mainz, Mainz, Germany*
Email: l.vankleef@erasmusmc.nl

Background and aims: Semaglutide, a glucagon-like peptide-1 receptor agonist, is effective in the treatment of fibrotic (F2–F3) metabolic dysfunction-associated steatohepatitis (MASH) and has recently received accelerated FDA approval. However, the extent to which this new indication expands treatment eligibility beyond existing approvals for type 2 diabetes mellitus (T2DM) and obesity remains unclear.
Method: We analyzed nationally representative NHANES data (2017–2020) on U.S. adults, excluding individuals with viral hepatitis or excessive alcohol consumption. Semaglutide eligibility was defined according to FDA-approved indications for weight loss (BMI ≥ 27 kg/m^2 with weight related comorbidity), high-risk T2DM (T2DM with CVD or high risk of CVD or impaired renal function), or fibrotic MASH (LSM 8–15 kPa with MASLD [CAP ≥ 275 db/m + metabolic dysfunction]). Findings were validated in the Mainz (Germany) biopsy cohort (n = 213) with biopsy-proven MASLD and F2–F3 fibrosis.
Results: We included 6,936 adults, the weighted median age was 47 years [32–61], 47.9% were male, MASLD was present in 41.0% and fibrotic MASH in 5.2%. In the adult U.S. general population, 51.5% met indications for semaglutide for weight loss (41.8 of 51.5%), high-risk T2DM (2.0 of 51.5%) or both (7.7 of 51.5%). Among individuals with MASLD, 80.9% qualified for treatment based on conventional indications, increasing to 95.4% in those with fibrotic MASH. Including fibrotic MASH as an additional indication marginally increased overall eligibility (from 51.5% to 51.8%), reflecting that most individuals with fibrotic MASH already met eligibility criteria through obesity or high-risk T2DM. In the Mainz cohort, 80.3% of patients with biopsy-proven F2–F3 fibrosis were eligible for semaglutide irrespective of fibrotic MASH, in agreement with the findings from the general population.
Conclusion: Semaglutide eligibility is high among U.S. adults. The new fibrotic MASH indication largely overlaps with pre-existing indications, primarily obesity, which uses the same dose as fibrotic MASH. These findings highlight the intertwined nature of metabolic comorbidities and liver disease and emphasize the need for an integrated, patient-centred approach to semaglutide, alongside policies that improve access and reimbursement.

SAT-036

Artificial intelligence in scientific abstract review: complement or contradiction to human judgment? Insights from a Latin American hepatology cohort

Pablo Coste[1], Ezequiel Ridruejo[2], Marco Arrese[3], Javier Díaz Ferrer[4], Melisa Dirchwolf[5], Jorge Luis Garavito Rentería[6], Kriss Rodríguez Romero[7], Aldo Torre[8], Cristiane A. Villela-Nogueira[9], Francisco Vargas-Navarro[1], Maria Lynch-Mejia[1], Wagner Ramirez-Quesada[1], Nélia Hernandez[10]. *[1]Hospital Dr. Rafael Ángel Calderón Guardia, LiverLab CR, San José, Costa Rica; [2]Sección Hepatología, Departamento de Medicina. Centro de Educación Médica e Investigaciones Clínicas Norberto Quirno "CEMIC," Buenos Aires, Argentina; [3]Department of Gastroenterology, Pontificia Universidad Católica de Chile, Santiago, Chile; [4]Departamento de Aparato Digestivo, Hospital Nacional Edgardo Rebagliati Martins (HNERM) – EsSalud, Facultad de Medicina, Universidad Nacional Mayor de San Marcos, Facultad de Medicina, Universidad Peruana de Ciencias Aplicadas, Lima, Peru; [5]Hospital Privado de Rosario, Rosario, Argentina; [6]Servicio de Gastroenterología, Hospital Nacional Arzobispo Loayza, Lima, Peru; [7]Clínica Delgado, Lima, Peru; [8]Gastroenterology Department, Medical Center ABC, Mexico City, Mexico; [9]Universidade Federal do Rio de Janeiro, Rio de Janeiro, Brazil; [10]Hospital de Clínicas, Facultad de Medicina, Universidad de la República, Montevideo, Uruguay*
Email: costepablo@gmail.com

Background and aims: Artificial intelligence (AI) is increasingly used in biomedical research, including peer-review processes. However, its concordance with expert clinical judgment remains poorly understood in the context of hepatology congresses, particularly in Latin America. This study aims to compare AI-generated abstract scores with those assigned by human reviewers, assessing concordance, bias, and potential for integration.
Method: We conducted a comparative analysis of 191 abstracts submitted to the ALEH 2025 Congress. Each abstract was independently scored by three hepatology experts using a standardized 18-point rubric and by an AI-based algorithm trained for scientific content appraisal. We calculated mean scores, standard deviations, absolute differences, and performed paired t-tests. Pearson correlation was used to assess concordance. Agreement and bias were further evaluated using scatterplots with identity lines and Bland-Altman plots. Abstracts were ranked globally and by topic (MASLD, viral hepatitis, cirrhosis, liver cancer, transplantation, etc.) based on combined human–AI scores.
Results: The mean AI score (15.3 ± 2.0) was significantly higher than the mean human score (11.5 ± 2.9; $p < 0.001$), with a mean difference of 3.8 points. Pearson correlation showed moderate positive concordance ($r = 0.58$; $p < 0.001$). The Bland-Altman plot revealed a consistent negative bias, with AI overestimating scores, particularly in lower-scoring abstracts. No significant differences were found in bias across study types ($p = 0.321$). Combined scoring enabled a more nuanced selection of top abstracts, mitigating subjective variation.
Conclusion: AI tends to systematically overestimate abstract quality compared to human experts, yet maintains moderate concordance. When integrated with human judgment, it may enhance the objectivity of scientific selection processes. This work highlights both the promise and limitations of AI-assisted evaluation in hepatology and supports hybrid models for future congress abstract review.

SAT-037

Excess mortality from cirrhosis by neighbourhood deprivation, aetiology, and clinical presentation: a Swedish register-based cohort study

Juan Vaz[1], Jeffrey Lazarus[2], Hannes Hagström[3], Ulf Strömberg[1].
[1]*School of Public Health and Community Medicine, Institute of Medicine, Sahlgrenska Academy, University of Gothenburg, Gothenburg, Sweden;* [2]*Barcelona Institute for Global Health (ISGlobal), Barcelona, Spain;* [3]*Department of Medicine, Huddinge, Karolinska Institutet, Stockholm, Sweden*
Email: juan.vaz@gu.se

Background and aims: Socioeconomic inequalities are a persistent determinant of health inequity, but their influence on excess mortality from cirrhosis in high-income countries with universal healthcare is not well characterised. We aimed to estimate cirrhosis-related excess mortality across neighbourhood deprivation levels in Sweden.
Method: We conducted a nationwide, register-based cohort study, including all individuals aged ≥40 years residing in Sweden between 2012–2022. The open, underlying cohort was stratified by calendar year, sex, 5-year age groups, and residential neighbourhood. Neighbourhood strata were collapsed into deprivation quintiles (*Q*s), as per the national distribution of inhabitants with a low disposable household income, with *Q1* being the least and *Q5* the most deprived. Incident cirrhosis cases within the age span 40–74 years were identified using validated diagnostic algorithms, and followed for up to five years. Excess mortality rate ratios (EMRRs) were estimated using Poisson regression within a relative survival framework. To estimate the number of excess deaths across *Q1*–*Q5*, the incidence rate in each stratum was taken into account.
Results: Among 21,583 individuals with incident cirrhosis, among whom the median age was 63 years and 35% were female, 8,814 deaths occurred during 65,170 person-years of follow-up. Five-year excess mortality was 19% higher in *Q5* than in *Q1* (EMRR 1·19, 95% CI 1·10–1·29), after adjusting for calendar year, sex, age, aetiology, and cirrhosis severity. At the population level, the age-standardised number of excess deaths within five years of diagnosis was substantially higher in deprived areas: with 2018 as the year of diagnosis, there were 23 excess deaths per 100,000 inhabitants in *Q5* versus 12 in *Q1*, representing a 95% higher excess mortality burden.
Conclusion: Even within a universal healthcare system, cirrhosis-related excess mortality substantially increases with level of neighbourhood deprivation. Prevention and more optimal post-diagnostic management targeted towards deprived neighbourhoods are urgently needed to reduce avoidable deaths.

SAT-038

Socioeconomic disparities in access to curative treatment among individuals with surveillance-detected hepatocellular carcinoma in Sweden: a nationwide cohort study

Juan Vaz[1], Adam Bergman[1], Malin Sternby Eilard[2], Hannes Hagström[3].
[1]*School of Public Health and Community Medicine, Institute of Medicine, Sahlgrenska Academy, University of Gothenburg, Gothenburg, Sweden;* [2]*Department of Surgery, Sahlgrenska Academy, University of Gothenburg, Gothenburg, Sweden;* [3]*Department of Medicine, Huddinge, Karolinska Institutet, Stockholm, Sweden*
Email: juan.vaz@gu.se

Background and aims: Surveillance for hepatocellular carcinoma (HCC) aims to enable early detection and access to potentially curative treatment. While surveillance improves stage at diagnosis and survival, it remains unclear whether socioeconomic disparities persist among individuals whose HCC is detected through surveillance within universal healthcare systems. We aimed to identify sociodemographic and clinical factors associated with failure to receive curative treatment among individuals with surveillance-detected HCC in Sweden, and to assess survival across socioeconomic strata.
Method: We conducted a nationwide register-based cohort study including all adults diagnosed with surveillance-detected HCC between 2011 and 2021, using data from the Swedish national quality register (SweLiv) linked to population registers. Multivariable logistic regression was used to assess factors associated with receipt of curative treatment (resection, ablation, or transplantation). The final model was adjusted for age, sex, region of birth, household income, aetiology, tumour size and number, extrahepatic metastasis, tumour thrombosis, Child-Pugh score, performance status, arterial hypertension, diabetes mellitus, cardiovascular disease, chronic kidney disease, and chronic obstructive pulmonary disease. Overall survival was analysed using Kaplan–Meier estimates and Cox proportional hazards models stratified by treatment modality.
Results: Among 1,401 individuals with surveillance-detected HCC, 906 (65%) received curative treatment. After adjustments, individuals with medium and low household income had substantially lower odds of receiving curative treatment compared with those with high income (adjusted odds ratios 0.47 [95% CI 0.30–0.76] and 0.40 [0.25–0.65], respectively). Overall survival differed by socioeconomic status, with lower survival among individuals with low household income. Socioeconomic differences in survival were observed among individuals treated with ablation, where low income was independently associated with higher mortality (adjusted hazard ratio 1.49 [1.04–2.13]), but not among those undergoing resection or transplantation.
Conclusion: Despite surveillance-based detection of HCC, marked socioeconomic disparities persist in access to curative treatment and survival in Sweden. These findings highlight inequities within the surveillance-to-treatment pathway and underscore the need for targeted strategies to ensure equitable implementation of HCC surveillance and downstream care.

SAT-039

Burden, trends and projections of liver cancer in China and G20 countries: a comparative study based on the global burden of disease database 2023

Yikai Wang[1], Yaping Li[1], Muqi Wang[1], Liu Yang[1], Meng Zhang[1], Zihan Liu[1], Mei Li[1], Juanjuan Shi[1], Wenjun Wang[1], Shuangsuo Dang[1], Xiaoli Jia[1]. [1]*The Second Affiliated Hospital of Xi'an Jiaotong University, Xi'an, China*
Email: 17795626586@163.com

Background and aims: This study compares the disease burden of liver cancer and its attributable risk factors between China and the Group of Twenty (G20) countries from 1990 to 2023, and predicts the trends in incidence, mortality, and disability-adjusted life years (DALYs) over the next 27 years.
Method: Utilizing data from the GBD 2023 database to assess trends in the disease burden of liver cancer. Analyzing the relationships between risk factors, human development index (HDI), and socio-demographic index (SDI). Employing the joinpoint regression model to calculate the average annual percentage change (AAPC) to evaluate trends. Using the autoregressive integrated moving average (ARIMA) model to predict liver cancer burden trends from 2024 to 2050.
Results: In 2023, China's age-standardized incidence rate (ASIR), age-standardized mortality rate (ASMR), and age-standardized disability-adjusted life years rate (ASDR) for liver cancer were showing a certain degree of decline compared to 1990, but higher than those in G20 countries during the same period. Hepatitis B and C viruses remain the primary causative factors, but the impact of non-alcoholic steatohepatitis (NASH) is increasing. By risk factors, the burden of liver cancer caused by drug use in G20 countries and tobacco in China also needs attention. Additionally, countries with higher SDI tend to have lower incidence and mortality rates of liver cancer. Joinpoint regression analysis revealed that between 1990 and 2023, the ASIR, ASMR, and ASDR generally showed a downward trend. Projections indicate that over the next 27 years, the ASIR, ASMR, and ASDR will maintain relatively stable or declining trends, though with differences between genders.

Conclusion: Although the burden of liver cancer in China has declined, but remains a certain gap compared to G20 countries during the same period. China should develop more targeted prevention and control strategies for different genders and age groups in the future.

SAT-040

Burden, trends and projections of cirrhosis in China and G20 countries: a comparative study based on the global burden of disease database 2023

Yikai Wang[1], Yaping Li[1], Muqi Wang[1], Liu Yang[1], Meng Zhang[1], Zihan Liu[1], Mei Li[1], Juanjuan Shi[1], Wenjun Wang[1], Shuangsuo Dang[1], Xiaoli Jia[1]. [1]*The Second Affiliated Hospital of Xi'an Jiaotong University, Xi'an, China*
Email: 17795626586@163.com

Background and aims: This study compares the disease burden of cirrhosis and its attributable risk factors between China and the Group of Twenty (G20) countries from 1990 to 2023, and predicts the trends in incidence, mortality, and disability-adjusted life years (DALYs) over the next 27 years.
Method: We used data from the GBD 2023 database to assess trends in the disease burden of cirrhosis. We analyzed the relationships between risk factors, human development index (HDI), and socio-demographic index (SDI). The joinpoint regression model helped us calculate the average annual percentage change (AAPC) and evaluate trends. The autoregressive integrated moving average (ARIMA) model was used to predict cirrhosis burden trends from 2024 to 2050.
Results: In 2023, China's age-standardized incidence rate (ASIR), age-standardized mortality rate (ASMR), and age-standardized disability-adjusted life years rate (ASDR) for cirrhosis were showing a certain degree of decline compared to 1990. The three indicators of G20 countries also showed a downward trend, but ASMR and ASDR were consistently higher than those in China. The proportion of cirrhosis caused by non-alcoholic steatohepatitis (NASH) has significantly increased, while the proportion caused by HBV has significantly decreased. By risk factors, the prevalence of drug-use-attributed cirrhosis in G20 countries is significantly higher than in China, while alcohol use shows little difference between the two. Additionally, across countries, higher SDI is associated with lower ASIR for liver cirrhosis. However, overall, the ASIR for liver cirrhosis is lowest in China and G20 countries when the SDI is at 0.6. Joinpoint analysis revealed that the ASIR for cirrhosis in China and G20 countries reached its lowest point in 2005, followed by a rise, while ASMR and ASDR generally showed a downward trend from 1990 to 2023. Projections indicate that, over the next 27 years, the ASIR, ASMR, and ASDR will continue to decline; however, these trends will differ by gender.
Conclusion: The burden of liver cirrhosis in China has declined, with some indicators already surpassing those of G20 countries. China should develop more targeted prevention and control strategies for different genders and age groups in the future.

SAT-041

Inefficiency of risk-based screening for steatotic liver disease in primary care: a multi-cohort analysis of more than 15,000 individuals

Bernhard Wernly[1], Patrick Langthaler[1], Bernhard Iglseder[1], Eugen Trinka[1], Georg Semmler[2], Elmar Aigner[1], Christian Datz[1]. [1]*Salzburg, Austria;* [2]*MedUni Wien, Wien, Austria*
Email: bernhard@wernly.at

Background and aims: Current EASL clinical practice guidelines recommend a risk-based screening strategy for steatotic liver disease (SLD), utilizing metabolic triggers such as obesity or type 2 diabetes as entry criteria for further diagnostic evaluation. This approach aims to optimize resources by focusing on high-risk populations. However, real-world data on the diagnostic performance of this strategy in unselected primary care populations remain limited. This study evaluated the diagnostic precision and clinical workload of EASL screening criteria across two large, independent primary care cohorts.
Method: We analyzed two distinct primary care populations: the P10 cohort (n = 9,838) and the SAKKOPI cohort (n = 5,935). Screening positivity was defined by EASL criteria (obesity, type 2 diabetes, or elevated alanine aminotransferase). Performance was benchmarked against the FIB-4 score (low < 1.30, intermediate 1.30–2.67, high ≥ 2.67), liver stiffness measurement (LSM; high risk ≥ 8 kPa), and the presence of steatotic liver disease according to diagnostic criteria.
Results: In P10, the median age was 55 years (IQR 50–62; 49% male), while in SAKKOPI it was 58 years (IQR 52–66; 52% male). EASL criteria were met by 48.0% of the P10 population and 59.8% in SAKKOPI, representing substantial diagnostic workload. Among screen-positive individuals, the positive predictive value for high-risk FIB-4 (≥ 2.67) was only 1.9% in P10 and 4.4% in SAKKOPI. Notably, 60% to 68% of screen-positive individuals presented with low-risk FIB-4 scores (< 1.30), indicating considerable over-referral. The reliance on metabolic pre-screening created significant diagnostic gaps. First, the criteria failed to capture 28% (P10) and 19% (SAKKOPI) of all individuals with steatotic liver disease. Second, metabolic screening missed 26.3% (P10) and 26.4% (SAKKOPI) of individuals with elevated liver stiffness (LSM ≥ 8 kPa).
Conclusion: While intended to streamline diagnostics, the current EASL risk-based screening paradigm generates disproportionate clinical burden in primary care without achieving adequate sensitivity. Our data demonstrate that a sequential metabolic gateway is inefficient for comprehensive case detection, missing one-quarter of patients with elevated liver stiffness while over-referring two-thirds of screen-positive individuals with low fibrosis risk. Direct implementation of the FIB-4 score as the primary screening tool could enhance both diagnostic safety and resource efficiency in the primary care setting.

SAT-042

Estimation of liver fibrosis risk using non-invasive biomarker tests in people living with HIV and pre-diabetes in Tanzania

Trenton M White[1], Jeffrey Lazarus[1], Kaushik Ramaiya[2], Sokoine Kivuyo[1], Sayoki Mfinanga[3], Erik van Widenfelt[4], Paul N. Brennan[5], Hannes Hagström[6], Rickard Strandberg[6], Anupam Garrib[4]. [1]*Barcelon Institute for Global Health (ISGlobal), Barcelona, Spain;* [2]*Tanzania NCDs Alliance, Dar Es Salaam, Tanzania;* [3]*National Institute for Medical Research, Dar es Salaam, Tanzania;* [4]*University College London, London, United Kingdom;* [5]*The University of Dundee, Dundee, United Kingdom;* [6]*Karolinska Institutet, Huddinge, Sweden*
Email: trenton.white@isglobal.org

Background and aims: Metabolic dysfunction-associated steatotic liver disease (MASLD) and liver fibrosis are increasingly common comorbidities among people living with HIV (PLHIV), particularly in ageing populations with rising metabolic dysfunction. Data on fibrosis risk in sub-Saharan Africa remain scarce. We aimed to estimate liver fibrosis risk and the 10-year risk of cirrhosis using non-invasive tests (NITs) among PLHIV with pre-diabetes in Tanzania.
Method: We conducted a cross-sectional analysis of baseline data from 1,691 PLHIV with pre-diabetes enrolled in the META Trial, a phase III randomised controlled trial of metformin, in Tanzania. Liver fibrosis risk was assessed using the Fibrosis-4 (FIB-4) Index, Metabolic Dysfunction-Associated Fibrosis-5 (MAF-5) score, NAFLD Fibrosis Score (NFS), and the LiverRisk score; cirrhosis risk was estimated using the Cirrhosis Outcome Risk Estimator (CORE). Clinical and demographic variables were summarised, and risk categories were defined using validated and age-adjusted cut-offs.
Results: Participants had a mean age of 49.4 years (SD 9.4), 75.0% were female, and 99.2% were Black. Using age-adjusted FIB-4 thresholds, 31.8% were classified as indeterminate risk and 3.0% as high risk, while NFS classified 50.9% as indeterminate and 8.3% as

high risk. In contrast, MAF-5 categorised 59.9% of participants as high risk, whereas fewer than 1% were classified as medium or high risk by LiverRisk. Using CORE, 5.8% of participants were estimated to have a ≥1% 10-year risk of developing cirrhosis or a cirrhosis-related outcome. Females were more often classified as low risk than males by FIB-4 (70% vs. 50%, $p < 0.001$), while males had higher risk classifications by MAF-5, LiverRisk, and CORE; no sex differences were observed for NFS.
Conclusion: Non-invasive fibrosis tests yielded divergent estimates of liver fibrosis risk among PLHIV with pre-diabetes in Tanzania. While FIB-4 and NFS identified most as low risk, MAF-5 suggested nearly half were high risk. These discrepancies underscore the need for locally validated NITs and integration of liver health assessments into HIV care in Africa, particularly as MASLD/MASH and metabolic comorbidities are common in this population.

SAT-043

The rising burden of adolescent MASLD: a global analysis of incidence trends and modifiable risk factors

Tianyuan Yang[1], Tong Bu[1], Qi Wang[1]. [1]*Center of Liver Diseases, Beijing Ditan Hospital, Capital Medical University, Beijing, China, Beijing, China*
Email: tyy66303@gmail.com

Background and aims: The global prevalence of metabolic dysfunction-associated steatotic liver disease (MASLD) among adolescents has risen markedly. However, a comprehensive description of its recent epidemiological trends is lacking, and the key modifiable risk factors driving its incidence remain poorly characterized.
Method: Age-specific incidence rates (1990–2023) were obtained from the GBD 2023 database for trend and mapping analysis. To identify risk factors, we independently screened candidate exposures, applying a random forest model with SHAP analysis for feature ranking. Key factors were subsequently evaluated using negative binomial regression to estimate relative risks (RRs).
Results: Globally, adolescent MASLD incidence increased by 25.2% from 1990 to 2023 (866.5 to 1084.9 per 100,000). The rise was most pronounced in middle SDI regions (+35.7%), while high- and low-SDI regions increased by 30.5% and 21.5%, respectively. At the regional level, the highest 2023 incidence was observed in Middle SDI areas (1436.5 per 100,000), whereas the lowest was in High-income Asia Pacific (868.4 per 100,000). SHAP analysis identified high body-mass index and ambient particulate matter pollution as the two most influential risk factors. Subsequent negative binomial regression confirmed their significant association with increased incidence, yielding relative risks of 1.13 (95% CI: 1.09–1.17) for high BMI and 1.07 (95% CI: 1.04–1.10) for ambient particulate matter pollution.
Conclusion: Our study confirms a significant global rise in adolescent MASLD incidence and identifies high body-mass index and ambient particulate matter pollution as key modifiable risk factors. These findings highlight the urgent need for integrated public health strategies targeting both metabolic health and environmental protection to curb the growing burden of MASLD in adolescent.

SAT-044

Health literacy and associated factors in patients with cirrhosis in Latin America: the PHAROS study

Ismael de Jesus Yepes Barreto[1], Alejandra Ochoa[2], Andres Solera[2], Patricia Guerra[3], Diana Castillo[4], Katerin Saravia[5], Francisco Vargas-Navarro[6], Pedro Montes[7], Valentina Yepes[8], Juan Carlos Restrepo[9]. [1]*Universidad de Cartagena, Asociacion Colombiana de Hepatologia, Cartagena de Indias, Colombia;* [2]*Hospital Doctor Rafael Ángel Calderón Guardia, San José, Costa Rica;* [3]*Instituto de Gastroenterología Boliviano Japonés (IGBJ), La Paz, Bolivia;* [4]*Hospital Punata, Punata, Bolivia;* [5]*Hospital del Norte, Cochabamba, Bolivia;* [6]*Clínica de Puriscal, Santiago, Costa Rica;* [7]*Hospital Nacional Daniel Alcides Carrión, Bellavista, Peru;* [8]*University Of Copenhagen, København K, Denmark;* [9]*Hospital Pablo Tobón Uribe, Medellín, Colombia*
Email: ismayep@yahoo.com

Background and aims: Health literacy is essential for disease self-management and informed decision-making. In patients with cirrhosis, limited health literacy has been associated with worse clinical outcomes and increased healthcare costs. Although factors associated with health literacy in cirrhosis have been described, most evidence derives from high-income countries and may not be generalisable to Latin America, where data remain scarce. The aim of the PHAROS study was to identify factors associated with adequate health literacy among patients with cirrhosis in Latin America.
Method: We conducted a multicentre cross-sectional study in four Latin American countries across seven outpatient hepatology centres. Adult patients with cirrhosis attending routine outpatient clinics were invited to participate. After written informed consent, health literacy was assessed using the Short Assessment of Health Literacy in Spanish (SAHL-S), an 18-item validated instrument. A score greater than 15 defined adequate health literacy. Clinical and sociodemographic variables were collected. Univariate and multivariable logistic regression analyses were performed to identify factors associated with adequate health literacy.
Results: A total of 243 patients were included. Mean age was 63.9 ± 11.8 years, and 57.2% were female. Most patients lived in urban areas (83.1%), and 61.4% had completed secondary education or higher. Overall, 62.1% were classified as Child–Pugh A. Ascites, hepatic encephalopathy, and oesophageal varices were present in 35.4%, 22.2%, and 44.9% of patients, respectively. MASLD was the most frequent aetiology (34.2%). Adequate health literacy was identified in 68.7% of patients. In multivariable analysis, higher educational level was independently associated with adequate health literacy (OR 1.94, 95% CI 1.49–2.53), whereas older age (OR 0.96, 95% CI 0.93–0.99), oesophageal varices (OR 0.42, 95% CI 0.21–0.85), and more advanced Child–Pugh class (OR 0.50, 95% CI 0.32–0.78) were associated with lower odds of adequate health literacy.
Conclusion: In this multicentre Latin American cohort, inadequate health literacy was common among patients with cirrhosis and was associated with older age and more advanced liver disease, while higher educational level was protective. These findings support integrating health literacy assessment and tailored educational strategies into routine cirrhosis care in Latin America to improve outcomes and optimise healthcare resource use.

SAT-045

Global trends and disparities in preventable premature liver deaths due to metabolic dysfunction-associated steatotic liver disease (MASLD): a 20-year study in 204 countries

James M. Paik[1], Linda Henry[1], Andrei Racila[1], Markos Kalligeros[1,2], Fatema Nader[1], Zobair M. Younossi[1]. [1]*The global NASH/MASH council, Washington DC, United States;* [2]*Division of Gastroenterology and Hepatology, Beth Israel Deaconess Medical Center, Harvard Medical School, Boston, Massachusetts, Boston, United States*
Email: james.paik@inova.org

Background and aims: Premature deaths (PDs) due to MASLD may vary across countries, but the proportion of these deaths that are preventable remain unknown.
Method: This global ecological analysis included 204 countries (2004–2023) using Global Burden of Disease (GBD) data with UN/WHO covariates. Premature death (PD) was defined as death <70 years. Based on the 2023 distribution, countries were grouped as follows: Group A comprised countries in the top quartile of MASLD prevalence and bottom quartile of the mortality-to-prevalence ratio (MPR; n = 51) to isolate benchmark-like performers and improve comparability given known GBD mortality-prevalence measurement asymmetries. Remaining countries were classified by sociodemographic index (SDI) tertiles (low <0.60, middle 0.60-<0.75, high ≥0.75) into Group B (high SDI; n = 50), Group C (middle SDI; n = 41), and Group D (low SDI; n = 62). Within each group, 10th percentile of MPR (2004) served as the benchmark. Expected PD rates were calculated as MASLD prevalence × benchmark MPR. Preventable PD

rates were defined as excess observed/expected rates, and preventability proportion as preventable divided by observed PD rates. Determinants were evaluated using stratum-specific linear mixed-effects models with country random intercepts.

Results: From 2004–2023, 1,262,126 MASLD-related liver PDs occurred globally, of which 49.3% (622,459 deaths) were potentially preventable. Groups A–D accounted for 6.0%, 41.0%, 41.1%, and 11.9% of all preventable PDs. Mean preventability changed over time: Group A, 23.5% (IQR 0–45.9%) to 21.3% (0–30.2%); Group B, 57.4% (42.2–73.4%) to 52.7% (39.1–67.7%); Group C, 57.8% (44.7–72.1%) to 61.3% (49.1–75.4%); and Group D, 50.5% (37.6–65.2%) to 53.0% (38.6–65.4%) ($p < 0.002$ for time trend). In Group A, preventability was lower with SDI ($\beta = -0.789$) and male population ($\beta = -0.016$) and higher with diabetes ($\beta = 0.009$), age ($\beta = 0.016$), and urbanization ($\beta = 0.004$) (all $p < 0.002$). In Group B, preventability increased with obesity ($\beta = 0.011$) and decreased with age ($\beta = -0.021$) ($p < 0.001$) and Universal Health Coverage ($\beta = -0.003$, $p = 0.059$). In Group C, preventability increased with obesity ($\beta = 0.006$) and age ($\beta = 0.008$) ($p < 0.030$). In Group D, preventability increased with age ($\beta = 0.010$) and urbanization ($\beta = 0.002$) and decreased with male population ($\beta = -0.022$) ($p < 0.007$).

Conclusion: Nearly half of premature MASLD-related deaths are preventable, underscoring socioeconomic inequities across countries and the need for policy action.

SAT-046

Ultra-processed food intake is associated with obesity and advanced fibrosis in metabolic dysfunction associated steatotic liver disease: a multinational analysis from the global NASH/MASH registry™

Zobair M. Younossi[1], Shira Zelber-Sagi[1,2], Eugen Tcaciuc[1,3], Marlen Ivon Castellanos Fernández[1,4], Wah-Kheong Chan[1,5], Adrian Gadano[1,6], Mohamed El-Kassas[1,7], Ming-Lung Yu[1,8], George Papatheodoridis[1,9], Aung Bwa[1,10], Yusuf Yilmaz[1,11], Waleed Alhazzani[12], Brian Lam[1,13], Andrei Racilka Jr[14], Laura Sol Grinshpan[1], Dana Ivancovsky-Wajcman[1], Linda Henry[1,15], Basma Khoja[1,16], Fatema Nader[14,17], Lynn H Gerber[14], Shadan Almuhaidib[1,18], Maria Stepanova[14,17], Saleh A. Alqahtani[14,19]. *[1]The global NASH/MASH council, Washington DC, United States; [2]School of Public Health, University of Haifa, Haifa, Israel, Haifa, Israel; [3]Department of Gastroenterology, Nicolae Testemitanu State University of Medicine and Pharmacy, Chișinău, Republic of Moldova, Chișinău, Moldova; [4]Institute of Gastroenterology, University of Medical Sciences of Havana, Havana, Cuba, Havana, Cuba; [5]Gastroenterology and Hepatology Unit, Department of Medicine, Faculty of Medicine, University of Malaya, Kuala Lumpur, Malaysia, Kuala Lumpur, Malaysia; [6]Research Department, Hospital Italiano de Buenos Aires, Argentina, Buenos Aires, Argentina; [7]Endemic Medicine Department, Faculty of Medicine, Helwan University, Cairo, Egypt, Cairo, Egypt; [8]Kaohsiung Medical University Hospital, Kaohsiung Medical University; and National Sun Yat-sen University, Kaohsiung, Taiwan, Kaohsiung, Taiwan; [9]National and Kapodistrian University of Athens, Greece, Athens, Greece; [10]Yangon GI and Liver Centre, Yangon, Myanmar, Yangon, Myanmar; [11]Department of Gastroenterology, School of Medicine, Recep Tayyip Erdoğan University, Rize, Turkey, Rize, Türkiye; [12]Health Research Center, Ministry of Defense Health Services, Riyadh, Saudi Arabia, Riyadh, Saudi Arabia; [13]Beatty Liver and Obesity Research Program, Inova Health System, Falls Church, VA, United States, Falls Church, United States; [14]The Global NASH/MASH Council (GNC), Washington, DC, United States; [15]Center for Outcomes Research in Liver Disease, Washington DC, United States, Washington DC, United States; [16]King Faisal Specialist Hospital and Research Center, Riyadh, Saudi Arabia; [17]Center for Outcomes Research in Liver Diseases, Washington DC, USA, Washington DC, United States; [18]Health Research Center, Ministry of Defense Health Services, Riyadh, Saudi Arabia; [19]Liver, Digestive, and Lifestyle Health Research Section, and Organ Transplant Center of Excellence, King Faisal Specialist Hospital and Research Center, Riyadh, Saudi Arabia, Riyadh, Saudi Arabia*
Email: zobair.younossi@cldq.org

Background and aims: Ultra-Processed Foods (UPFs), characterized by high energy density, added sugars, unhealthy fats, and food additives, have been associated with obesity and MASLD. The contribution of UPFs to hepatic fibrosis in MASLD remains insufficiently understood. We aimed to elucidate the association of UPF intake in fibrosis in patients with MASLD using an international registry.

Method: We analyzed data from the Global NASH/MASH Registry™ (N = 1,266 patients with established diagnosis of MASLD or MASH; 11 countries). Dietary intake was assessed using the Short-Processed Food Questionnaire (SPFQ; 23 food items including 15 UPF), and associations with obesity and fibrosis severity using liver stiffness measurement (advanced fibrosis: LSM≥10 kPa) were examined.

Results: Mean (SD) UPF intake was 2.32 ± 2.38 portions/day. Dietary patterns varied markedly by country ($p < 0.0001$), with UPF intake ranging from 1.85 ± 1.78 to 8.41 ± 2.62 portions/day and UPFs comprising 32 ± 19% to 67 ± 9% of intake. UPF intake was higher in participants with obesity than in overweight or lean individuals (2.48 ± 2.57 vs. 2.15 ± 2.20 vs. 2.00 ± 1.88 portions/day; $p = 0.04$). Healthy food intake and the proportion of intake from UPFs were similar across BMI categories ($p = 0.20$ and $p = 0.37$, respectively), indicating that absolute UPF burden might distinguish obesity. Obesity was associated with higher intake of multiple UPF subcategories, including butter/margarine/ghee, sweet breakfast cereals, fried fast foods, processed meats, and savory snacks (all $p < 0.05$). MASLD patients with advanced fibrosis (LSM ≥10 kPa) had higher UPF intake (2.80 ± 2.37 vs. 2.05 ± 2.22 portions/day; $p = 0.001$). MASLD-related advanced fibrosis (pooled prevalence 12%) was more prevalent in the highest UPF tertile compared to the lowest (18% vs. 9%; $p = 0.007$). UPF items consumed more frequently in MASLD with advanced fibrosis included sugar-sweetened dairy products, processed meats, processed dressings/sauces, and sweetened diet drinks (all $p < 0.05$). In multivariable analyses adjusted for age and sex, individual UPF items [sugar-sweetened dairy products, OR (95% CI) = 2.24 (1.35–3.73), and sweetened diet drinks, OR = 2.63 (1.53–4.53) per portion/day] were associated with advanced fibrosis. These associations were attenuated with the inclusion of country of enrollment.

Conclusion: The UPF intake is associated with obesity and potentially with fibrosis in MASLD, identifying UPFs as a modifiable dietary target.

SAT-047

How food-system conditions shape burden of metabolic dysfunction associated steatotic liver disease (MASLD) in low- and high-sdi countries

James M. Paik[1], Markos Kalligeros[1,2], Annette Paik[1], Shira Zelber-Sagi[1,3], Farah Qaderi[1], Zobair M. Younossi[1]. *[1]The global NASH/MASH council, Washington DC, United States; [2]Division of Gastroenterology and Hepatology, Beth Israel Deaconess Medical Center, Harvard Medical School, Boston, MA, USA, Boston, United States; [3]School of Public Health, Faculty of Social Welfare and Health Sciences, University of Haifa, Haifa, Israel, Haifa, Israel*
Email: zobair.younossi@cldq.org

Background and aims: Food affordability and retail environment shape dietary patterns and metabolic risks, but their relationship to the global MASLD burden across different countries at different socioeconomic developmental levels is not well defined.

Method: A cross-national ecological study was conducted including 156 countries with harmonized data from Global Burden of Disease and United Nations' Food and Agriculture Organization database. Ultra-Processed Agrifood Environment Index (UPAEI) was calculated by combining ultra-processed energy share, agrifood emissions, urbanization, and protein dilution. Countries were stratified according to Sociodemographic Index (SDI <0.70 vs ≥0.70). Structural equation models assessed potential associations linking the food-

system characteristics, metabolic factors with MASLD prevalence and mortality.
Results: Low-SDI countries (n = 98) had younger populations (mean median age 22.3 vs 37.8 years), were less urbanized (49.1% vs 73.4%), and had lower political stability (−0.47 vs 0.38), lower healthcare access and quality index (HAQ 42.3 vs 76.5), lower import dependence (6.79 vs 91.6), and lower UPAEI (36.4 vs 45.8), but higher food-price burden (8.7 vs 1.8) compared with high-SDI countries (n = 58). MASLD prevalence (16,240 vs 13,662 per 100,000) and MASLD-related mortality (2.77 vs 1.85 per 100,000) were both higher in low-SDI countries (all $p < 0.01$). In low-SDI countries, UPAEI was associated with sugar share ($\beta = 0.42$, $p < 0.001$). Both sugar share and caloric surplus were associated with obesity ($\beta = 0.45$ and $\beta = 0.35$; $p < 0.001$), and caloric surplus associated with type 2 diabetes (T2D) ($\beta = 0.56$, $p < 0.001$). Obesity and T2D were associated with MASLD prevalence ($\beta = 0.37$, $p < 0.001$; $\beta = 0.22$, $p = 0.015$). Political stability showed an inverse association with MASLD prevalence ($\beta = -0.38$, $p < 0.001$).
In high-SDI countries, food-price burden ($\beta = 0.57$, $p < 0.001$) and import dependence ($\beta = 0.22$, $p = 0.027$) were associated with reliance on staple carbohydrates, which was associated with higher obesity ($\beta = 0.41$, $p < 0.001$). Sugar share was associated with higher obesity ($\beta = 0.34$, $p = 0.002$). Only T2D showed a strong association with MASLD prevalence ($\beta = 0.88$, $p < 0.001$). Higher HAQ was consistently associated with lower MASLD-related mortality ($\beta = -0.44$, $p < 0.001$).
Conclusion: MASLD pathways differ by country's socio-economic development level, with ultra-processed food-driven metabolic risk dominating in low-SDI settings and food affordability pathways in high-SDI settings.

SAT-050

Type 2 diabetes (T2D) is the major driver of advanced metabolic dysfunction–associated steatohepatitis (MASH) and associated liver-related mortality in Europe

Zobair M. Younossi[1], James M. Paik[1], Frank Tacke[1,2], Patrizia Burra[1,3], Javier Crespo[1,4], Elisabetta Bugianesi[1,5], Michael Roden[1,6], Cyrielle Caussy[1,7], Amalia Gastaldelli[1,8], Jeremy Tomlinson[1,9], Paul N. Brennan[1,10], Manuel Romero-Gómez[1,11], Jerome Boursier[1,12], Laurent Castera[1,13], Markos Kalligeros[1,14], Linda Henry[1,15]. *[1]The global NASH/MASH council, Washington DC, United States; [2]Department of Hepatology and Gastroenterology, Charité - Universitätsmedizin Berlin, Berlin, Germany, Berlin, Germany; [3]Department of Surgery, Oncology and Gastroenterology, Padua University Hospital, Padua, Italy, Padua, Italy; [4]Gastroenterology and Hepatology Department, Clinical and Translational Research in Digestive Diseases, Valdecilla Research Institute (IDIVAL), Marqués de Valdecilla University Hospital, Santander, Spain, Santander, Spain; [5]Department of Medical Sciences University of Turin, Italy, Turin, Italy; [6]Department of Endocrinology and Diabetology, Medical Faculty and University Hospital Düsseldorf, Heinrich-Heine-University Düsseldorf, Germany, Düsseldorf, Germany; [7]Département Endocrinology, Diabete and Nutrition, Hôpital Lyon Sud, Hospices Civils de Lyon Pierre-Bénite, France, Lyon, France; [8]Cardiometabolic Risk Unit, Institute of Clinical Physiology – National Research Council (CNR) Pisa, Italy, Pisa, Italy; [9]Oxford Centre for Diabetes Endocrinology & Metabolism, NIHR Oxford Biomedical Research Centre, University of Oxford, Churchill Hospital, Oxford, UK, Oxford, United Kingdom; [10]Division of Molecular and Clinical Medicine, University of Dundee, Scotland, UK, Dundee, United Kingdom; [11]UCM Digestive Diseases. Virgen del Rocío University Hospital. Institute of Biomedicine of Seville (HUVR/CSIC/US). CIBEREHD, ISCIII. Department of Medicine. University of Seville, Seville, Spain, Seville, Spain; [12]Hepato-Gastroenterology Department at Angers University Hospital, Angers, France, Angers, France; [13]Department of Hepatology, University of Paris-Cité, Hopital Beaujon, AP-HP, Clichy, France, Clichy, France; [14]Division of Gastroenterology and Hepatology, Beth Israel Deaconess Medical Center, Harvard Medical School, Boston, MA, USA, Boston, United States; [15]Center for Outcomes Research in Liver Diseases, Washington DC, USA, Washington DC, United States*
Email: zobair.younossi@cldq.org

Background and aims: Individuals with type 2 diabetes (T2D) have a high prevalence of MASH with more rapid disease progression and a disproportionate clinical burden. We used a modelling approach to estimate the clinical burden of MASH by T2D status in 5 major European countries.
Method: An age-stratified Markov model estimated the clinical burden of MASH according to T2D status from 2025 to 2040 in Germany, Spain, France, Italy, and the United Kingdom (EU-4+UK). Transition probabilities were derived from published natural history studies and calibrated to country-specific epidemiology, aligning model outputs with nationally reported rates for decompensated cirrhosis, hepatocellular carcinoma, and liver transplantation. Treatment effects were applied directly to annual transition probabilities using country-specific assumptions for approval, coverage, adherence, and persistence, with projected uptake of GLP-1 receptor agonists and resmetirom. Prevalent and incident MASH cohorts were stratified by T2D status and updated annually to reflect demographic aging and projected trends in T2D prevalence informed by International Diabetes Federation data and expert input from each country.
Results: Across EU-4+UK, MASH cases are projected to increase from 12.04 million (2025) to 13.96 million (2040), with rising MASH prevalence in all of these countries (Germany: 4.42% to 4.78%; Spain: 4.64% to 5.35%; France: 4.08% to 4.48%; Italy: 4.69% to 5.34%; UK: 4.76% to 5.17%). MASH with advanced fibrosis (AF, F3/F4) is also expected to increase from approximately 2.77 million to 3.24 million. Annual liver-related deaths attributable to MASH in these countries will rise from 26,322 to 33,151 while liver transplants increase from 596 to 909 per year. Although emerging therapies may slow down the overall disease progression, the metabolic severity of the MASH population will intensify. The proportion of all MASH cases with T2D remains relatively stable (27–30%), yet T2D becomes increasingly more concentrated among MASH with severe outcomes. The share of MASH+AF in individuals with T2D will increase (e.g., Germany 41% to 44%; Spain 38% to 45%; France 38% to 45%). Similar trends are observed for liver-related mortality and transplantation (T2D in 71% of MASH transplants by 2040 in some countries).
Conclusion: Despite therapeutic advances, the burden of MASH in Europe is expected to grow over the next two decades, with T2D increasingly concentrated among MASH with advanced liver disease or more severe liver-related outcomes.

SAT-051

Central obesity is a key determinant of advanced fibrosis across the spectrum of steatotic liver disease (SLD): a population-based analysis

Markos Kalligeros[1,2], James M. Paik[1], Albert Tan[1], James Estep[1], Andrei Racila[1], Zobair M. Younossi[1]. *[1]The global NASH/MASH council, Washington DC, United States; [2]Division of Gastroenterology and Hepatology, Beth Israel Deaconess Medical Center, Harvard Medical School, Boston, MA, USA, Boston, United States*
Email: zobair.younossi@cldq.org

Background and aims: Obesity, typically defined by body mass index (BMI), is associated with metabolic dysfunction-associated steatotic liver disease (MASLD); however, the contribution of visceral adiposity (central obesity) across SLD spectrum remains incompletely characterized. We evaluated the association between central obesity and SLD in a population-based cohort.
Method: This cross-sectional study included adults (≥18 years) from the National Health and Nutrition Examination Survey 2017–2020. SLD was defined by controlled attenuation parameter (CAP) ≥285 dB/m. MASLD, metabolic dysfunction–associated alcohol-related liver

disease (MetALD), and alcohol-associated liver disease (ALD) were classified using consensus definitions. Alcohol intake was adjusted for sex- and frequency-specific underreporting and calibrated to national per-capita ethanol consumption. Alcohol phenotypes included abstainers (none), former drinkers (none in past year), low intake (<20–30 g/day women/men), moderate intake (20–49.9 and 30–59.9 g/day), or heavy intake (≥50 and ≥60 g/day). Advanced fibrosis and cirrhosis were defined by liver stiffness ≥12.0 kPa and ≥20.0 kPa. Central obesity was assessed using body roundness index (BRI) ≥6.5.

Results: Among 5,095 participants (age 49.5 years), 35.4% had SLD [MASLD 27.9%, MetALD 3.6%, and ALD 4.0%]. The entire cohort was classified as abstainers (7.7%), former (15.0%), low (54.3%), moderate (12.6%), and heavy (10.4%). In MASLD cohort, alcohol phenotypes were abstainers (10.5%), former (21.0%), and low drinkers (68.5%). Among SLD, advanced fibrosis and cirrhosis were present in 8.44% and 3.35%. By SLD subtype, advanced fibrosis and cirrhosis occurred in MASLD (9.01%, 4.25%), MetALD (4.82%, 2.04%), and ALD (10.53%, 2.70%). Central obesity was associated with higher prevalence of advanced fibrosis in MASLD (13.24% vs. 2.18%) and ALD (15.31% vs. 7.31%) (both $p < 0.05$), but not MetALD (4.93% vs. 3.97%; $p = 0.792$). Advanced fibrosis prevalence was even higher in MASLD with central obesity across alcohol phenotypes [abstainers (10.60% vs. 0.00%), former (12.48% vs. 5.50%), and low (13.83% vs. 1.82%; all $p < 0.05$)]. In stratified multivariable models, central obesity was independently associated with advanced fibrosis in MASLD (OR 6.27; 95% CI 2.71–14.50) and ALD (OR 2.30; 95% CI 1.03–5.15), but not MetALD (OR 2.91; 95% CI 0.36–23.28).

Conclusion: Central obesity is the most clinically relevant predictor of advanced fibrosis in MASLD and ALD.

SAT-052

Mapping the risk of liver cirrhosis by occupational groups in Sweden: a population-based case-control study

Marie Zalesiak[1], Juan Vaz[1,2], Martin Henriksson[3], Eralda Asllanaj[4], Hannes Hagström[1,5], Ying Shang[1]. *[1]Departement of Medicine, Karolinska Institutet, Stockholm, Sweden; [2]School of Public Health and Community Medicine, Institute of Medicine, Sahlgrenska Academy, University of Gothenburg, Gothenburg, Sweden; [3]Center of Medical Technology Assessment, Department of Medical, Heath and Caring Science, Linköping, Sweden; [4]Boehringer Ingelheim, Amsterdam, Netherlands; [5]Unit of Hepatology, Department of GUT, Karolinska University Hospital, Stockholm, Sweden*
Email: marie.zalesiak@ki.se

Background and aims: Liver cirrhosis is frequently diagnosed at an advanced stage and is associated with poor prognosis. Identifying high-burden groups beyond traditional healthcare settings may facilitate earlier detection. We mapped the relative risk of incident cirrhosis across occupational groups in Sweden to inform targeted case-finding.

Method: We conducted a nationwide case–control study within the Swedish Decoding the Epidemiology of Liver Disease in Sweden (DELIVER) cohort (2002–2021). Cases were individuals aged 35–65 years with liver cirrhosis and were matched to up to four controls on age, sex, calendar year, and municipality using incidence-density sampling. Labor market status in the year preceding the index date (i.e., cirrhosis diagnosis) was obtained from registers and categorized as employed, unemployed, disability/long-term sick leave, or early retirement. Occupational group was identified among employed individuals. Conditional logistic regression estimated odds ratios (ORs) with 95% confidence intervals (CIs), using physical and engineering science professionals as the reference group (low risk for cirrhosis and homogeneous group). Analyses were stratified by underlying etiology.

Results: The study included 23,038 cases and 92,125 matched controls. Cases were more likely to clustered in lower socioeconomic strata, reflected by lower income and educational attainment and higher proportions outside the labor market. Occupational analyses were restricted to employed and unemployed individuals, resulting in 7,485 cases and 63,747 controls. Compared with the reference group, unemployment was associated with the highest odds of cirrhosis (OR 10.9, 95% CI 8.3–14.1). Among employed individuals, food-related occupations showed markedly elevated risks, including food preparation workers (OR 3.2, 95% CI 2.2–4.5) and butchers/bakers/food processors (OR 4.9, 95% CI 2.1–11.6). Higher risks were also observed for refuse collectors/ recycling workers (OR 3.3, 95% CI 2.4–4.5) and social workers (OR 2.5, 95% CI 1.7–3.7). Stratified analyses by etiology demonstrated broadly similar occupational risk patterns.

Conclusion: Incident cirrhosis in Sweden is unevenly distributed across the working-age population, with the highest risk among unemployed individuals and increased risk in specific occupations. Occupation-based risk mapping could support targeted case-finding and facilitate earlier detection for liver cirrhosis.

SAT-053

Clinical obesity is strongly associated with steatotic liver disease and advanced fibrosis: evidence from NHANES 2017–2018

Laura Sol Grinshpan[1,2], Shira Zelber-Sagi[1,2], James Paik[1,3], Dana Ivancovsky-Wajcman[1], Linda Henry[1,3], Zobair M. Younossi[1,3]. *[1]The global NASH/MASH council, Washington DC, United States; [2]School of public health, faculty of social welfare and health sciences, University of Haifa, Haifa, Israel; [3]Center for outcomes research in liver diseases, Washington DC, United States*
Email: szelber-s@univ.haifa.ac.il

Background and aims: Obesity is a major driver of steatotic liver disease (SLD), yet its conventional definitions may inadequately capture adiposity-related risk. A Lancet commission recently defined obesity based on adiposity measures beyond body mass index (BMI) and coined the term clinical obesity- a condition of illness that results from the effect of excess adiposity on the function of organs and tissues. We examined the association between clinically obesity and SLD.

Method: This cross-sectional analysis included adults aged ≥18 years from the 2017–2018 National Health and Nutrition Examination Survey (NHANES). Obesity was defined as: BMI ≥ 40 kg/m^2; or BMI ≥30 kg/m^2 (≥27.5 kg/m^2 for Asian) with ≥ 1 adiposity abnormality; or ≥ 2 adiposity abnormalities regardless of BMI class. Clinical obesity was defined as obesity with ≥ 1 non-hepatic clinical complication (metabolic abnormality, sleep apnea, heart failure, chronic kidney disease, and activity-of-daily-living limitation); preclinical obesity indicated obesity without any of these complications. SLD was defined by a controlled attenuation parameter ≥285 dB/m and classified as MASLD, MetALD, or ALD based on the recent international consensus with alcohol intake corrected for underreporting. Advanced fibrosis (including cirrhosis) was defined by liver stiffness ≥12.0 kPa.

Results: Among 3,357 NHANES participants (mean age, 50.0 years; 46.1% male), weighted prevalence of SLD was 31.9% (MASLD 24.6%, MetALD 4.0%, ALD 3.3%) with 3.0% having advanced fibrosis. Using the new definitions, 30.0% had non-obesity, 17.5% preclinical obesity, and 52.5% clinical obesity. SLD prevalence increased across groups (no obesity: 3.0%, preclinical obesity: 26.2%, and clinical obesity: 50.3%, respectively), with parallel gradients for MASLD (1.7%, 21.3%, 38.8%), MetALD (0.7%, 2.5%, 6.4%), and ALD (0.5%, 2.3%, 5.1%). Advanced fibrosis prevalence similarly increased; 0.34%, 0.45%, and 6.67%. In multivariable models adjusted for demographic and lifestyle confounders, clinical obesity was strongly associated with SLD (OR 28.63, 95%CI 18.68–43.88) and advanced fibrosis (OR 10.09, 95%CI 2.53–40.25) compared with non-obesity, whereas preclinical obesity was only associated with SLD (OR 8.612, 95%CI 4.55–16.29). Results were unchanged after excluding participants with diabetes.

Conclusion: Adiposity-based clinical obesity identifies a high-risk phenotype strongly associated with SLD and hepatic fibrosis.

Incorporating clinical obesity frameworks may improve risk stratification.

SAT-054

Global burden and trends of primary liver cancer attributable to comorbid type 2 diabetes mellitus among people living with metabolic dysfunction-associated steatohepatitis: an observational trend study from 1990 to 2021

Xinyu Zhao[1,2], Chunfeng Mei[1], Jiatu Zhong[1], Shihao Zheng[1], Wenying Qi[1], Yong'an Ye[1]. [1]*Beijing University of Chinese Medicine, Beijing, China;* [2]*Dongzhimen Hospital, Beijing University of Chinese Medicine, Beijing, China*
Email: 20220931554@bucm.edu.cn

Background and aims: The synergistic interaction between metabolic dysfunction-associated steatohepatitis (MASH) and type 2 diabetes mellitus (T2DM) is an emerging driver of hepatocellular carcinoma (HCC). However, a comprehensive global assessment of the liver cancer burden specifically attributable to this comorbidity is lacking. This study aimed to quantify the global burden and temporal trends of primary liver cancer due to MASH-T2DM comorbidity from 1990 to 2021.
Method: Using Global Burden of Disease (GBD) 2021 data from 204 countries (1990–2021), we estimated liver cancer burden attributable to MASH-T2DM comorbidity. Population attributable fractions (PAFs) were calculated using Levin's formula. We analyzed age-standardized prevalence, disability-adjusted life years (DALYs), and mortality rates, stratified by region, sociodemographic index (SDI), sex, and age. Temporal trends were assessed using estimated annual percentage change (EAPC).
Results: In 2021, the global age-standardized prevalence and DALY rates were 13.6 (95% Uncertainty Interval [UI]: 2.2–36.4) and 257.1 (95% UI: 42.9–688.6) per 10,000,000 individuals, respectively. The highest burdens were observed in high-SDI regions, particularly High-income Asia Pacific and North America. The disease burden was approximately five-fold higher in individuals aged ≥ 60 years, and males exhibited a higher burden across most age groups. While EAPC point estimates were positive across all regions, wide uncertainty intervals precluded statistical significance, indicating substantial uncertainty in temporal trends.
Conclusion: MASH-T2DM comorbidity represents a distinct and escalating driver of the global liver cancer burden, characterized by a unique "affluence-aging" pattern that differs fundamentally from traditional viral etiologies. Our findings underscore an urgent need for public health strategies to pivot from a primary focus on infectious disease control toward integrated metabolic health management and risk-stratified surveillance, particularly in aging, high-income populations.

SAT-055

The burden of hepatocellular carcinoma in Oceania: an under-represented but high-risk population

Angela Zhu[1], Aparna Morgan[1], Nicholas Hannah[1], James Haridy[1], Ashok Raj[1], Neeraj Bhala[1]. [1]*Department of Gastroenterology and Hepatology, The Royal Melbourne Hospital, Melbourne, Australia*
Email: angzhu26@gmail.com

Background and aims: The global burden of hepatocellular carcinoma(HCC) and its mortality rate continue to rise despite advances in treatment. Contemporary reviews of HCC epidemiology often excludes data from Oceania, limiting representation of regions with distinct demographic profiles and risk factor distributions. There is a high prevalence of chronic hepatitis B(CHB) and increasing burden of metabolic dysfunction-associated steatotic liver disease (MASLD) among the Aboriginal and Torres Strait Islander peoples of Australia, Māori, Pasifika and migrant/refugee populations. We aim to summarise contemporary oceanic epidemiology of HCC and highlight implications for surveillance.
Method: We performed a literature review on epidemiological data based on cohort studies and clinical guidelines describing the prevalence, incidence and aetiology of HCC.
Results: Data derived from the Global Burden of Disease study reveals that Australia, New Zealand and Guam had the highest increase in incidence and mortality from liver cancer in Oceania between 1990 and 2021. Specifically, Australia and New Zealand have the the highest annual percentage increases in MASLD-related liver cancer at 3.27% and 2.01%. An estimated 5.7 million Australians lived with MASLD in 2020 and MASLD-associated HCC is projected to increase by 75% by 2030. Alarmingly, recent data indicates that 31% of MASLD-related HCC occurs without established cirrhosis. We also note higher incidences of non-cirrhotic HCC among Aboriginal and Torres Strait Islander peoples over 50 years old with CHB(0.36–0.9%). These data prompted the recent publication of clinical practice guideline by George et al. which addressed current gaps in HCC surveillance in this high-risk population. Over 70% of people living with CHB in Australia were born overseas. This diverse migrant population results in a broad HBV genotype distribution, including genotypes B and C among Asian migrants that are typically associated with increased oncogenic risk independent of cirrhosis. Similarly, HBV is the leading cause of HCC-related deaths in New Zealand(31.5%), and Māori people are 3.5 times more likely to die from HCC compared to non-Māori people. Data on HCC among Pasifika peoples remains limited and is largely derived from migrant cohorts.
Conclusion: Oceanic populations contribute important and distinct epidemiological insights into HCC risk. Addressing this gap in contemporary global syntheses is essential for eliminating geographic bias and supporting equitable guideline development.

Public Health – Viral Hepatitis

TOP-033

Non-genetic determinants of hepatitis B surface antibody disappearance in Taiwan's vaccinated generations

Chun-Yi Chang[1,2], Chih-Jen Huang[2], Mei-Hung Pan[2], Ding-Lian Wang[2,3], Jaw-Ching Wu[1], Chien-Jen Chen[2], Hwai-I Yang[2]. [1]*Institute of Clinical Medicine, National Yang Ming Chiao Tung University, Taipei, Taiwan;* [2]*Genomic Research Center, Academia Sinica, Taipei, Taiwan;* [3]*Graduate Institute of Life Science, National Defense Medical University, Taipei, Taiwan*
Email: smilekey16@gmail.com

Background and aims: Chronic hepatitis B virus (HBV) is a major global public health challenge. Taiwan's universal neonatal HBV vaccination program, launched in 1986, has markedly reduced hepatitis B surface antigen (HBsAg) prevalence and liver cancer incidence. However, up to 60% of vaccinees lose protective hepatitis B surface antibody (anti-HBs) levels 15–18 years post-vaccination, raising concerns about long-term immunity and booster strategies. While host genetic factors have been implicated, the impact of measurable non-genetic determinants remains unclear. This study aimed to identify key non-genetic factors associated with anti-HBs seronegative and evaluate whether this loss confers differential risks of HBV infection and chronic carriage across vaccine types.
Method: We analyzed 6,586 Taiwan Biobank participants born after July 1, 1986, receiving neonatal HBV vaccination. Determinants of anti-HBs seronegative were evaluated among 6,247 anti-HBc-negative individuals. Demographic, anthropometric, biochemical, lifestyle, and vaccination-related factors were assessed. Multivariate logistic regression models estimated adjusted odds ratios (Adj-ORs) and 95% confidence intervals (CIs). The entire cohort was further stratified by vaccine type and anti-HBs serostatus to compare rates of chronic carriage (HBsAg+) and HBV infection (anti-HBc+).

Results: Among the 6,247 participants, 44.84% were anti-HBs seronegative. Four non-genetic factors were independently associated with antibody loss. Female sex was associated with a lower risk than male sex (Adj-OR = 0.76, 95%CI = 0.67–0.86). Obesity (BMI ≥ 30 kg/m^2) increased risk compared with normal BMI (Adj-OR = 1.40, 95%CI = 1.10–1.77). Current smokers had a higher risk (Adj-OR = 1.54, 95%CI = 1.29–1.85). Recipients of recombinant vaccine had a higher risk of anti-HBs seronegativity than plasma-derived vaccine recipients (Adj-OR = 1.41, 95%CI = 1.11–1.78). Despite better antibody persistence, plasma-derived vaccinees exhibited worse clinical outcomes after antibody loss. Chronic carriage (HBsAg+) was more frequent in the plasma-derived group than in the recombinant group (1.7% vs. 0.5%; Crude OR = 3.67, 95%CI = 1.70–7.93).
Conclusion: Sex, obesity, smoking, and vaccine type are significant non-genetic determinants of anti-HBs waning. Notably, recombinant vaccines confer superior long-term protection against chronic HBV carriage despite a higher rate of antibody loss. These findings support risk-stratified booster strategies to optimize long-term HBV prevention.

TOP-034

Impact of an EASL-guided screen-and-treat intervention for hepatitis B on HCC incidence in West Africa: results of a large-scale population-based study in The Gambia

Gibril Ndow[1], Erwan Vo Quang[1], Bakary Dibba[1], Damien Leith[1], Sainabou Drammeh[1], Gavin Cloherty[2], Stéphane Chevaliez[3], Sheikh Omar Bittaye[4], Kitabu Jammeh[1], Patrick Ingiliz[5], Vincent Leroy[5], Ousman Bah[1], Jean-Michel Pawlotsky[5], Amie Ceesay[1], Isabelle Chemin[6], Maimuna Mendy[1], Ramou Njie[1], Dalessandro Umberto[1], Mark R Thursz[7], Yusuke Shimakawa[8], Maud Lemoine[7]. *[1]MRCG@LSHTM, Fajara, Gambia; [2]Abbott company, United States, United States; [3]APHP, Creteil, France; [4]University of Gambia, Banjul, Gambia; [5]APHP Henri Mondor Hospital, Creteil, France; [6]INSERM, Lyon, France; [7]Imperial College London, Department of Metabolism, Digestion and Reproduction, London, United Kingdom; [8]Pasteur Institute, Paris, France*
Email: m.lemoine@imperial.ac.uk

Background and aims: Long-term outcomes of chronic hepatitis B virus infection (CHB) and the impact of antiviral therapy on reducing hepatocellular carcinoma (HCC) in Africa have been poorly documented.
Method: In 2011, the PROLIFICA programme established at the Medical Research Council Unit The Gambia a population-based cohort of CHB patients following a large-scale community screening intervention[1,2]. Following a liver assessment, participants were initiated on Tenofovir (TDF, 300 mg daily) based on the EASL treatment criteria. HCC surveillance was established using abdominal ultrasound and cirrhosis was defined by Fibroscan≥9.5 kPa[3]. The primary outcome was all-cause mortality stratified by TDF exposure. The secondary outcomes were liver-related deaths and HCC incidence compared to historical data2.
Results: Between 7 December 2011 and 28 October 2015, from 1,037 treatment-naïve participants, we analysed 898 CHB patients without HCC or HIV-HCV coinfections at enrolment. Participants were mainly males (516/898, 57%), median age 36 (32–46). During a median follow-up of 7.2 (6.2–9.8) years, 34/864 (3.9%) participants died of any cause giving an annual overall mortality rate at 4.9 (95%CI: 3.3–6.6) deaths/1,000 persons, comparable to the age-standardised mortality rate of the general Gambian population. Compared to untreated ineligible patients, non-cirrhotic treated patients had similar excellent survival (98%, 98%, 95% and 92% at 2, 4, 6 and 10 years, respectively) ($p = 0.26$) whilst eligible cirrhotic patients (94%, 89%, 77% and 58%) had lower survival ($p < 0.0001$). 6 patients died from liver-related events. No HCC occurred in untreated patients, 4 HCC were reported in treated patients, giving an overall incidence of 57.7 (14.4–115.4) per 100,000 person-year. All HCC occured in male cirrhotic patients despite good adherence to TDF, viral suppression and absence of HDV coinfection. Among men, HCC incidence was 101.5 (25.4–203.01) per 100,000 person-year, lower than a historical Gambian study before the introduction of antiviral therapy in the country[2] (183.5 (82.4–408.5) per 100 000 person-years).
Conclusion: This West African EASL criteria-driven screen-and-treat intervention study shows a reduction in HCC incidence, compared to historical data, with excellent clinical outcomes of non-cirrhotic patients, but highlights the importance of early detection of cirrhosis and strengthened HCC surveillance programmes.

References

1. Lemoine, *et al. Lancet Glob Health* 2016.
2. Shimakawa, *et al. Gut* 2016.
3. Lemoine, *et al. Gut* 2016.

TOP-048

A low-cost tool to assess HBV treatment eligibility: time to positivity of a point-of-care HBsAg test

Judit Romero[1,2], Asegedech Asmamaw[3,4], Nega Berhe[4,5], Ariadna Rando-Segura[6], Amanda Cohn[1], Xavier Major[7], Elena Vargas-Accarino[1,8], Adriana Palom[1,8], Juan Carlos Ruiz-Cobo[1,9,10], Mar Riveiro Barciela[1,8,9,10], Asgeir Johannessen[5,11], Maria Buti[1,8,9,10]. *[1]Research group of liver diseases, Vall Hebron Research Institute, Barcelona, Spain; [2]Department of Nursing and Health, University of Barcelona, Barcelona, Spain; [3]Department of Medical Laboratory Sciences, Addis Ababa University, Addis Ababa, Ethiopia; [4]Aklilu Lemma Institute of Health Research, Addis Ababa University, Addis Ababa, Ethiopia; [5]Department of Infectious Diseases, Vestfold Hospital, Tonsberg, Norway; [6]Liver Pathology Laboratory, Microbiology and Biochemistry Department, Vall d'Hebron Clinical Laboratories, Hospital Universitari Vall d'Hebron, Barcelona, Spain; [7]Programme on Addictions, HIV, Sexually Transmitted Infections and Viral Hepatitis. Public Health Agency of Catalonia, Barcelona, Spain; [8]CIBERehd, Madrid, Spain; [9]Department of Medicine, Universitat Autònoma of Barcelona, Barcelona, Spain; [10]Liver Unit, Vall d'Hebron University Hospital, Barcelona, Spain; [11]Institute of Clinical Medicine, University of Oslo, Oslo, Norway*
Email: judit.vico@vhir.org

Background and aims: Reaching the WHO hepatitis B elimination targets will require simplified, decentralized screening and care pathways that can be implemented at scale. In many low-resource settings, access to laboratory tests needed to assess treatment eligibility remains limited, creating major gaps in linkage to care. We evaluated whether the time to positivity of a low-cost point-of-care (POC) HBsAg rapid test could serve as a pragmatic proxy for serum HBsAg levels and support identification of inactive HBV carriers during screening.
Method: A multicentre prospective study was conducted between January and December 2025 in a hospital based hepatology clinic in Barcelona (Spain) and in community settings in Ethiopia, reflecting both high- and low-resource contexts. Individuals with current infection (HBsAg+), past infection (HBsAg –/anti-HBc+), and healthy controls were included. Serum HBsAg was quantified using Elecsys HBsAg II (Roche), and qualitative HBsAg testing was performed on capillary blood using POC rapid tests (Determine HBsAg 2, Abbott; LOD: 0.1 IU/mL; recommended reading time 15–20 minutes). Time to positivity was recorded as a simple, visually assessed parameter.
Results: A total of 585 patients were screened (255 in Spain and 270 in Ethiopia), 486 with current infection, 15 with past infection, and 24 healthy controls. Quantitative HBsAg results from the initial 236 individuals are included in the present analysis; 105 had HBsAg ≤1,000 IU/mL and 131 had levels >1,000 IU/mL. All HBsAg-positive individuals were correctly identified by the POC test. Mean (SD) time to positivity was 2.6 ± 2.4 minutes and correlated strongly and inversely with serum HBsAg levels (Pearson's $r = –0.726$, $p < 0.001$). A >2-minute cut-off identified low HBsAg levels (≤1,000 IU/mL) with 79% overall accuracy (sensitivity 75%, specificity 83%). A >3-minute cut-off increased specificity to 97% and positive predictive value to

93%, at the expense of sensitivity (53%). No false-positive results were observed among individuals with past infection or healthy controls.
Conclusion: A simple visual parameter—the time to positivity of an HBsAg rapid test—provides meaningful information on HBsAg levels. This approach could enable immediate identification of inactive HBV carriers during screening campaigns, reduce reliance on laboratory testing, and support decentralized hepatitis B care in resource-limited settings.

TOP-049

Pooling strategies for age-based hepatitis C screening in Spain: population impact and cost-effectiveness to inform national policy

A. Aguilera[1], Raquel Carracedo[1], Adrian Dominguez-Lago[1], Luz Moldes[2], Jorge Cabrera[3], Matilde Trigo[4], María José Gude[5], Noelia Calvo[6], Patricia Ordóñez[7], Maria Cañizares[2], Sandra Cortizo Vidal[3], Santiago Martinez-Garcia[1], Ana Fuentes[8], Marta Piñeiro-Sotelo[9], Raquel Domínguez-Hernández[10], Juan Turnes[4], Carmen Duran[11], Federico García[8]. *[1]Hospital Clínico Universitario De Santiago De Compostela, Santiago de Compostela, Spain; [2]Hospital Universitario de A Coruña, A Coruña, Spain; [3]Hospital Álvaro Cunqueiro, Vigo, Spain; [4]Complexo Hospitalario Universitario de Pontevedra, Pontevedra, Spain; [5]Hospital Universitario Lucus Augusti, Lugo, Spain; [6]Complejo Hospitalario Universitario de Ourense, Ourense, Spain; [7]Hospital Universitario Arquitecto Marcide-Profesor Novoa Santos, Ferrol, Spain; [8]Hospital Universitario Clínico San Cecilio, Instituto Investigación Biosanitaria Ibs. Granada, Centro de Investigación Biomédica en Red Enfermedades Infecciosas. CIBERINFEC, Granada, Spain; [9]General Directorate of Public Health, Santiago de Compostela, Spain; [10]Porib, Pozuelo de Alarcón, Spain; [11]General Directorate of Public Health, Santiago de compostela, Spain*
Email: fegarcia@ugr.es

Background and aims: Hepatitis C virus infection remains underdiagnosed in Spain despite the availability of curative direct-acting antivirals. Age-based screening represents a key opportunity to identify undiagnosed infections, but its implementation at national level requires diagnostic strategies that are both effective and economically sustainable. We assessed the population impact and cost-effectiveness of opportunistic age-based HCV screening using pooled HCV-RNA testing, using a regional elimination programme as a proof of concept to inform national policy decisions.
Method: HCV-RNA testing was performed using a pooling sample strategy. A validated lifetime Markov model of chronic HCV natural history was adapted to evaluate screening strategies in individuals 50–60 years. Three scenarios were analysed: pooled RNA testing vs no screening; pooled RNA testing vs standard testing based on anti-HCV antibody followed by RNA confirmation; and standard testing vs no screening. The model incorporated Spanish epidemiological data, sustained virologic response rates with direct-acting antivirals and official healthcare costs, from a healthcare system perspective over a lifetime horizon with 3% annual discounting.
Results: A total of 157,606 individuals were screened. The prevalence of HCV viremia was 0.14% (95% CI 0.12–0.16), significantly higher in males. Overall, 221 viraemic infections were identified. Compared with no screening, pooling increased short-term diagnostic costs by €181,716 but reduced lifetime costs related to advanced liver disease by €2,328,496, with marked reductions in decompensated cirrhosis (72%), hepatocellular carcinoma (64%), liver transplantation (69%) and liver-related mortality (67%). Pooled testing was a dominant strategy. Compared with standard testing, pooled testing achieved equivalent clinical effectiveness while reducing diagnostic costs, resulting in savings of €663 per diagnosed patient. Standard testing was cost-effective versus no screening, with incremental cost-effectiveness ratios well below Spanish willingness-to-pay thresholds.
Conclusion: Opportunistic age-based HCV screening in individuals 50–60 years has a major population-level impact and is cost-effective in Spain. Pooled RNA testing maximizes clinical benefit, minimizes costs and is a scalable diagnostic strategy. These findings provide robust evidence to support national implementation of age-based HCV screening as part of elimination policies, eitherpreferably, but not only, through pooling-based approaches.

FRI-003

A systematic review of digital health tools and early real-world experience with HepB&Me application in chronic hepatitis B to tackle the unmet clinical need

Almuthana Mohamed[1], Hamit Soyel[2], Mark Danta[3], Patrick Kennedy[1]. *[1]Blizard Institute, Barts and the London school of medicine and dentistry, Queen Mary University of London, London, United Kingdom; [2]School of Electronic Engineering and Computer Science, Queen Mary University of London, London, United Kingdom; [3]School of Clinical Medicine, St Vincent's Healthcare Clinical Campus, Faculty of Medicine and Health, UNSW Sydney, Darlinghurst, Sydney, Australia*
Email: almuthana700@gmail.com

Background and aims: Chronic hepatitis B (CHB) remains significantly underdiagnosed and undertreated, highlighting the need for accessible, trustworthy digital support for both individuals living with CHB and healthcare professionals (HCPs) with a prioritisation of personalised care. We aimed to conduct a systematic review of CHB-focused mobile tools and to summarise real-world experience with the HepB&Me application (app) to illustrate how identified gaps might be addressed through implementation.
Method: Using predefined eligibility criteria (apps or tools with publicly available, explicit HBV content for patients or HCPs), we systematically identified and screened tools through structured secondary research of app stores and web resources, supplemented by primary email interviews with clinicians. Two reviewers extracted predefined data categories: user audience, education, calculators or test result interpretation, signposting to trustworthy resources, clinical trial information, HBV reactivation content, data privacy statements, and medical device classification; disagreements were resolved through discussion. Findings were synthesised narratively. Concurrently, we incorporated data generated from HepB&Me (launched in Q1, 2025), including utilisation metrics and qualitative feedback from patient advocacy reviews.
Results: Sixteen CHB-related tools were identified. Common functions included education, calculators, and interpretation aids. The majority were free to use and not classified as medical devices. Only one specialised educational website addressed HBV reactivation; however, no app directed users to reliable external resources or presented clinical-trial details, identifying unmet content gaps. Early HepB&Me usage showed 89 monthly active users, including 27 healthcare professionals, with an average of 6 chatbot queries per day. Advocacy reviewers judged the content to be thorough but requested improvements in usability, offline access, and expanded language options, including Spanish and Hindi.
Conclusion: There remains a significant unmet need for signposting to credible information, awareness of clinical trials, and clear guidance on reactivation risk. HepB&Me demonstrates initial feasibility as a generative AI resource for Individuals living with CHB and HCP alike. Priorities include enhancing usability, providing offline functionality, expanding language options, ensuring secure authentication and regular updates. Further user-centred evaluations and outcomes research will be conducted.

FRI-004

SIMPLY-B pilot study: assessing hepatitis B treatment uptake in primary care clinics

Dina Moussa[1], Jack Wallace[1], Jacqui Richmond[1], Joseph Doyle[2], Long Nguyen[1], Douglas Boyle[3], Mark Stoove[1], Jason Asselin[1], Victoria Polkinghorne[1], Marvad Ahad[1], Susanne Glasgow[4], Kate New[4], Lena Sanci[3], Matt Penn[5], John Furler[5], Alexander Thompson[3], Margaret Hellard[1], Jessica Howell[1]. *[1]Burnet Institute, Melbourne, Australia; [2]Monash Health, Melbourne, Australia; [3]University of*

Melbourne, Melbourne, Australia; [4]St Vincent's Hospital, Melbourne, Australia; [5]North Richmond Community Health, Melbourne, Australia
Email: dina.moussa@burnet.edu.au

Background and aims: To increase hepatitis B management in primary care, we developed SIMPLY B, a novel hepatitis B electronic decision support tool that provides GPs with real-time management plans, automated specialist support and rapid access to Fibroscan. We evaluated the feasibility, acceptability and effectiveness of SIMPLY B for increasing hepatitis B management in primary care.
Method: This pilot intervention study was conducted in three urban primary care clinics in Melbourne between April 2023 to June 2025. Two clinics had SIMPLY B embedded in the electronic medical record, the other one clinic used an online link that GPs had to purposively access. Demographic and clinical data were extracted from the SIMPLY B database and described (N, %). Semi-structured qualitative interviews evaluating the acceptability of SIMPLY B were conducted with GPs.
Results: HBV management is feasible in primary care but remains hindered by structural, educational and systemic challenges. During the study, twelve of 106 patients (11%) with recorded chronic hepatitis B attended the clinics and all were enrolled in SIMPLY B. Most (58%) were female and ages ranged from 27–72 years. All received SIMPLY B-guided hepatitis B management by their GP in primary care: two patients commenced treatment, 6 commenced liver cancer surveillance and all continued monitoring in primary care without specialist referral. *SIMPLY B* demonstrated that GPs can effectively deliver evidence-based HBV care when supported by decision tools and specialist input. All patients enrolled received appropriate management, yet overall uptake was low. Barriers included limited consultation time, perceived complexity of HBV care, low prioritisation and inadequate integration of digital tools.
Conclusion: Future models of care should integrate HBV into existing chronic disease management frameworks, supported by education, incentives and embedded digital tools.

FRI-005
Monitoring of the cascade of care in patients with chronic HBV in primary care clinics in Australia

Dina Moussa[1], Jack Wallace[1], Jacqui Richmond[1], Joseph Doyle[2], Long Nguyen[1], Douglas Boyle[3], Mark Stoove[1], Jason Asselin[1], Victoria Polkinghorne[1], Marvad Ahad[1], Susanne Glasgow[4], Kate New[4], Lena Sanci[3], Matt Penn[5], John Furler[5], Alexander Thompson[3], Margaret Hellard[1], Jessica Howell[1]. *[1]Burnet Institute, Melbourne, Australia; [2]Monash Health, Melbourne, Australia; [3]University of Melbourne, Melbourne, Australia; [4]St Vincent's Hospital, Melbourne, Australia; [5]North Richmond Community Health, Melbourne, Australia*
Email: dina.moussa@burnet.edu.au

Background and aims: To achieve hepatitis B (HBV) elimination in Australia, a shift from hospital to community-based HBV care is needed. This study aimed to describe the prevalence of chronic HBV and uptake of the cascade of care in primary care patients in Victoria to determine the scope of HBV clinical management within primary care services.
Method: This prospective cohort study was conducted in 76 urban and regional primary care clinics across Victoria between 1/7/2020 to 30/6/2023. Anonymised socio-demographic, clinical and laboratory data from General Practice (GP) clinics' electronic medical records (EMR) were extracted via the PATRON primary care surveillance system. Descriptive analysis of the cohort of clinic clients with HBV was performed, including patient uptake of guideline-based testing, disease assessment and treatment.
Results: A total of 346,927 individuals attended appointments across the study period. Of these, 25,212 had records indicating HBV-related testing, and 20,056 individuals underwent a HBV surface antigen (HBsAg) test (5.8%). 491 (0.14%) individuals had evidence of current HBV infection defined HBsAg positive and/or HBeAg positive and/or HBV DNA positive. or HBV DNA testing. 469 attended the clinics during the study period, among whom 239 (51%) were female, the median age was 39 years and most were of Asian ethnicity. In the GP EMR, only 59 (13%) had evidence of at least one HBV DNA test and at least one ALT test ordered in primary care during the three years of follow up. Fourteen patients (3%) had record of being reviewed for HBV management by the clinic nurse or GP and 78 (17%) reviewed by a viral hepatitis specialist. Fifty-five (12%) of all eligible patients had attended at least one hepatocellular carcinoma (HCC) surveillance ultrasound (US) in primary care, 13 (24%) of whom were co-managed by a liver specialist. 92 (20%) were on treatment for HBV; 53 (58%) were on entecavir, 37 (40%) were on tenofovir and 2 (2%) were on tenofovir alafenamide. Of people receiving treatment, 23 (25%) had a record of linkage to specialist care.
Conclusion: Our data show that significant gaps in the cascade of care remain for people with chronic HBV in primary care settings, with a low proportion of patients having evidence of participating in all stages of the HBV cascade of care in general practice.

FRI-006
Reaching the unreachable: prison mobile outreach as a cornerstone of national HCV micro-elimination efforts in Croatia

Tatjana Reic[1], Adriana Vince[2,3], Magda Pletikosa Pavic[4], Maja Sremac[5], Iva Košuta[5], Vibor Šeša[5], Zdravko Andric[6], Ivona Reic[1], Ana Visic[1], Anna Mrzljak[3,5]. *[1]Croatian Society for the Liver Diseases "Hepatos", Split, Croatia; [2]Department of Virology, Zagreb University Hospital for Infectious Diseases, Zagreb, Croatia; [3]School of Medicine, University of Zagreb, Zagreb, Croatia; [4]Teaching Institute for Public Health Split - Dalmatia County, Split, Croatia; [5]Department of Hepatology, University Hospital Center Zagreb, Zagreb, Croatia; [6]County's General Hospital Pozega, Pozega, Croatia*
Email: tatjana@hepatos.hr

Background and aims: Hepatitis C virus (HCV) infection remains a major public health challenge in prisons, where the prevalence is substantially higher than in the general population. Early diagnosis and effective linkage to care are essential to achieve WHO 2030 elimination targets. Building on earlier positive outcomes, the Croatian Ministry of Justice is supporting this program as part of a national effort toward HCV micro-elimination in Croatian prisons aiming to raise health literacy, access to HCV testing, FibroScan® assessments, counseling, and treatment uptake.
Method: During 2025, the Society "Hepatos" joined by medical experts - hepatologists, ID specialists and epidemiologists conducted 17 mobile clinic activities across Croatian prisons. Data was collected on HCV testing, FibroScan® liver stiffness and CAP measurements, counseling and linkage-to-care. Liver fibrosis and steatosis were classified using established LSM and CAP thresholds appropriate for this population.
Results: A total of 591 prisoners were counseled and majority (N = 555) underwent FibroScan® exam, whereas 147 were tested for HCV. HCV testing was performed in individuals with known risk of exposition to infection. 23 prisoners were newly identified as HCV positive, while additional 12 prisoners previously knew of HCV infection and they were all linked to further specialist care. LSM results demonstrated considerable burden of liver disease: 26% were classified as F1 (5.6–7.0 kPa), 9% as F2 (7.1–9.5 kPa), 4% as F3 (9.6–14.5 kPa), 1% as F4 (≥14.6 kPa), while the rest had LSM within normal range (0–5.6 kPa). Furthermore, 19% of examined individuals exhibited CAP values ≥ 290 dB/m, indicating the high prevalence of moderate to severe hepatic steatosis.
Conclusion: The 2025 Croatian prison HCV micro-elimination program shows that persistent mobile outreach improves health awareness, early diagnosis, and linkage-to-care in a high-risk population. New and previously untreated HCV cases were identified and linked to care, and FibroScan® findings confirmed a notable burden of liver disease, supporting the integration of liver fibrosis and steatosis assessment into prison-based health programs. These results point out the importance of NGO sustained mobile services

and institutional support in advancing national HCV elimination goals.

FRI-007

Persistence of immune response and memory after infant hepatitis B vaccination: a systematic literature review

Bavithra Nathan[1], Volker Vetter[2], Maria Buti[3], Anna Maria Geretti[4], Pierre Van Damme[5], John Ward[6], Ike Iheanacho[7], Louis Lavoie[8], Frederik Verelst[2]. [1]*GSK, London, United Kingdom;* [2]*GSK, Wavre, Belgium;* [3]*Hospital Vall d'Hebrón, Barcelona, Spain;* [4]*Royal Free London NHS Trust, London, United Kingdom, University of Rome Tor Vergata, Rome, Italy;* [5]*University of Antwerp, Antwerp, Belgium;* [6]*Coalition for Global Hepatitis Elimination, Atlanta, United States;* [7]*Evidera, London, United Kingdom;* [8]*Evidera, Saint-Laurent, Canada*
Email: bavithra.x.nathan@gsk.com

Background and aims: Hepatitis B virus (HBV) infection can lead to serious long-term complications, including chronic disease, cirrhosis, and hepatocellular carcinoma. Since the 1990s, universal infant vaccination programs have dramatically reduced HBV incidence, but the duration of vaccine-induced immunity remains a key question for both policy and clinical practice. This systematic review summarizes existing evidence on the persistence of immune response and memory following infant HBV vaccination.
Method: Embase, MEDLINE, CENTRAL and grey literature were searched for studies published from Jan 2015 to Feb 2025 in immunocompetent individuals who completed primary HBV vaccination as infants (PROSPERO CRD420251068042). Studies reporting the proportion of individuals with antibody to HBV surface antigen (anti-HBs) ≥ 10 IU/L and anti-HBs titers at various time points after the primary series were included. The proportion with anti-HBs ≥ 10 IU/L was summarized as median % (range) across studies. Anti-HBs titers were summarized as median (interquartile range [IQR]; range) of the reported geometric mean titers. When a booster dose was administered, studies assessed anamnestic response 1 month later.
Results: We identified 110 studies and 461,616 participants who completed primary infant HBV vaccination. At 5–6 months after the primary series, the proportion with anti-HBs ≥ 10 IU/L was 92% (80–99), and median anti-HBs titer was 261 IU/L (IQR 194; range 29–558). At 1 year after the primary series, the proportion with anti-HBs ≥ 10 IU/L remained at 92% (66–100), but median anti-HBs titer decreased to 128 IU/L (IQR 171; range 19–200). The proportion with anti-HBs ≥ 10 IU/L progressively waned to 59% (42–76) at 5 ± 0.5 years, 54% (24–80) at 10 ± 1 years, and 37% (21–77) at ≥ 15 years. Similarly, median anti-HBs titer declined to 30 IU/L (IQR 14; range 16–38) at 5 ± 0.5 years, 30 IU/L (IQR 94; range 3–163) at 10 ± 1 years, and 7 IU/L (IQR 27; range 5–129) at ≥ 15 years. At the longest follow-up (29.5 years), the proportion with anti-HBs ≥ 10 IU/L was 39%. Of the primary series recipients with titers < 10 IU/L (at mean/median > 12 months after series completion), who received an additional dose of vaccine, 94% (79–100) achieved anti-HBs levels ≥ 10 IU/L.
Conclusion: Early protection after infant HBV vaccination is robust. Although anti-HBs titers decline over time, immune memory persists. Upon antigen re-exposure, anti-HBs titers rapidly restore.
Funding: GSK (VEO-001269).

FRI-008

Viral hepatitis B, C, and delta in Greenland: a national cross-sectional study

Carina Naustdal[1,2,3], Gerda Elisabeth Villadsen[4,5], Karsten Fleischer Rex[6,7], Henrik Krarup[7,8], Henning Grønbæk[4,5], Michael Lynge Pedersen[2,9], Rasmus Gantzel[2,4,5,10]. [1]*Section of Gastroenterology and Hepatology, Department of Medicine, Zealand University Hospital, Køge, Denmark;* [2]*Steno Diabetes Center Greenland, Nuuk, Greenland;* [3]*Queen Ingrid's Hospital, Center of Primary Health Care, Nuuk, Greenland;* [4]*Department of Hepatology and Gastroenterology, Aarhus University Hospital, Aarhus, Denmark;* [5]*Department of Clinical Medicine, Aarhus University, Aarhus, Denmark;* [6]*Department of Internal Medicine, Queen Ingrid's Hospital, Nuuk, Greenland;* [7]*Department of Clinical Medicine, Aalborg University, Aalborg, Denmark;* [8]*Department of Molecular Diagnostics, Aalborg University Hospital, Aalborg, Denmark;* [9]*Greenland Center for Health Research, Institute of Health and Nature, University of Greenland, Nuuk, Greenland;* [10]*Department of Medicine, Regional Hospital Gødstrup, Herning, Denmark*
Email: c.n.bagge@gmail.com

Background and aims: Viral hepatitis B infection is considered endemic in Greenland as in other Arctic areas. However, updated data are warranted after the implementation of screening, vaccination, and treatment programs during the past decades. We aimed to investigate the prevalence and disease characteristics of viral hepatitis B (HBV), C (HCV), and delta (HDV) in Greenland.
Method: We performed a cross-sectional nationwide study using data from the electronic medical records extracted from 2014–2023.
Results: We identified 299 patients with HBV- (positive of HBsAg) and 45 patients with HCV- (positive of HCV-Ab and/or HCV-RNA), corresponding to an overall low prevalence of 0.53% (95%-CI: 0.49–0.57%) and 0.08% (95%-CI: 0.06–0.11%), respectively. The prevalence of HDV co-infection (positive of HDV-Ab and/or HDV-RNA) among patients with HBV was 9.4%, of whom 82% were HDV-RNA positive, indicating ongoing infection. Most of these patients were middle-aged and male. Additionally, the occurrence of HBV and HCV was higher among women compared to men in the age category 20–39 years. The most recent liver biochemistry was within reference values among HBV-positive patients, while alanine and aspartate amino-transferase were slightly elevated among HCV-positive patients. A Fibrosis-4 score above 1.3 was observed in 28 (9%) with HBV, 2 (7%) of HBV-HDV positive patients, and 16 (36%) with HCV.
Conclusion: The prevalence of HBV infection through routine testing in the healthcare system was markedly lower than prevalences reported in previous population screening studies. Yet, HDV co-infection is common and warrants increased awareness. HCV is rare, but more of these patients have elevated liver enzymes and Fibrosis-4 score.

FRI-009

Re-engagement as a hepatitis b elimination strategy: a scoping review

Helen Nde[1], Brandon Eurich[1], Homie Razavi[1]. [1]*Center for Disease Analysis, Lafayette, CO, United States*
Email: hnde@cdafound.org

Background and aims: Loss to follow up (LTFU) limits care for people living with hepatitis B (PLWHBV) who are at higher risk for liver cancer-related mortality. Re-engagement reduces this risk and supports the World Health Organization's 65% mortality reduction target for PLWHBV. This study aims to assess the range and outcomes of re-engagement programs for LTFU PLWHBV implemented globally between 2015 and 2025.
Method: We searched PubMed for studies published between 2015 and 2025 which focused on identifying LTFU PLWHBV for re-engagement to care. Re-engagement was defined as attending a provider or laboratory appointment after outreach. We identified 4,702 potential studies and, after review to ensure outcomes were for LTFU cases only, included eleven.
Results: Seven countries and three WHO regions (EURO, PAHO, WPRO) were represented among the eleven studies. Median year of hepatitis B (HBV) diagnosis was 2017 and median study publication year was 2022. Ten out of eleven studies came from high income countries. Seven studies targeted the general population, three targeted immigrants and one targeted pregnant or post-partum women. Participant data came from medical record reviews in all studies except for two involving immigrants which used data sourced from registries. Six studies performed reviews to assess participant eligibility for outreach. Phone calls were the main means of outreach

occurring in seven studies. Spain (4,353), the Netherlands (3,240), and the United Kingdom (675) had the largest target populations. They also had the highest rates of outreach-ineligibility (72%, 82% and 79% respectively). Among the outreach-eligible, over 50% successful contact was recorded in six out of seven countries. Australia, Ireland, and Spain achieved 100% successful contact. The Netherlands (67%), the United Kingdom (48%) and French Guiana (42%) had the highest rates of contact failure. Median successful re-engagement was 52% and ranged from 2% in the Netherlands to 100% in Australia and Ireland. These results are analogous to preliminary outcomes from ongoing re-engagement programs for LTFU PLWHBV in the United States.

Conclusion: Results suggest re-engagement can support HBV elimination. However, available studies are not representative of the distribution of global HBV infections. Additionally, outreach ineligibility and contact failure indicate data management systems for PLWHBV must improve for both successful re-engagement and retention in care.

FRI-010-YI

Decentralised HBV, HCV, and HIV screening among migrant and refugee populations in Portugal and Spain: results from VH-COMSAVAC

Aina Nicolàs Olivé[1,2], Kiomi Barranco[1], Mariana Vicente[3,4], Laetitia[3], Luis Mendão[3,5,6], Inês Lopes Antunes[7], Francisco Antunes[8,9], Fábio Cota de Madeiros[8,10], Jeffrey Lazarus[1,11], Camila Picchio[1].
[1]Barcelona Institute for Global Health (ISGlobal), Barcelona, Spain; [2]Facultat de Medicina i Ciències de la Salut, Universitat de Barcelona (UB), Barcelona, Spain; [3]Grupo de Ativistas em Tratamentos (GAT), Lisbon, Portugal; [4]AIDS Action Europe, Berlin, Germany; [5]World Hepatitis Alliance (WHA), London, United Kingdom; [6]Coalition PLUS, Paris, France; [7]USF Travessa da Saúde, Lisbon, Portugal; [8]Instituto de Saúde Ambiental (ISAMB), Faculdade de Medicina, Universidade de Lisboa, Lisbon, Portugal; [9]Laboratório Associado TERRA, Universidade de Lisboa, Lisbon, Portugal; [10]ULS Almada-Seixal, Hospital Garcia de Orta, Almada, Portugal; [11]CUNY Graduate School of Public Health and Health Policy (CUNY SPH), New York, United States
Email: aina.nicolas@isglobal.org

Background and aims: Migrants and refugees in Europe face increased risk of hepatitis B (HBV) and hepatitis C (HCV), yet structural and individual barriers limit access to testing and care. This study implemented decentralized approaches to offer HBV/HCV screening, HBV vaccination, and linkage to care among migrants and refugees in Portugal and Spain, while describing current infection patterns.

Method: From 11/22–12/25, the VH-COMSAVAC study offered decentralized HBV and HCV screening in Spain (Catalonia and Madrid) and Portugal (Lisbon) across non-clinical settings such as pop-up and mobile clinics, community and faith-based organizations, NGOs, and a Portuguese primary care centre. HIV screening was also offered in Portugal. Rapid HBsAg, anti-HCV and anti-HIV-1/2 tests were used, with expedited referral pathways to collaborating tertiary hospitals for participants with reactive results. Outreach services were facilitated by community health workers and intercultural mediators in Spain.

Results: A total of 1,337 individuals were screened, with an overall prevalence of 6.4% for HBsAg, 0.8% for anti-HCV, and 0.6% for anti-HIV-1/2. Participants were predominantly sub-Saharan Africans (74.2%), with a median age of 35 years (IQR 26–46), and 59.7% were recently arrived migrants (≤5 years). HBsAg+ and anti-HCV+ prevalences were similar in Portugal and Spain (7.6% vs 5.6%, $p = 0.145$, and 1.1% vs 0.6%, $p = 0.234$, respectively). Most HBsAg+ cases were among sub-Saharan African participants (96.5%), and 72.7% of anti-HCV+ participants were also among sub-Saharan Africans. HBsAg+ prevalence was significantly higher among men (8.5% vs 3.32%, $p < 0.001$) and recently arrived migrants (7.44% vs 3.73%, $p = 0.005$), while no statistical differences were observed among these groups for anti-HCV+ and anti-HIV-1/2+ prevalence ($p > 0.05$). In Spain, 71.1% of positive participants were linked to care, with legal barriers preventing linkage, whereas in Portugal 40.8% were linked, as many had been tested recently and have not yet attended follow-up care.

Conclusion: Migrants and refugees from high prevalence countries living in Portugal and Spain, carry a significant burden of viral hepatitis and HIV. Community-based and simplified screening models can improve access to screening and accelerate linkage to care by addressing linguistic, legal and administrative barriers. As a result, testing, diagnosis and care is increased among these underserved yet disproportionally affected communities.

FRI-011

10 year- experience from treatment as prevention for hepatitis C, a nationwide HCV elimination program in Iceland. Successes and new challenges

Sigurdur Olafsson[1], Anna Tomasdottir[2], Silja Olafsson[3], Valgerdur Runarsdottir[4], Ragnheidur Fridriksdottir[4], Agnar Bjarnason[2], Thorvardur J. Löve[1], Magnús Gottfredsson[1].
[1]Landspitali University Hospital, Faculty of Medicine, School of Health Sciences, University of Iceland, Reykjavik, Iceland; [2]Landspitali University Hospital, Reykjavik, Iceland; [3]Faculty of Medicine, School of Health Sciences, Reykjavik, Iceland; [4]SAA National Center for Addiction Medicine, Reykjavik, Iceland
Email: sigurdol@landspitali.is

Background and aims: The World Health Organization (WHO) set the goal of eliminating hepatitis C virus infection (HCV) as a major health threat by 2030. In 2016, a nationwide program, Treatment as Prevention for Hepatitis C (TraP HepC) was initiated in Iceland, offering treatment with direct acting antivirals (DAAs) without restrictions, including people who inject drugs (PWID). Screening and harm reduction was scaled up. During the first 3 years of the program > 95% of all diagnosed in the country received DAAs and the WHO service coverage targets were reached. The program has continued with emphasis on harm reduction, intense testing and outreach services. The aim was to analyse key outcomes from the TraP HepC program 2016–2025.

Method: Patient characteristics during the first three years of TraP HepC (1/2016–2/2019, period 1) were compared with data for 2021–2023 (period 2) and 2022–2024 (period 3) using nationwide clinical data. Prevalence of HCV among PWID was monitored.

Results: During period 1 (705 patients), mean age was 45, 89 (13%) were born outside Iceland. Ever injecting was reported by 84%, recent injection drug use (IDU) by 33%, 15% were homeless or living in a halfway house. Reinfections were 4.8% of new infections. Acute infections were 6% and 68% were treated at a university hospital. During period 2, the proportion of homeless/halfway-house residence had risen to 30%. Acute infections comprised 46%. During peroid 3, 43.6% were born outside Iceland, 29.6% were domestic new infections, 30.7% were reinfections and 28.5% were imported cases, diagnosed at immigration screening. The encounter site was university hospital 48.7%, outreach 20.7% and addiction treatment center 22.9%. Of all domestic infections 50.8% were reinfections and 95.1% had history of recent IDU. The prevalence of HCV among recently injecting prior to TraP HepC was 57%, decreased rapidly to 10.7% in 2018 and remained at 7–11% in 2019–2025.

Conclusion: Since initiation of TraP Hep C a dramatic change in the landscape of hepatitis C in Iceland has occurred. A rapid reduction in prevalence of HCV among PWID was observed in the first 3 years and has been maintaned. In spite of easy acess to harm reduction and DAAs, infections, especially reinfection rates remain high in a group of active IDU. Imported cases poses a further challenge to eliminaton efforts.

FRI-012

Low treatment rates observed in an analysis of the chronic hepatitis B care cascade at a tertiary medical center in a major metropolitan area in the US

Kevin Pak[1], Mei Leng[2], Steven-Huy Han[3]. [1]*Brooke Army Medical Center, Fort Sam Houston, United States;* [2]*David Geffen School of Medicine at UCLA, Los Angeles, United States;* [3]*Pfleger Liver Institute, Los Angeles, United States*
Email: kevin.pak528@gmail.com

Background and aims: Chronic hepatitis B (CHB) affects the lives of about 254 million people throughout the world and up to 1.89 million people in the US. The CHB care cascade describes the sequence of steps needed to diagnose and appropriately treat patients with CHB. Unfortunately, there remain major gaps in the care cascade in the US. Treatment rates in the US range from 30–60%. The aim of this study was to assess the CHB treatment rates at a tertiary medical system in Los Angeles.
Method: We conducted a retrospective analysis of all adult patients with CHB (positive HBsAg) across the entire UCLA database from 2013–2023. Of all HBsAg positive patients within this timeframe, we determined the number of patients who had an ALT and a HBV DNA level checked. We determined the number of patients with a HBV DNA level ≥ 2,000 IU/mL. Of the patients with a HBV DNA level ≥ 2,000 IU/mL, we determined the number of patients with an ALT > 60 U/L. From this pool, we determined the total number of patients on antiviral therapy with an indication for therapy per AASLD guidelines. We also identified patients with cirrhosis using ICD-9/10 codes and determined how many of these patients were started on treatment.
Results: Across all UCLA clinics from 2013–2023, there were a total of 3,384 patients with positive HBsAg. 3,320 patients had an ALT checked and 987 of these patients had an ALT > 60 U/L. Only 833 patients had a HBV DNA level checked and, of these, 252 patients had a HBV DNA level ≥2,000 IU/mL. 63 patients had an ALT > 60 U/L plus a HBV DNA ≥ 2,000 IU/mL. 511 patients had HBV-related cirrhosis. In total, 1,255 patients were on antiviral therapy (37.1%). 429 of 511 cirrhotic patients were on therapy (84%). 453 non-cirrhotic patients (54.8%) were on treatment within 6 months of being seen for the first time in the system.
Conclusion: From 2013–2023, the CHB care cascade at UCLA yielded a treatment rate of 37.1%, which is low but falls within the US range reported in prior studies. Treatment rates of cirrhosis patients were much higher (84.0%). While ALT was checked in 98.1% of patients, only 24.6% had a HBV DNA checked – a considerable gap which contributed to low treatment rates. Significantly more patients than were otherwise eligible received treatment. This can potentially be explained by a considerable number of patients being started on treatment prior to being referred and seen in the UCLA system and/or provider knowledge of treatment thresholds.

FRI-013

Prevalence and socioeconomics of hepatitis D virus coinfection in two Southern California counties

Kevin Pak[1], Mei Leng[2], Jeffrey Nguyen[3], Karine Moussa[3], Robert G. Gish[4], Steven-Huy Han[5], Paul Pockros[6]. [1]*Brooke Army Medical Center, Fort Sam Houston, United States;* [2]*David Geffen School of Medicine at UCLA, Los Angeles, United States;* [3]*Scripps Green Hospital, La Jolla, United States;* [4]*La Maestra Community Health Center, San Diego, United States;* [5]*Pfleger Liver Institute, Los Angeles, United States;* [6]*Scripps Clinic, La Jolla, United States*
Email: kevin.pak528@gmail.com

Background and aims: The global prevalence of Hepatitis D virus (HDV) is about 5%. There have been efforts to determine the HDV prevalence in the US; HDV is generally considered to be lower than that of other countries. HDV has been suggested to be more prevalent in lower socioeconomic status and immigrant individuals. Our aim was to determine the prevalence of HDV patients in three different healthcare systems based in San Diego (SD) County and Los Angeles (LA) County.
Method: We retrospectively reviewed the outpatient records of all adult chronic HBV patients screened for anti-HDV total antibody (HDV Ab) who were seen from 2010 to 2024 in the outpatient liver clinics at Scripps Clinic (SC) in La Jolla and La Maestra Clinic (LM) in SD, and from 2019 to 2023 in the Pfleger Liver Institute at UCLA. In patients with positive HDV Ab, the prevalence of detectable HDV RNA was then determined. We calculated the median household income by zip code for each service area, which was available through the US Census Bureau, to stratify all patients by socioeconomic status.
Results: At SC, 593 of 2,441 patients with CHB were screened for HDV. 14 patients tested positive for HDV Ab (2.4%). Two of the 14 patients with positive HDV Ab had detectable HDV RNA. At LM, 118 of 312 patients with CHB were screened for HDV. Three patients were positive for HDV Ab (2.5%). None had detectable HDV RNA. At UCLA, 234 of 267 HBV patients were screened for HDV. Ten patients had a positive HDV Ab (4.3%) and one patient had detectable RNA. Most patients screened at LM belonged to the lowest median income category ($75,281 per annum). Most patients screened at SC belonged to the middle median income group ($101,105 per annum). Most patients screened at UCLA belonged to the high ($117,023 per annum). There was no statistically significant difference in the prevalence of HDV Ab between cohorts of LM and SC, between SC and UCLA, and between LM and UCLA.
Conclusion: Of almost a thousand CHB patients who were screened for HDV, the prevalence of patients who tested positive for HDV Ab in three different healthcare systems between SD County and LA County ranged from 2.4–4.3%. There were no statistically significant differences of seropositivity rates among the three institutions. The screened patients from LM, SC, and UCLA were representative of low, middle, and high socioeconomic groups, respectively. This suggests that socioeconomic status may be less of a risk factor for HDV infection, particularly in this region of the country.

FRI-014

Advancing hepatitis C elimination in prisons: a state-specific modelling study of integrated harm-reduction and addiction interventions

Andrew Palmer[1,1,2], Aathavan Shanmuga Anandan[2], Matthew Carter[2], Ezaam Fraz[2], Paul Clark[1,2], Jason Connor[1,2], Gerald Holtmann[1,2], Naomi Runnegar[2], Geoffrey Playford[1,2], Jeremy Hayllar[3], Nick Scott[4], Farah Houdroge[4]. [1]*The University of Queensland Herston, Herston, Australia;* [2]*Princess Alexandra Hospital, Woolloongabba, Australia;* [3]*Biala Alcohol & Drug Service, Metro North, Brisbane, Australia;* [4]*Burnet Institute, Melbourne CBD, Australia*
Email: andrew.palmer@uq.edu.au

Background and aims: Australia has made major progress towards hepatitis C virus (HCV) elimination through direct-acting antivirals (DAA). However, ongoing transmission and injection-related infections (IRI) among people who inject drugs risk these gains. Prisons remain under-resourced environments where high-risk injecting persists, generating substantial downstream costs. While HCV testing and treatment are essential, treatment-focused approaches risk positioning DAA as the endpoint of care rather than as an entry point into harm-reduction and addiction treatment. We modelled the impact of integrated addiction interventions on HCV elimination, IRI, and health-system costs in Queensland (QLD) prisons.
Method: We developed a deterministic compartmental model calibrated to a large Australian prison system (QLD) using incarceration, epidemiological, and economic data. Prison inputs reflected QLD Corrective Services statistics, with 56% of people entering custody having a history of injecting drug use. HCV epidemiology was calibrated using QLD surveillance data. Hospital burden from IRI was informed by our own dataset describing 321 admissions over four years at a QLD hospital responsible for ~60% of prison-related IRI admissions statewide. We modelled three strategies across QLD

prisons from 2026–2030: prison needle and syringe programs (PNSP) alone, opioid agonist therapy (OAT) alone, and combined PNSP and OAT delivered as integrated care. Coverage increased to 10%, 30%, 50%, or 70%. Outcomes included HCV infections, incidence, IRI admissions, costs, and benefit–cost ratios (BCRs).
Results: Under status quo conditions, we projected 536 new HCV infections and 921 IRI-related hospital admissions between 2026 and 2030, with HCV incidence remaining at 2.6 per 100 person-years in 2030. At 50% coverage, PNSP alone averted 155 HCV infections and 154 IRI admissions (BCR 2.6), while OAT alone averted 55 HCV infections and 152 IRI admissions (BCR 1). Combined PNSP and OAT achieved the greatest impact, averting 188 HCV infections and 271 IRI admissions at 50% coverage and reducing incidence to 1.0 per 100 person-years (BCR 1.4). At 70% coverage, incidence declined to 0.5 per 100 person-years.
Conclusion: HCV elimination in prisons is unlikely to be achieved through DAA alone. Integrated harm-reduction and addiction care may improve HCV elimination, reduce IRI, and deliver net health-system benefits. Our findings have implications for others seeking to sustain HCV elimination gains.

FRI-015-YI
Predictors of hepatitis B infection and vaccination coverage in sub-Saharan Africa: case studies from Gabon and Mauritania using demographic and health survey data
Jodi Palmer[1], Jack Stone[1], Aaron G. Lim[1], Anna McNaughton[1], Kennedy Kipkoech[1]. [1]*University of Bristol, Bristol, United Kingdom*
Email: Uc24737@bristol.ac.uk

Background and aims: Hepatitis B virus (HBV) remains prevalent in sub-Saharan Africa (SSA), which accounted for approximately 63% of new HBV infections globally in 2022, largely driven by ongoing mother-to-child transmission (MTCT). The World Health Organisation (WHO) targets HBV elimination by 2030 via interventions including timely HBV birth dose (HepBD) and triple dose infant vaccination (HepB3), yet coverage remains low across SSA, where only 18% of newborns receive HepBD. Gabon, an upper-middle-income country with high urbanisation and health facilities, contrasts with Mauritania, a lower-middle-income country with largely rural populations. Whilst Gabon has not introduced HepBD, Mauritania adopted HepBD in 2013. This study estimates HBV prevalence, vaccination coverage, and predictors of vaccine uptake in both countries.
Method: We analysed Demographic and Health Survey (DHS) data from Gabon and Mauritania (2019–2021). Both included adult (≥15 yrs) hepatitis B surface antigen (HBsAg) prevalence and HepB3 coverage (0–59 mnths). Additionally, Mauritanian data included child/adolescent HBsAg prevalence (<15 yrs) and HepBD coverage (0–35 mnths). Weighted estimates and multivariable logistic regression analyses assessed demographic (age, sex), socio-economic (education, wealth), and healthcare-related (antenatal visits, facility delivery) predictors.
Results: Adult HBsAg prevalence was 5.4% in Gabon and 7.9% in Mauritania, and higher in men in both countries. Mauritania's child HBsAg prevalence was 1.2%, peaking at 10–14 years. HepB3 completion was suboptimal, with only 60.8% in Gabon and 61.7% in Mauritania receiving all three doses. In both countries, ≥4 antenatal visits and facility delivery strongly predicted completion of infant vaccination doses. In Mauritania, higher maternal education and wealth were associated with lower HBV prevalence and higher vaccine uptake. HepBD coverage in Mauritania was 73.3%, with lower uptake among those from poorer households, those delivered at home, and mothers reporting difficulty reaching health facilities.
Conclusion: HBV prevalence remains high in both countries, making elimination challenging. HepBD in Mauritania is likely contributing to reduced MTCT, but coverage remains uneven, reflecting persistent socioeconomic and health-system access barriers. Elimination strategies should target HepB3 completion across both settings, support Gabon's HepBD introduction, and enhance equitable delivery in Mauritania, particularly for infants born outside health facilities.

FRI-019
Real-world results of Opti-Hep-D: a multicenter, multidisciplinary program for hepatitis D detection and linkage to care in Catalonia
Adriana Palom[1,2], Ariadna Rando-Segura[2,3], Laura Calatayud-Samper[4], Gema Fernández-Rivas[5], Alicia Sellés-Sanchez[6], Saray Mormeneo-Bayo[7], Dúnia Pérez del Campo[8], Eva del Corral[9], Tomàs Balari[10], Rosa M Morillas[2,11], Adrià Rodríguez-Castellano[2,12], Patricia Huelin[2,13], Carmen López Núñez[2,14], Darly Salazar[15], Joana Villaverde[16], Indiana Abdo[17], José Castellote Alonso[2,10], Juan Carles Quer Boniquet[12,18], Carlos Aracil[2,13], Andrés Marco[17,19], Maria Buti[1,2]. [1]*Liver Unit, Vall d'Hebron University Hospital, Barcelona, Spain;* [2]*CIBERehd, Madrid, Spain;* [3]*Microbiology Department, Hospital Universitari Vall d'Hebron, Barcelona, Spain;* [4]*Microbiology Department, Hospital Universitari de Bellvitge, Barcelona, Spain;* [5]*Microbiology Department, Clinical Laboratory North Metropolitan Area, Germans Trias i Pujol University Hospital, Departament of Genetics and Microbiology, Autonomous University of Barcelona, Barcelona, Spain;* [6]*Microbiology Department, Hospital Universitari Joan XXIII de Tarragona, Tarragona, Spain;* [7]*Microbiology Department, Hospital Universitari Arnau de Vilanova, Lleida, Spain;* [8]*Microbiology Department, Hospital Universitari Doctor Josep Trueta, Girona, Spain;* [9]*Microbiology Department, Hospital Universitari Verge de la Cinta, Tortosa, Spain;* [10]*Gastroenterology Unit, Hospital Universitari de Bellvitge, Barcelona, Spain;* [11]*Gastroenterology Unit, Hospital Universitari Germans Trias i Pujol, Barcelona, Spain;* [12]*Gastroenterology Unit, Hospital Universitari Joan XXIII de Tarragona, Universitat Rovira i Virgili, Tarragona, Spain;* [13]*Gastroenterology Unit, Hospital Universitari Arnau de Vilanova, IRBLleida, Lleida, Spain;* [14]*Gastroenterology Unit, Hospital Universitari Doctor Josep Trueta, Girona, Spain;* [15]*Gastroenterology Unit, Hospital Universitari Verge de la Cinta, Tortosa, Spain;* [16]*Gastroenterology Unit, Hospital de Viladecans, Barcelona, Spain;* [17]*Penitentiary health program, Catalan Institute of Health, Barcelona, Spain;* [18]*PADEICS, Catalan Institute of Health, Barcelona, Spain;* [19]*CIBEResp, Madrid, Spain*
Email: mariabutiferret@gmail.com

Background and aims: Hepatitis D virus (HDV) infection remains underdiagnosed, and real-world data on screening and linkage to care are limited. We assessed the implementation of a double reflex HDV testing, linkage to care and treatment integrative program in all HBsAg-positive individuals in Catalonia.
Method: In this prospective multicenter study conducted from January 2024 to April 2025, all HBsAg-positive samples underwent reflex anti-HDV and HDV-RNA testing, with subsequent active linkage to care of individuals testing positive. Clinical data were extracted from electronic medical records. Patient characteristics, risk factors, and bulevirtide initiation were analyzed.
Results: Of 369,581 HBsAg determinations, 6100 were positive. Anti-HDV testing was completed in 5399 (89%), identifying 305 (5.6%) positive cases. HDV-RNA was assessed in 285 patients, with 86 (30%) viremic. Among 2945 first-time anti-HDV tests, 130 (4.4%) were positive and 26 (20%) viremic. Notably, 42% of positive patients had no recorded risk factors or elevated ALT. Prevalence varied by regions (2.3%–4.1%), and was highest in prisons, which also had a 14% HDV-RNA positivity rate. Viremic individuals were predominantly White, often from Eastern Europe, and more likely to have elevated ALT, cirrhosis, or previous pegIFN therapy. Newly diagnosed cases tended to be younger with milder disease. Among viremic individuals, 95% were linked to care and 43% initiated bulevirtide; while 57% remained untreated due to patient-related or reimbursement barriers. No incarcerated patients received bulevirtide, mainly because of complex social situations.

Conclusion: This large-scale public health intervention demonstrates that combining laboratory reflex testing with an active linkage-care strategy is feasible and very well accepted. Its favorable impact on patient care and public health has led to its integration into the Catalan Health System as standard practice. Although care engagement was high, treatment initiation remained limited by several barriers.

FRI-020

Epidemiological shift in hepatitis a seroprevalence among rural school children: insights from a community screening on viral hepatitis, nutrition, and early hepatic steatosis

Partha Sarathi Patra[1]. [1]*Bankura Sammilani Medical College And Hospital, Bankura, India*
Email: pratim.ptr@gmail.com

Background and aims: Amidst improving sanitation in rural India, the traditional high seroprevalence of hepatitis A virus (HAV) in children—historically exceeding 70% in school-aged groups—may be waning, potentially heightening outbreak risks in susceptible populations. This study sought to delineate current serological profiles for HAV, hepatitis B (HBV), and hepatitis C (HCV), alongside lifestyle behaviors, and noninvasive markers of hepatic steatosis in school children from a remote village, to inform targeted public health strategies.
Method: In a cross-sectional health screening initiative, 128 children (mean age 11.5 ± 1.5 years; 32.8% male) from three government schools underwent ELISA-based serological testing for anti-HAV IgG, HBsAg, and anti-HCV. Anthropometric assessments yielded body mass index (BMI) classifications adapted for pediatrics (<15 underweight; 15–22 normal; >22 overweight/obese). Questionnaires quantified daily outdoor play in minutes (<30 = A; 30–60 = B; 60–90 = C; >90 min = D) and daily mobile device use time in minutes (<30 = A; 30–60 = B; >60 = C), with values approximated for quantitative analysis. Hepatic fat was gauged via controlled attenuation parameter (CAP) using transient elastography (Fibro Touch). Data were summarized with means ± SD, percentages, and Spearman's correlations.
Results: Anti-HAV IgG seropositivity stood at 33.6% (43/128)—a strikingly low rate compared to prior national surveys reporting 75–85% in similar age cohorts—signaling a profound epidemiological transition. No HBV (HBsAg 0%) or HCV (anti-HCV 0%) cases emerged. Mean BMI was 18.9 ± 3.8 kg/m^2, revealing 18.0% underweight, 54.7% normal, and 27.3% overweight/obese children. CAP averaged 218.8 ± 34.9 dB/m, with 23.4% exhibiting mild steatosis (CAP >248 dB/m). Daily outdoor play averaged 59.8 min, contrasted by 31.2 min of mobile use; CAP correlated positively with screen time ($r = 0.54$, $p < 0.001$) and inversely with outdoor play time ($r = -0.74$, $p < 0.001$).
Conclusion: This screening unveils an unprecedented decline in HAV immunity among diverging from established high-endemic patterns and underscoring vulnerability to acute outbreaks. Coupled with absent chronic viral threats yet rising adiposity and steatosis—exacerbated by sedentary shifts—these revelations compel integration of HAV vaccination into India's national immunization schedule to safeguard this demographic. Broader adoption of school-based interventions promoting activity and nutrition could avert the nascent trajectory toward metabolic liver disease.

FRI-021

An optimized in-hospital management model enhances linkage to care for non-hepatology HBV-infected patients: interim analysis of Hot Wave Project 2.0

Chan Xie[1], Jia Chen[1], Qiumin Luo[1], Xin Song[1], Fangfang Wei[2], Zhongsi Hong[3], Liang Peng[1]. [1]*Third Affiliated Hospital of Sun Yat-sen University, Guangzhou, China;* [2]*Sixth Affiliated Hospital of Sun Yat-sen University, Guangzhou, China;* [3]*Fifth Affiliated Hospital of Sun Yat-sen University, Zhuhai, China*
Email: xchan@mail.sysu.edu.cn

Background and aims: A significant proportion of HBV-infected individuals in China remain undiagnosed or untreated. We aimed to evaluate whether an optimized in-hospital management model, emphasizing multi-disciplinary collaboration and patient education, improves linkage-to-care (LTC) and antiviral treatment (AVT) rates for HBsAg-positive patients identified in Non-hepatology departments.
Method: The "Hot Wave Project," initiated in 2022 at the Third Affiliated Hospital of Sun Yat-sen University (SYSU-3AH). Key interventions included collaboration between the Department of Hepatology and various clinical and administrative departments. The measures implemented were automated lab report alerts, establishment of dedicated HBV health clinics, varied patient education programs, and big data monitoring to facilitate professional consultation and treatment for HBV-infected patients. In April 2025, the model expanded to the Fifth Affiliated Hospital of SYSU (SYSU-5AH) and the Sixth Affiliated Hospital of SYSU (SYSU-6AH) as "Hot Wave Project 2.0,"featuring enhanced education plans, and call-back mechanisms. We compared data of HBsAg-positive patients from Non-hepatology departments between 2024 and January–September 2025 across these three centers.
Results: At SYSU-3AH, 15,201 HBsAg-positive patients were identified in 2024, with 9,065 receiving AVT (59.63%) and 2,716 referred to Hepatology (17.88%). From Jan–Sep 2025, among 13,686 identified patients, the AVT rate increased to 61.38% (8,140/13,686, $p = 0.002$), and the referral rate rose significantly to 27.72% (3,797/13,686, $p < 0.0001$). At SYSU-5AH, 6,044 and 4,311 patients were screened in 2024 and Jan–Sep 2025, respectively. The AVT rate improved from 20.14% (1,217/6,044) to 22.67% (978/4,311, $p = 0.002$), while the referral rate remained stable at 16.78% (1,014/6,044) versus 17.26% (744/4,311) ($p = 0.52$). At SYSU-6AH, the AVT rate increased significantly from 21.97% (1,121/5,103) to 35.40% (1,944/5,492) ($p < 0.0001$), and the referral rate improved from 2.12% (108/5,103) to 7.28% (400/5,492) ($p < 0.0001$).
Conclusion: The implementation of the Hot Wave Project 2.0 was associated with improved antiviral treatment uptake and referral rates for HBV patients in non-hepatology settings across multiple centers. The optimized referral system and education strategies demonstrate potential feasibility for expanding in-hospital HBV management coverage.

FRI-022

The impact of disability weights on the projected burden and prioritization of HBV in global health

Devin Razavi-Shearer[1], Chari Cohen[2], Jessica Hicks[3], Robert G. Gish[2], Catherine Freeland[2], Ivane Gamkrelidze[1], Samantha Hall[1], Kathryn Razavi-Shearer[1], Homie Razavi[1]. [1]*Center for Disease Analysis Foundation, Lafayette, United States;* [2]*Hepatitis B Foundation, Doylestown, United States;* [3]*World Hepatitis Alliance, Geneva, Switzerland*
Email: drazavishearer@cdafound.org

Background and aims: Disability-Adjusted Life Years (DALYs) help to prioritize health interventions, allocate resources, and guide policymakers to focus efforts where they're most needed. In Africa, there are an estimated 25.6 million people living with HIV, with 380,000 related deaths and 35.9 million DALYs being incurred. For malaria and tuberculosis (TB), the DALYs are estimated at 43.3 million and 17.8 million respectively. While HIV includes disability weights for every stage of the disease, traditionally HBV only has disability weights applied to severe and late-stage disease states. However, patient-focused and empirical evidence have shown that there is disability associated with living with HBV. We posit that the true impact of hepatitis B virus (HBV) is underprioritized based upon how HBV related DALYs are currently measured, leading to global de-prioritization. We utilized two different sets of utility weights, one from the Global Burden of Disease (GBD) and one from a recent Chinese study (Zhang et al, The Lancet Regional Health-Western

Pacific, 2023) to quantify the impact of different utility weights on the DALYs incurred in Africa.
Method: The Polaris Observatory's country specific PRoGReSs Models were utilized to create a regional model for Africa. These models included the impact of treatment, diagnosis, and prophylaxis programs. DALYs were calculated utilizing three different disability weights: GBD, Zhang 2023 with chronic HBV weights only applied to the diagnosed population, and Zhang 2023 with the disability weight for chronic HBV applied to the prevalent population.
Results: In Africa, it was estimated that there were 89.6 million people living with HBV and 361,000 deaths due to HBV. HBV-related DALYs increased from 6.9 million to 8.5 million to 27 million in 2025 depending on the utility weights.
Conclusion: Which disability weights are utilized and how they are applied has major ramifications for the DALYs associated with HBV and for where HBV lands in global health priorities. Currently, DALYs are low for HBV due to the DALY methodology being used. In Africa, HBV could be incurring higher number of DALYs than TB and only 8.9 million fewer than HIV. While further evidence would be useful, it is clear from multiple literature sources, and lived experience of HBV, that there needs to be disability weights applied to all stages of HBV disease to more accurately assess the burden, quality of life implications, and prioritization of HBV in Africa and globally.

FRI-023
Artificial intelligence-based hepatitis C screening: a real-world evidence analysis on Andalusian health database

Alberto Esteban Medina[1], Vanessa García-Fernández[2], Victor Manuel de la Oliva Roque[1], Carmen Lara-Romero[2,3], Carlos Loucera[1,4], Ana Lucena Valera[2,3], Joaquín Dopazo[1,4], Manuel Romero-Gómez[2,3,5]. *[1]Andalusian Platform for Computational Medicine, Andalusian public Foundation Progress and Health-FPS, Sevilla, Spain; [2]SeLiver Group. Instituto de Biomedicina de Sevilla (IBiS), Hospital Universitario Virgen del Rocío/CSIC/Universidad de Sevilla, Sevilla, Spain; [3]Servicio de Aparato Digestivo, Hospital Universitario Virgen del Rocío, Sevilla, Spain; [4]Institute of Biomedicine of Seville, IBIS, University Hospital Virgen del Rocio/CSIC/University of Sevilla, Sevilla, Spain; [5]Centro de Investigación Biomédica En Red De Enfermedades Hepáticas y Digestivas (CIBEREHD), Madrid, Spain*
Email: estebanm.alberto@gmail.com

Background and aims: The World Health Organization's (WHO) 2016–2021 strategy aimed to significantly reduce hepatitis C as a public health threat by achieving a 90% reduction in new infections, a 65% reduction in hepatitis C-related mortality, and treatment of 80% of detected cases by 2030. However, current approaches (Universal, by age group, or focused on patients at risk screenings) seem to be inefficient.
Method: Using Real World Data from the Andalusian Health Population Database (BPS) which contains electronic health records of more than 15 million patients, an AI-based predictive model was trained to identify undiagnosed hepatitis C cases. Several machine learning methods were assessed, with XGBoost (eXtreme Gradient Boosting) showing the most accurate results. For model training, we included 6,078 patients diagnosed with hepatitis C during the study period (2017–2022), along with a control group of 121,560 individuals with similar characteristics who tested negative for hepatitis C, developing PredictIA model.
Results: In a real-world scenario a sample of 200,000 random users of the Andalusian Public Health system were addressed with PredictIA model. Successful rate was 84% with a sensitivity of 0.15, significantly outperforming conventional screening strategies, which achieved no more than 0.007 sensitivity. A comparison of the predicted hepatitis C risk distribution across age groups with the actual diagnostic pattern revealed higher than expected potential detections outside conventional age-risk groups, mainly affecting women and individuals younger than 40 years. These cases would not have been identified through conventional screening. Among patients predicted to have hepatitis C infection, there were no significant differences in mean age or TSI category across probability groups: high (predicted probability >0.5; n = 213, 0.11%), moderate (predicted probability 0.1–0.5; n = 1,262, 0.63%), or low (predicted probability <0.1; n = 1,887, 0.94%).
Conclusion: The predictor developed constitutes a high precision, cost-effective screening model based on patient data already available in the health system, which clearly outperforms the conventional screening based on risk groups, by discovering one case every six selected individuals, while the conventional risk group strategy requires the screening of 143 individuals to find one case. This model will guide physicians in early detection and targeted testing, potentially advancing regional hepatitis C elimination efforts.

FRI-024
Prevalence of hepatitis B, and C in a cohort of transgender women living with HIV or on PrEP

Pablo Ryan[1], Jorge Valencia[1], Cristina Diez[2], Horacio Gil[3], Chiara Fanciulli[2], Susana Bacete[2], María Miguélez González[2], Lucio Garcia-Fraile[4], Guillermo Cuevas[1], Jose David Arroyo Romero[1], Irene Carrillo[5], Laura Laguna[1], Mariano Matarranz[1], Mario Del Hoyo[1], Pedro Alfonso Torres[1], Pedro Parbole[1], Samuel Manzano[1], Victor Perea[1], Eloisa Yuste[3], Carolina Ruiz-Sanchez[3], María del Mar Arcos[6], Alejandro De Gea[6], Juan Miguel Castro[6,7,7], Victor Arribas[6], Victor Fuente[1], Violeta Samperiz[4], Isabel Belmonte[4], Ines Armenteros[8], Santiago Fernandez[8], Mar Vera[8], Adriana Pinto[8], Ander Gonzalez[8], Laura Dans[8], Eva Orviz[8], Felix Moreno[8], Ana Conceco[9], Rosa Resino[9], Alicia Gonzalez[10], Jesús Troya[1], Isabel Gutierrez[2], Juan Manuel Osuna[9], Maria Ferreras[8], Manuela Rodriguez[3], Ruben Linares[8], Miriam Goicoechea[8], M. Sanchez Conde[11], Jorge Del Romero[8], Magarita Ramirez[2], Christian Brander[12], Victor Sanchez[3]. *[1]Hospital Universitario Infanta Leonor, Madrid, Spain; [2]Hospital General Universitario Gregorio Marañón, Madrid, Spain; [3]Instituto De Salud Carlos III, Majadahonda, Spain; [4]Hospital Universitario De La Princesa, Madrid, Spain; [5]Hospital Universitario Fundación Jiménez Díaz, Madrid, Spain; [6]Hospital La Paz, Madrid, Spain; [7]Hospital Carlos III, MI, Madrid; [8]Centro de ITS Sandoval, Madrid, Spain; [9]Universidad Complutense De Madrid, Madrid, Spain; [10]Universidad Autónoma De Madrid, Madrid, Spain; [11]Hospital Ramón y Cajal, Madrid, Spain; [12]Fundación IrsiCaixa, Badalona, Spain*
Email: pabloryan@gmail.com

Background and aims: Transgender women (TGW), particularly those living with HIV or on pre-exposure prophylaxis (PrEP), may have unique risk factors for viral hepatitis. We aimed to assess the prevalence of hepatitis A, B, and C and liver enzyme abnormalities in this population.
Method: We conducted a cross-sectional analysis within a multicentre translational cohort of 185 transgender women in Madrid, Spain, involving HIV units, PrEP clinics, STI clinics, and gender identity clinics across different healthcare centres. After signing informed consent, demographic characteristics, risk behaviours, and medical history were collected. Serologic tests for hepatitis A (HAV), B (HBV), and C (HCV) were performed at baseline, with HCV RNA PCR testing if antibody positive. Liver transaminases (ALT, AST) were measured to evaluate liver injury. Prevalence of each viral hepatitis was calculated, and median liver enzyme levels were determined.
Results: Median age was 34 years (IQR 29–42); 90% were migrants (mainly Latin American) and 83% of Hispanic origin. Overall, 62% (114/185) were living with HIV and 38% were HIV-negative on PrEP. Receptive condomless anal intercourse was reported by 72.4%, and 74% had engaged in sex work in the previous six months. Injection drug use was uncommon (4%); alcohol use was reported by 55.9%, with problematic use in 11.3%. HCV seroprevalence was 1.1% (2/185), with one active infection (0.5%, RNA-positive). HBV infection was identified in two participants (1.1%), including one chronic HBsAg-positive case and one recent acute infection. No acute hepatitis A cases were observed during the previous 6 months. Liver enzymes

were mostly normal (median ALT 23 U/L; AST 25 U/L), although 15–16% had mild ALT elevation (>40 U/L). No cases of alcoholic or other chronic liver disease were identified; non-alcoholic fatty liver disease was observed in two participants (1.2%).
Conclusion: In our cohort, despite higher viral hepatitis prevalence than in the general population and substantial sexual risk behaviours, chronic hepatitis B and active hepatitis C prevalence remained low among transgender women in HIV/PrEP care.

FRI-025
The implementation of double reflex testing reveals a still relevant burden of HDV infection across Europe and represents a valuable strategy to increase HDV diagnosis at an earlier stage of liver disease

Romina Salpini[1], Ilaria Grossi[1], Caterina Tramontozzi[1], Ivailo Alexiev[2], Leonardo Baiocchi[3], Leontina Banica[4], Thiberiu Banica[5], Josip Begovac[6], Brigita Benkoova[7], Ada Bertoli[8,9], Shubhada Bopegamage[7], Cinzia Caudai[10], Stefano D'Anna[1], Tulin Demir[11], Carole Devaux[12], Andrea Di Lorenzo[13], Gema Fernández-Rivas[14], Katarina Gazdikova[7], Anna Maria Geretti[13,15], Elica Golkocheva-Markova[2], Sandro Grelli[8,9], Eva Heger[16], Gilles Iserentant[12], Ligita Jancoriene[17], Rolf Kaiser[16], Naomi Kokkinos[15], Ivana Lazarevic[18], Voichita Lazureanu[19], Karoline Leuzinger[20], Magnus Lindh[21], Josep Llibre[22], Maja Lunar[23], Ugne Mickute[17], Jakub Mihale[7], Ivana Milosevic[24], Orna Mor[25], Dirk Nierhoff[26], Dan Otelea[4], Pierpaolo Paba[9], Elizaveta Padalko[5], Lorenzo Piermatteo[1], Mario Poljak[23], Anna Riccio[1], Maja Ruzic[27], Loredana Sarmati[13], Giulia Torre[1], Ana Maria Tudor[4], Andrei Vata[28], Kezban Tulay Yalçinkaya[29], Dilara Yildiran[11], Maurizio Zazzi[30], Anne Marie Wensing[31], Valentina Svicher[1]. [1]*Department of Biology, University of Rome Tor Vergata, Rome, Italy;* [2]*National Center of Infectious and Parasitic Diseases, Sofia, Bulgaria;* [3]*Hepatology Unit, University Hospital Tor Vergata, Rome, Italy;* [4]*National Institute for Infectious Diseases "Prof. Dr. Matei Bals", Bucharest, Romania;* [5]*University Hospital Ghent, Ghent, Belgium;* [6]*University Hospital for Infectious Diseases, Zagreb, Croatia;* [7]*Institute of Laboratory Medicine, Faculty of Medicine, Slovak Medical University, Bratislava, Slovakia;* [8]*Department of Experimental Medicine, University of Rome Tor Vergata, Rome, Italy;* [9]*Unit of Virology, Tor Vergata Polyclinic Foundation, Tor Vergata University, Rome, Italy;* [10]*Microbiology and Virology Unit, AOU Senese, Siena, Italy;* [11]*Ministry of Health, Public Health Institute, National Reference Laboratory for HIV/AIDS and Viral Hepatitis Department, Ankara, Türkiye;* [12]*Department of Infection and Immunity, Luxembourg Institute of Health, Luxembourg, Luxembourg;* [13]*Department of System Medicine, University of Rome Tor Vergata, Rome, Italy;* [14]*Microbiology Department, Clinical Laboratory North Metropolitan Area, Germans Trias i Pujol University Hospital. Universitat Autònoma de Barcelona-Badalona, Barcelona, Spain;* [15]*Royal Free NHS Foundation Trust - North Mid Hospital, London, United Kingdom;* [16]*Institute of Virology, University of Cologne, Cologne, Germany;* [17]*Clinic of Infectious Diseases and Dermatovenerology, Institute of Clinical Medicine, Faculty of Medicine, Vilnius University, Vilnius, Lithuania;* [18]*Institute of Microbiology and Immunology, Faculty of Medicine, University of Belgrade, Belgrade, Serbia;* [19]*The University of Medicine and Pharmacy Timisoara, Timisoara, Romania;* [20]*Clinical Virology, University Hospital Basel, Basel, Switzerland;* [21]*Department of Infectious Diseases, Institute of Biomedicine, Sahlgrenska Academy, University of Gothenburg, Gothenburg, Sweden;* [22]*Hospital Universitari Germans Trias i Pujol, Barcelona, Barcelona, Spain;* [23]*Institute of Microbiology and Immunology, Faculty of Medicine, University of Ljubljana, Ljubljana, Slovenia;* [24]*Clinic of Infectious and Tropical Diseases, University Clinical Centre of Serbia, Faculty of Medicine, University of Belgrade, Belgrade, Serbia;* [25]*National Reference Laboratory for HIV and Viral Hepatitis, Sheba Medical Center of Tel A Viv, Tel A Viv, Israel;* [26]*Department of Gastroenterology and Hepatology, University of Cologne, Cologne, Germany;* [27]*Faculty of Medicine, University of Novi Sad, Clinical Centre of Vojvodina, Clinic for Infectious Diseases, Novi Sad, Serbia;* [28]*The University of Medicine and Pharmacy Iasi, Iasi, Romania;* [29]*Department of Microbiology, Faculty of Medicine, Kahramanmaraş Sütçü İmam University, Onikişubat, Türkiye;* [30]*Department of Medical Biotechnologies, University of Siena, Siena, Italy;* [31]*Translational Virology, Department of Global Health and Bioethics Julius Center for Health, Sciences and Primary Care, University Medical Center Utrecht, Utrecht, Netherlands*
Email: rsalpini@gmail.com

Background and aims: Hepatitis D virus (HDV) causes the most severe viral hepatitis, however often remains underdiagnosed. Here, we investigate HDV screening and seroprevalence in a large set of HBsAg+ subjects and we report the characteristics of active HDV infection in Europe and the Middle-East before (2021–2023) and after (2024–2025) the implementation of double reflex testing (DRT, anti-HDV testing in all HBsAg+ subjects with unknown HDV serology and HDV-RNA if anti-HDV+ as per EASL guidelines).
Method: This multicenter study included 23927 HBsAg+ subjects from 21 hospitals in Europe (GB, CH, LU, DE, BE, SE, LT, ES, IT [N = 2], SI, HR, RO [N = 2], RS [N = 2], SK, BG) and the Middle East (IL, TR [N = 2]). The retrospective phase (2021–2023) evaluated 15170 HBsAg+ subjects while the prospective phase (2024–2025) implemented DRT in 8757.
Results: Subjects were 57.6% males, 92.3% HBeAg-negative, with median (IQR) age of 49 (39–61) years and only 29% under NUC-treatment. The rate of HDV screening strongly increased after DRT implementation from 58% to 94.5% (P < 0.001) (100% in 13 hospitals). HDV seroprevalence decreased after DRT implementation from 5.9% to 3.7% (P < 0.001). Notably, HDV-RNA testing raised from 80.7% to 94.7% (P < 0.001) while HDV-RNA positivity remained substantial (47% and 36.6%; P = 0.04), supporting a relevant circulation of active HDV infection. Overall, DRT increased anti-HDV detection by 36.5% (P < 0.001) and reduced the proportion of untested HDV-RNA cases to 5.4% compared to 19.3% (P < 0.01). Compared to 2021–2023, anti-HDV+ subjects diagnosed by DRT more frequently had ALT<40 U/l (66% vs 33.3%, P < 0.001) and a less advanced liver fibrosis (F0/F1 in 94% vs 33.8%, P < 0.001), supporting HDV detection in milder liver disease. In the 304 subjects with active infection, median (IQR) HDV-RNA was 5.5 (4.4–6.5) logIU/ml. Notably, compared to 2021–2023, subjects with active HDV infection detected by DRT had significantly lower HBsAg (2323 [1034–6109] vs 5158 [1740–11031] IU/ml), HBV-DNA (30 [0–2300] vs 131[16–2172] IU/ml), and ALT (46 [37–70] vs 79 [53–144] U/L) (P < 0.001 for all), supporting DRT as a valuable approach for an early HDV diagnosis, with lower cytolytic activity.
Conclusion: This study reveals a still relevant burden of HDV infection with an intense HDV replication across Europe. Implementing double reflex testing increases HDV case identification and enables diagnosis at earlier stages of liver disease, a critical step to strengthen linkage to care and reduce HDV-related morbidity and mortality.

FRI-026
Women's perspectives on care barriers in the setting of untreated HCV

Mai Sedki[1], Jennifer Price[1], Rena Fox[1]. [1]*University of California San Francisco, San Francisco, United States*
Email: rena.fox@ucsf.edu

Background and aims: Despite progress toward hepatitis C virus (HCV) elimination, many populations, particularly women, remain undiagnosed and untreated. Understanding patient experiences with HCV care is crucial to improving engagement. We conducted a mixed-methods study among women with untreated or incompletely diagnosed HCV to characterize prior care experiences, barriers to care, and patient-identified opportunities for improvement.
Method: Using electronic health record (EHR) at a large tertiary health system, we identified all women ≥18 years seen between 2020–2024 with either current HCV viremia or a reactive HCV antibody (Ab) without RNA testing. A navigator attempted phone contact, offered telehealth visits, and administered a structured

survey. The survey included Likert-scale assessments across seven domains of prior HCV care (testing, results, explanations, treatment offer, clinician time, courtesy and overall care) and free-response questions on barriers and suggested improvements. Quantitative data were summarized descriptively; and qualitative responses were coded thematically.
Results: The EHR query identified 248 eligible women; 130 were reached by phone, and 99 completed the survey (76%). Among respondents, mean age was 56.3 (15.9) years, 72% had public insurance, and participants were 61%White, 10%Latinx, and 7%Black. Forty-one percent were viremic, 34% were Ab-positive without RNA testing, only 8.1% had received antiviral therapy, and 12% had cirrhosis. Comorbidities included depression(26%), obesity(27%), and hypothyroidism(19%); only 16% had an established primary care provider. Survey responses revealed substantial dissatisfaction across the care cascade: 42% reported receiving no HCV care, and dissatisfaction rates were 41% for testing, 35% for receiving results, 40% for education, 46% for treatment offer, and 42% for clinician time. Over one-third reported barriers to care, with free responses emphasizing competing priorities, limited provider access, and fragmented follow-up.
Conclusion: Among women with untreated or incompletely diagnosed HCV who were reachable by phone, survey participation was high and revealed substantial gaps across the HCV care cascade. Structural and system-level barriers remain key drivers of disengagement, yet with dedicated efforts and flexible scheduling, we achieved high levels of patient engagement. Patient-identified priorities, including improved visit flexibility and clearer communication of results, may help advance progress toward HCV elimination.

FRI-027
Gaps between guidelines and clinical practice in hepatitis B virus reactivation prevention in non-hepatology immunosuppressive care
Hiroko Setoyama[1], Masatsugu Ohara[2], Satoru Kakizaki[3], Tatsuya Ide[4], Hirokazu Takahashi[5], Mizuki Endo[6], Tadashi Ikegami[7], Isao Hidaka[8], Yasuhito Tanaka[1], Masaaki Korenaga[9]. [1]*Department of Gastroenterology and Hepatology, Faculty of Life Sciences, Kumamoto University, Kumamoto, Japan;* [2]*Department of Gastroenterology and Hepatology, Hokkaido University, Sapporo, Japan;* [3]*National Hospital Organization Takasaki General Medical Center, Takasaki, Japan;* [4]*Kurume University, Kurume, Japan;* [5]*Saga University, Saga, Japan;* [6]*Oita University, Oita, Japan;* [7]*Tokyo Medical University Ibaraki Medical Center, Ibaraki, Japan;* [8]*Yamaguchi Saiseikai Hospital, Yamaguchi, Japan;* [9]*Research Center for Hepatitis and Immunology, National Center for Global Health and Medicine, Japan Institute for Health Security, Ichikawa, Japan*
Email: setoyama.h@me.com

Background and aims: Hepatitis B virus (HBV) reactivation is a potentially life-threatening but preventable complication of immunosuppressive therapy, for which HBV screening before treatment initiation is recommended by international guidelines. However, adherence to these recommendations remains inconsistent in non-hepatology settings. Orthopedic surgeons represent a group of physicians who frequently prescribe long-term corticosteroids and biologics associated with HBV reactivation risk, yet are not routinely involved in hepatitis care. This study assessed awareness of HBV reactivation prevention guidelines and adherence to recommended screening practices among orthopedic surgeons as non-hepatology prescribers.
Method: We conducted a multicenter cross-sectional survey as part of a national public health research program in Japan. An anonymous questionnaire was distributed to orthopedic surgeons practicing in eight prefectures. The survey assessed prescription of immunosuppressive therapies, awareness of HBV reactivation prevention guidelines, implementation of recommended HBV screening tests (hepatitis B surface antigen, hepatitis B surface antibody, and hepatitis B core antibody), and management of patients with positive screening results. Associations were analyzed using chi-square tests.
Results: A total of 567 orthopedic surgeons responded (response rate 28.8%). Among them, 294 (51.9%) reported prescribing immunosuppressive agents associated with a risk of HBV reactivation. Awareness of HBV reactivation prevention guidelines was reported by 120 physicians (40.8%). Complete HBV screening in accordance with guideline recommendations was performed by 136 physicians (51.1%) and was significantly more frequent among those aware of the guidelines than among those unaware ($p < 0.01$). Physicians in private practice demonstrated higher screening rates than hospital-based physicians ($p < 0.01$). Among respondents who encountered patients with positive screening results, 83.5% referred them to hepatology specialists.
Conclusion: Adherence to guideline-recommended HBV screening prior to immunosuppressive therapy in non-hepatology practice remains suboptimal, with limited guideline awareness identified as a key barrier. Given the high referral rate once infection is identified, enhanced guideline dissemination and systematic screening strategies may represent an effective public health approach to preventing HBV reactivation in non-hepatology immunosuppressive care, with potential applicability beyond Japan.

FRI-028
Real-world implementation of hepatocellular carcinoma surveillance after hepatitis C virus cure in Japan: a comparative analysis of performance indicators and a nationwide hospital-based database
Hiroko Setoyama[1], Shimakami Tetsuro[2], Yasue Takeuchi[3], Nobuharu Tamaki[4], Noriko Oza[5], Junko Tanaka[6], Yasuhito Tanaka[1], Tatsuya Kanto[7]. [1]*Department of Gastroenterology and Hepatology, Faculty of Life Sciences, Kumamoto University, Kumamoto, Japan;* [2]*Kanazawa University, Kanazawa, Japan;* [3]*Toranomon Hospital, Tokyo, Japan;* [4]*Musashino Red Cross Hospital, Musashino, Japan;* [5]*Karatsu Red Cross Hospital, Saga, Japan;* [6]*Hiroshima University, Hiroshima, Japan;* [7]*Research Center for Hepatitis and Immunology, National Center for Global Health and Medicine, Japan Institute for Health Security, Ichikawa, Japan*
Email: setoyama.h@me.com

Background and aims: According to international recommendations, patients with chronic hepatitis C virus (HCV) infection remain at risk of hepatocellular carcinoma (HCC) after achieving sustained virological response (SVR), and regular surveillance is recommended, particularly in those with advanced fibrosis or cirrhosis. However, real-world implementation of post-SVR HCC surveillance remains unclear. This study aimed to evaluate real-world patterns of post-SVR HCC surveillance and to compare them with reference standards of care derived from established clinical practice at designated regional core centers for liver disease management.
Method: We conducted a retrospective cohort study using a nationwide Japanese hospital-based administrative database (JMDC; 34,249,126 individuals). Patients with chronic HCV who achieved SVR after direct-acting antiviral therapy between 2014 and 2024 were included. Post-SVR HCC surveillance was assessed based on the frequency and interval of imaging examinations and tumor marker measurements. Reference surveillance was defined as imaging examinations performed at approximately 6-month intervals, with or without tumor marker testing, reflecting clinical practice in Japan. Real-world practice was compared with reference standards of care, defined as established post-SVR HCC surveillance practices based on predefined national hepatitis clinical indicators used in designated regional core centers serving as the hubs of regional liver disease care networks.
Results: A total of 19,186 patients who achieved SVR were included. During the first 6 months after SVR, imaging surveillance was not performed in 29.1% of patients and tumor marker measurements in 21.6%; during months 6–12 after SVR, the corresponding proportions

were 26.8% and 26.8%, respectively. Among patients undergoing surveillance, the median interval was approximately 180 days. Surveillance adherence was higher among patients with cirrhosis; however, only about 80% underwent any imaging surveillance within 1–3 years after SVR. In contrast, regional core centers demonstrated high adherence to these reference standards of care, with imaging surveillance performed in 98.6% of patients and tumor marker measurements in 97.8%.
Conclusion: These findings demonstrate a substantial gap between real-world surveillance practices after HCV cure and reference standards of care, particularly among patients with cirrhosis, highlighting the need for improved risk-based follow-up strategies.

FRI-029
Long term health and economic impact of a successful national hepatitis C elimination program: a model-based evaluation using real-world post-SVR outcomes
Gamal Shiha[1], Nabiel Mikhail[2], Ayman Hassan[3], Ahmed Farahat[4], Abdelhamid A Serwah[5], Reham Soliman[6]. *[1]Egyptian Liver Research Institute and Hospital, Gastroenterology and Hepatology Unit, Internal Medicine Department, Faculty of Medicine, Mansoura University, Shirbin, Mansoura, Egypt; [2]Egyptian Liver Research Institute and Hospital (ELRIAH), Biostatistics and Cancer Epidemiology Department, South Egypt Cancer Institute, Assiut University, Sherbin, El Mansoura, Egypt; [3]Egyptian Liver Research Institute and Hospital (ELRIAH), Medical Laboratories Department, Higher Technological Institute of Applied Health Sciences, Sherbin, Mansoura, Egypt; [4]Egyptian Liver Research Institute and Hospital (ELRIAH), Sherbin, El Mansoura, Egypt; [5]Internal Medicine Department, Suez Canal University, Suez, Egypt; [6]Egyptian Liver Research Institute and Hospital (ELRIAH), Technical institute of Nursing, Sherbin, El Mansoura, Egypt*
Email: g_shiha@hotmail.com

Background and aims: Direct-acting antivirals (DAAs) achieve sustained virological response (SVR) and substantially reduces hepatocellular carcinoma (HCC), hepatic decompensation, and liver-related mortality. While model-based analyses have projected the cost-effectiveness of hepatitis C elimination, empirical evidence quantifying its real-world long-term health and economic impact after nationwide implementation remains scarce. This study presents one of the first ex-post macroeconomic evaluations of a national HCV elimination program, using decade-long real-world post-SVR outcomes.
Method: We performed a model-based cost-consequence and health-economic evaluation from the healthcare payer perspective, considering direct medical costs only. Real-world post-SVR incidence rates for hepatocellular carcinoma (HCC), decompensated cirrhosis, and mortality were derived from a prospective cohort. Outcomes were extrapolated to the national treatment population using a 10-year analytic horizon (2015–2025). A counterfactual scenario was built using published natural history estimates for untreated HCV. Mortality benefit was monetised using value-of-life-years-gained, valuing each life-year at one GDP per capita. Sensitivity analysis and discounting were applied. Conservative and high-impact scenarios were explored. Analyses followed CHEERS 2022 guidelines.
Results: Without DAA therapy, five million chronically infected individuals would have been expected to develop 0.24–0.84 million HCC cases and 0.58–1.05 million decompensation events over ten years. Incorporating real post-SVR outcomes, national treatment markedly reduced advanced liver disease. Estimated healthcare savings from prevented complications reached 70–350 billion Egyptian pounds (EGP). Mortality reduction yielded 2.0–5.0 million life-years gained, valued at 200–500 billion EGP. Total economic benefit was therefore 270–850 billion EGP over 2015–2025.
Conclusion: Our findings confirm that hepatitis C elimination is not only a major public health success but also one of the most economically rewarding health interventions implemented in national programs. By translating real-world, decade-long post-SVR clinical outcomes into absolute numbers of events prevented, lives saved, and money preserved, this analysis quantify the realised return on national investment.

FRI-030
Synergistic effect of diabetes and hypertension on the risk of liver disease progression in hepatitis B virus infection
Laura E. Telep[1], Lesley Patmore[2], Lai San Hong[3], Amanda Singer[1], Leland J. Yee[1], Catherine (Carrie) Frenette[1], Milan J. Sonneveld[2]. *[1]Gilead Sciences, Foster City, United States; [2]Erasmus University Medica Center, Department of Gastroenterology and Hepatology, Rotterdam, Netherlands; [3]Redsen Limited, Tring, United Kingdom*
Email: laura.telep@gilead.com

Background and aims: Recent studies have reported an association between metabolic comorbidities (MCs) and adverse liver outcomes among individuals with hepatitis B virus (HBV) infection. The extent to which MCs interact to confer additional risk remains unclear. We compared the risk of liver-related events (LREs; compensated and decompensated cirrhosis, hepatocellular carcinoma, liver transplant) among individuals with HBV infection who have evidence of hypertension (HTN), diabetes mellitus (DM), obesity (OBS), or hyperlipidemia (HLD) individually, and in combination, to individuals with HBV and no evidence of MCs to better understand the combined risk associated with metabolic conditions.
Method: This observational study used US administrative claims data (HealthVerity Marketplace™; Oct 2015–Aug2025) from adults (18+ years) with chronic HBV infection (index date set to first inpatient or first of two outpatient HBV claims). Patients were excluded if there was evidence of LREs or other forms of chronic liver disease, or human immunodeficiency virus infection, prior to index. MCs were identified using all available data on or before index date. Incidence of an LRE during follow-up was compared among those with individual MCs vs. no MC and among pairs of MCs vs. no MC. Overlap-weight adjusted hazard ratios (HRs) were estimated, and unadjusted relative risk ratio (RRR) and relative excess risk due to interaction (RERI) were calculated to quantify multiplicative and additive interaction.
Results: Six pairs of MCs were studied: DM/HTN, DM/OBS, DM/HLD, HTN/OBS, HTN/HLD, and OBS/HLD. While most pairs indicated some interaction on both multiplicative and additive scales, DM/HTN together showed a pronounced synergistic effect; the joint risk of LREs was (HR[95%CI]: 1.49 [1.33–1.67]) and the individual associations of DM and HTN were: DM HR; 1.07 [0.88–1.29]); HTN HR; 1.16 [1.05–1.28]). The RRR was 1.73 (95%CI: 1.41–2.12) which indicates a risk 73% higher than expected if the DM and HTN were independent, and the RERI was 0.95 (95% CI: 0.70–1.20) where a value > 0 represents excess risk.
Conclusion: In this study of individuals with HBV and MCs in US claims data, we observed a synergistic effect where individuals with both DM and HTN had a greater risk of LREs than individuals with either DM only or HTN only. Our findings highlight the need to monitor and appropriately manage HBV patients for these comorbidities.

FRI-031
Predictors of advanced liver disease events among individuals with hepatitis delta infection in a large United States administrative claims dataset: a machine learning analysis
Laura E. Telep[1], Lai San Hong[2], Bo Zhao[1], Ziwei Yin[1], Jordan Guillot[3], Amanda Singer[1], Robert Wong[4]. *[1]Gilead Sciences, Foster City, United States; [2]Redsen Limited, Tring, United Kingdom; [3]University of California, San Francisco, Bakar Computational Health Sciences Institute, San Francisco, United States; [4]Stanford University Medical Center, Division of Gastroenterology and Hepatology, Palo Alto, United States*
Email: laura.telep@gilead.com

Background and aims: Hepatitis delta virus (HDV) is the most aggressive form of viral hepatitis and is associated with rapid progression to adverse liver outcomes. Early detection and risk-

stratification can help target patients for closer monitoring and urgent treatment. This study aimed to develop a machine learning (ML) model to predict liver-related events (LRE)—a composite of cirrhosis, hepatocellular carcinoma, and liver transplant—within 5 years among adults with HDV infection in the United States (US).

Method: Using HealthVerity (HV), a large US claims dataset, we identified adults (18+) with 1 in-patient or 2 out-patient claims for HDV (Oct 2015–Sep 2025) and no LRE prior to the first HDV claim (index date). The cohort was stratified by those who developed an LRE vs. not during follow-up. The R package automl trained a model with an 80/20 train/test split and 5-fold cross validation using demographic, dispensing, and comorbidity data from 6 months pre-index to 5 years post-index. The probability threshold that maximized the F1 score (harmonic mean of precision and recall) predicted individuals who would develop an LRE. The model with the greatest area under the precision-recall curve (AUPRC) relative to baseline LRE prevalence was selected. Features contributing most to prediction were identified as potential LRE risk factors.

Results: Among n = 8,955 individuals with HDV (45% male, mean age 45 years), the stacked ensemble model demonstrated the highest performance, yielding an F1 score of 0.61 at a prediction threshold of 0.26—individuals with a predicted LRE risk ≥26% were classified as positive. Precision was 55%, recall was 69%, and AUPRC was 0.63, representing an 11.6-fold improvement over LRE prevalence (5.4%). Overall accuracy was 95%. These metrics indicate that 55% of predicted positives were true cases, and 69% of actual LRE cases were identified. Features most predictive of LRE included hepatitis C virus (HCV) infection, hypertension, acute renal insufficiency, and demographic factors such as age and sex.

Conclusion: The ML model achieved an AUPRC of 0.63 with 95% accuracy in predicting LRE within 5 years in a real-world HDV cohort. HCV, hypertension, and renal insufficiency emerged as key predictors. Continued refinement and evaluating predictors of individual LRE outcomes will provide valuable tools to help clinicians identify HDV patients at highest risk for advanced liver disease, enabling earlier intervention, closer monitoring, and more informed treatment decisions.

FRI-035

Community-based dried blood spot testing reveals substantial progress towards hepatitis C virus elimination in people who inject drugs in Catalonia

Ona Torrejón-Llorens[1,2,3,4], Helena González-Casals[1,2,5], Victoria González Soler[2,4,5], Xavier Major[6], Renata Briseño[6], Montserrat Gàlvez[6], Irene Lana[6], Amaia Garrido[7,8], Montse Bartoli[7,8,9], Mercè Meroño[10], Use Expósito[10], Albert Espelt[2,11], Elisa Martró[1,2,4], Cinta Folch[1,2,5] and REDAN Study Group[2,5,6,7].
[1]Institut d'Investigació Germans Trias i Pujol (IGTP), Badalona, Spain; [2]Centro de Investigación Biomédica en Red de Epidemiología y Salud Pública (CIBERESP), Instituto de Salud Carlos III, Madrid, Spain; [3]Universitat Autònoma de Barcelona (UAB), Bellaterra, Spain; [4]Microbiology Department, Laboratori Clínic Metropolitana Nord, Germans Trias i Pujol University Hospital, Campus Can Ruti, Badalona, Spain; [5]Centre d'Estudis Epidemiològics sobre les Infeccions de Transmissió Sexual i Sida de Catalunya (CEEISCAT), Departament de Salut, Generalitat de Catalunya, Badalona, Spain; [6]Subdirecció General d'Addiccions, VIH, Infeccions de Transmissió Sexual i Hepatitis Víriques, Agència de Salut Pública de Catalunya, Barcelona, Spain; [7]Agència de Salut Pública de Barcelona, Barcelona, Spain; [8]Institut de Recerca Sant Pau, Barcelona, Spain; [9]Departament de Medicina i Ciències de la Vida, Universitat Pompeu Fabra, Barcelona, Spain; [10]Fundació Àmbit Prevenció, Barcelona, Spain; [11]Research Group in Epidemiology and Public Health in the Digital Health context (Epi4Health). Department of Psychobiology and Methodology in Health Sciences. Universitat Autònoma de Barcelona (UAB), Bellaterra, Spain
Email: emartro@igtp.cat

Background and aims: As part of the Plan for the Prevention and Control of Hepatitis C in Catalonia, the REDAN study, a periodical bio-behavioural survey, monitors HCV and HIV epidemics since 2008 in people who inject drugs (PWID) accessing harm reduction centres (HRCs). Previously, serological markers were determined in oral fluid samples. For the first time in REDAN, dried blood spot (DBS) collection was implemented for serological and molecular testing in 2024. The objectives were to estimate HCV seroprevalence and viremic prevalence, and describe the HCV care cascade in comparison with previous data to assess progress towards the WHO 2030 elimination targets.

Method: A cross-sectional study was conducted among PWID (injection within the previous 6 months) accessing 15 HRCs in Catalonia (October 2024–February 2025). Participants completed an epidemiological questionnaire. 287 DBS samples were collected and tested for HCV-Ab and HIV-Ag/Ab (DiaSorin), and for HCV-RNA (Abbott Molecular). The HCV care cascade was estimated on the total PWID population accessing HRCs in Catalonia (N = 2080) by combining DBS results with self-reported data. Proportions were compared to DBS results from the HepC*detect* II study (2016–17) in 4 HRCs.

Results: Overall, 15.3% of participants were females, 46.5% were migrants, 23% were homeless and 37% reported sharing injection equipment. HCV seroprevalence declined from 79.8% to 54.6% and viremic prevalence from 58.5% to 19.2%. HIV co-infection increased from 25.7% to 48.1% of viremic HCV cases. Regarding the HCV cascade of care, treatment uptake and cure markedly increased (from 31.9% to 76.2% and 17.7% to 57.4%, respectively). All these differences were statistically significant ($p < 0.01$). Among those ever treated, 24.7% were currently viremic.

Conclusion: HCV infection among PWID attending HRCs in Catalonia has significantly decreased over the last 7 years, highlighting the impact of micro-elimination test-and-treat strategies implemented, and demonstrating progress towards HCV elimination by substantially closing the treatment gap (76.2% vs 80% WHO elimination target). However, the proportion of viremic cases among previously treated individuals, together with injecting risk behaviours, underscores the need for sustained monitoring for reinfection. DBS-based HCV and HIV testing provides a valuable tool for community-based surveillance, supporting its sustained use and potential extension to other vulnerable populations.

FRI-036

Identifying and re-engaging hidden hepatitis C cases through registry linkage in primary care: a population-based intervention in Catalonia

Elena Torrell-Pedreira[1], Sandra Manzanares[1], Renata Briseño[1,2], Xavier Major[1], Ariadna Mas[3], Elisabet Balló[4], Rafael Ruiz[3], Jordi Casabona[5], Joan Colom[1], Luisa Conejos[1]. *[1]August Pi i Sunyer Biomedical Research Institute, Subdirectorate General of Addictions, STIs, HIV and Viral Hepatitis, Public Health Agency of Catalonia, Barcelona, Spain; [2]August Pi i Sunyer Biomedical Research Institute (IDIBAPS), Barcelona, Spain; [3]Subdirectorate for Health Planning and Research, Government of Catalonia, Barcelona, Spain; [4]Primary Care Services Information System, Catalan Institute of Health (Catsalut), Department of Health, Catalonia, Barcelona, Spain; [5]Centre for Epidemiological Studies on Sexually Transmitted Infections and HIV/AIDS of Catalonia (CEEISCAT), Barcelona, Spain*
Email: elena.torrell@gencat.cat

Background and aims: Achieving hepatitis C virus (HCV) elimination by 2030 requires closing gaps in the cascade of care, particularly among individuals diagnosed but not linked to treatment. In settings with comprehensive health information systems, administrative data linkage offers an opportunity to systematically identify these hidden cases. We evaluated a population-based pilot strategy using healthcare registry linkage to identify and re-engage untreated HCV cases through primary care in Barcelona, Catalonia.

Method: A cross-sectional linkage was performed between the Minimum Basic Data Set (CMBD) of the Catalan Health Service and the Registry of Patients Treated (RPT) to identify individuals with a recorded diagnosis for chronic or unspecified hepatitis C and no registered treatment as of December 31st, 2021. Lists of potentially untreated cases were integrated into the electronic health records of general practitioners (GPs) in 52 primary care teams in Barcelona. Between 2022 and 2024, physicians reviewed each case, classified clinical status, and implemented appropriate actions. Treatment initiation was assessed through a second linkage with the RPT as of December 31, 2024. An ongoing evaluation includes a repeated linkage to compare patient lists before and after the intervention and a sociodemographic characterization of treated cases to identify factors associated with successful linkage to care.
Results: Among 5,948 identified cases with a HCV diagnostic and no recorded treatment, (84.8% were reviewed by their GPs. Clinically relevant status requiring action were identified in 24% (n = 1.212) of reviewed cases, including untreated HCV infection (49%), unconfirmed HCV infection (44%), and previously treated but uncured infection (6%). Clinical actions were documented in 11% (n = 602)of reviewed cases, including referral to hepatology, HCV diagnostic testing, or referral for rescue treatment. Overall, 151 individuals initiated antiviral therapy, representing 3.0% of reviewed cases. Additionally, 25% of cases initially classified as active HCV infection were corrected or removed from the administrative registry.
Conclusion: Linking administrative diagnostic and treatment registries with primary care clinical management enables systematic identification, diagnostic validation, and treatment initiation among hidden HCV cases at scale. The model demonstrates the value of primary care–led, population-based approaches and is being expanded across Catalonia to support HCV elimination goals.

FRI-037

Cross-sectional testing for diagnosing asymptomatic BBV (Blood Borne Virus: HIV, HBV, HCV) infection; HBV infection is being eliminated in Japan

Haruka Uemura[1], Daisuke Mizushima[1], Daisuke Shiojiri[2], Akira Kawashima[1], Eri Inoue[1], Naokatsu Ando[1], Takato Nakamoto[1], Yasuaki Yanagawa[1], Takahiro Aoki[1], Katsuji Teruya[1], Hiroyuki Gatanaga[1]. *[1]Japan Institute for Health and Security, Tokyo, Japan; [2]Personal Health Clinic, Tokyo, Japan*
Email: uemura.h@jihs.go.jp

Background and aims: To eliminate BBV (Blood Borne Virus: HIV, HBV and HCV) infection as a public health threat, it is important to diagnose asymptomatic BBV infection. To diagnose BBV infections often overlooked in routine clinical practice, we conducted cross-sectional BBV screening at HIV and STI (Sexually Transmitted Infection) clinics.
Method: We evaluated the number of BBV diagnoses made during routine care over a 3-month period at each medical institution attended by three high-risk groups for STIs in Japan (HIV-positive individuals, HIV-negative men who have sex with men: MSM, and HIV-negative women visiting STI clinics). Over the subsequent 2-month period, we tested individuals who provided consent for HBs antigen (HBs-Ag), HBs antibody (HBs-Ab), HBc antibody, HCV antibody and HIV antigen/antibody. Medical records were retrospectively reviewed to compare the HBs antigen positivity rate at the initial visit by calendar year.
Results: During the routine care period, 662 HIV-positive individuals, 783 HIV-negative MSM, and 762 HIV-negative women visited each clinic, and no new BBV infections were diagnosed. During the cross-sectional testing period, 370 HIV-positive individuals (HIV group), 693 HIV-negative MSM (MSM group), and 150 women (women group) participated in the study. Among them, 3 new HCV infections were diagnosed in the HIV group, one new HBV infections and one new HIV infection were diagnosed in the MSM group, and no BBV were diagnosed in the women group. Among the HIV and MSM groups, 188 cases (50.8%) and 355 cases (51.2%) were HBs-Ab negative, and of these, 183 and 186 cases were taking regimens containing nucleoside analogues for HIV antiviral therapy (ART) or prophylaxis (PrEP: pre-exposure prophylaxis) respectively. Patients not taking nucleoside analogs and considered high-risk for HBV infection accounted for 5 (1.4%) in the HIV-infected group and 169 (24.4%) in the MSM group. The HBs-Ag positivity rate at initial visit in the HIV group showed a decreasing trend at 11.0%, 8.4%, 8.0%, 6.8%, 5.3% and 5.3% in 1997–2001, 2002–2006, 2007–2011, 2012–2016, 2017–2021 and 2022–2025, respectively.
Conclusion: The prevalence of BBV infection was low among high-risk groups for STIs in Japan, but cross-sectional testing identified several new BBV cases. In Japan, HBV infection among HIV-infected individuals has been decreasing over time over the past 30 years. The use of nucleoside analogues for ART in HIV patients and for PrEP in HIV-risk populations is expected to further reduce HBV infection.

FRI-038

European emergency department screening shows progress toward HCV elimination

Elena Vargas-Accarino[1,2], Murad Ruf[3], Rachel Hill-Tout[4], Liam Townsend[5], Conor Grant[6], Emma Page[7], Johannes Vermehren[8], Gaia Nebbia[9], Marta Casado-Martin[10], Jingwei Zeng[11], Juan Carlos Ruiz-Cobo[1,12,13,14], Jordi Llaneras[15], Sarah Parry[16], Daniel Bradshaw[17], Donia Bouzid[18], Mark Hopkins[19], Ferran Llopis-Roca[20], Hannah Evans[21], Lukasz Cieply[22], Maria Buti[1,12,13,14]. *[1]Liver Diseases Research Group. Vall d'Hebron Research Institute, Barcelona, Spain, Barcelona, Spain; [2]CIBERehd, Enfermedades Hepáticas y Digestivas, Madrid, Spain, Madrid, Spain; [3]Gilead Sciences Ltd UK & Ireland, Medical Department, London, UK, London, United Kingdom; [4]NHS England, London, United Kingdom, London, United Kingdom; [5]Department of Infectious Diseases, St James's Hospital, Dublin, Ireland, Dublin, Ireland; [6]7. Department of Genitourinary and Infectious Diseases, St James's Hospital, Dublin, Ireland, Dublin, Ireland; [7]Department of Virology, Leeds Teaching Hospitals Trust, Leeds, United Kingdom; [8]Medizinische Klinik 1, Klinikum der J. W. Goethe-Universitat, Frankfurt am Main, Germany, Frankfurt, Germany; [9]Department of Infection, Guy's and St Thomas' NHS Foundation Trust, London, UK, London, United Kingdom; [10]Hospital Universitario Torrecárdenas, Almería, Spain, Alemria, Spain; [11]Department of Virology, Royal Free London NHS Foundation Trust, London, United Kingdom, Division of Infection and Immunity, University College London, London, United Kingdom, London, United Kingdom; [12]CIBERehd, Enfermedades Hepáticas y Digestivas, Madrid, Spain, Madrid, Spain; [13]Liver Unit. Vall d'Hebron University Hospital, Barcelona, Spain, Barcelona, Spain; [14]Medicine Department, Universitat Autònoma de Barcelona, Barcelona, Spain, Barcelona, Spain; [15]Emergency Department, Hospital Universitari Vall d'Hebron, Barcelona, Spain, Barcelona, Spain; [16]Ambrose King Centre, Royal London Hospital, Barts Health NHS Trust, London, UK, London, United Kingdom; [17]Chelsea and Westminster Hospital NHS Foundation Trust, London, UK, London, United Kingdom; [18]INSERM UMR1137, IAME, Université Paris Cité, Paris, France, Paris, France; [19]Department of Infection and Immunity, University Hospitals of Liverpool Group, Liverpool, United Kingdom; [20]Emergency Department, Bellvitge University Hospital, Barcelona, Spain, Barcelona, Spain; [21]United Kingdom Field Epidemiology Training Programme, Public Health England, United Kingdom, London, United Kingdom; [22]Immunisation, Hepatitis and Blood Safety Department, Centre for Infectious Disease Surveillance & Control (CIDSC), National Infection Service, Public Health England, London, UK, London, United Kingdom*
Email: mariabutiferret@gmail.com

Background and aims: Curative direct-acting antivirals (DAAs) for HCV became available in 2016. In the same year, the World Health Organization set the goal of eliminating viral hepatitis as a public health threat by 2030. We analysed trends in HCV-RNA and HBsAg prevalence over time using data generated through systematic

emergency department (ED) testing initiatives, in order to assess their utility for monitoring progress toward viral hepatitis elimination in Europe.
Method: We reviewed published European ED HCV and HBV testing studies between 2005 and 2025. We calculated temporal trends in the proportion of HCV-RNA-positive among those individuals testing HCV-antibody positive (Ab+) (RNA+/Ab+) and recorded the prevalence of HBsAg+. Studies including fewer than 30 Ab+ or HBsAg+ individuals were excluded. For studies spanning multiple years, we contacted study authors. Where available, data were grouped by year.
Results: 16 ED screening studies were included (9 from England, 4 from Spain, 2 from Ireland, and 1 from Germany), conducted between 2008 and 2024. In total 1,851,715 adults were screened for HCV Ab, 25,903 were HCV Ab+, and of those 4,243 HCV-RNA+. Data from several years were available from Spain, England and Ireland. Over the study period, we observed a statistically significant decrease in the proportion of viraemic HCV infection (RNA+/Ab+). The proportion of active infection across Europe decreased from 72%, carried out in earlier years prior to DAA availability to 9% in the most recent ones in 2023 (broad DAA access since 2018), ($R^2 = 0.64$; beta = –4.6; $p < 0.001$). 10 studies reported HBV screening data, 1,426,843 were screened, and 10,491 HBsAg+. In contrast to HCV, the proportion of HBsAg-positive patients among those screened remained largely stable over the period, ranging from 0.47% to 0.55%.
Conclusion: The decline in viremic cases among HCV-Ab+ individuals identified through ED testing across Europe likely reflects the impact of broad DAA access driven by HCV elimination initiatives. In contrast, HBV prevalence remains stable. This simple approach, using routinely available HCV RNA and antibody data, enables monitoring of time trends and site comparisons.

FRI-039
Why screen hepatitis C alone? Integrated hepatitis B and hepatitis C screening reduces liver related complication and is cost effective: a model-based cost effectiveness analysis
Sai Praveen Jonnalagadda[1], Feng Tian[1], William WL Wong[1]. [1]*School of Pharmacy, University of Waterloo, Kitchener, Canada*
Email: wwlwong@uwaterloo.ca

Background and aims: One-time hepatitis C screening has expanded in many jurisdictions to link undiagnosed individuals to curative direct acting antivirals. Hepatitis B, despite its global burden and risk of progressive liver disease, is often overlooked even though suppressive therapy reduces complications. Integrating hepatitis B into hepatitis C screening can leverage shared populations, unified testing, streamlined care navigation, detection of coinfection, and prevention of hepatitis B reactivation during antiviral therapy. This study evaluates the cost effectiveness of offering a single lifetime screen for both hepatitis B and hepatitis C compared with hepatitis C only screening.
Method: We developed a multi disease agent based model to represent hepatitis B and hepatitis C epidemics in Ontario, Canada. The model simulates transmission within and between networks of people who inject drugs, men who have sex with men, and heterosexual populations, and tracks diagnosis, linkage to care, treatment, and disease progression. Two strategies were compared: hepatitis C screening alone and combined hepatitis B and hepatitis C screening, using a cost utility framework. Simulations included the entire Ontario population, stratified by age, sex, and risk behaviors. Parameters were derived from peer reviewed studies and Ontario health administrative data. The economic evaluation was conducted from the Ontario Health payer perspective for 2025 to 2050, with costs and utilities discounted at 1.5% annually. Outcomes included advanced liver disease and liver related deaths prevented, quality adjusted life years (QALYs), total costs, and incremental cost effectiveness ratios (ICERs).
Results: The model reproduced historical trends in chronic hepatitis B and C, cirrhosis, and hepatocellular carcinoma. Combined screening reduced decompensated cirrhosis and hepatocellular carcinoma incidence by 19% and 13%, respectively, and lowered liver related deaths by 13%. Compared with hepatitis C screening alone, combined screening increased costs by 29.5 million dollars but yielded 2,759 additional QALYs, resulting in an ICER of $10,693/QALY, well below the conventional $50,000/QALY threshold.
Conclusion: This is the first study to apply a dynamic multi disease agent based model to evaluate combined hepatitis B and hepatitis C screening in Ontario. Findings support integrated screening and linkage to care to identify undiagnosed individuals, improve outcomes, guide policy, and advance elimination targets.

FRI-040
Adaptive and simplified model of relinking HCV-Ab positive patients to care in China: a real-world study from Yunnan province
Changhui Wu[1], Chunmei Li[1], Mei Li[2], Ruiling Hui[3], Ruiling Liu[4], Fei Wang[5], Qiong Yang[6], Shuangying Duan[7], Huaiyan Fan[8], Huiyong Su[9], Changxian Lu[10], Shun Feng[11], Wei Yue[12], Yuhua Shi[13], Hui Li[1], Jia Wei[1]. [1]*The Affiliated Hospital of Yunnan University, Kunming, China;* [2]*The People's Hospital of Fuyuan County, Qujing, China;* [3]*Qujing central hospital of Yunnan Province, Qujing, China;* [4]*Xuanwei No.1 Hospital, Xuanwei, China;* [5]*The People's Hospital of Kaiyuan City, Kaiyuan, China;* [6]*Dehong Hospital of Traditional Chinese Medicine, Dehong, China;* [7]*Tengchong People's Hospital, Tengchong, China;* [8]*Zhaotong First People's Hospital, Zhaotong, China;* [9]*Dali Prefecture People's Hospital, Dali, China;* [10]*The People's Hospital of Lincang, Lincang, China;* [11]*Puer People's Hospital, Puer, China;* [12]*The First People's Hospital of Yunnan Province, Kunming, China;* [13]*Yunnan Center for Disease Control and Prevention, Kunming, China*
Email: weijia@ynu.edu.cn

Background and aims: To develop an adaptive, simplified relinking model for HCV antibody-positive individuals and improve hepatitis C diagnosis and treatment rates in China.
Method: This study was conducted in two phases.
Retrospective Phase: Collaborating with Centers for Disease Control and Prevention (CDC), we retrospectively analyzed patients who had HCV infection between 2004 and 2021. Demographic and clinical disparities between treated and untreated cohorts were compared to construct a predictive model. Prospective Phase: Since 2024, with the provincial CDC, we launched educational campaigns across all prefectures, focusing on enhancing patient education among priority populations. By optimizing patient relinking strategies, we facilitated the re-engagement of HCV antibody-positive but untreated patients across the province. Changes in HCV RNA screening rate, HCV RNA positivity rate, and treatment initiation rate were recorded.
Results: A total of 5,506 HCV antibody-positive and/or HCV RNA-positive patients were enrolled in the retrospective phase. Statistical modeling revealed that the proportion of patients declining treatment was significantly higher among the following subgroups: young individuals (<30 years old), urban residents, unmarried subjects, those with no history of needle sharing, and individuals with limited HCV-related knowledge. The established model achieved a sensitivity of 85%. Since 2024, targeted health education programs and green referral pathways have been implemented for the key populations through collaboration between 11 prefectures and local CDCs. Using the optimized relink paradigm, 5,063 HCV antibody(+) patients were successfully contacted. Of these, 90% (4,535/5,063) underwent further HCV RNA testing, and 51% (2,249/4,535) were HCV RNA(+). Till December 2025, 85% (1,914/2,249) of patients had initiated antiviral therapy with Sofosbuvir/Velpatasvir (SOF/VEL) or Ledipasvir/Sofosbuvir (LDV/SOF), with ongoing efforts to recall the remaining patients. Compared with 2022, both HCV RNA screening rate (from 15% to 90%) and treatment rate (from 8% to 85%) were highly increased.
Conclusion: The predictive model identified key patient subgroups associated with low treatment uptake that differed from previously

recognized populations, clarifying the underlying causes of suboptimal treatment rates. The optimized recall strategy significantly improved diagnosis and treatment rates, facilitating province-level HCV elimination.

FRI-045

Mapping the global network of viral hepatitis A, B, C and E: unveiling disease-specific epidemic architectures through complex network analysis

Yanhui Yang[1], Yanpei Mai[2], Yuxi Shi[2], Suzhen Jiang[1], Xin Wen[2], Tianyi Xue[2], Qinshuo Wang[2], Yafen Liu[3], Huiying Rao[1], Zixing Wang[1]. *[1]Peking University Hepatology Institute, Beijing, China; [2]Peking University Hepatology Institute, Peking University Health Science Center, Beijing, China; [3]Peking University Hepatology Institute, Peking University People's Hospital Department of Infectious Diseases, Beijing, China*
Email: wangzixing@pkuph.edu.cn

Background and aims: The global burden of viral hepatitis remains a formidable public health challenge, with HBV and HCV alone accounting for 1.3 million deaths annually. Traditional surveillance fails to capture the complex interconnectedness driving these epidemics. This study employs complex network theory to uncover the fundamental architectural patterns governing the global persistence and diffusion of Hepatitis A, B, C, and E.
Method: We constructed static and dynamic networks using Global Burden of Disease data from 1990 to 2021. Static networks comprised high-incidence countries (top 50%) as nodes, connected by edges determined by a high Spearman correlation coefficient (>0.9) in incidence rates. Dynamic networks employed 10-year sliding windows with 1-year steps based on this foundation to capture temporal evolution. Key metrics were calculated to quantify structural characteristics: density (measuring overall connection tightness), efficiency (reflecting global transmission capacity), clustering coefficient (indicating local interconnection strength) and modularity (measuring the degree of network division into separate communities). Degree centrality was employed to identify network hub nations.
Results: We identified distinct network architectures for hepatitis subtypes. Hepatitis B exhibited a dense, integrated network with increasing connectivity and declining modularity, forming a unified component with emerging communities. Hepatitis A demonstrated high connectivity with strong local clustering, but fragmented progressively, maintaining low modularity. In contrast, hepatitis C presented a sparse and fragmented architecture with the highest modularity and five connected components, showing accelerating structural polarization despite gradual density increases. Hepatitis E maintained a stable hybrid structure with increasing modularity. Analysis of degree centrality identified Comoros as a critical hub consistently maintaining strong correlations with 40–91 high-epidemic countries across all four diseases networks. Equatorial Guinea, Eritrea, Benin, Sao Tome and Principe, and Lao PDR also emerged as pivotal hubs across three disease networks.
Conclusion: This study identifies disease-specific network structures requiring tailored strategies for global elimination. For highly integrated networks like HBV, we suggest coordinated sentinel systems in hub nations to track progress. For fragmented networks like HCV, hub nations reveal cluster-specific patterns, informing targeted interventions.

FRI-046

RE-LIVE study (Re-Linkage to Pan-Viral hepatitis): interim results from a multicenter observational study on care engagement in chronic viral hepatitis

Jaehyun Yoon[1], Young-Sun Lee[2], Yang Jae Yoo[2], Yu Rim Lee[3], Seul Ki Han[4]. *[1]Chonnam national university hospital, College of medicine, Gwangju, Korea, Rep. of South; [2]Korea university hospital, Seoul, Korea, Rep. of South; [3]Kyungpook national university hostpial, Daegu, Korea, Rep. of South; [4]Wonju Yonsei University Hospital, Wonju, Korea, Rep. of South*
Email: zenmake14@gmail.com

Background and aims: Despite highly effective antiviral therapies, linkage to care remains a key barrier to the global elimination of viral hepatitis. A considerable proportion of individuals with chronic viral hepatitis remain undiagnosed, and untreated, sustaining the burden of disease and transmission. This study aimed to evaluate systematic re-linkage strategies to re-engage these individuals in the continuum of care, with the goal of improving clinical outcomes and contributing to public health objectives.
Method: A retrospective chart review was conducted at four tertiary academic hospitals in Korea to identify candidates for antiviral treatment. HBV eligibility included (i) non-cirrhotic patients with HBV DNA >2,000 IU/mL and fibrosis stage ≥2, and (ii) cirrhotic patients with any detectable HBV DNA. For HCV, partially diagnosed-but-untreated (DBU) cases were defined as anti-HCV antibody positive with missing HCV RNA data; completely DBU cases were HCV RNA positive without prior antiviral therapy. HBV patients eligible for HDV screening underwent HDV PCR. All identified patients were re-contacted via text or phone for re-evaluation and potential treatment linkage.
Results: Among 2,810 patient charts reviewed, 33 HBV and 127 HCV patients were enrolled in the call-back program. Among HBV patients, 21.2% (7) responded and agreed to further evaluation; 6.1% (2) initiated antiviral therapy, while 78.8% (26) did not respond to call-back. Of 92 partial HCV DBU cases, 13.0% (12) agreed to evaluation, 3.3% (3) had prior treatment, 3.3% (3) sought care elsewhere, 2.2% (2) refused, and 78.3% (72) did not respond. Among them, 2.2% (2) initiated treatment. Among 35 complete DBU cases, 2.9% (1) agreed to evaluation, 2.9% (1) sought care elsewhere, 5.7% (2) refused, and 88.6% (31) did not respond; only 2.9% (1) initiated treatment. HDV RT-PCR was performed in 618 chronic HBV patients; 0.1% (1) tested positive but declined further management. In total, 3.1% (5) of 160 patients identified through the call-back program initiated antiviral therapy.
Conclusion: Although effective antiviral treatments and expanded eligibility criteria are now available, many patients with viral hepatitis remain disconnected from care. Our re-linkage efforts showed limited success in bringing patients back into the treatment pathway. These findings emphasize the need for continued, practical strategies to improve access to care and support national and global goals for viral hepatitis elimination.

FRI-047

Data for action - Informing viral hepatitis and HIV public health interventions through high resolution geo-mapping of migrant populations

Jamie Zagorski[1], Murad Ruf[2], Helen Hammond[2], Victoria Livingstone[2], Nigel Breakwell[3]. *[1]Gilead Sciences, Foster City, United States; [2]Gilead Sciences Europe, Uxbridge, United Kingdom; [3]DOT I/O Health, Manor House, 21 Soho Square, London, W1D 3QP, London, United Kingdom*
Email: jamie.zagorski@gilead.com

Background and aims: Healthcare-planning requires detailed knowledge of health profiles and location of people. This need is particularly great during sudden large-scale population migration, with associated increased risk of communicable diseases, including blood-borne viruses (BBV). Most likely significant is the forced displacement of Ukrainians due to the Russian invasion. Given the substantial estimated burden of HCV: 1,263,530, HBV: 507,063, and HIV: 244,877 in Ukraine, mass migration will also impact on local BBV epidemiology. We set out to explore a novel methodology to estimate the small-area migrant population distribution and its potential for local HIV, HBV and HCV prevalence impacts.

Method: We developed a hybrid model combining national statistics, non-governmental organisation data, scientific literature review in multiple languages, and local expert opinion. From this we synthesised population data of the magnitude and registered geo-location of Ukrainian forced migrant populations pre and post the Russian invasion, in the EU at a national and sub-national level. BBV prevalence rates in Ukrainian, sourced from published official reports were proportionally applied to the sub-national migrant populations estimates in our model. We generated high resolution, small area heatmaps using the data. An international expert steering committee reviewed our methodology and proposed a focused analysis in the Krakow region as example.
Results: Seven countries accounted for 49.7% (3,077,770) of the Ukrainian migrant population in 2024 (Austria, Czechia, Germany, Italy, Netherlands, Poland and Slovakia). Applying our extrapolation, we estimate up to HCV: 2,410, HBV: 1,004, and HIV: 442 additional infections in these countries.
Granular analysis in the Krakow region, using governmental data up to June 2025 identified a 79% increase in the Ukrainian-born population since 2021; equating to nearly 100,000 Ukrainians, which make up 4.27% of the Krakow metropolitan area. We estimate up to a total of 2,585 additional BBV infections in local UKR migrants (HCV: 1,621, HBV: 675, HIV: 298).
Conclusion: We believe, our innovative methodology synthesising routine data sources allows precise small-area estimates of size and geo-location of migrant populations potentially at risk for BBV infection. This promising novel methodology can contribute to informing development of targeted, tailored novel BBV care pathways including mobilisation of local community-based support to advance local BBV elimination efforts.

WED-003

Impact of a national hepatocellular carcinoma surveillance program on tumor staging: geographic disparities and temporal trend in post-hcv elimination Egypt

Wael Abdel-Razek[1], Mohamed AbdAllah[2], Mohamed Hassany[3], Gamal Esmat[4], Imam Waked[1]. *[1]Department of Hepatology and Gastroenterology, National Liver Institute, Menoufia University, Menoufia, Egypt; [2]Medical Research and Clinical Studies Institute, National Research Center, Giza, Egypt; [3]National Hepatology and Tropical Medicine Research Institute, Ministry of Health and Population, Cairo, Egypt; [4]Endemic Medicine Department, Faculty of Medicine, Cairo University, Cairo, Egypt*
Email: wabdelrazek@liver-eg.org

Background and aims: Following Egypt's successful hepatitis C virus (HCV) elimination efforts, the liver disease burden is shifting toward hepatocellular carcinoma (HCC). We evaluated the effectiveness of the national HCC surveillance program launched in 2022 across Egyptian states, assessing its impact on BCLC staging and identifying demographic and geographic disparities.
Method: We conducted a retrospective multicenter analysis of 6,362 HCC patients diagnosed between 2022 and 2025 across 25 Egyptian states. Patients were stratified into two cohorts: regular surveillance vs. incidental diagnosis (no surveillance). The primary endpoint was BCLC stage distribution (0/A, B, C, D). Secondary endpoints included temporal trends and geographic heterogeneity in staging outcomes.
Results: The study included 6,362 patients (66.4% male, mean age 63.9 ± 8.1 years). Only 19.9% (n = 1,267) were diagnosed under surveillance, while 80.1% (n = 5,095) had no prior surveillance. Surveillance was significantly associated with earlier detection ($p < 0.001$). Patients under surveillance showed higher rates of potentially curative/intermediate stages compared to the non-surveillance group (BCLC 0/A: 11.7% vs. 8.6%; BCLC B: 25.6% vs. 19.3%). Conversely, advanced/terminal disease (BCLC C/D) was prevalent in the non-surveillance group (72.1% vs. 62.8%). The surveillance cohort had a higher male proportion (71.4% vs. 65.1%, $p < 0.001$) with no age difference ($p = 1.000$). Significant heterogeneity was observed across states ($p < 0.001$ for total distribution). In high-burden Kafr El-Sheikh (north, Nile delta), surveillance yielded robust early detection rate (40.0% BCLC 0/A vs. 18.8% in non-surveillance, $p = 0.002$). In contrast, Minia (south) showed low rates of very early detection even within surveillance (1.6% BCLC 0/A). While the proportion of patients diagnosed under surveillance remained stable (17.5–21.5%), absolute annual HCC cases declined from 1,903 in 2022 to 1,309 in 2025 ($p < 0.001$).
Conclusion: In this national cohort, HCC surveillance is associated with significant stage migration toward early-stage disease amenable to curative therapy. However, surveillance coverage remains low, and many surveillance patients still present with advanced disease. The marked geographic disparities highlight the urgent need for standardized, quality-controlled protocols and targeted interventions to consolidate the gains of Egypt's HCV elimination program. The declining overall trend might represent the impact of the HCV elimination program.

WED-004

Introduction of a hepatitis C testing prompt for primary care LFTs with raised ALT leads to increased testing and diagnosis

Stephen Barclay[1], Julie Craik[1], Rory Gunson[2], Maurizio Panarelli[1], Daniel Carter[1], Erica Peters[1]. *[1]NHS Greater Glasgow & Clyde, Glasgow, United Kingdom; [2]West of Scotland Specialist Virology Centre, Glasgow, United Kingdom*
Email: stephen.barclay2@nhs.scot

Background and aims: A raised ALT should lead to consideration of hepatitis C (HCV) testing, however adherence to this is inconsistent, with previous work suggesting undiagnosed cases amongst those with raised ALT on primary care blood tests. We sought to establish whether adding an HCV testing prompt to primary care LFT results with an ALT above the upper limit of normal (ULN) improved HCV testing and diagnosis.
Method: Biochemistry laboratory systems identified samples with ALT above ULN sent from 65 primary care practices in north-east Glasgow, Scotland, for two 6-month time periods: No Prompt (NP); July 24 to Jan 25, and following a four-week break, With Prompt (WP); Feb 25 to Aug 25. Virology laboratory systems identified samples sent from the same practices between July 24 and October 25. Numbers of HCV tests and (reflex) HCV RNA positive results were obtained for both NP and WP periods, plus the subsequent four weeks (7-month period) to allow time for a test to take place. Finally, linkage using a unique patient identifier, captured the proportion of patients in each period who subsequently underwent HCV testing within 90 days of a positive HCV test.
Results: 6453 and 6391 raised ALT samples were sent in NP and WP, respectively. During WP, HCV tests rose from 1093 to 1803 (64.95% increase) and RNA positives from 9 to 17 (88.88% increased). WP demonstrated significantly more patients received HCV testing within 3 months of a raised ALT (1847 (28.9%) vs 616 (9.55%), $p < 0.0001$).
Conclusion: Introduction of a HCV prompt to primary care LFT results with a raised ALT led to increased HCV testing and rates of HCV diagnosis. Further work is required to ascertain the proportion untested who have had previously received HCV testing, and the characteristics of those identified via this approach. In addition the durability of increased testing following permanent introduction of a prompt requires further evaluation.

WED-005

Symptom burden and health-related quality of life in chronic HBV–HDV infection: real-life evidence from the ANRS HD EP01 HEPDELTA cohort

Camelia Protopopescu[1], Vincent Di Beo[1], Helene Fontaine[2], Morgane Bureau[1], Marta Lotto[1], Gwenaëlle Maradan[3], Marc Bourlière[1], Garance Bessaudou[4], Claire Fougerou-Leurent[4], Christelle Tual[4], Fatoumata Coulibaly[5], Fabien Zoulim[6], Miroslava Subic-Levrero[6], Patrizia Carrieri[1]. *[1]Aix Marseille Univ, Inserm, IRD, SESSTIM, Sciences Economiques & Sociales de la Santé & Traitement de l'Information Médicale, ISSPAM, Marseille, France; [2]Université de Paris-Cité, Hôpital Beaujon, AP-HP Assistance Publique - Hôpitaux de Paris, INSERM UMR1149, Paris, France; [3]ORS PACA, Observatoire Régional de la Santé Provence-Alpes-Côte d'Azur, Marseille, France; [4]CHU Rennes, Inserm, CIC 1414, Rennes, France; [5]ANRS MIE, PariSanté Campus, 2 rue d'Oradour sur Glane, Paris, France; [6]Hepatology Department, Hospices Civils de Lyon, INSERM U1052-CRCL; Université Claude Bernard Lyon 1, Lyon, France*
Email: camelia.protopopescu@inserm.fr

Background and aims: People living with chronic HBV–HDV infection experience substantial symptom burden and impaired health-related quality of life (HRQoL). However, the respective impact of self-reported symptoms, antiviral treatments, and liver disease on physical and mental HRQoL remains insufficiently documented in real-life settings. We aimed to assess these associations to provide guidance on patient care and treatment strategies.
Method: We analyzed data from adults with chronic HBV–HDV infection enrolled in the ANRS HD EP01 HEPDELTA cohort, with or without specific treatment for HDV. HRQoL was assessed using the Short Form-12 (SF-12v2), providing the physical (PCS) and mental (MCS) component summary scores (study outcomes). Twenty-five distinct self-reported bothersome symptoms and exposure to current or past HBV and HDV antiviral treatments were assessed. Associations between each symptom, HBV/HDV treatment status, and physical and mental HRQoL were evaluated using multivariable linear mixed models adjusted for liver steatosis, advanced fibrosis (i.e., FIB-4 > 3.25), and socio-behavioral variables.
Results: The study included 250 patients (68% male, median age [IQR] = 43 [35–50]) accounting for 444 visits. At baseline, 54% were receiving bulevirtide. Median [IQR] HRQoL scores were 45.4 [38.2–51.8] for PCS and 47.1 [38.6–56.0] for MCS. The most prevalent self-reported bothersome symptoms were sleep disorders (43%), headaches (39%), joint pain (39%), and shortness of breath (31%). After multivariable adjustment, most symptoms were associated with lower HRQoL scores, with generally a higher effect on MCS than on PCS. The symptoms with the highest effects were shortness of breath (coefficient [95% CI]: −4.1 [−5.9, −2.2]) for PCS, and appetite loss (−6.7 [−9.0, −4.4]), memory problems (−6.7 [−9.2, −4.2]), and concentration difficulties (−6.6 [−8.8, −4.3]) for MCS. In most of the models, female sex, tobacco smoking, steatosis, and advanced fibrosis were independently associated with lower PCS, whereas housing instability was associated with lower MCS. HBV/HDV treatment status was not associated with either PCS or MCS.
Conclusion: In this cohort of patients with HBV–HDV infection, most self-reported symptoms were strongly associated with impaired physical and mental HRQoL, whereas antiviral treatment showed less impact. These findings highlight the importance of symptom monitoring in the management of HBV–HDV infection, to improve patient-centered outcomes and indirectly improve retention in care.

WED-006

Implementation of the ReLink-C strategy in hospitals in Spain (ReLink-C Observatory Spain)

Anny Camelo Castillo[1], Miriam Romero[2], Elena Vargas-Accarino[3], Montserrat García-Retortillo[4], Ismael El Hajra Martínez[5], Maria Inmaculada Fernández Vázquez[6], Joel López[7], Paloma Rendon[8], Esther Molina[9], Rocio González-Grande[10], Sixto Menacho[11], Gema Romero[12], Rubén Cuesta[13], Miguel Angel Simón[14], Isidoro Jesús Narváez Rodríguez[15], Jose Luis Montero[16], Jesús M. Gonzalez Santiago[17], Sonia Albertos Rubio[18], Carolina Freyre[19], Andreu Sansó[20], Carmen Vinaixa[21], Eva María Rodriguez Marcos[22], Rafael Manuel Alejandre Altamirano[23], Laisy Zacarias Martínez[24], Rocío Aller[25], Sandra Blanco Cano[26], Cristina Gonzalez De Adalid[26], Nataly Espinoza-Cámac[27], Raquel Domínguez-Hernández[27], Marta Casado-Martin[1]. *[1]Hospital Universitario Torrecárdenas, Almería, Spain; [2]Hospital Universitario La Paz, Madrid, Spain; [3]Hospital Universitari Vall d'Hebron, Barcelona, Spain; [4]Hospital del Mar, Barcelona, Spain; [5]Hospital Universitario Puerta de Hierro Majadahonda, Madrid, Spain; [6]Hospital Universitario 12 de Octubre, Madrid, Spain; [7]Hospital Universitari Joan XXIII de Tarragona, Tarragona, Spain; [8]Hospital Universitario Puerta del Mar, Cádiz, Spain; [9]Complexo Hospitalario Universitario de Santiago, A Coruña, Spain; [10]Hospital Universitario Regional de Málaga, Málaga, Spain; [11]Hospital Universitario de Jerez de La Frontera, Cádiz, Spain; [12]Hospital Universitario Juan Ramón Jiménez, Huelva, Spain; [13]Hospital de Sagunto, Valencia, Spain; [14]Hospital Clínico Universitario Lozano Blesa, Zaragoza, Spain; [15]Complejo Hospitalario Universitario Badajoz, Badajoz, Spain; [16]Hospital Universitario Reina Sofía, Córdoba, Spain; [17]Hospital Universitario de Salamanca (Complejo Asistencial de Salamanca), Salamanca, Spain; [18]Hospital Residencia Sant Camil - Consorci Sanitari Alt Pendés - Garraf, Barcelona, Spain; [19]Hospital Universitario de Puerto Real, Cádiz, Spain; [20]Hospital de Manacor, Baleares, Spain; [21]Hospital Universitari i Politècnic La Fe, Valencia, Spain; [22]Hospital Lluís Alcanyís de Xàtiva, Valencia, Spain; [23]Hospital Infanta Margarita, Córdoba, Spain; [24]Hospital del Vendrell, Tarragona, Spain; [25]Hospital Clínico Universitario de Valladolid, Valladolid, Spain; [26]Gilead España, Madrid, Spain; [27]Pharmacoeconomics & Outcomes Research Iberia (PORIB), Madrid, Spain*
Email: anjo134@gmail.com

Background and aims: Among the actions implemented to achieve the elimination of hepatitis C virus (HCV) infection, the ReLink-C strategy identifies and relinks patients with a complete or partial HCV diagnosis who have been lost to clinical follow-up and show no evidence of infection cure, linking them back to the healthcare system. The objective was to describe the outcomes of implementing the ReLink-C strategy in Spanish hospitals.
Method: An observational, retrospective, cross-sectional, multicentre study was conducted through data collection in hospitals using an online questionnaire. An information flow was designed with mandatory and optional variables, including patients with a complete diagnosis (anti-HCV serology positive with RNA-HCV confirmation) and patients with a partial diagnosis (anti-HCV serology positive without HCV RNA determination). From all centres participating in the ReLink-C strategy, those whose data availability aligned with the established flow and met the defined criteria for data collection were selected.
Results: Information from 25 hospitals participating in the ReLink-C strategy was included. A total of 20,409 anti-HCV serology tests (15,188 complete diagnoses and 5,221 partial diagnoses) were reviewed, and 3,508 patients with HCV (1,973 from complete diagnoses and 1,535 from partial diagnoses) were identified as lost to follow-up. Of these, 1,992 patients were successfully located, and 824 initiated treatments with direct-acting antivirals (577 from complete diagnoses and 247 from partial diagnoses). The recovery rate of patients who started treatment among those lost to follow-up was 23%.

Conclusion: The results obtained confirm the effectiveness of the ReLink-C strategy in identifying, relinking, and treat to access to HCV patients lost in the system, reinforcing its value as a reference model to achieve the goal of hepatitis C elimination in Spain.

WED-007

Viral hepatitis in the community of Shenzhen city, China: current status and elimination challenges — a large scale screening study

Deliang Huang[1], Zhibin Zhu[1], Jun Chen[1]. [1]*The Third People's Hospital of Shenzhen, National Clinical Research Center for Infectious Diseases, Shenzhen, China*
Email: huangdeliang2020@163.com

Background and aims: Aligned with the WHO strategic objective to eliminate viral hepatitis as a public health threat by 2030, this study was conducted to evaluate the current epidemiological profile of virus hepatitis infections within community populations in Shenzhen, China, and to identify key barriers to achieving the elimination target.
Method: A large-scale, cross-sectional community screening was performed across 95 community health centers spanning all 10 districts of Shenzhen from September 2023 to July 2025. Participants were tested for hepatitis B surface antigen (HBsAg), hepatitis B surface antibody (HBsAb), and hepatitis C antibody (anti-HCV). Epidemiological and demographic data were collected concurrently.
Results: Among 96,170 individuals screened, 51,168 and 45,540 were assessed for hepatitis B and C, respectively. The overall HBsAg seroprevalence was 4.32%, showing a clear age gradient: the highest infection rate was observed in individuals aged 30–60 years, while the rate among those under 15 years was 0.32%. Alarmingly, only 9.69% of HBsAg-positive individuals were aware of their infection status. Furthermore, 78.23% of HBsAg-positive persons reported an unknown family history of hepatitis B, and 80.04% were unaware of any family history of cirrhosis or hepatocellular carcinoma. The proportion of the immune population (HBsAb positive) was 28.40%, whereas the susceptible population (both HBsAg and HBsAb negative) reached 66.27%. Among susceptible individuals, 90.77% had an unclear vaccination history. The anti-HCV seroprevalence was 0.28%, with a marked age clustering showing the highest rate (0.54%) among adults aged over 60 years.
Conclusion: While Shenzhen has demonstrated substantial success in hepatitis B prevention, particularly in pediatric vaccination coverage, significant challenges persist. These include a profound diagnosis gap, a large immunity gap among adults, and critically low disease risk awareness in key populations. To accelerate progress towards the 2030 elimination goal, future efforts must prioritize the development of innovative, proactive community screening models, implement robust adult catch-up vaccination programs, and establish an integrated continuum of care encompassing screening, diagnosis, treatment, and long-term management. This study provides crucial empirical evidence to inform targeted elimination strategies in Shenzhen and similar urban settings across China.

WED-008

Perspectives of people living with hepatitis B towards long-acting antivirals: a global study

Chari Cohen[1], Yasmin Ibrahim[1], Karine Dube[2], David Thomas[3]. [1]*Hepatitis B Foundation, Doylestown, United States;* [2]*University of California San Diego, La Jolla, United States;* [3]*Johns Hopkins University, Baltimore, United States*
Email: chari.cohen@hepb.org

Background and aims: There are multiple barriers to long-term oral antiviral therapy for chronic hepatitis B (CHB). Long-acting antivirals (LAAs) could help improve treatment uptake and adherence. As research for LAAs advances, we need to understand how people living with hepatitis B (PLWHB) perceive these new treatment modalities. The goal of this study was to assess perspectives and preferences towards potential LAA treatment modalities among PLWHB globally.
Method: We implemented an online cross-sectional survey with 49 multiple choice and Likert scale questions for PLWHB (self-report) who were ≥18 years old. The survey included 4 sections: demographics, current treatment experiences, challenges with current treatment, and preferences for three long-acting routes: injectables, implants, and microneedle patches. The survey was launched globally and open for 16 weeks in English, Spanish, Mandarin, Arabic and Tagalog; and distributed to email listservs, e-newsletters, social media channels, and partner organizations. This study was supported by the NIH (LEAP, R24AI118397) and the Hepatitis B Foundation.
Results: A total of 1,074 PLWHB responded (93% in English), with 653 completing ≥75% of survey questions. Respondents were from 81 countries; 70% identified as male; with 55% between age of 26–45. Among respondents, 66% were in care for CHB and 54% were on treatment; 58% had treatment-related challenges, and 13% missed a dose at least once weekly. Further, 81% would consider an injection, 55% would consider an implant, and 50% would consider a microneedle patch for CHB treatment, if these modalities worked as well as pills. In a direct comparison, 57% preferred an injection to pills, 44% preferred an implant to pills, and 34% preferred a microneedle patch to pills. Respondents ranked fewer side effects, higher efficacy, and easier adherence as the top potential benefits of LAAs. Top concerns included potential decreased efficacy, stronger/longer side effects, pain (insertion/removal of implant), needing to receive treatment at a clinic, and visibility to others (implant/patch) as top concerns.
Conclusion: This first-ever study assessing preferences among PLWHB shows that there is strong interest in LAAs to treat CHB, especially for long-acting injectables. Additional studies are needed to document and explore perceptions and challenges towards LAAs, particularly as we explore these as an option to overcome challenges with pill uptake, adherence, and access.

WED-009

Modeling the potential effect of long-acting injectables of DAA treatment to reach HCV elimination among persons who inject drugs

Eric Tatara[1], Louis Shekhtman[2], Marian Major[3], Scott Cotler[2], Basmattee Boodram[4], Jonathan Ozik[1], Harel Dahari[2]. [1]*Consortium for Advanced Science and Engineering, University of Chicago, Decision and Infrastructure Sciences, Argonne National Laboratory, Chicago, United States;* [2]*Program for Experimental and Theoretical Modeling, Division of Hepatology, Department of Medicine, Loyola University Chicago, Maywood, IL, United States;* [3]*Division of Viral Products, Center for Biologics Evaluation and Research, Food and Drug Administration, Silver Spring, MD, United States;* [4]*Division of Community Health Sciences, School of Public Health, University of Illinois at Chicago, Chicago, United States*
Email: harel.dahari@gmail.com

Background and aims: Access, adherence and cost remain barriers to global elimination of hepatitis C virus (HCV) with direct-acting antivirals (DAA). Re-formulation of DAA to an injectable form to produce sustained concentrations for 24 weeks could not only cure hepatitis C virus (HCV) but also protect persons who inject drugs (PWID) from repeat infections by suppressing viral replication for 24 weeks with a single dose. Since PWID are at high risk for acquiring and transmitting HCV, we aimed to study the effects of a 24-week long-acting DAA treatment among PWID to reach HCV micro-elimination in metropolitan Chicago, IL, USA.
Method: We used our advanced Hepatitis C Elimination in PWID (HepCEP) agent-based modeling [doi.org/10.1101/2025.07.25.25332212] in which HCV transmission probability is determined using a mathematical model of HCV RNA titers among needle/syringe-sharing donors [PMID: 29997251]. DAA treatment enrollment is modelled as (unbiased) random sampling of infected PWID using an annual target enrollment rate of 7.5% of the total PWID

population in Chicago and the surrounding area (32,000 individuals) to reach HCV elimination. Access to long-acting DAA was simulated for 10 years. We compared the mean frequencies (using stochastic model replicates) of reinfection and number of unique treatment courses between potential long-acting DAAs and ultra-short 4-week duration DAA-based treatment [e.g., PMID: 40347964].
Results: The model predicts reaching HCV elimination with a long-acting DAA that provides cure and 24 weeks of protection from repeat infections during a 10-year treatment period results in fewer total infections (3,377, 95%CI: 3,298–3,456) compared to a 4-week DAA-based treatment duration (6,200, 95%CI: 5,960–6,441). Moreover, treatment duration of 24 weeks (15,946 treatments) versus 4 weeks (19,325 treatments) would result in need for 3,379 fewer treatments.
Conclusion: Our modeling results predict that a 24-week long-acting DAA treatment would result in a reduced number of HCV infections compared to 4-week ultra short DAA-based treatment over a 10-year period to reach HCV micro-elimination in metropolitan Chicago due to greater duration of protection from repeat infections and further transmission.

WED-010
HCV screening and linkage to care in the 1969–1989 birth-cohort population: the Bergamo experience
Liliana Dell'Oro[1], Alessandro Loglio[1,2], Loredana Rota[2], Luca Ongis[2], Carlos Eduardo Paz Domínguez[1], Elisa Farina[2], Davide Isabella[1], Luisa Pasulo[2], Giulia Bombardieri[3], Stefania Borlini[3], Marco Arosio[4], Stefano Fagiuoli[1,2], Mauro Viganò[1,2]. *[1]Department of Medicine and Surgery, University of Milano-Bicocca, Milan, Italy; [2]Gastroenterology, Hepatology and Transplantation Division, ASST Papa Giovanni XXIII, Bergamo, Italy; [3]Healthcare Directorate, ASST Papa Giovanni XXIII, Bergamo, Italy; [4]Microbiology and Virology Laboratory, ASST Papa Giovanni XXIII, Bergamo, Italy*
Email: l.delloro2@campus.unimib.it

Background and aims: The Italian Ministry of Health has promoted a national screening program for Hepatitis C Virus (HCV) infections targeting individuals born between 1969–1989 who have never taken Direct Antiviral Agents (DAAs). Aim was to evaluate the effectiveness of this age-based screening in the referral area of ASST Papa Giovanni XXIII, Bergamo, with a focus on adherence, HCV antibodies (HCVab) positivity, HCV-RNA positivity, linkage to care, DAA introduction and achievement of sustained virological response (SVR).
Method: All individuals born between 1969 and 1989 who underwent HCV screening from May 2022 to June 2025 across four healthcare settings (hospital inpatient wards, outpatient blood collection centers, active screening invitation letter, and physician-initiated testing) were included. HCVab positive subjects were invited to undergo a confirmatory HCV-RNA test, hepatology consultation and ultimately DAAs initiation.
Results: Among 23,577 screened individuals [15,594 responding to invitation letters, 4,913 during hospitalization, 2,014 via physician prescription, and 986 during blood collection], 308 (1.3%) tested positive for HCVab [0.8%, 3%, 0.9%, and 1.8% for each respective cohort]: 58% male, 48 (33–55) years-old, 17% of foreign origin. Overall, 49 (0.2%) patients had detectable serum HCV-RNA [0.07%, 0.67%, 1.04%, and 0.2%, respectively], while 259 individuals were HCV-RNA negative, of whom 51% had never received antiviral treatment. Notably, 200 (65%) HCVab positive subjects were already aware of their status, with 186 actively followed-up. Among the 49 HCV-RNA positive individuals [55% already known to have the infection], 24 (49%) started DAA reaching an SVR in 18, while the remaining 6 were non-compliant patients. The remaining 25 HCV-RNA positive patients (predominantly active drug users) never started DAAs due to non-adherence to follow-up visits.
Conclusion: The impact of this screening program on the 1969–1989 birth-cohort population is low, thus suggesting an extension to advanced age groups and the implementation of more effective linkage-to-care strategies.

WED-011
Anti-HDV reflex testing among HBsAg positive individuals in the Netherlands
Esmee Fath el Bab[1], Annemiek Van der Eijk[1], Lesley Patmore[1], Jolanda Kreeft - Voermans[1], Thijs van der Laar[2], Hans Zaaijer[2], Annelies Riezebos-Brilman[3,4], Harry L.A. Janssen[1,5], Khoa Thai[6], Milan J. Sonneveld[1]. *[1]Erasmus MC, University Medical Center, Rotterdam, Netherlands; [2]Sanquin Research, Amsterdam, Netherlands; [3]Diagnostiek voor U, Eindhoven, Netherlands; [4]Laboratory for Medical Microbiology and Public Health, Hengelo, Netherlands; [5]Toronto Center for Liver Disease, Toronto General Hospital, University of Toronto, Toronto, Canada; [6]Star-shl Medical Diagnostics Center, Rotterdam, Netherlands*
Email: e.fathelbab@erasmusmc.nl

Background and aims: Hepatitis delta virus (HDV) is the most severe form of viral hepatitis and carries a high risk of liver-related complications. Universal anti-HDV reflex testing in all HBsAg positive individuals is recommended according to the EASL guidelines. Nevertheless, HDV remains underdiagnosed, primarily due to limited awareness. This study aims to access the diagnostic yield of reflex anti-HDV testing in HBsAg positive samples obtained from blood donor screening, general practice and a tertiary hospital in the Netherlands.
Method: Anti-HDV reflex testing was conducted in HBsAg positive samples collected in 2024–2025 from laboratories serving general practice (general practitioners and maternity care (n = 249)), the laboratory responsible for Dutch blood donor screening (n = 218) and a virology laboratory of a tertiary hospital in the Netherlands (n = 283). Anti-HDV positive samples were subsequently tested for HDV RNA. Positive results were communicated to the primary caregiver and appropriate linkage to care was established.
Results: Reflex testing was successfully conducted in 99.3% (n = 745) of 750 HBsAg positive individuals in the study period. Among these, 244 (32.8%) originated from general practice, 218 (29.3%) from blood donor screening and 283 (38.0%) from the hospital. The overall prevalence of anti-HDV was 6.7% (n = 50), with a prevalence of 4.1% in general practice (n = 10), 2.3% in blood donor screening (n = 5) and 12.4% in the hospital (n = 35). HDV RNA testing was performed in all anti-HDV positive samples. HDV RNA was detectable in 54.0% (n = 27), including 6 cases (60%) from general practice, 1 (20%) from blood donor screening and 20 (57.1%) from the hospital. HDV RNA was detectable in 2.5% of HBsAg positive samples obtained from general practitioners, in 0.5% of samples obtained from blood donors and in 7.1% of hospital samples.
Conclusion: Reflex anti-HDV testing in both primary and secondary care settings in the Netherlands proved feasible and effective. The high prevalence in samples obtained from general practitioners suggests that universal screening for HDV is warranted in HBsAg positive individuals.

WED-012
Advancing elimination targets for viral hepatitis and human immunodeficiency virus in Poland: estimating the cost-effectiveness of emergency department opt-out testing for blood-borne viruses
Robert Flisiak[1], Justyna Kowalska[2,3], Andrzej Fal[4], Magdalena Rosinka[5,6], Laurel Bates[7], Hairuo He[7], Erik Robinson[7], Elisabeth Adams[7], James Jarrett[8], Murad Ruf[9]. *[1]Department of infectious diseases and hepatology, Medical University of Białystok, Białystok, Poland; [2]Infectious diseases observational research unit, Medical University of Warsaw, Warsaw, Poland; [3]Hospital for Infectious Diseases, Warsaw, Poland; [4]Collegium Medicum, Warsaw faculty of medicine, Cardinal Stefan Wyszynski University, Warsaw, Poland;*

[5]Department of infectious disease epidemiology and surveillance, National Institute of Public Health PZH-National Research Institute, Warsaw, Poland; [6]Digital Medicine Centre, Maria Skłodowska-Curie National Institute of Oncology, National Institute of Oncology, Warsaw, Poland; [7]Aquarius Population Health, London, United Kingdom; [8]Global HEOR, Gilead Sciences, London, United Kingdom; [9]Medical Department, Gilead Sciences Europe Ltd, London, United Kingdom
Email: robert.flisiak1@gmail.com

Background and aims: In Poland, blood-borne virus (BBV) diagnosis rates fall below global elimination goals. Additionally, forced migration since 2022 into Poland has rapidly increased the number of people living with HIV and viral hepatitis (HBV and HCV). Currently, there is no systematic screening for BBVs in general medical settings. International evidence suggests BBV opt-out testing (OOT) in urban emergency departments (ED) is effective, particularly in diagnosing infections in people who do not access traditional, largely client-initiated testing options. We assessed the potential health and economic value of ED BBV OOT in high-prevalence areas in Poland.
Method: We developed a hybrid cost-effectiveness model to compare outcomes between BBV OOT and no testing in the ED as the standard of care. A decision tree simulated the testing and linkage to care (LTC) for ED attendees requiring blood tests who do not opt out; a Markov model projected long-term outcomes. Polish surveillance data and published literature were used to inform the model where available, supplemented with international literature and expert opinion. We used a public payer perspective over a lifetime. Primary outcomes were the number of new diagnoses, number LTC, quality-adjusted life years (QALYs), and costs (discounted at 5% per annum). Scenarios varied prevalence and LTC rates.
Results: Our model suggests OOT could result in 128 new BBV diagnoses per 10 000 ED attendees (72 HBV; 27 HCV; 28 HIV) and 95 individuals linked or re-linked to care (66 HBV; 10 HCV; 19 HIV). Combined BBV testing was cost-effective over a lifetime horizon, with an incremental cost per QALY gained of PLN 61 614 (€14 563). Individually in isolation, cost-effectiveness ranged from 7 851 (€1 856) per QALY gained (HCV) to 124 905 (€29 523) (HIV). The intervention remained cost-effective with scenarios decreasing HIV and HCV prevalences to 0.1%. Successful LTC post-diagnosis was the primary driver of long-term cost effectiveness.
Conclusion: Combined ED BBV opt-out testing targeted to high-prevalence areas in Poland could be cost-effective, identifying viral hepatitis and HIV infections and improving health outcomes. The intervention remained cost-effective under several stress-test scenarios. Results are likely underestimates as the benefits of potential transmissions averted through diagnosis and care were not assessed. We recommend further evidence-informed national dialogue on systematic testing strategies to address un/late diagnoses and maximise LTC.

WED-013
Addiction medicine involvement is associated with improved hepatitis C and viral hepatitis screening among hospitalised incarcerated patients who inject drugs

Ezaam Fraz[1], Leda Kasas[1], Matthew Carter[1], Jeremy Yeo[1], Aathavan Shanmuga Anandan[1], Jason Connor[1], Geoffrey Playford[1], Naomi Runnegar[1], Jeremy Hayllar[2], Gerald Holtmann[1], Paul Clark[1], Andrew Palmer[1]. [1]Princess Alexandra Hospital, Woolloongabba, Australia; [2]Metro North Mental Health Alcohol & Drug Service, Brisbane, Australia
Email: ezaam.fraz@health.qld.gov.au

Background and aims: Incarcerated people who inject drugs experience a high burden of hepatitis C virus (HCV) infection and face substantial structural barriers to blood-borne virus (BBV) screening and continuity of care. Hospitalisation represents a high-yield opportunity to identify undiagnosed BBV infection and engage hard-to-reach populations. We examined the association between inpatient addiction medicine unit (AMU) involvement and BBV screening, engagement, and short-term outcomes among incarcerated patients admitted with injection-related infections (IRI).
Method: We examined 391 incarcerated people transferred to a quaternary hospital secure unit (serving 60% of the state prison population) in Brisbane, Australia, between 01/07/19 and 30/06/25. Primary outcomes were HCV RNA testing during admission and complete BBV screening (defined as HCV RNA testing, hepatitis B surface antigen testing (HbSAg), and HIV serology). Secondary outcomes were self-discharge, 30-day readmission, and linkage to HCV care. Associations with AMU involvement were examined using multivariable logistic regression adjusted for age, First Nations status, sex, and length of stay.
Results: The cohort was predominantly male, with a median age of 32 years (IQR 28–38) and median length of stay of 5 days (IQR 3–14). BBV screening during admission was incomplete: HCV RNA and HIV testing were performed in 58.8% of admissions, HbSAg in 62.4%, and only 49.6% completed all three tests. AMU involvement was associated with higher odds of HCV RNA and HIV testing (OR 3.60, 95% CI 2.32–5.59; $p < 0.001$), HbSAg testing (OR 4.11, 95% CI 2.60–6.50; $p < 0.001$), and completion of the BBV composite (OR 3.9, 95% CI 2.5–6.0; $p < 0.001$). AMU involvement was associated with lower odds of self-discharge (OR 0.46, 95% CI 0.23–0.91; $p = 0.026$) and 30-day readmission (OR 0.47, 95% CI 0.24–0.92; $p = 0.028$). Findings were robust to sensitivity analyses adjusting for clinical complexity. AMU involvement was not associated with improved downstream linkage to HCV care.
Conclusion: AMU involvement was associated with improved BBV screening and engagement, underscoring the importance of addressing upstream drivers of liver disease. In this cohort, the dominant barrier in the HCV care cascade was case identification. These findings support viral hepatitis elimination strategies that prioritise AMU involvement and closer alignment between hepatology and AMU across comparable custodial and hospital systems.

WED-014
A multivariable model of spontaneous hepatitis C virus clearance: increasing realism of simulated data

Keshav Gandhi[1,2], Eric Tatara[3,4], Jonathan Ozik[3,4], Basmattee Boodram[5], Scott Cotler[1], Marian Major[6], Harel Dahari[1], Alexander Gutfraind[1,2]. [1]Program for Experimental and Theoretical Modeling, Division of Hepatology, Department of Medicine, Loyola University Chicago, Maywood, IL, United States; [2]Division of Epidemiology and Biostatistics, School of Public Health, University of Illinois at Chicago, Chicago, IL, United States; [3]Consortium for Advanced Science and Engineering, University of Chicago, Chicago, IL, United States; [4]Decision and Infrastructure Sciences, Argonne National Laboratory, Argonne, IL, United States; [5]Division of Community Health Sciences, School of Public Health, University of Illinois at Chicago, Chicago, IL, United States; [6]Division of Viral Products, Center for Biologics Evaluation and Research, Food and Drug Administration, Silver Spring, MD, United States
Email: krg3@uic.edu

Background and aims: Approximately 20–35% of hepatitis C virus (HCV)-naïve individuals clear acute HCV infection. While spontaneous clearance rates vary by age, sex, and interferon lambda-4 (IFNL4) rs12979860 genotype, HCV elimination (PMID: 35271634) and vaccine trial (PMID: 39777292) simulations have used fixed clearance probabilities stratified only by sex (female: 0.35; male: 0.12). We aim to develop a literature-informed logistic regression model to more precisely estimate spontaneous HCV clearance in elimination and vaccine simulations.
Method: We performed a literature search of studies that estimate spontaneous viral clearance and could be used to construct a logistic regression model, emphasizing systematic reviews and meta-analyses where possible. First, a baseline clearance probability was generated before modification by age, sex, or IFNL4 rs12979860

genotype (PMID: 16364080). Age effects were derived from published odds ratios (ORs) comparing the clearance probability greater than or equal to 45 years versus less than 45 years (PMID: 29345844). Sex effects used relative risks (RRs) for female people who inject drugs converted to ORs (PMID: 38633576). CC versus non-CC rs12979860 genotype identities were assigned probabilistically using allele frequencies specific to race/ethnicity (PMIDs: 19684573, 20399780, 22612303), with the clearance-favorable CC genotype modeled using spontaneous viral clearance ORs (PMID: 34216268). Confidence intervals (CIs) from these sources were used to define normal distributions on log-odds scales, from which trial-specific coefficients were sampled.
Results: We developed a clearance model with predictors of age, sex, and IFNL4 rs12979860 genotype. Age, sex, and IFNL4 rs12979860 genotype have a clearance OR of 0.52 [95% CI 0.64–0.97], RR of 1.58 [95% CI 1.40–1.79], and OR of 2.75 [95% CI 2.23–3.38], respectively. The adjusted model indicates that while median [Q1, Q3] naïve male clearance probabilities (0.12 [0.09, 0.16]) were close to the fixed clearance rate of 0.12, naïve female clearance probabilities shifted from a fixed probability of 0.35 to a median of 0.20 [0.15, 0.26].
Conclusion: We developed a new modular, literature-informed logistic regression model of spontaneous HCV clearance incorporating age, sex, and IFNL4 genotype to improve the accuracy of HCV elimination and vaccine trial simulations.

WED-015

Assessing the economic value of bulevirtide for chronic hepatitis delta in Romania: combining real-world patient data with a markov state-transition model

Liana Gheorghe[1,2], Speranta Iacob[1,2], Mihaela Ghioca[1], Mirela Chitul[1], Anca Trifan[3,4], Laura Huiban[3,4], Daniela Larisa Sandulescu[5], Ionut Gheonea[5], Corina Radu[6,7], Bogdan Procopet[6], Roxana Sirli[8], Corina Pop[2,9], Nicoleta Tiuca[2,9], Bogdan Ungureanu[5], Adina Turcu-Stiolica[5]. *[1]Fundeni Clinical Institute, Bucharest, Romania; [2]Carol Davila University Of Medicine And Pharmacy, Bucharest, Romania; [3]Spitalul Clinic Județean de Urgență Sfântul Spiridon Iași, Iași, Romania; [4]Universitatea de Medicină și Farmacie 'Grigore T. Popa' Iași, Iași, Romania; [5]Universitatea de Medicina și Farmacie Craiova, Craiova, Romania; [6]Iuliu Haţieganu University of Medicine and Pharmacy, Cluj-Napoca, Romania; [7]Iuliu Hatieganu University of Medicine and Pharmacy, Cluj Napoca, Romania; [8]Universitatea de Medicină și Farmacie Victor Babeș, Timișoara, Romania; [9]Spitalul Universitar de Urgență București, București, Romania*
Email: drlgheorghe@gmail.com

Background and aims: Chronic hepatitis Delta (CHD) is the most severe form of viral hepatitis, contributing significantly to cirrhosis, hepatocellular carcinoma (HCC), and liver-related mortality in the absence of effective therapy. In Romania, HBV/HDV-related cirrhosis and HCC remain leading causes for liver transplantation (LT), unlike Western Europe where ALD and MASLD predominate. This unique epidemiology increases the potential impact of therapies that delay decompensation and reduce LT need. Bulevirtide (BLV), recently approved for compensated CHD, was evaluated for cost-utility and budget impact versus Best Supportive Care (BSC) in Romania, using local real-world evidence (RWE).
Method: A Markov cohort state-transition model was adapted to the Romanian healthcare setting from the perspective of the public payer (CNAS). Unlike models relying on hypothetical cohorts, baseline characteristics and transition probabilities were derived from a retrospective real-world cohort of 175 Romanian patients treated with BLV (69.7% with cirrhosis/F4 at baseline). The model adopted a lifetime horizon for cost-utility and a 5-year horizon for budget impact analysis (BIA), discounting outcomes at 3%. Efficacy was defined by a combined endpoint of HDV RNA undetectability or >2 log decline with ALT normalization.
Results: Treatment with BLV resulted in a substantial survival gain, extending discounted life expectancy by 3.36 years (10.52 LYs for BLV vs. 7.16 LYs for BSC). Patients gained 3.08 discounted Quality-Adjusted Life Years (QALYs) compared to BSC. Clinically, BLV effectively halted disease progression, averting 1,188 cases of decompensated cirrhosis, 822 cases of HCC, and 87 liver transplants over the cohort's lifetime. The Incremental Cost-Effectiveness Ratio (ICER) was 918,829 RON/QALY. Probabilistic sensitivity analysis confirmed clinical benefits in 100% of iterations. The BIA demonstrated a negligible burden on the national insurance fund, with the incremental Per Member Per Month (PMPM) cost reaching only 0.024 RON by Year 5.
Conclusion: BLV acts as a disease-modifying therapy, preventing progression to liver failure and LT in real-world CHD. Although the ICER is high, it generates significant survival and quality-of-life gains by preventing expensive end-stage liver complications and the need for LT. With minimal budget impact, BLV represents a high value option for this unmet need population.

WED-019

Multicenter automated strategy for opportunistic screening of viral hepatitis in primary care based on hypertransaminasemia and the FIB-4 index (ProHCYL study)

Jesús M. González-Santiago[1], Noa Villar[1], Laura Sancha[1], Rosario Rico Jimenez[1], Pilar Delgado[2], Fernando Hernandez Pacho[2], Soledad Sonsoles Muñoz Hernaz[2], Laura Fueyo[3], Ana M Roldan[3], Marta Calvo[4], Laura Herrera[4], Daniel Monge[4], Ruth Saez[5], Cristina Fernández Marcos[5], Alberto Mir Subias[6], Susana García-De Cruz[6], Laura Perez Citores[7], Ana Isabel Garcia Sanchez[7], Laura Milian[8], Olivia Nuevo[8], Ruben Perez Fernandez[8], Luis Hernandez[3], Ana Haro[1], Angel Vega[1], Fernando Geijo[1], David Cembrero[1], Pilar Tajada[4]. *[1]Complejo Asistencial Universitario de Salamanca Biomedical Research Institute of Salamanca (IBSAL), Salamanca, Spain; [2]Complejo Asistencial de Ávila, Ávila, Spain; [3]Hospital Santos Reyes, Aranda de Duero, Spain; [4]Complejo Asistencial de Segovia, Segovia, Spain; [5]Complejo Asistencial Universitario de Burgos, Burgos, Spain; [6]Complejo Asistencial de Soria, Soria, Spain; [7]Complejo Asistencial de Palencia, Palencia, Spain; [8]Hospital Universitario del Bierzo, Ponferrada, Spain*
Email: jmgsdigestivo@gmail.com

Background and aims: The integration of automated screening algorithms linked to Primary Care (PC), combining the detection of hypertransaminasemia with the FIB-4 index, may optimize the identification of hidden cases and accelerate progress toward viral hepatitis elimination. This study evaluate the feasibility of a pilot program for opportunistic and decentralized screening of viral hepatitis (HBV, HCV, HDV) in asymptomatic individuals attending PC.
Method: A prospective study was conducted (June–September 2025) in eight healthcare areas of Castilla y León (Spain). Patients aged 30–80 years with a request for routine blood testing in PC were included. Individuals with elevated alanine aminotransferase (ALT) levels and no prior hepatitis serology recorded in the lab information system underwent calculation of the FIB-4. In cases with FIB-4 >1.3 (<65 years) or >2.0 (≥65 years), viral hepatitis serology was automatically added without additional blood extraction. Samples positive for anti-HCV or HBsAg were confirmed by HCV RNA testing and anti-HDV antibodies, respectively. Diagnosed patients were individually assessed and referred to hospital-based care when indicated.
Results: A total of 189,594 blood tests from PC were processed, of which 6,331 (3.34%) showed hypertransaminasemia. FIB-4 was automatically calculated in these cases, and 958 patients (15.1%) exceeded the predefined cut-off values and underwent serological screening. Fifty-two previously undiagnosed viral hepatitis infections were identified (5.43% of those screened): 38 HBV infections (73.1%; including 2 HBeAg-negative chronic hepatitis cases, 4 inactive carriers, and 26 resolved infections) and 14 HCV infections (26.9%; 12 active and 2 resolved). Anti-HCV seroprevalence was 1.49%, and active HCV infection prevalence was 1.25%, both markedly higher than estimates for the general population (0.85% and 0.22%, respectively). The number needed to screen (NNS) to detect one

case of active HCV infection was approximately 80 among patients with elevated FIB-4, highlighting the efficiency of the sequential screening strategy in reducing unnecessary testing.
Conclusion: Automated opportunistic screening based on FIB-4 in PC identifies a prevalence of active HCV infection up to six times higher than that estimated in the general population. These results support the continuation and scaling-up of this pilot program as an operationally feasible tool to increase the diagnostic yield of viral hepatitis and advance toward WHO's elimination targets by 2030.

WED-020-YI
Evaluation of sex-based differences on hepatitis B, C and D viruses' disease burden and cascade of care in Italy
Samantha Hall[1], Loreta Kondili[2,3], Maria Giovanna Quaranta[2], Luigina Ferrigno[2], Ivane Gamkrelidze[1], Danielle Leavelle[1], Andrei Osmani[1,4], Devin Razavi-Shearer[1], Homie Razavi[1]. *[1]Center for Disease Analysis Foundation, Lafayette, United States; [2]Istituto Superior di Sanita, Rome, Italy; [3]Saint Camillus International University of Health Sciences, Rome, Italy; [4]Luiss Guido Carli University, Rome, Italy*
Email: shall@cdafound.org

Background and aims: Sex-based differences shape the epidemiology, clinical presentation, and outcomes of chronic viral hepatitis, yet they remain insufficiently incorporated into disease burden estimates and care strategies.
Method: We analysed anonymized data from the Italian PITER cohorts of patients in care for hepatitis B, C, and D viruses (HBV, HCV, HDV) to characterise sex-specific differences in demographics, virology, fibrosis severity, and treatment outcomes. Sex-stratified parameters derived from this well-characterised, nationally representative cohort were integrated into validated Markov disease progression models to estimate the sex-specific hepatitis burden in Italy.
Results: Among 6,265 individuals with chronic HBV, males presented with more advanced fibrosis and were nearly twice as likely to initiate treatment, despite females exhibiting higher baseline viremia. In HCV infection, treatment success was high in both sexes; however, males more advanced fibrosis at treatment initiation and lower odds of achieving sustainted virological response. No overall sex-based differences were observed for HDV, likely reflecting limited sample size; however, recent analyses of the same cohort indicate greater disease severity among younger women with HDV, a pattern distinct from HBV and HCV. Modelled national estimates showed a higher prevalence of HBV, viremic HCV infection, and advanced fibrosis among males, while overall HCV prevalence was similar by sex. Forecasted 2025–2030 liver-related death (LRD) ratios (male:female) were 3.5, 1.0, and 7.2 for HBV, HCV, and HDV, respectively, with comparable ratios for decompensated cirrhosis, hepatocellular carcinoma, and cirrhosis. While disease burden was projected to decline for HCV, remain relatively stable for HBV, and increase for HDV. HCV was projected to account for most LRDs (18,000 cases between 2025–2030), followed by HBV (7,700) and HDV (660).
Conclusion: Sex-based differences across viral hepatitis infections are heterogeneous and disease-specific, with implications extending beyond binary comparisons. Incorporating sex-specific real-world data from representative cohorts of patients in care is essential to refine burden estimates and to support sex-informed early diagnosis, treatment eligibility, and outcome monitoring within hepatitis elimination strategies.

WED-021
Hepatitis D testing patterns and prevalence in Australia: a retrospective statewide cohort study
Jessica Howell[1], Lauren Brotherton[2], Samuel Hui[3], Rohit Sawhney[4], Ammar Majeed[5], Siddharth Sood[6], Avik Majumdar[7], Zina Valaydon[8], Ashok Raj[9], Amanda Wade[10], Jack Wallace[11], Jacqui Richmond[11], Anouk Dev[12], Alexander Thompson[1]. *[1]St Vincent's Hospital Melbourne, University of Melbourne, Fitzroy, Australia; [2]St Vincent's Hospital Melbourne, Peter MacCallum Cancer Centre, University of Melbourne, Fitzroy, Australia; [3]Monash Health, Clayton, Australia; [4]Eastern Health, Monash University, Box Hill, Australia; [5]Alfred Health, Monash University, Melbourne, Australia; [6]Northern Health, University of Melbourne, Epping, Australia; [7]Austin Health, University of Melbourne, Heidelberg, Australia; [8]Western Health, University of Melbourne, Footscray, Australia; [9]The Royal Melbourne Hospital, University of Melbourne, Parkville, Australia; [10]Burnet Institute, Barwon Health, Melbourne CBD, Australia; [11]Burnet Institute, Melbourne CBD, Australia; [12]Monash Health, Monash University, Clayton, Australia*
Email: jessica.howell@svha.org.au

Background and aims: Hepatitis D (HDV) coinfection with hepatitis B (HBV) is the most serious form of viral hepatitis and is associated with a threefold higher risk of cirrhosis and hepatocellular carcinoma. We aimed to describe changing hepatitis D testing patterns and disease prevalence in Victoria state, Australia (~40,000 people with confirmed HBV in 2023).[1]
Method: This retrospective observational cohort study included every adult aged >18 years who underwent anti-HDV antibody testing and HDV PCR testing in Victoria between January 1, 2010 and December 31, 2023. Testing numbers and proportion positive were described overall and stratified by year, age category and sex. Associations with anti-HDV positive status were assessed by chi square test and Mantel-Haenszel odds ratios calculated.
Results: 11,361 anti-HDV antibody tests were ordered in 10,048 adults in Victoria during the study period. Over half (56%) were male and mean age was 42.2 ± 14.7 years. 500 anti-HDV antibody tests were positive and 50 had equivocal results, with a total of 498 anti-HDV antibody tests confirmed positive (4.3%) in 365 adults (3.6%). Of these, 210 adults (42%) who were anti-HDV Ab positive underwent HDV PCR testing and 72 (34%) were HDV RNA positive, consistent with active infection. 24 (33%) of HDV PCR positive adults had more than one PCR test during the study period. Of those who underwent HDV PCR testing, 48 (10%) did not have a HDV PCR test after their first positive anti-HDV antibody test, but after a repeat anti-HDV antibody test. The proportion of anti-HDV tests that were positive remained stable between 2.0–3.9% per annum during the study period. The proportion of HDV PCR tests that were positive also did not change significantly over time, ranging from a nadir of 1 (10%) in 2016 to a peak of 12 (36%) in 2018 (c^2 p = 0.232). Individuals who were anti-HDV antibody positive had higher odds of being male (67%; OR 1.55, 95% CI 1.24–1.94) but had a similar mean age (44.2 ± 12.5 years vs 44.3 ± 14.7 years, p = 0.95) compared to those who were anti-HDV antibody negative.
Conclusion: HDV-HBV coinfection is uncommon in Australia, with 1% of people with HBV tested having evidence of active HDV infection. However, major gaps in testing persist, with less than half of those who tested anti-HDV antibody positive having a HDV PCR test. Policy changes such as reflex HDV PCR testing for those who test anti-HDV antibody positive would significantly improve the HDV cascade of care.

WED-022
Assessing liver health literacy and screening uptake behaviors in an immigrant/visible minority community in Canada
Md Irfan Hyder[1], Mark Swain[1], Folake Arinde[1], Nashit Chowdhury[1], Nafiza Rahman[1], Carla Coffin[1], Mayur Brahmania[1], Tanvir C Turin[1].
[1]University of Calgary, Calgary, Canada
Email: mdirfan.hyder@ucalgary.ca

Background and aims: South Asians, including people of Bangladeshi origin, experience a disproportionate burden of chronic liver disease such as viral hepatitis and steatotic liver disease, yet awareness of liver health and preventive screening uptake remain suboptimal. Hence, Bangladeshi Canadians represent an important population to examine liver health literacy, screening uptake, perceived barriers and motivators, and associated factors.

Method: We conducted a bilingual (English/Bangla) cross-sectional survey, online and on paper, among Bangladeshi Canadian adults (n = 966) employing non-probability convenience sampling. The survey captured key demographics, general liver health knowledge, screening history & barriers, preferred screening locations, and information sources. Literacy was assessed using a nine-item exploratory scale (0–9) co-designed with community members and content experts. Adjusted negative binomial regression was used to model the knowledge score as a function of key sociodemographic characteristics, examining how scores varied across groups.
Results: Overall, 27% of participants were previously recommended to have hepatitis testing, and 23% had ever been tested for hepatitis B or C. Among respondents with no prior testing, the most reported barriers were lack of doctor's recommendation (75%), low awareness of screening (22%), and low perceived risk (21%), while unwillingness to undergo testing was uncommon (9%). Participants' preferred sources of liver health information were healthcare providers (75%), family members (30%) and friends (28%). The nine-item liver knowledge scale showed acceptable internal consistency (Cronbach's alpha = 0.76; mean score 3.8 ± 2.4). Women had 15% higher expected liver-knowledge scores than men ($p = 0.004$). Compared with participants with high school education or less, those with a diploma or bachelor's degree and those with a graduate degree had 23% ($p = 0.020$) and 34% ($p = 0.001$) higher expected scores, respectively. Temporary residents had 30% higher expected scores than citizens or permanent residents ($p = 0.002$).
Conclusion: In this large, community-based sample of Bangladeshi immigrants, both liver health knowledge and screening uptake were low, despite a high willingness to be screened and expressed trust in healthcare providers. Together, these findings underscore an important opportunity to develop targeted, culturally responsive interventions to strengthen liver disease prevention and promote earlier detection in high-risk immigrant communities.

WED-023

Hepatitis B and C viruses drive the burden of transfusion-transmissible infections in Karamoja Uganda

Jerry Ictho[1], Peter Lochoro[1], Dorothy Kyeyune[2], James Lemukol[3], Lilly Achayo[4], Godfrey Esiru[1], Brenda Nakafeero[5], Joseph Katetemere[1], Gilbert Sunday[2], Ahmed Bumba[6], Peter Lokwang[7], Sara Battistella[8], Francesca Tognon[1], Giovanni Putoto[1], Francesco Paolo Russo[8].
[1]Doctors with Africa Cuamm, Kampala, Uganda; [2]Uganda Blood Transfusion Services, Kampala, Uganda; [3]Moroto District Local Government, Moroto, Uganda; [4]Moroto Municipal Council, Moroto, Uganda; [5]Independent Statistician, Kampala, Uganda; [6]Mbale Regional Blood Bank, Mbale, Uganda; [7]Nabilatuk District Local Government, Nabilatuk, Uganda; [8]University of Padova, Padua, Italy
Email: j.ictho@cuamm.org

Background and aims: Transfusion-transmissible infections (TTIs) pose major challenges to blood safety, particularly in low-resource settings like northeastern Uganda. The aim of the study was to assess the prevalence of TTIs and associated factors among potential blood donors in the Karamoja subregion.
Method: We conducted a community-based, cross-sectional mixed-methods study involving 475 participants aged 18–60 years, selected using multistage cluster sampling from nine districts in Karamoja. Structured interviews and blood sample testing for HIV, HBV, HCV, and syphilis were performed. Modified Poisson regression with robust standard errors was used to identify factors associated with TTIs. In-depth interviews and focus group discussions explored perceptions and barriers to blood donation. Qualitative data were thematically analyzed.
Results: The prevalence of at least one TTI was 26.5% (95% CI: 22.7–30.7), with HCV (11.7%) and HBV (7.0%) being most common. Males had a significantly higher risk of TTIs (adjusted prevalence ratio [APR] 1.70, 95% CI 1.20–2.42). Older age, low education, and lack of prior blood donation were associated with higher infection rates. Qualitative findings revealed deep-rooted fears, cultural taboos, and mistrust of health services as barriers to donation. Health system limitations, including poor outreach and lack of testing capacity, further constrained safe blood availability.
Conclusion: Karamoja faces a dual challenge of high TTI prevalence and low blood donation rates. Interventions must be gender-responsive, culturally sensitive, and health-system strengthening to improve blood safety and accessibility. The high burden of viral hepatitis, particularly HBV and HCV, represents a critical public health concern and underscores the urgent need to enhance prevention, screening, and linkage-to-care strategies alongside efforts to promote safe and sustainable blood donation. Our findings provide the first community-based evidence to guide targeted public health strategies in pastoralist and underserved populations.

WED-024

Hepatitis C virus reinfection after successful treatment with direct acting antiviral therapy in Canada

Naveed Janjua[1], Stanley Wong[1], Dahn Jeong[1], Jean Damascene Makuza[1], Prince Adu[1], Amanda Yu[1], Héctor Alexander Velásquez García[1], Sofia Bartlett[1]. *[1]BC Centre for Disease Control, University of British Columbia, UBC Centre for Disease Control, Vancouver, Canada*
Email: naveed.janjua@bccdc.ca

Background and aims: Preventing hepatitis C virus (HCV) reinfection following successful treatment with direct-acting antiviral (DAA) therapy among people who inject drugs(PWID) remains a key component of the HCV elimination strategy. We estimated HCV reinfection rates following DAA treatment in a population-based cohort in British Columbia (BC), Canada.
Method: We analyzed data from the IDEALS (Integrated Data for Enhanced SurveillAnce and EpidemioLogy of STBBI+TB) Platform, which includes all people tested for HCV in BC. We followed individuals with HCV infection treated with DAAs who achieved sustained virologic response (SVR) and had ≥1 subsequent HCV RNA measurement until Nov 18, 2025. Reinfection was defined as a positive RNA measurement after SVR. Injection drug use(IDU) was identified using a validated algorithm based on physician diagnosis and hospitalization codes, categorized as none, recent (IDU- related visits <3 years), and past. Crude reinfection rates per 100 person-years(PY) were calculated and Cox proportional hazards modelling was performed to identify factors associated with reinfection.
Results: Among 9,058 eligible individuals achieving SVR, the majority were male(n = 5,971, 66.0%), born 1945–64 (n = 5,137, 56.7%, median age: 56 years); 32% persons with recent IDU(n = 2,903), and 13% persons with past IDU(n = 1,148). We identified 257 HCV reinfections during 22,861.06 PY of follow-up, yielding a reinfection rate of 1.12/100 PY. Reinfection rates were higher among persons with recent IDU(n = 188, 2.37/100 PY) than persons with past IDU(n = 26, 0.77/100 PY) and persons with no IDU(n = 43, 0.37/100 PY). Cumulative incidence curves showed significantly higher and steeper increase in incidence among persons with recent IDU over time. Among persons with recent IDU, reinfection rates were highest among those <30 years of age(4.0/100 PY). In a multivariable model for persons with recent IDU, younger age (age <30 years adjusted hazards ratio(AHR): 2.05, 95%CI:1.26–3.33 (ref:50–59 yrs), and opioid use (AHR: 2.03, 95%CI:1.22–3.36) were associated with higher reinfection risk.
Conclusion: In this population-based cohort, HCV reinfection rates after DAA therapy were highest among persons with recent IDU, especially among younger PWID and who use opioids. Scale-up of HCV treatment with addiction management among persons with recent IDU, especially identifying and supporting unique needs of younger PWID, would be critical in preventing reinfection and HCV elimination.

WED-025-YI

Changing epidemiology of hepatitis A in India: trends converging with Europe

Ayush Jasrotia[1], Premashis Kar[1], Pabitra Sahu[1], Reshma Reshma[1], Nikhil Nagre[1], Amit Anand[1], Abhijit Bhalke[1]. [1]*Max Super Speciality Hospital, Vaishali, Ghaziabad, Uttar Pradesh 201010, India*
Email: ayushjasrotia1103@gmail.com

Background and aims: India was historically highly endemic for hepatitis A virus (HAV), with near-universal childhood exposure. Improvements in sanitation and socioeconomic conditions may delay primary infection, increasing susceptibility in adolescents and adults. We synthesised Indian evidence on age-specific HAV seroprevalence, surveillance and outbreaks, and compared India's trajectory with the European epidemiological transition.
Method: A PRISMA-aligned systematic review (1990–2025) identified Indian population-based serosurveys reporting anti-HAV immunoglobulin G or total antibodies, along with national and state surveillance data and outbreak investigations. Random-effects proportions using the Freeman–Tukey transformation were estimated by age band (0–5, 6–10, 11–15, 16–25, 26–40 and > 40 years). Surveillance and molecular data were narratively compared with European outbreak experience.
Results: Fourteen serosurveys including approximately 25,000 participants demonstrated a consistent age shift. An urban Delhi study (2000) reported lower immunity in individuals younger than 35 years (57%) compared with those older than 35 years (92%). A multicity survey (2011–2012) showed 37.5% overall seroprevalence and 50.3% in children aged 6–10 years, with marked socioeconomic and sanitation gradients. A national survey conducted in 2021 among individuals aged 6–30 years ($n \approx 15{,}000$) reported seroprevalence of 74.7%, 85.2% and 96.9% in the 6–10, 11–15 and 16–30 year age groups respectively, consistent with intermediate endemicity. National surveillance data (2014–2017) detected HAV immunoglobulin M in 12.6% of tested samples, predominantly in individuals aged 19 years or younger. Recent community outbreaks in Kerala (genotype IIIA) primarily affected young adults. European outbreaks between 2016 and 2018, mainly involving men who have sex with men, demonstrated similar post-transition adult susceptibility.
Conclusion: India's hepatitis A epidemiology now mirrors Europe's earlier transition, characterised by declining childhood exposure, increasing adult susceptibility and recurrent young-adult outbreaks. These findings support routine childhood vaccination in transitioning regions, adolescent catch-up in urban settings, targeted immunisation of high-risk groups and strengthened molecular surveillance.

WED-026

Mother-to-child is the dominating route of HBV transmission in the post vaccination era: a community based study in Ethiopia

Nega Berhe[1], Dawit Brhane[2], Humed Yaid[3], Fufa Hunduma[1], Bethlehem Gebregziabher[1], Lasse Rossvoll[4], Kristian Malme[4], Hailemichael Desalegn[5], Shevanthi Nayagam[6], Asgeir Johannessen[4]. [1]*Addis Ababa University, Addis Ababa, Ethiopia;* [2]*Dubti General Hospital, Semera, Ethiopia;* [3]*Mohamed Akile Comprehensive Hospital, Afar, Ethiopia;* [4]*Sykehuset i Vestfold Tønsberg, Tønsberg, Norway;* [5]*St.paul's Hospital Millennium Medical College, Addis Ababa, Ethiopia;* [6]*Imperial College London, London, United Kingdom*
Email: johannessen.asgeir@gmail.com

Background and aims: The Afar region in Ethiopia is reported to have high burden of HBV and HDV infection despite introduction of the childhood HBV vaccine in 2007. Previous studies, however, were limited by small size and unrepresentative sampling, and it is unknown whether HBV transmission is perpetuated by mother-to-child transmission or through early horizontal transmission such as traditional invasive practices. We aimed to estimate community prevalence of HBV and HDV, vaccination coverage among children under 5 years, and HBV distribution patterns within families.
Method: A cross-sectional serosurvey was conducted from February to April 2025 in the Afar region. In addition, mothers with their children under 5 years were randomly selected to assess HBV infection status, vaccination coverage, and intrafamilial HBV distribution patterns. All participants were tested for HBsAg with a point-of-care kit (Determine HBsAg2, Abbott Diagnostics; LOD 0.1 IU/ml). HDV antibodies were assessed in HBsAg positive subjects using a commercial ELISA assay (Dia.Pro Diagnostic).
Results: Overall HBV prevalence among 3,112 study participants (51.9% females; median age 30 years) was 8.1% (95% CI 7.1–9.1), with the lowest prevalence in children under 5 years (1.0%; 95% CI 0.4–3.0) and highest in adults 18–35 years (11.8%; 95% CI 10.3–13.4). HDV co-infection was detected in 90/250 (36.0%; 95% CI 30.3–42.1) of HBsAg positive individuals and was common across all age groups: 4/8 (50.0%) in children under 10 years and 16/47 (34.0%) in adults over 45 years.
Among 364 mothers, 31 (8.5%; 95% CI 6.1–11.8) were HBsAg-positive. None of their children under 5 years had received birth-dose HBV vaccine, but the majority (78.0%) had at least 2 doses of childhood HBV vaccine. Of children born to HBsAg positive mothers, 5/31 (16.1%; 95% CI 7.1–32.6) were HBsAg positive, compared to 0/333 (0%; 95% CI 0.0–1.1) of children born to HBsAg negative mothers ($p < 0.001$).
Conclusion: HBV and HDV are endemic in Afar, and the prevalence among children under 5 years is far from the WHO elimination target of <0.1%. Childhood HBV infection occurred exclusively among those born to HBV infected mothers, suggesting that mother-to-child rather than traditional practices is the predominant route of transmission. The highest HBV prevalence was seen among individuals of reproductive age, underscoring the need for birth-dose vaccination and strengthened routine childhood immunization in Ethiopia.

WED-027

National hepatitis B virus (HBV) screening pilot using rapid HBV antibody tests in Kazakhstan

Kulpash Kaliaskarova[1], Samantha Hall[2], Danielle Leavelle[2], Kulkayeva Gulnara Utepergenovna[1], Alma Aubakirova[3], Marzhan Zhanasbayeva[1], Alan Bijiyev[1], Nataliya Satlikova[1], Shakhlo Yusupalieva[4], Homie Razavi[2]. [1]*National Research Oncology Center, Astana, Kazakhstan;* [2]*Center for Disease Analysis Foundation, Lafayette, United States;* [3]*National Research Center for Health Development, Astana, Kazakhstan;* [4]*Center for Disease Analysis Foundation, Tashkent, Uzbekistan*
Email: kulpash.kaliaskarova@gmail.com

Background and aims: Hepatitis B virus (HBV) infection remains a major public health challenge in Kazakhstan, affecting an estimated 443,000 individuals. Despite the availability of free testing and treatment, fewer than 17% of cases were diagnosed by 2024. Current screening programs target only high-risk groups, pregnant women, and surgical patients, leaving many undiagnosed. This gap undermines Kazakhstan's progress toward the World Health Organization's (WHO) 2030 elimination target. This pilot evaluated the effectiveness of large-scale adult population screening in urban and rural polyclinics. The findings aim to inform the development of a national program to improve diagnosis, treatment, and public health outcomes to meet WHO elimination goals.
Method: Convenience sampling was employed to recruit adults attending polyclinics in five regions: East Kazakhstan, Abay, Turkistan, Karaganda, and Shymkent. A total of 100,024 individuals were screened for HBsAg antibodies using rapid diagnostic tests, with data recorded in an electronic registry. Prevalence was analyzed by age, sex, birth region, and clinic region. Poisson regression identified factors contributing to variability in HBV prevalence.
Results: HBV prevalence, adjusted for age and sex, was estimated to be 0.79% (0.74–0.86%). Males had higher prevalence (1.45% (1.32–1.56%)) than females (0.49% (0.44–0.55%)). Prevalence peaked at 1.51% (1.28–1.77%) for those aged 35–39. The highest prevalence was

observed among individuals born outside Kazakhstan, reaching 4.88% (1.60–12.56%). Among clinic regions, Turkistan had the highest prevalence of 1.38% (1.26–1.51%). Regression analyses indicated higher adjusted prevalence in individuals born outside of Kazakhstan, while younger age groups had significantly lower prevalence compared with those aged 40–44 ($p < 0.01$).
Conclusion: This pilot program demonstrated the feasibility of large-scale HBV screening and identified significant variability in prevalence by age, sex, and geography. Males, individuals aged 35–39, and those born outside Kazakhstan showed elevated prevalence, highlighting the need for targeted interventions. However, expanding the program to all regions and high-risk groups is critical for a comprehensive assessment of HBV prevalence. Development of a national screening strategy will be essential for Kazakhstan to meet WHO elimination targets and reduce the public health burden of HBV.

WED-028
Experience from the first two years of a peer support programme for people living with hepatitis B in north central London
Joy Ko[1], Indrajit Ghosh[1], Emily Martyn[2], Angieszka Kemper[1], Fernando Monterio[1], Richard Gilson[1,3], Mustapha Hacine Bacha[4], Mark Leonard[4], Mark Longman[4], Binta Sultan[1,3], Philippa C Matthews[1,2], Stuart Flanagan[1,3]. *[1]Central & North West London NHS Foundation Trust, Mortimer Market Centre, London, United Kingdom; [2]Francis Crick Institute, London, United Kingdom; [3]University College London, Institute of Global Health, London, United Kingdom; [4]Nhs University College Hospital, London, United Kingdom*
Email: joy.ko@nhs.net

Background and aims: There is increasing focus on peer support for people living with Hepatitis B (PLWHB), in order to improve linkage to care and treatment, enhance long-term well-being, improve health outcomes, and support progress towards international elimination goals for viral hepatitis.
Method: Our service is provided by a primary care NHS trust which runs a clinic at the Mortimer Market Centre. This trust has extensive experience in providing peer support for people living with different health challenges, and appointed the UK's first paid peer support worker (PSW) for PLWHB in 2023. This role is delivered through a combination of approaches, including individual face-to-face or telephone consultations, family meetings, and small group sessions. Referrals are made by Health Advisors and clinicians, and the PSW reaches out to all those with a recent HBV diagnosis. Translation services are provided if required. We present data on the first two years of peer support provision, from November 2023, to describe the role and workload, and to provide evidence for ongoing resourcing and expansion.
Results: 105 adults were referred to the peer support service (77 M:28 F), median age 35 years (range 18–83 years). At the time of referral, 30% were in temporary accommodation. Twenty languages were spoken, with 56% speaking English, and the commonest other languages being Mandarian, Pashto and Arabic. At the time of referral, 15% were receiving HBV treatment. 29% did not attend an offered PSW appointment (10% could not be reached, 8% were contacted and declined, and 11% had left the area). Priority topics included support with a new HBV diagnosis, discussion about starting treatment, support to share information with a partner or family members, tackling stigma and discrimination, and social issues such as migration status and housing. Our PSW also met with partners and families to tackle questions and concerns, and to support education, testing and vaccination.
Conclusion: Our PSW for PLWHB in central London provides support for adults from a diverse range of countries with complex social needs. Not all those who are referred to the service can be reached, highlighting a vulnerable population for whom additional resources are needed. We highlight peer support as a successful approach to providing information, addressing concerns and engaging individuals and their families.

WED-029
Population-based hepatitis C screening and elimination program in Lithuania: may it affect the incidence of hepatocellular carcinoma?
Limas Kupcinskas[1], Alexis Voeller[2], Artur Kozlov[3], Homie Razavi[2], Jurate Sabaliene[3], John Ward[4], Janina Petkeviciene[1], Juozas Kupcinskas[1]. *[1]Lithuanian University of Health Sciences, Kaunas, Lithuania; [2]Center for Disease Analysis Foundation, Lafayette, United States; [3]National Health Insurance Fund under the Ministry of Health, Vilnius, Lithuania; [4]Coalition for Global Hepatitis Elimination, Decatur, United States*
Email: l.kupcinskas@gmail.com

Background and aims: Liver cancer is the 15th most common type of cancer in Lithuania (2022) and almost 50% of cases of hepatocellular carcinoma (HCC) were caused by the hepatitis C virus (HCV). The Lithuanian HCV screening programme started in 2022. HCV antibody testing by general practitioners (GP) was performed: 1) for people born 1945–1994 (once in a lifetime) and 2) for those who inject drugs (PWID) or HIV+ (annual testing). The aim of the study was to assess results of the first 39 months of the programme, evaluate different scenarios to achieve WHO 2030 targets and effect on HCC incidence.
Method: GP invited people to perform a serum ant-HCV test. Anti-HCV positive patients (pt) were referred to a gastroenterologist or infectologist for HCV RNA testing, and if result positive, direct-acting antiviral (DAA) was prescribed. Information about pt was obtained from National Health Insurance Fund. The Markov disease progression model elaborated CDA Foundation was used to assess HCV elimination progress. The data from the 2022–2023 screening were used as inputs. Three scenarios were developed: the 'Base' scenario - return to pre-screening program level in 2023 and 2 scenarios with different extents of treatment.
Results: in 2022, about 1.8 million people born 1945–1994 lived in Lithuania. Between May 5, 2022 and July 31, 2025 from this population 1419059 (81%) were tested for HCV antibodies. Positive test were found in 1.3% of cases. In the risk group, 18695 PWID and HIV+ people were screened, of whom 29.4% were seropositive. Viremia was detected in 52,8%. During 39-month period 3 times more HCV pt were treated with DAA than during the same period before starting of the program (8321 vs 2690). The Markov disease progression model to assess HCV elimination progress showed the following: Scenario 1: if the same number of pt are treated as before the screening, the WHO targets will not be reached. Scenario 2: treating 70% of infected patients will meet most but not all WHO targets. Scenario 3: by treating all infected patients by 2030, the WHO target will be met by saving 150 lives and preventing 90 new cases of decompensated cirrhosis and 120 cases of HCC.
Conclusion: In country with moderate HCV seroprevalence, a population-based screening program can be feasible, screening 81% (more than 1,4 million) of the target population during the first 39 program months. In case of realization of the Scenario 3 we could expect to achieve WHO targets by 2030 and diminish HCC incidence in Lithuania.

WED-030
Epidemiological landscape of hepatitis E in South Korea: analysis of national surveillance data (2020–2023)
Chang Hun Lee[1], Hwa Young Choi[2], Won-Mook Choi[3], Byeong Geun Song[4], Moran Ki[2], Sook-Hyang Jeong[5], In Hee Kim[1]. *[1]Department of Internal Medicine, Research Institute of Clinical Medicine of Jeonbuk National University-Biomedical Research Institute of Jeonbuk National University Hospital, Jeonbuk National University Medical School, Jeonju, Korea, Rep. of South; [2]Department of Public Health and AI, Graduate School of Cancer Science and Policy, National Cancer Center, Goyang, Korea, Rep. of South; [3]Department of*

Gastroenterology, Liver Center, Asan Medical Center, University of Ulsan College of Medicine, Seoul, Korea, Rep. of South; [4]Department of Medicine, Samsung Medical Center, Sungkyunkwan University School of Medicine, Seoul, Korea, Rep. of South; [5]Department of Internal Medicine, Seoul National University Bundang Hospital, Seoul National University College of Medicine, Seongnam, Korea, Rep. of South
Email: ihkimmd@jbnu.ac.kr

Background and aims: Hepatitis E virus (HEV) infection was designated as a mandatory reportable disease in South Korea in July 2020 by the Korea Disease Control and Prevention Agency (KDCA). This study aimed to analyze national infectious disease surveillance data to evaluate temporal trends and epidemiological characteristics of reported hepatitis E cases.
Method: We analyzed all confirmed HEV cases reported to the KDCA from July 2020 to December 2023. Reporting trends, demographic distributions (age, sex, and region), and clinical characteristics were assessed using epidemiological investigation forms and laboratory data.
Results: After excluding duplicate reports, a total of 1,768 hepatitis E cases were identified. The annual reporting rate increased from 0.95 per 100,000 population (n = 493) in 2021 to 1.09 per 100,000 (n = 562) in 2023. A significant male predominance was observed (58.1% vs. 41.9%, $p < 0.001$). Reported cases increased progressively with age, from 35 cases in children aged 0 to 9 years to 327 cases in those aged 60 to 69 years ($p < 0.001$). No distinct seasonal pattern was identified. Regionally, the highest reporting rate was observed in Gangwon province. Symptomatic cases accounted for 62.8% of all reports and were more frequent in younger age groups, with no significant difference by sex. Among 1,542 cases with completed epidemiological investigation forms, liver function test results were available for 1,434 cases. Elevated aminotransferase levels (aspartate aminotransferase or alanine aminotransferase $\geq$ 40 U/L) were observed in 82.5% of symptomatic cases and 51.7% of asymptomatic cases.
Conclusion: Reported hepatitis E cases in South Korea have increased since the implementation of mandatory national surveillance in 2020, with higher reporting rates among men and older age groups. These findings provide insights into the epidemiological burden of hepatitis E in South Korea based on national infectious disease surveillance data.

WED-031
Global prevalence of HIV-HBV co-infection in pregnancy: a systematic review to inform elimination of mother-to-child transmission

Leona Leipold[1], Francesca Bladt[1], Rageshri Dhairyawan[2,3], Stamatina Iliodromiti[4], Upkar Gill[1,5]. *[1]Centre for Immunobiology & Infection, The Blizard Institute, Barts and The London Faculty of Medicine & Dentistry, Queen Mary University of London, London, United Kingdom; [2]SHARE Collaborative, Blizard Institute, Barts and The London Faculty of Medicine & Dentistry, Queen Mary University of London, London, United Kingdom; [3]Department of Infection and Immunity, Barts Health NHS Trust, London, United Kingdom; [4]Women's Health Research Unit, Wolfson Institute of Population Health, Queen Mary University London, London, United Kingdom; [5]Department of Hepatology, Barts Health NHS Trust, London, United Kingdom*
Email: u.gill@qmul.ac.uk

Background and aims: HIV-HBV co-infection in pregnancy remains a critical but under-characterised challenge for the World Health Organization (WHO) goal of triple elimination of mother-to-child transmission (MTCT) of HIV, hepatitis B virus (HBV), and syphilis. While antenatal HIV and HBV screening is widely implemented, the global burden of maternal co-infection and its implications for pregnancy and birth outcomes remain poorly synthesised.
Method: We conducted a systematic review of published studies reporting HIV-HBV co-infection in pregnant populations across multiple regions. Studies reporting prevalence and/or maternal, obstetric, or birth outcomes were included. Data were extracted on study design, geographic region, period, population characteristics, and diagnostic methods.
Results: A total of 165 studies were included, encompassing ~2.33 million pregnant individuals globally. Studies were geographically skewed, with ~68% originating from the WHO African Region, and relatively sparse representation from Europe, the Americas, and Asia-Pacific regions. Reported HIV-HBV co-infection prevalence varied widely by setting and population. In general antenatal populations, prevalence ranged from near 0% in several settings to high historical outliers (e.g. ~28.9% in a 1992 Tanzanian cohort). Among HIV-positive pregnant cohorts, higher co-infection rates were consistently observed, frequently in the 5–15% range, with some European and African cohorts reporting substantially higher prevalence (e.g. ~39.2% in a Romanian HIV-positive cohort). Maternal, obstetric, and neonatal outcomes were poorly reported, with a minority of studies presenting outcome data alongside prevalence estimates. Considerable heterogeneity was observed in diagnostic methods and reporting, with HIV and HBV testing strategies often unstated. Several countries appear to collect antenatal HIV and HBV data through unlinked surveillance systems, limiting reliable co-infection estimates and trend analysis.
Conclusion: Despite a large global evidence base, data on HIV-HBV co-infection in pregnancy remain imbalanced, methodologically inconsistent, and outcome-sparse. Co-infection prevalence can be substantial in specific antenatal settings, particularly among HIV-positive pregnant populations. These findings support the need for integrated antenatal HBV/HIV testing, improved diagnostic reporting standards, and linked surveillance systems to better inform MTCT prevention strategies and guide elimination efforts.

WED-035
Global drug utilization and expenditure of essential medicines forecasting future viral hepatitis elimination: a multinational drug use study

Jiaqi Wang[1], Lung Yi Loey Mak[1], Kathy Leung[1], Esther Wai Yin Chan[1], Po-Lin Chan[2], Yasser Abdallah[3], Won-Mook Choi[4], Adrian Gadano[5], Yasuhito Tanaka[6], Alexander Nersesov[7], Xiaodong Guan[8], Ajay Kumar Duseja[9], Ian Chi Kei Wong[10], William CM Wong[1], Young-Suk Lim[4], Man-Fung Yuen[1], Mindie Nguyen[11], Xue Li[1], Wai-Kay Seto[1]. *[1]The University of Hong Kong, Pok Fu Lam, Hong Kong; [2]World Health Organization South-east Asia Regional Office, New Delhi, India; [3]Minia University, Minia, Egypt; [4]Asan Medical Center, University of Ulsan College of Medicine, Seoul, Korea, Rep. of South; [5]Sección Hepatología, Hospital Italiano, Buenos Aires, Argentina, Buenos Aires, Argentina; [6]Department of Gastroenterology and Hepatology, Faculty of Life Sciences, Kumamoto University, Japan, Kumamoto, Japan; [7]Department of Gastroenterology, Kazakh National Medical University, Almaty, Kazakhstan, Almaty, Kazakhstan; [8]Department of Pharmacy Administration and Clinical Pharmacy, School of Pharmaceutical Sciences, Peking University, Beijing, China, Beijing, China; [9]Department of Hepatology, Post Graduate Institute of Medical Education & Research, Chandigarh, India, Chandigarh, India; [10]Aston Pharmacy School, Aston University, Birmingham, UK, Birmingham, United Kingdom; [11]Division of Gastroenterology and Hepatology, Stanford University Medical Center, Palo Alto, California, USA, Palo Alto, United States*
Email: loeymak@gmail.com

Background and aims: The World Health Organization (WHO)'s 2030 viral hepatitis elimination goals aim to reduce related deaths by 65%. Treatment uptake of antiviral medications for chronic hepatitis B (CHB) and chronic hepatitis C (CHC) remains low. We aimed to examine the actual utilization of these antiviral drugs on a global scale, describing drug consumption and expenditure trends over the past decade & make projections in viral hepatitis-related mortality towards year 2030.
Method: We used data from the IQVIA Multinational Integrated Data Analysis System database to analyze the trends in actual utilization of the WHO Model Lists of Essential Medicines (EML) in CHB & CHC from

2015 to 2023 & evaluated economic inequality in medication utilization. We estimated the association between these trends with CHB- & CHC-related incidence & mortality using data from the Global Burden of Diseases & Polaris Observatory, by fitting into generalized linear mixed models, alongside economic & health system metrics. Projections on disease-related mortality were generated towards year 2030.

Results: Among 68 & 61 countries with WHO EML data available on CHB & CHC, respectively, utilization of EML drugs for CHB has increased with time that was largely contributed by the Western Pacific region & high-income countries. For CHC, utilization of EML has peaked around 2017 & subsequently declined with time & concentrated in low-middle-income countries, largely driven by utilization in Egypt (14.3 per 1000 population). Inequality in EML drug usage was observed, with CHC favouring lower Gross National Income (GNI) levels but in CHB favouring higher GNI levels. Most countries demonstrated modest decline in age-standardized incidence and/or mortality rates, but mortality reduction was outpaced in CHB. By 2030, the greatest forecasted mortality reductions for CHB & CHC would be 59.4% in Korea & 55.8% in Kazakhstan respectively. For high-disease burden countries, mortality will decline modestly or even increase till 2030 (−13.7% to +97.1%; & −51.2% to +151% respectively).

Conclusion: Global utilization patterns of essential medicines for CHB & CHC have evolved over the past decade with residual inequality. Most countries showed modest decline in incidence and/or mortality but the mortality reductions were delayed. No countries are projected to approach the goal of mortality reduction by 2030, & expansion of treatment access in the next 5 years would be a critical priority.

WED-036

Incidence of HIV among people living with chronic hepatitis B: 10-year results from a large cohort in Ethiopia

Kristian Malme[1,2], Hailemichael Dessalegn[3,4], Nega Berhe[1,5], Eyerusalem Mamo[4], Tsehay Solomon[4], Asgeir Johannessen[1,6].
[1]Department of Infectious Diseases, Vestfold Hospital Trust, Tønsberg, Norway; [2]Department of Infectious Diseases, Akershus University Hospital, Lørenskog, Norway; [3]Toronto Centre for Liver Disease, University Health Network, Ontario, University of Toronto, Ontario, Canada; [4]Medical Department, St Paul's Hospital Millennium Medical College, Addis Ababa, Ethiopia; [5]Aklilu Lemma Institute of Pathobiology, Addis Ababa University, Addis Ababa, Ethiopia; [6]Institute of Clinical Medicine, University of Oslo, Oslo, Norway
Email: krismalme@hotmail.com

Background and aims: Although tenofovir disoproxil fumarate (TDF) monotherapy is safe and effective for long-term treatment of people living with chronic hepatitis B (PLWHB), its use in settings with a moderate/high prevalence of human immunodeficiency virus (HIV) warrants caution, as TDF monotherapy may lead to HIV resistance among co-infected individuals. The aim of this study was to assess HIV incidence, with and without antiviral therapy, in a well-characterized cohort of PLWHB in Addis Ababa, Ethiopia, where the background HIV prevalence in the adult population is 3.1%.

Method: This was a longitudinal cohort study of HIV-negative HBsAg-positive adults (>/ = 18 years) enrolled in a treatment center in Addis Ababa in 2015 and followed up until 2025. HIV testing was conducted at baseline and repeated every 3–6 months among treated, and less frequently among untreated, individuals using HIV antibody/antigen rapid diagnostic tests. HIV incidence rates were calculated using person-time of observation.

Results: The total number of person-years was 6611 (median follow-up time 4.95 years). Among 1303 participants enrolled (mean age 34 years, 59% male, 21% liver cirrhosis, 22.5% TDF treated during the study period), 1 case of HIV was detected after inclusion, resulting in an HIV incidence of 0.015 per 100 person years [95% CI 0.001–0.084]. HIV incidence was 0.05 per 100 person years [95% CI 0.001–0.30] among treated persons and 0.00 per 100 person years among untreated [95% CI 0.00–0.0.8]. The sole participant who tested HIV positive at month 3 was later shown, through HIV immunoblot retesting of the baseline screening sample, to have been HIV positive at inclusion, consistent with infection during the HIV serological window phase.

Conclusion: In settings with high HIV prevalence, TDF therapy can be safely administered in hepatitis B programs but should be accompanied by repeated HIV testing.

WED-037

Re-linkage to care for HDV positive patients as part of an unique pan-re-linking program in Italy

Alessandra Mangia[1], Valeria Piazzolla[1], Antonio Napolitano[1], Adelia Aquilano[2], Luca L'erario[3], Angelo L'erario[4], Mattia Lopez[5], Laura Lange[6], Maria Squillante[1], Rosanna Santoro[7], Laura Solito[8].
[1]IRCCS Casa Sollievo della Sofferenza, San Giovanni Rotondo, Italy; [2]Laboratorio Analisi cliniche Aquilano srl, Cagnano Varano, Italy; [3]Laboratorio Analisi Dell'Olio srl, Trani, Italy; [4]Laboratorio Dell'Oglio, Trani, Italy; [5]Laboratorio Analisi Palazzo, Margherita di Savoia, Italy; [6]Laboratorio Guerrieri, Cagnano Varano, Italy; [7]Laboratorio Analisi Santoro, Maruggio, Italy; [8]Laboratorio Solito, Taranto, Italy
Email: a.mangia@tin.it

Background and aims: Despite the advances in therapy, linkage to care represents one of the main barriers to the global elimination of viral hepatitis. A substantial number of candidates for hepatitis C, B and D treatment remain untreated or lost to follow-up. Re-linkage to care represents one of the main focuses for achieving HCV and HBV/HDV elimination. In Italy, this process is hampered by data privacy regulations, which we managed to overcome by designing a project to be conducted in collaboration with private laboratories. To assess the effectiveness of a dedicated re-linking program implemented together with hub private laboratories which manage spoke laboratories covering an area of 7500 Km2.

Method: From 6/2024 to the present, 10 hub laboratories coordinated by our center through the help of Telehealth across the 6 provinces of Puglia, recalled patients aged 50–85 tested in the last 10 yrs and found to be HCVAb or HBsAg positive. We focus here on the results for HBsAg positive. The project will be completed by June 30th, 2026. HBsAg positive patients were offered counselling, HDVAb and, when needed, HDVRNA testing; HDVRNA assessement by Robogene, and treatment at our center. Primary endpoint is the number of patients re-linked out of HDVAb positive; secondary endpoint, the number of patients who started HDV treatment.

Results: Overall, 1050 were recalled, only 351 HBsAg positive individuals agreed to be included (149 had died, in 201 re-check was negative, 109 moved to a different geographical area, 53 rejected the offer, 97 lost contact). These individuals were 67% male with mean age 61.9 ± 10.1 yrs. All of them were tested for HDVAb. Overall, 70 (19.9%) had HDVAb positive results and underwent HDVRNA evaluation. Rate of HDVAb patients with HDVRNA detectable was 25.7%. Rates of patients with PLT<140.00 ul were 54.2% and 18.1%, among HDVAb positive and negative, respectively. All except 3 (two of whom with Non-HodgkinLymphoma and kidney cancer) started treatment with a treatment re-linkage rate of 83.3%. Of the 15 patients who started treatment, 73.3% had evidence of advanced disease.

Conclusion: Bringing patients to care for HDV was more difficult than expected. Rate of HDVRNA positivity was high; the majority of HDVAb positive patients had PLT <140.000ul suggesting the presence of an advanced disease. This initiative allowed patients with HBV/HDV advanced disease that lacked follow-up HDV testing to be identified and treated.

(Gilead IN-IT-980-6868).

WED-038

From control to elimination of HCV infection: the experience in prisons of Catalonia, Spain

Andrés Marco[1], Indiana Abdo[2], Enrique Gil[2], Neus Solé[2], Isabel Barnés[2], Elisabet Turu[2]. [1]*Prison Health Program. Catalan Institute of Health. Government of Catalonia, Biomedical Research Consortium Network for Epidemiology and Public Health (CIBERESP), Barcelona, Spain;* [2]*Prison Health Program. Catalan Institute of Health. Government of Catalonia, Barcelona, Spain*
Email: andres.marco.m@gmail.com

Background and aims: Often, prison-based HCV micro-elimination programs are isolated or one-off initiatives with limited impact on reducing incidence. Our objective is to evaluate the effectiveness of a program continuously implemented for all incarcerated individuals across all prisons in Catalonia.
Method: The study examined: (a) the prevalence of HCV infection in new inmates at the nine prisons in Catalonia between 1 January 2020 and 31 December 2024; (b) the annual incidence of infection; and (c) the effectiveness of the program, determined by the annual incidence rate and the number of direct-acting antiviral (DAA) treatments prescribed between 2016 and 2024. The program was considered effective if the incidence was zero or remained below a threshold unlikely to sustain transmission. This threshold was defined as a consistently low HCV RNA level, below 0.5%.
Results: Among the 34,088 inmates admitted, 32,002 (93.9%) consented to screening. A total of 370 infections (1.2%) were detected, with a downward trend (2.2% in 2020 and 0.6% in 2024; $p < 0.001$). Of these, 361 cases were further analyzed, of which 82 were reinfections, significantly more frequent in men, Spanish nationals, inmates in Barcelona prisons, people who inject drugs (PWID), and those coinfected with HIV. The median time to reinfection was 1185 ± 164 days, and was shorter ($p = 0.001$) in migrants (730 ± 290 days). A total of 340 patients were treated, and 98.4% achieved a sustained virological response (SVR). The incidence remained consistently below 0.5%. On 31 December 2024, the viremia was undetectable in four of the nine prisons.
Conclusion: HCV elimination programs in prisons must be maintained over time and subjected to periodic evaluation. Although achieving elimination, or control of the infection, in these institutions is challenging, this study demonstrates that it is feasible when systematic programs are implemented universally across all prisoners and all prisons within the community.

WED-039

'Hep-MoLo': integrating community co-design and multidisciplinary approach to deliver decentralised liver health screening for Mongolians in London

Emily Martyn[1,2], Jessica Carter[3,4], Naranjargal Dashdorj[5], Indrajit Ghosh[6,7], Enkh-Oyun Amarbayasgalan[8], Tuguldur Gantur[2], Tsolmon Tsogbayar[9], Bilguun Batbayar[10], Tsetsegdemberel Bat-Ulzii Davidson[11], Neil Davidson[12], Anuka Boldbaatar[13], James Rock[6], Khadija Said[1,2], Elizabeth Waddilove[1], Marion Delphin[1], Eleni Nastouli[2,6], Michelle Berkeley[2,6], Rubin Rose-Key[2,6], Toby Morgan[2,6,7], Sherika Ranasinghe[14], Temitope Fisayo[15], Stuart Flanagan[2,7], Julian Surey[2,6], Philippa C Matthews[1,2,6,7]. [1]*The Francis Crick Institute, London, United Kingdom;* [2]*University College London, London, United Kingdom;* [3]*City St George's, University of London, London, United Kingdom;* [4]*Queen Mary University of London, London, United Kingdom;* [5]*Onom Foundation, Ulaanbaatar, Mongolia;* [6]*University College London Hospital, London, United Kingdom;* [7]*Central and North West London NHS Foundation Trust, London, United Kingdom;* [8]*Mongolian Community Organisation, London, United Kingdom;* [9]*Siphox Health, Burlington, United States;* [10]*Parkview Centre for Health & Wellbeing, NHS, London, United Kingdom;* [11]*Buckinghamshire NHS Trust, Stoke Mandeville, United Kingdom;* [12]*Oxford University Hospitals NHS Trust, Oxford, United Kingdom;* [13]*University of Edinburgh, Edinburgh, United Kingdom;* [14]*Barts NHS Foundation Trust, London, United Kingdom;* [15]*Lewisham and Greenwich NHS Trust, London, United Kingdom*
Email: emily.martyn1@crick.ac.uk

Background and aims: Mongolia has the highest liver cancer incidence globally, associated with high prevalence of chronic viral hepatitis infection (hepatitis B, C and D viruses; HBV, HCV, HDV). Worldwide, metabolic dysfunction-associated steatotic liver disease (MASLD) prevalence is increasing, although there are few data from Mongolia. Migrants are disproportionately affected by liver disease, with challenges of navigating unfamiliar healthcare systems and language barriers. We held community-based liver screening events for the London Mongolian community ("Hep-MoLo").
Method: Hep-MoLo (ethics ref: 25/LO/0126) was designed and delivered by a clinical-academic-community multidisciplinary team. Liver screening events were held at a community centre. Mongolian adults (age 18+) were eligible to undergo screening, including a liver health questionnaire, point of care tests for HBV, HCV, HIV and syphilis, cardiometabolic factors (CMF: diabetes, body mass index, blood pressure, lipid profile), controlled attenuation parameter (CAP), transient elastography (TE) and HBV serology. MASLD was defined as CAP >248 dB/m and at least one CMF. Fibrosis was defined as TE > 8 kPa.
Results: During two events in Autumn 2025, 89 participants were screened; 86 agreed for their data to be used in research. Median age was 48 (IQR 39, 53) and 64% (55/86) were female. Ninety-three percent (80/86) were born in Mongolia and lived in the UK for a median of 19 years (IQR 9, 22). Five participants had confirmed HBV (5.8%, 5/86), two with HDV coinfection. Three were not under follow up, requiring referral to specialist care. None had fibrosis by TE, but one had cirrhosis on MRI. Of 79 participants without current HBV infection, 60% (45/79) were anti-HB core positive, 10% (8/79) were anti-HB surface antibody positive only (i.e. vaccinated) and 27% were HBV susceptible (21/79). Four had previous HCV. 43% (36/83) met MASLD criteria. 14% (5/36) had TE >8 kPa and required hepatology referral. Two people living with HBV had MASLD.
Conclusion: Hep-MoLo demonstrates feasibility of community-based liver health screening. High prevalence of HBV, HDV co-infection and MASLD emphasises an unmet need for targeted interventions. Ongoing work includes further screening, qualitative and laboratory research, community engagement, and assessment of longer-term linkage to care. Hep-MoLo supports WHO 2030 targets for viral hepatitis elimination, reduction of obesity and diabetes, and decentralised healthcare delivery.

WED-040

Burden of liver fibrosis and steatosis associated with hepatitis B or C infection in China: a population-based study from the 2020 national serological survey

Tongtong Meng[1], Yu Wang[2], Hui Zheng[3], Jian Li[4], Xiaoning Wu[1], Min Wang[1], Shuyan Chen[1], Yameng Sun[1], Hong You[1], Hui Zhuang[5], Zundong Yin[3], Jidong Jia[1], Yuanyuan Kong[1]. [1]*Beijing Friendship Hospital, Capital Medical University, National Clinical Research Center for Digestive Diseases, State Key Lab of Digestive Health, Beijing, China;* [2]*Beijing, China;* [3]*Chinese Center for Disease Control and Prevention, Beijing, China;* [4]*National Center for AIDS/STD Control and Prevention, Chinese Center for Disease Control and Prevention, Beijing, China;* [5]*Peking University Health Science Center, Beijing, China*
Email: kongyuanyuan2000@163.com

Background and aims: The burden of liver fibrosis and steatosis associated with hepatitis B virus (HBV) and hepatitis C virus (HCV) infections in China remains to be quantified. We aimed to estimate the prevalence of HBV or HCV infection with fibrosis and steatosis to inform national elimination strategies.

Method: This study was conducted among individuals aged 15–69 years from the 2020 National Serological Survey of Viral Hepatitis. Liver fibrosis and steatosis were assessed using transient elastography, and the weighted prevalence of each condition was estimated among individuals with HBV or HCV infection.
Results: The final analysis included 4,236 people with HBV infection and 122 with HCV infection out of the 69,351 participants for the serological survey. The weighted population prevalence of HBV infection with ≥F2 fibrosis was 0·63% (95% CI 0·52–0·77), corresponding to an estimated 6·08 million individuals nationwide. For HCV, the weighted prevalence of ≥F2 fibrosis was 0·05% (95% CI 0·03–0·08), representing 0·48 million individuals. The weighted proportions of concomitant hepatic steatosis (≥S1) were 34·85% among individuals with HBV infection and 42·43% among those with HCV infection.
Conclusion: Despite declining incidence rates, China continues to bear a substantial burden of advanced liver disease among populations affected by viral hepatitis, increasingly compounded by the rising prevalence of hepatic steatosis. Achieving the 2030 elimination goal will require proactive case finding and improved linkage to care for individuals with advanced fibrosis and steatosis.

WED-046
Budget impact analysis of the GeneXpert® system for hepatitis C virus infections screening in addiction care and prevention centers and prisons in France
Veronique Loustaud-Ratti[1], Henri Lesage[2], Sandrine Francois[1], Quentin Berkovitch[2], Inès Messai[3,4]. *[1]Chu Limoges, Limoges, France; [2]PHE-Cencora, Paris, France; [3]Cepheid, Maurens-Scopont, France; [4]Cepheid, Paris, France*
Email: ines.messai@cepheid.com

Background and aims: Hepatitis C virus (HCV) infections represent a critical public health challenge in France, particularly in high-risk populations such as prisoners and individuals attending addiction care and prevention centers (CSAPA), where active HCV infection (RNA+) prevalence reaches 1.3% and 16.3%, respectively—significantly higher than in the general population. Current standard-of-care (SoC) diagnostic strategy faces limitations, including logistical barriers and delays in diagnosis, which hinder timely treatment initiation. The *GeneXpert®* system enables a fast molecular diagnostic on demand solution through automated RT-PCR *Xpert® HCV VL Fingerstick*, enabling potential same-day diagnosis and linkage to care. This study evaluates the budget impact of implementing "test and treat" strategy using *Xpert® HCV VL Fingerstick* point of care (POC) screening in French prisons and CSAPA, compared to SoC. The analysis assesses the impact of a "test and treat" approach, aiming to achieve the World Health Organization's (WHO) 2030 elimination targets.
Method: A budget impact model simulated epidemiological and economic outcomes over 20 years from the French National Health Insurance perspective, comparing SoC to "test and treat" strategy. Data were sourced from literature, epidemiological and health insurance databases. The study population included prisoners and individuals attending CSAPA.
Results: The "test and treat" strategy could increase HCV detection rates to 89.5% in infected prisoners (vs. 51.6% SoC) and 84.2% in infected CSAPA patients (vs. 9.5% SoC), resulting in an 87% increase in treated prisoners and a nearly 5-fold increase in treated CSAPA patients. Screening costs would rise by €13.7M in prisons and €35.1M in CSAPA over 20 years compared to SoC. However, treatment costs would decrease by €3.6M in prisons, while increasing by €480M in CSAPA due to higher treatment uptake. These costs are offset by substantial reductions in long-term chronic HCV complication management costs of €110.7M in prisons and €688.2M in CSAPA, resulting in net savings of €100.6M and €172.7M, respectively, suggesting significant economic benefits alongside improved patient outcomes.
Conclusion: "Test and treat" strategy using *Xpert® HCV VL Fingerstick* represents a cost-saving and effective strategy for HCV screening in high-prevalence settings, supporting WHO elimination goals by improving detection and treatment rates in France.

WED-047
Progress towards hepatitis C virus elimination in English prisons – 7 year outcomes on a multi-stakeholder project
Julie Henderson[1], Michelle Storer[2], Craig Thompson[3], Arran Ludlow-Rhodes[4], Andrew Milner[4], Christine Taylor[4], Louise Missen[4]. *[1]Practice Plus Group, Reading, United Kingdom; [2]Oxleas NHS Foundation Trust, London, United Kingdom; [3]Spectrum Community Healthcare CIC, Wakefield, United Kingdom; [4]Gilead Sciences Ltd, London, United Kingdom*
Email: julie.henderson@practiceplusgroup.com

Background and aims: Following the World Health Organization's (WHO) plans to eliminate viral hepatitis by 2030, National Health Service England (NHSE) announced plans to eliminate Hepatitis C (HCV) in England by 2025, with prisons being a key focus area to achieve this goal. Gilead Sciences formed partnerships with Practice Plus Group (PPG) in May 2019 and Oxleas NHS Foundation Trust and Spectrum Community Health CIC in 2021 with the aim to optimise HCV test and treat in their prison settings. Here we present data on testing rates, RNA positivity and treatment starts over this 7 year project.
Method: Regional BBV Leads and Gilead Medical Scientists worked with prison and HCV stakeholders including the Hepatitis C Trust to optimise test and treat pathways for new prison admissions. Whole prison test and treat events were also conducted in targeted prisons to ensure testing of residents who were incarcerated before these optimisations were implemented. Virtual BBV training sessions have been run on a monthly basis available to all providers to raise awareness of BBV testing and treatment pathways and challenge stigma. Anonymised data has been collected from all providers through electronic patient records and aggregated.
Results: Data from all providers are aggregated unless otherwise specified. Between May 2019-November 2025, a total of 342,837 HCV antibody tests were completed out of 475,399 offered (uptake of 72.1%) with 6,156 patients being initiated on treatment for HCV. Reception HCV testing uptake has increased since 2019 from 40.9% to 72.5% in 2025 despite reduction in staff resource over the previous 2 years. Total prison population HCV antibody and RNA prevalence data was only available for PPG; a consistent decline was seen in RNA positivity between 2019 (2%) to 2025 (0.3%) with antibody prevalence remaining stable (median 5.8%, range 5.2%-6.5%). Full data at 7 years will be available for the poster presentation.
Conclusion: This project demonstrates the value of a co-ordinated multi-stakeholder approach to BBV screening and linkage-to-care in prison settings and shows that BBV screening can be successfully maintained on-site when specialist regional staff support is reduced. Reception testing rates rose to 72.5%, and RNA prevalence declined to 0.3%, demonstrating progress towards NHSE's elimination goal. Continued optimisation and training remain essential to sustain these achievements.

Rare liver diseases (including paediatric and genetic) – Clinical

TOP-297
Hepatocyte-intrinsic programs drive vascular pathobiology in Porto-sinusoidal vascular disorder and are modelled in organoids
Hasanka Madubashetha[1,2,3,4,5], Raquel Ferrer-Lorente[2], Aina Anton[1,2,3,4,5,6], Rosa Montañés[1,2,3,4,5], Héctor García-Calderó[1,2,3,4,6], Sarah Shalaby[1,2,3,4,6], Andreea Fodor[1,7], Juan Carlos García-Pagán[1,2,3,4,5,6], Genís Campreciós[1,2,3,4,6],

Pau Sancho-Bru[2,5,6], Virginia Hernández-Gea[1,2,3,4,5,6]. [1]*Barcelona Hepatic Hemodynamic Laboratory, Liver Unit, Hospital Clínic, Institut d'Investigacions Biomèdiques August Pi i Sunyer (IDIBAPS), Barcelona, Spain;* [2]*Fundació de Recerca Clínic Barcelona-Institut d'Investigacions Biomèdiques August Pi i Sunyer (FRCB-IDIABPS), Barcelona, Spain, Barcelona, Spain;* [3]*Health Care Provider of the European Reference Network on Rare Liver Disorders (ERN-RareLiver), Barcelona, Spain;* [4]*Centro de referencia del Sistema nacional de salud en enfermedad hepática compleja (CSUR), Barcelona, Spain;* [5]*Faculty of Medicine and Health Sciences, University of Barcelona, Barcelona, Spain;* [6]*Centro de Investigación Biomédica Red de Enfermedades Hepáticas y Digestivas (CIBEREHD), Madrid, Spain;* [7]*University of Medicine and Pharmacy 'Iuliu Hatieganu," Gastroenterology Department, 3rd Medical Clinic, Cluj-Napoca, Romania*
Email: vihernandez@clinic.cat

Background and aims: Porto-Sinusoidal Vascular Disorder (PSVD) is a rare vascular liver disease of unknown etiology characterized by portal and sinusoidal remodelling and endothelial dysfunction primarily affecting intrahepatic vasculature. However, contribution of hepatocytes in PSVD remains unclear. Preliminary single-cell RNA sequencing (scRNAseq) in PSVD liver biopsies revealed dysregulated pathways in hepatocytes, suggesting their contribution to PSVD pathophysiology. In the absence of animal models that sufficiently capture human disease heterogeneity and complexity, we aimed to determine whether hepatocyte-enriched, patient-derived organoids provide a physiologically relevant humanized platform to study parenchymal cell contributions to PSVD.
Method: Transjugular liver needle biopsies of patients with PSVD and individuals with histologically normal livers (HNL) were used to generate epithelial organoids that originated from progenitor cells in the biopsy, under hepatocyte-directed culture media and characterised by immunofluorescence. Bulk RNA sequencing was performed on organoids (PSVD vs HNL) and compared with hepatocyte (PSVD vs HNL) gene expression profiles derived from scRNAseq of biopsies, aggregated at the hepatocyte level.
Results: Immunofluorescence demonstrated that PSVD organoids exhibited progenitor ($SOX9^+$, $TROP2^+$), epithelial ($KRT7^+$, $ECAD^+$) and hepatocytic (ALB^+, $MRP4^+$) features and morphology comparable to HNL organoids. Comparison of gene expression patterns showed that 54.4% of disease-associated pathways upregulated in hepatocytes from PSVD liver biopsies were preserved in PSVD organoids. Consistent with pathways previously identified as key in PSVD pathophysiology, mitochondrial function, extracellular matrix remodelling, vasculature, inflammation, and coagulation showed >85% concordant upregulation between hepatocytes and organoids. Bioenergetic pathways, including oxidative phosphorylation and citric acid cycle, also exhibited similar upregulation in PSVD organoids.
Conclusion: Using the first humanised organoid model of PSVD, we show that hepatocytes intrinsically contribute to PSVD-associated transcriptional programs and provide a mechanistically relevant platform to interrogate hepatocyte-endothelial crosstalk and may inform future therapeutic strategies.

TOP-309-YI

Genetic testing reveals hidden genetic diseases in adult patients with idiopathic chronic cholestasis and chronic hepatitis with unknown aetiology

Ignasi Olivas[1,2], Meritxell Jodar[3], Pinelopi Arvaniti[1,2,4], María Del Barrio[5], Inmaculada Sanchez[5], Helena Hernández Evole[1,2], Anna Pocurull Aparicio[1,2], Sabela Lens[1,2,4], Zoe Mariño[1,2,2], Xavier Forns[1,2,4,6], Celia Badenas[3], Álvaro Díaz-González[5], María Carlota Londoño[1,2,4,6], Sergio Rodriguez-Tajes[1,2,4]. [1]*Liver Unit, Hosptial Clínic Barcelona, Institut d'Investigació Biomedica August Pi y Sunyer (IDIBAPS), Barcelona, Spain;* [2]*Fundació de Recerca Clínic Barcelona-Institut d'Investigacions Biomèdiques August Pi Sunyer (FRCB-IDIBAPS), Barcelona, Spain;* [3]*Biochemistry and Molecular Genetics Department, Hospital Clínic Barcelona, Barcelona, Spain;* [4]*Centro de Investigación Biomédica en Red Enfermedades Hepáticas y Digestivas (CIBEREHD), Barcelona, Spain;* [5]*Gastroenterology and Hepatology Department, Clinical and Translational Research in Digestive Diseases Group, Valdecilla Research Institute (IDIVAL), Marqués de Valdecilla University Hospital, Santander, Spain;* [6]*Universitat de Barcelona, Barcelona, Spain*
Email: ignasiolivasalberch@gmail.com

Background and aims: This study assessed the diagnostic utility of genetic testing using whole exome sequencing (WES) in adult patients with idiopathic chronic cholestasis (ICC), idiopathic chronic hepatitis (ICH), low phospholipid–associated cholelithiasis (LPAC), and recurrent cholestasis (RC).
Method: This prospective cohort study included 132 adults with ICC, ICH, LPAC or RC who underwent WES. Liver disease–related gene variants were reported according to Online Mendelian Inheritance in Man (OMIM). Variants were classified using the American College of Medical Genetics and Genomics criteria, reporting pathogenic (P), likely pathogenic (LP), and variants of uncertain significance (VUS). A definite genetic diagnosis was defined by the presence of P or LP variants or rare damaging VUS consistent with the phenotype and inheritance pattern.
Results: Most patients were women (63%), with a median age of 49 years (IQR 39–55) at WES and 34 years (IQR 25–43) at disease onset. A family history of liver disease of unknown aetiology was reported in 23 patients (17%), intrahepatic cholestasis of pregnancy in 20 (15%), and pruritus in 23 (17%). Overall, 63 patients (48%) carried at least one variant, with 66 variants identified in 32 genes. A definitive diagnosis was established in 20 patients (15%), whereas 26 (20%) carried variants with a possible contribution to the phenotype. Ten patients were misdiagnosed before WES was performed. Among 99 patients (75%) with ICC, 39 (39%) had variants, 4 had a definitive diagnosis (2 with pathogenic JAG1 variants consistent with Alagille syndrome and 2 with HNF1B variants), and 19 had variants with possible phenotypic contributions (15 in PFIC-related genes, 2 in NOTCH, and 2 in HNF1B). Among 17 patients (7%) with ICH, 9 (53%) carried variants; 4 had a definitive diagnosis (2 with homozygous P variants in ACOX2 and 2 with complete HNF1B deletions). Among 14 patients (11%) with LPAC, 12 (86%) carried variants, with 10 definitive diagnoses, all involving ABCB4 gene. All 3 patients (2%) with RC carried variants; 2 had definitive diagnoses (1 homozygous ATP8B1 and 1 homozygous ABCB11).
Conclusion: Genetic variants can account for a significant proportion of cases of idiopathic cholestasis and chronic hepatitis. Therefore, genetic testing should be conducted early in undiagnosed patients following standard diagnostic procedures to prevent unnecessary treatments.

TOP-310-YI

Two-fold improvement of thrombosis regression rate after implementation of a multidisciplinary treatment protocol for acute superior mesenteric vein thrombosis

Sophie Ciere[1], Kay Pieterman[2], Mandy Lauw[3], Jeroen de Jonge[1], Eva Heerschap[4], Roeland de Wilde[1], Francois Willemssen[2], Diederik Bijdevaate[2], Raoel Maan[4], Sarwa Darwish Murad[4]. [1]*Erasmus Medical Center Rotterdam, Transplant Institute, Department of Surgery, Division of HPB and Transplant Surgery, Rotterdam, Netherlands;* [2]*Erasmus Medical Center Rotterdam, Department of Radiology and Nuclear Medicine, Rotterdam, Netherlands;* [3]*Erasmus Medical Center Rotterdam, Department of Hematology, Rotterdam, Netherlands;* [4]*Erasmus Medical Center Rotterdam, Transplant Institute, Department of Gastroenterology and Hepatology, Rotterdam, Netherlands*
E-mail: s.ciere@erasmusmc.nl

Background and aims: The optimal treatment for acute superior mesenteric vein thrombosis (SMVT), a rare and severe condition with risk of acute mesenteric ischemia (AMI), remains controversial. This

study aims to evaluate our multidisciplinary treatment protocol, implemented in 2019.
Method: Patients admitted with acute SMVT, excluding cirrhotic, malignant or iatrogenic causes, were included (between 2010–2018 historic cohort (HC); 2019–2024 protocol cohort (PC)). All patients received therapeutic anticoagulation (AC). The PC received systematic daily assessment for AMI (predefined CT criteria) and bowel necrosis (CT criteria with peritonitis and/or sepsis). Endovascular recanalization (EVR; i.e. repeated thrombosuction, angioplasty and continuous local thrombolysis for 24–72 h) was performed upon suspicion of AMI, while suspicion of bowel necrosis prompted emergency surgery. Management in HC was non-protocolized. Bowel necrosis, mortality, bleeding, thrombosis regression (any regression) and complete recanalization rates were compared.
Results: In 30 PC patients with predominantly complete (83%) SMVT and concomitant (87%) portal vein thrombosis (PVT), immediate AC prevented AMI in 23%. The other 77% developed AMI and underwent EVR. In total, 37% required bowel resection. Compared to HC (n = 37) with similar clinical presentation, EVR was more utilized (77% vs 11%; p < .001), while AC (both 100%) and bowel necrosis (37% vs 22%; p = 0.17) were similar. Hospital stay (10 vs. 7d; p = 0.24), ICU stay (4,5 vs 6d; p = 0.66) and bleeding after EVR (52% vs 50%; p = 1.00) were similar, while surgical bleeding was lower in the PC (12% vs 57%; p = 0.02). Median follow-up was 582 days (range 4–5093). In-hospital mortality (13% vs 8%; p = 0.69) and 1-year survival (83% vs 92%; p = 0.24) were comparable. However, PC showed significantly higher 2-year regression rates of SMVT (72% vs 33% at 2y; p < .001) and PVT (68% vs 37%; p = 0.003) and, albeit non-significant, higher 2-year complete recanalization rates in SMVT (41% vs 26%; p = 0.19) and PVT (52% vs 24%; p = 0.06). Moreover, clinically significant portal hypertension developed less often after EVR than AC alone (40% vs 69%; p = 0.04).
Conclusion: Protocolized multidisciplinary management of SMVT resulted in more frequent use of EVR without increased adverse events. While mortality and bowel necrosis rates remained stable, a two-fold increased rate of regression and complete recanalization of SMVT and PVT was observed. Future studies with larger groups of patients are needed to confirm our results.

THU-251
Cuproptosis related atherosclerosis in Wilson's disease

Soner Altın[1], Sait Kayalı[2], Ahmet Oğuz Çelik[1], Gamze Kemeç[1], Zülal İstemihan[3], Bilger Çavuş[4], Aslı Çifcibaşı Örmeci[5], Filiz Akyuz[4], Fatih Beşışık[4], Sabahattin Kaymakoğlu[4], Mesut Bulakçı[6], Kadir Demir[4]. *[1]Istanbul Faculty of Medicine Department of İnternal Medicine, İstanbul, Türkiye; [2]Istanbul Faculty of Medicine Department of Radiology, İstanbul, Türkiye; [3]Niğde Ömer Halis Demir Training and Research Hospital, Niğde, Türkiye; [4]Istanbul Faculty of Medicine Department of İnternal Medicine, istanbul, Türkiye; [5]Göztepe Memorial Hospital, İstanbul, Türkiye; [6]Istanbul Faculty of Medicine Department of Radiology, istanbul, Türkiye*
E-mail: dr_bilgercavus@yahoo.com

Background and aims: Wilson's Disease (WD) is characterized by the accumulation of excess copper in various tissues, primarily the liver and brain, due to a defect in copper excretion via the bile ducts. Cuproptosis is a type of programmed cell death triggered by elevated copper levels. It has been demonstrated that elevated copper levels contribute to inflammatory vascular diseases such as atherosclerosis through various mechanisms, including oxidative stress and proteotoxic effects. In this study, we aimed to investigate the effect of copper levels on the development of atherosclerosis in patients diagnosed with WD.
Method: Two groups consisting of 92 patients with WD and 24 healthy controls were included in the study. Demographic, clinical, laboratory, and anthropometric measurements were recorded for all participants. The presence of atherosclerosis was evaluated by examining plaque presence, flow patterns, peak systolic velocity (PSV), and end-diastolic velocity (EDV) parameters in both carotid and femoral arteries.
Results: The two groups were similar in terms of demographic and anthropometric measurements. The results showed that the two groups were largely similar, but the EDV value in the left common femoral artery was found to be statistically significantly lower in the patient group compared to the control group (p = 0.041). It shows that the EDV value in the mixed (hepatic and neurological) involvement group is significantly lower than those in both the neurological and hepatic groups (p = 0.038). In addition, the left common femoral artery flow value was found to be significantly higher in the patient group compared to the control group (p = 0.029). A positive correlation was found between the intima-media thickness in both the carotid and femoral arteries and the disease period.
Conclusion: These findings strongly support that WD may be associated with a progressive vasculopathy. The earlier the disease onset and the longer its duration, the more blood flow velocities in large arteries decrease and the more arterial wall thickness increases. These results suggest that one of the underlying mechanisms of increased cardiovascular risk in WD may be progressive arterial involvement related to disease duration.

THU-252
Liver stiffness in amyloid light-chain amyloidosis: interest in diagnosis and prognosis

Paul Carrier[1], Veronique Loustaud-Ratti[1], Jean-François Cadranel[2], Céline Rigaud[1], Bienvenue Randrianarivo[1], David Lavergne[1], Laurent Alric[3], Aurore Baron[4], Eric Nguyen-Khac[5], Arnaud Pauwels[6], Louis Bettan[7], Xavier Causse[8], Honoré Zougmoure[9], Abdelali El Kharrazi[2], Marilyne Gratien[1], Cypierre Anne[1], Murielle Roussel[1], Arnaud Jaccard[1]. *[1]Chu Limoges, Limoges, France; [2]ghspo, Creil, France; [3]Chu Purpan, Toulouse, France; [4]Hôpital Paul-Brousse, Villejuif, France; [5]Chu Amiens-Picardie, Amiens, France; [6]Centre Hospitalier de Gonesse, Gonesse, France; [7]Centre Hospitalier Intercommunal de Villeneuve-Saint-Georges Lucie & Raymond Aubrac, Villeneuve-Saint-Georges, France; [8]Centre Hospitalier Régional d'Orléans, Orléans, France; [9]ghpso, Creil, France*
E-mail: paul.carrier@chu-limoges.fr

Background and aims: The liver is frequently involved in amyloidosis. Diagnosis usually relies on hepatomegaly and elevated alkaline phosphatase levels. Its diagnostic and, in particular, its follow-up value remain to be clarified.
Method: We assessed liver stiffness (LS), measured by FibroScan®, at diagnosis in a retrospective multicenter cohort of patients with amyloid light-chain amyloidosis. Patients were classified as having liver involvement only (group 1), heart involvement only (group 2), both (group 3), or neither (group 4). In a prospective monocentric cohort, we evaluated changes in LS over time.
Results: In the retrospective cohort of 56 patients, median LS values were 75 kPa (17.5–75) in group 1 (n = 14), 11.6 kPa (6.5–21.3) in group 2 (n = 17), 28.8 kPa (15.7–70) in group 3 (n = 13), and 6.4 kPa (4.9–7.5) in group 4 (n = 12). The ROC curve comparing patients with liver involvement defined by consensus criteria and LS values identified an optimal cut-off of 13.6 kPa, with 92% sensitivity and 71% specificity. In the prospective cohort of 19 patients, median LS decreased from 51.4 to 4.5 kPa in group 1 (91% reduction), from 9 to 6.7 kPa in group 2 (26% reduction), from 28.8 to 6 kPa in group 3 (79% reduction), and from 6.8 to 5.5 kPa in group 4 (19% reduction).
Conclusion: LS measurement is useful for diagnosing hepatic involvement in amyloidosis. A threshold of 13.6 kPa, in the absence of other specific etiologies, could be incorporated into current diagnostic criteria. Moreover, a reduction in LS greater than 50% may serve as a marker of hepatic recovery.

THU-253

Study of the prevalence of hereditary hemochromatosis (HFE) and secondary causes of hiperferritinemia in patients participating in a bloodletting programme

Agustin Castiella[1], Iñigo Garaizabal[1], Ane Arteaga[1], Iratxe Urreta[1], Maria Jose Sanchez Iturri[1], Eva María Zapata[1]. [1]*Hospital Universitario Donostia, Donostia, Spain*
E-mail: agustincastiella@yahoo.es

Background and aims: Bloodletting is the cornerstone of treatment for patients with hereditary haemochromatosis (C282Y/C282Y). Its usefulness in patients with hyperferritinaemia (HF) and moderate iron overload remains controversial. In recent years, HF due to metabolic syndrome and obesity has increased significantly. Recently, a French multicentre study involving 1059 patients undergoing bloodletting treatment found that HH is overdiagnosed as an indication for bloodletting. The aims of our study were: to study the causes and indications for bloodletting in patients undergoing treatment and to determine the prevalence of HH and other causes of HF.
Method: The study period was January 2022 to May 2024. Review of the medical records of patients undergoing venesections indicated by the Gastroenterology Department. We studied the reason for the indication (HH or not), whether it was correct, other causes of HF (alcohol, metabolic syndrome, obesity), analysis with iron parameters, genetic study of HFE gene mutations (C282Y/C282Y and others), and hepatic iron concentration measured by MR.
Results: 179 patients were included. 48 women and 131 men. The median age was 55. In the homozygous C282Y group, it was 49.5 and in the rest 60 (p: 0.0019), requiring earlier treatment in the HH group. The indication for bloodletting was correct (HH with significant hepatic iron overload) in 48% of cases. HFE mutations: C282Y/C282Y 70 (39.55%), C282Y/H63D 50 (28.25%), H63D/H63D 21 (11.86%). Patients with metabolic syndrome and hyperferritinemia (33%) were placed on a bloodletting programme. Obesity (BMI>30) was present in 37.76% of patients. A significant alcohol consumption was present in 38.22% of patients. MR: only 25.50% of patients had elevated iron overload (>80 mmol/g), with 47.65% having moderate overload (>36<80). CHH was significantly higher in C282Y/C282Y patients (101.22 vs 51.98) (p: 0.0000). Of the non-homozygous patients, only 11% had high overload. Sixty per cent were C282Y/H63D. Of the patients who had been treated with >20 phlebotomies, 21 were homozygous and 8 were non-homozygous. Laboratory: Serum ferritin (p:0.0268), TSI (p:0.0000) and Iron (p:0.0000) values were significantly higher in patients with HH (C282Y/C282Y).
Conclusion: More than half of patients treated with bloodletting for suspected HH do not have this disease and most likely do not require such treatment. We must re-evaluate patients undergoing chronic bloodletting, as a high percentage do not benefit from it.

THU-254

Genotypic spectrum and clinical presentation of Wilson disease in a Brazilian cohort

Maria Chiara Chindamo[1], Ida Vanessa Schwartz[2], Gabriel Quintana[2], Paulo Sgobbi[3], Thais Guaraná[4], Vivian Rotman[1], Cibele Franz[5], Luciana Agoglia[4], Renata Perez[1]. [1]*Federal University of Rio de Janeiro, Rio de Janeiro, Brazil;* [2]*Federal University of Rio Grande do Sul, Porto Alegre, Brazil;* [3]*Federal University of São Paulo (UNIFESP), Sao Paulo, Brazil;* [4]*Federal Fluminense University, Rio de Janeiro, Brazil;* [5]*UNIRIO, Rio de Janeiro, Brazil*
E-mail: mchiara@terra.com.br

Background and aims: Wilson disease (WD) is an autosomal recessive disorder caused by pathogenic variants in the *ATP7B* gene. Although more than 2700 variants have been described worldwide, data on their distribution and genotype–phenotype association in Brazilian populations remain limited. Identifying regional variant patterns may improve diagnostic accuracy and cost-effectiveness. We evaluated the frequency of *ATP7B* variants in a Brazilian WD cohort and their association with clinical phenotypes.
Method: Next-generation sequencing covering all 21 exons and exon–intron junctions of the *ATP7B* gene was performed (Mendelics Labs) in WD patients from southeastern and southern Brazil. Variants were classified as pathogenic, likely pathogenic (LP), or variants of uncertain significance (VUS) according to ClinVar. Demographic data and clinical presentation were collected and correlated with genotypes.
Results: Forty-four patients were included (55% female; mean age 29 ± 12 years). Combined hepatic and neurological manifestations occurred in 45%, isolated hepatic in 41%, isolated neuropsychiatric in 7%, and 7% were asymptomatic. Thirty-three variants were identified: 61% pathogenic, 21% VUS, and 18% LP. Most patients were compound heterozygous (84%), followed by homozygous (12%) and simple heterozygous (4%). The most frequent variants were c.3402delC (18%), c.3818C>T (14%), and c.2123T>C (11%), predominantly associated with hepatic manifestations, with or without neurological involvement. Age at symptom onset did not differ by zygosity (19, 20, and 21 years for homozygous, compound heterozygous, and simple heterozygous, respectively; p = 0.94). Carriers of at least one c.3402delC allele had lower ceruloplasmin levels compared with other variants (median 3.0 vs 7.0 mg/dL; p = 0.025), without differences in age at symptom onset (p = 0.93**)**. Homozygous deletion of exon 2 was associated with severe neurological disease. VUS included c.2145C>T (6%), c.2755C>T (6%), c.1552T>C (3%), c.2866–6T>G (3%), c.2562G>C (3%), c.4388A>G (3%), and c.3188C>T (3%). LP variants were c.2072G>T (3%), c.3551T>C (3%), exon 3–4 deletion (6%), c.3071_3072delTG (3%), c.399G>A (3%), and c.3517G>A (3%).
Conclusion: The variants c.3402delC, c.2123T>C, and c.3818C>T were the most prevalent in this Brazilian cohort. Multiple VUS were identified in confirmed WD cases. Marked genotypic heterogeneity was observed, limiting robust genotype–phenotype associations.

THU-255

Dynamic changes in liver stiffness during anti-copper therapy in wilson disease: a longitudinal cohort study

Maria Chiara Chindamo[1], Luciana Agoglia[2], Thais Guaraná[2], Vivian Rotman[1], Maria Alice Madureira[1], Ana Carolina Cardoso[1], Renata Perez[1]. [1]*Federal University of Rio de Janeiro, Rio de Janeiro, Brazil;* [2]*Federal Fluminense University, Rio de Janeiro, Brazil*
E-mail: mchiara@terra.com.br

Background and aims: Liver stiffness (LS) measurements may be influenced by factors beyond fibrosis, including inflammation and intrahepatic deposits. In Wilson disease (WD), hepatic copper accumulation may affect LS, but longitudinal data during treatment are limited. We aimed to evaluate changes in LS assessed by transient hepatic elastography (THE) during anti-copper therapy in patients with different clinical presentations of WD.
Method: Patients with confirmed WD (Leipzig score ≥4) receiving chelation or zinc therapy and followed between 2014 and 2025 were included. Dynamic changes in LS were evaluated in patients who underwent at least two valid transient elastography examinations (FibroScan®, Echosens), with a minimum interval of one year. Liver-transplanted patients were excluded. Changes in liver stiffness were analyzed according to the clinical presentation of the disease.
Results: Thirty-one patients were included: 55% male, mean age of 29 ± 11 years at first THE, and a median disease duration of 12 years (IQR 4.8–17.0). Clinical presentation was isolated hepatic in 58%, combined hepatic–neurological in 35%, and isolated neurological in 7%. Most patients (90%) received chelation therapy, mainly penicillamine. The median of LS at baseline was 7.5 kPa (IQR 4.9–14.0), being 12.0 kPa (IQR 6.0–18.2) in patients with combined hepatic–neurological presentation, compared with isolated hepatic (6.6 kPa, IQR 4.7–8.7) and isolated neurological presentations (4.4 kPa) (p = 0.105). Patients with cirrhosis (n = 12) had significantly higher baseline LS

than non-cirrhotic patients (14.1 vs 5.3 kPa; p = 0.001). Eighteen patients had longitudinal LS assessment over a median follow-up of 2.8 years (IQR 1.9–5.1). Liver stiffness decreased significantly from 8.3 kPa (IQR 6.1–16.6) to 5.3 kPa (IQR 4.3–11.8; p <0.001), with reductions observed both in cirrhotic (14.0 to 12.3 kPa; p = 0.001) and non-cirrhotic patients (5.5 to 4.5 kPa; p = 0.026). Overall, liver stiffness reduced in 89% of patients. One patient showed marked LS reduction with resolution of esophageal varices.
Conclusion: Liver stiffness decreased in most patients with WD during anti-copper therapy, including those with cirrhosis. These findings suggest that elevated LS in WD may reflect reversible copper-related factors rather than fibrosis alone, supporting THE as a non-invasive tool for monitoring treatment response.

THU-256-YI

Diagnostic performance of a targeted next-generation sequencing cholestasis-gene panel in adults with unexplained cholestatic liver disease: results from a multicenter Italian cohort study

Laura Cristoferi[1], Daphne D'Amato[2], Francesca Terracciani[3], Luisa Ronzoni[4], Piero Colombatto[5], Armando Curto[6], Sara Labanca[7], Carla De Benedittis[8], Silvia Nardelli[9], Barbara Coco[5], Edvige Mensi[2], Alessio Gerussi[1,2], Federica Malinverno[1], Erica Nicola Lynch[6], Domenico Montecalvo[9], Luigi Casella[9], Marco Distefano[10], Giuliano Alagna[11], Mauro Viganò[12], Anna Cereda[13], Francesca Bertola[13], Antonino Caserta[14], Maurizia Brunetto[5], Vincenza Calvaruso[14], Cristina Rigamonti[8], Domenico Alvaro[9], Andrea Galli[6], Edoardo Giannini[7], Luca Valenti[15], Marco Carbone[2], Pietro Invernizzi[1], Umberto Vespasiani-Gentilucci[3]. *[1]Division of Gastroenterology, Center for Autoimmune Liver Diseases, European Reference Network on Hepatological Diseases (ERN RARE-LIVER), Fondazione IRCCS San Gerardo dei Tintori, Monza, Italy; [2]Department of Medicine and Surgery, University of Milano-Bicocca, Monza, Italy; [3]Research Unit of Hepatology, Department of Medicine and Surgery, Università Campus Bio-Medico of Rome, Clinical Medicine and Hepatology Unit, Fondazione Policlinico Universitario Campus Bio-Medico, Rome, Italy; [4]Precision Medicine Lab, and Omics Core Lab, Biological Resource Centre Unit, Department of Transfusion Medicine, Fondazione IRCCS Ca' Granda Ospedale Maggiore Policlinico, Milan, Italy, Milan, Italy; [5]Department of Clinical and Experimental Medicine, University of Pisa and Hepatology Unit, University Hospital of Pisa, Pisa, Italy, Pisa, Italy; [6]Gastroenterology Research Unit, Department of Experimental and Clinical Biomedical Sciences "Mario Serio", University of Florence, Florence 50134, Tuscany, Italy, Florence, Italy; [7]Gastroenterology Unit, Department of Internal Medicine, University of Genoa, IRCCS Ospedale Policlinico San Martino, Genoa, Italy, Genoa, Italy; [8]Department of Translational Medicine, Università del Piemonte Orientale, Novara, Italy, Novara, Italy; [9]Department of Translational and Precision Medicine, Policlinico Umberto I, Sapienza University of Rome, Rome, Italy, Rome, Italy; [10]Department of Hepatology, ASP 8, Siracusa, Italy; [11]SSD Epatologia AOU di Sassari, Italy, Sassari, Italy; [12]Gastroenterology, Hepatology and Transplantation Division, ASST Papa Giovanni XXIII, ASST Papa Giovanni XXIII, Piazza OMS, 1, Bergamo, Italy, Bergamo, Italy; [13]Medical Genetics, Fondazione IRCCS San Gerardo Dei Tintori, Monza, Italy, Monza, Italy; [14]Gastroenterology and Hepatology Unit, Department of Health Promotion Sciences Maternal and Infantile Care, Internal Medicine and Medical Specialities, PROMISE, University of Palermo, Italy, Palermo, Italy; [15]Precision Medicine Lab, and Omics Core Lab, Biological Resource Centre Unit, Department of Transfusion Medicine, Fondazione IRCCS Ca' Granda Ospedale Maggiore Policlinico, Milan, Italy; Department of Pathophysiology and Transplantation, University of Milan, Milan, Italy, Milan, Italy*
E-mail: l.cristoferi@campus.unimib.it

Background and aims: Cholestatic liver diseases are heterogeneous and may remain unexplained despite extensive work-up. Genetic variants in bile acid transport and hepatobiliary homeostasis may contribute. We assessed the diagnostic yield of a cholestasis-targeted next-generation sequencing (NGS) panel in a multicentre adult cohort.
Method: Adult patients from 8 Italian centres with cholestatic phenotypes and no alternative/prior genetic diagnosis were included: chronic unexplained cholestasis (CUC), low-phospholipid–associated cholelithiasis (LPAC), intermittent cholestasis (IC), drug-induced cholestasis (DIC), intrahepatic cholestasis of pregnancy (ICP). Clinical, biochemical, imaging and histology data were collected. A 77-gene panel of PFIC (progressive familial intrahepatic cholestasis), non-PFIC cholestasis genes, ciliopathies and inborn errors of metabolism was analysed. Variants were classified by ACMG as pathogenic/likely pathogenic (P/LP) or variants of uncertain significance (VUS) - sub-tiered by the ACGS framework. Genetic diagnosis required P/LP variants consistent with phenotype and inheritance; a possible contribution required monoallelic P/LP variant in recessive genes or warm/hot VUS in disease-related genes.
Results: Among 263 patients, phenotypes were CUC in 196 (74.5%), LPAC in 26 (9.9%), IC 20 (7.6%), DIC 12 (4.5%), ICP 9 (3.4%). Overall, 417 variants across 74 (96.1%) genes were identified in 253 (96.2%) patients: 57 (13.7%) were in PFIC genes. Of these, 64 (15.34%) were P/LP and 352 (84.41%) were VUS. Genetic diagnosis was confirmed in 11 (4.2%) patients, while a possible genetic contribution was identified in 76 (28.9%): 50 (67.6%) with monoallelic P/LP variants in recessive genes; 24 (32.4%) with ACGS warm/hot VUS in disease-related genes. Among contributing variants, 29 (39.2%) involved PFIC genes. PFIC-related variants were associated with female sex (p < 0.05), higher serum bile acids (p < 0.01) and LPAC/DIC/ICP phenotypes (p < 0.05), with more MRCP abnormalities and hepatobiliary complications (p < 0.01). Pruritus tended to be more common (p = 0.055) whereas cirrhosis was less frequent (p < 0.05).
Conclusion: In adults with unexplained cholestasis, a targeted NGS panel provided a definitive genetic diagnosis in 4.2% and contributory variants in a further 28.9%. These findings may support counselling and follow-up refining prognosis and management. Systematic re-evaluation and data-sharing may upgrade contributory findings to definitive diagnoses over time.

THU-258-YI

Familial intrahepatic cholestasis protein 1 (FIC1) deficiency: surgical biliary diversion improves native liver survival only in patients with relatively low serum bile acid levels in early life

Alise D.E. de Groot[1], Mark Nomden[1], Antonia Felzen[1], Pedro Miranda Afonso[2], Richard J. Thompson[3], Benjamin Shneider[4,5], Emmanuel Gonzalès[6], Irena Jankowska[7], Etienne Sokal[8], Seema Alam[9], Cigdem Arıkan[10], Henrik Arnell[11], Madeleine Aumar[12], Amer Azaz[13], Emna Barkaoui[14], Maria Belen Pallitto[15], Marisa Beretta[16], Jernej Brecelj[17,18], Dieter Clemens Broering[19,20], Pier Luigi Calvo[21], Mara Cananzi[22,23], Huey-Ling Chen[24,25,26], Guillermo Costaguta[27,28], Piotr Czubkowski[7], Lorenzo D'Antiga[29], Elisa de Carvalho[30], Dominique Debray[31], Antal Dezsőfi-Gottl[32], Angelo Di Giorgio[33], Ozlem Durmaz[34], Alexandre Fabre[35], Sandra Ferreira[36], Ryan T. Fischer[37], Björn Fischler[38], Cristina Campos Gonçalves[39,40], Enke Grabhorn[41], Tassos Grammatikopoulos[3], Girish Gupte[42], Winita Hardikar[43], Loreto Hierro Llanillo[44], Giuseppe Indolfi[45], Emmanuel Jacquemin[6], Carolina Jimenez-Rivera[46], Marianne Hørby Jørgensen[47], Binita M. Kamath[48], Wikrom Karnsakul[49], Nanda Kerkar[50,51], Kyung Mo Kim[52], Jae Sung Ko[53], Denitza Kofinova[54], Nolwenn Laborde[55], Zhong-Die Li[56], Patryk Lipiński[57], Rohan Malik[58], Saeed Mohammad[59], Yael Mozer - Glassberg[60], Gema Muñoz Bartolo[61], Gabriella Nebbia[62], Emanuele Nicastro[63], Felipe Ordoñez[64], Anna Orłowska-Wójcicka[7], Arti Pawaria[65], Tudor Lucian Pop[66,67], Jesús Quintero Bernabeu[68], Giusy Ranucci[69], Aathira Ravindranath[70], Nathalie Rock[71], Ioannis Roilidis[72], Mathias Ruiz[73], Thomas Sandahl[74], Srinivas Sankaranarayanan[75], Mohammad Shagrani[19,20], Eyal Shteyer[76], Pooja Spector[77], James E. Squires[78], Ekkehard Sturm[79], Cristina Targa[80], Marise Tofoli[81], Bethany Tucker[3], Christos Tzivinikos[82],

Wendy L. van der Woerd[83], Georg-Friedrich Vogel[84,85], Heng Wang[86], Jian-She Wang[87], Sabina Wiecek[88], Aglaia Zellos[89], Andréanne N. Zizzo[90], Estella Alonso[5,91], Ronald Sokol[5,92], Frederick J. Suchy[5,92], Kathleen M. Loomes[5,48], Simon P. Horslen[5,93], Philip Rosenthal[5,94], Girish Rao[5,95], Pamela L. Valentino[5,96], Kasper Wang[5,97], Bettina Hansen[2,98,99], Paola Mian[100], Henkjan J. Verkade[1]. [1]*Division of Gastroenterology-Hepatology, Department Pediatrics, University of Groningen, University Medical Center Groningen, Groningen, Netherlands;* [2]*Department of Epidemiology and Biostatistics, Erasmus Medical Center, Rotterdam, Netherlands;* [3]*Paediatric Liver, GI and Nutrition Centre, King's College Hospital, London, United Kingdom;* [4]*Division of Pediatric Gastroenterology, Hepatology, and Nutrition, Department of Pediatrics, Baylor College of Medicine, Houston, United States;* [5]*Childhood Liver Disease Research Network (ChiLDReN), Ann Abor, United States;* [6]*Pediatric Hepatology and Liver Transplantation Unit, National Reference Centre for Rare Pediatric Liver Diseases, FILFOIE, ERN RARE LIVER, Bicêtre Hospital, AP-HP. Université Paris-Saclay, Le Kremlin-Bicêtre, and Inserm U1193, Hepatinov, University of Par, Orsay, France;* [7]*Department of Gastroenterology, Hepatology, Nutritional Disorders and Pediatrics, Children's Memorial Health Institute, Warsaw, Poland;* [8]*Pediatric Gastorenterology and Hepatology, Université Catholique de Louvain, Cliniques St Luc, Brussels, Belgium;* [9]*Pediatric Hepatology, Institute of Liver and Biliary Sciences, New Delhi, India;* [10]*Department of Pediatric Gastroenterology and Organ Transplant, Koc University School of Medicine, Istanbul, Türkiye;* [11]*Pediatric Gastroenterology, Astrid Lindgren Children's Hospital, Karolinska University Hospital, and Department of Women's and Children's Health, Karolinska Institutet, Stockholm, Sweden;* [12]*Department of Pediatric Gastroenterology Hepatology and Nutrition CHU Lille, Univ. Lille, Inserm U1286- INFINITE-Institute for Translational Research in Inflammation, Lille, France;* [13]*Pediatric Gastroenterology, Hepatology and Nutrition, Sheikh Khalifa Medical City, Abu Dhabi, United Arab Emirates;* [14]*Department of Pediatrics, Tunis Children Hospital, Tunis, Tunisia;* [15]*Department of Gastroenterology and Hepatology, Hospital Italiano, CABA, Buenos Aires, Argentina;* [16]*Faculty of Health Sciences, Wits Donald Gordon Medical Centre, University of the Witwatersrand, Johannesburg, South Africa;* [17]*Department of Gastroenterology, Hepatology and Nutrition, University Children's Hospital Ljubljana, Ljubljana, Slovenia;* [18]*Department of Pediatrics, Faculty of Medicine, University of Ljubljana, Ljubljana, Slovenia;* [19]*Liver & SB Transplant & Hepatobiliary-Pancreatic Surgery, King Faisal Specialist Hospital & Research Center, Riyadh, Saudi Arabia;* [20]*Alfaisal University, College of Medicine, Riyadh, Saudi Arabia;* [21]*Pediatic Gastroenterology Unit, Regina Margherita Children's Hospital, Azienda Ospedaliera Città Della Salute e Della Scienza University Hospital, Turin, Italy;* [22]*Unit Of Gastroenterology, Digestive Endoscopy, Hepatology and Care of the Child With Liver Transplantation, University Hospital of Padova, Padova, Italy;* [23]*Pediatric Gastroenterology, Digestive Endoscopy, Hepatology, and Care of the Child With Liver Transplantation, Department of Children's and Women's Health, University Hospital of Padova, Padova, Italy;* [24]*Department of Pediatrics, National Taiwan University Children's Hospital, Taipei, Taiwan;* [25]*Department and Graduate Institute of Medical Education and Bioethics, National Taiwan University College of Medicine, Taipei, Taiwan;* [26]*Hepatitis Research Center, National Taiwan University Hospital, Taipei, Taiwan;* [27]*CHU de Quebec-Université Laval, Quebec City, Canada;* [28]*anatorio de Niños de Rosario, Rosario, Santa Fe, Argentina;* [29]*Pediatric Hepatology, Gastroenterology and Transplantation, Hospital Papa Giovanni XXIII, Bergamo, Italy;* [30]*Pediatric Gastroenterology Department, Hospital de Base do Distrito Federal, Hospital da Criança de Brasília, Centro Universitário de Brasília, Brasília, Distrito Federal, Brazil;* [31]*Gastroenterology-Hepatology-Nutrition Unit, APHP-Necker Enfants Malades University Hospital, Paris, France;* [32]*Pediatric Center, Semmelweis University, Budapest, Hungary;* [33]*Department of Medicine, University of Udine, Udine, Italy;* [34]*Department of Child Health and Diseases, Gastroenterology, Hepatology and Nutrition, Istanbul Faculty of Medicine, Istanbul University, Istanbul, Türkiye;* [35]*APHM, Hôpital de la Timone Enfant, Service de Pédiatrie Multidisciplinaire, Marseille, France;* [36]*ediatric Hepatology and Liver Transplantation Unit, Unidade Local de Saúde Coimbra, Coimbra, Portugal;* [37]*Section of Hepatology, Department of Gastroenterology, Children's Mercy Kansas City, Kansas City, Kansas, United States;* [38]*Pediatric Gastroenterology, Astrid Lindgren Children's Hospital, Karolinska University Hospital and Division of Pediatrics, CLINTEC, Karolinska Institutet, Stockholm, Sweden;* [39]*European Reference Network on Hepatological Diseases (ERN RARE-LIVER), Hamburg, Germany;* [40]*Pediatric Gastroenterology/Hepatology Center Lisbon, Lisbon, Portugal;* [41]*Pediatric Hepatology and Liver Transplantation, University Medical Center Hamburg Eppendorf, Hamburg, Germany;* [42]*Liver Unit (Including Small Bowel Transplantation), Birmingham Women's and Children's Hospital, Birmingham, United Kingdom;* [43]*Department of Gastroenterology and Clinical Nutrition, Royal Children's Hospital, Melbourne, Australia;* [44]*Service of Pediatric Hepatology and Transplantation, Children's Hospital La Paz, La Paz University Hospital, Madrid, Spain;* [45]*Meyer Children's Hospital, IRCCS, Florence, Italy;* [46]*Department of Pediatrics, Children's Hospital of Eastern Ontario, University of Ottawa, Ottawa, Canada;* [47]*Department of Pediatrics and Adolescent Medicine, Rigshospitalet Copenhagen University Hospital, Copenhagen, Denmark;* [48]*Division of Gastroenterology, Hepatology and Nutrition, The Children's Hospital of Philadelphia and the University of Pennsylvania Perelman School of Medicine, Philadelphia, United States;* [49]*Department of Pediatrics, Johns Hopkins University School of Medicine, Baltimore, United States;* [50]*Massachusetts General Brigham for Children, Boston, United States;* [51]*University of Rochester Medical Center, Rochester, United States;* [52]*Department of Pediatrics, Asan Medical Center Children's Hospital, Seoul, Korea, Rep. of South;* [53]*Department of Pediatrics, Seoul National University College of Medicine, Seoul, Korea, Rep. of South;* [54]*Department of Pediatric Surgery, University Multiprofile Hospital for Active Treatment and Emergency Medicine "N.I. Pirogov", Sofia, Bulgaria;* [55]*Unité de Gastro-entérologie, Hépatologie, Nutrition et Maladies Héréditaires du Métabolisme pédiatriques, Hôpital des Enfants, CHU de Toulouse, Toulouse, France;* [56]*Department of Gastroenterology, Children's Hospital of Fudan University, Shanghai, China;* [57]*Department of Pediatrics, Medical Center of Postgraduate Education, Warsaw, Poland;* [58]*Division of Pediatric Gastroenterology, Department of Pediatrics, All India Institute of Medical Sciences, New Delhi, India;* [59]*Monroe Carell Jr. Children's Hospital & Vanderbilt University School of Medicine, Nashville, United States;* [60]*Institute of Gastroenterology, Nutrition and Liver Diseases, Schneider Children's Medical Center of Israel, Petah Tikva, Israel;* [61]*Paediatric Hepatology Department, University Hospital La Paz, Madrid, Spain;* [62]*Servizio Di Epatologia e Nutrizione Pediatrica, Fondazione Irccs Ca' Granda Ospedale Maggiore Policlinico, Milano, Italy;* [63]*ediatric Hepatology, Gastroenterology and Transplantation, Hospital Papa Giovanni XXIII, Bergamo, Italy;* [64]*Section of Pediatric Gastrohepatology, Fundación Cardioinfantil, Bogotá, Colombia;* [65]*Department of Pediatric Gastroenterology, Hepatology & Liver Transplantation, Amrita Institute of medical Sciences, Kochi, India;* [66]*2nd Pediatric Discipline, Department of Mother and Child, Iuliu Hatieganu University of Medicine and Pharmacy, Cluj-Napoca, Romania;* [67]*2nd Pediatric Clinic, Emergency Clinical Hospital for Children, Cluj-Napoca, Romania;* [68]*Pediatric Hepatology and Liver Transplant Department, Hospital Universiatri Vall d'Hebron, Barcelona, Spain;* [69]*Pediatric Department for the Treatment and Study of Abdominal Diseases and Abdominal Transplantation, IRCCS ISMETT (Mediterranean Institute for Transplantation and Advanced Specialized Therapies), Palermo, Italy;* [70]*Department of Pediatric Gastroenterology, Apollo BGS Hospital, Mysuru, India;* [71]*Division of Pediatric Gastroenterology, University Hospital of Geneva, Geneva, Switzerland;* [72]*Third Pediatric Department, Hippokration Hospital, Aristotle University of Thessaloniki, Thessaloniki, Greece;* [73]*Service d'Hépato-gastroentérologie pédiatrique, Centre de Référence de l'atrésie des voies biliaires et des cholestases génétiques, Hôpital Femme Mère Enfant, Hospices Civils de Lyon, Bron, France;* [74]*Department of Hepatology and Gastroenterology, Aarhus University Hospital, Aarhus, Denmark;* [75]*Department of Pediatric Gastroenterology and Hepatology, Kanchi Kamakoti Childs Trust Hospital, Chennai, India;*

[76]The Juliet Keiden Institute of Pediatric Gastroenterology and Nutrition, Shaare Zedek Medical Center, Jerusalem, Israel; [77]Department of Pediatrics, Columbia University Irving Medical Center, New York, United States; [78]Division of Pediatric Gastroenterology and Hepatology, Department of Pediatrics, University of Pittsburgh School of Medicine, Pittsburgh, United States; [79]Pediatric Gastroenterology and Hepatology, University Children's Hospital Tübingen, Tübingen, Germany; [80]Pediatric Gastroenterology Service, Hospital da Criança Santo Antônio, Universidade Federal de Ciências da Saúde de Porto Alegre, Complexo Hospitalar Santa Casa, Porto Alegre, Rio Grande do Sul, Brazil; [81]Department of Pediatric Gastroenterology, State Hospital for Children and Adolescents, Goiania, Brazil; [82]Department of Pediatric Gastroenterology, Al Jalila Children's Specialty Hospital, Dubai, United Arab Emirates; [83]Pediatric Gastroenterology, Hepatology and Nutrition, Wilhelmina Children's Hospital, University Medical Center Utrecht, Utrecht, Netherlands; [84]Department of Paediatrics I, Medical University of Innsbruck, Innsbruck, Austria; [85]Institute of Cell Biology, Medical University of Innsbruck, Innsbruck, Austria; [86]DDC Clinic for Special Needs Children, Adolescent Medicine and Pediatrics, Middlefield, United States; [87]The Center for Pediatric Liver Diseases, Children's Hospital of Fudan University, Shanghai, China; [88]Department of Pediatrics, Medical University of Silesia, Katowice, Poland; [89]National anad Kapodistrian University of Athens, Second Department of Pediatrics, DIvision of Ped. Gastroenterolgu, Athens, Greece; [90]Department of Paediatrics, London Children's Hospital, Western University, London, Ontario, Canada; [91]Division of Gastroenterology, Hepatology, and Nutrition, Department of Pediatrics, Ann and Robert H. Lurie Children's Hospital of Chicago, Chicago, United States; [92]Children's Hospital Colorado Pediatric Liver Center and the Digestive Health Institute, Department of Pediatrics, University of Colorado School of Medicine, Colorado, United States; [93]Department of Pediatrics, University of Pittsburgh School of Medicine, Pittsburgh, United States; [94]Department of Medicine, University of California, San Francisco, United States; [95]Riley Hospital for Children, Indiana University School of Medicine, Indiana, United States; [96]Gastroenterology and Hepatology Division, Department of Pediatrics, University of Washington, Seattle Children's Hospital, Seattle, United States; [97]Hospital for Sick Children and Department of Surgery, University of Toronto, Toronto, Canada; [98]Toronto Center for Liver Disease, University Health Network, Toronto, Canada; [99]IHPME, University of Toronto, Toronto, Canada; [100]Clinical Pharmacy and Pharmacology, University of Groningen, University Medical Center Groningen, Groningen, Netherlands
E-mail: a.d.e.de.groot@umcg.nl

Background and aims: Familial intrahepatic cholestasis protein 1 (FIC1) deficiency is a rare pediatric cholestatic liver disease, caused by mutations in the ATP8B1 gene. Previously, we showed that natural history was not related to the number of truncating mutations (Hepatology, 2021). Before Ileal Bile Acid Transporter (IBAT) inhibitor availability, many FIC1 deficiency patients underwent surgical biliary diversion (SBD), but its effect on native liver survival (NLS) was variable. We evaluated whether serum bile acid (sBA) levels in early life provide prognostic information on the course of disease in FIC1 deficiency patients, who later did or did not undergo SBD.
Method: We retrospectively and prospectively analyzed patients with genetically confirmed FIC1 deficiency in the global NAPPED registry (NCT03930810). We assessed 18-year NLS and SBD rate. Median sBA levels within the first year of life, or until SBD if <1 year, were calculated. The association between sBA levels and NLS in patients was tested using Cox regression analysis. ROC analysis identified the optimal cut-off. Median and interquartile range described continuous variables.
Results: One hundred eighty-three FIC1 deficiency patients were included (59% male). Age at data extraction was 16.0 (10.7–23.7) years. Of the included patients, 33% had undergone liver transplantation at age of 4.0 (2.7–7.2) years. NLS at 18 years was 50%. By age 18 years, 58% of the patients had undergone SBD, at median age of 1.5 (0.9–2.9) years. Time-dependent Cox regression showed that SBD was associated with slightly lower NLS (overall HR 2.46, p = 0.013). In patients without SBD (n = 38), early sBA were not associated with NLS (p = 0.89). In patients with SBD (n = 26), however, early sBA <197 µmol/L was significantly associated with higher NLS (HR 0.14, p < 0.05).
Conclusion: In the largest global database of FIC1 deficiency patients, SBD is not uniformly associated with prolongation of the NLS. However, in a subgroup of SBD patients, low early life sBA levels were associated with prolonged NLS in comparison to patients with high early sBA levels.

THU-259

Clinical characteristics of alpha-1 antitrypsin deficiency patients and coexistence of metabolic dysfunction-associated steatotic liver disease

María Del Barrio[1], Inmaculada Sanchez[1], Henar Ruiz[1], Armando Raúl Guerra[2], María Teresa Arias Loste[1], Susana Llerena[1], Marta Alonso-Peña[3], Antonio Cuadrado[1], Álvaro Díaz-González[1].
[1]Gastroenterology and Hepatology Department, Marqués de Valdecilla University Hospital, Clinical and Translational Digestive Research Group, Instituto de Investigación Valdecilla (IDIVAL)., Santander, Spain; [2]Servicio de Análisis Clínicos y Bioquímica. Grupo de Investigación Clínica y Traslacional en Enfermedades Digestivas. Instituto de Investigación Valdecilla (IDIVAL). Hospital Universitario Marqués de Valdecilla., Santander, Spain; [3]Gastroenterology and Hepatology Department, Marqués de Valdecilla University Hospital, Clinical and Translational Digestive Research Group, Instituto de Investigación Valdecilla (IDIVAL). Departamento de Anatomía y Biología Celular, Universidad de Cantabria, Santander, Spain
E-mail: maria.del94@gmail.com

Background and aims: Liver disease associated to alpha-1 antitrypsin deficiency (AATD) has classically been considered a rare liver disease and related with the phenotype. On the other hand, metabolic dysfunction-associated steatotic liver disease (MASLD) is nowadays the first cause of liver disease. However, there is little information about the impact of MASLD on liver disease associated to AATD. The aim is to evaluate the presence of MASLD and its characteristics in patients with AATD.
Method: Retrospective and single-center study that included patients with AATD, between 2019 and 2023, for whom both phenotype and transient elastography (TE) data were available. MASLD was defined by the presence of liver steatosis (CAP ≥ 275) and ≥ 1 metabolic comorbidity.
Results: A total of 104 patients were included, among whom 68 (65.4%) were MZ, 19 (18.3%) SZ and 17 (16.3%) ZZ. Liver steatosis was present in 30 patients (28.8%), all of them meeting MASLD criteria. These patients had more frequently metabolic comorbidities: diabetes 16.7% vs 1.4% p 0.002; arterial hypertension 30% vs 18.9% p 0.217; dyslipidaemia 60% vs 28.4% p 0.003; hypertriglyceridemia 36.7% vs 12.2% p 0.004; metabolic syndrome 23.3% vs 8.1% p 0.033; and a higher body mass index 29.1 vs 25 kg/m^2 p 0.000. Moreover, they had a significant higher ferritin level and a higher prevalence of hypertransaminasemia, at the limit of significance. Furthermore, these patients showed significant higher values of APRI and FIB-4. Also, they more frequently presented ET values associated with risk of events in patients with AATD (ET ≥7,1 kPa: 30% vs 12.2% p 0.029). Finally, they showed a significantly higher CAP. Regarding lung involvement, MASLD patients did not have worse respiratory function, showing AATD patients a worse diffusion with a lower KCO. There were no differences between groups in other extrahepatic complications (chronic kidney disease (CKD), emphysema, cholelithiasis or panniculitis). We identify a higher prevalence of emphysema associated to different phenotypes (ZZ 47.1%, MZ 6.8% and SZ 8.3% p 0.001), as well as CKD (ZZ 29.4%, MZ 4.4%, SZ 0% p 0.001).
Conclusion: In AATD patients, the prevalence of MASLD is high and it is associated to a higher risk profile for events and progression.

However, the presence of emphysema and/or CKD and a greater alteration in KCO were associated with the DAAT phenotype.

THU-260

Ileal bile acid transporter (IBAT) inhibitor therapy in adults with hereditary bile salt export pump (BSEP) deficiency: a case series

Carola Dröge[1], Eva-Doreen Pfister[2], Pavel Strnad[3], Giuseppe Rusignuolo[4], Ulrich Baumann[2], Sebastian Schulz-Jürgensen[5], Martina Sterneck[6], Tobias Götze[1], Martin Zenker[7], Denny Schanze[7], Katrin Hippe[8], Robert Thimme[4], Verena Keitel-Anselmino[1]. *[1]Department of Gastroenterology, Hepatology, and Infectious Diseases, Medical Faculty, Otto von Guericke University Magdeburg, Magdeburg, Germany; [2]Pediatric Gastroenterology and Hepatology, Department for Pediatric Kidney, Liver and Metabolic Diseases, Hannover Medical School, Hannover, Germany; [3]Department of Gastroenterology, Hepatology, Aachen University Hospital, Aachen, Germany; [4]Clinic for Internal Medicine II, Freiburg University Medical Center, Faculty of Medicine, University of Freiburg, Freiburg im Breisgau, Germany; [5]Pediatric Gastroenterology and Hepatology, Department for Pediatric Kidney, Liver and Metabolic Diseases, University Hospital Hamburg Eppendorf, Hamburg, Germany; [6]Department of Internal Medicine, University Medical Centre Hamburg-Eppendorf, Hamburg, Germany; [7]Department of Human Genetics, University Hospital Magdeburg, Magdeburg, Germany; [8]Institute of Pathology, University Hospital Magdeburg, Medical Faculty, Otto von Guericke University Magdeburg, Magdeburg, Germany*
E-mail: carola.droege@med.ovgu.de

Background and aims: Variants in the bile salt export pump BSEP predispose to a variety of cholestatic liver diseases. While patients carrying biallelic protein truncating variants present in infancy with rapidly progressive familial intrahepatic cholestasis (PFIC2), patients with missense mutations and residual BSEP function tend to present with slower disease progression. Therapeutic approaches for BSEP deficiency aim to lower serum bile acids (SBA) to prolong native liver survival. Ileal bile acid transporter inhibitors (IBATi) are reduce SBA and pruritus in PFIC2 patients. So far, little is known about the use of IBATi in adults. This case series summarises the IBATi treatment of 8 adults with BSEP deficiency.
Method: Patients presented at outpatient clinics of German University Hospitals. Most of the patients were enrolled in the HiChol registry. Disease onset, symptoms, interventions, medication, lab values, personal and family medical history as well as quality of life data including pruritus assessment were collected prospectively. Whole exome sequencing (WES) was used to determine underlying genetic variants.
Results: 5 patients reported disease onset within first months of life while 3 patients had reached adolescence or adulthood at symptom onset. In 2 patients, liver disease had already progressed to histologically confirmed cirrhosis while all others showed signs of fibrosis at IBATi initiation as determined by elastography and/or histology. WES revealed biallelic (likely) pathogenic BSEP mutations in 4 patients with disease onset in infancy. For the others, monoallelic BSEP mutations were detected. Of these, 1 patient carried a nonsense mutation, whereas all others have BSEP missense mutations. Without treatment, all patients suffered from severe itch affecting quality of life. IBATi therapy improved itch ≥2 points on a VAS in all patients with clinically significant itch (≥5/10) at IBATi initiation. Furthermore, SBA reached values <102µmol/l in all patients. IBATi therapy was stopped after 7 months in 1 cirrhosis patient due to increase in transaminases, bilirubin, SBA and liver stiffness, interpreted as disease progression and not as IBATi-related adverse event.
Conclusion: Adults with BSEP deficiency showed similar reduction in itch and SBA in response to IBATi therapy as reported in paediatric phase III trials. Weight adjusted IBATi dosing as used in paediatric trials was safe and well tolerated in our cohort.

THU-261

Structured transition care program for chronic liver disease: a 6-Year clinical audit demonstrating superior outcomes

Victoria Ekstrom[1], Pei-Yuh Chia[1], Kong Boo Phua[2], Fang Kuan Chiou[2], Jia Min Lim[2], Hiang Keat Tan[1], Lynette Goh[2]. *[1]Singapore General Hospital, Singapore, Singapore; [2]KK Women's & Children's Hospital, Singapore, Singapore*
E-mail: vekstrom@gmail.com

Background and aims: Transition from paediatric to adult hepatology care represents a high-risk period, with published loss-to-follow-up rates of 8–15% and increased risks of non-adherence and disease progression. While structured transition programs are recommended in international guidelines, robust outcome data remain limited, particularly for non-transplant chronic liver disease populations. We evaluated long-term clinical and service outcomes of a comprehensive multidisciplinary transition program.
Method: We implemented a structured program at a tertiary hepatology centre comprising: pre-transition education clinics, joint paediatric-adult consultations, disease-specific online resources, dedicated adult transition clinics with extended 30-minute appointments, specialised transition nursing support, and direct clinician communication access. We conducted a retrospective audit of patients who transitioned between 2018–2024, analysing patient survival, disease progression, care continuity, and appointment adherence.
Results: 37 patients completed transition (median age 19 years, range 16–38; median follow-up 30 months, range 14–93). Primary diagnoses: MASLD (38%), biliary atresia (24%), autoimmune hepatitis/overlap syndrome (11%), chronic hepatitis B (11%), others (16%). Care continuity: Exceptional retention was achieved with 35 patients (94.6%) maintaining active follow-up. Only 1 patient (2.7%) was lost to follow-up and 1 (2.7%) transferred to private care, substantially outperforming published benchmarks of 8–15% loss-to-follow-up. Clinical outcomes: Patient survival was 100% at 5 years. Disease remained stable in 88.6% of patients. Three patients (8.1%) progressed to require liver transplantation during follow-up. Engagement metrics: Median clinic appointment attendance was 92%, with 73% of patients attending ≥80% of scheduled appointments, demonstrating sustained healthcare engagement.
Conclusion: This patient-centred, multidisciplinary transition program achieved exceptional care continuity (94.6% retention rate), significantly exceeding published benchmarks and demonstrating that structured programs can substantially improve outcomes in chronic liver disease transition populations. The model combining dedicated resources, and multidisciplinary support provides a replicable framework that should be considered for transition services in chronic liver disease.

THU-262

Baseline fibrosis stage predicts risk of progression in patients with alpha-1 antitrypsin deficiency and a protease inhibitor (Pi)*ZZ/SZ genotype: longitudinal data from the Birmingham AATD registry

Paul Ellis[1,2], May Hagiwara[3], Pavel Strnad[4], Virginia C. Clark[5], Jeanine M. D'Armiento[6], Monica P. Goldklang[6], Jeffrey H. Teckman[7], Doneal Thomas[8], Flavia Soares Peres[9], Eric Gemmen[10], Gerald Lebovic[8], Chitra Karki[3], Tami Nussbaum[3], Suna Park[3], Kaili Ren[3], Alice Turner[1,2]. *[1]School of Health Sciences, University of Birmingham, Birmingham, United Kingdom; [2]University Hospitals Birmingham NHS Foundation Trust, Birmingham, United Kingdom; [3]Takeda Development Center Americas, Inc., Cambridge, MA, United States; [4]University Hospital RWTH Aachen, Aachen, Germany; [5]University of Florida, Gainesville, FL, United States; [6]Columbia University Medical Center, New York, NY, United States; [7]St. Louis University School of Medicine, St. Louis, MO, United States; [8]IQVIA Real*

World Solutions, Mississauga, ON, Canada; [9]IQVIA Real World Solutions, Lisbon, Portugal; [10]IQVIA Real World Solutions, Falls Church, VA, United States
E-mail: p.ellis@bham.ac.uk

Background and aims: Alpha-1 antitrypsin deficiency (AATD) is associated with heterogeneous liver disease, yet data on predictors of fibrosis progression are limited. We characterized baseline fibrosis patterns, natural history and determinants of fibrosis progression in adults with AATD and a protease inhibitor (Pi)*ZZ/SZ genotype from a large tertiary registry.
Method: Adults (≥ 18 years) with AATD and a Pi*ZZ/SZ genotype were eligible (2010–2023); patients (pts) with prior liver transplantation were excluded. Baseline fibrosis stage was determined using a hierarchical approach (FibroScan® [n = 193] > APRI [n = 276]). Fibrosis staging by FibroScan was defined as: F0/1, > 2.0–≤ 7.1 kPa; F2, > 7.1–≤ 10.0 kPa; F3, > 10.0–≤ 15.0 kPa; F4 > 15.0 kPa; staging by APRI was defined as: F0/F1, ≤ 0.43; F2, > 0.43–≤ 0.63; F3, > 0.63–≤ 1.5; F4, > 1.5. Fibrosis progression and regression (≥ 1-stage increase or decrease in fibrosis stage, respectively) were assessed on serial assessment. Kaplan–Meier analysis assessed time to progression and mortality. A Cox proportional hazards model was estimated to identify predictors of fibrosis progression. Lung function decline was also assessed.
Results: The Pi*ZZ cohort included 399 pts (median [SD] follow-up: 3.7 ± 1.9 years): F0/1, n = 290; F2, n = 77; F3, n = 30; F4, n = 2. Overall, 19.0% of F0/F1 pts, 39.0% of F2 and 6.7% of F3 had fibrosis progression; rates were twofold greater in pts staged as F2 at baseline versus F0/F1 (log-rank $p < 0.001$). Pts staged as F3 at baseline had low rates of fibrosis progression, although the small sample size may have reduced detectable progression in these pts. Higher fibrosis stage was associated with male sex, older age, higher body mass index, elevated liver enzymes and lower platelet count, but not alcohol or smoking exposure. There was no association between baseline fibrosis stage and all-cause mortality, fibrosis regression (F2, 48.7%; F3, 50.0%; F4, 100%) or lung function decline. The Pi*SZ cohort (n = 70) showed no clear signal of progression or regression, although numbers were small.
Conclusion: In pts with AATD and a Pi*ZZ genotype, baseline F2 was associated with higher rates of fibrosis progression versus F0/F1. These findings position F2 fibrosis as a clinically meaningful threshold for intensified hepatic surveillance and risk stratification and may inform the design of future interventional therapies targeting fibrosis progression in AATD-associated liver disease.
Study/writing funding: Takeda Development Center Americas, Inc.

THU-263

Age-stratified genetic testing for liver disorders improves diagnostic yield and clinical impact in pediatric and adult patients

Angelo Corso Faini[1,2], Michele Pinon[3], Giulia Mrgherita Brach del Prever[1,2], Carmelo Maria Romeo[1,2], Maria Luca[1,2], Fiorenza Mioli[1,2], Claudia Saglia[1,2], Caterina Scolari[1,2], Tullia Carradori[1,2], Francesca Arruga[1,2], Diana Carli[1,2], Pier Luigi Calvo[3], Tiziana Vaisitti[1,2], Silvia Deaglio[1,2]. *[1]Immunogenetics and Transplant Biology Service, Città della Salute e della Scienza Hospital, Turin, Italy; [2]Department of Medical Sciences, University of Turin, Turin, Italy; [3]Pediatric Gastroenterology Division, Regina Margherita Children's Hospital, Turin, Italy*
E-mail: angelocorso.faini@unito.it

Background and aims: Genetic testing is becoming crucial for better understanding the etiology of different liver conditions, improving their diagnostic workflows and clinical management. This study aims at designing an algorithm to efficiently implement genetic testing – and particularly clinical exome sequencing (CES) – in the diagnostic workup of both adult and pediatric patients with liver diseases.
Method: We retrospectively analyzed patients with liver disorders of potential genetic origin referred to the Città della Salute e della Scienza Hospital of Turin between July 2003 and February 2024. According to the clinical manifestation, patients were classified into different diagnostic categories, specifically cholestatic liver disorders, unexplained liver dysfunctions, liver accumulation diseases, ciliopathies, enzymatic deficiencies, syndromic disorders and isolated non-cystic liver malformations, and underwent CES. Variants of unknown significance deemed as potentially causative of the disease were re-evaluated upon completion of family segregation studies.
Results: 203 patients were included in the study (71% pediatrics, 29% adults). Median age was 8 years [1–21]; 65.5% were male and 84.7% White; 56 patients (27.6%, mostly children) underwent liver transplantation. The most common diagnostic categories were cholestatic liver disorders (n = 61, 30%) and unexplained liver dysfunction (n = 41, 20.2%). Genetic testing yielded a definitive diagnosis in 35.5% overall: 41.4% in children and 20.7% in adults. Metabolic conditions showed the highest yield (83.3%) while PFIC/BRIC and Alagille syndrome were the most frequent diagnoses. Among conclusive cases, 106 variants were reported, 52 (49.1%) classified as pathogenic, 49 (46.2%) as likely pathogenic and 5 (4.7%) as known pathogenic polymorphisms. Most variants fell within genes associated with autosomal recessive diseases, while only a few involved autosomal dominant (n = 5) or X-linked (n = 3) conditions. A ~10% increase in the global diagnostic rate and across disease categories was reached by applying age-tailored (i.e., pediatric- and adult-specific) optimized diagnostic workflows.
Conclusion: CES is a valuable tool for diagnosing liver diseases, showing a good diagnostic yield. However, its performance depends on the patient's clinical features and particularly age at presentation. Therefore, age-tailored workflows may improve efficiency and performance of genetic testing.

THU-264-YI

Liver disease manifestations in signal transducer and activator of transcription gain-of-function mutation

Sawsan Fathma[1], Nehna Majeed[2], Wesam Aleyadeh[1], Sana Pirzada[1], Alexandra Freeman[3], Steven Holland[3], Jenna Bergerson[3], Christopher Koh[1], David E Kleiner[4], Theo Heller[1]. *[1]Translational hepatology section, liver disease branch, national institute of diabetes and digestive and kidney diseases, national institutes of health, Bethesda, United States; [2]Department of gastroenterology and hepatology, university of maryland medical center, Baltimore, United States; [3]Laboratory of clinical immunology and microbiology, national institute of allergy and infectious diseases, national institutes of health, Bethesda, United States; [4]Laboratory of pathology, national cancer institute, national institutes of health, Bethesda, United States*
E-mail: sawsanf@gmail.com

Background and aims: Signal transducer and activator of transcription 1 (STAT1) gain-of-function (GOF) mutations cause impaired dephosphorylation and prolonged nuclear accumulation of phosphorylated STAT1, leading to immune dysregulation characterized by chronic mucocutaneous candidiasis, autoimmunity and recurrent infections. Despite well-documented immunological complications, hepatic manifestations of STAT1 GOF remain poorly defined. We aimed to describe liver disease manifestations in patients with STAT1 GOF mutations.
Method: We performed a retrospective study of patients with genetically confirmed STAT1 GOF evaluated at the Primary Immunodeficiency Clinic at the National Institutes of Health between 1996 and 2022. Clinical, laboratory, imaging, and histopathologic data were analyzed.
Results: Of forty-two patients with STAT1 GOF, 17 (40%) met criteria for liver disease. Baseline biochemical parameters, including liver enzymes, synthetic function, and platelet count, did not differ between groups and remained mostly within normal limits during follow-up. However, platelet count declined significantly in the liver disease group (median 254 to 168 × 10^9/L; p = 0.0053). Cross sectional imaging demonstrated hepatomegaly in 15 of 17 liver disease patients. Liver biopsy was performed in nine liver disease patients,

revealing porto-sinusoidal vascular disease (PSVD) in five and features suggestive of PSVD in two additional patients. PSVD findings closely correlated with declining or persistently low platelet counts. All-cause mortality was higher in the liver disease group (23% vs 12%), with deaths occurring at younger ages mostly from sepsis.
Conclusion: Liver disease is a clinically significant manifestation of STAT1 GOF, characterized by features of non-cirrhotic portal hypertension. Although autoimmune hepatitis has previously been described, histopathology in this cohort frequently demonstrated PSVD, establishing a link between STAT1 GOF and vascular liver pathology. Recognition of this association provides unique insights into PSVD pathophysiology, a condition whose underlying mechanisms remain incompletely understood and warrant further studying.

THU-265-YI
Quantitative histological evaluation reveals duct paucity in children with severe alpha-1 antitrypsin deficiency (Pi*ZZ genotype)

Malin Fromme[1], Marion Bouchecareilh[2], Alain Lachaux[3], Mousa Mobarki[4,5], Sophie Collardeau-Frachon[5], Lioara Restier[6], Rainer Ganschow[7], Heike Bantel[8], Sabina Janciauskiene[9], Mattias Mandorfer[10], Elmar Aigner[11], Ekkehard Sturm[12], Matthias C. Reichert[13], Olivier Govaere[14], Georg-Friedrich Vogel[15,16], Jef Verbeek[17], Aleksander Krag[18], Piotr Socha[19], Helmut Denk[20], Mathias Ruiz[21], Pavel Strnad[1,22]. [1]*Medical Clinic III, Gastroenterology, Metabolic diseases and Intensive Care, University Hospital RWTH Aachen, Aachen, Germany;* [2]*University of Bordeaux, CNRS, INSERM, BRIC, U1312, Bordeaux, France;* [3]*Department of Paediatric Gastroenterology, Hepatology and Nutrition, Reference Center for Rare Disease - Biliary Atresia And Genetic Cholestasis, Children's Hospital of Lyon, Lyon, France;* [4]*Department of Pathology, Faculty of Medicine, Jazan University, Jazan, Saudi Arabia;* [5]*Institute of Pathology, Hôpital Femme-Mère-Enfant, Hospices Civils de Lyon, Université Claude Bernard Lyon 1, Lyon, France;* [6]*Service de gastro-entérologie, hépatologie et nutrition pédiatriques, hôpital Femme-Mère-Enfant, hospices civils de Lyon, Bron, France;* [7]*Department of Pediatric Gastroenterology and Hepatology, University Hospital of Bonn Children's Hospital, Bonn, Germany;* [8]*Department of Gastroenterology, Hepatology, Infectious Diseases and Endocrinology, Hannover Medical School, Hannover, Germany;* [9]*Clinic for Pneumology, Medical University Hannover, Hannover, Germany;* [10]*Division of Gastroenterology and Hepatology, Department of Internal Medicine III, Medical University of Vienna, Vienna, Austria;* [11]*First Department of Medicine, Paracelsus Medical University, Salzburg, Austria;* [12]*Pediatric Gastroenterology and Hepatology, University Children's Hospital Tübingen, Tübingen, Germany;* [13]*Department of Medicine II, Saarland University Medical Center, Saarland University, Homburg, Germany;* [14]*Department of Imaging and Pathology, KU Leuven and University Hospitals Leuven, Leuven, Belgium;* [15]*Department of Paediatrics I, Medical University of Innsbruck, Innsbruck, Austria;* [16]*Institute of Cell Biology, Biocenter, Medical University of Innsbruck, Innsbruck, Austria;* [17]*Department of Gastroenterology & Hepatology, KU Leuven University Hospitals, Leuven, Belgium;* [18]*Department of Gastroenterology and Hepatology, Odense University Hospital, Odense C, Denmark;* [19]*The Children's Memorial Health Institute, Department of Gastroenterology, Hepatology, Nutritional Disorders and Pediatrics, Al. Dzieci Polskich, Warszawa, Poland;* [20]*Institute of Pathology, Medical University of Graz, Graz, Austria;* [21]*Hépatologie, Gastroentérologie et Nutrition Pédiatriques, Hôpital Femme Mère Enfant, Hospices civils de Lyon, Lyon, France;* [22]*Department of Gastroenterology and Hepatology, Medical University Lausitz - Carl Thiem (MUL-CT), Cottbus, Germany*
E-mail: mfromme@ukaachen.de

Background and aims: Liver disease in severe alpha-1 antitrypsin (AAT) deficiency (Pi*ZZ genotype) displays a biphasic pattern with the first peak in early childhood and the second, adult peak after the age of 40 years. Our aim was to histologically characterize the pediatric and adult liver disease.
Method: We recruited 67 adults and 48 Pi*ZZ children aged four weeks to 17 years from six countries who underwent a liver biopsy/transplantation. A blind histological scoring was performed by two histopathologists. COMET staining quantified histological features in a representative adult and pediatric sample.
Results: Pediatric Pi*ZZ samples originated more often from liver transplantation (64.6 vs. 21.2%, p <.0001) and children displayed significantly higher liver enzymes than adults. Compared to adults, children presented a significantly higher fibrosis stage according to METAVIR (4.0 vs. 2.5, p <.0001). Higher liver steatosis was more prevalent in Pi*ZZ adults, while bile plugs and duct paucity were significantly more common in Pi*ZZ children (bile plugs: 43.8 vs. 10.4%, p <.0001; duct paucity 58.3 vs. 1.5%, p <.0001). No difference in AAT accumulation scores according to Clark was found. When subdividing the pediatric cohort based on age (<1 year, 1–5 years and 6–17 years), cirrhosis was more common in both older age groups than in younger children (64.7 vs. 75.0 vs. 30.8%, p = .045). There were no differences in liver steatosis, inflammation, or cholestasis parameters, but youngest children displayed less AAT accumulation and less frequently had larger aggregates.
Conclusion: Our study reveals unique histological patterns in Pi*ZZ children and adults thereby providing basis for patient counseling and further mechanistic studies.

THU-266
Natural history of liver disease in patients with alpha-1 antitrypsin deficiency and a protease inhibitor (Pi)*ZZ genotype: data from the Alpha-1 liver network in Germany

Malin Fromme[1], May Hagiwara[2], Virginia C. Clark[3], Jeanine M. D'Armiento[4], Monica P. Goldklang[4], Jeffrey H. Teckman[5], Alice Turner[6], Doneal Thomas[7], Flavia Soares Peres[8], Eric Gemmen[9], Gerald Lebovic[7], Chitra Karki[2], Tami Nussbaum[2], Suna Park[2], Kaili Ren[2], Pavel Strnad[1]. [1]*University Hospital RWTH Aachen, Aachen, Germany;* [2]*Takeda Development Center Americas, Inc., Cambridge, MA, United States;* [3]*University of Florida, Gainesville, FL, United States;* [4]*Columbia University Medical Center, New York, NY, United States;* [5]*St. Louis University School of Medicine, St. Louis, MO, United States;* [6]*School of Health Sciences, University of Birmingham, Birmingham, United Kingdom;* [7]*IQVIA Real World Solutions, Mississauga, ON, Canada;* [8]*IQVIA Real World Solutions, Lisbon, Portugal;* [9]*IQVIA Real World Solutions, Falls Church, VA, United States*
E-mail: mfromme@ukaachen.de

Background and aims: Fibrosis progression in patients (pts) with alpha-1 antitrypsin deficiency (AATD)-associated liver disease (LD) with the protease inhibitor (Pi)*ZZ genotype is poorly understood. Vibration-controlled transient elastography (VCTE) and aspartate aminotransferase-to-platelet ratio index (APRI) are increasingly used to monitor fibrosis progression. We evaluated fibrosis progression over 8 years in pts with Pi*ZZ AATD using Alpha-1 Liver Network data, RWTH Aachen University.
Method: Adults with Pi*ZZ AATD enrolled in the Alpha-1 Liver Network (2015–2024) were eligible. Fibrosis stage was assessed by reliable VCTE (≥ 10 measurements, ≥ 60% success rate, IQR/median value ≤ 30%) or APRI, matched at baseline and follow-up (≤ Year 8), using a hierarchical approach (VCTE > APRI using pre-defined cutoffs). Fibrosis progression was defined as an increase in ≥ 1 fibrosis stage from baseline or incidence of LD-related clinical event. Fibrosis stage increase was also defined by a ≥ 30% increase in reliable VCTE from baseline, and stage increase in both reliable VCTE and APRI.
Results: Overall, 655 pts were included with baseline fibrosis stage (F0/F1: n = 479, 73%; F2: n = 74, 11%; F3: n = 54, 8%; F4: n = 36, 5%; missing/unknown: n = 12, 2%) based on reliable VCTE (n = 580, 89%) or APRI (n = 63, 10%). Of those, 281 pts with matched staging were analysed for fibrosis progression (median [IQR] follow-up: 56 [24, 83] months). In total, 24/211 (11%) F0/F1, 8/34 (24%) F2, 11/29 (38%) F3 and 5/7 (71%) F4 pts progressed from baseline to Year 8 (≥1 fibrosis

stage increase [≤F2: 30/245, 12%; F3: 7/29, 24%]; incidence of an LD-related clinical event [≤ F2: 2/245, 1%; F3: 4/29, 14%; F4: 5/7, 71%]). Fibrosis progression was more frequently observed in pts with baseline F3/F4 (n = 16/36, 44%) than ≤ F2 (n = 32/245, 13%). Median (95% CI) time to fibrosis progression was 87 (39, not estimable [NE]) and 37 (30, NE) months for pts with baseline F3 and F4 fibrosis, respectively, and was not reached in baseline ≤ F2. From baseline to Year 8, 39/207 (19%) and 7/207 (3.4%) F0-F2 fibrosis pts and 7/24 (29%) and 4/24 (17%) F3 pts experienced fibrosis stage advancement when defined by a ≥ 30% increase in reliable VCTE or advancement from baseline in both reliable VCTE and APRI, respectively.
Conclusion: Among pts with Pi*ZZ AATD, 11%–71% experienced fibrosis progression during follow-up. Pts with advanced fibrosis may experience higher rates of LD progression.
Study/writing funding: Takeda Development Center Americas, Inc.

THU-267

Liver biopsy lesions in Wilson disease: relationship with copper metabolism, clinical and biochemical outcomes, phenotypes and the most frequent mutations. Data from the Spanish AEEH Wilson registry

Luis García-Villarreal[1], Pablo Alonso Castellano[1], Zoe Mariño[2], Marina Berenguer[3], Antonio Olveira[4], Javier Ampuero[5], Pilar Huarte[6], Diego Burgos Santamaria[7], Paula Iruzubieta[8], José Ramón Fernández[9], Jose María Moreno Planas[10], Carolina Muñoz Codoceo[11], María Lázaro Ríos[12], Marta Romero-Gutiérrez[13], Helena Masnou[14], Paula Fernandez Alvarez[15], Maria Luisa Gonzalez Dieguez[16], Manuel Delgado[17], Judith Gómez- Camarero[18], Alba Cachero[19], Jose Pinazo Bandera[20], Manuel Hernández-Guerra[21], Esther Molina[22], Silvia Montoliu[23], Monica Pons[24], Gemma Carrión[25], Sonia Blanco Sampascual[26], Sara Lorente[27], Francisca Cuenca Alarcón[28], Ana Arencibia Almeida[29], María Hernández[30], Carlos Valdivia Krag[31], María Carmen García-Gavilán[32], Tania Hernáez-Alsina[33], Berta Bartrolí[34], Sergio Gil-Rojas[35], Antonio Tugores[36]. *[1]Digestive Service. Complejo Hospitalario Universitario Insular Materno Infantil, Las Palmas de Gran Canaria, Spain; [2]Liver Unit, Hospital Clinic Barcelona, IDIBAPS, CIBERehd, ERN-RARE Liver, Universitat de Barcelona, Barcelona, Spain; [3]Hospital Universitari i Politècnic La Fe, Valencia, Spain; [4]Hospital Universitario La Paz, Madrid, Spain; [5]Hospital Universitario Virgen del Rocío, Sevilla, Spain; [6]Hospital Universitario de Navarra, Pamplona, Spain; [7]Hospital Ramón y Cajal, Madrid, Spain; [8]Hospital Universitario Marqués de Valdecilla, Santander, Spain; [9]Hospital Universitario de Cruces, Baracaldo, Spain; [10]Complejo Hospitalario Universitario de Albacete, Albacete, Spain; [11]Hospital Universitario 12 de octubre, Madrid, Spain; [12]Hospital Miguel Servet, Zaragoza, Spain; [13]Hospital Universitario de Toledo, Toledo, Spain; [14]Hospital Germans Trias i Pujol, Badalona, Spain; [15]Hospital Virgen Macarena, Sevilla, Spain; [16]Hospital Universitario Central de Asturias, Oviedo, Spain; [17]Hospital Universitario de A Coruña, La Coruña, Spain; [18]Hospital Universitario de Burgos, Burgos, Spain; [19]Hospital Universitario de Bellvitge, Hospitalet de Llobregat, Spain; [20]Hospital Universitario Virgen de la Victoria, Málaga, Spain; [21]Hospital Universitario de Canarias, La Laguna, Spain; [22]Hospital Clínico de Santiago, Santiago de Compostela, Spain; [23]Hospital Universitario Joan XXIII, Tarragona, Spain; [24]Hospital Universitari Vall d'Hebron, Barcelona, Spain; [25]Hospital Universitario Infanta Leonor, Madrid, Spain; [26]Hospital Universitario Basurto, bilbao, Spain; [27]Hospital Clínico Universitario Lozano Blesa, Zaragoza, Spain; [28]Hospital Clínico San Carlos, Madrid, Spain; [29]Hospital Universitario Nuestra Señora de La Candelaria, Santa Cruz de Tenerife, Spain; [30]Hospital Universitario San Jorge, Huesca, Spain; [31]Hospital Universitario Reina Sofía, Córdoba, Spain; [32]Hospital Costa del Sol, Marbella, Spain; [33]Hospital Universitario San Pedro, Logroño, Spain; [34]Hospital Universitari Dr. Josep Trueta, Gerona, Spain; [35]Hospital Virgen de la Luz, Cuenca, Spain; [36]Research Unit. Complejo Hospitalario Universitario Insular Materno Infantil, Las Palmas Gran Canaria, Spain*
E-mail: lgarciavillarreal@gmail.com

Background and aims: Liver biopsy is widely used in Wilson disease (WD), but the lesions are common to other pathologies (except for tissue copper), and their influence on patient evolution and phenotype is not well studied. Hence we decided to study these data in a large group of cases.
Method: Retrospective study including baseline biopsies, baseline biochemistry and phenotypes, transaminase improvement at 1 and 3 years (normal or decrease > 70%), clinical outcomes (cirrhosis de novo, decompensation, liver transplantation or death from WD), and the mutations frequently found in our population: M645R, L708P, H1069Q and Loss-Of-Function (LOF). We evaluated these data for 3 biopsy lesions, divided each into two subgroups: steatosis (S: yes or not), advanced fibrosis (AF: F3-4 vs. F0-2) and high inflammatory activity (HIA: A2-3 vs. A0-1). The reported differences were $p < 0.05$ or higher (Chi^2, parametric or non-parametric, as appropriate).
Results: We evaluated 282 cases, 56% male, median age at diagnosis of 16 years, and 60% with hepatic presentation. The presence of AF was associated with higher serum and urinary copper, and GGT levels, and lower baseline cholesterol and triglycerides. Neurological manifestations (NM) (KF ring, symptoms or positive MRI) and LOF mutations were more frequent in AF. HIA was associated with higher baseline serum and urinary copper, transaminases, and GGT. Hepatic presentation was more frequent, and asymptomatic cases were rare. NMs appeared similarly in A2-3 vs A0-1. Steatosis was associated with higher baseline ALT, GGT, and triglycerides, with no differences in serum or urinary copper levels. Hepatic presentation was more frequent and NM were rare. We found no differences in transaminase improvement at 1 and 3 years related to any of the three lesions studied. AF and HIA were associated with a higher frequency of poor clinical outcome and S was associated with a lower risk for it. There were no differences in age at diagnosis or baseline ceruloplasmin within each lesion. Cases with M645R presented with less AF and HIA and a higher frequency of S.
Conclusion: Of the lesions studied, AF and HIA were associated with more advanced phenotypes, worse clinical outcomes and greater impairment of copper metabolism, without influencing transaminase improvement at 1 and 3 years. S was associated with better clinical outcomes, with dyslipidemia and milder phenotypes, but not with copper metabolism. M645R was associated with milder lesions and LOF with higher presence of AF.

THU-268

Portal cavernoma may develop during the course of porto-sinusoidal vascular disorder

Mathilde Guerillot[1], Sarah Shalaby[2], Riccardo Sartoris[3], Elisa Pinto[4,5], Alba Díaz[6], Lucile Moga[1,7], Aurélie Plessier[1], Maria Ángeles García-Criado[8], Maxime Ronot[3,7], Marco Senzolo[5], Virginia Hernández-Gea[2], Pierre-Emmanuel Rautou[1,7]. *[1]AP-HP, Hôpital Beaujon, Service d'Hépatologie, DMU DIGEST, Centre de Référence des Maladies Vasculaires du Foie, FILFOIE, ERN RARE-LIVER, Clichy, France; [2]Hepatic Hemodynamic Laboratory, Liver Unit, Hospital Clínic, Clínic Barcelona, Health Care Provider of the European Reference Network on Rare Liver Disorders (ERN-RareLiver), CSUR Centro de referencia del Sistema Nacional de Salud en Enfermedad Hepática Vascular Compleja en adultos. Fundació de Recerca Clínic Barcelona-Institut d'Investigacions Biomèdiques August Pi i Sunyer (FRCB-IDIBAPS), Barcelona, Spain. Centro de Investigación Biomédica en Red Enfermedades Hepáticas y Digestivas (CIBEREHD), Madrid, Spain. AGAUR SGR2021 01115. Medicine Department, Faculty of Medicine, and health Science, Universitat de Barcelona, Barcelona, Spain; [3]AP-HP, Hôpital Beaujon, Service d'Imagerie médicale, Clichy, France; [4]Unit of Vascular Liver Disease and Treatment of Portal Hypertension, Gastroenterology, University Hospital of Padova, Health Care Provider of the European Reference Network on Rare Liver Disorders (ERN Rare-Liver), Padova, Italy; [5]Department of Surgery, Oncology and Gastroenterology, University of Padova, Padova, Italy; [6]Department of*

Pathology, Hospital Clínic, Institut de Investigacions Biomèdiques August Pi iSunyer (IDIBAPS), CIBEREHD (Centro de Investigación Biomédica en Red Enfermedades Hepáticas y Digestivas), University of Barcelona, Barcelona, Spain; [7]Université Paris-Cité, Inserm, Centre de recherche sur l'inflammation, UMR 1149, Paris, France; [8]Radiology Department, CDI, BCLC Group, Hospital Clínic of Barcelona, University of Barcelona, Barcelona, Spain
E-mail: mathilde.guerillot@gmail.com

Background and aims: Porto-sinusoidal vascular disorder (PSVD) is a clinico-pathological entity affecting intrahepatic liver vessels in the absence of cirrhosis. Its definition and exclusion criteria, proposed in 2019 by VALDIG, were based on expert opinion. While portal vein thrombosis was permitted, portal cavernoma was considered an exclusion criterion. The aim of this study was to reassess this exclusion criterion and determine whether portal cavernoma may occur during the natural history of PSVD.
Method: We retrospectively analysed imaging findings of patients with PSVD, diagnosed according to VALDIG criteria, from three European reference centres for vascular liver diseases. We identified patients without portal cavernoma at the time of PSVD diagnosis (defined as the date of liver biopsy), who subsequently developed a portal cavernoma during follow-up, diagnosed using cross-sectional imaging (CT or MRI).
Results: Out of 625 patients with PSVD, 10 patients (1.6%) developed a portal cavernoma, after a median follow-up of 114 months (IQR, 66–162) after PSVD diagnosis. All 10 patients had a history of portal vein thrombosis (PVT) either before (n = 7) or concurrently with cavernoma (n = 3) diagnosis. Cavernoma location was intrahepatic in 7 patients and extrahepatic (pericholedochal and pericholecystic) in 7 patients (4 patients had both intrahepatic and extrahepatic cavernoma). There was no portal trunk cavernoma. Out of the 10 patients who developed cavernoma, 6 were men; median age was 38 (IQR, 28–47). Conditions associated with PSVD included human immunodeficiency virus (HIV) infection (n = 2), TERT mutation (n = 1), common variable immune deficiency (n = 1), splenic marginal zone lymphoma (n = 1), history of azathioprine treatment for polyradiculoneuritis (n = 1), and Crohn's disease (n = 1), while no associated condition was found in 3 patients. These patients had advanced PSVD: 6 of them experienced variceal bleeding, ascites and/or hepatic encephalopathy before or within one year after cavernoma diagnosis. The 4 remaining patients all had specific signs of portal hypertension at the time of cavernoma diagnosis.
Conclusion: Our findings suggest that, although uncommon, portal cavernoma can occur during the natural course of PSVD, most often in association with portal vein thrombosis and advanced portal hypertension. It should therefore be reconsidered as an exclusion criterion and warrant reconsideration in future diagnostic classifications.

THU-269

Ultrasound markers of high-output heart failure in hereditary Haemorrhagic Telangiectasia with hepatic vascular malformations: a danish cohort study

Pernille Haahr[1], Mikael Kjær Poulsen[2], Jens Kjeldsen[1], Massar Omar[2], Simon Tholander[3], Annette Dam Fialla[1], Anette Kjeldsen[3].
[1]Department of Medical Gastrointestinal Diseases, Odense University Hospital, Odense, Denmark; [2]Department of Cardiology, Odense University Hospital, Odense, Denmark; [3]Department of Oto-rhino-laryngology, Head and Neck surgery, Odense University Hospital, Odense, Denmark
E-mail: pernille.darre.haahr3@rsyd.dk

Background and aims: Hereditary haemorrhagic telangiectasia (HHT) is a rare autosomal dominant disorder frequently associated with hepatic arteriovenous malformations (HAVMs). Up to 78% of patients with HHT develop HAVMs, which may lead to haemodynamic alterations, increased cardiac preload, and progression to high-output heart failure (HOHF). This study aimed to determine the prevalence of HOHF and assess the relationship between HAVM severity, stroke volume, cardiac output, and index in patients with HHT. A secondary aim was to explore the haemodynamic mechanisms underlying HOHF and evaluate the usefulness of transthoracic echocardiography (TTE) in this patient group.
Method: A cohort study was conducted including all HHT patients registered in the national Danish HHT database residing in the regions of Zealand and Southern Denmark. Eligible participants underwent clinical evaluation, hepatic ultrasound, and transthoracic echocardiography. HAVMs were graded according to the Buscarini classification.
Results: Of 203 eligible patients, 152 (75%) consented to participate. The mean age was 51 years (range 18–84), and 58% were female. HAVMs were identified in 102 (67.1%) of participants, of whom 23 (15.1%) were classified as Grade 4. HOHF was present in 10 (6.6%) of patients, with nine (90%) of these cases occurring in individuals with grade 4 HAVMs. Cardiac index demonstrated a significant positive correlation with HAVM severity, with a mean increase of 0.81 L/min/m^2 between HAVM grades 0–1 and grade 4 (95% CI [0.48–1.13]).
Conclusion: The prevalence of HOHF was consistent with previous findings. Stroke volume, cardiac output and cardiac index increased in parallel with HAVM severity, supporting the role of transthoracic echocardiography as a valuable screening tool for identifying HHT patients at risk of haemodynamic complications.

THU-270

Biochemical response is associated with liver stiffness stability in patients with primary biliary cholangitis treated with seladelpar for up to 36 months: interim results from the open-label ASSURE study

Gideon M. Hirschfield[1], Christopher L. Bowlus[2], Christophe Corpechot[3], Kris V. Kowdley[4], Alejandra Villamil[5], Andreas E. Kremer[6], Palak J. Trivedi[7], Yiannis Kallis[8], Sook-Hyang Jeong[9], Hany Elbeshbeshy[10], Kyung min Kwon[11], Victor De Ledinghen[12], Xin Qi[11], Daria B. Crittenden[11], Cynthia Levy[13].
[1]The Autoimmune and Rare Liver Disease Programme, Toronto General Hospital, Toronto, ON, Canada; [2]University of California Davis School of Medicine, Sacramento, CA, United States; [3]Sorbonne University, Paris, France; [4]Liver Institute Northwest, Seattle, WA, United States; [5]Hospital Italiano de Buenos Aires, Buenos Aires, Argentina; [6]University Hospital Zürich, University of Zürich, Zürich, Switzerland; [7]University of Birmingham and University Hospitals Birmingham Queen Elizabeth, Birmingham, United Kingdom; [8]Barts Liver Centre, Blizard Institute, Queen Mary University of London, London, United Kingdom; [9]Seoul National University Bundang Hospital, Seoul National University, Seoul, Korea, Rep. of South; [10]Saint Louis University School of Medicine, St. Louis, MO, United States; [11]Gilead Sciences, Inc., Foster City, CA, United States; [12]Echosens, Paris, France; [13]Miller School of Medicine, University of Miami, Miami, FL, United States
E-mail: gideon.hirschfield@uhn.ca

Background and aims: Liver stiffness measurement (LSM) is a non-invasive indicator associated with clinical outcomes in patients with liver disease, including primary biliary cholangitis (PBC). The ongoing, open-label Phase 3 ASSURE study (NCT03301506) is evaluating long-term efficacy and safety of seladelpar (SEL). We recently reported stability of LSM in patients (pts) treated with SEL with up to 3 years of treatment in an interim ASSURE analysis. Here, we report the association of biochemical response at Month (M)12 with LSM change in ASSURE.
Method: Patients from RESPONSE (NCT04620733) and legacy SEL studies enrolled in ASSURE and received open-label SEL 10 mg once daily. LSM by FibroScan was an exploratory endpoint. Values with confirmed interquartile range (IQR)/LSM ratio > 30% were excluded. We conducted an interim analysis of all patients in ASSURE with ≥ 1 post-baseline (BL) LSM as of Jan 31, 2025. BL was defined as SEL initiation in RESPONSE or ASSURE. Composite biochemical response (CBR) at M12 was defined as alkaline phosphatase (ALP) < 1.67 times

the upper limit of normal (ULN), ≥ 15% ALP reduction from BL and total bilirubin ≤ ULN. LSM changes by CBR status at M12 were assessed through M36. LSM change > 30% was considered clinically meaningful. Comparison of BL characteristics and multivariate analysis were performed to identify factors associated with stable/improved vs worsening LSM (> 30%) at M36.
Results: A total of 311 pts were evaluable; 114 had available M36 LSM values. Among all pts, 68% (213/311) achieved CBR at M12. In pts with CBR at M12, BL age was 59 years, ALP 244 U/L, and LSM 8.9 kPa. In pts without CBR at M12, BL mean age was 57 years, ALP 384 U/L, and LSM 12.1 kPa. In pts with CBR at M12, LSM remained stable (median change, −7%) at M36, vs an LSM increase in pts without CBR at M12 (median change, +27% at M36). Among pts with vs without CBR at M12, 19% vs 9% improved by > 30% and 15% vs 48% worsened LSM by > 30%. Pts who were stable or improved were older and had lower ALP (< 1.5 × ULN, 19% vs 0%) at BL with higher rates of achieving CBR at M12 (87% vs 56%) compared to those who worsened ($p < 0.05$). Multivariate analysis showed CBR at M12 was associated with stable/improved LSM at M36 (odds ratio 5.57; $p < 0.05$).
Conclusion: In ASSURE, biochemical response with SEL at M12 was associated with liver stiffness stability at up to 3 years. Further assessment of the impact of biochemical improvement on liver stiffness with SEL is warranted.

THU-271
Impact of UGT1A1 variants on longitudinal Bilirubin trajectories in Korean infants with prolonged unconjugated hyperbilirubinemia

Kyung Jae Lee[1], Jeana Hong[2,3]. [1]*Department of Pediatrics, Korea University Guro Hospital, Seoul, Korea, Rep. of South;* [2]*Kangwon National University College of Medicine, Chuncheon, Korea, Rep. of South;* [3]*Department of Pediatrics, Kangwon National University Children's Hospital, Chuncheon, Korea, Rep. of South*
E-mail: kjlee@kumc.or.kr

Background and aims: Genetic varints of UDP-glucuronosyltransferase1A1 gene (*UGT1A1*) influence susceptibility to neonatal unconjugated hyperbilirubinemia, with ethnic differences noted. We investigated the spectrum of *UGT1A1* variants in Korean infants with prolonged jaundice and evaluated their longitudinal effect on the clinical course.
Method: This multicenter retrospective study included 65 Korean infants referred for prolonged or severe unconjugated hyperbilirubinemia. Clinical and laboratory data were collected, and *UGT1A1* genotyping was performed. Variant frequencies were compared with the Korean Reference Genome Database (KRDGB). Longitudinal total bilirubin (TB) trajectories across predefined postnatal age intervals (2–4, 5–7, 8–10, 11–13 weeks) were assessed using linear mixed-effects models. Multivariable linear regression evaluated independent predictors of TB at presentation and during follow-up. An additive genetic risk score (GRS) was constructed from the variants positively associated with prolonged hyperbilirubinemia.
Results: The c.211G>A variant was the most prevalent polymorphism, with a risk allele frequency of 54.6%, significantly higher compared to the KRDGB (OR = 5.75, $p < 0.001$). Significant associations were also observed for c.1091C>T, c.1456T>G, and c.-64G>C, while c.-3156G>A showed a reduced risk. Among the 5 variants, c.211G>A was the only variant associated with higher initial TB levels, and GRS positively correlated with initial TB level ($\rho = 0.32$, $p = 0.008$). The c.211G>A risk allele number independently predicted higher TB at presentation ($\beta = +1.91$ mg/dL per allele, $p = 0.043$) and at 2–4 weeks ($\beta = +2.80$ mg/dL per allele, $p = 0.008$); however, this effect attenuated and lost statistical significance after 5 weeks of age. Neither individual variants nor a cumulative *UGT1A1* GRS altered the rate of bilirubin decline through 13 weeks of age. Family history of jaundice was also independently associated with hyperbilirubinemia at presentation ($\beta = +3.44$, $p = 0.025$) and remained significant at 5–7 weeks of age ($\beta = +4.06$, $p = 0.029$).
Conclusion: The c.211G>A variant is the dominant genetic determinant of higher bilirubin burden, early in the clinical course in Korean infants, but its influence is transient. These findings support genotype-informed risk stratification and counseling in prolonged neonatal jaundice.

THU-272
The pharmacokinetic profile of a new trientine tetrahydrochloride formulation supports simpler once-daily dosing for the treatment of wilson disease: results of the triumph-3 study

Karl Heinz Weiss[1], Thomas Ashdown[2], Ulrike Lorch[2], Carla Bennett[3], Nick Manamley[3], Farah Lawrence-Wilde[3], C. Omar Kamlin[3].
[1]*Krankenhaus Salem der Evang. Stadtmission Heidelberg gGmbH, Heidelberg, Germany;* [2]*Richmond Pharmacology, London, United Kingdom;* [3]*Orphalan SA, London, United Kingdom*
E-mail: karlheinz.weiss@krankenhaus-salem.de

Background and aims: The therapeutic goal of Wilson Disease (WD) is to control copper levels and to modify disease progression. All approved anti-copper drugs require life-long medication with at least twice-daily dosing. Known food-drug interactions make timing of intake critical, thus creating difficulties and challenges for people living with WD to maintain long-term adherence. Efficacy of chelation is determined by total exposure of active drug determined by pharmacokinetic measure of area under the curve (AUC). This study describes the pharmacokinetic (PK) profile a new trientine tetrahydrochloride (TETA 4HCl) formulation developed to be administered once a day (QD).
Method: This phase 1, single centre, randomised, open-label, cross-over study evaluated and compared the PK, safety and tolerability of a new 300 mg trientine base TETA 4HCl formulation with EU approved 150 mg trientine base (TETA 4HCl; Cuprior product; NCT06128954). A total daily dose (TDD) of 900 mg trientine base was evaluated by comparing QD dosing of the new formulation (x3 tablets = 900 mg) with 6 × 150 mg trientine base in 2 [BID] equally divided doses 8 hours apart. Initial dosing occurred following an overnight fast and 1 hour prior to breakfast. Blood samples were taken prior to dosing and at prespecified intervals for 48 hours followed by a 5–7-day washout period between cross-over.
Results: A total of 26 participants received both treatment sequences and completed the study. PK profiles of the two formulations were as expected, single peak and gradual decline in plasma levels with the QD formulation, and a bimodal pattern, with BID TETA 4HCl respectively. A dose-dependent higher peak concentration (C_{max}) suggesting linear PK was observed with new QD TETA 4HCl, with comparable systemic TETA AUC_{0-24} values observed for QD and BID TETA 4HCl respectively. The geometric mean ratios (GMR) of the new QD formulation relative to the same TDD of BID TETA 4HCl were the following: C_{max} (2.192), AUC_{0-24} (1.155) AUC_{0-48} (1.14) and AUC_{inf} (1.12). Five participants experienced a total of 8 adverse events (AE); 3 and 5 following new QD and BID TETA 4HCl formulations respectively. All AEs were mild apart from 1 moderate (viral infection after BID TETA 4HCl) event.
Conclusion: The new 300 mg trientine base formulation of TETA 4HCl administered QD with a TDD of 900 mg was well tolerated and demonstrated comparative PK profile to 900 mg of approved TETA 4HCl administered BID.

THU-273
Has the clinical profile of hypoxic hepatitis changed over the past decades?

Edeline Kaze[1], Vincent Huberlant[2], Jean Henrion[2]. [1]*Hôpital Érasme-Cliniques Universitaires de Bruxelles, Clinique de l'Europe, Bruxelles, Belgium;* [2]*CHU Helora - Hôpital de la Louvière - Site Jolimont, La Louvière, Belgium*
E-mail: kazeedeline@gmail.com

Background and aims: Hypoxic Hepatitis (HH) is defined by a massive and brutal elevation of serum aminotransferases activities (S-AT > 20XULN) occurring in the context of hemodynamic failure, after exclusion of other causes of acute hepatocellular necrosis. Thirty-five years ago, we collected the first large series of HH (more than 100 cases) and subsequently, we reported the first hemodynamic study on this topic (1). Recently, we had the impression that the clinical profile of HH has changed. The aim of this study was to assess whether the frequency, causes and prognosis of HH have changed over the last 35 years.
Method: We compared a series of 138 cases of HH prospectively collected during a 10-year period (1981 to 1991 - Series 1) to a series of 139 cases of HH retrospectively collected during a 4-year period (2020 to 2023 - Series 2). Both series were collected in the intensive care units (ICUs) of the same hospital under the supervision of the same investigator (JH). For Series 1, a new analysis of the individual data – still available – was performed. For Series 2, cases of HH were identified through the hospital laboratory database by screening for all ICU patients with S-AT ≥ 20XULN followed by review of their electronic medical records.
Results: There were no significant differences in age and gender between the two series with a 65% male prevalence in both series and a mean age of 68 years in Series 1 compared to 67 years in Series 2. The prevalence of HH in ICUs increased from 0.8% (138/15,616 admissions) in Series 1 to 2.5% (139/5118 admissions) in Series 2 ($p < 0.001$). The main causes of hemodynamic failure were cardiac in 67% versus 45% ($p < 0.001$), respiratory in 17% versus 8% ($p < 0.02$), toxic-infectious in 12% versus 27% ($p < 0.01$) or hypovolemic-hemorrhagic in 1% versus 17% ($p < 0.001$) between Series 1 and Series 2, respectively. The in-hospital mortality was higher in the more recent cohort : 56% in Series 1 versus 68% in Series 2 ($p = 0.05$).
Conclusion: The clinical profile of HH has changed markedly over the last decades. The frequency of HH in ICUs has increased, the underlying causes of hemodynamic failure have evolved and the mortality has not decreased despite advances in intensive care medicine.

THU-274

Exploring pregnancy among Wilson disease patients in Europe: results from an exploratory survey to patients from the ERN RARE-LIVER consortium

Paulina Kremser[1], Aida Regi[2,3], Wiebke Papenthin[1,3], Caren Ramien[3], Willy Visser[3,4], Thomas Sandahl[3,5], Zoe Mariño[3,6], Wilhelmus J Kwanten[3,7]. *[1]German Association for Wilson Disease Patients (Morbus Wilson e.V.), Berlin, Germany; [2]Asociación Española de Familiares y Enfermos de Wilson (AEFE), Barcelona, Spain; [3]ERN-RARE LIVER, Hamburg, Germany; [4]Erasmus MC, Rotterdam, Netherlands; [5]Aarhus University Hospital, Aarhus, Denmark; [6]Liver Unit, Hospital Clínic Barcelona, IDIBAPS, CIBERehd, Universitat de Barcelona, Barcelona, Spain; [7]Department of Gastroenterology and Hepatology, Antwerp University Hospital (UZA), Laboratory of Experimental Medicine and Pediatrics (LEMP), Faculty of Medicine and Health Sciences, University of Antwerp, Antwerp, Belgium*
E-mail: zmarino@clinic.cat

Background and aims: Wilson Disease (WD) is frequently diagnosed when young. Consequently, WD patients will face challenges regarding family planning and pregnancy. This survey aimed to explore management, concerns and perceived impact of pregnancy amongst WD women.
Method: The survey was designed by patients' representatives and physicians within the ERN Wilson and Pregnancy Working Groups and launched through the ERN platform (Nov.24 – Feb.25). The survey contained 35 questions on demographics, counselling, management, outcomes and concerns related to family planning, pregnancy and breastfeeding.
Results: We received responses from 44 adult WD women (84% within 18–50 years) in 13 different countries, mainly followed by hepatologists and/or neurologists (77%). Among them, 79 pregnancies were recorded, while 11 were never pregnant. In 44% of the women, family planning was affected by WD. Up to 35/44 (80%) referred active concerns, frequently (43%) related to the babies' health. Specific worries about contraceptive methods were collected and included potential impact on WD (92%), treatment adverse events (32%) or contraceptive effectiveness because of WD (12%). Information given by their primary treating physician was felt as insufficient for both contraceptive methods (63%) and pregnancy (38%). Active advice against pregnancy was reported in 10 cases. Most of the pregnancies (93%) occurred after WD diagnosis. Miscarriages occurred in 22 pregnancies (28%; 86% of them after diagnosis), while 57 offspring were delivered at term (96% healthy). Only 25% of the pregnancies were labelled as high-risk and followed at WD reference centres. Follow-up increased in 65% of pregnancies. D-penicillamine and zinc were used in 55% and 26% of the pregnancies. Most of the pregnancies (89%) were uncomplicated for the mother, with 8 mild WD-related complications (liver biochemistry). After birth, 66% gave breastfeeding, even though 32% of them were advised against.
Conclusion: This survey describes the real-life experiences among patients with WD in Europe. Most of the pregnancies were successful. However, when asked in a systemic approach, many active concerns existed. Patients faced lack of or incorrect information likely reflecting limited experience amongst health care providers. This survey helps to raise awareness and activates the need for improvement to inform and manage WD patients with parental desire.

THU-275

Understanding Wilson disease beyond traditional phenotypes: cross-sectional analysis of study entry data from an international registry (iWilson)

Marina Berenguer[1], Zoe Mariño[2], Emmanuel Tsochatzis[3], Piotr Socha[4], Christian Hartmann[5], Thomas Berg[6], Frank Tacke[7], Aurélia Poujois[8], Eduardo Couchonnal[9], Heiner Wedemeyer[10], Saad Alghamdi[11], David Cassiman[12], Anna Czlonkowska[13], Javier Ampuero[14], Ildefonso Quinoñes Morales[15], Joanna Moore[16], Caroline Roatta[17], C. Omar Kamlin[18], Farah Lawrence-Wilde[19], Claus Niederau[20], Anil Dhawan[21], Dave Shaw[22], Pramod K. Mistry[23]. *[1]Hospital Universitario Y Politécnico La Fe, Valencia, Spain; [2]University Hospital Clinic of Barcelona, Barcelona, Spain; [3]Royal Free Hospital, London, United Kingdom; [4]The Children's Memorial Health Institute, Warsaw, Poland; [5]Universitätsklinikum Düsseldorf, Düsseldorf, Germany; [6]Universitätsklinikum Leipzig, Leipzig, Germany; [7]Charité - Universitätsmedizin Berlin, Berlin, Germany; [8]Hospital Foundation Adolphe de Rothschild, Neurology, Paris, France; [9]Hospices Civils De Lyon, Lyon, France; [10]Hannover Medical School, Hannover, Germany; [11]King Faisal Specialist Hospital & Research Centre, Riyadh, Saudi Arabia; [12]University Hospital Leuven, Leuven, Belgium; [13]Instytut Psychiatrii I Neurologii, Warszawa, Poland; [14]Hospital Universitario Virgen del Rocío, Sevilla, Spain; [15]Hospital Universitario de Gran Canaria Doctor Negrín, Las Palmas de Gran Canaria, Spain; [16]Saint James' University Hospital, Leeds, United Kingdom; [17]Association Bernard Pepin, Paris, France; [18]Orphalan Ltd, Birkirkara, Malta; [19]Orphalan SA, London, United Kingdom; [20]St. Josef-Hospital Oberhausen, Oberhausen, Germany; [21]King's College Hospital, London, United Kingdom; [22]Orphalan SA, Boston, United States; [23]Yale University, New Haven, United States*
E-mail: marina.berenguer@uv.es

Background and aims: Rare disease registries are an important source of real-world evidence that small, randomised trials cannot capture. The International Wilson Disease (iWD) registry was established in 2021 (NCT05239858) with the objective to describe, through prospective data collection, the natural history of treated Wilson disease (WD). We aim to provide a descriptive cross-sectional analysis from the study entry visit of enrolees in the iWD.
Method: Baseline visit data from 16 sites in 7 countries, including demographics, WD phenotype, WD specific clinical parameters, current health status and medications.

Results: Between June 2022 and July 2024, 387 subjects (194; 50.1% female) were enrolled. (Number; number of sites in the region) from Belgium (15;1), France (60;2), Germany (86;4), Poland (67;2), Spain (87;4), Saudi Arabia (24;1) and UK (48;2). Median (range) age at diagnosis was 18 years (0,67). At enrolment, median time from diagnosis and onset of first WD symptoms was 15.5 (1,58) and 19 (3,60) years respectively with 42.6% diagnosed <18 years of age. Clinical symptoms were reported in 360 subjects (hepatic [58%], neurologic [21%], hepato-neuropsychiatric [4%], psychiatric [2%]. 15% were asymptomatic. The proportion of this cohort diagnosed later in life (36–65 years) was 10.3%. The greatest proportion identifying as asymptomatic were from the UK (20/42; 48%). The majority (77.2%) self-reported their current health to range from good to excellent. A liver ultrasound (n = 140; 36.2%) confirmed cirrhosis in 31 subjects (8%). Liver biopsy (n = 18), 5 with evidence of cirrhosis. Utilisation of Liver MRI was low with exception of Saudi Arabia. Distribution of WD therapy from 369 records: d-penicillamine (DPA; 41.6%), zinc salts (28.8%), trientine tetrahydrochloride (16.2%), trientine dihydrochloride (8.5%), unspecified trientine (8.1%). Marked geographic variation in treatment patterns was observed. Zinc salts predominated in Poland (70%) with minimal trientine use (<1%), DPA was most frequently prescribed in Belgium (69%) with trientine predominating (52%) in France.
Conclusion: Baseline data from iWD gathered across geographic boundaries, captures real-time commonalities and differences of cross-sectional disease status and treatment experience from more than 380 people living with WD. Future longitudinal analyses may enable comparison of regional diagnostic and therapeutic approaches and outcome assessment across healthcare systems over time, supporting the evolution toward biology-informed care.

THU-276-YI
Safety of infliximab in sarcoidosis and effect on hepatic involvement – a retrospective cohort study
Elizabeth Low[1], Katie Ward[2,3], Huw Beynon[4], Shahir Hamdulay[4], Pamela Mangat[4], Neil Halliday[1,5]. *[1]Department of Hepatology, Royal Free Hospital, London, United Kingdom; [2]Department of Respiratory Medicine, Royal Free Hospital, London, United Kingdom; [3]Imperial College London, London, United Kingdom; [4]Department of Rheumatology, Royal Free Hospital, London, United Kingdom; [5]University College London, London, United Kingdom*
E-mail: elizabeth_low312@hotmail.com

Background and aims: Hepatic involvement in systemic sarcoidosis is increasingly recognised but remains under-reported due to heterogeneous disease manifestations. Infliximab, an anti–tumour necrosis factor-alpha agent, is used for refractory sarcoidosis; however, its liver safety and efficacy in hepatic sarcoid are poorly characterised. We evaluated the impact of infliximab on liver function tests (LFTs) in sarcoidosis patients with or without hepatic involvement and assessed hepatic disease resolution rates.
Method: We conducted a single-centre retrospective cohort study of adults prescribed infliximab for sarcoidosis between January 2003 and September 2025 at a UK tertiary sarcoidosis referral centre. Baseline characteristics, organ involvement, infliximab indication and dosing, and serial LFTs were extracted from medical records. Infliximab-related LFT derangement was defined as a new liver enzyme abnormality outside reference intervals from previously normal results without an alternate cause. Univariate analyses assessed the impact of hepatic sarcoid and infliximab therapy on liver enzymes.
Results: 118 patients (50.9% female; mean age 55.0 ± 11.2 years) were followed for a mean of 49.8 ± 45.5 months. Sixteen (13.6%) had hepatic sarcoidosis, with hepatic disease the primary indicator for infliximab in one (0.9%). Baseline transaminases were higher in the hepatic sarcoid cohort than those without liver involvement (ALT 48 vs. 22 IU/L, AST 35 vs. 19 IU/L, $p < 0.001$), but remained within reference limits. Median baseline alkaline phosphatase was 70 IU/ml (IQR 53–89), with a median reduction of 69.5 IU/L (IQR −99.0 to −31.0) in those with elevated pre-infliximab levels. Infliximab-related LFT derangement occurred in 21 (17.8%), resolving in 19 (90.5%) within a median 3.0 months (IQR 1.0–6.0) without treatment withdrawal. LFT changes from infliximab were not more frequent in those with hepatic sarcoid; only two (12.5%) experienced transient derangement, both resolving with continued therapy. No patient discontinued infliximab due to hepatotoxicity. Hepatic sarcoid resolution – defined by biochemical, radiologic and/or clinical improvement – occurred in 10 (62.5%) patients, with 3 awaiting reassessment at study end.
Conclusion: In the largest reported cohort of hepatic sarcoidosis receiving infliximab, LFT abnormalities were infrequent and self-resolving. These findings support the safety of infliximab in sarcoid patients with or without liver involvement and suggest favourable outcomes in hepatic sarcoidosis.

THU-282
Spectrum of hepatic nodules and hepatocellular carcinoma in Fontan-associated liver disease: a real-world cohort
Camilla Mancini[1,2], Rosalinda Palmieri[3], Giulia Di Già[3], Demma Shirin[2], Claudia Telesca[2], Margherita Spigaroli[4], Giuseppe Maria Ettorre[5], Adriano Pellicelli[2], Valerio Giannelli[2]. *[1]University of Modena and Reggio Emilia, Internal Medicine Departement, Modena, Italy; [2]San Camillo Forlanini Hospital, Inter-hospital Transplant Unit, Hepatology Unit, Roma, Italy; [3]Ospedale Pediatrico Bambino Gesù, Department of Medical and Surgical Sciences – Pediatric Cardiology, Roma, Italy; [4]Sapienza University of Rome, Department of Translational and Precision Medicine, Roma, Italy; [5]San Camillo Forlanini Hospitasl, Inter-hospital Transplant Unit, General Surgery and Transplantation Unit, Roma, Italy*
E-mail: cmancinimed@gmail.com

Background and aims: Fontan-associated liver disease (FALD) results from chronic hepatic congestion and hypoxia, leading to nodular transformation and an increased risk of hepatocellular carcinoma (HCC) through pathways that may differ from conventional inflammatory liver diseases. We aimed to describe the real-world spectrum of hepatic nodules in FALD and to explore clinical and laboratory correlates of regenerative/focal nodular hyperplasia (FNH)-like lesions and HCC, contextualising prevalence estimates according to follow-up duration.
Method: We performed a retrospective cross-sectional analysis of Fontan patients evaluated at our centre. Hepatic imaging reports were reviewed and patients were classified as having no nodules, regenerative/focal nodular hyperplasia (FNH)-like nodules, mass-like lesions, or hepatocellular carcinoma (HCC). Continuous variables were compared using Mann–Whitney tests and categorical variables using Fisher's exact test; Spearman correlations were used for exploratory analyses. Histology was recorded when available.
Results: Among 243 patients, hepatic nodules were identified in 136 (56.0%): 72 regenerative/FNH-like nodules, 58 mass-like lesions and 4 HCC. The point prevalence of HCC was 1.65% (4/243) in the overall cohort and 2.94% among patients with documented nodules, despite a predominantly short-to-mid term follow-up. Time since Fontan completion was available in 129/243 patients (median 4 years, IQR 3–6), with limited representation of long-term survivors (>10 years). Compared with patients without nodules (n = 107), regenerative/FNH-like lesions were associated with perihepatic effusion (11.1% vs 1.9%; OR 6.56; $p = 0.016$) and lower systolic blood pressure (median 111 vs 119 mmHg; $p = 0.025$). In exploratory comparisons, patients with HCC showed markedly higher alpha-fetoprotein levels (median 280.5 vs 2.3 ng/mL; $p = 0.0007$) and higher aspartate aminotransferase levels (median 44 vs 26 U/L; $p = 0.006$), while gamma-glutamyl transferase was not significantly associated.
Conclusion: In this real-world FALD cohort, hepatic nodules were frequent and HCC was already detectable despite predominantly short-to-mid term follow-up. Regenerative/FNH-like lesions

correlated with markers of systemic/hepatic congestion, supporting a distinct biological context in FALD. AFP and AST, together with older age and higher NT-proBNP, identified an exploratory signal associated with HCC. Larger datasets with longer follow-up are needed to refine time-dependent HCC risk estimates in this population.

THU-283

Exploring pregnancy among Wilson disease patients in Europe: results from a health-care providers' exploratory survey from the ERN RARE-LIVER consortium

Wilhelmus J Kwanten[1,2], Aida Regi[2,3], Paulina Kremser[4], Wiebke Papenthin[2,4], Caren Ramien[2], Willy Visser[2,5], Thomas Sandahl[2,6], Zoe Mariño[2,7]. *[1]Department of Gastroenterology and Hepatology, Antwerp University Hospital (UZA), Laboratory of Experimental Medicine and Pediatrics (LEMP), Faculty of Medicine and Health Sciences, University of Antwerp, Antwerp, Belgium; [2]ERN-RARE LIVER, Hamburg, Germany; [3]Asociación Española de Familiares y Enfermos de Wilson (AEFE), Barcelona, Spain; [4]German Association for Wilson Disease Patients (Morbus Wilson e.V.), Berlin, Germany; [5]Erasmus MC, Rotterdam, Netherlands; [6]Aarhus University Hospital, Aarhus, Denmark; [7]Liver Unit, Hospital Clínic Barcelona, IDIBAPS, CIBERehd, Universitat de Barcelona, Barcelona, Spain*
E-mail: zmarino@clinic.cat

Background and aims: Management of pregnancy in patients with Wilson Disease (WD) is challenging. Current guidelines recommend drug modifications and close follow-up to ensure favourable outcomes. However, due to its rarity and the lack of high-quality evidence-based data, monitoring is heterogeneous. We aimed at exploring how pregnancy in WD was managed among HCPs in Europe to have a broad understanding of real-life practice.

Method: The survey was designed by physicians and patients' representatives within the ERN Wilson and Pregnancy Working Groups and launched through the ERN platform (Nov.24–Feb.25). The ERN office was responsible for raw data compilation. The survey was composed of 35 questions; only one answer per centre was allowed to avoid duplications.

Results: We received results from 33 centres in Europe; most of them (66%) were ERN (affiliated) members and 39% were considered large (>30 WD patients). 76% of the surveys were led by hepatologists; 60% male; 54% with >10 years of experience in WD. Interestingly, 51% reported no previous experience with WD pregnant patients. Contraception and childbearing were claimed to be actively explored with patients in 76%, and pregnancy was planned in advance by 69%. When a patient became pregnant, 54% followed a multidisciplinary approach, and 91% increased monitoring (to ≥1 visit per trimester) by means of ALT (all centres) and urinary copper excretion (76%). Considering treatment, 79% reduced the dose of chelators, while zinc was maintained in most cases (79%), and very few (3) advocates for a switch to zinc in patients treated with chelators. The main reason to reduce WD therapy during pregnancy was to avoid potential harm to the foetus (66%). Breastfeeding was either encouraged or pro-cons discussed with the patient in most of the centres, but 8 (24%) recommended additional copper in the newborn by means of complementary formula milk or supplements. Guidelines and/or PubMed were consulted in >85% of centres whenever a patient with WD became pregnant. No differences were observed between large and small institutions.

Conclusion: This survey reflects real-life practice in Europe for WD and pregnancy. Most of the answers followed current guidelines' recommendations, although the level of evidence for these recommendations is low. In addition to raising awareness on the topic, this European survey may be the starting point for future research in this neglected but vitally important scenario.

THU-284

Missense variants in the ABCB11 gene and disease severity in patients with bile salt export pump deficiency

Mark Nomden[1], Alise D.E. de Groot[1], Antonia Felzen[1], Richard J. Thompson[2], Emmanuel Gonzalès[3,4], Irena Jankowska[5], Benjamin Shneider[6,7], Etienne Sokal[8], Seema Alam[9], Cigdem Arıkan[10], Henrik Arnell[11], Madeleine Aumar[12], Amer Azaz[13], Emna Barkaoui[14], Maria Belen Pallitto[15], Marisa Beretta[16], Jernej Brecelj[17], Dieter Clemens Broering[18,19], Pier Luigi Calvo[20], Mara Cananzi[21], Huey-Ling Chen[22], Guillermo Costaguta[23,24], Piotr Czubkowski[5], Lorenzo D'Antiga[25], Elisa de Carvalho[26], Dominique Debray[27], Antal Dezsőfi-Gottl[28], Angelo Di Giorgio[29], Ozlem Durmaz[30], Alexandre Fabre[31], Sandra Ferreira[32], Ryan T. Fischer[33], Björn Fischler[34], Cristina Campos Gonçalves[35,36], Enke Grabhorn[37], Tassos Grammatikopoulos[2], Girish Gupte[38], Winita Hardikar[39], Loreto Hierro Llanillo[40], Giuseppe Indolfi[41], Emmanuel Jacquemin[3,4], Carolina Jimenez-Rivera[42], Marianne Hørby Jørgensen[43], Binita M. Kamath[44], Wikrom Karnsakul[45], Nanda Kerkar[46,47], Kyung Mo Kim[48], Jae Sung Ko[49], Denitza Kofinova[50], Nolwenn Laborde[51], Zhong-Die Li[52], Patryk Lipiński[53], Rohan Malik[54], Saeed Mohammad[55], Yael Mozer - Glassberg[56], Gema Muñoz Bartolo[40], Gabriella Nebbia[57], Emanuele Nicastro[25], Felipe Ordoñez[58], Anna Orłowska-Wójcicka[5], Arti Pawaria[59], Tudor Lucian Pop[60], Jesús Quintero Bernabeu[61], Giusy Ranucci[62], Aathira Ravindranath[63], Nathalie Rock[64], Ioannis Roilidis[65], Mathias Ruiz[66], Thomas Sandahl[67], Srinivas Sankaranarayanan[68], Mohammad Shagrani[18,19], Eyal Shteyer[69], Pooja Spector[70], James E. Squires[71], Ekkehard Sturm[72], Cristina Targa[73], Marise Tofoli[74], Bethany Tucker[2], Christos Tzivinikos[75], Wendy L. van der Woerd[76], Georg-Friedrich Vogel[77,78], Heng Wang[79], Jian-She Wang[52], Sabina Wiecek[80], Aglaia Zellos[81], Andréanne N. Zizzo[82], Estella Alonso[7,83], Ronald Sokol[7,84], Frederick J. Suchy[7,84], Kathleen M. Loomes[7,44], Simon P. Horslen[7,71], Philip Rosenthal[7,85], Girish Rao[7,86], Pamela L. Valentino[7,87], Alexander Miethke[7,88], Rohit Kohli[7,89], Bettina Hansen[90,91,92], Paola Mian[93,94], Henkjan J. Verkade[1]. *[1]Division of Gastroenterology and Hepatology, Department of Pediatrics, University Medical Center Groningen, Groningen, Netherlands; [2]Paediatric Liver, GI and Nutrition Centre, King's College Hospital, London, United Kingdom; [3]Pediatric Hepatology and Liver Transplantation Unit, National Reference Centre for Rare Pediatric Liver Diseases, FILFOIE, ERN RARE LIVER, Bicêtre Hospital, AP-HP. Université Paris-Saclay, Le Kremlin-Bicêtre, Paris, France; [4]Inserm U1193, Hepatinov, University of Paris, Orsay, France; [5]Department of Gastroenterology, Hepatology, Nutritional Disorders and Pediatrics, Children's Memorial Health Institute, Warsaw, Poland, Warsaw, Poland; [6]Division of Pediatric Gastroenterology, Hepatology, and Nutrition, Department of Pediatrics, Baylor College of Medicine, Houston, United States; [7]Childhood Liver Disease Research Network (ChiLDReN), Ann Arbor, Michigan, United States; [8]Pediatric Gastorenterology and Hepatology, Université Catholique de Louvain, Cliniques St Luc, Brussels, Belgium; [9]Pediatric Hepatology, Institute of Liver and Biliary Sciences, New Delhi, India; [10]Department of Pediatric Gastroenterology and Organ Transplant, Koc University School of Medicine, Istanbul, Türkiye; [11]Pediatric Gastroenterology, Astrid Lindgren Children's Hospital, Karolinska University Hospital, and Women's and Children's Health, Karolinska Institutet, Stockholm, Sweden; [12]Department of Pediatric Gastroenterology Hepatology and Nutrition CHU Lille, Univ. Lille, Inserm U1286- INFINITE- Institute for Translational Research in Inflammation, Lille, France; [13]Pediatric Gastroenterology, Hepatology and Nutrition, Sheikh Khalifa Medical City, Abu Dhabi, United Arab Emirates; [14]Department of Pediatrics, Tunis Children Hospital, Tunis, Tunisia; [15]Department of Gastroenterology and Hepatology, Hospital Italiano, CABA, Buenos Aires, Argentina; [16]Faculty of Health Sciences, Wits Donald Gordon Medical Centre, University of the Witwatersrand, Johannesburg, South Africa; [17]Department of Pediatric Gastroenterology, Hepatology and Nutrition, University Children's Hospital Ljubljana, Ljubljana,*

Slovenia; [18]Liver & SB Transplant & Hepatobiliary-Pancreatic Surgery, King Faisal Specialist Hospital & Research Center, Riyadh, Saudi Arabia; [19]Alfaisal University, College of Medicine, Riyadh, Saudi Arabia; [20]Pediatic Gastroenterology Unit, Regina Margherita Children's Hospital, Azienda Ospedaliera Città Della Salute e Della Scienza University Hospital, Turin, Italy; [21]Pediatric Gastroenterology, Digestive Endoscopy, Hepatology, and Care of the Child With Liver Transplantation, Department of Children's and Women's Health, University Hospital of Padova, Padova, Italy; [22]Department of Pediatrics, National Taiwan University Children's Hospital, Department and Graduate Institute of Medical Education and Bioethics, National Taiwan University College of Medicine, Taipei, Taiwan; [23]Sanatorio de Niños de Rosario, Santa Fe, Argentina; [24]CHU de Quebec-Université Laval, Quebec City, Canada; [25]Pediatric Hepatology, Gastroenterology and Transplantation, Hospital Papa Giovanni XXIII, Bergamo, Italy; [26]Pediatric Gastroenterology Department, Hospital de Base do Distrito Federal, Hospital da Criança de Brasília, Centro Universitário de Brasília, Brasília, Brazil; [27]Pediatric Liver Unit, National Reference Centre for Rare Pediatric Liver Diseases (Biliary Atresia and Genetic Cholestasis), FILFOIE, ERN RARE LIVER, Necker-Enfants Malades Hospital, University of Paris, Paris, France; [28]First Department of Paediatrics, Semmelweis University, Budapest, Hungary; [29]Department of Medicine, University of Udine, Udine, Italy; [30]Department of Child Health and Diseases, Gastroenterology, Hepatology and Nutrition, Istanbul Faculty of Medicine, Istanbul University, Istanbul, Türkiye; [31]APHM, Hôpital de la Timone Enfant, Service de Pédiatrie Multidisciplinaire, Marseille, France; [32]Pediatric Hepatology and Liver Transplantation Unit. Unidade Local de Saúde Coimbra, Coimbra, Portugal; [33]Section of Hepatology, Department of Gastroenterology, Children's Mercy Kansas City, Kansas City, Kansas, United States; [34]Department of Paediatric Gastroenterology, Hepatology and Nutrition, Astrid Lindgren Children's Hospital, Karolinska University Hospital and CLINTEC, Karolinska Institutet, Stockholm, Sweden; [35]Pediatric Gastroenterology/Hepatology Center Lisbon, Lisbon, Portugal; [36]European Reference Network on Hepatological Diseases (ERN RARE-LIVER), Hamburg, Germany; [37]Pediatric Hepatology and Liver Transplantation, University Medical Center Hamburg Eppendorf, Hamburg, Germany; [38]Liver Unit (Including Small Bowel Transplantation), Birmingham Women's and Children's Hospital, Birmingham, United Kingdom; [39]Department of Gastroenterology and Clinical Nutrition, Royal Children's Hospital, Melbourne, Australia; [40]Service of Pediatric Hepatology and Transplantation, Children's Hospital La Paz, La Paz University Hospital, Madrid, Spain; [41]Meyer Children's Hospital, IRCCS, Florence, Italy; [42]Department of Pediatrics, Children's Hospital of Eastern Ontario, University of Ottawa, Ottawa, Canada; [43]Department of Pediatrics and Adolescent Medicine, Rigshospitalet Copenhagen University Hospital, Copenhagen, Denmark; [44]Division of Gastroenterology, Hepatology and Nutrition, The Children's Hospital of Philadelphia and the University of Pennsylvania Perelman School of Medicine, Philadelphia, Pennsylvania, United States; [45]Department of Pediatrics, Johns Hopkins University School of Medicine, Baltimore, Maryland, United States; [46]Massachusetts General Brigham for Children, Boston, Massachusetts, United States; [47]University of Rochester Medical Center, Rochester, New York, United States; [48]Department of Pediatrics, Asan Medical Center Children's Hospital, Seoul, Korea, Rep. of South; [49]Department of Pediatrics, Seoul National University College of Medicine, Seoul, Korea, Rep. of South; [50]Department of Pediatric Surgery, University Multiprofile Hospital for Active Treatment and Emergency Medicine "N.I. Pirogov", Sofia, Bulgaria; [51]Unité de Gastro-entérologie, Hépatologie, Nutrition et Maladies Héréditaires du Métabolisme pédiatriques, Hôpital des Enfants, CHU de Toulouse, Toulouse, France; [52]The Center for Pediatric Liver Diseases, Children's Hospital of Fudan University, Shanghai, China; [53]Department of Pediatrics, Medical Center of Postgraduate Education, Warsaw, Poland; [54]Division of Pediatric Gastroenterology, Department of Pediatrics, All India Institute of Medical Sciences, New Delhi, India; [55]Monroe Carell Jr. Children's Hospital & Vanderbilt University School of Medicine, Nashville, Tennessee, United States; [56]Institute of Gastroenterology, Nutrition and Liver Diseases, Schneider Children's Medical Center of Israel, Petah Tikva, Israel; [57]Servizio Di Epatologia e Nutrizione Pediatrica, Fondazione Irccs Ca' Granda Ospedale Maggiore Policlinico, Milano, Italy; [58]Section of Pediatric Gastrohepatology, Fundación Cardioinfantil, Bogotá, Colombia; [59]Department of Pediatric Gastroenterology, Hepatology & Liver Transplantation, Amrita Institute of medical Sciences, New Delhi, India; [60]Second Pediatric Discipline, "Iuliu Hatieganu" University of Medicine and Pharmacy Cluj-Napoca, Center of Expertise in Pediatric Liver Rare Disorders, Emergency Clinical Hospital for Children Cluj-Napoca, Cluj-Napoca, Romania; [61]Pediatric Hepatology and Liver Transplant Department, Hospital Universiatri Vall d'Hebron, Barcelon, Spain; [62]Pediatric Department for the Treatment and Study of Abdominal Diseases and Abdominal Transplantation, IRCCS ISMETT (Mediterranean Institute for Transplantation and Advanced Specialized Therapies), Palermo, Italy; [63]Department of Pediatric Gastroenterology, Apollo BGS Hospital, Mysuru, India; [64]ediatric Gastroenterology, Hepatology and Nutrition Unit, Division of Pediatric Specialties, Department of Pediatrics, Gynecology and Obstetrics, University Hospitals of Geneva, Geneva, Switzerland; [65]Third Pediatric Department, Hippokration Hospital, Aristotle University of Thessaloniki, Thessaloniki, Greece; [66]Service d'Hépato-gastroentérologie pédiatrique, Centre de Référence de l'atrésie des voies biliaires et des cholestases génétiques, Hôpital Femme Mère Enfant, Hospices Civils de Lyon, Bron, France; [67]Department of Hepatology and Gastroenterology, Aarhus University Hospital, Aarhus, Denmark; [68]Department of Pediatric Gastroenterology and Hepatology, Kanchi Kamakoti Childs Trust Hospital, Chennai, India; [69]The Juliet Keiden Institute of Pediatric Gastroenterology and Nutrition, Shaare Zedek Medical Center, Jerusalem, Israel; [70]Department of Pediatrics, Columbia University Irving Medical Center, New York, New York, United States; [71]Division of Pediatric Gastroenterology and Hepatology, Department of Pediatrics, University of Pittsburgh School of Medicine, Pittsburgh, Pennsylvania, United States; [72]Pediatric Gastroenterology and Hepatology, University Children's Hospital Tübingen, Tübingen, Germany; [73]Pediatric Gastroenterology Service, Hospital da Criança Santo Antônio, Universidade Federal de Ciências da Saúde de Porto Alegre, Complexo Hospitalar Santa Casa, Porto Alegre, Brazil; [74]Department of Pediatric Gastroenterology, State Hospital for Children and Adolescents, Goiania, Brazil; [75]Department of Paediatric Gastroenterology, Al Jalila Children's Specialty Hospital, Mohammed Bin Rashid University of Medicine and Health Sciences, Dubai, United Arab Emirates; [76]Pediatric Gastroenterology, Hepatology and Nutrition, Wilhelmina Children's Hospital, University Medical Center Utrecht, Utrecht, Netherlands; [77]Department of Paediatrics I, Medical University of Innsbruck, Innsbruck, Austria; [78]Institute of Cell Biology, Medical University of Innsbruck, Innsbruck, Austria; [79]DDC Clinic - Center for Special Needs Children, Adolescent Medicine and Pediatrics, Middlefield, Ohio, United States; [80]Department of Pediatrics, Medical University of Silesia, Katowice, Poland; [81]First Department of Pediatrics, Aghia Sophia Children's Hospital, National and Kapodistrian University of Athens, Athens, Greece; [82]Department of Paediatrics, London Children's Hospital, Western University, London, Canada; [83]Division of Pediatric Gastroenterology, Hepatology and Nutrition, Ann & Robert H. Lurie Children's Hospital, Chicago, IL, United States; [84]Section of Pediatric Gastroenterology, Hepatology and Nutrition, Department of Pediatrics, Children's Hospital Colorado, University of Colorado School of Medicine, Aurora, Colorado, United States; [85]Department of Pediatrics, UCSF Benioff Children's Hospital, University of California San Francisco School of Medicine, San Franscisco, California, United States; [86]Riley Hospital for Children, Indiana University School of Medicine, Indianapolis, Indiana, United States; [87]Division of Gastroenterology and Hepatology, Department of Pediatrics, Seattle Children's Hospital, University of Washington School of Medicine, Seattle, Washington, United States; [88]Cincinnati Children's Hospital Medical Center and Department of Pediatrics, University of Cincinnati School of Medicine, Cincinnati, Ohio, United States; [89]Department of Pediatrics, University of Southern California School of Medicine, Los Angeles, California, United States; [90]Department of Epidemiology and Biostatistics, Erasmus Medical Center, Rotterdam, Netherlands; [91]Toronto Center for Liver Disease,

University Health Network, Toronto, Canada; [92]IHPME, University of Toronto, Toronto, Canada; [93]Clinical Pharmacy and Pharmacology, University of Groningen, University Medical Center Groningen, Groningen, Netherlands; [94]Department of Pediatrics, University of Groningen, University Medical Center Groningen, Groningen, Netherlands
E-mail: m.nomden@umcg.nl

Background and aims: Patients with Bile Salt Export Pump (BSEP) deficiency have variable native liver survival (NLS) and serum bile acid (sBA) response to interruption of the enterohepatic circulation (iEHC) via surgical biliary diversion (SBD) or ileal bile acid transporter inhibition (IBATi). The missense variants E297G and D482G (ED) retain some BSEP transport functionality: patients carrying these variants have higher sBA responsiveness to iEHC and longer NLS. We aim to identify whether missense variants other than E297G and D482G (OMS) are associated with sBA response to iEHC and NLS, compatible with residual BSEP transport functionality.
Method: In the global NAPPED registry (NCT03930810), we categorized ABCB11 variants as ED, OMS or variants leading to a truncated protein (T). Based on the combination of two allelic variants, 6 genotype groups were then compared: ED/ED, ED/OMS, ED/T, OMS/OMS, OMS/T, and T/T. We analyzed sBA response rate after iEHC (sBA concentration <102 uM or decrease ≥75% within two post iEHC visits) and 5-year NLS without iEHC. Five-year NLS was assessed by Cox regression, and patients were grouped based on sBA response to iEHC.
Results: We included 75 BSEP-deficient patients with iEHC (59 SBD, 16 IBATi) and available sBA levels, and 204 without iEHC. The sBA response to iEHC was ≤20% in ED/T and T/T patients, but ≥50% in ED/ED, ED/OMS, OMS/OMS and OMS/T patients. Among patients without iEHC, the group of ED/ED, ED/OMS, OMS/OMS & OMS/T patients had a significantly higher 5-year NLS rate than ED/T and T/T (HR: 0.48 [0.32–0.72]; $p < 0.001$).
Conclusion: In BSEP deficiency, missense variants other than E297G and D482G are associated with sBA responsiveness to iEHC and with 5-year NLS without iEHC, compatible with relatively high residual BSEP functionality. We expect that the further identification of these variants will allow to optimize treatment strategies in patients with BSEP deficiency.

THU-285
Alpha-1 foundation research registry: highlighting pulmonary manifestations among liver-affected alpha-1 antitrypsin deficiency patients in the United States

Alison Keaveny[1], Nadine Nuchovich[1], Jennifer Illarramendi[1], Randel Plant[1], Jeanine M. D'Armiento[2], Monica P. Goldklang[2]. *[1]Alpha-1 Foundation, Coral Gables, FL, United States; [2]Columbia University Irving Medical Center, New York, NY, United States*
E-mail: akeaveny@alpha1.org

Background and aims: Alpha-1 Antitrypsin Deficiency (AATD) is a rare genetic disorder that is characterized by misfolding and retention of AAT protein in hepatocytes, predisposing patients to liver disease. Many individuals with AATD-related liver disease also experience pulmonary manifestations due to low circulating AAT protein. We therefore analyzed liver-affected individuals and assessed pulmonary comorbidities among this population.
Method: Utilizing REDCap, the Alpha-1 Research Registry (A1F Registry) has enrolled 3395 AATD patients who completed a liver specific questionnaire between June 2019 to December 2025. We identified 1656 liver-affected patients, defined as those who reported a positive history of abnormal liver function tests, liver symptoms, cirrhosis, MASH /MASLD, ascites, cholestasis, hepatopulmonary syndrome, portopulmonary hypertension, or bacterial peritonitis.
Results: Liver-affected A1F Registry participants identify largely as female (68.5%), white (97.3%) with a mean age of 50.53 ± 16.5 years. Nearly half of liver-affected individuals reported pulmonary symptoms including coughing most or several days a week (48.9%) and/ or experience shortness of breath most or several days a week (45.1%), while wheezing attacks occurring most or several days a week were seen in only 16.8% of participants. Diagnoses of obstructive lung disease were reported in 60% of liver- affected AATD participants, with COPD reported in 34.5%, emphysema in 25.8%, bronchiectasis 17.8% and adult asthma 37.3%. Among liver-affected participants with pulmonary comorbidities, PiZZ genotype was reported most frequently (43.3%), followed by PiMZ (28.1%) and PiSZ (9.4%). Common current pulmonary pharmacologic use in liver-affected AATD participants overall include corticosteroids (oral 10.2%, inhaled 33.8%), anticholinergics (15.0%), beta agonists (41.5%), and oxygen therapy (16%). Current or prior alpha-1 antitrypsin protease inhibitor therapy usage was reported in 32.2% of liver-affected AATD participants.
Conclusion: A considerable proportion of liver-affected AATD participants reported pulmonary involvement and therapy usage. Given this overlap, it is imperative that AATD liver affected patients be routinely screened for lung disease, and for pulmonologists and hepatologists to work collaboratively for comprehensive patient care. The A1F Registry continues to be a valuable resource that can use patient reported data to identify liver-affected AATD patients and support a comprehensive analysis of AATD comorbidities.

THU-286
Immunological landscape of autoimmune hepatitis: clinical insights from a retrospective cohort of 48 patients

Dahri Ouafae[1], Mohamed Borahma[1], Fatima Zahra Chabib[1], Nawal Lagdali[1], Sabbah Selma[1], Fatima Zahra Ajana[1], Maryeme Kadiri[1]. *[1]Mohammed V University, Ibn Sina Hospital, Gastroenterology C department, Rabat, Morocco*
E-mail: dahriouafae1@gmail.com

Background and aims: Autoimmune hepatitis (AIH) is a chronic immune-mediated liver disease characterized by hepatocellular injury, circulating autoantibodies and hypergammaglobulinemia. While immunological markers are central to diagnosis, their relationship with disease severity, biochemical activity and liver fibrosis remains incompletely understood. This study aimed to characterize the immunological profile of AIH patients and evaluate its association with clinical presentation, laboratory parameters and fibrosis severity.
Method: We conducted an 8-year retrospective single-center cohort study including 48 AIH patients. Immunological assessment included anti nuclear antibodies (ANA), anti-smooth muscle antibodies (ASMA/AML), anti-SLA, anti-LKM1, anti-LC1 antibodies and serum IgG levels. Liver biopsy findings were reviewed when available, with advanced fibrosis defined as F3–F4. Hepatic decompensation was defined by ascites, variceal bleeding or hepatic encephalopathy. Associations were analyzed using Fisher's exact test; $p < 0.05$ was considered statistically significant.
Results: The cohort comprised 48 patients (83.3% female), mean age 39.5 ± 16.8 years. Serum IgG was elevated in 65.9% of patients. Immunologically, ANA were detected in 63.4%, ASMA/AML in 36.6%, anti-SLA in 7.7%, anti-LKM1 and anti-LC1 in 3.8% of patients, confirming the predominance of type 1 AIH. Histological evaluation showed that a substantial proportion of patients already had significant liver damage at diagnosis. Advanced fibrosis was present in 63.4%, including cirrhosis in 9.8%. ASMA/AML positivity was significantly associated with advanced fibrosis, observed in 92.3% of ASMA/AML-positive patients versus 54.5% in ASMA/AML-negative patients (OR 10.0, $p = 0.027$). ANA, IgG elevation and other autoantibodies were not significantly associated with fibrosis severity. Hepatic decompensation occurred in a considerable proportion of patients. ASMA/AML-positive patients showed a higher rate of decompensation (66.7% vs 34.6%; OR 3.78, $p = 0.059$), representing a strong trend toward significance.
Conclusion: This cohort confirms the predominance of ANA and ASMA/AML in AIH and the frequent presence of elevated IgG and

advanced fibrosis at diagnosis. Importantly, ASMA/AML positivity was significantly associated with advanced fibrosis and tended to predict hepatic decompensation, highlighting its potential as a prognostic marker. These findings underscore the value of immunological profiling in AIH and warrant validation in larger prospective studies.

THU-287

Machine learning–based prediction of immunosuppressive treatment response in autoimmune hepatitis

Azzaoui Oumaima[1], Mohamed Borahma[1], Fatima Zahra Chabib[1], Nawal Lagdali[1], Sabbah Selma[1], Fatima Zahra Ajana[1], Maryeme Kadiri[1]. [1]*Mohamed V university, Ibn Sina Hospital, Rabat, Morocco*
E-mail: oumaimaazzaoui12@gmail.com

Background and aims: Autoimmune hepatitis (AIH) is a rare, immune-mediated liver disease with heterogeneous clinical presentation and variable response to immunosuppressive therapy. Early identification of patients at risk of suboptimal response is crucial to optimize management. Recent advances in artificial intelligence, particularly machine learning (ML), offer promising tools to integrate multidimensional clinical, biological and histological data to predict treatment outcomes. This study aimed to evaluate the performance of a ML-based model in predicting complete biochemical response to immunosuppressive therapy in AIH patients.
Method: A retrospective monocentric study included 37 patients diagnosed with AIH according to international criteria. Variables collected encompassed demographics, clinical presentation, relapses, treatment-related adverse events, laboratory data (serum transaminases, bilirubin, IgG), histopathology (fibrosis stage), and therapeutic details (duration of therapy, corticosteroid use, second-line treatment). The primary endpoint was complete biochemical response. Data preprocessing included encoding categorical variables, normalization, and exclusion of cases with missing target values. A Random Forest algorithm was trained using stratified cross-validation. Model performance was assessed via accuracy, sensitivity (recall), and area under the receiver operating characteristic curve (AUC-ROC). Feature importance analysis identified key predictors of treatment response.
Results: The Random Forest model achieved an accuracy of 86% and sensitivity of 84% in predicting complete response. The AUC-ROC was 0.90, reflecting excellent discrimination between responders and non-responders. Key predictive factors included marked IgG hypergammaglobulinemia, advanced fibrosis (F3–F4), severe hepatocellular injury (ALT >5 × ULN), presence of autoimmune thyroiditis, and early corticosteroid initiation. Variables such as isolated AST elevation, post-withdrawal relapse and type 2 diabetes mellitus were not significant predictors.
Conclusion: Machine learning models show strong potential to predict response to immunosuppressive treatment in AIH, enabling early identification of patients at risk of non-response and supporting precision medicine approaches. Despite limitations related to small sample size and monocentric design, these results warrant multicenter validation in larger cohorts. The integration of AI tools into autoimmune hepatology could improve therapeutic efficacy and patient management.

THU-288

Seladelpar vs Elafibranor as second-line treatments for primary biliary cholangitis: asystematic review and meta-analysis

Naren Nallapeta[1], Shayan Mahapatra[2], Bharadwaj Jilakaraju[3], Aiken Muratova[4], Adarsh Gande[5], Rakhshanda Khan[6], Dhanraj Ramteke[7], Sahana Parthasarathy[1], Yashaswi Koguru[1], Gary Drew[1], Brenden Pearce[1]. [1]*Grand Strand Medical Center, Myrtle Beach, United States;* [2]*Aiken Regional Medical Centers, Aiken, United States;* [3]*Archbold Medical Center, Thomasville, United States;* [4]*Adventhealth Orlando, Orlando, United States;* [5]*Jipmer Hospital, Puducherry, India;* [6]*Ayaan Institute of Medical Sciences, Moinabad, India;* [7]*Anhui medical university, Hefei, China*
E-mail: naren.nallapeta@Gmail.com

Background and aims: Primary biliary cholangitis (PBC) requires second-line therapy in up to 40% of patients with inadequate UDCA response. Seladelpar and elafibranor, newly approved PPAR-targeted agents, significantly reduce ALP and improve symptoms. Their comparative effectiveness is unknown. This meta-analysis evaluates biochemical response, ALP normalization, pruritus, and safety to determine the superior second-line option.
Method: A systematic search of five databases was performed using predefined terms through December 2025 to identify eligible RCTs. Statistical analyses were conducted using STATA 18.0, and risk of bias was assessed using the ROB 2.0 tool.
Results: A total of 5 RCTs involving 426 patients were included (Seladelpar n = 265; Elafibranor n = 161), of whom 94.5% were female and 5.5% male, with a mean age of 56.4 ± 9.1 years and baseline ALP 2.3 ± 0.7 × ULN. Seladelpar achieved a higher composite biochemical response than elafibranor (70.1% vs 56.3%; OR 1.78, 95% CI 1.22–2.61) and greater ALP normalization (29.9% vs 16.5%; OR 2.19, 95% CI 1.31–3.66), while mean ALP reduction was similar (−41.3% ± 12.6 vs −44.3% ± 14.1). Pruritus improvement favored seladelpar (−3.14 ± 1.8 vs −1.93 ± 1.4; MD −1.21, 95% CI −1.98 to −0.44), and bilirubin and ALT remained stable in both groups. Drug-level pooled adverse events showed lower overall AE incidence with seladelpar (86.7% vs 96.3%; RR 0.90, 95% CI 0.83–0.97). Specific AEs also favored seladelpar, including pruritus (RR 0.23, 95% CI 0.10–0.55), diarrhea (RR 0.56, 95% CI 0.24–1.33), nausea (RR 0.56, 95% CI 0.24–1.33), abdominal pain (RR 0.63, 95% CI 0.28–1.44), and fatigue (RR 0.68, 95% CI 0.28–1.65). Serious AEs were similar (RR 0.69, 95% CI 0.30–1.60), discontinuations remained low (RR 1.05, 95% CI 0.62–1.78), and no drug-related hepatotoxicity was identified.
Conclusion: Seladelpar demonstrated superior biochemical and symptomatic efficacy compared with elafibranor, with comparable safety, and all included trials showed a low risk of bias.

THU-289

Utility of using modified Leipzig score for diagnosis of Wilson's disease in a resource-limited setting

Yumnah Riaz[1], Ammara Naveed[1], Bilal Ahmad Shoukat[1], Ahmad Malik[1], Fatima Chaudry[1], Usman Aujla[1]. [1]*Pakistan Kidney and Liver Institute and Research Center, Lahore, Pakistan*
E-mail: yumnahriaz7@outlook.com

Background and aims: Wilson's disease is an autosomal recessive disorder diagnosed with a Leipzig score of 4 or more. This scoring system uses complex criteria which are not entirely available in many resource-limited countries. A modified Leipzig has been proposed by Nagral et al. with more weightage to serum ceruloplasmin less than 5, family history and presence of neurobehavioral symptoms irrespective of severity. We aimed to evaluate the utility of the modified Leipzig scoring system in our cohort to improve the diagnostic accuracy of the disease.
Method: This is a retrospective study of 120 patients who presented to our centre from 2017 to 2025 with high clinical suspicion of Wilson's disease and were treated based on suggestive clinical and laboratory parameters. We assessed the modified Leipzig score's ability to establish the diagnosis of Wilson disease in patients who remained indetermined on Leipzig score due to unavailability of advanced tests like genetic testing, relative exchangeable copper and hepatic copper quantification.
Results: Of 120 patients, 87 (72.5%) were male. The median age of patients was 15.5 (IQR 10.96–21.80). Pediatric population (aged less than 15) was 52 (43.3%). In patients who were assessed, hepatic manifestations were n = 92 (76.6%), neurological n = 29 (46%), psychiatric n = 12 (31.6%). Of the overall cohort n = 77 (%) were cirrhotic at the time of presentation and n = 42 (54.5%) had model for end-stage liver disease score of >15 and were transplant candidates. Only 14 out of 42 eligible patients underwent liver transplantation. 100 out of 120 patients had a Leipzig score of 4 or more confirming definitive diagnosis. A modified Leipzig score was applied, and

among 20 indeterminate cases, 5 were classified as definitive Wilson's disease. Thus the modified Leipzig score identified 25% additional cases as definitive Wilson's disease.
Conclusion: Given the challenges of diagnosing Wilson's disease, a modified Leipzig score offers an improved diagnostic criteria in a resource-limited setting; however, there still is a need for a simplified diagnostic algorithm.

THU-290
Changes in gastroenterology and hepatology practice through primary biliary cholangitis education
S Christy Rohani-Montez[1], Marinella Calle[1], Margaux Le Berre[1], Adriaan J. van der Meer[2], Emma Culver[3], David E. Jones[4]. *[1]Medscape Education Global, London, United Kingdom; [2]Erasmus MC, Rotterdam, Netherlands; [3]John Radcliffe Hospital, Oxford, United Kingdom; [4]University of Newcastle, Newcastle upon Tyne, United Kingdom*
E-mail: srohani@medscape.net

Background and aims: With the recent EU withdrawal of obeticholic acid and approval of peroxisome proliferator-activated receptor (PPAR) agonists for primary biliary cholangitis (PBC) in Europe, second-line therapy has had an overhaul. We sought to improve physicians' confidence and behaviours in implementing these new therapies in real-world practice through accredited education.
Method: Gastroenterologists & hepatologists (gastro/heps) participated in a 38-minute, debate-style video-based online CME activity about whether patients with PBC need to be evaluated for second line therapy now (available at: www.medscape.org/viewarticle/1002006). Education effects were assessed in part A using a 3-question, repeated pairs, directly pre- & post-assessment study; and part B using a performance survey 30–60 days after participation. The activity launched in 12–2024, and data collected through 10-2025.
Results: Of 1413 gastro/heps who had engaged with the program, 58 completed all questions in part A and 33 in part B. 52% were community practitioners, 39% in academic settings, and 8% other. In part A, overall 54% had correct responses at pre-assessment vs 70% at post-assessment; p <.001, Cohen's d = 0.77, N = 58. At this time, although 84% pre- and 90% post-assessment understood that response to UDCA should be regularly monitored, 16% at pre- and 45% at post-assessment were not clear on which specific patient characteristics (age and liver stiffness) inform the need for second-line therapy; and 62% at pre- and 76% at post-assessment were unfamiliar with the expectations of PPAR agonists. 49 participants (84%) indicated they had patients with PBC they felt should be reassessed for second line therapy; and directly after participating, 36% had measurable improved confidence regarding which patients should be evaluated. Survey results 30–60 days after participation for 18 gastros and 15 heps revealed that 94% modified their practice, implemented a new practice, or had their practice reinforced as a result of the education. Specifically, 14 (78%) gastros and 9 (60%) heps had reassessed their PBC patients for second line treatment, and 67% of gastros and 60% of heps had discussed PPAR agonists with patients experiencing an inadequate response to UDCA. Key barriers to implementing changes included capacity challenges and access to PPAR agonists.
Conclusion: This study demonstrates that online video-based education can impact gastroenterology and hepatology practice regarding second line PPAR agonist therapy for PBC.

THU-291
Non-ceruloplasmin bound copper measured by speciation assay: prospective evaluation over 12 months in real world setting of unstable Wilson disease patients
Michael Schilsky[1], Amanda Cheung[2], Valentina Medici[3], Regino Gonzalez-Peralta[4], James Hamilton[5], Cynthia Levy[6], Kalyan Bhamidimarri[7], Steven Lobritto[8], Amy Brown[9], C. Omar Kamlin[10], Jamie Heise[11], Nick Manamley[10], Fred Askari[12]. *[1]Divisions of Digestive Disease and Transplant and Immunology, Yale University Medical Center, New Haven, CT, United States; [2]Northwestern University, Evanston, United States; [3]University of California Davis, Gastroenterology and Hepatology, Sacramento, United States; [4]AdventHealth for Children, AdventHealth Transplant Institute, Orlando, United States; [5]The Johns Hopkins University School of Medicine, Division of Gastroenterology and Hepatology, Baltimore, United States; [6]Division of Digestive Health and Liver Diseases, University of Miami Miller School of Medicine, Schiff Center for Liver Diseases, University of Miami Miller School of Medicine, Miami, United States; [7]Cleveland Clinic, Cleveland, United States; [8]NY Presbyterian, Columbia University Irving Medical Center, New York, United States; [9]Vanderbilt University, Nashville, United States; [10]Orphalan, London, United Kingdom; [11]Orphalan, Boston, United States; [12]Gastroenterology and Hepatology, University of Michigan Health, Michigan, United States*
E-mail: michael.schilsky@yale.edu

Background and aims: Accurate assessment of copper status is critical for guiding therapy in Wilson disease (WD), yet no universally accepted biomarker exists. Non-Ceruloplasmin bound Copper (NCC) is the labile, bioavailable form of copper found in serum and implicated in organ injury seen in WD. Estimation of NCC is unreliable due to limitations with ceruloplasmin measurement. A novel method using anion exchange chromatography followed by inductively coupled plasma mass spectroscopy (ICPMS) quantifies NCC by copper protein speciation (NCC-Sp). Laboratory validated NCC-Sp was used as a primary endpoint in a Phase 3 (NCT03539952**)** study in stable WD. NCC-Sp data in biochemically unstable WD is limited. Our aim was to describe NCC-Sp in biochemically unstable WD.
Method: The REASON study (NCT05783687) was a prospective, non-interventional study conducted across 9 U.S. sites designed to evaluate the clinical utility of NCC-Sp in monitoring adult WD patients (Leipzig score ≥4) if either newly diagnosed within 28 days of baseline visit or biochemically unstable, defined by urinary copper excretion (UCE) outside the recommended therapeutic range or AST/ALT >1.5× upper limit of normal. During standard of care (SoC) visits an additional blood sample was collected for NCC-Sp over a12-month period. Clinical management was not protocolized, followed SoC and NCC-Sp was evaluated at end of study.
Results: In all, fifty-two patients were enrolled of which 43 (83%) met criteria for biochemical instability. Enrolees were 22/43 (51%) female with mean (SD) age of 37.1 (14.4) years. Baseline treatments included trientine (N = 29), zinc salts (N = 8) and d-penicillamine (N = 6). Baseline median (IQR) NCC-Sp concentrations were higher in newly diagnosed vs biochemically unstable patients: 183.0 (124.0, 241.0) vs 96.0 (70.8, 116.0) mcg/L respectively. Mean (SD) baseline and end of study ALT were 79.3 (59.2) vs 63.4 (39.9), for AST 54.5 (37.3) vs 39.3 (17.0), respectively. Mean (SD) change from baseline in ALT and AST were −22.0 (57.9) and −21.9 (53.3) IU/L respectively. End of study median NCC-Sp values declined across both groups 66.45 (57.95, 98.15) and 64.6 (50.7, 94.3) mg/L for newly diagnosed and unstable patients, respectively.
Conclusion: Observed NCC-Sp reductions support the potential clinical utility of NCC-Sp as a treatment responsive, clinically meaningful biomarker for monitoring response to, adherence and guiding treatment decisions in biochemically unstable WD.

THU-298
Non-ceruloplasmin bound copper measured by speciation assay: response to therapy over 12 months in real world setting of newly diagnosed Wilson disease patients
Michael Schilsky[1], Amanda Cheung[2], Valentina Medici[3], Regino Gonzalez-Peralta[4], James Hamilton[5], Cynthia Levy[6], Kalyan Bhamidimarri[7], Steven Lobritto[8], Amy Brown[9], C. Omar Kamlin[10], Jamie Heise[11], Nick Manamley[10], Fred Askari[12]. *[1]Divisions of Digestive Disease and Transplant and Immunology, Yale University Medical Center, New Haven, CT, United States; [2]Northwestern University, Evanston, IL, United States; [3]University of California Davis, Gastroenterology and Hepatology, Sacramento, United States;*

[4]AdventHealth for Children, Orlando, United States; [5]The Johns Hopkins University School of Medicine, Baltimore, United States; [6]Division of Digestive Health and Liver Diseases, University of Miami Miller School of Medicine, Miami, United States; [7]The Cleveland Clinic, Cleveland, United States; [8]NY Presbyterian, Columbia University Irving Medical Center, New York, United States; [9]Vanderbilt University, Nashville, United States; [10]Orphalan, London, United Kingdom; [11]Orphalan, Boston, United States; [12]Gastroenterology and Hepatology, University of Michigan Health, Michigan, United States
E-mail: michael.schilsky@yale.edu

Background and aims: Wilson disease (WD) is a rare genetic disorder of impaired copper transport. Non-Ceruloplasmin bound Copper (NCC), the labile form of copper found in serum contributes to organ injury. Serum NCC and tissue copper levels are in dynamic equilibrium with elevated NCC observed in symptomatic individuals at diagnosis. Estimation of NCC is unreliable due to limitations with ceruloplasmin measurement. A novel method was developed and validated to quantify NCC using anion exchange chromatography followed by copper protein speciation (NCC-Sp) with inductively coupled plasma mass spectroscopy (ICPMS). NCC-Sp was used as a primary endpoint in a Phase 3 (NCT03539952) study in stable WD patients. Our aim was to evaluate and monitor NCC-Sp in newly diagnosed WD.
Method: The REASON study (NCT05783687) was a prospective, non-interventional study conducted across 9 U.S. sites between June 2023 and October 2025 designed to evaluate the clinical utility of NCC-Sp in monitoring adult WD patients (Leipzig score ≥4) newly diagnosed (within 28 days) or if biochemically unstable. The primary objective was to describe NCC-Sp values during standard of care (SoC) visits when an additional blood sample was collected for NCC-Sp and analysed (Quotient laboratories, Alnwick, UK) over a12-month period. Clinical management was not protocolized and NCC-Sp was evaluated at the end of study.
Results: The study enrolled a total of 52 patients of whom 9 (17%) were newly diagnosed. Seven of these 9 were male (78%) with mean (SD) age of 29.7 (9.0) years. Most common first line therapy was zinc salts (N = 6) followed by d-penicillamine (N = 2) and trientine (N = 1). Baseline median (IQR) NCC-Sp was 183.0 (124.0, 241.0) mcg/L; change from baseline was −59.85 (−101.50, −21.50) and −64.35 (−184.55, −19.60) mcg/L at 6 months and end of study visit respectively. At baseline and end of study mean (SD) ALT was 35.0 (23.7), 34.1 (13.6) and for AST 37.0 (25.6), 28.6 (9.6) with change from baseline of −1.4 (15.7) and −3.0 (10.5) IU/L respectively.
Conclusion: NCC-Sp is elevated in newly diagnosed WD and falls in response to treatment in the first 6 months. Liver enzymes are modestly elevated at diagnosis and remain static over 12 months. NCC-Sp has the potential, if confirmed in future studies, to be an accurate and precise biomarker to monitor de-coppering and facilitate response-based titration of medication.

THU-299

Genome-wide association study to identify novel genetic variants associated with primary Budd-Chiari syndrome

Shalimar[1], Sonu Kumar[1], Sagnik Biswas[1], Samagra Agarwal[1], Ayush Agarwal[1], Anzar Ashraf[1], Dibyabhaba Pradhan[1], Baibaswat Nayak[1]. [1]All India Institute of Medical Science, New Delhi, India
E-mail: drshalimar@yahoo.com

Background and aims: Primary Budd-Chiari Syndrome (BCS) is rare hepatic vascular disorder characterized by obstruction of hepatic venous outflow, involving the hepatic veins (HV) and/or inferior vena cava (IVC). There is marked geographic variation in vascular anatomy and prothrombotic profile, suggesting an underlying genetic predisposition. We aimed to identify genetic variants associated with primary BCS using a genome-wide association study (GWAS) and to characterize implicated biological pathways.
Method: In a case–control study (June 2020–May 2022), 310 adults with primary BCS and 312 age- and sex-matched healthy controls were recruited; after quality control, 262 cases and 265 controls were included. We performed GWAS using an Illumina bead array-based high-density whole-genome single nucleotide polymorphism (SNP) genotyping. Rigorous quality control excluded SNPs with high missingness, low minor allele frequency, or Hardy–Weinberg disequilibrium, and samples with excess missing genotypes. Identified SNPs were annotated with their respective genes, and functionally analyzed for molecular pathways, gene ontology and organ-specific expression.
Results: A total of 778 783 high-quality SNPs were analysed; 1549 were associated with BCS at $p < 0{\cdot}05$, and 340 lead SNPs had $p < 0.001$. Fifteen top SNPs ($p < 5 \times 10^{-5}$) were mainly intronic, intergenic, or regulatory, mapping to genes including rs13164180, rs6883351, rs1558294, rs2656107, rs1413229, rs2903138, rs4919217, rs11948339, rs6936121, rs62218439, rs12966305, rs1609245, rs965428, rs697957, and rs34176204. Gene ontology analysis implicated these variants in extracellular matrix constitution, cell-cell junctions, focal adhesion and vasoconstriction pathways. No overlap was seen between lead SNPs and canonical hypercoagulable genes (e.g., protein C/S, antithrombin III, Factor V, JAK2, Calreticulin).
Conclusion: This GWAS with primary BCS identified novel germline loci predominantly in non-coding and regulatory regions, implicating extracellular matrix remodelling, vascular tone, and cell-adhesion pathways rather than classical thrombophilia genes. These findings highlight a distinct pathogenesis of BCS and support further functional and multi-ethnic studies to validate candidate genes and refine genetic risk stratification.

THU-300

Fazirsiran treatment reduces serum biomarkers that predict major adverse liver outcomes in patients with alpha-1 antitrypsin deficiency-associated liver disease

Jen-Chieh Chuang[1], Ying-Wooi Wan[1], Maria D. Paraskevopoulou[1], Ruixue Hou[1], Pedrum Mohammadi-Shemirani[1], Abeer Zeitone[1], Banishree Saha[1], Vinayagam Arunachalam[1], Susana Gonzalez[1], Nirav K. Desai[1], James Hamilton[2], Thomas Schluep[2], Malin Fromme[3], Virginia C. Clark[4], Pavel Strnad[3]. [1]Takeda Development Center Americas, Inc., Cambridge, MA, United States; [2]Arrowhead Pharmaceuticals, Inc., Pasadena, CA, United States; [3]University Hospital RWTH Aachen, Aachen, Germany; [4]University of Florida, Gainesville, FL, United States
E-mail: jen-Chieh.chuang@takeda.com

Background and aims: Alpha-1 antitrypsin deficiency-associated liver disease (AATD-LD) results from the hepatic accumulation of misfolded alpha-1 antitrypsin (Z-AAT) leading to liver fibrosis in patients (pts) with the protease inhibitor (Pi)*ZZ genotype. Fazirsiran, an investigational siRNA targeting Z-AAT, is in phase 3 development for the treatment of AATD-LD. Prior analysis of plasma proteomics data from the UK Biobank Pharma Proteomics Project (UKB-PPP) identified biomarkers predicting major adverse liver outcomes (MALOs; Balasubramani S *et al. medRxiv* 2025). Using data from phase 2 clinical trials, we assessed if fazirsiran treatment changes levels of predictive biomarkers for MALOs in pts with AATD-LD.
Method: Baseline (BL) and post-treatment (Month 6, Year 1 and Year 2) serum samples from pts with AATD-LD and a Pi*ZZ genotype treated with fazirsiran (n = 32) or placebo (n = 9) in AROAAT-2001/-2002 (NCT03945292/NCT03946449) were included in the proteomics analysis using the Olink Explore HT platform (~5400 unique proteins). Predictive biomarkers for MALOs from the UKB-PPP data were ranked and selected based on the combined ranking of the average log2-fold change and false discovery rate (FDR). Change from BL in levels of all, and the top 10, 30 and 50, predictive biomarkers were evaluated in pts treated with fazirsiran or placebo using a linear

mixed effect model for repeated measures (FDR ≤ 0.05 and ≥ 5% expression change from BL).
Results: Overall, 1410 predictive proteins for MALOs were identified from the UKB-PPP data (FDR < 0.05). Fazirsiran treatment (placebo-corrected) led to significant reductions in 176, 382 and 411 proteins at Month 6, Year 1 and Year 2, respectively. From BL up to Year 2 after fazirsiran treatment, there were significant reductions in 80% of the top 10 predictive proteins, 77% of the top 30 and 76% of the top 50 proteins. The top predictive biomarkers reduced by fazirsiran treatment included ADAMTSL2, GDF15, IGFBP7, ITGBL1, KRT18 and THBS2, associated with hepatocyte apoptosis, inflammation, fibrogenesis and fibrosis.
Conclusion: Fazirsiran treatment in pts with AATD-LD reduced levels of circulating biomarkers that predicted MALOs from the UKB-PPP data, supporting evaluation of the therapeutic potential of fazirsiran in a phase 3 clinical trial. Cell-type enrichment and pathway analyses are ongoing to better understand the biological and clinical relevance of these proteins following fazirsiran treatment.
Study/writing funding: Takeda Development Center Americas, Inc.

THU-301
Novel serum proteomic signatures associated with disease burden in alpha-1 antitrypsin deficiency-associated liver disease
Ying-Wooi Wan[1], Jen-Chieh Chuang[1], Abeer Zeitone[1], Ruixue Hou[1], Banishree Saha[1], Maria D. Paraskevopoulou[1], Vinayagam Arunachalam[1], Susana Gonzalez[1], Nirav K. Desai[1], James Hamilton[2], Thomas Schluep[2], Virginia C. Clark[3], Pavel Strnad[4]. *[1]Takeda Development Center Americas, Inc., Cambridge, MA, United States; [2]Arrowhead Pharmaceuticals, Inc., Pasadena, CA, United States; [3]University of Florida, Gainesville, FL, United States; [4]University Hospital RWTH Aachen, Aachen, Germany*
E-mail: ying-wooi.wan@takeda.com

Background and aims: In patients with alpha-1 antitrypsin deficiency-associated liver disease (AATD-LD) and a protease inhibitor (Pi)*ZZ genotype, hepatic misfolded alpha-1 antitrypsin (Z-AAT) aggregates can cause cell stress, inflammation, apoptosis and ultimately liver fibrosis/cirrhosis. Blood proteomic signatures associated with the Pi*ZZ genotype were previously identified (Chuang *et al. J Hepatol* 2024;80:S696–7; Balasubramani S *et al. medRxiv* 2025), but association with disease burden remains unclear. This study delineated serum proteomic profiles associated with AATD-LD clinical burden parameters.
Method: Baseline serum samples from 41 adults with fibrosis and a Pi*ZZ genotype from phase 2 trials (AROAAT-2001/-2002 [NCT03945292/NCT03946449]) of fazirsiran (an investigational siRNA therapy) were used for biomarker discovery via Olink Explore HT (~5400 unique proteins). Correlations between serum proteomics and parameters of AATD-LD clinical burden (Z-AAT burden [assessed by periodic acid-Schiff staining with diastase, total intrahepatic Z-AAT, serum Z-AAT], fibrogenesis [Pro-C3], fibrosis severity [METAVIR and liver stiffness measured by FibroScan®] and liver enzyme levels [ALT, AST, GGT]) were examined using Spearman's correlations. Pathway analysis (Reactome and Kyoto Encyclopedia of Genes and Genomes) was conducted for proteins with adjusted p-values (Benjamini-Hochberg method) ≤ 0.1.
Results: Serum proteomics correlations (adjusted p-value ≤ 0.1) were identified for 89 proteins (63 positive/26 negative) associated with all Z-AAT burden parameters, 171 (157 positive/14 negative) associated with fibrogenesis, 113 (96 positive/17 negative) associated with both fibrosis severity parameters, and 421 (336 positive/85 negative) associated with liver enzymes. Fifteen proteins (including ACY1, ADAMTSL2, HAO1, ITGBL1, FSTL1, FGFR2, FABP1) associated with ≥ 1 AATD-LD burden parameter overlapped with proteomic signatures identified in other fibrotic liver diseases (e.g. MASH). Pathway analysis suggests that these proteins are involved in hepatocyte function disruption and fibrosis (e.g. insulin-like growth factor signalling, extracellular membrane interactions).
Conclusion: This study identified novel serum proteins correlated with AATD-LD disease burden, advancing understanding of AATD-LD pathophysiology. Possible use of these markers for diagnosis, prognosis and/or monitoring treatment response in AATD-LD will be investigated in future studies.
Study/writing funding: Takeda Development Center Americas, Inc.

THU-302
Prevalence and risk factors of hemochromatosis arthropathy in HFE p.Cys282Tyr homozygotes: a cross-sectional study using adapted EULAR criteria
Maria Rosina Troppmair[1], Daniel Theurl[1], Lorenz Pammer[1], Bernhard Glodny[2], Gerald Degenhart[2], Laura Stein[1], David Haschka[3], Benedikt Schaefer[1], Heinz Zoller[1], Herbert Tilg[1]. *[1]university clinic innsbruck internal medicine 1, Innsbruck, Austria; [2]university clinic innsbruck department for radiology, Innsbruck, Austria; [3]university clinic innsbruck internal medicine 2, Innsbruck, Austria*
E-mail: m.troppmair@i-med.ac.at

Background and aims: Hemochromatosis arthropathy (HA) represents an unmet medical need, because phlebotomy rarely improves associated symptoms and affected patients often require premature joint replacement. Prevalence and understanding of risk factors for the development of HA is incomplete. The European Alliance of Associations for Rheumatology (EULAR) has recently proposed classification criteria for HA. The aim of the present study was to assess the prevalence and risk factors associated with HA among patients homozygous for the common disease-associated HFE genotype.
Method: Individuals with known homozygosity for p.Cys282Tyr in HFE were invited to participate in this cross-sectional study on HA. Participants underwent comprehensive clinical, radiological and biochemical assessment for the presence of HA, which was diagnosed when study participants had a score of greater or equal to 5 points on the adapted EULAR score.
Results: The prevalence of HA among 105 individuals (40% females) homozygous for p.Cys282Tyr was 25% (26/105). Mean age of the study population was 59 years (95% confidence interval 39; 80 years). Patients with HA were significantly more likely to be male (80%; 21/26), older (57 vs 67 years; p = 0.012) and had significantly higher transferrin saturation (58.5% vs 83%; p < 0.001) than patients without HA. Binary logistic regression analysis showed that age, sex, serum iron, transferrin saturation, but not ferritin of transferrin were independently associated with HA.
Conclusion: In this study one quarter of individuals with p.Cys282Tyr homozygosity meets the adapted EULAR diagnostic criteria for HA, where older age, male sex and higher transferrin saturation are risk factors for the disease. Patient recruitment by invitation could have resulted in selection bias and thereby resulted in a higher HA prevalence than in unselected p.Cys282Tyr homozygous populations.

THU-304
Multidisciplinary care in adult patients with Fontan-associated liver disease
Gabriella Tomaiuolo[1], Margherita Saracco[1], Silvia Strona[1], Chiara Manuli[1], Roberta Lasco[1], Michela Helga Falzone[1], Rachele Gastaldi[1], Elena Gribaudo[2], Giuseppe Annoni[2], Francesca Ferroni[2], Carlo Pace Napoleone[3], Massimo Boffini[4], Mauro Rinaldi[4], Renato Romagnoli[5], Silvia Martini[1]. *[1]SSD Insufficienza Epatica e Trapianto Epatico, AOU Città della Salute e della Scienza di Torino, University of Turin, Torino, Italy; [2]Division of Pediatric Cardiology, AOU Città della Salute e della Scienza di Torino, Torino, Italy; [3]Department of Pediatric Cardiac Surgery, AOU Città della Salute e della Scienza di Torino, Torino, Italy; [4]Cardiac Surgery Division, Surgical Sciences Department, AOU Città della Salute e della Scienza di Torino, Torino, Italy; [5]General Surgery 2U and Liver Transplant Center, AOU Città della Salute e della Scienza di Torino, Torino, Italy*
E-mail: gabriella.tomaiuolo@gmail.com

Background and aims: Survival into adulthood after palliative Fontan surgery for univentricular heart disease is increasing. Chronic hemodynamic changes can lead to multiorgan complications, including Fontan-associated liver disease (FALD) with risk of hepatocellular carcinoma (HCC) and hepatic decompensation. We report our experience in adult FALD patients (pts).
Method: All pts referred from Cardiology to our Liver Clinic since 2024 were included. Comorbidities screening followed EASL-ERN recommendations (*Téllez L. J Hepatol 2018)*. Disease severity was classified by VAST score (1 point each for esophageal varices, ascites, splenomegaly, platelets < 150.000). Follow-up closed at 31/12/25.
Results: From 01/2024 to 12/2025, 24 FALD pts were evaluated. 20 pts (83.3%) underwent extracardiac and 4 (16.7%) intracardiac Fontan surgery in childhood (median age 6 years - y - [IQR 3.8–7]). At our first evaluation, median age was 29 y [26.5–37]; median time from Fontan surgery 23 y [18.8–25]; 70.8% male. NYHA class I in 15 pts (62.5%), II in 8 (33.3%), III in 1 (4.2%). 8 pts (33.3%) were on anticoagulants, 10 (41.7%) on pulmonary vasodilators and 10 (41.7%) on diuretics. Extrahepatic complications included 8 (33.3%) tachyarrhythmia, 3 (12.5%) sinus node dysfunction, 1 (4.2%) plastic bronchitis and 2 (8.3%) protein-losing enteropathy. 5 pts (20.8%) had implanted pacemakers, 4 pts (16.7%) experienced ischemic strokes, 3 peri-Fontan surgery or Fontan conduit replacement. VAST score was 0 in 6 pts (25%), 1 in 12 pts (50%), 2 in 5 pts (20.8%) and 4 in 1 pt (4.7%) with median time from Fontan surgery of 23.5 y [21.5–29.5], 23.5 y [22.8–25.3], 19 y [17–19] and 19 y, respectively. Notably, 5 pts (20.8%) had esophageal varices, 2 (13.6%) ascites, 8 (33.3%) splenomegaly and 11 (45.8%) thrombocytopenia. 21 pts (87.5%) underwent liver stiffness measurement (LSM), median of 20.9 kPa [16.0–26.4], without significant differences among VAST groups (p = 0.53, ANOVA test). 2 pts were referred due to HCC (Up-to-Seven in; AFP 1042 and 2.4 ng/mL at referral): both underwent combined heart-liver transplant (CHLT) after HCC downstaging and bridge therapy respectively. 1 pt had CHLT due to liver failure (NaMELD 24). The 3 transplanted pts are alive after 15 months, 13 days and 13 months respectively.
Conclusion: FALD is a major long-term complication in adult Fontan pts. Multidisciplinary follow-up is essential for early complication detection and timely CHLT referral. The role of LSM remains debated.

THU-305-YI

Dysregulation of hepcidin in hemochromatosis: results from a multinational cross-sectional study on serum iron parameters and MRI

Maria Rosina Troppmair[1], Lorenz Pammer[1], Jeremy Shearman[2], Dimitris Grammatopoulos[3], Sonia Distante[4], Andrea Ricci[5], Graca Porto[6], Benedikt Schaefer[1], John Ryan[7], Edouard Bardou-Jacquet[8], Fabiana Busti[9], Domenico Girelli[9], Elena Corradini[5], Heinz Zoller[1]. *[1]Medical University of Innsbruck, Department of Internal Medicine I – Gastroenterology, Hepatology and Endocrinology, Innsbruck, Austria; [2]Department of Gastroenterology, South Warwickshire University NHS Foundation Trust, Warwick, United Kingdom; [3]Warwick Medical School, University of Warwick, Coventry, United Kingdom; [4]Oslo University Hospital, Oslo, Norway; [5]Department of Medical and Surgical Sciences for Children and Adults, University of Modena and Reggio Emilia, Modena, Italy; [6]Serviço de Imuno-hemoterapia, Centro Hospitalar Universitário de Santo António, Unidade Local de Saúde de Santo António, Porto, Portugal; [7]Hepatology Unit, Beaumont Hospital/RCSI University of Medicine and Health Sciences, Dublin, Ireland; [8]Department of Liver Diseases CHU de Rennes, Rennes 1 University, Pontchaillou Hospital, Rennes, France; [9]Department of Medicine, Section of Internal Medicine, University of Verona and Azienda Ospedaliera Universitaria Integrata of Verona, ERN-EuroBloodNet, Verona, Italy*
E-mail: m.troppmair@i-med.ac.at

Background and aims: Hemochromatosis results from genetic dysregulation of the hepcidin–ferroportin axis, which precedes the development of overt iron overload. Homozygosity for p.Cys282Tyr in *HFE* is present in >80% of patients with hemochromatosis and UK Biobank data suggest a cumulative incidence of hemochromatosis of 56.4% in males and 40.5% in females by age 80. Elevated ferritin is a non-specific finding and is frequently observed in the context of inflammation or metabolic syndrome, limiting its diagnostic utility. The objective of this study was to assess markers of an inappropriately blunted hepcidin response in relation to serum iron parameters as well as liver and spleen iron concentrations to validate the concept that hemochromatosis is a state of hepcidin deficiency.
Method: Hepcidin, serum iron parameters and liver and spleen iron assessed by magnetic resonance imaging (MRI) were collected in a multinational cohort including 8406 individuals with *HFE* p.Cys282Tyr homozygosity and control participants with a normal *HFE* genotype and high ferritin in the majority in both groups.
Results: When patients were grouped by *HFE* genotype as p.Cys282Tyr homozygotes and controls, regression analysis of serum ferritin with hepcidin demonstrated a significantly shallower slope of the regression line in p.Cys282Tyr homozygous, consistent with an inappropriately low hepcidin response in this group. Ferritin and transferrin saturation (TSAT) showed log-linear correlations, with 20% higher TSAT values in p.Cys282Tyr homozygotes than in controls. Liver iron concentration (LIC), assessed by R2*-weighted MRI, was associated with ferritin in both groups; however, p.Cys282Tyr homozygotes exhibited higher LIC despite comparable ferritin values. Spleen iron was also related to systemic iron measures, but p.Cys282Tyr homozygotes consistently showed lower spleen iron, indicating relative iron sparing of the spleen.
Conclusion: This study confirms that the principal biochemical manifestation of hemochromatosis is elevated TSAT and a blunted hepcidin response to iron loading. Additional surrogates of this dysregulation include altered relationships between ferritin, liver iron and spleen iron. Based on these findings, phenotypic criteria supporting the diagnosis of hemochromatosis could include high TSAT, elevated liver iron and inappropriately low spleen iron and/or hepcidin.

THU-306-YI

Prevalence and risk factors of sarcopenia throughout the disease spectrum of symptomatic polycystic liver disease: a retrospective multicentre cohort study

Nele Van Horebeek[1], Ozgur Koc[1], Walter Coudyzer[1], Antoon Billiet[2], Isabelle Colle[3], Filip Janssens[4], Stephane Demaeght[5], Hans Orlent[6], Sofie Decock[7], Jean Delwaide[8], Charlotte De Vloo[9], Sven Francque[10], Christophe Moreno[11], Dirk Sprengers[12], Diethard Monbaliu[1], Jacques Pirenne[1], Frederik Nevens[1], Jef Verbeek[1]. *[1]UZ Leuven, Leuven, Belgium; [2]AZ Oostende, Oostende, Belgium; [3]Azorg, Aalst, Belgium; [4]Jessa Hospital, Hasselt, Belgium; [5]Grand Hopital de Charleroi, Charleroi, Belgium; [6]AZ Sint-Jan, Brugge, Belgium; [7]AZ Sint-Lucas, Brugge, Belgium; [8]CHU, Liège, Belgium; [9]AZ Delta, Roeselare, Belgium; [10]Antwerp University Hospital, Edegem, Belgium; [11]ULB Erasme, Bruxelles, Belgium; [12]ZAS, Antwerpen, Belgium*
E-mail: nelevanhorebeek@hotmail.com

Background and aims: The severity of symptoms and complications such as malnutrition are key indications for volume-reducing therapy in patients with polycystic liver disease (PLD). Malnutrition is traditionally assessed by the mid–upper arm circumference (MUAC), although skeletal muscle index at the third lumbar vertebra (SMI-L3) is increasingly recognized as a more accurate marker of sarcopenia. This study aimed to determine the prevalence and clinical predictors of sarcopenia in patients with PLD, and assess whether sarcopenia predicts the need for volume-reducing therapy.
Method: This multicentre retrospective cohort study included 296 adult patients with symptomatic PLD. Sarcopenia was defined using SMI-L3 on CT: <39 cm^2/m^2 for females and <50 cm^2/m^2 for males. Reference values for MUAC were <23.1 cm for females and <23.8 cm for males. Additional variables included BMI, height-adjusted total liver volume (htLV), symptom severity (POLCA score), creatinine

levels and Charlson Comorbidity Index (CCI). Associations between sarcopenia and therapeutic needs were assessed using univariate tests and multivariable logistic regression adjusting for confounders (age, sex, BMI, ADPKD, malnutrition, POLCA score, htLV, creatinine levels and CCI).
Results: SMI-L3 was available for 137/296 (46.3%) patients of whom 80 (58.3%) had sarcopenia. Patients with and without sarcopenia showed no significant differences in MUAC value (39.4% vs 32.6%), POLCA score (22 ± 18 vs 20 ± 17), htLV (2667 ± 1675 mL vs 2539 ± 2048 mL) or CCI (2 ± 3 vs 3 ± 4); p-values all > 0.05. There was a significant difference in BMI (22 ± 4 vs 24 ± 5 kg/m^2, p = 0.009) and creatinine levels (1.01 ± 0.63 vs 1.14 ± 3.05 mg/dL, p = 0.040) among patients with and without sarcopenia respectively. In multivariable analysis only BMI (OR 0.81, p = 0.008) was an independent predictor for sarcopenia. The need for volume-reducing therapy was high (86.8%): somatostatin analogue (46.7%), resection/sclerotherapy (11.0%) and LTx (42.6%) (multiple treatments possible). After multivariable adjustment, sarcopenia independently predicted the need for volume-reducing therapy (OR 8.49, p = 0.018), alongside htLV (OR 1.001, p = 0.038) and CCI (OR 2.56, p = 0.033).
Conclusion: Sarcopenia is highly prevalent in patients with symptomatic PLD and predicts the need for volume-reducing therapy, whereas MUAC does not. Therefore, we recommend prioritizing sarcopenia measured by L3-SMI over MUAC in the management of PLD patients, especially in determining transplant eligibility.

THU-307

Genotype phenotype correlations and clinical presentation patterns in Wilson disease in a Sardinian cohort

Alberto Civolani[1], Emanuela Vargiu[2], Rocco Civolani[2], Orazio Sorbello[2], Erica Loddo[2], Michela Fansecco[2], Massimo Fantini[2]. *[1]AOU CAGLIARI, UOC Gastroenterology, Cagliari, Italy; [2]Azienda Ospedaliero Universitaria Cagliari "Duilio Casula", Cagliari, Italy*
E-mail: alberto.civolani@virgilio.it

Background and aims: Wilson disease results from ATP7B mutations and presents with variable clinical expression. Sardinia shows a unique genetic profile dominated by the c.-436_-422del15 promoter deletion. This study aimed to evaluate genotype-phenotype associations, age at onset and clinical presentation patterns in a large Sardinian cohort.
Method: We retrospectively analyzed 118 patients with Wilson disease (Leipzig score >=4) followed between 1978 and 2024. Clinical, biochemical, neurological, radiological and genetic data were collected. Liver fibrosis was assessed using Metavir. Patients were classified by genotype, phenotype (hepatic or neurological) and outcome (alive, transplanted, deceased). Statistical analyses included chi-square, t-test and ANOVA (p < 0.05).
Results: The Sardinian promoter deletion accounted for 89.5% of genotypes and was strongly associated with a hepatic phenotype (84%) and lower aspartate aminotransferase and alanine aminotransferase values compared with non-Sardinian genotypes. Variants p.V1146M and p.R778W showed higher neurological involvement (52% and 67%). The mean age at diagnosis was 24.5 years, with 76% diagnosed <=35 years. Early diagnosis correlated with milder fibrosis (p = 0.02). Patients alive at last follow-up were diagnosed significantly earlier than transplanted or deceased patients (p = 0.003). Histology showed milder fibrosis in the promoter deletion, while non-Sardinian genotypes exhibited more advanced staging.
Conclusion: The Sardinian promoter deletion is associated with hepatic involvement, lower necro-inflammatory activity and a more favorable clinical course. Non-Sardinian genotypes display a higher neurological burden and more severe fibrosis. Early diagnosis remains a key determinant of outcome, supporting targeted screening in genetically enriched regions.

THU-308

Characteristics of the adolescent population with Alagille syndrome and their liver survival

Nitika Gupta[1], Dominika Wojdyla[2], Bettina E. Hansen[2,3,4], Quinn Rabenau-McDonnell[5], Desiree Vaz[6], Morgan Faist[5], Jian-She Wang[7], Zhihong Guan[7], Irena Jankowska[8], Piotr Czubkowski[8], Dorota Gliwicz-Miedzińska[8], Kathleen M. Loomes[9], David A. Piccoli[9], Elizabeth B. Rand[9], Emmanuel Gonzalès[10,11], Emmanuel Jacquemin[10,11], Jérôme Bouligand[12], Lorenzo D'Antiga[13,14], Emanuele Nicastro[13], Étienne Sokal[15], Giulia Jannone[15], Noelle H. Ebel[16], Jeffrey A. Feinstein[17], Andrew Wehrman[18], Björn Fischler[19,20], Henrik Arnell[19,21], Susan M. Siew[22], Michael Stormon[22], Kyung Mo Kim[23], Seak Hee Oh[23], Rene Romero[1], Florence Lacaille[24], Muriel Girard[25], Amin J. Roberts[26], Helen M. Evans[26], Winita Hardikar[27], Sahana Shankar[28], M. Kyle Jensen[29], Catalina Jaramillo[29], Nehal M. El-Koofy[30], Mohamed A. Elmonem[31], Maria Camila Sanchez[32], Maria Lorena Cavalieri[32], Shikha S. Sundaram[33], Jane Hartley[34], Henkjan J. Verkade[35], Way Seah Lee[36], Henry C. Lin[37], Christina Hajinicolaou[38], Chatmanee Lertudomphonwanit[39], Ryan T. Fischer[40], Catherine Larson-Nath[41], Yael Mozer-Glassberg[42], Cigdem Arıkan[43], James E. Squires[44], Nathalie Rock[45], Seema Alam[46], Jesus Quintero-Bernabeu[47], Mureo Kasahara[48], Elisa de Carvalho[49], Ruben E. Quiros-Tejeira[50], Taisa Kohut[51], Melina Melere[52], Giuseppe Indolfi[53], Pinar Bulut[54], Pier Luigi Calvo[55], Zerrin Önal[56], Rima Fawaz[57], Amal A. Aqul[58], Aglaia Zellos[59], Wikrom Karnsakul[60], Antal Dezsőfi-Gottl[61], Sabina Wiecek[62], Victorien M. Wolters[63], John Eshun[64], Giulia Paolella[65], Raquel Borges Pinto[66], Maria Rogalidou[67], María Legarda Tamara[68], Andréanne N. Zizzo[69], Jennifer Garcia[70], Paulina Ordonez-Naranjo[71], Pamela L. Valentino[72], Marisa Beretta[73], Thomas Damgaard Sandahl[74], Georg-Friedrich Vogel[75,76], Cristina Campos Gonçalves[77,78], Jernej Brecelj[79], Cristina Molera Busoms[80], Eberhard Lurz[81], Ermelinda Santos-Silva[82,83], Nanda Kerkar[84,85], Quais Mujawar[86], Christos Tzivinikos[87], Simone Kortbeek[88], Richard J. Thompson[89], Deirdre A. Kelly[90,91], Binita M. Kamath[92,93]. *[1]Children's Healthcare of Atlanta, Emory University School of Medicine, Division of Pediatric Gastroenterology, Hepatology and Nutrition, Atlanta, United States; [2]Erasmus Medical Center, Department of Epidemiology and Biostatistics, Rotterdam, Netherlands; [3]Toronto General Hospital University Health Network, Toronto, Canada; [4]IHPME, University of Toronto, Toronto, Canada; [5]Children's Hospital of Philadelphia, Department of Pediatrics, Division of Gastroenterology, Hepatology, & Nutrition, Philadelphia, United States; [6]The Hospital for Sick Children, Department of Pediatrics, Division of Gastroenterology, Hepatology and Nutrition, Toronto, Canada; [7]The Center for Pediatric Liver Diseases, Children's Hospital of Fudan University, Shanghai, China; [8]The Children's Memorial Health Institute, Department of Gastroenterology, Hepatology, Nutritional Disorders and Pediatrics, Warsaw, Poland; [9]The Children's Hospital of Philadelphia and the University of Pennsylvania Perelman School of Medicine, Department of Pediatrics, Division of Gastroenterology, Hepatology and Nutrition, Philadelphia, United States; [10]Pediatric Hepatology and Liver Transplantation Unit, National Reference Centre for Rare Pediatric Liver Diseases, FILFOIE, ERN RARE LIVER, Bicêtre Hospital, AP-HP, Université Paris-Saclay, Le Kremlin-Bicêtre, France; [11]Inserm U1193, University of Paris-Saclay, Orsay, France; [12]Hopitaux Universitaires Paris-Saclay, AP-HP, Centre Hospitalier, Universitaire de Bicêtre, Service de Génétique Moléculaire, Pharmacogénétique et Hormonologie, Le Kremlin-Bicêtre, France; [13]Ospedale Papa Giovanni XXIII, Pediatric Hepatology, Gastroenterology and Transplantation, Bergamo, Italy; [14]University of Milano-Bicocca, Department of Medicine and Surgery, Milan, Italy; [15]Cliniques Universitaires Saint-Luc, Pediatric Gastroenterology and Hepatology Unit, Brussels, Belgium; [16]Stanford University School of Medicine, Division of Gastroenterology, Hepatology and Nutrition, Department of Pediatrics, Palo Alto, United States; [17]Stanford University School of Medicine, Lucile Packard Children's*

Hospital, Department of Pediatrics (Cardiology), Palo Alto, United States; [18]Boston Children's Hospital and Harvard School of Medicine, Division of Gastroenterology, Hepatology and Nutrition, Boston, United States; [19]Astrid Lindgren Children's Hospital, Karolinska University Hospital, Department of Pediatric Gastroenterology, Hepatology and Nutrition, Stockholm, Sweden; [20]Karolinska Institutet, European Reference Network for Rare Liver Diseases, CLINTEC, Stockholm, Sweden; [21]Karolinska Institutet, European Reference Network on Hepatological Diseases, Department of Women and Children's Health, Stockholm, Sweden; [22]The Children's Hospital at Westmead, Department of Gastroenterology, Sydney, Australia; [23]University of Ulsan College of Medicine, Asan Medical Center Children's Hospital, Department of Pediatrics, Seoul, Korea, Rep. of South; [24]Necker-Enfants Malades Hospital, University of Paris, Pediatric Gastroenterology, Hepatology and Nutrition, Paris, France; [25]Institut Necker-Enfants Malades, Paris, France; [26]Starship Child Health, Department of Paediatric Gastroenterology, Auckland, New Zealand; [27]Royal Children's Hospital, Department of Gastroenterology and Clinical Nutrition, Melbourne, Australia; [28]Mazumdar Shaw Medical Center, Narayana Health, Bangalore, India; [29]Primary Children's Hospital, University of Utah, Division of Pediatric Gastroenterology, Hepatology and Nutrition, Salt Lake City, United States; [30]Cairo University, Department of Pediatrics, Faculty of Medicine, Cairo, Egypt; [31]Cairo University, Department of Clinical and Chemical Pathology, Faculty of Medicine, Cairo, Egypt; [32]Hospital Italiano Buenos Aires, Pediatric Gastroenterology and Hepatology Division, Buenos Aires, Argentina; [33]Children's Hospital of Colorado and University of Colorado School of Medicine, Section of Gastroenterology, Hepatology and Nutrition, Department of Pediatrics and the Digestive Health Institute, Aurora, United States; [34]Liver Unit, Birmingham Women's and Children's Hospital, NHS Trust, and University of Birmingham, Birmingham, United Kingdom; [35]University Medical Center Groningen, University of Groningen, Department of Pediatrics, Groningen, Netherlands; [36]University of Malaya, Faculty of Medicine, Department of Paediatrics, Kuala Lumpur, Malaysia; [37]Oregon Health and Science University, Division of Pediatric Gastroenterology, Department of Pediatrics, Portland, United States; [38]Chris Hani Baragwanath Academic Hospital, University of the Witwatersrand, Department of Paediatrics and Child Health, Division of Paediatric Gastroenterology, Johannesburg, South Africa; [39]Ramathibodi Hospital, Mahidol University, Division of Gastroenterology, Department of Pediatrics, Bangkok, Thailand; [40]Children's Mercy Kansas City, Section of Hepatology, Department of Gastroenterology, Kansas City, United States; [41]University of Minnesota, Division of Pediatric Gastroenterology, Hepatology, and Nutrition, Minneapolis, United States; [42]Institute of Gastroenterology, Nutrition and Liver Diseases, Schneider Children's Medical Center of Israel, Petah Tikva, Israel; [43]Koc University School of Medicine, Department of Pediatric Gastroenterology and Organ Transplant, Istanbul, Türkiye; [44]University of Pittsburgh School of Medicine, Division of Pediatric Gastroenterology and Hepatology, Department of Pediatrics, Pittsburgh, United States; [45]University Hospitals Geneva and University of Geneva, Swiss Pediatric Liver Center, Division of Pediatric Specialties, Department of Pediatrics, Gynecology, and Obstetrics, Geneva, Switzerland; [46]Institute of Liver and Biliary Sciences, Department of Pediatric Hepatology, New Delhi, India; [47]Hospital Universiatri Vall d'Hebron, Barcelona, ERN Rare Liver - ERN TransplantChild, Pediatric Hepatology and Liver Transplant Department, Barcelona, Spain; [48]National Center for Child Health and Development, Organ Transplantation Center, Tokyo, Japan; [49]Hospital da Criança de Brasília, Centro Universitário de Brasília de Brasilia, Pediatric Gastroenterology Department, Brasilia, Brazil; [50]Children's Nebraska and University of Nebraska Medical Center, Omaha, United States; [51]AdventHealth for Children, Orlando, United States; [52]Hospital da Crianca Santo Antonio, Universidade Federeal de Ciencias da Saude de Porto Alergre, Complexo Hospitalar Santa Casa, Pediatric Gastroenterology Service, Porto Alegre, Brazil; [53]Liver Unit, Meyer Children's University Hospital IRCCS, Florence, Italy; [54]Phoenix Children's Hospital, Division of Pediatric Gastroenterology and Hepatology, Phoenix, United States; [55]Paediatic Gastroenterology Unit, Regina Margherita Children's Hospital, Azienda Ospedaliera Città Della Salute e Della Scienza University Hospital, Turin, Italy; [56]Istanbul University, Istanbul Faculty of Medicine, Pediatric Gastroenterology, Hepatology and Nutrition, Istanbul, Türkiye; [57]Yale University School of Medicine, Department of Pediatrics, New Haven, United States; [58]University of Texas Southwestern Medical Center and Children's Health, Dallas, United States; [59]Mitera Children's Hospital, Athens, Greece; [60]Johns Hopkins University School of Medicine, Department of Pediatrics, Baltimore, United States; [61]Semmelweis University, First Department of Paediatrics, Budapest, Hungary; [62]Medical University of Silesia in Katowice, Department of Pediatrics, Katowice, Poland; [63]University Medical Center Utrecht, Department of Pediatric Gastroenterology, Utrecht, Netherlands; [64]Le Bonheur Children's Hospital, The University of Tennessee Health Science Center, Division of Pediatric Gastroenterology, Memphis, United States; [65]Fondazione IRCCS Ca' Granda Ospedale Maggiore Policlinico, Pediatria-Gastroenterologia, Epatologia, Transplanto Pediatrico e Fibrosi, Milan, Italy; [66]Hospital Criança Conceição, Grupo Hospitalar Conceição, Division of Pediatric Gastroenterology, Porto Alegre, Brazil; [67]"Aghia Sofia" Children's Hospital, University of Athens, Department of Pediatrics, Division of Gastroenterology and Hepatology, Athens, Greece; [68]Cruces University Hospital, Paediatric Gastroenterology Unit, Bilbao, Spain; [69]Children's Hospital, London Health Sciences Centre, Western University, Division of Pediatric Gastroenterology and Hepatology, London, Canada; [70]Miami Transplant Institute, University of Miami, Division of Pediatric Gastroenterology, Hepatology and Nutrition, Miami, United States; [71]Sanford Consortium of Regenerative Medicine, University of California San Diego Rady Children's Health, San Diego, United States; [72]Seattle Children's Hospital, Seattle, United States; [73]Wits Donald Gordon Medical Centre, University of the Witwatersrand, Faculty of Health Sciences, Johannesburg, South Africa; [74]Aarhus University Hospital, Aarhus, Denmark; [75]Pediatrics I, Medical University of Innsbruck, Innsbruck, Austria; [76]Institute of Cell Biology, Medical University of Innsbruck, Innsbruck, Austria; [77]European Reference Network on Hepatological Diseases (ERN RARE-LIVER), Lisbon, Portugal; [78]Pediatric Gastroenterology/Hepatology Center, Lisbon, Portugal; [79]University Children's Hospital Ljubljana, Department of Pediatric Gastroenterology, Hepatology and Nutrition, Ljubljana, Slovenia; [80]Hospital Sant Joan de Deu, Pediatric Gastroenterology, Hepatology and Nutrition Unit, Esplugues De Llobregat, Spain; [81]Dr. von Hauner Children's Hospital, University Hospital Munich, Division of Pediatric Gastroenterology and Hepatology, Munich, Germany; [82]Centro Hospitalar Universitario de Santo Antonio, Centro Materno-Infantil do Norte Albino Aroso, Porto, Portugal; [83]Universidade do Porto, UCIBIO–Applied Molecular Biosciences Unit, Biochemistry Laboratory, Department of Biological Sciences, Faculdade de Farmacia, Porto, Portugal; [84]University of Rochester Medical Center, Rochester, United States; [85]Massachusetts General Hospital for Children, Boston, United States; [86]University of Manitoba, Department of Pediatrics, Section of Pediatric Gastroenterology, Winnipeg, Canada; [87]Al Jalila Children's Specialty Hospital, Mohammed Bin Rashid University of Medicine and Health Sciences, Department of Paediatric Gastroenterology, Dubai, United Arab Emirates; [88]Cumming School of Medicine, University of Calgary, Alberta Children's Hospital, Section of Gastroenterology, Hepatology and Nutrition, Calgary, Canada; [89]Institute of Liver Studies, King's College London, London, United Kingdom; [90]Liver Unit, Birmingham Women's and Children's Hospital, Birmingham, United Kingdom; [91]University of Birmingham, Birmingham, United Kingdom; [92]The Children's Hospital of Philadelphia and the Perelman School of Medicine, Pediatrics, Division of Gastroenterology, Hepatology and Nutrition, Philadelphia, United States; [93]The Hospital for Sick Children and the University of Toronto, Division of Gastroenterology, Hepatology and Nutrition, Toronto, Canada
E-mail: nitika.gupta@emory.edu

Background and aims: Alagille Syndrome (ALGS) is a genetic disorder that mostly manifests in infancy. The ALGS trajectory is evolving with the emergence of new therapies, yet little is known

about ALGS adolescence patients. This study provides descriptive data on ALGS in adolescents.
Method: We analysed data from the Global ALagille Alliance study, which contains 1535 patients from 79 centers/34 countries. ALGS patients surviving 12 years with their native liver were included. Variables analysed included age, platelets and bilirubin at presentation, site, clinical interventions, and sentinel events (transplant and death). Cox Regression with Kaplan-Meier and log-rank test evaluated hazard ratios and survival.
Results: 58% (95% CI: 54–61%) of children survived until 12 years with their native liver. This study analysed 248 patients (55% males). 40% were from North America, 37% from Europe and 23% from elsewhere. At 12 years median bilirubin was 1.56 mg/dL (IQR: 0.51–3.14) and median platelets were 239×10^9/L (IQR:182–303). 21 patients had interventions before inclusion: 4 had Kasai portoenterostomy, 13 had biliary diversion and 4 had endoscopic intervention for varices. 29 events occurred during follow-up. Event-free survival at 21 years was 72% (95% CI: 62–85). The most striking difference in survival at 18 years was between patients with prior clinical intervention (56%) compared to those without (87%) ($p < 0.0001$). Patients with platelets $< 150 \times 10^9$/L or bilirubin > 2 mg/dL at 12 years had worse survival than patients with higher platelets ($p < 0.0013$) or lower bilirubin ($p < 0.0001$). These results are compatible with the risks of events. Patients with prior clinical intervention, higher bilirubin, and lower platelets at 12 years had a higher risk of event (HR = 4.91 for children with prior intervention, 95% CI2.162–11.13, $p < 0.0001$, HR = 1.61 per 1 mg/dL of bilirubin increase, 95%CI 1.328–1.948, $p < 0.0001$, HR = 0.93 per 10×10^9/L platelets increase, 95%CI 0.87–0.99, $p < 0.04$). The differences in survival between the groups at the clinically meaningful cut-off points (platelets $< 150 \times 10^9$/L and bilirubin > 2 mg/dL) were significant. No significant differences between geographical location or mutation type were observed.
Conclusion: After 12 years, patients remain at high risk for an event. Platelets and bilirubin appear to be useful indicators of disease progression. Survival is better in those with a milder phenotype and without surgical interventions in childhood.

Rare liver diseases (including paediatric and genetic) – Experimental and pathophysiology

TOP-311
Lymphatic endothelium reprograms cholangiocytes in biliary atresia

Milad Rezvani[1], Lorenz Chua[2], Leonie Schumm[3], Mijuna Meindl[3], Julian Weihs[3], Susanna Quach[3], Katharina Jechow[2], Alexander Sudy[2], Johannes Liebig[2], Matylda Zofia Kuzinska[3], Reinhild Duennebacke[3], Philip Bufler[3], Christian Conrad[2]. *[1]Department of Pediatric Gastroenterology, Nephrology and Metabolic Medicine, Berlin, Germany, Berlin Institute of Health (BIH) at Charité-Universitätsmedizin Berlin, Berlin, Germany, Der Simulierte Mensch (Si-M), Joint Research Center of Technische Universität Berlin and Charité - Universitätsmedizin Berlin, Amrumer Str. 33, 13353 Berlin, Berlin, Germany; [2]Berlin Institute of Health (BIH) at Charité-Universitätsmedizin Berlin, Berlin, Germany, Berlin, Germany; [3]Charité – Universitätsmedizin Berlin, Department of Pediatric Gastroenterology, Nephrology and Metabolic Medicine, Berlin, Germany, Berlin, Germany*
Email: milad.rezvani@charite.de

Background and aims: Biliary Atresia (BA) is the leading cause of pediatric liver transplantation. Peribiliary signals governing jaundice clearance after a Kasai hepatoportoenterostomy remain unclear.
Method: A multidimensional workflow of BA patients at "Kasai" and cholestatic controls (total n = 46) investigated liver samples via 3D-light-sheet microscopy, multiplexed immunofluorescence (mpIF), single-nuclei RNA sequencing (snRNA-Seq), and spatial transcriptomics (10X VisiumHD & Stereo-Seq). To identify biliary niche signals dictating clinical outcomes, the stratification divided BA patients at the timepoint of Kasai into those who later proceeded to spontaneously clear jaundice within 100 days post-Kasai and those who required liver transplantation. Intrahepatic cholangiocyte organoids (ICOs), human induced pluripotent stem cell-derived hepatocytes (iHeps), and multicellular fetal liver-like organoids (FLOs) validated the impact of lymphatic signaling on various developmental epithelial compartments.
Results: snRNA-seq data established profound molecular dysregulation of lymphatic endothelial cells (LECs) in BA patients with poor outcomes. Light-sheet imaging and mpIF revealed expansion and 3D remodeling of the liver's lymphatic system, characterized by disorganized, simplified lumina within BA tissue. Lymphatic endothelial cell (LEC) hyperplasia at the Kasai timepoint predicted inability to clear jaundice and progression to liver transplant. Within LECs, snRNA-Seq, spatial transcriptomics and mpIF identified a surge in the chemokine CCL21 in patients with poor outcomes. To interrogate the impact of secreted mediators, we first added BA tissue secretome collected from incubated liver explants to FLO cultures. Within this multicellular organoid, cholangiocytes dedifferentiated and delumenized into tissue-like CK19+ conglomerates in a ductular-like reaction. Focusing on CCL21, we treated ICOs and iHeps with increasing doses of CCL21, consistently upregulating *SOX9* and *LGR5,* respectively, in biliary progenitor and stemness programs. Importantly, the co-culture of BA patient-derived hepatic LECs with ICOs recapitulated this result, confirming lymphatic-to-epithelial fate regression in BA.
Conclusion: An expanding, CCL21-enriched hepatic lymphatic vasculature predicts outcomes after Kasai. LECs reprogram cholangiocytes into reactive progenitors via CCL21, explaining the severe ductular reaction and impaired bile clearance in BA. Restoring dysfunctional LEC signaling may be a future avenue in BA treatment.

TOP-312
Precision gene-edited and functionally enhanced human hepatic organoids establish a novel therapeutic strategy for Wilson disease

Jiaqi Li[1], Pengfei Yu[1], Jiateng Zhang[1], Huaibin Zou[1], Yu Chen[1], Zhongping Duan[1]. *[1]Beijing You'an Hospital, Capital Medical University, Beijing Key Laboratory of Liver Regeneration and Artificial Liver Transformation Research, Beijing, China, Beijing, China*
Email: jairalee@163.com

Background and aims: Wilson disease (WD), caused by *ATP7B* mutations, lacks curative treatments. Cell therapy is limited by poor engraftment of 2D hepatocytes. 3D liver organoids, mimicking native tissue, offer a superior platform. We aimed to develop gene-corrected, patient-derived hepatic organoids and evaluate their therapeutic potential.
Method: Isogenic iPSC lines (CRISPR-corrected *ATP7B* R778L and uncorrected) from a WD patient were differentiated into hepatocyte-like cells (HLCs). Both lines were differentiated into hepatocyte-like cells (HLCs). The HLCs were then mixed with a growth factor-reduced (GFR), phenol red-free Matrigel matrix on ice and plated as three-dimensional domes to mimic a basal membrane microenvironment. Organoids were expanded and maintained in HepatiCult™ Organoid Growth Medium (OGM), a system designed to preserve a hepatic progenitor state. In vitro, we systematically compared the 3D organoids to their originating 2D monolayer HLCs, assessing key hepatic functions including albumin secretion, urea synthesis, and CYP3A4 enzymatic activity, as well as the formation of complex bile canalicular networks via immunofluorescence imaging. For in vivo evaluation, organoids were transplanted via intraperitoneal injection into ATP7B-knockout M-NSG mice (a WD model). Serum/urinary copper and liver function were monitored. Liver tissues were

analyzed by histopathology (H&E, Masson's, Oil Red O), transmission electron microscopy, and multi-omics.
Results: Using the optimized GFR Matrigel/OGM system, we generated proliferative 3D hepatic organoids. These organoids exhibited significantly enhanced functional maturity over 2D HLCs, with superior albumin secretion, urea production, and CYP3A4 activity. High-resolution imaging revealed the formation of highly organized, apicobasally polarized bile canalicular networks within organoids. In WD model mice, the gene-corrected organoid treatment group showed restored serum copper/ceruloplasmin levels, increased urinary copper excretion, and marked amelioration of liver histopathology (reduced damage, inflammation, fibrosis, and steatosis). Supporting analyses indicated the restoration of ultrastructural polarity and molecular shifts towards copper homeostasis and metabolic remodeling.
Conclusion: This study establishes that gene-corrected hepatic organoids exhibit superior functional and structural maturity over conventional hepatocytes and can reverse systemic copper dysregulation and liver injury in a WD model.

WED-282-YI
Visualizing retention of brain copper in a rat model of Wilson disease: a 64Cu PET study
Nicole Antolini[1,2], Vasileios Theologidis[2], Nana Christensen[3], Julie Loft Nagel[1,2], Aage Kristian Olsen Alstrup[2,3], Hans Zischka[4], Peter Ott[1,2], Mikkel Holm Vendelbo[3,5], Thomas Sandahl[1,2].
[1]Department of Hepatology and Gastroenterology, Aarhus University Hospital, Department of Clinical Medicine, Aarhus University, Aarhus, Denmark; [2]Department of Clinical Medicine, Aarhus University, PACE - Lundbeck Foundation Parkinson's Disease Research Center, Aarhus University, Denmark, Core Center for Molecular Morphology, Department of Clinical Medicine, Aarhus University, Aarhus, Denmark, Aarhus, Denmark; [3]Department of Nuclear Medicine, Aarhus University Hospital, Aarhus, Denmark, Aarhus, Denmark; [4]Institute of Molecular Toxicology and Pharmacology, Helmholtz Center Munich, Institute of Toxicology and Environmental Hygiene, School of Medicine and Health, Technical University, Munich, Germany; [5]Department of Biomedicine, Aarhus University, Aarhus, Denmark
Email: nicole.antolini@clin.au.dk

Background and aims: Wilson disease (WD) is caused by loss of function of the copper transporter ATP7B, leading to copper accumulation primarily in the liver and brain. While hepatic copper overload reflects impaired biliary excretion, it remains debated whether cerebral copper accumulation is secondary to hepatic spillover or due to impaired ATP7B-dependent copper clearance within the central nervous system. Using intracerebroventricular (ICV) ^{64}Cu, we aimed to assess cerebral copper clearance dynamics independently of systemic copper metabolism in a WD rat model.
Method: Atp7b LPP rats of both sexes were used as a model of WD. ^{64}Cu was administered ICV to access the cerebrospinal fluid (CSF) and bypass systemic copper transport. Copper distribution and retention were assessed using PET-MRI immediately after injection and at 4 and 24 hours. Homozygous (−/−) WD rats were compared with heterozygous (+/−) and wild-type (+/+) controls. Group comparisons of copper retention at 24 hours were performed using the Kruskal-Wallis test. The study was approved by the local animal ethics committee.
Results: WD rats (Atp7b −/−) showed increased cerebral copper retention, compared with heterozygous (Atp7b +/−) and wild-type (Atp7b +/+) controls. At 24 hours, the median (IQR) percentage of injected ^{64}Cu retained within the CSF and brain parenchyma was 65% (63.1–66.8%) in Atp7b −/− rats (n = 4) in contrast to 44.9% (33.2–56.7%) in Atp7b +/− (n = 4) and 53.9% (53.0–54.9%) in Atp7b +/+ LPP rats (n = 3). Genotype-dependent differences were statistically significant, p = 0.030.
Conclusion: By isolating cerebral copper kinetics from systemic copper metabolism, this study provides first in vivo evidence that loss of ATP7B function directly impairs copper clearance from the brain. These findings support a primary role of ATP7B in CNS copper homeostasis. ^{64}Cu PET-MRI represents a promising translational tool for investigating neurological Wilson disease and evaluating therapies targeting brain copper clearance.

WED-283
Loss of STN1 expression due to bi-allelic intronic mutations induces a pro-inflammatory liver sinusoidal endothelial cell phenotype and drives porto-sinusoidal vascular disease development
Lise Bertin[1], Nadia Ciriaci[1], Hammoutene Adel[1], Samira Laouirem[1], Alexandre Sayadi[1], Antoine Wawrzyniak[1], Emmanuel Gonzalès[2], Anne Spraul[2], Elodie Lainey[3], Helene Morel[4], Kannengiesser Caroline[4], Patrick Revy[5], Valerie Paradis[1], Pierre-Emmanuel Rautou[6]. *[1]Centre de recherche sur l'inflammation, INSERM U1149, Paris, France; [2]Hopital Bicêtre, Le Kremlin-Bicêtre, France; [3]Hopital Robert Debré, Paris, France; [4]Hopital Bichat, Paris, France; [5]Institut Imagine, Paris, France; [6]Hopital Beaujon, Clichy, France*
Email: lise.bertin@inserm.fr

Background and aims: Porto-sinusoidal vascular disease (PSVD) is a rare liver disorder that predominantly affects young or middle-aged adults. Pathophysiology of PSVD remains elusive. In this study, we took advantage of a monogenic form of PSVD to get insight into mechanisms leading to PSVD.
Method: Whole genome sequencing was performed in a 19-year-old patient with PSVD and his relatives. Proband's and his relatives' lymphocytes were immortalised. Following liver transplantation, proband's liver sinusoidal endothelial cells (LSECs) and whole liver tissue were isolated from the explanted liver. Western blot and RNA sequencing were performed on whole liver and LSECs from the proband as well as from patients with mild or with advanced liver fibrosis.
Results: Whole genome sequencing revealed compound heterozygous deep intronic mutations in the *STN1* gene, encoding a component of the CST-telomere complex. The proband had PSVD complicated with recurrent portal hypertensive bleeding, ascites and finally partial portal vein thrombosis. Extrahepatic features associated with *STN1* mutations in this patient included premature greying of hair and intestinal vascular ectasias. Immortalised lymphocytes from the proband showed a virtual absence of STN1 protein expression. Each parent of the proband (each carrying one of both *SNT1* mutation) had reduced STN1 expression compared with immortalised lymphocytes from healthy donors. STN1 protein expression was also markedly reduced in whole-liver tissue and undetectable in LSECs of the proband, as compared with preserved expression in corresponding samples from patients undergoing surgery for benign hepatocellular adenoma *(no or mild liver fibrosis, n = 3)*. We then compared transcriptomics results of the proband with those of 17 patients with no or mild liver fibrosis and those of 16 patients with advanced liver fibrosis. While no major difference was observed on whole-liver transcriptomic profile, proband's LSECs exhibited a marked deregulation of inflammatory pathways, including complement activation, IL-6 signalling, interferon and TNF-alpha response and vascular pathways, such as coagulation and Notch activation.
Conclusion: We identified novel bi-allelic deep intronic *STN1* mutations that result in a virtual loss of STN1 expression and are associated with PSVD. Transcriptomics results suggest that LSECs are particularly affected in this setting. The identified LSEC proinflammatory phenotype observed may suggest an immune component to PSVD.

WED-284

High copper levels induce oxidative stress and inflammatory processes in a cell culture model of Wilson's disease

Martha-Julia Sasula[1], Anna Held[1], Stefan Schefczyk[1], Marcin Krawczyk[1], Andree Zibert[2], Hartmut Schmidt[1], Ruth Broering[1].
[1]*Dept. of Gastroenterology, Hepatology and Transplantation Medicine, Medical Faculty, University Duisburg-Essen, Essen, Germany;* [2]*Department of Internal Medicine B, University Hospital Muenster, Muenster, Germany*
Email: ruth.broering@uni-due.de

Background and aims: Wilson's disease (WD) is a genetic disorder resulting from mutations in the *ATP7B* gene that lead to copper overload in hepatocytes. This study aims to address WD-associated cellular mechanisms in HepG2 ATP7B knockout (ATP7B-KO) cells, increasing its significance for the development and testing of direct-acting therapeutic targets.
Method: To gain a deeper understanding of the cellular mechanisms underlying WD, a reanalysis of the GSE1073236 dataset was conducted. Gene expression of selected genes in immunity and oxidative was validated by quantitative PCR in HepG2 and HepG2 ATP7B-KO cells, as well as in primary hepatocytes from WD patients and controls. NFκB and AP1 luciferase reporter, oxidative stress and functional assays were performed in HepG2 and HepG2 ATP7B-KO cells.
Results: Increased expression levels of genes associated with autophagy, oxidative stress and inflammation were observed in copper-treated HepG2 ATP7B-KO cells and in primary hepatocytes from patients with WD. Furthermore, copper increased the secretion of IL1B, TNF, GM-CSF, and IL8 in HepG2 ATP7B-KO cells. Accordingly, copper exposure enhanced NFKB promoter activity 6 h after treatment. However, the transcriptional activity of AP1 and NFKB was reduced in these cells 24 h after treatment with 0.6 mM $CuCl_2$. In addition, both HepG2 and HepG2 ATP7B-KO cells showed increased oxidative stress and H_2O_2 levels after copper treatment, indicating that reactive oxygen species could play a role in WD.
Conclusion: In the cell culture model of Wilson's disease, excessive copper accumulation unleashed a cascade of cellular stress responses, including autophagy, oxidative stress, and inflammation driven in part by the dysregulation of key signalling hubs such as NFKB and AP1. These critical mechanisms behind copper-related cell death underscore the importance of this model for developing molecular targets for future therapeutic strategies aimed at halting WD progression at its core.

WED-285

Decoding the molecular and histological architecture of liver yolk sac tumor and its patient-derived cell line reveals c-MYC–FOXM1 oncogenic dependencies

Darko Castven[1], Diana Becker[2], Nathalie Martin[1], Megan Sondermann[1], Jovana Castven[1], Carolin Zimpel[1], Stefanie Heilmann-Heimbach[3], Wilfried Roth[2], Nils Hartmann[2], Beate Straub[2], Hauke Lang[2], Peter R. Galle[2], Jens U. Marquardt[1].
[1]*University Hospital Schleswig-Holstein, Lübeck, Germany;* [2]*University Medical Center Mainz, Mainz, Germany;* [3]*University Hospital Bonn, Bonn, Germany*
Email: castvendarko@gmail.com

Background and aims: Primary yolk sac tumor of the liver (HYST) is uncommon disease with less than 20 cases reported worldwide and is often misdiagnosed as HCC. Therefore, in-depth molecular and histological characterization of HYST and development of representative models are essential for better diagnosis and development of patient-specific therapies.
Method: Samples of adjacent liver and tumor tissue were collected and processed after surgery. Long-term culture of the primary cell line (PCL) was established. Histological characteristics of tissues and PCL were analyzed by immunohistochemistry (IHC) and immunofluorescence (IF). Key oncogenic networks and actionable mutations were identified by NGS (DNA/RNA-seq) and SNP arrays and validated by western blot. Dose-response and synergistic approaches were applied to target the identified onco-networks.
Results: Tumor tissue showed solid trabecular growth without presence of Schiller-Duval bodies. IF and IHC displayed typical YST markers (AFP/CK19), which were effectively preserved in xenografts, PCL and spheroids. Transcriptomic profiling confirmed activation of embryonic markers, reduction of macrophages, enrichment of T cells and FOXM1 activation, also sustained in PCL. GISTIC analysis unveiled MYC amplification (8q24.3), validated by WB, as a potential regulator of FOXM1. NGS further showed presence of TP53 and KDR mutations which were highly conserved in PCL. Specific targeting of FOXM1-MYC network, as well as KDR mutation, confirmed sustained sensitivity to specific inhibition in PCL.
Conclusion: For the first time, we were able to dissect HYST at unprecedented molecular level and to establish primary cell line. We identified molecular alterations that could be used for targeted therapy and established cellular model for this extremely rare disease.

WED-286

Exploring the role of the c.41_40dup heterozygous UGT1A1 variant as an alternative polymorphism impacting on young-adult cryptogenic cholestasis phenotype

Fiammetta Di Nardo[1], Mario Romeo[1], Carmine Napolitano[1], Claudio Basile[1], Giusy Senese[1], Alessia Silvestrin[1], Paolo Vaia[1], Simone Olivieri[1], Marcello Dallio[1], Alessandro Federico[1].
[1]*Hepatogastroenterology Division, Department of Precision Medicine, University of Campania Luigi Vanvitelli, Piazza Miraglia 2, 80138, Naples (Italy), Naples, Italy*
Email: fiammetta.dinardo@studenti.unicampania.it

Background and aims: Unexplained chronic cholestasis (UCC) in young adults represents a diagnostic challenge. Uridine diphosphate glucuronosyltransferase-glucuronosyltransferase A1 (UGT1A1), by directly contributing to the bilirubin conjugation, is a crucial enzyme. The heterozygous *UGT1A1 c.41_40dup* variant is classically associated with Gilbert Syndrome (GS). However, a relevant proportion of carriers do not present GS but display reduced UGT1A1 activity, an increased proportion of bilirubin monoglucuronide (BMG) in bile, and enhanced lithogenesis. This research investigates the role of the *UGT1A1 c.41_40dup variant* as an alternative polymorphism in shaping the UCC features.
Method: Seventeen UDCA-naïve GS-free UCC young adults were consecutively enrolled and stratified into: Group A (UGT1A1 c.41_40dup alone), Group B (UGT1A1 c.41_40dup plus other variants), and Group C (other variants only). Pruritus severity, biochemical, and histological data were evaluated. HPLC analysis assessed biliary and intrahepatic bilirubin conjugate proportion (BMG%), as well as hepatic UGT1A1 activity. UDCA's "early" response was evaluated over six months.
Results: Groups A and B showed higher ALT levels and advanced fibrosis (p: 0.0022). Both bile and hepatic samples demonstrated increased BMG/BDG ratio with reduced UGT1A1 activity ($p < 0.0001$). UDCA response was insufficient in 70% of patients carrying c.41_40dup variant. Multivariate analysis confirmed genotype (aSHR: 1.184; p: 0.002) and enzyme activity (aSHR: 2.051; $p < 0.0001$) as independent predictors of this outcome.
Conclusion: The heterozygous *UGT1A1 c.41_40dup* variant delineates a distinct cholestatic phenotype characterized by altered bile composition, hepatic inflammation, and poor UDCA response. These findings support its role as a non-canonical modifier in young-adult UCC and warrant further investigation.

WED-287-YI

Hepatocyte-specific CNNM4 silencing alleviates liver injury in alpha-1 antitrypsin deficiency

Nerea Ferreiro[1], José García Consuegra[2], Carolina Conter[1], Amaia Navarro-Corcuera[1], Leidy Estefanía Zapata-Pavas[1], Maria Mercado[1], Jon Ander Barrenechea-Barrenechea[1], Nazli Khodayari[3], Regina Oshins[3], Mark Brantly[3], Pavel Strnad[4], Irene González-Recio[1], Naroa Goikoetxea-Usandizaga[1], Sara Cogliati[2], María Luz Martínez-Chantar[1]. *[1]CICbioGUNE, Basque Research and Technology Alliance (BRTA), Derio, Spain; [2]Centro de Biología Molecular Severo Ochoa, Madrid, Spain; [3]Nctc Gainesville Campus, Gainesville, United States; [4]University Hospital Aachen, Aachen, Germany*
Email: nferreiro@cicbiogune.es

Background and aims: Alpha-1 antitrypsin deficiency (AATD), most commonly caused by the PiZZ genotype, is a hereditary disorder in which misfolded alpha-1 antitrypsin (AAT) accumulates in the hepatocyte endoplasmic reticulum (ER), driving chronic liver inflammation, fibrosis, and increased risk of hepatocellular carcinoma. Altered magnesium homeostasis has been described in liver disease, but its role in AATD remains unclear. This study investigates the contribution of the magnesium exporter Cyclin M4 (CNNM4) to AAT-driven liver pathology and evaluates hepatocyte-targeted CNNM4 silencing to reduce protein aggregation, ER stress, and liver injury.
Method: CNNM4 expression was evaluated by immunohistochemistry in liver samples from PiZZ patients. In vivo, 6-month-old C57BL/6J mice carrying the SERPINA1*E366 K (PiZZ) mutation were treated with hepatocyte-specific N-acetylgalactosamine–conjugated siRNA targeting CNNM4. Liver tissue was collected to characterize immune cell activation by FACS, and bone marrow–derived macrophages and neutrophils were exposed to hepatocyte-derived conditioned media to evaluate inflammatory responses. ER stress and mitophagy-related markers were analyzed in liver tissue and isolated hepatocytes.
Results: Hepatic CNNM4 expression was upregulated in PiZZ patients and mice. CNNM4 silencing in PiZZ mice restored magnesium homeostasis and increased circulating AAT levels, while reducing total and aggregated AAT in the liver. These effects were associated with a significant reduction of ER stress and mitophagy and notably increased mitochondrial activity in liver tissue and isolated hepatocytes. Regarding inflammation, treated mice showed a significant decrease in infiltrating $CD8^+$ T cells and $CD11c^+/CD11b^+$ inflammatory myeloid cell populations. Conditioned media from treated hepatocytes led to a reduction in proinflammatory and activation markers in macrophages and neutrophils, indicating attenuation of the inflammatory response.
Conclusion: CNNM4 modulates magnesium-dependent stress and inflammatory pathways in AAT–driven liver injury; therefore, hepatocyte-targeted CNNM4 silencing is a promising therapeutic approach to decrease aggregation, reduce ER stress, and improve liver function in AATD.

WED-288

Utility of mRNA analysis in nasopharyngeal brushings from Wilson disease patients and carriers of ATP7B mutations to detect alterations in gene splicing

Luis García-Villarreal[1], Lenka Mrazova[2], Antonio Tugores[1], Maria Viera[1], Alena Cizkova[2], Filip Majer[2], Jakub Sikora[2], Viktor Stranecky[2], Ivana Jedlickova[2], Pablo Alonso Castellano[1], Alberto Monescillo[1], Paola Saiz Udaeta[1], Elena Jimenèz Mutiloa[1], Ildefonso Quiñones-Morales[3], Ana Cruz[1]. *[1]Digestive Service. Complejo Hospitalario Universitario Insular Materno Infantil, Las Palmas de Gran Canaria, Spain; [2]Research Unit for Rare Disease, Department of Pediatrics and Metabolic Disorders, First Faculty of Medicine, Charles University, Prague, Czech Republic; [3]Hospital Universitario Dr Negrín, Las Palmas de Gran Canaria, Spain*
Email: lgarciavillarreal@gmail.com

Background and aims: Some studies indicate that splicing errors may be the genetic mechanism responsible for cases of Wilson disease. This has been proposed for the most frequent mutation in the Spanish population (p.M645R) and also suggested as a possible mechanism for other mutations, even synonymous, in exons 6–8. A method has recently been designed to assess these errors using nasopharyngeal brushings (1) and we decided to analyze the effect of variants c.1934T>G (p.M645R), c.2123T>C (p.L708P) - most prevalent in Gran Canaria - and c.3061-12T>A, on mRNA processing using our novel protocol to extend previous findings.
Method: Total RNA was isolated from nasopharyngeal swabs, reverse transcribed into cDNA, and the target region encompassing exons 3–21 was amplified and the product analyzed using long-read sequencing on the Oxford Nanopore platform. Generated FastQ files were aligned to the human reference genome (hg19) for downstream analysis (1).
Results: Subjects analyzed included two homozygotes and three carriers for p.L708P, five carriers of c.3061-12T>A, and four carriers and one compound heterozygote for p.M645R. Splicing defects were evident for the p.M645R allele, showing exons 6 and 7 skipping and a variable reduction in exon 8, while the presence of p.L708P allele led to a complete exon 8 skipping, showing 50% of mRNA in carriers and 0% in homozygous patients. Carriers of c.3061-12T>A showed a decrease of 50% of mRNA at exon 14.
Conclusion: We show the usefulness of the isolation of mRNA from nasopharyngeal swabs, followed by long-read sequencing to study splicing alterations associated with ATP7B mutations. Using this strategy, we discovered that p.M645R, most common in the Spanish population, is associated with skipping in exons 6 and 7 and in 8 of variable intensity, that may contribute to the different phenotypes in patients carrying this mutation We also show that the most prevalent mutation in Gran Canaria (p.L708P), leads to a complete exon 8 skipping, indicating that the pathogenicity of this variant lies beyond the Leu to Pro substitution. Our novel approach could also be applied to other mutations not studied yet presenting variable phenotypes.
Grant number: NW24-04-00067 from the Ministry of Health of the Czech Republic.

Reference

1. Steiner MrázováL, *et al.*: Analyses of ATP7B mRNA in nasopharyngeal swab samples increase yields of Wilson disease molecular genetic diagnostics. *Human Mutation* 2025 In press.

WED-289

Loss-of-function mutations in Wilson disease: frequency and relationship with phenotype and prognosis (Spanish Wilson AEEH registry)

Luis García-Villarreal[1], Zoe Mariño[2], Pablo Alonso Castellano[1], Marina Berenguer[3], Antonio Olveira[4], Pilar Huarte[5], José Ramón Fernández[6], María Lázaro Ríos[7], Manuel Hernández-Guerra[8], Maria Luisa Gonzalez Dieguez[9], Jose María Moreno Planas[10], Manuel Delgado[11], Paula Iruzubieta[12], Helena Masnou[13], Paula Fernandez Alvarez[14], Carlos Valdivia Krag[15], Javier Ampuero[16], Marta Romero-Gutiérrez[17], Jose Pinazo Bandera[18], Sonia Blanco Sampascual[19], Judith Gómez-Camarero[20], Alba Cachero[21], Monica Pons[22], Gemma Carrión[23], Francisca Cuenca Alarcón[24], Jesús Rivera Esteban[25], Antonio Diaz[26], Esther Molina[27], Ana Arencibia Almeida[28], María Hernández[29], María Carmen García-Gavilán[30], Tania Hernáez-Alsina[31], Berta Bartrolí[32], Sergio Gil-Rojas[33], Beatriz Álvarez-Suárez[34], Antonio Tugores[35]. *[1]Digestive Service, Complejo Hospitalario Universitario Insular Materno Infantil, Las Palmas de Gran Canaria, Spain; [2]Liver Unit, Hospital Clinic Barcelona, IDIBAPS, CIBERehd, ERN-RARE Liver, Universitat de Barcelona, Barcelona, Spain; [3]Hospital Universitari i Politècnic La Fe, Valencia, Spain; [4]Hospital Universitario La Paz, Madrid, Spain; [5]Hospital Universitario de Navarra, Pamplona, Spain; [6]Hospital Universitario de Cruces, Baracaldo, Spain; [7]Hospital*

Miguel Servet, Zaragoza, Spain; [8]Hospital Universitario de Canarias, La Laguna, Spain; [9]Hospital Universitario Central de Asturias, Oviedo, Spain; [10]Complejo Hospitalario Universitario de Albacete, Albacete, Spain; [11]Hospital Universitario de A Coruña, La Coruña, Spain; [12]Hospital Universitario Marqués de Valdecilla, Santander, Spain; [13]Hospital Germans Trias i Pujol, Badalona, Spain; [14]Hospital Virgen Macarena, Sevilla, Spain; [15]Hospital Universitario Reina Sofía, Córdoba, Spain; [16]Hospital Universitario Virgen del Rocío, Sevilla, Spain; [17]Hospital Universitario de Toledo, Toledo, Spain; [18]Hospital Universitario Virgen de la Victoria, Málaga, Spain; [19]Hospital Universitario Basurto, Bilbao, Spain; [20]Hospital Universitario de Burgos, Burgos, Spain; [21]Hospital Universitario de Bellvitge, Hospitalet de Llobregat, Spain, [22]Hospital Universitari Vall d'Hebron, Barcelona, Spain; [23]Hospital Universitario Infanta Leonor, Madrid, Spain; [24]Hospital Clínico San Carlos, Madrid, Spain; [25]Hospital Universitario Puerta de Hierro, Madrid, Spain; [26]Hospital Universitario del Sureste, Madrid, Spain; [27]Hospital Clínico de Santiago, Santiago de Compostela, Spain; [28]Hospital Universitario Nuestra Señora de La Candelaria, Santa Cruz de Tenerife, Spain; [29]Hospital Universitario San Jorge, Huesca, Spain; [30]Hospital Costa del Sol, Marbella, Spain; [31]Hospital Universitario San Pedro, Logroño, Spain; [32]Hospital Universitari Dr. Josep Trueta, Gerona, Spain; [33]Hospital Virgen de la Luz, Cuenca, Spain; [34]Hospital Universitario Lucus Augusti, Lugo, Spain; [35]Research Unit. Complejo Hospitalario Universitario Insular Materno Infantil, Las Palmas Gran Canaria, Spain
Email: lgarciavillarreal@gmail.com

Background and aims: Loss-of-function (LOF) mutations in Wilson disease (WD) have been proposed as highly penetrant, with different copper metabolism and increased risk of transplantation and death. We hence decided to study them in a large sample of our Registry.
Method: Clinical, analytical and outcome data and the presence of LOF mutations and the prevalent M645R, L708P, and H1069Q, in cases with both known alleles, were collected. We compared both homozygotes (HO) and compound heterozygotes (HE), excluding combinations among the four mutations studied. We defined biochemical response (BR) as normalization of transaminase levels or a decrease >70% at 1 or 3 years, and lack of BR or the development of cirrhosis, decompensation, transplantation or death from WD defined clinical-biochemical progression (CBP).
Results: Of 512 patients, we reviewed 322 cases: 276 had two known alleles (study group); 46 had only one (of these 46 alleles, 87% were not LOF). LOF were present in 36% of the patients (116/322) and in 23% of the alleles (138/598). There were 22 cases with double LOF (14 HO of 4 mutations and 8 with other combinations) and 94 HE. We found 35 deletions, 10 insertions, 32 terminations and 60 splicings (53 in introns). In the two-allele group, patients with double LOFs had higher ceruloplasmin concentrations and less cases with levels <10 mg/dL; higher baseline copper excretion; younger age at diagnosis, fewer cases over 40 years of age and more cases with neurological manifestations. The BR was similar among mutations, both in the HO and HE groups. Double LOF cases showed a worse CBP than the HO M645R group and similar to the HO L708P group. The HE groups behaved similarly, but without reaching statistical significance. Combining HO and HE from mutations, the LOF and L708P groups continued to show worse CBP compared to M645R group (all contrasts, $p < 0.05$). No differences in copper content in liver biopsy, presence of cirrhosis at diagnosis nor in the de novo cirrhosis were detected.
Conclusion: LOF mutations in WD are frequent in our population; since they require more complex detection techniques, this may explain some of the alleles not yet classified. These mutations exhibit certain peculiarities on copper metabolism. They do not appear to affect the biochemical response, and they present a similar CBP to penetrant mutations like L708P. These findings need to be confirmed given the great heterogeneity of existing LOF variants.

WED-290

A determination of ATP7B peptides in dried blood spots from patients with Wilson disease: a feasibility study in a high-prevalence population (Gran Canaria) and potential utility in neonatal screening

Luis García-Villarreal[1], Antonio Tugores[2], Pablo Alonso Castellano[1], Tim Grotzer[3], Kayla Croney[3], Maria Viera[1], Alberto Monescillo[1], Paola Saiz Udaeta[1], Elena Jimenèz Mutiloa[1], Ana Cruz[1], Ildefonso Quiñones-Morales[4], Jiwoon Park[5], Claire Klippel[5], Sihoun Hahn[6]. *[1]Digestive Service, Complejo Hospitalario Universitario Insular Materno Infantil, Las Palmas de Gran Canaria, Spain; [2]Research Unit, Complejo Hospitalario Universitario Insular Materno Infantil, Las Palmas Gran Canaria, Spain; [3]Seattle Children's Research Institute, Seattle, United States; [4]Hospital Universitario Dr Negrín, Las Palmas de Gran Canaria, Spain; [5]Key Proteo, Seattle, United States; [6]Seattle Children's Hospital/University of Washington, Seattle, United States*
Email: lgarciavillarreal@gmail.com

Background and aims: Wilson disease is a genetic disease that meets the clinical requirements for neonatal screening (NS): available treatments and excellent outcomes with early treatment,but still with no accepted method for NS. Recently (1), quantification of peptides (P) from the ATP7B protein in DBS has been proposed as a technique applicable to NS.
Method: The blood samples from patients and family members (all genotyped) were processed according to the protocol published (1), and the cutoff points (CP) for peptides 887 and 1056 were obtained from the samples corresponding to 9 controls without mutations. A positive result was with considered when one or two P were below the cutoff point (CP) and negative when both were above CP, in each patient.
Results: Fifty patients, 21 carriers and 9 controls were included. The most frequent mutations were: p.L708P (18 homozygotes, 17 compound heterozygotes, and 9 carriers); p.M645R (8 heterozygotes), and c.-436-422del15 (3 homozygotes, 7 heterozygotes, and 5 carriers). Five false negatives (FN) and 9 false positives (FP) were obtained, with a sensitivity of 90.0%, a specificity of 70%, a PPV of 83.3%, and a NPV of 80.8%. Among the FPs, 5/9 were carriers of the p.L708P mutation. The FNs were compound heterozygotes with mutations of very low allele frequency (AF <0.0003): 2 p.N1270S, p.M769V, and p.T1031. All but one patient with the most frequent mutations (p.L708P and p.M645R) were correctly detected, as were the case who only had one known mutant allele in ATP7B.
Conclusion: It is critical to account for the expected variability when establishing the range for the cell-based proteomic assay. Although the CP might be not very reliable yet, the feasibility study shows that in our population the technique has very high sensitivity, although low specificity; its implementation will be decided after establishing a reliable control range in the region, followed by the cost-effectiveness and cost-utility studies. In other populations the specificity and sensibility may vary and the screening program will depend on these results. It is necessary to increase the number of healthy controls to better adjust the CP for any population.

Reference

1. KlippelC, ParkJ, *et al.* Advancing Newborn Screening in Washington State: A Novel Multiplexed LC-MS/MS Proteomic Assay for Wilson Disease and Inborn Errors of Immunity. *Int. J. Neonatal Screen.* 2025, 11 (1), 6; PMID: 39846592.

WED-291

Neutrophil extracellular traps activation in porto-sinusoidal vascular disorder: a novel mechanism linking intestinal permeability to vascular damage

Stefania Gioia[1], Oliviero Riggio[1], Diletta Overi[1], Roberto Carnevale[1], Silvia Nardelli[1], Graziella Basili[1], Lorenzo Ridola[1], Valerio Giannelli[2], Giulia d'Amati[1], Andrea Baiocchini[2], Alessio Aghemo[3], Luca Di Tommaso[3], Luigi Terracciano[3], Guido Carpino[1], Nicola Pugliese[3]. *[1]Sapienza, Università di Roma, Roma, Italy; [2]Azienda*

Ospedaliera San Camillo Forlanini, Roma, Italy; [3]Humanitas University, Rozzano, Italy
Email: stensgioia@hotmail.com

Background and aims: Etiopathogenesis of porto-sinusoidal vascular disorder (PSVD) is poorly understood. Our previous studies indicated the crucial role of endotoxemia in PSVD vascular lesions, demonstrating that patients exhibit increased intestinal permeability, bacterial translocation as well as pro-aggregating/pro-thrombotic state before portal hypertension (PH) onset. However, the mechanisms linking endotoxemia to vascular injury downstream have not been completely elucidated. Neutrophil extracellular traps (NETs)-web-like chromatin structures released by activated neutrophils in response to infectious/inflammatory stimuli-are known to contribute to sinusoidal endothelial damage, hepatic inflammation and fibrosis, but their role in PSVD remains unexplored. This study aimed to assess circulating NETs markers and their correlation with intestinal permeability and pro-thrombotic state in PSVD.
Method: Serum levels of citrullinated histone H3 (citH3), neutrophil elastase (NE), and myeloperoxidase (MPO) were measured in 51 patients with PSVD (34 with PH, 17 without PH) and 33 healthy controls. Correlations between NETs markers and markers of intestinal permeability (zonulin and lipopolysaccharides-LPS), platelet aggregation and microvascular inflammation (soluble glycoprotein VI, soluble P-selectin, ADAMTS13, and von Willebrand factor-vWF), and hypercoagulability (factor VIII and prothrombin fragment F1+2) were analyzed.
Results: Compared to healthy controls, PSVD patients exhibited significantly higher serum levels of citH3, MPO, and NE. Mean citH3 level (ng/dl) was 2.5 ± 0.5 in controls, 3.4 ± 0.4 in PSVD without PH, and 4.8 ± 1.2 in PSVD with PH ($p < 0.0001$). MPO (ng/dl) levels were 44.4 ± 11, 56.4 ± 11, and 71.8 ± 14 ($p < 0.0001$), respectively; NE (ng/dl) levels 68.9 ± 11.9, 84 ± 9, and 128 ± 36.2 ($p < 0.0001$). Serum LPS and zonulin correlated positively with citH3 ($r = 0.32$, $p = 0.01$; $r = 0.24$, $p = 0.04$), MPO ($r = 0.37$, $p < 0.005$; $r = 0.23$, $p = 0.04$) and NE ($r = 0.53$, $p < 0.001$; $r = 0.48$, $p < 0.001$). vWF and FVIII showed positive correlations with NETs markers, whereas ADAMTS13 correlated negatively. SP-selectin correlated significantly with MPO and NE.
Conclusion: PSVD patients displayed elevated markers of NETs, detectable even before the development of PH and further amplified thereafter. Their association with increased intestinal permeability, bacterial translocation, endothelial dysfunction and pro-thrombotic features, suggests that NETosis contributes to the cascade of events leading to vascular alterations in PSVD.

WED-298
Proteomic quantification of ATP7B in dried blood spots: a feasibility study in a high-prevalence sardinian population and implications for newborn screening of Wilson disease

Sihoun Hahn[1], Kayla Croney[2], Tim Grotzer[2], Phi Duong[2], Salvatore Zaru[3], Alberto Civolani[4], Georgios Loudianos[5]. *[1]Seattle Children's Hospital, University of Washington School of Medicine, Seattle Children's Research Institute, Seattle, United States; [2]Seattle Children's Research Institute, Seattle, United States; [3]UOC Medicina Interna e Gastroenterologia, Nuoro, Italy; [4]UOC Gastroenterologia, Cagliari, Italy; [5]Microcythemic Paediatric Hospital, Cagliari, Italy*
Email: sihahn@uw.edu

Background and aims: Wilson disease (WD) is an autosomal recessive disorder of copper transport caused by pathogenic variants in the *ATP7B* gene, with an estimated global incidence of approximately 1 in 30,000. In contrast, multiple studies have reported a markedly elevated prevalence in Sardinia—approximately 1 in 2700–3000 individuals—representing one of the highest known regional prevalences worldwide. We previously demonstrated that quantification of ATP7B peptides in dried blood spots (DBS) using liquid chromatography–tandem mass spectrometry (LC-MS/MS) is a promising approach for newborn screening (NBS) of WD. Recently, Washington State added WD to its existing newborn screening panel following a large-scale pilot study that screened over 30,000 newborns, further supporting the feasibility of population-based screening.
Method: A multiplexed proteomic assay using LC-MS/MS was applied to quantify ATP7B peptides as surrogate biomarkers in DBS. Seventy-five non-Sardinian unaffected samples were used to establish control distributions and preliminary cutoff values. A total of 52 blind samples from Sardinia were analyzed, including 6 individuals homozygous for the founder deletion variant (*c.-441_472del*) and 22 compound heterozygotes carrying one founder variant and one additional rare variant. Three heterozygous carriers were included, as well as one individual in whom a second pathogenic variant had not been identified.
Results: ATP7B peptide concentrations below the established cutoff were observed in 45 of 52 WD samples. All three heterozygous carriers demonstrated peptide levels within the normal range. Six WD samples were classified as false negatives; all were compound heterozygotes carrying one founder variant and one rare variant. Two additional cases with suspected large second deletions showed markedly reduced ATP7B peptide levels, consistent with a true WD biochemical phenotype despite incomplete molecular characterization.
Conclusion: Establishing population-specific reference ranges is critical in regions with high genetic heterogeneity and prevalent founder mutations. While refinement of cutoff values is ongoing, this feasibility study demonstrated a detection rate comparable to our previously reported results. Although WD has not yet been universally adopted into newborn screening panels worldwide, our findings support continued evaluation and potential implementation of ATP7B proteomic screening as part of newborn screening programs in Sardinia.

WED-299
In vivo determination of the transport capacity of bile salt export pump: a breakthrough for testing novel drugs for progressive familial intrahepatic cholestasis type 2

Willemien Hof[1], Ione Grammatikopoulos Pallidis[1], Hilde de Vries[1], Milaine Hovingh[1], Rick Havinga[1], Niels Mulder[1], Krisztina de Bruyn[2], Folkert Kuipers[1,3], Jan Freark de Boer[1,2], Henkjan J. Verkade[1]. *[1]Groningen, Netherlands; [2]Department of Laboratory Medicine, University of Groningen, University Medical Centre Groningen, Groningen, Netherlands; [3]European Research Institute for the Biology of Aging (ERIBA), University of Groningen, University Medical Centre Groningen, Groningen, Netherlands*
Email: w.f.j.hof@umcg.nl

Background and aims: The bile salt export pump (BSEP) transports conjugated bile acids (BAs) from hepatocytes into the bile canaliculi. Mutations in the *ABCB11* gene cause BSEP deficiency, also known as progressive familial intrahepatic cholestasis type 2 (PFIC2). This cholestatic liver disease is characterized by disrupted bile formation, leading to BA accumulation and severe liver injury. Many *ABCB11* mutations have been identified, a part of which appear to be associated with residual BSEP activity. Pharmacological stimulation of residual BSEP transport activity represents a potential treatment option for patients with such mutations. However, a model system to accurately quantify BSEP-mediated BA transport capacity and assess the impact of its pharmacological stimulation *in vivo* is currently lacking. We aimed to establish an approach to quantify the BA transport capacity of BSEP *in vivo*.
Method: Male and female anaesthetized *Abcb11*$^{+/+}$, *Abcb11*$^{+/-}$ and *Abcb11*$^{-/-}$ mice (11–15 weeks old) were infused with the bile acid tauroursodeoxycholic acid (TUDCA) via the jugular vein while the secreted bile was collected to determine the maximum hepatobiliary BA secretion rate.
Results: Hepatic BSEP protein levels were ±50% lower in *Abcb11*$^{+/-}$ mice than in *Abcb11*$^{+/+}$ controls, confirming the impact of gene copy number on protein abundance. Infusing 1200 nmol/min TUDCA for

60 minutes was well-tolerated and allowed to assess the maximum hepatobiliary BA secretion rate of *Abcb11*$^{+/-}$, mice. In male mice, maximum hepatobiliary BA secretion rates of 5019 ± 606 nmol/min/100 g BW, 2984 ± 458 nmol/min/100 g BW and 512 ± 121 nmol/min/100 g BW were observed in the *Abcb11*$^{+/+}$, *Abcb1*$^{+/-}$ and *Abcb1*$^{-/-}$ groups, respectively. In female mice, maximum hepatobiliary BA secretion rates of 4793 ± 281 nmol/min/100 g BW, 2929 ± 603 nmol/min/100 g BW and 330 ± 194 nmol/min/100 g BW were observed in the *Abcb11*$^{+/+}$, *Abcb1*$^{+/-}$ and *Abcb1*$^{-/-}$ groups, respectively. Comparison with wildtype mice confirmed the impaired BA transport capacity of *Abcb11*$^{+/-}$, mice and their suitability as model for genetic insufficiency. Moreover, male and female mice of the same genotype showed similar baseline and maximum BA secretion rates.
Conclusion: We have developed a quantitative assessment model for BSEP transport capacity. The model will for allow to test candidate drugs for therapeutic correction and potentiation of BSEP variants with decreased functionality, such as found in patients with BSEP deficiency (PFIC2).

WED-300-YI

Using an in vitro bile duct on a chip to study the mechanisms and treatment of biliary atresia

Henry Hoyle[1,2,3,4], Mughilan Selvarajah[1,2,3,4], Enya Amundsen-Isaksen[1,2,3,4], Sarah Peisl[1,2,5,6], Jeremy Yeoh[1,2,3,4], Anna Katharina Frank[1,2,3,4], Stefan Krauss[3,7], Espen Melum[1,2,3,4,8].
[1]*Norwegian PSC Research Center, Department of Transplantation Medicine, Division of Surgery and Specialized Medicine, Oslo University Hospital Rikshospitalet, Oslo, Norway;* [2]*Research Institute of Internal Medicine, Division of Surgery and Specialized Medicine, Oslo University Hospital Rikshospitalet, Oslo, Norway;* [3]*Hybrid Technology Hub, Institute of Basic Medical Sciences, Faculty of Medicine, University of Oslo, Oslo, Norway;* [4]*Institute of Clinical Medicine, Faculty of Medicine, University of Oslo, Oslo, Norway;* [5]*Department of Visceral Surgery and Medicine, Bern University Hospital, University of Bern, Bern, Switzerland;* [6]*Graduate School for Cellular and Biomedical Sciences, University of Bern, Bern, Switzerland;* [7]*Department of Immunology and Transfusion Medicine, Oslo University Hospital, Oslo, Norway;* [8]*Section of Gastroenterology, Department of Transplantation Medicine, Division of Surgery and Specialized Medicine, Oslo University Hospital Rikshospitalet, Oslo, Norway*
Email: h.w.hoyle@medisin.uio.no

Background and aims: Biliary atresia is a pediatric disease of the bile ducts with limited therapeutic treatments available which requires surgical intervention within months of birth for the best outcome. Due to the need to perform surgery in a short timeframe, studies of alternative treatment options are difficult to perform. Animal models can be used in the laboratory, with induction of biliary atresia through the addition of the toxin biliatresone, however these do not fully recapitulate human biology. We have previously developed an *in vitro* human bile duct on a chip which we aim to use in this work to model biliary atresia through the addition of biliatresone. Potential treatment of this *in vitro* bile duct injury can then be investigated.
Method: A microfluidic chip was 3D printed and a collagen gel containing a hollow channel formed within it. Primary human cholangiocytes were derived from endoscopic retrograde cholangiopancreatography (ERCP) brushings and propagated as organoids before being seeded into the channel as a single cell suspension. Experiments were performed at day 10 once cells had formed a mature epithelium. Treatment was performed with different doses of biliatresone (2, 5, 10 µg/mL) in the presence or absence of N-acetyl-L-cysteine. The properties of the bile duct on a chip system after treatment were investigated using brightfield and confocal microscopy along with biochemical assays.
Results: Treatment with biliatresone had a dose-dependent impact on the viability of *in vitro* bile ducts when measured using a tetrazolium reduction assay (~70% at 2 µg/mL, <10% at 5 µg/mL). The formation of organoid-like structures within the duct channel was also observed, with more such structures at higher doses of biliatresone. Within these structures, abnormal polarization of cells was observed when stained for actin. Treatment of the channels with 100 µM N-acetyl-L-cysteine led to a complete rescue of the phenotype with 2 µg/mL biliatresone treatment and partial rescue with 5 µg/mL biliatresone.
Conclusion: We have demonstrated that an abnormal phenotype is induced in an *in vitro* bile duct on a chip after treatment with biliatresone. The partial rescue of the model with N-acetyl-L-cysteine shows that this could be an effective platform for preclinical testing of novel therapeutic treatments and future studies could look into probing the mechanisms involved in biliary atresia progression in more depth.

WED-301

Heterozygous variants in NOTCH2 among a cohort of juvenile and adult patients with cholestatic liver disease: Disease modifiers or innocent bystanders?

Roman Liebe[1], Amelie Stalke[2], Hartmut Schmidt[1], Frank Lammert[3], Marcin Krawczyk[1]. [1]*Essen University Hospital, Department of Gastroenterology, Hepatology and Transplant Medicine, Medical Faculty, University of Duisburg-Essen, Essen, Germany;* [2]*Hannover Medical School, Hannover, Germany;* [3]*Center for Health Economics Research Hannover (CHERH), Hannover Medical School, Hannover, Germany*
Email: marcinjan.krawczyk@uk-essen.de

Background and aims: Genetic cholestatic liver disease is increasingly stratified using NGS, and the resulting information can be used to guide treatment with new drugs such as IBAT inhibitors, which have proven efficacious in congenital liver diseases such as Alagille Syndrome and PFIC. We hypothesised that hypomorphic variants in NOTCH2 or JAG1 may predispose affected patients for later-onset multifactorial cholestasis.
Method: We re-analysed NGS data from 128 patients with cholestatic liver disease of various aetiologies using a targeted sequencing panel of 36 candidate genes involved in hereditary cholestasis. Variants of interest were characterised by filtering allele frequencies in the gnomAD V4.1.0 database, and assessed for potential pathogenicity using various bioinformatic tools e.g. CADD, REVEL, and popEVE.
Results: Missense *NOTCH2* variants were identified in twelve patients (age range 26–83 y.o., 10 women), whereas no pathogenic variants in *JAG1* were detected. None of the private or very rare *NOTCH2* variants had been previously observed in paediatric patients with Alagille syndrome. Additional high-impact pro-cholestatic *ABCB4* variants occurred in three patients, lower-impact *ABCB4* variants in another three, and one patient carried an *ABCC2* variant associated with Dubin–Johnson syndrome. Low-impact single nucleotide polymorphisms predisposing for cholestatic conditions were identified in five patients. Among the twelve patients with *NOTCH2* variants, three exhibited phenotypes consistent with the co-inherited pathogenic *ABCB4* variants (i.e., PFIC or LPAC syndrome). Filtering allele frequencies of five *NOTCH2* variants in six patients ranged from 0.12%–5.05% suggesting that they were not associated with (a modest or highly penetrant) disease. In the remaining three patients, the predicted functional impact, low allele frequency, and absence of alternative explanatory variants support a plausible contribution of *NOTCH2* variants to the pathogenesis of episodic intrahepatic cholestasis, in line with their clinical presentations.
Conclusion: We show that rare heterozygous variants in *NOTCH2* might predispose their carriers for juvenile- or adult-onset recurrent intrahepatic cholestasis, possibly through bile duct paucity.

WED-302

Multimodal definition of the cytokine milieu predicting impaired jaundice clearance in biliary atresia

Matylda Zofia Kuzinska[1,2,3], Lorenz Chua[2], Susanna Quach[1,3], Leonie Schumm[1,4], Katharina Jechow[2], Alexander Sudy[2], Johannes Liebig[2], Reinhild Duennebacke[1], Philip Bufler[1],

Christian Conrad[2], Milad Rezvani[1,4,5,6,7]. [1]*Charité – Universitätsmedizin Berlin, Department of Pediatric Gastroenterology, Nephrology and Metabolic Medicine, Berlin, Germany, Berlin School for Regenerative Therapies (BSRT), Berlin, Germany, Berlin Institute of Health, Center for Digital Health, Berlin, Germany, Berlin, Germany;* [2]*Berlin Institute of Health at Charité, Center for Digital Health, Intelligent Imaging, Berlin, Germany;* [3]*Berlin School for Regenerative Therapies (BSRT), Berlin, Germany;* [4]*Berlin Institute of Health, BIH Charité Clinician Scientist Program, Berlin, Germany;* [5]*Division of Gastroenterology, Hepatology and Nutrition, Cincinnati Children's Hospital Medical Center, Cincinnati, Ohio, United States;* [6]*Berlin Institute of Health, Center for Regenerative Therapies (BCRT), Berlin, Germany;* [7]*Der Simulierte Mensch (Si-M), Joint Research Center of Technische Universität Berlin and Charité - Universitätsmedizin Berlin, Berlin, Germany*
Email: matylda.kuzinska@charite.de

Background and aims: Biliary atresia (BA) is a common pediatric cholangiopathy in which, following hepatoportoenterostomy ("Kasai" procedure), approximately 50% of patients fail to resolve jaundice. The precise cytokine environment underlying this clinical divergence remains unidentified.
Method: Liver tissue single-nucleus RNA sequencing (snRNAseq) was stratified by clinical jaundice clearance and native liver survival at 100 days after Kasai. Controls were non-BA-cholestatic patients (total n = 12, n = 4/group). A multiplex cytokine assay using flow cytometry and tissue secretome analysis was performed by incubating liver tissue and collecting liver-conditioned media (LCM) from BA patients and controls (n = 6/group). Patient-derived intrahepatic cholangiocyte organoids (ICOs) functionally modeled epithelial phenotypes *in vitro*.
Results: Cholangiocytes from patients failing to clear jaundice enriched the expression of the receptors *IL6R, IFNAR1/2*, *IL17R,* and *IL12RB1*. On the protein level, BA-derived LCM enriched IL-6, TNFα, IFNγ, IFNα2, IL-12, and IL-17 compared with controls ($p < 0.05$). Further, cholangiocytes from patients with persistent jaundice exhibited a pronounced interferon-responsive, epithelial remodeling transcriptional state, marked by upregulation of *IFI44L, CXCL9, CXCL10, KRT17, COL2A1*, and MMP7. BA-derived ICOs demonstrated reduced epithelial lumen diameter, impaired expandability, and sustained interferon-responsive gene enrichment across passaging. Additional growth suppression occured when TNFα and IL1β were added to ICOs at concentrations in the same log-fold as native BA-LCM tissue levels, indicating that both epithelial-intrinsic and cytokine-mediated effects govern epithelial dysfunction in BA.
Conclusion: We delineated the biliary cytokine milieu and cholangiocyte transcriptional states that dictate the inability to resolve jaundice, which may inform future immune-targeting therapeutic strategies.

WED-303
Multi-omics analysis reveals ECM defects and TGF-β signaling in biliary atresia

Qiongfen Lin[1], Zuyi Ma[1], Vincent CH Lui[1,2], Pak Chung Sham[3], Paul KH Tam[4], Clara Sze-man Tang[1,2]. [1]*Department of Surgery, Li Ka Shing Faculty of Medicine, The University of Hong Kong, Hong Kong SAR, China;* [2]*Dr Li Dak-Sum Research Centre, The University of Hong Kong-Karolinska Instituted Collaboration in Regenerative Medicine, Hong Kong SAR, China;* [3]*The University of Hong Kong, Hong Kong SAR, China;* [4]*Precision Regenerative Medicine Research Centre, Medical Sciences Division, Macau University of Science and Technology, Macau SAR, China*
Email: qiongfen@hku.hk

Background and aims: Biliary atresia (BA) is a severe cholangiopathy characterized by progressive fibrosclerosing and inflammatory obstruction of the bile ducts, which is caused by genetic predisposition (e.g., *ADD3*, *PKHD1*) to developmental defects in hepatobiliary development and plausibly triggered by environmental insults (e.g., viral infections). Liver fibrosis, marked by excessive deposition of abnormal extracellular matrix (ECM), and cirrhosis are the main contributors to morbidity in BA. In this study, we aimed to utilize multi-omics approaches—including whole exome and genome sequencing, RNA sequencing, and others—to investigate the role of ECM in the development of BA.
Method: To uncover novel disease-susceptibility genetic factors, rare damaging mutations were analyzed in a dataset comprising whole exome and genome sequencing data from 303 BA patients, including 228 trios (probands and unaffected parents).
Results: This analysis revealed a significant enrichment of rare, potentially damaging mutations in ECM-related genes, with approximately 30% of cases harboring at least one ECM mutation. To explore the regulatory landscape of ECM-related genes, we performed protein-protein interaction network and hub gene analyses, which uncovered a highly interconnected network composed of structural ECM components—such as laminins and collagens—and key TGF-β signaling activators, including integrins, thrombospondin-1 (THBS1), and members of the ADAMTS family (ADAMTS2, 5, 6, ADAMTSL1, and 17). Functional studies further elucidated the role of these components: dual luciferase reporter assays showed that wild-type THBS1 activates TGF-β signaling by directly binding to latent TGF-β, whereas BA-associated THBS1 variants impair this activation. Similarly, variants in ADAMTS5 and ADAMTSL1 linked to BA were found to reduce TGF-β activation. To investigate the developmental implications, CRISPR/Cas9-mediated knockdown of *thbs1a* and *thbs1b* in zebrafish resulted in reduced liver size and decreased density of biliary epithelial cells and ducts, indicating that impaired THBS1 function disrupts biliary development.
Conclusion: Collectively, these findings suggest that genetic disruptions in ECM components may contribute to BA pathogenesis by impairing biliary development through the dysregulation of TGF-β signaling.

WED-304
Variation of management in Wilson's disease in England: results from the first national audit

James Liu Yin[1], William J. H. Griffiths[2], Oliver Bandmann[3], Aftab Ala[1]. [1]*Institute of Liver Studies, King's College Hospital, London, United Kingdom;* [2]*Cambridge Liver Unit, Addenbrooke's Hospital, Cambridge, United Kingdom;* [3]*Division of Neuroscience, University of Sheffield, Sheffield, United Kingdom*
Email: aftab.ala1@nhs.net

Background and aims: Wilson's disease (WD) is a rare genetic metabolic liver disease which affects around 1 in 30,000 people. In England, patients have been managed in specialist centres which are able to provide 2nd line therapy.
Recently guidance has been released by international and national liver associations to help standardise patient care. We undertook a national audit of specialist centres to assess the current management of WD patients, as well as use of and alignment with society guidance.
Method: We conducted an online survey from 2024–25, which gathered information on the number of patients managed with WD at the centre, the presence and staffing of their multidisciplinary team, information on their 5 most recent patients (including medication regime, symptoms, and presence of cirrhosis or neurological symptoms) and the awareness of current guidance.
Results: We had responses from 80% of the clinical commissioned centres for Trientine prescriptions in 2019. 55% of centres had multidisciplinary teams mostly including a Gastroenterologist and Neurologist. Centre-reported patient numbers were 536 in total with mean age of 34 (range 9–50). D-penicillamine was the most commonly prescribed medication with 57% also prescribed pyridoxine (75% daily dosage compared to weekly). 37% of patients were on some form of Trientine with the remaining on zinc. Side effects were reported in 13% of the audited patients and 15% reported neurological deterioration. 24hr urinary copper was performed within 12 months in 83% of patients, with one third whilst off their chelator treatment. Treatment was titrated in 15% as a result of UCE. 38% of patients were

cirrhotic with two thirds having regular ultrasound surveillance. All clinicians reported following guidance, with only 1 reporting practice outside of guidance. Clinicians reported following; British 84% European 66% and American 42%.
Conclusion: Despite the high usage of published guidance there remained significant disparity in management regimes, in particular with treatment monitoring and titration. We will engage with clinicians at participating centres to explore the rationale leading to current practice. We hope to then achieve a level of standardisation of management of WD in line with current recommendations to elevate patient care.
This WD survey and engagement framework could then be adapted in other rare liver diseases, including WD, with the aim of it being utilised internationally within the EASL-ERN.

WED-305
Exploring causes of excess mortality in the Wilson's disease psychiatric cohort in the largest psychiatric centre in the UK
James Liu Yin[1], David Okai[2], Richard Thompson[1], Aftab Ala[1]. [1]*Institute of Liver Studies, King's College Hospital, London, United Kingdom;* [2]*Institute of Psychiatry, Psychology and Neuroscience, South London and Maudsley NHS Foundation Trust, London, United Kingdom*
Email: aftab.ala1@nhs.net

Background and aims: Wilson's disease (WD) is a genetic metabolic disease that leads to accumulation of copper in the body. Copper is deposited in the brain and the liver giving rise to a number of neurological, liver and psychiatric symptoms. Preliminary work exploring the data from the largest psychiatric centre (Maudsley Hospital, London) in the UK found a significant cohort of WD patients with a mortality rate of 27%. Our work investigated the cause of death of these patients and explored any contributing factors that could be related to the mortality rate.
Method: We identified our cohort of WD patients from the Maudsley hospital, part of the South London and Maudsley trust, by using hospital episodes statistic (HES) data coded as E83.0 as well as free text mention of WD. We then further used HES data to gather mortality status, coded cause of death, co-mobidities and medications.
Results: There were 81 WD patients identified within records with 22 deaths in total. Mean time to death was 83 months from time of referral (7–204), with a raised standarised mortality ratio. Cause of death data was available on 91% of patients. We found a variable cause of death across available data. The most common cause of death was infection, followed by overdose, renal failure and cirrhosis. Within patients with infection as cause of death, 3 had been liver transplant recipients and therefore would have been on a form of immunosuppression. There was a high rate of liver disease listed as a contributory cause of death within this cohort at 30%. On review of coded co-morbidities, liver disease was the highest co-morbidity at 34%, with mental and behaviours disorders at 31%. Cerebrovascular disease, ischaemic heart disease or hypertension were present in 38% of patients. 51% of patients were on a form of antipsychotic, anxiolytic or antidepressant with >50% of patients on 4 different types of these medications.
Conclusion: Patient with psychiatric conditions can often have a high rate of mortality due to cardiovascular disease, however our cohort, despite having risk factors and presence of these co-morbidities, did not follow this trend. We observed a high rate of liver disease or alcohol as contributing factors in mortality in the WD population. A higher rate of co-existing liver disease in those presenting with psychiatric symptoms should be therefore considered. This highlights the need to screen the psychiatric population for WD, as its prevalence is underestimated, to aid in decreasing liver related mortality.

WED-306
Genetic dysregulation of methionine metabolism in the pathogenesis and progression of biliary atresia
Zuyi Ma[1], Pak Chung Sham[2], Paul Kwong-Hang Tam[3], Vincent Ch Lui[1], Clara Sze-man Tang[1]. [1]*Department of Surgery, Li Ka Shing Faculty of Medicine, The University of Hong Kong, Hong Kong SAR, China;* [2]*Department of Psychiatry, Li Ka Shing Faculty of Medicine, The University of Hong Kong, Hong Kong SAR, China;* [3]*Precision Regenerative Medicine Research Centre, Medical Sciences Division, Macau University of Science and Technology, Macau SAR, China*
Email: u3013448@connect.hku.hk

Background and aims: Biliary Atresia (BA) is a life-threatening fibroinflammatory disease of the biliary tree, with the highest incidence in Asians. Its pathogenesis remains unknown, but it is thought to result from a combination of genetic predisposition and hepatobiliary injury and immune response. Our group previously conducted a sequencing study on BA patients, whereby we identified enrichment of rare damaging mutations in multiple genes associated with methionine metabolism in BA patients. We hypothesize that genetic predisposition to methionine metabolic dysfunction is a key pathological mechanism for BA. In this study, we aim to employ *Mat1a* knockout mice to elucidate the underlying molecular mechanisms by which reduced *Mat1a* expression leads to BA.
Method: We established a BA model in *Mat1a*–/–, *Mat1a*+/–, and wild-type mice through rhesus rotavirus (RRV) inoculation to investigate if deletion of *Mat1a* increases susceptibility to RRV-induced BA and disease severity. We will also inject SAMe and/or GSH supplements to the BA mice to determine if these supplements ameliorate disease development and alleviates the morbidity and mortality in RRV-induced BA mice.
Results: BA-like phenotypes were observed in RRV-injected *Mat1a* –/–, *Mat1a*+/–, and wild-type littermates. Homozygous deletion of *Mat1a* increased susceptibility to RRV-induced BA and exacerbated disease severity, as evidenced by pale, nodular livers and an obstructed extrahepatic bile duct. Histology revealed increased inflammatory cell infiltration and fibrosis in portal areas, accompanied by significantly elevated alkaline phosphatase (ALP) and aspartate aminotransferase (AST) levels. The effect of SAMe and/or GSH supplements will be discussed.
Conclusion: Loss function of *Mat1a* increased susceptibility to RRV-induced BA and exacerbated disease severity, indicating that genetic predisposition to dysregulation of methionine metabolism may be a key pathological mechanism in BA development.

WED-307
RNA - based CRISPR/Cas9 - mediated genetic modification of the copper transporter ATP7B in Wilson disease
Moritz Marciniak[1], Andree Zibert[1], Oksana Nadzemova[1], Hartmut Schmidt[2], Phil Robin Tepasse[1], Jonel Trebicka[1], Vanessa Sandfort[1]. [1]*University Hospital Münster, Münster, Germany;* [2]*University Hospital Essen, Essen, Germany*
Email: vanessa.sandfort@ukmuenster.de

Background and aims: Toxic copper (Cu) accumulations in the liver are described in Wilson disease (WD), a monogenic disorder characterized by mutations in Cu transporting protein ATP7B. H1069Q is the most common point mutation in *ATP7B* in Western Europe and the USA. A previous study by our group demonstrated the feasibility of H1069Q correction using plasmid-based CRISPR/Cas9 (Clustered Regularly Interspaced Short Palindromic Repeats/Caspase 9) molecules in WD-specific induced pluripotent stem cells (iPSCs). The corrected cells differentiated into hepatocyte-like cells (HLCs) and showed a higher resistance to high Cu concentrations (Iwan et al. in revision). However, an application of RNA-based CRISPR/Cas9 molecules would bring this technology one step closer to potential clinical application in WD.
Method: A single-guide RNA (sgRNA) targeting the ATP7B H1069Q locus was designed. HEK293 cells were lipofected with sgRNA and

Cas9 mRNA to induce a double-stranded DNA cleavage. Individual HEK293 clones were analysed by Sanger sequencing. ATP7B expression was assessed by Western blotting (WB) and quantitative PCR (qPCR), and cellular tolerance to high copper concentrations was evaluated using MTT assays. In parallel, HepG2 cells were subjected to the same CRISPR/Cas9 editing procedure, and individual clones were analysed by Sanger sequencing.
Results: In HEK293 cells, RNA-based CRISPR/Cas9 editing generated several ATP7B knockout (KO) clones with distinct homozygous and heterozygous insertions and deletions, as shown by Sanger sequencing. Reduced ATP7B expression in these clones was confirmed by WB and qPCR analysis. MTT assays indicated a functional impact on the cellular response to high Cu concentrations. In HepG2 cells, Sanger sequencing identified a first ATP7B KO clone.
Conclusion: This study demonstrates that RNA-based CRISPR/Cas9 molecules target and cleave the H1069Q-specific locus in ATP7B, leading to diverse ATP7B KOs. ATP7B loss was supported by concordant reductions in ATP7B expression by WB and qPCR. MTT assays revealed metabolic effects of Cu sensitivity in HEK293 KO clones, indicating a functional alteration of ATP7B. This RNA-based approach provides a proof of principle in terms of CRISPR/Cas9-mediated genetic modification in ATP7B. In future experiments, these molecules will also be applied to WD-specific iPSCs in combination with previously validated repair template molecules.

WED-308
New mouse strains recapitulating biliary atresia and Alagille syndrome-associated variants of JAGGED1 reveal a dual role of Jagged1 in liver development and biliatresone-induced injury response

Anna Maria Frontino[1], Daniel V. Oliveira[1,2], Mitra Tavakoli[3], Oren Gozlan[4], Eliška Trampotová[1], Kristyna Neffeova[5], Noémi K. M. Van Hul[6], Emma Andersson[6], Gabriela Pavlinková[3], Hana Kolesova[5], David Sprinzak[4], Jan Mašek[1,2]. [1]*Charles University, Faculty of Science, Department of Cell Biology, Prague, Czech Republic;* [2]*Institute of Organic Chemistry and Biochemistry, Prague, Czech Republic;* [3]*Institute of Biotechnology of the Czech Academy of Sciences, Prague, Czech Republic;* [4]*Jan Koum Center for Nanoscience and Nanotechnology, Tel Aviv University, Tel Aviv, Israel;* [5]*1st Faculty of Medicine, Charles University, Prague, Czech Republic;* [6]*Karolinska Institutet, Biomedicum, Solna, Sweden*
Email: jan.masek@natur.cuni.cz

Background and aims: Therapeutic solutions for disorders with complex genetic/environmental etiology, such as biliary atresia (BA)—the most common pediatric cholangiopathy—are hindered by the lack of suitable animal models. While *JAGGED1*(*JAG1*)|*NOTCH2* loss-of-function variants are the major driver of Alagille syndrome (ALGS), several distinct JAG1 missense variants have also been identified in BA, suggesting that JAG1 may exert context- or cell-type-specific effects during liver development. This study aimed to determine how human disease-associated Jag1 variants affect development of mouse liver, extrahepatic bile duct (EHBD), and their responses to injury.
Method: We recapitulated JAG1 variants associated with ALGS (R1097W (RW)) and BA (R1213Q (RQ)) in mice using CRISPR/Cas9. Notch activity luciferase reporter *assays* using mouse and human cells were used to measure the activity of JAG1 variants. Developing liver, heart and inner ear of the control and mutant mice were assessed using immunohistochemistry. To study biliary injury responses, postnatal day 1 (P1) C57BL/6J mice were administered biliatresone (70 μg/pup), and bulk RNA transcriptomic analyses of the EHBDs were performed at P10 (n = 3 for each treatment and genotype).
Results: While neonatal *Jag1*$^{RW/RW}$ mice manifested transient cardiac defects, hepatic artery loss, and bile duct disorganization, the *Jag1*$^{RQ/RQ}$ mice bile ducts were largely unaffected, with pronounced periportal arterial hyperplasia, indicating distinctly disrupted biliary–vascular development. Interestingly, the differently expressed genes (DEGs) in EHBD of WT mice treated with biliatresone showed little overlap with transcriptomic changes observed in BA liver biopsies, or RRV- and BDL-induced EHBD injury (1 up-/9 down-regulated, 10 up-/18 down-regulated, respectively). The overlap was low also for the EHBDs of biliatresone-treated *Jag1*$^{RW/RW}$ pups (0 up/12 down, 0 up/1 down, respectively), but much higher when compared with *Jag1*$^{RQ/RQ}$ mice (26 up/57 down, 3 up/28 down, respectively), indicating disrupted integrin and Akt signaling. Of note, neither the transcriptomics nor *in vitro* reporter assays indicated a disrupted Notch activity.
Conclusion: These findings demonstrate that Jag1 variants associated with distinct pediatric cholangiopathies differentially instruct liver development and EHBD injury responses. The results advance our understanding of Jag1's role in disease pathogenesis, potentially through mechanisms that are independent of canonical Notch signaling.

WED-313
Spatially resolved transcriptomics identifies disease-specific hepatic microenvironments in Fontan-associated liver disease

Yukie Nakadai[1], Nobuhito Taniki[1], Shuhei Tanemura[1], Junko Kuramoto[1], Naofumi Sumitomo[1], Masaaki Kodaira[1], Toshiyuki Yamagishi[1], Ryosuke Kasuga[1], Makoto Ueno[1], Tabuchi Takaya[1], Haruka Okada[1], Usui Shingo[1], Keisuke Ojiro[1], Takanori Kanai[1], Nobuhiro Nakamoto[1]. [1]*Keio University, Tokyo, Japan*
Email: yukie-t.1223@keio.jp

Background and aims: Fontan-associated liver disease (FALD) is a late complication after the Fontan procedure and is characterized by progressive hepatic fibrosis and an increased risk of hepatocellular carcinoma. However, the molecular mechanisms underlying disease progression remain poorly understood. We aimed to investigate its spatial molecular landscape using high-resolution spatial transcriptomic analysis (Visium HD) of human liver tissue.
Method: We enrolled 70 patients who had undergone the Fontan procedure at our institution. Among them, patients were clinically classified as high risk for FALD based on age and laboratory abnormalities. Of those patients considered to be at high risk, liver biopsy was performed in individuals who provided informed consent (n = 16). Bulk RNA sequencing was conducted using biopsy-derived liver tissue from these FALD patients. As disease controls, liver biopsy samples from 8 patients with chronic hepatitis C who had achieved sustained virologic response were analyzed by bulk RNA sequencing. In addition, for high-resolution spatial transcriptomic analysis, representative cases were selected from both disease groups: FALD patients with mild fibrosis and advanced fibrosis, as well as fibrosis stage–matched HCV-SVR patients. Formalin-fixed paraffin-embedded liver sections from these selected cases were subjected to high-resolution spatial transcriptomic analysis using the Visium HD platform.
Results: Bulk RNA sequencing demonstrated upregulation of genes associated with fibrosis, extracellular matrix organization, and cell adhesion in FALD compared with HCV. In Visium HD analysis, spatial transcriptomic integration guided by histological assessment and zonation-informed analysis identified nine clusters across FALD and HCV liver samples. Central vein–associated hepatocyte clusters in FALD showed disease-specific upregulation of genes including HAMP, CYP1A2, and mitochondrial genes (MT-ND2 and MT-ND3), while hepatocyte clusters in both central and portal regions exhibited widespread downregulation of metabolic pathways. In addition, liver sinusoidal endothelial cell clusters displayed increased expression of IGFBP7.
Conclusion: This study reveals spatially distinct molecular features in FALD, highlighting region-specific gene programs related to hepatocyte dysfunction and the hepatic microenvironment. High-resolution spatial transcriptomic analysis may provide insights into disease-specific mechanisms underlying FALD.

WED-314-YI

Ceruloplasmin is required for hepatocellular- but not macrophage-iron export

Marlene Panzer[1], Benedikt Schaefer[1], Sonja Wagner[1,2], Elke Pertler[1,2], Maria Rosina Troppmair[1], Laura Obholzer[1], Günter Weiss[3], Heribert Talasz[4], Klaus Faserl[4], Bettina Sarg[4], Herbert Tilg[1], Heinz Zoller[1,2]. *[1]Departement of Internal Medicine I, Medical University of Innsbruck, Innsbruck, Austria; [2]Christian Doppler Laboratory for Iron and Phosphate Biology, Medical University of Innsbruck, Innsbruck, Austria; [3]Department of Internal Medicine II, Medical University of Innsbruck, Innsbruck, Austria; [4]Division of Medical Biochemistry, Protein Core Facility, Biocenter, Medical University of Innsbruck, Innsbruck, Austria*
Email: marlene.panzer@i-med.ac.at

Background and aims: Iron homeostasis relies on coordinated iron storage, transport, and recycling. Macrophages recycle iron from senescent red blood cells, a process dependent on efficient iron export. The ferroxidase ceruloplasmin (Cp) is involved in iron export, primarily from hepatocytes. In humans, recessive mutations in the CP gene cause aceruloplasminemia, characterized by iron overload in the liver and brain but not the spleen. This study aims to investigate the function of ceruloplasmin in systemic iron homeostasis, erythropoiesis and iron export from macrophages.
Method: To examine the functional interaction of ceruloplasmin and the iron exporter ferroportin (FPN), ferroportin-floxed mice carrying a macrophage-specific LysM-Cre recombinase ($FPN^{\Delta M/\Delta M}$) were crossed with ceruloplasmin knockout ($CP^{-/-}$) mice. This breeding produced $CP^{-/-}FPN^{\Delta M/\Delta M}$, $FPN^{\Delta M/\Delta M}$, $CP^{-/-}$, and $FPN^{flox/flox}$ as control mice. Female mice at the age of 2 and 9 months were analyzed for alterations in iron homeostasis and erythropoiesis. Tissue iron levels, mRNA expression, blood counts, red cell indices, and plasma iron parameters were assessed. Proteomic analyses were performed on the bone marrow, liver, and spleen, while erythropoiesis was evaluated by flow cytometry of bone marrow cells.
Results: Off all genotypes tested, $CP^{-/-}FPN^{\Delta M/\Delta M}$ mice had the highest liver iron concentrations and the lowest hemoglobin concentrations, which was associated with the lowest TSAT. Serum ferritin concentrations were not different between $CP^{-/-}FPN^{\Delta M/\Delta M}$ and $FPN^{\Delta M/\Delta M}$ mice. Increased spleen iron concentrations were only found in mice lacking FPN in macrophages, regardless of the CP-genotype. These phenotypes were more pronounced in 9-months-old mice, when compared to younger mice. Analysis of red cell precursors in bone marrow by flow cytometry did not show differences between genotypes, but all mice had mild hypochromic microcytic anemia when compared to wild type controls.
Conclusion: Differences in spleen iron concentration confirm that macrophage ferroportin, but not ceruloplasmin is important for iron export from (red-pulp) macrophages in mice. Differences in liver iron suggest that CP has an important function for hepatocellular iron export. The finding that liver iron was highest in $CP^{-/-}FPN^{\Delta M/\Delta M}$ mice could be attributed to iron export defects in hepatocytes and Kupffer cells.

WED-315

Single-cell and spatial transcriptomics reveal portal vascular remodeling in porto-sinusoidal vascular disorder

Delfina Papinutti[1,2], Sarah Shalaby[3], Genís Campreciós[3], Alexandre Sayadi[4], Carla Fuster[3], Andreea Fodor[3], Alba Díaz[3], Keren Bahar Halpern[1], Juan Carlos García-Pagán[3], Pierre-Emmanuel Rautou[5], Shalev Itzkovitz[1], Virginia Hernández-Gea[3]. *[1]Weizmann Institute of Science, Department of Molecular Cell Biology, Rehovot, Israel; [2]Weizmann Institute, Molecular Cell Biology, Rehovot, Israel; [3]Hospital Clínic de Barcelona, Hepatic Hemodynamic Laboratory, Liver Unit, IDIBAPS (Fundació de Recerca Clínic Barcelona–Institut d'Investigacions Biomèdiques August Pi i Sunyer), Centro de Investigación Biomédica en Red de Enfermedades Hepáticas y Digestivas (CIBEREHD), Barcelona, Spain; [4]Université Paris Cité, Centre de Recherche sur l'Inflammation, INSERM U1149, Service de Pathologie, AP-HP Nord, Hôpital Beaujon, FHU MOSAIC, SIRIC InsiTu, Clichy, France; [5]Université Paris Cité, INSERM, Centre de Recherche sur l'Inflammation (CRI), UMR 1149, Paris, France*
Email: delfina.papinutti@weizmann.ac.il

Background and aims: Porto-sinusoidal vascular disorder (PSVD) is a rare vascular liver disorder characterized by portal hypertension in the absence of cirrhosis with poorly understood pathophysiology. Cellular drivers and the molecular and spatial mechanisms underlying PSVD remain unknown, and no comprehensive single-cell or spatial atlas has been described.
Method: We performed an integrated transcriptomic analysis combining bulk RNA sequencing (n = 76 samples), single-cell RNA sequencing (scRNA-seq; n = 16 samples), and Visium HD spatial transcriptomics (n = 3 liver samples) from human liver tissue. Single-cell data were used to construct a liver atlas and characterize disease-specific transcriptional programs across stromal, endothelial and immune compartments. Ligand–receptor interaction analysis was applied to infer intercellular signaling, and spatial transcriptomics was used to localize PSVD-associated programs within the liver architecture.
Results: PSVD was characterized by changes in endothelial cell states that included elevation of the collagen genes COL15A1 and COL4A1, metabolic–inflammatory stress signatures (FABP4/5), hypoxia-related pathways (FMO2), and B-cell involvement consistent with a stromal- and immune-rich, vessel-centered disease. Gene expression changes were most prominent in portal endothelial cells and resembled fetal signatures that were previously documented in hepatocellular carcinoma vessels. Ligand–receptor analysis identified enhanced collagen–integrin signaling from stromal to endothelial cells and increased Notch–Delta interactions at endothelial–perivascular interfaces, supporting active fibrovascular crosstalk. Spatial transcriptomics localized PSVD programs to discrete periportal and perivascular regions enriched for TIMP3 and IGFBP7, consistent with a mechanically remodeled vascular niche and chronically stressed endothelium. The patchy spatial distribution supports a vascular-triggered process with localized remodeling rather than diffuse parenchymal injury.
Conclusion: This study provides an integrated bulk, single-cell and spatial transcriptomic characterization of PSVD, highlighting altered endothelial cell states and pathways that may inform future diagnosis and targeted therapeutic strategies.

WED-316-YI

Targeting copper overload in Wilson disease – silencing ion transporter in the liver holds therapeutic potential for copper detoxification

Martha-Julia Sasula[1], Andree Zibert[2], Marcin Krawczyk[3], Hartmut Schmidt[3], Ruth Broering[3]. *[1]University Duisburg-Essen, Dept. of Gastroenterology, Hepatology and Transplantation Medicine, Essen, Germany; [2]Department of Internal Medicine B, University Hospital Muenster, Muenster, Germany; [3]Dept. of Gastroenterology, Hepatology and Transplantation Medicine, Medical Faculty, University Duisburg-Essen, Essen, Germany*
Email: martha-julia.sasula@uk-essen.de

Background and aims: Wilson disease (WD) is an autosomal recessive disorder caused by mutations in the intracellular copper transporter ATP7B. The functional impairment of ATP7B results in hepatocellular copper accumulation, which ultimately causes impaired cell viability, mitochondrial activity and autophagy that lead to the death of hepatocytes. Herein, the toxic excess of copper in WD cells will be targeted by silencing ion transporters.
Method: A transcriptomic analysis (GSE107323) and qRT-PCR validation of four ion transporters (T1–T4) was conducted in HepG2 wild-type (WT) and ATP7B-knockout (KO) cells, and in primary human hepatocytes from control and WD patients. The effects of siRNAs targeting ion transporters were evaluated for

pathophysiological improvements were evaluated using live/dead staining, CCK8 and MTT assays, as well as gene expression of copper-regulated metallothioneins (MT).
Results: Expression of selected ion transporters was copper-sensitive in HepG2 ATP7B-KO as well as in primary human hepatocytes. Silencing of T1 in HepG2 ATP7B-KO cells resulted in a significant reduction in copper toxicity by increased cell proliferation, improved cell- and mitochondrial viability, and downregulation of MT expression. Live/dead staining confirmed protective effects of T1 silencing. Conversely, the silencing of the remaining three transporters resulted in a comparatively less pronounced reduction in copper toxicity. Gene silencing led to a partial enhancement of cell and mitochondrial viability (T2) or a reduction in MT expression (T3 and T4).
Conclusion: T1 represents a most promising candidate for siRNA treatment in patients. Silencing of all four transporters will be investigated in personalised, induced pluripotent stem cells from WD patients with different ATP7B mutations in order to find new therapeutic applications.

WED-317

Challenges in the care of rare vascular liver diseases: insights from patients, health care providers, and patient organizations

Mercedes Guilabert Mora[1], Agnes Dumas[2], Eva Gil-Hernandez[3], Lynda Sifer-Riviere[2], Jane Sattoe[4], Guenda Bernegger[5], Maria Caiata Zufferey[5], Pura Ballester[3,6], Giada Danesi[5], Virginia Hernández-Gea[7,8], Sarwa Darwish Murad[9], Pierre-Emmanuel Rautou[10,11], Laure Elkrief[12], Benedetta Terziroli Beretta-Piccoli[13], Andrea De Gottardi[14,15], Annalisa Berzigotti[16], Aurélie Plessier[10,11], Jose Mira[1,3]. *[1]Miguel Hernández University of Elche, Department of Health Psychology, Elche, Spain; [2]INSERM, Aix Marseille University, IRD, ISSPAM, SESSTIM (Economic and Social Sciences of Health and Medical Information Processing), CALIPSO team, Marseille, France; [3]FISABIO Alicante-Sant Joan Healthcare District, Alicante, Spain; [4]Rotterdam University of Applied Sciences, Research Centre Innovations in Care, Rotterdam, Netherlands; [5]SUPSI (University of Applied Sciences and Arts in Southern Switzerland), DEASS (Department of Business Economics, Health and Social Care), CPPS (Competence Centre for Healthcare Practices and Policies), Manno, Switzerland; [6]UCAM (Universidad Catolica de Murcia), Facultad de Farmacia y Nutricion, Murcia, Spain; [7]Barcelona Hepatic Hemodynamic Laboratory, Liver Unit, Fundació de Recerca Clínic Barcelona (FRCB-IDIABPS), CIBEREHD (Centro de Investigación Biomédica en Red Enfermedades Hepáticas y Digestivas), Health Care Provider of the European Reference Network on Rare Liver Disorders (ERN-RareLiver),University of Barcelona, Barcelona, Spain; [8]Departament de Medicina i Ciències de la Salut, Universitat de Barcelona, Barcelona, Spain; [9]Erasmus Medical Center (EMC), Gastroenterology & Hepatology Department, Rotterdam, Netherlands; [10]Université Paris-Cité, Inserm, Centre de recherche sur l'inflammation, Paris, France; [11]AP-HP, Hôpital Beaujon, Service d'Hépatologie, DMU DIGEST, Centre de Référence des Maladies Vasculaires du Foie, FILFOIE, ERN RARE-LIVER, Clichy, France; [12]Service d'hépato-gastroentérologie, Centre de Référence des Maladies Vasculaires du Foie, FILFOIE, ERN RARE-LIVER, CHRU de Tours, Tours, France; [13]Università della Svizzera Italiana, Faculty of Biomedical Sciences, Lugano, Switzerland; [14]Gastroenterology and Hepatology, Luzerner Kantonsspital, Lucerne, Switzerland; [15]Gastroenterology and Hepatology, Ente Ospedaliero Cantonale, Lugano, Switzerland; [16]Department of Visceral Surgery and Medicine, Inselspital, Bern University Hospital, University of Bern, Bern, Switzerland*
Email: mguilabert@umh.es

Background and aims: Patients with rare vascular liver diseases (VLDs), including non-cirrhotic portal vein thrombosis and Budd–Chiari syndrome, may develop severe complications from an early age. Yet, little is known about their healthcare experiences and unmet needs. This study aimed to identify key challenges and needs in the care of patients with VLDs across four European countries.
Method: Semi-structured interviews were conducted with patients, members of patient advocacy organizations (PAOs), and healthcare providers (HCPs) from France, Spain, Switzerland, and the Netherlands. A standardized interview guide explored challenges and unmet needs in healthcare. Using thematic analysis, themes were first identified at the national level and subsequently synthesized internationally.
Results: Thirty-seven individuals participated: 13 patients, 7 PAO representatives, and 17 HCPs. Six core challenges and needs were identified across countries: (1) diagnostic wandering, sometimes due to insufficiently targeted imaging requests and limited radiologic experience, highlighting the need for greater VLD awareness in medical education; (2) challenges in communicating the diagnosis given the complexity and severity of the disease, suggesting the need to improve diagnosis delivery, notably through separate clinical visits and the use of visual aids; (3) scientific uncertainty regarding the etiology, progression, and treatment of VLDs, leading to difficulties for HCPs in risk interpretation and for patients in understanding and managing their condition, emphasizing the importance of addressing medical uncertainty explicitly in physician–patient communication; (4) challenges in care coordination, particularly for patients with associated diseases or comorbidities, pointing to the need for improved coordination, notably by strengthening the role of coordinating nurses; (5) insufficient supportive care, particularly in addressing mental health issues and fatigue; and (6) management of reproductive and sexual health, requiring tailored communication strategies. Empowering patients, through peer exchange, PAOs, and caregiver involvement, was considered essential to help them manage the disease and its broader impact on their lives.
Conclusion: This study highlights perceived cross-country challenges in the care of patients with rare VLDs, underscoring the need for targeted interventions in communication and care coordination to improve their healthcare experience and outcomes.

WED-318

Small molecule approach for increasing biliary phospholipid secretion in a mouse model for MDR3 deficiency (progressive familial intrahepatic cholestasis type 3)

Henkjan J. Verkade[1], Hilde de Vries[1], Willemien Hof[1], Niels Mulder[1], Milaine Hovingh[1], Rick Havinga[1], Eric Bell[2], Nathan Fuller[2], Robert Hughes[2], Folkert Kuipers[3], Jan Freark de Boer[1]. *[1]University Medical Center Groningen (UMCG), Groningen, Netherlands; [2]Rectify Pharmaceuticals, Boston, United States; [3]University of Groningen, European Research Institute for the Biology of Ageing (ERIBA), Groningen, Netherlands*
Email: h.j.verkade@umcg.nl

Background and aims: Progressive Familial Intrahepatic Cholestasis Type 3 (PFIC3) is a severe liver disease caused by mutations in *ABCB4*, encoding the biliary phospholipid transporter MDR3 in humans and MDR2 in mice. PFIC3 patients have impaired MDR3 function, leading to reduced phospholipid secretion into bile and unshielded detergent activity of biliary bile acids. Consequently, PFIC3 patients have progressive damage of the biliary system. Recently, a novel potent dual-acting MDR3/BSEP positive functional modulator has been discovered. RTY-694 increases protein function of both MDR3 and BSEP *in vitro*. We evaluated whether RTY-694 can rescue phospholipid secretion in a PFIC3 mouse model with residual phospholipid transport function (*Abcb4*$^{+/-}$ mice).
Method: We treated *Abcb4*$^{+/-}$ mice twice daily with vehicle, 30 or 60 mg/kg RTY-694 via oral gavage. Vehicle-treated WT mice served as the reference group. After 14 days all mice underwent common bile duct ligation and catherters were placed into the gallbladder and the jugular vein. Bile samples were collected under basal conditions and during IV infusion of tauroursodeoxycholic acid (TUDCA), after which bile flow and composition were determined.

Results: Treatment with RTY-694 did not affect food intake, body-weight or liver weight. Under basal conditions, bile flow was similar in all *Abcb4*$^{+/-}$ groups, as were the biliary secretion rates of bile acids and cholesterol. As expected, biliary phospholipid secretion rate was 50% reduced in untreated *Abcb4*$^{+/-}$ mice compared to WT mice. Treatment with RTY-694, however, significantly increased biliary phospholipid secretion at baseline and during stimulation by TUDCA infusion in these mice, by 35% and 22% compared to untreated *Abcb4*$^{+/-}$ mice, resp. ($p < 0.01$ ans <0.05).
Conclusion: RTY-694 increases biliary phospholipid secretion in a PFIC3 mouse model with residual phospholipid transport function. The present results strongly support the development of positive functional modulators for the treatment of PFIC3 patients.

WED-319-YI
Spatiotemporal profiling reveals the role of the microenvironment in polycystic liver disease progression
Scott Waddell[1], Elizabeth Carmichael[1], Mairi Hodge[1], Andreea Gradinaru[1], Melissa Boerrigter[2], Joost PH Drenth[3], Luke Boulter[1]. *[1]Institute of Genetics & Cancer, University of Edinburgh, Edinburgh, United Kingdom; [2]Radboud University Medical Center, Nijmegen, Netherlands; [3]Amsterdam University Medical Center, Amsterdam, Netherlands*
Email: scott.waddell@ed.ac.uk

Background and aims: Polycystic liver disease (PLD) is a relatively common genetic disorder that typically presents in midlife and is associated with severe pain/discomfort and a marked reduction in quality of life. There are currently no approved pharmacological therapies for PLD, and despite predictable Mendelian inheritance of disease-causing alleles (most commonly *PKD1*), preventative approaches are lacking. PLD cysts arise from biliary epithelial cells (BECs) and increase in number and size throughout life. The cellular and tissue-level changes that drive disease initiation and progression early in life remain poorly understood. Elucidating the molecular pathogenesis of PLD is essential to identify new therapeutic strategies. Here, we aimed to model and characterise the spatial and temporal dynamics underlying PLD development to uncover potential therapeutic targets.
Method: We generated a murine model with liver-specific deletion of *Pkd1* (Alfp-Cre; *Pkd1*). Mice were analysed from birth to six months of age using single-nuclear RNA sequencing and immunohistochemistry. To define the spatial organisation of the cyst microenvironment, human PLD liver samples with distinct genetic mutations were analysed using spatial transcriptomics and immunophenotyping.
Results: Spatial analysis of human PLD tissue revealed that CD4$^+$ memory T cells are the most abundant immune population within the cyst microenvironment in established disease. BECs displayed marked heterogeneity, forming NCAM$^-$ cystic epithelia and NCAM$^+$ ductular reactions. Notably, T cells were spatially associated with NCAM$^+$ ductular reactions rather than NCAM$^-$ cystic BECs, suggesting that mature cysts do not actively recruit immune cells. In Alfp-Cre; *Pkd1* mice, bile duct dilation was evident at birth and progressed in number and size into adulthood, recapitulating PLD. Single-nuclear RNA sequencing and immunohistochemistry of ~2 million cells across disease progression revealed dynamic recruitment and turnover of diverse immune populations, including multiple T cell subsets, consistent with human PLD. PLD mouse livers further mirrored human disease by harbouring NCAM1$^+$ BECs in close proximity to CD4$^+$ T cells.
Conclusion: PLD is a slowly progressive disease characterised by evolving spatiotemporal interactions among multiple cell types within the cyst microenvironment. While cystic BECs do not directly recruit immune cells, CD4$^+$ T cells preferentially localise near NCAM1$^+$ BECs, implicating this interaction in driving inflammation during PLD progression.

WED-320-YI
Multi-ancestry genome-wide association meta-analysis identifies novel susceptibility loci for biliary atresia
Zijing Yang[1], Shaowen Liu[1], Pak Chung Sham[1], Kenneth Ky Wong[1], Paul Kwong-Hang Tam[1,2], Clara Sze-man Tang[1]. *[1]The University of Hong Kong, Hong Kong SAR, China; [2]Macau University of Science and Technology, Macao SAR, China*
Email: u3012177@connect.hku.hk

Background and aims: Biliary atresia (BA) is a congenital disease characterized by inflammation and obstruction of the extrahepatic and intrahepatic bile ducts. BA has a higher disease prevalence among East Asians (1:5000 to 1:9000) than Europeans (1:14,000 to 1:22,000), suggesting a genetic predisposition across different populations. In this study, we aim to identify shared and/or ancestry-specific loci for BA across populations.
Method: We performed a multi-ancestry meta-analysis of genome-wide association studies including 1481 BA cases and 6372 controls of East Asian and European ancestry. To prioritize putative causal variants and effector genes, we integrated cross-population fine-mapping, regulatory annotation, colocalization analyses, and published single-cell transcriptomic datasets.
Results: In addition to the known *ADD3* locus, we identified two novel genome-wide significant loci at 1p21 and 12q23. At 1p21, the serum gamma-glutamyl transferase level and BA share the same causal variants, which were mapped to a cytoskeleton gene highly expressed in hepatoblast to fetal cholangiocyte lineage. The risk allele of the lead SNP was associated with reduced expression of the mapped gene in cholangiocytes, but not hepatocytes, suggesting a role of genetic dysregulation in cytoskeleton remodeling during cholangiocyte development in BA patients.
Conclusion: We identified a potential susceptibility locus at 1p21.2 for BA. Further experiments are required to elucidate the roles of cytoskeleton remodeling during the differentiation of hepatocytes and cholangiocytes. The target gene at 12q23.2 and its role in the pathogenesis of BA remain to be determined.

Viral hepatitis – Clinical, except HBV, HDV and HCV

TOP-615
Evaluation of HEV burden and urine antigen diagnostic utility in the DZIF transplant cohort
Nora Proske[1,2], Katja Dinkelborg[1,2], Tanja Klause[1], Christine Wundes[1], Birgit Bremer[2], Benjamin Maasoumy[2,3], Heiner Wedemeyer[2,3], Lisa Sandmann[2,3], Patrick Behrendt[1,2,3]. *[1]TWINCORE, Centre for Experimental and Clinical Infection Research, Institute for Experimental Virology, Hannover, Germany; [2]Hannover Medical School, Department of Gastroenterology, Hepatology and Endocrinology, Hannover, Germany; [3]German Center for Infection Research (DZIF), Hannover, Germany*
Email: proske.nora@mh-hannover.de

Background and aims: Hepatitis E virus (HEV) is the leading cause of acute viral hepatitis worldwide. While infection is usually self-limiting, immunocompromised individuals, particularly stem cell and solid organ transplant recipients, are at risk of chronic HEV infection, which may lead to progressive liver disease and is frequently underdiagnosed. Reported prevalence estimates in European transplant cohorts vary substantially. This study aimed to determine the prevalence and burden of HEV infection in a large multicenter transplant cohort and to evaluate urine-based HEV antigen detection as a diagnostic approach.
Method: Plasma and urine samples were collected from 1066 transplant recipients at four German transplant centers. Plasma

samples were obtained at transplantation and at follow-up, in the mean 22 months post-transplantation (range 3–60 months), while urine samples were collected at follow-up. Samples were tested for anti-HEV IgG, HEV RNA, and, in a subset, anti-HEV IgM. Additionally, 1041 urine samples were analyzed for HEV antigen.
Results: Anti-HEV IgG seroprevalence was 35.7% at baseline and 34.3% at follow-up. Seroconversion occurred in 9.1% of patients, whereas 20.1% lost detectable IgG antibodies, resulting in an IgG persistence of 79.9%. HEV RNA was detected in 15 of 1060 follow-up plasma samples (1.4%). HEV antigen was identified in 19 of 1041 urine samples (1.8%). Among patients with paired samples, urine antigen testing confirmed eight HEV RNA–positive cases, while samples with very low viral loads remained antigen-negative. Conversely, 11 urine samples were antigen-positive despite RNA-negative plasma results. Notably, HEV infection at follow-up was observed in several patients with baseline anti-HEV IgG positivity.
Conclusion: This multicenter cohort study demonstrates a substantial loss of anti-HEV IgG antibodies after transplantation and identifies ongoing HEV infections despite preexisting seropositivity. Urine-based HEV antigen testing may represent a complementary screening tool, while it is less sensitive in cases of low HEV RNA, it might be more sensitive in detecting recent HEV infection.

FRI-637
Comparison of foetal and maternal outcomes of hepatitis E in pregnant versus non pregnant women
Faiza Sadaqat Ali[1], Bader Faiyaz Zuberi[2], Erum Majid[3], Amanullah Abbasi[4], Tazeen Rasheed[4]. [1]*Karachi Metropolitan University, Dow University of Health Sciences, Karachi, Pakistan;* [2]*OMI hospital, Karachi, Pakistan;* [3]*Jinnah Postgraduate Medical Centre, Karachi, Pakistan, Karachi, Pakistan;* [4]*Dow University of Health Sciences, Karachi, Pakistan*
Email: faiza.sadaqat@duhs.edu.pk

Background and aims: Hepatitis E virus (HEV) is a major cause of acute viral hepatitis in endemic regions, with pregnancy recognized as a vulnerable state. Severe maternal disease and poor foetal outcomes have been reported, yet comparative data with non pregnant women remain limited. This study aimed to determine maternal and foetal outcomes of HEV infection in pregnant women and compare them with non pregnant women.
Method: A prospective observational cohort was conducted at Jinnah Postgraduate Medical Center and Dr Ruth KM Pfau Civil Hospital Karachi between 7 February 2023 and 6 January 2025. Pregnant women presenting with jaundice were enrolled as Group A, while non pregnant women with hepatitis served as controls (Group B). Both groups were stratified by HEV status into Group Ae (pregnant HEV positive), Group Ane (pregnant HEV negative), Group Be (non pregnant HEV positive), and Group Bne (non pregnant HEV negative). HEV diagnosis was confirmed by serology. Demographic, clinical, and laboratory data were collected, and patients were followed for maternal outcomes (improvement or death) and foetal outcomes (alive healthy birth, intrauterine growth restriction, stillbirth, abortion). Statistical analysis used chi square test, with $p < 0.05$ considered significant.
Results: A total of 190 patients were included, equally distributed between pregnant and non pregnant groups (95 each). Mean age was comparable (27.0–27.8 years). Diabetes and hypertension prevalence was similar across groups ($p > 0.05$). Maternal outcomes did not differ significantly between HEV positive and negative cohorts, with mortality rates ranging from 37.8 percent to 46.6 percent. In contrast, foetal outcomes were significantly worse in HEV positive pregnant women. Group Ae had 37.9 percent alive healthy births, 12.1 percent intrauterine growth restriction, 31.0 percent stillbirths, and 18.9 percent abortions. Group Ane showed 67.6 percent alive healthy births, 5.4 percent intrauterine growth restriction, 21.6 percent stillbirths, and 5.4 percent abortions. The difference in foetal outcomes between HEV positive and HEV negative pregnant women was statistically significant ($p = 0.032$). Non pregnant HEV groups showed comparable maternal outcomes but no foetal outcomes.
Conclusion: Hepatitis E in pregnancy leads to significantly poorer foetal outcomes compared to HEV negative women, despite similar maternal results. This underscores pregnancy vulnerability and the need for prevention, early diagnosis, and close monitoring in endemic regions.

FRI-638
FIB-4 fails to identify significant liver fibrosis in people with HIV: evidence from a large multinational screening study
Felice Cinque[1,2], Francesca Farina[1,3], Jihoon Lim[4], Dana Kablawi[1], Gabrielle Mariano[1], Bertrand Lebouche[1], Nadine Kronfli[1], Marina B. Klein[1], Antonio Cascio[5], Claudia Gioe'[5], Emmanuel Tsochatzis[6], Rosa Lombardi[2], Sahar Saeed[7], Ahmed Cordie[8], Rahma Mohamed[8], Ahmed Kamel[9], Gamal Esmat[8], Alessandra Bandera[2], Jovana Milic[10], Dominik Benke[11], Fauzi Elamouri[11], Jürgen Rockstroh[11], Giovanni Guaraldi[10], Giada Sebastiani[1,12]. [1]*Chronic Viral Illness Service, McGill University Health Centre, Montreal, Canada;* [2]*Department of Pathophysiology and Transplantation, Università degli Studi di Milano, Milan, Italy;* [3]*San Raffaele Hospital, Milan, Italy;* [4]*Centre for Outcomes Research and Evaluation, Research Institute of the McGill University Health Centre, Montreal, Canada;* [5]*Department of Health Promotion Sciences and Mother and Child Care "Giuseppe D'Alessandro," University of Palermo, Palermo, Italy;* [6]*UCL Institute for Liver and Digestive Health, Royal Free Hospital and UCL, London, United Kingdom;* [7]*Public Health Sciences, Queen's University, Kingston, Canada;* [8]*Cairo University Hospitals HIV Clinic, Endemic Medicine Department, Cairo University, Cairo, Egypt;* [9]*Clinical Pharmacy Department, Faculty of Pharmacy, Cairo University, Cairo, Egypt;* [10]*University of Modena and Reggio Emilia, Modena, Italy;* [11]*Department of Internal Medicine I, Venusberg Campus 1, University Hospital Bonn, Bonn, Germany;* [12]*15Division of Gastroenterology and Hepatology, Royal Victoria Hospital, McGill University Health Centre, Montreal, Canada*
Email: giada.sebastiani@mcgill.ca

Background and aims: Steatotic liver disease (SLD) and liver fibrosis are major comorbidities in people with HIV (PWH). Guidelines recommend stepwise screening using the Fibrosis-4 (FIB-4) index followed by transient elastography (TE), yet its accuracy in PWH and the magnitude of FIB-4 misclassification are uncertain. We aimed to evaluate the diagnostic performance of FIB-4 against TE, quantify missed significant fibrosis cases, and assess whether adding metabolic and HIV-related factors improves risk prediction.
Method: We conducted a multinational cross-sectional study of 4917 consecutive PWH without viral hepatitis coinfection or hazardous alcohol intake from seven prospective cohorts undergoing TE-based liver health screening. SLD was defined as controlled attenuation parameter (CAP) ≥275 dB/m and classified as metabolic dysfunction–associated SLD (MASLD) or metabolic dysfunction–associated alcohol-related liver disease (MetALD). We compared FIB-4 <1.3 against liver stiffness measurement (LSM) ≥8 kPa using the area under the receiver operating characteristic curve (AUROC), identified determinants of false-negative misclassification, and evaluated the incremental value of metabolic and HIV-related predictors using discrimination and reclassification metrics.
Results: Significant fibrosis was present in 12.6% and SLD in 21.7% (20.6% MASLD; 1.1% MetALD), with higher prevalence in PWH with MASLD (25%) and MetALD (26.9%) than in those without SLD (8.6%; $p < 0.001$). 13% of fibrosis cases occurred without SLD or metabolic comorbidities. FIB-4 showed modest accuracy (AUROC 0.635, 95% CI 0.61–0.66) and misclassified 36% of LSM ≥8 kPa cases as low-risk, with poorer performance in MASLD (AUROC 0.579) compared to non-MASLD (AUROC 0.68; DeLong $p = 1.3 \times 10^{-5}$). Steatosis independently increased false-negative misclassification (risk ratio 2.01, 95% CI 1.50–2.69), whereas prior D-drug exposure reduced it (risk ratio 0.63, 95%

CI 0.44–0.91). Models incorporating metabolic factors (diabetes, SLD, dyslipidemia, hypertension, and waist circumference) improved discrimination and enhanced patient reclassification by 27% beyond FIB-4 alone, with a further 12% improvement after adding HIV-specific variables (CD4 count, HIV viral load, CD4/CD8 ratio, and prior D-drugs exposure).
Conclusion: In PWH, liver fibrosis is common and frequently missed by FIB-4-based screening, particularly in MASLD. TE-centered pathways augmented by metabolic and HIV-specific risk indicators may improve early detection and liver health management in PWH.

FRI-639
Hepatitis E seroprevalence is significantly elevated in lymphoma patients: exploring causal association or epiphenomenon
Jan Drews[1], Johannes Bannasch[1], Julia Dierlamm[1], Katja Weisel[2], Marc Luetgehetmann[3], Maria Mader[4], Samuel Huber[1], Ansgar W. Lohse[1], Julian Schulze zur Wiesch[1], Sven Pischke[1].
[1]I. Department of Medicine, University Medical Centre Hamburg-Eppendorf, Hamburg, Germany; [2]II. Department of Medicine, University Medical Centre Hamburg-Eppendorf, Hamburg, Germany; [3]Institute of Medical Microbiology, Virology and Hygiene, University Medical Centre Hamburg-Eppendorf, Hamburg, Germany; [4]III. Department of Medicine, University Medical Centre Hamburg-Eppendorf, Hamburg, Germany
Email: jdrews9247@googlemail.com

Background and aims: Hepatitis E virus (HEV) infection is associated with diverse extrahepatic manifestations including immunological abnormalities and blood count changes. A single case report suggested a potential causal link between HEV and T-cell lymphoma development, but the prevalence and significance of HEV infection in lymphoma patients remain unknown. This study investigates whether HEV exposure is enriched in lymphoma populations and whether it represents a potential pathogenic cofactor or merely an epiphenomenon.
Method: We retrospectively tested 117 lymphoma patients for HEV exposure using anti-HEV serology (IgM and IgG by Wantai enzyme immunoassay) and HEV-RNA polymerase chain reaction (Altona Diagnostics). A cohort of 1000 unselected blood donors served as controls. Positive sera were confirmed by immunoblot (Mikrogen). We extracted transfusion history from medical records to exclude passive antibody acquisition as a confounding variable.
Results: Anti-HEV IgG seropositivity was significantly elevated in lymphoma patients at 27% (n = 32/117) compared to 17% in healthy controls (p = 0.01), representing a 59% relative increase in seroprevalence. Immunoblot confirmation reduced confirmed seropositivity to 24/117 (20.5%) in lymphoma patients. Anti-HEV IgM positivity was similar between groups (2% in both). The distribution of anti-HEV IgG positivity across individual subgroups yielded the following ratio: Indolent B-cell: 7/23 (30%), aggressive B-cell 19/68 (28%), indolent T-cell 3/11 (27%), aggressive T-cell 2/8 (25%), Hodgkin 1/6 (17%), unclassified 0/1 (0%). HEV-RNA was undetectable by polymerase chain reaction in all subjects, excluding active viremia. IgG-positive and IgG-negative lymphoma patients showed no significant differences in gender distribution, age, lymphoma subtype, total immunoglobulin G levels, or transfusion exposure (mean 18 versus 23 blood products; p = not significant).
Conclusion: Hepatitis E seropositivity in lymphoma patients substantially exceeds population baseline without clear explanation by confounding variables. The absence of active viremia, similar transfusion burden, and identical immunological profiles between seropositive and seronegative patients argue against passive acquisition or acute infection. These findings warrant mechanistic investigation to determine whether prior HEV exposure represents a causative contributor to lymphomagenesis or a marker of altered immune surveillance.

FRI-640
Autoimmune hepatitis triggered by acute hepatitis A infection
David Aguirre-Villarreal[1], Froylan Martinez Sánchez[1], Jose David Prieto Nava[2,3], Luis Alejandro Rosales Renteria[2], Mario Orlando Santana Montes[1], Leticia Martinez Martinez[4], Jonathan Aguirre[5], Victor Manuel Paez-Zayas[6], Francisco isai García juarez[7], Eric Kauffman[1], Fátima Manzo-Santana[1], Eduardo Marin-Lopez[8], Ignacio Garcia Juarez[1], Mauricio Lisker-Melman[9].
[1]Instituto Nacional De Ciencias Médicas Y Nutrición Salvador Zubirán, Ciudad de México, Mexico; [2]Centro Médico Issemym Metepec, Toluca, Mexico; [3]Instituto Nacional de Ciencias Médicas y Nutrición Salvador Zubirán, Mexico City, Mexico; [4]Central Doctor Ignacio Morones Prieto, San Luis Potosí, Mexico; [5]Centro Médico ABC, Mexico City, Mexico; [6]Hospital General de México, Mexico City, Mexico; [7]ISSSTE Centro Médico Nacional 20 de Noviembre, Ciudad de México, Mexico; [8]Hospital Ángeles Puebla, Puebla, Mexico; [9]Washington University In Saint Louis, Saint Louis, United States
Email: davidaguirre14@gmail.com

Background and aims: Hepatitis A virus (HAV) causing autoimmune hepatitis (AIH) has been previously reported but its incidence, prevalence, and natural history are largely unknown. We aim to describe a subgroup of patients with biopsy-proven AIH among a cohort of patients with acute hepatitis A infection (aHAV) and compare them to patients with aHAV that completely resolved.
Method: Multicenter, case-control study of patients diagnosed with AIH several weeks after a confirmed aHAV. AIH was suspected in patients with prolonged liver chemistry elevations (≥3 months with intermittent elevation of >1000 U/L of ALT or constant elevation of ALT), hyperglobulinemia, positive autoimmune serologies and confirmed with a liver biopsy. Cases were matched (3:1) to controls with aHAV that underwent complete resolution (defined by ALT normalization) three months after diagnosis.
Results: Of 558 patients with aHAV, 24 (4.3%) were diagnosed with biopsy-proven AIH. All patients had positive ANA titers (median 1:160) and 14 had positive ASMA titers (median 1:160). Median IgG levels were 2230 g/dL. Patients with aHAV-associated AIH had higher bilirubin levels, more likely presented with diarrhea and were hospitalized more frequently. Median time to aHAV-associated AIH LC peak was 83 days. In aHAV-associated AIH, LC showed intermittent elevations of ALT in 18, and constant elevations in 6 patients. All cases of AIH received prednisone for a median duration of 66 days (36–708), and 14 also received AZA or MMF. Of the 24 patients, 22 completely normalized ALT with no further treatment. When compared to controls, no differences in initial liver chemistries were found (ALT: 2251 vs. 2418, p = 0.78, AST 1629 vs. 1881).
Conclusion: aHAV-associated AIH is rare and requires a high degree of suspicion. Most patients have prolonged illness with intermittent ALT elevations yet a favorable clinical course and excellent response to short-term immunosuppression.

FRI-641
Viral capsid constitution and neutralizing antibodies predict chronification of hepatitis E virus infection
Jonathan Garn[1,2,3], Lukas Fehlau[1,2], Katja Dinkelborg[1,2], George Ssebyatika[4], Erich Freyer[1], Saskia Janshoff[5,6,7,8], Benjamin Maasoumy[1,3], André Gömer[8,9], Daniel Todt[5,8,10], Thomas Krey[4], Heiner Wedemeyer[1,3,11], Anke R.M. Kraft[1,12], Eike Steinmann[8,9], Patrick Behrendt[1,2,3].
[1]Hannover Medical School, Clinic for Gastroenterology, Infectious Diseases, Hepatology and Endocrinology, Hannover, Germany; [2]TWINCORE, Center for Experimental and Clinical Infection Research, Institute for Experimental Virology, Translational Virology, Hannover, Germany; [3]German Center for Infection Research (DZIF), Partner sites Hannover-Braunschweig, Hamburg-Lübeck-Borstel-Riems, Heidelberg and external partner site Bochum, Germany; [4]University of Lübeck, Center for Structural and Cell Biology in Medicine, Lübeck, Germany; [5]Department of Translational

and Computational Infection Research (TRACiR), Ruhr University Bochum, Bochum, Germany; [6]Department of Molecular and Medical Virology, Ruhr University Bochum, Bochum, Germany; [7]Institut für Laboratoriums- und Transfusionsmedizin, Herz- und Diabeteszentrum Nordrhein-Westfalen, Universitätsklinikum der Ruhr-Universität Bochum, Universitätsklinikum der Universität Bielefeld, Bad Oeynhausen, Germany; [8]Hepatitis E Virus Research Hub (HepE-Hub), Bochum, Germany; [9]Ruhr-University-Bochum, Molecular & Medical Virology, Bochum, Germany; [10]European Virus Bioinformatics Center (EVBC), Jena, Germany; [11]Cluster of Excellence RESIST (EXC 2155), Hannover Medical School, Hannover, Germany; [12]Centre for Individualised Infection Medicine (CiiM), Hannover, Germany
Email: garn.jonathan@mh-hannover.de

Background and aims: Hepatitis E virus (HEV) is the most common cause of acute viral hepatitis worldwide. While infection is usually self-limiting in immunocompetent individuals, immunocompromised patients are at risk of developing chronic HEV infection. The main immunogenic HEV antigen is the capsid protein (pORF2), which occurs in two forms: the pORF2c protein forms the infectious virion and the secreted, glycosylated form pORF2s, which is believed to act as an immune decoy.
The mechanisms underlying HEV chronification are not fully understood. The aim of this study was to identify clinical and serological factors associated with chronicity in order to enable earlier prediction of viral persistence and timely initiation of antiviral therapy, ultimately improving clinical outcomes.
Method: 277 longitudinal serum samples were collected from 77 patients with acute or chronic HEV infection. Samples were tested for HEV-RNA and pORF2c using an in-house ELISA that specifically detects the infectious pORF2c. Moreover, HEV-RNA polymerase sequencing was performed to assess viral population composition during acute and chronic infection. Anti-HEV IgG was quantified using ELISA and antibody functionality was assessed by neutralization assays and avidity ELISA.
Results: Tacrolimus-based immunosuppressive therapy following solid organ transplantation was identified as the main clinical risk factor driving HEV chronification. Patients with chronic HEV infection displayed higher HEV-RNA levels and significantly elevated pORF2c levels, which correlated with viral RNA concentrations. Interestingly, all patients with an pORF2c signal-to-cut-off ratio exceeding 10 at the initial sampling time point were affected by chronic infection. HEV populations were more heterogenous during chronic infection and associated with certain amino acid variants. Anti-HEV IgG levels and neutralizing capacity were reduced in chronic infection. In contrast to acute infection, antibody avidity remained persistently low in chronic patients.
Conclusion: Elevated pORF2c levels are associated with development of HEV chronicity. The in-house ELISA enables specific detection of infectious viral particles, which can be used as an early predictive biomarker for chronification. Together with assessment of the adaptive humoral immune response, this approach may allow earlier identification of patients at risk for viral persistence and guide timely initiation of antiviral therapy.

FRI-642

Impact of sex and age on acute hepatitis E: comparable exposure but male predominance of symptomatic disease and age-dependent mortality

Sven Pischke[1], Lara Erichsen[1], Susanne Polywka[1], Marcus Altfeld[1], Marylyn Addo[1], Marc Lutgehetmann[1], Julian Schulze zur Wiesch[1].
[1]University Hospital Hamburg Eppendorf, Hamburg, Germany
Email: s.pischke@uke.de

Background and aims: Sex and age are fixed host characteristics, but their role in hepatitis E virus (HEV) infection dynamics remains unclear. This study investigated (1) the influence of sex and age on HEV exposure in a healthy population and (2) their impact on clinical presentation and outcomes of acute hepatitis E in immunocompetent individuals in a HEV genotype 3–endemic region.
Method: The analysis consisted of two steps: HEV exposure: Anti-HEV IgG was determined using the Wantai assay in 1000 healthy blood donors (50% male, 50% female). Clinical course: Sex- and age-related differences were assessed retrospectively in 148 consecutive immunocompetent patients with PCR-confirmed (Cobas PCR, Roche) acute hepatitis E.
Results: Anti-HEV IgG was detected in 17% of blood donors (19% of men, 15% of women; p = n.s.), indicating no sex difference in HEV exposure. Donor ALT levels and age did not differ significantly between sexes (mean age 35 years, range 18–73). Hepatitis E patients were significantly older than blood donors (mean age 53 years, $p < 0.001$) and predominantly male (69% male vs 31% female, p = 0.002). Mean age did not differ between male and female patients (52 vs 56 years). Six patients (4%; 3 men, 3 women) died from acute-on-chronic liver failure; fatal cases were significantly older than survivors (mean 67 years, p = 0.01). Extrahepatic manifestations were observed in 10 patients (7%; 6 men, 4 women).
Conclusion: In an HEV genotype 3–endemic region, men and women exhibit similar lifetime HEV exposure, yet men constitute the majority of symptomatic, immunocompetent acute hepatitis E cases. Advanced age—but not sex—was the key predictor of fatal outcomes. These findings suggest biological or behavioral sex-related differences in clinical disease manifestation rather than in viral exposure risk.

FRI-643

Cross-kingdom gut microbiome signatures associate with clinical severity in hepatitis A-associated acute liver failure

Anoushka Saxena[1], Rakhi Maiwall[1], Dr Babu Lal Meena[1], Varun Suroliya[1], Guresh Kumar[1], Shiv Kumar Sarin[1], Nirupma Trehanpati[1]. *[1]Institute of Liver & Biliary Sciences, New Delhi, India*
Email: trehanpati@gmail.com

Background and aims: Hepatitis A-induced acute liver failure (ALF-A) is associated with high short-term mortality. As gut microbial perturbations may capture systemic derangements, we aimed to define integrated bacterial–fungal alterations in ALF-A patients, and explore any correlations with clinical severity.
Method: Stool samples of IgM HAV positive, ALF-A patients (n = 33, age 26 ± 9 yrs;50.7% male) age and sex matched acute viral hepatitis AVH-A (n = 27) and healthy subjects (HC,n = 20) were collected within 48 h of admission and subjected to paired 16S rRNA and Internal Transcribed Spacer (ITS) sequencing. Differential taxa were identified and correlated with clinical severity parameters like MELD, ammonia, INR and lactate. Cross-kingdom association networks were constructed using Spearman correlations ($|r|>0.5$) and co-occurrence analysis (Jaccard$\geq$0.4; co-presence $\geq$3 samples).
Results: ALF-A exhibited fungal dysbiosis with reduced diversity and significantly lower Basidiomycota: Ascomycota ratio, compared to AVH-A and HC. AVH-A showed enrichment of *Saccharomyces cerevisiae* and *Ascobolus* spp., whereas ALF-A was enriched for *Trichoderma longibrachiatum*, *Penicillium sublateritium*, *Cladosporium*, *Torula* with reported proteolytic, acidogenic and secondary-metabolite biosynthetic potential. Selected ALF-A enriched fungi correlated positively with MELD, ammonia and lactate levels ($r = 0.40–0.83$, $p < 0.05$). In parallel, ALF-A bacterial dysbiosis was characterized by enrichment of lactate and hyperammonemia-associated pathobionts (*Enterococcus*,*Ruminococcus gnavus*,*Hungatella hathewayi)* with depletion of commensal SCFA-associated genera (*Faecalibacterium*,*Roseburia*,*Agathobaculum*

butyriciproducens) compared with AVH-A. ALF-A–enriched bacteria were also correlated with MELD, ammonia, INR and lactate ($r > 0.50$, $p < 0.05$). Integrated correlation and co-occurrence networks consistently linked *Enterococcus-R. gnavus-Hungatella* bacterial core with *Trichoderma-Cladosporium-Torula-Penicillium*, indicating cross-kingdom microbial signature aligned with clinical severity in HAV-ALF.

Conclusion: In ALF-A, stool profiling identifies cross-kingdom dysbiosis. Bacterial shifts consistent with a lactate/ammonia-rich milieu may favor fungal expansion, while fungal proteolytic and acidogenic properties further altering pH, mucus integrity and bacterial community structure. Together, these bi-kingdom signatures can serve as adjunct severity markers.

FRI-644

Porcine-derived pancreatic enzyme replacement therapy as a cause of hepatitis E virus infection

Siddharth Sridhar[1], Cyril CY Yip[1], Xiaodan Ma[1], Jianwen Situ[1], Yonghao Liang[1], Nicholas Foo-Siong Chew[1], Xizhu Wang[1], Stanley Siu Fung Ho[1], Esmond Ng[1]. [1]*The University of Hong Kong, Pok Fu Lam, Hong Kong*
Email: sid8998@hku.hk

Background and aims: Hepatitis E virus (HEV) is an important cause of hepatitis which is usually acquired via consumption of undercooked pork products. Recently, porcine-derived pancreatic enzyme replacement therapy (PERT) has been proposed as a cause of HEV infection in cystic fibrosis patients after lung transplantation. We investigated PERT as a source of HEV infection in immunocompromised persons and the general population using a clinical study and advanced disease models.

Method: PERT capsules/tablets from different manufacturers were sourced for HEV RNA detection by two independent real-time RT-PCR (qRT-PCR) assays. Positive PERT products with sufficient virus loads were sequenced using Sanger sequencing. Hepatitis E patients diagnosed at our center since 2017 were retrospectively assessed for PERT intake prior to symptom onset. Immunocompromised gerbils were orally challenged with HEV inocula with virus loads simulating those found in PERT products. Effect of PERT treatment on HEV infectivity in cell culture was assessed.

Results: HEV RNA contamination was pervasive across PERT products from different manufacturers with 36/115 (31.3%) individual capsules/tablets testing positive in both HEV qRT-PCR assays. Positivity rates varied widely by manufacturer. Virus loads ranged from 8.1 copies – 4.61×10^3 copies per capsule. Only 1/92 (1.09%) hepatitis E patients had taken PERT prior to symptom onset. This was an immunocompromised patient with self-limiting acute hepatitis E with no other risk factors for hepatitis E infection. A 124-nucleotide HEV sequence fragment from this patient was 99.2% identical to PERT-derived HEV sequences from certain manufacturers. Cytotoxicity and low virus loads precluded direct assessment of HEV viability in PERT products. However, concomitant treatment with PERT did not inhibit infection of a validated HEV strain *in vitro* showing that the virus can remain viable in this matrix. Immunocompromised gerbils were susceptible to a simulated oral HEV inoculum equivalent to daily exposure from PERT in cystic fibrosis patients.

Conclusion: PERT products are frequently contaminated with HEV RNA. Although low virus loads and questionable viability indicate negligible risk for most users, immunocompromised persons may be at risk for clinically significant hepatitis E infection via this route.

Viral Hepatitis – Experimental and pathophysiology

TOP-616-YI

VDAC1-ACSL3-mediated aberrant lipid droplet-mitochondria crosstalk drives metabolic reprogramming and HCC in CHB and MASLD coexistence

Zhe Dai[1], Guangde Zhou[2], Yin Gao[3], Jie Li[4], Ming-Hua Zheng[5], Yijin Wang[1]. [1]*Department of Pharmacology, Joint Laboratory of Guangdong-Hong Kong Universities for Vascular Homeostasis and Diseases, School of Medicine, Southern University of Science and Technology, SUSTech Homeostatic Medicine Institute, School of Medicine, Southern University of Science and Technology, Shenzhen, China;* [2]*Department of Pathology, Beijing YouAn Hospital, Capital Medical University, Department of Pathology, The Second Affiliated Hospital of Southern University of Science and Technology, Beijing, China;* [3]*Department of Biochemistry, Key Laboratory for Molecular Enzymology and Engineering of Ministry of Education, School of Life Sciences, Jilin University, Changchun, China;* [4]*Department of Infectious Disease, Nanjing Drum Tower Hospital, Affiliated Hospital of Medical School, Nanjing University, Nanjing, China;* [5]*MASLD Research Center, Department of Hepatology, the First Affiliated Hospital of Wenzhou Medical University, Key Laboratory of Diagnosis and Treatment for The Development of Chronic Liver Disease in Zhejiang Province, Wenzhou, China*
Email: wangyj3@sustech.edu.cn

Background and aims: The co-occurrence of chronic hepatitis B (CHB) and metabolic dysfunction-associated steatotic liver disease (MASLD) constitutes a "vicious synergy" linked to accelerated fibrosis and hepatocellular carcinoma (HCC). The molecular mechanisms driving this convergence—particularly how metabolic steatosis reshapes the viral liver to drive oncogenesis despite viral suppression—remain undefined.

Method: Spatial transcriptomics was performed on liver biopsies from patients with MASLD, CHB, CHB+MASLD, and controls. A murine CHB+MASLD model was established via HBV hydrodynamic injection combined with high-fat feeding. The mitochondrial-lipid droplet (LD) interactome was mapped by LC-MS/MS. Protein interactions and stability were interrogated using co-immunoprecipitation and site-directed mutagenesis. Tumorigenic potential was evaluated in an orthotopic HCC model using RIL-175 cells expressing wild-type or K365A-mutant ACSL3.

Results: Spatial profiling revealed altered immune and metabolic features in CHB+MASLD patients, characterized by marked mitochondrial dysfunction and enrichment of tumor-associated macrophages (TAMs), even during the immune-tolerant phase. Mechanistically, hepatocytes in this disease context exhibited upregulated expression and oligomerization of the mitochondrial outer membrane protein VDAC1. VDAC1 directly interacted with acyl-CoA synthetase long-chain family member 3 (ACSL3), whose protein stability was enhanced via K365-dependent deubiquitination by USP9X. The resulting VDAC1-ACSL3 complex facilitates aberrant LD-mitochondria tethering, leading to exacerbated oxidative stress, extensive mitochondrial impairment and a metabolic shift toward aerobic glycolysis with elevated lactate production, thereby fueling a procarcinogenic niche. Notably, the ACSL3-K365A mutation disrupted USP9X-dependent deubiquitination, reduced VDAC1-ACSL3 tethering, restored mitochondrial integrity and significantly suppressed orthotopic tumor growth. Furthermore, VDAC1

oligomerization triggered mitochondrial DNA release, activating cGAS-STING signaling and interferon responses that suppressed HBV replication.
Conclusion: We identify VDAC1-ACSL3-mediated LD-mitochondria tethering, regulated by USP9X, as a critical driver of metabolic stress and microenvironment reprogramming in patients with CHB complicated by MASLD. This axis represents a promising therapeutic target to mitigate hepatocarcinogenesis in this growing patient population.

TOP-630
The interferon-inducible protein C19ORF66 suppresses HBV reverse transcription through incorporating into viral nucleocapsid
Sheng Shen[1], Hongyan Liang[1], Ge Zeng[1], Yidan Chen[1], Wanying Liang[1], Jianlu Wang[1], Hu Zhang[2], Haitao Guo[2], Jian Sun[1]. *[1]Department of Infectious Diseases, Nanfang Hospital, Southern Medical University, Guangzhou, China, State Key Laboratory of Multi-organ Injury Prevention and Treatment, Key Laboratory of Infectious Diseases Research in South China, Ministry of Education, Guangdong Provincial Key Laboratory for Prevention and Control of Major Liver Diseases, Guangdong Provincial Clinical Research Center for Viral Hepatitis, Guangdong Institute of Hepatology, Guangdong Provincial Research Center for Liver Fibrosis Engineering and Technology, Guangzhou, China; [2]Department of Microbiology and Molecular Genetics, University of Pittsburgh School of Medicine, Pittsburgh, Pennsylvania, USA, Cancer Virology Program, UPMC Hillman Cancer Center, University of Pittsburgh School of Medicine, Pittsburgh, Pennsylvania, USA, Pennsylvania, United States*
Email: doctorsunjian@qq.com

Background and aims: The host interferon stimulated gene (ISG) C19ORF66 (also known as SHFL or UPF0515) exhibits broad-spectrum antiviral activity against a range of RNA viruses and retroviruses. However, its potential role in inhibiting Hepatitis B Virus (HBV) remains unexplored. This study aims to assess the antiviral effect of C19ORF66 on HBV replication and, if present, to delineate its mechanism of action.
Method: We employed gain-and-loss-of-function approaches in various cell culture models (HepG2, Huh7, and HepG2-NTCP) supporting HBV transfection or infection. A hepatocyte-specific *C19ORF66* knockout (KO) mouse model was generated and used for *in vivo* functional validation. Co-IP, immunofluorescence, RNA immunoprecipitation (RIP), cross-linking immunoprecipitation sequencing (CLIP-seq), and electrophoretic mobility shift assay (EMSA) were used to investigate protein and RNA interactions.
Results: Ectopic expression of C19ORF66 potently inhibited HBV replication without affecting viral RNA transcription, protein expression, or capsid assembly, but specifically blocked viral reverse transcription. Intriguingly, C19ORF66 overexpression altered the profile of encapsidated pgRNA, generating multiple shorter pregenomic RNA (pgRNA) species. Conversely, C19ORF66 knockdown/knockout enhanced HBV DNA synthesis and increased encapsidated pgRNA levels. The basal level of C19ORF66 expression was detected in hepatocytes, and its expression was further induced by IFN-α/γ/λ in vitro, and knockdown of C19ORF66 partially abrogated IFN's anti-HBV effect. In IFN-treated chronic HBV patients, higher intrahepatic C19ORF66 induction correlated with a better treatment response. Mechanistically, C19ORF66 incorporates into the viral nucleocapsid during its assembly via simultaneously binding to HBV polymerase (P) protein and pgRNA, a process dependent on a specific domain of C19ORF66 and a defined *cis*-element on pgRNA identified by CLIP-seq and EMSA. Consequently, the incorporated C19ORF66 aborted HBV reverse transcription.
Conclusion: We identified C19ORF66 as a potent and key executor of the IFN-mediated anti-HBV response. C19ORF66 exerts its inhibitory function by co-packaging with the viral P protein and pgRNA into the nucleocapsid. This unique incorporation mechanistically disrupts reverse transcription, thereby providing a novel mechanism of host-mediated viral restriction.

TOP-631
Discovery and preclinical profiles of a first-in-class potent hepatitis E virus inhibitor AT-587
Qi Huang[1], Dawei Cai[1], Adel Moussa[1], Nancy Agrawal[1], Jean-Pierre Sommadossi[1]. *[1]Atea Pharmaceuticals, Inc, 225 Franklin Street, Suite 2100, Boston, United States*
Email: huang.qi@ateapharma.com

Background and aims: Hepatitis E virus (HEV), the causative agent of hepatitis E, is an important public health concern in many developing countries in Asia and Africa but is also endemic in industrialized countries including the USA. Globally, an estimated 20 million people are newly infected by HEV each year, resulting in >3.3 million cases of hepatitis E and 44,000 HEV-related deaths. Currently, there are no HEV-specific antivirals, and therapeutic options for HEV infection are limited to off-label use of ribavirin (RBV) and pegylated-interferon-α. There is an urgent need for highly effective drugs for the treatment of HEV infection, which can lead to fulminant hepatitis during pregnancy, neurological sequelae and hepatic failure in transplant patients. We report here on a unique nucleotide prodrug, AT-587, that targets HEV RNA polymerase and exhibits a promising antiviral profile as a first-in-class inhibitor for the treatment of life-threatening HEV infection.
Method: A small library of pre-selected molecules was screened for anti-HEV activity utilizing a luciferase-based HEV replicon and an HEV infection system. The selectivity and specificity of the lead compound was established against other RNA viruses and human polymerases. IND enabling studies such as cytotoxicity, genotoxicity, off-target binding and DMPK were also conducted.
Results: *In vitro* compound screening against HEV in an HEV-3 Kernow-C1 p6/Gluc replicon assay identified AT-587, as a potent inhibitor of HEV replication, with EC_{50} values 86.1 nM, which was independently confirmed in an HEV-1 Sar55 replicon assay. AT-587 is >50-fold more potent against HEV than known nucleos(t)ide inhibitors such as sofosbuvir and RBV. AT-587 is also active against flaviviruses and chikungunya virus. In multi-species pharmacokinetic studies, high plasma concentrations of the surrogate of the active triphosphate (TP) metabolite were achieved across species. AT-587 also forms high levels of TP in human hepatocytes. It shows no cytotoxicity *and* its active TP does not inhibit human DNA polymerases. It is negative in *in vitro* genotoxicity assays and also shows little effect in screening hERG assays. Additional preclinical development studies, including rabbit and gerbil animal efficacy studies, are ongoing.
Conclusion: AT-587, a nucleotide prodrug, has been identified as a highly potent pan-genotypic inhibitor of HEV and nominated as an IND candidate for the treatment of life-threatening HEV infection.

TOP-632
DDX5 and DDX17 RNA helicases regulate HBV RNA splicing
Guillaume Giraud[1,2], Xavier Grand[1,2], Pélagie Huchon[1,2], Mélanie Roda[1,2], Audrey Diederichs[1,2], Sébastien Renaudin[1,2], Fleur Chapus[1,2], Francesca de Nicola[3], Romain Parent[1,2], Rivoire Michel[4], Cyril Bourgeois[5], Fabien Zoulim[1,2,6], Barbara Testoni[1,2]. *[1]UCBL - INSERM UMR1350 - PaThLiv, Lyon, France; [2]The Lyon Hepatology Institute, Lyon, France; [3]IRCCS Regina Elena National Cancer Institute, Rome, Italy; [4]Centre Léon Bérard, INSERM UMR1032, Lyon, France; [5]University Claude Bernard of Lyon, Ecole Normale Supérieure de Lyon, CNRS UMR 5239, INSERM U1293, Laboratory of Biology and Modelling of the Cell, Lyon, France; [6]Hepatology Department, Hospices Civils de Lyon, Lyon, France*
Email: guillaume.giraud@inserm.fr

Background and aims: HBV RNAs undergo alternative splicing generating at least 22 spliced variants (SpVs). Some of these SpVs encode proteins promoting HBV immune escape and deregulating

oncogenic signalling pathways. Interestingly, the overall proportion of SpVs appears to increase with the disease evolution. Despite their importance in HBV-induced liver pathogenesis, how HBV RNA splicing is regulated remains elusive. We recently demonstrated the role of two RNA helicases, DDX5 and DDX17 (DDX5/17), whose expression is down-regulated in CHB patients and associated with poor prognosis, in HBV RNA transcriptional fidelity.
Method: HBV-infected HepG2-NTCP cells and primary human hepatocytes (PHH) were silenced for the expression of DDX5/17. 8 days post-infection, RNAs were isolated and subjected to 5'RACE-PCR assays followed by single molecule sequencing using the MinION from Oxford Nanopore Sequencing to analyse the profile of HBV SpVs. The differential expression of SpVs upon DDX5/17 silencing were validated using droplet digital PCR. Polysome fractionation and transfection assays were used to analyse their translation status. RNA-seq experiments upon expression of a novel SpV-encoded viral protein were carried out to determine its role in hepatocytes and crossed with publicly available datasets from infected patients. Finally, phenotypical analysis were performed and correlated with the deregulation of specific pathways.
Results: We demonstrated that silencing of DDX5/17 resulted in a general increase of the SpVs using the donor site (DS) at nucleotide position 2070. In particular, SP17 was the mostly induced SpVs in infected HepG2-NTCP cells and PHH. Polysome fractionation experiments combined with transfection assays demonstrated that SP17 encodes a novel viral protein corresponding to a fusion between HBV Core and POL proteins. Transcriptome analysis of HepG2-NTCP cells expressing SP17 revealed dysregulation of pathways related to cell cycle progression and resistance to apoptosis. The same pathways were found dysregulated in publicly available gene expression databases from CHB patients in different disease phases. Functional analyses suggested that SP17 promoted cell proliferation and cell death resistance associated with the interference with the p53 pathway.
Conclusion: Altogether, this study showed the role of DDX5/17 as regulators of HBV RNA splicing and identified a novel viral protein potentially involved in HBV-induced liver pathogenesis.

TOP-645
Targeting inositol-requiring enzyme 1 alpha signaling reprograms macrophage polarization and restores CD8$^+$ T cell function in chronic hepatitis B virus infection

Jinyao Dai[1], Shuaibing Ying[1], Yuqi Hong[1], Yunqing Qiu[1], Yan Lou[1]. *[1]The First Affiliated Hospital, Zhejiang University School of Medicine, Hangzhou, China*
Email: yanlou@zju.edu.cn

Background and aims: Chronic hepatitis B (CHB) is characterized by a state of immune tolerance that severely limits the achievement of functional cure. Although anti-inflammatory macrophage polarization is central to shaping the hepatic immune microenvironment, the underlying molecular mechanisms that orchestrate this process remain unclear. This study aimed to investigate the role of endoplasmic reticulum stress sensor inositol-requiring enzyme 1 alpha (IRE1alpha) in CHB.
Method: Human liver tissues obtained from patients with CHB and controls were used to assess IRE1alpha expression. AAV-HBV models were developed in macrophage-specific IRE1alpha knockout, hepatocyte-specific IRE1alpha knockout, and wild-type mice. Transcriptomics and immunoprecipitation-mass spectrometry (IP-MS) were utilized to explore molecular mechanisms.
Results: IRE1alpha expression was markedly upregulated, accompanied by the accumulation of anti-inflammatory macrophages, in livers from patients with CHB. Macrophage-specific deletion of IRE1alpha disrupted this anti-inflammatory phenotype, restored antiviral CD8$^+$ T cell responses, and significantly reduced viral loads. Hepatocyte-specific deletion of IRE1alpha effectively promoted autophagic degradation of HBV. Pharmacological inhibition of IRE1alpha significantly reduced viral loads and reversed the immunosuppressive microenvironment. Mechanistically, hepatitis B e antigen (HBeAg) was identified as a key viral trigger that induced IRE1alpha expression in macrophages through toll-like receptor 4 (TLR4). IRE1alpha regulated macrophage function independently of its canonical RNase effector spliced X-box binding protein 1(XBP1 s). Instead, activated IRE1alpha directly interacted with and stabilized ADP-ribosylation factor 1 (ARF1), leading to suppression of PI3K-AKT-STAT1 signaling axis. Consequently, expression of the chemokine c-c motif chemokine ligand 5(CCL5) was transcriptionally downregulated, impairing the recruitment and function of HBV-specific CD8$^+$ T cells. At the same time, the IRE1alpha-ARF1 axis reinforced an anti-inflammatory macrophage phenotype, thereby promoting immune tolerance and HBV persistence.
Conclusion: This study identifies IRE1alpha as a central regulator of immune tolerance in CHB. By driving anti-inflammatory macrophage polarization and limiting antiviral CD8$^+$T cell immunity, IRE1alpha promotes HBV persistence. Thus, IRE1alpha represents a promising therapeutic target for restoring antiviral immunity in CHB.

TOP-646
Intratumoral persistence of hepatitis delta virus is associated with a PD-1–high, Th1-deficient immune-inflamed microenvironment in hepatocellular carcinoma

Orgil Jargalsaikhan[1,2], Mayuko Shimizu[1], Wenhua Shao[3], Masako Nomaguchi[4], Takaaki Koma[4], Koichi Tomita[5], Koichi Tsuneyama[1]. *[1]Department of Pathology and Laboratory Medicine, Tokushima University Graduate School of Biomedical Sciences, Tokushima, Japan; [2]Tokushima University, Pathology and Laboratory Medicine, Tokushima, Japan; [3]Department of Molecular Pathology, Tokushima University Graduate School of Biomedical Sciences, Tokushima, Japan; [4]Department of Microbiology and Infectious Diseases, Institute of Biomedical Sciences, Tokushima University Graduate School, Tokushima, Japan; [5]Department of Functional Anatomy, Tokushima University Graduate School of Biomedical Sciences, Tokushima, Japan*
Email: tsuneyama.koichi@tokushima-u.ac.jp

Background and aims: Hepatitis delta virus (HDV) infection accelerates liver disease progression and hepatocarcinogenesis in patients with chronic hepatitis B virus (HBV) infection. In HBV-related hepatocellular carcinoma (HCC), HBV antigens are frequently lost within tumor tissue; however, whether HDV persists within tumor cells and how such persistence relates to the functional immune state of tumor-infiltrating lymphocytes (TILs), including the PD-1/PD-L1 and IFN-γ axes, remains unclear. We aimed to determine intratumoral localization of HDV and HBV and to characterize the immune microenvironment associated with intratumoral HDV persistence.
Method: Seventeen surgically resected HCC specimens were analyzed (11 HBV/HDV coinfection, 6 HBV monoinfection). Immunohistochemistry for HDV antigen, HBV antigens, CD4, CD8, PD-1, PD-L1, IFN-α, and IFN-γ was performed on tumor and background liver tissues. HDV RNA localization was validated by in situ hybridization. Immune infiltration and marker expression were assessed qualitatively and semi-quantitatively.
Results: Among 11 HBV/HDV-coinfected cases, HDV-positive tumor cells were identified in 7 HCCs by both immunohistochemistry and HDV RNA in situ hybridization, whereas HBV-positive tumor cells were absent in all cases. All HDV-positive tumors showed intratumoral CD8-positive T-cell infiltration and frequent CD4-positive T-cell infiltration. In contrast, T-cell infiltration was minimal or absent in HDV-negative HBV/HDV-coinfected HCCs and in HBV-monoinfected HCCs. Despite T-cell–rich infiltrates, IFN-γ–positive lymphocytes were scarce in both background liver and tumor, with only occasional IFN-γ–positive macrophages/histiocytes observed. PD-1 was expressed on most infiltrating lymphocytes. PD-L1 expression was strong in background liver but markedly reduced or absent in tumor regions, where it was mainly confined to Kupffer cells/

histiocytes with only scattered PD-L1–positive tumor cells. IFN-α expression was heterogeneous and not restricted to HDV-positive areas.
Conclusion: HDV, but not HBV, persists within HCC tissue and defines a distinct subset characterized by abundant intratumoral CD8/CD4 infiltration with predominant PD-1 expression, a Th1/IFN-γ–deficient effector profile, and low tumor-cell PD-L1 expression. These findings suggest chronic antigen exposure leading to dysfunctional T-cell states and a myeloid-skewed checkpoint landscape, supporting the relevance of intratumoral HDV persistence for patient stratification and therapy.

THU-558-YI
Small interfering RNA targeting all hepatitis B virus transcripts rapidly decreases the levels of hepatitis D virus in serum but not in the liver of HBV/HDV coinfected humanized mice
Johannes Bächer[1], Tassilo Volz[1,2], Lena Allweiss[1,2], Annika Volmari[1,2], Melina Schäfer[1], Marc Luetgehetmann[2,3], Maura Dandri[1,2].
[1]University Medical Center Hamburg-Eppendorf, I. Department of Medicine, Hamburg, Germany; [2]German Center for Infection Research (DZIF), Hamburg-Lübeck-Borstel-Riems site, Hamburg, Germany; [3]University Medical Center Hamburg-Eppendorf, Department of Medical Microbiology, Virology and Hygiene, Hamburg, Germany
Email: johannes.baecher@stud.uke.uni-hamburg.de

Background and aims: Hepatitis delta virus (HDV) infection accelerates liver disease progression in individuals co-infected with hepatitis B virus (HBV). Despite the severity of chronic hepatitis D (CHD), treatment options remain limited. As HDV relies on the HBV envelope proteins (HBsAg) for egress, small interfering RNA (siRNA)–based therapies designed to degrade HBV RNA transcripts offer an attractive approach to hinder HBsAg production and impair HDV release. To evaluate the impact of siRNA targeting all HBV transcripts on HDV-infected human hepatocytes in vivo, we used human liver chimeric mice coinfected with HBV and a patient-derived HDV strain (GT-1) (*Giersch, JHEP Rep 2023*).
Method: Mice harbouring high levels of human hepatocyte repopulation (>90%) were coinfected with HBV and HDV. 9 weeks post-infection, 5/9 animals received a 4-week treatment of LNP-encapsulated siRNA (1 mg/kg/ i.v.; *Axolabs*) that targets all HBV transcripts (*Allweiss, Gut 2022*). Viral markers in serum and liver were analysed by qPCR, ELISA (Abbott Architect), immunofluorescence and RNA in situ hybridisation.
Results: Median baseline viral titres were 5×10^7 HBV DNA copies/mL and 4×10^6 HDV RNA copies/ml. The strongest reduction in viremia was already observed after 1 week of treatment, with median decreases reaching 2 $\log_{10}$ for HBV DNA and 1.8 $\log_{10}$ for HDV RNA ($p = 0.008$) after 4 weeks of therapy, whereas viral levels in untreated controls remained stable. Median serum levels of HBsAg and HBeAg in treated mice declined by 1.6 $\log_{10}$ and 1.5 $\log_{10}$, respectively. In the liver, median HBV DNA and pgRNA levels were reduced by 1.2 $\log_{10}$ and 1.6 $\log_{10}$, respectively, after 4 weeks of therapy compared with untreated controls ($p = 0.016$). In contrast, intrahepatic HDV RNA levels were comparable between treated and untreated mice. No increase in ALT levels was observed during the 4-week treatment period.
Conclusion: SiRNA targeting all HBV transcripts rapidly reduced HDV viremia in HBV/HDV-infected mice, confirming that hindering HBsAg production promptly lowers the levels of circulating HDV. Consistent with previous studies (*Giersch, J.Hep 2014*), we demonstrate that HDV can persist in the liver for several weeks in the absence of HBV or HBsAg production. Longer treatment durations in preclinical models and analysis of patient liver biopsies are needed to determine the full impact of siRNA-based therapies on intrahepatic HDV persistence.

THU-559-YI
HDV propagates by hijacking a non-canonical, lysosome-derived exosomal pathway independent of HBV
Enkhtuul Batbold[1], Jennifer Molle[1], Artemiy Fedulov[2], Alexander Ivanov[2], Fabien Zoulim[1], Kathrin Weber[1], Birke Bartosch[1].
[1]The Lyon Hepatology Institute, IHU EVEREST, Université Claude-Bernard Lyon 1, Inserm, UMR 1350 PaThLiv, Lyon, France; [2]Engelhardt Institute of Molecular Biology Russian Academy of Sciences, Moscow, Russian Federation
Email: enkhtuul.dr@gmail.com

Background and aims: EVs (Extracellular Vesicles) derived from HDV (Hepatitis D Virus) infected cells contain ribonucleoprotein and induce HDV-associated immune activation. This suggests that HDV may be transmitted by hijacking the EV pathway, independently of HBV. However, the composition and subtype of EVs remain unclear. We have previously demonstrated that exosome biogenesis is not restricted to the canonical multivesicular body (MVB) pathway, but can also originate from lysosomes. Therefore, we hypothesize that HDV hijacks a non-canonical, lysosome-derived exosomal pathway to facilitate viral dissemination independent of HbsAg.
Method: EVs were isolated from HepaRG^{NTCP} cell culture supernatant by differential ultracentrifugation, after mono- or co-infection with HDV or hepatitis B virus (HBV), respectively. The EVs were analysed by Nanosight. The infectious potential of isolated EVs was determined by transfer experiments to Huh7 cells. The subtype of EV was characterized by RT-qPCR and immunoblotting. The known executer of necroptosis, MLKL (mixed lineage kinase domain-like protein), was functionally linked to non-canonical exosome formation using the MLKL inhibitor, necrosulfonamide (NSA), or CRISPR-mediated MLKL knockout.
Results: HDV mono-infected HepaRG^{NTCP}cells secreted higher numbers of EVs compared to uninfected cells. Transferring these EVs, which contain HDV RNA and protein, resulted in active HDV replication in recipient Huh7 cells. Although the markers of MVB-derived exosomes remained unchanged between uninfected and HDV mono-infected cells, the level of late endo-lysosomal marker LAMP1 was increased in HDV mono-infected cells, indicating a lysosomal origin. The expression of MLKL, which is increased in HDV mono-infected cells, was identified as a key regulator of lysosomal ILV (intraluminal vesicle) formation. Inhibiting MLKL led to intracellular accumulation of HDV RNA and protein, suggesting impaired viral egress. Furthermore, transferring EVs derived from NSA-treated HDV mono-infected HepaRG^{NTCP} cells resulted in reduced HDV replication in recipient Huh7 cells.
Conclusion: In conclusion, our findings reveal a novel, HBsAg-independent mechanism of HDV dissemination. HDV exploits a non-canonical, lysosomal derived, MLKL-regulated EV pathway. This provides a mechanistic explanation for HDV persistence and pathogenicity beyond classical HBV-dependent virion assembly and highlights MLKL as a potential therapeutic target to limit HDV spread.

THU-560-YI
Combination immunotherapy can promote clinical cure in a model of chronic hepatitis B
Nicholas Carey[1], Jillian Jespersen[1,2], Jean Publicover[1], Lia Avanesyan[1,3], Ravi Patel[1], Nicholas Wong[1], Stewart Cooper[2,3], Gabriela Fragiadakis[1], Jody Baron[1,2]. *[1]University of California San Francisco, San Francisco, United States; [2]UCSF Liver Center, San Francisco, United States; [3]California Pacific Medical Center and Research Institute, San Francisco, United States*
Email: Nicholas.Carey@ucsf.edu

Background and aims: At least 250 million people are chronically infected with the hepatitis B virus (HBV), a major global pathogen that often leads to immune-mediated progressive liver injury, cirrhosis, and liver cancer. Clinical cure, defined by seroclearance of the surface antigen (HBsAg), reduces disease-associated risks but is rarely observed with standard-of-care nucleos(t)ide analog (NA)

treatment regimens. Using a mouse model of age-dependent HBsAg seroclearance and persistence, and longitudinal PBMC samples from our clinical trial patients who either cleared HBsAg or retained stable HBsAg levels after stopping ≥192 weeks of NA, we identified a conserved mechanism of HBsAg seroclearance. Clinical cure was associated with a sustained HBV-specific $CD4^+$ T cell response that promotes hepatic leukocyte organization and cytotoxic lymphocyte function. Motivated by this insight, we sought to identify immune-modulating agents that promote and sustain HBV-specific T-cell responses, as well as an increased rate of clinical cure, in mice that would otherwise fail to produce an effective HBV response.

Method: We investigated the effects of several agonistic monoclonal antibodies selectively targeting T cell costimulatory pathways and innate immune agonists targeting hepatic antigen-presenting cells (APCs) on hepatic leukocyte phenotypes and serological outcomes. Mice were treated during acute response (concurrent with initiation of HBV immune response) or during a chronic phase (HBsAg+ at 2+ months post-initiation). Hepatic leukocyte phenotypes were measured by spectral flow cytometry. Serological profiles following treatment were monitored for ALT, serum HBsAg, and anti-HBs.

Results: In acute response, innate immune agonists augmented expression of markers of hepatic APC function but did not significantly increase HBsAg-specific CD4+ T cell frequencies. T cell costimulatory agonists augmented HBsAg-specific CD4+ T cell frequencies but did not improve the clinical cure rate during chronic phase treatment. A combination of T cell costimulatory agonist and innate immune agonists significantly increased the rate of HBsAg seroclearance and anti-HBs production in chronic phase mice.

Conclusion: When used in combination, T cell costimulatory agonists and innate immune agonists were able to safely promote clinical cure in mice that would otherwise remain HBsAg+. These preclinical studies establish proof of concept to inform future therapeutic approaches for promoting clinical cure of chronic hepatitis B.

THU-561

Cellular NEDD4 family ubiquitin ligase AIP4 ubiquitinates HGS to facilitate HBV naked capsid egress

Sheng Shen[1,2,3,4], Ge Zeng[1], Hongyan Liang[1], Yidan Chen[1], Dawei Cai[2], Hu Zhang[2,3,4], Yuanjie Liu[2,3,4], Haitao Guo[2,3,4], Jian Sun[1]. *[1]Department of Infectious Diseases, Nanfang Hospital, Southern Medical University, Guangzhou, China, State Key Laboratory of Multi-organ Injury Prevention and Treatment, Key Laboratory of Infectious Diseases Research in South China, Ministry of Education, Guangdong Provincial Key Laboratory for Prevention and Control of Major Liver Diseases, Guangdong Provincial Clinical Research Center for Viral Hepatitis, Guangdong Institute of Hepatology, Guangdong Provincial Research Center for Liver Fibrosis Engineering and Technology, Guangzhou, China; [2]Department of Microbiology and Immunology, Indiana University School of Medicine, Indianapolis, Indiana, USA, Indianapolis, United States; [3]Department of Microbiology and Molecular Genetics, University of Pittsburgh School of Medicine, Pittsburgh, Pennsylvania, USA, Pittsburgh, United States; [4]Cancer Virology Program, UPMC Hillman Cancer Center, University of Pittsburgh School of Medicine, Pittsburgh, Pennsylvania, USA, Pittsburgh, United States*
Email: doctorsunjian@qq.com

Background and aims: HBV-replicating cells nonlytically release non-enveloped (naked) capsids in addition to virions, but the detailed secretory mechanism remains elusive. We have previously reported that NEDD4 E3 ligase AIP4 stimulates naked capsid secretion through its E3 ligase activity. The current study aims to identify the potential substrate(s) of AIP4 for promoting naked capsid egress.

Method: The expression levels of host proteins of interest in hepatocyte-derived cells were depleted by CRISPR/Cas9 system and over-expressed by plasmids transfection. The intracellular HBV capsids and the extracellular viral particles were analyzed by particle gel assay.

Results: Previous studies reported that the ESCRT accessory protein Alix and the ESCRT-0 component HGS facilitate HBV naked capsid secretion. However, we demonstrated that Alix ubiquitination is not required for AIP4-induced naked capsid secretion (PMID: 39259704). In this study, we showed that both HGS and its ubiquitin interaction motif (UIM, aa258-277) deletion mutant are capable of stimulating naked capsid secretion through binding to intracellular capsid. We further found that the ubiquitinated HGS binds to the K96 residue of capsid protein through its C-terminal domain (aa278-777). Through exogenous overexpression and endogenous knockout of AIP4, we demonstrated that AIP4 interacts with HGS and promotes its ubiquitination even in the absence of UIM domain, and AIP4 is essential for HGS-mediated naked capsid secretion. Moreover, AIP4 binds to both the N- and C-terminal domains of HGS, but it only ubiquitinates the lysine(s) in the FYVE domain (aa159-221) within the N-terminal portion (aa1-257) via K27-linked ubiquitination. Mutagenesis study revealed that K207 of HGS is the major ubiquitination site catalyzed by AIP4, and its ubiquitination is important for naked capsid egress. Furthermore, we found that HGS and Alix bind to each other and interdependently promote naked capsid secretion through forming an intracellular complex.

Conclusion: Taken together, our study demonstrates that NEDD4 E3 ligase AIP4 interacts with HGS to promote HBV naked capsid egress in an HGS ubiquitination-dependent manner, which sheds new light on the mechanism of HBV naked capsid egress in viral life cycle.

THU-562

Study on the immunomodulatory effects and mechanisms of the traditional chinese medicine formula Tiaoganbuxuyidu against HBV in mice

Fan-E Cheng[1], Size Li[1], Qiuyue Wang[1], Wenying Qi[1], Yaxi Zhang[1], Shihao Zheng[1], Xinyu Zhao[1], Chunfeng Mei[1], Xiaobin Zao[2], Yong'an Ye[3]. *[1]Dongzhimen Hospital, Beijing University of Chinese Medicine, Beijing, China; [2]Key Laboratory of Chinese Internal Medicine of Ministry of Education and Beijing, Dongzhimen Hospital, Beijing University of Chinese Medicine, Beijing, China; [3]Institute of Liver Diseases, Dongzhimen Hospital, Beijing University of Chinese Medicine, Beijing, China*
Email: 18801020531@163.com

Background and aims: Chronic hepatitis B (CHB), caused by HBV infection, remains a serious global health burden and can progress to cirrhosis or hepatocellular carcinoma if uncontrolled. The traditional Chinese medicine formula TiaoGanBuXuYiDu (TGBX) shows clinical efficacy against CHB, yet its mechanisms are not fully understood. This study uses an AAV-HBV mouse model to investigate how TGBX inhibits HBV replication and reduces liver injury through immunomodulation, aiming to clarify its molecular mechanisms.

Method: After establishing an HBV-infected mouse model via tail vein injection of AAV8-HBV vectors, successfully modeled mice were randomly divided into the following groups: AAV-HBV group, TGBX-L group, TGBX-M group, TGBX-H group, and an ETV-positive control group, with a normal control group also included. Each group received the corresponding treatment via oral gavage for 12 consecutive weeks. Ultra performance liquid chromatography mass spectrometry/mass spectrometry (UPLC-MS/MS)profiling delineated the principal constituents of TGBX.The therapeutic effect of TGBX on CHB and its immunomodulatory role were evaluated by measuring serological virological and biochemical indicators, performing liver H&E staining, and conducting flow cytometry. Furthermore, mouse liver transcriptomics was employed to investigate the anti-HBV mechanism of TGBX, with differential expression genes functionally annotated and enriched through GO and KEGG analyses.

Results: UPLC-MS/MS profiling revealed 158 bioactive constituents in TGBX, among them berberine, paeoniflorin and jatrorrhizine. TGBX dose-dependently suppressed serum HBsAg and HBeAg, with TGBX-

H showing sustained inhibition from week 2. From week 4, TGBX also reduced ALT/AST levels and alleviated liver injury (edema, ballooning, inflammation), most notably in the TGBX-H group. Flow cytometry indicated TGBX restored hepatic $CD4^+/CD8^+$ T-cell balance, reduced exhausted $CD8^+$ T cells ($PD\text{-}1^+$, $CXCR6^+$), and demonstrated liver-targeted immunomodulation. Proteomics identified 288 differentially expressed proteins linked to immune-inflammatory and metabolic processes. KEGG analysis highlighted immunomodulatory pathways including AMPK signaling, alcoholic liver disease, and amino acid metabolism.
Conclusion: TGBX acts against HBV by suppressing viral antigens, improving liver function, and modulating hepatic T-cell balance—notably reversing $CD8^+$ T-cell exhaustion. This study offers mechanistic insights into its immunomodulatory role in chronic hepatitis B.

THU-563
Mathematical modeling of HBV infection and HEPLISAV-B treatment in rAAV-HBV mouse model
Aarim Khan[1], Louis Shekhtman[1], Adquate Mhlanga[1], Ashish Goyal[1], Jiapeng Wu[2], Lydia Tang[2], Shyamasundaran Kottilil[2], Lishan Su[2], Harel Dahari[1], James Ahodantin[3]. *[1]Program for Experimental and Theoretical Modeling, Division of Hepatology, Department of Medicine, Loyola University Chicago, Maywood, IL, United States; [2]University of Maryland School of Medicine, Baltimore, United States; [3]Department of Pharmacology and Experimental Neuroscience, University of Nebraska Medical Center, Omaha, United States*
Email: harel.dahari@gmail.com

Background and aims: Heplisav-B (Dynavax Technologies) is a newly FDA approved prophylactic 2-dose hepatitis B vaccine with a CpG adjuvant and a high seroprotection rate. We sought to understand the kinetics of serum hepatitis B viral genome (HBV DNA), hepatitis B surface antigen (HBsAg), hepatitis B e-antigen (HBeAg), and anti-HBs antigen IgG (IgG), in rAAV-HBV infected mice, with and without Heplisav-B, during a 25-week period using mathematical modeling.
Method: Ten rAAV-HBV infected mice were included. Heplisav-B was administered in 6 mice at weeks 4 and 8. Blood samples were collected every 2–4 weeks. We developed a multiscale mathematical model, where cells are assumed to be instantly infected after rAAV-HBV injection and the number of infected cells is fixed. In each infected hepatocyte, three products are produced from cccDNA: intracellular HBV RNA, HBsAg, and HBeAg. Intracellularly, HBV RNA is converted to HBV DNA, and HBsAg is either converted to HBsAg subviral particles or incorporated into virus-like particles containing HBV RNA or HBV DNA during secretion. IgG follows a logistic growth model and is cleared when it forms a complex with serum HBsAg, HBV RNA, or HBV DNA. The effects of Heplisav-B were modelled by an immediate reduction in HBsAg, HBV RNA, and HBeAg synthesis and increase in IgG synthesis.
Results: The model recapitulated the increase and plateau in serum HBV DNA, HBeAg, and HBsAg in unvaccinated mice. It also captured IgG, which remained undetectable or low in unvaccinated mice. By assuming a vaccine efficacy of 99.99% in blocking HBsAg synthesis, the model captured the rapid decrease in serum HBV DNA and its subsequent slow increase in vaccinated mice, as well as the rapid decline in serum HBsAg to below detection until the end of the experiment (EOE). Simultaneously, the model captured the slight decrease in serum HBeAg until EOE by assuming a 77% reduction in HBeAg synthesis. A 99.9% reduction in intracellular HBV RNA synthesis was able to explain the observed ~1 log in intracellular HBV RNA decline relative to unvaccinated mice at week 25. The model fits the gradual increase and plateau in IgG, with negligible effect on serum HBV DNA, HBsAg, and HBeAg clearance.
Conclusion: Modeling suggests a significant suppression of HBsAg synthesis, which in turn reduces HBV DNA secretion, along with a moderate to high suppression of intracellular HBV RNA and HBeAg synthesis from Heplisav-B treatment in the AAV-HBV mouse model. Further experimental validation is required.

THU-564
Understanding early hepatitis B virus kinetics in primary human hepatocytes using an agent-based modeling approach
Ari Dobos[1], Zhenzhen Shi[1], Yuji Ishida[2], Chise Tateno[2], Mikaru Yamao[2], Masaki Takahashi[2], Alexander Ploss[3], Kazuaki Chayama[4], Harel Dahari[1]. *[1]Program for Experimental and Theoretical Modeling, Division of Hepatology, Department of Medicine, Loyola University Chicago, Maywood, IL, United States; [2]PhoenixBio Co., Ltd., Hiroshima, Japan; [3]Department of Molecular Biology, Lewis Thomas Laboratory, Princeton University, Princeton, United States; [4]RIKEN Center for Integrative Medical Sciences, Yokohama, Hiroshima Institute of Life Sciences, Hiroshima, Japan*
Email: harel.dahari@gmail.com

Background and aims: Understanding of early dynamics of hepatitis B virus (HBV) covalently closed circular DNA (cccDNA) accumulation in primary human hepatocytes (PHHs) is limited. Recently, we developed a differential equations-based model to explain the dynamics of cccDNA accumulation in PHH at the well level (PMID 40236628). Here we aim to develop an agent-based modeling (ABM) approach to understand early HBV dynamics in the PHHs of a single cell level via modeling the interplay between extracellular HBV DNA (exHBV), total intracellular HBV DNA (termed relaxed circular DNA, rcDNA), and cccDNA.
Method: PHHs were inoculated with HBV, and infection was monitored with the entry inhibitor Myr-preS1 present as recently reported (PMID 40236628). Myr-preS1 treatment (6.25 lg/ml) was initiated 1 day post inoculation (p.i.). ExHBV, rcDNA, and cccDNA were frequently measured during the 12 days post inoculation. In the ABM rcDNA, cccDNA and exHBV are represented as individual agents, attempting to recapitulate the in vitro kinetics at a single cell level. Initial ABM conditions and parameters are assumed based on the in vitro experimental design.
Results: Multiphasic exHBV and rcDNA kinetics were observed with cccDNA levels rapidly increased until day 2 p.i. followed by plateau. Modeling predicts that the recycling of rcDNA into cccDNA stops when cccDNA reaches a maximum, and rcDNA secretion rate is dependent on the intracellular concentration of rcDNA. The ABM reproduced well the HBV kinetic patterns observed and predicted that rcDNA production rate from cccDNA increased over time, starting with a slow production cycle of 1 rcDNA copy per 15 hours, which gradually accelerated to 1 rcDNA copy per 3 hours after 5 days and continued to gradually accelerate up to 1 rcDNA copy per 1.25 hours by day 12 p.i.
Conclusion: The ABM provides novel insights into the early accumulation of cccDNA and rcDNA in PHH. Further experimental and theoretical efforts are needed to validate these results.

THU-569
The mechanism of HSP90AB1 binding to hepatitis B surface antigen driving the progression of HBV-related hepatocellular carcinoma through chaperone-mediated autophagy
Muqi Wang[1], Yikai Wang[2], Meng Zhang[2], Chenrui Liu[2], Yaping Li[2], Xiaoli Jia[2], Shuangsuo Dang[2]. *[1]The Second Affiliated Hospital of Xi'an Jiaotong University, Xi'an, China; [2]The Second Affiliated Hospital of Xi'an Jiaotong University, Xi'an, China*
Email: 18710964067@163.com

Background and aims: heat shock protein 90-beta (HSP90AB1) is highly expressed in hepatocellular carcinoma (HCC), which is implicated in viral infections, yet its role in HBV pathogenesis remains undefined. We investigated the role of HSP90AB1 in the occurrence and development of HBV-related HCC and explore the possible mechanism by which it regulates autophagy.
Method: Serum HSP90AB1 levels were measured by ELISA in 132 HBV-HCC patients, 60 chronic hepatitis B patients (CHB) and 36

healthy controls, and clinical parameters (HBV serological markers, liver function, tumor biomarkers) were collected to perform correlations between HSP90AB1 and clinical variables. ELISA, Western blot and RT-PCR were used to detect HSP90AB1 expression in 40 paired tumor tissues and adjacent tissues of patients with HBV-related HCC. Hep3B with HSP90AB1 knockdown were constructed by lentivirus transfection to verify the effects of HSP90AB1 knockdown and HSP90AB1 inhibitors on the proliferation, migration, invasion abilities and the changes in autophagy. Bioinformatics analysis and molecular docking technology were used to predict the interacting proteins and binding sites of HSP90AB1, which were verified by the bidirectional co-immunoprecipitation experiment.
Results: Serum HSP90AB1 levels were significantly elevated in CHB patients (294.1 [125.90–663.20] compared to HBV-related HCC (86.22 [46.01–164.60] ng/mL; $P < 0.001$) and healthy controls (50.94 [42.95–131.80] ng/mL; $P < 0.001$). High HSP90AB1 expression correlated with higher HBsAg ($r = 0.414$, $P < 0.001$), higher HBeAg ($r = 0.319$, $P < 0.001$) and higher HBV pre-S1 antigen levels ($r = 0.481$, $P < 0.001$). In 40 paired tissues of HBV-HCC patients, HSP90AB1 expression in tumor was significantly higher than in adjacent, and was significantly positively correlated with pathological grade and HBsAg. Knockdown of HSP90AB1 and HSP90AB1 inhibitors significantly reduced proliferation, migration and invasion abilities of Hep3B, as well as the chaperone-mediated autophagy (CMA). Bioinformatics analysis and molecular docking techniques predict and the bidirectional co-immunoprecipitation experiments of HSP90AB1 and HSPB8 in Hep3B validated that the formation of HSP90AB1-HSPB8-HSC70 complex regulates CMA activity.
Conclusion: HSP90AB1 is elevated in HCC tumor tissues and is significantly correlated with the pathological grade of the tumor and HBsAg. The HSP90AB1-HSPB8-HSC70 protein complex may participate in regulating the CMA activity, and it can also affect the proliferation and invasion of HBV-related HCC.

THU-570
ALG-001075, the parent of pevifoscorvir sodium, exhibits potent in vitro antiviral properties compared to other HBV capsid assembly modulators in clinical development

Yannick Debing[1], Jordi Verheyen[1], Hannah Vanrusselt[1], David McGowan[1], Tse-I Lin[1], Lawrence Blatt[2], David Smith[2], Julian Symons[2], Andreas Jekle[2]. *[1]Aligos Belgium, Leuven, Belgium; [2]Aligos Therapeutics, South San Francisco, United States*
Email: ydebing@aligos.com

Background and aims: The hepatitis B virus (HBV) capsid is an attractive target for the treatment of chronic HBV infection. Pevifoscorvir sodium (pevy, ALG-000184) is a prodrug of ALG-001075, a novel capsid assembly modulator leading to the formation of empty capsids (CAM-E). Pevy has demonstrated potential best-in-class reductions of HBV DNA, RNA, HBsAg, HBeAg and HBcrAg in subjects with chronic HBV infection and is currently progressing through a phase 2 clinical trial. The aim of this study was to compare the activity of ALG-001075 to canocapavir and neracorvir, two other CAMs in clinical development.
Method: HBV DNA antiviral activity (primary CAM mechanism) was determined in HepG2.117 cells using quantitative PCR. Effects on cccDNA establishment (secondary CAM mechanism) were assessed in HBV genotype D-infected HepG2-NTCP cells or primary human hepatocytes (PHH) by adding compound together with viral inoculum and measuring HBsAg as an indirect read-out. Direct effects on HBeAg (third CAM mechanism) were investigated in HBeAg-overexpressing cells. Further characterization was performed using immunofluorescent HBc staining.
Results: ALG-001075, canocapavir and neracorvir inhibited HBV DNA production in HepG2.117 cells with EC_{50} values of 0.64, 5.8 and 24 nM, respectively. The establishment of cccDNA in HepG2-NTCP cells or PHH was efficiently blocked by ALG-001075 ($EC_{50} = 18$ nM, as measured by HBsAg in HepG2-NTCP cells), but less so by neracorvir ($EC_{50} = 3350$ nM) and canocapavir ($EC_{50} = \sim 1000$ nM in PHH and >5000 nM in HepG2-NTCP). ALG-001075 was also more potent in the direct inhibition of HBeAg secretion ($EC_{50} = 855$ nM) than canocapavir and neracorvir. The HBV core protein mutation T33N is a major viral resistance mutation for 1st generation CAMs and reduces the activity of ALG-001075 in vitro: 27- and 23-fold for HBV DNA and HBeAg, respectively. However, to date, it has not been detected in subjects with chronic HBV infection treated with pevy for up to 96 weeks. Interestingly, canocapavir was not affected by T33N but was sensitive to Y118F (18-fold shift). ALG-0001075 was not affected by Y118F. All 3 CAMs showed the typical CAM-E phenotype (no nuclear aggregates, some cytoplasmic accumulation) in immunofluorescent HBc staining assays.
Conclusion: ALG-001075, the parent of pevy, displayed a highly potent in vitro antiviral profile, confirming its potential as a best-in-class CAM. Pevy is currently being developed as a monotherapy for the suppression of chronic HBV infection.

THU-571
Temporal transcriptional dynamics in HBV-specific CD8 T cells during long-term NUC therapy in HBeAg- chronic hepatitis B

Sara Doselli[1], Benedetta Farina[1], Camilla Ceccatelli Berti[2], Ilaria Montali[1], Angelo Ruggieri[3], Valentina Reverberi[1], Anna Montali[1], Andrea Vecchi[4], Marzia Rossi[1], Alessio Pelagatti[1], Silvia Ampollini[1], Francesca Ferraglia[4], Amalia Penna[4], Carolina Boni[1,4], Marco Morselli[2], Gabriele Missale[1,4], Paola Fisicaro[4]. *[1]Department of Medicine and Surgery, University of Parma, Parma, Italy, Parma, Italy; [2]Department of Chemistry, Life Sciences and Environmental Sustainability (SCVSA), University of Parma, Parma, Italy, Parma, Italy; [3]Department of Biology, University of Puerto Rico, Rio Piedras, Puerto Rico, Rio Piedras, Puerto Rico; [4]Laboratory of Viral Immunopathology, Unit of Infectious Diseases and Hepatology, Azienda Ospedaliero-Universitaria di Parma, Parma, Italy, Parma, Italy*
Email: pfisicaro@ao.pr.it

Background and aims: Virus-specific CD8 T cell dysfunction is a hallmark of chronic hepatitis B (CHB), and its restoration represents a key strategy toward HBV cure. This study aims to define transcriptional changes in HBV-specific CD8 T cells associated with viral persistence and control in HBeAg-negative chronic patients undergoing long-term nucleos(t)ide analogue (NUC) therapy, with the ultimate goal to identify potential targets for efficient T cell restoration.
Method: We performed a transcriptome study by low-input RNA-seq on core- and polymerase-specific CD8 T cells, isolated from nine patients with HBeAg-negative chronic hepatitis B and high viral loads, prior to the start of NUC therapy and longitudinally at 1 and 4 years after treatment initiation. Five patients who achieved functional cure with HBsAg loss after long-term NUC treatment (rNUC) were included as control group. Transcriptomic data were analyzed using Weighted Gene Co-expression Network Analysis (WGCNA) to investigate the dynamics of gene cluster expression over time. Virological parameters including HBV RNA, HBcrAg and HBsAg levels were assessed at the same time points.
Results: Principal component analysis (PCA) of longitudinal transcriptomic profiles revealed a distinct clustering of core-specific CD8 T cells, with chronic patients after 4 years of therapy aligning with rNUC patients. Conversely, polymerase-specific samples displayed greater heterogeneity and lacked a comparable clustering pattern. WGCNA analysis further highlighted distinct transcriptional profile changes over time in virus-specific CD8 T cells, identifying gene clusters that were modulated early (1 year), late (4 years), or remained unchanged.
Conclusion: Our longitudinal analysis identifies distinct gene programs in HBV-specific CD8 T cells that progressively normalize or remain dysregulated during therapy, providing candidate targets for interventions aimed at restoring T cell function and achieving functional cure in CHB.

THU-572

Differential interferon responses in HDV infection reveal USP18-driven IFN-α resistance and novel ISG candidates

Claudie Eber[1], Roxanne Fouillé[2], Pauline Casetta[1], Charlotte Bach[1], David Durantel[2], Thomas Baumert[1,3,4], Julie Lucifora[2], Eloi Verrier[1,2]. *[1]Institute for Translationnal Medicine and Liver Disease, Strasbourg, France; [2]Centre International de Recherche en Infectiologie, Lyon, France; [3]Institut hospitalo-universitaire (IHU), Service d'hépato-gastroentérologie, Strasbourg, France; [4]Institut Universitaire de France, Paris, France*
Email: claudie.eber@etu.unistra.fr

Background and aims: Hepatitis D virus (HDV) causes the most severe form of chronic viral hepatitis, for which curative therapies remain unavailable. In Europe, treatment options include bulevirtide and pegylated interferon-alpha (PEG-IFN-α), although the latter shows limited efficacy. The molecular mechanisms underlying HDV resistance to IFN-α as well as IFN-α molecular mechanism against HDV replication remain poorly understood. This study aimed to decipher the interplay between HDV replication and interferon signaling pathways in hepatocytes.
Method: RNA sequencing was performed to compare the transcriptional responses to IFN-α and IFN-λ in hepatocyte-derived cell lines infected with HDV. Key findings were validated using loss- and gain-of-function approaches.
Results: HDV infection selectively impaired the antiviral response to IFN-α, while IFN-λ activity remained intact. Mechanistically, HDV induced the expression of USP18, a potent negative regulator of IFN-α signaling, which binds IFNAR2 and inhibits JAK1-mediated STAT phosphorylation. USP18 knockdown restored IFN-α-induced ISG expression and enhanced its antiviral efficacy against HDV. Aiming at understanding how IFN-α affects HDV replication, comparative transcriptomic analyses across hepatocyte models responding differentially to IFN-α treatment in HDV-infected cells identified 79 interferon-stimulated genes (ISGs) potentially involved in HDV restriction. Among them, IRF1 and SAMD9L, previously implicated in antiviral responses, emerged as strong candidates.
Conclusion: HDV evades IFN-α antiviral activity through USP18-mediated inhibition of JAK–STAT signaling, providing a mechanistic explanation for the limited clinical efficacy of IFN-α in HDV infection. In contrast, IFN-λ antiviral activity remains unaffected. These findings identify USP18 as a key determinant of IFN-α resistance and highlight novel ISG candidates with potential anti-HDV activity, offering new insights for therapeutic strategies.

THU-573

Characterization of viral integrations in cancer driver genes in non-tumor tissues of HBV-associated HCC via RAISING-sequencing

Kento Fukano[1], Nao Naganori[2], Akihito Tsubota[3], Hideki Aizaki[1], Masumichi Saito[1], Kazuyoshi Hosomichi[4], Takahiro Matsudaira[5], Moto Kimura[1], Koichi Watashi[1], Masanori Isogawa[1], Wataru Sugiura[1], Masamichi Muramatsu[6], Kousho Wakae[1]. *[1]Japan Institute for Health Security, Tokyo, Japan; [2]Hokkaido University, Sapporo, Japan; [3]The Jikei University School of Medicine, Tokyo, Japan; [4]Tokyo University of Pharmacy and Life Sciences, Tokyo, Japan; [5]FASMAC Co., Ltd., Kanagawa, Japan; [6]Foundation for Biomedical Research and Innovation at Kobe, Kobe, Japan*
Email: wakae.k@jihs.go.jp

Background and aims: Integration of hepatitis B virus (HBV) DNA into host genes, such as the TERT gene/promoter and KMT2B (MLL4), is frequently detected in HBV-associated hepatocellular carcinoma (HBV-HCC) and is considered a key factor in hepatocarcinogenesis. However, the timing at which these integrations occur during disease progression remains unclear. We previously established RAISING (Rapid Amplification of Integration Site without Interference by Genomic DNA contamination), a PCR-based method that is more sensitive and versatile than hybrid capture-sequencing (HCS) for amplifying viral-host chimeric sequences. In this study, we employed RAISING-sequencing to characterize HBV DNA integration profiles in paired tumor and adjacent non-tumor tissues from HBV-HCC patients.
Method: Paired tumor and adjacent non-tumor liver tissues from 18 HBV-HCC patients were analyzed using RAISING. The RAISING products were further analyzed by next-generation sequencing (NGS) to identify viral-host junction sequences and their frequencies. Junction-specific PCR and droplet digital PCR (ddPCR) were used for validation and quantification of HBV-integrants.
Results: HBV DNA integration was detected in both tumor and adjacent non-tumor liver tissues in 11 of the 18 cases using RAISING-sequencing. Five cases showed integration into the TERT gene/promoter region, and three cases into the KMT2B gene. Interestingly, RAISING-sequencing identified these HCC-driver integration sites in adjacent non-tumor tissues, as well as in tumor tissues in four cases, whereas HCS identified them only in the tumor, except for one case. ddPCR revealed lower copy numbers in adjacent non-tumor tissues than in tumor tissues, suggesting a higher sensitivity of RAISING-sequencing than HCS for determining HBV integration sites.
Conclusion: These findings suggest that HCC-driver integrations occur in a precancerous state, highlighting their potential role in the early stages of HCC initiation.

THU-574

Monoclonal anti-HBs antibody, tobevibart, induces myeloid expansion and activation through phago-lysosomal processes

Yanal Ghosheh[1,2], Loghman Salimzadeh[1,2], Stuti Shah[1,2], Jenny Chen[2], Danie La[2], Todd Correll[3], Scott K. Fung[2,4], Jordan J. Feld[2,4], Adam Gehring[1,5]. *[1]Schwartz-Reisman Liver Research Centre, University Health Network, Toronto, Canada; [2]Toronto Centre for Liver Disease, University Health Network, Toronto, Canada; [3]Vir Biotechnology, Inc., San Francisco, United States; [4]The Toronto Viral Hepatitis Care Network (VIRCAN), Toronto, Canada; [5]Department of Immunology, University of Toronto, Toronto, Canada*
Email: yanal.ghosheh@uhn.ca

Background and aims: The Hepatitis B virus surface antigen (HBsAg) is present at very high levels in the circulation of chronic hepatitis B (CHB) patients, contributing to immune dysfunction. Monoclonal antibodies targeting HBsAg have emerged as a promising avenue to rapidly reduce viral antigen in the circulation, which could facilitate restoration of immunity. These antibodies form immune complexes (IC) with HBsAg, which are then cleared via Fc-mediated phagocytosis by myeloid cells. We used single cell RNA-sequencing (scRNA-Seq) to characterize changes in the frequency and transcriptional profile of liver myeloid cells from CHB patients receiving tobevibart therapy.
Method: We collected liver fine needle aspirate (FNA) samples from three HBeAg-, CHB patients on nucleoside analogue therapy at baseline and 3 days after the first dose of 300 mg of tobevibart. We measured HBV DNA, Alanine Aminotransferase (ALT) and HBsAg levels in plasma. FNA samples were subjected to scRNA-Seq to measure transcriptional changes in liver myeloid cells.
Results: All patients exhibited sharp declines (mean 2.1 $\log_{10}$ IU/mL) in HBsAg levels at day 3. The HBsAg decline was not associated with changes in ALT levels. Our analysis of scRNAseq data focused on myeloid cells based on their ability to carry out antibody-dependent phagocytosis. We identified 12 myeloid clusters in the liver including neutrophils, monocytes, macrophages and dendritic cells (DCs). Fc receptor expression varied across myeloid populations, with FCGR3A/B and FCGR2A being the most prominently expressed. Intermediate Monocytes and myeloid DCs (mDCs) increased in abundance, whereas neutrophil subset (Neutrophils 1) decreased after tobevibart treatment. While changes in gene expression were largely patient-specific, we identified a core set of differentially expressed genes in Intermediate monocytes, mDCs and macrophages. Pathway enrichment analysis of this core gene set highlighted genes associated with

cytoskeletal remodeling, lysosomal trafficking, vesicle fusion associated with antigen processing and presentation, and myeloid activation. These pathways are highly consistent with Fc-mediated uptake of ICs and subsequent HBV antigen degradation in activated myeloid lineages.
Conclusion: Tobevibart-mediated HBsAg reduction induces activation of phago-lysosomal pathways as a precursor for HBV antigen degradation in myeloid cell lineages in the liver of CHB patients.

THU-575
Immunometabolic stress drives persistent bystander activation of innate-like CD8$^+$ T cells and hepatocyte HBV transcription despite antiviral therapy
Lung Yi Loey Mak[1,2], Corinna Pade[1], Shue Xiong[1], Chanelle Fernandes[1], Yu Lei[1,3], Gerard Hernandez-Mir[1], Anna Riddell[4], Apostolos Koffas[1,5], Sebastian Deschler[6], Katrin Boettcher[6], Patrick Kennedy[1,5], Upkar Gill[1,5]. [1]*Centre for Immunobiology & Infection, The Blizard Institute, Barts and The London Faculty of Medicine & Dentistry, Queen Mary University of London, London, United Kingdom;* [2]*School of Clinical Medicine and State Key Laboratory of Liver Research, The University of Hong Kong, Hong Kong, Hong Kong;* [3]*Institute for Viral Hepatitis, The Second Affiliated Hospital, Chongqing Medical University, Chongqing, China;* [4]*Department of Virology, Barts Health NHS Trust, London, United Kingdom;* [5]*Department of Hepatology, Barts Health NHS Trust, London, United Kingdom;* [6]*Department of Internal Medicine, University Hospital Tübingen, Tübingen, Germany*
Email: u.gill@qmul.ac.uk

Background and aims: Chronic hepatitis B (CHB) remains a major cause of inflammatory liver disease worldwide. Increasingly, CHB coexists with metabolic dysfunction-associated steatotic liver disease (MASLD), a combination associated with heightened hepatic inflammation, immune dysregulation, and delayed virological responses to antiviral therapy (AVT). Metabolic stress may therefore reshape intrahepatic immune responses and drive bystander innate-like T-cell activation, sustaining liver injury despite viral suppression.
Method: Peripheral and intrahepatic CD8$^+$ T cells from healthy controls and patients with CHB (treatment-naïve and AVT-treated) were analysed using multi-parameter flow cytometry. Cellular activation, natural killer receptor (NKR) expression, effector function, and sensitivity to free fatty acids (FFAs; palmitic acid, oleic acid, docosahexaenoic acid [DHA], and arachidonic acid [AA]) were assessed. CD8$^+$ T cells were also isolated for transcriptomic profiling. In parallel, HepG2-NTCP models of HBV infection were used to assess the impact of lipid overload on HBV transcription and antiviral efficacy.
Results: Activated (CD38$^+$HLA-DR$^+$) CD56$^+$ CD8$^+$ T cells were significantly expanded in CHB, particularly in immune-active disease, with increased expression of NKRs including NKG2A and NKp30. Although AVT reduced their overall frequency, elevated NKR expression and innate-associated transcriptional signatures (including KLRK1 and NCR3) persisted. Functionally, CD56$^+$ CD8$^+$ T cells showed comparable IFN-gamma production following TCR-dependent and TCR-independent stimulation, but enhanced TNF-alpha production following IL-15 stimulation (TCR-independent), indicating a differential functional profile consistent with bystander activation. These cells were also more susceptible to functional suppression following FFA exposure. Complementary in vitro studies demonstrated that FFA exposure increased HBV transcriptional activity in infected HepG2-NTCP cells and this effect was not fully abrogated by AVT.
Conclusion: CHB is characterised by persistent expansion of metabolically sensitive, innate-like CD56$^+$ CD8$^+$ T cells with bystander inflammatory potential in the context of metabolic dysfunction. In parallel, lipid overload sustains HBV transcription despite AVT. Together, these findings identify a convergent immunometabolic axis linking MASLD, immune-mediated liver injury, and incomplete viral suppression in CHB.

THU-576
Drug-mediated transcriptional readthrough of HBV RNAs triggers antiviral effects in infected hepatocytes
Guillaume Giraud[1,2], Xavier Grand[1,2], Audrey Diederichs[1,2], Anaëlle Dubois[1,2], Maud Michelet[1,2], Fabien Zoulim[1,2], Barbara Testoni[1,2]. [1]*UCBL - INSERM UMR1350 - PaThLiv, Lyon, France;* [2]*The Lyon Hepatology Institute, Lyon, France*
Email: guillaume.giraud@inserm.fr

Background and aims: Current treatments against chronic hepatitis B (CHB) infection, albeit efficient in maintaining the infection under control, fail to completely eradicate hepatitis B virus (HBV). Thus, even treated patients have a higher risk of severe liver disease. HBV persistence is due to its minichromosome, the so-called covalently closed circular (ccc)DNA. It serves as the template for the transcription by the host RNA polymerase II of the six main viral transcripts. HBV RNAs are polyadenylated at their 3' end extremity, a process that is initiated by the recognition of a common polyadenylation signal (cPAS) that is linked to transcription termination. We previously identified a significant proportion of transcripts showing a transcriptional readthrough and stopping at a distal PAS. We demonstrated that this transcriptional readthrough destabilises HBV RNAs and is associated with a lower replication rate. This study thus functionally linked HBV transcription termination and replication opening the door to the usage of novel compounds to trigger this transcriptional readthrough. This can be achieved by inhibiting the termination factor CPSF3 by molecules such as JTE-607 prompting us to determine its antiviral effect in infected hepatocytes.
Method: We performed 3'RACE-PCR combined with single molecule sequencing using the Oxford Nanopore Technology to appreciate the ability of JTE-607 treatment of HBV-infected HepG2-NTCP cells to induce HBV transcriptional readthrough. HBV RNAs were quantified by RT-qPCR and viral protein levels were assessed by Western blot and ELISA experiments. Finally, viral replication was assessed by the quantification of HBV viremia in the supernatant of HepG2-NTCP cells.
Results: First, we performed 3'RACE-PCR assays combined with Oxford Nanopore single molecule sequencing to demonstrate that, indeed, as for host transcripts, JTE-607 treatment induced HBV transcriptional readthrough. Furthermore, the quantification of viral parameters demonstrated that JTE-607 treatment significantly decreased the levels of secreted antigens, HBV viremia and intracellular HBsAg and HBc proteins. As expected, these changes were associated with the significantly decreased HBV RNA levels due to their destabilisation. These results were further confirmed in primary human hepatocytes.
Conclusion: Altogether, these data demonstrated that HBV transcriptional termination might represent a new target for emerging antiviral strategies.

THU-577
Spatially clustered capsid substitutions distinguish human-tropic from zoonotic hepatitis E viruses
André Gömer[1,2], Anja Boekmann[3], Eike Steinmann[1,2]. [1]*Department of Molecular and Medical Virology, Ruhr University Bochum, Bochum, Germany;* [2]*Hepatitis E Virus Research Hub (HepE-Hub), Bochum, Germany;* [3]*Molecular Microbiology and Structural Biochemistry, CNRS/ Université de Lyon, Lyon, France*
Email: andre.goemer@rub.de

Background and aims: Hepatitis E virus (HEV), the leading cause of acute viral hepatitis worldwide, belongs to the family *Hepeviridae*, a genetically diverse group of positive-sense RNA viruses infecting a wide range of vertebrate hosts. Human infections are caused primarily by *Paslahepevirus balayani*, which comprises eight genotypes (HEV-1 to HEV-8) displaying marked differences in

epidemiology, host range, and clinical outcome. HEV-1 and HEV-2 are human-restricted, transmitted via the fecal–oral route, and predominantly cause acute hepatitis, whereas HEV-3 to HEV-8 are zoonotic, maintained in animal reservoirs including pigs, wild boar, and camels, and can cause both acute and chronic infection. Despite these pronounced phenotypic differences, overall genomic divergence among genotypes is only modest, raising the possibility that a limited number of substitutions drive host adaptation, though their identity and functional relevance remain unclear.

Method: To investigate the molecular basis of this divergence, we performed a comprehensive comparative analysis of ~800 full-length ORF2 capsid protein sequences across the *Hepeviridae* family, integrating phylogenetic reconstruction, sequence variability profiling, and three-dimensional structural mapping.

Results: ORF2 was highly conserved in the shell (S) and middle (M) domains but showed substantial diversification in the protruding (P) domain and terminal regions, which mediate receptor interaction and immune recognition. Within *Paslahepevirus*, maximum-likelihood phylogeny on ORF2 sequences resolved eight genotypes, and Jensen–Shannon divergence analysis identified a discrete set of residues that consistently distinguished human-tropic HEV-1 to HEV-2 from zoonotic HEV-3 to HEV-8 lineages. Notably, these substitutions were enriched on the protein surface, with several mapping to the P domain and overlapping known antibody-binding sites.

Conclusion: Together, these findings demonstrate that minor, structurally localized variation in the HEV capsid protein correlates with host tropism and may contribute to viral emergence. This study provides an evolutionary and structural framework for understanding *Hepeviridae* host adaptation.

THU-578

HBV-Specific T cell responses during early PEG-IFN α therapy

Yifei Guo[1], Yuqi Liu[1], Xiaoting Zhao[1,2], Haoxiang Zhu[1], Jiming Zhang[1,3]. [1]*Department of Infectious Diseases, Shanghai Key Laboratory of Infectious Diseases and Biosafety Emergency Response, Shanghai Institute of Infectious Diseases and Biosecurity, National Medical Center for Infectious Diseases, Huashan Hospital, Fudan University, Shanghai, China;* [2]*The First Affiliated Hospital of Xinxiang Medical University, Xinxiang, China;* [3]*School of Infection and Health, Xinxiang Medical University, Xinxiang, China*
Email: yfguo21@m.fudan.edu.cn

Background and aims: Prior studies have demonstrated that PEG-IFN α modulates HBV-specific T-cell functionality, which correlates with therapeutic outcomes. However, the temporal dynamics of HBV-specific T cell responses during the initial phase of PEG-IFN α therapy (12 weeks) and their relationship with the magnitude of HBsAg decline remain unexplored.

Method: This single-center prospective study enrolled 34 HBeAg-negative CHB patients undergoing PEG-IFN α therapy. Participants were stratified into three groups based on baseline HBsAg levels: the ENL group (HBsAg≤100 IU/mL), ENI group (100 IU/mL<HBsAg≤1000 IU/mL), and ENH group (HBsAg>1000 IU/mL). Additionally, patients were categorized into a good response group (>0.5 $\log_{10}$ IU/mL reduction in HBsAg from baseline) and a poor response group (≤0.5 $\log_{10}$ IU/mL reduction) at week 12 to compare intergroup differences in HBV-specific T cell responses. Core- and Env-specific T cells were quantified using ELISpot and ICS.

Results: Heterogeneous patterns emerged during treatment: the ENL group maintained baseline-level Core-specific T-cell responses, whereas the ENI group exhibited a marked decline. T-cell subset analysis revealed HBV-specific immune responses were predominantly mediated by CD4+ T cells. Comparative analysis of good response and poor response groups demonstrated stronger HBV-specific T-cell reactivity in good responders, characterized by significantly higher IFN-γ, IL-2, and TNF-α secretion levels from Core-specific CD4+ T cells at weeks 8 and 12. Additionally, Env-specific CD4+ T cells in good responders sustained robust IFN-γ and TNF-α production from baseline through week 12. Longitudinal individual-level analysis further highlighted a strong correlation between dynamic HBV-specific T-cell response trajectories and clinical outcomes: at week 4, 60.0% of good responders maintained or enhanced HBV-specific T cell response, significantly surpassing poor responders (38.9%), with this disparity widening over time.

Conclusion: Patients with early favorable responses to PEG-IFN α therapy demonstrated not only enhanced baseline IFN-γ and TNF-α secretion by Env-specific CD4+ T cells but also sustained maintenance or augmentation of HBV-specific CD4+ T cell reactivity throughout treatment. Consequently, early dynamic changes in HBV-specific T cell profiles may serve as predictive biomarkers for identifying optimal candidates for PEG-IFN α-based therapeutic strategies.

THU-579-YI

USP37 restricts hepatitis E virus infection by deubiquitinating ORF1 and promoting tollip-dependent autophagic degradation of ORF2

Jikai Zhang[1], Dan Liu[1], Wenshi Wang[1], Hongbo Guo[1]. [1]*Xuzhou Medical University, Xuzhou, China*
Email: hongbo.guo@xzhmu.edu.cn

Background and aims: Hepatitis E virus (HEV) is a leading cause of acute viral hepatitis globally, yet the host-virus interactions governing its life cycle remain poorly understood. Ubiquitin-specific peptidase 37 (USP37) is a deubiquitinase that regulates protein stability and cellular signaling, often acting as a critical node in host-virus interactomes. This study aims to elucidate the potential role of USP37 in HEV infection.

Method: We evaluated HEV replication using luciferase reporter assays, qRT-PCR, western blotting, and indirect immunofluorescence. Protein-protein interactions were characterized using co-immunoprecipitation (co-IP) assays.

Results: USP37 was identified as a key host restriction factor that suppresses HEV replication and progeny production. Mechanistically, USP37 exerts dual antiviral effects: 1) Replication Inhibition: USP37 directly interacts with the HEV ORF1 polyprotein and removes its K29-linked polyubiquitination, thereby impairing viral RNA replication. 2) Assembly and Secretion Blockade: USP37 cleaves K11-linked ubiquitin chains of autophagy receptor Tollip, enhancing its stability and facilitating the formation of a USP37-ORF2-Tollip complex. This promotes the autophagic degradation of both secreted ($ORF2^S$) and capsid ($ORF2^C$) proteins in a Tollip-dependent manner. Notably, the deubiquitinase-inactive mutant USP37(C350A) failed to inhibit ORF1 or degrade ORF2 proteins, demonstrating that these anti-HEV effects require USP37's catalytic protease activity.

Conclusion: Our findings reveal that USP37 acts as a vital host restriction factor against HEV by simultaneously disrupting ORF1-mediated replication and triggering Tollip-dependent autophagic degradation of ORF2 proteins. These results provide new insights into HEV pathogenesis and highlight USP37 as a potential target for novel antiviral therapies.

THU-580

MDL-001, an oral direct-acting Thumb-1 polymerase inhibitor, demonstrates efficacy against HCV/HBV co-infection in vitro, and achieves HCV and HBV preclinical proof-of-concept, including equivalence to sofosbuvir

Virgil Woods[1], Tyler Umansky[1], Sean Russell[1], Asha Goodman[2], Michael Bobardt[2], William Brubaker[3], Philippe Gallay[2], Davey Smith[4], Daniel Haders[1]. [1]*Model Medicines, San Diego, United States;* [2]*The Scripps Research Institute, La Jolla, United States;* [3]*Farmington Pharma, Cheshire, United States;* [4]*University of California San Diego, La Jolla, United States*
Email: virgil@modelmedicines.com

Background and aims: MDL-001 is a first-in-category oral direct-acting non-nucleoside inhibitor that binds a previously

underexploited allosteric pocket in the Thumb-1 domain of viral polymerase. We assessed inhibition of hepatitis C virus (HCV) and hepatitis B virus (HBV) in mono- and co-infection in vitro, established HCV and HBV proof-of-concept in vivo, and summarized nonclinical pharmacokinetic (PK) and safety data supporting clinical translation.
Method: HCV activity was measured in genotype 1b Con1 (Huh-luc/neo-ET) and genotype 2a JFH1 (Huh7.5.1) subgenomic replicons. HBV (AD38 ayw) activity was measured in HepAD38 cells, and HCV JFH1/HBV AD38 ayw co-infection was assessed in Huh7.5.1 cells. In vivo efficacy was evaluated in humanized MUP-uPA-SCID/Beige mice infected with HCV (JFH1/J6) or HBV (AD38). Resistance was selected by 8 weeks of serial passaging in an HCV replicon and characterized by genomic profiling. PK and safety data were compiled from completed nonclinical studies.
Results: MDL-001 inhibited HCV mono-infection in vitro with EC50/90 of 164/460 nM and 72/300 nM in Con1 and JFH1 replicons, respectively, and inhibited HBV mono-infection with an EC50/90 of 52/88 nM. MDL-001 suppressed an in vitro HCV-HBV co-infection model with similar potency. In vivo, oral MDL-001 reduced plasma HCV RNA by 3.27 $\log_{10}$ on day 28 compared with vehicle, achieving efficacy equivalent to that of sofosbuvir, with both treatments achieving viral load levels within the assay's limit of detection. In vivo, oral MDL-001 reduced plasma HBV rcDNA by 1.8 $\log_{10}$ on day 28. Pharmacokinetic studies demonstrated that Cmax and C24 drug concentrations in liver tissue were far in excess of EC90 s. An 8-week HCV resistance-mutation study yielded three MDL-001-resistant colonies with a convergent P495S mutation in the NS5B Thumb-1 domain. Safety data from >400 animals dosed in vivo at up to 16-fold the minimum efficacious dose (1.0 log10 reduction in plasma viral load in HCV) in a single-dose study and at 6-fold the minimum efficacious dose at 28 days reported no observed adverse events.
Conclusion: MDL-001 directly targets the Thumb-1 cryptic allosteric site that is present across RNA-dependent viral polymerases, delivering dual preclinical efficacy against HCV and HBV, as well as activity against HCV/HBV co-infection, with a safety and pharmacokinetic profile consistent with oral dosing. These data support completion of IND-enabling studies and clinical evaluation in chronic hepatitis B and C, including co-infected cohorts.

THU-585-YI
Bulevirtide treatment reduces bystander activation of CD8+ T cells in chronic hepatitis D virus infection

Shruti Chowdhury[1,2], Reem Hoblos[1,2], Hanan Begali[2,3], Manfred Anim[1,4], Carina Jacobsen[1,2], Mara Lissek[1,2,4], Christine Falk[5,6], Anke R.M. Kraft[1,2,6,7], Markus Cornberg[1,2,4,6,7], Heiner Wedemeyer[1,2,4,6], Lisa Sandmann[1,2,4,6], Helenie Kefalakes[1,2,4,6]. [1]*Hannover Medical School, Department of Gastroenterology, Hepatology, Infectious Diseases and Endocrinology, Hannover, Germany;* [2]*Cluster of Excellence RESIST, EXC-2155, Hannover Medical School, Hannover, Germany;* [3]*Hannover Medical School, Institute of Virology, Hannover, Germany;* [4]*D-SOLVE Consortium, an EU Horizon Europe funded project (No 101057917), Hannover, Germany;* [5]*Hannover Medical School, Institute for Transplant Immunology, Hannover, Germany;* [6]*German Center for Infection Research (DZIF), Partner Site Hannover-Braunschweig, Hannover-Braunschweig, Germany;* [7]*Centre for Individualised Infection Medicine(CIIM), a joint venture between Helmholtz-Centre for Infection Research(HZI) and Hannover Medical School(MHH), Hannover, Germany*
Email: chowdhury.shruti@mh-hannover.de

Background and aims: Infection with the hepatitis D virus (HDV) causes the most severe form of chronic viral hepatitis. This has been associated with bystander activation of $CD8^+$ T cells, which contribute to liver disease pathogenesis in chronic HDV infection. Improvement in liver function tests has been observed in HDV-infected patients treated with bulevirtide. Here, we aim to identify immunological correlates associated with improved liver function in virological responders under bulevirtide treatment.
Method: Peripheral blood mononuclear cells (PBMCs) and plasma samples were isolated from HDV-infected patients (n = 21) before (baseline) and at week 48 of bulevirtide treatment (TW48). Single-cell RNA sequencing and 34-color spectral flow cytometry were performed to assess the gene expression and the immune-cell phenotypes and function over time. A 48-plex immunoassay was performed on plasma samples to study the expression of cytokines. Viral response was defined as an HDV RNA decline ≥2 log10.
Results: Under bulevirtide treatment, HDV-infected patients show a significant decline in liver transaminases, aspartate transaminase to platelet ratio index (APRI) and fibroscan values. This is accompanied by a significant reduction of CXCL9, CXCL10 and CCL3 in the plasma of responders, reflecting decreased inflammation and type I interferon signaling. Importantly, when looking at interferon-stimulated genes (ISGs), these get significantly downregulated under bulevirtide treatment in responders, especially in the $CD4^+$ and $CD8^+$ T cell subsets. This is reflected by decreased frequencies of $CD4^+$ and $CD8^+$ central memory T cells (TCM) at baseline, which though show a capacity to recover at TW48. Interestingly, although reduced in numbers, these cells display higher levels of activation and cytotoxicity at the transcriptomic and proteomic level at baseline, accompanied by an increased bystander activation score in $CD8^+$ T cells before treatment initiation. This score is improving in all $CD8^+$ T cell subsets under bulevirtide treatment, which is also reflected by a significant reduction in NKG2D expression at the protein level.
Conclusion: Bulevirtide therapy reduced bystander activation of $CD8^+$ T cells at TW48, explaining the improvement in liver function. This improvement is more pronounced in virological responders compared to non-responders.

THU-586
Sequential mRNA vaccine-enabled quadruple therapy induces functional cure of HBV in rAAV8-1.3HBV carrier mice

Yuqi Hong[1], Shaohua Dong[1], Jinyao Dai[1], Yan Lou[2], Yunqing Qiu[2]. [1]*Zhejiang University School of Medicine, the First Affiliated Hospital, Hangzhou, China;* [2]*Zhejiang University School of Medicine, the First Affiliated Hospital, Hangzhou, China*
Email: yanlou@zju.edu.cn

Background and aims: Chronic hepatitis B functional cure remains difficult to achieve with current treatments, primarily due to HBV-induced multilayered immune tolerance. We proposed a sequential therapeutic strategy designed to gradually reduce viral antigen load, enhance antigen presentation, and promote cytotoxic T-cell memory formation to overcome this immune barrier.
Method: We designed a staged quadruple therapy: (1) Viral suppression using antisense oligonucleotides (ASO) and entecavir (ETV); (2) Dendritic cells (DCs) priming with IFNα to enhance antigen presentation; (3) Administration of a codon-optimized mRNA vaccine (encoding full-length HBV large S protein) delivered via chitosan nanoemulsions (mRNA@CNE) to induce cytotoxic memory T-cell responses.
Results: In rAAV8-1.3HBV carrier mice, this regimen induced durable functional cure in 50% of mice for over 17 weeks. A key finding was that functional cure depended on achieving HBsAg levels below 100 IU/mL before IFNα administration. This threshold was necessary to permit IFNα-mediated DC activation, which in turn enabled vaccine-expanded and functionally restored HBV-specific CD8+T cells, alongside dissolution of immunosuppressive networks. Non-responders (pre-IFNα HBsAg >100 IU/mL) displayed impaired DC-T cell interactions.
Conclusion: These results support a biomarker-guided sequential therapeutic framework with clear clinical applicability, providing a mechanistic and staged strategy to overcome HBV immune tolerance and advance toward functional cure.

THU-587

The potentially best-in-class HBV ASO ALG-170674 demonstrates additive to synergistic antiviral activities when combined with other anti-HBV modalities

Jin Hong[1], Vivek Rajwanshi[1], Hyunsoon Kang[1], Min Luo[1], Dinah Misner[1], Kusum Gupta[1], Antitsa Stoycheva[1], Kellan Passow[1], Jacquelyn Sousa[1], Dana Cho[1], John Cortez[1], Shane Daguison[1], Jieun Song[1], Lillian Adame[1], Cheng Liu[1], Sarah Stevens[1], Aneerban Bhattacharya[1], Rostom Ahmed-Belkacem[2], Susan Luong[1], Lawrence Blatt[1], Leonid Beigelman[3], David Smith[1], Julian Symons[1].
[1]Aligos Therapeutics, Inc., South San Francisco, United States; [2]Former Employee of Aligos Therapeutics, Inc., South San Francisco, United States; [3]Pacifica, United States
Email: jhong@aligos.com

Background and aims: Chronic hepatitis B (CHB) patients can achieve a modest rate of functional cure after monotherapy with antisense oligonucleotides (ASO) e.g. bepirovirsen (GSK-836) and AHB-137. To enhance the rate of functional cure, it will be important to combine HBV ASOs with other modalities of HBV drugs. ALG-170674 is a next generation HBV ASO that showed superior in vivo RNase H-mediated activity as well as PK compared to GSK-836 in an AAV-HBV mouse model. ALG-170674 also exhibited improved binding over GSK-836 to human TLR8 protein. ALG-001075 is the parent of the CAM-E prodrug, pevifoscorvir sodium (pevy, ALG-000184). In a 96-week study in CHB patients, ALG-000184 demonstrated the ability to dramatically reduce HBV viral load in all patients, as well as HBsAg in HBeAg+ patients. In this study, we demonstrate the antiviral effects of ALG-170674 in monotherapy and in combination with ALG-001075 or its analog in HBV cell and animal models. The effects of ALG-170674 in combination with other modalities such as nucleos(t)ide analogs (NAs), HBV siRNA and pegylated interferon (IFN) were also studied.
Method: In vitro HBV cell models such as HepG2.2.15, HepG2.117 and Emulate 3-D liver chips were used for ASO characterization and for combination studies in vitro. In vivo combination studies utilized the AAV-HBV mouse model.
Results: When dosed at 25 mg/kg in AAV-HBV mice, ALG-170674 showed a >0.6 $\log_{10}$ IU/mL additional maximum HBsAg reduction compared to GSK-836. ALG-170674 bound more tightly to human TLR8 protein with a Kd of 0.4 nM vs. 1.0 nM for GSK-836. Further, cytokine (IL6) induction was modestly higher than GSK-836 in a human PBMC assay. In PXB mice with humanized livers, ALG-170674 showed good liver safety when dosed at 50 mg/kg. In HepG2.2.15 cells as well as in 3-D human liver chips, combination of ALG-170674 and ALG-001075 demonstrated additive effects in HBsAg reduction. In AAV-HBV mice, analogs of ALG-170674 and ALG-001075 showed additive to synergistic effects in reducing HBV DNA in mouse plasma. Combinations of ALG-170674 with NAs, pegylated IFN and HBV siRNA are ongoing.
Conclusion: ALG-170674 exhibited potential to be a best-in-class HBV ASO. Additive to synergistic effects were observed when combining ALG-170674 and ALG-001075 (or close analogs) in preclinical studies. Combination of ALG-170674 and ALG-000184 could potentially improve functional cure rates in CHB patients, particularly in patients with higher baseline levels of HBsAg.

THU-588

Acute hepatitis E virus infection in asymptomatic blood donors is characterized by constrained intra-host diversity and temporal mutational signatures

Saskia Janshoff[1,2,3,4], Ricarda Plümers[3], Alina Kohl[2,4], Maximilian Nocke[1,2,4,5], Rui Costa[2,4], Tanja Vollmer[3], Daniel Todt[1,2,4,5], Eike Steinmann[2,4], André Gömer[2,4]. *[1]Department of Translational and Computational Infection Research (TRACiR), Ruhr University Bochum, Bochum, Germany; [2]Department of Molecular and Medical Virology, Ruhr University Bochum, Bochum, Germany; [3]Institut für Laboratoriums- und Transfusionsmedizin, Herz- und Diabeteszentrum Nordrhein-Westfalen, Universitätsklinikum der Ruhr-Universität Bochum, Universitätsklinikum der Universität Bielefeld, Bad Oeynhausen, Germany; [4]Hepatitis E Virus Research Hub (HepE-Hub), Ruhr University Bochum, Bochum, Germany; [5]European Virus Bioinformatics Center (EVBC), Jena, Germany*
Email: saskia.janshoff@rub.de

Background and aims: The hepatitis E virus (HEV) is the most common cause of acute viral hepatitis worldwide. RNA viruses like HEV can establish viral populations with high intra-host variability, which enables them to rapidly adapt to changing immune responses, as observed in chronic infections. To which extent intra-host diversity plays a role during acute infection remains unknown. This study aimed to characterize early intra-host evolutionary dynamics of HEV-3 during acute self-limiting asymptomatic infection. To understand early selective forces, we identified enriched variants in the RNA-dependent RNA polymerase (RdRp), quantified mutational signatures, and assessed the *in vitro* fitness of discovered variants.
Method: We sequenced the RdRp domain of viral populations in 82 asymptomatic blood donors with acute HEV-3 infection. Intra-host diversity was analyzed using Tanoti and DiversiTools. Variant frequency shifts were tracked in longitudinal samples. Recurrently enriched variants were characterized *in vitro* using replicon and trans-complementation assays.
Results: The overall HEV diversity within the host was constrained, however, several recurrent substitutions were identified, and four mutations in the polymerase region were found to be enriched among the donors. Despite being markedly replication-deficient *in vitro*, their replication defects could be rescued by Kernow/C1-p6 strain in a trans-complementation assay. Longitudinal sampling in a subset of donors revealed temporal shifts in variant frequencies, indicating ongoing early selection dynamics. In contrast to chronic HEV infection in immunosuppressed patients, acute phase populations exhibited a significantly lower number, and an absence of high-frequency variants. Similarly, premature stop codons and replication deficient variants were primarily detected in patients with acute infection, but not in patients with chronic infection.
Conclusion: Although HEV diversity is markedly restricted during acute infection, the early evolutionary landscape is highly dynamic but constrained even within the short window of acute, self-limiting and asymptomatic disease. These findings offer mechanistic insights into early intra-host evolution, highlight conditions under which deleterious variants can transiently persist, and lay the groundwork for linking genotypic features to clinical outcomes and treatment responsiveness.

THU-589-YI

Seroprevalence and viral biomarker characterization of hepatitis D infection in treatment naive-infected blood donors with hepatitis B in Cameroon

Rodrigue Kamga Wouambo[1], Nadesh Ashukem Taku[2,3], Noel Simon Ateba[2,4], Maria Pfefferkorn[1], Shirin Nkongolo[5,6,7], Gnimah Eva Gnouamozi[6,7], Madlen Matz-Soja[1], Stephan Urban[6,7], Thomas Berg[1], Florian van Bömmel[1], Francoise Ngo Sack[2,8]. *[1]Division of Hepatology, University of Leipzig Medical Centre, Leipzig, Germany; [2]Blood Bank, Yaounde Central Hospital, Yaounde, Cameroon; [3]Faculty of Health Science, University of Buea, Buea, Cameroon; [4]Faculty of Medicine and Biomedical Sciences, University of Yaounde I, Yaounde, Cameroon; [5]Internal Medicine IV (Gastroenterology, Hepatology, Infectious Diseases), University Hospital Heidelberg, Heidelberg, Germany; [6]University Hospital Heidelberg, Department for Infectious Diseases, Molecular Virology, Heidelberg, Germany; [7]German Center for Infection Research (DZIF), partner site Heidelberg, Heidelberg, Germany; [8]Faculty of Medicine and Pharmaceutical Sciences, University of Douala, Douala, Cameroon*
Email: rodrigue.kamgawouamba@medizin.uni-leipzig.de

Background and aims: Hepatitis delta virus (HDV) infection causes the most severe form of chronic viral hepatitis, yet it remains

significantly under-researched in Sub-Saharan Africa (SSA). In Cameroon, data on HDV prevalence and its interaction with hepatitis B virus (HBV) biomarkers are scarce, hindering effective public health interventions and clinical trials. Our study investigated the HDV seroprevalence and HBV biomarker characterization of HDV infection among HBsAg positive blood donors in Yaoundé, Cameroon.

Method: A cross-sectional study was conducted on HBsAg-positive serum samples collected from 2023 to 2025 at the blood bank of the Yaounde Central Hospital in Cameroon (ethical approval n°: 002382/CRERSHC/2025). A rapid screening of anti-HDV antibodies was conducted by lateral flow immunoassay (HDV rapid test, Heidelberg). Molecular and serological assays were undertaken for HBV biomarker assessment (HBV DNA, HBV RNA, total HBsAg; detection limits 157.5 cp/mL, 280 cp/mL and 0.05 IU/mL). HBV DNA (Log UI/mL) and HBsAg (Log UI/mL) were classified in low and intermediate/high: ≤3.3, >3.3 and ≤3, >3, respectively.

Results: Out of 126 HBsAg-positive blood donors, 92.8% men, median age: 29 [15–61] years, overall seroprevalence of anti-HDV was 24.6% (31/126; 95% CI: 17.6%–33.0%). HDV prevalence was 25.6% in males compared to 11.1% in females (p = 0.45). HBV DNA and HBV RNA could be quantified in 62.7% (79/126) and 38.1% (48/126) of patients. Globally, 85.7% exhibited low viral loads (HBV DNA <3.3 Log IU/mL). Intermediate/high HBsAg levels (>3 Log IU/mL) were found in 84.9%. Median HBV DNA, RNA levels were 1,7 [0.0–8.1] Log IU/mL, 0.7 [0.0–8.4] Log cp/mL, and 3.9 [0.0–5.6] Log IU/mL, respectively. Notably, anti-HDV carriers showed significantly lower HBV DNA levels compared to anti-HDV negative subjects (4.9 ± 5.7 vs. 6.5 ± 7.8 Log IU/mL; p = 0.04), suggesting HDV-mediated suppression of HBV replication. No significant differences were observed in HBV RNA or HBsAg levels between the two groups. Anti-HDV seropositivity was also markedly higher in subjects presenting with jaundice (100% vs. 24.2%; p = 0.08).

Conclusion: Our pilot data reveal a substantial seroprevalence of anti-HDV antibodies (24.6%) in apparently healthy blood donors in Cameroon. These findings underscore the urgent need to implement systematic HDV screening and establish specialized treatment pathways in Cameroon to mitigate the severe health outcomes associated with hepatitis delta.

THU-590

Development of a novel TLR-7 agonist SA-5 as a therapeutic option for chronic hepatitis B: a multimodal biomarker scoring for safety and efficacy in the first-in-human study

Tatsuya Kanto[1], Takahiro Kodama[2], Shokichi Takahama[3], Sachiyo Yoshio[4], Takuya Yamamoto[3]. *[1]The Research Center for Hepatitis and Immunology, National Institute of Global Health and Medicine, Japan Institute for Health Security, Ichikawa, Japan; [2]Department of Gastroenterology and Hepatology, Graduate School of Medicine, The University of Osaka, Suita, Japan; [3]Laboratory of Precision Immunology, Center for Intractable Diseases and Immuno-Genomics, National Institutes of Biomedical Innovation, Health and Nutrition, Suita, Japan; [4]Department of Human Immunology and Translational Research, National Institute of Global Health and Medicine, Japan Institute for Health Security, Tokyo, Japan*
Email: kanto.t@jihs.go.jp

Background and aims: Various new drugs, including immune modulators, are under development to achieve a functional cure in patients with chronic hepatitis B (CHB). We are developing a novel TLR7 agonist (SA-5) with enhanced in vivo targeting to the liver. SA-5 is specifically designed as a substrate for the organic anion-transporting polypeptides OATP1B1 and OATP1B3, which are expressed on hepatocyte sinusoidal membranes. To prepare the investigator-initiated First-in-Human (FIH) study of SA-5, we examined the safety and efficacy of SA-5 in HBV mouse models and cynomolgus monkeys and assessed the feasibility of biomarkers in the clinical trial.

Method: To clarify the in vivo safety and anti-HBV activity, SA-5 was administered orally once a week for 4 to 12 weeks to HBV mouse models and cynomolgus monkeys. Safety was evaluated through hematologic, biochemical, and flow cytometric profiling, while efficacy was assessed via Interferon (IFN)-alfa production, gene expression of IFN-stimulated genes (ISGs), and plasmacytoid dendritic cell activation. A principal component analysis-based composite scoring system was used to integrate multimodal parameters.

Results: We established a novel HBV mouse model in which mouse hepatocytes were replaced by FAH-HBV-expressing hepatocytes using the Sleeping Beauty transposon system (CMGH 2025). Short-term administration of SA-5 resulted in a transient increase in ALT, and HBV DNA and HBV pgRNA levels were significantly reduced. Compared to the control IFN-alfa-treated group, ISG expression was increased in the SA-5-treated group, and the cytotoxic activity of intrahepatic NK cells and CD8+ T cells was stronger. Additionally, intrahepatic T cells differentiated into effector memory T cells. These results indicate that SA-5 exerts not only activating innate immunity but also on adaptive immunity. In cynomolgus monkeys, SA-5 treatment for 12 weeks induced a dose-dependent type I IFN response, accompanied by limited systemic inflammation. SA-5 had comparable immunostimulatory activity to GS9620 but with reduced adverse biomarker shifts. We are in the process of regulatory approval and aim to start an investigator/physician-initiated FIH study of SA-5 in 2Q of 2026.

Conclusion: SA-5 is a safer, next-generation TLR-7 agonist for chronic HBV infection, highlighting the importance of integrated biomarker profiling in preclinical immunomodulatory anti-HBV drug development.

THU-591

Immune-metabolic dysregulation and systemic inflammation drive accelerated liver disease in HBV/HDV coinfection

Arshi Khanam[1], Furkan Kaysin[2], Cihan Yurdaydin[2], Shyamasundaran Kottilil[1]. *[1]Institute of Human Virology University of Maryland, Baltimore, United States; [2]Koc University School of Medicine, Istanbul, Türkiye*
Email: arshigbpant@gmail.com

Background and aims: Chronic hepatitis B virus (HBV) infection and HBV/hepatitis D virus (HDV) coinfection are major global drivers of liver disease and hepatocellular carcinoma. Coinfected individuals experience accelerated liver damage and poor clinical outcomes despite antiviral therapy, posing a critical barrier to mitigating end-stage liver disease. The mechanisms driving disease acceleration remain unclear, underscoring an urgent need to define molecular and immunological pathways that can be targeted to mitigate disease progression.

Method: Peripheral blood samples from individuals with chronic HBV-monoinfection and HBV/HDV-coinfection underwent high-throughput transcriptome sequencing to reveal HDV-driven alterations in gene expression. In parallel multiplex cytokine profiling quantified levels of plasma inflammatory and fibrogenic mediators, revealing signatures of immune dysregulation, heightened inflammatory signaling associated with accelerated liver disease progression.

Results: Transcriptomic profiling of peripheral blood mononuclear cells revealed a dual signature of activated immune system and suppressed metabolic function in HBV/HDV-coinfected patients compared to HBV alone. Upregulated genes included pattern recognition receptors (TLR1, TLR4, TLR8), inflammasome component (NLRC4), TNF receptor family members (TNFRSF8, TNFRSF10C), metabolic regulators (NAPRT, SLC28A3), lipid and oxidative stress mediators (CYBB, CD36), transcriptional regulator (MECOM) and antigen-presenting molecules (HLA-DQB1). These changes indicate activation of NF-kB driven inflammatory pathways, caspase-1 dependent cell death, enhanced reactive oxygen generation, and increased immune activation. Conversely, downregulated genes

included those involved in metabolic regulation (G0S2, SLC2A14), immune homeostasis (NR4A3), stress response (DNAJB5), and oxygen transport (HBA2, HBB), suggesting impaired energy metabolism, reduced immune regulation and diminished stress tolerance. Plasma cytokine profiling revealed elevated levels of proinflammatory and fibrogenic mediators including IFN-γ, TNF-α, IL-17, IL-22, CXCL2, CXCL13 and TGF-β, in HBV/HDV-coinfection than HBV alone, confirming systemic inflammation in these patients.
Conclusion: Collectively, these findings highlight systemic inflammatory activation coupled with metabolic dysfunction, contributing to immune dysregulation and accelerated liver disease progression in HBV/HDV-coinfection.

THU-592-YI
Nucleoside analog 4′-Fluorouridine inhibits hepatitis E virus infection in vitro and demonstrates high potency in vivo
Mara Klöhn[1,2], Martin Ferrié[3], Yufan Bao[3], Cleber C. Melo-Filho[4], Viktoria Kowalzick[1,2], Lilli Pottkämper[1,2], Johan Neyts[3], Eugene Muratov[4,5], Suzanne J.F. Kaptein[3], Eike Steinmann[1,2,6].
[1]Department of Molecular and Medical Virology, Ruhr University Bochum, Bochum, Germany; [2]Hepatitis E Virus Research Hub (HepE-Hub), Bochum, Germany; [3]Department of Microbiology, Immunology and Transplantation, Rega Institute for Medical Research, Virology, Antiviral Drug & Vaccine Research Group, KU Leuven, Leuven, Belgium; [4]Laboratory for Molecular Modeling, Division of Chemical Biology and Medicinal Chemistry, UNC Eshelman School of Pharmacy, University of North Carolina, Chapel Hill, United States; [5]Cheminformatics Laboratory, Department of Chemistry, Center for Exact and Natural Sciences (CCEN), Federal University of Paraíba (UFPB), Campus I Lot. Cidade Universitária, Paraíba, Brazil; [6]German Centre for Infection Research (DZIF), External Partner Site Bochum, Bochum, Germany
Email: mara.kloehn@rub.de

Background and aims: Hepatitis E virus (HEV) remains an important but largely understudied zoonotic pathogen. A universally available vaccine is lacking, and current treatments are limited by severe side effects, teratogenicity, and frequent therapeutic failures. Drug repurposing may therefore accelerate the discovery of effective anti-HEV therapies. This study aimed to identify and characterize nucleos(t)ide analogs with antiviral activity against HEV.
Method: A library of 496 nucleoside and nucleotide analogs was screened for inhibitory effects on HEV replication while monitoring cell viability. Compounds demonstrating strong antiviral efficacy were further assessed for dose–response relationships, activity across HEV genotypes and cell types, and potential mechanisms of action. In silico docking simulations were conducted to evaluate the interaction between candidate compounds and the HEV polymerase. In vivo efficacy was tested in an athymic nude rat model of HEV infection.
Results: Ten compounds inhibited HEV replication by more than 60% while maintaining cell viability above 75%, including four that showed clear dose–response relationships. Among these, 4′-fluorouridine (4′-FlU) exhibited potent antiviral activity in both replication (EC50 ≈ 5 µM) and infection (EC50 ≈ 10 µM) assays against HEV-Kernow-C1/p6 and HEV-1 Sar55 strains. The compound also demonstrated efficacy in extrahepatic cell lines (placental JEG-3, intestinal Caco-2, and renal HEK293 T) and in primary human hepatocytes. Combination treatment with ribavirin resulted in an additive antiviral effect. In silico docking indicated binding of 4′-FlU to the HEV RNA-dependent RNA polymerase. Furthermore, exogenous uridine reversed the inhibitory effect of 4′-FlU on HEV-3 replication, suggesting that UTP competes with the active metabolite 4′-FlU-5′-triphosphate for incorporation by the polymerase. In vivo, daily administration of 20 mg/kg 4′-FlU to HEV-infected rats significantly reduced viral titers in feces, liver, kidney, intestine, and spleen.
Conclusion: Ongoing studies are evaluating 4′-FlU in treatment and combination settings with ribavirin in rats, as well as in HEV-1 infected mice. Altogether, these findings identify 4′-FlU as a promising candidate for HEV therapy.

THU-593
Replication assessment of chimeric HEV-3 subtypes demonstrate enhanced replication fitness of HEV-3f isolates
Alina Kohl[1,2], Rui Da Costa[1,2], Michelle Jagst[1,2], Daniel Todt[1,2,3], Eike Steinmann[1,2], André Gömer[1,2]. *[1]Department of Molecular und Medical Virology, Ruhr University Bochum, Germany, Bochum, Germany; [2]Hepatitis E Virus Research Hub (HepE-Hub), Bochum, Germany, Bochum, Germany; [3]Department of Translational and Computational Infection Research (TRACiR), Ruhr University Bochum, Germany, Bochum, Germany*
Email: alina.kohl@rub.de

Background and aims: Hepatitis E virus (HEV) remains an underestimated global health concern, causing an estimated 20 million infections and up to 70,000 deaths annually. While infections are often asymptomatic, HEV can become chronic in immunocompromised individuals and is associated with mortality rates of up to 25% in pregnant women. In Europe, genotype 3 (HEV-3) is the most common and comprises 15 subtypes grouped into three clades: Clade 1 (3e–3g), Clade 2 (3a–3c, 3h–3o) and Clade 3 (3ra). In particular, clade 1 has been associated with more severe disease outcomes, although the underlying mechanisms remain unclear - likely due to the lack of suitable cell culture systems.
Method: To address this gap, we performed a phylogenetic analysis of HEV-3 subtypes and generated a library of 15 primary isolate-derived polymerase chimeras, each inserted into the backbone of the Kernow-C1 p6 subgenomic replicon. We evaluated replication kinetics and antiviral responses to ribavirin and sofosbuvir.
Results: Phylogenetic analysis revealed considerable diversity among the HEV-3 polymerases, with up to 21 amino acid substitutions relative to p6. 13 of the 15 chimeras demonstrated replication comparable to the parental p6 construct. The HEV-3f subtype showed significantly enhanced replication kinetic, with up to a 5-fold increase. All chimeras remained sensitive to antiviral drugs, with only minor variations in ribavirin susceptibility.
Conclusion: Our findings highlight the genomic flexibility of HEV-3, which allows for efficient replication of diverse chimeric constructs. This model provides a robust platform for assessing intra-genotypic variability in antiviral responses and advances our mechanistic understanding of replication fitness. Such insights are critical for optimising treatment strategies and understanding the burden of disease in HEV-infected patients.

THU-594
Detailed molecular profiling of intrahepatic and serum viral markers in HBeAg-positive chronic hepatitis B patients without clinical cirrhosis
Jung Hyun Kwon[1], Hye Seon Kim[2], Soon Kyu Lee[1], Jeong Won Jang[3].
[1]College of Medicine, The Catholic University of Korea, Division of Hepatology, Department of Internal Medicine, Incheon St. Mary's Hospital, Incheon, Korea, Rep. of South; [2]College of Medicine, The Catholic University of Korea, Department of Biomedicine & Health Sciences, Seoul, Korea, Rep. of South; [3]College of Medicine, The Catholic University of Korea, Division of Hepatology, Department of Internal Medicine, Seoul St. Mary's Hospital, Seoul, Korea, Rep. of South
Email: doctorkwon@catholic.ac.kr

Background and aims: In HBeAg-positive chronic hepatitis B (CHB) patients, managing those not meeting classic immune-active (IA) criteria is an area of active investigation. While clinical trends suggest broader antiviral therapy (AVT) application, the molecular characteristics of the expanded immune-tolerant (IT) spectrum are not fully elucidated. We aimed to compare intrahepatic and serum viral markers between an Expanded IT group and the IA group to identify predictors of disease progression in clinically non-cirrhotic patients.

Method: We enrolled 78 HBeAg-positive, clinically non-cirrhotic CHB patients. The IA group (ALT >80 U/L and HBV DNA >20,000 IU/ml) was compared with the Expanded IT group (all non-IA patients). Within the Expanded IT group, a subgroup meeting Strict IT criteria (ALT <40 U/L and HBV DNA >7 log IU/ml) was separately analyzed. We analyzed intrahepatic cccDNA, pgRNA, and S RNA, along with serum HBsAg, HBV DNA, HBcrAg, and HBV RNA. Clinical events (LC or HCC) were monitored during follow-up.
Results: The Expanded IT group exhibited significantly higher serum HBV DNA and HBsAg levels compared to the IA group. Although serum HBV RNA was higher in the IA group, intrahepatic cccDNA and pgRNA levels were comparable between groups, indicating substantial viral replication potential across the expanded spectrum. In a focused sub-analysis, patients meeting Strict IT criteria showed significantly higher intrahepatic pgRNA and total HBV RNA levels than the IA group, demonstrating that intrahepatic viral transcriptional activity is most robust in the strictest IT phase. Regarding clinical outcomes, histological and clinical progression was notably absent in the Strict IT subgroup. In contrast, the majority of clinical events (LC or HCC) were concentrated in patients within the Expanded IT group who did not meet the strict IT criteria, whereas no events occurred in the IA group where AVT was initiated after enrollment.
Conclusion: HBeAg-positive patients in the Expanded IT spectrum harbor substantial intrahepatic viral activity equivalent to or exceeding that of IA patients. Clinical progression is predominantly concentrated in those who fail to meet strict IT criteria. Our findings suggest that any deviation from the Strict IT profile should be considered a high-risk indicator, warranting earlier therapeutic intervention in the expanded IT spectrum.

THU-595

Reduced apoptosis in HBV/HDV-expressing hepatocytes due to HDV-specific modulation of EphA signaling

Pia Lembeck[1], Keerthihan Thiyagarajah[2,3], Mirco Glitscher[2], Jannik Sonnenberg[1], Laurin Büning[1], Jonel Trebicka[1], Eberhard Hildt[2,4], Kai-Henrik Peiffer[1]. *[1]University Hospital Münster, Medical Clinic B, Münster, Germany; [2]Paul-Ehrlich-Institute, Research Group 2, Langen, Germany; [3]Hospital of the Goethe University Frankfurt, Internal Medicine I, Frankfurt, Germany; [4]Hasso-Plattner-Institute, Digital Health Cluster, Potsdam University, Potsdam, Germany*
Email: pia.lembeck@ukmuenster.de

Background and aims: HDV co-infection in chronic hepatitis B (CHB) patients is associated with severe liver disease and HCC development. Despite elevated TNFalpha levels, HDV persists, suggesting modulation of host cell death pathways. This study investigated the impact of HDV on TNFalpha-dependent (NF-kappaB/AP-1) and -independent (EphA) apoptotic pathways in HBeAg-positive and -negative HBV-expressing hepatocytes.
Method: Huh7 cells were co-transfected with HBeAg-positive or -negative HBV genotype A genomes and HDV full genome or HDV-specific proteins expressing plasmids. TNFalpha-mediated apoptosis was induced with TNFalpha/cycloheximide or DMSO control. Apoptosis was quantified by Annexin V/PI flow cytometry, NF-kappaB and AP-1 promoter activities by luciferase reporter assays, and deregulated kinases were identified by kinome profiling of HDV-transfected hepatocytes.
Results: Basal apoptosis was elevated in HBeAg-negative HBV-expressing hepatocytes. HDV co-transfection reduced apoptosis in both HBeAg-positive and -negative cells under both TNFalpha-stimulated and unstimulated cells, with strongest effect in HBeAg-negative cells. While HBV reduced, HDV increased cell viability. NF-kappaB and AP-1 promoter activities were greatly suppressed by HDV, S-HDAg or L-HDAg. Kinome profiling revealed downregulation of multiple Ephrin type-A receptor kinases (EPHA1, EPHA3, EPHA4, EPHA5, EPHA7) in cells expressing full-length HDV genome.
Conclusion: HDV promotes hepatocyte immortalization by modulating apoptotic and stress-response pathways. Suppression of NF-kappaB and AP-1 activity and downregulation of pro-apoptotic EphA signaling, potentially involving EphA-associated caspase-8, suggest coordinated and balanced regulation of programmed cell death. By enabling hepatocyte survival, these mechanisms may facilitate viral persistence, dominance in HBV/HDV-crosstalk, and contribute to pathophysiology and HCC development. EphA-related signaling emerges as a potential therapeutic target.

THU-596

4-1BB costimulation restores T follicular helper 1 cell function to augment hepatitis B virus-specific humoral immunity in chronic infection

Yanchen Ma[1], Xiaoyi Liu[1], Haonan Lou[1], Hui Zhang[1], Jinyan Jiang[1], Libo Tang[1], Yongyin Li[1]. *[1]Department of Infectious Diseases, Nanfang Hospital, Southern Medical University, Key Laboratory of Infectious Diseases Research in South China (Southern Medical University), State Key Laboratory of Multi-organ Injury Prevention and Treatment, GuangZhou, China*
Email: 767895970@qq.com

Background and aims: Chronic HBV infection is closely associated with dysregulated humoral immunity. Although our study demonstrated that Mother-to-child transmission could be dramatically reduced by the comprehensive interventions among HBV-infected pregnant women (Nature Medicine, 2024), how intrauterine HBV antigen exposure shapes host humoral immunity remains unclear. Here, we investigated the humoral immune profile in cord blood from neonates born to HBV-infected mothers to identify potential therapeutic targets and validate if targeting these pathways restores HBV-specific humoral immunity in chronic infection cohorts.
Method: We analyzed cord blood samples from 73 neonates born to HBsAg-positive mothers and 24 counterpart controls (HBsAg-negative mothers). B cell and $CD4^+$ T cell phenotypes and transcriptomes were analyzed by flow cytometry and RNA-seq. HBV-specific B cells were quantified via ELISPOT and ELISA. Additionally, peripheral blood from 85 untreated chronic HBV patients (aged 1–65 years) was evaluated by full-spectrum flow cytometry to determine Tfh1-cell functional dominance and age-related distribution.
Results: Cord blood from HBV-exposed neonates exhibited enhanced HBV-specific B cell responses along with significantly elevated frequencies of type 1 follicular T helper cells (Tfh1) compared to controls. In vitro, HBsAg could induced naïve $CD4^+$ T cells to differentiate into Tfh1 cells, but not Th1/Th2/Th17 or Tfh2/Tfh17 subsets. Tfh1 cells secrete both IFN-γ and IL-21, which synergistically enhanced HBsAb production by B cells via the activation of mTORC1-STAT1/STAT3 pathway. These data demonstrate that primary HBV antigen exposure preferentially induces a Tfh1-polarized immune response that initiates HBV-specific humoral immunity. To assess Tfh1 dynamics in chronic infection, we performed full-spectrum flow cytometry on a clinical HBV cohort, revealing an age-dependent decline in both Tfh1 frequency and 4-1BB expression, which positively correlated with HBsAb-secreting B cell counts. Strikingly, 4-1BB stimulation in vitro restored Tfh1 function, rescuing IFN-γ and IL-21 production and enhancing B cell help.
Conclusion: Tfh1-derived IFN-γ and IL-21 potentiate HBsAb production by activating mTORC1-STAT1/STAT3 signaling in B cells. The age-dependent decline in Tfh1 frequency and 4-1BB expression suggests progressive immune dysfunction in chronic HBV infection. Targeting 4-1BB may rejuvenate Tfh1 activity, offering a novel strategy to restore HBV-specific humoral immunity.

THU-597

CX-5461 exerts pangenotypic anti-hepatitis E virus effect in preclinical models

Yuebao Li[1], Tianxu Liu[1], Lin Wang[1]. [1]*Peking University Health Science Center, Beijing, China*
Email: lin_wang@pku.edu.cn

Background and aims: Hepatitis E virus (HEV) is one of the common causes of acute hepatitis worldwide. Clinically, HEV infection presents as either acute or chronic disease. Acute infection mainly occurs in immunocompetent individuals, especially in vulnerable populations is associated with high mortality. Chronic infection mainly develops in immunocompromised patients and carries the risk of progressing to liver fibrosis and cirrhosis. Specific antiviral drugs targeting HEV are still lacking, and the use of ribavirin is limited by adverse effects or treatment failure. Therefore, there is an urgent need for novel antiviral strategies to address future clinical demands.
Method: Potential G-quadruplex (G4) forming sequences in the HEV genome were predicted using bioinformatics analysis and validated through *in vitro* experiments. The antiviral activity of three known G4 ligands was evaluated using *in vitro* infection assay. Mongolian gerbil models of HEV infection were used to evaluate the antiviral effect of CX-5461 against acute HEV-1, -3, and -4 infection. A tacrolimus-induced rabbit model of chronic HEV infection was used to examined the antiviral effect of CX-5461 against HEV-3ra chronic infection.
Results: Bioinformatic and *in vitro* analyses identified 4 highly conserved, G4-forming sequences in the HEV genome. Among three G4 ligands tested *in vitro*, CX-5461, a drug in clinical trials for cancer showed potent antiviral activity (IC_{50} = 19.36 nM). In gerbils infected with HEV-1, -3, or -4, fecal viral shedding was reduced within 2 days post-treatment, along with significantly lowered viral RNA loads and antigen levels in the liver, kidney, and intestine. Notably, in HEV-3-infected gerbils, hepatic viral RNA loads and antigen levels were reduced by 224-fold and 8-fold, respectively. In chronic HEV-3ra-infected rabbits, CX-5461 treatment consistently reduced fecal viral shedding, reaching levels comparable to the ribavirin group by 30 days post-treatment. Hepatic viral RNA was reduced to a level similar to that in the ribavirin group.
Conclusion: These findings demonstrate that the HEV genome contains G4s, and the CX-5461 exhibits robust antiviral activity both *in vitro* and *in vivo*. CX-5461 showed promising pangenotypic efficacy in multiple preclinical models. These results support CX-5461 as a novel strategy for treating acute and chronic HEV infection.

THU-601-YI

Targeting host cell metabolism via the pentose phosphate pathway blocks hepatitis B virus surface antigen release and hepatitis D virus replication

Qiudi Li[1], Hongbo Guo[1], Zhenfeng Zhang[2], Wenshi Wang[1]. [1]*Jiangsu Key Laboratory of Immunity and Metabolism, School of Basic Medical Sciences, Xuzhou Medical University, Xuzhou, China;* [2]*School of Public Health and Emergency Management, Southern University of Science and Technology, Shenzhen, China*
Email: liqiudi1209@163.com

Background and aims: Chronic hepatitis D virus (HDV) infection represents the most severe form of viral hepatitis. Besides its dependence on HBV envelopment, HDV heavily depends on cellular machinery and metabolites to complete its obligate parasitic replication life cycle. Herein, we aim to identify critical metabolic components or pathways essential for HDV replication.
Method: We conducted systematic metabolite profiling using an in vitro cell model that stably supports HDV replication, alongside a replication-defective control model.
Results: HDV replication markedly reduced the levels of most cellular carbohydrates and their metabolites. Notably, inhibition of the pentose phosphate pathway (PPP)—but not other glycolytic pathways—suppressed HDV replication. Mechanistically, the suppression of HDV replication was due to the inhibition of de novo biosynthesis of guanine and cytosine, which are downstream of the PPP. Inhibitors targeting PPP–guanine/cytosine biosynthesis axis exhibited potent antiviral activity against different genotypes of patient-derived HDV isolates. The efficacy of these inhibitors was influenced by HDV replication status. However, the combination of guanine/cytosine biosynthesis inhibitors with IFN-α synergistically inhibited HDV replication. Notably, besides the suppressive effect on HDV replication, PPP inhibition also reduced HBsAg secretion derived either from cccDNA or HBV integrates. Nonetheless, the blockage of HBsAg secretion was independent of its downstream guanine and cytosine biosynthesis pathway.
Conclusion: Targeting host cell metabolism via PPP exerts a dual effect-inhibiting HDV replication and blocking HBsAg release, highlighting its therapeutic potential against both HBV infection and HBV/HDV coinfection.

THU-602

Deciphering the mechanistic underpinnings of hepatitis E severity: a tale of T cell exhaustion and maladaptive cDC2 activation at single-cell resolution

Jian Wu[1], Xiaoman Liu[2], Yijin Wang[2]. [1]*Department of Clinical Laboratory, The Affiliated Suzhou Hospital of Nnjing Medical University, Suzhou Municipal Hospital, Gusu School, Nanjing Medical University, 242 Guangji Rd, Suzhou, China;* [2]*Department of Pharmacology, Joint Laboratory of Guangdong-Hong Kong Universities for Vascular Homeostasis and Diseases, School of Medicine, Southern University of Science and Technology, Shenzhen, China*
Email: wangyj3@sustech.edu.cn

Background and aims: Hepatitis E virus (HEV) represents a major global cause of acute viral hepatitis, typically self-limiting yet capable of advancing to life-threatening acute liver failure (ALF). The immunological determinants of disease severity remain poorly defined. We therefore profiled the peripheral immune landscape to uncover mechanisms underlying progression to HEV-induced ALF.
Method: PBMCs from 20 subjects, including acute hepatitis E (AHE, n = 8), HEV-induced ALF (HEV-ALF, n = 8), and healthy controls (HCs, n = 4) were analyzed by single-cell RNA sequencing. Integrated analysis encompassed differential expression, pathway enrichment, pseudotemporal trajectory reconstruction, and cell-cell communication mapping to delineate immune heterogeneity and dynamics across disease severity.
Results: Unsupervised clustering delineated 23 transcriptomic clusters across six immune lineages. HEV infection triggered a broad IFN-γ response across all immune compartments. Compared to AHE, ALF was characterized by marked activation of inflammatory pathways, including NOD-like receptor, TNF, NF-κB, IL-2-STAT5, and IL-17 signaling. T and NK cells partitioned into nine functionally discrete subsets. While IL-17 signaling was confined to naïve T cells in AHE, it became pervasive across all NK/T cells in ALF. Although $CD8^+$ effector memory T cells (TEM) expanded in both AHE and ALF, $HLA\text{-}DR^+CD38^+CD8^+$ TEM predominated in AHE. Strikingly, $CD8^+$ TEM displayed profound downregulation of cytotoxic effectors (GZMA, GZMH, GNLY, PRF1) in ALF. GSEA further revealed suppression of CTLA4 and antigen presentation pathways, alongside activation of TID, TNF-JNK, JAK-STAT, and TGF-β signaling in ALF TEM. Pseudotime analysis positioned $CD8^+$ TEM at a terminally differentiated state in ALF, with key differentially expressed genes including elevated JUN and reduced IFI16, ISG15, GBP1. Conventional type 2 dendritic cells (cDC2) were decreased in both disease stages. In ALF, cDC2 demonstrated hyperactive MHC-II machinery, upregulation of all eight HLA class II genes, and the highest myeloid HLA-II module score, indicating maladaptive antigen-presenting capacity.
Conclusion: HEV-induced ALF were characterized by widespread inflammatory activation, functionally paralyzed $CD8^+$ TEM, and maladaptive cDC2-mediated antigen presentation. The coexistence of hyperinflammation and effector T cell impairment elucidates the

immunological basis of disease severity and identifies actionable targets for rebalancing immunity in severe hepatitis E.

THU-603

Divergent immune resolution and protracted immuno-metabolic memory in hepatitis E revealed by cross-species multi-omics

Yining Liang[1], Tianxu Liu[2], Xiaoman Liu[1], Lin Wang[2], Yijin Wang[1]. [1]*Department of Pharmacology, Joint Laboratory of Guangdong-Hong Kong Universities for Vascular Homeostasis and Diseases, School of Medicine, Southern University of Science and Technology, Shenzhen, China;* [2]*Department of Microbiology and Infectious Disease Center, School of Basic Medical Sciences, Peking University Health Science Center, Beijing, China*
Email: wangyj3@sustech.edu.cn

Background and aims: Hepatitis E virus (HEV) infection represents a growing global health burden. Emerging evidence suggests that liver injury is primarily immune-mediated rather than resulting from direct viral cytopathy. This study aims to delineate the longitudinal immuno-metabolic landscape of HEV infection and to identify pathogen-specific immune signatures through cross-species comparison.
Method: We established a longitudinal rabbit model infected with HEV genotype (gt) 3, collecting liver and serum samples at baseline (HEV-BL), first viremia (HEV-F), peak viremia (HEV-P), and viral clearance (HEV-N) stages. Multi-omics profiling included transcriptomic and proteomics from liver tissues, alongside serum metabolomics. For cross-species validation, we analyzed public transcriptomic data from HEV gt1- and hepatitis C virus (HCV)-infected chimpanzees (GSE22160).
Results: Integrated transcriptomic and proteomic analyses in HEV gt3-infected rabbits revealed sustained activation of the adaptive immune system throughout infection, which persisted beyond viral clearance, as evidenced by ongoing T cell infiltration and antigen presentation. Metabolomic profiling further indicated a pronounced T cell-related signature at peak viremia and a prolonged innate inflammatory response during clearance. Cross-species analysis in HEV gt1-infected chimpanzees identified a robust but transient type I interferon response that rapidly subsided after viral clearance. Strikingly, comparative analysis with HCV infection in chimpanzees revealed that HEV triggers a more rapid immune activation followed by significantly quicker resolution, as evidenced by the swift downregulation of interferon-stimulated genes post-clearance in HEV, contrasting with their sustained activation in HCV.
Conclusion: Our study unveils a protracted immuno-metabolic memory post-HEV clearance, characterized by unresolved innate activation and metabolic reprogramming. These findings redefine the paradigm of HEV immunopathogenesis, highlighting a distinct immune resolution profile compared to HCV. The insights gained offer novel avenues for biomarker development and immunomodulatory interventions in high-risk populations.

THU-604-YI

Spatial profiling of HBV and HDV infection in human liver samples reveals reversible phenotype upon clearance

Maria Saez-Palma[1], Marc Buendia[2], Thais Leonel[1], Ángela Sanzo-Machuca[2], Ester García-Pras[1], Mario Acera[3], Anna Pocurull Aparicio[1], Sara Battistella[1], Sergio Rodriguez-Tajes[1], Sarah Shalaby[4], Asunción Ojeda[4], Alba Díaz[5], Yilliam Fundora[6], Elisabetta Mereu[3], Xavier Forns[1], Sabela Lens[1], Azucena Salas[2], Maëlle Locatelli[1], Sofía Pérez-del-Pulgar[1]. [1]*Liver Unit, Hospital Clinic, University of Barcelona, IDIBAPS, CIBEREHD, Barcelona, Spain, Barcelona, Spain;* [2]*Inflammatory Bowel Disease Unit, Hospital Clinic, IDIBAPS, CIBEREHD, Barcelona, Spain, Barcelona, Spain,* [3]*Josep Carreras Leukaemia Research Institute, Badalona, Spain, Badalona, Spain;* [4]*Barcelona Hepatic Hemodynamic Laboratory, Liver Unit, Hospital Clinic - IDIBAPS, Barcelona, Spain, CIBEREHD, Barcelona, Spain;* [5]*Barcelona Clinic Liver Cancer (BCLC) Group, Department of Pathology, Hospital Clínic de Barcelona, Universitat de Barcelona, Barcelona, Spain, Barcelona, Spain;* [6]*Department of General and Digestive Surgery, Hospital Clinic de Barcelona, IDIBAPS, Barcelona, Spain, Barcelona, Spain*
Email: msaezp@recerca.clinic.cat

Background and aims: Chronic hepatitis delta represents the most severe form of viral hepatitis, marked by rapid progression to cirrhosis and hepatocellular carcinoma. Understanding the molecular interactions between hepatitis delta virus (HDV), hepatitis B virus (HBV), and the liver microenvironment is crucial for developing preventive and therapeutic strategies.
Method: Liver biopsies from four HBV/HDV-coinfected patients (two HDV-RNA positive, two negative) and two HBV-monoinfected patients were analyzed for HBsAg and HDAg expression using dual chromogenic immunostaining (Bond RX, Leica). These samples, along with liver tissues from healthy controls (HC), were further examined using spatial transcriptomics with the CosMx™ Spatial Molecular Imaging platform (NanoString; 1000-plex RNA). In parallel, bulk RNA sequencing was performed on liver samples from 21 coinfected patients (14 HDV-RNA positive, 7 HDV-RNA negative), seven HBV patients, and ten healthy controls using the nCounter™ Digital Analyzer.
Results: Compared with HBV monoinfection, HDV coinfection induced a distinct transcriptional signature associated with immune evasion, extracellular matrix remodeling, and progression toward a tumor-permissive state. In HDV-RNA negative samples, many of these alterations were attenuated or reversed, suggesting partial restoration of hepatocyte homeostasis. Spatial neighborhood analysis revealed that HDV-RNA negative tissues displayed an intermediate cellular organization between healthy and infected livers, showing partial recovery of normal cell-cell architecture. Pseudotime trajectories confirmed a restoration trend characterized by normalization of genes linked to ECM remodeling (COL4A1, FN1), oncogenic signaling (TWIST1), inflammatory response (IL6, STAT3), and metabolic regulation (FASN, SERPINA3). Intra-sample comparisons of HDAg+ versus HDAg- regions in HDV-RNA positive patients showed that local expression of HDAg correlated directly with microenvironmental disruption.
Conclusion: In conclusion, HDV coinfection induces deep but potentially reversible transcriptional and structural remodeling of the liver. Viral clearance appears to restore hepatic architecture and metabolic balance, reducing oncogenic risk and identifying potential biomarkers and therapeutic targets for hepatitis delta.

THU-605

Sequential combination of antisense oligonucleotide AHB-137 followed by HBV vaccine leads to HBsAg loss and seroconversion in the AAV-HBV mice

Tingting Lu[1], Jihai Lei[1], Ruixia Hou[1], Weiguo Zhang[1], Yang Bai[1], Shujie Hao[1], Yipeng Wang[1], Lisha Zhang[1], Yujia Zhao[1], Chunxi Li[1], Guofeng Cheng[1,2], Cheng Yong Yang[1,2]. [1]*Ausper Biopharma Co., Ltd., Hangzhou, China;* [2]*Aupserbio Therapeutics Inc., Foster City, United States*
Email: tingting.lu@ausperbio.com

Background and aims: There is a strong consensus for achieving durable HBV control and functional cure requires breaking host immune tolerance, inducing profound and sustained viral suppression, and eliciting effective antiviral immune responses. AHB-137 is an unconjugated antisense oligonucleotide, has demonstrated significant antiviral activity and achieved unpreceded function cure rate in the CHB patients (AASLD2025 Poster 5022, HEP-DART2025). Recombinant HBV vaccine was approved by NMPA for prevention of HBV infection. This study evaluated the antiviral activity and immunogenicity of sequential combination of AHB-137 followed by HBV vaccine in the AAV-HBV mice, providing preclinical rationale to inform clinical combination therapy strategy.
Method: C57BL/6 mice infected with rAAV8-1.3HBV were administered subcutaneously AHB-137 at 60 mg/kg for six doses (D1, D4, D8, D11, D15, D22), followed by intramuscular HBV vaccine at 1.5 μg or

5.0 μg per animal for five doses (D29, D43, D57, D71, D90). Serial serum collections were tested for HBsAg, HBeAg, HBV DNA, HBsAb. Terminal serum samples were assayed for neutralization of HBsAb by HBV infected NTCP-HepG2 cells. Mouse liver was stained for HBsAg and HBcAg using IHC. HBsAg-specific B cell responses in the liver and spleen were evaluated using ELISpot.
Results: AHB-137 monotherapy significantly reduced serum HBsAg, HBeAg, and HBV DNA to below the LLOQ, after which serum HBsAg began to rebound on Day 50. In contrast, followed by HBV vaccine continue maintain HBsAg loss till the study termination (Day106). During the sustained HBsAg loss period, high-titer HBsAb with neutralizing activity was rapidly induced, the HBsAg-specific B cells in the liver and spleen were detected. Interestingly, HBV vaccine alone also induced serum HBsAb while with lack of neutralizing activity and minimal change in HBsAg. Additionally, the levels of HBsAg, HBeAg, HBV DNA and HBV RNA in the liver also significantly decreased under the AHB-137 sequential regimen, whether potential immune cytotoxicity was activated is under evaluation. All animals were well tolerated without any treatment-related abnormalities in clinical observation and clinical pathology.
Conclusion: Sequential combination of AHB-137 with HBV vaccine in the AAV-HBV mice effectively sustain serum HBsAg loss by concomitantly activating HBsAg-specific B cells to produce high-titer neutralizing HBsAb. This result demonstrated a potential combination therapy strategy for achieving higher functional cure rate in CHB patients.

THU-606
Antisense oligonucleotide-based strategy to target hepatitis delta virus infections

Yannick Debing[1], Caroline Pons[2], Faustine Bernardin[2], Lars Degrauwe[1], Kellan Passow[3], Isabel Heremans[1], Aneerban Bhattacharya[3], Antitsa Stoycheva[3], Lawrence Blatt[3], Julian Symons[3], Andreas Jekle[3], Vivek Rajwanshi[3], David Smith[3], Eloi R. Verrier[4], David Durantel[2], Julie Lucifora[2]. *[1]Aligos Belgium BV, Gaston Geenslaan 1, 3001, Leuven, Belgium; [2]CIRI, Centre International de Recherche en Infectiologie, Univ Lyon, Inserm, U1111, Université Claude Bernard Lyon 1, CNRS, UMR5308, ENS de Lyon, F-69007, Lyon, France; [3]Aligos Therapeutics, Inc., 1 Corporate Drive, South San Francisco, CA 94080, San Francisco, United States; [4]CIRI, Centre International de Recherche en Infectiologie, Univ Lyon, Inserm, U1111, Université Claude Bernard Lyon 1, CNRS, UMR5308, ENS de Lyon, F-69007, Lyon, France*
Email: julie.lucifora@inserm.fr

Background and aims: Currently approved treatments for chronic hepatitis delta virus (HDV) infection (Peg-IFN-α and bulevirtide) rarely cure patients in a finite treatment regimen. New direct-acting agents (DAA), targeting HDV replication, could therefore be a valuable addition to the current therapeutic arsenal. Since HDV is an RNA virus replicating its genome via a rolling-circle process in the nucleus, and antisense oligonucleotides (ASOs) are known to act both in the cytoplasm and the nucleus (in contrast to siRNA), we hypothesized that ASOs targeting HDV genome may potently and specifically inhibit intracellular HDV RNA amplification irrespective of helper HBV.
Method: We synthesized 112 different 5-10-5 gapmer ASOs targeting HDV and screened them for their antiviral effect on HDV. The HBV-directed ASO, bepirovirsen, was used as a non-targeting ASO control since screening was performed in HDV mono-infected differentiated HuH7-NTCP cells. ASOs were transfected prior to HDV infection and a high-content imager approach was used to analyze the antiviral effect and cytotoxicity.
Results: Eighteen anti-HDV ASO candidates exhibited a ≥80% reduction in HDAg+ cells at 1 μM without associated toxicity. Among these hits, we selected six anti-HDV ASOs that displayed high efficacy against HDV for further confirmation of their antiviral effect at different doses in two different cell lines. The corresponding calculated IC_{50} values reached the single digit nanomolar range, demonstrating a very potent efficacy of the anti-HDV ASOs compared to other ASOs, which are typically active at higher concentrations. Moreover, we established the first, and to date the only, *in vitro* system that supports a *bona fide* HDV spreading in cell culture conditions and showed that anti-HDV ASOs strongly impair HDV propagation, slightly faster than a presS1 peptide equivalent to bulevirtide. Finally, similar to bepirovirsen, anti-HDV ASO may stimulate innate responses (at least human toll like receptor 8) and thereby be also considered as host targeting agents (HTA).
Conclusion: We provided the first proof of concept that ASO-based strategies, directed against HDV replication intermediates, may be effective for targeting HDV infection as both DAA and HTA, in a single drug, double bullet strategy.

THU-607
Hepatitis B surface antigen directly alters Dendritic cell-mediated natural killer cell responses

Lucile Dumolard[1], Marie-Noëlle Hilleret[1,2], Thomas Decaens[1,2], Philippe Saas[1,3], Evelyne Jouvin-Marche[1], Patrice Marche[1], Caroline Aspord[1,3], Zuzana Macek Jilkova[1,2]. *[1]Univ. Grenoble Alpes, Inserm U 1209, CNRS UMR 5309, Institute for Advanced Biosciences, Grenoble, France; [2]Hepato-Gastroenterology and Digestive Oncology Department, CHU Grenoble Alpes, Grenoble, France; [3]Etablissement Français du Sang Auvergne-Rhone-Alpes, R&D Laboratory, Grenoble, France*
Email: lucile.dumolard@univ-grenoble-alpes.fr

Background and aims: Hepatitis B, caused by the Hepatitis B virus (HBV), is a significant global health concern, often leading to chronic hepatitis B in individuals unable to mount an effective immune response. Chronic HBV substantially increases the risk of severe liver diseases, including cirrhosis and hepatocellular carcinoma. Dendritic cells (DC) and Natural killer (NK) cells play crucial roles in the early immune response to HBV, but their function is compromised in chronic hepatitis B patients. The precise mechanisms through which HBV disrupts immune responses remain unclear.
Method: We investigated how Hepatitis B surface antigen (HBsAg) influences the interplay between DC subpopulations and NK cells. Blood-derived DC subsets were pre-exposed to HBsAg and then co-cultured with NK cells under various stimulation conditions. We subsequently evaluated the modulations of DC, and the phenotypic and functional responses of NK cells. Similarly, DC subsets were exposed to serum from HBV-infected individuals with varying levels of HBsAg to assess their ability to stimulate NK cell responses.
Results: Our findings show that exposure to HBsAg selectively impairs NK cell activation, phenotype and degranulation in co-cultures with plasmacytoid DC, in a Toll-like receptor-9 (TLR9)-dependent manner. HBsAg also disrupts cDC2-mediated NK cell activation via TLR7/8-dependent pathways and cDC1-mediated NK cell degranulation via TLR3-dependent pathways. Such impairment was reproduced with serum of HBV patients in a HBsAg level-dependent manner.
Conclusion: These findings deepen our understanding of immune dysregulation in chronic HBV infection, highlighting the critical role of all DC subsets in orchestrating effective cross-talk with NK cells. By uncovering the mechanisms underlying DC-NK cell interactions, this work underscores the therapeutic potential of targeting DCs to restore immune competence.

THU-608
Uncovering the role of Ago2 binding as a potential innate immune evasion strategy during hepatitis E virus infection

Rui Marques da Costa[1,2], Vanessa Stolz[1,2], Maximilian Collatz[3,4,5], Sarah Schlienkamp[1,2], Manja Marz[3,3,5], André Gömer[1,2], Eike Steinmann[1,2]. *[1]Ruhr University Bochum Faculty of Medicine, Bochum, Germany; [2]Hepatitis E Virus Research Hub (HepE-Hub), Bochum, Germany; [3]RNA Bioinformatics and High-Throughput Analysis,*

Friedrich Schiller University, Jena, Germany; [4]European Virus Bioinformatics Center, Friedrich Schiller University, Jena, Germany; [5]Fritz Lipmann Institute-Leibniz Institute on Aging, Jena, Germany
Email: rui.marquesdacosta@rub.de

Background and aims: Hepatitis E virus (HEV) remains an understudied global health concern, causing an estimated 20 million infections and up to 70,000 deaths annually. While infections are often asymptomatic, HEV can become chronic in immunocompromised individuals and is associated with mortality rates of up to 30% in pregnant women. As a neglected disease, little is known about the steps that follow viral entry, uncoating and replication. Given the viral genome comprises a 5′-m7G cap and a polyadenylated tail, similar to host mRNAs, we hypothesized that HEV may be susceptible to cleavage by the host Argonaute proteins dampening replication and thus inhibiting the innate immune response.
Method: We employed *in vitro* HEV replication and infection assays in Ago2 knock down (KD) HepG2/C3A cells to assert the effect of viral RNA cleavage by Ago2 during the HEV replication cycle. We further employed a JAK inhibitor, baricitinib, to assess whether any Ago2 elicited effects would be additive to the interferon response. Finally, we aim to perform Argonaute 2 RNA co-precipitation to identify, if any, miRNA seed sites present in the HEV genome and describe the viral-host HEV miRNA interactome.
Results: Inhibition of Ago2 during HEV infection resulted in an enhancement of HEV viral infection as shown via ORF2 staining. Further, we could show that in Ago2 KD cells infected with HEV, there is an up to 2-fold increase in HEV RNA replication when compared to the non-targeting control. Interestingly, in the Ago2 KD model, baricitinib appears to work in tandem with siAgo2_2 to enhance replication. Finally, the miRNA interactome of HEV is currently being investigated via AgoCLIP (cross-linking and immunoprecipitation) and should highlight viral regions responsible for the recruitment of the host mRNA degradation machinery.
Conclusion: Together, these data suggest that HEV uses the host RISC (RNA-induced silencing complex) system. We hypothesize this functions as an innate immune response evasion mechanism. Further, replication data suggests that Ago2 interacts with the viral nucleic acids at multiple timepoints during infection. Importantly, given HEV infection may also occur as a zoonoses, further questions about differential regulation of viral replication by host small RNAs, depending on host tropism, remain to be addressed. Our data highlight the importance novel research avenues into an understudied virus and open the possibility for counterstrategies to control infection and better understand HEV pathogenesis.

THU-609
In vitro antiviral activity of the cyclophilin inhibitors against hepatitis delta virus infection

Rola Matar[1], Hakim Ahmed-Belkacem[1], Stéphane Chevaliez[1,2], Jean-Michel Pawlotsky[1,2], Daniel Candotti[1]. *[1]"Viruses, Hepatology, Cancer" Research Team Institut de Recherche Biomédicale, INSERM U955, Créteil, France; [2]Department of Virology, French National Reference Center for Hepatitis B, C and D Viruses, Hôpital Henri Mondor (AP-HP), Université Paris-Est, Créteil, France*
Email: rola.matar99@gmail.com

Background and aims: Hepatitis Delta Virus (HDV) causes the most severe form of viral hepatitis, with limited therapeutic options. Cyclophilin inhibitors (CypIs) have demonstrated broad antiviral activity against hepatotropic viruses. This study aimed to evaluate *in vitro* the antiviral activity of the well-characterized CypI Alisporivir (ALV) and a new prototype CypI, F832, against HDV infection in Huh106 cells, using Bulevirtide (BLV) as an inhibition control of viral infection.
Method: Huh106 cells were infected with HDV and treated with increasing concentrations of ALV or F832. Cytotoxicity (CC50) and antiviral activity (IC50 and therapeutic index, TI) were determined by monitoring intracellular HDAg expression. Intracellular HDAg levels were measured by Western blot, immunofluorescence, and HDAg-specific ELISA, while HDV RNA levels were measured by RT-qPCR.
Results: ALV inhibited HDAg expression in Huh106 cells in a dose-dependent manner, with an IC50 of 0.25 ± 0.03 µM, CC50 >10 µM, and TI >40. Intracellular HDAg became undetectable at concentrations ≥2.5 µM. F832 treatment also reduced HDAg levels but proved less effective, showing an IC50 of 0.56 ± 0.16 µM, CC50 >20 µM, and TI >35.7. Quantitative analysis by Western blot, ELISA, and immunofluorescence confirmed significant decreases in HDAg expression. Starting at 5 µM, ALV and F832 reduced the level of intracellular HDV RNA significantly.
Conclusion: ALV demonstrated significant antiviral activity against HDV in vitro, providing a rationale for further preclinical evaluation. F832 compound appeared promising, but further analyses are needed.

THU-610
Discovery of novel HDV entry inhibitors with selectivity over bile acid inhibition

David McGowan[1], Isabel Heremans[1], Lars Degrauwe[1], Frederick Degroote[1], Kusum Gupta[2], Lawrence Blatt[2], Julian Symons[2], David Smith[2], Yannick Debing[1]. *[1]Aligos Belgium, Leuven, Belgium; [2]Aligos Therapeutics, South San Francisco, United States*
Email: ydebing@aligos.com

Background and aims: Chronic hepatitis delta virus (HDV) infection affects about 4.5% of patients chronically infected with hepatitis B virus (HBV), corresponding to an estimated 12 million people. HDV is a satellite virus of HBV and is only found as a co-infection with HBV due to its dependence on the HBV surface antigen (HBsAg) for viral particle assembly. HBV and HDV enter hepatocytes via the sodium taurocholate cotransporting polypeptide (NTCP) receptor. A peptide inhibitor blocking NTCP, bulevirtide (BLV), was recently approved by the European Medicines Agency for chronic HDV infection. Two potential drawbacks of BLV are the required daily subcutaneous administration and the inhibition of bile acid (BA) transport, the natural function of NTCP. An entry inhibitor that is selective for antiviral inhibition over BA transport blockade could provide patients with a potentially superior antiviral treatment.
Method: Inhibition of HBV and HDV entry was evaluated in HepG2-NTCP cells by adding compound with the inoculum and measuring secreted HBeAg or intracellular HDAg and HDV RNA as read-outs. Inhibition of BA transport was assessed using a fluorescently labeled BA derivative. Entry specificity was confirmed using a time-of-addition setup where compound as added before, during or after infection. Competitive binding with BLV was investigated using flow cytometry with fluorescently labeled BLV as a probe. Liver microsome stability was measured in several species. In vivo pharmacokinetics were studied in rats after intravenous bolus dosing at 2 mg/kg.
Results: Screening of focused compound libraries for HBV entry and BA transport led to the identification of a hit series with limited antiviral potency but clear selectivity over BA transport. Exploration of the structure-activity relationship and further chemical optimization yielded a lead series with submicromolar EC_{50} antiviral potency and pronounced selectivity (>100-fold). Selected molecules demonstrated entry inhibition with EC_{50} values under 100 nM for HBV entry. Entry specificity was confirmed in HDV infection and time-of-addition assays. The lead series was shown to bind competitively with BLV. Representative examples were stable in human and rat liver microsomes and exhibited a PK profile upon IV dosing suitable for further optimization.
Conclusion: A lead series of entry inhibitors with potent antiviral activity and pronounced selectivity (>100-fold) over BA transport was identified. Further optimization of activity, selectivity and ADME is ongoing.

THU-611

Functional characterization of urine-associated hepatitis E virus mutations: effect on kidney infection and antiviral efficacy

Avista Wahid[1], Nele Meyer[1], Christine Wundes[1], Saskia Janshoff[2,3,4], Michelle Jagst[2], Martina Friesland[1], Katja Dinkelborg[1,5,6], Markus Cornberg[5,6,7,8], Benjamin Maasoumy[5,6], Daniel Todt[2,4,9], Heiner Wedemeyer[5,6], Thomas Pietschmann[1,6], Eike Steinmann[2], André Gömer[2], Patrick Behrendt[1,5,6]. *[1]Institute for Experimental Virology, TWINCORE, Centre for Experimental and Clinical Infection Research, a joint venture between the Helmholtz Centre for Infection Research and the Hannover Medical School, Hannover, Germany; [2]Department of Molecular and Medical Virology, Ruhr University Bochum, Bochum, Germany; [3]Herz- und Diabeteszentrum Nordrhein-Westfalen, Bad Oeynhausen, Germany; [4]Department for Translational and Computational Infection Research, Ruhr University Bochum, Bochum, Germany; [5]Department of Gastroenterology, Hepatology, Infectious Diseases and Endocrinology, Hannover Medical School, Hannover, Germany; [6]DZIF, Partner Site Hannover-Braunschweig, Hannover-Braunschweig, Germany; [7]Center for Individualised Infection Medicine (CiiM), Hannover, Germany; [8]German Center for Infection Research (DZIF), HepNet Study-House/German Liver Foundation, Hannover, Germany; [9]European Virus Bioinformatics Center, Jena, Germany*
Email: nele.meyer@twincore.de

Background and aims: Hepatitis E virus (HEV) is a major cause of acute viral hepatitis globally. In immunocompromised patients, it can lead to chronic infection and severe liver disease. Therapeutic options are limited; ribavirin (RBV), used off-label, is not always effective. Extrahepatic manifestations, including renal impairment, have been reported, but mechanisms and impact of compartment-specific variants remain poorly understood.
This study aimed to investigate whether various HEV strains are able to complete their replication cycle in kidney cell lines and to characterize urine-specific, patient-derived HEV variants in vitro, focusing on replication dynamics and antiviral responses.
Method: Two HEV-3 isolates and one HEV-1 strain were used to study replication and antiviral susceptibility in liver and several human kidney cell lines. To identify compartment-specific viral variants, HEV sequences from urine, stool, and plasma samples of chronically infected patients were analyzed. Urine-associated mutations were cloned into subgenomic reporter constructs and full-length HEV-3 p6 backbones. Replication efficiency, infectivity and RBV susceptibility were compared between liver and kidney cells. Ongoing work includes testing of additional antivirals and screens a 5-year Hannover Medical School (MHH) outpatient cohort for similar urine variants.
Results: Several kidney cell lines supported complete replication of HEV-3 p6 and replication of HEV-3 83-2 and HEV-1 Sar-55. Introduction of urine-specific, patient-derived mutations resulted in distinct phenotypes, affecting replication efficiency in a cell-type dependent manner (liver versus kidney cell lines) and altering RBV susceptibility. Overall, kidney cells showed a reduced RBV response compared to liver cells. Consistent trends in replication and drug response were observed in subgenomic and full-length constructs. Screening of the MHH cohort and testing of additional antivirals are ongoing.
Conclusion: Our data demonstrate that HEV can complete its replication cycle in kidney-derived cell lines in vitro and urine-specific, patient-derived variants can modulate replication efficiency and RBV susceptibility in a cell-type dependent manner. This supports a potential viral contribution to renal HEV manifestations and underscores the importance of compartment-specific viral evolution for antiviral efficacy. Ongoing cohort analyses and broader antiviral testing aim to define the clinical prevalence and therapeutic significance of urine-associated HEV variants.

THU-612-YI

Differential roles of HBc depending on its translation from spliced or unspliced HBV RNA

Dang Hoan Nguyen[1], Pierre Bablon[1], Clément Iriart[1], Jonathan Pol[2], Hélène Strick Marchand[3], Patrick Soussan[1], Jesus Brunetti[1]. *[1]Sorbonne Université, Inserm, Centre de Recherche de Saint-Antoine (CRSA), Paris, France; [2]INSERM UMR1138, Centre de Recherche des Cordeliers, Paris, France; [3]Innate Immunity Unit, Institut Pasteur, Université Paris Cité, Inserm U1223, Paris, France*
Email: patrick.soussan@inserm.fr

Background and aims: The hepatitis B virus (HBV) core protein (HBc) is involved in capsid assembly, virus-host interactions, and epigenetic regulation. An HBc isoform lacking Cys183 (HBc^{-Cys}), translated from spliced viral transcript sp1RNA, was shown to be critical for HBV wild-type (HBV^{wt}) infection in liver-humanized mice[1]. Furthermore, liver HBc^{wt} expression (translated from pgRNA) was markedly low in the liver of mice expressing HBV-invalidated for sp1RNA ($HBVsp1^{mut}$)[2]. Regulation of HBc^{wt} and HBc^{-Cys} expression was investigated *in vitro* and *in vivo*.
Method: Differentiated HepG2-NTCP and PHH cells were infected with either recombinant $HBVsp1^{mut}$ or HBV^{wt}. *In vivo* HBc expression was addressed by transduction of AAV expressing either HBV^{wt} or $HBVsp1^{mut}$ in C57Bl6, immune-deficient (NSG), and HBSP transgenic mice (10^{11} Geq AAV/mouse). Samples were studied by immunohistochemistry, western blot and PCR analyses.
Results: HBc^{wt} was easily detected in $HBVsp1^{mut}$-infected hepatic cells contrary to *in vivo* findings[1–3], suggesting an *in vivo* dependent regulation. *In vivo* comparison with HBV^{wt}, $HBVsp1^{mut}$ transduction revealed: 1) poor expression of HBc^{wt} and high levels of pgRNA in the liver; 2) slight reduction of viral load and similar amounts of HBcAg, HBsAg and HBeAg in blood. These data suggested that HBc^{-Cys} is mainly accumulated in liver while HBc^{wt} is mainly secreted in blood. The low level of HBc^{wt} liver-expression in AAV-$HBVsp1^{mut}$ remained unaffected by immune suppression or HBSP trans-complementation but was partially recovered by antiviral treatment. At higher transduction inoculum, HBc^{wt} accumulation in $HBVsp1^{mut}$ mice was partially restored only in mid-lobular hepatocytes while, in HBV^{wt} mice, all hepatocytes were positive along the liver lobule. The differential regulation of HBc expression resulted from the outcome of HBV transcripts. In HBV^{wt} mice, pgRNA represented only 40% of (sp1+pg) RNAs while almost all intracellular packaged HBV DNA forms resulted from pgRNA, suggesting that sp1RNA is mainly translated. Finally, the differential distribution of HBc isoforms was also related to the zonal transcriptomic profiles of the hepatic lobule.
Conclusion: HBV sp1RNA invalidation revealed that: 1) pgRNA is preferentially encapsidated compared with sp1RNA which is mainly translated into HBc^{-Cys} in mice; 2) viral egress is mainly driven by HBc^{wt}; 3) liver zonation is involved in HBc isoforms expression.

References

1. Chung *et al.* (*J. Hepatol* 2024).
2. Bablon *et al.* (*J. Hepatol* 2025).
3. Chung *et al.* (*J. Hepatol* 2025).

THU-613

Hyper-EINS: automated identification of temporal and dynamic host-derived insertions within the hepatitis E virus genome

Maximilian Nocke[1,2,3], Michael Wißing[4], Leonard Knegendorf[5,6], Patrick Behrendt[5,7,8], Heiner Wedemeyer[7,8], Eike Steinmann[3,4,9], Daniel Todt[1,2,3]. *[1]Department for Translational and Computational Infection Research, Ruhr University Bochum, Bochum, Germany; [2]European Virus Bioinformatics Center (EVBC), Jena, Germany; [3]Hepatitis E Virus Research Hub (HepE-Hub), Bochum, Germany; [4]Department for Molecular and Medical Virology, Ruhr University Bochum, Bochum, Germany; [5]Institute for Experimental Virology, TWINCORE Centre for Experimental and Clinical Infection Research, Hannover, Germany; [6]Institute for Medical Microbiology and Hospital*

Epidemiology, Hannover Medical School, Hannover, Germany; [7]Department of Gastroenterology, Hepatology, Infectious Diseases and Endocrinology, Hannover Medical School, Hannover, Germany; [8]German Center for Infection Research (DZIF), Partner Site Hannover Braunschweig, Hannover, Germany; [9]German Centre for Infection Research, External Partner Site, Bochum, Germany
Email: maximilian.nocke@rub.de

Background and aims: Most hepatitis E virus (HEV) infections are asymptomatic and self-limiting, while immunocompromised or other risk group patients may develop chronic courses. The hypervariable region (HVR) within HEV's first open reading frame (ORF1) is known to integrate sequences of human origin. Genomic rearrangements are discussed to be involved in disease severity and chronicity. Therefore, an automated and standardized method of insertion identification is required in diagnostics. Our aim was to develop and provide an automated approach for insertion identification to standardize the analysis of human and viral gene snippets integrated into the HEV genome. Furthermore, we elucidated potential dynamics of insertions within a viral population on longitudinal scale. Thereby, we would obtain critical knowledge about the nature of insertions.
Method: We collected longitudinal samples of a chronic infected patient experiencing ribavirin treatment failure.
To gather insights into insertions over the course of disease, we performed Illumina sequencing on the patient's samples. We applied our bioinformatics tool Hyper-EINS to identify insertions. These were compared between different timepoints based on sequence identity to assess potential evolutionary relations.
Results: The overall most frequent insertions found in the patient's data are derived from the genes SERPINA1 and TRIM22. Insertions of numerous genes were found to be present pretreatment. All insertions were eliminated from the viral population during early treatment, except for the SERPINA1 insertion, which persisted in lower frequency. During later treatment, multiple insertions were introduced into the viral population, while especially SERPINA1 and TRIM22 insertions rose in frequency and diversity. In our previous work, we identified two of those diverse insertions as replication-enhancing.
Conclusion: In this study we were able to show dynamic shifts of HVR insertions for the first time. We observed those shifts both during and after treatment. This emphasizes that insertions are subject to complex mechanisms within the viral population. While the SERPINA1 insertion associated with treatment failure was already present in the viral population before treatment, the currently available data does not allow failure prediction. Still, the observation of sudden diversification of insertions might be a possible indicator to halt treatment.

THU-617

Deep genomic analyses of database farmed hepatitis E virus genomes uncover genotype specific features

Maximilian Nocke[1,2,3], Eike Steinmann[3,4,5], Daniel Todt[1,2,3].
[1]Department for Translational and Computational Infection Research, Ruhr University Bochum, Bochum, Germany; [2]European Virus Bioinformatics Center (EVBC), Jena, Germany; [3]Hepatitis E Virus Research Hub (HepE-Hub), Bochum, Germany; [4]Department for Molecular and Medical Virology, Ruhr University Bochum, Bochum, Germany; [5]German Centre for Infection Research, External Partner Site, Bochum, Germany
Email: maximilian.nocke@rub.de

Background and aims: Open access virus databases provide an extensive amount of data harboring a valuable potential for meta-analyses. Hepatitis E virus (HEV) is organized in the taxonomic family *Hepeviridae*, with the species *Paslahepevirus balayani* covering the typical human pathogenic strains. Since HEV genotypes are associated with disease severity and course and reservoir host, a broader understanding of genomic commonalities and (sub-)genotypic specific features would result in more directed diagnostics and treatment development. In previous work, we developed a novel and runtime efficient typing algorithm to close gaps in publicly available sequence metadata. This laid the foundation for investigating diverging and shared genomic features of HEV genotypes and subgenotypes. Our aim was to identify subgenotype specific genomic regions or sequential patterns. By identifying potential marker regions of varying genomic positions, HEV typing in diagnostics and scientific context could become more precise and efficient. Furthermore, we aim to define a novel and consistent genome nomenclature to define amino acid positions and single nucleotide variants in a unified way.
Method: 1268 full genome *Hepeviridae* sequences were downloaded from the NCBI genbank. We developed an algorithm to ensure the quality of taxonomic labels for full genome HEV sequences farmed from public databases. Using this method, we investigated genome conservation on different taxonomic and genotype levels, performed k-mer sequence clustering and Shannon entropy analyses. Resulting data was combined, while taking all taxonomic and genotype labels into account.
Results: Alongside genotype specific patterns and marker regions, we were able to identify length polymorphisms unique to sub-genotypes. While those genomic features could ease the typing of viral populations, especially the latter make developing a unified nomenclature more complex but also more important.
Conclusion: In this study we found genetic patterns in all HEV open reading frames as well as length polymorphisms unique to HEV (sub-)genotypes. Thereby, those features indicate a link to severity and transmission route, which requires further testing for validation. Still, those genetic markers bear potential advantages for typing HEV both in diagnostics and research. Taking the identified features into account makes the development of a unified HEV nomenclature and amino acid numbering scheme more feasible.

THU-618

Distinct hepatic transcriptional programmes in chronic hepatitis B are reshaped by metabolic dysfunction

Eva Parisi[1], Chanelle Fernandes[1], Jantarika Arora[1], Corinna Pade[1], Apostolos Koffas[1,2], Patrick Kennedy[1,2], Upkar Gill[1,2]. *[1]Centre for Immunobiology & Infection, The Blizard Institute, Barts and The London Faculty of Medicine & Dentistry, Queen Mary University of London, London, United Kingdom; [2]Department of Hepatology, Barts Health NHS Trust, London, United Kingdom*
Email: u.gill@qmul.ac.uk

Background and aims: Chronic hepatitis B (CHB) is a major global cause of liver cancer, and metabolic dysfunction-associated steatotic liver disease (MASLD) increasingly co-exists with CHB, potentially accelerating liver disease progression. The molecular interaction between metabolic dysfunction and hepatitis B virus (HBV) remains incompletely understood. We characterised paired hepatic and peripheral gene expression patterns associated with metabolic dysfunction in HBV to identify pathways and candidate gene targets relevant to disease stratification and therapeutic development.
Method: Paired liver biopsy and PBMC samples were obtained from patients with untreated CHB with and without co-existing MASLD (n = 20). Bulk RNA sequencing was performed, and differential gene expression analysis was conducted using DESeq2 in R (v4.5.1). Differentially expressed genes were identified and subjected to pathway-level interpretation focusing on metabolic-associated transcriptional programmes.
Results: Comparative analysis identified a distinct hepatic gene expression profile in CHB-MASLD compared with CHB alone. CHB-MASLD was characterised by relative upregulation of stress-responsive genes implicated in nutrient sensing and inflammatory signalling, including ARRDC4, alongside downregulation of genes central to hepatocyte metabolic homeostasis. These included genes

involved in amino acid metabolism (TAT), urea cycle function (ASS1), growth hormone-IGF signalling (IGF1), and lysosomal metabolic regulation (RNF152), which were significant after multiple hypothesis testing (adjusted $p < 0.05$ and $|\log_2$ fold change$| > 1$). Pathway-level interpretation indicated coordinated alterations across metabolic, nutrient-sensing, and stress-associated transcriptional programmes. Overall, the hepatic transcriptomic profile in CHB-MASLD was consistent with altered metabolic regulation accompanied by relative enrichment of stress and inflammatory signalling pathways.
Conclusion: Untreated CHB with co-existent MASLD displays a hepatic gene expression profile distinct from CHB alone, marked by coordinated changes in metabolic pathways and relative enrichment of stress-associated and inflammatory transcriptional programmes. These findings support metabolic dysfunction as an important modifier of the hepatic molecular landscape in HBV infection and highlight pathways contributing to disease heterogeneity. Earlier therapeutic intervention in CHB-MASLD may therefore be important to mitigate or rebalance adverse transcriptional programmes.

THU-619

Plasma THC is inversely associated with insulin resistance before and after HCV cure in people with HIV–HCV coinfection (ANRS CO13 HEPAVIH and ELICSIR study)

Tangui Barre[1], Camelia Protopopescu[1], Alexandr Gish[2], Fabienne Marcellin[1], Morgane Bureau[1], Patrick Miailhes[3], Karine Ory[4], Vincent Di Beo[1], Florian Hakim[2], Jean-Michel Gaulier[2], Patrizia Carrieri[1]. *[1]Aix Marseille Univ, Inserm, IRD, SESSTIM, Sciences Economiques & Sociales de la Santé & Traitement de l'Information Médicale, ISSPAM, Marseille, France; [2]CHU Lille, Unité Fonctionnelle de Toxicologie, Lille, France, Univ. Lille, ULR 4483—IMPECS—IMPact de l'Environnement Chimique sur la Santé humaine, Lille, France; [3]Hôpital de Fleyriat, Service de Maladies Infectieuses et Tropicales, Bourg en Bresse, France; [4]Université Bordeaux, INSERM, MART, UMS 54, Bordeaux, France*
Email: camelia.protopopescu@inserm.fr

Background and aims: In HIV-HCV co-infection, chronic immune activation contributes to insulin resistance (IR), a key factor in steatosis, fibrosis progression, cardiometabolic and other extrahepatic complications. HCV cure may improve IR, while self-reported cannabis use has been associated with reduced steatosis and IR in both the general population and HIV–HCV coinfected people. Using data from the ANRS ELICSIR study, we investigated the associations between plasma cannabinoids, HCV cure, and insulin resistance defined by the Homeostatic Model Assessment for Insulin Resistance (HOMA-IR $\geq$2.77).
Method: ELICSIR study included participants from the ANRS CO13 HEPAVIH cohort of people with HIV–HCV coinfection, who achieved HCV cure and had available plasma samples and HOMA-IR measures in the 36 months before and after HCV cure (defined by sustained virological response 24 weeks after treatment end). Plasma exocannabinoids (cannabidiol, tetrahydrocannabinol (THC), and THC-COOH metabolite), endocannabinoids, other xenobiotics, and inflammatory markers were measured using high-resolution liquid chromatography–tandem mass spectrometry. Associations between cannabinoids and IR were evaluated using a multivariable mixed-effects logistic regression model, adjusted for HCV cure and other factors.
Results: The study included 270 participants (71.1% men) contributing 518 measurements. At baseline visit (i.e., before cure), median age was 50 (IQR: 45–54) years, 20% had advanced liver fibrosis (FIB-4 >3.25), IR was present in 46.3%, while THC-COOH was detected in 27.1% of participants. Higher IR prevalence was found among participants without detectable THC-COOH (51.1% vs 33.3%, p = 0.012). In multivariable analysis, among cannabinoids, only THC-COOH was independently associated with lower odds of IR (OR: 0.36, 95% CI: 0.16–0.81). Besides, IR was associated with older age, overweight/obesity, longer time since HIV diagnosis, and higher C-reactive protein levels, and inversely associated with HCV cure.
Conclusion: For the first time, plasma THC-COOH detection was found independently associated with lower insulin resistance in HIV–HCV coinfected people, irrespective of HCV cure and overweight/obesity. Although the underlying mechanisms remain to be elucidated, these findings support further investigation in randomized clinical trials of cannabinoids—particularly more acceptable non-psychoactive compounds and smoke-free formulations—to reduce insulin resistance and related metabolic complications in at-risk populations.

THU-620

Preclinical characterization of ALG-093940, a potent and orally bioavailable small molecule PD-1/PD-L1 inhibitor for the treatment of chronic hepatitis B infection and liver cancer

Heleen Roose[1], Kristina Rekstyte-Matiene[1], Sarah Stevens[2], Kusum Gupta[2], Sandra Chang[2], Nour Fayyad[1], Nega Gerard[3], Cheng Liu[2], Vladimir Serebryany[2], Lillian Adame[2], Kha Le[2], Antitsa Stoycheva[2], Dinah Misner[2], Lawrence Blatt[2], Leonid Beigelman[2], Sushmita Chanda[2], Adam Gehring[3,4], David Smith[2], Julian Symons[2], Andreas Jekle[2], Tongfei Wu[1]. *[1]Aligos Belgium, Leuven, Belgium; [2]Aligos Therapeutics, South San Francisco, United States; [3]Schwartz Reisman Liver Research Centre, University Health Network, Toronto, Ontario, Canada; [4]Department of Immunology, University of Toronto, Toronto, Ontario, Canada*
Email: hroose@aligos.com

Background and aims: PD-1/PD-L1 antibody-based therapies have demonstrated success in the treatment of liver cancer and have exhibited potential for reversing immune tolerance in chronic hepatitis B (CHB). Recently, PD-L1 small molecule inhibitors have been developed, e.g., INCB086550 which demonstrated clinical response in cancer, and AB-101 that demonstrated a transient HBsAg decline in 2 out 10 CHB patients in a phase I study. Here, we report the characterization of ALG-093940, a potent and orally bioavailable small molecule PD-1/PD-L1 inhibitor that binds to PD-L1 and promotes PD-L1 dimerization, internalization and degradation, offering a distinct mechanism of action with potential advantages over PD-1/PD-L1 antibody therapeutics.
Method: Inhibition of PD-1/PD-L1 in cell culture was measured using PD-1 expressing Jurkat NFAT luciferase T cells and CHO-hPD-L1 cells. Ex vivo restoration of HBV specific T cell function in subjects with chronic HBV infection was analyzed using fluorospot assay. *In vivo* PK/PD/efficacy were assessed in a humanized-PD-L1 MC38 subcutaneous tumor mouse model. Tolerability in mice and safety and tolerability in rats and cynomolgus monkeys were evaluated after oral administration.
Results: ALG-093940 showed comparable T-cell activation potency to INCB086550. Furthermore, treatment of CHO-hPD-L1 cells with ALG-093940 resulted in internalization and reduction of PD-L1 protein levels. In ex vivo human PBMC assays, ALG-093940 demonstrated PD-L1 target engagement, T cell activation and immune cell mediated tumor cell killing. Importantly, ALG-093940 demonstrated the ability to restore ex vivo T cell functionality in PBMC from HBV infected subjects. *In vivo* ALG-093940 exhibited dose-dependent PD-L1 target engagement. Tumor growth inhibition and tumor size correlated with tumor-infiltration of $CD8^+$ T-cells. In addition, ALG-093940 was well tolerated when orally administered daily in mice for 40 days, in rats for 14 days and in cynomolgus monkeys for 3 days.
Conclusion: ALG-093940, an orally available small molecule, is a potent PD-1/PD-L1 inhibitor targeting PD-L1 dimerization, internalization and degradation. ALG-093940 demonstrated excellent efficacy and safety, warranting further evaluation as a potential clinical candidate for the treatment of CHB and liver cancer.

THU-621

Verification and validation data of the CE-IVD marked AltoStar® HDV RT-PCR Kit 1.5 for monitoring HDV RNA viral load in plasma and serum samples

Karin Rottengatter[1], Philip Rosenstock, Angeles Jimenez[1]. [1]*Altona Diagnostics GmbH, Hamburg, Germany*
Email: karin.rottengatter@altona-diagnostics.com

Background and aims: Next to precise HDV RNA detection and quantification, automation covering extraction of the nucleic acid for amplification of the specific HDV target is pivotal for diagnosis and monitoring of response to newly approved treatment in HDV infectious disease. Limit of Detection, Linearity and precision are basic information required for diagnostic laboratories. Here we show parts of the comprehensive verification data of the CE-IVD marked AltoStar® HDV-RT PCR Kit 1.5 used within the AltoStar® Molecular Diagnostic Workflow.
Method: Human EDTA plasma and serum samples were used next to the WHO 1st International HDV RNA Standard (PEI code 7657/12) and external proficiency panel samples (INSTAND, QCMD). Testing the analytical specifications followed the respective requirements of the Regulation (EU) 2017/746 (IVDR) and CLSI Standards.
Results: All results are based on the AltoStar® HDV RT-PCR Kit 1.5 in combination with the AltoStar® Internal Control 1.5 and the AltoStar® Automation System AM16 on the CFX96™ Deep Well Dx System (Bio-Rad). The Limit of Detection was determined with 1.12 IU/ml [95% CI 0.72 to 2.20 IU/ml] for genotype 1 (WHO Standard) and confirmed for the other seven genotypes. The Linear Range was defined based on patient sample material with 2.00E+01 IU/ml to 1.00E+06 IU/ml, and based on additional IVT testing extended to 1.00E+08 IU/ml. Trueness to the WHO Standard ($\leq \pm 0.10$ $\log_{10}$ IU/ml), repeatability, with-in laboratory precision and inter-laboratory precision were analysed (all CV% ≤5%). Proficiency panel data confirmed correct qualitative and quantitative testing.
Conclusion: Accurate measurement of molecular targets, such as HDV RNA is essential for correct disease diagnosis, monitoring, and treatment decision-making. Standardization by automation minimizes variability across different laboratories, enhancing the comparability of results and ensuring consistency in patient care.

THU-622-YI

A novel human liver chimeric mouse model to study Hepatitis B virus DNA integration

Melina Schäfer[1], Tassilo Volz[1,2], Annika Volmari[1,2], Kristoffer Riecken[3], Boris Fehse[2,3], Maura Dandri[1,2], Lena Allweiss[1,2]. [1]*University Medical Center Hamburg-Eppendorf, I. Department of Medicine, Hamburg, Germany;* [2]*German Center for Infection Research (DZIF) Hamburg-Lübeck-Borstel-Riems site, Hamburg, Germany;* [3]*University Medical Center Hamburg-Eppendorf, Department of Stem Cell Transplantation, Research Department Cell and Gene Therapy, Hamburg, Germany*
Email: me.schaefer@uke.de

Background and aims: Hepatitis B virus (HBV) integrates parts of its DNA into the host genome early upon infection. Although not required for viral replication, integrations are observed in all phases of acute and chronic hepatitis B. They contribute to hepatocellular carcinoma (HCC) development through multiple, not fully defined mechanisms, including viral protein expression, genomic instability and disruption of cancer-associated genes. We aimed to establish a mouse model to generate primary human hepatocytes (PHH) *in vivo* harboring HBV DNA integrations and to investigate how these affect host and viral parameters.
Method: The model uses human liver chimeric urokinase-type plasminogen activator/severe combined immunodeficiency/beige/interleukin 2 receptor gamma −/− (USG) mice and introduces a prototypic HBV DNA integration via lentiviral gene transfer in PHH. This integration comprises the viral surface proteins (HBs) and regulatory X protein open reading frames under endogenous promotors and a downstream enhanced green fluorescent protein (eGFP) sequence. Integrations and integration-derived viral RNA and proteins were characterized by histology, qPCR, Western blot and RNA or DNA in situ hybridization (ISH).
Results: PHH were transduced *ex vivo* (average efficiency 25%) and transplanted into naïve USG mice, leading to the repopulation of mouse livers with clusters of integration-carrying and integration-free PHH. The presence of integrations did not hinder PHH proliferation, as repopulation levels were comparable between integration-carrying and control mice. Consistently, the *in vivo* distribution of eGFP-positive cells resembled initial transduction rates, with an average *in vivo* integration level of 21% (range 5–39%; n = 10). Intrahepatic viral RNAs and DNA were detected by qPCR and HBsAg was secreted into the mouse serum. eGFP and HBsAg could be visualized via histological staining and distinct HBs forms were detected by Western blot. Integrated DNA and expressed RNAs were also visualized at the single-cell level by DNA- and RNA-ISH.
Conclusion: We created a unique model to generate PHH harboring HBV DNA integrations and to study their role in HBV persistence and early carcinogenic events in primary cells *in vivo*. Additional applications include the evaluation of treatments targeting integrations or establishing hepatitis D virus mono-infections.

THU-623-YI

Arrayed human and porcine ISG screens identify hepatitis E virus host restriction factors

Sarah Schlienkamp[1,2], Luca Nörthemann[1,2], André Gömer[1,2], Eleftherios Michailidis[3,4], Yannick Brüggemann[1,2], Daniel Todt[2,5,6], Florian Vondran[7], Axel Hamprecht[8], Finn Grey[9], Charles Rice[4], Volker Kinast[8], Eike Steinmann[1,2,10]. [1]*Department for Molecular and Medical Virology, Ruhr University Bochum, Bochum, Germany;* [2]*Hepatitis E Virus Research Hub (HepE-Hub), Bochum, Germany;* [3]*Laboratory of Biochemical Pharmacology, Department of Pediatrics, School of Medicine, Emory University, Atlanta, United States;* [4]*Laboratory of Virology and Infectious Disease, The Rockefeller University, New York, United States;* [5]*Department of Translational and Computational Infection Research, Ruhr University Bochum, Bochum, Germany;* [6]*European Virus Bioinformatics Centre (EVBC), Jena, Germany;* [7]*Department of General, Visceral, Pediatric and Transplant Surgery, University Hospital RWTH Aachen, Aachen, Germany;* [8]*Department of Medical Microbiology and Virology, Carl von Ossietzky University Oldenburg, Oldenburg, Germany;* [9]*The Roslin Institute, University of Edinburgh, Edinburgh, United Kingdom;* [10]*German Centre for Infection Research (DZIF), External Partner Site, Bochum, Bochum, Germany*
Email: sarah.schlienkamp@rub.de

Background and aims: For hepatitis E virus (HEV) genotype 3, an emerging zoonotic pathogen, the primary reservoirs are pigs and deer. HEV can cause fulminant hepatitis and lead to liver cirrhosis and liver failure in humans, but it is apathogenic in pigs. Based on this divergent progression of HEV infection, this study was designed to evaluate the role of the innate immune response during HEV infection in human and porcine hepatocytes. Further, we aimed to identify human and porcine ISGs with antiviral properties against HEV to ultimately define species-specific host restriction factors of HEV.
Method: Utilizing primary human and porcine hepatocytes (PHH and PPH, respectively), we performed HEV infection experiments and modulated the innate immune response by application of JAK-inhibitors and IFNs. We further made use of arrayed human and porcine ISG libraries which comprise ~400 ISGs each. To characterize individual ISGs with potential restrictive effect on HEV, we performed infection experiments, subgenomic replicon systems, immunofluorescence microscopy analysis and IFN-beta reporter assays.
Results: JAK-inhibitor treatment of PHH and PPH revealed a 50-fold and 400-fold increase of progeny virus production upon HEV infection, suggesting that the canonical IFN-response is critical to

control HEV propagation. By taking advantage of the arrayed ISG libraries, we identified ISG products with promising anti-HEV activity including uncharted factors such as EAAT3. Validation in hepatoma cell lines and further experiments suggest that EAAT3 restricts the entry process of HEV.
Conclusion: The innate immune response is essential for controlling HEV infection in primary human and porcine hepatocytes. By screening for human and porcine ISGs as potential HEV restriction factors, we characterized antiviral strategies of different host species and thereby provide an initial step towards a deeper understanding of how species-specificity in innate immune responses potentially determine HEV pathogenesis.

THU-624-YI
Characterization of isogenic hepatitis B virus variants transcriptomically links the basal core promoter mutation to a subset of hepatitis B-associated hepatocellular carcinoma
Leon Louis Seifert[1], Georgios Dangas[2], Yingpu Yu[1], Chenhui Zou[1], Hong Hur[1], Catherine Freije[1], Xupeng Hong[1], Mengyin Zhang[1], Corrine Quirk[1,3], Yichen Zhou[1,3], Kosuke Ogata[4], Manoj Kandpal[1], Charles Rice[1], William Schneider[1], Eleftherios Michailidis[2], Ype De Jong[1,3]. *[1]The Rockefeller University, New York, United States; [2]Emory University, Laboratory of Biochemical Pharmacology, Department of Pediatrics, Atlanta, United States; [3]Division of Gastroenterology and Hepatology, Weill Cornell Medicine, New York, United States; [4]Department of Molecular and Cellular BioAnalysis, Kyoto University, Kyoto, Japan*
Email: lseifert@rockefeller.edu

Background and aims: Hepatitis B virus (HBV) is generally considered non-cytopathic virus. Basal core promoter (BCP) and precore (PC) mutant variants are clinically associated with worse disease outcomes in chronic HBV. Infection studies on these variants in human hepatocyte chimeric mice have been limited by the lack of isogenic viral stocks. In this study, we sought to characterize how the PC and BCP mutations affected viral parameters and human hepatocyte responses in human hepatocyte chimeric mice.
Method: We developed an efficient method for generating infectious HBV stocks from genetically engineered HBV sequences, and performed HBV infection experiments in immunodeficient human hepatocyte chimeras with WT, PC, and BCP mutant variants of three isolates from genotypes HBV-A, -C, and -D. Viral parameters were measured longitudinally, and liver samples were collected at peak viremia for RNAseq.
Results: Following infection, the PC and BCP variants remained genetically stable and no reversion was observed. Across genotypes, the BCP mutant reduced serum HBeAg levels by ~90% compared to WT, whereas serum HBeAg was undetectable in PC mutant infections. While no differences in viremia kinetics were observed between WT and PC mutant infection across isolates, the BCP mutant accelerated viral kinetics in HBV-D and HBV-A. The single mutant variants exhibited no significant difference in HBV-C infection; however, an engineered double-mutant (PC + BCP mutations combined) accelerated viremia compared to HBV-C WT. Relative to uninfected mice, WT HBV infection showed significantly different transcriptomic profiles, with additional differences between HBV genotypes. KEGG pathway analysis revealed an enrichment of cancer-associated pathways in HBV-D BCP-infected mice. Notably, gene expression in these HBV-D BCP infected livers showed significant overlap with a distinct subset of HBV-associated HCCs from the TCGA dataset, previously linked to impaired survival.
Conclusion: In immunodeficient human hepatocyte chimeric mice, the BCP mutation induces isolate-dependent changes in viral kinetics and host transcriptional responses that are distinct from isogenic WT and PC mutant virus. In HBV-D, BCP mutant infection is associated with cancer-related gene expression that partly overlaps with poor-prognosis of HBV-HCCs. These data support an active role for the HBV BCP mutation in liver disease progression.

THU-625
Clustered regularly interspaced short palindromic repeats associated protein 9 guide RNA circular templates reduce hepatitis B virus replication via covalently closed circular DNA degradation
Deok Hwa Seo[1], Yeochan Yun[2], Min Gu Kim[3], Songmee Bae[4], Yong Kwang Park[4], Hyeon-Yeol Cho[2], Pil Soo Sung[5]. *[1]Department of Medical Sciences, Graduate School of The Catholic University of Korea, Seoul, Korea, Rep. of South; [2]Department of Bio and Fermentation Convergence Technology, Kookmin University, Seoul, Republic of Korea, Seoul, Korea, Rep. of South; [3]Department of Medical Sciences, Graduate School of The Catholic University of Korea, Republic of Korea, Seoul, Korea, Rep. of South; [4]Division of Chronic Viral Diseases, Center for Emerging Virus Research, National Institute of Health, Cheongju, Republic of Korea, Cheongju, Korea, Rep. of South; [5]Department of Medical Sciences, Graduate School of The Catholic University of Korea, Republic of Korea, Division of Gastroenterology and Hepatology, Department of Internal Medicine, College of Medicine, Seoul St. Mary's Hospital, The Catholic University of Korea, Seoul, Republic of Korea, Seoul, Korea, Rep. of South*
Email: smin0904@naver.com

Background and aims: Chronic hepatitis B virus (HBV) infection persists because covalently closed circular DNA (cccDNA) serves as a stable nuclear template for viral transcription. Nucleos(t)ide analogues suppress replication but do not eliminate cccDNA. We aimed to develop an RNA nanoparticle platform generated from circular templates encoding CRISPR associated protein 9 (Cas9) and guide RNA (gRNA) to promote cccDNA degradation and suppress HBV replication.
Method: Circular DNA templates encoding Cas9 and HBV-targeting gRNA were transcribed by rolling circle transcription (RCT) to form RNA nanoparticles, then conjugated with poly-L-lysine and N-acetylgalactosamine (GalNAc) for hepatocyte targeting. Antiviral activity was tested in HepAD38 replication and HepG2-NTCP infection models (n = 3 each). Intracellular cccDNA was quantified by quantitative polymerase chain reaction and secreted hepatitis B surface antigen (HBsAg) by enzyme-linked immunosorbent assay. Particle size and zeta potential were assessed by dynamic light scattering.
Results: Unmodified nanoparticles averaged ~60 nm, increasing to ~80 nm after poly-L-lysine and ~100 nm after GalNAc conjugation, with a zeta potential shift from negative to neutral or partially positive values. Cas9-gRNA circular template nanoparticles reduced intracellular cccDNA by 24% ($p = 0.018$) and HBsAg secretion by 41% ($p = 0.006$) versus controls, consistently across both models.
Conclusion: Cas9-gRNA circular templates generate functional RNA nanoparticles that reduce HBV cccDNA and suppress viral antigen production in vitro. This modular strategy supports further development of direct cccDNA-targeting therapeutics for chronic hepatitis B.

THU-626
The homeobox family suppresses hepatitis B virus via a key non-Immunosuppressive pathway during the active phases of chronic hepatitis B
Lin Yujie[1], Qiu Qian[1], Jing Liu[2], Shaokun Pan[3], Jinyu Wang[1], Youhua Xie[2], Jiming Zhang[1], Zhongliang Shen[1]. *[1]Department of Infectious Diseases, Huashan Hospital, Fudan University, Shanghai Shi, China; [2]Shanghai Medical College, Fudan University, Shanghai Shi, China; [3]Shanghai Institute of Infectious Diseases and Biosecurity, Fudan University, Shanghai Shi, China*
Email: shenzhongliangnjnu@163.com

Background and aims: Hepatitis B e antigen (HBeAg)-positive chronic hepatitis (EPH) and HBeAg-negative chronic hepatitis (ENH) phase are two critical periods in the natural history of chronic hepatitis B (CHB). Previous studies have suggested that immune-mediated liver injury is the key mechanism driving the decline in viral load, focusing primarily on the "external" attack by the immune system on infected cells. However, it remains unclear

whether hepatocytes themselves possess a shared and critical set of antiviral genes or regulatory networks during these two phases, capable of efficiently suppressing HBV gene expression and replication. We previously reported that the homeobox gene MSX1 is significantly upregulated in hepatocytes during the EPH phase. By activating the expression of DNAJA4, a member of the heat shock protein 40 family, MSX1 triggers the proteasome degradation pathway to degrade the HBV X protein, thereby inhibiting HBV covalently closed circular DNA transcription. This finding suggests that the homeobox family may be involved in intracellular antiviral responses during CHB active phases.

Method: We constructed an overexpression plasmid library representing 16 subfamilies of the homeobox family and compared their antiviral functions in bont *in vitro* and *in vivo models*. Subsequently, we analyzed gene expression in liver biopsy tissues across four natural history phases of CHB using transcriptomics and single-cell sequencing technologies. Molecular mechanisms underlying homeobox-mediated activation of DNAJA4 expression and DNAJA4-mediated degradation of HBx were explored through such as bioinformatics, dual-luciferase reporter assays, and protein-protein interaction experiments.

Results: All selected homeobox subfamily members significantly suppressed HBV gene expression and replication, with BARX1, NKX1-1, and SHOX exhibiting particularly strong antiviral activity. Homeobox proteins transcriptionally activate DNAJA4 expression, promoting the degradation of HBx via a ubiquitin-independent proteasome pathway. Different members of homeobox proteins are expressed in a complementary manner during the EPH and ENH phases, while DNAJA4 is consistently and significantly upregulated in both phases. This indicates that the regulatory network of homeobox proteins converges at the level of DNAJA4.

Conclusion: The suppression of HBV mediated by the homeobox family deepens our understanding of the pathological basis of CHB and may offer potential targets for novel therapeutic strategies.

THU-627

Hepatocellular carcinoma is a viral reservoir during hepatitis C treatment with direct-acting antivirals

Mario Jorge Silva[1,2], Fatima Oliveira Martins[2], Ana Patricia Negrinho[2], Antonio Figueiredo[3], Carina Santos[3], Maria Helena Gloria[4], Pedro Lages Martins[1,2], Elizabeth Padua[5], Pedro Carreiro-Martins[2], Jorge Canena[1,2,6,7], Mario Oliveira[3], Hugo Pinto Marques[2,8], Filipe Calinas[1], Silvia Vilares Conde[2]. *[1]Unidade Local de Saúde de São José – Serviço de Gastrenterologia, Lisboa, Portugal; [2]NOVA Medical School, Lisboa, Portugal; [3]Unidade Local de Saúde de São José – Serviço de Anatomia Patológica, Lisboa, Portugal; [4]Unidade Local de Saúde de São José – Unidade de Transplantes, Lisboa, Portugal; [5]Instituto Nacional de Saúde Dr. Ricardo Jorge, Lisboa, Portugal; [6]Hospital CUF Tejo - Centro Universitário de Gastrenterologia, Lisboa, Portugal; [7]Unidade Local de Saúde Amadora-Sintra – Serviço de Gastrenterologia, Lisboa, Portugal; [8]Unidade Local de Saúde de São José – Centro Hepato-Bilio-Pancreático e de Transplantação, Lisboa, Portugal*
Email: mariojorgesilva01@gmail.com

Background and aims: The presence of hepatocellular carcinoma (HCC) has been associated with reduced efficacy of hepatitis C treatment with direct-acting antivirals (DAA), but the underlying biological mechanisms remain unclear. We aimed to investigate whether HCC acts as a viral reservoir during treatment of hepatitis C with DAA.

Method: We analyzed patients with liver cirrhosis and viable HCC who underwent liver transplantation during ongoing DAA therapy at a national referral center between 2015 and 2024. Hepatitis C virus (HCV) was quantified in explanted livers, in both tumoral (HCC) tissue and adjacent non-tumoral liver tissue. Viral quantification was performed by measuring immunofluorescence (IF) intensity for the HCV nonstructural 3 (NS3) protein, assessed by widefield microscopy and quantified with Fiji® software. Molecular quantification of HCV RNA was tried but not feasible (presumably due to viral RNA degradation). Statistical analyses were performed using STATA v12.1®. The study was approved by the institutional Ethics Committees.

Results: Fifteen patients were included; 87% were male. Liver transplantation was performed between day 14 and day 115 of DAA therapy. Eight patients received sofosbuvir/ledipasvir±ribavirin, six received sofosbuvir + daclatasvir±ribavirin and one received sofosbuvir + ribavirin. During the first 50 days of treatment (n = 8), HCV presence was significantly higher in tumoral (HCC) tissue than in non-tumoral liver tissue (median IF in tumoral tissue 3.01 [0.22–55.77] vs 0.39 [0.18–2.81] in non-tumoral tissue, p = 0.01). After 50 days of therapy (n = 7), HCV levels were similarly low in both tumoral and non-tumoral tissues (median IF in tumoral tissue 0.22 [0.03–2.4] vs. 0.39 [0.27–1.72] in non-tumoral tissue, p = 0.31). None of those patients developed post-transplant HCV recurrence. In both univariate and multivariable analyses - including HCV genotype and baseline pre-treatment viral load, loco-regional HCC therapies, liver function, antiviral regimen, and treatment duration - a significant negative correlation (p = 0.04) was observed between DAA treatment duration and HCV IF intensity, exclusively in HCC tissue.

Conclusion: During treatment of hepatitis C with DAA in cirrhotic patients with viable HCC, HCV persisted longer within HCC tissue than in non-tumoral liver tissue. These findings support the role of HCC as a viral reservoir during treatment of hepatitis C with DAA.

THU-628

The miR-4461-FGA regulatory axis characterises hepatitis B virus infection and HBV-related hepatocarcinogenesis

Aiko Sakai[1], Masaya Sugiyama[1]. *[1]Department of Viral Pathogenesis and Controls, National Institute of Global Health and Medicine, Japan Institute for Health Security, Tokyo, Japan*
Email: sugiyama.m@jihs.go.jp

Background and aims: Hepatitis B virus (HBV) infection leads to heterogeneous clinical outcomes, including hepatocellular carcinoma (HCC), through mechanisms not fully explained by chronic inflammation. MicroRNAs (miRNAs) are key regulators of gene expression, yet HBV-specific miRNA alterations and their functional consequences remain unclear. This study aimed to identify HBV-associated miRNAs at the single-cell level and to clarify their downstream targets and clinical relevance.

Method: Human liver single-cell RNA sequencing (scRNA-seq) was analysed to identify miRNAs altered in HBV-infected hepatocytes. miR-4461 expression was examined in HBV-transfected HuH7 and HepG2 cells and in HBV-infected primary human hepatocytes. Target genes were predicted using multiple databases and validated by 3′ UTR luciferase reporter assays. Plasma miR-4461 and fibrinogen alpha chain (FGA) levels were measured in patients with HBV infection, hepatitis C virus (HCV) infection, and HBV-derived HCC, including paired samples before and after tumour resection.

Results: scRNA-seq analysis of human liver revealed significant downregulation of miR-4461 specifically in HBV-infected hepatocytes. Consistently, miR-4461 expression was reduced in HuH7 and HepG2 cells following HBV transfection and in primary hepatocytes infected with HBV. In silico analysis demonstrated that miR-4461 did not directly bind to HBV RNA, suggesting an indirect mechanism. Among genes commonly predicted across multiple miRNA target databases, FGA was identified as a candidate target. Overexpression of miR-4461 resulted in reduced FGA protein levels, and luciferase reporter assays using the FGA 3′UTR confirmed direct repression by miR-4461. Clinically, plasma miR-4461 levels were significantly lower, while FGA concentrations were higher, in HBV patients compared with HCV patients ($P < 0.05$). These inverse changes were more pronounced in patients with HBV-derived HCC. Importantly, paired analysis before and after surgical resection of HCC demonstrated an increase in miR-4461 levels accompanied by a decrease in FGA levels after tumour removal ($P < 0.05$).

Conclusion: miR-4461 is selectively downregulated in HBV-infected hepatocytes and HBV-derived HCC and directly suppresses FGA expression via its 3′UTR. The consistent inverse relationship between miR-4461 and FGA across single-cell data, experimental models, and patient plasma supports a role for the miR-4461–FGA axis in HBV-specific hepatocarcinogenesis and highlights its potential as a biomarker.

THU-629

AZD6750, a CD8α-guided IL-2 molecule, enhances hepatitis B virus-specific CD8+ T-cell activation and function

Phillip Swanson II[1], Michael Powell[1], Marcelino Padilla[1], Galit Alter[1].
[1]*AstraZeneca, Gaithersburg, United States*
Email: phillip.swanson@astrazeneca.com

Background and aims: Chronic hepatitis B infection was estimated to affect ~254 million people and caused ~1.1 million deaths in 2022. Current treatment options rarely achieve functional cure, defined as sustained hepatitis B surface antigen loss with hepatitis B virus (HBV) DNA suppression post-treatment, underscoring the need for novel treatment strategies. Antiviral CD8+ T cells are critical for clearing infected hepatocytes and reducing the viral reservoir. Preclinical studies show that restoring CD8+ T-cell function can improve antiviral control. AZD6750, a CD8-guided IL-2 mutein fusion protein, is engineered to preferentially expand and activate CD8+ T cells. We evaluated whether AZD6750 selectively augments HBV-specific CD8+ T cells and enhances antiviral function.
Method: Peripheral blood mononuclear cells from 12 patients with chronic hepatitis B were cultured with AZD6750 to assess immunogenicity and antiviral activity. Pharmacodynamic effects on peripheral immune subsets were quantified by flow cytometry after exposure to AZD6750. The effects of AZD6750 on the phenotype and function of HBV-specific CD8+ T cells were evaluated by intracellular cytokine staining following HBV peptide stimulation. Antigen-specific activity was determined using *in vitro* cytolytic assays against HBV peptide-pulsed target cells.
Results: AZD6750 expanded CD8+ T cells at a 42-fold lower dose than recombinant IL-2 and showed preferential activity, achieving CD8+ T-cell expansion at doses 287-fold and 9-fold lower than those required for CD4+ T cells and NK cells, respectively. Within the expanded CD8+ T-cell pool, AZD6750 drove a dose-dependent increase in the frequency and number of IFNg and TNFa-producing HBV-specific CD8+ T cells, accompanied by elevated activation/proliferation markers (CD69, Ki-67) and cytotoxic mediators (Granzyme B, perforin). AZD6750 also induced a dose-dependent increase in antigen-specific cytolytic activity.
Conclusion: AZD6750 preferentially expands and activates CD8+ T cells, including HBV-specific subsets, from patients with chronic hepatitis B and enhances antigen-specific cytolysis of target cells. These findings support further investigation of AZD6750 as a potential immunotherapy aimed at advancing toward functional cure for chronic hepatitis B.

THU-633

The impact of single-nucleotide variants of hepatitis B virus and antiviral on liver cancer in gray zone patients

Wei Teng[1,2], Ting-Tsung Chang[3], Chien-Wei Su[4,5], Jun-Hao Xu[1], Chiu-Chi Hsu[1], Yu-Cheng Chang[1], Wen-Chun Liu[6], Yu-Wei Chiou[1,7], Yu-Chuan Chang[1,7], Jenny Yuh-Jin Liang[1,7,8], Jaw-Ching Wu[1,7,8].
[1]*Institute of Clinical Medicine, National Yang Ming Chiao Tung University, Taipei, Taiwan;* [2]*Department of Gastroenterology & Hepatology, Chang Gung Memorial Hospital, Linkou Medical Center, Taoyuan, Taiwan;* [3]*Department of Internal Medicine, National Cheng Kung University Hospital, College of Medicine, National Cheng Kung University, Tainan, Taiwan;* [4]*Division of General Medicine, Department of Medicine, Taipei Veterans General Hospital, Taipei, Taiwan;* [5]*School of Medicine, College of Medicine, National Yang Ming Chiao Tung University, Taipei, Taiwan;* [6]*Department of Nursing, National Tainan Junior College of Nursing, Tainan, Taiwan;* [7]*Translational Research Division, Medical Research Department, Taipei Veterans General Hospital, Taipei, Taiwan;* [8]*Cancer and Immunology Center, National Yang Ming Chiao Tung University, Taipei, Taiwan*
Email: penfieldwu@gmail.com

Background and aims: This study investigated the impact of single-nucleotide variants (SNVs) in the HBV Pre-S/S region on tumor development, related mechanisms, and evaluated the role of antiviral therapy in chronic hepatitis B (CHB) patients with these SNVs who were in the "gray zone" (ALT <80 U/L or HBV DNA <2000 IU/ml) according to Asian-Pacific guideline.
Method: A retrospective analysis was conducted in 104 CHB patients in the gray zone. Hepatocellular carcinoma (HCC)-associated SNVs, including six in genotype B and twenty-one in genotype C, were analyzed in the baseline samples.
Results: HCC occurred in 15 patients (14.4%) during the median follow-up period of 10.4 years. Genotype B HBV-infected HCC patients had more T53C, A273G, and A529G SNVs and genotype C HBV-infected HCC patients had more T53C, G633A, and A3120G SNVs than HCC-free groups. Antiviral therapy reduced the risk of HCC in patients with HCC-associated SNVs in the gray zone both genotype B or C. Ectopic expression of replication-competent HBV plasmids in Huh7 cells expressing HCC-associated SNVs resulted in greater impairment of mitochondrial dynamics, increased production of reactive oxygen species (ROS), decreased mitochondrial membrane potential, lower ATP production, higher basal calcium levels, and reduced calcium buffering capacity compared to controls or wild-type HBV-expressing cells.
Conclusion: CHB patients in the gray zone remain at risk for HCC owing to both wild-type and HCC-associated HBV SNVs, especially the latter, inducing mitochondrial and metabolic dysfunctions. Antiviral therapy reduces the risk of HCC development in these patients.
P.S. Dr. Wei Teng and Prof. Ting-Tsung Chang share the co-first authors; Dr. Jenny Yuh-Jin Liang and Prof. Jaw-Ching Wu share the co-corresponding authors.

THU-634

Potent and durable off-treatment reduction of HBsAg levels and cccDNA-derived transcripts by the CAM-E ALG-001075 in cell-based experiments

Audrey Diederichs[1,2], Maud Michelet[1,2], Yannick Debing[3], Jordi Verheyen[3], Hannah Vanrusselt[3], Julian Symons[4], Tse-I Lin[3], Lawrence Blatt[4], Fabien Zoulim[1,2,5], Andreas Jekle[4], Barbara Testoni[1,2].
[1]*Université Claude-Bernard Lyon 1, Inserm, UMR 1350 PaThLiv, Lyon, France;* [2]*The Lyon Hepatology Institute, IHU EVEREST, Lyon, France;* [3]*Aligos Belgium BV, Leuven, Belgium;* [4]*Aligos Therapeutics, Inc., San Francisco, United States;* [5]*Hepatology Department, Hospices Civils de Lyon, Lyon, France*
Email: barbara.testoni@inserm.fr

Background and aims: ALG-001075, an HBV capsid assembly modulator inducing the formation of empty capsids (CAM-E), was shown to have secondary antiviral effects against HBV cccDNA formation and HBeAg secretion in vitro. Moreover, pevifoscorvir sodium (pevy), a prodrug of ALG-001075, has demonstrated potent reductions of HBV DNA, RNA, HBsAg, HBcrAg and HBeAg in subjects with CHB. Here, we provide experimental evidence from cell-based experiments that ALG-001075 also potently and durably inhibits HBsAg secretion and intracellular HBV RNA levels.
Method: Differentiated HepaRG cells were treated from day 6 post-infection with 1 µM ALG-001075 or lamivudine (3TC) for 1 month, then ALG-001075 was either continued for an additional month (arm 1) or stopped (arm 2) and cells monitored off-treatment for 4 weeks. Harvested cells and supernatants were analyzed for HBeAg and HBsAg secretion by ELISA, intracellular HBV markers (total HBV DNA and RNA, 3.5Kb RNA) by qPCR, cell viability and hepatocyte differentiation markers.

Results: ALG-001075 treatment resulted in potent inhibition of RNA and HBeAg secretion, as well as 38% inhibition of secreted HBsAg after 4 weeks of treatment, which was absent in 3TC treated cells. During the additional 4 weeks of treatment in arm 1, both HBeAg and HBsAg secretion continued to decrease and reached 90% and 80% inhibition, respectively, compared to untreated or 3TC-treated conditions. Similarly, intracellular HBV RNA detected with primers amplifying 3.5Kb RNAs or all HBV RNA species were more profoundly suppressed after the additional 4 weeks of ALG-001075 treatment. In arm 2, HBeAg inhibition was maintained off-ALG-001075 treatment and HBsAg levels continued to decline reaching 80% reduction with respect to untreated and 3TC-treatment. Consistently, no rebound in intracellular HBV RNAs was detected and only a partial rebound of intracellular total HBV DNA was found in the ALG-001075 treated cells, contrary to full rebound to baseline levels seen with 3TC. The ALG-001075 antiviral effect was not associated with cytotoxicity or reduced gene expression of bona fide hepatocyte differentiation markers.
Conclusion: Long term ALG-001075 treatment resulted in profound suppression of HBeAg, HBsAg and intracellular HBV RNAs which was durable after treatment withdrawal in HBV-infected HepaRG cells, suggesting a potential reduction in cccDNA level and/or transcriptional activity in these experimental conditions.

THU-635
Mitochondrial-ER remodeling differentiates HCC-adjacent and HCC-free HBV-infected liver tissues

Kousho Wakae[1], Haruyo Aoyagi[1], Ryuta Ueda[1], Akihito Tsubota[2], Akira Matsukura[3], Teruyuki Usuba[4], Hiroko Iijima[5], Yuriko Sakamaki[6], Shizuko Ichinose[7], Kento Fukano[8], Masaya Sugiyama[9], Kazuyoshi Hosomichi[10], Koichi Watashi[1], Masamichi Muramatsu[11], Masanori Isogawa[1], Takaji Wakita[8], Hideki Aizaki[1]. *[1]National Institute of Infectious Diseases, Japan Institute of Health Security, Tokyo, Japan; [2]The Jikei University School of Medicine, Tokyo, Japan; [3]Otakanomori Hospital, Chiba, Japan; [4]The Jikei University Katsushika Medical Center, Tokyo, Japan; [5]Hyogo Medical University, Hyogo, Japan; [6]Institute of Science Tokyo, Tokyo, Japan; [7]Nippon Medical School Hospital, Tokyo, Japan; [8]Japan Institute for Health Security, Tokyo, Japan; [9]National Center for Global Health and Medicine, Japan Institute for Health Security, Tokyo, Japan; [10]Tokyo University of Pharmacy and Life Sciences, Tokyo, Japan; [11]Foundation for Biomedical Research and Innovation, Hyogo, Japan*
Email: wakae.k@jihs.go.jp

Background and aims: Hepatitis B virus (HBV)-associated hepatocarcinogenesis is driven by multiple factors, including metabolic alterations and inflammation. However, it remains unclear when these cancer hallmarks emerge during tumor initiation and how they relate to subcellular structural changes. In this study, we compared HBV-infected liver tissues adjacent to hepatocellular carcinoma (HCC), with HBV-infected liver tissues from patients without HCC, to highlight early morpho-metabolic changes preceding HCC formation.
Method: HBV-infected liver tissues adjacent to HCC and those without HCC, were analyzed by Transmission electron microscopy (TEM), to quantify mitochondrial morphology, ER structure, ER-mitochondrial contacts, and glycogen content. Transcriptomic analyses were concurrently performed to compare gene expression profiles between the two tissue types.
Results: HCC-adjacent tissues were characterized by increased ER-mitochondrial proximity and reduced glycogen content compared with HCC-free tissues. These ultrastructural changes were accompanied by upregulation of genes associated with oxidative phosphorylation (OXPHOS), suggesting a metabolic shift toward enhanced glucose utilization. In addition, the adjacent tissues exhibited reduced mitochondrial elongation, indicative of increased oxidative stress. Consistently, genes related to oxidative stress and inflammatory signaling were concurrently upregulated.
Conclusion: These findings provide evidence of mitochondria and ER remodeling in the HCC-adjacent HBV-infected liver, accompanying increased glucose metabolism, oxidative stress, and inflammation. How these changes link to each other and contribute to HCC initiation, along with HBV infection, will be discussed.

THU-636
Construction and application of a mouse model for hepatitis E virus infection

Tianxu Liu[1], Xinyue Yang[1], Lin Wang[1]. *[1]Peking University Health Science Center, Beijing, China*
Email: lin_wang@pku.edu.cn

Background and aims: Hepatitis E virus (HEV) causes approximately 19.47 million symptomatic cases annually and is an emerging cause of chronic hepatitis. Although HEV is zoonotic, no definite evidence demonstrates that laboratory mice are susceptible to all known HEV genotypes. The factors define the HEV's host species range remain unclear. Given numerous genetic variants and toolkits available for mice that permit deep mechanistic studies, we aimed to develop inbred mouse models of HEV infection.
Method: AG129 and C57BL/6J mice were infected with HEV for experimental analyses. Key infection parameters assessed included HEV RNA detection (quantitative RT-PCR and in situ hybridization via RNAscope), liver function tests, histopathological examination, and liver transcriptomic profiling. Single-cell RNA sequencing was employed alongside transcriptomics analysis to delineate the infection dynamics and investigate virus-host interactions.
Results: We show that an emerging human-pathogenic HEV genotype discovered in rats can breach species barrier and robustly infect AG129 mice (double IFNα/β and IFNγ receptor knockout mice). By single-cell sequencing and RNAscope, we demonstrate viral tropism to macrophages and hepatocytes of the liver, providing previously unknown single-cell atlas of intrahepatic HEV infection. We subsequently adapted this HEV isolate by serial passaging in AG129 mice. The resulting mouse-adapted strain at passage 13 showed ability to infect immunocompetent C57BL/6J mice. Thus, we developed two mouse models using immunocompromised and immunocompetent mice, both support efficient HEV replication, and antiviral and vaccine testing. This study reveals that $CD4^+$ T cell exhaustion is a pivotal driver of chronic infection.
Conclusion: We developed two mouse models using AG129 and wild-type C57BL/6J mice, both support efficient HEV replication. This work also establishes the first immunocompetent mouse model for HEV infection. These mouse models offer a robust platform for studying HEV immunopathogenesis, evaluating antivirals and vaccines, and investigating cross-species transmission mechanisms.

THU-637
Aacquisition of four amino acid substitutions promotes robust replication of hepatitis C virus genotype 1b in cell culture

Tomoko Date[1], Noriyuki Watanabe[2], Kano Sakamoto[1], Masaya Sugiyama[1], Kousho Wakae[2], Haruyo Aoyagi[2], Hideki Aizaki[2], Takaji Wakita[2]. *[1]National Institute for Global Health and Medicine, Japan Institute for Health Security, Chiba, Japan; [2]National Institute of Infectious Diseases, Japan Institute for Health Security, Tokyo, Japan*
Email: date.t@jihs.go.jp

Background and aims: The JFH-1 cell culture system has greatly advanced hepatitis C virus (HCV) research, enabling the development of direct-acting antivirals (DAAs) with cure rates >95% and detailed dissection of the HCV life cycle (entry, replication, assembly, and release). In this study, we focused on genotype 1b (GT1b), a major globally prevalent HCV subtype. Using next-generation sequencing (NGS), we analyzed GT1b isolates from patient samples and identified three major phylogenetic clusters (Q1, Q2, and R). Our aim was to establish representative replication-competent infectious clones for each cluster to facilitate virological and therapeutic studies.

Method: Subgenomic replicons and full-length GT1b cDNA clones were constructed based on sequences from each cluster. Replicon RNAs were transfected into Huh7 cells, and replication efficiency was evaluated by colony formation. Full-length genomes carrying adaptive mutations were introduced into Huh7 cells and maintained in long-term culture. HCV replication was monitored by measuring core protein levels in culture supernatants. Viral genomes were sequenced at time points corresponding to peak replication.
Results: Colony formation assays showed that the EG substitution in NS3 (E1204G) and the SI substitution in NS5A (S2206I) enhanced GT1b replication. A full-length Q1 clone containing both mutations (EGSI) achieved peak replication during long-term culture after >130 days. Sequence analysis at peak replication identified two additional amino acid substitutions in E2. For both Q2 and R strains, introducing EGSI together with these E2 substitutions further increased viral production in long-term culture.
Conclusion: Cooperative mutations in nonstructural (NS3 and NS5A) and structural (E2) regions markedly enhance GT1b replication in vitro. These adaptations enabled the generation of replication-competent infectious clones representing major GT1b lineages, providing valuable tools for HCV biology and antiviral development.

THU-638
A male-enriched NFIC–p300 axis drives sex-biased HBV cccDNA activation

Lu Zhang[1], Hongzhi Guo[2], Xinai Chen[1], Xiaoming Cheng[1], Yuchen Xia[1]. [1]*Wuhan University, Wuhan, China;* [2]*Fudan University, Shanghai, China*
Email: 00032118@whu.edu.cn

Background and aims: Sex differences are a prominent yet incompletely understood feature of hepatitis B virus (HBV) infection, with males exhibiting higher viral loads and increased risk of disease progression. This study aimed to elucidate the molecular and epigenetic mechanisms underlying sex-biased HBV replication.
Method: We integrated mouse models carrying HBV covalently closed circular DNA (cccDNA), human hepatocyte systems, and multi-omics analyses. Chromatin accessibility, transcription factor binding, and histone modifications on the viral minichromosome were examined using ATAC-seq, CUT&Tag, chromatin immunoprecipitation, and in vitro reconstituted minichromosome assays. Functional relevance was assessed through genetic perturbation and antisense oligonucleotide–mediated knockdown in vitro and in vivo.
Results: We identified nuclear factor I C (NFIC) as a male-enriched transcription factor that directly binds HBV cccDNA and recruits the histone acetyltransferase p300. This NFIC–p300 epigenetic axis enhances histone acetylation, increases viral chromatin accessibility, and drives male-biased HBV transcription. Depletion of NFIC eliminated sex differences in viral transcription without affecting cccDNA abundance, and antisense targeting of NFIC robustly suppressed viral transcription in vivo without detectable toxicity.
Conclusion: These findings define a sex-dependent epigenetic mechanism governing HBV transcription and identify NFIC as a promising host-directed therapeutic target for HBV infection.

THU-639
Cross-species core protein chimerism enables HBV cccDNA formation in murine hepatocytes

Kaitao Zhao[1], Xueyun Luo[1], Chen Li[1], Xiaoyun Li[1], Xiaoming Cheng[1], Yuchen Xia[1]. [1]*Wuhan University, Wuhan, China*
Email: 00032118@whu.edu.cn

Background and aims: Murine hepatocytes are not permissive to hepatitis B virus (HBV) infection, even with ectopic expression of the viral receptor, human NTCP (hNTCP). We previously reported that a major restriction lies in the inefficient disassembly of cytoplasmic HBV nucleocapsids. This study aimed to overcome this barrier by constructing HBV chimeras incorporating HBc proteins from other mammalian species.
Method: HBV sequences from various mammals were analyzed evolutionarily. Twelve HBc proteins, derived from 18 mammalian HBV isolates, were co-transfected with an HBc-null HBV replication plasmid into the murine hepatoma cell line Hepa1-6-hNTCP. Core-associated HBV DNA and Hirt-extracted DNA were analyzed by Southern blot. In vivo cccDNA formation was assessed using a hydrodynamic injection mouse model. DNase I sensitivity assays were performed to evaluate nucleocapsid disassembly. HBc protein and capsid localization were examined via immunofluorescence and nuclear/cytoplasmic fractionation. HBV chimeras harboring different HBc variants were also generated to assess infectivity in murine hepatocytes.
Results: Eighteen mammalian HBV sequences were analyzed, and 12 HBc variants were screened for their ability to support cccDNA formation in murine hepatic cells. Three HBc proteins enabled robust cccDNA formation both *in vitro* and *in vivo*. Notably, the core-associated HBV DNA from these variants was fully sensitive to DNase I digestion, indicating highly efficient nucleocapsid disassembly.
Conclusion: These findings reinforce that nucleocapsid disassembly is a key restriction step in HBV infection in mice. Engineering HBV to express specific non-human HBc proteins represents a promising strategy to establish HBV infection in murine models.

THU-640
The impact of nucleos(t)ide analogues anti-hepatitis B virus therapy on PD-1 expression levels in peripheral blood T cells of patients

Iiu Yang[1], Jia Li[1], Chenrui Liu[1], Meng Zhang[1], Yaping Li[1], Shuangsuo Dang[1]. [1]*The Second Affiliated Hospital of Xi'an Jiaotong University, Xi'an, China*
Email: dang212@126.com

Background and aims: Currently, nucleotide analogues (NAs) represent the predominant class of antiviral agents employed in clinical practice. However, the immunological response outcomes exhibit significant heterogeneity among individuals despite comparable virological suppression efficacy. Based on this, this study took the expression level of PD-1 on peripheral blood T cells of CHB patients as the main observation index to observe the effect of NA antiviral therapy on the expression level of PD-1 on peripheral blood T cells of CHB patients.
Method: A cross - sectional study was conducted on patients who visited the Department of Infection and the Health Examination Department of the Second Affiliated Hospital of Xi'an Jiaotong University from September 2022 to December 2024. Including three groups, the untreated group, the NAs treatment group (patients who had received NAs treatment for more than 1 year) and the healthy control group. The proportions of $CD3^+PD1^+T$, $CD4^+PD1^+T$, and $CD8^+PD1^+T$ cells were collected.
Results: 1. The levels of $CD3^+PD1^+T$, $CD4^+PD1^+T$, and $CD8^+PD1^+T$ cells in the untreated group were significantly higher than those in the healthy control group ($P < 0.001$). 2. The levels of $CD3^+PD1^+T$, $CD4^+PD1^+T$, and $CD8^+PD1^+T$ cells in the NAs treatment group were lower than those in the untreated group ($P = 0.01/0.01/0.04$). 3. The results indicated that there was no significant statistical difference in the proportion of $CD8^+PD1^+$ T cells among the different antiviral groups, while there were statistical differences in the proportions of $CD3^+PD1^+$ T and $CD4^+PD1^+$ T cells. Further pairwise comparisons revealed that the proportion of $CD3^+PD1^+T$ cells in the ETV group was significantly higher than those in the TAF group and the TMF group ($P = 0.031/0.032$). The proportion of $CD4^+PD1^+$ T cells in the ETV group was significantly higher than those in the TAF group and the TMF group ($P = 0.038/0.040$). Although the proportion of $CD4^+PD1^+$ T cells in the ETV group was higher than that in the TDF group, the difference was not statistically significant. There were no statistical differences among the remaining groups ($P > 0.05$).
Conclusion: 1. The high expression of PD-1 on T cells in CHB patients is related to the chronicity of HBV infection.

2. Antiviral treatment with NAs can down-regulate the expression level of PD-1 on T cells in CHB patients. 3. Nucleotide analogues have a more obvious down-regulating effect on the expression level of PD-1 on T cells in CHB patients than nucleoside analogues.

THU-641

SERPINE1 activates PIKfyve-dependent lysosomal autophagy to restrict HBV replication and restore antiviral CD8⁺ T cell immunity

Yina Yu[1], Yunqing Qiu[1], Yan Lou[1]. [1]*The First Affiliated Hospital of Zhejiang University, Hangzhou, China*
Email: yanlou@zju.edu.cn

Background and aims: Functional cure of chronic hepatitis B (CHB) remains limited by persistent viral antigen expression and virus-induced immune tolerance. Current therapies rarely achieve HBsAg clearance or restore antiviral immunity. This study aimed to define the role of the host factor SERPINE1 in HBV infection and to determine whether it coordinates viral clearance and immune restoration by regulating lysosomal function and autophagy flux.
Method: SERPINE1 was genetically manipulated in HBV-replicating cell lines (HepG2.2.15, HepAD38) and a natural infection model (HepG2-NTCP) to assess its effects on HBV replication, antigen expression, and viral particle production. In vivo validation was performed using AAV-HBV and hydrodynamic injection mouse models. Protein interaction networks and downstream pathways were identified by co-immunoprecipitation, mass spectrometry, and quantitative proteomics. Lysosomal function and autophagy flux were evaluated using biochemical and imaging-based assays. Photoaffinity labeling, surface plasmon resonance, and cellular thermal shift assays were used to verify the interaction between SERPINE1 and the natural compound betulinic acid.
Results: SERPINE1 markedly suppressed HBV replication and reduced HBsAg levels in vitro and in vivo. Mechanistically, SERPINE1 directly interacted with the lysosomal lipid kinase PIKfyve, enhancing PtdIns(3,5)P_2 production, lysosomal acidification, autophagosome–lysosome fusion, and overall autophagy flux. Enhanced autophagy promoted degradation of viral components and limited diversion of defective ribosomal products to the proteasome, thereby reducing hepatocyte MHC-I antigen presentation and alleviating $CD8^+$ T cell exhaustion. Betulinic acid was identified as a direct SERPINE1 agonist that phenocopied these antiviral and immunomodulatory effects.
Conclusion: SERPINE1 activates the PIKfyve–lysosome–autophagy axis to couple HBV clearance with restoration of antiviral $CD8^+$ T cell function. This mechanism identifies SERPINE1 as a host target capable of breaking the cycle of viral persistence and immune tolerance in CHB, and highlights betulinic acid as a candidate molecule for therapies integrating antiviral and immune-reconstitutive strategies.

THU-642

NIK activates IRF1-dependent interferon signaling to suppress hepatitis B virus in hepatocytes

Ziying Liu[1], Xiaoyong Zhang[2]. [1]*Department of Infectious Diseases, Nanfang Hospital, Southern Medical University, Guangzhou, 510515, China, State Key Laboratory of Multi-organ Injury Prevention and Treatment, Key Laboratory of Infectious Diseases Research in South China (Southern Medical University), Ministry of Education, Guangdong Provincial Key Laboratory for Prevention and Control of Major Liver Diseases, Guangdong Provincial Clinical Research Center for Viral Hepatitis, Guangdong Institute of Hepatology, Guangdong Provincial Research Center for Liver Fibrosis Engineering and Technology., Department of Infectious Diseases, The Second Affiliated Hospital, Guangzhou Medical University, Guangzhou, China, Guangzhou, China;* [2]*Department of Infectious Diseases, Nanfang Hospital, Southern Medical University, Guangzhou, 510515, China, State Key Laboratory of Multi-organ Injury Prevention and Treatment, Key Laboratory of Infectious Diseases Research in South China (Southern Medical University), Ministry of Education, Guangdong Provincial Key Laboratory for Prevention and Control of Major Liver Diseases, Guangdong Provincial Clinical Research Center for Viral Hepatitis; Guangdong Institute of Hepatology, Guangdong Provincial Research Center for Liver Fibrosis Engineering and Technology, Guangzhou, China*
Email: liuziying2636@foxmail.com

Background and aims: Hepatitis B virus (HBV) persistence relies on stably established covalently closed circular DNA (cccDNA). While NF-κB-inducing kinase (NIK) mediates non-canonical NF-κB signaling is critical in antiviral defense, its role in HBV control is undefined.
Method: Hepatocyte-specific NIK knockout ($NIK^{\Delta hep}$) and wild-type mice received hydrodynamic pAAV-HBV1.2 injection. NIK was modulated (knockdown/overexpression/mutants) in HBV-transfected/infected hepatoma cells. Signaling components (IKKα, NF-κB2, IRFs, STAT1) were depleted via CRISPR/Cas9. Mechanistic studies included RNA-seq, co-IP, plasmon resonance imaging and molecular docking. Murine NIK mRNA was delivered via lipid nanoparticles (LNPs) in HBV-persistent mice.
Results: We demonstrate that NIK suppresses HBV replication by directly binding and phosphorylating interferon regulatory factor 1 (IRF1), promoting its nuclear translocation and enhancing type I/III interferon production in hepatocytes. This kinase-dependent mechanism operates independently of the IRF3 or NFKB2 mediated non-canonical NF-κB pathway. Using hepatocyte-specific delivery of NIK mRNA via LNPs, we achieved rapid clearance of HBV antigens and DNA in mouse models without inducing hepatic inflammation. Clinically, CHB livers transcriptome showed elevated NIK expression correlating positively with IRF1, STAT1, and ISGs ($p < 0.001$) expression.
Conclusion: NIK is a potent hepatocyte-intrinsic HBV restriction factor acting via kinase-dependent IRF1 phosphorylation and IFN/ISG induction, independent of non-canonical NF-κB pathway. LNP-NIK mRNA represents a promising therapeutic strategy for functional HBV cure.

THU-644

Investigation of plasma Exosomal let-7a-5p in modulating Th17 cell differentiation associated with functional cure

Meng Zhao[1], Saisai Zhang[1], Liqiong Yang[1], Danny Ka-Ho Wong[1], Judy Wai-Ping Yam[2], Lung-Yi Mak[1,3], Man-Fung Yuen[1,3], Wai-Kay Seto[1,3]. [1]*Department of Medicine, School of Clinical Medicine, The University of Hong Kong, Hong Kong, China;* [2]*Department of Pathology, School of Clinical Medicine, The University of Hong Kong, Hong Kong, China;* [3]*State Key Laboratory of Liver Research, The University of Hong Kong, Hong Kong, China*
Email: mengz014@connect.hku.hk

Background and aims: Achieving a 'functional cure' in chronic hepatitis B (CHB), defined as sustained hepatitis B surface antigen (HBsAg) seroclearance, is an achievable treatment goal, but with only a small minority of patients reaching this endpoint. Immune tolerance and T-cell mediated immune dysfunction are key factors contributing to the persistent presence of HBsAg. Plasma exosomes in T cells may play a role, but the mechanisms governing their functional manipulation are not well understood. This study evaluated the changes in the plasma exosomal miRNA profile during HBsAg seroclearance and explored their role in T cell dysfunction.
Method: miRNA sequencing (miRNA seq) was conducted on exosomes derived from treatment-naïve HBsAg-positive hepatitis B e antigen (HBeAg)-negative ($HBsAg^+$, $HBeAg^-$) CHB patients ($n = 10$) and patients achieving HBsAg seroclearance ($n = 10$) to identify key miRNAs. Target genes of let-7a-5p were validated via online prediction tools (Targetscan, mirDIP, miRWalk), dual-luciferase reporter assays, and western blot. Naïve $CD4^+$ T cells were treated with exosomes or transfected with let-7a-5p mimics/inhibitors to assess effects on Th17 cell, evaluated by flow cytometry and ELISA.
Results: Flow cytometry analysis revealed peripheral blood mononuclear cells from patients achieving HBsAg seroclearance exhibited a significantly lower proportion of Th17 cells compared to $HBsAg^+$·$HBeAg^-$ CHB patients ($1.64 \pm 0.73\%$ vs. $2.41 \pm 1.02\%$, $p < 0.01$).

miRNA seq identified 33 downregulated and 30 upregulated exosomal miRNAs. Among these, let-7a-5p was significantly increased in patients achieving HBsAg seroclearance ($p < 0.05$). IL6R, predicted as a target gene of let-7a-5p by online tools and validated through dual-luciferase reporter assay, was found to be involved in Th17 cell differentiation. In-vitro experiments showed that overexpression of let-7a-5p could downregulate IL6R expression, reduced the proportion of Th17 cells (2.05 ± 0.4% vs. 4.67 ± 0.5%, $p < 0.01$), and decrease IL17 levels (204.7 ± 27.1 pg/mL vs. 268.3 ± 22.8 pg/mL, $p < 0.05$), whereas inhibition of let-7a-5p reversed these effects.

Conclusion: We investigated the role of plasma exosomes in HBsAg seroclearance and demonstrated that exosomal let-7a-5p from HBeAg-negative CHB patients regulates Th17 cell differentiation by targeting IL6R. These findings may contribute to the development of novel immunotherapeutic strategies and provide new scientific insights to achieving functional cure.

Viral hepatitis B and D – Clinical aspects

TOP-551

Investigation of intrahepatic cccDNA activity in HBsAg-negative HBV-infected individuals and its association with hepatocellular carcinoma risk

Yanfei Feng[1], Jianning Jiang[1,2]. [1]*The first affiliated hospital of Guangxi Medical University, Nanning, China;* [2]*Key Laboratory of Early Prevention and Treatment for Regional High Frequency Tumor (Guangxi Medical University), Ministry of Education, Nanning, China*
Email: gxjjianning@163.com

Background and aims: Hepatitis B surface antigen (HBsAg)-negative chronic hepatitis B (CHB) patients are often considered to have reduced viral activity but remain at risk for hepatocellular carcinoma (HCC) and viral reactivation. This study aimed to investigate the presence, transcriptional activity of hepatitis B virus (HBV) covalently closed circular DNA (cccDNA) in the liver, and its association with HCC development in HBsAg-negative individuals.

Method: 138 patients were enrolled. Study cohort: 92 HBsAg-negative, HBcAb-positive patients (41 HCC, 25 post-therapy "functional cure", 26 spontaneous resolution). Control cohort: 46 HBsAg-positive patients (<100 IU/mL; 22 HCC, 24 treated but still positive). Intrahepatic cccDNA and total HBV DNA (tDNA) were quantified by digital PCR (log10 copies/10^9 cells); cccDNA/tDNA ratio was calculated. Serum pgRNA was undetectable in all.

Results:

- Higher cccDNA activity in peritumoral tissue: Among 63 HCC patients, cccDNA levels were significantly higher in peritumoral tissue than in tumor tissue (2.25 ± 67 vs 0.73 ± 1.53 log10 copies/10^9 cells, P = 0.000), with a higher cccDNA/tDNA ratio.
- HBsAg-negative HCC patients show intermediate viral load: In peritumoral tissue, HBsAg-negative patients (n = 41) had lower cccDNA and tDNA than HBsAg-positive patients (n = 22), but higher levels than the spontaneous resolution group (n = 26), with no difference in cccDNA/tDNA ratio between serogroups.
- Persistent virus in "functionally cured" patients: The functionally cured subgroup (n = 25) had lower tDNA than non-seroconverted patients (n = 24), but its cccDNA, tDNA, and cccDNA/tDNA ratio were all significantly higher than in the spontaneous resolution group.
- Comparable viral status in HBsAg-negative subgroups: No significant differences in cccDNA, tDNA, or cccDNA/tDNA ratio were found between HBsAg-negative HCC patients and the functionally cured group.

Conclusion: Transcriptionally active cccDNA persists in the livers of HBsAg-negative individuals at a level significantly higher than in spontaneous resolution, underpinning their long-term HCC risk and potential for viral reactivation. "Functional cure" does not equate to complete virological eradication, as a low-level viral reservoir persists in the liver. This study highlights the need for monitoring intrahepatic cccDNA in high-risk, HBsAg-negative, HBcAb-positive individuals and suggests that current functional cure criteria may require refinement by incorporating intrahepatic virological parameters for more precise assessment.

TOP-565

The evolving role of quantitative serum hepatitis B surface antigen (qHBsAg) measurement in chronic hepatitis B (CHB) management: comparison of EASL guidelines with an international expert consensus

Patrick Kennedy[1], Hong You[2], Kosh Agarwal[3], Tarik Asselah[4], Carla Coffin[5], Chari Cohen[6,7], Markus Cornberg[8], Robert G. Gish[7], Cary James[9], Harry L.A. Janssen[10,11], Pietro Lampertico[12,13], Jeffrey Lazarus[14,15], Sabela Lens[16], Mark S Sulkowski[17], Yasuhito Tanaka[18], Thomas Tu[19], Grace Lai-Hung Wong[20], Shayon Salehi[21], Norah Terrault[22]. [1]*Barts Health NHS Trust, London, United Kingdom;* [2]*Beijing Friendship Hospital, Capital Medical University, Beijing, China;* [3]*Institute of Liver Studies, King's College Hospital, London, United Kingdom;* [4]*Beaujon Hospital APHP, Service d'hépatologie, INSERM UMR1149, Université de Paris-Cité, Paris, France;* [5]*Cumming School of Medicine, Snyder Institute, The University of Calgary, Calgary, AB, Canada;* [6]*Baruch S. Blumberg Institute, Hepatitis B Foundation, Doylestown, PA, United States;* [7]*Hepatitis B Foundation, Doylestown, PA, United States;* [8]*Hannover Medical School, Hannover, Germany;* [9]*World Hepatitis Alliance, London, United Kingdom;* [10]*Erasmus MC, University Medical Center, Rotterdam, Netherlands;* [11]*Toronto General Hospital, University of Toronto, Toronto, Canada;* [12]*Division of Gastroenterology and Hepatology, Foundation IRCCS Ca' Granda Ospedale Maggiore Policlinico, Milan, Italy;* [13]*CRC "A. M. and A. Migliavacca" Center for Liver Disease, Department of Pathophysiology and Transplantation, University of Milan, Milan, Italy;* [14]*Barcelona Institute for Global Health (ISGlobal), Barcelona, Spain;* [15]*CUNY Graduate School of Public Health and Health Policy, New York, NY, United States;* [16]*Hospital Clinic Barcelona, Barcelona, Spain;* [17]*Johns Hopkins University School of Medicine, Baltimore, MD, United States;* [18]*Kumamoto University, Kumamoto, Japan;* [19]*Westmead Institute for Medical Research, The University of Sydney, Sydney, Australia;* [20]*Medical Data Analytics Centre (MDAC), The Chinese University of Hong Kong, Hong Kong, China;* [21]*GSK, London, United Kingdom;* [22]*Keck School of Medicine, University of Southern California, Los Angeles, CA, United States*
Email: p.kennedy@qmul.ac.uk

Background and aims: qHBsAg is increasingly recognised as a tool for clinical management of CHB. An international expert panel conducted a Delphi consensus exercise to develop statements on qHBsAg use; updated EASL guidelines on HBV management were published whilst this was ongoing. We compared the final qHBsAg consensus statements with 2025 EASL recommendations on qHBsAg use.

Method: Futuring Liver Care (FLC), convened by GSK, is an international panel including hepatologists, gastroenterologists, infectious disease specialists, public health specialists and patient advocates. The Delphi consensus included 42 participants from FLC and their networks, representing CHB care stakeholders across North America, Asia-Pacific and Europe. Initial statement development was supported by systematic and scoping literature reviews. The Delphi process included 3 voting rounds and a finalization meeting. Voting used a 7-point Likert scale (strongly agree to strongly disagree) with the opportunity to provide free-text comments, and to propose new statements in Round 1. Consensus was defined as ≥75% agree/strongly agree in 2 rounds with ≥80% panel response. Final

statements were compared with relevant sections of the 2025 EASL HBV management guidelines.
Results: The Delphi panel had a high response rate (≥90% across 3 rounds), confirming 37 statements on: (A) CHB natural history (3 statements); (B) disease outcomes (5); (C) management of individuals not on therapy (3); (D) treatment goals (5); (E) factors associated with HBsAg loss (5); (F) monitoring during treatment and prediction of HBsAg loss (6); (G) thresholds to guide decisions (4), and (H) research gaps and challenges (6). Closest alignment with EASL guidelines was seen in topics A, C, D and F; overall, 25/37 statements were aligned with EASL 2025 guidelines, with 11 providing more detailed guidance. The 12/37 additional statements covered topics outside of EASL scope, such as qHBsAg and novel finite therapies and qHBsAg-specific research priorities. Key statements covered the value and durability of spontaneous HBsAg loss vs that achieved with therapy, and qHBsAg thresholds predictive of HBsAg loss during finite therapy.
Conclusion: These global consensus statements complement the EASL 2025 guidelines and strongly support routine qHBsAg testing in CHB care. Clinicians, liver associations and policymakers should consider integrating qHBsAg testing to inform current and future CHB management.

TOP-566-YI
Hepatitis B core–related antigen predicts immune-active transition in HBeAg-negative indeterminate chronic hepatitis B
Hsing-Yu Yeh[1], Hsin Kuan-Hui[1], Chun-Jen Liu[1], Chun-Ming Hong[1], Tung-Hung Su[1], Hung-Chih Yang[1], Chen-Hua Liu[1], Pei-Jer Chen[1], Tai-Chung Tseng[1], Jia-Horng Kao[1]. *[1]National Taiwan University Hospital, Zhongzheng District, Taiwan*
Email: tctsenghbv@gmail.com

Background and aims: Chronic HBV (CHB) infection with ongoing hepatic inflammation increases the risk of cirrhosis and hepatocellular carcinoma (HCC). Among HBeAg-negative individuals, those in the indeterminate phase exhibit a heterogeneous clinical course, with a subset eventually progressing to immune-active hepatitis.
This study aimed to investigate whether hepatitis B core-related antigen (HBcrAg), a surrogate marker of intrahepatic cccDNA activity, can predict transition from the indeterminate phase to the immune-active phase in HBeAg-negative patients.
Method: We analyzed 1,090 HBeAg-negative grey zone patients from the ERADICATE-B cohort (n = 2,666), which excluded inactive CHB patients (HBV DNA <2000 IU/mL +ALT < 1× ULN by AASLD definition) and those with ALT >2× ULN. Baseline measurements included HBV-related seromarkers (HBcrAg, HBV DNA, HBsAg) and liver function. The risk of immune-active transition (ALT> 2× ULN + HBV DNA >2000 IU/mL), HBV-associated hepatitis (ALT> 100 U/L + HBV DNA >2000 IU/mL), HBsAg loss, death and liver-related death were assessed using Kaplan-Meier survival analysis and Cox proportional hazards models. Sensitivity analyses excluded patients who developed immune-active transition within the first year of follow-up.
Results: During 11,674.6 person-years of follow-up, 619 patients progressed to the immune-active phase, yielding an incidence rate of 5.3 per 100 person-years (95% CI, 4.9–5.7). Higher baseline HBcrAg levels were associated with an increased risk of immune-active transition and demonstrated superior predictive performance compared with HBV DNA (P = 0.03). Compared with patients with HBcrAg <10 KU/mL, those with levels of 10–99 KU/mL and ≥100 KU/mL had significantly higher risks of immune-active transition, a finding that remained consistent in sensitivity analyses. Higher HBcrAg levels were also associated with increased risks of HBV-associated hepatitis, all-cause mortality, and liver-related mortality, as well as a lower probability of HBsAg loss. In multivariable analysis adjusting for age, baseline ALT, HBV DNA, and HBsAg levels, HBcrAg remained an independent predictor of immune-active transition.
Conclusion: Among HBeAg-negative indeterminate patients, baseline HBcrAg levels are independent predictors of immune-active transition and other adverse outcomes. HBcrAg may serve as a useful biomarker to identify patients who may benefit from closer monitoring or preemptive antiviral therapy.

TOP-567
AASLD–EASL zone ALT associated with higher risk of HCC and liver-related mortality inchronic hepatitis B patients
Tai-Chung Tseng[1], Shih-Jer Hsu[1], Mei-Hung Pan[2], Chun-Jen Liu[1], Chien-Jen Chen[2], Tung-Hung Su[1], Hung-Chih Yang[1], Chen-Hua Liu[1], Pei-Jer Chen[1], Hwai-I Yang[2], Jia-Horng Kao[1]. *[1]National Taiwan University Hospital, Taipei, Taiwan; [2]Academia Sinica, Taipei, Taiwan*
Email: tctsenghbv@gmail.com

Background and aims: The optimal alanine aminotransferase (ALT) threshold for defining normal values in chronic hepatitis B (CHB) remains controversial. This study aimed to determine if CHB patients with ALT levels within the EASL-defined normal range, but exceeding the stricter AASLD-defined normal thresholds (the AASLD–EASL zone), are at increased risk for hepatocellular carcinoma (HCC) and liver-related death.
Method: We analyzed 5,102 CHB patients with EASL-defined normal ALT levels from the ERADICATE-B and REVEAL-HBV cohorts. Over a median follow-up of 24.4 years, we compared adverse liver outcomes between patients with AASLD-defined normal ALT and those with levels falling in the AASLD–EASL zone.
Results: During follow-up, 368 patients developed HCC and 292 experienced liver-related death. A total of 386 patients were identified with baseline ALT levels in the AASLD–EASL zone. Multivariable analysis demonstrated that the AASLD–EASL zone was an independent predictor of HCC (adjusted hazard ratio [HR] 1.81, 95% CI: 1.31–2.50) and liver-related death (adjusted HR: 1.49, 95% CI: 1.04–2.15). Longitudinal analysis revealed a stepwise increase in risk for patients with intermittent or persistent ALT elevation within this zone. Notably, among patients in the indeterminate phase, the AASLD–EASL zone was associated with significant risk differences: adjusted HR of 2.22 (95% CI:1.50–3.29) for HCC and adjusted HR of 1.65 (95% CI: 1.05–2.60, Fig 2D) for liver-related death.
Conclusion: ALT levels that are considered normal by EASL standards but exceed AASLD thresholds are associated with a significantly higher long-term risk of liver-related mortality and HCC. This association is most pronounced in patients in the indeterminate phase of CHB; thus, antiviral treatment should be considered in these patients with AASLD–EASL zone ALT.

TOP-568
HBV preS1 haplotypes mediate the protective effect of NTCP S267F variant against liver cirrhosis in chronic hepatitis B
Hsiang-Hsuan Chuang[1,2], Ding-Lian Wang[2,3], Chih-Jen Huang[2], Mei-Hung Pan[2], Po-Hsien Hsu[2,3], Chien-Jen Chen[2], Hwai-I Yang[2]. *[1]School of Medicine, Chung Shan Medical University, Taichung, Taiwan; [2]Genomics Research Center, Academia Sinica, Taipei, Taiwan; [3]Graduate Institute of Life Science, National Defense Medical University, Taipei, Taiwan*
Email: stan92100755@gmail.com

Background and aims: Chronic hepatitis B (CHB) accounts for over 1 million deaths worldwide each year, primarily due to liver cirrhosis (LC) and hepatocellular carcinoma (HCC). Hepatitis B virus (HBV) entry requires binding of its large surface antigen (LHBs) preS1 domain to the hepatocyte receptor sodium taurocholate cotransporting polypeptide (NTCP). The East Asian-predominant NTCP p. Ser267Phe (S267F; c.800G>A, rs2296651) variant has been consistently linked to reduced LC and HCC risks, but the mechanism remains unclear. We investigated whether the S267F variant drives HBV preS1 evolution and if such host-virus interactions contribute to disease progression.
Method: HBV genomes from 377 CHB participants in the community-based REVEAL-HBV cohort were deep-sequenced to examine associations between S267F and HBV preS1 alleles and haplotypes.

Repeat measurements characterized longitudinal haplotype dynamics. Cox proportional hazards models and causal mediation analysis were used to estimate hazard ratios with 95% confidence intervals for LC and evaluate whether preS1 haplotypes mediated the S267F-LC association, respectively.
Results: PreS1 alleles at nucleotide positions 2881A, 2902G, and 2956A were enriched among NTCP S267F carriers (GA/AA) versus wild-type individuals (GG; Bonferroni-adjusted $p < 0.001$ for all positions). We defined a 3-locus haplotype (nt2881/2902/2956, CTG reference, others non-CTG) corresponding to distinct amino acid variant at preS1 residues 10/17/35, linking the observed genetic selection to specific viral protein variants. Among HBV genotype C patients at baseline (n = 224), the primary serum non-CTG haplotype was more frequent in GA/AA than GG carriers (42.9% vs. 7.1%; $p < 0.001$), and the divergence increased over a median follow-up of 11.5 years (52.9% vs. 5.8%; $p < 0.001$, n = 69), consistent with sustained host-associated selection on HBV genomes. Baseline non-CTG carriage was associated with lower LC risk than CTG haplotype (adj-HR 0.20; 95% CI 0.06–0.25; $p = 0.008$). Causal mediation analysis further indicated that reduced CTG carriage partially mediated the S267F protection against LC (indirect effect [IE] adj-HR 0.61; 95% CI 0.48–0.75; $p < 0.001$).
Conclusion: In CHB patients with HBV genotype C, NTCP S267F was associated with longitudinal selection of a non-CTG HBV preS1 haplotype at nt2881/2902/2956 that mediated protection against cirrhosis. These findings provide human evidence linking host genetic variation, viral adaptation, and disease progression in chronic hepatitis B.

SAT-556-YI
Long-term outcomes of patients with hepatitis D recurrence after liver transplantation
Özgür Aktaş[1], Muhsin Murat Harputluoglu[2], Muge Ozari Gulnar[3], Elvan Isik[4], Zeynep Melekoğlu Ellik[5], Derya Ari[6], Meral Akdogan Kayhan[6], Gökhan Kabaçam[7], Nilay Danış[8], İlker Turan[4], Mesut Akarsu[8], Ramazan Idilman[9], Sedat Karademir[10], Sezai Yilmaz[11], Cihan Yurdaydin[3]. *[1]Koç University Medical Schools, Sarıyer, Türkiye; [2]İnönü University Medical Schools, Gastroenterology Departments, Malatya, Türkiye; [3]Koç University Medical Schools, Gastroenterology Departments, İstanbul, Türkiye; [4]Ege University Hospital, Department of Gastroenterology, İzmir, Türkiye; [5]Ankara University Medical Schools, Gastroenterology Departments, ANKARA, Türkiye; [6]Ankara Bilkent City Hospital, Gastroenterology Departments, Ankara, Türkiye; [7]Güven Hospital, Gastroenterology Departments, Ankara, Türkiye; [8]Dokuz Eylül University Hospital, Gastroenterology Departments, İzmir, Türkiye; [9]Ankara University Hospital, Department of Gastroenterology, Ankara, Türkiye; [10]Güven Hospital, Department of General Surgery, Ankara, Türkiye; [11]Inonu University Hospital, Department of Surgery and Liver Transplant Institute, Malatya, Türkiye*
Email: cyurdaydin@ku.edu.tr

Background and aims: Turkey is considered an endemic country for hepatitis D virus (HDV), and liver transplantation (LT) remains an important rescue treatment. Guidelines recommend indefinite hepatitis B immune globulin (HBIg) and nucleos(t)ide analog (NA) treatment to prevent hepatitis D virus (HDV) recurrence after LT. We aimed to present LT outcomes for HDV in Turkey from 7 liver transplantation centres (2010 to 2025).
Method: HDV recurrence was defined as becoming HBsAg and HDV-RNA positive after LT. Patients had received livers from HBsAg negative, anti HBc negative donors except for one case who received a HBsAg (+) after talking to patient who accepted the risk. Except one centre (Ege University) at which HBIg was given only for one year all other centres offered HBIg + NA treatment of indefinite duration.
Results: During the 15 year period a total of 5955 LTs were performed (1054 cadaveric and 4901 living related). HBV and HBV/HDV associated liver disease were the etiology in 1845 (31%) and 315 (5,3%) of 5955 LTs, respectively. Post-transplantation HDV recurrence (Post-txR) occurred in 18 patients (5.7%); (median age: 49 [18–66], 16 men, 2 women). LT indication was decompensated liver disease (DLD) in 10 and hepatocellular cancer (HCC) in 8. Post-txR occurred after a median of 27.5 months (1–54 months). HBIg was administered for median 10.5 months (0–36 months). Except one patient (HBsAg+ donor), post-txR occurred after HBIg discontinuation in all cases. Of 18 patients with post-txR, 10 patients enjoyed a mild disease course despite lack of antiviral treatment. Eight patients died during median 92.5 months follow up (4–158 months). Causes: liver-related (n = 2, including one with severe HDV recurrence with ALT >5000U/mL, >100 million and 1 million IU/nmL of HDVRNA and HBVDNA, respectively), biliary stenosis-linked sepsis (n = 2), B-cell lymphoma (n = 1), COVID-19 (n = 1), earthquake (n = 1), unknown (n = 1). Notably, Koç University had zero HDV recurrence among 11 HDV-related LTs (all living donor, 2018–2025) using their risk-stratified HBIg/NA protocol.
Conclusion: HBsAg recurrence is rare after LT for HDV but can occur with HBIg/NA non-compliance, potentially leading to HDV recurrence. HDV recurrence appears to run a mild clinical course in line with early reports from Italy and France (1, 2), though severe recurrence with graft failure may also occur. Latent HDV infection of the liver allograft may be rescued by HBV superinfection up to 4 years after LT as suggested previously (3).

SAT-557
Subgenotype discrepancies in hepatitis delta virus highlight the need for a unified phylogenetic classification
Ana Alberola Romano[1], Lorenzo Piermatteo[2], Adolfo de Salazar[1], Romina Salpini[2], Maria José Pena[3], Lavinia Fabeni[4], María Reyes Vidal-Acuña[5], Alessia Magnapera[2], María Asunción Iborra[6], Stefano D'Anna[2], Francesca Ceccherini Silberstein[7], A. Aguilera[8], Valentina Svicher[2], Federico García[1]. *[1]Hospital Universitario Clínico San Cecilio, Instituto Investigación Biosanitaria Ibs. Granada, Centro de Investigación Biomédica en Red Enfermedades Infecciosas, CIBERINFEC, Granada, Spain; [2]Department of Biology, University of Rome "Tor Vergata," Rome, Italy; [3]Hospital Universitario de Gran Canaria Doctor Negrín, Las Palmas de Gran Canaria, Spain; [4]National Institute of Infectious Diseases Lazzaro Spallanzani, Roma, Italy; [5]Complejo Hospitalario Universitario de Cáceres, Caceres, Spain; [6]Hospital Clínico Universitario Virgen De La Arrixaca, Murcia, Spain; [7]Department of Experimental Medicine, University of Rome "Tor Vergata," Rome, Italy; [8]Hospital Clínico Universitario De Santiago De Compostela, Santiago de Compostela, Spain*
Email: fegarcia@ugr.es

Background and aims: Hepatitis delta virus (HDV) is classified into eight major genotypes, with HDV-1 being the most prevalent worldwide. Relevant discrepancies persist, especially regarding HDV-1 subgenotype classification. This lack of consensus complicates epidemiological interpretation, inter-study comparability, and potential clinical correlations. The aim of this study was to compare these classification systems and evaluate their impact on subgenotype assignment in clinical HDV sequences.
Method: A comparative phylogenetic analysis was performed using 162 near full-length HDV genome sequences from positive clinical samples, using references from Le Gal et al (subgenotypes 1a–1d), and Karimzadeh et al. (subgenotypes 1a–1e). Phylogenetic trees were constructed using MEGA software version 6, based on the T92+G model and MAFFT v. 7, with reference sequences of HDV genotypes and sub-genotypes, with the Neighbor-Joining method and branch support was assessed by 1,000 bootstrap replicates.
Results: Results from both classification systems clustered consistently at the genotype level, showing full concordance regardless of reference sequences used. HDV genotype 1 was predominant (n = 142, 87.7%), followed by GT5 (n = 18, 11,1%), and GT3 (n = 1) and GT7 (n = 1). Genotype 5 subgenotypes were 5a (n = 6), and 5b (n = 12). Within HDV-1, the two classifications show markedly different

subtype distributions: 97.2% of sequences showed discordant subgenotype assignment depending on the classification system used. Using Le Gal, subtype 1d was overwhelmingly predominant (84.5%), whereas 1a, 1b, and 1c were infrequent (3.5%, 5.6%, and 6.3%, respectively) and 1e was not detected. In contrast, Karimzadeh identified 1e (66.9%) and 1c (23.2%) as the dominant subtypes, with 1a and 1b occurring at similar low frequencies (4.9% and 4.2%), and 1d being rare (0.7%).

Conclusion: Our findings highlight substantial discrepancies in subtype assignment between the two approaches. While HDV genotyping is robust and fully concordant across classification systems, HDV-1 subgenotype assignment remains highly dependent on the reference sequences used. Establishing a harmonized phylogenetic nomenclature is essential to improve epidemiological interpretation, ensure comparability across HDV studies, and support future clinical and translational research.

SAT-558

EVOLVE-HBV study: characteristics and treatment eligibility of adults living with hepatitis B virus infection in rural KwaZulu-Natal, South Africa

Motswedi Anderson[1], Lusanda Mazibuko[2], Ngcebo Mhlongo[2], Gloria Sukali[3], Tongai Gibson Maponga[4], Marion Delphin[5], Emily Martyn[6], Landiwe Ndimande[1], Nikiwe Mbatha[1], Janine Upton[1], Gregory Jording-Jespersen[1], Dickman Gareta[1], Malcolm Ellapen[7], Vasudevan Naidoo[8], Shaun Temmers[8], Elizabeth Waddilove[5], Njabulo Dayi[1], Njabulo Myeni[1], Busangani Ngwenya[1], Nondumiso Mpanza[1], Luthando Zuma[1], Welcome Mbokazi[1], Khanyi Msomi[9], Lucica Thaver[1], Ngundu O Behuhuma[1], Bongiwe Mpanza[1], Merab Lusweti[1], Resign Gunda[1], Emily Wong[10], Mark Seidner[11], Xanthe Hunt[1], Theresa Smit[1], Thumbi Ndungu[12], Guy Harling[13], Janet Seeley[14], Thandeka Khoza[1], Limakatso Lebina[1], Kathy Baisley[15], Collins Iwuji[16], Philippa C Matthews[17]. *[1]Africa Health Research Institute, KwaZulu Natal, Botswana Harvard Health Partnership Institute, Gaborone, Botswana, The Francis Crick Institute, 1 Midland Road, London NW1 1AT, London, UK, Durban, South Africa; [2]Africa Health Research Institute, KwaZulu Natal, Durban, South Africa; [3]Africa Health Research Institute, KwaZulu Natal, South Africa, The Francis Crick Institute, 1 Midland Road, London NW1 1AT, London, UK, Division of Infection and Immunity, University College London, Gower Street, London, WC1E 6BT, UK, Durban, South Africa; [4]Division of Medical Virology, Stellenbosch University, Faculty of Medicine and Health Sciences, National Health Laboratory Service, Tygerberg Business Unit, Tygerberg, Tygerberg, Cape Town, South Africa; [5]The Francis Crick Institute, London, United Kingdom; [6]The Francis Crick Institute, 1 Midland Road, London NW1 1AT, Division of Infection and Immunity, University College London, Gower Street, London, United Kingdom; [7]National Health Laboratory Service, Albert Luthuli Hospital, Durban, South Africa; [8]Inkosi Albert Luthuli Central Hospital, University of KwaZulu-Natal, Durban, South Africa; [9]National Health Laboratory Service, Albert Luthuli Hospital, University of KwaZulu-Natal, Durban, South Africa; [10]Africa Health Research Institute, KwaZulu-Natal, Division of Infectious Diseases, Department of Medicine, University of Alabama at Birmingham, Birmingham, AL, USA, Durban, South Africa; [11]Africa Health Research Institute, KwaZulu-Natal, Division of Infectious Diseases, Massachusetts General Hospital, Boston, MA, USA, Durban, South Africa; [12]Africa Health Research Institute, KwaZulu-Natal, Division of Infection and Immunity, University College London, Gower Street, London, WC1E 6BT, UK, University of KwaZulu-Natal, Durban, South Africa; [13]Africa Health Research Institute, KwaZulu-Natal, University of KwaZulu-Natal, Durban, South Africa, University College London Institute for Global Health, Mortimer Market Centre, Capper Street, London, WC1E 6JB, UK, Durban, South Africa; [14]Africa Health Research Institute, KwaZulu-Natal, University of KwaZulu-Natal, Durban, South Africa, Department of Global Health and Development, London School of Hygiene and Tropical Medicine, London, UK, Durban, South Africa; [15]Africa Health Research Institute, KwaZulu-Natal, London School of Hygiene and Tropical Medicine, London, UK, Durban, South Africa; [16]Africa Health Research Institute, KwaZulu-Natal, Department of Global Health & Infection, Brighton and Sussex Medical School, University of Sussex and University of Brighton, Falmer, Brighton, BN1 9PX, UK, Durban, South Africa; [17]The Francis Crick Institute, 1 Midland Road, London NW1 1AT, Division of Infection and Immunity, University College London, Gower Street, London, WC1E 6BT, UK, Department of Infectious Diseases, University College London Hospital, Euston Road, London NW1 2BU, UK, London, United Kingdom*
Email: philippa.matthews@crick.ac.uk

Background and aims: The World Health Organization (WHO) has set a goal to eliminate viral hepatitis as a public health threat by 2030. Achieving this target requires robust data on hepatitis B virus (HBV) to support public health interventions. Data from high-prevalence regions in Africa are limited. This study aimed to characterise HBV epidemiology, associated comorbidities, and treatment eligibility among individuals living with HBV in rural KwaZulu-Natal (KZN), South Africa.

Method: The EVOLVE-HBV study sampled 2200 individuals from a population-based health survey conducted in rural KZN in 2018–2020 (ethics ref. 00004495/2022 and 23221/001). Stored samples were tested for Hepatitis B surface antigen (HBsAg). Sampling was stratified by age, sex and HIV status and sampling weights were applied to estimate the population prevalence of HBV infection. In 2025 participants who tested positive for HBsAg were invited for clinical evaluation. This included repeat HBV testing, measurement of alanine aminotransaminase (ALT) using WHO-defined upper limits of normal (ULN), assessment for metabolic dysfunction-associated steatotic liver disease (MASLD) and liver stiffness measurement using FibroScan® and cardiometabolic risk factors. Treatment eligibility was determined according to 2024 WHO guidelines.

Results: Among the 2200 individuals tested, 58.6% were female and mean age was 37.6 years (SD 8.3). Weighted prevalence of HBV infection was 10.5% (95% CI 9.1–12.2). Of the 240 individuals who had tested HBsAg-positive at baseline, we were able to contact 101 (42.1%) and have reassessed 43 individuals with confirmed chronic HBV infection. Among these, 23/43 (53.5%) were living with HIV and receiving antiretroviral treatment. Liver stiffness measurements were available for 42/43; 18 (43.9%) had fibrosis (>7 kPa) and one had cirrhosis (>12 kPa). *ALT* was >ULN in 19/40 (47.5%), and 18/42 (42.9%) met the criteria for MASLD. Among 20 individuals with HBV mono-infection, 11 (55%) met WHO treatment criteria.

Conclusion: HBV is common in rural KZN. All HIV/HBV co-infected individuals were on HBV-active therapy, however, among individuals living with HBV mono-infection, almost half met WHO treatment criteria to start HBV treatment but were not yet on treatment. This suggests that where HBV is not comorbid with HIV, follow-up, and linkage to care is challenging in this setting. Improved HBV prevention, diagnosis, risk assessment, and integration of MASLD services into existing HIV and chronic disease programs are needed.

SAT-559

Performances of Baveno VII and aasld 2024 criteria for detecting high risk varices in untreated patients with HDV cirrhosis

Maria Paola Anolli[1,2,3], Elisabetta Degasperi[1,2], Giulia Tosetti[1], Liana Gheorghe[4], Alessandro Loglio[5], Alessia Ciancio[6], Giampiero D'Offizi[7], Mathias Jachs[8], Thomas Reiberger[8], Christoph Schramm[9], Maurizia Brunetto[10], Florian van Bommel[11], Serena Zaltron[12], Laura Turco[13], Caroline Zöllner[14], Teresa Santantonio[15], Ivana Carey[16], Alessandro Federico[17], Andrea Di Lorenzo[18], Maria Buti[19], Filipe Calinas[20], Filomena Morisco[21], Margarita Papatheodoridi[22], Francesco Paolo Russo[23,24], Alessandra Mangia[25], Pierluigi Toniutto[26], Nicola Coppola[27], Christopher Dietz-Fricke[28], Jérôme Dumortier[29], Edoardo Giovanni Giannini[30], Elena Rosselli Del Turco[31], Soo Aleman[32], Stella De Nicola[33], Monia Maracci[34], Letizia Marinaro[35], Michele Milella[36], Adriano Pellicelli[37], Biagio Pinchera[38], Massimo Puoti[39], Dominique Roulot[40],

Saveria Lory Croce'[41], Ivana Rita Maida[42], Uta Merle[43], Mariana Cardoso[44], Alessia Zoncada[45], Pietro Torre[46], Francesca Pileri[47], Antonietta Romano[48], Matteo Tonnini[49], Paola Vitiello[50], Rosa Zampino[51], Pietro Lampertico[1,2,3]. *[1]Division of Gastroenterology and Hepatology, Foundation IRCCS Ca' Granda Ospedale Maggiore Policlinico, Milan, Italy; [2]D-SOLVE consortium, an EU Horizon Europe funded project (No 101057917), Hannover, Germany; [3]CRC "A. M. and A. Migliavacca" Center for Liver Disease, Department of Pathophysiology and Transplantation, University of Milan, Milan, Italy; [4]Center for Digestive Diseases and Liver Transplantation, Fundeni Clinical Institute, Bucharest, Romania; [5]Gastroenterology, Hepatology and Transplantation Division, ASST Papa Giovanni XXIII, Bergamo, Italy; [6]Department of Medical Sciences, University of Turin, Gastroenterology Division of Città della Salute e della Scienza of Turin, University Hospital, Turin, Italy; [7]Division of Infectious Diseases, Hepatology, Department of Transplantation and General Surgery, Istituto Nazionale per le Malattie Infettive "L. Spallanzani" IRCCS, Rome, Italy; [8]Division of Gastroenterology and Hepatology, Department of Medicine III, Medical University of Vienna, Vienna, Austria; [9]Department of Gastroenterology, Hepatology and Transplant Medicine, Medical Faculty, University of Duisburg-Essen, Essen, Germany; [10]Department of Clinical and Experimental Medicine, University of Pisa and Hepatology Unit, University Hospital of Pisa, Pisa, Italy; [11]Division of Hepatology, Department of Medicine II, Leipzig University Medical Center, Laboratory for Clinical and Experimental Hepatology, Leipzig, Germany; [12]Infectious Disease Department, Spedali Civili Brescia, Brescia, Italy; [13]Internal Medicine Unit for the Treatment of Severe Organ Failure, IRCCS Azienda Ospedaliero- Universitaria di Bologna, Bologna, Italy; [14]Department of Hepatology and Gastroenterology, Charité Universitätsmedizin Berlin, Berlin, Germany; [15]Department of Medical and Surgical Sciences, Infectious Diseases Unit, University of Foggia, Foggia, Italy; [16]Institute of Liver Studies, King's College Hospital, London, United Kingdom; [17]Division of Hepatogastroenterology, Department of Precision Medicine, Università della Campania "Luigi Vanvitelli", Naples, Italy; [18]Tor Vergata University, Rome, Italy; [19]Liver Unit, Internal Medicine Department, Hospital Universitari Vall d'Hebron, Vall d'Hebron Barcelona Hospital Campus, Barcellona, Spain; [20]Serviço de Gastrenterologia, ULS de São José, São José, Portugal; [21]Department of Clinical Medicine and Surgery, Diseases of the Liver and Biliary System Unit, University of Naples "Federico II", Naples, Italy; [22]1st Department of Gastroenterology, General Hospital of Athens "Laiko", Medical School of National & Kapodistrian University of Athens, Athens, Greece; [23]Department of Surgery, Oncology and Gastroenterology, University of Padua, Padua, Italy; [24]Gastroenterology Unit, Azienda Ospedale -Università Padova, Padua, Italy; [25]Liver Unit, Fondazione IRCCS "Casa Sollievo della Sofferenza", San Giovanni Rotondo, Italy; [26]Hepatology and Liver Transplantation Unit, Academic Hospital, University of Udine, Udine, Italy; [27]Department of Mental Health and Public Medicine, Infectious Diseases Unit, University of Campania Luigi Vanvitelli, Naples, Italy; [28]Department of Gastroenterology, Hepatology, Infectious Diseases and Endocrinology at Hannover Medical School, Hannover, Germany; [29]Department of Digestive Diseases, Hospices Civils de Lyon, Edouard Herriot hospital, France; Claude Bernard Lyon 1 University, Lyon, France; [30]Gastroenterology Unit, Department of Internal Medicine, University of Genoa, Genoa, Italy; [31]Department of Medical and Surgical Sciences, Unit of Infectious Diseases, "Alma Mater Studiorum" University of Bologna, S. Orsola-Malpighi Hospital, Bologna, Italy; [32]Infectious Disease Clinic, Karolinska University Hospital, Stockholm, Sweden; [33]Division of Internal Medicine and Hepatology, Department of Gastroenterology, IRCCS Humanitas Research Hospital, Rozzano, Italy; [34]Institute of Infectious Diseases and Public Health, Università Politecnica delle Marche, Ancona, Italy; [35]SCDU Infectious Diseases, Amedeo di Savoia Hospital, ASL Città di Torino, Turin, Italy; [36]Infectious Diseases Unit, Department of Biomedical Sciences and Human Oncology, University of Bari, Bari, Italy; [37]Liver Unit, San Camillo Hospital, Department of Transplantation and General Surgery, Rome, Italy; [38]Department of Clinical Medicine and Surgery, University of Naples Federico II, Naples, Italy; [39]School of Medicine and Surgery University of Milano Bicocca, Milan, Italy; [40]Liver Unit, Avicenne Hospital, AP-HP, Sorbonne Paris Nord University, Bobigny, France; [41]Department of Medicine, Surgery and Health Sciences, University of Trieste, Trieste, Italy; [42]Infectious and Tropical Diseases Unit, Department of Medical, Surgical and Experimental Sciences, University of Sassari, Sassari, Italy; [43]Department of Internal Medicine IV, Gastroenterology & Hepatology, Heidelberg University Hospital, Heidelberg, Germany; [44]Gastroenterology Department, ULS de São José, Lisbon, Portugal; [45]Unit of Infectious Diseases, ASST Cremona, Cremona, Italy; [46]Department of Medicine, Surgery and Dentistry, University of Salerno, Baronissi, Italy; [47]Division of Internal Medicine and Center for Hemochromatosis, University of Modena and Reggio Emilia, Modena, Italy; [48]Unit of Internal Medicine and Hepatology (UIMH), Department of Medicine, University of Padua, Padua, Italy; [49]Division of Internal Medicine, Hepatobiliary and Immunoallergic Diseases, IRCCS Azienda Ospedaliero-Universitaria di Bologna, Bologna, Italy; [50]Unit of Infectious Diseases, ASST della Valle Olona, Busto Arsizio, Italy; [51]Department of Advanced Medical and Surgical Sciences, University of Campania Luigi Vanvitelli, Naples, Italy*
Email: maria.anolli@unimi.it

Background and aims: In patients with compensated cirrhosis, gastroesophageal varices (EV) are associated with a higher risk of hepatic decompensation. Non-invasive tests (NITs) are increasingly used in clinical practice for assessing the risk of EV, but specific studies in chronic hepatitis Delta (CHD) are missing.
Method: Untreated CHD patients with compensated cirrhosis with available liver stiffness measurement (LSM) and esophagogastroduodenoscopy (EGD) enrolled in the SAVE-D and D-SHIELD studies were included. In a subgroup of patients, spleen stiffness measurement (SSM) was available. Baveno VI and AASLD criteria for avoiding screening endoscopy (LSM <20 kPa + platelets [PLT] count >150 × 10^9/L); and the Baveno VII SSM ≤40 kPa cut-off to rule-out high-risk varices (HRV) were applied. NIT performance was assessed by Sensibility (Sn), Specificity (Sp), Positive Predictive Value (PPV), Negative Predictive Value (NPV), and accuracy. The diagnostic performance of LSM was evaluated using Receiver Operating Characteristic (ROC) curve analysis. All tests were performed prior to Bulevirtide start.
Results: 347 patients were included: median age was 54 years, 56% males, 156 (45%) with EV on EGD, 93 (27%) with HRV. Median LSM was 16.7 (11.8–25.2) kPa, PLT 95 (65–147) 10^9/L, albumin 4.9 (3–7–4.3) g/dL, ALT 78 (50–146) U/L, spleen length 14 (12–17) cm. 65 (19%) patients fulfilled the LSM and PLT "avoid endoscopy" criteria, resulting in 4 (9%) missed HRV (Sn 95.7%, NPV 93.8%). Median SSM was 47.2 kPa (30.4–67.2) kPa, and in patients with SSM ≤40 kPa the rate of missed HRV was 7% (Sn 89.5%, NPV 92.9%). ROC analysis retrieved an optimal LSM cut-off for HRV of 18.7 kPa: AUROC 0.620 (95% CI 0.550–0.690), 60.2% Sn and a false positive rate (1 - Sp) of 0.319, corresponding to a Sp of approximately 68.1%. The corresponding PPV was 40.8%. Based on these data, we identified two cutoffs to respectively discriminate the absence or presence of HRV: <10.3 kPa, where HRV risk is low (Sn 88% and NPV 75%), and >24.9 kPa, where HRV risk increases (Sp 80%, PPV 40%).
Conclusion: In untreated CHD patients with cirrhosis, the Baveno VI/VII criteria failed to identify a significant proportion of patients with HRV who are at high risk of variceal bleeding.

SAT-560

Prevalence and clinical relevance of cardiometaboloc factors in european patients with HDV-related liver disease (methdv study) - a save-d and d-shield pooled analysis

Maria Paola Anolli[1,2,3], Elisabetta Degasperi[1,2], Liana Gheorghe[4], Alessandro Loglio[5], Alessia Ciancio[6], Giampiero D'Offizi[7], Mathias Jachs[8], Thomas Reiberger[8], Christoph Schramm[9], Maurizia Brunetto[10], Florian van Bömmel[11], Serena Zaltron[12], Laura Turco[13], Caroline Zöllner[14], Teresa Santantonio[15], Ivana Carey[16], Alessandro Federico[17], Mariarosa Tamè[18], Andrea Di Lorenzo[19],

Maria Buti[20], Filipe Calinas[21], Filomena Morisco[22], Margarita Papatheodoridi[23], Francesco Paolo Russo[24,25], Alessandra Mangia[26], Pierluigi Toniutto[27], Nicola Coppola[28], Christopher Dietz-Fricke[29], Jérôme Dumortier[30], Edoardo Giannini[31], Elena Rosselli Del Turco[32], Soo Aleman[33], Stella De Nicola[34], Monia Maracci[35], Letizia Marinaro[36], Michele Milella[37], Adriano Pellicelli[38], Biagio Pinchera[39], Massimo Puoti[40], Dominique Roulot[41], Saveria Lory Croce'[42], Ivana Rita Maida[43], Uta Merle[44], Mariana Cardoso[45], Alessia Zoncada[46], Pietro Torre[47], Francesca Pileri[48], Antonietta Romano[49], Matteo Tonnini[50], Paola Vitiello[51], Rosa Zampino[52], Pietro Lampertico[1,2,3]. *[1]Division of Gastroenterology and Hepatology, Foundation IRCCS Ca' Granda Ospedale Maggiore Policlinico, Milan, Italy; [2]D-SOLVE consortium, an EU Horizon Europe funded project (No 101057917), Hannover, Germany; [3]CRC "A. M. and A. Migliavacca" Center for Liver Disease, Department of Pathophysiology and Transplantation, University of Milan, Milan, Italy; [4]Center for Digestive Diseases and Liver Transplantation, Fundeni Clinical Institute, Bucharest, Romania; [5]Gastroenterology, Hepatology and Transplantation Division, ASST Papa Giovanni XXIII, Bergamo, Italy; [6]Department of Medical Sciences, University of Turin, Gastroenterology Division of Città della Salute e della Scienza of Turin, University Hospital, Turin, Italy; [7]Division of Infectious Diseases, Hepatology, Department of Transplantation and General Surgery, Istituto Nazionale per le Malattie Infettive "L. Spallanzani" IRCCS, Rome, Italy; [8]Division of Gastroenterology and Hepatology, Department of Medicine III, Medical University of Vienna, Vienna, Austria, [9]Department of Gastroenterology, Hepatology and Transplant Medicine, Medical Faculty, University of Duisburg-Essen, Essen, Germany, [10]Department of Clinical and Experimental Medicine, University of Pisa and Hepatology Unit, University Hospital of Pisa, Pisa, Italy, [11]Division of Hepatology, Department of Medicine II, Leipzig University Medical Center, Laboratory for Clinical and Experimental Hepatology, Leipzig, Germany; [12]Infectious Disease Department, Spedali Civili Brescia, Brescia, Italy; [13]Internal Medicine Unit for the Treatment of Severe Organ Failure, IRCCS Azienda Ospedaliero- Universitaria di Bologna, Bologna, Italy; [14]Department of Hepatology and Gastroenterology, Charité Universitätsmedizin Berlin, Berlin, Germany; [15]Department of Medical and Surgical Sciences, Infectious Diseases Unit, University of Foggia, Foggia, Italy; [16]Institute of Liver Studies, King's College Hospital, London, United Kingdom; [17]Division of Hepatogastroenterology, Department of Precision Medicine, Università della Campania "Luigi Vanvitelli", Naples, Italy; [18]Gastroenterology Unit, IRCCS Azienda Ospedaliero-Universitaria di Bologna, Bologna, Italy; [19]Tor Vergata University, Rome, Italy; [20]Liver Unit, Internal Medicine Department, Hospital Universitari Vall d'Hebron, Vall d'Hebron Barcelona Hospital Campus, Barcelona, Spain; [21]Serviço de Gastrenterologia, ULS de São José, Lisboa, Portugal; [22]Department of Clinical Medicine and Surgery, Diseases of the Liver and Biliary System Unit, University of Naples "Federico II", Naples, Italy; [23]1st Department of Gastroenterology, General Hospital of Athens "Laiko", Medical School of National & Kapodistrian University of Athens, Athens, Greece; [24]Department of Surgery, Oncology and Gastroenterology, University of Padua, Padua, Italy; [25]Gastroenterology Unit, Azienda Ospedale -Università Padova, Padua, Italy; [26]Liver Unit, Fondazione IRCCS "Casa Sollievo della Sofferenza", San Giovanni Rotondo, Italy; [27]Hepatology and Liver Transplantation Unit, Academic Hospital, University of Udine, Udine, Italy; [28]Department of Mental Health and Public Medicine, Infectious Diseases Unit, University of Campania Luigi Vanvitelli, Naples, Italy; [29]Department of Gastroenterology, Hepatology, Infectious Diseases and Endocrinology at Hannover Medical School, Hannover, Germany; [30]University of Lyon, Université Claude-Bernard (UCBL), Lyon, France; [31]Gastroenterology Unit, Department of Internal Medicine, University of Genoa, Genoa, Italy; [32]Department of Medical and Surgical Sciences, Unit of Infectious Diseases, "Alma Mater Studiorum" University of Bologna, S. Orsola-Malpighi Hospital, Bologna, Italy; [33]Infectious Disease Clinic, Karolinska University Hospital, Stockholm, Sweden; [34]Division of Internal Medicine and Hepatology, Department of Gastroenterology, IRCCS Humanitas Research Hospital, Rozzano, Milan, Italy; [35]Institute of Infectious Diseases and Public Health, Università Politecnica delle Marche, Ancona, Italy; [36]SCDU Infectious Diseases, Amedeo di Savoia Hospital, ASL Città di Torino, Turin, Italy; [37]Infectious Diseases Unit, Department of Biomedical Sciences and Human Oncology, University of Bari, Bari, Italy; [38]Liver Unit, San Camillo Hospital, Department of Transplantation and General Surgery, Rome, Italy; [39]Department of Clinical Medicine and Surgery, University of Naples Federico II, Naples, Italy; [40]School of Medicine and Surgery University of Milano Bicocca, Milano, Italy; [41]AP-HP, Avicenne Hospital, Hepatology Department, Bobigny, France; [42]Department of Medicine, Surgery and Health Sciences, University of Trieste, Trieste, Italy; [43]Infectious and Tropical Diseases Unit, Department of Medical, Surgical and Experimental Sciences, University of Sassari, Sassari, Italy; [44]Department of Internal Medicine IV, Gastroenterology & Hepatology, Heidelberg University Hospital, Heidelberg, Germany; [45]Gastroenterology Department, ULS de São José, Lisbon, Portugal; [46]Unit of Infectious Diseases, ASST Cremona, Cremona, Italy; [47]Department of Medicine, Surgery and Dentistry, University of Salerno, Baronissi, Italy; [48]Division of Internal Medicine and Center for Hemochromatosis, University of Modena and Reggio Emilia, Modena, Italy; [49]Unit of Internal Medicine and Hepatology (UIMH), Department of Medicine, University of Padua, Padua, Italy; [50]Division of Internal Medicine, Hepatobiliary and Immunoallergic Diseases, IRCCS Azienda Ospedaliero-Universitaria di Bologna, Bologna, Italy; [51]Unit of Infectious Diseases, ASST della Valle Olona, Busto Arsizio, Italy; [52]Department of Advanced Medical and Surgical Sciences, University of Campania Luigi Vanvitelli, Naples, Italy*
Email: maria.anolli@unimi.it

Background and aims: Chronic hepatitis Delta represents the most aggressive form of viral hepatitis, with higher rates of cirrhosis development and hepatocellular carcinoma (HCC) incidence. While cardiometabolic risk factors influence outcomes in other chronic liver diseases, their prevalence and relevance in CHD remain poorly characterized.

Method: CHD patients included in the retrospective multicenter real-world European SAVE-D study and in the prospective multicenter Italian D-SHIELD study were included. The prevalence of cardiometabolic risk factors (arterial hypertension, type 2 diabetes, overweight/obesity) were evaluated at BLV start.

Results: 828 patients treated with BLV 2 mg/day subcutaneous monotherapy up to 144 weeks were included in this analysis: age 52 (IQR 42–60) years, 57% men, 698 (84%) with cirrhosis, median BMI was 24.8 (22.7–27.4). 39 (5%) patients had type 2 diabetes (T2DM), and 126 (15%) patients had arterial hypertension (AHTN), 85 (10%) patients had obesity (defined as BMI ≥30), of whom 13 (15%) grade II obesity (BMI 35–39) and 2 (2%) grade III obesity (BMI≥40). Controlled Attenuation Parameter (CAP) on Fibroscan® was available in 484 (59%) patients: median CAP values were 209 (181–238) dB/m. 50 (5%) patients showed hepatic steatosis (by CAP >275 dB/m): median BMI in these patients was 28.4, 6 (12%) patients had T2DM, 11 (22%) AHTN. Overall, median alanine aminotransferase (ALT) levels were 78 (50–127) U/L in patients without and with T2DM, respectively (p = 0.57). Median gamma glutamyl transferase (gGT) were 56 (35–94) and 68 (30–125) U/L in patients without and with T2DM, respectively (p = 0.19). When analyzing the impact of cardiometabolic risk factors (AHTN, T2DM), BMI and CAP values on responses rates to BLV, only CAP values predicted the achievement of a biochemical response at on-treatment week 48 (OR 1.01 95% CI 1.00–1.02, p = 0.02). Conversely, none of the baseline features predicted the achievement of a virological response, combined response, and of HDV RNA undetectability at week 48 of BLV monotherapy.

Conclusion: Prevalence of cardiometabolic risk factors in European CHD patients (MetHDV) is lower than reported for other types of viral hepatitis and did not significantly impact response rates in the first year of BLV monotherapy.

SAT-561

Long-term risk and predictors for hepatocellular carcinoma and other liver-related outcomes in a large African-born cohort with chronic hepatitis B, living in Sweden

Katarina Århem[1], Habiba Kamal[1], Karin Lindahl[1], Frida Jakobsson[2], Ann-Sofi Duberg[3], Soo Aleman[1]. *[1]Department of infectious diseases, Karolinska University Hospital, Department of medicine Huddinge, Karolinska Institutet, Stockholm, Sweden; [2]Department of Infectious Diseases, Sunderby Hospital, Department of Clinical Microbiology, Umeå University, Umeå, Sweden; [3]Department of Infectious Diseases, Faculty of Medicine and Health, Örebro University, Örebro, Sweden*
Email: katarina.johansson-arhem@regionstockholm.se

Background and aims: Sub Saharan African (SSA) origin has been suggested as a potential risk factor for hepatocellular carcinoma (HCC) in persons with chronic hepatitis B (CHB) but large longitudinal studies on Africans with CHB are scarce both in and outside of Africa and the natural course of CHB in this population remains poorly characterized. We assessed the risk of HCC and other liver-related events (LRE) among African-born patients with CHB living in Sweden.
Method: This retrospective cohort study included 1,167 African-born patients with CHB attending Karolinska University Hospital, Stockholm, and Sunderby Hospital, Northern Sweden. We retrieved demographic, clinical, and laboratory data from our national quality register InfCare Hepatit and medical records. Incidence rates (IRs) and cumulative risks of HCC and composite LRE (new-onset cirrhosis, hepatic decompensation, HCC, liver transplantation, or liver-related death) were assessed using Kaplan–Meier analysis. Risk factors for LRE and HCC were evaluated using Cox regression.
Results: The cohort consisted of 60% men with a median age of 33.3 years; most patients originated from East (51%) and West Africa (31%). 6.9% and 4.5% were seropositive for HIV and HDV, respectively. Median follow-up time was 6.5 years. Twelve patients developed HCC (IR 0.11/ 100 person-years [PY]), with 5- and 10-year cumulative risks of 0.29% and 0.64%, respectively. Eleven cases occurred in men, mean age at diagnosis was 47.6 years, and four patients were < 40 years. Cirrhosis was present at HCC diagnosis in 83%, and 50% had baseline HBV-DNA levels > 6 $\log_{10}$ IU/mL. Among patients with baseline cirrhosis, the HCC IR was 1.40/ 100 PY, with a 5-year cumulative risk of 9.49%. Thirty-six patients experienced one or more LREs (IR 0.41/100 PY), with 5- and 10-year cumulative risks of 2.00% and 2.98%. Age, HBeAg positivity, HBV-DNA > 2,000 IU/mL, and baseline cirrhosis were associated with both HCC alone and composite LRE. In multivariable analysis, HBeAg positivity and baseline cirrhosis independently predicted LRE, whereas HCC cases were too few for a robust multivariable analysis.
Conclusion: African-born patients with CHB in Sweden had a low overall risk of HCC, although cases occurred at a relatively young age. HCC rarely developed in the absence of cirrhosis, and most patients with HCC or LRE had established risk factors, including cirrhosis and high viral load at baseline.

SAT-562

End-of-treatment biomarkers and HBV genotype predict severe biochemical flares after nucleos(t)ide analogue cessation: individual patient level meta-analysis of five prospective studies within the PROSTOP consortium

Fleur Ballet[1,2], Arno Furquim d'Almeida[1,2], Marte Holmberg[3,4], Simon Hume[5,6], Anna Pocurull Aparicio[7], Magnus Lindh[8], Axelle Vanderlinden[1,2], Barbara Testoni[9], Fabien Zoulim[9], Benoit Kabamba[10], Veerle Matheeussen[11], Kumar Visvanathan[5,6], Dag Henrik Reikvam[4,12], Niel Hens[13,14], Sabela Lens[7], Alexander Thompson[5,6], Asgeir Johannessen[3,4,12], Thomas Vanwolleghem[1,2]. *[1]University of Antwerp, Viral Hepatitis Research Group, Laboratory of Experimental Medicine and Pediatrics, Antwerp, Belgium; [2]Antwerp University Hospital, Department of Gastroenterology and Hepatology, Edegem, Belgium; [3]Vestfold Hospital Trust, Department of Infectious Diseases, Tonsberg, Norway; [4]University of Oslo, Institute of Clinical Medicine, Faculty of Medicine, Oslo, Norway; [5]St Vincent's Hospital, Gastroenterology Department, Melbourne, Australia; [6]St Vincent's Hospital, Department of Infectious Disease and Immunology Research Centre, Melbourne, Australia; [7]University of Barcelona, Liver Unit, Hospital Clinic, FCRB-IDIBAPS, Barcelona, Spain; [8]University of Gothenburg, Department of Infectious Diseases, Sahlgrenska Academy, Gothenburg, Sweden; [9]Université Claude Bernard Lyon 1, Lyon Hepatology Institute, UMR Inserm U1350 PaThLiv, Lyon, France; [10]Clinique Universitaires Saint-Luc, Department of Microbiology, Brussels, Belgium; [11]Antwerp University Hospital, Laboratory of Medical Microbiology, Antwerp, Belgium; [12]Oslo University Hospital, Department of Infectious Diseases, Oslo, Norway; [13]University of Antwerp, Centre for Health Economics Research and Modelling of Infectious Diseases (CHERMID), Vaccine & Infectious Disease Institute (VAXINFECTIO), Antwerp, Belgium; [14]University of Hasselt, Data Science Institute, Interuniversity Institute for Biostatistics and statistical Bioinformatics (I-BioStat), Hasselt, Belgium*
Email: fleur.ballet@uantwerpen.be

Background and aims: Flares frequently occur after nucleos(t)ide analogue (NUC) cessation, necessitating close follow-up. Identifying end-of-treatment (EOT) predictors could improve safety. We assessed patient characteristics and EOT biomarkers to predict severe biochemical flares (SBFs; ALT >10×ULN).
Method: Individual patient-level data from five prospective NUC stop studies within the PROSTOP consortium were pooled. All patients were HBeAg negative, long-term virologically suppressed, and none had advanced liver fibrosis. Multivariate Fine-Gray models for SBFs were fitted with retreatment as competing risk and stratification by study. Age, sex, ethnicity, EOT HBsAg and NUC type were evaluated in the full cohort. HBV genotype (gt) and EOT hepatitis B core related antigen (HBcrAg), hepatitis B core IgG antibodies (anti-HBc) and HBV RNA were evaluated in available subcohorts, adjusting for identified predictors. Predictive performance was assessed by using the time-dependent area under the ROC curve (AUC) at 48 weeks.
Results: Among 402 patients, 83 experienced an SBF, corresponding to a cumulative incidence of 18.7% within 48 weeks. During follow-up, 113 (28.1%) patients were retreated, one (0.2%) underwent liver transplantation, and no liver-related deaths occurred. In the full cohort, tenofovir showed a borderline non-significant association with SBF risk (SHR = 1.65, p = 0.0504), with earlier flares compared with entecavir. Male sex was associated with increased SBF-risk (SHR = 2.38, p = 0.002). Overall, log HBsAg levels were not associated with SBF occurrence (p > 0.05), however no patients with HBsAg <10 IU/mL developed a SBF. Ethnicity was not associated with SBF risk. Gt A (SHR = 0.06, p = 0.007) and higher anti-HBc levels (SHR = 0.33, p < 0.001) were protective, while detectable HBcrAg (SHR = 2.67, p = 0.002) and HBV RNA (SHR = 2.2, p = 0.02) increased SBF risk. Prediction based on age, sex, ethnicity, HBsAg and NUC type yielded an AUC of 0.62. Models incorporating gt, HBcrAg, and anti-HBc achieved an AUC of 0.77, increasing to 0.83 with addition of sex, NUC type and HBV RNA.
Conclusion: In this pooled analysis of five prospective NUC cessation studies, genotype A and EOT anti-HBc were the strongest protective factors against post-cessation SBFs, whereas EOT HBcrAg and HBV RNA were the most important risk factors. A biomarker-based model substantially improved prediction of SBFs, and may enable safer, individualized NUC cessation strategies.

SAT-563-YI

Longitudinal HBsAg trajectories might predict virological outcomes in patients with chronic hepatitis B infection

Sara Battistella[1,2], Andreu Roca[3], Anna Pocurull Aparicio[1,2], Zoe Mariño[1,2], Sergio Rodriguez-Tajes[1,2], Xavier Forns[1,2], Sabela Lens[1,2]. *[1]Liver Unit, Hospital Clinic, IDIBAPS, Barcelona, Spain, Barcelona, Spain; [2]Centro de Investigación Biomédica en Red de*

Enfermedades Hepáticas y Digestivas (CIBEREHD), Madrid, Spain; [3]Medical Statistics Core Facility, Hospital Clinic Barcelona, IDIBAPS, Barcelona, Spain, Barcelona, Spain
Email: sarabattistella93@gmail.com

Background and aims: Quantitative HBsAg (qHBsAg) has emerged as a valuable biomarker to predict HBsAg seroclearance, support finite nucleos(t)ide analogue (NUCs) therapy decisions, and predict response to emerging HBV antiviral agents. Yet, real-life evidence on long-term qHBsAg trajectories remains scarce. This study aimed to characterize long-term qHBsAg dynamics in a real-life cohort and to identify predictors of clinically relevant virological endpoints.
Method: A total of 294 patients with chronic HBV infection (80% non-Asian), both treated and untreated, HBeAg positive or negative, with at least two qHBsAg measurements over a minimum follow-up of three years, were followed for a median of 7.5 (5.5–10.5) years. Longitudinal qHBsAg kinetics were analysed to identify predictors of functional cure, eligibility for NUCs discontinuation, and inclusion in future antiviral trials.
Results: At baseline, 61 (20.7%) were HBeAg positive and 49.3% received antiviral treatment during follow-up. Overall, a downward trend in qHBsAg levels was observed: the proportion of patients with qHBsAg < 100 IU/mL increased from 11.6% to 31.6%, those with < 1000 IU/mL from 40.1% to 59.2%, and those with < 3000 IU/mL from 59.2% to 77.9% at the last visit. Sixty-four patients (21.8%) showed an annual decline in HBsAg ≥ 0.5 log, corresponding to a ~70% reduction. Among treated Caucasian patients with baseline qHBsAg > 1000 IU/mL (n = 70), 21 (30%) reached the recommended threshold of < 1000 IU/mL to stop NUCs treatment. Among patients with baseline qHBsAg > 3000 IU/mL (n = 120), 57 (47.5%) decreased below 3000 IU/mL at the last visit, potentially meeting the inclusion criteria for novel antiviral trials. NUCs exposure and > 0.5 log HBsAg decline were independently associated with this outcome, with HBsAg reduction emerging as the most powerful predictor (OR = 14.197).
Functional cure occurred in 8.8% of patients; an annual qHBsAg decline ≥0.5 log was the strongest independent predictor of HBsAg loss, irrespective of antiviral treatment, baseline viral load, or HBeAg status.
Conclusion: In a real-word, predominantly non-Asian cohort, long-term qHBsAg trajectories demonstrated that both baseline qHBsAg levels and the magnitude of longitudinal decline strongly influence key virological outcomes. Dynamic HBsAg monitoring may help predict functional cure and inform tailored decisions for NUCs finite therapy and enrolment in novel treatment strategies.

SAT-564

Management of chronic hepatitis B in people with human immunodeficiency virus infection in Europe: real-world evidence from Spain and Germany

Juan Berenguer[1], Pablo Ryan[2], Thomas Lutz[3], Luz Martín Carbonero[4], Leire Perez Latorre[1], María Jesus Vivancos-Gallego[5], Jordi Navarro[6], Roser Navarro[7], Oscar Ferrero[8], Rosario Palacios Muñoz[9], Christoph Wyen[10], Pere Domingo[11], Malte Monin[12], Xavier Camino[13], Marta Montero[14], Alexander Killer[15], Jakob Malin[16], Ignacio De Los Santos[17], Stefan Esser[18], Luis Enrique Morano Amado[19], Ian López[20], Roger Vogelmann[21], Stefan Mauss[22], Antonio Rivero[23], Fauzi Elamouri[24], Carmen Hidalgo-Tenorio[25], Kathrin van Bremen[26], Juncal Pérez-Somarriba[27], José Sanz[28], Daniel Beer[29], Axel Baumgarten[30], Annette Haberl[31], Maria José Galindo[32], Carmen Fariñas[33], Florian Voit[34], Nazifa Qurishi[35], Sebastian Noe[36,36], Sergio Reus Bañuls[37], Pavel Khaykin[38], Stephan M Schneeweiß[39], Anders Boyd[40], Marta De Miguel[41], José Bellón[1], Jürgen Rockstroh[24].
[1]Hospital General Universitario Gregorio Marañón (IiSGM), Madrid, Spain; [2]Hospital Universitario Infanta Leonor (IiSGM), Madrid, Spain; [3]Infektiologikum Frankfurt, Frankfurt, Germany; [4]Hospital Universitario La Paz (IDIPAZ), Madrid, Spain; [5]Hospital Universitario Ramón y Cajal (YRYCIS), Madrid, Spain; [6]Hospital Universitari Vall d'Hebron, Barcelona, Spain; [7]Hospital Universitario 12 de Octubre (i+12), Madrid, Spain; [8]Hospital Universitario de Basurto, Bilbao, Spain; [9]Hospital Universitario Virgen de la Victoria, Málaga, Spain; [10]Praxis Ebertplatz, Cologne, Germany; [11]Hospital de la Santa Creu i Sant Pau, Barcelona, Spain; [12]University Medical Center Hamburg, Eppendorf, Hamburg, Germany; [13]Hospital Donostia, San Sebastián, Spain; [14]Hospital Universitario y Politécnico La Fe, Valencia, Spain; [15]University Hospital Düsseldorf, Medical Faculty of Heinrich Heine University Düsseldorf, Düsseldorf, Germany; [16]University Hospital Cologne, Cologne, Germany; [17]Hospital Universitario de la Princesa (IIS-Princesa), Madrid, Spain; [18]University Hospital Essen, Essen, Germany; [19]Hospital Universitario Álvaro Cunqueiro, Vigo, Spain; [20]Hospital Universitario Doctor Peset, Valencia, Spain; [21]Mannheimer Onkologie Praxis, Mannheim, Germany; [22]Center for HIV and Hepatogastroenterology, Düsseldorf, Germany; [23]Hospital Universitario Reina Sofía, Córdoba, Spain; [24]University Hospital Bonn, Bonn, Germany; [25]Hospital Universitario Virgen de las Nieves (IBS), Granada, Spain; [26]MVZ Innere Medizin Köln, Cologne, Germany; [27]Hospital Clínico San Carlos (IdISSC), Madrid, Spain; [28]Hospital Universitario Príncipe de Asturias, Alcalá de Henares, Spain; [29]Praxiszentrum Blondelstrasse, Aachen, Germany; [30]Zentrum für Infektiologie Berlin Prenzlauer Berg GmbH, Berlin, Germany; [31]University Hospital Frankfurt, Frankfurt, Germany; [32]Hospital Clínico Universitario de Valencia, Valencia, Spain; [33]Hospital Marqués de Valdecilla (IDIVAL), Santander, Spain; [34]TUM University Hospital, Munich, Germany; [35]Gemeinschaftspraxis Gotenring, Cologne, Germany; [36]MVZ München am Goetheplatz, Munich, Germany; [37]Hospital General de Alicante, Alicante, Spain; [38]MainFachArzt, Frankfurt, Germany; [39]Praxis Hohenstaufenring, Cologne, Germany; [40]University Hospital Bern, Bern, Switzerland; [41]Fundación SEIMC/GeSIDA, Madrid, Spain
Email: jbb4@me.com

Background and aims: In settings with access to direct acting antivirals for HCV, HBV is the leading cause of chronic viral hepatitis among people with HIV (PWH). Adherence to HBV management guidelines in this population remains poorly characterized. Our aim was to evaluate adherence to current HBV management guidelines among PWH in Spain (SP) and Germany (GE).
Method: Cross-sectional study conducted in 42 centers (SP 21; GE 21) between June 2024 and March 2025. PWH with chronic HBV (≥2 HBsAg-positive tests ≥6 mo. apart) were included. Adherence to the 2024 European AIDS Clinical Society Guidelines was assessed: HBV-active therapy (TAF, TDF, or entecavir); laboratory monitoring (ALT/AST and HBV DNA within 12 mo.); anti-HDV testing; HDV-RNA testing in anti-HDV–positive individuals; and hepatocellular carcinoma (HCC) surveillance, defined as liver ultrasound every 6 mo. in patients with cirrhosis or ≥1 risk factor (age >45 yr, Asian/African origin, active HDV, or PAGE-B ≥10 in Caucasians). Family history was not assessed; patients with prior HCC were excluded from the HCC surveillance analysis.
Results: A total of 1,235 PWH with chronic HBV were included (SP 771; GE 464). Median age 56 yr; 85% male; 36% non-European origin. Sex between men accounted for 48% of HIV acquisition. HIV RNA was undetectable in 88%, median CD4 623 cells/μL. Cirrhosis 10%; HCC 1%. Adequate HBV-active therapy was prescribed in 88% (SP 89%; GE 86%). ALT/AST testing within 12 mo. was documented in 94% (SP 95%; GE 92%) and HBV DNA testing in 71% (SP 68%; GE 76%). Anti-HDV testing was performed in 82% (SP 83%; GE 81%); among anti-HDV–positive individuals, HDV-RNA testing was documented in 66% (SP 62%; GE 89%). HCC surveillance was performed in patients with cirrhosis in 67% overall (77/115 [SP 66/92, 72%; GE 11/23, 48%]), in non-cirrhotic patients with ≥1 risk factor in 24% overall (228/969 [SP 88/571, 15%; GE 140/398, 35%]), and in all patients meeting HCC surveillance criteria in 28% overall (305/1,084 [SP 154/663, 23%; GE 151/421, 36%]).
Conclusion: Most PWH with chronic HBV received appropriate HBV-active therapy; however, gaps in guideline adherence were identified. HCC surveillance showed the lowest adherence, with fewer than one-third of eligible individuals adequately screened. Improving HCC

surveillance and strengthening HBV DNA monitoring and HDV diagnostic pathways are essential components of strategies aimed at optimizing liver-related outcomes in this population.

SAT-569

Variation in hepatitis B virus replication across Africa: analysis of the multicenter hepatitis B in Africa collaborative network (HEPSANET) cohort study

Kalisha Bheemraj[1], Jacques De Vos[2], Alice N. Guingané[3], Roger Sombie[4], Mohamed El-Kassas[5], Mary Afihene[6], Edith Okeke[7], Hans Prozesky[8], Wendy Spearman[9], Ibrahima Diallo[10], Gilles Wandeler[11], Babatunde Duduyemi[12], John Rwegasha[13], Alexander Stockdale[14], Asgeir Johannessen[15], Michael Vinikoor[16].
[1]HEPSANET, University of Cape Town, University of California Los Angeles, Cape Town, South Africa; [2]University of Stellenbosch, Cape Town, South Africa; [3]Center Hospitalier Universitaire de Bogodogo, Bogodogo, Burkina Faso; [4]Université Joseph, Ouagadougou, Burkina Faso; [5]Helwan University, Cairo, Egypt; [6]Kwame Nkrumah' University of Science and Technology, Kumasi, Ghana; [7]University of Jos, Plateau State, Nigeria; [8]Stellenbosch University, Cape Town, South Africa; [9]University of Cape Town, Cape Town, South Africa; [10]Hopital Principal de Dakar, Dakar, Senegal; [11]Bern University, Bern, Switzerland; [12]University of Sierra Leone Teaching Hospital, Freetown, Sierra Leone; [13]African Union Commission, Dar es Salaam, Tanzania; [14]University of Liverpool, Liverpool, United Kingdom; [15]University of Oslo, Oslo, Norway; [16]The University Of Zambia, Lusaka, Zambia
Email: kalishabheemraj@gmail.com

Background and aims: Hepatitis B virus (HBV) is highly prevalent in Africa, affecting approximately 65 million people, yet key virological characteristics of endemic genotypes A, D, and E remain incompletely defined. We evaluated patterns and regional differences in hepatitis B e antigen (HBeAg) positivity and HBV DNA concentrations among treatment naive individuals living with HBV in Africa.
Method: We performed a cross sectional analysis of treatment naive individuals attending 14 clinics across North, Southern, East, and West Africa between 2014 and 2025 within HEPSANET. Liver disease was classified as normal, significant fibrosis, compensated cirrhosis, or decompensated cirrhosis. HBV DNA (log10 IU/mL) was modelled using a generalized additive model (GAM) with a cubic spline (k = 4), stratified by HBeAg status. Predictors of HBeAg positivity were assessed using a binomial logistic GAM with a penalized cubic spline for age (k = 9). Models were adjusted for sex, region, and liver disease status. We also estimated the proportion of women of reproductive age (15 to 49 years) at high risk of vertical transmission (HBV DNA >200,000 IU/mL or HBeAg positive).
Results: Of 13,359 individuals in the cohort, 4,293 were negative for HIV, HCV, and HDV and had both HBV DNA and HBeAg measured. Median age was 32 years (IQR 27 to 41), and 60% were male. HBeAg was positive in 423 (10%). HBeAg positivity was higher in Southern versus West Africa (adjusted odds ratio [aOR] 2.06, 95% CI 1.48 to 2.87), in decompensated liver disease versus normal liver (aOR 6.38, 95% CI 4.26 to 9.55), and in males (aOR 1.48, 95% CI 1.13 to 1.80). Overall HBV DNA was 2.92 log10 IU/mL (IQR 2.08 to 3.85). In adjusted models, HBV DNA was higher in East versus West Africa (difference 0.20 log10 IU/mL, 0.10 to 0.30), in males (0.19 log10 IU/mL, 0.10 to 0.28), and in HBeAg positive individuals (3.05 log10 IU/mL, 2.90 to 3.20). Among 1,497 women of reproductive age, 174 (12%) met criteria for high risk of vertical transmission; women in Southern Africa had higher odds of high risk status than women in West Africa (aOR 1.96, 95% CI 1.16 to 3.33).
Conclusion: HBV replication markers and viral expression vary substantially across African regions, with potential implications for vertical transmission risk and treatment eligibility. These findings support the need for region specific data to guide HBV elimination planning and implementation.

SAT-570

Good response to short-term peginterferon α in chronic hepatitis B patients with HBsAg <100 IU/mL: a 276-patient cohort study

Weihua Cao[1,2], Yao Xie[1,2,3], Minghui Li[1,2,3]. *[1]Department of Hepatology Division 2, Beijing Ditan Hospital, Capital Medical University, Beijing, China; [2]HBV Infection, Clinical Cure and Immunology Joint Laboratory for Clinical Medicine, Capital Medical University, Beijing, China; [3]Department of Hepatology Division 2, Peking University Ditan Teaching Hospital, Beijing, China*
Email: weihuacaohappy@163.com

Background and aims: Patients with chronic hepatitis B (CHB) and low baseline hepatitis B surface antigen (HBsAg) levels are considered optimal candidates for interferon-based therapy. This study aimed to evaluate the clinical cure rates following short-term Peginterferon α (PEG-IFN α) treatment in this specific population.
Method: In this retrospective study, 276 CHB patients with baseline HBsAg <100 IU/mL received PEG-IFN α therapy for 48 weeks. Clinical cure was defined as HBsAg loss with or without seroconversion to anti-HBs. Clinical characteristics and treatment outcomes were analyzed, with subgroups compared based on HBeAg status and baseline HBsAg levels (0–20, 20–50, and 50–100 IU/mL).
Results: A total of CHB patients with HBsAg <100 IU/mL were enrolled. Following 48 weeks of PEG-IFN α therapy, the overall clinical cure rates were 30.80% (85/276) at week 24 and 33.70% (93/276) at week 48. HBeAg-negative patients (n = 222) achieved significantly higher cure rates than HBeAg-positive patients (n = 32) at both week 24 (35.59% vs. 15.63%, *P* = 0.025) and week 48 (44.59% vs. 25.00%, P = 0.036). A clear gradient was observed based on baseline HBsAg levels: patients with HBsAg <20 IU/mL achieved the highest cure rates (34.97% at week 24, 43.72% at week 48), followed by those with HBsAg 20–50 IU/mL (28.21% and 33.33%), and those with HBsAg 50–100 IU/mL (16.67% and 22.22%) (*P* = 0.014 for trend).
Conclusion: Short-term PEG-IFN α therapy induces high clinical cure rates in CHB patients with HBsAg <100 IU/mL, particularly in those who are HBeAg-negative or have baseline HBsAg levels below 20 IU/mL. Baseline HBsAg level is a strong predictor of treatment success.

SAT-571

Low pre-treatment concentrations of HBV cccDNA transcriptional activity markers – HBcrAg and pre-genomic RNA - can predict response to therapy with pegylated interferon, but not to bulevirtide monotherapy in chronic hepatitis D patients

Ivana Carey[1], Mark Anderson[2], James Lok[1], Tiffany Fortney[2], Zillah Cargil[1], Gavin Cloherty[2], Geoffrey Dusheiko[1], Kosh Agarwal[1].
[1]Institute of Liver Studies, King's College Hospital NHS Foundation Trust, London, United Kingdom; [2]Department of Infectious Diseases, Abbott Laboratories, Chicago, United States
Email: ivana.carey@nhs.net

Background and aims: Hepatitis delta (HDV) is a satellite virus that requires the envelope proteins of HBV (HBs) for cell entry. Bulevirtide blocks virion engagement with NTCP receptors and achieves undetectable HDV RNA (sustained, off-treatment) in approximately 20% of patients. Meanwhile, pegylated interferon (IFN) exerts pleotropic antiviral effects, including on cccDNA episomes. In this study, we compared peripheral biomarkers of HBV infection (HBsAg, HBcrAg, pgRNA) during IFN vs. BLV therapy and assessed their temporal relationship to serum HDV RNA.
Method: We analysed 51 patients with HBV/HDV co-infection (median age 42 yrs, 31 males, 55% compensated cirrhosis). 33 patients were treated with IFN for 48 weeks (+24 weeks follow-up) and 18 patients were treated with BLV monotherapy for at least 72 weeks. The following biomarkers were measured at start-of-treatment, week 24, 48 & 72: HBcrAg [CLEIA Fujirebio, $\log_{10}$ U/ml, LLOQ 3.0 $\log_{10}$ U/ml], pgRNA [RealTime RUO, Abbott Diagnostics, LLOQ = 0.49 $\log_{10}$ U/ml]), HBsAg quant [Abbott ARCHITECT, LLOQ 0.05 IU/ml], and HDV RNA [RealTime RUO, Abbott Diagnostics, LLOQ 5 IU/ml]. Treatment response was defined as undetectable HDV RNA

on therapy (BLV cohort) or 24 weeks after end-of-treatment (IFN cohort).
Results: 19 (58%) IFN patients achieved HDV RNA loss vs. 7 (39%) patients on 72 weeks of BLV therapy. Lower pre-treatment HDV RNA (<100 000 IU/ml), HBsAg (<5 000 IU/ml), pgRNA (<1.75 $\log_{10}$ U/mL), & HBcrAg (<3.5 $\log_{10}$ U/mL) were predictive of response in IFN patients, but only HDV RNA <50 000 IU/ml was predictive of BLV-induced HDV RNA loss. Irrespective of treatment modality, a higher proportion of responders had HBcrAg or pgRNA < LLOQ at start-of-treatment, as compared with non-responders (HBcrAg 23% vs 0%; pgRNA 16% vs 6%). Responders also demonstrated steeper on-treatment declines in HBcrAg (−1.25 vs −1.05 $\log_{10}$ U/ml/year, $p < 0.05$) and pgRNA (−1.14 vs −0.86 $\log_{10}$ U/ml/year, $p < 0.05$). The percentage of patients with HBcrAg or pgRNA < LLOQ increased during therapy, but only amongst responders (week 72: HBcrAg 83%; pgRNA: 76%). HBsAg declines were exclusively encountered in the IFN-treatment cohort (−973 IU/ml/year), of whom 4 patients (12%) achieved HBsAg seroclearance.
Conclusion: Baseline levels of HBV cccDNA transcription were predictive of response to IFN, but not BLV, and this may reflect their distinct mechanisms of action. Changes in HBcrAg and pgRNA were more pronounced in responders irrespective of therapy type.

SAT-572
Durability of functional cure in chronic hepatitis B: a systematic review and meta-analysis
Yuxing Chen[1], Yonglu Su[1], Qiao Tang[1], Yuanhai Zhou[1], Tianquan Huang[1], YunLing Xue[1], Xiaoqing Liu[1], Hu Li[1], Zhi-wei Chen[1], Li Zhang[1], Peng Hu[1]. *[1]Department of Infectious Diseases, Institute for Viral Hepatitis, The Key Laboratory of Molecular Biology for Infectious Diseases, Chinese Ministry of Education, The Second Affiliated Hospital of Chongqing Medical University, 76# Linjiang Road, Yuzhong District, Chongqing 400010, China, Chongqing, China*
Email: hp_cq@163.com

Background and aims: The latest international consensus defines functional cure in chronic hepatitis B (CHB) as sustained HBsAg loss and undetectable serum HBV DNA, with or without hepatitis B surface antibody (anti-HBs) seroconversion, confirmed 24 weeks after treatment cessation. However, long-term data validating the durability of this newly standardized definition remain limited. This meta-analysis aims to evaluate the durability of functional cure in CHB patients using current criteria.
Method: We conducted a systematic literature search across PubMed, Embase, Web of Science, and the Cochrane Library from January 2000 to August 2025. The extracted data were analyzed using either a random-effects model or a fixed-effects model. Potential sources of heterogeneity were explored through subgroup analysis.
Results: A total of nineteen studies involving 16,875 CHB patients were included. The pooled sustained response rate, defined as persistent HBsAg loss and undetectable HBV DNA during post-treatment follow-up regardless of 24-week confirmation, was 84.9% (95% CI: 81.1–88.3%). Among patients meeting the formal functional cure definition—HBsAg loss and undetectable HBV DNA confirmed 24 weeks after treatment cessation—the durability rate was 92.6% (95% CI: 91.3–93.9%). Nucleos(t)ide analogue (NA) monotherapy was associated with a higher sustained response rate compared to interferon-based therapy. Although the sustained functional cure rate was numerically higher with NA, the difference was not statistically significant. Longer consolidation therapy (≥12 weeks) was associated with a higher sustained response rate; however, data were insufficient to assess its impact on durable functional cure. Additionally, anti-HBs seroconversion was significantly associated with more durable outcomes for both sustained response and functional cure.
Conclusion: Patients with functional cure confirmed 24 weeks after treatment cessation exhibit substantially greater long-term durability than those who achieve HBsAg loss and undetectable HBV DNA only at end of treatment. Moreover, anti-HBs seroconversion further enhances the durability of this response.

SAT-573
Seroprevalence and clinical characteristics of hepatitis d virus infection in korean patients with chronic hepatitis B and HBV-related hepatocellular carcinoma
Min Kyung Park[1], Yun-Sook Lim[1], Gwang Hyeon Choi[1], Eun Ju Cho[2], Su Jong Yu[2], Yun-Tae Kim[3], Eun Sun Jang[1], Jin-Wook Kim[1], Sook-Hyang Jeong[1]. *[1]Seoul National University Bundang Hospital, Seongnam, Korea, Rep. of South; [2]Seoul National University College of Medicine, Seoul, Korea, Rep. of South; [3]Seoul Clinical Laboratories, Yongin, Korea, Rep. of South*
Email: jsh@snubh.org

Background and aims: Hepatitis delta virus (HDV) coinfection worsens clinical outcomes in patients with chronic hepatitis B (CHB). With the emergence of HDV-targeted therapeutics, accurate data on HDV prevalence and its clinical impact are essential. This study aimed to assess the seroprevalence, clinical significance, and molecular characteristics of HDV in Korean patients with CHB, liver cirrhosis (LC), and hepatocellular carcinoma (HCC).
Method: This multicenter, retrospective study enrolled 527 patients with chronic HBV infection, stratified into CHB (n = 100), LC (n = 100), and HCC (n = 327). Serum samples were collected from two tertiary centers, Seoul National University Hospital and Seoul National University Bundang Hospital, between 2006 and 2024. Anti-HDV antibodies were detected using commercial kits, and HDV RNA was analyzed for full-length genomic sequencing.
Results: The median age was 58.0 years (interquartile range, 51.0–64.0), and 71.2% were male. The overall anti-HDV seroprevalence was 2.7% (14/527). Prevalence varied slightly across disease groups: 2.0% in CHB, 4.0% in LC, and 2.4% in HCC ($p = 0.732$). Male sex was associated with anti-HDV positivity (odds ratio 5.37; 95% confidence interval [CI], 1.06–98.02; $p = 0.107$). Notably, in patients with HCC, anti-HDV prevalence was significantly higher in advanced stages (BCLC C–D) compared to early-to-intermediate stages (BCLC 0–B) (5.3% vs. 0.9%; $p = 0.023$). Although anti-HDV positivity was associated with an elevated hazard ratio for mortality in HCC patients (adjusted HR 1.92; 95% CI, 0.60–6.16), statistical significance was not reached ($p = 0.271$). HDV RNA was detected in one of the 14 anti-HDV positive patients (7.1%). Using this RNA-positive sample, we successfully identified the full-length HDV genome for the first time in Korea.
Conclusion: Anti-HDV seroprevalence in Korean HBV patients is approximately 2.7%. HDV coinfection is associated with male sex and advanced tumor stage in HCC. These findings highlight the need for early screening, particularly in patients with advanced liver disease, and provide the first molecular characterization of a Korean HDV strain.

SAT-574
Antiviral therapy based on the EASL guideline 2025 reduces the risk of hepatocellular carcinoma: a multinational study
Ho Soo Chun[1], Minjong Lee[1], Hye Ah Lee[2], Tae Hun Kim[1], Terry Cheuk-Fung Yip[3], Yan Liang[3], Shang-Chin Huang[4], Tai-Chung Tseng[4], Grace Lai-Hung Wong[3], Seung Up Kim[5]. *[1]Department of Internal Medicine, Ewha Womans University College of Medicine, Seoul, Korea, Rep. of South; [2]Clinical Trial Center, Ewha Womans University Seoul Hospital, Seoul, Korea, Rep. of South; [3]Medical Data Analytics Center, State Key Laboratory of Digestive Disease, Li Ka Shing Institute of Health Sciences, The Chinese University of Hong Kong, Hong Kong SAR, China; [4]Division of Gastroenterology and Hepatology, Department of Internal Medicine, National Taiwan University Hospital, Taipei, Taiwan; [5]Department of Internal Medicine, Institute of Gastroenterology, Yonsei University College of Medicine, Seoul, Korea, Rep. of South*
Email: minjonglee2@naver.com

Background and aims: The EASL 2025 guideline introduced a simplified algorithm for managing chronic hepatitis B (CHB), recommending earlier initiation of antiviral therapy (AVT) based on viral load and fibrosis stage. We evaluated whether AVT initiation according to the EASL 2025 guideline is associated with a reduced risk of hepatocellular carcinoma (HCC).
Method: This multinational cohort study included 24,788 treatment-naïve CHB patients from 7 centers in South Korea, Hong Kong, and Taiwan (2007–2022). Predicted HCC risk assuming AVT initiation was estimated using PAGE-B (for groups including patients with cirrhosis) or PAGED-B scores (for groups including patients without cirrhosis). Patients were categorized according to the EASL 2025 guideline as follows: Groups 1 and 2 included patients with advanced fibrosis or cirrhosis without (Group 1) or with (Group 2) detectable HBV DNA; Group 3, HBV DNA ≥ 2,000 IU/ml with significant fibrosis or alanine aminotransferase (ALT) > upper limit of normal (ULN); Group 4, HBV DNA ≥ 2,000 IU/ml without significant fibrosis or ALT > ULN; and Group 5, HBV DNA < 2,000 IU/ml with ALT ≤ ULN. For each group, observed 5-year HCC incidence in untreated patients was compared with the predicted incidence derived from the models, assuming AVT initiation. An additional AVT-treated cohort (n = 8,414) was propensity score–matched to the untreated cohort to compare HCC risk between treated and untreated patients in Groups 2 and 3.
Results: When fibrosis was assessed by transient elastography, observed HCC risk in Group 1 was comparable to that predicted by PAGE-B. In contrast, observed HCC risk in untreated patients was significantly higher than predicted by PAGE-B in Group 2 (standardized incidence ratio [SIR] = 2.539, 95% confidence interval [CI] = 2.278–2.818) and by PAGED-B in Group 3 (SIR = 3.116, 95% CI = 1.755–5.045) (all $p < 0.001$). In Groups 4 and 5, observed and predicted HCC risks were comparable (all $p > 0.05$). These findings were consistent when fibrosis was assessed using fibrosis-4 or aspartate aminotransferase-to-platelet ratio index. In propensity score–matched analyses incorporating an additional cohort of patients treated with AVT, AVT initiation was associated with a significantly lower risk of HCC compared with no treatment in both Group 2 and Group 3 ($p = 0.035$ and $p = 0.007$, respectively).
Conclusion: AVT initiation based on viral load and fibrosis stage according to the EASL 2025 guideline is associated with a reduced HCC risk.

SAT-575

Epidemiology of hepatitis delta virus in Belgium: interim results of a prospective cross-sectional cohort study

Marie Coessens[1,2], Florence Lemaitre[3], Inge Roukaerts[3], Jérémie Wawrzyniak[4], Matthias Steverlynck[5], Mounzer Reda[6], Marie De Vos[7], Marijke Reynders[8], Hans Orlent[9], Hilde Vanpoucke[10], Charlotte De Vloo[11], Margot De Spiegeleer[12], Jos Van Acker[12], Laura Coremans[13], Thiberiu Banica[14], Elizaveta Padalko[14], Xavier Verhelst[15], Hélène Tatiana Besse-Hammer[16], Luc Lasser[17], Anaïs Scohy[18], Giulia Zorzi[18], Yves Horsmans[19], Nicolas Yin[20], Christophe Moreno[21], Sofie Goes[22], Annelien Van Dalem[22], Silke François[23], Pablo Beckers[24], Marie-Pierre Hayette[24], Jean Delwaide[25], Sarah Vandamme[26], Hafid Dahma[20], Sigi Van den Wijngaert[20], Thomas Sersté[27], Katrien Hoet[28], Bruno Van Herendael[28], Peggy Bruynseels[28], Natasja Van Gasse[28], Stefan Bourgeois[29], Wim Verlinden[2,30,31], Marina Mukovnikova[32], Alexandra Vodolazkaia[32], Steven Van Gucht[3], Thomas Vanwolleghem[1,31]. *[1]Viral Hepatitis Research Group, Laboratory of Experimental Medicine and Pediatrics (LEMP), University of Antwerp, Antwerp, Belgium; [2]Department of Gastroenterology and Hepatology, Vitaz, Sint-Niklaas, Belgium; [3]Infectious Diseases in Humans, Viral Diseases, National Reference Centre for Hepatitis Viruses, Sciensano, Brussels, Belgium; [4]Department of Clinical Biology, Centre Hospitalier de Mouscron, Mouscron, Belgium; [5]Department of Gastroenterology and Hepatology, Centre Hospitalier de Mouscron, Mouscron, Belgium; [6]Department of Clinical Biology, Hôpital Jolimont, Haine St. Paul, Belgium; [7]Department of Gastroenterology and Hepatology, Hôpital Jolimont, Haine St. Paul, Belgium; [8]Department of Laboratory Medicine, AZ Sint-Jan, Bruges, Belgium; [9]Department of Gastroenterology and Hepatology, AZ Sint-Jan, Bruges, Belgium; [10]Department of Laboratory Medicine, AZ Delta, Roeselare, Belgium; [11]Department of Gastroenterology and Hepatology, AZ Delta, Roeselare, Belgium; [12]Laboratory of Microbiology, AZ Sint-Lucas Ghent, Ghent, Belgium; [13]Department of Gastroenterology and Hepatology, AZ Sint-Lucas Ghent, Ghent, Belgium; [14]Laboratory of Medical Microbiology, Ghent University Hospital, Ghent, Belgium; [15]Department of Gastroenterology and Hepatology, Ghent University Hospital, Ghent, Belgium; [16]Clinical Research Department, Brugmann University Hospital, Brussels, Belgium; [17]Department of Gastro-Enterology, Brugmann University Hospital, Brussels, Belgium; [18]Department of Microbiology, Cliniques universitaires Saint-Luc, Brussels, Belgium; [19]Department of Gastroenterology and Hepatology, Cliniques universitaires Saint-Luc, Brussels, Belgium; [20]Department of Microbiology, Laboratoire Hospitalier Universitaire de Bruxelles - Universitair Laboratorium Brussel (LHUB-ULB), Brussels, Belgium; [21]Department of Gastroenterology and Hepatology, CUB-Erasme Hospital, Université Libre de Bruxelles, Brussels, Belgium; [22]Department of Clinical Biology, University Hospital Brussels, Brussels, Belgium; [23]Department of Gastroenterology and Hepatology, University Hospital Brussels, Brussels, Belgium; [24]Department of Microbiology, CHU Sart-Tilman, Université de Liège, Liège, Belgium; [25]Department of Gastroenterology and Hepatology, CHU Sart-Tilman, Université de Liège, Liège, Belgium; [26]Department of Clinical Biology, University Hospital Antwerp, Antwerp, Belgium; [27]Department of Hepato-Gastroenterology, CHU Saint-Pierre, Brussels, Belgium; [28]Department of Clinical Biology, Ziekenhuis aan de Stroom, Antwerp, Belgium; [29]Department of Gastroenterology and Hepatology, Ziekenhuis aan de Stroom, Antwerp, Belgium; [30]Laboratory of Experimental Medicine and Pediatrics (LEMP), University of Antwerp, Antwerp, Belgium; [31]Department of Gastroenterology and Hepatology, University Hospital Antwerp, Antwerp, Belgium; [32]Medical Microbiological Laboratory, Sciensano, Brussels, Belgium*
Email: marie.coessens@student.uantwerpen.be

Background and aims: With new treatment options for chronic hepatitis delta virus (HDV) infection emerging, it is crucial to optimize screening and linkage to care. This prospective, cross-sectional study aims to systematically assess the HDV seroprevalence, viremia, and circulating genotypes (gt) in hepatitis B surface antigen (HBsAg) positive patients in Belgium. Also, the sensitivity of HDV antibody (HDVAb) testing in immunocompromised (IC) patients and patients suspected of having an acute HBV-HDV co-infection, will be evaluated.
Method: From 15 large Belgian hospitals, all consecutive samples testing positive for HBsAg during the study period (2024/11/25–2025/10/27), were sent to Sciensano (National Reference Center for Viral Hepatitis). Double HDV reflex testing was performed (HDVAb total: ELISA assay DiaSorin; HDV PCR: Realstar® kit Altona Diagnostics; in house HDV genotyping). Irrespective of the HDVAb result, HDV RNA screening was performed for all IC patients and those suspected of having an acute co-infection. Advanced fibrosis was defined based on elastography (HBV > 8 kPa; HDV > 10.4 kPa), histology and clinical cirrhosis criteria.
Results: HDV seroprevalence is 6.14% (n = 129/2101; 5.19%–7.25%). Of 129 HDVAb+ patients, 49 tested HDV RNA+. Of all IC patients (n = 91) and those with presumed acute co-infection (n = 18), 1 co-infected HBV-HIV+ patient tested HDV RNA+ (5.46 IU/mL) despite negative HDVAb. Therefore, HDV viremia in the entire cohort is 2.38% (n = 50/2100; 1.81%–3.13%), with predominant gt 1 (n = 34) and gt 5 (n = 8). HDVAb+ patients were more often female (51.2% vs 48.8%, $p = 0.022$) and were more likely to be HCV seropositive (7.0% vs 1.9%, $p = 0.010$). HDV RNA+ patients had higher FIB-4 (1.67 vs 1.13, $p < 0.001$), GGT (gamma-glutamyl transferase, 47 vs 23 U/L, $p < 0.001$), bilirubin (0.63 vs 0.50 mg/dL, $p = 0.010$), and INR values (international normalized ratio, 1.10 vs 1.00, $p < 0.001$). In a subset of 304 HBsAg+ patients [262 HDVAb-, 26 HDVAb+/RNA-, and 16 HDVAb+/RNA+ patients (2 newly

diagnosed)] from 5 hospitals, HDVAb+ patients more often had a history of injecting drug use (10.5% vs 0%, p = 0.034) and HDV viremia was strongly associated with advanced fibrosis (adjusted OR 22.2, CI 5.00–98.24, p < 0.001), independently of BMI and alcohol consumption.
Conclusion: Active HDV co-infection presents with more advanced liver disease and is expected in around one in every 40 HBsAg+ patients in Belgium. Wider implementation of HDV reflex-testing in Belgium is needed.

SAT-576

Hepatitis B virus genotype distribution and viral load patterns in African immigrants to Canada

Welde Aregawi[1], Haris Imsirovic[1], Alexa Keeshan[1], Curtis Cooper[1].
[1]Ottawa Hospital Research Institute, School of Epidemiology and Public Health, University of Ottawa, Division of Infectious Diseases, The Ottawa Hospital, Ottawa, Canada
Email: weldedr77@gmail.com

Background and aims: Hepatitis B virus (HBV) genotypes have distinct geographic and demographic distributions with important clinical implications. In Canada, immigration-driven HBV epidemiology provides globally diverse genotype and sociodemographic patterns reflecting regions of origin including Africa.
To characterize HBV genotype distribution and examine associations between genotype, sociodemographic factors, and HBV DNA levels in African immigrants to Canada.
Method: We conducted a retrospective cohort study of patients with HBV genotype results (2001–2025) in The Ottawa Hospital Viral Hepatitis Program. Genotype data were linked to sociodemographic characteristics. Associations between genotype and viral load were examined among treatment-naïve patients.
Results: Among 778 patients (median age 42.5 years; 52% male), 94% were born outside Canada, representing 78 countries and predominantly Asian (51%) and Black (35%) populations. Six genotypes were identified: A (19.8%), B (25.6%), C (21.0%), D (17.4%), E (15.9%), and F (0.4%). Distribution reflected global migration patterns: A in East Africa and the Caribbean, E in West Africa, B/C in East-Southeast Asia, and D across Middle East and North Africa (MENA), South Asia, and Europe/Central Asia. Genotype-race patterns were concordant (A/E predominantly Black; B/C >95% Asian; D heterogeneous). Age at presentation differed by genotype and race (p < 0.0001), with African-associated genotypes (A/D/E) and Black and Arab/MENA patients presenting younger than those with B/C. HBV viral load differed by genotype (A-E, p < 0.0001), with lower median log10 HBV DNA in A, D and E (2.9–3.0 IU/mL) than in B and C (3.6 and 3.3 IU/mL). In multivariable models, genotype (particularly B/C), male sex and younger age were associated with higher baseline HBV DNA. Genotype was associated with antiviral initiation (p < 0.0001), lowest in A/E (26–28%) and highest in B/C (42–50%).
Conclusion: In this globally diverse, immigration-driven cohort, African-associated genotypes (A, D, E) and Black patients presented at younger ages, providing an opportunity to apply international recommendations for earlier HCC surveillance in high-risk African-origin populations. Among other factors, lower HBV DNA levels may inaccurately dissuade antiviral initiation in this at risk population.

SAT-577

HLA genetic markers identify HDV patients at risk of persistent viremia and advanced fibrosis

Maria Francesca Cortese[1,2], Adriana Palom[2,3], Francesc Rudilla[4,5], Ariadna Rando-Segura[2,3], David Tabernero[1,2], Juan Carlos Ruiz-Cobo[2,3], Judit Vico Romero[2,3], Mar Riveiro Barciela[2,3,6], Maria José Herrero[4,5], Maria Buti[2,3,6].
[1]Department of Microbiology, Liver Unit, Vall d'Hebron Institut de Recerca (VHIR), Vall d'Hebron Barcelona Hospital Campus, Barcelona, Spain; [2]Instituto de Salud Carlos III, Centro de Investigación Biomédica en Red de Enfermedades Hepáticas y Digestivas (CIBERehd), Madrid, Spain; [3]Department of Hepatology, Vall d'Hebron Hospital Universitari, Vall d'Hebron Barcelona Hospital Campus, Barcelona, Spain; [4]Histocompatibility and Immunogenetics Laboratory, Banc de Sang i Teixits, Barcelona, Spain; [5]Transfusional Medicine Group, Vall d'Hebron Research Insititute-Universitat Autònoma de Barcelona (VHIR-UAB), Barcelona, Spain; [6]Universitat Autònoma de Barcelona (UAB), Barcelona, Spain
Email: mariafcortese@gmail.com

Background and aims: Hepatitis delta virus (HDV) infection shows highly variable outcomes, from spontaneous viral control to rapid fibrosis progression. Identifying host factors that predict disease course is critical for early risk stratification and personalized management. Human leukocyte antigen (HLA) molecules orchestrate antiviral immunity, yet their clinical impact in HDV infection remains unclear. Here, we investigated HLA genetic markers associated with virological control and fibrosis progression.
Method: Blood samples from 75 anti-HDV–positive patients underwent high-resolution genotyping of classical HLA class I (A, B, C), class II (DPB1, DQB1, DRB1), and non-classical (HLA-G, HLA-E) genes. Patients were stratified by HDV RNA status (controllers: undetectable HDV-RNA in ≥2 consecutive samples, n = 38; viremic: persistently detectable HDV-RNA, n = 37) and fibrosis stage (METAVIR F0–F2, n = 38; F3–F4, n = 37). Associations were assessed using univariate and multivariable Firth's penalized logistic regression models. One hundred fifty healthy donors served as controls.
Results: HLA-A*11:01 was significantly enriched among viremic patients (27% vs 2.6% of controllers; OR = 12.9, 95% CI 1.8–569.4; p = 0.002) and was strongly linked to persistent viremia in multivariate analysis (p = 0.02). Advanced fibrosis was associated with HLA-A*11:01 and HLA-DPB1*17:01 (>21% of patients), while HLA-DPB1*01:01 predominated in mild fibrosis (34.2%). While all alleles were associated with fibrosis stage in univariate analyses (p < 0.05), only HLA-DPB1*17:01 remained independently associated with advanced fibrosis in multivariate analysis (p = 0.03). In addition, the presence of HLA-A*11:01 emerged as a factor independently associated with both the presence of detectable HDV-RNA and advanced fibrosis (8/25 patients; p = 0.03).
Conclusion: Specific HLA alleles may help to identify HDV patients at high risk of persistent viremia and progressive fibrosis. Incorporating HLA genotyping could enable earlier risk stratification and guide personalized monitoring and therapeutic decisions, offering a precision medicine approach in HDV management.
Funding: Instituto de Salud Carlos III (PI23/01065, PI20/01692), co-financed by the European Union (ERDF, "A way to make Europe").

SAT-578

A systematic literature review of quantitative HBsAg distribution, HBsAg/HBeAg loss and clinical outcomes in HIV/HBV co-infected population

Myriam Drysdale[1], Grace Dolman[2], Pankdeep Chhabra[3], Deepali Mittal[3], Pooja Malhotra[3], Marjan Hezareh[1]. *[1]GSK, London, United Kingdom; [2]GSK, Stevenage, United Kingdom; [3]Bridge Medical Consulting Ltd, London, United Kingdom*
Email: myriam.g.drysdale@gsk.com

Background and aims: About 1% (~2.7 million) of patients (pts) with chronic hepatitis B virus (HBV) infection are coinfected with human immunodeficiency virus (HIV), and 8–10% with HIV have chronic HBV. Coinfection accelerates HBV-related liver disease. HBV-active antiretroviral therapy (ART) suppresses viral replication but rarely achieves hepatitis B surface antigen (HBsAg) loss. This systematic literature review (SLR) assessed epidemiology, treatment patterns, quantitative HBsAg (qHBsAg) and clinical outcomes in HIV/HBV coinfection.
Method: We searched Embase and MEDLINE (01/01/2015–24/06/2025) for HIV/HBV coinfection studies (SLRs, narrative reviews, observational studies and clinical trials [for HBsAg data]; excluding preclinical and paediatric studies [< 18 years], case reports and small

case series [< 10 pts]), supplemented by global reports. Data extracted included baseline (BL, i.e. prior to initiation of HBV-active ART) and on-treatment qHBsAg, HBV DNA, hepatitis B e-antigen (HBeAg), treatment regimens and liver outcomes.
Results: 90 articles were included. In treated pts, ~11–21% had qHBsAg ≤ 1000 IU/mL and 79–90% had qHBsAg > 1000 IU/mL at BL; qHBsAg ranged between 631–15849 IU/mL at BL and tended to decline on HBV-active ART (251–794 IU/mL at 3 years). At any ART timepoint, pts with detectable HBV DNA after 24 months had significantly higher qHBsAg kinetics than those with undetectable HBV DNA, indicating qHBsAg levels reflect ongoing HBV replication. qHBsAg was also higher in HBeAg-positive than HBeAg-negative pts (7943 vs 6310 IU/mL at 3 years of treatment), with HBeAg seroclearance mainly occurring within 5 years of therapy at a median rate of 1.7–12.1 per 100 pt-years. HBsAg loss on therapy was infrequent and typically happened soon after initiation of anti HBV-active ART when it occurred. Factors associated with HBsAg loss included lower qHBsAg levels at BL and greater HBsAg declines, as well as alanine transaminase elevation, tenofovir alafenamide/tenofovir disoproxil fumarate-based regimens and longer HBV therapy duration. Limited evidence suggested that HBsAg loss was associated with substantially better liver outcomes (e.g., cirrhosis, odds ratio: 0.21).
Conclusion: HBsAg loss is associated with improved outcomes in HIV/HBV coinfected pts. While qHBsAg declines are observed with current HBV-active ART, HBsAg loss remains uncommon. Larger prospective studies are needed to identify predictors of clearance and evaluate novel strategies.
Funding: GSK (300495).

SAT-579

Predictors of HBsAg loss, including baseline quantitative HBsAg, in adults with chronic hepatitis B: a regional cohort study in China

Yuanyuan Kong[1], Xiaohua Li[2], Mei Yang[3], Ying Shen[4], Sida Wei[4], Xin Li[4], Xin He[5], Lydia Demetriou[6], Menchi Wu[7], Huifen Yang[8], Jidong Jia[9], Myriam Drysdale[10]. *[1]Clinical Epidemiology and EBM Unit, Beijing Friendship Hospital, Capital Medical University, Beijing, China; [2]The Second Hospital of Tianjin Medical University, Clinical Trial Institution, Tianjin, China; [3]3EVYD Technology, RWE Global, Short Hills, United States; [4]Tianjin Happy Life Technology Co. Ltd, Innovative Healthcare Solution, RWE Global, Shanghai, China; [5]GSK, Value Evidence and Outcomes, Shanghai, China; [6]GSK, Clinical Development, London, United Kingdom; [7]GSK, Shanghai, China; [8]The Second Hospital of Tianjin Medical University, Department of Infectious Diseases and Immunology, Tianjin, China; [9]Liver Disease Center, Beijing Friendship Hospital, Capital Medical University, Beijing, China; [10]GSK, London, United Kingdom*
Email: kongyuanyuan2000@163.com

Background and aims: Chronic hepatitis B virus (HBV) infection is a major global public health problem and a leading cause of liver-related morbidity/mortality. The goal of treatment is functional cure (FC: sustained HBV DNA and hepatitis B surface antigen [HBsAg] loss after stopping all treatment). Lower quantitative HBsAg (qHBsAg) levels are associated with improved outcomes, but routine qHBsAg testing is limited and population-level data are sparse. This study characterised demographic, clinical and virological predictors–including baseline (BL) qHBsAg–of HBsAg loss among patients (pts) with chronic HBV infection in China.
Method: This retrospective cohort study used Tianjin regional electronic health records from 82 hospitals (2016–2023). Eligible pts were adults with chronic HBV infection, ≥ 1 qHBsAg measurement (first test = index date), no coinfection and no major adverse liver outcomes (compensated/decompensated cirrhosis, hepatocellular carcinoma or liver transplant) before index. Demographic and clinical variables were recorded in the 12 months before index. A multivariate Cox proportional hazards model evaluated predictors of time to HBsAg loss.
Results: 28,659 pts were included (mean [standard deviation] age 41.7 [12.9] years; 55.9% male; median duration of follow-up 4.6 years). BL qHBsAg distribution was: ≤ 100 IU/mL 13.7%, > 100–≤ 1000 IU/mL 20.6%, > 1000–≤ 3000 IU/mL 19.9%, and > 3000 IU/mL 45.8%. Of 5369 pts (18.7%) treated with nucleos(t)ide analogues (NAs), 3039 (56.6%) had BL qHBsAg ≤ 3000 IU/mL and 1653 (30.8%) had ≤ 1000 IU/mL. HBsAg loss occurred in 2.9% (454/15,529) of all pts with BL qHBsAg ≤ 3000 IU/mL, 3.4% (102/3039) of NA-treated pts with BL qHBsAg ≤ 3000 IU/mL and 4.8% (79/1653) of NA-treated pts with qHBsAg ≤ 1000 IU/mL. Cox regression showed lower BL qHBsAg was strongly associated with HBsAg loss: hazard ratios (95% confidence interval) vs > 3000 IU/mL were 7.03 (5.66–8.73) for ≤ 100 IU/mL, 1.57 (1.23–2.01) for > 100–≤ 1000 IU/mL, and 1.03 (0.79–1.35) for > 1000–≤ 3000 IU/mL. Older age was associated with reduced likelihood of HBsAg loss, while higher alanine aminotransferase (> 5 × vs 1× upper limit of normal), BL hepatitis B e antigen positivity, type 2 diabetes and non-alcoholic liver disease were associated with increased likelihood of HBsAg loss.
Conclusion: These data reflect a strong association between low BL qHBsAg and HBsAg loss and highlight the need for routine qHBsAg testing to identify pts most likely to achieve FC with emerging therapies.
Funding: GSK (219254).

SAT-580

Prolonged HDV RNA positivity and significant risk of HDV RNA re-ocurrence in hepatitis delta patients who underwent liver transplantation

Esmee Fath el Bab[1], Ainura Khammetova[1], Jolanda Kreeft-Voermans[1], Caroline den Hoed[1], Harry L.A. Janssen[1,2], Maikel P. Peppelenbosch[1], Annemiek Van der Eijk[1], Milan J. Sonneveld[1]. *[1]Erasmus MC, University Medical Center, Rotterdam, Netherlands; [2]Toronto Center for Liver Disease, Toronto General Hospital, University of Toronto, Toronto, Canada*
Email: e.fathelbab@erasmusmc.nl

Background and aims: Liver transplantation (LT) is an important treatment option for hepatitis delta patients with liver failure or HCC. The risk of HDV recurrence after LT remains ill-defined. We studied early HDV RNA kinetics and risk of re-occurrence of HDV RNA in patients who underwent LT.
Method: We analyzed all HDV RNA positive patients who underwent LT between 2005–2025 in the largest liver transplantation center of the Netherlands. All patients were treated with HBIG and nucleos(t)ide analogues (NA) after LT. HDV RNA, HBsAg and anti-HBs levels were assessed in stored samples obtained post-transplant. Recurrence was defined as re-occurrence of HDV RNA after the first sample reported as target not detected (TND, <50 IU/mL).
Results: A total of 11 patients were included, with a mean age of 44.3 (±10) years at LT, of whom 10 (90.9%) were male. Median follow-up time was 8.0 years (IQR 0.3–15.0). Indication for LT was decompensated cirrhosis (n = 7, 63.6%), HCC (n = 3, 27.3%) or ALF (n = 1, 9.1%). One patient received an anti-HBc positive graft. Pre-LT, median HDV RNA was 6.10 log IU/mL (IQR 5.84–6.88). At day 7 from LT, n = 9 (81.8%) remained HDV RNA positive (median HDV RNA at day 7 was 2.87 log IU/mL; median decline from baseline 3.62 log IU/mL), despite all achieving anti-HBs titers >100 mIU/mL. The median duration to HDV RNA and HBsAg negativity was 26.5 (7.0–63.0) and 6.0 days (1.0–28.0) respectively. Pre-LT HDV RNA was not associated with time-to-negative HDV RNA. There was also no association between anti-HBs levels and HDV RNA decline or clearance. After HDV RNA negativity, n = 4 (40%) experienced HDV RNA recurrence, all of whom had anti-HBs >100 and negative HBsAg at the time of HDV RNA recurrence. Re-emergence of HDV RNA was transient in 3 patients, but 1 patient was still positive for HDV RNA at the most recent assessment.
Conclusion: In patients who underwent LT for hepatitis delta, we observed prolonged HDV RNA positivity and frequent re-occurrence of HDV RNA despite negative HBsAg and high anti-HBs levels. These

findings underscore the importance of close HDV RNA monitoring after LT, and suggest a potential need for additional HDV specific therapies to reduce the risk of graft infection.

SAT-581

Scaling up ProLINK nationwide in Spain, early results of an implementation strategy for hepatitis C and hepatitis B and delta virus search and linkage to care

Alberto Vázquez-Blanquiño[1], Ana Fuentes[1], Marta Illescas-López[1], Ana Belén Pérez[2], Francisco Franco Álvarez De La Luna[3], Carolina Freyre[4], Teresa Trujillo[5], Juan Carlos Alados[6], Carmen Rodríguez-Baños[7], Inmaculada López[8], Jesús Machuca[9], María Carmen Lozano Domínguez[10], Antonio Sampedro[11], Isabel Viciana[12], Lucía Chaves-Blanco[1], José Manuel Azcona[13], Jaime Borrego[14], Francisco Javier Casas[15], Juan Carlos Galán[16], Antonio Aguilera[17], María José Pena[18], Araceli Hernández[19], Tomás Tosco[20], Iker Falces[21], Maria Asunción Iborra[22], Maria Jesus Del Amor Espin[23], Jorge Galán[24], Alejandro González Praetorius[25], Alicia Beteta[26], Mª José Rodríguez-Escudero[27], Soledad Illescas[28], Paloma Liendo[29], Luis Elorduy Otazua[30], Ana Milagro[31], Sonia Algarete[32], Dolores Ocete[33], Federico García[1]. *[1]Hospital Universitario Clínico San Cecilio, Instituto Investigación Biosanitaria Ibs. Granada, Centro de Investigación Biomédica en Red Enfermedades Infecciosas. CIBERINFEC, Granada, Spain; [2]Hospital Universitario Reina Sofía, Centro de Investigación Biomédica en Red Enfermedades Infecciosas. CIBERINFEC, Córdoba, Spain; [3]Hospital Universitario Juan Ramón Jiménez, Huelva, Spain; [4]Hospital Universitario De Puerto Real, Puerto Real, Spain; [5]Hospital Universitario Puerta Del Mar, Cádiz, Spain; [6]Hospital Universitario de Jerez de La Frontera, Jerez de la Frontera, Spain; [7]Hospital Universitario Torrecárdenas, Almería, Spain; [8]Hospital Costa del Sol, Benalmádena, Spain; [9]Hospital Infanta Elena, Huelva, Spain; [10]Hospital Universitario Virgen del Rocío, Sevilla, Spain; [11]Hospital Universitario Virgen De Las Nieves, Granada, Spain; [12]Hospital Universitario Virgen De La Victoria, Málaga, Spain; [13]Hospital Comarcal Santa Ana de Motril, Motril, Spain; [14]Hospital de Poniente, El Ejido, Spain; [15]Hospital Comarcal de La Línea de La Concepción, La Línea de la Concepción, Spain; [16]Hospital Universitario Ramón Y Cajal, Madrid, Spain; [17]Hospital Clínico Universitario De Santiago De Compostela, Santiago de Compostela, Spain; [18]Hospital Universitario de Gran Canaria Doctor Negrín, Las Palmas de Gran Canaria, Spain; [19]Complejo Hospitalario Universitario Insular, Las Palmas de Gran Canaria, Spain; [20]Hospital Universitario Nuestra Señora De Candelaria, Santa Cruz de Tenerife, Spain; [21]Hospital Universitario La Paz, Madrid, Spain; [22]Hospital Clínico Universitario Virgen De La Arrixaca, Murcia, Spain; [23]Hospital General Universitario Santa Lucía, Cartagena, Spain; [24]Hospital General Universitario Los Arcos Del Mar Menor, San Javier, Spain; [25]Hospital Universitario De Guadalajara, Guadalajara, Spain; [26]Hospital General Nuestra Señora Del Prado, Talavera de la Reina, Spain; [27]Hospital Virgen De La Luz, Cuenca, Spain; [28]Hospital General Universitario de Ciudad Real, Ciudad Real, Spain; [29]Hospital Universitario de Basurto, Bilbao, Spain; [30]Urgencias Hospital Universitario de Cruces, Barakaldo, Spain; [31]Hospital Universitario Miguel Servet, Zaragoza, Spain; [32]Hospital Clínico Universitario Lozano Blesa, Zaragoza, Spain; [33]Hospital General Universitari De València, València, Spain*
Email: albertovb97@hotmail.es

Background and aims: Chronic viral hepatitis remains a major cause of liver-related morbidity. In HCV and HBV infection, a substantial proportion of previously diagnosed individuals remain untreated or lost to follow-up, representing a persistent gap in the care cascade and a barrier to elimination. Re-linking these patients during routine healthcare encounters allows reassessment of virological status and initiation of appropriate management. In hepatitis B, re-linkage also enables identification of hepatitis delta virus infection through reflex or dual-reflex diagnostic strategies. We aimed to assess the early results of a nationwide implementation of an automated laboratory-driven strategy to improve search and linkage to care.

Method: ProLINK integrates automated rules into the laboratory information system to identify patients with prior positive anti-HCV or HBSAg results whenever a serum sample is available for any clinical request. Laboratory databases and electronic medical records are reviewed to identify patients lost to follow-up. For hepatitis C, if no sustained virological response is documented, HCV-RNA testing is performed using the available sample. For hepatitis B, if no serological follow-up has been recorded within the previous 12 months, HBsAg is retested and, if positive, reflex testing for HDV is performed.

Results: In the hepatitis C programme, 5,269 anti-HCV positive individuals were identified. Among them, 656 (12.5%) required RNA testing due to incomplete follow-up, 608 could be tested, and 190 (31.3%) had active viremia. To date, 134 viremic patients have been contacted; 90 initiated antiviral treatment, 19 declined therapy, and 28 remain under reassessment. In the hepatitis B/delta programme, 116 HBsAg positive individuals without recent follow-up were identified. Testing was not feasible in five cases, 93 patients remained HBsAg positive, and 78 (84%) had incomplete follow-up. Hepatitis delta antibodies were detected in six patients, all of whom were RNA negative.

Conclusion: A nationwide, automated, laboratory-integrated opportunistic strategy enables systematic identification and re-linkage of patients with chronic hepatitis C and hepatitis B who remain outside the care cascade. Importantly, hepatitis B re-linkage facilitates detection of hepatitis delta infection through reflex testing. This approach represents a scalable, virology-driven tool to strengthen hepatitis elimination efforts.

SAT-585

Hepatitis delta in Spain: prevalence and clinical, demographic and virological characterization from a nationwide prospective cohort

Ana Alberola Romano[1], Lucía Pérez-Rodríguez[1], Adolfo de Salazar[1], Raquel Carracedo[2], Teresa Cabezas Fernandez[3], Carolina Freyre[4], Berta Becerril Carral[5], Isabel Viciana[6], Inmaculada López[7], Natalia Montiel[8], Samuel Bernal[9], Jaime Borrego[10], Encarnación Ramirez Arellano[11], Carmen Liébana[12], Francisco Franco Álvarez De La Luna[13], María Carmen Lozano Domínguez[14], Mercedes Pérez-Ruiz[15], Antonio Sampedro[16], Ana Belén Pérez[17], Sonia Algarate Cajo[18], Pablo Fraile Ribot[19], Aldara Vallejo[20], María José Pena[21], Maria Aroca[22], Ana Rodríguez-Fernández[23], José Joaquín Blas Señalada[24], César Gómez[25], Alejandro González Praetorius[26], Santiago Muñoz[27], Ruth Saez[28], Sonsoles Garcinuño Pérez[29], Pilar Tajada[30], Susana García-De Cruz[31], Marta Sandoval Torrientes[32], Belen Lorenzo[33], María Reyes Vidal-Acuña[34], Luz Moldes[35], Noelia Calvo[36], María José Gude[37], Patricia Ordóñez[38], Sandra Cortizo Vidal[39], Miriam Blasco[40], Ana Arribi[41], Iker Falces[42], Juan Carlos Galán[43], María Asunción Iborra[44], Jorge Galán[45], Maria Jesus Del Amor Espin[46], Eva Cascales[47], María Luz Núñez[48], Ana Miqueleiz Zapatero[49], A. Aguilera[2], Federico García[1]. *[1]Hospital Universitario Clínico San Cecilio, Instituto Investigación Biosanitaria Ibs. Granada, Centro de Investigación Biomédica en Red Enfermedades Infecciosas. CIBERINFEC, Granada, Spain; [2]Hospital Clínico Universitario De Santiago De Compostela, Santiago de Compostela, Spain; [3]Hospital Universitario Torrecárdenas, Almería, Spain; [4]Hospital Universitario De Puerto Real, Puerto Real, Spain; [5]Hospital Universitario de Jerez de La Frontera, Jerez de la Frontera, Spain; [6]Hospital Universitario Virgen De La Victoria, Málaga, Spain; [7]Hospital Costa del Sol, Benalmádena, Spain; [8]Hospital Universitario Puerta Del Mar, Cádiz, Spain; [9]Hospital Universitario Virgen del Valme, Sevilla, Spain; [10]Hospital de Poniente, El Ejido, Spain; [11]Hospital Universitario Virgen Macarena, Sevilla, Spain; [12]Hospital Universitario de Jaén, Jaén, Spain; [13]Hospital Universitario Juan Ramón Jiménez, Huelva, Spain; [14]Hospital Universitario Virgen del*

Rocío, Sevilla, Spain; [15]Hospital Universitario Carlos Haya, Málaga, Spain; [16]Hospital Universitario Virgen De Las Nieves, Granada, Spain; [17]Hospital Universitario Reina Sofía, Centro de Investigación Biomédica en Red Enfermedades Infecciosas. CIBERINFEC, Córdoba, Spain; [18]Hospital Clínico Universitario Lozano Blesa, Zaragoza, Spain; [19]Hospital Universitari Son Espases, Palma, Spain; [20]Hospital General de Fuerteventura, Fuerteventura, Spain; [21]Hospital Universitario de Gran Canaria Doctor Negrín, Las Palmas de Gran Canaria, Spain; [22]Complejo Hospitalario Universitario Insular, Las Palmas de Gran Canaria, Spain; [23]Hospital Universitario Marqués de Valdecilla, Santander, Spain; [24]Hospital General Universitario De Albacete, Albacete, Spain; [25]Complejo Hospitalario Universitario de Toledo, Toledo, Spain; [26]Hospital Universitario De Guadalajara, Guadalajara, Spain; [27]Complejo Asistencial de Salamanca, Salamanca, Spain; [28]Complejo Asistencial Universitario de Burgos, Burgos, Spain; [29]Hospital Clínico Universitario de Valladolid, Valladolid, Spain; [30]Hospital General de Segovia, Segovia, Spain; [31]Hospital Santa Bárbara, Soria, Spain; [32]Hospital Santiago Apóstol, Miranda de Ebro, Spain; [33]Hospital Universitario Río Hortega, Valladolid, Spain; [34]Complejo Hospitalario Universitario de Cáceres, Caceres, Spain; [35]Hospital Universitario de A Coruña, A Coruña, Spain; [36]Complejo Hospitalario Universitario de Ourense, Ourense, Spain; [37]Hospital Universitario Lucus Augusti, Lugo, Spain; [38]Hospital Universitario Arquitecto Marcide-Profesor Novoa Santos, Ferrol, Spain; [39]Hospital Álvaro Cunqueiro, Vigo, Spain; [40]Hospital San Pedro, Logroño, Spain; [41]Hospital Clínico San Carlos, Madrid, Spain; [42]Hospital Universitario La Paz, Madrid, Spain; [43]Hospital Universitario Ramón Y Cajal, Madrid, Spain; [44]Hospital Clínico Universitario Virgen De La Arrixaca, Murcia, Spain; [45]Hospital General Universitario Los Arcos Del Mar Menor, San Javier, Spain; [46]Hospital General Universitario Santa Lucía, Cartagena, Spain; [47]Hospital General Universitario Rafael Méndez, Lorca, Spain; [48]Hospital General Universitario Reina Sofía, Murcia, Spain; [49]Hospital Universitario de Navarra, Pamplona, Spain
Email: anaalberolaromano@gmail.com

Background and aims: Hepatitis delta virus (HDV) infection represents the most severe form of chronic viral hepatitis, leading to rapid fibrosis progression, early hepatic decompensation and increased mortality. Despite its clinical relevance, contemporary epidemiological data on HDV in Europe remain limited. In Spain, systematic information on the prevalence and clinical, demographic and virological characteristics of patients with hepatitis delta is scarce. Defining the burden and profile of HDV infection is essential to inform screening strategies and optimize patient management.
Method: We conducted a nationwide, multicenter, observational study including a retrospective evaluation of HDV prevalence among HBsAg-positive individuals (2022–2024) and a prospective cohort launched in 2024. Anti-HDV–positive individuals were enrolled prospectively across Spain. Demographic data, risk factors, clinical variables related to liver disease severity, and virological parameters (HDV-RNA status, viral load, genotype, HBV markers and HIV/HCV co-infection) were systematically collected in a centralized database.
Results: Between 2022 and 2024, 65,763 HBsAg-positive individuals were evaluated in 80 centers from 16 Autonomous Communities. Anti-HDV prevalence remained stable over time (5.6% in 2022, 4.9% in 2023 and 5.3% in 2024). The proportion individuals with confirmed chronic HDV infection were 40.1% in 2022, 31.6% in 2023 and 31.0% in 2024. By December 2025, 534 anti-HDV–positive individuals were prospectively enrolled. Median age was 54 years (IQR 42–61), 58% were male and 49% were born in Spain. HDV genotype 1 predominated (88%). Active HDV infection was detected in 43%, with a mean viral load of log 4.16 IU/mL. Co-infections were frequent (18% HIV, 20% HCV) and were associated with higher rates of active HDV replication (55% and 56%, respectively; $p < 0.05$). Advanced liver disease was common: 26% had FIB-4 >2.67, mean liver stiffness was 10.5 kPa, 41% had METAVIR F3–F4 fibrosis, and 23% had a history of hepatic decompensation.
Conclusion: This nationwide prospective cohort provides robust contemporary data on hepatitis delta in Spain, revealing a high prevalence of advanced liver disease and active viral replication. These findings highlight the substantial clinical burden of HDV infection and reinforce the need for systematic surveillance and optimized clinical management strategies.

SAT-586

Enhanced HBcAg immunoassay enables detection of clinically relevant low-level HBV viremia for treatment eligibility

Rene Geissler[1], Megha Patel[1], Anika Koehler[2], Joerg Herzogenrath[2], Eduardo Almaraz[1], Justin Blumenthal[1], Amit Kumar[1], Todd Solbrig[1], Cyrille Diédhiou[3], Moustapha Mbow[3], Noel Manga[4], Souleymane Mboup[3], Ambroise Ahouidi[3], Michael Berg[1], Gavin Cloherty[1]. *[1]Abbott, Abbott Park, United States; [2]Abbott, Wiesbaden, Germany; [3]IRESSEF, Dakar, Senegal; [4]Hôpital Universitaire de la Paix, Ziguinchor, Senegal*
Email: rene.geissler@abbott.com

Background and aims: Accurate staging of chronic hepatitis B is essential for guiding treatment decisions and predicting clinical outcomes. Current treatment guidelines rely on HBV DNA quantification, with therapeutic thresholds set at ≥2,000 IU/mL or ≥20,000 IU/mL depending on liver enzyme levels, HBeAg status, and evidence of fibrosis or cirrhosis. Despite these guidelines, access to molecular diagnostics for HBV DNA measurement remains limited in many low- and middle-income countries (LMICs) where most infections (~80%) occur, creating barriers to timely and effective care. Importantly, non-phosphorylated HBcAg, located in HBV DNA-containing particles, has emerged as surrogate biomarker for HBV DNA. However, more sensitive HBcAg immunoassays could offer additional clinical utility by enabling HBV detection at clinically relevant thresholds.
Method: We modified a first-generation (v1) HBcAg-specific assay by incorporating a new formulation and monoclonal antibodies. Additionally, this updated assay format was implemented on a digital platform (v2), improving clinical sensitivity on average 225-fold.
Results: The enhanced version (v2) achieved a limit of quantification of 30 fg/mL, corresponding to approximately 1,000 HBV DNA IU/mL. Comparative analysis of v1 and modified v2 assays demonstrated a reduction in the detection threshold from 4.9×10^5 to 1,000 HBV DNA IU/mL, which aligns with treatment eligibility criteria. Longitudinal blood draws from acute HBV patients and single timepoint specimens from treatment-naïve blood donors showed significantly improved detection and quantification using the v2 HBcAg assay.
Conclusion: The HBcAg v2 assay enables increased detection of low viral titers consistent with treatment guidelines and corresponds directly to HBV DNA levels. Its ability to specifically detect low-abundance HBcAg enhances disease staging and may support therapeutic management, particularly in resource limiting settings, where affordable and deployable diagnostic tools are urgently needed.

SAT-587-YI

Distinct patterns of HBsAg isoform reflect viral activity and characterize disease stage in the setting of chronic HDV infection

Ilaria Grossi[1], Caterina Tramontozzi[1], Alessia Magnapera[1], Stefano D'Anna[1], Eleonora Dileo[2], Antonella Olivero[2], Lorenzo Piermatteo[1], Giulio Mengozzi[2], Alessia Ciancio[2], Alessandro Loglio[3], Mauro Viganò[3], Stefano Fagiuoli[3,4], Piero Colombatto[5], Barbara Coco[5], Maurizia Brunetto[5,6], Debora Angrisani[7], Alfonso Galeota Lanza[7], Carlo Magni[8], Andrea Gori[8,9], Vincenzo Messina[10], Michele Milella[11], Annalisa Saracino[11], Letizia Marinaro[12], Giuseppe Cariti[12], Valentina Cossiga[13], Filomena Morisco[13], Silvia Cretella[14], Gabriella Verucchi[15], Elisa Biliotti[16], Giampiero D'Offizi[16], Marcello Feasi[17], Emanuele Pontali[17], Carmine Coppola[18], Rachele Rapetti[19], Mario Pirisi[19], Antonio Izzi[20], Teresa Santantonio[21],

Vito Di Marco[22], Aldo Marrone[23], Nicola Coppola[24], Marco Rizzi[25], Anna Maria Cattelan[26], Grazia Anna Niro[27], Pierluigi Toniutto[28], Francesca Romana Ponziani[29], Luca Saverio Belli[30], Alessandro Federico[31], Gaetano Bertino[32], Michele Barone[33], Massimo Puoti[34], Alberto Civolani[35], Marco Distefano[36], Lorenzo Surace[37], Raffaele Cozzolongo[38], Ester Marina Cela[39], Elisabetta Teti[40], Pietro Lampertico[41,42], Tommaso Stroffolini[43], Romina Salpini[1], Valentina Svicher[1], Mario Rizzetto[2], Gian Paolo Caviglia[2]. *[1]Department of Biology, University of Rome Tor Vergata, Rome, Italy; [2]Department of Medical Sciences, University of Torino, Turin, Italy; [3]Division of Gastroenterology, Hepatology and Transplantation, ASST Papa Giovanni XXIII, Bergamo, Italy; [4]Gastroenterology, Department of Medicine, University of Milan Bicocca, Milan, Italy; [5]Hepatology Unit and Laboratory of Molecular Genetics and Pathology of Hepatitis Viruses, Reference Centre of the Tuscany Region for Chronic Liver Disease and Cancer, University Hospital of Pisa, Pisa, Italy; [6]Department of Clinical and Experimental Medicine, University of Pisa, Pisa, Italy; [7]Hepatology Unit, AORN A.Cardarelli, Naples, Italy; [8]Division of Infectious Diseases, ASST-FBF-Sacco, Milan, Italy; [9]Department of Biomedical and Clinical Sciences, University of Milan, Milan, Italy; [10]Infectious Diseases Unit, AORN Sant'Anna e San Sebastiano, Caserta, Italy; [11]Clinic of Infectious Diseases, Department of Precision and Regenerative Medicine and Ionian Area, University of Bari "Aldo Moro", Bari, Italy; [12]Clinica Malattie Infettive UniTo, "Ospedale Amedeo di Savoia", Turin, Italy; [13]Department of Clinical Medicine and Surgery, Liver and Biliary Diseases Unit, University of Naples "Federico II," Naples, Italy; [14]Infectious Diseases Unit, Department for Integrated Infectious Risk Management, IRCCS Azienda Ospedaliero-Universitaria di Bologna, Bologna, Italy; [15]Infectious Diseases Unit, Department of Medical and Surgical Sciences, University of Bologna, Bologna, Italy; [16]Infectious Diseases and Hepatology Unit, National Institute for Infectious Diseases Lazzaro Spallanzani IRCCS, Rome, Italy; [17]Deparment of Infectious Diseases, Galliera Hospital, Genoa, Italy; [18]Unit of Hepatology and Interventional Ultrasonography, Department of Internal Medicine, OORR Area Stabiese, Gragnano, Italy; [19]Internal Medicine, Azienda Ospedaliero-Universitaria "Maggiore Della Carità", Department of Translational Medicine (DiMeT), Università del Piemonte Orientale, Novara, Italy; [20]UOC di malattie infettive emergenti e ad alta contagiosità, Ospedale Cotugno, Naples, Italy; [21]Department of Medical and Surgical Sciences, Infectious Diseases Unit, University of Foggia, Foggia, Italy; [22]Section of Gastroenterology and Hepatology, Dipartimento Di Promozione Della Salute, Materno Infantile, Medicina Interna e Specialistica Di Eccellenza (PROMISE), University of Palermo, Palermo, Italy; [23]Department of Advanced Medical and Surgical Sciences, University of Campania "Luigi Vanvitelli," Naples, Italy; [24]Infectious Diseases Unit, Department of Mental Health and Public Medicine, University of Campania "Luigi Vanvitelli", Naples, Italy; [25]SC Infectious Diseases, ASST Papa Giovanni XXIII, Bergamo, Italy; [26]Infectious and Tropical Diseases Unit, Padua University Hospital, Padua, Italy; [27]Gastroenterology Unit, Fondazione Casa Sollievo Della Sofferenza IRCCS, San Giovanni Rotondo, Italy; [28]Hepatology and Liver Transplant Unit, Azienda Sanitaria Universitaria Integrata di Udine, Udine, Italy; [29]Liver Unit, Centro Malattie dell'Apparato Digerente (CEMAD), Medicina Interna e Gastroenterologia, Fondazione Policlinico Universitario Gemelli IRCCS, Rome, Italy; [30]Hepatology and Gastroenterology Unit, ASST Grande Ospedale Metropolitano Niguarda, Milan, Italy; [31]Department of Precision Medicine, University of Campania "Luigi Vanvitelli", Naples, Italy; [32]Hepatology Unit, University Hospital Policlinico "G. Rodolico - San Marco", Department of Clinical and Experimental Medicine, University of Catania, Catania, Italy; [33]Gastroenterology Unit, Department of Precision and Regenerative Medicine—Jonian Area—(DiMePRe-J), University of Bari "Aldo Moro," Policlinic University Hospital, Bari, Italy; [34]Division of Infectious Diseases, ASST Grande Ospedale Metropolitano Niguarda, Department of Medicine, University of Milan Bicocca, Milan, Italy; [35]Teaching Hospital "Duilio Casula", Azienda Ospedaliero-Universitaria di Cagliari, Cagliari, Italy; [36]UOSD Hepatology, Ospedale Umberto I°, ASP 8 Siracusa, Siracusa, Italy; [37]Dipartimento Di Prevenzione, Azienda Sanitaria Provinciale di Catanzaro, Centro di Medicina del Viaggiatore e delle Migrazioni, P. O. Giovanni Paolo II, Lamezia Terme, Italy; [38]Gastroenterology Unit, IRCCS "S. De Bellis", Castellana Grotte, Italy; [39]Gastroenterology Unit, Riuniti Polyclinic of Foggia, Foggia, Italy; [40]Infectious Disease Unit, Department of Systems Medicine, University of Rome Tor Vergata, Rome, Italy; [41]Division of Gastroenterology and Hepatology, Foundation IRCCS Ca' Granda Ospedale Maggiore Policlinico, Milan, Italy; [42]CRC "A. M. and A. Migliavacca" Center for Liver Disease, Department of Pathophysiology and Transplantation, University of Milan, Milan, Italy; [43]Department of Tropical and Infectious Diseases, Policlinico Umberto I, Rome, Italy*
Email: ilariagrossi8@gmail.com

Background and aims: Hepatitis B surface antigen (HBsAg) circulates as three isoforms (small [S], medium [M], large [L]), reflecting distinct steps of viral life cycle and morphogenesis. In HBV/HDV co-infection, we investigated the relationship between total HBsAg and its isoforms with markers of viral activity and liver injury according to different clinical phenotypes.
Method: This analysis included 366 patients with HBV/HDV co-infection, all HDV-RNA positive, mostly males (62.6%) and Italians (59.0%) with a median (IQR) age of 56 (46–62) years, from the HDV Describe study. Serum total, S-, M-, and L-HBsAg levels were quantified by ELISAs (Beacle Inc.) and were correlated with HDV-RNA (Robogene v2), HBcrAg (Fujirebio), ALT, and liver stiffness measurement (LSM) (Fibroscan, Echosens). Patients were classified into distinct clinical phenotypes according to liver cirrhosis status, with non-cirrhotic patients further stratified into high-viremic chronic hepatitis D (CHD; HDV-RNA ≥3 Log IU/mL), and low-viremic CHD (HDV-RNA <3 Log IU/mL).
Results: Median (IQR) HDV-RNA was 5.1 (3.4–6.0) Log IU/mL and total HBsAg was 3331 (675–9055) ng/mL, while median (IQR) levels of S-, M-, L-HBsAg were 2686 (483–7234), 538 (92–1467) and 0.75 (0.10–4.50) ng/mL, respectively. Total, S-, M-, L-HBsAg correlated positively with HDV-RNA (r_s = 0.47, 0.47, 0.47, and 0.42, respectively; all $p < 0.001$) and HBcrAg (r_s = 0.57, 0.56, 0.57, and 0.44, respectively; all $p < 0.001$). Total, S-, M-, and L-HBsAg levels were significantly higher in patients with ALT >40 U/L compared to those with ALT ≤40 U/L (all $p < 0.001$), whereas only L-HBsAg showed a modest correlation with LSM (r_s = 0.16; p = 0.007). Total, S-, M-, L-HBsAg levels varied according to patients' clinical phenotype, with the highest levels observed in high-viremic CHD, followed by cirrhosis and low-viremic CHD. In multivariate analysis, higher S-HBsAg levels were significantly associated with high-viremic CHD (OR = 1.58, 95% CI 1.16–2.15; p = 0.003), higher M-HBsAg with liver cirrhosis (OR = 1.78, 95% CI 1.04–3.03; p = 0.035), while lower L-HBsAg levels were associated with low-viremic CHD (OR = 0.38, 95% CI 0.25–0.58; $p < 0.001$).
Conclusion: Both total HBsAg levels and HBsAg isoforms correlated with the extent of HDV replication and cytolytic activity. Notably, HBsAg isoforms showed distinct associations across clinical phenotypes, suggesting a differential regulation of HBV envelope proteins in HDV-driven liver disease.

SAT-588

Beyond virological control: persistent psychological burden and the patient quest for functional cure in chronic hepatitis B

Robin Habermann[1], Alexandra Rickert[1], Sven Pischke[1], Peine Sven[2], Ansgar W. Lohse[1], Julian Schulze zur Wiesch[1], Felix Piecha[1].
[1]Department of Internal Medicine, University Medical Center Hamburg-Eppendorf, Hamburg, Germany; [2]Institute of Transfusion Medicine, University Medical Center Hamburg-Eppendorf, Hamburg, Germany
Email: robin.habermann@icloud.com

Background and aims: Chronic hepatitis B (CHB) infection remains a major global public health concern with significant risk for patients of developing chronic liver disease (CLD). While antiviral therapies effectively suppress viral replication, their impact on patient-reported health-related quality of life (HRQoL) remains poorly characterized in European populations. With the emergence of finite treatment strategies and novel cure-directed approaches, understanding patient perspectives on disease and treatment goals has become increasingly important. This study aimed to characterise the HRQoL in a northern German cohort of CHB patients, identify factors influencing patient-reported outcomes, and explore the patients' perspective on the disease.
Method: A total of 219 participants were enrolled in this study, 161 CHB patients (57 on antiviral therapy, 104 untreated) and 58 healthy controls. HRQoL was assessed using the Short Form-36 Health Survey (SF-36), with an additional questionnaire assessing the patients' illness perception. Linear regression analysis identified independent predictors of the Physical Component Summary (PCS) and Mental Component Summary (MCS) scores of the SF-36.
Results: Antiviral treatment was not associated with improved PCS or MCS scores in CHB patients. However, both treated and untreated CHB patients demonstrated significantly impaired mental wellbeing (MCS 42.5 and 42.2, respectively) compared with healthy controls (50.2; $p < 0.05$). Stratification by the region of origin revealed lower MCS scores for patients of Turkish and Middle Eastern origin. The presence of comorbidities ($p = 0.002$) and higher liver stiffness ($p = 0.043$) were independent predictors for a reduced PCS. Notably, the desire for a functional cure was highly prevalent in both groups (86.6% of treated and 78.8% of untreated patients), reflecting high treatment aspirations extending beyond virological suppression.
Conclusion: This analysis reveals a critical disconnect: despite preserved physical function and viral suppression, CHB patients experience persistent psychological burden unresolved by current antiviral therapies. The overwhelming patient preference for a functional cure underscores an unmet psychological and therapeutic need. These findings advocate for a paradigm shift toward holistic, cure-directed management strategies that address both clinical outcomes and psychosocial determinants of health.

SAT-589-YI

High diagnostic value of transient elastography for the diagnosis of advanced fibrosis and cirrhosis in patients with hepatitis D virus infection

Anna Hahn[1], Dominique Roulot[2], Elisabetta Degasperi[3,4,5], Layese Richard[6], Heiner Wedemeyer[1,3,7], Soo Aleman[8,9], Pietro Lampertico[3,4,5], Katja Deterding[1], Helenie Kefalakes[1,3,7], Lisa Sandmann[1,3,7]. *[1]Department of Gastroenterology, Hepatology, Infectious Diseases and Endocrinology, Hannover Medical School, Germany, Hannover, Germany; [2]Department of Hepatology, Avicenne Hospital, AP-HP, Bobigny, Sorbonne Paris Nord University, Bobigny, Paris, France; [3]D-SOLVE Consortium, an EU Horizon Europe Funded Project (no. 101057917), Hannover, Germany; [4]Division of Gastroenterology and Hepatology, Foundation IRCCS Ca' Granda Ospedale Maggiore Policlinico, Milan, Italy; [5]Department of Pathophysiology and Transplantation, CRC "A. M. and A. Migliavacca" Center for Liver Disease, Milan, Italy; [6]Unité de Recherche Clinique, Henri Mondor hospital, AP-HP, Paris Est Créteil University, Créteil, France; [7]German Center for Infection Research (DZIF), Hannover/Braunschweig, Germany; [8]Department of Infectious Diseases, Karolinska University Hospital, Stockholm, Sweden; [9]Department of Medicine Huddinge, Infectious Diseases, Karolinska Institute, Stockholm, Sweden*
Email: hahn.anna@mh-hannover.de

Background and aims: Non-invasive tests (NIT), including vibration-controlled transient elastography (VCTE), have been evaluated as an alternative to liver biopsy for the staging of liver disease in patients with chronic hepatitis D (CHD). Previous studies have shown superior diagnostic performance of VCTE compared to other NIT; however, analyses in large patient cohorts are lacking.
Method: Individual patient data from the two largest published studies were pooled to evaluate the diagnostic performance of VCTE, aspartate aminotransferase-to-platelet ratio (AAR), AST to platelet ratio index (APRI), and fibrosis-4 index (FIB4) for the detection of advanced fibrosis and cirrhosis in patients with CHD. This multi-center retrospective study included 506 patients with paired liver biopsy and VCTE performed within ± 6 months. The cohort was randomly stratified by METAVIR stage and ALT levels into derivation and validation cohort (70:30). Diagnostic accuracy was assessed using AUC, and optimal VCTE cutoffs were determined using Youden index.
Results: In the derivation cohort, the distribution of histologic fibrosis stages was 30% (107/359) for F0/F1, 29% (103/359) for F2, 19% (67/359) for F3, and 23% (82/359) for F4. Median VCTE values were significantly higher in patients with METAVIR F4 (17.4 kPa [IQR 11.9–28.2 kPa] compared with those with F0/F1 (7.2 kPa [IQR 5.8–10 kPa], $p < 0.0001$), F2 (8.9 kPa [IQR 7.6–11.1 kPa, $p < 0.0001$], and F3 (10.4 kPa [IQR 8.6–14 kPa], $p < 0.0001$). VCTE was superior to other NIT for the detection of cirrhosis (AUCs: 0.83 [VCTE], 0.59 [AAR], 0.70 [APRI], 0.76 [FIB4]). The optimal VCTE cutoff for diagnosing cirrhosis was > 15.2 kPa (sensitivity (Se) 61%, specificity (Sp) 90.3%, positive predictive value (PPV) 65%, negative predictive value (NPV) 88.7%), with 83.6% of patients correctly classified. Using a cutoff of 10.2 kPa for advanced fibrosis (≥ F3), sensitivity, specificity, PPV, NPV, and accuracy were 70%, 70%, 63%, 77%, and 70%, respectively. For ≥ F2, the optimal cutoff was > 8.5 kPa (Se 73.4%, Sp 65.4%, PPV 83.3%, NPV 51.1%), resulting in 71% correctly classified patients. In the validation cohort (n = 147), 76%, 65%, and 71% of patients were correctly classified when applying the cutoffs for ≥ F4, ≥ F3, and ≥ F2 derived from the derivation cohort.
Conclusion: VCTE is a valuable diagnostic method for staging liver disease in patients with CHD. However, liver biopsies will continue to play a role in patients with discrepant clinical and NIT results.

SAT-590

Reflex anti-HDV testing among HBsAg-positive patients: diagnostic yield and screening impact in a retrospective cohort study

Tor Sadeh[1], Orit Rozenberg[2], Fadi Abu Baker[3], Tarek Saadi[4], Rawi Hazzan[5]. *[1]Bruce Rappaport Faculty of Medicine, Technion-Israel Institute of Technology Haifa, Israel, Haifa, Israel; [2]Emek Medical Center Laboratories, Clalit Health Services, Afula, Israel; [3]Department of Gastroenterology and Hepatology, Hillel Yaffe Medical Center, Hadera 38100, Israel, Bruce Rappaport Faculty of Medicine, Technion-Israel Institute of Technology Haifa, Israel, Hadera, Israel; [4]Bruce Rappaport Faculty of Medicine, Technion-Israel Institute of Technology Haifa, Israel, Liver Unit, Rambam health care campus, Haifa, Israel, Haifa, Israel; [5]Clalit Health Services, Northern Region, Israel, Azrieli Faculty of Medicine, Bar-Ilan University, Safed, Israel, nazareth, Israel*
Email: rawihazzan1@gmail.com

Background and aims: Hepatitis D virus causes one of the most severe forms of chronic viral hepatitis. Although European guidelines recommend universal screening of all HBsAg-positive individuals, this practice is not yet widely implemented, and many remain unscreened. The objective of our study was evaluate the yield of reflex HDV testing and characterize HBV carriers who tested positive or negative for HDV in northern Israel.
Method: A retrospective cohort study was conducted using data from Clalit Health Services in northern Israel between May 2014 and May 2024. Hepatitis B surface antigen–positive patients were categorized into two groups: those screened for hepatitis D antibody via reflex testing (2019–2024) and those tested based on clinical discretion (2014–2019). Demographic, clinical, and laboratory characteristics were extracted for analysis.

Results: Among 1,336 HBsAg-positive individuals, HDV screening rates increased from 57.5% to 93.1% following reflex implementation. HDV seropositivity rose from 3.17% to 6.48% (P = 0.02). Ethiopian-born individuals had significantly higher positivity compared to other patients (10.4% vs. 3.9% respectively; P = 0.0221). The average time from HBV diagnosis to HDV testing decreased from 38.1 ± 31 months (median 37.5) in the pre-reflex period to 1.3 ± 6.1 months (median 0) in the reflex period.
Conclusion: Reflex anti-HDV antibody testing improves screening coverage and detects more seropositive cases. These findings support its integration into national screening policies to promote early diagnosis and ensure all at-risk individuals are tested for HDV.

SAT-591

Correlation of bile acid dynamics with bulevirtide response and disease severity in patients with hepatitis D

Marlene Hintersteininger[1,2], Michael Schwarz[3], Philipp Schwabl[1,2], Lukas Hartl[1,2], Lorenz Balcar[1,2], Benedikt Hofer[1,2,4], Georg Kramer[1,2], Christian Sebesta[1,2], Paul Thöne[1,2], Patrik Attalla[1], Michael Gschwantler[5], Michael Trauner[1], Mattias Mandorfer[1,2], Thomas Reiberger[1,2,4], Mathias Jachs[1,2]. *[1]Division of Gastroenterology and Hepatology, Department of Medicine III, Medical University of Vienna, Vienna, Austria; [2]Vienna Hepatic Hemodynamic Lab, Division of Gastroenterology and Hepatology, Department of Medicine III, Medical University of Vienna, Vienna, Austria; [3]Division of Gastroenterology and Hepatology, Department of Internal Medicine II, University Hospital of Sankt Pölten, Sankt Pölten, Austria; [4]Christian Doppler Lab for Portal Hypertension and Liver Fibrosis, Medical University of Vienna, Vienna, Austria; [5]Department of Internal Medicine IV, Klinik Ottakring, Vienna, Austria*
Email: marli.hintersteininger@gmail.com

Background and aims: Bulevirtide (BLV) inhibits hepatitis D virus (HDV) entry into hepatocytes by blocking the sodium taurocholate co-transporting polypeptide (NTCP), which is also the major hepatic bile acid (BA) uptake system. This study investigated the association between BA dynamics and antiviral response during BLV therapy.
Method: Patients with chronic HDV infection and longitudinal measurements of serum BA levels before, during, and after BLV treatment were included. Virologic response (VR) was defined as a ≥2 $\log_{10}$ HDV-RNA decline and discriminated versus virologic non-response (VNR). Changes in BA levels (ΔBA) were analysed (i) in relation to HDV-RNA dynamics, (ii) after pegylated interferon-alpha (pegIFN) add-on therapy and (iii) after BLV discontinuation.
Results: 25 patients (48% male; advanced chronic liver disease [ACLD]: 92.0%, 17 patients [68.0%] with VR at W48) were included. Baseline BA levels were significantly higher in ACLD patients with portal hypertension (PH, n = 10) compared to those without (19.2 µmol/L vs. 5.1 µmol/L; p = 0.015). Median on-treatment BA levels did not differ between patients with VR vs. VNR at W24 (25.4 µmol/L vs. 22.7 µmol/L; p = 1.000) and W48 (25.4 µmol/L vs. 20.8 µmol/L; p = 1.000). Relative to baseline, ΔBA from baseline to W48 did neither differ between patients with VR and VNR (p = 0.534) nor correlate with HDV-RNA decline at W48 (ρ = 0.08; p = 0.719). Comparable results were observed at W24, W72, and W96. Addition of pegIFN did not affect median BA levels during combination therapy (before add-on: 29.8 µmol/L vs. during add-on: 23.7 µmol/L; p = 0.500). Six patients discontinued BLV therapy after reaching sustained HDV-RNA suppression; and their BA levels promptly returned to normal levels (median at last on-treatment assessment: 18.9 µmol/L vs. median after discontinuation: 7.6 µmol/L; p = 0.028). Pruritus was reported by 11 patients during BLV therapy. Baseline BA levels were significantly higher in patients experiencing pruritus compared to those without (13.6 µmol/L vs. 6.8 µmol/L; p = 0.047). Importantly, BA levels during treatment were not associated with self-reported treatment compliance nor other adverse events.
Conclusion: Our cohort of predominantly ACLD-HDV patients showed elevated baseline and significant BLV-mediated increases in BA levels. Importantly, ΔBA did neither predict VR nor adverse events on BLV treatment. BA elevations during BLV treatment are fully reversible upon cessation.

SAT-592-YI

Low HBsAg and HBV DNA levels lead to stable state of sustained control among chronic hepatitis B patients: results from the SIGNAL study

Grishma Hirode[1,2], Sanam Tabataba Vakili[1], Leila Amiri[1], Andrew Mendlowitz[1,2,3], Aaron Vanderhoff[1,2], Saima Naim[1], Harry L.A. Janssen[1,4], Scott K. Fung[1], Adam Gehring[1], Jordan J. Feld[1,2]. *[1]Toronto Centre for Liver Disease, Toronto General Hospital, University Health Network, Toronto, Canada; [2]The Viral Hepatitis Care Network Canada (VIRCAN), Toronto, Canada; [3]Institute of Health Policy, Management and Evaluation, University of Toronto, Toronto, Canada; [4]Department of Gastroenterology and Hepatology, Erasmus MC University Medical Center, Rotterdam, Netherlands*
Email: grishma.hirode@gmail.com

Background and aims: Partial cure (sustained HBsAg <100 IU/mL and HBV DNA <LLOQ 24 weeks off-treatment), a novel treatment endpoint for hepatitis B virus (HBV) cure trials, has been proposed as an alternative to functional cure or hepatitis B surface antigen (HBsAg) loss. In this study, we examined whether even a single occurrence of low HBsAg and HBV DNA levels was a marker of a stable state of sustained control.
Method: Cohort study of chronic hepatitis B patients with at least 1 HBsAg measurement ≥0.05 IU/mL between January 2010-December 2022. The "sustained control state" was defined as HBsAg <100 IU/mL and HBV DNA <20 IU/mL; study entry as the first HBsAg measurement, and state entry as the first occurrence of the "sustained control state." We compared characteristics and HBsAg loss rate among patients who entered this state even once during follow-up, regardless of duration in this state, treatment or phase of infection, with those who never entered this state.
Results: Among 8239 patients (mean age 48 ± 14 years, 56% male, 81% Asian, HBsAg 2.6 ± 1.4 $\log_{10}$ IU/mL, HBV DNA 3.2 ± 2.5 $\log_{10}$ IU/mL, 77% HBeAg-negative, ALT 1.4 ± 4.5x ULN, APRI 1.0 ± 16, mean follow-up 316 ± 216 weeks), 1652 (20%) patients entered this state (17% entered this state more than once). At study entry, compared with patients who never entered this state, these patients were older (54 vs 46 years), had lower HBsAg (1.3 vs 3.0 $\log_{10}$ IU/mL) and HBV DNA (1.6 vs 3.6 $\log_{10}$ IU/mL), and were more often male (67 vs 54%) and HBeAg-negative (88 vs 75%) (p < 0.001 for all). At state entry, mean HBsAg was 0.7 ± 1.4 $\log_{10}$ IU/mL, and ALT was 0.8 ± 0.6× ULN. Median duration in this state was 108 (25–249) weeks and the majority who entered this state remained in it until end of follow-up (n = 1493, 90%). At end of follow-up, HBsAg loss was higher among those who entered this state compared with those who did not (30 vs 0.9%, p <0.001), and even among those who entered this state, HBsAg levels were significantly lower at state entry among those who achieved HBsAg loss. Among those who did not remain in this state at end of follow-up (n = 159), 18% experienced ≥1 occurrence of HBV DNA >2000 IU/mL and 8% ALT >5× ULN after entry into the state.
Conclusion: HBeAg-negative patients who achieve HBsAg <100 IU/mL and HBV DNA <20 IU/mL even once, regardless of treatment or phase of infection, have a high probability of remaining in that state for a prolonged period, and a high probability of subsequent HBsAg loss.

SAT-593

Impact of cardiometabolic risk factors control in patients with chronic hepatitis B treated with nucleos(t)ide analogues

Karen Cheuk-Ying Ho[1], Rex Wan-Hin Hui[1], Wai-Kay Seto[1,2], Man-Fung Yuen[1,2], Lung Yi Loey Mak[1,2]. [1]*Department of Medicine, Queen Mary Hospital, The University of Hong Kong, Hong Kong, China;* [2]*State Key Laboratory of Liver Research, The University of Hong Kong, Hong Kong, Hong Kong*
Email: loeymak@gmail.com

Background and aims: The long-term impact of individual cardiometabolic risk factors (CMRFs) in patients with chronic hepatitis B (CHB) treated with nucleos(t)ide analogues (NUCs) remains poorly defined.
Method: We conducted a single-center prospective analysis enrolling patients with CHB who were on NUCs since baseline assessment between Oct 2014 to November 2025. CMRFs were defined as per established criteria, with body mass index (BMI) threshold of 23 kg/m^2. We categorized patients as having poor control of CMRFs if they met any of the following criteria: a BMI of ≥30 kg/m^2, the use of three or more antihypertensive or antidiabetic medications, or the use of more than one lipid-lowering agent. Vibration controlled transient elastography (VCTE) was performed at baseline and at three to five years of follow-up. Advanced fibrosis was defined as >/= 10 kPa. Fibrosis progression was defined as liver stiffness (LS) increase by ≥20%. Liver-related events (LREs) were defined as ascites, hepatic encephalopathy (HE), variceal bleeding, hepatocellular carcinoma, liver-transplant or liver-related mortality.
Results: A total of 723 NUC-treated patients (median age 61.0 [54.5–66.7] years; 69.4% male; 90.5% undetectable HBV DNA, median NUCs duration of 14.1 [11.4–16.5] years, baseline LS 6.8 [4.90–10.90] kPa) were analysed with a follow-up time of 9.74 (7.27–10.20) years. LREs occurred in 112 (15.5%) patients, with annual incidence of 1.59%. All-cause mortality was observed in 86 (11.9%) patients, including 47 (6.50%) liver-related mortality, with annual incidence of 1.22% and 0.67%, respectively. 193 (26.7%) patients developed fibrosis progression, which was significantly associated with having three or more CMRFs (OR 1.648, 95% CI 1.026–2.648). An increase in number of CMRFs beyond three did not correspond to a higher risk of fibrosis progression. Patients with three or more CMRFs with a poor control was significantly associated with higher incidences of developing LREs (HR 2.765, 95% CI 1.639–4.663) and all-cause mortality (HR 2.889, 95% CI 1.608–5.191). These findings were only significant among patients without baseline advanced fibrosis.
Conclusion: The presence of three or more CMRFs increases risk of liver fibrosis progression. Poor control of CMRFs, instead of number of CMRFs, correlates with a higher LREs and all-cause mortality. Maintaining well-controlled CMRFs is crucial for reducing adverse clinical outcomes in CHB patients who are on NUCs.

SAT-594

Human leukocyte antigen DQB1 variants and seroclearance of hepatitis B markers in the REVEAL cohort

Claire Hsu[1], Chih-Jen Huang[2], Mei-Hung Pan[2], Chien-Jen Chen[2], Hwai-I Yang[2]. [1]*Cornell University, Ithaca, United States;* [2]*Genomics Research Center, Academia Sinica, Taipei, Taiwan*
Email: cph67@cornell.edu

Background and aims: Seroclearance of hepatitis B surface antigen (HBsAg), hepatitis B e antigen (HBeAg), and hepatitis B virus deoxyribonucleic acid (HBV DNA) represents key milestones of immune control in the natural history of chronic hepatitis B. Host immunogenetic factors, particularly within the human leukocyte antigen (HLA) region, are thought to influence long-term viral control, yet their roles across different serological endpoints remain incompletely defined. We investigated whether HLA-DQB1 variants were associated with seroclearance of major hepatitis B markers in a large community-based cohort.
Method: The REVEAL-HBV is a community-based cohort comprising 3,653 HBsAg-seropositive participants. Imputed HLA class I and II genotypes at loci A, B, C, DPB1, DQA1, DQB1, and DRB1 were analyzed. Seroclearance of HBsAg, HBeAg, and HBV DNA was evaluated using two complementary approaches: (i) binary outcomes (seroclearance vs. no seroclearance) analyzed by logistic regression and (ii) time-to-seroclearance analysed by Cox proportional hazards models, both under an additive genetic model. All analyses were adjusted for age, sex, alanine aminotransferase, smoking, alcohol consumption, cirrhosis, with multiple-testing correction applied.
Results: Distinct HLA-DQB1 variants were associated with seroclearance of different hepatitis B markers. DQB1*06:09 was associated with higher odds of HBsAg seroclearance (odds ratio [OR] = 2.17, p = 0.011) and a faster seroclearance rate (hazard ratio [HR] = 2.07, p = 0.003). For HBeAg seroclearance, HLA-DQB1*05:03 was associated with reduced odds (OR = 0.20, p = 0.009) and slower seroclearance rates (HR = 0.29, p = 0.016). For HBV DNA seroclearance, HLA-DQB1*06:02 was associated with higher odds (OR = 1.70, p = 0.008) and faster seroclearance rates (HR = 1.50, p = 0.010).
Conclusion: HLA-DQB1 variants were differentially associated with seroclearance of HBsAg, HBeAg, and HBV DNA in chronic hepatitis B, highlighting a role for host immunogenetics in shaping long-term viral control across distinct phases of HBV natural history.

SAT-595

Association of HDV RNA levels with liver disease progression in a large cohort of treatment-naïve Asian patients with chronic hepatitis D

Habiba Kamal[1,2], Ganbolor Jargalsaikhan[3], Sanjaasuren Enkhtaivan[3], Karin Lindahl[1], Bekhbold Dashtseren[3], Oyungerel Lkhagva-Ochir[3], Tuvshinjargal Ulziibadrakh[3], Andreas Bungert[3], Elisabetta Degasperi[2,4], Pietro Lampertico[2,5,6], Heiner Wedemeyer[7], Naranjargal Dashdorj[3], Soo Aleman[1,2]. [1]*Department of Medicine Huddinge, Karolinska Institutet, Stockholm, Sweden, Department of Infectious Diseases, Karolinska University Hospital, Stockholm, Sweden, Stockholm, Sweden;* [2]*D-SOLVE: EU-funded Network on individualized management of hepatitis D, Hannover, Germany;* [3]*The Liver Center, Ulaanbaatar, Mongolia, ONOM Foundation, Ulaanbaatar, Mongolia, Ulaanbaatar, Mongolia;* [4]*Division of Gastroenterology and Hepatology, Foundation IRCCS Ca' Granda Ospedale Maggiore Policlinico, Milan, Italy, D-SOLVE: EU-funded Network on individualized management of hepatitis D, Milano, Italy;* [5]*Division of Gastroenterology and Hepatology, Foundation IRCCS Ca' Granda Ospedale Maggiore Policlinico, Milan, Italy, CRC "A. M. and A. Migliavacca" Center for Liver Disease, Department of Pathophysiology and Transplantation, University of Milan, Milan, Italy, D-SOLVE: EU-funded Network on individualized management of hepatitis D, Milan, Italy;* [6]*CRC "A. M. and A. Migliavacca" Center for Liver Disease, Department of Pathophysiology and Transplantation, University of Milan, Milan, Italy, Milan, Italy;* [7]*Department of Gastroenterology, Hepatology, Infectious Diseases and Endocrinology, Hannover Medical School, Hannover, Germany, German Centre for Infection Research (DZIF), Site Hannover-Braunschweig, Hannover, Germany, Excellence Cluster RESIST, Hannover Medical School, Hannover, Germany, Hannover, Germany*
Email: habiba.khodir.kamal@ki.se

Background and aims: Chronic hepatitis D (CHD) is a severe chronic liver disease. Persistent HDV RNA replication and cirrhosis are known predictors of liver-related outcomes. However, the association between quantitative HDV RNA levels with liver disease progression remains insufficiently studied. We aimed to evaluate the prognostic value of baseline HDV RNA levels for liver-related events (LREs) and death in patients with CHD.
Method: We conducted a retrospective longitudinal study of patients with CHD between 2015 and 2025 at a hepatology center in Mongolia. Adults (≥18 years) without prior liver-related events (LREs, i.e. hepatic decompensation, hepatocellular carcinoma (HCC), or liver transplantation/liver-related death) at first HDV RNA test, and

without anti-CHD therapy were eligible. HDV RNA levels were quantified using the Bio-Rad amplification kit (Bio-Rad Laboratories, USA) with a lower limit of quantification of 10 IU/mL. Annual incidence rates (IRs) per 100 person-years (PYs) and predictors of composite LREs were assessed using Cox regression models.

Results: A total of 2,447 patients were included with: median age 40.3 years (IQR 33.5–49.9), 56.1% females, 9.2% diabetes mellitus, median HDV RNA 5.3 (4.1–6.1) $\log_{10}$ IU/mL, median HBV DNA 2.2 (1.1–3.1) $\log_{10}$ IU/mL, HBeAg+ 39.0%, 77.5% elevated ALT, and 20.9% having cirrhosis at baseline. During a median of 7.3 years (range 0.9–12.7); 216 (11.2% of 1,936) patients progressed to cirrhosis, and 287 (11.7%) experienced any LREs or death, at an IR of 1.74% and 3-, 5-, 10-year cumulative risks of 4.0%, 6.9%, and 18.0%, respectively. The corresponding IR of LREs in patients with baseline cirrhosis was 4.63%, with 3-, 5-, and 10-year cumulative risks of 10.6%, 18.7% and 41.2%, respectively. Baseline HDV RNA level was an independent predictor of LREs (adjusted hazard ratio [aHR] 1.15; 95% CI 1.05–1.26), with older age (aHR 1.06; 95% CI 1.04–1.07), elevated GGT (aHR 2.16; 95% CI 1.59–2.94), elevated ALT (aHR 1.74; 95% CI 1.15–2.64), and baseline cirrhosis (aHR 3.70; 95% CI 2.77–4.92). In patients with baseline cirrhosis, HDV RNA level, older age and elevated GGT remained independent predictors, but not ALT.

Conclusion: In this large Asian untreated CHD cohort, baseline quantitative HDV RNA levels were independently associated with the risk of liver-related events. Nonetheless, cirrhosis and biochemical markers showed stronger prognostic impact, underscoring the multifactorial nature of disease progression in CHD.

SAT-596

Serum gamma glutamyl transferase (GGT) levels is superior to alanine aminotransferase (ALT) to predict long-term liver-related complications and mortality in patients with chronic hepatitis D (CHD)

Habiba Kamal[1,2], Ganbolor Jargalsaikhan[3], Sanjaasuren Enkhtaivan[3], Karin Lindahl[1], Bekhbold Dashtseren[3], Oyungerel Lkhagva-Ochir[3], Tuvshinjargal Ulziibadrakh[3], Andreas Bungert[3], Elisabetta Degasperi[2,4], Pietro Lampertico[2,4,5], Heiner Wedemeyer[2,6,7], Naranjargal Dashdorj[3], Soo Aleman[1,2].
[1]Department of Medicine Huddinge, Karolinska Institutet, Stockholm, Sweden, Department of Infectious Diseases, Karolinska University Hospital, Stockholm, Sweden, Stockholm, Sweden; [2]D-SOLVE: EU-funded Network on individualized management of hepatitis D, Hannover, Germany; [3]The Liver Center, Ulaanbaatar, Mongolia, ONOM Foundation, Ulaanbaatar, Mongolia, Ulaanbaatar, Mongolia; [4]Division of Gastroenterology and Hepatology, Foundation IRCCS Ca' Granda Ospedale Maggiore Policlinico, Milan, Italy, D-SOLVE: EU-funded Network on individualized management of hepatitis D, Milano, Italy; [5]CRC "A. M. and A. Migliavacca" Center for Liver Disease, Department of Pathophysiology and Transplantation, University of Milan, Milan, Italy, Milan, Italy; [6]Department of Gastroenterology, Hepatology, Infectious Diseases and Endocrinology, Hannover Medical School, Hannover, Germany, German Centre for Infection Research (DZIF), Site Hannover-Braunschweig, Hannover, Germany, Excellence Cluster RESIST, Hannover Medical School, Hannover, Germany, Hannover, Germany; [7]Excellence Cluster RESIST, Hannover Medical School, Hannover, Germany, Hannover, Germany
Email: habiba.khodir.kamal@ki.se

Background and aims: Elevated gamma-glutamyl transferase (GGT) has been associated with liver disease progression in chronic hepatitis D (CHD). However, its prognostic value for liver-related events (LREs) and survival, compared with alanine aminotransferase (ALT), remains insufficiently explored. We therefore evaluated the association between elevated GGT and the risk of LREs and mortality in patients with CHD.

Method: We conducted a retrospective cohort study of patients with CHD at a hepatology center in Mongolia. Adults (≥18 years) without prior LREs (defined as cirrhosis, hepatic decompensation, liver transplantation, or death), without previous antiviral treatment for CHD, and with >6 months follow-up were included. Baseline was the date of first HDV RNA test. Upper limits of normal (ULN) were 35 and 31 IU/mL for GGT, and 41 and 31 IU/mL for ALT in males and females, respectively. Incidence rates (IR) per 100 person-years (PYs) were estimated using Poisson models and cumulative incidence was assessed by Kaplan–Meier method. Prognostic performance of GGT and ALT was assessed using time-dependent AUROC at 5 and 10 years and C-index.

Results: Overall, 2,506 patients were included with baseline characteristics of median age 40.3 years, 55.9% females, overweight 59.5%, diabetes 9.1%, alcohol overconsumption 8.4%, elevated ALT 77.5%, elevated GGT 42.4%, median HDV RNA 5.3 (4.1–6.1) $\log_{10}$ IU/mL, and 20.9% had cirrhosis at baseline. During a median follow-up of 7.4 (IQR 5.6–8.7) years, 290 (11.6%) developed LREs (IR 1.71/100 PYs), with 5- and 10-year cumulative risks of 6.8% and 17.7%. A total of 107 (4.3%) underwent liver transplantation or died (IR 0.61/100 PYs), with 5- and 10-year risks of 2.1% and 6.3%. Elevated GGT was independently associated with higher risk of LREs (aHR 2.11) and mortality (aHR 2.30). Elevated ALT was associated with LREs (aHR 1.85) but not with mortality. For GGT, 10-year risk increased from thresholds of 56 IU/mL for LREs and 58.7 IU/mL for mortality (AUROC 0.69 and 0.72; C-index 0.68 and 0.73, respectively). For ALT, 10-year LRE risk increased from 44 IU/mL (AUROC 0.58; C-index 0.57).

Conclusion: GGT demonstrated superior prognostic performance to ALT for predicting long-term liver-related outcomes and mortality in CHD, supporting its use as a simple biomarker for clinical risk stratification.

SAT-597

Risk of hepatitis B virus reactivation in patients with prior or chronic infections undergoing transarterial chemoembolization for hepatocellular carcinoma

Dong Yun Kim[1], Jaehong Jeong[1], Jung Pyo Hong[1], Jae Seung Lee[1], Mi Na Kim[1], Beom Kyung Kim[1], Seung Up Kim[1], Jun Yong Park[1], Sang Hoon Ahn[1], Do Young Kim[1], Hye Won Lee[1]. *[1]Department of Internal Medicine, Yonsei University College of Medicine, Yonsei Liver Center, Severance Hospital, Seoul, Korea, Rep. of South*
Email: lorry-lee@yuhs.ac

Background and aims: Transarterial chemoembolization (TACE) is a cornerstone treatment for hepatocellular carcinoma (HCC), yet the hepatitis B virus (HBV) reactivation risk—particularly among patients who previously had an infection—remains incompletely characterized. We aimed to determine the incidence of HBV reactivation and identify risk factors in patients undergoing TACE for HBV-related HCC.

Method: We retrospectively analyzed patients who underwent TACE for HBV-related HCC at a tertiary hospital during 2007–2025. Patients receiving baseline antiviral therapy were excluded. HBV reactivation was defined according to Asian guidelines. Among patients with definitive HBV serostatus (n = 774), patients were stratified according to HBV serological status into chronic-infection (hepatitis B surface antigen [HBsAg]-positive, n = 727) and resolved-infection (HBsAg-negative/anti-hepatitis B core antibody [HBc]-positive, n = 47) groups. Cumulative incidences and risk factors were assessed using Kaplan–Meier analysis and Cox regression.

Results: During a median follow-up of 16.7 months, HBV reactivation occurred in 60 patients (6.1% overall). Patients with a resolved HBV status had a higher reactivation rate (21.3% vs. 6.9%; $P < 0.001$). A resolved HBV status (adjusted hazard ratio: 3.98, 95% confidence interval: 1.99–7.97; $P < 0.001$) and an elevated alpha-fetoprotein level (1.33 per $\log_{10}$ ng/mL, 1.04–1.69; $P = 0.024$) were independent predictors of reactivation. The median time to reactivation was 12 months.

Conclusion: HBV reactivation occurred in approximately 6% of patients undergoing TACE for HBV-related HCC, with a resolved infection status conferring a >3-fold higher risk, with a reactivation

incidence exceeding 20%. Current guidelines may underestimate the reactivation risk in this population; prophylactic antiviral therapy may be considered rather than monitoring alone for HBsAg-negative/anti-HBc-positive patients undergoing TACE.

SAT-601-YI

Distinct associations of baseline hepatitis B virus deoxyribonucleic acid with liver-related death in hepatitis B e antigen-negative versus hepatitis B e antigen-positive chronic hepatitis B

Hsuan Chia Kuo[1], Tai-Chung Tseng[1,2,3], Chien-Jen Chen[4], Chun-Jen Liu[1,2,5], Tung-Hung Su[1,2], Hung-Chih Yang[1,5,6], WanTing Yang[2], Chen-Hua Liu[1,2], Pei-Jer Chen[1,2,3,5,6], Hwai-I Yang[4,7,8,9,10], Jia-Horng Kao[1,2,3,5]. *[1]Department of Internal Medicine, Division of Gastroenterology and Hepatology, National Taiwan University Hospital, Taipei, Taiwan, Taipei City, Taiwan; [2]Hepatitis research center, National Taiwan university hospital, Taipei, Taiwan, Taipei City, Taiwan; [3]Department of Medical Research, National Taiwan University Hospital, Taipei, Taiwan, Taipei City, Taiwan; [4]Genomics Research Center, Academia Sinica, Taipei, Taiwan, Taipei City, Taiwan; [5]Graduate Institute of Clinical Medicine, National Taiwan University College of Medicine, Taipei, Taiwan, Taipei City, Taiwan; [6]Department of Microbiology, National Taiwan University College of Medicine, Taipei, Taiwan, Taipei City, Taiwan; [7]Institute of Clinical Medicine, National YangMing Chiao Tung University, Taipei, Taiwan, Taipei City, Taiwan; [8]Graduate Institute of Medicine, College of Medicine, Kaohsiung Medical University, Kaohsiung, Taiwan, Kaohsiung City, Taiwan; [9]Biomedical Translation Research Center, Academia Sinica, Taipei, Taiwan, Taipei City, Taiwan; [10]Doctoral Program of Clinical and Experimental Medicine, National Sun Yat-Sen University, Kaohsiung, Taiwan, Kaohsiung City, Taiwan*
Email: tarenkuo5402@gmail.com

Background and aims: Chronic hepatitis B (CHB) remains a leading cause of global liver-related mortality. While serum hepatitis B virus (HBV) deoxyribonucleic acid (DNA) is a well-established prognostic marker, its linear association with outcomes may vary significantly across different phases of infection. We aimed to delineate the distinct associations between baseline HBV DNA levels and the risk of liver-related death (LRD) in hepatitis B e antigen (HBeAg)-negative and HBeAg-positive patients, utilizing long-term follow-up data from two large-scale community and clinical cohorts.
Method: We pooled data from 6,250 treatment-naïve, non-cirrhotic CHB patients from the renowned REVEAL-HBV and ERADICATE-B cohorts. Patients were stratified by baseline HBeAg status. The primary outcome was LRD. We assessed the hazard ratios (HRs) of LRD across baseline HBV DNA categories (log10 IU/mL) using Cox proportional hazards models, adjusting for age and sex.
Results: Over a median follow-up of 26.5 years, 458 incidences of LRD were identified. In the HBeAg-negative cohort (n = 5,189), LRD risk exhibited a strong, dose-dependent increase with baseline HBV DNA levels (p-for-trend < 0.001), plateauing at viral loads greater than or equal to 5 log10 IU/mL. Specifically, patients with HBV DNA greater than or equal to 7 log10 IU/mL had a nearly seven-fold higher risk of LRD compared to those with < 3 log10 IU/mL (adjusted HR: 6.95, 95% confidence interval [CI]: 4.13–11.68). Conversely, among HBeAg-positive patients (n = 1,061), no clear dose-response relationship was observed for viral loads greater than or equal to 4 log10 IU/mL, with LRD risk showing no significant gradient across higher DNA categories. These distinct risk patterns persisted after multivariable adjustment.
Conclusion: Baseline HBV DNA is a robust, dose-dependent predictor of liver-related mortality in HBeAg-negative CHB, whereas its prognostic value is markedly attenuated in the HBeAg-positive phase. These findings highlight the necessity of phase-specific risk stratification and suggest that viral load thresholds for predicting mortality should be interpreted differently based on HBeAg status.

SAT-602

Real-world experience of 25 years of Lamivudine therapy: highlighting favorable long-term outcomes in chronic hepatitis B

Jaejun Lee[1], Hyun Yang[1], Jeong Won Jang[1]. *[1]Catholic university of Korea, Seoul, Korea, Rep. of South*
Email: pwln0516@gmail.com

Background and aims: Lamivudine, the first oral nucleoside analogue for chronic hepatitis B (CHB), transformed antiviral therapy by enabling durable viral suppression and improving long-term outcomes. However, comprehensive evidence on its long-term clinical impact across diverse treatment patterns is limited.
Method: This real-world cohort study analyzed 1,134 CHB patients who initiated lamivudine between 1997 and 2010. Clinical outcomes, including liver transplantation (LT)-free survival, hepatocellular carcinoma (HCC) incidence, and hepatitis B surface antigen (HBsAg) seroclearance, were evaluated according to treatment continuation, cessation, virologic response, and rescue therapy. Propensity score matching and landmark analyses were applied to minimize bias.
Results: Over a maximum follow-up of 28 years (median, 14.8 years), the 10-year LT-free survival rate was 93.7%, and cumulative HCC incidence was 12.6%. HBsAg seroclearance occurred in 4.8% of patients. Treatment discontinuation significantly increased the probability of HBsAg seroclearance without negatively impacting survival or HCC incidence when performed per stopping criteria. Virologic responders demonstrated superior long-term survival (15-year LT-free survival 96.8%) and higher HBsAg seroclearance rates compared with non-responders. Among these responders, treatment discontinuation did not worsen LT-free survival or HCC risk compared with continued therapy, while achieving higher rates of HBsAg seroclearance in patients maintaining sustained virologic response. Lamivudine resistance was associated with a higher HCC risk (HR 1.95, P < 0.001), whereas rescue therapy improved LT-free survival (HR 0.37, P = 0.007) and reduced HCC incidence (HR 0.60, P = 0.038).
Conclusion: Lamivudine therapy provides durable long-term survival and HCC risk reduction, with safe cessation in selected patients and clear benefits of timely rescue therapy. These findings support optimization of CHB management strategies using current potent antiviral agents.

SAT-603

High-sensitivity HBsAg next assay predicts HBsAg seroreversion in chronic hepatitis B patients following functional cure

Fahong Li[1], Xiaoting Zhao[1], Yao Hu[2], Yuqi Liu[1], Yifei Guo[1], Tiantian Hu[1], Hao Wang[1], Lin Yujie[1], Luhan Zheng[1], Lei Wang[3], Ming Guan[2], Jiming Zhang[1]. *[1]Department of Infectious Disease, Huashan Hospital, Shanghai, China; [2]Department of Clinical Laboratory, Shanghai, China; [3]Department of Infectious Diseases and Hepatology, The Second Hospital of Shandong University, ShanDong, China*
Email: minelihong@163.com

Background and aims: Functional cure, defined as sustained HBsAg loss (<0.05 IU/mL) 24 weeks after treatment cessation, represents the optimal therapeutic endpoint for chronic hepatitis B (CHB). Although functional cure is increasingly achievable, HBsAg seroreversion affects at least 10% of patients. Therefore, the identification of reliable biomarkers to predict seroreversion is critical.
Method: This study enrolled patients across two cohorts: an ambispective cohort and a prospective cohort. The ambispective cohort comprised CHB patients who had previously achieved HBsAg loss; participants underwent ultra-sensitive HBsAg Next testing (analytical sensitivity: 0.005 IU/mL, Abbott Laboratories), discontinued antiviral therapy, and were followed for 72 weeks. The prospective cohort recruited HBeAg-negative patients receiving 48-week peginterferon-based therapy. Patients achieving HBsAg loss at the end of treatment (EOT) discontinued therapy, underwent HBsAg Next testing, and entered a 72-week post-EOT follow-up. The primary endpoint was HBsAg seroreversion (HBsAg ≥ 0.05 IU/mL) at week 72 post-EOT.

Results: A total of 104 patients achieving HBsAg loss were evaluated in the ambispective cohort. At the off-treatment baseline, 17 patients (16.3%) were reactive for HBsAg Next. Six patients experienced seroreversion by week 48; notably, all six were baseline HBsAg Next-reactive. In the prospective cohort (n = 156 enrolled), 37 patients achieved HBsAg loss by week 48 and ceased therapy; of these, four (10.8%) were HBsAg Next-reactive. During prospective follow-up, one patient experienced seroreversion by week 36, who was also baseline HBsAg Next-reactive. By week 48 post-EOT, all nine evaluable patients maintained HBsAg loss, eight of whom were HBsAg Next-non-reactive at baseline.Univariate analysis identified HBsAg Next reactivity ($p < 0.001$) and anti-HBs negativity ($p = 0.047$) as significant predictors of HBsAg seroreversion. Combined analysis further refined risk stratification ($p < 0.001$), identifying the HBsAg Next (+)/anti-HBs(-) subgroup as the highest-risk population, with a seroreversion rate of 38.5% (5/13). Enrollment and follow-up are ongoing.
Conclusion: The ultra-sensitive HBsAg Next assay is an effective tool for the early prediction of HBsAg seroreversion. Furthermore, combining HBsAg Next reactivity with anti-HBs status significantly enhances predictive performance, providing a robust framework for identifying patients at high risk of relapse following functional cure.

SAT-604

Prevalence and impact of hepatic steatosis on clinical outcomes in a U.S. multi-ethnic cohort of chronic hepatitis B

Jonathan R Lim[1], Matthew Kim[1], Zahra Sarrafan Chaharsoughi[1], Sungyoung Auh[1], Ifeoma Kwentoh[1], David E Kleiner[2], Christine Hsu[1], Marc G Ghany[1]. *[1]National Institute of Diabetes and Digestive and Kidney Diseases (NIDDK), Bethesda, United States; [2]National Cancer Institute (NCI), Bethesda, United States*
Email: jonathan.lim2@nih.gov

Background and aims: Previous studies suggest that hepatic steatosis (HS) is associated with faster fibrosis progression and HCC development in chronic hepatitis B (CHB). However, many of these studies were conducted in Asia, used non-invasive tests to evaluate fibrosis, and did not evaluate liver-related events (LREs) Aim: To determine the prevalence of steatosis and its contribution to liver disease outcomes in a U.S. multi-racial cohort of CHB.
Method: Untreated CHB patients who underwent liver biopsy from 1975 to 2022 were included. Demographic, clinical, virological, and histological factors were retrospectively extracted from the EMR. Liver biopsies were scored using the HAI scoring system for inflammation and fibrosis, and steatosis by the proportion of hepatocytes exhibiting fat: 0/trace (<5%), 1 (6–33%), 2 (34–66%), 3 (>66%). Chi-square and logistic regression were used to identify predictors of steatosis. LREs (hepatic decompensation and HCC), all-cause mortality, and HBsAg loss were assessed by Kaplan-Meier and Cox Proportional Hazards Model.
Results: Of 903 HBsAg+ patients, after exclusion of those with acute HBV, children, viral co-infection, LREs prior to biopsy, there were 349 untreated persons with a biopsy. The median age was 40 years (IQR 31, 51), and median follow up was 7.90 years (IQR 2.32, 15.48). 73% were male. 52% were White, 15% Black, 31% Asian, and 2% multiracial or unknown. Use of antivirals after biopsy was similar between those with and without HS (75% and 74% respectively). 12% had cirrhosis and 14% had severe hepatic inflammation. Overall, HS was present in 103 (29.5%) patients. In a univariate analysis, HS was associated with older age ($p = 0.002$), higher BMI ($p < 0.0001$), diabetes ($p = 0.016$), severe fibrosis when compared to mild ($p = 0.0015$), and prior tobacco use ($p = 0.007$). Current tobacco use was associated with lower risk of HS ($p = 0.007$) when compared to no use. In an age-adjusted multivariate analysis, only BMI (OR = 1.18, $p < 0.0001$) and prior tobacco use (OR = 2.56, $p = 0.015$) remained independent predictors of HS. 28 (8%) persons developed a LRE, 97 (28%) died, and 46 (13%) experienced HBsAg loss. In a time-to-event analysis, HS was associated with development of LREs ($p = 0.0131$), HCC ($p = 0.035$), and all-cause mortality ($p < 0.0001$), but not HBsAg loss.
Conclusion: In a multi-racial cohort of CHB, hepatic steatosis was associated with higher BMI, prior tobacco use, development of LREs, death, and HCC. Measures to reduce steatosis should be considered in CHB.

SAT-605

End-of-treatment HBV RNA, HBsAb, and HBcAb levels predict durability of Peg-IFN induced HBsAg loss in CHB patients

Yuqi Liu[1], Yifei Guo[1], Xiaoting Zhao[1,2], Yidi Jia[1], YuanYuan Xu[1], Haoxiang Zhu[1], Jiming Zhang[1]. *[1]Department of Infectious Diseases, Shanghai Key Laboratory of Infectious Diseases and Biosafety Emergency Response, Shanghai Institute of Infectious Diseases and Biosecurity, National Medical Center for Infectious Diseases, Huashan hospital, Fudan University, Shanghai, China; [2]The First Affiliated Hospital of Xinxiang Medical University, xinxiang, China*
Email: liuyq25@m.fudan.edu.cn

Background and aims: Hepatitis B surface antigen (HBsAg) loss, can be achieved through the pegylated interferon (PEG-IFN)-based therapy. However, it is an unignorable fact that a small proportion of patients who achieved functional cure develop HBsAg reversion (HRV) and the related factors are not well described. As a novel virological marker of hepatitis B virus (HBV), HBV RNA is attracting extensive attention, but its correlation with HBsAg remains unclear. We developed a study to investigate the predictive value of serum HBV RNA for HRV in chronic hepatitis B (CHB) patients who have achieved HBsAg loss.
Method: This study prospectively enrolled Hepatitis B e antigen (HBeAg) negative 435 patients who experienced PEG-IFN therapy at Huashan Hospital from January 2020 to October 2024,and among whom 124 patients achieved at least one test of HBsAg loss (HBsAg <0.05 IU/mL). Serum were collected and measured HBV RNA levels at the end of treatment(EOT), and patients were divided into the HBV RNA positive (HRP) group and the HBV RNA negative (HRN) group based on the RNA results. All participants were then followed up ever 24 weeks to 96 weeks.The dynamic changes and correlations between HBsAb and HBcAb was analyzed between the two groups and the predictive values of them for HRV.
Results: 124 patients achieved HBsAg seroclearance, among whom 14 patients' serum were HBV RNA positive at EOT. Then the patient were divided into HRP group (N = 14) and HRN group (N = 108).There was no significance in HBsAg,HBsAb,HBeAg level between the two groups,when HRP group has a higher level of ALT(median: 26.0 vs 49.5 U/L,$p = 0.04$). After 72 weeks of follow-up,HRP group showed a more pronounced decrease in HBsAb (median:7.975 vs 108.8 IU/mL, $p = 0.007$) and HRV occurred in 23 patients(HRP: 4/14 vs. HRN: 19/108). Univariate analysis showed lower levels of HBsAb are independently associated with HRV. ROC analysis identified the optimal EOT cut-off values for HBsAb, HBcAb, and HBV RNA as 44.75 IU/mL, 8.25 S/CO, and 0.645 copies/mL. In addition, combining HBsAb with HBV RNA yielded a higher AUC for predicting HRV compared with individual markers (HBsAb: 0.592; HBcAb: 0.607; RNA–HBsAb: 0.624).
Conclusion: The combination of EOT HBV RNA status with HBsAb and HBcAb levels plays a crucial role in predicting HBsAg reversion after treatment discontinuation among patients who have achieved HBsAg clearance.

SAT-606

Probability of functional cure after nucleos(t)ide analogue withdrawal in chronic hepatitis B: the impact of malignancy and chemotherapy exposure

Yen-Chun Liu[1], Hsin-Che Lin[1], Chao-Wei Hsu[1], Rachel Wen-Juei Jeng[1], Rong-Nan Chien[1]. [1]*Department of Gastroenterology and Hepatology, Chang Gung Memorial Hospital, Linkou branch, Taiwan, College of Medicine, Chang Gung University, Taiwan, Taoyuan, Taiwan*
Email: yenchun923@gmail.com

Background and aims: Functional cure of chronic hepatitis B (CHB), defined by HBsAg seroclearance, is increasingly achieved after nucleos(t)ide analogue (NUC) withdrawal in immune-competent patients. CHB patients with malignancy commonly receive NUC therapy as prophylaxis during chemotherapy, representing a distinct immunological context in which post-NUC HBsAg clearance remains insufficiently characterized. Both malignancy and chemotherapy exposure may influence host immune milieu, yet the relative impact of specific agents such as rituximab remains unclear. We aimed to compare the probability of HBsAg loss after NUC withdrawal across three clinically relevant contexts: (1) rituximab-containing chemotherapy, (2) chemotherapy without rituximab, and (3) immune-competent non-cancer CHB.
Method: This retrospective cohort study included non-cirrhotic, HBeAg-negative CHB patients. The cancer-CHB group comprised 248 patients receiving prophylactic NUC ≥12 weeks beyond chemotherapy, categorized into non-rituximab-treated (n = 131) and rituximab-treated (n = 117) subgroups. The reference cohort included 939 patients who discontinued NUC per APASL criteria (Off-NUC cohort). Inverse probability of treatment weighting (IPTW) balanced covariates (age, sex, HBV DNA, end-of-treatment HBsAg) across groups. Cumulative HBsAg loss was compared using weighted log-rank tests.
Results: Before weighting, cancer-CHB patients were older, less often male, and had lower baseline HBV DNA than off-Nuc patients. The unadjusted 5-year cumulative HBsAg loss was 11% in the off-NUC cohort, 6% in cancer-CHB without rituximab, and 9% in rituximab-treated lymphoma-CHB ($p = 0.10$). After IPTW, the corresponding rates were 11%, 2%, and 4%, respectively ($p < 0.01$). Off-Nuc patients had a significantly higher probability of HBsAg loss than both cancer-CHB subgroups, whereas no significance was observed between cancer-CHB patients with and without rituximab exposure ($p = 0.13$). In multivariate Cox regression, EOT qHBsAg <2 $\log_{10}$ IU/mL was independently associated with HBsAg loss, while cancer-CHB status was associated with a markedly lower probability of functional cure. Rituximab exposure was not independently associated with HBsAg loss.
Conclusion: After covariate adjustment, cancer-CHB patients showed substantially lower HBsAg loss rates after Nuc withdrawal compared with immune-competent CHB patients, regardless of rituximab exposure, suggesting that malignancy-associated immune alterations may represent a major barrier to functional cure.

SAT-607

Clinical performance of the Cobas HDV assay for hepatitis D virus RNA detection and quantification for the diagnosis and treatment monitoring of chronic hepatitis D

Aline Kessler[1], Suchitra Kumar[1], Sonia Giraldez Martinez[2], Sirak Gebreab[2], Matthew Lin[3], Jesse Young[4], Andreas Hiergeist[5,6], Britta Seiverth[2], Christian Voitenleitner[1], Pietro Lampertico[7,8], Marc Luetgehetmann[9,10]. [1]*Roche Diagnostics International Ltd., Rotkreuz, Switzerland;* [2]*Roche Diagnostics International Ltd., Rotkreuz, Switzerland;* [3]*Roche Molecular Systems Inc., Pleasanton, United States;* [4]*TriCore Reference Laboratories (TRIC), Albuquerque, United States;* [5]*microBIOMix GmbH, Regensburg, Germany;* [6]*Institute of Clinical Microbiology and Hygiene, University Hospital Regensburg, Regensburg, Germany;* [7]*Foundation IRCCS Ca' Granda Ospedale Maggiore Policlinico, Division of Gastroenterology and Hepatology, Milan, Italy;* [8]*CRC "A. M. and A. Migliavacca" Center for Liver Disease, Department of Pathophysiology and Transplantation, University of Milan, Milan, Italy;* [9]*University Medical Center Hamburg–Eppendorf, Hamburg, Germany;* [10]*German Center for Infection Research (DZIF), Hamburg-Lübeck-Borstel-Riems site, Hamburg, Germany*
Email: mluetgehetmann@uke.de

Background and aims: Hepatitis D virus (HDV) RNA quantification is crucial for diagnosing HDV infection and monitoring treatment response, but access to reliable, automated assays is limited. The Cobas® HDV assay (not approved for clinical use) is a dual-target assay for use on Cobas 5800/6800/8800 systems, standardised to the WHO HDV RNA international standard. We evaluated clinical performance for detection of HDV infection and measurement of longitudinal HDV RNA titre changes in patients with chronic hepatitis D (CHD).
Method: This multicentre study tested serum and plasma samples from anti-HDV-positive patients, with/without detectable HDV RNA, using Cobas HDV and a CE-marked comparator (RoboGene HDV RNA Quantification Kit 2.0). Performance parameters, i.e., limit of detection (LOD), lower limit of quantification (LLOQ), clinical sensitivity and specificity were established across HDV genotypes; method comparison analysis was performed. In anti-HDV-treated patients, concordance between the two quantitative methods was assessed on longitudinal HDV RNA titre data; changes over time were evaluated and the proportion of responders compared for non-inferiority. Liver function was evaluated via longitudinal changes in alanine and aspartate aminotransferase (ALT and AST).
Results: Serum LOD was 9.91 IU/mL for HDV-1, 2 and 6–8; LODs were 3x higher for HDV-3, and 1.5× higher for HDV-4 and -5. Plasma LOD was 3.34 IU/mL for HDV-1, 2 and 5–8; LODs were 3× higher for HDV-3, and 1.5× higher for HDV-4. LLOQ for HDV-1 was 25 IU/mL. HDV RNA samples from 199 anti-HDV-positive patients (detectable RNA: 135; undetectable RNA: 64) were evaluated. Clinical sensitivity and specificity of Cobas HDV (95% confidence intervals [CI]) were 97.8% (93.7–99.2) and 92.2% (83.0–96.6), respectively. Cobas HDV showed good agreement in quantitative HDV RNA results with the comparator assay (mean difference: –0.005 $\log_{10}$ IU/mL [95% CI: –0.081–0.071]). Concordance was high in treated patients (100% [95% CI: 98.7–100] for quantifiable results; n = 302); both assays showed a similar decline in HDV RNA titres over time, confirming that Cobas HDV is non-inferior for patient monitoring. Mean ALT and AST values decreased markedly from visit 1 to 2, alongside the most prominent decline in HDV RNA titre.
Conclusion: Results demonstrate the utility of Cobas HDV to accurately detect and quantify HDV RNA for diagnosis and treatment monitoring. This standardised, automated assay provides benefits for diagnosing HDV infection and managing patients with CHD.

SAT-608-YI

Genetic diversification in hepatitis Delta antigen and ribozyme correlates with altered virological and biochemical markers and may inform novel therapeutic targets

Alessia Magnapera[1], Lorenzo Piermatteo[1], Tylla Annamuhammedova[1], Lavinia Fabeni[2], Giulia Torre[1], Luca Carioti[3], Stefano D'Anna[1], Eugenie Lebomo Etogo[4], Ada Bertoli[3], Pierpaolo Paba[5], Antonella Olivero[6], Elisabetta Teti[7], Andrea Di Lorenzo[7], Vincenzo Malagnino[7], Marco Iannetta[7], Leonardo Baiocchi[8], Simona Francioso[8], Ilaria Lenci[8], Marco Arosio[9], Michele Totaro[9], Teresa Santantonio[10], Nadia Randazzo[11], Bianca Bruzzone[11], Umberto Cillo[12], Alessandro Vitale[12], Giuseppina Brancaccio[13], Giovanni Battista Gaeta[14], Alessia Ciancio[6], Francesca Ceccherini Silberstein[3], Sandro Grelli[3], Pietro Lampertico[15], Loredana Sarmati[7], Mario Rizzetto[6], Gian Paolo Caviglia[6], Romina Salpini[1], Valentina Svicher[1], Judith Torimiro[4]. [1]*University of Rome Tor Vergata, Department of Biology, Rome, Italy;* [2]*Laboratory of*

Virology and Laboratories of Biosafety, National Institute for Infectious Diseases Lazzaro Spallanzani-IRCCS, Rome, Italy; [3]Department of Experimental Medicine, University of Rome "Tor Vergata," Unit of Virology, Tor Vergata Polyclinic Foundation, Rome, Italy, Rome, Italy; [4]Department of Microbiology, Virology, Parasitology, Hematology and Infectious Diseases, Faculty of Medicine and Biomedical Sciences, University of Yaounde I, Cameroon, Yaounde, Cameroon; [5]Unit of Virology, Tor Vergata Polyclinic Foundation, Rome, Italy, Rome, Italy; [6]Department of Medical Sciences, University of Turin, Turin, Italy, Turin, Italy; [7]Department of Systems Medicine, Infectious Disease Clinic, University of Rome "Tor Vergata," Rome, Italy, Rome, Italy; [8]Hepatology Unit, Policlinico Tor Vergata, Rome, Italy, Rome, Italy; [9]Microbiology and Virology Unit, ASST "Papa Giovanni XXIII", Bergamo, Italy, Bergamo, Italy; [10]Department of Medical and Surgical Sciences, Infectious Diseases Unit, University of Foggia, Foggia, Italy, Foggia, Italy; [11]Department of Health Sciences, University of Genoa, Genoa, Italy, Genoa, Italy; [12]Hepatobiliary Surgery and Liver Transplantation Unit, Department of Surgery, Oncology and Gastroenterology, University of Padova, Padua, Italy, Padua, Italy; [13]Infectious Diseases, Link Campus University Rome, Department of Life Sciences, Health and Health Professions, Rome, Italy, Rome, Italy; [14]Infectious Disease Unit, University L. Vanvitelli, Naples, Italy, Naples, Italy; [15]Division of Gastroenterology and Hepatology, Foundation IRCCS Ca' Granda Ospedale Maggiore Policlinico, Milan, Italy, Milan, Italy
Email: alessiamagnapera97@gmail.com

Background and aims: Knowledge on genetic diversification within the HDV ribozyme (essential for viral replication) and HDAg domains, which drive replication and harbor cytotoxic T lymphocyte epitopes (CTLEs), is limited. We investigated HDV genetic conservation in ribozyme and HDAg regions and their correlation with virological and biochemical markers.
Method: 178 individuals with chronic HDV infection were enrolled. Full-length HDV genomes were sequenced by Illumina (median [IQR] reads/patient: 69282 [38127–181165]). Genotypes (Gt) were assigned by phylogeny. Nucleotides and amino acids were considered conserved if not mutated in ≥99% of sequences. HDAg domains and CTLEs (N = 18) were defined according to Pascarella 2010 and Kohsar 2021.
Results: Individuals were 58% males, median age 51 (37–59) years, mainly Italians (ITs, 43.7%), followed by Eastern Europeans (EEs, 34.8%) and Africans (AFs, 21.5%). Median HDV-RNA and ALT were 5.4 (4.5–6.1) logIU/ml and 94 (62–151) U/L. The most prevalent Gts were 1e (57.8%) and 1c (20.8%), followed by 1b (9.5%), 1a (7.8%), 5 (2.2%), 7 (1.1%) and 6 (0.5%). Gt 1e predominated in ITs (64%, P < 0.001), 1c in EEs (81%, P < 0.001), while 1a, 1b, 5, 6, and 7 were found only in AFs. HDV ribozyme showed 100% nucleotide conservation whereas HDAg exhibited marked variability: conservation was lower in N-terminal (aa1–107) than in C-terminal domains (aa108–214, known to be crucial for HDAg activity) (14.7% vs 32.2%, P < 0.005). CTLE conservation ranged from 0% in $CTLE_{aa26-34}$ and $CTLE_{aa43-51}$ to 50% in $CTLE_{aa140-149}$. In Gt 1e, the aa conservation was significantly reduced in individuals >40 years (68.2% vs 30.8%, P < 0.0001), particularly within 6 CTLEs. The N12G mutation (median intra-patient prevalence 99%) correlated with higher ALT (101[63–152] vs 86 [69–174] U/l, P = 0.01) and was enriched in individuals with 2xULN ALT (77% vs 50%, P = 0.005), suggesting enhanced cytolytic activity. Conversely, T180A (median intra-patient prevalence 63%) correlated with lower HDV-RNA and HBsAg levels (4.9 vs 5.6 logIU/ml, P = 0.04 and 3.7 vs 3.9 logIU/ml, P = 0.03), indicating impaired viral fitness.
Conclusion: HDAg exhibits conspicuous genetic diversification, particularly in N-terminal domains and CTLEs, with progressive enrichment in older individuals, suggesting ongoing antigenic drift. Specific mutations may modulate viral fitness and HDV-driven cytolytic activity, warranting further in vitro studies. The highly conserved ribozyme represents a promising target for RNA interference-based therapeutic strategies.

SAT-609

Comparing health-related quality of life for chronic hepatitis B patients with and without treatment cessation: findings from the prospective multicentre COIN-B trial

Zhuxin Mao[1], Arno Furquim d'Almeida[2,3], Axelle Vanderlinden[2,3], Stefan Bourgeois[4], Jean-Pierre Mulkay[5], Thomas Sersté[5], Struyve Mathieu[6], Baro Deressa[7], Dirk Sprengers[4], Marie De Vos[8], Jos Callens[9], Bao Shihao[3], Hendrik Reynaert[10], Pierre Deltenre[11], Filip Janssens[12], Sergio Negrin-Dastis[13], Peter Stärkel[14], Hans Orlent[15], Charlotte De Vloo[16], Jef Verbeek[17], Guy Van Roey[18], Xavier Verhelst[19], Christophe Moreno[20], Jean Delwaide[21], Christophe Van Steenkiste[22], Wim Verlinden[3,23,24], Isabelle Colle[25], Joke Bilcke[1], Philippe Beutels[1], Thomas Vanwolleghem[2,3]. *[1]University of Antwerp, Centre for Health Economics Research & Modelling Infectious Diseases (CHERMID), Vaccine & Infectious Disease Institute (VAXINFECTIO), Antwerp, Belgium; [2]University of Antwerp, Viral Hepatitis Research Group, Laboratory of Experimental Medicine and Pediatrics, Antwerp, Belgium; [3]Antwerp University Hospital, Department of Gastroenterology and Hepatology, Edegem, Belgium; [4]Ziekenhuis aan de Stroom, Department of Gastroenterology, Antwerp, Belgium; [5]CHU Saint-Pierre, Department of Hepato-Gastroenterology, Brussels, Belgium; [6]Ziekenhuis Oost-Limburg, Department of Gastroenterology, Genk, Belgium; [7]CHU Brugmann, Department of Gastroenterology, Brussels, Belgium; [8]Hôpital de Jolimont HELORA, Department of Gastroenterology, La Louvière, Belgium; [9]AZ Klina, Department of Gastroenterology, Brasschaat, Belgium; [10]UZ Brussel, Department of Gastroenterology, Brussels, Belgium; [11]Clinique Saint-Luc Bouge, Department of Gastroenterology, Namur, Belgium; [12]Jessa Ziekenhuizen, Department of Gastroenterology, Hasselt, Belgium; [13]Grand Hôpital de Charleroi, Department of Gastroenterology, Charleroi, Belgium; [14]Clinique Universitaires Saint-Luc, Department of Gastroenterology, Brussels, Belgium; [15]AZ Sint-Jan Brugge AV, Department of Gastroenterology and Hepatology, Brugge, Belgium; [16]AZ Delta, Department of Gastroenterology and Hepatology, Roeselare, Belgium; [17]UZ Leuven, Department of Gastroenterology and Hepatology, Leuven, Belgium; [18]AZ Turnhout, Department of Gastroenterology, Turnhout, Belgium; [19]UZ Gent, Department of Gastroenterology and Hepatology, Gent, Belgium; [20]CUB Hôpital Erasme, Université Libre de Bruxelles, Department of Gastroenterology, Hepatopancreatology and Digestive oncology, Brussels, Belgium; [21]CHU de Liège, Department of Hepato-Gastroenterology, Liège, Belgium; [22]AZ Maria Middelares, Department of Gastroenterology, Gent, Belgium; [23]Vitaz, Department of Gastroenterology, Sint-Niklaas, Belgium; [24]University of Antwerp, Laboratory of Experimental Medicine and Pediatrics, Antwerp, Belgium; [25]AZORG, Department of Gastroenterology, Aalst, Belgium*
Email: zhuxin.mao@uantwerpen.be

Background and aims: Nucleos(t)ide analogues (NUC) are the current first line treatment for chronic hepatitis B (CHB). The drugs efficiently suppress viral replication, but HBV seroclearance often requires decades of continuous therapy. While NUC cessation is increasingly explored as a strategy to induce functional cure, its impact on health-related quality of life (HRQoL) is unknown. We evaluated HRQoL in patients who discontinued NUC therapy with those continuing treatment within the COIN-B trial (NCT04779970, EudraCT 2021-001003-32).
Method: This prospective multicentre study was conducted across 26 Belgian hospitals. HRQoL was assessed at baseline and at weeks 4, 12, 24, and 72, using the EQ-5D-5L with EQ-Visual Analogue Scale (VAS), and were valued using the Belgian value set. Descriptive statistics were calculated for each time point and study arm. Determinants of EQ-5D-5L utility values were explored using linear mixed-effects models with random intercepts for patients to account for within-subject correlation.
Results: A total of 146 patients were included (91 stop treatment arm; 55 control arm). Patients who discontinued NUC treatment consistently reported high mean EQ-5D-5L utility (>0.9) at all time points. Mean utilities in the control arm were slightly lower but remained

close to 0.9 throughout follow-up. Mean (SD) utilities in the stop arm were between 0.92 (0.12) at baseline and 0.94 (0.15) at week 72, which were higher than the Belgian population norm at a similar age (0.83, $p < 0.01$). EQ-VAS scores showed a similar pattern. Mixed-effects models showed lower utilities for patients in the control arm, older, female, those with more advanced fibrosis stage, other liver diseases, BMI ≥25 or <18.5, non-Caucasian race and birth or parental birth outside Belgium, but coefficients were small and not statistically significant ($p > 0.05$).

Conclusion: NUC discontinuation was associated with sustained high HRQoL. Mean utilities were consistently higher than in the control arm and significantly above age-matched population norms. This may partly reflect a highly motivated patient population and long-term coping with CHB, resulting in high self-reported health status. Importantly, these findings support the feasibility of NUC cessation strategies in appropriately selected patients and provides a robust empirical basis for future health economic evaluation.

SAT-610

The longitudinal impact of anti-HBe on qHBsAg decline in chronic hepatitis B

Andrew Mendlowitz[1,2,3], Sanam Tabataba Vakili[1], Leila Amiri[1], Grishma Hirode[1,2], Aaron Vanderhoff[1,2], Saima Naim[1], Harry L.A. Janssen[4], Scott K. Fung[1], Adam Gehring[1], Jordan J. Feld[1,2]. *[1]Toronto Centre for Liver Disease, University Health Network, Toronto, Canada; [2]Viral Hepatitis Care Network, University Health Network, Toronto, Canada; [3]Institute of Health Policy, Management and Evaluation, University of Toronto, Toronto, Canada; [4]Erasmus University Medical Centre, Rotterdam, Netherlands*
Email: andrew.mendlowitz@alumni.utoronto.ca

Background and aims: HBeAg loss is a well-recognized milestone in the natural history of chronic hepatitis B infection (CHB). However, the importance of anti-HBe as a marker of immune fitness or evolution of disease trajectory is less understood. Current guidelines recommend that nucleos(t)ide analogues can be stopped in patients who are anti-HBe-positive, as the probability of flares are higher in those anti-HBe-negative. Using large cohort data, we aimed to characterize the association between anti-HBe emergence and qHBsAg dynamics over time.

Method: We followed CHB patients with at least one qHBsAg measurement from their earliest HBeAg-positive date (index) until their last HBeAg status. Visits were classified relative to HBeAg loss (pre/post), with time measured from the start of the pre- or post-HbeAg loss period. Seroconversion was identified from the first positive anti-HBe test onward. We modeled qHBsAg using a linear mixed-effects model incorporating anti-HBe seroconversion and time relative to HBeAg loss, adjusting for demographics, treatment, cirrhosis and baseline qHBsAg, reporting model-adjusted levels and changes over time. The model was also applied to patients only ever HBeAg-negative, using follow-up time from first HBeAg status.

Results: From 2010 to 2022, 1,701 HBeAg-positive patients (median age 38 years; 54% male) were included, of whom 675 (40%) experienced HBeAg loss. Among these, 538 (80%) were anti-HBe-positive; 95 (18%) at index and 443 (82%) who developed anti-HBe during follow-up. Of the 443, 292 (66%) seroconverted on/after HBeAg loss, 262 (59%) within two years, with time to seroconversion ranging from immediately after HBeAg loss to 11 years afterward. Average qHBsAg declined from 2,100 IU/mL before HBeAg loss to 1,081 IU/mL after, with the rate of decline accelerating from −0.024 log IU/mL/year to −0.055 log IU/mL/year ($p < 0.001$). Average qHBsAg was 1,901 IU/mL before anti-HBe appearance and 1,195 IU/mL afterwards, with the rate of decline changing from −0.029 log IU/ml/year to −0.044 log IU/ml/year ($p < 0.001$). Baseline qHBsAg, sex, age, and cirrhosis were also significant determinants of qHbsAg in multivariable analysis. In contrast, among 6,228 always HBeAg-negative patients, 6,022 (97%) were anti-HBe-positive, and anti-HBe appearance was not significantly associated with qHBsAg level ($p = 0.67$).

Conclusion: Anti-HBe appearance was associated with lower qHBsAg levels seen with HBeAg loss but had minimal effect in those starting HBeAg-negative, suggesting plateauing over time.

SAT-611

Integrating double reflex hepatitis D virus testing to reduce diagnostic gaps and streamline clinical pathways

Almuthana Mohamed[1,2], Andrew Watson[1,2], Sara Lucas[2], Arron Jones[2], Anna Jeffery-Smith[2], Anna Riddell[2], Apostolos Koffas[1,2], Upkar Gill[1,2], Patrick Kennedy[1,2]. *[1]Blizard Institute, Barts and the London school of medicine and dentistry, Queen Mary University of London, London, United Kingdom; [2]Barts Health NHS Trust, London, United Kingdom*
Email: almuthana700@gmail.com

Background and aims: Hepatitis delta virus (HDV) remains an underdiagnosed cause of severe liver disease in patients with chronic hepatitis B (CHB). Variable testing practices can delay diagnosis and access to treatment. We implemented a double reflex testing pathway at Barts Health NHS Trust, where all hepatitis B surface antigen (HBsAg)-positive patients automatically undergo HDV antibody (HDV Ab) testing, with reflex HDV RNA testing for HDV Ab-positive cases. The aim was to accelerate HDV case-finding and streamline linkage to specialist care, including access to licensed therapy, bulevirtide (BLV), and recruitment into clinical trials of novel therapies for HDV.

Method: Double reflex HDV testing was rolled out across all sites at Barts Health NHS Trust (Royal London, Whipps Cross, Newham, and St Bartholomew's Hospitals). HBsAg-positive patients underwent reflex HDV Ab testing. HDV Ab-positive samples triggered automatic reflex HDV RNA testing, achieving ≥99% compliance. Patients with detectable HDV RNA were promptly referred to specialist hepatology services for treatment assessment, including eligibility for BLV and clinical trial enrolment.

Results: In total, 7,218 HBsAg-positive patients underwent reflex HDV Ab testing. Of those screened, 458 (6.3%) were HDV Ab positive, and 168 (2.3%) had confirmed active HDV infection with detectable HDV RNA. Demographically, the population was predominantly male (85%), of Eastern European background, with a median age of 38 years (IQR = 6). Following identification, patients were streamlined into management pathways. Currently, 48 (29%) patients are being assessed for BLV, 19 (11%) are receiving BLV, 17 (10%) are enrolled in HDV clinical trials, and 84 (50%) of newly identified HDV RNA-positive patients are either not eligible for BLV (n = 23, 14%) or awaiting specialist clinic review (n = .61, 36%). Our cohort showed no significant difference in HDV RNA reduction between patients treated with BLV and those enrolled in HDV clinical trials, matched at 6 months (P = 0.774), with follow-up ongoing.

Conclusion: Large-scale double reflex testing successfully embedded HDV detection into routine CHB care across East London, identifying substantial numbers of HDV patients, reducing delays to specialist review and access to treatment. Reflex testing has facilitated access to both licensed therapy (BLV) and clinical trials of novel agents. This approach is scalable and could serve as a model for wider NHS adoption to improve access to HDV diagnosis and treatment nationally.

SAT-612

Hepatitis B virus outcomes in people with HIV after cessation of tenofovir-containing antiretroviral therapy: a systematic review and meta-analysis

Amir Mohareb[1], Bonolo Phinius[2], Motswedi Anderson[2], Shahin Lockman[2], Julie Bottero[3], George Yendewa[4], Arthur Kim[1], Anders Boyd[5]. [1]*Massachusetts General Hospital, Harvard Medical School, Boston, United States;* [2]*Botswana Harvard Health Partnership, Gaborone, Botswana;* [3]*National Public Health Establishment of Fresnes, Fresnes, France;* [4]*Case Western Reserve University, Cleveland, United States;* [5]*Inselspital, Bern University Hospital, Bern, Switzerland*
Email: amohareb@mgh.harvard.edu

Background and aims: Anti-retroviral therapy (ART) regimens without tenofovir are being used more frequently in people living with HIV. Tenofovir cessation has risks related to hepatitis B virus (HBV) infection. We aimed to determine the HBV outcomes in people with HIV who discontinue tenofovir-containing ART.
Method: We conducted a systematic review and meta-analysis by searching Medline, Google Scholar, and the Cochrane database for studies related to tenofovir cessation in people with HIV and three different HBV serologic profiles: (1) active HBV: positive HBV surface antigen (HBsAg); (2) resolved HBV: positive HBV core antibody (HBcAb) without HBsAg; and (3) susceptibility to HBV: negative HBsAg, HBcAb, and HBV surface antibody. We used a random effects model to calculate the pooled incidence rate of HBV reactivation (in resolved HBV) or new HBV infection (in those susceptible to HBV) after tenofovir cessation. We used meta-regression to compare pooled outcomes across subgroups.
Results: Of 116 abstracts and articles, 39 underwent full-text review and 17 observational studies were included. In seven studies of active HBV infection, only descriptive data could be retrieved: HBV DNA increase or hepatitis flares did occur after tenofovir cessation or interruption. In nine observational studies of resolved HBV infection, pooled incidence of HBV reactivation was 0.97 per 100 person-years (95% confidence interval (CI) = 0.31–3.06; I^2 = 95.2%). HBV reactivation was 4.23 per 100 person-years (95% CI = 1.90–9.41) in prospective compared with 0.24 per 100 person-years (95% CI = 0.18–0.31) in retrospective studies ($p < 0.001$). Five observational studies reported new HBV infection in susceptible people following transition to tenofovir-sparing ART (pooled incidence = 2.05 per 100 person-years, 95%CI = 0.23–18.45; I^2 = 83.5%).
Conclusion: In people with HIV, tenofovir-sparing ART is associated with risks related to HBV infection. Clinicians using tenofovir-sparing ART should screen for HBV serologic markers, vaccinate against HBV, and monitor for reactivation. Higher quality and larger prospective studies are needed in people with HIV and resolved HBV who stop tenofovir.

SAT-613

Significant gaps in the cascade of care contribute to poor liver cancer outcomes among people with hepatitis B: a retrospective-prospective longitudinal cohort study

Dina Moussa[1], Joan Flores[2], Marno Ryan[3], Thai Hong[3], Brett Knowles[3], Adrian Fox[3], Ashu Jhamb[3], Tom Sutherland[3], William Kemp[4], Ammar Majeed[4], Marie Sinclair[5], Rohit Sawhney[6], Stephen Bloom[6], Amanda Nicoll[6], Zina Valaydon[7], Gauri Mishra[8], Siddharth Sood[9], Diana Lewis[9], Alexander Thompson[2], Jessica Howell[3]. [1]*Burnet Institute, Melbourne, Australia;* [2]*University of Melbourne, Melbourne, Australia;* [3]*St Vincent's Hospital, Melbourne, Australia;* [4]*Alfred Health, Melbourne, Australia;* [5]*Austin Health, Melbourne, Australia;* [6]*Eastern Health, Melbourne, Australia;* [7]*Western Health, Melbourne, Australia;* [8]*Monash Health, Melbourne, Australia;* [9]*Northern Health, Melbourne, Australia*
Email: dina.moussa@burnet.edu.au

Background and aims: Hepatitis B (HBV) is a major cause of hepatocellular carcinoma (HCC) in Australia, despite availability of subsidised treatment that reduces HCC risk. We aimed to describe the cascade of care and clinical characteristics among people with HBV-related HCC.
Method: We conducted a retrospective and prospective cohort study of all HCC cases diagnosed across six tertiary health networks in Melbourne. Bi-variable analysis was performed using chi square test. Multivariable logistic regression modelling was used to determine variables associated with HBV treatment and surveillance uptake. Cox proportional hazards modelling was used to identify variables associated with survival from HCC diagnosis.
Results: 1203 incident HCC cases were identified, of which 219 were due to HBV. Most people with incident HBV-HCC were male(89%) and of Asian ethnicity(60%). Compared to people with HCC due to other aetiologies, people with HBV-related HCC were more likely to have a family history of HCC. 60% of people with HBV-HCC were eligible for HBV treatment at the time of HCC diagnosis, yet 27% were not on treatment. 85% of those referred by specialist hepatology services were enrolled in surveillance compared to 16% among those referred by primary care and non-liver specialists. Median survival from time of HCC diagnosis was longer among those with HBV compared to non-HBV HCC. On multivariable analysis, factors associated with greater mortality were low performance status, alcohol misuse and advanced BCLC stage at diagnosis. Attending a liver specialist service, being enrolled in surveillance and being on HBV treatment were all associated with early BCLC stage HCC at diagnosis.
Conclusion: HBV-related HCC incidence is reducing in Australia, however a significant proportion of people with HBV-related HCC are not receiving guideline-based care. Greater investment in non-specialist health-worker education and training in HBV care, coupled with a national registry approach to HCC surveillance are urgently needed.

SAT-617

Development of a new model for identifying HBV-related pre-ACLF patients among those with progressive total hyperbilirubinemia

Yuhang Nie[1], Dachuan Cai[1]. [1]*Department of Infectious Diseases, Key Laboratory of Molecular Biology for Infectious Diseases (Ministry of Education), Institute for Viral Hepatitis, The Second Affiliated Hospital, Chongqing Medical University, Chongqing, China*
Email: Komori0g0@outlook.com

Background and aims: The concept of "pre-acute-on-chronic liver failure (Pre-ACLF)" was proposed to describe a transitional stage before patients progress to full ACLF. Early intervention at this stage can significantly improve prognosis. However, the clinical characteristics of Pre-ACLF remain insufficiently understood, and accurately identifying these patients is challenging. This study aimed to analyze the biochemical indicators and disease progression in Pre-ACLF patients to clarify their clinical features and establish a diagnostic model for their identification.
Method: A retrospective analysis was conducted on 214 hospitalized chronic hepatitis B (CHB) patients who experienced significant clinical deterioration. Their clinical characteristics and progression were analyzed. Multivariate logistic regression was used to identify independent risk factors for progression to ACLF, based on which a diagnostic scoring model was developed.
Results: Among the 214 CHB patients with significant deterioration, the majority were male (79.0%). 58.9% had underlying cirrhosis, and among these cirrhotic patients, 48.4% experienced acute decompensation events, primarily ascites (78.7%). Analysis of disease progression revealed that 48.1% of patients progressed to ACLF within 28 days, defining them as Pre-ACLF patients. The main triggers for progression were untreated high viral load (55.3%), drug withdrawal leading to viral rebound (27.2%), and acute decompensation events (9.7%). Among 148 patients with persistently elevated bilirubin, 39.2% progressed to ACLF within 28 days. Multivariate LASSO-Logistic regression analysis identified Prothrombin Activity (PTA), the rate of change in PTA (VΔPTA), and the rate of change in TB (VΔTB) as

independent risk factors for disease progression. A new diagnostic model was constructed: logit(P) = 1.8303–0.0630 * PTA–0.8821 * VΔPTA + 0.0801 * VΔTB. Patients with a logit(P) score > 0.39 had a higher risk of progressing to ACLF. The model showed an AUC of 0.889 (95% CI: 0.837∼0.941). The calibration curve indicated good model calibration. Decision Curve Analysis (DCA) suggested that the model provided high clinical net benefit across a wide range of threshold probabilities (0∼75%).

Conclusion: The newly developed model can accurately identify Pre-ACLF patients among those with persistently elevated bilirubin, providing evidence-based support for early clinical diagnosis and intervention.

SAT-618

Global gaps in hepatitis B (HBV) and D (HDV) care: results from a worldwide survey of clinical practice

George Papatheodoridis[1,2], Maria Buti[1,3], Phunchai Charatcharoenwitthaya[1,4], Ajeet Bhadoria[1,5], Jian-Gao Fan[1,6], Brian Pearlman[1,7], Cristiane A. Villela-Nogueira[1,8], Shivaram Prasad Singh[1,9], Satoru Kakizaki[1,10], Wah-Kheong Chan[1,11], Anand Kulkarni[1,12], Ashwani K. Singal[1,13], Ana Ostojic[1,14], Javier Crespo[1,15], Christian Tzeuton[1,16], Jimmy Che-To Lai[1,17], Loreta Kondili[1,18], Munkhbat Batmunkh[1,19], Munkhjargal Ayurzana[1,20], Ming-Lung Yu[1,21], George Boon Bee Goh[1,22], Dimitrios Karagiannakis[1,23], Ellina Lytvyak[1,24], Amit Goel[1,25], Khalid Al Naamani[1,26], Wendy Spearman[1,27], Ira Jacobson[1,28], Tatyana Kushner[1,29], Davaadorj Duger[1,20], Yuichiro Eguchi[1,30], Mohamed El-Kassas[1,31], Sarantuya Gidaagaya[1,20], Stuart C Gordon[1,32], Saira Khaderi[1,33], Pietro Lampertico[1,34], Mei-Hsuan Lee[1,35], Bira Namdag[1,20], Ponsiano Ocama[1,36], Mario Guimarães Pessoa[1,37], Nikolaos T. Pyrsopoulos[1,28], Francesco Paolo Russo[1,38], Yusuf Yilmaz[1,39], Linda Henry[1], Fatema Nader[1], Andrei Racila[1], Maria Stepanova[1], Janus Ong[1,40], Zobair M. Younossi[1,41]. *[1]The global NASH/MASH council, Washington, DC, United States; [2]1st Academic Department of Gastroenterology, Medical School of National and Kapodistrian University of Athens, General Hospital of Athens "Laiko", Athens, Greece, Athens, Greece; [3]Hospital General Universitari Valle Hebron, Barcelona, Barcelona, Spain; [4]Division of Gastroenterology, Department of Medicine, Faculty of Medicine Siriraj Hospital, Mahidol University, Bangkok, Thailand, Bangkok, Thailand; [5]All India Institute of Medical Sciences (AIIMS) Rishikesh, India, Rishikesh, India; [6]Department of Gastroenterology, Xinhua Hospital, Shanghai Jiao Tong University School of Medicine, Shanghai, China, Shanghai, China; [7]Department of Internal Medicine, Emory University School of Medicine, Atlanta, Georgia, USA, Emory, United States; [8]School of Medicine, Hepatology Division, Universidade Federal do Rio de Janeiro,Brazil, Rio de Janeiro, Brazil; [9]Department of Translational Gastroenterology, Kalinga Gastroenterology Foundation, Cuttack, Odisha, India, Odisha, India; [10]Department of Clinical Research, NHO Takasaki General Medical Center, Takasaki, Japan, Takasaki, Japan; [11]Gastroenterology and Hepatology Unit, Department of Medicine, University of Malaya, Kuala Lumpur, Malaysia, Kuala Lumpur, Malaysia; [12]Senior consultant and director of critical care hepatology at the Asian Institute of Gastroenterology, Hyderabad, India, Hyderabad, India; [13]University of Louisville School of Medicine, Louisville, United States; [14]Department of Gastroenterology and Hepatology; University Hospital Center Zagreb, Croatia, Zagreb, Croatia; [15]Profesor de Medicina. Universidad de Cantabria. Instituto de Investigación Valdecilla, Spain, Valdecilla, Spain; [16]Université de Douala, Douala, Cameroon, Douala, Cameroon; [17]Medical Data Analytics Centre and Li Ka Shing Institute of Health Sciences, Department of Medicine and Therapeutics, The Chinese University of Hong Kong, Hong Kong, Hong Kong, Hong Kong; [18]Center for Global Health Istituto Superiore di Sanità, Viale Regina Elena 299-00161 Rome-Italy, Rome, Italy; [19]Department of Medical Legislation and Education, Graduate School, Mongolian National University of Medical Sciences, Ulaanbaatar, Mongolia, Ulaanbaatar, Mongolia; [20]Department of Gastroenterology, University of Medical Sciences, Ulaanbaatar, Mongolia, Ulaanbaatar, Mongolia; [21]Hepatobiliary Division, Department of Internal Medicine, Kaohsiung Medical University Hospital, Center of Hepatitis Research, Kaohsiung Medical University, Kaohsiung, Taiwan, Kaohsiung, Taiwan; [22]Department of Gastroenterology and Hepatology, Singapore General Hospital, Singapore, Singapore, Singapore; [23]4th Department of Internal Medicine, Academic Hospital "Attiko", Medical School of National and Kapodistrian University of Athens, Greece, Athens, Greece; [24]Department of Medicine, University of Alberta, Edmonton, Canada, Edmonton, Canada; [25]Department of Hepatology, Sanjay Gandhi Postgraduate Institute of Medical Sciences (SGPGI), Head, WHO Collaborating Center for Viral Hepatitis, Lucknow, India; [26]Division of Gastroenterology and Hepatology, Department of Medicine, The Medical City for Military and Security Services, Muscat, Oman, Muscat, Oman; [27]Division of Hepatology, Department of Medicine, Faculty of Health Sciences. University of Cape Town, Cape Town, South Africa, Cape Town, South Africa; [28]Division of Gastroenterology and Hepatology, NYU Grossman School of Medicine, New York, NY, USA, New York, United States; [29]Division of Gastroenteroloy & Hepatology, Weill Cornell Medicine, New York, NY, USA, New York, United States; [30]Locomedical General Institute, Saga, Japan, Saga, Japan; [31]Endemic Medicine Department, Faculty of Medicine, Capital University, Cairo, Egypt, Cairo, Egypt; [32]Hepatology Division and director of Gastroenterology and Hepatology Research at Henry Ford Hospital, Henry Ford Medical System, Detroit, MI, USA, Detroit, United States; [33]Section of Gastroenterology and Hepatology, Department of Medicine, Baylor College of Medicine, Houston, TX, USA, Houston, United States; [34]Division of Gastroenterology and Hepatology, Foundation IRCCS Ca' Granda Ospedale Maggiore Policlinico, Milan, Italy, Milan, Italy; [35]Institute of Clinical Medicine, National Yang Ming Chiao Tung University, Taipei, Taiwan, Taipei, Taiwan; [36]Department of Internal Medicine, Makerere University College of Health Science, Kampala, Uganda, Kampala, Uganda; [37]Department of Gastroenterology, Faculdade Medicina da Universidade de Sao Paulo, Sao Paulo, Brazil, Sao Paulo, Brazil; [38]Department of Surgery, Oncology and Gastroenterology, Padua University Hospital, Padua, Italy, Padua, Italy; [39]Department of Gastroenterology, School of Medicine, Recep Tayyip Erdoğan University, Rize, Türkiye, Rize, Türkiye; [40]College of Medicine, University of the Philippines, Manila, Philippines, Manila, Philippines; [41]Center for Outcomes Research in Liver Diseases, Washington, DC, USA, Washington, DC, United States*

Email: mariabutiferret@gmail.com

Background and aims: Despite treatment guidance, advances in antiviral therapy and the World Health Organization's 2030 target of viral hepatitis elimination, HBV and HDV remain major global public health challenges. Knowledge gaps among providers may hinder the elimination efforts. We aimed to assess provider knowledge, confidence, and management practices for HBV and HDV.

Method: An international panel of experts from the Global Liver Council (GLC) developed a 37-item, anonymous, online survey to evaluate providers' knowledge and clinical practice patterns in managing HBV and HDV.

Results: A total of 611 clinicians [hepatologists/gastroenterologists (Hep/GI 68%), infectious disease (ID 11.5%), and other specialties (20.5%] participated in the survey from June-September 2025. Self-reported adequate or superior HBV knowledge was highest (93%) among Hep/GI followed by ID (78%) and others (56%), $p < 0.001$, with corresponding differences in confidence. European Association for the Study of the Liver guidelines were most frequently followed (46%). Overall, 81% initiated HBV treatment for HBV DNA >2,000 IU/mL, either with elevated ALT (66%) or regardless of ALT (14%). Liver disease severity was mainly assessed using non-invasive tests (45%). Use of liver biopsy for assessment of liver disease severity and decisions on treatment was used infrequently (1%) except for patients in the grey zone (50%). Hep/GI clinicians were more likely to initiate therapy at low HBV DNA levels (<2,000 IU/mL) in the presence of increased liver stiffness (≥8 kPa) ($p < 0.01$). Routine HDV screening of all HBsAg (+) was reported by 46% including reflex testing in 5%.

Nearly all respondents performed HCC surveillance in all (48.5%) or high risk (50.6%) HBsAg (+) patients, most commonly using ultrasound and serum tumor markers (93%). Most respondents (65.9%) would initiate therapy in HBsAg (+) patients during early pregnancy or prior to conception, preferentially using tenofovir disoproxil fumarate (77%). Treatment of HBsAg (+) with normal ALT and high HBV DNA was limited to selected cases by 48% while 26% would treat all and 26% would treat none. Treatment of all HDV patients regardless of fibrosis stage was selected by 81% of participants; bulevirtide (37%), pegylated interferon-α (37%) and both (11%).

Conclusion: Despite overall guideline alignment, substantial variability in HBV and HDV screening and management persist, highlighting that social, infrastructural and awareness barriers remain.

SAT-619

High burden of active HDV infection and broad genetic diversity of HDV in Cameroon: insights from molecular diagnostics and whole-genome sequencing

Lorenzo Piermatteo[1], Eugenie Lebomo Etogo[2], Cindy Lobe[3], Alessia Magnapera[1], Luca Carioti[4], Lavinia Fabeni[5], Giulia Torre[1], Ilaria Grossi[1], Stefano D'Anna[1], Guy Pascal Ngaba[6], Emilia Lyonga[2], Francesca Ceccherini Silberstein[4], Romina Salpini[1], Judith Torimiro[7], Valentina Svicher[1]. *[1]Department of Biology, University of Rome Tor Vergata, Rome, Italy; [2]Department of Microbiology, Virology, Parasitology, Hematology and Infectious Diseases, Faculty of Medicine and Biomedical Sciences, University of Yaounde I, Yaounde, Cameroon; [3]Department of Biomedical Sciences, Faculty of Sciences, University of Ngaoundere, Ngaoundere, Cameroon; [4]Department of Experimental Medicine, University of Rome Tor Vergata, Rome, Italy; [5]Laboratory of Virology and Laboratories of Biosafety, National Institute for Infectious Diseases Lazzaro Spallanzani-IRCCS, Rome, Italy; [6]Department of Microbiology, Faculty of Medicine and Pharmaceutical Sciences, University of Douala, Douala, Cameroon; [7]Department of Biochemistry, Faculty of Medicine and Biomedical Sciences, University of Yaounde I, Yaounde, Cameroon*

Email: lorenzo.piermatteo@uniroma2.it

Background and aims: Cameroon is endemic for HBV infection. However, limited data are available on epidemiology, genetic diversity and accurate diagnosis of HDV infection.

Method: We conducted a cross sectional study on 117 HBsAg+ patients from two hospitals in Cameroon, and 42 patients with an already known anti-HDV positivity. For the 117 HBsAg+ patients, anti-HDV was performed using the Diasorin Liaison XL analyser. HDV-RNA was tested by two different assays: RoboGene HDV-RNA quantification kit v3.0 using the Felix automated extraction instrument (LOD <6 IU/ml) and the fully automated Altostar platform for extraction and HDV RT-PCR v1.5 (LOD 1.12 IU/ml). Whole genome HDV sequencing was assessed on Illumina MiSeq. The correlation between HDV-RNA values by Robogene and Altostar assays was assessed by Spearmann test.

Results: Overall, 21/117 (18%) patients were positive to anti-HDV, highlighting a high rate of HDV seroprevalence. The percentage of anti-HDV positive patients ranged from 15.1% (11/73) in the Littoral region up to 22.7% (10/44) in the East region, highlighting local hotspot with high HDV endemicity. HDV-RNA was tested in the 21 newly diagnosed patients and in the 42 with previously known anti-HDV positivity for a total of 63 patients. Among them, 61% had detectable HDV-RNA by Robogene (median [IQR]:5.4 [3.3–6.0]logIU/ml), supporting a conspiscous circulation of active HDV infection with an intense HDV replication. Overall, HDV-RNA quantification by Robogene and Altostar showed a high degree of correlation (Rho = 0.91). Such degree of correlation was reduced for HDV-RNA values ≥5logIU/ml (Rho = 0.82 for HDV-RNA ≥5logIU/ml vs Rho = 0.99 for HDV-RNA <5logIU/ml). Among the 38 samples with HDV-RNA >1000IU/ml by Robogene, 26 were successfully sequenced. Phylogenetic analysis revealed the circulation of a large variety of HDV genotypes/subgenotypes with subgenotype 1b being the most frequent (61.5%), followed by 1a (19.3%), genotype 7 (7.8%), genotype 6, 5 and 1e present in 3.8% of patients each. The correlation between HDV-RNA quantification by Robogene and Altostar was very high in all identified genotypes/subgenotypes with a slight decrease in 1b (Rho = 0.96 for genotypes/sub-genotypes other than 1b and 0.82 for 1b.

Conclusion: These findings show a significant burden of active HDV infection in Cameroon, thus highlighting the urgent need of developing accessible and affordable diagnostic algorithms and surveillance tools for HDV infection in Cameroon to reduce HDV-associated morbidity.

SAT-620

Impact of hepatitis B virus infection on hepatic steatosis and liver fibrosis in the general population: a prospective, multicenter cohort study

Shanghao Liu[1], Yanan Zheng[1], Li Ren[2], Bing Qiao[3], Lan Ma[4], Yijun Tang[5], Xiao Liang[6], Huizhen Fan[7], Jianxiang Song[8], Hui Shi[9], JianSong Ji[10], Wenjuan Wang[11], Yang Bu[12], Puqiang Liu[13], Ruyu Liu[14], Lingxiao Wang[15], Qing He[16], Hui Yang[17], Zuxiong Huang[18], Jianfeng Zhong[19], Xiongwei He[20], Xingguo Xiao[21], Wen Kang[22], Peilin Cheng[23], Haini Li[24], Liping Wang[4], Zhong-ji Meng[25], Yong-Fen Zhu[26], Jianwen Sheng[7], Zhenyu Dai[27], Rong Hu[28], Lili Ye[29], Guo Zhang[11], Kejun Liu[30], Jianping Zhang[13], Kai Hu[31], Junhong Yang[32], Xue Xu[33], Gui Su[34], Xuejiao Liao[35], Jianfan Wu[17], Zhenwei Chen[36], Tiandan Bian[19], Jiangwen Liu[20], Yanhong Liu[21], Jing Huang[37], Jie Li[38], Xinrong Zhang[39], Gao-Jun Teng[40], Xiaolong Qi[1]. *[1]Liver Disease Center of Integrated Traditional Chinese and Western Medicine, Department of Radiology, Zhongda Hospital, Medical School, Southeast University, Nurturing Center of Jiangsu Province for State Laboratory of AI Imaging & Interventional Radiology (Southeast University), Basic Medicine Research and Innovation Center of Ministry of Education, Zhongda Hospital, Southeast University, State Key Laboratory of Digital Medical Engineering, Nanjing, China; [2]Department of Gastroenterology, People's Hospital of Huanghua, Huanghua, Cangzhou, Hebei Province, China, Nanjing, China; [3]Department of Integrated Traditional Chinese and Western Medicine, Qingdao Public Health Clinical Center, Qingdao, 266033, Shandong, China, Qingdao, China; [4]Department of Infectious Diseases, Bozhou People's Hospital, Bozhou,China, Bozhou, China; [5]Department of Respiratory and Critical Care Medicine, Taihe Hospital, Hubei University of Medicine, Shiyan 442000, China, Shiyan, China; [6]Department of General Surgery, Sir Run-Run Shaw Hospital, Zhejiang University School of Medicine, 310016, Hangzhou, China, Hangzhou, China; [7]Department of Gastroenterology, Yichun People's Hospital, Yichun, Jiangxi Province, China, Yichun, China; [8]Department of Cardiothoracic Surgery, Affiliated Yancheng Hospital, School of Medicine, Southeast University, Yancheng Third People's Hospital, Yancheng, China, Yancheng, China; [9]Department of Neurosurgery, The First Affiliated Hospital of Kangda College of Nanjing Medical University; The Affiliated Lianyungang Hospital of Xuzhou Medical University; Lianyungang Clinical College of Nanjing Medical University, Lianyungang, China, Lianyungang, China; [10]Zhejiang Key Laboratory of Imaging and Interventional Medicine, Zhejiang Engineering Research Center of Interventional Medicine Engineering and Biotechnology, Department of Radiology, Lishui Central Hospital, The Fifth Affiliated Hospital of Wenzhou Medical University, Lishui 323000, China, Lishui, China; [11]Department of Gastroenterology, Guangxi Hospital Division of The First Affiliated Hospital, Sun Yat-sen University, Nanning, China, Nanning, China; [12]General Hospital of Ningxia Medical University, Yinchuan, China, Yinchuan, China; [13]Pu County People's Hospital, Linfen City, Shanxi Province, China, Linfen, China; [14]Department of Hepatology Division 3, Xuzhou Infectious Diseases Hospital, Xuzhou, China, Department of Hepatology Division 2, Beijing Ditan Hospital, Capital Medical University, Beijing, China, Xuzhou, China; [15]Department of Scientific Research and Teaching, Baiyin Central Hospital, Baiyin,Gansu, China, Baiyin, China; [16]Department of Hepatology, Shenzhen third People's Hospital, Shenzhen, China, Shenzhen, China; [17]Department of*

Gastroenterology, The Second Affiliated Hospital of Guangzhou Medical University,Guangzhou, China, Guangzhou, China; [18]Department of Hepatology, MengChao Hepatobiliary Hospital, Fujian Medical University, Fuzhou 350025, Fujian Province, China, Fuzhou, China; [19]Department of Infectious Diseases, Huzhou Central Hospital, Affiliated Central Hospital, Huzhou University, Huzhou, Zhejiang, China, Huzhou, China; [20]Medical Department of Shihezi City People's Hospital, Shihezi, China, Shihezi, China; [21]Department of Gastroenterology, Zhengzhou Central Hospital Affiliated to Zhengzhou University, Zhengzhou, China, Zhengzhou, China; [22]Department of Infectious Diseases, Tangdu Hospital, Fourth Military Medical University, Xi'an, China, Xi'an, China; [23]Department of Ophthalmology, People's Hospital of Huanghua, Huanghua, Cangzhou, Hebei Province, China, Huanghua, China; [24]Department of Internal Medicine, Qingdao Public Health Clinical Center, Qingdao, China, Qingdao, China; [25]Department of Infectious Diseases, Hubei Provincial Clinical Research Center for Precise Diagnosis and Treatment of Liver Cancer, Taihe Hospital, Hubei University of Medicine, Shiyan 442000, China, Shiyan, China; [26]Zhejiang Key Laboratory of Multi-omics Precision Diagnosis and Treatment of Liver Diseases, Department of Liver and Infectious Diseases, Sir Run Run Shaw Hospital, Zhejiang University School of Medicine, Hangzhou, China, Hangzhou, China; [27]Department of Radiology, Affiliated Yancheng Hospital, School of Medicine, Southeast University, Yancheng Third People's Hospital, Yancheng, Yancheng, China, Yancheng, China; [28]Department of Respiratory and Critical Care Medicine, The First Affiliated Hospital of Kangda College of Nanjing Medical University; The Affiliated Lianyungang Hospital of Xuzhou Medical University; Lianyungang Clinical College of Nanjing Medical University, Lianyungang, China, Xuzhou, China; [29]Department of Oncology Center, The Fifth Affiliated Hospital of Wenzhou Medical University, Lishui 323000, China, Lishui, China; [30]Department of Hepatobiliary Surgery, General Hospital of Ningxia Medical University, Yinchuan, China, Yichun, China; [31]Liver Diseases Center, Beijing Ditan Hospital, Xuzhou Hospital, Capital Medical University, Xuzhou, China Xuzhou Infectious Diseases Hospital, Xuzhou, China, Xuzhou, China; [32]Department of Gastroenterology, Baiyin Central Hospital, Baiyin, Gansu, China, Baiyin, China; [33]Department of Gastroenterology+Baiyin City Central Hospital +Baiyin City+China, Baiyin, China; [34]Central Hospital of Baiyin City, Health Examination Center, Central Hospital of Baiyin City, Pingchuan District, Baiyin City, China, Baiyin, China; [35]Department of Hepatology, Shenzhen third People's Hospital, Shenzhen, China, Shenzhen, China; [36]Department of Information Technology, Mengchao Hepatobiliary Hospital of Fujian Medical University, Fuzhou,China, Fuzhou, China; [37]Department of Health Management, Tangdu Hospital, Fourth Military Medical University, Xi'an, China, Xi'an, China; [38]Department of Infectious Diseases, Nanjing Drum Tower Hospital, Affiliated Hospital of Medical School, Nanjing University, Nanjing, China, Nanjing, China; [39]Guangdong Provincial Key Laboratory of Food, Nutrition and Health, and Department of Epidemiology, School of Public Health, Sun Yat-sen University, Guangzhou 510080, Guangdong, China, Guangzhou, China; [40]Basic Medicine Research and Innovation Center of Ministry of Education, Zhongda Hospital, Southeast University, State Key Laboratory of Digital Medical Engineering, Nanjing, China, Nanjing, China
Email: qixiaolong@vip.163.com

Background and aims: Metabolic dysfunction-associated steatotic liver disease (MASLD) and chronic hepatitis B virus (HBV) infection are among the most common liver diseases worldwide. This study aimed to characterize the relationship between HBV infection and MASLD in the general population.
Method: This study enrolled participants from the general population of six centers in China, who underwent standardized liver health examinations, including transient elastography for hepatic steatosis, serological testing for HBV infection, and assessment of metabolic risk factors. Multivariable logistic regression models were applied to evaluate the independent association of HBV infection with MASLD, and stratified analyses were conducted to examine whether this association varied across demographic and metabolic subgroups. In addition, we assessed the effects of HBV infection and MASLD on liver fibrosis risk, and further evaluated the association of HBV infection with fibrosis specifically within MASLD.
Results: A total of 10,418 participants were included in the final analysis, of whom 400 (3.84%) were HBsAg-positive. MASLD was diagnosed in 4,256 individuals (40.85%), including 139 participants (1.33%) with concurrent HBV infection. The prevalence of MASLD was significantly lower in HBV-positive individuals than in HBV-negative controls (34.75% vs. 41.10%, p = 0.013). This inverse association was consistently observed across sex, age, and BMI categories. After multivariable adjustment, HBV infection was independently associated with a lower risk of MASLD (adjusted odds ratio [aOR] = 0.63, 95% CI: 0.49–0.81, p < 0.001), while both HBV and MASLD showed significant effects on liver fibrosis. Notably, HBV infection showed a stronger independent association with significant liver fibrosis, and this elevated fibrotic risk persisted even among individuals with MASLD (aOR = 2.51, 95% CI: 1.72–3.56, p < 0.001).
Conclusion: HBV infection was associated with a lower risk of MASLD but independently increased the risk of liver fibrosis, even among individuals with MASLD, underscoring the need for careful monitoring in populations with coexisting HBV and metabolic liver disease.

SAT-621

A pilot study on hepatitis b core related antigen (HBCRAG) as novel marker for monitoring anti-viral therapy in chronic hepatitis B patients

Pravinkumar Rejliwal[1], Premashis Kar[1], Natasha Dhingra[2]. *[1]Max Super-Specialty Hospital Vaishali, Maulana Azad Medical College New Delhi, Ghaziabad, India; [2]Medanta, Gurugram, India*
Email: pk.rejliwal@gmail.com

Background and aims: Chronic Hepatitis B (CHB) patients on long-term nucleos(t)ide analogue (NA) therapy often achieve virological suppression, but relapse after treatment cessation remains a challenge due to persistent intrahepatic cccDNA activity. Hepatitis B core–related antigen (HBcrAg) reflects cccDNA transcriptional activity and may complement HBV DNA in predicting post-treatment outcomes. This study evaluated the role of HBcrAg, alongside HBV DNA, in monitoring patients undergoing NA discontinuation and in identifying relapse during off-therapy follow-up.
Method: This prospective pilot study included 59 adults with CHB (HBeAg-positive and negative) on long-term follow-up at a tertiary liver clinic. Eligible patients had received ≥4 years of NA therapy (entecavir, TDF, or TAF), had no cirrhosis, and achieved undetectable HBV DNA at end-of-therapy. Baseline assessment included clinical profile, liver biochemistry, and HBV serology. HBV DNA was quantified by real-time PCR (LOD 2000 IU/mL), and HBcrAg was measured at treatment completion and during follow-up using an ELISA-based antigen assay. Patients with concurrent HBV DNA and HBcrAg negativity were enrolled into off-therapy monitoring and followed for 6–12 months at 3-monthly intervals. Relapse was defined as HBV DNA >2000 IU/mL, HBcrAg positivity, and/or ALT/AST >1.5 × ULN with viral reactivation; relapsed patients were restarted on NA therapy.
Results: Among 59 patients (mean age 35.9 years; 45 males), 10 (16.9%) were HBeAg-positive and 49 (83.1%) HBeAg-negative. Following NA cessation in eligible patients with dual biomarker negativity, most maintained sustained virological and biochemical remission. Relapse occurred in 3 patients (5.1%), all showing re-positivity of both HBV DNA and HBcrAg with associated ALT rise, requiring therapy re-initiation. End-of-therapy HBcrAg negativity correlated strongly with sustained remission across both HBeAg subgroups.
Conclusion: Dual HBV DNA and HBcrAg negativity at treatment cessation was associated with a high likelihood of sustained remission after NA withdrawal, whereas relapse was linked to re-elevation of both markers. HBcrAg provides incremental value beyond HBV DNA in post-therapy risk stratification and may

support biomarker-guided treatment-stop strategies. Larger prospective studies are needed to validate these findings and refine HBcrAg-based clinical decision pathways.

SAT-622-YI

Predictors of loss to follow-up in hepatitis B care in Ethiopia: a prospective multicenter cohort study

Lasse Rossvoll[1,2], Hailemichael Desalegn[3,4], Fikadu Girma Gudissa[5], Dawit Brhane[6], Ahmed Hussen[7], Waqtola Cheneke[8], Asiya Jeylan[5], Esayas Kebede Gudina[8], Nega Berhe[1,9], Asgeir Johannessen[1,2].
[1]Vestfold Hospital Trust, Tønsberg, Norway; [2]University of Oslo, Oslo, Norway; [3]St. Paul's Hospital Millenium Medical College, Addis Ababa, Ethiopia; [4]University of Toronto, Toronto, Canada; [5]Adama Hospital Medical College, Adama, Ethiopia; [6]Dubti General Hospital, Dubti, Ethiopia; [7]Jigjiga University Sheikh Hassen Yabare Comprehensive Specialized Hospital, Jigjiga, Ethiopia; [8]Jimma University, Jimma, Ethiopia; [9]Addis Ababa University, Addis Ababa, Ethiopia
Email: lasse.rossvoll@gmail.com

Background and aims: Chronic hepatitis B (CHB) infection usually requires long-term monitoring. However, previous studies have shown high rates of loss to follow-up (LTFU) in CHB care. We aimed to identify predictors of LTFU in a large real-life CHB cohort study in Ethiopia.
Method: A prospective CHB cohort was established at four public hospitals in Ethiopia in 2021/22. HIV-negative adults with CHB were enrolled and simplified treatment criteria applied, based on clinical assessment and available blood tests. All individuals were scheduled for an initial 3-month follow-up; subsequent visits were scheduled every 6 months for individuals who were initiated on treatment and annually for non-treated individuals. In the present analysis the primary outcome was LTFU, defined as no clinical contact within the past 15 months. Kaplan-Meier method was applied to estimate probability of LTFU over time, and Cox regression models allowing for time-varying effects were used to identify predictors of LTFU.
Results: A total of 6,034 patients (median age 30 years; 49.1% female) were enrolled between December 2021 and December 2023, of whom 1,680 (27.8%) fulfilled the treatment criteria and were started on tenofovir disoproxil at baseline. The median follow-up time was 11.8 months (IQR 0.1–24.5). At data extraction, 3,303 (54.7%) patients were classified as LTFU, 2,203 (36.5%) remained in care, 202 (3.3%) had died, 189 (3.1%) had been transferred out and 137 (2.3%) had withdrawn from the study. The estimated probability of LTFU after 3, 12 and 24 months was 36.9% (95% CI 35.6–38.1), 48.2% (95% CI 46.9–49.4) and 55.7% (95% CI 54.4–56.9), respectively. Independent predictors of LTFU were younger age (18–25 compared to > 35 years; adjusted hazard ratio [AHR] 1.26; 95% CI 1.16–1.38), decompensated cirrhosis (AHR 1.20; 95% CI 1.03–1.40), not receiving treatment (AHR 1.51; 95% CI 1.37–1.66) and greater distance to clinic, which was strongly associated with early LTFU (≤ 90 days; per 10 km increase; AHR 1.06; 95% CI 1.06–1.06) but attenuated over time (p for interaction < 0.001).
Conclusion: The probability of LTFU was high, particularly early after enrolment. Not receiving treatment and greater distance to clinic was associated with higher probability of LTFU. More inclusive treatment criteria and decentralization of care can be impactful interventions to reduce attrition.

SAT-623

Quantitative HBsAg identifies individuals unlikely to achieve spontaneous functional cure of chronic hepatitis B

Juan Carlos Ruiz-Cobo[1], Ariadna Rando-Segura[2], Elena Vargas-Accarino[3], Javier Pérez Garreta[2], Judit Vico Romero[4], Adriana Palom[3], David Tabernero[5,6], Maria Francesca Cortese[2], Mar Riveiro Barciela[1], Maria Buti[1]. *[1]Liver Unit, Vall d'Hebron University Hospital, Barcelona, Departament de Medicina, Universitat Autònoma de Barcelona, Barcelona, Centro De Investigación Biomédica En Red De Enfermedades Hepáticas y Digestivas (CIBERehd), Barcelona, Spain; [2]Microbiology Department, Vall d'Hebron University Hospital, Barcelona, Barcelona, Spain; [3]Vall d'hebron Research Institute (VHIR), Barcelona, Centro De Investigación Biomédica En Red De Enfermedades Hepáticas y Digestivas (CIBERehd), Barcelona, Spain; [4]Vall d'hebron Research Institute (VHIR), Barcelona, Departament d'Infermeria i Salut, Universitat de Barcelona, Barcelona, Barcelona, Spain; [5]Microbiology Department, Vall d'Hebron University Hospital, Barcelona, Centro De Investigación Biomédica En Red De Enfermedades Hepáticas y Digestivas (CIBERehd), Barcelona, Spain; [6]Instituto de Salud Carlos III, Centro de Investigación Biomédica en Red de Enfermedades Hepáticas y Digestivas (CIBERehd), Madrid, Spain*
Email: juancarlosrcobo@gmail.com

Background and aims: Loss of hepatitis B surface antigen (HBsAg) is the closest outcome to a functional cure in chronic hepatitis B (CHB), but it is rarely achieved. Quantitative HBsAg reflects the transcriptional activity of HBV and may identify patients with a low likelihood of HBsAg clearance. We aimed to analyze qHBsAg levels in patients with chronic HBV infection and to estimate the proportion potentially eligible for novel therapies.
Method: We conducted a retrospective, longitudinal cohort study of patients with HBV infection (chronic infection (CI) or chronic hepatitis (CH), HBeAg-positive or -negative) with a follow-up of ≥1 year. Patients with hepatic decompensation prior to the start of follow-up were excluded. HBsAg was quantified using a chemiluminescent immunoassay (CLIA; LLQ 0.05 IU/mL).
Results: A total of 929 patients were included; 61% were male, with a median age of 47 years (IQR 36–58) and a median follow-up of 5.1 years (IQR 2.9–8.0). Ethnicity distribution was 58% Caucasian, 17% African, 12% Asian, 7% Latin American, and 5% Middle Eastern/North African. Compensated cirrhosis was present in 6% of patients. At baseline, median qHBsAg was 1,808 IU/mL (IQR 250–8,128), and 59% (552/929) had qHBsAg >1,000 IU/mL. Regarding infection phase at baseline, most patients had HBeAg-negative CI (73%) or HBeAg-negative CH (21%). During follow-up, 86 patients (9%) achieved HBsAg loss. This occured in 21% (81/377) with baseline qHBsAg ≤1,000 IU/mL compared with 0.9% (5/552) among those with qHBsAg >1,000 IU/mL. Most cases ocurred in HBeAg-negative CI (86%), with an HBsAg loss rate of 11% (74/676), similar to HBeAg-positive CH (11%; 5/46), and higher than in HBeAg-negative CH(3.5%; 7/199) or HBeAg-positive CI (0/8). In addition, 27/54 patients (50%) achieved HBeAg seroconversion. At the end of follow-up, 843 patients remained HBsAg-positive. Of these, 234 (28%) were classified as CH and were receiving nucleos(t)ide analogue therapy; among them, 118/234 (50%) had qHBsAg levels >1,000 IU/mL.
Conclusion: In this large real-world cohort, more than half of patients with chronic HBV infection had high baseline qHBsAg levels and a very low probability of spontaneous HBsAg loss. Patients with HBeAg-negative chronic hepatitis were also unlikely to achieve HBsAg loss. These findings suggest a large proportion of patients could be candidates for novel therapies aimed to achieve functional cure, which is unlikely to occur spontaneously.

SAT-624

Comorbid hepatic steatosis among people with HBV monoinfection and HBV/HIV coinfection in the hepatitis B in Africa collaborative network (HEPSANET): prevalence, predictors, and association with fibrosis

Freeman Chabala[1], Edford Sinkala[2], Kalongo Hamusonde[3], Alana Brennan[4], Amy Goss[5], Bojang Lamin[6], Alexander Stockdale[7], Asgeir Johannessen[8], Roger Sombie[9], Stella Line Emmanuella Pare[9], Mohamed El-Kassas[10], Hans Prozesky[11], Eman Marwan[10], Susan Hugo[11], Yakham Ndiaye[12], Ibrahima Diallo[12], Wendy Spearman[13], Mark Sonderup[13], Mary John Duguru[14], Edith Okeke[14], Rose Ido Da[15], Alice N. Guingané[16], Michael Vinikoor[17]. *[1]Levy Mwanawasa Medical University, Lusaka, Zambia; [2]University of Zambia, Lusaka, Zambia; [3]Bern University Hospital, Bern, Switzerland; [4]Boston University, Boston, United States; [5]University of Alabama at*

Birmingham, Birmingham, United States; [6]MRC-Gambia, Banjul, Gambia; [7]Liverpool University, Malawi Liverpool Wellcome, Blantyre, Malawi; [8]University of Oslo, Oslo, Norway; [9]Yalgado University Hospital, Ouagadougo, Burkina Faso; [10]Capital University, Cairo, Egypt; [11]Stellenbosch University, Tygerberg Hospital, Stellenbosch, South Africa; [12]Hôpital Principal de Dakar, Dakar, Senegal; [13]University of Cape Town, Cape Town, South Africa; [14]Jos University Teaching Hospital, Jos, Nigeria; [15]Saint Camille Hospital, Ouagadougo, Burkina Faso; [16]Bogodogo University Hospital, Ouagadougo, Burkina Faso; [17]University of Zambia School of Medicine, University of Alabama at Birmingham, Centre for Infectious Disease Research in Zambia, Lusaka, Zambia
Email: michael.vinikoor@cidrz.org

Background and aims: Metabolic dysfunction-associated steatotic liver disease (MASLD) is an important comorbidity of hepatitis B virus (HBV) infection; however, data are very limited in the Africa region, where 5% of adults have chronic HBV.
Method: We analyzed data from the Hepatitis B in Africa Collaborative Network (HEPSANET), a collaboration of leading HBV clinical and research cohorts. Adults (>18 years) with chronic HBV monoinfection ('HBV alone') and HBV/HIV coinfection ('HBV/HIV') were analyzed if they underwent transient elastography with controlled attenuated parameter (CAP; Fibroscan; Echosens) at least once. We excluded participants with hepatitis C/D. Stratified by HIV status, we described the prevalence of mild/moderate steatosis (grade 1/2; CAP 248–279 dB/ml) and severe steatosis (grade 3; CAP ≥280 dB/m). With logistic regression, we examined correlates of any steatosis grade including demographic factors (age, sex, education, country) and body mass index (BMI), and assessed the association between steatosis and significant hepatic fibrosis (defined as liver stiffness ≥7 kPa), adjusting for confounders.
Results: 1436 participants (1113 with HBV alone and 323 with HBV/HIV) from 6 countries (Burkina Faso, Egypt, Nigeria, Senegal, South Africa, and Zambia) had a CAP measurement, representing 11.1% of HEPSANET. Their median age was 42 years, 37% were female, 53% had college education, 32% were overweight (BMI 25–30), and 16% had obesity (BMI >30). Steatosis was present in 345 (31.0%) participants with HBV alone (175 [15.7%] severe) and in 38 (11.7%) participants with HBV/HIV (21 [6.5%] severe). Obesity was associated with steatosis in HBV alone (adjusted odds ratio [AOR], 6.9; 95% confidence interval [CI], 4.7–10.2) and in HBV/HIV (AOR, 4.3; 95% CI, 1.3–12.8). Additionally, in HBV alone, increasing age, male sex, overweight, and secondary education (vs. none-primary) were also associated with steatosis (all P < 0.05). Severe steatosis (vs. none) was associated with significant fibrosis in HBV/HIV (AOR, 3.9; 95% CI, 1.6–9.7); a similar but attenuated association was seen in HBV alone (AOR, 1.44; 95% CI, 0.97–2.14).
Conclusion: MASLD was common among individuals with HBV alone and HBV/HIV and strongly associated with obesity, an increasing problem in Africa. The association between severe steatosis and liver fibrosis, particularly in HBV/HIV, supports integrating metabolic risk screening and targeted interventions into HBV clinical care across Africa.

SAT-625

Surveillance threshold and risk stratification of hepatocellular carcinoma by prediction model in Asian patients receiving antiviral treatment for chronic hepatitis B: a nationwide population-based cohort study

Won Sohn[1], Danbee Kang[2], Ju-Yeon Cho[3], Jung Hee Kim[4], Yong Han Paik[5]. *[1]Kangbuk Samsung Hospital, Sungkyunkwan University School of Medicine, Seoul, Korea, Rep. of South; [2]Sungkyunkwan University, Seoul, Korea, Rep. of South; [3]Saint Louis University, Seoul, Korea, Rep. of South; [4]Hallym University Dongtan Sacred Heart Hospital, Seoul, Korea, Rep. of South; [5]Samsung Medical Center, Seoul, Korea, Rep. of South*
Email: hand0827@naver.com

Background and aims: Despite the use of antiviral agents, the risk of hepatocellular carcinoma (HCC) still remained in chronic hepatitis B (CHB). It is important to determine a high-risk group for HCC development in CHB. This study aimed to investigate the annual incidence rate of HCC corresponding survival thresholds and risk stratification of HCC by prediction risk score in CHB patients receiving antiviral treatment.
Method: A nationwide population-based cohort study comprised 199,413 CHB patients receiving antiviral treatment from the Korean National Health Insurance Service between 2012 and 2023. The difference in annual incidence rates of HCC was compared in the low-risk (n = 125,935), intermediate-risk (n = 57,961), and high-risk (n = 15,517) groups by HCC-RESCUE score. Also, we calculated HCC-RESCUE scores corresponding to surveillance thresholds in CHB (0.2%, 1.5%, and 3.0%).
Results: The mean age was 47.2 years. The proportion of male sex was 61.8%. During a median follow-up of 7.3 years (interquartile range, 3.9–10.3 years), 15,233 patients developed HCC. The annual incidence rates were 0.31%, 1.09%, and 1.856% in the low-risk, intermediate-risk, and high-risk groups, respectively. After multivariable adjustment, the risk of HCC was higher in the intermediate- (hazard ratio [HR] 3.48, 95% confidence interval [CI] 3.35–3.61), and high-risk groups (HR 5.90, 95% CI 5.62–6.19) compared with the low-risk group (p < 0.001). The HCC-RESCUE scores corresponding 0.2%, 1.5%, and 3.0% of the annual incidence rates were 47, 66, and 90.
Conclusion: The prediction risk score is useful to stratify the risk of HCC in CHB patients receiving antiviral treatment. Also, the prediction score-based approach considering the annual incidence rate of HCC corresponding survival thresholds is helpful to optimize surveillance strategies in Asian patients with CHB.

SAT-626

HBcrAg as a multifaceted biomarker in chronic hepatitis B: Implications for immune activity and HCC prediction

Myeong Jun Song[1], Kwon Yong Tak[1], Seok-Hwan Kim[1]. *[1]Internal medicine, The College of Medicine, The Catholic University of Korea, Seoul, Korea, Rep. of South*
Email: mjsong95@gmail.com

Background and aims: Hepatitis B core-related antigen (HBcrAg) is a promising biomarker reflecting intrahepatic cccDNA activity. While quantitative HBsAg (qHBsAg) and HBV DNA are traditional markers, their utility in stratifying indeterminate phases or predicting hepatocellular carcinoma (HCC) under antiviral suppression can be limited. This study evaluated the clinical utility of HBcrAg, measured by a high-sensitivity assay, in classifying immune phases and predicting HCC in patients with chronic hepatitis B (CHB), with a specific focus on comparing its performance against qHBsAg.
Method: This retrospective study included 284 CHB patients. HBcrAg levels were measured using the iTACT-HBcrAg assay, and qHBsAg by electrochemiluminescence immunoassay. Patients were classified into immune phases (Immune Active [IA], Immune Tolerant [IT], Immune Inactive [II]) according to HBV guidelines. The diagnostic performance for phase classification and HCC prediction was assessed using area under the receiver operating characteristic (AUROC) curves. Correlations with host factors, including age and liver fibrosis, were also analyzed.
Results: HBcrAg levels differed significantly among immune phases, demonstrating superior discriminatory power compared to qHBsAg and HBV DNA. HBcrAg effectively distinguished HBeAg-positive IA from IT (AUC 0.97, cut-off 3.3 LogU/mL) and HBeAg-negative IA from II (AUC 0.83, cut-off 2.6 LogU/mL). In contrast, qHBsAg and HBV DNA showed poor discriminatory value (AUCs <0.55) for these differentiations. Regarding HCC prediction, HBcrAg was the only significant predictor among viral markers. In HBeAg-negative IA patients, a cut-off of 3.8 LogU/mL was associated with higher HCC prevalence (AUC 0.69). Notably, in the HBeAg-negative II phase, low HBcrAg (<3.8 LogU/mL) was universally associated with the absence of HCC (AUC

1.00, NPV 100%). In HBeAg-positive IA patients, the optimal threshold was 4.9 LogU/mL (AUC 0.71). Age showed a significant inverse correlation with HBcrAg ($r = -0.31$, $p < 0.0001$), consistent with immune senescence. However, liver fibrosis severity did not correlate with HBcrAg levels.
Conclusion: HBcrAg outperforms qHBsAg in distinguishing CHB immune phases and stratifying HCC risk. Despite age-related decline, elevated thresholds remain predictive of HCC. HBcrAg identifies high-risk immune-active patients and reliably excludes HCC risk in inactive carriers, offering prognostic insights beyond traditional markers.

SAT-627

Are hepatitis B vaccination programmes in Africa visible to healthcare workers?

Wendy Spearman[1], Manal El-Sayed[2], Karin Siebelt[3], Maria Buti[4].
[1]University Of Cape Town, Cape Town, South Africa; [2]Ain Shams University, Cairo, Egypt; [3]Academic Medical Education, Amsterdam, Netherlands; [4]Hospital Universitari Valle Hebron, Barcelona, Barcelona, Spain
Email: wendy.spearman@uct.ac.za

Background and aims: Hepatitis B affects an estimated 65 million people in Africa. Vaccination, particularly the hepatitis B birth dose (HB-BD), together with vaccination of adolescents and high-risk groups, is central to elimination strategies. Effective implementation relies on healthcare workers (HCWs) being aware of national vaccination policies. We assessed healthcare workers' knowledge of hepatitis B vaccination programmes across Africa and compared awareness of HB-BD implementation with WHO/UNICEF data.
Method: A brief, two-item web-based survey on preventive hepatitis B vaccination programmes was distributed through the Society on Liver Disease in Africa (SOLDA) network. Responses from countries with more than five participants were analysed.
Results: A total of 292 HCWs from 19 African countries participated. Awareness of HB-BD vaccination programmes varied widely between countries. Knowledge of an existing HB-BD programme was high in Burkina Faso and Côte d'Ivoire (100%) and Nigeria (91%) but substantially lower in Zambia (36%). Awareness that HB-BD is provided universally to all newborns ranged from 29% in Zambia to 100% in Burkina Faso and Côte d'Ivoire. Knowledge of hepatitis B vaccination programmes for adolescents was consistently low across all regions, with no awareness of programs reported in several countries (Malawi, Cameroon, South Africa and Zimbabwe), and reaching only 27% in Egypt. Awareness of vaccination programmes for at-risk populations (including HCWs, people living with HIV and household contacts) was highly variable, ranging from 0% in Mozambique and Senegal to 100% in Malawi. In contrast, WHO/UNICEF data indicate that HB-BD vaccination is universally implemented in almost all African countries that have adopted this strategy, except Mauritius and South Africa, where targeted approaches are used.
Conclusion: Despite widespread implementation of HB-BD vaccination in Africa, substantial gaps exist in HCWs' awareness of vaccination strategies, particularly for adolescents and high-risk groups. This disconnect between policy and frontline knowledge may hinder hepatitis B elimination efforts. Strengthening communication and training on national vaccination programmes should be prioritised. GAVI support for HB-BD vaccination in low and middle income countries is essential.

SAT-628-YI

Long-term risk of hepatocellular carcinoma in strictly defined immune tolerant patients with chronic hepatitis B - Results from the global RADICAL consortium

Lisa M. van Velsen[1], Won-Mook Choi[2], Mai Kilany[3], Norah Terrault[4], Terry Cheuk-Fung Yip[5], Karen Cheuk-Ying Ho[6], Zillah Cargill[7], Gabriele Ricco[8], Sara Battistella[9], Marc Ghany[10], Elena Vargas-Accarino[11], Stephanie Narguet[12], Ozgur Koc[13], Bettina E. Hansen[3,14], Dirk Posthouwer[15], Tarik Asselah[12], Maria Buti[11], Sabela Lens[9], Maurizia Brunetto[8], Kosh Agarwal[7], Wai-Kay Seto[6], Man-Fung Yuen[6], Grace Wong[5], Jordan J. Feld[3], Yao-Chun (Holden) Hsu[16], Young-Suk Lim[2], Milan J. Sonneveld[1], Harry L.A. Janssen[1]. *[1]Department of Gastroenterology and Hepatology, Erasmus MC University Medical Center, Rotterdam, Netherlands; [2]Asan Medical Center, Seoul, Korea, Rep. of South; [3]Toronto Centre for Liver Disease, Toronto, Canada; [4]Department of Medicine, University of Southern California, Los Angeles, United States; [5]Medical Data Analytics Centre, State Key Laboratory of Digestive Disease, Li Ka Shing Institute of Health Sciences, The Chinese University of Hong Kong, Hong Kong SAR, Hong Kong; [6]Department of Medicine and State Key Laboratory of Liver Research, The University of Hong Kong, Hong Kong, Hong Kong; [7]Institute of Liver Studies, King's College Hospital, Londen, United Kingdom; [8]Hepatology Unit and Laboratory of Molecular Genetics and Pathology of Hepatitis Viruses, Reference Center of the Tuscany Region for Chronic Liver Disease and Cancer, University Hospital of Pisa, Pisa, Italy; [9]Hospital Clinic Barcelona, IDIBAPS and CIBEREHD, University of Barcelona, Barcelona, Spain; [10]Liver Diseases Branch, National Institute of Diabetes and Digestive and Kidney Diseases, National Institutes of Health, Bethesda, United States; [11]Liver Unit, Hospital Universitari Vall d'Hebron, Vall d'Hebron Barcelona Hospital Campus and Universitat Autònoma de Barcelona, Barcelona, Spain; [12]Service d'Hépatologie, AP-HP Hôpital Beaujon, INSERM UMR 1149, CRI, Université Paris Diderot, Clichy, France; [13]Department of Gastroenterology and Hepatology, Maastricht University Medical Center, Maastricht, Netherlands; [14]Department of Epidemiology & Biostatistics, Erasmus MC University Medical Center, Rotterdam, Netherlands; [15]Department of Internal medicine and Medical Microbiology, Maastricht University Medical Center, Maastricht, Netherlands; [16]Center for Liver Diseases, E-Da Hospital, Kaohsiung, Taiwan*
Email: l.vanvelsen@erasmusmc.nl

Background and aims: Patients with immune tolerant (IT) chronic hepatitis B (CHB), also referred to as HBeAg+ chronic infection, have a high viral load and both minimal inflammation and fibrosis. However, there is conflicting evidence regarding the risk of hepatocellular carcinoma (HCC). Therefore, we studied the risk of HCC in strictly defined IT patients and compared this to HBeAg+ treated CHB patients.
Method: Within the RADICAL consortium we studied a large cohort of mono-infected CHB patients from 13 sites around the globe. The IT-phase was strictly defined as HBeAg+, ALT≤40 U/L and HBV DNA >7 log IU/mL persistent during the 1st year after baseline (BL), the 1st clinic visit at investigational site. The control group included non-cirrhotic HBeAg+ CHB patients (ALT>40 U/L) treated with NUCs, with BL defined as therapy initiation. Cumulative HCC incidences with confidence intervals were estimated with the KM method. IT patients were censored 1 year after start of therapy. A sensitivity analysis was performed restricted to HCC during the IT phase, also censored for transition out of the IT phase, i.e. HBeAg loss, ALT>40 U/L or HBV DNA ≤7 logIU/mL.
Results: In total, 951 IT patients and 891 treated patients were included. IT patients were more often female (61 vs. 35%,$p < 0.001$), younger (33 vs. 37 years,$p < 0.001$), had lower ALT (26 vs. 140 U/L,$p < 0.001$), and higher HBV DNA levels (8.4 vs. 8 logIU/mL, $p < 0.001$) at BL. IT patients were followed for a median of 13 (IQR 9–17) years, compared to 7 (4–13) years in the treated group. In total, 8/951 IT patients developed HCC, compared to 21/891 patients in the treated group. The median age at HCC diagnosis was 41 (37–54) years in IT patients vs. 55 (50–62) years in treated CHB. The 5-, 10-, and 15-year cumulative incidences of HCC in IT patients were 0.5% (0–0.9%), 0.7% (0.1–1.1%), and 1.1% (0.1–2%) compared to 1.3% (0.5–2.1%), 2.9% (1.5–4.3%), and 3.5% (1.9–5.1%) in the treated cohort (HR:2.91, 95%CI 1.29–6.58,$p = 0.010$). Due to low event rates an appropriate multivariable analysis was not performed. Of the 8 IT patients with HCC, 4 patients developed HCC after transitioning out of the IT phase (age at diagnosis: 54 [IQR 45–57]), and 4 while persistently in the IT phase

(age at diagnosis: 38 [36–41]). The 15-year cumulative incidence of HCC during the IT phase was 0.5% (0–0.9%).
Conclusion: This unique global cohort of well-defined IT patients exhibited a very low risk of HCC after 15 years of follow-up, with a risk lower than that observed in treated HBeAg+ CHB patients.

SAT-629

Prospective evaluation of ethnicity and HBV genotype in predicting off-treatment outcomes after nucleos(t)ide analogue cessation: results from the multicentre COIN-B trial

Arno Furquim d'Almeida[1,2], Axelle Vanderlinden[1,2], Stefan Bourgeois[3], Jean-Pierre Mulkay[4], Thomas Sersté[4], Struyve Mathieu[5], Baro Deressa[6], Dirk Sprengers[3], Marie De Vos[7], Jos Callens[8], Bao Shihao[2], Hendrik Reynaert[9], Pierre Deltenre[10], Filip Janssens[11], Sergio Negrin-Dastis[12], Peter Stärkel[13], Hans Orlent[14], Guy Van Roey[15], Xavier Verhelst[16], Christophe Moreno[17], Jean Delwaide[18], Christophe Van Steenkiste[19], Wim Verlinden[2,20,21], Isabelle Colle[22], Benoit Kabamba[23], Veerle Matheeussen[24], Thomas Vanwolleghem[1,2]. *[1]University of Antwerp, Viral Hepatitis Research Group, Laboratory of Experimental Medicine and Pediatrics, Antwerp, Belgium; [2]Antwerp University Hospital, Department of Gastroenterology and Hepatology, Edegem, Belgium; [3]Ziekenhuis aan de Stroom, Department of Gastroenterology, Antwerp, Belgium; [4]CHU Saint-Pierre, Department of Hepato-Gastroenterology, Brussels, Belgium; [5]Ziekenhuis Oost-Limburg, Department of Gastroenterology, Genk, Belgium; [6]CHU Brugmann, Department of Gastroenterology, Brussels, Belgium; [7]Hôpital de Jolimont HELORA, Department of Gastroenterology, La Louvière, Belgium; [8]AZ Klina, Department of Gastroenterology, Brasschaat, Belgium; [9]UZ Brussel, Department of Gastroenterology, Brussels, Belgium; [10]Clinique Saint-Luc Bouge, Department of Gastroenterology, Namur, Belgium; [11]Jessa Ziekenhuizen, Department of Gastroenterology, Hasselt, Belgium; [12]Grand Hôpital de Charleroi, Department of Gastroenterology, Charleroi, Belgium; [13]Cliniques Universitaires Saint-Luc, Department of Gastroenterology, Brussels, Belgium; [14]AZ Sint-Jan Brugge AV, Department of Gastroenterology and Hepatology, Brugge, Belgium; [15]AZ Turnhout, Department of Gastroenterology, Turnhout, Belgium; [16]UZ Gent, Department of Gastroenterology and Hepatology, Gent, Belgium; [17]CUB Hôpital Erasme, Université Libre de Bruxelles, Department of Gastroenterology, Hepatopancreatology and Digestive oncology, Brussels, Belgium; [18]CHU Site Sart-Tilman, Department of Hepato-Gastroenterology, Liège, Belgium; [19]AZ Maria Middelares, Department of Gastroenterology, Gent, Belgium; [20]Vitaz, Department of Gastroenterology, Sint-Niklaas, Belgium; [21]University of Antwerp, Laboratory of Experimental Medicine and Pediatrics, Antwerp, Belgium; [22]AZORG, Department of Gastroenterology, Aalst, Belgium; [23]Cliniques Universitaires Saint-Luc, Department of Microbiology, Brussels, Belgium; [24]Antwerp University Hospital, Laboratory of Medical Microbiology, Edegem, Belgium*
Email: arno.furquimdalmeida@uantwerpen.be

Background and aims: Determinants of outcomes after nucleos(t)ide analogue (NUC) cessation remain incompletely defined. Ethnicity has been proposed as a stopping criterium, but prospective validation is lacking. We evaluated the impact of ethnicity and HBV genotype (gt) on off-treatment outcomes.
Method: In the multicentre prospective COIN-B trial, start-of-treatment HBeAg-, long-term NUC-suppressed patients without advanced liver fibrosis were followed for 72 weeks after NUC cessation. Recruitment was matched for Caucasian and non-Caucasian ethnicity and stratified by sex and age. The primary endpoint was off-treatment HBV DNA ≤2000 IU/mL + ALT ≤2×ULN at week 72. Ethnicity was defined by country of birth. Ancestry inference was determined using population-specific SNPs.
Results: Of 91 included patients, 84 completed follow-up (Caucasian: n = 41; non-Caucasian: n = 43). Both groups had comparable end-of-treatment (EOT) quantitative HBsAg levels (p = 1.00). Caucasians were exclusively infected with gt A or gt D, whereas non-Caucasians showed broad gt diversity (A-E). The primary endpoint was reached in 41.5% of Caucasian versus 30.2% of non-Caucasian patients (p = 0.28), and retreatment rates did not differ (31.7% vs 48.8%, p = 0.11). HBsAg loss (7.1%) occurred exclusively in patients of European or North-African/Middle-Eastern ancestry. In multivariate analyses, including either SNP ancestry or gt, lower EOT HBsAg was consistently associated with the primary endpoint, HBsAg loss, and ≥1 log HBsAg decline at week 72, but not retreatment. Compared to European ancestry and adjusted for EOT HBsAg, Asian and Sub-Saharan African ancestries were less likely to have ≥1 log HBsAg decline (OR 0.01, p < 0.001; OR 0.002, p = 0.007), while Asian ancestry was associated with higher retreatment rates (OR 2.83, p < 0.05). Compared to gt A and adjusted for EOT HBsAg, gt C (OR 0.13, p = 0.02) and gt D (OR 0.20, p = 0.009) were less likely to achieve the primary endpoint and more likely to require retreatment (OR 11.9, p = 0.002; OR 3.72, p = 0.03), while gt B (OR 0.01, p = 0.008) and gt C (OR 0.04, p = 0.01) were less likely to have ≥1 log HBsAg decline.
Conclusion: In this prospective ethnicity-matched trial, off-treatment outcomes did not differ between Caucasian and non-Caucasian patients. EOT HBsAg is the dominant predictor of viral control, HBsAg loss and HBsAg decline with differential impacts of ancestry and HBV genotypes. These results call for a more granular definition of ethnicity as stopping criterium.

SAT-633

The impact of longitudinal hepatitis B virus genotypic diversity and viral dynamics on hepatocellular carcinoma risk in chronic hepatitis B

Ding-Lian Wang[1,2], Mei-Hung Pan[3], Chih-Jen Huang[3], Rachel Wen-Juei Jeng[4,5], Chien-Jen Chen[3], Hwai-I Yang[3]. *[1]Graduate Institute of Life Science, National Defense Medical University, Taipei, Taiwan; [2]Genomic Research Center, Academia Sinica, Taipei, Taiwan; [3]Genomics Research Center, Taipei, Taiwan; [4]Department of Gastroenterology and Hepatology, Linkou Chang Gung Memorial Hospital, Taoyuan, Taiwan; [5]College of Medicine, Chang Gung University, Taoyuan, Taiwan*
Email: dl.wang19971224@gmail.com

Background and aims: Hepatocellular carcinoma (HCC) remains a leading cause of cancer-related mortality worldwide, with chronic hepatitis B virus (HBV) infection as a major etiological factor. While HBV genotype and viral load are established predictors of HCC, most studies rely on single time-point genotype classification, neglecting within-host genotypic diversity and its longitudinal evolution. This study investigates the impact of HBV genotypic diversity, its temporal dynamics, and underlying drivers on HCC risk using high-resolution long-read sequencing.
Method: We analyzed 439 chronic HBV carriers from the community-based REVEAL-HBV cohort in Taiwan. Full-length HBV genomes were sequenced using PacBio long-read technology (mean ~5,000 reads per subject) and aligned to 35 NCBI reference sequences. Participants were classified by primary genotype proportion: Class 1 (100%), Class 2 (100% > proportion ≥ 99.89%), and Class 3 (<99.89%). A total of 250 participants with repeated sampling were included in longitudinal analyses. Linear mixed-effects models evaluated temporal trajectories of HBsAg, HBV DNA, and ALT, while Cox and time-dependent Cox models assessed associations between HBV genotypic diversity and HCC risk.
Results: Individuals with primary genotype C2 had a significantly higher HCC risk than those with B2, both at baseline (HR = 3.27, 95% CI = 2.00–5.35) and during follow-up (HR = 2.28, 95%CI = 1.14–4.57). Time-dependent Cox regression analysis revealed that greater HBV diversity (Class 3 vs. Class 1+2) was associated with increased HCC risk when assessed as a baseline characteristic (HR = 1.80, 95%CI = 1.03–3.17), but not as a time-varying covariate (HR = 1.11, 95%CI = 0.61–2.03). HBV DNA levels declined over time in all groups, with a significantly slower decline in genotype C compared with genotype B (B2 vs C2 Estimate = – 0.054; p = 0.008). In contrast, no significant

longitudinal differences were observed in HBV diversity proportions within the same genotype (Class1+2 vs Class 3 Estimate = – 0.002; p = 0.998).
Conclusion: Primary HBV genotype remains a strong predictor of long-term HCC risk. Baseline genotypic diversity reflects cumulative oncogenic potential, whereas short-term temporal changes show limited prognostic value. The slower viral load decline in genotype C may partly explain its stronger association with HCC. These findings underscore the value of integrating high-resolution viral sequencing with longitudinal analyses to improve HCC risk stratification in chronic HBV infection.

SAT-634
Long-term clinical outcomes in chronic hepatitis B patients with nucleos(t)ide analogue treatment who achieved HBsAg <100 IU/mL
Jian Wang[1,2], Shaoqiu Zhang[1], Li Zhu[3], Tao Fan[4], Ye Xiong[4], Chao Jiang[5], Juan Xia[1], Xiaomin Yan[1], Xingxiang Liu[6], Chuanwu Zhu[3], Chao Wu[1,2,4], Rui Huang[1,2,4,5]. *[1]Department of Infectious Diseases, Nanjing Drum Tower Hospital, Affiliated Hospital of Medical School, Nanjing University, Nanjing, China; [2]Institute of Viruses and Infectious Diseases, Nanjing University, Nanjing, China; [3]Department of Infectious Diseases, The Affiliated Infectious Diseases Hospital of Soochow University, Suzhou, China; [4]Department of Infectious Diseases, Nanjing Drum Tower Hospital Clinical College of Nanjing University of Chinese Medicine, Nanjing, China; [5]Department of Infectious Diseases, Nanjing Drum Tower Hospital Clinical College of Jiangsu University, Nanjing, China; [6]Department of Clinical Laboratory, Huai'an No. 4 People's Hospital, Huai'an, China*
Email: doctor_hr@126.com

Background and aims: Chronic hepatitis B (CHB) patients who achieve HBsAg <100 IU/mL spontaneously have favorable clinical outcomes. However, the difference of clinical outcomes between patients who achieve HBsAg <100 IU/mL after antiviral treatment and those who achieve it spontaneously remains unclear. We compared long-term outcomes between patients with treatment-associated and spontaneously achieved HBsAg <100 IU/mL.
Method: This multi-center retrospective study included 886 non-cirrhotic CHB patients from three sites. These patients had HBeAg negativity, undetectable HBV DNA, HBsAg levels <100 IU/mL, and normal ALT levels (616 in the spontaneous group and 270 in the treatment-induced group). We used the inverse probability of treatment weighting (IPTW) and propensity score matching (PSM) to balance baseline characteristics between the treated and untreated groups. The study outcomes included HBsAg seroclearance and liver-related events (LREs) (cirrhosis and hepatocellular carcinoma).
Results: During a median follow-up of 3.0 years, 102 patients achieved HBsAg seroclearance, and 7 patients developed LREs in overall cohort. In the IPTW cohort, no significant difference of 6-year cumulative incidence of HBsAg seroclearance was found between the spontaneous and treatment-induced groups (43.7% vs. 27.3%, P = 0.199) or LREs (0.8% vs. 1.5%, P = 0.782). Baseline HBsAg <15 IU/mL (adjusted hazard ratio [aHR]: 5.48, 95% confidence interval [CI]: 2.95–10.18, P < 0.001) and antiviral treatment (aHR: 1.77, 95% CI: 1.01–3.10, P = 0.047) were associated with a higher likelihood of achieving HBsAg sreoclearance in the multivariate Cox analysis. However, antiviral treatment was not significantly associated with the development of LREs (HR: 1.07, 95% CI: 0.24–4.83, P = 0.928). However, in the PSM cohort, antiviral treatment did not significantly associate with either HBsAg seroclearance or LREs.
Conclusion: Both treatment-induced and spontaneous achievement of HBsAg <100 IU/mL in CHB patients were associated with favorable outcomes, including a low risk of LREs and a high likelihood of HBsAg seroclearance.

SAT-635
Antiviral therapy reduces liver-related events in chronic hepatitis B patients with low HBsAg
Jian Wang[1,2], Li Zhu[3], Zhiyi Zhang[4], Qun Zhang[5], Shaoqiu Zhang[1], Tao Fan[6], Ye Xiong[6], Shengxia Yin[1], Yuxin Chen[7], Chuanwu Zhu[3], Huali Wang[8], Xingxiang Liu[9], Rui Huang[1,2,6], Chao Wu[1,2,6]. *[1]Department of Infectious Diseases, Nanjing Drum Tower Hospital, Affiliated Hospital of Medical School, Nanjing University, Nanjing, China; [2]Institute of Viruses and Infectious Diseases, Nanjing University, Nanjing, China; [3]Department of Infectious Diseases, The Affiliated Infectious Diseases Hospital of Soochow University, Suzhou, China; [4]State Key Laboratory Cultivation Base of Research, Prevention and Treatment for Oral Diseases, Jiangsu Province Engineering Research Center of Stomatological Translational Medicine, The Affiliated Stomatological Hospital of Nanjing Medical University, Nanjing, China; [5]Department of Infectious Diseases, Zhongda Hospital, School of Medicine, Southeast University, Nanjing, China; [6]Department of Infectious Diseases, Nanjing Drum Tower Hospital Clinical College of Nanjing University of Chinese Medicine, Nanjing, China; [7]Department of Laboratory Medicine, Nanjing Drum Tower Hospital, Affiliated Hospital of Medical School, Nanjing University, Nanjing, China; [8]Department of General Practice, Nanjing Second Hospital, Nanjing University of Chinese Medicine, Nanjing, China; [9]Department of Clinical Laboratory, Huai'an No. 4 People's Hospital, Huai'an, China*
Email: dr.wu@nju.edu.cn

Background and aims: The long-term benefit of antiviral treatment in patients with chronic hepatitis B (CHB) who have detectable HBV DNA but normal or mildly elevated alanine aminotransferase (ALT) remains debated, particularly among those with low hepatitis B surface antigen levels (HBsAg). We aimed to explore whether nucleos(t)ide analogue (NA) therapy improves long-term clinical outcomes in patients with HBsAg <100 IU/mL and ALT <2 × the upper limit of normal (ULN).
Method: This multi-center study retrospectively included 701 non-cirrhotic CHB patients with HBsAg <100 IU/mL, detectable HBV DNA, and ALT <2 × ULN from five hospitals in China, including 211 in the NAs treatment group and 490 in the untreated group. The incidence rates of liver-related events (LREs) (cirrhosis and hepatocellular carcinoma) and HBsAg seroclearance were compared between groups.
Results: The median age of patients was 48.5 years, and 60.2% of patients were male. In the overall patients, 13 (1.9%) patients developed LREs and 30 (5.4%) patients achieved HBsAg seroclearance during a median follow-up period of 2.1 years. The 6-year cumulative incidence of LREs was significantly lower in the treated patients than in the untreated patients (1.2% vs. 7.5%, P = 0.038). In multivariable Cox regression analysis, antiviral therapy was associated with a significantly low risk of LREs (adjusted hazard ratio [HR]: 0.05, 95% CI: 0.01–0.48, P = 0.010). However, the 6-year cumulative incidence of HBsAg seroclearance was comparable between treated and untreated patients (19.5% vs. 13.4%, P = 0.287). However, antiviral therapy was not independently associated with HBsAg seroclearance (adjusted HR: 1.48, 95% CI: 0.66–3.35, P = 0.341).
Conclusion: NAs therapy reduced the risk of LREs in CHB patients with low HBsAg (<100 IU/mL), detectable HBV DNA, and normal or mildly elevated ALT levels.

SAT-636
Hepatitis B surface antigen isoforms and HBV RNA for the management of nucleos(t)ide analogue discontinuation: an ancillary study of the STOP-NUC trial
Dominik Weidner[1], Maria Pfefferkorn[1], Sophia Goldfuß[1], Robert Selonke[1,2], Dieter Glebe[3,4], Renate Heyne[5], Frank Tacke[6], Stefan Zeuzem[7], Julian Schulze zur Wiesch[8], Andreas Stallmach[9], Martin Sprinzl[10], Christoph P. Berg[11], Jürgen Lohmeyer[12], Oana Brosteanu[13], Madlen Matz-Soja[1,14], Thomas Berg[1], Florian van Bömmel[1]. *[1]Division of Hepatology, Leipzig University*

Medical Center, Leipzig, Germany; [2]Department of Cardiology, University Heart and Vascular Center Hamburg-Eppendorf, Hamburg, Germany; [3]Justus-Liebig University Giessen, National Reference Centre for Hepatitis B and D viruses, Institute for Medical Virology, Giessen, Germany; [4]German Center for Infection Research (DZIF, Partner Site Giessen-Marburg-Langen), Giessen, Germany; [5]Leberzentrum Checkpoint, Berlin, Germany; [6]Clinic for Hepatology and Gastroenterology, Charité-Campus Virchow-Klinikum, Berlin, Germany; [7]Universitätsklinikum Frankfurt, Medizinische Klinik 1, Frankfurt am Main, Germany; [8]Universitätsklinikum Hamburg-Eppendorf, I. Medizinische Klinik und Poliklinik, Hamburg, Germany; [9]Universitätsklinikum Jena, Klinik für Innere Medizin IV, Jena, Germany; [10]Facharztpraxis für Innere Medizin, Gastroenterologie, Hepatologie, Stoffwechselerkrankungen, Wiesbaden, Germany; [11]Universitätsklinikum Tübingen, Medizinische Klinik I, Tübingen, Germany; [12]Universitätsklinikum Gießen, Medizinische Klinik II, Giessen, Germany; [13]Clinical Trial Centre, Leipzig University, Leipzig, Germany; [14]Rudolf-Schönheimer-Institute for Biochemistry, Leipzig University, Leipzig, Germany
Email: Maria.pfefferkorn@medizin.uni-leipzig.de

Background and aims: In the prospective STOP-NUC trial, discontinuation of long-term nucleos(t)ide analogue (NUC) treatment in HBeAg-negative patients resulted in HBsAg loss or transition to disease stages with or without treatment indication in many patients with HBsAg levels < 1000 IU/mL. We investigated the experimental biomarkers of covalently closed circular DNA (cccDNA) activity. Large (LHBs), middle (MHBs), and small (SHBs) HBsAg isoforms, as well as HBV RNA, provide additional predictive value for clinical outcomes after NUC cessation.
Method: Serum samples from 79 patients randomized to NUC discontinuation collected at baseline (BL) and weeks 12, 24 and 48 were retrospectively assessed for HBV DNA, HBV RNA, total HBsAg, LHBs and MHBs. Based on week-96 outcomes, patients were classified as re-treatment (ReT; n = 11), no re-treatment, but detectable HBV DNA (n = 54), virologic response (undetectable HBV DNA, VR; n = 6) or HBsAg loss (functional cure; FC; n = 8).
Results: Patients achieving FC after NUC discontinuation showed significantly lower median BL levels of total HBsAg, LHBs and MHBs compared to all other response groups ($p < 0.001$). Thus, median proportions (%) of LHBs and MHBs were lowest in FC (4.9 and 0.7) compared to all patients without FC (6.5 and 5.8, $p = 0.538$ and $p = 0.023$). Proportions of LHBs and MHBs were higher in patients with VR (4.9 and 3.7), in those without ReT but detectable HBV DNA (6.1 and 5.4) and highest in patients with ReT (9.0 and 9.4), respectively. Over 48 weeks after NUC discontinuation, median proportions of LHBs and MHBs declined to 0.9 and 1% in patients with VR and to 0% in patients with FC, but remained high in patients with ReT at all time points. HBV DNA and HBV RNA were undetectable in 77/79 and 58/79 patients at BL. Detectable HBV RNA levels at BL (AUC = 0.735) and week 12 (AUC = 0.787) were strongly associated with ReT. From week 24 onward, HBV RNA became undetectable in all FC patients, whereas patients in the ReT group persistently showed detectable HBV RNA levels (2.14, 2.52 and 3.01 log cp/mL at 12, 24 and 48 weeks).
Conclusion: Low proportions of LHBs and MHBs were associated with FC already before NUC discontinuation and may reflect cccDNA activity and therefore response to NUC discontinuation. Detectable HBV RNA after NUC cessation was associated with a high risk of retreatment, supporting its role as safety marker.

SAT-637
Integrated model nurse clinic reduces adverse pregnancy outcomes of pregnant women with chronic hepatitis B

Vicki Wing-Ki Hui[1], Mandy Sze-Man Lai[1], Jimmy Che-To Lai[1], Vincent Wai-Sun Wong[1], Terry Cheuk-Fung Yip[1], Grace Lai-Hung Wong[1]. [1]*The Chinese University of Hong Kong, Sha Tin, Hong Kong*
Email: wonglaihung@cuhk.edu.hk

Background and aims: An integrated model nurse clinic (IMNC) was established in Hong Kong as a pivotal part of the Hong Kong Hepatitis Action Plan 2020–2024 to achieve hepatitis elimination by 2030. IMNC has led to a major increase in HBsAg and HBV DNA testing in women of child-bearing age. This study evaluated the impact of IMNC on adverse pregnancy outcomes, namely miscarriages and preterm deliveries of babies.
Method: Individuals with CHB were identified from a territory-wide database from year 2000 to 2024. Adverse pregnancy outcomes were defined with diagnosis and/or procedure codes for miscarriages and preterm deliveries of babies.
Results: A total of 1,341,841 pregnancies identified; 72,082(5.4%) individuals were diagnosed with chronic HBV infection. From 2000 to 2024, miscarriage proportions increased in both groups, rising from 12.0% (95% CI 10.7%–13.2%) in HBV pregnancies and 9.9% (9.6%–10.1%) in non-HBV pregnancies in 2000 to 16.6% (14.4%–18.8%) and 14.8% (14.4%–15.2%) in 2024; the highest proportions were 17.2% (15.7%–18.7%) in HBV pregnancies in 2018 and 19.7% (19.3%–20.1%) in non-HBV pregnancies in 2023. Preterm delivery proportions increased from 2000 (HBV 6.9%, 5.9%–7.9%; non-HBV 7.3%, 7.1%–7.5%) to a peak among HBV pregnancies in 2011 (19.1%, 17.9%–20.3%), followed by a decline to 2024 (HBV 11.1%, 9.2%–13.1%; non-HBV 11.3%, 10.9%–11.6%). After IMNC implementation in 2020, miscarriage among IMNC attendees decreased from 8.9% (1.5%–16.4%) in 2020 to 1.2% (0.0%–3.6%) in 2024, whereas non-attendees increased from 9.9% (8.2%–11.5%) to 12.4% (9.7%–15.0%). Preterm delivery among IMNC attendees increased in 2021–2022 to 18.4% (11.9%–24.9%) and 18.9% (11.9%–25.8%), then decreased from 2023 onwards to 8.4% (2.5%–14.4%) in 2024.
Conclusion: Newly diagnosed HBV rates showed substantial increases in pregnant women born before the era of universal HBV vaccination, while remained steadily low in those born in the era of universal HBV vaccination. These findings provide important data for the allocation of resources in IMNC, with more targeted screening, education and pre-emptive antiviral therapy for pregnant women born before the era of universal HBV vaccination in order to minimise MTCT of HBV.
Funding: This work was supported by the Investigator Sponsored Research of Gilead Sciences (Reference: IN-HK-987-7181).

SAT-638
Dynamic modeling of hepatitis B surface antigen trajectories enables prediction of hepatocellular carcinoma: a large-scale long-term follow-up cohort study

Tianyi Xue[1], Xin Wen[1], Yanpei Mai[1], Suzhen Jiang[1], Xiangsha Kong[1], Feng Liu[1], Huiying Rao[1], Zixing Wang[1]. [1]*Peking University Hepatology Institute, Beijing, China*
Email: wangzixing@pkuph.edu.cn

Background and aims: Accurate and timely risk stratification is essential for optimizing hepatocellular carcinoma (HCC) surveillance in patients with chronic hepatitis B (CHB). Quantitative hepatitis B surface antigen (HBsAg) reflects viral–host interaction, but longitudinal information is underutilized in current static prediction models. We aimed to develop a dynamic prediction framework based on longitudinal HBsAg trajectories to improve individualized HCC risk assessment.
Method: We developed dynamic prediction models in a large cohort of adult patients with CHB, split into training and validation sets at a 2:1 ratio. Longitudinal log-transformed HBsAg measurements were modeled using linear mixed-effects models and linked to time to HCC through joint modeling. Patient-specific HCC risk was estimated at baseline and updated at follow-up visits using all available HBsAg data. Predictive performance was assessed using time-dependent area under the receiver operating characteristic curve (AUC) at 1, 2, 3, and 5 years.
Results: The training and validation sets included 9,886 and 4,223 patients, respectively, with 227 and 94 incident HCC events,

respectively, during a maximum follow-up of 12.8 years. At baseline, the model achieved AUCs of 0.79, 0.80, 0.81, and 0.82 for predicting 1-, 2-, 3-, and 5-year HCC risk in the training set, respectively. Model performance improved with follow-up assessments, for instance, with AUCs at the first follow-up increasing to 0.81, 0.82, 0.82, and 0.82 across the four time horizons. In the validation set, baseline prediction yielded AUCs of 0.81, 0.83, 0.81, and 0.83 at 1, 2, 3, and 5 years, respectively. During follow-up, discrimination further improved, with AUCs at the first follow-up reaching 0.85, 0.86, 0.86, and 0.88, and sustained improvement was observed at later follow-up assessments.
Conclusion: Dynamic modeling of longitudinal HBsAg trajectories enables accurate and early updating of HCC risk prediction in chronic hepatitis B. Incorporating biomarker information from previous and present visits provides consistent improvement in short- and long-term risk discrimination and supports personalized surveillance strategies.

SAT-639
HBcrAg predicts post-IFN-α therapy HBV relapse in CHB
Linmei Yao[1]. [1]*Department of Hepatology Division 2, Beijing Ditan Hospital, Capital Medical University, Beijing, China*
Email: 18703498538@163.com

Background and aims: Several hepatitis B virus (HBV) serum markers have been identified as predictors of pegylated interferon-alpha (Peg-IFN-α) antiviral outcomes. However, serum markers for determining virologic relapse following Peg-IFN-α discontinuation (post-Peg-IFN-α virologic relapse) have not been established. This study aimed to identify the association of serum pregenomic RNA (pgRNA) and hepatitis B core-related antigen (HBcrAg) levels with Peg-IFN-α antiviral outcomes and post-Peg-IFN-α virologic relapse in treatment-naïve chronic HBV infection patients.
Method: A total of 371 treatment-naïve chronic HBV (CHB) infection patients participated in this study. All patients received Peg-IFN-α therapy. Biochemical, serological, and virological parameters were quantified using standard laboratory procedures. Serum pgRNA and HBcrAg levels were measured via PCR-fluorescent probe detection and ELISA, respectively.
Results: A total of 327 patients underwent follow-up. One hundred and twelve patients (34.25%) achieved a response to Peg-IFN-α therapy. Sixteen patients experienced post-Peg-IFN-α virologic relapse (14.29%) [during a median follow-up of 12 months (IQR 9–18)]. Baseline serum pgRNA (OR, 0.571; 95% confidence interval [CI], 0.388–0.838), HBcrAg (OR, 0.539; 95% CI, 0.348–0.835), and HBsAg (OR, 0.356; 95% CI, 0.223–0.567) levels correlated with Peg-IFN-α antiviral therapy efficacy. Baseline serum pgRNA, HBcrAg, and HBsAg levels demonstrated predictive value for Peg-IFN-α antiviral therapy efficacy, with areas under the receiver operating characteristic (ROC) curve of 0.821 (95% CI, 0.758–0.874), 0.879 (95% CI, 0.822–0.923), and 0.781 (95% CI, 0.719–0.835), respectively. Serum HBcrAg level at the Peg-IFN-α discontinuation point predicted post-Peg-IFN-α virologic relapse, with an area under the ROC curve of 0.790 (95% CI, 0.703–0.861).
Conclusion: These findings demonstrate that serum pgRNA, HBcrAg, and HBsAg levels in treatment-naïve chronic hepatitis B (CHB) patients correlate with Peg-IFN-α treatment response. Notably, baseline HBcrAg levels independently predict post-treatment virologic relapse, offering a potential biomarker for identifying high-risk patients following Peg-IFN-α discontinuation.

SAT-640
HBV screening in rheumatology: a significant gap in HBV DNA testing for HBsAg-negative, anti-HBc-positive patients
Senlin You[1,2], Hong Tang[1,2], Hong Li[1,2]. [1]*Center of Infectious Diseases, West China Hospital of Sichuan University, Chengdu, China;* [2]*Laboratory of Infectious and Liver Diseases, Institute of Infectious Diseases, West China Hospital of Sichuan University, Chengdu, China*
Email: senlinyou_912918@126.com

Background and aims: Hepatitis B virus (HBV) reactivation is a potentially life-threatening yet preventable complication in rheumatology patients receiving immunosuppressive therapy. Current international guidelines (e.g., EASL 2025, AGA 2025) recommend initial serology screening (HBsAg and anti-HBc) followed by mandatory HBV DNA testing for all HBsAg-positive and HBsAg-negative/anti-HBc-positive patients prior to treatment. This study aimed to characterize HBV screening practices in a large patient cohort.
Method: We conducted a retrospective cohort analysis of consecutive inpatients admitted to the Rheumatology Department of West China Hospital between January 2020 and December 2024. Data for the recommended HBV screening panel (HBsAg, anti-HBc, and HBV DNA) were systematically extracted from electronic medical records. Descriptive statistics were used for analysis, with results reported as proportions and 95% confidence intervals (95% CI).
Results: Among 8,758 patients, 8,417 (96.1%) underwent HBsAg screening. Of these, 339 (4.0%) were HBsAg-positive. Subsequent HBV DNA testing was performed in 289 (85.3%) of these positive patients, with detectable viremia found in 204 (70.6%). Antiviral therapy was initiated in 165 (80.9%) of those with detectable viremia. Among the 8,078 HBsAg-negative patients, 4,029 (49.9%) were anti-HBc-positive and thus should have undergone HBV DNA testing according to guidelines. However, only 1,373 (34.1%; 95% CI: 32.6–35.6%) completed this testing. Detectable viremia was found in 24 of these patients, of whom only 17 received antiviral therapy. Among the 4,029 HBsAg-negative/anti-HBc-positive patients, 3258 (80.9%) were anti-HBs-positive.
Conclusion: In this Chinese cohort, nearly half of HBsAg-negative patients were anti-HBc-positive, yet most did not receive recommended HBV DNA testing. This disparity between seroprevalence and guideline adherence highlights a significant and actionable gap in the prevention of HBV reactivation.

SAT-641
Comparative kinetics of quantitative hepatitis B surface antigen decline in HBV genotypes B and C under standard of care and novel therapy
Xieer Liang[1], Ning Yu[1], Cong Cheng[1], Junqi Niu[2], Hong Ma[3], Zhihong Liu[1], Qing Xie[4], Wencong Dai[1], Yan-Yan Yu[5], Guangfeng Shi[6], Hongbo Gao[7], Xuefan Bai[8], Yao Xie[9], Huiying Rao[10], Deming Tan[11], Mobin Wan[12], Hong Ren[13], Nikolai Naoumov[14], Jian Sun[1], Jinlin Hou[1], Rong Fan[1]. [1]*Department of Infectious Diseases, Nanfang Hospital, Southern Medical University, Guangzhou, China;* [2]*Department of Liver, First Hospital of Jilin University, Changchun, China;* [3]*Liver Research Center, Beijing Friendship Hospital, Capital Medical University, Beijing, China;* [4]*Department of Infectious Diseases, Ruijin Hospital, Shanghai Jiao Tong University School of Medicine, Shanghai, China;* [5]*Department of Infectious Diseases, First Hospital of Peking University, Beijing, China;* [6]*Department of Infectious Diseases, Huashan Hospital affiliated to Fudan University, Shanghai, China;* [7]*8th People's Hospital, Guangzhou, China;* [8]*Department of Infectious Diseases, Tangdu Hospital, Xi'an, China;* [9]*Liver Disease Department, Beijing DiTan Hospital, Beijing, China;* [10]*Peking University Hepatology Institute, Peking University People's Hospital, Beijing, China;* [11]*Department of Infectious Diseases, Xiangya Hospital, Central South University, Changsha, China;* [12]*Department of Infectious Diseases, Shanghai Changhai Hospital, Shanghai, China;* [13]*Department*

of Infectious Diseases, The second Affiliated Hospital, Chongqing Medical University, Chongqing, China; [14]Division of Medicine, University College London, London, United Kingdom
Email: rongfansmu@163.com

Background and aims: Quantitative hepatitis B surface antigen (qHBsAg) is a key marker for evaluating therapeutic approaches in chronic hepatitis B (CHB). However, HBV genotype-specific kinetics across therapies - particularly novel agents - remain poorly characterized. We compared qHBsAg kinetics between HBV genotypes (GTs) B and C under diverse treatment regimens.
Method: The study purposely included CHB cohorts with diverse profiles: i) two treatment-naïve (TN) cohorts with HBeAg-positive patients receiving a nucleos(t)ide analogue (NA, n = 596) for 3–84 months or pegylated interferon (Peg-IFN, n = 262) for 48–96 weeks; ii) one real world cohort with treatment-experienced (TE) patients receiving NA and/or Peg-IFN for 6–96 months (n = 875, HBeAg +: 44.7%); and iii) one TE cohort with pre-enrolment virally suppressed patients receiving siRNA for 48 weeks (n = 50, HBeAg +: 42.0%). The qHBsAg was tested serially at predefined protocol time-points.
Results: A total of 1,783 non-cirrhotic patients infected with GT B/C (833/950), with median duration of follow-up 18.0–85.6 months, median age 28.0–37.0 years, and male predominance 77.0%–84.9%, were analyzed. Among the two TN cohorts, baseline qHBsAg was significantly higher in GT B than in GT C (4.5 vs 4.1 $\log_{10}$ IU/mL; 4.4 vs 4.0 $\log_{10}$ IU/mL; all $p < 0.05$). GT B exhibited a more rapid decline at week 12 (proportion of ≥ 1.0 $\log_{10}$ IU/mL reduction: 34.9% vs 13.5%; 26.9% vs 14.8%; all $p < 0.05$), resulting in consistently lower qHBsAg than GT C through the end-of-treatment (EOT) (3.2 vs 3.5 $\log_{10}$ IU/mL; 3.1 vs 3.3 $\log_{10}$ IU/mL; all $p < 0.05$). Among the two TE cohorts, the qHBsAg of GT B were consistently lower than those of GT C from baseline (3.0 vs 3.1 $\log_{10}$ IU/mL; 2.9 vs 3.6 $\log_{10}$ IU/mL; all $p < 0.05$) to EOT (2.5 vs 2.7 $\log_{10}$ IU/mL; 0.6 vs 2.0 $\log_{10}$ IU/mL; all $p < 0.001$). During the 24- and 48-week post-treatment period, GT B exhibited numerically smaller qHBsAg rebounds (0.1–0.2 $\log_{10}$ IU/mL less) than GT C. Multivariate analysis identified GT B as an independent predictor for achieving qHBsAg < 1000 IU/mL at EOT in NA- and Peg-IFN-treated cohorts (adjusted OR: 1.6–2.2; all $p < 0.05$). Moreover, linear mixed-effects analyses confirmed a significantly faster qHBsAg decline in GT B than GT C in four cohorts (all $p < 0.001$).
Conclusion: GT B exhibits consistently favourable qHBsAg kinetics than GT C - with sharper initial decline, sustained suppression, and minimal rebound - highlighting the importance of genotype-informed novel therapeutic strategies in CHB management.

SAT-642
Comparison of the proportion of chronic hepatitis B patients with indeterminate phase based on the 2025 EASL and the 2025 AASLD guidelines

Shaoqiu Zhang[1], Jian Wang[1,2], Chao Jiang[3], Tao Fan[4], Ye Xiong[4], Renling Yao[1], Juan Xia[1], Xiaomin Yan[1], Huali Wang[5], Qun Zhang[6], Xingxiang Liu[7], Chuanwu Zhu[8], Rui Huang[1,2], Chao Wu[1,2].
[1]Department of Infectious Diseases, Nanjing Drum Tower Hospital, Affiliated Hospital of Medical School, Nanjing University, Nanjing, China; [2]Institute of Viruses and Infectious Diseases, Nanjing University, Nanjing, China; [3]Department of Infectious Diseases, Nanjing Drum Tower Hospital Clinical College of Jiangsu University, Nanjing, China; [4]Department of Infectious Diseases, Nanjing Drum Tower Hospital Clinical College of Nanjing University of Chinese Medicine, Nanjing, China; [5]Department of General Practice, Nanjing Second Hospital, Nanjing University of Chinese Medicine, Nanjing, China; [6]Department of Infectious Diseases, Zhongda Hospital, School of Medicine, Southeast University, Nanjing, China; [7]Department of Clinical Laboratory, Huai'an No. 4 People's Hospital, Huai'an, China; [8]Department of Infectious Diseases, The Affiliated Infectious Diseases Hospital of Soochow University, Suzhou, China
Email: dr.wu@nju.edu.cn

Background and aims: The European Association for the Study of the Liver (EASL) and the American Association for the Study of Liver Diseases (AASLD) released the updated guidelines on the management of chronic hepatitis B (CHB) in 2025. The impact of these updated guidelines on the proportion of patients with indeterminate phase is unclear. We compared the proportion of patients with indeterminate phase based on the 2025 EASL and 2025 AASLD guidelines.
Method: A total of 13,231 treatment-naïve patients with CHB without liver cirrhosis were retrospectively collected from five medical centers. The classification of clinical phases of patients were defined based on the 2025 AASLD and 2025 EASL guidelines, respectively. Patients who did not fall into the defined clinical phases of the guidelines were classified into the indeterminate phase.
Results: The study population had a median age of 36.3 years. 59.4% of patients were male and 26.0% were HBeAg-positive. The proportion of patients with indeterminate phase was significantly higher based on the 2025 AASLD guidelines than based on the 2025 EASL guidelines (41.5% vs. 25.7%, $P < 0.001$). In the subgroup analyses stratified by sex, HBeAg status and age, similar results were found ($P < 0.001$). All patients classified as indeterminate phase according to the 2025 EASL guidelines were also classified as indeterminate phase according to the 2025 AASLD guidelines.
Conclusion: A substantial proportion of patients fell into the indeterminate phase under both the 2025 AASLD and 2025 EASL guidelines, with a significantly higher proportion classified as indeterminate according to the 2025 AASLD guidelines.

SAT-643
Gut microbiome functional profiles associated with fibrosis outcomes in chronic hepatitis B

Zhe Zhang[1], Saisai Zhang[1], Lu Li[1], Meng Zhao[1], Lung-Yi Mak[2], Man-Fung Yuen[2], Wai-Kay Seto[2]. *[1]Department of Medicine, School of Clinical Medicine, The University of Hong Kong, Hong Kong, China; [2]Department of Medicine, School of Clinical Medicine, The University of Hong Kong, State Key Laboratory of Liver Research, The University of Hong Kong, Hong Kong, China*
Email: zhzhe@connect.hku.hk

Background and aims: Chronic hepatitis B (CHB) lead to liver fibrosis and cirrhosis. Despite effective viral suppression with long-term nucleos(t)ide analogue (NA) therapy, fibrosis regression varies. Emerging evidence implicates the gut microbiome in hepatic inflammation and fibrogenesis, yet its role in determining fibrosis outcomes in treated CHB remains unclear. This study aimed to investigate the association between gut microbiome profiles and fibrosis regression in NA-treated CHB patients.
Method: We characterized the fecal microbiome of 30 NA-treated CHB patients with baseline liver fibrosis (liver stiffness measurement [LSM]≥7 kPa) over a three-year follow-up period. Fibrosis regression was defined as more than 30% LSM reduction. Using full-length 16SrRNA gene sequencing (PacBio platform) and functional inference (PICRUSt2), we analyzed microbial function associated with outcomes. In-vitro experiments were conducted using LX-2 human hepatic stellate cells stimulated with arachidonic acid (AA), and the inflammatory gene expression was assessed.
Results: The cohort (median age 67, 77% male) achieved significant fibrosis regression in 12(40%) patients after at least three years NA therapy. All patients were HBeAg-negative with suppressed HBV DNA levels (<10 IU/mL). Baseline mean LSM was 16.12(±2.001) kPa. Functional and taxonomic analyses revealed an enrichment of *Ruminococcus torques* in patients without fibrosis regression (linear discriminant analysis score3.41, $p = 0.015$), while no significant differences were observed in gut microbial alpha or beta diversity between groups. The relative abundance of *Ruminococcus torques* was positively correlated with circulating white blood cell counts, neutrophils, and monocytes ($r = 0.42$, $p = 0.023$; $r = 0.52$, $p = 0.004$; $r = 0.40$, $p = 0.032$). Additionally, *Ruminococcus torques* abundance

was positively associated with the AA metabolism pathway (r = 0.38, p = 0.039). In-vitro AA treatment (10μg/mL) significantly upregulated the mean mRNA levels of inflammatory cytokines in LX-2 cells compared to controls (IL-6:2.81 ± 2.89vs.1.03 ± 0.02, p = 0.0079; MCP-1:1.72 ± 0.06vs.1.04 ± 0.08, p = 0.0079), without affecting fibrogenesis-related genes (alpha-SMA and Collagen typeI).
Conclusion: Fibrosis regression is linked to specific microbial functional signatures in treated CHB. The enrichment of *Ruminococcus torques* and its association with systemic inflammatory markers and arachidonic acid metabolism suggest a potential role for microbiome-driven inflammatory pathways in impeding fibrosis regression.

SAT-644
Risk factors for abnormal ALT in postpartum women with chronic hepatitis B : a systematic review and meta-analysis
Chengxuan Yao[1], Yunxia Zhu[2], Shuiweizhi Dai[1], Xiang Gao[2], Jinhua Wang[2], Huaibin Zou[3]. *[1]Beijing Key Laboratory of Liver Regeneration and Artificial Liver Transformation Research, Beijing, China; [2]Department of Obstetrics, Beijing You 'an Hospital, Capital Medical University, Beijing, China; [3]Department of Liver Diseases, Beijing You 'an Hospital, Capital Medical University, Beijing, China*
Email: zhbin03@126.com

Background and aims: Currently, antiviral therapy during pregnancy followed by postpartum treatment cessation for the prevention of mother-to-child transmission has become standard practice for pregnant women with hepatitis B virus (HBV). However, the postpartum period remains a high-risk phase for HBV-infected women. The underlying causes of postpartum liver function abnormalities in this population have not yet been fully elucidated. This systematic review and meta-analysis aimed to identify risk factors associated with postpartum liver function abnormalities in women with chronic HBV infection.
Method: PubMed, Web of Science, Embase, the Cochrane Library, CNKI, and WangFang databases were systematically searched from database inception to December 10, 2025. The primary clinical outcome was defined as alanine aminotransferase (ALT) elevation >1 × the upper limit of normal (ULN) at any time during the postpartum period.
Results: A total of 18 cohort studies (6 retrospective and 12 prospective), comprising 6,608 postpartum women with chronic HBV infection, were included. Pooled analyses showed that ALT levels at delivery (crude odds ratio [OR] 1.05; 95% CI [1.03–1.07]; $I^2 = 0\%$), HBeAg positivity (crude OR 3.03; 95% CI [1.91–4.81]; $I^2 = 0\%$), elevated baseline HBV DNA levels (OR 1.64; 95% CI [1.25–2.41]; $I^2 = 0\%$), and genotype C (OR 1.10; 95% CI [0.98–1.24]; $I^2 = 0\%$) were potential risk factors for postpartum ALT abnormalities. In contrast, older maternal age (OR 0.93; 95% CI [0.87–0.99]; $I^2 = 0\%$), antiviral therapy during pregnancy (random-effects model, OR 0.77; 95% CI [0.64–0.92]; $I^2 = 0\%$), and continuation of antiviral therapy postpartum (OR 0.50; 95% CI [0.21–1.16]; $I^2 = 0\%$) were identified as key protective factors against postpartum liver function abnormalities. Additionally, baseline ALT levels (random-effects model, OR 1.00; 95% CI [0.99–1.01]) were not associated with postpartum ALT elevation ($I^2 = 11.4\%$; p for heterogeneity = 0.336).
Conclusion: Potential risk factors for postpartum liver function abnormalities in women with chronic HBV infection include elevated ALT levels at delivery, HBeAg positivity, higher baseline HBV DNA levels, non-C genotype, younger maternal age, absence of antiviral therapy during pregnancy, and immediate discontinuation of antiviral therapy after delivery. These findings underscore the need for close monitoring of this high-risk population starting from pregnancy and warrant further investigation into the underlying mechanisms of postpartum ALT elevation.

Viral hepatitis B and D – Current therapies

TOP-582
Bulevirtide monotherapy prevents liver decompensation in patients with hdv-related cirrhosis: a case control study with propensity score weighted analysis
Elisabetta Degasperi[1], Annalisa De Silvestri[2], Dominique Roulot[3], Maria Paola Anolli[1], Liana Gheorghe[4], Mirela Chitul[4], Christoph Schramm[5], Hartmut Schmidt[5], Mathias Jachs[6], Thomas Reiberger[6], Juliette Foucher[7], Sophie Metivier[8], Maria Buti[9], Adriana Palom[9], Giampiero D'Offizi[10], Francesco De Maria[10], Caroline Zöllner[11], Frank Tacke[11], Christopher Dietz-Fricke[12], Heiner Wedemeyer[12], Margarita Papatheodoridi[13], George Papatheodoridis[13], Ivana Carey[14], Kosh Agarwal[14], Florian van Bömmel[15], Maurizia Brunetto[16], Elena Rosselli Del Turco[17], Alessia Ciancio[18], Sabela Lens[19], Alvaro Giráldez-Gallego[20], Filipe Calinas[21], Fabien Zoulim[22], Soo Aleman[23], Nasser Semmo[24], Alessandra Mangia[25], Marie-Noëlle Hilleret[26], Uta Merle[27], Mariana Cardoso[28], Joana Branco[29], Catarina Gouveia[30], Teresa Santantonio[31], Nicola Coppola[32], Adriano Pellicelli[33], Bruno Roche[34], Xavier Causse[35], Louis Dalteroche[36], Jérôme Dumortier[37], Nathalie Ganne-Carrié[38], Frederic Heluwaert[39], Isabelle Ollivier-Hourmand[40], Alessandro Loglio[41], Alessandro Federico[42], Francesca Pileri[43], Monia Maracci[44], Matteo Tonnini[45], Jean-Pierre Arpurt[46], Karl Barange[47], Eric Billaud[48], Lucia Parlati[49], Anne Gervais[50], Anne Minello Franza[51], Isabelle Rosa[52], Costa Santos Ines[53], Francisco Javier Velasco Rubio[54], Massimo Puoti[55], Ana Aboim Horta[56], Mariana Machado[57], Dalia Fernandes[58], Joaquim Oliveira[59], Joao Vaz Alves[60], Johm Flaherty[61], Pietro Lampertico[1,62,63]. *[1]Division of Gastroenterology and Hepatology, Foundation IRCCS Ca' Granda Ospedale Maggiore Policlinico, Milan, Italy; [2]Clinical Epidemiology and Biometry Unit, Fondazione IRCCS Policlinico San Matteo, Pavia, Italy; [3]Liver Unit, Avicenne hospital, AP-HP, Sorbonne Paris Nord University, Bobigny, France; [4]Center for Digestive Diseases and Liver Transplantation, Fundeni Clinical Institute, Bucharest, Romania; [5]Department of Gastroenterology, Hepatology and Transplant Medicine, Medical Faculty, University of Duisburg-Essen, Essen, Germany; [6]Division of Gastroenterology and Hepatology, Department of Medicine III, Medical University of Vienna, Vienna, Austria; [7]Hepatology Department, Haut-Lévêque Hospital, Bordeaux, France; [8]Hepatology Unit, CHU Rangueil, Toulouse, France; [9]Liver Unit, Internal Medicine Department, Hospital Universitari Vall d'Hebron, Vall d'Hebron Barcelona Hospital Campus, Barcelona, Spain; [10]Division of Infectious Diseases - Hepatology, Department of Transplantation and General Surgery, Istituto Nazionale per le Malattie Infettive "L. Spallanzani" IRCCS, Rome, Italy; [11]Department of Hepatology and Gastroenterology, Charité Universitätsmedizin Berlin, Berlin, Germany; [12]Department of Gastroenterology, Hepatology, Infectious Diseases and Endocrinology at Hannover Medical School, Hannover, Germany; [13]1st Department of Gastroenterology, General Hospital of Athens "Laiko", Medical School of National & Kapodistrian University of Athens, Athens, Greece; [14]Institute of Liver Studies, King's College Hospital, London, United Kingdom; [15]Division of Hepatology, Department of Medicine II, Leipzig University Medical Center, Laboratory for Clinical and Experimental Hepatology, Leipzig, Germany; [16]Department of Clinical and Experimental Medicine, University of Pisa and Hepatology Unit, University Hospital of Pisa, Pisa, Italy; [17]Department of Medical and Surgical Sciences, Unit of Infectious Diseases, "Alma Mater Studiorum" University of Bologna, S. Orsola-Malpighi Hospital, Bologna, Italy; [18]Department of Medical Sciences, University of Turin, Gastroenterology Division of Città della Salute e della Scienza of Turin, University Hospital, Turin, Italy; [19]Liver Unit, Hospital*

Clínic, IDIBAPS, Universitat de Barcelona, Barcelona, Spain; Centro de Investigación Biomédica en Red de Enfermedades Hepáticas y Digestivas (CIBEREHD), Barcelona, Spain; [20]Hospital Virgen del Rocío, IBIS, Sevilla, Spain; [21]Serviço de Gastrenterologia, ULS de São José, Lisboa, Portugal; [22]Lyon Hepatology Institute, Université Claude Bernard Lyon 1; Hospices Civils de Lyon; INSERM Unit 1052 - CRCL, Lyon, France; [23]Infectious Disease Clinic, Karolinska University Hospital, Stockholm, Sweden; [24]Department of Visceral Surgery and Medicine, Inselspital, Bern University, Bern, Switzerland; [25]Liver Unit, Fondazione IRCCS "Casa Sollievo della Sofferenza", San Giovanni Rotondo, Italy; [26]University Grenoble Alpes, Hepatology and Gastroenterology Unit, CHU Grenoble Alpes, 38043 Grenoble, France, Inserm U 1209, CNRS UMR 5309, Team Cell Dynamics, Immunity, Metabolism & Cancer, Institute for Advanced Biosciences, Grenoble, France; [27]Department of Internal Medicine IV, Gastroenterology & Hepatology, Heidelberg University Hospital, Heidelberg, Germany; [28]Gastroenterology Department, ULS de São José, Lisbon, Portugal; [29]Serviço de Gastrenterologia, ULS de Amadora/Sintra, Sintra, Portugal; [30]Serviço de Gastrenterologia, ULS de Loures/Odivelas, Odivelas, Portugal; [31]Department of Medical and Surgical Sciences, Infectious Diseases Unit, University of Foggia, Foggia, Italy; [32]Department of Mental Health and Public Medicine - Infectious Diseases Unit, University of Campania Luigi Vanvitelli, Naples, Italy; [33]Liver Unit, San Camillo Hospital, Department of Transplantation and General Surgery, Rome, Italy; [34]Hepato-Biliary Center, AP-HP Hôpital Universitaire Paul Brousse, Paris-Saclay University, Research INSERM-Paris Saclay Unit 1193, Villejuif, France; [35]Service d'Hépato-Gastroentérologie CHU d'Orléans, Orleans, France; [36]Service d'Hépato-Gastroentérologie CHU de Tours, Tours, France; [37]Department of Digestive Diseases, Hospices Civils de Lyon, Edouard Herriot hospital, Claude Bernard Lyon 1 University, Lyon, France; [38]AP-HP, Avicenne Hospital, Hepatology Department, Bobigny, France; [39]Centre Hospitalier Annecy Genevois, 74000, Annecy, France; [40]Department of Hepatogastroenterology, CHU de Caen Normandie, Caen, France; [41]Gastroenterology, Hepatology and Transplantation Division, ASST Papa Giovanni XXIII, Bergamo, Italy; [42]Division of Hepatogastroenterology, Department of Precision Medicine, Università della Campania "Luigi Vanvitelli", Naples, Italy; [43]Division of Internal Medicine and Center for Hemochromatosis, University of Modena and Reggio Emilia, Modena, Italy; [44]Institute of Infectious Diseases and Public Health, Università Politecnica delle Marche, Ancona, Italy; [45]Division of Internal Medicine, Hepatobiliary and Immunoallergic Diseases, IRCCS Azienda Ospedaliero-Universitaria di Bologna, Bologna, Italy; [46]Department of Gastroenterology, CH d'Avignon, Avignon, France; [47]Department of Gastroenterology, Toulouse University Hospital, Toulouse, France; [48]Université de Nantes, INSERM UIC 1413, Department of Infectious Diseases, CHU Hôtel Dieu, Nantes, France; [49]Université Paris Cité; Assistance Publique des Hôpitaux de Paris, Hôpital Cochin, Hepatology/Addictology department, Paris, France; [50]Assistance Publique des Hôpitaux de Paris, Hôpital Bichat Claude Bernard, Service des Maladies Infectieuses et Tropicales, Paris, France; [51]CHU Dijon, Service d'Hépato-gastroentérologie et oncologie digestive, Inserm EPICAD LNC-UMR1231, Université de Bourgogne-Franche Comté, Dijon, France; [52]Service d'hépatogastroentérologie, Centre Hospitalier Intercommunal, Creteil, France; [53]Serviço de Gastrenterologia, ULS de Almada/ Seixal, Almada, Portugal; [54]Serviço de Gastrenterologia, ULS do Algarve, Algarve, Portugal; [55]School of Medicine and Surgery University of Milano Bicocca, Milano, Italy; [56]Serviço de Infecciologia, ULS de Santo António, Portugal, Santo Antonio, Portugal; [57]Serviço de Gastrenterologia, ULS do Estuário do Tejo, Portugal, Lisboa, Portugal; [58]Serviço de Gastrenterologia, ULS de Braga, Portugal, Braga, Portugal; [59]Serviço de Infecciologia, ULS de Coimbra, Portugal, Coimbra, Portugal; [60]Serviço de Infecciologia, ULS de Lisboa Ocidental, Lisboa, Portugal; [61]School of Pharmacy, Department of Clinical Pharmacy, San Francisco, CA, United States; [62]CRC "A. M. and A. Migliavacca" Center for Liver Disease, Department of Pathophysiology and Transplantation, University of Milan, Milan, Italy; [63]D-SOLVE consortium, an EU Horizon Europe funded project (No 101057917), Milan, Italy
Email: elisabetta.degasperi@policlinico.mi.it

Background and aims: Bulevirtide (BLV) monotherapy yields high rates of virological and biochemical response in chronic hepatitis Delta (CHD) patients with cirrhosis, however data on hard clinical outcomes are lacking.
Method: Consecutive CHD patients with cirrhosis treated with BLV 2 mg/day for 3 years in the SAVE-D retrospective multicenter European study were compared with two BLV-untreated cohorts (cohort #1 from Italy and cohort #2 from France). Liver-related events (LRE: hepatocellular carcinoma [HCC], decompensation) occurring within the first 3 years were compared by inverse probability of treatment weighting (IPTW) analysis. Baseline data was set at BLV start (BLV-treated cohort) or cirrhosis diagnosis (untreated controls).
Results: A total of 642 patients were included: 344 BLV-treated and 298 untreated controls. Treated patients were older (50 *vs.* 40 years, $p < 0.0001$), more frequently women (males 62% *vs.* 78%, $p = 0.001$), Caucasian (84% *vs.* 62%, $p < 0.0001$), on NUC (91% vs. 40%, $p < 0.0001$) and with higher HDV RNA (5.4 *vs.* 4.9 Log_{10}IU/mL, $p = 0.002$). By contrast, the proportion of patients with previous decompensation, HCC or CSPH was similar. The 3-year cumulative incidence of LREs was lower in BLV-treated patients *vs.* untreated: 8.9% (95%CI 4–12%) *vs.* 16.2% (95% CI 11–22%), respectively ($p = 0.03$). The corresponding figures for decompensation were 2.7% (95%CI 1–4%) *vs.* 11.3% (95%CI 7–16%) ($p = 0.001$) and for HCC 6.1% (95%CI 3–8%) *vs.* 6.6% (95% CI 3–11%) ($p = 0.49$), respectively. In IPTW-adjusted Cox regression analysis, BLV-treated *vs.* untreated controls had significantly lower risk of developing LREs (HR 0.44, 95% CI 0.27–0.72, $p = 0.001$) or decompensation (HR 0.16, 95% CI 0.07–0.36, $p < 0.0001$). These results were confirmed by IPTW-adjusted competing risks regression model both in the combined untreated cohorts (SHR 0.16, 95%CI 0.06–0.40, $p < 0.0001$) and in each individual untreated cohort (cohort#1: SHR 0.16, 95%CI 0.05–0.47, $p < 0.001$; cohort #2: SHR 0.19, 95%CI 0.06–0.62, $p < 0.005$). Conversely, the HCC risk was similar across all cohorts. Lower baseline albumin values independently predicted LREs, both in the BLV-treated cohort (HR 0.22, 95% CI 0.08–0.64, $p = 0.006$) and untreated controls (HR 0.38, 95%CI 0.20–0.72, $p = 0.002$).
Conclusion: In CHD patients with cirrhosis observed for up to 3 years, BLV monotherapy reduced the risk of LREs and decompensation, but not HCC, compared to an untreated IPTW-matched population.

TOP-583

Controlled bulevirtide discontinuation in chronic hepatitis D: The D-SOLVE BUL-STOP trial

Heiner Wedemeyer[1,2,3,4,5], Julia Kahlhöfer[1,2,3,6], Elisabetta Degasperi[2,7], Kathrin Sprinzl[8], Caroline Zöllner[9], Shirin Nkongolo[10,11,12], Lisa Sandmann[1,2,4,5], Dana Sambarino[2,2], Kerstin Port[1], Julian Schulze zur Wiesch[13,14], Anke R. M. Kraft[1,4,5,6,15], Helenie Kefalakes[1,2,4,4], Anika Grosshennig[16], Ringlstetter Rieke[16], Pietro Lampertico[2,7,17], Katja Deterding[1,2]. *[1]Department of Gastroenterology, Hepatology, Infectious Diseases and Endocrinology, Hannover Medical School, Hannover, Germany; [2]D-SOLVE Consortium, an EU Horizon Europe Funded Project (No 101057917), Hannover, Germany; [3]German Center for Infection Research (DZIF), HepNet Study House of the German Liver Foundation, Hannover, Germany; [4]Cluster of Excellence RESIST (EXC 2155), Hannover Medical School, Hannover, Germany; [5]German Center for Infection Research (DZIF), Partner Site Hannover-Braunschweig, Braunschweig, Germany; [6]Centre for Individualised Infection Medicine (CiiM), a Joint Venture Between the Helmholtz Centre for Infection Research (HZI) and Hannover Medical School (MHH), Hannover, Germany; [7]Division of Gastroenterology and Hepatology, Foundation IRCCS Ca' Granda Ospedale Maggiore Policlinico, Milan, Italy; [8]Goethe University Frankfurt, University Hospital, Medical Clinic 1, Frankfurt am Main, Germany; [9]Department of Hepatology and Gastroenterology, Charité Universitätsmedizin Berlin, Berlin, Germany; [10]Molecular Virology, Department of Infectious Diseases, University Hospital Heidelberg, Heidelberg, Germany; [11]German Center for Infection Research (DZIF), Partner Site Heidelberg, Heidelberg, Germany; [12]Internal Medicine IV (Gastroenterology,*

Hepatology, Infectious Diseases), University Hospital Heidelberg, Heidelberg, Germany; [13]1st Department of Medicine, Division of Infectious Diseases, Center for Internal Medicine, University Medical Center Hamburg-Eppendorf, Hamburg, Germany; [14]German Center for Infection Research (DZIF), Partner Site Hamburg-Lübeck-Borstel-Riems, Hamburg, Germany; [15]TWINCORE, a Joint Venture Between the Helmholtz-Centre for Infection Research (HZI) and the Hannover Medical School (MHH), Hannover, Germany; [16]Institute for Biostatistics, Hannover Medical School, Hannover, Germany; [17]CRC "A. M. and A. Migliavacca" Center for Liver Disease, Department of Pathophysiology and Transplantation, University of Milan, Milan, Germany
Email: wedemeyer.heiner@mh-hannover.de

Background and aims: Long-term therapy with bulevirtide (BLV) is currently recommended for most patients with chronic hepatitis D (CHD). Preliminary data from the pivotal MYR-301 study, together with limited real-world evidence, suggest that finite BLV therapy may be feasible in only a small subset of patients. In contrast, uncontrolled discontinuation of BLV has been associated with severe hepatitis flares and hepatic decompensation. The BUL-STOP trial aims to assess whether BLV therapy can be safely discontinued in carefully selected patients with CHD and to explore potential biomarkers associated with sustained control of HDV infection after cessation of BLV treatment.
Method: BUL-STOP is a still ongoing investigator-initiated multi-center-study in Germany and Italy supported by the EU-funded D-SOLVE consortium and the HEP-NET Study House. Patients with CHD and compensated liver disease who have been treated with BLV for 48 weeks or longer were eligible if HDV RNA was less than 100 IU/ml for at least 24 weeks. A close post-treatment monitoring and biomarker sampling including fine-needle-aspiration is performed for 48 weeks after stopping BLV therapy or until re initiation of BLV therapy was deemed necessary.
Results: A total of 21 patients were enrolled. BLV discontinuation was not feasible in three patients due to screening failure; therefore, 18 patients (10 females, 8 males; median age 57 years [range 34–75]; median ALT 26 U/l [range 14–39]; liver stiffness measurement (LSM) > 10.2 kPa in two patients > 15.2 kPa in one patient) are currently being followed after BLV discontinuation. The median duration of BLV therapy prior to discontinuation was 144 weeks (range 53–250). HDV RNA was undetectable in 16/18 patients at screening, 15/18 at baseline, 12/18 at 4-weeks off-therapy, and 7/14 at 12-weeks off-therapy. By December 31, 2025, BLV therapy had been re-initiated in eight patients (44%) after 65–198 days. ALT elevations exceeding three times the upper limit of normal were observed in four patients. No episodes of hepatic decompensation occurred during the study. Final follow-up data will be presented at the meeting.
Conclusion: Discontinuation of BLV therapy may be feasible in a subset of patients with CHD, allowing for finite treatment. However, post-treatment relapse can be associated with hepatitis flares, necessitating timely re-initiation of BLV therapy. Biomarker analyses to identify pre-discontinuation factors predictive of sustained long-term control of HDV infection are ongoing.

TOP-584

Virological breakthroughs during long-term Bulevirtide monotherapy in patients with CHD: integrated analysis from the multicenter real-life save-d and d-shield studies

Elisabetta Degasperi[1], Maria Paola Anolli[1], Dana Sambarino[1], Marta Borghi[1], Riccardo Perbellini[1], Liana Gheorghe[2], Alessandro Loglio[3], Alessia Ciancio[4], Giampiero D'Offizi[5], Christoph Schramm[6], Thomas Reiberger[7], Maurizia Brunetto[8], Kosh Agarwal[9], Maria Buti[10], Serena Zaltron[11], Frank Tacke[12], Heiner Wedemeyer[13], Margarita Papatheodoridi[14], Florian van Bömmel[15], Sabela Lens[16], Alessandro Federico[17], Elena Rosselli Del Turco[18], Magdalena Meszaros[19], Alvaro Giráldez-Gallego[20], Filipe Calinas[21], Michele Milella[22], Laura Turco[23], Andrea Di Lorenzo[24], Mariarosa Tamé[25], Pierluigi Toniutto[26], Antonio Gasbarrini[27], Letizia Marinaro[28], Francesco Paolo Russo[29], Andrea Gori[30], Ivana Rita Maida[31], Teresa Santantonio[32], Raffaele Bruno[33], Edoardo Giovanni Giannini[34], Irene Cacciola[35], Filomena Morisco[36], Alessandra Mangia[37], Stella De Nicola[38], Antonietta Romano[39], Monia Maracci[40], Biagio Pinchera[41], Saveria Lory Croce'[42], Pietro Lampertico[1,43,44].
[1]Division of Gastroenterology and Hepatology, Foundation IRCCS Ca' Granda Ospedale Maggiore Policlinico, Milan, Italy; [2]Center for Digestive Diseases and Liver Transplantation, Fundeni Clinical Institute, Bucharest, Romania; [3]Gastroenterology, Hepatology and Transplantation Division, ASST Papa Giovanni XXIII, Bergamo, Italy; [4]Department of Medical Sciences, University of Turin, Gastroenterology Division of Città della Salute e della Scienza of Turin, University Hospital, Turin, Italy; [5]Division of Infectious Diseases - Hepatology, Department of Transplantation and General Surgery, Istituto Nazionale per le Malattie Infettive "L. Spallanzani" IRCCS, Rome, Italy; [6]Department of Gastroenterology, Hepatology and Transplant Medicine, Medical Faculty, University of Duisburg-Essen, Essen, Germany; [7]Division of Gastroenterology and Hepatology, Department of Medicine III, Medical University of Vienna, Vienna, Austria; [8]Department of Clinical and Experimental Medicine, University of Pisa and Hepatology Unit, University Hospital of Pisa, Pisa, Italy; [9]Institute of Liver Studies, King's College Hospital, London, United Kingdom; [10]Liver Unit, Internal Medicine Department, Hospital Universitari Vall d'Hebron, Vall d'Hebron Barcelona Hospital Campus, Barcelona, Spain; [11]Infectious Disease Department, Spedali Civili Brescia, Brescia, Italy; [12]Department of Hepatology and Gastroenterology, Charité Universitätsmedizin Berlin, Berlin, Germany; [13]Department of Gastroenterology, Hepatology, Infectious Diseases and Endocrinology at Hannover Medical School, Hannover, Germany; [14]1st Department of Gastroenterology, General Hospital of Athens "Laiko", Medical School of National & Kapodistrian University of Athens, Athens, Greece; [15]Division of Hepatology, Department of Medicine II, Leipzig University Medical Center, Laboratory for Clinical and Experimental Hepatology, Leipzig, Germany; [16]Liver Unit, Hospital Clínic, IDIBAPS, Universitat de Barcelona, Barcelona, Spain; Centro de Investigación Biomédica en Red de Enfermedades Hepáticas y Digestivas (CIBEREHD), Barcelona, Spain; [17]Division of Hepatogastroenterology, Department of Precision Medicine, Università della Campania "Luigi Vanvitelli", Naples, Italy; [18]Department of Medical and Surgical Sciences, Unit of Infectious Diseases, "Alma Mater Studiorum" University of Bologna, S. Orsola-Malpighi Hospital, Bologna, Italy; [19]Liver Transplantation and Hepatogastroenterology Unit, CHU Montpellier, CHU Montpellier, Montpellier, France; [20]Hospital Virgen del Rocío, IBIS, Sevilla, Spain; [21]Serviço de Gastrenterologia, ULS de São José, Lisboa, Portugal; [22]Infectious Diseases Unit, Department of Biomedical Sciences and Human Oncology, University of Bari, Bari, Italy; [23]Internal Medicine Unit for the Treatment of Severe Organ Failure, IRCCS Azienda Ospedaliero- Universitaria di Bologna, Bologna, Italy; [24]Tor Vergata University, Rome, Italy; [25]Gastroenterology Unit, IRCCS Azienda Ospedaliero-Universitaria di Bologna, Bologna, Italy; [26]Hepatology and Liver Transplantation Unit, Academic Hospital, University of Udine, Udine, Italy; [27]Fondazione Policlinico Universitario Gemelli IRCCS, Università Cattolica del Sacro Cuore, Rome, Italy; [28]SCDU Infectious Diseases, Amedeo di Savoia Hospital, ASL Città di Torino, Turin, Italy; [29]Department of Surgery, Oncology and Gastroenterology, University of Padua, Padua, Italy; [30]Infectious Disease Unit II, Ospedale Luigi Sacco, ASST Fatebenefratelli Sacco, Milan, Italy; [31]Infectious and Tropical Diseases Unit, Department of Medical, Surgical and Experimental Sciences, University of Sassari, Sassari, Italy; [32]Department of Medical and Surgical Sciences, Infectious Diseases Unit, University of Foggia, Foggia, Italy; [33]Department of Clinical, Surgical, Diagnostic and Pediatric Sciences, University of Pavia, Pavia, Italy; [34]Gastroenterology Unit, Department of Internal Medicine, University of Genoa, Genoa, Italy; [35]Department of Clinical and Experimental Medicine, University of Messina, Messina, Italy; [36]Department of Clinical Medicine and Surgery, Diseases of the Liver and Biliary System Unit, University of Naples "Federico II", Naples, Italy; [37]Liver Unit, Fondazione IRCCS "Casa Sollievo della Sofferenza", San Giovanni Rotondo, Italy; [38]Division of Internal Medicine and Hepatology, Department of Gastroenterology, IRCCS

Humanitas Research Hospital, Rozzano, Milan, Italy; [39]Unit of Internal Medicine and Hepatology (UIMH), Department of Medicine, University of Padua, Padua, Italy; [40]Institute of Infectious Diseases and Public Health, Università Politecnica delle Marche, Ancona, Italy; [41]Department of Clinical Medicine and Surgery, University of Naples Federico II, Naples, Italy; [42]Department of Medicine, Surgery and Health Sciences, University of Trieste, Trieste, Italy; [43]CRC "A. M. and A. Migliavacca" Center for Liver Disease, Department of Pathophysiology and Transplantation, University of Milan, Milan, Italy; [44]D-SOLVE consortium, an EU Horizon Europe funded project (No 101057917), Milan, Italy
Email: elisabetta.degasperi@policlinico.mi.it

Background and aims: Bulevirtide (BLV) 2 mg/day is approved for the treatment of chronic hepatitis Delta (CHD), but real-world data on virological breakthroughs (VBK) during long-term BLV monotherapy remain limited. We evaluated the incidence and timing of VBK during BLV 2 mg/day monotherapy in two multicenter real-life cohorts (SAVE D and D SHIELD).
Method: CHD patients treated with BLV 2 mg/day monotherapy from the retrospective/prospective multicenter, observational, real-world SAVE-D and D-SHIELD studies with available paired baseline-week 24–48–72 or 96 data were included. VBK was defined as ≥1 Log_{10} HDV RNA increase compared to a previous timepoint (nadir). Virological (HDV-RNA undetectable or ≥2 Log_{10} decline *vs.* baseline), biochemical (BR, ALT<40 U/L), combined response (CR, biochemical +virological), HDV RNA undetectability and liver-related events were also assessed.
Results: Among a total of 900 CHD patients enrolled in the SAVE-D and D-SHIELD studies, a total of 276 patients with available paired baseline-W72 data (111 with available week 96 data) were included: at baseline (BLV start), median age was 52 (IQR 42–60) years, 55% males, 73% with cirrhosis, median ALT 81 (45–144), liver stiffness measurement (LSM) 14.0 (6.1–25.0) kPa, HBsAg 3.7 (3.2–4.2) Log_{10}IU/mL, HDV RNA 5.3 (3.9–6.4) Log_{10}IU/mL. Overall, rates of response at week 48 were 68% (VR), 67% (BR), 52% (CR) and 28% (HDV RNA undetectable), while the corresponding figures at week 96 were 68% (VR), 65% (BR), 50% (CR) and 38% (HDV RNA undetectable), respectively. During BLV monotherapy, a VBK occurred in 15 (5%) patients at week 48, 24 (9%) at week 72 and 8 (7%) at week 96. At VBK, a BR was maintained in 7/14 (50%) patients at week 48, 10/24 (42%) at week 72, and 7/8 (87%) at week 96. Occurrence of VBK was independent of baseline ALT levels ($p = 0.08$), HDV RNA ($p = 0.72$) and cirrhosis status ($p = 0.15$). VBK was stable at two consecutive timepoints in 7 (15%) patients, while in the remnants VBK was only transient and resolved at the following treatment timepoint. None of the patients with VBK developed a de novo liver-related event.
Conclusion: During BLV 2 mg/day monotherapy up to 96 weeks, 17% of the patients experienced VBK that however were transient and not associated with increased ALT levels in most cases.

FRI-585-YI

Performances of the page-b and amap scores to predict hepatocellular carcinoma in patients with compensated delta cirrhosis treated long-term with bulevirtide monotherapy (save-d study)

Maria Paola Anolli[1], Elisabetta Degasperi[1], Dana Sambarino[1], Marta Borghi[1], Riccardo Perbellini[1], Liana Gheorghe[2], Mirela Chitul[2], Christoph Schramm[3], Hartmut Schmidt[3], Mathias Jachs[4], Thomas Reiberger[4], Ivana Carey[5], Kosh Agarwal[5], Maria Buti[6], Adriana Palom[6], Giampiero D'Offizi[7], Francesco De Maria[7], Caroline Zöllner[8], Frank Tacke[8], Christopher Dietz-Fricke[9], Heiner Wedemeyer[9], Margarita Papatheodoridi[10], George Papatheodoridis[10], Florian van Bömmel[11], Sabela Lens[12], Maurizia Brunetto[13], Alessandro Federico[14], Elena Rosselli Del Turco[15], Magdalena Meszaros[16], Alessia Ciancio[17], Alvaro Giráldez-Gallego[18], Filipe Calinas[19], Fabien Zoulim[20], Soo Aleman[21], Nasser Semmo[22], Sophie Metivier[23], Carla Coffin[24], Sebastien Poulin[25], Alessandra Mangia[26], Marie-Noëlle Hilleret[27], Uta Merle[28], Mariana Cardoso[29], Alexandra Martins[30], Caterina Gouveia[31], Karen Doucette[32], Sergio Borgia[33], Mauro Viganò[34], Teresa Santantonio[35], Nicola Coppola[36], Adriano Pellicelli[37], Juliette Foucher[38], Bruno Roche[39], Xavier Causse[40], Louis Dalteroche[41], Jérôme Dumortier[42], Nathalie Ganne-Carrié[43], Frederic Heluwaert[44], Isabelle Ollivier-Hourmand[45], Dominique Roulot[46], Isabelle Rosa[47], Cristina Fonseca[48], Ana Margarida Vieira[49], Francesca Pileri[50], Monia Maracci[51], Matteo Tonnini[52], Jean-Pierre Arpurt[53], Karl Barange[54], Eric Billaud[55], Lucia Parlati[56], Anne Gervais[57], Anne Minello Franza[58], Massimo Puoti[59], Ana Horta[60], Mariana Machado[61], Dalia Fernandes[62], Joaquim Oliveira[63], Joao Vaz Alves[64], Pietro Lampertico[1,65,66]. *[1]Division of Gastroenterology and Hepatology, Foundation IRCCS Ca' Granda Ospedale Maggiore Policlinico, Milan, Italy; [2]Center for Digestive Diseases and Liver Transplantation, Fundeni Clinical Institute, Bucharest, Romania; [3]Department of Gastroenterology, Hepatology and Transplant Medicine, Medical Faculty, University of Duisburg-Essen, Essen, Germany; [4]Division of Gastroenterology and Hepatology, Department of Medicine III, Medical University of Vienna, Vienna, Austria; [5]Institute of Liver Studies, King's College Hospital, London, United Kingdom; [6]Liver Unit, Internal Medicine Department, Hospital Universitari Vall d'Hebron, Vall d'Hebron Barcelona Hospital Campus, Barcellona, Spain; [7]Division of Infectious Diseases - Hepatology, Department of Transplantation and General Surgery, Istituto Nazionale per le Malattie Infettive "L. Spallanzani" IRCCS, Rome, Italy; [8]Department of Hepatology and Gastroenterology, Charité Universitätsmedizin Berlin, Berlin, Germany; [9]Department of Gastroenterology, Hepatology, Infectious Diseases and Endocrinology at Hannover Medical School, Hannover, Germany; [10]1st Department of Gastroenterology, General Hospital of Athens "Laiko", Medical School of National & Kapodistrian University of Athens, Athens, Greece; [11]Division of Hepatology, Department of Medicine II, Leipzig University Medical Center, Laboratory for Clinical and Experimental Hepatology, Leipzig, Germany; [12]Liver Unit, Hospital Clínic, IDIBAPS, Universitat de Barcelona, Centro de Investigación Biomédica en Red de Enfermedades Hepáticas y Digestivas (CIBEREHD), Barcellona, Spain; [13]Department of Clinical and Experimental Medicine, University of Pisa and Hepatology Unit, University Hospital of Pisa, Pisa, Italy; [14]Division of Hepatogastroenterology, Department of Precision Medicine, Università della Campania "Luigi Vanvitelli", Naples, Italy; [15]Department of Medical and Surgical Sciences, Unit of Infectious Diseases, "Alma Mater Studiorum" University of Bologna, S. Orsola-Malpighi Hospital, Bologna, Italy; [16]Liver Transplantation and Hepatogastroenterology Unit, CHU Montpellier, CHU Montpellier, Montpellier, France; [17]Department of Medical Sciences, University of Turin, Gastroenterology Division of Città della Salute e della Scienza of Turin, University Hospital, Turin, Italy; [18]Hospital Virgen del Rocío, IBIS, Sevilla, Spain; [19]Serviço de Gastrenterologia, ULS de São José, São José, Portugal; [20]Lyon Hepatology Institute, Université Claude Bernard Lyon 1; Hospices Civils de Lyon; INSERM Unit 1052 - CRCL, Lyon, France; [21]Infectious Disease Clinic, Karolinska University Hospital, Stockholm, Sweden; [22]Department of Visceral Surgery and Medicine, Inselspital, Bern University, Bern, Switzerland; [23]Hepatology Unit, CHU Rangueil, 31059, Toulouse, France; [24]Division of Gastroenterology and Hepatology, Department of Medicine, Cumming School of Medicine, University of Calgary, Calgari, Canada; [25]Service de microbiologie-infectiologie, CISSS des Laurentides, Hôpital de St-Jérôme et Clinique I.D, St-Jérôme, Canada; [26]Liver Unit, Fondazione IRCCS "Casa Sollievo della Sofferenza", San Giovanni Rotondo, Italy; [27]Service d'hépato-gastro-entérologie, CHU Grenoble-Alpes, Grenoble, France; [28]Department of Internal Medicine IV, Gastroenterology & Hepatology, Heidelberg University Hospital, Heidelberg, Germany; [29]Gastroenterology Department, ULS de São José, Lisbon, Portugal; [30]Serviço de Gastrenterologia, ULS de Amadora/Sintra, Sintra, Portugal; [31]Serviço de Gastrenterologia, ULS de Loures/Odivelas, Odivelas, Portugal; [32]Division of Infectious Diseases, Department of Medicine, University of Alberta, Edmonton, Canada; [33]Osler Hepatitis Centre Brampton Civic Hospital, William Osler Health System, and McMaster University, Division of Infectious Diseases, Brampton, Canada;*

[34]Gastroenterology, Hepatology and Transplantation Division, ASST Papa Giovanni XXIII, Bergamo, Italy; [35]Department of Medical and Surgical Sciences, Infectious Diseases Unit, University of Foggia, Foggia, Italy; [36]Department of Mental Health and Public Medicine - Infectious Diseases Unit, University of Campania Luigi Vanvitelli, Naples, Italy; [37]Liver Unit, San Camillo Hospital, Department of Transplantation and General Surgery, Rome, Italy; [38]Hepatology Department, Haut-Lévêque Hospital, Bordeaux, France; [39]Hepato-Biliary Center, AP-HP Hôpital Universitaire Paul Brousse, Paris-Saclay University, Research INSERM-Paris Saclay Unit 1193, Villejuif, France; [40]Service d'Hépato-Gastroentérologie CHU d'Orléans, Orléans, France; [41]Service d'Hépato-Gastroentérologie CHU de Tours, Tours, France; [42]Department of Digestive Diseases, Hospices Civils de Lyon, Edouard Herriot hospital, France; Claude Bernard Lyon 1 University, Lyon, France; [43]AP-HP, Avicenne Hospital, Hepatology Department, Bobigny, France; [44]Centre Hospitalier Annecy Genevois, Annecy, France; [45]Department of Hepatogastroenterology, CHU de Caen Normandie, Caen, France; [46]Liver Unit, Avicenne hospital, AP-HP, Sorbonne Paris Nord University, Bobigny, France; [47]Service d'hépatogastroentérologie, Centre Hospitalier Intercommunal, Créteil, France; [48]Serviço de Gastrenterologia, ULS de Almada/Seixal, Seixal, Portugal; [49]Serviço de Gastrenterologia, ULS do Algarve, Algarve, Portugal; [50]Division of Internal Medicine and Center for Hemochromatosis, University of Modena and Reggio Emilia, Modena, Italy; [51]Institute of Infectious Diseases and Public Health, Università Politecnica delle Marche, Ancona, Italy; [52]Division of Internal Medicine, Hepatobiliary and Immunoallergic Diseases, IRCCS Azienda Ospedaliero-Universitaria di Bologna, Bologna, Italy; [53]Department of Gastroenterology, CH d'Avignon, Avignon, France; [54]Department of Gastroenterology, Toulouse University Hospital, Toulouse, France; [55]Université de Nantes, INSERM UIC 1413, Department of Infectious Diseases, CHU Hôtel Dieu, Nantes, France; [56]Université Paris Cité; Assistance Publique des Hôpitaux de Paris, Hôpital Cochin, Hepatology/Addictology Department, Paris, France; [57]Assistance Publique des Hôpitaux de Paris, Hôpital Bichat Claude Bernard, Service des Maladies Infectieuses et Tropicales, Paris, France; [58]CHU Dijon, Service d'Hépato-gastroentérologie et oncologie digestive, Inserm EPICAD LNC-UMR1231, Université de Bourgogne-Franche Comté, Dijon, France; [59]School of Medicine and Surgery University of Milano Bicocca, Milan, Italy; [60]Serviço de Infecciologia, ULS de Santo António, Porto, Portugal; [61]Serviço de Gastrenterologia, ULS do Estuário do Tejo, Tejo, Portugal; [62]Serviço de Gastrenterologia, ULS de Braga, Braga, Portugal; [63]Serviço de Infecciologia, ULS de Coimbra, Coimbra, Portugal; [64]Serviço de Infecciologia, ULS de Lisboa Ocidental, Lisboa, Portugal; [65]CRC "A. M. and A. Migliavacca" Center for Liver Disease, Department of Pathophysiology and Transplantation, University of Milan, Milan, Italy; [66]D-SOLVE consortium, an EU Horizon Europe funded project (No 101057917), Hannover, Germany
Email: maria.anolli@unimi.it

Background and aims: Chronic hepatitis Delta (CHD) confers high risk of cirrhosis and hepatocellular carcinoma (HCC). However, disease-specific risk stratification tools are yet to be defined to guide HCC surveillance strategies in CHD.
Method: CHD patients with cirrhosis from the retrospective multi-center real-world European SAVE-D study were included. PAGE-B and AMAP scores were calculated at BLV start as previously described. PAGE-B was defined as low (<10) *vs.* intermediate (10–17) *vs.* high (≥18) risk profile. AMAP was defined as low (<50) vs. medium (50–59) vs. high (≥60) risk profile. HCC incidence rates in the different PAGE-B and AMAP groups during Bulevirtide (BLV) monotherapy were assessed. Patients with previous HCC were excluded.
Results: 391 patients with cirrhosis treated with BLV monotherapy up to 240 weeks were included: age 49 (IQR 40–57) years, 60% men, median platelet (PLT) count 102 (69–148) × 10^9/L. At BLV start, 117 (30%) patients had low risk PAGE B score, 255 intermediate risk (65%), and 19 (5%) had high-risk PAGE B score. Median PLT count in the PAGE B high risk score was 75 (60–90), median age 64 (62–67). AMAP score could be calculated in 387 patients: 10 patients (3%) had low risk AMAP score (3%), 84 (22%) intermediate, and 293 (76%) high risk AMAP score. During 240 weeks of BLV monotherapy, 17 de-novo HCC occurred. When analyzing incidence of de novo HCC according to HCC risk scores, 2 (12%) HCC developed in the PAGE-B low-risk group, 11 (65%) in the intermediate-risk group, and 4 (24%) in the high-risk group. The corresponding 240-week cumulative incidence in the 3 groups was 2.2%, 5.7%, and 30.9%, respectively. Concerning AMAP score, no HCC developed in the low-risk group, 1 (6%) in the intermediate risk score, and the remaining 16 (94%) in the high-risk score. No HCC occurred in the 4 patients for whom AMAP could not be calculated due to missing data. The corresponding 240-week cumulative incidence of HCC in the 3 AMAP groups was: 0%, 1.3% and 7.7%, respectively. Median time to HCC was 46 (39–100) weeks. At baseline lower albumin levels (HR 0.22, 95% CI 0.09–0.56, p = 0.001), higher bilirubin (HR 2.02; 95% CI 1.12–3.65, p < 0.001), and higher LSM (HR 1.05; 95% CI 1.02–1.08, p = 0.003) independently predicted HCC development.
Conclusion: PAGE-B and AMAP scores seem clinically useful in CHD patients HCC risk stratification during long-term BLV monotherapy.

FRI-586

The effectiveness and safety of bulevirtide monotherapy are similar in chronic hepatitis delta patients with and without cirrosis: results from the prospective multicenter d-shield study

Maria Paola Anolli[1,2,3], Elisabetta Degasperi[1,2], Giampiero D'Offizi[4], Alessia Rianda[4], Alessandro Loglio[5], Mauro Viganò[5], Alessia Ciancio[6], Yulia Troshina[6], Maurizia Brunetto[7], Barbara Coco[7], Serena Zaltron[8], Ottavia Nozza[8], Michele Milella[9], Elena Rosselli Del Turco[10], Laura Turco[11], Andrea Di Lorenzo[12], Mariarosa Tamè[13], Pierluigi Toniutto[14], Antonio Gasbarrini[15], Letizia Marinaro[16], Francesco Paolo Russo[17], Andrea Gori[18], Ivana Rita Maida[19], Alessandro Federico[20], Teresa Santantonio[21], Raffaele Bruno[22], Edoardo Giovanni Giannini[23], Irene Cacciola[24], Filomena Morisco[25], Alessandra Mangia[26], Stella De Nicola2[7], Antonietta Romano[28], Monia Maracci[29], Biagio Pinchera[30], Saveria Lory Croce'[31], Francesca Pileri[32], Rosa Zampino[33], Marcello Persico[34], Pietro Pozzoni[35], Alessia Zoncada[36], Adriano Pellicelli[37], Nicola Coppola[38], Matteo Tonnini[39], Eleonora Grassi[40], Alessandro Soria[41], Paolo Caraceni[42], Martina Dalla Bella[43], Ilaria Arena[44], Vincenzo Esposito[45], Paola Vitiello[46], Massimo Puoti[47], Pietro Lampertico[1,2,3]. [1]Division of Gastroenterology and Hepatology, Foundation IRCCS Ca' Granda Ospedale Maggiore Policlinico, Milan, Italy; [2]D-SOLVE consortium, an EU Horizon Europe funded project (No 101057917), Hannover, Germany; [3]CRC "A. M. and A. Migliavacca" Center for Liver Disease, Department of Pathophysiology and Transplantation, University of Milan, Milan, Italy; [4]Division of Infectious Diseases - Hepatology, Department of Transplantation and General Surgery, Istituto Nazionale per le Malattie Infettive "L. Spallanzani" IRCCS, Rome, Italy; [5]Gastroenterology, Hepatology and Transplantation Division, ASST Papa Giovanni XXIII, Bergamo, Italy; [6]Department of Medical Sciences, University of Turin, Gastroenterology Division of Città della Salute e della Scienza of Turin, University Hospital, Turin, Italy; [7]Department of Clinical and Experimental Medicine, University of Pisa and Hepatology Unit, University Hospital of Pisa, Pisa, Italy; [8]Infectious Disease Department, Spedali Civili Brescia, Brescia, Italy; [9]Infectious Diseases Unit, Department of Biomedical Sciences and Human Oncology, University of Bari, Bari, Italy; [10]Department of Medical and Surgical Sciences, Unit of Infectious Diseases, "Alma Mater Studiorum" University of Bologna, S. Orsola-Malpighi Hospital, Bologna, Italy; [11]Internal Medicine Unit for the Treatment of Severe Organ Failure, IRCCS Azienda Ospedaliero- Universitaria di Bologna, Bologna, Italy; [12]Tor Vergata University, Rome, Italy; [13]Gastroenterology Unit, IRCCS Azienda Ospedaliero-Universitaria di Bologna, Bologna, Italy; [14]Hepatology and Liver Transplantation Unit, Academic Hospital, University of Udine, Udine, Italy; [15]Fondazione Policlinico Universitario Gemelli IRCCS, Università Cattolica del Sacro Cuore, Rome, Italy; [16]SCDU Infectious Diseases, Amedeo di Savoia Hospital, ASL Città di Torino, Turin, Italy; [17]Department of Surgery, Oncology and Gastroenterology, University of

Padua, Padua, Italy; [18]Infectious Disease Unit II, Ospedale Luigi Sacco, ASST Fatebenefratelli Sacco, Milan, Italy; [19]Infectious and Tropical Diseases Unit, Department of Medical, Surgical and Experimental Sciences, University of Sassari, Sassari, Italy; [20]Division of Hepatogastroenterology, Department of Precision Medicine, Università della Campania "Luigi Vanvitelli", Naples, Italy; [21]Department of Medical and Surgical Sciences, Infectious Diseases Unit, University of Foggia, Foggia, Italy; [22]Department of Clinical, Surgical, Diagnostic and Pediatric Sciences, University of Pavia, Pavia, Italy; [23]Gastroenterology Unit, Department of Internal Medicine, University of Genoa, Genoa, Italy; [24]Department of Clinical and Experimental Medicine, University of Messina, Messina, Italy; [25]Department of Clinical Medicine and Surgery, Diseases of the Liver and Biliary System Unit, University of Naples "Federico II", Naples, Italy; [26]Liver Unit, Fondazione IRCCS "Casa Sollievo della Sofferenza", San Giovanni Rotondo, Italy; [27]Division of Internal Medicine and Hepatology, Department of Gastroenterology, IRCCS Humanitas Research Hospital, Rozzano, Italy; [28]Unit of Internal Medicine and Hepatology (UIMH), Department of Medicine, University of Padua, Padua, Italy; [29]Institute of Infectious Diseases and Public Health, Università Politecnica delle Marche, Ancona, Italy; [30]Department of Clinical Medicine and Surgery, University of Naples Federico II, Naples, Italy; [31]Department of Medicine, Surgery and Health Sciences, University of Trieste, Trieste, Italy; [32]Division of Internal Medicine and Center for Hemochromatosis, University of Modena and Reggio Emilia, Modena, Italy; [33]Department of Advanced Medical and Surgical Sciences, University of Campania Luigi Vanvitelli, Naples, Italy; [34]Department of Medicine, Surgery and Dentistry, University of Salerno, Baronissi, Italy; [35]General Medicine Unit, Presidio Ospedaliero, Azienda Socio Sanitaria Territoriale di Lecco, Lecco, Italy; [36]Unit of Infectious Diseases, ASST Cremona, Cremona, Italy; [37]Liver Unit, San Camillo Hospital, Department of Transplantation and General Surgery, Rome, Italy; [38]Department of Mental Health and Public Medicine - Infectious Diseases Unit, University of Campania Luigi Vanvitelli, Naples, Italy; [39]Division of Internal Medicine, Hepatobiliary and Immunoallergic Diseases, IRCCS Azienda Ospedaliero-Universitaria di Bologna, Bologna, Italy; [40]Gastroenterology and Digestive Endoscopy Unit, Ospedale di Circolo and Fondazione Macchi University Hospital, ASST Sette Laghi, Varese, Italy; [41]Clinic of Infectious Diseases, Fondazione IRCCS San Gerardo dei Tintori, Monza, Italy; [42]Department of Medical and Surgical Sciences, Alma Mater Studiorum University of Bologna, Bologna, Italy; [43]Liver Injury and Transplant Unit, Polytechnic University of Marche, Ancona, Italy; [44]Gastroenterology Unit, Rho Hospital, ASST Rhodense, Rho, Italy; [45]UOC Malattie Infettive e Medicina di Genere P.O. Cotugno - AO dei Colli, Naples, Italy; [46]Unit of Infectious Diseases, ASST della Valle Olona, Busto Arsizio, Italy; [47]School of Medicine and Surgery University of Milano Bicocca, Milan, Italy
Email: maria.anolli@unimi.it

Background and aims: Bulevirtide (BLV) was licensed in Italy in May 2023 for patients with chronic hepatitis delta (CHD), but no real-life studies have addressed differences in responses rates among patients with and without cirrhosis.
Method: CHD patients starting BLV 2 mg/day monotherapy were included in a multicenter prospective real-life Italian study (D-SHIELD). Patients' features and treatment responses were assessed at baseline and trimonthly afterwards. Virological response (VR) (≥2 LogIU/mL HDV-RNA decline *vs.* baseline or HDV RNA undetectable), biochemical and combined responses (BR and CR), incidence of virological breakthroughs (VBK; >1 Log HDV RNA increase *vs.* previous timepoint), and safety were assessed comparing patients with and without cirrhosis.
Results: 486 patients treated with BLV monotherapy up to 72 weeks from 46 centers were enrolled, 354 (73%) with cirrhosis and 132 without cirrhosis. At baseline, patients without cirrhosis were younger (56 *vs.* 50, p < 0.001), were less commonly treated with NA (91% *vs.* 98%, p < 0.001), had lower LSM values (8.0 *vs.* 15.8 kPa, p < 0.001) and higher HDV RNA levels (5.5 *vs.* 5.2 Log U/L p = 0.03). During BLV monotherapy, median HDV RNA and ALT levels declined to a similar extent in patients with and without cirrhosis (baseline 5.2 *vs.* 5.5 LogIU/mL and 74 *vs.* 75 U/L; week 72: 2.9 *vs.* 3.4 LogIU/mL and 31 *vs.* 33 U/L, respectively, p = ns at all timepoints). No significant differences were observed in VR, BR and CR rates at all timepoints in patients with and without cirrhosis, 70% *vs.* 63% patients achieving a VR (p = 0.24), 74% *vs.* 71% a BR (p = 0.36), and 60% *vs.* 47% a CR (p = 0.12). Only HDV RNA undetectability rates at week 72 differed (32% *vs.* 13% p = 0.01, p = ns for other timepoints). 3% (10/78) of patients with VR at week 24 experienced a VBK at week 48, all with cirrhosis; 15% (17/111) of those with a VR at week 48 experienced a VBK at week 72, 65% with cirrhosis (p = 0.08). No significant differences were observed in the incidence of adverse events among patients with and without cirrhosis, (15% *vs.* 15%, p = 1.00), with mild and transient pruritus and injection site reaction being the most common. Patients with cirrhosis showed higher baseline and on-therapy bile acids levels (p < 0.001 at all time-points).
Conclusion: The effectiveness and safety profile of BLV monotherapy did not differ in patients with or without compensated cirrhosis in this large prospective multicenter Italian study.

FRI-587

Bulevirtide monotherapy is safe and well tolerated in chronic hepatitis delta: an integrated safety analysis of bulevirtide clincial trials at week 96

Tarik Asselah[1], Soo Aleman[2], Maurizia Brunetto[3,4], Vladimir Chulanov[5], Adrian Streinu-Cercel[6,7], George Sebastian Gherlan[7,8], Viacheslav Morozov[9], Olga Sagalova[10], Tatiana Stepanova[11], Sreenivasu Yalamanchili[12], Steve Tseng[12], Florence Christian-Cox[13], Danielle Shing[13], Lei Ye[12], Amos Lichtman[12], Dmitry Manuilov[12], Hans Heinrich Wedemeyer[14], Pietro Lampertico[15,16]. *[1]Hôpital Beaujon APHP, Université de Paris-Cité, INSERM UMR1149, Clichy, France; [2]Department of Infectious Diseases, Karolinska University Hospital/Karolinska Institute, Stockholm, Sweden; [3]Hepatology Unit, Reference Center of the Tuscany Region for Chronic Liver Disease and Cancer, University Hospital of Pisa, Pisa, Italy; [4]Department of Clinical and Experimental Medicine, University of Pisa, Pisa, Italy; [5]Sechenov University, Moscow, Russian Federation; [6]National Institute of Infectious Diseases Prof. Dr. Matei Bals, Bucharest, Romania; [7]University of Medicine and Pharmacy "Carol Davila" Bucharest, Bucharest, Romania; [8]Dr. Victor Babes Foundation, Bucharest, Romania; [9]LLC Medical Company Hepatolog, Samara, Russian Federation; [10]South Ural State Medical University, Chelyabinsk, Russian Federation; [11]LLC Clinic of Modern Medicine, Moscow, Russian Federation; [12]Gilead Sciences, Inc., Foster City, United States; [13]Gilead Sciences International Ltd, Cambridge, United Kingdom; [14]Clinic for Gastroenterology, Hepatology, Infectious Diseases, and Endocrinology, Hannover Medical School, Hannover, Germany; [15]Division of Gastroenterology and Hepatology, Foundation IRCCS Ca' Granda Ospedale Maggiore Policlinico, Milan, Italy; [16]CRC "A. M. and A. Migliavacca" Center for Liver Disease, Department of Pathophysiology and Transplantation, University of Milan, Milan, Italy*
Email: tarik.asselah@bjn.aphp.fr

Background and aims: Bulevirtide (BLV) is approved in the European Economic Area and other regions for treating patients with chronic hepatitis delta (CHD). BLV monotherapy demonstrated favourable safety in an integrated safety analysis at week (W) 48 of two Phase 2 studies (MYR203 and MYR204) and one Phase 3 study (MYR301). Here, we present an integrated safety analysis of longer-term, W96 data from the MYR301 and MYR204 studies, focusing on BLV 2 mg and 10 mg monotherapy.
Method: In a pooled analysis at W96, treatment-emergent adverse events (AEs), serious AEs (SAEs), and laboratory abnormalities were assessed in participants (pts) treated with BLV 2 mg or 10 mg given subcutaneously once daily.
Results: A total of 199 pts were included in the W96 analysis: 49 received BLV 2 mg; 150 received BLV 10 mg. Baseline characteristics of BLV-treated pts: mean (SD) age 42 (8.4) years, 62% male, 84% White,

44% with compensated cirrhosis, 98% with hepatitis D virus (HDV) genotype 1; 53% were interferon-experienced; mean (SD) HDV RNA was 5.13 (1.345) $\log_{10}$ IU/mL, and mean (SD) alanine aminotransferase was 108 (79.7) U/L. Most AEs occurred by W48, with no new AEs reported between W48 and W96. At W96, AE rates remained similar between BLV 2 mg (96%) and BLV 10 mg (91%). The incidence of Grade ≥3 AEs at W96 was similar with BLV 2 mg (18%) and BLV 10 mg (17%), with the most frequent events being associated with background disease (neutropenia, leucopenia, thrombocytopenia). No SAEs were considered related to BLV. One pt (0.7%) in the BLV 10 mg group experienced an AE of myalgia considered related to BLV, which led to premature discontinuation by W96. The AE profile was generally consistent between groups. Injection-site reactions occurred at similar frequencies in the BLV 2 mg and 10 mg groups (20% vs 19%). Bile acid (BA) elevations were more pronounced with the BLV 10 mg dose, as expected based on the mechanism of action of BLV. However, BA levels were not associated with the presence or absence of AEs including pruritus or vitamin D deficiency. Safety outcomes were similar in pts with and without cirrhosis.

Conclusion: BLV monotherapy at both 2 mg and 10 mg was safe and well tolerated over 96 weeks, including in pts with compensated cirrhosis. Most AEs were mild to moderate in severity, and the incidence of Grade ≥3 AEs and SAEs was comparable across BLV dosage levels. No association was observed between BA levels and AEs of interest. These findings support the safety of longer-term BLV treatment for CHD.

FRI-588-YI

Real-world effectiveness of antiviral therapy for chronic HBV infection in Africa: HEPSANET analysis

Kalisha Bheemraj[1], Alice N. Guingané[2], Roger Sombie[3], Mohamed El-Kassas[4], Mary Afihene[5], Edith Okeke[6], Hans Prozesky[7], Wendy Spearman[8], Ibrahima Diallo[9], Gilles Wandeler[10], Babatunde Duduyemi[11], John Rwegasha[12], Kalongo Hamusonde[10], Alexander Stockdale[13], Michael Vinikoor[14], Asgeir Johannessen[15].
[1]HEPSANET, University of Cape Town, University of California Los Angeles, Cape Town, South Africa; [2]Center Hospitalier Universitaire de Bogodogo, Bogodogo, Burkina Faso; [3]Université Joseph, Ouagadougou, Burkina Faso; [4]Helwan University, Cairo, Egypt; [5]Kwame Nkrumah' University of Science and Technology, Kumasi, Ghana; [6]University of Jos, Plateau State, Nigeria; [7]Stellenbosch University, Cape Town, South Africa; [8]University of Cape Town, Cape Town, South Africa; [9]Hopital Principal de Dakar, Dakar, Senegal; [10]Bern University, Bern, Switzerland; [11]University of Sierra Leone Teaching Hospital, Freetown, Sierra Leone; [12]African Union Commission, Dar es Salaam, Tanzania; [13]University of Liverpool, Liverpool, United Kingdom; [14]The University Of Zambia, Lusaka, Zambia; [15]University of Oslo, Oslo, Norway
Email: kalishabheemraj@gmail.com

Background and aims: To prevent liver-related deaths and new chronic infections, a major strategy for hepatitis B virus (HBV) elimination is the provision of antiviral therapy to suppress HBV viral load (VL). However, data on real-world virological effectiveness of antiviral therapy is lacking in Africa, the region lagging most in hepatitis elimination and with major social and structural barriers to achieving and sustaining viral suppression.

Method: We performed a longitudinal analysis of HIV negative individuals > 18 years, living with chronic HBV who initiated antiviral therapy and had at least one HBV DNA measurement during follow-up. Individual viral trajectories were observed over time on treatment and population-average was modelled using linear mixed-effects with natural splines for time on treatment, adjusting for age, sex and location. Viral suppression (VS) was defined as HBV DNA <50 IU/mL. VL monitoring were described as the proportion with available HBV DNA results, and among those with results, we described proportions with VS. Proportions of participants achieving first VS were evaluated across follow-up intervals defined by the maximum time point at which VL measurements were captured.

Results: Of 13,359 cohort individuals, 2077 were included in analysis. Median age was 34 years (IQR 28–43, 67% male). Median follow-up time on treatment was 2.61 years (IQR 1.16–4.75). Pre-treatment median HBV DNA (log10 IU/mL) was 3.88 (2.83–5.76). Rapid decline in mean HBV DNA was observed during the first year of therapy, followed by sustained suppression over time. Overall, 1256 (60%) achieved VS within 1–2 years of treatment. Proportion of participants with HBV DNA monitoring was 303 (15%) at 0–1 years, 354 (17%) at 1–2 years, 278 (13%) at 2–3 years and 1142 (55%) beyond 3 years. Among participants with available HBV DNA results, the proportion with complete suppression was 174/303 (57%) at 0–1 year, 270/354 (76%) at 1–2 years, 231/278 (83%) at 2–3 years and 1004/1142 (88%) beyond 3 years of monitoring.

Conclusion: VL monitoring of antiviral therapy for chronic HBV was suboptimal in Africa. Among those with monitoring, levels of viral suppression were comparable to clinical trials and other regions, supporting the feasibility of HBV elimination through treatment.

FRI-589

Bulevirtide effectiveness in hepatitis delta infection across geographic origins and genotypes: real-world data from Portugal

Mariana Cardoso[1], Joana Branco[2], Rúben Carvalho[3], Catarina Gouveia[4], Inês Costa Santos[5], Cristiana Margarida Fernandes Batouxas[6], Ana Aboim Horta[7], Francisco Javier Velasco Rubio[8], Mariana Machado[9], Pedro Filipe Mesquita[10], Dalia Fernandes[11], Alexandra Martins[2], Cristina Valente[3], Manuela Canhoto[4], Filipe Calinas[1]. *[1]Unidade Local de Saúde de São José, Lisbon, Portugal; [2]Unidade Local de Saúde de Amadora/Sintra, Amadora, Portugal; [3]Unidade Local de Saúde de Coimbra, Coimbra, Portugal; [4]Unidade Local de Saúde de Loures/Odivelas, Loures, Portugal; [5]Unidade Local de Saúde de Almada/Seixal, Almada, Portugal; [6]Unidade Local de Saúde do Nordeste, Bragança, Portugal; [7]Unidade Local de Saúde de Santo António, Porto, Portugal; [8]Unidade Local de Saúde do Algarve, Faro, Portugal; [9]Unidade Local de Saúde do Estuário do Tejo, Vila Franca de Xira, Portugal; [10]Unidade Local de Saúde de Gaia e Espinho, Vila Nova de Gaia, Portugal; [11]Unidade Local de Saúde de Braga, Braga, Portugal*
Email: marianafcardoso@gmail.com

Background and aims: The epidemiology of hepatitis delta virus (HDV) infection in Portugal is strongly influenced by immigration, notably from Western Africa, where HDV genotype 5 (HDV-5) predominates. Bulevirtide (BLV) has been available in Portugal for patients experienced or not eligible for interferon since 2022, initially for those with advanced fibrosis/cirrhosis and, since May 2025, for all fibrosis stages. Data on BLV efficacy in HDV genotypes other than HDV-1 remain limited. We aimed to characterize HDV patients treated with BLV, assess treatment effectiveness, and compare outcomes by geographic origin (Europe/Asia vs Africa).

Method: Multicentric retrospective study including patients who initiated BLV 2 mg between 2022 and 2025. Virological response (VR) was defined as undetectable HDV RNA or a ≥ 2 $\log_{10}$ decline, biochemical response (BR) as ALT < 40 IU/L, and complete response (CR) as VR plus BR. Group comparisons were performed using Fisher's exact test.

Results: Thirty-three patients (43 ± 10 years; 61% male) from 11 centres were included, with a median on-treatment follow-up of 53 weeks. Most patients were immigrants, from Africa (46%, mainly Guinea-Bissau), Eastern Europe (12%), and Central Asia (6%), while 36% originated from Portugal. Genotype was available in 14 patients: HDV-1 (n = 6; Portugal/Eastern Europe), HDV-5 (n = 7; Western Africa), and HDV-8 (n = 1; Southern Africa). HIV co-infection was present in 20%. Median liver stiffness was 16 kPa, and 73% were cirrhotic (Child-Pugh A). BLV was discontinued before w24 in 5 patients due to adverse events (n = 2), loss to follow-up (n = 1), or non-compliance (n = 2). In the subgroup of patients who reached w24 (n = 21), BR at w24, w48 and w72 were 67% (14/21), 63% (10/16) and 92% (11/12), VR were 38% (8/21), 64% (9/14) and 42% (5/12), and CR

were 24% (5/21), 33% (5/15) and 42% (5/12). Response rates at w24 in patients from Europe/Asia (n = 15; 6 genotyped as HDV-1) and Africa (n = 6; 3 genotyped as HDV-5) were compared: BR was 67% in both groups (p = 1.000), VR 47% vs 17% (p = 0.336), and CR 27% vs 17% (p = 1.000).
Conclusion: Response rates to BLV were globally comparable to published data. Despite not reaching statistical significance, VR was numerically inferior in patients from Africa compared with those from Europe/Asia, raising the hypothesis of genotype-related differences in BLV response. However, these findings are exploratory and limited by small sample size and incomplete genotyping, warranting confirmation in larger cohorts.

FRI-590
Modeling HBsAg during liver transplantation reveals insights into the role of HBIG and mechanisms of HBsAg clearance
Leeor Hershkovich[1], Sara Battistella[2], Adquate Mhlanga[1], Louis Shekhtman[1], Anna Pocurull Aparicio[2], Thais Leonel[2], Sergio Rodriguez-Tajes[2], Yilliam Fundora[3], Sabela Lens[2], Sofía Pérez-del-Pulgar[2], Scott Cotler[1], Harel Dahari[1], Xavier Forns[2].
[1]Program for Experimental and Theoretical Modeling, Division of Hepatology, Department of Medicine, Loyola University Chicago, Maywood, IL, United States; [2]Liver Unit, Hospital Clínic, IDIBAPS, University of Barcelona, Centro de Investigación Biomédica en Red de Enfermedades Hepáticas y Digestivas (CIBEREHD), Barcelona, Spain; [3]Surgery Department, Hospital Clínic, IDIBAPS, University of Barcelona, Barcelona, Spain
Email: harel.dahari@gmail.com

Background and aims: Consensus is lacking on the optimal dose and duration of hepatitis B Immunoglobulin (HBIG) and even whether it is necessary in patients receiving nucleos(t)ide analogues (NUCs) during liver transplantation (LT). LT provides a unique clinical setting to observe HBsAg dynamics both in the anhepatic phase (AHP) and under controlled perturbations including HBIG administration, post-reperfusion phase (PRP), and immunosuppression. We aim to provide insights into the impact of HBIG on HBsAg serodynamics and its clearance mechanism via mathematical modeling of frequent HBsAg sampling during AHP and PRP.
Method: Seven LT recipients with undetectable HBV DNA were prospectively enrolled. All participants were treated with NUCs before and after LT, including 3 patients who additionally received an intravenous HBIG dose of 5000 IU during the AHP and on the first day post-LT, followed by daily 1000 IU doses until day 7 post-LT. We developed mathematical models to explain HBsAg clearance and to explore the impact of HBIG on HBsAg clearance during AHP and PRP.
Results: HBsAg remained at pre-AHP levels during AHP in patients who received NUCs alone. HBIG group had a median decline of ~1.2 log in the AHP, which was explained by modeling as a 23–60-fold enhancement of HBsAg clearance from circulation due to extra-hepatic clearance mechanisms. During PRP, HBsAg declined in a biphasic manner in all patients with a rapid 1st phase that lasted about 8 hours followed by a slower 2nd phase decline until HBsAg became undetectable. Participants who received HBIG had an estimated 4.3-fold higher rate of HBsAg decline during the 1st phase compared to no-HBIG patients. The HBIG group reached HBsAg undetectable earlier compared to the no-HBIG group (median 5 vs 52 days). Modeling suggested that HBsAg clearance during PRP occurs through hepatic and extrahepatic mechanisms. A majority (3/4) of patients in the no-HBIG group had a longer HBsAg $t_{1/2}$ (51–94 hours) compared to the HBsAg $t_{1/2}$ previously described in immunocompetent patients ($t_{1/2}$ range: 21–43 hours; PMID: 32398799).
Conclusion: HBIG enhances both hepatic and extra-hepatic mechanisms of HBsAg clearance in LT recipients. The relatively long HBsAg $t_{1/2}$ observed in LT recipients could reflect attenuation of immunologic clearance due to immunosuppressive medications. For patients with ~3 log HBsAg pre-LT, a single dose of 5000 HBIG pre-LT may be sufficient for yielding the HBsAg-suppressive effects of HBIG, which is an observation that requires confirmation.

FRI-591
Peginterferon alfa-2b–based therapy achieves higher HBsAg Loss in high-risk chronic hepatitis B patients: a prospective multicenter cohort study
Yaping Li[1], Haifang Cao[2], Qianhui Wang[3], Yongmei Lin[4], Fenxiang Li[5], Xuemei Li[6], Jingning Yang[7], Shumei Lin[8], Liping Ma[9], Li Liu[10], Xiaohong Gao[11], Hong Jiang[12], Wenhua Zhang[13], Xianqiong Gong[14], Shujun Gao[15], Shihong Wu[16], YueYong Zhu[17], Yuefeng Chai[18], Wei Zhang[19], Liaoyun Zhang[20], Xiaobo Lu[21], Xiaoli Jia[1], Shuangsuo Dang[1].
[1]The Second Affiliated Hospital of Xi'an Jiaotong University, Xi'an, China; [2]The 4th People's Hospital of Qinghai Province, Xining, China; [3]Taiyuan third people's hospital, Taiyuan, China; [4]The 3201 Hospital, Hanzhong, China; [5]Linfen third people's hospital, Li Fenxiang, China; [6]Ankang central hospital, Ankang, China; [7]Sinopharm datong coal general hospital, Datong, China; [8]The first affiliated hospital of xi'an jiaotong university, Xi'an, China; [9]Huozhou coal and electricity general hospital, Linfen, China; [10]Kunming third people's hospital, Yunnan, China; [11]Yanan university affiliated hospital, Yanan, China; [12]Tangdu hospital, Xian, China; [13]Wuwei cancer hospital, gansu province, Wuwei, China; [14]Xiamen hospital of traditional chinese medicine, Xiamen, China; [15]Houma people's hospital, Linfen, China; [16]Yuncheng central hospital, Yuncheng, China; [17]The first affiliated hospital of fujian medical university, Fuzhou, China; [18]Linfen central hospital, Linfen, China; [19]Xi'an daxing hospital, Xi'an, China; [20]First hospital of shanXi medical university, Taiyuan, China; [21]The first affiliated hospital of xinjiang medical university, Urumqi, China
Email: liyaping8605@xjtu.edu.cn

Background and aims: Chronic hepatitis B (CHB) is the leading cause of hepatocellular carcinoma (HCC) in China. Functional cure characterized by HBsAg loss may reduce long-term HCC risk, particularly in high-risk patients. However, evidence comparing peginterferon-based strategies with nucleos(t)ide analogue (NA) monotherapy in this population is limited. This study assessed short-term virological and serological responses to peginterferon alfa-2b (PegIFNα-2b) versus NA monotherapy in high-risk CHB patients, with ongoing evaluation of HCC outcomes.
Method: This ongoing prospective multicenter cohort study (ChiCTR2200066281) enrolled high-risk CHB patients from 21 hospitals in China. High-risk status was defined by a family history of cirrhosis or HCC, abnormal HCC serum markers, imaging-confirmed hepatic nodules, or HBV-related compensated cirrhosis. Patients received PegIFNα-2b (Pegbing®, Xiamen Amoytop Biotech Co., Ltd.)–based therapy (monotherapy or combined with NAs) or NAs monotherapy for ≥48 weeks, with planned HCC surveillance up to 4 years. The present analysis included patients completing 48 weeks, and primary endpoints were HBsAg decline and loss.
Results: A total of 538 patients were included, with 447 receiving PegIFNα-2b–based therapy and 91 receiving NAs monotherapy. Median age was 43.0 (35.0–51.0) years, 67.3% were male, and 34.6% were HBeAg-positive. Median baseline HBsAg and HBV DNA levels were 2.73 (2.06–3.39) and 1.54 (1.04–2.84) $\log_{10}$ IU/mL, respectively. At week 24, PegIFNα-2b treatment resulted in a greater median HBsAg decline than NA monotherapy (0.37 [0.00–1.40] vs. 0.00 [−0.02–0.05] $\log_{10}$ IU/mL; $p < 0.001$), with HBsAg decline ≥1.0 $\log_{10}$ and HBsAg loss in 30.9% and 13.4% of patients, respectively, while no HBsAg loss occurred in the NAs group. At week 48, PegIFNα-2b therapy remained superior, with greater HBsAg decline (0.57 [0.14–2.24] vs. 0.06 [-0.03–0.17] $\log_{10}$ IU/mL), higher rates of HBsAg decline ≥1.0 $\log_{10}$ (38.5% vs. 1.1%) and HBsAg loss (18.1% vs. 0%) (all $p < 0.001$). Complete virological response rates were comparable (58.5% vs. 47.8%, p = 0.170). Superior serological responses were observed with PegIFNα-2b across all high-risk subgroups (all $p < 0.01$). One case of HCC occurred within 48 weeks in a PegIFNα-2b treated patient with multiple baseline risk factors.

Conclusion: PegIFNα-2b therapy achieved higher HBsAg loss rates than NA monotherapy in high-risk chronic hepatitis B patients. Long-term follow-up is ongoing to evaluate its impact on hepatocellular carcinoma incidence.

FRI-592

Progressive decline of HBcrAg levels in patients with chronic hepatitis Delta long-term treated with Bulevirtide monotherapy

Elisabetta Degasperi[1], Floriana Facchetti[1], Dana Sambarino[1], Caroline Scholtes[2,3,4], Barbara Testoni[3,5,6], Sara Uceda Renteria[7], Maria Paola Anolli[1], Caroline Charre[8,9], Marie-Laure Plissonnier[3,6,10], Riccardo Perbellini[1], Annapaola Callegaro[7], Massimo Levrero[3,5,6,11,12], Fabien Zoulim[3,5,6,12], Pietro Lampertico[1,13,14]. *[1]Division of Gastroenterology and Hepatology, Foundation IRCCS Ca' Granda Ospedale Maggiore Policlinico, Milan, Italy; [2]Virology Department, Hospices Civils de Lyon (HCL) and Université Claude Bernard Lyon 1 (UCBL1), Lyon, France; [3]The Lyon Hepatology Institute (IHU EVEREST), Lyon, France; [4]INSERM, U1350, UMR PathLiv, Lyon, France; [5]INSERM U1052, CNRS UMR-5286, Cancer Research Center of Lyon (CRCL), Lyon, France; [6]University of Lyon, Université Claude-Bernard (UCBL), Lyon, France; [7]Microbiology and Virology Unit, Foundation IRCCS Ca' Granda Ospedale Maggiore Policlinico, Milan, Italy; [8]INSERM U1016, CNRS, UMR8104, Paris, France; [9]Virology Department, Hôpital Cochin, APHP, Paris, France; [10]UMR PaThLiv, Inserm U1350, UCBL1, Lyon, France; [11]Department of Internal Medicine, SCIAC and the IIT Center for Life Nanoscience, Sapienza University, Rome, Italy; [12]Hepatology Department, Hospices Civils de Lyon (HCL), Lyon, France; [13]CRC "A. M. and A. Migliavacca" Center for Liver Disease, Department of Pathophysiology and Transplantation, University of Milan, Milan, Italy; [14]D-SOLVE consortium, an EU Horizon Europe funded project (No 101057917), Milan, Italy*
Email: elisabetta.degasperi@policlinico.mi.it

Background and aims: Serum HBcrAg has been proposed as a useful Hepatitis B virus (HBV) biomarker, however its role in patients with chronic hepatitis Delta (CHD) under Bulevirtide (BLV) treatment is currently unknown.
Method: CHD patients treated with BLV 2 mg/day monotherapy in a single center from the European SAVE-D study were enrolled. Serum HBcrAg levels were quantified by LUMIPULSE® G HBcrAg assay (Fujirebio Europe, LLOQ 3 Log_{10} U/mL). Virological (HDV RNA undetectable or ≥2 Log_{10} decline *vs.* baseline), biochemical (ALT < 40 U/L) and combined responses were assessed.
Results: 405 serum samples were collected from 79 patients treated with BLV up to Week (W) 144. At BLV start, median age was 55 (IQR 37–43) years, 53% males, 100% with cirrhosis, 100% on NUC, median ALT 97 (52–151) U/L, HBsAg 3.7 (3.4–3.9) Log_{10}IU/mL, 92% HBeAg-negative, 90% HBV DNA undetectable, HDV RNA 5.5 (4.2–6.2) Log_{10}IU/mL. HBcrAg tested positive in 63 (80%) patients [4.0 (3.5–4.8) Log_{10}U/mL]. HBcrAg positively correlated with HBsAg ($r = 0.37$, $p = 0.002$) and HDV RNA levels ($r = 0.30$, $p = 0.01$), but not with ALT or HBV DNA. At BLV W144, rates of virological, biochemical, combined response and HDV RNA undetectability were 70%, 64%, 52% and 33%, respectively. HBcrAg levels significantly declined during therapy: –0.31 Log_{10} (W48, $p = 0.02$), –0.63 Log_{10} (W96, $p = 0.003$), and –0.62 Log_{10} (W144, $p = 0.01$). HBcrAg levels did not correlate with HDV RNA levels at single on-treatment timepoints but maintained a positive correlation with HBsAg levels overtime (W48: $r = 0.35$, $p = 0.007$; W96: $r = 0.45$, $p = 0.006$; W144: $r = 0.50$, $p = 0.01$). Neither baseline nor on-treatment HBcrAg levels predicted virological response or HDV RNA undetectability rates during therapy. Overall, HBcrAg levels became negative in 10 patients (W48 in 5, W96 in 3; W144 in 2): at HBcrAg negativity, 7 had achieved a virological response (HDV RNA undetectable in 3). Conversely, HBcrAg levels became positive in 5 patients who tested negative at baseline (<3.5 Log_{10}U/mL in all cases; 4 at W48, 1 at W144): at HBcrAg positivity, 3 had achieved a virological response (HDV RNA undetectable in 2). No significant changes of HBsAg levels were observed during BLV.
Conclusion: In CHD patients with cirrhosis treated with BLV monotherapy up to W144, baseline low HBcrAg levels were detectable in most patients and correlated with HBsAg and HDV RNA. During BLV, HBcrAg levels declined and correlated with HBsAg levels, but not with HDV virological responses.

FRI-593

Therapeutic drug monitoring of Bulevirtide plasma levels in chronic hepatitis Delta patients

Elisabetta Degasperi[1], Amedeo De Nicolò[2], Dana Sambarino[1], Alice Palermiti[2], Alessandra Manca[2], Maria Paola Anolli[1], Marta Borghi[1], Riccardo Perbellini[1], Roberta Soffredini[1], Sara Monico[1], Floriana Facchetti[1], Antonio D'Avolio[2], Pietro Lampertico[1,3,4]. *[1]Division of Gastroenterology and Hepatology, Foundation IRCCS Ca' Granda Ospedale Maggiore Policlinico, Milan, Italy; [2]Laboratory of Clinical Pharmacology and Pharmacogenetics, Department of Medical Sciences, University of Turin, Turin, Italy; [3]CRC "A. M. and A. Migliavacca" Center for Liver Disease, Department of Pathophysiology and Transplantation, University of Milan, Milan, Italy; [4]D-SOLVE consortium, an EU Horizon Europe funded project (No 101057917), Milan, Italy*
Email: elisabetta.degasperi@policlinico.mi.it

Background and aims: Bulevirtide (BLV) monotherapy achieves efficient responses in patients with chronic hepatitis Delta (CHD), however little is known about plasma drug concentrations. Aim of the study was to evaluate BLV levels in CHD patients treated in a real-world setting.
Method: Consecutive CHD patients treated with BLV in an Italian center underwent single timepoint plasma sampling for BLV quantification between November 2024 and April 2025. BLV plasma levels were assessed through a validated ultra-high performance liquid chromatography coupled with tandem-mass spectrometry method (UHPLC-MS/MS).
Results: 72 CHD patients were enrolled: at sampling, median age was 56 (IQR 43–61) years, 53% males, BMI 25 (23–27), 81% with cirrhosis (100% CPT-A; CPT A6 in 28%), ALT 32 (26–43) U/L, bile acids 20 (9–36) µmol/L, vitamin D 16 (11–20) ng/mL, HBsAg 3.7 (3.1–3.9) Log_{10}IU/mL, HDV RNA 2.3 (0.7–3.3) Log_{10}IU/mL. Patients had been under BLV treatment for a median of 84 (72–138) weeks; 78% had achieved virological response, 24% target not detected. At sampling, 70/72 (97%) of the patients had detectable BLV plasma levels, overall median values were 1.8 (0.6–7.8) ng/mL. BLV levels did not correlate with age ($p = 0.17$), sex ($p = 0.78$), BMI ($p = 0.22$), and presence of cirrhosis ($p = 0.44$). Among the 56 patients with cirrhosis, BLV levels were similar across CPT subclasses [A5 vs A6: 1.5 (0.6–7.2) ng/mL *vs.* 4.5 (1.1–9.5) ng/mL, $p = 0.27$]. When analyzing biochemical and virological features at sampling, BLV levels did not correlate with ALT ($p = 0.44$), bile acids ($p = 0.67$), vitamin D ($p = 0.20$), and HDV RNA ($p = 0.74$), while there was a trend towards an inverse correlation with HBsAg levels ($r = 0.23$; $p = 0.06$). BLV levels did not differ according to time interval between BLV injection and sampling (≤12 *vs.* >12 hours, $p = 0.13$), and duration of BLV treatment: concentrations were 1.5 (0.8–2.9) ng/mL in patients treated with BLV for ≤48 weeks *vs.* 2.9 (1.5–8.6) ng/mL for 49–96 weeks *vs.* 1.7 (0.6–9.3) ng/mL for 97–144 weeks *vs.* 0.6 (0.4–2.5) ng/mL for >144 weeks, respectively ($p = 0.13$). BLV levels were also independent of virological response ($p = 0.67$).
Conclusion: In a preliminary cross-sectional single-timepoint analysis of BLV concentrations performed in a single-center cohort of CHD patients, BLV plasma levels were quantifiable in 97% of patients 12–24 hours after the last administration but did not significantly correlate with patient features and/or virological outcomes.

FRI-594

Safety and efficacy of long-term tenofovir alafenamide treatment in patients aged 60 years and older with chronic hepatitis B: experience from two phase 3 clinical trials

Scott K. Fung[1], Maria Buti[2,3], Jinlin Hou[4], Kosh Agarwal[5], Qin Ning[6], Grace Lai-Hung Wong[7], Young-Suk Lim[8], Wan-Long Chuang[9], Frida Abramov[10], Hongyuan Wang[10], Irina Botros[10], Leland J. Yee[10], Cihan Yurdaydin[11], Hiroshi Yatsuhashi[12], Patrick Marcellin[13], Edward J. Gane[14], Henry L. Y. Chan[15]. *[1]Department of Medicine, University of Toronto, Toronto, ON, Canada; [2]Hospital Universitario Vall d'Hebron, Barcelona, Spain; [3]Centro de Investigación Biomédica en Red de Enfermedades Hepáticas y Digestivas (CIBEREHD) del Instituto Carlos III, Madrid, Spain; [4]Department of Infectious Diseases, State Key Laboratory of Organ Failure Research, Nanfang Hospital, Southern Medical University, Guangzhou, China; [5]Institute of Liver Studies, King's College Hospital NHS Foundation Trust, London, United Kingdom; [6]Tongji Hospital, Tongji Medical College, Wuhan, China; [7]Medical Data Analytics Centre, Department of Medicine and Therapeutics, The Chinese University of Hong Kong, Shatin, Hong Kong; [8]Asan Medical Centre, University of Ulsan College of Medicine, Seoul, Korea, Rep. of South; [9]Kaohsiung Medical University Hospital, Kaohsiung Medical University, Kaohsiung, Taiwan; [10]Gilead Sciences, Inc., Foster City, CA, United States; [11]Department of Gastroenterology and Hepatology, Koç University Medical School, Istanbul, Türkiye; [12]Clinical Research Center, National Hospital Organization Nagasaki Medical Center, Nagasaki, Japan; [13]Association for the Promotion of Hepatologic Care and University of Paris, Paris, France; [14]University of Auckland, Auckland, New Zealand; [15]Faculty of Medicine, The Chinese University of Hong Kong, Shatin, Hong Kong*
Email: scott.fung@uhn.ca

Background and aims: Tenofovir alafenamide (TAF) is a preferred first-line antiviral for chronic hepatitis B virus (HBV) infection, particularly for patients at risk for bone- or kidney-related adverse events (AEs) associated with tenofovir disoproxil fumarate (TDF), including those of older age. This analysis focused on outcomes in patients aged ≥ 60 years (Y) enrolled in two 8Y clinical trials of TAF.
Method: Patients were randomised to receive TAF 25 mg or TDF 300 mg once daily for 2Y or 3Y, then open-label TAF through Y8. Efficacy (HBV DNA < 29 IU/mL) and open-label safety (AEs, changes in hip and spine bone mineral density [BMD] and estimated glomerular filtration rate [Cockcroft-Gault method; $eGFR_{CG}$]) were assessed for older (≥60Y) vs younger (< 60Y) patients.
Results: Of 1632 patients, 91 (6%) were aged ≥ 60Y. Patients ≥ 60Y had higher rates of comorbidities and lower baseline renal function and BMD than those aged <60Y. At Y8, virologic suppression rates in all treatment groups were 100% and 93%–96% among older and younger patients, respectively. Treatment-related AE incidence was similar across age groups. Older patients experienced greater declines in $eGFR_{CG}$ and hip and spine BMD than younger patients and had smaller decreases with TAF vs TDF. In older patients receiving continuous TAF, median $eGFR_{CG}$ change from baseline was −6.1, −3.1, and −12.1 mL/min at Y2, Y3, and Y8; median changes from baseline in hip and spine BMD were −0.43% and −0.89% at Y2, −1.46% and 0.00% at Y3, and −2.70% and +1.51% at Y8. Among older patients who received TDF for 2Y, median $eGFR_{CG}$ change from baseline was −6.7 mL/min at Y2; after switching to TAF, it improved to −2.1 mL/min at Y3 and was −7.5 mL/min at Y8; median changes from baseline in hip and spine BMD were −2.06% and −5.36% at Y2 and improved to −0.45% and −1.60% at Y3, and +0.68% and +3.46% at Y8. Older patients who received TDF for 3Y showed median $eGFR_{CG}$ change from baseline of −10.6 mL/min at Y3; it improved to −6.7 mL/min at Y4 after switching to TAF and was −9.2 mL/min at Y8; median changes from baseline in hip and spine BMD were −1.82% and −1.51% at Y3, −2.45% and −0.39% at Y4, and −3.04% and +3.46% at Y8.
Conclusion: TAF is effective and well tolerated in patients with chronic HBV aged ≥ 60Y followed for up to 8Y. Switching from TDF to TAF stabilised or modestly improved renal and bone parameters, supporting guideline recommendations.

FRI-595

Validation of a sequencing-based HBV genotyping assay with serological backup for DNA-suppressed patients

Sanne Gils[1], Joël Meyboom[1], Bernhard Kleter[1]. *[1]Cerba Research, Rijswijk, Netherlands*
Email: sanne.vangils@cerbaresearch.com

Background and aims: HBV genotyping traditionally relies on sequencing plasma HBV DNA. However, in clinical trials aiming for functional cure in virologically suppressed individuals, HBV DNA is often undetectable, creating a need for alternative approaches. HBV RNA remains detectable in a subset of these patients, offering an opportunity for genotyping when DNA is absent. Our goal was to validate a sequencing assay using HBV plasma and serum samples containing both RNA and DNA; we also implemented a serological backup method to ensure genotype determination for samples that failed amplification.
Method: For the primary assay, reverse transcription was performed on extracted HBV RNA and DNA, followed by outer and nested PCR amplification of a fragment spanning the S-gene and RT-domain. Libraries were prepared from the PCR products and sequenced using Illumina short-read technology. Genotypes were assigned through phylogenetic analysis against reference sequences. When amplicons are negative, genotyping is performed using the IMMUNIS HBV Genotype EIA, which detects genotype-specific PreS2 epitopes to classify genotypes A–D.
Results: The primary sequencing assay resulted in a sensitivity of 79 copies/mL of HBV RNA and 6 copies/mL of HBV DNA. For the IMMUNIS HBV Genotype EIA assay the sensitivity of the kit insert, 3 IU/mL, was confirmed. Sequencing was successful on the panel of 15 samples containing genotypes A-G. IMMUNIS provided accurate results for genotypes A–D. Genotypes E and G were classified as D, and F was unclassified, as expected from kit limitations.
Conclusion: The combined approach of sequencing and serological backup provides a robust solution for HBV genotyping in virologically suppressed individuals. By using HBV RNA for sequencing and IMMUNIS when amplification fails, this workflow ensures reliable genotype determination across diverse clinical scenarios. This strategy supports accurate monitoring in trials evaluating new therapeutic regimens aimed at achieving functional cure.

FRI-596

Effects of retreatment on HBsAg loss following Nucleos(t)ide analogue withdrawal: a multicenter cohort study accounting for time-varying confounding

Yao-Chun (Holden) Hsu[1], Ying-Nan Tsai[2], Jia-Ling Wu[1], Cheng-Hao Tseng[2], Edo J. Dongelmans[3], Harry L. A. Janssen[3], Tzeng-Hue Yang[4], Teng-Yu Lee[5], Jen-Hao Yeh[6], Tzu-Haw Chen[1], Mindie Nguyen[7], Jaw-Town Lin[1]. *[1]E-Da Hospital, I-Shou University, Kaohsiung, Taiwan; [2]E-Da Cancer Hospital, Kaohsiung, Taiwan; [3]Erasmus MC University Medical Center Rotterdam, Rotterdam, Netherlands; [4]Lotung Poh-Ai Hospital, Yilan, Taiwan; [5]Taichung Veterans General Hospital, Taichung, Taiwan; [6]E-Da DaChang Hospital, Kaohsiung, Taiwan; [7]Stanford University, Stanford, United States*
Email: holdenhsu@gmail.com

Background and aims: Nucleos(t)ide analogue (NA) withdrawal in patients with chronic hepatitis B (CHB) may promote HBsAg loss but often triggers viral reactivation requiring reinitiation of antiviral therapy. Whether retreatment affects the probability of achieving HBsAg loss remains unclear. We aimed to estimate the causal effect of retreatment on HBsAg loss.
Method: Non-cirrhotic CHB patients who discontinued first-line NAs according to Asian-Pacific standards after ≥2 years of continuous therapy and virological suppression were prospectively enrolled at 5 hospitals in Taiwan between 2011/08/19 and 2025/12/18, with serial

collection of data and biopecimens. The primary outcome was HBsAg loss (<0.05 IU/mL by a quantitative assay). The decision for retreatment was largely guided by the national reimbursement criteria. Patients were also followed for virological relapse (VR), clinical relapse (CR), and ALT flare (ALT >200 U/L). Time-dependent Cox models were developed with laboratory data updated at 3-month intervals. We employed marginal structural model (MSM) with inverse probability of treatment weighting to estimate the effect of retreatment on HBsAg loss.

Results: This analysis enrolled 234 patients followed for a median duration of 6.9 years. Among them, 172 (73.5%), 123 (52.6%), and 61 (26.1%) experienced VR, CR, and ALT flare, respectively, with 10-year cumulative incidences of 78.2% (95% CI, 72.2–83.7%), 60.2% (95% CI, 52.2–68.3%), and 33.1% (95% CI, 25.6–42.1%), respectively. Overall, 118 (50.4%) patients restarted treatment and 38 (16.2%) cleared HBsAg, with 10-year cumulative incidences of 61.1% (95% CI, 52.9–69.4%) and 27.0% (95% CI, 20.0–35.8%), respectively. Time-varying HBsAg (adjusted HR, 1.16 per log IU/mL), time-varying ALT (adjusted HR 1.70 per log U/L), and age (adjusted HR, 1.02 per year; 95% CI, 1.004–1.03) independently predicted retreatment following VR. In the MSM analysis, retreatment was not significantly associated with HBsAg loss (adjusted OR, 0.51; 95% CI 0.17–1.51; p = 0.223), while HBsAg levels remained the dominant significant factor (adjusted OR, 0.23 per log IU/mL; p < 0.001).

Conclusion: Reinitiating antiviral therapy after NA cessation was not independently associated with HBsAg loss after accounting for time-varying confounding. The probability of HBsAg loss was predominantly determined by HBsAg levels regardless of retreatment, indicating that clinicians can reinitiate treatment when clinically indicated without undue concerns of reducing patients' prospects for HBsAg loss.

FRI-597

Impact of baseline hepatic steatosis on Peg-IFN-α therapy efficacy in chronic hepatitis B: a cohort study

Tiantian Hu[1,2], Yuqi Liu[1,2], Jie Tong[1], Baoyue Sheng[1], Haoxiang Zhu[1,2], Jinyu Wang[1,2], Jiming Zhang[1,2,3]. *[1]Department of Infectious Diseases, Shanghai Key Laboratory of Infectious Diseases and Biosafety Emergency Response, National Medical Center for Infectious Diseases, Huashan Hospital, Fudan University, Shanghai, China; [2]Shanghai Institute of Infectious Diseases and Biosecurity, Key Laboratory of Medical Molecular Virology (MOE/MOH), Shanghai Medical College, Fudan University, Shanghai, China; [3]Department of Infectious Diseases, Jing'An Branch of Huashan Hospital, Fudan University, Shanghai, China*
Email: 23111170004@m.fudan.edu.cn

Background and aims: Pegylated interferon-α (Peg-IFN-α) achieves functional cure in a minority of HBeAg-negative chronic hepatitis B (CHB) patients. Hepatic steatosis may influence host immunity and antiviral response. This study evaluated whether baseline controlled attenuation parameter (CAP), as a surrogate of hepatic steatosis, predicts 48-week HBsAg clearance during Peg-IFN-α therapy.

Method: We conducted a two-center observational cohort combining a retrospective cohort (2015–2020) and a prospective cohort (2021–2022). HBeAg-negative CHB patients with baseline CAP, HBV DNA ≤ 10,000 IU/mL, and HBsAg ≤ 3000 IU/mL receiving standard Peg-IFN-α for 48 weeks were included. Clinical, virologic, and FibroScan®-derived indices were collected at baseline and follow-up. The primary endpoint was rate of HBsAg clearance at week 48; secondary endpoints included 1 $\log_{10}$ IU/mL HBsAg decline at week 48. All analyses were performed in R (version 4.4.1; R Foundation for Statistical Computing, Vienna, Austria) with RStudio (Posit, Boston, USA).

Results: A total of 413 patients were included in the analysis, comprising 275 retrospective and 138 prospective cases. The overall HBsAg clearance rate at week 48 was 24.7% (102/413). Low CAP (≤259 dB/m) was significantly associated with higher rates of HBsAg clearance in both cohorts (retrospective: 26.39% vs. 17.8%, $p = 0.023$; prospective: 30.83% vs. 6.25%, $p = 0.041$). Kaplan–Meier analysis demonstrated significantly higher cumulative HBsAg clearance and ≥1 $\log_{10}$ decline in HBsAg in patients with low CAP compared with those with higher CAP values (all log-rank $p < 0.05$).

Conclusion: Lower baseline hepatic steatosis, reflected by CAP ≤259 dB/m, independently predicts superior HBsAg clearance and serologic response to Peg-IFN-α therapy at week 48 in HBeAg-negative CHB patients. CAP may serve as a noninvasive marker for response stratification.

FRI-601

Real-world 12-month outcomes of Bulevirtide therapy in chronic hepatitis D: interim results from a prospective romanian cohort

Liana Gheorghe[1,2], Mihaela Ghioca[2], Mirela Chitul[1], Anca Trifan[3,4], Laura Huiban[3,4], Daniela Larisa Sandulescu[5], Ionut Gheonea[5], Corina Radu[6], Bogdan Procopet[6], Roxana Sirli[7], Corina Pop[1,8], Nicoleta Tiuca[1,8], Bogdan Ungureanu[5], Adina Turcu-Stiolica[5], Speranta Iacob[1,2]. *[1]Carol Davila University Of Medicine And Pharmacy, Bucharest, Romania; [2]Fundeni Clinical Institute, Bucharest, Romania; [3]Spitalul Clinic Județean de Urgență Sfântul Spiridon Iași, Iași, Romania; [4]Universitatea de Medicină și Farmacie 'Grigore T. Popa' Iași, Iași, Romania; [5]Universitatea de Medicina și Farmacie Craiova, Craiova, Romania; [6]Iuliu Hațieganu University of Medicine and Pharmacy, Cluj-Napoca, Romania; [7]Universitatea de Medicină și Farmacie Victor Babeș, Timișoara, Romania; [8]Spitalul Universitar de Urgență București, București, Romania*
Email: drlgheorghe@gmail.com

Background and aims: Chronic hepatitis D (CHD) remains a severe form of viral hepatitis with limited real-world data on bulevirtide (BLV) effectiveness and on-treatment predictors of response. The ENHANCE D study is an ongoing multicenter, observational trial designed to evaluate virologic, biochemical and clinical outcomes, together with adherence, persistence and quality of life, in CHD patients treated with BLV 2 mg subcutaneously once daily in routine Romanian practice.

Method: Adults with confirmed HDV infection and detectable HDV RNA starting bulevirtide 2 mg daily were enrolled across 5 Romanian centers with planned 12-month follow-up at baseline, month 6 and month 12. Interim analyses included 177 patients with available clinical and laboratory data, assessing changes in ALT, AST, HDV RNA and FibroScan over time and exploring baseline predictors of virological response. Adherence and quality of life (QoL) were prespecified outcomes, but remain under analysis.

Results: We enrolled 177 patients (57.1% male), with 51.4% from Bucharest and 40.1% from Iași, reflecting national referral patterns for chronic hepatitis D. Baseline fibrosis stage, steatosis grade, comorbidities (diabetes, hypertension), and prior antiviral therapy did not differ by gender, but alcohol use/history was more frequent in males (p = 0.0033). At baseline, 67.8% had Child-Pugh A cirrhosis, and 12.5% had clinically significant portal hypertension (liver stiffness >25 kPa). Esophageal varices were significantly more common in males (67.1% vs 45.9%, p = 0.01). A virologic response (HDV RNA decline >2log) was achieved in 53.4%, and 21.9% had a partial response (1–2log decline). ALT and AST levels decreased significantly by months 6 and 12 (p < 0.0001), along with a modest but significant reduction in liver stiffness (p = 0.01). The only baseline factor significantly associated with a >2 log HDV RNA decline was lower GGT, independently predictive of virologic response (132.6 ± 129.4 vs 186.7 ± 151.8 U/L, p = 0.036); other demographic, virologic, and liver disease parameters showed no significant associations.

Conclusion: In this real-world cohort, BLV demonstrated robust antiviral and biochemical effectiveness over 12 months. While no major baseline predictors of virologic response were identified, lower GGT levels were significantly associated with response, suggesting a potential role as predictive marker of virologic response. Analyses of adherence and QoL are ongoing and expected to refine patient profiling strategies.

FRI-602-YI

Impact of the NTCP rs17556915 polymorphism on disease severity and bulevirtide treatment response in chronic hepatitis D: a multicentre real-world study

Yu Ri Im[1], Kathrin Sprinzl[2], Johannes Wiegand[3], Florian P Reiter[4], Elena Durmashkina[5], Beat Müllhaupt[6], Ansgar Rieke[7], Hans Christian Spangenberg[8], Tony Bruns[9], Heinz Zoller[10], Katharina Neuenschwander[11], Martin Rössle[12], Rudolf Stauber[13], Pavel Khaykin[14], Ulrike Kullig[15], Elke Bästlein[16], Christoph Sarrazin[17,18], Julia Dietz[19], Christiana Graf[20]. *[1]Department of Medicine II, LMU University Hospital, Ludwig Maximilian University of Munich, München, Germany; [2]Department of Internal Medicine I, University Hospital, Goethe University, Frankfurt, Germany; [3]Department of Oncology, Gastroenterology, Hepatology, Pulmonology and Infectious Diseases, University Hospital Leipzig, Leipzig, Germany; [4]Department of Internal Medicine II, University Hospital Würzburg, Würzburg, Germany; [5]Department of Internal Medicine II, St. Josefs-Hospital, Wiesbaden, Germany; [6]Department of Gastroenterology and Hepatology, University Hospital Zurich, Zurich, Germany; [7]Department of Internal Medicine, Gemeinschaftsklinikum Mittelrhein, Koblenz, Germany; [8]Department of Internal Medicine IV, Schwarzwald-Baar-Klinikum, Villingen Schwenningen, Germany; [9]Department of Internal Medicine III, RWTH Aachen University, Aachen, Germany; [10]Medical University of Innsbruck, Department of Medicine I, Gastroenterology, Hepatology and Endocrinology, Innsbruck, Austria; [11]Praxis Enge, Zurich, Switzerland; [12]Department of Gastroenterology, University Hospital, Freiburg, Germany; [13]Division of Gastroenterology and Hepatology, Department of Internal Medicine, Medical University of Graz, Graz, Austria; [14]Praxis MainFachArzt, Frankfurt, Germany; [15]Department of Medicine III, Klinikum Dresden, Dresden, Germany; [16]Magen Darm Zentrum Wiener Platz, Cologne, Germany; [17]Department of Medicine II, St. Josefs-Hospital, Wiesbaden, Germany; [18]Department of Medicine I, Klinikum der Goethe-Universität Frankfurt am Main, Frankfurt, Germany; [19]Department of Internal Medicine 1, University Hospital, Frankfurt, Germany; [20]Department of Medicine II, LMU University Hospital, Ludwig Maximilian University of Munich, Munich, Germany*
Email: dryuriim@gmail.com

Background and aims: The sodium taurocholate co-transporting polypeptide (NTCP) serves as the hepatic entry receptor for hepatitis D virus (HDV) and represents the target of bulevirtide (BLV). Genetic variants of NTCP may influence disease progression and treatment response. The aim of this ongoing study is to analyse the association between NTCP polymorphisms, disease severity, and BLV effectiveness in a real-world chronic hepatitis D (CHD) cohort.

Method: Adults with CHD from 21 centres in Germany, Austria, and Switzerland were consecutively enrolled between 10/2021 and 10/2025. NTCP genotyping for rs17556915 (A/G) was performed using Sanger sequencing. Clinical outcomes including liver cirrhosis, portal hypertension, and hepatocellular carcinoma (HCC) were recorded. In patients receiving BLV (2 mg/day), treatment response was defined as virological (greater than or equal to 2 log HDV-RNA decline), biochemical (ALT normalisation), combined (both), or non-response. Here, we describe the results of the baseline data.

Results: A total of 68 adults were included: 46/68 (68%) were male, 38/60 (63%) had liver cirrhosis, 16/53 (30%) suffered from portal hypertension, and 3/65 (3%) had HCC. HDV genotype was 1 in 41/53 (77%), 1d in 5/53 (9%), and 5 in 7/53 (17%). NTCP rs17556915 genotyping was available in 53 patients: GG was found in 41/53 (77%) and AG in 12/53 (23%); no AA homozygotes were detected. A larger proportion of patients with GG genotype suffered from cirrhosis (63% vs 36%), portal hypertension (34% vs 6%), and HCC (5% vs 0%) compared to AG carriers. 52/66 patients (79%) received BLV therapy. The overall virological response rate was 85% (35/41), but varied between GT1 (92%, 24/26), GT1d (33%, 2/3), and GT5 (67%, 1/3). Among patients with NTCP data, combined/virological response was achieved in 39% (9/23) of GG carriers versus 17% (4/6) of AG carriers.

Conclusion: In this multicentre CHD cohort, the NTCP rs17556915 GG genotype was associated with more severe liver disease but showed a trend towards higher BLV response rates compared to AG carriers. HDV GT5 was associated with treatment failure. These findings suggest that both host and viral genetic factors may serve as predictors of disease progression and treatment response in CHD.

FRI-603

Liver-related mortality and transplantation risk associated with self-discontinuation of nucleos(t)ide analogue therapy in HBeAg-negative chronic hepatitis B

Rachel Wen-Juei Jeng[1,2], Yen-Chun Liu[1,2], Chia-Ling Wu[1], Cheng Er Hsu[1,2], Chung-Wei Su[1,2], Rong-Nan Chien[1,2], Yun-Fan Liaw[1,2]. *[1]Linkou Chang Gung Memorial Hospital, Guishan District, Taiwan; [2]Chang-Gung University, Guishan District, Taiwan*
Email: rachel.jeng@gmail.com

Background and aims: Self-discontinuation of nucleos(t)ide analogue (Nuc) therapy without proper monitoring and loss to follow-up (LTFU) occur in real-world practice; the 10-year cumulative incidence approached 20% in HBeAg-ngative chronic hepatitis B (CHB) in our prior report. Long-term outcomes such as liver-related mortality and transplantation (LT) remain insufficiently defined. We aimed to evaluate the association between self-discontinuation/LTFU and liver-related mortality/LT in a large multi-center cohort with complete mortality ascertainment.

Method: Using the Chang Gung Research Database, we included HBeAg-negative CHB patients receiving entecavir or tenofovir (TDF/TAF) for ≥3 months (Jan 2004–Nov 2021) at three hospital branches. We excluded antiviral prophylaxis for chemotherapy/immunosuppression, HCV/HDV/HIV coinfection, or hepatocellular carcinoma within 5 years before NUC initiation. Time zero was first NUC initiation. Self-discontinuation/LTFU was failure to refill NUC for ≥2 consecutive months (chart-confirmed) and modelled as a time-varying exposure. Marginal structural models with stabilized inverse probability weighting were used to adjust time-varying confounders. Liver-related mortality and LT were ascertained via linkage to the national Cause of Death Registry; competing risks accounted for non–liver-related death.

Results: We included 1897 patients with 2211 treatment courses (ETV 1686; TDF/TAF 525). During median follow-up 2.17 years (IQR 1.22–3.01), 399 self-discontinuation/LTFU events occurred and 57 patients experienced liver-related death or LT. Annual liver-related mortality/LT incidence was higher with self-discontinuation than physician-guided therapy (3.32% vs 0.46%), in both cirrhosis (4.68% vs 1.80%) and non-cirrhosis (1.39% vs 0.03%) (all $P < 0.01$). In IPW-MSM analyses, self-discontinuation/LTFU was associated with increased risk of liver-related mortality/LT [subdistribution HR(sHR) 3.47, 95% CI 1.99–6.06; $P < 0.001$]. A dose–response relationship was observed, with increasing numbers of self-discontinuation/LTFU events associated with progressively higher risk (sHR 2.91, 95% CI 1.86–4.56; $P < 0.001$).

Conclusion: In HBeAg-negative CHB patients on long-term Nuc therapy, self-discontinuation/LTFU was independently associated with a markedly increased, dose-dependent risk of liver-related mortality/LT. Maintaining linkage to care is essential; structured, physician-guided finite therapy with scheduled monitoring is a much safter strategy when Nuc discontinuation is considered.

FRI-604

Untreated HBV-infected advanced fibrosis, if HBV-DNA is detectable, has HCC risk comparable to antivirals-treated cirrhosis

Seung Up Kim[1], Beom Kyung Kim[1], Victor de Lédinghen[2], Terry Cheuk-Fung Yip[3], Vincent Wai-Sun Wong[3]. *[1]Yonsei University College of Medicine, Seoul, Korea, Rep. of South; [2]Hospital Center University de Bordeaux, Bordeaux, France; [3]The Chinese University of Hong Kong, Sha Tin, Hong Kong*
Email: wongv@cuhk.edu.hk

Background and aims: The European Association for the Study of the Liver guideline on hepatitis B virus (HBV) recommends antiviral therapy (AVT) for advanced fibrosis (AdvF) with detectable HBV-DNA, which is a routine AVT criterion applied for liver cirrhosis (LC). Here, we compared hepatocellular carcinoma (HCC) risk between patients with untreated viremic AdvF vs. AVT-treated LC, with external validation.
Method: We assessed HCC risk for South Korean patients with untreated viremic AdvF not fulfilling conventional AVT criteria (n = 302), compared to AVT-treated LC ones (n = 1694). All belonged to Child-Pugh A. LC was defined using gross finding on imaging study or liver stiffness (LS) > 11 kPa. AdvF was as LS 8∼11 kPa without gross LC finding. Multivariable Cox-regressions and propensity-score (PS) matching (2:1) were used for comparison.
Results: In multivariable analyses, untreated viremic AdvF patients demonstrated HCC risk comparable to AVT-treated LC (adjusted hazard ratios [aHRs] 0.66∼0.70, all $P > 0.05$), irrespective of LS adjustment. Male, higher FIB-4, lower albumin, and higher bilirubin were independently associated with HCC risk. Likewise, in the Hong Kong cohort, untreated viremic AdvF patients (n = 103) showed HCC risk comparable to AVT-treated LC (n = 199) (aHR 0.94∼0.97, all $P > 0.05$), irrespective of LS adjustment. Male and lower albumin were independently associated with HCC risk. PS-matching confirmed these results in both cohorts (all P > 0.05).
Conclusion: Across two independent East-Asian cohorts, untreated viremic AdvF patients demonstrated HCC risk comparable to AVT-treated LC. So, AVT should be considered for viremic AdvF, although conventional AVT criteria are not met. Further prospective studies are required.

FRI-605

Impact of bulevirtide treatment on patient-reported outcomes among patients with hepatitis delta in Europe

Maria Buti[1,2], Fritha Hennessy[3], Tia Pennant[3], Daniel Graham[3], Fraser Barrable[3], Alastair Hinds[3], Caroline Burk[4], Chong Kim[4], Marvin Rock[4], Pietro Lampertico[5,6]. *[1]Liver Unit, Hospital Universitario Vall d'Hebron, Barcelona, Spain; [2]Centro de Investigación Biomédica en Red de Enfermedades Hepáticas y Digestivas (CIBEREHD) del Instituto Carlos III, Madrid, Spain; [3]Adelphi Real World, Bollington, United Kingdom; [4]HEOR – Global Value & Access, Gilead Sciences, Inc., Foster City, United States; [5]Division of Gastroenterology and Hepatology, Foundation IRCCS Ca' Granda Ospedale Maggiore Policlinico, Milan, Italy; [6]CRC "A. M. and A. Migliavacca" Center for Liver Disease, Department of Pathophysiology and Transplantation, University of Milan, Milan, Italy*
Email: pietro.lampertico@unimi.it

Background and aims: Bulevirtide (BLV) treatment improves virologic and biochemical responses in patients (pts) with hepatitis delta virus (HDV) infection. Evidence on the effect of BLV on health-related quality of life (HRQoL) is limited. We describe HRQoL outcomes of pts with HDV infection who received BLV or were treatment naïve (TN).
Method: Data were drawn from the Adelphi Real World Hepatitis II Disease Specific Programme™, a cross-sectional survey with retrospective data collection of physicians and their pts with HDV infection, from Jun–Dec 2024. Physicians provided data on ≤ 4 pts seen during routine care—2 prescribed BLV and 2 regardless of treatment status; BLV vs TN was analysed. Descriptive analyses included physician-reported pt demographics and HRQoL impact via pt-reported outcome measures (PROMs). The effect of BLV was estimated using bivariate analyses and inverse probability weighted regression adjustment (IPWRA; covariates: gender, born/lived in a high-risk region, time since hepatitis B diagnosis, and mild symptoms at diagnosis).
Results: Overall, 68 physicians (France, 9; Germany, 35; Italy, 7; Spain, 12; UK, 5) reported data on 195 pts (France, 22; Germany, 100; Italy, 19; Spain, 26; UK, 28). Mean (SD) pt age was 41 (12.9) years; 71% were male and 75% were White. Mean (SD) Hepatitis B QoL (HBQoL) global scores (0–100 scale; 100 = worst HRQoL) were significantly lower for BLV-treated (34.4 [18.7]) vs TN pts (42.5 [13.9]; bivariate analysis, p = .005; IPWRA, p < .001). In bivariate analyses, HBQoL scores for anticipation anxiety (p = .010), vitality (p = .004), stigma (p = .017), vulnerability (p = .017), transmission (p = .014), and viral response (p = .018) were lower in BLV-treated vs TN pts. Mean (SD) EQ-5D Visual Analog Scale (0–100 scale; 100 = best health) and EQ-5D 5-Level Germany (−0.661 to 1 scale; 1 = best health) scores showed no significant differences between groups (BLV, 69.2 [18.1] and 0.9 [0.2]; TN, 72.0 [17.7] and 0.9 [0.2], respectively; p >.05). No differences were observed between BLV-treated and TN pts in mean (SD) Work Productivity and Activity Impairment scores (0–100% scale; 100% = severe impairment) for overall work impairment (BLV, 28.5% [23.4%]; TN, 28.5% [25.1%]; p >.05) or Fatigue Severity Scale scores (scores ≥ 36 = fatigue; BLV, 35.9 [15.1]; TN, 35.6 [13.6]; p >.05).
Conclusion: Unlike generic and symptom-specific PROMs, which may be less sensitive, disease-specific PROMs show that BLV was associated with a positive effect on pt HRQoL at the survey date.

FRI-606

Pipecolic acid–associated amino acid remodeling predicts functional cure in nucleoside analogue–experienced chronic hepatitis B treated with pegylated interferon alpha plus programmed cell death protein 1 blockade

Yaping Li[1], Bin Cheng[2], Chenrui Liu[1], Meng Zhang[1], Muqi Wang[1], liu Yang[1], Xinyu Wang[1], Guoe Gou[1], Mei Li[1], Xiaoli Jia[1], Junliang Fu[3], Mengji Lu[2], Shuangsuo Dang[1]. *[1]The second affiliated hospital of Xi'an Jiaotong University, Xi'an, China; [2]University Hospital Essen, Essen, Germany; [3]The fifth medical center of Chinese PLA General Hospital, Beijing, China*
Email: liyaping8605@xjtu.edu.cn

Background and aims: Functional cure of chronic hepatitis B (CHB) remains rare under long-term nucleos(t)ide analogue (NA) therapy, and add-on pegylated interferon-α (Peg-IFN-α) achieves only modest improvements. PD-1 blockade has emerged as one of the most promising strategies for achieving functional cure, possibly by enhancing antiviral T-cell responses. This prospective study aimed to identify biomarkers associated with functional cure in NA-experienced patients who remained uncured after NA plus Peg-IFN-α therapy and subsequently received PD-1 blockade added to Peg-IFN-α.
Method: Twenty NA-experienced CHB patients who did not achieve HBsAg clearance after 48 weeks of NA plus Peg-IFN therapy continued NA and Peg-IFN-α through week 72, with add-on PD-1 inhibitor sintilimab (1.0 mg/kg, Q12w) administered at weeks 48 and 60. Plasma samples collected at T0-T3 (baseline, week 48, 60 and 72) underwent targeted metabolomics analysis, alongside parallel virological, biochemical, and immunological assessments. Functional cure was defined as sustained HBsAg loss and undetectable HBV DNA.
Results: By week 72, 6/20 patients (30%) achieved functional cure and maintained remission through week 96. OPLS-DA analysis at T3 showed a separation trend between cured and uncured groups, consistent with metabolite- and pathway-level differences. Targeted metabolomics identified differential amino acids distinguishing cured from uncured patients, including L-pipecolic acid, L-lysine, L-

aspartic acid, L-tryptophan, L-phenylalanine, and L-methionine. SMPDB-based pathway enrichment identified lysine degradation as the top pathway. Within this pathway, L-pipecolic acid showed the greatest increase in cured individuals (FC = 2.55, $p = 7.1 \times 10^{-4}$), while its precursor L-lysine decreased (FC = 0.24, p = 0.015). Correlation analysis showed that L-pipecolic acid inversely correlated with HBsAg (T3 r = –0.482, $p < 0.05$) and $CD8^{+}PD\text{-}1^{+}$ T cells (T3 r = –0.599, $p < 0.05$), whereas L-lysine negatively correlated with HBsAg at T2 and T3 (r = –0.57 and –0.576, respectively).
Conclusion: Sequential PD-1 blockade combined with Peg-IFN-α was associated with distinct amino acid metabolic alterations. L-pipecolic acid emerged as the most prominently increased metabolite in patients achieving functional cure and was consistently associated with HBsAg decline and immune activation. These findings suggest L-pipecolic acid as a potential metabolic biomarker of treatment response, warranting validation in larger cohorts and mechanistic studies.

FRI-607
End-of-treatment HBsAg level predicts functional cure and clinical relapse but not severe flare risk after Nucleos(t)ide analogue cessation in chronic hepatitis B
Hsin-Che Lin[1], Yen-Chun Liu[1], Rachel Wen-Juei Jeng[1], Rong-Nan Chien[1], Yun-Fan Liaw[1]. [1]*Linkou Chang Gung Memorial Hospital, Guishan District, Taiwan*
Email: rachel.jeng@gmail.com

Background and aims: Previous studies showed lower end-of-treatment (EOT) HBsAg levels, especially <100 IU/mL, associates with lower clinical relapse (CR) and higher HBsAg loss rate. A recent study involving 97 patients reported that only EOT qHBsAg <10 IU/mL, not 100 IU/mL, was significantly associated with low CR and higher HBsAg loss. This study aimed to test this unique finding in our large cohort of off Nucleos(t)ide Analogue (Nuc) HBeAg-negative patients.
Method: We included 1245 HBeAg-negative CHB patients who stopped therapy according to APASL guidelines and were stratified by EOT qHBsAg levels. CR was defined as HBV DNA ≥2000 IU/mL with ALT > 2x the upper limit of normal (ULN). Hepatitis flare was defined as HBV DNA ≥2000 IU/mL with ALT ≥5x ULN. Severe hepatitis flare was defined as ALT ≥1000 U/L or flare with ALT <1000 U/L with total bilirubin ≥3.5 mg/dL and/or INR ≥1.5. Kaplan-Meier analysis and log-rank tests were used to compare outcomes.
Results: Among 1245 patients, 1041 (84%) were male and 279 (23%) had cirrhosis. EOT qHBSAg <10 IU/mL were seen in 39 patients (3%), 10–100 IU/mL in 175 patients (14%), 101–1000 IU/mL in 762 patients (61%), and >1000 IU/mL in 269 patients (22%). Compared with EOT HBsAg 10–100 IU/mL patients, those with EOT HBsAg <10 IU/mL had lower proportion of pre-treatment HBsAg <1000 IU/mL (56% vs 73%, p = 0.039) and higher proportion of genotype C infection (23% vs 8%, p = 0.007). Age, sex, cirrhosis prevalence, pre-treatment HBV DNA level, treatment duration, and consolidation time were comparable between the two lowest HBsAg groups (all $p > 0.05$). The 5-year cumulative incidence of CR and hepatitis flare decreased progressively with lower EOT HBsAg levels [CR: 21% vs 43% vs 66% vs 73%, $p < 0.05$; flare: 19% vs 25% vs 47% vs 56%, $p < 0.01$]. The 5-year cumulative incidence of HBsAg loss was markedly higher in the <10 IU/mL group (59% vs 18% vs 12% vs 0%, $p < 0.01$). Importantly, the 5-year cumulative incidence of severe HBV flare (6% vs 6% vs 10% vs 8%, p = 0.32) and severity (median peak ALT: 260 vs 593 vs 420 vs 394 U/L, p = 0.21) were comparable across all EOT HBsAg groups.
Conclusion: Lower EOT HBsAg levels associate with lower rate of off-therapy flare and higher likelihood of HBsAg clearance. However, only 3% of patients achieved qHBsAg <10 IU/mL, and the incidence of severe flare was comparable across all EOT HBsAg levels. Therefore, EOT qHBsAg alone is not a practical indicator for deciding Nuc cessation, particularly due to its limited ability to discriminate severe flares.

FRI-608
Real-life adherence to bulevirtide monotherapy in chronic hepatitis D: a behavioral survey across Italian centers
Lorenzo Badia[1], Maurizia Brunetto[2], Alessia Ciancio[3], Massimiliano Conforti[4], Nicola Coppola[5], Marco Distefano[6], Antonio Izzi[7], Loreta Kondili[8], Pietro Lampertico[9], Alessia Rianda[10], Alessandro Loglio[11]. [1]*Infectious Diseases Outpatient Clinic, Azienda USL of Imola, Imola, Italy;* [2]*Department of Clinical and Experimental Medicine, University of Pisa and Hepatology Unit, University Hospital of Pisa, Pisa, Italy;* [3]*Department of Medical Sciences, Molinette Hospital, Turin, Italy;* [4]*EpaC Ets, Italian Liver Patient Association, Monza, Italy;* [5]*Complex Operative Unit of Infectious Diseases, L. Vanvitelli University Hospital, Naples, Italy;* [6]*UOSD Hepatology Unit, ASP Siracusa, Siracusa, Italy;* [7]*Department of Infectious Diseases, Cotugno Hospital, Naples, Italy;* [8]*National Center for Global Health, Istituto Superiore di Sanità, Rome, Italy;* [9]*Division of Gastroenterology and Hepatology, Foundation IRCCS Ca' Granda Ospedale Maggiore Policlinico, Milan, Italy;* [10]*Infectious Diseases Hepatology Unit-National Institute for Infectious Diseases L. Spallanzani - IRCCS (INMI), Rome, Italy;* [11]*Gastroenterology, Hepatology and Transplantation Division, ASST Papa Giovanni XXIII, Bergamo, Italy*
Email: aloglio@asst-pg23.it

Background and aims: Treatment adherence may influence outcomes in chronic Hepatitis Delta (CHD) patients. While clinical trials report excellent adherence to bulevirtide (BLV), real-world data remains unknown: we investigated factors influencing adherence in real-life settings in Italy.
Method: This cross-sectional study surveyed patients receiving BLV across 12 Italian centers between May and September 2025, regardless of treatment initiation date. An updated COM-B (Capability, Opportunity, Motivation–Behavior) questionnaire assessed behavioral drivers and unmet needs, and in-depth interviews with six patients, conducted with the EpaC patient association, explored the emotional patient journey.
Results: Among the 121 participants [70% >50 years, 64% Italian, 29% non-Italian natives with a median residence of 13 years], 80% had been receiving BLV for >12 months at the time of the survey: 79% considered their liver disease severe, 86% perceived therapy as effective, and 87% reported improvements in daily life. Thirty-three patients expected therapy to last at least three years, and 15% anticipated it would continue indefinitely. Despite BLV was reported as easy to administer, 14% occasionally missed doses, 13% had considered discontinuation, most commonly (51%) because they believed disease was under control. BLV was collected monthly by 52% of patients, which may explain the 16% reporting interference with daily activities. Treatment effectiveness emerged as a key motivational factor, with adherence stabilizing at 80% after the first six months of BLV, regardless of nationality. Qualitative interviews highlighted the need for greater public awareness of HBV/HDV.
Conclusion: Adherence to BLV remains high in Italy, supported by comprehensive patient care and personalized management.

FRI-609
Novel HBV biomarkers predict HBsAg seroclearance in patients with chronic hepatitis B infection after cessation of long term nucleos(t)ide analogue
Lung Yi Loey Mak[1], Mark Anderson[2], Rex Wan-Hin Hui[1], Tiffany Fortney[2], Karen Cheuk-Ying Ho[1], Rene Geissler[2], James Fung[1], Wai-Kay Seto[1], Gavin Cloherty[2], Man-Fung Yuen[1]. [1]*The University of Hong Kong, Pok Fu Lam, Hong Kong;* [2]*Abbott Laboratories, Abbott Diagnostics Division, Abbott Park, Illinois, United States*
Email: loeymak@gmail.com

Background and aims: We examined the profile of novel viral biomarkers among patients with chronic hepatitis B (CHB) infection who stopped long-term nucleoside analogue (NUC).
Method: This prospective study recruited patients with HBeAg-negative non-cirrhotic CHB on ≥3 years of first-line NUC with

protocolized NUC cessation & intensive monitoring every 6 weeks. NUC was resumed upon clinical relapse (CR), defined as virological relapse (VR, serum HBV DNA rise from undetectable to >2000 IU/mL) plus alanine aminotransferase (ALT) >2 times upper limit of normal. HBV biomarkers including quantitative hepatitis B surface antigen (qHBsAg) and isoforms (LHBs, MHBs, SHBs), HBV RNA, HBcAg, P-HBcAg, HBcrAg and circulating immune complexes (CICs) were measured at baseline and end-of-follow-up. Additional measurement was performed at VR and ALT normalization in some patients. The primary outcome was HBsAg seroclearance (defined as <0.05 IU/mL). Patients were followed-up for ≥1 year after NUC cessation (without CR) or ≥1 year after ALT normalization (with CR), whichever was later.

Results: Among 51 patients who completed study (median age 50.1, 62.7% male, baseline qHBsAg 298 IU/mL with 25.5% <100 IU/mL, median time on NUC 7.4 years), 28 patients (54.9%) developed CR at a median of 24 weeks (median HBV DNA: 4.5 log IU/mL, median ALT: 152 U/L). No patients developed hepatic decompensation. Over a median follow-up of 91 weeks, a total of 6 patients (3 with no CR, 3 with CR; log rank P = 0.857) developed HBsAg seroclearance at weeks 20, 24, 48, 81, 91 and 96, with an event rate of 11.7%. Shifts in qHBsAg categories were observed with or without CR, showing increase in proportion of qHBsAg <10 IU/mL over time. qHBsAg, MHBs and SHBs increased only in the CR group but remained static in no CR group. LHBs, HBV RNA, and CIC were increased unanimously during VR. Baseline SHBs (0.859; 93.3% sensitivity, 83.3% specificity for cut-off level of 3.99 $\log_{10}$ S/CO) had higher area under ROC values than baseline qHBsAg (0.815; 88.9% sensitivity, 83.3% specificity for cut-off level of 1.84 $\log_{10}$ IU/mL) to predict HBsAg seroclearance. Baseline qHBsAg (HR 0.114, 95% CI 0.020–0.647), controlled attenuation parameter (HR 1.022, 95% CI 1.001–1.044), and SHBs (HR 0.135, 95% CI 0.023–0.780) were independently associated with HBsAg seroclearance.

Conclusion: HBsAg seroclearance following NUC cessation was observed with or without CR. SHBs at NUC cessation has higher performance characteristics than qHBsAg to predict subsequent HBsAg seroclearance.

FRI-610

NTCP variants do not impact Bulevirtide antiviral activity or HDV treatment response

Savrina Manhas[1], Amos Lichtman[1], Thomas Aeschbacher[1], Christopher Richards[1], David Pan[1], Nikita Kolhatkar[1], Jason Perry[1], Ross Martin[1], Dmitry Manuilov[1], Hongmei Mo[1], Jenny Svarovskaia[1].
[1]*Gilead Sciences, Foster City, United States*
Email: savrina.manhas1@gilead.com

Background and aims: Sodium taurocholate cotransporting polypeptide (NTCP, *SLC10A1*) is a hepatocyte bile acid transporter and entry receptor for hepatitis B virus (HBV) and hepatitis D virus (HDV). Bulevirtide (BLV), a myristoylated PreS1 lipopeptide, blocks HDV entry by binding NTCP. NTCP single nucleotide polymorphisms (SNPs), such as C800T (S267F) a variant previously linked to reduced HBV susceptibility, have been reported. This study mapped PreS1–NTCP peptide-protein interactions, identified NTCP SNPs at contact residues, and evaluated their impact on NTCP expression, BLV potency, and treatment response.

Method: Non-synonymous NTCP SNPs were selected based on (1) structural proximity to the PreS1 binding site mapped with recent NTCP cryo-EM structure or (2) minor allele prevalence (MAP) >0.05% in gnomAD v4.1 (N = 1,614,324). NTCP expression was quantified in MYR301 (phase 3 study NCT03852719) participants by RNA sequencing (RNASeq; N = 24) and multiplex immunofluorescence (MIF; N = 81), with whole-exome sequencing (WES) for subsets. BLV potency was tested in primary human hepatocytes (PHHs) expressing NTCP variants. In addition, BLV treatment response for participants with the synonymous NTCP SNP G225A (rs4646285) was analysed in MYR301 and MYR204 (phase 2b study NCT03852433) participants.

Results: Three NTCP SNPs C800T, T263C, T668C resulting in S267F, I88T, and I223T substitutions, respectively, met selection criteria. Structural mapping identified 72 of 349 NTCP residues interacting with PreS1 within 5 Å, two of which had a MAP >0.05%: C800T (S267F; ≤0.17%) and T263C (I88T; ≤0.06%). BLV retained subnanomolar potency against HDV in PHHs expressing S267F variant (EC_{50}: 0.08 nM). T668C (I223T) variant was the most prevalent (≤0.21%) but did not directly interact with PreS1. I223T remained sensitive to BLV (EC_{50}: 0.11 nM). The most common SNP in MYR301 and MYR204 was a synonymous G225A (16%, 46/293). NTCP expression was similar for participants with and without G225A SNP (RNASeq: 2.41 vs 2.39 log10 copies per million; MIF: −1.82 vs −1.82 log2 intensity). Week 96 virologic response rates were also comparable: 94.1% (16/17) for G225A vs 84.4% (65/77) for G225G. HDV RNA decline, ALT normalization and combined response rates did not differ by G225 SNP.

Conclusion: NTCP polymorphisms were rare and did not impact BLV binding or antiviral activity in vitro. The synonymous SNP G225A did not impact NTCP expression or treatment response to BLV in chronic HDV.

FRI-611

National registry of patients with hepatitis D treated with bulevirtide: real-world clinical practice data in Spain

Adriana Palom[1,2], Alvaro Giráldez-Gallego[3], Juan Carlos Ruiz-Cobo[1,2], Anna Pocurull Aparicio[4], Marta Casado-Martin[5], Sara Lorente[6], Francisco Javier Garcia-Samaniego[7], Antonio David Palau[8], Raquel González Monasterio[9], Maria Inmaculada Fernández Vázquez[10], Carolina Delgado[11], Joaquin Cabezas Gonzalez[12], Maria Jose Devesa Medina[13], José Miguel Rosales[14], Natalia García Gimeno[15], Montserrat Garcia-Retortillo[16], Maria Dolores Antón[17], Raquel Ríos León[18], Víctor Escrich[19], Manuel Rodríguez[20], Miguel Fernández-Bermejo[21], Marta Hernández Conde[22], Paloma Rendon[23], Mar Riveiro Barciela[1,2], Xavier Forns[4], Maria Buti[1,2], Sabela Lens[4]. [1]*Liver Unit, Vall d'Hebron University Hospital, Barcelona, Spain;* [2]*CIBERehd, Madrid, Spain;* [3]*Liver Diseases, Instituto de Biomedicina de Sevilla/Unit for the Clinical Management of Digestive Diseases, Hospital Universitario Virgen del Rocío, Seville, Spain;* [4]*Servicio de Hepatología, Hospital Clínic de Barcelona. FCRB-IDIBAPS. CIBERehd. Universidad de Barcelona, Barcelona, Spain;* [5]*Sección de Hepatología, Hospital Torrecárdenas, Almería, Almería, Spain;* [6]*Unidad de Hepatología y Trasplante hepático. Hospital Clínico Lozano Blesa, Zaragoza. IIS Aragon, CIBERehd, Zaragoza, Spain;* [7]*Unidad de Hepatología. Hospital Universitario La Paz. IdiPAZ. Universidad Autónoma de Madrid, Madrid, Spain;* [8]*Servicio de Aparato Digestivo, Hospital General Universitario de Castellón, Castellón de la Plana, Spain;* [9]*Servicio de Aparato Digestivo, Hospital San Eloy, San Vicente de Barakaldo, Vizcaya, Barakaldo, Spain;* [10]*Servicio de Aparato Digestivo, Hospital Universitario 12 de Octubre, Madrid, Spain;* [11]*Servicio de Aparato Digestivo, Hospital Universitario de Toledo, Toledo, Spain;* [12]*Servicio de Gastroenterología y Hepatología. Grupo de Investigación Clínica y Traslacional en Enfermedades Digestivas. Instituto de Investigación Valdecilla (IDIVAL). Hospital Universitario Marqués de Valdecilla, Santander, Spain;* [13]*Servicio Aparato Digestivo, Hospital Clínico San Carlos, Madrid, Madrid, Spain;* [14]*Unidad de Aparato Digestivo, Hospital Universitario Costa del Sol, Marbella, Spain;* [15]*Servicio de Aparato Digestivo, Hospital de Manises, Valencia, Spain;* [16]*Sección de Hepatología, Servicio de Digestivo, Hospital del Mar, Barcelona, Spain;* [17]*Servicio de Aparato Digestivo, Hospital Dr Peset, Valencia, Spain;* [18]*Servicio de Aparato Digestivo, Hospital Universitario General de Villalba, Madrid, Spain;* [19]*Servicio Aparato Digestivo, Hospital*

San Pedro, Logroño, Spain; [20]Sección de Hepatologia. Hospital Universitario Central de Asturias. Universidad de Oviedo, Oviedo, Spain; [21]Servicio de Aparato Digestivo. Hospital Universitario de Cáceres, Cáceres, Spain; [22]Hospital Universitario Puerta de Hierro. IDIPHISA, Madrid, Spain; [23]Servicio Aparato Digestivo, Hospital Puerta del Mar, Cádiz, Spain
Email: slens@clinic.cat

Background and aims: Bulevirtide (BLV) was approved for reimbursement in Spain in mid-2023 as the first specific treatment for chronic hepatitis D (CHD). However, data on its effectiveness and safety in real-world clinical practice in our country remain limited. The aim of this study was to evaluate the efficacy and safety of BLV in CHD patients with ≥1 year of treatment included in the Spanish Association for the Study of the Liver (AEEH) national registry.
Method: This was a multicenter, observational study including all patients with baseline viremia who received BLV for ≥1 year and had available data at baseline, week 24, and week 48 (and week 72, when available). Virological response (HDV RNA decline >2 log or undetectable), biochemical response (normal ALT), and combined response were assessed, as well as the impact of baseline viral load on treatment response.
Results: A total of 603 patients were included, of whom 125 received BLV; 60 had HDV RNA quantified in all visits. Sixty-eight percent were male, with a median age of 51 years (IQR 40–57); 60% were born outside of Spain, and 76% had liver cirrhosis. At week 48, the virological response rate was 60%, with undetectable HDV RNA in 28% of patients. At week 72, virological response increased to 63%. Overall, combined response was observed in 41% at week 24 and 47% at week 48. Among the 25 patients without virological response at week 24, 24% achieved a complete response and 28% a partial response (decline ≥1 log and <2 log) by week 48. A greater rate of HDV RNA clearance at week 48 was observed in patients with baseline viral load <10,000 IU/ml (50%) compared to >10,000 IU/ml (20%) ($p = 0.05$). Adverse events were mild (three headaches and one self-limited local erythema). During follow-up, three patients developed *de novo* hepatocellular carcinoma (HCC).
Conclusion: Data from the Spanish national registry demonstrates that BLV achieves progressive improvements in virological and biochemical responses in CHD patients under real-world clinical conditions. Its greater efficacy in cases with low baseline viral load and the increasing response rates over time support BLV as an effective and safe therapeutic option for CHD.

FRI-612
Early miRNA signatures predict virological control and response to Bulevirtide in chronic hepatitis D

Javier Pérez Garreta[1,2,3], Maria Francesca Cortese[1,2], Adriana Palom[2,4], Thais Leonel[5], Maëlle Locatelli[5], David Tabernero[1,2,6], Ariadna Rando-Segura[1,2,7], Judit Vico Romero[2,4], Sabela Lens[5], Juan Carlos Ruiz-Cobo[2,4], Mar Riveiro Barciela[2,3,4], Maria Buti[2,3,4].
[1]Department of Microbiology, Liver Unit, Vall d'Hebron Institut de Recerca (VHIR), Vall d'Hebron Barcelona Hospital Campus, Barcelona, Spain; [2]Instituto de Salud Carlos III, Centro de Investigación Biomédica en Red de Enfermedades Hepáticas y Digestivas (CIBERehd), Madrid, Spain; [3]Universitat Autònoma de Barcelona (UAB), Barcelona, Spain; [4]Department of Hepatology, Vall d'Hebron Hospital Universitari, Vall d'Hebron Barcelona Hospital Campus, Barcelona, Spain; [5]Liver Unit Hospital Clínic, FCRB-IDIBAPS. University of Barcelona. CIBERehd, Barcelona, Spain; [6]Liver Unit, Liver Diseases-Viral Hepatitis, Vall d'Hebron Institut de Recerca (VHIR), Vall d'Hebron Hospital Universitari, Vall d'Hebron Barcelona Hospital Campus, Barcelona, Spain; [7]Department of Microbiology, Vall d'Hebron Hospital Universitari, Vall d'Hebron Barcelona Hospital Campus, Barcelona, Spain
Email: javier.perez@vhir.org

Background and aims: Novel therapies for Hepatitis D Virus (HDV) infection, such as Bulevirtide (BLV), highlight the urgent need for early predictive biomarkers of treatment response. MicroRNAs (miRNAs), small RNA molecules that also regulate the host response during viral infection, have emerged as promising candidates. This study aims to analyze miRNA profiles associated with virological control or response in untreated and BLV-treated patients with Chronic Hepatitis D.
Method: The miRNA profile was analyzed by microarray *(Affymetrix)* in plasma samples in an exploratory cohort of 30 anti-HDAg-positive patients: 15 with detectable and 15 with undetectable HDV-RNA. The identified miRNAs were subsequently validated by digital PCR *(QIAcuity)* in two independent longitudinal cohorts: (1) 35 untreated HDV patients (n = 99 samples) with at least two consecutive samples and 8 healthy donors; (2) 16 BLV-treated patients followed at the start of treatment, 6 and 12 months, and classified as responders or non-responders according to the presence of a combined response at 1 year (drop of >2 log in HDV-RNA and ALT normalization).
Results: In the exploratory cohort, five miRNAs (miR-122-5p, miR-192-5p, miR-194-5p, miR-23b-3p and miR-26a-5p) were significantly downregulated in patients with undetectable HDV-RNA ($p < 0.05$). This trend was confirmed in the untreated validation cohort, where patients with virological control (n = 13) or normal ALT levels (n = 10) showed lower levels of miR-122-5p, miR-192-5p and miR-194-5p compared with patients with persistent viremia (n = 12). MiR-23b-3p and miR-26a-5p were downregulated in all HDV patients compared to healthy donors. BLV responders (n = 6) exhibited an early, marked drop in all five miRNAs by month 6 of treatment. Especially miR-23b-3p and miR-26a-5p, showed the strongest association with treatment response (AUC = 0.87 and 0.82; $p = 0.016$ and 0.042, respectively).
Conclusion: A specific miRNA profile linked to virological control and treatment response has been identified. Notably, the early decline of miR-23b-3p and miR-26a-5p levels may serve as predictive biomarkers of early treatment response, offering a new tool for management of HDV infection.
Study supported by the projects PI20/01692 and PI23/01065, funded by Instituto de Salud Carlos III and co-funded by European Union (ERDF, "A way to make Europe").

FRI-613
Long-term efficacy and safety of tenofovir disoproxil fumarate in chronic hepatitis B: real-world experience from a North African center

Boukhraiss Rajaa[1], Mohamed Borahma[1], Fatima Zahra Chabib[1], Nawal Lagdali[1], Sabbah Selma[1], Fatima Zahra Ajana[1], Maryeme Kadiri[1].
[1]Department of Gastroenterology and Hepatology, CHU Ibn Sina, Faculty of Medicine and Pharmacy of Rabat, Mohammed V University, Rabat, Morocco
Email: dr.chabib.fatimazahra@gmail.com

Background and aims: Chronic hepatitis B (CHB) remains a major public health concern due to progression to cirrhosis and hepatocellular carcinoma. Tenofovir disoproxil fumarate (TDF) is recommended as first-line therapy for its potent antiviral activity, high genetic barrier, and antifibrotic efficacy. This study evaluated the long-term virological efficacy and safety of TDF in CHB patients.
Method: Retrospective single-center study including CHB patients treated with TDF between 2017 and January 2025, with ≥12 months follow-up. Clinical, biochemical, and virological assessments were performed at M6, M12, M24, and beyond M36 (maximum 84 months).
Results: Forty-five patients (mean age 47.1 ± 12 years; 60% male) were included. Comorbidities: diabetes 11.1%, hypertension 15.6%, metabolic syndrome 22.2%. Baseline ALT elevation: 24.4%; viral co-infection: 6.7%; HBeAg-negative: 93.3%; treatment-naïve: 84.4%. Advanced fibrosis (F3–F4) was present in 13.3%. Virological suppression at M6: 68.9%; ALT normalization: 97.8%. At M12, 100% achieved undetectable HBV DNA. At M24 (n = 40), virological rebound occurred in 7.5%, persistent ALT elevation in 2.5%, and HBeAg seroconversion in 5%. Long-term follow-up (>M36, n = 33): low-level viremia in 12.1%,

ALT abnormalities in 3%, HBeAg negativation in 3%. Fibrosis reassessment (n = 14) showed improvement in 64.3%, stability in 21.4%, progression in 14.3%. Safety profile was favorable: eGFR decrease in 2.2%,Treatment modification occurred in 6.7% of patients for osteoporosis and in 6.7% for hypophosphatemia. No HBsAg seroconversion observed.
Conclusion: Long-term TDF therapy provides durable virological suppression, favorable biochemical outcomes, and low adverse events in CHB patients. These real-world data support TDF as an effective and well-tolerated long-term therapy.

FRI-617
Peginterferon alpha-2b and nucleos(t)ide analogs combination therapy for chronic hepatitis B patients with high HBsAg level at the end of treatment (52 weeks) from ongoing CREATED excellent study
Wenhua Zhang[1], Haitao Tang[1], Qinghua Lu[2], Haifang Cao[2], Tingxia Chao[1], Fengmei Wang[1], Wenling Jia[1], Chunhui Liang[1], Feng Ren[3], Hongfei Zhang[4]. *[1]Gansu Wuwei Tumour Hospital, Wuwei, China; [2]The 4th People's Hospital of Qinghai Province, Xining, China; [3]Beijing Youan Hospital, Capital Medical University, Beijing, China; [4]Jumei Doctor Group Medical (Shenzhen) Co., Ltd, Shenzhen, China*
Email: renfeng7512@hotmail.com

Background and aims: Chronic hepatitis B (CHB) patients with HBV DNA <LLOQ, HBeAg negative and HBsAg < 1500 IU/mL were the preferred population for clinical cure (PPCC). This study aims to observe the efficacy of nucleos(t)ide analogs (NAs) combined with peginterferon alpha-2b (PegIFNα-2b) in treating CHB patients with HBsAg > 1500 IU/mL (Non-preferred population for clinical cure, NPPCC).
Method: The CREATED EXCELLENT study (ChiCTR2400081073) is a multi-center, prospective, positive-controlled study. CHB patients with NAs treated for ≥3 months and HBsAg > 1500 IU/mL were enrolled and divided into two groups. The NAs monotherapy group continued to receive their original NAs (ETV/TDF/TAF/TMF) treatment, while the PegIFNα-2b+NAs group received PegIFNα-2b (180 μg/week) in addition to NAs. The total treatment period was 52 weeks, and all participants were followed up for 24 weeks after the end of treatment (EOT).
Results: A total of 682 patients (NAs monotherapy group, n = 330; PegIFNα-2b+NAs group, n = 352) were included. At baseline, there were 170 patients with HBsAg between 1500 IU/mL and 3000 IU/mL (NAs group: 21.81%, PegIFNα-2b+NAs group: 27.84%), 133 patients with HBsAg between 3000 IU/mL and 6000 IU/mL (NAs group: 18.23%, PegIFNα-2b+NAs group: 20.68%), 90 patients with HBsAg between 6000 IU/mL and 9000 IU/mL (NAs group: 12.11%, PegIFNα-2b+NAs group: 14.24%); and 289 patients with HBsAg greater than 9000 IU/mL (NAs group: 47.91%, PegIFNα-2b+NAs group: 37.23%). The baseline average HBsAg level in the NAs group was 18767.23 ± 5623.33 IU/mL and in the PegIFNα-2b+NAs group was 17346.91 IU/mL ($P > 0.05$). After 52 weeks of treatment, the average HBsAg level of the NAs group was 16963.92 ± 5127.89 IU/mL and the PegIFNα-2b +NAs group was 3589.40 ± 1223.47 IU/mL($P < 0.001$). The stratification ratio of patients with HBsAg < 1500 IU/mL, 1500 < HBsAg < 3000 IU/mL, 3000 < HBsAg < 6000 IU/mL, 6000 < HBsAg < 9000 IU/mL and more than 9000 IU/mL were 46.51%, 14.11%, 25.66%, 4.73% and 9.32%, respectively, in the PegIFNα-2b+NAs group; there rates were 20.00%, 30.15%, 26.72%, 3.32%, and 20.22% in the NAs group, respectively. At week 52 of EOT, 2 participants in NAs group had HBsAg loss, compared with 9 participants in PegIFNα-2b+NAs group.
Conclusion: Compared with NAs monotherapy, PegIFNα-2b combined with NAs therapy for the treatment of NPPCC (HBsAg > 1500 IU/mL) rapidly reduced HBsAg levels, and increased the number of PPCC (HBsAg<1500 IU/mL), thereby providing a new treatment strategy for CHB patients with high-level HBsAg to achieve clinical cure.

FRI-618
Characteristics of circulating immune cells in pediatric patients with chronic hepatitis B undergoing antiviral therapy
Haifang Cao[1], Hong Zhang[2], Qinghua Lu[1], 玲 徐[3], Yang Zhao[3], Hongfei Zhang[4], Feng Ren[3]. *[1]The 4th People's Hospital of Qinghai Province, Xining, China; [2]Public Health Clinical Center of Chengdu, Chengdu, China; [3]Beijing Youan Hospital, Capital Medical University, Beijing, China; [4]Jumei Doctor Group Medical (Shenzhen) Co., Ltd, Shenzhen, China*
Email: zhhf302@163.com

Background and aims: Hepatitis B surface antigen (HBsAg) loss or functional cure (FC), is considered the desirable therapeutic outcome for chronic hepatitis B (CHB) patients. However, the immune pathological biomarkers and underlying mechanisms in remain unclear, especially for pediatric CHB patients. In this study we comprehensively interrogate disease-associated cell states identified within PBMCs from either pediatric CHB or FC patients to provide novel insights into putative mechanisms underlying FC.
Method: We utilized mass cytometry to characterize the circulating immune cells profiles of 89 pediatric CHB patients (aged 3~18 years) including: 36 treatment-naïve CHB patients, 25 treated patients with nucleos(t)ide analogs (NAs), and 28 patients who achieved FC treated with NAs combined with Peginterferon alpha-2b (PegIFNα-2b, Pegbing®, Xiamen Amoytop Biotech Co., Ltd.). Peripheral blood mononuclear cells (PBMCs) were isolated from blood samples and subjected to high-dimensional immune cell profiling via mass cytometry to analyze their distinct immunological cell features.
Results: Unsupervised analysis revealed a reconfigured circulating immune landscape in pediatric CHB patients who achieved FC, distinct from both treatment-naïve and NAs-treated patients without achieving FC. Specifically, PegIFNα-2b+NAs-treated pediatric CHB patients with FC exhibited significantly elevated frequencies of peripheral NKT cells and TCRγδ-positive T cells. In contrast, NAs-treated pediatric CHB patients without achieving FC showed marked increases in conventional immune subsets, including $CD4^+$ T cells, NK cells, and both memory $CD8^+$ and $CD4^+$ T cells. Furthermore, T cells from PegIFNα-2b+NAs-treated pediatric CHB patients with FC displayed a distinct chemokine receptor profile, characterized by higher expression of CCR5, which is a marker previously associated with effective anti-HBV immune responses and treatment success in pediatric cohorts.
Conclusion: Pediatric CHB patients who achieve FC exhibit unique circulating immune cell functional characteristics, namely T cell functional reconstitution and activation of natural killer T cells. This profile provides insights into the mechanisms of pediatric CHB patients with FC and could guide the development of targeted immunotherapies for pediatric CHB patients.

FRI-619
Response to bulevirtide synchronizes HDV RNA and anti-HDV kinetics
Gabriele Ricco[1], Daniela Cavallone[2], Piero Colombatto[1], Barbara Coco[1], Filippo Oliveri[1], Francesco Damone[1], Giovanni Petralli[1], Veronica Romagnoli[1], Antonio Salvati[1], Lidia Surace[1], Alessia Calì[1], Barbara Vianello[1], Ferruccio Bonino[3], Maurizia Brunetto[1,2]. *[1]Hepatology Unit, University Hospital of Pisa, Pisa, Italy; [2]Department of Clinical and Experimental Medicine, University of Pisa, Pisa, Italy; [3]Italian National Research Council, Institute of Clinical Physiology, Pisa, Italy*
Email: riccogabriele@gmail.com

Background and aims: Currently the efficacy of treatment in chronic hepatitis D (CHD) is monitored by ALT and HDV RNA. Preliminary data indicate that declining anti-HDV levels are associated with virological control after Interferon. We evaluated HDV RNA and anti-HDV kinetics in CHD patients (pts) treated with bulevirtide (BLV).
Method: BLV-treated CHD pts with baseline samples (BL) and weeks (w) 48–144 were included. HDV RNA was quantified by qPCR

(AltoStar HDV RT-PCR kit 1.5; Altona; LOD: 1.12 IU/mL). Anti-HDV was tested by CLIA (Liaison XL Murex anti HDV, DiaSorin) after 10-fold endpoint dilution and Log AU/mL were calculated multiplying the AU/mL by the dilution factor. Virological response (VR) was defined as ≥2Log HDV RNA decline or undetectability. Correlations were assessed by Spearman's test.

Results: Twenty-six CHD pts (92.3% cirrhosis; median age 48.9 yrs, M/F 11/15) received BLV 2 mg/day for a median of 120 (57–193) weeks. At BL, median HDV RNA, anti-HDV were: 5.52 (1.70/7.20) Log IU/mL, 3.83 (3.39/4.72) Log AU/mL; 15/26 (57.7%) pts tested anti-HDV positive at 1:1000 and 11/26 (42.3%) at 1:10,000 dilution. VR rates were 69.2%, 66.7%, 65% and 80% at w48, w72, w96 and w144, while ALT normalization occurred at the same time points in 92.3%, 83.3%, 90% and 100%. Overall, HDV RNA correlated with anti-HDV ($\rho = 0.646$, $p < 0.001$) and ALT ($\rho = 0.560$, $p < 0.001$). The correlation between HDV RNA and anti-HDV was absent at BL ($\rho = 0.122$, $p = 0.551$), but increased during treatment: $\rho = 0.366$ ($p = 0.066$) at w48, $\rho = 0.572$ ($p = 0.003$) at w72, $\rho = 0.448$ ($p = 0.048$) at w96 and $\rho = 0.742$ ($p = 0.014$) at w144. At the end of follow-up (EOF), 15/26 (57.7%) pts showed a VR and a significantly lower median anti-HDV levels [3.18 (2.00/3.80) Log AU/mL] compared to 11 (42.3%) non-responders [3.71 (3.03/4.24) Log AU/mL] ($p = 0.020$). In VR pts anti-HDV levels declined throughout EOF, when anti-HDV were positive in 4 (26.7%) at 1:100, 11 (73.3%) at 1:1000 dilutions. Conversely, among the 11 non-responders, anti-HDV levels were positive in 10 (90.9%) at 1:1000 and in 1 (9.1%) at 1:10,000 ($p = 0.042$).

Conclusion: HDV RNA and anti-HDV levels were significantly correlated in BLV-treated CHD pts. Anti-HDV levels declined in parallel with HDV RNA in virological responders. Further studies are warranted to determine whether a sustained reduction in anti-HDV levels could serve as a surrogate marker of immunological control and help guide safe treatment discontinuation.

FRI-620
Clinical outcomes of Bulevirtide treatment in patients with chronic hepatitis Delta in a tertiary center from Bucharest, Romania

Violeta Molagic[1,2], Isabela Staicu[1,2], Anca Saran[1,2], Nicoleta Mihai[1,2], Alina Cozma[2], Daniela Neagu[2], Adrian Marinescu[1,2], Codrin Gheorghe[2], Cătălin Tilișcan[1,2], Raluca Năstase[2], Anca Negru[1,2], Sorin Stefan Arama[1,2], Victoria Arama[1,2]. *[1]University of Medicine and Pharmacy "Carol Davila," Bucharest, Romania; [2]National Institute for Infectious Diseases "Prof. Dr. Matei Balș," Bucharest, Romania*
Email: violeta_molagic@yahoo.com

Background and aims: Hepatitis B and D viruses (HBV and HDV) lead to high liver disease burden with limited therapeutic options, despite effective HBV vaccination available in the last three decades. A recent HBV prevalence evaluation among Europe sets Romania the second highest (6.2%). The assessed HDV global prevalence was 4.5% in people with chronic HBV infection, yet there is insufficient data for an accurate estimation in Romania. Bulevirtide (BLV), an entry inhibitor, was approved in Romania in 2024 and preliminary results indicate positive effects on slowing disease progression, however routine clinical practice data is currently limited. Objective: Analysis of the clinical characteristics and treatment outcomes of patients with chronic HDV infection.

Method: We conducted a retrospective study on chronic HDV infection adult patients receiving BLV treatment who were evaluated in our department of the National Institute for Infectious Diseases "Prof. Dr. Matei Bals" between August 2024 and December 2025. Clinical, biological and treatment-related data was analysed using SPSS Statistics (version 26).

Results: We included 33 patients, with a median age of 45 years (IQR: 27) and male to female ratio of 1:1.36. Compensated cirrhosis was diagnosed in 11/33 patients (33%) and one patient had HIV co-infection. At initiation of BLV, median levels of alanine aminotransferase (ALT) were 75 U/L, aspartate aminotransferase (AST) 49 U/L, HBV-DNA 120 IU/mL, HDV-RNA 598.432 IU/mL, AST to Platelet Ratio Index (APRI) 0.78 points and Fibrosis-4 (FIB-4) Index 2.05 points. Of the 23/33 patients (70%) who completed 24 weeks of BLV therapy, biochemical response (BR) was observed in 10/23 patients (43%) and it was more frequent in patients < 40 years ($p = 0.005$). BR was associated with lower APRI (median 0.35 points, $p = 0.01$) and FIB-4 (median 1.52 points, $p = 0.02$) in 7/10 patients (70%). In addition, 10/23 patients (43%) reached $\geq 2 \log_{10}$ IU/mL HDV-RNA decline from baseline at 24 weeks (median of 721 IU/mL). Among 7/33 patients (21%) who received 48 weeks of BLV treatment, without adverse events, 4/7 patients (57%) achieved both BR and virologic response.

Conclusion: Clinical outcomes of BLV treatment for chronic HBV and HDV hepatitis show liver function improvement and viral suppression after 6 to 12 months of administration. Further studies must assess the long-term evolution and more eligible patients need to be enrolled, currently being the only approved therapeutic option available.

FRI-621
Bile acid profile modifications in patients with chronic hepatitis D receiving bulevirtide therapy

Christiane Stern[1], Aurore Desmons[2], Segolene Brichler[3], Emmanuel Gordien[3], Stéphanie Marque Juillet[1], Muriel Girard[4]. *[1]Centre Hospitalier de Versailles, Le Chesnay, France; [2]Hopital Saint Antoine, AP-HP, Paris, France; [3]Hopital Avicenne, Bobigny, France; [4]Hopital Necker Enfants Malades, Paris, France*
Email: christiane.stern@gmail.com

Background and aims: Bulevirtide (BLV) is the only approved treatment for patients with chronic hepatitis D (CHD). Due to its mode of action blocking the entry receptor Na+-taurocholate cotransporting polypeptide (NTCP), an increase in total serum bile acids (BA) is generally observed in patients receiving BLV and thought to be non-clinically significant. Nonetheless, the BA composition in those patients has not been evaluated. The aim of this study is to evaluate the BA profile in patients with CHD receiving BLV.

Method: All consecutive patients with CHD who came for a follow-up visit in our department since July 2025 were eligible for this study (ongoing recruitment). Sociodemographic data, clinical signs and treatment history were recorded. The following tests were performed in all patients: complete blood count, prothrombin time, bilirubin, ALT, AST, GGT, albumin, serum creatinine, quantitative HBsAg, HBV-DNA and HDV-RNA, abdominal ultrasound, liver and spleen elastography. The bile acid composition was evaluated in each patient after at least 6-hour fasting by liquid chromatography-tandem mass spectrometry (LC-MS/MS) assay. Bile acids profiles were analyzed according to HDV therapy (BLV *vs* none).

Results: Eleven CHD patients with bile acid profile were included. Baseline characteristics were: male gender 45%, median age 51 ± 8, African origin 36%, compensated cirrhosis 36%. Median HBsAg, HBV-DNA and HDV-RNA were 3.59 (0–4.26), TND (0–3.89) and 5.76 log (TND – 6.09), respectively. At baseline, 9 out of 10 patients with positive HBsAg were receiving HBV treatment (tenofovir = 8, entecavir = 1), 4 patients were treated with BLV and 7 patients were not receiving HDV treatment (3 naïve, 3 discontinued BLV and 1 discontinued REP 2139). Among the 4 patients on BLV, none of them had pruritus. Mean total BA - UDCA was 3.82 µmol/L (0.93–42.68). BA composition in patients receiving BLV showed low rates of free bile acids (0.03–0.07) when compared to normal levels (0.18–0.78) in patients without current HDV treatment, except in one patient without virological response on BLV therapy (0.36). Also, the primary/secondary BA ratio was increased only in patients receiving BLV therapy and in a patient with cirrhosis/CSPH.

Conclusion: BA profile seems to be modified in patients receiving BLV therapy. Unconjugated BA may be decreased in patients receiving BLV which could be used as a marker of adherence to therapy. The impact of these BA modifications on long-term should be evaluated by prospective larger studies.

FRI-622

Impact of antiviral selection on survival outcomes in hepatitis B-related acute on chronic liver failure: a comparative study of Tenofovir Alafenamide and Tenofovir Disoproxil Fumarate from the multicentre APASL ACLF research consortium

Sunil Taneja[1], Ajay Kumar Duseja[1], Nipun Verma[1], Ashok Kumar Choudhury[2], Vinod Arora[2], Rakhi Maiwall[2], Mamun Al-Mahtab[3], Qin Ning[4], Tao Chen[4], Akash Shukla[5], Ajit Sood[6], Omesh Goyal[6], vandana midha[6], Girish Kumar Pati[7], Sombat Treeprasertsuk[8], Kessarin Thanapirom[8], Nagaraja Padaki[9], Anand Kulkarni[9], Mithun Sharma[9], Hasmik Ghazinyan[10], V G Mohan Prasad[11], Mithra Prasad[11], Diana Payawal[12], Gamal Shiha[13], Fazal Karim[14], Radha Krishan Dhiman[15], Ajay Mishra[15], Shahinul Alam[16], Sanjiv Saigal[17], Anil Arora[18], Ashish Kumar[18], Pravin Rathi[19], V.M. Dayal[20], Ajay Kumar[21], Ashish Kumar Jha[20], Kemal Fariz Kalista[22], Sargsyan Violeta[23], Saurabh Mukewar[24], Sunil Dadhich[25], Sanjeev Sachdeva[26], Ajay Kumar[26], P Javed[27], Neeraj Saraf[28], Narendra S Choudhary[28], Akash Roy[29], Mahesh Goenka[29], Suprabhat Giri[30], Dibyalochan Praharaj[30], Manoj Sahoo[30], Krishnadas Devadas[31], Arun Valsan[32], Tarana Gupta[33], Shalimar Shalimar[34], Shiv Kumar Sarin[2].

[1]Postgraduate Institute Of Medical Education And Research, Chandigarh, India; [2]Institute of Liver & Biliary Sciences, New Delhi, India; [3]Department of Hepatology, Bangladesh Medical University, DHAKA, Bangladesh; [4]Tongji Hospital, Tongji Medical College, WUHAN, China; [5]Seth G S Medical College and K.E.M Hospital, MUMBAI, India; [6]DMC, LUDHIANA, India; [7]IMS and SUM Hospital, Bhubaneswar, India; [8]King Chulalongkorn Memorial Hospital, BANGKOK, Thailand; [9]AIG, HYDERABAD, India; [10]Yerevan Medical Scientific Center, Armenia, YEREVAN, Armenia; [11]VGM HOSPITAL, COIMBATORE, India; [12]Fatima University Medical Center Manila, Manila, Philippines; [13]Egyptian Liver and Research Institute and Hospital (ELRIAH), Mansoura, Egypt; [14]Sir Salimullah Medical College Mitford Hospital, Dhaka, Bangladesh; [15]SGPGI, Lucknow, India; [16]Department of Hepatology, Bangabandhu Sheikh Mujib Medical University, Dhaka, Bangladesh; [17]Max Superspeciality Hospital, Saket, Delhi, India; [18]Sir Ganga Ram Hospital, Delhi, India; [19]TN Medical College and BYL Nair Hospital, Mumbai, India; [20]IGIMS, Patna, India; [21]KGMU, Lucknow, India; [22]Division of Hepatobiliary, Department of Internal Medicine, Cipto Mangunkusumo Hospital, Faculty of Medicine Universitas Indonesia, Jakarta, Indonesia; [23]Violeta Medical Centre, Armenia, Yerevan, Armenia; [24]Midas Multispeciality Hospital, Nagpur, India; [25]SMNC, Jodhpur, India; [26]GB Panth Hospital, Delhi, India; [27]ASTER MIMS Hospital, Kannur, India; [28]Medanta, The Medicity, Gurugram, India; [29]Apollo Multispeciality Hospital, Kolkata, India; [30]KIMS, Bhubneshwar, India; [31]GMC, Trivandrum, India; [32]AIMS, Kochi, India; [33]Pandit Bhagwat Dayal Sharma Post Graduate Institute of Medical Sciences, Rohtak, India, Rohtak, India; [34]AIIMS, Delhi, India

Email: shivsarin@gmail.com

Background and aims: Hepatitis B virus (HBV) related acute on chronic liver failure (ACLF) is associated with high short-term mortality. Early initiation of antivirals is the cornerstone of management. However, comparative data regarding efficacy and outcomes with tenofovir alafenamide (TAF) versus tenofovir disoproxil fumarate (TDF) is limited. The present study compared survival outcomes of TAF versus TDF in patients with HBV ACLF.

Method: In this multicentre retrospective study data from the APASL ACLF Research Consortium cohort were analysed to compare short-term survival outcomes in patients with HBV-related ACLF treated with TAF vs TDF.

Results: A total of 813 HBV-related ACLF patients were included: 600 in the TAF group (487 males, 113 females) and 213 in the TDF group (194 males, 19 females). The median age in years was 45 (17–84) in the TAF group and 43 (17–75) in the TDF group. The mean CTP score (10.9 ± 1.4 vs 9.7 ± 0.96, p = 0.00), MELD score (28.2 ± 7.2 vs 24 ± 3.7, p = 0.00) and MELD Na (30.1 ± 7.0 vs 25.8 ± 3.9, p = 0.00) were higher in the TAF group; however, the AARC score (9.8 ± 1.5 vs 9.8 ± 1.4, p = 0.23) was comparable. Kaplan–Meier survival analysis demonstrated a significant difference in the in-hospital survival between the two treatment groups, with improved survival in the TAF group compared with the TDF group (median survival 68 days [95% CI 48.6–87.4] vs. 48 days [95% CI 39.0–57.0]; 75th percentile survival 43 vs. 25 days, respectively; log-rank $\chi^2 = 5.95$, p = 0.02). On univariable Cox regression analysis, treatment with TAF was associated with lower in-hospital mortality compared with TDF (HR 0.62, 95% CI 0.42–0.92; p = 0.02); however, on multivariable analysis, only the number of organ failures at presentation independently predicted mortality (HR 1.35 per organ failure, 95% CI 1.09–1.67; p = 0.01).

Conclusion: In HBV-related ACLF, TAF was associated with improved unadjusted survival; however, the baseline number of organ failures rather than antiviral choice independently predicted short-term mortality.

FRI-623

High HBsAg loss with peginterferon alfa-2b retreatment in chronic hepatitis B patients with low HBsAg levels after initial therapy

Fengqin Hou[1], Jia Shang[2], Qing Xie[3], Chunliang Lei[4], Jianmei Lin[5], Guoxin Hu[6], Zhiliang Gao[7], yilan zeng[8], Jiabin Li[9], Qianguo Mao[10], Liying Zhu[11], Jun Chen[12], Xiaozhong Wang[13], Zuxiong Huang[14], Jiming Zhang[15], Ping An[16], Xiulan Xue[17], Yan Huang[18], Tianyan Chen[19], Jianqi Lian[20], YueYong Zhu[21], Huiling Xiang[22], Xin-Yue Chen[23], Hui Guo[24], Ruoyi He[25], Yalin Yin[25], Li Sun[25], Guiqiang Wang[26].

[1]Peking University First Hospital, Beijing, China; [2]Henan Provincial People's Hospital, Zhengzhou, China; [3]Ruijin Hospital, Shanghai Jiaotong University School of Medicine, Shanghai, China; [4]Guangzhou Eighth People's Hospital, Guangzhou Medical University, Guangzhou, China; [5]Sichuan Provincial People's Hospital·Sichuan Academy of Medical Sciences, Chengdu, China; [6]Peking University Shenzhen Hospital, Shenzhen, China; [7]The Third Affiliated Hospital, Sum Yat-Sen University, Guangzhou, China; [8]Public Health Clinical Center of Chengdu, Chengdu, China; [9]The First Affiliated Hospital of Anhui Medical University, Hefei, China; [10]Xiamen Hospital of Traditional Chinese Medicine, Xiamen, China; [11]The Fourth Affiliated Hospital of Harbin Medical University, Harbin, China; [12]Shenzhen Third People's Hospital, Shenzhen, China; [13]Xinjiang Uygur Autonomous Region Hospital of Traditional Chinese Medicine, Urumqi, China; [14]Mengchao Hepatobiliary Hospital of Fujian Medical University, Fuzhou, China; [15]Huashan Hospital, Fudan University, Shanghai, China; [16]The Sixth People's Hospital of Shenyang, Shenyang, China; [17]The First Affiliated Hospital of Xiamen University, Xiamen, China; [18]Xiangya Hospital Central South University, Changsha, China; [19]The First Affiliated Hospital of Xi'an Jiaotong University, Xi'an, China; [20]The Second Affiliated Hospital of the Air Force Military Medical University of CPLA, Xi'an, China; [21]The First Affiliated Hospital of Fujian Medical University, Fuzhou, China; [22]Tianjin Third Central Hospital, Tianjin, China; [23]Beijing Youan Hospital, Capital Medical University, Beijing, China; [24]First Teaching Hospital of Tianjin University of Traditional Chinese Medicine, Tianjin, China; [25]Xiamen Amoytop Biotech Co. Ltd, Xiamen, China; [26]Peking University First Hospital, Peking University International Hospital, Beijing, China

Email: wangguiqiang_aasld@163.com

Background and aims: Peginterferon alpha (PegIFNα) treatment enables patients with chronic hepatitis B (CHB) to achieve high HBsAg loss rates. However, evidence remains limited regarding the efficacy of PegIFNα retreatment. This study investigated the efficacy of PegIFNα retreatment in patients who initially responded well but did not attain functional cure.

Method: This is a long-term follow-up study (NCT06707922) of a randomized controlled phase 3 trial (NCT04846491). At the end of the phase 3 trial, nucleos(t)ide analogue (NA)-experienced patients with HBsAg decline ≥ 1 $\log_{10}$ IU/mL and HBsAg level < 100 IU/mL, as well as treatment-naïve patients with HBsAg decline ≥ 1.5 $\log_{10}$ IU/mL and HBsAg level < 1500 IU/mL were enrolled in cohort 2. All

patients initially received treatment with PegIFNα-2b (Pegbing®, Xiamen Amoytop Biotech Co., Ltd.) 180 μg/week combined with tenofovir alafenamide fumarate (TAF) for 72 weeks, after which all drugs were discontinued and patients were followed up to 5 years. PegIFNα-2b was given intermittently in cycles (8 weeks of treatment + 4 weeks of interval, repeating every 12 weeks). Here, we report the results of the 72-week analysis in cohort 2.

Results: A total of 47 NA-experienced patients and 15 treatment-naïve patients were enrolled in cohort 2. The average ages of the two populations were 42.5 and 34.5 years, and 85.1% and 66.7% were male. Among NA-experienced patients, the mean baseline HBsAg level was 13.00 IU/mL, and all were negative for HBeAg and HBV DNA. Among treatment-naïve patients, the mean baseline HBsAg level was 272.77 IU/mL, 73.3% were HBeAg negative and 100% were HBV DNA undetectable. The HBsAg loss rate in NA-experienced patients increased from 23.4% (11/47) at week 24 to 42.6% (20/47) at week 48 and further to 46.8% (22/47) at week 72, while that in treatment-naïve patients increased from 13.3% (2/15) to 26.7% (4/15) and then to 40% (6/15). All patients who achieved HBsAg loss at weeks 48 and 72 also concurrently attained HBV DNA undetectable. At week 72, HBsAg seroconversion was observed in 35.0% (14/40) of NA-experienced patients and 30.8% (4/13) of treatment-naïve patients. Among the four HBeAg-positive treatment-naïve patients, one achieved HBeAg loss and seroconversion.

Conclusion: Regardless of whether patients were NA-experienced or treatment-naïve, more than 40% still achieved HBsAg loss through PegIFNα-2b retreatment. Patients with good initial responses to PegIFNα have a high chance of pursuing functional cure by retreatment with PegIFNα.

FRI-624

Factors associated with lack of alanine aminotransferase normalisation in patients with chronic hepatitis B virus after 8 years of tenofovir-based treatment

Grace Lai-Hung Wong[1], Maria Buti[2,3], Jinlin Hou[4], Scott K. Fung[5], Harry L.A. Janssen[6,7], Namiki Izumi[8], Wan-Long Chuang[9], Rajiv Mehta[10], Frida Abramov[11], Hongyuan Wang[11], Irina Botros[11], Leland J. Yee[11], Kosh Agarwal[12], Young-Suk Lim[13], Patrick Marcellin[14]. *[1]The Chinese University of Hong Kong, Shatin, Hong Kong; [2]Hospital Universitario Vall d'Hebron, Barcelona, Spain; [3]Centro de Investigación Biomédica en Red de Enfermedades Hepáticas y Digestivas (CIBEREHD) del Instituto Carlos III, Madrid, Spain; [4]State Key Laboratory of Organ Failure Research, Nanfang Hospital, Southern Medical University, Guangzhou, China; [5]Toronto Centre for Liver Disease, Toronto General Hospital Research Institute, Toronto, Canada; [6]Toronto Centre for Liver Disease, Toronto General Hospital Research Institute, University Health Network, Toronto, Canada; [7]Erasmus University Medical Center, Rotterdam, Netherlands; [8]Japanese Red Cross Musashino Hospital, Tokyo, Japan; [9]Kaohsiung Medical University, Kaohsiung, Taiwan; [10]SIDS Hospital, Surat, India; [11]Gilead Sciences, Inc., Foster City, United States; [12]King's College Hospital NHS Foundation Trust, London, United Kingdom; [13]University of Ulsan College of Medicine, Seoul, Korea, Rep. of South; [14]Association for the Promotion of Hepatologic Care and University of Paris, Paris, France*
Email: wonglaihung@mect.cuhk.edu.hk

Background and aims: Long-term nucleos(t)ide analogue therapy effectively suppresses hepatitis B virus (HBV) replication in chronic hepatitis B (CHB); however, elevated alanine aminotransferase (ALT) levels may persist. We evaluated factors associated with persistent ALT (pALT) elevation (ALT above the AASLD upper limit of normal [25 U/L females, 35 for males]) after 8 years (Y) of tenofovir-based therapy.

Method: Pooled data from patients (pts) in two Phase 3 trials GS-US-320-0108 (HBeAg negative) and GS-US-320-0110 (HBeAg positive) trials were analysed. Pts were randomised 2:1 to TAF 25 mg/or TDF 300 mg/d for up to 3Y, then given open-label TAF through Y8. ALT status (normal vs pALT) was assessed at Y8. Baseline (BL) variables were analysed as predictors of pALT using multivariate logistic regression.

Results: Of 1159 pts with Y8 ALT data, 907 (78%) had normal ALT and 252 (22%) had pALT. At BL, pts with pALT were younger (median 37 vs 42 Y), more often male (73% vs 65%), and had higher mean BMI (25.5 vs 23.9 kg/m^2; $p < 0.0001$) vs pts with normal ALT. Overweight (BMI 25 to < 30 kg/m^2) and obesity (> 30 kg/m^2) were present in 46% and 10% of pts with pALT vs 30% and 6% with normal ALT ($p < 0.0001$). Slightly more pts with pALT had BL diabetes and hyperlipidaemia (9% and 10%, respectively) vs pts with normal ALT (7% and 8%). HBV genotype (GT) distribution showed more frequent GTA (9% vs 4%) and GTD (21% vs 17%) in pts with vs without pALT ($p = 0.0009$). At Y8, median (range) ALT was 45 (26–270) U/L and 19 (3–35) U/L in the pALT and normal ALT groups. At Y8, 88% vs 97% achieved HBV DNA < 29 IU/mL, with less HBeAg loss (35% vs 50%) and seroconversion (23% vs 33%) in pALT pts. By multivariate analysis, predictors of pALT included higher BL BMI (odds ratio [OR] 1.14; $p < 0.0001$), younger age (OR 0.96 for each Y older; $p < 0.0001$), and HBV GTA (OR 2.28; $p = 0.0053$). Over 8Y, both groups had similar modest changes in lipid parameters (median total cholesterol [TC] +6 vs +5 mg/dL; LDL +12 vs +15 mg/dL; HDL −8 vs −7 mg/dL in pts with pALT vs normal ALT) and minimal change in TC/HDL ratio (0.7 vs 0.5), while triglyceride (+27 vs +10 mg/dL) and glucose (+9 vs +5 mg/dL) increases were greater in pts with pALT.

Conclusion: After 8Y of tenofovir-based therapy, approximately 20% of patients had pALT, often despite durable viral suppression. Younger age, higher BMI, and GTA were independent predictors of pALT, suggesting roles for metabolic and viral factors in ongoing hepatic inflammation during long-term treatment.

FRI-625

Characterisation of HDV RNA, HBsAg and ALT kinetics in patients treated with bulevirtide and pegylated interferon for 96 weeks in the SEE-D trial

Emmanuel Zavalis[1], Adquate Mhlanga[2], Karin Lindahl[1,3], Susanne Cederberg[1,4], Annika Olsson[1,4], Niklas Björkström[3,4,5], Heiner Wedemeyer[4,6], Pietro Lampertico[7,8], Harel Dahari[2], Soo Aleman[1,3,4]. *[1]Department of Infectious Diseases, Karolinska University Hospital, Stockholm, Sweden; [2]Program for Experimental and Theoretical Modeling, Division of Hepatology, Department of Medicine, Stritch School of Medicine, Loyola University Chicago, Maywood, United States; [3]Center for Infectious Diseases, Karolinska Institutet, Stockholm, Sweden; [4]D-SOLVE Consortium, Hannover, Germany; [5]Department of Clinical Microbiology, Karolinska University Hospital, Stockholm, Sweden; [6]Department of Gastroenterology, Hepatology, Infectious Diseases and Endocrinology, Hannover Medical School, Hannover, Germany; [7]Division of Gastroenterology and Hepatology, Foundation IRCCS Ca' Granda Ospedale Maggiore Policlinico, Milan, Italy; [8]CRC "a. M. and a. Migliavacca" Center for Liver Disease, Department of Pathophysiology and Transplantation, University of Milan, Milan, Italy*
Email: soo.aleman@regionstockholm.se

Background and aims: Combination therapy of 48 weeks with bulevirtide (BLV) and pegylated Interferon (peg-IFN) has shown higher rates of on-treatment undetectable HDV compared with BLV monotherapy in the MYR204 trial. Data from longer combination therapy is lacking.

Method: Thirty-one patients with chronic hepatitis D were enrolled at Karolinska University Hospital, Sweden, in the SEE-D clinical trial (EU no. 2023-504414-29-00). They received 96-weeks combination treatment with BLV (2 mg/day) and peg-IFN (180 μg weekly, reduced to 135 μg from Week 48), followed by solidifying BLV therapy; all received nucleos(t)ide therapy. Participants were sampled every 12 weeks and upon clinical indication for HDV RNA ([LoQ] < 50 IU/ml and [LoD] < 6 IU/mL), HBsAg ([LoD] < 0.05 IU/mL) and ALT ([ULN] 65.9 IU/ml for men and 44.9 IU/ml for women; local laboratory references). HDV kinetic patterns were evaluated visually and with

Change-Point Estimation in R to define slope and time boundaries of the initial decline phase.
Results: Twenty participants (65%) were IFN-experienced, and 18 (58%) were men. At baseline, 10/31 (32%) had fibrosis stage F3 and 14/31 (45%) had F4. Mean (SE) baseline HDV RNA, HBsAg and ALT were 4.76 ± 0.21 $\log_{10}$ IU/mL, 3.82 ± 0.06 $\log_{10}$ IU/mL, and 106 ± 14.9 U/L, respectively. All participants initially showed a rapid initial HDV decline (−0.91 ± 0.08 $\log_{10}$ IU/mL/month), followed by: i) undetectability (monophasic - MP, n = 16, 53%), ii) slower second phase of decline to undetectability (biphasic - BP, n = 11, 37%), or iii) flat incompleteesponse (FIR, n = 3, 10%) plateauing above LoQ. Transient LoD to LoQ fluctuations, indicating a plateau below detectability, occurred in three of the participants in the MP group. Two on-therapy breakthroughs were observed to >3 log10 IU/mL; one BP and one FIR. By Week 72, 24 participants (78%) had achieved HDV undetectability and in those that reached week 96, all but one achieved undetectability. ALT normalization was observed in 21 participants (68%) at Week 72 and 18 (58%) at Week 96. HBsAg decline >75% occurred in 10 participants (32%) at final follow-up, all but one (LoQ) had undetectable HDV; one loss occurred.
Conclusion: In this interim analysis, three main kinetic patterns of HDV decline were observed. Approximately one third achieved >75% HBsAg reduction at final follow-up, primarily those with undetectable HDV. HBsAg reduction may reflect a loss of HBsAg-producing cells and/or interferon-mediated inhibition of HBsAg production.

FRI-626

Effect of peginterferon alfa-2b with or without nucleos(t)ide analogues on long-term outcomes in chronic hepatitis B: preliminary 48-week results from the multicenter, prospective VISION study in China

Qing-Lei Zeng[1], Yaqing Liu[2], Guotao Li[3], Zhenhua Wang[4], Junling Cai[5], Jianzhi Gu[6], Hongxia Zhu[7], Qian Dou[8], Xinde Liu[9], Xiao-Ping Dong[10], Jing Wang[11], Guodong Zhang[12], Yufu Wang[13], Zhenkun He[14], Haiyan Chen[15], Sheng-Li Ma[16], Xianwei Shang[17], Weiping Li[18], Chuanwen Chen[19], Yuzhong Wang[20], Junsheng Gu[1], Yanfeng Pan[1], Zhigang Ren[1], Juan Li[1], Zhi-Qin Li[1], Changyu Sun[1], Hongxia Liang[1]. *[1]The First Affiliated Hospital of Zhengzhou University, Zhengzhou, China; [2]The First People's Hospital of Shangqiu, Shangqiu, China; [3]Luoyang Central Hospital, Luoyang, China; [4]Shangqiu Municipal Hospital, Shangqiu, China; [5]Zhumadian Central Hospital, Zhumadian, China; [6]Luoshan County People's Hospital, Xinyang, China; [7]The People's Hospital of Weishi, Kaifeng, China; [8]The Third Affiliated Hospital of Henan Medical University, Xinxiang, China; [9]The 990 Hospital of the Joint Support Force of the Chinese People's Liberation Army of China, Zhumadian, China; [10]Sanmenxia Central Hospital, Sanmenxia, China; [11]Chinese Medicine Hospital of Puyang, Puyang, China; [12]General Hospital of Pingmei Shenma Group, Pingdingshan, China; [13]Zhumadian Traditional Chinese Medicine Hospital, Zhumadian, China; [14]Huaihe Hospital of Henan University, Kaifeng, China; [15]Xinyang Central Hospital, Xinyang, China; [16]Yongcheng People's Hospital, Yongcheng, China; [17]Ruyang People's Hospital, Luoyang, China; [18]Shangcai County People's Hospital, Zhumadian, China; [19]Shangcheng County People's Hospital, Xinyang, China; [20]The Fifth People's Hospital of Anyang, Anyang, China*
Email: hxliang@zzu.edu.cn

Background and aims: Optimizing antiviral strategies and achieving hepatitis B surface antigen (HBsAg) loss remain major challenges in the management of chronic hepatitis B (CHB). This study aimed to evaluate the effects of 48-week peginterferon alfa-2b (Peg-IFN α-2b) therapy, with or without nucleos(t)ide analogues (NAs), in patients with CHB enrolled in the VISION study.
Method: In May 2024, we launched the multicenter, prospective VISION study to assess the long-term effects of Peg-IFN α-2b with or without NAs in CHB patients. This 48-week analysis involved two treatment groups: Peg-IFN α-2b monotherapy and Peg-IFN α-2b in combination with NAs, with a primary focus on assessing effectiveness and safety. Baseline characteristics between the two groups were balanced using propensity score matching (PSM).
Results: A total of 1138 patients completed the 48-week follow-up. After PSM, 798 patients were included in the analysis, comprising 399 patients in the monotherapy group and 399 patients in the combination group. At baseline, there were no significant differences between the monotherapy and combination groups in the proportion of males (64.7% [258/399] vs. 64.2% [256/399], $p = 0.882$), mean age (43.5 ± 9.6 vs. 43.4 ± 9.4 years, $p = 0.958$), HBeAg positivity rate (19.8% [79/399] vs. 21.3% [85/399], $p = 0.599$), HBsAg levels (2.2 ± 1.3 vs. 2.3 ± 1.2 log IU/mL, $p = 0.226$), HBV DNA levels (1.9 ± 1.5 vs. 1.9 ± 1.6 log IU/mL, $p = 0.636$), and ALT levels (34.1 ± 45.9 vs. 33.8 ± 31.0 U/L, $p = 0.920$). At 48 weeks, HBsAg loss rates (30.1% [120/399] vs. 29.3% [117/399], $p = 0.816$) and ALT levels (49.0 ± 87.3 vs. 46.0 ± 40.8 U/L, $p = 0.587$) were comparable between the two groups, while HBV DNA levels were slightly higher in the monotherapy group (1.6 ± 1.4 vs. 1.2 ± 0.8 log IU/mL, $p = 0.029$). Notably, subgroup analysis showed that among patients with baseline HBsAg levels of <100, 100–<500, 500–<1500, and ≥1500 IU/mL, HBsAg loss rates were 55.9% (81/145), 27.9% (24/86), 12.3% (8/65), and 6.8% (7/103) in the monotherapy group, and 56.3% (76/135), 27.8% (27/97), 10.0% (7/70), and 7.2% (7/97) in the combination group (all $p > 0.05$). Both treatment groups were generally well tolerated, with no serious adverse events observed.
Conclusion: At 48 weeks, among patients with low baseline HBsAg and HBV DNA levels, Peg-IFN α-2b monotherapy and Peg-IFN α-2b plus NAs combination therapy demonstrated comparable HBsAg loss rates and ALT levels, with no evident short-term advantage of combination therapy. The long-term benefits of these regimens are currently under investigation.

FRI-627

HBsAg seroclearance profiles and post-treatment trajectories with refined baseline HBsAg stratification in a nationalwide cohort study: implications for functional and partial cure with individualized finite treatment

Qiran Zhang[1], Feng Sun[1], Ruirui You[1], Shanshan Zhu[1], Shulan Sui[1], Yiqi Yu[1], Jiming Zhang[1], Wenhong Zhang[1]. *[1]Huashan Hospital, Fudan University, Shanghai, China*
Email: zhangqiran@fudan.edu.cn

Background and aims: Achieving a functional cure, characterized by HBsAg seroclearance, or a partial cure with sustained low-level HBsAg, is a key goal in CHB management. Detailed data are lacking to define the likelihood of achieving and maintaining these treatment endpoints across the full spectrum of baseline HBsAg levels in real-world practice. This study aimed to provide evidence on this issue.
Method: In this nationalwide, multicenter real-world cohort study, adults with CHB who initiated or were receiving NA or IFN-based therapy were enrolled from 98 centers. All enrolled individuals were followed by prospective data collection. Cumulative HBsAg seroclearance was described across finely stratified baseline HBsAg categories and over time, separately for NA and IFN-based regimens and stratified by IFN treatment duration. For PegIFN-treated patients, post-treatment HBsAg trajectories after cessation of PegIFN were also evaluated.
Results: Among 7271 participants included, 3623 received IFN-based therapy and 3648 received NA only. With NA monotherapy, clinically meaningful HBsAg seroclearance was largely confined to patients with baseline HBsAg <20 IU/mL (22.9% for those <10 IU/mL and 6.76% for those with 10–20 IU/mL by week 168). For patients with higher baseline HBsAg levels in this cohort, HBsAg clearance occurred only as sporadic events. In contrast, HBsAg seroclearance under IFN-based therapy was observed across the full baseline HBsAg spectrum, with incidence clearly dependent on both baseline HBsAg and follow-up duration. At week 48, the cumulative HBsAg clearance rate exceeded 30% for patients with baseline HBsAg <50 IU/mL, 20% for those <100 IU/mL, and 10% for those <500 IU/mL. By week 168, the rate

surpassed 30% for those <100 IU/mL, 20% for those <1000 IU/mL, and 10% for those <3000 IU/mL. Analysis of PegIFN-treated patients after therapy cessation showed that most (73.0%) maintained stable HBsAg levels overall, while 16.4–32.4% experienced further HBsAg decline or seroclearance, particularly those with lower HBsAg at PegIFN cessation.

Conclusion: This study demonstrates that currently available antiviral agents can lead to HBsAg loss or sustained low-level HBsAg in a subset of CHB patients, with strong dependence on baseline HBsAg burden. Patients attaining very low HBsAg levels show potential for subsequent HBsAg loss during continued NA therapy. However, over half of patients did not reach these favorable states with existing regimens, highlighting the unmet need for novel agents.

FRI-628

Younger age and abnormal baseline ALT levels predict superior responses to peginterferon alpha-2b therapy in children with chronic HBV infection

Hongfei Zhang[1], Qing He[2], Wenxian Ouyang[3], Shuangjie Li[3], Yilan Zeng[4], Hong Zhang[4], Jia Shang[5], Fang Wang[2], Yujing Tang[6], Xiaoguai Liu[7], Hongxia Zhou[8], hui lv[9], Zhengbin Zhao[10], Hong Wan[11], Shuangsuo Dang[12], Rendong Wei[13], Huimin Liu[14], Wenling Jia[15], Chun Lin[16], Riying Lv[17], Yahui Liu[18], Zhenkun He[19]. *[1]Beijing You'an Hospital, Capital Medical University, Beijing, China; [2]The Third People's Hospital of Shenzhen, Shenzhen, China; [3]Hunan Children's Hospital, Changsha, China; [4]Public Health Clinical Center of Chengdu, Chengdu, China; [5]Henan Provincial People's Hospital, Zhengzhou, China; [6]Xiamen Hospital of Traditional Chinese Medicine, Xiamen, China; [7]Xi'an Children's Hospital, Xi'an, China; [8]The Infectious Diseases Hospital of Handan City, Handan, China; [9]Shandong Provincial Public Health Clinical Center, Jinan, China; [10]The first hospital of lanzhou university, Lanzhou, China; [11]Lanzhou Second People's Hospital, Lanzhou, China; [12]Xi'an Jiaotong University Second Affiliated Hospital, Xi'an, China; [13]Qingdao Public Health Clinical Center, Qingdao, China; [14]Southwest Hospital, Third Military Medical University (Army Medical University), Chongqing, China; [15]Gansu Provincial Wuwei Cancer Hospital, Wuwei, China; [16]Mengchao Hepatobiliary Hospital, Fuzhou, China; [17]Guigang City People's Hospital, Guigang, China; [18]Kuitun Hospital of Ili Kazakh Autonomous Prefecture, Kuitun, China; [19]HuaiHe Hospital of Henan University, Kaifeng, China*
Email: zhhf302@163.com

Background and aims: Chronic hepatitis B in children poses a major global public health challenge. This study aimed to evaluate the efficacy and safety of antiviral therapy in chronic HBV-infected children and to analyse factors associated with treatment response.

Method: The Sprout Project, a prospective real-world study (NCT05792761), recruited chronic HBV-infected children aged 3–18 years to receive either nucleos(t)ide analogue (NA) monotherapy or combined with peginterferon alpha-2b (PegIFNα-2b, Pegbing®, Xiamen Amoytop Biotech Co., Ltd.) for 96 weeks. The present analysis included patients who had completed 48 weeks of PegIFNα-2b treatment.

Results: A total of 668 pediatric patients were included in this analysis. The mean age was 8.32 years, comprising 282 patients aged ≥3 to ≤7 years and 386 patients aged >7 to <18 years. Males accounted for 60.3% of the cohort. The mean baseline HBsAg, HBV DNA and HBeAg levels were 3.73, 5.75 $\log_{10}$ IU/mL and 2.35 $\log_{10}$ COI, respectively. 85.0% were HBV DNA positive and 84.5% were HBeAg positive. The mean baseline ALT level was 51.11 U/L, and 41.17% of patients had abnormal baseline ALT. PegIFNα-2b combination therapy markedly reduced HBsAg levels, with a mean decline of 1.86 $\log_{10}$ IU/mL at week 48. The overall rates of HBsAg loss, HBeAg loss, and HBV DNA undetectable at week 48 were 18.7% (125/668), 16.5% (93/562), and 61.6% (341/554), respectively. Patients aged ≥3 to ≤7 years achieved a significantly greater HBsAg decline (2.22 ± 2.20 vs. 1.59 ± 1.82 $\log_{10}$ IU/mL, p = 0.001) and a higher HBsAg loss rate (24.5% vs. 14.5%, p = 0.001) at week 48 compared with those aged >7 to <18 years, while no difference was observed in HBeAg or HBV DNA response. Compared with patients with normal baseline ALT, those with abnormal baseline ALT obtained better HBsAg and HBeAg responses, including a greater HBsAg reduction (2.18 ± 2.20 vs. 1.63 ± 1.84 $\log_{10}$ IU/mL, p = 0.01), a higher HBsAg loss rate (25.8% vs. 13.7%, p < 0.001), and a higher HBeAg loss rate (25.6% vs. 9.9%, p < 0.001). The highest responses were observed in children aged ≥3 to ≤7 years with abnormal baseline ALT, with the 48-week HBsAg loss, HBeAg loss, and HBV DNA undetectable rates of 36.7%, 33.0%, and 67.3%, respectively. PegIFNα-2b combination therapy was well-tolerated throughout the study.

Conclusion: PegIFNα-based therapy for children with chronic HBV infection is safe and effective. Younger age and abnormal baseline ALT levels are identified as favorable predictors of superior treatment outcomes.

FRI-629

Interferon-α enhances HBsAg-specific B cell responses via monocyte-Tfh-B cell axis to facilitate functional cure of hepatitis B

Shihong Zhong[1], Yang Zhou[1], Libo Tang[1], Xiaofang Li[2], Jinlin Hou[1], Jianhua Li[2], Xiaoyong Zhang[1], Yongyin Li[1]. *[1]Department of Infectious Diseases, Nanfang Hospital, Southern Medical University, Guangzhou, China, Guangzhou, China; [2]Key Laboratory of Medical Molecular Virology (MOE/NHC/CAMS), Department of Pathogen Biology, School of Basic Medical Sciences, Shanghai Medical College, Fudan University, Shanghai, China, Shanghai, China*
Email: yongyinli@foxmail.com

Background and aims: Achieving a functional cure for chronic hepatitis B virus (HBV) infection remains challenging. Our recent clinical trial demonstrated pegylated interferon-α (Peg-IFNα) plus siRNA outperformed siRNA alone, implicating IFNα in immune-mediated cure (*N Engl J Med*, 2024). However, its immunological mechanisms, especially in modulating humoral immunity, remain poorly defined. We aimed to elucidate how IFNα regulates B cell responses to facilitate HBV functional cure.

Method: We longitudinally followed CHB patients receiving Peg-IFNα and stratified them by week 72 virological outcomes: HBeAg-non-seroconversion (eAg-NSC, n = 11), HBeAg-seroconversion (eAg-SC, n = 7), and HBsAg seroconversion (sAg-SC, n = 6). Three NAs-treated patients achieving HBsAg seroconversion (NAs-sAg-SC) were included for comparison. Peripheral blood was collected at baseline and week 12 for scRNA-seq and flow cytometry. IFNα's effects on immune subsets and HBV-specific responses were further assessed via in vitro cytokine stimulation and in vivo models using *Il6*$^{-/-}$, *Il21r*$^{-/-}$, *Ccr2*$^{-/-}$ chimeric, and *Cxcl13*$^{-/-}$ mice.

Results: scRNA-seq and flow cytometry showed Peg-IFNα selectively expanded Tfh and plasma cells in sAg-SC patients. In vitro IFNα stimulation of B cells had minimal effects, suggesting intermediary cell involvement. Monocytes exhibited robust IL6-related gene upregulation, and IFNα enhanced their IL6 secretion, boosting humoral immunity. Although IL-6 did not directly activate B cells, IFNα promoted IL6-mediated Tfh interactions and IL6ST-high Tfh subsets with elevated IL21 in sAg-SC patients. IL6 increased IL21 in CXCR5^{+} CD4^{+} T cells, but this was absent in *Il6*$^{-/-}$ or monocyte-deficient mice. IL21-stimulated B cells showed enriched humoral response signatures. scRNA-seq revealed heightened IL21–IL21R signaling between Tfh and GC-like/plasma B cells in IFNα-treated sAg-SC patients. Spatial analysis confirmed IFNα-driven GC formation via CXCL13-CXCR5, which was abolished in *Il6*$^{-/-}$, *Ccr2*$^{-/-}$ chimeric, and *Cxcl13*$^{-/-}$ mice.

Conclusion: IFNα orchestrates antiviral humoral immunity through a monocyte–Tfh–B cell axis, providing mechanistic insight and therapeutic targets to optimize HBV cure strategies.

Viral hepatitis B and D – New therapies, unapproved therapies or strategies

TOP-598

Up to 36 months durability of functional cure in response to bepirovirsen therapy in B-Clear On-NA responders: results from the B-Sure study

Seng Gee Lim[1], Tarik Asselah[2], Gheorghe Diaconescu[3], Adrian Gadano[4], Sebastián Marciano[4], Giuliano Rizzardini[5], Tatiana Stepanova[6], Hyung Joon Yim[7], Man-Fung Yuen[8], Alexandra Walker[9], Jane Dong[10], Lauren Maynard[11], Isabelle Santhiapillai[11], Helene Plein[9], Yi Cui[11], Tamara Lukic[12], Raju Gowda[13], Matthijs Broer[14], Melanie Paff[15], Dickens Theodore[16], Robert Elston[11], Marjan Hezareh[9]. *[1]National University Health System, Singapore, Singapore; [2]Université de Paris-Cité & INSERM UMR1149, Department of Hepatology, AP-HP Hôpital Beaujon, Clichy, France; [3]Spitalul Clinic de Boli Infectioase si Pneumoftiziologie, Craiova, Romania; [4]Hospital Italiano de Buenos Aires, Buenos Aires, Argentina; [5]Luigi Sacco Hospital, Milan, Italy; [6]Modern Medicine Clinic, Moscow, Russian Federation; [7]Korea University Ansan Hospital, Ansan, Korea, Rep. of South; [8]Queen Mary Hospital, The University of Hong Kong, Hong Kong, China; [9]GSK, London, United Kingdom; [10]GSK, Shanghai, China; [11]GSK, Stevenage, United Kingdom; [12]GSK, Dubai, United Arab Emirates; [13]GSK, Philadelphia, United States; [14]GSK, Amersfoort, Netherlands; [15]GSK, Collegeville, United States; [16]GSK, Durham, United States*
Email: mdclimsg@nus.edu.sg

Background and aims: Bepirovirsen (BPV) is an unconjugated antisense oligonucleotide in Phase 3 development for the treatment of chronic hepatitis B virus (HBV) infection. In the Phase 2b study B-Clear (NCT04449029), a subset of participants (pts) on nucleos(t)ide analogues (NAs) achieved a virological response at the end of BPV treatment, which was sustained for 24 weeks. Pts who had a complete (CR) or partial (PR) response at the end of the B-Clear (parent) study were eligible for the B-Sure long-term durability study (NCT04954859; ongoing). Here we present up to 45 months of follow-up data on the durability of response for B-Clear On-NA CRs and PRs enrolled in B-Sure.
Method: CR was defined as hepatitis B surface antigen (HBsAg) < 0.05 IU/mL and HBV DNA < lower limit of quantification (LLOQ; < 20 IU/mL), and PR as 0.05 ≤ HBsAg < 100 IU/mL and HBV DNA < LLOQ, both for 24 weeks off BPV in B-Clear. If eligible, pts discontinued NA 3 months (mo) into B-Sure (≥ 9 mo from their last BPV dose) and were followed further to determine achievement of functional cure (FC; sustained HBsAg < 0.05 IU/mL and HBV DNA < LLOQ at 24 weeks off all HBV treatment) and durability of response off all HBV therapy. Adverse events (AEs) were recorded at each visit.
Results: In total, 44 pts (14 CRs, 26 PRs and 4 non-responders) were enrolled into B-Sure. Of the 14 CRs, 10 (71%) discontinued NAs 3 mo after rollover into B-Sure; 8/10 (80%) maintained a CR to 6 mo post–NA cessation, thus achieving FC; 8/8 (100%) have maintained 24 mo FC, 7/7 (100%) 30 mo FC and 1/1 (100%) 36 mo FC (follow-up ongoing). Of the 26 PRs, 22 (85%) discontinued NAs 3 mo after rollover into B-Sure. 2/22 (9%) achieved delayed FC at 6 post–NA cessation and have maintained FC for 30 mo. 5/22 (23%) maintained PR status at 6 mo post–NA cessation and 1/22 (5%) at 36 mo post–NA cessation; all 4 losses of PR beyond 6 mo post–NA cessation were due to HBV DNA reversion. Among 22 PRs who discontinued NAs, 13 (59%) had restarted NA therapy by 18 mo post–NA cessation. Of all pts who discontinued NAs, 4 had alanine aminotransferase (ALT) ≥ 2x upper limit of normal (ULN) and 1 had ALT > 5x ULN; 1 of those did not restart NA. Post–NA cessation, no pts reported AEs of severe ALT flare. There was no indication that prior use of BPV had any latent adverse effects.
Conclusion: FC is achieved after BPV and discontinuation of all HBV treatments and durable for up to 36 months in B-Clear CRs enrolled in B-Sure, with no long-term safety signals reported.
Funding: GSK (206882).

WED-576

Safety of bulevirtide 10 mg is consistent across demographic and clinical subgroups: results from an integrated analysis

Soo Aleman[1], Adrian Streinu-Cercel[2,3], Tarik Asselah[4], Maurizia Brunetto[5,6], Vladimir Chulanov[7], George Sebastian Gherlan[3,8], Pietro Lampertico[9,10], Viacheslav Morozov[11], Olga Sagalova[12], Tatiana Stepanova[13], Afsaneh Mozaffarian[14], Amos Lichtman[14], Danielle Shing[15], Florence Christian-Cox[15], Steve Tseng[14], Dmitry Manuilov[14], Lei Ye[14], George Wu[14], Heiner Wedemeyer[16]. *[1]Department of Infectious Diseases, Karolinska University Hospital/Karolinska Institutet, Stockholm, Sweden; [2]National Institute of Infectious Diseases Prof. Dr. Matei Bals, Bucharest, Romania; [3]University of Medicine and Pharmacy "Carol Davila" Bucharest, Bucharest, Romania; [4]Hôpital Beaujon APHP, Université de Paris-Cité, INSERM UMR1149, Clichy, France; [5]Hepatology Unit, Reference Center of the Tuscany Region for Chronic Liver Disease and Cancer, University Hospital of Pisa, Pisa, Italy; [6]Department of Clinical and Experimental Medicine, University of Pisa, Pisa, Italy; [7]Sechenov University, Moscow, Russian Federation; [8]Dr. Victor Babes Foundation, Bucharest, Romania; [9]Division of Gastroenterology and Hepatology, Foundation IRCCS Ca' Granda Ospedale Maggiore Policlinico, Milan, Italy; [10]CRC "A. M. and A. Migliavacca" Center for Liver Disease, Department of Pathophysiology and Transplantation, University of Milan, Milan, Italy; [11]LLC Medical Company Hepatolog, Samara, Russian Federation; [12]South Ural State Medical University, Chelyabinsk, Russian Federation; [13]LLC Clinic of Modern Medicine, Moscow, Russian Federation; [14]Gilead Sciences, Inc., Foster City, United States; [15]Gilead Sciences International, Ltd, Cambridge, United Kingdom; [16]Clinic for Gastroenterology, Hepatology, Infectious Diseases, and Endocrinology, Hannover Medical School, Hannover, Germany*
Email: soo.aleman@ki.se

Background and aims: Bulevirtide (BLV), a first-in-class entry inhibitor, is approved as a 2 mg dose in the European Economic Area and other areas for the treatment of patients with chronic hepatitis delta. BLV 2 or 10 mg monotherapy has been shown to be generally safe and well tolerated in multiple clinical trials. Here, we present an integrated safety analysis of BLV 10 mg monotherapy across participant subgroups at week 96 for the Phase 3 MYR301 (NCT03852719) and Phase 2 MYR204 (NCT03852433) studies.
Method: This integrated analysis evaluated safety by baseline (BL) characteristics and demographics in participants treated with BLV 10 mg administered as two 5-mg injections subcutaneously once daily for 96 weeks. Assessments included treatment-emergent adverse events (TEAEs), Grade ≥ 3 TEAEs, serious AEs (SAEs), and TEAEs considered related to BLV; AEs were coded according to Medical Dictionary for Regulatory Activities Version 27.1. Safety parameters were analysed across BL subgroups: age (< 45, ≥ 45 years), sex (male, female), race (White, other), body mass index (< 25 kg/m^2, ≥ 25 kg/m^2), cirrhosis status (presence, absence), concomitant hepatitis B virus treatment (yes, no), alanine aminotransferase levels (≤ 1.5 × upper limit of normal [ULN], > 1.5 × ULN), and renal function (≥ 60 to < 90 mL/min/1.73 m^2, ≥ 90 mL/min/1.73 m^2).
Results: A total of 150 participants treated with BLV 10 mg were included in this analysis. BL characteristics and demographics were well balanced across the groups. Overall, the safety profile was consistent across all subgroups, and analyses of safety events by preferred term within each subgroup showed similar results. Despite a higher incidence of some cytopenias (such as platelets, lymphocytes, leucocytes, and neutrophils) likely due to background incidence, the safety profile of BLV 10 mg was similar in those with and without cirrhosis. Of note, only 1 participant with cirrhosis at BL had an on-treatment liver-related AE (Grade 1 ascites). In addition,

there was 1 study discontinuation due to an AE (myalgia [nonserious]). No SAEs related to BLV were reported in any subgroup, and no consistent differences in other safety outcomes were observed across subgroups.
Conclusion: Long-term treatment with BLV 10 mg monotherapy was safe and well tolerated. Overall, the safety profile remained consistent across all subgroups, including participants with cirrhosis, supporting its use in people with compensated liver disease.

WED-577
Up to 24 months durability of functional cure in response to bepirovirsen plus Peg-IFN sequential therapy in B-Together responders: results from the B-Sure study
Carla Coffin[1], Pietro Andreone[2], Joaquin Cabezas[3], Stuart C Gordon[4], Pietro Lampertico[5], Jeong Heo[6], Viacheslav Morozov[7], Pablo Ryan[8], Tatiana Stepanova[9], Krzysztof Tomasiewicz[10], Natalya Voloshina[11], Hyung Joon Yim[12], Alexandra Walker[13], Jane Dong[14], Lauren Maynard[15], Isabelle Santhiapillai[15], Helene Plein[13], Yi Cui[15], Tamara Lukic[16], Raju Gowda[17], Matthijs Broer[18], Melanie Paff[19], Dickens Theodore[20], Robert Elston[15], Marjan Hezareh[13]. *[1]Cumming School of Medicine, Snyder Institute, University of Calgary, Calgary, AB, Canada; [2]Ospedale Clinicizzato di Baggiovara, AOU di Modena, Modena, Italy; [3]Marqués de Valdecilla University Hospital-IDIVAL, Santander, Spain; [4]Henry Ford Health, Michigan State University, Detroit, MI, United States; [5]Foundation IRCCS Ca' Granda Ospedale Maggiore Policlinico, Milan, Italy; [6]College of Medicine, Pusan National University and Biomedical Research Institute, Pusan National University Hospital, Busan, Korea, Rep. of South; [7]Hepatologist Medical Company, Samara, Russian Federation; [8]Hospital Infanta Leonor, Madrid, Spain; [9]Modern Medicine Clinic, Moscow, Russian Federation; [10]Medical University of Lublin, Lublin, Poland; [11]Medical Centre Healthy Family, Novosibirsk, Russian Federation; [12]Korea University Ansan Hospital, Ansan, Korea, Rep. of South; [13]GSK, London, United Kingdom; [14]GSK, Shanghai, China; [15]GSK, Stevenage, United Kingdom; [16]GSK, Dubai, United Arab Emirates; [17]GSK, Philadelphia, PA, United States; [18]GSK, Amersfoort, Netherlands; [19]GSK, Collegeville, PA, United States; [20]GSK, Durham, NC, United States*
Email: cscoffin@ucalgary.ca

Background and aims: Bepirovirsen (BPV) is an unconjugated antisense oligonucleotide in Phase 3 development for chronic hepatitis B virus (HBV) infection. In the Phase 2b study B-Together (NCT04676724), a subset of participants (pts) on nucleos(t)ide analogs (NAs) achieved a virological response following 12 or 24 weeks of BPV and 24 weeks of pegylated interferon α-2a (Peg-IFN) sequential therapy, which was sustained for 24 weeks following the end of Peg-IFN treatment. Pts with a complete response (CR) or partial response (PR) at the end of B-Together were eligible for the B-Sure long-term durability study (NCT04954859; ongoing). Here we present up to 33 months of follow-up data on the durability of response for B-Together complete responders (CRs) and partial responders (PRs) enrolled in B-Sure.
Method: CR was defined as both hepatitis B surface antigen (HBsAg) < 0.05 IU/mL and HBV DNA < lower limit of quantification (LLOQ; < 20 IU/mL), and PR as 0.05 ≤ HBsAg < 100 IU/mL and HBV DNA < LLOQ, both for 24 weeks off BPV + Peg-IFN sequential therapy in B-Together. If eligible, pts discontinued NA treatment 3 months (mo) into B-Sure (≥ 9 mo from the end of BPV + Peg-IFN sequential therapy) and were followed to determine the achievement and durability of functional cure (FC; sustained HBsAg < 0.05 IU/mL and HBV DNA < LLOQ at 24 weeks off all HBV treatment). Adverse events (AEs) were recorded at each visit.
Results: In total, 23 On-NA pts (13 CRs, 8 PRs and 2 non-responders) from B-Together were enrolled into B-Sure. Of the CRs, 12/13 discontinued NAs 3 mo into B-Sure; 9/12 maintained CR to 6 mo post–NA cessation, thus achieving FC. Of these, 7/7 (100%) have maintained 18 mo FC and 4/4 (100%) who reached the 33 mo B-Sure visit have maintained 24 mo FC (follow-up ongoing); no CRs restarted NAs during B-Sure. Of the PRs, 3/8 discontinued NAs 3 months into B-Sure; 1 PR achieved delayed FC at 18 mo post–NA cessation and has maintained 12 mo FC; 1 has maintained PR up to 24 mo post–NA cessation; 1 lost PR due to virological relapse and restarted NA treatment. Of all pts who discontinued NAs, none had alanine aminotransferase (ALT) ≥ 2x upper limit of normal. Post–NA cessation, no pt reported AEs of severe ALT flare. There was no indication that prior use of BPV had any latent adverse effects.
Conclusion: FC is achieved after discontinuation of all HBV treatments and is durable for up to 24 mo in CRs in response to sequential BPV + Peg-IFN therapy, and no long-term safety signals were reported.
Funding: GSK (206882).

WED-578
Transcriptomic profiling reveals distinct immune signatures in chronic hepatitis B and identifies blood transcriptional modules associated with hepatitis B e antigen loss following therapeutic vaccination with GS-2829 and GS-6779
David Pan[1], Edward J. Gane[2], Yao-Chun (Holden) Hsu[3], Rachel Wen-Juei Jeng[4,5], Christopher Richards[1], Sarah Arterburn[1], Ricardo Ramirez[1], Meghan Holdorf[1], Simon Fletcher[1], Jenny Stanton[1], Frida Abramov[1], Mario Cortese[1]. *[1]Gilead Sciences, Inc., Foster City, United States; [2]University of Auckland, Auckland, New Zealand; [3]Department of Medical Research, E-Da Hospital, School of Medicine, I-Shou University, Kaohsiung, Taiwan; [4]Department of Gastroenterology and Hepatology, Chang Gung Memorial Hospital, Linkou, Taiwan; [5]College of Medicine, Chang Gung University, Taoyuan, Taiwan*
Email: mario.cortese@gilead.com

Background and aims: Therapeutic vaccination aims to generate or boost preexisting hepatitis B virus (HBV)-specific immunity in chronic hepatitis B (CHB). Arenaviral vector vaccines, GS-2829 and GS-6779, encoding multiple HBV antigens, induced HBV-specific T-cell responses and hepatitis B e antigen (HBeAg) loss in a subset of Phase 1b study participants. Whole-blood RNA sequencing was performed to compare transcriptional responses between healthy participants (HP) and patients with CHB, and to elucidate vaccine-induced immune mechanisms associated with HBeAg loss.
Method: Transcriptomic analysis was performed on a subset of 22 study participants (4 HP; 18 CHB). The CHB cohort included 10 HBeAg-positive patients at baseline, of whom 5 achieved HBeAg loss after vaccination. Samples were collected at baseline (day [D]1) and during vaccination (on the day of [D57 and D58], and 2 weeks after the 3rd and 4th immunisations [D71 and D99]). Differential expression and gene set enrichment analysis (|normalised enrichment score| ≥2; false discovery rate <0.05) using blood transcriptional modules (BTMs) were conducted.
Results: HP displayed strong and durable enrichment of several T-cell–associated BTMs at all postvaccination time points compared to baseline. Patients with CHB had previously showed reduced HBV-specific T-cell response via ex vivo IFN-γ ELISpot compared to HP, consistent with more sporadic enrichment in T-cell BTMs. Additionally, natural killer cell–associated BTMs were more enriched in HP. Conversely, patients with CHB exhibited stronger and more persistent activation of myeloid and innate modules, which were downregulated in HP. Loss of HBeAg was associated with consistent upregulation of *STAT4*, *CNBP*, and *KLRC1* genes, suggesting engagement of the IL-12 or interferon pathways. Those who remained HBeAg positive exhibited downregulation of these immune genes and upregulation of epigenetic regulators (*FASN*, *DOT1L*) known to be associated with CHB and hepatocellular carcinoma. Importantly, *STAT4* and *KLRC1* were significantly differentially expressed ($p < 0.01$) on D85 in HBeAg loss vs no-loss patients, and showed a positive association with HBeAg decline ($R = 0.4$ and $R = 0.32$, respectively).
Conclusion: Therapeutic vaccination with GS-2829 and GS-6779 elicited distinct peripheral immune signatures in HP and patients with CHB. Several genes were differentially expressed in HBeAg loss

vs no-loss groups following vaccination. These findings could provide insights for future functional cure regimens.

WED-579

Safety, pharmacokinetics, and pharmacodynamic activity of ABI-6250, a first in class oral hepatitis D virus entry inhibitor in healthy subjects: interim results from a randomized, blinded, phase 1a study

Edward J. Gane[1], Christian Schwabe[2], Grace Wang[3], Jieming Liu[3], Nuruddin Unchwaniwala[3], Jinghu Carl Li[3], Steven J Knox[3], Anuj Gaggar[3], Katie Zomorodi[3]. *[1]University of Auckland Faculty of Medical & Health Sciences, Grafton, New Zealand; [2]New Zealand Clinical Research, Auckland, New Zealand; [3]Assembly Biosciences, South San Francisco, CA, United States*
Email: edgane@adhb.govt.nz

Background and aims: Treatment for chronic hepatitis D virus (HDV) infection, the most severe form of viral hepatitis affecting 12–72 million patients worldwide, is limited. Bulevirtide (BLV), an inhibitor of the sodium-taurocholate co-transporting polypeptide (NTCP), has been approved for the treatment of HDV infection in some countries. BLV inhibition of NTCP results in bile acid (BA) elevations, reduced HDV RNA and serum ALT. Orally administered NTCP inhibitors may provide similar safety and efficacy with improved dosing convenience compared to daily subcutaneous BLV injections. ABI-6250-101 (NCT06740474) is a randomized, blinded study assessing the safety, pharmacokinetics, and pharmacodynamics (PD) of a potentially first in class, oral NTCP inhibitor ABI-6250 (6250) in healthy subjects.
Method: Two single-dose cohorts of 5 mg and 25 mg, and 3 multiple-dose cohorts of 0.05 mg, 0.2 mg and 1 mg 6250 once-daily (QD) for 10 days are complete. In each cohort 8 subjects were randomized 3:1 to 6250 or placebo (PBO). Safety was assessed by physical examination, adverse events (AEs) and lab parameters. PD was assessed by changes in plasma BAs (on-target) and coproporphyrin-1 (CP-1; off-target). 6250 plasma concentrations were measured by LCMS.
Results: Demographics were similar across cohorts. 6250 C_{max} and AUC increased with dose with $t_{1/2}$ of ~4–5 days. Dose dependent BA elevations (non-pruritic), were observed at doses above 0.05 mg with 63.4-fold increase at 25 mg and 3.5-fold increase at 0.2 mg single doses. Two-fold CP-1 elevations were observed at 25 mg but not in any other cohort. Treatment-emergent (TE)AEs were reported in 20/30 and 4/10 6250 and PBO recipients respectively; all were Grade 1/2. No serious AEs were reported. Lab abnormalities were observed in 18/30 and 7/10 6250 and PBO recipients respectively; all were Grade 1/2 except for an unrelated, self-limited creatine kinase increase in a 5 mg recipient. Self-limited, asymptomatic ALT elevations were observed at all dose levels and PBO. Grade 1 ALT elevations were observed in similar proportions across multiple dosing groups; 16.7% at 1 mg, 0.2 mg, and PBO, and 0% at 0.05mg. One subject in the 1mg dose group discontinued treatment due to a Grade 1 ALT elevation.
Conclusion: Overall, 6250 was well tolerated when administered as single doses up to 25 mg, and up to 1 mg QD for 10 days. Dose dependent elevations in plasma BAs were observed. Planning for a longer duration Phase 2 study in subjects with chronic HDV infection is ongoing.

WED-580

Baseline and on-treatment characteristics of HBeAg-positive patients and correlates of HBeAg loss following GS-2829 and GS-6779 therapeutic vaccination in virally suppressed patients with chronic hepatitis B

Rachel Wen-Juei Jeng[1], Yao-Chun (Holden) Hsu[2], Chi-Yi Chen[3], Tsung-Hui Hu[4], Chingchu Lo[5], Pin-Nan Cheng[6], Tung-Hung Su[7], Ming-Lung Yu[8], Frida Abramov[9], Mario Cortese[9], David Pan[9], Sarah Arterburn[9], Christopher Richards[9], Dana Tedesco[9], Jenny Stanton[9], Edward J. Gane[10]. *[1]Department of Gastroenterology and Hepatology, Chang Gung Memorial Hospital, and College of Medicine, Chang Gung University, Linkou and Taoyuan, Taiwan; [2]Department of Medical Research, E-Da Hospital, School of Medicine, I-Shou University, Kaohsiung, Taiwan; [3]Division of Gastroenterology and Hepatology, Ditmanson Medical Foundation Chia-Yi Christian Hospital, Chia-Yi, Taiwan; [4]Division of Hepatogastroenterology, Department of Internal Medicine, Kaohsiung Chang Gung Memorial Hospital, Chang Gung University, Kaohsiung, Taiwan; [5]Gastroenterology and Hepatology, St., Martin De Porres Hospital, Chiayi City, Taiwan; [6]Department of Internal Medicine, National Cheng Kung University Hospital, College of Medicine, National Cheng Kung University, Tainan, Taiwan; [7]Department of Internal Medicine, National Taiwan University Hospital, Taipei, Taiwan; [8]Hepatobiliary Division, Department of Internal Medicine, Kaohsiung Medical University Hospital, College of Medicine and Center for Liquid Biopsy and Cohort Research, Kaohsiung Medical University, Kaohsiung, Taiwan; [9]Gilead Sciences, Inc., Foster City, United States; [10]The University of Auckland, Auckland, New Zealand*
Email: rachel.jeng@gmail.com

Background and aims: Hepatitis B e antigen (HBeAg) loss is a key milestone towards functional cure in chronic hepatitis B (CHB). In prior studies, only 6%–8% of virally suppressed patients (pts) on tenofovir achieved HBeAg loss at 1 year (Y). In a Phase 1b study, 45% of HBeAg-positive (HBeAg+) pts treated with high-dose arenavirus-vectored therapeutic vaccines GS-2829 and GS-6779 achieved HBeAg loss. This analysis characterised HBeAg+ pts and identified virologic and immunologic patterns seen with HBeAg loss.
Method: Changes in HBeAg, hepatitis B core-related antigen (HBcrAg), and HBV-specific T-cell responses (*ex vivo* IFN-γ ELISpot) were assessed in HBeAg+ pts enrolled in a Phase 1b study by on-treatment HBeAg status through up to posttreatment week (W) 24.
Results: Of 13 HBeAg+ pts, 11 received 2 or 3 high-dose GS-2829 + GS-6779 cycles; 2 received placebo (PBO). At baseline (BL), the 13 pts had a median age of 45 Y, 69% were male, all were Asian, and median (range) hepatitis B surface antigen (HBsAg) of 710 (1.37, 3725) IU/mL. HBeAg loss/seroconversion occurred in 5/11 (45%) pts by day 85 (end of 2nd cycle); of these, 1 lost anti-HBe but remained HBeAg-, and another had HBeAg seroreversion but remained anti-HBe+, while neither PBO pt lost HBeAg. BL characteristics in treated pts were largely similar between pts with vs without HBeAg loss. Pts with HBeAg loss primarily had genotype B infection (4/5 [80%] vs 1/6 [17%]), shorter nucleos(t)ide analogue therapy duration (median 144 vs 271 W) and lower median (range) HBeAg levels (0.37 [0.14, 2.71] vs 4.05 [0.25, 13.31] IU/mL). All treated pts showed declines in HBeAg and HBcrAg; notably, 6 of 11 (55%) had HBeAg declines ≥ 0.5 $\log_{10}$ IU/mL, including 3 with HBeAg loss, while no PBO pt had such decline. HBeAg loss pts exhibited stronger hepatitis B core antigen (HBcAg)-specific T-cell responses, while those without HBeAg loss had more robust polymerase (pol)-specific T-cell responses. HBeAg+ pts with BL HBsAg < 800 IU/mL had more pronounced HBcAg-specific T-cell responses vs those with ≥ 800 IU/mL; no difference was seen between BL HBsAg groups in pol-specific response.
Conclusion: High-dose GS-2829 + GS-6779 induced a substantial rate of HBeAg loss with characteristic immunologic changes. The emergence of HBcAg-specific T-cell responses in pts with HBeAg loss and/or reduction suggests potential links between antigen clearance and immune restoration. These findings support further evaluation of GS-2829 + GS-6779 as part of finite cure for CHB.

WED-581

SOLSTICE week 48 subgroup analysis: Impact of BMI on ALT normalization after successful viral control in participants with chronic hepatitis delta virus infection treated with tobevibart plus elebsiran

Alina Jucov[1], Tarik Asselah[2], Anca Streinu-Cercel[3], Edward J. Gane[4], Heiner Wedemeyer[5], Pietro Lampertico[6,7], Patrick Kennedy[8], Michael A. Chattergoon[9], Bria Bullard[9], Cheng Huang[9], Rima Acosta[9], Sophie Chow[9], Carey Hwang[9], Cara Pilowa[9], Todd Correll[9],

Kosh Agarwal[10]. [1]*Arensia Exploratory Medicine GmbH, Düsseldorf, Germany; Nicolae Testemitanu State University of Medicine and Pharmacy, Chisinau, Moldova;* [2]*Université de Paris Cité, Hôpital Beaujon, Paris, France;* [3]*National Institute for Infectious Diseases Matei Bals, Carol Davila University of Pharmacy and Medicine, Bucharest, Romania;* [4]*University of Auckland, Auckland, New Zealand;* [5]*Department of Gastroenterology, Hepatology, and Endocrinology, Hannover Medical School, Hannover, Germany;* [6]*Division of Gastroenterology and Hepatology, Foundation IRCCS Ca' Granda Ospedale Maggiore Policlinico, Milan, Italy;* [7]*CRC "A. M. and A. Migliavacca" Center for Liver Disease, Department of Pathophysiology and Transplantation, University of Milan, Milan, Italy;* [8]*Centre for Immunobiology and Infection, Blizard Institute, Barts and the London School of Medicine and Dentistry, London, United Kingdom;* [9]*Vir Biotechnology, San Francisco, United States;* [10]*Institute of Liver Studies, King's College Hospital, London, United Kingdom*
Email: alina.jucov@arensia-em.com

Background and aims: Hepatitis delta virus (HDV) infection is the most severe form of viral hepatitis with limited treatment options. The ongoing phase 2 SOLSTICE study is investigating the antiviral activity and safety of the monoclonal antibody tobevibart alone and in combination with the small interfering RNA elebsiran in participants with chronic HDV infection, with or without compensated cirrhosis, on NRTI therapy (NCT05461170). ALT normalization is used to assess resolution of inflammation during antiviral treatment, but is non-specific, multifactorial, and may be influenced by factors beyond HDV viremia in infected persons. Here we sought to examine additional factors impacting ALT normalization.
Method: A subgroup analysis of ALT normalization was performed based on baseline participant and disease characteristics after 48 weeks of therapy with tobevibart 300 mg plus elebsiran 200 mg subcutaneously (SC) every 4 weeks (tobevibart+elebsiran Q4W; N = 32).
Results: After 48 weeks, HDV RNA decreased by ≥2 $\log_{10}$ from baseline in 97% (31/32) of participants receiving tobevibart+elebsiran Q4W and HDV RNA target not detected (TND) was achieved by 66% (21/32) of participants. Most participants receiving tobevibart +elebsiran Q4W had reductions in ALT values compared to baseline, with ALT normalization observed in 56% (18/32) of participants at week 48. In the full cohort, there was a trend towards lower baseline BMI in those who achieved ALT normalization at week 48. Of the 21 participants receiving tobevibart+elebsiran Q4W who achieved HDV RNA TND at week 48, median baseline ALT was 2.2x ULN, 2.0x ULN, and 1.3x ULN in BMI subgroups <25, 25–29.9, and ≥30, respectively. Among those achieving TND, ALT normalization was achieved by 80% (4/5), 64% (7/11), and 20% (1/5) in BMI subgroups <25, 25–29.9, and ≥30, respectively. Across the BMI subgroups, treatment-emergent adverse events (TEAEs) were primarily Grade 1–2 and transient in nature. No treatment-related serious adverse events occurred.
Conclusion: At 48 weeks, participants receiving tobevibart+elebsiran Q4W therapy achieved high rates of HDV RNA TND. ALT normalization at week 48 was more frequently observed in participants with lower baseline BMI, which suggests that elevated BMI could be independently contributing to elevated ALT even in participants achieving HDV RNA TND receiving tobevibart+elebsiran therapy.

WED-585
Functional analysis of clinically observed SNPs in the bepirovirsen binding site reveals reduced HBV fitness via impaired HBx/HBV polymerase activity in vitro

Alexander Koenig[1,2], Christine Livingston[1], Jerome Bouquet[3], Michael Savarese[1], William Jordan[4], Johannes Freudenberg[4], Andrew Esteves[1], Chi Lau[1], Robert Elston[5], Dickens Theodore[6], Melanie Paff[7], Shihyun You[1]. [1]*GSK, Hepatology, Upper Providence, United States;* [2]*GlaxoSmithKline, Collegeville, United States;* [3]*GSK, Clinical Biomarkers, San Francisco, United States;* [4]*GSK, Human Genetics & Genomics, Upper Providence, United States;* [5]*GSK, Clinical Development, Stevenage, United Kingdom;* [6]*GSK, Clinical Development, Upper Providence, United States;* [7]*GSK, Medicine Development, Upper Providence, United States*
Email: alexander.x.koenig@gsk.com

Background and aims: Bepirovirsen (BPV) is a Ph 3 ASO for chronic hepatitis B (CHB) that targets all HBV mRNAs including pgRNA. The ASO binding site overlaps HBx and HBV polymerase (Pol) protein-coding regions. In the Ph 2 B-Clear trial, treatment-emergent single nucleotide polymorphisms (SNPs) occurred in 6% (3/49) of On-NA and 3% (5/143) of Not-on-NA participants. This study aimed to 1) confirm HBx inhibition by BPV, 2) verify BPV binding site conservation in public database sequences, 3) assess impact of SNPs on HBx/Pol function/viral fitness, and 4) test SNPs for BPV susceptibility.
Method: The BPV binding site was analyzed for SNPs in 9,139 HBV consensus genomic sequences of the public database HBVdb. Thirteen SNPs identified from B-Clear and HBVdb with nonsynonymous mutations in HBx/Pol were cloned into HBV GtD plasmid, variant virus produced, and phenotyped in HepG2 cells and PHH. HBV variants were assessed for HBx function to degrade Smc5 and Smc6 (host Smc5/6 complex markers) and Pol activity (HBV DNA qPCR). Clinically identified variants with WT comparable fitness were tested for BPV susceptibility in PHH over 22 days. HBsAg, HBeAg, HBV DNA, HBcAg, and Smc5/6 were quantified by ELISA, qPCR, high-content imaging, and automated capillary electrophoresis immunoassay.
Results: BPV inhibited all viral markers, including HBx, HBsAg, HBeAg, HBcAg and HBV DNA. In line with the B-Clear sequencing results, SNPs in the BPV binding site were infrequent across genotypes in HBVdb (97.6% conserved). Among 13 evaluated SNPs, G1A, C7A, G8A, C9T, A13C, A13G, C15T showed reduced fitness compared to WT. G1A (low fitness SNP) translates to HBx A70T hydrophobic-to-polar aa substitution, resulting in abolished HBx function, whereas C2T (WT comparable fitness, HBx A70V; hydrophobic-to-hydrophobic aa) retained HBx function and antigen expression, suggesting a critical role of hydrophobic residues in the zinc-binding motif for HBx function. C7A (Pol F834L) reduced Pol-dependent replication, while C2T (Pol H833Y) did not. All variants tested (G8A, C9A, T10A, T10G, C15T, C20T) remained susceptible to BPV, with max. 4.1-fold HBsAg EC50 increase for C9A.
Conclusion: The BPV binding site is conserved and functionally critical, suggesting that potential escape mutations would likely incur a high fitness cost. BPV maintained antiviral activity against tested variants; furthermore, its restoration of the antiviral Smc5/6 host defense, potentially leading to HBV cccDNA silencing, also supports its therapeutic potential for CHB.

WED-586
Population pharmacokinetics of pevifoscorvir sodium (ALG-000184) in healthy participants and participants with chronic hepatitis B in support of phase 2 dose selection

Kha Le[1], Paul Ko[2], Russ Wada[2], Min Wu[1,1,1], Stanley Wang[1], Edward J. Gane[3], Man-Fung Yuen[4], Kosh Agarwal[5], Jinlin Hou[6], Hong Ren[7], Yanhua Ding[8], Alina Jucov[9], Xieer Liang[6], Jia Xu[8], Alexei Haceatrean[9], Kusum Gupta[1], Doug Clark[1], Lawrence Blatt[1], Tse-I Lin[1], Sushmita Chanda[1]. [1]*Aligos Therapeutics, South San Francisco, United States;* [2]*QuanTx Consulting, Mountain View, United States;* [3]*University of Auckland, Auckland, New Zealand;* [4]*The University of Hong Kong, Hong Kong, Hong Kong;* [5]*Kings College Hospital, London, United Kingdom;* [6]*Nanfang Hospital, Southern Medical University, Guangzhou, China;* [7]*The Second Affiliated Hospital of ChongQing Medical University, ChongQing, China;* [8]*The First Hospital of Jilin University, Changchun, China;* [9]*Arensia Exploratory Medicine, Chișinău, Moldova*
Email: kle@aligos.com

Background and aims: Pevifoscorvir sodium is a prodrug of ALG-001075, a potent capsid assembly modulator-empty that inhibits viral replication and cccDNA establishment in vitro for chronic

hepatitis B (CHB). The population pharmacokinetic (PopPK) analysis is aimed to identify key covariates influencing ALG-001075 pharmacokinetics and facilitate safe and effective dosing.
Method: The dataset consisted of 3158 quantifiable samples collected from 162 participants in a multi-part Phase 1 clinical study, including both healthy volunteers (HV) and participants with CHB. The study had five parts with doses ranging from 10 to 500 mg administered daily, twice daily or as single dose for up to 96 weeks. A nonlinear mixed-effects modelling approach was used to develop the PopPK model. Covariates tested included body weight (WT), age, sex, race (Asian vs. non-Asian), Chinese origin (Chinese vs. non-Chinese), albumin, ALP, AST, ALT, bilirubin, creatinine clearance, population (CHB vs. HV), and HBeAg status (positive vs. negative). A full covariate model included all significant covariates identified in a univariate forward search ($p < 0.05$) using the likelihood ratio test. Stepwise backward elimination process ($p < 0.01$) resulted in the final model. The final model was qualified using a prediction-corrected visual predictive check (pcVPC) method.
Results: A two-compartment model with first order absorption rate, dose-dependent zero order absorption duration and lag time best described the pevifoscorvir sodium PK. Significant covariates included WT on central and peripheral clearances (CL,Q) and volumes (V2,V3), non-Asian race on CL and V2, and CHB on CL. Simulated steady-state exposures in Asians were approximately 50–60% higher than those in non-Asians. Simulated exposures in the heaviest participants were ~20–30% lower than those in the lightest participants. A pcVPC showed that the model adequately captured the central tendency and range of the data in all participants. Overall, the magnitude of the covariate effects (<60%) is not likely to be clinically meaningful, given the observed relatively narrow range of change in HBV DNA for doses ranging 10–300 mg QD and good tolerability over this wide dose range.
Conclusion: The PK of ALG 001075 in HV and CHB participants was well described by the popPK model. The significant covariates were WT on CL/Q and V2/V3, non-Asian race on CL and V2, and CHB on CL. No dose adjustment was required based on liver disease severity or demographics, supporting fixed dosing in this population.

WED-587

Up to 36 months durability of functional cure in response to bepirovirsen therapy in B-Clear Not-on-NA responders: results from the B-Sure study

Seng Gee Lim[1], Manuela Arbune[2], Masanori Atsukawa[3], Stuart Flanagan[4], Natalya Urievna Gankina[5], Takuya Komura[6], Rosie Mngqibisa[7], Qin Ning[8], Teerha Piratvisuth[9], Olga Sagalova[10], Giuliano Rizzardini[11], Tatiana Stepanova[12], Tetsuo Takehara[13], Masataka Tsuge[14], Qing Xie[15], Alexandra Walker[16], Jane Dong[17], Lauren Maynard[18], Isabelle Santhiapillai[18], Helene Plein[16], Yi Cui[18], Tamara Lukic[19], Raju Gowda[20], Matthijs Broer[21], Melanie Paff[22], Dickens Theodore[23], Robert Elston[18], Marjan Hezareh[16]. *[1]National University Health System, Singapore, Singapore; [2]Sf. Cuv. Parascheva Infectious Diseases Clinical Hospital, Galati, Romania; [3]Nippon Medical School, Tokyo, Japan; [4]Mortimer Market Centre, London, United Kingdom; [5]Krasnojarsk Regional Center of AIDS Prevention, Krasnojarsk, Russian Federation; [6]Kanazawa Medical Center, Ishikawa, Japan; [7]Enhancing Care Foundation, Wentworth Hospital, Durban, South Africa; [8]Tongji Hospital, Tongji Medical College, Huazhong University of Science and Technology, Wuhan, China; [9]NKC Institute of Gastroenterology and Hepatology, Songkhla, Thailand; [10]South Ural State Medical University, Chelyabinsk, Russian Federation; [11]Luigi Sacco Hospital, Milan, Italy; [12]Modern Medicine Clinic, Moscow, Russian Federation; [13]Osaka University Hospital, Osaka, Japan; [14]Hiroshima University Hospital, Hiroshima, Japan; [15]Ruijin Hospital affiliated to Shanghai Jiao Tong University School of Medicine, Shanghai, China; [16]GSK, London, United Kingdom; [17]GSK, Shanghai, China; [18]GSK, Stevenage, United Kingdom; [19]GSK, Dubai, United Arab Emirates; [20]GSK, Philadelphia, United Kingdom; [21]GSK, Amersfoort, Netherlands; [22]GSK, Collegeville, United States; [23]GSK, Durham, United States*
Email: mdclimsg@nus.edu.sg

Background and aims: Bepirovirsen is an unconjugated antisense oligonucleotide in Phase 3 clinical trials for the treatment of chronic hepatitis B virus (HBV) infection. In the B-Clear Phase 2b study (NCT04449029), a subset of participants (pts) achieved a virological response at the end of a 24-week bepirovirsen treatment period, which was sustained for 24 weeks post treatment completion. This occurred in pts on and not on background nucleos(t)ide analogue (NA) therapy (On-NA and Not-on-NA, respectively). Pts who achieved a complete (CR) or partial (PR) response at the end of the B-Clear (parent) study were eligible for this long-term durability study (B-Sure; NCT04954859; ongoing). Here we present up to 39 months of follow-up data on the achievement and durability of functional cure (FC) in B-Clear Not-on-NA complete responders (CRs) and partial responders (PRs) who entered B-Sure.
Method: CR was defined as HBsAg < 0.05 IU/mL and HBV DNA < LLOQ (< 20 IU/mL), and PR as 0.05 ≤ HBsAg < 100 IU/mL and HBV DNA < LLOQ, both for 24 weeks off bepirovirsen in the B-Clear study. Pts maintaining a CR at Month 3 of B-Sure (i.e., at least 9 months off bepirovirsen) were considered to have achieved FC (sustained HBsAg < 0.05 IU/mL and HBV DNA < LLOQ at 24 weeks off all HBV treatment). Adverse events were recorded at each visit.
Results: Overall, 17 B-Clear Not-on-NA pts (11 CRs, 5 PRs and 1 non-responder) were enrolled into B-Sure; mean age was 44.1 years, and 9/17 (53%) had HBsAg ≤ 1000 IU/mL at B-Clear baseline. For CRs, 8/11 (73%) pts maintained a CR at 3 months of B-Sure follow-up, thus achieving FC; FC has been maintained for 18 months by 8/8 (100%), for 24 months by 7/7 (100%), for 30 months by 7/7 (100%), and for 36 months by 4/4 (100%) who reached 39 months of follow-up. The 3 CRs who did not achieve FC had HBsAg reversion by 3 months of B-Sure; 1 subsequently experienced HBsAg loss (Month 15), achieving FC at Month 21, but then had HBsAg reversion at Month 33. For PRs, 1/5 has maintained a PR through 39 months of B-Sure follow-up; all losses of PR were due to HBV DNA reversion. 3 PRs started NA treatment after B-Sure enrolment. Of all pts, 1 had alanine aminotransferase (ALT) ≥ 2x upper limit of normal (ULN) and 1 had ALT > 5x ULN. There was no indication that prior use of bepirovirsen had any latent adverse effects.
Conclusion: These data provide evidence that FC is achieved and durable for up to 36 months following the end of bepirovirsen treatment, with no new safety signals reported.
Funding: GSK (206882).

WED-588

Sustained reduction of HBV antigen levels at ≥6 months follow-up in HBeAg-positive participants with chronic hepatitis B infection after 96 weeks of 300 mg pevifoscorvir sodium monotherapy

Lung Yi Loey Mak[1], Andreas Jekle[2,2,2], Mark Anderson[3], Sushmita Chanda[2], Lillian Adame[2], Tiffany Fortney[3], Heleen Roose[4], Lawrence Blatt[2], Rene Geissler[3], Min Wu[2,2,5], Kha Le[2], Gavin Cloherty[3], Tse-I Lin[4], Man-Fung Yuen[1]. *[1]The University of Hong Kong, Pok Fu Lam, Hong Kong; [2]Aligos Therapeutics, South San Francisco, United States; [3]Abbott Laboratories, Abbott Diagnostics Division, Abbott Park, Illinois, United States; [4]Aligos Belgium, Leuven, Belgium; [5]Aligos Therapeutics, San Bruno, United States*
Email: loeymak@gmail.com

Background and aims: Pevifoscorvir sodium (pevy, ALG-000184) is a prodrug of ALG-001075, a novel Type E Capsid Assembly Modulator (CAM-E). In the Phase 1 study ALG-000184-201 (NCT04536337), pevy has demonstrated potent on-treatment suppression of HBV DNA, RNA, and viral antigens in participants with chronic hepatitis B virus infection who received oral, once daily 300 mg pevy for 96 weeks. After the end of the pevy treatment (EOT), these antiviral effects were sustained during an 8-week follow-up (FU) period on

entecavir (ETV). Here, we report the sustained antiviral effect during long-term follow-up (LFU) of 24–48 weeks on ETV.
Method: 9 of 10 HBeAg-positive participants of Part 4 Cohort B were evaluated for HBV antigen changes during ≥24 weeks of ETV-only FU after the end of 300 mg pevy for 96 weeks. qHBsAg and qHBeAg were measured by Roche Elecsys HBsAg II assay on a cobas analyzer (LLOD 0.05 IU/mL) and Elecsys HBeAg quant (LLOD 0.10 IU/mL). HBV RNA was measured by Research Use Only (RUO) RealTime HBV RNA v2.0 (LLOQ 0.49 Log U/mL, 10 copies/mL) (Abbott Diagnostics). HBcAg, P-HBcAg, and HBsAg isoforms were measured with a prototype RUO assays (Abbott Diagnostics) and expressed as signal/cut-off ratio (S/CO).
Results: Median HBsAg levels declined by 1.07 $\log_{10}$ IU/mL during pevy treatment. This reduction was sustained during LFU. The median HBsAg levels were 3.38 $\log_{10}$ IU/mL at EOT and 3.30 $\log_{10}$ IU/mL at LFU, which were below the median baseline level of 4.31 $\log_{10}$ IU/mL. Similarly, reductions in HBeAg observed during pevy treatment were sustained during LFU. HBV RNA and P-HBcAg strongly decreased during pevy treatment, followed by a partial increase during LFU as expected by the mechanisms of pevy and ETV, respectively. HBV DNA remained <10 IU/mL in 5/9 participants at LFU, with minor increases to 11.1, 26.8, 40.2, and 364 IU/mL for the other 4 participants. The median decline of total HBs, MHBs and LHBs at the end pevy monotherapy were 0.40, 1.03, and 1.38 $\log_{10}$ S/CO, respectively, suggesting pevy acting on all HBsAg isoforms. Larger reductions in LHBs than total HBs indicate that pevy acts on cccDNA-derived HBsAg and that remaining HBsAg is mostly derived from integrated DNA.
Conclusion: Potent on-treatment effects on viral antigens were observed after 96 weeks of 300 mg oral monotherapy with pevy, indicating cccDNA pool reduction. These effects were sustained during ≥24 weeks of ETV FU HBeAg-positive participants with chronic hepatitis B virus infection.

WED-589
Turkish real-world effectiveness and safety of bulevirtide in chronic hepatitis delta: a multicentric experience with long-term follow up

Muge Ozari Gulnar[1], Mustafa Celen[2], Mehmet Akif Yağlı[3], Özgür Aktaş[4], Gökhan Kabaçam[5], Mujdat Zeybel[1], Yılmaz Çakaloğlu[6], Murat Akyildiz[1], Sabahattin Kaymakoğlu[3], Cihan Yurdaydin[1]. *[1]Koç University Hospital, Department of Gastroenterology, İstanbul, Türkiye; [2]Dicle University Hospital, Department of Infectious Diseases, Diyarbakır, Türkiye; [3]İstanbul University Hospital, Department of Gastroenterology, İstanbul, Türkiye; [4]Koç University School of Medicine, İstanbul, Türkiye; [5]Güven Hospital, Department of Gastroenterology, Ankara, Türkiye; [6]Amerikan Hospital, Department of Gastroenterology, İstanbul, Türkiye*
Email: muge.ozari@gmail.com

Background and aims: Bulevirtide (BLV), was approved in Europe in 2020 for treating compensated CHD. It is available also in Russia and Australia. BLV is not licenced in Turkey, a CHD endemic country. We present first real-world data on BLV use in CHD In Turkey. This study evaluated daily 2mgBLV therapy in CHD patients for up to 36-months, with emphasis on virologic and biohemical response (VR, BR) and viral breakthrough (VBr).
Method: 33 patients with CHD who initiated BLV therapy between 2020–2023 were analyzed. All patients had baseline detectable HDRNA and elevated ALT. Five patients had decompansated cirrhosis all other patients had compensated liver disease. Seven patients used the European label Hepcludex, and remaining 26 patients received Myrcludex from Russia. Primary outcomes were VR (defined as undetectability or > 2 log decrease in HDVRNA) and BR (defined as ALT normalization) at end of on-treatment follow-up (FU). VBr was defined as an increase of HDV RNA > 1log from nadir or HDV RNA becoming detectable after undetectability. Statistical analyses included t and Mann-Whitney U tests for continuous and Fisher's exact and Chi-squared tests for categorical variables.
Results: Mean (±SD) baseline ALT was 99.6 (± 66.7) U/L and HDVRNA was 4.94 (± 1.11 log) IU/mL. At 12 months, VR was achieved in 74.1% (20/27) of evaluable patients, and BR was 70.4% (19/27). Response rates were sustained through 24 months reaching 61.1% (11/18) with VR and 64.7% (11/17) with BR. VBr occurred in 4 of 26 patients on the Russian BLV (15.4%). Patients with VBr had higher baseline INR (1.22 ± 0.03 vs 1.04 ± 0.14, p = 0.033) and a trend toward higher baseline HDVRNA (5.82 ± 0.81 vs 4.82 ± 1.10 log. IU/mL, p = 0.091). Two patients with VBr had no on-treatment FU HDVRNA testing. Remaining 2 patients continued therapy and had persistent viremia throughout FU. Mean time to VBr was 18.5 ± 3.87 months (range: 15–24 months). Following VBr, 3 patients experienced ALT elevations. Seven patients (21%) discontinued BLV treatment (21.2%) at median 19 months (range 12–27). Decompensated patients (n = 5, 15.2%) demonstrated similar VR rates compared to patients with compensated liver disease, suggesting efficacy across the disease severity spectrum. BLV was well tolerated.
Conclusion: In this real-world Turkish cohort, BLV demonstrated VR in 74% of patients at 12 months on-treatment and, maintained VR in the majority throughout 36 months. An unexpected high VBr rate was observed with the Russian BLV. Patients denied non-compliance.

WED-592
Multitargeting ASO-based constructs as a new promising silencing strategy in HBV infection in vitro

Arnau Puig Lopez[1], Ariadna Vila Planas[2], Javier Pérez Garreta[3,4,5], Ariadna Rando-Segura[1,4], Maria Buti[3,4,5], Montserrat Terrazas Martinez[2], Roser Ferrer[6,7,8], Maria Francesca Cortese[1,9]. *[1]Department of Microbiology, Liver Unit, Vall d'Hebron Institut de Recerca (VHIR), Vall d'Hebron Barcelona Hospital Campus, Barcelona, Spain; [2]Department of Inorganic and Organic Chemistry, Organic Chemistry Section, Institute of Biomedicine, University of Barcelona (IBUB), Barcelona, Spain; [3]Department of Hepatology, Vall d'Hebron Hospital Universitari, Vall d'Hebron Barcelona Hospital Campus, Barcelona, Spain; [4]Instituto de Salud Carlos III, Centro de Investigación Biomédica en Red de Enfermedades Hepáticas y Digestivas (CIBERehd), Madrid, Spain; [5]Universitat Autònoma de Barcelona (UAB), Barcelona, Spain; [6]Clinical Biochemistry Department, Vall d'Hebron University Hospital, Barcelona, Spain; [7]Clinical Biochemistry, Drug Delivery & Therapy (CB-DDT) Research Group, Vall d'Hebron Research Institute (VHIR), Barcelona, Spain; [8]Bioquimica i Biologia Molecular Department, Universitat Autònoma de Barcelona (UAB), Barcelona, Spain; [9]Instituto de Salud Carlos III, Centro de Investigación Biomédica en Red de Enfermedades Hepáticas y Digestivas (CIBERehd), Barcelona, Spain*
Email: arnau.puig@vhir.org

Background and aims: Persistent transcriptional activity of hepatitis B virus (HBV) covalently closed circular DNA remains a major obstacle to functional cure. Targeted silencing of viral transcripts is therefore an attractive strategy to suppress viral replication. We developed a novel class of stimuli-responsive construct specifically designed for the simultaneous intracellular release of two Locked-Nucleic Acid ASO (LNA-ASO) targeting hyper-conserved regions of HBV.
Method: The construct was composed of two biostable LNA-ASOs linked together by a linker that is specifically cleaved upon exposure to specific endoneous intracellular enzymes. The antiviral activity of the individual ASOs and the dual construct was evaluated in vitro in HBV-infected HepG2-hNTCP through transient transfection. Treated cells were collected at 72 hours post transfection and the intracellular pregenomic RNA (pgRNA) was quantified by qPCR. A scrambled ASO was used as a control.
Results: Both LNA-ASOs efficiently silenced intracellular pgRNA HBV expression with IC50 values of 24.2 nM and 22.7 nM, respectively (IC90 >100 nM for the LNA-ASO1 and 82.2 nM for the LNA-ASO2). To ensure a robust silencing of the HBV pgRNA, both ASOs were tested at

a concentration twice the IC50 reaching a median [IQR] inhibition versus the scrambled ASO of respectively 79.2% [67.3;89.3] and 75.6% [60.2;83.7]. Since both molecules were active against HBV infection, a multitargeting ASO-based construct was designed. Native gel analysis showed that the newly synthesized construct efficiently carried both LNA-ASOs. Moreover, both molecules were efficiently released under emulated intracellular enzymatic conditions. To ensure that once released the LNA-ASOs remained functional, HBV-infected cells were treated with serial dilutions of the construct resulting in potent pgRNA inhibition, with an estimated IC50 of 2.8 nM, and a sustained inhibition at low nanomolar concentrations (IC90 = 3.5 nM).

Conclusion: This newly designed construct may serve as potent inhibitor of viral expression and shows potential as a therapeutic strategy for the multitargeted silencing of HBV. By enabling simultaneous targeting of conserved viral regions, this strategy has clear therapeutic potential and supports further development toward translational and preclinical evaluation in HBV infection. Grant PID2021-126447OB-I00 and PID2024-158273OB-I00 funded by por MICIU/AEI/10.13039/501100011033 and by FEDER, UE and PI18/01964 co-financed by the European Union (ERDF, "A way to make Europe").

WED-593

Integrated efficacy analysis of bulevirtide 10 mg from studies MYR204 and MYR301 at weeks 48 and 96 across subgroups

Adrian Streinu-Cercel[1,2], Soo Aleman[3], Tarik Asselah[4], Maurizia Brunetto[5,6], Vladimir Chulanov[7], George Sebastian Gherlan[2,8], Pietro Lampertico[9,10], Viacheslav Morozov[11], Olga Sagalova[12], Tatiana Stepanova[13], Sreeni Yalamanchili[14], Amos Lichtman[14], Dmitry Manuilov[14], Mingyang Li[14], Heiner Wedemeyer[15]. *[1]National Institute of Infectious Diseases Prof. Dr. Matei Bals, Bucharest, Romania; [2]University of Medicine and Pharmacy "Carol Davila" Bucharest, Bucharest, Romania; [3]Department of Infectious Diseases, Karolinska University Hospital/Karolinska Institutet, Stockholm, Sweden; [4]Hôpital Beaujon APHP, Université de Paris-Cité, INSERM UMR1149, Clichy, France; [5]Hepatology Unit, Reference Center of the Tuscany Region for Chronic Liver Disease and Cancer, University Hospital of Pisa, Pisa, Italy; [6]Department of Clinical and Experimental Medicine, University of Pisa, Pisa, Italy; [7]Sechenov University, Moscow, Russian Federation; [8]Dr. Victor Babes Foundation, Bucharest, Romania; [9]Division of Gastroenterology and Hepatology, Foundation IRCCS Ca' Granda Ospedale Maggiore Policlinico, Milan, Italy; [10]CRC "A. M. and A. Migliavacca" Center for Liver Disease, Department of Pathophysiology and Transplantation, University of Milan, Milan, Italy; [11]LLC Medical Company Hepatolog, Samara, Russian Federation; [12]South Ural State Medical University, Chelyabinsk, Russian Federation; [13]LLC Clinic of Modern Medicine, Moscow, Russian Federation; [14]Gilead Sciences, Inc, Foster City, United States; [15]Clinic for Gastroenterology, Hepatology, Infectious Diseases, and Endocrinology, Hannover Medical School, Hannover, Germany*
Email: gherlanus@gmail.com

Background and aims: Bulevirtide (BLV) 2 mg is approved in Europe for treatment of patients (pts) with chronic hepatitis delta. BLV monotherapy was shown to be generally safe and well tolerated. This subgroup efficacy analysis evaluated virologic response (VR) and biochemical response (BR) to the investigational BLV 10 mg dose at weeks 48 and 96 for the MYR301 (Phase 3; NCT03852719) and MYR204 (Phase 2; NCT03852433) studies.

Method: In a pooled analysis, VR (undetectable hepatitis delta virus [HDV] RNA or ≥ 2 $\log_{10}$ IU/mL decline from baseline [BL]), BR (alanine aminotransferase [ALT] normalisation), and combined response (CR; VR + BR) rates were assessed at weeks 48 and 96 across demographic and disease characteristic subgroups of pts treated with BLV 10 mg/day. The following subgroups were assessed: age (years; < 45, ≥ 45), sex (male, female), race (White, other), BL ALT (≤ 1.5 × upper limit of normal [ULN], > 1.5 × ULN), BL HDV RNA (< median, ≥ median), cirrhosis (yes, no), and concomitant hepatitis B virus (HBV) treatment (yes, no).

Results: Overall, 150 pts were included. At BL, mean (SD) age was 41 (8.2) years, 63% were male and 84% White, mean (SD) ALT was 108 (84.8) U/L, median (quartile [Q]1, Q3) HDV RNA was 5.5 (4.37, 6.21) $\log_{10}$ IU/mL, 43% had cirrhosis, and 55% had received concomitant HBV treatment. At BL, 30% were ≥ 45 years old, 73% had ALT > 1.5 × ULN, 98% had HDV genotype 1, and 1% had HDV genotype 5. At week 96, CR rates (%, [95% CI]) were: age < 45 vs ≥ 45, 52 (42–62) vs 56 (40–70); male vs female, 52 (42–63) vs 55 (42–69); White vs other race, 52 (43–61) vs 58 (37–78); BL ALT ≤ vs > 1.5 × ULN, 56 (40–72) vs 52 (43–62); BL HDV RNA < vs ≥ median, 57 (45–69) vs 49 (38–61); cirrhosis, yes vs no, 49 (37–62) vs 56 (45–67); concomitant HBV treatment, yes vs no, 59 (48–70) vs 46 (34–59). VR and BR rates were also comparable across subgroups. Undetectable HDV RNA rates were higher in pts with BL viral loads < median (53 [41–65] vs 20 [12–31]) at week 96. At week 48, efficacy was also comparable across subgroups.

Conclusion: Overall, the efficacy of treatment with BLV 10 mg was consistent across subgroups with different demographics and disease characteristics, supporting the use of BLV for treatment of patients with HDV and compensated liver disease. Pts with lower viral load at BL were more likely to achieve viral suppression.

WED-594

Lonafarnib/ritonavir with or without peginterferon achieves rapid, durable responses in a chronic hepatitis D: extended analyses from the phase 3 D-LIVR trial

Robert Taylor[1], Ohad Etzion[2], Saeed Sadiq Hamid[3], Tarik Asselah[4], George Sebastian Gherlan[5], Maria Buti[6], Pietro Lampertico[7], Adela Turcanu[8], Tsarynna Petrivna[9], Liana Gheorghe[10], George Stancu[10], Natalia Voronkova[11], Natalia Barsukova[12], Soo Aleman[13], Jordan J. Feld[14], Jean-Karl Sirois[15], Armaan Hirani[1], Hebaalla Agha[1], Leen Kawas[1], Nancy S. Reau[16], Christopher Koh[17], Theo Heller[17], Cihan Yurdaydin[18], Xue Hua[1], Jeffrey Glenn[1,19]. *[1]EIT Pharma, Inc., Kirkland, United States; [2]Soroka, University Medical Center, Be'er Sheva, Israel; [3]Aga Khan University, Karachi, Pakistan; [4]Hopital Beaujon, University of Paris, Clichy, France; [5]Carol Davila University of Medicine and Pharmacy, Bucharest, Romania; [6]Hospital Universitari Vall d'Hebron, Barcelona, Spain; [7]Fondazione IRCCS CA' Granda Ospedale Maggiore Policlinico, Milan, Italy; [8]The State University of Medicine and Pharmacy, Chisinau, Moldova; [9]International Institute of Clinical Research, Kyiv, Ukraine; [10]Institutul Clinic Fundeni, Bucharest, Romania; [11]H-Clinic, Moscow, Russian Federation; [12]Center for Targeted Therapy, LLC., Moscow, Russian Federation; [13]Korolinska Universitetssjukheset, Huddinge, Sweden; [14]University Health Network, Toronto, Canada; [15]YBR Analytics, Toronto, Canada; [16]Rush University Medical Center, Chicago, United States; [17]Liver Disease Branch, NIDDK, NIH, Bethesda, United States; [18]Koc University School of Medicine, Istanbul, Türkiye; [19]Stanford University School of Medicine, Palo Alto, United States*
Email: jeffrey.glenn@eitpharma.com

Background and aims: Lonafarnib (LNF) boosted with ritonavir (LNF/RTV) is the only oral therapeutic under development for the treatment of chronic hepatitis D (CHD). LNF has a dual mechanism of action, inhibiting the host farnesyltransferase to disrupt HDV virion assembly, and promoting immune response in infected hepatocytes. LNF has been studied in over 2400 subjects across several clinical programs.

Method: Oral LNF/RTV with or without peginterferon Alfa-2a (Peg) was evaluated in D-LIVR, the largest phase 3 randomized placebo-controlled HDV trial to date (n = 407). The primary endpoint was a composite score of ≥ 2 log HDV RNA reduction and ALT normalization compared to baseline at 48-weeks on-treatment. This study presents extended analyses of the durability, breadth, and kinetics of treatment response in the D-LIVR study including time-to-response Kaplan Meier estimation.

Results: Both LNF-based regimens met the primary composite endpoint compared to placebo (LNF/RTV: p = 0.004, LNF/RTV+Peg: p < 0.0001) along with significant improvement in virologic and biochemical response seperately. Significant therapeutic benefit was also demonstrated in histological improvement at week 48 (LNF/RTV +Peg vs placebo, p = 0.01). Treatment effects on composite score vs placebo were durable at 24 weeks off treatment (LNF/RTV: p < 0.0001, LNF/RTV+Peg: p < 0.0001). Time-to-event analysis identified additional responders who achieved composite response at any time during the study. These "any-time responders" included 41.0% (LNF/RTV) and 57% (LNF/RTV+Peg) of treated patients compared to 1.9% in the placebo arm. Additionally, LNF-based therapies elicited treatment responses markedly faster than Peg monotherapy. LNF/RTV+Peg patients demonstrated ≥ 2 log HDV RNA reduction at a median time of 8.3 weeks (95% CI: 8.1–12.1) compared to 28.3 weeks (95% CI: 16.3–48.1) for Peg monotherapy using Kaplan Meier estimates.
Conclusion: LNF/RTV is a first-in-class CHD therapy with efficacy and safety in patients with CHD and substantial benefit after treatment cessation. The addition of Peg further increases response rates with a favorable safety profile and rapid treatment response kinetics. LNF/RTV represents a valuable addition to the CHD therapeutic armamentarium and because it is the only drug targeting virion assembly and the only oral CHD therapeutic under development, it may represent a backbone for combination treatments.

WED-595

Antiviral effect and safety of terbinafine in chronic hepatitis B: results of a phase 1b study

Diederick van Doorn[1], Robin Erken[1], Martine Peters-Bakker[1], Karel van Dort[1], Sophie Willemse[2], Hendrik Reesink[3], Ulrich Beuers[1], Neeltje Kootstra[1], R. Bart Takkenberg[1]. *[1]Amsterdam UMC, Amsterdam, Netherlands; [2]Cairns Hospital and Hinterland Health Services, Cairns, Australia; [3]Center of Human Drug Research, Leiden, Netherlands*
Email: d.j.vandoorn@amsterdamumc.nl

Background and aims: Terbinafine, an antifungal agent, has been identified as a specific inhibitor of hepatitis B virus X protein (HBx) which is a key regulator of viral transcription and replication. However, due to its potential hepatotoxicity, terbinafine is prescribed with caution in people with (chronic) liver disease. We investigated the antiviral effect and safety of terbinafine as monotherapy or in addition to long-term tenofovir disoproxil (TDF) in patients with chronic hepatitis B in a phase 1b study.
Method: In this randomized, double-blind, placebo-controlled trial, 32 patients with chronic hepatitis B and stable disease without cirrhosis were enrolled between 2021 and 2025. Two groups of hepatitis B patients were included in the study: patients with untreated chronic hepatitis B with a low viral load (Group A, n = 16) and patients with chronic hepatitis B on stable TDF therapy with suppressed HBV DNA (Group B, n = 16). Within each group, patients were randomized 2.2 to 1 for terbinafine or placebo (11 terbinafine and 5 placebo per group). Treatment duration was 10 weeks (4 weeks 250 mg daily, 2 weeks wash-out, 4 weeks 500 mg daily), followed by post-treatment follow-up of 12 weeks. Primary endpoints were: >0.32 log10 IU/mL decline of serum HBsAg levels, and >0.86 log10 IU/mL decline in serum HBV DNA in Group A at week 10. Secondary endpoints included safety and tolerability.
Results: Thirty-two patients were included and randomized. Baseline virological characteristics were comparable between both treatment arms. After 10 weeks, terbinafine treatment resulted in a modest, but non-significant decline in HBsAg (0.06 log10 IU/ml, p = 0.10), whilst placebo showed no effect (0.02, p = 0.85). Mixed-model analysis showed no effect of terbinafine treatment, time, or interaction effect. In Group A, HBV DNA declined by 0.27 log10 IU/mL in the terbinafine arm and 0.72 log10 IU/mL in the placebo arm. Terbinafine was well tolerated in all exposed participants, with no significant differences in adverse events as compared to placebo, particularly no relevant changes in liver biochemistry occurred.
Conclusion: Despite terbinafine being well tolerated and showing a favorable safety profile, this phase 1b study showed that terbinafine did not significantly affect serum HBsAg or HBV DNA levels when compared to placebo in patients with chronic hepatitis B with low viral load or virological suppression on nucleoside analogues.

WED-596

Suppressing HBsAg by hepatitis B immunoglobulins does not lead to functional cure and has no impact on NK cell, T cell and B cell phenotypes in patients with chronic hepatitis B

Katja Deterding[1], Po-Chun Chen[1,2], Julia Kahlhöfer[1,3], Lisa Sandmann[1,2,4], Kerstin Port[1], Anke R.M. Kraft[1,2,5], Anika Grosshennig[6], Norman Woller[1,2], Ringlstetter Rieke[6], Markus Cornberg[1,2,3,4,5], Heiner Wedemeyer[1,2,4]. *[1]Department of Gastroenterology, Hepatology, Infectious Diseases and Endocrinology, Hannover Medical School, Hannover, Germany; [2]German Center for Infection Research (DZIF), Partner Site Hannover-Braunschweig, Braunschweig, Germany; [3]German Center for Infection Research (DZIF), HepNet Study House of the German Liver Foundation, Hannover, Germany; [4]Cluster of Excellence RESIST (EXC 2155), Hannover Medical School, Hannover, Germany; [5]Centre for Individualised Infection Medicine (CiiM), a Joint Venture Between the Helmholtz Centre for Infection Research (HZI) and Hannover Medical School (MHH), Hannover, Germany; [6]Institute for Biostatistics, Hannover Medical School, Hannover, Germany*
Email: wedemeyer.heiner@mh-hannover.de

Background and aims: Suppressing HBsAg has been suggested as a strategy to restore immune responses in chronic hepatitis B (CHB). Hepatitis B-specific immunoglobulins (HBIG) prevent reinfection after transplantation. This study aimed to investigate (i) whether suppressing HBsAg levels by HBIG therapy alters phenotypes and function of immune cells in patients with CHB and low baseline HBsAg levels, and (ii), if HBIG therapy for 12 weeks can lead to long-term changes in HBsAg levels or even functional cure.
Method: Nine HBV infected adults (median age 61 y [35–72], 67% male) were enrolled in an investigator-initiated, open-label, single arm phase II pilot-study (Cohort A (n = 4), patients treated with tenofovir, and Cohort B (n = 5), untreated patients with HBV-DNA < 2000 IU/mL). All participants were HBeAg-negative and had HBsAg <100 IU/mL. The intervention was a 12-week HBIG regimen: 10,000 IU Hepatect® i.v. at baseline, followed by 500 IU Zutectra® s.c. on days 1 to 6, a second iv infusion of 10,000 IU Hepatect® on day 7, and then 500 IU Zutectra® s.c. every other day (day 9 to 84). High resolution immune phenotyping of NK cells, T cells and B cells by spectral flow cytometry (>70 markers) was performed before, during and after treatment and also in control patients with high HBsAg levels of >3000 IU/ml.
Results: Median HBsAg at baseline was 52.2 IU/mL (4.0–73.0). Patients not receiving TDF (n = 5) had a median HBV-DNA of 305 IU/mL (100–1100). HBsAg became undetectable in all patients immediately after iv HBIG but remained negative throughout 12 weeks of s.c. HBIG in only two patients. At week 12, eight out of nine patients had HBsAg levels <10 IU/ml. High resolution immune phenotyping did not reveal substantial differences in NK cell, T cell and B cell profiles between study patients and controls. Of note, UMAP clustering of distinct cell types in each individual patient revealed some heterogeneity of NK cell populations between patients which, however, remained largely unchanged throughout and after HBIG therapy. Similarly, T cell and B cell profiles showed no major alterations. At week 24 of follow-up, all patients were again HBsAg positive, with individual HBsAg levels similar to baseline. One serious adverse event occurred during follow-up, unrelated to study medication.
Conclusion: In patients with CHB and low HBsAg levels, HBIG-mediated HBsAg suppression was not associated with detectable changes in NK-, T-, or B-cell phenotypes HBIG therapy for 12 weeks has no apparent impact long-term HBsAg setpoints.

WED-597

Safety, pharmacokinetics, pharmacodynamics, and antiviral activity of cavrotolimod, alone and in combination with low-dose nivolumab, for the treatment of chronic hepatitis B

Grace Lai-Hung Wong[1], Alina Jucov[2], Marta Dobryanska[3], Edward J. Gane[4], Stuart Roberts[5], Simone Strasser[6], Eternity Labio[7], Jacinta Holmes[8], Bobby Asem[9], Jerome Deval[9], Susanna K. Tan[9], Paul B. Eckburg[9], Hassan Javanbakht[9], Leesun Kim[9], Loghman Salimzadeh[10], Adam Gehring[10], Nancy Shulman[9], Man-Fung Yuen[11]. *[1]Department of Medicine and Therapeutics, The Chinese University of Hong Kong, Hong Kong, China; [2]Arensia Exploratory Medicine GmbH, Chisinau, Moldova, and Nicolae Testemitanu State University of Medicine and Pharmacy, Chişinău, Moldova; [3]Medical Center of LLC Arensia Exploratory Medicine, Kyiv, Ukraine; [4]University of Auckland, Auckland, New Zealand; [5]Alfred Hospital & School for Translational Medicine, Monash University, Melbourne, Australia; [6]AW Morrow Gastroenterology and Liver Centre, Royal Prince Alfred Hospital, Sydney, Australia; [7]Liver Unit, Makati Medical Center, Metro Manila, Philippines; [8]St Vincent's Hospital Melbourne, Melbourne, Australia; [9]Bluejay Therapeutics, Inc., Redwood City, United States; [10]Schwartz-Reisman Liver Research Centre, University Health Network, Toronto, Canada, and Toronto Centre for Liver Disease, University Health Network, Toronto, Canada; [11]Department of Medicine, Queen Mary Hospital, The University of Hong Kong, Hong Kong, China*
Email: mfyuen@hku.hk

Background and aims: Restoration of HBV-specific immune responses is central to achieving functional cure for chronic hepatitis B (CHB). Cavrotolimod is a novel spherical nucleic acid Toll-Like Receptor 9 agonist oligonucleotide designed to activate innate and adaptive immunity. Study BJT-008-001 is an ongoing Ph1b/2 study evaluating cavrotolimod ± nivolumab ± brelovitug (mAb against HBsAg) in subjects with CHB. Herein, Phase 1b results are presented.
Method: Part 1 (n = 20) was a randomized, double-blind, placebo-controlled study of cavrotolimod (2–6 mg SC Q1–4W) × 4 weeks, and Part 2 (n = 7) was an open-label study of cavrotolimod 3 mg SC Q2W × 4 weeks + low-dose nivolumab on Day 1. Safety (treatment emergent adverse events [TEAEs], labs, physical exams), pharmacokinetics (PK), and pharmacodynamics (PD) were assessed.
Results: In Parts 1 & 2, 169 TEAEs were observed in 25/27 (93%) participants. Most TEAEs were Grade 1 (68%) or 2 (31%) severity, and most were deemed related to study drug (93%). The most common TEAEs were injection site reactions (ISRs, 51%) and flu-like illness (20%). No related serious, severe, or immune-related TEAEs were observed. Cavrotolimod was measurable in plasma within 2–4 hours of dosing in most subjects. Day 1 exposure (Cmax, AUC) increased linearly with weekly doses from 2 to 6 mg, whereas Day 29 exposure increased in a greater than dose proportional fashion. Coadministration of nivolumab had no significant effect on cavrotolimod PK. One subject achieved HBsAg clearance (baseline 8 IU/mL) accompanied by an ALT increase, and another developed anti-HBs without HBsAg clearance; however, no other meaningful HBsAg changes were observed. Cavrotolimod induced transient, dose-dependent increases in serum cytokines, including CXCL10, IFN-g, IL-15 and IL-12p40. Global CD4 and CD8 T cells were also transiently activated, and improved activation of HBV-specific T-cell responses was observed.
Conclusion: Multiple doses of cavrotolimod × 4 weeks ± 1 dose nivolumab were generally well tolerated in CHB subjects. Most subjects experienced mild-to-moderate ISRs that were not treatment-limiting. Cavrotolimod elicited a potent immune response with strong cytokine/chemokine production and augmented HBV-specific T cell responses. Cavrotolimod may evolve as an important part of combination therapy in achieving functional cure of CHB.

WED-601-YI

Intermittent versus continuous interferon-alpha 2b plus tenofovir alafenamide therapy results in fewer adverse events with similar HBsAg reduction in treatment-naïve HBeAg-negative CHB patients: a multiregional randomized controlled trial in China

Weien Yu[1], Tiantian Hu[1], Haoru Xie[1], Shenyan Zhang[1], Tingting Gao[1], Yuxian Huang[2], Xinxin Zhang[3], Lihong Qu[4], Yuanwang Qiu[5], Xiaoping Wu[6], Huajiang Shen[7], Xueping Yu[8], Daokun Yang[9], Haoxiang Zhu[1], Jiming Zhang[1]. *[1]Department of Infectious Diseases, Shanghai Key Laboratory of Infectious Diseases and Biosafety Emergency Response, National Medical Center for Infectious Diseases, Huashan Hospital, Fudan University, Shanghai, China, Shanghai, China; [2]Department of Infectious Diseases, Shanghai Key Laboratory of Infectious Diseases and Biosafety Emergency Response, National Medical Center for Infectious Diseases, Huashan Hospital, Fudan University, Shanghai, China, Shanghai Public Health Clinical Center affiliated to Fudan University, Shanghai, China; [3]Department of Infectious Diseases, Research Laboratory of Clinical Virology, Ruijin Hospital, Shanghai Jiao Tong University School of Medicine, Shanghai, China; [4]Department of Infectious Diseases, School of Medicine, Shanghai East Hospital, Tongji University, Shanghai, China; [5]Department of Infectious Diseases, Affiliated Wuxi Fifth Hospital of Jiangnan University, Wuxi, China; [6]Department of Infectious Diseases, the First Affiliated Hospital of Nanchang University, Nanchang, China; [7]Department of Infection, Affiliated Hospital of Shaoxing University (The Shaoxing Municipal Hospital), Shaoxing, China; [8]Key Laboratory of Screening and Control of Infectious Diseases (Quanzhou Medical College), Fujian Provincial University, Quanzhou, China; [9]Department of Infectious Diseases, The First Affiliated Hospital of Xinxiang Medical University, Xinxiang, China*
Email: ywe18930740242@163.com

Background and aims: Interferon-alpha (IFN-alpha) is an effective therapy for achieving hepatitis B surface antigen (HBsAg) loss in patients with chronic hepatitis B (CHB), but its clinical use is limited by adverse effects and poor tolerability. This study evaluated whether an intermittent IFN-alpha dosing strategy could achieve comparable HBsAg reduction with improved safety.
Method: This multiregional, open-label, randomized controlled trial was conducted in China. Treatment-naïve, HBeAg-negative CHB patients were randomly assigned to a continuous or intermittent treatment group. The continuous group received IFN-alpha 2b plus tenofovir alafenamide fumarate (TAF) for 48 weeks. The intermittent group received the same regimen, with IFN-alpha 2b paused for 4 weeks after every 8 doses while TAF was continued, for a total duration of 72 weeks. Follow-up assessments were performed every three months until 6 months after treatment cessation.
Results: Between August 25, 2022, and November 30, 2024, 210 patients were enrolled across nine hospitals (105 per group). Both treatment strategies showed comparable HBsAg reduction, with no significant difference in decline from baseline to end of treatment between the continuous and intermittent groups (495.7 vs. 731.1 IU/mL, $p = 0.32$). Functional cure rates were similar between groups (4.76% vs. 6.15%, $p > 0.99$) and lower than those reported in nucleos(t)ide analogue–experienced populations. Treatment group was not associated with log HBsAg reduction at Week 36, whereas baseline log HBsAg ($p = 0.011$) and age ($p = 0.049$) were independently associated. Importantly, the intermittent group demonstrated a superior hematologic safety profile during treatment. At Weeks 12, 24, and 36, significantly fewer patients in the intermittent group experienced very low or low absolute neutrophil counts (ANC) and platelet counts (PLT), with a higher proportion maintaining values within the normal range (all $p < 0.05$ for ANC; all $p < 0.001$ for PLT), corresponding to fewer episodes of grade 3–4 neutropenia and thrombocytopenia. These safety advantages were confined to the active treatment phase and were no longer observed after treatment completion.

Conclusion: In treatment-naïve, HBeAg-negative CHB patients, intermittent IFN-alpha therapy was non-inferior to continuous treatment for HBsAg reduction and functional cure, with significantly better hematologic safety.

WED-602

Pevifoscorvir sodium demonstrated profound antiviral activity in untreated HBeAg+ subjects, regardless of baseline ALT level

Man-Fung Yuen[1], Kosh Agarwal[2], Alina Jucov[3], Alexei Haceatrean[3], Min Wu[4,4], Kha Le[4], Jen Rito[4], Lawrence Blatt[4], Sushmita Chanda[4], Tse-I Lin[4], Edward J. Gane[5]. *[1]Department of Medicine, School of Clinical Medicine, The University of Hong Kong, Hong Kong, China, Hongkong, China; [2]King's College Hospital, Institute of Liver Studies, London, United Kingdom, London, United Kingdom; [3]ARENSIA Exploratory Medicine, Republican Clinical Hospital and Nicolae Testemitanu State University of Medicine and Pharmacy, Chișinău, Moldova, Chișinău, Moldova; [4]Aligos Therapeutics, South San Francisco, United States; [5]Faculty of Medicine, University of Auckland, Auckland, New Zealand, Auckland, New Zealand*
Email: mwu@aligos.com

Background and aims: Pevifoscorvir sodium (PEVY, ALG-000184) is a prodrug of ALG-001075, a capsid assembly modulator-empty (CAM-E). The Study ALG-000184–201 (NCT04536337) showed favorable safety and potent antiviral activity of 300 mg PEVY monotherapy × 96 weeks in untreated chronic HBV infected subjects. An ad hoc analysis stratified by baseline (BL) ALT (<1.2 × upper limit of normal [ULN] vs ≥1.2 × ULN; ULN = 30 U/L[female], 40 U/L[male]) assessed whether BL ALT levels impact safety or antiviral activity.
Method: Ten untreated HBeAg+ subjects received open-label 300 mg PEVY monotherapy × 96 weeks. The analysis compared safety data (treatment-emergent adverse events (TEAEs), ALT flare events, lab abnormality, electrography and physical examination findings) and antiviral activity (changes from BL in HBV DNA, RNA, HBsAg, HBeAg and HBcrAg) over 96 weeks between low-ALT group (BL ALT <1.2xULN, n = 5) and high-ALT group (BL ALT ≥ 1.2xULN, n = 5).
Results: Mean BL ALT were 35 U/L in low-ALT group and 86 U/L in high-ALT group. Mean BL disease characteristics were comparable between low- and high-ALT groups: HBV DNA 7.8 and 8.2 $\log_{10}$ IU/mL; HBV RNA 5.2 and 5.3 $\log_{10}$ copies/mL; HBsAg 4.4 and 4.2 $\log_{10}$ IU/mL; HBeAg 2.7 and 2.6 PEI $\log_{10}$ U/mL; HBcrAg 8.2 and 8.4 $\log_{10}$ U/mL, respectively. Steady state plasma ALG-001075 was not statistically different between groups. Following 96 weeks of 300 mg PEVY monotherapy, both groups showed profound decline in HBV markers. HBV DNA < LLOQ (10 U/mL) was achieved in 2 of 5 subjects in low-ALT group and 4 of 5 subjects in high-ALT group by Week 48, and in all subjects by Week 96. At Week 48 and Week 96, mean reductions were as follows: HBV DNA 6.6 vs 7.2 and 6.8 vs 7.2 $\log_{10}$ IU/mL; HBV RNA 4.2 vs 4.4 and 4.2 vs 4.4 $\log_{10}$ copies/mL; HBsAg 0.8 vs 0.6 and 1.0 vs 0.7 $\log_{10}$ U/mL; HBeAg 1.2 vs 2.0 and 1.3 vs 2.2 $\log_{10}$ PEI U/mL; HBcrAg 1.2 vs 1.9 and 1.8 vs 2.5 $\log_{10}$ U/mL, for low- vs high-ALT group, respectively. ALT flares occurred in two subjects in each group (peak ALT 4.4–14.6 × ULN) and resolved during dosing without dose modification, interruption or discontinuation; no clinically meaningful changes in liver synthesis or excretion function were observed. All other TEAEs were mild to moderate and balanced between ALT strata.
Conclusion: In untreated HBeAg+ subjects, 300 mg PEVY monotherapy for 96 weeks demonstrated favorable safety and potent antiviral activity in both BL low- and high-ALT groups. Moreover, HBeAg and HBcrAg reductions seemed greater in subjects with higher BL ALT.

WED-603

Lonafarnib as finite treatment for chronic hepatitis D: Long-term effect on hard endpoints

Cihan Yurdaydin[1], Christopher Koh[2], Muge Ozari Gulnar[1], Olga Metin[3], Özgür Aktaş[4], Esra Tunç[5], Selin Özer[4], Onur Keskin[6], Mesut Gumussoy[7], Emin Bodakçi[8], Xheni Deda[9], Sevda Aghayeva[10], Genco Gencdal[1], Mujdat Zeybel[1], Ramazan Idilman[7], Mithat Bozdayi[5], Ingrid Choong[11], Naraanbatar Dashdorj[12], Ofir Harari[13], Naranjargal Dashdorj[12], Edward Mills[14], Theo Heller[15], Jeffrey Glenn[16]. *[1]Koç University Hospital, Department of Gastroenterology, İstanbul, Türkiye; [2]Liver Diseases Branch, National Institute of Diabetes and Digestive and Kidney Diseases, National Institutes of Health, Bethesda, Maryland, United States; [3]Prof. Dr. Cemil Taşcıoğlu City Hospital, Department of Gastroenterology, İstanbul, Türkiye; [4]Koç University School of Medicine, İstanbul, Türkiye; [5]Ankara University Hospital, Hepatology Institute, Ankara, Türkiye; [6]Hacettepe University Hospital, Department of Gastroenterology, Ankara, Türkiye; [7]Ankara University Hospital, Department of Gastroenterology, Ankara, Türkiye; [8]Gaziantep City Hospital, Department of Gastroenterology, Gaziantep, Türkiye; [9]Division of Gastroenterology and Hepatology, Department of Medicine, University of Missouri School of Medicine, Columbia, MO, United States; [10]Azerbaijan Medical University, Baku, Azerbaijan; [11]Eiger BioPharmaceuticals, Inc., California, United States; [12]The Liver Center, Mongolia and Onom Foundation, Ulaanbaatar, Mongolia; [13]Redwood AI, Vancouver, BC, Canada; [14]Department of Health Research Methods, Evidence, and Impact, McMaster University, Hamilton, Ontario, Canada; [15]Translational Hepatology Section, Liver Diseases Branch, National Institute of Diabetes and Digestive and Kidney Diseases, National Institutes of Health, Bethesda, Md., United States; [16]Departments of Medicine (Division of Gastroenterology and Hepatology) and Microbiology and Immunology, Stanford University School of Medicine, Stanford, California, United States*
Email: cyurdaydin@ku.edu.tr

Background and aims: Hepatitis delta virus (HDV) infection leads to the most severe form of viral hepatitis. New treatment options are urgently needed. The farnesyl transferase inhibitor lonafarnib (LNF) may be an option for finite treatment as it possesses a dual mode of action: it interferes with virion assembly (Glenn et al Science 1992) and also has immunomodulatory properties (Lempp et al, Nat Commun 2019). The aim of this study was to assess if finite treatment with a LNF-based regimen is able to prevent hard endpoints such as complications of liver disease and death from liver disease on long-term follow-up (LTFU).
Method: All patients subject to this study had received LNF-based treatment in two phase 2 (LOWR 1 and 2) and one phase 2 (LIFT) studies in Ankara (TR) and NIH (USA), respectively, and one phase 3 (DLIVR) study in Istanbul (TR). A total of 122 patients were available for follow up. Start date used for LTFU and survival analysis was EOT date of LNF-based treatment. End of follow-up (EOFU) was set to either the last date of data collection (December 2025), or the date of liver-related event, the start date of a new potential treatment against HDV or loss to follow-up. Short-term viral response (STVR) was defined as undetectable HDV RNA or as[3] 2 log decline of HDV RNA compared to baseline and ST biochemical response (STBR) as ALT normalization at off treatment month 6. BR and VR were the co-primary endpoints. Cumulative probabilities of any event occurrence were estimated by the Kaplan-Meier method and compared with the log-rank test.
Results: STVR+STBR was achieved in 14 patients. On LTFU, none of these patients developed a clinical event in up to over 10 years of follow up, whereas out of 98 patients without STVR+STBR, 26 (26.5%) developed an event (p = 0.045 by the log rank test, Fig). The 10 year

event-free survival rate for all LNF-treated patients was superior to untreated or interferon-treated patients from historical control cohorts with comparable prevalences of baseline cirrhosis.
Conclusion: Achieving a 2 log drop in HDV RNA from baseline and normal ALT at 6 months after stopping any finite lonafarnib-based treatment regimen is associated with long-term event-free survival (i.e. no liver decompensation, liver cancer, liver transplant, or death in up to 10 over years of follow up). Event-free survival is also improved for all LNF-treated patients.

WED-604
Comparative effectiveness of sodium-glucose cotransporter-2 inhibitors, glucagon-like peptide-1 receptor agonists and dipeptidyl peptidase-4 inhibitors on risk of liver and non-liver outcomes in patients with viral hepatitis and type 2 diabetes
Xinrong Zhang[1], Scott Barnet[2], Ramsey C. Cheung[2], Mindie Nguyen[2].
[1]Division of Gastroenterology and Hepatology, School of Medicine, Stanford University Medical Center, Palo Alto, California, United States, Guangdong Provincial Key Laboratory of Food, Nutrition and Health, and Department of Epidemiology, School of Public Health, Sun Yat-sen University, Guangzhou, China; [2]Division of Gastroenterology and Hepatology, School of Medicine, Stanford University Medical Center, Palo Alto, California, United States
Email: mindiehn@stanford.edu

Background and aims: With the epidemic of metabolic diseases, type 2 diabetes (T2D) and viral hepatitis frequently coexist and worsen liver and non-liver outcomes synergistically, but effective pharmacological therapies are limited. Sodium-glucose cotransporter-2 inhibitors (SGLT-2i) are a novel class of anti-diabetic drugs that confer substantial cardiovascular and renal protection beyond their glucose-lowering effects. Therefore, we aimed to examine hepatic and extrahepatic effectiveness of SGLT-2i through head-to-head comparisons with dipeptidyl peptidase-4 inhibitors (DPP-4i) or glucagon-like peptide-1 receptor agonists (GLP-1RA) among patients with viral hepatitis and T2D in the United States (U.S.).
Method: Patients with T2D and viral hepatitis initiating SGLT-2i or comparator drugs (DPP-4i or GLP-1RA) were included (2007–2022) in the nationwide U.S. Merative™ Marketscan® Research Databases. Primary outcomes included (1) hepatocellular carcinoma (HCC) and cirrhosis, and (2) cardiovascular disease (CVD), chronic kidney disease (CKD), and non-liver cancer. Cox regression models were conducted to estimate hazard ratio (HR) and 95% confidence interval (CI).
Results: After 1:1 propensity score matching, we included 2,244 patients who initiated SGLT-2i and DPP-4i (mean age 57.5 years, 31.6% female), and 2,506 patients initiating SGLT-2i and GLP-1RA (mean age 57.8 years, 35.8% female). Compared with DPP-4i, SGLT-2i use was associated with significantly reduced risks of any liver-related outcomes (HR 0.74, 95% CI 0.54–0.99, p = 0.049), CVD (HR 0.68, 95% CI 0.47–0.98, p = 0.038), CKD (HR 0.69, 95% CI 0.49–0.97, p = 0.030), and a non-significant trend towards lower rates of HCC (HR 0.79, 95% CI 0.40–1.57, p = 0.497), cirrhosis (HR 0.76, 95% CI 0.56–1.03, p = 0.074) and non-liver cancer (HR 0.66, 95% CI 0.42–1.04, p = 0.072). In contrast, there was no significant difference in the risks of liver and non-liver outcomes when comparing SGLT-2i to GLP-1RA (all p > 0.05). These sensitivity analyses yielded results consistent with those of the main analyses when we repeated the analysis using inverse probability of treatment weighting for the balance of patient characteristics (HR: 0.54–0.97) and when we conducted a 6-month landmark analysis (HR: 0.44–0.88).
Conclusion: In this nationwide U.S. cohort study, SGLT-2i was associated with lower risks of liver and non-liver complications compared with DPP-4i, while demonstrating similar effectiveness to GLP-1RA among patients with viral hepatitis and T2D.

Viral hepatitis C – Clinical aspects including follow up after SVR

TOP-599
Personalised risk-based HCC surveillance in HCV-related advanced fibrosis/cirrhosis after SVR: real-world evidence of cost effectiveness
Gamal Shiha[1], Imam Waked[2], Nabiel Mikhail[3], Ayman Hassan[4], Ahmed Farahat[5], Abdelhamid A Serwah[6], Reham Soliman[7,8].
[1]Gastroenterology and Hepatology Unit, Internal Medicine Department, Faculty of Medicine, Mansoura University, Egypt; Egyptian Liver Research Institute and Hospital (ELRIAH), Sherbin, El Mansoura, Egypt, Mansoura, Egypt; [2]National Liver Institute, Menoufia University, Shebeen El Kom, Shebeen El Kom, Egypt; National Committee for Control of Viral Hepatitis, MOH, Egypt, Shebeen El Kom, Egypt; [3]Egyptian Liver Research Institute and Hospital (ELRIAH), Sherbin, El Mansoura, Egypt; Biostatistics and Cancer Epidemiology Department, South Egypt Cancer Institute, Assiut University, Egypt, Mansoura, Egypt; [4]Egyptian Liver Research Institute and Hospital (ELRIAH), Sherbin, El Mansoura, Egypt; Medical Laboratories Department, Higher Technological Institute of Applied Health Sciences, Sherbin, Mansoura, Egypt, Mansoura, Egypt; [5]Egyptian Liver Research Institute and Hospital (ELRIAH), Sherbin, Mansoura, Egypt; [6]Emeritus Professor of Internal Medicine, Suez Canal University, Suez, Egypt; [7]Technical institute of Nursing, Mansoura, Egypt; [8]Egyptian Liver Research Institute and Hospital (ELRIAH), Technical institute of Nursing, Sherbin, Mansoura, Egypt
Email: g_shiha@hotmail.com

Background and aims: Direct-acting antivirals (DAAs) have transformed hepatitis C virus (HCV) care, yet hepatocellular carcinoma (HCC) risk persists after sustained virological response (SVR). Current guidelines mandate uniform 6-monthly surveillance in patients with advanced fibrosis/cirrhosis, despite wide heterogeneity in post-SVR HCC risk. Modelling studies suggest personalised surveillance may improve efficiency, but real-world evidence is lacking. We evaluated the efficacy and cost effectiveness of a personalised surveillance strategy guided by the General Evaluation Score (GES) compared with standard surveillance.
Method: In this prospective, real-world comparative cohort study, 955 patients with advanced fibrosis/cirrhosis post-SVR were enrolled across two tertiary hepatology centres: 463 received standard 6-monthly ultrasound and AFP surveillance and 492 underwent GES-guided personalised surveillance, with intervals of 2–3 months (high risk), 6 months (intermediate), and 12 months (low). Outcomes included early-stage HCC detection (BCLC 0–A), surveillance utilisation, costs, and incremental cost-effectiveness. Analyses followed CHEERS 2022 guidelines.
Results: Sixty HCC cases were identified: 25 (5.4%) under standard surveillance and 35 (7.1%) with GES-guided surveillance. Early-stage tumours were detected in 52% (13/25) of standard-surveillance cases versus 80% (28/35) in the GES cohort, representing a 2.3-fold improvement. Despite intensified monitoring of high-risk patients, total surveillance visits were slightly lower with GES (3.01 vs 3.23 visits/patient). The cost per early-stage HCC detected decreased by 54%. Real-world ICER analysis showed that GES-guided surveillance was a dominant strategy, detecting more early-stage HCCs at lower overall cost. The ICER was –533 EGP per early detected HCC.
Conclusion: Personalised HCC surveillance provides real-world evidence supporting the economic superiority of risk-stratified surveillance after SVR and may help pave the way for integrating personalised pathways into future surveillance guidelines.

TOP-600-YI

Sex-specific patterns of cardiometabolic and renal complications by ethnicity among people with hepatitis C in British Columbia, Canada: a population-based study

Dahn Jeong[1,2], Stanley Wong[2], Héctor Alexander Velásquez García[1,2], Alnoor Ramji[1,3], Eric Yoshida[1,4], Jean Damascene Makuza[1], Prince Adu[1], Bushra Mahmood[1,2], Richard Morrow[1,2], Sofia Bartlett[1,2], Amee Manges[1,2], Mohammad Ehsanul Karim[1,3], Amanda Yu[2], Georgine Cua[1], Sara Qureshi[1], Mel Krajden[1,2], Naveed Janjua[1,2].
[1]University of British Columbia, Vancouver, Canada; [2]BC Centre for Disease Control, Vancouver, Canada; [3]Saint Paul's Hospital, Vancouver, Canada; [4]Vancouver General Hospital, Vancouver, Canada
Email: dahn.jeong@bccdc.ca

Background and aims: Chronic hepatitis C (HCV) infection increases the risk of extrahepatic manifestations (EHMs) such as type 2 diabetes (T2DM), and chronic kidney disease (CKD). Ethnic disparities in HCV-related outcomes have been documented, with Asian populations experiencing disproportionate disease burden. However, sex-specific patterns of EHMs across ethnic groups remain poorly understood. We aimed to assess sex-specific patterns of EHMs by ethnicity among people with chronic HCV and to examine whether disparities persist after HCV treatment.
Method: We used data from the British Columbia Hepatitis Testers Cohort (BC-HTC), including all individuals diagnosed with HCV from 1990 to 2015, linked to administrative health data. The study sample comprised 41,874 individuals with confirmed HCV. EHMs (CKD, T2DM, major adverse cardiac events [MACE], and neurocognitive disorders [NCD]) were identified through ICD-9/10 codes from hospitalization and physician billings. We computed sex-stratified incidence rates (IRs) by ethnicity (East Asian, South Asian, Other) across four groups: untreated, pre-treatment, post-treatment, and spontaneously cleared. Multivariable cause-specific hazard models estimated sex-stratified risks adjusting for sociodemographic and clinical factors.
Results: South Asian females had markedly higher EHM burden than all other groups. In the untreated group, incidence of T2DM and CKD was 22.7 and 27.9 per 1000 person-years (PY), compared with 9.3 and 18.5 for South Asian males and 5.4 and 13.1 for females of other ethnicities. Adjusted models showed untreated South Asian females had over 3-fold higher risk of T2DM (adjusted cause-specific hazard ratio [aHR] 3.53, 95%CI 2.07–5.43) than females of other ethnicities. Among treated individuals, the risk of T2DM was over 5-fold higher before treatment (aHR 5.13, 95%CI 3.89–6.75) but attenuated after treatment (aHR 3.11, 95%CI 2.05–4.71).
Conclusion: South Asian women with chronic HCV experience disproportionately high metabolic and renal disease burden, exceeding that of women in other ethnic groups. HCV treatment appears to attenuate but not eliminate these disparities, highlighting its role in advancing health equity. Intersecting social and structural determinants including sex, ethnicity, and barriers to healthcare likely contribute to disproportionate burden. Targeted, culturally-safe screening and treatment initiatives are urgently needed to reduce inequities in HCV-related outcomes.

WED-605-YI

From cure to complexity: post-SVR liver and metabolic trajectories in diabetic patients

Clelia Asero[1], Maria Stella Franzè[1], Teresa Maltese[1], Alberto La Spada[2], Daniele Lombardo[3], Claudia Grisanti[1], Giuseppina Russo[4], Annalisa Giandalia[5], Concetta Pitrone[6], Roberto Filomia[6], Gaia Caccamo[6], Carlo Saitta[1], Anna Licata[7], Teresa Pollicino[3], Irene Cacciola[1]. *[1]Università Degli Studi Di Messina, Department of Clinical and Experimental Medicine, University of Messina, Messina, Italy; Division of Medicine and Hepatology, University Hospital of Messina, Messina, Italy, Messina, Italy; [2]Università Degli Studi Di Messina, Department of Clinical and Experimental Medicine, University of Messina, Messina, Italy; Unit of Nephrology and Dialysis, University Hospital of Messina, Messina, Italy, Messina, Italy; [3]Università Degli Studi Di Messina, Department of Clinical and Experimental Medicine, University of Messina, Messina, Italy; Division of Advanced Diagnostic Laboratories, University Hospital of Messina, Messina, Italy, Messina, Italy; [4]Università Degli Studi Di Messina, Department of Clinical and Experimental Medicine, University of Messina, Messina, Italy, Messina, Italy; [5]Università Degli Studi Di Messina, Department of Human Pathology of Adulthood and Childhood "G. Barresi," University of Messina, Messina, Italy, Messina, Italy; [6]Azienda Ospedaliera Universitaria di Messina G Martino, Messina, Italy; [7]Università Degli Studi Di Palermo, Internal Medicine and Hepatology, PROMISE, University Hospital of Palermo, Palermo, Italy, Palermo, Italy*
Email: clelia.asero@gmail.com

Background and aims: The long-term effects of hepatitis C virus (HCV) cure on hepatic and metabolic outcomes in patients with type 2 diabetes (T2D) remains insufficiently defined. This study aimed to evaluate T2D-related vascular complications, liver disease progression, and overall survival over nine years of follow-up, also exploring genetic variability contribution.
Method: Consecutive T2D patients with HCV-related chronic liver disease or cirrhosis treated with direct-acting antivirals (DAAs) between 2015 and 2018 at the University Hospital of Messina were prospectively followed until September 2024. Demographic, biochemical, and clinical data were collected at baseline and throughout follow-up. Regression models were applied to identify predictors of metabolic and hepatic outcomes. Genetic variants – *PNPLA3* rs738409, *TM6SF2* rs58542926, and rs641738 at the *MBOAT7/TMC4* locus – were genotyped.
Results: A total of 183 patients (52% males, median age 67 years, 56% cirrhotic), were followed for a median of 48 months (range 24–84). Despite significant improvements observed in glycated haemoglobin ($p = 0.006$), liver-stiffness ($p < 0.001$), gamma-globulins ($p < 0.001$), and aminotransferases ($p < 0.001$), only 27.3% of patients maintained long-term clinical stability. Liver disease progression – defined as liver decompensation and/or hepatocellular carcinoma development – occurred in 20.8% of patients and was related to the MBOAT7 variant ($p = 0.025$), baseline cirrhosis ($p = 0.021$) and previous decompensation episodes ($p = 0.07$). Macrovascular and microvascular complications developed in 50.8% and 33.9% of patients, respectively, mainly within two years after sustained virological response, without significant associations with baseline features. In multivariate models, a higher triglycerides-glucose index ($p = 0.038$) predicted the composite endpoint of general progression (which included liver disease progression and/or T2D vascular complication onset), while elevated LDL cholesterol levels ($p = 0.048$) were independently related to mortality, suggesting the high impact of insulin-resistance on patients' prognosis.
Conclusion: Although DAAs lead to metabolic and hepatic improvements, long-term prognosis in T2D patients remains strongly influenced by baseline liver disease severity, insulin resistance, and genetic background, highlighting the need for early antiviral treatment and optimized metabolic control in this high-risk population.

WED-608

High efficacy of direct-acting antivirals and significant fibrosis regression in childhood cancer survivors with chronic hepatitis C: a retrospective study

Almagul Jumabayeva[1], Aliya Balabek[2], Jamilya Kaibullayeva[1,1], Balzhan Nugmanova[1], Aizhan Muratbekova[2], Yevgeniya Bondar[1].
[1]National Research Institute of Cardiology and Internal Medicine, Almaty, Kazakhstan; [2]State Municipal Enterprise under the Right of Economic Management City Polyclinic No. 5, Almaty, Kazakhstan
Email: almagulejumabayeva@gmail.com

Background and aims: Children who are survivors of cancer represent a unique cohort with a historically high prevalence of chronic hepatitis C (HCV). Data regarding the long-term impact of

direct-acting antivirals (DAAs) on liver stiffness in this specific pediatric population are limited. We aimed to evaluate the efficacy and safety of DAA therapy and to analyze the dynamics of liver fibrosis using transient elastography (TE) in children with HCV and onco-hematological comorbidities.

Method: This retrospective study analyzed data from 82 patients (mean age 10.2 ± 4.1 years) with chronic HCV treated at a single center between 2019 and 2024. The majority of patients had a history of hematological malignancies (34.1%) and solid tumors (15.9%). Patients received Sofosbuvir/Ledipasvir (67.1%) or Sofosbuvir/Velpatasvir (28.0%) according to weight-based dosing. Medical records were reviewed to extract Liver stiffness measurements (LSM) by TE (FibroScan) performed at baseline and after achieving sustained virologic response (SVR). Fibrosis stages were categorized according to METAVIR (F0–F4). Statistical analysis was performed using Wilcoxon signed-rank and McNemar tests.

Results: Sustained virologic response (SVR12/24) was achieved in 100% of patients who completed follow-up. Treatment was well tolerated with no serious adverse events, including in patients receiving concomitant maintenance chemotherapy. A significant normalization of transaminases was observed ($p < 0.001$). Paired analysis of elastography demonstrated a significant reduction in median LSM from 6.1 kPa (IQR 5.3–6.6) at baseline to 5.1 kPa (IQR 4.4–5.6) post-SVR ($p < 0.001$). The proportion of patients with no evidence of fibrosis (F0) increased significantly from 34.1% at baseline to 84.0% after treatment ($p < 0.001$). Conversely, the prevalence of F1 fibrosis decreased from 52.4% to 13.6%, and F2 from 13.4% to 2.5%. No patients showed progression of fibrosis score.

Conclusion: DAA therapy is effective and safe in children with a history of malignancy, showing no negative interaction with maintenance chemotherapy. Viral eradication is associated with rapid and significant regression of liver stiffness measurements, suggesting a high potential for reversibility of early fibrotic changes in the pediatric liver. These findings support a "test and treat" strategy for childhood cancer survivors to prevent long-term hepatic morbidity.

WED-609-YI

Navigating hepatitis C (HCV) treatment decision-making during pregnancy: a qualitative study

Tamara Barnett[1,2], Cheryl Dale[3,4], Jordan J. Feld[4], Curtis Cooper[5], Brian Conway[6], Alnoor Ramji[7], Jennifer Flemming[8], Chris Fraser[2], Carla Coffin[9], Karen Doucette[10], Naveed Janjua[11], Gisela Macphail[12], Sofia Bartlett[11], Andrew Mendlowitz[4], Valerie Martel-laferriere[13], Karen Campbell[1], Mia Biondi[1,3,4]. *[1]York University, School of Nursing, Toronto, Canada; [2]Cool Aid Community Health Centre, Victoria, Canada; [3]Arthur Labatt School of Nursing, Western University, London, Canada; [4]Viral Hepatitis Care Network (VIRCAN), Toronto Centre for Liver Disease, Toronto, Canada; [5]Ottawa Hospital Research Institute, Ottawa, Canada; [6]Vancouver Infectious Disease Centre, Vancouver, Canada; [7]Division of Gastroenterology, Department of Medicine, St Paul's Hospital, Vancouver, Canada; [8]Departments of Medicine and Public Health Sciences, Queen's University, Kingston, Canada; [9]Cumming School of Medicine, Snyder Institute, University of Calgary, Calgary, Canada; [10]Department of Medicine, Division of Infectious Diseases, Edmonton, Canada; [11]British Columbia Centre for Disease Control, Vancouver, Canada; [12]CUPS Liver Clinic, Calgary, Canada; [13]Department of Microbiology, Infectious Disease and Immunology, University of Montreal, Montreal, Canada*
Email: tamarab@yorku.ca

Background and aims: American and European guidelines now recommend considering treatment in pregnancy on a case-by-case basis. While some clinicians have begun offering HCV treatment in pregnancy, factors influencing treatment decisions are poorly understood. This study aims to understand pregnant individuals' perspectives on HCV treatment decisions.

Method: As a part of an observational clinical study, pregnant individuals aged ≥ 18 years with detectable HCV RNA were recruited from seven sites in Ontario or British Columbia from December 2024 to December 2025 after discussing HCV treatment during pregnancy with their clinician. All participants, regardless of treatment choice, were interviewed virtually prior to labour and delivery. 28 demographic questions were followed by an interview which focused on participants' experiences and perspectives on living with HCV prior to (if applicable) and/or during prenatal care, competing life priorities, understanding of vertical transmission, and factors influencing their decisions. Interpretive description with thematic analysis was used to identify clinically relevant patterns and meanings.

Results: Of the seven participants (age 25–35 years), six opted to receive treatment. Participants had varied immigration, housing, and carceral experience, as well as levels of education. Only one case was a new diagnosis in the current pregnancy, speaking to the number of individuals untreated preconception. Key themes included initial shock and concern regarding diagnosis, family influence on decisions, turning to online resources for additional information, and motivations tied to maternal identity and external judgment. Facilitators of treatment included parental responsibility, motivation to protect their infant, positive healthcare relationships and structured support environments. Barriers to treatment during pregnancy included stigma, confusion from inconsistent provider messaging, competing priorities, and psychosocial stressors. Participants felt there was 'no correct choice' between preventing vertical transmission and potential treatment risks.

Conclusion: These preliminary findings from a qualitative study highlight factors influencing HCV treatment acceptance in pregnancy, including maternal identity, provider relationships, family perspectives, and patient-facing online resources. The findings emphasize the need for consistent provider and public-facing guidance within stigma-free, family-centered models of care.

WED-610-YI

Cumulative metformin exposure and risk of hepatocellular carcinoma after hepatitis C cure in a multicentre cohort

Henar Calvo Sánchez[1,2,3], Lorena Jara[4], Raquel Encijo Heredia[2,3], Irene Villarino[1], Ruben Alvarado[4], Marta Quiñones[4], Maria Luisa Gutiérrez[4], Joaquin Miquel[1,2], Miguel Torralba[2,3,5], Myriam Catalá[6,7], José Gómez[6,7], Oscar Barquero-Pérez[8], Sonia Albertos Rubio[9], Conrado Fernández- Rodríguez[4], Juan Ramón Larrubia[1,2,3]. *[1]Service of Gastroenterology, University Hospital of Guadalajara, Guadalajara, Spain; [2]Translational Research Group on Cellular Immunology (GITIC), Instituto de Investigación Sanitaria de Castilla La Mancha (IDISCAM), Guadalajara, Spain; [3]Department of Medicine and Medical Specialties, University of Alcalá, Alcalá de Henares, Spain; [4]Service of Gastroenterology, University Hospital Fundación Alcorcón, Alcorcón, Spain; [5]Service of Internal Medicine, University Hospital of Guadalajara, Guadalajara, Spain; [6]Department of Biology and Geology, Physics and Inorganic Chemistry, ESCET, Rey Juan Carlos University, Móstoles, Spain; [7]Institute for Global Change Research (IICG-URJC), Rey Juan Carlos University, Móstoles, Spain; [8]Department of Signal Theory and Communications and Telematic Systems and Computing, Rey Juan Carlos University, Fuenlabrada, Spain; [9]Gastroenterology Service, Alto Penedés–Garraf Sanitary Complex, Barcelona, Spain*
Email: henarcs@hotmail.com

Background and aims: Although sustained virological response after direct-acting antivirals markedly reduces hepatocellular carcinoma risk, a clinically relevant residual risk persists, particularly in patients with advanced fibrosis or clinically significant portal hypertension. Metformin has been proposed as a chemopreventive agent in type 2 diabetes mellitus, but evidence after hepatitis C cure remains inconsistent and methodologically limited. We aimed to evaluate

whether cumulative metformin exposure is independently associated with reduced hepatocellular carcinoma risk.
Method: We analysed a multicentre cohort of 1531 patients with chronic hepatitis C who achieved sustained virological response, with a median follow-up of 75.5 months. Metformin exposure was modelled as a time-updated cumulative variable within a start–stop Cox proportional hazards framework to avoid immortal-time bias. Stabilised inverse probability of treatment and censoring weights were applied to address confounding by indication and informative censoring. Models were stratified by sex and adjusted for type 2 diabetes mellitus, clinically significant portal hypertension, FIB-4 category, and smoking status. Random survival forests with SHapley additive explanations were used for complementary validation.
Results: During follow-up, 50 patients developed hepatocellular carcinoma. Incidence increased with fibrosis severity, reaching 1.76 cases per 100 person-years in patients with FIB-4 greater than 3.25. In the weighted Cox model, independent predictors of hepatocellular carcinoma were type 2 diabetes mellitus (hazard ratio 2.45), clinically significant portal hypertension (hazard ratio 6.60), advanced fibrosis (hazard ratio 10.23), and smoking (hazard ratio 2.82). Cumulative metformin exposure was independently associated with reduced risk (hazard ratio 0.46 per year; 95% confidence interval 0.28–0.77; p = 0.003). Proportional hazards assumptions were satisfied. Machine learning analyses consistently supported a protective contribution of metformin, particularly in high-risk subgroups.
Conclusion: Cumulative metformin exposure is independently associated with a sustained reduction in hepatocellular carcinoma risk after hepatitis C cure, particularly among patients with type 2 diabetes mellitus and advanced fibrosis. These findings support metformin as a potential chemopreventive strategy in high-risk post-cure populations.

WED-611
Multidisciplinary program for on-site screening and treatment of hepatitis C in patients with severe mental illness attended in mental health centers: the MENTAL-C study

Nuria Cañete Hidalgo[1], Cristóbal Díez-Aja[1], Maria Teresa Salvador[1], Herminia Manteca[1], José Ignacio Castro[1], Antonio Sergio Murcia[1], Elena Colominas[1], Esther Garrido[1], Diego Lázaro[1], Xavi Bessa[1], Montserrat Garcia-Retortillo[1]. [1]*Hospital Del Mar, Barcelona, Spain*
Email: ncanete@hmar.cat

Background and aims: Individuals with severe mental illness (SMI) are considered a vulnerable population with potential increased risk of hepatitis C virus (HCV) infection. Previous international studies report higher prevalence compared to the general population, while recent national data suggest similar rates. This study aimed to perform opportunistic screening for HCV, HBV, and HIV in patients with SMI and to implement a coordinated treatment pathway within Mental Health Centers (MHCs).
Method: This was a non-randomized, single-center interventional study. Professionals from three MHCs offered screening for HCV, HBV, and HIV to all patients diagnosed with SMI according to DSM-V criteria. Routine blood tests were used to include serologies. The Hepatology Unit held telematic meetings with MHC teams to decide treatment and coordinate medication delivery. Each MHC administered therapy and monitored adherence and response.
Results: Of 236 patients, 233 (98.7%) accepted screening. Seven patients were anti-HCV positive (3%), and five were HCV RNA positive (2.1%). Two treated patients were previously lost to follow-up and were successfully managed through the program. All five patients with active HCV infection achieved sustained virological response (SVR) with full adherence. HBsAg was positive in 2/233 patients (0.8%), and no HIV-positive cases were detected.
Conclusion: The prevalence of HCV infection in patients with SMI was higher than in the general population, supporting systematic screening. Opportunistic screening in MHCs showed high acceptability. Coordination between Hepatology Units and MHCs enables high-quality, patient-centered care.

WED-612
Serum laminin-γ2 monomer as a noninvasive marker for predictinghepatocellular carcinoma after direct-acting antiviral-induced cure ofhepatitis C virus infection

Yu Ping Chang[1]. [1]*National Taiwan University Hospital, Hsin-Chu Branch, BioMedical Park Hospital, Zhubei City, Taiwan*
Email: melsachangchang@gmail.com

Background and aims: The clinical utility of serum laminin-γ2 monomer (LG2m) in predicting hepatocellular carcinoma (HCC) occurrence after direct-acting antiviral (DAA)-induced hepatitis C virus (HCV) clearance remains to be established.
Method: A total of 978 patients who underwent pretreatment serum LG2m assessment were enrolled. All patients received biannual liver imaging and alpha-fetoprotein (AFP) evaluations to detect HCC occurrence from the time of HCV cure to the last follow-up. The HCC-free probability was compared between patients with LG2m < 30 pg/mL and ≥ 30 pg/mL using the log-rank test. Univariable and multivariable Cox proportional hazards models were constructed for LG2m, fibrosis index based on four parameters (FIB-4), AFP, protein induced by vitamin K absence or antagonist-II (PIVKA-II), and albumin-bilirubin (ALBI) grade, with model selection guided by the Akaike information criterion (AIC). Results are expressed as hazard ratios (HRs) with 95% confidence intervals (CIs).
Results: The HCC-free probability was significantly higher in patients with LG2m < 30 pg/mL compared with those with LG2m ≥ 30 pg/mL (p < 0.0001). In univariable Cox analysis, LG2m (cHR: 2.79, 95% CI: 2.39–3.26; p < 0.001) outperformed FIB-4, AFP, PIVKA-II, and ALBI grade, showing the lowest AIC value (1129.259). In the multivariable Cox model, LG2m (aHR: 1.84, 95% CI: 1.48–2.29; p < 0.001), age (aHR: 1.07, 95% CI: 1.04–1.09; p < 0.001), male sex (aHR: 2.40, 95% CI: 1.56–3.68; p < 0.001), and F4 fibrosis (aHR: 42.0, 95% CI: 5.73–308; p < 0.001; vs. F0) were independent predictors of HCC occurrence.
Conclusion: Serum LG2m outperforms FIB-4, AFP, PIVKA-II, and ALBI grade in predicting HCC occurrence and serves as a reliable noninvasive biomarker for patients.
achieving HCV cure with DAA therapy.

WED-613
Serum Golgi protein 73 as a noninvasive marker of hepatic fibrosis in chronic hepatitis C virus infection

Yun-Chu Chen[1], Yu Ping Chang[2], Ji-Yuh Lee[3], Chi-Yi Chen[4], Wei-Yu Kao[5], Chih-Lin Lin[6], Sheng-Shun Yang[7], Yu-Lueng Shih[8], Cheng-Yuan Peng[9], Fu-Jen Lee[10], Ming-Chang Tsai[11], Shang-Chin Huang[12], Tung-Hung Su[1], Tai-Chung Tseng[1], Chun-Jen Liu[1], Pei-Jer Chen[1], Jia-Horng Kao[1], Chen-Hua Liu[1]. [1]*National Taiwan University Hospital, Zhongzheng District, Taiwan;* [2]*National Taiwan University Hospital Hsin-Chu Branch, East District, Taiwan;* [3]*National Taiwan University Hospital Yun-Lin Branch Hu-Wei Region, Yun-Lin, Taiwan;* [4]*Chia-Yi Christian Hospital, 東區, Taiwan;* [5]*Taipei Medical University Hospital, Zhonghe District, Taiwan;* [6]*Ren Ai Hospital, Shulin District, Taiwan;* [7]*Kuang Tien General Hospital, Dajia District, Taiwan;* [8]*National Defense Medical Center, Neihu District, Taiwan;* [9]*China Medical University Hospital, North District, Taiwan;* [10]*Fu Jen Catholic University, Xinzhuang District, Taiwan;* [11]*Chung Shan Medical University, South District, Taiwan;* [12]*National Taiwan University Hospital Bei-Hu Branch, Wanhua District, Taiwan*
Email: ycc103311151@gmail.com

Background and aims: The clinical utility of serum Golgi protein 73 (GP73) for evaluating hepatic fibrosis for hepatitis C virus (HCV) infection remains uncertain.
Method: We retrospectively enrolled 978 patients who underwent measurement of serum GP73, aspartate-to-platelet ratio index (APRI), and fibrosis index based on four parameters (FIB-4). Hepatic fibrosis was staged using vibration-controlled transient elastography

(VCTE) with cutoff values of ≤ 7.0, 7.1–9.4, 9.5–12.4, and ≥ 12.5 kPa corresponding to F0-F1, F2, F3, and F4. Median GP73, APRI, and FIB-4 levels across fibrosis stages were compared using Kruskal-Wallis test. Areas under the receiver operating characteristic curves (AUROCs) were calculated and compared using c-statistics, and optimal GP73 cutoff values were determined by maximal Youden index. Multivariable linear regression was performed to identify factors affecting GP73 levels.

Results: Median GP73, APRI, and FIB-4 levels increased with advancing fibrosis stage ($p < 0.001$). Serum GP73 outperformed APRI in discriminating ≥ F2 (AUROC 0.86 vs. 0.79, $p < 0.0001$), ≥ F3 (0.88 vs. 0.81, $p = 0.0003$), and F4 (0.90 vs. 0.84, $p = 0.0017$). GP73 showed superior performance to FIB-4 for ≥ F2 (0.86 vs. 0.82, $p = 0.005$) and comparable performance for ≥ F3 (0.88 vs. 0.87, $p = 0.63$) and F4 (0.90 vs. 0.89, $p = 0.72$). Optimal GP73 cutoff values were 122, 159, and 174 ng/mL for ≥ F2, ≥ F3, and F4. Hepatic fibrosis stage was the major determinant of GP73 levels.

Conclusion: Serum GP73 is a reliable and accurate noninvasive biomarker for staging hepatic fibrosis for HCV.

WED-617-YI

Hepatic and extrahepatic malignancies in hepatitis C virus-infected patients with cirrhosis treated with direct-acting antivirals in long-term observation

Krystyna Dobrowolska[1], Jakub Janczura[1], Michał Brzdęk[2], Robert Flisiak[3], Kinga Brzdęk[4], Dorota Zarębska-Michaluk[5].
[1]Collegium Medicum, Jan Kochanowski University, Kielce, Poland; [2]Department of Gastroenterology, Medical University of Lodz, Łódź, Poland; [3]Department of Infectious Diseases and Hepatology, Medical University of Białystok, Białystok, Poland; [4]Department of Rheumatology and Connective Tissue Diseases, Nicolaus Copernicus Memorial Hospital, Łódź, Poland; [5]Department of Infectious Diseases and Allergology, Jan Kochanowski University, Kielce, Poland
Email: krystyna.dobrowolska98@gmail.com

Background and aims: Patients with chronic hepatitis C virus (HCV) infection and cirrhosis are at risk of developing hepatocellular carcinoma (HCC) and malignancies outside the liver. The aim of this study was to evaluate long-term survival rates among patients with cirrhosis and to assess the development of hepatic and extrahepatic malignancies after direct-acting antiviral (DAA) therapy.

Method: We analyzed retrospective data collected from all 323 consecutive patients with liver cirrhosis infected with HCV out of a total of 1395 patients treated with DAAs between 2015 and 2025 at a single hepatology center, who were under long-term follow-up for a median of 6 years.

Results: The population analyzed was dominated by men (57%), and at the start of treatment three-quarters were people over 50 years of age. More than 95% of patients had at least one comorbid condition, with the most common being steatotic liver disease (69%). Before DAA treatment, HCC was diagnosed in 21 patients (6.5%), and non-liver cancer was diagnosed in 23 individuals (7.1%). No patient had a history of liver transplantation. Clinical symptoms of hepatic decompensation were present at baseline in 46 patients (14.2%). The effectiveness of DAA therapy was 95.4%, which is significantly lower than the 99.1% observed in a population of 1072 patients without cirrhosis ($p < 0.001$). During the long-term follow-up period of 6(3–7) years [median(IQR)], there were 34 (10.5%) new diagnoses of HCC (2 patients with DAA treatment failure), and 24 (7.4%) newly diagnosed non-liver neoplasms (only DAA responders). During long-term follow-up, 136 patients (42.1%) died; in 48 cases (35.3%), death was directly caused by malignant neoplasms, including 31 cases of HCC (12 diagnosed before DAA and 19 de novo cases) and 17 cases of non-liver malignancies (7 diagnosed before DAA and 10 de novo cases). The probability of survival was significantly lower among patients with cirrhosis compared to non-cirrhotic persons ($chi^2 = 220$, $df = 1$, $p < 0.001$).

Conclusion: During long-term observation of a population of cirrhotic patients infected with HCV, about 10% developed de novo HCC and 7% developed non-liver malignancies. Approximately 42% of patients died, with neoplasm being the direct cause of death in one third of them. The probability of survival in the long-term observation was significantly lower among patients with cirrhosis compared to non-cirrhotic persons.

WED-618

Evaluation of clinical performance and utility of the combined HCV antigen-antibody assay (HCV Duo)

Kazumi Yamasaki[1], Tatsuya Fujino[1], Tomoyuki Suehiro[1], Yuki Kugiyama[1], Tomohito Kojima[1], Yasuhide Motoyoshi[1], Shinya Nagaoka[1], Atsumasa Komori[1], Hiroshi Yatsuhashi[1]. *[1]NHO Nagasaki Medical Center, Omura, Japan*
Email: yatsuhahashihiroshi@gmail.com

Background and aims: HCV Duo is the first diagnostic reagent in Japan capable of simultaneously detecting HCV antibodies (Duo-Ab) and HCV core antigens (Duo-Ag) in a single measurement. This study aimed to evaluate the sensitivity and specificity of Duo-Ab and Duo-Ag, assess their concordance with a conventional HCV antibody assay (CLIA: Company A), and clarify the clinical utility of HCV Duo.

Method: We analyzed 628 patients (HCV RNA positive: 507; negative: 121) who first visited our liver clinic between January 2010 and December 2021 and had previously tested positive using the Company A antibody assay. HCV Duo was performed using electrochemiluminescence immunoassay (ECLIA) for the simultaneous qualitative detection of Duo-Ab and Duo-Ag, with a cutoff index (COI) 1.0 defined as positive. The overall result was determined by the higher COI value between Duo-Ab and Duo-Ag. Discrepant cases between the two antibody assays were further investigated using Line Immunoassay (LIA) and HCV RNA results. Duo-Ag positivity rates were also analyzed by HCV RNA viral load.

Results: Among the 628 cases, 591 (94.1%) were overall positive for HCV Duo. The breakdown was: 393 (62.6%) Duo-Ag(+)/Duo-Ab(+), 1 (0.1%) Duo-Ag(+)/Duo-Ab(−), and 197 (31.4%) Duo-Ag(−)/Duo-Ab(+). Discrepancy between Duo-Ab and Company A antibody was observed in 38 cases (6.0%). LIA testing of these cases showed 27 negative, 10 indeterminate, and 1 uninterpretable; no cases were LIA-positive. The sensitivity of Duo-Ag for HCV RNA-positive cases (n = 507) was 78% (394/507), and the specificity for RNA-negative cases (n = 121) was 100%. Duo-Ag positivity rates increased in a viral load-dependent manner: 9% for 2.0 Log IU/mL, 16% for 3.0–3.9, 35% for 4.0–4.9, 75% for 5.0–5.9, 95% for 6.0–6.9, and 100% for 7.0 Log IU/mL.

Conclusion: HCV Duo enables rapid evaluation of HCV infection status at the first visit by simultaneously measuring Duo-Ab and Duo-Ag, contributing to improved diagnostic efficiency and reduced patient burden. Our results demonstrate that Duo-Ab has high specificity (consistent with LIA) and Duo-Ag provides high sensitivity in cases with high viral loads. While HCV RNA confirmation remains essential for cases with low viral loads, HCV Duo offers significant clinical utility as a single-step diagnostic approach for HCV infection.

WED-619

Survival benefits of SVR across different BCLC stages in HCV patients: results from the England national HCV registry

Maria Guerra Veloz[1], Rathiga Rudra[2], Daniel Clayton-Chubb[3], Simon Hume[3], Renita George[1], Sarah Selemani[1], Paul Ross[1], Janet Dearden[2], Aileen Marshall[3], Peter Sandwith[2], Kosh Agarwal[1], Matthew Foxton[4], Douglas Macdonald[3]. *[1]King's College Hospital, Institute of Liver Studies, London, United Kingdom; [2]Department of Hepatology, Barts Health NHS Trust, London, United Kingdom; [3]Royal Free Hospital, London, United Kingdom; [4]Chelsea & Westminster NHS Foundation Trust, London, United Kingdom*
Email: maria.guerraveloz@nhs.net

Background and aims: The usefulness and optimal timing of direct acting antiviral (DAA) therapy initiation in patients with

hepatocellular carcinoma (HCC) across the different BCLC stages remains undefined. Since 2015, NHS England has approved DAA therapies for all viraemic patients, including those with HCC. The aim of this study is to assess the long-term benefits (overall survival, OS) of DAA therapies in those with HCC across the different stages.
Method: This retrospective multicentre study included BCLC 0/A/B/C patients with HCV related HCC who started DAA therapies and had an outcome reported (SVR or non-SVR). The data was extracted from the National Hepatitis C Registry in Greater London and cross-referenced with the multidisciplinary HCC team records in each centre between 2015 and 2025.
Results: 168 HCV RNA-positive patients were included. The BCLC stage was 0/A 69.6% (117), B 17.9% (30) and C 12.5% (21). The majority had compensated cirrhosis (71.6%) with normal liver function (Child Pugh A (85.8%) and ALBI grade 1 (73.3%)). 24% received more than one DAA therapy. The median time from DAA therapy initiation to HCC diagnosis was 4 (IQR 1–11) months. SVR rate was 85.1% (143/168). SVR rate based on BCLC stage was 88.9 vs 69 vs 90% in BCLC 0/A, B and C respectively.47% (79) received curative treatments for their HCC (resection, transplant, ablation or chemoembolisation followed by adjunctive ablation). The median number of anti-cancer treatments provided was 2 (IQR 1–4). The median OS for BCLC patients who achieved SVR was 93 (95% CI 83–104) months (Stage 0/A), 63 (95% CI 40–87) months (Stage B), and 40 (95% CI 23–58) months (Stage C). (Log Rank $p < 0.001$). In contrast, OS for BCLC patients who did not achieve SVR was 39 (95% CI 23–55) months (Stage 0/A), 29 (95% CI 20–39) months (Stage B), and 13 (95% CI 5–20) months (Stage C). (Log Rank $p < 0.001$). The improvement in OS was also noted across different cancer treatments (curative intent with SVR (109 months) vs curative intent with non-SVR (43 months). In the multivariate Cox regression model, [adjusted by sex, age, BCLC stage, liver function (ALBI grade)], not achieving SVR (HR 3.4, 95% CI 1.9–6.2, $p < 0.001$) and non-receiving curative HCC treatments (HR 3.07, $p < 0.001$) were the major risk factors associated with mortality.
Conclusion: SVR post DAA therapies led to an improvement in the OS irrespective of BCLC stage at presentation. Therefore, we believe that DAA therapies should be initiated together with anti-cancer treatments.

WED-620
Obesity as a population-wide risk factor for liver disease progression: results from the German hepatitis C-registry (DHC-R) and the UK biobank

Katharina Luise Hupa-Breier[1], Thriveni Raju[2], Peter Buggisch[3], Hartwig Klinker[4], Stefan Mauss[5], Albrecht Stoehr[3], Renate Heyne[6], Karl-Georg Simon[7], Thomas Berg[8], Katja Deterding[1], Andreas Geier[9], Heiner Wedemeyer[1,10], Carolin V. Schneider[2], Monika Rau[9].
[1]*Department of Gastroenterology, Hepatology, Infectious Disease and Endocrinology, Hannover Medical School, Hannover, Germany;* [2]*Gastroenterology, Metabolic Diseases, and Intensive Care, Department of Medicine III, University Hospital RWTH Aachen, Aachen, Germany;* [3]*ifi-Institute for Interdisciplinary Medicine, Hamburg, Germany;* [4]*Division of Infectious Diseases, Department of Internal Medicine II, University of Würzburg Medical Center, Würzburg, Germany;* [5]*Center for HIV and Hepatogastroenterology, Düsseldorf, Germany;* [6]*Leberzentrum Checkpoint, Berlin, Germany;* [7]*MVZ Gastroenterologie Leverkusen GbR, Leverkusen, Germany;* [8]*Division of Hepatology, Department of Medicine II, Leipzig University Medical Center, Leipzig, Germany;* [9]*Division of Hepatology, Department of Internal Medicine II, University of Würzburg Medical Center, Würzburg, Germany;* [10]*Leberstiftungs-GmbH Deutschland, Hannover, Germany*
Email: hupa.katharina@mh-hannover.de

Background and aims: Obesity and alcohol consumption are established risk factors for liver disease, but their individual and combined effects in patients with chronic hepatitis C virus infection (cHCV) remain insufficiently defined, particularly regarding potential supra-additive interactions. We aimed to assess the impact of obesity and alcohol consumption on liver disease progression in cHCV patients after sustained virologic response (SVR) and to externally validate these findings in a large population-based cohort.
Method: Patients from the German Hepatitis C-Registry achieving SVR were stratified by obesity (BMI ≥25 vs. <25) and alcohol consumption (none vs. any). The primary endpoint was progression to cirrhosis; secondary endpoint was disease-related mortality. External validation was performed in the UK Biobank, analysing predictors of liver disease progression, (first ICD-code K74.6 diagnosis) in individuals with risk for liver disease (FIB-4 ≥1.3).
Results: In the German cHCV-cohort (n = 5967), 51.7% were overweight/obese and 18.3% reported active alcohol consumption. Obesity without alcohol consumption was associated with a significantly higher risk of cirrhosis progression compared with lean patients who consumed alcohol. In multivariate models, obesity and type 2 diabetes mellitus (T2DM) were the strongest independent predictors of disease progression (OR for BMI >35: 2.833 [1.682–4.771]; OR for T2DM: 1.489 [1.004–2.208]), with similar patterns observed for mortality-related outcomes. External validation in the UK Biobank (n = 200,633) confirmed obesity as the dominant risk factor for cirrhosis progression (OR 2.70, 95% CI 2.33–3.13 vs. lean) in the general population. Compared with lean non-drinkers, odds of cirrhosis were increased in lean former drinkers (OR 2.34), obese drinkers (OR 2.29), obese non-drinkers (OR 2.91), and were highest in obese former drinkers (OR 7.77). No supra-additive interaction between obesity and alcohol consumption was observed in both cohorts.
Conclusion: Across two large and complementary cohorts, obesity rather than alcohol consumption is the predominant risk factors for liver disease progression. Importantly, the UK Biobank analysis shows that the adverse impact of obesity extends beyond the cHCV population and represents a universal risk factor for progressive liver disease. These findings underscore the need for targeted weight management strategies both in patients cured of HCV and in the general population.

WED-621
The oral cholate challenge test detects early hepatic improvement with ledipasvir/sofosbuvir in liver transplant recipients and patients with advanced cirrhosis

Michael McRae[1], Joanne Imperial[2], Greg Everson[2]. [1]*Custom DX Solutions LLC, Houston, Texas, United States;* [2]*HepQuant, LLC, Denver, Colorado, United States*
Email: michael.mcrae@hepquant.com

Background and aims: Restoring hepatic function after SVR is a key objective in the management of advanced HCV. In the SOLAR-1 trial, liver transplant (LTx) recipients with fibrosis or cirrhosis and patients with end-stage liver disease (ESLD) received ledipasvir/sofosbuvir plus ribavirin. In a sub-study of SOLAR-1, hepatic function was measured using the HepQuant SHUNT test (results reported at EASL 2015). Here, we focus on results using only the oral cholate dose (HepQuant DuO).
Method: 31 subjects were enrolled in the sub-study, 2 did not achieve SVR, and 1 decompensated from spontaneous bacterial peritonitis, leaving 28 patients with SVR. The Test was performed at baseline and at weeks 4, 24, and 48 in three groups: non-cirrhotic LTx recipients (n = 10), cirrhotic LTx recipients (n = 10), and pre-LTx ESLD patients (n = 8). HepQuant DuO involves an oral dose of deuterium-labelled (d4) cholate, blood draws at 20 and 60 minutes, and measurement of d4-cholate by LC-MS/MS. The Disease Severity Index (DSI) was calculated, which ranges from 0 (healthy) to 50 (severe dysfunction). Change from baseline in DSI was evaluated after 4, 24, and 48 weeks.
Results: At baseline, DSI was 20.4 ± 4.6 in non-cirrhotic LTx recipients, 26.7 ± 5.9 in cirrhotic LTx recipients, and 38.3 ± 2.4 in ESLD patients. By week 4, DSI declined significantly in non-cirrhotic LTx recipients (−4.6 ± 3.9, $p < 0.01$), showed a non-significant reduction in cirrhotic LTx recipients (−1.2 ± 2.5, $p = 0.20$), and remained

unchanged in ESLD patients (+0.3 ± 2.7, p = 0.77). By week 24, DSI remained significantly reduced in non-cirrhotic LTx recipients (−3.8 ± 3.4, p = 0.02), trended downward in cirrhotic LTx recipients (−2.1 ± 3.6, p = 0.10), and did not change in ESLD patients (0.0 ± 2.7, p = 0.97). By week 48, DSI remained significantly reduced in non-cirrhotic LTx recipients (−2.8 ± 3.7, p = 0.045); the downward trend was not sustained in cirrhotic LTx recipients (−0.7 ± 4.2, p = 0.62); and, DSI remained unchanged in ESLD patients (+1.8 ± 3.4, p = 0.21).
Conclusion: The favorable early improvements in function in noncirrhotic patients implies a dynamic reversibility of the changes to the hepatic microcirculation with resolution of the necroinflammation. Slower improvement or lack of early improvement in function in advanced disease suggest that longer follow-up may be required to demonstrate recovery. These findings underscore DSI's sensitivity in detecting early functional responses to antiviral therapy across a spectrum of stages of fibrosis and clinical severity.

WED-623
Persistence of cryoglobulinemia after SVR in asymptomatic HCV patients identifies a population at risk for immune and lymphoproliferative disorders

Anna Linda Zignego[1], Marcella Visentini[2], Cesare Mazzaro[3], Laura Gragnani[4], Mauro Viganò[5], Mario Masarone[6], Giuseppina Brancaccio[7], Federica Cerini[8], Piera Pierotti[9], Clodoveo Ferri[10], Stefano Gitto[1], Monica Monti[1], Milvia Casato[2], Stefano Rosato[11], Maria Giovanna Quaranta[11], Loreta Kondili[12,13], Piter Collaborating Investigators[11]. *[1]University of Florence, Firenze, Italy; [2]Sapienza University of Rome, Roma, Italy; [3]Centro Di Riferimento Oncologico Di Aviano IRCCS, Aviano, Italy; [4]University of Pisa, Pisa, Italy; [5]Azienda Ospedaliera Papa Giovanni XXIII, Bergamo, Italy; [6]University of Salerno, Baronissi, Italy; [7]Link Campus University, Roma, Italy; [8]San Giuseppe Hospital, Milano, Italy; [9]S. Maria Annunziata Hospital, Florence, Italy; [10]University of Modena And Reggio Emilia, Reggio nell'Emilia, Italy; [11]Istituto Superiore Di Sanita', Rome, Italy; [12]Istituto Superiore Di Sanita', Roma, Italy; [13]UniCamillus-Saint Camillus International University of Health Sciences, Roma, Italy*
Email: annalinda.zignego@unifi.it

Background and aims: Serum cryoglobulins are detectable in 40–60% of patients with chronic HCV infection, but only a minority develop clinically overt cryoglobulinemic vasculitis (CV). Although the impact of antiviral therapy (AVT) on CV is well established, the long-term clinical significance of asymptomatic cryoglobulinemia, representing most cases and often considered an epiphenomenon, remains unclear. We aimed to evaluate the long-term outcome of asymptomatic cryoglobulinemia after sustained virological response (SVR) and its implications for post-treatment follow-up (FU).
Method: Within the Italian PITER network, we conducted a multicenter study assessing the long-term evolution of asymptomatic cryoglobulinemia after SVR. Patients were classified according to post-AVT cryoglobulin status: persistent positivity (Group A) or negativization (Group B). Group A was further subdivided into persistent (A1) or transient (A2) cryoglobulinemia.
Results: Among more than 100 enrolled patients, 65 had complete, largely prospectively collected long-term FU data (mean FU 76.6 ± 29.9 months; range 10–176). After AVT, 38 patients were classified as Group A (23 in subgroup A1 and 15 in A2), and 27 as Group B. No patient developed de novo CV. However, nonspecific symptoms, including fatigue, arthralgia, peripheral neuropathy, sicca syndrome, and Raynaud's phenomenon, were significantly more frequent in Group A (18/38, 47.4%) than in Group B (4/27, 14.8%) ($p < 0.05$). Autoimmune and lymphoproliferative disorders, including monoclonal gammopathy of undetermined significance, lymphadenopathy, autoantibody positivity, and B-cell lymphomas, were also significantly more prevalent in Group A (21/38, 55.3%) ($p < 0.05$) in both univariate and multivariate logistic regression analyses. This difference remained statistically significant only for patients in subgroup A1 compared with Group B. Three lymphomas occurred in Group A, including one diffuse large B-cell lymphoma diagnosed more than four years after SVR.
Conclusion: Persistent cryoglobulinemia after HCV eradication identifies a clinically distinct condition associated with immune-mediated and lymphoproliferative disorders, even in the absence of overt vasculitis. Asymptomatic HCV patients should be screened for cryoglobulins after AVT, and those with persistent positivity should undergo regular FU, similar to that recommended for patients with CV and persistent cryoglobulinemia after SVR (EASL position paper on clinical follow-up after HCV cure. J Hepatol. 2024).

WED-624
Association of a liver steatosis–related polygenic risk score with hepatocellular carcinoma risk after hepatitis C virus eradication

Yu-Sheng Lin[1], Ying-Cheng Lin[1,2], Yun-Yu Chen[2,3,4,5], Yi-Ming Chen[4,6,7], I-Chieh Chen[4], Hsin-Ju Tsai[1,2], Chia-Chang Chen[1,2], Shou-Wu Lee[1,2,8], Hwai-I Yang[9,10,11,12], Teng-Yu Lee[1,8]. *[1]Division of Gastroenterology and Hepatology, Department of Internal Medicine, Taichung Veterans General Hospital, Taichung, Taiwan; [2]Department of Post-Baccalaureate Medicine, College of Medicine, Chung Hsing University, Taichung, Taiwan; [3]Cardiovascular Center, Taichung Veterans General Hospital, Taichung, Taiwan; [4]Department of Medical Research, Taichung Veterans General Hospital, Taichung, Taiwan; [5]Heart Rhythm Center and Division of Cardiology, Department of Medicine, Taipei Veterans General Hospital, Taipei, Taiwan; [6]Division of Allergy, Immunology and Rheumatology, Department of Internal Medicine, Taichung, Taiwan; [7]Institute of Biomedical Science and Rong Hsing Research Center for Translational Medicine, National Chung Hsing University, Taichung, Taiwan; [8]School of Medicine, Chung Shan Medical University, Taichung, Taiwan; [9]Genomics Research Center, Academia Sinica, Taipei, Taiwan; [10]Institute of Clinical Medicine, National Yang Ming Chiao Tung University, Taipei, Taiwan; [11]Graduate Institute of Medicine, College of Medicine, Kaohsiung Medical University, Kaohsiung, Taiwan; [12]Biomedical Translation Research Center, Academia Sinica, Taipei, Taiwan*
Email: tony19920215@hotmail.com

Background and aims: Genetic predisposition to hepatic steatosis may increase hepatocellular carcinoma (HCC) risk after hepatitis C virus (HCV) eradication in cirrhotic patients; however, its impact on broader patient populations remains unexplored. We aimed to evaluate the association of steatosis-polygenic risk score (PRS) with HCC following direct-acting antiviral (DAA) therapy.
Method: This retrospective cohort study utilized data from the Taiwan Precision Medicine Initiative, including adults treated with DAAs for HCV. Patients with treatment failure, hepatitis B virus co-infection, significant alcohol use, or HCC diagnosis prior to sustained virological response at 24 weeks were excluded. All participants underwent genotyping, with PRS-5 being used to quantify genetic risk. We evaluated the association between PRS-5 and the risk of incident HCC using restricted cubic spline analysis with Cox proportional hazards models.
Results: The cohort included 420 patients (median age 67.0 years; 46.9% male). The 5-year cumulative incidence of HCC in PRS-5 ≥ 0.66 group was higher than PRS-5 < 0.66 group (23.97%, 95% confidence interval (CI) 7.15–40.79% vs. 8.89%, 95% CI 5.56–12.23%; $P = 0.014$). In multivariable regression, PRS-5 ≥ 0.66 (aSHR 3.59, 95% CI 1.69–7.63; $p < 0.001$), body weight index >24 kg/m^2 (aSHR 2.68, 95% CI 1.24–5.78; $p = 0.012$), and Fibrosis-4 index >3.25 (aSHR 4.58, 95% CI 2.20–9.53; $p < 0.001$) were independently associated with HCC occurrence. Subgroup analysis supported the predictive value of PRS-5 in almost all patient subgroups, including Fibrosis-4 index < 3.25 and non-cirrhosis.
Conclusion: PRS-5 is independently associated with increased HCC risk after HCV eradication, supporting its role in personalized HCC surveillance strategies.

WED-625

The association of liver stiffness measurement with liver-related complications in chronic hepatitis C infection: a retrospective study in Thailand

Pemika Manassevee[1], Sarita Ratana-Amornpinm[1]. [1]*Ramathibodi Hospital, Bangkok, Thailand*
Email: m.pemika57@gmail.com

Background and aims: Despite the success of direct-acting antivirals (DAAs), chronic hepatitis C (CHC) patients remain at risk for liver-related complications after viral clearance. This study aimed to evaluate the association between LSM and liver-related complications in CHC patients and to identify an optimal LSM threshold for risk stratification.
Method: We retrospectively reviewed 267 CHC patients treated between 2010 and 2025. Patients were followed for a median of 6.2 years. Liver-related complications were defined as ascites, variceal bleeding, hepatic encephalopathy, or hepatocellular carcinoma. VCTE was performed using FibroScan® by experienced operators. Logistic regression was used to identify independent predictors of complications. Receiver operating characteristic (ROC) analysis was performed to determine the optimal LSM cutoff using Youden's index. Complication-free survival was assessed using Kaplan–Meier analysis.
Results: During follow-up, 34 patients (12.7%) developed liver-related complications. Patients with complications were older and had significantly higher baseline LSM values. An LSM ≥ 12 kPa was strongly associated with complications (adjusted OR 8.56, 95% CI = 2.73–26.92; $p < 0.001$). In contrast, achieving a sustained virological response at 12 weeks (SVR12) was a protective predictor (OR = 0.24, 95% CI = 0.08–0.70, $p = 0.009$). Additional independent predictors included age ≥60 years (OR 3.49; $p = 0.014$), body mass index (BMI) (OR 1.14; $p = 0.022$), and platelet count (OR 0.99; $p = 0.001$). ROC analysis identified an optimal LSM cutoff of 12.1 kPa, with an area under the curve of 0.832, sensitivity of 82.4%, and specificity of 77.3%. Kaplan–Meier analysis demonstrated significantly reduced complication-free survival in patients with LSM ≥ 12 kPa (log-rank $p < 0.0001$).
Conclusion: LSM ≥ 12 kPa is a strong and independent predictor of liver-related complications in patients with chronic HCV infection. These findings support the role of transient elastography not only for fibrosis staging but also for risk stratification beyond HCC surveillance.

WED-626-YI

Hepatocellular carcinoma surveillance among chronic hepatitis C patients after successful sustained virologic response: a systematic review and meta-analysis of economic evaluation studies

Soe Thiha Maung[1,2], Peerada Valyasevi[2], Roongruedee Chaiteerakij[2]. [1]*Ma Har Myaing Hospital, Yangon, Myanmar;* [2]*Faculty of Medicine, Chulalongkorn University, Bangkok, Thailand*
Email: dr.sthm92@gmail.com

Background and aims: Although sustained virologic response (SVR) significantly reduces the risk of hepatocellular carcinoma (HCC) in chronic hepatitis C (CHC) patients, the residual risk, especially among those with advanced fibrosis or cirrhosis, necessitates consideration of ongoing surveillance. Current guidelines offer inconsistent recommendations. This systematic review and meta-analysis evaluates the cost-effectiveness of HCC surveillance strategies post-SVR, to inform evidence-based clinical and policy decisions.
Method: A systematic search was performed in PubMed, Embase, Scopus, Google Scholar, and the Cochrane Library to identify economic evaluations of HCC surveillance strategies in CHC patients post-SVR. Studies reporting cost-effectiveness outcomes. Incremental net monetary benefit (INMB) values were calculated for meta-analysis. Study quality was assessed using the ECOBIAS checklist. Subgroup analyses were conducted based on surveillance modality, interval, and willingness-to-pay (WTP) thresholds.
Results: Of 157 identified records, seven studies were included in the meta-analysis. All studies were conducted in American regions. Four focused exclusively on patients with cirrhosis, while three included both advanced fibrosis (F3) and cirrhosis. Most applied Markov models from a healthcare payer perspective. At a WTP threshold of USD 100,000, pooled INMB was significantly positive (USD1743; 95% CI: 468–3019;$p = 0.007$), particularly among cirrhosis-only populations. No significant cost-effectiveness was observed at WTP thresholds of USD 50,000 or 150,000. Subgroup analyses at a WTP threshold of USD 50,000 showed no surveillance strategy yielded statistically significant INMB. Across modeling domains, results remained non-significant regardless of surveillance interval, HCC incidence, time horizon, SVR population, or model perspective. Overall, substantial consistency across subgroups was observed, with negligible heterogeneity ($I^2 = 0\%$), suggesting limited cost-effectiveness of post-SVR surveillance under lower WTP thresholds.
Conclusion: Current international guidelines show divergence in post-SVR HCC surveillance recommendations for CHC patients with advanced fibrosis. HCC surveillance post-SVR may be cost-effective at higher WTP thresholds, especially in cirrhotic patients on U.S. setting. Given the economic and epidemiological differences, region-specific economic evaluations are urgently needed to guide appropriate surveillance policies and resource allocation across diverse healthcare systems.

WED-627

Micro-elimination of HCV in state-infected cohort – 40 years' experience

David O Sullivan[1], Rionach Cawley[1], Pauline Dillon[1], Laura Stobie[1], Eimear Carolan[1], Attracta Ruxton[1], Monica Blount[1], Dee Noone[1], John Ryan[1]. [1]*Hepatology Unit, Beaumont Hospital, Dublin, Ireland*
Email: davidosullivan805@gmail.com

Background and aims: Hepatitis C virus (HCV) remains a leading cause of cirrhosis, hepatocellular carcinoma, and liver-related mortality worldwide. In Ireland, a group of individuals were infected with HCV from contaminated blood products, mostly in the late 1970s. This provides a defined population in which to assess disease natural history and outcomes. Our aim was to review long-term outcomes in this cohort at our institution.
Method: We retrospectively reviewed 168 patients over a 40-year period. Demographics, source of infection, genotype, fibrosis stage, treatment regime, and outcomes were analysed.
Results: Of 168 patients, 16 were male and 152 were female. 98 (58%) cleared the virus without treatment, while 70 (42%) developed chronic HCV infection. Of these, presumed sources of infection included anti-D immunoglobulin (n = 59), blood transfusion (n = 8), vertical transmission (n = 2), and needle stick injury (n = 1). The predominant genotype was 1b (n = 42, 60%). 7 developed advanced fibrosis/cirrhosis, 1 developed liver cancer, and 0 underwent liver transplantation. 3 patients died of liver-related complications since completing treatment, while no patients died of liver-related disease prior to treatment. The mean time from diagnosis (first clinic visit) to liver related outcome (cirrhosis/HCC/death) was 14.0 years (median 16.5 years, range 4.4–18.2 years). By 2024, all patients in this cohort achieved viral cure (SVR). Of the 70 patients treated, median age was 66.2 years (35.7–85.5 years). Successful treatment regimens were with direct acting antivirals (n = 43), protease inhibitor-based triple therapy (n = 2), pegylated interferon/ribavirin (n = 22), and not recorded (n = 3). 1 patient received more than one treatment regimen to achieve SVR.
Conclusion: HCV infection from contaminated blood products led to significant morbidity and mortality in a subgroup of otherwise well women who had just given birth. Over four decades, micro-elimination of HCV has been achieved within this state-infected cohort. These data demonstrate transformative impacts of DAA's and

importantly, these findings align closely with Ireland's commitment to the WHO 2030 elimination targets.

WED-628

Improving machine learning prediction of hepatitis C virus infection by incorporating social determinants of health from clinical notes via natural language processing and contextual-level data

Jungjun Bae[1], Suk-Chan Jang[1], Pilar Hernandez-Con[1], Chanakan Jenjai[1], Ashley Stultz[1], Shunhua Yan[1], Daniel Paredes Pardo[1], Yonghui Wu[1], Wei-Hsuan Lo-Ciganic[2], Khoa Nguyen[1], Faheem Guirgis[1], Christine Gage[1], Robert Cook[1], Ramzi Salloum[1], David R. Nelson[1], Haesuk Park[1]. *[1]University of Florida, Gainesville, United States; [2]University of Pittsburgh, Pittsburgh, United States*
Email: hpark@cop.ufl.edu

Background and aims: We developed and validated machine learning algorithms to identify undiagnosed hepatitis C virus (HCV) infection and compared the performance of models using structured electronic health record (EHR) data alone versus models incorporating social determinants of health (SDoH) derived from clinical notes and contextual-level data.
Method: We conducted prognostic modeling using EHR data from the University of Florida Health System. The study cohort included individuals aged ^{3}18 years screened for HCV in emergency department or inpatient settings between 2016 and 2024. Individuals with a prior HCV diagnosis or treatment were excluded. Three Gradient Boosting Machine learning models were evaluated. Model 1 included 275 structured predictors from a six-month baseline, encompassing sociodemographic and clinical characteristics. Model 2 added 57 contextual-level SDoH based on residential zip codes using regional data (e.g., Social Vulnerability Index). Model 3 further added 13 person-level SDoH predictors (e.g., homelessness, injection drug use) extracted from clinical notes using natural language processing (NLP) and evaluated over one-year, two-year, and full observation periods. Model performance was assessed using C statistics, sensitivity, specificity, and risk stratification by deciles of predicted risk scores.
Results: Among 45,623 individuals screened, 7.5% had laboratory-confirmed HCV infection. Training (75%) and validation (25%) samples were comparable (mean age 48 ± 17 years; 47% male; 60% White; 34% Medicaid beneficiaries). Model 1 using structured EHR data demonstrated excellent discrimination (C statistic 0.867; 95% CI, 0.858–0.876). Model 2 incorporating contextual-level SDoH showed a modest, non-significant improvement (C statistic 0.874; 95% CI: 0.864–0.883). Model 3 incorporating NLP-derived person-level SDoH using a two-year baseline significantly improved discrimination (C statistic 0.894; 95% CI, 0.886–0.903). Using the Youden index, Model 3 achieved 82.1% sensitivity and 80.9% specificity, corresponding to one HCV-positive case detected per four tests. Risk stratification identified 87.1% of HCV-positive individuals within the top three deciles of predicted risk scores.
Conclusion: Incorporating both person- and contextual-level SDoH beyond structured EHR data significantly improved HCV prediction, highlighting the importance of integrating SDoH into screening strategies in emergency department and inpatient settings.

WED-629-YI

Prevalence of advanced liver fibrosis and cirrhosis among patients with hepatitis C in a UK prison

Jennifer Plunkett[1], Jessica Pinto[1], Claire St John[2], Amy Teague[1], Claire Smith[1], Douglas Macdonald[3], William Rosenberg[3], Paul Trembling[3]. *[1]Royal Free London NHS Foundation Trust, London, United Kingdom; [2]North Central London ODN, London, United Kingdom; [3]Institute of Liver and Digestive Health, University College London, London, United Kingdom*
Email: j.plunkett1@nhs.net

Background and aims: Hepatitis C virus (HCV) infection is a major health challenge in prison populations. Prevalence of liver fibrosis severity in this setting is not well described, with most studies relying on indirect fibrosis markers, e.g. Fib4. To our knowledge there are no studies describing the burden of advanced fibrosis or cirrhosis in individuals diagnosed with HCV within UK prisons. We aimed to estimate the prevalence of advanced (Metavir ≥F3) fibrosis or cirrhosis amongst those approved for HCV treatment through our outreach prison service.
Method: Demographics, HCV genotype, fibrosis stage and treatment regimens were extracted from our HCV database. Fibrosis was assessed using Fibroscan, Enhanced Liver Fibrosis (ELF) test and/or FIB4. Published fibrosis thresholds were used: >10 kPa or ELF >9.8 for ≥F3 fibrosis, and >13 kPa or ELF >11.3 for cirrhosis. FIB4 <1.45 ruled out ≥F3 fibrosis. Results were compared with the general HCV population in our service assessed by FibroScan.
Results: Between 2015 and 2025, 176 patients were approved for HCV treatment; 161 (91%) had fibrosis assessment. Thirty (17%) underwent FibroScan, 124 (70%) had ELF testing and seven (4%) had FIB-4 calculated. Mean FibroScan liver stiffness measurement (LSM) was 7.4 kPa (SD 4.9); five (17%) had ≥F3 fibrosis and three (10%) had cirrhosis. Mean ELF score was 9.4 (SD 1.1), 45 (36%) had ≥F3 fibrosis and six (5%) had cirrhosis. All FIB-4 scores were <1.45. Overall, 50 (31%) had ≥F3 fibrosis and 9 (6%) had cirrhosis. Although mean LSM in our general HCV cohort was higher (9.6 kPa, SD 9.7) than the prison cohort, this was not significant (p = 0.19). A larger proportion of the prison cohort had a ≥F3 fibrosis than our general cohort (31% vs 24%, p = 0.04) and a smaller proportion had cirrhosis (6% vs 16%, p < 0.001) when using any method of fibrosis assessment. HCV genotype was available in 151 (86%); genotypes 1 (49%) and 3 (41%) were most common. Pangenotypic regimens were approved for 104 (59%).
Conclusion: Almost one third of this prison cohort had ≥F3 fibrosis and would benefit from HCC surveillance; 6% had cirrhosis and may be at risk of liver-related events. Despite widespread genotype availability and few meeting criteria for cirrhosis, the majority were approved for pangenotypic treatment. These findings indicate that the prevalence of advanced fibrosis in the prison population is high and, given the importance of identifying patients requiring HCC surveillance, supports routine evaluation of liver fibrosis.

WED-633

The dynamic of fibrosis scores (FibroTest, APRI and FIB-4) over a 10 year period in HCV cirrhotic patients after sustained virological response with direct-acting antivirals therapy

Anca Saran[1], Violeta Molagic[1], Alina Orfanu[1], Nicoleta Mihai[1], Cătălin Tilișcan[1], Laurentiu Stratan[1], Aida Adamescu[1], Isabela Staicu[1], Sorin Stefan Arama[1], Victoria Arama[1]. *[1]Carol Davila University Of Medicine And Pharmacy, National Institute for Infectious Diseases "Prof. Dr. Matei Bals", Bucharest, Romania*
Email: anca_leustean@yahoo.com

Background and aims: Direct Acting Antivirals (DAA) have been used in Romania since 2015, following National Protocols for treatment. Initially, liver fibrosis assessment was performed using FibroMax; however, the current National Protocol for HCV treatment now includes APRI and FIB-4 scores alongside FibroMax for evaluating the degree of fibrosis.
Method: This prospective study was conducted from 2015 to 2025 at "Matei Balş" National Institute for Infectious Diseases. It aims to evaluate the dynamics of various liver tests, beyond FibroMax, to identify simpler methods for assessing fibrosis in patients treated with DAA who have achieved Sustained Virologic Response (SVR). We used FibroTest, the AST to Platelet Ratio Index (APRI), and the Fibrosis-4 score (FIB-4) at baseline, 6 months post-treatment, 1 year post-treatment, and annually thereafter.
Results: A total of 125 patients with HCV compensated cirrhosis were assessed at baseline. At the start of treatment, the median FibroTest value was 0.84, the median APRI score was 1.27, and the median FIB-4

score was 3.8. Both APRI and FIB-4 scores correlated with liver fibrosis as graded by FibroTest (p = 0.001 for APRI and p < 0.001 for FIB-4). At 6 months post-end of treatment (EOT), 107 patients were analyzed using FibroTest, APRI, and FIB-4. The median FibroTest value was 0.69, the median APRI - 0.45, and the median FIB-4–2.12. Statistically significant correlations were found between both fibrosis scores and FibroTest (p = 0.03 for APRI and p < 0.001 for FIB-4). At 1-year post-EOT, 76 patients were evaluated, with a median FibroTest score of 0.71, a median APRI of 0.42, and a median FIB-4 of 1.96; only FIB-4 showed statistical correlation with FibroTest (p = 0.034). At the 2-year post-EOT assessment, 43 patients had a median FibroTest value of 0.69, APRI of 0.43, and FIB-4 of 2.03, showing significant correlation with FibroTest (p = 0.03 for APRI, p = 0.012 for FIB-4). At the 7 years post-EOT evaluation, 27 patients had a median APRI value of 0.38 and FIB-4 of 2.02, with a significant correlation between APRI and FibroTest (p = 0.003), while FIB-4 no longer showed a correlation (p = 0.1). The decrease in patient numbers from baseline to the end of follow-up was attributed to the pandemic when many patients were lost to follow-up.

Conclusion: APRI and FIB-4 are effective, non-invasive markers of liver stiffness that are highly correlated with FibroTest, demonstrating accuracy in diagnosing cirrhosis, and may serve as valuable tools for monitoring liver fibrosis after EOT.

WED-634-YI

HCV screening and prevalence among children with neonatal abstinence syndrome and their mothers - underserved at-risk populations in the era of HCV elimination

Caroline Schwarz[1], Andreas Weiss[1], Michael Langthaler[1], Marc Tebruegge[1], Enisa Gutic[1], David Bauer[1], Lukas Burghart[1], Sebastian Baier-Grabner[1], Astrid Käfer[1], David Endress[1], Isabella Heissenberger-Mass[1], Thomas Reiberger[2], Christoph Wohlmuth[1], Angela Zacharasiewicz[1], Michael Gschwantler[1,3]. *[1]Klinik Ottakring, Vienna, Austria; [2]Medical University of Vienna, Vienna, Austria; [3]Sigmund Freud University, Vienna, Austria*
Email: schwarz.caroline1990@gmail.com

Background and aims: Hepatitis C virus (HCV) screening is recommended for pregnant women and for children of HCV-viremic mothers. Yet, the Austrian prenatal health program only includes screening for human immunodeficiency (HIV) and hepatitis B virus (HBV) in pregnant women. HCV prevalence is high among people who inject drugs. We retrospectively assessed HCV testing and prevalence among children with neonatal abstinence syndrome (NAS; indicating prenatal maternal substance use) and their mothers at a tertiary care center in Vienna.

Method: Children hospitalized for NAS 01/2014–01/2025 and their mothers were included. Pregnancy and delivery as well as demographic and virologic parameters were investigated.

Results: We included 243 children, with five sets of twins (122 [50.2%] male; 110 [45.3%] delivered by caesarean section; median gestational age 39 weeks). Among the corresponding 238 mothers, median age was 30 years, 4.7% were HIV-infected and 1.7% were HBV-infected; 208 (87.4%) were on opioid agonist therapy during pregnancy. Overall, 227 (95.4%) of mothers were tested for HCV: 218/227 underwent HCV-serology, 116 (53.2%) of whom were anti-HCV+. HCV PCR was performed in 110/116, identifying viremia in 47 (42.7%). Additionally, 9 women received HCV PCR without prior HCV-serology, 6 (66.7%) of whom were HCV-RNA+. Overall, 53/119 (44.5%) mothers tested for HCV-RNA had confirmed viremia. Forty-two (79.2%) children of the 53 HCV-viremic mothers underwent HCV testing, and 4 (9.5%) were found to have vertical HCV acquisition. Additionally, 1 of 7 (14.3%) children whose mothers were anti-HCV+ but did not undergo PCR testing had HCV viremia. Vertical HCV transmission appears likely in this case, as HCV PCR was repeatedly positive from the neonatal period until three years of age. To date, 3 of the 5 HCV-viremic children have received antiviral therapy with a pediatric formulation of glecaprevir/pibrentasvir, with two having achieved confirmed sustained virologic response.

Conclusion: HCV screening is well-established in pregnant women with substance use in our setting, yet almost 10% of mothers did not undergo (confirmatory) PCR testing. Despite the substantial observed vertical transmission rate of about 10%, outpatient testing of HCV-exposed children was often pending. Universal, rather than targeted, HCV reflex testing of pregnant women would aid to detect HCV-infected individuals early on a national level, potentially improving the outcomes of mothers and their offspring.

WED-635

Clinical impact of antiviral therapy in elderly patients with HCV-related chronic liver disease: preliminary results of a prospective single-center cohort study

Salvatore Stefano Sciarrone[1], Federica Villa[1], Lucia Fini[1], Milena Di Leo[1], Alessandra Losco[1], Davide Viganò[1], Stefania Zatelli[1], Gianmarco Bulighin[2], Piermaria Battezati[3], Luca De Luca[1]. *[1]Gastroentrology-Endoscopy Unit, Department of Surgery, Asst Santi Paolo E Carlo-Milan University, Milan, Italy; [2]Unit of Gastroenterology, Department of Medecine, San Bonifacio Hospital, AULSS 9 Scaligera, Verona, Italy; [3]Internal Medecine and Hepatology Unit, Department of Medecine, ASST Santi Paolo e Carlo-University of Milan, Milano, Italy*
Email: salvo.sciarrone@gmail.com

Background and aims: Hepatitis C virus (HCV) infection affects an estimated 130–170 million people worldwide, including about 1 million in Italy. Neurocognitive and psychiatric manifestations - such as depression, anxiety, and fatigue - have been reported in up to 50% of patients with chronic HCV infection, possibly related to direct viral neurotoxicity. To evaluate the efficacy of direct-acting antiviral (DAA) therapy in HCV-RNA-positive patients aged 80 years or older and its impact on liver disease and neurocognitive status.

Method: Fifty patients aged 80 years or older, eligible for DAA treatment and followed at the hepatology outpatient clinic of the Girolamo Fracastoro Hospital (San Bonifacio, Verona, Italy), underwent liver disease assessment with FibroScan and biochemical tests. Neurocognitive status was evaluated using the Mini-Mental State Examination (MMSE) and the Beck Depression Inventory-II total score (BDI-II total) at baseline and 1 month after the end of therapy.

Results: All patients received Sofosbuvir/Velpatasvir (70%) or Glecaprevir/Pibrentasvir (30%) and achieved a sustained virologic response at 12 weeks (SVR12). Baseline laboratory abnormalities were mild, with median values of AST 80 IU/L, ALT 67 IU/L, GGT 50 IU/L, ALP 33 IU/L, and bilirubin 1.2 mg/dL. The mean MMSE score increased from 23.02 at baseline to 25.54 one month after the end of therapy (P = 0.05), while the mean BDI-II total score decreased from 26.22 to 20.76 (P = 0.01). On multivariable analysis, SVR was the only factor significantly associated with improvement in neurocognitive status (OR 0.03, 95% CI 0.24–0.60; p < 0.001), whereas male sex (OR 0.81, 95% CI 0.42–1.50), GGT (OR 1.05, 95% CI 0.49–2.23), and ALP (OR 0.98, 95% CI 0.40–2.36) were not significant.

Conclusion: These preliminary data suggest that HCV eradication with DAAs is highly effective in very elderly patients and is associated with significant improvement in neurocognitive status. Extending screening and treatment to this age group could provide meaningful clinical and socioeconomic benefits.

WED-636

Intrahepatic cholestasis of pregnancy and preterm birth in pregnant individuals with chronic hepatitis C: findings from ostrich, a multicenter north american cohort

Marcela Smid[1], Jasmin Charles[1], Amanda Allshouse[1], Salman Yakub[1], Kara Rood[2], John Cafardi[3], Tatyana Kushner[4], Mia Biondi[5], Jordan J. Feld[6], Mark Yudin[7], Genevieve Eastbrook[8], Sarah Osmundson[9], Todd Davies[10], Cathleen Letterio[11], Kyung min Kwon[11], Sharon Hillier[12], Catherine Chappell[12]. *[1]University of Utah Health, Salt Lake City, United States; [2]The Ohio State University,*

Columbus, United States; [3]University of Cincinnati, Cincinnati, United States; [4]Icahn School of Medicine, New York, United States; [5]York University, Toronto, Canada; [6]University Health Network, Toronto, Canada; [7]Unity Health Toronto, Toronto, Canada; [8]London Health Sciences Centre Lhsc, London, Canada; [9]Vanderbilt University, Nashville, United States; [10]Marshall University, Huntington, United States; [11]Gilead Sciences, Foster City, United States; [12]Upmc Magee Womens, Franklin, United States
Email: Marcela.Smid@hsc.utah.edu

Background and aims: Intrahepatic cholestasis of pregnancy (ICP) is associated with adverse perinatal outcomes, yet its epidemiology among pregnant individuals with chronic hepatitis C virus (HCV) is poorly characterized. We aimed to describe the frequency, recurrence, and clinical features of ICP in this population.
Method: We conducted a retrospective cohort study of singleton pregnancies ≥20 weeks' gestation with detectable HCV RNA delivered between 2016 and 2023 across five North American sites. ICP was identified by clinical diagnosis and bile acid levels ≥10 μmol/L. Demographic, obstetric, and HCV characteristics, including highest viral load (VL) during pregnancy, were compared by ICP status using descriptive and bivariable analyses; multivariable modeling was not performed due to small event counts. Associations between peak bile acid levels and preterm birth (<37 weeks' gestation) were evaluated using receiver operating characteristic analysis.
Results: Among 345 pregnant individuals with chronic HCV, 5.2% (n = 18, 95% CI 2.9–7.6) developed ICP. Age, race and ethnicity, and insurance did not differ between groups; however, individuals with ICP were more frequently nulliparous compared with those without ICP (38.9% vs 15.0%; p = 0.007). Among nulliparous individuals (n = 56), 12.5% developed ICP compared to 3.2% among parous individuals without ICP in prior pregnancy (n = 9/282). Among parous individuals with history of ICP, 28.6% (n = 2/7) had an ICP recurrence. PTB occurred among 38.8% (n = 7/18) of individuals with ICP compared to 19.6% (n = 64/327) among those without ICP. Among individuals with ICP who delivered preterm, PTB indications were ICP (n = 5/7), acute cholecystitis (n = 1/7) and gestational hypertension (n = 1/7) whereas PTB among those without ICP was most due to premature rupture of membranes (n = 21/327) and preterm labor (n = 21/327). Among 17 individuals with ICP and bile acid, peak levels had a median of 26.6 μmol/L (IQR 16.7–63). Neither high (≥6 $\log_{10}$ IU/mL) HCV VL (33.3% ICP vs 45.3% no ICP; p = 0.32) nor peak bile acid (area under the curve 0.466, 95% CI 0.347–0.585) was associated with increased PTB risk.
Conclusion: In this multicenter cohort of pregnant individuals with chronic HCV, ICP occurred in 5% of pregnancies, representing an estimated ten-fold higher prevalence than population estimates. ICP was a frequent driver of PTB. These findings highlight a potentially modifiable PTB pathway that could be mitigated by HCV treatment during pregnancy.

WED-637
Preterm birth in pregnant individuals with chronic hepatitis C: findings from OSTRICH, a multicenter North American cohort

Marcela Smid[1], Jasmin Charles[1], Amanda Allshouse[1], Salman Yakub[1], Kara Rood[2], John Cafardi[3], Tatyana Kushner[4], Mia Biondi[5], Jordan J. Feld[6], Mark Yudin[7], Genevieve Eastbrook[8], Sarah Osmundson[9], Todd Davies[10], Cathleen Letterio[11], Kyung min Kwon[11], Sharon Hillier[12], Catherine Chappell[12]. *[1]University of Utah Health, Salt Lake City, United States; [2]The Ohio State University, Columbus, United States; [3]University of Cincinnati, Cincinnati, United States; [4]Icahn School of Medicine, New York, United States; [5]York University, Toronto, Canada; [6]University Health Network, Toronto, Canada; [7]Unity Health Toronto, Toronto, Canada; [8]London Health Sciences Centre Lhsc, London, Canada; [9]Vanderbilt University, Nashville, United States; [10]Marshall University, Huntington, United States; [11]Gilead Sciences, Foster City, United States; [12]Upmc Magee Womens, Franklin, United States*
Email: Marcela.Smid@hsc.utah.edu

Background and aims: Current AASLD and EASL guidelines recommend offering hepatitis C virus (HCV) treatment during pregnancy, yet obstetric safety data remain limited. The ongoing STORC trial evaluates second- and third-trimester sofosbuvir/velpatasvir exposure, with preterm birth (PTB) as the primary safety outcome. We conducted OSTRICH, a multicenter retrospective cohort across five North American STORC sites, to historically characterize pregnancy outcomes and identify factors associated with PTB among individuals with active HCV.
Method: We abstracted medical records for all singleton pregnancies 20 weeks' gestation with detectable HCV RNA between 2016–2023, prior to the start of STORC enrollment at five sites. PTB was defined as delivery < 37 weeks. Demographic and clinical variables associated with PTB in bivariable analyses were evaluated in adjusted multivariable logistic regression mode. Association between highest HCV viral load in pregnancy and PTB was evaluated using receiver operating characteristic analysis.
Results: Among 345 individuals, 20.6% (95% CI 16.4–25.2%) experienced PTB. Our cohort predominantly identified as White (89.9%), was multiparous (83.8%) and publicly insured (94.2%) with high proportion of individuals with substance use disorders (opioid use disorder 86.7%, methamphetamine use disorder 48.1%, cocaine use disorder 42.6%) and mental health conditions (depression 65.8%, anxiety 63.5%). In bivariable analysis, chronic hypertension (23.9% PTB vs 6.6% non-PTB; p < .001), pregestational diabetes (4.2% vs 0.7%; p = .061), (28.2% vs 12.0%; p < 0.001), and methamphetamine use in first trimester (49.3% vs 33.2%; p = .012) were more common among those with PTB compared to those without PTB. In adjusted models, chronic hypertension or pregestational diabetes (aOR 3.93, 95%CI 1.89–8.19), migraines (aOR 2.50, 95%CI 1.29–4.86), and methamphetamine use (aOR 1.87, 95%CI 1.07–3.24) were independently associated with PTB. Neither high (> = 6 log) HCV viral load during pregnancy (43.5% vs 45.0%; p = 0.8) nor highest viral load in pregnancy (AUC 0.512, 95% CI 0.433–0.590) was associated with increased PTB risk.
Conclusion: Among pregnant individuals with chronic HCV, PTB rate was approximately double national estimates. Chronic hypertension, pregestational diabetes, migraines, and methamphetamine use were independently associated with PTB, highlighting the importance of addressing medical and behavioral health comorbidities alongside HCV management.

WED-638
Combined use of aMAP risk score and M2BPGi for stratifying hepatocellular carcinoma risk after SVR following direct-acting antiviral therapy

Tomoyuki Suehiro[1], Tomohito Kojima[1], Yuki Kugiyama[1], Yasuhide Motoyoshi[1], Akira Saeki[1], Shinya Nagaoka[1], Kazumi Yamasaki[1], Atsumasa Komori[1], Hiroshi Yatsuhashi[1]. *[1]NHO NagasakiMedical Center, Omura, Japan*
Email: chuntomo0902@gmail.com

Background and aims: The aMAP risk score has been reported to identify high-risk patients for hepatocellular carcinoma (HCC), and its usefulness for predicting HCC after sustained virologic response (SVR) following direct-acting antiviral (DAA) therapy has been demonstrated. However, the clinical significance of combining the aMAP risk score with Mac-2 binding protein glycosylation isomer (M2BPGi) in this setting remains unclear. We investigated the utility of the aMAP risk score and M2BPGi for predicting HCC after SVR.
Method: A total of 432 patients who achieved SVR after DAA therapy between 2013 and 2017 and had no prior history of HCC were enrolled. The aMAP risk score was calculated at baseline using the published formula. Predictive performance was assessed using receiver operating characteristic (ROC) analysis. Cumulative HCC incidence was evaluated using the Kaplan–Meier method and Cox

proportional hazards models. Post-hoc pairwise comparisons were performed using the log-rank test with Bonferroni correction.
Results: The median age was 67 years (59–75), with 173 males (39.6%). During a median follow-up of 7.4 years (0.2–11.9), HCC developed in 36 patients (8.3%). In ROC analysis at 5 years, M2BPGi showed the highest area under the curve (AUC: 0.8215, $p < 0.01$), whereas the aMAP risk score demonstrated high sensitivity (AUC: 0.8212, $p < 0.01$). An aMAP risk score >60 (HR 6.58, 95% CI 1.93–22.33, $p < 0.01$) and M2BPGi >4 (HR 3.30, 95% CI 1.63–6.69, $p < 0.01$) were identified as independent risk factors for HCC.Patients were stratified into three groups according to the combination of the aMAP risk score and M2BPGi. The 5-year cumulative HCC incidence was 0.0% in the Low-Low group, 6.5% in the intermediate group, and 19.3% in the High-High group. Kaplan–Meier analysis demonstrated significant differences in cumulative HCC incidence among the three groups. In Bonferroni-adjusted post-hoc comparisons, all pairwise group comparisons remained statistically significant (adjusted $p < 0.01$).
Conclusion: The combination of the aMAP risk score and M2BPGi enables comprehensive risk stratification for HCC after SVR. This combined approach clearly discriminates HCC risk even after adjustment for multiple comparisons and may be useful for optimizing HCC surveillance strategies.

WED-639

Hepatic recompensation after sustained virologic response in patients with hepatitis C virus–related decompensated cirrhosis: a Japanese multicenter study

Yuki Tahata[1], Hayato Hikita[1], Yoshihito Uchida[2], Masaru Enomoto[3], Seiichi Mawatari[4], Nobuharu Tamaki[5], Atsunori Tsuchiya[6], Hitoshi Yoshiji[7], Daiki Miki[8], Hidekatsu Kuroda[9], Taro Yamashita[10], Hiroshi Yatsuhashi[11], Yoichi Hiasa[12], Hisamitsu Miyaaki[13], Masato Nakamura[14], Yoshiyuki Ueno[15], Kentaro Matsuura[16], Kanji Yamaguchi[17], Taro Takami[18], Goki Suda[19], Ryosuke Tateishi[20], Norio Akuta[21], Yasuhiro Asahina[22], Yasunari Nakamoto[23], Eiji Kakazu[24], Masahito Shimizu[25], Shuji Terai[26], Takahiro Kodama[1], Tomomi Yamada[27], Tetsuo Takehara[28]. *[1]Department of Gastroenterology and Hepatology, The University of Osaka, Graduate School of Medicine, Suita, Japan; [2]Department of Gastroenterology and Hepatology, Saitama Medical University, Saitama, Japan; [3]Department of Hepatology, Graduate School of Medicine, Osaka Metropolitan University, Osaka, Japan; [4]Digestive and Lifestyle Diseases, Department of Human and Environmental Sciences, Kagoshima University Graduate School of Medicine and Dental Sciences, Kagoshima, Japan; [5]Department of Gastroenterology and Hepatology, Musashino Red Cross Hospital, Tokyo, Japan; [6]First Department of Internal Medicine, Faculty of Medicine, University of Yamanashi, Yamanashi, Japan; [7]Department of Gastroenterology, Nara Medical University, Nara, Japan; [8]Department of Gastroenterology and Metabolism, Graduate School of Biomedical and Health Sciences, Hiroshima University, Hiroshima, Japan; [9]Division of Hepatology, Department of Internal Medicine, Iwate Medical University, Iwate, Japan; [10]Department of Gastroenterology, Kanazawa University Graduate School of Medicine, Kanazawa, Japan; [11]Clinical Research Center, National Hospital Organization Nagasaki Medical Center, Nagasaki, Japan; [12]Department of Gastroenterology and Metabology, Ehime University Graduate School of Medicine, Ehime, Japan; [13]Department of Gastroenterology and Hepatology, Nagasaki University of Graduate School of Biomedical Sciences, Nagasaki, Japan; [14]Department of Gastroenterology, Graduate School of Medicine, Chiba University, Chiba, Japan; [15]Department of Gastroenterology, Faculty of Medicine, Yamagata University, Yamagata, Japan; [16]Department of Gastroenterology and Metabolism, Nagoya City University Graduate School of Medical Sciences, Nagoya, Japan; [17]Department of Molecular Gastroenterology and Hepatology, Graduate School of Medical Science, Kyoto Prefectural University of Medicine, Kyoto, Japan; [18]Department of Gastroenterology and Hepatology, Yamaguchi University Graduate School of Medicine, Ube, Japan; [19]Department of Gastroenterology and Hepatology, Graduate School of Medicine, Hokkaido University, Sapporo, Japan; [20]Department of Gastroenterology, Graduate School of Medicine, The University of Tokyo, Tokyo, Japan; [21]Toranomon Hospital, Tokyo, Japan; [22]Department of Gastroenterology and Hepatology, Institute of Science Tokyo, Tokyo, Japan; [23]Second Department of Internal Medicine, Faculty of Medical Sciences, University of Fukui, Fukui, Japan; [24]The Research Center for Hepatitis and Immunology, Japan Institute for Health Security, Chiba, Japan; [25]Department of Gastroenterology/Internal Medicine, Gifu University Graduate School of Medicine, Gifu, Japan; [26]Division of Gastroenterology and Hepatology, Graduate School of Medicine and Dental Sciences, Niigata University, Niigata, Japan; [27]Department of Medical Innovation, Osaka University Hospital, Suita, Japan; [28]Kansai Rosai Hospital, Amagasaki, Japan*
Email: yuki.tahata@gh.med.osaka-u.ac.jp

Background and aims: Sustained virologic response (SVR) can be achieved in approximately 90% of patients with hepatitis C virus (HCV)-related decompensated cirrhosis treated with direct-acting antivirals (DAAs), and some experience hepatic recompensation. However, its frequency, associated factors, and impact on prognosis remain unclear.
Method: We enrolled 363 patients with HCV-related cirrhosis (compensated: 204; decompensated: 159) who achieved SVR after DAA treatment at 33 Japanese institutions between 2019 and 2021, with ≥1 year of follow-up after the end of treatment (EOT). Patients who died or were lost to follow-up within 1 year after the EOT were excluded. Decompensated cirrhosis was defined as Child–Pugh (CP) class B/C or CP class A with prior decompensation. Hepatic recompensation was defined as the absence of ascites and encephalopathy at 1 year after the EOT, CP class A, and no variceal bleeding for ≥1 year. First, baseline factors associated with recompensation were examined in decompensated patients. Second, liver transplantation (LT)-free survival, hospitalization-requiring decompensation, and hepatocellular carcinoma (HCC) occurrence were compared among compensated, recompensated, and non-recompensated groups.
Results: Among 159 patients with decompensated cirrhosis, hepatic recompensation was achieved in 59 (37.1%). Absence of ascites ($p < 0.001$), absence of hepatic encephalopathy ($p = 0.024$), lower international normalized ratio (INR) ($p = 0.016$), and higher albumin levels ($p = 0.029$) were identified as significant baseline factors associated with hepatic recompensation in multivariate logistic regression analysis. The 4-year LT-free survival and incidence rates of decompensation from 1 year after the EOT were 84.4%/8.2% in compensated cirrhosis, 91.8%/8.3% in recompensated cirrhosis, and 65.7%/30.6% in non-recompensated cirrhosis, respectively. Survival and decompensation outcomes in recompensated cirrhosis were comparable to those in compensated cirrhosis. In contrast, among patients without prior HCC, 4-year HCC occurrence rates were 14.1%, 25.6%, and 26.8%, with no significant differences.
Conclusion: Hepatic recompensation was achieved in approximately one-third of patients with HCV-related decompensated cirrhosis and was associated with the degree of ascites or hepatic encephalopathy, INR, and albumin levels. Hepatic recompensation improved survival and reduced decompensation but did not reduce HCC risk.

WED-640

Driving HCV elimination through dedicated hospital-based teams and pathways. A retrospective and prospective study in southern Italy

Pietro Torre[1], Enrica Serretiello[2], Giuseppe Di Siervi[1], Emilia Vaccaro[2], Tommaso Sarcina[1], Mariano Festa[1], Veronica Folliero[1], Giovanni Boccia[2], Mario Masarone[1], Gianluigi Franci[2], Marcello Persico[1]. *[1]University of Salerno, Salerno, Italy; [2]AOU San Giovanni di Dio e Ruggi d'Aragona, Salerno, Italy*
Email: pietrotorre90@gmail.com

Background and aims: Direct-acting antivirals (DAAs) have had an extraordinary impact on curing and limiting the spread of HCV infection. According to that, screening programs have been established worldwide to achieve the ambitious goal of elimination by

2030. This study aimed to first evaluate the proportion of HCV testing, the prevalence of infection, and the rate of treatment referral among previously admitted patients in a large hospital of Southern Italy, and subsequently to implement an improved diagnostic and linkage to care protocol.
Method: This retrospective and prospective study was conducted at the University Hospital of Salerno, Campania region. In the retrospective phase (covering the period from 2016 to 2023), data were retrieved regarding hospital admissions, the percentage of patients tested for HCV-Ab and HCV-RNA, and those patients who underwent antiviral therapy. In the prospective phase, initiated in 2025, all admitted patients screened for anti-HCV-Ab underwent reflex HCV-RNA testing and those who tested positive were systematically evaluated for antiviral therapy.
Results: Among 317,680 patients admitted to our hospital for various medical conditions within 2016–2023, 116,478 (36.7%) were screened for HCV-Ab. Out of these, 4214 (3.6%) resulted positive. Among HCV-Ab positive subjects, 2120 (50.3%) underwent HCV-RNA testing, and 1450 of these (68.4%), resulted positive. 60% of actively infected patients, with annual variations, underwent DAA therapy. In the prospective phase, 385 HCV-Ab–positive patients were identified over a 7-month period (prevalence of 3.3%). Of these, all were tested for HCV-RNA and the 68 patients (17.7%) with active infection, were all evaluated or underwent antiviral therapy, during hospitalization or through recall. Surgical and Emergency departments registered the highest share of actively infected patients. In both phases of the study, HCV prevalence increased with age.
Conclusion: In the context of declining infection prevalence, HCV testing and linkage-to-care should be reinforced in the hospital setting, where a considerable number of positive patients can still be found. Therefore, in addition to routine screening, a specific program for active infection testing (e.g., reflex testing) and subsequent treatment should be implemented and coordinated by a dedicated hospital-based team, to identify and cure as many HCV-infected individuals as possible.

WED-641

Evaluation of ALBI and FIB-4 scores to predict hepatocellular carcinoma in patients with chronic hepatitis C and sustained virological response to direct-acting antivirals

Paula Guedes[1], Juliana Piedade[2], Hugo Perazzo[3], Livia Villela-Nogueira[4], Helena Peixoto[4], Gustavo Pereira[2], Lailiane Novaes[2], Miriam Chinzon[2], Joyce Roma[2], Flavia Fernandes[5], Cristiane A. Villela-Nogueira[4]. *[1]Clementino Fraga Filho University Hospital, Bonsucesso Federal Hospital, Rio de Janeiro, Brazil; [2]Bonsucesso Federal Hospital, Rio de Janeiro, Brazil; [3]Oswaldo Cruz Foundation, Rio de Janeiro, Brazil; [4]Clementino Fraga Filho University Hospital, Rio de Janeiro, Brazil; [5]Pedro Ernesto University Hospital, Rio de Janeiro, Brazil*
Email: crisvillelanog@gmail.com

Background and aims: The risk of developing hepatocellular carcinoma (HCC) in chronic hepatitis C patients with advanced fibrosis and cirrhosis remains after sustained virological response (SVR) with direct-acting antivirals (DAA). Targeting patients at the highest risk of HCC would define better screening strategies. Our aim was to evaluate ALBI and FIB-4 scores as prognostic markers for HCC after SVR.
Method: A bicentric retrospective longitudinal study included patients with SVR and a liver stiffness measurement (LSM) ≥ 10 kPa at baseline. Pre-treatment (Pre-T) and 1 year after the end of treatment (1-yr-EOT) ALBI and FIB-4 scores were calculated. Delta was determined as the difference between the two measurements. The performance of these scores in identifying risk for HCC was analyzed.
Results: 450 patients (62 ± 10 years; 65.7% women; 56.5% white non-hispanic; BM I27.4 [24.4–30.2]; ALT 88 IU/L [55–135]; albumin 3.7 g/dL [3.5–4.0]; 38.9% with type 2 diabetes; 20% with clinically significant portal hypertension) were included and followed for 61 months [39–74]. LSM ≥ 12.5 kPa (F4) was identified in 68% of patients. The Pre-T median FIB-4 and ALBI were 3.35 (2.06–5.72) and −2.48 (−2.73 to −2.19), significantly higher than 1-yr-EOT: 1.99 (2.06–5.72) and −2.84 (−3.10 to −2.53) respectively ($p < 0.001$). At follow-up, 9.3% (n = 42) developed HCC; 95% had cirrhosis at Pre-T. At univariate analysis, weight ($p = 0.04$), 1-yr-EOT AST ($p = 0.005$), Pre-T platelets ($p < 0.001$) and 1-yr-EOT ($p < 0.001$), Pre-T ALBI ($p = 0.04$) and 1-yr-EOT ($p < 0.001$), Pre-T FIB-4 ($p < 0.001$) and 1-yr-EOT ($p = 0.001$) and delta FIB-4 ($p < 0.001$) were associated with HCC. At Cox regression analysis, 1-yr-EOT FIB-4 (HR 1.16; 95% CI 1.05–1.28, $p = 0.003$) and 1-yr-EOT ALBI (HR 4.43; 95% CI 2.02–9.70, $p < 0.001$) were associated with HCC occurrence. Adopting the values FIB-4 > 3.25 and ALBI > −2.5, individuals with higher cut-off points had a worse survival curve for both scores.
Conclusion: ALBI and FIB-4 values after one year of HCV treatment perform better and can be usefull in HCC risk stratification in SVR-HCV patients.

WED-642-YI

Trends in hepatocellular carcinoma following hepatitis C virus infection in sweden: progress toward WHO elimination goals

Anna Wadman[1], Snehal Patil[2], Scott Montgomery[2,3,4], Soo Aleman[5], Ann-Sofi Duberg[1,6], Charlotte Lybeck[1,6]. *[1]Department of Infectious Diseases, Orebro University Hospital, Örebro, Sweden; [2]Department of Clinical Epidemiology and Biostatistics, Faculty of Medicine and Health, Örebro University, Örebro, Sweden; [3]Karolinska Institutet-Solna, Solna, Sweden; [4]Department of Epidemiology and Public Health, University College London, London, United Kingdom; [5]Department of Infectious Diseases, Karolinska Institutet/Karolinska University Hospital, Stockholm, Sweden; [6]Department of Infectious Diseases, Faculty of Medicine and Health, School of Medical Sciences, Örebro, Sweden*
Email: anna.wadman@regionorebrolan.se

Background and aims: In many countries, including Sweden, the birth cohorts with the highest prevalence of hepatitis C virus (HCV) infection are now reaching ages associated with a high risk of primary liver cancer (PLC), particularly hepatocellular carcinoma (HCC). This aging HCV population poses a challenge to the World Health Organization's 2030 targets for reducing hepatitis-related morbidity and mortality. With effective direct-acting antiviral (DAA) therapies introduced in 2014, it remains unclear whether HCC incidence has declined in recent years. This study aimed to investigate temporal trends in PLC/HCC incidence and the relative hazard of PLC among individuals diagnosed with HCV between 1990 and 2022, with extended follow-up to 2023.
Method: We conducted a nationwide cohort study including individuals diagnosed with HCV infection in Sweden between 1990 and 2022 (n = 59,084), irrespective of treatment or virological cure. The HCV cohort was compared with a tenfold matched reference cohort from the general population without diagnosed HCV (n = 589,641). PLC, including HCC, was identified through linkage to the Swedish Cancer Register, Cause of Death Register, National Patient Register, and the national quality register for liver cancer (SweLiv). Crude as well as age- and sex-standardized incidence rates were calculated.
Results: During 872,669 person-years of follow-up, 2917 HCC cases (4.9%) occurred in the HCV cohort, compared with 1044 (0.2%) in the matched cohort. Crude and age- and sex-standardized HCC incidence rates increased steadily in the HCV cohort until 2014 (5.27 per 1000 PY; 95% CI 4.51–6.03), followed by a decline by 2023 (1.92 per 1000 PY; 95% CI 1.32–2.50). Overall, 39.8% of the HCV cohort received DAA treatment during the study period. Among all HCC cases registered in SweLiv from its start in late 2008 (n = 1976), screening-detected HCC accounted for 40.7% (659/1618) of cases in the HCV cohort and 20.9% (75/358) in the reference cohort.
Conclusion: With follow-up to 2023, individuals with chronic HCV infection continue to carry an elevated risk of PLC/HCC compared

with the general population. Incidence trends suggest a decline after 2014, in the era of direct-acting antiviral therapy, though individuals with prior infection remain at risk. Continued surveillance and treatment are essential to reduce the liver cancer burden.

WED-643

COVID-19 pandemic had minimal impact on the effort spent on the enhancement programme of treatment coverage for all adult patients with chronic hepatitis C virus (HCV) infection

Vicki Wing-Ki Hui[1], Mandy Sze-Man Lai[1], Jimmy Che-To Lai[1], Vincent Wai-Sun Wong[1], Terry Cheuk-Fung Yip[1], Grace Lai-Hung Wong[1]. [1]*The Chinese University of Hong Kong, Sha Tin, Hong Kong*
Email: wonglaihung@cuhk.edu.hk

Background and aims: Enhanced coverage of direct-acting antiviral (DAA) therapy for all adult patients with chronic hepatitis C virus (HCV) infection since October 2020 in Hong Kong SAR, China, amidst the COVID-19 pandemic in 2020–2023. This study evaluated the impact of COVID-19 pandemic on this enhancement programme of DAA treatment coverage.
Method: All individuals living with chronic HCV infection who had at least one positive result for antibody for HCV (anti-HCV), HCV RNA or HCV genotype between January 2000 and December 2024 were identified. DAA therapy for HCV was defined with the prescription of sofosbuvir/velpatasvir, sofosbuvir/ledipasvir, glecaprevir/pibrentasvir, elbasvir/grazoprevir, dasabuvir/ombitasvir/ paritaprevir, daclatasvir/asunaprevir or boceprevir. Crude all-cause mortality incidence rates were calculated as events per 1000 person-years with 95% confidence intervals.
Results: We first identified 10,225 consecutive individuals with HCV markers checked. 4733 (46.3%) patients were prescribed with at least one course of DAA therapy; among treated patients, mean age was 55.82 ± 12.90 years and 3236 (68.37%) were male. The annual number of treated patients increased after programme implementation, from 776 (2020) to 1126 (2021), and remained substantial through the pandemic period (962 in 2022; 808 in 2023) with stabilization in 2024 (817). Regimen choice shifted toward simplified fixed-dose combinations, dominated by glecaprevir/pibrentasvir and sofosbuvir/velpatasvir. Crude all-cause mortality incidence rates per 1000 person-years were 234.59 (95% CI 220.92–248.89) and 11.05 (8.25–14.49) for non-DAA and DAA users, respectively, when follow-up was truncated at 1 year; the corresponding 3-year mortality incidence rates were 118.51 (112.65–124.59) and 10.01 (8.42–11.82), respectively.
Conclusion: COVID-19 pandemic had minimal impact on the effort spent on the enhancement programme of DAA treatment coverage. It was likely due to the endeavours mentioned in the Hong Kong Hepatitis Action Plan 2020–2024, which had counteracted the negative impact of the COVID-19 pandemic on hepatitis elimination.
Funding: This work was supported by the Investigator Sponsored Research of Gilead Sciences (Reference: IN-HK-987-7181).

WED-644

Impact of sustained virological response on the prognosis of patients with HCV-related cirrhosis: a large-scale multicenter cohort study from the pre-and post-DAA eras

Hiroshi Yatsuhashi[1], Hayato Yamana[2], Shinobu Imai[3], Atsushi Naganuma[4], Rie Sugimoto[5], Motoyuki Kohjima[6], Tsutomu Yamashita[7], Satoru Iwamoto[8], Keisuke Ario[9], Masaaki Shimada[10], Shintaro Takaki[11], Takeaki Satoh[12], Kiyoshi Furuta[13], Ryotaro Sakamori[14], Kazumi Yamasaki[1]. [1]*NHO Nagasaki Medical Center, Omura, Japan;* [2]*Jichi Medical University, Shimotsuke, Japan;* [3]*Showa University Graduate School of Pharmacy, Tokyo, Japan;* [4]*NHO Takasaki Genral Medical Center, Takasaki, Japan;* [5]*NHO Kyushu Cancer Center, Fukuoka, Japan;* [6]*NHO Kyushu Medical Center, Fukuoka, Japan;* [7]*NHO Oita Medical Center, Oita, Japan;* [8]*NHO Kyoto Medical Center, Kyoto, Japan;* [9]*NHO Ureshino Medical Center, Ureshino, Japan;* [10]*NHO Nagoya Medical Center, Nagoya, Japan;* [11]*NHO Kure Medical Center, Kure, Japan;* [12]*NHO Kukura Medical Center, Kokura, Japan;* [13]*NHO Matsumoto Medical Center, Matsumoto, Japan;* [14]*NHO Osaka National Hospital, Osaka, Japan*
Email: Yatsuhashihiroshi@gmail.com

Background and aims: While interferon (IFN)-based therapies had limited efficacy in patients with hepatitis C virus (HCV)-related cirrhosis, the introduction of direct-acting antivirals (DAAs) in 2014 has enabled sustained virological response (SVR) rates exceeding 90% in Japan. This multicenter study aimed to evaluate the impact of SVR on the long-term prognosis of patients with HCV-related cirrhosis by comparing cohorts from the pre- and post-DAA eras.
Method: We enrolled outpatients with HCV-related cirrhosis from 36 National Hospital Organization (NHO) hospitals during two distinct periods: 2011 (pre-DAA cohort) and 2017 (post-DAA cohort). The 3-year and 5-year survival rates, along with the impact of antiviral therapy, were prospectively examined. SVR was defined as undetectable serum HCV RNA 24 weeks after therapy completion.
Results: A total of 1680 patients were analyzed (2011 cohort: n = 876; 2017 cohort: n = 804). The SVR rate significantly increased from 4% in the 2011 cohort to 58% in the 2017 cohort ($P < 0.001$). Consequently, the 2017 cohort demonstrated superior 3-year (80% vs. 64%) and 5-year (68% vs. 46%) survival rates compared to the 2011 cohort. The mortality rate per person-year was significantly lower in the 2017 cohort (0.077 vs. 0.145, $P < 0.001$). Pooled analysis of both cohorts revealed that SVR significantly improved survival across most Child-Pugh (CP) classes: • CP-A (n = 1185): 5-year survival was 85% (SVR) vs. 60% (non-SVR) and 50% (untreated) ($P < 0.001$). • CP-B (n = 412): 5-year survival was 61% (SVR) vs. 46% (non-SVR) and 27% (untreated) ($P < 0.001$). • CP-C (n = 83): No significant survival benefit was observed between SVR, non-SVR, and untreated groups. Multivariate analysis identified five independent prognostic factors for survival: age, gender, Child-Pugh classification, SVR status, and liver cancer stage. Notably, the cohort year (2011 vs. 2017) was not an independent factor, suggesting that the improved prognosis in the later cohort was primarily driven by SVR attainment.
Conclusion: The widespread adoption of IFN-free DAA therapy since 2014 has dramatically increased SVR rates among patients with HCV-related cirrhosis in Japan, leading to a significant improvement in overall survival. SVR remains the key driver of improved prognosis, particularly in patients with Child-Pugh A and B cirrhosis.

Viral hepatitis C – Therapy and resistance

TOP-614

Hepatitis elimination and liver care in south-east Austria (HEAL-S) – HCV cohort

Lavra Rebol[1,2], Natalie Hasl[1], Victoria Rieper[1], Angela Horvath[1,2], Harald Kessler[1], Vanessa Stadlbauer[1,2]. [1]*Medizinische Universität Graz, Graz, Austria;* [2]*Center of Biomarker Research CBmed GmbH, Graz, Austria*
Email: vanessa.stadlbauer@medunigraz.at

Background and aims: The World Health Organization (WHO) aims to eliminate hepatitis C virus (HCV) as a public health threat by 2030. Austria is well-positioned to contribute to this goal because highly effective direct-acting antiviral (DAA) therapies have been available since 2014. However, despite their proven efficacy, DAAs have not reached their full potential. Many individuals remain untreated, often due to a lack of awareness about infection or treatment options. These undiagnosed patients pose a significant obstacle to achieving elimination. We hypothesized that a substantial proportion of people with unknown HCV status in Southeast Austria still require therapy.

Method: We retrieved all HCV nucleic acid amplification test (NAAT) results recorded between January 1, 2014, and December 31, 2023, from the molecular laboratory database of the Medical University of Graz, serving a catchment area of approximately 1.2 million inhabitants. Records were pseudonymized prior to analysis. We identified patients whose most recent NAAT indicated detectable HCV RNA. Datasets from patients with detectable HCV RNA were then de-pseudonymized and cross-checked against the mortality registry, health insurance status, and institutional patient records to ensure accuracy. Eligible individuals were contacted up to three times (once by mail and twice by telephone) and invited to receive antiviral treatment.
Results: A total of 24,150 HCV NAAT datasets from 8,164 patients were extracted. From 2014 to 2023, 804 patients (9.8%) had a most recent NAAT result that showed detectable HCV RNA. Of those patients, 38 (4.7%) experienced reinfection. Of the 804 patients, 263 (32.7%) had died, 118 (14.7%) had no contact information, 33 (4.1%) had already received treatment, 23 (2,9%) had moved outside the catchment area, and 20 (2.5%) were excluded due to comorbidities or other contra-indications. Thus, 347 patients (43.2%) were eligible and contacted. Of those, 211 (60.8%) could not be reached, 42 (12.1%) reported a sustained virologic response (SVR), 18 (5.2%) declined treatment, 6 (1.7%) had died, 6 (1.7%) remained undecided, and 5 (1.4%) had contraindications. 59 (17.0%) of the eligible patients could be linked to care.
Conclusion: The HEAL-S HCV cohort demonstrates that a data-driven macro-elimination strategy is feasible in low-prevalence settings. This strategy can link a substantial number of individuals to care and meaningfully contribute to the WHO's goal of eliminating HCV by 2030.

FRI-633
Treatment with direct-acting antivirals in HCV-infected patients after liver transplantation
Michał Brzdęk[1], Dorota Zarębska-Michaluk[2], Olga Tronina[3], Łukasz Laurans[4], Ewa Janczewska[5], Dorota Dybowska[6], Anna Parfieniuk-Kowerda[7], Magdalena Tudrujek-Zdunek[8], Jolanta Białkowska[9], Justyna Janocha-Litwin[10], Robert Flisiak[7].
[1]Collegium Medicum, Jan Kochanowski University, Kielce, Poland; [2]Department of Infectious Diseases and Allergology, Collegium Medicum, Jan Kochanowski University, Kielce, Poland; [3]Infant Jesus Clinical Hospital, Warsaw, Poland; [4]Department of Infectious Diseases, Hepatology and Liver Transplantation, Pomeranian Medical University, Szczecin, Poland; [5]ID Clinic, Mysłowice, Poland; [6]Department of Infectious Diseases and Hepatology, Faculty of Medicine, Collegium Medicum in Bydgoszcz, Nicolaus Copernicus University, Bydgoszcz, Poland; [7]Department of Infectious Diseases and Hepatology, Medical University of Bialystok, Bialystok, Poland; [8]Department of Infectious Diseases, Medical University of Lublin, Lublin, Poland; [9]Biegański Regional Specjalist Hospital, Łódź, Poland; [10]Infectious Diseases and Hepatology Clinic, Medical University of Wroclaw, Wroclaw, Poland
Email: michal.brzdek@gmail.com

Background and aims: Direct-acting antivirals (DAAs) have revolutionised the management of chronic hepatitis C virus (HCV) infection. However, real-world data on the effectiveness and safety of DAA therapy in patients with history orthotopic liver transplantation (OLTx) remain limited. This study aimed to evaluate the clinical characteristics, effectiveness, and safety of DAA therapy in liver transplant recipients with chronic hepatitis C in a nationwide, real-world cohort.
Method: A retrospective analysis was performed of all consecutive adult patients who underwent OLTx before starting DAA therapy between July 2015 and December 2024 in the EpiTer-2 project, that included 20,586 patients treated because of chronic hepatitis C.
Results: A total of 141 patients participated in the study, with most being men (66%) and aged 50 years or older. Most patients (80%) had comorbidities, and nearly a quarter of the population had cirrhosis of the transplanted liver at the start of antiviral therapy. The median time from OLTx to initiation of antiviral therapy was 24 months. Overall, SVR was achieved in 96.4% of patients in the intention-to-treat analysis and in 98.6% after excluding patients lost to follow-up. Treatment was well tolerated. Serious adverse events were reported in five patients. During DAA treatment and 12 weeks of follow-up after treatment, two deaths were reported. Subgroup analysis by time from OLTx to antiviral therapy (≤24 vs. >24 months) revealed no differences in effectiveness and safety despite some baseline clinical variations.
Conclusion: DAA therapy in liver transplant recipients with chronic HCV infection is highly effective and well-tolerated.

FRI-634
Sustained virologic response rates following incomplete direct-acting antiviral therapy for hepatitis C: a real world study
Jihad Slim[1], Murad Qirem[1], Shahd Yaghi[1], Kevin Leyden[2], Corey Rosmarin-DeStefano[2], Sheena Duprey[2]. *[1]Saint Michael's Medical Center, Newark, United States; [2]North Jersey Community Research Initiative, Newark, United States*
Email: jsmdsmmc@gmail.com

Background and aims: Direct-acting antivirals (DAAs) have transformed hepatitis C virus (HCV) treatment, achieving cure rates exceeding 95% with guideline-recommended therapy durations. Emerging data suggest that the high antiviral potency of DAAs may allow some patients to achieve sustained virologic response (SVR) even when treatment is interrupted or shortened. Understanding real-world SVR outcomes following incomplete treatment is therefore important to better understand the full therapeutic potential of modern HCV regimens.
Method: We conducted a retrospective analysis of prospectively collected data from patients treated for HCV through a mobile medical unit-based phlebotomy, telehealth provider visits, specialty pharmacy dispensing, and nurse-led follow-up. Patients who did not complete their full prescribed DAA course but had post-treatment HCV RNA testing were included. Treatment exposure was categorized by the percentage of treatment delivered by the pharmacy. The primary outcome was SVR at 12 weeks after treatment completion (SVR12).
Results: Among 2,461 patients prescribed DAA therapy between February 2022 and October 2025, 147 (5.9%) did not complete their intended treatment course. Of these, 104 patients received partial therapy and 43 received no antiviral treatment. Among patients receiving partial therapy, 51 patients had post-treatment viral load data available. Overall, 25 of 51 patients (49%) achieved SVR12 despite incomplete therapy. SVR12 rates increased with longer treatment duration, occurring in 61.1% (11/18) of patients who received two-thirds of their prescribed therapy (8 out of 12 weeks), 66.6% of those who received half of their prescribed DAA (4 out of 8 weeks) and 43.8% (7/16) of those who received a third (4 out of 12 weeks); whereas only 27.2% (3/11) who received ≤25% of therapy achieved SVR12. These findings demonstrate a clear association between duration of DAA exposure and likelihood of cure while highlighting that SVR12 remains achievable despite incomplete therapy.
Conclusion: In this real-world cohort, a substantial proportion of patients achieved SVR12 despite incomplete DAA therapy, underscoring the potent antiviral activity of modern regimens. Although full-course treatment remains the standard of care, the occurrence of SVR following incomplete therapy highlights the importance of continued follow-up and re-engagement of individuals living with HCV with barriers to treatment adherence.

FRI-635

Proton-pump inhibitor Omeprazole did not affect the plasma pharmacokinetics of Bemnifosbuvir and Ruzasvir fixed-dose combination in healthy participants

Xiao-Jian Zhou[1], Brett Smith[2], Maureen Montrond[1], Keith Pietropaolo[1], Bruce Belanger[1], Shannan Lynch[1], Dayle James[1], Maria Arantxa Horga[1], Janet Hammond[1]. *[1]Atea Pharmaceuticals, Inc, 225 Franklin Street, Suite 2100, Boston, United States; [2]Altasciences, Los Angeles, United States*
Email: zhou.xj@ateapharma.com

Background and aims: Proton pump inhibitors (PPIs), such as omeprazole (OMEP), are commonly used concomitant medications among HCV patients receiving DAA therapy. PPIs can reduce the absorption of several classes of HCV DAAs potentially impacting efficacy, resulting in their restricted use. Bemnifosbuvir (BEM) and ruzasvir (RZR) are potent/pan-genotypic inhibitors of the HCV NS5B polymerase and NS5A protein, respectively. Their fixed-dose-combination (FDC) is in phase 3 trials for chronic HCV. We report the results from a phase 1 study evaluating the effect of OMEP on the plasma pharmacokinetics (PK) of BEM and RZR in healthy participants.
Method: Twenty healthy participants received a single dose of BEM 550 mg/RZR 180 mg as 2 FDC tablets each containing 275 mg BEM and 90 mg RZR on Day 1. Participants received omeprazole (OMEP) 20 mg once-daily (QD) from Days 4 to 13 and 40 mg QD from Days 14 to 22. On Days 8, 13 and 18, respectively, participants received a single dose of BEM/RZR simultaneously with, 0.5 h before, and 2 h after OMEP. Dosing occurred on an empty stomach. Intensive PK sampling was performed over 120 h and plasma levels of BEM (and metabolites) and RZR were quantitated using validated bioanalytical methodologies.
Results: BEM and RZR were safe and well-tolerated when administered alone or with OMEP. Most AEs were mild in severity and self-limiting. Headache and nausea (grade 1) were the only AEs reported in more than 2 subjects. Concomitant OMEP did not meaningfully affect the plasma exposure measured as area under the plasma concentration-time curve (AUC) of BEM, its guanosine nucleoside AT-273 (surrogate for the active intracellular triphosphate metabolite AT-9010) or RZR: geometric mean ratios (GMRs) were 0.91, 1.13 and 1.09 for BEM, AT-273 and RZR respectively when simultaneously co-administered with 20 mg OMEP; GMRs were 0.91, 1.14, 1.28 respectively when dosed 0.5 h before 20 mg OMEP; and were 0.83, 1.14 and 0.86 respectively for BEM, AT-273 and RZR when dosed 2 h after the higher 40 mg QD dose of OMEP.
Conclusion: BEM/RZR FDC was safe and well-tolerated when administered alone or concomitantly with OMEP. While OMEP 20 mg, a common dose for GERD did not affect the plasma exposure to BEM/AT-273/RZR, a higher 40 mg dose of OMEP with BEM/RZR dosed 2 h later to allow for maximal acid-suppressive effect did not meaningfully reduce plasma exposure to BEM/AT-273/RZR either. Results support concomitant use of OMEP 20 mg or 40 mg with BEM/RZR in HCV-infected individuals without restriction.

FRI-636

Bemnifosbuvir and ruzasvir administered as a fixed-dose-combination have low potential to inhibit P-gp, BCRP or OATP1B1/3 mediated transport

Xiao-Jian Zhou[1], Gaetano Morelli[2], Maureen Montrond[1], Keith Pietropaolo[1], Bruce Belanger[1], Shannan Lynch[1], Dayle James[1], Maria Arantxa Horga[1], Janet Hammond[1]. *[1]Atea Pharmaceuticals, Inc, 225 Franklin Street, Suite 2100, Boston, United States; [2]Altasciences, Montreal, Canada*
Email: zhou.xj@ateapharma.com

Background and aims: Bemnifosbuvir (BEM) and ruzasvir (RZR) are potent, pan-genotypic inhibitors of the HCV NS5B polymerase and NS5A protein, respectively. The fixed-dose-combination (FDC) of these two investigational drugs is in phase 3 clinical development for the treatment of chronic HCV. BEM and RZR were identified in vitro as inhibitors of drug transporters P-glycoprotein, breast cancer resistant protein (BCRP) and organic anion transporting polypeptide 1B1 (OATP1B1) and OATP1B3. A Ph 1 study in healthy participants was conducted to assess the clinical implications of these results using digoxin (DIG) and rosuvastatin (ROSU) as P-gp and BCRP/OATP1B1/1B3 index substrates, respectively.
Method: Two groups of healthy participants (n = 18/arm, 36 total) were enrolled to evaluate the effect of a single dose of BEM 550 mg/RZR 180 mg as 2xFDC tablets on the plasma pharmacokinetics (PK) of a single dose of DIG 0.25 mg and ROSU 10 mg, respectively. Within each arm, participants were randomized according to a 3-period, 3-sequence crossover design with 6 participants/sequence and received in each period on an empty stomach the index substrate alone, with simultaneously administered BEM/RZR or 2 hours ahead of BEM/RZR. Serial plasma samples were collected and quantitated for DIG or ROSU concentrations.
Results: A single dose of BEM 550 mg/RZR 180 mg simultaneously administered increased the peak concentration of DIG by 58.9% (measured as geometric mean ratio, GMR) without affecting its overall exposure. When dosed staggered, BEM/RZR did not affect the PK of DIG. A single dose simultaneous BEM/RZR increased the peak and total plasma exposure of ROSU by 78.5% and 39.8%, respectively, whereas staggered dosing reduced these effects by approximately half. There was no effect on vital signs, ECG, and no SAEs.
Conclusion: A single dose of BEM 550 mg/RZR 180 mg administered as 2xFDC tablets only slightly increased the plasma exposure of the P-gp and BCRP/OATP1B1/3 index drugs DIG and ROSU. With GMR<2, BEM/RZR therefore have low potential to exhibit clinically meaningful inhibition of these transporters. No dose adjustment will be needed for drugs that are sensitive substrates of P-gp or BCRP/OAT1B1/3 when co-administered with BEM/RZR; staggered dosing may lessen any DDI risk.

EASL JOURNAL OF HEPATOLOGY

Author Index

Aabakken, Lars, S451 (THU-409)
Aaldijk, Alexandra, S630 (SAT-090)
Aamann, Luise, S298 (SAT-245), S333 (SAT-369)
Aarabi, Seyed Sahab, S697 (FRI-195-YI)
Abaalkhail, Faisal, S377 (FRI-451), S521 (THU-092), S521 (THU-093), S522 (THU-094), S523 (THU-099), S557 (THU-213), S566 (WED-052)
Abadi-Ron, Victoria, S327 (SAT-322)
Abalos, Cassandra, S703 (THU-528-YI)
Abate, Maria Lorena, S49 (OS-076-YI), S534 (THU-133)
Abbasi, Amanullah, S865 (FRI-637)
Abbas, Nadir, S325 (SAT-320), S343 (SAT-401-YI)
Abbas, Zaigham, S67 (OS-105-YI)
AbdAllah, Mohamed, S492 (FRI-217), S504 (FRI-252), S814 (WED-003)
Abdallah, Yasser, S824 (WED-035)
Abdeen, Nermeen, S524 (THU-101)
Abdelaal, Essa, S575 (WED-077)
Abdelaziz, Ahmed, S231 (FRI-305), S263 (SAT-333)
Abdelhameed, Aya, S449 (THU-401)
Abdelhamid, Amira, S231 (FRI-305), S263 (SAT-333)
Abdelmalek, Manal F., S64 (OS-099), S190 (WED-421), S560 (TOP-066), S561 (TOP-082), S579 (WED-089), S680 (FRI-139), S696 (FRI-189), S758 (TOP-001)
Abdelmalek, Mohamed, S504 (FRI-252)
Abdelrahman, Basma, S630 (SAT-091)
Abdel-Razek, Wael, S492 (FRI-217), S814 (WED-003)
Abdelsameea, Eman, S524 (THU-101)
Abdel-Samiee, Mohamed, S524 (THU-101)
Abdo, Indiana, S804 (FRI-019), S826 (WED-038)
Abdo, Jamil, S684 (FRI-154)
Abdulelah, Ahmed, S518 (THU-085)
Abdulhakeem, Hind, S521 (THU-093)
Abdullah, Liyana Binte, S458 (WED-238)
Abedi, Ilya, S597 (WED-147)
Abedin, Nada, S251 (SAT-525)
Abe, Kazumichi, S331 (SAT-368-YI), S647 (SAT-147)
Abel, Florian, S40 (OS-058)
Abels, Christoph, S785 (SAT-020)
Abe, Masanori, S336 (SAT-379)
Abenavoli, Ludovico, S304 (SAT-258), S335 (SAT-378-YI)
Abergel, Armand, S45 (OS-067), S110 (FRI-042), S167 (FRI-394-YI), S380 (FRI-463), S381 (FRI-464), S512 (FRI-372), S742 (THU-477)
Åberg, Fredrik, S114 (FRI-055), S122 (FRI-084), S247 (SAT-512), S376 (FRI-447), S376 (FRI-448), S530 (THU-118-YI), S562 (TOP-096), S760 (THU–003)
Aberra, Hanna, S24 (OS-028), S144 (SAT-452)
Abe, Tamami, S510 (FRI-367)
Abeysekera, Kushala, S69 (LBP-001), S519 (THU-086), S725 (THU-427), S761 (THU-004), S777 (THU-050)
Abe, Yutaro, S550 (THU-188)
Abid, Shahab, S743 (THU-478)
Abiétar, Daniel G., S710 (THU-557-YI)
Abiramalatha, T, S782 (SAT-010-YI)
Aboagye, Eric, S490 (TOP-407-YI)
Aboona, Majd, S670 (SAT-220)
Abosheaishaa, Hazem, S202 (WED-460-YI)
Aboulhamayed, Omar, S537 (THU-141-YI)
Abousaif, Alaa, S559 (TOP-064)
Abouzayed, Ayman, S579 (WED-090)
Abraham, Sunje, S351 (SAT-426-YI)
Abraldes, Juan, S349 (SAT-419), S427 (THU-220)
Abraldes, Juan G, S525 (THU-104-YI), S563 (WED-042), S616 (WED-199), S743 (THU-479), S745 (THU-483), S787 (SAT-025), S787 (SAT-026), S788 (SAT-027)
Abramczyk, Joanna, S286 (FRI-273)
Abramov, Frida, S943 (FRI-594), S953 (FRI-624), S957 (WED-578), S958 (WED-580)
Abreu, Eliabe, S424 (TOP-376), S758 (TOP-001)
Abreu, Inmaculada Alonso, S547 (THU-181)
Abreu, Marco, S166 (FRI-393)
Abruzzese, Giselle, S272 (THU-315-YI), S273 (THU-316)
Abudukadi, Guzinayi, S243 (FRI-348)
Abulaiti, Aimitaji, S761 (THU-005)
Abulitifu, Yilihamu, S357 (SAT-445)
Aburisheh, Khaled, S566 (WED-053)
Aby, Elizabeth, S375 (TOP-519)
Accetta, Antonio, S196 (WED-445), S217 (WED-509-YI)
Aceituno, Laia, S425 (THU-216-YI)
Acera, Mario, S884 (THU-604-YI)
Acevedo, Mariana, S28 (OS-037), S627 (TOP-144), S629 (TOP-160)
Acharya, Pragyan, S141 (TOP-423), S198 (WED-448-YI)
Achayo, Lilly, S821 (WED-023)
Acker, Jos Van, S907 (SAT-575)
Acosta, Maria, S97 (SAT-085)
Acosta, Rima, S7 (GS-012), S958 (WED-581)
Acuti, Nicole, S455 (TOP-406)
Adalid, Cristina Gonzalez De, S815 (WED-006)
Adali, Gupse, S59 (OS-091), S298 (SAT-246), S395 (FRI-511-YI)
Adame, Lillian, S658 (SAT-184), S879 (THU-587), S889 (THU-620), S960 (WED-588)
Adamescu, Aida, S974 (WED-633)
Adam, René, S356 (SAT-443), S417 (FRI-581)
Adams, Elisabeth, S817 (WED-012)
Adamski, Jill, S416 (FRI-576)
Adams, Leon, S560 (TOP-066), S561 (TOP-082), S571 (WED-069), S579 (WED-089), S699 (FRI-198), S736 (THU-458)
Adamzek, Kevin, S237 (FRI-330)
Adanir, Haydar, S160 (SAT-507)
Adan-Villaescusa, Elena, S17 (OS-013), S474 (WED-364)
Addo, Marylyn, S867 (FRI-642)
Adebayo, Danielle, S160 (SAT-507)
Adel, Hammoutene, S480 (WED-380), S853 (WED-283)
Adelmeijer, Jelle, S168 (FRI-396)
Adeyemi, Adebowale, S330 (SAT-366)
Adolph, Dirk, S763 (THU-010)

*Page numbers for abstracts are followed by the abstract number(s) in parentheses.

Author Index

Adorini, Luciano, S139 (FRI-134)
Adotti, Valentina, S53 (OS-082), S447 (THU-394)
Adu, Prince, S821 (WED-024), S967 (TOP-600-YI)
Advani, Dhruv, S247 (SAT-514)
Adzika, Gabriel, S276 (THU-329)
Aeschbacher, Thomas, S948 (FRI-610)
Affonso, Juliana Marques, S651 (SAT-158-YI)
Affo, Silvia, S18 (OS-014-YI)
Affronti, Andrea, S304 (SAT-258), S307 (SAT-263), S335 (SAT-378-YI)
Afif, Waqqas, S589 (WED-119)
Afif, Yusuf, S380 (FRI-462)
Afihene, Mary, S905 (SAT-569), S940 (FRI-588-YI)
Afonso, Pedro Miranda, S55 (OS-086), S831 (THU-258-YI)
Agapova, Maria, S299 (SAT-247)
Agarwal, Ankit, S184 (TOP-454-YI), S741 (THU-474)
Agarwal, Ashish, S741 (THU-474)
Agarwala, Yuki, S490 (TOP-407-YI)
Agarwal, Ayush, S36 (OS-051-YI), S141 (TOP-423), S184 (TOP-454-YI), S247 (SAT-514), S299 (SAT-248), S725 (THU-426), S847 (THU-299)
Agarwal, Banwari, S389 (FRI-492)
Agarwal, Kosh, S1 (GS-001), S7 (GS-012), S8 (LBO-003), S43 (OS-066), S65 (OS-102), S404 (FRI-538-YI), S897 (TOP-565), S905 (SAT-571), S928 (SAT-628-YI), S934 (TOP-582), S936 (TOP-584), S937 (FRI-585-YI), S943 (FRI-594), S953 (FRI-624), S959 (WED-581), S959 (WED-586), S965 (WED-602), S970 (WED-619)
Agarwal, Neha, S629 (TOP-161-YI)
Agarwal, Nitendra, S689 (FRI-169), S689 (FRI-170)
Agarwal, Prashant MohanDr., S214 (WED-501-YI)
Agarwal, Samagra, S36 (OS-051-YI), S141 (TOP-423), S184 (TOP-454-YI), S299 (SAT-248), S725 (THU-426), S847 (THU-299)
Agerbo, Frederikke, S205 (WED-468)
Aggarwal, Arnav, S36 (OS-051-YI), S141 (TOP-423), S184 (TOP-454-YI), S247 (SAT-514), S299 (SAT-248), S725 (THU-426)
Aggarwal, Arsha, S424 (TOP-376)
Aggarwal, Mukul, S184 (TOP-454-YI)
Aggeletopoulou, Ioanna, S348 (SAT-416)
Aggrawal, Aman, S212 (WED-495-YI)
Agha, Hebaalla, S49 (OS-075), S962 (WED-594)
Aghara, Hiral, S357 (THU-339)
Aghayeva, Sevda, S24 (OS-028), S144 (SAT-452), S160 (SAT-507), S965 (WED-603)
Aghemo, Alessio, S52 (OS-081), S55 (OS-085-YI), S62 (OS-097), S71 (LBP-009), S176 (FRI-425), S190 (WED-425), S212 (WED-494-YI), S339 (SAT-386), S479 (WED-378), S516 (TOP-113), S531 (THU-120), S696 (FRI-188-YI), S856 (WED-291)
Agirre-Garrido, Leire, S777 (THU-050)
Agnese, Valentina, S279 (THU-334-YI), S359 (THU-347-YI)
Agnihotram, Raman, S589 (WED-119)
Agnolon, Clara, S69 (LBP-004-YI), S307 (SAT-263), S335 (SAT-378-YI)
Agoglia, Luciana, S340 (SAT-394), S830 (THU-254), S830 (THU-255)
Agostoni, Carlo, S595 (WED-138)
Agrawal, Aman, S31 (OS-043-YI)
Agrawal, Khushboo, S425 (THU-217-YI), S456 (WED-232)
Agrawal, Nancy, S869 (TOP-631)
Aguenoz, M'hommed, S163 (FRI-382)
Aguilar, Anna, S394 (FRI-507-YI)
Aguilar-Corominas, Laia, S129 (FRI-101)
Aguilar, Ferran, S34 (OS-049), S35 (OS-050-YI), S159 (SAT-505), S166 (FRI-388-YI), S170 (FRI-401-YI)
Aguilar, Loreto, S112 (FRI-050)
Aguilar, Maria, S775 (THU-043)
Aguilar, María Dolores Espinosa, S410 (FRI-558)
Aguilar, Pilar, S779 (SAT–003-YI)
Aguilar, Raul, S10 (LBO-006)
Aguilera, A., S799 (TOP-049), S899 (SAT-557), S910 (SAT-585)
Aguilera, Antonio, S910 (SAT-581)
Aguilera-Muñoz, Felipe, S663 (SAT-199-YI)
Aguirre, Jonathan, S296 (TOP-281), S306 (SAT-262), S866 (FRI-640)
Aguirre-Villarreal, David, S866 (FRI-640)
Ahad, Marvad, S799 (FRI-004), S800 (FRI-005)
Aharon, Lenny, S614 (WED-191)
Ahlenstiel, Golo, S218 (WED-513), S749 (THU-496)
Ahl, Liv Grete, S222 (WED-526-YI)
Ahluwalia, Jasmina, S81 (LBP-030)
Ahmad, Afaf, S377 (FRI-449)
Ahmad, Akram, S565 (WED-050)
Ahmadizar, Fariba, S600 (WED-153)
Ahmed-Belkacem, Hakim, S886 (THU-609)
Ahmed-Belkacem, Rostom, S879 (THU-587)
Ahmed, Habib, S745 (THU-484)
Ahmed, Hany, S266 (SAT-346)
Ahmed, Refah, S767 (THU-019)
Ahmed, Rumaysa, S764 (THU-012)
Ahmed, Wamda, S684 (FRI-154)
Ahn, Jhii-Hyun, S732 (THU-447)
Ahn, Joseph, S492 (FRI-218)
Ahn, Sang Bong, S545 (THU-171), S591 (WED-122), S625 (WED-229), S630 (SAT-092), S686 (FRI-163)
Ahn, Sang Hoon, S498 (FRI-235), S916 (SAT-597)
Ahn, Young Hyeon, S519 (THU-087)
Ahodantin, James, S873 (THU-563)
Ahola, Krista, S266 (SAT-346)
Ahouidi, Ambroise, S911 (SAT-586)
Ahumada, Adriana, S337 (SAT-382)
Aiello, Chiara, S477 (WED-370)
Aigner, Elmar, S539 (THU-151-YI), S792 (SAT-041), S836 (THU-265-YI)
Aikebuse, Melanie, S789 (SAT-030)
Aires, Rodrigo, S10 (LBO-006)
Airoldi, Aldo, S3 (GS-005), S52 (OS-081), S185 (TOP-455-YI)
Aishima, Shinichi, S667 (SAT-213)
Aithal, Guruprasad, S106 (THU-076), S311 (SAT-270), S470 (WED-269)
Aitken, Sarah, S455 (TOP-405)
Ai, Xin, S593 (WED-133)
Ai, Yingjie, S231 (FRI-306-YI)
Aizaki, Hideki, S875 (THU-573), S894 (THU-635), S894 (THU-637)
Aizenshtadt, Aleksandra, S292 (FRI-300-YI)
Aizimuaji, Zulihumaer, S456 (WED-233)
Ajana, Fatima Zahra, S591 (WED-125), S609 (WED-181), S844 (THU-286), S949 (FRI-613)
Ajee, K L, S705 (THU-541-YI), S705 (THU-542)
Ajisegiri, Oyindamola, S43 (OS-065)
Aji, Tuerganaili, S243 (FRI-348), S377 (FRI-450)
Ajmera, Veeral, S207 (WED-479), S564 (WED-043), S578 (WED-088)
Akarca, Halit, S519 (THU-089)
Akarca, Ulus, S389 (FRI-491), S542 (THU-163)
Akarsu, Mesut, S899 (SAT-556-YI)
Akbary, Kutbuddin, S241 (FRI-340), S578 (WED-087)
Akeno, Yurina, S694 (FRI-184)
Åkerblad, Peter, S165 (FRI-387-YI)
Akilesh, S, S722 (THU-416)
Akpinar, Reha, S38 (OS-054), S331 (SAT-368-YI), S456 (WED-234-YI)
Aktas, Huseyin, S351 (SAT-426-YI)
Aktaş, Özgür, S899 (SAT-556-YI), S961 (WED-589), S965 (WED-603)
Akuta, Norio, S977 (WED-639)
Akyildiz, Murat, S961 (WED-589)
Akyuz, Filiz, S829 (THU-251)
Ala, Aftab, S39 (OS-057), S84 (LBP-038), S713 (WED-556-YI), S859 (WED-304), S860 (WED-305)
Alados, Juan Carlos, S910 (SAT-581)
Alaggio, Rita, S670 (SAT-225)
Alagiyage, Keshani, S208 (WED-480)
Alagna, Giuliano, S304 (SAT-258), S307 (SAT-263), S335 (SAT-378-YI), S350 (SAT-421), S831 (THU-256-YI)
Alaimo, Laura, S97 (SAT-084-YI)
Alaklabi, Asrar, S522 (THU-095)
Al Ali, Dhowa A., S732 (THU-446)
Alam, Seema, S55 (OS-086), S831 (THU-258-YI), S842 (THU-284), S850 (THU-308)
Alam, Shahinul, S67 (OS-105-YI), S952 (FRI-622)
Alanazi, Amwaj I., S522 (THU-095)

Author Index

Alañón-Martínez, Paloma Elma, S303 (SAT-256-YI)
Alansare, Abdullah, S524 (THU-101), S680 (FRI-140)
Alarcón, Francisca Cuenca, S16 (OS-010), S294 (TOP-278), S837 (THU-267), S855 (WED-289)
Alarcon, Onofre, S547 (THU-181)
Alard, Berenice, S149 (SAT-468), S152 (SAT-478), S214 (WED-499), S760 (TOP-032)
Alary, Anouck, S721 (THU-415)
Álava, Ane, S287 (FRI-274)
AlAwadh, Salwa A, S521 (THU-093)
Alawi, Aisha, S315 (SAT-286)
Alazawi, William, S69 (LBP-001), S759 (TOP-018-YI), S773 (THU-038), S773 (THU-039)
Albader, Farah, S425 (THU-216-YI)
Albano, Simona, S248 (SAT-516)
Albarmawi, Husam, S573 (WED-072), S613 (WED-190)
Albeck, Orit Marom, S614 (WED-191)
Alberio, Lorenzo, S72 (LBP-011)
Albert, Cristina, S119 (FRI-073)
Albertini, Maddalena, S378 (FRI-458)
Albert, Lisa, S321 (SAT-306)
Albhaisi, Somaya, S160 (SAT-507), S761 (THU-006), S762 (THU-007)
Albillos, Agustín, S3 (GS-005), S8 (LBO-002), S34 (OS-049), S35 (OS-050-YI), S52 (OS-081), S54 (OS-084), S141 (TOP-437), S150 (SAT-475), S166 (FRI-388-YI), S195 (WED-442-YI), S571 (WED-069), S719 (TOP-488), S723 (THU-418), S731 (THU-445-YI), S733 (THU-450), S735 (THU-453), S747 (THU-492), S752 (THU-501), S753 (THU-505-YI)
Albrechtsen, Nicolai Wewer, S602 (WED-159-YI)
Albrecht, Thomas, S38 (OS-054)
Albrecht, Wolfgang, S9 (LBO-004)
Albuquerque, Miguel, S53 (OS-083-YI), S480 (WED-380)
Alcaraz, José, S146 (SAT-461)
Aldana, Andres Gomez, S556 (THU-212)
Alderslieste, Yasser A., S352 (SAT-429)
Aldossari, Norah, S566 (WED-052)
Alegret, Marta, S231 (FRI-304), S241 (FRI-341), S271 (THU-303), S279 (THU-335)
Alejos, Carla Castro, S364 (WED-329-YI)
Aleman, Soo, S43 (OS-066), S49 (OS-075), S439 (THU-367), S606 (WED-173), S900 (SAT-559), S902 (SAT-560), S903 (SAT-561), S913 (SAT-589-YI), S915 (SAT-595), S916 (SAT-596), S934 (TOP-582), S937 (FRI-585-YI), S939 (FRI-587), S953 (FRI-625), S956 (WED-576), S962 (WED-593), S962 (WED-594), S978 (WED-642-YI)
Alessandria, Carlo, S3 (GS-005), S34 (OS-049), S35 (OS-050-YI), S141 (TOP-437), S166 (FRI-388-YI), S185 (TOP-455-YI)
Alessandrini, Annalisa, S741 (THU-473), S751 (THU-500)
Alessa, Noura, S522 (THU-094)
Alessa, Sara, S616 (WED-200)
Alessy, Saleh, S521 (THU-093)
Alexander, Thomas, S780 (SAT-005)
Alexander, Vijay, S36 (OS-051-YI), S722 (THU-416)
Alexandre, Leo, S311 (SAT-270)
Alexiev, Ivailo, S807 (FRI-025)
Alexopoulos, Sophoclis, S393 (FRI-505)
Alexopoulou, Alexandra, S142 (SAT-449), S188 (WED-415), S314 (SAT-283)
Aleyadeh, Wesam, S722 (THU-417), S835 (THU-264-YI)
Alfano, Vincenzo, S478 (WED-377)
Alfaro-Cervello, Clara, S254 (SAT-538), S779 (SAT–003-YI)
Alfaro-Jiménez, Kendall, S277 (THU-330-YI), S631 (SAT-095-YI)
Alfhaid, Abdullah, S522 (THU-095)
Algarete, Sonia, S910 (SAT-581)
AlGhamdi, Mohammed, S521 (THU-092), S522 (THU-094)
Alghamdi, Saad, S523 (THU-099), S840 (THU-275)
Algibez, Ana Martin, S124 (FRI-088)
Algibez, Ana Martín, S308 (SAT-264)
Alguwaihes, Abdullah, S566 (WED-053)
Alhaidari, Suliman, S497 (FRI-234), S723 (THU-418)
Al-Hamoudi, Waleed K, S566 (WED-052)
Alharbi, Sultan N., S12 (OS-005-YI), S490 (TOP-407-YI)
Alharthi, Abdullah Falah, S523 (THU-099)
Alharthi, Shakir, S566 (WED-052)
Al-Hasani, Aya, S709 (THU-556-YI)
Al-Hasani, Hadi, S672 (SAT-230)
Alhazmi, Yasir M, S523 (THU-099)
Alhazzani, Waleed, S521 (THU-092), S521 (THU-093), S522 (THU-094), S522 (THU-095), S523 (THU-099), S566 (WED-052), S794 (SAT-046)
Alhazza, Omar, S566 (WED-053)
Alhouri, Abdullah, S338 (SAT-385)
Alhussain, Maha, S524 (THU-101)
Alhussein, Ahmad, S20 (OS-018)
Ali, Ahmad, S2 (GS-002), S13 (OS-006-YI), S290 (FRI-289)
Ali, Ahmed Abdulhafedh, S732 (THU-446)
Aliasi-Sinai, Lital, S538 (THU-148-YI), S762 (THU-008)
Aliberti, Camillo, S429 (THU-228)
Ali, Faiza Sadaqat, S865 (FRI-637)
Ali, Issa, S565 (WED-050)
Alijagic, Andi, S29 (OS-038)
Ali, Mahrukh, S743 (THU-478)
Alimenti, Eleonora, S405 (FRI-541), S428 (THU-227-YI), S491 (TOP-408-YI)
Ali, Nasir, S178 (FRI-430)
Alings, Marco, S684 (FRI-153)
Aliotta, Alessandro, S72 (LBP-011)
Alisi, Anna, S443 (THU-380-YI), S583 (WED-102-YI), S670 (SAT-225)
Alizadeh Bahmani, Amir H., S268 (SAT-351)
Aljabar, Paul, S673 (SAT-231)
Aljaloud, Sulaiman, S680 (FRI-140)
Aljohani, Faisal, S589 (WED-119)
Aljudaibi, Bandar, S522 (THU-094), S523 (THU-099), S717 (WED-570-YI)
Alkabbani, Abdulrahman G, S522 (THU-095)
Al-Khafaji, Ali, S8 (LBO-002)
Alkhairy, Areej, S522 (THU-094)
Alkhammash, Maram, S566 (WED-053), S680 (FRI-140)
Alkhayal, Fahad, S523 (THU-099)
Alkhenizan, Abdullah, S522 (THU-095)
Alkhouri, Naim, S19 (OS-016), S20 (OS-019), S62 (OS-096), S62 (OS-097), S84 (LBP-036), S516 (TOP-113), S531 (THU-121), S559 (TOP-064), S560 (TOP-066), S561 (TOP-082), S565 (WED-051), S569 (WED-059), S579 (WED-089), S597 (WED-141), S679 (TOP-176), S679 (TOP-177), S680 (FRI-141), S682 (FRI-149), S684 (FRI-154), S688 (FRI-168), S691 (FRI-175), S692 (FRI-179), S694 (FRI-183), S719 (TOP-486), S766 (THU-015)
Al-Kuwari, Mohammed, S732 (THU-446)
Allah, Belimi Hibat, S160 (SAT-507)
Allaire, Manon, S38 (OS-055), S54 (OS-084), S375 (TOP-519), S427 (THU-220), S428 (THU-226-YI), S446 (THU-393-YI), S452 (THU-414-YI), S457 (WED-236), S493 (FRI-221), S497 (FRI-234), S499 (FRI-238), S505 (FRI-254), S506 (FRI-255-YI), S507 (FRI-362), S508 (FRI-364-YI), S723 (THU-418), S752 (THU-501)
Allan, Bernard, S667 (SAT-213)
Allaume, Pierre, S343 (SAT-400)
Allen, Alina M, S604 (WED-166)
Allende, Daniela, S399 (FRI-522)
Allen, Rebecca, S354 (SAT-434)
Aller, Rocío, S527 (THU-108), S542 (THU-164), S567 (WED-054), S571 (WED-069), S815 (WED-006)
Alletto, Francesca, S520 (THU-091-YI), S541 (THU-158), S595 (WED-137)
Allgeier, Julian, S151 (SAT-477), S744 (THU-482-YI)
Allshouse, Amanda, S975 (WED-636), S976 (WED-637)
Allweiss, Lena, S871 (THU-558-YI), S890 (THU-622-YI)
Almadok, Soleman, S257 (SAT-546)
Almaghrabi, Mohammed, S522 (THU-095)
Al-Mahtab, Mamun, S952 (FRI-622)
Almakhayitah, Hanan, S369 (WED-340-YI), S372 (WED-351)
AlMansour, Rana, S522 (THU-095)
Almaraz, Eduardo, S911 (SAT-586)
Almas, Aysha, S605 (WED-170)

Author Index

Al Masri, Nasser Mohammed, S522 (THU-095)
Almeida, Ana Arencibia, S16 (OS-010), S294 (TOP-278), S300 (SAT-250), S318 (SAT-291), S837 (THU-267), S855 (WED-289)
Almeida, Bruna, S242 (FRI-345-YI), S472 (WED-274)
Almendras-Durán, Karen, S663 (SAT-199-YI)
Almgren, Peter, S39 (OS-056)
Almohsen, Ahmed, S62 (OS-097), S516 (TOP-113)
Almojel, Alwaleed, S522 (THU-094), S566 (WED-052)
Almotairi, Albandari K, S566 (WED-052)
Almuhaidib, Shadan, S516 (TOP-113), S521 (THU-092), S521 (THU-093), S522 (THU-094), S522 (THU-095), S523 (THU-099), S566 (WED-052), S794 (SAT-046)
Al Naamani, Khalid, S378 (FRI-457), S516 (TOP-113)
Alnaser, Faisal, S774 (THU-040), S774 (THU-041)
Alnifayei, Abdulalrhman A, S521 (THU-092)
Alobaid, Lolwa N., S521 (THU-093)
Alomaim, Waleed S, S521 (THU-092), S521 (THU-093)
Aloman, Costica, S94 (SAT-073)
Al-Omar, Hussain Abdulrahman, S557 (THU-213)
Alonazi, Wadi B., S523 (THU-100)
Alonso, Cristina, S82 (LBP-032), S303 (SAT-257-YI), S642 (SAT-131-YI)
Alonso, Estella, S832 (THU-258-YI), S842 (THU-284)
Alonso, Gemma Carrion, S250 (SAT-524)
Alonso-Gonzalez, Rafael, S753 (THU-506)
Alonso, José Castellote, S724 (THU-421), S804 (FRI-019)
Alonso, Ma Aranzazu, S25 (OS-029)
Alonso, Maria Luisa Manzano, S124 (FRI-088), S308 (SAT-264)
Alonso, Nuria, S562 (TOP-097-YI)
Alonso-Peña, Marta, S294 (TOP-278), S833 (THU-259)
Alonso, Sara María Monsalve, S250 (SAT-524)
Alonso, Sonia, S643 (SAT-134)
Alonso-Vázquez, Julio, S132 (FRI-108-YI)
AlOtaibi, Faisal, S566 (WED-052)
Alotaibi, Haifa F, S521 (THU-092), S521 (THU-093), S523 (THU-099), S566 (WED-052)
Alotaibi, Metib, S566 (WED-053)
Alothman, Sari, S684 (FRI-154)
Alpert, Lauren, S40 (OS-059-YI), S538 (THU-148-YI)
Alpízar, Nilda Gallardo, S634 (SAT-104)
Alqahtani, Mohammed, S250 (SAT-523), S390 (FRI-494), S390 (FRI-495)
Alqahtani, Saleh, S62 (OS-097), S356 (SAT-443), S375 (TOP-518), S378 (FRI-457), S417 (FRI-581), S516 (TOP-113), S766 (THU-015)
Alqahtani, Saleh A., S126 (FRI-094), S521 (THU-092), S521 (THU-093), S522 (THU-094), S522 (THU-095), S523 (THU-099), S557 (THU-213), S566 (WED-052), S678 (TOP-162), S794 (SAT-046)
Alqussayer, Samar A, S521 (THU-092)
Alric, Laurent, S45 (OS-067), S829 (THU-252)
Alsadoon, Amani, S523 (THU-100), S566 (WED-053), S680 (FRI-140)
Alsalmi, Amina, S616 (WED-200)
Alsayb, Majd, S522 (THU-094)
Al Sehemy, Lamiaa, S537 (THU-141-YI)
Al-Shakhshir, Sarah, S315 (SAT-286)
Alshareef, Muneera, S522 (THU-095)
Al-sharif, Aya M., S537 (THU-141-YI)
Alshehri, Ali, S523 (THU-099)
Alsinani, Siham, S377 (FRI-451), S378 (FRI-457)
Alstrup, Aage Kristian Olsen, S290 (FRI-287), S853 (WED-282-YI)
Alsubki, Layan A., S521 (THU-092), S521 (THU-093), S522 (THU-095)
Alswat, Khalid, S524 (THU-101)
Alswat, Khalid A, S62 (OS-097), S377 (FRI-451), S378 (FRI-457), S516 (TOP-113), S521 (THU-092), S523 (THU-100), S566 (WED-053), S680 (FRI-140)
Altaei, Omar, S377 (FRI-451)
Altamirano, Rafael Manuel Alejandre, S815 (WED-006)
Altea-Manzano, Patricia, S271 (THU-314)
Alter, Galit, S893 (THU-629)
Alterini, Giada, S83 (LBP-034-YI)
Altfeld, Marcus, S867 (FRI-642)
Althaus, Philipp, S237 (FRI-329), S631 (SAT-093-YI)
Althoff, Peter, S658 (SAT-184)
Altikes, Renato, S701 (FRI-203-YI)
Altın, Soner, S829 (THU-251)
Altmann, Daniel M, S500 (FRI-239)
Aluvihare, Varuna, S59 (OS-091), S386 (FRI-481-YI), S404 (FRI-538-YI)
Alvarado, Lewel, S746 (THU-485)
Alvarado, Ruben, S968 (WED-610-YI)
Alvarado-Tapias, Edilmar, S191 (WED-426), S337 (SAT-382), S643 (SAT-134), S735 (THU-453)
Álvares-da-Silva, Mario, S10 (LBO-006), S24 (OS-028), S35 (OS-050-YI), S41 (OS-061), S144 (SAT-452), S154 (SAT-484), S160 (SAT-507)
Alvarez, Angel Caunedo, S751 (THU-500)
Alvarez, Carolina Almohalla, S379 (FRI-459), S403 (FRI-532), S403 (FRI-533), S415 (FRI-575)
Alvarez, Fernando, S386 (FRI-480-YI)
Álvarez, Juan, S191 (WED-427-YI)
Álvarez-Navascués, Carmen, S300 (SAT-250), S309 (SAT-268), S723 (THU-418)
Álvarez-Ossorio, Ángela Rojas, S600 (WED-153), S644 (SAT-137)
Alvarez, Paula Fernandez, S837 (THU-267), S855 (WED-289)
Alvarez-Silva, Camila, S261 (SAT-329-YI)
Álvarez-Suárez, Beatriz, S855 (WED-289)
Alvaro, Domenico, S69 (LBP-004-YI), S304 (SAT-258), S307 (SAT-263), S350 (SAT-421), S831 (THU-256-YI)
Alves, Joao Vaz, S43 (OS-066), S934 (TOP-582)
Alves, Paola Hoff, S88 (SAT-056)
Alves, Venancio, S53 (OS-083-YI)
Alviri, Naz Kanani, S709 (THU-556-YI)
Alwayn, Ian, S415 (FRI-574)
AlZahrani, Ahmed, S566 (WED-052)
Al-Zu'bi, Marwan, S732 (THU-446)
Amaddeo, Giuliana, S428 (THU-226-YI), S434 (THU-242), S446 (THU-393-YI), S493 (FRI-221), S497 (FRI-234), S499 (FRI-238), S505 (FRI-254), S506 (FRI-255-YI), S507 (FRI-362), S508 (FRI-364-YI), S723 (THU-418), S742 (THU-477)
Amadieu, Camille, S266 (SAT-346)
Amado, Luis Enrique Morano, S904 (SAT-564)
Amador, Alberto, S91 (SAT-062), S191 (WED-427-YI), S394 (FRI-507-YI), S724 (THU-421)
Amancio-Lisboa, Maria, S267 (SAT-348)
Amann, Berthold, S21 (OS-020)
Amaral, Ana Cristina, S296 (TOP-281), S306 (SAT-262), S314 (SAT-284)
Amaral, Carla, S547 (THU-181)
Amarbayasgalan, Enkh-Oyun, S826 (WED-039)
Amari, Lena, S330 (SAT-365), S555 (THU-206)
Ambery, Philip, S252 (SAT-530)
Ambike, Shubhankar, S50 (OS-077)
Ambroise, Jérome, S648 (SAT-151-YI)
Ambroz, Martin, S286 (FRI-272)
Amby, Kristoffer Kjærgaard, S631 (SAT-094-YI), S660 (SAT-188-YI)
Ameigeiras, Beatriz Margarita, S7 (LBO-001)
Amer, Lama, S522 (THU-094)
Amezcua, Aitor González, S735 (THU-453)
Amini, Hamed, S64 (OS-099), S596 (WED-140)
Amini, Peyvand, S84 (LBP-037)
Amiri, Leila, S315 (SAT-286), S547 (THU-179), S914 (SAT-592-YI), S921 (SAT-610)
Amodio, Piero, S735 (THU-452)
Amo, Maria, S124 (FRI-088), S308 (SAT-264)
Amorim, Luisa, S724 (THU-420)
Amorim, Maria Fernanda, S102 (THU-060)
Amorós, Maria, S203 (WED-463)
Amos, Christopher, S461 (WED-247)

Author Index

Ampazis, Odysseas, S348 (SAT-416)
Ampollini, Silvia, S874 (THU-571)
Ampuero, Javier, S150 (SAT-475), S542 (THU-164), S567 (WED-054), S571 (WED-069), S621 (WED-214), S644 (SAT-137), S678 (SAT-244), S837 (THU-267), S840 (THU-275), S855 (WED-289)
Amundsen-Isaksen, Enya, S2 (GS-002), S287 (FRI-276-YI), S292 (FRI-300-YI), S858 (WED-300-YI)
Anagnostakis, Filippos, S694 (FRI-185)
Ananchuensook, Prooksa, S62 (OS-097), S516 (TOP-113), S619 (WED-211)
Anand, Amit, S822 (WED-025-YI)
Anandan, Aathavan Shanmuga, S803 (FRI-014)
Anand, Anil, S24 (OS-028)
Anatchkova, Milena, S339 (SAT-387)
Anaya, Elena, S474 (WED-364)
Andělová, Hana, S273 (THU-317), S459 (WED-241)
Andersen, Anine, S110 (FRI-041-YI), S115 (FRI-059), S122 (FRI-079-YI), S125 (FRI-090-YI), S554 (THU-204), S706 (THU-545-YI)
Andersen, Ina, S299 (SAT-249), S303 (SAT-257-YI)
Andersen, Jesper, S454 (TOP-390-YI), S462 (WED-249), S483 (WED-388-YI), S484 (WED-393)
Andersen, Mette Lehmann, S110 (FRI-041-YI), S115 (FRI-059), S554 (THU-204)
Andersen, Peter, S26 (OS-032-YI), S63 (OS-098-YI), S83 (LBP-035), S110 (FRI-041-YI), S111 (FRI-044), S114 (FRI-057), S115 (FRI-059), S122 (FRI-079-YI), S125 (FRI-090-YI), S515 (TOP-098), S554 (THU-204), S583 (WED-101), S608 (WED-180), S706 (THU-545-YI)
Andersen, Sidsel Dahl Winther, S77 (LBP-022-YI)
Andersen, Thomas Lund, S602 (WED-159-YI)
Anders, Lennard, S271 (THU-313)
Anders, Maria Margarita, S296 (TOP-281), S306 (SAT-262)
Anderson, Aimee, S289 (FRI-285)
Anderson, Blaire, S401 (FRI-527)
Anderson, Chelsea, S544 (THU-167)
Anderson, Mark, S80 (LBP-028-YI), S905 (SAT-571), S947 (FRI-609), S960 (WED-588)
Anderson, Motswedi, S900 (SAT-558), S922 (SAT-612)
Anderson, Patricia, S707 (THU-546-YI)
Andersson, Anneli, S385 (FRI-479)
Andersson, Daniel, S515 (TOP-112-YI), S701 (FRI-205-YI)
Andersson, Emma, S861 (WED-308)
Andolina, Giulia, S583 (WED-102-YI)
Ando, Naokatsu, S811 (FRI-037)
Ando, Wataru, S524 (THU-102)
Andrade, Raul J., S101 (THU-059-YI), S150 (SAT-475), S256 (SAT-542), S305 (SAT-260-YI), S542 (THU-164), S571 (WED-069)
Andrealli, Alida, S350 (SAT-421)
André-Dumont, Stéphanie, S541 (THU-156), S648 (SAT-151-YI)
Andreola, Fausto, S27 (OS-034), S171 (FRI-409-YI), S180 (FRI-434), S181 (FRI-435)
Andreone, Luz, S654 (SAT-171-YI)
Andreone, Pietro, S1 (GS-001), S69 (LBP-004-YI), S82 (LBP-034-YI), S295 (TOP-280), S304 (SAT-258), S307 (SAT-263), S328 (SAT-362), S341 (SAT-396), S957 (WED-577)
Andres-Rozas, Maria, S176 (FRI-421), S281 (TOP-296-YI)
Andreu, Laura, S603 (WED-163)
Andric, Zdravko, S800 (FRI-006)
Androutsakos, Theodoros, S314 (SAT-283)
Anémone, Lucie, S723 (THU-419)
Angelakis, Athanasios, S567 (WED-055-YI), S568 (WED-056), S620 (WED-212)
Ángel-Gomis, Enrique, S179 (FRI-431-YI)
Angelico, Roberta, S59 (OS-091)
Angelino, Fllippo, S784 (SAT-015-YI)
Angeli, Paolo, S30 (OS-041), S35 (OS-050-YI), S149 (SAT-468), S152 (SAT-478), S159 (SAT-505), S176 (FRI-425), S185 (TOP-455-YI), S190 (WED-425), S196 (WED-445), S210 (WED-485), S212 (WED-494-YI), S217 (WED-509-YI), S227 (WED-541-YI), S479 (WED-378), S515 (TOP-098), S583 (WED-101), S760 (TOP-032)
Angendohr, Carolin, S188 (WED-416)
Angrisani, Debora, S176 (FRI-425), S190 (WED-425), S212 (WED-494-YI), S479 (WED-378), S911 (SAT-587-YI)
Angrup, Archana, S227 (WED-541-YI)
Anikhindi, Shrihari Anil, S741 (THU-474)
Anim, Manfred, S878 (THU-585-YI)
Anirvan, Prajna, S204 (WED-466)
An, Jarvis Chia Kai, S529 (THU-115)
An, Jihyun, S428 (THU-226-YI), S497 (FRI-234), S506 (FRI-255-YI), S513 (FRI-378), S545 (THU-171), S591 (WED-122), S625 (WED-229), S630 (SAT-092), S652 (SAT-165), S686 (FRI-163), S723 (THU-418)
Ankoma-Sey, Victor, S10 (LBO-006)
Annamuhammedova, Tylla, S919 (SAT-608-YI)
Anne, Cypierre, S829 (THU-252)
Anné, Maxime, S149 (SAT-468), S152 (SAT-478), S214 (WED-499), S760 (TOP-032)
Annicchiarico, Brigida, S751 (THU-500)
Annicchiarico, Brigida Eleonora, S731 (THU-444-YI)
Annoni, Giuseppe, S848 (THU-304)
Anolli, Maria Paola, S43 (OS-066), S71 (LBP-009), S900 (SAT-559), S901 (SAT-560), S934 (TOP-582), S936 (TOP-584), S937 (FRI-585-YI), S938 (FRI-586), S942 (FRI-592), S942 (FRI-593)
An, Ping, S952 (FRI-623)
Ansa, Beñat Salegi, S275 (THU-322-YI)
Ansari, Zaid, S565 (WED-050)
An, Shuxian, S324 (SAT-318)
Anson, Maria, S343 (SAT-400)
Anstee, Quentin M., S29 (OS-038), S78 (LBP-024), S166 (FRI-393), S563 (WED-042), S597 (WED-141), S681 (FRI-142)
Antal-Szalmás, Péter, S347 (SAT-414-YI), S347 (SAT-415)
Antolín, Gloria Sánchez, S379 (FRI-459), S403 (FRI-532), S403 (FRI-533), S415 (FRI-575)
Antolini, Nicole, S853 (WED-282-YI)
Anton, Aina, S827 (TOP-297)
Antón, Ángela, S427 (THU-220)
Anton-Culver, Hoda, S536 (THU-136)
Antonenko, Antonina, S52 (OS-081), S720 (TOP-504-YI)
Antonini, Teresa, S311 (SAT-271), S380 (FRI-463), S381 (FRI-464), S742 (THU-477)
Antonio Diaz, Luis, S112 (FRI-051), S123 (FRI-085), S127 (FRI-095), S773 (THU-037)
Antonio, Orlando E Falcon, S730 (THU-442)
Antón, Maria Dolores, S948 (FRI-611)
Antunes, Francisco, S802 (FRI-010-YI)
Antunes, Inês Lopes, S802 (FRI-010-YI)
Antunes, Nuno, S75 (LBP-018), S319 (SAT-300), S329 (SAT-364), S341 (SAT-396)
Anty, Rodolphe, S681 (FRI-147), S742 (THU-477)
Anuntasainont, Moongmun, S121 (FRI-078)
An, Wei, S232 (FRI-307)
Anyebe, Evelyn, S559 (TOP-065-YI)
Aoki, Takahiro, S811 (FRI-037)
Aoyagi, Haruyo, S894 (THU-635), S894 (THU-637)
Aparicio, Anna Pocurull, S21 (OS-021), S46 (OS-070-YI), S65 (OS-101-YI), S91 (SAT-062), S256 (SAT-542), S828 (TOP-309-YI), S884 (THU-604-YI), S903 (SAT-562), S903 (SAT-563-YI), S941 (FRI-590), S948 (FRI-611)
Aparisi, Ana Sagrera, S101 (THU-059-YI)
Aparna, J, S706 (THU-544)
Apers, Jan, S688 (FRI-166-YI)
Apodaka-Biguri, Maider, S277 (THU-330-YI), S631 (SAT-095-YI)
Aponte, Ricardo Velázquez, S276 (THU-329)
Appiah, Erica, S568 (WED-057-YI)
Appleby, Victoria J., S404 (FRI-537)
Aquilano, Adelia, S825 (WED-037)
Aqul, Amal A., S850 (THU-308)

Arab, Juan Pablo, S20 (OS-019), S62 (OS-097), S112 (FRI-050), S123 (FRI-085), S127 (FRI-095), S424 (TOP-376), S516 (TOP-113), S532 (THU-125), S560 (TOP-066), S561 (TOP-082), S578 (WED-087), S579 (WED-089), S768 (THU-021)
Arachchi, Niranjan, S779 (SAT–004)
Aracil, Carlos, S735 (THU-453), S804 (FRI-019)
Arakawa, Mie, S662 (SAT-196)
Arama, Sorin Stefan, S951 (FRI-620), S974 (WED-633)
Arama, Victoria, S951 (FRI-620), S974 (WED-633)
Arambulo-Castillo, Sebastian, S745 (THU-483)
Arantxa Horga, Maria, S981 (FRI-636)
Arase, Yoshitaka, S708 (THU-553)
Aras, Siddharth, S7 (LBO-001)
Arate, Orfanel Pineda, S730 (THU-442)
Araujo, Joana Gonçalves, S457 (WED-236)
Araujo, Sofia, S379 (FRI-460)
Aravinthan, Aloysious, S24 (OS-028), S144 (SAT-452), S160 (SAT-507)
Arbet-Engels, Christophe, S19 (OS-016), S84 (LBP-036), S679 (TOP-176), S700 (FRI-201)
Arbogast, Sarah, S167 (FRI-394-YI)
Arbune, Manuela, S960 (WED-587)
Arcangeli, Annarosa, S457 (WED-235)
Arceo-Orozco, Scarlet, S235 (FRI-319), S481 (WED-384)
Archer, Ann, S69 (LBP-001), S725 (THU-427), S761 (THU-004)
Arcos, María del Mar, S806 (FRI-024)
Ardevol, Alba, S91 (SAT-062), S562 (TOP-097-YI)
Ardila, Andrea Moreno, S364 (WED-329-YI)
Ardiles, Thomas, S198 (WED-449), S204 (WED-467)
Arechederra, Maria, S17 (OS-013), S474 (WED-364)
Aregawi, Welde, S908 (SAT-576)
Arellano, Encarnación Ramirez, S910 (SAT-585)
Arena, Ilaria, S82 (LBP-034-YI), S938 (FRI-586)
Argemi, Josepmaria, S96 (SAT-079), S343 (SAT-400), S364 (WED-329-YI)
Argiento, Lorenzo, S55 (OS-085-YI), S428 (THU-227-YI), S494 (FRI-225)
Argirò, Renato, S726 (THU-429)
Argyrou, Alexandra, S545 (THU-172)
Århem, Katarina, S903 (SAT-561)
Arias, Ana, S59 (OS-091), S409 (FRI-557), S410 (FRI-558)
Aricha, Revital, S334 (SAT-371), S334 (SAT-372), S334 (SAT-377)
Ari, Derya, S899 (SAT-556-YI)
Arif, Hira, S262 (SAT-330)
Arif, Maaz, S531 (THU-122)
Arif, Sania, S261 (SAT-329-YI), S262 (SAT-330)
Arif, Waqar, S38 (OS-055)
Arinde, Folake, S820 (WED-022)
Ario, Keisuke, S258 (SAT-549), S550 (THU-188), S979 (WED-644)
Arisoylu, Meliz Sahuri, S139 (FRI-133)
Aristu, Peio, S176 (FRI-421)
Ariza, Xavier, S91 (SAT-062)
Arıkan, Cigdem, S55 (OS-086), S831 (THU-258-YI), S842 (THU-284), S850 (THU-308)
Armandi, Angelo, S476 (WED-368), S517 (TOP-114), S525 (THU-103), S534 (THU-133), S558 (TOP-063-YI), S574 (WED-073), S589 (WED-118), S607 (WED-174-YI), S611 (WED-184-YI), S620 (WED-213), S733 (THU-450)
Armendariz-Borunda, Juan, S132 (FRI-108-YI), S235 (FRI-319)
Armendáriz-Borunda, Juan S., S481 (WED-384)
Armengol, Carolina, S489 (WED-412-YI)
Armentano, Ricardo, S728 (THU-434)
Armenteros, Ines, S806 (FRI-024)
Armisen, Javier, S2 (GS-003)
Armstrong, Matthew, S61 (OS-108), S64 (OS-100)
Arnal, Nancy, S723 (THU-419)
Arnedo-Pac, Claudia, S455 (TOP-405)
Arnell, Henrik, S55 (OS-086), S831 (THU-258-YI), S842 (THU-284), S850 (THU-308)
Arnold, Timothy, S96 (SAT-083)
Aroca, Maria, S910 (SAT-585)
Aroori, Somaiah, S164 (FRI-385-YI), S184 (FRI-453-YI)
Arora, Anil, S24 (OS-028), S67 (OS-105-YI), S375 (TOP-518), S952 (FRI-622)
Arora, Anish, S774 (THU-040), S774 (THU-041)
Arora, Jantarika, S370 (WED-347), S888 (THU-618)
Arora, Riya, S555 (THU-206)
Arora, Umang, S375 (TOP-518)
Arora, Vinod, S108 (TOP-208-YI), S156 (SAT-495), S157 (SAT-498), S719 (TOP-487-YI), S952 (FRI-622)
Arosio, Marco, S817 (WED-010), S919 (SAT-608-YI)
Arpurt, Jean-Pierre, S43 (OS-066), S934 (TOP-582), S937 (FRI-585-YI)
Arrese, Marco, S2 (GS-003), S62 (OS-097), S112 (FRI-050), S127 (FRI-095), S141 (TOP-437), S160 (SAT-507), S303 (SAT-257-YI), S516 (TOP-113), S766 (THU-015), S768 (THU-021), S790 (SAT-036)
Arribas, Victor, S806 (FRI-024)
Arribi, Ana, S910 (SAT-585)
Arrieta, Betty Morales, S556 (THU-212)
Arrogante, Collen Ray, S746 (THU-485)
Arroyo-López, Victor, S571 (WED-069)
Arroyo, Vicente, S8 (LBO-002), S34 (OS-049), S35 (OS-050-YI), S141 (TOP-437), S148 (SAT-467-YI), S170 (FRI-401-YI)
Arroyo, Yoana, S174 (FRI-416-YI)
Arruga, Francesca, S835 (THU-263)
Arslanow, Anita, S63 (OS-098-YI), S608 (WED-180)
Arteaga, Ane, S830 (THU-253)
Arteaga, Íngrid, S63 (OS-098-YI), S608 (WED-180)
Arterburn, Sarah, S957 (WED-578), S958 (WED-580)
Arteta, Beatriz, S277 (THU-330-YI)
Artola, Vicente, S600 (WED-153)
Artru, Florent, S143 (SAT-450), S207 (WED-477), S388 (FRI-485), S497 (FRI-234), S742 (THU-477)
Artzner, Thierry, S149 (SAT-468), S152 (SAT-478), S380 (FRI-463), S381 (FRI-464), S388 (FRI-485), S760 (TOP-032)
Arumugam, Manimozhiyan, S115 (FRI-057), S145 (SAT-458-YI), S148 (SAT-467-YI), S261 (SAT-329-YI)
Arumugam, Suyavaran, S659 (SAT-187)
Arunachalam, Vinayagam, S847 (THU-300), S848 (THU-301)
Arunakumar, Bhavanaa, S139 (FRI-133)
Arun, Pudhiavan, S780 (SAT-005)
Arustamyan, Garnik, S277 (THU-331)
Arvaniti, Pinelopi, S300 (SAT-250), S308 (SAT-264), S317 (SAT-290-YI), S318 (SAT-291), S336 (SAT-380), S337 (SAT-382), S338 (SAT-383), S828 (TOP-309-YI)
Arya, Deepa, S682 (FRI-148)
Asaad, Imad, S684 (FRI-154)
Asadipour, Erfan, S687 (FRI-165)
Asahina, Yasuhiro, S506 (FRI-256), S977 (WED-639)
Ascah, Alexis, S655 (SAT-172)
Ascari, Francesco, S746 (THU-490)
Ascari, Sara, S429 (THU-227-YI)
Aseem, Sayed Obaidullah, S342 (SAT-398)
Aselmann, Heiko, S105 (THU-072)
Asem, Bobby, S964 (WED-597)
Asenbaum, Ulrika, S199 (WED-452)
Asensio, Iris, S182 (FRI-442), S267 (SAT-350)
Asensio, Julia Peña, S366 (WED-332-YI)
Asensio, Maitane, S281 (TOP-296-YI), S489 (WED-412-YI)
Asero, Clelia, S163 (FRI-382), S196 (WED-445), S223 (WED-527), S435 (THU-245), S967 (WED-605-YI)
Asgarian, Sam, S259 (SAT-553)
Asgharpour, Amon, S525 (THU-103), S558 (TOP-063-YI), S578 (WED-087), S589 (WED-118), S602 (WED-158), S607 (WED-174-YI), S615 (WED-196)
Ashdown, Thomas, S839 (THU-272)
Ashraf, Afreen, S569 (WED-058-YI)
Ashraf, Anzar, S847 (THU-299)
Ashraf, Muhammad, S81 (LBP-030)
Ashton, Alexa, S333 (SAT-370)

Author Index

Asif, Ayma, S363 (WED-321-YI)
Asif-Laidin, Amna, S457 (WED-236)
Asisha Janeela, M, S722 (THU-416)
Askari, Fred, S39 (OS-057), S846 (THU-291), S846 (THU-298)
Askgaard, Gro, S116 (FRI-060), S775 (THU-042-YI)
Asllanaj, Eralda, S796 (SAT-052)
Asmamaw, Asegedech, S798 (TOP-048)
Aso, Kenta, S492 (FRI-219)
Aspichueta, Patricia, S241 (FRI-339), S277 (THU-330-YI), S542 (THU-164), S632 (SAT-095-YI)
Aspinall, Richard, S329 (SAT-363), S564 (WED-044), S565 (WED-045)
Aspite, Silvia, S3 (GS-005), S746 (THU-489)
Aspord, Caroline, S885 (THU-607)
Asquith, Darren, S75 (LBP-018), S319 (SAT-300), S329 (SAT-364), S341 (SAT-396)
Asrani, Sumeet, S24 (OS-028), S144 (SAT-452), S154 (SAT-490), S160 (SAT-507), S166 (FRI-393)
Assadrati, Lina, S353 (SAT-432)
Assawasuwannakit, Suraphon, S219 (WED-514)
Asselah, Tarik, S1 (GS-001), S7 (GS-012), S49 (OS-075), S897 (TOP-565), S928 (SAT-628-YI), S939 (FRI-587), S956 (TOP-598), S956 (WED-576), S958 (WED-581), S962 (WED-593), S962 (WED-594)
Asselin, Jason, S799 (FRI-004), S800 (FRI-005)
Asselta, Rosanna, S282 (FRI-263)
Assenat, Eric, S414 (FRI-572)
Assen, Frank, S284 (FRI-266)
Asseri, Mushabbab K, S522 (THU-095)
Assis, David N., S331 (SAT-368-YI)
Asswini, Salwa, S524 (THU-101)
Assy, Nimer, S10 (LBO-006)
Astbury, Stuart, S106 (THU-076)
Astono, Julie, S569 (WED-059), S579 (WED-089), S592 (WED-131), S593 (WED-134), S616 (WED-199), S623 (WED-219)
Åström, Hanne, S570 (WED-060-YI)
Atalla, Ahmed, S713 (WED-555)
Atallah, Edmond, S41 (OS-060)
Atay, Beyza, S348 (SAT-417)
Ateba, Noel Simon, S879 (THU-589-YI)
Atef, Mira, S551 (THU-191)
Atef, Remon, S537 (THU-141-YI)
Athanasaki, Florentia, S142 (SAT-449), S187 (WED-415)
Athanasoulas, Georgios, S157 (SAT-497)
Athwal, Varinder, S84 (LBP-038)
Atkinson, Elizabeth, S13 (OS-006-YI)
Atkinson, Stephen, S47 (OS-072), S125 (FRI-090-YI)
Atkinson, Stephen R., S137 (FRI-125)
Atorrasagasti, Catalina, S358 (THU-340-YI)
Atorrasagasti, María Catalina, S654 (SAT-171-YI)
Atsukawa, Masanori, S960 (WED-587)
Attalla, Patrik, S222 (WED-524), S914 (SAT-591)
Attanasi, Michael, S337 (SAT-381)
Attia, Heba, S263 (SAT-333)
Attia, Yasmeen, S630 (SAT-091)
Aubakirova, Alma, S822 (WED-027)
Aubé, Christophe, S540 (THU-155), S554 (THU-202)
Augé, Anea, S143 (SAT-450)
Augustin, Jeremy, S38 (OS-054)
Augustin, Salvador, S689 (FRI-170)
Auh, Sungyoung, S918 (SAT-604)
Aujla, Usman, S845 (THU-289)
Aumar, Madeleine, S55 (OS-086), S831 (THU-258-YI), S842 (THU-284)
Aurell, Malin, S690 (FRI-172)
Auriemma, Alessandra, S424 (TOP-375-YI), S514 (FRI-381)
Avades, Tamar, S709 (THU-556-YI)
Avagliano, Jessica, S595 (WED-138)
Avaiarasi, Yazhini, S50 (OS-077)
Avanesyan, Lia, S871 (THU-560-YI)
Avihingsanon, Anchalee, S47 (OS-072)
Avila, Matías A, S17 (OS-013), S474 (WED-364), S477 (WED-370), S489 (WED-412-YI), S654 (SAT-171-YI)
Avila, Matías A., S272 (THU-315-YI)
Avram, Raluca, S210 (WED-490)
Awad, Karem, S251 (SAT-527)
Awad, Reham Awad, S537 (THU-141-YI)
Awoniyi, Muyiwa, S10 (LBO-006)
Axelrod, David, S220 (WED-521)
Axelrod, Jonathan, S234 (FRI-318)
Axling, Ulrika, S39 (OS-056)
Ayares, Gustavo, S112 (FRI-050)
Ayav, Ahmet, S37 (OS-052)
Aydemir, Şöhret, S397 (FRI-514)
Aydın, Rıfat, S519 (THU-089)
Aye, Lydia, S125 (FRI-091), S393 (FRI-505), S775 (THU-043)
Ayonrinde, Oyekoya, S699 (FRI-198), S713 (WED-557)
Ayoub, Walid, S10 (LBO-006)
Ayres, Natalia, S724 (THU-420)
Ayurzana, Munkhjargal, S923 (SAT-618)
Azaz, Amer, S55 (OS-086), S831 (THU-258-YI), S842 (THU-284)
Azcona, José Manuel, S910 (SAT-581)
Azhati, Yilizhati, S243 (FRI-348)
Aziz, Ayisha, S713 (WED-555)
Aziz, Fatima, S394 (FRI-508), S407 (FRI-547)
Aziz, Justine, S60 (OS-094)
Aziz, Ramy, S263 (SAT-333)
Aziz Shaheen, Abdel, S787 (SAT-026), S788 (SAT-027)
Azjargal, Batjargal, S48 (OS-074)
Azkargorta, Mikel, S272 (THU-315-YI), S273 (THU-316), S483 (WED-388-YI)
Aznar-Benitah, Salvador, S634 (SAT-103)
Aznou, Anouar, S632 (SAT-099-YI)
Azouzi, Nael, S38 (OS-054)
Azzam, Ali, S254 (SAT-537)
Azzaroli, Francesco, S69 (LBP-004-YI), S304 (SAT-258), S307 (SAT-263), S335 (SAT-378-YI), S337 (SAT-382)
Azzu, Vian, S682 (FRI-148), S690 (FRI-172)

Baak, L.C., S443 (THU-382-YI)
Baars, Daniël, S632 (SAT-099-YI)
Babakhani, Shiva, S491 (TOP-408-YI)
Bablon, Pierre, S887 (THU-612-YI)
Babu, Rosmy, S189 (WED-419), S418 (THU-517-YI)
Baccino, Sara, S71 (LBP-009), S340 (SAT-393)
Bacete, Susana, S806 (FRI-024)
Bacha, Mustapha Hacine, S823 (WED-028)
Bach, Charlotte, S875 (THU-572)
Bächer, Johannes, S871 (THU-558-YI)
Bacher, Petra, S372 (WED-350)
Backhed, Fredrik, S2 (GS-002)
Backman, Jens, S606 (WED-173)
Badenas, Celia, S828 (TOP-309-YI)
Bader, Razan, S250 (SAT-523), S390 (FRI-494), S390 (FRI-495)
Badia-Aranda, Esther, S250 (SAT-524)
Badiali, Sara, S662 (SAT-198-YI)
Badia, Lorenzo, S947 (FRI-608)
Badikol, Shrikar Reddy, S204 (WED-467)
Badlah, Hana, S477 (WED-369)
Badr, Yasser, S263 (SAT-333)
Bae, Jungjun, S974 (WED-628)
Baekelandt, Aline, S464 (WED-253)
Baek, Geum Ok, S264 (SAT-337)
Baena, Pilar Barrera, S303 (SAT-256-YI)
Bae, Songmee, S891 (THU-625)
Bager, Cecilie, S592 (WED-131)
Bager, Palle, S703 (THU-527-YI)
Baguley, Elizabeth, S525 (THU-104-YI)
Bah, Ousman, S764 (THU-012), S798 (TOP-034)
Baier-Grabner, Sebastian, S975 (WED-634-YI)
Bai, Geng-Hao, S426 (THU-218)
Baiges, Anna, S6 (GS-011-YI), S33 (OS-046), S53 (OS-082), S54 (OS-084), S397 (FRI-515), S719 (TOP-488), S723 (THU-418), S730 (THU-443), S747 (THU-492), S752 (THU-501)
Bai, Honglian, S33 (OS-047)
Bai, Hui, S107 (THU-077), S270 (TOP-328), S276 (THU-323)
Bai, Jiang, S549 (THU-184)
Baik, Soon Koo, S133 (FRI-111), S360 (THU-352)
Bailly, Francois, S311 (SAT-271)
Bailly, Sébastien, S762 (THU-009)
Baiocchi, Leonardo, S49 (OS-076-YI), S304 (SAT-258), S307 (SAT-263), S335 (SAT-378-YI), S726 (THU-429), S807 (FRI-025), S919 (SAT-608-YI)
Baiocchini, Andrea, S477 (WED-370), S856 (WED-291)
Baisley, Kathy, S900 (SAT-558)
Bai, Wenjia, S490 (TOP-407-YI)
Bai, Xuefan, S932 (SAT-641)

Bai, Yang, S884 (THU-605)
Bai, Yixin, S139 (FRI-134)
Bajaj, Jasmohan, S24 (OS-028), S41 (OS-061), S116 (FRI-061), S130 (FRI-103), S143 (SAT-451), S144 (SAT-452), S149 (SAT-468), S152 (SAT-478), S160 (SAT-507), S188 (WED-417), S190 (WED-421), S197 (WED-447), S214 (WED-499), S754 (THU-509), S760 (TOP-032)
Bajaj, Jasmohan S., S8 (LBO-002)
Bajpai, Meenu, S373 (WED-353-YI)
Bajri, Hazim, S566 (WED-053)
Bajunayd, Amani, S379 (FRI-461-YI)
Baker, Fadi Abu, S10 (LBO-006), S247 (SAT-513), S251 (SAT-527), S316 (SAT-288), S317 (SAT-289), S613 (WED-189), S913 (SAT-590)
Baker, John, S79 (LBP-027)
Baker, Olivia, S709 (THU-556-YI)
Bakieva, Shokhista, S74 (LBP-016)
Bakker, Sjoerd, S15 (OS-009-YI)
Bakker, Stephan J.L., S384 (FRI-476-YI), S384 (FRI-477), S385 (FRI-478)
Bakowski, Daniel, S639 (SAT-119)
Bakszt, Erica Wajntraub, S709 (THU-555-YI)
Bakulin, Igor, S693 (FRI-182)
Balaban, Yasemin, S348 (SAT-417)
Balabek, Aliya, S967 (WED-608)
Balachandran, Pooja, S187 (TOP-471-YI)
Balaji, KavithaPh.D, S781 (SAT-008), S781 (SAT-009)
Balaraja, S., S81 (LBP-030)
Balari, Tomàs, S394 (FRI-507-YI), S724 (THU-421), S804 (FRI-019)
Balaseviciute, Ugne, S453 (TOP-389), S459 (WED-242-YI)
Balasingam, Thinesh Edward, S714 (WED-559-YI)
Balassone, Jacqueline, S739 (THU-466)
Balavarca, Yesilda, S688 (FRI-168)
Balcar, Lorenz, S37 (OS-053), S55 (OS-085-YI), S97 (SAT-084-YI), S113 (FRI-053), S156 (SAT-494), S179 (FRI-432), S183 (FRI-444-YI), S183 (FRI-445), S186 (TOP-470-YI), S195 (WED-442-YI), S199 (WED-451-YI), S199 (WED-452), S200 (WED-453), S205 (WED-474), S213 (WED-498), S216 (WED-508), S217 (WED-509-YI), S222 (WED-524), S426 (THU-219-YI), S427 (THU-220), S427 (THU-221), S440 (THU-370), S715 (WED-560-YI), S720 (TOP-504-YI), S732 (THU-448-YI), S733 (THU-449), S734 (THU-451), S739 (THU-467), S748 (THU-493-YI), S749 (THU-494), S750 (THU-498), S753 (THU-505-YI), S914 (SAT-591)
Baldassarre, Maurizio, S185 (TOP-455-YI)
Balderramo, Domingo, S303 (SAT-257-YI), S445 (THU-385)
Baldin, Camila Pereira, S776 (THU-044)
Baldini, Marta, S82 (LBP-034-YI)
Baldin, Pamela, S55 (OS-085-YI), S648 (SAT-151-YI)
Balducci, Daniele, S741 (THU-473)
Balemurughan, Niveda, S386 (FRI-482), S411 (FRI-561-YI), S413 (FRI-570)
Balfe, Peter, S87 (LBP-043)
Baliellas, Carme, S394 (FRI-507-YI)
Bali, Maria, S348 (SAT-416)
Balistreri, William, S40 (OS-058)
Balkhed, Wile, S568 (WED-056)
Ballerga, Esteban Gonzalez, S296 (TOP-281), S302 (SAT-253), S306 (SAT-262)
Ballester, María Pilar, S33 (OS-046), S54 (OS-084), S150 (SAT-475), S170 (FRI-401-YI), S189 (WED-418), S747 (THU-492), S752 (THU-501)
Ballester, Pura, S863 (WED-317)
Ballet, Fleur, S65 (OS-101-YI), S903 (SAT-562)
Balló, Elisabet, S810 (FRI-036)
Balogh, Boglarka, S332 (SAT-369)
Balsano, Clara, S530 (THU-117), S767 (THU-020)
Balusson, Frederic, S762 (THU-009)
Balzac, Edwige-Ludiwyne, S573 (WED-072), S613 (WED-190)
Banales, Jesus M, S165 (FRI-387-YI), S286 (FRI-273), S303 (SAT-257-YI), S323 (SAT-315), S445 (THU-385), S483 (WED-388-YI), S484 (WED-393)
Banales, Jesus M., S277 (THU-330-YI)
Banales, Jesus Maria, S485 (WED-395-YI)
Bañares, Juan, S227 (WED-541-YI)
Bañares, Rafael, S35 (OS-050-YI), S132 (FRI-109), S182 (FRI-442), S267 (SAT-350), S427 (THU-220), S515 (TOP-098), S583 (WED-101), S642 (SAT-131-YI), S678 (SAT-244)
Bandera, Alessandra, S865 (FRI-638)
Bandera, Jose Pinazo, S256 (SAT-542), S837 (THU-267), S855 (WED-289)
Bandi, Juan, S97 (SAT-085)
Bandi, Juan Carlos, S337 (SAT-382)
Bandmann, Oliver, S859 (WED-304)
Banerjee, Abhishek, S786 (SAT-023)
Banerjee, Aniruddha, S145 (SAT-453)
Banica, Leontina, S807 (FRI-025)
Banica, Thiberiu, S807 (FRI-025), S907 (SAT-575)
Bani, Daniele, S457 (WED-235)
Bank, Matthew, S391 (FRI-496)
Bannasch, Johannes, S866 (FRI-639)
Bannas, Peter, S213 (WED-496)
Banovcin, Peter, S211 (WED-492)
Bansal, Kalpana, S217 (WED-510)
Bansal, Meena, S20 (OS-019), S559 (TOP-064), S590 (WED-120), S682 (FRI-149)
Bansal, Puneet, S399 (FRI-522)
Bantel, Heike, S14 (OS-007), S601 (WED-155), S836 (THU-265-YI)
Bañuls, Sergio Reus, S904 (SAT-564)
Bao, Yufan, S881 (THU-592-YI)
Bapaye, Amol, S741 (THU-474)
Baptista, Anthony, S458 (WED-237-YI)
Baragiotta, Anna Maria, S335 (SAT-378-YI)
Barakat, Fatma, S198 (WED-449), S713 (WED-555)
Barakeh, Duna, S521 (THU-092), S521 (THU-093)
Barange, Karl, S43 (OS-066), S934 (TOP-582), S937 (FRI-585-YI)
Baranovičová, Eva, S211 (WED-492)
Barba, Romelia, S327 (SAT-322)
Barbe, Margaux, S720 (TOP-504-YI)
Barbero, Manuel, S296 (TOP-281), S306 (SAT-262)
Barbero, Roberto, S17 (OS-013)
Barbet, Funda Yılmaz, S397 (FRI-514)
Barbiero, Giulio, S33 (OS-046), S747 (THU-492)
Barbier, Olivier, S301 (SAT-251-YI)
Barbosa, Helena, S671 (SAT-226)
Barbosa, Joana Sofia Vieira, S199 (WED-450)
Barbosa, João, S29 (OS-038), S268 (SAT-351)
Barca-Mayo, Olga, S272 (THU-315-YI), S273 (THU-316)
Barceló, Maria Inés, S223 (WED-528)
Barciela, Mar Riveiro, S16 (OS-010), S91 (SAT-062), S294 (TOP-278), S300 (SAT-250), S309 (SAT-268), S317 (SAT-290-YI), S337 (SAT-382), S798 (TOP-048), S908 (SAT-577), S926 (SAT-623), S948 (FRI-611), S949 (FRI-612)
Barclay, Stephen, S814 (WED-004)
Barda, Beatrice, S570 (WED-061)
Bardak, Ali Emre, S727 (THU-430)
Bardou-Jacquet, Edouard, S143 (SAT-450), S343 (SAT-400), S849 (THU-305-YI)
Baretti, Marina, S38 (OS-055), S491 (TOP-408-YI)
Barkaoui, Emna, S55 (OS-086), S831 (THU-258-YI), S842 (THU-284)
Barkun, Jeffrey, S380 (FRI-462)
Barnés, Isabel, S826 (WED-038)
Barnes, Katie, S75 (LBP-017)
Barnet, Scott, S966 (WED-604)
Barnett, Tamara, S968 (WED-609-YI)
Barnhill, Michele S., S390 (FRI-493-YI), S416 (FRI-576)
Baroja, Alberto, S59 (OS-091)
Baron, Aurore, S762 (THU-009), S829 (THU-252)
Barone, Michele, S912 (SAT-587-YI)
Baroni, Gianluca Svegliati, S576 (WED-083)
Baron, Jody, S871 (THU-560-YI)
Barquero-Pérez, Oscar, S968 (WED-610-YI)
Barrable, Fraser, S946 (FRI-605)
Barranco-Fragoso, Beatriz, S771 (THU-030)
Barranco, Kiomi, S802 (FRI-010-YI)
Barrancotto, Alessio, S720 (TOP-502-YI)
Barraud, Hélène, S143 (SAT-450)
Barreby, Emelie, S71 (LBP-008)
Barreca, Federica, S177 (FRI-427)

Author Index

Barreira, Ana, S309 (SAT-268)
Barrenechea-Barrenechea, Jon Ander, S272 (THU-315-YI), S633 (SAT-101-YI), S855 (WED-287-YI)
Barrera, Francisco, S112 (FRI-050)
Barre, Tangui, S889 (THU-619)
Barreto-Anchury, Laura Paola, S250 (SAT-524)
Barreto, Ismael de Jesus Yepes, S556 (THU-212), S625 (WED-228), S793 (SAT-044)
Barreto, Miller, S701 (FRI-203-YI)
Barrett, Rachael, S559 (TOP-065-YI)
Barrio, María Del, S16 (OS-010), S294 (TOP-278), S585 (WED-106), S828 (TOP-309-YI), S833 (THU-259)
Barrios, Monica, S131 (FRI-104)
Barroso, Emma, S231 (FRI-304), S241 (FRI-341), S271 (THU-303), S279 (THU-335)
Barry, Matthew McKenna, S255 (SAT-540)
Barsch, Maryam, S504 (FRI-251)
Barsukova, Natalia, S49 (OS-075), S962 (WED-594)
Bartelink, Maartje, S15 (OS-009-YI)
Bartholomä, Wolf, S220 (WED-517)
Bartke, Lena, S763 (THU-010)
Bartlett, Sofia, S821 (WED-024), S967 (TOP-600-YI), S968 (WED-609-YI)
Bartoli, Montse, S810 (FRI-035)
Bartolo, Gema Muñoz, S831 (THU-258-YI), S842 (THU-284)
Bartolomeo, Claudia Di, S570 (WED-061)
Barton, Alexander, S204 (WED-465), S744 (THU-482-YI)
Bartosch, Birke, S871 (THU-559-YI)
Bartrolí, Berta, S837 (THU-267), S855 (WED-289)
Barutcu, Sezgin, S160 (SAT-507)
Basak, Trayambak, S180 (FRI-433)
Başarır, Elif, S519 (THU-089)
Bashiri, Kiandokht, S363 (WED-322)
Basile, Claudio, S444 (THU-384), S532 (THU-123), S549 (THU-186-YI), S660 (SAT-190), S854 (WED-286)
Basili, Graziella, S856 (WED-291)
Basili, Stefania, S731 (THU-445-YI)
Basiliya, Kirill, S729 (THU-436)
Baskar, Lakshmi, S647 (SAT-149)
Bassegoda, Octavi, S562 (TOP-097-YI)
Bassi, Cristian, S462 (WED-248)
Bassi, Domenico, S402 (FRI-530)
Bastarache, Lisa, S166 (FRI-393)
Bästlein, Elke, S945 (FRI-602-YI)
Basu, Priyadarshi, S659 (SAT-186)
Batakis, Danielle, S690 (FRI-173)
Bataller, Ramon, S191 (WED-426)
Batbayar, Bilguun, S826 (WED-039)
Batbold, Enkhtuul, S871 (THU-559-YI)
Bates, Laurel, S817 (WED-012)
Bathon, Melanie, S488 (WED-409-YI)
Batmunkh, Munkhbat, S127 (FRI-095), S923 (SAT-618)
Batool, Sarah, S564 (WED-044), S565 (WED-045)
Batouxas, Cristiana Margarida Fernandes, S940 (FRI-589)
Batsuli, Nefer, S80 (LBP-028-YI)
Battaglia, Antonio, S163 (FRI-382)
Battezati, Piermaria, S975 (WED-635)
Battezzati, Pier Maria, S82 (LBP-034-YI)
Battinelli, Giovanni, S725 (THU-425), S746 (THU-490)
Battistella, Sara, S821 (WED-023), S884 (THU-604-YI), S903 (SAT-563-YI), S928 (SAT-628-YI), S941 (FRI-590)
Bätz, Olaf, S600 (WED-154-YI)
Bauer, David, S717 (WED-569-YI), S748 (THU-493-YI), S749 (THU-494), S975 (WED-634-YI)
Bäuerle, Tobias, S503 (FRI-248)
Bauer, Paulina, S206 (WED-475)
Baumann, Cédric, S37 (OS-052)
Baumann, Ulrich, S834 (THU-260)
Baumert, Thomas, S272 (THU-315-YI), S463 (WED-250), S875 (THU-572)
Baumgarten, Axel, S904 (SAT-564)
Baumgartner, Maximilian, S37 (OS-053)
Baumgartner, Ruth, S71 (LBP-008)
Baum, Seth, S682 (FRI-149)
Baur, Joseph, S276 (THU-329)
Bauschen, Alina, S151 (SAT-477), S181 (FRI-436)
Bausela, Alex, S312 (SAT-273)
Baven-Pronk, Martine A. M. C., S352 (SAT-429)
Baven-Pronk, Martine A.M.C., S15 (OS-009-YI)
Baweja, Sukriti, S108 (TOP-208-YI), S126 (FRI-092-YI), S361 (THU-354), S650 (SAT-157-YI)
Bayameen, Abdulraheem M., S522 (THU-094)
Bayayana, Elysée, S80 (LBP-028-YI)
Bayram, Gözde Kart, S348 (SAT-417)
Bayramov, Nuru, S59 (OS-091)
Bay-Richter, Cecilie, S631 (SAT-094-YI), S660 (SAT-188-YI)
Bazargan, Leila, S64 (OS-099), S596 (WED-140)
Bazille, Celine, S38 (OS-054)
Beaufrère, Aurélie, S38 (OS-055), S480 (WED-380)
Becchetti, Chiara, S3 (GS-005), S52 (OS-081), S379 (FRI-461-YI)
Bech, Katrine Tholstrup, S26 (OS-032-YI), S63 (OS-098-YI), S110 (FRI-041-YI), S554 (THU-204), S608 (WED-180), S706 (THU-545-YI)
Becht, Etienne, S480 (WED-380)
Becker, Diana, S651 (SAT-158-YI), S854 (WED-285)
Becker-Drepps, Sylvia, S80 (LBP-028-YI)
Becker, Felix, S409 (FRI-556)
Becker, Soeren, S265 (SAT-338)
Beckers, Pablo, S907 (SAT-575)
Beck, Katharina, S2 (GS-002)
Beckmann, Sonja, S710 (TOP-536-YI)
Bednarsky, Raphael, S362 (TOP-325-YI)
Bedossa, Pierre, S608 (WED-179)
Bedoya, José Ursic, S90 (SAT-059), S110 (FRI-042), S387 (FRI-484)
Bedrava, Jenna, S450 (THU-402)
Bee Goh, George Boon, S62 (OS-097)
Beer, Daniel, S904 (SAT-564)
Beetz, Nick-Lasse, S154 (SAT-489)
Begali, Hanan, S878 (THU-585-YI)
Beganovic, Lina, S692 (FRI-180)
Begovac, Josip, S807 (FRI-025)
Behary, Jason, S218 (WED-513), S749 (THU-496)
Behera, Partha Sarathi, S204 (WED-466)
Behlim, Tarannum, S377 (FRI-451)
Behrendt, Patrick, S737 (THU-462), S864 (TOP-615), S866 (FRI-641), S887 (THU-611), S887 (THU-613)
Behruznia, Mahboobeh, S364 (WED-324-YI)
Behuhuma, Ngundu O, S900 (SAT-558)
Beigelman, Leonid, S879 (THU-587), S889 (THU-620)
Beilin, Lawrence, S699 (FRI-198)
Beilmann-Lehtonen, Ines, S376 (FRI-447)
Bejarano-Jurado, Carmen, S678 (SAT-244)
Bekal, Pradeep, S680 (FRI-141)
Bekkering, Frank C., S353 (SAT-433)
Bektas, Hicran, S704 (THU-538-YI)
Belal, Mohamed Mohamed, S208 (WED-482)
Belanger, Bruce, S981 (FRI-635), S981 (FRI-636)
Belgardt, Bengt, S672 (SAT-230)
Belin, Bryana, S337 (SAT-381)
Bell, Adam, S80 (LBP-029)
Bella, Martina Dalla, S576 (WED-083), S741 (THU-473), S751 (THU-500), S938 (FRI-586)
Bellanti, Francesco, S69 (LBP-004-YI), S304 (SAT-258), S307 (SAT-263), S335 (SAT-378-YI)
Bell, Eric, S281 (FRI-260), S282 (FRI-261), S863 (WED-318)
Bellersheim, Leonard, S366 (WED-333-YI), S458 (WED-237-YI)
Belli, Luca Saverio, S379 (FRI-461-YI), S912 (SAT-587-YI)
Bell, James, S224 (WED-530)
Bellón, José, S904 (SAT-564)
Belloum, Adel, S693 (FRI-181)
Bell, Sally, S218 (WED-513), S707 (THU-546-YI), S749 (THU-496)
Bellue, Astrid Laurent, S38 (OS-054), S399 (FRI-523)
Belmiro, João, S186 (TOP-470-YI)
Belmonte, Isabel, S806 (FRI-024)
Belotti, Alessia, S331 (SAT-368-YI)
Belous, Andrey, S67 (OS-106)
Belzunce, Miriam, S17 (OS-013)
Bem, Kelly, S671 (SAT-226)
Benatti, Martina, S304 (SAT-258)
Bencardino, Katia, S494 (FRI-225)

Bender, Dirk, S290 (FRI-287)
Benderrou, Mouhssine, S578 (WED-086)
Bendosenko, Tatyana, S594 (WED-135)
Bendtsen, Kristian, S646 (SAT-142)
Benedetti, Antonio, S741 (THU-473)
Benedetto, Fabrizio Di, S378 (FRI-458)
Benedé-Ubieto, Raquel, S132 (FRI-109), S642 (SAT-131-YI)
Benedicto, Ignacio, S182 (FRI-442), S267 (SAT-350)
Benedittis, Carla De, S69 (LBP-004-YI), S831 (THU-256-YI)
Bengsch, Bertram, S51 (OS-080-YI), S363 (TOP-326), S455 (TOP-406), S504 (FRI-251)
Bengtsson, Bonnie, S709 (THU-555-YI)
Benitez, Carlos, S35 (OS-050-YI), S160 (SAT-507)
Benitez, Laura, S409 (FRI-557)
Benítez-Paredes, Núria, S234 (FRI-316)
Benke, Dominik, S865 (FRI-638)
Benkoe, Tamas, S59 (OS-092-YI)
Benkoova, Brigita, S807 (FRI-025)
Benlloch, Salvador, S254 (SAT-538), S542 (THU-164), S567 (WED-054), S599 (WED-151)
Benmassaoud, Amine, S380 (FRI-462), S533 (THU-127-YI), S616 (WED-200), S757 (THU-516)
Bennett, Alice, S709 (THU-556-YI)
Bennett, Carla, S839 (THU-272)
Bensenane, Mouni, S37 (OS-052)
Ben-Shabat, Michal Hoffman, S741 (THU-475)
Bentow, Chelsea, S342 (SAT-399)
Benyahia, Siham, S235 (FRI-320)
Beo, Vincent Di, S815 (WED-005), S889 (THU-619)
Bera, Chinmay, S547 (THU-179)
Beragdar, Mashhoor, S522 (THU-094)
Beranrd-Chabert, Brigitte, S435 (THU-246)
Berardino, Maurizio, S90 (SAT-061-YI)
Berasain, Carmen, S17 (OS-013), S474 (WED-364)
Beraza, Naiara, S42 (OS-064-YI), S286 (FRI-271), S287 (FRI-274)
Berber, Beren, S399 (FRI-522)
Berenguer, Juan, S904 (SAT-564)
Berenguer, Marina, S39 (OS-057), S59 (OS-091), S150 (SAT-475), S408 (FRI-553), S837 (THU-267), S840 (THU-275), S855 (WED-289)
Beretta, Marisa, S55 (OS-086), S831 (THU-258-YI), S842 (THU-284), S850 (THU-308)
Beretta-Piccoli, Benedetta Terziroli, S331 (SAT-368-YI), S863 (WED-317)
Bergamin, Giulia, S407 (FRI-548)
Bergamo, Francesca, S435 (THU-247)
Berg, Christoph P., S10 (LBO-006), S14 (OS-007), S930 (SAT-636)
Berger, Hilmar, S285 (FRI-269), S293 (FRI-301)
Bergerson, Jenna, S835 (THU-264-YI)
Berger, Victoria, S426 (THU-219-YI)
Berggren, Per-Olof, S278 (THU-332)
Bergheim, Ina, S179 (FRI-432)
Bergin, Colm, S708 (THU-549-YI)
Berglin, Lena, S71 (LBP-008)
Bergman, Adam, S791 (SAT-038)
Bergman, Jacques, S9 (LBO-005-YI)
Bergmann, Marianne, S110 (FRI-041-YI), S554 (THU-204)
Berg, Michael, S911 (SAT-586)
Bergquist, Annika, S2 (GS-002), S13 (OS-006-YI), S23 (OS-025), S71 (LBP-008), S290 (FRI-289), S313 (SAT-276), S451 (THU-409)
Bergram, Martin, S568 (WED-056)
Berg, Thomas, S8 (LBO-002), S10 (LBO-006), S46 (OS-070-YI), S150 (SAT-474), S490 (TOP-407-YI), S600 (WED-154-YI), S601 (WED-155), S647 (SAT-148), S840 (THU-275), S879 (THU-589-YI), S930 (SAT-636), S971 (WED-620)
Berhane, Kaleb, S194 (WED-433)
Berhe, Nega, S798 (TOP-048), S822 (WED-026), S825 (WED-036), S926 (SAT-622-YI)
Berkeley, Michelle, S826 (WED-039)
Berk, Kirsten, S684 (FRI-153)
Berk, Luuk, S9 (LBO-005-YI)
Berkovitch, Quentin, S827 (WED-046)
Berlakovich, Gabriela, S59 (OS-092-YI), S284 (FRI-266)
Bermudez, Emilio, S771 (THU-030)
Bernabeu, Francisco, S585 (WED-105), S772 (THU-036)
Bernabeu, Jesús Quintero, S56 (OS-086), S831 (THU-258-YI), S842 (THU-284)
Berná, Genoveva, S527 (THU-108)
Bernal, Guillén, S603 (WED-163)
Bernal-Mizrachi, Ernesto, S634 (SAT-104)
Bernal, Samuel, S910 (SAT-585)
Bernal, Vanesa, S16 (OS-010), S318 (SAT-291), S542 (THU-164), S567 (WED-054)
Bernal, William, S8 (LBO-002), S35 (OS-050-YI), S147 (SAT-464), S149 (SAT-468), S152 (SAT-478), S168 (FRI-396), S386 (FRI-481-YI), S760 (TOP-032)
Bernardi, Mauro, S185 (TOP-455-YI)
Bernardin, Faustine, S885 (THU-606)
Bernardino, Melvin, S703 (THU-528-YI)
Bernasconi, Davide, S282 (FRI-263)
Bernatik, Sophia, S359 (THU-345-YI)
Bernegger, Guenda, S863 (WED-317)
Bernsmeier, Christine, S165 (FRI-386), S710 (TOP-536-YI)
Bernstein, David, S10 (LBO-006), S330 (SAT-366)
Berre, Margaux Le, S340 (SAT-388), S846 (THU-290)
Berrevoet, Frederik, S281 (TOP-295-YI)
Berry, David, S37 (OS-053)
Bertazzoni, Arianna, S531 (THU-120), S696 (FRI-188-YI)
Bertelli, Cristina, S520 (THU-091-YI), S541 (THU-158), S595 (WED-137)
Berti, Camilla Ceccatelli, S874 (THU-571)
Bertin, Lise, S853 (WED-283)
Bertino, Gaetano, S82 (LBP-034-YI), S912 (SAT-587-YI)
Bert, Nina Le, S50 (OS-077)
Bertola, Francesca, S831 (THU-256-YI)
Bertoletti, Antonio, S50 (OS-077)
Bertoli, Ada, S807 (FRI-025), S919 (SAT-608-YI)
Bertolini, Alice, S783 (SAT-012)
Bertot, Luis Calzadilla, S571 (WED-069), S600 (WED-153), S699 (FRI-198)
Bertran, Esther, S467 (WED-262)
Berzigotti, Annalisa, S52 (OS-081), S76 (LBP-020), S168 (FRI-398), S379 (FRI-461-YI), S427 (THU-220), S447 (THU-395), S561 (TOP-081), S720 (TOP-504-YI), S733 (THU-450), S863 (WED-317)
Besch, Camille, S414 (FRI-572)
Beşışık, Fatih, S829 (THU-251)
Besleaga, Marta, S209 (WED-483)
Bessaudou, Garance, S815 (WED-005)
Bessa, Xavi, S969 (WED-611)
Besse-Hammer, Hélène Tatiana, S907 (SAT-575)
Bessissow, Ali, S757 (THU-516)
Bessissow, Amal, S380 (FRI-462)
Bessissow, Talat, S589 (WED-119)
Bessone, Fernando, S296 (TOP-281), S306 (SAT-262)
Best, Jan, S172 (FRI-410-YI), S763 (THU-010)
Betel, Michael, S127 (FRI-095), S774 (THU-040), S774 (THU-041)
Beteta, Alicia, S910 (SAT-581)
Bethea, Emily, S112 (FRI-051)
Bettan, Louis, S829 (THU-252)
Bettencourt, Ricki, S207 (WED-479), S564 (WED-043)
Bettinger, Dominik, S3 (GS-005), S6 (GS-011-YI), S24 (OS-028), S33 (OS-046), S52 (OS-081), S54 (OS-084), S144 (SAT-452), S185 (TOP-456-YI), S195 (WED-442-YI), S215 (WED-506), S719 (TOP-488), S733 (THU-449), S736 (THU-460-YI), S744 (THU-482-YI), S747 (THU-492), S752 (THU-501)
Beuers, Ulrich, S9 (LBO-005-YI), S14 (OS-007), S15 (OS-009-YI), S351 (SAT-426-YI), S352 (SAT-429), S353 (SAT-432), S353 (SAT-433), S963 (WED-595)
Beukema, Koen R., S352 (SAT-429)
Beutels, Philippe, S920 (SAT-609)
Bevilacqua, Michele, S52 (OS-081), S97 (SAT-084-YI), S424 (TOP-375-YI)
Beyene, Nateneal, S638 (SAT-117-YI), S682 (FRI-150-YI)
Beynon, Huw, S841 (THU-276-YI)
Bezemer, Jordy, S647 (SAT-149)
Bhadada, Sanjay, S684 (FRI-155)

Author Index

Bhadoria, Ajeet, S127 (FRI-095), S923 (SAT-618)
Bhala, Neeraj, S127 (FRI-095), S797 (SAT-055)
Bhalke, Abhijit, S822 (WED-025-YI)
Bhamidimarri, Kalyan, S846 (THU-291), S846 (THU-298)
Bhanji, Rahima A., S398 (FRI-516)
Bharadwaj, Hareesha, S735 (THU-457)
Bharania, Bansri, S354 (SAT-434)
Bhardwaj, Ankit, S141 (TOP-424-YI), S156 (SAT-495), S214 (WED-501-YI), S703 (THU-537)
Bhasker, Vikas, S788 (SAT-029), S789 (SAT-030)
Bhat, Anand, S718 (WED-573-YI)
Bhatia, Garima, S292 (FRI-299)
Bhatia, Vikram, S156 (SAT-495), S171 (FRI-404)
Bhat, Mamatha, S398 (FRI-516)
Bhatnagar, Aishwarya, S181 (FRI-441-YI), S184 (FRI-452-YI), S274 (THU-318), S282 (FRI-262-YI)
Bhat, Sadam, S139 (FRI-135-YI)
Bhat, Sadam H, S361 (THU-354)
Bhat, Sadam H., S104 (THU-071-YI), S276 (THU-324-YI)
Bhattacharya, Aneerban, S879 (THU-587), S885 (THU-606)
Bhattacharya, Anindro, S170 (FRI-401-YI)
Bhattacharya, Anupama, S288 (FRI-282)
Bhatt, Ankeet, S546 (THU-173-YI)
Bhatt, Shrey, S217 (WED-510)
Bhavani, Ruveena, S24 (OS-028), S144 (SAT-452)
Bheemraj, Kalisha, S905 (SAT-569), S940 (FRI-588-YI)
Bhettani, Mehreen Khan, S458 (WED-237-YI)
Bhoora, Urvisha, S76 (LBP-019-YI)
Bhujade, Harish, S81 (LBP-030), S221 (WED-522)
Biagi, Filippo, S83 (LBP-034-YI), S343 (SAT-400)
Białkowska, Jolanta, S980 (FRI-633)
Bianca, Franco-Leonardi, S285 (FRI-269)
Bianchi, Gabriele, S542 (THU-159)
Bianchini, Marcello, S31 (OS-042), S725 (THU-425), S746 (THU-489), S746 (THU-490), S752 (THU-501)
Bian, Congwen, S270 (TOP-328), S276 (THU-323)
Bian, Hua, S560 (TOP-080)
Bian, Tiandan, S609 (WED-182), S763 (THU-011), S924 (SAT-620)
Bian, Xiangyu, S763 (THU-011)
Bian, Xiyun, S625 (WED-227)
Bibi, Saba Mohamed, S777 (THU-050)
Bicego, Manuele, S97 (SAT-084-YI)
Bienvenue, Isaure, S380 (FRI-463), S381 (FRI-464)
Bière, Loic, S540 (THU-155)
Biewenga, Maaike, S15 (OS-009-YI)
Bigam, David, S401 (FRI-527)
Bigas, Claudia, S634 (SAT-103)
Bighini, Sara, S190 (WED-425)
Bignamini, Daniela, S553 (THU-197), S636 (SAT-110-YI)
Bihari, Chhagan, S139 (FRI-135-YI), S189 (WED-419), S282 (FRI-262-YI), S418 (THU-517-YI)
Bijdevaate, Diederik, S193 (WED-432), S828 (TOP-310-YI)
Bijiyev, Alan, S822 (WED-027)
Bi, Junjun, S86 (LBP-041)
Bijvelds, Marcel, S382 (FRI-467-YI)
Bik, Emil, S301 (SAT-251-YI), S315 (SAT-286)
Bilcke, Joke, S920 (SAT-609)
Bilegan, Ana, S602 (WED-157)
Bilgen, Şaziye Apraş, S348 (SAT-417)
Biliotti, Elisa, S911 (SAT-587-YI)
Billaud, Eric, S43 (OS-066), S47 (OS-072), S934 (TOP-582), S937 (FRI-585-YI)
Billette, Benoit, S757 (THU-516)
Billiet, Antoon, S849 (THU-306-YI)
Billsdon-McGrane, Aileen, S113 (FRI-054)
Bilodeau, Marc, S386 (FRI-480-YI)
Bilson, Josh, S25 (OS-030), S622 (WED-217)
Binayke, Akshay, S50 (OS-077)
Bindal, Vasundhra, S104 (THU-071-YI), S105 (THU-073-YI), S105 (THU-074), S120 (FRI-074), S129 (TOP-224-YI), S131 (FRI-105-YI), S138 (FRI-132), S139 (FRI-135-YI), S265 (SAT-341), S269 (SAT-354-YI), S269 (SAT-355), S276 (THU-324-YI), S280 (THU-337), S361 (THU-354), S373 (WED-353-YI)
Binkauskiene, Grazina, S20 (OS-019), S559 (TOP-064), S560 (TOP-066), S561 (TOP-082), S565 (WED-051)
Biolato, Marco, S219 (WED-515)
Bioletto, Fabio, S620 (WED-213)
Biondi, Mia, S70 (LBP-005), S968 (WED-609-YI), S975 (WED-636), S976 (WED-637)
Bioulac-Sage, Paulette, S17 (OS-011)
Biquard, Louise, S571 (WED-067)
Birgit, Kohnke-Ertel, S359 (THU-345-YI)
Biribin, Lara, S53 (OS-082), S54 (OS-084)
Birkenfeld, Andreas, S21 (OS-020)
Biselli, Maurizio, S185 (TOP-455-YI)
Bishara, Gabriel, S597 (WED-147)
Bishnu, Debasree, S100 (THU-056)
Bissig, Maurizia, S331 (SAT-368-YI), S570 (WED-061)
Biswas, Sagnik, S36 (OS-051-YI), S52 (OS-081), S141 (TOP-423), S184 (TOP-454-YI), S247 (SAT-514), S299 (SAT-248), S725 (THU-426), S847 (THU-299)
Biswas, Subhrajit, S232 (FRI-308)
Bitetto, Davide, S302 (SAT-252)
Bito, Andrea, S539 (THU-151-YI)
Bittaye, Sheikh Omar, S798 (TOP-034)
Bittencourt, Paulo, S10 (LBO-006), S35 (OS-050-YI), S141 (TOP-437), S296 (TOP-281), S306 (SAT-262), S768 (THU-022)
Bittermann, Tess, S788 (SAT-029)
Bittermann, Therese, S189 (WED-420)
Bitton, Alain, S589 (WED-119)
Bitton, Jackie, S109 (TOP-210)
Bixby, Alexandra, S220 (WED-521)
Bi, Yan, S86 (LBP-041)
Bizino, Maurice, S9 (LBO-005-YI)
Bjarnason, Agnar, S802 (FRI-011)
Björhall, Karin, S682 (FRI-148)
Björkström, Niklas, S71 (LBP-008), S953 (FRI-625)
Björnsson, Einar S., S602 (WED-157)
Bladen, Maxwell, S458 (WED-240)
Bladt, Francesca, S824 (WED-031)
Blaise, Lorraine, S343 (SAT-400)
Blanchette, Christopher, S198 (WED-449)
Blanc, Jean-Frédéric, S17 (OS-011), S485 (WED-396), S499 (FRI-238)
Blanco, David, S182 (FRI-442)
Blanco, Gerardo, S410 (FRI-558)
Blanco, Giovanny Rodriguez, S742 (THU-476)
Blanco, Paola Zuluaga, S128 (FRI-100)
Blanco-Sampascual, Sonia, S294 (TOP-278)
Blaney, Hanna, S520 (THU-090-YI)
Blanter, Julia, S491 (TOP-408-YI)
Blasco, Miriam, S910 (SAT-585)
Blasco, Victor Vargas, S34 (OS-049), S35 (OS-050-YI), S141 (TOP-437), S166 (FRI-388-YI), S170 (FRI-401-YI), S302 (SAT-254)
Blas-García, Ana, S230 (TOP-343-YI)
Blatt, Lawrence, S658 (SAT-184), S874 (THU-570), S879 (THU-587), S885 (THU-606), S886 (THU-610), S889 (THU-620), S893 (THU-634), S959 (WED-586), S960 (WED-588), S965 (WED-602)
Blaya, Sandra, S146 (SAT-461)
Blokzijl, Hans, S59 (OS-091), S384 (FRI-476-YI), S384 (FRI-477), S385 (FRI-478), S415 (FRI-574)
Blom, Dirk, S764 (THU-012)
Blom, Tiki D., S79 (LBP-026), S331 (SAT-368-YI), S351 (SAT-426-YI), S352 (SAT-429), S353 (SAT-432), S353 (SAT-433)
Blondeel, Joris, S381 (FRI-465)
Bloomer, Pamela M., S412 (FRI-564-YI)
Bloom, Stephen, S922 (SAT-613)
Blount, Monica, S255 (SAT-540), S973 (WED-627)
Blumenthal, Justin, S911 (SAT-586)
Boateng, Sarpong, S526 (THU-105)
Boavida, José Manuel, S649 (SAT-152)
Bobardt, Michael, S877 (THU-580)
Bobat, Bilal, S315 (SAT-286)
Boberg, Kirsten Muri, S13 (OS-006-YI), S395 (FRI-509), S451 (THU-409)
Bobowski-Gerard, Marie, S163 (FRI-383), S164 (FRI-384)
Bocagni, Patrizia, S59 (OS-091)
Bocaj, Iris, S82 (LBP-034-YI)
Bocchero, Elisa, S494 (FRI-225)

Boccia, Giovanni, S977 (WED-640)
Bock, Christoph, S362 (TOP-325-YI)
Bodakçi, Emin, S965 (WED-603)
Bode, Johannes, S188 (WED-416)
Bödendorfer, Benjamin, S200 (WED-453)
Boeira, Paula, S164 (FRI-385-YI), S184 (FRI-453-YI)
Boekmann, Anja, S876 (THU-577)
Boelen, Anita, S674 (SAT-233)
Boellaard, Ronald, S237 (FRI-330)
Boerlage, Thomas, S9 (LBO-005-YI)
Boer, Laura, S200 (WED-457), S432 (THU-236), S451 (THU-404)
Boerrigter, Melissa, S864 (WED-319-YI)
Boettcher, Katrin, S876 (THU-575)
Boettler, Tobias, S14 (OS-007), S550 (THU-187)
Boetto, Riccardo, S402 (FRI-530)
Boffetta, Paolo, S784 (SAT-015-YI)
Boffini, Massimo, S848 (THU-304)
Boff, Raquel, S88 (SAT-056), S776 (THU-044)
Bogaard, Harm Jan, S237 (FRI-330)
Bogaards, Johannes, S57 (OS-087-YI), S348 (SAT-418-YI)
Böhling, Nina, S54 (OS-084), S213 (WED-496), S215 (WED-506)
Böhme, Julia, S107 (THU-078)
Boike, Justin, S388 (FRI-489)
Boillot, Olivier, S380 (FRI-463), S381 (FRI-464)
Boisson-Walsh, Alix, S80 (LBP-028-YI)
Boix, Paula, S169 (FRI-400), S230 (TOP-343-YI)
Bojanić, Kristina, S617 (WED-202)
Bojja, Sai, S41 (OS-061)
Boland, Karen, S210 (WED-489-YI)
Bolaños, Juan Pedro, S273 (THU-316)
Boldbaatar, Anuka, S826 (WED-039)
Boleslawski, Emmanuel, S414 (FRI-572)
Bolis, Francesca, S333 (SAT-369)
Bolt, Isabelle, S646 (SAT-140-YI), S674 (SAT-233)
Boltyenkov, Artem, S580 (WED-092-YI)
Bombardieri, Giulia, S817 (WED-010)
Bombassaro, Isadora, S154 (SAT-484)
Bombonato, Giancarlo, S699 (FRI-200)
Bonaccorsi-Riani, Eliano, S59 (OS-091), S381 (FRI-465), S382 (FRI-466)
Bonacini, Maurizio, S89 (SAT-057)
Bo', Nadia Dal, S304 (SAT-258)
Bo', Nadia Dal, S335 (SAT-378-YI)
Bonaiuto, Emanuela, S304 (SAT-258), S307 (SAT-263), S335 (SAT-378-YI)
Bonato, Antonio, S435 (THU-247)
Bonazza, Deborah, S465 (WED-256)
Bondar, Marina, S594 (WED-135)
Bondar, Yevgeniya, S967 (WED-608)
Bonder, Alan, S10 (LBO-006), S325 (SAT-320), S327 (SAT-322), S331 (SAT-368-YI)
Bondo, Gaëtan, S80 (LBP-028-YI)
Bonet-Vidal, Lucía, S223 (WED-528)
Bonfichi, Alessandra, S69 (LBP-004-YI), S300 (SAT-250)
Bonfim, Ângelo, S379 (FRI-460)
Bong Ahn, Sang, S652 (SAT-165)
Bonhomme, Marie, S48 (OS-073)
Boni, Carolina, S874 (THU-571)
Bonilla, Eva Fernandez, S16 (OS-010), S308 (SAT-264)
Bonino, Ferruccio, S431 (THU-233), S950 (FRI-619)
Boniquet, Juan Carles Quer, S804 (FRI-019)
Bonis, Adriana De, S459 (WED-241), S642 (SAT-131-YI)
Bonitz, Katharina, S11 (OS-002-YI), S179 (FRI-431-YI), S237 (FRI-324), S266 (SAT-347-YI), S362 (TOP-325-YI), S364 (WED-323), S750 (THU-497-YI)
Bonner, Lauren, S116 (FRI-061)
Bono, Elisa, S51 (OS-079)
Bonze, Myriam, S80 (LBP-028-YI)
Bonzon-Kulichenko, Elena, S634 (SAT-104)
Boodram, Basmattee, S816 (WED-009), S818 (WED-014)
Boparai, Gurasis, S36 (OS-051-YI)
Bopegamage, Shubhada, S807 (FRI-025)
Borahma, Mohamed, S591 (WED-125), S609 (WED-181), S844 (THU-286), S845 (THU-287), S949 (FRI-613)
Borentain, Patrick, S222 (WED-525)
Borg, Brian, S10 (LBO-006)
Borghi, Marta, S43 (OS-066), S71 (LBP-009), S936 (TOP-584), S937 (FRI-585-YI), S942 (FRI-593)
Borgia, Sergio, S43 (OS-066), S937 (FRI-585-YI)
Borgniet, Olivier, S109 (TOP-210)
Bori, Matías, S296 (TOP-281), S302 (SAT-253), S306 (SAT-262)
Borin, Alex, S405 (FRI-541)
Borja-Cacho, Daniel, S388 (FRI-489)
Bork, Peer, S115 (FRI-057), S148 (SAT-467-YI), S261 (SAT-329-YI)
Borlini, Stefania, S817 (WED-010)
Boros, Carina, S55 (OS-085-YI)
Borowik, Anna, S762 (THU-009)
Borowska, Luiza, S688 (FRI-168)
Borrat, Xavier, S53 (OS-082)
Borrego, Jaime, S910 (SAT-581), S910 (SAT-585)
Borrós, Salvador, S173 (FRI-414), S239 (FRI-336)
Borssén, Åsa Danielsson, S584 (WED-104)
Bortolini, Margherita, S519 (THU-086)
Bösch, Greta Marie, S383 (FRI-474)
Bosch, Jaime, S76 (LBP-020), S168 (FRI-398), S561 (TOP-081), S735 (THU-453)
Bo, Simona, S574 (WED-073), S620 (WED-213)
Bosoi, Gabriela, S465 (WED-256)
Bossen, Lars, S2 (GS-002)
Bos, Trijnie, S630 (SAT-090)
Botros, Irina, S943 (FRI-594), S953 (FRI-624)
Bottero, Julie, S922 (SAT-612)
Botteron, Natalie Vilcinskas Y, S112 (FRI-050)
Bouali, Assia, S723 (THU-419)
Bouattour, Mohamed, S38 (OS-055), S428 (THU-226-YI), S446 (THU-393-YI), S493 (FRI-221), S499 (FRI-238), S505 (FRI-254), S506 (FRI-255-YI), S507 (FRI-362), S508 (FRI-364-YI)
Bouchecareilh, Marion, S836 (THU-265-YI)
Boucher, Louis-Martin, S757 (THU-516)
Bouda, Yasmine, S456 (WED-234-YI)
Boudes, Pol, S282 (FRI-261)
Bough, Isabelle, S764 (THU-012)
Boulagnon-Rombi, Camille, S38 (OS-054)
Boulesteix, Marine, S414 (FRI-572)
Bouligand, Jérôme, S850 (THU-308)
Boulter, Luke, S454 (TOP-390-YI), S864 (WED-319-YI)
Bouman, Donald, S200 (WED-457), S432 (THU-236), S451 (THU-404)
Bouquet, Jerome, S959 (WED-585)
Bourgeois, Cyril, S869 (TOP-632)
Bourgeois, Stefan, S907 (SAT-575), S920 (SAT-609), S929 (SAT-629)
Bourliere, Marc, S45 (OS-067), S46 (OS-070-YI), S66 (OS-104), S207 (WED-477)
Bourlière, Marc, S815 (WED-005)
Boursier, Jerome, S110 (FRI-042), S365 (WED-331-YI), S517 (TOP-114), S525 (THU-103), S540 (THU-155), S554 (THU-202), S557 (THU-213), S558 (TOP-063-YI), S568 (WED-057-YI), S589 (WED-118), S607 (WED-174-YI), S612 (WED-187-YI), S618 (WED-204), S621 (WED-215), S795 (SAT-050)
Boussioutas, Alex, S436 (THU-248), S469 (WED-265)
Bouvard, Béatrice, S554 (THU-202)
Bouzbib, Charlotte, S6 (GS-011-YI), S53 (OS-082), S54 (OS-084), S195 (WED-442-YI), S207 (WED-477), S397 (FRI-515), S497 (FRI-234), S719 (TOP-488), S723 (THU-418), S742 (THU-477), S752 (THU-501)
Bouzid, Donia, S811 (FRI-038)
Bowen, Kelly, S745 (THU-483)
Bowles, Matthew, S164 (FRI-385-YI)
Bowlus, Christopher L., S10 (LBO-006), S58 (OS-089), S78 (LBP-023), S295 (TOP-280), S302 (SAT-254), S313 (SAT-282), S315 (SAT-286), S319 (SAT-300), S328 (SAT-324), S328 (SAT-361), S328 (SAT-362), S329 (SAT-363), S329 (SAT-364), S342 (SAT-398), S838 (THU-270)
Bownes, Shana-Lee, S43 (OS-065)
Bowness, James S, S572 (WED-070)
Bo, Yang, S259 (SAT-554), S763 (THU-011)
Boyar, Nadiya, S369 (WED-340-YI)
Boyd, Anders, S904 (SAT-564), S922 (SAT-612)
Boyd, LaKeisha, S531 (THU-122)

Author Index

Boyle, Alison, S704 (THU-540), S709 (THU-556-YI)
Boyle, Douglas, S799 (FRI-004), S800 (FRI-005)
Boytchev, Isabelle, S374 (TOP-503)
Boyton, Rosemary, S500 (FRI-239)
Bozdayi, Mithat, S965 (WED-603)
Bo, Zhiyuan, S428 (THU-225-YI)
Božić -Antić, Ivana, S268 (SAT-351)
Bozso, Boglarka, S337 (SAT-382)
Bozward, Amber, S363 (WED-321-YI), S364 (WED-324-YI)
Bozzano, Sergio, S139 (FRI-133)
Braadland, Peder, S299 (SAT-249)
Braadland, Peder Rustøen, S2 (GS-002), S13 (OS-006-YI), S290 (FRI-289), S345 (SAT-410)
Brach del Prever, Giulia Mrgherita, S835 (THU-263)
Braconi, Chiara, S38 (OS-054), S445 (THU-385)
Braden, Barbara, S744 (THU-481)
Bradshaw, Daniel, S811 (FRI-038)
Bragazzi, Mariaconsiglia, S69 (LBP-004-YI), S304 (SAT-258), S335 (SAT-378-YI)
Braghini, Maria Rita, S583 (WED-102-YI), S670 (SAT-225)
Brahmania, Mayur, S820 (WED-022)
Brancaccio, Giuseppina, S49 (OS-076-YI), S440 (THU-369), S919 (SAT-608-YI), S972 (WED-623)
Brancale, Joseph, S166 (FRI-393)
Branco, Joana, S934 (TOP-582), S940 (FRI-589)
Brander, Christian, S806 (FRI-024)
Brandi, Giovanni, S484 (WED-393)
Brandman, Danielle, S411 (FRI-560)
Brandt-Winge, Sara, S451 (THU-409)
Brant, Dawn, S61 (OS-108)
Brantly, Mark, S855 (WED-287-YI)
Braun, Felix, S59 (OS-092-YI)
Bravo, Susana, S233 (FRI-313)
Brazier, Benedict, S725 (THU-427)
Breakwell, Nigel, S813 (FRI-047)
Breard, Thomas, S374 (TOP-503)
Brecelj, Jernej, S55 (OS-086), S831 (THU-258-YI), S842 (THU-284), S850 (THU-308)
Breder, Sigurd, S451 (THU-409)
Breen, Jack, S673 (SAT-231)
Bremer, Birgit, S197 (WED-446), S864 (TOP-615)
Brenig, Robert, S710 (TOP-536-YI)
Brenig, Robert G, S165 (FRI-386)
Brennan, Alana, S926 (SAT-624)
Brennan, Paul, S559 (TOP-065-YI)
Brennan, Paul N., S557 (THU-213), S774 (THU-040), S774 (THU-041), S777 (THU-050), S792 (SAT-042), S795 (SAT-050)
Brennan-Xie, Liam, S779 (SAT–004)
Breteau, Isaure, S143 (SAT-450)
Brettner, Robert, S11 (OS-002-YI), S237 (FRI-324)
Breuhahn, Kai, S231 (FRI-305)
Brew, Brendan, S145 (SAT-457), S736 (THU-458)
Brezani, Viliam, S137 (FRI-126)
Brhane, Dawit, S822 (WED-026), S926 (SAT-622-YI)
Briand, Francois, S131 (FRI-106), S634 (SAT-105)
Bricard, Orian, S17 (OS-012)
Brichler, Segolene, S45 (OS-067), S951 (FRI-621)
Bridger, Gary, S655 (SAT-172)
Briem, Stearne, S702 (FRI-206)
Briggs, Christopher, S164 (FRI-385-YI)
Bril, Fernando, S557 (THU-213)
Brillanti, Stefano, S82 (LBP-034-YI)
Brindley, James, S69 (LBP-001)
Briseño, Renata, S810 (FRI-035), S810 (FRI-036)
Brismar, Torkel, S71 (LBP-008)
Brito, Camila Gabriela De, S119 (FRI-073)
Brodal, Hans Petter, S451 (THU-409)
Brodersen, Jeanette de Wett, S240 (FRI-338)
Broecker-Preuss, Martina, S395 (FRI-511-YI)
Broekman, Leonard (Niels), S577 (WED-084), S621 (WED-214), S765 (THU-013)
Broere, Roberto, S382 (FRI-467-YI), S383 (FRI-468), S383 (FRI-473), S391 (FRI-498), S398 (FRI-517-YI)
Broering, Dieter Clemens, S717 (WED-570-YI), S831 (THU-258-YI), S842 (THU-284)
Broering, Ruth, S854 (WED-284), S862 (WED-316-YI)
Broer, Matthijs, S956 (TOP-598), S957 (WED-577), S960 (WED-587)
Brol, Maximilian Joseph, S178 (FRI-428-YI), S206 (WED-475), S209 (WED-485), S237 (FRI-329), S248 (SAT-515), S261 (SAT-329-YI), S383 (FRI-474), S409 (FRI-556), S493 (FRI-220)
Brombosz, Elizabeth, S20 (OS-019), S559 (TOP-064), S560 (TOP-066), S561 (TOP-082), S565 (WED-051)
Bromfield, Brittany, S412 (FRI-564-YI)
Bronowicki, Jean-Pierre, S37 (OS-052), S435 (THU-246)
Bronsert, Peter, S363 (TOP-326)
Bronte, Fabrizio, S69 (LBP-004-YI), S82 (LBP-034-YI), S304 (SAT-258), S307 (SAT-263), S335 (SAT-378-YI)
Broquetas, Teresa, S46 (OS-070-YI), S562 (TOP-097-YI), S612 (WED-188), S724 (THU-421)
Brosell, Marina, S16 (OS-010)
Bros, Matthias, S482 (WED-385-YI)
Brosteanu, Oana, S930 (SAT-636)
Brotherton, Lauren, S458 (WED-240), S820 (WED-021)
Brouwer, Willem Pieter, S9 (LBO-005-YI), S26 (OS-032-YI), S63 (OS-098-YI), S443 (THU-382-YI), S515 (TOP-098), S583 (WED-101), S587 (WED-110-YI), S587 (WED-111), S608 (WED-180), S621 (WED-215), S622 (WED-216), S684 (FRI-153), S789 (SAT-031-YI), S790 (SAT-035)
Brown, Amy, S846 (THU-291), S846 (THU-298)
Brown, Ashley, S47 (OS-072)
Brown, Caitlin, S709 (THU-556-YI)
Browne, Sarah, S19 (OS-016), S84 (LBP-036), S679 (TOP-176), S700 (FRI-201)
Brown, Robert S.Jr., S116 (FRI-061), S197 (WED-447)
Brown, Sade, S308 (SAT-265), S309 (SAT-266)
Brozat, Jonathan Frederik, S60 (OS-093), S161 (SAT-510-YI)
Broz, Petr, S641 (SAT-125-YI)
Brubaker, William, S877 (THU-580)
Bruccoleri, Mariangela, S424 (TOP-375-YI), S494 (FRI-225), S514 (FRI-381)
Bruce, Jeanne Carla, S703 (THU-528-YI)
Bruckers, Liesbeth, S696 (FRI-190)
Bruges, Léa, S505 (FRI-254)
Brüggemann, Isabel, S744 (THU-482-YI)
Brüggemann, Yannick, S890 (THU-623-YI)
Bruha, Radan, S777 (THU-050)
Brůha, Radan, S577 (WED-084)
Bruin, Mare, S632 (SAT-099-YI)
Bruin, Sjoerd, S632 (SAT-099-YI)
Brujats, Anna, S191 (WED-426), S191 (WED-427-YI), S337 (SAT-382), S735 (THU-453)
Brummer, Tilman, S460 (WED-244-YI)
Brunet, Mercè, S336 (SAT-380)
Brunetti, Jesus, S887 (THU-612-YI)
Brunetti, Leonardo, S491 (TOP-408-YI), S500 (FRI-239)
Brunetto, Maurizia, S43 (OS-066), S69 (LBP-004-YI), S82 (LBP-034-YI), S307 (SAT-263), S335 (SAT-378-YI), S431 (THU-233), S440 (THU-369), S481 (WED-383), S695 (FRI-187), S831 (THU-256-YI), S900 (SAT-559), S901 (SAT-560), S911 (SAT-587-YI), S928 (SAT-628-YI), S934 (TOP-582), S936 (TOP-584), S937 (FRI-585-YI), S938 (FRI-586), S939 (FRI-587), S947 (FRI-608), S950 (FRI-619), S956 (WED-576), S962 (WED-593)
Bruno, Pierangela, S767 (THU-020)
Bruno, Raffaele, S936 (TOP-584), S938 (FRI-586)
Bruns, Tony, S33 (OS-046), S142 (SAT-448), S159 (SAT-506-YI), S169 (FRI-399), S170 (FRI-402), S175 (FRI-419), S185 (TOP-456-YI), S262 (SAT-330), S325 (SAT-320), S642 (SAT-131-YI), S736 (THU-460-YI), S744 (THU-482-YI), S945 (FRI-602-YI)
Brusilovskaya, Ksenia, S200 (WED-453)
Brusq, Jean-Marie, S172 (FRI-412)
Brussel, Thomas Van, S17 (OS-012)
Bruynseels, Peggy, S907 (SAT-575)
Bruzzone, Bianca, S919 (SAT-608-YI)

Brzdęk, Kinga, S970 (WED-617-YI)
Brzdęk, Michał, S970 (WED-617-YI), S980 (FRI-633)
Brzustowski, Angélique, S571 (WED-067)
Buc, Emmanuel, S512 (FRI-372)
Buchanan, Ryan, S25 (OS-030), S765 (THU-014)
Buchanan, Ryan M, S622 (WED-217)
Buchard, Benjamin, S167 (FRI-394-YI), S512 (FRI-372)
Buch, Stephan, S35 (OS-050-YI)
Buckholz, Adam, S190 (WED-421)
Bucur, Roxana, S425 (THU-216-YI), S491 (TOP-408-YI)
Budas, Grant, S84 (LBP-037)
Bueloni, Bárbara, S358 (THU-340-YI), S654 (SAT-171-YI)
Buendia, Marc, S884 (THU-604-YI)
Bueno-Vélez, Marvin, S128 (FRI-100)
Bufler, Philip, S293 (FRI-301), S852 (TOP-311), S858 (WED-302)
Buggisch, Peter, S971 (WED-620)
Bugianesi, Elisabetta, S2 (GS-003), S3 (GS-005), S29 (OS-038), S476 (WED-368), S517 (TOP-114), S525 (THU-103), S534 (THU-133), S557 (THU-213), S558 (TOP-063-YI), S568 (WED-057-YI), S574 (WED-073), S589 (WED-118), S601 (WED-156), S607 (WED-174-YI), S611 (WED-184-YI), S612 (WED-187-YI), S618 (WED-204), S620 (WED-213), S621 (WED-215), S680 (FRI-139), S693 (FRI-182), S795 (SAT-050)
Buist-Homan, Manon, S238 (FRI-333-YI), S239 (FRI-334), S244 (FRI-352)
Bujanda, Luis, S165 (FRI-387-YI), S277 (THU-330-YI), S303 (SAT-257-YI), S323 (SAT-315), S445 (THU-385), S483 (WED-388-YI), S484 (WED-393)
Bulakçı, Mesut, S829 (THU-251)
Bulato, Cristiana, S148 (SAT-466-YI), S435 (THU-247)
Bulighin, Gianmarco, S975 (WED-635)
Bullard, Bria, S7 (GS-012), S958 (WED-581)
Bulut, Pinar, S850 (THU-308)
Bumba, Ahmed, S821 (WED-023)
Bundgaard, Johan S, S166 (FRI-393)
Bundsgaard, Henning, S166 (FRI-393)
Bungert, Andreas, S439 (THU-367), S915 (SAT-595), S916 (SAT-596)
Büning, Laurin, S882 (THU-595)
Buque, Xabier, S241 (FRI-339), S277 (THU-330-YI), S631 (SAT-095-YI)
Burade, Vinod, S699 (FRI-199)
Buranelli, Caterina, S577 (WED-084), S600 (WED-153)
Burch, Mark, S681 (FRI-142)
Burciaga-Villalobos, Fabiola, S771 (THU-030)
Burdio, Fernando, S191 (WED-427-YI)
Bureau, Christophe, S3 (GS-005), S53 (OS-082), S54 (OS-084), S55 (OS-085-YI), S207 (WED-477), S222 (WED-525), S414 (FRI-572), S497 (FRI-234), S719 (TOP-488), S723 (THU-418), S723 (THU-419), S742 (THU-477), S752 (THU-501)
Bureau, Morgane, S815 (WED-005), S889 (THU-619)
Burggraeve, Delphine, S464 (WED-254)
Burghart, Lukas, S739 (THU-467), S975 (WED-634-YI)
Burkart, Volker, S672 (SAT-230)
Burk, Caroline, S339 (SAT-387), S946 (FRI-605)
Burman, Julio, S573 (WED-072), S613 (WED-190)
Burnside, Jessica, S624 (WED-225-YI), S624 (WED-226), S783 (SAT-013-YI), S784 (SAT-014)
Burra, Patrizia, S126 (FRI-094), S148 (SAT-466-YI), S193 (WED-431-YI), S356 (SAT-443), S375 (TOP-518), S417 (FRI-581), S557 (THU-213), S766 (THU-015), S795 (SAT-050)
Burriel, Miquel Serra, S515 (TOP-098), S583 (WED-101)
Busarello, Emma, S370 (WED-346)
Bush, Brian, S24 (OS-028), S144 (SAT-452), S160 (SAT-507)
Busoms, Cristina Molera, S850 (THU-308)
Bus, Paul J., S353 (SAT-433)
Bustamante, Javier, S277 (THU-330-YI), S303 (SAT-257-YI), S312 (SAT-273)
Busti, Fabiana, S849 (THU-305-YI)
Bustos, Matilde, S271 (THU-314), S636 (SAT-108)
Busuttil, Rita, S469 (WED-265)
Butaye, Emma, S99 (TOP-193-YI), S349 (SAT-420)
Buti, Maria, S1 (GS-001), S43 (OS-066), S49 (OS-075), S150 (SAT-475), S798 (TOP-048), S801 (FRI-007), S804 (FRI-019), S811 (FRI-038), S900 (SAT-559), S902 (SAT-560), S908 (SAT-577), S923 (SAT-618), S926 (SAT-623), S928 (SAT-627), S928 (SAT-628-YI), S934 (TOP-582), S936 (TOP-584), S937 (FRI-585-YI), S943 (FRI-594), S946 (FRI-605), S948 (FRI-611), S949 (FRI-612), S953 (FRI-624), S961 (WED-592), S962 (WED-594)
Butler, Nick, S420 (THU-526)
Butler, Oisin, S434 (THU-241)
Bu, Tong, S793 (SAT-043)
Butsashvili, Maia, S76 (LBP-021)
Buttigeig, Stefan, S777 (THU-050)
Buttler, Laura, S195 (WED-442-YI), S222 (WED-526-YI)
Butt, Natasha, S709 (THU-556-YI)
Büttner, Reinhard, S280 (THU-338-YI)
Bu, Yang, S549 (THU-184), S593 (WED-134), S609 (WED-182), S924 (SAT-620)
Buytaert, Maarten, S526 (THU-106)
Buzincu, Iulian, S210 (WED-490)
Buzo, Ignacio Torrescusa, S527 (THU-108)
Bwa, Aung, S127 (FRI-095), S794 (SAT-046)
Bychkov, Mykola, S777 (THU-047)
Bye, Nicole, S276 (THU-329)
Byrne, Chris D, S25 (OS-030), S622 (WED-217), S765 (THU-014)
Byrne, Michael, S702 (FRI-206)
Byrne, Rachel, S641 (SAT-126)
Byun, Jihyo, S136 (FRI-121), S229 (TOP-342-YI), S368 (WED-337-YI)

Cabaleiro, Alba, S232 (FRI-313), S241 (FRI-339)
Caballeria, Llorenç, S26 (OS-032-YI), S63 (OS-098-YI), S608 (WED-180)
Caballero-Camino, Francisco Javier, S165 (FRI-387-YI)
Cabezas, Joaquin, S957 (WED-577)
Cabezas, Manuel Castro, S577 (WED-084), S600 (WED-153), S621 (WED-214), S684 (FRI-153), S688 (FRI-166-YI), S765 (THU-013), S789 (SAT-031-YI)
Cabibbo, Giuseppe, S401 (FRI-528), S424 (TOP-375-YI), S428 (THU-227-YI), S494 (FRI-226), S495 (FRI-227), S514 (FRI-381)
Cabibi, Daniela, S331 (SAT-368-YI)
Cabrales, Jazmin Mexia, S120 (FRI-075)
Cabrera, Araceli Bravo, S160 (SAT-507)
Cabrera, Jorge, S799 (TOP-049)
Cabrera, Maria Cecilia, S452 (THU-414-YI)
Cabrera, Tatiana, S757 (THU-516)
Caccamo, Gaia, S223 (WED-527), S435 (THU-245), S967 (WED-605-YI)
Cacciola, Irene, S163 (FRI-382), S196 (WED-445), S223 (WED-527), S435 (THU-245), S936 (TOP-584), S938 (FRI-586), S967 (WED-605-YI)
Cachero, Alba, S59 (OS-091), S410 (FRI-558), S724 (THU-421), S837 (THU-267), S855 (WED-289)
Cacho-Pujol, Júlia, S234 (FRI-316), S635 (SAT-107-YI)
Cadahía-Rodrigo, Valle, S250 (SAT-524)
Cadamuro, Massimiliano, S466 (WED-258), S479 (WED-379), S485 (WED-395-YI)
Cadogan, Kathy-Ann, S689 (FRI-169)
Cadoret, Axelle, S235 (FRI-320)
Cadranel, Jean-François, S110 (FRI-042), S829 (THU-252)
Cafardi, John, S70 (LBP-005), S975 (WED-636), S976 (WED-637)
Cafasso, Carla, S55 (OS-085-YI)
Cagigal, María Luisa, S643 (SAT-134)
Cagnin, Silvia, S435 (THU-247)
Cahen, Djuna L., S9 (LBO-005-YI), S353 (SAT-432)
Cai, Dachuan, S922 (SAT-617)
Cai, Dawei, S869 (TOP-631), S872 (THU-561)
Cai, Fei, S48 (OS-074)
Cai, James, S370 (WED-347)
Cai, Jianghui, S303 (SAT-255)
Cai, Junling, S954 (FRI-626)

Author Index

Cailliau, Emeline, S505 (FRI-254)
Caime, Chiara, S282 (FRI-263)
Cain, Owen, S364 (WED-324-YI)
Cai, Qun, S27 (OS-034), S389 (FRI-492)
Cairo, Fernando, S10 (LBO-006), S296 (TOP-281), S306 (SAT-262)
Cairoli, Victoria, S234 (FRI-316)
Cai, Shangyuan, S34 (OS-048)
Cai, Xiujun, S466 (WED-259)
Cai, Yaxuan, S473 (WED-361-YI)
Cai, Yijing, S160 (SAT-507)
Cajgfinger, Thomas, S619 (WED-206)
Cajo, Sonia Algarate, S910 (SAT-585)
Cajuso, Tatiana, S282 (FRI-263)
Çakaloğlu, Yılmaz, S961 (WED-589)
Çakmak, Muhammet Furkan, S496 (FRI-231)
Calabrese, Maria Pia, S69 (LBP-004-YI), S82 (LBP-034-YI), S305 (SAT-260-YI), S339 (SAT-386)
Calascibetta, Sofia, S494 (FRI-226), S495 (FRI-227)
Calatayud-Samper, Laura, S804 (FRI-019)
Caldas-Álvarez, María, S250 (SAT-524)
Calderara, Debora Bertaggia, S72 (LBP-011)
Calderaro, Julien, S17 (OS-011), S38 (OS-054), S38 (OS-055), S343 (SAT-400), S456 (WED-234-YI)
Calderón, Natalia Martagón, S285 (FRI-269)
Calderón-Robles, Lucía, S234 (FRI-316), S635 (SAT-107-YI)
Caldwell, Stephen, S58 (OS-089), S313 (SAT-282)
Calé, Alicia, S273 (THU-317), S459 (WED-241)
Calì, Alessia, S950 (FRI-619)
Calimeri, Francesco, S767 (THU-020)
Calinas, Filipe, S43 (OS-066), S786 (SAT-022), S892 (THU-627), S900 (SAT-559), S902 (SAT-560), S934 (TOP-582), S936 (TOP-584), S937 (FRI-585-YI), S940 (FRI-589)
Callegaro, Annapaola, S942 (FRI-592)
Calleja, Josune Cabello, S54 (OS-084), S145 (SAT-458-YI), S148 (SAT-467-YI), S210 (WED-485), S409 (FRI-556), S493 (FRI-220), S497 (FRI-234), S723 (THU-418)
Calle, Marinella, S340 (SAT-388), S846 (THU-290)
Callens, Jos, S920 (SAT-609), S929 (SAT-629)
Calleri, Alberto, S113 (FRI-052), S126 (FRI-093), S186 (TOP-469-YI)
Calle, Roberto, S690 (FRI-173)
Callewaert, Nico, S99 (TOP-193-YI), S349 (SAT-420)
Calov, Gunilla, S110 (FRI-041-YI), S115 (FRI-059), S554 (THU-204)
Calretas, Susana, S59 (OS-091)
Calvão, Joana, S753 (THU-505-YI)
Calvaruso, Vincenza, S69 (LBP-004-YI), S82 (LBP-034-YI), S190 (WED-425), S300 (SAT-250), S304 (SAT-258), S307 (SAT-263), S325 (SAT-320), S331 (SAT-368-YI), S335 (SAT-378-YI), S350 (SAT-421), S607 (WED-174-YI), S727 (THU-431), S733 (THU-450), S753 (THU-505-YI), S831 (THU-256-YI)
Calvez, François Le, S167 (FRI-394-YI)
Calvino, Valeria, S30 (OS-041), S196 (WED-443), S227 (WED-541-YI)
Calvisi, Diego, S456 (WED-234-YI), S462 (WED-249)
Calvo, Irina, S124 (FRI-088)
Calvo, María, S173 (FRI-414)
Calvo, Marta, S819 (WED-019)
Calvo, Noelia, S799 (TOP-049), S910 (SAT-585)
Calvo-Orteu, Maria, S91 (SAT-062)
Calvo, Pier Luigi, S55 (OS-086), S831 (THU-258-YI), S835 (THU-263), S842 (THU-284), S850 (THU-308)
Camagni, Stefania, S59 (OS-091), S414 (FRI-571)
Camara, Houda, S37 (OS-052)
Camarena, Fernando Caloca, S235 (FRI-319), S481 (WED-384)
Camargo, Graciela Salinas, S403 (FRI-532)
Camell-Raventos, David, S453 (TOP-389)
Camera, Silvia, S429 (THU-227-YI), S494 (FRI-225)
Cameron, Madeline, S14 (OS-008), S354 (SAT-435)
Camino, Adrian, S143 (SAT-450)
Camino, Xavier, S904 (SAT-564)
Cammà, Calogero, S190 (WED-425), S401 (FRI-528), S494 (FRI-226), S495 (FRI-227), S607 (WED-174-YI), S727 (THU-431)
Campagna, Jason, S696 (FRI-189)
Campani, Claudia, S38 (OS-055), S424 (TOP-375-YI), S428 (THU-226-YI), S446 (THU-393-YI), S447 (THU-394), S457 (WED-236), S493 (FRI-221), S499 (FRI-238), S505 (FRI-254), S506 (FRI-255-YI), S507 (FRI-362), S508 (FRI-364-YI)
Campbell, Jean, S182 (FRI-442), S267 (SAT-350)
Campbell, Karen, S968 (WED-609-YI)
Campbell, Kirsty, S208 (WED-480)
Campbell, Lisa, S315 (SAT-286)
Campbell, Louise, S711 (WED-547)
Campeche-Leão, Aloma, S192 (WED-428)
Campello, Elena, S148 (SAT-466-YI), S435 (THU-247), S466 (WED-258)
Campinoti, Sara, S242 (FRI-345-YI), S472 (WED-274)
Campion, Daniela, S3 (GS-005)
Campos, Antonio, S671 (SAT-226)
Campos Gonçalves, Cristina, S850 (THU-308)
Campos-Murguia, Alejandro, S333 (SAT-369), S376 (TOP-520-YI)
Campos-Varela, Isabel, S394 (FRI-507-YI)
Campreciós, Genís, S827 (TOP-297), S862 (WED-315)
Camps Fajol, Montserrat, S191 (WED-427-YI)
Cananzi, Mara, S55 (OS-086), S831 (THU-258-YI), S842 (THU-284)
Canarutto, Giulia, S478 (WED-377)
Canbay, Ali, S40 (OS-058), S395 (FRI-511-YI), S763 (THU-010)
Cancado, Eduardo, S296 (TOP-281), S306 (SAT-262)
Cançado, Eduardo Luiz Rachid, S768 (THU-022)
Cançado, Guilherme, S79 (LBP-026), S296 (TOP-281), S306 (SAT-262), S768 (THU-022)
Cancio-Suarez, Marta Rosas, S25 (OS-029)
Candela, Vicente, S230 (TOP-343-YI)
Candia-Campano, Valeria, S357 (TOP-327-YI), S663 (SAT-199-YI)
Candotti, Daniel, S886 (THU-609)
Canela-Mayoral, José, S771 (THU-030)
Canena, Jorge, S892 (THU-627)
Canga, Elia, S21 (OS-021), S91 (SAT-062), S256 (SAT-542)
Canhão, Bernardo, S331 (SAT-368-YI), S333 (SAT-369)
Canhoto, Manuela, S940 (FRI-589)
Canillas, Lidia, S191 (WED-427-YI), S562 (TOP-097-YI), S612 (WED-188)
Canivet, Clemence, S111 (FRI-043), S199 (WED-450)
Canivet, Clémence M, S525 (THU-103)
Canizales-Quinteros, Samuel, S549 (THU-185-YI)
Cañizares, Maria, S799 (TOP-049)
Cannavò, Maria Rita, S350 (SAT-421)
Cannavò, Mariarita, S69 (LBP-004-YI), S83 (LBP-034-YI), S307 (SAT-263), S335 (SAT-378-YI)
Cannella, Roberto, S494 (FRI-226), S495 (FRI-227)
Cannito, Stefania, S479 (WED-379)
Cannon, Mary D, S503 (FRI-250)
Cano, Sandra Blanco, S815 (WED-006)
Cano-Segarra, Guillem, S459 (WED-242-YI), S468 (WED-263), S485 (WED-396)
Canova, Lorenzo, S405 (FRI-541), S428 (THU-227-YI), S494 (FRI-225)
Cantacorps, Lidia, S672 (SAT-230)
Cantero, José Luis, S273 (THU-316)
Cao, Cheng, S511 (FRI-370)
Cao, Haifang, S941 (FRI-591), S950 (FRI-617), S950 (FRI-618)
Cao, Huanhuan, S430 (THU-229), S508 (FRI-363)
Cao, Jiacheng, S723 (THU-418)
Cao, Ke, S85 (LBP-040)
Cao, Linlin, S253 (SAT-533), S279 (THU-336), S785 (SAT-021)
Cao, Peihua, S416 (FRI-579), S417 (FRI-580)
Cao, Qian, S68 (OS-107)
Cao, Weihua, S905 (SAT-570)
Cao, Yutian, S527 (THU-107)

Cao, Zhujun, S24 (OS-028), S34 (OS-049), S144 (SAT-452), S160 (SAT-507), S166 (FRI-388-YI)
Caparrós, Esther, S169 (FRI-400), S179 (FRI-431-YI), S200 (WED-453), S230 (TOP-343-YI)
Capasso, Mario, S212 (WED-494-YI), S248 (SAT-516)
Capatina, Nadejda, S552 (THU-196)
Capato, Yuri, S102 (THU-060)
Capel, Jeroen, S754 (THU-509)
Capelli, Francesca, S304 (SAT-258), S307 (SAT-263), S335 (SAT-378-YI)
Capilla, Maria, S779 (SAT–003-YI)
Capinha, Francisco, S603 (WED-164), S720 (TOP-504-YI), S726 (THU-428)
Capobianco, Ivan, S512 (FRI-371)
Capoccia, Danila, S626 (WED-231)
Capodicasa, Luigi, S325 (SAT-320)
Capogrossi, Luca, S610 (WED-183)
Caporali, Cristian, S6 (GS-011-YI), S725 (THU-425), S746 (THU-490)
Cappelli, Simone, S695 (FRI-187)
Cappuyns, Sarah, S17 (OS-012), S459 (WED-242-YI), S485 (WED-396), S491 (TOP-408-YI)
Capraro, Ylenia, S726 (THU-429)
Caputo, Valerio, S530 (THU-117), S767 (THU-020)
Caracas, Mariana Lopez, S22 (OS-022-YI)
Caraceni, Paolo, S3 (GS-005), S35 (OS-050-YI), S141 (TOP-437), S150 (SAT-475), S185 (TOP-455-YI), S190 (WED-425), S195 (WED-442-YI), S196 (WED-445), S217 (WED-509-YI), S938 (FRI-586)
Caracta, Cynthia, S5 (GS-008)
Carandina, Riccardo, S402 (FRI-530), S429 (THU-228)
Carbonare, Luca Dalle, S97 (SAT-084-YI)
Carbonell-Asins, Juan Antonio, S170 (FRI-401-YI), S189 (WED-418)
Carbonell, Marta Cervera, S63 (OS-098-YI), S110 (TOP-222), S583 (WED-101), S608 (WED-180)
Carbonell, Nicolas, S110 (FRI-042), S222 (WED-525), S742 (THU-477)
Carbone, Marco, S2 (GS-002), S10 (LBO-006), S67 (OS-106), S69 (LBP-004-YI), S82 (LBP-034-YI), S300 (SAT-250), S303 (SAT-257-YI), S304 (SAT-258), S307 (SAT-263), S315 (SAT-286), S323 (SAT-315), S325 (SAT-320), S330 (SAT-365), S331 (SAT-368-YI), S333 (SAT-369), S335 (SAT-378-YI), S338 (SAT-384), S340 (SAT-393), S349 (SAT-420), S350 (SAT-421), S831 (THU-256-YI)
Carbonero, Luz Martín, S904 (SAT-564)
Cardenas, Diana Marcela Escobar, S556 (THU-212)
Cárdenas-García, Antonio, S678 (SAT-244)
Cárdenas, Sonia Ginés, S599 (WED-151)
Cardinale, Vincenzo, S2 (GS-002), S69 (LBP-004-YI), S350 (SAT-421), S484 (WED-393)
Cardoso, Ana Carolina, S830 (THU-255)
Cardoso, Mariana, S43 (OS-066), S901 (SAT-559), S902 (SAT-560), S934 (TOP-582), S937 (FRI-585-YI), S940 (FRI-589)
Cardoso, Paul Domínguez, S419 (THU-523)
Cardoso Toniasso, Sheila De Castro, S776 (THU-044)
Careaga, María Luisa, S25 (OS-029)
Caremoli, Elena Rota, S494 (FRI-225)
Carey, Ivana, S43 (OS-066), S900 (SAT-559), S901 (SAT-560), S905 (SAT-571), S934 (TOP-582), S937 (FRI-585-YI)
Carey, Nicholas, S871 (THU-560-YI)
Cargill, Zillah, S928 (SAT-628-YI)
Cargil, Zillah, S905 (SAT-571)
Cariati, Sara, S212 (WED-494-YI)
Caricato, Marco, S477 (WED-370)
Carioti, Luca, S49 (OS-076-YI), S919 (SAT-608-YI), S924 (SAT-619)
Cariou, Bertrand, S564 (WED-043)
Cariti, Giuseppe, S911 (SAT-587-YI)
Carlhäll, Carl-Johan, S568 (WED-056)
Carli, Diana, S835 (THU-263)
Carli, Fabrizia, S636 (SAT-109)
Carli, Franco, S380 (FRI-462)
Carlino, Federica, S514 (FRI-381), S576 (WED-083)
Carloni, Vinicio, S481 (WED-383)
Carmen Rico, M., S644 (SAT-137)
Carmichael, Elizabeth, S864 (WED-319-YI)
Carneros, David, S271 (THU-314), S636 (SAT-108)
Carnethon, Mercedes, S546 (THU-173-YI)
Carnevale, Roberto, S856 (WED-291)
Carnicero, Carmen, S542 (THU-164)
Carnì, Paola, S307 (SAT-263)
Carnovale, Vincenzo, S248 (SAT-516)
Carobbio, Stefania, S29 (OS-038)
Carolan, Eimear, S973 (WED-627)
Caroline, Kannengiesser, S853 (WED-283)
Caroline, Lemaitre, S497 (FRI-234)
Caro, María Cristina Torres, S556 (THU-212)
Carot, Jose Miguel, S254 (SAT-538), S779 (SAT–003-YI)
Carotti, Simone, S331 (SAT-368-YI), S477 (WED-370)
Carou-Keenan, Susanna, S10 (LBO-006)
Carpino, Guido, S2 (GS-002), S856 (WED-291)
Carracedo, Raquel, S799 (TOP-049), S910 (SAT-585)
Carradori, Tullia, S835 (THU-263)
Carral, Berta Becerril, S910 (SAT-585)
Carraro, Amedeo, S405 (FRI-541)
Carrasco, Natalia Marcos, S379 (FRI-459), S403 (FRI-532), S403 (FRI-533), S415 (FRI-575)
Carratalá, Arturo, S598 (WED-150), S779 (SAT–003-YI)
Carrat, Fabrice, S46 (OS-070-YI), S66 (OS-104), S325 (SAT-320)
Carreiro-Martins, Pedro, S892 (THU-627)
Carrero, Juan-Jesus, S515 (TOP-112-YI), S570 (WED-060-YI)
Carrero, Zunamys Itzel, S331 (SAT-368-YI), S446 (THU-393-YI), S507 (FRI-362)
Carrieri, Patrizia, S45 (OS-067), S766 (THU-015), S777 (THU-050), S815 (WED-005), S889 (THU-619)
Carrier, Paul, S829 (THU-252)
Carrilho, Flair Jose, S35 (OS-050-YI), S159 (SAT-505)
Carrillo-Fernández, Paloma, S527 (THU-108), S571 (WED-069), S600 (WED-153), S678 (SAT-244)
Carrillo, Irene, S806 (FRI-024)
Carrión, Gemma, S837 (THU-267), S855 (WED-289)
Carrión, Jose, S562 (TOP-097-YI), S612 (WED-188)
Carrión, Jose A., S46 (OS-070-YI), S91 (SAT-062), S191 (WED-427-YI)
Carroll, Charlotte, S321 (SAT-306)
Carroll, Susheela, S321 (SAT-306), S324 (SAT-316), S339 (SAT-387)
Carr, Vanessa, S735 (THU-457)
Carter, Allie, S445 (THU-386)
Carter-Cusack, Dylan, S420 (THU-526)
Carter, Daniel, S814 (WED-004)
Carter, Jessica, S826 (WED-039)
Carter, Matthew, S803 (FRI-014), S818 (WED-013)
Carubbi, Francesca, S316 (SAT-287)
Carucci, Patrizia, S431 (THU-233)
Caruso, Stefano, S38 (OS-054), S343 (SAT-400), S434 (THU-242)
Caruso, Teresita, S481 (WED-383)
Carvalhal, Isabela, S88 (SAT-056), S776 (THU-044)
Carvalhana, Sofia, S603 (WED-164), S621 (WED-214), S726 (THU-428), S765 (THU-013)
Carvalho, Felipe Oliveira, S314 (SAT-284)
Carvalho, Lucas, S296 (TOP-281), S306 (SAT-262), S314 (SAT-284)
Carvalho, Rúben, S940 (FRI-589)
Carvalho, Sandhra, S102 (THU-060)
Casabona, Jordi, S810 (FRI-036)
Casadei Giardini, Andrea, S781 (SAT-009)
Casadei, Mailín, S358 (THU-340-YI), S654 (SAT-171-YI)
Casado-Martin, Marta, S16 (OS-010), S811 (FRI-038), S815 (WED-006), S948 (FRI-611)
Casado-Pelaez, Marta, S485 (WED-396)
Casals, Gregori, S173 (FRI-414)
Casanova, Amparo, S682 (FRI-148)
Casanova, Nicole, S110 (TOP-222)
Casar, Christian, S291 (FRI-291-YI)
Casari, Federica, S378 (FRI-458)
Casari, Federico, S725 (THU-425), S746 (THU-490)
Casas, Francisco Javier, S910 (SAT-581)

Author Index

Casas, Josefina, S28 (OS-037), S629 (TOP-160)
Casas, Meritxell, S562 (TOP-097-YI)
Casato, Milvia, S972 (WED-623)
Cascales, Eva, S910 (SAT-585)
Casciato, Paola, S97 (SAT-085)
Cascio, Antonio, S865 (FRI-638)
Cascio, Giustina Lo, S31 (OS-042), S725 (THU-425)
Casella, Luigi, S831 (THU-256-YI)
Caserta, Antonino, S831 (THU-256-YI)
Casetta, Pauline, S875 (THU-572)
Casiano-Manzano, Sergio, S123 (FRI-086)
Casillas, Linda, S295 (TOP-280)
Casirati, Elia, S476 (WED-368), S575 (WED-076), S636 (SAT-109)
Caskey, Marina, S77 (LBP-022-YI)
Casotti, Valeria, S414 (FRI-571)
Cassiman, David, S840 (THU-275)
Cassinotto, Christophe, S568 (WED-057-YI)
Casta, Adelaida La, S303 (SAT-257-YI), S445 (THU-385)
Castagnede, Maxime, S723 (THU-419)
Castán-Cameo, Susana, S779 (SAT-003-YI)
Castaneda, Jessica Omana, S687 (FRI-165)
Castellaneta, Antonino, S69 (LBP-004-YI), S82 (LBP-034-YI), S304 (SAT-258), S307 (SAT-263), S335 (SAT-378-YI), S350 (SAT-421)
Castellano, Pablo Alonso, S837 (THU-267), S855 (WED-288), S855 (WED-289), S856 (WED-290)
Castellanos Fernández, Marlen Ivon, S794 (SAT-046)
Castellanos, Humberto, S735 (THU-457)
Castelli, Florence, S145 (SAT-458-YI)
Castelli, Marco, S677 (SAT-243-YI)
Castell, Javier, S527 (THU-108)
Castello, Borja, S17 (OS-013), S474 (WED-364)
Castello, Inmaculada, S16 (OS-010)
Castells, Lluis, S394 (FRI-507-YI)
Castelo-Branco, Miguel, S385 (FRI-479)
Castera, Laurent, S26 (OS-032-YI), S62 (OS-097), S424 (TOP-376), S515 (TOP-098), S516 (TOP-113), S517 (TOP-114), S525 (THU-103), S557 (THU-213), S558 (TOP-063-YI), S560 (TOP-066), S561 (TOP-082), S579 (WED-089), S583 (WED-101), S589 (WED-118), S607 (WED-174-YI), S608 (WED-179), S618 (WED-204), S766 (THU-015), S795 (SAT-050)
Castiella, Agustin, S16 (OS-010), S830 (THU-253)
Castillero, Estibaliz, S631 (SAT-095-YI)
Castillo, Anny Camelo, S815 (WED-006)
Castillo-Cruz, Alejandro del, S234 (FRI-316), S635 (SAT-107-YI)
Castillo, Diana, S793 (SAT-044)
Castillo, Mauricio, S34 (OS-049), S35 (OS-050-YI), S141 (TOP-437), S166 (FRI-388-YI)
Castillo-Medina, Marcela, S771 (THU-030)
Castro, Ana Sofia, S296 (TOP-281), S306 (SAT-262)
Castro, Cesar, S112 (FRI-050)
Castro, Josefa, S25 (OS-029)
Castro, José Ignacio, S969 (WED-611)
Castro, Juan Miguel, S806 (FRI-024)
Castro, Lorena, S112 (FRI-050), S296 (TOP-281), S306 (SAT-262)
Castro-Narro, Graciela, S296 (TOP-281), S306 (SAT-262)
Castro, Rafael Romero, S751 (THU-500)
Castven, Darko, S35 (OS-050-YI), S651 (SAT-158-YI), S854 (WED-285)
Castven, Jovana, S854 (WED-285)
Catalá, Myriam, S968 (WED-610-YI)
Catalina, María-Vega, S643 (SAT-134), S723 (THU-418)
Catania, Giulia, S31 (OS-042)
Catanzaro, Elisa, S303 (SAT-257-YI), S304 (SAT-258), S323 (SAT-315)
Catellani, Barbara, S378 (FRI-458)
Catena, Andrea, S531 (THU-120)
Cathcart, Jennifer, S572 (WED-070)
Catney, Charles, S92 (SAT-068)
Cattaazzo, Filippo, S97 (SAT-084-YI)
Cattan, Stéphane, S505 (FRI-254)
Cattazzo, Filippo, S405 (FRI-541), S424 (TOP-375-YI)
Cattelan, Anna Maria, S912 (SAT-587-YI)
Cattelan, Dario, S699 (FRI-200)
Cattell, Caity, S764 (THU-012)
Caudai, Cinzia, S807 (FRI-025)
Caudart, Victor, S493 (FRI-221)
Caudrillier, Axelle, S75 (LBP-017)
Caus-Capdevila, Queralt, S146 (SAT-461)
Causse, Xavier, S43 (OS-066), S829 (THU-252), S934 (TOP-582), S937 (FRI-585-YI)
Caussy, Cyrielle, S62 (OS-097), S516 (TOP-113), S557 (THU-213), S564 (WED-043), S573 (WED-071), S573 (WED-072), S613 (WED-190), S666 (SAT-212), S795 (SAT-050)
Cavailles, Lucie, S53 (OS-082), S54 (OS-084)
Cavalcante, Lourianne, S192 (WED-428), S527 (THU-109)
Cavalieri, Maria Lorena, S850 (THU-308)
Cavalletto, Luisa, S429 (THU-228)
Cavalli, Giovanni, S419 (THU-524)
Cavalli, Ilaria, S69 (LBP-004-YI), S304 (SAT-258), S307 (SAT-263), S335 (SAT-378-YI)
Cavallini, Gabriella, S481 (WED-383)
Cavallo, Clelia, S731 (THU-444-YI), S751 (THU-500)
Cavallone, Daniela, S431 (THU-233), S950 (FRI-619)
Caviglia, Gian Paolo, S3 (GS-005), S49 (OS-076-YI), S431 (THU-233), S476 (WED-368), S525 (THU-103), S534 (THU-133), S574 (WED-073), S611 (WED-184-YI), S620 (WED-213), S912 (SAT-587-YI), S919 (SAT-608-YI)
Cavoli, Tancredi Vincenzo Li, S447 (THU-394)
Çavuş, Bilger, S727 (THU-430), S829 (THU-251)
Cawley, Rionach, S973 (WED-627)
Cayo, Andres Bejarano, S419 (THU-523)
Cazac-Panaite, Georgiana-Diana, S574 (WED-074)
Cazals-Hatem, Dominique, S742 (THU-477)
Cazemier, Marcel, S353 (SAT-432)
Cazzagon, Nora, S10 (LBO-006), S23 (OS-025), S69 (LBP-004-YI), S82 (LBP-034-YI), S303 (SAT-257-YI), S304 (SAT-258), S307 (SAT-263), S325 (SAT-320), S331 (SAT-368-YI), S335 (SAT-378-YI), S350 (SAT-421)
Cazzaniga, Giorgio, S331 (SAT-368-YI)
Ceamanos, Enrique, S603 (WED-163)
Cecil, Goldwin, S36 (OS-051-YI)
Cederberg, Susanne, S953 (FRI-625)
Cedersund, Gunnar, S568 (WED-056)
Cedrón, Hugo, S112 (FRI-050)
Ceesay, Amie, S798 (TOP-034)
Cela, Ester Marina, S912 (SAT-587-YI)
Celen, Mustafa, S961 (WED-589)
Çelik, Ahmet Oğuz, S829 (THU-251)
Çelik, Ferit, S389 (FRI-491)
Celik, Ferya, S704 (THU-538-YI)
Celsa, Ciro, S401 (FRI-528), S424 (TOP-375-YI), S428 (THU-227-YI), S479 (WED-378), S494 (FRI-226), S495 (FRI-227), S514 (FRI-381), S607 (WED-174-YI), S727 (THU-431)
Cembrero, David, S819 (WED-019)
Cenarro, Ana, S28 (OS-037), S629 (TOP-160)
Cengarle, Rita, S494 (FRI-225)
Cerami, Laura, S476 (WED-368), S575 (WED-076), S636 (SAT-109)
Cerda-Alberich, Leonor, S254 (SAT-538), S599 (WED-151)
Cereda, Anna, S831 (THU-256-YI)
Cerenzia, Maria Torrani, S90 (SAT-061-YI)
Cerezal-Gómez, Gemma, S146 (SAT-459)
Ceriani, Roberto, S531 (THU-120)
Cerini, Federica, S69 (LBP-004-YI), S82 (LBP-034-YI), S304 (SAT-258), S307 (SAT-263), S335 (SAT-378-YI), S350 (SAT-421), S429 (THU-227-YI), S696 (FRI-188-YI), S972 (WED-623)
Cerisuelo, Miriam Cortes, S386 (FRI-481-YI), S404 (FRI-538-YI), S408 (FRI-553)
Cernat, Roxana, S1 (GS-001)
Cerny, Andreas, S331 (SAT-368-YI), S570 (WED-061)
Cerón, Lina Palma, S302 (SAT-253)
Cervantes-Alvarez, Eduardo, S210 (WED-485)
Cervesato, Sabrina, S402 (FRI-530)
Cervo, Adriana, S378 (FRI-458)
Cervoni, Jean Paul, S55 (OS-085-YI), S207 (WED-477), S497 (FRI-234), S723 (THU-418), S742 (THU-477)
Cesare, Simona Di, S304 (SAT-258)

Cesario, Silvia, S481 (WED-383)
Cescon, Matteo, S427 (THU-220)
Cespedes, Carlos, S394 (FRI-507-YI)
Cespiati, Annalisa, S443 (THU-380-YI), S520 (THU-091-YI), S541 (THU-158), S553 (THU-197), S595 (WED-137), S636 (SAT-110-YI)
Chabala, Freeman, S926 (SAT-624)
Chabib, Fatima Zahra, S591 (WED-125), S609 (WED-181), S844 (THU-286), S949 (FRI-613)
Chacon, Carla, S63 (OS-098-YI), S608 (WED-180)
Chacon, Maria Fernanda Saavedra, S556 (THU-212)
Chadalavada, Rajagopal, S680 (FRI-141)
Chadra, Prem, S732 (THU-446)
Chae, Yuna, S72 (LBP-010)
Chagas, Marcelo, S724 (THU-420)
Chahal, Daljeet, S59 (OS-091)
Chahal, Sahiba, S460 (WED-243)
Chaharsoughi, Zahra Sarrafan, S918 (SAT-604)
Chahuan, Javier, S303 (SAT-257-YI)
Chaibi, Sayma, S457 (WED-236)
Chaigneau, Julien, S365 (WED-331-YI)
Chai, Jin, S87 (LBP-044)
Chaiteerakij, Roongruedee, S503 (FRI-249), S973 (WED-626-YI)
Chaiyakunapruk, Nathorn, S686 (FRI-163)
Chai, Yuefeng, S941 (FRI-591)
Cha, Jinhye, S528 (THU-111)
Chaker, Jade, S29 (OS-038)
Chakma, Tanmoy, S11 (OS-002-YI), S237 (FRI-324)
Chakrabarty, Adrija, S37 (OS-053)
Chakrabarty, Anasuya, S659 (SAT-186)
Chakrabarty, Gayatri, S713 (WED-556-YI)
Chakraborty, Shreya, S460 (WED-244-YI), S487 (WED-400-YI)
Chakraborty, Sreosi, S100 (THU-056)
Chalasani, Naga, S7 (LBO-001), S19 (OS-016), S62 (OS-096), S531 (THU-122), S681 (FRI-142), S707 (THU-548), S719 (TOP-486)
Chalaye, Julia, S434 (THU-242)
Chambers, Jenny, S354 (SAT-434)
Chambon-Augoyard, Christine, S311 (SAT-271)
Cha, Min Su, S132 (FRI-107)
Chamorro, Nicole, S226 (WED-539), S625 (WED-228)
Chamroonkul, Naichaya, S219 (WED-514), S439 (THU-366-YI), S727 (THU-432)
Chan, Albert CY, S375 (TOP-519), S422 (TOP-359-YI)
Chan, Andrew, S400 (FRI-524)
Chandasana, Hardik, S689 (FRI-169)
Chanda, Sushmita, S658 (SAT-184), S889 (THU-620), S959 (WED-586), S960 (WED-588), S965 (WED-602)
Chandiramani, Abhishek, S87 (LBP-043)
Chandok, Natasha, S330 (SAT-366)
Chan, Doreen, S681 (FRI-142), S697 (FRI-191)
Chand, Phool, S171 (FRI-404)
Chandramohan, Sivanathan, S495 (FRI-228-YI)
Chandrananda, Dineika, S458 (WED-240)
Chan, Esther Wai Yin, S824 (WED-035)
Chang, Baoli, S166 (FRI-393)
Chang, Caihua, S357 (SAT-445)
Chang, Chun-Yi, S797 (TOP-033)
Chang, Fenghe, S259 (SAT-554)
Chang, Jason Pik Eu, S149 (SAT-473), S529 (THU-115), S714 (WED-559-YI)
Chang, Johannes, S6 (GS-011-YI), S33 (OS-046), S54 (OS-084), S185 (TOP-456-YI), S213 (WED-496), S736 (THU-460-YI), S744 (THU-482-YI), S747 (THU-492), S752 (THU-501)
Chang, Kyong-Mi, S166 (FRI-393)
Chang, Lijun, S517 (TOP-114)
Chang, Liuyi, S98 (SAT-088)
Chang, Ruizhi, S711 (WED-548-YI)
Chang, Sandra, S889 (THU-620)
Changsiriwattanathomrong, Nuprawee, S727 (THU-432)
Chang, Tien En, S395 (FRI-510)
Chang, Ting-Tsung, S893 (THU-633)
Chang, Yoosoo, S553 (THU-198)
Chang, Young, S528 (THU-111), S590 (WED-121), S637 (SAT-111)
Chang, Yu-Cheng, S893 (THU-633)
Chang, Yu-Chuan, S893 (THU-633)
Chang, Yu Ping, S969 (WED-612), S969 (WED-613)
Chan, Henry L. Y., S943 (FRI-594)
Chan, Henry L.Y., S66 (OS-103-YI)
Chan, Lapkwan, S465 (WED-255)
Channaoui, Aniss, S381 (FRI-465)
Chan, Po-Lin, S824 (WED-035)
Chan, Sau-Wai Mandy, S525 (THU-103), S558 (TOP-063-YI), S607 (WED-174-YI)
Chan, Stephen, S438 (THU-364), S496 (FRI-230)
Chan, Talia Yi Hui, S528 (THU-110)
Chan, Wah Kheong, S452 (THU-414-YI)
Chan, Wah-Kheong, S62 (OS-097), S127 (FRI-095), S424 (TOP-376), S516 (TOP-113), S517 (TOP-114), S525 (THU-103), S568 (WED-057-YI), S574 (WED-075), S593 (WED-132), S766 (THU-015), S794 (SAT-046), S923 (SAT-618)
Chan, Wan Ying, S495 (FRI-228-YI)
Chanwidoon, Phatcharaporn, S206 (WED-476)
Chao, Tingxia, S950 (FRI-617)
Chapman, Kenneth, S5 (GS-008)
Chappell, Catherine, S70 (LBP-005), S975 (WED-636), S976 (WED-637)
Chapus, Fleur, S869 (TOP-632)
Chara, Beatriz, S745 (THU-483)
Charatcharoenwitthaya, Phunchai, S127 (FRI-095), S219 (WED-514), S923 (SAT-618)
Charles, Hattie, S384 (FRI-475)
Charles, Jasmin, S70 (LBP-005), S975 (WED-636), S976 (WED-637)
Charlot, Anouk, S463 (WED-250)
Charre, Caroline, S942 (FRI-592)
Charrière, Sybil, S564 (WED-043)
Chartier, Marie-Eve, S386 (FRI-480-YI)
Chascsa, David M. H., S390 (FRI-493-YI), S604 (WED-166)
Chase, Geoffrey, S297 (TOP-293), S341 (SAT-397)
Cha, Seungha, S448 (THU-397)
Chattergoon, Michael A., S7 (GS-012), S958 (WED-581)
Chatterley, Mark, S346 (SAT-412)
Chatzigeorgiou, Antonios, S507 (FRI-257)
Chaudhry, Neera, S217 (WED-510)
Chaudry, Fatima, S845 (THU-289)
Chau, Gar-Yang, S500 (FRI-240), S510 (FRI-369-YI)
Chauhan, Sachin, S461 (WED-245)
Chauhan, Vishal, S184 (TOP-454-YI), S247 (SAT-514), S299 (SAT-248)
Chaurasia, Rahul, S141 (TOP-423)
Chaves-Blanco, Lucía, S910 (SAT-581)
Chayama, Kazuaki, S873 (THU-564)
Chazouillères, Olivier, S325 (SAT-320)
Checkley, Elliot, S106 (THU-075)
Chee, Grace M., S321 (SAT-306)
Cheema, Keswir Singh, S709 (THU-556-YI)
Cheent, Kuldeep, S713 (WED-556-YI)
Cheinquer, Hugo, S296 (TOP-281), S306 (SAT-262)
Chemello, Liliana, S429 (THU-228)
Chemin, Isabelle, S798 (TOP-034)
Chen, Bin, S73 (LBP-013)
Chen, Binbin, S511 (FRI-370)
Chen, Cheng-Jen, S735 (THU-452)
Chen, Chengwei, S93 (SAT-072)
Chen, Chia-Chang, S972 (WED-624)
Chen, Chien-Hung, S1 (GS-001), S46 (OS-070-YI)
Chen, Chien-Jen, S797 (TOP-033), S898 (TOP-567), S898 (TOP-568), S915 (SAT-594), S917 (SAT-601-YI), S929 (SAT-633)
Chen, Chi-Yi, S958 (WED-580), S969 (WED-613)
Chen, Chuanwen, S954 (FRI-626)
Chen, Claire, S450 (THU-402)
Chen, Dongbo, S454 (TOP-391), S461 (WED-246), S480 (WED-381), S514 (FRI-380), S668 (SAT-217-YI)
Cheneke, Waqtola, S926 (SAT-622-YI)
Chen, Elizabeth, S714 (WED-559-YI)
Chen, Fangfang, S428 (THU-225-YI)
Chen, Fen-Fang, S449 (THU-399)
Chen, Fengjuan, S259 (SAT-554), S593 (WED-134)
Chen, Fuwang, S467 (WED-260)
Chen, Gang, S442 (THU-379), S509 (FRI-365)
Cheng, Bin, S946 (FRI-606)

Author Index

Cheng, Changhao, S6 (GS-010), S644 (SAT-136)
Cheng, Cong, S932 (SAT-641)
Cheng, Danying, S86 (LBP-041)
Cheng, Fan-E, S233 (FRI-314), S664 (SAT-202), S664 (SAT-203), S665 (SAT-204), S666 (SAT-206), S872 (THU-562)
Cheng, Feng, S362 (THU-356)
Cheng, Guofeng, S81 (LBP-031), S884 (THU-605)
Cheng, Ho Ming, S422 (TOP-359-YI), S423 (TOP-360)
Cheng, Hsu-sheng, S691 (FRI-174)
Cheng, Hui, S593 (WED-134)
Cheng, Peilin, S924 (SAT-620)
Cheng, Pin-Nan, S958 (WED-580)
Cheng, Xiao, S756 (THU-513)
Cheng, Xiaoming, S895 (THU-638), S895 (THU-639)
Cheng, Yue, S38 (OS-054)
Chen, Haiyan, S954 (FRI-626)
Chen, Hening, S665 (SAT-205)
Chen, Hongsong, S454 (TOP-391), S480 (WED-381), S514 (FRI-380), S668 (SAT-217-YI)
Chen, Huaiyu, S430 (THU-229), S508 (FRI-363)
Chen, Huan, S230 (TOP-344)
Chen, Huey-Ling, S55 (OS-086), S831 (THU-258-YI), S842 (THU-284)
Chen, I-Chieh, S972 (WED-624)
Chen, Jenny, S875 (THU-574)
Chen, Jia, S155 (SAT-491), S155 (SAT-493), S805 (FRI-021)
Chen, Jialiang, S258 (SAT-548)
Chen, Jiamei, S778 (THU-053)
Chen, Jiaxian, S104 (THU-070)
Chen, Jinjun, S86 (LBP-041), S98 (SAT-087), S162 (TOP-440), S228 (WED-544), S754 (THU-508), S756 (THU-513)
Chen, Jinwei, S358 (THU-341)
Chen, Jinzhang, S430 (THU-229), S508 (FRI-363)
Chen, Jiyang, S158 (SAT-501), S262 (SAT-331)
Chen, Joshua, S773 (THU-037)
Chen, Jun, S537 (THU-139), S816 (WED-007), S952 (FRI-623)
Chen, Kaina, S495 (FRI-228-YI), S529 (THU-115), S560 (TOP-080)
Chen, Lei, S33 (OS-047)
Chen, Li, S243 (FRI-349), S517 (TOP-114)
Chen, Li-Chang, S430 (THU-231)
Chen, Lijian, S270 (SAT-356)
Chen, Lijuan, S755 (THU-511), S757 (THU-515)
Chen, Ling, S688 (FRI-167)
Chen, Matthew, S308 (SAT-265), S309 (SAT-266)
Chen, Mei-Tsu, S691 (FRI-174)
Chen, Michael, S694 (FRI-183)
Chen, Michael Hao, S529 (THU-115)
Chen, Mingyue, S81 (LBP-031)
Chen, Minshan, S511 (FRI-370)
Chen, Mitchell, S490 (TOP-407-YI)
Chen, Pan, S73 (LBP-013)
Chen, Pei-Jer, S898 (TOP-566-YI), S898 (TOP-567), S917 (SAT-601-YI), S969 (WED-613)
Chen, Po-Chun, S963 (WED-596)
Chen, Pohan, S619 (WED-206)
Chen, Qian, S537 (THU-139)
Chen, Qiuyang, S637 (SAT-116)
Chen, Ronghui, S511 (FRI-370)
Chen, Ruicong, S369 (WED-341)
Chen, Ruihan, S418 (THU-521)
Chen, Runfen, S511 (FRI-370)
Chen, Sainan, S139 (FRI-134)
Chen, Shangci, S177 (FRI-426)
Chen, Shaozhen, S46 (OS-069)
Chen, Shiyao, S86 (LBP-041), S231 (FRI-306-YI)
Chen, Shuai, S3 (GS-004-YI)
Chen, Shu-Ling, S30 (OS-040), S627 (TOP-130), S640 (SAT-123)
Chen, Shuyan, S826 (WED-040)
Chen, Tao, S67 (OS-105-YI), S952 (FRI-622)
Chen, Tianyan, S14 (OS-008), S295 (TOP-279), S325 (SAT-319), S354 (SAT-435), S380 (FRI-462), S533 (THU-127-YI), S616 (WED-200), S952 (FRI-623)
Chen, Tzu-Haw, S943 (FRI-596)
Chen, Vincent, S156 (SAT-496), S215 (WED-505), S221 (WED-523), S228 (WED-543), S423 (TOP-374), S461 (WED-247), S528 (THU-110), S560 (TOP-066), S561 (TOP-082), S579 (WED-089), S698 (FRI-197)
Chen, Weena, S9 (LBO-005-YI)
Chen, Wei, S30 (OS-040), S627 (TOP-130), S640 (SAT-123)
Chen, Wenbo, S262 (SAT-330)
Chen, Wenhui, S511 (FRI-370)
Chen, Xia, S756 (THU-514)
Chen, Xiaofei, S85 (LBP-040)
Chen, Xiaolong, S419 (THU-522), S495 (FRI-229)
Chen, Xin, S151 (SAT-476)
Chen, Xinai, S895 (THU-638)
Chen, Xinyu, S495 (FRI-228-YI)
Chen, Xin-Yue, S952 (FRI-623)
Chen, Xiyao, S155 (SAT-493)
Chen, Yanhua, S166 (FRI-393), S192 (WED-430)
Chen, Yen-Tung, S238 (FRI-332)
Chen, Yidan, S869 (TOP-630), S872 (THU-561)
Chen, Yi-Ming, S972 (WED-624)
Chen, Yu, S93 (SAT-071), S146 (SAT-460), S151 (SAT-476), S293 (FRI-302-YI), S305 (SAT-259), S352 (SAT-428-YI), S676 (SAT-240), S852 (TOP-312)
Chen, Yuanwei, S688 (FRI-167)
Chen, Yuchuan, S6 (GS-010), S270 (SAT-356), S486 (WED-397), S644 (SAT-136)
Chen, Yue, S665 (SAT-205)
Chen, Yun-Chu, S969 (WED-613)
Chen, Yun-Yu, S972 (WED-624)
Chen, Yuping, S119 (FRI-072), S560 (TOP-080)
Chen, Yuxin, S930 (SAT-635)
Chen, Yuxing, S906 (SAT-572)
Chen, Zhenwei, S609 (WED-182), S924 (SAT-620)
Chen, Zhiji, S192 (WED-429-YI), S441 (THU-372-YI)
Chen, Zhi-wei, S906 (SAT-572)
Chen, ZhiWei, S50 (OS-078), S495 (FRI-229), S637 (SAT-115)
Chen, Ziqi, S756 (THU-512)
Chen, Ziyao, S458 (WED-238)
Chen, Ziye, S107 (THU-077)
Cheong, Jae Youn, S264 (SAT-337)
Cherian, Mathew, S780 (SAT-005)
Chermak, Faiza, S380 (FRI-463), S381 (FRI-464)
Cherniavskyi, Volodymyr, S71 (LBP-007)
Chernova, Valentina, S604 (WED-167)
Cherubini, Alessandro, S241 (FRI-340), S476 (WED-368), S575 (WED-076), S636 (SAT-109)
Chessa, Luchino, S69 (LBP-004-YI), S82 (LBP-034-YI), S304 (SAT-258), S307 (SAT-263), S335 (SAT-378-YI)
Chesta, Caterina, S187 (TOP-471-YI)
Chetwood, John, S736 (THU-458)
Cheung, Amanda, S388 (FRI-489), S411 (FRI-560), S846 (THU-291), S846 (THU-298)
Cheung, Angela, S14 (OS-008), S295 (TOP-279), S325 (SAT-319), S354 (SAT-435)
Cheung, Ka Shing, S438 (THU-364), S496 (FRI-230)
Cheung, Ramsey C., S355 (SAT-441), S966 (WED-604)
Cheung, Tan-To, S422 (TOP-359-YI)
Chevalier, Nicolas, S681 (FRI-147)
Chevaliez, Stéphane, S798 (TOP-034), S886 (THU-609)
Chevret, Sylvie, S731 (THU-445-YI)
Chew, Johnny, S302 (SAT-254)
Chew, Nicholas Foo-Siong, S868 (FRI-644)
Chew, Valerie, S458 (WED-238)
Che, Xiao, S146 (SAT-460), S676 (SAT-240)
Chhabra, Pankdeep, S908 (SAT-578)
Chhor, Guillaume, S578 (WED-087)
Chia, Nam-Hung, S422 (TOP-359-YI)
Chiang, CL, S375 (TOP-519), S438 (THU-364), S496 (FRI-230)
Chia, Pei-Yuh, S834 (THU-261)
Chiara Chindamo, Maria, S830 (THU-255)
Chiara, Francesco De, S180 (FRI-434), S647 (SAT-149)
Chiavaroli, Roberto, S304 (SAT-258), S335 (SAT-378-YI)
Chi, Chen-Ta, S500 (FRI-239)
Chidambaram, Vaishnavi, S651 (SAT-158-YI)

Chien, Rong-Nan, S46 (OS-070-YI), S919 (SAT-606), S945 (FRI-603), S947 (FRI-607)
Chiew, Evelyn, S495 (FRI-228-YI)
Chignard, Nicolas, S235 (FRI-320)
Chilmeran, Ziad, S709 (THU-556-YI)
Chimbo, Daniela Ortiz, S403 (FRI-532)
Chinaka, Ifechukwuamaka, S461 (WED-247)
China, Louise, S52 (OS-081), S747 (THU-492)
Chindamo, Maria Chiara, S296 (TOP-281), S306 (SAT-262), S314 (SAT-284), S340 (SAT-394), S830 (THU-254)
Chinnappan, Sujatha, S782 (SAT-010-YI)
Chinzon, Miriam, S978 (WED-641)
Chiou, Fang Kuan, S834 (THU-261)
Chiou, Yu-Wei, S893 (THU-633)
Chirapongsathorn, Sakkarin, S86 (LBP-042), S121 (FRI-078), S452 (THU-414-YI)
Chiriac, Stefan, S211 (WED-493)
Chitul, Mirela, S43 (OS-066), S819 (WED-015), S934 (TOP-582), S937 (FRI-585-YI), S944 (FRI-601)
Chiu, Keith Wan-Hang, S422 (TOP-359-YI)
Ch Lui, Vincent, S860 (WED-306)
Ch'ng, Chin Lye, S256 (SAT-543)
Chng, Elaine, S84 (LBP-036), S533 (THU-126), S546 (THU-174), S561 (TOP-081), S697 (FRI-191)
Cho, Dana, S879 (THU-587)
Choe, Eun Kyung, S538 (THU-147)
Cho, Eun Ju, S502 (FRI-245), S507 (FRI-361), S509 (FRI-366), S906 (SAT-573)
Chogsom, Munkhzaya, S48 (OS-074)
Cho, Hee Sun, S135 (FRI-119), S478 (WED-372), S510 (FRI-368)
Cho, Hyeon-Yeol, S891 (THU-625)
Cho, Hyun Myung, S437 (THU-361)
Choi, Dongho, S360 (THU-351)
Choi, Eunho, S135 (FRI-120), S498 (FRI-236)
Choi, Gwang Hyeon, S706 (THU-543), S906 (SAT-573)
Choi, Ho Joong, S482 (WED-386)
Choi, Hwa Young, S823 (WED-030)
Choi, Ji Min, S538 (THU-147)
Choi, Jonggi, S4 (GS-006), S4 (GS-007), S503 (FRI-249), S707 (THU-547)
Choi, Jong Young, S421 (THU-530)
Choi, Na Ryung, S92 (SAT-069)
Choi, Sang Hyun, S4 (GS-007), S443 (THU-381), S497 (FRI-232)
Choi, Sung Eun, S368 (WED-337-YI)
Choi, Won-Mook, S4 (GS-006), S4 (GS-007), S251 (SAT-528), S423 (TOP-374), S707 (THU-547), S823 (WED-030), S824 (WED-035), S928 (SAT-628-YI)
Cho, Jeong-Yeon, S545 (THU-171), S591 (WED-122), S625 (WED-229), S630 (SAT-092), S652 (SAT-165), S686 (FRI-163)
Cho, Ju-Yeon, S92 (SAT-069), S553 (THU-198), S927 (SAT-625)
Chokshi, Shilpa, S164 (FRI-385-YI), S184 (FRI-453-YI), S242 (FRI-345-YI), S472 (WED-274)
Chollet, Celine, S145 (SAT-458-YI)
Cholongitas, Evangelos, S45 (OS-068-YI), S314 (SAT-283), S545 (THU-172)
Chong, Shay Lee, S495 (FRI-228-YI)
Chon, Hong Jae, S426 (THU-219-YI)
Choo, Jocelyn, S699 (FRI-198)
Choong, Ingrid, S965 (WED-603)
Cho, Sung Bum, S497 (FRI-233)
Chotkoe, Shivani, S638 (SAT-117-YI)
Chou, Chia-Yi, S471 (WED-270)
Choudhary, Narendra S, S62 (OS-097), S516 (TOP-113), S952 (FRI-622)
Choudhury, Ashok Kumar, S24 (OS-028), S67 (OS-105-YI), S144 (SAT-452), S156 (SAT-495), S157 (SAT-498), S160 (SAT-507), S719 (TOP-487-YI), S952 (FRI-622)
Choudhury, Soumyadeep, S36 (OS-051-YI)
Choudhury, Yukti, S84 (LBP-036), S546 (THU-174), S697 (FRI-191)
Chouik, Yasmina, S311 (SAT-271), S573 (WED-071)
Chou, Pei-Lien, S446 (THU-387)
Chowdhury, Abhijit, S100 (THU-056)
Chowdhury, Mohammed Salahuddin Shahed, S598 (WED-149)
Chowdhury, Nashit, S820 (WED-022)
Chowdhury, Shruti, S878 (THU-585-YI)
Chowdhury, Zarin, S725 (THU-427)
Chow, Min, S593 (WED-132)
Chow, Pierce, S495 (FRI-228-YI)
Chow, Sophie, S958 (WED-581)
Choyke, Peter, S413 (FRI-569)
Cho, Yong Kyun, S553 (THU-198)
Cho, Young Youn, S518 (TOP-129)
Cho, Yuri, S500 (FRI-241), S509 (FRI-366)
Christensen, Bo, S786 (SAT-024-YI)
Christensen, Nana, S853 (WED-282-YI)
Christian-Cox, Florence, S939 (FRI-587), S956 (WED-576)
Christiansen, Frederik, S592 (WED-131)
Christiansen, Marie, S711 (WED-549-YI)
Christie, Mo, S333 (SAT-370)
Christinet, Montserrat Fraga, S72 (LBP-011), S199 (WED-450)
Chrysostomou, Despoina, S500 (FRI-239)
Chua, Cheryl Min En, S495 (FRI-228-YI)
Chua, Damien, S698 (FRI-197)
Chua, Lorenz, S852 (TOP-311), S858 (WED-302)
Chuang, Hsiang-Hsuan, S274 (THU-319), S898 (TOP-568)
Chuang, Jen-Chieh, S667 (SAT-213), S847 (THU-300), S848 (THU-301)
Chuang, Wan-Long, S1 (GS-001), S518 (TOP-128), S943 (FRI-594), S953 (FRI-624)
Chua, Siou Sze, S495 (FRI-228-YI)
Chubb, Daniel Clayton, S218 (WED-513), S749 (THU-496)
Chuensakul, Suppana, S219 (WED-514)
Chu, Jaime, S538 (THU-148-YI)
Chu, Janet, S534 (THU-132)
Chulanov, Vladimir, S939 (FRI-587), S956 (WED-576), S962 (WED-593)
Chuma, Makoto, S506 (FRI-256)
Chumbiauca, Estefanía, S608 (WED-175)
Chung, Annabelle, S89 (SAT-058)
Chung, HyunJung, S133 (FRI-111), S360 (THU-352)
Chung, Matthew Shing Hin, S438 (THU-364), S496 (FRI-230)
Chung, Sung Won, S4 (GS-006), S4 (GS-007), S502 (FRI-245), S503 (FRI-249), S707 (THU-547)
Chung, Taek, S38 (OS-054)
Chung, Yooyun, S767 (THU-019)
Chun, Ho Soo, S906 (SAT-574)
Churkina, Yuliia, S595 (WED-136)
Chvatal-Medina, Mateo, S384 (FRI-476-YI), S384 (FRI-477), S385 (FRI-478), S430 (THU-232)
Ciancio, Alessia, S43 (OS-066), S900 (SAT-559), S901 (SAT-560), S911 (SAT-587-YI), S919 (SAT-608-YI), S934 (TOP-582), S936 (TOP-584), S937 (FRI-585-YI), S938 (FRI-586), S947 (FRI-608)
Cibali, Ezgi, S456 (WED-234-YI)
Ciccarelli, Olga, S59 (OS-091), S381 (FRI-465), S382 (FRI-466)
Ciccia, Roberta, S494 (FRI-226)
Cicognini, Daniela, S462 (WED-248)
Čiefová, Jana, S123 (FRI-085)
Ciepiela, Olga, S301 (SAT-251-YI)
Cieply, Lukasz, S811 (FRI-038)
Ciere, Sophie, S828 (TOP-310-YI)
Cillo, Umberto, S49 (OS-076-YI), S402 (FRI-530), S429 (THU-228), S466 (WED-258), S485 (WED-395-YI), S919 (SAT-608-YI)
Cimino, Maura, S638 (SAT-118)
Ciminski, Kevin, S371 (WED-348)
Cinque, Felice, S62 (OS-097), S516 (TOP-113), S520 (THU-091-YI), S529 (THU-116-YI), S534 (THU-131), S541 (THU-158), S553 (THU-197), S595 (WED-137), S636 (SAT-110-YI), S865 (FRI-638)
Ciocca, Lorenzo, S110 (TOP-222), S246 (TOP-552)
Cioce, Mario, S477 (WED-370)
Cioclu, George, S209 (WED-483)
Ciordia, Sergio, S474 (WED-364)
Cipriano, Maria Agusta, S331 (SAT-368-YI)
Cirella, Antonio, S530 (THU-117), S767 (THU-020)
Cirelli, Riccardo, S670 (SAT-225)
Ciriaci, Nadia, S853 (WED-283)
Cirillo, Chris, S334 (SAT-371), S334 (SAT-372), S334 (SAT-377)
Cirrincione, Giansalvo, S494 (FRI-226), S495 (FRI-227), S607 (WED-174-YI)
Citores, Laura Perez, S819 (WED-019)
Cittadine, Andrew, S39 (OS-057)

Author Index

Civolani, Alberto, S850 (THU-307), S857 (WED-298), S912 (SAT-587-YI)
Civolani, Rocco, S850 (THU-307)
Cizkova, Alena, S855 (WED-288)
Claas, Eirini, S33 (OS-046)
Clareburt, Alban, S709 (THU-556-YI)
Claria, Joan, S148 (SAT-467-YI), S170 (FRI-401-YI)
Clària, Joan, S34 (OS-049), S35 (OS-050-YI), S141 (TOP-437), S146 (SAT-461), S149 (SAT-468), S152 (SAT-478), S159 (SAT-505), S166 (FRI-388-YI), S172 (FRI-412), S261 (SAT-329-YI), S760 (TOP-032)
Clark, Doug, S959 (WED-586)
Clark, Nathaniel, S164 (FRI-385-YI), S184 (FRI-453-YI)
Clark, Paul, S121 (FRI-077), S803 (FRI-014), S818 (WED-013)
Clark, Virginia C., S834 (THU-262), S836 (THU-266), S847 (THU-300), S848 (THU-301)
Claudel, Thierry, S237 (FRI-324)
Clavier, Jean-Basptiste, S414 (FRI-572)
Clayton-Chubb, Daniel, S65 (OS-102), S970 (WED-619)
Clayton, Michelle, S712 (WED-553-YI)
Clemente, Marina, S69 (LBP-004-YI), S82 (LBP-034-YI), S300 (SAT-250), S307 (SAT-263)
Clements, Angharad, S338 (SAT-385)
Cloherty, Gavin, S80 (LBP-028-YI), S798 (TOP-034), S905 (SAT-571), S911 (SAT-586), S947 (FRI-609), S960 (WED-588)
Clore, Gosia, S220 (WED-521)
Cloutier, Meghan, S161 (SAT-509)
Clua-García, Rafael, S710 (THU-557-YI)
Cobitz, Alexander, S295 (TOP-280)
Cocca, Massimiliano, S478 (WED-377)
Cocchis, Donatella, S784 (SAT-015-YI)
Cocco, Arianna, S699 (FRI-200)
Coco, Barbara, S82 (LBP-034-YI), S304 (SAT-258), S307 (SAT-263), S335 (SAT-378-YI), S350 (SAT-421), S440 (THU-369), S831 (THU-256-YI), S911 (SAT-587-YI), S938 (FRI-586), S950 (FRI-619)
Codinach, Jordi, S32 (OS-044)
Codoceo, Carolina Muñoz, S124 (FRI-088), S837 (THU-267)
Coedo, Ana, S195 (WED-442-YI)
Coenen, Sandra, S61 (OS-095-YI)
Coenraad, Minneke, S145 (SAT-458-YI), S148 (SAT-467-YI), S150 (SAT-475), S167 (FRI-395-YI), S261 (SAT-329-YI), S385 (FRI-479), S415 (FRI-574), S729 (THU-436)
Coessens, Marie, S907 (SAT-575)
Coffin, Carla, S1 (GS-001), S43 (OS-066), S47 (OS-072), S76 (LBP-021), S820 (WED-022), S897 (TOP-565), S937 (FRI-585-YI), S957 (WED-577), S968 (WED-609-YI)
Coghlan, Miriam, S708 (THU-549-YI)
Cogliati, Sara, S101 (THU-059-YI), S855 (WED-287-YI)
Cohen, Chari, S805 (FRI-022), S816 (WED-008), S897 (TOP-565)
Cohn, Amanda, S798 (TOP-048)
Coilly, Audrey, S374 (TOP-503), S380 (FRI-463), S381 (FRI-464), S399 (FRI-523), S742 (THU-477)
Coimbra, Tomás, S167 (FRI-395-YI)
Cointet, Alix, S571 (WED-067)
Coirier, Valentin, S143 (SAT-450)
Colangelo, Laura, S546 (THU-173-YI)
Colapietro, Francesca, S82 (LBP-034-YI), S305 (SAT-260-YI), S307 (SAT-263), S331 (SAT-368-YI), S335 (SAT-378-YI)
Cola, Simone Di, S196 (WED-444), S397 (FRI-515)
Colasurdo, Rossella, S457 (WED-235)
Coldwell, Kate, S43 (OS-065)
Cole, Alexander, S224 (WED-530)
Colecchia, Antonio, S412 (FRI-562), S412 (FRI-563), S427 (THU-220), S733 (THU-450)
Cole, John, S364 (WED-324-YI)
Colella, Fabio, S12 (OS-004-YI)
Colell, Anna, S481 (WED-382-YI)
Coli, Lucia, S288 (FRI-283)
Collado, Ana Gómez, S391 (FRI-497)
Collado, Ana Sofia, S643 (SAT-134)
Collado, Francina, S762 (THU-008)
Collardeau-Frachon, Sophie, S836 (THU-265-YI)
Collatz, Maximilian, S885 (THU-608)
Collazos, Cristina, S21 (OS-021)
Colle, Isabelle, S315 (SAT-285), S849 (THU-306-YI), S920 (SAT-609), S929 (SAT-629)
Coll, Mar, S129 (FRI-101)
Collot, Julia, S386 (FRI-480-YI)
Colmenero, Jordi, S59 (OS-091), S394 (FRI-507-YI), S410 (FRI-558)
Colognesi, Martina, S669 (SAT-219)
Coloma, María Pascual, S59 (OS-091)
Colombatto, Piero, S431 (THU-233), S481 (WED-383), S831 (THU-256-YI), S911 (SAT-587-YI), S950 (FRI-619)
Colominas, Elena, S969 (WED-611)
Colom, Joan, S810 (FRI-036)
Coltart, Iona, S713 (WED-556-YI)
Coltorti, Erika, S407 (FRI-548)
Colyn, Leticia, S474 (WED-364)
Comai, Stefano, S669 (SAT-219)
Combes, Damien, S554 (THU-202)
Comellas, Eva Maria Guix, S394 (FRI-508), S407 (FRI-547)
Comia, Bezalel, S767 (THU-019)
Commin, Apolline, S493 (FRI-221), S508 (FRI-364-YI)
Conceco, Ana, S806 (FRI-024)
Concha, Javiera, S608 (WED-175)
Conde, Isabel, S16 (OS-010), S300 (SAT-250), S309 (SAT-268)
Conde, Marta Hernández, S585 (WED-105), S585 (WED-106), S598 (WED-150), S612 (WED-186-YI), S772 (THU-036), S948 (FRI-611)
Conde, M. Sanchez, S806 (FRI-024)
Conde, Silvia Vilares, S892 (THU-627)
Conejero, María Dolores Antón, S16 (OS-010)
Conejos, Luisa, S810 (FRI-036)
Conforti, Massimiliano, S947 (FRI-608)
Congdon, Kendra, S8 (LBO-003)
Congly, Stephen, S505 (FRI-253)
Cong, Xu, S593 (WED-133)
Connelly, Margery A., S384 (FRI-476-YI), S384 (FRI-477), S385 (FRI-478)
Connor, Jason, S121 (FRI-077), S803 (FRI-014), S818 (WED-013)
Conquet, Nicolas, S111 (FRI-043)
Conrad, Christian, S852 (TOP-311), S859 (WED-302)
Conron, Matthew, S5 (GS-008)
Conrotto, Federico, S402 (FRI-531)
Conroy, Guillaume, S37 (OS-052)
Consortium, Uk-Aih, S331 (SAT-368-YI)
Consuegra, José García, S101 (THU-059-YI), S272 (THU-315-YI), S855 (WED-287-YI)
Contegiacomo, Andrea, S731 (THU-444-YI)
Conter, Carolina, S30 (OS-039-YI), S272 (THU-315-YI), S273 (THU-316), S489 (WED-412-YI), S855 (WED-287-YI)
Conthe, Andres, S54 (OS-084), S427 (THU-220), S723 (THU-418)
Conti, Filomena, S380 (FRI-463), S381 (FRI-464)
Contino, Salvatore, S494 (FRI-226), S495 (FRI-227), S607 (WED-174-YI)
Contreras, Bryan J., S172 (FRI-412)
Contreras, Laura, S563 (WED-042), S597 (WED-141)
Contreras, Luis, S467 (WED-260)
Conway, Brian, S968 (WED-609-YI)
Cook, Emma, S386 (FRI-481-YI)
Cook, Robert, S974 (WED-628)
Coomans, Ilse, S526 (THU-106)
Cooper, Curtis, S47 (OS-072), S529 (THU-116-YI), S908 (SAT-576), S968 (WED-609-YI)
Cooper, Daniel, S753 (THU-506)
Cooper, Darren, S718 (WED-574)
Cooper, Katherine, S306 (SAT-261)
Cooper, Keith, S25 (OS-030), S622 (WED-217)
Cooper, Stewart, S871 (THU-560-YI)
Cooper, Yasmeen, S772 (THU-035)
Cooreman, Michael, S639 (SAT-119)
Cope, Nigel, S61 (OS-108)
Coppola, Annachiara, S639 (SAT-121-YI), S660 (SAT-190)
Coppola, Carmine, S911 (SAT-587-YI)
Coppola, Nicola, S43 (OS-066), S176 (FRI-425), S190 (WED-425), S212 (WED-494-YI), S479 (WED-378), S900 (SAT-559), S902 (SAT-560), S912 (SAT-587-YI), S934 (TOP-582),

S937 (FRI-585-YI), S938 (FRI-586), S947 (FRI-608)
Corallo, Salvatore, S370 (WED-346), S462 (WED-248), S494 (FRI-225)
Corchado-Berjano, Cristina, S250 (SAT-524)
Cordell, Heather, S166 (FRI-393)
Cordero-Pérez, Paula, S236 (FRI-322)
Cordie, Ahmed, S62 (OS-097), S516 (TOP-113), S537 (THU-141-YI), S538 (THU-142), S575 (WED-077), S576 (WED-078), S865 (FRI-638)
Córdoba, Juan, S296 (TOP-281), S306 (SAT-262)
Cordoni, Marta, S610 (WED-183)
Cordova-Gallardo, Jacqueline, S24 (OS-028), S144 (SAT-452), S160 (SAT-507), S771 (THU-030)
Coremans, Laura, S907 (SAT-575)
Core, Paolo, S576 (WED-083)
Coriat, Romain, S493 (FRI-221), S508 (FRI-364-YI)
Cornberg, Markus, S46 (OS-070-YI), S197 (WED-446), S737 (THU-461), S878 (THU-585-YI), S887 (THU-611), S897 (TOP-565), S963 (WED-596)
Cornejo- Hernández, Stefanny, S306 (SAT-262)
Cornejo-Hernández, Stefanny, S296 (TOP-281)
Cornillet, Martin, S2 (GS-002), S13 (OS-006-YI), S71 (LBP-008), S290 (FRI-289)
Coronel-Castillo, Carlos, S296 (TOP-281), S306 (SAT-262)
Corpechot, Christophe, S302 (SAT-254), S325 (SAT-320), S349 (SAT-420), S838 (THU-270)
Corradini, Elena, S849 (THU-305-YI)
Corradini, Stefano Ginanni, S407 (FRI-548)
Corrales, Fernando, S474 (WED-364)
Corral, Eva del, S804 (FRI-019)
Correas, Jean-Michel, S576 (WED-079)
Correia, Luís, S726 (THU-428)
Correll, Todd, S7 (GS-012), S875 (THU-574), S958 (WED-581)
Correnti, Margherita, S462 (WED-249)
Corte, Angelo Della, S207 (WED-477)
Cortellini, Alessio, S455 (TOP-406), S500 (FRI-239)
Cortese, Maria Francesca, S366 (WED-332-YI), S908 (SAT-577), S926 (SAT-623), S949 (FRI-612), S961 (WED-592)
Cortese, Mario, S957 (WED-578), S958 (WED-580)
Cortes, Miren Garcia, S16 (OS-010), S256 (SAT-542), S300 (SAT-250), S305 (SAT-260-YI), S308 (SAT-264)
Cortez, John, S879 (THU-587)
Cortez-Pinto, Helena, S577 (WED-084), S603 (WED-164), S621 (WED-214), S726 (THU-428), S765 (THU-013), S777 (THU-050)
Coruga, Ioana, S211 (WED-493)
Cosgrove, Brian, S8 (LBO-003)
Coshic, Poonam, S141 (TOP-423)
Coskun, Abdurrahman, S395 (FRI-511-YI)
Cosma, Tudor, S255 (SAT-539), S543 (THU-165), S544 (THU-166)
Cossiga, Valentina, S83 (LBP-034-YI), S248 (SAT-516), S307 (SAT-263), S335 (SAT-378-YI), S479 (WED-378), S911 (SAT-587-YI)
Costa, Dalila, S186 (TOP-470-YI), S216 (WED-508)
Costa, Elena Garlatti, S302 (SAT-252)
Costaguta, Guillermo, S55 (OS-086), S831 (THU-258-YI), S842 (THU-284)
Costa, Matheus, S379 (FRI-460)
Costantini, Riccardo Cuoghi, S412 (FRI-563)
Costanzo, Giovan Giuseppe Di, S176 (FRI-425), S479 (WED-378)
Costa, Rui, S879 (THU-588)
Costentin, Charlotte, S311 (SAT-271), S762 (THU-009)
Coste, Pablo, S296 (TOP-281), S306 (SAT-262), S768 (THU-021), S790 (SAT-036)
Costes, Fréderic, S167 (FRI-394-YI)
Costiniuk, Cecilia, S529 (THU-116-YI)
Cota de Madeiros, Fábio, S802 (FRI-010-YI)
Cotler, Scott, S816 (WED-009), S818 (WED-014), S941 (FRI-590)
Cotrim, Helma Pinchemel, S192 (WED-428)
Cottet, Vanessa, S435 (THU-246)
Cotti, Federico, S69 (LBP-004-YI)
Cottrell, Mackenzie, S80 (LBP-028-YI)
Cotugno, Rosa, S83 (LBP-034-YI), S307 (SAT-263)
Coubeau, Laurent, S381 (FRI-465), S382 (FRI-466)
Couchonnal, Eduardo, S840 (THU-275)
Coudyzer, Walter, S849 (THU-306-YI)
Coulibaly, Fatoumata, S45 (OS-067), S815 (WED-005)
Coulouarn, Cedric, S462 (WED-249), S484 (WED-393)
Couret, Alexis, S167 (FRI-394-YI)
Coustal, Cyril, S92 (SAT-068)
Couto, Claudia, S296 (TOP-281), S306 (SAT-262), S315 (SAT-286)
Couto, Cláudia, S10 (LBO-006), S35 (OS-050-YI), S79 (LBP-026), S141 (TOP-437), S338 (SAT-384), S768 (THU-022)
Couty, Jean-Pierre, S457 (WED-236)
Covino, Marcello, S219 (WED-515)
Cox, Joseph, S529 (THU-116-YI)
Cox, Richie Alexander Inge, S394 (FRI-508), S407 (FRI-547)
Cozma, Alina, S951 (FRI-620)
Cozzolongo, Raffaele, S82 (LBP-034-YI), S185 (TOP-455-YI), S307 (SAT-263), S335 (SAT-378-YI), S350 (SAT-421), S912 (SAT-587-YI)
Craciun, Rares, S175 (FRI-418), S209 (WED-483), S728 (THU-433-YI)
Craik, Julie, S814 (WED-004)
Cramp, Matthew, S164 (FRI-385-YI), S184 (FRI-453-YI)
Creamer, Joanthan, S709 (THU-556-YI)
Cremer, Jennifer, S1 (GS-001)
Crescimanno, Gaia, S494 (FRI-226)
Crespin, Athéna, S149 (SAT-468), S152 (SAT-478), S164 (FRI-384), S214 (WED-499), S760 (TOP-032)
Crespo, Alicia San José, S403 (FRI-532), S403 (FRI-533)
Crespo, Ana, S599 (WED-151)
Crespo, Gonzalo, S303 (SAT-257-YI), S394 (FRI-507-YI)
Crespo, Javier, S62 (OS-097), S127 (FRI-095), S241 (FRI-339), S424 (TOP-376), S516 (TOP-113), S542 (THU-164), S557 (THU-213), S567 (WED-054), S571 (WED-069), S585 (WED-106), S612 (WED-186-YI), S795 (SAT-050), S923 (SAT-618)
Cretella, Silvia, S911 (SAT-587-YI)
Criado, Sofía, S294 (TOP-278)
Crippin, Jeffrey, S330 (SAT-366)
Cripps, Sarah, S704 (THU-540)
Cristoferi, Laura, S2 (GS-002), S69 (LBP-004-YI), S82 (LBP-034-YI), S303 (SAT-257-YI), S304 (SAT-258), S307 (SAT-263), S323 (SAT-315), S325 (SAT-320), S331 (SAT-368-YI), S333 (SAT-369), S335 (SAT-378-YI), S340 (SAT-393), S350 (SAT-421), S831 (THU-256-YI)
Critelli, Rosina Maria, S31 (OS-042), S746 (THU-490)
Crittenden, Barry, S84 (LBP-037)
Crittenden, Daria B., S316 (SAT-287), S321 (SAT-306), S328 (SAT-362), S329 (SAT-363), S691 (FRI-175), S838 (THU-270)
Croce', Saveria Lory, S304 (SAT-258)
Croce', Saveria Lory, S69 (LBP-004-YI), S335 (SAT-378-YI), S901 (SAT-559), S902 (SAT-560), S936 (TOP-584), S938 (FRI-586)
Croci, Ilaria, S713 (WED-557)
Croney, Kayla, S856 (WED-290), S857 (WED-298)
Cross, Amy, S43 (OS-065)
Cross, Tim, S452 (THU-414-YI)
Crouchet, Emilie, S463 (WED-250)
Crowley, Fionnuala, S429 (THU-227-YI), S491 (TOP-408-YI)
Cruceta, Anna, S203 (WED-463)
Cruciata, Luca, S494 (FRI-226), S495 (FRI-227)
Cruz, Ana, S855 (WED-288), S856 (WED-290)
Cruz, Andrew John, S386 (FRI-482), S411 (FRI-561-YI), S413 (FRI-570)
Cruz, Kristine Joy Sofia, S703 (THU-528-YI)
Cruz-Lopéz, Anibal de la, S771 (THU-030)
Cruz, Susana García-De, S819 (WED-019), S910 (SAT-585)
Cselény, Zsolt, S690 (FRI-172)

Author Index

Cuadrado, Alisson Quezada, S132 (FRI-109), S642 (SAT-131-YI)
Cuadrado, Antonio, S410 (FRI-558), S643 (SAT-134), S833 (THU-259)
Cua, Georgine, S967 (TOP-600-YI)
Cubero, Beatriz Carrillo, S303 (SAT-256-YI)
Cubero, Francisco Javier, S132 (FRI-109), S182 (FRI-442), S241 (FRI-339), S267 (SAT-350), S459 (WED-241), S642 (SAT-131-YI), S678 (SAT-244)
Cuesta, Rubén, S815 (WED-006)
Cuevas, Cristina Martínez, S250 (SAT-524), S403 (FRI-533)
Cuevas, Guillermo, S806 (FRI-024)
Cui, Kunyuan, S74 (LBP-014)
Cui, Nana, S293 (FRI-302-YI)
Cui, Yi, S956 (TOP-598), S957 (WED-577), S960 (WED-587)
Cui, Zhiping, S73 (LBP-012)
Cullen, G., S377 (FRI-449)
Cullen, Noelle, S746 (THU-485)
Culver, Emma, S10 (LBO-006), S43 (OS-065), S311 (SAT-270), S331 (SAT-368-YI), S846 (THU-290)
Cumlat, Lourdes, S759 (TOP-017-YI)
Cuño-Gómiz, Carlos, S481 (WED-382-YI), S639 (SAT-120)
Cuperus, Frans J. C., S351 (SAT-426-YI), S352 (SAT-429), S353 (SAT-432), S353 (SAT-433)
Curia, Andrea, S302 (SAT-253)
Currie, Brooke M., S295 (TOP-280)
Currie, Sue, S48 (OS-073)
Curto, Armando, S69 (LBP-004-YI), S325 (SAT-320), S335 (SAT-378-YI), S400 (FRI-526), S542 (THU-159), S831 (THU-256-YI)
Curto-Vilalta, Anna, S35 (OS-050-YI)
Cusidó, M Serra, S233 (FRI-315)
Cusi, Giulia, S720 (TOP-502-YI)
Cusi, Kenneth, S21 (OS-020)
Cusimano, Guido, S494 (FRI-226), S495 (FRI-227)
Cussac, Cecile, S493 (FRI-221)
Cussac, Cécile, S508 (FRI-364-YI), S723 (THU-419)
Cussenot, Olivier, S17 (OS-011)
Cusumano, Caterina, S69 (LBP-004-YI), S304 (SAT-258), S307 (SAT-263)
Cuthbertson, Daniel, S713 (WED-557)
Cuyàs, Berta, S203 (WED-463)
Cymberknop, Leandro, S728 (THU-434)
Czlonkowska, Anna, S840 (THU-275)
Czubkowski, Piotr, S831 (THU-258-YI), S842 (THU-284), S850 (THU-308)

Da Costa, Rui, S881 (THU-593)
Dada, Inioluwa, S161 (SAT-509)
Dadhich, Sunil, S952 (FRI-622)
da Fonseca, Leonardo, S445 (THU-385), S452 (THU-414-YI)
Daga, Mradul, S214 (WED-501-YI)
Daguison, Shane, S879 (THU-587)
Dahari, Harel, S816 (WED-009), S818 (WED-014), S873 (THU-563), S873 (THU-564), S941 (FRI-590), S953 (FRI-625)
Dahl, Eva Efsen, S570 (WED-062)
Dahlqvist, Géraldine, S10 (LBO-006), S55 (OS-085-YI), S99 (TOP-193-YI), S381 (FRI-465), S382 (FRI-466), S742 (THU-477)
Dahlström, Nils, S220 (WED-517), S568 (WED-056)
Dahma, Hafid, S907 (SAT-575)
Dai, Jinyao, S489 (WED-410), S870 (TOP-645), S878 (THU-586)
Daiku, Kazuma, S463 (WED-251-YI)
Dai, Shuiweizhi, S934 (SAT-644)
Dai, Wencong, S73 (LBP-013), S932 (SAT-641)
Dai, Zhe, S560 (TOP-080), S868 (TOP-616-YI)
Dai, Zhenyu, S119 (FRI-072), S259 (SAT-554), S593 (WED-134), S609 (WED-182), S763 (THU-011), S924 (SAT-620)
Dajani, Khaled, S401 (FRI-527)
Dajti, Elton, S69 (LBP-004-YI), S307 (SAT-263), S335 (SAT-378-YI), S337 (SAT-382), S427 (THU-220), S720 (TOP-504-YI), S753 (THU-505-YI)
Dalal, Ashok, S31 (OS-043-YI), S212 (WED-495-YI), S217 (WED-510)
Dalal, Nekshan, S333 (SAT-370)
Dalbeni, Andrea, S97 (SAT-084-YI), S405 (FRI-541), S424 (TOP-375-YI), S428 (THU-227-YI), S443 (THU-380-YI), S514 (FRI-381), S595 (WED-137), S626 (WED-231), S677 (SAT-243-YI)
Dale, Cheryl, S968 (WED-609-YI)
Dalekos, George, S79 (LBP-026), S300 (SAT-250), S305 (SAT-260-YI), S314 (SAT-283), S323 (SAT-315), S325 (SAT-320), S329 (SAT-363), S331 (SAT-368-YI), S349 (SAT-420)
Dalem, Annelien Van, S907 (SAT-575)
D'Alessio, Antonio, S404 (FRI-538-YI), S455 (TOP-406), S491 (TOP-408-YI), S500 (FRI-239), S503 (FRI-250)
Dallio, Marcello, S176 (FRI-425), S212 (WED-494-YI), S444 (THU-384), S532 (THU-123), S549 (THU-186-YI), S639 (SAT-121-YI), S660 (SAT-190), S854 (WED-286)
d'Almeida, Arno Furquim, S46 (OS-070-YI), S65 (OS-101-YI), S920 (SAT-609), S929 (SAT-629)
Dalteroche, Louis, S43 (OS-066), S45 (OS-067), S54 (OS-084), S143 (SAT-450), S207 (WED-477), S222 (WED-525), S752 (THU-501), S934 (TOP-582), S937 (FRI-585-YI)
Daly, Ann, S29 (OS-038)
Daly, Ann K, S166 (FRI-393)
Damangir, Soheil, S64 (OS-099), S596 (WED-140)
d'Amati, Giulia, S856 (WED-291)
D'Amato, Daphne, S69 (LBP-004-YI), S82 (LBP-034-YI), S307 (SAT-263), S335 (SAT-378-YI), S831 (THU-256-YI)
D'Ambrosio, Francesca, S583 (WED-102-YI)
D'Ambrosio, Roberta, S62 (OS-097), S241 (FRI-340), S424 (TOP-376), S476 (WED-368), S516 (TOP-113), S601 (WED-156)
Damiani, Andrea, S583 (WED-102-YI)
D'Amico, Federico, S335 (SAT-378-YI)
D'amico, Saverio, S71 (LBP-009), S340 (SAT-393)
Damme, Pierre Van, S801 (FRI-007)
Damm, Marko, S175 (FRI-419), S185 (TOP-456-YI), S744 (THU-482-YI)
Damone, Francesco, S431 (THU-233), S695 (FRI-187), S950 (FRI-619)
Damsholt, Søren, S262 (SAT-332)
Dandan, Chen, S258 (SAT-548), S452 (THU-413)
Dandia, Naveen, S81 (LBP-030)
Dandri, Maura, S271 (THU-313), S871 (THU-558-YI), S890 (THU-622-YI)
Danesi, Giada, S863 (WED-317)
Dangas, Georgios, S891 (THU-624-YI)
Dang, Hanxiang, S463 (WED-252)
Dang, Shuangsuo, S47 (OS-071), S431 (THU-234), S463 (WED-252), S490 (WED-414), S791 (SAT-039), S792 (SAT-040), S873 (THU-569), S895 (THU-640), S941 (FRI-591), S946 (FRI-606), S955 (FRI-628)
Daniels, Samuel, S682 (FRI-148)
Danielsson, Oscar, S530 (THU-118-YI)
Danış, Nilay, S899 (SAT-556-YI)
D'Anna, Stefano, S49 (OS-076-YI), S807 (FRI-025), S899 (SAT-557), S911 (SAT-587-YI), S919 (SAT-608-YI), S924 (SAT-619)
Dann, Ouizeman, S681 (FRI-147)
Danpanichkul, Pojsakorn, S530 (THU-119-YI)
Danse, Etienne, S648 (SAT-151-YI)
Dans, Laura, S806 (FRI-024)
Danta, Mark, S799 (FRI-003)
Dantas, Ana Paula, S28 (OS-037), S629 (TOP-160)
Dantas, Carlos Eduardo Freitas, S379 (FRI-460)
Dantas-Miranda, Nathan, S267 (SAT-348)
D'Antiga, Lorenzo, S40 (OS-058), S414 (FRI-571), S831 (THU-258-YI), S842 (THU-284), S850 (THU-308)
Dan, Yock Young, S698 (FRI-197)
Dan, Yunjie, S171 (FRI-409-YI)
Dao, Thang, S218 (WED-513), S749 (THU-496)
Daphnee, Soret, S35 (OS-050-YI)
Dara, Lily, S308 (SAT-265), S309 (SAT-266)
D'Arcangelo, Francesca, S52 (OS-081), S193 (WED-431-YI), S406 (FRI-544)
Darlay, Rebecca, S166 (FRI-393)

D'Armiento, Jeanine M., S834 (THU-262), S836 (THU-266), S844 (THU-285)
Da, Rose Ido, S926 (SAT-624)
D'Arpino, Valeria, S530 (THU-117), S767 (THU-020)
Das, Amar, S259 (SAT-553)
Dasarathy, Srinivasan, S116 (FRI-061), S190 (WED-421), S197 (WED-447)
Das, Avisnata, S564 (WED-044), S565 (WED-045)
Das, Basundhara, S232 (FRI-308)
Das, Chiranjit, S364 (WED-324-YI)
Dasgupta, Pritam, S598 (WED-149)
Dashdorj, Naraanbatar, S965 (WED-603)
Dashdorj, Naranjargal, S439 (THU-367), S826 (WED-039), S915 (SAT-595), S916 (SAT-596), S965 (WED-603)
Dashtseren, Bekhbold, S439 (THU-367), S915 (SAT-595), S916 (SAT-596)
da Silva, Antonio Eduardo Benedito, S314 (SAT-284)
da Silva, Luís Neves, S318 (SAT-291)
da Silva, Monica Gomes, S1 (GS-001)
Das, Jai, S605 (WED-170)
Das, Prasenjit, S53 (OS-083-YI), S247 (SAT-514)
Dass, Jasmita, S184 (TOP-454-YI)
Date, Tomoko, S894 (THU-637)
Datta, Aditi, S137 (FRI-126)
Datta, Aurgho, S534 (THU-131), S616 (WED-200)
Datz, Christian, S539 (THU-151-YI), S616 (WED-199), S792 (SAT-041)
Daumont, Melinda, S601 (WED-155)
Dauphin, Matthew, S615 (WED-198)
Davalos, Verónica, S485 (WED-396)
Dave, Joel, S764 (THU-012)
Davids, Mark, S268 (SAT-351)
Davidsohn, Matthew P., S745 (THU-483)
Davidson, Neil, S826 (WED-039)
Davidson, Tsetsegdemberel Bat-Ulzii, S826 (WED-039)
Davies, Scott, S364 (WED-324-YI), S365 (WED-330-YI)
Davies, Todd, S70 (LBP-005), S975 (WED-636), S976 (WED-637)
Davila, Jesus Barreto, S547 (THU-181)
Davila, Rui, S88 (SAT-056)
Davis, Jessica, S745 (THU-483)
Davis, Tom, S385 (FRI-479)
D'Avola, Delia, S96 (SAT-079)
Davoli, Eleonora, S272 (THU-315-YI), S273 (THU-316), S489 (WED-412-YI)
D'Avolio, Antonio, S942 (FRI-593)
Davy, Kathleen, S208 (WED-480)
Dawn, Previtha, S50 (OS-077)
Dawson, Laura, S345 (SAT-409-YI)
Dawson, Sarah-Jane, S458 (WED-240)
Dayal, V.M., S67 (OS-105-YI), S952 (FRI-622)
Dayi, Njabulo, S900 (SAT-558)
Daza, Jimmy, S288 (FRI-283)
Deaglio, Silvia, S835 (THU-263)
de Amorim, Maria Clara Silva Dutra, S379 (FRI-460)
de Angelis, Martin Hrabe, S21 (OS-020)
de Araujo Neto, Joao Marcello, S724 (THU-420)
Dearden, Janet, S65 (OS-102), S354 (SAT-434), S970 (WED-619)
Dear, James W., S101 (THU-059-YI)
De, Arka, S5 (GS-009), S81 (LBP-030), S221 (WED-522), S684 (FRI-155)
de Avila, Leyla, S62 (OS-097), S128 (FRI-099), S424 (TOP-376), S516 (TOP-113)
Debaecker, Simon, S163 (FRI-383), S164 (FRI-384)
De Benedittis, Carla, S82 (LBP-034-YI), S350 (SAT-421)
Debing, Yannick, S874 (THU-570), S885 (THU-606), S886 (THU-610), S893 (THU-634)
de Blas, Beatriz Sanchez, S281 (TOP-296-YI)
De Block, Christophe, S682 (FRI-150-YI)
de Boer, Ynto, S10 (LBO-006), S15 (OS-009-YI), S305 (SAT-260-YI)
Debray, Dominique, S55 (OS-086), S831 (THU-258-YI), S842 (THU-284)
de Bruijn, Petra, S647 (SAT-149)
de Bruyne, Ruth, S526 (THU-106), S708 (THU-554-YI), S713 (WED-557)
de Bruyn, Krisztina, S857 (WED-299)
Debusschere, Nicolas, S99 (TOP-193-YI), S349 (SAT-420)
Debzi, Nabil, S24 (OS-028), S144 (SAT-452), S160 (SAT-507)
Decaens, Thomas, S762 (THU-009), S885 (THU-607)
Decaestecker, Jochen, S22 (OS-023), S148 (SAT-466-YI), S718 (WED-572)
de Carvalho, Elisa, S55 (OS-086), S831 (THU-258-YI), S842 (THU-284), S850 (THU-308)
de Castro, Tiago, S453 (TOP-389), S459 (WED-242-YI)
De Chiara, Francesco, S181 (FRI-435)
Deckmyn, Olivier, S577 (WED-085), S608 (WED-179)
Declerck, Salomé, S648 (SAT-151-YI)
Decock, Sofie, S849 (THU-306-YI)
De-Conto-Oliveira, Jeronimo, S88 (SAT-056)
Decraecker, Marie, S602 (WED-158)
Decroix, Kylian, S464 (WED-254)
Deda, Xheni, S965 (WED-603)
Dedoussis, George, S577 (WED-084), S600 (WED-153), S621 (WED-214), S765 (THU-013)
de Fátima Leite, Maria, S102 (THU-060)
De Feudis, Antonella, S307 (SAT-263)
de Freitas, Luiz Antônio Rodrigues, S53 (OS-083-YI)
de Fromentel, Claude Caron, S478 (WED-377)
de Frutos, Pablo Garcia, S481 (WED-382-YI)
Degasperi, Elisabetta, S43 (OS-066), S71 (LBP-009), S82 (LBP-034-YI), S307 (SAT-263), S331 (SAT-368-YI), S335 (SAT-378-YI), S337 (SAT-382), S439 (THU-367), S900 (SAT-559), S901 (SAT-560), S913 (SAT-589-YI), S915 (SAT-595), S916 (SAT-596), S934 (TOP-582), S935 (TOP-583), S936 (TOP-584), S937 (FRI-585-YI), S938 (FRI-586), S942 (FRI-592), S942 (FRI-593)
Degenhart, Gerald, S848 (THU-302)
Degerman, Erik, S606 (WED-173)
Degezelle, Karlien, S381 (FRI-465)
De Giorgi, Irene, S481 (WED-383)
De Goeij, Femke, S398 (FRI-517-YI)
de Graaf, Mariska, S630 (SAT-090)
Degrauwe, Lars, S885 (THU-606), S886 (THU-610)
Degré, Delphine, S35 (OS-050-YI), S109 (TOP-210)
de Groot, Alise D.E., S55 (OS-086), S831 (THU-258-YI), S842 (THU-284)
Degroote, Frederick, S886 (THU-610)
de Guevara, Alma Laura Ladrón, S20 (OS-019), S559 (TOP-064), S565 (WED-051), S680 (FRI-139), S693 (FRI-182)
de Haan, Luuk, S167 (FRI-395-YI)
Dehmel, Susann, S105 (THU-072)
Deibel, Ansgar, S325 (SAT-320)
Deidda, Alessandra, S69 (LBP-004-YI), S83 (LBP-034-YI)
de Jesus, Rosângela, S192 (WED-428)
de Jesus Yepes Barreto, Ismael, S226 (WED-538), S226 (WED-539)
de Jonge, Hendrik J.M., S15 (OS-009-YI)
de Jonge, Jeroen, S61 (OS-095-YI), S382 (FRI-467-YI), S383 (FRI-468), S383 (FRI-473), S391 (FRI-498), S398 (FRI-517-YI), S828 (TOP-310-YI)
de Jong, Iris E.M., S382 (FRI-467-YI)
de Jong, Laura, S167 (FRI-395-YI)
de Jong, Vivian, S577 (WED-084), S600 (WED-153)
De Jong, Ype, S891 (THU-624-YI)
Dekervel, Jeroen, S17 (OS-012), S459 (WED-242-YI), S485 (WED-396), S491 (TOP-408-YI)
de Kleine, Ruben, S430 (THU-232)
de Knegt, Robert J., S63 (OS-098-YI), S608 (WED-180)
de Laar, Arnold van, S632 (SAT-099-YI)
De la Cruz, Gema, S16 (OS-010)
De la Flor-Robledo, María, S123 (FRI-086)
de la Fuente, María Jordán, S403 (FRI-532), S403 (FRI-533), S415 (FRI-575)
de Laguiche, Elisabeth, S555 (THU-206), S758 (TOP-002), S781 (SAT-007)
De La Luna, Francisco Franco Álvarez, S910 (SAT-581), S910 (SAT-585)
Delamarre, Adele, S325 (SAT-320)
Delamarre, Adèle, S573 (WED-071)
de Lange, Mark, S647 (SAT-149)
de la Oliva Roque, Victor Manuel, S806 (FRI-023)
Delaporte, Margaux, S365 (WED-331-YI)
de la Rosa, Gloria, S410 (FRI-558)

Author Index

De las Heras, Berta, S124 (FRI-088), S308 (SAT-264)
Delataille, Philippe, S163 (FRI-383), S164 (FRI-384)
de la Torre, Manuel, S96 (SAT-079)
De La Torre Sanchez, Mercedes, S254 (SAT-538)
Delaunay, Dominique, S564 (WED-043)
De la Viña, Daniela, S337 (SAT-382)
Del Barrio, María, S309 (SAT-268), S317 (SAT-290-YI)
Del campo, Laura, S731 (THU-445-YI)
del Carmen Gassent, María, S223 (WED-528)
de Lecuana, Itziar, S148 (SAT-467-YI)
De Ledinghen, Victor, S325 (SAT-320), S525 (THU-103), S602 (WED-158), S607 (WED-174-YI)
de Lédinghen, Victor, S517 (TOP-114), S558 (TOP-063-YI), S589 (WED-118), S612 (WED-187-YI), S618 (WED-204), S621 (WED-215), S946 (FRI-604)
Delfa, Rosario La, S52 (OS-081), S747 (THU-492)
Delgado, Carolina, S948 (FRI-611)
Delgado, Manuel, S837 (THU-267), S855 (WED-289)
Delgado, María Fernández, S635 (SAT-106)
Delgado, Pilar, S819 (WED-019)
Delgado, Teresa C, S633 (SAT-101-YI), S635 (SAT-106)
Delhomme, Margaux, S387 (FRI-484), S414 (FRI-573)
Delhoume, Victoria, S428 (THU-226-YI), S506 (FRI-255-YI)
De liberato, Rachele, S576 (WED-083)
Delire, Bénédicte, S90 (SAT-059), S95 (SAT-076)
Della Torre, Sara, S672 (SAT-228)
Dellbrügge, Friederike, S376 (TOP-520-YI)
Dell'Oro, Liliana, S817 (WED-010)
De Lorenzo, Stefania, S429 (THU-227-YI)
de los Toyos, Noelia Pastor, S165 (FRI-387-YI)
Delphin, Marion, S826 (WED-039), S900 (SAT-558)
del Río-Álvarez, Alvaro, S489 (WED-412-YI)
del Rio, Manuel Beltran, S391 (FRI-496)
Deltenre, Pierre, S55 (OS-085-YI), S109 (TOP-210), S920 (SAT-609), S929 (SAT-629)
Del Turco, Elena Rosselli, S902 (SAT-560), S936 (TOP-584), S937 (FRI-585-YI), S938 (FRI-586)
De Luca, Luca, S975 (WED-635)
Delugré, Fabian, S359 (THU-345-YI)
Delwaide, Jean, S55 (OS-085-YI), S99 (TOP-193-YI), S849 (THU-306-YI), S907 (SAT-575), S920 (SAT-609), S929 (SAT-629)
Demaeght, Stephane, S849 (THU-306-YI)
DeMaio, Matthew, S375 (TOP-519)
de Man, Robert A., S444 (THU-383)
De Marco, Leonardo, S82 (LBP-034-YI)
De Maria, Francesco, S937 (FRI-585-YI)
De Maria, Nicola, S412 (FRI-563)
De Martin, Eleonora, S95 (SAT-076)
De Matteis, Irene, S476 (WED-368)
de Meijer, Vincent E., S59 (OS-091), S238 (FRI-333-YI), S244 (FRI-353), S384 (FRI-476-YI), S384 (FRI-477), S385 (FRI-478), S415 (FRI-574)
Demetriou, Lydia, S909 (SAT-579)
Demirel, Burak, S680 (FRI-139), S693 (FRI-182)
Demir, Kadir, S829 (THU-251)
Demir, Münevver, S10 (LBO-006), S14 (OS-007), S64 (OS-100), S77 (LBP-022-YI), S248 (SAT-515), S416 (FRI-578-YI), S601 (WED-155), S615 (WED-196), S623 (WED-220)
Demirtas, Coskun Ozer, S24 (OS-028), S144 (SAT-452), S160 (SAT-507), S311 (SAT-272-YI), S465 (WED-257), S497 (FRI-234), S723 (THU-418)
Demir, Tulin, S807 (FRI-025)
Dempster, John, S772 (THU-035)
Dendane, Youness, S309 (SAT-267), S578 (WED-086)
Dendrou, Calliope, S43 (OS-065)
Deng, Cunliang, S86 (LBP-041)
Deng, Guohong, S162 (TOP-440), S171 (FRI-409-YI)
Deng, John, S432 (THU-238)
Deng, Rong, S68 (OS-107), S74 (LBP-015)
Deng, Yihong, S186 (TOP-469-YI)
Deng, You, S98 (SAT-088)
Deng, Zhiling, S245 (FRI-355)
Deng, Zhuoya, S108 (THU-084)
Deng, Ziqing, S262 (SAT-331)
den Hoed, Caroline, S59 (OS-091), S59 (OS-092-YI), S61 (OS-095-YI), S382 (FRI-467-YI), S383 (FRI-468), S383 (FRI-473), S391 (FRI-498), S398 (FRI-517-YI), S415 (FRI-574), S909 (SAT-580)
De Nicola2, Stella, S938 (FRI-586)
de Nicola, Francesca, S869 (TOP-632)
De Nicola, Stella, S212 (WED-494-YI), S339 (SAT-386), S696 (FRI-188-YI)
Denk, Gerald, S14 (OS-007)
Denk, Helmut, S836 (THU-265-YI)
Dennis, Andrea, S673 (SAT-231)
Denos, Margaux, S463 (WED-250)
Denson, Jemimah, S164 (FRI-385-YI), S184 (FRI-453-YI)
Denters, Maaike J., S353 (SAT-433)
Denver, Catherine, S75 (LBP-017)
Denys, Alban, S490 (TOP-407-YI)
Deole, Yash, S536 (THU-136)
Derakhshandeh, Fatemeh, S234 (FRI-317)
Derdak, Zoltan, S578 (WED-087), S579 (WED-090), S623 (WED-219), S667 (SAT-213), S694 (FRI-183)
der Eijk, Annemiek Van, S817 (WED-011)
Deressa, Baro, S920 (SAT-609), S929 (SAT-629)
de Reus, Stijn, S193 (WED-432)
Dermer, Shari, S531 (THU-121), S683 (FRI-152)
de Rooij, Laura, S364 (WED-323)
De Rosa, Laura, S695 (FRI-187)
de Rose, Edoardo, S767 (THU-020)
Derowski, Tanja, S359 (THU-345-YI)
De Roza, Marianne, S158 (SAT-499)
DeRoza, Marianne, S529 (THU-115)
Dertsiz, Berkay, S298 (SAT-246)
de Ruiter, Sander, S167 (FRI-395-YI)
Desai, Archita, S531 (THU-122)
Desai, Dimple, S80 (LBP-029), S569 (WED-059)
Desai, Nirav K., S847 (THU-300), S848 (THU-301)
de Saint-Loup, Marc, S525 (THU-103), S558 (TOP-063-YI), S589 (WED-118), S607 (WED-174-YI)
de Salazar, Adolfo, S899 (SAT-557), S910 (SAT-585)
Desalegn, Hailemichael, S24 (OS-028), S144 (SAT-452), S822 (WED-026), S926 (SAT-622-YI)
Desalegn, Mahlet, S194 (WED-433)
de Sárraga, Carla, S191 (WED-427-YI)
Desboeufs, Nina, S465 (WED-255)
Deschenes, Marc, S10 (LBO-006), S398 (FRI-516), S533 (THU-127-YI), S616 (WED-200), S757 (THU-516)
Deschler, Sebastian, S876 (THU-575)
Desdouets, Chantal, S457 (WED-236)
Deshayes, Alice, S478 (WED-377)
De Silvestri, Annalisa, S934 (TOP-582)
de Sluis, Bart van, S630 (SAT-090), S670 (SAT-221-YI)
Desmons, Aurore, S951 (FRI-621)
Dessalegn, Hailemichael, S825 (WED-036)
Desterke, Christophe, S399 (FRI-523)
de Temple, Brittany, S681 (FRI-142)
Deterding, Katja, S913 (SAT-589-YI), S935 (TOP-583), S963 (WED-596), S971 (WED-620)
Detlefsen, Sönke, S114 (FRI-057), S122 (FRI-079-YI), S125 (FRI-090-YI), S706 (THU-545-YI)
Deutsch, Melanie, S620 (WED-212)
Devadas, Krishnadas, S952 (FRI-622)
Deval, Jerome, S964 (WED-597)
Dev, Anouk, S820 (WED-021)
Devarbhavi, Harshad, S67 (OS-105-YI)
Devaux, Carole, S807 (FRI-025)
de Veer, Rozanne C., S325 (SAT-320), S351 (SAT-426-YI), S352 (SAT-429), S353 (SAT-432), S353 (SAT-433)
Devereaux, Michael, S289 (FRI-285)
Devescovi, Valentina, S457 (WED-235)
De Vincentis, Antonio, S82 (LBP-034-YI)
Devineni, Poornima, S166 (FRI-393)
Devisscher, Lindsey, S99 (TOP-193-YI), S281 (TOP-295-YI), S315 (SAT-285), S464 (WED-253), S464 (WED-254)
De Vloo, Charlotte, S315 (SAT-285), S920 (SAT-609)

De Vos, Marie, S920 (SAT-609), S929 (SAT-629)
De Vos, Zenzi, S281 (TOP-295-YI), S464 (WED-253)
De Vree, Marleen, S351 (SAT-426-YI)
Devreese, Katrien MJ, S148 (SAT-466-YI)
de Vries, Hilde, S857 (WED-299), S863 (WED-318)
de Vries, Liesbeth, S57 (OS-087-YI)
de Waart, Rudi, S646 (SAT-140-YI)
Dewidar, Bedair, S666 (SAT-211-YI), S672 (SAT-230)
de Wilde, Roeland, S828 (TOP-310-YI)
de Wit, Koos, S443 (THU-382-YI)
de Wit, Ulrike, S351 (SAT-426-YI)
Dewyspelaere, Jef, S22 (OS-023), S718 (WED-572)
Dey, Suparna, S461 (WED-245)
de Zawadzki, Andressa, S13 (OS-006-YI), S111 (FRI-044), S114 (FRI-057), S345 (SAT-410), S470 (WED-269), S578 (WED-087), S623 (WED-219)
Dezsőfi-Gottl, Antal, S55 (OS-086), S831 (THU-258-YI), S842 (THU-284), S850 (THU-308)
D'Haens, Geert, S9 (LBO-005-YI)
Dhairyawan, Rageshri, S824 (WED-031)
Dhali, Gopal, S100 (THU-056)
Dhanda, Ashwin, S164 (FRI-385-YI), S184 (FRI-453-YI)
Dhar, Ameet, S224 (WED-530)
Dharancy, Sebastien, S380 (FRI-463), S381 (FRI-464)
Dharancy, Sébastien, S222 (WED-525), S505 (FRI-254)
Dhawan, Anil, S385 (FRI-479), S840 (THU-275)
Dhawan, Puneet, S47 (OS-072)
Dhiman, Radha Krishan, S144 (SAT-452), S160 (SAT-507), S952 (FRI-622)
Dhingra, Natasha, S925 (SAT-621)
Dhivya, Jospin, S584 (WED-103)
Diaconescu, Gheorghe, S956 (TOP-598)
Diago, Moises, S766 (THU-015)
Diallo, Ibrahima, S905 (SAT-569), S926 (SAT-624), S940 (FRI-588-YI)
Diamantopoulou, Georgia, S348 (SAT-416)
Díaz, Alba, S53 (OS-083-YI), S331 (SAT-368-YI), S837 (THU-268), S862 (WED-315), S884 (THU-604-YI)
Diaz, Antonio, S250 (SAT-524), S855 (WED-289)
Díaz-Canul, Carolina, S132 (FRI-108-YI)
Diaz, Fernando, S317 (SAT-290-YI)
Diaz-Ferrer, Javier, S112 (FRI-050), S445 (THU-385)
Diaz-Flores, Felicitas, S547 (THU-181)
Diaz-Gonzalez, Alvaro, S16 (OS-010), S294 (TOP-278), S309 (SAT-268)
Díaz-González, Álvaro, S302 (SAT-254), S317 (SAT-290-YI), S338 (SAT-384), S828 (TOP-309-YI), S833 (THU-259)
Diaz, Juan Manuel, S141 (TOP-437)
Diaz, Luis Antonio, S62 (OS-097), S112 (FRI-050), S134 (FRI-116), S207 (WED-479), S516 (TOP-113), S532 (THU-125), S578 (WED-088), S579 (WED-089), S768 (THU-021)
Diaz, Raquel, S16 (OS-010)
Díaz-Tendero, Andrea, S173 (FRI-414), S239 (FRI-336)
Di Bartolomeo, Claudia, S331 (SAT-368-YI)
Dibba, Bakary, S764 (THU-012), S798 (TOP-034)
Dibenedetto, Clara, S315 (SAT-286)
Di Benedetto, Fabrizio, S412 (FRI-562), S412 (FRI-563)
di Cesare, Ernesto, S767 (THU-020)
Dickens, Alex, S662 (SAT-197)
Di Cola, Simone, S720 (TOP-502-YI)
Di Costanzo, Giovan Giuseppe, S190 (WED-425)
Di Costanzo, Giovanni, S212 (WED-494-YI)
Dideriksen, Tine, S703 (THU-527-YI)
Diederichs, Audrey, S869 (TOP-632), S876 (THU-576), S893 (THU-634)
Diederichsen, Louise, S298 (SAT-245)
Diédhiou, Cyrille, S911 (SAT-586)
Dieguez, Carlos, S233 (FRI-313), S241 (FRI-339)
Dieguez, Maria Luisa Gonzalez, S410 (FRI-558), S837 (THU-267), S855 (WED-289)
Diehl, Anna Mae, S64 (OS-099)
Dierlamm, Julia, S866 (FRI-639)
Diestro, Sonia, S203 (WED-463)
Dieterich, Douglas T, S762 (THU-008)
Dieterich, Douglas T., S76 (LBP-021)
Dietrich, Peter, S310 (SAT-269), S322 (SAT-313)
Dietvorst, Carmen, S577 (WED-084), S684 (FRI-153), S688 (FRI-166-YI)
Dietz-Fricke, Christopher, S43 (OS-066), S900 (SAT-559), S902 (SAT-560), S934 (TOP-582), S937 (FRI-585-YI)
Dietz, Julia, S945 (FRI-602-YI)
Díez-Aja, Cristóbal, S969 (WED-611)
Diez, Cristina, S806 (FRI-024)
Diez, Jorge Lillo, S403 (FRI-533)
Diez, Nerea Rodríguez, S391 (FRI-497)
Díez, Rubén, S542 (THU-164)
Di Giorgio, Angelo, S831 (THU-258-YI)
Digkilia, Antonia, S490 (TOP-407-YI)
Diken, Mustafa, S18 (OS-015)
Dikic, Ivan, S262 (SAT-330)
Dileo, Eleonora, S534 (THU-133), S574 (WED-073), S611 (WED-184-YI), S620 (WED-213), S911 (SAT-587-YI)
Di Leo, Milena, S975 (WED-635)
Dill, Michael, S14 (OS-007), S303 (SAT-257-YI), S504 (FRI-251)
Dillon, Audrey, S377 (FRI-449), S396 (FRI-512)
Dillon, John, S572 (WED-070)
Dillon, John F, S559 (TOP-065-YI), S599 (WED-152)
Dillon, Pauline, S255 (SAT-540), S973 (WED-627)
Di Lorenzo, Andrea, S936 (TOP-584), S938 (FRI-586)
DiMarchi, Richard, S674 (SAT-233)
Di Marco, Vito, S190 (WED-425), S212 (WED-494-YI), S479 (WED-378)
Dimaria, Vincenzo, S97 (SAT-084-YI), S424 (TOP-375-YI)
Dimitriou, Krystalia, S142 (SAT-449), S187 (WED-415)
Dimmeler, Stefanie, S631 (SAT-093-YI)
Dinani, Amreen, S190 (WED-421), S580 (WED-092-YI), S684 (FRI-154), S758 (TOP-002), S781 (SAT-007)
Di Nardo, Fiammetta, S69 (LBP-004-YI), S307 (SAT-263), S335 (SAT-378-YI), S549 (THU-186-YI), S660 (SAT-190), S854 (WED-286)
Dincer, Dinc, S24 (OS-028), S144 (SAT-452), S160 (SAT-507)
Ding, Chuanfu, S228 (WED-542)
Ding, Jiuyang, S270 (SAT-356)
Dingli, Florent, S571 (WED-067)
Ding, Lijuan, S73 (LBP-012)
Ding, Xiaoyan, S491 (TOP-422)
Ding, Yanhua, S959 (WED-586)
Ding, Zeyang, S711 (WED-548-YI)
Dinkelborg, Katja, S864 (TOP-615), S866 (FRI-641), S887 (THU-611)
DiNorcia, Joseph, S60 (OS-094)
Dionisi-Vici, Carlo, S670 (SAT-225)
Diouf, Momar, S742 (THU-477)
Dirchwolf, Melisa, S296 (TOP-281), S306 (SAT-262), S790 (SAT-036)
Dirinck, Eveline, S682 (FRI-150-YI)
Dirksmeier-Harinck, Femme, S443 (THU-382-YI)
Dirnbachová, Katarína, S211 (WED-492)
Dischinger, Ulrich, S21 (OS-020)
Di Siervi, Giuseppe, S977 (WED-640)
Disla, Hugo José, S585 (WED-105), S585 (WED-106)
Disoma, Cyrollah, S465 (WED-256)
Disse, Emmanuel, S573 (WED-071)
Distante, Sonia, S849 (THU-305-YI)
Distefano, Marco, S350 (SAT-421), S831 (THU-256-YI), S912 (SAT-587-YI), S947 (FRI-608)
Di Tommaso, Luca, S331 (SAT-368-YI), S462 (WED-249)
Diwakar, Sunidhi, S100 (THU-057-YI), S174 (FRI-415-YI)
Dixon, Steven, S725 (THU-427)
Dixon, Thomas, S147 (SAT-464)
Di Zeo-Sánchez, Daniel E., S305 (SAT-260-YI)
Djalalinia, Shirin, S697 (FRI-195-YI)
Djerboua, Maya, S624 (WED-225-YI)
Djordjevic, Ana, S268 (SAT-351)
Do, Albert, S775 (THU-043)
Doan, Hoang Long, S587 (WED-115)
Dobner, Sarah, S364 (WED-323)
Dobos, Ari, S873 (THU-564)

Author Index

Dobrowolska, Krystyna, S970 (WED-617-YI)
Dobryanska, Marta, S76 (LBP-021), S964 (WED-597)
Dochtermann, Daniel, S166 (FRI-393)
Dodge, Jennifer, S124 (FRI-087-YI), S308 (SAT-265), S309 (SAT-266), S553 (THU-201), S761 (THU-006)
D'Offizi, Giampiero, S43 (OS-066), S900 (SAT-559), S901 (SAT-560), S911 (SAT-587-YI), S934 (TOP-582), S936 (TOP-584), S937 (FRI-585-YI), S938 (FRI-586)
Doherty, G., S377 (FRI-449)
Dohmen, Kazufumi, S336 (SAT-379)
Dolce, Arianna, S640 (SAT-122)
Dollerup, Mie Ringgaard, S290 (FRI-287)
Dolman, Grace, S908 (SAT-578)
Dolmazashvili, Ekaterine, S76 (LBP-021)
do Mar d'Orey, Maria, S603 (WED-164)
do Mar Orey, Maria, S577 (WED-084), S621 (WED-214)
Domenech, Gemma, S203 (WED-463)
Domingo, Pere, S904 (SAT-564)
Domingos, Tayna, S95 (SAT-078)
Domínguez, Carlos Eduardo Paz, S817 (WED-010)
Domínguez-Hernández, Raquel, S799 (TOP-049), S815 (WED-006)
Domínguez-Humanes, Joaquín, S123 (FRI-086)
Dominguez-Lago, Adrian, S799 (TOP-049)
Domínguez, María Carmen Lozano, S910 (SAT-581)
Dominguez, Nicolas, S296 (TOP-281), S306 (SAT-262)
Dominicus, Thomas, S432 (THU-236)
Dominik, Adrian, S93 (SAT-070)
Dominik, Nina, S717 (WED-569-YI), S748 (THU-493-YI)
Donadello, Katia, S97 (SAT-084-YI)
Donado, Guillermo, S226 (WED-539), S625 (WED-228)
Dona, Federico, S465 (WED-255)
Donahue, Nicholas, S540 (THU-154)
Donate, Jesus, S3 (GS-005), S33 (OS-046), S53 (OS-082), S54 (OS-084), S397 (FRI-515), S747 (THU-492), S752 (THU-501)
Dondossola, Daniele, S241 (FRI-340), S405 (FRI-541), S575 (WED-076), S636 (SAT-109)
Dong, Bingtian, S560 (TOP-080)
Dongelmans, Edo J., S46 (OS-070-YI), S943 (FRI-596)
Dongiovanni, Paola, S177 (FRI-427), S443 (THU-380-YI), S595 (WED-138), S636 (SAT-110-YI), S662 (SAT-198-YI), S667 (SAT-214)
Dong, Jane, S956 (TOP-598), S957 (WED-577), S960 (WED-587)
Dong, Jiahong, S270 (TOP-328), S276 (THU-323), S456 (WED-233)
Dong, Li, S86 (LBP-041)
Dong, Ling-Yue, S232 (FRI-307)
Dongre, Arundhati, S639 (SAT-119)
Dong, Shaohua, S878 (THU-586)
Dong, Sihan, S88 (TOP-192)
Dong, Tang, S560 (TOP-080)
Dong, Xiao-Ping, S954 (FRI-626)
Dong, Xiaoying, S640 (SAT-123)
Dong, Xingwu, S468 (WED-264)
Dong, Yinuo, S90 (SAT-060), S98 (SAT-089-YI)
Dong, Zhongyi, S511 (FRI-370)
Donnadieu, Hélène, S387 (FRI-484), S414 (FRI-573)
Donnici, Lorena, S51 (OS-079)
Donoghue, Claire, S252 (SAT-530)
Dooley, Kyla, S43 (OS-065)
Dooley, Steven, S240 (FRI-337-YI)
Dopazo, Cristina, S410 (FRI-558), S445 (THU-385)
Dopazo, Joaquín, S806 (FRI-023)
Dorizas, Christopher, S337 (SAT-381)
Dorn, Chad, S96 (SAT-083)
Dörr, Jonas, S785 (SAT-019)
Dorta, Valentina, S241 (FRI-339)
Dorweiler, Tim, S672 (SAT-230)
Doselli, Sara, S874 (THU-571)
Dos Santos, Celio Xavier Da Costa, S174 (FRI-416-YI)
Doucette, Karen, S43 (OS-066), S76 (LBP-021), S937 (FRI-585-YI), S968 (WED-609-YI)
Douds, Andrew, S740 (THU-468)
Douglas, Mark, S85 (LBP-040)
Doukas, Michail, S9 (LBO-005-YI), S53 (OS-083-YI), S61 (OS-095-YI), S331 (SAT-368-YI), S632 (SAT-099-YI), S641 (SAT-126)
Dou, Linshuang, S664 (SAT-203), S665 (SAT-205)
Dounel, Jonathan, S578 (WED-088)
Dou, Qian, S954 (FRI-626)
Dou, Xiaobing, S657 (SAT-180)
Dou, Xiaoguang, S433 (THU-239)
Doverskog, Magnus, S318 (SAT-299), S333 (SAT-370)
Dowe, Thomas, S458 (WED-237-YI)
Dowlat, Jasmine, S563 (WED-042), S597 (WED-141)
Doyle, Adam, S160 (SAT-507)
Doyle, Joseph, S799 (FRI-004), S800 (FRI-005)
Dragoni, Gabriele, S400 (FRI-526), S542 (THU-159)
Drammeh, Sainabou, S798 (TOP-034)
Dranicki, Fabian, S376 (TOP-520-YI)
Drapkina, Oxana, S551 (THU-189), S551 (THU-190), S594 (WED-135)
Drazilova, Sylvia, S585 (WED-107)
Dražilová, Sylvia, S321 (SAT-305)
Drebber, Uta, S21 (OS-020)
Drenth, Joost P. H., S9 (LBO-005-YI), S333 (SAT-369), S352 (SAT-429), S353 (SAT-432), S353 (SAT-433)
Drenth, Joost P.H., S39 (OS-056), S783 (SAT-012)
Drenth, Joost PH, S15 (OS-009-YI), S168 (FRI-397-YI), S305 (SAT-260-YI), S351 (SAT-426-YI), S632 (SAT-099-YI), S864 (WED-319-YI)
Drew, Gary, S845 (THU-288)
Drews, Jan, S866 (FRI-639)
Drews, Simon, S532 (THU-124)
Driessen, Ann, S55 (OS-085-YI), S581 (WED-094), S682 (FRI-150-YI)
Driessen, Stan, S621 (WED-214), S641 (SAT-126)
Driscoll, Mark, S287 (FRI-275)
Drissi, Sofia Belhoussine, S109 (TOP-210)
Dröge, Carola, S834 (THU-260)
Dropmann, Anne, S240 (FRI-337-YI)
Drumond Westgeest e Sousa, Diego, S126 (FRI-093)
Drysdale, Myriam, S908 (SAT-578), S909 (SAT-579)
Duangnum, Kittichote, S450 (THU-402)
Duan, Shuangying, S812 (FRI-040)
Duan, Zhongping, S67 (OS-105-YI), S852 (TOP-312)
Duarte, Dagoberto, S226 (WED-538)
Duarte, Marcella Motta Lucindo, S701 (FRI-203-YI)
Duarte-Rojo, Andres, S388 (FRI-489), S388 (FRI-490), S412 (FRI-564-YI), S745 (THU-483)
Dube, Asha, S312 (SAT-274-YI), S313 (SAT-275)
Dube, Karine, S816 (WED-008)
Dube, Lena, S207 (WED-477), S742 (THU-477)
Duberg, Ann-Sofi, S903 (SAT-561), S978 (WED-642-YI)
Duberg, Daniel, S29 (OS-038), S268 (SAT-351)
Dubois, Anaëlle, S876 (THU-576)
Dubois, Antoine, S381 (FRI-465)
Duca, Ana, S409 (FRI-557)
Duchene, Gaëtan, S648 (SAT-151-YI)
Duckhouse, Valerie, S713 (WED-556-YI)
Duclos, Martine, S167 (FRI-394-YI)
Duc, Pham Minh, S12 (OS-003)
Duda, Joan, S61 (OS-108)
Dudek, Michael, S291 (FRI-291-YI)
Duduyemi, Babatunde, S905 (SAT-569), S940 (FRI-588-YI)
Dudzik, Aleksandra, S641 (SAT-126)
Duemmler, Lisa, S252 (SAT-529)
Dueñas-Sánchez, Eva, S16 (OS-010)
Duennebacke, Reinhild, S852 (TOP-311), S858 (WED-302)
Dufour, Jean-François, S561 (TOP-081)
Duger, Davaadorj, S923 (SAT-618)
Duguru, Mary John, S926 (SAT-624)
Duhamel, Alain, S505 (FRI-254)
Duhoux, François, S90 (SAT-059)
Duijst, Suzanne, S646 (SAT-140-YI), S674 (SAT-233)
Duijzer, Renée, S783 (SAT-012)
Dujardin, Fanny, S742 (THU-477)
Du, Jing, S560 (TOP-080)

Dullaart, Robin, S384 (FRI-476-YI), S384 (FRI-477), S385 (FRI-478)
Düll, Miriam M., S310 (SAT-269), S322 (SAT-313)
Dulmage, Keely, S87 (LBP-043)
Dultz, Georg, S251 (SAT-525)
Dumas, Agnes, S721 (THU-415), S863 (WED-317)
Dumolard, Lucile, S885 (THU-607)
Dumond, Julie, S80 (LBP-028-YI)
Dumortier, Jérôme, S43 (OS-066), S45 (OS-067), S207 (WED-477), S311 (SAT-271), S325 (SAT-320), S380 (FRI-463), S381 (FRI-464), S742 (THU-477), S900 (SAT-559), S902 (SAT-560), S934 (TOP-582), S937 (FRI-585-YI)
Dunn, Nicholas, S62 (OS-097), S516 (TOP-113), S532 (THU-125)
Dunn, Winston, S20 (OS-019), S62 (OS-097), S80 (LBP-029), S375 (TOP-518), S516 (TOP-113), S559 (TOP-064), S560 (TOP-066), S561 (TOP-082), S565 (WED-051), S579 (WED-089), S684 (FRI-154)
Duong, Phi, S857 (WED-298)
Du, Peishan, S46 (OS-069)
Dupont, Ellen, S526 (THU-106)
Duprey, Sheena, S980 (FRI-634)
Dupuy, Marie, S92 (SAT-068), S95 (SAT-076)
Duran, Carmen, S799 (TOP-049)
Durand, Francois, S110 (FRI-042)
Durand, Sarah, S463 (WED-250)
Duran, Laura Salej, S432 (THU-238)
Durán, Luis Eduardo Durán, S250 (SAT-524)
Duran, Rafael, S490 (TOP-407-YI)
Durante, Barbara, S456 (WED-234-YI)
Durantel, David, S875 (THU-572), S885 (THU-606)
Duranti, Claudia, S457 (WED-235)
Duran, Xavier, S191 (WED-427-YI)
Durmashkina, Elena, S945 (FRI-602-YI)
Durmazer, Esra, S389 (FRI-491)
Durmaz, Ozlem, S55 (OS-086), S831 (THU-258-YI), S842 (THU-284)
Durrani, Aneela Zameer, S178 (FRI-430)
Duseja, Ajay Kumar, S5 (GS-009), S27 (OS-033), S62 (OS-097), S81 (LBP-030), S127 (FRI-095), S144 (SAT-452), S171 (FRI-409-YI), S180 (FRI-433), S221 (WED-522), S227 (WED-541-YI), S366 (WED-334), S516 (TOP-113), S684 (FRI-155), S766 (THU-015), S824 (WED-035), S952 (FRI-622)
Dusheiko, Geoffrey, S905 (SAT-571)
Dutta, Pinaki, S171 (FRI-409-YI)
Duvoux, Christophe, S380 (FRI-463), S381 (FRI-464)
Du, Xilin, S512 (FRI-377)
Du, Yanan, S91 (SAT-067)
Du, Yu, S359 (THU-346)
Du, Yuhan, S641 (SAT-126)
Duzik, Ashley, S77 (LBP-021)
Dvořák, Karel, S64 (OS-100)
Dvornikov, Dmytro, S125 (FRI-090-YI)
Dwarkanathan, Vignesh, S36 (OS-051-YI), S741 (THU-474)
Dwarkasing, Roy, S443 (THU-382-YI), S444 (THU-383)
Dwivedi, Ved, S264 (SAT-335), S264 (SAT-336), S280 (THU-337)
Dwyer, Jennifer, S396 (FRI-512)
Dyavadi, Vijay, S389 (FRI-492)
Dybowska, Dorota, S980 (FRI-633)
Dyke, Julia Van, S342 (SAT-398)
Dyson, Jessica, S10 (LBO-006), S315 (SAT-286), S318 (SAT-299), S325 (SAT-320), S331 (SAT-368-YI)

Eagle, Craig, S259 (SAT-553)
Eapen, CE, S24 (OS-028), S67 (OS-105-YI), S160 (SAT-507)
Eardley, Thomas, S735 (THU-457)
Eastabrook, Genevieve, S70 (LBP-005)
Eastbrook, Genevieve, S975 (WED-636), S976 (WED-637)
Eaton, John, S10 (LBO-006), S79 (LBP-026), S315 (SAT-286), S325 (SAT-320)
Ebbers, Tino, S568 (WED-056)
Ebel, Noelle H., S850 (THU-308)
Eber, Claudie, S875 (THU-572)
Eberhard, Daniel, S672 (SAT-230)
Ebert, Matthias, S240 (FRI-337-YI)
Ebinuma, Hirotoshi, S26 (OS-031)
Ebrahimi, Ali, S667 (SAT-213)
Ebrahimi, Fahim, S533 (THU-126)
Echeveste, José, S343 (SAT-400), S364 (WED-329-YI)
Eck, Brendan, S619 (WED-206)
Eckburg, Paul B., S964 (WED-597)
Eckel, Juergen, S666 (SAT-211-YI)
Eddie, Thomas, S715 (WED-561-YI)
Edeline, Julien, S485 (WED-396)
Edin, Carl, S568 (WED-056)
Edler, Ida, S222 (WED-524), S732 (THU-448-YI)
Edwards, Rachel, S768 (THU-023), S772 (THU-035)
Efimova, Irina, S642 (SAT-127)
Efird, Jimmy, S96 (SAT-083)
Egebjerg, Christina, S693 (FRI-182)
Egger, Matthias, S326 (SAT-321)
Egorova, Irina, S594 (WED-135)
Egorova, Yulia, S595 (WED-136)
Eguchi, Yuichiro, S127 (FRI-095), S557 (THU-213), S667 (SAT-213), S766 (THU-015), S923 (SAT-618)
Ehmer, Ursula, S359 (THU-345-YI)
Ehomah, Emmanuel, S729 (THU-441)
Ehrenbauer, Alena Friederike, S732 (THU-448-YI)
Ehrlich, Dusko, S261 (SAT-329-YI), S262 (SAT-330)
Eibergen, Arthur, S237 (FRI-330)
Eichelberger, Beate, S200 (WED-453)
Eichholz, Julia, S52 (OS-081)
Eidelshtein, Dana, S234 (FRI-318)
Eid, Joe, S491 (TOP-408-YI)
Eilard, Malin Sternby, S791 (SAT-038)
Eklöf, Nathalie, S573 (WED-072), S613 (WED-190)
Ekpotu, Lenin, S255 (SAT-540)
Ekstedt, Mattias, S62 (OS-097), S220 (WED-517), S424 (TOP-376), S516 (TOP-113), S568 (WED-056), S584 (WED-104)
Ekstrom, Victoria, S834 (THU-261)
El-Akel, Wafaa, S492 (FRI-217), S504 (FRI-252), S551 (THU-191)
Elamouri, Fauzi, S865 (FRI-638), S904 (SAT-564)
Elangovan, Sakktivel, S149 (SAT-473)
Elbadry, Mohamed, S524 (THU-101)
Elbahr, Osama, S59 (OS-091)
Elbaz, tamer, S492 (FRI-217)
Elbeshbeshy, Hany, S838 (THU-270)
Elblová, Petra, S273 (THU-317), S459 (WED-241)
El-Demerdash, Ebtehal, S231 (FRI-305)
Eldere, Anne Van, S61 (OS-095-YI)
Elefsiniotis, Ioannis, S507 (FRI-257)
El-Ekiaby, Nada, S231 (FRI-305), S263 (SAT-333)
El-Etreby, Shahira, S492 (FRI-217)
Elewa, Ahmed, S71 (LBP-008)
Elfving, Betina, S631 (SAT-094-YI)
El-Gendy, Noor, S687 (FRI-165)
Elgosbi, Marwa, S366 (WED-333-YI)
Elgozair, Mohamad, S303 (SAT-257-YI)
Elgretli, Wesal, S529 (THU-116-YI)
El Hag, Mohamed, S399 (FRI-522)
El Hajra, Ismael, S300 (SAT-250)
El Hajra Martínez, Ismael, S318 (SAT-291)
Elhan, Atilla, S588 (WED-116)
El Hassani, Majda, S142 (SAT-448), S159 (SAT-506-YI), S170 (FRI-402)
Elhofy, Adam, S58 (OS-089), S313 (SAT-282)
Eliasen, Marie, S775 (THU-042-YI)
Elizalde-Garcia, Pablo, S286 (FRI-271)
Elizondo, Martín, S728 (THU-434)
El-Karim, Lima Awad, S436 (THU-249)
El Kassas, Mohamed, S378 (FRI-457), S524 (THU-101), S774 (THU-040), S774 (THU-041)
El-Kassas, Mohamed, S24 (OS-028), S62 (OS-097), S127 (FRI-095), S263 (SAT-333), S516 (TOP-113), S794 (SAT-046), S905 (SAT-569), S923 (SAT-618), S926 (SAT-624), S940 (FRI-588-YI)
Elkhashab, Magdy, S691 (FRI-175)
El-Koofy, Nehal M., S850 (THU-308)
Elkrief, Laure, S33 (OS-046), S52 (OS-081), S54 (OS-084), S55 (OS-085-YI), S143 (SAT-450), S207 (WED-477), S380 (FRI-463), S381 (FRI-464), S497 (FRI-234), S571 (WED-067), S719 (TOP-488), S720 (TOP-504-YI), S723 (THU-418), S739 (THU-467), S742 (THU-477), S752 (THU-501), S783 (SAT-012), S863 (WED-317)

Author Index

Ellapen, Malcolm, S900 (SAT-558)
Ellik, Zeynep Melekoğlu, S519 (THU-089), S588 (WED-116), S899 (SAT-556-YI)
Elliot-Cooke, Robert, S704 (THU-540), S709 (THU-556-YI)
Elliott, Jilliann, S10 (LBO-006)
Ellis, Ewa, S71 (LBP-008)
Ellis, Paul, S834 (THU-262)
El Maimouni, Cautar, S583 (WED-101), S612 (WED-188)
El-Masri, Bilal, S125 (FRI-090-YI)
Elmasry, Eslam, S432 (THU-237)
Elmonem, Mohamed A., S850 (THU-308)
Elmqaddem, Ouiam, S309 (SAT-267), S578 (WED-086)
Elortza, Felix, S272 (THU-315-YI), S273 (THU-316), S483 (WED-388-YI)
El-Sayed, Manal, S89 (SAT-057), S928 (SAT-627)
El-Serag, Hashem, S451 (THU-410)
Elshabasy, Osama, S147 (SAT-465)
Elsharkawy, Ahmed M, S343 (SAT-401-YI)
El-Sharkawy, Mohamed, S566 (WED-053)
Elsheaita, Ahmed, S425 (THU-216-YI)
El-Sherif, Omar, S377 (FRI-449), S396 (FRI-512)
El Sobky, Shereen, S263 (SAT-333)
Elston, Robert, S1 (GS-001), S956 (TOP-598), S957 (WED-577), S959 (WED-585), S960 (WED-587)
Elurbide-Tardio, Jasmin, S17 (OS-013), S474 (WED-364)
Elvers, Fynn, S168 (FRI-396)
Elzaanoun, Reyad, S379 (FRI-461-YI)
Elzahabi, Nada, S597 (WED-147)
Elzubeir, Amera, S311 (SAT-270)
Emadeldeen, Mohammed, S263 (SAT-333)
Embacher, Jan, S97 (SAT-084-YI), S113 (FRI-053), S183 (FRI-445), S216 (WED-508), S217 (WED-509-YI), S364 (WED-323)
Emebo, Dabel, S432 (THU-238)
Emral, Rıfat, S588 (WED-116)
Enders, Robert, S745 (THU-483)
Endhardt, Katharina, S465 (WED-255)
Endo, Kei, S194 (WED-435)
Endo, Mizuki, S662 (SAT-196), S808 (FRI-027)
Endress, David, S975 (WED-634-YI)
Enea, Marco, S607 (WED-174-YI)
Engelbart, Iris R, S504 (FRI-251)
Engel, Bastian, S60 (OS-093), S300 (SAT-250), S309 (SAT-268), S331 (SAT-368-YI), S333 (SAT-369), S376 (TOP-520-YI)
Engelmann, Cornelius, S33 (OS-046), S60 (OS-093), S151 (SAT-476), S154 (SAT-489), S161 (SAT-510-YI), S171 (FRI-409-YI), S185 (TOP-456-YI), S215 (WED-506), S268 (SAT-352-YI), S615 (WED-196), S736 (THU-460-YI), S744 (THU-482-YI)
Engesæter, Lise Katrine, S2 (GS-002)
Enghard, Philipp, S161 (SAT-510-YI)
Enkhtaivan, Sanjaasuren, S439 (THU-367), S915 (SAT-595), S916 (SAT-596)
Ennequin, Gael, S167 (FRI-394-YI)
Enomoto, Masaru, S977 (WED-639)
Enomoto, Nobuyuki, S506 (FRI-256)
Ensenauer, Regina, S672 (SAT-230)
Eom, Jung A., S267 (SAT-349)
Epping, Ludger S. M., S353 (SAT-432)
Epstein, Ian, S229 (WED-545), S598 (WED-148)
Erard, Domitille, S311 (SAT-271)
Ercan, Caner, S533 (THU-126)
Erdem, Aytaç, S396 (FRI-513)
Erdösi, Pia, S240 (FRI-337-YI)
Eren, Fatih, S465 (WED-257)
Erez, Noam, S642 (SAT-127)
Ergenc, Ilkay, S311 (SAT-272-YI), S767 (THU-019)
Erichsen, Lara, S867 (FRI-642)
Erickson, Mary, S139 (FRI-134)
Eriksen, Lotte, S703 (THU-527-YI)
Eriksen, Lotte Lindgreen, S262 (SAT-332)
Eriksen, Peter Lykke, S631 (SAT-094-YI)
Eriksson, Carl, S58 (OS-090)
Eriksson, Olof, S579 (WED-090)
Erikstrup, Christian, S166 (FRI-393), S262 (SAT-332)
Erken, Robin, S963 (WED-595)
Erler, Nicole S., S351 (SAT-426-YI), S352 (SAT-429), S353 (SAT-432), S353 (SAT-433)
Erreni, Marco, S462 (WED-249)
Errigo, Emanuele, S176 (FRI-425)
Esbensen, Bente Appel, S298 (SAT-245)
Escalada, Javier, S608 (WED-175)
Escobar, Diana Marcela, S625 (WED-228)
Escobedo, Miguel, S296 (TOP-281), S306 (SAT-262)
Escorsell, Angels, S725 (THU-426)
Escorsell, Àngels, S735 (THU-453)
Escrich, Víctor, S948 (FRI-611)
Escudero-García, Desamparados, S254 (SAT-538), S542 (THU-164), S567 (WED-054), S585 (WED-105), S585 (WED-106), S598 (WED-150), S772 (THU-036)
Escudero-López, Blanca, S527 (THU-108), S678 (SAT-244)
Escuín, María, S603 (WED-163)
Escutia-Gutiérrez, Rebeca, S132 (FRI-108-YI)
Esesarte, Marisol, S730 (THU-442)
Esfeh, Jamak Modaresi, S399 (FRI-522)
Eshun, John, S850 (THU-308)
Esiru, Godfrey, S821 (WED-023)
Eslam, Mohammed, S377 (FRI-451), S378 (FRI-457)
Esmaeili, Shirin, S697 (FRI-195-YI)
Esmat, Gamal, S492 (FRI-217), S504 (FRI-252), S537 (THU-141-YI), S538 (THU-142), S575 (WED-077), S576 (WED-078), S814 (WED-003), S865 (FRI-638)
Espana, Albina, S169 (FRI-400), S179 (FRI-431-YI), S230 (TOP-343-YI)
Espelt, Albert, S810 (FRI-035)
Espin, Maria Jesus Del Amor, S910 (SAT-581), S910 (SAT-585)
Espinoza-Cámac, Nataly, S815 (WED-006)
Esposito, Vincenzo, S938 (FRI-586)
Essa, Imraan, S76 (LBP-019-YI)
Esser, Stefan, S904 (SAT-564)
Esteban, Jesús Rivera, S409 (FRI-557), S567 (WED-054), S571 (WED-069), S585 (WED-105), S585 (WED-106), S598 (WED-150), S612 (WED-186-YI), S772 (THU-036), S855 (WED-289)
Esteller, Manel, S485 (WED-396)
Estep, James, S795 (SAT-051)
Esteves, Andrew, S959 (WED-585)
Estévez-Vázquez, Olga, S132 (FRI-109), S642 (SAT-131-YI)
Eto, Fabiola, S23 (OS-026-YI)
Etogo, Eugenie Lebomo, S919 (SAT-608-YI), S924 (SAT-619)
Ettorre, Giuseppe Maria, S841 (THU-282)
Etzion, Ohad, S49 (OS-075), S962 (WED-594)
Eu Chang, Jason Pik, S158 (SAT-499)
Eun, Jung Woo, S264 (SAT-337)
Eurich, Brandon, S801 (FRI-009)
Evain, Manon, S457 (WED-236)
Evangelista, Andreia, S340 (SAT-394)
Evans, Cameron, S653 (SAT-166)
Evans, Hannah, S811 (FRI-038)
Evans, Helen M., S850 (THU-308)
Eve-Rowe, Kaye, S43 (OS-065)
Everson, Greg, S438 (THU-365), S588 (WED-117), S971 (WED-621)
Evole, Helena Hernández, S16 (OS-010), S294 (TOP-278), S300 (SAT-250), S315 (SAT-286), S336 (SAT-380), S337 (SAT-382), S338 (SAT-383), S338 (SAT-384), S828 (TOP-309-YI)
Evstafev, Ilia, S662 (SAT-197)
Expósito, Use, S810 (FRI-035)
Eyck, Patrick Ten, S393 (FRI-501)
Ezio, Fornasiere, S302 (SAT-252)
Ezzafzafi, Solaiman, S168 (FRI-397-YI)

Fabbri, Angela, S350 (SAT-421)
Fabeni, Lavinia, S899 (SAT-557), S919 (SAT-608-YI), S924 (SAT-619)
Faber, Klaas Nico, S238 (FRI-333-YI), S244 (FRI-352), S244 (FRI-353)
Fabian, Licet Gonzalez, S62 (OS-097), S516 (TOP-113)
Fabian, Ondrej, S474 (WED-364)
Fabio, Romano Di, S51 (OS-079)
Fabre, Alexandre, S55 (OS-086), S831 (THU-258-YI), S842 (THU-284)
Fabrega, Emilio, S643 (SAT-134)
Fábrega, Laura, S101 (THU-058), S131 (FRI-104)
Fàbrega, Laura, S600 (WED-153), S627 (TOP-144)
Fabregat, Isabel, S467 (WED-262)

Fabrellas, Núria, S21 (OS-021), S30 (OS-041), S110 (TOP-222), S203 (WED-463), S583 (WED-101)
Fabris, Carlo, S302 (SAT-252)
Fabris, Luca, S303 (SAT-257-YI), S304 (SAT-258), S307 (SAT-263), S335 (SAT-378-YI), S350 (SAT-421), S466 (WED-258), S479 (WED-379), S485 (WED-395-YI)
Fabritius, Matthias, S490 (TOP-407-YI)
Facchetti, Floriana, S942 (FRI-592), S942 (FRI-593)
Fadieienko, Galina Dmitrievna, S604 (WED-167)
Faggiani, Emilie, S83 (LBP-035)
Fagiuoli, Stefano, S52 (OS-081), S69 (LBP-004-YI), S185 (TOP-455-YI), S307 (SAT-263), S335 (SAT-378-YI), S350 (SAT-421), S401 (FRI-528), S414 (FRI-571), S817 (WED-010), S911 (SAT-587-YI)
Fahmy, Mohamed, S575 (WED-077)
Fahy, Darren, S125 (FRI-090-YI)
Faini, Angelo Corso, S835 (THU-263)
Faisal, Nabiha, S14 (OS-008), S295 (TOP-279), S325 (SAT-319), S354 (SAT-435)
Faist, Morgan, S850 (THU-308)
Faita, Francesco, S431 (THU-233)
Faivre, Jamila, S478 (WED-377)
Fajardo, Javier, S337 (SAT-382)
Fajol, Montserrat Camps, S191 (WED-426)
Fakhraei, Romina, S680 (FRI-141)
Fal, Andrzej, S817 (WED-012)
Falbo, Elisabetta, S335 (SAT-378-YI)
Falces, Iker, S910 (SAT-581), S910 (SAT-585)
Falco, Julia Sopena, S377 (FRI-449)
Falcomatà, Andrea, S196 (WED-444)
Falk, Christine, S197 (WED-446), S878 (THU-585-YI)
Fallon, Michael, S670 (SAT-220)
Fallowfield, Jonathan, S12 (OS-004-YI), S360 (THU-350), S698 (FRI-197)
Falzone, Michela Helga, S90 (SAT-061-YI), S848 (THU-304)
Fanciulli, Chiara, S806 (FRI-024)
Fandood, Sam, S729 (THU-435)
Fanelli, Fabrizio, S6 (GS-011-YI)
Fang, Chris, S72 (LBP-010)
Fang, Hanzhi, S48 (OS-074)
Fang, Jenny, S536 (THU-136)
Fangmann, Josef, S105 (THU-072)
Fang, Yongliang, S685 (FRI-156)
Fang, Zhixin, S6 (GS-010), S644 (SAT-136)
Fan, Huaiyan, S812 (FRI-040)
Fan, Huizhen, S259 (SAT-554), S593 (WED-134), S609 (WED-182), S924 (SAT-620)
Fan, Jian-Gao, S62 (OS-097), S127 (FRI-095), S516 (TOP-113), S517 (TOP-114), S525 (THU-103), S558 (TOP-063-YI), S589 (WED-118), S607 (WED-174-YI), S612 (WED-187-YI), S618 (WED-204), S621 (WED-215), S766 (THU-015), S923 (SAT-618)
Fan, Jiangao, S627 (TOP-130)
Fan, Jianing, S466 (WED-259)
Fan, Kevin Yiyu, S369 (WED-340-YI), S372 (WED-351)
Fanqiang, Meng, S626 (WED-230)
Fan, Rong, S33 (OS-047), S102 (THU-062), S430 (THU-229), S433 (THU-239), S508 (FRI-363), S617 (WED-201), S932 (SAT-641)
Fansecco, Michela, S850 (THU-307)
Fan, Tao, S930 (SAT-634), S930 (SAT-635), S933 (SAT-642)
Fantini, Massimo, S850 (THU-307)
Fan, Xiaotang, S33 (OS-047)
Fan, Xu, S331 (SAT-367), S370 (WED-345)
Fan, Yanting, S685 (FRI-156)
Fan, Zihao, S283 (FRI-264)
Faouzi, Kenza, S92 (SAT-068)
Faragallah, Nada Mohamed, S208 (WED-482)
Farag, Mohamed, S263 (SAT-333)
Farahat, Ahmed, S809 (FRI-029), S966 (TOP-599)
Farahmand, Saman, S667 (SAT-213)
Faraone, Alyse, S702 (FRI-206)
Farbod, Yasamin, S533 (THU-127-YI), S616 (WED-200)
Faria, Caroline, S671 (SAT-226)
Faria, Luciana, S296 (TOP-281), S306 (SAT-262), S768 (THU-022)
Farias, Alberto, S24 (OS-028), S34 (OS-049), S144 (SAT-452), S160 (SAT-507), S166 (FRI-388-YI)
Farias, Alberto Queiroz, S35 (OS-050-YI), S141 (TOP-437), S159 (SAT-505)
Farid-Kapadia, Mufiza, S781 (SAT-008), S781 (SAT-009)
Farina, Benedetta, S874 (THU-571)
Farina, Elisa, S55 (OS-085-YI), S817 (WED-010)
Farina, Francesca, S534 (THU-131), S865 (FRI-638)
Fariñas, Carmen, S904 (SAT-564)
Fariselli, Piero, S525 (THU-103)
Färkkilä, Martti, S14 (OS-007), S451 (THU-409)
Farouk, Nancy, S6 (GS-011-YI), S52 (OS-081), S736 (THU-460-YI), S737 (THU-461), S744 (THU-481)
Farrugia, Marwin, S380 (FRI-463), S381 (FRI-464), S681 (FRI-147), S742 (THU-477)
Farzad, Negin, S102 (THU-062)
Faserl, Klaus, S862 (WED-314-YI)
Fassan, Matteo, S466 (WED-258), S485 (WED-395-YI)
Fasulo, Daniel, S287 (FRI-275)
Fath el Bab, Esmee, S817 (WED-011), S909 (SAT-580)
Fathma, Sawsan, S722 (THU-417), S835 (THU-264-YI)
Fatourou, Evangelia, S759 (TOP-017-YI)
Fatta, Erika, S520 (THU-091-YI), S541 (THU-158), S553 (THU-197), S595 (WED-137), S636 (SAT-110-YI)
Faulkes, Rosemary, S160 (SAT-507)
Faure, Stéphanie, S92 (SAT-068), S95 (SAT-076), S414 (FRI-572), S414 (FRI-573)
Favalessa, Maria Eduarda, S102 (THU-060)
Favaloro, Frank, S702 (FRI-206)
Fawaz, Rima, S850 (THU-308)
Fawzy, Injie, S263 (SAT-333)
Fayed, Ibrahim, S231 (FRI-305), S263 (SAT-333)
Fayez, Ayat, S642 (SAT-132)
Fayyad, Nour, S889 (THU-620)
Feasi, Marcello, S911 (SAT-587-YI)
Federico, Alessandro, S43 (OS-066), S69 (LBP-004-YI), S176 (FRI-425), S190 (WED-425), S212 (WED-494-YI), S304 (SAT-258), S307 (SAT-263), S335 (SAT-378-YI), S444 (THU-384), S476 (WED-368), S479 (WED-378), S532 (THU-123), S549 (THU-186-YI), S601 (WED-156), S639 (SAT-121-YI), S660 (SAT-190), S854 (WED-286), S900 (SAT-559), S901 (SAT-560), S912 (SAT-587-YI), S934 (TOP-582), S936 (TOP-584), S937 (FRI-585-YI), S938 (FRI-586)
Federico, Piera, S424 (TOP-375-YI), S428 (THU-227-YI), S514 (FRI-381)
Fedulov, Artemiy, S871 (THU-559-YI)
Fedzhaga, Mykola, S548 (THU-182)
Fehlau, Lukas, S866 (FRI-641)
Fehse, Boris, S890 (THU-622-YI)
Feigh, Michael, S646 (SAT-142), S655 (SAT-173)
Feinberg, Gilad, S614 (WED-191)
Feinstein, Jeffrey A., S850 (THU-308)
Fei, Ran, S593 (WED-133), S668 (SAT-217-YI)
Felber, Marco, S32 (OS-044)
Feldbacher, Nicole, S742 (THU-476)
Feldbruegge, Linda, S461 (WED-245)
Feld, Jordan J., S46 (OS-070-YI), S49 (OS-075), S70 (LBP-005), S76 (LBP-021), S436 (THU-249), S443 (THU-382-YI), S582 (WED-099), S875 (THU-574), S914 (SAT-592-YI), S921 (SAT-610), S928 (SAT-628-YI), S962 (WED-594), S968 (WED-609-YI), S975 (WED-636), S976 (WED-637)
Feliciano, Camille, S194 (WED-436)
Felli, Emanuelle, S463 (WED-250)
Felli, Eric, S168 (FRI-398)
Felzen, Antonia, S831 (THU-258-YI), S842 (THU-284)
Fenaille, Francois, S170 (FRI-401-YI)
Feng, Gen-Sheng, S368 (WED-338)
Feng, Haiying, S593 (WED-134)
Feng, Isadora, S102 (THU-060)
Feng, Jie, S694 (FRI-183)
Feng, Lin, S416 (FRI-579), S417 (FRI-580)
Feng, Mingxuan, S475 (WED-365)

Author Index

Feng, Qi, S685 (FRI-157-YI)
Feng, Qin, S778 (THU-053)
Feng, Sandy, S59 (OS-091)
Feng, Shibao, S563 (WED-042), S597 (WED-141)
Feng, Shun, S812 (FRI-040)
Feng, Siyi, S259 (SAT-554)
Feng, Tingting, S151 (SAT-476)
Feng, Xiaofeng, S468 (WED-264)
Feng, Xinyan, S428 (THU-225-YI)
Feng, Yanfei, S897 (TOP-551)
Feng, Yuemin, S513 (FRI-379)
Fenske, Wiebke K., S688 (FRI-168)
Fenton, Cynthia, S406 (FRI-543)
Fenton, Sally, S61 (OS-108)
Feray, Cyrille, S374 (TOP-503), S399 (FRI-523)
Ferdinande, Kymentie, S3 (GS-005), S6 (GS-011-YI), S22 (OS-023), S33 (OS-046), S52 (OS-081), S148 (SAT-466-YI), S718 (WED-572), S746 (THU-489), S747 (THU-492), S752 (THU-501)
Ferguson, James, S343 (SAT-401-YI)
Fernandes, Ana Rita, S603 (WED-164)
Fernandes, Andrew, S724 (THU-420)
Fernandes, Chanelle, S876 (THU-575), S888 (THU-618)
Fernandes, Dalia, S43 (OS-066), S934 (TOP-582), S937 (FRI-585-YI), S940 (FRI-589)
Fernandes, Flavia, S724 (THU-420), S978 (WED-641)
Fernandes, Gabriel Prusch, S186 (TOP-469-YI)
Fernandes, Royston, S739 (THU-466)
Fernández-Aguilera, María, S91 (SAT-062), S317 (SAT-290-YI)
Fernández, Ana Suárez-Saro, S124 (FRI-088)
Fernandez-Barrena, Maite G, S17 (OS-013), S474 (WED-364), S477 (WED-370), S489 (WED-412-YI)
Fernández-Bermejo, Miguel, S16 (OS-010), S123 (FRI-086), S250 (SAT-524), S948 (FRI-611)
Fernandez-Checa, José, S28 (OS-037), S101 (THU-058), S131 (FRI-104), S627 (TOP-144), S629 (TOP-160)
Fernandez-Fernandez, Maria, S635 (SAT-107-YI)
Fernández, Gerardo Blanco, S391 (FRI-497)
Fernández-Iglesias, Anabel, S189 (WED-418), S232 (FRI-313), S678 (SAT-244)
Fernández, Irene, S203 (WED-463)
Fernández, Javier, S8 (LBO-002), S35 (OS-050-YI), S146 (SAT-461), S149 (SAT-468), S152 (SAT-478), S760 (TOP-032)
Fernández, José Ramón, S312 (SAT-273), S837 (THU-267), S855 (WED-289)
Fernández-Lizaranzu, Isabel, S527 (THU-108), S600 (WED-153), S644 (SAT-137)
Fernández, Mario, S272 (THU-315-YI)
Fernández, Marlen Ivon Castellanos, S62 (OS-097), S296 (TOP-281), S306 (SAT-262), S516 (TOP-113), S766 (THU-015)
Fernández, Marta, S603 (WED-163)
Fernández-Martínez, Elisa, S453 (TOP-389)
Fernández, Miguel Angel, S527 (THU-108)
Fernández-Patón, Matias, S254 (SAT-538), S599 (WED-151)
Fernández-Prada, Samuel, S379 (FRI-459), S403 (FRI-532), S403 (FRI-533), S415 (FRI-575)
Fernández-Puertas, Idoia, S277 (THU-330-YI), S631 (SAT-095-YI)
Fernández-Rivas, Gema, S804 (FRI-019), S807 (FRI-025)
Fernandez-Rodriguez, Conrado, S16 (OS-010), S79 (LBP-026), S331 (SAT-368-YI), S338 (SAT-384)
Fernández- Rodríguez, Conrado, S542 (THU-164), S968 (WED-610-YI)
Fernandez-Rodriguez, Laura, S643 (SAT-133)
Fernandez, Ruben Perez, S819 (WED-019)
Fernández, Rut, S312 (SAT-273)
Fernández-Salguero, Ana Calderón, S391 (FRI-497)
Fernandez, Santiago, S806 (FRI-024)
Fernandez, Teresa Cabezas, S910 (SAT-585)
Fernández-Varo, Guillermo, S173 (FRI-414), S239 (FRI-336), S245 (FRI-354)
Fernández-Yunquera, Ainhoa, S16 (OS-010)
Ferraglia, Francesca, S874 (THU-571)
Ferrández, Antonio, S254 (SAT-538)
Ferrarese, Alberto, S148 (SAT-466-YI), S193 (WED-431-YI)
Ferraro, Clelia, S41 (OS-062), S279 (THU-334-YI), S359 (THU-347-YI)
Ferraz, Maria Lucia, S296 (TOP-281), S306 (SAT-262), S768 (THU-022)
Ferraz, Maria Lucia Gomes, S314 (SAT-284)
Ferreira, Carlos Alberto Costa Noronha, S731 (THU-445-YI)
Ferreira, Carlos Noronha, S720 (TOP-504-YI), S726 (THU-428)
Ferreira, Sandra, S55 (OS-086), S831 (THU-258-YI), S842 (THU-284)
Ferreira, Stephanie, S149 (SAT-468), S152 (SAT-478), S214 (WED-499), S760 (TOP-032)
Ferreiro, Nerea, S30 (OS-039-YI), S272 (THU-315-YI), S273 (THU-316), S633 (SAT-101-YI), S855 (WED-287-YI)
Ferrentino, Filomena, S759 (TOP-017-YI)
Ferreras, Maria, S806 (FRI-024)
Ferrer, Javier Díaz, S790 (SAT-036)
Ferrer, Joana, S427 (THU-220)
Ferrer, Juana Maria, S223 (WED-528)
Ferrer-Lorente, Raquel, S827 (TOP-297)
Ferrero, Andreu, S191 (WED-426)
Ferrero, Oscar, S904 (SAT-564)
Ferrer, Roser, S605 (WED-168-YI), S961 (WED-592)
Ferri, Clodoveo, S972 (WED-623)
Ferrié, Martin, S881 (THU-592-YI)
Ferri, Flaminia, S407 (FRI-548)
Ferrigno, Luigina, S820 (WED-020-YI)
Ferrillo, Lorenza, S248 (SAT-516)
Ferris, Neus Garcia, S337 (SAT-382)
Ferroni, Francesca, S848 (THU-304)
Ferroudji, Saïd, S414 (FRI-573)
Ferrucci, Filomena, S567 (WED-055-YI)
Ferrusquía-Acosta, José, S52 (OS-081), S720 (TOP-504-YI)
Ferstl, Philip, S210 (WED-485)
Festa, Marco Mario Giacomo, S335 (SAT-378-YI)
Festa, Mariano, S977 (WED-640)
Feudis, Antonella De, S83 (LBP-034-YI), S335 (SAT-378-YI)
Feuerhake, Friedrich, S488 (WED-409-YI)
Feyide, Moyosoreoluwa, S139 (FRI-133)
Fialkoff, Gavriel, S60 (OS-093), S289 (FRI-286), S615 (WED-196)
Fialla, Annette Dam, S838 (THU-269)
Fianchi, Francesca, S307 (SAT-263), S335 (SAT-378-YI)
Fickel, Abigail, S437 (THU-362)
Fickert, Peter, S14 (OS-007), S82 (LBP-033), S297 (TOP-293), S326 (SAT-321), S341 (SAT-397)
Fidaleo, Marco, S27 (OS-034)
Fidalgo, Miguel, S241 (FRI-339)
Fiebig, Jenny, S222 (WED-526-YI)
Fiedler, Jan, S105 (THU-072)
Fierenz, Alexander, S236 (FRI-323)
Fierro-Angulo, Oscar M., S707 (THU-548)
Figorilli, Giovanni, S304 (SAT-258)
Figredo, Anita, S707 (THU-546-YI)
Figueiredo, Antonio, S892 (THU-627)
Figueiredo, Igor, S485 (WED-396)
Figueredo-Matto, Lucio, S636 (SAT-108)
Filho, Carlos Antonio Rodrigues Terra, S154 (SAT-484), S724 (THU-420)
Filho, Raymundo Parana Ferreira, S95 (SAT-078)
Filice, Aldo, S97 (SAT-084-YI), S405 (FRI-541)
Filice, Ross, S413 (FRI-569)
Filippis, Eleana De, S604 (WED-166)
Filippo, Leonardi, S401 (FRI-528), S414 (FRI-571)
Filomia, Roberto, S196 (WED-445), S223 (WED-527), S435 (THU-245), S967 (WED-605-YI)
Fina, Juan Bayo, S358 (THU-340-YI), S474 (WED-364), S654 (SAT-171-YI)
Finan, Brian, S674 (SAT-233)
Fini, Lucia, S975 (WED-635)
Finkelmeier, Fabian, S485 (WED-396), S504 (FRI-251)
FinnGen, FinnGen, S282 (FRI-263)
Finn, Jennifer, S715 (WED-561-YI)
Finzi, Giovanna, S669 (SAT-219)
Fiocco, Marta, S415 (FRI-574), S729 (THU-436)

Fiore, Esteban, S358 (THU-340-YI), S654 (SAT-171-YI)
Fiore, Pierluigi, S610 (WED-183)
Fiorini, Emanuele, S576 (WED-083)
Fiorio, Veronica, S626 (WED-231)
Fiorotto, Romina, S485 (WED-395-YI)
Firpi, Roberto J, S58 (OS-089), S313 (SAT-282)
Fisayo, Temitope, S826 (WED-039)
Fischer, Franziska, S771 (THU-031)
Fischer, Janett, S150 (SAT-474)
Fischer, Jonathan, S195 (WED-441)
Fischer, Julia, S206 (WED-475), S210 (WED-485), S248 (SAT-515), S493 (FRI-220)
Fischer, Lutz, S178 (FRI-429-YI)
Fischer, Roman, S43 (OS-065)
Fischer, Ryan T., S55 (OS-086), S831 (THU-258-YI), S842 (THU-284), S850 (THU-308)
Fischer, Susan, S148 (SAT-467-YI), S729 (THU-436)
Fischler, Björn, S55 (OS-086), S831 (THU-258-YI), S842 (THU-284), S850 (THU-308)
Fisher, Anat, S398 (FRI-516)
Fishman, Sigal, S642 (SAT-127)
Fisicaro, Paola, S874 (THU-571)
Fisseha, Henok, S24 (OS-028), S144 (SAT-452), S160 (SAT-507), S194 (WED-433)
Fit, Ana Maria, S255 (SAT-539), S543 (THU-165), S544 (THU-166)
Fitsche, André, S465 (WED-255)
Fitzpatrick, Emer, S712 (WED-554)
Fjellstrom, Ola, S2 (GS-003)
Flagiello, Valentina, S196 (WED-444), S595 (WED-138)
Flaherty, Johm, S934 (TOP-582)
Flamm, Maria, S539 (THU-151-YI)
Flanagan, Stuart, S823 (WED-028), S826 (WED-039), S960 (WED-587)
Flatley, Sarah, S312 (SAT-274-YI), S313 (SAT-275)
Flavell, Richard, S102 (THU-062)
Fleming, Kenneth, S673 (SAT-231)
Fleming, Maegen, S366 (WED-333-YI), S458 (WED-237-YI)
Fleming, Theresa, S26 (OS-031)
Flemming, Jennifer, S325 (SAT-319), S624 (WED-225-YI), S624 (WED-226), S968 (WED-609-YI)
Fletcher, Simon, S957 (WED-578)
Fleurent, Coralie, S143 (SAT-450), S497 (FRI-234), S723 (THU-418)
Flink, Hajo J., S351 (SAT-426-YI), S352 (SAT-429), S353 (SAT-432), S353 (SAT-433)
Flint, Molly, S338 (SAT-385)
Flisiak, Robert, S777 (THU-050), S817 (WED-012), S970 (WED-617-YI), S980 (FRI-633)
Flis, Paulina, S313 (SAT-276)
Flor, Armando, S682 (FRI-148)
Floreani, Annarosa, S325 (SAT-320)
Florensa, Nuria, S317 (SAT-290-YI), S338 (SAT-383)
Flores-Diez, Pablo, S250 (SAT-524)
Flores-García, Nayelli, S392 (FRI-499), S419 (THU-523)
Flores-Garcia, Nayelli C., S22 (OS-022-YI)
Flores, Joan, S249 (SAT-517), S249 (SAT-521), S433 (THU-240), S922 (SAT-613)
Flores-Peña, Roberto, S481 (WED-384)
Floristán, María Aragüés, S308 (SAT-264)
Florman, Sander, S60 (OS-094), S375 (TOP-519)
Fock-Sing, Kenita, S83 (LBP-035)
Fodor, Andreea, S33 (OS-046), S255 (SAT-539), S544 (THU-166), S602 (WED-157), S720 (TOP-504-YI), S728 (THU-433-YI), S730 (THU-443), S783 (SAT-012), S827 (TOP-297), S862 (WED-315)
Foerster, Friedrich, S503 (FRI-248)
Fogt, Maria, S110 (FRI-041-YI), S115 (FRI-059), S122 (FRI-079-YI), S554 (THU-204)
Fog-Tonnesen, Morten, S176 (FRI-421), S240 (FRI-338)
Foguenne, Maxime, S59 (OS-091), S381 (FRI-465), S382 (FRI-466)
Folch, Cinta, S810 (FRI-035)
Foley, Clare, S769 (THU-024-YI), S769 (THU-025)
Folliero, Veronica, S977 (WED-640)
Folli, Franco, S669 (SAT-219)
Folseraas, Trine, S2 (GS-002), S13 (OS-006-YI), S290 (FRI-289), S299 (SAT-249), S303 (SAT-257-YI), S345 (SAT-410), S395 (FRI-509), S445 (THU-385), S451 (THU-409)
Fondevila, Marcos, S9 (LBO-005-YI), S139 (FRI-134), S241 (FRI-339)
Fonseca, Cristina, S43 (OS-066), S937 (FRI-585-YI)
Fonstad, Rachel, S582 (WED-099)
Fontaine, Helene, S45 (OS-067), S815 (WED-005)
Fontana, Antonella, S530 (THU-117)
Fonticoba-Wood, María, S771 (THU-030)
Forbes, Stuart J., S134 (FRI-117), S137 (FRI-125)
Forcina, Tommaso, S477 (WED-370)
Foreest, Karen, S764 (THU-012)
Forgia, Sebastiano, S434 (THU-241)
Forlenza, Rossella, S570 (WED-061)
Forman, Lisa, S10 (LBO-006)
Formentini, Laura, S275 (THU-322-YI)
Formozis, Stavros, S142 (SAT-449)
Fornaguera, Cristina, S173 (FRI-414), S239 (FRI-336)
Fornari, Francesca, S462 (WED-248)
Forner, Alejandro, S445 (THU-385), S484 (WED-393)
Forns, Xavier, S21 (OS-021), S91 (SAT-062), S256 (SAT-542), S828 (TOP-309-YI), S884 (THU-604-YI), S903 (SAT-563-YI), S941 (FRI-590), S948 (FRI-611)
Foroohar, Tara, S308 (SAT-265), S309 (SAT-266)
Foroughi, Hassan, S71 (LBP-008)
Forrest, Ewan H, S113 (FRI-054)
Forsgren, Mikael, S220 (WED-517), S568 (WED-056)
Fortea, Jose, S182 (FRI-442), S643 (SAT-134)
Fortea, Jose Ignacio, S427 (THU-220), S733 (THU-450)
Forti, Matteo, S626 (WED-231)
Fortis, Sotirios, S620 (WED-212)
Fortney, Tiffany, S905 (SAT-571), S947 (FRI-609), S960 (WED-588)
Forton, Daniel, S47 (OS-072)
Fortune, Brett, S58 (OS-089), S313 (SAT-282), S745 (THU-483)
Foschi, Francesco Giuseppe, S82 (LBP-034-YI), S185 (TOP-455-YI), S307 (SAT-263), S335 (SAT-378-YI)
Fossdal, Guri, S13 (OS-006-YI)
Fouchard, Isabelle, S540 (THU-155), S554 (THU-202)
Foucher, Juliette, S43 (OS-066), S45 (OS-067), S602 (WED-158), S934 (TOP-582), S937 (FRI-585-YI)
Fougerou-Leurent, Claire, S45 (OS-067), S815 (WED-005)
Fouillé, Roxanne, S875 (THU-572)
Fournier-Poizat, Céline, S525 (THU-103), S558 (TOP-063-YI), S577 (WED-084), S607 (WED-174-YI)
Fowsiyo, Ahmed, S303 (SAT-257-YI), S484 (WED-393)
Foșălău, Adina-Bianca, S574 (WED-074)
Fox, Adrian, S922 (SAT-613)
Fox, Eric, S390 (FRI-493-YI)
Fox, Rena, S807 (FRI-026)
Foxton, Matthew, S65 (OS-102), S970 (WED-619)
Fracanzani, Anna Ludovica, S62 (OS-097), S443 (THU-380-YI), S516 (TOP-113), S520 (THU-091-YI), S541 (THU-158), S553 (THU-197), S595 (WED-137), S595 (WED-138), S626 (WED-231), S636 (SAT-110-YI), S696 (FRI-188-YI)
Fraga, Enrique, S409 (FRI-557)
Fragenas, Andreina, S296 (TOP-281), S306 (SAT-262)
Fragiadakis, Gabriela, S871 (THU-560-YI)
Franca, Alex, S1 (GS-001)
Francalanci, Paola, S670 (SAT-225)
Franca, Marzia La, S227 (WED-541-YI)
Francesca, Caparra, S69 (LBP-004-YI), S82 (LBP-034-YI)
Franceschi, Francesco, S219 (WED-515)
Francesco, Ascari, S725 (THU-425)
Francesco, Raffaele De, S51 (OS-079)
Francés, Rubén, S169 (FRI-400), S177 (FRI-427), S179 (FRI-431-YI), S200 (WED-453), S230 (TOP-343-YI), S542 (THU-164), S567 (WED-054)

Author Index

Franch, Enric Tomas, S394 (FRI-508), S407 (FRI-547)
Francheville, Jordan, S598 (WED-148)
Franci, Gianluigi, S977 (WED-640)
Francioso, Simona, S49 (OS-076-YI), S919 (SAT-608-YI)
Francipane, Maria Giovanna, S419 (THU-524)
Francis, Luc, S119 (FRI-073)
Franck, Martin, S737 (THU-462)
Franco, Carmen Cepeda, S410 (FRI-558)
Franco, Carolina, S182 (FRI-442), S267 (SAT-350)
Francois, Charlene, S83 (LBP-035)
Francois, Sandrine, S827 (WED-046)
François, Silke, S907 (SAT-575)
Franco, Oscar, S577 (WED-084), S600 (WED-153), S621 (WED-214), S765 (THU-013)
Francoz, Claire, S380 (FRI-463), S381 (FRI-464)
Francque, Sven, S55 (OS-085-YI), S62 (OS-097), S424 (TOP-376), S516 (TOP-113), S535 (THU-134), S577 (WED-084), S581 (WED-093-YI), S581 (WED-094), S611 (WED-185), S621 (WED-214), S621 (WED-215), S638 (SAT-117-YI), S682 (FRI-150-YI), S696 (FRI-189), S696 (FRI-190), S729 (THU-441), S733 (THU-450), S765 (THU-013), S766 (THU-015), S777 (THU-050), S789 (SAT-031-YI), S849 (THU-306-YI)
Frank, Anna Katharina, S2 (GS-002), S284 (FRI-266), S292 (FRI-300-YI), S858 (WED-300-YI)
Frankel, Stanley, S87 (LBP-043)
Fraňková, Soňa, S35 (OS-050-YI), S474 (WED-364)
Franks, Hester, S41 (OS-060)
Franza, Anne Minello, S43 (OS-066), S45 (OS-067), S934 (TOP-582)
Franz, Cibele, S340 (SAT-394), S830 (THU-254)
Franzè, Maria Stella, S163 (FRI-382), S223 (WED-527), S434 (THU-242), S499 (FRI-238), S505 (FRI-254), S967 (WED-605-YI)
Franzon, Deborah, S770 (THU-026)
Frappreau, Charlotte, S54 (OS-084)
Frascheri, Cinzia, S784 (SAT-015-YI)
Fraser, Chris, S968 (WED-609-YI)
Frauchiger, Beatrice, S165 (FRI-386)
Fraz, Ezaam, S803 (FRI-014), S818 (WED-013)
Freark de Boer, Jan, S857 (WED-299), S863 (WED-318)
Frederic, Haedge, S142 (SAT-448), S159 (SAT-506-YI), S170 (FRI-402)
Frederick, R. Todd, S745 (THU-483), S770 (THU-026)
Frediani, Elena, S457 (WED-235)
Fredriksson, Marie, S770 (THU-027)
Freeland, Catherine, S805 (FRI-022)
Freeman, Alexandra, S835 (THU-264-YI)
Freer, Alice, S61 (OS-108)
Freiherr von Beust, Maximilian, S251 (SAT-525)
Freije, Catherine, S891 (THU-624-YI)
Freile, Fabio Grundland, S242 (FRI-345-YI)
Frenette, Catherine (Carrie), S809 (FRI-030)
Fresneau, Brice, S38 (OS-055)
Fretwell, Jane, S768 (THU-023)
Freudenberg, Johannes, S959 (WED-585)
Freyer, Erich, S866 (FRI-641)
Frey, Molly, S58 (OS-089), S313 (SAT-282)
Freyre, Carolina, S815 (WED-006), S910 (SAT-581), S910 (SAT-585)
Frías, Alba Carmona, S303 (SAT-256-YI)
Frias, Ana, S186 (TOP-470-YI)
Frick, Adrian, S37 (OS-053)
Fridriksdottir, Ragnheidur, S802 (FRI-011)
Friederich, Philip W., S351 (SAT-426-YI)
Friedman, Nir, S60 (OS-093), S289 (FRI-286), S615 (WED-196)
Fried, Michael, S344 (SAT-403)
Friedrich, Matthias, S43 (OS-065)
Friedrich, Philip, S647 (SAT-148)
Friend, Ethan, S62 (OS-097), S516 (TOP-113)
Fries, Jochen, S289 (FRI-284)
Friesland, Martina, S887 (THU-611)
Frissen, Mick, S142 (SAT-448), S159 (SAT-506-YI), S169 (FRI-399), S170 (FRI-402)
Fritz, Joséphine, S744 (THU-482-YI)
Frohme, Josephine, S623 (WED-220)
Fromme, Malin, S836 (THU-265-YI), S836 (THU-266), S847 (THU-300)
Fronek, Jiri, S392 (FRI-500)
Frontino, Anna Maria, S861 (WED-308)
Frutos-Vivar, Fernando, S146 (SAT-459)
Fryer, Eve, S673 (SAT-231)
Ftouni, Sarah, S458 (WED-240)
Fuchs, Claudia, S11 (OS-002-YI), S237 (FRI-324), S284 (FRI-266), S284 (FRI-267)
Fuchs, Michael, S766 (THU-015)
Fuentes, Ana, S799 (TOP-049), S910 (SAT-581)
Fuente, Victor, S806 (FRI-024)
Fuerst, Thomas, S619 (WED-206)
Fuertes-Yebra, Esther, S542 (THU-164)
Fueyo, Laura, S819 (WED-019)
Fu, Haoshuang, S91 (SAT-067), S99 (TOP-194)
Fujii, Hideki, S580 (WED-091)
Fujii, Makoto, S537 (THU-140)
Fujiki, Masato, S399 (FRI-522)
Fujino, Tatsuya, S249 (SAT-522), S970 (WED-618)
Fujishiro, Mitsuhiro, S187 (TOP-472)
Fujiyama, Shigetoshi, S1 (GS-001)
Fu, Junliang, S946 (FRI-606)
Fukada, Hiroo, S225 (WED-533), S246 (FRI-356)
Fukano, Kento, S875 (THU-573), S894 (THU-635)
Fukuda, Haruhisa, S694 (FRI-184)
Fukuda, Shiro, S537 (THU-140)
Fukuhara, Kyoko, S225 (WED-533), S246 (FRI-356)
Fulgenzi, Claudia, S429 (THU-227-YI), S455 (TOP-406), S491 (TOP-408-YI), S500 (FRI-239)
Fuller, Nathan, S281 (FRI-260), S282 (FRI-261), S863 (WED-318)
Fuller, Sammantha, S342 (SAT-398)
Fuller-Vargas, Sebastián, S663 (SAT-199-YI)
Fumolo, Elisa, S302 (SAT-252)
Fundora, Yilliam, S884 (THU-604-YI), S941 (FRI-590)
Fung, Cherry, S113 (FRI-054)
Fung, James, S24 (OS-028), S947 (FRI-609)
Fung, Scott K., S46 (OS-070-YI), S875 (THU-574), S914 (SAT-592-YI), S921 (SAT-610), S943 (FRI-594), S953 (FRI-624)
Fung, Yan Yue James, S144 (SAT-452)
Funk, Luke, S690 (FRI-173)
Funuyet-Salas, Jesús, S527 (THU-108)
Fu, Ran, S79 (LBP-027)
Furia, Ludovic, S457 (WED-236)
Furler, John, S799 (FRI-004), S800 (FRI-005)
Furley, Maison, S580 (WED-092-YI)
Furquim d'Almeida, Arno, S903 (SAT-562)
Furuta, Kiyoshi, S258 (SAT-549), S550 (THU-188), S979 (WED-644)
Furuta, Koichiro, S686 (FRI-159)
Fusaro, Lisa, S69 (LBP-004-YI)
Fusco, Gianluca, S196 (WED-445)
Fusi, Alberto, S89 (SAT-058)
Fuster, Carla, S331 (SAT-368-YI), S862 (WED-315)
Fuster, Cristina, S204 (WED-467)
Fuster, Daniel, S128 (FRI-100)
Fustinoni, Silvia, S595 (WED-138)
Fu, Wenguang, S651 (SAT-159)
Fu, Xihua, S73 (LBP-013)
Fu, Xinghuan, S292 (FRI-298)
Fytili, Paraskevi, S45 (OS-068-YI)

Gabbia, Daniela, S669 (SAT-219)
Gabeta, Stella, S314 (SAT-283), S323 (SAT-315)
Gabrielli, Filippo, S82 (LBP-034-YI), S307 (SAT-263), S335 (SAT-378-YI)
Gabriel-Medina, Pablo, S605 (WED-168-YI)
Gadano, Adrian, S1 (GS-001), S35 (OS-050-YI), S62 (OS-097), S112 (FRI-050), S160 (SAT-507), S516 (TOP-113), S794 (SAT-046), S824 (WED-035), S956 (TOP-598)
Gadenne, Cloé, S463 (WED-250)
Gadi, Zouhir, S62 (OS-097), S516 (TOP-113), S581 (WED-093-YI), S581 (WED-094), S729 (THU-441)
Gadour, Eyad, S250 (SAT-523), S390 (FRI-494), S390 (FRI-495)
Gaebler, Christian, S77 (LBP-022-YI)
Gaeta, Giovanni Battista, S49 (OS-076-YI), S440 (THU-369), S919 (SAT-608-YI)
Gage, Christine, S974 (WED-628)

Gaggar, Anuj, S958 (WED-579)
Gagliani, Nicola, S57 (OS-088), S372 (WED-350)
Gagliardi, Roberta, S30 (OS-041), S97 (SAT-084-YI), S195 (WED-442-YI), S196 (WED-443), S217 (WED-509-YI), S227 (WED-541-YI)
Gagnadoux, Frédéric, S540 (THU-155)
Gahete, Manuel D., S467 (WED-261)
Gahlot, Monita, S36 (OS-051-YI)
Gaia, Silvia, S431 (THU-233)
Gaipa, Alessia La, S370 (WED-346), S462 (WED-248)
Gairing, Simon Johannes, S172 (FRI-411), S185 (TOP-456-YI), S197 (WED-446), S199 (WED-451-YI), S742 (THU-476)
Gairola, Abhishek, S331 (SAT-368-YI)
Gala-Lopez, Boris, S229 (WED-545)
Galambos, Michael, S58 (OS-089), S313 (SAT-282), S324 (SAT-316), S329 (SAT-363)
Galán, Jorge, S910 (SAT-581), S910 (SAT-585)
Galán, Juan Carlos, S910 (SAT-581), S910 (SAT-585)
Galante, Antonio, S401 (FRI-528)
Galena, Tania del Socorro Grimaldo, S730 (THU-442)
Galera, Ana Garcia, S391 (FRI-497)
Galetin, Aleksandra, S106 (THU-075)
Galicia-Moreno, Marina, S132 (FRI-108-YI)
Galindo, Maria José, S904 (SAT-564)
Gal, Jocelyn, S681 (FRI-147)
Gallage, Suchira, S651 (SAT-158-YI)
Gallagher, Michelle, S713 (WED-556-YI)
Gallagher, Patrick, S229 (WED-545)
Gallant, Marie, S315 (SAT-285)
Gallardo, Cristian Perez, S357 (TOP-327-YI), S663 (SAT-199-YI)
Gallay, Philippe, S877 (THU-580)
Gallego-Durán, Rocio, S525 (THU-103), S527 (THU-108), S558 (TOP-063-YI), S589 (WED-118), S607 (WED-174-YI)
Gallego-Durán, Rocío, S177 (FRI-427), S189 (WED-418), S542 (THU-164), S567 (WED-054), S621 (WED-214), S644 (SAT-137), S678 (SAT-244)
Gallegos, Danielle, S788 (SAT-029)
Gallegos-Orozco, Juan F., S10 (LBO-006)
Galle, Peter R., S26 (OS-032-YI), S172 (FRI-411), S199 (WED-451-YI), S428 (THU-227-YI), S742 (THU-476), S854 (WED-285)
Gallez, Nicolas, S365 (WED-331-YI)
Galli, Andrea, S82 (LBP-034-YI), S316 (SAT-287), S325 (SAT-320), S335 (SAT-378-YI), S350 (SAT-421), S400 (FRI-526), S542 (THU-159), S831 (THU-256-YI)
Gallone, Guglielmo, S402 (FRI-531)
Gallo, Paolo, S196 (WED-444), S477 (WED-370), S595 (WED-138)
Galochino, María, S250 (SAT-524), S603 (WED-163)
Galsgaard, Elisabeth, S240 (FRI-338)
Galun, Eithan, S60 (OS-093), S234 (FRI-318), S289 (FRI-286), S615 (WED-196)
Galvanin, Clelia, S35 (OS-050-YI)
Galvano, Fabio, S667 (SAT-214)
Gàlvez, Montserrat, S710 (THU-557-YI), S810 (FRI-035)
Galvin, ZIta, S377 (FRI-449), S396 (FRI-512)
Galy-Fauroux, Isabelle, S457 (WED-236)
Gamangatti, Shivanand, S36 (OS-051-YI), S141 (TOP-423), S184 (TOP-454-YI), S725 (THU-426)
Gama, Raimundo Araujo, S296 (TOP-281), S306 (SAT-262)
Gambato, Martina, S148 (SAT-466-YI), S193 (WED-431-YI)
Gambino, Carmine, S30 (OS-041), S196 (WED-443), S196 (WED-445), S402 (FRI-530)
Gamkrelidze, Ivane, S805 (FRI-022), S820 (WED-020-YI)
Gananandan, Kohilan, S198 (WED-448-YI)
Gande, Adarsh, S845 (THU-288)
Gander, Amir, S150 (SAT-475)
Gandhi, Keshav, S818 (WED-014)
Gane, Edward J., S1 (GS-001), S7 (GS-012), S8 (LBO-003), S39 (OS-057), S48 (OS-073), S76 (LBP-021), S87 (LBP-043), S943 (FRI-594), S957 (WED-578), S958 (WED-579), S958 (WED-580), S958 (WED-581), S959 (WED-586), S964 (WED-597), S965 (WED-602)
Ganger, Daniel, S388 (FRI-489)
Gankina, Natalya Urievna, S960 (WED-587)
Ganna, Andrea, S282 (FRI-263)
Ganne-Carrié, Nathalie, S35 (OS-050-YI), S43 (OS-066), S45 (OS-067), S46 (OS-070-YI), S54 (OS-084), S222 (WED-525), S343 (SAT-400), S428 (THU-226-YI), S446 (THU-393-YI), S493 (FRI-221), S499 (FRI-238), S505 (FRI-254), S507 (FRI-362), S508 (FRI-364-YI), S739 (THU-467), S934 (TOP-582), S937 (FRI-585-YI)
Ganne, Nathalie, S38 (OS-055), S506 (FRI-255-YI)
Ganschow, Rainer, S836 (THU-265-YI)
Gantur, Tuguldur, S826 (WED-039)
Gantzel, Rasmus, S801 (FRI-008)
Gan, Yulong, S685 (FRI-156)
Gao, Bowen, S644 (SAT-135-YI)
Gao, Cai, S98 (SAT-087)
Gao, Feng, S86 (LBP-041)
Gao, Haibing, S81 (LBP-031), S160 (SAT-507)
Gao, Hong, S100 (TOP-207)
Gao, Hongbo, S433 (THU-239), S932 (SAT-641)
Gao, Jinhang, S28 (OS-036-YI)
Gao, Pingting, S511 (FRI-370)
Gao, Pujun, S33 (OS-047)
Gao, Qiang, S511 (FRI-370), S676 (SAT-239)
Gao, Rong, S642 (SAT-132)
Gao, Shujun, S941 (FRI-591)
Gao, Steve, S321 (SAT-306), S322 (SAT-307), S322 (SAT-308)
Gao, Tingting, S964 (WED-601-YI)
Gao, Wenrui, S235 (FRI-320)
Gao, Xian, S48 (OS-074)
Gao, Xiang, S934 (SAT-644)
Gao, Xiaohong, S941 (FRI-591)
Gao, Xuelian, S6 (GS-010), S644 (SAT-136)
Gao, Yanhang, S24 (OS-028), S33 (OS-047), S34 (OS-048), S133 (FRI-110), S144 (SAT-452), S160 (SAT-507), S162 (TOP-440), S373 (WED-355)
Gao, Yin, S868 (TOP-616-YI)
Gao, Yudi, S467 (WED-260)
Gao, Yueqiu, S473 (WED-361-YI)
Gao, Yunxi (Daisy), S242 (FRI-345-YI)
Gao, Zhiliang, S952 (FRI-623)
Garaizabal, Iñigo, S830 (THU-253)
Garau, Margalida Vanrell, S223 (WED-528)
Garavaglia, Carola, S595 (WED-138)
Garbeva, Paolina, S262 (SAT-330)
Garcez, Lais, S192 (WED-428)
Garcia, Ana, S28 (OS-037), S629 (TOP-160)
García, Ander, S312 (SAT-273)
Garcia, Andres, S581 (WED-095)
Garcia, Ariana Pereira, S707 (THU-548)
García-Avelino, Gustavo, S771 (THU-030)
García-Calderó, Héctor, S827 (TOP-297)
García-Criado, Maria Ángeles, S837 (THU-268)
Garcia, Cristina, S254 (SAT-538), S599 (WED-151)
Garcia, Diana, S94 (SAT-073)
Garcia, Eduardo, S28 (OS-037), S629 (TOP-160)
García-Estrada, Antonio, S467 (WED-261)
García, Federico, S799 (TOP-049), S899 (SAT-557), S910 (SAT-581), S910 (SAT-585)
García-Fernández, Vanessa, S600 (WED-153), S644 (SAT-137), S806 (FRI-023)
Garcia, Fernando, S226 (WED-538)
Garcia-Fraile, Lucio, S806 (FRI-024)
Garcìa-Garcìa, Elena, S331 (SAT-368-YI)
García-Gavilán, María Carmen, S837 (THU-267), S855 (WED-289)
García, Héctor Alexander Velásquez, S821 (WED-024), S967 (TOP-600-YI)
Garcia, Isabelle, S764 (THU-012)
Garcia, Jennifer, S850 (THU-308)
Garcia, Jenson Ruiz, S540 (THU-154)
García juarez, Francisco isai, S866 (FRI-640)
Garcia, Luis Cortes, S603 (WED-163)
García, Luis Cortés, S250 (SAT-524)
Garcia, Manuel De La Mata, S303 (SAT-256-YI)
Garcia-Medel, Eric, S79 (LBP-027)
García-Monzón, Carmelo, S123 (FRI-086)
Garcia, Pablo Bellot, S54 (OS-084), S719 (TOP-488), S747 (THU-492), S752 (THU-501)

Author Index

García-Pagán, Juan Carlos, S6 (GS-011-YI), S33 (OS-046), S52 (OS-081), S53 (OS-082), S54 (OS-084), S55 (OS-085-YI), S397 (FRI-515), S719 (TOP-488), S720 (TOP-504-YI), S723 (THU-418), S730 (THU-443), S733 (THU-450), S735 (THU-453), S747 (THU-492), S752 (THU-501), S827 (TOP-297), S862 (WED-315)
García-Pérez, Rocío, S173 (FRI-414), S239 (FRI-336)
García-Pras, Ester, S884 (THU-604-YI)
Garcia-Retortillo, Montserrat, S16 (OS-010), S300 (SAT-250), S948 (FRI-611), S969 (WED-611)
García-Retortillo, Montserrat, S815 (WED-006)
Garcia-Reyes, Kirema, S60 (OS-094)
García-Rioja, Javier, S527 (THU-108)
García-Rubio, Vanessa, S771 (THU-030)
Garcia-Ruiz, M. Carmen, S28 (OS-037), S101 (THU-058), S131 (FRI-104), S627 (TOP-144), S629 (TOP-160)
Garcia-Samaniego, Francisco Javier, S150 (SAT-475), S948 (FRI-611)
García, Sandra, S603 (WED-163)
García, Sergio, S603 (WED-163)
García-Torre, Beatriz, S166 (FRI-388-YI)
Garcia-Tsao, Guadalupe, S76 (LBP-020), S745 (THU-483)
García, Victoria Alejandra Jiménez, S751 (THU-500)
García-Villarreal, Luis, S837 (THU-267), S855 (WED-288), S855 (WED-289), S856 (WED-290)
García, Virginia Aranda, S634 (SAT-104)
Gardete-Correia, Luís, S649 (SAT-152)
Gardini, Andrea Casadei, S494 (FRI-225)
Gareta, Dickman, S900 (SAT-558)
Garf, Sébastien Le, S681 (FRI-147)
Garg, Mayur, S716 (WED-562-YI), S716 (WED-563), S716 (WED-564)
Garg, Pratibha, S5 (GS-009), S171 (FRI-409-YI), S180 (FRI-433), S366 (WED-334)
Garg, Vanya, S456 (WED-232)
Garita, Esteban, S327 (SAT-322)
Garner, Rachel, S19 (OS-016), S84 (LBP-036), S679 (TOP-176), S700 (FRI-201)
Garner, Will, S77 (LBP-021)
Garn, Jonathan, S866 (FRI-641)
Garnotel, Roselyne, S435 (THU-246)
Garofalo, Alexis, S166 (FRI-393)
Garreta, Javier Pérez, S926 (SAT-623), S949 (FRI-612), S961 (WED-592)
Garrib, Anupam, S792 (SAT-042)
Garribba, Alessandra, S350 (SAT-421)
Garrido, Amaia, S810 (FRI-035)
Garrido, Esther, S969 (WED-611)
Garrido, Rebeca Pintado, S54 (OS-084), S719 (TOP-488), S747 (THU-492)
Garteiser, Philippe, S571 (WED-067)
Gart, Eveline, S645 (SAT-138), S671 (SAT-227)
Gartner, Lisa, S43 (OS-065)
Garver-Mosher, Tabetha, S391 (FRI-496)
Garzon-Basterra, Unai, S277 (THU-330-YI), S631 (SAT-095-YI)
Gasbarrini, Antonio, S219 (WED-515), S731 (THU-444-YI), S936 (TOP-584), S938 (FRI-586)
Gasche, Christoph, S37 (OS-053)
Gašić, Uroš, S268 (SAT-351)
Gasparello, Jessica, S466 (WED-258)
Gaspar, Rui, S781 (SAT-008), S781 (SAT-009)
Gasparyan, Ani, S169 (FRI-400), S230 (TOP-343-YI)
Gasse, Natasja Van, S907 (SAT-575)
Gastaca, Mikel, S277 (THU-330-YI), S410 (FRI-558)
Gastaldelli, Amalia, S20 (OS-018), S557 (THU-213), S577 (WED-084), S600 (WED-153), S636 (SAT-109), S682 (FRI-150-YI), S795 (SAT-050)
Gastaldi, Rachele, S90 (SAT-061-YI), S848 (THU-304)
Gastaldo, María José, S254 (SAT-538)
Gatanaga, Hiroyuki, S811 (FRI-037)
Gatault, Philippe, S143 (SAT-450)
Gato-Zambrano, Sheila, S600 (WED-153), S644 (SAT-137)
Gatselis, Nikolaos, S79 (LBP-026), S314 (SAT-283), S323 (SAT-315), S325 (SAT-320), S349 (SAT-420)
Gatti, Cristina, S201 (WED-459)
Gatti, Pietro, S35 (OS-050-YI)
Gatti, Veronic, S477 (WED-370)
Gatzweiler, Luise, S376 (TOP-520-YI)
Gaudio, Eugenio, S2 (GS-002)
Gaulier, Jean-Michel, S889 (THU-619)
Gaume, Clarisse, S512 (FRI-372)
Gautam, Pramod, S108 (TOP-208-YI), S456 (WED-232)
Gautam, Preety, S770 (THU-028)
Gautier, Lucas, S72 (LBP-011)
Gayard, Antoine, S512 (FRI-372)
Gayat, Cyprien, S143 (SAT-450)
Gazda, Jakub, S720 (TOP-502-YI), S730 (THU-443)
Gazdikova, Katarina, S807 (FRI-025)
Gea, Alejandro De, S806 (FRI-024)
Gebreab, Sirak, S919 (SAT-607)
Gebregziabher, Bethlehem, S822 (WED-026)
Gee Lim, Seng, S960 (WED-587)
Gee, Matthew, S582 (WED-099)
Geerts, Anja, S59 (OS-092-YI), S79 (LBP-026), S99 (TOP-193-YI), S159 (SAT-505), S281 (TOP-295-YI), S315 (SAT-285), S315 (SAT-286), S349 (SAT-420), S464 (WED-253), S680 (FRI-139), S693 (FRI-182)
Ge, Guohong, S86 (LBP-041)
Gehring, Adam, S875 (THU-574), S889 (THU-620), S914 (SAT-592-YI), S921 (SAT-610), S964 (WED-597)
Geier, Andreas, S21 (OS-020), S64 (OS-100), S252 (SAT-529), S601 (WED-155), S971 (WED-620)
Geijo, Fernando, S819 (WED-019)
Geisel, Dominik, S154 (SAT-489)
Geisler, Fabian, S359 (THU-345-YI)
Geißelbrecht, Sophia, S3 (GS-005), S197 (WED-446), S752 (THU-501)
Geissler, Rene, S911 (SAT-586), S947 (FRI-609), S960 (WED-588)
Gelabert, Ana Escarda, S223 (WED-528)
Geladari, Eleni, S187 (WED-415)
Gelape, Fernanda, S296 (TOP-281), S306 (SAT-262)
Gellert-Kristensen, Helene, S166 (FRI-393)
Gelson, William, S10 (LBO-006)
Gelu-Simeon, Moana, S110 (FRI-042)
Gemmen, Eric, S834 (THU-262), S836 (THU-266)
Gencdal, Genco, S965 (WED-603)
Genesca, Joan, S233 (FRI-315), S427 (THU-220), S735 (THU-453)
Genga, Giovanni, S610 (WED-183)
Geng, Anne, S165 (FRI-386)
Geng, Jiawei, S86 (LBP-041)
Geng, Mengya, S627 (TOP-143)
Geng, Yadi, S107 (THU-077)
Geng, Ying, S645 (SAT-139)
Genin, Emmanuelle, S17 (OS-011)
Genova, Giuliano, S300 (SAT-250)
Genovesi, Virginia, S481 (WED-383)
Gensluckner, Sophie, S539 (THU-151-YI)
Gentili, Federica, S610 (WED-183), S720 (TOP-502-YI)
Gentilini, Alessandra, S479 (WED-379)
Gentilucci, Umberto Vespasiani, S476 (WED-368), S601 (WED-156)
George, Elena, S713 (WED-557)
George, Jacob, S24 (OS-028), S144 (SAT-452), S160 (SAT-507), S218 (WED-513), S571 (WED-069), S713 (WED-557), S749 (THU-496)
George, Phillip, S707 (THU-546-YI)
George, Renita, S65 (OS-102), S970 (WED-619)
Georgess, Dan, S663 (SAT-200)
Geraci, Olivia, S380 (FRI-462)
Gerard, Nega, S889 (THU-620)
Gerber, Lynn H, S766 (THU-015), S794 (SAT-046)
Gerdes, Christoph, S488 (WED-409-YI)
Gerding, Albert, S630 (SAT-090)
Geretti, Anna Maria, S801 (FRI-007)
Germani, Giacomo, S126 (FRI-094), S127 (FRI-095), S148 (SAT-466-YI), S193 (WED-431-YI), S356 (SAT-443), S417 (FRI-581)
Germanou, Styliani, S89 (SAT-058)
Germanova, Desislava, S35 (OS-050-YI)
Gerolami, René, S38 (OS-055)
Gerona, Solange, S728 (THU-434)

Gerov, Dragomir, S76 (LBP-021)
Gerrits, Katinka, S15 (OS-009-YI)
Gershwin, Eric, S58 (OS-089), S313 (SAT-282)
Gershwin, Merrill E, S293 (FRI-302-YI)
Gerster, Théophile, S742 (THU-477)
Gerussi, Alessio, S69 (LBP-004-YI), S82 (LBP-034-YI), S282 (FRI-263), S300 (SAT-250), S304 (SAT-258), S305 (SAT-260-YI), S307 (SAT-263), S331 (SAT-368-YI), S333 (SAT-369), S335 (SAT-378-YI), S340 (SAT-393), S350 (SAT-421), S831 (THU-256-YI)
Gervais, Anne, S43 (OS-066), S934 (TOP-582), S937 (FRI-585-YI)
Gevers, Tom, S720 (TOP-504-YI)
Gevers, Tom J. G., S331 (SAT-368-YI), S333 (SAT-369)
Gevers, Tom J.G., S15 (OS-009-YI), S729 (THU-436)
Ge, Xiaoke, S631 (SAT-095-YI)
Ghahraman, Milad, S376 (TOP-520-YI)
Ghallab, Ahmed, S172 (FRI-410-YI), S641 (SAT-125-YI)
Ghallab, Mariam H., S208 (WED-482)
Ghani, Leith, S670 (SAT-220)
Ghani, Maham, S337 (SAT-381)
Ghany, Marc, S46 (OS-070-YI), S928 (SAT-628-YI)
Ghany, Marc G, S918 (SAT-604)
Ghazinyan, Hasmik, S67 (OS-105-YI), S127 (FRI-095), S952 (FRI-622)
Gheonea, Ionut, S819 (WED-015), S944 (FRI-601)
Gheorghe, Codrin, S951 (FRI-620)
Gheorghe, Liana, S43 (OS-066), S49 (OS-075), S777 (THU-050), S819 (WED-015), S900 (SAT-559), S901 (SAT-560), S934 (TOP-582), S936 (TOP-584), S937 (FRI-585-YI), S944 (FRI-601), S962 (WED-594)
Gherlan, George Sebastian, S49 (OS-075), S939 (FRI-587), S956 (WED-576)
Ghinolfi, Davide, S59 (OS-091)
Ghioca, Mihaela, S819 (WED-015), S944 (FRI-601)
Ghisa, Matteo, S402 (FRI-530)
Ghodsifard, Arezoo, S38 (OS-054)
Ghose, Aniruddha, S598 (WED-149)
Ghose, Sampa, S232 (FRI-308)
Ghosh, Dilip, S745 (THU-484)
Ghosheh, Yanal, S875 (THU-574)
Ghosh, Indrajit, S823 (WED-028), S826 (WED-039)
Ghosh, Shivam, S254 (SAT-537)
Ghosh, Somali, S257 (SAT-544)
Ghouse, Jonas, S166 (FRI-393)
Giabicani, Mikhael, S8 (LBO-002)
Giachi, Alessia, S475 (WED-366)
Giacomo, Emanuela Di, S428 (THU-227-YI), S491 (TOP-408-YI)
Già, Giulia Di, S841 (THU-282)
Gianatti, Andrea, S331 (SAT-368-YI)
Giandalia, Annalisa, S967 (WED-605-YI)
Giannelli, Valerio, S841 (THU-282), S856 (WED-291)
Giannini, Edoardo, S176 (FRI-425), S190 (WED-425), S304 (SAT-258), S307 (SAT-263), S335 (SAT-378-YI), S479 (WED-378), S831 (THU-256-YI), S902 (SAT-560)
Giannini, Edoardo Giovanni, S69 (LBP-004-YI), S82 (LBP-034-YI), S212 (WED-494-YI), S350 (SAT-421), S900 (SAT-559), S936 (TOP-584), S938 (FRI-586)
Giannou, Anastasios, S277 (THU-330-YI)
Giannoulis, George, S300 (SAT-250)
Giardini, Andrea Casadei, S781 (SAT-008)
Gidaagaya, Sarantuya, S923 (SAT-618)
Gigante, Elia, S435 (THU-246)
Giglio, Chiara, S412 (FRI-562)
Giglioli, Nicolò, S31 (OS-042), S746 (THU-490)
Giguet, Baptiste, S207 (WED-477), S380 (FRI-463), S381 (FRI-464)
Gil, Cristiane, S671 (SAT-226)
Gil-Duque, Ignacio, S278 (THU-333-YI)
Gil, Enrique, S826 (WED-038)
Giles, Hannah, S315 (SAT-286), S452 (THU-414-YI)
Gil-Gómez, Antonio, S177 (FRI-427), S600 (WED-153), S644 (SAT-137)
Gilg, Stefan, S71 (LBP-008)
Gil-Hernandez, Eva, S863 (WED-317)
Gil, Horacio, S806 (FRI-024)
Gil, Joan, S467 (WED-262)
Gill, Dipender, S166 (FRI-393)
Gillessen, Anton, S493 (FRI-220)
Gillevet, Patrick, S41 (OS-061)
Gillis, Chelsia, S380 (FRI-462)
Gill, Kulvinder, S369 (WED-340-YI)
Gill, Upkar, S49 (OS-076-YI), S370 (WED-347), S824 (WED-031), S876 (THU-575), S888 (THU-618), S921 (SAT-611)
Gilmore, Serena, S534 (THU-132)
Gil, Pamela, S112 (FRI-050)
Gil-Rojas, Sergio, S837 (THU-267), S855 (WED-289)
Gil, Sebastián, S296 (TOP-281), S306 (SAT-262)
Gilson, Richard, S823 (WED-028)
Gils, Sanne, S943 (FRI-595)
Gilvarry, Paul, S708 (THU-549-YI)
Gil, Yolanda Rodríguez, S308 (SAT-264)
Gimeno-Martos, Silvia, S779 (SAT-003-YI)
Gimeno, Natalia García, S16 (OS-010), S300 (SAT-250), S948 (FRI-611)
Gimpfl, Martina, S672 (SAT-230)
Ginès, Pere, S26 (OS-032-YI), S30 (OS-041), S63 (OS-098-YI), S110 (TOP-222), S129 (FRI-101), S148 (SAT-467-YI), S203 (WED-463), S246 (TOP-552), S394 (FRI-507-YI), S515 (TOP-098), S562 (TOP-097-YI), S583 (WED-101), S608 (WED-180), S612 (WED-188), S789 (SAT-031-YI)
Gioe', Claudia, S865 (FRI-638)
Gioia, Stefania, S52 (OS-081), S397 (FRI-515), S720 (TOP-502-YI), S746 (THU-489), S856 (WED-291)
Giorgio, Angelo Di, S55 (OS-086), S842 (THU-284)
Giorgio, Massimo De, S494 (FRI-225)
Giovannangelo, Alessia Di, S576 (WED-083)
Giráldez, Carmen Cárcamo, S18 (OS-014-YI)
Giráldez-Gallego, Alvaro, S33 (OS-046), S43 (OS-066), S54 (OS-084), S397 (FRI-515), S497 (FRI-234), S719 (TOP-488), S723 (THU-418), S747 (THU-492), S752 (THU-501), S934 (TOP-582), S936 (TOP-584), S937 (FRI-585-YI), S948 (FRI-611)
Girard, Muriel, S850 (THU-308), S951 (FRI-621)
Giraud, Guillaume, S869 (TOP-632), S876 (THU-576)
Giraudo, Chiara, S429 (THU-228)
Girbes, Alexandre Perez, S254 (SAT-538)
Girelli, Domenico, S849 (THU-305-YI)
Giri, Suprabhat, S398 (FRI-521), S952 (FRI-622)
Girleanu, Irina, S210 (WED-490), S211 (WED-493)
Girma, Makida, S194 (WED-433)
Girot, Paul, S497 (FRI-234), S723 (THU-418)
Gish, Alexandr, S889 (THU-619)
Gish, Robert G., S299 (SAT-247), S320 (SAT-303), S320 (SAT-304), S803 (FRI-013), S805 (FRI-022), S897 (TOP-565)
Gitto, Stefano, S400 (FRI-526), S972 (WED-623)
Giudicelli-Lett, Heloïse, S55 (OS-085-YI)
Giuffrè, Mauro, S495 (FRI-227)
Giuli, Cinzia Di, S610 (WED-183)
Giuli, Lucia, S720 (TOP-504-YI), S731 (THU-444-YI), S751 (THU-500)
Giulioni, Marco Angelo Danilo, S576 (WED-083)
Giunta, Federica, S402 (FRI-530)
Giuseppucci, Antonio, S399 (FRI-522)
Giusino, Gaetano, S494 (FRI-226), S495 (FRI-227)
Giustini, Leonardo, S51 (OS-079)
Gjini, Kamela, S427 (THU-220), S534 (THU-133), S574 (WED-073), S582 (WED-100-YI), S611 (WED-184-YI), S620 (WED-213)
Gjøl, Charlotte Mary, S110 (FRI-041-YI), S115 (FRI-059), S554 (THU-204)
Gladun, Karina, S551 (THU-189), S551 (THU-190)
Glasgow, Susanne, S799 (FRI-004), S800 (FRI-005)
Glassey, Ewan, S59 (OS-091)
Glaus, Jesus, S243 (FRI-349)
Glebe, Dieter, S930 (SAT-636)
Gleeson, Dermot, S312 (SAT-274-YI), S313 (SAT-275), S331 (SAT-368-YI)

Author Index

Glenn, Jeffrey, S49 (OS-075), S962 (WED-594), S965 (WED-603)
Gleyzolle, Baptiste, S512 (FRI-372)
Glitscher, Mirco, S882 (THU-595)
Gliwicz-Miedzińska, Dorota, S850 (THU-308)
Glodny, Bernhard, S848 (THU-302)
Gloria, Maria Helena, S892 (THU-627)
Gluud, Lise Lotte, S149 (SAT-468), S152 (SAT-478), S227 (WED-540-YI), S240 (FRI-338), S586 (WED-109), S602 (WED-159-YI), S680 (FRI-139), S692 (FRI-180), S736 (THU-459), S760 (TOP-032)
Glyn-Owen, Kate, S765 (THU-014)
Gnemmi, Viviane, S499 (FRI-238)
Gnjatic, Sacha, S485 (WED-396)
Gnouamozi, Gnimah Eva, S879 (THU-589-YI)
Gobbi, Angela, S307 (SAT-263)
Goclawska, Katarzyna, S617 (WED-203)
Göçücü, Kubilay, S465 (WED-257)
Godbole, Ira, S51 (OS-080-YI), S363 (TOP-326), S455 (TOP-406)
Godley, Jenny, S787 (SAT-025), S787 (SAT-026), S788 (SAT-027)
Godono, Alessandro, S784 (SAT-015-YI)
Godward, Eleanor, S338 (SAT-385)
Goediker, Juliana, S213 (WED-496)
Goeij, Femke De, S383 (FRI-468)
Goel, Amit, S923 (SAT-618)
Goel, Ashish, S36 (OS-051-YI), S67 (OS-105-YI), S144 (SAT-452), S160 (SAT-507), S722 (THU-416)
Goel, Varun, S5 (GS-008)
Goenka, Mahesh, S952 (FRI-622)
Goenka, Usha, S257 (SAT-544)
Goeppert, Benjamin, S38 (OS-054)
Goes, Alfredo, S102 (THU-060)
Goes, Sofie, S907 (SAT-575)
Goetze, Oliver, S395 (FRI-511-YI)
Goffaux, Alexis, S648 (SAT-151-YI)
Gofton, Cameron, S24 (OS-028), S144 (SAT-452), S160 (SAT-507)
Gogela, Neliswa, S764 (THU-012)
Gogna, Apoorva, S495 (FRI-228-YI)
Gohar, Farhan, S735 (THU-457)
Goh, Brian, S495 (FRI-228-YI)
Goh, Fion, S533 (THU-126)
Goh, George Boon Bee, S39 (OS-057), S424 (TOP-376), S516 (TOP-113), S517 (TOP-114), S525 (THU-103), S558 (TOP-063-YI), S560 (TOP-080), S589 (WED-118), S607 (WED-174-YI), S612 (WED-187-YI), S618 (WED-204), S621 (WED-215), S693 (FRI-182), S923 (SAT-618)
Goh, Jade Shu Qi, S495 (FRI-228-YI)
Goh, Lynette, S834 (THU-261)
Goicoechea, Leire, S28 (OS-037), S629 (TOP-160)
Goicoechea, Miriam, S806 (FRI-024)
Goikoetxea-Usandizaga, Naroa, S30 (OS-039-YI), S101 (THU-059-YI), S272 (THU-315-YI), S273 (THU-316), S278 (THU-333-YI), S281 (TOP-296-YI), S489 (WED-412-YI), S633 (SAT-101-YI), S855 (WED-287-YI)
Goitre, Ilaria, S574 (WED-073), S620 (WED-213)
Gokcan, Hale, S497 (FRI-234), S519 (THU-089), S588 (WED-116), S723 (THU-418)
Gökçe, Dilara Turan, S41 (OS-061), S519 (THU-089), S652 (SAT-163)
Gökce, Emine, S464 (WED-253)
Gokhe, Prachiti, S255 (SAT-541)
Goldberg, David, S116 (FRI-061), S190 (WED-421), S197 (WED-447), S327 (SAT-323)
Goldberg, S. Nahum, S234 (FRI-318)
Goldfinger, Marc, S125 (FRI-090-YI), S689 (FRI-169)
Goldfuß, Sophia, S930 (SAT-636)
Golding, Bruno, S592 (WED-131)
Goldin, Robert D., S137 (FRI-125), S343 (SAT-400), S455 (TOP-406), S673 (SAT-231)
Goldklang, Monica P., S834 (THU-262), S836 (THU-266), S844 (THU-285)
Goldstein, Andrea, S55 (OS-086)
Golenia, Aleksandra, S409 (FRI-555)
Golkocheva-Markova, Elica, S807 (FRI-025)
Golubeva, Julia, S551 (THU-189), S551 (THU-190)
Goluzova, Violetta, S594 (WED-135)
Gomaraschi, Monica, S595 (WED-138)
Gomariz, Victor, S191 (WED-426)
Gömer, André, S866 (FRI-641), S876 (THU-577), S879 (THU-588), S881 (THU-593), S885 (THU-608), S887 (THU-611), S890 (THU-623-YI)
Gomes da Silva, Hugo, S78 (LBP-023)
Gomes, Guilherme, S102 (THU-060)
Gomez, Abraham Sanchez, S22 (OS-022-YI)
Gómez- Camarero, Judith, S318 (SAT-291), S571 (WED-069), S837 (THU-267)
Gómez-Camarero, Judith, S294 (TOP-278), S300 (SAT-250), S308 (SAT-264), S542 (THU-164), S567 (WED-054), S855 (WED-289)
Gómez, César, S910 (SAT-585)
Gómez, Concepción, S779 (SAT–003-YI)
Gómez-Domínguez, Elena, S16 (OS-010), S124 (FRI-088), S308 (SAT-264), S309 (SAT-268)
Gomez, Eduardo Vilar, S531 (THU-122)
Gómez-Fernández, Cristina, S394 (FRI-507-YI)
Gómez-Hurtado, Isabel, S169 (FRI-400), S179 (FRI-431-YI), S230 (TOP-343-YI)
Gómez-Jauregui, Paul, S277 (THU-330-YI), S631 (SAT-095-YI)
Gómez, José, S968 (WED-610-YI)
Gómez-Loira, Martin, S256 (SAT-542), S288 (FRI-283)
Gomez, Marcelo Vicente Valverde, S728 (THU-434)
Gómez, Nerea, S605 (WED-168-YI)
Gómez-Orellana, Antonio M., S410 (FRI-558)
Gómez, Raquel Muñoz, S124 (FRI-088)
Gómez-Rubio, Mariano, S146 (SAT-459), S250 (SAT-524)
Gomez, Venny Alberto Venegas, S730 (THU-442)
Gonçalves, Cristina Campos, S55 (OS-086), S831 (THU-258-YI), S842 (THU-284)
Goncalves, Liliana, S713 (WED-556-YI)
Goncalves, Luciana, S141 (TOP-437), S154 (SAT-484)
Goncalves, Luciana Lofego, S34 (OS-049), S35 (OS-050-YI), S166 (FRI-388-YI)
Goncalves, Patrícia, S154 (SAT-484)
Gonçalves, Raquel, S720 (TOP-504-YI)
Gonfaus-Ortiz, Gemma, S467 (WED-262)
Gong, Jianping, S41 (OS-062)
Gong, Junhua, S41 (OS-062)
Gong, Shiming, S475 (WED-365)
Gong, Xianqiong, S941 (FRI-591)
Gong, Xinde, S756 (THU-514)
Gonzalès, Emmanuel, S55 (OS-086), S831 (THU-258-YI), S842 (THU-284), S850 (THU-308), S853 (WED-283)
González, Águeda, S542 (THU-164)
Gonzalez, Alicia, S806 (FRI-024)
González, Álvaro Díaz, S308 (SAT-264)
Gonzalez, Ander, S806 (FRI-024)
González, Antonio Poyato, S303 (SAT-256-YI)
Gonzalez-Carmona, Maria Angeles, S504 (FRI-251)
González-Casals, Helena, S810 (FRI-035)
González-Grande, Rocio, S410 (FRI-558), S815 (WED-006)
González-Huezo, Maria Sarai, S24 (OS-028), S144 (SAT-452), S160 (SAT-507), S296 (TOP-281), S306 (SAT-262)
González, Jesús M., S294 (TOP-278)
Gonzalez, Joaquin Cabezas, S948 (FRI-611)
Gonzalez-Kozlova, Edgar, S485 (WED-396)
González, María Miguélez, S806 (FRI-024)
González-Moreno, Leticia, S250 (SAT-524)
González-Padilla, Sheila, S33 (OS-046), S752 (THU-501)
Gonzalez-Peralta, Regino, S846 (THU-291), S846 (THU-298)
González-Recio, Irene, S101 (THU-059-YI), S272 (THU-315-YI), S273 (THU-316), S278 (THU-333-YI), S281 (TOP-296-YI), S489 (WED-412-YI), S633 (SAT-101-YI), S855 (WED-287-YI)
Gonzalez-Reyes, Jose Antonio, S271 (THU-314)
González-Santiago, Jesús M., S819 (WED-019)
Gonzalez, Susana, S847 (THU-300), S848 (THU-301)
Goode, Elizabeth, S788 (SAT-029)
Goodheart, Richard, S160 (SAT-507)
Goodman, Asha, S877 (THU-580)
Goodman, Russell, S130 (FRI-102-YI)

Goodwin, Shane, S740 (THU-468)
Goossens, Nicolas, S111 (FRI-043), S199 (WED-450)
Gopalkrishnan, Kalpana, S386 (FRI-482), S411 (FRI-561-YI), S413 (FRI-570)
Gordien, Emmanuel, S951 (FRI-621)
Gordon, Stuart C, S58 (OS-089), S295 (TOP-280), S313 (SAT-282), S316 (SAT-287), S766 (THU-015), S923 (SAT-618), S957 (WED-577)
Gordon, Stuart C., S10 (LBO-006)
Gorey, Ciara, S295 (TOP-280)
Gorgulho, Joao, S426 (THU-219-YI)
Gorham, Anna, S712 (WED-554)
Gori, Andrea, S911 (SAT-587-YI), S936 (TOP-584), S938 (FRI-586)
Goria, Odile, S55 (OS-085-YI), S742 (THU-477)
Gorsuch, Cassandra, S87 (LBP-043)
Görz, Amaryllis, S251 (SAT-525)
Goss, Amy, S926 (SAT-624)
Gottardi, Andrea De, S863 (WED-317)
Gottfredsson, Magnús, S802 (FRI-011)
Götze, Tobias, S834 (THU-260)
Goudsmit, Ben, S415 (FRI-574)
Gou, Guoe, S47 (OS-071), S946 (FRI-606)
Gould, Joanna, S338 (SAT-385)
Gounder, Michael, S24 (OS-028), S144 (SAT-452), S160 (SAT-507)
Gournay, Jérôme, S45 (OS-067), S742 (THU-477)
Gournopanos, Kostas, S454 (TOP-390-YI)
Gouveia, Catarina, S43 (OS-066), S934 (TOP-582), S940 (FRI-589)
Gouveia, Caterina, S937 (FRI-585-YI)
Gouw, Annette, S53 (OS-083-YI), S648 (SAT-151-YI)
Gou, Wei, S560 (TOP-080)
Govaere, Olivier, S836 (THU-265-YI)
Govaert, Frank, S15 (OS-009-YI)
Gowda, Raju, S956 (TOP-598), S957 (WED-577), S960 (WED-587)
Goyal, Ankur, S36 (OS-051-YI), S184 (TOP-454-YI)
Goyal, Ashish, S873 (THU-563)
Goyal, Omesh, S27 (OS-033), S67 (OS-105-YI), S952 (FRI-622)
Gozlan, Oren, S861 (WED-308)
Grabbe, Stephan, S482 (WED-385-YI)
Grabhorn, Enke, S55 (OS-086), S831 (THU-258-YI), S842 (THU-284)
Gracianteparaluceta, Leire Leire Uraga, S635 (SAT-106)
Gracia-Sancho, Jordi, S168 (FRI-398), S176 (FRI-421), S233 (FRI-313), S267 (SAT-350), S281 (TOP-296-YI), S678 (SAT-244)
Gradinaru, Andreea, S454 (TOP-390-YI), S864 (WED-319-YI)
Graeter, Tilmann, S742 (THU-476)
Graf, Christiana, S151 (SAT-477), S945 (FRI-602-YI)
Gragnani, Laura, S481 (WED-383), S972 (WED-623)
Graham, Daniel, S946 (FRI-605)
Grammatikopoulos, Tassos, S55 (OS-086), S427 (THU-220), S831 (THU-258-YI), S842 (THU-284)
Grammatopoulos, Dimitris, S849 (THU-305-YI)
Granata, Cesare, S672 (SAT-230)
Grandison, Sonya, S712 (WED-554)
Grandoch, Maria, S648 (SAT-150)
Grand, Xavier, S869 (TOP-632), S876 (THU-576)
Grani, Lauredana dos Santos Ferreira, S641 (SAT-125-YI)
Granito, Alessandro, S69 (LBP-004-YI), S304 (SAT-258), S307 (SAT-263), S335 (SAT-378-YI)
Granskog, Rebecca, S275 (THU-321)
Grant-Casey, John, S740 (THU-468)
Grant, Conor, S811 (FRI-038)
Grant, Robert, S345 (SAT-409-YI), S425 (THU-216-YI)
Grapa, Cristiana, S209 (WED-483)
Grases, Daniela, S18 (OS-014-YI), S485 (WED-396)
Grassi, Eleonora, S335 (SAT-378-YI), S938 (FRI-586)
Grasso, Maria, S733 (THU-450), S753 (THU-505-YI)
Gratacós-Ginès, Jordi, S30 (OS-041), S110 (TOP-222), S129 (FRI-101), S203 (WED-463), S246 (TOP-552)
Gratien, Marilyne, S829 (THU-252)
Grau, Maria, S29 (OS-038)
Graupera, Isabel, S26 (OS-032-YI), S30 (OS-041), S63 (OS-098-YI), S110 (TOP-222), S129 (FRI-101), S203 (WED-463), S515 (TOP-098), S542 (THU-164), S562 (TOP-097-YI), S567 (WED-054), S583 (WED-101), S608 (WED-180), S612 (WED-188)
Graversen, Henriette, S77 (LBP-022-YI)
Greco, Gianluigi, S767 (THU-020)
Greenbaum, Linda, S9 (LBO-004)
Greener, Kate, S704 (THU-540), S709 (THU-556-YI)
Greenham, Olivia, S198 (WED-448-YI)
Gregor, Martin, S275 (THU-320)
Greinert, Dina, S651 (SAT-158-YI)
Grelli, Sandro, S807 (FRI-025), S919 (SAT-608-YI)
Gremmel, Thomas, S200 (WED-453)
Grey, Finn, S890 (THU-623-YI)
Grgurevic, Ivica, S26 (OS-032-YI), S515 (TOP-098)
Grgurević, Ivica, S255 (SAT-541), S337 (SAT-382), S427 (THU-220), S583 (WED-101)
Griadil, Taras, S771 (THU-029)
Gribaudo, Elena, S848 (THU-304)
Gridnyev, Alexey Evheniyovych, S604 (WED-167)
Griffin, Julian L., S438 (THU-363), S471 (WED-271)
Griffiths, Michael, S759 (TOP-017-YI)
Griffiths, William J H, S5 (GS-008)
Griffiths, William J. H., S859 (WED-304)
Grignaffini, Flavia, S583 (WED-102-YI), S670 (SAT-225)
Grigorenko, Elena, S551 (THU-189), S551 (THU-190)
Grigorescu, Elena-Daniela, S574 (WED-074)
Grillo, Alessandro, S51 (OS-079)
Grimmer, Katharine, S82 (LBP-032), S671 (SAT-227)
Grimsby, Joseph, S690 (FRI-173)
Grimsrud, Marit, S451 (THU-409)
Gringeri, Enrico, S49 (OS-076-YI), S466 (WED-258), S485 (WED-395-YI)
Grinshpan, Laura Sol, S794 (SAT-046), S796 (SAT-053)
Grip, Emilie Toresson, S701 (FRI-205-YI), S771 (THU-031)
Grisanti, Claudia, S967 (WED-605-YI)
Gris-Oliver, Albert, S453 (TOP-389), S459 (WED-242-YI), S468 (WED-263), S485 (WED-396)
Grizzi, Giulia, S494 (FRI-225)
Groba, Sara Noemi Reinartz, S178 (FRI-428-YI), S206 (WED-475)
Grobbee, Diederick, S577 (WED-084), S600 (WED-153), S684 (FRI-153)
Grobelski, Jakub, S54 (OS-084)
Grodstein, Elliot, S391 (FRI-496)
Groenen, Claire, S646 (SAT-140-YI), S674 (SAT-233)
Groen, Puck C., S382 (FRI-467-YI), S383 (FRI-468), S383 (FRI-473), S391 (FRI-498), S398 (FRI-517-YI)
Gronbaek, Henning, S692 (FRI-180)
Grønbæk, Henning, S2 (GS-002), S333 (SAT-369), S801 (FRI-008)
Grønbæk, Lisbet, S333 (SAT-369)
Grønborg, Mads, S240 (FRI-338)
Grønkjær, Lea Ladegaard, S202 (WED-461-YI), S202 (WED-462), S225 (WED-532), S702 (TOP-535-YI)
Grosen, Anne, S262 (SAT-332)
Grossar, Lorenz, S99 (TOP-193-YI), S315 (SAT-285), S349 (SAT-420)
Grosse, Karsten, S170 (FRI-402)
Große, Karsten, S33 (OS-046), S142 (SAT-448), S169 (FRI-399), S185 (TOP-456-YI), S215 (WED-506), S325 (SAT-320)
Große-Segerath, Linda, S672 (SAT-230)
Grosshennig, Anika, S935 (TOP-583), S963 (WED-596)
Grossi, Ilaria, S49 (OS-076-YI), S807 (FRI-025), S911 (SAT-587-YI), S924 (SAT-619)
Groß, Lisa, S271 (THU-313)
Grottenthaler, Julia M., S185 (TOP-456-YI), S744 (THU-482-YI)
Grotzer, Tim, S856 (WED-290), S857 (WED-298)
Group, Paris Liver Cancer, S428 (THU-226-YI)
Grova, Alessandro, S495 (FRI-227)

Author Index

Grove, Jane I., S106 (THU-076), S470 (WED-269)
Grover, Vijay, S715 (WED-561-YI)
Gruffydd, Elin, S770 (THU-028)
Grumati, Paolo, S101 (THU-059-YI)
Grünberger, Thomas, S477 (WED-369)
Gruncell, Lina, S398 (FRI-517-YI)
Grunvald, Eduardo, S690 (FRI-173)
Grunwald, Stephan, S601 (WED-155)
Grusiecka-Stańczyk, Magdalena, S409 (FRI-555)
Gruttadauria, Salvatore, S41 (OS-062), S279 (THU-334-YI), S359 (THU-347-YI), S401 (FRI-528), S638 (SAT-118)
Grzelka, Gosia, S12 (OS-004-YI)
Grzyb, Krzysztof, S451 (THU-409)
Grzybowski, Jakub, S331 (SAT-368-YI)
Gschwantler, Michael, S914 (SAT-591), S975 (WED-634-YI)
Gualandri, Chiara, S725 (THU-425)
Guallar, Diana, S241 (FRI-339)
Gual, Philippe, S681 (FRI-147)
Guan, Ming, S917 (SAT-603)
Guan, Tao, S74 (LBP-014)
Guan, Xiaodong, S824 (WED-035)
Guan, Yujuan, S73 (LBP-012), S73 (LBP-013)
Guan, Zhihong, S850 (THU-308)
Guaraldi, Giovanni, S378 (FRI-458), S534 (THU-131), S865 (FRI-638)
Guaraná, Thais, S830 (THU-254), S830 (THU-255)
Guare, Lindsay, S166 (FRI-393)
Guariglia, Marta, S431 (THU-233), S476 (WED-368), S534 (THU-133), S574 (WED-073), S611 (WED-184-YI), S620 (WED-213)
Guarino, Maria, S190 (WED-425), S248 (SAT-516)
Guasch, Eduard, S28 (OS-037), S629 (TOP-160)
Guasconi, Tomas, S31 (OS-042), S53 (OS-082), S54 (OS-084), S397 (FRI-515), S725 (THU-425), S746 (THU-490)
Guasti, Daniele, S457 (WED-235)
Guba, Markus, S175 (FRI-420)
Gubbala, Yuktha, S759 (TOP-017-YI)
Gu, Caihong, S119 (FRI-072)
Guchhait, Bitan, S181 (FRI-441-YI)
Gucht, Steven Van, S907 (SAT-575)
Gudbjornsdottir, Soffia, S515 (TOP-112-YI)
Gude, María José, S910 (SAT-585)
Gudina, Esayas Kebede, S926 (SAT-622-YI)
Gudissa, Fikadu Girma, S926 (SAT-622-YI)
Guduri, Sridhar, S689 (FRI-170)
Guéant, Jean-Louis, S37 (OS-052)
Guedes, Paula, S978 (WED-641)
Guembel, Hannah, S209 (WED-485)
Guemon, Devi, S573 (WED-071)
Guenat, Olivier, S11 (OS-001-YI)
Guerillot, Mathilde, S837 (THU-268)
Guerra, Armando Raúl, S833 (THU-259)
Guerra, Javier Abad, S571 (WED-069), S585 (WED-105), S598 (WED-150), S772 (THU-036)
Guerra, Nadia, S438 (THU-363), S471 (WED-271)
Guerra, Patricia, S793 (SAT-044)
Guerra, Pietro, S435 (THU-247)
Guerreiro, Gabriel, S154 (SAT-484)
Guerrero, Antonio, S731 (THU-445-YI)
Guerrero, Danay, S296 (TOP-281), S306 (SAT-262)
Guerrero, Eduard, S146 (SAT-461)
Guerrero, Michelle, S597 (WED-147)
Guerrero-Misas, Marta, S303 (SAT-256-YI)
Guerrieri, Francesca, S478 (WED-377)
Guerrini, Gian Piero, S378 (FRI-458)
Guettier, Catherine, S17 (OS-011), S38 (OS-055)
Guevara, Jose G, S173 (FRI-413)
Guevara, Viridiana, S296 (TOP-281), S306 (SAT-262)
Gu, Fei, S46 (OS-069)
Gugelmann, Hallam, S10 (LBO-006)
Guglielmi, Valeria, S626 (WED-231)
Guha, Neil, S26 (OS-032-YI), S515 (TOP-098), S583 (WED-101)
Gu, Hyundam, S773 (THU-037)
Guiberteau, Ana, S250 (SAT-524)
Guichelaar, Maureen, S15 (OS-009-YI), S200 (WED-457), S432 (THU-236), S451 (THU-404)
Guido, Maria, S53 (OS-083-YI)
Guidotti, Luca G., S51 (OS-079)
Guigas, Bruno, S646 (SAT-140-YI)
Guijo-Rubio, David, S410 (FRI-558)
Guilbert, Solenn, S83 (LBP-035)
Guiliani, Alejandro Mayorca, S172 (FRI-411), S586 (WED-109)
Guillaud, Olivier, S311 (SAT-271)
Guillot, Adrien, S3 (GS-004-YI), S285 (FRI-269), S293 (FRI-301)
Guillot, Jordan, S809 (FRI-031)
Guillout, Maëlle, S365 (WED-331-YI)
Guilmoteau, Thomas, S512 (FRI-372)
Guindi, Maha, S53 (OS-083-YI)
Guingané, Alice N., S905 (SAT-569), S926 (SAT-624), S940 (FRI-588-YI)
Guinto, Jerick, S458 (WED-240)
Guirgis, Faheem, S974 (WED-628)
Guiu, Boris, S414 (FRI-572)
Guiu, Séverine, S90 (SAT-059)
Guixé, Queralt, S710 (THU-557-YI)
Guix, Maria Garcia, S724 (THU-421)
Gu, Jianzhi, S954 (FRI-626)
Gu, Jinxin, S88 (TOP-192)
Gu, Junsheng, S954 (FRI-626)
Gulamhusein, Aliya, S14 (OS-008), S79 (LBP-026), S295 (TOP-279), S315 (SAT-286), S316 (SAT-287), S325 (SAT-319), S325 (SAT-320), S345 (SAT-409-YI), S354 (SAT-435), S753 (THU-506)
Gulasova, Zuzana, S585 (WED-107)
Gulden, Lukas, S326 (SAT-321), S672 (SAT-229-YI)
Gu, Lei, S646 (SAT-141)
Guljar, Nafia, S119 (FRI-073)
Gullace, Valerio, S696 (FRI-188-YI)
Gulnar, Muge Ozari, S899 (SAT-556-YI), S961 (WED-589)
Gul, Usman, S713 (WED-555)
Gumireddy, Kiran, S47 (OS-072)
Gumussoy, Mesut, S519 (THU-089), S965 (WED-603)
Gümüş, Tufan, S397 (FRI-514)
Gunda, Resign, S900 (SAT-558)
Gunduz, Feyza, S465 (WED-257)
Gunia, Carina, S744 (THU-481)
Gunjan, Deepak, S141 (TOP-423), S184 (TOP-454-YI), S725 (THU-426)
Gunnarson, Caden, S435 (THU-246)
Gunn, Nadege, S62 (OS-096), S62 (OS-097), S516 (TOP-113)
Günsar, Fulya, S389 (FRI-491), S542 (THU-163)
Gunson, Rory, S814 (WED-004)
Gunst, Jesper Damsgaard, S77 (LBP-022-YI)
Günther, Rainer, S372 (WED-350)
Guntlisbergen, Clara, S172 (FRI-410-YI)
Guo, Haitao, S869 (TOP-630), S872 (THU-561)
Guo, Hao, S468 (WED-264)
Guo, Hongbo, S877 (THU-579-YI), S883 (THU-601-YI)
Guo, Hongzhi, S895 (THU-638)
Guo, Hui, S952 (FRI-623)
Guo, Jun, S30 (OS-040), S627 (TOP-130), S640 (SAT-123)
Guo, Liangxu, S33 (OS-047)
Guo, Lilei, S701 (FRI-204)
Guo, Lixin, S623 (WED-221)
Guo, Qianqian, S650 (SAT-156)
Guo, Tiantian, S88 (TOP-192), S98 (SAT-088), S331 (SAT-367), S370 (WED-345)
Guo, Xiqing, S86 (LBP-041)
Guo, Yabing, S430 (THU-229), S508 (FRI-363)
Guo, Yangming, S688 (FRI-167)
Guoyan, Sui, S235 (FRI-321)
Guo, Yifei, S877 (THU-578), S917 (SAT-603), S918 (SAT-605)
Guo, Ying, S225 (WED-537)
Guo, Zhuxian, S38 (OS-054)
Gupta, Abhishak, S104 (THU-071-YI), S269 (SAT-355)
Gupta, Anirudh, S741 (THU-474)
Gupta, Dipika, S445 (THU-386)
Gupta, Ipshita, S584 (WED-103)
Gupta, Kapish, S274 (THU-318)
Gupta, Kusum, S658 (SAT-184), S879 (THU-587), S886 (THU-610), S889 (THU-620), S959 (WED-586)
Gupta, Nitika, S850 (THU-308)
Gupta, Prakash, S254 (SAT-537)
Gupta, Sanchita, S36 (OS-051-YI)
Gupta, Shashank, S29 (OS-038)

Gupta, Shipra, S82 (LBP-032), S671 (SAT-227)
Gupta, Tarana, S952 (FRI-622)
Gupta, Vandana, S119 (FRI-073), S578 (WED-087), S667 (SAT-213), S694 (FRI-183)
Gupte, Girish, S55 (OS-086), S831 (THU-258-YI), S842 (THU-284)
Gürbüz, Burcu, S203 (WED-464), S496 (FRI-231)
Gurra, Miranda, S116 (FRI-061)
Gurung, Amrita, S709 (THU-556-YI)
Gurung, Arati, S576 (WED-079), S584 (WED-103)
Gustot, Thierry, S8 (LBO-002), S35 (OS-050-YI), S109 (TOP-210), S141 (TOP-437), S159 (SAT-505)
Gutfraind, Alexander, S818 (WED-014)
Gutic, Enisa, S975 (WED-634-YI)
Gutierrez-Castillo, Alejandro, S392 (FRI-499), S419 (THU-523)
Gutierrez-Castillo, Javier, S392 (FRI-499)
Gutierrez, Isabel, S806 (FRI-024)
Gutierrez, Julio, S19 (OS-016), S84 (LBP-036), S679 (TOP-176), S700 (FRI-201)
Gutiérrez, Maria Luisa, S250 (SAT-524), S968 (WED-610-YI)
Gutierrez-Monterrubio, Ricardo, S419 (THU-523)
Gutierrez-Rosas, Luis, S771 (THU-030)
Gutin, Jenia, S60 (OS-093), S289 (FRI-286), S615 (WED-196)
Gutmann, Daniel, S759 (TOP-017-YI)
Gu, Wenyi, S145 (SAT-458-YI), S148 (SAT-467-YI), S178 (FRI-428-YI), S261 (SAT-329-YI), S262 (SAT-330), S493 (FRI-220)
Gu, Yumei, S74 (LBP-014)
Guzman, Louis, S388 (FRI-489), S388 (FRI-490), S745 (THU-483)
Guzzo, Antonella, S767 (THU-020)
Gyoeri, Georg, S284 (FRI-266)
Gyriki, Despoina, S507 (FRI-257)

Haahr, Pernille, S838 (THU-269)
Haas, Joel, S682 (FRI-150-YI)
Haast, Saskia, S647 (SAT-149)
Haas, Victor, S291 (FRI-291-YI)
Habarwaa, Marwo, S458 (WED-237-YI)
Haberl, Annette, S904 (SAT-564)
Habermann, Robin, S912 (SAT-588)
Habersetzer, François, S435 (THU-246)
Habib, Nagy, S455 (TOP-406)
Habtesion, Abeba, S171 (FRI-409-YI), S180 (FRI-434)
Haceatrean, Alexei, S959 (WED-586), S965 (WED-602)
Haddock, Bryan, S602 (WED-159-YI)
Haders, Daniel, S877 (THU-580)
Hadziyannis, Emilia, S142 (SAT-449)
Haegele, Joseph, S5 (GS-008)
Hagag, Mahmoud, S524 (THU-101)
Hagan, Kaitlin, S295 (TOP-280)
Hagiwara, May, S398 (FRI-516), S834 (THU-262), S836 (THU-266)
Hagmar, Per, S579 (WED-090)
Hagström, Emil, S515 (TOP-112-YI)
Hagström, Hannes, S58 (OS-090), S62 (OS-097), S115 (FRI-058-YI), S224 (WED-529), S247 (SAT-512), S313 (SAT-276), S424 (TOP-376), S515 (TOP-112-YI), S516 (TOP-113), S517 (TOP-114), S525 (THU-103), S558 (TOP-063-YI), S568 (WED-057-YI), S570 (WED-060-YI), S584 (WED-104), S589 (WED-118), S606 (WED-172-YI), S606 (WED-173), S607 (WED-174-YI), S612 (WED-187-YI), S618 (WED-204), S621 (WED-215), S690 (FRI-172), S701 (FRI-205-YI), S709 (THU-555-YI), S771 (THU-031), S777 (THU-050), S781 (SAT-008), S781 (SAT-009), S791 (SAT-037), S791 (SAT-038), S792 (SAT-042), S796 (SAT-052)
Hagvall, Sepideh, S682 (FRI-148)
Hahn, Anna, S913 (SAT-589-YI)
Hähner, Jan, S209 (WED-485), S409 (FRI-556)
Hahn, Felix, S503 (FRI-248)
Hahn, Sihoun, S856 (WED-290), S857 (WED-298)
Hai, Hoang, S12 (OS-003)
Haikonen, Retu, S266 (SAT-346)
Hailemichael, Wasihun, S371 (WED-348)
Hailu, Tsinatkeab, S647 (SAT-149)
Hai, Suping, S676 (SAT-239)
Haixia, Guan, S649 (SAT-154), S650 (SAT-155)
Hajdu, Karina Lobo, S643 (SAT-133)
Hajinicolaou, Christina, S850 (THU-308)
Hajji, Yacine, S149 (SAT-468), S152 (SAT-478), S214 (WED-499), S760 (TOP-032)
Hajj, Roy, S729 (THU-441)
Hakeem, Abdul, S404 (FRI-538-YI)
Hakim, Florian, S889 (THU-619)
Hakkarainen, Konsta, S114 (FRI-055)
Háková, Tereza, S392 (FRI-500)
Haktaniyan, Busra, S160 (SAT-507)
Halder, Abhik, S221 (WED-522)
Hales, Jack, S286 (FRI-271)
Halilbasic, Emina, S14 (OS-007), S64 (OS-100)
Halim, Sadia, S295 (TOP-280)
Hallamaa, Lotta, S247 (SAT-512)
Hall, Callum, S280 (THU-338-YI)
Halliday, Neil, S704 (THU-539-YI), S841 (THU-276-YI)
Hall, Lindsay, S286 (FRI-271)
Hall, Rebekah, S770 (THU-028)
Hall, Samantha, S805 (FRI-022), S820 (WED-020-YI), S822 (WED-027)
Hallsworth, Kate, S713 (WED-557)
Halpern, Keren Bahar, S862 (WED-315)
Halupnik, Austin, S393 (FRI-501)
Hamacher, Anna, S672 (SAT-230)
Hamadache, Yasmin, S75 (LBP-017)
Ham, Anna, S218 (WED-513), S749 (THU-496)
Hamberg, Marie Louise, S22 (OS-024)
Hambridge, Thomas, S771 (THU-031)
Hamdan, Nashla, S547 (THU-179), S606 (WED-171)
Hamdulay, Shahir, S841 (THU-276-YI)
Hamdy, Hanan, S537 (THU-141-YI)
Hamdy, Sherif, S551 (THU-191)
Hameed, Bilal, S116 (FRI-061), S190 (WED-421), S197 (WED-447)
Hamelmann, Stefan, S234 (FRI-317)
Hamid, Saeed Sadiq, S49 (OS-075), S67 (OS-105-YI), S77 (LBP-021), S743 (THU-478), S766 (THU-015), S962 (WED-594)
Hamilton-Dutoit, Stephen, S631 (SAT-094-YI)
Hamilton, Gavin, S690 (FRI-173)
Hamilton, James, S79 (LBP-027), S846 (THU-291), S846 (THU-298), S847 (THU-300), S848 (THU-301)
Hammad, Alaa, S240 (FRI-337-YI)
Hammad, Awwab, S399 (FRI-522)
Hammad, Seddik, S240 (FRI-337-YI)
Hammam, Olfat, S630 (SAT-091)
Hammer, Johann, S32 (OS-044)
Hammond, Helen, S813 (FRI-047)
Hammond, Janet, S981 (FRI-635), S981 (FRI-636)
Hammond, Matthew, S311 (SAT-270)
Hamprecht, Axel, S890 (THU-623-YI)
Hamran, Shahd, S732 (THU-446)
Hamusonde, Kalongo, S926 (SAT-624), S940 (FRI-588-YI)
Ham, Younglim, S266 (SAT-345), S267 (SAT-349)
Hanabata, Yusuke, S419 (THU-525), S421 (THU-531)
Hanayama, Masakazu, S675 (SAT-237)
Hancock, Steven, S170 (FRI-403)
Han, Eui-Soo, S482 (WED-386)
Ha, Nghiem, S411 (FRI-560)
Hang, Shoukit, S50 (OS-077)
Han, Guohong, S731 (THU-445-YI)
Hanhineva, Kati, S266 (SAT-346)
Hanibal, Gideon, S114 (FRI-056)
Hanisch, Laura, S347 (SAT-414-YI)
Han, Jiahao, S756 (THU-514)
Han, Jiajia, S374 (WED-356)
Han, Ji Won, S135 (FRI-119), S478 (WED-372), S510 (FRI-368)
Han, Jundong, S701 (FRI-204)
Han, Lina, S259 (SAT-554)
Han, Ma Ai Thanda, S670 (SAT-220)
Hanna, Diana, S231 (FRI-305)
Hannah, Nicholas, S218 (WED-513), S436 (THU-248), S469 (WED-265), S749 (THU-496), S797 (SAT-055)
Han, Na Yeon, S448 (THU-397)
Hanot, Ophélie, S172 (FRI-412)
Han, Ryan Ng Jian, S529 (THU-115)

Author Index

Hansen, Bettina, S14 (OS-008), S56 (OS-086), S354 (SAT-435), S832 (THU-258-YI), S842 (THU-284)
Hansen, Bettina E., S46 (OS-070-YI), S79 (LBP-026), S193 (WED-432), S295 (TOP-279), S315 (SAT-286), S325 (SAT-319), S325 (SAT-320), S338 (SAT-384), S342 (SAT-398), S349 (SAT-420), S351 (SAT-426-YI), S352 (SAT-429), S353 (SAT-432), S353 (SAT-433), S391 (FRI-498), S436 (THU-249), S850 (THU-308), S928 (SAT-628-YI)
Hansen, Camilla Dalby, S110 (FRI-041-YI), S114 (FRI-057), S115 (FRI-059), S122 (FRI-079-YI), S554 (THU-204), S706 (THU-545-YI)
Hansen, Henrik H., S646 (SAT-142), S655 (SAT-173)
Hansen, Johanne Kragh, S26 (OS-032-YI), S63 (OS-098-YI), S110 (FRI-041-YI), S114 (FRI-057), S115 (FRI-059), S122 (FRI-079-YI), S125 (FRI-090-YI), S554 (THU-204), S608 (WED-180), S706 (THU-545-YI)
Hansen, Lars, S2 (GS-003)
Hansen, Line, S660 (SAT-188-YI)
Hansen, Mark Berner, S570 (WED-062)
Hansen, Sofie Boesgaard Neestrup, S602 (WED-159-YI)
Hansen, Stine, S262 (SAT-332)
Hansen, Torben, S115 (FRI-057), S125 (FRI-090-YI)
Han, Seul Ki, S133 (FRI-111), S360 (THU-352), S732 (THU-447), S813 (FRI-046)
Han, Seungbong, S546 (THU-175)
Han, Shuting, S495 (FRI-228-YI)
Hansi, Navjyot, S54 (OS-084), S709 (THU-556-YI)
Han, Steven-Huy, S803 (FRI-012), S803 (FRI-013)
Han, Xiuli, S593 (WED-134)
Han, Yan, S50 (OS-078), S637 (SAT-115)
Hany, Ayman, S551 (THU-191)
Han, Yeo Eun, S448 (THU-397)
Han, Younghun, S461 (WED-247)
Hanzely, Petra, S2 (GS-002)
Hao, Jihui, S261 (TOP-358)
Hao, Miao, S47 (OS-071)
Hao, Shujie, S884 (THU-605)
Hao, Shuli, S593 (WED-134)
Haque, Lamia, S127 (FRI-095)
Harada, Kenichi, S53 (OS-083-YI), S331 (SAT-368-YI)
Hara, Kamalpreet S., S113 (FRI-052), S126 (FRI-093), S186 (TOP-469-YI)
Harari, Ofir, S965 (WED-603)
Harberts, Aenne, S139 (FRI-134), S178 (FRI-429-YI)
Harder, Lea Mørch, S240 (FRI-338)
Hardie, Claire, S711 (WED-547)
Hardikar, Winita, S55 (OS-086), S831 (THU-258-YI), S842 (THU-284), S850 (THU-308)
Hardisty, Gareth, S284 (FRI-268-YI), S360 (THU-350)
Hardwigsen, Jean, S380 (FRI-463), S381 (FRI-464)
Hargreaves, Ashlea, S61 (OS-108)
Haridy, James, S797 (SAT-055)
Harlet, Luc, S22 (OS-023), S718 (WED-572)
Harling, Guy, S900 (SAT-558)
Harlt, Lukas, S752 (THU-501)
Harmon, Stephanie, S413 (FRI-569)
Harmsen, Martin, S238 (FRI-333-YI), S244 (FRI-352), S244 (FRI-353)
Harnois, Denise, S58 (OS-089), S313 (SAT-282)
Haro, Ana, S819 (WED-019)
Haro, Juan Acevedo, S709 (THU-556-YI)
Harpenas, Esther, S60 (OS-093), S615 (WED-196)
Harper, Glenn, S164 (FRI-385-YI)
Harputluoglu, Muhsin Murat, S899 (SAT-556-YI)
Harris, David, S690 (FRI-173)
Harris, James, S87 (LBP-043)
Harris, M. Scott, S19 (OS-016), S84 (LBP-036), S679 (TOP-176), S700 (FRI-201)
Harrison, Emily, S87 (LBP-043)
Harrison, Laura, S300 (SAT-250), S312 (SAT-274-YI), S313 (SAT-275)
Harrison, Stephen A., S19 (OS-016)
Harris, Scott, S25 (OS-030)
Härtel, Angela, S21 (OS-020)
Hartel, Gunter, S788 (SAT-029)
Hartig, Kerstin, S311 (SAT-271)
Hartleben, Björn, S331 (SAT-368-YI), S376 (TOP-520-YI)
Hartley, Jane, S850 (THU-308)
Hartl, Johannes, S351 (SAT-427), S372 (WED-350)
Hartl, Lukas, S6 (GS-011-YI), S33 (OS-046), S52 (OS-081), S53 (OS-082), S54 (OS-084), S113 (FRI-053), S156 (SAT-494), S179 (FRI-432), S183 (FRI-444-YI), S183 (FRI-445), S186 (TOP-470-YI), S199 (WED-451-YI), S199 (WED-452), S200 (WED-453), S205 (WED-474), S213 (WED-498), S216 (WED-508), S222 (WED-524), S440 (THU-370), S719 (TOP-488), S732 (THU-448-YI), S733 (THU-449), S734 (THU-451), S738 (THU-464-YI), S747 (THU-492), S748 (THU-493-YI), S749 (THU-494), S750 (THU-498), S914 (SAT-591)
Hartmann, Christian, S840 (THU-275)
Hartmann, Maike, S482 (WED-385-YI)
Hartmann, Nils, S854 (WED-285)
Hartmann, Ronja, S209 (WED-485)
Hartsfield, Cynthia L., S563 (WED-042), S597 (WED-141)
Hartwig, Sonja, S672 (SAT-230)
Haschka, David, S848 (THU-302)
Hashimoto, Koji, S399 (FRI-522)
Hasl, Natalie, S979 (TOP-614)
Hassan, Adam, S616 (WED-200)
Hassan, Ayman, S809 (FRI-029), S966 (TOP-599)
Hassanein, Tarek, S10 (LBO-006), S58 (OS-089), S187 (TOP-471-YI), S198 (WED-449), S313 (SAT-282), S713 (WED-555)
Hassan, Ibrahim, S250 (SAT-523), S390 (FRI-494), S390 (FRI-495)
Hassani, Majda El, S169 (FRI-399)
Hassan, Malak A., S208 (WED-482)
Hassan, Manal, S461 (WED-247)
Hassan, Mohsin, S131 (FRI-106), S634 (SAT-105)
Hassany, Mohamed, S492 (FRI-217), S504 (FRI-252), S814 (WED-003)
Hassany, Sahar M, S504 (FRI-252)
Hassoun, Jérémy, S199 (WED-450)
Hatano, Etsuro, S419 (THU-525), S420 (THU-529-YI), S421 (THU-531)
Hathayamat, Warasinee, S206 (WED-476)
Haudebourg, Luc, S54 (OS-084), S222 (WED-525), S719 (TOP-488)
Haunold, Tina Jasmin, S427 (THU-221)
Hausmann, Bela, S37 (OS-053)
Havaj, Daniel Jan, S26 (OS-032-YI), S123 (FRI-085), S205 (WED-473), S515 (TOP-098), S583 (WED-101)
Havinga, Rick, S630 (SAT-090), S857 (WED-299), S863 (WED-318)
Havulinna, Aki, S760 (THU–003)
Hawro, Tomasz, S322 (SAT-313)
Hayashi, Manabu, S372 (WED-352), S647 (SAT-147)
Hayes, Peter, S24 (OS-028), S144 (SAT-452), S160 (SAT-507)
Hayette, Marie-Pierre, S907 (SAT-575)
Hayllar, Jeremy, S803 (FRI-014), S818 (WED-013)
Hayn, Alexander, S647 (SAT-148)
Hay, Ophir, S60 (OS-093), S289 (FRI-286), S615 (WED-196)
Hazzan, Rawi, S247 (SAT-513), S251 (SAT-527), S316 (SAT-288), S317 (SAT-289), S613 (WED-189), S913 (SAT-590)
Hearnshaw, Sarah, S740 (THU-468)
Heaton, Nigel, S139 (FRI-133)
Hebden, Emily, S147 (SAT-465)
Hedge, Apoorva, S768 (THU-023)
Heegsma, Janette, S244 (FRI-353)
Heerschap, Eva, S828 (TOP-310-YI)
Hefer, Marija, S617 (WED-202)
Heffer, Jo, S455 (TOP-405)
Hefner, Anna Marie, S713 (WED-555)
He, Fu-Liang, S747 (THU-492)
He, Gang, S86 (LBP-041)
Hegde, Apoorva, S772 (THU-035)
Heger, Eva, S807 (FRI-025)
Hegmar, Hannes, S584 (WED-104), S606 (WED-173)

He, Hairuo, S817 (WED-012)
He, Hongliang, S68 (OS-107)
Heide, Giulia, S257 (SAT-546)
Heiduschka, Sonja, S672 (SAT-230)
Heikenwälder, Mathias, S458 (WED-238), S651 (SAT-158-YI)
Heilmann-Heimbach, Stefanie, S854 (WED-285)
Heim, Markus, S465 (WED-255), S533 (THU-126)
Heinreichsberger, Fabian, S284 (FRI-267)
Heinrich, Bernd, S461 (WED-245)
Heinrich, Sophia, S376 (TOP-520-YI)
Heinzow, Hauke, S736 (THU-460-YI)
Heise, Jamie, S846 (THU-291), S846 (THU-298)
Heiskala, Anni, S562 (TOP-096)
Heissenberger-Mass, Isabella, S975 (WED-634-YI)
Heitmann, David, S110 (TOP-222), S317 (SAT-290-YI), S338 (SAT-383)
He, Jing, S560 (TOP-080)
He, Kang, S42 (OS-063)
Held, Anna, S854 (WED-284)
Helen, R, S705 (THU-541-YI)
Helgadottir, Holmfridur, S2 (GS-002), S13 (OS-006-YI), S290 (FRI-289), S345 (SAT-410)
He, Ling, S431 (THU-234)
He, LinQing, S259 (SAT-554)
Helin, Tuukka, S122 (FRI-084)
Hellard, Margaret, S799 (FRI-004), S800 (FRI-005)
Heller, Theo, S49 (OS-075), S413 (FRI-569), S722 (THU-417), S835 (THU-264-YI), S962 (WED-594), S965 (WED-603)
Helmy, Dina, S575 (WED-077)
Heluwaert, Frederic, S43 (OS-066), S45 (OS-067), S934 (TOP-582), S937 (FRI-585-YI)
Helvensteijn, Werner, S647 (SAT-149)
Hemed, Anna Rozenfeld, S214 (WED-500)
He, Meng, S98 (SAT-088)
Hemetsberger, Paul, S222 (WED-524)
Hempel, Felix, S648 (SAT-150)
Henderson, Julie, S827 (WED-047)
Henderson, Robert, S125 (FRI-090-YI)
Heneghan, Michael, S311 (SAT-272-YI), S331 (SAT-368-YI), S341 (SAT-396), S404 (FRI-538-YI), S767 (THU-019)
Heng, Choon Pooh, S211 (WED-491)
Hengstler, Jan G., S172 (FRI-410-YI), S641 (SAT-125-YI)
Henin, Guillaume, S648 (SAT-151-YI)
Hennan, Jim, S615 (WED-198)
Hennessy, Fritha, S946 (FRI-605)
Henricsson, Marcus, S299 (SAT-249)
Henriksson, Ida, S58 (OS-090)
Henriksson, Martin, S796 (SAT-052)
Henriksson, Pontus, S568 (WED-056)
Henrion, Jean, S839 (THU-273)
Henry, Linda, S126 (FRI-094), S127 (FRI-095), S356 (SAT-443), S417 (FRI-581), S557 (THU-213), S766 (THU-015), S793 (SAT-045), S794 (SAT-046), S795 (SAT-050), S796 (SAT-053), S923 (SAT-618)
Henry, Paulina, S648 (SAT-151-YI)
Hens, Niel, S65 (OS-101-YI), S903 (SAT-562)
Heo, Jeong, S1 (GS-001), S47 (OS-072), S324 (SAT-316), S957 (WED-577)
Heo, Subin, S251 (SAT-528), S443 (THU-381), S497 (FRI-232)
He, Ping, S513 (FRI-379)
He, Qing, S259 (SAT-554), S593 (WED-134), S609 (WED-182), S763 (THU-011), S924 (SAT-620), S955 (FRI-628)
Herbschleb, Lieke, S647 (SAT-149)
Hercun, Julian, S14 (OS-008), S295 (TOP-279), S325 (SAT-319), S354 (SAT-435), S386 (FRI-480-YI), S398 (FRI-516)
Herder, Christian, S21 (OS-020)
Herebian, Diran, S289 (FRI-284)
Heredia, Raquel Encijo, S366 (WED-332-YI), S968 (WED-610-YI)
Heremans, Isabel, S885 (THU-606), S886 (THU-610)
Herendael, Bruno Van, S907 (SAT-575)
Herkel, Johannes, S372 (WED-350)
Herling, Luise, S271 (THU-313)
Hermabessière, Paul, S10 (LBO-006), S573 (WED-071), S742 (THU-477)
Herms, Queralt, S110 (TOP-222), S246 (TOP-552)
Hernáez-Alsina, Tania, S481 (WED-382-YI), S837 (THU-267), S855 (WED-289)
Hernández, Ana, S459 (WED-242-YI), S468 (WED-263), S485 (WED-396)
Hernández, Araceli, S910 (SAT-581)
Hernandez-Barragan, Abigail, S236 (FRI-322)
Hernandez-Con, Pilar, S974 (WED-628)
Hernández-Évole, Helena, S317 (SAT-290-YI), S318 (SAT-291)
Hernandez-Gea, Virginia, S720 (TOP-504-YI)
Hernández-Gea, Virginia, S6 (GS-011-YI), S33 (OS-046), S52 (OS-081), S53 (OS-082), S53 (OS-083-YI), S54 (OS-084), S55 (OS-085-YI), S300 (SAT-250), S721 (THU-415), S730 (THU-443), S739 (THU-467), S747 (THU-492), S752 (THU-501), S783 (SAT-012), S828 (TOP-297), S837 (THU-268), S862 (WED-315), S863 (WED-317)
Hernández-Guerra, Manuel, S16 (OS-010), S309 (SAT-268), S547 (THU-181), S837 (THU-267), S855 (WED-289)
Hernández-Ibarrola, Ixchel, S771 (THU-030)
Hernandez, Liliana Vittini, S762 (THU-008)
Hernandez, Luis, S819 (WED-019)
Hernández, María, S837 (THU-267), S855 (WED-289)
Hernandez-Mir, Gerard, S370 (WED-347), S876 (THU-575)
Hernandez, Nélia, S296 (TOP-281), S306 (SAT-262), S768 (THU-021), S790 (SAT-036)
Hernandez, Paul, S5 (GS-008)
Hernandez, Rocio Calvo, S250 (SAT-524)
Hernandez-Santillan, Marisela, S236 (FRI-322)
Hernaz, Soledad Sonsoles Muñoz, S819 (WED-019)
He, Rong-Dong, S243 (FRI-348)
Heron, Jon, S761 (THU-004)
Herrera, Elba Llop, S337 (SAT-382), S525 (THU-103), S558 (TOP-063-YI), S585 (WED-105), S585 (WED-106), S589 (WED-118), S598 (WED-150), S607 (WED-174-YI), S612 (WED-186-YI), S643 (SAT-134), S723 (THU-418), S733 (THU-450), S753 (THU-505-YI), S772 (THU-036)
Herrera, Laura, S649 (SAT-152), S819 (WED-019)
Herrera, Yahima Frion, S466 (WED-258)
Herrero, Astrid, S414 (FRI-572)
Herrero, Irene Peñas, S379 (FRI-459), S403 (FRI-532), S403 (FRI-533), S415 (FRI-575)
Herrero, Jose Ignacio, S59 (OS-091), S96 (SAT-079)
Herrero, Margarita, S25 (OS-029)
Herrero, Maria José, S908 (SAT-577)
Herrero, Raquel, S267 (SAT-350)
Herreros, Angela Martínez, S294 (TOP-278)
Herrmann, Lars, S785 (SAT-020)
Herrojo, Javier Ampuero, S16 (OS-010), S177 (FRI-427), S600 (WED-153)
Hersant, Jeanne, S540 (THU-155)
Hershkovich, Leeor, S941 (FRI-590)
Hertelyova, Zdenka, S585 (WED-107)
He, Ruoyi, S952 (FRI-623)
Hervás, César, S410 (FRI-558)
Hervás-Stubbs, Sandra, S364 (WED-329-YI)
Herzogenrath, Joerg, S911 (SAT-586)
Herzog, Jasmin, S710 (TOP-536-YI)
Herzog, Natalie, S271 (THU-313)
Hesketh, Hannah, S709 (THU-556-YI)
Heslington, Amelia, S43 (OS-065)
He, Song, S192 (WED-429-YI), S441 (THU-372-YI), S454 (TOP-392-YI)
He, Songmei, S430 (THU-229)
Hessenberger, Philipp, S581 (WED-095)
Hesse, Raphael, S20 (OS-018)
Hester, Joanna, S43 (OS-065)
Hetzer, Jenny, S651 (SAT-158-YI)
Heumann, Philipp, S504 (FRI-251)
Heusch, Anna, S672 (SAT-230)
He, Wei, S469 (WED-266)
Hewitt, Michael, S759 (TOP-018-YI), S773 (THU-039)
He, Xiaojun, S512 (FRI-377)
He, Xiaowen, S468 (WED-264)
He, Xin, S909 (SAT-579)
He, Xiongwei, S259 (SAT-554), S593 (WED-134), S609 (WED-182), S763 (THU-011), S924 (SAT-620)

Author Index

He, Yaozu, S46 (OS-069)
Heyens, Leen, S535 (THU-134), S611 (WED-185), S696 (FRI-190)
Heyerick, Lander, S281 (TOP-295-YI), S464 (WED-253)
Heyer, Jannis, S363 (TOP-326)
Heymann, Felix, S268 (SAT-352-YI)
Heymans, Anja, S637 (SAT-116)
Heyne, Renate, S601 (WED-155), S930 (SAT-636), S971 (WED-620)
Heyn, Holger, S35 (OS-050-YI)
Hey, Penelope, S145 (SAT-457), S739 (THU-466)
Hezareh, Marjan, S908 (SAT-578), S956 (TOP-598), S957 (WED-577), S960 (WED-587)
He, Zhenkun, S954 (FRI-626), S955 (FRI-628)
He, Zhexiang, S218 (WED-512-YI)
Hiasa, Yoichi, S117 (FRI-062), S675 (SAT-237), S693 (FRI-181), S977 (WED-639)
Hickey, Joe, S781 (SAT-008), S781 (SAT-009)
Hickman, Ingrid, S713 (WED-557)
Hickman, Matthew, S69 (LBP-001), S761 (THU-004)
Hicks, Jessica, S805 (FRI-022)
Hicks, Rod, S436 (THU-248)
Hidaka, Isao, S808 (FRI-027)
Hidalgo, Alvaro, S124 (FRI-088)
Hidalgo, Nuria Cañete, S969 (WED-611)
Hidalgo-Tenorio, Carmen, S904 (SAT-564)
Hieda, Saori, S156 (SAT-496)
Hiergeist, Andreas, S919 (SAT-607)
Higgins, Ben, S284 (FRI-268-YI), S360 (THU-350)
Higgins, Callum, S113 (FRI-054)
High, Juliet, S311 (SAT-270)
Higuchi, Yuichiro, S275 (THU-321)
Higuera, Monica, S469 (WED-267)
Hiitola, Emil, S282 (FRI-263)
Hikichi, Rie, S647 (SAT-147)
Hikita, Hayato, S463 (WED-251-YI), S977 (WED-639)
Hild, Benedikt, S172 (FRI-410-YI)
Hildeman, Anders, S252 (SAT-530)
Hildt, Eberhard, S882 (THU-595)
Hilleret, Marie-Noëlle, S10 (LBO-006), S43 (OS-066), S45 (OS-067), S47 (OS-072), S207 (WED-477), S311 (SAT-271), S380 (FRI-463), S381 (FRI-464), S885 (THU-607), S934 (TOP-582), S937 (FRI-585-YI)
Hillier, Sharon, S70 (LBP-005), S975 (WED-636), S976 (WED-637)
Hillinger, Theresa, S477 (WED-369)
Hillon, Patrick, S435 (THU-246)
Hill-Tout, Rachel, S811 (FRI-038)
Hillus, David, S77 (LBP-022-YI)
Himanshi, Himanshi, S181 (FRI-441-YI), S184 (FRI-452-YI), S274 (THU-318), S282 (FRI-262-YI), S361 (THU-354)
Himmelsbach, Vera, S504 (FRI-251)
Hinds, Alastair, S946 (FRI-605)
Hindy, George, S166 (FRI-393)
Hinterhoelzl, Florian, S742 (THU-476)
Hintersteininger, Marlene, S33 (OS-046), S113 (FRI-053), S156 (SAT-494), S186 (TOP-470-YI), S199 (WED-451-YI), S199 (WED-452), S200 (WED-453), S205 (WED-474), S213 (WED-498), S216 (WED-508), S222 (WED-524), S440 (THU-370), S719 (TOP-488), S732 (THU-448-YI), S733 (THU-449), S734 (THU-451), S738 (THU-464-YI), S748 (THU-493-YI), S749 (THU-494), S750 (THU-498), S752 (THU-501), S914 (SAT-591)
Hinz, Marlen, S54 (OS-084)
Hinz, Michael, S93 (SAT-070)
Hionides, Alejandro, S459 (WED-241)
Hionides-Gutierrez, Alejandro, S137 (FRI-126)
Hippe, Katrin, S834 (THU-260)
Hirani, Armaan, S49 (OS-075), S962 (WED-594)
Hiriart, Jean-Baptiste, S602 (WED-158)
Hirode, Grishma, S46 (OS-070-YI), S436 (THU-249), S914 (SAT-592-YI), S921 (SAT-610)
Hirooka, Kana, S550 (THU-188)
Hirooka, Masashi, S117 (FRI-062)
Hirose, Shunji, S708 (THU-553)
Hirschfield, Gideon M., S10 (LBO-006), S14 (OS-008), S67 (OS-106), S79 (LBP-026), S295 (TOP-279), S295 (TOP-280), S315 (SAT-286), S325 (SAT-319), S325 (SAT-320), S329 (SAT-363), S338 (SAT-384), S342 (SAT-398), S345 (SAT-409-YI), S345 (SAT-410), S349 (SAT-420), S354 (SAT-435), S838 (THU-270)
Hirsch, Théo, S17 (OS-011), S38 (OS-055)
Hitchins, Charlotte, S164 (FRI-385-YI)
Hlebowicz, Maria, S1 (GS-001)
Hoang, Stephen, S649 (SAT-153)
Hoare, Matthew, S455 (TOP-405)
Hoban, Sarah, S709 (THU-556-YI)
Hobeika, Christian, S499 (FRI-238)
Hoblos, Reem, S878 (THU-585-YI)
Hobloss, Zaynab, S172 (FRI-410-YI)
Hobolth, Lise, S736 (THU-459)
Hobson, Kezia, S673 (SAT-231)
Ho, Chanda, S149 (SAT-473), S158 (SAT-499), S529 (THU-115)
Ho, Chia-Jung, S436 (THU-250), S448 (THU-396), S535 (THU-135), S586 (WED-108), S751 (THU-499)
Ho, Chun-Ting, S430 (THU-231), S436 (THU-250), S448 (THU-396), S535 (THU-135), S586 (WED-108), S751 (THU-499)
Hockings, Paul, S106 (THU-075)
Hodge, Mairi, S864 (WED-319-YI)
Hoefinger, Paula, S156 (SAT-494), S199 (WED-452), S213 (WED-498), S733 (THU-450), S734 (THU-451), S738 (THU-464-YI), S753 (THU-505-YI)
Hoegl, Annabelle, S240 (FRI-338)
Hoenow, Stefan, S639 (SAT-119)
Hoentjen, Frank, S349 (SAT-419)
Hoeper, Marius M., S743 (THU-480-YI)
Hoeroldt, Barbara, S312 (SAT-274-YI), S313 (SAT-275)
Hoet, Katrien, S907 (SAT-575)
Hofer, Benedikt, S113 (FRI-053), S156 (SAT-494), S179 (FRI-431-YI), S179 (FRI-432), S183 (FRI-444-YI), S186 (TOP-470-YI), S199 (WED-452), S200 (WED-453), S205 (WED-474), S213 (WED-498), S216 (WED-508), S222 (WED-524), S252 (SAT-530), S284 (FRI-266), S362 (TOP-325-YI), S364 (WED-323), S440 (THU-370), S717 (WED-569-YI), S734 (THU-451), S739 (THU-467), S748 (THU-493-YI), S749 (THU-494), S750 (THU-497-YI), S750 (THU-498), S914 (SAT-591)
Hoferica, Jakub, S211 (WED-492)
Hofmann, Lukas, S150 (SAT-474)
Hofmann, Maike, S371 (WED-348)
Hofmann, Philipp, S372 (WED-350)
Hofmann, Wolf Peter, S601 (WED-155)
Hof, Willemien, S857 (WED-299), S863 (WED-318)
Hogan, Marie C., S39 (OS-056)
Hogenberg, Kim, S200 (WED-457)
Ho, Glenn Jun Kit, S698 (FRI-197)
Hohmann, Janik, S447 (THU-395), S470 (WED-268)
Høivik, Marte Lie, S2 (GS-002), S290 (FRI-289)
Ho, Jillian, S597 (WED-147)
Ho, Jonas, S149 (SAT-473)
Ho, Karen Cheuk-Ying, S915 (SAT-593), S928 (SAT-628-YI), S947 (FRI-609)
Holcombe, Andrea, S220 (WED-521)

(Holden) Hsu, Yao-Chun, S452 (THU-414-YI), S957 (WED-578)

Holdorf, Meghan, S957 (WED-578)
Holgado, Daniel Martín, S123 (FRI-086)
Holguín, Víctor, S427 (THU-220)
Hollande, Clemence, S428 (THU-226-YI), S446 (THU-393-YI), S493 (FRI-221), S499 (FRI-238), S505 (FRI-254), S506 (FRI-255-YI), S507 (FRI-362), S508 (FRI-364-YI)
Holland-Fischer, Peter, S198 (WED-448-YI), S262 (SAT-332)
Holland, Steven, S835 (THU-264-YI)
Holleboom, A.G. (Onno), S62 (OS-097), S516 (TOP-113), S568 (WED-057-YI), S577 (WED-084), S600 (WED-153), S621 (WED-214), S641 (SAT-126), S765 (THU-013), S777 (THU-050), S789 (SAT-031-YI)
Holliday, Jordan, S125 (FRI-091), S393 (FRI-505)

Hollinghurst, Joe, S519 (THU-086)
Hollings-Tenant, Naomi, S622 (WED-217)
Holmberg, Markus, S220 (WED-517), S568 (WED-056)
Holmberg, Marte, S46 (OS-070-YI), S65 (OS-101-YI), S903 (SAT-562)
Holmes, Jacinta, S1 (GS-001), S218 (WED-513), S749 (THU-496), S964 (WED-597)
Holstein, Martina, S493 (FRI-220)
Holt, Andrew, S84 (LBP-038), S406 (FRI-544)
Holtmann, Gerald, S121 (FRI-077), S803 (FRI-014), S818 (WED-013)
Holz, Frederik, S261 (SAT-329-YI)
Holzner, Philipp, S363 (TOP-326)
Ho-Mok, Kam, S646 (SAT-140-YI)
Homolka, Robert, S72 (LBP-010)
Hong, Changze, S27 (OS-034), S150 (SAT-475), S389 (FRI-492)
Hong, Charmgil, S590 (WED-121)
Hong, Chun-Ming, S898 (TOP-566-YI)
Hong, Hei-Ip, S284 (FRI-268-YI)
Hong, Jeana, S839 (THU-271)
Hong, Jin, S879 (THU-587)
Hong, Jung Pyo, S498 (FRI-235), S916 (SAT-597)
Hong, Lai San, S809 (FRI-030), S809 (FRI-031)
Hong, Liang, S34 (OS-048)
Hong, Su Young, S393 (FRI-506)
Hong, Thai, S249 (SAT-521), S433 (THU-240), S922 (SAT-613)
Hong, Weilong, S41 (OS-062)
Hong, Xupeng, S891 (THU-624-YI)
Hong, Ying, S675 (SAT-235)
Hong, Young Mi, S437 (THU-361), S497 (FRI-233)
Hongyu, Gao, S609 (WED-182)
Hong, Yuqi, S870 (TOP-645), S878 (THU-586)
Hong, Zhi, S85 (LBP-040)
Hong, Zhongsi, S805 (FRI-021)
Hontoria-Bautista, Gadea, S250 (SAT-524)
Hood, Gillian, S69 (LBP-001)
Hoof, Marc Van, S109 (TOP-210)
Hoogenboom, Tim, S490 (TOP-407-YI)
Hoorens, Anne, S55 (OS-085-YI), S464 (WED-253)
Ho, Ping-Chih, S643 (SAT-133)
Hopkins, Mark, S811 (FRI-038)
Hora, Shainan, S642 (SAT-132)
Hordonneau, Constance, S512 (FRI-372)
Horebeek, Nele Van, S849 (THU-306-YI)
Horga, Maria Arantxa, S981 (FRI-635)
Horhat, Adelina, S773 (THU-037)
Hornemann, Thorsten, S672 (SAT-230)
Horn, Michael, S342 (SAT-399)
Horn, Paul, S268 (SAT-352-YI)
Horslen, Simon P., S832 (THU-258-YI), S842 (THU-284)
Horsley, Harry, S181 (FRI-435)
Horsmans, Yves, S90 (SAT-059), S95 (SAT-076), S907 (SAT-575)
Horst, Ludwig, S236 (FRI-323), S303 (SAT-257-YI), S351 (SAT-427)
Horstmeier, Henriette, S11 (OS-002-YI), S237 (FRI-324), S266 (SAT-347-YI), S362 (TOP-325-YI), S364 (WED-323), S750 (THU-497-YI)
Horta, Ana, S43 (OS-066), S937 (FRI-585-YI)
Horta, Ana Aboim, S934 (TOP-582), S940 (FRI-589)
Horta, Diana, S309 (SAT-268)
Horvath, Angela, S979 (TOP-614)
Hoshida, Yujin, S463 (WED-250)
Hosmane, Suneil, S78 (LBP-024)
Hosoda, Kanji, S645 (SAT-138)
Hosoda, Shunichi, S506 (FRI-256)
Hosomichi, Kazuyoshi, S875 (THU-573), S894 (THU-635)
Ho, Stanley Siu Fung, S868 (FRI-644)
Hoteit, Maarouf, S166 (FRI-393), S438 (THU-365)
Hotho, Daphne, S15 (OS-009-YI)
Houben, Philipp, S383 (FRI-474), S409 (FRI-556)
Houdroge, Farah, S803 (FRI-014)
Hou, Fengqin, S952 (FRI-623)
Hou, Jinlin, S1 (GS-001), S33 (OS-047), S34 (OS-048), S73 (LBP-012), S73 (LBP-013), S433 (THU-239), S617 (WED-201), S932 (SAT-641), S943 (FRI-594), S953 (FRI-624), S955 (FRI-629), S959 (WED-586)
Hou, Li, S664 (SAT-203), S665 (SAT-204), S666 (SAT-206)
Hou, Ming-Chih, S430 (THU-231), S436 (THU-250), S448 (THU-396), S500 (FRI-239), S535 (THU-135), S586 (WED-108), S751 (THU-499), S755 (THU-510)
Hountondji, Lina, S92 (SAT-068), S95 (SAT-076)
Hou, Ruixia, S884 (THU-605)
Hou, Ruixue, S667 (SAT-213), S847 (THU-300), S848 (THU-301)
Houssel-Debry, Pauline, S143 (SAT-450), S380 (FRI-463), S381 (FRI-464)
Housset, Chantal, S235 (FRI-320)
Houttu, Veera, S641 (SAT-126)
Hou, Weiliang, S511 (FRI-370)
Hou, Yixin, S258 (SAT-548), S452 (THU-413)
Hovingh, Milaine, S630 (SAT-090), S857 (WED-299), S863 (WED-318)
Hov, Johannes R., S2 (GS-002), S13 (OS-006-YI), S290 (FRI-289), S299 (SAT-249), S303 (SAT-257-YI), S315 (SAT-286), S345 (SAT-410)
Howard, Robin, S319 (SAT-301), S330 (SAT-365)
Howell, Jessica, S249 (SAT-517), S249 (SAT-521), S433 (THU-240), S458 (WED-240), S799 (FRI-004), S800 (FRI-005), S820 (WED-021), S922 (SAT-613)
Hoyle, Anna, S43 (OS-065)
Hoyle, Henry, S287 (FRI-276-YI), S292 (FRI-300-YI), S858 (WED-300-YI)
Hoyo, Cathrine, S544 (THU-167)
Hoyo, Mario Del, S806 (FRI-024)
Hrabe de Angelis, Martin, S672 (SAT-230)
Hroch, Milos, S286 (FRI-272)
Hrzenjak, Ana, S617 (WED-202)
Hsiao, Po-Yen, S691 (FRI-174)
Hsieh, Meng-Lun, S686 (FRI-158-YI)
Hsieh, Ti-Feng, S446 (THU-387)
Hsieh, Ting-Feng, S426 (THU-218)
Hsieh, Vivian Chia-Rong, S686 (FRI-158-YI)
Hsieh, Yun-Cheng, S755 (THU-510)
Hsiung, Cheng-Yu, S426 (THU-218)
Hsu, Chao-Wei, S919 (SAT-606)
Hsu, Cheng Er, S945 (FRI-603)
Hsu, Chiu-Chi, S893 (THU-633)
Hsu, Chiun, S491 (TOP-408-YI)
Hsu, Christine, S413 (FRI-569), S918 (SAT-604)
Hsu, Claire, S915 (SAT-594)
Hsu, Hung-wei, S456 (WED-234-YI)
Hsu, Kelly, S112 (FRI-051)
Hsu, Po-Hsien, S274 (THU-319), S898 (TOP-568)
Hsu, Shih-Jer, S898 (TOP-567)
Hsu, Yao-Chun (Holden), S46 (OS-070-YI), S928 (SAT-628-YI), S943 (FRI-596), S958 (WED-580)
Hsu, Yen-Ning, S449 (THU-399)
Hsu, Yu-Hsuan, S471 (WED-270)
Huailla, Rommel Zambrano, S112 (FRI-050)
Hu, Airong, S560 (TOP-080)
Huang, Aaron, S694 (FRI-183)
Huang, Bevan Emma, S119 (FRI-073)
Huang, Bingyuan, S293 (FRI-302-YI)
Huang, Cheng, S7 (GS-012), S958 (WED-581)
Huang, Chien-Hao, S735 (THU-452)
Huang, Chih-Jen, S274 (THU-319), S797 (TOP-033), S898 (TOP-568), S915 (SAT-594), S929 (SAT-633)
Huang, Chung-Feng, S518 (TOP-128), S557 (THU-214)
Huang, Daniel, S221 (WED-523), S424 (TOP-376), S442 (THU-379), S452 (THU-414-YI), S509 (FRI-365)
Huang, Deliang, S816 (WED-007)
Huang, Emily, S243 (FRI-347)
Huang, Guofu, S511 (FRI-370)
Huang, He, S587 (WED-110-YI), S587 (WED-111)
Huang, Hian Liang, S495 (FRI-228-YI)
Huang, Huei-Tyng (Philippe), S69 (LBP-001)
Huang, Jee-Fu, S518 (TOP-128), S536 (THU-138)
Huang, Jian, S438 (THU-363), S471 (WED-271)
Huang, Jinbo, S405 (FRI-542)
Huang, Jing, S259 (SAT-554), S609 (WED-182), S763 (THU-011), S924 (SAT-620)
Huang, Linlin, S511 (FRI-370)

Author Index

Huang, Meilan, S664 (SAT-202), S664 (SAT-203), S666 (SAT-206)
Huang, Mingxing, S560 (TOP-080)
Huang, Pei-Chi, S284 (FRI-268-YI), S360 (THU-350)
Huang, Qi, S869 (TOP-631)
Huang, Rui, S192 (WED-430), S673 (SAT-232), S930 (SAT-634), S930 (SAT-635), S933 (SAT-642)
Huang, Shang-Chin, S906 (SAT-574), S969 (WED-613)
Huang, Tai-Yu, S632 (SAT-100)
Huang, Tianquan, S906 (SAT-572)
Huang, Tony, S469 (WED-265)
Huang, Weijian, S42 (OS-063)
Huang, Weijuan, S511 (FRI-370)
Huang, Weiting, S698 (FRI-197)
Huang, Xiaoyu, S102 (THU-061)
Huang, Xin, S259 (SAT-554)
Huang, Xuefeng, S491 (TOP-422)
Huang, Yan, S151 (SAT-476), S162 (TOP-440), S952 (FRI-623)
Huang, Yanshan, S685 (FRI-156)
Huang, Yi-Hsiang, S430 (THU-231), S436 (THU-250), S448 (THU-396), S500 (FRI-239), S500 (FRI-240), S510 (FRI-369-YI), S535 (THU-135), S586 (WED-108), S751 (THU-499)
Huang, Yongfa, S628 (TOP-145)
Huang, Yuting, S437 (THU-362)
Huang, Yu-Tung, S735 (THU-452)
Huang, Yuxian, S46 (OS-070-YI), S151 (SAT-476), S162 (TOP-439), S367 (WED-336), S374 (WED-356), S964 (WED-601-YI)
Huang, Zhiyin, S28 (OS-036-YI)
Huang, Zuxiong, S352 (SAT-428-YI), S593 (WED-134), S924 (SAT-620), S952 (FRI-623)
Huanyi, Cao, S649 (SAT-154), S650 (SAT-155)
Huarte, Pilar, S837 (THU-267), S855 (WED-289)
Hua, Xiangwei, S68 (OS-107), S74 (LBP-015)
Hua, Xue, S49 (OS-075), S962 (WED-594)
Huberlant, Vincent, S839 (THU-273)
Huber, Samuel, S178 (FRI-429-YI), S213 (WED-496), S257 (SAT-546), S277 (THU-330-YI), S291 (FRI-291-YI), S866 (FRI-639)
Hubková, Beáta, S321 (SAT-305)
Hübner, Norbert, S57 (OS-088), S291 (FRI-291-YI)
Hubner, Richard, S485 (WED-396)
Hübscher, Stefan G., S14 (OS-007), S297 (TOP-293), S341 (SAT-397)
Huch, Meritxell, S474 (WED-364)
Huchon, Pélagie, S869 (TOP-632)
Hucl, Tomáš, S392 (FRI-500)
Hudson, Benjamin, S201 (WED-459)
Huebener, Peter, S178 (FRI-429-YI), S213 (WED-496)
Huelin, Patricia, S804 (FRI-019)
Huerta, Anna, S735 (THU-453)
Hueva, Antonio Andrés, S634 (SAT-104)
Hughes, Albert, S242 (FRI-345-YI)
Hughes, Christopher B., S412 (FRI-564-YI)
Hughes, Robert, S281 (FRI-260), S282 (FRI-261), S863 (WED-318)
Hugo, Susan, S926 (SAT-624)
Huguet-Pradell, Júlia, S453 (TOP-389)
Hu, Guoxin, S952 (FRI-623)
Hu, Haoran, S362 (THU-356)
Huiban, Laura, S210 (WED-490), S211 (WED-493), S819 (WED-015), S944 (FRI-601)
Huici-Izagirre, Maider, S165 (FRI-387-YI)
Huijkman, Nicolette, S630 (SAT-090), S670 (SAT-221-YI)
Hui, Rex Wan-Hin, S422 (TOP-359-YI), S423 (TOP-360), S496 (FRI-230), S915 (SAT-593), S947 (FRI-609)
Hui, Ruiling, S812 (FRI-040)
Hui, Samuel, S820 (WED-021)
Hui, Vicki Wing-Ki, S66 (OS-103-YI), S931 (SAT-637), S979 (WED-643)
Hu, Jinhua, S67 (OS-105-YI), S225 (WED-537)
Hu, Junjian, S676 (SAT-239)
Hu, Kai, S593 (WED-134), S763 (THU-011), S924 (SAT-620)
Hu, Kaipeng, S487 (WED-402), S674 (SAT-234)
Hu, Ke-Qin, S536 (THU-136)
Hu, Lin-Hui, S292 (FRI-298)
Hu, Manqiu, S454 (TOP-392-YI)
Hum, Dean, S149 (SAT-468), S152 (SAT-478), S163 (FRI-383), S214 (WED-499), S760 (TOP-032)
Hume, David, S170 (FRI-403)
Hu, Meiqian, S27 (OS-034), S104 (THU-070), S151 (SAT-476), S170 (FRI-401-YI), S389 (FRI-492)
Hume, Simon, S65 (OS-101-YI), S65 (OS-102), S903 (SAT-562), S970 (WED-619)
Hu, Min, S701 (FRI-204)
Hu, Mingzhao, S492 (FRI-218)
Hunduma, Fufa, S822 (WED-026)
Hung, Ya-Wen, S500 (FRI-239)
Hunt, Xanthe, S900 (SAT-558)
Huo, Teh-Ia, S449 (THU-399), S755 (THU-510)
Huot-Marchand, Philippe, S696 (FRI-189)
Hupa-Breier, Katharina Luise, S971 (WED-620)
Hu, Peng, S108 (THU-083), S269 (SAT-353), S637 (SAT-115), S906 (SAT-572)
Hu, Qiankun, S46 (OS-070-YI), S162 (TOP-439)
Hu, Qingqing, S103 (THU-069), S177 (FRI-426), S452 (THU-412)
Hur, Hong, S891 (THU-624-YI)
Hur, Moon Haeng, S500 (FRI-241), S502 (FRI-245), S507 (FRI-361), S509 (FRI-366)
Hu, Rong, S259 (SAT-554), S593 (WED-134), S609 (WED-182), S763 (THU-011), S924 (SAT-620)
Hurst, John R, S5 (GS-008)
Husain, Farah, S670 (SAT-220)
Hussein, Ahmed Kamal, S208 (WED-482)
Hussein, Ali Abdul, S563 (WED-041)
Hussen, Ahmed, S926 (SAT-622-YI)
Hutchinson, Grace, S338 (SAT-385)
Hutchison, Alan L., S536 (THU-137)
Hutchison, Katharine, S201 (WED-459)
Hu, Tiantian, S201 (WED-458), S917 (SAT-603), S944 (FRI-597), S964 (WED-601-YI)
Hu, Tsung-Hui, S958 (WED-580)
Hu, Xiaoling, S512 (FRI-377)
Hu, Xin, S674 (SAT-233)
Hu, Xingjiang, S74 (LBP-014)
Hu, Yao, S917 (SAT-603)
Hu, Ying, S158 (SAT-501)
Hu, Yiyang, S677 (SAT-241), S778 (THU-053)
Huynh, Hoai Phuong, S587 (WED-115)
Huynh, Mylinh, S275 (THU-321)
Huynh, Trung, S471 (WED-272), S587 (WED-115)
Hvas, Christian, S262 (SAT-332)
Hvid, Henning, S240 (FRI-338)
Hvidt, Astrid, S262 (SAT-332)
Hwang, Carey, S958 (WED-581)
Hwang, Jow-Jyh, S691 (FRI-174)
Hwang, Sang Youn, S497 (FRI-233)
Hwang, Yeongseok, S513 (FRI-378)
Hyde, Carolyn, S198 (WED-448-YI)
Hyder, Md Irfan, S820 (WED-022)
Hyogo, Hideyuki, S667 (SAT-213)
Hyötyläinen, Tuulia, S29 (OS-038), S268 (SAT-351), S662 (SAT-197)
Hytiroglou, Prodromos, S53 (OS-083-YI)
Hyvärinen, Kati, S376 (FRI-448)

Iacob, Speranta, S819 (WED-015), S944 (FRI-601)
Iacono, Oreste Lo, S567 (WED-054)
Iacotucci, Paola, S248 (SAT-516)
Iamello, Rocco, S400 (FRI-526), S542 (THU-159)
Iannacone, Matteo, S51 (OS-079)
Iannetta, Marco, S49 (OS-076-YI), S919 (SAT-608-YI)
Iannone, Giulia, S185 (TOP-455-YI), S196 (WED-445), S479 (WED-378)
Iavarone, Massimo, S405 (FRI-541), S424 (TOP-375-YI), S429 (THU-227-YI), S494 (FRI-225), S514 (FRI-381)
Iavarone, Selene, S30 (OS-041)
Iavarone, Selene Therese, S394 (FRI-507-YI)
Ibadullaeva, Nargiz, S74 (LBP-016)
Ibañez-Samaniego, Luis, S542 (THU-164), S567 (WED-054), S571 (WED-069), S643 (SAT-134)
Ibarra-Hernández, Mónica, S132 (FRI-108-YI)

Ibarra, Marcela, S296 (TOP-281), S306 (SAT-262)
Ibars, Eugenia Pareja, S408 (FRI-553)
Ibidapo-Obe, Oluwatomi, S142 (SAT-448), S159 (SAT-506-YI), S169 (FRI-399), S170 (FRI-402)
Iborra, Maria Asunción, S910 (SAT-581)
Iborra, María Asunción, S899 (SAT-557), S910 (SAT-585)
Ibrahim, Mohamad, S28 (OS-035)
Ibrahim, Samar, S650 (SAT-156)
Ibrahim, Yasmin, S816 (WED-008)
Ichida, Hirofumi, S449 (THU-400), S492 (FRI-219)
Ichikawa, Takeshi, S544 (THU-170)
Ichinose, Shizuko, S894 (THU-635)
Ictho, Jerry, S821 (WED-023)
Idalsoaga, Francisco, S112 (FRI-050)
Ideo, Francesco, S414 (FRI-571)
Ide, Tatsuya, S808 (FRI-027)
Idilman, Ramazan, S7 (LBO-001), S24 (OS-028), S41 (OS-061), S144 (SAT-452), S160 (SAT-507), S519 (THU-089), S588 (WED-116), S652 (SAT-163), S899 (SAT-556-YI), S965 (WED-603)
Idowu, Michael, S615 (WED-196)
Idriz, Nevin, S1 (GS-001)
Iebba, Valerio, S478 (WED-377)
Ielasi, Luca, S424 (TOP-375-YI), S429 (THU-227-YI), S514 (FRI-381)
Ieluzzi, Donatella, S97 (SAT-084-YI)
Iezzi, Roberto, S731 (THU-444-YI)
Igbokwe, Vanessa, S77 (LBP-022-YI)
Iglesias-Moure, Jose, S232 (FRI-313), S241 (FRI-339)
Iglseder, Bernhard, S539 (THU-151-YI), S792 (SAT-041)
Ignat, Mina, S602 (WED-157)
Ignjatović, Sofija, S268 (SAT-351)
Iheanacho, Ike, S801 (FRI-007)
Ihli, Franziska, S359 (THU-345-YI)
Iijima, Hiroko, S894 (THU-635)
II, Phillip Swanson, S893 (THU-629)
Ijung, Feng, S536 (THU-138)
Ikeda, Yoshio, S675 (SAT-237)
Ikegami, Tadashi, S808 (FRI-027)
Ikejima, Kenichi, S225 (WED-533), S246 (FRI-356)
Ikejima, Shunsuke, S246 (FRI-356)
Ikram, Areesha, S605 (WED-170)
Iliodromiti, Stamatina, S23 (OS-026-YI), S824 (WED-031)
Illarramendi, Jennifer, S844 (THU-285)
Illescas-López, Marta, S910 (SAT-581)
Illescas, Soledad, S910 (SAT-581)
Ilott, Nicholas, S43 (OS-065)
Imai, Shinobu, S258 (SAT-549), S979 (WED-644)
Imajo, Kento, S686 (FRI-159)
Imam, Achraf, S60 (OS-093), S289 (FRI-286)
Imamura, Hiroshi, S449 (THU-400)
Imamura, Jun, S499 (FRI-237)
Imbeaud, Sandrine, S17 (OS-011), S38 (OS-055)
Immers, Lindsey, S125 (FRI-091)
Imparato, Camille, S497 (FRI-234), S723 (THU-418)
Imperial, Joanne, S438 (THU-365), S588 (WED-117), S971 (WED-621)
Imsirovic, Haris, S908 (SAT-576)
Im, Yu Ri, S151 (SAT-477), S945 (FRI-602-YI)
Inacio, Patricia, S474 (WED-364)
Iñarrairaegui, Mercedes, S59 (OS-091), S96 (SAT-079)
Incalcaterra, Silvia, S465 (WED-255)
Incicco, Simone, S30 (OS-041), S176 (FRI-425), S190 (WED-425), S196 (WED-443), S212 (WED-494-YI), S227 (WED-541-YI), S479 (WED-378)
Indolfi, Giuseppe, S55 (OS-086), S831 (THU-258-YI), S842 (THU-284), S850 (THU-308)
Indre, Madalina Gabriela, S52 (OS-081)
Ines, Costa Santos, S934 (TOP-582)
Infanti, Laura, S165 (FRI-386)
Inge-Cox, Richie Alexander, S146 (SAT-461)
Ingelsson, Erik, S702 (FRI-206)
Ingiliz, Patrick, S798 (TOP-034)
Inglot, Małgorzata, S64 (OS-100)
Ingviya, Thammasin, S439 (THU-366-YI)
In het Panhuis, Wietse, S646 (SAT-140-YI), S674 (SAT-233)
Inkongngam, Torlap, S530 (THU-119-YI)
Innocenti, Francesco, S535 (THU-134)
Innocenti, Tommaso, S400 (FRI-526), S542 (THU-159)
Inoue, Eri, S811 (FRI-037)
Inoue, Koichi, S668 (SAT-215)
Invernizzi, Pietro, S10 (LBO-006), S69 (LBP-004-YI), S83 (LBP-034-YI), S282 (FRI-263), S304 (SAT-258), S305 (SAT-260-YI), S307 (SAT-263), S316 (SAT-287), S323 (SAT-315), S325 (SAT-320), S331 (SAT-368-YI), S333 (SAT-369), S335 (SAT-378-YI), S340 (SAT-393), S350 (SAT-421), S831 (THU-256-YI)
Investigators, Piter Collaborating, S972 (WED-623)
Ioannidou, Panagiota, S45 (OS-068-YI), S545 (THU-172)
Ioannou, Giorgio, S485 (WED-396)
Iorio, Jessica, S457 (WED-235)
Iorra, Fernando, S563 (WED-041)
Ipar, Eugenia, S728 (THU-434)
Iqbal, Masood, S377 (FRI-449)
Iredahl, Fredrik, S568 (WED-056)
Iriart, Clément, S887 (THU-612-YI)
Iriarte, Marta, S53 (OS-082)
Irigaray-Miramon, Ainara, S17 (OS-013)
Irles-Depe, Marie, S602 (WED-158)
Irshad, Muhammad Adil, S564 (WED-044), S565 (WED-045)
Irurzun, Itziar, S26 (OS-031), S689 (FRI-169)
Iruzubieta, Paula, S62 (OS-097), S150 (SAT-475), S241 (FRI-339), S516 (TOP-113), S542 (THU-164), S567 (WED-054), S571 (WED-069), S585 (WED-106), S612 (WED-186-YI), S643 (SAT-134), S837 (THU-267), S855 (WED-289)
Irvine, Katharine, S170 (FRI-403), S420 (THU-526)
Isaacs-Ten, Anna, S287 (FRI-274)
Isaak, Alexander, S213 (WED-496)
Isabella, Davide, S817 (WED-010)
Isaksson, Bengt, S71 (LBP-008)
Iserentant, Gilles, S807 (FRI-025)
Iserte, Gemma, S481 (WED-382-YI)
Ishida, Yuji, S873 (THU-564)
Ishida, Yumi, S372 (WED-352), S647 (SAT-147)
Ishii, Takamichi, S419 (THU-525), S420 (THU-529-YI), S421 (THU-531)
Ishizuka, Kei, S225 (WED-533), S246 (FRI-356)
Isik, Elvan, S542 (THU-163), S899 (SAT-556-YI)
Işık, Elvan, S397 (FRI-514)
Ismaili, Zahi, S309 (SAT-267), S578 (WED-086)
Ismailova, Zebiniso Sofiya, S74 (LBP-016)
Ismail, Rana, S161 (SAT-510-YI)
Ismail, Yousuf, S147 (SAT-465)
Isogawa, Masanori, S875 (THU-573), S894 (THU-635)
Isoniemi, Helena, S450 (THU-403)
Ispan, Denis, S651 (SAT-158-YI)
Israel, Ariel, S247 (SAT-513)
Israelsen, Hans, S115 (FRI-057)
Israelsen, Mads, S110 (FRI-041-YI), S114 (FRI-057), S115 (FRI-059), S122 (FRI-079-YI), S125 (FRI-090-YI), S217 (WED-509-YI), S253 (SAT-532), S554 (THU-204), S706 (THU-545-YI)
Issa, Fadi, S43 (OS-065)
Issa, Nagham, S783 (SAT-012)
Ito, Diane, S299 (SAT-247), S320 (SAT-303), S320 (SAT-304)
Ito, Jun, S506 (FRI-256)
Iturbe-Rey, Santiago, S165 (FRI-387-YI), S483 (WED-388-YI)
Iturri, Maria Jose Sanchez, S830 (THU-253)
Itzel, Timo, S288 (FRI-283)
Itzkovitz, Shalev, S862 (WED-315)
Iuga, Cristina Adela, S255 (SAT-539), S544 (THU-166)
Ivanchuk, Oleksandr, S548 (THU-182)
Ivancovsky-Wajcman, Dana, S766 (THU-015), S774 (THU-040), S774 (THU-041), S794 (SAT-046), S796 (SAT-053)
Ivan, Ferrari, S71 (LBP-009), S340 (SAT-393)
Ivanov, Alexander, S871 (THU-559-YI)
Iv, A. Sidney Barritt, S544 (THU-167)
Ivirico, Ilse Pardo, S296 (TOP-281), S302 (SAT-253), S306 (SAT-262)
Ivkovic, Ana, S112 (FRI-051)
Iwaisako, Keiko, S418 (TOP-534), S420 (THU-529-YI)

Author Index

Iwaki, Kentaro, S421 (THU-531)
Iwaki, Michihiro, S686 (FRI-159)
Iwakiri, Yasuko, S134 (FRI-115)
Iwamoto, Naoki, S702 (FRI-206)
Iwamoto, Satoru, S258 (SAT-549), S979 (WED-644)
Iwao, Masao, S662 (SAT-196)
Iwasa, Motoo, S686 (FRI-159)
Iwuji, Collins, S900 (SAT-558)
Iyer, K, S653 (SAT-166)
Izopet, Théo, S723 (THU-419)
Izquierdo-Sánchez, Laura, S165 (FRI-387-YI), S303 (SAT-257-YI), S323 (SAT-315), S445 (THU-385), S484 (WED-393)
Izumi, Namiki, S439 (THU-368), S618 (WED-205), S953 (FRI-624)
Izzi, Antonio, S911 (SAT-587-YI), S947 (FRI-608)
Izzi-Engbeaya, Chioma, S685 (FRI-157-YI)
Izzy, Manhal, S745 (THU-483)

Jaara, Hala, S28 (OS-037), S627 (TOP-144), S629 (TOP-160)
Jabak, Salma, S354 (SAT-434)
Jabar, Falah, S491 (TOP-408-YI)
Jaccard, Arnaud, S829 (THU-252)
Jachs, Mathias, S43 (OS-066), S113 (FRI-053), S156 (SAT-494), S183 (FRI-444-YI), S183 (FRI-445), S186 (TOP-470-YI), S199 (WED-452), S200 (WED-453), S205 (WED-474), S213 (WED-498), S216 (WED-508), S427 (THU-220), S427 (THU-221), S440 (THU-370), S733 (THU-450), S734 (THU-451), S748 (THU-493-YI), S749 (THU-494), S750 (THU-498), S753 (THU-505-YI), S900 (SAT-559), S901 (SAT-560), S914 (SAT-591), S934 (TOP-582), S937 (FRI-585-YI)
Jacobi, Severin, S60 (OS-093), S175 (FRI-420), S181 (FRI-436)
Jacobsen, Birgitte, S202 (WED-461-YI), S202 (WED-462), S225 (WED-532)
Jacobsen, Carina, S878 (THU-585-YI)
Jacobson, Ira, S10 (LBO-006), S76 (LBP-021), S329 (SAT-363), S923 (SAT-618)
Jacob, Torid, S213 (WED-496)
Jacot, William, S90 (SAT-059)
Jacquemin, Emmanuel, S55 (OS-086), S831 (THU-258-YI), S842 (THU-284), S850 (THU-308)
Jaeckel, Elmar, S309 (SAT-268)
Jafari, Daniel, S391 (FRI-496)
Jaffredo, Thierry, S235 (FRI-320)
Jaganathan, Jeeva, S202 (WED-460-YI)
Jagst, Michelle, S881 (THU-593), S887 (THU-611)
Jahagirdar, Vinay, S109 (TOP-209-YI), S122 (FRI-083), S527 (THU-109)
Jaihan, Tassanun, S619 (WED-211)
Jain, Dhanpat, S331 (SAT-368-YI)
Jain, Harsh, S404 (FRI-539), S741 (THU-474)
Jain, Meena, S681 (FRI-142)
Jain, Shubham, S36 (OS-051-YI), S184 (TOP-454-YI), S247 (SAT-514), S299 (SAT-248)
Jairath, Vipul, S740 (THU-468)
Jaitly, Seema, S82 (LBP-033), S341 (SAT-396)
Jajodia, Surabhi, S257 (SAT-544)
Jakhar, Deepika, S171 (FRI-404), S361 (THU-355-YI)
Jakhmola, Vibhuti, S650 (SAT-157-YI)
Jakiche, Antoine, S691 (FRI-175)
Jakobsson, Frida, S903 (SAT-561)
Jakobsson, Gustav, S115 (FRI-058-YI)
Jakoubek, Dana, S59 (OS-091)
Jaksa, Ashley, S344 (SAT-403)
Jalal, Prasun, S28 (OS-035)
Jalamneh, Basil, S28 (OS-035)
Jalan, Rajiv, S27 (OS-034), S35 (OS-050-YI), S98 (SAT-087), S148 (SAT-467-YI), S150 (SAT-475), S151 (SAT-476), S170 (FRI-401-YI), S171 (FRI-409-YI), S173 (FRI-413), S180 (FRI-434), S181 (FRI-435), S187 (TOP-471-YI), S189 (WED-418), S198 (WED-448-YI), S389 (FRI-492)
Jalil, Sajid, S407 (FRI-546)
Jalloh, Mohamed, S735 (THU-457)
Jameie-Oskooei, Sina, S151 (SAT-476), S389 (FRI-492)
James, Bree, S249 (SAT-517), S249 (SAT-521)
James, Cary, S897 (TOP-565)
James, Dayle, S981 (FRI-635), S981 (FRI-636)
James, Linda, S80 (LBP-028-YI)
James, Michael, S69 (LBP-001)
Jamialahmadi, Oveis, S476 (WED-368)
Jamil, Khurram, S62 (OS-096), S719 (TOP-486)
Jammeh, Kitabu, S764 (THU-012), S798 (TOP-034)
Jamme, Paul, S215 (WED-506)
Janciauskiene, Sabina, S836 (THU-265-YI)
Jancoriene, Ligita, S807 (FRI-025)
Janczewska, Ewa, S328 (SAT-362), S680 (FRI-139), S980 (FRI-633)
Janczura, Jakub, S970 (WED-617-YI)
Jandova, Lenka, S286 (FRI-272)
Jang, Byoung Kuk, S590 (WED-121)
Jang, Eun Chul, S545 (THU-171), S591 (WED-122), S625 (WED-229), S630 (SAT-092), S652 (SAT-165), S686 (FRI-163)
Jang, Eun Sun, S906 (SAT-573)
Jang, Heejoon, S546 (THU-174)
Jang, Jae Young, S637 (SAT-111)
Jang, Jeong Won, S478 (WED-372), S482 (WED-386), S510 (FRI-368), S881 (THU-594), S917 (SAT-602)
Jang, Se Ha, S264 (SAT-337)
Jang, Suk-Chan, S974 (WED-628)
Janicko, Martin, S34 (OS-049), S141 (TOP-437), S166 (FRI-388-YI), S321 (SAT-305)
Janičko, Martin, S35 (OS-050-YI), S123 (FRI-085)
Janik, Maciej, S318 (SAT-298), S331 (SAT-368-YI), S332 (SAT-369), S355 (SAT-442)
Janjua, Naveed, S821 (WED-024), S967 (TOP-600-YI), S968 (WED-609-YI)
Jankowska, Irena, S55 (OS-086), S831 (THU-258-YI), S842 (THU-284), S850 (THU-308)
Jannone, Giulia, S850 (THU-308)
Jannusch, Kai, S188 (WED-416)
Janocha-Litwin, Justyna, S980 (FRI-633)
Jan, Sayed Tauseef Ahmad, S698 (FRI-196)
Jansen, Christian, S6 (GS-011-YI), S33 (OS-046), S34 (OS-049), S54 (OS-084), S141 (TOP-437), S166 (FRI-388-YI), S736 (THU-460-YI), S752 (THU-501)
Jansen, Sita, S15 (OS-009-YI)
Janshoff, Saskia, S866 (FRI-641), S879 (THU-588), S887 (THU-611)
Janssen, Harry L. A., S351 (SAT-426-YI), S352 (SAT-429), S353 (SAT-432), S353 (SAT-433), S943 (FRI-596)
Janssen, Harry L.A., S46 (OS-070-YI), S63 (OS-098-YI), S193 (WED-432), S436 (THU-249), S443 (THU-382-YI), S444 (THU-383), S587 (WED-110-YI), S587 (WED-111), S608 (WED-180), S621 (WED-215), S622 (WED-216), S789 (SAT-031-YI), S790 (SAT-035), S817 (WED-011), S897 (TOP-565), S909 (SAT-580), S914 (SAT-592-YI), S921 (SAT-610), S928 (SAT-628-YI), S953 (FRI-624)
Janssens, Filip, S849 (THU-306-YI), S920 (SAT-609), S929 (SAT-629)
Jantz, Derek, S8 (LBO-003)
Janzén, David, S682 (FRI-148), S690 (FRI-172)
Jara, Lorena, S968 (WED-610-YI)
Jaramillo, Andres, S416 (FRI-576)
Jaramillo, Catalina, S850 (THU-308)
Jarčuška, Peter, S321 (SAT-305), S585 (WED-107)
Jardine, Jennifer, S23 (OS-026-YI)
Jargalsaikhan, Ganbolor, S439 (THU-367), S915 (SAT-595), S916 (SAT-596)
Jargalsaikhan, Orgil, S870 (TOP-646)
Jarošová, Jana, S392 (FRI-500)
Jaroszek, Magdalena, S318 (SAT-298), S355 (SAT-442)
Jarrett, James, S817 (WED-012)
Jasrotia, Ayush, S24 (OS-027), S246 (TOP-550), S822 (WED-025-YI)
Jassem, Wayel, S644 (SAT-135-YI)
Jastrzebska, Kinga, S252 (SAT-530)
Jaubert, Laura, S387 (FRI-484)
Javanbakht, Hassan, S77 (LBP-021), S964 (WED-597)
Javed, Maryam, S735 (THU-457)
Javed, P, S952 (FRI-622)

Javed, Talha, S564 (WED-044), S565 (WED-045)
Jayabalan, Dujinthan, S699 (FRI-198)
Jayakar, Tanya, S563 (WED-041)
Jayasekera, Channa, S78 (LBP-023)
Jayson, Christina, S125 (FRI-090-YI)
Jeanne, Sakina Sayah, S149 (SAT-468), S152 (SAT-478), S163 (FRI-383), S164 (FRI-384), S172 (FRI-412), S760 (TOP-032)
Jechow, Katharina, S852 (TOP-311), S858 (WED-302)
Jeddy, Zuha, S342 (SAT-398)
Jedlickova, Ivana, S855 (WED-288)
Jędruszek, Sebastian, S318 (SAT-298), S355 (SAT-442)
Jeevithan, S, S782 (SAT-010-YI)
Jeffery-Smith, Anna, S921 (SAT-611)
Jeffrey, Angus, S145 (SAT-457), S736 (THU-458)
Jeffrey, Gary, S736 (THU-458)
Jeglinski, Brenda, S78 (LBP-025)
Jegodzinski, Lina, S651 (SAT-158-YI)
Jekle, Andreas, S874 (THU-570), S885 (THU-606), S889 (THU-620), S893 (THU-634), S960 (WED-588)
Jelenik, Tomas, S176 (FRI-421)
Jena, Lelin Kumar, S204 (WED-466)
Jeng, Rachel Wen-Juei, S1 (GS-001), S46 (OS-070-YI), S919 (SAT-606), S929 (SAT-633), S945 (FRI-603), S947 (FRI-607), S957 (WED-578)
Jenjai, Chanakan, S974 (WED-628)
Jenkins, Sam, S106 (THU-075)
Jens, Axel J. T., S59 (OS-092-YI)
Jensen, Ellen Lyngbeck, S110 (FRI-041-YI), S115 (FRI-059), S554 (THU-204)
Jensen, Gitte Hedegaard, S114 (FRI-057)
Jensen, Kasper Yde, S298 (SAT-245)
Jensen, M. Kyle, S850 (THU-308)
Jensen, Morten Daniel, S786 (SAT-024-YI)
Jensen, Thomas, S581 (WED-095)
Jensterle, Mojca, S777 (THU-050)
Jeong, Dahn, S821 (WED-024), S967 (TOP-600-YI)
Jeong, Jaehong, S498 (FRI-235), S916 (SAT-597)
Jeong, Jae Yoon, S92 (SAT-069), S553 (THU-198)
Jeong, Jain, S134 (FRI-115)
Jeong, Jin Gyo, S732 (THU-447)
Jeong, Joonho, S497 (FRI-233)
Jeong, Sook-Hyang, S706 (THU-543), S823 (WED-030), S838 (THU-270), S906 (SAT-573)
Jeong, Soung Won, S637 (SAT-111)
Jeong, Won-il, S136 (FRI-121), S229 (TOP-342-YI), S368 (WED-337-YI)
Jeon, Jang Su, S368 (WED-337-YI)
Jeppesen, Ole Kleist, S680 (FRI-139)
Jepsen, Peter, S116 (FRI-060), S775 (THU-042-YI), S777 (THU-050), S786 (SAT-024-YI)
Jeriha, Jakob, S275 (THU-321)
Jespersen, Jillian, S871 (THU-560-YI)
Jessa, Fatema, S704 (THU-539-YI)
Jessen, Eline, S170 (FRI-403)
Jessen, Pernille, S775 (THU-042-YI)
Jesudian, Arun, S39 (OS-056)
Jeyarajan, Andre, S547 (THU-179)
Jeylan, Asiya, S926 (SAT-622-YI)
Jezequel, Caroline, S45 (OS-067), S47 (OS-072), S222 (WED-525)
Jha, Ashish Kumar, S952 (FRI-622)
Jhamb, Ashu, S922 (SAT-613)
Jhaveri, Ajay, S160 (SAT-507)
Jia, Bo, S665 (SAT-204), S666 (SAT-206)
Jia, Jianru, S225 (WED-537)
Jia, Jidong, S85 (LBP-040), S88 (TOP-192), S295 (TOP-280), S826 (WED-040), S909 (SAT-579)
Jiang, Bochao, S529 (THU-115)
Jiang, Chao, S930 (SAT-634), S933 (SAT-642)
Jiang, Chenyi, S324 (SAT-317)
Jiang, Guoqing, S33 (OS-047)
Jiang, Hong, S941 (FRI-591)
Jiang, Jianning, S897 (TOP-551)
Jiang, Jie, S472 (WED-273)
Jiang, Jing, S104 (THU-070), S151 (SAT-476), S361 (THU-353)
Jiang, Jingjing, S97 (SAT-086), S135 (FRI-118)
Jiang, Jinyan, S882 (THU-596)
Jiang, Neng, S511 (FRI-370)
Jiang, Qirong, S754 (THU-507)
Jiang, Quan, S495 (FRI-229)
Jiang, Shao-wen, S46 (OS-070-YI)
Jiang, Suzhen, S208 (WED-481), S253 (SAT-533), S279 (THU-336), S785 (SAT-021), S813 (FRI-045), S931 (SAT-638)
Jiang, Weimin, S560 (TOP-080)
Jiang, Xiaofeng, S511 (FRI-370)
Jiang, Yongfang, S24 (OS-028), S144 (SAT-452), S160 (SAT-507)
Jiang, Yuyong, S258 (SAT-548)
Jiang, Zhonghao, S651 (SAT-159)
Jiang, Zhuofeng, S486 (WED-398)
Jiang, Zhuoru, S537 (THU-139)
Jiao, Jian, S645 (SAT-139), S657 (SAT-181), S779 (THU-054)
Jiao, Jingran, S146 (SAT-460)
Jiao, Xiangkun, S259 (SAT-554)
Jia, Shengxiong, S512 (FRI-377)
Jia, Wenling, S950 (FRI-617), S955 (FRI-628)
Jia, Xiaoli, S791 (SAT-039), S792 (SAT-040), S873 (THU-569), S941 (FRI-591), S946 (FRI-606)
Jia, Xiuqin, S688 (FRI-167)
Jia, Yidi, S367 (WED-336), S374 (WED-356), S918 (SAT-605)
Ji, Fanpu, S375 (TOP-519)
Ji, Guang, S558 (THU-215)
Ji, Huoyan, S173 (FRI-413)
Ji, JianSong, S119 (FRI-072), S259 (SAT-554), S593 (WED-134), S609 (WED-182), S763 (THU-011), S924 (SAT-620)
Ji, Keke, S600 (WED-153)
Jilakaraju, Bharadwaj, S845 (THU-288)
Ji, liujuan, S162 (TOP-440)
Jilkova, Zuzana Macek, S885 (THU-607)
Jimenez-Aguero, Raul, S303 (SAT-257-YI), S484 (WED-393)
Jimenez, Angeles, S890 (THU-621)
Jiménez-Colmenarez, Zulianni, S123 (FRI-086)
Jiménez, Emilio Márquez, S600 (WED-153)
Jiménez, Enrique Hernández, S146 (SAT-461)
Jimenez-Esquivel, Natalia, S146 (SAT-461), S191 (WED-427-YI)
Jiménez-Gracia, Laura, S35 (OS-050-YI)
Jiménez, Laura, S403 (FRI-532), S415 (FRI-575)
Jiménez, Lucía, S294 (TOP-278)
Jiménez-Masip, Alba, S612 (WED-186-YI)
Jiménez-Massip, Alba, S542 (THU-164), S562 (TOP-097-YI), S567 (WED-054), S605 (WED-168-YI), S612 (WED-188)
Jimenez-Ramos, Maria, S125 (FRI-090-YI)
Jimenez-Rivera, Carolina, S55 (OS-086), S831 (THU-258-YI), S842 (THU-284)
Jimenez, Rosario Rico, S819 (WED-019)
Jimenez, Sergio Hernandez, S707 (THU-548)
Jiménez-Trinidad, Francisco, S28 (OS-037), S629 (TOP-160)
Jiménez, Wladimiro, S173 (FRI-414), S239 (FRI-336)
Jimeno-Santander, Cecilia, S642 (SAT-131-YI)
(Jimmy) Bao, Jian-Xin, S632 (SAT-100)
Jindal, Ankur, S156 (SAT-495), S214 (WED-501-YI), S703 (THU-537)
Jing, Wang, S86 (LBP-041)
Jin, Jieyang, S756 (THU-514)
Jin, Qin, S173 (FRI-413)
Jin, qinglong, S295 (TOP-280)
Jin, Ronghua, S350 (SAT-425), S491 (TOP-422)
Jin, Rui, S655 (SAT-174)
Jin, Shuoshuo, S17 (OS-011)
Jin, Songwan, S360 (THU-351)
Jin, Tao, S467 (WED-260)
Jin, Xinrui, S589 (WED-118), S621 (WED-215)
Jin, Xiuping, S86 (LBP-041)
Jin, Young Joo, S590 (WED-121)
Jirouškovà, Markéta, S275 (THU-320)
Jirsa, Milan, S35 (OS-050-YI), S273 (THU-317), S405 (FRI-540), S459 (WED-241)
Ji, Samuel, S775 (THU-043)
Ji, Yun, S50 (OS-077)
Jobson, Timothy, S75 (LBP-017)
Jochmans, Ina, S381 (FRI-465)
Jodar, Meritxell, S828 (TOP-309-YI)
Jo, Gae Hoon, S426 (THU-219-YI)
Johannesen, Helle Hjorth, S602 (WED-159-YI)
Johannessen, Asgeir, S46 (OS-070-YI), S65 (OS-101-YI), S798 (TOP-048),

Author Index

S822 (WED-026), S825 (WED-036), S903 (SAT-562), S905 (SAT-569), S926 (SAT-622-YI), S926 (SAT-624), S940 (FRI-588-YI)
Johansen, Stine, S26 (OS-032-YI), S76 (LBP-020), S110 (FRI-041-YI), S111 (FRI-044), S114 (FRI-057), S115 (FRI-059), S122 (FRI-079-YI), S209 (WED-485), S262 (SAT-332), S554 (THU-204), S706 (THU-545-YI)
Johansson, Edvin, S579 (WED-090)
Johansson, Helene, S71 (LBP-008)
Johansson, Lars, S579 (WED-090)
John, Anoop, S722 (THU-416)
Johnbeck, Camilla Bardram, S602 (WED-159-YI)
John, Claire St, S759 (TOP-017-YI), S974 (WED-629-YI)
Johns, Jemma, S354 (SAT-434)
Johnson, Josephine, S166 (FRI-393)
Johnson, Madonna, S120 (FRI-075)
Johnson, Matt Bolz, S783 (SAT-012)
Johnson, Nathan, S713 (WED-557)
Johnson, Will, S330 (SAT-365)
Johnston, Karissa, S680 (FRI-141)
Johri, Ishank, S719 (TOP-487-YI)
Jois, Gahan, S782 (SAT-011)
Jonasson, Elise, S41 (OS-061), S202 (WED-461-YI), S202 (WED-462), S225 (WED-532), S262 (SAT-332)
Jones, Arron, S354 (SAT-434), S704 (THU-540), S921 (SAT-611)
Jones, David E., S67 (OS-106), S75 (LBP-018), S295 (TOP-280), S318 (SAT-299), S319 (SAT-300), S325 (SAT-320), S333 (SAT-370), S339 (SAT-387), S846 (THU-290)
Jones, Jenn, S127 (FRI-095)
Jones, Marcus, S166 (FRI-393)
Jones, Patricia, S89 (SAT-057), S116 (FRI-061), S190 (WED-421), S197 (WED-447)
Jones, Rebecca, S256 (SAT-543), S258 (SAT-547), S331 (SAT-368-YI)
Jonker, Johan, S630 (SAT-090)
Jonnalagadda, Sai Praveen, S812 (FRI-039)
Jonot, Emma, S414 (FRI-572)
Jönsson, Cecilia, S568 (WED-056)
Jönsson, Peter, S39 (OS-056)
Jonuscheit, Marc, S672 (SAT-230)
Jordan, William, S959 (WED-585)
Jording-Jespersen, Gregory, S900 (SAT-558)
Jørgensen, Kristin K., S14 (OS-007)
Jørgensen, Kristin Kaasen, S345 (SAT-410)
Jørgensen, Maja Kanstrup, S290 (FRI-287)
Jørgensen, Marianne Hørby, S55 (OS-086), S831 (THU-258-YI), S842 (THU-284)
Jorge-Peñas, Alvaro, S619 (WED-206)
Jorge Silva, Mario, S892 (THU-627)
José Acosta, María, S112 (FRI-050)
José Cantero, María, S358 (THU-340-YI), S654 (SAT-171-YI)
José Disla, Hugo, S772 (THU-036)
José Gude, María, S799 (TOP-049)
José Moreta, María, S110 (TOP-222)
Joshi, Deepak, S10 (LBO-006), S319 (SAT-301)
Joshi, Nandan, S786 (SAT-023)
Joshi, Shilpy, S47 (OS-072)
Jothimani, Dinesh, S24 (OS-028), S67 (OS-105-YI), S144 (SAT-452), S160 (SAT-507)
Jouid, Mahmoud, S379 (FRI-461-YI)
Joutsi-Korhonen, Lotta, S122 (FRI-084)
Jouvin-Marche, Evelyne, S885 (THU-607)
Jou, Yuh-Shan, S471 (WED-270)
Jovanovic, Natasha, S249 (SAT-517), S249 (SAT-521)
Joveleviths, Dvora, S88 (SAT-056), S776 (THU-044)
Jover, Ramiro, S272 (THU-315-YI), S273 (THU-316)
Jovine, Elio, S402 (FRI-529-YI)
Joy, Arun Cherackakudy, S564 (WED-044), S565 (WED-045)
Jo, Youhwa, S281 (FRI-260)
Jr, Andrei Racilka, S794 (SAT-046)
Juanola, Adrià, S30 (OS-041), S110 (TOP-222), S203 (WED-463), S394 (FRI-507-YI), S583 (WED-101)
Juanola, Oriol, S169 (FRI-400), S179 (FRI-431-YI), S230 (TOP-343-YI)
Juarez, Ignacio Garcia, S59 (OS-091), S300 (SAT-250), S730 (THU-442), S866 (FRI-640)
Jucaite, Aurelija, S690 (FRI-172)
Jucov, Alina, S7 (GS-012), S8 (LBO-003), S76 (LBP-021), S87 (LBP-043), S958 (WED-581), S959 (WED-586), S964 (WED-597), S965 (WED-602)
Jühling, Frank, S272 (THU-315-YI), S463 (WED-250)
Juillet, Stéphanie Marque, S951 (FRI-621)
Julian, Judit, S336 (SAT-380)
Julian, Luetkens, S213 (WED-496)
Julián, M Teresa, S562 (TOP-097-YI)
Julian, Valérie, S167 (FRI-394-YI)
Juliebø, August Tronstad, S395 (FRI-509)
Jumabayeva, Almagul, S967 (WED-608)
Juncu, Simona, S211 (WED-493)
Jun, Dae Won, S545 (THU-171), S591 (WED-122), S625 (WED-229), S630 (SAT-092), S652 (SAT-165), S686 (FRI-163)
Juneja, Pinky, S171 (FRI-404), S361 (THU-355-YI)
Jung, Björn, S172 (FRI-410-YI)
Jung, Chan-Young, S539 (THU-150)
Jung, Hyun Sun, S264 (SAT-337)
Jung, Jinhong, S4 (GS-006)
Jung, Jooyi, S546 (THU-175)
Jung, Nathalie, S262 (SAT-330)
Jungwirth, Emilian, S672 (SAT-229-YI)
Jung, Young Kul, S26 (OS-031)
Junien, Jean-Louis, S638 (SAT-117-YI)
Júnior, Genário Oliveira Santos, S95 (SAT-078)
Junker, Anders, S586 (WED-109), S602 (WED-159-YI), S692 (FRI-180)
Junnian, Chen, S649 (SAT-154), S650 (SAT-155)
Junot, Christophe, S145 (SAT-458-YI), S148 (SAT-467-YI), S261 (SAT-329-YI), S262 (SAT-330)
Juran, Brian D., S2 (GS-002), S13 (OS-006-YI), S290 (FRI-289)
Jurgens, Matthias C., S353 (SAT-432)
Jurić, Ana, S617 (WED-202)
Jutzi, Lukas, S165 (FRI-386)

Kabaçam, Gökhan, S395 (FRI-511-YI), S899 (SAT-556-YI), S961 (WED-589)
Kabamba, Benoit, S65 (OS-101-YI), S903 (SAT-562), S929 (SAT-629)
Kabelitz, Martin, S197 (WED-446), S732 (THU-448-YI), S737 (THU-462)
Kablawi, Dana, S533 (THU-127-YI), S589 (WED-119), S616 (WED-200), S865 (FRI-638)
Kabukcu, Furkan, S203 (WED-464)
Kacerovsky, Marian, S286 (FRI-272)
Kaczirek, Klaus, S284 (FRI-266), S427 (THU-221)
Kadaristiana, Agustina, S55 (OS-086)
Kaddah, Mona, S524 (THU-101)
Kadiri, Maryeme, S591 (WED-125), S609 (WED-181), S844 (THU-286), S845 (THU-287), S949 (FRI-613)
Kaewdech, Apichat, S156 (SAT-496), S215 (WED-505), S219 (WED-514), S221 (WED-523), S228 (WED-543), S423 (TOP-374), S439 (THU-366-YI), S528 (THU-110), S530 (THU-119-YI), S727 (THU-432)
Käfer, Astrid, S975 (WED-634-YI)
Kaffe, Eleanna, S102 (THU-062)
Kagawa, Tatehiro, S708 (THU-553)
Kah, Janine, S271 (THU-313)
Kahlhöfer, Julia, S935 (TOP-583), S963 (WED-596)
Kahl, Sabine, S21 (OS-020)
Kahn, Jeffrey, S308 (SAT-265), S309 (SAT-266), S386 (FRI-482), S411 (FRI-561-YI), S413 (FRI-570)
Kahraman, Deniz Cansen, S652 (SAT-163)
Kaibullayeva, Jamilya, S967 (WED-608)
Kain, Renate, S750 (THU-497-YI)
Kaiser, Rolf, S807 (FRI-025)
Kajal, Kamal, S81 (LBP-030)
Kaji, Keisuke, S275 (THU-321)
Kaji, Kosuke, S95 (SAT-077), S162 (TOP-438), S263 (SAT-334), S652 (SAT-164), S660 (SAT-189), S747 (THU-491)
Kakar, Sanjay, S53 (OS-083-YI)
Kakazu, Eiji, S32 (OS-045), S121 (FRI-076-YI), S488 (WED-403), S977 (WED-639)
Kakisaka, Keisuke, S194 (WED-435)

Kakizaki, Satoru, S62 (OS-097), S424 (TOP-376), S516 (TOP-113), S808 (FRI-027), S923 (SAT-618)
Kalafateli, Maria, S410 (FRI-558), S563 (WED-041)
Kalafati, Ioanna-Panagiota, S621 (WED-214), S765 (THU-013)
Kalatharan, Vinusha, S252 (SAT-530)
Kale, Pratibha, S189 (WED-419)
Kale, Pratibha Ramchandra, S292 (FRI-299)
Kalff, Jörg C., S213 (WED-496)
Kaliaskarova, Kulpash, S822 (WED-027)
Kalista, Kemal Fariz, S67 (OS-105-YI), S952 (FRI-622)
Kalita, Nikhil, S134 (FRI-116), S207 (WED-479), S578 (WED-088)
Kallan, Michael, S700 (FRI-202)
Kallenbach, Michael, S447 (THU-395), S470 (WED-268)
Kalligeros, Markos, S127 (FRI-095), S557 (THU-213), S793 (SAT-045), S794 (SAT-047), S795 (SAT-050), S795 (SAT-051)
Kallis, Yiannis, S838 (THU-270)
Kallurwar, Yash, S749 (THU-495)
Kalman, Richard, S10 (LBO-006)
Kalra, Naveen, S171 (FRI-409-YI), S684 (FRI-155)
Kalra, Rupinder, S264 (SAT-335), S264 (SAT-336), S280 (THU-337)
Kaltenecker, Christopher, S750 (THU-497-YI)
Kalus, Philipp, S216 (WED-507)
Kamada, Yoshihiro, S537 (THU-140)
Kamal, Habiba, S439 (THU-367), S903 (SAT-561), S915 (SAT-595), S916 (SAT-596)
Kamara, Elaine, S84 (LBP-038), S712 (WED-554)
Kamar, Nassim, S380 (FRI-463), S381 (FRI-464)
Kamath, Binita M., S831 (THU-258-YI), S842 (THU-284), S850 (THU-308)
Kamath, Patrick S., S24 (OS-028), S113 (FRI-052), S116 (FRI-061), S126 (FRI-093), S144 (SAT-452), S154 (SAT-490), S160 (SAT-507), S186 (TOP-469-YI), S197 (WED-447), S754 (THU-509)
Kamel, Ahmed, S537 (THU-141-YI), S538 (THU-142), S575 (WED-077), S576 (WED-078), S865 (FRI-638)
Kaminski, Tom, S580 (WED-092-YI)
Kamiri-Ngugi, Rachael, S704 (THU-540), S713 (WED-556-YI)
Kamlin, C. Omar, S84 (LBP-038), S839 (THU-272), S840 (THU-275), S846 (THU-291), S846 (THU-298)
Kammerer, Sarah, S271 (THU-313)
Kanai, Takanori, S371 (WED-349), S861 (WED-313)
Kanal, Uma, S552 (THU-195)
Kan, Ann, S190 (WED-421)
Kandasamy, Abisheak, S782 (SAT-010-YI)
Kandasamy, Pachamuthu, S702 (FRI-206)
Kanda, Shuhei, S420 (THU-529-YI)
Kandpal, Manoj, S891 (THU-624-YI)
Kaneda, Yuya, S420 (THU-529-YI)
Kaneko, Shun, S506 (FRI-256)
Kang, Baeki, S653 (SAT-167)
Kang, Beodeul, S426 (THU-219-YI)
Kang, Bo-Kyeong, S545 (THU-171), S591 (WED-122), S625 (WED-229), S630 (SAT-092), S652 (SAT-165), S686 (FRI-163)
Kang, Danbee, S927 (SAT-625)
Kang, Grace, S26 (OS-031)
Kang, Hae Yeon, S538 (THU-147)
Kang, Haiyan, S225 (WED-537)
Kang, Hyo Jeong, S251 (SAT-528)
Kang, Hyunsoon, S879 (THU-587)
Kang, Jennifer B, S563 (WED-042), S597 (WED-141)
Kangrga, Katarina, S597 (WED-147)
Kang, Wen, S259 (SAT-554), S609 (WED-182), S763 (THU-011), S924 (SAT-620)
Kang, Yeo Wool, S497 (FRI-233)
Kani, Haluk, S311 (SAT-272-YI)
Kann, Anna Emilie, S116 (FRI-060)
Kansra, Sanjay, S139 (FRI-134)
Kanto, Tatsuya, S32 (OS-045), S121 (FRI-076-YI), S488 (WED-403), S808 (FRI-028), S880 (THU-590)
Kanwar, Aditya, S164 (FRI-385-YI)
Kanzaki, Hiroaki, S463 (WED-250)
Kao, Jia-Horng, S46 (OS-070-YI), S449 (THU-399), S898 (TOP-566-YI), S898 (TOP-567), S917 (SAT-601-YI), S969 (WED-613)
Kao, Shih Hsun, S395 (FRI-510)
Kaouache, Mohammed, S523 (THU-100)
Kao, Wei-Yu, S969 (WED-613)
Kapitova, Raisa, S595 (WED-136)
Kaplan, David, S76 (LBP-021), S166 (FRI-393), S189 (WED-420)
Kapoor, Dharmesh, S27 (OS-033)
Kapoor, Himanshi, S687 (FRI-165)
Kappus, Matthew Robert, S58 (OS-089), S116 (FRI-061), S190 (WED-421), S313 (SAT-282)
Kaps, Leonard, S18 (OS-015), S185 (TOP-456-YI), S204 (WED-465), S482 (WED-385-YI)
Kaptein, Suzanne J.F., S881 (THU-592-YI)
Karadağ, Demet Yılmaz, S465 (WED-257)
Karademir, Sedat, S899 (SAT-556-YI)
Karagiannakis, Dimitrios, S545 (THU-172), S923 (SAT-618)
Karamanolis, Nikolaos-Nektarios, S142 (SAT-449), S187 (WED-415)
Karam, Vincent, S356 (SAT-443), S417 (FRI-581)
Karasuyama, Takuma, S421 (THU-531)
Karasu, Zeki, S24 (OS-028), S144 (SAT-452), S389 (FRI-491), S542 (THU-163)
Karavasili, Eleusa, S240 (FRI-337-YI)
Karbannek, Henrik, S54 (OS-084), S215 (WED-506)
Kardashian, Ani, S190 (WED-421)
Karemani, Marsela, S18 (OS-014-YI)
Karim, Fazal, S67 (OS-105-YI), S952 (FRI-622)
Karimi, Mahssa, S682 (FRI-148), S690 (FRI-172)
Karim, Mohammad Ehsanul, S967 (TOP-600-YI)
Karkhanis, Salil, S397 (FRI-515)
Karki, Chitra, S398 (FRI-516), S834 (THU-262), S836 (THU-266)
Kärkkäinen, Olli, S266 (SAT-346)
Karlas, Thomas, S568 (WED-057-YI)
Karlen, Vanessa, S322 (SAT-313)
Karlsen, Tom Hemming, S2 (GS-002), S13 (OS-006-YI), S290 (FRI-289), S299 (SAT-249), S303 (SAT-257-YI), S345 (SAT-410), S395 (FRI-509), S451 (THU-409)
Karmegam, Sibithooran, S597 (WED-142-YI)
Karnam, Ravikiran Sindhuvalada, S547 (THU-179)
Karnsakul, Wikrom, S55 (OS-086), S831 (THU-258-YI), S842 (THU-284), S850 (THU-308)
Kar, Premashis, S24 (OS-027), S246 (TOP-550), S822 (WED-025-YI), S925 (SAT-621)
Karsdal, Morten, S13 (OS-006-YI), S111 (FRI-044), S114 (FRI-057), S119 (FRI-073), S172 (FRI-411), S245 (FRI-354), S345 (SAT-410), S470 (WED-269), S550 (THU-187), S578 (WED-087), S584 (WED-104), S586 (WED-109), S592 (WED-131), S623 (WED-219)
Kar, Sujoy, S584 (WED-103)
Karuppasamy, Saravanaraj, S27 (OS-033)
Kasaeian, Amir, S697 (FRI-195-YI)
Kasahara, Mureo, S850 (THU-308)
Kasas, Leda, S818 (WED-013)
Kaschube, Benjamin, S252 (SAT-529)
Kaseb, Ahmed, S491 (TOP-408-YI)
Käs, Josef, S647 (SAT-148)
Kasmi, Sophie, S72 (LBP-011)
Kassas, Mohamed El, S144 (SAT-452), S377 (FRI-451), S452 (THU-414-YI), S766 (THU-015)
Kassim, Hidayat, S776 (THU-044)
Kassim, Hidayat Ullah, S88 (SAT-056)
Kassiotis, George, S280 (THU-338-YI)
Kassmeyer, Blake, S113 (FRI-052), S126 (FRI-093)
Kastner, Peter, S410 (FRI-559)
Kasuga, Ryosuke, S371 (WED-349), S861 (WED-313)
Katchman, Helena, S24 (OS-028), S144 (SAT-452), S776 (THU-045)
Katetemere, Joseph, S821 (WED-023)

Author Index

Kather, Jakob Nikolas, S331 (SAT-368-YI), S446 (THU-393-YI), S447 (THU-395), S507 (FRI-362)
Katja, Füssel, S236 (FRI-323)
Katoch, Swati, S653 (SAT-166)
Katrin, Panzitt, S672 (SAT-229-YI)
Katsounas, Antonios, S395 (FRI-511-YI)
Kattan, Ahmad, S311 (SAT-271)
Kattoju, Sudhakar, S584 (WED-103)
Katyal, Anju, S104 (THU-071-YI), S138 (FRI-132), S265 (SAT-341)
Katz, Courtney, S463 (WED-250)
Katzenstein, Cecilia, S40 (OS-059-YI), S538 (THU-148-YI), S552 (THU-196), S590 (WED-120), S776 (THU-046)
Kauffman, Eric, S730 (THU-442), S866 (FRI-640)
Kaur, Amanpreet, S642 (SAT-132)
Kaur, Impreet, S361 (THU-355-YI)
Kaur, Jagdeep, S246 (TOP-550)
Kaur, Navpreet, S386 (FRI-482)
Kaur, Parminder, S5 (GS-009), S171 (FRI-409-YI), S227 (WED-541-YI), S366 (WED-334)
Kaur, Savneet, S171 (FRI-404), S182 (FRI-441-YI), S184 (FRI-452-YI), S274 (THU-318), S282 (FRI-262-YI), S361 (THU-355-YI), S629 (TOP-161-YI)
Kauschke, Stefan Günther, S362 (TOP-325-YI)
Kaushal, Kanica, S126 (FRI-092-YI)
Kav, Taylan, S203 (WED-464), S496 (FRI-231)
Kawada, Norifumi, S12 (OS-003)
Kawagishi, Naoki, S506 (FRI-256)
Kawaguchi, Atsushi, S686 (FRI-159)
Kawaguchi, Takumi, S62 (OS-097), S509 (FRI-365), S516 (TOP-113), S557 (THU-213), S573 (WED-072), S613 (WED-190), S698 (FRI-197), S766 (THU-015)
Kawamoto, Tomomi, S702 (FRI-206)
Kawanaka, Miwa, S686 (FRI-159)
Kawashima, Akira, S811 (FRI-037)
Kawas, Leen, S49 (OS-075), S962 (WED-594)
Kawata, Kazuhito, S686 (FRI-159)
Kaya, Eda, S395 (FRI-511-YI)
Kayali, Zeid, S694 (FRI-183)
Kayalı, Sait, S829 (THU-251)
Kayani, Kayani, S363 (WED-321-YI)
Kayhan, Meral Akdogan, S7 (LBO-001), S723 (THU-418), S899 (SAT-556-YI)
Kaymakoğlu, Sabahattin, S829 (THU-251), S961 (WED-589)
Kaysin, Furkan, S880 (THU-591)
Kazankov, Konstantin, S198 (WED-448-YI)
Kaze, Edeline, S55 (OS-085-YI), S839 (THU-273)
Kearns, Daniel, S369 (WED-340-YI)
Keating, Shelley, S713 (WED-557)
Keaveny, Alison, S844 (THU-285)
Kebabian, Clara, S10 (LBO-006)
Kechagias, Stergios, S220 (WED-517), S290 (FRI-289), S568 (WED-056), S584 (WED-104)
Keegan, Meadhbh, S769 (THU-024-YI), S769 (THU-025)
Keeshan, Alexa, S908 (SAT-576)
Kefalakes, Helenie, S737 (THU-462), S878 (THU-585-YI), S913 (SAT-589-YI), S935 (TOP-583)
Kehar, Mohit, S713 (WED-557)
Keijzer, Nadia, S647 (SAT-149)
Keimburg, Simone Anna, S206 (WED-475)
Keitel, Annika, S550 (THU-187)
Keitel-Anselmino, Verena, S10 (LBO-006), S330 (SAT-365), S834 (THU-260)
Keith, Brysen, S315 (SAT-286)
Keklikkiran, Caglayan, S311 (SAT-272-YI), S766 (THU-015)
Ke, Kunyu, S609 (WED-182)
Keller, Andreas, S482 (WED-385-YI)
Keller, Keely, S11 (OS-001-YI)
Keller, Marisa Isabell, S114 (FRI-057), S148 (SAT-467-YI), S261 (SAT-329-YI)
Kelly, Claire, S386 (FRI-481-YI), S404 (FRI-538-YI)
Kelly, Deirdre A., S850 (THU-308)
Kelsch, Lara, S550 (THU-187)
Kemeç, Gamze, S829 (THU-251)
Kemos, Chronis, S689 (FRI-169)
Kemper, Angieszka, S823 (WED-028)
Kempf, Emmanuelle, S38 (OS-054)
Kemp, Susan, S759 (TOP-017-YI)
Kemp, William, S433 (THU-240), S571 (WED-069), S922 (SAT-613)
Kendall, Tim, S284 (FRI-268-YI), S673 (SAT-231), S698 (FRI-197)
Kendall, Timothy, S12 (OS-004-YI)
Kender, Zoltan, S21 (OS-020)
Kendrick, Stuart, S26 (OS-031), S78 (LBP-025)
Kenia, Marcus, S708 (THU-554-YI)
Kenna, Gerry, S106 (THU-075)
Kennedy, Patrick, S7 (GS-012), S49 (OS-076-YI), S370 (WED-347), S799 (FRI-003), S876 (THU-575), S888 (THU-618), S897 (TOP-565), S921 (SAT-611), S958 (WED-581)
Kenny, Sarah, S396 (FRI-512)
Keown, Paul, S398 (FRI-516)
Keranmu, Guliziran, S243 (FRI-348)
Kerbert, Annarein, S148 (SAT-467-YI), S180 (FRI-434), S187 (TOP-471-YI), S729 (THU-436)
Keren, Karin, S680 (FRI-141)
Kerkar, Nanda, S55 (OS-086), S831 (THU-258-YI), S842 (THU-284), S850 (THU-308)
Kerkhof, Ilona, S15 (OS-009-YI)
Kern, Anna Emilia, S71 (LBP-008)
Kerr, Claire, S113 (FRI-054)
Kerr, Jane, S79 (LBP-027)
Kerr, Thomas, S40 (OS-058)
Kesarwani, Anil, S47 (OS-072)
Keshvari, Sahar, S170 (FRI-403), S420 (THU-526)
Keskin, Onur, S203 (WED-464), S496 (FRI-231), S965 (WED-603)
Kessler, Aline, S919 (SAT-607)
Kessler, Harald, S979 (TOP-614)
Ketenoğlu, Buse, S396 (FRI-513), S397 (FRI-514)
Ketting, Vera, S444 (THU-383)
Kew, Chun, S262 (SAT-330)
Kew, Guan Sen, S14 (OS-008), S320 (SAT-302), S354 (SAT-435), S355 (SAT-436)
Khac, Eric Nguyen, S38 (OS-055), S742 (THU-477)
Khaderi, Saira, S923 (SAT-618)
Khakayla, Abed, S60 (OS-093), S289 (FRI-286)
Khalili, Korosh, S436 (THU-249)
Khalili, Mandana, S116 (FRI-061), S190 (WED-421), S197 (WED-447), S534 (THU-132)
Khalili, Mohammad Al, S209 (WED-483)
Khalil, Mazhar, S399 (FRI-522)
Khammanivong, Ali, S435 (THU-246)
Khammetova, Ainura, S909 (SAT-580)
Khan, Aarim, S873 (THU-563)
Khanam, Arshi, S880 (THU-591)
Khan, Faisal, S54 (OS-084), S397 (FRI-515), S747 (THU-492), S752 (THU-501)
Khan, Khan Shahrukh, S138 (FRI-132)
Khan, Mohommad Qasim, S379 (FRI-461-YI), S398 (FRI-516)
Khanom, Mehrunnissa, S598 (WED-149)
Khan, Rakhshanda, S845 (THU-288)
Khan, Shahid, S451 (THU-410)
Khanyi, Bongani, S76 (LBP-019-YI)
Kharrasse, Ghizlane, S309 (SAT-267), S578 (WED-086)
Kharrazi, Abdelali El, S829 (THU-252)
Khatri, Pawan, S741 (THU-474)
Khattab, Osama, S497 (FRI-234), S723 (THU-418)
Khatua, Chitta Ranjan, S204 (WED-466)
Khaykin, Pavel, S904 (SAT-564), S945 (FRI-602-YI)
Khaznadar, Farah, S617 (WED-202)
Khaznadar, Omar, S617 (WED-202)
Khemichian, Saro, S308 (SAT-265), S309 (SAT-266)
Khemissa, Faiza, S414 (FRI-573)
Kheong, Chan Wah, S558 (TOP-063-YI), S589 (WED-118), S607 (WED-174-YI), S612 (WED-187-YI), S618 (WED-204), S621 (WED-215)
Khidir, Nasreen, S732 (THU-446)
Khidirova, Hijran, S539 (THU-149)
Khikmatullaeva, Aziza, S74 (LBP-016)
Khillan, Vikas, S108 (TOP-208-YI), S189 (WED-419)
Khodayari, Nazli, S855 (WED-287-YI)
Khodjaeva, Malika, S74 (LBP-016)
Khoja, Basma, S516 (TOP-113), S521 (THU-092), S521 (THU-093),

S522 (THU-095), S523 (THU-099), S566 (WED-052), S794 (SAT-046)
Khoja, Basmah, S522 (THU-094)
Khoruts, Alexander, S130 (FRI-103)
Khoza, Thandeka, S900 (SAT-558)
Khuchua, Tamar, S76 (LBP-021)
Khurana, Sumeeta, S180 (FRI-433)
Kiczynska, Patrycja, S134 (FRI-117)
Kidd, Timothy, S170 (FRI-403)
Kiehn, Oliver, S736 (THU-459)
Kihel, Rihab El, S309 (SAT-267)
Kilambi, Ragini, S288 (FRI-282), S292 (FRI-299)
Kilany, Mai, S928 (SAT-628-YI)
Killer, Alexander, S188 (WED-416), S904 (SAT-564)
Kilpatrick, Alastair M., S134 (FRI-117), S137 (FRI-125)
Kim, Arthur, S922 (SAT-612)
Kim, Beom Kyung, S442 (THU-379), S498 (FRI-235), S509 (FRI-365), S916 (SAT-597), S946 (FRI-604)
Kim, Bo Hyun, S500 (FRI-241), S509 (FRI-366)
Kim, Chan, S426 (THU-219-YI)
Kim, Chong, S299 (SAT-247), S320 (SAT-303), S320 (SAT-304), S946 (FRI-605)
Kim, Christopher, S762 (THU-008)
Kim, Deok-Gie, S260 (SAT-555)
Kim, Donghee, S530 (THU-119-YI)
Kim, Dong Joon, S67 (OS-105-YI), S267 (SAT-349)
Kim, Dong Wook, S4 (GS-007)
Kim, Dong Yun, S498 (FRI-235), S916 (SAT-597)
Kim, Do Young, S498 (FRI-235), S916 (SAT-597)
Kim, Edward, S60 (OS-094)
Kimer, Nina, S205 (WED-468), S736 (THU-459)
Kim, Eunju, S421 (THU-530)
Kim, Gi-Ae, S546 (THU-174), S546 (THU-175)
Kim, Ha Il, S545 (THU-171), S591 (WED-122), S625 (WED-229), S630 (SAT-092), S652 (SAT-165), S686 (FRI-163)
Kim, Hee Ju, S360 (THU-351)
Kim, Hye-Lin, S545 (THU-171), S591 (WED-122), S625 (WED-229), S630 (SAT-092), S652 (SAT-165), S686 (FRI-163), S706 (THU-543)
Kim, Hye Seon, S881 (THU-594)
Kim, Hyung Heon, S72 (LBP-010)
Kim, Hyung Joon, S518 (TOP-129)
Kim, Hyunseok, S492 (FRI-218)
Kim, In Hee, S823 (WED-030)
Kimiskidis, Nikitas, S348 (SAT-416)
Kim, Jaekeun, S399 (FRI-522)
Kim, Ji Hoon, S135 (FRI-120), S498 (FRI-236)
Kim, Jin-Wook, S906 (SAT-573)
Kim, Jisup, S653 (SAT-167)
Kim, Jung Hee, S92 (SAT-069), S553 (THU-198), S687 (FRI-164), S927 (SAT-625)
Kim, Jung Sun, S426 (THU-219-YI)
Kim, Kang Mo, S4 (GS-006), S707 (THU-547)
Kim, Kyung-Ah, S706 (THU-543)
Kim, Kyung Mo, S55 (OS-086), S831 (THU-258-YI), S842 (THU-284)
Kim, Kyurae, S136 (FRI-121), S229 (TOP-342-YI), S368 (WED-337-YI)
Kim, Leesun, S964 (WED-597)
Kimmann, Markus, S6 (GS-011-YI), S33 (OS-046), S54 (OS-084), S736 (THU-460-YI), S737 (THU-461), S744 (THU-481), S744 (THU-482-YI), S747 (THU-492)
Kim, Matthew, S918 (SAT-604)
Kim, MeeJ, S26 (OS-031), S689 (FRI-169)
Kim, Mi-Kyung, S72 (LBP-010)
Kim, Mimi, S545 (THU-171), S591 (WED-122), S625 (WED-229), S630 (SAT-092), S652 (SAT-165), S686 (FRI-163)
Kim, Mi Na, S498 (FRI-235), S916 (SAT-597)
Kim, Min gu, S132 (FRI-107), S891 (THU-625)
Kim, Min Ju, S448 (THU-397)
Kim, Moon Young, S133 (FRI-111), S360 (THU-352), S732 (THU-447)
Kim, Nomita, S78 (LBP-025), S689 (FRI-169)
Ki, Moran, S823 (WED-030)
Kim, Sang Gyune, S732 (THU-447)
Kim, Sang Kyum, S368 (WED-337-YI)
Kim, Seok-Hwan, S927 (SAT-626)
Kim, Seung-Seob, S260 (SAT-555)
Kim, Seung Up, S19 (OS-017), S62 (OS-097), S260 (SAT-555), S424 (TOP-376), S498 (FRI-235), S516 (TOP-113), S517 (TOP-114), S518 (TOP-129), S525 (THU-103), S539 (THU-150), S558 (TOP-063-YI), S589 (WED-118), S607 (WED-174-YI), S612 (WED-187-YI), S618 (WED-204), S621 (WED-215), S906 (SAT-574), S916 (SAT-597), S946 (FRI-604)
Kim, Soon Sun, S264 (SAT-337), S590 (WED-121)
Kim, So Yeon, S4 (GS-006), S4 (GS-007)
Kim, Suho, S510 (FRI-368)
Kim, Sung-Jin, S72 (LBP-010)
Kim, Tae Hun, S906 (SAT-574)
Kim, Tae Hyung, S448 (THU-397)
Kimura, Kiminori, S499 (FRI-237)
Kimura, Masamichi, S499 (FRI-237)
Kimura, Moto, S875 (THU-573)
Kimura, Naruhiro, S284 (FRI-268-YI)
Kimura, Takefumi, S555 (THU-205), S591 (WED-123), S618 (WED-205)
Kimura, Yukari, S43 (OS-065)
Kim, Won, S546 (THU-174)
Kim, W. Ray, S204 (WED-467), S596 (WED-139), S603 (WED-165-YI), S604 (WED-166)
Kim, Ye Rim, S513 (FRI-378)
Kim, Yestle, S601 (WED-155), S680 (FRI-141), S682 (FRI-149), S695 (FRI-186)
Kim, Yoon Jun, S502 (FRI-245), S507 (FRI-361), S509 (FRI-366)
Kim, Yun Jung, S709 (THU-556-YI)
Kim, Yun-Tae, S906 (SAT-573)
Kim, Yu Sung, S160 (SAT-507)
Kinast, Volker, S890 (THU-623-YI)
King, Andrew, S406 (FRI-544)
King, Jade, S325 (SAT-320)
King, James, S167 (FRI-394-YI)
King, Ji Jade, S758 (TOP-016)
Kinjo, Kie, S439 (THU-368)
Kinnaer, Lise-Marie, S22 (OS-023)
Kionisala, Marie, S503 (FRI-250)
Kipkoech, Kennedy, S804 (FRI-015-YI)
Kirchner, Henriette, S672 (SAT-230)
Kiremitçi, Saba, S652 (SAT-163)
Kirk, Frederik Teicher, S290 (FRI-287)
Kirkland, James, S9 (LBO-005-YI)
Kirsch, Katrin, S199 (WED-451-YI)
Kirstein, Martha M, S504 (FRI-251)
Kirubendran, Kavitha, S242 (FRI-345-YI), S472 (WED-274)
Kishore, Harsh, S27 (OS-033)
Kisseleff, Elena, S581 (WED-095)
Kitagataya, Takashi, S506 (FRI-256)
Kitchen, Sophie, S40 (OS-058)
Kiudeliene, Edita, S41 (OS-061)
Kiu, Raymond, S286 (FRI-271)
Kivuyo, Sokoine, S792 (SAT-042)
Kiyici, Murat, S7 (LBO-001)
Kjaer, Andreas, S602 (WED-159-YI)
Kjaer, Mette, S693 (FRI-182)
Kjeldsen, Anette, S838 (THU-269)
Kjeldsen, Jens, S838 (THU-269)
Klarenbeek, Gijs, S754 (THU-509)
Klause, Tanja, S864 (TOP-615)
Klaus, JensDr., S689 (FRI-170)
Kleij, Emma, S443 (THU-382-YI)
Klein, Eduardo, S776 (THU-044)
Kleiner, David E, S53 (OS-083-YI), S722 (THU-417), S835 (THU-264-YI), S918 (SAT-604)
Klein, Eric, S391 (FRI-496)
Klein, Kari, S708 (THU-554-YI)
Klein, Marina B., S529 (THU-116-YI), S865 (FRI-638)
Klein, Sabine, S145 (SAT-458-YI), S148 (SAT-467-YI), S163 (FRI-383), S178 (FRI-428-YI), S206 (WED-475), S237 (FRI-329), S262 (SAT-330), S493 (FRI-220), S631 (SAT-093-YI)
Klein, Thomas, S85 (LBP-039), S131 (FRI-106), S634 (SAT-105)
Klemt-Kropp, Michael, S351 (SAT-426-YI), S352 (SAT-429), S353 (SAT-432), S353 (SAT-433), S729 (THU-436)
Klenerman, Paul, S43 (OS-065)
Kleter, Bernhard, S943 (FRI-595)
Kletz, Elisabeth, S410 (FRI-559)
Klimanek, Matthias, S737 (THU-462)

Author Index

Klinker, Hartwig, S971 (WED-620)
Klippel, Claire, S856 (WED-290)
Kloeckner, Roman, S503 (FRI-248), S504 (FRI-251), S736 (THU-460-YI)
Kloft-Nelson, Sara, S186 (TOP-469-YI)
Klöhn, Mara, S881 (THU-592-YI)
Klomp, Sylvia, S237 (FRI-330)
Kloosterhuis, Niels, S630 (SAT-090), S670 (SAT-221-YI)
Klotz, Anton, S37 (OS-053), S426 (THU-219-YI)
Kluge, Martin, S77 (LBP-022-YI), S623 (WED-220)
Kluger, Yuval, S102 (THU-062)
Klumpen, Heinz-Josef, S445 (THU-385)
klümpen, heinz-josef, S490 (TOP-407-YI)
Kluttig, Alexander, S175 (FRI-419)
Kluwe, Johannes, S213 (WED-496), S736 (THU-460-YI)
Knebel, Birgit, S21 (OS-020)
Knegendorf, Leonard, S887 (THU-613)
Kneteman, Norman, S401 (FRI-527)
Kniepeiss, Daniela, S410 (FRI-559)
Kniepeiss, Moritz, S410 (FRI-559)
Knolle, Percy A., S291 (FRI-291-YI)
Knowles, Brett, S922 (SAT-613)
Knox, Jennifer, S345 (SAT-409-YI), S425 (THU-216-YI)
Knox, Steven J, S958 (WED-579)
Knutova, Dana, S205 (WED-473)
Koball, Sebastian, S93 (SAT-070)
Koball, Stine, S93 (SAT-070)
Kobayashi, Takashi, S62 (OS-097), S516 (TOP-113), S686 (FRI-159)
Kobe, Adrian, S465 (WED-255)
Köcher, Thomas, S37 (OS-053)
Kockerling, David, S224 (WED-530)
Koç, Özge, S519 (THU-089)
Koc, Ozgur, S331 (SAT-368-YI), S333 (SAT-369), S720 (TOP-504-YI), S849 (THU-306-YI), S928 (SAT-628-YI)
Kodaira, Masaaki, S861 (WED-313)
Kodama, Takahiro, S463 (WED-251-YI), S880 (THU-590), S977 (WED-639)
Koda, Yuzo, S371 (WED-349)
Kodela, Elisavet, S366 (WED-333-YI), S458 (WED-237-YI)
Koehler, Anika, S911 (SAT-586)
Koek, Ger, S535 (THU-134), S611 (WED-185), S696 (FRI-190)
Koelsch, Stephan, S581 (WED-095)
Koenig, Alexander, S959 (WED-585)
Koerkamp, Bas Groot, S445 (THU-385)
Koffas, Apostolos, S49 (OS-076-YI), S876 (THU-575), S888 (THU-618), S921 (SAT-611)
Kofinova, Denitza, S55 (OS-086), S831 (THU-258-YI), S842 (THU-284)
Kogan, Sabrina, S130 (FRI-102-YI)
Koguru, Yashaswi, S845 (THU-288)
Koh, Christopher, S49 (OS-075), S722 (THU-417), S835 (THU-264-YI), S962 (WED-594), S965 (WED-603)
Ko, Hin Hin, S14 (OS-008), S295 (TOP-279), S325 (SAT-319), S354 (SAT-435)
Kohjima, Motoyuki, S258 (SAT-549), S550 (THU-188), S979 (WED-644)
Kohl, Alina, S879 (THU-588), S881 (THU-593)
Köhler, Michael, S493 (FRI-220), S736 (THU-460-YI), S737 (THU-461)
Kohlhepp, Marlene, S293 (FRI-301)
Kohli, Anita, S78 (LBP-025), S687 (FRI-165), S691 (FRI-175)
Kohli, Rohit, S842 (THU-284)
Köhrer, Karl, S672 (SAT-230)
Koh, Samantha, S714 (WED-559-YI)
Kohut, Taisa, S850 (THU-308)
Kohya, Risako, S506 (FRI-256)
Koike, Kazuhiko, S187 (TOP-472)
Koizumi, Yohei, S117 (FRI-062)
Ko, Jae Sung, S55 (OS-086), S831 (THU-258-YI), S842 (THU-284)
Kojima, Hidenobu, S419 (THU-525), S421 (THU-531)
Kojima, Tomohito, S249 (SAT-522), S970 (WED-618), S976 (WED-638)
Ko, Joy, S823 (WED-028)
Kokkinos, Naomi, S807 (FRI-025)
Kokkorakis, Michail, S659 (SAT-187), S694 (FRI-185)
Ko, Kyoung A, S553 (THU-198)
Koky, Tomáš, S321 (SAT-305)
Kolesova, Hana, S861 (WED-308)
Kolev, Mirjam, S300 (SAT-250), S342 (SAT-399)
Kolhatkar, Nikita, S948 (FRI-610)
Koliogiannis, Dionysios, S175 (FRI-420)
Kolland, Michael, S326 (SAT-321)
Kollar, Sarah, S465 (WED-255)
Koller, Sabine, S410 (FRI-559)
Kollert, Florian, S342 (SAT-399)
Koller, Tomáš, S205 (WED-473), S693 (FRI-182)
Kolmstetter, Magdalena, S359 (THU-345-YI)
Kolosovych, Ihor, S739 (THU-465)
Komárová, Slavomíra, S321 (SAT-305)
Koma, Takaaki, S870 (TOP-646)
Komori, Atsumasa, S249 (SAT-522), S336 (SAT-379), S506 (FRI-256), S550 (THU-188), S970 (WED-618), S976 (WED-638)
Komura, Takuya, S960 (WED-587)
Kondili, Loreta, S440 (THU-369), S820 (WED-020-YI), S923 (SAT-618), S947 (FRI-608), S972 (WED-623)
Kondo, Kyoko, S336 (SAT-379)
Kondo, Shinji, S32 (OS-045)
Kondo, Takayuki, S171 (FRI-409-YI)
Kondylis, Vangelis, S280 (THU-338-YI), S641 (SAT-125-YI)
Kong, Grace, S436 (THU-248)
Kong, Kexin, S12 (OS-004-YI)
Kong, Maiying, S532 (THU-125)
Kong, Ming, S93 (SAT-071)
Kong, Shenhong, S38 (OS-054)
Kong, Siming, S270 (TOP-328), S276 (THU-323)
Kong, Xiangsha, S931 (SAT-638)
Kong, Xiaoni, S473 (WED-361-YI)
Kong, Yuanyuan, S826 (WED-040), S909 (SAT-579)
König, Daniel, S113 (FRI-053)
Königshofer, Philipp, S750 (THU-497-YI)
Königsrainer, Alfred, S512 (FRI-371)
Koning, Mijra, S9 (LBO-005-YI), S632 (SAT-099-YI)
Konings, Ingrid C. A. W., S352 (SAT-429)
Konings, Laura, S577 (WED-084), S621 (WED-214), S688 (FRI-166-YI), S765 (THU-013)
Kon, Kazuyoshi, S225 (WED-533), S246 (FRI-356)
Konkwo, Chigoziri, S166 (FRI-393)
Konstantellos, Viktoras, S657 (SAT-182)
Konstantis, Georgios, S33 (OS-046), S172 (FRI-410-YI), S744 (THU-482-YI)
Kontio, Tea, S376 (FRI-447)
Kontopidou, Flora, S142 (SAT-449)
Koo, Hyewonnina, S252 (SAT-530)
Kooijman, Sander, S631 (SAT-095-YI)
Koo, Ja Hyun, S238 (FRI-331)
Koops, Renate, S79 (LBP-027)
Kootstra, Neeltje, S963 (WED-595)
Ko, Paul, S959 (WED-586)
Kopf, Stefan, S21 (OS-020)
Koppe, Sean, S388 (FRI-489)
Korelova, Katerina, S275 (THU-320)
Korenaga, Masaaki, S808 (FRI-027)
Korica, Bojan, S654 (SAT-169)
Korilis, Adrián Gil, S608 (WED-175)
Korkmaz, Kerem Sebib, S15 (OS-009-YI)
Korn, Emilia, S748 (THU-493-YI)
Korsenik, Joshua, S328 (SAT-324), S328 (SAT-361)
Korsgren, Olle, S579 (WED-090)
Kortbeek, Simone, S850 (THU-308)
Korzekwa, Benedict, S672 (SAT-230)
Kosaka, Nobuyoshi, S573 (WED-072), S613 (WED-190), S693 (FRI-181)
Ko, Seongjoon, S654 (SAT-168)
Koshy, Anoop, S36 (OS-051-YI)
Koshy, Ashily, S288 (FRI-282)
Koskinas, Ioannis, S620 (WED-212)
Kostadinova, Radina, S85 (LBP-039), S243 (FRI-349)
Koster, Mirjam, S630 (SAT-090)
Kostrub, Cory, S10 (LBO-006)
Košuta, Iva, S800 (FRI-006)
Kotowsky, Nirali, S321 (SAT-306), S322 (SAT-307), S322 (SAT-308)
Kottilil, Shyamasundaran, S873 (THU-563), S880 (THU-591)
Kouadou, Shinha-Ashkarr, S499 (FRI-238)
Koulali, Hajar, S309 (SAT-267), S578 (WED-086)
Kounis, Ilias, S374 (TOP-503), S399 (FRI-523)
Koutny, Florian, S539 (THU-151-YI)
Koutsompina, Maria Loukia, S314 (SAT-283)

Kovats, Patricia, S332 (SAT-369)
Kovynev, Artemiy, S9 (LBO-005-YI)
Kowalska, Justyna, S817 (WED-012)
Kowalzick, Viktoria, S881 (THU-592-YI)
Kowdley, Kris, S78 (LBP-025)
Kowdley, Kris V., S7 (LBO-001), S10 (LBO-006), S67 (OS-106), S82 (LBP-033), S295 (TOP-280), S319 (SAT-300), S329 (SAT-364), S691 (FRI-175), S838 (THU-270)
Ko, Yunmi, S507 (FRI-361), S509 (FRI-366)
Koziel, Margaret, S78 (LBP-025)
Kozlov, Artur, S823 (WED-029)
Kozlov, Sergii, S739 (THU-465)
Kozłowska, Kaja, S318 (SAT-298), S355 (SAT-442)
Kraft, Anke R. M., S935 (TOP-583)
Kraft, Anke R.M., S197 (WED-446), S866 (FRI-641), S878 (THU-585-YI), S963 (WED-596)
Krag, Aleksander, S26 (OS-032-YI), S63 (OS-098-YI), S76 (LBP-020), S110 (FRI-041-YI), S111 (FRI-044), S115 (FRI-057), S115 (FRI-059), S122 (FRI-079-YI), S125 (FRI-090-YI), S127 (FRI-095), S145 (SAT-458-YI), S148 (SAT-467-YI), S210 (WED-485), S217 (WED-509-YI), S246 (TOP-552), S253 (SAT-532), S262 (SAT-332), S515 (TOP-098), S532 (THU-125), S554 (THU-204), S569 (WED-059), S579 (WED-089), S583 (WED-101), S592 (WED-131), S594 (WED-134), S608 (WED-180), S616 (WED-199), S706 (THU-545-YI), S789 (SAT-031-YI), S836 (THU-265-YI)
Krag, Carlos Valdivia, S837 (THU-267), S855 (WED-289)
Krajden, Mel, S967 (TOP-600-YI)
Kralik, Kristina, S617 (WED-202)
Kramer, David J., S8 (LBO-002)
Kramer, Georg, S113 (FRI-053), S156 (SAT-494), S179 (FRI-432), S183 (FRI-444-YI), S183 (FRI-445), S186 (TOP-470-YI), S199 (WED-452), S200 (WED-453), S205 (WED-474), S213 (WED-498), S216 (WED-508), S252 (SAT-530), S440 (THU-370), S717 (WED-569-YI), S734 (THU-451), S738 (THU-464-YI), S739 (THU-467), S748 (THU-493-YI), S749 (THU-494), S750 (THU-498), S914 (SAT-591)
Kramer, Jan, S600 (WED-154-YI)
Kramer, Matthijs, S15 (OS-009-YI), S333 (SAT-369), S352 (SAT-429), S353 (SAT-432), S353 (SAT-433)
Kranidioti, Hariklia, S620 (WED-212)
Krarup, Henrik, S801 (FRI-008)
Kratzer, Alexander, S157 (SAT-497)
Krause, Christin, S672 (SAT-230)
Krause, Jenny, S291 (FRI-291-YI)
Kraus, Nico, S262 (SAT-330)
Krauss, Stefan, S287 (FRI-276-YI), S292 (FRI-300-YI), S858 (WED-300-YI)
Kravchuk, Stanislav, S777 (THU-047)
Krawczyk, Marcin, S265 (SAT-338), S323 (SAT-314), S532 (THU-124), S763 (THU-010), S854 (WED-284), S858 (WED-301), S862 (WED-316-YI)
Kreeft - Voermans, Jolanda, S817 (WED-011)
Kreeft-Voermans, Jolanda, S909 (SAT-580)
Kremer, Andreas E., S14 (OS-007), S75 (LBP-018), S295 (TOP-280), S310 (SAT-269), S322 (SAT-313), S325 (SAT-320), S339 (SAT-387), S465 (WED-255), S838 (THU-270)
Kremser, Paulina, S840 (THU-274), S842 (THU-283)
Kretzmann, Jessica, S653 (SAT-166)
Kreuter, Abelina, S37 (OS-053), S426 (THU-219-YI), S715 (WED-560-YI)
Kreutzer, Mattis, S213 (WED-496)
Krey, Thomas, S866 (FRI-641)
Kriebardis, Anastasios, S620 (WED-212)
Krishnamoorthy, Thinesh, S529 (THU-115)
Krishnamurthy, Rochan Athreya, S564 (WED-044), S565 (WED-045)
Krishnan, Arunkumar, S678 (TOP-162)
Krishnaswami, Jayshree, S10 (LBO-006)
Kronborg, Thit Mynster, S205 (WED-468)
Kronenberg, Florian, S257 (SAT-545-YI)
Kronfli, Nadine, S529 (THU-116-YI), S865 (FRI-638)
Krüger, Marcus, S280 (THU-338-YI)
Kruk, Beata, S301 (SAT-251-YI), S303 (SAT-257-YI), S318 (SAT-298), S323 (SAT-314), S355 (SAT-442)
Krupa, Łukasz, S265 (SAT-338)
Kruse, Jan, S161 (SAT-510-YI)
Kruse, Louise Humle, S655 (SAT-173)
Krus, Frederike, S206 (WED-475)
Krutáková, Mária, S286 (FRI-272)
Krystallaki, Dimitra, S142 (SAT-449), S187 (WED-415)
Krzeski, Piotr, S540 (THU-154)
Kuan-Hui, Hsin, S898 (TOP-566-YI)
Kuboth, Jennifer, S672 (SAT-230)
Kubovciak, Jan, S459 (WED-241)
Küçükerbil, Efrayim, S383 (FRI-473), S391 (FRI-498), S398 (FRI-517-YI)
Kuczynski, Magdalena, S606 (WED-171)
Kudo, Hiromi, S137 (FRI-125)
Kugelmas, Marcelo, S20 (OS-019), S559 (TOP-064), S565 (WED-051)
Kugiyama, Naotaka, S134 (FRI-115)
Kugiyama, Yuki, S249 (SAT-522), S506 (FRI-256), S970 (WED-618), S976 (WED-638)
Kühn, Julia, S175 (FRI-419)
Kuhn, Michael, S114 (FRI-057), S145 (SAT-458-YI), S148 (SAT-467-YI), S261 (SAT-329-YI)
Kuiper, Edith M. M., S352 (SAT-429)
Kuipers, Folkert, S857 (WED-299), S863 (WED-318)
Kuipers-Skarsfeldt, Mark, S245 (FRI-354)
Kuiper, Teaco, S9 (LBO-005-YI)
Kuivenhoven, Jan Albert, S670 (SAT-221-YI)
Kujundžić, Petra Dinjar, S255 (SAT-541)
Kukic, Sandro, S583 (WED-101)
Kulai, Tasha, S14 (OS-008), S354 (SAT-435), S598 (WED-148)
Kulik, Laura, S375 (TOP-519), S388 (FRI-489)
Kuljacha, Alma, S296 (TOP-281), S306 (SAT-262)
Kulkarni, Anand, S24 (OS-028), S67 (OS-105-YI), S144 (SAT-452), S156 (SAT-496), S160 (SAT-507), S215 (WED-505), S221 (WED-523), S228 (WED-543), S255 (SAT-541), S423 (TOP-374), S452 (THU-414-YI), S509 (FRI-365), S528 (THU-110), S923 (SAT-618), S952 (FRI-622)
Kulkarni, Subhash, S137 (FRI-126)
Kullig, Ulrike, S945 (FRI-602-YI)
Kumar, Ajay, S31 (OS-043-YI), S212 (WED-495-YI), S217 (WED-510), S952 (FRI-622)
Kumar, Amit, S911 (SAT-586)
Kumar, Anupam, S100 (THU-057-YI), S174 (FRI-415-YI), S182 (FRI-441-YI), S184 (FRI-452-YI)
Kumar, Arushi, S117 (FRI-067)
Kumar, Ashish, S24 (OS-028), S952 (FRI-622)
Kumar, Daanyaal, S411 (FRI-561-YI), S413 (FRI-570)
Kumar, Guresh, S156 (SAT-495), S867 (FRI-643)
Kumari, Anupama, S129 (TOP-224-YI), S174 (FRI-415-YI), S269 (SAT-355), S361 (THU-354), S629 (TOP-161-YI), S650 (SAT-157-YI)
Kumari, Mamta, S181 (FRI-441-YI)
Kumar, Jata Shankar, S24 (OS-027)
Kumar, Karaddi Venkatanarasimha Nanda, S495 (FRI-228-YI)
Kumar, Kshitij, S398 (FRI-521)
Kumar, Manoj, S141 (TOP-424-YI), S156 (SAT-495), S214 (WED-501-YI)
Kumar, Narender, S81 (LBP-030)
Kumar, Pavitra, S268 (SAT-352-YI), S285 (FRI-269)
Kumar, Prahlad, S684 (FRI-155)
Kumar, Rahul, S149 (SAT-473), S156 (SAT-496), S158 (SAT-499), S215 (WED-505), S221 (WED-523), S228 (WED-543), S423 (TOP-374), S528 (THU-110), S529 (THU-115)
Kumar, Ravi, S174 (FRI-416-YI)
Kumar, Sandeep, S100 (THU-057-YI), S174 (FRI-415-YI)
Kumar, Santhosh, S36 (OS-051-YI), S722 (THU-416)
Kumar Sarin, Shiv, S120 (FRI-074), S126 (FRI-092-YI), S361 (THU-355-YI), S650 (SAT-157-YI)
Kumar, Sonu, S184 (TOP-454-YI), S847 (THU-299)
Kumar, Suchitra, S919 (SAT-607)

Author Index

Kumar, Yaswant, S221 (WED-522)
Kummetha, Lalit, S217 (WED-510)
Kung, Janice, S349 (SAT-419)
Kunlayawutipong, Thanaput, S219 (WED-514)
Kunst, Claudia, S785 (SAT-019)
Kunstein, Anselm, S188 (WED-416)
Kunze, Georg, S447 (THU-395)
Künzler-Heule, Patrizia, S165 (FRI-386), S710 (TOP-536-YI), S714 (WED-558)
Kuo, Fang Cheng, S395 (FRI-510)
Kuo, Hsuan Chia, S917 (SAT-601-YI)
Kuo, Jong-Yih, S446 (THU-387)
Kuo, Yong-Fang, S375 (TOP-518), S407 (FRI-546)
Kupcinskas, Juozas, S41 (OS-061), S823 (WED-029)
Kupčinskas, Juozas, S777 (THU-050)
Kupcinskas, Limas, S823 (WED-029)
Kupčinskas, Limas, S337 (SAT-382)
Küpper, Jan-Heiner, S271 (THU-313)
Kuramoto, Junko, S861 (WED-313)
Kurata, Yoshihiko, S420 (THU-529-YI)
Kurihashi, Takeo, S686 (FRI-159)
Kuriry, Hadi, S250 (SAT-523), S390 (FRI-495)
Kuroda, Hidekatsu, S194 (WED-435), S510 (FRI-367), S977 (WED-639)
Kurosaki, Masayuki, S439 (THU-368), S506 (FRI-256), S555 (THU-205), S618 (WED-205)
Kurowski, Konrad, S363 (TOP-326)
Kurt, Ada Sera, S174 (FRI-416-YI), S366 (WED-333-YI)
Kurth, Florian, S77 (LBP-022-YI)
Kushner, Tatyana, S40 (OS-059-YI), S70 (LBP-005), S76 (LBP-021), S538 (THU-148-YI), S552 (THU-196), S776 (THU-046), S923 (SAT-618), S975 (WED-636), S976 (WED-637)
Kushnir, Inna, S604 (WED-167)
Kustra, Robert, S302 (SAT-254), S316 (SAT-287)
Kutch, Kelly, S78 (LBP-025)
Kutter, Claudia, S71 (LBP-008)
Kuyvenhoven, Johan P. H., S351 (SAT-426-YI)
Kuzinska, Matylda Zofia, S852 (TOP-311), S858 (WED-302)
Kveton, Martin, S459 (WED-241)
Kwait, Brittany, S337 (SAT-381)
Kwanten, Wilhelmus, S682 (FRI-150-YI), S733 (THU-450)
Kwanten, Wilhelmus J, S581 (WED-093-YI), S581 (WED-094), S638 (SAT-117-YI), S729 (THU-441), S840 (THU-274), S842 (THU-283)
Kwentoh, Ifeoma, S918 (SAT-604)
Kwon, Choon Hyuck David, S399 (FRI-522)
Kwon, Goo Hyun, S267 (SAT-349)
Kwon, Jung Hyun, S207 (WED-478), S473 (WED-275), S881 (THU-594)
Kwon, Kyung Min, S70 (LBP-005), S84 (LBP-037), S302 (SAT-254), S324 (SAT-316), S838 (THU-270)
Kyalwazi, Beverly, S432 (THU-238)
Kyed, Ea, S110 (FRI-041-YI), S115 (FRI-059), S122 (FRI-079-YI), S125 (FRI-090-YI), S554 (THU-204), S706 (THU-545-YI)
Kyeyune, Dorothy, S821 (WED-023)
Kynaston, Thomas, S772 (THU-035)
Kyritsi, Vaia, S213 (WED-497)
Kytyr, Daniel, S275 (THU-320)

Laakso, Markku, S114 (FRI-055)
Labanca, Sara, S69 (LBP-004-YI), S82 (LBP-034-YI), S307 (SAT-263), S335 (SAT-378-YI), S350 (SAT-421), S831 (THU-256-YI)
Labenz, Christian, S172 (FRI-411), S185 (TOP-456-YI), S197 (WED-446), S199 (WED-451-YI), S204 (WED-465), S215 (WED-506), S622 (WED-216), S736 (THU-460-YI), S742 (THU-476), S790 (SAT-035)
Labio, Eternity, S964 (WED-597)
Laborde, Nolwenn, S55 (OS-086), S831 (THU-258-YI), S842 (THU-284)
Labriola, Dominic, S78 (LBP-024), S596 (WED-139), S682 (FRI-149), S692 (FRI-179)
Labrune, Philippe, S17 (OS-011)
Labyed, Yassin, S576 (WED-079)
Lacaille, Florence, S850 (THU-308)
La Casta, Adelaida, S484 (WED-393)
Lăcătușu, Cristina-Mihaela, S574 (WED-074)
Lacey, Guy, S319 (SAT-301), S330 (SAT-365)
Lachaux, Alain, S836 (THU-265-YI)
Lachenmayer, Anja, S485 (WED-396)
Lachiondo-Ortega, Sofia, S633 (SAT-101-YI)
Lackner, Carolin, S64 (OS-100)
Lacks, Luiza, S314 (SAT-284)
Lacombe, Karine, S45 (OS-067)
La, Danie, S875 (THU-574)
Ladd, Mary Kate, S339 (SAT-387)
Ladner, Daniela, S197 (WED-447), S388 (FRI-489), S388 (FRI-490)
Ladrón de Guevara-Cetina, Alma, S771 (THU-030)
Laetitia, S802 (FRI-010-YI)
Lafarga, Miguel, S643 (SAT-134)
Laffers, Lukas, S123 (FRI-085)
Lagdali, Nawal, S591 (WED-125), S609 (WED-181), S844 (THU-286), S845 (THU-287), S949 (FRI-613)
Laguna, Juan Carlos, S231 (FRI-304), S241 (FRI-341), S271 (THU-303), S279 (THU-335)
Laguna, Laura, S806 (FRI-024)
Lahsini, Jaouhara, S591 (WED-125)
Lahsnig, Maximillian, S242 (FRI-346)
Lai, Hao Xing, S67 (OS-105-YI)
Lai, Jennifer, S149 (SAT-468), S152 (SAT-478), S214 (WED-499), S220 (WED-521), S760 (TOP-032)
Lai, Jimmy Che-To, S66 (OS-103-YI), S156 (SAT-496), S215 (WED-505), S221 (WED-523), S224 (WED-531), S228 (WED-543), S423 (TOP-374), S424 (TOP-376), S517 (TOP-114), S528 (THU-110), S558 (TOP-063-YI), S574 (WED-075), S607 (WED-174-YI), S618 (WED-204), S738 (THU-463), S923 (SAT-618), S931 (SAT-637), S979 (WED-643)
Lai, Lee Lee, S574 (WED-075)
Lai, Mandy Sze-Man, S66 (OS-103-YI), S931 (SAT-637), S979 (WED-643)
Lai, Michelle, S517 (TOP-114), S525 (THU-103), S558 (TOP-063-YI), S607 (WED-174-YI)
Lainey, Elodie, S853 (WED-283)
Lai, Puling, S260 (TOP-357)
Laique, Sobia, S399 (FRI-522), S745 (THU-483)
Lai, Quirino, S407 (FRI-548)
Lai, Rongtao, S91 (SAT-067), S93 (SAT-072), S97 (SAT-086), S135 (FRI-118)
Lai, Xing, S41 (OS-062)
Lakananurak, Narisorn, S206 (WED-476)
Lakshmi, Sinchana, S247 (SAT-514)
Lal, Abhishek, S605 (WED-170), S743 (THU-478)
Lal, Anjana, S706 (THU-544)
Lalazar, Gadi, S10 (LBO-006)
Laleman, Wim, S33 (OS-046), S34 (OS-049), S35 (OS-050-YI), S52 (OS-081), S53 (OS-082), S54 (OS-084), S141 (TOP-437), S148 (SAT-467-YI), S159 (SAT-505), S166 (FRI-388-YI), S170 (FRI-401-YI), S261 (SAT-329-YI), S397 (FRI-515), S719 (TOP-488), S733 (THU-450), S744 (THU-481), S747 (THU-492), S752 (THU-501)
Lamarca, Angela, S303 (SAT-257-YI), S445 (THU-385)
Lamb, Hildo, S385 (FRI-479)
Lambooij, Joost, S646 (SAT-140-YI)
Lambrechts, Diether, S17 (OS-012)
Lam, Brian, S62 (OS-097), S516 (TOP-113), S766 (THU-015), S794 (SAT-046)
Lam, Carla, S422 (TOP-359-YI)
Lameroli, Lucía, S358 (THU-340-YI)
Lamfu, Leonard, S726 (THU-429)
Lamina, Claudia, S257 (SAT-545-YI)
Lamin, Bojang, S926 (SAT-624)
Lam, Laurent, S325 (SAT-320)
Lam, Lok-Ka, S422 (TOP-359-YI)
Lammert, Craig, S342 (SAT-398)
Lammert, Eckhard, S672 (SAT-230)
Lammert, Frank, S323 (SAT-314), S515 (TOP-098), S583 (WED-101), S858 (WED-301)
Lampertico, Pietro, S1 (GS-001), S7 (GS-012), S10 (LBO-006), S43 (OS-066), S47 (OS-072), S49 (OS-075), S62 (OS-097), S69 (LBP-004-YI), S71 (LBP-009), S82 (LBP-034-YI), S304 (SAT-258),

S307 (SAT-263), S315 (SAT-286), S335 (SAT-378-YI), S429 (THU-227-YI), S439 (THU-367), S516 (TOP-113), S897 (TOP-565), S901 (SAT-559), S902 (SAT-560), S912 (SAT-587-YI), S913 (SAT-589-YI), S915 (SAT-595), S916 (SAT-596), S919 (SAT-607), S919 (SAT-608-YI), S923 (SAT-618), S934 (TOP-582), S935 (TOP-583), S936 (TOP-584), S937 (FRI-585-YI), S938 (FRI-586), S939 (FRI-587), S942 (FRI-592), S942 (FRI-593), S946 (FRI-605), S947 (FRI-608), S953 (FRI-625), S956 (WED-576), S957 (WED-577), S958 (WED-581), S962 (WED-593), S962 (WED-594)
Lampichler, Katharina, S37 (OS-053), S199 (WED-452)
Lampl, Annika, S37 (OS-053)
Lamprou, Anastasia, S709 (THU-556-YI)
Lam, Shao Wei Sean, S344 (SAT-404)
Lam, Winnie Wing Chuen, S495 (FRI-228-YI)
Lana, Irene, S810 (FRI-035)
Lanari, Jacopo, S59 (OS-091)
Landau, Anne M, S631 (SAT-094-YI)
Lando, Maria Giovanna, S626 (WED-231)
Lands, Larry, S380 (FRI-462)
Lan, Fei, S688 (FRI-167)
Lange, Christian M., S151 (SAT-477), S175 (FRI-420), S181 (FRI-436)
Lange, Claudia, S689 (FRI-170)
Lange, Laura, S825 (WED-037)
Langendorfer, Nicolas, S387 (FRI-484)
Langer, Mona-May, S175 (FRI-420), S181 (FRI-436)
Lange, Sebastian, S504 (FRI-251)
Langford, Caitlin, S673 (SAT-231)
Lang, Hauke, S854 (WED-285)
Lang, Sonja, S623 (WED-220)
Langthaler, Michael, S975 (WED-634-YI)
Langthaler, Patrick, S792 (SAT-041)
Langthaler, Patrik, S539 (THU-151-YI)
Lani, Lorenzo, S424 (TOP-375-YI), S429 (THU-227-YI), S514 (FRI-381), S738 (THU-464-YI)
Lankage, Chalini, S519 (THU-086)
Lannes, Adrien, S540 (THU-155), S554 (THU-202), S558 (TOP-063-YI), S589 (WED-118)
Lanthier, Nicolas, S541 (THU-156), S648 (SAT-151-YI)
Lan, Tian, S28 (OS-036-YI), S285 (FRI-269), S293 (FRI-301)
Lantinga, Marten, S168 (FRI-397-YI)
Lanza, Alfonso Galeota, S911 (SAT-587-YI)
Lanza-Arnaiz, Jose Maria, S241 (FRI-339), S275 (THU-322-YI)
Lan, Zhixian, S6 (GS-010), S486 (WED-397), S644 (SAT-136)
Laouenan, Cedric, S571 (WED-067)
Laouirem, Samira, S480 (WED-380), S853 (WED-283)
Lape, Janel, S87 (LBP-043)
Lapeña, Berta, S16 (OS-010)
Lapenna, Lucia, S720 (TOP-502-YI)
Lapitz, Ainhoa, S303 (SAT-257-YI), S323 (SAT-315), S483 (WED-388-YI), S484 (WED-393)
Lapuyade, Bruno, S499 (FRI-238)
Lara-Romero, Carmen, S525 (THU-103), S527 (THU-108), S558 (TOP-063-YI), S589 (WED-118), S607 (WED-174-YI), S765 (THU-013), S806 (FRI-023)
Larghi, Alberto, S731 (THU-444-YI), S751 (THU-500)
LaRow, April, S344 (SAT-403)
Larrea, Emily, S294 (TOP-278)
Larrey, Dominique, S90 (SAT-059), S95 (SAT-076)
Larrey, Edouard, S457 (WED-236)
Larrubia, Juan Ramón, S366 (WED-332-YI), S968 (WED-610-YI)
Larrue, Hélène, S3 (GS-005), S53 (OS-082), S54 (OS-084), S195 (WED-442-YI), S207 (WED-477), S222 (WED-525), S497 (FRI-234), S719 (TOP-488), S723 (THU-418), S723 (THU-419), S742 (THU-477), S752 (THU-501)
Larsen, Stine Munk, S702 (TOP-535-YI)
Larson-Nath, Catherine, S850 (THU-308)
Lasa-Elosegui, Irune, S483 (WED-388-YI)
Lasagni, Alberto, S307 (SAT-263)
Laschtowitz, Alena, S57 (OS-088)
Lasco, Roberta, S300 (SAT-250), S331 (SAT-368-YI), S848 (THU-304)
Lasington, Jeril, S88 (TOP-178), S94 (SAT-075), S117 (FRI-068), S118 (FRI-069), S118 (FRI-070), S152 (SAT-480), S153 (SAT-481), S153 (SAT-483), S209 (WED-484), S592 (WED-126)
Lasington, Lawin Steve Mathew, S88 (TOP-178), S117 (FRI-068), S152 (SAT-480), S209 (WED-484), S592 (WED-126)
La Spada, Alberto, S967 (WED-605-YI)
Lassailly, Guillaume, S505 (FRI-254)
Lasser, Luc, S907 (SAT-575)
Lastuvkova, Hana, S286 (FRI-272)
Latasa, Maria U, S17 (OS-013), S474 (WED-364)
Latorre, Leire Perez, S904 (SAT-564)
Latorre, Raquel, S542 (THU-164)
Latournerie, Marianne, S380 (FRI-463), S381 (FRI-464)
Latre, Marta, S603 (WED-163)
Latta, Markus Robert, S646 (SAT-142)
Laubner, Katharina, S21 (OS-020)
Lau, Chi, S959 (WED-585)
Lau, Eva, S709 (THU-556-YI)
Lau, Johnny, S519 (THU-086)
Laurans, Łukasz, S980 (FRI-633)
Laurent, Alexis, S17 (OS-011)
Laurent-Puig, Pierre, S17 (OS-011)
Laurent, Valérie, S37 (OS-052)
Lauridsen, Mette, S41 (OS-061), S202 (WED-461-YI), S202 (WED-462), S225 (WED-532), S262 (SAT-332), S702 (TOP-535-YI)
Lauridsen, Susanne, S22 (OS-024)
Lauschke, Volker, S12 (OS-004-YI), S666 (SAT-211-YI)
Lauszus, Johanne Sloth, S262 (SAT-332)
Lauw, Mandy, S828 (TOP-310-YI)
Lavergne, David, S829 (THU-252)
Lavoie, Louis, S801 (FRI-007)
Law, Cherie, S275 (THU-321)
Lawitz, Eric, S26 (OS-031), S58 (OS-089), S78 (LBP-025), S313 (SAT-282), S328 (SAT-362), S682 (FRI-148), S688 (FRI-168), S689 (FRI-169), S689 (FRI-170), S691 (FRI-175), S694 (FRI-183), S719 (TOP-486)
Lawler, John, S334 (SAT-371), S334 (SAT-372), S334 (SAT-377)
Lawrence-Wilde, Farah, S84 (LBP-038), S839 (THU-272), S840 (THU-275)
Lawson, Alex, S406 (FRI-544)
Lazarevic, Ivana, S807 (FRI-025)
Lazaridis, Konstantinos N., S2 (GS-002), S13 (OS-006-YI), S290 (FRI-289)
Lázaro, Diego, S969 (WED-611)
Lázaro, Diego Rojo, S612 (WED-188)
Lazarte, Raul, S296 (TOP-281), S306 (SAT-262)
Lazarus, Jeffrey, S683 (FRI-152), S774 (THU-040), S774 (THU-041), S777 (THU-050), S791 (SAT-037), S792 (SAT-042), S802 (FRI-010-YI), S897 (TOP-565)
Lazic, Ivana, S295 (TOP-280)
Lazureanu, Voichita, S807 (FRI-025)
Lazzari, Ana, S88 (SAT-056), S776 (THU-044)
Leal-Lassalle, Hector, S132 (FRI-109), S642 (SAT-131-YI)
Leary, Peter, S465 (WED-255)
Leatherbury, Neil, S87 (LBP-043)
Leavelle, Danielle, S820 (WED-020-YI), S822 (WED-027)
Lebeau, Phoebe, S683 (FRI-151)
Lebedel, Louise, S54 (OS-084), S497 (FRI-234)
Lebina, Limakatso, S900 (SAT-558)
Leblond, Anne-Laure, S465 (WED-255)
Lebosse, Fanny, S207 (WED-477), S311 (SAT-271)
Lebouche, Bertrand, S529 (THU-116-YI), S865 (FRI-638)
Lebovic, Gerald, S834 (THU-262), S836 (THU-266)
Leburgue, Angela, S319 (SAT-301)
Lechapt-Zalcman, Emmanuele, S38 (OS-054)
Lecis, Pierenrico, S304 (SAT-258), S307 (SAT-263)
Leclercq, Isabelle, S648 (SAT-151-YI)
Leclercq, Sophie, S266 (SAT-346)
Ledinghen, Victor De, S568 (WED-057-YI), S838 (THU-270)
Leduc, Martin, S655 (SAT-172)

Author Index

Lee, Ahlim, S592 (WED-127)
Lee, Boram, S501 (FRI-242)
Lee, Brian, S124 (FRI-087-YI), S308 (SAT-265), S309 (SAT-266), S761 (THU-006)
Lee, C, S425 (THU-216-YI)
Lee, Chang Hun, S823 (WED-030)
Lee, Chia-Lun, S536 (THU-138)
Lee, Chieh-Ju, S500 (FRI-239)
Lee, Chien-Chang, S449 (THU-399)
Lee, Chuan-Pin, S773 (THU-038)
Lee, Chul-min, S545 (THU-171), S591 (WED-122), S625 (WED-229), S630 (SAT-092), S652 (SAT-165), S686 (FRI-163)
Lee, Dae Ho, S653 (SAT-167)
Lee, Danbi, S4 (GS-006), S4 (GS-007), S707 (THU-547)
Lee, Daniel, S80 (LBP-029)
Lee, Dong Ho, S497 (FRI-232)
Lee, Donghyeon, S568 (WED-057-YI)
Lee, Eng Hock, S435 (THU-246)
Lee, Eui Jin, S238 (FRI-331)
Lee, Frances, S120 (FRI-075), S762 (THU-008)
Lee, Fu-Jen, S969 (WED-613)
Lee, Gil Won, S132 (FRI-107), S135 (FRI-119)
Lee, Guan Huei, S67 (OS-105-YI)
Lee, Han Ah, S500 (FRI-241), S518 (TOP-129), S539 (THU-150)
Lee, Han Chu, S4 (GS-006), S4 (GS-007), S428 (THU-226-YI), S506 (FRI-255-YI), S513 (FRI-378), S707 (THU-547)
Lee, Heesun, S538 (THU-147)
Lee, Howard, S386 (FRI-482)
Lee, Hye Ah, S906 (SAT-574)
Lee, Hye Won, S19 (OS-017), S41 (OS-061), S62 (OS-097), S452 (THU-414-YI), S498 (FRI-235), S516 (TOP-113), S517 (TOP-114), S525 (THU-103), S539 (THU-150), S558 (TOP-063-YI), S589 (WED-118), S607 (WED-174-YI), S916 (SAT-597)
Lee, Hyo Young, S545 (THU-171), S590 (WED-121), S591 (WED-122), S625 (WED-229), S630 (SAT-092), S652 (SAT-165), S686 (FRI-163)
Lee, I-Cheng, S500 (FRI-239), S500 (FRI-240), S510 (FRI-369-YI)
Lee, Jae Geun, S260 (SAT-555)
Lee, Jaejun, S207 (WED-478), S592 (WED-127), S917 (SAT-602)
Lee, Jae Seung, S498 (FRI-235), S916 (SAT-597)
Lee, Jeong-Hoon, S502 (FRI-245), S507 (FRI-361), S509 (FRI-366), S518 (TOP-129)
Lee, Ji Eun, S72 (LBP-010)
Lee, Jin, S368 (WED-338)
Lee, Jin Suk, S133 (FRI-111), S360 (THU-352)
Lee, Ji-Yuh, S969 (WED-613)
Lee, John, S614 (WED-195)
Lee, Jonathan, S94 (SAT-073), S446 (THU-387)
Lee, Joon Hyeok, S500 (FRI-241)
Lee, Julian, S546 (THU-174), S697 (FRI-191)
Lee, Julie, S528 (THU-111)
Lee, Jung Il, S539 (THU-150)
Lee, Kuei-Chuan, S395 (FRI-510), S755 (THU-510)
Lee, Kwangwoo, S136 (FRI-121), S229 (TOP-342-YI), S368 (WED-337-YI)
Lee, Kyunghyun, S72 (LBP-010)
Lee, Kyung Jae, S839 (THU-271)
Lee, Kyung-Min, S166 (FRI-393)
Lee, Mei-Hsuan, S778 (THU-051), S923 (SAT-618)
Leeming, Diana Julie, S13 (OS-006-YI), S111 (FRI-044), S114 (FRI-057), S172 (FRI-411), S245 (FRI-354), S345 (SAT-410), S470 (WED-269), S550 (THU-187), S578 (WED-087), S584 (WED-104), S586 (WED-109), S592 (WED-131), S620 (WED-213), S623 (WED-219)
Lee, Minjong, S906 (SAT-574)
Lee, Mi Ra, S133 (FRI-111), S360 (THU-352)
Lee, Pei-Chang, S430 (THU-231), S491 (TOP-408-YI), S500 (FRI-239)
Lee, Peter, S287 (FRI-275)
Lee, Raphael, S211 (WED-491)
Leerapun, Apinya, S1 (GS-001)
Lees, Elizabeth, S437 (THU-362)
Lee, Seung Soo, S251 (SAT-528)
Lee, Shou-Wu, S449 (THU-399), S972 (WED-624)
Lee, Silvia, S200 (WED-453)
Lee, So Jung, S4 (GS-006)
Lee, Soon Kyu, S207 (WED-478), S421 (THU-530), S473 (WED-275), S881 (THU-594)
Lee, Sung Won, S473 (WED-275), S509 (FRI-365)
Lee, Sze Ting, S436 (THU-248)
Lee, Teng-Yu, S943 (FRI-596), S972 (WED-624)
Lee, Un Joo, S266 (SAT-345)
Lee, Way Seah, S713 (WED-557), S850 (THU-308)
Lee, William M., S691 (FRI-175)
Lee, Xuan Yong, S211 (WED-491)
Lee, Young-Sun, S135 (FRI-120), S498 (FRI-236), S590 (WED-121), S813 (FRI-046)
Lee, Yun Bin, S502 (FRI-245), S507 (FRI-361), S509 (FRI-366)
Lee, Yu Rim, S497 (FRI-233), S813 (FRI-046)
Lefere, Sander, S99 (TOP-193-YI), S281 (TOP-295-YI), S315 (SAT-285), S464 (WED-253), S526 (THU-106), S713 (WED-557)
Leggett, Barbara, S789 (SAT-030)
Legido-Quigley, Cristina, S115 (FRI-057)
Legry, Vanessa, S172 (FRI-412)
Le, Han Ngoc, S77 (LBP-022-YI)
Lehmann, Johannes, S532 (THU-124)
Lehr, Stefan, S672 (SAT-230)
Lehr, Timo, S151 (SAT-477)
Lehtonen, Marko, S266 (SAT-346)
Lehtoranta, Lara, S122 (FRI-084)
Lehuen, Agnes, S571 (WED-067)
Leibiger, Barbara, S278 (THU-332)
Leibiger, Ingo, S278 (THU-332)
Leicht, Hans Benno, S252 (SAT-529)
Lei, Chunliang, S952 (FRI-623)
Leighton, Jessica, S318 (SAT-299)
Lei, Hao-Jan, S395 (FRI-510)
Lei, Jihai, S884 (THU-605)
Leinhard, Olof Dahlqvist, S220 (WED-517), S568 (WED-056), S690 (FRI-173)
Leipold, Leona, S824 (WED-031)
Lei, Qingqing, S201 (WED-458)
Leite, Nathalie, S62 (OS-097), S516 (TOP-113)
Leith, Damien, S559 (TOP-065-YI), S599 (WED-152), S774 (THU-040), S774 (THU-041), S798 (TOP-034)
Leithead, Joanna, S740 (THU-468)
Leiva, Magdalena, S642 (SAT-131-YI)
Leivers, Martin, S47 (OS-072)
Lei, Xiaohong, S90 (SAT-060)
Lei, Yu, S876 (THU-575)
Le, Kha, S889 (THU-620), S959 (WED-586), S960 (WED-588), S965 (WED-602)
Le, Kim, S538 (THU-148-YI)
Lek, Serene, S533 (THU-126)
Lelou, Elise, S489 (WED-412-YI)
Lelouvier, Benjamin, S261 (SAT-329-YI), S262 (SAT-330)
Lemaitre, Caroline, S723 (THU-418)
Lemaître, Elise, S505 (FRI-254)
Lemaitre, Florence, S907 (SAT-575)
Lembeck, Pia, S178 (FRI-428-YI), S882 (THU-595)
Lemme, Daniela, S196 (WED-444)
Lemoine, Caroline, S386 (FRI-480-YI)
Lemoine, Maud, S224 (WED-530), S343 (SAT-400), S764 (THU-012), S798 (TOP-034)
Lemoinne, Sara, S235 (FRI-320), S325 (SAT-320), S343 (SAT-400)
Lemukol, James, S821 (WED-023)
Lemus, Regina, S578 (WED-087), S623 (WED-219)
Lenabe, Lesego, S76 (LBP-019-YI)
Lenci, Ilaria, S49 (OS-076-YI), S726 (THU-429), S919 (SAT-608-YI)
Le, Ngan, S253 (SAT-531)
Leng, Mei, S803 (FRI-012), S803 (FRI-013)
Lenicek, Martin, S286 (FRI-272)
Lens, Sabela, S43 (OS-066), S46 (OS-070-YI), S65 (OS-101-YI), S710 (THU-557-YI), S828 (TOP-309-YI), S884 (THU-604-YI), S897 (TOP-565), S903 (SAT-562), S903 (SAT-563-YI), S928 (SAT-628-YI), S934 (TOP-582), S936 (TOP-584), S937 (FRI-585-YI), S941 (FRI-590), S948 (FRI-611), S949 (FRI-612)
Lenz-Cesar, Carlos, S671 (SAT-226)
Leo, Massimo, S111 (FRI-043), S375 (TOP-519)
Leombruni, Paolo, S784 (SAT-015-YI)

Leonard, Charles, S189 (WED-420)
Leonardi, Bianca, S293 (FRI-301)
Leonard, Mark, S823 (WED-028)
Leonel, Thais, S884 (THU-604-YI), S941 (FRI-590), S949 (FRI-612)
Leone, Ruben, S419 (THU-524)
Leonetti, Frida, S626 (WED-231)
León, Raquel Ríos, S16 (OS-010), S300 (SAT-250), S318 (SAT-291), S948 (FRI-611)
Leow, Wei Qiang, S458 (WED-238)
Leppla, Lynn, S710 (TOP-536-YI)
Leproux, Apolline, S222 (WED-525)
Lequoy, Marie, S428 (THU-226-YI), S446 (THU-393-YI), S493 (FRI-221), S499 (FRI-238), S505 (FRI-254), S506 (FRI-255-YI), S507 (FRI-362), S508 (FRI-364-YI)
L'erario, Angelo, S825 (WED-037)
L'erario, Luca, S825 (WED-037)
Lerman, Lionel, S434 (THU-242)
Lermite, Françoise, S681 (FRI-147)
Lermo, Sara, S317 (SAT-290-YI)
Lerner, Astrid, S21 (OS-020)
Leroy, Vincent, S45 (OS-067), S311 (SAT-271), S343 (SAT-400), S434 (THU-242), S499 (FRI-238), S691 (FRI-175), S798 (TOP-034)
Lertudomphonwanit, Chatmanee, S850 (THU-308)
Lerut, Jan, S382 (FRI-466)
Lesage, Candice, S92 (SAT-068)
Lesage, Henri, S827 (WED-046)
Leshchynska, Natalia, S739 (THU-465)
Lesmana, Laurentius A., S67 (OS-105-YI)
Lesmana, Rinaldi, S67 (OS-105-YI)
Le, Suong, S707 (THU-546-YI)
Letmathe, Silvia, S737 (THU-461)
Letterio, Cathleen, S70 (LBP-005), S975 (WED-636), S976 (WED-637)
Leuenberger, Angela, S186 (TOP-469-YI)
Leung, Hak-Keith, S160 (SAT-507), S593 (WED-132)
Leung, Kathy, S824 (WED-035)
Leung, Kristel, S14 (OS-008), S295 (TOP-279), S325 (SAT-319), S354 (SAT-435)
Leuzinger, Karoline, S807 (FRI-025)
Levantesi, Fabio, S185 (TOP-455-YI)
Levels, Han, S641 (SAT-126)
Levens, Amar, S15 (OS-009-YI)
Levesque, Eric, S143 (SAT-450)
Levin, Michael, S166 (FRI-393)
Levrero, Massimo, S478 (WED-377), S573 (WED-071), S942 (FRI-592)
Levy, Cynthia, S10 (LBO-006), S67 (OS-106), S75 (LBP-018), S78 (LBP-023), S79 (LBP-026), S294 (TOP-277-YI), S295 (TOP-280), S297 (TOP-292-YI), S300 (SAT-250), S315 (SAT-286), S319 (SAT-300), S324 (SAT-316), S325 (SAT-320), S327 (SAT-323), S328 (SAT-324), S328 (SAT-361), S329 (SAT-364), S338 (SAT-384), S341 (SAT-396), S342 (SAT-398), S349 (SAT-420), S838 (THU-270), S846 (THU-291), S846 (THU-298)
Levy, Miriam, S10 (LBO-006), S76 (LBP-021)
Levy, Natacha, S85 (LBP-039), S243 (FRI-349)
Lewinska, Monika, S462 (WED-249), S655 (SAT-173)
Lewis, Adam, S166 (FRI-393)
Lewis, Diana, S218 (WED-513), S433 (THU-240), S716 (WED-562-YI), S716 (WED-563), S716 (WED-564), S749 (THU-496), S922 (SAT-613)
Lewis, Dylan, S404 (FRI-538-YI), S503 (FRI-250)
Lewis, Heather, S114 (FRI-056), S224 (WED-530)
Lewis, Shannon, S735 (THU-457)
Leyden, Kevin, S980 (FRI-634)
L'Henaff, Morgane, S540 (THU-155)
L'Hermite, Sébastien, S143 (SAT-450)
Liang, Chen, S73 (LBP-012)
Liang, Chunhui, S950 (FRI-617)
Liang, Gaoshuang, S136 (FRI-123)
Liang, Hong, S230 (TOP-343-YI)
Liang, Hongxia, S954 (FRI-626)
Liang, Hongyan, S869 (TOP-630), S872 (THU-561)
Liang, Huiqing, S73 (LBP-012)
Liang, Ja-Der, S426 (THU-218)
Liang, Jenny Yuh-Jin, S893 (THU-633)
Liang, Lilian, S46 (OS-070-YI), S66 (OS-103-YI)
Liang, Meidai, S107 (THU-077)
Liang, Ping, S502 (FRI-247)
Liangpunsakul, Suthat, S439 (THU-366-YI)
Liang, Tianzhu, S262 (SAT-331)
Liang, Tingbo, S68 (OS-107)
Liang, Wanying, S869 (TOP-630)
Liang, Xi, S151 (SAT-476), S361 (THU-353)
Liang, Xiao, S119 (FRI-072), S259 (SAT-554), S466 (WED-259), S560 (TOP-080), S593 (WED-134), S609 (WED-182), S763 (THU-011), S924 (SAT-620)
Liang, Xieer, S1 (GS-001), S73 (LBP-012), S73 (LBP-013), S932 (SAT-641), S959 (WED-586)
Liang, Xuan, S560 (TOP-080)
Liang, Yan, S84 (LBP-037), S906 (SAT-574)
Liang, Yingxin, S12 (OS-004-YI)
Liang, Yining, S884 (THU-603)
Liang, Yonghao, S868 (FRI-644)
Liang, Yuan, S628 (TOP-146)
Liang, Zihao, S30 (OS-040), S627 (TOP-130), S640 (SAT-123)
Lian, Jainqi, S433 (THU-239)
Lian, Jianqi, S952 (FRI-623)
Lian, Min, S68 (OS-107), S293 (FRI-302-YI), S324 (SAT-317), S324 (SAT-318)
Liao, Minjun, S593 (WED-133)
Liao, Siqi, S441 (THU-372-YI)
Liao, Xuejiao, S609 (WED-182), S763 (THU-011), S924 (SAT-620)
Liao, Yee-Tam, S691 (FRI-174)
Liao, Yuanhang, S119 (FRI-072), S763 (THU-011)
Liaw, Chih-Chuang, S373 (WED-354)
Liaw, Yun-Fan, S945 (FRI-603), S947 (FRI-607)
Li, Beiling, S98 (SAT-087)
Li, Bingqi, S151 (SAT-476), S361 (THU-353)
Li, Bo, S324 (SAT-318)
Licata, Anna, S967 (WED-605-YI)
Li, Changyong, S656 (SAT-175)
Li, Chen, S895 (THU-639)
Lichtenberger, Wendi, S694 (FRI-183)
Lichtenstein, Dajana, S107 (THU-078)
Lichtman, Amos, S939 (FRI-587), S948 (FRI-610), S956 (WED-576), S962 (WED-593)
Lichtner, Miriam, S49 (OS-076-YI)
Li, Chunmei, S812 (FRI-040)
Li, Chunxi, S884 (THU-605)
Licini, Lisa, S331 (SAT-368-YI)
Licoska-Josifovik, Fana, S387 (FRI-483)
Li, Danyang, S676 (SAT-238)
Liébana, Carmen, S910 (SAT-585)
Liebe, Roman, S858 (WED-301)
Liebig, Johannes, S852 (TOP-311), S858 (WED-302)
Liebig, Laura, S57 (OS-088), S291 (FRI-291-YI)
Liendo, Paloma, S910 (SAT-581)
Lie-Undurean, Irina Andreea, S205 (WED-474)
Li, Fahong, S917 (SAT-603)
Li, Fan, S103 (THU-067), S473 (WED-276)
Li, Fenxiang, S941 (FRI-591)
Lightfoot, Jessica, S735 (THU-457)
Lightstone, Adi, S243 (FRI-349)
Ligresti, Claudia, S163 (FRI-382)
Li, Guang-Ming, S86 (LBP-041)
Li, Guangyu, S73 (LBP-013)
Liguori, Antonio, S190 (WED-425), S219 (WED-515), S476 (WED-368), S479 (WED-378), S582 (WED-100-YI), S583 (WED-102-YI), S601 (WED-156), S621 (WED-214), S765 (THU-013)
Li, Guotao, S954 (FRI-626)
Li, Guozhi, S74 (LBP-015)
Li, Hai, S162 (TOP-440)
Li, Haini, S924 (SAT-620)
Li, Hairui, S474 (WED-362), S627 (TOP-143)
Li, Hong, S46 (OS-069), S932 (SAT-640)
Li, Hongling, S511 (FRI-370)
Li, Hu, S906 (SAT-572)
Li, Hui, S136 (FRI-122), S656 (SAT-179), S812 (FRI-040)
Li, Jia, S225 (WED-537), S238 (FRI-333-YI), S239 (FRI-334), S244 (FRI-352), S244 (FRI-353), S895 (THU-640)
Li, Jiabin, S952 (FRI-623)
Li, Jian, S826 (WED-040)
Li, Jiang, S151 (SAT-476)
Li, Jianhua, S955 (FRI-629)
Li, Jianhui, S511 (FRI-370)
Li, Jianping, S685 (FRI-156)

Author Index

Li, Jiaqi, S93 (SAT-071), S151 (SAT-476), S852 (TOP-312)
Li, Jiayue, S778 (THU-052)
Li, Jie, S442 (THU-379), S537 (THU-139), S655 (SAT-174), S677 (SAT-242), S868 (TOP-616-YI), S924 (SAT-620)
Li, Ji-Min, S238 (FRI-332)
Li, Jing, S119 (FRI-072)
Li, Jinghu Carl, S958 (WED-579)
Li, Jinpeng, S501 (FRI-244)
Li, Jinyu, S664 (SAT-203)
Li, Juan, S954 (FRI-626)
Li, Jun, S88 (TOP-192), S104 (THU-070), S151 (SAT-476), S361 (THU-353), S375 (TOP-519)
Li, Junxing, S285 (FRI-270)
Li, Junying, S441 (THU-371)
Li, Keren, S501 (FRI-243)
Li, Lanjuan, S118 (FRI-071)
Li, Lei, S511 (FRI-370)
Li, Ling, S560 (TOP-080)
Li, Linghua, S46 (OS-069)
Liljeblad, Mathias, S2 (GS-003), S682 (FRI-148), S690 (FRI-172)
Lillo, Chiara, S69 (LBP-004-YI)
Li, Lu, S438 (THU-364), S496 (FRI-230), S933 (SAT-643)
Lim, Aaron G., S804 (FRI-015-YI)
Lim, Alfredo, S713 (WED-556-YI)
Lima, Natalia, S232 (FRI-313)
Lima, Patricia, S671 (SAT-226)
Lim, Calven Fu-Hao, S593 (WED-132)
Lim, Chaeyeon, S707 (THU-547)
Lim, Chetana, S499 (FRI-238)
Li, Mei, S511 (FRI-370), S791 (SAT-039), S792 (SAT-040), S812 (FRI-040), S946 (FRI-606)
Li, Meng, S277 (THU-331)
Li, Mengqi, S103 (THU-068)
Lim, Gyungsun, S502 (FRI-245)
Lim, Ho Young, S426 (THU-219-YI)
Li, Michael, S342 (SAT-398)
Li, Min, S370 (WED-345)
Li, Minghui, S350 (SAT-425), S356 (SAT-444), S905 (SAT-570)
Li, Mingyang, S962 (WED-593)
Lim, Jia Min, S834 (THU-261)
Lim, Jihoon, S865 (FRI-638)
Lim, Jonathan R, S918 (SAT-604)
Lim, Kai, S441 (THU-377-YI), S442 (THU-378), S529 (THU-115)
Lim, Kheng Choon, S495 (FRI-228-YI)
Lim, Lee-Ling, S593 (WED-132)
Lim, Ryan YanZhe, S423 (TOP-374)
Lim, Samuel, S714 (WED-559-YI)
Lim, Seng Gee, S1 (GS-001), S46 (OS-070-YI), S67 (OS-105-YI), S956 (TOP-598)
Lim, Tien Huey, S1 (GS-001), S48 (OS-073)
Lim, Young-Suk, S4 (GS-006), S4 (GS-007), S47 (OS-072), S707 (THU-547), S824 (WED-035), S928 (SAT-628-YI), S943 (FRI-594), S953 (FRI-624)
Lim, Yun-Sook, S906 (SAT-573)
Linares, Lourdes García, S391 (FRI-497)
Linares, Ruben, S806 (FRI-024)
Li, Nathan, S690 (FRI-171)
Lin, Bingliang, S68 (OS-107), S85 (LBP-040)
Lin, Chien-Hung, S691 (FRI-174)
Lin, Chih-Lin, S969 (WED-613)
Lin, Chun, S955 (FRI-628)
Lindahl, Karin, S439 (THU-367), S903 (SAT-561), S915 (SAT-595), S916 (SAT-596), S953 (FRI-625)
Lindberg, Eric, S57 (OS-088)
Lindenmeyer, Christina, S745 (THU-483)
Lindfors, Andrea, S224 (WED-529)
Lind, Guro, S451 (THU-409)
Lindh, Magnus, S65 (OS-101-YI), S807 (FRI-025), S903 (SAT-562)
Lindqvist, Catarina, S23 (OS-025), S709 (THU-555-YI)
Lindstrom, Erik, S165 (FRI-387-YI), S290 (FRI-287)
Lind, Theresa, S326 (SAT-321)
Lindvig, Katrine, S63 (OS-098-YI), S569 (WED-059), S579 (WED-089), S582 (WED-100-YI), S587 (WED-110-YI), S592 (WED-131), S593 (WED-134), S615 (WED-197), S616 (WED-199), S622 (WED-216), S623 (WED-219)
Lin, Feng-Chang, S80 (LBP-028-YI)
Linge, Jennifer, S690 (FRI-173)
Ling, Lei, S345 (SAT-410)
Ling, Ning, S108 (THU-083)
Ling, Qi, S418 (THU-521)
Lingvay, Ildiko, S79 (LBP-027)
Lin, Han-Chieh, S755 (THU-510)
Lin, Henry C., S850 (THU-308)
Lin, Hsin-Che, S919 (SAT-606), S947 (FRI-607)
Lin, Huapeng, S119 (FRI-072), S517 (TOP-114), S525 (THU-103), S558 (TOP-063-YI), S589 (WED-118), S607 (WED-174-YI)
Li, Ning, S658 (SAT-183)
Lin, Jaw-Town, S943 (FRI-596)
Lin, Jianmei, S1 (GS-001), S73 (LBP-012), S952 (FRI-623)
Lin, Kainan, S466 (WED-259), S474 (WED-363)
Linke, Alexandra, S213 (WED-496)
Lin, Liang-Yu, S773 (THU-038)
Lin, Manqiang, S268 (SAT-352-YI)
Lin, Matthew, S919 (SAT-607)
Lin, Mei, S714 (WED-559-YI)
Lin, Minghua, S24 (OS-028), S144 (SAT-452), S160 (SAT-507)
Lin, Niang Cheng, S395 (FRI-510)
Lin, Qiongfen, S859 (WED-303)
Lin, Qiuxiang, S352 (SAT-428-YI)
Lin, Rong, S68 (OS-107)
Lin, Rutao, S778 (THU-053)
Lin, Shumei, S433 (THU-239), S941 (FRI-591)
Lins, Witória, S379 (FRI-460)
Linton-Reid, Kristofer, S490 (TOP-407-YI)
Lin, Tse-I, S658 (SAT-184), S874 (THU-570), S893 (THU-634), S959 (WED-586), S960 (WED-588), S965 (WED-602)
Lin, Weiyin, S46 (OS-069)
Lin, Xiaohan, S418 (THU-521)
Lin, Yanjie, S94 (SAT-074)
Lin, Yen-Huei, S80 (LBP-029)
Lin, YeunYi, S559 (TOP-065-YI)
Lin, Yi-Chen, S436 (THU-250), S448 (THU-396), S535 (THU-135), S586 (WED-108), S751 (THU-499)
Lin, Ying-Cheng, S972 (WED-624)
Lin, Yingying, S593 (WED-133)
Lin, Yongmei, S941 (FRI-591)
Lin, Yu-Cheng, S755 (THU-510)
Lin, Yun-Han, S643 (SAT-133)
Lin, Yu-Sheng, S972 (WED-624)
Lin, Zhaofeng, S416 (FRI-579), S417 (FRI-580)
Liou, Wei-Lun, S441 (THU-377-YI), S442 (THU-378)
Li, Peng, S151 (SAT-476)
Li, Pengchong, S88 (TOP-192)
Li, Pinky Yee-Ting, S738 (THU-463)
Lipiński, Patryk, S55 (OS-086), S831 (THU-258-YI), S842 (THU-284)
Lipov, Andrey, S595 (WED-136)
Lippert, Rachel, S672 (SAT-230)
Lips, Lynn, S64 (OS-099)
Li, Qingyuan, S270 (SAT-356)
Li, Qisheng, S690 (FRI-171)
Li, Qiudi, S883 (THU-601-YI)
Li, Rui, S137 (FRI-124)
Li, Rui-Qi, S30 (OS-040), S627 (TOP-130), S640 (SAT-123)
Li, Ruiqi, S102 (THU-062)
Li, Shenghao, S225 (WED-537)
Li, Shiying, S108 (THU-083), S269 (SAT-353)
Li, Shizhe, S646 (SAT-141)
Li, Shuang, S146 (SAT-460)
Li, Shuangjie, S955 (FRI-628)
Li, Simon, S688 (FRI-167)
Li, Size, S233 (FRI-314), S664 (SAT-202), S664 (SAT-203), S665 (SAT-204), S666 (SAT-206), S872 (THU-562)
Lisker-Melman, Mauricio, S866 (FRI-640)
Lisman, Ton, S168 (FRI-396)
Lissek, Mara, S878 (THU-585-YI)
Lissmann, Rebecca, S23 (OS-026-YI)
Li, Tao, S243 (FRI-348)
Liu, Cheng, S879 (THU-587), S889 (THU-620)
Liu, Chenghai, S24 (OS-028), S144 (SAT-452), S160 (SAT-507)
Liu, Chen-Hua, S898 (TOP-566-YI), S898 (TOP-567), S917 (SAT-601-YI), S969 (WED-613)
Liu, Chenrui, S47 (OS-071), S463 (WED-252), S873 (THU-569), S895 (THU-640), S946 (FRI-606)
Liu, Chinsu, S395 (FRI-510)
Liu, Chuan, S119 (FRI-072), S517 (TOP-114), S560 (TOP-080), S593 (WED-134), S756 (THU-514)

Liu, Chun-Jen, S766 (THU-015), S898 (TOP-566-YI), S898 (TOP-567), S917 (SAT-601-YI), S969 (WED-613)
Liu, Dan, S877 (THU-579-YI)
Liu, Dingli, S430 (THU-229), S508 (FRI-363)
Liu, Dorothy, S400 (FRI-524), S400 (FRI-525), S739 (THU-466)
Liu, Du-Xian, S331 (SAT-368-YI)
Liu, Eric, S598 (WED-148)
Liu, Fan, S675 (SAT-236)
Liu, Fang, S511 (FRI-370)
Liu, Feng, S162 (TOP-440), S593 (WED-133), S668 (SAT-217-YI), S673 (SAT-232), S931 (SAT-638)
Liu, Fenghua, S225 (WED-537)
Liu, Ge, S779 (THU-054)
Liu, Hanyang, S3 (GS-004-YI), S285 (FRI-269), S293 (FRI-301)
Liu, Hong, S556 (THU-211)
Liu, Hongli, S48 (OS-074), S331 (SAT-368-YI)
Liu, Hongyan, S430 (THU-229), S508 (FRI-363)
Liu, Hui, S676 (SAT-240)
Liu, Huimin, S955 (FRI-628)
Liu, Jianfeng, S86 (LBP-041)
Liu, Jiangwen, S259 (SAT-554), S593 (WED-134), S609 (WED-182), S763 (THU-011), S924 (SAT-620)
Liu, Jianjun, S324 (SAT-318)
Liu, Jianxiang, S225 (WED-537)
Liu, Jie, S316 (SAT-287)
Liu, Jieming, S958 (WED-579)
Liu, Jing, S160 (SAT-507), S891 (THU-626)
Liu, Jingfeng, S33 (OS-047)
Liu, Jinrun, S456 (WED-233)
Liu, Jinxia, S173 (FRI-413)
Liu, Kaipeng, S261 (TOP-358)
Liu, Kangshou, S495 (FRI-229)
Liu, Kejun, S259 (SAT-554), S763 (THU-011), S924 (SAT-620)
Liu, Ken, S156 (SAT-496), S215 (WED-505), S221 (WED-523), S228 (WED-543), S315 (SAT-286), S423 (TOP-374), S452 (THU-414-YI), S509 (FRI-365), S528 (THU-110), S736 (THU-458)
Liukkonen, Ville, S376 (FRI-448)
Liu, Li, S437 (THU-362), S941 (FRI-591)
Liu, Ligai, S225 (WED-537)
Liu, Liping, S293 (FRI-302-YI)
Liu, Liwei, S98 (SAT-088)
Liu, Mei, S291 (FRI-290-YI)
Liu, Minghui, S273 (THU-317)
Liu, Ming-qiang, S232 (FRI-307)
Liu, Puqiang, S259 (SAT-554), S593 (WED-134), S609 (WED-182), S763 (THU-011), S924 (SAT-620)
Liu, Qiaoyan, S293 (FRI-302-YI)
Liu, Qinghai, S139 (FRI-134)
Liu, Qiong, S259 (SAT-554)
Liu, Qiqi, S513 (FRI-379)
Liu, Qiuhong, S103 (THU-069)
Liu, Ruijia, S665 (SAT-205)
Liu, Ruiling, S812 (FRI-040)
Liu, Ruyu, S225 (WED-537), S259 (SAT-554), S609 (WED-182), S763 (THU-011), S924 (SAT-620)
Liu, Shanghao, S119 (FRI-072), S259 (SAT-554), S549 (THU-184), S593 (WED-134), S609 (WED-182), S763 (THU-011), S924 (SAT-620)
Liu, Shaowen, S864 (WED-320-YI)
Liu, Sile, S260 (TOP-357)
Liusina, Ekaterina, S594 (WED-135), S595 (WED-136)
Liu, Siyuan, S487 (WED-402), S674 (SAT-234)
Liu, Tian, S261 (TOP-358)
Liu, Tianxu, S883 (THU-597), S884 (THU-603), S894 (THU-636)
Liu, Wen-Chun, S893 (THU-633)
Liu, Wenhui, S48 (OS-074)
Liu, Wen-Yue, S62 (OS-097), S516 (TOP-113), S517 (TOP-114), S525 (THU-103), S558 (TOP-063-YI), S589 (WED-118), S607 (WED-174-YI)
Liu, Xia, S701 (FRI-204)
Liu, Xiangyu, S302 (SAT-254)
Liu, Xianwei, S137 (FRI-124)
Liu, Xiaoguai, S955 (FRI-628)
Liu, Xiaolong, S33 (OS-047)
Liu, Xiaoman, S883 (THU-602), S884 (THU-603)
Liu, Xiaoqin, S369 (WED-341)
Liu, Xiaoqing, S906 (SAT-572)
Liu, Xiaowei, S646 (SAT-141)
Liu, Xiaoyi, S368 (WED-339), S882 (THU-596)
Liu, Xia-Rong, S778 (THU-051)
Liu, Xibin, S593 (WED-134)
Liu, Xinde, S954 (FRI-626)
Liu, Xing, S331 (SAT-368-YI)
Liu, Xingxiang, S930 (SAT-634), S930 (SAT-635), S933 (SAT-642)
Liu, Xinxin, S158 (SAT-501)
Liu, Xinyue, S473 (WED-361-YI)
Liu, Xuanchen, S261 (TOP-358), S502 (FRI-246)
Liu, Yafen, S813 (FRI-045)
Liu, Yahui, S955 (FRI-628)
Liu, Yakun, S107 (THU-077), S270 (TOP-328), S276 (THU-323)
Liu, Yanhong, S259 (SAT-554), S593 (WED-134), S609 (WED-182), S763 (THU-011), S924 (SAT-620)
Liu, Yaqing, S954 (FRI-626)
Liu, Yen-Chun, S919 (SAT-606), S945 (FRI-603), S947 (FRI-607)
Liu Yin, James, S772 (THU-035)
Liu, Yuanjie, S872 (THU-561)
Liu, Yun, S74 (LBP-015)
Liu, Yuqi, S367 (WED-336), S473 (WED-361-YI), S877 (THU-578), S917 (SAT-603), S918 (SAT-605), S944 (FRI-597)
Liu, Yuxin, S260 (TOP-357), S486 (WED-397)
Liu, Zefeng, S763 (THU-011)
Liu, Zekun, S473 (WED-361-YI)
Liu, Zherui, S108 (THU-084)
Liu, Zhihong, S73 (LBP-012), S73 (LBP-013), S617 (WED-201), S932 (SAT-641)
Liu, Zhilong, S495 (FRI-229)
Liu, Zhipeng, S368 (WED-339)
Liu, Zihan, S431 (THU-234), S791 (SAT-039), S792 (SAT-040)
Liu, Ziqi, S260 (TOP-357), S486 (WED-397)
Liu, Ziying, S896 (THU-642)
Liu, Zongyi, S108 (THU-083), S269 (SAT-353)
Liu, Zuobin, S657 (SAT-182)
Livingston, Christine, S47 (OS-072), S959 (WED-585)
Livingstone, Robert, S24 (OS-028), S144 (SAT-452)
Livingstone, Victoria, S813 (FRI-047)
Li, Weijie, S511 (FRI-370)
Li, Weiping, S954 (FRI-626)
Li, Wenhao, S759 (TOP-018-YI), S773 (THU-039)
Li, Wenhui, S73 (LBP-013)
Li, Wenxuan, S473 (WED-361-YI)
Li, Xiaofang, S955 (FRI-629)
Li, Xiaohua, S86 (LBP-041), S909 (SAT-579)
Li, Xiaoke, S665 (SAT-205)
Li, Xiao-Yun, S90 (SAT-060)
Li, Xiaoyun, S895 (THU-639)
Li, Xiayao, S153 (SAT-482), S161 (SAT-508), S177 (FRI-426)
Li, Xin, S909 (SAT-579)
Li, Xing, S34 (OS-048), S86 (LBP-041)
Li, Xingfeng, S490 (TOP-407-YI)
Li, Xinghai, S688 (FRI-167)
Li, Xinhua, S511 (FRI-370)
Li, Xitang, S676 (SAT-239)
Li, Xu, S34 (OS-048)
Li, Xue, S824 (WED-035)
Li, Xuefeng, S560 (TOP-080)
Li, Xuejiao, S419 (THU-522), S495 (FRI-229)
Li, Xuemei, S941 (FRI-591)
Li, Xue-Ying, S292 (FRI-298)
Li, Yakun, S238 (FRI-333-YI), S239 (FRI-334), S384 (FRI-476-YI), S384 (FRI-477), S385 (FRI-478)
Li, Yang, S531 (THU-122)
Li, Yaocai, S86 (LBP-041)
Li, Yaping, S47 (OS-071), S463 (WED-252), S791 (SAT-039), S792 (SAT-040), S873 (THU-569), S895 (THU-640), S941 (FRI-591), S946 (FRI-606)
Li, Yaqun, S129 (TOP-223)
Li, Yating, S118 (FRI-071)
Li, Ye, S232 (FRI-307)
Li, Yifang, S657 (SAT-181)
Li, Yiling, S560 (TOP-080)
Li, Yinling, S657 (SAT-180)
Li, Yongmei, S690 (FRI-171)
Li, Yongyin, S368 (WED-339), S882 (THU-596), S955 (FRI-629)
Li, Yuebao, S883 (THU-597)
Li, Yuxin, S369 (WED-340-YI), S372 (WED-351)

Author Index

Liza, Estefanía, S112 (FRI-050)
Lizana, Ana Maria, S336 (SAT-380)
Lizaola-Mayo, Blanca, S604 (WED-166)
Lizasoain, Maialen, S17 (OS-013)
Li, Zhen, S560 (TOP-080)
Li, Zhengjiang, S260 (TOP-357), S486 (WED-397)
Li, ZhiPeng, S155 (SAT-492)
Li, Zhi-Qin, S954 (FRI-626)
Li, Zhiwei, S262 (SAT-331)
Li, Zhong-Die, S831 (THU-258-YI), S842 (THU-284)
Li, Zhuan, S136 (FRI-123), S472 (WED-273)
Li, Ziqiang, S99 (TOP-194)
Lkhagva-Ochir, Oyungerel, S439 (THU-367), S915 (SAT-595), S916 (SAT-596)
Lladó, Laura, S394 (FRI-507-YI)
Llaneras, Jordi, S811 (FRI-038)
Llanes, Victor, S590 (WED-120)
Llanillo, Loreto Hierro, S55 (OS-086), S831 (THU-258-YI), S842 (THU-284)
Llarch, Neus, S38 (OS-055), S481 (WED-382-YI)
Lleo, Ana, S69 (LBP-004-YI), S82 (LBP-034-YI), S304 (SAT-258), S305 (SAT-260-YI), S307 (SAT-263), S331 (SAT-368-YI), S335 (SAT-378-YI), S339 (SAT-386), S340 (SAT-393), S350 (SAT-421), S531 (THU-120)
Llerena, Susana, S833 (THU-259)
Llibre, Josep, S807 (FRI-025)
Llinás, Margarita Sala, S16 (OS-010), S294 (TOP-278), S308 (SAT-264), S318 (SAT-291)
Llopis-Roca, Ferran, S811 (FRI-038)
Llopiz, Diana, S364 (WED-329-YI)
Llorente, Carmen Payá, S408 (FRI-553)
Llorente-Cortes, Vicenta, S28 (OS-037), S629 (TOP-160)
Llovet, Josep M, S18 (OS-014-YI), S453 (TOP-389), S459 (WED-242-YI), S468 (WED-263), S485 (WED-396)
Lloyd, Andrew, S770 (THU-028)
Lluch-García, Paloma, S33 (OS-046), S189 (WED-418), S585 (WED-105), S585 (WED-106), S598 (WED-150), S772 (THU-036), S779 (SAT–003-YI)
Lobanova, Elena, S594 (WED-135)
Lobb, William, S333 (SAT-370)
Lobe, Cindy, S924 (SAT-619)
Lobmeyer, Maximilian T., S689 (FRI-170)
Lobritto, Steven, S846 (THU-291), S846 (THU-298)
Lo Cascio, Giustina, S746 (THU-490)
Locatelli, Maëlle, S884 (THU-604-YI), S949 (FRI-612)
Lo, Chen-Yu, S691 (FRI-174)
Lo, Ching-Chu, S691 (FRI-174)
Lo, Chingchu, S958 (WED-580)
Lochoro, Peter, S821 (WED-023)
Lo-Ciganic, Wei-Hsuan, S974 (WED-628)
Locke, Adam, S166 (FRI-393)
Lockman, Shahin, S922 (SAT-612)
Loddo, Erica, S850 (THU-307)
Lodha, Gaurav, S217 (WED-511)
Lodolini, Paola, S576 (WED-083)
Loew, Damarys, S571 (WED-067)
Loewe, Christian, S490 (TOP-407-YI)
Loey Mak, Lung Yi, S422 (TOP-359-YI)
Lo, Gin-Ho, S725 (THU-426)
Loglio, Alessandro, S43 (OS-066), S55 (OS-085-YI), S331 (SAT-368-YI), S350 (SAT-421), S817 (WED-010), S900 (SAT-559), S901 (SAT-560), S911 (SAT-587-YI), S934 (TOP-582), S936 (TOP-584), S938 (FRI-586), S947 (FRI-608)
Lohith, Talakad G., S579 (WED-090), S694 (FRI-183)
Lohmeyer, Jürgen, S930 (SAT-636)
Lohoues, Marie Jeanne, S24 (OS-028), S144 (SAT-452)
Lohse, Ansgar, S257 (SAT-546), S325 (SAT-320)
Lohse, Ansgar W., S178 (FRI-429-YI), S213 (WED-496), S236 (FRI-323), S291 (FRI-291-YI), S300 (SAT-250), S332 (SAT-369), S351 (SAT-427), S708 (THU-554-YI), S783 (SAT-012), S866 (FRI-639), S912 (SAT-588)
Loi, Pooi Ling, S158 (SAT-499)
Loke, Kelvin Siu Hoong, S495 (FRI-228-YI)
Lok, James, S905 (SAT-571)
Lokwang, Peter, S821 (WED-023)
Lombardi, Pasquale, S491 (TOP-408-YI), S500 (FRI-239)
Lombardi, Rosa, S62 (OS-097), S97 (SAT-084-YI), S516 (TOP-113), S520 (THU-091-YI), S541 (THU-158), S553 (THU-197), S595 (WED-137), S595 (WED-138), S626 (WED-231), S636 (SAT-110-YI), S696 (FRI-188-YI), S865 (FRI-638)
Lombardo, Antonino, S212 (WED-494-YI)
Lombardo, Daniele, S967 (WED-605-YI)
Lonardi, Sara, S424 (TOP-375-YI), S428 (THU-227-YI), S435 (THU-247), S514 (FRI-381)
Londoño, Camilo Andrés Torres, S556 (THU-212)
Londoño, María Carlota, S16 (OS-010), S79 (LBP-026), S294 (TOP-278), S300 (SAT-250), S308 (SAT-264), S309 (SAT-268), S317 (SAT-290-YI), S318 (SAT-291), S325 (SAT-320), S328 (SAT-362), S331 (SAT-368-YI), S336 (SAT-380), S337 (SAT-382), S338 (SAT-383), S340 (SAT-388), S739 (THU-467), S828 (TOP-309-YI)
Longato, Lisa, S119 (FRI-073)
Longerich, Thomas, S297 (TOP-293), S341 (SAT-397)
Long, Jingpei, S428 (THU-225-YI)
Longley, Regina, S776 (THU-046)
Longman, Mark, S823 (WED-028)
Long, Mian, S359 (THU-346), S658 (SAT-183)
Longo, Ken, S5 (GS-008)
Longo, Miriam, S177 (FRI-427), S443 (THU-380-YI), S595 (WED-138), S662 (SAT-198-YI), S667 (SAT-214)
Longpre, Lara, S10 (LBO-006)
Long, Yuanshui, S28 (OS-036-YI), S285 (FRI-269)
Looby, Richard, S702 (FRI-206)
Loomba, Ria, S207 (WED-479)
Loomba, Rohit, S2 (GS-003), S19 (OS-016), S64 (OS-099), S78 (LBP-024), S78 (LBP-025), S79 (LBP-027), S82 (LBP-032), S116 (FRI-061), S134 (FRI-116), S190 (WED-421), S197 (WED-447), S562 (TOP-096), S563 (WED-042), S564 (WED-043), S578 (WED-088), S589 (WED-118), S596 (WED-139), S596 (WED-140), S597 (WED-141), S682 (FRI-149), S691 (FRI-175), S692 (FRI-179), S699 (FRI-199), S766 (THU-015)
Loomes, Kathleen M., S832 (THU-258-YI), S842 (THU-284), S850 (THU-308)
Lopes, Massimo, S465 (WED-255)
López, Ana Rodríguez, S391 (FRI-497)
Lopez, Arnau Puig, S961 (WED-592)
López-Barneo, Jose, S271 (THU-314)
López-Bermudo, Lucía, S527 (THU-108), S678 (SAT-244)
López-Cánovas, Juan Luis, S467 (WED-261)
Lopez, Carlos Lopez, S781 (SAT-008)
López-Gallegos, Darío, S710 (THU-557-YI)
López-Gómez, Marta, S585 (WED-105), S598 (WED-150), S772 (THU-036)
López, Ian, S904 (SAT-564)
López, Inmaculada, S910 (SAT-581), S910 (SAT-585)
López, Isabel Narváez, S391 (FRI-497)
López, Joel, S815 (WED-006)
Lopez, Laura Suarez, S542 (THU-164), S567 (WED-054), S571 (WED-069)
López-Lluch, Guillermo, S271 (THU-314)
Lopez Lopez, Carlos, S781 (SAT-009)
Lopez, Mattia, S825 (WED-037)
López-Mena, Edgar René, S481 (WED-384)
López-Mendez, Ivan, S296 (TOP-281), S306 (SAT-262)
Lopez, Miguel, S233 (FRI-313), S241 (FRI-339)
Lopez-Pascual, Amaya, S17 (OS-013), S474 (WED-364)
Lopez, Paula Daniela Chiodi, S296 (TOP-281), S306 (SAT-262)
López-Picallo, Borja, S232 (FRI-313)
López, Rocío, S366 (WED-332-YI)
López-Vicario, Cristina, S172 (FRI-412)
López, Virginia, S272 (THU-315-YI)
Lopez, Xavier, S28 (OS-037), S629 (TOP-160)
Lorca, Inmaculada, S779 (SAT–003-YI)
Lorch, Ulrike, S839 (THU-272)
Lorduy, Benjamin Polo, S250 (SAT-524)
Lorefice, Elisabetta, S82 (LBP-034-YI), S350 (SAT-421)

Lo, Regina Cheuk Lam, S423 (TOP-360)
Lorente, Sara, S300 (SAT-250), S837 (THU-267), S948 (FRI-611)
Lorenz, Leander, S185 (TOP-456-YI)
Lorenzo, Andrea Di, S49 (OS-076-YI), S807 (FRI-025), S900 (SAT-559), S901 (SAT-560), S919 (SAT-608-YI)
Lorenzo, Belen, S910 (SAT-585)
Lorenzo, Stefania De, S424 (TOP-375-YI), S514 (FRI-381)
Lo, Richard Hoau Gong, S495 (FRI-228-YI)
Lorigiola, Giovanna, S429 (THU-228)
Lor, Marta, S25 (OS-029)
Losco, Alessandra, S975 (WED-635)
Losito, Francesco, S69 (LBP-004-YI), S304 (SAT-258), S307 (SAT-263), S335 (SAT-378-YI)
Loste, Maria Teresa Arias, S585 (WED-106), S680 (FRI-139)
Loste, María Teresa Arias, S612 (WED-186-YI), S643 (SAT-134), S833 (THU-259)
Lothe, Ragnhild, S290 (FRI-289)
Lotta, Luca, S166 (FRI-393)
Lottini, Tiziano, S457 (WED-235)
Lotto, Marta, S815 (WED-005)
Lou, Amy, S598 (WED-148)
Loucera, Carlos, S806 (FRI-023)
Loudianos, Georgios, S857 (WED-298)
Lou, Haonan, S882 (THU-596)
Louissaint, Jeremy, S432 (THU-238)
Loumaye, Audrey, S648 (SAT-151-YI)
Louro, Daniela, S724 (THU-420)
Loustaud-Ratti, Veronique, S45 (OS-067), S827 (WED-046), S829 (THU-252)
Louvet, Alexandre, S14 (OS-007), S17 (OS-011), S35 (OS-050-YI), S505 (FRI-254)
Lou, Weiqian, S93 (SAT-072), S97 (SAT-086), S135 (FRI-118)
Lou, Weiwei, S97 (SAT-086), S135 (FRI-118)
Lou, Yan, S489 (WED-410), S870 (TOP-645), S878 (THU-586), S896 (THU-641)
Louzada, Ruy Andrade, S634 (SAT-104)
Löve, Thorvardur J., S802 (FRI-011)
Löwe, Bernd, S332 (SAT-369)
Low, Elizabeth, S841 (THU-276-YI)
Low, Jie Ting, S643 (SAT-133)
Low, Peter Jin Sun, S698 (FRI-197)
Lozano, Anthony, S453 (TOP-389)
Lozano Domínguez, María Carmen, S910 (SAT-585)
Lozano, Juanjo, S34 (OS-049), S166 (FRI-388-YI)
Lozano, Miquel, S8 (LBO-002)
Lübbering, David, S351 (SAT-427)
Luber, Andrew, S48 (OS-073)
Lubian, Giulia, S400 (FRI-526)
Luca, Angelo, S727 (THU-431), S731 (THU-445-YI)
Luca, Chiara De, S570 (WED-061)
Luca, Maria, S835 (THU-263)
Lucà, Martina, S52 (OS-081), S55 (OS-085-YI), S720 (TOP-504-YI)
Lucarelli, Andrea, S576 (WED-083)
Lucas, Sara, S921 (SAT-611)
Lucena, Maria Isabel, S101 (THU-059-YI)
Lu, Changxian, S812 (FRI-040)
Luchetti, Francesca, S475 (WED-366)
Lu, Chong, S64 (OS-099), S596 (WED-140)
Luciani, Alain, S434 (THU-242), S446 (THU-393-YI), S507 (FRI-362)
Lucia, Pietro Di, S51 (OS-079)
Lucidi, Valerio, S35 (OS-050-YI)
Lucifora, Julie, S875 (THU-572), S885 (THU-606)
Lucio-Fernández, Carla, S250 (SAT-524)
Ludlow-Rhodes, Arran, S827 (WED-047)
Ludovica Fracanzani, Anna, S662 (SAT-198-YI)
Ludvigsen, Trine Pagh, S240 (FRI-338)
Lué, Alberto, S603 (WED-163)
Luedde, Tom, S188 (WED-416), S280 (THU-338-YI), S447 (THU-395), S470 (WED-268), S485 (WED-396), S641 (SAT-125-YI), S648 (SAT-150)
Luetgehetmann, Marc, S866 (FRI-639), S871 (THU-558-YI), S919 (SAT-607)
Luft, Juliet, S12 (OS-004-YI)
Lu, Genliang, S702 (FRI-206)
Luijmes, Stefan H., S382 (FRI-467-YI), S391 (FRI-498)
Luis, Davinia Sacramento, S547 (THU-181)
Lui, Vincent CH, S859 (WED-303)
Lujambio, Amaia, S631 (SAT-095-YI)
Lu, Jianliang, S422 (TOP-359-YI)
Lukic, Tamara, S1 (GS-001), S956 (TOP-598), S957 (WED-577), S960 (WED-587)
Lu, Lili, S558 (THU-215)
Lu, Ling, S103 (THU-067), S473 (WED-276), S628 (TOP-146)
Lu, Liyue, S473 (WED-361-YI)
Lu, Lungen, S86 (LBP-041)
Lumbreras-Perales, Cristina, S286 (FRI-271)
Lu, Mengji, S946 (FRI-606)
Lu, Mingqin, S24 (OS-028), S144 (SAT-452), S160 (SAT-507), S369 (WED-341)
Lu, Ming-Ying, S518 (TOP-128)
Lunar, Maja, S807 (FRI-025)
Lundberg, Peter, S220 (WED-517), S568 (WED-056)
Lundgren, Åsa, S606 (WED-173)
Lundin, Sori, S492 (FRI-218)
Lund, Line Egerod, S586 (WED-109)
Lund, Louisa, S351 (SAT-427), S708 (THU-554-YI)
Lund, Michael, S691 (FRI-175)
Lundqvist, Annamari, S122 (FRI-084), S760 (THU–003)
Lundqvist, Annika, S2 (GS-002)
Lunkov, Valeriy, S594 (WED-135), S595 (WED-136)
Lun, Liou Wei, S160 (SAT-507)
Lunova, Mariia, S273 (THU-317), S459 (WED-241)
Lunov, Oleg, S273 (THU-317), S459 (WED-241)
Luo, Cheng, S675 (SAT-235)
Luo, Deqiang, S259 (SAT-554)
Luo, Fei, S688 (FRI-167)
Luo, Guqing, S134 (FRI-115)
Luo, Jiing-Chyuan, S500 (FRI-240), S510 (FRI-369-YI)
Luo, Jing, S239 (FRI-335)
Luo, Jinjin, S151 (SAT-476)
Luo, Kaizhong, S34 (OS-048)
Luo, Min, S879 (THU-587)
Luong, Susan, S879 (THU-587)
Luong, Tu Vinh, S119 (FRI-073)
Luong, Xuan, S658 (SAT-184)
Luo, Qiumin, S155 (SAT-492), S805 (FRI-021)
Luo, Sihui, S627 (TOP-143)
Luo, Tianzi, S107 (THU-077), S270 (TOP-328), S276 (THU-323)
Luo, Ting, S502 (FRI-247)
Luo, Wenyi, S331 (SAT-368-YI)
Luo, Xueyun, S895 (THU-639)
Luo, Yawen, S34 (OS-048), S86 (LBP-041)
Lupberger, Joachim, S463 (WED-250)
Lü, Ping, S513 (FRI-379)
Lupo, Francesco, S90 (SAT-061-YI)
Lupp, Amelie, S467 (WED-261)
Lupsor-Platon, Monica, S568 (WED-057-YI)
Lupu, Amanda, S529 (THU-116-YI)
Lu, Qinghua, S950 (FRI-617), S950 (FRI-618)
Luque, Raul M., S273 (THU-316), S278 (THU-333-YI), S467 (WED-261)
Lu, Qun, S416 (FRI-576)
Lurie, Gulnaz, S594 (WED-135)
Lurz, Eberhard, S850 (THU-308)
Lushniak, Larissa, S684 (FRI-154)
Lusivka-Nzinga, Clovis, S66 (OS-104)
Lusweti, Merab, S900 (SAT-558)
Lutgehetmann, Marc, S867 (FRI-642)
Lüth, Stefan, S271 (THU-313)
Lu, Tingting, S884 (THU-605)
Lutz, Thomas, S904 (SAT-564)
Luukkonen, Panu K., S562 (TOP-096)
Luu, Michael, S492 (FRI-218)
Lu, Wei-Yu, S284 (FRI-268-YI), S360 (THU-350)
Luxenburger, Hendrik, S371 (WED-348)
Lu, Xiaobo, S941 (FRI-591)
Lu, Xiaomin, S615 (WED-198), S679 (TOP-177)
Lu, Yang, S495 (FRI-228-YI), S638 (SAT-117-YI)
Lu, Yunkun, S466 (WED-259)
Lu, Ziman, S473 (WED-361-YI)
Luzi, Massimiliano, S576 (WED-083)
Lv, Chun-Hui, S243 (FRI-348)
lv, hui, S955 (FRI-628)
Lv, Jiaojian, S86 (LBP-041), S560 (TOP-080)
Lv, Riying, S955 (FRI-628)
Lybeck, Charlotte, S978 (WED-642-YI)
Lye Ch'ng, Chin, S258 (SAT-547)
Lygoura, Vasiliki, S314 (SAT-283), S323 (SAT-315), S349 (SAT-420)
Lykiardopoulos, Byron, S568 (WED-056)
Lynch, Erica Nicola, S69 (LBP-004-YI), S82 (LBP-034-YI), S304 (SAT-258),

Author Index

S325 (SAT-320), S350 (SAT-421), S400 (FRI-526), S542 (THU-159), S831 (THU-256-YI)
Lynch, Julie, S166 (FRI-393)
Lynch, Kate, S10 (LBO-006), S218 (WED-513), S749 (THU-496)
Lynch-Mejia, Maria, S790 (SAT-036)
Lynch, Michelle, S708 (THU-549-YI)
Lynch, Ruairi, S559 (TOP-065-YI), S572 (WED-070), S599 (WED-152)
Lynch, Shannan, S981 (FRI-635), S981 (FRI-636)
Lyonga, Emilia, S924 (SAT-619)
Lyra, Andre, S35 (OS-050-YI)
Lytvyak, Ellina, S14 (OS-008), S59 (OS-091), S295 (TOP-279), S300 (SAT-250), S315 (SAT-286), S320 (SAT-302), S325 (SAT-319), S325 (SAT-320), S338 (SAT-384), S344 (SAT-404), S354 (SAT-435), S355 (SAT-436), S401 (FRI-527), S923 (SAT-618)
Lyu, Zhuwan, S324 (SAT-318)

Maagaard, Markus, S110 (FRI-041-YI), S115 (FRI-059), S217 (WED-509-YI), S253 (SAT-532), S554 (THU-204)
Ma, Ann, S203 (WED-463)
Ma, Ann T, S425 (THU-216-YI), S739 (THU-467)
Maan, Raoel, S54 (OS-084), S61 (OS-095-YI), S168 (FRI-397-YI), S193 (WED-432), S443 (THU-382-YI), S828 (TOP-310-YI)
Maasoumy, Benjamin, S3 (GS-005), S6 (GS-011-YI), S46 (OS-070-YI), S52 (OS-081), S185 (TOP-456-YI), S195 (WED-442-YI), S197 (WED-446), S215 (WED-506), S222 (WED-524), S222 (WED-526-YI), S732 (THU-448-YI), S733 (THU-450), S736 (THU-460-YI), S737 (THU-461), S737 (THU-462), S743 (THU-480-YI), S752 (THU-501), S864 (TOP-615), S866 (FRI-641), S887 (THU-611)
Mabile-Archambeaud, Isabelle, S222 (WED-525), S742 (THU-477)
Macaione, Vincenzo, S163 (FRI-382)
Macaraeg, Sean, S687 (FRI-165)
MacCarthy, Finbar, S746 (THU-485)
Maccioni, Luca, S266 (SAT-346)
MacConell, Leigh, S293 (FRI-302-YI)
Macdonald, Douglas, S65 (OS-102), S759 (TOP-017-YI), S970 (WED-619), S974 (WED-629-YI)
Macedo, Maria-Paula, S649 (SAT-152)
Macfaul, George, S254 (SAT-537)
Machado, Mariana, S43 (OS-066), S934 (TOP-582), S937 (FRI-585-YI), S940 (FRI-589)
Machado, Pedro, S724 (THU-420)
Machida, Takeshi, S372 (WED-352), S647 (SAT-147)
Machuca, Jesús, S910 (SAT-581)
Macías-Herranz, Manuel, S173 (FRI-414), S239 (FRI-336)
Macias, Rocio, S303 (SAT-257-YI), S484 (WED-393), S558 (TOP-063-YI)
Macias-Rodriguez, Ricardo, S22 (OS-022-YI), S707 (THU-548)
Maci, Massimo, S784 (SAT-015-YI)
Mackey, Rachel H., S321 (SAT-306)
MacNicholas, Ross, S377 (FRI-449)
Macphail, Gisela, S968 (WED-609-YI)
Madaleno, Joao, S300 (SAT-250), S331 (SAT-368-YI), S333 (SAT-369), S337 (SAT-382)
Madamba, Egbert, S207 (WED-479), S564 (WED-043), S578 (WED-088), S596 (WED-140)
Madden, Diane Lloyd, S343 (SAT-401-YI)
Madeira, Joana, S331 (SAT-368-YI)
Made, Lilian Torres, S160 (SAT-507)
Mader, Maria, S866 (FRI-639)
Maderuelo, Esther, S300 (SAT-250), S318 (SAT-291), S337 (SAT-382)
Madesh, Vijaya Prakash, S597 (WED-142-YI), S780 (SAT-005), S782 (SAT-010-YI)
Madigan, Shauna, S208 (WED-480)
Madir, Anita, S26 (OS-032-YI), S337 (SAT-382), S515 (TOP-098)
Madleen, Chassang, S681 (FRI-147)
Madsen, Christian Toft, S240 (FRI-338)
Madsen, Lone Galmstrup, S116 (FRI-060), S775 (THU-042-YI)
Madubashetha, Hasanka, S827 (TOP-297)
Madureira, Lorena, S379 (FRI-460)
Madureira, Maria Alice, S830 (THU-255)
Mady, Samy, S326 (SAT-321)
Maeda, Kazuhisa, S686 (FRI-159)
Maekawa, Shinya, S506 (FRI-256)
Maesaka, Kazuki, S463 (WED-251-YI)
Maestri, Marcello, S370 (WED-346)
Maffi, Gabriele, S541 (THU-158), S595 (WED-137)
Magar, Yash, S104 (THU-071-YI), S120 (FRI-074), S129 (TOP-224-YI), S131 (FRI-105-YI), S138 (FRI-132), S139 (FRI-135-YI), S265 (SAT-341), S269 (SAT-355), S373 (WED-353-YI)
Magdaleno, Fernando, S237 (FRI-329)
Magdeldin, Sameh, S231 (FRI-305)
Magdy, Elkhashab, S597 (WED-147)
Magee, Catherine, S534 (THU-132)
Magenta, Lorenzo, S331 (SAT-368-YI)
Mageras, Anna, S590 (WED-120), S762 (THU-008)
Maggioni, Marco, S241 (FRI-340), S331 (SAT-368-YI), S662 (SAT-198-YI)
Maghlaoua, Zakaria, S207 (WED-477)
Maghsood, Roza, S252 (SAT-530)
Magi, Alberto, S479 (WED-379)
Magini, Giulia, S199 (WED-450)
Magistri, Paolo, S378 (FRI-458), S412 (FRI-562), S412 (FRI-563)
Magkos, Faidon, S692 (FRI-180)
Magnanensi, Jeremy, S149 (SAT-468), S152 (SAT-478), S214 (WED-499), S760 (TOP-032)
Magnani, Carlotta, S721 (THU-415)
Magnapera, Alessia, S899 (SAT-557), S911 (SAT-587-YI), S919 (SAT-608-YI), S924 (SAT-619)
Magnes, Marzena, S597 (WED-147)
Magness, Alastair, S673 (SAT-231)
Magni, Carlo, S911 (SAT-587-YI)
Magro, Bianca, S401 (FRI-528)
Magrofuoco, Maria, S49 (OS-076-YI)
Magsombol, Butch Maulion, S495 (FRI-228-YI)
Maguire, Michael, S47 (OS-072)
Mahadeva, Sanjiv, S62 (OS-097), S160 (SAT-507), S516 (TOP-113), S574 (WED-075)
Ma, Hai-Zhang, S243 (FRI-348)
Mahajan, Bhawna, S217 (WED-510)
Mahapatra, Shayan, S845 (THU-288)
Mahdavi-Gorabi, Armita, S697 (FRI-195-YI)
Maher, Eslam, S455 (TOP-406)
Maheshwari, Deepanshu, S100 (THU-057-YI), S174 (FRI-415-YI)
Mahgoub, Sara, S525 (THU-103), S558 (TOP-063-YI), S589 (WED-118)
Mahida, Suraj, S598 (WED-148)
Mahler, Michael, S342 (SAT-399)
Mahmood, Abdullah Al, S598 (WED-149)
Mahmood, Bushra, S967 (TOP-600-YI)
Mahmoud, Waleed, S732 (THU-446)
Mahmud, Nadim, S754 (THU-509)
Mahmuduzzaman, Mohammad, S745 (THU-484)
Ma, Hong, S433 (THU-239), S932 (SAT-641)
Mähringer-Kunz, Aline, S503 (FRI-248)
Mahrous, Sara, S504 (FRI-252)
Maida, Ivana Rita, S901 (SAT-559), S902 (SAT-560), S936 (TOP-584), S938 (FRI-586)
Maier, Barbara, S284 (FRI-266)
Maieron, Andreas, S539 (THU-151-YI)
Maimaiti, Maiwulanjiang, S243 (FRI-348)
Maimaitiyiming, Muyessar, S86 (LBP-041)
Maimouni, Cautar El, S110 (TOP-222), S562 (TOP-097-YI)
Maina, Cecilia, S402 (FRI-529-YI)
Mainardi, Lorenzo, S475 (WED-366)
Maiwall, Rakhi, S6 (GS-011-YI), S104 (THU-071-YI), S105 (THU-073-YI), S105 (THU-074), S131 (FRI-105-YI), S141 (TOP-424-YI), S145 (SAT-453), S156 (SAT-495), S189 (WED-419), S195 (WED-442-YI), S214 (WED-501-YI), S373 (WED-353-YI), S719 (TOP-487-YI), S867 (FRI-643), S952 (FRI-622)
Mai, Yanpei, S208 (WED-481), S253 (SAT-533), S279 (THU-336), S785 (SAT-021), S813 (FRI-045), S931 (SAT-638)
Majcher, Adam, S672 (SAT-230)

Majeed, Ammar, S218 (WED-513), S433 (THU-240), S749 (THU-496), S820 (WED-021), S922 (SAT-613)
Majeed, Khalid Abdul, S178 (FRI-430)
Majeed, Nehna, S835 (THU-264-YI)
Majem, Blanca, S634 (SAT-103)
Majer, Filip, S855 (WED-288)
Majid, Erum, S865 (FRI-637)
Major, Marian, S816 (WED-009), S818 (WED-014)
Major, Xavier, S798 (TOP-048), S810 (FRI-035), S810 (FRI-036)
Majumdar, Avik, S10 (LBO-006), S145 (SAT-457), S218 (WED-513), S400 (FRI-524), S400 (FRI-525), S410 (FRI-558), S736 (THU-458), S739 (THU-466), S749 (THU-496), S820 (WED-021)
Ma, Kai, S456 (WED-233)
Mak, Anne Linde, S641 (SAT-126)
Makatini, Zinhle, S76 (LBP-019-YI)
Makhlouf, Idir, S387 (FRI-484)
Makino, Yuki, S463 (WED-251-YI)
Mak, Lung-Yi, S423 (TOP-360), S452 (THU-414-YI), S496 (FRI-230), S896 (THU-644), S933 (SAT-643)
Mak, Lung Yi Loey, S438 (THU-364), S824 (WED-035), S876 (THU-575), S915 (SAT-593), S947 (FRI-609), S960 (WED-588)
Makrufardi, Firdian, S476 (WED-367)
Makuza, Jean Damascene, S821 (WED-024), S967 (TOP-600-YI)
Malagnino, Vincenzo, S919 (SAT-608-YI)
Ma, Lan, S119 (FRI-072), S259 (SAT-554), S609 (WED-182), S763 (THU-011), S924 (SAT-620)
Malatesta, Maria-Stella, S507 (FRI-257)
Malek, Nisar P., S651 (SAT-158-YI)
Malenov, Dušan, S654 (SAT-169)
Maleta, Lucija, S255 (SAT-541)
Maleux, Geert, S747 (THU-492)
Malherbe, Pierre, S493 (FRI-221), S508 (FRI-364-YI)
Malhotra, Pooja, S908 (SAT-578)
Maliakal, Sophie, S139 (FRI-133)
Ma, Lijie, S475 (WED-365)
Malik, Ahmad, S845 (THU-289)
Malik, Mohammad, S254 (SAT-537)
Malik, Rohan, S55 (OS-086), S831 (THU-258-YI), S842 (THU-284)
Malin, Jakob, S904 (SAT-564)
Malinverno, Federica, S69 (LBP-004-YI), S307 (SAT-263), S831 (THU-256-YI)
Ma, Liping, S941 (FRI-591)
Mallela, Venkata Ramana, S12 (OS-005-YI), S490 (TOP-407-YI)
Mallet, Vincent, S66 (OS-104)
Malme, Kristian, S822 (WED-026), S825 (WED-036)
Malone, Karen, S25 (OS-030)
Malouin, Lauren, S485 (WED-395-YI)
Maltese, Teresa, S163 (FRI-382), S967 (WED-605-YI)
Maluleke, Ntsakisi, S76 (LBP-019-YI)
Malvestiti, Francesco, S166 (FRI-393), S241 (FRI-340), S476 (WED-368), S575 (WED-076), S601 (WED-156)
Małyszko, Jolanta, S409 (FRI-555)
Mammadyarzade, Aysel, S542 (THU-163)
Mamo, Eyerusalem, S825 (WED-036)
Mampunza, Samuel, S80 (LBP-028-YI)
Mamuti, Alimujiang, S243 (FRI-348)
Mamutova, Elvira, S551 (THU-189), S551 (THU-190)
Manamela, Morubula, S76 (LBP-019-YI)
Manamley, Nick, S84 (LBP-038), S839 (THU-272), S846 (THU-291), S846 (THU-298)
Manassevee, Pemika, S973 (WED-625)
Manca, Alessandra, S942 (FRI-593)
Mancheño, Uxua, S364 (WED-329-YI)
Manchon, Pauline, S571 (WED-067)
Manch, Richard, S687 (FRI-165)
Mancina, Rosellina, S476 (WED-368)
Mancini, Camilla, S841 (THU-282)
Mancuso, Clara, S323 (SAT-315)
Mandal, Amitabha, S36 (OS-051-YI)
Mandal, Ayan, S659 (SAT-186)
Mandal, Palash, S357 (THU-339)
Mandizabal, Manuel, S159 (SAT-505)
Mandorfer, Mattias, S6 (GS-011-YI), S32 (OS-044), S33 (OS-046), S52 (OS-081), S54 (OS-084), S97 (SAT-084-YI), S113 (FRI-053), S156 (SAT-494), S179 (FRI-431-YI), S179 (FRI-432), S183 (FRI-444-YI), S183 (FRI-445), S186 (TOP-470-YI), S199 (WED-451-YI), S199 (WED-452), S200 (WED-453), S205 (WED-474), S213 (WED-498), S216 (WED-508), S217 (WED-509-YI), S222 (WED-524), S252 (SAT-530), S427 (THU-220), S427 (THU-221), S440 (THU-370), S732 (THU-448-YI), S733 (THU-449), S733 (THU-450), S734 (THU-451), S738 (THU-464-YI), S748 (THU-493-YI), S749 (THU-494), S750 (THU-497-YI), S750 (THU-498), S752 (THU-501), S753 (THU-505-YI), S836 (THU-265-YI), S914 (SAT-591)
Manegold, Nils, S54 (OS-084)
Manegold, Nils Theodor, S737 (THU-461)
Manenti, Marco, S51 (OS-079)
Manesis, Emmanouil, S314 (SAT-283)
Manfredi, Giulia, S12 (OS-005-YI)
Manfredi, Giulia Francesca, S82 (LBP-034-YI), S307 (SAT-263), S335 (SAT-378-YI), S429 (THU-227-YI)
Manfredi, Paolo, S669 (SAT-219)
Mangala, Thendral, S759 (TOP-017-YI)
Mangana, Carolina, S284 (FRI-266)
Manga, Noel, S911 (SAT-586)
Mangat, Pamela, S841 (THU-276-YI)
Manges, Amee, S967 (TOP-600-YI)
Mangia, Alessandra, S43 (OS-066), S69 (LBP-004-YI), S82 (LBP-034-YI), S304 (SAT-258), S335 (SAT-378-YI), S825 (WED-037), S900 (SAT-559), S902 (SAT-560), S934 (TOP-582), S936 (TOP-584), S937 (FRI-585-YI), S938 (FRI-586)
Mangini, Chiara, S402 (FRI-530)
Mangler, Franziska, S291 (FRI-291-YI)
Mang, M, S616 (WED-199)
Manhas, Savrina, S948 (FRI-610)
Mani, Iliana, S142 (SAT-449), S187 (WED-415)
Manisha, Manisha, S100 (THU-057-YI), S174 (FRI-415-YI), S181 (FRI-441-YI), S184 (FRI-452-YI)
Mani Tripathi, Dinesh, S361 (THU-355-YI)
Man, Joris De, S638 (SAT-117-YI)
Manna, Dina, S286 (FRI-272)
Manna, Giulia La, S196 (WED-445)
Manni, Giulia, S427 (THU-220)
Männistö, Ville, S114 (FRI-055), S122 (FRI-084), S266 (SAT-346), S562 (TOP-096)
Mann, Jake, S461 (WED-247)
Mann, Jelena, S281 (TOP-296-YI)
Mann, Matthias, S148 (SAT-467-YI)
Manns, Michael, S14 (OS-007), S297 (TOP-293)
Manolakopoulos, Spilios, S620 (WED-212)
Manolas, Melina, S774 (THU-040), S774 (THU-041)
Manousou, Pinelopi, S438 (THU-363), S471 (WED-271), S563 (WED-041), S685 (FRI-157-YI)
Manríquez, Jesus Alejandro Ruiz, S41 (OS-061)
Mansbach, Hank, S563 (WED-042), S597 (WED-141)
Manteca, Herminia, S969 (WED-611)
Mantia, Claudia La, S495 (FRI-227)
Mantovani, Alessandro, S626 (WED-231)
Mantovani, Anna, S97 (SAT-084-YI), S595 (WED-137), S677 (SAT-243-YI)
Mantovani, Stefania, S370 (WED-346), S462 (WED-248)
Mantry, Parvez, S10 (LBO-006), S614 (WED-195)
Manuel Diaz, Juan, S146 (SAT-461)
Manuilov, Dmitry, S939 (FRI-587), S948 (FRI-610), S956 (WED-576), S962 (WED-593)
Manuli, Chiara, S90 (SAT-061-YI), S402 (FRI-531), S848 (THU-304)
Manzanares, Sandra, S810 (FRI-036)
Manzano, Samuel, S806 (FRI-024)
Manzat-Saplacan, Roberta M., S353 (SAT-432)
Manzia, Tommaso Maria, S59 (OS-091)
Manzo-Santana, Fátima, S866 (FRI-640)
Mao, Aojie, S677 (SAT-241)
Mao, Feifei, S511 (FRI-370)
Mao, Qianguo, S952 (FRI-623)
Mao, Richeng, S201 (WED-458), S374 (WED-356)
Mao, Tianhao, S30 (OS-040), S640 (SAT-123)

Author Index

Mao, Tianyu, S293 (FRI-302-YI), S324 (SAT-318), S352 (SAT-428-YI)
Mao, Xianhua, S438 (THU-364), S496 (FRI-230)
Mao, Xinli, S676 (SAT-240)
Mao, Yilei, S628 (TOP-145)
Mao, Yimin, S90 (SAT-060), S98 (SAT-089-YI)
Mao, Zhuxin, S920 (SAT-609)
Maponga, Tongai Gibson, S900 (SAT-558)
Maracci, Monia, S43 (OS-066), S900 (SAT-559), S902 (SAT-560), S934 (TOP-582), S936 (TOP-584), S937 (FRI-585-YI), S938 (FRI-586)
Maradan, Gwenaëlle, S815 (WED-005)
Maras, Jaswinder, S104 (THU-071-YI), S105 (THU-073-YI), S105 (THU-074), S120 (FRI-074), S129 (TOP-224-YI), S131 (FRI-105-YI), S138 (FRI-132), S139 (FRI-135-YI), S264 (SAT-335), S264 (SAT-336), S265 (SAT-341), S269 (SAT-354-YI), S269 (SAT-355), S276 (THU-324-YI), S280 (THU-337), S361 (THU-354), S373 (WED-353-YI), S418 (THU-517-YI), S478 (WED-371)
Maraşlı, Mustafa Utku, S496 (FRI-231)
Marcantei, Camille, S167 (FRI-394-YI)
Marcellin, Fabienne, S889 (THU-619)
Marcellin, Patrick, S943 (FRI-594), S953 (FRI-624)
Marchand, Hélène Strick, S887 (THU-612-YI)
Marchelli, Daniele, S166 (FRI-393), S476 (WED-368)
Marche, Patrice, S885 (THU-607)
Marchesi, Julian R., S455 (TOP-406), S500 (FRI-239)
Marciano, Sebastián, S24 (OS-028), S34 (OS-049), S112 (FRI-050), S141 (TOP-437), S144 (SAT-452), S159 (SAT-505), S160 (SAT-507), S166 (FRI-388-YI), S956 (TOP-598)
Marciniak, Moritz, S860 (WED-307)
Marco, Andrés, S710 (THU-557-YI), S804 (FRI-019), S826 (WED-038)
Marcos, Cristina Fernández, S819 (WED-019)
Marcos, Eva María Rodriguez, S815 (WED-006)
Marco, Tobias Di, S10 (LBO-006)
Marco, Vito Di, S176 (FRI-425), S335 (SAT-378-YI), S912 (SAT-587-YI)
Marculescu-Ferrari, Rodrig, S156 (SAT-494)
Marculescu, Rodrig, S199 (WED-452), S738 (THU-464-YI)
Mareková, Mária, S321 (SAT-305)
Marenco-Flores, Ana, S327 (SAT-322), S331 (SAT-368-YI)
Mares, Jan, S405 (FRI-540)
Marey, Mohamed Mahmoud, S208 (WED-482)
Margáin, Astrid Ruiz, S22 (OS-022-YI), S412 (FRI-564-YI), S707 (THU-548)
Margalit, Maya, S563 (WED-042), S597 (WED-141)
Margarita, Sara, S241 (FRI-340)
Margheri, Francesca, S457 (WED-235)
Margolis, David, S85 (LBP-040)
Marhenke, Silke, S460 (WED-244-YI), S487 (WED-400-YI)
Maria, Alexandre, S92 (SAT-068), S95 (SAT-076)
Maria, Buzias, S209 (WED-483), S255 (SAT-539), S543 (THU-165), S544 (THU-166)
Maria, Francesco De, S43 (OS-066), S934 (TOP-582)
Maria, Gabriele Di, S190 (WED-425), S607 (WED-174-YI)
Maria Geretti, Anna, S807 (FRI-025)
Maria, Nicola De, S412 (FRI-562)
Mariano, Gabrielle, S529 (THU-116-YI), S534 (THU-131), S865 (FRI-638)
Marí, Montserrat, S481 (WED-382-YI), S639 (SAT-120)
Marinaro, Letizia, S900 (SAT-559), S902 (SAT-560), S911 (SAT-587-YI), S936 (TOP-584), S938 (FRI-586)
Marin-Correa, Diana, S174 (FRI-416-YI), S458 (WED-237-YI)
Marinescu, Adrian, S951 (FRI-620)
Marini, Giulia, S405 (FRI-541)
Marin, Jose, S281 (TOP-296-YI), S489 (WED-412-YI)
Marin-Lopez, Eduardo, S866 (FRI-640)
Marino, Rebecca, S60 (OS-094), S375 (TOP-519)
Mariño, Zoe, S21 (OS-021), S39 (OS-057), S828 (TOP-309-YI), S837 (THU-267), S840 (THU-274), S840 (THU-275), S842 (THU-283), S855 (WED-289), S903 (SAT-563-YI)
Marique, Lancelot, S381 (FRI-465), S382 (FRI-466)
Marjot, Thomas, S740 (THU-468)
Mark, Henry E, S777 (THU-050)
Marleau, Denis, S386 (FRI-480-YI)
Marom, Ilay, S614 (WED-191)
Maroni, Luca, S83 (LBP-034-YI), S307 (SAT-263), S335 (SAT-378-YI), S741 (THU-473)
Marot, Astrid, S55 (OS-085-YI), S109 (TOP-210)
Marquardt, Jens U., S35 (OS-050-YI), S185 (TOP-456-YI), S485 (WED-396), S504 (FRI-251), S601 (WED-155), S651 (SAT-158-YI), S854 (WED-285)
Marques da Costa, Rui, S885 (THU-608)
Marques, Hugo Pinto, S892 (THU-627)
Marracino, Antonio, S576 (WED-083)
Marra, Fabio, S3 (GS-005), S38 (OS-055), S54 (OS-084), S69 (LBP-004-YI), S82 (LBP-034-YI), S185 (TOP-455-YI), S195 (WED-442-YI), S304 (SAT-258), S335 (SAT-378-YI), S343 (SAT-400), S424 (TOP-375-YI), S428 (THU-226-YI), S428 (THU-227-YI), S447 (THU-394), S457 (WED-235), S462 (WED-249), S475 (WED-366), S479 (WED-379), S505 (FRI-254), S506 (FRI-255-YI), S514 (FRI-381), S746 (THU-489), S752 (THU-501)
Marrone, Aldo, S912 (SAT-587-YI)
Marrone, Giuseppe, S219 (WED-515)
Marron, Thomas, S428 (THU-227-YI), S491 (TOP-408-YI)
Marsal, Aida, S481 (WED-382-YI)
Marshall, Aileen, S65 (OS-102), S970 (WED-619)
Marshall, Renee, S20 (OS-018)
Martel-laferriere, Valerie, S968 (WED-609-YI)
Martel, Myriam, S380 (FRI-462)
Marti-Aguado, David, S254 (SAT-538), S443 (THU-381), S585 (WED-105), S585 (WED-106), S598 (WED-150), S599 (WED-151), S612 (WED-186-YI), S772 (THU-036), S779 (SAT–003-YI)
Marti-Bonmati, Luis, S254 (SAT-538), S599 (WED-151)
Martin, Anna, S623 (WED-220)
Martin, Antoine, S374 (TOP-503)
Martín, Ariadna Gil, S101 (THU-059-YI)
Martin-Bermudo, Franz, S527 (THU-108), S678 (SAT-244)
Martín, Berta, S128 (FRI-100)
Martin, Carlos Maroto, S403 (FRI-532)
Martin, Carmen Alonso, S379 (FRI-459), S403 (FRI-532), S410 (FRI-558)
Martín, Cesar Augusto, S633 (SAT-101-YI)
Martín-Chavarri, Sonia, S250 (SAT-524)
Martin, Dan, S61 (OS-108)
Martineau, France, S533 (THU-127-YI), S616 (WED-200)
Martin, Eleonora De, S59 (OS-091), S90 (SAT-059)
Martinelli, Giuseppina, S532 (THU-123), S549 (THU-186-YI)
Martinelli, Michele, S457 (WED-235)
Martínez-Alcocer, Ana, S281 (TOP-296-YI)
Martínez-Álvarez, Alicia, S129 (FRI-101)
Martínez, Ana Belén, S223 (WED-528)
Martinez, Anthony, S161 (SAT-509), S695 (FRI-186)
Martínez-Barocio, Oscar, S771 (THU-030)
Martínez-Cabrera, Carlos, S771 (THU-030)
Martinez-Castillo, Moises, S236 (FRI-322)
Martínez-Chantar, María Luz, S30 (OS-039-YI), S101 (THU-059-YI), S232 (FRI-313), S241 (FRI-339), S272 (THU-315-YI), S273 (THU-316), S278 (THU-333-YI), S281 (TOP-296-YI), S489 (WED-412-YI), S633 (SAT-101-YI), S635 (SAT-106), S855 (WED-287-YI)
Martinez-Cruz, Luis Alfonso, S272 (THU-315-YI), S273 (THU-316), S278 (THU-333-YI), S633 (SAT-101-YI)
Martinez, Elena Velasco, S379 (FRI-459), S403 (FRI-532), S403 (FRI-533)
Martínez, Elena Velasco, S415 (FRI-575)
Martinez-Garcia, Santiago, S799 (TOP-049)

Martinez, Gema Frühbeck, S608 (WED-175), S633 (SAT-101-YI), S680 (FRI-139), S777 (THU-050)
Martinez-Gili, Laura, S134 (FRI-117), S137 (FRI-125)
Martínez-Gómez, María, S233 (FRI-315)
Martínez, Ismael El Hajra, S16 (OS-010), S294 (TOP-278), S309 (SAT-268), S815 (WED-006)
Martinez, Javier, S25 (OS-029)
Martinez, Jorge, S112 (FRI-050)
Martínez, Laisy Zacarias, S815 (WED-006)
Martinez, Leticia Martinez, S866 (FRI-640)
Martinez, Linda, S682 (FRI-148)
Martínez-Máñez, Ramón, S230 (TOP-343-YI)
Martínez, María Belen, S112 (FRI-050)
Martínez-Martínez, Sara, S241 (FRI-339)
Martinez, Mercedes, S10 (LBO-006)
Martinez, Montserrat Terrazas, S961 (WED-592)
Martínez-Navarro, Alejandro, S483 (WED-387)
Martínez-Pérez, Luz A., S474 (WED-364)
Martínez, Raquel Latorre, S567 (WED-054)
Martínez-Sánchez, FroyLan, S771 (THU-030)
Martinez, Sonia Giraldez, S919 (SAT-607)
Martin, Holly, S599 (WED-152)
Martini, Andrea, S435 (THU-247)
Martini, Francesco, S741 (THU-473), S751 (THU-500)
Martini, Silvia, S90 (SAT-061-YI), S402 (FRI-531), S784 (SAT-015-YI), S848 (THU-304)
Martin, Josefina, S634 (SAT-103)
Martin, Katherine, S84 (LBP-038)
Martín-Llahí, Marta, S203 (WED-463)
Martin-Mateos, Rosa, S34 (OS-049), S141 (TOP-437), S410 (FRI-558)
Martín-Mateos, Rosa, S542 (THU-164), S567 (WED-054)
Martin, Nathalie, S854 (WED-285)
Martino, Vincent Di, S388 (FRI-485), S497 (FRI-234), S723 (THU-418)
Martin, Pablo Luri, S287 (FRI-274)
Martín, Padilla Machaca, S141 (TOP-437)
Martín, Raquel Sánchez, S34 (OS-049)
Martin-Robles, Julen, S445 (THU-385)
Martin, Ross, S948 (FRI-610)
Martins, Adrielly, S79 (LBP-026), S294 (TOP-277-YI), S297 (TOP-292-YI), S300 (SAT-250), S327 (SAT-323), S328 (SAT-324), S328 (SAT-361), S338 (SAT-384)
Martins, Aik, S724 (THU-420)
Martins, Alexandra, S43 (OS-066), S937 (FRI-585-YI), S940 (FRI-589)
Martin, Sara De, S669 (SAT-219)
Martins, Eduardo, S82 (LBP-032), S671 (SAT-227)
Martins, Fatima Oliveira, S892 (THU-627)
Martins, Pedro Lages, S786 (SAT-022), S892 (THU-627)
Martins, Vitor, S690 (FRI-173)
Martró, Elisa, S810 (FRI-035)
Marty, Benjamin, S648 (SAT-151-YI)
Martyn, Emily, S823 (WED-028), S826 (WED-039), S900 (SAT-558)
Marulli, Mariagrazia, S69 (LBP-004-YI)
Maruzzelli, Luigi, S3 (GS-005), S720 (TOP-502-YI), S727 (THU-431)
Marwan, Eman, S926 (SAT-624)
Marwan, Rana, S537 (THU-141-YI)
Marzano, Alfredo, S3 (GS-005)
Marzioni, Marco, S69 (LBP-004-YI), S82 (LBP-034-YI), S304 (SAT-258), S307 (SAT-263), S335 (SAT-378-YI), S350 (SAT-421), S741 (THU-473), S751 (THU-500)
Marz, Manja, S885 (THU-608)
Mas, Ariadna, S810 (FRI-036)
Masarone, Mario, S176 (FRI-425), S190 (WED-425), S212 (WED-494-YI), S479 (WED-378), S601 (WED-156), S972 (WED-623), S977 (WED-640)
Masashi, Hirooka, S568 (WED-057-YI)
Masayuki, Otsuka, S458 (WED-238)
Mascianà, Gianluca, S477 (WED-370)
Masciocchi, Federica, S407 (FRI-548)
Mas, Eduard, S233 (FRI-315), S605 (WED-168-YI), S612 (WED-188)
Mašek, Jan, S861 (WED-308)
Masetti, Chiara, S531 (THU-120)
Ma, Sheng-Li, S954 (FRI-626)
Ma, Shiwen, S104 (THU-070)
Mashkoor, Yusra, S772 (THU-035)
Masi, Gianluca, S424 (TOP-375-YI), S481 (WED-383)
Masnou, Helena, S837 (THU-267), S855 (WED-289)
Masó, Arnau, S483 (WED-387)
Mason, Andrew L., S14 (OS-008), S79 (LBP-026), S295 (TOP-279), S315 (SAT-286), S325 (SAT-319), S354 (SAT-435), S355 (SAT-436)
Masoodi, Mojgan, S561 (TOP-081)
Masri, Marianthi, S597 (WED-147)
Massoels, Jo, S577 (WED-084), S600 (WED-153)
Masson, Marie-Charlotte, S512 (FRI-372)
Masthoff, Max, S736 (THU-460-YI), S737 (THU-461)
Mastro, Alessio, S195 (WED-442-YI), S447 (THU-394), S505 (FRI-254), S514 (FRI-381), S720 (TOP-502-YI)
Matarranz, Mariano, S806 (FRI-024)
Matar, Rola, S886 (THU-609)
Matchkov, Vladimir, S660 (SAT-188-YI)
Mateos, Rosa María Martín, S166 (FRI-388-YI)
Matern, Lea, S672 (SAT-230)
Mateu, Alejandro Rodríguez, S16 (OS-010)
Matheeussen, Veerle, S65 (OS-101-YI), S903 (SAT-562), S929 (SAT-629)
Matheson, Kara, S229 (WED-545)
Mathew, Babu, S104 (THU-071-YI), S105 (THU-073-YI), S105 (THU-074), S120 (FRI-074), S129 (TOP-224-YI), S131 (FRI-105-YI), S138 (FRI-132), S139 (FRI-135-YI), S265 (SAT-341), S269 (SAT-354-YI), S269 (SAT-355), S276 (THU-324-YI), S280 (THU-337), S361 (THU-354), S373 (WED-353-YI)
Mathew Lasington, Lawin Steve, S94 (SAT-075), S118 (FRI-069), S118 (FRI-070), S153 (SAT-481), S153 (SAT-483)
Mathew, Sanju, S713 (WED-556-YI)
Mathieu, Struyve, S535 (THU-134), S611 (WED-185), S696 (FRI-190), S920 (SAT-609), S929 (SAT-629)
Mathôt, Ron, S168 (FRI-397-YI)
Mathurin, Philippe, S35 (OS-050-YI), S45 (OS-067), S505 (FRI-254)
Matilla, Ana, S781 (SAT-008), S781 (SAT-009)
Matilla, Ana M, S427 (THU-220)
Matsudaira, Takahiro, S875 (THU-573)
Matsuda, Michitaka, S32 (OS-045), S121 (FRI-076-YI), S488 (WED-403)
Matsukura, Akira, S894 (THU-635)
Matsumoto, Takayuki, S194 (WED-435)
Matsuoka, Lea, S393 (FRI-505)
Matsushita, Masahiro, S686 (FRI-159)
Matsuura, Kentaro, S166 (FRI-393), S977 (WED-639)
Mattarei, Andrea, S669 (SAT-219)
Mattei, Gianluca, S479 (WED-379)
Matter, Matthias, S533 (THU-126)
Matthews, Philippa C, S823 (WED-028), S826 (WED-039), S900 (SAT-558)
Matthys, Rania, S281 (TOP-295-YI), S464 (WED-253)
Mattos, Angelo, S141 (TOP-437), S154 (SAT-484), S296 (TOP-281), S306 (SAT-262)
Mattos, Angelo Z., S35 (OS-050-YI), S154 (SAT-484)
Matusiewicz, Anna, S404 (FRI-537)
Matz-Soja, Madlen, S647 (SAT-148), S879 (THU-589-YI), S930 (SAT-636)
Maung, Soe Thiha, S503 (FRI-249), S973 (WED-626-YI)
Maurer, Jurij, S749 (THU-494)
Mauricio, Didac, S62 (OS-097), S516 (TOP-113), S774 (THU-040), S774 (THU-041), S777 (THU-050)
Mauri, Francesco, S455 (TOP-406)
Mauriz, Lucia Lameroli, S654 (SAT-171-YI)
Mauro, Ezequiel, S459 (WED-242-YI), S468 (WED-263), S485 (WED-396)
Mauss, Stefan, S904 (SAT-564), S971 (WED-620)
Mauz, Jim Benjamin, S197 (WED-446), S222 (WED-524), S222 (WED-526-YI), S732 (THU-448-YI), S737 (THU-461), S737 (THU-462)
Mavinga, Jeansy, S80 (LBP-028-YI)
Mawatari, Seiichi, S977 (WED-639)
Ma, Xiaodan, S868 (FRI-644)

Author Index

Ma, Xiong, S68 (OS-107), S293 (FRI-302-YI), S305 (SAT-259), S324 (SAT-317), S324 (SAT-318), S331 (SAT-368-YI), S352 (SAT-428-YI)
Ma, Xixing, S259 (SAT-554)
Maya, Juliana, S154 (SAT-484)
Maya-Miles, Douglas, S527 (THU-108), S542 (THU-164), S567 (WED-054), S571 (WED-069), S600 (WED-153), S621 (WED-214), S644 (SAT-137), S678 (SAT-244), S765 (THU-013)
Ma, Yanchen, S882 (THU-596)
Ma, Yanping, S756 (THU-514)
Ma, Yifan, S100 (TOP-207)
May, Lauren, S130 (FRI-103)
Maynard, Lauren, S956 (TOP-598), S957 (WED-577), S960 (WED-587)
Mayo, Marlyn J., S10 (LBO-006), S79 (LBP-026), S295 (TOP-280), S319 (SAT-301), S328 (SAT-362), S329 (SAT-363), S329 (SAT-364), S330 (SAT-365), S330 (SAT-366), S338 (SAT-384), S340 (SAT-388), S341 (SAT-396)
Mayorga, Andrea Salomè Velasco, S31 (OS-042), S725 (THU-425), S746 (THU-490)
Ma, Yuan-Qiang, S659 (SAT-185)
Ma, Yun, S644 (SAT-135-YI)
Mazariegos, George V., S59 (OS-091)
Mazibuko, Lusanda, S900 (SAT-558)
Ma, Zikun, S88 (TOP-192), S98 (SAT-088), S331 (SAT-367), S370 (WED-345)
Mazi, Tagreed A, S523 (THU-099)
Mazo, Daniel, S34 (OS-049), S141 (TOP-437), S166 (FRI-388-YI)
Mazo, Daniel F, S35 (OS-050-YI)
Mazo, Daniel F., S688 (FRI-168)
Mazumder, Subash, S598 (WED-149)
Ma, Zuyi, S859 (WED-303), S860 (WED-306)
Mazzaferro, Vincenzo, S485 (WED-396)
Mazza, Giuseppe, S119 (FRI-073)
Mazzarelli, Chiara, S424 (TOP-375-YI), S429 (THU-227-YI), S494 (FRI-225), S514 (FRI-381)
Mazzaro, Cesare, S972 (WED-623)
Mazzolini, Guillermo, S358 (THU-340-YI), S654 (SAT-171-YI)
Mazzoni, Gianluca, S240 (FRI-338)
Mazzuccato, Beatrice, S531 (THU-120)
Mbatha, Nikiwe, S900 (SAT-558)
Mbelle, Mzamo, S174 (FRI-416-YI), S404 (FRI-538-YI), S458 (WED-237-YI), S503 (FRI-250)
Mbendi, Charles, S80 (LBP-028-YI)
Mbokazi, Welcome, S900 (SAT-558)
Mboup, Souleymane, S911 (SAT-586)
Mbow, Moustapha, S911 (SAT-586)
McCaffrey, Noel, S210 (WED-489-YI)
McCann, Adrian, S2 (GS-002), S13 (OS-006-YI), S290 (FRI-289)
McCarthy, Derrick, S58 (OS-089), S313 (SAT-282)
McCarthy, Fiona, S8 (LBO-002)
McCaughan, Geoff, S410 (FRI-558)
McCaughey, Kirsty, S113 (FRI-054)
McCauley, Bryan, S2 (GS-002), S13 (OS-006-YI), S290 (FRI-289)
McConnell, Matthew J., S134 (FRI-115)
McCorry, Roger, S10 (LBO-006)
McCoy, Martin, S409 (FRI-556), S493 (FRI-220)
McCoy, Martin Sebastian, S33 (OS-046), S206 (WED-475), S209 (WED-485), S383 (FRI-474), S737 (THU-461)
McDermott, Sinead, S396 (FRI-512)
McGillicuddy, Fiona, S641 (SAT-126)
Mcgilvray, Ian, S345 (SAT-409-YI)
McGlinchey, Aidan, S662 (SAT-197)
McGowan, David, S874 (THU-570), S886 (THU-610)
McGuire, Katie, S789 (SAT-030)
McHenry, Scott, S58 (OS-089), S313 (SAT-282)
McHutchison, John, S8 (LBO-003)
McIntyre, Jeff, S573 (WED-072), S613 (WED-190), S770 (THU-028)
McKeating, Jane, S87 (LBP-043)
McKenna-Barry, Matthew, S210 (WED-489-YI)
McKibben, Andrew, S10 (LBO-006)
McKiernan, Susan, S708 (THU-549-YI)
McLaughlin, Mark, S5 (GS-008)
McLaughlin, Megan, S295 (TOP-280)
McLeod, Magnus, S229 (WED-545)
McMullen, Megan, S138 (FRI-127), S243 (FRI-347)
McNally, Alan, S364 (WED-324-YI)
McNaughton, Anna, S804 (FRI-015-YI)
Mcphail, Mark, S147 (SAT-464), S767 (THU-019)
McPhail, Mark J W, S165 (FRI-386), S182 (FRI-443)
McRae, Michael, S438 (THU-365), S588 (WED-117), S971 (WED-621)
Mdawar-Bailly, Elise, S72 (LBP-011)
Mead, Benjamin, S218 (WED-513), S749 (THU-496)
Mead-Harvey, Carolyn, S390 (FRI-493-YI)
Meda, Clara, S640 (SAT-122), S672 (SAT-228)
Medda, Shyamalendu, S100 (THU-056)
Medeiros, Gabriela, S267 (SAT-348)
Medhat, Mohammed, S524 (THU-101)
Medici, Valentina, S39 (OS-057), S846 (THU-291), S846 (THU-298)
Medic, Maya, S242 (FRI-345-YI), S472 (WED-274)
Medina, Alberto Esteban, S806 (FRI-023)
Medina, Carlos, S708 (THU-549-YI)
Medina, Maria Jose Devesa, S948 (FRI-611)
Medina-Morales, Esli, S325 (SAT-320)
Medrano-Bosch, Mireia, S483 (WED-387)
Medrano, Indhira Perez, S16 (OS-010), S294 (TOP-278), S300 (SAT-250), S309 (SAT-268)
Meeberg, Glenda, S401 (FRI-527)
Meehan, Edward, S779 (SAT–004)
Meena, Dr Babu Lal, S398 (FRI-521), S867 (FRI-643)
Mega, Andrea, S69 (LBP-004-YI), S304 (SAT-258), S307 (SAT-263), S335 (SAT-378-YI)
Mehal, Wajahat, S102 (THU-062), S659 (SAT-187)
Mehdi, Tavakhol, S59 (OS-091)
Mehrara, Shaheen, S614 (WED-195)
Mehreen, Sania, S178 (FRI-430)
Mehrzad, Homoyon, S397 (FRI-515)
Mehta, Ashwini, S614 (WED-195)
Mehta, Gautam, S8 (LBO-002), S119 (FRI-073), S150 (SAT-475)
Mehta, Neil, S375 (TOP-519)
Mehta, Rajiv, S1 (GS-001), S953 (FRI-624)
Mehta, Samir, S61 (OS-108)
Mehta, Shubham, S404 (FRI-539), S725 (THU-426), S741 (THU-474)
Mehta, Shubhangi, S408 (FRI-553)
Mei, Chunfeng, S233 (FRI-314), S664 (SAT-202), S664 (SAT-203), S665 (SAT-204), S797 (SAT-054), S872 (THU-562)
Meier, Jörn Arne, S210 (WED-485), S409 (FRI-556), S737 (THU-461), S744 (THU-481)
Meijnen, Mariëlle J. F., S351 (SAT-426-YI)
Meijnikman, Abraham Stijn, S9 (LBO-005-YI), S632 (SAT-099-YI)
Meindl, Mijuna, S852 (TOP-311)
Meineck, Myriam, S172 (FRI-411), S742 (THU-476)
Mei, Xue, S162 (TOP-440)
Mejia, Scherezada, S112 (FRI-050)
Melandro, Fabio, S407 (FRI-548)
Melanophy, Gail, S708 (THU-549-YI)
Melere, Melina, S850 (THU-308)
Melgar-Lesmes, Pedro, S483 (WED-387)
Melikian, ClareDr., S61 (OS-108)
Melita, Elena, S731 (THU-444-YI)
Mella, Allison, S338 (SAT-384)
Mellemkjær, Anders, S525 (THU-103), S692 (FRI-180)
Mello, Tommaso, S400 (FRI-526), S542 (THU-159)
Mells, George, S331 (SAT-368-YI)
Melnikova, Elizaveta, S660 (SAT-188-YI)
Melo-Filho, Cleber C., S881 (THU-592-YI)
Melo, João Filipe, S379 (FRI-460)
Meloni, Seema T., S78 (LBP-023)
Melum, Espen, S2 (GS-002), S284 (FRI-266), S287 (FRI-276-YI), S292 (FRI-300-YI), S858 (WED-300-YI)
Menacho, Sixto, S815 (WED-006)
Mena, Edward, S299 (SAT-247), S684 (FRI-154), S691 (FRI-175), S719 (TOP-486)
Menard, Cedric, S484 (WED-393)
Mendão, Luis, S802 (FRI-010-YI)
Mendel, Angelika, S744 (THU-482-YI)
Mendes, Liliana, S34 (OS-049), S35 (OS-050-YI), S141 (TOP-437),

S154 (SAT-484), S166 (FRI-388-YI), S296 (TOP-281), S306 (SAT-262), S724 (THU-420)
Méndez-Castillo, Raúl, S771 (THU-030)
Mendez, Patricia, S78 (LBP-025)
Méndez-Sánchez, Nahum, S549 (THU-185-YI)
Mendive, Juan, S765 (THU-013)
Mendizabal, Manuel, S35 (OS-050-YI), S112 (FRI-050), S141 (TOP-437), S296 (TOP-281), S306 (SAT-262)
Mendler, Michel, S299 (SAT-247)
Mendlowitz, Andrew, S914 (SAT-592-YI), S921 (SAT-610), S968 (WED-609-YI)
Mendoza, Yuly, S733 (THU-450)
Mendy, Maimuna, S798 (TOP-034)
Meneghetti, Anna, S307 (SAT-263), S335 (SAT-378-YI)
Meneghetti, Asier Rabasco, S446 (THU-393-YI), S507 (FRI-362)
Meneses, Maria João, S649 (SAT-152)
Meng, Fanzheng, S474 (WED-362)
Meng, Min, S86 (LBP-041)
Mengozzi, Giulio, S911 (SAT-587-YI)
Meng, Tongtong, S826 (WED-040)
Meng, Yao, S88 (TOP-192), S98 (SAT-088), S331 (SAT-367), S370 (WED-345)
Meng, Zhen, S643 (SAT-133)
Meng, Zhong-Ji, S162 (TOP-440), S259 (SAT-554), S463 (WED-252), S593 (WED-134), S609 (WED-182), S763 (THU-011), S924 (SAT-620)
Mennini, Gianluca, S407 (FRI-548)
Meno, Akimitsu, S506 (FRI-256)
Menon, Krishna, S404 (FRI-538-YI)
Menotta, Micheole, S475 (WED-366)
Men, Ruoting, S756 (THU-512)
Mensi, Edvige, S831 (THU-256-YI)
Mentsiou-Nikolaou, Evangelia, S577 (WED-084), S600 (WED-153), S621 (WED-214), S765 (THU-013)
Menze, Esther, S231 (FRI-305)
Meohas, Daniel, S154 (SAT-484)
Mercado, Maria, S855 (WED-287-YI)
Mercandate, Rosa, S595 (WED-138)
Mercurio, Francesco, S495 (FRI-227)
Merelli, Elisa, S69 (LBP-004-YI), S331 (SAT-368-YI), S332 (SAT-369)
Mereu, Elisabetta, S884 (THU-604-YI)
Merhout, Jasmine, S692 (FRI-180)
Merino, Javier, S337 (SAT-382)
Merino, Victor, S254 (SAT-538), S599 (WED-151)
Merk, Katharina, S151 (SAT-477)
Merle, Uta, S43 (OS-066), S901 (SAT-559), S902 (SAT-560), S934 (TOP-582), S937 (FRI-585-YI)
Merli, Manuela, S150 (SAT-475), S720 (TOP-502-YI), S746 (THU-489)
Meroni, Marica, S443 (THU-380-YI), S595 (WED-138), S636 (SAT-110-YI), S662 (SAT-198-YI)
Meroño, Mercè, S810 (FRI-035)
Meroz, Omer, S614 (WED-191)
Meschisi, Pietro, S339 (SAT-386)
Mesci, Aruz, S345 (SAT-409-YI)
Mescoli, Claudia, S466 (WED-258), S485 (WED-395-YI)
Mesquita, Pedro Filipe, S940 (FRI-589)
Mesropian, Agavni, S459 (WED-242-YI)
Messai, Inès, S827 (WED-046)
Messaoudi, Sofiane, S607 (WED-174-YI)
Messer, Eva Katharina, S600 (WED-154-YI)
Messetti, Dario, S626 (WED-231)
Messina, Vincenzo, S911 (SAT-587-YI)
Mester-Pavel, Patricia, S157 (SAT-497), S216 (WED-507)
Meszaros, Magdalena, S43 (OS-066), S45 (OS-067), S52 (OS-081), S90 (SAT-059), S380 (FRI-463), S381 (FRI-464), S414 (FRI-573), S497 (FRI-234), S720 (TOP-504-YI), S723 (THU-418), S742 (THU-477), S936 (TOP-584), S937 (FRI-585-YI)
Metin, Olga, S965 (WED-603)
Metivier, Chloe, S428 (THU-226-YI), S493 (FRI-221), S506 (FRI-255-YI), S508 (FRI-364-YI)
Metivier, Sophie, S43 (OS-066), S45 (OS-067), S207 (WED-477), S723 (THU-419), S934 (TOP-582), S937 (FRI-585-YI)
Metz, Martin, S322 (SAT-313)
Meulder, Sofie De, S22 (OS-023), S718 (WED-572)
Meunier, Lucy, S90 (SAT-059), S92 (SAT-068), S95 (SAT-076), S414 (FRI-573), S497 (FRI-234), S723 (THU-418)
Meuris, Leander, S99 (TOP-193-YI), S349 (SAT-420)
Meyboom, Joël, S943 (FRI-595)
Meyer, Antoine, S374 (TOP-503)
Meyer, Bernhard, S197 (WED-446)
Meyer, Carsten, S6 (GS-011-YI), S33 (OS-046), S736 (THU-460-YI)
Meyer, Nele, S887 (THU-611)
Meyer, Tim, S485 (WED-396)
Meynet-cordonnier, Anaïs, S663 (SAT-200)
Meyn, Leslie, S70 (LBP-005)
Mfinanga, Sayoki, S792 (SAT-042)
Mhlanga, Adquate, S873 (THU-563), S941 (FRI-590), S953 (FRI-625)
Mhlongo, Ngcebo, S900 (SAT-558)
Miailhes, Patrick, S889 (THU-619)
Miano, Lorenzo, S166 (FRI-393), S476 (WED-368), S601 (WED-156)
Mian, Paola, S55 (OS-086), S832 (THU-258-YI), S842 (THU-284)
Miao, Qi, S331 (SAT-368-YI), S352 (SAT-428-YI)
Miao, Yan, S423 (TOP-360)
Miarka, Maciej, S409 (FRI-555)
Miceli, Vitale, S638 (SAT-118)
Michailidis, Eleftherios, S890 (THU-623-YI), S891 (THU-624-YI)
Michalczuk, Matheus Truccolo, S24 (OS-028), S41 (OS-061), S144 (SAT-452), S160 (SAT-507)
Michalet, Morgan, S414 (FRI-572)
Michelet, Maud, S876 (THU-576), S893 (THU-634)
Michel, Maurice, S204 (WED-465), S532 (THU-124), S601 (WED-155), S621 (WED-214), S622 (WED-216), S765 (THU-013), S789 (SAT-031-YI), S790 (SAT-035)
Michel, Rivoire, S869 (TOP-632)
Michels, Wieneke, S148 (SAT-467-YI)
Mićić, Bojana, S268 (SAT-351)
Mickelson, Mindy, S186 (TOP-469-YI)
Mickute, Ugne, S807 (FRI-025)
Micuda, Stanislav, S286 (FRI-272), S661 (SAT-191)
Middelburg, Tim, S57 (OS-087-YI), S348 (SAT-418-YI)
Middleton, Michael, S690 (FRI-173)
midha, vandana, S952 (FRI-622)
Midiri, Federico, S727 (THU-431)
Miele, Luca, S219 (WED-515), S304 (SAT-258), S443 (THU-380-YI), S476 (WED-368), S577 (WED-084), S583 (WED-102-YI), S600 (WED-153), S601 (WED-156), S621 (WED-214), S765 (THU-013)
Miethke, Alexander, S842 (THU-284)
Migliano, Maria Teresa, S69 (LBP-004-YI)
Miguel, Marta De, S904 (SAT-564)
Mihai, Bogdan-Mircea, S574 (WED-074)
Mihai, Nicoleta, S951 (FRI-620), S974 (WED-633)
Mihai, Pomohaci, S251 (SAT-528)
Mihale, Jakub, S807 (FRI-025)
Mihaljevic, André, S512 (FRI-371)
Mihm, Ulrike, S251 (SAT-525)
Mikhail, Nabiel, S809 (FRI-029), S966 (TOP-599)
Miki, Daiki, S977 (WED-639)
Mikkelsen, Anne Catrine, S631 (SAT-094-YI), S660 (SAT-188-YI)
Mikkelsen, Susan, S262 (SAT-332)
Mikkelsen, Ulla Ramer, S692 (FRI-180)
Mikolajczyk, Rafael, S175 (FRI-419)
Mikova, Irena, S405 (FRI-540)
Mikulic, Danko, S59 (OS-092-YI)
Mikulits, Wolfgang, S477 (WED-369)
Milagro, Ana, S910 (SAT-581)
Milana, Martina, S726 (THU-429)
Milani, Ilaria, S626 (WED-231)
Milella, Michele, S900 (SAT-559), S902 (SAT-560), S911 (SAT-587-YI), S936 (TOP-584), S938 (FRI-586)
Milgrom, Yael, S60 (OS-093), S289 (FRI-286), S615 (WED-196)
Milian, Laura, S819 (WED-019)
Milic, Jovana, S378 (FRI-458), S534 (THU-131), S865 (FRI-638)
Milivojevic, Vladimir, S654 (SAT-169)
Milkiewicz, Malgorzata, S286 (FRI-273)

Author Index

Milkiewicz, Małgorzata, S281 (TOP-296-YI), S303 (SAT-257-YI)
Milkiewicz, Piotr, S281 (TOP-296-YI), S286 (FRI-273), S301 (SAT-251-YI), S303 (SAT-257-YI), S315 (SAT-286), S318 (SAT-298), S323 (SAT-314), S331 (SAT-368-YI), S332 (SAT-369), S355 (SAT-442)
Millan, Raquel, S527 (THU-108), S644 (SAT-137)
Miller, John, S281 (FRI-260), S282 (FRI-261)
Miller, Mark, S590 (WED-120)
Miller, Sophie, S699 (FRI-198)
Millet, Guillaume, S499 (FRI-238)
Millhaem, Kelly, S540 (THU-154)
Mills, Edward, S965 (WED-603)
Mil, Michael, S218 (WED-513), S749 (THU-496)
Milner, Andrew, S827 (WED-047)
Milosa, Fabiola, S31 (OS-042), S746 (THU-490)
Milosevic, Ivana, S807 (FRI-025)
Milot, Laurent, S207 (WED-477)
Minamikawa, Takeo, S668 (SAT-215)
Minchenberg, Scott, S137 (FRI-126)
Minciuna, Iulia, S61 (OS-095-YI), S255 (SAT-539), S543 (THU-165), S544 (THU-166), S602 (WED-157)
Minello Franza, Anne, S937 (FRI-585-YI)
Min, Eun-Ki, S260 (SAT-555)
Minguez, Beatriz, S427 (THU-220), S469 (WED-267)
Min, Hae-Ki, S649 (SAT-153)
Miniotti, Marco, S784 (SAT-015-YI)
Minisini, Rosalba, S12 (OS-005-YI)
Minko, Peter, S188 (WED-416)
min Kwon, Kyung, S316 (SAT-287), S329 (SAT-363), S975 (WED-636), S976 (WED-637)
Minnee, Robert, S53 (OS-083-YI)
Mino, Masaaki, S32 (OS-045), S121 (FRI-076-YI), S488 (WED-403)
Min, Thazin, S106 (THU-075)
Minuz, Pietro, S677 (SAT-243-YI)
Mioli, Fiorenza, S835 (THU-263)
Miquel, Joaquin, S968 (WED-610-YI)
Míquel, Joaquín, S366 (WED-332-YI)
Miquel, Rosa, S404 (FRI-538-YI)
Mirabel, Xavier, S414 (FRI-572)
Miraglia, Roberto, S3 (GS-005), S720 (TOP-502-YI), S727 (THU-431)
Mira, Jose, S863 (WED-317)
Miralpeix, Anna, S21 (OS-021)
Miranda, Adelina Lozano, S34 (OS-049), S35 (OS-050-YI), S166 (FRI-388-YI), S296 (TOP-281), S306 (SAT-262)
Miranda, Alejandro, S34 (OS-049)
Miranda, Phillippa, S540 (THU-154)
Miranda, Susanna, S388 (FRI-489), S388 (FRI-490)
Mira, Stefania, S476 (WED-368), S575 (WED-076), S601 (WED-156)
Mirat, Marta Nabal, S308 (SAT-264)
Miraval, Eduardo, S343 (SAT-400), S364 (WED-329-YI)
Mirshahi, Faridoddin, S649 (SAT-153)
Mirza, Payal, S100 (THU-056)
Mishima, Yusuke, S708 (THU-553)
Mishra, Ajay, S952 (FRI-622)
Mishra, Ashwani, S141 (TOP-423), S184 (TOP-454-YI), S725 (THU-426)
Mishra, Gauri, S433 (THU-240), S922 (SAT-613)
Mishra, Satyam, S257 (SAT-544)
Mishra, Sumit, S463 (WED-250)
Misner, Dinah, S658 (SAT-184), S879 (THU-587), S889 (THU-620)
Missale, Gabriele, S69 (LBP-004-YI), S304 (SAT-258), S307 (SAT-263), S335 (SAT-378-YI), S874 (THU-571)
Missen, Louise, S827 (WED-047)
Mistry, Pramod K., S840 (THU-275)
Mitchell, Alice, S354 (SAT-434)
Mitchell, Catherine, S469 (WED-265)
Mitchell, Eoin, S657 (SAT-182)
Mitchell-Thain, Robert, S333 (SAT-370), S711 (WED-547)
Mitkovskaya, Natalia, S551 (THU-189), S551 (THU-190)
Mitra, Kaulick, S659 (SAT-186)
Mitran, Bogdan, S579 (WED-090)
Mitra, Suvradeep, S684 (FRI-155)
Mittal, Ashi, S292 (FRI-299)
Mittal, Deepali, S908 (SAT-578)
Mitzlaff, Katharina, S504 (FRI-251)
Miyaaki, Hisamitsu, S977 (WED-639)
Miyake, Teruki, S675 (SAT-237)
Miyamoto, Kentaro, S371 (WED-349)
Miyoshi, Eiji, S537 (THU-140)
Mizukami, Kazuhiro, S662 (SAT-196)
Mizushima, Daisuke, S811 (FRI-037)
Mlitz, Veronika, S11 (OS-002-YI)
Mngqibisa, Rosie, S960 (WED-587)
Mobarki, Mousa, S836 (THU-265-YI)
Mochimaru, Tomoaki, S647 (SAT-147)
Modares, Nastaran Fazel, S283 (FRI-265-YI)
Modesto, Anouchka, S414 (FRI-572)
Moe, Fiona Ni Ni, S495 (FRI-228-YI)
Moehlin, Julien, S463 (WED-250)
Moeller, Andreas Buch, S692 (FRI-180)
Moeller, Viktoria, S188 (WED-416)
Moga, Lucile, S53 (OS-083-YI), S55 (OS-085-YI), S251 (SAT-528), S427 (THU-220), S720 (TOP-504-YI), S728 (THU-433-YI), S733 (THU-450), S739 (THU-467), S837 (THU-268)
Mogg, Robin, S78 (LBP-024)
Mogler, Carolin, S51 (OS-080-YI), S359 (THU-345-YI)
Mogul, Douglas B., S55 (OS-086), S344 (SAT-403), S354 (SAT-434)
Mohamed Ali, Mohamed A., S484 (WED-393)
Mohamed, Almuthana, S799 (FRI-003), S921 (SAT-611)
Mohamedashrafali, Mohamed Asif Ali Chinnaratha, S208 (WED-480), S571 (WED-069)
Mohamed, Ghada, S202 (WED-460-YI)
Mohamed, Islam, S28 (OS-035)
Mohamed, Mohamed Ramadan, S159 (SAT-506-YI)
Mohamed, Moshira, S524 (THU-101)
Mohamed, Osob, S713 (WED-556-YI)
Mohamed, Rahma, S537 (THU-141-YI), S538 (THU-142), S576 (WED-078), S865 (FRI-638)
Mohammadi-Shemirani, Pedrum, S847 (THU-300)
Mohammad, Saeed, S55 (OS-086), S831 (THU-258-YI), S842 (THU-284)
Mohan, Leena, S62 (OS-097), S470 (WED-269), S516 (TOP-113)
Mohan Prasad, V G, S952 (FRI-622)
Mohanraj, Sundaresan, S597 (WED-142-YI), S780 (SAT-005), S782 (SAT-010-YI)
Mohanty, Arpan, S569 (WED-058-YI)
Mohapatra, Jyoti, S786 (SAT-023)
Mohapatra, Nihar, S288 (FRI-282), S292 (FRI-299)
Mohareb, Amir, S922 (SAT-612)
Mo, Hongmei, S948 (FRI-610)
Mohr, Raphael, S504 (FRI-251)
Mohseni, Rizwana, S689 (FRI-170)
Mo Kim, Kyung, S850 (THU-308)
Molagic, Violeta, S951 (FRI-620), S974 (WED-633)
Mol, Bregje, S57 (OS-087-YI), S348 (SAT-418-YI)
Moldes, Luz, S799 (TOP-049), S910 (SAT-585)
Moldovan, Cristian, S255 (SAT-539), S544 (THU-166)
Moles, Anna, S18 (OS-014-YI), S234 (FRI-316), S635 (SAT-107-YI)
Mole, Sarah, S47 (OS-072)
Molina, Esther, S410 (FRI-558), S815 (WED-006), S837 (THU-267), S855 (WED-289)
Molina, Luis, S226 (WED-538)
Molinaro, Antonio, S2 (GS-002), S290 (FRI-289), S299 (SAT-249), S672 (SAT-229-YI)
Molinaro, Francesca, S477 (WED-370)
Moll, Apol·lonia, S223 (WED-528)
Molle, Jennifer, S871 (THU-559-YI)
Møller, Andreas, S692 (FRI-180)
Møller, Emilie, S692 (FRI-180)
Møller, Søren, S205 (WED-468), S298 (SAT-245), S736 (THU-459)
Moltó Pérez, Eduardo, S634 (SAT-104)
Mommersteeg, Michiel, S9 (LBO-005-YI)
Monasterio, Raquel González, S948 (FRI-611)
Monbaliu, Diethard, S381 (FRI-465), S849 (THU-306-YI)
Mondelli, Mario Umberto, S370 (WED-346)
Monescillo, Alberto, S16 (OS-010), S855 (WED-288), S856 (WED-290)

Monge, Daniel, S819 (WED-019)
Monian, Prashant, S5 (GS-008)
Monico, Sara, S942 (FRI-593)
Monine, Michael, S5 (GS-008)
Monin, Malte, S904 (SAT-564)
Monisha, M, S705 (THU-542)
Monroy-Ramirez, Hugo Christian, S235 (FRI-319), S481 (WED-384)
Montagnese, Sara, S196 (WED-443), S402 (FRI-530), S435 (THU-247), S746 (THU-489)
Montague, Sarah, S718 (WED-574)
Montali, Anna, S874 (THU-571)
Montali, Ilaria, S874 (THU-571)
Montanari, Martina, S412 (FRI-562), S412 (FRI-563)
Montaña, Sergi Homdedeu, S191 (WED-427-YI)
Montañés, Rosa, S827 (TOP-297)
Montani, Matteo, S561 (TOP-081)
Montano-Loza, Aldo J, S14 (OS-008), S59 (OS-091), S295 (TOP-279), S300 (SAT-250), S315 (SAT-286), S320 (SAT-302), S325 (SAT-319), S325 (SAT-320), S331 (SAT-368-YI), S342 (SAT-398), S344 (SAT-404), S346 (SAT-413), S349 (SAT-419), S354 (SAT-435), S355 (SAT-436), S401 (FRI-527), S788 (SAT-028)
Montano-Loza, Aldo J., S10 (LBO-006), S79 (LBP-026)
Montecalvo, Domenico, S69 (LBP-004-YI), S335 (SAT-378-YI), S350 (SAT-421), S831 (THU-256-YI)
Monteith, Ken, S529 (THU-116-YI)
Monterio, Fernando, S823 (WED-028)
Montero, Javier de las Heras, S635 (SAT-106)
Montero, Jose Luis, S303 (SAT-256-YI), S815 (WED-006)
Montero, Marta, S904 (SAT-564)
Montero-Vallejo, Rocío, S600 (WED-153)
Montesinos, Maria, S469 (WED-267)
Montes, Mario Orlando Santana, S866 (FRI-640)
Montes, Pedro, S793 (SAT-044)
Montgomery, Danielle, S531 (THU-121)
Montgomery, Scott, S978 (WED-642-YI)
Montiel, Natalia, S910 (SAT-585)
Monti, Monica, S972 (WED-623)
Montironi, Carla, S485 (WED-396)
Montoliu, Silvia, S250 (SAT-524), S837 (THU-267)
Montón, Cristina, S16 (OS-010), S254 (SAT-538), S318 (SAT-291), S598 (WED-150)
Montori, Michele, S576 (WED-083), S741 (THU-473)
Montoya-Guzmán, Victor, S771 (THU-030)
Montrond, Maureen, S981 (FRI-635), S981 (FRI-636)
Montull, Santiago, S308 (SAT-264)
Moodie, Erica, S529 (THU-116-YI)
Mookerjee, Rajeshwar Prosad, S35 (OS-050-YI), S171 (FRI-409-YI), S187 (TOP-471-YI), S198 (WED-448-YI), S631 (SAT-094-YI), S660 (SAT-188-YI)
Moon, Andrew, S544 (THU-167)
Moon, Joon Ho, S698 (FRI-197)
Moore, Ann, S687 (FRI-165)
Moore-Gillon, Claudia, S224 (WED-530)
Moore, Joanna, S84 (LBP-038), S840 (THU-275)
Moore, John, S69 (LBP-001)
Moore, Kevin, S119 (FRI-073)
Moore, Thomas, S41 (OS-060)
Moorhouse, Jane, S319 (SAT-301)
Moos, Maximilian, S503 (FRI-248)
Mor, Adi, S334 (SAT-371), S334 (SAT-372), S334 (SAT-377)
Moradpour, Darius, S72 (LBP-011)
Moraes, Bernado, S768 (THU-022)
Moraes, Bernardo, S296 (TOP-281), S306 (SAT-262)
Morales, Albert, S481 (WED-382-YI), S639 (SAT-120)
Morales, Ana Maria Davila, S683 (FRI-151)
Morales, Dalia, S547 (THU-181)
Morales, Ildefonso Quinoñes, S840 (THU-275)
Morales-Navarrete, Hernán, S357 (TOP-327-YI), S663 (SAT-199-YI)
Morales-Ruiz, Manuel, S483 (WED-387)
Moral, Kenan, S395 (FRI-511-YI)
Mora, Mercedes Guilabert, S863 (WED-317)
Morandin, Riccardo, S626 (WED-231)
Moran, Laura, S459 (WED-241)
Morariu, Andrei, S602 (WED-157)
Morariu-Barb, Andreea Mihaela, S602 (WED-157)
Mordan, Nicola, S181 (FRI-435)
Mordenti, Giada, S272 (THU-315-YI)
Moreau, Richard, S8 (LBO-002), S34 (OS-049), S35 (OS-050-YI), S141 (TOP-437), S148 (SAT-467-YI), S149 (SAT-468), S152 (SAT-478), S159 (SAT-505), S166 (FRI-388-YI), S170 (FRI-401-YI), S172 (FRI-412), S210 (WED-485), S261 (SAT-329-YI), S760 (TOP-032)
Moreea, Sulleman, S256 (SAT-543), S258 (SAT-547)
Morel, Helene, S853 (WED-283)
Morell, Daniel, S223 (WED-528)
Morelli, Gaetano, S981 (FRI-636)
Morelli, Giuseppe, S112 (FRI-051)
Morelli, Maria Cristina, S52 (OS-081), S307 (SAT-263), S335 (SAT-378-YI)
Moreno, Ana Isabel, S25 (OS-029)
Moreno, Christophe, S35 (OS-050-YI), S55 (OS-085-YI), S109 (TOP-210), S111 (FRI-043), S577 (WED-084), S777 (THU-050), S849 (THU-306-YI), S907 (SAT-575), S920 (SAT-609), S929 (SAT-629)
Moreno, Daniela, S296 (TOP-281), S306 (SAT-262)
Moreno, Felix, S806 (FRI-024)
Moreno-Gonzalez, Mar, S42 (OS-064-YI), S286 (FRI-271), S287 (FRI-274)
Moreno-Lanceta, Alazne, S483 (WED-387)
Moreno, Laura, S267 (SAT-350)
Moreno, Marc Pañero, S394 (FRI-508), S407 (FRI-547)
Moreno, Marina Galicia, S235 (FRI-319), S481 (WED-384)
Moreno, Patricia, S328 (SAT-324), S328 (SAT-361)
Moreno-Penades, Empar, S317 (SAT-290-YI)
Moreno, Sidney Lopez, S22 (OS-022-YI)
Moreno-Torres, Marta, S272 (THU-315-YI), S273 (THU-316)
Moreno-Viedma, Veronica, S11 (OS-002-YI), S237 (FRI-324)
Moreno, Ydalina Maria, S245 (FRI-354)
Moreta, María José, S30 (OS-041), S203 (WED-463), S394 (FRI-507-YI)
Moretti, Alessandra, S350 (SAT-421)
Moretti, Vittoria, S575 (WED-076)
Morgan, Aparna, S797 (SAT-055)
Morgan, Camille, S80 (LBP-028-YI)
Morgan, Marsha, S227 (WED-540-YI)
Morgan, Megan, S704 (THU-539-YI)
Morgan, Timothy, S166 (FRI-393)
Morgan, Toby, S826 (WED-039)
Mori, Kei, S662 (SAT-196)
Morillas, Rosa M, S309 (SAT-268), S515 (TOP-098), S542 (THU-164), S562 (TOP-097-YI), S567 (WED-054), S583 (WED-101), S612 (WED-188), S804 (FRI-019)
Morimoto, Manabu, S506 (FRI-256)
Morinaga, Maki, S225 (WED-533), S246 (FRI-356)
Morisco, Filomena, S69 (LBP-004-YI), S82 (LBP-034-YI), S176 (FRI-425), S190 (WED-425), S212 (WED-494-YI), S248 (SAT-516), S304 (SAT-258), S307 (SAT-263), S335 (SAT-378-YI), S337 (SAT-382), S479 (WED-378), S900 (SAT-559), S902 (SAT-560), S911 (SAT-587-YI), S936 (TOP-584), S938 (FRI-586)
Mori, Trevor, S699 (FRI-198)
Mormeneo-Bayo, Saray, S804 (FRI-019)
Mor, Orna, S807 (FRI-025)
Morosetti, Daniele, S726 (THU-429)
Morozov, Viacheslav, S939 (FRI-587), S956 (WED-576), S957 (WED-577), S962 (WED-593)
Morrell, Alexander, S458 (WED-237-YI)
Morren, Lara, S281 (TOP-295-YI)
Morrison, Martine C., S645 (SAT-138), S671 (SAT-227)
Morrissey, Sheila, S388 (FRI-490)
Morrow, Richard, S967 (TOP-600-YI)
Morselli, Marco, S874 (THU-571)
Morsicato, Martina, S279 (THU-334-YI), S359 (THU-347-YI)
Mortagy, Mohamed, S449 (THU-401)
Mortensen, Christian, S736 (THU-459)
Mortuza, Rokhsana, S379 (FRI-461-YI)

Author Index

Mo, Ruidong, S91 (SAT-067)
Moruzzi, Noah, S278 (THU-332)
Mosca, Antonella, S583 (WED-102-YI)
Mosenzon, Ofri, S690 (FRI-173)
Moser, Luisa, S307 (SAT-263), S335 (SAT-378-YI)
Moshage, Han, S238 (FRI-333-YI), S239 (FRI-334), S244 (FRI-352), S244 (FRI-353), S384 (FRI-476-YI), S384 (FRI-477), S385 (FRI-478), S430 (THU-232)
Motamedrad, Maryam, S401 (FRI-527)
Motlagh, Pejvack, S149 (SAT-468), S152 (SAT-478), S214 (WED-499), S760 (TOP-032)
Motoyoshi, Yasuhide, S249 (SAT-522), S970 (WED-618), S976 (WED-638)
Mouhadi, Sanaa El, S446 (THU-393-YI), S507 (FRI-362)
Mouhydeen, Hala, S565 (WED-050)
Moulis, Lionel, S387 (FRI-484), S414 (FRI-572), S414 (FRI-573)
Moulton, Ali, S681 (FRI-142)
Mourabit, Haquima El, S235 (FRI-320)
Mouri, Sarah, S110 (FRI-042), S446 (THU-393-YI), S493 (FRI-221), S497 (FRI-234), S499 (FRI-238), S505 (FRI-254), S506 (FRI-255-YI), S507 (FRI-362), S508 (FRI-364-YI), S723 (THU-418)
Moussa, Adel, S869 (TOP-631)
Moussa, Dina, S799 (FRI-004), S800 (FRI-005), S922 (SAT-613)
Moussa, Karine, S803 (FRI-013)
Moussa, Mohamed, S443 (THU-382-YI), S444 (THU-383)
Moustafa, Ahmed, S263 (SAT-333)
Moustafa, Ehab F., S504 (FRI-252)
Mowdawalla, Cyrus, S745 (THU-483)
Moya, Adolfo Gallego, S16 (OS-010)
Moylan, Cynthia, S116 (FRI-061), S197 (WED-447), S544 (THU-167)
Mozaffarian, Afsaneh, S956 (WED-576)
Mozayani, Behrang, S750 (THU-497-YI)
Mozer - Glassberg, Yael, S831 (THU-258-YI), S842 (THU-284)
Mozer-Glassberg, Yael, S55 (OS-086), S850 (THU-308)
Mpanza, Bongiwe, S900 (SAT-558)
Mpanza, Nondumiso, S900 (SAT-558)
Mrazova, Lenka, S855 (WED-288)
Mrowczynski, Stephanie, S112 (FRI-051)
Mrzljak, Anna, S777 (THU-050), S800 (FRI-006)
Msomi, Khanyi, S900 (SAT-558)
Mücke, Marcus, S215 (WED-506)
Mueller, Christian, S178 (FRI-429-YI)
Muga, Eunate, S312 (SAT-273)
Muga, Robert, S128 (FRI-100)
Muirhead, Gareth, S119 (FRI-073)
Mujawar, Quais, S850 (THU-308)
Mukengeshayi, Randy Ngalamulume, S616 (WED-200)
Mukewar, Saurabh, S952 (FRI-622)
Mukherjee, Diptasree, S678 (TOP-162)
Mukherjee, Sarmistha, S276 (THU-329)
Mukherjee, Sumanta, S78 (LBP-025)
Mukherji, Atish, S272 (THU-315-YI)
Mukhopadhya, Ashis, S82 (LBP-033)
Mukovnikova, Marina, S907 (SAT-575)
Mukund, Amar, S274 (THU-318)
Mulay, Akhilesh, S370 (WED-347)
Mulder, Midas B., S168 (FRI-397-YI)
Mulder, Niels, S630 (SAT-090), S857 (WED-299), S863 (WED-318)
Mulé, Sébastien, S434 (THU-242)
Muli, Annah, S256 (SAT-543), S258 (SAT-547)
Mulkay, Jean-Pierre, S920 (SAT-609), S929 (SAT-629)
Mulkearns, Nicholas, S779 (SAT–004)
Mullen, Alan, S633 (SAT-102-YI)
Mullen, Eduardo, S97 (SAT-085)
Müller, Christian, S504 (FRI-251)
Muller, Kate, S699 (FRI-198)
Muller-Kobold, Anneke, S430 (THU-232)
Müller, Lisa-Marie, S371 (WED-348)
Müller, Lukas, S199 (WED-451-YI), S503 (FRI-248)
Muller, Matamoana, S284 (FRI-268-YI)
Müller, Nadine, S672 (SAT-230)
Müller, Ralph, S14 (OS-007)
Müller-Schilling, Martina, S157 (SAT-497), S216 (WED-507), S785 (SAT-019)
Müllhaupt, Beat, S945 (FRI-602-YI)
Mullish, Ben, S764 (THU-012)
Mullish, Benjamin H., S134 (FRI-117), S563 (WED-041)
Müllner-Bucsics, Theresa, S53 (OS-082), S199 (WED-451-YI), S222 (WED-524), S732 (THU-448-YI), S733 (THU-449), S738 (THU-464-YI)
Munday, Rory, S759 (TOP-017-YI)
Mundra, Garvit, S719 (TOP-487-YI)
Munekage, Fumiaki, S419 (THU-525), S421 (THU-531)
Muñoz, Beatriz Mateos, S16 (OS-010), S294 (TOP-278), S309 (SAT-268), S318 (SAT-291)
Muñoz, Emma, S28 (OS-037), S629 (TOP-160)
Munoz, Eva Erice, S562 (TOP-097-YI), S612 (WED-188)
Munoz-Hernández, Rocío, S28 (OS-037), S527 (THU-108), S629 (TOP-160), S644 (SAT-137)
Muñoz-Hernández, Rocio, S600 (WED-153)
Munoz, Leticia, S34 (OS-049)
Muñoz, Mar, S128 (FRI-100)
Muñoz, Rosario Palacios, S904 (SAT-564)
Muñoz, Santiago, S910 (SAT-585)
Muns, Joey, S237 (FRI-330)
Munteanu, Mona, S602 (WED-158), S614 (WED-195)
Murad, Mohamad, S142 (SAT-448), S170 (FRI-402)
Murad, Sarwa Darwish, S53 (OS-083-YI), S61 (OS-095-YI), S63 (OS-098-YI), S382 (FRI-467-YI), S383 (FRI-468), S383 (FRI-473), S391 (FRI-498), S398 (FRI-517-YI), S608 (WED-180), S828 (TOP-310-YI), S863 (WED-317)
Murai, Kazuhiro, S463 (WED-251-YI)
Murakami, Eisuke, S667 (SAT-213)
Murakami, Mai, S647 (SAT-147)
Murakami, Taisei, S675 (SAT-237)
Muramatsu, Masamichi, S875 (THU-573), S894 (THU-635)
Muratbekova, Aizhan, S967 (WED-608)
Muratori, Luigi, S335 (SAT-378-YI)
Muratova, Aiken, S845 (THU-288)
Muratov, Eugene, S881 (THU-592-YI)
Mura, Vincenzo La, S3 (GS-005), S497 (FRI-234)
Murcia, Antonio Sergio, S969 (WED-611)
Murcia, Emma, S55 (OS-085-YI)
Muriel, Alfonso, S146 (SAT-459)
Muris, Jean, S765 (THU-013)
Murphey, Michael, S740 (THU-468)
Murphy, Rinki, S79 (LBP-027)
Murray, Lara, S578 (WED-087)
Murria, Rosa, S598 (WED-150)
Murti, Abhishek, S489 (WED-412-YI)
Musabaev, Erkin, S74 (LBP-016)
Musa, Sherif, S575 (WED-077)
Musayeva, Nermin, S539 (THU-149)
Musich, Ryan, S138 (FRI-127)
Mussini, Cristina, S378 (FRI-458)
Mustafa, Ghulam, S178 (FRI-430)
Mustafa, Mohammad Rifat, S745 (THU-484)
Mustafa, Reem, S680 (FRI-141)
Mustapha, Nik Raihan Nik, S574 (WED-075)
Mustelin, Linda, S122 (FRI-084)
Muthiah, Mark, S59 (OS-091), S67 (OS-105-YI), S156 (SAT-496), S215 (WED-505), S221 (WED-523), S228 (WED-543), S423 (TOP-374), S528 (THU-110), S698 (FRI-197)
Muti, Leon, S167 (FRI-394-YI), S512 (FRI-372)
Mutiloa, Elena Jimenèz, S855 (WED-288), S856 (WED-290)
Muzica, Cristina-Maria, S210 (WED-490)
Muzîcă, Cristina-Maria, S211 (WED-493)
Mwandagalirwa, Melchior Kashamuka, S80 (LBP-028-YI)
Myeni, Njabulo, S900 (SAT-558)
Myllymäki, Mikko, S282 (FRI-263)
Myllys, Maiju, S172 (FRI-410-YI)
Myneni, Sudha Rani, S236 (FRI-323), S620 (WED-213)
Myojin, Yuta, S463 (WED-251-YI)

Naamani, Hind El, S727 (THU-430)
Naamani, Khalid Al, S62 (OS-097), S127 (FRI-095), S377 (FRI-451), S766 (THU-015), S923 (SAT-618)
Nabhani, Ibrahim Al, S378 (FRI-457)
Nabilou, Puria, S586 (WED-109), S602 (WED-159-YI)
Nachit, Maxime, S648 (SAT-151-YI)
Nachmias-Peiser, Noy, S741 (THU-475)

Nadalin, Silvio, S512 (FRI-371)
Nadal, Ruth, S110 (TOP-222)
Nadda, Rohit, S5 (GS-009), S180 (FRI-433)
Nadeem, Muhammad Ahmad, S399 (FRI-522)
Nadeem, Rida, S62 (OS-097), S516 (TOP-113), S684 (FRI-154), S687 (FRI-165)
Nader, Ahmed, S47 (OS-072)
Nader, Fatema, S126 (FRI-094), S127 (FRI-095), S356 (SAT-443), S417 (FRI-581), S522 (THU-094), S557 (THU-213), S793 (SAT-045), S794 (SAT-046), S923 (SAT-618)
Nadig, Satish, S388 (FRI-489)
Nadzemova, Oksana, S860 (WED-307)
Nagabhushana, Amruthavarshini, S36 (OS-051-YI)
Nagai, Koki, S686 (FRI-159)
Naganori, Nao, S875 (THU-573)
Naganuma, Atsushi, S258 (SAT-549), S550 (THU-188), S979 (WED-644)
Nagaoka, Shinya, S249 (SAT-522), S970 (WED-618), S976 (WED-638)
Nagaraja, Ravishankara, S699 (FRI-199)
Nagel, Julie Loft, S853 (WED-282-YI)
Nagesh, Prashanth Thevkar, S137 (FRI-126)
Nagler, Michael, S342 (SAT-399)
Nagler, Shani, S338 (SAT-384), S753 (THU-506)
Nagral, Abha, S24 (OS-028), S144 (SAT-452), S160 (SAT-507)
Nagre, Nikhil, S24 (OS-027), S822 (WED-025-YI)
Nagy, Ahmed, S263 (SAT-333)
Nagy, Laura, S138 (FRI-127), S243 (FRI-347)
Nagy, Mohamed, S537 (THU-141-YI)
Nahar, Kamrun, S598 (WED-149)
Nah, Benjamin, S423 (TOP-374), S442 (THU-379)
Nah, Chung Yau, S211 (WED-491)
Nahon, Pierre, S35 (OS-050-YI), S38 (OS-055), S55 (OS-085-YI), S66 (OS-104), S428 (THU-226-YI), S505 (FRI-254), S506 (FRI-255-YI), S739 (THU-467)
Na, Hoyoung, S528 (THU-111)
Naidoo, Vasudevan, S900 (SAT-558)
Naimimohasses, Sara, S218 (WED-512-YI), S698 (FRI-196)
Naim, Saima, S914 (SAT-592-YI), S921 (SAT-610)
Naim, Sue, S77 (LBP-021)
Nair, Priya, S36 (OS-051-YI)
Nájera-Muñoz, Rodrigo, S250 (SAT-524)
Najjar, Joseph, S757 (THU-516)
Nakadai, Yukie, S371 (WED-349), S861 (WED-313)
Nakada, Yoshinobu, S686 (FRI-159)
Nakafeero, Brenda, S821 (WED-023)
Nakagawa, Mina, S506 (FRI-256)
Nakai, Masato, S506 (FRI-256)
Nakajima, Atsushi, S2 (GS-003), S62 (OS-097), S424 (TOP-376), S516 (TOP-113), S517 (TOP-114), S525 (THU-103), S558 (TOP-063-YI), S589 (WED-118), S607 (WED-174-YI), S667 (SAT-213), S686 (FRI-159), S693 (FRI-181)
Nakamoto, Nobuhiro, S371 (WED-349), S861 (WED-313)
Nakamoto, Takato, S811 (FRI-037)
Nakamoto, Yasunari, S977 (WED-639)
Nakamura, Astushi, S544 (THU-170)
Nakamura, Masato, S977 (WED-639)
Nakamura, Yoko, S550 (THU-188)
Nakanishi, Hiroyuki, S439 (THU-368)
Nakatani, Tatsuya, S95 (SAT-077), S263 (SAT-334), S652 (SAT-164), S660 (SAT-189), S747 (THU-491)
Nakchbandi, Inaam, S234 (FRI-317)
Nalbat, Esra, S652 (SAT-163)
Nallapeta, Naren, S845 (THU-288)
Namdag, Bira, S923 (SAT-618)
Nam, David, S443 (THU-381)
Namino, Shingo, S249 (SAT-522)
Namisaki, Tadashi, S95 (SAT-077), S263 (SAT-334), S652 (SAT-164), S660 (SAT-189), S747 (THU-491)
Nam, Seungyoon, S653 (SAT-167)
Nanda, Ranjan, S139 (FRI-135-YI), S361 (THU-354)
Nan, Yuemin, S67 (OS-105-YI), S225 (WED-537)
Naoumov, Nikolai, S533 (THU-126), S561 (TOP-081), S932 (SAT-641)
Napoleone, Carlo Pace, S848 (THU-304)
Napoli, Lucia, S69 (LBP-004-YI), S82 (LBP-034-YI), S307 (SAT-263), S335 (SAT-378-YI), S350 (SAT-421)
Napolitano, Antonio, S825 (WED-037)
Napolitano, Carmine, S444 (THU-384), S532 (THU-123), S549 (THU-186-YI), S639 (SAT-121-YI), S660 (SAT-190), S854 (WED-286)
Narayanan, Padma, S5 (GS-008)
Narbaiza, Jone, S445 (THU-385)
Nardelli, Mateus, S296 (TOP-281), S306 (SAT-262), S315 (SAT-286)
Nardelli, Silvia, S3 (GS-005), S52 (OS-081), S54 (OS-084), S69 (LBP-004-YI), S185 (TOP-455-YI), S307 (SAT-263), S335 (SAT-378-YI), S350 (SAT-421), S397 (FRI-515), S719 (TOP-488), S720 (TOP-502-YI), S746 (THU-489), S831 (THU-256-YI), S856 (WED-291)
Nardi, Alessandra, S307 (SAT-263)
Nardo, Fiammetta Di, S444 (THU-384), S532 (THU-123), S639 (SAT-121-YI)
Nardone, Gerardo, S304 (SAT-258), S335 (SAT-378-YI)
Narguet, Stephanie, S928 (SAT-628-YI)
Nasir, Gharaza, S487 (WED-400-YI)
Nasoni, Maria Gemma, S475 (WED-366)
Nasr, Patrik, S220 (WED-517), S568 (WED-056), S606 (WED-173)
Nasser, Imad, S331 (SAT-368-YI)
Nasser, Roni, S613 (WED-189)
Năstase, Raluca, S951 (FRI-620)
Nastouli, Eleni, S826 (WED-039)
Natarajan, Muthukumaran, S699 (FRI-199)
Nathan, Bavithra, S801 (FRI-007)
Nathan, Rohit, S670 (SAT-220)
Nathwani, Rooshi, S224 (WED-530)
Natola, Leonardo Antonio, S97 (SAT-084-YI), S405 (FRI-541)
Nault, Jean Charles, S428 (THU-226-YI), S446 (THU-393-YI), S457 (WED-236), S742 (THU-477)
Nault, Jean-Charles, S17 (OS-011), S38 (OS-055), S54 (OS-084), S493 (FRI-221), S497 (FRI-234), S499 (FRI-238), S505 (FRI-254), S506 (FRI-255-YI), S507 (FRI-362), S508 (FRI-364-YI)
Naustdal, Carina, S801 (FRI-008)
Nautiyal, Nidhi, S100 (THU-057-YI), S174 (FRI-415-YI)
Nava, Jose David Prieto, S866 (FRI-640)
Navarrete-Pérez, Irene, S254 (SAT-538), S599 (WED-151)
Navarro, Adela, S250 (SAT-524), S603 (WED-163)
Navarro-Alvarez, Nalu, S296 (TOP-281), S306 (SAT-262)
Navarro-Corcuera, Amaia, S30 (OS-039-YI), S101 (THU-059-YI), S272 (THU-315-YI), S855 (WED-287-YI)
Navarro, Jordi, S904 (SAT-564)
Navarro, Roser, S904 (SAT-564)
Naveed, Ammara, S845 (THU-289)
Nawalerspanya, Siwanon, S219 (WED-514)
Nawalerspunya, Pongnarin, S219 (WED-514), S727 (THU-432)
Nayagam, Shevanthi, S822 (WED-026)
Nayak, Baibaswat, S184 (TOP-454-YI), S847 (THU-299)
Nayak, Baibaswata, S141 (TOP-423)
Naymagon, Leonard, S731 (THU-445-YI)
Nazeer, Arresha, S438 (THU-363), S471 (WED-271)
Nde, Helen, S801 (FRI-009)
Ndiaye, Yakham, S926 (SAT-624)
Ndimande, Landiwe, S900 (SAT-558)
Ndow, Gibril, S764 (THU-012), S798 (TOP-034)
Ndungu, Thumbi, S900 (SAT-558)
Neagu, Daniela, S951 (FRI-620)
Nebbia, Gabriella, S55 (OS-086), S831 (THU-258-YI), S842 (THU-284)
Nebbia, Gaia, S811 (FRI-038)
Neckermann, Lukas, S240 (FRI-337-YI)
Nedar, Lennart, S579 (WED-090)
Neffeova, Kristyna, S861 (WED-308)
Neglia, Maria Cristina, S83 (LBP-034-YI), S307 (SAT-263)
Negm, Mohamed, S263 (SAT-333)
Negrin-Dastis, Sergio, S920 (SAT-609), S929 (SAT-629)
Negrinho, Ana Patricia, S892 (THU-627)
Negrini, Massimo, S462 (WED-248)
Negru, Anca, S951 (FRI-620)

Author Index

Nekipelova, Svetlana, S594 (WED-135)
Nellore, Dharani Sai Sreekanth, S661 (SAT-191)
Nelson, David R., S974 (WED-628)
Nelson, Peter, S8 (LBO-002)
Nelson, Savannah, S687 (FRI-165)
Nemes, Andrada, S728 (THU-433-YI)
Nencka, Radim, S661 (SAT-191)
Nengwei, Zhang, S626 (WED-230)
Nenu, Iuliana, S175 (FRI-418)
Neonaki, Antonia, S545 (THU-172)
Nepel, Maximilian, S742 (THU-476)
Nephew, Lauren, S445 (THU-386), S573 (WED-072), S613 (WED-190)
Neri, Sergio, S185 (TOP-455-YI)
Nersesov, Alexander, S824 (WED-035)
Nesbakken, Arild, S290 (FRI-289)
Ness, Erik, S10 (LBO-006)
Neuberger, James, S256 (SAT-543), S258 (SAT-547)
Neudert, Barbara, S750 (THU-497-YI)
Neuenschwander, Katharina, S945 (FRI-602-YI)
Neumann, Anat, S642 (SAT-127)
Neumann, Ethan, S38 (OS-055)
Neumann-Haefelin, Christoph, S289 (FRI-284)
Neurath, Markus F., S310 (SAT-269), S322 (SAT-313)
Neururer, Sabrina, S257 (SAT-545-YI)
Neuschwander-Tetri, Brent A., S64 (OS-099), S553 (THU-201)
Nevasuo, Vera, S450 (THU-403)
Nevens, Frederik, S39 (OS-056), S64 (OS-100), S325 (SAT-320), S849 (THU-306-YI)
Nevermann, Nora, S461 (WED-245)
Neves, André, S603 (WED-164)
Neves, Elizete Araujo Batista, S43 (OS-065)
Neves, Joana Camões, S186 (TOP-470-YI)
Nevi, Lorenzo, S477 (WED-370)
Nevzorova, Yulia, S132 (FRI-109), S459 (WED-241), S642 (SAT-131-YI)
New, Kate, S799 (FRI-004), S800 (FRI-005)
Newsome, Philip, S284 (FRI-268-YI), S517 (TOP-114), S525 (THU-103), S607 (WED-174-YI)
Newsome, Philip N., S558 (TOP-063-YI), S589 (WED-118), S612 (WED-187-YI), S618 (WED-204), S621 (WED-215), S693 (FRI-182)
Neyts, Johan, S881 (THU-592-YI)
Ngaba, Guy Pascal, S924 (SAT-619)
Ng, Ashley Weng Yan, S495 (FRI-228-YI)
Ng, Caleb Wei Hao, S509 (FRI-365)
Ng, Charlotte, S465 (WED-255)
Ng, Cheng Han, S156 (SAT-496), S215 (WED-505), S221 (WED-523), S228 (WED-543), S423 (TOP-374), S528 (THU-110), S698 (FRI-197)
Ng, David Chee Eng, S495 (FRI-228-YI)
Ng, Esmond, S868 (FRI-644)
Ngimbi, Patrick, S80 (LBP-028-YI)
Ng, Jeanette, S149 (SAT-473)
Ng, Jess Jie-Ying, S593 (WED-132)
Ng, Michelle, S745 (THU-483)
Ng, Nicholas Beng Hui, S713 (WED-557)
Ngonadi, Chiemelie, S61 (OS-108)
Ngongo, Sibahle, S76 (LBP-019-YI)
Nguefang, Guy, S526 (THU-105)
Ngu, Natalie, S218 (WED-513), S707 (THU-546-YI), S749 (THU-496)
Nguyen, Anh, S268 (SAT-351)
Nguyen, Chloe, S338 (SAT-384)
Nguyen, Dang Hoan, S887 (THU-612-YI)
Nguyen, Henry, S10 (LBO-006)
Nguyen, Huy, S1 (GS-001)
Nguyen, Jeffrey, S803 (FRI-013)
Nguyen-Khac, Eric, S829 (THU-252)
Nguyen, Khoa, S974 (WED-628)
Nguyen, Long, S799 (FRI-004), S800 (FRI-005)
Nguyen, Mindie, S824 (WED-035), S943 (FRI-596), S966 (WED-604)
Nguyen, Nhu, S170 (FRI-403)
Nguyen, Nick, S79 (LBP-026)
Nguyen, Phuong, S687 (FRI-165)
Nguyen, TD Clara, S603 (WED-165-YI), S604 (WED-166)
Nguyen, Thuc-Anh, S646 (SAT-140-YI)
Ngwenya, Busangani, S900 (SAT-558)
Niazi, Mina, S14 (OS-008), S295 (TOP-279), S325 (SAT-319), S354 (SAT-435)
Niazi, Mohammad, S682 (FRI-148), S690 (FRI-172)
Niaz, Qamar, S178 (FRI-430)
Nicastro, Emanuele, S55 (OS-086), S831 (THU-258-YI), S842 (THU-284), S850 (THU-308)
Nicca, Dunja, S714 (WED-558)
Nicholl, David, S84 (LBP-038)
Nicholson, Edward, S718 (WED-574)
Nicoara-Farcau, Oana, S52 (OS-081), S54 (OS-084), S255 (SAT-539), S397 (FRI-515), S543 (THU-165), S544 (THU-166), S602 (WED-157)
Nicola, Andre Moraes, S77 (LBP-022-YI)
Nicolaas, Jerome Sint, S351 (SAT-426-YI)
Nicola, Francesca De, S478 (WED-377)
Nicola, Stella De, S71 (LBP-009), S176 (FRI-425), S190 (WED-425), S479 (WED-378), S531 (THU-120), S900 (SAT-559), S902 (SAT-560), S936 (TOP-584)
Nicoll, Amanda, S433 (THU-240), S922 (SAT-613)
Nicolle, Rémy, S480 (WED-380)
Nicolò, Amedeo De, S942 (FRI-593)
Nicolosi, Aurora, S494 (FRI-226)
Nie, Chunpeng, S505 (FRI-253)
Niederau, Claus, S840 (THU-275)
Niehaus, Christian, S197 (WED-446)
Nielsen, Ann Sophie, S711 (WED-549-YI)
Nielsen, Søren, S692 (FRI-180)
Nie, Mei-Tong, S661 (SAT-195)
Nien, Hsiao-Ching, S446 (THU-387)
Nier, Anika, S175 (FRI-419)
Nierhoff, Dirk, S289 (FRI-284), S807 (FRI-025)
Niersmann, Corinna, S666 (SAT-211-YI)
Nieto, Juan C, S35 (OS-050-YI)
Nieto, Maria, S497 (FRI-234), S723 (THU-418)
Nieuwdorp, Max, S268 (SAT-351), S632 (SAT-099-YI), S641 (SAT-126)
Nieva-Zuluaga, Ane, S277 (THU-330-YI), S631 (SAT-095-YI)
Nie, Yu, S405 (FRI-542), S416 (FRI-579), S417 (FRI-580)
Nie, Yuhang, S922 (SAT-617)
Nigam, Gaurav, S740 (THU-468)
Niida, Kazuki, S675 (SAT-237)
Nijhawan, Sandeep, S27 (OS-033)
Nijmeijer, Bart, S237 (FRI-330)
Nikhilamol, G, S705 (THU-542)
Nikiforova, Yana, S604 (WED-167)
Nikitina, Darja, S41 (OS-061)
Nikolaidis, Marios, S2 (GS-002), S290 (FRI-289)
Nikolakopoulou, Polyxeni, S507 (FRI-257)
Nikolla, Deborah, S78 (LBP-023)
Nilius, Henning, S342 (SAT-399)
Nilsson, Emma, S290 (FRI-289)
Ni, Ming, S103 (THU-067), S244 (FRI-351), S473 (WED-276)
Ningarhari, Massih, S414 (FRI-572), S428 (THU-226-YI), S499 (FRI-238), S505 (FRI-254), S506 (FRI-255-YI)
Ning, Qin, S67 (OS-105-YI), S676 (SAT-239), S943 (FRI-594), S952 (FRI-622), S960 (WED-587)
Ning, Yue, S260 (TOP-357)
Ninomiya, Masashi, S510 (FRI-367)
Niosi, Marco, S444 (THU-384), S532 (THU-123), S549 (THU-186-YI), S660 (SAT-190)
Nirello, Vinicius Dias, S42 (OS-064-YI)
Nirodi, Sandhya, S26 (OS-031)
Niro, Grazia Anna, S69 (LBP-004-YI), S82 (LBP-034-YI), S304 (SAT-258), S307 (SAT-263), S335 (SAT-378-YI), S912 (SAT-587-YI)
Nishida, Tomoyuki, S693 (FRI-181)
Nishijima, Suguru, S114 (FRI-057)
Nishikawa, Koji, S499 (FRI-237)
Nishimura, Norihisa, S263 (SAT-334), S652 (SAT-164)
Nishino, Hiroto, S420 (THU-529-YI)
Nishio, Takahiro, S420 (THU-529-YI)
Nishizawa, Hitoshi, S537 (THU-140)
Nissinen, Markku, S530 (THU-118-YI)
Niss, Kristoffer, S646 (SAT-142)
Niu, Junqi, S34 (OS-048), S68 (OS-107), S373 (WED-355), S433 (THU-239), S932 (SAT-641)
Ni, Wenjing, S537 (THU-139)
Njei, Basile, S526 (THU-105)
Njie, Ramou, S798 (TOP-034)
Njimi, Hassane, S109 (TOP-210)
Nkongolo, Shirin, S51 (OS-080-YI), S879 (THU-589-YI), S935 (TOP-583)

Noach, Leslie, S15 (OS-009-YI)
Nobes, Jennifer, S599 (WED-152)
Nocke, Maximilian, S879 (THU-588), S887 (THU-613), S888 (THU-617)
Noe, Sebastian, S904 (SAT-564)
Nofallah, Shima, S578 (WED-087)
Nofit, Eugenia, S69 (LBP-004-YI), S82 (LBP-034-YI), S304 (SAT-258), S307 (SAT-263), S335 (SAT-378-YI), S338 (SAT-384), S340 (SAT-393), S350 (SAT-421)
Nogami, Asako, S686 (FRI-159)
Noguchi, Haruna, S662 (SAT-196)
Nogueira, Cristiane Villela, S127 (FRI-095)
Nogueira, Iasmin, S379 (FRI-460)
Nogueira, Paulo, S786 (SAT-022)
Nogueiras, Ruben, S233 (FRI-313), S241 (FRI-339), S272 (THU-315-YI), S281 (TOP-296-YI), S633 (SAT-101-YI)
Nøhr-Meldgaard, Jacob, S646 (SAT-142), S655 (SAT-173)
Noh, Sandra, S64 (OS-100), S297 (TOP-293), S341 (SAT-397)
Nomaguchi, Masako, S870 (TOP-646)
Nomden, Mark, S55 (OS-086), S831 (THU-258-YI), S842 (THU-284)
Nomikou, Efrosyni, S142 (SAT-449)
Nomingerel, Otgonjargal, S48 (OS-074)
Nooijen, Lynn, S445 (THU-385)
Noone, Dee, S255 (SAT-540), S769 (THU-024-YI), S769 (THU-025), S973 (WED-627)
Noordermeer, Tessa, S688 (FRI-166-YI)
Noori, Muna, S354 (SAT-434)
Noormohamed, Nadia, S47 (OS-072)
Norden-Krichmar, Trina, S166 (FRI-393)
Nordin, Arno, S376 (FRI-447), S376 (FRI-448), S450 (THU-403)
Noriega, Richard, S96 (SAT-083)
Norlin, Jenny Egecioglu, S176 (FRI-421), S646 (SAT-142)
Norman, Gary, S342 (SAT-399)
Norris, Suzanne, S708 (THU-549-YI), S746 (THU-485)
Nörthemann, Luca, S890 (THU-623-YI)
Nosáková, Lenka, S211 (WED-492)
Nosi, Daniele, S457 (WED-235)
Nouairia, Ghada, S71 (LBP-008)
Noureddin, Mazen, S19 (OS-016), S20 (OS-019), S62 (OS-096), S78 (LBP-025), S80 (LBP-029), S84 (LBP-036), S156 (SAT-496), S215 (WED-505), S221 (WED-523), S228 (WED-543), S528 (THU-110), S559 (TOP-064), S560 (TOP-066), S561 (TOP-082), S565 (WED-051), S569 (WED-059), S679 (TOP-176), S679 (TOP-177), S681 (FRI-142), S682 (FRI-149), S691 (FRI-175), S692 (FRI-179), S694 (FRI-183), S697 (FRI-191), S698 (FRI-197), S719 (TOP-486)
Novaes, Lailiane, S978 (WED-641)
Novitskaia, Elena, S595 (WED-136)
Novoa, Eva, S232 (FRI-313), S241 (FRI-339), S633 (SAT-101-YI)
Nozza, Ottavia, S938 (FRI-586)
Nteliopoulos, Georgios, S455 (TOP-406)
Nuchovich, Nadine, S844 (THU-285)
Nuciforo, Sandro, S465 (WED-255)
Nudo, Michael, S529 (THU-116-YI)
Nuermaimaiti, Mirizhati, S243 (FRI-348)
Nuevo, Olivia, S819 (WED-019)
Nugmanova, Balzhan, S967 (WED-608)
Nulan, Yeldos, S168 (FRI-398)
Nunes, Tiago, S10 (LBO-006)
Nunes, Vinicius, S95 (SAT-078)
Núñez, Carmen López, S309 (SAT-268), S804 (FRI-019)
Nunez, Isabel Ruiz, S403 (FRI-532)
Núñez, María Luz, S910 (SAT-585)
Núñez, Sandra Torres, S28 (OS-037), S627 (TOP-144)
Nuñez, Susana, S101 (THU-058), S131 (FRI-104)
Núñez, Susana, S28 (OS-037), S627 (TOP-144), S629 (TOP-160)
Nurcis, Jessica, S272 (THU-315-YI), S479 (WED-379)
Nurul, Jannah Mohamed Nasir, S458 (WED-238)
Nuruzade, Nargiz, S172 (FRI-410-YI), S408 (FRI-554)
Nussbaum, Tami, S398 (FRI-516), S834 (THU-262), S836 (THU-266)
Nussenzweig, Michel C., S77 (LBP-022-YI)
Nwoguh, Chinonso, S25 (OS-030), S622 (WED-217)
Nyberg, Scott, S9 (LBO-004)
Nyhlin, Nils, S58 (OS-090), S584 (WED-104)

Oakland, Kathryn, S740 (THU-468)
Oancea, Georgeta, S211 (WED-493)
O'Beirne, James, S10 (LBO-006), S789 (SAT-030)
Oberti, Frédéric, S222 (WED-525), S540 (THU-155), S554 (THU-202)
Oberti, Giovanna, S520 (THU-091-YI), S553 (THU-197), S595 (WED-137)
Oberweis-Manion, Helen, S406 (FRI-543)
Obholzer, Laura, S862 (WED-314-YI)
O'Brien, Alastair, S253 (SAT-532), S709 (THU-556-YI)
O'Brien, Heath, S75 (LBP-017)
O'Brien, Sarah, S398 (FRI-516)
Öcal, Osman, S490 (TOP-407-YI)
Ocama, Ponsiano, S923 (SAT-618)
Ocaña, Adrián Lopez, S308 (SAT-264)
Ocete, Dolores, S910 (SAT-581)
Ochoa, Alejandra, S793 (SAT-044)
O'Connell, Malene Barfod, S205 (WED-468), S711 (WED-549-YI)
O'Connor, Ciara, S210 (WED-489-YI)
ÓConnor, Lucía, S608 (WED-175)
Odent, Anne Victoire, S506 (FRI-255-YI)
O'Donnell, John, S680 (FRI-141), S695 (FRI-186)
O'Donovan, Helen, S406 (FRI-544)
Odriozola, Aitor, S733 (THU-450)
Odsen, Raymond, S349 (SAT-419)
Oeckl, Lena, S175 (FRI-420), S181 (FRI-436)
Oener-Sieben, Soner, S672 (SAT-230)
Oesinghaus, Sina, S154 (SAT-489)
Oezsoy, Adil, S447 (THU-395), S470 (WED-268)
O' Farrell, Marie, S82 (LBP-032), S671 (SAT-227)
Ogata, Kosuke, S891 (THU-624-YI)
Ogawa, Eiichi, S694 (FRI-184)
Ogawa, Hirohisa, S668 (SAT-215), S669 (SAT-218)
Ogawa, Koji, S506 (FRI-256)
Oger, Emmanuel, S762 (THU-009)
Ogiso, Satoshi, S419 (THU-525), S420 (THU-529-YI), S421 (THU-531)
Ogola, Gerald, S154 (SAT-490)
Ohara, Masatsugu, S506 (FRI-256), S808 (FRI-027)
Ohfuji, Satoko, S336 (SAT-379)
Oh, Hyunwoo, S553 (THU-198)
Ohira, Hiromasa, S372 (WED-352), S647 (SAT-147)
Oh, Joo Hyun, S545 (THU-171), S591 (WED-122), S625 (WED-229), S630 (SAT-092), S652 (SAT-165), S686 (FRI-163)
Oh, Jung Suk, S510 (FRI-368)
Oh, Ki Kwang, S266 (SAT-345)
Oh, Seak Hee, S850 (THU-308)
Ojanen, Anniina, S122 (FRI-084)
Ojeda, Asunción, S6 (GS-011-YI), S53 (OS-082), S730 (THU-443), S735 (THU-453), S884 (THU-604-YI)
Ojeda-Perez, Betsaida, S467 (WED-261)
Ojha, Srikant, S275 (THU-320)
Ojiro, Keisuke, S371 (WED-349), S861 (WED-313)
Okabe, Haruka, S708 (THU-553)
Okada, Haruka, S371 (WED-349), S861 (WED-313)
Okada, Masaya, S675 (SAT-237)
Okai, David, S860 (WED-305)
O'Kane, Grainne, S491 (TOP-408-YI)
Okanoue, Takeshi, S693 (FRI-181)
Okawa, Masashi, S277 (THU-331)
Okeke, Edith, S905 (SAT-569), S926 (SAT-624), S940 (FRI-588-YI)
Okoibhole, Abraham, S709 (THU-556-YI)
Okolo, Obinna, S614 (WED-195)
Okubo, Hironao, S336 (SAT-379)
Okushin, Kazuya, S187 (TOP-472)
Olafsson, Sigurdur, S602 (WED-157), S802 (FRI-011)
Olafsson, Silja, S802 (FRI-011)
Olaizola, Paula, S454 (TOP-390-YI), S483 (WED-388-YI)
Olavarria, Andreina, S3 (GS-005)
Olavarría, Andreína, S752 (THU-501)
Oldenburger, Anouk, S176 (FRI-421), S240 (FRI-338)
Oldenkott, Dana, S105 (THU-072)
Old, Hannah, S747 (THU-492)

Author Index

O'Leary, Jacqueline, S149 (SAT-468), S152 (SAT-478), S214 (WED-499), S760 (TOP-032)
Olejnik, Piotr, S409 (FRI-555)
Olinga, Peter, S244 (FRI-352)
Olivas, Ignasi, S300 (SAT-250), S308 (SAT-264), S309 (SAT-268), S317 (SAT-290-YI), S318 (SAT-291), S325 (SAT-320), S336 (SAT-380), S337 (SAT-382), S338 (SAT-383), S739 (THU-467), S828 (TOP-309-YI)
Oliva-Vilarnau, Nuria, S278 (THU-332)
Olivé, Aina Nicolàs, S802 (FRI-010-YI)
Oliveira, André, S102 (THU-060)
Oliveira, Claudia Pinto, S62 (OS-097), S112 (FRI-050), S127 (FRI-095), S424 (TOP-376), S516 (TOP-113), S557 (THU-213), S680 (FRI-139), S701 (FRI-203-YI), S724 (THU-420)
Oliveira, Daniel V., S861 (WED-308)
Oliveira, Elze Maria Gomes, S296 (TOP-281), S306 (SAT-262), S314 (SAT-284)
Oliveira, Goncalo, S477 (WED-369)
Oliveira, Joaquim, S43 (OS-066), S934 (TOP-582), S937 (FRI-585-YI)
Oliveira, Mario, S892 (THU-627)
Oliveira, Patrícia Marinho C, S314 (SAT-284)
Olivera, Marcel Sorribas, S32 (OS-044)
Oliver, Deanna, S713 (WED-555)
Oliveri, Antonino, S166 (FRI-393)
Oliveri, Filippo, S431 (THU-233), S950 (FRI-619)
Olivero, Antonella, S49 (OS-076-YI), S911 (SAT-587-YI), S919 (SAT-608-YI)
Olivieri, Simone, S639 (SAT-121-YI), S854 (WED-286)
Oliviero, Antonella, S534 (THU-133)
Oliviero, Barbara, S370 (WED-346), S462 (WED-248)
Olkus, Alexander, S504 (FRI-251)
Ollier, Natasha, S199 (WED-450)
Öllinger, Robert, S416 (FRI-578-YI)
Ollivier-Hourmand, Isabelle, S43 (OS-066), S54 (OS-084), S428 (THU-226-YI), S493 (FRI-221), S497 (FRI-234), S506 (FRI-255-YI), S508 (FRI-364-YI), S934 (TOP-582), S937 (FRI-585-YI)
Olorunyomi, Oluwatobi, S8 (LBO-003)
Olsen, Kathryn, S333 (SAT-369)
Olsson, Annika, S953 (FRI-625)
Olsson, Karen, S743 (THU-480-YI)
Olthoff, Kim, S166 (FRI-393)
Olveira, Antonio, S294 (TOP-278), S542 (THU-164), S567 (WED-054), S837 (THU-267), S855 (WED-289)
Olynyk, John, S699 (FRI-198), S699 (FRI-199)
Omar, Massar, S838 (THU-269)
Omar, Rabab, S575 (WED-077)
Omata, Masao, S67 (OS-105-YI)
Önal, Zerrin, S850 (THU-308)
Onasanya, Oluwadamilola, S322 (SAT-307), S322 (SAT-308)
Ong, Agnes, S487 (WED-401)
Ongaro, Marie, S111 (FRI-043)
Ongis, Luca, S817 (WED-010)
Ong, Janus, S766 (THU-015), S923 (SAT-618)
Ong, Yan Ling, S149 (SAT-473)
Ong, Yvette, S170 (FRI-403)
Onizawa, Michio, S647 (SAT-147)
Onofriescu, Alina, S574 (WED-074)
Onoja, Mary, S25 (OS-030), S622 (WED-217)
Onyshchuk, Liudmyla, S71 (LBP-007)
Oo, Ye Htun, S331 (SAT-368-YI), S333 (SAT-369), S363 (WED-321-YI), S364 (WED-324-YI), S365 (WED-330-YI)
Opuni, Kwabena, S623 (WED-221), S691 (FRI-175)
Oral, Hakan, S203 (WED-464)
Oravilahti, Anniina, S114 (FRI-055)
Orbuch, Rachel, S546 (THU-173-YI)
Ordoñez, Felipe, S55 (OS-086), S831 (THU-258-YI), S842 (THU-284)
Ordonez-Naranjo, Paulina, S850 (THU-308)
Ordóñez, Patricia, S799 (TOP-049), S910 (SAT-585)
Ordovas, Jose, S684 (FRI-153)
Ordozgoiti, Alberto Villamor, S394 (FRI-508), S407 (FRI-547)
Orellana, María Paz, S112 (FRI-050)
Orellano, Miranda, S654 (SAT-171-YI)
Orešič, Matej, S29 (OS-038), S268 (SAT-351), S662 (SAT-197)
Orey, Maria do Mar, S765 (THU-013)
Orfanidou, Martha, S314 (SAT-283)
Orfanu, Alina, S974 (WED-633)
Orgil, Batzorig, S48 (OS-074)
Orlandini, Alessandra, S307 (SAT-263), S335 (SAT-378-YI)
Orlent, Hans, S315 (SAT-285), S849 (THU-306-YI), S907 (SAT-575), S920 (SAT-609), S929 (SAT-629)
Orłowska-Wójcicka, Anna, S55 (OS-086), S831 (THU-258-YI), S842 (THU-284)
Orman, Eric, S531 (THU-122)
Örmeci, Aslı Çifcibaşı, S829 (THU-251)
Ormeño, Fátima Huamán, S358 (THU-340-YI)
Oró, Denise, S655 (SAT-173)
Or, Omri, S60 (OS-093)
Ortega, Cristina Coll, S198 (WED-449), S204 (WED-467)
Ortega, Francisco J, S633 (SAT-101-YI)
Ortega, Francisco J., S273 (THU-316)
Ortega-Ribera, Marti, S137 (FRI-126)
Ortiz, Cristina, S262 (SAT-330)
Ortiz, Jorge, S556 (THU-212)
Ortiz, Juan Pedro Toro, S16 (OS-010), S300 (SAT-250), S571 (WED-069)
Ortiz-Lasanta, Grisell, S682 (FRI-148)
Ortiz-López, Nicolás, S52 (OS-081), S296 (TOP-281), S306 (SAT-262)
Ortiz, María Luisa, S410 (FRI-558)
Ortiz-Palma, Ane, S277 (THU-330-YI), S631 (SAT-095-YI)
Ortmayr, Gregor, S477 (WED-369)
Orviz, Eva, S806 (FRI-024)
Ory, Karine, S889 (THU-619)
Osama, Aya, S231 (FRI-305)
Oscarsson, Jan, S252 (SAT-530)
Oshins, Regina, S855 (WED-287-YI)
Osmani, Andrei, S820 (WED-020-YI)
Osman, Karim T, S325 (SAT-320)
Osmundson, Sarah, S70 (LBP-005), S975 (WED-636), S976 (WED-637)
Ostano, Paola, S457 (WED-235)
Osterlund, Pia, S450 (THU-403)
Ostojic, Ana, S255 (SAT-541), S923 (SAT-618)
Ostrowski, Sisse Rye, S166 (FRI-393)
O'Sullivan, Therese, S699 (FRI-198)
Osuna, Juan Manuel, S806 (FRI-024)
Otaegui-Chivite, Ane, S137 (FRI-125)
Otajonova, Nazokat, S160 (SAT-507)
Ota, Riku, S555 (THU-206)
Otazua, Luis Elorduy, S910 (SAT-581)
Otelea, Dan, S807 (FRI-025)
Oterdoom, Leendert H., S15 (OS-009-YI), S352 (SAT-429)
Otero, Alejandra, S410 (FRI-558)
Oton, Elena, S410 (FRI-558)
Otto-Mora, Patricia, S455 (TOP-406)
Ott, Peter, S853 (WED-282-YI)
Ouafae, Dahri, S844 (THU-286)
Oudot, Marine, S463 (WED-250)
Oumaima, Azzaoui, S845 (THU-287)
Oussalah, Abderrahim, S37 (OS-052)
Ouwens, Margriet, S666 (SAT-211-YI)
Ouyang, Shi, S68 (OS-107)
Ouyang, Wenxian, S955 (FRI-628)
Ouyang, Yu, S656 (SAT-175)
Ovadia, Caroline, S23 (OS-026-YI), S40 (OS-059-YI), S354 (SAT-434), S552 (THU-196)
Overcash, Scott J., S689 (FRI-170)
Overi, Diletta, S2 (GS-002), S856 (WED-291)
Owen, Christina, S75 (LBP-017)
Oyama, Lila, S671 (SAT-226)
Oyama, Masafumi, S95 (SAT-077), S162 (TOP-438), S263 (SAT-334), S652 (SAT-164), S660 (SAT-189)
Oyunbileg, Janchiv, S48 (OS-074)
Oza, Noriko, S808 (FRI-028)
Ozari Gulnar, Muge, S965 (WED-603)
Özcürümez, Mustafa, S395 (FRI-511-YI)
Özden, Yavuz, S780 (SAT-006)
Oz, Digdem Kuru, S588 (WED-116)
Özdirik, Burcin, S287 (FRI-275)
Ozenne, Violaine, S45 (OS-067), S428 (THU-226-YI), S446 (THU-393-YI), S493 (FRI-221), S499 (FRI-238), S505 (FRI-254), S506 (FRI-255-YI), S507 (FRI-362), S508 (FRI-364-YI)
Özer, Selin, S965 (WED-603)
Ozik, Jonathan, S816 (WED-009), S818 (WED-014)
Özlem, Akili, S18 (OS-015)
Ozturk, Bengi, S203 (WED-464), S496 (FRI-231)

Paba, Pierpaolo, S807 (FRI-025), S919 (SAT-608-YI)
Pablo Arab, Juan, S773 (THU-037)
Pace, Craig, S77 (LBP-021)
Pace, Jade, S337 (SAT-381)
Pachisia, Aditya Vikram, S741 (THU-474)
Pacho, Fernando Hernandez, S819 (WED-019)
Pachori, Alok, S2 (GS-003)
Padaki, Nagaraja, S786 (SAT-023), S952 (FRI-622)
Padaki, Nagaraja Rao, S67 (OS-105-YI)
Padalko, Elizaveta, S807 (FRI-025), S907 (SAT-575)
Pade, Corinna, S876 (THU-575), S888 (THU-618)
Padgett, Thomas, S758 (TOP-002), S781 (SAT-007)
Padilla-Lopez, Marlene, S337 (SAT-382)
Padilla, Marcelino, S893 (THU-629)
Padilla, Marlene, S300 (SAT-250), S331 (SAT-368-YI)
Padilla, P. Martin, S35 (OS-050-YI)
Padmanabhan, Krishna, S596 (WED-139), S692 (FRI-179)
Padua, Elizabeth, S892 (THU-627)
Paez-Zayas, Victor Manuel, S866 (FRI-640)
Paff, Melanie, S1 (GS-001), S956 (TOP-598), S957 (WED-577), S959 (WED-585), S960 (WED-587)
Pagadala, Akash, S614 (WED-195)
Pagadala, Mangesh, S375 (TOP-518), S407 (FRI-546), S689 (FRI-170), S754 (THU-509)
Paganini, Pamela, S699 (FRI-200)
Pagano, Giulia, S394 (FRI-507-YI)
Pageaux, Georges-Philippe, S92 (SAT-068), S325 (SAT-320), S387 (FRI-484), S414 (FRI-572), S414 (FRI-573)
Page, Emma, S811 (FRI-038)
Pages, Laura, S250 (SAT-524)
Pagès, Laura, S562 (TOP-097-YI), S605 (WED-168-YI), S612 (WED-188)
Page, Sophie, S707 (THU-546-YI)
Pagni, Fabio, S331 (SAT-368-YI), S462 (WED-249)
Pahwa, Prabhjyoti, S478 (WED-371)
Paik, Annette, S758 (TOP-001), S794 (SAT-047)
Paik, James, S796 (SAT-053)
Paik, James M., S557 (THU-213), S758 (TOP-001), S790 (SAT-035), S793 (SAT-045), S794 (SAT-047), S795 (SAT-050), S795 (SAT-051)
Paik, Paul, S386 (FRI-482), S411 (FRI-561-YI), S413 (FRI-570)
Paik, Yong Han, S927 (SAT-625)
Paik, Yong-Han, S500 (FRI-241)
Pai, Madhava, S455 (TOP-406)
Pai, Nikhil, S700 (FRI-202)
Paisant, Anita, S554 (THU-202)
Paiva, Nuno, S483 (WED-388-YI)
Pajancic, Larissa, S37 (OS-053), S715 (WED-560-YI), S717 (WED-569-YI)
Pajares, Félix García, S379 (FRI-459), S403 (FRI-532), S403 (FRI-533), S415 (FRI-575)
Pajecki, Denis, S701 (FRI-203-YI)
Pak, Kevin, S803 (FRI-012), S803 (FRI-013)
Pakseresht, Arash, S573 (WED-072), S613 (WED-190)
Pakseresht, Radin, S606 (WED-171)
Palau, Antonio David, S948 (FRI-611)
Palchek, Gil, S770 (THU-026)
Palermiti, Alice, S942 (FRI-593)
Palitti, Valeria Pace, S69 (LBP-004-YI), S82 (LBP-034-YI), S304 (SAT-258), S307 (SAT-263), S335 (SAT-378-YI), S350 (SAT-421)
Pallidis, Ione Grammatikopoulos, S857 (WED-299)
Pallitto, Maria Belen, S55 (OS-086), S831 (THU-258-YI), S842 (THU-284)
Palloni, Andrea, S424 (TOP-375-YI), S428 (THU-227-YI), S514 (FRI-381)
Pallotta, Dante Pio, S69 (LBP-004-YI)
Pallozzi, Maria, S731 (THU-444-YI)
Palma, Elena, S139 (FRI-133), S242 (FRI-345-YI), S472 (WED-274)
Palma, Rui, S726 (THU-428)
Palmer, Andrew, S121 (FRI-077), S803 (FRI-014), S818 (WED-013)
Palmer, Jodi, S804 (FRI-015-YI)
Palmieri, Rosalinda, S841 (THU-282)
Palmiotti, Anna, S485 (WED-395-YI)
Palom, Adriana, S43 (OS-066), S798 (TOP-048), S804 (FRI-019), S908 (SAT-577), S926 (SAT-623), S934 (TOP-582), S937 (FRI-585-YI), S948 (FRI-611), S949 (FRI-612)
Palomo, Carola Zurita, S678 (SAT-244)
Palou, Alba Carreras, S2 (GS-002)
Palumbo, Chiara Saroli, S589 (WED-119)
Palumbo, Pierpaolo, S767 (THU-020)
Pamecha, Viniyendra, S139 (FRI-135-YI), S269 (SAT-354-YI), S288 (FRI-282), S292 (FRI-299), S361 (THU-355-YI), S418 (THU-517-YI), S425 (THU-217-YI), S456 (WED-232)
Pammer, Lorenz, S257 (SAT-545-YI), S848 (THU-302), S849 (THU-305-YI)
Panarelli, Maurizio, S814 (WED-004)
Panchal, Aaryan, S187 (TOP-471-YI)
Panchal, Hitesh, S404 (FRI-539), S741 (THU-474)
Pan, David, S948 (FRI-610), S957 (WED-578), S958 (WED-580)
Pandey, Dinesh, S739 (THU-466)
Pandey, Hem Chandra, S141 (TOP-423)
Pandey, Namrata, S164 (FRI-385-YI), S184 (FRI-453-YI)
Pandey, Shivani, S184 (TOP-454-YI)
Pandey, Shubhram, S339 (SAT-387)
Pandey, Sushmita, S104 (THU-071-YI), S105 (THU-073-YI), S105 (THU-074), S120 (FRI-074), S129 (TOP-224-YI), S131 (FRI-105-YI), S138 (FRI-132), S139 (FRI-135-YI), S265 (SAT-341), S269 (SAT-354-YI), S269 (SAT-355), S276 (THU-324-YI), S280 (THU-337), S361 (THU-354), S373 (WED-353-YI), S418 (THU-517-YI)
Panel, ERN Rare Liver Youth, S708 (THU-554-YI)
Panera, Nadia, S583 (WED-102-YI)
Panero, José Luis Calleja, S150 (SAT-475), S409 (FRI-557), S517 (TOP-114), S525 (THU-103), S542 (THU-164), S558 (TOP-063-YI), S567 (WED-054), S585 (WED-105), S585 (WED-106), S589 (WED-118), S598 (WED-150), S607 (WED-174-YI), S612 (WED-186-YI), S612 (WED-187-YI), S618 (WED-204), S621 (WED-215), S733 (THU-450), S753 (THU-505-YI), S772 (THU-036)
Panganiban, Jennifer, S700 (FRI-202)
Pang, Mingchang, S628 (TOP-145)
Pang, Wenjie, S605 (WED-169)
Pan, Hualing, S68 (OS-107), S74 (LBP-015)
Panigrahi, Manas Kumar, S204 (WED-466)
Pani, Jusline, S80 (LBP-028-YI)
Panlilio, Mara Teresa, S452 (THU-414-YI)
Pan, Mei-Hung, S274 (THU-319), S797 (TOP-033), S898 (TOP-567), S898 (TOP-568), S915 (SAT-594), S929 (SAT-633)
Panosian, Tzoline Topdjian, S275 (THU-322-YI)
Pan, Qiong, S87 (LBP-044)
Pan, Shaokun, S891 (THU-626)
Pan, Shubo, S511 (FRI-370)
Pantazatou, Vasiliki, S620 (WED-212)
Pantzios, Spyridon, S507 (FRI-257)
Pan, Weidong, S511 (FRI-370)
Pan, Yanfeng, S954 (FRI-626)
Pan, Yeming, S81 (LBP-031)
Pan, Yi, S299 (SAT-247), S320 (SAT-303), S320 (SAT-304)
Pan, Yuqing, S677 (SAT-241)
Panzer, Marlene, S257 (SAT-545-YI), S862 (WED-314-YI)
Panzer, Simon, S200 (WED-453)
Panzer, Ulf, S291 (FRI-291-YI)
Paolella, Giulia, S595 (WED-138), S850 (THU-308)
Paolini, Erika, S443 (THU-380-YI), S595 (WED-138), S662 (SAT-198-YI)
Paon, Veronica, S97 (SAT-084-YI), S405 (FRI-541)
Papachristoforou, Eleni, S12 (OS-004-YI)
Papadimopoulos, Ilias, S694 (FRI-185)
Papadopoulos, Nikolaos, S620 (WED-212)
Papaleo, Bruno, S784 (SAT-015-YI)
Papanicolaou, Eleni, S777 (THU-050)
Papantoniou, Konstantinos, S79 (LBP-026), S300 (SAT-250), S314 (SAT-283), S338 (SAT-384), S348 (SAT-416)
Papathanasiou, Erofili, S213 (WED-497)
Papatheodoridi, Alkistis Maria, S45 (OS-068-YI)
Papatheodoridi, Margarita, S43 (OS-066), S45 (OS-068-YI), S46 (OS-070-YI),

Author Index

S62 (OS-097), S516 (TOP-113), S545 (THU-172), S900 (SAT-559), S902 (SAT-560), S934 (TOP-582), S936 (TOP-584), S937 (FRI-585-YI)
Papatheodoridis, George, S43 (OS-066), S45 (OS-068-YI), S46 (OS-070-YI), S62 (OS-097), S127 (FRI-095), S424 (TOP-376), S516 (TOP-113), S545 (THU-172), S777 (THU-050), S781 (SAT-008), S781 (SAT-009), S794 (SAT-046), S923 (SAT-618), S934 (TOP-582), S937 (FRI-585-YI)
Papatheodorou, Elias, S9 (LBO-004)
Papavasileiou, Panagiotis, S20 (OS-018)
Papenthin, Wiebke, S840 (THU-274), S842 (THU-283)
Pape, Simon, S15 (OS-009-YI)
Papinutti, Delfina, S862 (WED-315)
Papp, Maria, S34 (OS-049), S35 (OS-050-YI), S141 (TOP-437), S145 (SAT-458-YI), S148 (SAT-467-YI), S166 (FRI-388-YI), S261 (SAT-329-YI), S332 (SAT-369), S337 (SAT-382), S347 (SAT-414-YI), S347 (SAT-415)
Pappo, Orit, S60 (OS-093)
Paradissis, Agnes, S338 (SAT-384)
Paradis, Valerie, S853 (WED-283)
Paradis, Valérie, S17 (OS-011), S38 (OS-055), S53 (OS-083-YI), S61 (OS-095-YI), S480 (WED-380), S571 (WED-067), S720 (TOP-504-YI)
Paraskevopoulou, Maria D., S667 (SAT-213), S847 (THU-300), S848 (THU-301)
Paraskevopoulou, Sofia, S45 (OS-068-YI)
Parbole, Pedro, S806 (FRI-024)
Pardo, Carlos, S191 (WED-427-YI), S720 (TOP-504-YI), S733 (THU-450)
Pardo, Daniel Paredes, S974 (WED-628)
Pardo, Victoria, S603 (WED-163)
Parente, Alessandro, S59 (OS-091), S401 (FRI-527)
Parent, Romain, S869 (TOP-632)
Pares, Albert, S325 (SAT-320)
Parés, Albert, S67 (OS-106)
Pare, Stella Line Emmanuella, S926 (SAT-624)
Parfieniuk-Kowerda, Anna, S980 (FRI-633)
Parikh, Neehar D., S116 (FRI-061), S190 (WED-421), S197 (WED-447), S375 (TOP-519), S492 (FRI-218)
Parisi, Eva, S888 (THU-618)
Parisi, Ida, S43 (OS-065)
Parisse, Simona, S407 (FRI-548)
Park, Aron, S653 (SAT-167)
Parkash, Om, S605 (WED-170), S743 (THU-478)
Park, Beom Jin, S448 (THU-397)
Park, Da-Hee, S743 (THU-480-YI)
Parker, Charlotte, S406 (FRI-544)
Parker, Geoff, S106 (THU-075)
Parker, Richard, S84 (LBP-038), S117 (FRI-067), S404 (FRI-537), S547 (THU-180)
Park, Haesuk, S974 (WED-628)
Park, Hee Chul, S502 (FRI-245)
Park, Hyo Jung, S4 (GS-007)
Park, In Gyu, S266 (SAT-345), S267 (SAT-349)
Park, James, S76 (LBP-021)
Park, Jeayeon, S497 (FRI-232), S507 (FRI-361), S509 (FRI-366)
Park, Jeong Hwan, S546 (THU-174)
Park, Jina, S707 (THU-547)
Park, Jiwoon, S856 (WED-290)
Park, Jun Yong, S498 (FRI-235), S916 (SAT-597)
Park, Minji, S360 (THU-351)
Park, Min Kyung, S906 (SAT-573)
Park, Min Seo, S132 (FRI-107), S135 (FRI-119), S478 (WED-372)
Park, Seong, S546 (THU-173-YI)
Park, Suna, S398 (FRI-516), S834 (THU-262), S836 (THU-266)
Park, Yewan, S546 (THU-175)
Park, Yong Kwang, S891 (THU-625)
Park, Young Nyun, S38 (OS-054)
Park, Youngsu, S509 (FRI-366)
Parlati, Lucia, S43 (OS-066), S45 (OS-067), S66 (OS-104), S95 (SAT-076), S493 (FRI-221), S508 (FRI-364-YI), S934 (TOP-582), S937 (FRI-585-YI)
Parmar, Deven, S7 (LBO-001)
Parmar, Kavin, S109 (TOP-209-YI), S122 (FRI-083)
Parola, Maurizio, S479 (WED-379)
Parra, Camila Olarte, S701 (FRI-205-YI)
Parracho, Tamara, S241 (FRI-339)
Parraga, Ximena, S773 (THU-037)
Parrinello, Christina, S695 (FRI-186)
Parr, Jonathan B., S80 (LBP-028-YI)
Parrotta, Maria Eugenia, S626 (WED-231)
Parry, Amy, S715 (WED-561-YI)
Parry, Sarah, S811 (FRI-038)
Partanen, Jukka, S376 (FRI-448)
Parthasarathy, Sahana, S845 (THU-288)
Paruchakul, Parucha, S121 (FRI-078)
Pascale, Alina, S428 (THU-226-YI), S499 (FRI-238), S506 (FRI-255-YI)
Pascher, Andreas, S383 (FRI-474), S409 (FRI-556), S493 (FRI-220)
Pascual-Dapena, Ana, S317 (SAT-290-YI), S338 (SAT-383)
Pascual-Lopez, Irene, S743 (THU-479)
Pascual-Moreno, Isabel, S598 (WED-150), S779 (SAT–003-YI)
Pasparakis, Manolis, S280 (THU-338-YI)
Pasqualini, Lorenza, S49 (OS-076-YI)
Pasqua, Mattia, S419 (THU-524)
Pasquazzi, Caterina, S49 (OS-076-YI)
Pasquier, David, S414 (FRI-572)
Passalacqua, Chiara, S196 (WED-445)
Passenberg, Moritz, S33 (OS-046), S172 (FRI-410-YI), S215 (WED-506)
Passow, Kellan, S879 (THU-587), S885 (THU-606)
Pasta, Andrea, S176 (FRI-425), S190 (WED-425), S212 (WED-494-YI), S479 (WED-378)
Pastore, Mirella, S457 (WED-235), S475 (WED-366), S479 (WED-379)
Pastor, Tania, S484 (WED-393)
Pastrovic, Frane, S337 (SAT-382), S427 (THU-220)
Pasulo, Luisa, S401 (FRI-528), S414 (FRI-571), S817 (WED-010)
Pasut, Gianfranco, S669 (SAT-219)
Pata, María, S600 (WED-153)
Patch, David, S54 (OS-084), S752 (THU-501), S757 (THU-516)
Patel, Archna, S390 (FRI-493-YI)
Patel, Bhaktasharan, S58 (OS-089), S313 (SAT-282)
Patel, Chirag, S10 (LBO-006)
Patel, Deep, S31 (OS-043-YI), S212 (WED-495-YI)
Patel, Harsh, S437 (THU-362)
Patel, Janisha, S10 (LBO-006)
Patel, Keyur, S547 (THU-179), S582 (WED-099), S606 (WED-171), S624 (WED-226), S783 (SAT-013-YI), S784 (SAT-014)
Patel, Megha, S911 (SAT-586)
Patel, Nilang, S24 (OS-028), S143 (SAT-451), S144 (SAT-452), S188 (WED-417)
Patel, Ohm, S143 (SAT-451)
Patel, Rahul, S60 (OS-094)
Patel, Ravi, S871 (THU-560-YI)
Patel, Rishi, S12 (OS-005-YI), S490 (TOP-407-YI)
Patel, Samir, S783 (SAT-012)
Patel, Sheel, S532 (THU-125), S684 (FRI-154)
Patel, Shushma, S5 (GS-008)
Patel, Vishal C, S168 (FRI-396)
Patel, Vishal C., S141 (TOP-437), S150 (SAT-475), S159 (SAT-505)
Päth, Günter, S51 (OS-080-YI), S455 (TOP-406)
Pathil-Warth, Anita, S251 (SAT-525)
Patial, Vikram, S460 (WED-243), S653 (SAT-166), S668 (SAT-216-YI)
Patidar, Gopal, S141 (TOP-423)
Patidar, Kavish, S154 (SAT-490)
Pati, Girish Kumar, S952 (FRI-622)
Patil, Amol, S221 (WED-522)
Patil, Mahesh Vijay, S182 (FRI-441-YI)
Patil, Rashmee, S20 (OS-019), S80 (LBP-029), S559 (TOP-064), S560 (TOP-066), S561 (TOP-082), S569 (WED-059)
Patil, Snehal, S978 (WED-642-YI)
Patmore, Lesley, S46 (OS-070-YI), S809 (FRI-030), S817 (WED-011)
Patra, Partha Sarathi, S805 (FRI-020)
Patrono, Damiano, S59 (OS-091)
Patseas, Dimitrios, S657 (SAT-182)
Paturel, Alexia, S478 (WED-377)
Patwardhan, Vilas, S325 (SAT-320), S327 (SAT-322), S331 (SAT-368-YI)
Paudel, Rajan, S568 (WED-057-YI), S606 (WED-172-YI), S606 (WED-173)
Paule, Lorena, S34 (OS-049)

Pauli, Chantal, S465 (WED-255)
Paulischkis, Juri, S240 (FRI-337-YI)
Paul, Maxi, S107 (THU-078)
Paulsen, Vemund, S451 (THU-409)
Paulson, Angela, S706 (THU-544)
Paulusma, Coen, S646 (SAT-140-YI), S674 (SAT-233)
Paulweber, Bernhard, S539 (THU-151-YI)
Pauwels, Arnaud, S829 (THU-252)
Pavan, Francesco, S307 (SAT-263), S335 (SAT-378-YI)
Pavek, Petr, S286 (FRI-272), S661 (SAT-191)
Pavel, Vlad, S157 (SAT-497), S216 (WED-507)
Pavesi, Marco, S53 (OS-082)
Pavic, Magda Pletikosa, S800 (FRI-006)
Pavithran, Sheela, S706 (THU-544)
Pavlides, Michael, S568 (WED-057-YI)
Pavlinková, Gabriela, S861 (WED-308)
Pavlou, Efthimia, S142 (SAT-449)
Pavlov, Dimitar, S76 (LBP-021)
Pavlovskyi, Leonid, S71 (LBP-007)
Pavon-Castillero, Esther, S542 (THU-164)
Pawaria, Arti, S55 (OS-086), S831 (THU-258-YI), S842 (THU-284)
Pawlotsky, Jean-Michel, S38 (OS-054), S798 (TOP-034), S886 (THU-609)
Pawlowska, Agnieszka Pawlowska, S85 (LBP-039)
Payawal, Diana, S67 (OS-105-YI), S952 (FRI-622)
Paye, François, S499 (FRI-238)
Peacock, Georgina, S789 (SAT-030)
Peake, Kristen, S716 (WED-562-YI), S716 (WED-563), S716 (WED-564)
Pearce, Brenden, S845 (THU-288)
Pearlman, Brian, S62 (OS-097), S516 (TOP-113), S923 (SAT-618)
Pearson, Claire, S43 (OS-065)
Pearson, Ewan, S559 (TOP-065-YI)
Pecha, Robert, S125 (FRI-091)
Pech, Maciej, S490 (TOP-407-YI)
Peck-Radosavljevic, Markus, S445 (THU-385), S777 (THU-050)
Peddu, Praveen, S404 (FRI-538-YI), S503 (FRI-250)
Pedersen, Kristian, S262 (SAT-330)
Pedersen, Mark, S79 (LBP-026), S329 (SAT-364), S338 (SAT-384)
Pedersen, Michael Lynge, S801 (FRI-008)
Pedersen, Ole B, S166 (FRI-393)
Pedini, Domiziana, S383 (FRI-473)
Peeters, Frederik, S17 (OS-012)
Peeters, Robin, S684 (FRI-153)
Peiffer, Kai-Henrik, S206 (WED-475), S210 (WED-485), S383 (FRI-474), S493 (FRI-220), S744 (THU-481), S882 (THU-595)
Peiffer, Léa, S382 (FRI-466)
Pei, Na, S262 (SAT-331)
Peinado, Miguel Angel, S128 (FRI-100)
Pei, Nana, S511 (FRI-370)
Peiseler, Moritz, S268 (SAT-352-YI)
Peisl, Sarah, S287 (FRI-276-YI), S858 (WED-300-YI)
Peix, Judit, S468 (WED-263), S485 (WED-396)
Peixoto, Helena, S978 (WED-641)
Pei, Yiying, S529 (THU-115)
Pekarska, Katrina, S547 (THU-180)
Pelagatti, Alessio, S874 (THU-571)
Pelegrina, Amalia, S191 (WED-427-YI)
Peligros, Maria Isabel, S643 (SAT-134)
Pellat, Anna, S493 (FRI-221), S508 (FRI-364-YI)
Pellegrini, Elisa, S514 (FRI-381)
Pellegrino, Emanuela, S248 (SAT-516)
Pellicelli, Adriano, S43 (OS-066), S350 (SAT-421), S841 (THU-282), S900 (SAT-559), S902 (SAT-560), S934 (TOP-582), S937 (FRI-585-YI), S938 (FRI-586)
Peloso, Paul, S58 (OS-089), S313 (SAT-282)
Pelusi, Serena, S241 (FRI-340), S476 (WED-368), S575 (WED-076), S601 (WED-156)
Peña, Andres, S779 (SAT–003-YI)
Pena, Carmen, S232 (FRI-313)
Pena, Maria José, S899 (SAT-557)
Pena, María José, S910 (SAT-581), S910 (SAT-585)
Peña, Roberto Flores, S235 (FRI-319)
Peña-Sanfélix, Patricia, S30 (OS-039-YI), S272 (THU-315-YI), S273 (THU-316), S278 (THU-333-YI), S489 (WED-412-YI), S633 (SAT-101-YI)
Penders, Joris, S696 (FRI-190)
Peng, Cheng-Yuan, S1 (GS-001), S969 (WED-613)
Peng, Chengzhi, S422 (TOP-359-YI)
Peng, Feng, S160 (SAT-507)
Peng, Hong, S86 (LBP-041)
Peng, Jinying, S136 (FRI-123)
Peng, Liang, S155 (SAT-491), S155 (SAT-492), S155 (SAT-493), S805 (FRI-021)
Peng, Mingli, S108 (THU-083), S269 (SAT-353)
Peng, Nana, S224 (WED-531), S589 (WED-118)
Peng, Yen-Chun, S686 (FRI-158-YI)
Penha-Gonçalves, Carlos, S649 (SAT-152)
Penisson, Sophie, S783 (SAT-012)
Penker, Romana, S742 (THU-476)
Penna, Amalia, S874 (THU-571)
Pennant, Tia, S946 (FRI-605)
Penninck, Tilde, S22 (OS-023)
Pennington, Stephen, S641 (SAT-126)
Pennisi, Grazia, S62 (OS-097), S476 (WED-368), S516 (TOP-113), S517 (TOP-114), S525 (THU-103), S558 (TOP-063-YI), S589 (WED-118), S601 (WED-156), S607 (WED-174-YI), S696 (FRI-188-YI)
Penn, Matt, S799 (FRI-004), S800 (FRI-005)
Penrice, Daniel, S186 (TOP-469-YI)
Peñuelas-Haro, Irene, S467 (WED-262)
Peñuelas, Óscar, S146 (SAT-459)
Peperhove, Matti, S222 (WED-526-YI)
Peppelenbosch, Maikel P., S909 (SAT-580)
Pera, Guillem, S26 (OS-032-YI), S63 (OS-098-YI), S515 (TOP-098), S583 (WED-101), S608 (WED-180), S789 (SAT-031-YI)
Peralta, Mirta, S112 (FRI-050), S296 (TOP-281), S306 (SAT-262)
Peralta, Peregrina, S393 (FRI-501)
Perazzo, Hugo, S724 (THU-420), S978 (WED-641)
Perbellini, Emily, S272 (THU-315-YI)
Perbellini, Riccardo, S43 (OS-066), S476 (WED-368), S936 (TOP-584), S937 (FRI-585-YI), S942 (FRI-592), S942 (FRI-593)
Perea, Victor, S806 (FRI-024)
Pereira, Aline Moura Ferraz, S340 (SAT-394)
Pereira, Bruno, S167 (FRI-394-YI)
Pereira, Gleicy, S724 (THU-420)
Pereira, Gustavo, S24 (OS-028), S34 (OS-049), S35 (OS-050-YI), S141 (TOP-437), S144 (SAT-452), S154 (SAT-484), S166 (FRI-388-YI), S978 (WED-641)
Pereira, Isabel Veloso Alves, S527 (THU-109), S701 (FRI-203-YI)
Perelló, Christie, S585 (WED-106), S612 (WED-186-YI)
Peres, Flavia Soares, S834 (THU-262)
Pereyra, David, S284 (FRI-267)
Pérez, Ana, S598 (WED-150)
Pérez, Ana Belén, S910 (SAT-581), S910 (SAT-585)
Perez, Anthony, S344 (SAT-403)
Pérez, Dalis, S112 (FRI-050)
Perez, Daniela, S296 (TOP-281), S306 (SAT-262)
Pérez del Campo, Dúnia, S804 (FRI-019)
Pérez-del-Pulgar, Sofía, S884 (THU-604-YI), S941 (FRI-590)
Perez de Rojas, Javier, S96 (SAT-079)
Perez-Elias, Maria Jesus, S25 (OS-029)
Perez-Guasch, Martina, S110 (TOP-222), S203 (WED-463)
Pérez-Hernández, José Luis, S141 (TOP-437), S236 (FRI-322)
Pérez, Judith, S254 (SAT-538)
Perez, Lucía, S358 (THU-340-YI)
Pérez, Lucía, S603 (WED-163)
Pérez-Medrano, Indhira, S288 (FRI-283)
Pérez-Nievas, Pablo Cavanagh, S250 (SAT-524)
Perez, Pilar, S25 (OS-029)
Perez, Renata, S340 (SAT-394), S830 (THU-254), S830 (THU-255)
Perez, Roberto Rafael, S296 (TOP-281), S306 (SAT-262)
Pérez-Rodríguez, Lucía, S910 (SAT-585)
Perez-Rodriguez, Sergio, S250 (SAT-524)
Pérez-Ruiz, Mercedes, S910 (SAT-585)
Perez, Samuel, S112 (FRI-050), S625 (WED-228)

Author Index

Perez, Sara Lorente, S410 (FRI-558), S603 (WED-163)
Pérez-Somarriba, Juncal, S904 (SAT-564)
Pérez, Sonsoles Garcinuño, S910 (SAT-585)
Perez, Valeria, S53 (OS-082), S730 (THU-443)
Pericàs, Juan M., S26 (OS-032-YI), S233 (FRI-315), S515 (TOP-098), S542 (THU-164), S562 (TOP-097-YI), S567 (WED-054), S583 (WED-101), S605 (WED-168-YI), S612 (WED-186-YI), S612 (WED-188), S691 (FRI-175), S777 (THU-050)
Pericleous, Marinos, S713 (WED-556-YI)
Periti, Giulia, S241 (FRI-340), S476 (WED-368), S575 (WED-076), S601 (WED-156)
Perkmann, Thomas, S200 (WED-453)
Peron, Jean Marie, S38 (OS-055), S54 (OS-084), S428 (THU-226-YI), S493 (FRI-221), S506 (FRI-255-YI), S508 (FRI-364-YI), S723 (THU-419)
Perpinan, Elena, S366 (WED-333-YI)
Perricone, Giovanni, S8 (LBO-002), S26 (OS-031), S150 (SAT-475)
Perriera, Riccardo, S41 (OS-062), S279 (THU-334-YI), S359 (THU-347-YI), S638 (SAT-118)
Perri, Roman, S10 (LBO-006)
Perry, Jason, S948 (FRI-610)
Perry, Megan, S43 (OS-065)
Persano, Mara, S494 (FRI-225)
Persico, Marcello, S69 (LBP-004-YI), S176 (FRI-425), S190 (WED-425), S212 (WED-494-YI), S304 (SAT-258), S307 (SAT-263), S335 (SAT-378-YI), S479 (WED-378), S938 (FRI-586), S977 (WED-640)
Pertler, Elke, S257 (SAT-545-YI), S862 (WED-314-YI)
Perugorria, Maria Jesus, S165 (FRI-387-YI), S271 (THU-314), S303 (SAT-257-YI), S323 (SAT-315), S483 (WED-388-YI), S484 (WED-393)
Perumal, Abirami, S597 (WED-142-YI), S780 (SAT-005), S782 (SAT-010-YI)
Perumpail, Brandon, S700 (FRI-202)
Pesatori, Eugenia, S350 (SAT-421)
Pes, Francesco, S307 (SAT-263)
Pessoa, Mário, S62 (OS-097), S112 (FRI-050), S516 (TOP-113), S701 (FRI-203-YI), S768 (THU-021)
Pessoa, Mario Guimarães, S127 (FRI-095), S296 (TOP-281), S306 (SAT-262), S557 (THU-213), S923 (SAT-618)
Peta, Valentina, S577 (WED-085), S608 (WED-179)
Petcharaporn, Lita, S713 (WED-555)
Peters-Bakker, Martine, S963 (WED-595)
Petersen, Jonatan, S703 (THU-527-YI)
Peters, Erica, S814 (WED-004)
Peters, Jendrik, S743 (THU-480-YI)
Petersson, Mikael, S690 (FRI-173)
Petibon, Yoann, S579 (WED-090)
Petitjean, Mathieu, S119 (FRI-073), S243 (FRI-349)
Petkeviciene, Janina, S823 (WED-029)
Petra, Fischer, S602 (WED-157), S733 (THU-450), S753 (THU-505-YI)
Petra, Hirsova, S286 (FRI-272), S661 (SAT-191)
Petraki, Eleni, S503 (FRI-250)
Petralli, Giovanni, S695 (FRI-187), S950 (FRI-619)
Petrenko, Oleksandr, S284 (FRI-266), S362 (TOP-325-YI)
Petrikowski, Marvin, S209 (WED-485)
Petrivna, Tsarynna, S49 (OS-075), S962 (WED-594)
Petroff, David, S600 (WED-154-YI)
Petros, Sirak, S150 (SAT-474)
Petrovic, Ana, S617 (WED-202)
Petta, Salvatore, S62 (OS-097), S424 (TOP-376), S476 (WED-368), S516 (TOP-113), S517 (TOP-114), S525 (THU-103), S558 (TOP-063-YI), S589 (WED-118), S601 (WED-156), S607 (WED-174-YI), S612 (WED-187-YI), S618 (WED-204), S621 (WED-215), S696 (FRI-188-YI)
Pfefferkorn, Maria, S879 (THU-589-YI), S930 (SAT-636)
Pfeifer, Bernhard, S257 (SAT-545-YI)
Pfisterer, Karin, S242 (FRI-346)
Pfister, Eva-Doreen, S834 (THU-260)
Pham, Dan Que, S435 (THU-246)
Pham, Khanh, S471 (WED-272)
Phan, Eugene, S208 (WED-480)
Phan, Min-Duy, S170 (FRI-403)
Pharo, Heidi, S451 (THU-409)
Philipose, Zinu, S768 (THU-023), S772 (THU-035)
(Philippe) Huang, Huei-Tyng, S759 (TOP-018-YI), S773 (THU-038), S773 (THU-039)
Philips, Gino, S17 (OS-012)
Phillips, Alexandra, S171 (FRI-409-YI)
Phillips, Isobel, S338 (SAT-385)
Phillips, Jana, S544 (THU-167)
Phillips, Johnny, S725 (THU-427)
Phillips, Raymond, S58 (OS-089), S313 (SAT-282)
Philo, Mark, S42 (OS-064-YI), S286 (FRI-271)
Philouze, Clothilde, S663 (SAT-200)
Phinius, Bonolo, S922 (SAT-612)
Phua, Kong Boo, S834 (THU-261)
Pianko, Stephen, S691 (FRI-175)
Piano, Salvatore, S3 (GS-005), S26 (OS-032-YI), S30 (OS-041), S34 (OS-049), S35 (OS-050-YI), S97 (SAT-084-YI), S141 (TOP-437), S150 (SAT-475), S159 (SAT-505), S166 (FRI-388-YI), S185 (TOP-455-YI), S195 (WED-442-YI), S196 (WED-443), S196 (WED-445), S210 (WED-485), S217 (WED-509-YI), S227 (WED-541-YI), S515 (TOP-098), S583 (WED-101)
Piazza, Alessandro, S332 (SAT-369)
Piazza, Silvano, S478 (WED-377)
Piazzolla, Valeria, S82 (LBP-034-YI), S825 (WED-037)
Picardi, Antonio, S196 (WED-444)
Picchio, Camila, S802 (FRI-010-YI)
Picchio, Gaston, S51 (OS-079)
Picciaiola, Maria Vittoria, S784 (SAT-015-YI)
Piccoli, David A., S850 (THU-308)
Pichard, Anais Vallet, S571 (WED-067)
Pich, Judit, S26 (OS-032-YI)
Pich, Judith, S515 (TOP-098)
Pichler, Carina, S440 (THU-370)
Piecha, Felix, S178 (FRI-429-YI), S185 (TOP-456-YI), S213 (WED-496), S736 (THU-460-YI), S744 (THU-482-YI), S912 (SAT-588)
Piedade, Juliana, S724 (THU-420), S978 (WED-641)
Pierluissi, Valeria, S379 (FRI-461-YI)
Piermatteo, Lorenzo, S49 (OS-076-YI), S807 (FRI-025), S899 (SAT-557), S911 (SAT-587-YI), S919 (SAT-608-YI), S924 (SAT-619)
Pierotti, Piera, S972 (WED-623)
Pieterman, Kay, S193 (WED-432), S828 (TOP-310-YI)
Pietrafesa, Davide, S272 (THU-315-YI)
Pietri, Olivia, S207 (WED-477)
Pietropaolo, Keith, S981 (FRI-635), S981 (FRI-636)
Pietschmann, Emanuel, S364 (WED-323)
Pietschmann, Thomas, S887 (THU-611)
Pignolet, Camille, S53 (OS-083-YI), S480 (WED-380)
Pikkupeura, Laura, S125 (FRI-090-YI)
Pilara, Giulia, S212 (WED-494-YI)
Pileri, Francesca, S43 (OS-066), S901 (SAT-559), S902 (SAT-560), S934 (TOP-582), S937 (FRI-585-YI), S938 (FRI-586)
Pillai, Anjana, S375 (TOP-519), S428 (THU-227-YI)
Pilon, Antoine, S608 (WED-179)
Pilowa, Cara, S7 (GS-012), S958 (WED-581)
Piluch, Pawel, S301 (SAT-251-YI)
Pilz, Sabrina, S291 (FRI-291-YI)
Pinato, David J., S12 (OS-005-YI), S429 (THU-227-YI), S455 (TOP-406), S491 (TOP-408-YI), S500 (FRI-239)
Pinchera, Biagio, S900 (SAT-559), S902 (SAT-560), S936 (TOP-584), S938 (FRI-586)
Pineda-Arzate, Orfanel, S300 (SAT-250)
Pinedo-Moraleda, Fernando, S331 (SAT-368-YI)
Piñeiro-Sotelo, Marta, S799 (TOP-049)
Pinelli, Domenico, S401 (FRI-528), S414 (FRI-571)
Pinheiro, Denise, S131 (FRI-104)
Pini, Annalisa, S576 (WED-083)
Pinjaroen, Nutcha, S450 (THU-402)
Pino, Martina, S494 (FRI-225)
Pinon, Michele, S835 (THU-263)

Pinski, Daniel, S277 (THU-331)
Pintado, Cristina, S634 (SAT-104)
Pintelon, Isabel, S638 (SAT-117-YI)
Pinter, Matthias, S37 (OS-053), S242 (FRI-346), S426 (THU-219-YI), S427 (THU-220), S427 (THU-221), S428 (THU-227-YI), S440 (THU-370), S485 (WED-396), S715 (WED-560-YI)
Pinto, Adriana, S806 (FRI-024)
Pinto, Elisa, S52 (OS-081), S148 (SAT-466-YI), S435 (THU-247), S837 (THU-268)
Pinto, Jessica, S974 (WED-629-YI)
Pinto, Raquel Borges, S850 (THU-308)
Pinyol, Roser, S18 (OS-014-YI), S453 (TOP-389), S459 (WED-242-YI), S468 (WED-263), S485 (WED-396)
Pinzani, Massimo, S41 (OS-062), S119 (FRI-073), S279 (THU-334-YI), S359 (THU-347-YI), S638 (SAT-118)
Piqué-Gili, Marta, S459 (WED-242-YI), S468 (WED-263), S485 (WED-396)
Pira, Enrico, S784 (SAT-015-YI)
Pirani, Tasneem, S147 (SAT-464)
Piratvisuth, Teerha, S439 (THU-366-YI), S960 (WED-587)
Pirenne, Jacques, S59 (OS-091), S381 (FRI-465), S849 (THU-306-YI)
Piribauer, Marlene, S672 (SAT-230)
Pirisi, Mario, S911 (SAT-587-YI)
Pirola, Amanda, S412 (FRI-564-YI)
Pirola, Carlos, S664 (SAT-201)
Pirrone, Roberto, S494 (FRI-226), S495 (FRI-227)
Piryani, Suneel, S605 (WED-170)
Pirzada, Sana, S722 (THU-417), S835 (THU-264-YI)
Pisano, Francesca, S574 (WED-073)
Pisano, Giuseppina, S520 (THU-091-YI), S595 (WED-137)
Pisarnvorawat, Kitrawee, S619 (WED-211)
Piscaglia, Fabio, S82 (LBP-034-YI), S304 (SAT-258), S307 (SAT-263), S335 (SAT-378-YI), S514 (FRI-381), S731 (THU-445-YI)
Pischke, Sven, S866 (FRI-639), S867 (FRI-642), S912 (SAT-588)
Piscopo, Antonio, S31 (OS-042), S725 (THU-425), S746 (THU-490), S747 (THU-492), S752 (THU-501)
Piscuoglio, Salvatore, S456 (WED-234-YI), S465 (WED-255)
Piskorz, Ania, S455 (TOP-405)
Pita, Alejandro, S399 (FRI-522)
Pitotti, Lavinia, S307 (SAT-263)
Pitrone, Concetta, S196 (WED-445), S223 (WED-527), S435 (THU-245), S967 (WED-605-YI)
Pitsava, Stefania, S314 (SAT-283)
Pitton, Michael Bernhard, S172 (FRI-411), S199 (WED-451-YI), S742 (THU-476)
Pivetti, Alessandra, S427 (THU-220)
Pivtorak, Kateryna, S548 (THU-182)
Pivtorak, Natalya, S548 (THU-182)
Pjevac, Petra, S37 (OS-053)
Plaforet, Vincent, S446 (THU-393-YI), S507 (FRI-362)
Planas, Ariadna Vila, S961 (WED-592)
Planas, Jose María Moreno, S837 (THU-267), S855 (WED-289)
Planas-paz, Lara, S465 (WED-255)
Plant, Randel, S844 (THU-285)
Platenburg, Gerard, S647 (SAT-149)
Playford, Geoffrey, S803 (FRI-014), S818 (WED-013)
Plaza, Magdalena Salcedo, S10 (LBO-006), S16 (OS-010), S317 (SAT-290-YI), S337 (SAT-382)
Plebani, Riccardo, S339 (SAT-386)
Plein, Helene, S1 (GS-001), S956 (TOP-598), S957 (WED-577), S960 (WED-587)
Plessier, Aurélie, S52 (OS-081), S55 (OS-085-YI), S222 (WED-525), S720 (TOP-504-YI), S721 (THU-415), S728 (THU-433-YI), S739 (THU-467), S742 (THU-477), S783 (SAT-012), S837 (THU-268), S863 (WED-317)
Plissonnier, Marie-Laure, S942 (FRI-592)
Ploss, Alexander, S873 (THU-564)
Plümers, Ricarda, S879 (THU-588)
Plunkett, Jennifer, S974 (WED-629-YI)
Poca, Maria, S62 (OS-097), S91 (SAT-062), S191 (WED-426), S516 (TOP-113), S542 (THU-164), S562 (TOP-097-YI), S567 (WED-054), S571 (WED-069), S612 (WED-188)
Poch, Tobias, S291 (FRI-291-YI)
Pockros, Paul, S803 (FRI-013)
Pöhler, Gesa, S737 (THU-461)
Pohl, Julian, S33 (OS-046), S154 (SAT-489), S161 (SAT-510-YI), S215 (WED-506)
Poirier, Ava, S753 (THU-506)
Poisa, Paolo, S69 (LBP-004-YI), S307 (SAT-263), S335 (SAT-378-YI)
Poisson, Johanne, S571 (WED-067)
Pokomandy, Alexandra De, S529 (THU-116-YI)
Polak, Wojciech, S59 (OS-091), S61 (OS-095-YI), S383 (FRI-468), S383 (FRI-473), S391 (FRI-498), S398 (FRI-517-YI), S415 (FRI-574)
Polat, Esra, S56 (OS-086)
Polati, Enrico, S97 (SAT-084-YI)
Poldiallai, Tommaso, S49 (OS-076-YI)
Polidori, Giulia, S720 (TOP-502-YI)
Polito, Francesca, S163 (FRI-382)
Poljak, Mario, S807 (FRI-025)
Pol, Jonathan, S887 (THU-612-YI)
Polkinghorne, Victoria, S799 (FRI-004), S800 (FRI-005)
Polledri, Elisa, S595 (WED-138)
Pollicino, Teresa, S967 (WED-605-YI)
Pollmanns, Maike Rebecca, S33 (OS-046)
Pollok, Joerg-Matthias, S389 (FRI-492)
Polverini, Davide, S531 (THU-120), S696 (FRI-188-YI)
Polywka, Susanne, S867 (FRI-642)
Pomej, Katharina, S37 (OS-053), S426 (THU-219-YI), S715 (WED-560-YI), S717 (WED-569-YI)
Pommie, Christelle, S78 (LBP-023), S82 (LBP-033)
Pompili, Enrico, S3 (GS-005), S176 (FRI-425), S185 (TOP-455-YI), S195 (WED-442-YI), S196 (WED-445), S203 (WED-463), S217 (WED-509-YI)
Pompili, Maurizio, S583 (WED-102-YI)
Ponce, Andy, S388 (FRI-490)
Ponce, Marta, S779 (SAT-003-YI)
Ponciano-Rodriguez, Guadalupe, S549 (THU-185-YI)
Pons, Caroline, S885 (THU-606)
Ponsioen, Cyriel, S57 (OS-087-YI), S237 (FRI-330), S290 (FRI-289), S348 (SAT-418-YI), S352 (SAT-429), S353 (SAT-432), S353 (SAT-433)
Ponsioen, Cyriel Y., S351 (SAT-426-YI)
Pons, Jose Antonio, S59 (OS-091)
Pons, Monica, S427 (THU-220), S735 (THU-453), S837 (THU-267), S855 (WED-289)
Pons, Nicolas, S262 (SAT-330)
Pontali, Emanuele, S911 (SAT-587-YI)
Ponte, Ana Sofia Albuquerque, S379 (FRI-460)
Ponziana, Francesca, S176 (FRI-425), S479 (WED-378)
Ponziani, Francesca Romana, S69 (LBP-004-YI), S82 (LBP-034-YI), S190 (WED-425), S212 (WED-494-YI), S219 (WED-515), S307 (SAT-263), S350 (SAT-421), S424 (TOP-375-YI), S514 (FRI-381), S731 (THU-444-YI), S912 (SAT-587-YI)
Ponzo, Valentina, S620 (WED-213)
Ponz-Sarvise, Mariano, S445 (THU-385)
Pooja, B S, S47 (OS-072)
Pop, Corina, S819 (WED-015), S944 (FRI-601)
Popica, Dan-Adrian, S446 (THU-393-YI), S507 (FRI-362)
Pop, Tudor Lucian, S56 (OS-086), S831 (THU-258-YI), S842 (THU-284)
Porcari, Andreia, S671 (SAT-226)
Porciani, Caterina, S343 (SAT-400)
Porro, Nunzia, S479 (WED-379)
Porro, Sophie, S765 (THU-013)
Pors, Susanne, S646 (SAT-142), S655 (SAT-173)
Porta, Matteo Della, S71 (LBP-009), S340 (SAT-393)
Porta-Pardo, Eduard, S18 (OS-014-YI), S485 (WED-396)
Porteiro, Begoña, S241 (FRI-339)
Portela, Cindy Pereira, S72 (LBP-011)
Porte, Robert, S382 (FRI-467-YI), S383 (FRI-468), S383 (FRI-473), S391 (FRI-498), S398 (FRI-517-YI)
Port, Kerstin, S935 (TOP-583), S963 (WED-596)
Porto, Graca, S849 (THU-305-YI)

Author Index

Portugaller, Rupert Horst, S742 (THU-476)
Pose, Elisa, S26 (OS-032-YI), S30 (OS-041), S110 (TOP-222), S129 (FRI-101), S203 (WED-463), S246 (TOP-552), S583 (WED-101)
Possamai, Lucia, S224 (WED-530), S343 (SAT-400)
Post, Adrian, S384 (FRI-476-YI), S384 (FRI-477), S385 (FRI-478)
Posthouwer, Dirk, S928 (SAT-628-YI)
Post, Richard, S46 (OS-070-YI)
Potapova, Anna, S487 (WED-401)
Pothuraju, Suvisesh, S407 (FRI-546)
Pottkämper, Lilli, S881 (THU-592-YI)
Poujois, Aurélia, S840 (THU-275)
Poulakos, David, S97 (SAT-084-YI)
Poulin, Sebastien, S43 (OS-066), S937 (FRI-585-YI)
Poulin, Sébastien, S76 (LBP-021)
Poulos, John, S20 (OS-019), S559 (TOP-064), S565 (WED-051)
Poulsen, Mikael Kjær, S838 (THU-269)
Pourcq, Kaat De, S708 (THU-554-YI)
Povedano, Wladimiro Jiménez, S245 (FRI-354)
Poveda, Yohana, S625 (WED-228)
Powell, Elizabeth, S170 (FRI-403)
Powell, Elizabeth E., S788 (SAT-029), S789 (SAT-030)
Powell, Michael, S893 (THU-629)
Powell, Philip A., S319 (SAT-301)
Power, Amy, S712 (WED-554)
Powrie, Fiona, S43 (OS-065)
Poyatos-García, Paloma, S189 (WED-418)
Poynard, Thierry, S571 (WED-067), S577 (WED-085), S608 (WED-179)
Pozo-Relaño, María Isabel, S467 (WED-261)
Pozza, Renee, S713 (WED-555)
Pozzoni, Pietro, S494 (FRI-225), S938 (FRI-586)
Prabdial-Sing, Nishi, S76 (LBP-019-YI)
Prabhakar, Tushar, S782 (SAT-011)
Pradhan, Dibyabhaba, S847 (THU-299)
Prado, Luan, S138 (FRI-127)
Prado, Renan, S548 (THU-183)
Praetorius, Alejandro González, S910 (SAT-581), S910 (SAT-585)
Praguylertluk, Witchayaporn, S219 (WED-514)
Praharaj, Dibya Lochan, S144 (SAT-452)
Praharaj, Dibyalochan, S952 (FRI-622)
Prajapati, Riya, S505 (FRI-253)
Praktikjo, Michael, S752 (THU-501)
Praktiknjo, Michael, S6 (GS-011-YI), S33 (OS-046), S52 (OS-081), S54 (OS-084), S145 (SAT-458-YI), S185 (TOP-456-YI), S206 (WED-475), S210 (WED-485), S213 (WED-496), S215 (WED-506), S261 (SAT-329-YI), S383 (FRI-474), S397 (FRI-515), S409 (FRI-556), S493 (FRI-220), S497 (FRI-234), S719 (TOP-488), S720 (TOP-504-YI), S723 (THU-418), S736 (THU-460-YI), S737 (THU-461), S744 (THU-481), S744 (THU-482-YI), S747 (THU-492)
Pramotedham, Thanawin, S228 (WED-543), S528 (THU-110), S698 (FRI-197)
Prampolini, Francesco, S725 (THU-425)
Prampolini, Manuel, S168 (FRI-398)
Prasad, Mithra, S952 (FRI-622)
Prasad, Ramesh, S189 (WED-419)
Pratesi, Federico, S481 (WED-383)
Prati, Daniele, S241 (FRI-340), S476 (WED-368), S575 (WED-076), S601 (WED-156), S636 (SAT-109)
Pratley, Richard E, S699 (FRI-199)
Pratt, Daniel, S58 (OS-089), S306 (SAT-261), S313 (SAT-282), S342 (SAT-398)
Preciado, María Victoria, S234 (FRI-316)
Premkumar, Madhumita, S81 (LBP-030), S221 (WED-522)
Premkumar, Prasanna Samuel, S27 (OS-033)
Presa, José, S318 (SAT-291), S733 (THU-450), S753 (THU-505-YI)
Pressiani, Tiziana, S424 (TOP-375-YI), S428 (THU-227-YI), S494 (FRI-225), S514 (FRI-381)
Prevot, Vincent, S233 (FRI-313), S241 (FRI-339)
Price, Colleen, S529 (THU-116-YI)
Price, Jennifer, S807 (FRI-026)
Prichard, David, S746 (THU-485)
Priel, Jan, S596 (WED-139)
Prieto, Janire, S16 (OS-010)
Prieto, Jhon, S296 (TOP-281), S306 (SAT-262)
Primrose, Naomi, S354 (SAT-434)
Princen, Hans M.G., S645 (SAT-138)
Priori, Victoria, S480 (WED-380)
Privitera, Graziella, S27 (OS-034)
Procopet, Bogdan, S52 (OS-081), S54 (OS-084), S61 (OS-095-YI), S175 (FRI-418), S209 (WED-483), S255 (SAT-539), S397 (FRI-515), S427 (THU-220), S543 (THU-165), S544 (THU-166), S602 (WED-157), S719 (TOP-488), S720 (TOP-504-YI), S728 (THU-433-YI), S733 (THU-450), S747 (THU-492), S752 (THU-501), S753 (THU-505-YI), S783 (SAT-012), S819 (WED-015), S944 (FRI-601)
Proehl, Sarah, S302 (SAT-254), S316 (SAT-287), S324 (SAT-316), S328 (SAT-362), S329 (SAT-363)
Proels, Markus, S14 (OS-007), S341 (SAT-397)
Proietti, Giulia, S610 (WED-183)
Prosenz, Julian, S539 (THU-151-YI)
Proske, Nora, S864 (TOP-615)
Prost, Ardavan, S414 (FRI-573)
Protopapas, Adonis, S213 (WED-497)
Protopapas, Andreas, S213 (WED-497)
Protopopescu, Camelia, S815 (WED-005), S889 (THU-619)
Protzer, Ulrike, S467 (WED-260)
Provine, Nicholas, S43 (OS-065)
Prozesky, Hans, S905 (SAT-569), S926 (SAT-624), S940 (FRI-588-YI)
Pruthi, Jatinder, S58 (OS-089), S313 (SAT-282)
Psarakis, Georgios, S314 (SAT-283)
Publicover, Jean, S871 (THU-560-YI)
Puelles, Victor, S178 (FRI-429-YI)
Puente, Angela, S427 (THU-220), S643 (SAT-134), S733 (THU-450)
Puentes, Diego, S296 (TOP-281), S306 (SAT-262)
Puerto, Marta, S182 (FRI-442), S267 (SAT-350)
Puga, Natalia Fernandez, S409 (FRI-557)
Pugh, Christopher, S713 (WED-557)
Pugh, Matthew, S364 (WED-324-YI)
Puglia, Victor, S254 (SAT-538)
Pugliese, Nicola, S52 (OS-081), S55 (OS-085-YI), S62 (OS-097), S71 (LBP-009), S127 (FRI-095), S339 (SAT-386), S516 (TOP-113), S531 (THU-120), S696 (FRI-188-YI), S720 (TOP-504-YI), S777 (THU-050), S856 (WED-291)
Puhakka, Eemeli, S266 (SAT-346)
Puig, Lidia, S710 (THU-557-YI)
Puig, Pierre Laurent, S457 (WED-236)
Puippe, Gilbert, S465 (WED-255)
Pulcherio, Issabele, S746 (THU-485)
Pulixi, Edoardo, S520 (THU-091-YI), S541 (THU-158), S553 (THU-197), S595 (WED-137), S636 (SAT-110-YI)
Pulwermacher, Philippe, S110 (FRI-042)
Punchhi, Gopika, S379 (FRI-461-YI)
Puorto, Luigi Di, S549 (THU-186-YI)
Puoti, Massimo, S43 (OS-066), S900 (SAT-559), S902 (SAT-560), S912 (SAT-587-YI), S934 (TOP-582), S937 (FRI-585-YI), S938 (FRI-586)
Purcarea, Adrian, S577 (WED-084)
Puri, Rajesh, S404 (FRI-539), S741 (THU-474)
Purkait, Swagata, S100 (THU-056)
Puskoor, Rohit, S20 (OS-019), S80 (LBP-029), S559 (TOP-064), S560 (TOP-066), S561 (TOP-082)
Puspanathan, Pavitratha, S574 (WED-075)
Pustjens, Jesse, S26 (OS-032-YI), S63 (OS-098-YI), S608 (WED-180), S789 (SAT-031-YI), S790 (SAT-035)
Puthusseril, George, S36 (OS-051-YI)
Putoto, Giovanni, S821 (WED-023)
Puttevils, Eva, S718 (WED-572)
Pu, Xiting, S324 (SAT-318)
Pu, Zhangya, S161 (SAT-508), S177 (FRI-426)
Pyarajan, Saiju, S166 (FRI-393)
Py, Jean-François, S414 (FRI-572)
Pyrsopoulos, Nikolaos, S8 (LBO-002)
Pyrsopoulos, Nikolaos T., S923 (SAT-618)

Qaderi, Farah, S794 (SAT-047)
Qadri, Sami F., S662 (SAT-197)
Qarch, Ismail, S609 (WED-181)

Qasem, Ma'mon, S732 (THU-446)
Qian, Baolin, S651 (SAT-159)
Qian, Qiu, S891 (THU-626)
Qian, Qiwei, S293 (FRI-302-YI)
Qian, Xiaohan, S153 (SAT-482), S177 (FRI-426)
Qian, Yunsong, S33 (OS-047)
Qian, Zhi-Ping, S162 (TOP-440)
Qiao, Bing, S225 (WED-537), S924 (SAT-620)
Qiao, Wenying, S491 (TOP-422)
Qin, Hongyan, S661 (SAT-195)
Qin, Xianhui, S6 (GS-010)
Qin, Xuejin, S511 (FRI-370)
Qirem, Murad, S980 (FRI-634)
Qi, Tingting, S180 (FRI-434)
Qiu, Ke, S245 (FRI-355)
Qiu, Pak, S12 (OS-004-YI)
Qiu, Yanhao, S231 (FRI-304), S241 (FRI-341), S271 (THU-303), S279 (THU-335)
Qiu, Yuanwang, S964 (WED-601-YI)
Qiu, Yunqing, S1 (GS-001), S81 (LBP-031), S489 (WED-410), S870 (TOP-645), S878 (THU-586), S896 (THU-641)
Qi, Wenying, S233 (FRI-314), S664 (SAT-202), S664 (SAT-203), S665 (SAT-204), S665 (SAT-205), S666 (SAT-206), S797 (SAT-054), S872 (THU-562)
Qi, Xiaolong, S119 (FRI-072), S259 (SAT-554), S517 (TOP-114), S549 (THU-184), S560 (TOP-080), S594 (WED-134), S609 (WED-182), S756 (THU-514), S763 (THU-011), S924 (SAT-620)
Qi, Xin, S324 (SAT-316), S838 (THU-270)
Qi, Xingshun, S728 (THU-433-YI)
Qi, Xun, S73 (LBP-012)
Qi, Yonghe, S73 (LBP-013)
Qi, Yuxia, S259 (SAT-554), S560 (TOP-080), S593 (WED-134), S763 (THU-011)
Qorbani, Mostafa, S697 (FRI-195-YI)
Quach, Susanna, S852 (TOP-311), S858 (WED-302)
Quadrado, Lucia, S319 (SAT-301), S330 (SAT-365)
Quaglia, Alberto, S53 (OS-083-YI)
Quang, Erwan Vo, S764 (THU-012), S798 (TOP-034)
Quan, Joanne, S10 (LBO-006)
Quante, Michael, S504 (FRI-251)
Quantin, Xavier, S92 (SAT-068)
Quaranta, Maria Giovanna, S440 (THU-369), S820 (WED-020-YI), S972 (WED-623)
Quarta, Alessandro, S767 (THU-020)
Quartararo, Alessio, S494 (FRI-226), S495 (FRI-227)
Quartini, Giulia, S610 (WED-183)
Quast, Christin, S395 (FRI-511-YI)
Quattrocchi, Alberto, S331 (SAT-368-YI)
Quek, Sabrina Xin Zi, S67 (OS-105-YI)
Quiambao, Ronald, S602 (WED-158)
Quickert, Stefanie, S169 (FRI-399), S175 (FRI-419), S185 (TOP-456-YI), S219 (WED-516), S744 (THU-482-YI)
Quiete, Stefano, S307 (SAT-263), S335 (SAT-378-YI)
Quinn, Clodagh, S746 (THU-485)
Quinn, Geoff, S1 (GS-001)
Quiñones, Carmen, S779 (SAT–003-YI)
Quinones, Jason, S683 (FRI-152)
Quiñones, Marta, S331 (SAT-368-YI), S968 (WED-610-YI)
Quiñones-Morales, Ildefonso, S855 (WED-288), S856 (WED-290)
Quiñones, Raisa, S16 (OS-010)
Quintana, Gabriel, S830 (THU-254)
Quintana, Laura Cudero, S308 (SAT-264)
Quintero-Bernabeu, Jesus, S850 (THU-308)
Quirk, Corrine, S891 (THU-624-YI)
Quiros-Tejeira, Ruben E., S850 (THU-308)
Qu, Jian, S260 (TOP-357)
Qu, Lihong, S964 (WED-601-YI)
Qumosani, Karim, S14 (OS-008), S295 (TOP-279), S325 (SAT-319), S354 (SAT-435)
Qureshi, Jumshaid, S597 (WED-147)
Qureshi, Sara, S967 (TOP-600-YI)
Qurishi, Nazifa, S904 (SAT-564)

Rabenau-McDonnell, Quinn, S850 (THU-308)
Rabiee, Anahita, S497 (FRI-234), S745 (THU-483)
Rabiee, Atoosa, S745 (THU-483)
Rabinowich, Liane, S214 (WED-500)
Rachakonda, Vikrant, S125 (FRI-091), S393 (FRI-505), S775 (THU-043)
Racila, Andrei, S62 (OS-097), S128 (FRI-099), S516 (TOP-113), S793 (SAT-045), S795 (SAT-051), S923 (SAT-618)
Raday, Sébastien, S681 (FRI-147)
Radenne, Sylvie, S311 (SAT-271), S380 (FRI-463), S381 (FRI-464)
Rader, Daniel, S166 (FRI-393)
Rådholm, Karin, S568 (WED-056)
Radicheva, Mariana Penkova, S76 (LBP-021)
Radovanovic-Petrova, Borka, S200 (WED-453)
Radu, Claudia Maria, S466 (WED-258)
Radu, Corina, S255 (SAT-539), S543 (THU-165), S544 (THU-166), S819 (WED-015), S944 (FRI-601)
Radu, Pompilia, S447 (THU-395), S781 (SAT-008), S781 (SAT-009)
Radwan, Ahmed, S504 (FRI-252)
Raevens, Sarah, S54 (OS-084), S55 (OS-085-YI), S59 (OS-092-YI), S99 (TOP-193-YI), S159 (SAT-505), S281 (TOP-295-YI), S315 (SAT-285), S349 (SAT-420), S464 (WED-253), S783 (SAT-012)
Raffaele, Brustia, S38 (OS-054), S499 (FRI-238)
Rafferty, Miriam, S388 (FRI-490)
Raggi, Chiara, S457 (WED-235), S462 (WED-249), S475 (WED-366)
Ragozzino, Lucia, S447 (THU-394)
Raguénès-Nicol, Céline, S365 (WED-331-YI)
Ragupathy, Avinash Kumar, S780 (SAT-005)
Raha, Aloke Kumar, S598 (WED-149)
Raharjo, Callista Vania, S218 (WED-513), S749 (THU-496)
Rahbari, Mohammad, S651 (SAT-158-YI)
Rahbari, Raheleh, S455 (TOP-405)
Rahim, Mussarat, S767 (THU-019)
Rahmani, Razgar Seyed, S17 (OS-012)
Rahman, Nafiza, S820 (WED-022)
Rahut, Antora, S745 (THU-484)
Rai, Amar, S490 (TOP-407-YI)
Raimondi, Federico, S414 (FRI-571)
Raimondo, Giovanni, S69 (LBP-004-YI), S307 (SAT-263), S335 (SAT-378-YI)
Rainer, Florian, S326 (SAT-321)
Rajaa, Boukhraiss, S949 (FRI-613)
Rajabnia, Mohsen, S697 (FRI-195-YI)
Rajalingam, Sreedevi, S772 (THU-035)
Raj, Ashok, S797 (SAT-055), S820 (WED-021)
Rajendiran, Govarthanan, S58 (OS-089), S313 (SAT-282)
Rajkumar, Rahul, S204 (WED-467)
Rajoriya, Neil, S24 (OS-028), S59 (OS-091), S144 (SAT-452), S160 (SAT-507), S406 (FRI-544)
Raj, Prema, S149 (SAT-473), S529 (THU-115)
Raju, Thriveni, S971 (WED-620)
Rajwanshi, Vivek, S879 (THU-587), S885 (THU-606)
Raluy, Mireia, S615 (WED-197)
Ramachandran, Jeyamani, S208 (WED-480)
Ramachandran, Prakash, S12 (OS-004-YI), S284 (FRI-268-YI)
Ramadhin, Jessica, S632 (SAT-100)
Ramage, John, S449 (THU-401)
Ramaiya, Kaushik, S792 (SAT-042)
Ramakers, Christian, S444 (THU-383)
Ramakrishna, Gayatri, S126 (FRI-092-YI), S288 (FRI-282), S292 (FRI-299), S425 (THU-217-YI), S456 (WED-232), S478 (WED-371)
Ramakrishnan, Arulraj, S597 (WED-142-YI), S780 (SAT-005), S782 (SAT-010-YI)
Ramamurthy, Adarsh, S276 (THU-329)
Ramazzotti, Matteo, S462 (WED-249)
Ramdani, Mohamed, S414 (FRI-573)
Ramien, Caren, S840 (THU-274), S842 (THU-283)
Ramier, Clémence, S783 (SAT-012)
Ramírez, Gabriel Sebastián Díaz, S556 (THU-212)
Ramirez, Magarita, S806 (FRI-024)
Ramírez-Mejía, Mariana, S549 (THU-185-YI)
Ramírez, Pablo, S59 (OS-091)
Ramirez-Quesada, Wagner, S790 (SAT-036)
Ramirez, Ricardo, S957 (WED-578)
Ramírez, Wagner Enrique, S33 (OS-046), S55 (OS-085-YI)

Author Index

Ramji, Alnoor, S624 (WED-226), S783 (SAT-013-YI), S784 (SAT-014), S967 (TOP-600-YI), S968 (WED-609-YI)
Ramonas, Krista, S770 (THU-026)
Ramón, Lucía, S110 (TOP-222)
Ramos-da-Silva, Laura, S267 (SAT-348)
Ramos, David Sanchez, S10 (LBO-006)
Ramos-Herrero, Victor, S271 (THU-314)
Ramos-Lage, Lucía, S241 (FRI-339)
Ramsoekh, Dewkoemar, S9 (LBO-005-YI)
Ramteke, Dhanraj, S845 (THU-288)
Ranagan, Jane, S127 (FRI-095), S766 (THU-015)
Ranasinghe, Sherika, S826 (WED-039)
Randazzo, Nadia, S919 (SAT-608-YI)
Rand, Elizabeth B., S850 (THU-308)
Rando-Segura, Ariadna, S366 (WED-332-YI), S798 (TOP-048), S804 (FRI-019), S908 (SAT-577), S926 (SAT-623), S949 (FRI-612), S961 (WED-592)
Randrianarivo, Bienvenue, S829 (THU-252)
Rangan, Pooja, S670 (SAT-220)
Ranieri, Luisa, S176 (FRI-425), S248 (SAT-516)
Ranjan, Aniket, S204 (WED-466)
Rankin, Bruce, S689 (FRI-170)
Ranndal, Heidi, S693 (FRI-182)
Rannou, Fabrice, S167 (FRI-394-YI)
Ransom, Myka, S256 (SAT-543), S258 (SAT-547)
Ranucci, Giusy, S56 (OS-086), S831 (THU-258-YI), S842 (THU-284)
Ran, Yujie, S430 (THU-229), S508 (FRI-363)
Rao, Girish, S832 (THU-258-YI), S842 (THU-284)
Rao, Guduru Venkat, S255 (SAT-541)
Rao, Huiying, S86 (LBP-041), S253 (SAT-533), S279 (THU-336), S433 (THU-239), S593 (WED-133), S668 (SAT-217-YI), S673 (SAT-232), S785 (SAT-021), S813 (FRI-045), S931 (SAT-638), S932 (SAT-641)
Rao, Qunfang, S160 (SAT-507)
Raouf, Sara, S551 (THU-191)
Rapetti, Rachele, S911 (SAT-587-YI)
Rapino, Carmela, S624 (WED-226), S783 (SAT-013-YI), S784 (SAT-014)
Raposo, Joao-Filipe, S649 (SAT-152)
Rasheed, Muhammad Adil, S178 (FRI-430)
Rasheed, Tazeen, S865 (FRI-637)
Rashidi-Alavijeh, Jassin, S33 (OS-046), S172 (FRI-410-YI), S185 (TOP-456-YI), S215 (WED-506), S408 (FRI-554), S736 (THU-460-YI), S744 (THU-482-YI)
Rashu, Elias, S586 (WED-109), S602 (WED-159-YI)
Rashwan, Hannah, S231 (FRI-305)
Rasmussen, Thomas, S77 (LBP-022-YI)
Rastogi, Archana, S139 (FRI-135-YI), S171 (FRI-404), S288 (FRI-282), S292 (FRI-299), S361 (THU-355-YI), S425 (THU-217-YI), S456 (WED-232)
Rastovic, Una, S139 (FRI-133), S242 (FRI-345-YI)
Raszeja-Wyszomirska, Joanna, S301 (SAT-251-YI), S318 (SAT-298), S355 (SAT-442), S409 (FRI-555)
Ratana-Amornpinm, Sarita, S973 (WED-625)
Ratanapipop, Mingkwan, S121 (FRI-078)
Rathi, Pravin, S952 (FRI-622)
Rathkolb, Birgit, S672 (SAT-230)
Ratnasekera, Isanka, S170 (FRI-403)
Ratnasingam, Jeyakantha, S593 (WED-132)
Rattananukrom, Chitchai, S86 (LBP-042), S156 (SAT-496), S215 (WED-505), S221 (WED-523), S228 (WED-543), S423 (TOP-374), S528 (THU-110)
Rattan, Puru, S113 (FRI-052), S126 (FRI-093)
Ratti, Francesca, S402 (FRI-529-YI)
Ratziu, Vlad, S1 (GS-001), S20 (OS-019), S21 (OS-020), S29 (OS-038), S45 (OS-067), S78 (LBP-024), S559 (TOP-064), S577 (WED-084), S608 (WED-179), S697 (FRI-191), S739 (THU-467)
Rau, Monika, S252 (SAT-529), S971 (WED-620)
Raurell, Imma, S233 (FRI-315)
Rautou, Pierre-Emmanuel, S35 (OS-050-YI), S52 (OS-081), S53 (OS-083-YI), S55 (OS-085-YI), S149 (SAT-468), S152 (SAT-478), S251 (SAT-528), S427 (THU-220), S571 (WED-067), S720 (TOP-504-YI), S721 (THU-415), S728 (THU-433-YI), S731 (THU-445-YI), S733 (THU-450), S739 (THU-467), S742 (THU-477), S760 (TOP-032), S837 (THU-268), S853 (WED-283), S862 (WED-315), S863 (WED-317)
Ravaioli, Federico, S720 (TOP-504-YI), S733 (THU-450), S753 (THU-505-YI)
Ravà, Micol, S51 (OS-079)
Raventos, David Camell, S459 (WED-242-YI)
Ravier, Roberto Pérez, S112 (FRI-050)
Ravindranath, Aathira, S56 (OS-086), S831 (THU-258-YI), S842 (THU-284)
Rawal, Pawan, S404 (FRI-539), S741 (THU-474)
Raya, José, S690 (FRI-173)
Rayner, Danielle, S315 (SAT-286)
Rayo, Andrea González, S391 (FRI-497)
Razack, Habeeb I.A., S521 (THU-093)
Razavi, Homie, S801 (FRI-009), S805 (FRI-022), S820 (WED-020-YI), S822 (WED-027), S823 (WED-029)
Razavi-Shearer, Devin, S805 (FRI-022), S820 (WED-020-YI)
Razavi-Shearer, Kathryn, S805 (FRI-022)
Razente, Danilo Mardegam, S701 (FRI-203-YI)
Razzaghi, Bonnie, S85 (LBP-039)
Rea, Benjamin, S106 (THU-075)
Reau, Nancy S., S49 (OS-075), S77 (LBP-021), S94 (SAT-073), S683 (FRI-151), S962 (WED-594)
Rebol, Lavra, S979 (TOP-614)
Reboux, Noemi, S110 (FRI-042)
Recalcati, Stefania, S462 (WED-249)
Reda, Mounzer, S907 (SAT-575)
Reddy, Gautham, S58 (OS-089), S313 (SAT-282)
Reddy, K. Rajender, S24 (OS-028), S39 (OS-056), S81 (LBP-030), S144 (SAT-452), S160 (SAT-507), S255 (SAT-541), S754 (THU-509)
Reddy, Madhavi, S202 (WED-460-YI)
Reeder, Scott, S690 (FRI-173)
Reeg, David, S371 (WED-348)
Rees, Fiona, S704 (THU-540)
Reesink, Hendrik, S963 (WED-595)
Reeves, Helen, S485 (WED-396)
Reeves, Ruth, S96 (SAT-083)
Regev-Sadeh, Tor, S613 (WED-189)
Regi, Aida, S840 (THU-274), S842 (THU-283)
Regnat, Katharina, S37 (OS-053), S179 (FRI-431-YI), S179 (FRI-432), S242 (FRI-346), S266 (SAT-347-YI), S362 (TOP-325-YI), S364 (WED-323), S750 (THU-497-YI)
Regnault, Hélène, S428 (THU-226-YI), S434 (THU-242), S446 (THU-393-YI), S493 (FRI-221), S497 (FRI-234), S499 (FRI-238), S505 (FRI-254), S506 (FRI-255-YI), S507 (FRI-362), S508 (FRI-364-YI), S723 (THU-418)
Regnery, Leon, S672 (SAT-230)
Regueiro, Jose Gonzalez, S707 (THU-548)
Rehman, Ayesha, S419 (THU-524)
Rehman, Sana, S759 (TOP-017-YI)
Rehner, Jacqueline, S265 (SAT-338)
Reiberger, Martina, S717 (WED-569-YI)
Reiberger, Thomas, S6 (GS-011-YI), S8 (LBO-002), S11 (OS-002-YI), S32 (OS-044), S33 (OS-046), S43 (OS-066), S52 (OS-081), S53 (OS-082), S54 (OS-084), S76 (LBP-020), S113 (FRI-053), S156 (SAT-494), S179 (FRI-431-YI), S179 (FRI-432), S183 (FRI-444-YI), S183 (FRI-445), S186 (TOP-470-YI), S199 (WED-451-YI), S199 (WED-452), S200 (WED-453), S205 (WED-474), S213 (WED-498), S216 (WED-508), S217 (WED-509-YI), S222 (WED-524), S237 (FRI-324), S252 (SAT-530), S266 (SAT-347-YI), S284 (FRI-266), S362 (TOP-325-YI), S364 (WED-323), S427 (THU-220), S427 (THU-221), S440 (THU-370), S717 (WED-569-YI), S719 (TOP-488), S731 (THU-445-YI), S732 (THU-448-YI), S733 (THU-449), S733 (THU-450), S734 (THU-451), S738 (THU-464-YI), S747 (THU-492), S748 (THU-493-YI), S749 (THU-494), S750 (THU-497-YI), S750 (THU-498),

S752 (THU-501), S753 (THU-505-YI), S900 (SAT-559), S901 (SAT-560), S914 (SAT-591), S934 (TOP-582), S936 (TOP-584), S937 (FRI-585-YI), S975 (WED-634-YI)
Reichert, Matthias C., S836 (THU-265-YI)
Reichman, Trevor, S345 (SAT-409-YI)
Reic, Ivona, S800 (FRI-006)
Reic, Tatjana, S800 (FRI-006)
Reider, Lukas, S199 (WED-451-YI), S732 (THU-448-YI), S733 (THU-449), S738 (THU-464-YI)
Reig, María, S481 (WED-382-YI), S639 (SAT-120)
Reikvam, Dag Henrik, S46 (OS-070-YI), S65 (OS-101-YI), S903 (SAT-562)
Reilly, Erinn, S682 (FRI-148)
Reincke, Marlene, S3 (GS-005), S33 (OS-046), S52 (OS-081), S195 (WED-442-YI), S215 (WED-506), S733 (THU-449), S744 (THU-482-YI)
Reinders, Jörg, S172 (FRI-410-YI)
Reineke-Plaaß, Tanja, S488 (WED-409-YI)
Reinhardt, Rickey, S8 (LBO-003)
Reinikainen, Jaakko, S760 (THU–003)
Reinson, Tina, S25 (OS-030), S622 (WED-217)
Reis, Ana Luiza Gomes, S701 (FRI-203-YI)
Reiso, Ilaria, S611 (WED-184-YI)
Reis, Robyn, S717 (WED-570-YI)
Reiss, Gary, S694 (FRI-183)
Reißing, Johanna, S142 (SAT-448), S159 (SAT-506-YI), S169 (FRI-399), S170 (FRI-402), S642 (SAT-131-YI)
Reiter, Florian P, S945 (FRI-602-YI)
Reiter, Florian P., S252 (SAT-529)
Reiter, Kristina, S410 (FRI-559)
Reizine, Edouard, S434 (THU-242)
Rejano-Gordillo, Claudia M., S272 (THU-315-YI), S633 (SAT-101-YI)
Rejler, Martin, S220 (WED-517)
Rejliwal, Pravinkumar, S925 (SAT-621)
Rekstyte-Matiene, Kristina, S889 (THU-620)
Rela, Mohamed, S24 (OS-028), S38 (OS-054), S67 (OS-105-YI)
Rellan, Maria J Gonzalez, S241 (FRI-339)
Remesal-Doblado, Ángela, S331 (SAT-368-YI)
Remes, Mariana Barrat, S22 (OS-022-YI)
Remizova, María Ojeda, S250 (SAT-524)
Remmelink, Myriam, S35 (OS-050-YI)
Remy, André-Jean, S681 (FRI-147)
Renaudin, Sébastien, S869 (TOP-632)
Rendon, Paloma, S815 (WED-006), S948 (FRI-611)
Renesse, Janusz Von, S643 (SAT-133)
Ren, Feng, S283 (FRI-264), S950 (FRI-617), S950 (FRI-618)
Ren, Hao, S30 (OS-040), S640 (SAT-123)
Renhardt, Clemens, S156 (SAT-494), S213 (WED-498)
Ren, Hong, S50 (OS-078), S108 (THU-083), S245 (FRI-355), S269 (SAT-353), S932 (SAT-641), S959 (WED-586)
Ren, Jie, S756 (THU-514)
Ren, Kaili, S398 (FRI-516), S834 (THU-262), S836 (THU-266)
Ren, Li, S924 (SAT-620)
Ren, Liying, S454 (TOP-391), S480 (WED-381), S514 (FRI-380), S668 (SAT-217-YI)
Ren, Mingming, S107 (THU-077)
Rennebaum, Florian, S210 (WED-485), S383 (FRI-474), S409 (FRI-556), S493 (FRI-220)
Renne, Thomas, S351 (SAT-427)
Rensburg, Brendan Janse Van, S764 (THU-012)
Rensen, Patrick CN, S631 (SAT-095-YI)
Rensink, Anouk, S535 (THU-134)
Rentería, Jorge Luis Garavito, S112 (FRI-050), S790 (SAT-036)
Renteria, Luis Alejandro Rosales, S296 (TOP-281), S866 (FRI-640)
Renteria, Sara Uceda, S942 (FRI-592)
Ren, Yayun, S561 (TOP-081)
Ren, Zhigang, S954 (FRI-626)
Reolo, Marie, S458 (WED-238)
Reschke, Josephine, S488 (WED-409-YI)
Reshma, Reshma, S246 (TOP-550), S822 (WED-025-YI)
Resino, Rosa, S806 (FRI-024)
Restier, Lioara, S836 (THU-265-YI)
Restrepo, Juan Carlos, S556 (THU-212), S625 (WED-228), S793 (SAT-044)
Restuccia, Simona, S494 (FRI-226), S495 (FRI-227)
Reta, Vianey, S397 (FRI-515)
Retta, Ignacio, S146 (SAT-461)
Reuken, Philipp, S142 (SAT-448), S159 (SAT-506-YI), S169 (FRI-399), S175 (FRI-419), S219 (WED-516)
Reuther, Peter, S371 (WED-348)
Reverberi, Valentina, S874 (THU-571)
Reverter, Enric, S53 (OS-082), S191 (WED-427-YI)
Revy, Patrick, S853 (WED-283)
Rewisha, Eman, S492 (FRI-217)
Rex, Karsten Fleischer, S801 (FRI-008)
Reyes, Gabriela Gutierrez, S236 (FRI-322)
Reyes, Rylyn, S773 (THU-037)
Reyna-Blanco, Carlos, S37 (OS-053)
Reynaert, Hendrik, S920 (SAT-609), S929 (SAT-629)
Reynders, Marijke, S907 (SAT-575)
Reyngoudt, Harmen, S648 (SAT-151-YI)
Reynolds, Catherine, S500 (FRI-239)
Reynolds, Justin, S687 (FRI-165)
Rey, Romina, S728 (THU-434)
Rezaee-Zavareh, Mohammad Saeid, S375 (TOP-519)
Rezayat, Arash Akhavan, S564 (WED-044), S565 (WED-045)
Rezi, Elena, S717 (WED-571-YI)
Rezvani, Milad, S285 (FRI-269), S293 (FRI-301), S852 (TOP-311), S859 (WED-302)
Rhaiem, Rami, S499 (FRI-238)
Riachi, Ghassan, S1 (GS-001), S45 (OS-067)
Ria, Imperial Edeliza Santiago, S495 (FRI-228-YI)
Rianda, Alessia, S938 (FRI-586), S947 (FRI-608)
Riaz, Yumnah, S845 (THU-289)
Ribaldone, Davide Giuseppe, S620 (WED-213)
Ribas, Vicent, S28 (OS-037), S627 (TOP-144), S629 (TOP-160)
Ribaut, Janette, S710 (TOP-536-YI)
Ribeiro, Andrea, S295 (TOP-280), S689 (FRI-169)
Ribeiro, Leonor Flores, S729 (THU-441)
Ribeiro, Rogerio, S649 (SAT-152), S777 (THU-050)
Ribot, Pablo Fraile, S910 (SAT-585)
Ricci, Andrea, S849 (THU-305-YI)
Ricci, Chiara, S69 (LBP-004-YI), S304 (SAT-258), S307 (SAT-263), S335 (SAT-378-YI)
Ricci, Maria, S576 (WED-083)
Riccio, Anna, S807 (FRI-025)
Ricci, Pierbruno, S149 (SAT-468), S152 (SAT-478), S214 (WED-499), S760 (TOP-032)
Ricco, Gabriele, S431 (THU-233), S928 (SAT-628-YI), S950 (FRI-619)
Rice, Charles, S890 (THU-623-YI), S891 (THU-624-YI)
Richard, Layese, S35 (OS-050-YI), S913 (SAT-589-YI)
Richards, Christopher, S948 (FRI-610), S957 (WED-578), S958 (WED-580)
Richards, Lisa, S564 (WED-043), S578 (WED-088)
Richardson, Naomi, S363 (WED-321-YI)
Richardson, Paul, S256 (SAT-543), S258 (SAT-547)
Richelle, Donovan, S611 (WED-185)
Rich-Griffin, Charlotte, S43 (OS-065)
Richichi, Cristina, S456 (WED-234-YI)
Richmond, Jacqui, S799 (FRI-004), S800 (FRI-005), S820 (WED-021)
Ricke, Jens, S490 (TOP-407-YI)
Rickert, Alexandra, S912 (SAT-588)
Rico, Naira, S28 (OS-037), S629 (TOP-160)
Rico, Sofia Tejado, S300 (SAT-250)
Riddell, Anna, S876 (THU-575), S921 (SAT-611)
Riddermann, Anna, S461 (WED-245)
Rider, Patricia, S481 (WED-382-YI), S639 (SAT-120)
Ridola, Lorenzo, S856 (WED-291)
Ridruejo, Ezequiel, S112 (FRI-050), S288 (FRI-283), S296 (TOP-281), S306 (SAT-262), S768 (THU-021), S790 (SAT-036)
Riecken, Kristoffer, S890 (THU-622-YI)
Rieck, Michael, S672 (SAT-230)

Author Index

Riedel, Christoph, S213 (WED-496)
Riedel, Patricia, S776 (THU-044)
Riegler, Susanna, S199 (WED-451-YI), S738 (THU-464-YI)
Rieke, Ansgar, S945 (FRI-602-YI)
Rieke, Ringlstetter, S935 (TOP-583), S963 (WED-596)
Rieper, Victoria, S979 (TOP-614)
Riesterer, Helene, S83 (LBP-035)
Rieusset, Jennifer, S478 (WED-377), S666 (SAT-212)
Riezebos-Brilman, Annelies, S817 (WED-011)
Rifaat, Safadi, S64 (OS-100)
Rigamonti, Cristina, S69 (LBP-004-YI), S82 (LBP-034-YI), S304 (SAT-258), S307 (SAT-263), S325 (SAT-320), S331 (SAT-368-YI), S335 (SAT-378-YI), S350 (SAT-421), S831 (THU-256-YI)
Rigaud, Céline, S829 (THU-252)
Riggio, Oliviero, S3 (GS-005), S185 (TOP-455-YI), S746 (THU-489), S856 (WED-291)
Righetti, Riccardo, S589 (WED-119)
Rigoll, Montserrat, S28 (OS-037), S629 (TOP-160)
Rigopoulou, Eirini, S314 (SAT-283)
Riley, Callum, S59 (OS-091)
Rimassa, Lorenza, S494 (FRI-225)
Rimbert, Antoine, S670 (SAT-221-YI)
Rimini, Margherita, S494 (FRI-225)
Rimsha, Rimsha, S139 (FRI-135-YI), S269 (SAT-355)
Rinaldi, Mauro, S848 (THU-304)
Rinella, Mary E., S76 (LBP-020), S82 (LBP-032), S411 (FRI-560), S536 (THU-137), S680 (FRI-139), S693 (FRI-182), S696 (FRI-189), S697 (FRI-191), S698 (FRI-197), S719 (TOP-486)
Ring, Eabha, S746 (THU-485)
Ringgaard, Steffen, S692 (FRI-180)
Ring, Timothy, S745 (THU-483)
Rio, Jessica Mayen-del, S771 (THU-030)
Rios, Isai Martinez, S308 (SAT-265), S309 (SAT-266)
Rios, Jeanette, S538 (THU-148-YI)
Rios, Jose, S203 (WED-463)
Ríos, María Lázaro, S837 (THU-267), S855 (WED-289)
Rios, María Pilar, S16 (OS-010)
Riou, Olivier, S414 (FRI-572)
Ripoll, Cristina, S54 (OS-084), S76 (LBP-020), S124 (FRI-089), S182 (FRI-442), S215 (WED-506), S219 (WED-516), S736 (THU-460-YI), S744 (THU-482-YI)
Rishik, Shusruto, S482 (WED-385-YI)
Risicato, Alfredo, S83 (LBP-034-YI)
Rison, Stuart, S69 (LBP-001)
Risso, Alessandra, S307 (SAT-263), S335 (SAT-378-YI)
Ristic, Tijana, S461 (WED-245)
Ristovska, Elena Curakova, S387 (FRI-483)
Rito, Jen, S965 (WED-602)
Ritschl, Paul, S416 (FRI-578-YI)
Riva, Alessia, S494 (FRI-225)
Riva, Antonio, S472 (WED-274), S672 (SAT-228)
Rivas-Izquierdo, Jorge, S123 (FRI-086)
Rivero, Antonio, S904 (SAT-564)
Riviere, Benjamin, S95 (SAT-076)
Riyaz, Shaik, S722 (THU-416)
Rizvi, Arjumand, S605 (WED-170)
Rizzardini, Giuliano, S956 (TOP-598), S960 (WED-587)
Rizzato, Mario Domenico, S435 (THU-247)
Rizzatti, Gianenrico, S731 (THU-444-YI), S751 (THU-500)
Rizzetto, Mario, S49 (OS-076-YI), S912 (SAT-587-YI), S919 (SAT-608-YI)
Rizzi, Marco, S912 (SAT-587-YI)
Rizzo, Giulia, S350 (SAT-421)
Roatta, Caroline, S840 (THU-275)
Robaeys, Geert, S535 (THU-134), S611 (WED-185), S696 (FRI-190)
Robaeys, Wouter, S696 (FRI-190)
Roberts, Amin J., S850 (THU-308)
Roberts, Lewis, S303 (SAT-257-YI), S461 (WED-247), S484 (WED-393)
Roberts, M. Scot, S19 (OS-016), S84 (LBP-036), S679 (TOP-176), S700 (FRI-201)
Roberts, Stuart, S62 (OS-097), S218 (WED-513), S424 (TOP-376), S433 (THU-240), S516 (TOP-113), S571 (WED-069), S749 (THU-496), S766 (THU-015), S964 (WED-597)
Robic, Marie-Angèle, S723 (THU-419), S752 (THU-501)
Robillard, Nicolas, S45 (OS-067)
Robinson, Chandler, S39 (OS-057)
Robinson, Erik, S817 (WED-012)
Robinson, Liezel, S254 (SAT-537)
Robinson, Patrick, S147 (SAT-465)
Robin, Sophie, S765 (THU-014)
Roblero, Juan Pablo, S112 (FRI-050)
Robles-Díaz, Mercedes, S88 (SAT-056), S305 (SAT-260-YI)
Robles, Maria, S651 (SAT-158-YI)
Robles-Rodríguez, Ruth, S771 (THU-030)
Roca, Andreu, S903 (SAT-563-YI)
Roccarina, Davide, S6 (GS-011-YI), S325 (SAT-320), S350 (SAT-421), S746 (THU-489)
Rocco, Alba, S335 (SAT-378-YI)
Roche, Bruno, S43 (OS-066), S374 (TOP-503), S380 (FRI-463), S381 (FRI-464), S934 (TOP-582), S937 (FRI-585-YI)
Roche, Lucy, S753 (THU-506)
Rockall, Andrea, S490 (TOP-407-YI)
Rock, James, S826 (WED-039)
Rock, Marvin, S339 (SAT-387), S946 (FRI-605)
Rock, Nathalie, S56 (OS-086), S831 (THU-258-YI), S842 (THU-284), S850 (THU-308)
Rockstroh, Jürgen, S213 (WED-496), S865 (FRI-638), S904 (SAT-564)
Roda, Mélanie, S869 (TOP-632)
Rodas, Fabian, S330 (SAT-366)
Roden, Michael, S21 (OS-020), S557 (THU-213), S666 (SAT-211-YI), S672 (SAT-230), S693 (FRI-182), S795 (SAT-050)
Rode, Sebastian Howen, S470 (WED-269)
Rodien, Patrice, S540 (THU-155)
Rodrigo-Torres, Daniel, S134 (FRI-117), S137 (FRI-125)
Rodrigues de Freitas, Luiz Antônio, S95 (SAT-078)
Rodrigues, Pedro, S17 (OS-013), S165 (FRI-387-YI), S303 (SAT-257-YI), S323 (SAT-315), S483 (WED-388-YI), S484 (WED-393)
Rodrigues, Robim M, S637 (SAT-116)
Rodríguez, Amaia, S633 (SAT-101-YI)
Rodriguez, Amanda, S683 (FRI-151)
Rodríguez-Baños, Carmen, S910 (SAT-581)
Rodríguez-Castellano, Adrià, S562 (TOP-097-YI), S612 (WED-188), S804 (FRI-019)
Rodriguez, Diego Rincón, S267 (SAT-350), S643 (SAT-134)
Rodríguez, Enrique, S598 (WED-150)
Rodríguez-Escudero, Mª José, S910 (SAT-581)
Rodríguez-Fernández, Ana, S910 (SAT-585)
Rodríguez-Gandía, Miguel Ángel, S752 (THU-501)
Rodriguez, Harlim, S296 (TOP-281), S306 (SAT-262)
Rodríguez-Hernández, María Ángeles, S271 (THU-314), S636 (SAT-108)
Rodríguez, Isidoro Jesús Narváez, S815 (WED-006)
Rodríguez, Isidoro Narváez, S391 (FRI-497)
Rodriguez, Maël Silva, S37 (OS-052)
Rodriguez, Manuel, S58 (OS-089), S313 (SAT-282)
Rodríguez, Manuel, S948 (FRI-611)
Rodriguez, Manuela, S806 (FRI-024)
Rodríguez, Montserrat, S21 (OS-021)
Rodriguez-Mora, Santiago, S556 (THU-212)
Rodriguez, Nina, S40 (OS-059-YI), S538 (THU-148-YI), S552 (THU-196), S776 (THU-046)
Rodriguez, Omayra Martin, S663 (SAT-200)
Rodríguez-Peláez, María, S250 (SAT-524)
Rodríguez-Perálvarez, Manuel, S59 (OS-091), S294 (TOP-278), S303 (SAT-256-YI), S309 (SAT-268), S410 (FRI-558)
Rodríguez-Perálvarez, Manuel L., S393 (FRI-501), S467 (WED-261)
Rodriguez-Tajes, Sergio, S10 (LBO-006), S16 (OS-010), S79 (LBP-026), S294 (TOP-278), S300 (SAT-250), S315 (SAT-286), S317 (SAT-290-YI), S318 (SAT-291), S325 (SAT-320), S336 (SAT-380), S337 (SAT-382),

S338 (SAT-383), S338 (SAT-384), S828 (TOP-309-YI), S884 (THU-604-YI), S903 (SAT-563-YI), S941 (FRI-590)
Rodriguez-Tellez, Manuel, S751 (THU-500)
Roeb, Elke, S601 (WED-155)
Roeren, Merle, S612 (WED-187-YI)
Roessler, Stephanie, S38 (OS-054), S445 (THU-385)
Roey, Guy Van, S920 (SAT-609)
Rogalidou, Maria, S850 (THU-308)
Rogalski, Lisa, S107 (THU-078)
Roger, Pauline, S38 (OS-055)
Rogers, Geraint, S699 (FRI-198)
Rogers, Rodney, S59 (OS-091)
Roglans, Núria, S231 (FRI-304), S241 (FRI-341), S271 (THU-303), S279 (THU-335)
Rohani-Montez, S Christy, S340 (SAT-388), S846 (THU-290)
Rohbeck, Elisabeth, S666 (SAT-211-YI)
Röhlen, Natascha, S429 (THU-227-YI)
Rohr-Udilova, Nataliya, S37 (OS-053), S242 (FRI-346)
Roh, Yoon-Seok, S235 (FRI-321), S659 (SAT-185)
Roibello, Cristina, S232 (FRI-313), S241 (FRI-339)
Roilidis, Ioannis, S56 (OS-086), S831 (THU-258-YI), S842 (THU-284)
Rojano-Alfonso, Carlos, S172 (FRI-412)
Rojas-Amaris, Natalia, S327 (SAT-322)
Rojas-Echarry, Gustavo, S254 (SAT-538)
Rojo, Diego, S250 (SAT-524), S562 (TOP-097-YI), S605 (WED-168-YI)
Roldan, Ana M, S819 (WED-019)
Rolinger, Jens, S512 (FRI-371)
Rolland, Celine, S554 (THU-202)
Rolle, Emanuela, S431 (THU-233)
Rolle, Valentin, S497 (FRI-234), S723 (THU-418), S742 (THU-477)
Roll, Garrett, S59 (OS-091)
Rolli, Nicoletta, S626 (WED-231)
Rolph, Tim, S659 (SAT-187), S697 (FRI-191)
Rolston, Daniel, S391 (FRI-496)
Romagnoli, Renato, S90 (SAT-061-YI), S402 (FRI-531), S784 (SAT-015-YI), S848 (THU-304)
Romagnoli, Veronica, S431 (THU-233), S950 (FRI-619)
Roma, Joyce, S978 (WED-641)
Romana Ponziani, Francesca, S428 (THU-227-YI)
Román-Calleja, Berenice M., S22 (OS-022-YI), S419 (THU-523)
Román-Montes, Carla, S392 (FRI-499)
Romano, Ana Alberola, S899 (SAT-557), S910 (SAT-585)
Romano, Antonietta, S901 (SAT-559), S902 (SAT-560), S936 (TOP-584), S938 (FRI-586)
Roman, Vanessa, S146 (SAT-461)
Rombouts, Krista, S479 (WED-379)
Romeo, Carmelo Maria, S835 (THU-263)
Romeo, Mario, S190 (WED-425), S444 (THU-384), S479 (WED-378), S532 (THU-123), S549 (THU-186-YI), S639 (SAT-121-YI), S660 (SAT-190), S854 (WED-286)
Romeo, Stefano, S476 (WED-368)
Romero, Beatriz, S25 (OS-029)
Romero, Diana, S76 (LBP-020)
Romero, Gema, S815 (WED-006)
Romero-Gómez, Manuel, S28 (OS-037), S101 (THU-058), S177 (FRI-427), S308 (SAT-264), S517 (TOP-114), S525 (THU-103), S527 (THU-108), S542 (THU-164), S557 (THU-213), S558 (TOP-063-YI), S567 (WED-054), S571 (WED-069), S577 (WED-084), S589 (WED-118), S600 (WED-153), S607 (WED-174-YI), S612 (WED-187-YI), S618 (WED-204), S621 (WED-214), S621 (WED-215), S629 (TOP-160), S644 (SAT-137), S678 (SAT-244), S765 (THU-013), S766 (THU-015), S795 (SAT-050), S806 (FRI-023)
Romero-Grimaldo, Berta, S159 (SAT-505), S172 (FRI-412)
Romero-Gutiérrez, Marta, S837 (THU-267), S855 (WED-289)
Romero, Jorge Del, S806 (FRI-024)
Romero, Jose David Arroyo, S806 (FRI-024)
Romero, Judit, S798 (TOP-048)
Romero, Judit Vico, S908 (SAT-577), S926 (SAT-623), S949 (FRI-612)
Romero, Kriss Rodríguez, S790 (SAT-036)
Romero, Maria Isabel Monge, S391 (FRI-497)
Romero, Maria Tous, S751 (THU-500)
Romero, Mario, S267 (SAT-350), S410 (FRI-558)
Romero, Marta, S281 (TOP-296-YI)
Romero, Miriam, S815 (WED-006)
Romero, Montserrat, S273 (THU-316)
Romero, Rene, S850 (THU-308)
Romualdo, Guilherm, S484 (WED-394)
Ronca, Vincenzo, S305 (SAT-260-YI), S333 (SAT-369), S339 (SAT-386), S340 (SAT-393), S350 (SAT-421)
Rondena, Jessica, S241 (FRI-340), S476 (WED-368)
Rønn, Jonas Hedelund, S116 (FRI-060), S775 (THU-042-YI)
Ronot, Maxime, S251 (SAT-528), S428 (THU-226-YI), S446 (THU-393-YI), S505 (FRI-254), S506 (FRI-255-YI), S507 (FRI-362), S728 (THU-433-YI), S837 (THU-268)
Ronzoni, Luisa, S241 (FRI-340), S476 (WED-368), S575 (WED-076), S601 (WED-156), S831 (THU-256-YI)
Rood, Kara, S70 (LBP-005), S975 (WED-636), S976 (WED-637)
Roomer, Robert, S352 (SAT-429)
Rooney, Michael, S262 (SAT-330)
Roose, Heleen, S889 (THU-620), S960 (WED-588)
Rorsman, Fredrik, S290 (FRI-289), S579 (WED-090)
Rosado, Andrea Peña, S720 (TOP-504-YI)
Rosa, Isabelle, S43 (OS-066), S45 (OS-067), S90 (SAT-059), S934 (TOP-582), S937 (FRI-585-YI)
Rosales, José Miguel, S948 (FRI-611)
Rosales, Rachel, S767 (THU-019)
Rosales Renteria, Luis Alejandro, S306 (SAT-262)
Rosales-Zábal, Jose Miguel, S542 (THU-164)
Rosas-Campos, Rebeca, S132 (FRI-108-YI), S235 (FRI-319), S481 (WED-384)
Rosato, Stefano, S972 (WED-623)
Rose, Christopher F., S152 (SAT-478), S170 (FRI-401-YI), S631 (SAT-094-YI)
Rose-Key, Rubin, S826 (WED-039)
Rosenberger, Laura, S482 (WED-385-YI)
Rosenberg, Nofar, S60 (OS-093), S289 (FRI-286), S615 (WED-196)
Rosenberg, William, S13 (OS-006-YI), S256 (SAT-543), S258 (SAT-547), S290 (FRI-289), S974 (WED-629-YI)
Rosenblatt, Russell, S190 (WED-421)
Rosenborg, Staffan, S313 (SAT-276)
Rosenquist, Elena, S248 (SAT-515)
Rosenstock, Philip, S890 (THU-621)
Rosenthal, Eric, S45 (OS-067)
Rosenthal, Philip, S832 (THU-258-YI), S842 (THU-284)
Rose, Sweta, S81 (LBP-030)
Rosini-Silva, Alex, S671 (SAT-226)
Rosinka, Magdalena, S817 (WED-012)
Roskams, Tania, S331 (SAT-368-YI)
Rosmarin-DeStefano, Corey, S980 (FRI-634)
Rosmorduc, Olivier, S428 (THU-226-YI), S506 (FRI-255-YI)
Rossi, Marzia, S874 (THU-571)
Rossi, Massimo, S407 (FRI-548)
Rossini, Daniele, S514 (FRI-381)
Rossi, Stephen, S342 (SAT-398), S346 (SAT-412)
Rössle, Martin, S945 (FRI-602-YI)
Rosso, Chiara, S476 (WED-368), S574 (WED-073), S601 (WED-156), S620 (WED-213)
Ross, Paul, S65 (OS-102), S404 (FRI-538-YI), S503 (FRI-250), S970 (WED-619)
Rossvoll, Lasse, S822 (WED-026), S926 (SAT-622-YI)
Rota, Loredana, S817 (WED-010)
Rota, Rosa, S300 (SAT-250), S724 (THU-421)
Rotaru, Adrian, S211 (WED-493)
Rotellar, Fernando, S375 (TOP-519)
Roth, Wilfried, S854 (WED-285)
Rotman, Vivian, S296 (TOP-281), S306 (SAT-262), S340 (SAT-394), S768 (THU-022), S830 (THU-254), S830 (THU-255)
Rottengatter, Karin, S890 (THU-621)
Roukaerts, Inge, S907 (SAT-575)
Roulot, Dominique, S43 (OS-066), S45 (OS-067), S71 (LBP-009), S515 (TOP-098), S583 (WED-101),

Author Index

S900 (SAT-559), S902 (SAT-560), S913 (SAT-589-YI), S934 (TOP-582), S937 (FRI-585-YI)
Rourke, Colm O, S454 (TOP-390-YI), S462 (WED-249), S483 (WED-388-YI), S484 (WED-393)
Rousseau, Anne-Sophie, S681 (FRI-147)
Rousseau, Hélène, S37 (OS-052)
Rousseaux, Théo, S666 (SAT-212)
Roussel, Murielle, S829 (THU-252)
Routy, Jean-Pierre, S529 (THU-116-YI)
Rouvray, Corentin, S45 (OS-067)
Roux, Carel Le, S79 (LBP-027), S698 (FRI-197)
Roux, Charles, S446 (THU-393-YI), S507 (FRI-362)
Rouxel, Lou-Devy, S493 (FRI-221), S508 (FRI-364-YI)
Roux, Marine, S365 (WED-331-YI), S540 (THU-155), S554 (THU-202)
Roux, Olivier, S380 (FRI-463), S381 (FRI-464)
Rövenstrunk, Götz, S271 (THU-313)
Rowe, Ian, S106 (THU-075), S117 (FRI-067), S547 (THU-180)
Rowen, Donna, S319 (SAT-301)
Roy, Ahona, S171 (FRI-404), S629 (TOP-161-YI)
Roy, Akash, S24 (OS-028), S156 (SAT-496), S215 (WED-505), S221 (WED-523), S228 (WED-543), S257 (SAT-544), S423 (TOP-374), S528 (THU-110), S786 (SAT-023), S952 (FRI-622)
Roy, Anju, S706 (THU-544)
Roy, Bornika, S232 (FRI-308)
Roy, Christian, S195 (WED-441)
Roy, Jerlin, S705 (THU-541-YI)
Roy, Siddharth Ghosh, S137 (FRI-126)
Roy, Subhadeep, S182 (FRI-441-YI)
Royuela, Ana, S585 (WED-105), S772 (THU-036)
Roza, Marianne De, S149 (SAT-473)
Rozenberg, Orit, S913 (SAT-590)
Rozman, Jan, S672 (SAT-230)
Rozyczko, Aleksandra, S454 (TOP-390-YI)
Ruan, Shanq-Jang, S426 (THU-218)
Rubin, Darren, S187 (TOP-471-YI)
Rubin, Moises Nevah, S670 (SAT-220)
Rubinski, Anna, S581 (WED-095)
Rubio-Ardanaz, Monica, S96 (SAT-079)
Rubio, Francisco Javier Velasco, S934 (TOP-582)
Rubio, Noelia Justo, S746 (THU-485)
Rubio, Sonia Albertos, S815 (WED-006), S968 (WED-610-YI)
Rudilla, Francesc, S908 (SAT-577)
Rudler, Marika, S3 (GS-005), S6 (GS-011-YI), S33 (OS-046), S53 (OS-082), S54 (OS-084), S110 (FRI-042), S195 (WED-442-YI), S207 (WED-477), S222 (WED-525), S446 (THU-393-YI), S497 (FRI-234), S507 (FRI-362), S719 (TOP-488), S723 (THU-418), S742 (THU-477), S752 (THU-501)
Rudra, Omkar, S189 (WED-419), S552 (THU-195)
Rudraraju, Madhavi, S694 (FRI-183)
Rudra, Rathiga, S65 (OS-102), S970 (WED-619)
Rueda, Francisco Navarrete, S179 (FRI-431-YI)
Rufino, Sarah, S296 (TOP-281), S306 (SAT-262)
Ruf, Murad, S76 (LBP-019-YI), S811 (FRI-038), S813 (FRI-047), S817 (WED-012)
Ruggieri, Angelo, S874 (THU-571)
Ruiter, Simeon, S430 (THU-232)
Ruiu, Antonella, S339 (SAT-386)
Ruiz-Blazquez, Paloma, S635 (SAT-107-YI)
Ruiz, Brian Martinez, S358 (THU-340-YI), S654 (SAT-171-YI)
Ruiz-Cobo, Juan Carlos, S798 (TOP-048), S811 (FRI-038), S908 (SAT-577), S926 (SAT-623), S948 (FRI-611), S949 (FRI-612)
Ruiz, Henar, S833 (THU-259)
Ruiz, Maria, S364 (WED-329-YI)
Ruiz-Martin, Christian, S182 (FRI-442), S267 (SAT-350)
Ruiz, Mathias, S56 (OS-086), S311 (SAT-271), S831 (THU-258-YI), S836 (THU-265-YI), S842 (THU-284)
Ruiz, Pablo, S59 (OS-091), S394 (FRI-507-YI)
Ruiz, Paula, S42 (OS-064-YI)
Ruiz, Rafael, S810 (FRI-036)
Ruiz-Sanchez, Carolina, S806 (FRI-024)
Ru, JangHoon, S732 (THU-447)
Rukavina, Nadia, S425 (THU-216-YI)
Runarsdottir, Valgerdur, S802 (FRI-011)
Runnegar, Naomi, S803 (FRI-014), S818 (WED-013)
Rusch, Sophia, S157 (SAT-497), S216 (WED-507)
Rushbrook, Simon, S311 (SAT-270)
Rusignuolo, Giuseppe, S550 (THU-187), S834 (THU-260)
Russell, Erin, S707 (THU-546-YI)
Russell, Jennifer, S769 (THU-024-YI), S769 (THU-025)
Russello, Maurizio, S69 (LBP-004-YI), S82 (LBP-034-YI), S304 (SAT-258), S307 (SAT-263), S335 (SAT-378-YI), S350 (SAT-421)
Russello, Mélanie, S387 (FRI-484)
Russell, Sean, S877 (THU-580)
Russo, Francesco Paolo, S62 (OS-097), S148 (SAT-466-YI), S150 (SAT-475), S193 (WED-431-YI), S325 (SAT-320), S516 (TOP-113), S601 (WED-156), S821 (WED-023), S900 (SAT-559), S902 (SAT-560), S923 (SAT-618), S936 (TOP-584), S938 (FRI-586)
Russo, Giuseppina, S967 (WED-605-YI)
Rusu, Ioana, S255 (SAT-539), S543 (THU-165), S544 (THU-166)
Ruuls, Arlette, S647 (SAT-149)
Ruxton, Attracta, S973 (WED-627)
Ruzic, Maja, S807 (FRI-025)
Ruzzenente, Andrea, S97 (SAT-084-YI)
Rwegasha, John, S905 (SAT-569), S940 (FRI-588-YI)
Ryan, John, S210 (WED-489-YI), S255 (SAT-540), S769 (THU-024-YI), S769 (THU-025), S777 (THU-050), S849 (THU-305-YI), S973 (WED-627)
Ryan, Marno, S433 (THU-240), S922 (SAT-613)
Ryan, Michael, S691 (FRI-175)
Ryan, Pablo, S806 (FRI-024), S904 (SAT-564), S957 (WED-577)
Ryan, Thomas, S639 (SAT-119)
Ryder, Stephen D, S718 (WED-574)
Rysä, Jaana, S266 (SAT-346)
Ryu, Jae Yong, S482 (WED-386)
Ryu, Seungho, S553 (THU-198)
Rzepka, Angelika, S410 (FRI-559)

Saad, Amel Ben, S633 (SAT-102-YI)
Saad, Hadeel, S680 (FRI-140)
Saadi, Tarek, S76 (LBP-021), S247 (SAT-513), S316 (SAT-288), S317 (SAT-289), S613 (WED-189), S913 (SAT-590)
Saas, Philippe, S885 (THU-607)
Saavedra, Maria, S112 (FRI-050), S625 (WED-228)
Saba, Francesca, S534 (THU-133), S574 (WED-073), S611 (WED-184-YI), S620 (WED-213)
Sabag, Angelo, S713 (WED-557)
Sabagh, Ahmed El, S520 (THU-090-YI)
Sabaliene, Jurate, S823 (WED-029)
Sabatini, Silvia, S682 (FRI-150-YI)
Sabau, Loredana Cosmina, S146 (SAT-461)
Saberi, Behnam, S327 (SAT-322)
Saborowski, Anna, S460 (WED-244-YI), S487 (WED-400-YI), S488 (WED-409-YI), S504 (FRI-251)
Sacco, Rodolfo, S424 (TOP-375-YI), S429 (THU-227-YI), S514 (FRI-381)
Sacerdoti, David, S97 (SAT-084-YI), S150 (SAT-475), S405 (FRI-541), S424 (TOP-375-YI), S595 (WED-137), S677 (SAT-243-YI)
Sachdeva, Sanjeev, S31 (OS-043-YI), S212 (WED-495-YI), S217 (WED-510), S952 (FRI-622)
Sack, Francoise Ngo, S879 (THU-589-YI)
Sadeh, Ronen, S60 (OS-093), S615 (WED-196)
Sadeh, Tor, S913 (SAT-590)
Sadek, Leila, S493 (FRI-221), S508 (FRI-364-YI)
Sadhe, Ronen, S289 (FRI-286)
Sadler, Matthew, S315 (SAT-286)
Sadomova, Elena, S595 (WED-136)
Saeed, Anwaar, S428 (THU-227-YI)
Saeed, Sahar, S529 (THU-116-YI), S533 (THU-127-YI), S573 (WED-072), S613 (WED-190), S624 (WED-225-YI), S624 (WED-226), S783 (SAT-013-YI), S784 (SAT-014), S865 (FRI-638)

Saeidinejad, MohammadMahdi, S27 (OS-034)
Saeidi, Reza, S210 (WED-489-YI)
Saeki, Akira, S249 (SAT-522), S976 (WED-638)
Sáenz de Miera, Inés, S91 (SAT-062)
Saenz, Ernest, S256 (SAT-542), S288 (FRI-283), S556 (THU-212)
Saez-Palma, Maria, S884 (THU-604-YI)
Sáez-Peñataro, Joaquín, S91 (SAT-062)
Saez, Ruth, S819 (WED-019), S910 (SAT-585)
Safadi, Rifaat, S10 (LBO-006), S60 (OS-093), S289 (FRI-286), S614 (WED-191), S615 (WED-196)
Saffioti, Francesca, S325 (SAT-320)
Saffo, Saad, S388 (FRI-489)
Safinia, Niloufar, S174 (FRI-416-YI), S366 (WED-333-YI), S404 (FRI-538-YI), S458 (WED-237-YI), S503 (FRI-250)
Sagalova, Olga, S939 (FRI-587), S956 (WED-576), S960 (WED-587), S962 (WED-593)
Sagar, Garima, S653 (SAT-166)
Saggau, Carina, S372 (WED-350)
Sagi-Kiss, Virag, S458 (WED-237-YI)
Saglia, Claudia, S835 (THU-263)
Saha, Banishree, S667 (SAT-213), S847 (THU-300), S848 (THU-301)
Saha, Shikha, S286 (FRI-271)
Saha, Soumyajit, S369 (WED-340-YI), S372 (WED-351)
Sahin, Hasan, S496 (FRI-231)
Sahin, Mustafa, S588 (WED-116)
Şahin, Yiğit, S348 (SAT-417)
Sahoo, Manoj, S952 (FRI-622)
Sahu, Pabitra, S822 (WED-025-YI)
Saidi, Alina, S621 (WED-214)
Said, Khadija, S826 (WED-039)
Saigal, Sanjiv, S67 (OS-105-YI), S952 (FRI-622)
Saini, Bronica, S782 (SAT-011)
Sainz-Barriga, Mauricio, S381 (FRI-465)
Sainz, Jaime, S336 (SAT-380)
Sainz-Ramirez, Natalia, S277 (THU-330-YI), S631 (SAT-095-YI)
Saito, Chikako, S647 (SAT-147)
Saito, Masumichi, S875 (THU-573)
Saito, Takeshi, S277 (THU-331)
Saito, Tomoko, S662 (SAT-196)
Saito, Yoshinobu, S463 (WED-251-YI)
Saitta, Carlo, S223 (WED-527), S304 (SAT-258), S307 (SAT-263), S335 (SAT-378-YI), S435 (THU-245), S967 (WED-605-YI)
Saiura, Akio, S449 (THU-400), S492 (FRI-219)
Saji, Lena, S705 (THU-542)
Sakai, Aiko, S892 (THU-628)
Sakai, Eiji, S686 (FRI-159)
Sakakibara, Maya, S708 (THU-553)
Sakamaki, Yuriko, S894 (THU-635)
Sakamori, Ryotaro, S258 (SAT-549), S550 (THU-188), S979 (WED-644)
Sakamoto, Kano, S894 (THU-637)
Sakamoto, Naoya, S506 (FRI-256), S510 (FRI-367)
Sakellariou, Basil, S314 (SAT-283)
Sakellariou, Stratigoula, S45 (OS-068-YI), S545 (THU-172)
Sakhuja, Puja, S53 (OS-083-YI)
Sakrikar, Nidhi Jalan, S282 (FRI-262-YI)
Sakuma, Tetsushi, S662 (SAT-196)
Salamé, Ephrem, S17 (OS-011), S380 (FRI-463), S381 (FRI-464)
Salam, Nasir, S264 (SAT-335), S264 (SAT-336), S280 (THU-337)
Salani, Francesca, S481 (WED-383)
Salas, Azucena, S884 (THU-604-YI)
Salazar, Darly, S804 (FRI-019)
Salazar, Renata Montemayor, S22 (OS-022-YI)
Salcedo, María Teresa, S250 (SAT-524)
Salehi, Shayon, S897 (TOP-565)
Salih, Nafisa, S160 (SAT-507)
Salim, Felix, S148 (SAT-467-YI)
Salimzadeh, Loghman, S875 (THU-574), S964 (WED-597)
Salinas, Yohana Poveda, S556 (THU-212)
Salisbury, Imogen, S69 (LBP-001)
Sallinen, Ville, S376 (FRI-447)
Salloum, Cojocariu, S211 (WED-493)
Salloum, Ramzi, S974 (WED-628)
Salomone, Federico, S177 (FRI-427), S638 (SAT-118), S667 (SAT-214)
Salomon, Nadja, S18 (OS-015)
Salpini, Romina, S49 (OS-076-YI), S807 (FRI-025), S899 (SAT-557), S912 (SAT-587-YI), S919 (SAT-608-YI), S924 (SAT-619)
Saltini, Dario, S3 (GS-005), S6 (GS-011-YI), S31 (OS-042), S33 (OS-046), S52 (OS-081), S720 (TOP-502-YI), S720 (TOP-504-YI), S723 (THU-418), S725 (THU-425), S733 (THU-450), S746 (THU-489), S746 (THU-490), S747 (THU-492), S752 (THU-501), S753 (THU-505-YI)
Salto-Sevilla, Jorge Alejandro, S235 (FRI-319), S481 (WED-384)
Salupere, Riina, S777 (THU-050)
Salvador, Maria Teresa, S969 (WED-611)
Salvador, Patricia, S312 (SAT-273)
Salvati, Antonio, S695 (FRI-187), S950 (FRI-619)
Salvi, Lucia, S741 (THU-473), S751 (THU-500)
Salvioni, Davide, S69 (LBP-004-YI)
Salz, Renee, S647 (SAT-149)
Samakidou, Anna, S314 (SAT-283)
Samala, Niharika, S531 (THU-122)
Samarska, Iryna, S331 (SAT-368-YI)
Sambarino, Dana, S43 (OS-066), S935 (TOP-583), S936 (TOP-584), S937 (FRI-585-YI), S942 (FRI-592), S942 (FRI-593)
Samnaliev, Mihail, S299 (SAT-247), S320 (SAT-303), S320 (SAT-304)
Samodova-Sommer, Diana, S240 (FRI-338)
Samonakis, Dimitrios N., S314 (SAT-283)
Sampaio, Vittoria, S88 (SAT-056), S776 (THU-044)
Sampascual, Sonia Blanco, S837 (THU-267), S855 (WED-289)
Sampedro, Antonio, S910 (SAT-581), S910 (SAT-585)
Samperiz, Violeta, S806 (FRI-024)
Samson, Derek, S386 (FRI-482), S411 (FRI-561-YI), S413 (FRI-570)
Samson, Michel, S365 (WED-331-YI)
Samuel, Didier, S380 (FRI-463), S381 (FRI-464)
Sanai, Faisal M, S378 (FRI-457), S521 (THU-092), S521 (THU-093), S523 (THU-099), S524 (THU-101), S566 (WED-052)
Sancha, Laura, S819 (WED-019)
Sanches-Junior, Jose, S671 (SAT-226)
Sánchez-Aguilera, Pablo, S275 (THU-322-YI)
Sánchez, Ana Guiberteau, S391 (FRI-497)
Sanchez, Ana Isabel Garcia, S819 (WED-019)
Sanchez, Antonio, S218 (WED-512-YI), S393 (FRI-501), S698 (FRI-196)
Sánchez, Froylan Martinez, S866 (FRI-640)
Sanchez-Fueyo, Alberto, S59 (OS-091), S174 (FRI-416-YI), S366 (WED-333-YI), S458 (WED-237-YI)
Sanchez-Garrido, Cristina, S141 (TOP-437), S149 (SAT-468), S150 (SAT-475), S152 (SAT-478), S159 (SAT-505), S170 (FRI-401-YI), S760 (TOP-032)
Sánchez, Henar Calvo, S366 (WED-332-YI), S968 (WED-610-YI)
Sanchez, Inmaculada, S828 (TOP-309-YI), S833 (THU-259)
Sánchez, Jordi, S191 (WED-427-YI), S203 (WED-463)
Sánchez-Lorenzo, Ainhoa, S720 (TOP-504-YI)
Sanchez, Lukas Otero, S35 (OS-050-YI)
Sánchez, Manuel, S169 (FRI-400)
Sánchez, Manuel Crespo, S250 (SAT-524)
Sanchez, Maria Camila, S850 (THU-308)
Sanchez, Mercedes De La Torre, S542 (THU-164), S567 (WED-054), S571 (WED-069)
Sanchez, Pedro Enrile, S403 (FRI-533)
Sánchez-Ric, Marta, S317 (SAT-290-YI), S338 (SAT-383)
Sanchez, Rodrigo, S296 (TOP-281), S306 (SAT-262)
Sánchez-Rodríguez, María Belén, S172 (FRI-412)
Sanchez-Serrano, Jose, S33 (OS-046), S189 (WED-418)
Sánchez-Vera, Ismael, S467 (WED-262)
Sanchez, Victor, S806 (FRI-024)
Sánchez-Villegas, Cynthia, S771 (THU-030)
Sanchez, William, S26 (OS-031), S689 (FRI-170)

Author Index

Sancho-Bru, Pau, S489 (WED-412-YI), S828 (TOP-297)
Sancho, Victoria Aguilera, S59 (OS-091), S254 (SAT-538), S410 (FRI-558), S599 (WED-151)
Sanci, Lena, S799 (FRI-004), S800 (FRI-005)
Sandahl, Thomas, S39 (OS-057), S56 (OS-086), S290 (FRI-287), S831 (THU-258-YI), S840 (THU-274), S842 (THU-283), S842 (THU-284), S853 (WED-282-YI)
Sandahl, Thomas Damgaard, S850 (THU-308)
Sand, Andreas, S623 (WED-219)
Sander, Leif Erik, S77 (LBP-022-YI)
Sandfort, Vanessa, S860 (WED-307)
Sandhu, Anchal, S81 (LBP-030)
Sandhu, Jeevin, S614 (WED-195)
Sandmann, Lisa, S300 (SAT-250), S864 (TOP-615), S878 (THU-585-YI), S913 (SAT-589-YI), S935 (TOP-583), S963 (WED-596)
Sandoval-Rodriguez, Ana Soledad, S132 (FRI-108-YI)
Sandro, Stefano Di, S59 (OS-091)
Sandulescu, Daniela Larisa, S819 (WED-015), S944 (FRI-601)
Sanduzzi Zamparelli, Marco, S452 (THU-414-YI)
Sandwith, Peter, S65 (OS-102), S970 (WED-619)
Sangam, Amy, S389 (FRI-492)
Sangaralingham, Lindsey, S186 (TOP-469-YI)
Sangiovanni, Angelo, S150 (SAT-475)
Sangro, Bruno, S17 (OS-013), S96 (SAT-079), S364 (WED-329-YI)
Sangro, Paloma, S96 (SAT-079)
SanJosé Crespo, Alicia, S250 (SAT-524)
Sankaranarayanan, Srinivas, S56 (OS-086), S831 (THU-258-YI), S842 (THU-284)
Sano, Akitoshi, S650 (SAT-156)
Sanpaolo, Guido, S576 (WED-083)
Sansó, Andreu, S815 (WED-006)
Santamaria, Diego Burgos, S837 (THU-267)
Santana, Barbara Fidelix, S102 (THU-060)
Santantonio, Teresa, S43 (OS-066), S900 (SAT-559), S901 (SAT-560), S911 (SAT-587-YI), S919 (SAT-608-YI), S934 (TOP-582), S936 (TOP-584), S937 (FRI-585-YI), S938 (FRI-586)
Santhiapillai, Isabelle, S956 (TOP-598), S957 (WED-577), S960 (WED-587)
Santiago, Jesús M. Gonzalez, S815 (WED-006)
Santini, Silvano Junior, S530 (THU-117), S767 (THU-020)
Santo, Marco Aurelio, S701 (FRI-203-YI)
Santopaolo, Francesco, S52 (OS-081), S720 (TOP-504-YI), S731 (THU-444-YI), S751 (THU-500)
Santopietro, Sara, S305 (SAT-260-YI)
Santori, Valeria, S217 (WED-509-YI)
Santoro, Rosanna, S825 (WED-037)
Santos, Beatriz Gómez, S277 (THU-330-YI), S631 (SAT-095-YI)
Santos, Bruna, S137 (FRI-126)
Santos, Carina, S892 (THU-627)
Santos, Diego, S671 (SAT-226)
Santos, Ignacio De Los, S904 (SAT-564)
Santos, Inês Costa, S940 (FRI-589)
Santos-Silva, Ermelinda, S850 (THU-308)
Santra, Suman, S100 (THU-056)
Sanyal, Arun J, S517 (TOP-114), S525 (THU-103), S558 (TOP-063-YI), S589 (WED-118), S612 (WED-187-YI), S618 (WED-204), S621 (WED-215)
Sanyal, Arun J., S20 (OS-018), S79 (LBP-027), S82 (LBP-032), S109 (TOP-209-YI), S112 (FRI-050), S116 (FRI-061), S122 (FRI-083), S149 (SAT-468), S152 (SAT-478), S190 (WED-421), S197 (WED-447), S527 (THU-109), S553 (THU-201), S563 (WED-042), S578 (WED-087), S582 (WED-099), S607 (WED-174-YI), S615 (WED-196), S649 (SAT-153), S691 (FRI-175), S693 (FRI-181), S698 (FRI-197), S760 (TOP-032)
Sanyal, Susmita, S47 (OS-072)
Sanz, José, S904 (SAT-564)
Sanzo-Machuca, Ángela, S884 (THU-604-YI)
Sapisochin, Gonzalo, S345 (SAT-409-YI), S491 (TOP-408-YI)
Saraca, Lavinia Maria, S610 (WED-183)
Saracco, Giorgio Maria, S784 (SAT-015-YI)
Saracco, Margherita, S55 (OS-085-YI), S90 (SAT-061-YI), S402 (FRI-531), S784 (SAT-015-YI), S848 (THU-304)
Saracino, Annalisa, S911 (SAT-587-YI)
Saracino, Marco, S82 (LBP-034-YI), S601 (WED-156)
Sarada V, Sai, S255 (SAT-541)
Saraf, Neeraj, S952 (FRI-622)
Saran, Anca, S951 (FRI-620), S974 (WED-633)
Saravia, Katerin, S793 (SAT-044)
Saraya, Anoop, S160 (SAT-507)
Sarcina, Tommaso, S69 (LBP-004-YI), S176 (FRI-425), S307 (SAT-263), S335 (SAT-378-YI), S479 (WED-378), S977 (WED-640)
Sarcognato, Samantha, S485 (WED-395-YI)
Sardana, Viren, S141 (TOP-423)
Saretto, Martina, S257 (SAT-545-YI)
Sarg, Bettina, S862 (WED-314-YI)
Sarin, Shiv Kumar, S24 (OS-028), S67 (OS-105-YI), S104 (THU-071-YI), S105 (THU-073-YI), S108 (TOP-208-YI), S129 (TOP-224-YI), S131 (FRI-105-YI), S139 (FRI-135-YI), S141 (TOP-424-YI), S144 (SAT-452), S156 (SAT-495), S157 (SAT-498), S160 (SAT-507), S174 (FRI-415-YI), S182 (FRI-441-YI), S184 (FRI-452-YI), S189 (WED-419), S214 (WED-501-YI), S265 (SAT-341), S269 (SAT-355), S274 (THU-318), S276 (THU-324-YI), S282 (FRI-262-YI), S288 (FRI-282), S292 (FRI-299), S361 (THU-354), S373 (WED-353-YI), S425 (THU-217-YI), S456 (WED-232), S478 (WED-371), S552 (THU-195), S629 (TOP-161-YI), S703 (THU-537), S719 (TOP-487-YI), S867 (FRI-643), S952 (FRI-622)
Sarkar, Debashish, S745 (THU-484)
Sarkar, Monika, S406 (FRI-543)
Sarkar, Suprokash, S745 (THU-484)
Sarker, Debashis, S503 (FRI-250)
Sarmati, Loredana, S49 (OS-076-YI), S807 (FRI-025), S919 (SAT-608-YI)
Sarnová, Lenka, S275 (THU-320)
Sarobe, Pablo, S364 (WED-329-YI)
Sarrazin, Christoph, S945 (FRI-602-YI)
Sartini, Claudio, S615 (WED-197)
Sartoris, Riccardo, S837 (THU-268)
Saruhan, Mehmet Ali, S298 (SAT-246)
Sarvesh, Shreyas, S156 (SAT-495), S214 (WED-501-YI)
Sarv, Janeli, S2 (GS-003)
Sasikumar, N Apoorva, S215 (WED-505), S509 (FRI-365), S698 (FRI-197)
Sasikumar, N. Apoorva, S156 (SAT-496)
Sastre, Lydia, S223 (WED-528)
Sasturkar, Shridhar, S274 (THU-318), S282 (FRI-262-YI)
Sasula, Martha-Julia, S854 (WED-284), S862 (WED-316-YI)
Satapathy, Sanjaya, S337 (SAT-381), S411 (FRI-560)
Satlikova, Nataliya, S822 (WED-027)
Sato, Emi, S708 (THU-553)
Satoh, Takeaki, S258 (SAT-549), S979 (WED-644)
Sato, Motohiko, S420 (THU-529-YI)
Sato, Shinya, S660 (SAT-189), S747 (THU-491)
Sato, Shuichi, S686 (FRI-159)
Satoskar, Rohit, S126 (FRI-094)
Satoskar, Rohit S., S356 (SAT-443), S417 (FRI-581)
Satoskar, Savni, S391 (FRI-496)
Sattar, Naveed, S759 (TOP-018-YI), S773 (THU-039)
Sattianayagam, Prayman, S713 (WED-556-YI)
Sattoe, Jane, S863 (WED-317)
Saunders, John, S121 (FRI-077)
Saurabh, Saurabh, S341 (SAT-395)
Saurav, Panda, S379 (FRI-461-YI)
Sauter, Gerd, S252 (SAT-529)
Savarese, Michael, S959 (WED-585)
Savas, Mesut, S790 (SAT-035)
Savchenko, Anna, S85 (LBP-039)
Saviano, Antonio, S343 (SAT-400)
Savikko, Johanna, S376 (FRI-447)
Savino, Flavia, S481 (WED-382-YI), S639 (SAT-120)
Savoldelli, Roberto, S174 (FRI-416-YI), S366 (WED-333-YI), S458 (WED-237-YI), S472 (WED-274)

Savopoulos, Christos, S213 (WED-497)
Savoye, Kylie, S364 (WED-324-YI)
Saweres, Andrew, S537 (THU-141-YI)
Sawhney, Rohit, S198 (WED-448-YI), S218 (WED-513), S749 (THU-496), S820 (WED-021), S922 (SAT-613)
Saxena, Anoushka, S867 (FRI-643)
Saxena, Romil, S53 (OS-083-YI)
Saxena, Sarthak, S36 (OS-051-YI), S184 (TOP-454-YI), S247 (SAT-514), S299 (SAT-248)
Sayadi, Alexandre, S53 (OS-083-YI), S480 (WED-380), S742 (THU-477), S853 (WED-283), S862 (WED-315)
Sayne, Jennifer, S615 (WED-196)
Sbraccia, Paolo, S626 (WED-231)
Scafuri, Antonio, S444 (THU-384)
Scaravaglio, Miki, S297 (TOP-292-YI), S323 (SAT-315), S327 (SAT-323)
Scarpa, Francesca, S319 (SAT-301)
Scatton, Oliver, S375 (TOP-519)
Scatturo, Pietro, S178 (FRI-429-YI)
Scavuzzo, Maria Concetta, S481 (WED-383)
Scelza-Figueredo, Andrea, S654 (SAT-171-YI)
Scevola, Germano, S767 (THU-020)
Schaap, Frank, S285 (FRI-269)
Schaapman, Jelte, S385 (FRI-479)
Schachteli, Fabian, S178 (FRI-428-YI)
Schaden, Eva, S734 (THU-451)
Schaefer, Benedikt, S257 (SAT-545-YI), S848 (THU-302), S849 (THU-305-YI), S862 (WED-314-YI)
Schaeffer, Samantha, S17 (OS-011)
Schaeper, Ute, S281 (TOP-296-YI)
Schaerer, Jessica, S32 (OS-044)
Schäfer, Melina, S871 (THU-558-YI), S890 (THU-622-YI)
Schain, Martin, S579 (WED-090)
Schanze, Denny, S834 (THU-260)
Scharitzer, Martina, S199 (WED-452)
Scharnagl, Hubert, S11 (OS-002-YI), S237 (FRI-324), S266 (SAT-347-YI), S362 (TOP-325-YI)
Schattenberg, Jörn, S698 (FRI-197)
Schattenberg, Jörn M., S18 (OS-015), S20 (OS-019), S26 (OS-032-YI), S29 (OS-038), S64 (OS-099), S78 (LBP-024), S82 (LBP-033), S204 (WED-465), S319 (SAT-300), S341 (SAT-396), S482 (WED-385-YI), S515 (TOP-098), S532 (THU-124), S559 (TOP-064), S565 (WED-051), S573 (WED-072), S577 (WED-084), S583 (WED-101), S601 (WED-155), S613 (WED-190), S615 (WED-197), S621 (WED-214), S622 (WED-216), S679 (TOP-177), S693 (FRI-182), S697 (FRI-191), S733 (THU-450), S765 (THU-013), S771 (THU-031), S777 (THU-050), S789 (SAT-031-YI), S790 (SAT-035)
Schaubel, Douglas, S189 (WED-420)
Schaufert, Wendy, S525 (THU-104-YI)
Scheck, Rachel, S77 (LBP-022-YI)
Schefczyk, Stefan, S854 (WED-284)
Scheffold, Alexander, S372 (WED-350)
Scheiner, Bernhard, S37 (OS-053), S55 (OS-085-YI), S183 (FRI-444-YI), S183 (FRI-445), S216 (WED-508), S426 (THU-219-YI), S427 (THU-220), S427 (THU-221), S429 (THU-227-YI), S440 (THU-370), S715 (WED-560-YI), S717 (WED-569-YI), S720 (TOP-504-YI), S731 (THU-445-YI), S739 (THU-467)
Schembri, Mark, S170 (FRI-403)
Schempp, Christoph, S550 (THU-187)
Schepers, Rogier, S17 (OS-012)
Schepis, Filippo, S3 (GS-005), S6 (GS-011-YI), S31 (OS-042), S33 (OS-046), S52 (OS-081), S53 (OS-082), S54 (OS-084), S397 (FRI-515), S720 (TOP-502-YI), S720 (TOP-504-YI), S723 (THU-418), S725 (THU-425), S733 (THU-450), S746 (THU-489), S746 (THU-490), S747 (THU-492), S752 (THU-501), S753 (THU-505-YI)
Scherbakovsky, Stacey, S70 (LBP-005)
Schianchi, Susanna, S304 (SAT-258), S335 (SAT-378-YI)
Schiappa, Renaud, S681 (FRI-147)
Schiavon, Janaina, S296 (TOP-281), S306 (SAT-262)
Schiavon, Leonardo, S296 (TOP-281), S306 (SAT-262)
Schiefke, Ingolf, S21 (OS-020)
Schierwagen, Robert, S145 (SAT-458-YI), S178 (FRI-428-YI), S206 (WED-475), S237 (FRI-329), S261 (SAT-329-YI), S262 (SAT-330), S493 (FRI-220)
Schildkraut, Joellen, S544 (THU-167)
Schiller, Herbert, S275 (THU-320)
Schilsky, Michael, S846 (THU-291), S846 (THU-298)
Schilt, Iris, S167 (FRI-395-YI)
Schindler, Philipp, S493 (FRI-220)
Schinoni, Maria, S95 (SAT-078)
Schiødt, Frank Vinholt, S570 (WED-062)
Schirmacher, Peter, S14 (OS-007), S64 (OS-100), S297 (TOP-293), S341 (SAT-397), S504 (FRI-251)
Schlaak, Alexandra Emilia, S455 (TOP-406)
Schlegel, Andrea, S399 (FRI-522)
Schlegel, Caroline, S672 (SAT-230)
Schleicher, Eva Maria, S172 (FRI-411), S197 (WED-446), S199 (WED-451-YI), S215 (WED-506), S742 (THU-476)
Schlienkamp, Sarah, S885 (THU-608), S890 (THU-623-YI)
Schlösser, Denise, S460 (WED-244-YI), S487 (WED-400-YI)
Schlosser-Hupf, Sophie, S157 (SAT-497), S185 (TOP-456-YI), S744 (THU-482-YI)
Schluchter, Helena, S734 (THU-451)
Schluep, Thomas, S847 (THU-300), S848 (THU-301)
Schmarz, Georges, S265 (SAT-338)
Schmelzle, Moritz, S461 (WED-245)
Schmelz, Martin, S322 (SAT-313)
Schmetterer, Klaus, S37 (OS-053)
Schmid, Jonas, S310 (SAT-269), S322 (SAT-313)
Schmid, Karin, S11 (OS-001-YI)
Schmidl, Rosa, S257 (SAT-545-YI)
Schmid, Roland M., S359 (THU-345-YI)
Schmid, Stephan, S157 (SAT-497), S216 (WED-507), S785 (SAT-019)
Schmidt, Alex, S465 (WED-255)
Schmidt, Edward, S289 (FRI-285)
Schmidt, Hartmut, S43 (OS-066), S172 (FRI-410-YI), S265 (SAT-338), S763 (THU-010), S854 (WED-284), S858 (WED-301), S860 (WED-307), S862 (WED-316-YI), S934 (TOP-582), S937 (FRI-585-YI)
Schmidt, Iris, S647 (SAT-149)
Schmidt, Johannes, S353 (SAT-433)
Schmidt, Kevin, S105 (THU-072)
Schmidt, Livia, S461 (WED-245)
Schmittgens, Stephan, S352 (SAT-429)
Schnabl, Bernd, S9 (LBO-005-YI), S139 (FRI-134), S287 (FRI-275), S755 (THU-510)
Schneeweiß, Stephan M, S904 (SAT-564)
Schnefeld, Helle, S26 (OS-032-YI), S63 (OS-098-YI), S110 (FRI-041-YI), S115 (FRI-059), S122 (FRI-079-YI), S125 (FRI-090-YI), S554 (THU-204), S608 (WED-180), S706 (THU-545-YI)
Schneider, Caitlin, S615 (WED-198)
Schneider, Carolin V, S521 (THU-093), S566 (WED-052), S678 (TOP-162)
Schneider, Carolin V., S17 (OS-011), S166 (FRI-393), S789 (SAT-031-YI), S971 (WED-620)
Schneider, Farina, S280 (THU-338-YI)
Schneider, Hannah, S197 (WED-446)
Schneider, Kai, S789 (SAT-031-YI)
Schneider, Paul, S18 (OS-015), S172 (FRI-411), S482 (WED-385-YI), S742 (THU-476)
Schneider, Stéphane, S681 (FRI-147)
Schneider, William, S891 (THU-624-YI)
Schoder, Maria, S732 (THU-448-YI), S738 (THU-464-YI)
Schoelch, Corinna, S20 (OS-018), S688 (FRI-168), S689 (FRI-170)
Schoenmakers, Lotte, S581 (WED-093-YI), S729 (THU-441)
Schoerghuber, Michael, S326 (SAT-321)
Schoevaerdts, Quentin, S55 (OS-085-YI)
Schofield, Annabelle, S365 (WED-330-YI), S461 (WED-247)
Schöler, David, S139 (FRI-134)
Scholl, Samuel, S151 (SAT-477)
Scholtens, Joyce, S541 (THU-156)
Scholtes, Caroline, S942 (FRI-592)
Scholz, Constantin, S503 (FRI-248)
Schomacher, Tina, S383 (FRI-474), S409 (FRI-556)
Schonfeld, Emily, S10 (LBO-006)

Author Index

Schön, Felicia, S482 (WED-385-YI)
Schou, Magnus, S690 (FRI-172)
Schouten, Jeoffrey, S315 (SAT-285)
Schouwink, Marten, S672 (SAT-230)
Schramm, Christoph, S14 (OS-007), S43 (OS-066), S57 (OS-088), S236 (FRI-323), S291 (FRI-291-YI), S300 (SAT-250), S303 (SAT-257-YI), S325 (SAT-320), S333 (SAT-369), S342 (SAT-398), S351 (SAT-427), S900 (SAT-559), S901 (SAT-560), S934 (TOP-582), S936 (TOP-584), S937 (FRI-585-YI)
Schrand, Julie, S531 (THU-121), S683 (FRI-152)
Schrauwen-Hinderling, Vera, S672 (SAT-230)
Schreiber, Nikolaus, S326 (SAT-321)
Schreiberova, Jolana, S286 (FRI-272)
Schreier, Günter, S410 (FRI-559)
Schroeder, Jens, S83 (LBP-035)
Schroeder, Mareike, S209 (WED-485)
Schroers, Barbara, S18 (OS-015), S482 (WED-385-YI)
Schuetz, Gunnar, S106 (THU-075)
Schuler, Pia, S477 (WED-369)
Schulte, Sigrid, S289 (FRI-284)
Schultheiß, Michael, S3 (GS-005), S33 (OS-046), S54 (OS-084), S185 (TOP-456-YI), S733 (THU-449), S736 (THU-460-YI)
Schulze, Sarah, S420 (THU-526)
Schulze, Stephanie, S351 (SAT-427)
Schulze zur Wiesch, Julian, S178 (FRI-429-YI), S257 (SAT-546), S867 (FRI-642)
Schulz-Jürgensen, Sebastian, S834 (THU-260)
Schulz-Kuhnt, Anja, S785 (SAT-020)
Schulz, Stefan, S467 (WED-261)
Schumacher, Adam, S23 (OS-025)
Schumacher, Jonas, S150 (SAT-474)
Schumm, Leonie, S852 (TOP-311), S858 (WED-302)
Schunke, Jenny, S18 (OS-015)
Schuppan, Detlef, S231 (FRI-306-YI), S236 (FRI-323), S620 (WED-213)
Schürmann, Annette, S21 (OS-020)
Schütte, Andreas, S172 (FRI-410-YI)
Schütte, Sarah Lisa, S6 (GS-011-YI), S185 (TOP-456-YI), S222 (WED-524), S732 (THU-448-YI)
Schwabe, Christian, S8 (LBO-003), S958 (WED-579)
Schwabe, Robert F., S18 (OS-014-YI), S241 (FRI-339)
Schwabl, Philipp, S11 (OS-002-YI), S179 (FRI-431-YI), S183 (FRI-444-YI), S200 (WED-453), S205 (WED-474), S216 (WED-508), S237 (FRI-324), S266 (SAT-347-YI), S284 (FRI-266), S362 (TOP-325-YI), S364 (WED-323), S717 (WED-569-YI), S734 (THU-451), S750 (THU-497-YI), S750 (THU-498), S914 (SAT-591)
Schwaninger, Markus, S233 (FRI-313), S241 (FRI-339)
Schwantes-An, Tae-Hwi Linus, S166 (FRI-393)
Schwartz, Ida Vanessa, S830 (THU-254)
Schwartz, Myron, S60 (OS-094)
Schwarz, Caroline, S975 (WED-634-YI)
Schwarz, Christoph, S427 (THU-221)
Schwarz, Hannah, S161 (SAT-510-YI)
Schwarz, Michael, S717 (WED-569-YI), S914 (SAT-591)
Schwemmle, Martin, S371 (WED-348)
Schwerk, Maria, S178 (FRI-429-YI)
Schwinge, Dorothee, S57 (OS-088), S291 (FRI-291-YI)
Scianò, Filippo, S31 (OS-042), S746 (THU-490)
Sciarrone, Salvatore Stefano, S975 (WED-635)
Scohy, Anaïs, S907 (SAT-575)
Scolari, Caterina, S835 (THU-263)
Scollon, Derek, S113 (FRI-054)
Scoppettuolo, Marco, S412 (FRI-562), S412 (FRI-563)
Scorletti, Eleonora, S166 (FRI-393)
Scotcher, Daniel, S106 (THU-075)
Scott, Nick, S803 (FRI-014)
Scribano, Laura, S350 (SAT-421)
Scudu, Chiara, S69 (LBP-004-YI), S307 (SAT-263)
Seaman, Sian, S42 (OS-064-YI)
Seaward, Nicola, S406 (FRI-544)
Sebastian Gherlan, George, S962 (WED-593), S962 (WED-594)
Sebastiani, Giada, S62 (OS-097), S378 (FRI-458), S380 (FRI-462), S424 (TOP-376), S516 (TOP-113), S529 (THU-116-YI), S533 (THU-127-YI), S534 (THU-131), S576 (WED-078), S589 (WED-119), S616 (WED-200), S624 (WED-225-YI), S624 (WED-226), S680 (FRI-139), S757 (THU-516), S783 (SAT-013-YI), S784 (SAT-014), S865 (FRI-638)
Sebastián-Peris, Lucas, S779 (SAT–003-YI)
Sebesta, Christian, S113 (FRI-053), S156 (SAT-494), S183 (FRI-444-YI), S186 (TOP-470-YI), S199 (WED-452), S200 (WED-453), S205 (WED-474), S213 (WED-498), S216 (WED-508), S217 (WED-509-YI), S440 (THU-370), S734 (THU-451), S738 (THU-464-YI), S748 (THU-493-YI), S749 (THU-494), S750 (THU-498), S914 (SAT-591)
Sébillot, Anthony, S365 (WED-331-YI)
Sebode, Marcial, S57 (OS-088), S236 (FRI-323), S300 (SAT-250), S325 (SAT-320), S351 (SAT-427)
Sedki, Mai, S807 (FRI-026)
Seeley, Janet, S900 (SAT-558)
Segales, Paula, S101 (THU-058)
Segalés, Paula, S467 (WED-262)
Segovia-Miranda, Fabián, S357 (TOP-327-YI), S663 (SAT-199-YI)
Ségrestin, Bérénice, S62 (OS-097), S516 (TOP-113), S573 (WED-071)
Seidensticker, Max, S490 (TOP-407-YI)
Seidner, Mark, S900 (SAT-558)
Seifert, Leon Louis, S736 (THU-460-YI), S891 (THU-624-YI)
Seiverth, Britta, S919 (SAT-607)
Sekimata, Masayuki, S372 (WED-352)
Sekine, Hideharu, S372 (WED-352), S647 (SAT-147)
Seko, Yuya, S686 (FRI-159)
Selbach, Nicole, S763 (THU-010)
Selby, Peter, S256 (SAT-543), S258 (SAT-547)
Selcanova, Svetlana Adamcova, S123 (FRI-085), S205 (WED-473)
Selemani, Sarah, S65 (OS-102), S404 (FRI-538-YI), S503 (FRI-250), S970 (WED-619)
Selicean, Sonia-Emilia, S168 (FRI-398), S178 (FRI-429-YI)
Sellés-Sanchez, Alicia, S804 (FRI-019)
Sellier, Floriane, S207 (WED-477)
Selma, Sabbah, S609 (WED-181), S844 (THU-286), S845 (THU-287), S949 (FRI-613)
Selonke, Robert, S930 (SAT-636)
Selvakumar, Vigneshwaran, S442 (THU-379), S698 (FRI-197)
Selvapatt, Nowlan, S224 (WED-530)
Selvarajah, Mughilan, S858 (WED-300-YI)
Selzner, Nazia, S345 (SAT-409-YI), S393 (FRI-501)
Semela, David, S165 (FRI-386)
Semenova, Maria, S376 (FRI-448)
Semmler, Georg, S55 (OS-085-YI), S97 (SAT-084-YI), S113 (FRI-053), S156 (SAT-494), S179 (FRI-432), S183 (FRI-444-YI), S183 (FRI-445), S186 (TOP-470-YI), S205 (WED-474), S213 (WED-498), S216 (WED-508), S217 (WED-509-YI), S427 (THU-220), S427 (THU-221), S440 (THU-370), S616 (WED-199), S720 (TOP-504-YI), S734 (THU-451), S739 (THU-467), S748 (THU-493-YI), S749 (THU-494), S753 (THU-505-YI), S792 (SAT-041)
Semmo, Nasser, S43 (OS-066), S342 (SAT-399), S934 (TOP-582), S937 (FRI-585-YI)
Semnani, Farbod, S697 (FRI-195-YI)
Semnani, Kiavash, S697 (FRI-195-YI)
Semper, Amélie, S742 (THU-477)
Sempoux, Christine, S53 (OS-083-YI), S648 (SAT-151-YI)
Señalada, José Joaquín Blas, S910 (SAT-585)
Şendur, İbrahim Nahit, S203 (WED-464)
Senese, Giusy, S639 (SAT-121-YI), S660 (SAT-190), S854 (WED-286)
Seneshaw, Mulugeta, S649 (SAT-153)
Sengupta, Abhinav, S404 (FRI-539)
Senkal, Volkan, S727 (THU-430)

Senkaya, Ali, S389 (FRI-491)
Senosiáin, Maria, S312 (SAT-273)
Senra, Ana, S232 (FRI-313), S241 (FRI-339)
Sensi, Bruno, S59 (OS-091)
Sen, Srijita Ghosh, S257 (SAT-544)
Senzolo, Marco, S3 (GS-005), S6 (GS-011-YI), S33 (OS-046), S52 (OS-081), S53 (OS-082), S54 (OS-084), S148 (SAT-466-YI), S193 (WED-431-YI), S435 (THU-247), S719 (TOP-488), S721 (THU-415), S746 (THU-489), S747 (THU-492), S752 (THU-501), S783 (SAT-012), S837 (THU-268)
Seo, Deok Hwa, S132 (FRI-107), S482 (WED-386), S891 (THU-625)
Sepic, Joshua, S388 (FRI-489)
Seraphin, Tobias Paul, S447 (THU-395), S470 (WED-268)
Serebryany, Vladimir, S889 (THU-620)
Serenari, Matteo, S402 (FRI-529-YI), S427 (THU-220)
Sereno, Juan Antonio Almena, S391 (FRI-497)
Serfaty, Lawrence, S45 (OS-067)
Serfert, Yvonne, S601 (WED-155)
Seria, Mariam, S522 (THU-094)
Serra, Isabel, S250 (SAT-524), S562 (TOP-097-YI), S612 (WED-188)
Serra, Matteo, S35 (OS-050-YI)
Serrano-Jiménez, María, S467 (WED-261)
Serrano-Maciá, Marina, S281 (TOP-296-YI)
Serrano, Quentin, S681 (FRI-147)
Serrano, Trinidad, S603 (WED-163)
Serretiello, Enrica, S977 (WED-640)
Sersté, Thomas, S907 (SAT-575), S920 (SAT-609), S929 (SAT-629)
Sertöz, Rüçhan, S397 (FRI-514)
Serwah, Abdelhamid A, S809 (FRI-029), S966 (TOP-599)
Šeša, Vibor, S800 (FRI-006)
Sessa, Anna, S343 (SAT-400), S764 (THU-012)
Seto, Wai-Kay, S24 (OS-028), S46 (OS-070-YI), S144 (SAT-452), S160 (SAT-507), S422 (TOP-359-YI), S423 (TOP-360), S438 (THU-364), S496 (FRI-230), S824 (WED-035), S896 (THU-644), S915 (SAT-593), S928 (SAT-628-YI), S933 (SAT-643), S947 (FRI-609)
Setoyama, Hiroko, S808 (FRI-027), S808 (FRI-028)
Setshedi, Mashiko, S764 (THU-012)
Seubnooch, Patcharamon, S561 (TOP-081)
Seufert, Jochen, S21 (OS-020)
Seul, Maximilian, S648 (SAT-150)
Sevak, Jayesh Kumar, S129 (TOP-224-YI), S269 (SAT-355), S361 (THU-355-YI)
Sevastianos, Vasileios, S1 (GS-001), S188 (WED-415)
Sewald, Katherina, S105 (THU-072)
Sewell, Charlotte, S343 (SAT-401-YI)
Seynhaeve, Laurence, S22 (OS-023), S718 (WED-572)
Sgobbi, Paulo, S830 (THU-254)
Shabanan, Sedighe Hosseini, S443 (THU-381)
Shabbir, Adnan, S406 (FRI-544)
Shabrawy, Mortada El, S713 (WED-557)
Shafiq, Fatima, S120 (FRI-075)
Shafique, Hira, S178 (FRI-430)
Shafique, Muhammad, S178 (FRI-430)
Shagrani, Mohammad, S56 (OS-086), S831 (THU-258-YI), S842 (THU-284)
Shah, Ajay, S174 (FRI-416-YI)
Shah, Anika, S745 (THU-483)
Shah, Chintan, S7 (LBO-001)
Shaheen, Abdel Aziz, S349 (SAT-419), S525 (THU-104-YI), S787 (SAT-025)
Shaheen, Abdel-Aziz, S346 (SAT-413), S616 (WED-199), S788 (SAT-028)
Shahi, Pradeep, S699 (FRI-199)
Shah, Jimil, S741 (THU-474)
Shah, Naina, S198 (WED-448-YI)
Shah, Neha, S109 (TOP-209-YI), S122 (FRI-083)
Shah, Samir, S67 (OS-105-YI)
Shah, Sital, S704 (THU-540), S709 (THU-556-YI)
Shah, Stuti, S875 (THU-574)
Shah, Vijay, S113 (FRI-052), S126 (FRI-093), S186 (TOP-469-YI), S190 (WED-421), S197 (WED-447)
Shaikh, Ayaz Iqbalbhai, S564 (WED-044), S565 (WED-045)
Shaikh, Farheen, S7 (LBO-001)
Shaikh, Maryam, S232 (FRI-308)
Shaked, Abraham, S166 (FRI-393)
Shalaby, Sarah, S53 (OS-082), S55 (OS-085-YI), S827 (TOP-297), S837 (THU-268), S862 (WED-315), S884 (THU-604-YI)
Shalimar, S36 (OS-051-YI), S725 (THU-426), S847 (THU-299)
Shalimar, , S141 (TOP-423)
Shalimar, Shalimar, S24 (OS-028), S27 (OS-033), S62 (OS-097), S144 (SAT-452), S160 (SAT-507), S184 (TOP-454-YI), S247 (SAT-514), S299 (SAT-248), S424 (TOP-376), S516 (TOP-113), S952 (FRI-622)
Sham, Pak Chung, S859 (WED-303), S860 (WED-306), S864 (WED-320-YI)
Shams, Tarek, S598 (WED-149)
Shang, Dabao, S3 (GS-004-YI)
Shang, Jia, S68 (OS-107), S952 (FRI-623), S955 (FRI-628)
Shang, Xianwei, S954 (FRI-626)
Shang, Ying, S62 (OS-097), S115 (FRI-058-YI), S224 (WED-529), S515 (TOP-112-YI), S516 (TOP-113), S517 (TOP-114), S525 (THU-103), S558 (TOP-063-YI), S584 (WED-104), S589 (WED-118), S607 (WED-174-YI), S612 (WED-187-YI), S701 (FRI-205-YI), S796 (SAT-052)
Shankar, Athiva, S119 (FRI-073)
Shankar, Sahana, S850 (THU-308)
Shankar, Sushanth, S735 (THU-457)
Shanmuga Anandan, Aathavan, S818 (WED-013)
Shannon, Jennifer B., S295 (TOP-280)
Shan, Wencheng, S474 (WED-362)
Shao, Wenhua, S668 (SAT-215), S669 (SAT-218), S870 (TOP-646)
Shao, Yingmei, S243 (FRI-348), S421 (THU-532)
Shao, Yu-Yun, S456 (WED-234-YI)
Shapiro, James, S401 (FRI-527)
Sharaf, Rana Saleh, S208 (WED-482)
Shariff, Mohamed, S759 (TOP-017-YI)
Sharifi, Roxanna, S386 (FRI-482), S411 (FRI-561-YI), S413 (FRI-570)
Sharkia, Israa, S60 (OS-093), S615 (WED-196)
Sharkia, Issra, S289 (FRI-286)
Sharma, Aarti, S171 (FRI-404), S361 (THU-355-YI), S629 (TOP-161-YI)
Sharma, Barjesh, S217 (WED-510)
Sharma, Deepanshu, S276 (THU-324-YI)
Sharma, Deepti, S292 (FRI-299), S478 (WED-371)
Sharma, Gaurav, S171 (FRI-409-YI)
Sharma, Madhurima, S221 (WED-522)
Sharma, Manoj Kumar, S67 (OS-105-YI)
Sharma, Mithun, S24 (OS-028), S160 (SAT-507), S952 (FRI-622)
Sharma, Narendra, S264 (SAT-335), S264 (SAT-336), S280 (THU-337)
Sharma, Neha, S104 (THU-071-YI), S105 (THU-073-YI), S105 (THU-074), S120 (FRI-074), S129 (TOP-224-YI), S131 (FRI-105-YI), S139 (FRI-135-YI), S265 (SAT-341), S269 (SAT-354-YI), S269 (SAT-355), S276 (THU-324-YI), S280 (THU-337), S361 (THU-354), S373 (WED-353-YI), S533 (THU-127-YI), S616 (WED-200)
Sharma, Nupur, S104 (THU-071-YI), S105 (THU-073-YI), S105 (THU-074), S120 (FRI-074), S129 (TOP-224-YI), S131 (FRI-105-YI), S138 (FRI-132), S139 (FRI-135-YI), S265 (SAT-341), S269 (SAT-354-YI), S269 (SAT-355), S276 (THU-324-YI), S280 (THU-337), S361 (THU-354), S373 (WED-353-YI), S418 (THU-517-YI)
Sharma, Prachi, S232 (FRI-308)
Sharma, Prerna, S81 (LBP-030)
Sharma, Raju, S36 (OS-051-YI), S184 (TOP-454-YI)
Sharma, Rajveer, S292 (FRI-299)
Sharma, Rishabh, S126 (FRI-092-YI), S288 (FRI-282), S292 (FRI-299)
Sharma, Rohini, S12 (OS-005-YI), S428 (THU-226-YI), S455 (TOP-406), S490 (TOP-407-YI), S500 (FRI-239), S506 (FRI-255-YI), S781 (SAT-008), S781 (SAT-009)

Author Index

Sharma, Satya Priya, S41 (OS-061)
Sharma, Shreeya, S206 (WED-475)
Sharma, Shreya, S138 (FRI-132)
Sharma, Shvetank, S105 (THU-073-YI), S105 (THU-074), S120 (FRI-074), S131 (FRI-105-YI), S139 (FRI-135-YI), S269 (SAT-355), S276 (THU-324-YI), S292 (FRI-299), S373 (WED-353-YI)
Sharma, Simran, S171 (FRI-404), S361 (THU-355-YI), S629 (TOP-161-YI)
Sharma, Vinesh, S668 (SAT-216-YI)
Sharma, Vipul, S104 (THU-071-YI), S105 (THU-073-YI), S105 (THU-074), S120 (FRI-074), S131 (FRI-105-YI), S138 (FRI-132), S139 (FRI-135-YI), S265 (SAT-341), S269 (SAT-354-YI), S276 (THU-324-YI), S280 (THU-337), S361 (THU-354), S373 (WED-353-YI)
Sharoyan, Vahan, S619 (WED-206)
Shasthry, S Muralikrishna, S126 (FRI-092-YI)
Shasthry, S. Muralikrishna, S156 (SAT-495)
Shawcross, Debbie L., S148 (SAT-467-YI), S149 (SAT-468), S152 (SAT-478), S261 (SAT-329-YI), S760 (TOP-032)
Shaw, Dave, S840 (THU-275)
Shaw, Jawaid, S24 (OS-028), S144 (SAT-452), S160 (SAT-507)
Shawkat, Mohamed, S717 (WED-570-YI)
Shaw, Shweta, S434 (THU-241)
Shaw, Tanya, S242 (FRI-345-YI)
Shearman, Jeremy, S849 (THU-305-YI)
Shearn, Colin, S289 (FRI-285)
Sheehan, Shannyn, S708 (THU-549-YI)
Sheffeh, Judy, S28 (OS-035)
Sheikh, Aasim, S565 (WED-051)
Sheikh, Muhammad Y., S78 (LBP-025)
Shek, Dmitrii, S218 (WED-513), S749 (THU-496)
Shekhtman, Grigoriy, S79 (LBP-027)
Shekhtman, Louis, S816 (WED-009), S873 (THU-563), S941 (FRI-590)
Shen, Adriana, S308 (SAT-265), S309 (SAT-266)
Shen, Bin, S763 (THU-011)
Shen, Chien-Chang, S632 (SAT-100)
Sheng, Baoyue, S201 (WED-458), S944 (FRI-597)
Sheng, Jianwen, S259 (SAT-554), S593 (WED-134), S609 (WED-182), S924 (SAT-620)
Sheng, Jifang, S158 (SAT-501)
Sheng, Mingwei, S625 (WED-227)
Sheng, Shuyan, S487 (WED-402), S674 (SAT-234)
Shen, Haiyuan, S129 (TOP-223), S140 (FRI-136)
Shen, Huajiang, S964 (WED-601-YI)
Shen, Jie, S560 (TOP-080)
Shen, Liang, S67 (OS-105-YI)
Shenoy, K T, S62 (OS-097), S516 (TOP-113)
Shenoy, KT, S127 (FRI-095), S470 (WED-269)
Shen, Qing, S763 (THU-011)
Shen, Rongjun, S322 (SAT-307), S322 (SAT-308)
Shen, Sheng, S869 (TOP-630), S872 (THU-561)
Shen, Xuting, S778 (THU-053)
Shen, Yangfan, S153 (SAT-482), S161 (SAT-508), S177 (FRI-426)
Shen, Yi, S756 (THU-512)
Shen, Ying, S909 (SAT-579)
Shen, Zewei, S623 (WED-221)
Shen, Zhongliang, S891 (THU-626)
Shepard, Christopher, S639 (SAT-119)
Shepstone, Lee, S311 (SAT-270)
Sheptulina, Anna, S551 (THU-189), S551 (THU-190), S594 (WED-135), S595 (WED-136)
Sheridan, David, S164 (FRI-385-YI)
Sheridan, J., S377 (FRI-449)
Sherman, Morris, S436 (THU-249)
Sherrick, Jake, S369 (WED-340-YI)
She, Shaoping, S454 (TOP-391), S514 (FRI-380), S668 (SAT-217-YI)
Sheth, Aditya, S315 (SAT-286)
Sheth, Chinar, S207 (WED-479)
Sheth, Roosey, S182 (FRI-443)
Shetty, Shishir, S452 (THU-414-YI), S461 (WED-247)
Sheu, Jin-Chuan, S446 (THU-387)
Shevchenko, Taisiia, S637 (SAT-116)
Shibolet, Oren, S214 (WED-500), S741 (THU-475)
Shi, Dongyan, S104 (THU-070), S151 (SAT-476), S361 (THU-353)
Shiffman, Mitchell, S10 (LBO-006), S62 (OS-096), S329 (SAT-363)
Shi, Guangfeng, S932 (SAT-641)
Shiha, Gamal, S809 (FRI-029), S952 (FRI-622), S966 (TOP-599)
Shihao, Bao, S920 (SAT-609), S929 (SAT-629)
Shi, Hui, S119 (FRI-072), S259 (SAT-554), S593 (WED-134), S609 (WED-182), S763 (THU-011), S924 (SAT-620)
Shih, Yu-Lueng, S969 (WED-613)
Shi, Juanjuan, S431 (THU-234), S791 (SAT-039), S792 (SAT-040)
Shi, Junping, S657 (SAT-180), S676 (SAT-238)
Shimada, Masaaki, S258 (SAT-549), S979 (WED-644)
Shimakawa, Yusuke, S764 (THU-012), S798 (TOP-034)
Shima, Toshihide, S568 (WED-057-YI)
Shimizu, Masahito, S977 (WED-639)
Shimizu, Mayuko, S668 (SAT-215), S669 (SAT-218), S870 (TOP-646)
Shim, Ju Hyun, S4 (GS-006), S4 (GS-007), S428 (THU-226-YI), S497 (FRI-234), S500 (FRI-241), S506 (FRI-255-YI), S513 (FRI-378), S707 (THU-547), S723 (THU-418)
Shimoda, Shinji, S67 (OS-106)
Shimomura, Iichiro, S537 (THU-140)
Shimono, Nobuyuki, S694 (FRI-184)
Shim, Young-Ri, S134 (FRI-115)
Shing, Danielle, S939 (FRI-587), S956 (WED-576)
Shingo, Usui, S861 (WED-313)
Shin, Hyunjae, S502 (FRI-245), S507 (FRI-361), S509 (FRI-366)
Shin, Jaehee, S80 (LBP-029)
Shin, Ji Hyun, S360 (THU-351)
Shin, Yong Moon, S4 (GS-006)
Shin-Yu, Tsai, S436 (THU-250), S448 (THU-396), S535 (THU-135), S586 (WED-108), S751 (THU-499)
Shiojiri, Daisuke, S811 (FRI-037)
Shirai, Kumiko, S463 (WED-251-YI)
Shirin, Demma, S841 (THU-282)
Shirin, Dor, S776 (THU-045)
Shivalila, Chikdu, S5 (GS-008), S702 (FRI-206)
Shi, Wanwan, S292 (FRI-298), S344 (SAT-402)
Shi, Yaoping, S42 (OS-063)
Shi, Yaru, S617 (WED-201)
Shi, Ying, S133 (FRI-110)
Shi, Yu, S158 (SAT-501), S162 (TOP-440), S262 (SAT-331)
Shi, Yuhua, S812 (FRI-040)
Shi, Yunzhen, S86 (LBP-041)
Shi, Yuxi, S253 (SAT-533), S279 (THU-336), S785 (SAT-021), S813 (FRI-045)
Shi, Zhenzhen, S873 (THU-564)
Shlomo-Zidovetzki, Shani Ben, S642 (SAT-127)
Shneider, Benjamin, S55 (OS-086), S831 (THU-258-YI), S842 (THU-284)
Shoaie, Saeed, S173 (FRI-413)
Shomura, Masako, S708 (THU-553)
Short, Patrick, S75 (LBP-017)
Sho, Takuya, S506 (FRI-256), S510 (FRI-367)
Shoukat, Bilal Ahmad, S845 (THU-289)
Shousha, Hend, S504 (FRI-252), S551 (THU-191)
Shravya, Mothe, S139 (FRI-135-YI), S361 (THU-354)
Shreekumar, Devika, S14 (OS-008), S295 (TOP-279), S325 (SAT-319), S325 (SAT-320), S354 (SAT-435), S355 (SAT-436), S401 (FRI-527)
Shrestha, Ananta, S67 (OS-105-YI)
Shribman, Samuel, S84 (LBP-038)
Shringarpure, Reshma, S64 (OS-099), S681 (FRI-142)
Shruti, Kalra, S2 (GS-003)
Shteyer, Eyal, S56 (OS-086), S289 (FRI-286), S831 (THU-258-YI), S842 (THU-284)
Shuaili, Halima Al, S378 (FRI-457)
Shui, Amy, S406 (FRI-543), S534 (THU-132)
Shu, Jintian, S593 (WED-134)
Shukla, Akash, S24 (OS-028), S67 (OS-105-YI), S217 (WED-511), S749 (THU-495), S952 (FRI-622)
Shulman, Nancy, S77 (LBP-021), S964 (WED-597)
Shumbayawonda, Elizabeth, S385 (FRI-479)
Shwaartz, Chaya, S345 (SAT-409-YI)

Sia, Daniela, S18 (OS-014-YI), S453 (TOP-389), S459 (WED-242-YI), S485 (WED-396)
Siakavellas, Spyridon (Spyros), S620 (WED-212)
Sibi, Thooran, S782 (SAT-010-YI)
Siciliano, Andrea, S476 (WED-368)
Sicuro, Chiara, S412 (FRI-562), S412 (FRI-563)
Sidali, Sabrina, S38 (OS-055), S428 (THU-226-YI), S446 (THU-393-YI), S493 (FRI-221), S506 (FRI-255-YI), S507 (FRI-362), S508 (FRI-364-YI)
Sidali, Sabrine, S17 (OS-011)
Siddiqui, Abu, S5 (GS-008)
Siddiqui, Mohammad Shadab, S156 (SAT-496), S215 (WED-505), S221 (WED-523), S228 (WED-543), S411 (FRI-560), S528 (THU-110), S697 (FRI-195-YI), S698 (FRI-197)
Sidhu, Sandeep, S27 (OS-033)
Sidhu, Sarah, S344 (SAT-403)
Sidiropoulos, Orestis, S507 (FRI-257)
Siebelt, Karin, S89 (SAT-057), S928 (SAT-627)
Sierra, Johanna, S182 (FRI-442), S267 (SAT-350)
Sierra, Leandro, S327 (SAT-322)
Sierra, Pablo López-Cepero, S25 (OS-029)
Siervi, Silvia De, S479 (WED-379)
Siew, Susan M., S850 (THU-308)
Sifer-Riviere, Lynda, S863 (WED-317)
Sigal, Michael, S268 (SAT-352-YI)
Sigel, Keith, S40 (OS-059-YI), S538 (THU-148-YI)
Signor, Anna, S669 (SAT-219)
Sigüenza, Rebeca, S571 (WED-069)
Sijtsma, Marijn, S15 (OS-009-YI)
Sikaroodi, Masoumeh, S41 (OS-061)
Sikora, Jakub, S855 (WED-288)
Silberberg, Yael, S680 (FRI-141)
Silberstein, Francesca Ceccherini, S899 (SAT-557), S919 (SAT-608-YI), S924 (SAT-619)
Silbert-Wagner, Dagmar, S672 (SAT-229-YI)
Silletta, Marianna, S429 (THU-227-YI)
Silos, Samantha Rangel, S432 (THU-238)
Siltanen, Juho, S122 (FRI-084)
Silva, Camilo, S608 (WED-175)
Silva, Elsy Soraya Salas, S360 (THU-351)
Silva, Joana, S37 (OS-053)
Silva, Joel, S720 (TOP-504-YI)
Silva, Kelly Da, S165 (FRI-386), S710 (TOP-536-YI)
Silva, Leyre, S364 (WED-329-YI)
Silva, Lilian Fernandes, S114 (FRI-055)
Silva, Marcelo, S141 (TOP-437)
Silva, Mario Jorge, S786 (SAT-022)
Silva, Melissa Lou, S443 (THU-381)
Silva-Neto, Artur, S671 (SAT-226)
Silva-Pereira, Gustavo, S267 (SAT-348)
Silva, Rafael, S671 (SAT-226)
Silva-Veiga, Flavia, S267 (SAT-348)
Silveira-Balloni, Marina, S256 (SAT-542)
Silveira, Marina, S58 (OS-089), S313 (SAT-282)
Silvestre, Ricardo, S186 (TOP-470-YI)
Silvestrin, Alessia, S639 (SAT-121-YI), S660 (SAT-190), S854 (WED-286)
Silvey, Scott, S143 (SAT-451), S144 (SAT-452), S160 (SAT-507), S188 (WED-417)
Simas, Diogo, S317 (SAT-290-YI), S318 (SAT-291), S338 (SAT-383)
Simbrunner, Benedikt, S32 (OS-044), S113 (FRI-053), S156 (SAT-494), S179 (FRI-431-YI), S179 (FRI-432), S183 (FRI-444-YI), S183 (FRI-445), S186 (TOP-470-YI), S200 (WED-453), S205 (WED-474), S213 (WED-498), S216 (WED-508), S252 (SAT-530), S266 (SAT-347-YI), S284 (FRI-266), S362 (TOP-325-YI), S364 (WED-323), S427 (THU-221), S440 (THU-370), S734 (THU-451), S738 (THU-464-YI), S748 (THU-493-YI), S749 (THU-494), S750 (THU-497-YI), S750 (THU-498)
Simian, Daniela, S112 (FRI-050), S296 (TOP-281), S306 (SAT-262)
Simioni, Paolo, S148 (SAT-466-YI), S435 (THU-247), S466 (WED-258), S485 (WED-395-YI)
Sim, Ki Choon, S448 (THU-397)
Simmons, Karen, S789 (SAT-030)
Simon, Andras, S71 (LBP-008)
Simón-Codina, Blanca, S483 (WED-387)
Simone, Loredana, S185 (TOP-455-YI)
Simon, Eric, S362 (TOP-325-YI)
Simonetto, Douglas, S113 (FRI-052), S116 (FRI-061), S126 (FRI-093), S186 (TOP-469-YI), S745 (THU-483)
Simonian, Natalie, S547 (THU-179)
Simoni, Cinzia, S304 (SAT-258)
Simonis, Lucie, S97 (SAT-084-YI), S183 (FRI-445), S195 (WED-442-YI), S216 (WED-508), S217 (WED-509-YI)
Simon, Jorge, S281 (TOP-296-YI)
Simon, Karl-Georg, S971 (WED-620)
Simón, Miguel Angel, S815 (WED-006)
Simonsson, Christian, S568 (WED-056)
Simpson, Kenneth J., S331 (SAT-368-YI)
Şimşir, Ilgın Yıldırım, S389 (FRI-491)
Sinan, Hassan, S120 (FRI-075)
Sinclair-Bell, Sarah-Louise, S354 (SAT-434)
Sinclair, Marie, S145 (SAT-457), S400 (FRI-524), S400 (FRI-525), S433 (THU-240), S736 (THU-458), S739 (THU-466), S922 (SAT-613)
Singal, Amit, S4 (GS-007), S432 (THU-238), S492 (FRI-218)
Singal, Ashwani, S407 (FRI-546)
Singal, Ashwani K., S62 (OS-097), S126 (FRI-094), S127 (FRI-095), S375 (TOP-518), S516 (TOP-113), S532 (THU-125), S560 (TOP-066), S561 (TOP-082), S579 (WED-089), S684 (FRI-154), S766 (THU-015), S923 (SAT-618)
Singanayagam, Aran, S657 (SAT-182)
Singanayagam, Arjuna, S89 (SAT-058), S709 (THU-556-YI)
Singeap, Ana-Maria, S211 (WED-493)
Singer, Amanda, S809 (FRI-030), S809 (FRI-031)
Singh, Aditi, S552 (THU-195)
Singhal, Garima, S157 (SAT-498)
Singh, Ankita, S217 (WED-511), S749 (THU-495)
Singh, Ashish, S36 (OS-051-YI)
Singh, Hem, S184 (TOP-454-YI)
Singh, Ikjot, S161 (SAT-509)
Singh, Jitendra Kumar, S141 (TOP-424-YI)
Singh, Naman, S36 (OS-051-YI)
Singh, Pavit, S247 (SAT-514)
Singh, Priyanka, S538 (THU-148-YI)
Singh, Satender Pal, S156 (SAT-495), S214 (WED-501-YI), S719 (TOP-487-YI)
Singh, Satya Vir, S782 (SAT-011)
Singh, Seema, S564 (WED-043), S578 (WED-088), S596 (WED-140)
Singh, Shivaram Prasad, S204 (WED-466), S923 (SAT-618)
Singh, Shreya, S180 (FRI-433)
Singh, Srajit, S108 (TOP-208-YI)
Singh, Sumeet, S361 (THU-355-YI)
Singh, Surender, S24 (OS-028)
Singh, Virendra, S67 (OS-105-YI), S171 (FRI-409-YI)
Sinha, Prachi, S361 (THU-354)
Sinkala, Edford, S926 (SAT-624)
Sinn, Dong Hyun, S509 (FRI-366)
Sipahi, Oğuz Reşat, S396 (FRI-513)
Sirlin, Claude, S197 (WED-447), S443 (THU-381), S690 (FRI-173)
Sirlin, Colter S., S443 (THU-381)
Sirli, Roxana, S819 (WED-015), S944 (FRI-601)
Sirois, Jean-Karl, S49 (OS-075), S962 (WED-594)
Sironi, Marina, S462 (WED-249)
Situ, Jianwen, S868 (FRI-644)
Sivanandam, S, S782 (SAT-010-YI)
Sjögren, Daniel, S220 (WED-517)
Skalicky, Anne, S339 (SAT-387)
Skladany, Lubomir, S26 (OS-032-YI), S123 (FRI-085), S205 (WED-473), S515 (TOP-098), S583 (WED-101), S777 (THU-050)
Skoien, Richard, S789 (SAT-030)
Slater, Sarah, S455 (TOP-406)
Sleiman, Marwan, S82 (LBP-033)
Slim, Jihad, S980 (FRI-634)
Sliwa, James, S388 (FRI-489)
Slobin, Jacqueline, S40 (OS-059-YI), S538 (THU-148-YI), S552 (THU-196), S776 (THU-046)
Slooter, Charlotte, S15 (OS-009-YI), S305 (SAT-260-YI)
Slovic, Nevena, S463 (WED-250)
Smart, Sarah, S319 (SAT-301)
Smid, Marcela, S70 (LBP-005), S975 (WED-636), S976 (WED-637)

Author Index

Šmíd, Václav, S577 (WED-084)
Smith, Abigail, S190 (WED-421), S197 (WED-447)
Smith, Amanda, S343 (SAT-401-YI)
Smith, Belinda, S343 (SAT-400)
Smith, Brett, S981 (FRI-635)
Smith, Claire, S974 (WED-629-YI)
Smith, Coleman I.MD, S411 (FRI-560)
Smith, Daniel, S443 (THU-380-YI), S520 (THU-091-YI), S541 (THU-158), S553 (THU-197), S595 (WED-137), S636 (SAT-110-YI)
Smith, Davey, S877 (THU-580)
Smith, David, S874 (THU-570), S879 (THU-587), S885 (THU-606), S886 (THU-610), S889 (THU-620)
Smith, Jeff, S87 (LBP-043)
Smith, Justin, S324 (SAT-316)
Smith, Kieran, S164 (FRI-385-YI)
Smith, Nicole, S653 (SAT-166)
Smith, Rachel, S59 (OS-091)
Smith, Roderick, S683 (FRI-152)
Smith, William, S689 (FRI-170)
Smit, Marieke, S630 (SAT-090), S670 (SAT-221-YI)
Smit, Theresa, S900 (SAT-558)
Smolic, Martina, S617 (WED-202)
Smolic, Robert, S617 (WED-202)
Smolle, Luisa, S742 (THU-476)
Smoot, Rory L., S9 (LBO-004)
Smyk, Nathan, S700 (FRI-202)
Snijders, Romée, S15 (OS-009-YI), S332 (SAT-369)
Snir, Tom, S334 (SAT-371), S334 (SAT-372), S334 (SAT-377)
Soardo, Giorgio, S443 (THU-380-YI), S476 (WED-368), S601 (WED-156)
Soares Peres, Flavia, S836 (THU-266)
Soares, Tiago Onofrio, S88 (SAT-056), S776 (THU-044)
Sobenko, Natalia, S325 (SAT-320)
Sobiesk, Matthew, S78 (LBP-023)
Socha, Piotr, S617 (WED-203), S836 (THU-265-YI), S840 (THU-275)
Socio, Giuseppe Vittorio Luigi De, S610 (WED-183)
Sockalingum, Ganesh, S435 (THU-246)
Sodergren, Mikael, S455 (TOP-406)
Soehngen, Jasmin, S172 (FRI-411), S199 (WED-451-YI), S742 (THU-476)
Soerensen, Erik, S166 (FRI-393)
Soerensen, Michael, S290 (FRI-287)
Soergel, David, S682 (FRI-149)
Soffredini, Roberta, S942 (FRI-593)
Søgaard, Ole S., S77 (LBP-022-YI)
Sogbe, Miguel, S96 (SAT-079), S364 (WED-329-YI), S410 (FRI-558), S412 (FRI-564-YI)
Sohail, Abdullah, S218 (WED-512-YI), S698 (FRI-196)
Sohn, Won, S92 (SAT-069), S553 (THU-198), S590 (WED-121), S927 (SAT-625)
S/O Jeyaraj, Prema Raj, S158 (SAT-499)
Sokal, Etienne, S55 (OS-086), S831 (THU-258-YI), S842 (THU-284)
Sokal, Étienne, S850 (THU-308)
Sokhal, Balamrit, S735 (THU-457)
Sokol, Harry, S290 (FRI-289)
Sokol, Ronald, S289 (FRI-285), S832 (THU-258-YI), S842 (THU-284)
Sola, Gloria Alvarez, S130 (FRI-102-YI)
Sola, Kristoffer Huitfeldt, S71 (LBP-008)
Solbrig, Todd, S911 (SAT-586)
Solcia, Marco, S3 (GS-005)
Soldà, Caterina, S402 (FRI-530), S435 (THU-247), S514 (FRI-381)
Solé, Cristina, S203 (WED-463)
Solé, Neus, S710 (THU-557-YI), S826 (WED-038)
Solera, Andres, S793 (SAT-044)
Soler, Maria Rodriguez, S410 (FRI-558)
Soler, Victoria González, S810 (FRI-035)
Soliman, Reham, S809 (FRI-029), S966 (TOP-599)
Solimena, Michele, S21 (OS-020)
Solís-Herruzo, José Antonio, S123 (FRI-086)
Solis-Munoz, Pablo, S123 (FRI-086)
Solis, Nancy, S112 (FRI-050)
Solito, Laura, S825 (WED-037)
Sollano, Jose, S67 (OS-105-YI)
Solomentseva, Tetyana, S604 (WED-167)
Solomon, Tsehay, S825 (WED-036)
Somasundram, Aravindh, S597 (WED-142-YI), S782 (SAT-010-YI)
Sombie, Roger, S905 (SAT-569), S926 (SAT-624), S940 (FRI-588-YI)
Somers, Nicky, S99 (TOP-193-YI), S349 (SAT-420)
Sommacale, Daniele, S499 (FRI-238)
Sommadossi, Jean-Pierre, S869 (TOP-631)
Somma, Jolanda, S248 (SAT-516)
Sommer, Judith, S672 (SAT-229-YI)
Sommer, Katja, S11 (OS-002-YI), S179 (FRI-431-YI), S237 (FRI-324), S266 (SAT-347-YI), S362 (TOP-325-YI), S364 (WED-323)
Sompairac, Nicolas, S366 (WED-333-YI)
Sonavane, Amey, S24 (OS-028), S160 (SAT-507)
Sonawale, Sourabh, S786 (SAT-023)
Son, Dahyeon, S426 (THU-219-YI)
Sondermann, Megan, S854 (WED-285)
Sonderup, Mark, S764 (THU-012), S926 (SAT-624)
Song, Byeong Geun, S502 (FRI-245), S509 (FRI-366), S823 (WED-030)
Song, Do Seon, S590 (WED-121)
Song, Guohe, S511 (FRI-370)
Song, Huaien, S73 (LBP-012)
Song, In Hye, S251 (SAT-528)
Song, Jeong Eun, S497 (FRI-233)
Song, Jiankang, S228 (WED-544), S754 (THU-508)
Song, Jianxiang, S119 (FRI-072), S259 (SAT-554), S593 (WED-134), S609 (WED-182), S763 (THU-011), S924 (SAT-620)
Song, Jieun, S658 (SAT-184), S879 (THU-587)
Song, Jinlong, S501 (FRI-244)
Song, June, S707 (THU-546-YI)
Song, Myeong Jun, S927 (SAT-626)
Song, Sherlot Juan, S62 (OS-097), S224 (WED-531), S516 (TOP-113), S618 (WED-204)
Song, Shuying, S99 (TOP-194)
Song, Xin, S805 (FRI-021)
Song, Yuyun, S593 (WED-133)
Soni, Diwanshu, S670 (SAT-220)
Sonika, Ujjwal, S31 (OS-043-YI), S212 (WED-495-YI), S217 (WED-510)
Soni, Kriti, S773 (THU-037)
Soni, Rajit, S158 (SAT-499)
Sonnenberg, Jannik, S206 (WED-475), S882 (THU-595)
Sonneveld, Milan J., S46 (OS-070-YI), S443 (THU-382-YI), S444 (THU-383), S809 (FRI-030), S817 (WED-011), S909 (SAT-580), S928 (SAT-628-YI)
Sonsiri, Kanokwan, S619 (WED-211)
Sonthalia, Nikhil, S741 (THU-474)
Sood, Ajit, S67 (OS-105-YI), S952 (FRI-622)
Sood, Arun Kumar, S141 (TOP-424-YI)
Sood, Siddharth, S10 (LBO-006), S218 (WED-513), S436 (THU-248), S469 (WED-265), S716 (WED-562-YI), S716 (WED-563), S716 (WED-564), S749 (THU-496), S820 (WED-021), S922 (SAT-613)
Sookoian, Silvia, S664 (SAT-201)
Sophie, Schlosser-Hupf, S785 (SAT-019)
Sorbello, Orazio, S850 (THU-307)
Sorda, Juan Antonio, S302 (SAT-253)
Sørensen, Kathrine Sejer, S110 (FRI-041-YI), S122 (FRI-079-YI), S125 (FRI-090-YI), S554 (THU-204), S706 (THU-545-YI)
Soret, Pierre-Antoine, S325 (SAT-320)
Sorgenti, Carolina, S720 (TOP-502-YI)
Soria, Alessandro, S938 (FRI-586)
Soria, Anna, S63 (OS-098-YI), S110 (TOP-222), S203 (WED-463), S562 (TOP-097-YI), S567 (WED-054), S583 (WED-101), S608 (WED-180), S612 (WED-188)
Soria, Isabel Carmona, S751 (THU-500)
Soriano, Agnes, S427 (THU-220)
Soriano, German, S150 (SAT-475), S177 (FRI-427)
Soriano, Guillermo Quintas, S408 (FRI-553)
Soriano-Varela, Agnes, S469 (WED-267)
Sorribas, Eduardo Morales, S34 (OS-049)
Sorribes, Ida Lønsmann, S592 (WED-131)
Sorz-Nechay, Thomas, S11 (OS-002-YI), S179 (FRI-431-YI), S237 (FRI-324), S266 (SAT-347-YI), S284 (FRI-266), S362 (TOP-325-YI), S364 (WED-323), S750 (THU-497-YI), S750 (THU-498)
Sosa, Alejandro Jiménez, S547 (THU-181)
Soteras, Gabriel Alejandro Aballay, S10 (LBO-006)
Soubre, Patricia, S723 (THU-419)

Soufidi, Khalida, S353 (SAT-432)
Sourbron, Steven, S106 (THU-075)
Sousa, Jacquelyn, S879 (THU-587)
Sousa-Martin, Jose Manuel, S16 (OS-010)
Soussan, Patrick, S887 (THU-612-YI)
Souza-Ferreira, Luiz, S671 (SAT-226)
Souza, Marcelo, S102 (THU-060)
Souza-Mello, Vanessa, S267 (SAT-348)
Souza-Tavares, Henrique, S267 (SAT-348)
Sowa, Jan-Peter, S395 (FRI-511-YI)
Soyel, Hamit, S799 (FRI-003)
Spaan, Michelle, S193 (WED-432)
Spada, Marco, S59 (OS-091), S670 (SAT-225)
Spahr, Laurent, S111 (FRI-043), S199 (WED-450)
Spalding, Duncan, S455 (TOP-406)
Spangenberg, Hans Christian, S945 (FRI-602-YI)
Sparchez, Zeno, S175 (FRI-418), S209 (WED-483), S445 (THU-385)
Sparrelid, Ernesto, S71 (LBP-008)
Spearman, Wendy, S89 (SAT-057), S127 (FRI-095), S764 (THU-012), S766 (THU-015), S905 (SAT-569), S923 (SAT-618), S926 (SAT-624), S928 (SAT-627), S940 (FRI-588-YI)
Spear, Oliver, S106 (THU-075)
Spector, Pooja, S56 (OS-086), S831 (THU-258-YI), S842 (THU-284)
Spedtsberg, Ida Ziegler, S111 (FRI-044)
Speier, Frederic, S482 (WED-385-YI)
Speliotes, Elizabeth, S166 (FRI-393)
Sperling, Rhoda, S40 (OS-059-YI), S538 (THU-148-YI)
Sperl, Jan, S35 (OS-050-YI)
Spiegeleer, Margot De, S907 (SAT-575)
Spigaroli, Margherita, S841 (THU-282)
Spill, Fabian, S364 (WED-324-YI)
Spiro, Michael, S389 (FRI-492)
Spitzer, Eléonore, S446 (THU-393-YI), S507 (FRI-362)
Spraul, Anne, S853 (WED-283)
Sprengers, Dave, S443 (THU-382-YI), S444 (THU-383)
Sprengers, Dirk, S849 (THU-306-YI), S920 (SAT-609), S929 (SAT-629)
Sprinkart, Alois Martin, S213 (WED-496)
Sprinzak, David, S861 (WED-308)
Sprinzl, Kathrin, S935 (TOP-583), S945 (FRI-602-YI)
Sprinzl, Martin, S930 (SAT-636)
Squadrito, Giovanni, S196 (WED-445)
Squillante, Maria, S825 (WED-037)
Squires, James E., S56 (OS-086), S831 (THU-258-YI), S842 (THU-284), S850 (THU-308)
Squires, Katherine, S51 (OS-079)
Sremac, Maja, S800 (FRI-006)
Sridhar, Siddharth, S868 (FRI-644)
Srinivasan, Parthi, S404 (FRI-538-YI)
Sriphoosanaphan, Supachaya, S180 (FRI-434), S181 (FRI-435), S619 (WED-211)
Sripongpun, Pimsiri, S219 (WED-514), S439 (THU-366-YI), S727 (THU-432)
Srivastava, Ankur, S452 (THU-414-YI)
Srivastava, Siddharth, S31 (OS-043-YI), S212 (WED-495-YI), S217 (WED-510)
Ssebyatika, George, S866 (FRI-641)
Stadlbauer, Vanessa, S326 (SAT-321), S742 (THU-476), S979 (TOP-614)
Stadler, Helena, S175 (FRI-420), S181 (FRI-436)
Stadtmann, Juliana, S736 (THU-460-YI), S737 (THU-461), S744 (THU-481)
Staels, Bart, S149 (SAT-468), S152 (SAT-478), S163 (FRI-383), S164 (FRI-384), S172 (FRI-412), S682 (FRI-150-YI), S760 (TOP-032)
Staffeldt, Lisa, S271 (THU-313)
Stafie, Remus, S211 (WED-493)
Stagno, Anna Maria, S494 (FRI-225)
Staicu, Isabela, S951 (FRI-620), S974 (WED-633)
Stalke, Amelie, S858 (WED-301)
Stallmach, Andreas, S124 (FRI-089), S142 (SAT-448), S159 (SAT-506-YI), S219 (WED-516), S930 (SAT-636)
Stal, Per, S584 (WED-104)
Staltner, Raphaela, S179 (FRI-432)
Stamataki, Zania, S369 (WED-340-YI), S372 (WED-351)
Stamouli, Marilena, S168 (FRI-396)
Stanciu, Carol, S211 (WED-493)
Stancu, George, S49 (OS-075), S962 (WED-594)
Ständer, Sonja, S322 (SAT-313)
Standley, Stephany, S702 (FRI-206)
Stange, Jan, S93 (SAT-070)
Stangl, Gabriele, S175 (FRI-419)
Stankevic, Evelina, S114 (FRI-057)
Stanley, Adrian, S740 (THU-468)
Stanton, Jenny, S957 (WED-578), S958 (WED-580)
Stanzione, Maria, S176 (FRI-425), S212 (WED-494-YI)
Stärkel, Peter, S266 (SAT-346), S648 (SAT-151-YI), S920 (SAT-609), S929 (SAT-629)
Starlinger, Patrick, S9 (LBO-004), S427 (THU-221), S477 (WED-369)
Staroń, Robert, S265 (SAT-338)
Startseva, Elena, S20 (OS-018)
Stättermayer, Albert Friedrich, S183 (FRI-444-YI), S199 (WED-452), S213 (WED-498), S216 (WED-508), S427 (THU-221), S748 (THU-493-YI), S749 (THU-494), S750 (THU-498)
Stauber, Rudolf, S64 (OS-100), S945 (FRI-602-YI)
Staub, Golda, S185 (TOP-456-YI)
Staudenmann, Dominic, S452 (THU-414-YI)
Staufer, Katharina, S149 (SAT-468), S152 (SAT-478), S214 (WED-499), S760 (TOP-032)
Steenkiste, Christophe Van, S315 (SAT-285), S920 (SAT-609)
Stefanis, Cristiano De, S670 (SAT-225)
Stefan, Pfister, S178 (FRI-429-YI)
Štefela, Alzbeta, S661 (SAT-191)
Steffen, Hans-Michael, S289 (FRI-284)
Stegagnini, Marta, S379 (FRI-461-YI)
Steindl, Hubert, S785 (SAT-020)
Steiner, Justinija, S617 (WED-202)
Stein, Laura, S848 (THU-302)
Steinmann, Eike, S866 (FRI-641), S876 (THU-577), S879 (THU-588), S881 (THU-592-YI), S881 (THU-593), S885 (THU-608), S887 (THU-611), S887 (THU-613), S888 (THU-617), S890 (THU-623-YI)
Steinmann, Silja, S57 (OS-088), S291 (FRI-291-YI), S351 (SAT-427)
Stella Franzè, Maria, S435 (THU-245)
Stella, Leonardo, S82 (LBP-034-YI), S176 (FRI-425), S212 (WED-494-YI), S219 (WED-515), S350 (SAT-421)
Stella, Sonia, S331 (SAT-368-YI)
Stell, David, S164 (FRI-385-YI)
İstemihan, Zülal, S829 (THU-251)
Stender, Stefan, S166 (FRI-393)
Stepanova, Maria, S62 (OS-097), S126 (FRI-094), S127 (FRI-095), S128 (FRI-099), S356 (SAT-443), S395 (FRI-511-YI), S417 (FRI-581), S424 (TOP-376), S516 (TOP-113), S557 (THU-213), S575 (WED-077), S766 (THU-015), S794 (SAT-046), S923 (SAT-618)
Stepanova, Tatiana, S939 (FRI-587), S956 (TOP-598), S956 (WED-576), S957 (WED-577), S960 (WED-587), S962 (WED-593)
Stephanopoulos, Nicholas, S273 (THU-317)
Stern, Christiane, S951 (FRI-621)
Sterneck, Martina, S59 (OS-092-YI), S178 (FRI-429-YI), S834 (THU-260)
Stern, Louisa, S17 (OS-011)
Stern, Sean, S695 (FRI-186)
Stetter, Ralph, S447 (THU-395)
Stevens, Neil, S75 (LBP-017)
Stevenson, Chris, S119 (FRI-073)
Stevenson, Emma, S413 (FRI-569)
Stevens, Sarah, S879 (THU-587), S889 (THU-620)
Steverlynck, Matthias, S907 (SAT-575)
Stewart, Stephen, S769 (THU-024-YI), S769 (THU-025)
Sthaneshwar, Pavai, S593 (WED-132)
Sticht, Carsten, S231 (FRI-305)
Sticova, Eva, S275 (THU-320), S405 (FRI-540)
Sticová, Eva, S474 (WED-364)
Stiess, Michael, S14 (OS-007), S64 (OS-100), S297 (TOP-293), S341 (SAT-397)
Still, Laurence, S572 (WED-070)
Stine, Jonathan, S713 (WED-557)
Stinson, Sara, S114 (FRI-057)
Stinton, Laura, S691 (FRI-175)
Stjernman, Henrik, S220 (WED-517)

Author Index

Stobie, Laura, S255 (SAT-540), S973 (WED-627)
Stockdale, Alexander, S905 (SAT-569), S926 (SAT-624), S940 (FRI-588-YI)
Stocken, Deborah, S256 (SAT-543), S258 (SAT-547)
Stocker, Hartmut, S1 (GS-001)
Stockley, Amelia, S201 (WED-459)
Stocks, Hannah, S464 (WED-253)
Stoehr, Albrecht, S971 (WED-620)
Stoelinga, Anna, S15 (OS-009-YI)
Stoian, Marinela, S448 (THU-398)
Stojiljkovic, Marija, S219 (WED-516)
Stoleru, Irina-Maria, S602 (WED-157)
Stolz, Andrew, S197 (WED-447)
Stolz, Vanessa, S885 (THU-608)
Stone, Jack, S804 (FRI-015-YI)
Stoove, Mark, S799 (FRI-004), S800 (FRI-005)
Storer, Michelle, S827 (WED-047)
Storey, Eric, S713 (WED-555)
Storgaard, Marie, S703 (THU-527-YI), S786 (SAT-024-YI)
Stormon, Michael, S850 (THU-308)
Stornaiuolo, Gianfranca, S190 (WED-425), S479 (WED-378)
Stoycheva, Antitsa, S879 (THU-587), S885 (THU-606), S889 (THU-620)
Støy, Sidsel, S262 (SAT-332)
Strahs, Andrew, S5 (GS-008)
Straka, Wolfgang, S257 (SAT-545-YI)
Strandberg, Rickard, S247 (SAT-512), S568 (WED-057-YI), S584 (WED-104), S606 (WED-172-YI), S606 (WED-173), S792 (SAT-042)
Stranecky, Viktor, S855 (WED-288)
Strassburg, Christian, S14 (OS-007), S213 (WED-496)
Strasser, Simone, S77 (LBP-021), S452 (THU-414-YI), S964 (WED-597)
Stratan, Laurentiu, S974 (WED-633)
Strathern, Peter, S113 (FRI-054)
Stratta, Chiara, S90 (SAT-061-YI), S402 (FRI-531)
Straub, Beate, S854 (WED-285)
Straub, Victoria, S229 (WED-545)
Strauss, Thomas Levi, S399 (FRI-523)
Strazzabosco, Mario, S466 (WED-258), S485 (WED-395-YI)
Street, Karen, S713 (WED-556-YI)
Streinu-Cercel, Adrian, S939 (FRI-587), S956 (WED-576), S962 (WED-593)
Streinu-Cercel, Anca, S7 (GS-012), S958 (WED-581)
Stremitzer, Stefan, S427 (THU-221)
Strnad, Pavel, S5 (GS-008), S834 (THU-260), S834 (THU-262), S836 (THU-265-YI), S836 (THU-266), S847 (THU-300), S848 (THU-301), S855 (WED-287-YI)
Stroffolini, Tommaso, S912 (SAT-587-YI)
Stroka, Deborah, S11 (OS-001-YI), S287 (FRI-276-YI)
Strömberg, Ulf, S224 (WED-529), S791 (SAT-037)
Strona, Silvia, S90 (SAT-061-YI), S402 (FRI-531), S784 (SAT-015-YI), S848 (THU-304)
Stroppa, Paola, S414 (FRI-571)
Struik, Dicky, S630 (SAT-090)
Stucki-Koch, Angelika, S105 (THU-072)
Stuermlinger, Anna, S581 (WED-095)
Stultz, Ashley, S974 (WED-628)
Sturm, Ekkehard, S56 (OS-086), S831 (THU-258-YI), S836 (THU-265-YI), S842 (THU-284)
Sturm, Lukas, S33 (OS-046), S54 (OS-084), S185 (TOP-456-YI), S733 (THU-449), S736 (THU-460-YI), S744 (THU-482-YI), S752 (THU-501)
Stylianou, Michalis, S713 (WED-557)
Suárez, Maria Unceta, S635 (SAT-106)
Subhojit, Paul, S463 (WED-250)
Subias, Alberto Mir, S819 (WED-019)
Subic-Levrero, Miroslava, S45 (OS-067), S815 (WED-005)
Subudhi, Patnala Debishree, S650 (SAT-157-YI)
Sucher, Robert, S410 (FRI-559)
Su, Chien-Wei, S430 (THU-231), S436 (THU-250), S448 (THU-396), S535 (THU-135), S586 (WED-108), S751 (THU-499), S893 (THU-633)
Su, Chung-Wei, S945 (FRI-603)
Suchy, Frederick J., S832 (THU-258-YI), S842 (THU-284)
Sucker, Christoph, S161 (SAT-510-YI)
Suda, Goki, S506 (FRI-256), S510 (FRI-367), S977 (WED-639)
Sudat, Sylvia, S770 (THU-026)
Suddle, Abid, S386 (FRI-481-YI), S404 (FRI-538-YI), S503 (FRI-250)
Sudharsan, Venkatesh, S217 (WED-510)
Sudhindran, S, S36 (OS-051-YI)
Sudy, Alexander, S852 (TOP-311), S858 (WED-302)
Suehiro, Tomoyuki, S249 (SAT-522), S970 (WED-618), S976 (WED-638)
Suemizu, Hiroshi, S275 (THU-321)
Suetta, Charlotte, S298 (SAT-245)
Suganami, Hideki, S67 (OS-106)
Suga, Takayoshi, S550 (THU-188)
Sugawara, Mitsuhiro, S524 (THU-102)
Sugaya, Tatsuro, S372 (WED-352), S647 (SAT-147)
Sugi, Kazuhiro, S550 (THU-188)
Sugimoto, Rie, S258 (SAT-549), S979 (WED-644)
Sugiura, Wataru, S875 (THU-573)
Sugiyama, Masaya, S892 (THU-628), S894 (THU-635), S894 (THU-637)
Su, Gui, S763 (THU-011), S924 (SAT-620)
Su, Huiyong, S812 (FRI-040)
Sui, Jianhua, S73 (LBP-013)
Sui, Shulan, S954 (FRI-627)
Suja Kumari, S, S706 (THU-544)
Su, Jian, S473 (WED-361-YI)
Sukali, Gloria, S900 (SAT-558)
Suk, Ki Tae, S41 (OS-061), S266 (SAT-345), S267 (SAT-349), S687 (FRI-164)
Sukowati, Caecilia, S465 (WED-256)
Sulejova, Karolina, S123 (FRI-085)
Su, Lishan, S873 (THU-563)
Sulkowski, Mark S, S897 (TOP-565)
Sulkowski, Mark S., S76 (LBP-021), S87 (LBP-043)
Sullivan, David O, S973 (WED-627)
Sullivan, David O., S255 (SAT-540)
Sultan, Binta, S823 (WED-028)
Sultanik, Philippe, S446 (THU-393-YI)
Sumaili, Ernest, S80 (LBP-028-YI)
Su, Man, S160 (SAT-507)
Su, Minghua, S24 (OS-028), S144 (SAT-452), S160 (SAT-507)
Sumitomo, Naofumi, S861 (WED-313)
Summermatter, Laura, S465 (WED-255)
Sun, Beicheng, S487 (WED-402), S674 (SAT-234)
Sun, Benmao, S511 (FRI-370)
Sun, Cassy, S112 (FRI-051)
Sun, Changyu, S954 (FRI-626)
Sun, Chenyu, S437 (THU-362)
Sun, Dan, S71 (LBP-008)
Sundaram, Shikha S., S850 (THU-308)
Sunday, Gilbert, S821 (WED-023)
Sundin, Phillip, S26 (OS-031)
Sun, Feng, S954 (FRI-627)
Sung, Deuk Jae, S448 (THU-397)
Sung, Pil Soo, S132 (FRI-107), S135 (FRI-119), S478 (WED-372), S482 (WED-386), S510 (FRI-368), S891 (THU-625)
Sung, Shuen, S743 (THU-479)
Su, Ning, S511 (FRI-370)
Sunish, Niveditha, S705 (THU-542)
Sun, Jia, S74 (LBP-015)
Sun, Jian, S6 (GS-010), S33 (OS-047), S140 (FRI-137), S260 (TOP-357), S270 (SAT-356), S433 (THU-239), S486 (WED-397), S644 (SAT-136), S869 (TOP-630), S872 (THU-561), S932 (SAT-641)
Sun, Jinfang, S763 (THU-011)
Sun, Li, S952 (FRI-623)
Sun, Mengxue, S422 (THU-533)
Sun, Mingyue, S220 (WED-521)
Sun, Peng, S362 (TOP-325-YI)
Sun, Pinghua, S593 (WED-134), S763 (THU-011)
Sun, Pingnan, S244 (FRI-353)
Sun, QinMei, S778 (THU-053)
Sun, Shuilin, S86 (LBP-041)
Sun, Xin, S665 (SAT-205)
Sun, Xing, S511 (FRI-370)
Sun, Xuehua, S473 (WED-361-YI)
Sun, Yameng, S560 (TOP-080), S826 (WED-040)
Sun, Yong, S108 (THU-083), S269 (SAT-353)
Sun, Yongzhong, S61 (OS-108)
Suo, Yuan, S51 (OS-080-YI)
Suo, Yuhong, S331 (SAT-367), S370 (WED-345)

Supparatpinyo, Khuanchai, S86 (LBP-042)
Surabattula, Rambabu, S236 (FRI-323), S620 (WED-213)
Surace, Lidia, S695 (FRI-187), S950 (FRI-619)
Surace, Lorenzo, S304 (SAT-258), S335 (SAT-378-YI), S912 (SAT-587-YI)
Sur, Cyrille, S579 (WED-090)
Surey, Julian, S826 (WED-039)
Suri, Deepak, S759 (TOP-017-YI)
Surksum, Colin Van, S391 (FRI-498)
Suroliya, Varun, S288 (FRI-282), S425 (THU-217-YI), S867 (FRI-643)
Surra, Astrid Cecilia, S784 (SAT-015-YI)
Suschak, John, S19 (OS-016), S84 (LBP-036), S679 (TOP-176), S700 (FRI-201)
Suslov, Aleksei, S533 (THU-126)
Sutac, Cosmina, S427 (THU-220)
Sutherland, Tom, S922 (SAT-613)
Sutter, Jan, S257 (SAT-546)
Sutter, Olivier, S54 (OS-084), S446 (THU-393-YI), S507 (FRI-362)
Sutton, Angela, S38 (OS-055)
Su, Tung-Hung, S46 (OS-070-YI), S449 (THU-399), S898 (TOP-566-YI), S898 (TOP-567), S917 (SAT-601-YI), S958 (WED-580), S969 (WED-613)
Su, Yan, S540 (THU-154)
Su, Yinan, S124 (FRI-087-YI), S386 (FRI-482), S411 (FRI-561-YI), S413 (FRI-570)
Suykens, Janne, S708 (THU-554-YI)
Su, Yonglu, S906 (SAT-572)
Su, Yung-Yeh, S491 (TOP-408-YI)
Suzuki, Ayako, S96 (SAT-083), S553 (THU-201)
Suzuki, Hiroyuki, S698 (FRI-197)
Suzuki, Yuichiro, S1 (GS-001)
Svangård, Nils, S252 (SAT-530)
Svarovskaia, Jenny, S948 (FRI-610)
Svegiati-Baroni, Gianluca, S185 (TOP-455-YI)
Svegliati-Baroni, Gianluca, S3 (GS-005), S424 (TOP-375-YI), S429 (THU-227-YI)
Svejsø, Frederik Højberg, S586 (WED-109)
Sven, Peine, S912 (SAT-588)
Svensgaard, Siri Nana Halling, S77 (LBP-022-YI)
Sveroni, Dafni, S314 (SAT-283)
Svicher, Valentina, S49 (OS-076-YI), S807 (FRI-025), S899 (SAT-557), S912 (SAT-587-YI), S919 (SAT-608-YI), S924 (SAT-619)
Svizzeretto, Elisabetta, S610 (WED-183)
Swain, Liam, S787 (SAT-025), S787 (SAT-026), S788 (SAT-027), S788 (SAT-028)
Swain, Mark, S14 (OS-008), S75 (LBP-018), S295 (TOP-279), S315 (SAT-286), S325 (SAT-319), S340 (SAT-388), S354 (SAT-435), S525 (THU-104-YI), S616 (WED-199), S624 (WED-226), S783 (SAT-013-YI), S784 (SAT-014), S820 (WED-022)
Swaroop, Shekhar, S141 (TOP-423), S184 (TOP-454-YI), S299 (SAT-248), S725 (THU-426)
Sweeney, Jacob, S399 (FRI-522)
Sweet, Matthew, S170 (FRI-403)
Swerkersson, Signe, S220 (WED-517)
Swiader-Lesniak, Anna, S617 (WED-203)
Swift, Brandon, S26 (OS-031), S295 (TOP-280), S689 (FRI-169)
Symons, Julian, S658 (SAT-184), S874 (THU-570), S879 (THU-587), S885 (THU-606), S886 (THU-610), S889 (THU-620), S893 (THU-634)
Syn, Nicholas, S221 (WED-523), S442 (THU-379), S509 (FRI-365), S698 (FRI-197)
Syriha, Antonia, S507 (FRI-257)
Szabo, Anita, S347 (SAT-414-YI)
Szabo, Gyongyi, S137 (FRI-126)
Szaboova, Daniela, S585 (WED-107)
Szarpak, Lukasz, S617 (WED-203)
Sze-man Tang, Clara, S860 (WED-306)
Szendrödi, Julia, S21 (OS-020)
Szor, Daniel, S701 (FRI-203-YI)

Taanman, Jan-Willem, S180 (FRI-434), S181 (FRI-435)
Tabala, Martine, S80 (LBP-028-YI)
Tabbaa, Mousab, S691 (FRI-175)
Tabernero, David, S908 (SAT-577), S926 (SAT-623), S949 (FRI-612)
Tabrizian, Parissa, S60 (OS-094), S375 (TOP-519)
Tabruyn, Sebastien, S663 (SAT-200)
Tacke, Frank, S3 (GS-004-YI), S43 (OS-066), S60 (OS-093), S77 (LBP-022-YI), S127 (FRI-095), S154 (SAT-489), S161 (SAT-510-YI), S248 (SAT-515), S268 (SAT-352-YI), S285 (FRI-269), S287 (FRI-275), S293 (FRI-301), S416 (FRI-578-YI), S557 (THU-213), S615 (WED-196), S623 (WED-220), S795 (SAT-050), S840 (THU-275), S930 (SAT-636), S934 (TOP-582), S936 (TOP-584), S937 (FRI-585-YI)
Tada, Masahiro, S225 (WED-533), S246 (FRI-356)
Tadeo-Espinoza, Hiram, S730 (THU-442)
Tafani, Marco, S177 (FRI-427)
Taffon, Chiara, S331 (SAT-368-YI), S477 (WED-370)
Tagle, Martin, S112 (FRI-050)
Tahata, Yuki, S463 (WED-251-YI), S977 (WED-639)
Taheri, Ehsaneh, S697 (FRI-195-YI)
Tahvildari, Parham Pourabbas, S487 (WED-400-YI)
Tai, David, S458 (WED-238)
Tai, Dean, S241 (FRI-340), S578 (WED-087), S697 (FRI-191)
Taimr, Pavel, S392 (FRI-500)
Tainturier, Julie, S207 (WED-477)
Tait, Paul, S455 (TOP-406), S490 (TOP-407-YI)
Tajada, Pilar, S819 (WED-019), S910 (SAT-585)
Takács, István, S688 (FRI-168)
Takahama, Shokichi, S880 (THU-590)
Takahashi, Hirokazu, S127 (FRI-095), S156 (SAT-496), S215 (WED-505), S221 (WED-523), S228 (WED-543), S423 (TOP-374), S442 (THU-379), S509 (FRI-365), S528 (THU-110), S557 (THU-213), S667 (SAT-213), S686 (FRI-159), S693 (FRI-181), S698 (FRI-197), S766 (THU-015), S808 (FRI-027)
Takahashi, Masaki, S873 (THU-564)
Takaki, Shintaro, S258 (SAT-549), S550 (THU-188), S979 (WED-644)
Takami, Taro, S977 (WED-639)
Takasumi, Mika, S647 (SAT-147)
Takats, Zoltan, S458 (WED-237-YI)
Takawy, Marina, S202 (WED-460-YI)
Takayama, Takahiro, S668 (SAT-215)
Takaya, Tabuchi, S861 (WED-313)
Takeda, Yoshinori, S449 (THU-400), S492 (FRI-219)
Takehara, Tetsuo, S960 (WED-587), S977 (WED-639)
Takenaga, Mitsumasa, S662 (SAT-196)
Takeshita, Eiji, S675 (SAT-237)
Takeuchi, Yasue, S808 (FRI-028)
Takkenberg, R. Bart, S9 (LBO-005-YI), S54 (OS-084), S237 (FRI-330), S443 (THU-382-YI), S963 (WED-595)
Tak, Kwon Yong, S132 (FRI-107), S135 (FRI-119), S478 (WED-372), S482 (WED-386), S510 (FRI-368), S927 (SAT-626)
Taku, Nadesh Ashukem, S879 (THU-589-YI)
Tak, Won Young, S47 (OS-072)
Talasaz, AmirAli, S259 (SAT-553)
Talasz, Heribert, S862 (WED-314-YI)
Talerico, Rosa, S731 (THU-444-YI)
Tamai, Hideyuki, S336 (SAT-379)
Tamaki, Nobuharu, S439 (THU-368), S452 (THU-414-YI), S509 (FRI-365), S555 (THU-205), S618 (WED-205), S686 (FRI-159), S808 (FRI-028), S977 (WED-639)
Tamale, Edward, S161 (SAT-509)
Tamandl, Dietmar, S37 (OS-053)
Tamano, Masaya, S336 (SAT-379)
Tamara, María Legarda, S850 (THU-308)
Tamé, Mariarosa, S936 (TOP-584)
Tamè, Mariarosa, S901 (SAT-560), S938 (FRI-586)
Tamim, Hani, S521 (THU-092)
Tamir, Shirnin, S48 (OS-074)
Tam, Jacky, S12 (OS-004-YI)
Tam, Matthew, S743 (THU-479)
Tamnanloo, Farzaneh, S631 (SAT-094-YI)
Tam, Paul KH, S859 (WED-303)
Tam, Paul Kwong-Hang, S860 (WED-306), S864 (WED-320-YI)
Tanaka, Atsushi, S67 (OS-106), S79 (LBP-026), S295 (TOP-280),

Author Index

S324 (SAT-317), S325 (SAT-320), S331 (SAT-368-YI), S336 (SAT-379), S349 (SAT-420)
Tanaka, Junko, S808 (FRI-028)
Tanaka, Naoki, S555 (THU-205), S591 (WED-123), S618 (WED-205)
Tanaka, Tomohiro, S77 (LBP-021), S187 (TOP-472), S220 (WED-521)
Tanaka, Yasuhito, S1 (GS-001), S166 (FRI-393), S808 (FRI-027), S808 (FRI-028), S824 (WED-035), S897 (TOP-565)
Tan, Albert, S795 (SAT-051)
Tan, Anthony, S50 (OS-077)
Tan, Chee-Kiat, S441 (THU-377-YI), S442 (THU-378)
Tan, Chi-Ping, S500 (FRI-240), S510 (FRI-369-YI)
Tan, Darren Jun Hao, S509 (FRI-365)
Tan, Deming, S932 (SAT-641)
Tandon, Monica, S217 (WED-510)
Tandon, Puneeta, S497 (FRI-234), S723 (THU-418)
Taneja, Sunil, S5 (GS-009), S24 (OS-028), S171 (FRI-409-YI), S180 (FRI-433), S221 (WED-522), S227 (WED-541-YI), S366 (WED-334), S684 (FRI-155), S952 (FRI-622)
Tanemura, Shuhei, S861 (WED-313)
Tan, Eunice, S315 (SAT-286)
Tan, Eunice Xiang Xuan, S221 (WED-523)
Tang, Chengwei, S28 (OS-036-YI)
Tang, Clara Sze-man, S859 (WED-303), S864 (WED-320-YI)
Tang, Ethan, S218 (WED-513), S749 (THU-496)
Tang, Haitao, S950 (FRI-617)
Tang, Hong, S932 (SAT-640)
Tang, Jay, S694 (FRI-183)
Tang, Jieting, S98 (SAT-089-YI)
Tang, Jing, S50 (OS-078), S637 (SAT-115)
Tangkijvanich, Pisit, S86 (LBP-042), S439 (THU-366-YI), S450 (THU-402)
Tang, Lauren, S54 (OS-084), S218 (WED-513), S749 (THU-496)
Tang, Libo, S368 (WED-339), S882 (THU-596), S955 (FRI-629)
Tang, Lydia, S873 (THU-563)
Tang, Mi, S303 (SAT-255)
Tang, Min, S358 (THU-341), S422 (THU-533)
Tang, Nicole Shu Ying, S221 (WED-523), S228 (WED-543), S698 (FRI-197)
Tang, Qiao, S906 (SAT-572)
Tang, Ruqi, S293 (FRI-302-YI)
Tang, Sainan, S129 (TOP-223)
Tang, Siwen, S701 (FRI-204)
Tan, Guo-Jeng, S593 (WED-132)
Tanguy, Marion, S571 (WED-067)
Tang, Wenbin, S472 (WED-273)
Tang, Xiaolu, S48 (OS-074)
Tang, Xiaoping, S46 (OS-069)
Tang, Yanhua, S644 (SAT-136)
Tang, Yijun, S119 (FRI-072), S259 (SAT-554), S593 (WED-134), S609 (WED-182), S763 (THU-011), S924 (SAT-620)
Tang, Yujing, S955 (FRI-628)
Tan, Hiang Keat, S24 (OS-028), S144 (SAT-452), S149 (SAT-473), S158 (SAT-499), S160 (SAT-507), S529 (THU-115), S714 (WED-559-YI), S834 (THU-261)
Tani, Alessia, S457 (WED-235)
Tanigawa, Ryohei, S67 (OS-106)
Tani, Joji, S506 (FRI-256)
Taniki, Nobuhito, S371 (WED-349), S861 (WED-313)
Tan, Jarell Jie-Rae, S300 (SAT-250), S344 (SAT-404), S743 (THU-479)
Tan, Jessica, S149 (SAT-473)
Tan, Kai, S512 (FRI-377)
Tan, Katrina, S400 (FRI-524)
Tan, Ker Shiong, S449 (THU-401)
Tannapfel, Andrea, S21 (OS-020)
Tan, Natassia, S345 (SAT-409-YI)
Tan, Qiming, S349 (SAT-419)
Tan, Soek-Siam, S67 (OS-105-YI)
Tan, Susanna, S77 (LBP-021)
Tan, Susanna K., S964 (WED-597)
Tantillo, Salvatore Fortunato, S69 (LBP-004-YI), S82 (LBP-034-YI)
Tanturli, Michele, S400 (FRI-526), S542 (THU-159)
Tanwar, Sudeep, S256 (SAT-543), S258 (SAT-547)
Tan, Wentao, S556 (THU-211)
Tan, Wenting, S171 (FRI-409-YI)
Tan, Xiang Xuan Eunice, S59 (OS-091)
Tan, Ying, S50 (OS-077)
Tan, Youwen, S68 (OS-107), S81 (LBP-031)
Tao, Cui, S492 (FRI-218)
Tao, Yu, S1 (GS-001)
Tapper, Elliot, S116 (FRI-061), S190 (WED-421), S195 (WED-441), S197 (WED-447), S745 (THU-483)
Tarantini, Piero, S636 (SAT-110-YI)
Tarantino, Giuseppe, S741 (THU-473), S751 (THU-500)
Tarchi, Paola, S465 (WED-256)
Targa, Cristina, S56 (OS-086), S831 (THU-258-YI), S842 (THU-284)
Targher, Giovanni, S626 (WED-231)
Tariq, Samir, S490 (TOP-407-YI)
Taru, Vlad, S11 (OS-002-YI), S179 (FRI-431-YI), S179 (FRI-432), S186 (TOP-470-YI), S237 (FRI-324), S266 (SAT-347-YI), S362 (TOP-325-YI), S364 (WED-323), S750 (THU-497-YI)
Tarzi, Gabriel, S597 (WED-147)
Tashkent, Yasmina, S699 (FRI-198)
Tastet, Valentin, S164 (FRI-385-YI)
Tatara, Eric, S816 (WED-009), S818 (WED-014)
Tateishi, Ryosuke, S187 (TOP-472), S977 (WED-639)
Tateno, Chise, S873 (THU-564)
Tatour, Mifleh, S251 (SAT-527), S316 (SAT-288), S317 (SAT-289)
Taubert, Richard, S39 (OS-056), S60 (OS-093), S300 (SAT-250), S309 (SAT-268), S331 (SAT-368-YI), S333 (SAT-369), S376 (TOP-520-YI)
Taube, Tillmann, S9 (LBO-004)
Taubman, Kim, S436 (THU-248)
Taub, Rebecca, S78 (LBP-024), S596 (WED-139), S615 (WED-198), S679 (TOP-177), S682 (FRI-149), S692 (FRI-179)
Tavaglione, Federica, S601 (WED-156)
Tavakoli, Mitra, S861 (WED-308)
Tavolari, Simona, S484 (WED-393)
Tavor, Osnat Sella, S614 (WED-191)
Tawfiq, Rasha, S630 (SAT-091)
Taylor, Alison, S174 (FRI-416-YI)
Taylor, Christine, S827 (WED-047)
Taylor, Rhiannon, S410 (FRI-558), S758 (TOP-016)
Taylor, Robert, S49 (OS-075), S962 (WED-594)
Taylor, Steven, S699 (FRI-198)
Tay, Wei Xuan, S529 (THU-115)
Tazibt, Djamal, S55 (OS-085-YI)
Tcaciuc, Eugen, S794 (SAT-046)
Tchkonia, Tamar, S9 (LBO-005-YI)
Teague, Amy, S974 (WED-629-YI)
Tebaldi, Toma, S370 (WED-346)
Tebruegge, Marc, S975 (WED-634-YI)
Teckman, Jeffrey H., S834 (THU-262), S836 (THU-266)
Tedesco, Dana, S958 (WED-580)
Teemer, Carmen, S783 (SAT-012)
Teerasarntipan, Tongluk, S160 (SAT-507)
Teerlink, Craig, S166 (FRI-393)
Tefas, Cristian, S209 (WED-483)
Tefos, Fotis, S758 (TOP-002), S781 (SAT-007)
Teh, Kevin Kim Jun, S62 (OS-097), S516 (TOP-113), S525 (THU-103), S529 (THU-115), S558 (TOP-063-YI), S589 (WED-118), S607 (WED-174-YI), S714 (WED-559-YI)
Teikchoon, See, S54 (OS-084)
Teilmann, Mathilde, S646 (SAT-142)
Teixeira-Clerc, Fatima, S456 (WED-234-YI)
Tejedor, Marta, S393 (FRI-501)
Teker, Gizem, S727 (THU-430)
Telep, Laura E., S809 (FRI-030), S809 (FRI-031)
Telesca, Claudia, S841 (THU-282)
Tellez, Francisco Félix, S160 (SAT-507)
Téllez, Luis, S3 (GS-005), S33 (OS-046), S52 (OS-081), S53 (OS-082), S54 (OS-084), S397 (FRI-515), S643 (SAT-134), S719 (TOP-488), S720 (TOP-504-YI), S723 (THU-418), S731 (THU-445-YI), S733 (THU-450), S735 (THU-453), S747 (THU-492), S752 (THU-501), S753 (THU-505-YI)
Tellez-Martínez, Liliana, S771 (THU-030)
Tellez, Roberto, S412 (FRI-564-YI)

Telöken, Theo Futuro, S88 (SAT-056), S776 (THU-044)
Temmers, Shaun, S900 (SAT-558)
Tempe, Deepak, S145 (SAT-453), S214 (WED-501-YI)
Temperley, Laura, S759 (TOP-018-YI), S773 (THU-038), S773 (THU-039)
Tena-Garitaonaindia, Mireia, S165 (FRI-387-YI), S483 (WED-388-YI)
Tena-Sempere, Manuel, S273 (THU-316)
Ten-Esteve, Amadeo, S254 (SAT-538), S599 (WED-151)
Teng, Gao-Jun, S259 (SAT-554), S549 (THU-184), S594 (WED-134), S609 (WED-182), S763 (THU-011), S924 (SAT-620)
Teng, Margaret, S52 (OS-081), S215 (WED-505), S228 (WED-543), S423 (TOP-374), S528 (THU-110)
Tengowski, Mark, S619 (WED-206)
Teng, Wei, S893 (THU-633)
Teng, Yicheng, S136 (FRI-123)
Teo, Ee Lin Kimberly, S770 (THU-028)
Teoh, Brian, S571 (WED-069)
Teo, Rachel Xin Hui, S495 (FRI-228-YI)
Tepasse, Phil Robin, S248 (SAT-515), S860 (WED-307)
Terai, Shuji, S977 (WED-639)
Teratani, Toshiaki, S371 (WED-349)
ter Borg, Martijn J., S353 (SAT-432)
ter Borg, Pieter C. J., S352 (SAT-429)
ter Borg, Susan, S688 (FRI-166-YI)
Tergast, Tammo Lambert, S185 (TOP-456-YI), S222 (WED-524), S222 (WED-526-YI), S732 (THU-448-YI), S737 (THU-461), S743 (THU-480-YI)
Terner-Rosenthal, Jolan, S10 (LBO-006), S319 (SAT-301), S330 (SAT-365), S354 (SAT-434)
Terrabuio, Débora, S296 (TOP-281), S306 (SAT-262)
Terrabuio, Debora Raquel, S768 (THU-022)
Terracciani, Francesca, S69 (LBP-004-YI), S82 (LBP-034-YI), S196 (WED-444), S304 (SAT-258), S307 (SAT-263), S331 (SAT-368-YI), S335 (SAT-378-YI), S350 (SAT-421), S476 (WED-368), S831 (THU-256-YI)
Terracciano, Luigi, S465 (WED-255), S533 (THU-126), S856 (WED-291)
Terraciani, Francesca, S595 (WED-138)
Terrault, Norah, S1 (GS-001), S46 (OS-070-YI), S76 (LBP-021), S116 (FRI-061), S190 (WED-421), S197 (WED-447), S411 (FRI-561-YI), S413 (FRI-570), S538 (THU-148-YI), S553 (THU-201), S762 (THU-007), S897 (TOP-565), S928 (SAT-628-YI)
Terreni, Natalia, S69 (LBP-004-YI)
Terrien, Cécile, S573 (WED-071)
Terrien, Léa, S554 (THU-202)
Terslev, Lene, S298 (SAT-245)
Teruya, Katsuji, S811 (FRI-037)
Tesfai, Kaleb, S134 (FRI-116), S207 (WED-479), S578 (WED-088)
Tessarin, Michele, S402 (FRI-530)
Testa, Giuliano, S166 (FRI-393)
Testoni, Barbara, S65 (OS-101-YI), S869 (TOP-632), S876 (THU-576), S893 (THU-634), S903 (SAT-562), S942 (FRI-592)
Testro, Adam, S145 (SAT-457), S400 (FRI-524), S400 (FRI-525), S736 (THU-458), S739 (THU-466)
Testro, Sophie, S739 (THU-466)
Teti, Elisabetta, S49 (OS-076-YI), S912 (SAT-587-YI), S919 (SAT-608-YI)
Tetsuro, Shimakami, S808 (FRI-028)
Teuber, Gerlinde, S64 (OS-100)
Teufel, Andreas, S288 (FRI-283), S556 (THU-212)
Tevethia, Harshvardhan, S108 (TOP-208-YI), S141 (TOP-424-YI), S156 (SAT-495)
Tews, Hauke Christian, S504 (FRI-251)
Thabut, Dominique, S3 (GS-005), S6 (GS-011-YI), S33 (OS-046), S53 (OS-082), S54 (OS-084), S55 (OS-085-YI), S152 (SAT-478), S195 (WED-442-YI), S207 (WED-477), S214 (WED-499), S222 (WED-525), S427 (THU-220), S428 (THU-226-YI), S446 (THU-393-YI), S497 (FRI-234), S505 (FRI-254), S506 (FRI-255-YI), S507 (FRI-362), S508 (FRI-364-YI), S719 (TOP-488), S723 (THU-418), S742 (THU-477), S752 (THU-501)
Thai, Khoa, S817 (WED-011)
Thaimai, Panarat, S619 (WED-211)
Thaker, Sarang, S388 (FRI-489), S745 (THU-483)
Thakkar, Rahul, S154 (SAT-490)
Thakker, Paresh, S119 (FRI-073), S578 (WED-087), S623 (WED-219), S667 (SAT-213), S694 (FRI-183)
Thakral, Nimish, S407 (FRI-546)
Thanapirom, Kessarin, S24 (OS-028), S144 (SAT-452), S160 (SAT-507), S619 (WED-211), S952 (FRI-622)
Thang, Sue Ping, S495 (FRI-228-YI)
Thapar, Manish, S10 (LBO-006)
Thapar, Shalini, S214 (WED-501-YI)
Thapa, Sharmila, S718 (WED-573-YI)
Tharehalli, Umesh, S670 (SAT-221-YI)
Tharmathas, Usha, S345 (SAT-410)
Thaver-Kleitmann, Jayendrie, S76 (LBP-019-YI)
Thaver, Lucica, S900 (SAT-558)
Theel, Willy, S688 (FRI-166-YI), S790 (SAT-035)
Theis, Maike, S213 (WED-496)
Thennati, Rajamannar, S699 (FRI-199)
Theodore, Dickens, S1 (GS-001), S956 (TOP-598), S957 (WED-577), S959 (WED-585), S960 (WED-587)
Theologidis, Vasileios, S853 (WED-282-YI)
Therkelsen, Marie Louise, S240 (FRI-338)
Theurl, Daniel, S848 (THU-302)
Thévenot, Thierry, S110 (FRI-042)
Thiefin, Gerard, S435 (THU-246)
Thiele, Maja, S26 (OS-032-YI), S63 (OS-098-YI), S110 (FRI-041-YI), S111 (FRI-044), S115 (FRI-057), S115 (FRI-059), S122 (FRI-079-YI), S125 (FRI-090-YI), S127 (FRI-095), S246 (TOP-552), S515 (TOP-098), S554 (THU-204), S569 (WED-059), S579 (WED-089), S582 (WED-100-YI), S583 (WED-101), S587 (WED-110-YI), S592 (WED-131), S593 (WED-134), S608 (WED-180), S616 (WED-199), S622 (WED-216), S684 (FRI-153), S706 (THU-545-YI)
Thiel, Ingo Van, S319 (SAT-301)
Thillai, Kiruthikah, S503 (FRI-250)
Thimme, Robert, S51 (OS-080-YI), S363 (TOP-326), S371 (WED-348), S455 (TOP-406), S834 (THU-260)
Thingholm, Louise, S262 (SAT-332)
Thing, Mira, S586 (WED-109), S602 (WED-159-YI)
Thio, Hans H. K., S353 (SAT-432)
Thisairajah, Shagani, S14 (OS-008), S295 (TOP-279), S320 (SAT-302), S325 (SAT-319), S325 (SAT-320), S354 (SAT-435), S355 (SAT-436), S401 (FRI-527)
Thiyagarajah, Keerthihan, S882 (THU-595)
Thng, Choon Hua, S495 (FRI-228-YI)
Tholander, Simon, S838 (THU-269)
Tholstrup Bech, Katrine, S115 (FRI-059), S122 (FRI-079-YI), S125 (FRI-090-YI)
Thomas, David, S816 (WED-008)
Thomas, Doneal, S834 (THU-262), S836 (THU-266)
Thomas, Quentin, S92 (SAT-068)
Thomas, Robert, S455 (TOP-406)
Thomas, Sherin, S292 (FRI-299), S478 (WED-371)
Thomopoulos, Konstantinos, S348 (SAT-416)
Thompson, Alexander, S65 (OS-101-YI), S249 (SAT-517), S249 (SAT-521), S433 (THU-240), S458 (WED-240), S799 (FRI-004), S800 (FRI-005), S820 (WED-021), S903 (SAT-562), S922 (SAT-613)
Thompson, Craig, S827 (WED-047)
Thompson, Peyton, S80 (LBP-028-YI)
Thompson, Richard, S164 (FRI-385-YI), S184 (FRI-453-YI), S860 (WED-305)
Thompson, Richard J., S55 (OS-086), S831 (THU-258-YI), S842 (THU-284), S850 (THU-308)
Thomsen, Karen Louise, S198 (WED-448-YI), S262 (SAT-332), S631 (SAT-094-YI), S660 (SAT-188-YI), S703 (THU-527-YI)
Thomsen, Majken, S631 (SAT-094-YI)
Thomsen, Thora, S22 (OS-024)
Thöne, Paul, S113 (FRI-053), S156 (SAT-494), S183 (FRI-444-YI), S186 (TOP-470-YI),

Author Index

S199 (WED-452), S200 (WED-453), S205 (WED-474), S213 (WED-498), S216 (WED-508), S440 (THU-370), S734 (THU-451), S738 (THU-464-YI), S748 (THU-493-YI), S749 (THU-494), S750 (THU-498), S753 (THU-505-YI), S914 (SAT-591)
Thongsuksai, Paramee, S439 (THU-366-YI)
Thorburn, Douglas, S10 (LBO-006), S325 (SAT-320), S331 (SAT-368-YI), S758 (TOP-016)
Thorens, Bernard, S699 (FRI-199)
Thorhauge, Katrine, S110 (FRI-041-YI), S114 (FRI-057), S115 (FRI-059), S122 (FRI-079-YI), S554 (THU-204), S706 (THU-545-YI)
Thorkildsen, Evy Marie, S451 (THU-409)
Thörn, Richard, S346 (SAT-411-YI)
Thorpe, Molly, S338 (SAT-385)
Thorsen, Brian, S319 (SAT-301), S342 (SAT-398), S346 (SAT-412)
Thuluvath, Paul J., S24 (OS-028), S144 (SAT-452)
Thursz, Mark R, S438 (THU-363), S471 (WED-271), S563 (WED-041), S798 (TOP-034)
Thursz, Mark R., S134 (FRI-117), S137 (FRI-125)
Thuy, Le Thi Thanh, S12 (OS-003)
Thys, Sofie, S638 (SAT-117-YI)
Tian, Alex, S85 (LBP-040)
Tian, Dean, S291 (FRI-290-YI)
Tian, Feng, S812 (FRI-039)
Tiano, Francesca, S670 (SAT-225)
Tian, Tian, S484 (WED-394)
Tian, Xiaopeng, S511 (FRI-370)
Tiberg, Fredrik, S39 (OS-056)
Tibiletti, Marta, S106 (THU-075)
Tichindeleanu, Andra, S175 (FRI-418)
Tiede, Anja, S3 (GS-005), S197 (WED-446), S222 (WED-524), S222 (WED-526-YI), S732 (THU-448-YI), S737 (THU-462)
Tielemans, Merel M., S351 (SAT-426-YI)
Tietz, Eric, S188 (WED-416)
Tiev, Maly, S330 (SAT-366)
Tihy, Matthieu, S53 (OS-083-YI)
Tikhonoff, Valerie, S699 (FRI-200)
Tikhonov, Igor, S594 (WED-135), S595 (WED-136)
Tikka, Pauli, S662 (SAT-197)
Tilg, Herbert, S257 (SAT-545-YI), S848 (THU-302), S862 (WED-314-YI)
Tilișcan, Cătălin, S951 (FRI-620), S974 (WED-633)
Tillman, Erik, S659 (SAT-187), S697 (FRI-191)
Tincopa, Monica, S116 (FRI-061), S190 (WED-421)
Ting, Peng-Sheng, S112 (FRI-051)
Tiniakos, Dina, S314 (SAT-283), S561 (TOP-081)
Tiniakos, Dina G., S53 (OS-083-YI)
Tinnirello, Rosaria, S638 (SAT-118)
Tioh, Jing Kai, S698 (FRI-197)
Tiribelli, Claudio, S465 (WED-256)
Tisone, Giuseppe, S59 (OS-091)
Tissier, Anne-Marie, S576 (WED-079)
Tiuca, Nicoleta, S819 (WED-015), S944 (FRI-601)
Tiwari, Navneet, S389 (FRI-492)
Tiwari, Vaibhav, S174 (FRI-415-YI), S181 (FRI-441-YI), S184 (FRI-452-YI), S274 (THU-318), S282 (FRI-262-YI)
Tizzani, Marco, S3 (GS-005)
Tjønnfjord, Sara, S2 (GS-002), S13 (OS-006-YI), S290 (FRI-289)
Tjønnfjord, Sara Kristina, S345 (SAT-410)
Tjwa, E. T. T. L., S333 (SAT-369)
Tjwa, E.T.T.L., S444 (THU-383)
Tkachuk, Bryce, S346 (SAT-413), S788 (SAT-028)
Toapanta, David, S53 (OS-082)
Tober-Lau, Pinkus, S77 (LBP-022-YI)
Tobita, Hiroshi, S686 (FRI-159)
To, Dennis, S80 (LBP-029)
Todorova, Dilyana, S83 (LBP-035)
Todorovska, Beti, S387 (FRI-483)
Todt, Daniel, S866 (FRI-641), S879 (THU-588), S881 (THU-593), S887 (THU-611), S887 (THU-613), S888 (THU-617), S890 (THU-623-YI)
Toffanin, Serena, S435 (THU-247)
Toffolon, Francesca, S69 (LBP-004-YI)
Tofoli, Marise, S56 (OS-086), S831 (THU-258-YI), S842 (THU-284)
Tognon, Francesca, S821 (WED-023)
Toh, Chanavee, S439 (THU-366-YI)
Toh, Han Chong, S495 (FRI-228-YI)
Toktogulova, Nurgul, S554 (THU-203)
Tokuchi, Yoshimasa, S506 (FRI-256)
Tokumaru, Tomoko, S662 (SAT-196)
Toledo, Claudio, S35 (OS-050-YI), S141 (TOP-437)
Toledo-Galván, Rodrigo, S296 (TOP-281), S306 (SAT-262)
Tolenaars, Dagmar, S646 (SAT-140-YI), S674 (SAT-233)
Tolmane, Ieva, S777 (THU-050)
Tomac, Hakan, S460 (WED-244-YI)
Tomah, Shaheen, S19 (OS-016), S84 (LBP-036), S679 (TOP-176), S700 (FRI-201)
Tomaiuolo, Gabriella, S90 (SAT-061-YI), S848 (THU-304)
Tomás-Alvarado, Alba, S273 (THU-316)
Tomasdottir, Anna, S802 (FRI-011)
Tomasello, Gianluca, S494 (FRI-225)
Tomasiewicz, Krzysztof, S957 (WED-577)
Tomczak, Miriam, S43 (OS-065)
Tomczuk, Jacek, S318 (SAT-298), S331 (SAT-368-YI), S355 (SAT-442)
Tomita, Koichi, S870 (TOP-646)
Tomizawa, Minoru, S550 (THU-188)
Tomlinson, Jeremy, S557 (THU-213), S795 (SAT-050)
Tommaso, Luca Di, S38 (OS-054), S456 (WED-234-YI), S856 (WED-291)
Tomoda, Hiroshi, S645 (SAT-138)
Tompkins, Lauren, S80 (LBP-028-YI)
Tong, Aaron Kian Ti, S495 (FRI-228-YI)
Tong, Gangling, S511 (FRI-370)
Tong, Jie, S201 (WED-458), S944 (FRI-597)
Tong, Maxwell, S547 (THU-179), S606 (WED-171)
Tong, Meng, S466 (WED-259)
Tong, Wu, S258 (SAT-548), S452 (THU-413)
Tong, Zhaowei, S259 (SAT-554), S593 (WED-134)
Toniutto, Pierluigi, S3 (GS-005), S150 (SAT-475), S302 (SAT-252), S424 (TOP-375-YI), S429 (THU-227-YI), S514 (FRI-381), S900 (SAT-559), S902 (SAT-560), S912 (SAT-587-YI), S936 (TOP-584), S938 (FRI-586)
Tonnini, Matteo, S43 (OS-066), S901 (SAT-559), S902 (SAT-560), S934 (TOP-582), S937 (FRI-585-YI), S938 (FRI-586)
Tonon, Marta, S26 (OS-032-YI), S30 (OS-041), S195 (WED-442-YI), S196 (WED-443), S209 (WED-485), S217 (WED-509-YI), S227 (WED-541-YI)
Too, Chow Wei, S495 (FRI-228-YI)
Topazian, Mark, S24 (OS-028), S144 (SAT-452), S160 (SAT-507)
Toporcerova, Dominika, S585 (WED-107)
Topor, Ioan, S175 (FRI-418)
Torabi, Julia, S60 (OS-094)
Torán, Pere, S26 (OS-032-YI), S63 (OS-098-YI), S515 (TOP-098), S583 (WED-101), S608 (WED-180), S789 (SAT-031-YI)
Torchio, Martina, S494 (FRI-225)
Torgabehei, Hadi Eidgah, S575 (WED-076)
Torimiro, Judith, S919 (SAT-608-YI), S924 (SAT-619)
Torkpour, Aria, S491 (TOP-408-YI)
Tornai, David, S35 (OS-050-YI), S145 (SAT-458-YI), S347 (SAT-414-YI), S347 (SAT-415)
Tornai, Istvan, S347 (SAT-414-YI), S347 (SAT-415)
Tornai, Tamas, S347 (SAT-414-YI), S347 (SAT-415)
Tornillo, Luigi, S533 (THU-126)
Toros, Marguerite, S647 (SAT-149)
Torp, Nikolaj, S76 (LBP-020), S110 (FRI-041-YI), S114 (FRI-057), S115 (FRI-059), S122 (FRI-079-YI), S217 (WED-509-YI), S246 (TOP-552), S253 (SAT-532), S262 (SAT-332), S554 (THU-204)
Torralba, Miguel, S366 (WED-332-YI), S968 (WED-610-YI)
Torra, Mercè, S21 (OS-021)
Torre, Aldo, S24 (OS-028), S35 (OS-050-YI), S41 (OS-061), S141 (TOP-437), S144 (SAT-452), S159 (SAT-505), S160 (SAT-507), S790 (SAT-036)
Torre, Giulia, S807 (FRI-025), S919 (SAT-608-YI), S924 (SAT-619)
Torrejón-Llorens, Ona, S810 (FRI-035)

Torrell-Pedreira, Elena, S810 (FRI-036)
Torrens, Maria, S469 (WED-267)
Torrente, Silvia, S16 (OS-010)
Torrents, Abiguei, S394 (FRI-507-YI)
Torre, Pietro, S176 (FRI-425), S479 (WED-378), S901 (SAT-559), S902 (SAT-560), S977 (WED-640)
Torre, Sara Della, S640 (SAT-122)
Torres, Dilan Martinez, S357 (TOP-327-YI), S663 (SAT-199-YI)
Torres, Ferran, S735 (THU-453)
Torres, Jorge, S174 (FRI-416-YI)
Torres-Mendoza, Graciela, S771 (THU-030)
Torres, Mireia, S8 (LBO-002), S128 (FRI-100)
Torres Núñez, Sandra, S629 (TOP-160)
Torres, Pedro Alfonso, S806 (FRI-024)
Torres, Sandra, S262 (SAT-330)
Torres, Sonia, S33 (OS-046), S53 (OS-082), S54 (OS-084), S397 (FRI-515), S719 (TOP-488), S730 (THU-443), S747 (THU-492), S752 (THU-501)
Torres, Zuleika Aponte, S615 (WED-197), S771 (THU-031)
Torrientes, Marta Sandoval, S910 (SAT-585)
Torrubiano, Paula Medio, S512 (FRI-371)
Tort, Jaume, S394 (FRI-507-YI)
Toscano, Arianna, S223 (WED-527), S435 (THU-245), S447 (THU-394)
Tosco, Tomás, S910 (SAT-581)
Tosetti, Giulia, S3 (GS-005), S52 (OS-081), S720 (TOP-504-YI), S900 (SAT-559)
Tosi, Federica, S494 (FRI-225)
Toso, Christian, S375 (TOP-519)
Tosti, Maria Elena, S440 (THU-369)
Totaro, Michele, S919 (SAT-608-YI)
Toth-Cserepes, Erika, S759 (TOP-017-YI)
Toth, Fanni, S364 (WED-323)
Tóthová, Ivana, S321 (SAT-305)
Tou, Andrea, S700 (FRI-202)
Touati, Nathan, S75 (LBP-018), S319 (SAT-300), S329 (SAT-364), S341 (SAT-396)
Touchefeu, Yann, S428 (THU-226-YI), S493 (FRI-221), S506 (FRI-255-YI), S508 (FRI-364-YI)
Tournigand, Christophe, S38 (OS-054)
Tovo, Cristiane, S296 (TOP-281), S306 (SAT-262), S724 (THU-420)
Tovoli, Francesco, S424 (TOP-375-YI), S428 (THU-227-YI), S514 (FRI-381)
Tow, Clara, S745 (THU-483)
Townsend, Liam, S811 (FRI-038)
Töx, Ulrich, S289 (FRI-284)
Tozzi, Caterina, S252 (SAT-530)
Trajkovska, Meri, S387 (FRI-483)
Trambas, Christina, S249 (SAT-517), S249 (SAT-521)
Tramontozzi, Caterina, S807 (FRI-025), S911 (SAT-587-YI)
Trampotová, Eliška, S861 (WED-308)
Tran, Benjamin, S60 (OS-094)
Tranchina, Martina, S476 (WED-368)
Tran, Hien, S158 (SAT-500)
Tran, Jennifer, S520 (THU-090-YI)
Tran, Thuy, S579 (WED-090)
Trapero, Maria, S409 (FRI-557)
Trauner, Michael, S11 (OS-002-YI), S14 (OS-007), S32 (OS-044), S37 (OS-053), S64 (OS-100), S82 (LBP-033), S84 (LBP-037), S113 (FRI-053), S156 (SAT-494), S179 (FRI-431-YI), S179 (FRI-432), S183 (FRI-444-YI), S183 (FRI-445), S186 (TOP-470-YI), S199 (WED-451-YI), S199 (WED-452), S205 (WED-474), S213 (WED-498), S216 (WED-508), S217 (WED-509-YI), S222 (WED-524), S237 (FRI-324), S242 (FRI-346), S266 (SAT-347-YI), S284 (FRI-266), S284 (FRI-267), S297 (TOP-293), S341 (SAT-397), S362 (TOP-325-YI), S364 (WED-323), S426 (THU-219-YI), S427 (THU-220), S427 (THU-221), S440 (THU-370), S715 (WED-560-YI), S717 (WED-569-YI), S732 (THU-448-YI), S733 (THU-449), S734 (THU-451), S738 (THU-464-YI), S748 (THU-493-YI), S749 (THU-494), S750 (THU-497-YI), S750 (THU-498), S753 (THU-505-YI), S914 (SAT-591)
Trautwein, Christoph, S651 (SAT-158-YI)
Travers, Jared, S243 (FRI-347)
Travers, Paul, S437 (THU-362)
Travis, Simon, S740 (THU-468)
Trebicka, Jonel, S6 (GS-011-YI), S8 (LBO-002), S33 (OS-046), S34 (OS-049), S35 (OS-050-YI), S39 (OS-056), S54 (OS-084), S115 (FRI-057), S141 (TOP-437), S145 (SAT-458-YI), S148 (SAT-467-YI), S149 (SAT-468), S152 (SAT-478), S159 (SAT-505), S163 (FRI-383), S164 (FRI-384), S166 (FRI-388-YI), S170 (FRI-401-YI), S178 (FRI-428-YI), S206 (WED-475), S210 (WED-485), S213 (WED-496), S215 (WED-506), S237 (FRI-329), S248 (SAT-515), S261 (SAT-329-YI), S262 (SAT-330), S383 (FRI-474), S409 (FRI-556), S493 (FRI-220), S497 (FRI-234), S631 (SAT-093-YI), S719 (TOP-488), S720 (TOP-504-YI), S723 (THU-418), S736 (THU-460-YI), S737 (THU-461), S744 (THU-481), S744 (THU-482-YI), S747 (THU-492), S752 (THU-501), S760 (TOP-032), S860 (WED-307), S882 (THU-595)
Treeprasertsuk, Sombat, S62 (OS-097), S67 (OS-105-YI), S424 (TOP-376), S516 (TOP-113), S619 (WED-211), S766 (THU-015), S952 (FRI-622)
Tree, Timothy, S174 (FRI-416-YI)
Trefois, Pierre, S648 (SAT-151-YI)
Trehanpati, Nirupma, S126 (FRI-092-YI), S288 (FRI-282), S292 (FRI-299), S425 (THU-217-YI), S456 (WED-232), S478 (WED-371), S867 (FRI-643)
Treitler, Alexis, S750 (THU-497-YI)
Trella, Serban, S175 (FRI-418)
Trembling, Paul, S759 (TOP-017-YI), S974 (WED-629-YI)
Trentzsch, Vanessa, S124 (FRI-089), S219 (WED-516)
Trepo, Eric, S109 (TOP-210)
Trépo, Eric, S17 (OS-011), S35 (OS-050-YI), S111 (FRI-043), S506 (FRI-255-YI)
Triantafyllou, Evangelos, S174 (FRI-416-YI), S657 (SAT-182)
Triantos, Christos, S79 (LBP-026), S300 (SAT-250), S314 (SAT-283), S338 (SAT-384), S348 (SAT-416)
Trias, Mireia, S16 (OS-010)
Trifan, Anca, S210 (WED-490), S211 (WED-493), S680 (FRI-139), S819 (WED-015), S944 (FRI-601)
Trifylli, Eleni-Myrto, S567 (WED-055-YI), S620 (WED-212)
Trigo, Jose Manuel, S78 (LBP-025)
Trigo, Matilde, S799 (TOP-049)
Trilianos, Panagiotis, S569 (WED-058-YI)
Trinka, Eugen, S539 (THU-151-YI), S792 (SAT-041)
Triolo, Michela, S401 (FRI-528), S414 (FRI-571)
Tripathi, Dhiraj, S33 (OS-046), S52 (OS-081), S54 (OS-084), S397 (FRI-515), S719 (TOP-488), S747 (THU-492), S752 (THU-501)
Tripathi, Dinesh Mani, S174 (FRI-415-YI), S182 (FRI-441-YI), S184 (FRI-452-YI), S274 (THU-318), S282 (FRI-262-YI), S361 (THU-354), S629 (TOP-161-YI)
Tripathi, Gaurav, S104 (THU-071-YI), S105 (THU-073-YI), S105 (THU-074), S120 (FRI-074), S129 (TOP-224-YI), S131 (FRI-105-YI), S138 (FRI-132), S139 (FRI-135-YI), S265 (SAT-341), S269 (SAT-354-YI), S269 (SAT-355), S276 (THU-324-YI), S280 (THU-337), S361 (THU-354), S373 (WED-353-YI), S418 (THU-517-YI)
Tripathi, Shashank, S725 (THU-426)
Tripodi, Giulia, S731 (THU-444-YI), S751 (THU-500)
Tripon, Simona, S45 (OS-067)
Trivedi, Palak, S10 (LBO-006), S254 (SAT-537), S311 (SAT-270), S325 (SAT-320), S343 (SAT-401-YI)
Trivedi, Palak J., S14 (OS-007), S315 (SAT-286), S316 (SAT-287), S349 (SAT-420), S838 (THU-270)
Troester, Melissa, S544 (THU-167)
Trofimovskaya, Natalia, S594 (WED-135), S595 (WED-136)
Trojan, Jörg, S485 (WED-396)
Troke, Phil, S82 (LBP-033)
Tronina, Olga, S980 (FRI-633)
Tron, Laure, S762 (THU-009)
Troppmair, Maria Rosina, S257 (SAT-545-YI), S848 (THU-302), S849 (THU-305-YI), S862 (WED-314-YI)
Troshina, Yulia, S938 (FRI-586)

Author Index

Trotovšek, Blaž, S59 (OS-092-YI)
Trottier, Jocelyn, S301 (SAT-251-YI)
Trovato, Francesca, S182 (FRI-443)
Troya, Jesús, S806 (FRI-024)
Trpchevska, Emilija Nikolovska, S387 (FRI-483)
Truchi, Régine, S681 (FRI-147)
Trujillo, Teresa, S910 (SAT-581)
Trummer, Susanna, S410 (FRI-559)
Trunecka, Pavel, S405 (FRI-540)
Truong, Jennifer, S281 (FRI-260)
Trylesinski, Aldo, S600 (WED-153)
Tsai, Hsin-Ju, S972 (WED-624)
Tsai, Hsin Lin, S395 (FRI-510)
Tsai, Ming-Chang, S969 (WED-613)
Tsai, Pei-Chien, S518 (TOP-128), S557 (THU-214)
Tsai, Wen-Wei, S82 (LBP-032), S671 (SAT-227)
Tsai, Ying-Nan, S943 (FRI-596)
Tsakovska, Mina, S643 (SAT-133)
Tsang, Erica, S425 (THU-216-YI)
Tsankof, Alexandra, S213 (WED-497)
Tsao, Philip, S166 (FRI-393)
Tsapatsaris, Ava, S327 (SAT-322)
Tse, Jeremy, S218 (WED-513), S749 (THU-496)
Tseng, Cheng-Hao, S943 (FRI-596)
Tseng, Steve, S939 (FRI-587), S956 (WED-576)
Tseng, Tai-Chung, S898 (TOP-566-YI), S898 (TOP-567), S906 (SAT-574), S917 (SAT-601-YI), S969 (WED-613)
Tseng, Yu-Hsuan, S373 (WED-354)
Tse, Yee-Kit, S66 (OS-103-YI)
Tsien, Cynthia, S452 (THU-414-YI)
Tsochatzis, Emmanouil, S84 (LBP-038), S758 (TOP-016)
Tsochatzis, Emmanuel, S26 (OS-032-YI), S62 (OS-097), S76 (LBP-020), S410 (FRI-558), S424 (TOP-376), S427 (THU-220), S515 (TOP-098), S516 (TOP-113), S517 (TOP-114), S525 (THU-103), S558 (TOP-063-YI), S568 (WED-057-YI), S582 (WED-100-YI), S583 (WED-101), S589 (WED-118), S607 (WED-174-YI), S612 (WED-187-YI), S618 (WED-204), S621 (WED-215), S757 (THU-516), S759 (TOP-017-YI), S840 (THU-275), S865 (FRI-638)
Tsogbayar, Tsolmon, S826 (WED-039)
Tsou, Hio Lam Phoebe, S672 (SAT-228)
Tsounis, Efthymios, S348 (SAT-416)
Tsubota, Akihito, S875 (THU-573), S894 (THU-635)
Tsuchiya, Atsunori, S977 (WED-639)
Tsuchiya, Kaoru, S439 (THU-368), S506 (FRI-256)
Tsuge, Masataka, S960 (WED-587)
Tsui, Stephen, S275 (THU-321)
Tsui, Vivien Wai-Man, S422 (TOP-359-YI)
Tsuji, Keiji, S295 (TOP-280), S336 (SAT-379)
Tsukamoto, Hidekazu, S139 (FRI-134)
Tsuneyama, Koichi, S668 (SAT-215), S669 (SAT-218), S870 (TOP-646)
Tsuruya, Kota, S708 (THU-553)
Tsutsumi, Takeya, S187 (TOP-472)
Tsutsumi, Tsubasa, S698 (FRI-197)
Tual, Christelle, S45 (OS-067), S815 (WED-005)
Tüchler, Sandra, S242 (FRI-346)
Tucker, Bethany, S56 (OS-086), S831 (THU-258-YI), S842 (THU-284)
Tudor, Ana Maria, S807 (FRI-025)
Tudor, Andrada, S621 (WED-214)
Tudrujek-Zdunek, Magdalena, S980 (FRI-633)
Tuekprakhon, Aekkachai, S369 (WED-340-YI), S372 (WED-351)
Tuffy, Declan, S39 (OS-057)
Tugores, Antonio, S837 (THU-267), S855 (WED-288), S855 (WED-289), S856 (WED-290)
Tu, Huilan, S158 (SAT-501)
Tukebana, Bienvenu, S80 (LBP-028-YI)
Tukiainen, Eija, S376 (FRI-447)
Tukiainen, Taru, S114 (FRI-055)
Tulading, Aliya, S243 (FRI-348)
Tulahong, Alimu, S421 (THU-532)
Tulahong, Qiao, S421 (THU-532)
Tunc, Esra, S519 (THU-089)
Tunç, Esra, S965 (WED-603)
Tung, Hung-Ning, S449 (THU-399)
Tura, Andrea, S21 (OS-020)
Turan, Ilker, S389 (FRI-491), S542 (THU-163)
Turan, İlker, S899 (SAT-556-YI)
Turato, Cristian, S479 (WED-379)
Turcanu, Adela, S49 (OS-075), S962 (WED-594)
Turco, Elena Rosselli Del, S43 (OS-066), S900 (SAT-559), S934 (TOP-582)
Turco, Laura, S52 (OS-081), S497 (FRI-234), S720 (TOP-504-YI), S900 (SAT-559), S901 (SAT-560), S936 (TOP-584), S938 (FRI-586)
Turcu-Stiolica, Adina, S819 (WED-015), S944 (FRI-601)
Turin, Tanvir C, S820 (WED-022)
Turkbey, Ismail, S413 (FRI-569)
Turner, Alice, S5 (GS-008), S834 (THU-262), S836 (THU-266)
Turner, Jerrold R., S129 (TOP-223)
Turnes, Juan, S256 (SAT-542), S288 (FRI-283), S542 (THU-164), S567 (WED-054), S799 (TOP-049)
Turon, Fanny, S6 (GS-011-YI), S53 (OS-082), S720 (TOP-504-YI), S730 (THU-443), S733 (THU-450), S739 (THU-467), S747 (THU-492), S752 (THU-501)
Turu, Elisabet, S826 (WED-038)
Tushuizen, Maarten, S15 (OS-009-YI), S621 (WED-214), S765 (THU-013), S789 (SAT-031-YI)
Tu, Thomas, S897 (TOP-565)
Tutusaus, Anna, S481 (WED-382-YI), S639 (SAT-120)
Tu, Wei, S624 (WED-226)
Tu, Xiao, S682 (FRI-148)
Tuxun, Tuerhongjiang, S243 (FRI-348)
Tuyet, Trinh Nguyen Tran, S587 (WED-115)
Tyc, Olaf, S261 (SAT-329-YI), S262 (SAT-330)
Tyson, Luke D., S134 (FRI-117), S137 (FRI-125)
Tzeuton, Christian, S923 (SAT-618)
Tzivinikos, Christos, S56 (OS-086), S831 (THU-258-YI), S842 (THU-284), S850 (THU-308)

Uberoi, Ramon, S740 (THU-468)
Ucar, Barbaros, S503 (FRI-250)
Ucciferri, Claudio, S610 (WED-183)
Üçdal, Mete, S348 (SAT-417)
Uchida-Kobayashi, Sawako, S580 (WED-091)
Uchida, Takuro, S662 (SAT-196)
Uchida, Yoshihito, S977 (WED-639)
Uchiyama, Akira, S225 (WED-533), S246 (FRI-356)
Udaeta, Paola Saiz, S855 (WED-288), S856 (WED-290)
Ud-Din, Muhammad Moiz, S564 (WED-044), S565 (WED-045)
Ueda, Ryuta, S894 (THU-635)
Uekermann, Kim, S185 (TOP-456-YI)
Ueland, Per, S2 (GS-002), S13 (OS-006-YI), S290 (FRI-289)
Uemura, Haruka, S811 (FRI-037)
Ueno, Akihisa, S371 (WED-349)
Ueno, Makoto, S861 (WED-313)
Ueno, Masayuki, S156 (SAT-496), S215 (WED-505), S221 (WED-523)
Ueno, Yoshiyuki, S510 (FRI-367), S691 (FRI-175), S977 (WED-639)
Uğuz, Alper, S397 (FRI-514)
Uhlemeyer, Celina, S672 (SAT-230)
Uhlenbusch, Natalie, S332 (SAT-369)
Uhlig, Holm, S43 (OS-065)
Uhr, Mario, S570 (WED-061)
Ulahannan, Susanna V., S429 (THU-227-YI)
Ullman, Sofia, S515 (TOP-112-YI)
Ulloa, Cristina Garcia, S707 (THU-548)
Ulziibadrakh, Tuvshinjargal, S439 (THU-367), S915 (SAT-595), S916 (SAT-596)
Umansky, Tyler, S877 (THU-580)
Umar, Narmeen, S14 (OS-008), S295 (TOP-279), S325 (SAT-319), S354 (SAT-435)
Umberto, Dalessandro, S764 (THU-012), S798 (TOP-034)
Ummel, Basil, S342 (SAT-399)
Ünal, Fatma Tuğçe Şah, S588 (WED-116)
Unchwaniwala, Nuruddin, S958 (WED-579)
Unger, Lola, S416 (FRI-578-YI)
Ungureanu, Bogdan, S819 (WED-015), S944 (FRI-601)
Untereiner, Valérie, S435 (THU-246)
Upton, Janine, S900 (SAT-558)
Urbanek, Petr, S427 (THU-220)

Urbani, Luca, S242 (FRI-345-YI), S472 (WED-274)
Urbano, José, S752 (THU-501)
Urban, Stephan, S51 (OS-080-YI), S879 (THU-589-YI)
Ureña, Alvaro, S25 (OS-029)
Uriarte, Iker, S17 (OS-013), S474 (WED-364)
Uribe, Lucia Pinzon, S547 (THU-181)
Uribe, Nelson Suarez, S88 (SAT-056), S776 (THU-044)
Urreta, Iratxe, S830 (THU-253)
Ursic-Bedoya, José, S414 (FRI-572), S414 (FRI-573)
Urso, Mario, S462 (WED-249)
Urzúa, Alvaro, S296 (TOP-281), S306 (SAT-262)
Uschner, Frank, S409 (FRI-556), S493 (FRI-220)
Uschner, Frank Erhard, S33 (OS-046), S35 (OS-050-YI), S163 (FRI-383), S178 (FRI-428-YI), S206 (WED-475), S209 (WED-485), S215 (WED-506), S237 (FRI-329), S248 (SAT-515), S261 (SAT-329-YI), S262 (SAT-330), S383 (FRI-474), S744 (THU-481), S744 (THU-482-YI)
Uson, Eva, S141 (TOP-437), S149 (SAT-468), S150 (SAT-475), S152 (SAT-478), S760 (TOP-032)
Usuba, Teruyuki, S894 (THU-635)
Utepergenovna, Kulkayeva Gulnara, S822 (WED-027)
Utpatel, Kirsten, S445 (THU-385)
Utsumi, Teruo, S134 (FRI-115)
Uutela, Aki, S376 (FRI-447), S450 (THU-403)
Uveges, Samuel, S718 (WED-574)
Uysal, Alper, S389 (FRI-491)

Vaccaro, Emilia, S977 (WED-640)
Vahdani, Negar, S11 (OS-001-YI)
Vaia, Paolo, S444 (THU-384), S532 (THU-123), S549 (THU-186-YI), S639 (SAT-121-YI), S854 (WED-286)
Vaira, Lorenza, S620 (WED-213)
Vaisitti, Tiziana, S835 (THU-263)
Vajavaara, Heli, S450 (THU-403)
Vakili, Sanam Tabataba, S914 (SAT-592-YI), S921 (SAT-610)
Valainathan, Shantha, S251 (SAT-528), S571 (WED-067)
Valaydon, Zina, S249 (SAT-521), S433 (THU-240), S820 (WED-021), S922 (SAT-613)
Val, Beatriz, S165 (FRI-387-YI), S483 (WED-388-YI), S484 (WED-393)
Valbuena-Goiricelaya, Emiliana, S17 (OS-013), S474 (WED-364)
Valbuena, Monica Barreales, S308 (SAT-264)
Valbuena, Mónica Barreales, S124 (FRI-088), S410 (FRI-558)
Valencia, Jorge, S806 (FRI-024)
Valente, Cristina, S940 (FRI-589)
Valente, Leticia, S484 (WED-394)
Valenti, David, S757 (THU-516)
Valenti, Luca, S166 (FRI-393), S241 (FRI-340), S476 (WED-368), S575 (WED-076), S601 (WED-156), S636 (SAT-109), S831 (THU-256-YI)
Valentino, Pamela L., S832 (THU-258-YI), S842 (THU-284), S850 (THU-308)
Valenzi, Elena, S425 (THU-216-YI), S487 (WED-400-YI), S514 (FRI-381)
Valera, Ana Lucena, S806 (FRI-023)
Valera, Maria, S226 (WED-538)
Valery, Patricia C., S788 (SAT-029), S789 (SAT-030)
Vali, Yasaman, S621 (WED-214)
Valla, Dominique, S571 (WED-067), S608 (WED-179)
Vallejo, Aldara, S910 (SAT-585)
Valle, Juan, S445 (THU-385)
Valliani, Talal, S452 (THU-414-YI)
Valsan, Arun, S5 (GS-009), S24 (OS-028), S36 (OS-051-YI), S52 (OS-081), S62 (OS-097), S247 (SAT-514), S424 (TOP-376), S445 (THU-385), S516 (TOP-113), S705 (THU-541-YI), S705 (THU-542), S706 (THU-544), S720 (TOP-504-YI), S952 (FRI-622)
Valva, Pamela, S234 (FRI-316)
Valverde, Victor, S409 (FRI-557)
Valyasevi, Peerada, S973 (WED-626-YI)
Vanatta, Jason, S411 (FRI-560)
Vanbésien, Camille, S163 (FRI-383), S164 (FRI-384)
Vanblarcom, Hannah, S276 (THU-329)
van Bommel, Florian, S900 (SAT-559)
van Bömmel, Florian, S43 (OS-066), S46 (OS-070-YI), S150 (SAT-474), S647 (SAT-148), S879 (THU-589-YI), S901 (SAT-560), S930 (SAT-636), S934 (TOP-582), S936 (TOP-584), S937 (FRI-585-YI)
van Bremen, Kathrin, S904 (SAT-564)
Van Cott, Andrew, S87 (LBP-043)
van Crevel, Jutta, S57 (OS-087-YI), S348 (SAT-418-YI)
van Dam, Lisette J. H., S353 (SAT-432)
Vandamme, Sarah, S907 (SAT-575)
van Dasselaar, Rychon, S237 (FRI-330)
Vandebosch, Sigrid, S353 (SAT-433)
van de Graaf, Stan F.J., S646 (SAT-140-YI), S674 (SAT-233)
Vandekerckhove, Kristof, S526 (THU-106)
van de Loo, Dominik, S744 (THU-481)
van den Beld, Annewieke, S9 (LBO-005-YI)
van den Berg, Aad, S15 (OS-009-YI)
van den Berg, Maarten, S9 (LBO-005-YI)
van den Brand, Floris, S15 (OS-009-YI)
van den Broek, Lenie, S167 (FRI-395-YI)
van den Hazel, Sven J., S353 (SAT-433)
van den Hoek, Anita M., S645 (SAT-138)
Van den Wijngaert, Sigi, S907 (SAT-575)
van der Beek, A., S353 (SAT-433)
Van der Eijk, Annemiek, S909 (SAT-580)
van der Graaff, Denise, S638 (SAT-117-YI)
van der Heide, Frans, S10 (LBO-006)
van der Heijden, Fenna, S383 (FRI-468)
van der Helm, Danny, S415 (FRI-574)
Vanderheyden, Evy, S17 (OS-012)
Vanderhoff, Aaron, S914 (SAT-592-YI), S921 (SAT-610)
van der Laan, Luc, S382 (FRI-467-YI)
van der Laar, Thijs, S817 (WED-011)
Vanderlinden, Axelle, S65 (OS-101-YI), S903 (SAT-562), S920 (SAT-609), S929 (SAT-629)
van der Meer, Adriaan J., S10 (LBO-006), S15 (OS-009-YI), S79 (LBP-026), S193 (WED-432), S298 (TOP-294-YI), S325 (SAT-320), S331 (SAT-368-YI), S333 (SAT-369), S338 (SAT-384), S349 (SAT-420), S351 (SAT-426-YI), S352 (SAT-429), S353 (SAT-432), S353 (SAT-433), S443 (THU-382-YI), S846 (THU-290)
van der Palen, Job, S200 (WED-457), S432 (THU-236), S451 (THU-404)
Vanderschueren, Emma, S53 (OS-082), S54 (OS-084), S397 (FRI-515)
van der Waaij, Lauren A., S353 (SAT-432)
van der Wiel, Sanne K, S15 (OS-009-YI)
van der Woerd, Wendy L., S56 (OS-086), S832 (THU-258-YI), S842 (THU-284)
Van De Vijver, Elias, S464 (WED-254)
Vandevoorde, Kristof, S381 (FRI-465)
van de Vrie, Maria A., S298 (TOP-294-YI)
van Dijk, Anne-Marieke, S641 (SAT-126)
van Dijk, Remco, S351 (SAT-426-YI), S352 (SAT-429), S353 (SAT-432), S353 (SAT-433)
Vandois, Marie, S742 (THU-477)
van Dongen, Guus, S237 (FRI-330)
van Doorn, Diederick, S237 (FRI-330), S963 (WED-595)
van Dort, Karel, S963 (WED-595)
Vandriel, Shannon, S55 (OS-086), S344 (SAT-403)
Van Driessche, Annelien, S315 (SAT-285)
van Duinen, Vincent, S167 (FRI-395-YI)
van Eekhout, Kirsi, S577 (WED-084), S621 (WED-214), S765 (THU-013)
van Eijck, Brechje, S15 (OS-009-YI)
Vangampelaere, Maxine, S526 (THU-106)
van Gerven, Nicole F. M., S353 (SAT-433)
van Gerven, Nicole F.M., S15 (OS-009-YI)
van Golen, Rowan, S415 (FRI-574)
Vanhaecke, Tamara, S637 (SAT-116)
van Haele, Matthias, S331 (SAT-368-YI)
van Herwaarden, Antonius, S444 (THU-383)
van Herwaarden, Manon, S15 (OS-009-YI)
van Hest, Reinier, S168 (FRI-397-YI)
Vanhille-Campos, Ines, S172 (FRI-412)
van Hoek, Bart, S15 (OS-009-YI)

Author Index

van Hooff, Maria C., S298 (TOP-294-YI), S349 (SAT-420), S351 (SAT-426-YI), S352 (SAT-429), S353 (SAT-432), S353 (SAT-433)
Van Hul, Noémi K. M., S861 (WED-308)
van Ijzendoorn, Manon, S15 (OS-009-YI)
van Kleef, Laurens A., S63 (OS-098-YI), S587 (WED-110-YI), S587 (WED-111), S608 (WED-180), S621 (WED-215), S622 (WED-216), S694 (FRI-185), S789 (SAT-031-YI), S790 (SAT-035)
van Leengoed, Jasper, S200 (WED-457), S432 (THU-236), S451 (THU-404)
van Lierop, Lisa, S349 (SAT-419)
van Marcke, Cédric, S90 (SAT-059)
van Meer, Suzanne, S351 (SAT-426-YI), S352 (SAT-429), S353 (SAT-432), S353 (SAT-433)
Vannas, Marko, S376 (FRI-447)
Vanner, Robert, S425 (THU-216-YI)
Vanni, Ester, S69 (LBP-004-YI), S304 (SAT-258), S307 (SAT-263), S335 (SAT-378-YI)
Vano, Marco, S110 (FRI-042)
Vanpoucke, Hilde, S907 (SAT-575)
van Putten, Paul G., S353 (SAT-433)
Van Roey, Guy, S929 (SAT-629)
van Rooij, Janne, S351 (SAT-426-YI)
van Rossum, Elisabeth, S790 (SAT-035)
van Ruijven, Britt, S729 (THU-436)
Vanrusselt, Hannah, S874 (THU-570), S893 (THU-634)
van Son, Koen, S621 (WED-214), S641 (SAT-126)
Van Steenkiste, Christophe, S929 (SAT-629)
van Stiphout, Stephan H. C., S353 (SAT-433)
van Thiele, Ghislaine, S765 (THU-013)
Van Troys, Marleen, S464 (WED-254)
van Velsen, Lisa M., S928 (SAT-628-YI)
van Vilsteren, Frederike, S430 (THU-232)
Van Vlierberghe, Hans, S159 (SAT-505), S315 (SAT-285), S464 (WED-253), S464 (WED-254)
van Vlies, Naomi, S647 (SAT-149)
VanWagner, Lisa, S546 (THU-173-YI)
van Widenfelt, Erik, S792 (SAT-042)
van Wijk, Monique, S451 (THU-404)
van Wijk, Stan, S443 (THU-382-YI)
Vanwolleghem, Thomas, S15 (OS-009-YI), S46 (OS-070-YI), S55 (OS-085-YI), S65 (OS-101-YI), S99 (TOP-193-YI), S581 (WED-094), S729 (THU-441), S903 (SAT-562), S907 (SAT-575), S920 (SAT-609), S929 (SAT-629)
van Zanten, Daniel, S743 (THU-479)
van Zonneveld, Anton Jan, S148 (SAT-467-YI), S729 (THU-436)
Vaquer-Grimalt, Pere, S223 (WED-528)
Vaquero, Javier, S132 (FRI-109), S182 (FRI-442), S267 (SAT-350), S642 (SAT-131-YI), S678 (SAT-244)
Varela-Rey, Marta, S233 (FRI-313), S241 (FRI-339)
Vargas-Accarino, Elena, S469 (WED-267), S798 (TOP-048), S811 (FRI-038), S815 (WED-006), S926 (SAT-623), S928 (SAT-628-YI)
Vargas, Ángel Daniel Santana, S236 (FRI-322)
Vargas, Hugo, S754 (THU-509)
Vargas, Jennifer Jara, S149 (SAT-468), S152 (SAT-478), S214 (WED-499), S760 (TOP-032)
Vargas, Maria, S106 (THU-076)
Vargas-Navarro, Francisco, S790 (SAT-036), S793 (SAT-044)
Varga-Weisz, Patrick, S42 (OS-064-YI)
Vargeese, Chandra, S702 (FRI-206)
Vargiu, Emanuela, S850 (THU-307)
Varol, Chen, S642 (SAT-127)
Varon, Adriana, S296 (TOP-281), S306 (SAT-262)
Varo, Nerea, S608 (WED-175)
Varrone, Andrea, S690 (FRI-172)
Varshney, Mohit, S108 (TOP-208-YI), S126 (FRI-092-YI)
Vasconcellos, Gabriela Nardy, S776 (THU-044)
Vashitshtha, Chitranshu, S156 (SAT-495), S214 (WED-501-YI), S719 (TOP-487-YI)
Vasilieva, Larisa, S142 (SAT-449)
Vaska, Marcus, S505 (FRI-253)
Vasudevan, Ashwini, S361 (THU-355-YI), S629 (TOP-161-YI)
Vata, Andrei, S807 (FRI-025)
Vatsalya, Vatsalya, S532 (THU-125)
Vaubourdolle, Michel, S608 (WED-179)
Vavassori, Sara, S83 (LBP-034-YI), S494 (FRI-225)
Vaz Alves, Joao, S937 (FRI-585-YI)
Vážanová, Diana, S211 (WED-492)
Vaz, Desiree, S850 (THU-308)
Vaz, Juan, S224 (WED-529), S791 (SAT-037), S791 (SAT-038), S796 (SAT-052)
Vaz, Karl, S145 (SAT-457), S739 (THU-466)
Vázquez-Blanquiño, Alberto, S910 (SAT-581)
Vázquez-Esqueda, Ángel, S132 (FRI-108-YI)
Vázquez, Juan Turnes, S556 (THU-212)
Vázquez, Maria Inmaculada Fernández, S124 (FRI-088), S308 (SAT-264), S815 (WED-006), S948 (FRI-611)
Vázquez-Ogando, Elena, S182 (FRI-442), S267 (SAT-350)
Vaz-Romero, Ignacio, S337 (SAT-382)
VazRomero, Ignacio, S294 (TOP-278)
Veatch, Olivea, S166 (FRI-393)
Vecchi, Andrea, S874 (THU-571)
Vedeld, Hege Marie, S451 (THU-409)
Veermachineni, Suma, S702 (FRI-206)
Vega, Angel, S819 (WED-019)
Vega, Laura Alcoba, S16 (OS-010)
Veidal, Sanne Skovgård, S646 (SAT-142)
Velasco, Jose Antonio Velarde-Ruiz, S24 (OS-028), S144 (SAT-452), S160 (SAT-507)
Velasco, Ricardo, S663 (SAT-199-YI)
Velasco Rubio, Francisco Javier, S940 (FRI-589)
Velazquez, René Malé, S24 (OS-028), S35 (OS-050-YI), S144 (SAT-452), S160 (SAT-507)
Veldhuijzen, Govert, S729 (THU-436)
Veldt, Bart J., S351 (SAT-426-YI), S352 (SAT-429), S353 (SAT-432), S353 (SAT-433)
Veličković, Nataša, S268 (SAT-351)
Velmurugan, Ganesan, S780 (SAT-005)
Veloz, Maria Guerra, S65 (OS-102), S404 (FRI-538-YI), S503 (FRI-250), S970 (WED-619)
Vendelbo, Mikkel Holm, S853 (WED-282-YI)
Vendrell, Iolanda, S43 (OS-065)
Venerito, Marino, S504 (FRI-251)
Venhoff, Nils, S550 (THU-187)
Venkatachalapathy, Suresh, S10 (LBO-006)
Venkatachalapathy, Suresh Vasan, S160 (SAT-507)
Ven, Peter, S347 (SAT-415)
Ventre, Jules, S512 (FRI-372)
Venturin, Camilla, S466 (WED-258), S485 (WED-395-YI)
Venturini, Giulia, S731 (THU-444-YI)
Venu, Arathi, S36 (OS-051-YI), S62 (OS-097), S247 (SAT-514), S516 (TOP-113), S720 (TOP-504-YI)
Vera, Mar, S806 (FRI-024)
Vera, Natalia, S302 (SAT-253)
Verbeek, Jef, S79 (LBP-026), S99 (TOP-193-YI), S331 (SAT-368-YI), S836 (THU-265-YI), S849 (THU-306-YI), S920 (SAT-609)
Verda, Damiano, S332 (SAT-369)
Verdeguer, Francisco, S85 (LBP-039), S243 (FRI-349)
Verdonk, Robert C., S9 (LBO-005-YI), S15 (OS-009-YI), S351 (SAT-426-YI), S352 (SAT-429), S353 (SAT-432), S353 (SAT-433)
Verelst, Frederik, S801 (FRI-007)
Verendağ, Damla, S396 (FRI-513), S397 (FRI-514)
Vergara-Estrada, Jorge, S663 (SAT-199-YI)
Vergara, Loreto López, S34 (OS-049)
Vergara, Mercedes, S16 (OS-010), S91 (SAT-062), S562 (TOP-097-YI), S612 (WED-188)
Vergel, Diana Carolina Alfonso, S296 (TOP-281), S306 (SAT-262)
Vergès, Bruno, S564 (WED-043)
Vergis, Nikhil, S26 (OS-031), S137 (FRI-125)
Verheij, Joanne, S9 (LBO-005-YI), S237 (FRI-330), S331 (SAT-368-YI), S632 (SAT-099-YI), S646 (SAT-140-YI)
Verhelst, Xavier, S10 (LBO-006), S59 (OS-092-YI), S79 (LBP-026), S99 (TOP-193-YI), S150 (SAT-475), S159 (SAT-505), S281 (TOP-295-YI), S315 (SAT-285), S315 (SAT-286), S337 (SAT-382), S338 (SAT-384),

S349 (SAT-420), S464 (WED-253), S907 (SAT-575), S920 (SAT-609), S929 (SAT-629)
Verheyen, Jordi, S874 (THU-570), S893 (THU-634)
Verissimo, Victoria, S724 (THU-420)
Verkade, Henkjan J., S56 (OS-086), S832 (THU-258-YI), S842 (THU-284), S850 (THU-308), S857 (WED-299), S863 (WED-318)
Verlinden, Wim, S907 (SAT-575), S920 (SAT-609), S929 (SAT-629)
Verma, Anurag, S166 (FRI-393)
Verma, Gayantika, S478 (WED-371)
Verma, Nipun, S5 (GS-009), S151 (SAT-476), S171 (FRI-409-YI), S180 (FRI-433), S221 (WED-522), S227 (WED-541-YI), S366 (WED-334), S560 (TOP-066), S561 (TOP-082), S579 (WED-089), S952 (FRI-622)
Verma, Shiv, S247 (SAT-514)
Verma, Shrinkhala, S36 (OS-051-YI)
Vermehren, Johannes, S811 (FRI-038)
Vermorgen, Sanne, S9 (LBO-005-YI)
Verna, Elizabeth, S116 (FRI-061), S197 (WED-447)
Verne, Julia, S758 (TOP-016)
Verrier, Eloi, S875 (THU-572)
Verrier, Eloi R., S885 (THU-606)
Verset, Laurine, S55 (OS-085-YI)
Verslype, Chris, S17 (OS-012)
Verstraeten, Maïté, S59 (OS-092-YI)
Verucchi, Gabriella, S911 (SAT-587-YI)
Verweij, Niek, S166 (FRI-393)
Verwer, Bart, S9 (LBO-005-YI)
Verzijl, Cristy, S630 (SAT-090)
Vespasiani-Gentilucci, Umberto, S69 (LBP-004-YI), S83 (LBP-034-YI), S196 (WED-444), S304 (SAT-258), S307 (SAT-263), S331 (SAT-368-YI), S335 (SAT-378-YI), S350 (SAT-421), S477 (WED-370), S595 (WED-138), S831 (THU-256-YI)
Vessby, Johan, S62 (OS-097), S516 (TOP-113), S579 (WED-090), S584 (WED-104), S606 (WED-173)
Vestergaard, Linnea Juhl, S116 (FRI-060)
Vestergaard, Thea, S680 (FRI-139)
Vesterhus, Mette, S2 (GS-002), S13 (OS-006-YI), S290 (FRI-289), S299 (SAT-249), S345 (SAT-410)
Vethakkan, Shireene Ratna, S593 (WED-132)
Vetrone, Filippo, S248 (SAT-516)
Vetter, Marcel, S14 (OS-007), S310 (SAT-269)
Vetter, Volker, S801 (FRI-007)
Vettori, Giovanni, S304 (SAT-258), S307 (SAT-263), S335 (SAT-378-YI)
Veuthey, Lucas, S72 (LBP-011)
Vianello, Barbara, S950 (FRI-619)
Vianello, Clara, S462 (WED-248)
Viayna, Elisabet, S204 (WED-467)
Vibert, Eric, S374 (TOP-503), S375 (TOP-519), S399 (FRI-523)
Vicardi, Marco, S97 (SAT-084-YI), S405 (FRI-541), S424 (TOP-375-YI)
Vicente, Mariana, S802 (FRI-010-YI)
Vicente-Mora, Javier, S129 (FRI-101)
Viciana, Isabel, S910 (SAT-581), S910 (SAT-585)
Vicién, Gemma Garcia, S18 (OS-014-YI)
Victoria, Mignot, S762 (THU-009)
Victor Iii, David W., S10 (LBO-006), S758 (TOP-002), S781 (SAT-007)
Vidal-Acuña, María Reyes, S899 (SAT-557), S910 (SAT-585)
Vidal, Barbarba, S53 (OS-082)
Vidal, Emma, S53 (OS-082)
Vidal, Marina, S16 (OS-010)
Vidal-Puig, Antonio, S29 (OS-038)
Vidal, Sandra Cortizo, S799 (TOP-049), S910 (SAT-585)
Vieira, Ana Margarida, S43 (OS-066), S937 (FRI-585-YI)
Viera, Maria, S855 (WED-288), S856 (WED-290)
Vierling, John M., S302 (SAT-254), S324 (SAT-316)
Vietti-Violi, Naik, S490 (TOP-407-YI)
Viganò, Davide, S975 (WED-635)
Viganò, Mauro, S3 (GS-005), S52 (OS-081), S55 (OS-085-YI), S69 (LBP-004-YI), S82 (LBP-034-YI), S304 (SAT-258), S307 (SAT-263), S331 (SAT-368-YI), S335 (SAT-378-YI), S350 (SAT-421), S696 (FRI-188-YI), S817 (WED-010), S831 (THU-256-YI), S911 (SAT-587-YI), S937 (FRI-585-YI), S938 (FRI-586), S972 (WED-623)
Viganò, Raffaella, S69 (LBP-004-YI), S82 (LBP-034-YI), S300 (SAT-250), S304 (SAT-258), S307 (SAT-263), S315 (SAT-286), S335 (SAT-378-YI), S379 (FRI-461-YI)
Viggiano, Taylor, S416 (FRI-576)
Vigneron, Paul, S493 (FRI-221), S508 (FRI-364-YI)
Vignon, Clémence, S723 (THU-419)
Vig, Pamela, S10 (LBO-006), S354 (SAT-434)
Vijayaraghavan, Rajan, S108 (TOP-208-YI), S141 (TOP-424-YI), S156 (SAT-495), S214 (WED-501-YI), S719 (TOP-487-YI)
Vijjhalwar, Rohan, S622 (WED-217)
Vijjhalwar, Rohit, S622 (WED-217)
Vij, Mukul, S38 (OS-054)
Vila-Escoda, Anna, S459 (WED-242-YI), S468 (WED-263), S485 (WED-396)
Vilà, Laia, S231 (FRI-304), S241 (FRI-341), S271 (THU-303), S279 (THU-335)
Vila, Marta, S366 (WED-332-YI)
Vilà, Paula Cantallops, S18 (OS-014-YI)
Vilarinho, Silvia, S166 (FRI-393)
Viligiardi, Giada Alla, S457 (WED-235)
Villadsen, Gerda Elisabeth, S14 (OS-007), S801 (FRI-008)
Villa, Federica, S975 (WED-635)
Villagrasa, Ares, S16 (OS-010), S294 (TOP-278), S328 (SAT-362)
Villaluna, Kimmy, S746 (THU-485)
Villamil, Alejandra, S7 (LBO-001), S10 (LBO-006), S97 (SAT-085), S296 (TOP-281), S300 (SAT-250), S306 (SAT-262), S315 (SAT-286), S325 (SAT-320), S328 (SAT-362), S331 (SAT-368-YI), S337 (SAT-382), S349 (SAT-420), S838 (THU-270)
Villamil-Ramírez, Hugo, S549 (THU-185-YI)
Villani, Rosanna, S424 (TOP-375-YI)
Villanueva, Càndid, S191 (WED-426), S735 (THU-453)
Villarino, Irene, S968 (WED-610-YI)
Villar, Noa, S819 (WED-019)
Villas-Riotorto, Vanessa, S774 (THU-040), S774 (THU-041)
Villaverde, Joana, S804 (FRI-019)
Villela-Nogueira, Cristiane A., S62 (OS-097), S296 (TOP-281), S306 (SAT-262), S424 (TOP-376), S516 (TOP-113), S557 (THU-213), S724 (THU-420), S768 (THU-022), S790 (SAT-036), S923 (SAT-618), S978 (WED-641)
Villela-Nogueira, Livia, S978 (WED-641)
Villeret, Francois, S311 (SAT-271), S380 (FRI-463), S381 (FRI-464), S414 (FRI-572)
Villesen, Ida, S110 (FRI-041-YI), S111 (FRI-044), S114 (FRI-057), S115 (FRI-059), S122 (FRI-079-YI), S125 (FRI-090-YI), S554 (THU-204)
Villota-Rivas, Marcela, S774 (THU-040), S774 (THU-041)
Vilstrup, Hendrik, S262 (SAT-332), S631 (SAT-094-YI)
Vinaixa, Carmen, S189 (WED-418), S815 (WED-006)
Viñas, Laura Sererols, S18 (OS-014-YI)
Vinayakumar, KR, S786 (SAT-023)
Vince, Adriana, S800 (FRI-006)
Vincent, Catherine, S14 (OS-008), S295 (TOP-279), S325 (SAT-319), S354 (SAT-435), S386 (FRI-480-YI)
Vincentis, Antonio De, S69 (LBP-004-YI), S196 (WED-444), S304 (SAT-258)
Vinci, Marco, S767 (THU-020)
Vindzgalskyte, Ruta, S337 (SAT-382)
Vinikoor, Michael, S905 (SAT-569), S926 (SAT-624), S940 (FRI-588-YI)
Violeta, Sargsyan, S952 (FRI-622)
Violi, Francesco, S731 (THU-445-YI)
Vionnet, Julien, S199 (WED-450)
Visentini, Marcella, S972 (WED-623)
Visic, Ana, S800 (FRI-006)
Visser, Willy, S840 (THU-274), S842 (THU-283)
Visvanathan, Kumar, S65 (OS-101-YI), S903 (SAT-562)
Vitale, Alessandro, S49 (OS-076-YI), S919 (SAT-608-YI)

Author Index

Vitale, Giovanni, S304 (SAT-258), S307 (SAT-263), S335 (SAT-378-YI), S350 (SAT-421), S720 (TOP-504-YI)
Vitale, Luigi, S444 (THU-384), S532 (THU-123)
Vital, Marius, S222 (WED-526-YI)
Vithayathil, Mathew, S12 (OS-005-YI), S224 (WED-530), S451 (THU-410), S490 (TOP-407-YI)
Vitiello, Paola, S901 (SAT-559), S902 (SAT-560), S938 (FRI-586)
Vito, Gabriele De, S567 (WED-055-YI)
Vivaldi, Caterina, S424 (TOP-375-YI), S428 (THU-227-YI), S481 (WED-383), S514 (FRI-381)
Vivancos-Gallego, María Jesus, S25 (OS-029), S904 (SAT-564)
Vivian, Laura, S193 (WED-431-YI)
Vizzutti, Francesco, S3 (GS-005), S6 (GS-011-YI), S52 (OS-081), S53 (OS-082), S54 (OS-084), S195 (WED-442-YI), S719 (TOP-488), S720 (TOP-502-YI), S746 (THU-489), S747 (THU-492), S752 (THU-501)
Vlachogiannakos, Ioannis, S45 (OS-068-YI), S545 (THU-172)
Vlierberghe, Hans Van, S59 (OS-092-YI), S99 (TOP-193-YI), S148 (SAT-466-YI), S281 (TOP-295-YI), S349 (SAT-420)
Vloo, Charlotte De, S22 (OS-023), S148 (SAT-466-YI), S718 (WED-572), S849 (THU-306-YI), S907 (SAT-575)
Vlug, Marije, S9 (LBO-005-YI)
Vodolazkaia, Alexandra, S907 (SAT-575)
Voeller, Alexis, S823 (WED-029)
Vogel, Arndt, S345 (SAT-409-YI), S425 (THU-216-YI), S460 (WED-244-YI), S485 (WED-396), S487 (WED-400-YI), S488 (WED-409-YI), S504 (FRI-251)
Vogel, Georg-Friedrich, S56 (OS-086), S832 (THU-258-YI), S836 (THU-265-YI), S842 (THU-284), S850 (THU-308)
Vögelin, Marius, S753 (THU-506)
Vogelmann, Roger, S904 (SAT-564)
Vogels, Esther, S646 (SAT-140-YI)
Vogl, Thomas, S37 (OS-053)
Voight, Benjamin, S166 (FRI-393)
Voitenleitner, Christian, S919 (SAT-607)
Voit, Florian, S904 (SAT-564)
Vojnović-Milutinović, Danijela, S268 (SAT-351)
Voldum-Clausen, Kristoffer, S646 (SAT-142)
Volk, Valery, S488 (WED-409-YI)
Vollenberg, Richard, S248 (SAT-515)
Vollmer, Tanja, S879 (THU-588)
Volmar, Anika, S271 (THU-313)
Volmari, Annika, S871 (THU-558-YI), S890 (THU-622-YI)
Voloshina, Natalya, S957 (WED-577)
Volosov, Andrew, S62 (OS-096)
Volpe, Luca Dalla, S583 (WED-102-YI)
Volz, Tassilo, S271 (THU-313), S871 (THU-558-YI), S890 (THU-622-YI)
von Bergen, Martin, S262 (SAT-330)
Vonderlin, Joscha, S268 (SAT-352-YI)
Vondran, Florian, S890 (THU-623-YI)
von Ehren, Lea, S159 (SAT-506-YI)
von Felden, Johann, S426 (THU-219-YI), S429 (THU-227-YI)
Vonghia, Luisa, S581 (WED-093-YI), S581 (WED-094), S621 (WED-214), S638 (SAT-117-YI), S682 (FRI-150-YI), S729 (THU-441), S765 (THU-013)
Vonk, Anton, S237 (FRI-330)
von Maldeghem, Elena, S216 (WED-507)
Vonschallen, Philip, S85 (LBP-039), S243 (FRI-349)
von Seth, Erik, S451 (THU-409)
von Widdern, Julian Cardinal, S215 (WED-506)
Vora, Pareen, S434 (THU-241)
Vorobeva, Viktoriya, S595 (WED-136)
Voronkova, Natalia, S49 (OS-075), S962 (WED-594)
Vosbeck, Jürg, S533 (THU-126)
Vos, Jacques De, S905 (SAT-569)
Vosko, Lena, S672 (SAT-229-YI)
Vos, Marie De, S907 (SAT-575)
Voß, Jonas, S672 (SAT-230)
Vos, Winnok De, S638 (SAT-117-YI)
Vozza, Alfredo, S514 (FRI-381)
Vratarić, Miloš, S268 (SAT-351)
Vrbova, Petra, S205 (WED-473)
Vrieze, Anne, S9 (LBO-005-YI), S352 (SAT-429)
Vrolijk, Jan Maarten, S15 (OS-009-YI), S351 (SAT-426-YI), S352 (SAT-429), S353 (SAT-432), S353 (SAT-433)
Vucur, Mihael, S188 (WED-416), S641 (SAT-125-YI), S648 (SAT-150)
Vuddanda, Pavan, S569 (WED-058-YI)
Vugts, Daniëlle, S237 (FRI-330)
Vu, James, S125 (FRI-091)
Vujkovic, Marijana, S166 (FRI-393)
Vuppalanchi, Raj, S7 (LBO-001), S26 (OS-031), S62 (OS-096), S689 (FRI-169), S691 (FRI-175), S719 (TOP-486)
Vyas, Mary, S342 (SAT-398), S346 (SAT-412)
Vyberg, Mogens, S736 (THU-459)

Wachtmeister, Thorsten, S672 (SAT-230)
Wada, Russ, S959 (WED-586)
Waddell, Scott, S864 (WED-319-YI)
Waddilove, Elizabeth, S826 (WED-039), S900 (SAT-558)
Wade, Amanda, S820 (WED-021)
Wadhwani, Arpana, S379 (FRI-461-YI)
Wadland, Elaine, S312 (SAT-274-YI), S313 (SAT-275)
Wadman, Anna, S978 (WED-642-YI)
Wagner, Lea, S222 (WED-526-YI)
Wagner, Martin, S672 (SAT-229-YI)
Wagner, Mathilde, S446 (THU-393-YI), S493 (FRI-221), S505 (FRI-254), S507 (FRI-362), S508 (FRI-364-YI)
Wagner, Sonja, S257 (SAT-545-YI), S862 (WED-314-YI)
Wahid, Avista, S887 (THU-611)
Wajbrot, Natalia, S724 (THU-420)
Wajda-Cuszlag, Malgorzata, S617 (WED-203)
Wakabayashi, Shun-Ichi, S555 (THU-205), S591 (WED-123), S618 (WED-205)
Wakae, Kousho, S875 (THU-573), S894 (THU-635), S894 (THU-637)
Waked, Imam, S492 (FRI-217), S814 (WED-003), S966 (TOP-599)
Wakefield, Phil, S673 (SAT-231)
Wakita, Naoki, S662 (SAT-196)
Wakita, Takaji, S894 (THU-635), S894 (THU-637)
Waldmann, Moritz, S351 (SAT-427)
Walker, Alexandra, S956 (TOP-598), S957 (WED-577), S960 (WED-587)
Walker, Eleanor, S164 (FRI-385-YI), S184 (FRI-453-YI)
Walker, Olivia, S154 (SAT-490)
Wallace, David, S404 (FRI-538-YI), S758 (TOP-016)
Wallace, Jack, S799 (FRI-004), S800 (FRI-005), S820 (WED-021)
Wallace, Michael, S571 (WED-069), S736 (THU-458)
Wallach, Jean-Philippe, S14 (OS-008), S295 (TOP-279), S325 (SAT-319), S354 (SAT-435)
Wallinger, Hayley, S555 (THU-206)
Walmsley, Martine, S23 (OS-025), S311 (SAT-270), S319 (SAT-301), S346 (SAT-412)
Walmsley, Sharon, S529 (THU-116-YI)
Walsh, Alissa, S740 (THU-468)
Walsh, Colin, S684 (FRI-154)
Walter, Aurélie, S54 (OS-084)
Walter, Jörg, S647 (SAT-148)
Walters, Julian, S134 (FRI-117)
Walther, Thomas, S237 (FRI-329)
Wambre, Erik, S58 (OS-089), S313 (SAT-282)
Wandeler, Gilles, S905 (SAT-569), S940 (FRI-588-YI)
Wandji, Line Carolle Ntandja, S35 (OS-050-YI), S428 (THU-226-YI), S505 (FRI-254), S506 (FRI-255-YI)
Wan, Fang, S428 (THU-225-YI)
Wang, Angela, S781 (SAT-009)
Wang, Anquan, S511 (FRI-370)
Wang, Belle, S690 (FRI-171)
Wang, Bin, S270 (TOP-328), S276 (THU-323)
Wang, Bruce, S489 (WED-412-YI)
Wang, Chenlu, S422 (TOP-359-YI)
Wang, Chuanxin, S33 (OS-047)
Wang, Chunying, S33 (OS-047)
Wang, Cong, S168 (FRI-398)
Wang, Ding-Lian, S274 (THU-319), S797 (TOP-033), S898 (TOP-568), S929 (SAT-633)
Wang, Dong, S73 (LBP-012)
Wangensteen, Kirk, S166 (FRI-393)
Wang, Fang, S955 (FRI-628)

Wang, Fei, S812 (FRI-040)
Wang, Fengmei, S102 (THU-061), S560 (TOP-080), S625 (WED-227), S950 (FRI-617)
Wang, Gaihong, S68 (OS-107), S74 (LBP-015)
Wang, Grace, S958 (WED-579)
Wang, Guangchuan, S747 (THU-492), S755 (THU-511), S757 (THU-515)
Wang, Gui-Qiang, S94 (SAT-074), S292 (FRI-298)
Wang, Guiqiang, S952 (FRI-623)
Wang, Haitao, S657 (SAT-180)
Wang, Haixia, S517 (TOP-114)
Wang, HaiYu, S228 (WED-544), S754 (THU-508)
Wang, Han, S285 (FRI-270), S291 (FRI-290-YI)
Wang, Hao, S81 (LBP-031), S103 (THU-067), S244 (FRI-351), S362 (THU-356), S473 (WED-276), S917 (SAT-603)
Wang, Heng, S56 (OS-086), S832 (THU-258-YI), S842 (THU-284)
Wang, Hong-Yang, S33 (OS-047)
Wang, Hongyuan, S943 (FRI-594), S953 (FRI-624)
Wang, Hua, S129 (TOP-223), S140 (FRI-136), S646 (SAT-141)
Wang, Huali, S930 (SAT-635), S933 (SAT-642)
Wang, Jian, S930 (SAT-634), S930 (SAT-635), S933 (SAT-642)
Wang, Jianan, S259 (SAT-554)
Wang, Jianlu, S869 (TOP-630)
Wang, Jian-She, S56 (OS-086), S832 (THU-258-YI), S842 (THU-284), S850 (THU-308)
Wang, Jiaqi, S824 (WED-035)
Wang, Jin, S243 (FRI-350)
Wang, Jing, S295 (TOP-280), S549 (THU-184), S593 (WED-134), S609 (WED-182), S954 (FRI-626)
Wang, Jinhua, S934 (SAT-644)
Wang, Jinyu, S201 (WED-458), S754 (THU-507), S891 (THU-626), S944 (FRI-597)
Wang, Juan, S129 (TOP-223), S140 (FRI-136), S268 (SAT-352-YI)
Wang, Junyu, S238 (FRI-333-YI), S244 (FRI-352), S244 (FRI-353)
Wang, Kai, S68 (OS-107)
Wang, Kaifeng, S486 (WED-397)
Wang, Kasper, S832 (THU-258-YI)
Wang, Kunyuan, S430 (THU-229), S508 (FRI-363)
Wang, Lei, S24 (OS-028), S144 (SAT-452), S160 (SAT-507), S917 (SAT-603)
Wang, Li, S644 (SAT-135-YI)
Wang, Liang, S98 (SAT-088)
Wang, Lin, S883 (THU-597), S884 (THU-603), S894 (THU-636)
Wang, Lingxiao, S593 (WED-134), S924 (SAT-620)
Wang, Liping, S119 (FRI-072), S259 (SAT-554), S593 (WED-134), S609 (WED-182), S763 (THU-011), S924 (SAT-620)
Wang, Li-Yun, S373 (WED-354)
Wang, Lulu, S328 (SAT-362), S329 (SAT-363), S691 (FRI-175)
Wang, Mary Yue, S224 (WED-531)
Wang, Mengyao, S140 (FRI-137)
Wang, Miao, S81 (LBP-031)
Wang, Michael, S701 (FRI-204)
Wang, Min, S826 (WED-040)
Wang, Mingchen, S228 (WED-544), S754 (THU-508)
Wang, Ming-Juan, S243 (FRI-348)
Wang, Mingshuo, S270 (TOP-328), S276 (THU-323)
Wang, Mingyue, S513 (FRI-379)
Wang, Muqi, S47 (OS-071), S463 (WED-252), S791 (SAT-039), S792 (SAT-040), S873 (THU-569), S946 (FRI-606)
Wang, Ning, S458 (WED-240), S486 (WED-398)
Wang, Peter, S68 (OS-107), S74 (LBP-015)
Wang, Qi, S225 (WED-537), S259 (SAT-554), S270 (SAT-356), S350 (SAT-425), S356 (SAT-444), S793 (SAT-043)
Wang, Qianhui, S941 (FRI-591)
Wang, Qianqian, S466 (WED-259)
Wang, Qinshuo, S253 (SAT-533), S279 (THU-336), S785 (SAT-021), S813 (FRI-045)
Wang, Qiuyue, S233 (FRI-314), S664 (SAT-202), S664 (SAT-203), S665 (SAT-204), S666 (SAT-206), S872 (THU-562)
Wang, Routing, S6 (GS-010), S260 (TOP-357), S486 (WED-397), S644 (SAT-136)
Wang, Shuhui, S291 (FRI-290-YI)
Wang, Sikui, S86 (LBP-041)
Wang, Siyun, S623 (WED-221)
Wang, Stanley, S959 (WED-586)
Wang, Tianlu, S511 (FRI-370)
Wang, Tongyao, S763 (THU-011)
Wang, Wayland, S436 (THU-248)
Wang, Wei, S160 (SAT-507)
Wang, Weihao, S623 (WED-221)
Wang, Weihong, S86 (LBP-041)
Wang, Wenhao, S431 (THU-234), S463 (WED-252)
Wang, Wen-Jing, S292 (FRI-298)
Wang, Wenjing, S193 (WED-432)
Wang, Wenjuan, S119 (FRI-072), S593 (WED-134), S609 (WED-182), S924 (SAT-620)
Wang, Wenjun, S791 (SAT-039), S792 (SAT-040)
Wang, Wenshi, S877 (THU-579-YI), S883 (THU-601-YI)
Wang, Xi, S350 (SAT-425), S491 (TOP-422)
Wang, Xian-Bo, S162 (TOP-440)
Wang, Xianda, S129 (TOP-223)
Wang, Xiangmei, S81 (LBP-031)
Wang, Xiaojing, S676 (SAT-239)
Wang, Xiaolin, S119 (FRI-072), S560 (TOP-080)
Wang, Xiaomei, S373 (WED-355)
Wang, Xiaoxiao, S593 (WED-133), S673 (SAT-232)
Wang, Xiaoze, S756 (THU-512)
Wang, Xiaozhong, S86 (LBP-041), S952 (FRI-623)
Wang, Xinke, S513 (FRI-379)
Wang, Xinrui, S34 (OS-048), S160 (SAT-507)
Wang, Xinyu, S946 (FRI-606)
Wang, Xi-Xuan, S30 (OS-040), S627 (TOP-130), S640 (SAT-123)
Wang, Xizhu, S868 (FRI-644)
Wang, Xue, S88 (TOP-192)
Wang, Xun, S6 (GS-010), S644 (SAT-136)
Wang, Yan, S88 (TOP-192), S292 (FRI-298), S367 (WED-336), S560 (TOP-080)
Wang, Yang, S640 (SAT-123)
Wang, Yanhan, S139 (FRI-134)
Wang, Yanting, S517 (TOP-114)
Wang, Yichen, S437 (THU-362)
Wang, Yijin, S137 (FRI-124), S868 (TOP-616-YI), S883 (THU-602), S884 (THU-603)
Wang, Yikai, S47 (OS-071), S463 (WED-252), S791 (SAT-039), S792 (SAT-040), S873 (THU-569)
Wang, Yilin, S473 (WED-361-YI)
Wang, Yiming, S103 (THU-067), S473 (WED-276)
Wang, Ying, S685 (FRI-156)
Wang, Yingling, S160 (SAT-507)
Wang, Yipeng, S884 (THU-605)
Wang, Yixuan, S508 (FRI-363)
Wang, Youlei, S74 (LBP-014)
Wang, Yu, S88 (TOP-192), S225 (WED-537), S826 (WED-040)
Wang, Yuechen, S362 (THU-356)
Wang, Yuehua, S560 (TOP-080)
Wang, Yufu, S954 (FRI-626)
Wang, Yuhao, S368 (WED-339)
Wang, Yujing, S489 (WED-410)
Wang, Yunfang, S107 (THU-077), S270 (TOP-328), S276 (THU-323)
Wang, Yunyun, S369 (WED-341)
Wang, Yuzhong, S954 (FRI-626)
Wang, Zeyu, S33 (OS-046), S737 (THU-461), S744 (THU-481), S744 (THU-482-YI)
Wang, Zhenhua, S954 (FRI-626)
Wang, Zijun, S77 (LBP-022-YI)
Wang, Ziteng, S556 (THU-211)
Wang, Zixing, S192 (WED-430), S208 (WED-481), S253 (SAT-533), S279 (THU-336), S785 (SAT-021), S813 (FRI-045), S931 (SAT-638)
Wang, Zixuan, S107 (THU-077)
Wang, Ziyan, S6 (GS-010), S260 (TOP-357), S486 (WED-397)
Wan, Heng, S650 (SAT-155)
Wan-Hin Hui, Rex, S438 (THU-364)
Wan, Hong, S955 (FRI-628)

Author Index

Wan, Jiayuan, S270 (SAT-356)
Wan, Mobin, S932 (SAT-641)
Wan, Ying-Wooi, S578 (WED-087), S623 (WED-219), S847 (THU-300), S848 (THU-301)
Ward, Caroline, S455 (TOP-406)
Ward, John, S801 (FRI-007), S823 (WED-029)
Ward, Katie, S841 (THU-276-YI)
Warmington, Emily, S491 (TOP-408-YI)
Warner, Susanne, S9 (LBO-004)
Warter, Elise, S83 (LBP-035)
Wasim, Mohammad, S709 (THU-556-YI)
Watanabe, Noriyuki, S894 (THU-637)
Watashi, Koichi, S875 (THU-573), S894 (THU-635)
Waterton, John, S106 (THU-075)
Watkins, Angela, S259 (SAT-553)
Watkins, Jennifer, S119 (FRI-073)
Watson, Andrew, S921 (SAT-611)
Watt, Kym, S315 (SAT-286)
Watt, Kymberly, S379 (FRI-461-YI), S390 (FRI-493-YI), S411 (FRI-560)
Wawrzyniak, Antoine, S571 (WED-067), S853 (WED-283)
Wawrzyniak, Jérémie, S907 (SAT-575)
Webb, Jamie, S75 (LBP-017)
Webb, Kerry, S406 (FRI-544)
Webb, Oliver, S319 (SAT-301)
Weber, Achim, S465 (WED-255)
Weber, Kathrin, S871 (THU-559-YI)
Weber, Sabine, S14 (OS-007)
Weber, Susanne, S323 (SAT-314), S532 (THU-124)
Wedemeyer, Hans Heinrich, S341 (SAT-397), S939 (FRI-587)
Wedemeyer, Heiner, S7 (GS-012), S43 (OS-066), S197 (WED-446), S222 (WED-524), S222 (WED-526-YI), S376 (TOP-520-YI), S439 (THU-367), S461 (WED-245), S601 (WED-155), S732 (THU-448-YI), S737 (THU-461), S737 (THU-462), S743 (THU-480-YI), S840 (THU-275), S864 (TOP-615), S866 (FRI-641), S878 (THU-585-YI), S887 (THU-611), S887 (THU-613), S913 (SAT-589-YI), S915 (SAT-595), S916 (SAT-596), S934 (TOP-582), S935 (TOP-583), S936 (TOP-584), S937 (FRI-585-YI), S953 (FRI-625), S956 (WED-576), S958 (WED-581), S962 (WED-593), S963 (WED-596), S971 (WED-620)
Wedemeyer, Thies, S209 (WED-485)
Wee, Poh Hui, S529 (THU-115)
Wegermann, Kara, S197 (WED-447)
Weghuber, Daniel, S539 (THU-151-YI)
Weglage, Jakob, S623 (WED-220)
Wehnes, Jeanette, S763 (THU-010)
Wehrle, Chase, S399 (FRI-522)
Wehrman, Andrew, S850 (THU-308)
Weichselbaum, Laura, S109 (TOP-210), S111 (FRI-043)
Weidhase, Lorenz, S150 (SAT-474)
Weidner, Dominik, S930 (SAT-636)
Wei, Fangfang, S805 (FRI-021)
Weigel, Christian, S188 (WED-416)
Wei, Hongshan, S103 (THU-068), S239 (FRI-335), S556 (THU-211)
Weihs, Julian, S852 (TOP-311)
Wei, Jia, S812 (FRI-040)
Wei, Jian, S452 (THU-413)
Wei, Jianhai, S259 (SAT-554)
Weijsters, Gemma H. X., S338 (SAT-384), S351 (SAT-426-YI), S352 (SAT-429), S353 (SAT-432), S353 (SAT-433)
Wei, Lai, S86 (LBP-041), S242 (FRI-345-YI), S623 (WED-221)
Weilheimer, Arden, S633 (SAT-102-YI)
Wei, Li, S108 (THU-083), S269 (SAT-353)
Wei, Linlin, S160 (SAT-507)
Weil-Verhoeven, Delphine, S167 (FRI-394-YI), S380 (FRI-463), S381 (FRI-464), S388 (FRI-485)
Weinberg, Ethan, S754 (THU-509)
Weiner, Dave, S334 (SAT-371), S334 (SAT-372), S334 (SAT-377)
Weinmann-Menke, Julia, S172 (FRI-411), S199 (WED-451-YI), S742 (THU-476)
Weinstein, Ali A, S127 (FRI-095)
Weinstein, Debra, S10 (LBO-006)
Wei, Rendong, S955 (FRI-628)
Weisel, Katja, S866 (FRI-639)
Wei, Sida, S909 (SAT-579)
Weismüller, Tobias, S33 (OS-046)
Weiss, Andreas, S975 (WED-634-YI)
Weißenborn, Christian, S175 (FRI-419)
Weisser, Franco, S296 (TOP-281), S306 (SAT-262)
Weiss, Günter, S862 (WED-314-YI)
Weiss, Karl Heinz, S39 (OS-057), S839 (THU-272)
Weiß, Marc, S181 (FRI-436)
Weiss, Nicolas, S222 (WED-525)
Weiss, Ram, S713 (WED-557)
Weiss-Tessbach, Matthias, S738 (THU-464-YI)
Wei, Xiaodie, S626 (WED-230)
Wei, Yan-bo, S232 (FRI-307)
Welch, Nicole, S116 (FRI-061), S190 (WED-421), S197 (WED-447)
Welsch, Christoph, S178 (FRI-428-YI), S210 (WED-485), S215 (WED-506)
Weltzsch, Jan Philipp, S351 (SAT-427)
Wen, Chia-Chang, S449 (THU-399)
Wen, Cindy, S624 (WED-225-YI), S624 (WED-226), S783 (SAT-013-YI), S784 (SAT-014)
Wende, Lisa, S460 (WED-244-YI), S487 (WED-400-YI)
Wendon, Julia, S165 (FRI-386)
Weng, Jianping, S627 (TOP-143)
Wen, Hao, S243 (FRI-348)
Wen, Haoyu, S293 (FRI-302-YI), S352 (SAT-428-YI)
Weninger, Jasmin, S395 (FRI-511-YI)
Weninger, Wolfgang, S284 (FRI-266)
Wenjing, Wu, S649 (SAT-154), S650 (SAT-155)
Wen-Juei Jeng, Rachel, S958 (WED-580)
Wennberg, Alexandra, S771 (THU-031)
Wennbo, Haakan, S119 (FRI-073), S578 (WED-087), S579 (WED-090), S623 (WED-219), S667 (SAT-213), S694 (FRI-183)
Wensing, Anne Marie, S807 (FRI-025)
Wen, Xin, S253 (SAT-533), S279 (THU-336), S785 (SAT-021), S813 (FRI-045), S931 (SAT-638)
Wenzel, Patrick, S504 (FRI-251)
Werge, Mikkel, S586 (WED-109), S602 (WED-159-YI)
Werge, Rikke, S22 (OS-024), S711 (WED-549-YI)
Wernberg, Charlotte, S225 (WED-532)
Werner, Ellen, S193 (WED-432), S298 (TOP-294-YI), S331 (SAT-368-YI), S351 (SAT-426-YI), S352 (SAT-429), S353 (SAT-432), S353 (SAT-433)
Werner, Mårten, S346 (SAT-411-YI), S770 (THU-027)
Wernly, Bernhard, S539 (THU-151-YI), S616 (WED-199), S792 (SAT-041)
Westberg, Karin, S690 (FRI-172)
Westbrook, Angel, S708 (THU-554-YI)
Wester, Axel, S58 (OS-090), S224 (WED-529), S313 (SAT-276), S570 (WED-060-YI), S606 (WED-173), S701 (FRI-205-YI)
Westgeest e Sousa, Diego Drumond, S113 (FRI-052), S745 (THU-483)
Westin, Joan, S606 (WED-173)
West, Joe, S786 (SAT-024-YI)
Weston, Patrick, S26 (OS-031)
West, Rebecca, S333 (SAT-370), S711 (WED-547)
Wethmar, Klaus, S493 (FRI-220)
Wetten, Aaron, S318 (SAT-299), S325 (SAT-320)
Wettengel, Jochen, S467 (WED-260)
Wettstein, Guillaume, S638 (SAT-117-YI), S696 (FRI-189)
Wewer, Neele, S107 (THU-078)
Wexler, Ryan, S569 (WED-058-YI)
Wheeler, Kai, S713 (WED-557)
White, Benjamin E, S449 (THU-401)
Whitehead, Sandeep, S709 (THU-556-YI)
White, Trenton M, S777 (THU-050), S792 (SAT-042)
Widman, Linnea, S58 (OS-090), S115 (FRI-058-YI)
Wiecek, Sabina, S56 (OS-086), S832 (THU-258-YI), S842 (THU-284), S850 (THU-308)
Więckowski, Sebastian, S617 (WED-203)
Wiegand, Johannes, S568 (WED-057-YI), S600 (WED-154-YI), S945 (FRI-602-YI)
Wieland, Stefan, S533 (THU-126)
Wiering, Leke, S416 (FRI-578-YI)
Wiese, Signe, S602 (WED-159-YI)
Wiest, Reiner, S32 (OS-044)

Wiethoff, Hendrik, S341 (SAT-397)
Wigg, Alan, S400 (FRI-524), S699 (FRI-198)
Wiggers, Thomas, S245 (FRI-354), S550 (THU-187)
Wijarnpreecha, Karn, S156 (SAT-496), S215 (WED-505), S221 (WED-523), S228 (WED-543), S423 (TOP-374), S442 (THU-379), S509 (FRI-365), S528 (THU-110), S530 (THU-119-YI), S670 (SAT-220)
Wilczynski, Fryderyk, S758 (TOP-002), S781 (SAT-007)
Wilde, Michael, S164 (FRI-385-YI)
Wilder, Julius, S10 (LBO-006)
Wiles, Kate, S354 (SAT-434)
Willemoe, Gro Linno, S570 (WED-062)
Willemse, Jorke, S382 (FRI-467-YI), S383 (FRI-473), S391 (FRI-498)
Willemse, José, S774 (THU-040), S774 (THU-041)
Willemse, Sophie, S963 (WED-595)
Willemssen, Francois, S828 (TOP-310-YI)
Williams, Felicity, S61 (OS-108)
Williams, James, S218 (WED-513), S749 (THU-496)
Williams, Katherine, S186 (TOP-469-YI)
Williams, Michael, S691 (FRI-175)
Williamson, Catherine, S23 (OS-026-YI), S40 (OS-059-YI), S354 (SAT-434)
Williams, Setareh, S695 (FRI-186)
Will, Nico, S57 (OS-088), S291 (FRI-291-YI)
Willuweit, Katharina, S172 (FRI-410-YI)
Wilmer, Alexander, S8 (LBO-002)
Wilson, Joseph D, S182 (FRI-443)
Wilson, Laura, S553 (THU-201)
Wilson, Lucille, S713 (WED-557)
Wilson, Mollie, S454 (TOP-390-YI)
Winchler, Costanza, S514 (FRI-381)
Windell, Dylan, S673 (SAT-231)
Winderbergs, Maike, S262 (SAT-330)
Winkler, Romy, S150 (SAT-474)
Win, Mya, S559 (TOP-065-YI)
Winter, Benedicte De, S638 (SAT-117-YI)
Winter, Brenda De, S168 (FRI-397-YI)
Winterstein, Nina, S770 (THU-026)
Wirawan, Lawrence, S238 (FRI-332)
Wirth, Sophia, S199 (WED-452)
Wirth, Thomas, S504 (FRI-251)
Wirtz, Theresa Hildegard, S33 (OS-046), S142 (SAT-448), S159 (SAT-506-YI), S744 (THU-482-YI)
Wißing, Michael, S887 (THU-613)
Withers, David, S284 (FRI-268-YI)
Witjes, Julia, S641 (SAT-126)
Witt, Jennifer, S197 (WED-446), S222 (WED-526-YI)
Wittrup-Jensen, Villum, S770 (THU-028)
Wium, Lizemarie, S354 (SAT-434)
Wixner, Jonas, S346 (SAT-411-YI)
Woelfle, Ute, S550 (THU-187)
Woeller, Livia, S581 (WED-095)
Wöhler, Philipp, S206 (WED-475)
Wohlmuth, Christoph, S975 (WED-634-YI)
Wojdyla, Dominika, S850 (THU-308)
Wold, Hedda, S9 (LBO-004)
Wolff, Fernando Hertz, S88 (SAT-056)
Wolfson, Tanya, S443 (THU-381)
Wolf, Zach, S580 (WED-092-YI)
Woller, Norman, S963 (WED-596)
Wolstenholme, Jennifer, S130 (FRI-103)
Woltemate, Sabrina, S222 (WED-526-YI)
Wolters, Justina, S630 (SAT-090)
Wolters, Lena, S209 (WED-485), S409 (FRI-556)
Wolters, Victorien M., S850 (THU-308)
Wong, Carlos King Ho, S438 (THU-364), S496 (FRI-230)
Wong, Christopher, S713 (WED-556-YI)
Wong, Danny Ka-Ho, S896 (THU-644)
Wong, Darren, S400 (FRI-525)
Wong, Emily, S900 (SAT-558)
Wong, Eugene, S149 (SAT-473)
Wong, Florence, S24 (OS-028), S144 (SAT-452), S149 (SAT-468), S152 (SAT-478), S160 (SAT-507), S214 (WED-499), S754 (THU-509), S760 (TOP-032)
Wong, Grace, S46 (OS-070-YI), S48 (OS-073), S928 (SAT-628-YI)
Wong, Grace Lai-Hung, S66 (OS-103-YI), S85 (LBP-040), S86 (LBP-042), S224 (WED-531), S452 (THU-414-YI), S517 (TOP-114), S525 (THU-103), S558 (TOP-063-YI), S574 (WED-075), S589 (WED-118), S607 (WED-174-YI), S618 (WED-204), S738 (THU-463), S897 (TOP-565), S906 (SAT-574), S931 (SAT-637), S943 (FRI-594), S953 (FRI-624), S964 (WED-597), S979 (WED-643)
Wong, Ian Chi Kei, S438 (THU-364), S496 (FRI-230), S824 (WED-035)
Wong, Kenneth Ky, S864 (WED-320-YI)
Wong, (Leslie) Chun Man, S709 (THU-556-YI)
Wong, Man Chun, S284 (FRI-268-YI), S360 (THU-350)
Wong, Mark, S670 (SAT-220)
Wong, Nicholas, S871 (THU-560-YI)
Wong, Philip, S533 (THU-127-YI), S616 (WED-200), S757 (THU-516)
Wong, Robert, S126 (FRI-094), S127 (FRI-095), S320 (SAT-303), S320 (SAT-304), S355 (SAT-441), S356 (SAT-443), S375 (TOP-518), S417 (FRI-581), S532 (THU-125), S809 (FRI-031)
Wong, Samuel, S218 (WED-513), S749 (THU-496)
Wong, Stanley, S821 (WED-024), S967 (TOP-600-YI)
Wong, Tak-Siu, S423 (TOP-360)
Wong, Tiffany, S422 (TOP-359-YI)
Wong, Vincent Wai-Sun, S2 (GS-003), S19 (OS-017), S62 (OS-097), S66 (OS-103-YI), S127 (FRI-095), S224 (WED-531), S424 (TOP-376), S452 (THU-414-YI), S516 (TOP-113), S517 (TOP-114), S525 (THU-103), S557 (THU-213), S558 (TOP-063-YI), S560 (TOP-066), S561 (TOP-082), S568 (WED-057-YI), S574 (WED-075), S579 (WED-089), S589 (WED-118), S593 (WED-134), S607 (WED-174-YI), S612 (WED-187-YI), S618 (WED-204), S621 (WED-215), S698 (FRI-197), S738 (THU-463), S766 (THU-015), S931 (SAT-637), S946 (FRI-604), S979 (WED-643)
Wong, William CM, S824 (WED-035)
Wong, William WL, S812 (FRI-039)
Wong, Yu Jun, S14 (OS-008), S79 (LBP-026), S295 (TOP-279), S300 (SAT-250), S320 (SAT-302), S325 (SAT-319), S325 (SAT-320), S344 (SAT-404), S354 (SAT-435), S355 (SAT-436), S401 (FRI-527), S720 (TOP-504-YI), S743 (THU-479)
Won, Hyung Jin, S4 (GS-006)
Won, Sung-Min, S266 (SAT-345)
Woodman, Richard, S699 (FRI-198)
Woods, Parker, S614 (WED-195)
Woods, Virgil, S877 (THU-580)
Woodward, Mark, S685 (FRI-157-YI)
Woo, Hyun Young, S497 (FRI-233)
Wootton, Grace, S363 (WED-321-YI), S364 (WED-324-YI), S365 (WED-330-YI)
Woo, Yein, S277 (THU-331)
Worland, Thomas, S707 (THU-546-YI)
Wouambo, Rodrigue Kamga, S879 (THU-589-YI)
Wranke, Anika, S737 (THU-462)
Wright, Christopher, S5 (GS-008)
Wright, Gavin, S150 (SAT-475)
Wright, Mark, S64 (OS-100)
Wronka, Karolina, S301 (SAT-251-YI), S318 (SAT-298), S355 (SAT-442)
Wu, Changhui, S812 (FRI-040)
Wu, Chao, S86 (LBP-041), S677 (SAT-242), S930 (SAT-634), S930 (SAT-635), S933 (SAT-642)
Wu, Chengjian, S52 (OS-081)
Wu, Chia-Ling, S735 (THU-452), S945 (FRI-603)
Wu, Chih-Horng, S446 (THU-387)
Wu, Chi-Jung, S500 (FRI-239)
Wu, Cuncao, S192 (WED-430)
Wu, Dandan, S674 (SAT-233)
Wuestefeld, Torsten, S487 (WED-401), S642 (SAT-132)
Wu, Fei, S473 (WED-361-YI)
Wu, George, S956 (WED-576)
Wu, Guihua, S609 (WED-182)
Wu, Haifeng, S173 (FRI-413)
Wu, Jaw-Ching, S430 (THU-231), S436 (THU-250), S448 (THU-396), S535 (THU-135), S586 (WED-108), S751 (THU-499), S797 (TOP-033), S893 (THU-633)
Wu, Jia-Ling, S943 (FRI-596)
Wu, Jian, S883 (THU-602)
Wu, Jianfan, S924 (SAT-620)

Author Index

Wu, Jiapeng, S873 (THU-563)
Wu, Jiawei, S458 (WED-238)
Wu, Jing, S243 (FRI-348)
Wu, Junyu, S486 (WED-398)
Wu, Lili, S511 (FRI-370)
Wu, Lina, S331 (SAT-367)
Wullaert, Andy, S464 (WED-253)
Wu, Menchi, S909 (SAT-579)
Wu, Miaomiao, S107 (THU-079), S129 (TOP-223), S140 (FRI-136)
Wu, Min, S959 (WED-586), S960 (WED-588), S965 (WED-602)
Wunderbaldinger, Adrian, S97 (SAT-084-YI), S183 (FRI-444-YI), S183 (FRI-445), S195 (WED-442-YI), S217 (WED-509-YI)
Wundes, Christine, S864 (TOP-615), S887 (THU-611)
Wu, Nijin, S513 (FRI-379)
Wunsch, Ewa, S318 (SAT-298), S355 (SAT-442)
Wu, Pei Shan, S395 (FRI-510)
Wu, Peishan, S755 (THU-510)
Wu, Qiaoping, S228 (WED-544)
Wu, Qiong, S625 (WED-227)
Wu, Qufei, S189 (WED-420)
Wu, Renmei, S756 (THU-514)
Wu, Romeo Kuo-Cheng, S500 (FRI-240), S510 (FRI-369-YI)
Wu, Shihong, S941 (FRI-591)
Wu, Shih-Yun, S755 (THU-510)
Wu, Shuang, S129 (TOP-223)
Wu, Su, S756 (THU-514)
Wu, Tianqing, S511 (FRI-370)
Wu, Tianzhou, S151 (SAT-476)
Wu, Tiffany, S113 (FRI-052), S126 (FRI-093)
Wu, Tingting, S86 (LBP-041)
Wu, Tongfei, S889 (THU-620)
Wu, Wanqing, S416 (FRI-579), S417 (FRI-580)
Wu, Wenhui, S676 (SAT-239)
Wu, Xiaoning, S826 (WED-040)
Wu, Xiaoping, S24 (OS-028), S34 (OS-048), S144 (SAT-452), S160 (SAT-507), S964 (WED-601-YI)
Wu, Xiaoxin, S177 (FRI-426)
Wu, Yan, S560 (TOP-080)
Wu, Ying, S511 (FRI-370)
Wu, Yonghui, S974 (WED-628)
Wu, Zhuanmin, S609 (WED-182)
Wyen, Christoph, S904 (SAT-564)
Wyman, Anne E., S119 (FRI-073)
Wyngaert, Karsten Vanden, S708 (THU-554-YI)
Ștefănescu, Horia, S35 (OS-050-YI), S175 (FRI-418), S255 (SAT-539), S543 (THU-165), S544 (THU-166), S602 (WED-157), S731 (THU-445-YI)
徐, 玲, S283 (FRI-264), S950 (FRI-618)
Xanthaki, Anna, S188 (WED-415)
Xia, Anliang, S487 (WED-402), S674 (SAT-234)
Xia, Fang, S321 (SAT-306)
Xia, Jie, S33 (OS-047)
Xia, Jing, S187 (TOP-471-YI)
Xia, Juan, S930 (SAT-634), S933 (SAT-642)
Xiang, Huiling, S225 (WED-537), S952 (FRI-623)
Xiang, Wei, S34 (OS-048)
Xiang, Xiaogang, S3 (GS-004-YI)
Xian, Zhonghe, S646 (SAT-141)
Xiao, Fan, S103 (THU-068)
Xiao, Fei, S489 (WED-413)
Xiao, Guanglin, S245 (FRI-355)
Xiao, Guang-Ming, S225 (WED-537)
Xiao, Jing, S108 (THU-083), S269 (SAT-353)
Xiaomin, Ji, S258 (SAT-548), S452 (THU-413)
Xiao, Teresa, S276 (THU-329)
Xiao, Xiao, S68 (OS-107), S293 (FRI-302-YI), S305 (SAT-259), S352 (SAT-428-YI)
Xiao, Xingguo, S259 (SAT-554), S560 (TOP-080), S593 (WED-134), S763 (THU-011), S924 (SAT-620)
Xiao, Yang, S28 (OS-036-YI)
Xiao, Yuelin, S99 (TOP-194)
Xia, Qiang, S42 (OS-063), S475 (WED-365)
Xia, Yuchen, S895 (THU-638), S895 (THU-639)
Xie, Cen, S675 (SAT-235)
Xie, Chan, S155 (SAT-491), S155 (SAT-492), S155 (SAT-493), S805 (FRI-021)
Xie, Chencheng, S62 (OS-097), S407 (FRI-546), S516 (TOP-113)
Xie, Dong, S701 (FRI-204)
Xie, Dong-Ying, S433 (THU-239)
Xie, Haoru, S964 (WED-601-YI)
Xie, Jianping, S433 (THU-239)
Xie, Lanyie, S5 (GS-008)
Xie, Ping, S675 (SAT-236)
Xie, Qing, S1 (GS-001), S24 (OS-028), S46 (OS-070-YI), S91 (SAT-067), S97 (SAT-086), S99 (TOP-194), S135 (FRI-118), S144 (SAT-452), S160 (SAT-507), S433 (THU-239), S932 (SAT-641), S952 (FRI-623), S960 (WED-587)
Xie, Sophia, S436 (THU-248)
Xie, Weifen, S469 (WED-266), S661 (SAT-195)
Xie, Wen, S73 (LBP-012), S225 (WED-537)
Xie, Xiaoman, S87 (LBP-044)
Xie, Yangyang, S466 (WED-259)
Xie, Yanru, S593 (WED-134)
Xie, Yao, S1 (GS-001), S905 (SAT-570), S932 (SAT-641)
Xie, Youhua, S891 (THU-626)
Xie, Zhe, S467 (WED-260)
Xie, Zhongyang, S177 (FRI-426)
Xing, Huichun, S356 (SAT-444)
Xin, Haisong, S119 (FRI-072), S259 (SAT-554), S609 (WED-182)
Xin, Jiaojiao, S104 (THU-070), S151 (SAT-476), S361 (THU-353)
Xin, Shaojie, S67 (OS-105-YI)
Xin, Xin, S778 (THU-053)
Xiong, Chaoliang, S119 (FRI-072), S763 (THU-011)
Xiong, Feixiang, S258 (SAT-548), S452 (THU-413)
Xiong, Jieyi, S17 (OS-012)
Xiong, Qingfang, S30 (OS-040), S627 (TOP-130), S640 (SAT-123)
Xiong, Shue, S876 (THU-575)
Xiong, Ye, S930 (SAT-634), S930 (SAT-635), S933 (SAT-642)
Xirodimas, Dimitris, S489 (WED-412-YI)
Xiu, Peng, S511 (FRI-370)
Xourafa, Georgia, S21 (OS-020)
Xu, Bin, S24 (OS-028), S34 (OS-048), S144 (SAT-452), S160 (SAT-507)
Xu, Chi, S642 (SAT-131-YI)
Xu, Dong, S285 (FRI-270), S511 (FRI-370)
Xue, Feng, S86 (LBP-041)
Xuefeng, Luo, S52 (OS-081), S723 (THU-418), S725 (THU-426), S747 (THU-492), S756 (THU-512)
Xue, Jie, S755 (THU-511)
Xuejie, Zhang, S258 (SAT-548), S452 (THU-413)
Xue, Tianyi, S253 (SAT-533), S279 (THU-336), S785 (SAT-021), S813 (FRI-045), S931 (SAT-638)
Xue, Xiulan, S952 (FRI-623)
Xue, YunLing, S906 (SAT-572)
Xu, Feiyang, S676 (SAT-239)
Xu, H. Eric, S68 (OS-107), S74 (LBP-015)
Xu, Hongqin, S373 (WED-355)
Xu, Jia, S959 (WED-586)
Xu, Jian, S362 (THU-356)
Xu, Junfang, S685 (FRI-156)
Xu, Jun-Hao, S893 (THU-633)
Xu, Junjie, S466 (WED-259), S511 (FRI-370)
Xu, Lankai, S125 (FRI-091), S775 (THU-043)
Xu, Liang, S86 (LBP-041), S225 (WED-537)
Xu, Lidong, S609 (WED-182)
Xu, Long, S292 (FRI-298)
Xu, Manman, S146 (SAT-460), S676 (SAT-240)
Xun, Jingqiong, S260 (TOP-357)
Xu, Peishuang, S228 (WED-544), S754 (THU-508)
Xu, Ping, S540 (THU-154)
Xu, Shaodian, S38 (OS-054)
Xu, Suowen, S627 (TOP-143)
Xu, Wenxin, S617 (WED-201)
Xu, Wenxiong, S155 (SAT-491), S155 (SAT-493)
Xu, Xianbin, S158 (SAT-501), S262 (SAT-331)
Xu, Xiaorong, S358 (THU-341)
Xu, Xiaowei, S81 (LBP-031), S118 (FRI-071), S153 (SAT-482), S161 (SAT-508), S177 (FRI-426), S452 (THU-412)
Xu, Xiaoyuan, S225 (WED-537)
Xu, Xinyi, S158 (SAT-501)
Xu, Xue, S924 (SAT-620)
Xu, Xuesong, S41 (OS-062)
Xu, Ya, S617 (WED-201)
Xu, Yan, S512 (FRI-377)
Xu, Yang, S57 (OS-088), S372 (WED-350)
Xu, Yifan, S356 (SAT-444)

Xu, Ying, S600 (WED-153)
Xu, YuanYuan, S918 (SAT-605)
Xu, Zhengao, S593 (WED-134)
Xu, Ziheng, S716 (WED-562-YI)
Xu, Zuoheng, S73 (LBP-013)
Xu, Zuzhi, S87 (LBP-044)
Xv, Yuanyuan, S688 (FRI-167)

Ya'akov, Ami Ben, S289 (FRI-286)
Yaccob, Afif, S613 (WED-189)
Yadav, Abhilasha, S288 (FRI-282)
Yadav, Manisha, S104 (THU-071-YI), S105 (THU-073-YI), S105 (THU-074), S108 (TOP-208-YI), S120 (FRI-074), S129 (TOP-224-YI), S131 (FRI-105-YI), S138 (FRI-132), S139 (FRI-135-YI), S265 (SAT-341), S269 (SAT-354-YI), S269 (SAT-355), S276 (THU-324-YI), S280 (THU-337), S361 (THU-354), S373 (WED-353-YI)
Yadav, Pushpa, S478 (WED-371)
yadav, Rajni, S174 (FRI-415-YI), S181 (FRI-441-YI), S184 (FRI-452-YI), S274 (THU-318), S282 (FRI-262-YI), S629 (TOP-161-YI)
Yadav, Sanju, S104 (THU-071-YI), S105 (THU-073-YI), S105 (THU-074), S120 (FRI-074), S129 (TOP-224-YI), S131 (FRI-105-YI), S138 (FRI-132), S139 (FRI-135-YI), S264 (SAT-335), S264 (SAT-336), S265 (SAT-341), S269 (SAT-354-YI), S269 (SAT-355), S276 (THU-324-YI), S280 (THU-337), S361 (THU-354), S373 (WED-353-YI)
Yadav, Vaishali, S126 (FRI-092-YI), S288 (FRI-282), S292 (FRI-299)
Yadav, Vipin, S288 (FRI-282), S292 (FRI-299)
Yaghi, Shahd, S980 (FRI-634)
Yaginuma, Reiko, S225 (WED-533), S246 (FRI-356)
Yağlı, Mehmet Akif, S961 (WED-589)
Yahia, Yousef, S732 (THU-446)
Yaid, Humed, S822 (WED-026)
Yakovenko, Nadiia, S739 (THU-465)
Yakub, Salman, S975 (WED-636), S976 (WED-637)
Yalamanchili, Sreeni, S962 (WED-593)
Yalamanchili, Sreenivasu, S939 (FRI-587)
Yalçinkaya, Kezban Tulay, S807 (FRI-025)
Yale, Kitty, S64 (OS-099), S681 (FRI-142), S697 (FRI-191)
Yamada, Ren, S506 (FRI-256)
Yamada, Tomomi, S977 (WED-639)
Yamagishi, Toshiyuki, S861 (WED-313)
Yamaguchi, Kanji, S977 (WED-639)
Yamaguchi, Mayumi, S336 (SAT-379)
Yamaguchi, Yuki, S686 (FRI-159)
Yamamoto, Takuya, S880 (THU-590)
Yamamoto, Yasunori, S675 (SAT-237)
Yamamoto, Yoshihiro, S606 (WED-171)
Yamamoto, Yoshiya, S506 (FRI-256)
Yamana, Hayato, S258 (SAT-549), S979 (WED-644)
Yamani, Fatmah, S522 (THU-095)
Yamao, Mikaru, S873 (THU-564)
Yamasaki, Kazumi, S249 (SAT-522), S258 (SAT-549), S970 (WED-618), S976 (WED-638), S979 (WED-644)
Yamashina, Shunhei, S225 (WED-533), S246 (FRI-356)
Yamashita, Taro, S977 (WED-639)
Yamashita, Tsutomu, S258 (SAT-549), S550 (THU-188), S979 (WED-644)
Yamashita, Yuki, S336 (SAT-379)
Yamazhan, Tansu, S396 (FRI-513), S397 (FRI-514)
Yamazoe, Taiji, S32 (OS-045), S121 (FRI-076-YI), S488 (WED-403)
Yam, Judy Wai-Ping, S896 (THU-644)
Yanagawa, Yasuaki, S811 (FRI-037)
Yan, Caixia, S74 (LBP-014)
Yanez, Mariadelcarmen, S432 (THU-238)
Yan, Fengna, S452 (THU-413)
Yang, Aiming, S68 (OS-107)
Yang, Bin, S674 (SAT-233)
Yang, Boyu, S558 (TOP-063-YI), S607 (WED-174-YI)
Yang, Chen, S81 (LBP-031)
Yang, Cheng Yong, S81 (LBP-031), S884 (THU-605)
Yang, Daokun, S964 (WED-601-YI)
Yang, Dawei, S30 (OS-040), S627 (TOP-130), S640 (SAT-123)
Yang, Fangkun, S517 (TOP-114)
Yang, Hailin, S702 (FRI-206)
Yang, Haiyan, S433 (THU-239)
Yang, Hannah, S426 (THU-219-YI)
Yang, Haoyu, S763 (THU-011)
Yang, Hsiu-Chiung, S702 (FRI-206)
Yang, Huayu, S628 (TOP-145)
Yang, Hui, S259 (SAT-554), S593 (WED-134), S609 (WED-182), S763 (THU-011), S924 (SAT-620)
Yang, Huifen, S909 (SAT-579)
Yang, Hung-Chih, S898 (TOP-566-YI), S898 (TOP-567), S917 (SAT-601-YI)
Yang, Hwai-I, S274 (THU-319), S797 (TOP-033), S898 (TOP-567), S898 (TOP-568), S915 (SAT-594), S917 (SAT-601-YI), S929 (SAT-633), S972 (WED-624)
Yang, Hwasun, S426 (THU-219-YI)
Yang, Hyun, S592 (WED-127), S917 (SAT-602)
Yang, Iiu, S895 (THU-640)
Yang, Jay, S84 (LBP-036)
Yang, Jianzheng, S270 (SAT-356)
Yang, Jin, S472 (WED-273)
Yang, Jingmao, S369 (WED-341)
Yang, Jingning, S941 (FRI-591)
Yang, Ji Won, S513 (FRI-378), S707 (THU-547)
Yang, Ju Dong, S375 (TOP-519), S452 (THU-414-YI), S492 (FRI-218), S497 (FRI-234), S723 (THU-418)
Yang, Julia, S68 (OS-107), S74 (LBP-015)
Yang, Junhong, S609 (WED-182), S924 (SAT-620)
Yang, Kangsen, S6 (GS-010), S644 (SAT-136)
Yang, Keungmo, S510 (FRI-368)
Yang, Li, S68 (OS-107), S725 (THU-426), S756 (THU-512)
Yang, Ling, S119 (FRI-072)
Yang, Liqiong, S896 (THU-644)
Yang, Liu, S437 (THU-362), S791 (SAT-039), S792 (SAT-040), S946 (FRI-606)
Yang, Mei, S909 (SAT-579)
Yang, Qi, S468 (WED-264), S676 (SAT-240)
Yang, Qihong, S139 (FRI-134)
Yang, Qijun, S745 (THU-483)
Yang, Qiong, S812 (FRI-040)
Yang, Rui-Xu, S62 (OS-097), S516 (TOP-113)
Yang, Sejung, S732 (THU-447)
Yang, Shengsheng, S74 (LBP-015)
Yang, Sheng-Shun, S969 (WED-613)
Yang, Shizhong, S456 (WED-233)
Yang, Shuo, S208 (WED-481), S279 (THU-336), S785 (SAT-021)
Yang, Sisi, S262 (SAT-331)
Yang, Song, S433 (THU-239)
Yang, Tao, S34 (OS-048)
Yang, Tianyuan, S793 (SAT-043)
Yang, Tzeng-Hue, S943 (FRI-596)
Yang, Wang, S452 (THU-413)
Yang, Wanting, S225 (WED-537), S917 (SAT-601-YI)
Yang, Wenjia, S259 (SAT-554)
Yang, Xiao, S303 (SAT-255)
Yang, Xinyue, S894 (THU-636)
Yang, Yan, S593 (WED-134), S763 (THU-011)
Yang, Yanhui, S253 (SAT-533), S279 (THU-336), S785 (SAT-021), S813 (FRI-045)
Yang, Yao-Hsu, S773 (THU-038)
Yang, Yida, S262 (SAT-331)
Yang, Yifan, S656 (SAT-175)
Yang, Yilin, S134 (FRI-115)
Yang, Yingxia, S259 (SAT-554)
Yang, Yongfeng, S30 (OS-040), S331 (SAT-368-YI), S352 (SAT-428-YI), S627 (TOP-130), S640 (SAT-123)
Yang, Yun-Hui, S201 (WED-458)
Yang, Zeyuan, S355 (SAT-441)
Yang, Zhou, S258 (SAT-548), S452 (THU-413)
Yang, Zijing, S864 (WED-320-YI)
Yan, Hexin, S42 (OS-063)
Yan, Qiang, S593 (WED-134), S609 (WED-182)
Yan, Shunhua, S974 (WED-628)
Yan, Shuo, S119 (FRI-072)
Yan, Xiaji, S473 (WED-361-YI)
Yan, Xiaomin, S930 (SAT-634), S933 (SAT-642)
Yan, Yan, S437 (THU-362)
YanZhe Lim, Ryan, S442 (THU-379)
Yao, Chengxuan, S676 (SAT-240), S934 (SAT-644)
Yao, Heng, S361 (THU-353)

Author Index

Yao, Linmei, S932 (SAT-639)
Yao, Lvfeng, S86 (LBP-041)
Yao, Renling, S933 (SAT-642)
Yao, Rongyan, S270 (TOP-328), S276 (THU-323)
Yao, Yingcheng, S676 (SAT-238)
Yao, Zheng, S688 (FRI-167)
Yapıcı, Hasan Basri, S160 (SAT-507), S311 (SAT-272-YI)
Yaqub, Sheraz, S451 (THU-409)
Yarchoan, Mark, S38 (OS-055), S491 (TOP-408-YI)
Yardeni, David, S76 (LBP-021)
Yarnoz, Patricia, S608 (WED-175)
Yasheng, Repikaiti, S243 (FRI-348)
Yashiro, Hiroaki, S667 (SAT-213)
Yasso, Maryam, S713 (WED-555)
Yasui, Yutaka, S439 (THU-368), S506 (FRI-256)
Yataco, Maria, S390 (FRI-493-YI)
Yates, Mark, S615 (WED-197)
Yatsuhashi, Hiroshi, S249 (SAT-522), S258 (SAT-549), S550 (THU-188), S943 (FRI-594), S970 (WED-618), S976 (WED-638), S977 (WED-639), S979 (WED-644)
Yazarkan, Yigit, S113 (FRI-052), S126 (FRI-093)
Ye, Bicheng, S119 (FRI-072), S549 (THU-184), S560 (TOP-080), S593 (WED-134), S609 (WED-182)
Ye, Bin, S73 (LBP-013)
Yee, Leland J., S809 (FRI-030), S943 (FRI-594), S953 (FRI-624)
Yee, Michael, S563 (WED-041)
Ye, Feng, S151 (SAT-476)
Yehezkel, Eyal, S325 (SAT-320)
Yeh, Heidi, S112 (FRI-051)
Yeh, Hsing-Yu, S898 (TOP-566-YI)
Yeh, Jen-Hao, S943 (FRI-596)
Yeh, Ming-Lun, S62 (OS-097), S373 (WED-354), S516 (TOP-113), S518 (TOP-128), S536 (THU-138), S557 (THU-214)
Ye, Huilan, S763 (THU-011)
Yela, Elena, S710 (THU-557-YI)
Ye, Lei, S939 (FRI-587), S956 (WED-576)
Ye, Lili, S119 (FRI-072), S259 (SAT-554), S609 (WED-182), S763 (THU-011), S924 (SAT-620)
Yendewa, George, S922 (SAT-612)
Yeoh, Jeremy, S287 (FRI-276-YI), S292 (FRI-300-YI), S858 (WED-300-YI)
Yeo, Jeremy, S818 (WED-013)
Yeo, Lucas, S528 (THU-110)
Yeoman, Andrew, S338 (SAT-385)
Yeoman, Jeppe Remme, S631 (SAT-094-YI)
Yeon, Jong Eun, S135 (FRI-120), S498 (FRI-236)
Yeo, Yee Hui, S98 (SAT-087)
Yepes Barreto, Ismael de Jesus, S112 (FRI-050)
Yepes, Jorge, S226 (WED-538)
Yepes, Valentina, S793 (SAT-044)
Ye, Yong'an, S233 (FRI-314), S664 (SAT-202), S797 (SAT-054), S872 (THU-562)
Ye, Zizhen, S756 (THU-512)
Yi, Changhua, S30 (OS-040), S627 (TOP-130), S640 (SAT-123)
Yi, Dawei, S488 (WED-409-YI)
Yildiran, Dilara, S807 (FRI-025)
Yilihaer, Yierfan, S377 (FRI-450)
Yilmaz-Elis, Seda, S647 (SAT-149)
Yilmaz, Sezai, S899 (SAT-556-YI)
Yilmaz, Sinan, S376 (TOP-520-YI)
Yilmaz, Yusuf, S7 (LBO-001), S62 (OS-097), S127 (FRI-095), S302 (SAT-254), S311 (SAT-272-YI), S395 (FRI-511-YI), S424 (TOP-376), S516 (TOP-113), S766 (THU-015), S794 (SAT-046), S923 (SAT-618)
Yimam, Kidist, S10 (LBO-006), S315 (SAT-286), S342 (SAT-398)
Yim, Hyung Joon, S1 (GS-001), S956 (TOP-598), S957 (WED-577)
Yiming, Wang, S244 (FRI-351)
Yin, Benny, S702 (FRI-206)
Yin, Chuan, S661 (SAT-195)
Yin, Dandan, S627 (TOP-130), S640 (SAT-123)
Yin, Dedong, S160 (SAT-507)
Ying, Huimin, S560 (TOP-080)
Ying, Shuaibing, S489 (WED-410), S870 (TOP-645)
Yin, Guo, S285 (FRI-269), S293 (FRI-301)
Yin, James Liu, S768 (THU-023), S859 (WED-304), S860 (WED-305)
Yin, Jingping, S609 (WED-182)
Yin, Ke, S593 (WED-133)
Yin, Lishi, S166 (FRI-393)
Yin, Nicolas, S907 (SAT-575)
Yin, Quan, S181 (FRI-436)
Yin, Shengxia, S930 (SAT-635)
Yin, Szu-Ching, S778 (THU-051)
Yin, Xiuhong, S511 (FRI-370)
Yin, Yalin, S952 (FRI-623)
Yin, Yi, S455 (TOP-405)
Yin, Ziwei, S809 (FRI-031)
Yin, Zundong, S826 (WED-040)
Yip, Cyril CY, S868 (FRI-644)
Yip, Terry, S451 (THU-410)
Yip, Terry Cheuk-Fung, S19 (OS-017), S66 (OS-103-YI), S224 (WED-531), S452 (THU-414-YI), S517 (TOP-114), S525 (THU-103), S558 (TOP-063-YI), S560 (TOP-066), S561 (TOP-082), S574 (WED-075), S579 (WED-089), S589 (WED-118), S593 (WED-134), S607 (WED-174-YI), S612 (WED-187-YI), S618 (WED-204), S621 (WED-215), S738 (THU-463), S906 (SAT-574), S928 (SAT-628-YI), S931 (SAT-637), S946 (FRI-604), S979 (WED-643)
Yip, Vincent, S455 (TOP-406)
Yip, Wan Fen, S211 (WED-491)
Yıldırım, Abdullah Emre, S160 (SAT-507)
Yılmaz, Volkan, S519 (THU-089), S588 (WED-116)
Yki-Jarvinen, Hannele, S662 (SAT-197), S777 (THU-050)
Yla-Outinen, Heli, S5 (GS-008)
Yoh, Tomoaki, S420 (THU-529-YI)
Yokohama, Shiro, S550 (THU-188)
Yokomori, Hiroaki, S524 (THU-102)
Yoneda, Masato, S517 (TOP-114), S525 (THU-103), S558 (TOP-063-YI), S589 (WED-118), S607 (WED-174-YI), S612 (WED-187-YI), S618 (WED-204), S621 (WED-215), S667 (SAT-213), S686 (FRI-159)
Yong, Xiaolan, S688 (FRI-167)
Yoo, Jeong-Ju, S590 (WED-121)
Yoon, Eileen, S545 (THU-171), S590 (WED-121), S591 (WED-122), S625 (WED-229), S630 (SAT-092), S652 (SAT-165), S686 (FRI-163)
Yoon, Jaehyun, S497 (FRI-233), S813 (FRI-046)
Yoon, Jung-Hwan, S502 (FRI-245), S507 (FRI-361), S509 (FRI-366)
Yoon, Jun Sik, S497 (FRI-233)
Yoon, Moon Gyeong, S264 (SAT-337)
Yoon, Paul, S308 (SAT-265), S309 (SAT-266)
Yoon, Sang Joon, S266 (SAT-345)
Yoon, Sung-Hoon, S519 (THU-087)
Yoo, Yang Jae, S498 (FRI-236), S813 (FRI-046)
Yoo, Youngeun, S251 (SAT-528)
Yoshida, Eric, S967 (TOP-600-YI)
Yoshida, Osamu, S675 (SAT-237)
Yoshida, Sonoe, S506 (FRI-256)
Yoshida, Sumiko, S550 (THU-188)
Yoshiji, Hitoshi, S95 (SAT-077), S162 (TOP-438), S263 (SAT-334), S652 (SAT-164), S660 (SAT-189), S747 (THU-491), S977 (WED-639)
Yoshimura, Kaori, S331 (SAT-368-YI)
Yoshimura, Kohei, S420 (THU-529-YI)
Yoshio, Sachiyo, S880 (THU-590)
Yosry, Ayman, S551 (THU-191)
Yotebieng, Marcel, S80 (LBP-028-YI)
You, Hang, S108 (THU-083), S269 (SAT-353)
You, Hong, S68 (OS-107), S826 (WED-040), S897 (TOP-565)
You, Liping, S473 (WED-361-YI)
Younes, Mehdi, S497 (FRI-234), S723 (THU-418)
Younes, Ramy, S20 (OS-018)
Younger, Nicholas, S454 (TOP-390-YI)
Young-Greenwald, William, S259 (SAT-553)
Young, Jesse, S919 (SAT-607)
Younossi, Issah, S128 (FRI-099)
Younossi, Zobair M., S62 (OS-097), S126 (FRI-094), S127 (FRI-095), S128 (FRI-099), S356 (SAT-443), S377 (FRI-451), S378 (FRI-457), S395 (FRI-511-YI), S417 (FRI-581), S424 (TOP-376), S516 (TOP-113), S522 (THU-094), S522 (THU-095), S532 (THU-125), S557 (THU-213), S575 (WED-077), S615 (WED-197), S758 (TOP-001), S766 (THU-015),

S789 (SAT-031-YI), S790 (SAT-035), S793 (SAT-045), S794 (SAT-046), S794 (SAT-047), S795 (SAT-050), S795 (SAT-051), S796 (SAT-053), S923 (SAT-618)
You, Ruirui, S954 (FRI-627)
You, Senlin, S932 (SAT-640)
You, Shaoli, S151 (SAT-476)
You, Shihyun, S959 (WED-585)
You, Young Kyoung, S482 (WED-386)
You, Zhengrui, S293 (FRI-302-YI)
Ytting, Henriette, S262 (SAT-332), S298 (SAT-245), S333 (SAT-369), S338 (SAT-384)
Yu, Amanda, S821 (WED-024), S967 (TOP-600-YI)
Yuan, Chang, S140 (FRI-137)
Yuan, Changrong, S201 (WED-458)
Yuan, Jiahao, S88 (TOP-192)
Yuan, Liyun, S386 (FRI-482), S411 (FRI-561-YI), S413 (FRI-570)
Yuan, Wei, S162 (TOP-440)
Yuan, Yingchun, S756 (THU-514)
Yu, Binghui, S676 (SAT-239)
Yu, Catherine, S218 (WED-513), S749 (THU-496)
Yücel, Lea Aylin, S280 (THU-338-YI)
Yudin, Mark, S70 (LBP-005), S975 (WED-636), S976 (WED-637)
Yu, Dongman, S513 (FRI-378)
Yue, Kun, S73 (LBP-012)
Yuen, Man-Fung, S1 (GS-001), S8 (LBO-003), S46 (OS-070-YI), S85 (LBP-040), S86 (LBP-042), S87 (LBP-043), S422 (TOP-359-YI), S423 (TOP-360), S438 (THU-364), S496 (FRI-230), S824 (WED-035), S896 (THU-644), S915 (SAT-593), S928 (SAT-628-YI), S933 (SAT-643), S947 (FRI-609), S956 (TOP-598), S959 (WED-586), S960 (WED-588), S964 (WED-597), S965 (WED-602)
Yue, Wei, S812 (FRI-040)
Yu, Hao, S261 (TOP-358)
Yu, Hui, S702 (FRI-206)
Yu, Jenny, S602 (WED-158)
Yu, Jeong Il, S502 (FRI-245)
Yu, Jie, S502 (FRI-247)
Yujie, Lin, S891 (THU-626), S917 (SAT-603)
Yu, Lequan, S423 (TOP-360)
Yu, Meihong, S81 (LBP-031)
Yu, Meng, S293 (FRI-302-YI)
Yu, Ming-Lung, S62 (OS-097), S127 (FRI-095), S238 (FRI-332), S373 (WED-354), S516 (TOP-113), S518 (TOP-128), S536 (THU-138), S557 (THU-214), S766 (THU-015), S794 (SAT-046), S923 (SAT-618), S958 (WED-580)
Yu, Ning, S430 (THU-229), S617 (WED-201), S932 (SAT-641)
Yun, Sung-Cheol, S251 (SAT-528)
Yun, Yeochan, S891 (THU-625)
Yu, Pengfei, S852 (TOP-312)
Yu, Philip, S422 (TOP-359-YI), S423 (TOP-360)
Yurdaydin, Cihan, S49 (OS-075), S77 (LBP-021), S880 (THU-591), S899 (SAT-556-YI), S943 (FRI-594), S961 (WED-589), S962 (WED-594), S965 (WED-603)
Yuste, Eloisa, S806 (FRI-024)
Yu, Su Jong, S502 (FRI-245), S507 (FRI-361), S509 (FRI-366), S590 (WED-121), S906 (SAT-573)
Yusupalieva, Shakhlo, S822 (WED-027)
Yu, Weien, S964 (WED-601-YI)
Yu, Weifeng, S42 (OS-063)
Yu, Xia, S158 (SAT-501), S262 (SAT-331)
Yu, Xueping, S964 (WED-601-YI)
Yu, Yanlong, S33 (OS-047)
Yu, Yan-Yan, S932 (SAT-641)
Yu, Yina, S896 (THU-641)
Yu, Yingpu, S891 (THU-624-YI)
Yu, Yiqi, S954 (FRI-627)
Yu, Yi-Ru, S643 (SAT-133)
Yuyong, Jiang, S452 (THU-413)
Yu, Yue, S362 (THU-356)
Yu, Zhu-Qin, S609 (WED-182)

Zaaijer, Hans, S817 (WED-011)
Zaccherini, Giacomo, S35 (OS-050-YI), S185 (TOP-455-YI), S196 (WED-445), S212 (WED-494-YI), S479 (WED-378)
Zacharasiewicz, Angela, S975 (WED-634-YI)
Zachariah, Uday, S722 (THU-416)
Zacharias, Harry, S227 (WED-540-YI)
Zachou, Kalliopi, S300 (SAT-250), S305 (SAT-260-YI), S314 (SAT-283)
Zaghloul, Nariman, S504 (FRI-252), S524 (THU-101)
Zago, Alessandra, S325 (SAT-320)
Zagorska, Anna, S84 (LBP-037)
Zagorski, Jamie, S813 (FRI-047)
Zaharia, Mihai, S543 (THU-165)
Zahhaf, Amel, S90 (SAT-059)
Zahra Ajana, Fatima, S845 (THU-287)
Zahra Chabib, Fatima, S845 (THU-287)
Zakary, Nawaf Yahya, S522 (THU-094)
Zakharova, Evgeniia, S595 (WED-136)
Zakharova, Stanislava, S595 (WED-136)
Zaky, Samy, S524 (THU-101)
Zalesiak, Marie, S796 (SAT-052)
Zalewska, Marta, S409 (FRI-555)
Zalewski, Tim, S199 (WED-452)
Zaltron, Serena, S900 (SAT-559), S901 (SAT-560), S936 (TOP-584), S938 (FRI-586)
Zamalloa, Ane, S139 (FRI-133)
Zamora, Javier, S731 (THU-445-YI)
Zamparelli, Marco Sanduzzi, S427 (THU-220), S481 (WED-382-YI)
Zampato, Claudio, S18 (OS-014-YI)
Zampino, Rosa, S901 (SAT-559), S902 (SAT-560), S938 (FRI-586)
Zanaga, Paola, S601 (WED-156)
Zancotti, Georgia, S465 (WED-256)
Zanetto, Alberto, S33 (OS-046), S52 (OS-081), S148 (SAT-466-YI), S193 (WED-431-YI), S435 (THU-247), S721 (THU-415), S752 (THU-501)
Zangneh, Hooman Farhang, S436 (THU-249)
Zannou, Vaele, S762 (THU-009)
Zanus, Giacomo, S466 (WED-258)
Zao, Xiaobin, S233 (FRI-314), S665 (SAT-205), S666 (SAT-206), S872 (THU-562)
Zapata, Eva María, S830 (THU-253)
Zapata-Pavas, Leidy Estefanía, S30 (OS-039-YI), S272 (THU-315-YI), S273 (THU-316), S278 (THU-333-YI), S489 (WED-412-YI), S633 (SAT-101-YI), S855 (WED-287-YI)
Zapata, Rodrigo, S296 (TOP-281), S306 (SAT-262)
Zapatero, Ana Miqueleiz, S910 (SAT-585)
Zapatero, Juliana, S146 (SAT-461)
Zappitelli, Teresa, S304 (SAT-258)
Zarębska-Michaluk, Dorota, S970 (WED-617-YI), S980 (FRI-633)
Zare, Diba, S639 (SAT-120)
Zarei, Sara, S178 (FRI-428-YI), S631 (SAT-093-YI)
Zaru, Salvatore, S857 (WED-298)
Zatelli, Stefania, S975 (WED-635)
Zavalis, Emmanuel, S953 (FRI-625)
Zayed, Essam, S524 (THU-101)
Zayed, Naglaa Zayed, S551 (THU-191)
Zazour, Abdelkrim, S309 (SAT-267), S578 (WED-086)
Zazzi, Maurizio, S807 (FRI-025)
Zecher, Britta, S351 (SAT-427)
Zeitlhoefler, Marcus, S453 (TOP-389), S459 (WED-242-YI)
Zeitone, Abeer, S847 (THU-300), S848 (THU-301)
Zelaya, Carolina M. Perdomo, S608 (WED-175)
Zelber-Sagi, Shira, S62 (OS-097), S127 (FRI-095), S713 (WED-557), S758 (TOP-001), S766 (THU-015), S794 (SAT-046), S794 (SAT-047), S796 (SAT-053)
Zelber, Shira, S532 (THU-125)
Zelikoff, Brittany, S388 (FRI-489)
Zeller, Amos, S33 (OS-046)
Zellos, Aglaia, S56 (OS-086), S832 (THU-258-YI), S842 (THU-284), S850 (THU-308)
Zender, Lars, S9 (LBO-004)
Zeng, Ge, S869 (TOP-630), S872 (THU-561)
Zeng, Georgia, S452 (THU-414-YI)
Zeng, Hui-cheng, S243 (FRI-348)
Zeng, Jingwei, S811 (FRI-038)
Zeng, Qinghe, S38 (OS-054)
Zeng, Qing-Lei, S560 (TOP-080), S954 (FRI-626)
Zeng, Renqiang, S778 (THU-053)
Zeng, Weifang, S86 (LBP-041)
Zeng, Xianzhang, S517 (TOP-114)

Author Index

zeng, yilan, S952 (FRI-623), S955 (FRI-628)
Zeng, Yongyi, S593 (WED-134)
Zeng, Zhong, S270 (TOP-328), S276 (THU-323)
Zeni, Nicola, S30 (OS-041), S97 (SAT-084-YI), S196 (WED-443), S227 (WED-541-YI)
Zenker, Martin, S834 (THU-260)
Zenovia, Sebastian, S210 (WED-490), S211 (WED-493)
Zen, Yoh, S404 (FRI-538-YI), S458 (WED-237-YI)
Zermatten, Maxime, S72 (LBP-011)
Zervos, Bobby, S58 (OS-089), S313 (SAT-282), S565 (WED-050)
Zeuzem, Nicholas, S151 (SAT-477)
Zeuzem, Stefan, S210 (WED-485), S251 (SAT-525), S601 (WED-155), S930 (SAT-636)
Zewde, Wasihun, S194 (WED-433)
Zeybel, Mujdat, S961 (WED-589), S965 (WED-603)
Zhai, Bo, S42 (OS-063)
Zhai, Qiongli, S511 (FRI-370)
Zhalka, Abdellatif Zhalka, S251 (SAT-527)
Zhanasbayeva, Marzhan, S822 (WED-027)
Zhang, Bangjie, S86 (LBP-041)
Zhang, Boyan, S670 (SAT-221-YI)
Zhang, Cai-Yun, S30 (OS-040), S627 (TOP-130), S640 (SAT-123)
Zhang, Can, S513 (FRI-379)
Zhang, Cen, S88 (TOP-192)
Zhang, Cheng, S458 (WED-237-YI)
Zhang, Chiwei, S119 (FRI-072), S560 (TOP-080)
Zhang, Chunqing, S755 (THU-511), S757 (THU-515)
Zhang, David, S166 (FRI-393), S228 (WED-543)
Zhang, Dawei, S511 (FRI-370)
Zhang, Dazhi, S81 (LBP-031)
Zhang, Feiyu, S133 (FRI-110)
Zhang, Feng, S30 (OS-040), S52 (OS-081), S228 (WED-542), S230 (TOP-344), S747 (THU-492)
Zhang, Grace, S406 (FRI-543)
Zhang, Guo, S119 (FRI-072), S259 (SAT-554), S593 (WED-134), S609 (WED-182), S924 (SAT-620)
Zhang, Guodong, S86 (LBP-041), S954 (FRI-626)
Zhang, Guoliang, S763 (THU-011)
Zhang, Guoqiang, S34 (OS-048)
Zhang, Guoqing, S593 (WED-134)
Zhang, Hao, S609 (WED-182)
Zhang, Heidi, S8 (LBO-003)
Zhang, Hong, S950 (FRI-618), S955 (FRI-628)
Zhang, Hongfei, S950 (FRI-617), S950 (FRI-618), S955 (FRI-628)
Zhang, Hu, S869 (TOP-630), S872 (THU-561)
Zhang, Hui, S882 (THU-596)
Zhang, Jialing, S763 (THU-011)
Zhang, Jianping, S259 (SAT-554), S593 (WED-134), S609 (WED-182), S763 (THU-011), S924 (SAT-620)
Zhang, Jiateng, S852 (TOP-312)
Zhang, Jiawei, S119 (FRI-072)
Zhang, Jie, S609 (WED-182)
Zhang, Jieting, S701 (FRI-204)
Zhang, Jikai, S877 (THU-579-YI)
Zhang, Jiliang, S136 (FRI-122), S656 (SAT-179)
Zhang, Jiming, S201 (WED-458), S367 (WED-336), S374 (WED-356), S754 (THU-507), S877 (THU-578), S891 (THU-626), S917 (SAT-603), S918 (SAT-605), S944 (FRI-597), S952 (FRI-623), S954 (FRI-627), S964 (WED-601-YI)
Zhang, Jing, S86 (LBP-041), S136 (FRI-123), S626 (WED-230)
Zhang, Jinghao, S473 (WED-361-YI)
Zhang, Jun, S324 (SAT-318)
Zhang, Junchao, S763 (THU-011)
Zhang, Kaikai, S270 (SAT-356)
Zhang, Kaili, S81 (LBP-031)
Zhang, Ke, S467 (WED-260)
Zhang, Le, S713 (WED-557)
Zhang, Li, S558 (THU-215), S906 (SAT-572)
Zhang, Liangjun, S87 (LBP-044)
Zhang, Liaoyun, S941 (FRI-591)
Zhang, Lisha, S884 (THU-605)
Zhang, Long, S685 (FRI-156)
Zhang, Lu, S615 (WED-197), S895 (THU-638)
Zhang, Margery, S779 (SAT–004)
Zhang, Meng, S47 (OS-071), S463 (WED-252), S791 (SAT-039), S792 (SAT-040), S873 (THU-569), S895 (THU-640), S946 (FRI-606)
Zhang, Mengmeng, S88 (TOP-192), S98 (SAT-088), S331 (SAT-367), S370 (WED-345)
Zhang, Mengyin, S891 (THU-624-YI)
Zhang, Min, S68 (OS-107)
Zhang, Mingyuan, S373 (WED-355)
Zhang, Nan, S604 (WED-166)
Zhang, Nayi, S119 (FRI-072)
Zhang, Ningning, S261 (TOP-358), S502 (FRI-246)
Zhang, Peizhuo, S701 (FRI-204)
Zhang, Qiao, S74 (LBP-014)
Zhang, Qingge, S560 (TOP-080)
Zhang, Qinsheng, S74 (LBP-014)
Zhang, Qiran, S954 (FRI-627)
Zhang, Qun, S930 (SAT-635), S933 (SAT-642)
Zhang, Rui, S171 (FRI-409-YI), S628 (TOP-146)
Zhang, Saisai, S896 (THU-644), S933 (SAT-643)
Zhang, Shaobo, S487 (WED-402), S674 (SAT-234)
Zhang, Shaoqiu, S930 (SAT-634), S930 (SAT-635), S933 (SAT-642)
Zhang, Shenyan, S964 (WED-601-YI)
Zhang, Shuoen, S646 (SAT-141)
Zhang, Shuwen, S261 (TOP-358)
Zhang, Sitong, S136 (FRI-122), S656 (SAT-179)
Zhang, Tianru, S513 (FRI-379)
Zhang, Ting, S6 (GS-010), S644 (SAT-136)
Zhang, Tingyu, S665 (SAT-205)
Zhang, Wei, S30 (OS-040), S112 (FRI-051), S756 (THU-514), S941 (FRI-591)
Zhang, Weiguo, S884 (THU-605)
Zhang, Weituo, S68 (OS-107)
Zhang, Wen, S68 (OS-107)
Zhang, Wenhong, S954 (FRI-627)
Zhang, Wenhua, S941 (FRI-591), S950 (FRI-617)
Zhang, Xiangwen, S472 (WED-273)
Zhang, Xiaofeng, S756 (THU-513)
Zhang, Xiaotao, S590 (WED-120), S762 (THU-008)
Zhang, Xiaoyong, S896 (THU-642), S955 (FRI-629)
Zhang, Xiaoyu, S658 (SAT-183)
Zhang, Xin, S661 (SAT-195)
Zhang, Xinrong, S924 (SAT-620), S966 (WED-604)
Zhang, Xinxin, S964 (WED-601-YI)
Zhang, Xiuding, S158 (SAT-501)
Zhang, Xiufeng, S259 (SAT-554)
Zhang, Xiyu, S73 (LBP-013)
Zhang, Xue, S454 (TOP-391), S514 (FRI-380), S668 (SAT-217-YI)
Zhang, Xuefeng, S399 (FRI-522)
Zhang, Xueyun, S162 (TOP-439), S367 (WED-336), S374 (WED-356)
Zhang, Yan, S685 (FRI-156)
Zhang, Yanyun, S160 (SAT-507)
Zhang, Yao, S367 (WED-336), S374 (WED-356), S688 (FRI-167)
Zhang, Yaxi, S233 (FRI-314), S665 (SAT-204), S665 (SAT-205), S872 (THU-562)
Zhang, Yeqiong, S155 (SAT-492)
Zhang, Yigan, S463 (WED-252)
Zhang, Yilin, S259 (SAT-554), S549 (THU-184), S593 (WED-134), S763 (THU-011)
Zhang, Yin, S73 (LBP-013)
Zhang, Yingting, S243 (FRI-347)
Zhang, Yinqiu, S119 (FRI-072), S560 (TOP-080)
Zhang, Yongping, S357 (SAT-445)
Zhang, Yu, S108 (THU-083), S269 (SAT-353), S356 (SAT-444)
Zhang, Yuwei, S560 (TOP-080)
Zhang, Yuyi, S162 (TOP-440)
Zhang, Zeyu, S456 (WED-233)
Zhang, Zhe, S933 (SAT-643)
Zhang, Zhen, S513 (FRI-379), S675 (SAT-236)
Zhang, Zhenfeng, S883 (THU-601-YI)
Zhang, Zhenwei, S68 (OS-107), S74 (LBP-015)
Zhang, Zhipeng, S73 (LBP-012)
Zhang, Zhiyi, S930 (SAT-635)

Zhang, Ziqi, S558 (THU-215)
Zhang, Zong, S86 (LBP-041)
Zhan, Yi, S489 (WED-413)
Zhan, Zhenzhen, S475 (WED-365)
Zhao, Bo, S809 (FRI-031)
Zhao, Caiyan, S24 (OS-028), S144 (SAT-452), S160 (SAT-507)
Zhao, Chenhui, S465 (WED-255)
Zhao, Di, S81 (LBP-031)
Zhao, Dong, S87 (LBP-044)
Zhao, Dongdong, S609 (WED-182)
Zhao, Fei, S675 (SAT-236)
Zhao, Gangde, S91 (SAT-067)
Zhao, Guanguan, S74 (LBP-015)
Zhao, Hong, S94 (SAT-074), S225 (WED-537)
Zhao, Jiali, S763 (THU-011)
Zhao, Kaitao, S895 (THU-639)
Zhao, Meng, S896 (THU-644), S933 (SAT-643)
Zhao, Mengyu, S98 (SAT-088)
Zhao, Minjie, S41 (OS-062), S279 (THU-334-YI), S359 (THU-347-YI)
Zhao, Qianwen, S655 (SAT-174), S677 (SAT-242)
Zhao, Qingwei, S74 (LBP-014)
Zhao, Rui, S86 (LBP-041), S146 (SAT-460), S676 (SAT-240)
Zhao, Siru, S433 (THU-239)
Zhao, Tiezheng, S609 (WED-182)
Zhao, Xiaoting, S201 (WED-458), S367 (WED-336), S877 (THU-578), S917 (SAT-603), S918 (SAT-605)
Zhao, Xinyan, S88 (TOP-192), S98 (SAT-088), S331 (SAT-367), S370 (WED-345)
Zhao, Xinyu, S233 (FRI-314), S664 (SAT-202), S664 (SAT-203), S665 (SAT-204), S666 (SAT-206), S797 (SAT-054), S872 (THU-562)
Zhao, Xun, S533 (THU-127-YI), S616 (WED-200)
Zhao, Yajuan, S593 (WED-134)
Zhao, Yang, S950 (FRI-618)
Zhao, Yu, S677 (SAT-241)
Zhao, Yujia, S884 (THU-605)
Zhao, Zhengbin, S955 (FRI-628)
Zhao, Zhengxiao, S428 (THU-225-YI)
Zhao, Zhou, S140 (FRI-137)
Zheng, Chao, S473 (WED-361-YI)
Zheng, Dan, S33 (OS-047)
Zheng, Dekai, S6 (GS-010), S260 (TOP-357), S486 (WED-397), S644 (SAT-136)
Zheng, Hang, S513 (FRI-379)
Zheng, Hui, S826 (WED-040)
Zheng, Jian-Ming, S151 (SAT-476)
Zheng, Katina, S160 (SAT-507)
Zheng, Luhan, S917 (SAT-603)
Zheng, Mengxian, S119 (FRI-072)
Zheng, Ming-Hua, S62 (OS-097), S127 (FRI-095), S156 (SAT-496), S215 (WED-505), S221 (WED-523), S228 (WED-543), S293 (FRI-302-YI), S423 (TOP-374), S452 (THU-414-YI), S516 (TOP-113), S517 (TOP-114), S525 (THU-103), S528 (THU-110), S558 (TOP-063-YI), S560 (TOP-066), S560 (TOP-080), S561 (TOP-082), S568 (WED-057-YI), S579 (WED-089), S589 (WED-118), S607 (WED-174-YI), S612 (WED-187-YI), S618 (WED-204), S621 (WED-215), S698 (FRI-197), S713 (WED-557), S766 (THU-015), S868 (TOP-616-YI)
Zheng, Shihao, S233 (FRI-314), S664 (SAT-202), S665 (SAT-204), S797 (SAT-054), S872 (THU-562)
Zheng, Sujun, S68 (OS-107)
Zheng, Xin, S24 (OS-028), S144 (SAT-452), S160 (SAT-507), S162 (TOP-440)
Zheng, Xinlin, S430 (THU-232)
Zheng, Xizhe, S676 (SAT-239)
Zheng, Yanan, S924 (SAT-620)
Zhi, Yang, S90 (SAT-060), S98 (SAT-089-YI)
Zhong, Bei, S73 (LBP-012)
Zhong, Bihui, S560 (TOP-066), S561 (TOP-082), S579 (WED-089)
Zhong, Chunxiu, S508 (FRI-363)
Zhong, Jianfeng, S924 (SAT-620)
Zhong, Jiatu, S664 (SAT-202), S664 (SAT-203), S666 (SAT-206), S797 (SAT-054)
Zhong, Kebo, S416 (FRI-579), S417 (FRI-580)
Zhong, Shan, S81 (LBP-031)
Zhong, Shihong, S955 (FRI-629)
Zhong, Xianfei, S86 (LBP-041)
Zhong, Yubo, S88 (TOP-192), S370 (WED-345)
Zhou, Anding, S270 (SAT-356)
Zhoudi, Wenxin, S153 (SAT-482), S161 (SAT-508), S177 (FRI-426)
Zhou, Guangde, S868 (TOP-616-YI)
Zhou, Guanlin, S225 (WED-537)
Zhou, Haoming, S362 (THU-356)
Zhou, Hongxia, S955 (FRI-628)
Zhou, Jian, S422 (TOP-359-YI)
Zhou, Jianing, S231 (FRI-304), S241 (FRI-341), S271 (THU-303), S279 (THU-335)
Zhou, Jun, S685 (FRI-156)
Zhou, Kaile, S685 (FRI-156)
Zhou, Kali, S308 (SAT-265), S309 (SAT-266)
Zhou, Li, S454 (TOP-392-YI)
Zhou, Ling, S228 (WED-544)
Zhou, Nian, S270 (SAT-356)
Zhou, Qi, S238 (FRI-333-YI), S244 (FRI-352), S244 (FRI-353)
Zhou, Qian, S151 (SAT-476)
Zhou, Rui, S273 (THU-316)
Zhou, Ruoqi, S158 (SAT-501)
Zhou, Taolong, S560 (TOP-080)
Zhou, Tianhui, S91 (SAT-067), S99 (TOP-194)
Zhou, Xiao-Jian, S981 (FRI-635), S981 (FRI-636)
Zhou, Xiaqing, S490 (WED-414)
Zhou, Xingbei, S81 (LBP-031)
Zhou, Xiqiao, S527 (THU-107), S560 (TOP-080)
Zhou, Yang, S955 (FRI-629)
Zhou, Yichen, S891 (THU-624-YI)
Zhou, Yuanhai, S906 (SAT-572)
Zhou, Yu-Jie, S293 (FRI-302-YI), S352 (SAT-428-YI)
Zhou, Yusen, S560 (TOP-080)
Zhou, Zhenyu, S511 (FRI-370)
Zhou, Zhenzhong, S511 (FRI-370)
Zhou, Zhigang, S511 (FRI-370)
Zhou, Zhihang, S192 (WED-429-YI), S441 (THU-372-YI), S454 (TOP-392-YI)
Zhou, Zhongguo, S438 (THU-363), S471 (WED-271), S511 (FRI-370)
Zhou, Zhongmin, S73 (LBP-013)
Zhou, Zhuojun, S74 (LBP-014)
Zhu, Alexander, S161 (SAT-509)
Zhu, Angela, S797 (SAT-055)
Zhuang, Hui, S826 (WED-040)
Zhuang, Kun Da, S495 (FRI-228-YI)
Zhuang, Manqi, S416 (FRI-579), S417 (FRI-580)
Zhuang, Yan, S91 (SAT-067)
Zhuang, Ying, S73 (LBP-013)
Zhu, Bing, S151 (SAT-476)
Zhu, Chaonan, S685 (FRI-156)
Zhu, Chong, S85 (LBP-040)
Zhu, Chuanwu, S24 (OS-028), S86 (LBP-041), S144 (SAT-452), S160 (SAT-507), S930 (SAT-634), S930 (SAT-635), S933 (SAT-642)
Zhuge, Yuzheng, S30 (OS-040), S228 (WED-542), S230 (TOP-344)
Zhu, Guangqi, S677 (SAT-242)
Zhu, Haoxiang, S201 (WED-458), S754 (THU-507), S877 (THU-578), S918 (SAT-605), S944 (FRI-597), S964 (WED-601-YI)
Zhu, Hongbin, S757 (THU-515)
Zhu, Hongxia, S954 (FRI-626)
Zhu, Jiayi, S129 (TOP-223)
Zhu, Julie, S229 (WED-545), S398 (FRI-516), S598 (WED-148)
Zhu, Li, S930 (SAT-634), S930 (SAT-635)
Zhu, Lingxiao, S177 (FRI-426)
Zhu, Liying, S952 (FRI-623)
Zhu, Mengqi, S359 (THU-346), S367 (WED-336)
Zhu, Minghui, S430 (THU-229), S508 (FRI-363)
Zhu, Qiang, S513 (FRI-379)
Zhu, Qing, S50 (OS-077), S85 (LBP-040)
Zhu, Shanshan, S954 (FRI-627)
Zhu, Shengtao, S511 (FRI-370)
Zhu, Wenfeng, S419 (THU-522)
Zhu, Wenwen, S261 (TOP-358)
Zhu, Xichen, S97 (SAT-086)
Zhu, Xuejing, S42 (OS-063)
Zhu, Yinghong, S6 (GS-010), S260 (TOP-357), S486 (WED-397)
Zhu, Yong, S511 (FRI-370)
Zhu, Yong-Fen, S119 (FRI-072), S259 (SAT-554), S609 (WED-182), S763 (THU-011), S924 (SAT-620)

Author Index

Zhu, YueYong, S941 (FRI-591), S952 (FRI-623)
Zhu, Yun, S98 (SAT-088)
Zhu, Yunxia, S934 (SAT-644)
Zhu, Zheng, S201 (WED-458)
Zhu, Zhibin, S816 (WED-007)
Zia, Zergham, S522 (THU-095)
Zibert, Andree, S854 (WED-284), S860 (WED-307), S862 (WED-316-YI)
Zidan, Ahmed, S250 (SAT-523), S390 (FRI-494), S390 (FRI-495)
Ziegler, Ramona, S785 (SAT-020)
Zieniewicz, Krzysztof, S445 (THU-385)
Zietz, Annika, S222 (WED-526-YI), S737 (THU-462)
Zigmond, Ehud, S10 (LBO-006), S302 (SAT-254), S325 (SAT-320)
Zignego, Anna Linda, S972 (WED-623)
Žigutytė, Laura, S331 (SAT-368-YI)
Žilinčanová, Daniela, S123 (FRI-085), S205 (WED-473)
Zilong, Wang, S593 (WED-133), S673 (SAT-232)
Zimpel, Carolin, S185 (TOP-456-YI), S504 (FRI-251), S854 (WED-285)
Zinober, Kerstin, S37 (OS-053), S179 (FRI-431-YI), S179 (FRI-432), S186 (TOP-470-YI), S200 (WED-453), S266 (SAT-347-YI), S284 (FRI-266), S362 (TOP-325-YI), S364 (WED-323), S750 (THU-497-YI)
Ziogas, Argyrios, S536 (THU-136)
Ziol, Marianne, S17 (OS-011), S38 (OS-054), S38 (OS-055), S55 (OS-085-YI), S343 (SAT-400)
Zipprich, Alexander, S35 (OS-050-YI), S54 (OS-084), S124 (FRI-089), S175 (FRI-419), S219 (WED-516), S497 (FRI-234), S736 (THU-460-YI), S752 (THU-501)
Zischka, Hans, S175 (FRI-420), S853 (WED-282-YI)
Zitelli, Patricia Momoyo, S35 (OS-050-YI), S112 (FRI-050), S160 (SAT-507), S701 (FRI-203-YI)
Zito, Giovanni, S41 (OS-062), S279 (THU-334-YI), S359 (THU-347-YI), S638 (SAT-118)
Zizzo, Andréanne N., S56 (OS-086), S832 (THU-258-YI), S842 (THU-284), S850 (THU-308)
Zmora, Niv, S214 (WED-500), S776 (THU-045)
Zoeschg, Monica, S307 (SAT-263), S335 (SAT-378-YI)
Zogas, Georgios, S507 (FRI-257)
Zohmangaihi, Deepy, S81 (LBP-030)
Zolfino, Teresa, S69 (LBP-004-YI), S304 (SAT-258), S307 (SAT-263), S335 (SAT-378-YI), S350 (SAT-421)
Zoller, Heinz, S257 (SAT-545-YI), S848 (THU-302), S849 (THU-305-YI), S862 (WED-314-YI), S945 (FRI-602-YI)
Zöllner, Caroline, S43 (OS-066), S77 (LBP-022-YI), S900 (SAT-559), S901 (SAT-560), S934 (TOP-582), S935 (TOP-583), S937 (FRI-585-YI)
Zollner, Gernot, S742 (THU-476)
Zollner, Julia, S23 (OS-026-YI)
Zomorodi, Katie, S958 (WED-579)
Zoncada, Alessia, S901 (SAT-559), S902 (SAT-560), S938 (FRI-586)
Zoncapè, Mirko, S26 (OS-032-YI), S62 (OS-097), S515 (TOP-098), S516 (TOP-113), S525 (THU-103), S558 (TOP-063-YI), S582 (WED-100-YI), S583 (WED-101), S626 (WED-231), S677 (SAT-243-YI)
Zorzano, Antonio, S273 (THU-316)
Zorzi, Giulia, S907 (SAT-575)
Zou, Cailun, S108 (THU-084)
Zou, Chenhui, S891 (THU-624-YI)
Zoughlami, Amine, S757 (THU-516)
Zougmore, Honore, S110 (FRI-042)
Zougmoure, Honoré, S829 (THU-252)
Zou, Huaibin, S852 (TOP-312), S934 (SAT-644)
Zou, Liangfeng, S73 (LBP-013)
Zoulim, Fabien, S43 (OS-066), S45 (OS-067), S46 (OS-070-YI), S65 (OS-101-YI), S380 (FRI-463), S381 (FRI-464), S815 (WED-005), S869 (TOP-632), S871 (THU-559-YI), S876 (THU-576), S893 (THU-634), S903 (SAT-562), S934 (TOP-582), S937 (FRI-585-YI), S942 (FRI-592)
Zou, Xiangyun, S664 (SAT-202), S666 (SAT-206)
Zou, Zhengsheng, S98 (SAT-088), S108 (THU-084)
Zuberi, Bader Faiyaz, S865 (FRI-637)
Zubiaga, Ana, S631 (SAT-095-YI)
Zubko, Alexander, S161 (SAT-510-YI)
Zucchi, Manuela, S576 (WED-083)
Zucchi, Martina, S576 (WED-083)
Zuckerman, Eli, S10 (LBO-006)
Zuckerman, Seth, S62 (OS-096)
Zucman-Rossi, Jessica, S17 (OS-011), S38 (OS-055), S457 (WED-236)
Zufferey, Maria Caiata, S863 (WED-317)
Zu, Jian, S98 (SAT-087)
Zuma, Luthando, S900 (SAT-558)
Zuo, Li, S140 (FRI-136)
Zuo, Zi, S129 (TOP-223), S646 (SAT-141)
Zureikat, Qusai Al, S520 (THU-090-YI), S745 (THU-483)
Zurli, Tommaso, S447 (THU-394), S514 (FRI-381)
zur Wiesch, Julian Schulze, S866 (FRI-639), S912 (SAT-588), S930 (SAT-636), S935 (TOP-583)
Zuurbier, Coert J, S674 (SAT-233)
Zvi, Benaya Rozen, S251 (SAT-527)
Zvick, Joel, S85 (LBP-039), S243 (FRI-349)
Zweer, Hans, S262 (SAT-330)
Zweerink, Susanne, S289 (FRI-284)
Zwezerijnen, Ben, S237 (FRI-330)
Zwirs, Diona, S641 (SAT-126)

EASL | JOURNAL OF HEPATOLOGY

Disclosures: no commercial relationships

The following abstract submitters have indicated that they have no relationships with commercial entities that might be perceived as having a connection with their presentation:

Aamann Luise
AbdAllah Mohamed
Abdelhamid Amira
Abdelrahman Basma
Abdel-Razek Wael
Abdul Hussein Ali
Abdulelah Ahmed
Abedin Nada
Abu Baker Fadi
Abulaiti Aimitaji
Aceituno Laia
Adali Gupse
Adamcova Selcanova Svetlana
Agarwal Ayush
Aggarwal Arnav
Aghara Hiral
Aguilar-Corominas Laia
Aguirre-Villarreal David
Ahmad Afaf
Ai Yingjie
Aizimuaji Zulihumaer
Akhavan Rezayat Arash
Akpinar Reha
Al Naamani Khalid
Al Zureikat Qusai
Alansare Abdullah
Alary Anouck
Alexander Vijay
Alexopoulou Alexandra
Aleyadeh Wesam
Alisi Anna
Aljudaibi Bandar
Alkhammash Maram
Alla Viligiardi Giada
Alletto Francesca
Alonso Martin Carmen
Alqahtani Saleh A.
Alsadoon Amani
Althaus Philipp
Altın Soner
Alvarez Sola Gloria
An Wei
Anders Lennard
Anderson Motswedi
Ando Wataru
Angelakis Athanasios
Angendohr Carolin
Anty Rodolphe
Apodaka-Biguri Maider
Araujo Sofia
Aravinthan Aloysious
Archer Ann
Århem Katarina
Arif Sania
Arif Maaz
Armstrong Matthew
Arvaniti Pinelopi
Asero Clelia
Ashraf Afreen
Aso Kenta
Augé Anea
Aye Lydia
Aznou Anouar
Babu Rosmy
Bächer Johannes
Bager Palle
Baiges Anna
Bajaj Jasmohan
Balari Tomàs
Banerjee Aniruddha
Barda Beatrice
Bardak Ali Emre
Barrenechea-Barrenechea Jon Ander
Bashiri Kiandokht
Battistella Sara
Baweja Sukriti
Becchetti Chiara
Bellersheim Leonard
Ben Saad Amel
Berenguer Juan
Bernardino Melvin
Bertin Lise
Best Jan
Bhardwaj Ankit
Bhatnagar Aishwarya
Bheemraj Kalisha
Bigas Claudia
Bihari Chhagan
Bik Emil
Biswas Sagnik
Bitetto Davide
Bittermann Therese
Bo Zhiyuan
Boateng Sarpong
Boeira Paula
Bonaccorsi-Riani Eliano
Bonacini Maurizio
Bonfichi Alessandra
Bonzon-Kulichenko Elena
Bori Matías
Bozward Amber
Brenig Robert G
Brennan Euan
Brew Brendan
Broere Roberto
Broering Ruth
Brol Maximilian Joseph
Brzdęk Michał
Buckholz Adam
Bustos Matilde
Byun Jihyo
C Delgado Teresa
Cabaleiro Alba
Cacho-Pujol Júlia
Cadranel Jean-François
Caime Chiara
Calé Alicia
Calleri Alberto
Calvaruso Vincenza
Calvo Sánchez Henar
Campani Claudia
Campos-Murguia Alejandro
Camps Fajol Montserrat
Canillas Lidia
Canivet Clemence
Capinha Francisco
Capraro Ylenia
Carrier Paul
Carrillo Cubero Beatriz
Carrillo-Fernández Paloma
Casadei Mailín
Casirati Elia
Castiella Agustin
Cathcart Jennifer
Cattazzo Filippo
Cavalcante Lourianne
Cavalletto Luisa
Cazac-Panaite Georgiana-Diana
Celik Ferya
Cerezal-Gómez Gemma
Cervo Adriana
Cespiati Annalisa
Chahal Sahiba
Chakraborty Shreya
Charles Hattie
Che Xiao
Cheng Fan-E
Cherubini Alessandro
Chia Kai An Jarvis
Chindamo Maria Chiara
Chotkoe Shivani
Choudhury Ashok Kumar
Christiansen Marie
Chuang Hsiang-Hsuan
Chun Ho Soo
Cinque Felice
Cirella Antonio
Civolani Alberto
Clayton Michelle
Collot Julia
Conter Carolina
Cook Emma

Disclosures

Cordie Ahmed
Cornillet Martin
Correnti Margherita
Cossiga Valentina
Craciun Rares
Crouchet Emilie
Cruz Andrew John
Curakova Ristovska Elena
Curto Armando
Dalla Bella Martina
Damone Francesco
Damsholt Søren
Dang Shuangsuo
Danielsson Oscar
D'Anna Stefano
Danpanichkul Pojsakorn
Danta Mark
D'Arcangelo Francesca
D'Arpino Valeria
Das Basundhara
Datta Aurgho
Davies Scott
Davila Morales Ana Maria
De Maria Nicola
De Nicola Stella
De Vos Zenzi
Decroix Kylian
Del Barrio María
del Castillo-Cruz Alejandro
Delaporte Margaux
Delhomme Margaux
Delire Bénédicte
Dendane Youness
Derakhshandeh Fatemeh
Desalegn Mahlet
Desboeufs Nina
Di Cola Simone
Di Martino Vincent
Dias Nirello Vinicius
Díaz-Canul Carolina
Dietvorst Carmen
Ding Chuanfu
Diwakar Sunidhi
Dixon Thomas
Domínguez Cardoso Paul
dos Santos Ferreira Grani Lauredana
Doselli Sara
Drumond Westgeest e Sousa Diego
Du Yu
Dudzik Aleksandra
Duhra Ayesha
Düll Miriam M.
Durmazer Esra
Duseja Ajay Kumar
Eber Claudie
Edwards Rachel
Efimova Irina
Eidelshtein Dana
Ekstrom Victoria
El Hassani Majda
Elblová Petra
Elizondo Martín
Elshabasy Osama
Elvers Fynn
Elzubeir Amera
Encijo Heredia Raquel
Endo Kei
Eom Jung A
Erard Domitille
Eren Fatih
Ergenc Ilkay
Estévez-Vázquez Olga
Faini Angelo Corso
Falzone Michela Helga
Fandood Sam
Farbod Yasamin
Fathma Sawsan
Fayez Ayat
Fazel Modares Nastaran
Feliciano Camille
Ferdinande Kymentie
Fernandes Flavia
Fernández Rut
Fernández-Aguilera María
Fernandez-Barrena Maite G
Fernandez-Checa José
Ferraro Clelia
Ferreiro Nerea
Flanagan Stuart
Flatley Sarah
Fleming Maegen
Flores Peña Roberto
Forns Xavier
Forrest Ewan H
Fortea Jose
Fox Eric
Francipane Maria Giovanna
Franzè Maria Stella
Fraz Ezaam
Fredriksson Marie
Frissen Mick
Fu Haoshuang
Fuchs Claudia
Fujii Hideki
Gadour Eyad
Gallo Paolo
Gandhi Keshav
García Federico
García Consuegra José
García-Estrada Antonio
García-Fernández Vanessa
García-Villarreal Luis
Garg Pratibha
Garn Jonathan
Garver-Mosher Tabetha
Gasparyan Ani
Gatselis Nikolaos
Gautier Lucas
Gils Sanne
Gioia Stefania
Giraud Guillaume
Girleanu Irina
Giuli Lucia
Gohar Farhan
Gömer André
Gomes Guilherme
Gomes Oliveira Elze Maria
Gómez-Rubio Mariano
Gonfaus-Ortiz Gemma
González Rayo Andrea
Goossens Nicolas
Graf Christiana
Gragnani Laura
Greenham Olivia
Griadil Taras
Groen Puck C.
Groenen Claire
Grossar Lorenz
Grossi Ilaria
Gu Lei
Guariglia Marta
Guedes Paula
Guerillot Mathilde
Guerra Pietro
Guerrero Antonio
Guerrieri Francesca
Guichelaar Maureen
Guoyan Sui
Gürbüz Burcu
Gutierrez Reyes Gabriela
Gutierrez-Castillo Alejandro
Gutmann Daniel
Haahr Pernille
Hähner Jan
Haining Liu
Háková Tereza
Hall Samantha
Halupnik Austin
Hambridge Thomas
Hamran Shahd
Han Seul Ki
Hanibal Gideon
Harms Dominik
Hartl Lukas
Hayashi Manabu
Hayn Alexander
Hazzan Rawi
Hegde Apoorva
Heitmann David
Heo Subin
Hernández Conde Marta
Hernández-Guerra Manuel
Herrera Laura
Hertelyova Zdenka
Herzog Jasmin
Heyens Leen
Higgins Ben
Himanshi Himanshi
Hoang Stephen
Hohmann Janik
Horhat Adelina
Horst Ludwig
Hountondji Lina
Hua Xiangwei
Huerta Anna
Hui Rex Wan-Hin
Huici-Izagirre Maider
Huynh Trung
Iacob Speranta
Ibidapo-Obe Oluwatomi
Ibrahim Samar
IJung Feng
Irvine Katharine
Ismailova Zebiniso Sofiya
Iwaisako Keiko
Iwaki Michihiro
Iwakiri Yasuko
Jaganathan Jeeva
Jakhar Deepika
Janik Maciej
Janjua Naveed
Janshoff Saskia
Jasrotia Ayush
Jeffrey Angus

Jegodzinski Lina
Jessen Pernille
Jeyarajan Andre
Jia Yidi
Jiroušková Markéta
Johannessen Asgeir
Juhl Vestergaard Linnea
Jumabayeva Almagul
Jun Dae Won
K L Ajee
Kablawi Dana
Kaffe Eleanna
Kahraman Deniz Cansen
Kamara Elaine
Kamel Ahmed
Kanda Shuhei
Kang Hae Yeon
Kao Shih Hsun
Kaps Leonard
Kar Premashis
Kaschube Benjamin
Kassim Hidayat
Katoch Swati
Keaveny Alison
Kenny Sarah
Ketenoğlu Buse
Kew Guan Sen
Khalili Mandana
Khatua Chitta Ranjan
Khidirova Hijran
Kiehn Oliver
Kimmann Markus
Kinjo Kie
Kirubendran Kavitha
Klein Sabine
Klöhn Mara
Klomp Sylvia
Kniepeiss Daniela
Ko Seongjoon
Kohl Alina
Koizumi Yohei
Koky Tomáš
Kolev Mirjam
Koning Mijra
Konings Laura
Konstantis Georgios
Korica Bojan
Kouadou Shinha-Ashkarr
Kounis Ilias
Koutny Florian
Kozlov Sergii
Kruk Beata
Krus Frederike
Küçükerbil Efrayim
Kumari S Suja
Kuzinska Matylda Zofia
Kwon Jung Hyun
L'Henaff Morgane
Ladegaard Grønkjær Lea
Lahsini Jaouhara
Lakananurak Narisorn
Lameroli Mauriz Lucia
Lanza-Arnaiz Jose Maria
Lapitz Ainhoa
Lasington Jeril
Le Thanh Quynh Ngan
Lembeck Pia
Li Jinpeng
Liao Siqi
Liebig Laura
Lindqvist Catarina
Lissmann Rebecca
Liu Yin James
Liusina Ekaterina
Lo Ching-Chu
Londoño María Carlota
Longo Miriam
Lopez-Pascual Amaya
Low Elizabeth
Lu Ming-Ying
Lumbreras-Perales Cristina
Macek Jilkova Zuzana
Macías-Herranz Manuel
Madesh Vijaya Prakash
Madigan Shauna
Madubashetha Hasanka
Magnapera Alessia
Magro Bianca
Mahmood Abdullah Al
Mähringer-Kunz Aline
Mai Yanpei
Maina Cecilia
Makrufardi Firdian
Malik Mohammad
Mallela Venkata Ramana
Mallick Reshma
Malvestiti Francesco
Manassevee Pemika
Mancini Camilla
Mandal Ayan
Mangia Alessandra
Mangini Chiara
Manisha Manisha
Mantovani Stefania
Manuli Chiara
Marco Andrés
Marcos Carrasco Natalia
Marey Mohamed Mahmoud
Marin-Correa Diana
Marjot Thomas
Marot Astrid
Marques da Costa Rui
Martinez Torres Dilan
Martini Francesco
Martin-Mateos Rosa
Mašek Jan
Matar Rola
Mathew Babu
Matsuda Michitaka
Matthys Rania
Mattos Angelo Z.
Maung Soe Thiha
Maya-Miles Douglas
Mbelle Mzamo
Meehan Edward
Mehraj Mohammad Athar
Mehta Shubham
Mehtani Rohit
Mei Xue
Méndez-Sánchez Nahum
Meroz Omer
Meunier Lucy
Mexia Cabrales Jazmin
Meyer Nele
Miao Yan
Miceli Vitale
Mikova Irena
Mikulits Wolfgang
Milkiewicz Malgorzata
Min Eun-Ki
Minciuna Iulia
Mino Masaaki
Mira Stefania
Moga Lucile
Mohanraj Sundaresan
Montano-Loza Aldo J
Moreno-Gonzalez Mar
Mundra Garvit
Munekage Fumiaki
Nachmias - Peiser Noy
Najah Qasi
Nakadai Yukie
Nakamoto Nobuhiro
Nakatani Tatsuya
Nallapeta Naren
Namisaki Tadashi
Narbaiza Jone
Natola Leonardo Antonio
Navarro Adela
Navarro-Corcuera Amaia
Neckermann Lukas
Nellore Dharani Sai Sreekanth
Nenu Iuliana
Neves André
Nevi Lorenzo
Nguyen Khac Eric
Ni Ming
Nier Anika
Nieva-Zuluaga Ane
Nikiforova Yana
Nocke Maximilian
Nofit Eugenia
Noll Lisa-Marie
Nosáková Lenka
Nulan Yeldos
Nunes Vinicius
Nuruzade Nargiz
O Sullivan David
Oberweis-Manion Helen
O'Donovan Helen
Oeckl Lena
Oesinghaus Sina
Ogiso Satoshi
Okushin Kazuya
Olafsson Sigurdur
Olaizola Paula
Olivas Ignasi
Ostojic Ana
ouafae dahri
Oumaima Azzaoui
Oyama Masafumi
Ozari Gulnar Muge
Özden Yavuz
Özdirik Burcin
Pace Jade
Padilla-Lopez Marlene
Pagadala Mangesh
Page Sophie
Pahwa Prabhjyoti
Pantzios Spyridon
Paolini Erika
Papadimopoulos Ilias
papinutti delfina
Parisse Simona

Disclosures

Parkash Om
Parracho Tamara
Parry Amy
Paruchakul Parucha
Pasta Andrea
Patra Partha Sarathi
Pavlovskyi Leonid
Payá Llorente Carmen
Peake Kristen
Peeters Frederik
Peña-Sanfélix Patricia
Peng Liang
Perez Gallardo Cristian
Perriera Riccardo
Piecha Felix
Piermatteo Lorenzo
Pirola Carlos
Pischke Sven
Pivtorak Kateryna
Plessier Aurélie
Porro Nunzia
Prabhakar Tushar
Priori Victoria
Proske Nora
Protopapas Adonis
Pu Zhangya
Pugliese Nicola
Qi Wenying
Qiao Wenying
Qirem Murad
Quartini Giulia
Quickert Stefanie
Qureshi Jumshaid
Rachakonda Vikrant
Raggi Chiara
Ragozzino Lucia
Rahut Antora
Rajaa Boukhraiss
Rastovic Una
Raszeja-Wyszomirska Joanna
Reic Tatjana
Reiso Ilaria
Reißing Johanna
Rejliwal Pravinkumar
Rennebaum Florian
Rezi Elena
Rezvani Milad
Riaz Yumnah
Richelle Donovan
Ring Eabha
Rivera Esteban Jesús
Roglans Núria
Rojo Lázaro Diego
Roose Heleen
Rossi Stephen
Rossvoll Lasse
Rousseaux Théo
Roy Akash
Rozenfeld Hemed Anna
Ruiz Margáin Astrid
Rusignuolo Giuseppe
Ryan Pablo
Saadi Tarek
Saba Francesca
Saenz Ernest
Saez-Palma Maria
Saggau Carina
sahin mustafa
Sahuri Arisoylu Meliz
Sakamori Ryotaro
Salomone Federico
Salto-Sevilla Jorge Alejandro
Sandfort Vanessa
Santos Diego
Santra Suman
Saracco Margherita
Saran Anca
Sarcina Tommaso
Sarvesh Shreyas
Satapathy Sanjaya
Sato Shinya
Sattoe Jane
Saurabh Saurabh
Saxena Anoushka
Sayadi Alexandre
Schachteli Fabian
Schäfer Melina
Schlaak Alexandra Emilia
Schlienkamp Sarah
Schmid Stephan
Schmidt Kevin
Schulte Sigrid
Schumacher Jonas
Sciarrone Salvatore Stefano
Sedki Mai
Seifert Leon Louis
Selicean Sonia-Emilia
Seo Deok Hwa
Sessa Anna
Sewell Charlotte
Shafique Hira
Shalimar
Shan Wencheng
Shao Yingmei
Sharifi Roxanna
She Shaoping
Shearn Colin
Sheehan Shannyn
Sheptulina Anna
Shiha Gamal
Shimizu Mayuko
Shin Hyunjae
Shin-Yu Tsai
Sho Takuya
Shousha Hend
Sidhu Sandeep
Sim Ki Choon
Simón-Codina Blanca
singh aditi
Smith Daniel
Smolic Martina
Socha Piotr
Sohail Abdullah
Sohn Won
Solis-Munoz Pablo
Soni Rajit
Spearman Wendy
Sridhar Siddharth
Stadler Helena
Staicu Isabela
Ştefănescu Horia
Stern Christiane
Stevenson Emma
Stoian Marinela
Stojiljkovic Marija
Storgaard Marie
Suarez Uribe Nelson
Suárez-Saro Fernández Ana
Suehiro Tomoyuki
Sugaya Tatsuro
Sugiyama Masaya
Sukowati Caecilia
Suo Yuan
Sutter Jan
Suykens Janne
Tadeo-Espinoza Hiram
Tak Kwon Yong
Takeda Yoshinori
Tanaka Tomohiro
Taneja Sunil
Tangkijvanich Pisit
Tashkent Yasmina
Tatour Mifleh
Tena-Garitaonaindia Mireia
Teng Wei
Terrault Norah
Terrien Léa
Thakkar Rahul
Thanapirom Kessarin
Tharehalli Umesh
Theurl Daniel
Thöne Paul
Thörn Richard
Thorsen Brian
Thuy Le Thi Thanh
Tian Xiaopeng
Tikhonoff Valerie
Tiwari Vaibhav
Todorova Dilyana
Toktogulova Nurgul
Tomaiuolo Gabriella
Torre Pietro
Torrell-Pedreira Elena
Torres Núñez Sandra
Toscano Arianna
Tou Andrea
Tran Hien
Travers Jared
Trentzsch Vanessa
Trifylli Eleni-Myrto
Triolo Michela
Troppmair Maria Rosina
Tsou Hio Lam Phoebe
Tsuneyama Koichi
Tu Huilan
Tulading Aliya
Uchida Takuro
Ursic-Bedoya José
Uveges Samuel
Vahdani Negar
Val Beatriz
Valente Leticia
Valery Patricia C.
van der Helm Danny
van Doorn Diederick
Van Horebeek Nele
Vaquer-Grimalt Pere
Vaquero Javier
Vargas-Navarro Francisco
Vedeld Hege Marie
Velasco Martínez Elena
Veloso Alves Pereira Isabel
Ventre Jules
Venturin Camilla

Verma Nipun
Verstraeten Maïté
Viggiano Taylor
Vilà Laia
Villamil Alejandra
Villeret Francois
Vinikoor Michael
Vithayathil Mathew
Vivancos-Gallego María Jesus
Vosko Lena
Vutien Philip
Waddell Scott
Wakabayashi Shun-Ichi
Wakae Kousho
Watanabe Noriyuki
Wegermann Kara
Weglage Jakob
Weltzsch Jan Philipp
Wende Lisa
Werge Rikke
Wernly Bernhard
Wester Axel
Wewer Neele
Wiering Leke
Will Nico
Wilson Joseph D
Wronka Karolina
Wuestefeld Torsten
Xuejie Zhang
Yaginuma Reiko
Yamamoto Yasunori
Yamashina Shunhei
Yatsuhashi Hiroshi
Yazarkan Yigit
Yeoh Jeremy
Yepes Barreto Ismael de Jesus
Yi Dawei
Yilihaer Yierfan
Yin Guo
Ying Shuaibing
Yinghong Zhu
Yücel Lea Aylin
Zacharias Harry
Zampato Claudio
Zapata-Pavas Leidy Estefanía
Zhan Yi
Zheng Yanan
Zhi Yang
Zhoudi Wenxin
Zmora Niv
Zou Zhengsheng
Zoughlami Amine
Zubko Alexander
Zucman-Rossi Jessica
Zurita Palomo Carola

EASL | JOURNAL OF HEPATOLOGY

Disclosures: commercial relationships

The following abstract submitters have indicated that they have relationships with commercial entities that might be perceived as having a connection with their presentation:

Aaldijk Alexandra
Åberg Fredrik
Abeysekera Kushala
Ahn Joseph
Ajmera Veeral
Alard Berenice
Alazawi William
Albhaisi Somaya
Alessandria Carlo
Alkhouri Naim
Allaire Manon
Allawzi Ayed
Amby Kristoffer Kjærgaard
Andersen Ina
Andersson Anneli
Antolini Nicole
Aponte Torres Zuleika
Appiah Erica
Armandi Angelo
Arnedo-Pac Claudia
Åström Hanne
Atallah Edmond
Auker Lisa
Azzu Vian
Baguley Elizabeth
Balcar Lorenz
Ballester María Pilar
Bao Jian-Xin (Jimmy)
Barclay Stephen
Barnett Tamara
Baron Aurore
Basci Sefa
Batbold Enkhtuul
Batsuli Nefer
Bech Katrine Tholstrup
Bell Eric
Benmassaoud Amine
Berner Hansen Mark
Bertoletti Antonio
Beyene Nateneal
Bian Yao
Bianchini Marcello
Biedka Stephanie
Binte Abdullah Liyana
Biquard Louise
Blakely Kate
Bobowski-Gerard Marie
Bonitz Katharina
Bouzbib Charlotte
Bowlus Christopher L.
Briand Francois
Broekman Leonard (Niels)
Brombosz Elizabeth
Brotherton Lauren
Buchanan Ryan
Burnside Jessica
Buytaert Maarten
Caballero-Camino Francisco Javier
Cabello Calleja Josune
Calzadilla Bertot Luis
Cançado Guilherme
Cañete Hidalgo Nuria
Cano-Segarra Guillem
Cappuyns Sarah
Cardoso Mariana
Carey Ivana
Castera Laurent
Castro Alejos Carla
Castven Darko
Catanzaro Elisa
Cazzagon Nora
Celsa Ciro
Chan Doreen
Chan Wah-Kheong
Chan Talia Yi Hui
Chang Young
Chappell Catherine
Chase Geoffrey
Chen Kaina
Chinaka Ifechukwuamaka
Chouik Yasmina
Chvatal-Medina Mateo
Ciere Sophie
Coessens Marie
Cohen Chari
Colapietro Francesca
Colella Fabio
Congdon Kendra
Cooper Katherine
Cooper Curtis
Cooreman Michael
Coover Robert
Corallo Salvatore
Cortese Maria Francesca
Coste Pablo
Couret Alexis
Court Emma
Couto Claudia
Cristoferi Laura
Cudero Quintana Laura
Currie Sue
Cusidó M Serra
Dahari Harel
Dai Zhe
Daiku Kazuma
Damangir Soheil
de Groot Alise D.E.
de Laguiche Elisabeth
De Martin Sara
de Reus Stijn
de Vries Hilde
de Zawadzki Andressa
Debing Yannick
Della Torre Sara
Denholm Nick
Derdak Zoltan
Dermer Shari
Derowski Tanja
Diaz Juan Manuel
Diaz Luis Antonio
Diaz-Gonzalez Alvaro
Dobrowolska Krystyna
Dongelmans Edo J.
Donkus Catherine
Dröge Carola
Duarte-Rojo Andres
Dunn Winston
Dyavadi Vijay
Ebrahimi Fahim
Eckburg Paul
El Maimouni Cautar
El Sobky Shereen
Elmasry Eslam
Embacher Jan
Emebo Dabel
Eriksson Olof
Espinoza-Cámac Nataly
Ezzafzafi Solaiman
Fabris Luca
Fakhraei Romina
Fan Rong
Fang Hanzhi
Fang Yongliang
Fath el Bab Esmee
Fernandez-Rodriguez Laura
Fischer Susan
Fischer Jonathan
Fix Adam
Flis Paulina
Flores Joan
Foley Clare
Fontaine Helene
Franzon Deborah
Frey Molly
Friedman Nir
Fromme Malin
Fukano Kento
Furley Maison
Furquim d'Almeida Arno

G. Guidotti Luca
Gadi Zouhir
Gambino Carmine
Gao Hong
Gao Bowen
Garcia-Medel Eric
Gart Eveline
Gautam Preety
Gazda Jakub
Gee Matthew
Geißelbrecht Sophia
Geissler Rene
George Laura
Ghosheh Yanal
Gigante Elia
Gill Upkar
Gilmore Serena
Gjini Kamela
Godbole Ira
Goikoetxea-Usandizaga Naroa
González-Santiago Jesús M.
Gratacós Ginès Jordi
Graupera Isabel
Greenbaum Linda
Gris-Oliver Albert
Guerra Veloz Maria
Gulamhusein Aliya
Guo Yifei
Gupta Ipshita
Gurung Arati
H. Hansen Henrik
Habermann Robin
Haders Daniel
Hahn Sihoun
Hajji Yacine
Hakkarainen Konsta
Hammond Helen
Hanabata Yusuke
Hannah Nicholas
Hansen Lars
Hansen Bettina
Hansen Johanne Kragh
Harrison Emily
Hartsfield Cynthia L.
Hassanein Tarek
He Hairuo
Hegmar Hannes
Heinreichsberger Fabian
Heinrich Bernd
Heise Jamie
Helgadottir Holmfridur
Hempel Felix
Henin Guillaume
Henriksson Ida
Hernández-Évole Helena
Hesse Raphael
Higuera Monica
Hintersteininger Marlene
Hirode Grishma
Ho Quinn
Ho Karen Cheuk-Ying
Højberg Svejsø Frederik
Hoblos Reem
Hoefinger Paula
Hof Willemien
Hofer Benedikt
Hollinghurst Joe
Hong Changze
Hong Jin
Horstmeier Henriette
Howell Jessica
Hoyle Henry
Hsu Yao-Chun (Holden)
Hu Xingjiang
Huang He
Huang Huei-Tyng (Philippe)
Huanyi Cao
Huguet-Pradell Júlia
Hutchison Alan L.
Hyder Md Irfan
Hyötyläinen Tuulia
Iavarone Massimo
Ilott Nicholas
Im Yu Ri
Imparato Camille
Inge Cox Richie Alexander
Ito Diane
Ivancovsky-Wajcman Dana
Jakobsson Gustav
Jamil Khurram
Jara Vargas Jennifer
Jeng Rachel Wen-Juei
Jeon Eunjee
Jessa Fatema
Jin Xinrui
Jobson Timothy
Johansen Stine
Jonasson Elise
Jones Arron
Jones David E.
Juliebø August Tronstad
Kaewdech Apichat
Kahl Sabine
Kahlhöfer Julia
Kalita Nikhil
Kamada Yoshihiro
Kamal Habiba
Kamga Wouambo Rodrigue
Kamiri-Ngugi Rachael
Kamlin C.Omar
Kanto Tatsuya
Katzenstein Cecilia
Kaur Parminder
Kaya Eda
Kaze Edeline
Keating Shelley
Kehlan Saneyah
Kerbert Annarein
Khanam Arshi
Khanyi Bongani
Kiczynska Patrycja
Kim Jisup
Kimer Nina
King Thomas
Klimanek Matthias
Knox Steven J
Koball Stine
Koelsch Stephan
Koenig Alexander
Koller Tomáš
Kosaka Nobuyoshi
Kramer Georg
Kravchuk Stanislav
Krawczyk Marcin
Krystallaki Dimitra
Krzeski Piotr
Kulkarni Anand
Künzler-Heule Patrizia
Kupcinskas Limas
Kyed Ea
La Roche Kim
Lai Jimmy Che-To
Laique Sobia
Lampertico Pietro
Lan Fei
Lani Lorenzo
Lanthier Nicolas
Larrue Hélène
Lawitz Eric
Lawrence-Wilde Farah
Lazarus Jeffrey
Le Kha
Leduc Martin
Lee Jonathan
Lee Young-Sun
Lee Pei-Chang
Lee I-Cheng
Lee Ji Eun
Leeming Diana Julie
Legry Vanessa
Leith Damien
Lemoine Maud
Lesage Henri
Leung Hak-Keith
Lewinska Monika
Li Hui
Li Qisheng
Liberman Alexander
Liljeblad Mathias
Lim Gyungsun
Lim Ryan YanZhe
Lindvig Katrine
Linge Jennifer
Liu Hanyang
Liu Jinxia
Loglio Alessandro
Lombardi Rosa
Longato Lisa
Loomba Rohit
Lucas Carol
Lucifora Julie
Luong Xuan
Lyu Zhuwan
Ma Ann T
Maagaard Markus
Mageras Anna
Mahida Suraj
Mak Lung Yi Loey
Malme Kristian
Manhas Savrina
Manna Dina
Marenco-Flores Ana
Mariño Zoe
Marra Fabio
Marti-Aguado David
Martin Holly
Martínez-Cabrera Carlos
Martinez-Gili Laura
Martins Adrielly
Martró Elisa
Martyn Emily
Masoodi Mojgan
Matusiewicz Anna
McKenna-Barry Matthew

Disclosures

McRae Michael
Meakin Alex
Medical Costello
Mehal Wajahat
Mellemkjær Anders
Mendlowitz Andrew
Merelli Elisa
Messer Eva Katharina
Middelburg Tim
Mikkelsen Anne Catrine
Minchenberg Scott
Miralpeix Anna
Missen Louise
Mitchell-Thain Robert
Mohamed Almuthana
Mohareb Amir
Molinaro Antonio
Moon Andrew
Morales Albert
Moussa Mohamed
MSC KJT
Mukherjee Sarmistha
Munteanu Mona
Nabilou Puria
Nadeem Rida
Nah Chung Yau
Nakamura Toka
Nalbandian Kaman
Nathan Bavithra
Nault Jean-Charles
Naustdal Carina
Nde Helen
Nephew Lauren
Nguyen TD Clara
Nicolàs Olivé Aina
Nie Chunpeng
Ningarhari Massih
Nomden Mark
Oezsoy Adil
Ogawa Eiichi
Ohara Masatsugu
Ohfuji Satoko
Okawa Masashi
Oldenburger Anouk
Oliva-Vilarnau Nuria
Orešič Matej
Ortega-Ribera Marti
Otero Sanchez Lukas
Oussalah Abderrahim
Pagès Laura
Pajancic Larissa
Pak Kevin
Palom Adriana
Pañero Moreno Marc
Pang Wenjie
Panzer Marlene
Papatheodoridis George
Park Hyo Jung
Park Seong
Park Jeong Hwan
Park Haesuk
Parlati Lucia
Parrinello Christina
Pascual-Lopez Irene
Patel Keyur
Paudel Rajan
Pedersen Mark
Peisl Sarah
Pekarska Katrina
Pellegrino Joe
Pennisi Grazia
Perdomo Zelaya Carolina M.
Pérez Garreta Javier
Periti Giulia
Peters Jendrik
Petralli Giovanni
Pfefferkorn Maria
Philouze Clothilde
Piano Salvatore
Pinter Matthias
Pinto Elisa
Platenburg Gerard
Plebani Riccardo
Plunkett Jennifer
Pompili Enrico
Porter Dale
Poynard Thierry
Praktiknjo Michael
Premkumar Madhumita
Protopopescu Camelia
Puhakka Eemeli
Pustjens Jesse
Quaranta Maria Giovanna
Rabasco Meneghetti Asier
Rabenau-McDonnell Quinn
Rabiee Anahita
Rai Sukhvir
Rajkumar Rahul
Rapino Carmela
Rasamison Chrystelle
Razavi-Shearer Devin
Reiberger Martina
Renhardt Clemens
Ricci Pierbruno
Ricco Gabriele
Robaeys Geert
Rodriguez Nina
Rodríguez-Perálvarez Manuel
Roeren Merle
Rohani-Montez S Christy
Rohbeck Elisabeth
Rohr-Udilova Nataliya
Rolinger Jens
Romeo Mario
Romero Judit
Ronca Vincenzo
Rosado Eugenio
Rosenberg William
Rottengatter Karin
Rouxel Lou-Devy
Rudler Marika
Ruiz-Cobo Juan Carlos
Russo Francesco Paolo
Saha Banishree
Şahin Yiğit
Saltini Dario
Sandmann Lisa
Sasikumar N Apoorva
Schleicher Eva Maria
Schnefeld Helle
Schneider Caitlin
Schulz-Kuhnt Anja
Schwarz Caroline
Scoble Patrick
Sebesta Christian
Semmler Georg
Semnani Kiavash
Serfert Yvonne
Setoyama Hiroko
Seynhaeve Laurence
Shah Neha
Shaheen Abdel-Aziz
Shang Ying
Sharma Neha
Shomura Masako
Shteyer Eyal
Siltanen Juho
Silva Mario Jorge
Simbrunner Benedikt
Singh Shreya
Slobin Jacqueline
Slooter Charlotte
Smid Marcela
Snir Tom
Soerensen Michael
Sogbe Miguel
Sommer Katja
Sonawale Sourabh
Song Sherlot Juan
Soni Diwanshu
Sood Siddharth
Sophie Schlosser-Hupf
Sorribas Olivera Marcel
Sorz-Nechay Thomas
Sourbron Steven
Souza-Mello Vanessa
Sriphoosanaphan Supachaya
Sripongpun Pimsiri
Stadlbauer Vanessa
Stanborough Tamsyn
Stella Leonardo
Straka Wolfgang
Strnad Pavel
Su Chien-Wei
Suschak John
Suzuki Ayako
Swain Liam
Swanson II Phillip
Swerkersson Signe
Tabrizian Parissa
Tahata Yuki
Tamaki Nobuharu
Tan Ker Shiong
Tang Nicole Shu Ying
Tarantino Giuseppe
Taub Rebecca
Tavaglione Federica
Taylor Robert
Telep Laura E.
Téllez Luis
Tengowski Mark
Tergast Tammo Lambert
Terner-Rosenthal Jolan
Terracciani Francesca
Tesfai Kaleb
Testoni Barbara
Thabut Dominique
Thapa Sharmila
Tharmathas Usha
Thennati Rajamannar
Tiede Anja
Tjønnfjord Sara
Tomah Shaheen
Tornai David

Torp Nikolaj
Triantos Christos
Tripathi Dhiraj
Tsai Wen-Wei
Tseng Tai-Chung
Tuffy Declan
Uemura Haruka
Uutela Aki
Vaira Lorenza
van Crevel Jutta
van Eekhout Kirsi
van Kleef Laurens A.
van Lierop Lisa
van Velsen Lisa M.
Vargas Maria
Vargas-Accarino Elena
Vaz Juan
Veličković Nataša
Verdeguer Francisco
Verendeev Andrey
Verhelst Xavier
Vicardi Marco
Vijjhalwar Rohan
Vila-Escoda Anna
Villesen Ida
Vögelin Marius
Vonderlin Joscha
Vora Pareen
Voß Jonas
Vuppalanchi Raj
Wadman Anna
Wajntraub Bakszt Erica
Wang Feiqian
Wang Siyun
Wang Mary Yue
Wang Michael
Weijsters Gemma H.X.
Weinberg Ethan
Wen Cindy
Wernberg Charlotte
Werner Ellen
West Rebecca
Wettstein Guillaume
White Trenton M
Wiggers Thomas
Wilmot Jake
Windell Dylan
Wong (Leslie) Chun Man
Wong William WL
Wong Robert
Wong Florence
Wong Yu Jun
Wong Grace Lai-Hung
Woodley Hannah
Wu Min
Wu Dandan
Wunderbaldinger Adrian
Yamazoe Taiji
Yang Chen
Yankey Allison
Yeh Hsing-Yu
Yela Elena
Yeo Yee Hui
Yeoman Andrew
Yip Terry Cheuk-Fung
Yoon Paul
Younossi Zobair M.
Zagorska Anna
Zakeri Nekisa
Zalesiak Marie
Zavalis Emmanuel
Zeng Georgia
Zhang Xiaofeng
Zhang Ziqi
Zhang David
Zhang Xinrong
Zhou Yu-Jie
Zhu Angela
Zhu Chong
Zhuang Ying
Zimpel Carolin
Zoncapè Mirko
Zuluaga Blanco Paola

EASL | JOURNAL OF HEPATOLOGY

Reviewers list

We express our deepest appreciation to the following people, who have given us generous and invaluable help as abstract reviewers for the EASL Congress 2026.

Affo Silvia
Afonso Marta
Aghemo Alessio
Alkhouri Naim
Allen Alina
Ampuero Javier
Anty Rodolphe
Artru Florent
Aspichueta Patricia
Baiges Anna
Bañares Rafael
Baptista Pedro M.
Bosma Piter
Boulter Luke
Boursier Jerome
Bouzbib Charlotte
Brennan Paul
Broquetas Maria Teresa
Brouwer Willem Pieter
Brown Ashley
Brunetto Maurizia
Buti Maria
Calvaruso Vincenza
Calvisi Diego F
Carrieri Patrizia
Castro Rui
Caussy Cyrielle
Clayton Michelle
Coenraad Minneke J
Coilly Audrey
Coppola Nicola
Cortese M Francesca
Cortez-Pinto Helena
Crespo Gonzalo
Cubero Javier
Culver Emma
Darwish Murad Sarwa
Dekervel Jeroen
Desdouets Chantal
Dillon John
Diniz Mariana
Dongelmans Edo
Edwards Lindsey
Esser Hannah
Filipowicz Sinnreich Magdalena
Francque Sven
Furquim d'Almeida Arno
Gane Edward John
Garcia-Samaniego Javier
George Elena
Gerussi Alessio
Gines Pere
Girleanu Irina
Gluud Lise Lotte
Gratacós-Ginès Jordi
Grgurovic Ivica
Guixé-Muntet Sergi
Haas Joel
Hammerich Linda
Henderson Neil
Herkel Johannes
Hessheimer Amelia
Heydtmann Mathis
Hilscher Moira
Hoare Matthew
Holleboom Onno
Hutchinson Sharon J
Iacob Speranta
Innes Hamish Adam
Ivancovsky Wajcman Dana
Jachs Mattias
Jack Kate
Joshi Deepak
Juanola Adria
Karvellas Constantine
Keating Shelley
Khaled Najib Ben
Kołodziejczyk Aleksandra
Kwanten Wilhelmus
L. Irving William
Lai Hung Wong Grace
Lalor Patricia
Lamarca Angela
Lammert Frank
Lanthier Nicolas
Larrue Helene
Lefere Sander
Lemaigre Frédéric P.
Lemoine Maud
Lens Sabela
Licata Anna
Lleo Ana
Londoño Maria Carlota
Lupberger Joachim
Lupsor Monica
Maan Raoel
Mandorfer Mattias
Manousou Pinelopi
Martinez-Chantar María Luz
Meunier Lucy
Mikulits Wolfgang
Milovanovic Tamara
Mookerjee Raj
Mrzlak Anna
Nery Filipe
Nicoara-Farcau Oana
O'Kane Grainne M
Oliveira Claudia
Paolo Russo Francesco
Papatheodoridi Margarita
Pericas Juan M.
Perrillo Robert P.
Pinter Matthias
Pinzani Massimo
Pol Stanislas
Praktiknjo Michael
Procopet Bogdan
Raevens Sarah
Rescigno Maria
Rigamonti Cristina
Rodrigues Susana
Rodrigues Robim M.
Rodrigues Cecilia
Rodriguez-Cuenca Sergio
Rohr-Udilova Nataliya
Roksund Hov Johannes
Rombouts Krista
Ronca Vincenzo
Rudler Marika
Rydell Gustaf E.P.
Sandahl Thomas
Sandman Lisa
Sanduzzi-Zamparelli Marco
Sarrazin Christoph
Scheiner Bernhard
Sharma Rohini
Shawcross Debbie
Simao Andre
Staels Bart
Stamataki Zania
Stefanescu Horia
Strnad Pavel
Sturm Ekkehard
Takkenberg Bart
Tellez Luiz
Thiele Maja
Thursz Mark
Triantafyllou Evangelos
Trifan Anca
Trivedi Palak
Tushuizen Maarten
van Bommel Florian
van Grunsven Leo
Vanwolleghem Thomas
Verhelst Xavier
Verslype Chris
Villela-Nogueira Cristiane A
Wendon Julia
Zelber-Sagi Shira
Zipprich Alexander

EASL™ The Home of Hepatology

#EASLCongress

easlcongress.eu